Precision
Partnership
Purpose

Advancing
Cancer Science
to Save Lives
Globally

AACR American Association for Cancer Research

Annual Meeting

April 17-22, 2026

SAN DIEGO

SAN DIEGO CONVENTION CENTER

Proceedings

Sunday, April 19, 2026

: AACR Project GENIE: Predictive Models and AI
Poster Session

#0001 Synapse.org as a foundational platform supporting multicenter cancer data coordination, benchmarking, and broad community reuse.

Adam Taylor, Gaia Andreoletti, Robert Allaway, Jineta Banerjee, Orion Banks, Angie Bowen, Kevin Boske, Aditi Gopalan, Ashley Clayton, Xindi Guo, Savitha Sangameswaran, Amber Nelson, Aditya Nath, Milen Nikolov, Anh Nguyet Vu, Ziwei Pan, Alex Paynter, Chelsea Nayan, Thomas Yu, Bishoy Kamel, Serghei Mangul, Alberto Pepe, Luca Foschini, Susheel Varma

Sage Bionetworks, Seattle, WA

Collaborative cancer research requires a shared data infrastructure that functions across institutions, modalities, and funders. Synapse.org, developed by Sage Bionetworks, is a versatile public data platform used by research consortia, real-world data efforts, and computational challenges. We describe the use of Synapse to support diverse cancer research communities.
Synapse provides tools for validated metadata, provenance, versioning, and fine-grained access control. For supported communities we provide curation and validation apps, domain-specific portals, dashboards, and challenge frameworks. APIs and clients connect Synapse to local compute and trusted research environments (Cavatica, Terra, Pluto, SevenBridges CGC) via GA4GH DRS. Recent enhancements include human-guided, AI-powered curation, OpenSearch-based discovery, and natural-language data search. Data arrive through contributor uploads (web, CLI, APIs), programmatic ETL pipelines, and indexing of external repositories (GEO, dbGaP).. Curated datasets are indexed for discovery and surfaced through program portals. Community use and feedback guide curation priorities, maintaining a continuous improvement cycle.
The Synapse platform hosts >3.6 PB data used by >6,000 monthly users. The Cancer Complexity Knowledge Portal links 160 grants, 4,178 publications, 1,039 datasets, and 321 tools focused on cancer biology. The Human Tumor Atlas Network DCC manages 334 TB of harmonized omics data (0.23M files from 2,372 cases and 11,378 biospecimens across >60 diseases and 25 assays), with >2,500 annual users. The NF Data Portal integrates over 200 TB data from 312 neurology and oncology studies, and catalogues >1,100 tools spanning NF1, NF2, and schwannomatosis. As part of the coordinating center for AACR Project GENIE we have supported the ETL and sharing of clinico-genomic data from 19 centers, including 211,527 patients and 250,018 samples. DREAM cancer challenges run on Synapse have established benchmarks including in AML subtyping, prostate cancer survival, immunotherapy response and digital mammography. Independent Synapse users have contributed >1.2M public files (>95 TB) across 400+ cancer-related projects.
A user-friendly generalist data platform and a set of proven data coordination and challenge operations lower the activation energy for new cancer collaborations, from independent projects to large, multi-institutional networks. We invite researchers to explore Synapse.org and our data portals.
AI was used to summarize metrics and refine wording Authors reviewed and approved all content.

#0002 Variant interpretation web services for precision oncology: Genome Nexus and reVUE.

Xiang Li[1], Alexandria Dymun[1], Benjamin Preiser[1], Reshma Ramaiah[1], Allison Richards[1], Walid Chatila[1], Moriah Nissan[1], Amanda Dhaneshwar[2], Sara E. DiNapoli[3], Erika Gedvilaite[1], Thomas Y. Cong[4], Hongxin Zhang[5], Bryan Lai[1], Selcuk Onur Sumer[1], Aditi Gopalan[6], Tonatiuh Gonzalez[7], Madelaine Rangel[8], Trevor J. Pugh[9], Rose Brannon[1], Michael Berger[1], Debyani Chakravarty[1], Nikolaus Schultz[1], Jianjiong Gao[1], Ino de Bruijn[1]

[1]Memorial Sloan Kettering Cancer Center, New York, NY,[2]St. John's University, New York, NY,[3]Melanoma Research Alliance, New York, NY,[4]Massachusetts Institute of Technology, Cambridge, MA,[5]Oracle, New York, NY,[6]Sage Bionetworks, New York, NY,[7]Weill Cornell Grad. School of Medical Sci., New York, NY,[8]University of Rochester Medical Center, Rochester, NY,[9]UHN Princess Margaret Cancer Centre, Toronto, ON, Canada

Accurate interpretation of genomic alterations is essential for precision oncology, yet variant information remains dispersed across heterogeneous resources. To streamline access to high-quality annotations, we present recent advancements to Genome Nexus (genomenexus.org) and reVUE (cancerrevue.org), two complementary open-source web services that together provide an integrated ecosystem for interpreting both canonical and atypical cancer variants.

Genome Nexus aggregates functional, structural, population, and clinical evidence from a broad collection of cancer- and genome-focused databases. Through a unified API and intuitive interface, it harmonizes variant effect predictions, protein annotations, variant population frequencies, mutational hotspot and driver information, and clinical actionability from resources such as VEP, UniProt, Pfam, gnomAD, Cancer Hotspots, CIViC, OncoKB, and ClinVar. Recent enhancements include improved selection of canonical transcripts for routine clinical cancer care, expanded handling of transcript versioning, and optimized annotation performance. Genome Nexus enables high-throughput variant annotation, supports interactive browsing, and is integrated into cBioPortal and used by AACR Project GENIE.

A subset of genomic alterations exhibit variants with unexpected effects (VUEs), whose molecular consequences diverge from those predicted by standard annotation rules. These variants are frequently mis-annotated despite documented functional evidence in the literature. To address this gap, we developed reVUE, an open-source curated repository and API cataloging experimentally validated VUEs, including therapeutically relevant alterations in genes such as KIT, MET, ATM, EGFR, and BRCA1/2. The resource continues to expand, with several newly curated VUEs added across multiple cancer-associated genes. reVUE is fully integrated into Genome Nexus, ensuring that both predictable and atypical variant effects are captured within a unified interpretation workflow.

Together, Genome Nexus and reVUE advance the accuracy and completeness of cancer variant interpretation by consolidating diverse evidence sources, incorporating expert-curated annotations for complex variant classes, and providing scalable programmatic access. As open-source resources, they support transparent, reproducible, and extensible workflows that enhance precision oncology research and clinical reporting.

#0003 Evaluation of an agentic LLM chatbot for clinico-genomic analysis of AACR GENIE BPC data.

Likhita Thiriveedi, Kenneth L. Kehl

Dana-Farber Cancer Institute, Boston, MA

Purpose
The significant volume and complexity of genomic and clinical data can hinder efficient research based on clinico-genomic datasets, requiring manual effort and specialized expertise. Agentic large language model (LLM) workflows may help accelerate data processing, but the performance of existing LLMs for this task is not well-characterized.
Methods
An agentic large language model-based chatbot was developed to leverage the Gemini-2.5-pro LLM to interpret oncology research queries and autonomously execute sequential analytic tasks based on the AACR GENIE BPC NSCLC cohort (version 2.0 public). The LLM's performance was assessed against a curated benchmark set of 125 expert-reviewed clinical and genomic questions derived from a published study (https://pubmed.ncbi.nlm.nih.gov/37223888/), with accuracy defined as numerical concordance within ±10% of manuscript-reported reference values.
Results
The chatbot was used to ask 118 questions manually extracted from the publication, including questions broadly categorized as quantifying cohort sizes (n=92) or conducting statistical analyses (n=26). The overall accuracy rate was 42.37%. Inaccurate responses were manually reviewed and assigned to the following categories: no obvious source of error or discrepancy (33.8%), where 39.1% of these deviated < 20% from the reference value; chatbot reasoning faulty (36.8%); chatbot failed to clarify a concept in the user question (22.1%); reference publication analysis insufficiently specified to replicate (7.4%); user error in response to chatbot (4.4%); chatbot did not interpret analysis question as intended (1.5%); and unclear/other (1.5%).
Conclusion
Agentic LLM data analysis workflows hold potential for automating components of oncology data interpretation, but current performance limitations, attributable to inconsistent reasoning, incomplete clarification of clinical concepts, and a need for clear specification of published analysis plans for reproducibility and evaluation, highlight the need for further model refinement in these specific areas before these systems can be reliably integrated into real-world clinical research pipelines.

#0004 A multi-agent conversational artificial intelligence ecosystem for real-time integration of clinical, genomic, and social determinants of health data in colorectal cancer precision oncology.

Enrique Velazquez-Villarreal[1], Brigette Waldrup[2]

[1]Integrative Transaltional Sciences, City of Hope Comprehensive Cancer Ctr., Duarte, CA,[2]Integrative Translational Sciences, Beckman Research Institute, City of Hope, Duarte, CA

Introduction: The rapid expansion of clinical, genomic, and social determinants of health (SDoH) data has outpaced traditional analytic approaches, creating an urgent need for intelligent systems capable of integrating and interpreting complex oncology datasets at scale. To address this challenge, our team developed a suite of domain-specific conversational AI agents that enable real-time, natural language-driven exploration of multi-omic colorectal cancer (CRC) data. These agents facilitate discovery of population-specific molecular alterations and treatment-response patterns.

Methods: Each agent leverages fine-tuned biomedical LLaMA-3 models, a natural language-to-code interpreter, and a backend statistical engine linked to harmonized datasets from TCGA, AACR Project GENIE, and cBioPortal. The platform automates cohort creation, mutation profiling, survival analysis, odds ratio testing, and integration of clinical and SDoH variables. Specialized agents include AI-HOPE-PI3K, TGFβ, TP53, RTK-RAS, JAK-STAT, MAPK, WNT, and AI-HOPE-PM, the latter uniquely integrating clinical, genomic, and SDoH features. A core agent maintains data interoperability across the ecosystem. All analyses are triggered by plain-language prompts and return visual and narrative outputs within seconds.

Results:AI-agents successfully reproduced established clinical-genomic associations and uncovered novel, clinically meaningful insights. AI-HOPE-PI3K identified INPP4B mutations enriched in Hispanic/Latino early-onset CRC; AI-HOPE-TGFβ detected MSI-associated survival benefits in SMAD4-mutant tumors; and AI-HOPE-PM revealed worse survival in TP53-mutant CRC cases experiencing financial strain, along with differences in chemotherapy access linked to food insecurity. Additional agents identified prognostic variation across stage, treatment exposure, and demographic groups within MAPK, RTK-RAS, and WNT pathways. Accuracy exceeded 90% across use cases, with all analyses completed in real time without requiring programming expertise.

Conclusions: Multi-agent conversational artificial intelligence ecosystem provides a scalable, interoperable, and population-informed multi-agent architecture for precision oncology. Development of Agent-to-Agent (A2A) and Modular Collaborative Protocols (MCPs) will enable coordinated, cross-domain analysis and hypothesis generation, advancing a collaborative AI ecosystem for cancer research. By unifying clinical, molecular, and SDoH data under a conversational interface, AI-agents ecosystem introduces a new paradigm for data intelligence, accelerates biomarker discovery, and supports population-informed precision oncology across populations.

#0005 Artificial intelligence-driven precision medicine identifies prognostic WNT pathway alterations in African American colorectal cancer patients treated with FOLFOX.

Tsion Z. Minas[1], Brigette Waldrup[2], Francisco G. Carranza[2], Sophia Manjarrez[2], **Enrique Velazquez-Villarreal**[3]

[1]Department of Pathology, Johns Hopkins School of Medicine, Baltimore, MD,[2]Integrative Translational Sciences, Beckman Research Institute, City of Hope, Duarte, CA,[3]Integrative Translational Sciences, City of Hope Comprehensive Cancer Ctr., Duarte, CA

Background: African Americans (AA) experience disproportionate burden of colorectal cancer. Dysregulation of the Wingless-related integration site (WNT) and transforming growth factor-beta (TGF-β) pathways contributes to tumor progression, yet their prognostic roles in FOLFOX-treated CRC among AA patients remain understudied.
Methods: We analyzed 2,562 colorectal cancer cases stratified by ancestry, age at onset, and FOLFOX treatment using Fisher's exact, chi-square, and Kaplan-Meier analyses from AACR Project GENIE andcBioPortal databases. To enhance data integration and interpretation, we applied AI-HOPE and AI-HOPE-WNT/TGFβ, conversational artificial intelligence (AI) platforms designed to integrate clinical, genomic, and treatment data through natural language-driven queries.
Results: Overall survival analyses showed that early-onset AA patients treated with FOLFOX who had WNT pathway alterations experienced significantly better survival ($p = 0.035$). WNT pathway alterations were less frequent in late-onset AA patients treated with FOLFOX compared to those not treated (80% vs. 92%; $p = 0.05$). Similarly, TGF-β pathway alterations were reduced in late-onset non-Hispanic White (NHW) patients receiving FOLFOX compared to untreated cases (23% vs. 31%; $p = 0.0005$).
Conclusions: Chemotherapy exposure may influence pathway-specific mutation frequencies across ancestry and disease stage. AI-enabled integrative analyses highlight the potential of conversational AI platforms to accelerate biomarker discovery and reveal ancestry- and treatment-specific vulnerabilities in colorectal cancer.

#0006 Empowering populations at risk through conversational artificial intelligence: a framework for patient advocacy and precision oncology.

Araceli Estrada[1], Brigette Waldrup[2], Francisco G. Carranza[2], Sophia Manjarrez[3], **Enrique Velazquez-Villarreal**[4]

[1]Office of Science Policy and Government Affairs, AACR, Baltimore, MD,[2]Integrative Translational Sciences, Beckman Research Institute of City of Hope, Duarte, CA,[3]Beckman Research Institute of City of Hope, Duarte, CA,[4]Integrative Translational Sciences, City of Hope Comprehensive Cancer Ctr., Duarte, CA

Background:
Populations at risk for colorectal and other cancers continue to face barriers to equitable healthcare, including limited health literacy, fragmented communication, and underrepresentation in genomic research. Traditional approaches to patient engagement often overlook cultural and linguistic variety, leaving many patients without the knowledge or tools to fully participate in their care. To address this gap, we developed a Conversational AI-Patient Advocacy framework designed to help patients understand, access, and benefit from precision oncology in a personalized informed way.

Methods:
Built upon our validated AI-HOPE ecosystem, which has been successfully implemented and tested across several precision oncology research applications, this innovative platform functions as a digital patient advocate that integrates insights from the AACR Project GENIE database—a global cancer registry linking clinical and genomic data from all populations. Using natural language processing and explainable AI, the system translates complex cancer related questions into accessible, plain-language explanations, supports patient comprehension of diagnostics and treatment options, and connects users to advocacy and educational resources. The framework emphasizes empathy-driven dialogue, cultural adaptability, and accessibility for all populations, including those historically underrepresented in precision medicine.

Results:
Preliminary implementation using GENIE-derived datasets enabled population-level insights into cancer mutation patterns that were then translated into conversational narratives for patients. Early testing demonstrated improved understanding of genomic results, enhanced confidence in patient-provider communication, and increased engagement with advocacy resources and clinical trial information.

Conclusions:
Conversational AI-Patient Advocacy represents a new paradigm for virtual patient advocacy, combining patient education with precision oncology insights derived from large-scale databases like AACR GENIE. By acting as a virtual advocate, this technology empowers patients to navigate their care journey with clarity and trust—bridging the gap between complex cancer data and actionable understanding for all populations.

#0007 Molecularly-informed prediction of treatment efficacy in the GENIE BPC NSCLC cohort using computational reasoning.

Barbara Vodicska[1], Eniko Kispeter[1], Dora Lakatos[1], Gabor Gy Kalmar[1], Robert Doczi[1], Dora Gorog-Tihanyi[1], Anna Dirner[1], Reka Szalkai-Denes[1], William T. Beck[2], Arkadiusz Z. Dudek[3], Christophe Le Tourneau[4], Istvan Petak[1]

[1]Genomate Health, Cambridge, MA,[2]University of Illinois at Chicago, Chicago, IL,[3]Division of Oncology, Mayo Clinic, Rochester, MN,[4]Gustave Roussy, Villejuif, France

Background: Digital Drug Assignment (DDA) is a computational reasoning model that scores cancer therapies based on the complete molecular profile of a tumor, and stratifies them by predicted efficacy (Petak et al., 2021). In a prior study of 111 lung cancer patients, DDA-derived high-score molecularly targeted agents (MTAs) were associated with improved clinical outcomes (Dirner et al., 2025). Here, we extend this analysis to the GENIE BPC NSCLC cohort to assess the broader clinical validity of DDA.
Methods: From the GENIE BPC NSCLC cohort data available on Synapse, we included 1,078 patients with a single-sample genomic profile, available primary treatment data and survival outcomes (total 2,103 treatment lines, therapies included: afatinib, erlotinib, osimertinib, crizotinib, nivolumab, pembrolizumab, atezolizumab, bevacizumab+chemo, ramucirumab+chemo; and chemotherapy alone). DDA scores were generated for all cases, and the individual score of the administered MTAs (incl. immune checkpoint inhibitors) was used to stratify outcomes into low (<0), intermediate, and high DDA-score (≥1000) tiers. Progression-free survival (PFS, by imaging) and overall survival (OS) were analyzed using Kaplan-Meier statistics.
Results: Median PFS and OS differed significantly across DDA score tiers, increasing with higher scores (see table). Intermediate-tier drugs had similar mPFS values as chemotherapies (3.9 vs 4.2 months). Six-month PFS and twelve-month OS rates increased with DDA-tiers and were all significantly different by χ^2 test. DDA-high therapies provided greater benefit across treatment types than lower-score counterparts.
Conclusions: Across a large, real-world NSCLC cohort, DDA effectively distinguished therapies with higher clinical efficacy based on the full molecular profile of each patient. These results reinforce the potential of DDA to enhance personalized treatment selection based on NGS diagnostics in precision oncology.

	DDA-low	DDA-intermediate	DDA-high	Statistical test	Chemo
mPFS (months)	1.7 (n = 72)	3.9 (n = 303)	5.1 (n = 554)	log-rank p<0.0001; HR high vs low = 0.52	4.2 (n = 709)
mOS (months)	9.0 (n = 74)	16.2 (n = 327)	23.3 (n = 601)	log-rank p<0.0001; HR high vs low = 0.49	23.5 (n = 1094)
6-month PFS rate	14%	28%	40%	X^2 p<0.0001	25%
12-month OS rate	36%	53%	63%	X^2 p<0.0001	65%

#0008 Using *in vitro* models to predict imatinib responses in PDGFRA-mutant gastrointestinal stromal tumor.

Homma M. Khosroyani[1], Alina Teuber[2], Ajia Town[1], Lillian Klug[1], Denisse Evans[3], Jerry Call[3], Sara Rothschild[3], Neeta Somaiah[4], Prapassorn Thirasastr[4], Ping Chi[2], Marion Liu[2], Peter Hohenberger[5], Piotr Rutkowski[6], Patrick Schoffski[7], Abbas Agaimy[8], Mehdi Brahmi[9], Carol Beadling[10], Sebastian Bauer[11], Johanna Falkenhorst[11], Michael C. Heinrich[1]

[1]Portland VA Health Care System and OHSU Knight Cancer Institute, Portland, OR,[2]Memorial Sloan Kettering Cancer Center, New York, NY,[3]Life Raft Group, Wayne, NJ,[4]UT MD Anderson Cancer Center, Houston, TX,[5]Mannheim University Medical Center, Mannheim, Germany,[6]Maria Sklodowska-Curie Memorial Cancer Center and Institute of Oncology, Warsaw, Poland,[7]KU Leuven Cancer Center, Leuven, Belgium,[8]University of Erlangen, Erlangen, Germany,[9]Centre Leon Berard, Lyon, France,[10]Knight Diagnostic Laboratories- OHSU Knight Cancer Institute, Portland, OR,[11]West German Cancer Ctr., Essen, Germany

Gastrointestinal stromal tumor (GIST) is the most common sarcoma, and 85% of cases harbor mutations in KIT or PDGFRA receptor tyrosine kinases. Imatinib (IM), a type II TKI, can treat many KIT-mutant GIST, but not GIST with the most common PDGFRA mutation, exon 18 D842V. D842V is resistant to all type II TKIs. Avapritinib (AVA), a type I TKI, was developed and is FDA-approved for all PDGFRA exon 18 mutant GIST but is costly and has severe cognitive side effects in some patients. AVA is also not widely available outside the United States, leaving many exon 18 mutant GIST patients without treatment options. However, limited clinical evidence reports the usage of IM to treat non-D842V exon 18 mutations. As IM is a more tolerable, cost-effective, and accessible drug than AVA, utilizing IM therapy in certain cases would provide treatment for those who cannot access or tolerate AVA. As it is not feasible to model every observed mutation, we utilized *in vitro* models to predict exon 18 mutations that could be treated with IM. Through collaboration and AACR GENIE, we curated a cohort of 1000+ PDGFRA-mutant GIST. 66% had D842V while the remaining had non-D842V point mutations and complex in/dels. Strikingly, 78% of mutations involved the D842 residue, which plays a key role in the autoinhibition of PDGFRA, and mutations like D842V disrupt this. As nearly every single amino acid substitution at the 842-residue was observed in our cohort, we hypothesized that the characteristics of the 842-position amino acid determine IM sensitivity and will predict treatment responses for any exon 18 mutation. To test our hypothesis, we used Ba/F3 and CHO cells to express every possible D842X and D842_D846delinsX mutation. This 4-residue deletion was the most common in/del in the cohort; therefore, we chose to profile this mutation backbone as well. IM sensitivity was determined by calculating an IC_{50} value using immunoblotting for phosphorylated and total PDGFRA. We observed similar trends in IM sensitivity depending on the class of amino acid at the 842-position, with little difference between D842X and D842_D846delinsX mutant kinases. Seven out of eight hydrophobic residues conferred IM resistance while amino acids from other classes (polar, +/- charged, special case) conferred IM sensitivity/intermediate sensitivity. Notably, alanine conferred IM sensitivity, different than the other hydrophobic substitutions and *in silico* modeling revealed how the side chain structure at the 842-position affects IM binding/activity. Lastly, we determined that our results are concordant with first-line IM response data, as patients with predicted IM-sensitive mutations experienced a longer median progression-free survival than those with predicted or known IM-resistant mutations (30 vs 4 months, $p < 0.0001$). Our work highlights an approach to optimize clinical guidelines for the TKI treatment for PDGFRA-mutant GIST based on specific patient mutations.

#0009 ShinyEvents: Harmonizing real-world longitudinal data for clinical insights and survival analytics.

Alyssa Obermayer[1], Joshua Davis[2], Roger Li[3], Rodrigo Rodrigues Pessoa[3], Brandon J. Manley[3], G. Daniel Grass[3], Aik Choon Tan[4], Dung-Tsa Chen[3], Timothy Shaw[3]

[1]Biostatistics and Bioinformatics, H. Lee Moffitt Cancer Center & Research Institute, Tampa, FL,[2]H. Lee Moffitt Cancer Center & Research Institute, Hudson, FL,[3]H. Lee Moffitt Cancer Center & Research Institute, Tampa, FL,[4]University of Utah Huntsman Cancer Institute, Salt Lake City, UT

Background: Harmonizing patient longitudinal data is critical to uncovering variables and events that can influence outcomes or molecular data, yet existing tools have significant limitations in integrating multilayered time-series data, particularly in linking treatment events with survival outcomes. Due to their observational nature, real-world data (RWD) can be comprehensive and heterogeneous, posing a challenge when visualizing and interpreting the data. We developed ShinyEvents, an open-source tool and application to facilitate interaction and exploration of longitudinal data, which we demonstrate in the application of the AACR Project GENIE a global consortium that pools real-world cancer genomic and clinical data to advance precision oncology.

Methods: ShinyEvents is a web-based framework that allows users to upload longitudinal data and generate interactive patient timelines to view clinical events and perform cohort-level analyses through treatment clustering and endpoint assignment. The tool provides informative cohort visualizations, such as a Sankey diagram of the treatment line, swimmer diagrams of the clinical course and treatment duration, as well as heatmaps to view unsupervised clustering on patient treatments. Our tool can infer real-world progression-free survival (rwPFS) based on user-defined endpoints and perform Kaplan-Meier and Cox proportional hazards regression analysis. We incorporated the AACR Project GENIE data on non-small cell lung cancer (NSCLC) and colorectal cancer (CRC) into a dedicated wed instance to visualize and interact with the data. The application is publicly accessible at the following link: https://shawlab-moffitt.shinyapps.io/ShinyEvents_AACR_GENIE/.

Conclusions: ShinyEvents provides a unified framework integrating longitudinal real-world data with survival analytics to facilitate transparent and reproducible collaboration between clinicians and data scientists. Based on the GENIE data, the tool is able to provide dynamic longitudinal visualization on the patient treatment regimen and relate back to the molecular data by identifying complexities surrounding sample collection in relation to treatment regimens. This standardized approach to RWD analysis will facilitate additional collaboration across the global GENIE network.

#0010 A continuous modeling framework for age-dependent selection on melanoma driver mutations.

Yihan Liu[1], Moein Rajaei[1], Jeffrey D. Mandell[1], Jorge Alfaro-Murillo[2], Jeffrey P. Townsend[1]

[1]Yale University, New Haven, CT,[2]Universidad de Costa Rica, San Jose, Costa Rica

Aging is a major risk factor for melanoma, yet whether age alters tumor evolution by altering mutation rates, the strength of selection on drivers—or both—has not been investigated. We developed a continuous age-selection modeling framework that estimates strength of selection as a function of patient age from large-scale sequencing data. Using whole-exome (TCGA) and targeted-panel (AACR Project GENIE) data from 5,472 melanomas, we inferred neutral mutation rates from synonymous substitution counts and mutational covariate data within <40, 40-59, and ≥60 year age groups, calibrating site-specific rates within each tumor using COSMIC mutational signatures. Age-dependent selection on individual variants was then modeled within a shared Poisson-likelihood framework using three parametric forms—linear, logistic, and generalized sigmoid—allowing flexible continuous relationships between age and the strength of selection. Model fits were evaluated by likelihood-ratio tests. To quantify uncertainty, we used adaptive Metropolis-Hastings sampling around the maximum-likelihood estimates to build likelihood-ratio-based confidence intervals and to estimate the posterior probability that the inferred age effect reverses direction. Applied to melanoma, neutral mutation rates rose modestly with age, and UV-associated signatures dominated at all ages, but endogenous processes (SBS1, SBS3) increased in older tumors. In contrast, this framework revealed strongly age-dependent and variant-specific selection: BRAF V600E exhibited a steep, continuous decline in selection with age; NRAS Q61 substitutions showed the opposite pattern, with increasing selection in older patients; and TERT-promoter mutations (C228T, C250T) became more frequent yet conferred weaker selective advantage with age. Gene-level analyses of TP53, PTEN, and CDKN2A revealed monotonic declines in selection, consistent with convergently lower oncogenicity in late-life tumors. At BRAF codon 600, single- and double-base substitutions (DBS) producing V600E provided similar selective benefits, despite the rarity of DBS events, whereas the DBS variant V600K showed increasing selection with age. Together, these results demonstrate that age shapes the somatic evolution of melanoma primarily through age-dependent selection rather than mutation supply or identity, mechanistically tying the differing burdens of BRAF- versus NRAS-driven disease across the lifespan to the differential state of aging tissues and providing a framework for age-aware cancer prevention, molecular testing, and therapeutic strategies.

#0011 Artificial intelligence-based spatial analysis of the local tumor microenvironment in relation to c-MET expression in non-small cell lung cancer.

Ji-Hyang Lee[1], Joshua Littrell[2], Chiyoon Oum[1], Taebum Lee[1], Sanghoon Song[1], Yoojoo Lim[1], Chang Ho Ahn[1], Jim Christian[2], Seokwhi Kim[3], Siraj M. Ali[1]

[1]Lunit, Seoul, Korea, Republic of,[2]Agilent Technologies, Inc., Carpinteria, CA,[3]Department of Pathology, Ajou University School of Medicine, Suwon, Korea, Republic of

Introduction: MET is a well-known oncogenic driver that confers various genomic aberrations. Recent approval of antibody drug conjugates has expanded therapeutic options for c-MET expressing non-small cell lung cancer (NSCLC). However, the relationship between MET expression, tumor microenvironment (TME), and immunotherapy response remains unclear. This study explores the association between c-MET expression and spatial TME features in NSCLC to better understand its immunologic behavior.
Methods: This study analyzed a total of 25,674 NSCLC samples from various cohorts, including AACR GENIE, TCGA, Ajou University Medical Center (AUMC), and Agilent Technologies. AI-powered analyzers (Lunit SCOPE IO and SCOPE uIHC) were previously developed using 19,112 H&E and 4,638 IHC whole slide images of 25 cancer types, stained with over 20 different antibodies. These platforms enabled the quantitative assessment of both the TME, and subcellular expression levels detected by IHC staining.
Results: MET alterations occurred in 27 (2.9%) of TCGA and 909 (3.8%) of GENIE, including exon 14 skipping (n=388, 1.5%), amplification (n=380, 1.5%), and others (n=223, 0.9%). MET-altered tumors had higher MET RNA expression compared with wild-types (median: 0.4 vs. -0.2, $p<0.001$). TME analysis of samples with high (Z-score ≥2) and low RNA expression showed no significant difference in tumor-infiltrating lymphocyte (TIL) density (/mm^2, median: 851 vs. 673, $p=0.46$). In 640 pairs of H&E and IHC slides from AUMC and Agilent, c-MET positive (3+, ≥50%) samples tended to have lower TIL density across the whole slide compared to c-MET negative samples (median, AUMC, 78.5 vs. 79.2, $p=0.16$; Agilent, 80.6 vs. 211.3, $p=0.23$, respectively). This trend became significant with cell and subcellular spatial analysis. The density of TIL was markedly reduced within 30um of tumor cells exhibiting strong (3+) c-MET expression (median:85.5 vs. 121.6, $p<0.001$; 132.2 vs. 162, $p=0.013$, respectively). Notably, a similar reduction in TIL density was also observed around tumor cells with membrane-specific c-MET expression (median: 106.6 vs. 122.3, $p<0.001$; 144.9 vs. 165.8, $p=0.002$, respectively).
Conclusion: Spatial analysis of IHC demonstrated sparse immune cells near tumor cells with strong c-MET expression or membrane-specific localization. These findings suggest a mechanistic link between c-MET overexpression and immune evasion, indicating the potential benefit of combining MET-targeted and immunotherapy.

#0012 Integrative spatial multi-omics profiling enhanced by artificial intelligence reveals ancestry-associated molecular features in early-onset colorectal cancer among Southern California patients.

Francisco G. Carranza, Brigette Waldrup, Yuxin Jin, Yonatan Amzaleg, David Craig, John Carpten, PE-CGS Network, Enrique I. Velazquez Villarreal

Department of Integrative Translational Sciences, City of Hope National Medical Center, Duarte, CA

Introduction: Colorectal cancer (CRC) is the third most common malignancy and the second leading cause of cancer-related mortality worldwide. Although overall CRC incidence has stabilized in many high-income countries, early-onset CRC (EOCRC; <50 years) continues to rise. This increase is especially noticeable in our catchment area, the greater Los Angeles, CA region. Despite this trend, little is known about this population at risk, limiting insight into ancestry-associated biological factors and tumor microenvironment (TME) features.
Methods: A total of 2,730 colorectal cancer (CRC) tumor samples were analyzed from patients in our NIH Cancer Moonshot COPECC PE-CGS Network and from public data repositories, including the AACR Project GENIE database. High-resolution spatial transcriptomics (10x Genomics Visium HD), together with whole-exome sequencing (WES) and RNA sequencing (RNA-seq), was used to assess regional gene expression patterns. Compartment-specific signatures were quantified using SpaCET, focusing on CRC-related genes and pathways. Clinical and molecular datasets were harmonized and analyzed through an AI-driven multi-omics platform, enabling natural-language-based exploration of genomic, transcriptomic, and clinical features.
Results: EOCRC tumors showed a high median genetic similarity to the 1000 Genomes Peruvian-in-Lima (1KG-PEL) reference population. Key CRC-associated mutations were more frequent in EOCRC, particularly among patients with stronger 1KG-PEL-like similarity. Integrated analyses revealed ancestry-associated differences in gene expression between EOCRC and late-onset CRC within the catchment cohort. Spatial transcriptomics demonstrated marked variation in pathway activity across malignant, immune, and stromal regions, with EOCRC displaying distinct compartment-specific patterns.
Conclusions: EOCRC in populations from our catchment area is defined by ancestry-associated genomic alterations and notable spatial heterogeneity in CRC-relevant pathways. These findings underscore the importance of ancestry-informed CRC molecular profiling to advance precision oncology.

#0013 Integrating transcriptomic data to improve multi-omic tumor-of-origin classification.

Pranav Gadde, Naga Mudda, Pratayanch Sav, Krithik Senthilkumar, Aadarsh Sivaraman, Krithik Mudda

Illinois Mathematics and Science Academy, Aurora, IL

Background: Cancers of Unknown Primary (CUP) make up approximately 2-5% of malignancies with a poor prognosis due to empirical therapy. Existing genomic classifiers only have approximately 60-75% accuracy. The AACR Project GENIE consortium and database provide large-scale and real-world genomic data, but there are currently no integrated transcriptomic features with AACR GENIE data. We hypothesized that developing a validated multi-omic framework on TCGA data could create an approach for integrating transcriptomic data into GENIE, with the expected outcome of improving the precision of the tumor-of-origin classification.
Method: We examined a cohort of 1,556 solid tumors from the TCGA PanCancer Atlas, via cBioPortal, across four cancer types: COAD (n=76 test), HNSC (n=103), LUAD (n=102), and READ (n=31). Two XGBoost classifiers were trained (80/20 held-out split) with SMOTE: (1) Genomic-Only baseline classifier (Tumor Mutation Burden, MSI Score, Aneuploidy Score) and (2) Multi-Omic (same genomic features plus 20,506 RNA-Seq genes). Performance was evaluated on a held-out test set (n=312).
Results: The Multi-Omic classifier achieved 93.0% accuracy compared to 52.2% for the Genomic-Only classifier (40.7% improvement). Per-class F1 scores were: COAD=0.86, HNSC=1.00, LUAD=1.00, and READ=0.58. The baseline classifier demonstrated near random performance (COAD F1=0.50 and READ F1=0.33). A feature importance analysis also confirmed known lineage markers as the top predictive features, KRT5 (9.2% importance, HNSC squamous marker), SFTPB (6.1% importance, LUAD lung surfactant), GPA33 (2.9% importance, COAD/READ intestinal marker), CDX1 (2.7% importance, intestinal transcription factor), HOXB13, NAPSA, and EVX2, therefore demonstrating meaningful biological pattern recognition.
Conclusions: Multi-omic integration significantly increases tumor-of-origin classification compared to genomic methods. Its reliance on established, tissue-specific biomarkers provides biological validity critical for diagnostics. READ performance was lower (F1=0.58) due to the limited number of samples and the similarity to COAD. Overall, the framework showed good discrimination across other cancer types. This TCGA proof-of-concept establishes a validated pipeline for expanding to 15-20 cancer types using the AACR Project GENIE, helping advance clinical diagnosis of CUP and precision oncology.

#0014 Mutational profiling of chondrosarcoma across multicenter cohorts.

Luyuan Li[1], Wensi Tao[2], Robert L. Walker[3], Manish KC[1], Darshan Gundala[2], Josiane E. Eid[3], Zhenfeng Duan[3], Jonathan C. Trent[3]

[1]North Alabama Medical Center, Florence, AL,[2]Nova Southeastern University Dr. Kiran C. Patel College of Osteopathic Medicine, Fort Lauderdale, FL,[3]University of Miami Miller School of Medicine, Miami, FL

Background: Molecular therapies for chondrosarcomas remain limited, in part due to the rarity of these cancers, which hampers efforts at broad genomic characterization. The establishment of large, standardized, multicenter databases, such as the AACR Project GENIE, along with subsequent individual studies, has begun to assemble an extensive mutational profile of this disease. This abstract provides a preliminary analysis of the mutational data from these studies.

Methods: The GENIE Cohort v18.0, MSK Nature Communications Sarcoma 2022, and UCLA Cell 2024 sarcoma datasets, accessed via cBioPortal, were collated and analyzed. These datasets included patient information for conventional chondrosarcoma (CS), dedifferentiated chondrosarcoma (DDCS), and mesenchymal chondrosarcoma (MCS). Available data included patient age, sex, race, mutational profiles, and, for CS and DDCS, survival outcomes.

Results: In total, the datasets encompassed 518 patients with chondrosarcoma: 428 CS, 38 DDCS, and 52 MCS. The average age at biopsy was 52 for CS patients, 63 for DDCS patients, and 33 for MCS patients. Women comprised 40.4%, 54.1%, and 55.8% of CS, DDCS, and MCS patients, respectively. Among patients with recorded race, the racial distribution was 74% White, 5% Black, 10% Asian, and 12% Other for CS; 89% White, 5% Black, 3% Asian, and 3% Other for DDCS; and 83% White, 13% Black, and 4% Other for MCS. The average mutation count per patient sample was 10.1 for CS, 5.4 for DDCS, and 2.6 for MCS. The top five most frequently mutated genes for each disease were as follows - CS:*TP53* (124/439), *IDH1* (113/437), *IDH2* (35/423), *KMT2D* (15/186), and *TERT* (14/179); DDCS:*TP53* (24/40), *IDH1* (18/40), *TERT* (13/38), *IDH2* (12/40), *FLT4* (8/40); MCS: *MAP3K13* (5/18), *INSR* (4/17), *SDHA* (5/23), *KMT2D* (4/24), and *KMT5A* (2/13). Median overall survival was 58 months for CS patients versus 25 months for DDCS patients. Notably, many of the most frequently mutated genes beyond *TP53*, *IDH1*, and *IDH2* are involved in chromatin regulation and genomic stability (*KMT2A*, *KMT2D*, *TERT*, etc.), and these mutations are more common in DDCS.

Conclusion: This multicenter mutational analysis confirms that, after *TP53*, the most frequently mutated genes in CS and DDCS are *IDH1* and *IDH2*. Mutations in genes involved in chromatin regulation and genomic stability are more prevalent in DDCS, which may contribute to its increased aggressiveness. These findings support ongoing efforts to target these pathways in chondrosarcoma.

: DNA Damage and Repair 1
Poster Session

#0230 AZD4956, a potent and selective inhibitor of DNA polymerase theta, enhances the activity of DNA-damaging agents in HRR defective cellular backgrounds and improves efficacy of the new generation PARP1-selective inhibitor, saruparib.

Josep V. Forment[1], Lee Mulderrig[1], Christelle de Renty[1], Harriet Southgate[1], Gemma Jones[2], Martina Gesu[3], Rebecca Sargeant[3], Daniel Sutton[3], Lenka Oplustil O'Connor[4], Susan Critchlow[1], Sabina Cosulich[5]

[1]Oncology Targeted Discovery, AstraZeneca R&D, Cambridge, United Kingdom,[2]Cancer Biomarker Development, AstraZeneca R&D, Cambridge, United Kingdom,[3]Clinical Pharmacology and Safety Sciences, AstraZeneca R&D, Cambridge, United Kingdom,[4]Oncology Translational Medicine, AstraZeneca R&D, Cambridge, United Kingdom,[5]Early Oncology Programs Group, AstraZeneca R&D, Cambridge, United Kingdom

Introduction: Loss-of-function mutations in the tumour suppressors *BRCA1*/*BRCA2* inactivate the homologous recombination repair (HRR) pathway, driving genomic instability and cancer progression but conferring sensitivity to DNA double-strand break–inducing agents such as platinum salts and poly(ADP-ribose) polymerase inhibitors (PARPi). *BRCA1*/*BRCA2* mutations are frequent in ovarian, breast, pancreatic, and prostate cancers, underpinning approvals of PARPi in these settings. Despite strong activity in HRR-defective tumours, PARPi responses vary and resistance emerges. Attempts to boost efficacy by combining PARPi with other DNA damage response inhibitors have been limited by enhanced myelosuppression, constraining dose intensity and benefit.**Results:** AZD4956 is a novel, potent, and selective inhibitor of the polymerase activity of DNA polymerase theta (Polθ), a key effector of microhomology-mediated end joining—a repair pathway critical when HRR is compromised. Combining AZD4956 with the PARP1-selective inhibitor saruparib improves efficacy versus either agent alone across HRR-defective cellular backgrounds, with no activity in HRR-proficient settings. Enhanced efficacy correlates with increased genomic instability: in HRR-deficient cells, the combination produces a ~4-fold rise in chromosomal aberrations. AZD4956 also potentiates other DNA-damaging agents (e.g., cisplatin, TOP1 inhibitors) specifically in HRR-deficient lines.AZD4956 shows single-agent *in vitro* activity in the low-nanomolar range in cell lines with *PALB2*, *BRCA2*, and *RAD51C* mutations, like PARPi, but no single-agent activity in *BRCA1*-mutant cells. *In vivo*, AZD4956 monotherapy yields modest tumour growth inhibition (TGI ~50–80%) in some *BRCA2* and *PALB2* mutant models. By contrast, AZD4956 (≥10 mg/kg BID) combined with the maximal efficacious mouse dose of saruparib (1 mg/kg QD) consistently outperforms either monotherapy. Increased efficacy aligns with pharmacodynamic modulation: the combination drives an average ~2-fold increase in micronuclei in red blood cells versus monotherapy. Combination activity is observed in both *BRCA1*- and *BRCA2*-mutant patient-derived xenografts from diverse tissues (breast, prostate) and is restricted to HRR-deficient models where PARPi alone confers some TGI. Notably, maximal combination benefit requires the maximal efficacious saruparib dose.**Conclusions:** Preclinical pharmacology supports AZD4956 selectivity and its potential to amplify antitumour activity when combined with PARPi in HRR-defective cancers. AZD4956 is being evaluated in PARTHENON, a first-in-human, open-label, multicentre, phase 1/2a study of AZD4956 plus saruparib in patients with HRR-deficient solid tumours.

#0231 Polymerase iota drives aberrant mitotic DNA synthesis and replication stress in BRCA2 deficient human mammary epithelial cells.

Kavya Vipparthi[1], Ariana Bellare[2], Resul Ozbilgic[1], **Mihriban Karaayvaz**[1]

[1]Cancer Sciences, Cleveland Clinic, Cleveland, OH,[2]Biochemistry, Case Western Reserve University, Cleveland, OH

Germline mutations in *BRCA2* greatly increase breast cancer risk, yet the early molecular events preceding tumor initiation remain incompletely defined. Prior work shows that mammary epithelial cells with compromised BRCA2 function, including cells from mutation carriers, exhibit replication-associated genome instability. Here, we investigated the role of polymerase iota (Pol ι), an error-prone translesion polymerase upregulated in breast cancer and linked to replication stress.Using primary human mammary epithelial cells (HMECs) from *BRCA2* mutation carriers and *BRCA2*-silenced MCF10A cells, we found that loss of BRCA2 augments Pol ι expression at both mRNA and protein levels. We demonstrate that Pol ι is required for mitotic DNA synthesis (MiDAS), a compensatory pathway engaged when DNA under-replication persists into mitosis. Pol ι silencing significantly reduced MiDAS in BRCA2-silenced cells, but not in wild-type cells, revealing a context-specific dependency on Pol ι for completing mitotic replication.Unexpectedly, silencing Pol ι in BRCA2-silenced cells *reduced* chromosomal breaks, 53BP1 bodies, and micronuclei, lesions typically associated with impaired MiDAS. Moreover, Pol ι loss markedly decreased replication stress markers, including phosphorylated γH2AX and RPA. These findings indicate that Pol ι -mediated MiDAS in the setting of BRCA2 deficiency is not protective but instead amplifies replication stress and genome instability.Our results uncover a previously unrecognized regulatory interaction in which BRCA2 restrains Pol ι, and loss of this restraint permits aberrant Pol ι -driven MiDAS that exacerbates genome instability. This work identifies Pol ι as a potential early intervention target for reducing replication stress in individuals carrying *BRCA2* mutations.

#0232 IDE034, A bispecific antibody-drug conjugate co-targeting PTK7 and B7-H3, exhibits avidity-driven selectivity and enhanced antitumor activity versus mono-specific ADCs.

Diana M Munoz Delgado[1], Ying Zhu[2], Yanan Guo[2], Yuelei Shen[2], Peiran Li[2], Reeja Maskey[1], Pei Xin Lim[1], Megan Conway[1], Marcus M. Fischer[1], Vidhya Nagarajan[1], Arjun A. Rao[1], Christian Frey[1], Yuchen Bai[1], Paul A. Barsanti[1], Claire Neilan[1], Mike A. White[1]

[1]IDEAYA Biosciences, South San Francisco, CA,[2]Biocytogen, Beijing, China

IDE034 is a humanized IgG1 bispecific antibody-drug conjugate (bsADC) that co-targets protein tyrosine kinase 7 (PTK7) and B7-homolog 3 (B7-H3), two tumor-associated antigens broadly expressed across refractory solid tumors but largely absent from normal tissues. Dual-antigen engagement by IDE034 is designed to enhance tumor cell-specific binding, avidity-driven internalization, and intracellular payload release relative to monospecific ADCs, thereby maximizing tumor payload exposure while minimizing normal tissue uptake. IDE034 binds human and cynomolgus PTK7 and B7-H3 with sub-nanomolar affinity and shows no cross-reactivity with other B7-family members. In dual-antigen-positive tumor cells, IDE034 exhibits saturable co-binding and superior internalization kinetics compared with B7-H3- or PTK7-monospecific ADCs. Target-dependent intracellular release of its topoisomerase I inhibitor (TOP1i) payload induces S-phase enrichment, G_2/M arrest, and apoptosis, with bystander cytotoxicity. *In-vivo*, IDE034 produced rapid and durable tumor regressions across PTK7/B7-H3 co-expressing xenograft models and consistently outperformed monospecific comparators. Because poly(ADP-ribose) glycohydrolase (PARG) is essential for resolving TOP1-DNA cleavage complexes, its inhibition has emerged as a strategy to amplify TOP1i-induced DNA damage. The clinical-stage PARG inhibitor IDE161 enhances accumulation of TOP1-DNA crosslinks and replication stress, resulting in deep and durable responses when combined with TOP1 inhibition. The combination of IDE034 with IDE161 reproduced the enhanced antitumor activity observed with TOP1 inhibitors, demonstrating that blockade of PARG-dependent DNA repair can maximize the therapeutic benefit of bispecific TOP1i-ADC-mediated DNA damage. By coupling dual-antigen recognition with a cleavable, membrane-permeable TOP1i payload, IDE034 has the potential to broaden the therapeutic window and address intratumoral heterogeneity. Given the reported frequency of detection of B7H3 and PTK7 protein expression across numerous tumor samples, double positive disease is anticipated to be prevalent in colorectal, non-small cell lung, and breast cancers. Together, these findings support IDE034 as a potential first-in-class bispecific TOP1i-ADC with broad opportunity across disease indications as a monotherapy and in combination with IDE161.

#0233 Preclinical development of EIK1005, a potent and selective inhibitor of Werner helicase.

Fernando Rodriguez Perez[1], Danny Murnock[2], Juanita Ezemba[2], Tamer Ahmed[2], Jose Ortega[1], Huntly M. Morrison[1], Rafael Miranda[1], Taylor Heuer[2], Stephen Jones[2], Brenda Smith[1], Ali Tabatabaei[1], Stephen Basham[1], Melissa Dumble[2], **Marcus P. Kelly**[2]

[1]Eikon Therapeutics, Millbrae, CA,[2]Eikon Therapeutics, New York, NY

The RecQ Werner (WRN) helicase plays a critical role in DNA repair and genomic stability and has been identified as a promising synthetic lethal target in microsatellite instability-high (MSI-H) cancers. Here we present preclinical cellular and in vivo data demonstrating the potent and selective activity of WRN inhibitor EIK1005 across multiple MSI-H cancer models. EIK1005 potently inhibited the biochemical activity of WRN (IC_{50} = 30 nM), with no activity against BLM and other related RecQ helicases. In MSI-H HCT116 cells, EIK1005 induced DNA damage (EC_{50} = 90 nM) that correlated with significant anti-proliferative effect (EC_{50} = 28 nM). Mechanistic studies using our cellular Single Molecule Tracking platform revealed that EIK1005 potently decreased WRN motion, traps WRN on chromatin and promotes WRN degradation, illustrating robust target engagement. No effects of EIK1005 could be measured in microsatellite stable cell lines. EIK1005 has robust pharmaceutical properties including high bioavailability across preclinical species and dose proportional PK. As such, EIK1005 was tested in several mouse models of cancer. In HCT116 xenografted mice, once-daily oral dosing of EIK1005 at 15 and 30 mg/kg induced tumor regression of 48.7% and 47.6%, respectively. In RKO and IGROV-1 MSI-H models that are less sensitive to WRN inhibition, EIK1005 showed dose-dependent tumor growth inhibition across the 30, 90 and 180 mg/kg dose levels assessed. Robust dose-dependent pharmacodynamic activity of EIK1005 was observed in the HCT116 and RKO tumor models, with significant degradation of WRN protein (~ 70%, 8 h post dosing) observed at 15 and 90 mg/kg EIK1005 dose levels respectively. EIK1005 also mediated consistent elevation of DNA damage response markers in these models. A significant increase in GDF-15 was observed in vitro and in mouse plasma following EIK1005, suggesting GDF-15 elevations as a possible peripheral biomarker of WRN inhibition. The pharmacodynamic changes observed at the 15 and 90 mg/kg dose levels correlated with robust and dose responsive plasma concentrations. Further studies elucidated several mechanisms of potential resistance to WRN inhibition. Overall, our preclinical characterization of EIK1005 demonstrates its strong activity and favorable pharmacologic profile that provide impetus to the ongoing clinical development of EIK1005 in patients with MSI-H cancers.

#0234 Proteomic profiling of FEN1 inhibition by BSM-1516 reveals chromatin-associated biomarkers for preclinical pharmacodynamic evaluation.

Jason Munguia[1], Sanjay Agarwalla[1], Dave Martin[1], Junhua Fan[1], Jack Schultz[2], Celeste Giansanti[2], David Cortez[2], David Puerta[1], Zachary Zimmerman[1], **Konstantin Taganov**[1]

[1]Blacksmith Medicines, San Diego, CA,[2]Vanderbilt-Ingram Cancer Center, Vanderbilt University, Nashville, TN

Flap endonuclease 1 (FEN1) is a structure-specific metallonuclease essential for Okazaki fragment maturation and DNA repair. We previously reported the discovery of BSM-1516, a potent and selective small-molecule FEN1 inhibitor that synergizes with PARP-targeted and other DNA damage response therapies and exhibits favorable in vivo pharmacokinetic properties. Pharmacologic inhibition of FEN1 increases its chromatin association, induces poly(ADP-Ribosyl)ation and ssDNA gaps, and is selectively cytotoxic to cells with homologous recombination deficiency. To characterize chromatin protein dynamics following FEN1 inhibition and identify potential pharmacodynamic (PD) biomarkers of target engagement, we employed isolation of Proteins On Nascent DNA (iPOND) coupled to mass spectrometry in proliferating cells treated with BSM-1516, alone or in combination with olaparib. FEN1 inhibition reproducibly enriched replication and DNA repair proteins, including FEN1, PARP1/2, LIG3, XRCC1, and CHD1L, reflecting PARP-dependent engagement of an alternative Okazaki fragment maturation pathway that was abrogated by co-treatment with olaparib. Orthogonal assays for chromatin-bound proteins confirmed selective enrichment of several iPOND-identified hits, establishing tractable PD biomarker candidates. Collectively, these findings delineate a proteomic signature of FEN1 inhibition at the replication forks and lay the groundwork for ongoing in vivo studies assessing these markers as indicators of target engagement in preclinical models.

#0235 Cellular comparison of a covalent and non-covalent WRN inhibitor reveals shared and unique response biomarkers.

Gerarda van de Kamp, Daphne J. F. Kluitmans, Tsang W. Lam, Jeroen A. D. M. de Roos, Janneke J. T. M. Melis, Jeffrey J. Kooijman, **Jorg C. J. Benningshof**

Oncolines B.V., Oss, Netherlands

Werner Syndrome ATP-dependent helicase (WRN) is crucial for preserving genome integrity through its involvement in key cellular processes such as DNA repair and DNA replication. The WRN helicase has emerged as a promising target for cancer therapy since the discovery of the synthetic lethal interaction between WRN deficiency and microsatellite instability. Although no WRN inhibitors have been approved to date, several candidates, including HRO761 and VVD-214 (RO7589831), have entered clinical trials. HRO761 inhibits WRN non-covalently by interacting with its D1 and D2 helicase domains, while VVD-214 covalently binds to cysteine 727 within an allosteric pocket of WRN. This study aimed to find shared and unique predictive response biomarkers for these two WRN inhibitors. HRO761 and VVD-214 were profiled on a panel of 114 cancer cell lines in cell viability assays using ATP as readout. Response data were related to the microsatellite status of the cell lines as well as to publicly available basal gene expression levels, protein expression levels and *WRN* dependency based on CRSIPR knock-out and RNAi knock-down screens. Additionally, a selection of microsatellite stable (MSS) and microsatellite instable (MSI) cell lines was used to assess sensitivity to the WRN inhibitors in colony formation unit assays and to evaluate DNA damage induction using fluorescent imaging. Despite their distinct binding mechanisms, the two WRN inhibitors showed nearly identical response patterns across the 114 cancer cell lines. Notably, VVD-214 was 1.7 times more potent than HRO761. The response to the two inhibitors did not correlate well with basal *WRN* gene expression and WRN protein expression, but showed a significant positive correlation with *WRN* dependency from a CRISPR knock-out screen and RNAi knock-down screen. The gene expression analysis identified *MLH1* expression as a potential resistance marker for both WRN inhibitors. After splitting the 114 cell lines into an MSS and an MSI group, all cell lines in the MSS group were found to be insensitive to the WRN inhibitors, as expected. Surprisingly, the MSI group included both sensitive and non-sensitive cell lines for the two inhibitors. Within the MSI group, VVD-214 was 2.9-fold more potent than HRO761, whereas in the MSS group the difference was only 1.5-fold. Colony formation unit assays and DNA damage imaging further confirmed the differential responses to the WRN inhibitors between MSS and MSI cell lines. The WRN inhibitors HRO761 and VVD-214 showed similar response profiles in the tested cancer cell lines, although some differences were observed. This study highlights potential shared and unique response biomarkers for the WRN inhibitors HRO761 and VVD-214.

#0236 Targeting DNA damage sensors (DDS) to enhance Osimertinib response in EGFR-driven cancers.

Pamela L. Mendoza-Munoz[1], Madison E. Gerbig[1], John J. Turchi[2], Shadia I. Jalal[1]

[1]Department of Medicine, Indiana University School of Medicine, Indianapolis, IN,[2]Department of Biochemistry, Molecular Biology & Pharmacology, Indiana University School of Medicine, Indianapolis, IN

Lung cancer remains the leading cause of cancer-related mortality worldwide. Approximately 85% of cases are classified as non-small cell lung cancer (NSCLC) and activating mutations in the epidermal growth factor receptor (EGFR) are present in about 16% of metastatic NSCLC tumors. The development of EGFR tyrosine kinase inhibitors (EGFR-TKIs) including the third-generation agent Osimertinib, have significantly improved patient outcomes. Nonetheless, its efficacy is limited by both on-target and off-target resistance mechanisms, including the C797S mutation, MET amplification, and histological transformation. Emerging evidence has shown that EGFR signaling influences DNA repair, and that persistent proliferative signaling in EGFR-driven tumors elevates replication stress (RS), making them uniquely vulnerable to inhibition of the DNA damage response (DDR). While prior approaches have primarily targeted DDR kinases such as ATR, CHK1, and WEE1, the role of DNA damage sensors (DDS), including replication protein A (RPA) and the Ku70/80 complex, remains largely unexplored. In this study, we focus on this strategy by targeting RPA and Ku70/80, which recognize DNA structures generated by direct DNA damage or RS and initiate the DDR. Using small molecule inhibitors that target RPA and Ku-DNA binding in combination with clinically relevant EGFR-TKIs, we aimed to dissect the mechanistic interactions between DDR pathways and EGFR signaling to elucidate how DDR modulation impact therapeutic response and resistance in EGFR-driven NSCLCs. Our results show that the DDS inhibitors NERx-329 (RPAi) and Ku-DBi 3392 (Ku70/80) in combination with Osimertinib further enhances antiproliferative and cytotoxic effects in TKI-sensitive, EGFR-mutant NSCLC cells in an additive manner. Our data demonstrate that DDR inhibition is effective in TKI-sensitive EGFR-driven models potentiating Osimertinib activity. Importantly, this is independent of a DNA damaging agent, suggesting that inhibition of DDR itself is enough to increase the therapeutic effect of Osimertinib. This effect appears to be EGFR-specific, as no potentiation of Alectinib activity was observed in an EML4-ALK driven NSCLC model. These preliminary findings support a functional crosstalk between DDS-mediated DDR pathways and EGFR signaling highlighting a potential therapeutic strategy to overcome, delay, or prevent the recurrence of resistance in EGFR-driven NSCLC cancers.

#0237 Selective Cytotoxicity of Base Excision Repair Inhibitor, TRC102, in DNA Damage Response Hyperactivated Glioblastoma.

Shaunak Sathe, Qi Li, Jinkyu Jung, Peng Lu, Zach Sergi, Herui Wang, Jing Wu

National Cancer Institute, National Institutes of Health, Bethesda, MD

Background Glioblastoma is the most aggressive and lethal type of brain tumor. Tumor heterogeneity and DNA repair pathways contribute strongly to poor outcomes, highlighting the need for more personalized approaches. TRC102 (methoxyamine hydrochloride) is a small-molecule inhibitor of base excision repair that acts by covalently binding to abasic sites and preventing downstream repair enzymes from repairing the lesion. Clinical studies utilizing TRC102 in glioblastoma have identified hyperactivated DNA damage response (DDR) gene signature among exceptional responders, suggesting DDR-hyperactivity as a potential clinical biomarker. Here, we evaluated whether glioblastoma cells reliant on DDR signaling are particularly vulnerable to TRC102 treatment. *Methods* We performed gene set enrichment analysis using RNA-seq data across 24 glioblastoma cell lines within the NCI, Neuro Oncology Branch database and identified three patient-derived cell lines (L0, L1, GSC627) with hyperactivated DDR signature. Treatment efficacy was evaluated using cell viability, colony formation, DNA damage, repair and immunofluorescence assays. *Results* TRC102 treatment alone induced significant DNA damage and cell death in DDR-hyperactivated glioblastoma cell lines, whereas DDR-hypoactivated cells showed minimal sensitivity. In L0 and L1 cell lines, TRC102 treatment significantly inhibited colony formation and cell proliferation over 72-hour treatment. Mechanistic studies through western blotting revealed that TRC102 led to significant suppression of CHK2 activity, a key kinase involved in the DDR that controls cell cycle progression. Abrogation of cell cycle checkpoint blockades through CHK2 depletion may allow glioblastoma cells to initiate mitosis without fully resolving DNA damage, leading to mitotic catastrophe and cell death. Interestingly, TRC102 also suppressed HIF protein expression in hypoxic conditions, leading to eventual cell death. *Conclusions* The antitumor effect of TRC102 appears to be mediated through targeting of the newly identified ATM-CHK2-HIF axis, allowing for selective cytotoxicity in DDR-hyperactivated glioblastoma. These results suggest a specific vulnerability to TRC102 in DDR-hyperactivated glioblastoma that are typically resistant to conventional chemotherapy and radiation therapy, supporting biomarker-driven patient selection in future clinical studies.

#0238 Targeted degradation of DNA ligase IV through a double-stranded DNA-based PROTAC for precision radiosensitization.

Monica Pandey, Daniel S Higginson

Radiation Oncology, Memorial Sloan Kettering Cancer Center, New York, NY

DNA ligase IV (LIG4), the terminal ligase of the non-homologous end-joining (NHEJ) pathway, represents one of the most potent yet least druggable radiosensitization targets in double-strand break repair. To overcome this challenge, we designed a first-in-class, double-stranded DNA-based proteolysis-targeting chimera (PROTAC; termed as NHEJ-P) that couples a short 32-bp duplex “DNA bait” to a cereblon-binding E3 ligase ligand, enabling selective proteasomal degradation of LIG4. NHEJ-P achieves near-complete loss of endogenous LIG4 at ~10 nM, verified by western blot and rescued by MG132, confirming proteasome dependence. In vitro, NHEJ-P induces sustained γH2AX and 53BP1 foci with no effects on RAD51 foci, disrupts end-joining kinetics, and enhances radiation-induced cytotoxicity in U2OS and HeLa cells but not in non-transformed RPE1 or HEK293T models, defining a favorable tumor-to-normal therapeutic index. These results suggest that genomically unstable cancer cells are uniquely dependent on LIG4 for survival under replication stress. Building on this foundation, we are conjugating NHEJ-P to trastuzumab using a site-directed enzymatic approach to generate t-NHEJ-P, a HER2-directed antibody-oligonucleotide conjugate (AOC) for tumor-restricted delivery. Planned studies will assess pharmacokinetics, tissue-selective LIG4 degradation, and radiosensitization in $HER2^{+}$ xenografts, along with prospective safety in gastrointestinal, cardiac, pulmonary, and skin radiation-toxicity models. Together, these findings establish targeted LIG4 degradation as a new paradigm for DNA-damage-response modulation and lay the groundwork for next-generation, bystander-limited radiosensitizers that integrate molecular precision with translational safety.

#0239 Potent synergy between CHK1/2 inhibitor ACR-368 and the ADC payload topoisomerase I inhibitor: Rationale for ADC + ACR-368 combination therapy.

Portia Lombardo[1], Ahmed Youssef[1], Mohamed Eldeeb[2], Nina Lipjankic[3], Martina Pasetto[3], Ruban Cornelius[3], Sofija Skoric[3], Ignacio Arribas Diez[3], Zachary Best[1], Anna-Maria Alves[1], Subodh Kumar[1], Kate Rappard[1], Calvin Yang[1], Corey Xu[1], Emma Ahrman[3], Valentina Siino[3], Taronish Dubash[1], Joelle Baddour-Sousounis[1], Reina Improgo[1], Magnus E. Jakobsson[3], Ayesha Murshid[1], Helen Asa Nilsson[3], Lei Shi[1], **Caroline Maria Wigerup**[3], Michail Shipitsin[1], Joon Jung[1], David Proia[1], Erick Gamelin[1], Mansoor Mirza[1], Kristina Masson[1], Peter Blume-Jensen[1]

[1]Acrivon Therapeutics, Watertown, MA,[2]Acrivon AB, Lund, Sweden,[3]Acrivon Therapeutics, Lund, Sweden

Antibody-drug conjugates (ADCs) enable targeted delivery of cytotoxic payloads to tumor cells, improving the therapeutic index compared with conventional chemotherapy. Topoisomerase I (Topo I) inhibitors are potent ADC payloads that trap the Topo 1-DNA cleavage complex, leading to replication-fork collapse and tumor cell death. However, this also activates the DNA damage response through CHK1/2-dependent cell cycle checkpoints, attenuating cytotoxicity and enhancing resistance to Topo1-containing ADCs. CHK1/2 inhibition exploits this therapeutic vulnerability, abrogating these checkpoints, increasing replication stress, and hence enhancing the efficacy of Topo I inhibitors across multiple tumor models. Consistent with this, treatment with the potent, selective CHK1/2 inhibitor ACR-368 combined with irinotecan has demonstrated encouraging clinical activity in heavily pretreated patients with sarcomas who had progressed on prior irinotecan therapy. Combined, these data provide a strong rationale for combining ACR-368 with Topo I inhibitor-based therapies.

Using the Acrivon Predictive Precision Proteomics (AP3) platform for “Indication Finding”, we previously identified endometrial cancer as a tumor type predicted to be particularly sensitive to ACR-368, which has been shown and is being further evaluated in a Phase 2 registrational trial. In a panel of endometrial cancer cell lines, the combination of ACR-368 with exatecan or SN38 demonstrated synergy in a majority of these, with comparable synergy scores between both Topo I inhibitors. Synergy was observed in both Topo I-sensitive and -resistant lines, supporting the potential to overcome resistance to Topo I inhibitor-based ADCs. To elucidate the pathway mechanisms underlying Topo I inhibitor sensitivity and resistance and the potent, synergistic activity with ACR-368, results from our AP3 Generative Phosphoproteomics approach applied to endometrial cancer will be presented.

Combined, these findings demonstrate that CHK1/2 inhibition with ACR-368 synergizes with Topo I inhibitors to enhance cytotoxicity and overcome resistance mechanisms, supporting a mechanistically rational combination strategy with potential to improve the therapeutic benefit of Topo I inhibitor-based ADC therapies.

#0240 Allele-specific sensitization of pancreatic ductal adenocarcinoma to PARP inhibition via adenine base editing.

Jin Zhang[1], Jingrui Yan[2], Tianxing Zhou[2], Xiuchao Wang[2], Chao Yang[2], Jun Yu[2], Jihui Hao[2]

[1]Tianjin Medical University Cancer Institute and Hospital, Tianjin, China,[2]Tianjin Medical Univ. Cancer Inst. & Hospital, Tianjin, China

Synthetic lethality represents a promising therapeutic paradigm in oncology, particularly for pancreatic ductal adenocarcinoma (PDAC) patients with BRCA1/2 mutations, who demonstrate increased sensitivity to PARP inhibitors (PARPi) like olaparib. However, the broader application of this strategy is constrained by the limited incidence of homologous recombination deficiency (HRD) in PDAC that parallels BRCA loss. To address this, we employed SpRY-mediated adenine base editing (ABE) to screen for allele-specific mutations in HR-related genes across normal pancreatic epithelial (HPNE) and PDAC cell lines, including both KRAS-G12D mutant (PANC-1) and wild-type (BxPC-3) models. These edited cells were subjected to olaparib treatment at three escalating doses. A subsequent slope-based analysis of viability reduction identified several mutations that specifically sensitized PDAC cells to PARPi. Strikingly, the NBN-X mutation conferred robust olaparib hypersensitivity in KRAS-wild-type BxPC-3 cells, while PALB2-Y and RAD50-Z mutations markedly enhanced olaparib efficacy in KRAS-G12D mutant PANC-1 cells compared to normal HPNE controls. Mechanistically, the NBN-X variant sensitizes non-KRAS mutant PDAC by disrupting MYC-driven homologous recombination (HR) repair. In contrast, the RAD50-Z variant synergizes with KRAS-driven suppression of HR to potentiate PARPi efficacy. These allele-specific effects were functionally validated, demonstrating up to a 4.1-fold decrease in olaparib IC50 and a 2.5-fold increase in apoptosis. Critically, this potent sensitization was highly tumor-specific, yielding a significantly improved safety profile over conventional BRCA-mutant models both in vitro and in vivo. Leveraging these findings, we are using virtual screening and AI-driven drug design to develop small molecules that mimic the PARPi-hypersensitivity induced by our identified mutations. These lead compounds will be advanced for evaluation in sophisticated PDAC models, including patient-derived xenografts (PDX) and genetically engineered mice. Our results highlight a novel strategy for personalizing PARPi therapy in PDAC and suggest a substantially expanded therapeutic window that could improve outcomes for patients with this aggressive disease.

#0241 Targeted drug screening identifies novel compounds enabling accelerated mismatch repair deficiency (MMRd) for immunotherapy sensitization.

Benoit Rousseau[1], Miteshkumar Patel[1], Karthik Rangavajhula[1], Lin Zhang[1], David Mieles[1], James R. White[2], Oliver Artz[1], Shrey Patel[1], Somer Abdelfattah[1], Neil Segal[3], Luis A. Diaz[1]

[1]Memorial Sloan Kettering Cancer Center, New York, NY,[2]Resphera Biosciences, Baltimore, MD,[3]Memorial Sloan Kettering Cacner Center, New York, NY

Background: MMRd tumors respond exceptionally to immunotherapy, and pharmacologic MMR inactivation has the potential to improve immunosensitivity of MMR-proficient tumors. We previously showed that temozolomide plus cisplatin (TMZ+CDDP) induces MMRd through MSH2 silencing. However, clinical translation revealed limited efficacy, potentially due to delayed MMR inactivation preventing sufficient tumor mutational burden (TMB) and microsatellite instability (MSI) accumulation on treatment. We hypothesized that compounds enabling rapid MMR inactivation could overcome this limitation.
Methods: Preclinical models treated with TMZ+CDDP were analyzed longitudinally for TMB and MSI. Clinical trial data (NCT04457284) combining TMZ+CDDP with nivolumab in metastatic colorectal cancer patients were assessed using serial ctDNA profiling. We performed computational screening of open-source databases to identify compounds inducing rapid *MLH1* or *MSH2* downregulation (≤3 days) across cancer cell lines. Candidates were studied using CT26 cells transfected with an out-of-frame luciferase-microsatellite reporter, where MSI-induced frameshift mutations restore luciferase expression, enabling real-time MSI monitoring. These repurposed compounds underwent MMR expression analyses.
Results: In vivo, TMZ+CDDP induced MSH2 loss only after 4 weeks (W) of treatment, with MMRd genotype recapitulated only after 8W. Clinical trial analysis of 16 evaluable patients revealed that only 5 patients (31%) developed a MMRd-like genotype with gains in TMB and MSI at a median of 8W, which associated with improved survival. Critically, patients failing to increase TMB and/or MSI developed aneuploid gains in MMR genes on treatment suggesting a compensatory resistance mechanism to mutagenesis. These findings indicate that delayed MMR inactivation with TMZ+CDDP limits clinical efficacy. To address this limitation, our drug screen identified 6 compounds inhibiting significantly *Msh2* and/or *Mlh1* after short course treatment. Three compounds were confirmed to generate sustained bioluminescence increases within 1-2W compared to 4-8W with TMZ+CDDP. Two compounds were showed to completely abolish *Msh2* expression by 1 or 2W, while the third reduced expression by 70%. The three other agents showed only transient *Msh2* or *Mlh1* downregulation without change in bioluminescence. These novel compounds demonstrate substantially accelerated MMR inactivation kinetics compared to TMZ+CDDP.
Conclusions: While TMZ+CDDP can induce a MMRd genotype in patients, delayed MMR inactivation and compensatory MMR gene amplification limit therapeutic efficacy. Repurposed compounds enabling rapid MSH2 inhibition may prevent adaptive resistance mechanisms and improve clinical responses when combined with immunotherapy, warranting further preclinical/clinical development.

#0242 Targeting the DNA damage response sensor replication protein A for first in class cancer therapy.

Pamela VanderVere-Carozza[1], Matthew R. Jordan[1], Katherine Pawelczak[2], **John J. Turchi**[1]

[1]Indiana University School of Medicine, Indianapolis, IN,[2]Nerx Biosciences, Inc., Indianapolis, IN

The DNA damage response (DDR) and replication stress response (RSR) are validated pathways for targeted cancer therapy, particularly through the exploitation of synthetic lethal interactions. We have pursued the discovery and development of DDR and RSR sensor protein inhibitors to disrupt these dysregulated pathways in cancer. We have demonstrated the therapeutic efficacy of the novel Replication Protein A inhibitor (RPAi), NERx-329, which disrupts the RPA-DNA interaction, induces chemical exhaustion of RPA function, and exhibits potent anticancer activity in vivo. We identified a series of synthetic lethal interactions that revealed the RPAi mechanism of action and therapeutic efficacy is primarily mediated by molecular events at the replication fork in response to replication stress (RS). These studies showed that RPAi exacerbates both genetically and pharmacologically induced RS via chemical RPA exhaustion resulting in further genomic instability, replication catastrophe, and cell death of cancer cells, with minimal toxicity in vivo. Data presented demonstrate the development of a combined treatment regimen targeting RPA and PARP that abrogates cancer growth in an in vivo BRCA1-deficient breast cancer model and ovarian cancer cell line. To assess markers of genome instability, we performed metaphase spreads on single agent- and combination agent-treated TNBC MDA-MB-436 cells. Single-agent RPAi treatment had no observable effect on the chromosome structure, whereas olaparib treatment increased chromosome pulverization. However, the combination strikingly induced chromosome pulverization. Taken together, NERx-329 chemically exhausts RPA such that olaparib-induced ssDNA gaps are degraded, and chromosomal integrity is compromised. Considering the induction of chromosome pulverization, we assessed the generation of micronuclei (MN) following RPAi treatment in combination with olaparib and the PARP1-specific PARPi saruparib. The data revealed that PARPi treatment resulted in a significant increase in MN, whereas treatment with RPAi alone did not affect MN formation. The combination of RPAi-PARPi treatment did not significantly alter MN occurrence. These results indicate that MN formation is not required for the enhanced cell killing effect of the combination treatment. Overall, these data support a model in which loss of BRCA1 and its prevention of ssDNA gaps during replication is further exacerbated by PARP inhibition. This data suggests that RPAi-PARPi combination enhances therapeutic efficacy and offers a strategy to overcome PARPi resistance by targeting gap protection mechanisms.

#0243 DNA fiber-based replication phenotypes distinguish WEE1-inhibitor response in high-grade endometrial cancer patient-derived organoids (PDOs) treated with azenosertib.

Elena Ivanova[1], Ke Cong[1], Shrabasti Roychoudhury[1], David Han[1], Magdalena Zielinska[1], Minh Ha[1], Abrielle Jens[1], Vaishnavi Anand[1], Bose S. Kochupurakkal[1], Courtney H. Qi[1], Arunika Shee[1], Maureen Mulready[1], Madison Zizzo[1], Alexis Rabbitt[1], Jennifer D. Curtis[1], Nabihah Tayob[1], Marisa R. Nucci[2], Cam A. Tran[1], Panagiotis A. Konstantinopoulos[1], Geoffrey I. Shapiro[1], Dipanjan Chowdhury[1], Cloud P. Paweletz[1], Ursula Matulonis[1], Joyce Liu[1]

[1]Dana-Farber Cancer Institute, Boston, MA,[2]Brigham and Women's Hospital, Boston, MA

Background: High-grade endometrial cancers (EC), including serous, carcinosarcoma, and clear cell subtypes, frequently harbor *TP53* mutations, replication stress (RS), and cell-cycle dysregulation, suggesting vulnerability to WEE1 inhibition. We conducted a translational study to define RS-linked pharmacodynamics and *ex vivo* correlates of response in high-grade EC PDOs.

Methods: PDOs from high-grade EC biopsies and surgical samples were treated *ex vivo* with azenosertib (200 nM, 24 h). DNA-fiber assays measured: (i) fork speed (CldU+IdU as ongoing replication forks), (ii) replication fork stability under RS caused by hydroxyurea (HU), using the IdU:CldU ratio after WEE1i+HU, and (iii) single-stranded (ss)DNA gap formation via the S1 nuclease assay (WEE1i±S1).

Results: Four PDOs were profiled: DF4850 and DF4161 (WEE1i-sensitive; IC50s<100nM) and DF042 and DF4968 (insensitive; IC50s>1500nM). Across all four models, fork speed decreased after azenosertib, consistent with on-target effects on RS. However, fork degradation and gap formation aligned with viability. Specifically, under WEE1i+HU, the sensitive models (DF4850, DF4161) showed a significant reduction in the IdU:CldU ratio, indicating impaired fork restart/stability. The insensitive models (DF042, DF4968) were able to protect forks from degradation despite WEE1 inhibition and showed no change. In the S1 gap assay, DF4850/DF4161 exhibited shorter fiber tracts with WEE1i+S1 vs WEE1i alone, consistent with increased ssDNA gaps, whereas DF042/DF4968 again showed no difference, indicating the ability to tolerate WEE1i-induced stress. Thus, while fork slowing is a uniform pharmacodynamic effect of WEE1 inhibition, HU-sensitive fork instability and S1-sensitive gap formation are enriched in sensitive PDO models.

Conclusions: In high-grade EC PDOs, azenosertib uniformly slows replication forks, but fork stability under HU and S1-detectable gap formation distinguish WEE1i-sensitive (DF4850, DF4161) from insensitive (DF042, DF4968) models. These mechanism-anchored DNA-fiber readouts merit prospective evaluation as predictive and pharmacodynamic biomarkers for WEE1 inhibitors in high-grade EC. Additional biomarker analyses, including immunohistochemical analyses of RS proteins, are ongoing and will be presented.

#0244 DHX9 inhibition is synthetically lethal with homologous recombination deficient and dMMR/MSI-H cancers and synergizes with PARP1 inhibition and chemotherapy.

Samantha S. Hodge, Natalie Hill, Jhansi L. Leslie, **Umida Djakbrova**, Logan Chinn, Saranya Chandrasekar, Susan Paprcka, Ester Fernandez-Salas

Arcus Biosciences Inc., Hayward, CA

BACKGROUND: DHX9 is an RNA/DNA helicase that unwinds various RNA/DNA secondary structures, including R-loops and G-quadruplexes, which increase replication stress and transcription-replication collisions if not properly resolved. Homologous recombination deficient (HRD) and mismatch repair deficient/microsatellite instability-high (dMMR/MSI-H) cancer cells exhibit dependence on DHX9 due to enhanced formation of RNA/DNA secondary structures. PARP inhibitors (PARPi) are a front-line standard of care (SOC) for BRCA-deficient and HRD cancers but exhibit limited efficacy and durability. Topoisomerase 1 (TOP1) inhibitors are commonly used in dMMR/MSI-H cancers post-immunotherapy and in PARP and chemo-refractory HRD cancers. Both PARP1 and TOP1 have roles in R-loop prevention and resolution. We hypothesized that DHX9 inhibition combined with PARP or TOP1 inhibition might elicit deeper responses in a greater fraction of HRD or dMMR/MSI-H tumors than SOC therapy alone.
METHODS: Cell lines were categorized as HRD based on genomic scar scores or as dMMR/MSI-H based on MMR LOF or MSISensor scores. Sensitivity of cell lines to siDHX9, DHX9 inhibition, or WRN inhibition was assessed using viability assays. Cell cycle changes after DHX9 or WRN inhibition were monitored using the PIP-FUCCI sensor using live cell imaging. Combined inhibition of DHX9 and PARP or TOP1 was evaluated using a viability assay, and synergy was quantified using Bliss Synergy scores.
RESULTS: siDHX9 decreased cell viability in HRD and dMMR/MSI-H cells with no effect on homologous recombination proficient (HRP), microsatellite stable (MSS), and non-tumorigenic cells. Similarly, DHX9 inhibition altered the cell cycle and decreased viability in HRD and dMMR/MSI-H cell lines while sparing HRP, MSS, and non-tumorigenic cells. DHX9 inhibition exhibited synergism with both saruparib (PARPi) in HRD cell lines and with SN38 (TOP1i) in HRD and dMMR/MSI-H cell lines. On the other hand, WRN inhibition had no effect on the cell cycle or viability of HRD cell lines. While WRN inhibition reduced viability in a subset of dMMR/MSI-H cell lines, a greater number of dMMR/MSI-H cell lines were sensitive to DHX9 inhibition.
CONCLUSION: These data support that DHX9 inhibition is synthetically lethal in HRD and dMMR/MSI-H cancers and demonstrate that DHX9 inhibition synergizes with SOC therapies. For the first time, these data highlight that DHX9 inhibition synergizes with both PARPi or TOP1i to elicit robust tumor cell killing in HRD and dMMR/MSI-H cancers. Additionally, these data demonstrate that DHX9 inhibition is a superior synthetic lethal target compared to WRN inhibition in both HRD and dMMR/MSI-H cancers.

#0245 Expanding the therapeutic window of PARP inhibitors by co-administering PARG inhibitors.

Giacomo G. Rossetti[1], Michalis Petropoulos[1], Theodoros Rampias[2], Thanos D. Halazonetis[3]

[1]University of Bern, Bern, Switzerland,[2]Biomedical Research Foundation Academy of Athens, Athens, Greece,[3]Cancentus Pharma and University of Bern, Bern, Switzerland

Background:
Homologous recombination (HR) deficiency sensitizes tumors to PARP inhibitors (PARPi), which are standard-of-care for HR-deficient cancers. Despite their efficacy, clinical use of PARPi is limited by on-target toxicity, particularly anemia, leading to dose reductions and drug holidays in about half of treated patients. To address these limitations and expand the therapeutic window of PARPi, we investigated co-administration with selective PARG inhibitors (PARGi).
Methods:
Cell survival assays were used to evaluate the interaction between potent PARP inhibitors (talazoparib, saruparib), less potent PARP inhibitors (niraparib, olaparib, rucaparib), and selective PARG inhibitors in HR-deficient cell lines. Bone marrow toxicity was assessed in mice and rats treated with talazoparib (0.2-0.25 mg/kg) or saruparib (0.1 mg/kg), administered alone or in combination with selective PARG inhibitors undergoing clinical development, using a 4-days-on/2-days-off/4-days-on regimen. Red blood cell counts, hematocrit, and body weight were measured one day after treatment. Antitumor efficacy was evaluated in DLD1-BRCA2-knockout cell line-derived xenografts (CDX) using a 3-days-on/4-days-off dosing schedule, administered alone or in combination with PARG inhibitors.
Results:
In cell survival assays, PARG inhibitors did not antagonize the cytotoxicity of potent PARPi in HR-deficient cells. In vivo, PARPi monotherapy induced anemia, weight loss, and mortality. Co-administration of PARG inhibitors rescued anemia, attenuated weight loss, and prevented treatment-related deaths. CDX studies demonstrated that tumor growth inhibition by PARPi was maintained or enhanced in combination with PARG inhibitors, allowing higher PARPi dosing without compromising safety. In rats, anemia induced by PARPi was similarly rescued by a PARG inhibitor. Overall, the combination improved the therapeutic window, enabling enhanced efficacy at higher PARPi doses.
Conclusions:
PARG inhibition selectively mitigates PARPi-induced toxicity without compromising anticancer efficacy in HR-deficient tumors, thereby expanding the therapeutic window. This approach enables higher PARPi dosing for improved tumor control or equivalent efficacy with fewer adverse events, particularly anemia. By reducing PARPi-associated toxicity, PARG inhibition may also facilitate combination therapies, warranting further investigation.

#0246 Discovery and mechanistic characterisation of the first oral bioavailable FEN1 inhibitor for treatment of HRD and EWS cancers and combination with various DDR inhibitors.

Lars T. Burgdorf[1], Julien Lefranc[1], Lucy Armstrong[2], Roch Boivin[3], Joerg Bomke[1], Xiaoling Chen[3], Paula Costales[2], Owen A. Davis[2], Lizbeth DeSelm[3], Elias Elinati[2], Maria Filipa Pinto[2], Bruce Follows[3], Alessandro Galbiati[2], Catherine Jorand-Lebrun[3], Timothea Konstantinou[2], Julian Kreis[1], Claudio A. Lademann[1], Birgitta Leuthner[1], Jayesh B. Majithiya[2], Balca R. Mardin[1], Bethany Mason[2], Claire L. McWhirter[2], Djordje Musil[1], Ulrich Pehl[1], David Perera[2], Silvia Peripolli[2], Carl Petersson[1], Eeson Rajendra[2], Christin Rakers[1], Ada Sala-Hojman[1], Graeme C. M. Smith[2], Fiona Sorrell[1], Ana Toste Rego[2], Helen M. R. Robinson[2], Frank T. Zenke[1], Robert A. Heald[2], Sam E. Mann[2]

[1]Merck Healthcare KGaA, Darmstadt, Germany,[2]Artios Pharma Ltd., Cambridge, United Kingdom,[3]EMD Serono Research & Development Institute, Billerica, MA

Flap endonuclease 1 (FEN1) has emerged as a critical target in the DNA damage response (DDR) landscape, particularly due to its synthetic lethal interactions with homologous recombination-deficient (HRD) cancers, such as those harboring BRCA mutations. Despite the therapeutic potential of FEN1 inhibition, the development of effective small molecule inhibitors has been limited, with existing compounds exhibiting modest selectivity and lacking oral bioavailability. In this presentation, we highlight the discovery of MSC778, the first potent, selective, and orally bioavailable FEN1 inhibitor and its mechanistic characterization. Utilizing a metal-chelating fragment-based screening approach combined with structure-based optimization, we successfully identified MSC778, which demonstrates strong cellular activity and selectivity and induces cell death in BRCA-deficient cancer cells. Our medicinal chemistry optimization campaign led to the development of oral bioavailable compounds that potentiate the activity of the PARPi niraparib *in vivo* to induce tumor stasis in a *BRCA2* KO DLD-1 mouse xenograft model. Mechanistically we could demonstrate that MSC778 enhances FEN1 retention on chromatin and disrupts active DNA replication, leading to S-phase accumulation and subsequent DNA damage. Our findings also reveal a novel sensitization of Ewing sarcoma (EWS) cells to FEN1 inhibition, driven by the expression of SLFN11. Through CRISPR and drug combination screening, we elucidate a spectrum of synthetic lethal interactions between FEN1 and key DDR factors, including PARP1, USP1, PARG, and ATR, highlighting the synergistic potential of combining FEN1 inhibition with existing and emerging DDR-targeting agents. Together, these data underscore the relevance of FEN1 inhibition as a precision oncology strategy, with significant implications for the treatment of HRD and EWS cancers, as well as potential for combination therapies that leverage the DDR landscape.

#0247 Multiomic and preclinical assessment of ATR and Aurora kinase inhibitors in diverse TNBC models.

Nathan M. Merrill, Hamadi Madhi, Nathalie M. Vandecan, Athena Marie Apfel, Habib Serhan, Peter J. Ulintz, Liwei Bao, Aki Morikawa, Matthew B. Soellner, Soffia D. Merajver

University of Michigan, Ann Arbor, MI

Introductory Sentence: This study investigated the efficacy of combined ATR and Aurora kinase (AK) inhibition in triple-negative breast cancer (TNBC), emphasizing racially diverse patient-derived models and mechanisms of therapeutic resistance.
Pertinent experimental procedures: Through high throughput screening, we identified an ATR inhibitor, berzosertib, that targets the DNA damage response (DDR) pathway, and whose efficacy correlates with AK expression and activity. When combined with danusertib, a pan-AK inhibitor, berzosertib produced synergistic cell death across a broad range of TNBC cell lines. To validate this drug combination, we initiated a 1x1x1x1 patient-derived xenograft (PDX) trial using 30 racially diverse PDX models (15 from Caucasian and 15 from African descent patients), allowing assessment of potential ethnicity-based differences in response, given the higher TNBC incidence in African American women of West African ancestry. Mice were first exposed to the berzosertib-danusertib combination to evaluate toxicity and optimize dosing. Once dosing was established, PDX tumors were serially implanted and treated with berzosertib, danusertib, their combination, or vehicle control for 21 days. After treatment, tumors were collected for single-cell RNA sequencing and spatial transcriptomics analysis. Finally, baseline DNA and RNA sequencing will be conducted across all PDX models to identify predictive biomarkers of therapeutic response.
Summary of new unpublished data: Initial experiments in NSG mice revealed unexpected toxicity with the combination therapy, which was resolved by switching to NRG mice without RAG1 knockout. Screening four PDX models showed synergistic effects in three, indicating strong anti-cancer potential. Single-cell and spatial transcriptomic analysis of treated tumors revealed enrichment of extracellular matrix remodeling genes, especially MMP7, and proliferation genes at the tumor periphery. This upregulation suggests possible activation of pro-invasive pathways and increased metastatic risk with the combination treatment. These preliminary studies established workable experimental protocols, but further testing in additional models with deeper sequencing is needed. While initial transcriptomic studies compared combination therapy to vehicle controls, it will be important to perform similar analyses for danusertib and berzosertib monotherapies to determine if either drug alone is responsible for the increased proliferation and extracellular remodeling observed with the combination.
Statement of the conclusions: Overall, these findings suggest that dual ATR and Aurora kinase inhibition benefits select TNBC models and uncover gene expression changes, highlighting the need for ongoing surveillance for metastatic indicators.
AI disclosure: AI was used for language editing only; content was verified by the authors

#0248 Nesuparib (JPI-547), a dual tankyrase/PARP inhibitor, exhibits potent antitumor activity in small-cell lung cancer models by modulating Wnt and Hippo signaling pathways.

Jun Kim[1], Joon-Hyung Lee[1], John Kim[1], Hyunju Cha[1], Seounghun Kang[2]

[1]Onconic Therapeutics, Seoul, Korea, Republic of,[2]Soongsil University, Seoul, Korea, Republic of

Objectives: Small-cell lung cancer (SCLC) accounts for 13-15% of lung cancers and remains an aggressive malignancy with rapid progression and poor prognosis, as median survival for extensive-stage disease is below 10 months. Nesuparib (JPI-547) is a potent, orally active dual inhibitor of Tankyrase-1/2 (TNKS1/2) and Poly (ADP-ribose) Polymerase-1/2 (PARP1/2). This study evaluated in vitro cytotoxicity and in vivo antitumor efficacy of nesuparib in BRCA wild-type SCLC models. The research aimed to characterize the antitumor activity and mechanism of nesuparib compared with olaparib and irinotecan and assess the synergistic efficacy of nesuparib combined with irinotecan. These investigations sought to clarify the mechanistic and therapeutic potential of dual TNKS1/2-PARP1/2 inhibition in SCLC.
Methods: Human SCLC NCI-H146 cells were treated with nesuparib, olaparib, or irinotecan to assess in vitro cytotoxicity by CellTiter-Glo assay. For in vivo evaluation, two independent xenograft studies were performed: a mono-treatment study comparing each agent's antitumor efficacy and a combination study assessing synergistic activity of nesuparib with irinotecan. Tumors from nesuparib-treated mice were analyzed by RT-qPCR, Western blot, and IHC to elucidate molecular mechanisms.
Results: In vitro, nesuparib showed the strongest potency among tested agents (IC_{50} = 2.4 nM), being ~133-fold and ~25-fold more potent than olaparib and irinotecan, respectively. In vivo, nesuparib exhibited a clear dose-dependent tumor-growth inhibition in the NCI-H146 xenograft model. At 50 mg/kg, nesuparib achieved a TGI of 65.4%, exceeding the efficacy of olaparib (36.0%) and irinotecan 10 mg/kg (42.9%). Combination with irinotecan produced a significant synergistic effect, resulting in enhanced and sustained tumor regression, which was superior to the combination of olaparib with irinotecan. Mechanistic analyses revealed that nesuparib suppressed Wnt and Hippo signaling pathways, leading to inhibition of tumor growth, as confirmed by qPCR, Western blot, and IHC.
Conclusions: Nesuparib (JPI-547), a dual TNKS1/2-PARP1/2 inhibitor, showed strong dose-dependent antitumor activity in BRCA wild-type SCLC. Combination with irinotecan produced a synergistic tumor-suppressive effect. Mechanistic studies indicated that nesuparib inhibited tumor growth by suppressing Wnt and Hippo signaling, supporting its potential as a novel therapeutic strategy for SCLC alone or with DNA-damaging agents.

#0249 MOMA-313, an inhibitor of the DNA polymerase theta helicase domain, prevents BRCA reversions in preclinical models.

Giulia Bottoni, Anthony Tubbs, Kelly McGlynn, Vinny Motwani, Michael Reutershan, Timothy Guzi, Erica Evans, Peter Hammerman, **Jordan A. Krall**

MoMa Therapeutics, Cambridge, MA

MOMA-313 is a small molecule inhibitor of the DNA polymerase theta (Polθ) helicase domain in development for the treatment of homologous recombination (HR)-deficient tumors. Polθ repairs DNA double-strand breaks (DSBs) by annealing flanking regions of microhomology, a process called theta-mediated end-joining (TMEJ). In preclinical models, MOMA-313 synergizes with PARP inhibitors to drive deeper responses both in vitro and in vivo, demonstrating the potential for combination benefit in the clinic. Clinical resistance to PARP inhibitors is caused by BRCA reversions – secondary mutations that restore BRCA function – that often have the hallmarks of Polθ-mediated DNA repair. It has been hypothesized that, in addition to providing mechanistic synergy, inhibiting Polθ may extend the duration of PARP inhibitor responses by preventing or delaying the emergence of BRCA reversions. However, due to the challenge of creating reversion mutations via a clinically relevant mechanism, this hypothesis has not been experimentally addressed. Here, we use genetic tools to create targeted DNA single-strand breaks (SSBs) – the most common form of endogenous DNA damage – which can be converted to DSBs during DNA replication and are efficiently repaired by HR. As expected, SSBs in HR-proficient cells show no evidence of mutagenic DNA repair. In contrast, we find that in the context of HR deficiency, SSBs are repaired as genomic deletions flanked by regions of microhomology, suggesting a specific role for Polθ in the DNA repair process. Using MOMA-313 to inhibit Polθ activity, we demonstrate a broad role for Polθ in DNA repair initiated by SSBs in HR-deficient models, with MOMA-313 preventing the vast majority of DNA repair products. The extent of Polθ-mediated repair was unexpectedly broad, extending beyond canonical TMEJ products to include a large proportion of repair products with only one base pair of DNA microhomology. Importantly, the induction of SSBs adjacent to the pathogenic BRCA2 mutation in Capan-1 cells produced genomic deletions that restored the BRCA2 reading frame and caused cellular resistance to PARP inhibitor treatment. MOMA-313 dramatically reduced the frequency of these BRCA reversion mutations, preventing the emergence of PARP inhibitor resistance. These data provide experimental evidence that Polθ activity is a key contributor to PARP inhibitor resistance and provide a strong rationale for early and sustained Polθ inhibition in BRCA-mutant tumors to drive deeper and more durable clinical responses.

#0250 Targeting DNA damage repair pathway and CCR2$^+$ myeloid cell to overcome radioimmunotherapy resistance in small cell lung cancer.

Zhuoran Yao[1], Hui Wang[2], Kai Kang[1], Min Yu[2], Feifei Na[2], Ren Luo[2], Linglu Yi[2], Ruizhan Tong[3], Jianxin Xue[4], You Lu[5]

[1]West China Hospital, Sichuan University, Chengdu, China,[2]Department of Thoracic cancer, West China Hospital, Sichuan University, Chengdu, China,[3]Department of Thoracic cancer, West China Hospital, Chengdu, China,[4]Department of Thoracic Oncology, West China Hospital, Sichuan University, Philadelphia, PA,[5]Sichuan University West China School of Medicine, Chengdu, China

Background: Small cell lung cancer (SCLC) is a highly aggressive neuroendocrine carcinoma characterized by rapid progression and a high relapse rate. Although the combination of immune checkpoint inhibitors (ICIs) with radiotherapy (RT) has improved patient outcomes, acquired resistance remains inevitable. This study aims to elucidate the underlying mechanisms of radioimmunotherapy resistance and explore potential novel strategies.
Methods: We established a murine SCLC model of acquired radioimmunotherapy resistance by subjecting tumor-bearing mice to multiple cycles of RT + ICI until resistance developed. Subsequently, longitudinal single-cell RNA sequencing (scRNA-seq) analysis of tumor specimens was performed to validate the findings. The DNA damage repair (DDR) pathway was investigated using Western Blot, ELISA, and Transwell assays. The efficacy of adding PARP inhibitor (PARPi) to RT+ICI was evaluated *in vivo*.
Results: Analysis of the radioimmunotherapy-resistant murine SCLC model revealed that enhanced DDR activity, elevated CCL2 secretion, and increased of infiltration of CCR2$^+$ myeloid-derived suppressor cells (MDSCs), which were further validated by longitudinal scRNA-seq. Targeting the CCL2-CCR2 axis significantly delayed tumor relapse following RT + ICI treatment. Next, i*n vitro*, combining PARPi with RT synergistically suppressed DDR activation and inhibited CCL2-dependent MDSC migration. *In vivo*, concurrent administration of PARPi with RT + ICI was essential for achieving better tumor control and survival benefit compared with RT + ICI treatment, whereas delayed intervention of PARPi proved ineffective. Tumor microenvironment analysis demonstrated that the triple therapy (RT + ICI + concurrent PARPi) effectively suppressed the DDR pathway, significantly reduced CCR2$^+$ MDSC infiltration, and increased effector T cell recruitment.
Conclusion: DDR-driven CCL2 secretion recruits CCR2$^+$ MDSCs to mediate radioimmunotherapy resistance in SCLC. PARPi disrupts this axis through dual blockade of tumor DDR and MDSC recruitment. Our data revealed that the combination of concurrent PARPi with radio-chemo-immunotherapy as first line therapy in ES-SCLC is worth exploring and a prospective clinical trial is ongoing (NCT06217757).

#0251 Targeting cyclin K-CDK12 synergizes with ATR inhibition by limiting RPA chromatin loading in triple-negative breast cancer.

Eun-Bee Choi[1], Sophia Podeszwa[1], Ah-Ram Kim[2], Ashwani Bahl[3], Geoffrey I. Shapiro[1]

[1]Department of Medical Oncology, Dana-Farber Cancer Institute, Boston, MA,[2]Department of Genetics, Blavatnik Institute, Harvard Medical School, Boston, MA,[3]Carrick Therapeutics, Dublin, Ireland

Targeting cyclin K-CDK12 is a promising therapeutic due to its ability to induce homologous recombination (HR) repair deficiency through transcriptional regulation. Reduced CDK12 activity sensitizes HR repair-proficient tumor cells to PARP inhibitors (PARPi) and DNA-damaging agents. However, recent studies show that *CDK12*-mutant cancers lack the genomic signatures associated with HR repair deficiency and derive limited therapeutic benefit from PARPi. It is therefore essential to understand additional mechanisms by which cyclin K-CDK12 depletion promotes genomic instability beyond impaired HR repair. Here, we demonstrate that cyclin K-CDK12 depletion drives a replication stress (RS)-associated vulnerability and synergizes with ATR inhibition, using CT7311 (Carrick Therapeutics), a protein degrader of cyclin K. Triple-negative breast cancer (TNBC) cells, especially those with high *MYC* expression, were the most sensitive to CT7311 compared with estrogen receptor-positive (ER+) BC and non-transformed breast cells. Notably, CT7311 sensitivity did not correlate with HR repair status. In a DNA damage response-focused CRISPR screen with CT7311, DNA replication-related genes were highly enriched among the sensitizers, with effects stronger than those of HR repair-related factors. We validated three sensitizers, *TOPBP1*, *PRIM2*, and *PRPF19*, which are closely linked to ATR activation, a central RS regulator. Consistent with the screen, cyclin K-CDK12 depletion yielded synergistic cytotoxicity with ATR inhibition only in TNBC, not in ER+ BC cells. Mechanistically, CT7311 induces transcription-replication conflicts (TRCs), a known RS source, but fails to robustly activate ATR. Rather, it limits ATR activation by reducing the chromatin loading of Replication Protein A (RPA). This impaired ATR activation is further exacerbated when combined with tuvusertib (ATRi), leading to marked DNA damage specifically in replicating cells. Strikingly, RPA overexpression conferred resistance to the combination, indicating that the synergy arises from impaired availability of RPA. We further show that cyclin K-CDK12 regulates RPA chromatin loading via the PRPF19 E3-ligase complex. AlphaFold-Multimer predictions revealed interactions between cyclin K-CDK12 and the PRPF19 complex. CT7311 disrupted PRPF19 complex assembly, compromising its activity and impairing RPA ubiquitination. Notably, CDK12-mediated phosphorylation of CDC5L, a PRPF19 complex subunit, was required for RPA chromatin loading. Collectively, our work identifies cyclin K-CDK12 as a critical regulator of RPA dynamics and uncovers ATR dependency driven by cyclin K-CDK12 depletion. These insights extend the rationale for cyclin K-CDK12 targeted therapy beyond HR repair-focused applications, supporting its use in RS-high tumors including TNBC, as monotherapy or in combination with ATR inhibition.

#0252 Targeting replication stress promotes immunogenic cell death in chordoma.

Nindo Punturi[1], Arijit Ghosh[2], Caitlin King[1], Wendy Leung[3], Joan B. Levy[4], Lee Zou[2], Gregory M. Cote[3], Dan Freed[1]

[1]Chordoma Foundation, Durham, NC,[2]Duke University School of Medicine, Durham, NC,[3]Massachusetts General Hospital, Boston, MA,[4]Melanoma Research Alliance, Hamden, CT

Chordoma is a rare bone cancer with a high rate of recurrence and no approved systemic therapies. Target discovery efforts have uncovered complex genomic rearrangements, alterations in DNA damage response (DDR) and chromatin-remodeling genes, and a reliance on DDR pathways that stabilize stalled replication forks. Additionally, a subset of chordomas is highly infiltrated by multicellular immune aggregates, but the underlying mechanisms driving an antitumor immune response remain unclear. We hypothesized that replication stress presents an actionable therapeutic vulnerability in chordoma and that targeting this pathway could induce lethal DNA damage and immunogenic cell death. To assess the effects of exacerbating replication stress in chordoma, a panel of 14 cell lines was treated with the DNA synthesis inhibitor gemcitabine or the ATR inhibitor elimusertib (BAY 1895344). Most lines were highly sensitive, with 9 of 14 showing EC_{50} values below 10 nM (gemcitabine) or 100 nM (elimusertib). Biochemical analysis showed that gemcitabine-induced DNA damage leads to activation of Chk1 in an ATR-dependent manner, with DNA fiber assays revealing decreased replication fork speed, symmetry, and stability following ATR inhibition (ATRi). Sensitivity to ATRi or gemcitabine was mirrored in chordoma PDX models, with ATRi promoting 85–90% tumor growth inhibition in sensitive models and gemcitabine driving tumor regressions. Exceptional synergy was observed in vitro when these therapies were combined, with significant reductions in cell viability, enhanced DNA double-strand breaks, and near-complete S-phase collapse. Moreover, treatment with either drug resulted in the accumulation of double-stranded DNA in the cytoplasm, along with upregulation of type I interferon, immunomodulatory chemokines CXCL10 and CCL5, and cell surface PD-L1. These findings are consistent with a model where ATRi or gemcitabine treatment promotes lethal DNA damage and immunogenic cell death in chordoma, which may be further augmented by PD-1 checkpoint blockade.

#0253 Antitumor activity of PARP inhibitors in combination with Temozolomide in fumarate hydratase-deficient RCC.

Sameer Issaq, Kylie Enten, Emily Hnath, **Komal Rawal**, Ramaprasad Srinivasan

Urologic Oncology Branch, National Cancer Institute, National Institutes of Health,, Bethesda, MD

Hereditary Leiomyomatosis and Renal Cell Cancer (HLRCC) is a rare form of RCC associated with an aggressive clinical course. Despite the recent availability of therapeutic approaches active in FH-deficient RCC, most patients with advanced HLRCC die from their disease; identification of additional effective treatment strategies for these patients is, therefore, a therapeutic imperative. HLRCC is characterized by germline pathogenic variants in the *fumarate hydratase (FH)* gene, that encodes a key Tricarboxylic Acid (TCA) Cycle enzyme. Loss of FH activity leads to the accumulation of its substrate, fumarate. Excess fumarate serves as an oncometabolite and has been reported to suppress DNA damage repair. We evaluated the activity of PARP inhibitor-based combinations in preclinical models of HLRCC. The antitumor activity of two PARP inhibitors, Talazoparib and Niraparib, either as single agents or in combination with the alkylating chemotherapy agent temozolomide, was evaluated in several patient-derived HLRCC cell lines. In vitro viability assays demonstrated that both PARP inhibitors induced dose-dependent growth inhibition in HLRCC lines. The addition of temozolomide to either PARP inhibitor led to more pronounced reductions in cell proliferation across the HLRCC lines tested, compared to control single PARP inhibitors or temozolomide alone. At the molecular level, western blot analysis demonstrated that PARP inhibitors inhibited PARylation with concomitant upregulation of phosphorylated (γ) H2AX expression, and increased apoptosis. Furthermore, the effects on PARylation, γH2AX accumulation, and apoptosis were more pronounced in the PARP inhibitor/temozolomide combinations than with PARP inhibitors alone and were accompanied by substantial increases in cleaved PARP. These results demonstrate that PARP inhibitors have antitumor activity against HLRCC cells and that their activity is potentiated by the addition of the alkylating agent temozolomide. Additional in vitro and in vivo studies are ongoing to further define the activity of these combinations and to better understand the underlying molecular mechanisms. This study highlights the potential therapeutic utility of PARP inhibitor-based combinations in targeting DNA repair defects in HLRCC and provides the impetus for further exploration of this strategy.

#0254 The PARP1-selective inhibitor and trapper saruparib achieves extended PARP1 target engagement *in vitro*, *in vivo* and in the clinic.

Mark Robert Albertella[1], Giuditta Illuzzi[1], Anna D. Staniszewska[1], Domenic Pilger[1], Sophie Cooke[1], Spiros Linardopoulos[2], Anna Beckett[1], Christopher Stubbs[3], Ganesh Moorthy[4], Mark J. O'Connor[1]

[1]Bioscience, AstraZeneca Oncology R&D, Cambridge, United Kingdom,[2]Translational Medicine, AstraZeneca Oncology R&D, Cambridge, United Kingdom,[3]Discovery Sciences, AstraZeneca R&D, Cambridge, United Kingdom,[4]AstraZeneca Oncology R&D, Boston, MA

Saruparib (AZD5305) is a potent and selective inhibitor and trapper of PARP1 which is currently in ph3 clinical development. Initial preclinical characterisation highlighted nanomolar PARP1 inhibition potency and differentiated PARP1 binding profile with longer residence time kinetics compared with approved non-selective PARP inhibitors (PARPi). Here we describe the consequences of this in pre-clinical and clinical studies where we analysed PARP1 inhibition duration and phenotypic effects after different exposure times to saruparib. Surface plasmon resonance (SPR) of purified PARP1 showed that saruparib has a very slow dissociation rate, K_{off}, and extended residence time on purified PARP1 protein (>5 days) compared to approved PARP1/2 inhibitors (hours). In cellular assays, saruparib treatment followed by wash-off resulted in sustained suppression of Poly ADP Ribose (PAR) over several days, whereas PAR levels recovered within 24 hours after olaparib exposure. We explored the duration of *in vivo* pharmacodynamic effects by monitoring PAR levels after steady state dosing of saruparib to mice bearing BRCA1-mutant MDA-MB-436 tumours, for up to 7 days after cessation of dosing. Saruparib at 0.01, 0.03 or 0.1mg/kg maintained PAR inhibition of >90% for up to 7 days, although the drug levels were not detectible in plasma after 2 days, confirming this extended duration of action *in vivo*. In contrast, PAR levels were substantially recovered by 24 hours after olaparib dosing. The functional consequences of the extended duration of action of saruparib were evaluated for *in vivo* efficacy. Multiple intermittent schedules of saruparib, compared to olaparib or talazoparib were evaluated in the BRCA1m-MDA-MB-436 model. Strong regressions were observed with saruparib on intermittent schedules where even 1 wk on, 2 wk off schedule at 1mg/kg (equivalent to the clinical RP2D dose of 60mg) gave durable regressions. A reduced dose of saruparib of 0.1mg/kg was still effective on an intermittent schedule, but lost significant activity compared to the higher dose. Intermittent dosing schedules of saruparib were clearly superior to the same schedules of olaparib or talazoparib at clinically equivalent doses. The long duration of activity of saruparib observed in preclinical studies were also observed in the PETRA clinical study (NCT04644068). A single dose of saruparib resulted in >90% PAR inhibition for up to 7 days, despite no drug being detected in plasma after 48 hours. These data suggest that short-term dose interruptions are unlikely to result in reduced efficacy, in contrast to approve non-selective PARPi where dose interruptions have been shown to reduce efficacy. These data also suggest that intermittent scheduling may be effective for saruparib in circumstances where minimising exposure may provide an optimal risk-benefit - for example cancer prevention.

: Gene and Vector-Based Therapy
Poster Session

#0258 Preclinical study of nucleic acid therapeutics targeting the Warburg effect.

Keita Matsumoto, Hirokatsu Hayashi, Seito Fujibayashi, Noriki Mitsui, Takeshi Horaguchi, Yuji Hatanaka, Ryoma Yokoi, Ayana Yokoyama, Chika Mizutani, Masashi Kuno, Masahiro Fukada, Ryuichi Asai, Itaru Yasufuku, Yuta Sato, Jesse Yu Tajima, Yoshihiro Tanaka, Nobuhisa Matsuhashi

Gifu Univ. Hospital, Gifu, Japan

[Background] Cancer cells rely on glycolysis for energy, known as the Warburg effect, which supports survival by promoting nucleotide synthesis, reducing oxidative stress, and inhibiting cell death.
Polypyrimidine tract-binding protein 1 (PTBP1) regulates pyruvate kinase muscle (PKM1/PKM2) splicing, maintaining a PKM2-dominant state. Suppressing PTBP1 shifts cellular metabolism to a PKM1-dominant state, reduces glycolysis, alters ATP production, and increases oxidative stress, ultimately resulting in cell death.
We developed optimized chemically modified siR-PTBP1 derivatives to evaluate their therapeutic potential.
[Methods] Anti-proliferative activity in human colorectal DLD-1 cells was tested by chemically modified siR-PTBP1 derivatives. Cell viability was assessed by CVS assay, and PTBP1, PKM1/PKM2, and cleaved PARP protein levels were analyzed by Western blotting and immunostaining after the transfection. ATP production and oxidative stress assay were performed to examine the alternation from glycolysis-dominant to oxidative phosphorylation via TCA cycle. Metabolome analysis was also examined.
[Results] Among 14 derivatives, the derivative siR-2-6 significantly suppressed PTBP1, increased PKM1 expression, and raised the PKM1/PKM2 ratio. Increased cleaved PARP expression indicated apoptosis induction and Warburg effect suppression. Also, siR-2-6 increased ATP production and oxidative stress, resulting in apoptosis. The higher RNase resistance and biological activity under RNase-containing conditions were shown in comparison to those of the SiR-2-1 that is not chemically modified.
[Conclusion] Optimized siR-PTBP1 derivatives increased the PKM1/PKM2 ratio and partially shifted cellular metabolism from glycolysis dependence to oxidative phosphorylation, highlighting their potential as nucleic acid therapeutics.
The enhanced RNase resistance of siR-2-6 further supports its promise for in vivo application and clinical translation.

#0259 Targeted STEAP2 knockdown with self-delivering antisense oligonucleotide reduces cancer malignant behavior.

Nagesh K. Panchal[1], Araceli Bernal[1], Brittany Michelle Barre[1], Francisco Cigarroa[2], LuZhe Sun[1]

[1]Cell System and Antomy, The University of Texas Health Science Center At San Antonio, San Antonio, TX,[2]Transplant Center, The University of Texas Health Science Center At San Antonio, San Antonio, TX

Background: The STEAP (Six-Transmembrane Epithelial Antigen of Prostate) family encodes metalloreductases involved in iron and copper metabolism, with increasing evidence linking dysregulated metal homeostasis to tumor progression. Increased STEAP2 expression has been implicated in the development and progression of several cancers, with enhanced cellular proliferation, migration, but its precise role in cancer remains obscure. The goal of this project is to investigate the significance and prognostic potential of targeting STEAP2 in oncogenesis.

Methods: Our study investigated a self-delivering antisense oligonucleotide (ASO) targeting STEAP2 in cancer. Human liver cancer SNU398 and prostate cancer PC3 cells were treated with increasing ASO concentrations (0.25, 0.5, 1 and 5 μM) for 92 hours, followed by assessment of cell viability (WST-1), migration (transwell), and anchorage-independent growth (soft agar). For the in vivo study, orthotopic xenografts were created by injecting SNU398-luc/GFP cells into the livers of immunodeficient mice. Beginning on day 7, mice received 12 doses of the STEAP2-ASO or scrambled control (5 mg/kg, every two days). Tumor growth was monitored non-invasively via IVIS imaging. Upon treatment completion, tumors and adjacent liver tissues were harvested. Expression of EMT markers (Vimentin and SNAIL1) was evaluated in cell and tissue lysates using western blot analysis.

Results: ASO mediated KD of STEAP2 induced a dose dependent reduction in STEAP2 expression, leading to significantly reduced cell viability, migration, and anchorage-independent growth in both SNU398 and PC3 cell lines. In addition, STEAP2 knockdown resulted in decreased expression of key EMT markers, including Vimentin and SNAIL1. *In vivo* analysis demonstrated that treatment with STEAP2 targeting ASOs resulted in a substantial decrease in tumor size, together with downregulation of STEAP2 levels, highlighting a clear association between STEAP2 suppression and inhibition of cancer progression. Consistent with the in vitro findings, tumors from ASO-treated mice also showed reduced Vimentin and SNAIL1 expression, further supporting EMT attenuation. Thus, our findings emphasize STEAP2 as an essential regulator of cancer development and progression as well as the therapeutic promise of the ASO-based STEAP2 silencing for abrogating the progression of liver and prostate cancer.

Conclusion: Overall, these findings establish STEAP2 as a potential biomarker and therapeutic target for the intervention of various cancers.

#0260 EpCAM-CD3 bispecific antibody-encoding mRNA delivered by lung targeted lipid nanoparticles suppresses orthotopic lung tumor growth.

Dong Wang[1], Gang Liu[1], Yuhe Han[2], Maorong Fu[3], Tingting Li[3], Xiangnan Qiang[1], Shunchuan Zhang[3], Zhixiang Zhang[1], Letian Kuai[1]

[1]WuXi AppTec, Shanghai, China,[2]WuXi AppTec, Nantong, China,[3]WuXi AppTec, Chengdu, China

The therapeutic use of bispecific T-cell engaging (BiTE) antibodies has shown great potential for treating malignancies. However, full exploitation of the potential of BsAbs is hindered by manufacturing challenges and short serum half-lives. In contrast, mRNA therapeutics have emerged as a powerful approach for treating a wide range of diseases. Their applications are increasingly linked to advancements in targeted delivery technologies and the production of mRNA encoded antibody is more flexible and cost-effective than the traditional method. In this work, We developed a lung selective organ targeting lipid nanoparticles (SORT LNPs)-formulated RNA (RNA-LNP) encoding a T cell-engaging bispecific antibody that binds the T cell marker CD3 and bivalently binds epithelial cell adhesion molecule (EpCAM), an epithelial antigen that is expressed on various solid tumors. We first performed *In vitro* flow cytometry analysis, which revealed that mRNA lipid nanoparticles (LNP) effectively mediated the killing of EpCAM positive tumor cells and activated human T cells. Then we established NCI-H441 lung orthotopic tumor model in PBMC humanized mice. We observed robust antitumor efficacy of mRNA LNP in this tumor model. To assess mRNA distribution, we quantified its content in various organs using qPCR. Results confirmed the lung targeting specificity of LNP. Moreover, we analyzed the activation of tumor-infiltrating T cells post mRNA LNP treatment. Finally, we conducted histopathological examination of various organs and we didn't find signs of adverse effects from LNP formulated mRNA administration. In this comprehensive preclinical evaluation, we demonstrated that mRNA-encoded bispecific antibody promoted the activation and cytotoxicity of human T cells, exhibiting significant inhibition of orthotopic lung tumor growth *in vivo*. These findings underscore the potential research value of mRNA-encoded CD3-EpCAM T cell engager in treating solid tumors, marking a potential shift in the clinical application of protein-based T-cell engagers.

#0261 A mRNA-encoded trispecific CD19xBCMAxCD3 T cell engager to treat cancer and autoimmunity.

Beibei Cao[1], Bingxu Zhang[1], Shuting Yao[1], Qiang Zhang[2], Shanshan Zhou[1], Lun Zhang[1], Lei Li[2], Chenxing Ni[2], Jianqi Zhang[2], Ya Zhou[1], Xiaoyun Ma[2], Xiaoju Zhang[1], Hongya Han[1], **Wei Xu**[1]

[1]METiS TechBio, Hangzhou, China,[2]METiS TechBio, Beijing, China

Background: B-cell-directed therapies have transformed treatment for B-cell-driven cancers and autoimmune diseases, yet current T-cell-based modalities, including CAR-T cells and T-cell engagers (TCEs), are limited by safety concerns such as cytokine release syndrome (CRS)—a particular risk for autoimmune patients requiring wide safety margins. In addition, plasma cells drive disease progression and relapse but are not efficiently eliminated by CD19-targeted treatments. To overcome these limitations, we developed a first-in-class mRNA-encoded trispecific TCE targeting CD19, BCMA, and CD3 to achieve broad B-cell and plasma-cell depletion with improved safety.

Methods: The TCE was constructed by fusing a CD3-binding scFv with VHH domains targeting CD19 and BCMA. The encoding mRNA was optimized through codon and structural engineering to balance Codon Adaptation Index (CAI) and Minimal Free Energy (MFE) across untranslated regions and the coding sequence. The optimized mRNA was formulated in a novel lipid nanoparticle (LNP) designed for preferential biodistribution to secondary lymphoid organs, including spleen, bone marrow, and lymph nodes. B-cell cytotoxicity was evaluated using PBMCs from healthy donors, autoimmune patients, or in BCMA+ multiple myeloma co-culture assays. In vivo B-cell depletion, pharmacokinetics, biodistribution, and safety were tested in humanized immune-deficient mice reconstituted with CD34+ HSCs or systemic lupus erythematosus (SLE) PBMCs, in human CD19/CD3 transgenic mice, and in non-human primates (NHPs). Activity against BCMA+ tumors was assessed in PBMC-reconstituted multiple myeloma xenografts.

Results: The mRNA-encoded TCE induced potent B-cell killing in human PBMC assays, achieving an EC50 of ~0.1 pM. Robust B-cell depletion was confirmed across multiple mouse models. In the SLE-PBMC model, treatment significantly reduced autoantibody levels. In OPM2 tumor-bearing mice, the TCE induced profound CD19+ B-cell depletion in blood and lymphoid tissues and complete regression of BCMA+ tumors. In NHPs, ultra-low mRNA-LNP dosing (5 μg/kg) produced complete peripheral B-cell depletion within 6 hours, with broad depletion of naïve, memory, and plasma cell compartments in spleen, lymph nodes, and bone marrow by day 15. B-cell reconstitution began ~3 weeks post-dose and was dominated by naïve phenotypes, suggesting immune resetting. Subcutaneous dosing achieved efficacy comparable to intravenous delivery but with markedly reduced cytokine release, consistent with the favorable pharmacokinetic profile of mRNA translation. No toxicity or clinical pathology abnormalities were observed at doses up to 100 μg/kg.

Conclusion: This mRNA-encoded trispecific CD19×BCMA×CD3 TCE demonstrates potent and broad B-cell and plasma-cell depletion, anti-tumor activity, and an improved safety profile, supporting ongoing First-in-Human clinical evaluation.

#0262 Leveraging cancer-activated gene expression and cGAS-STING activation for efficient tumor killing via a DNA-LNP delivery platform.

Moataz Reda, Evan Bishop, Priyanka Balasubrahmanyam, Blaine McCarthy, Sushil Lathwal, Robby Chandra, Audrey Smith, Xiao Wu, Jesse Simons, Kim Tran, Ajda Rojc, Jayalakshmi Ramani, Suyog Shaha, Dang Dang, David Rosen, Badri Ananthanarayanan, Nadege Morisot, David Suhy

Earli Inc., Redwood City, CA

Background: Despite rapid advances in immunotherapy, the clinical use of potent immune-modulating agents remains constrained by systemic toxicities. Earli is developing a DNA-based immunotherapy platform that uses synthetic cancer-activated promoters (CAPs) to drive selective expression of therapeutic payloads in malignant cells, while remaining silent in normal tissues and benign lesions. DNA is delivered systemically to the tumor cells by lipid nanoparticles (LNPs). The platform also engages innate immunity via the immunostimulatory nature of DNA. This study highlights the dual mechanism of combining 1) CAP-driven expression of a potent immunostimulatory payload such as IL-12 with 2) cGAS-STING-induced innate immune activation.
Methods: Naïve or tumor-bearing mice were treated with LNPs encapsulating either a DNA nanoplasmid encoding IL-12 under a cancer-activated promoter (CAP-IL-12) or a matched construct with three stop codons (Control-DNA). Mice were assessed for tumor growth inhibition, cytokines (IL-6, IL-1β, TNF-α), and IL-12 levels in tumor and serum.
Results: LNP encapsulating Control-DNA increased transcript levels of STING downstream targets and triggered a transient rise in pro-inflammatory cytokines. This innate immune response resulted in a partial (i.e. non-durable) inhibition of tumor growth across multiple syngeneic tumor models and showed enhanced efficacy when combined with PD-1 checkpoint blockade. Importantly, in STING knockout mice, the anti-tumor response to the formulated Control-DNA was completely lost. In contrast, IV treatment with an LNP encapsulating CAP-IL-12 DNA led to complete and durable tumor regression. Surprisingly, although modest IL-12 protein was detectable in tumors, there were no substantial IL-12 levels measured in serum, demonstrating the platform's ability to concentrate a highly potent therapeutic at the tumor site while avoiding systemic exposure. Further, immune profiling showed both IL-12 and STING induced changes including increases in T cell and NK cell proliferation, granzyme B upregulation, and enhanced myeloid activation and antigen presentation. Importantly, the anti-tumor efficacy of CAP-IL-12 was retained in syngeneic tumors in STING knockout mice, demonstrating that cancer-specific payload expression is sufficient to drive efficacy even in the absence of adjuvant STING agonism. Our current work focuses on modulating STING agonism through LNP engineering approaches to fine-tune its activity in the tumor for a balanced therapeutic response.
Conclusions: Overall, our findings highlight the dual-function nature of Earli’s DNA-LNP platform: a programmable, tumor-selective gene therapy system with built-in innate immune activation through STING agonism. The approach supports a new class of immunotherapies that combine precision and potency in a single genetic modality.

#0263 Towards personalized cancer vaccines: LNP-mediated delivery of multi-epitope mRNA extends survival in aggressive melanoma cancer model.

Jay Paquette, Gayatri Namala, Leanna Yee, Sams MA Sadat, Ruchi Sharma, Darius Menezes, Pierrot Harvie, Nikita Jain, Zhengyu Chen, Malathi Anantha, Tony Wu, Vicente Lacap, Richard Jiang, Vinay Mayya, Sijo Chemmannur, Avisek Deyati, Anitha Thomas

Cytiva, Vancouver, BC, Canada

Personalized cancer vaccines (PCVs) open new doors for immunotherapy by harnessing the immune system to target tumor specific neoantigens — mutated proteins — unique to an individual's cancer. Lipid nanoparticle (LNP)-based mRNA vaccines, shown to be effective against COVID-19, serve as a suitable platform for delivering multi-epitope neoantigen mRNA payloads. LNP drug product for PCV applications however, may require optimization of the multi-antigenic mRNA cargo, target tissue uptake, and endosomal release, along with frequent therapeutic dosing. We identified 10 melanoma-specific antigens and synthesized multiple multi-antigen mRNA constructs encoding various antigen combinations, with and without marker epitopes such as ovalbumin (OVA), eGFP, and firefly luciferase (Fluc). We developed proprietary ionizable lipids and encapsulated the various multi-epitope mRNA constructs in LNPs and evaluated their performance in well-established *in vitro* cell based assays and a B16F10 syngeneic mouse melanoma model. The *in vitro* cell-based assays confirmed effective LNP-mediated delivery, mRNA translation, and antigen presentation via major histocompatibility complex (MHC) molecules. *In vivo* imaging demonstrated payload expression 6 hours post-injection. Selected multi-epitope mRNA-LNP formulations were administered intramuscularly in B16F10 tumor-bearing mice. Multi-epitope comprising LNPs significantly reduced mean tumor growth rate and extended survival in vaccinated mice compared to controls. Additionally, repeated dosing regimens showed favorable safety profiles. These results demonstrate that our proprietary LNP platform efficiently delivers multi-epitope mRNA LNPs, eliciting potent anti-tumor immune responses in a relevant melanoma model and demonstrating safety of repeated LNP administrations for shared or individualized cancer vaccine applications. This positions our LNP as a promising candidate for further developing PCVs and accelerating new personalized medicine to clinic.

#0264 A novel gene therapy approach for treating breast cancer through the overexpression of mutant estrogen receptor.

Seung-hwan Jeong[1], Seokbong Hong[2], Hyeong Dong Yuk[2], Cheol Kwak[2]

[1]Seoul National University, Seoul, Korea, Republic of,[2]Seoul National University Hospital, Seoul, Korea, Republic of

Background: Endocrine therapy (ET) is the primary treatment for hormone receptor-positive (HR+) breast cancer, but resistance inevitably develops, leading to endocrine-resistant breast cancer. While agents like tamoxifen and aromatase inhibitors improve outcomes, resistance mechanisms remain significant challenges. This suggests a complex role for estrogen receptor (ER) signaling. We hypothesized that maintaining a non-functional, mutant ER (mER) could overcome this resistance.
Methods: We synthesized a full-length ER (ESR1) gene with a mutation in the DNA-binding domain (DBD). To ensure targeted delivery, the mER-encoding plasmid was encapsulated within poly(lactic-co-glycolic acid) (PLGA) nanoparticles. These nanoparticles were surface-functionalized with 4-carboxyl-17beta-estradiol, an ER ligand, to facilitate active targeting to ER-positive breast cancer cells. The effects of mER overexpression were investigated in vitro using HER2-ER+PR+ MCF7 and T47D cell lines, as well as their tamoxifen-resistant (TamR) counterparts. In vivo antitumoral effects were assessed using xenograft mouse models.
Results: The ER-targeted PLGA nanoparticles effectively delivered the mER plasmid to ER-expressing breast cancer cells in vitro and in vivo. Overexpression of mER did not activate estrogen-responsive genes and exerted a potent antiproliferative effect in both MCF7 and T47D cells. Notably, mER overexpression maintained its strong antitumoral activity in tamoxifen-resistant (TamR) MCF7 and T47D cells. Mechanistically, mER overexpression led to a reduction in wild-type ER (wtER) levels and suppressed DNA replication-related gene pathways. In vivo, mER treatment significantly inhibited the growth of both standard and tamoxifen-resistant tumors. Furthermore, a synergistic antitumoral effect was observed when mER was combined with tamoxifen.
Conclusions: Overexpression of a mutant ER with a non-functional DBD, delivered via an ER-targeted nanoparticle system, represents a novel therapeutic strategy for advanced HR+ breast cancer, including endocrine-resistant and tamoxifen-resistant disease. By suppressing wtER, disrupting DNA replication, and maintaining activity in resistant models, mER effectively inhibits tumor growth and overcomes therapeutic resistance.

#0265 Engineering robust AAV vectors: Addressing ITR instability for effective cancer gene therapy.

Crystal Richardson, Sofija Markovic, Cassandra Koole, Andrea O'Hara, Sumit Kumar

Azenta Life Sciences, Burlington, MA

Introduction: Cancer remains one of the most challenging diseases to treat due to the complexity of tumor biology and barriers to effective drug delivery. Gene therapy using adeno-associated viruses (AAVs) offers a promising approach for oncology, particularly with the development of engineered capsids such as AAV-DJ, which demonstrate enhanced tissue penetration and targeted gene expression in tumor microenvironments. Importantly, AAV-based strategies are also being explored in neuro-oncology, where capsid variants capable of crossing the blood-brain barrier provide new opportunities for treating aggressive brain tumors such as glioblastoma. The AAV genome consists of a therapeutic transgene flanked by 145 bp inverted terminal repeats (ITRs), which are prone to mutations and deletions but also essential for viral packaging. While capsid engineering has improved tumor targeting and systemic delivery, ITR instability remains a critical challenge for consistent therapeutic outcomes.
Methods: In this study, we evaluated the impact of five common ITR mutations on vector integrity and performance. HEK293T cells were co-transfected with transfer, Rep/Cap (AAV-DJ), and helper plasmids for viral packaging. ITR mutations were confirmed via Sanger sequencing, and purified vectors were assessed for viral titers using qPCR and transduction efficiency via GFP fluorescence microscopy. Mutant ITRs were subsequently repaired to wild-type sequences to compare recovery of function. To model therapeutic relevance, AAV vectors were tested in tumor-bearing mice using immunofluorescence markers to assess transgene expression within cancerous tissues.
Results: Even minor ITR alterations, such as single base pair deletions, demonstrated significantly reduced viral titers and transduction efficiency, with more pronounced effects in constructs carrying large therapeutic cassettes. Although mutant vectors retained some tumor-targeting capability, wild-type ITR constructs achieved the highest efficiency.
Conclusion: This work underscores the critical role of ITR integrity in AAV-based oncology applications, including neuro-oncology. Even small sequence disruptions can compromise vector potency, highlighting the need for rigorous quality control during vector design and production. These findings inform the development of robust AAV platforms for cancer gene therapy, ensuring optimal delivery and therapeutic impact.

#0266 Redtail: A dual-programmable virotherapy platform for systemic tumor targeting and localized gene delivery.

Yunyi Kang[1], **Duong H. Nguyen**[1], Stephanie Songco[1], Trevor Smith[1], David Nguyen[1], Yan Pang[1], Lina Schulte[2], Hongli Zhang[2], Sinje Tigges[2], Fabian Kortum[2], Daniela Kleinholz[2], Susan Tamraz[2], Ivelina Minev[1], Evan Cassavaugh[1], Travis Clifton[1], Thomas Herrmann[2], Barbara Hartl[2], Antonio F. Santidrian[1]

[1]Calidi Biotherapeutics, San Diego, CA,[2]StemVAC GmbH, Bernried, Germany

RedTail is a next-generation gene therapy platform combining systemic delivery with tumor selectivity. Unlike conventional oncolytic viruses, RedTail integrates programmable targeting for precise tumor specificity and genetic payload delivery for immune modulation of the tumor microenvironment (TME). It employs a tumor-specific, replicating extracellular enveloped vaccinia virus (EEV) cloaked in a second human cell-derived membrane (the “Envelope”) from engineered host cell lines; chimeric CD55 overexpression in the Envelope confers resistance to complement and neutralizing antibodies, enabling systemic administration. The Envelope can be further designed to express targeting proteins. The viral genome can be modified to deliver immune-cell activating therapeutic payloads such as IL-15 Superagonist along with bispecific T-cell engagers (BiTEs) for localized expression in the tumor microenvironment. Delivering BITEs at high concentrations to the tumor while simultaneously activating T-cells in the TME through in situ expression of an immunostimulatory payload may overcome the challenges seen to date with T-cell engagers in solid tumors.
Methods: RedTail EEVs were produced using engineered host cell lines expressing chimeric antigen receptors (CARs). The RedTail EEVs were further engineered to express BITEs and T-cell activating payloads at high concentrations in situ. Tumor targeting, viral amplification, and transgene expression were assessed by viral titers, ELISA, flow cytometry, and immunohistochemistry.
Results: The first programmable characteristic of RedTail is its extracellular membrane. RedTail EEVs were manufactured using host cell lines engineered to express CARs, producing particles that displayed CARs (e.g., anti-HER2, anti-Trop2) on their surface with corresponding tropism.The second programmable characteristic is the viral genome, engineered to express genetic payloads including BiTEs targeting tumor antigens along with CD3 to recruit and activate T cells. A T-cell activating payload was also included. Viral infection was enhanced for tumor cells that displayed the cognate target, and resulted in tumor cell lysis along with high levels of expression of the BITE and the immune stimulating payload.This dual programmability—membrane engineering for targeting and genome programming for payload delivery—represents a unique approach among systemic virotherapies.
Conclusions: This dual programmability enables systemic tumor targeting, immune priming, and localized expression of both a T-cell engager and an immune priming payload, positioning RedTail as a next-generation systemic platform with a unique approach to T-cell targeting in solid tumors.

#0268 Engineering a novel epithelial-tropic pseudovirus platform for targeted gene therapy to carcinomas.

Kendall Wesley Knechtel, Daniel Pelaez

University of Miami Miller School of Medicine, Miami, FL

Carcinomas represent over 80% of all cancer diagnoses and remain difficult to treat due to genetic heterogeneity, acquired drug resistance, and limited therapeutic specificity. Oncolytic viral therapies (OVTs) have shown promise for many cancers; however, current platforms such as the modified herpes simplex virus rely on intratumoral delivery and remain highly immunogenic, restricting their use against deep-seated and metastatic epithelial malignancies. To address this, we developed a non-replicative pseudotyped lentiviral platform designed with epithelial tropism and stable genomic integration. Our engineered chimeric envelope surface receptor retains key native receptor interactions of the L1 capsid protein of the human papilloma virus, designed in-silico to exploit functional domains, while preserving vital molecular mechanisms. This glycoprotein, combined with lentiviral backbone elements, yields a morphologically intact virion, confirmed by negative-stain TEM, that avoids virus-like-particle formation prior to plasma membrane trafficking. Transduction assays demonstrated selective infection and sustained transgene expression in epithelial cell lines as opposed to non-epithelial controls. To enhance selectivity, cancer-specific promoters would further confine payload expression to malignant epithelial cells. The pseudovirus can deliver a larger payload (8-10 kb) greater than that of Adeno-Associated Virus (≤ 4.7 kb) supporting complex therapeutic cassettes, including suicide genes and barrier-repair payloads. Our ongoing in-vitro and in-vivo studies are evaluating therapeutic delivery and efficacy in specific carcinoma models.

#0269 Functionalization of virus-like particles for improved *in vivo* immune cell engineering.

Frances Rocamora[1], Matthew S. Kim[1], Barbara S. Perez[2], Vivian Le[1], Trinidad Kellemen[1], Enaaya Mahmood[1], Dan Kaufman[1]

[1]UC San Diego School of Medicine, La Jolla, CA,[2]UC San Francisco, San Francisco, CA

To address the limitations of conventional chimeric antigen receptor (CAR) T cell manufacturing, we developed a novel *in vivo* CAR engineering platform based on functionalized virus-like particles (VLPs) that self-assemble with a minimal viral genome to efficiently package and deliver mRNA payloads. Our initial studies compared the level and stability of transgene (GFP) expression in primary human T cells transduced with VSV-G pseudotyped lentivirus (LV) with those transduced with our mRNA-delivering VLPs and circular DNA-forming non-integrating LV (NILV). In these studies, our VLPs transduce over 20% more cells at an equivalent titer than both LV and NILV. As expected, GFP expression from VLP-treated and NILV-treated T cells declined 72 hours after VLP removal, consistent with transient transgene expression. To further improve the platform, we modified the VLP envelope in two ways. First, we added an anti-CD3-targeting single-chain variable fragment (scFv) fused to a low-density lipid (LDL) receptor-blind mutant of the VSV-G fusogen protein (VSVg mut). This construct promotes T cell-specific targeting without non-specific cell binding. In a co-culture model of T cells and Raji B cells, we demonstrated that our scFv-coated VLPs can transduce up to 15% of T cells while less than 1% of B cells are transduced. Because the targeting molecule is derived from blinatumomab, anti-CD3 scFv-coated VLPs also induced upregulation of activation markers CD69 and CD25 in primary human T cells relative to a non-functionalized VLP control. Second, we engineered our VLPs to express an immune-enhancing molecule to both improve mRNA delivery and augment the cytotoxic activity of engineered T cells. While scFv-coated VLPs delivering an anti-CD19 CAR transduced less than 5% of rested primary T cells, enhancer-coated VLPs transduced about 35% of cells and dual-functionalized VLPs (scFv + enhancer) transduced approximately 24% of cells. Next, we used *in vitro* live cell imaging assays (Incucyte) to quantify killing of CD19+ Nalm6 cells with functionalized VLP-treated rested T cells over 72 hours. While the cells treated with only anti-CD3 scFv-coated VLPs did not elicit a significant anti-tumor activity (demonstrated by continued growth of the tumor cells), targeting T cells using just the enhancer-coated VLPs lead to ~75% decrease in tumor cells compared to control targeted T cells. Notably, T cells treated with dual functionalized VLPs (anti-CD3 scFv plus enhancer) led to almost complete tumor cell killing (>95%). In conclusion, our novel VLP system with using dual immune cell targeting via anti-CD3 and functionalized envelope enhances mRNA delivery and anti-CD19 CAR-T cell-mediated cytotoxicity *in vitro*. In vivo studies using humanized mouse models are underway to validate this *in vivo* engineering and anti-tumor efficacy.

#0270 pIR-a new antibiotic free plasmid production platform for non-viral DNA delivery.

Dan Zhao, Yifei Wang, Junhao Wang, Zak D. Carden, Perry Ayn Mayson Maza, Dana Rae Cyril-Ramirez, Yong Li

Baylor College of Medicine, Houston, TX

Plasmid-based non-viral DNA delivery systems are widely utilized in gene therapy and cancer immunotherapy due to their safety and scalability. However, conventional production depends on antibiotic resistance markers, creating regulatory hurdles and complicating manufacturing. To overcome these limitations, we developed pIR, an antibiotic-free plasmid production platform that employs an arabinose-inducible Cre recombinase system to excise the antibiotic resistance gene during amplification. This system uses a pir+ bacterial strain supporting replication of R6K-origin plasmids, enabling high-yield production of antibiotic-free DNA suitable for clinical applications. We first verified that pIR generates high-purity DNA with over 80% of the final product in supercoiled form. Next, we compared pIR-derived plasmids to the traditional gWiz vector using Firefly luciferase (Fluc) and NanoLuc reporters in both in vitro and in vivo models. Our plasmids exhibited superior transgene expression and favorable safety profiles. Further comparison with the commercially available Nanoplasmid™ NTC9385R revealed comparable performance, with slightly higher NanoLuc expression in vitro and in vivo. To demonstrate versatility, we applied pIR to produce a plasmid encoding LINE1 ORF1p, a transposable element protein implicated in aging and cancer that constitutes ~20% of the human genome. In vitro studies confirmed robust ORF1p expression, and in vivo immunization via electroporation elicited a significantly stronger immune response compared to gWiz. By eliminating antibiotic sequences, pIR reduces the risk of horizontal gene transfer and aligns with regulatory requirements for clinical-grade DNA. Its ability to produce high-performance plasmids for both reporter and immunogenic payloads underscores its potential for gene therapy and cancer vaccine development. As non-viral DNA delivery gains momentum in oncology and personalized medicine, platforms that combine safety, efficiency, and compliance will be essential for accelerating translation. In conclusion, we establish pIR as an alternative to existing technologies, offering broad applications in cancer immunotherapy and beyond.

#0271 IL-7-secreting *Salmonella* synergizes with PD-L1 blockade to induce durable antitumor immune memory.

Minju Han

Chungnam National University, Yuseong, Daejeon, Korea, Republic of

Background: Interleukin-7 (IL-7) is a key cytokine that maintains the survival and homeostasis of T cells and induces antitumor immune responses. This study investigated the antitumor effects of attenuated *Salmonella* genetically engineered to secrete IL-7 against cancer by activating immune cell responses.

Methods: Mouse colorectal cancer cell line CT26 and *S. typhimurium* were used. The *S. typhimurium* was engineered to secrete IL-7 based on an arabinose induction system. The anti-tumor effect of the engineered *Salmonella* was examined *in vitro* and *in vivo*, both alone and in combination with anti-PD-L1 treatment. Flow cytometry was performed to analyze immune cell populations in tumors and spleens to elucidate the underlying mechanisms.

Results: The genetically engineered *Salmonella* secreted IL-7 upon arabinose induction without affecting its growth. IL-7 secretion in response to arabinose was confirmed via ELISA. In *in vivo* experiments, the arabinose-induced group exhibited enhanced antitumor effects and improved survival compared to the non-induced group, with body weight recovery observed within five days post-*Salmonella* injection. TUNEL analysis showed increased apoptosis in tumor tissues following arabinose induction, along with a significant reduction in Ki67 expression. On days 3 and 7 post-induction, flow cytometry revealed an increased T cell population. The activation of cytotoxic T cells was confirmed by elevated levels of granzyme B, perforin, and IFN-γ. Co-administration of IL-7-secreting *Salmonella* with anti-PD-L1 antibody resulted in significantly greater tumor suppression compared to *Salmonella* secreting IL-7 alone. Notably, in the arabinose-induced group, complete tumor regression was observed in 4 out of 5 mice. When tumor cells were re-challenged on the opposite flank 60 days later, no tumor recurrence was detected, indicating the establishment of long-term antitumor immunity. Subsequent flow cytometric analysis of splenocytes confirmed an increased population of memory T cells, supporting the development of durable immune memory following IL-7 secretion. Biodistribution analysis showed that *Salmonella* was cleared from other organs over time, with predominant accumulation in tumor tissue. Biochemical analyses of liver and kidney function revealed no abnormalities in the arabinose-treated group. The biological safety of the *Salmonella* strain was confirmed through biodistribution studies and H&E staining.

Conclusion: The *Salmonella* secreting IL-7 enhances antitumor activity by inducing T cell-mediated immune responses, particularly showing potential as an immunotherapy strategy for solid tumors when combined with anti-PD-L1 antibodies. Further research is needed to evaluate its efficacy in various tumor models, long-term safety, and the potential for combination with other immune checkpoint inhibitors.

#0272 Attenuated *Salmonella* secreting IFN-β via the flagellar secretion system enhances antitumor immunity and therapeutic efficacy.

Kim Eunji

Chungnam National University, Yuseong, Daejeon, Korea, Republic of

Purpose: Bacterial cancer therapy offers a unique approach to target tumor tissues and modulate the immune microenvironment. Here, we aimed to establish an attenuated *Salmonella* platform capable of secreting interferon-β(IFN-β) through the flagellar type III secretion system(FT3SS) to potentiate antitumor immunity, and to evaluate its therapeutic efficacy as monotherapy and in combination with PD-L1 blockade.

Methods: The attenuated *Salmonella Typhimurium* strain was constructed by deleting the *rcsB* gene from the parental *BRD509* background and engineered to secrete IFN-β through the FT3SS under L-arabinose induction. IFN-β secretion was verified by Western blot and ELISA. The biodistribution of the strain was evaluated using IVIS bioluminescence imaging. The antitumor efficacy and immune activation induced by the IFN-β secreting *Salmonella* were assessed in CT26 tumor-bearing mice by evaluating tumor growth inhibition, apoptosis, and immune cell activation. Combination therapy with an anti-PD-L1 antibody was performed to potentiate the therapeutic effect. In addition, the *in vivo* safety of the strain was confirmed by monitoring serum liver and kidney function markers, body weight, and H&E histology of major organs.

Results: In this study, we developed an attenuated *Salmonella* strain capable of secreting IFN-β through the FT3SS. IFN-β secretion was regulated by L-arabinose induction without affecting the viability of the *Salmonella* strain. *In vivo* bioluminescence imaging of Lux-expressing IFN-β secreting *Salmonella* demonstrated rapid tumor colonization and selective intratumoral proliferation, confirming its tumor-targeting capability. In CT26 tumor-bearing mice, treatment with the IFN-β secreting strain followed by L-arabinose induction from day 3 post-injection inhibited tumor growth and induced tumor cell apoptosis. The therapy also promoted N1-type neutrophil infiltration and activation of antitumor immune responses, and its safety was confirmed *in vivo*. However, IFN-β monotherapy did not completely eradicate tumors, and PD-L1 expression was upregulated in the tumor tissues after bacterial injection. Therefore, combination therapy with the IFN-β secreting *Salmonella* and an anti PD-L1 antibody resulted in synergistic antitumor effects, including markedly enhanced tumor regression and prolonged survival compared to either monotherapy. These results highlight the clinical potential of this controllable bacterial platform for next-generation cancer immunotherapy.

Conclusion: Overall, these findings demonstrate that the FT3SS-based IFN-β secreting *Salmonella* represents a safe, potent, and versatile therapeutic platform that enhances antitumor immunity and synergizes with immune checkpoint blockade.

#0273 High-avidity reversible engager proteins efficiently redirect the entry of intravenously delivered lentiviral vectors, simplifying the direct *in vivo* delivery of CAR-T cell therapy.

Gopal Naik Nenavath[1], Nandakumar Packiriswamy[1], Diana Gataulin[2], Md Sharif Hasan[1], Tatenda Kadungure[1], Harshitha Anantharama[1], Pragati Jain[1], Kyle Gromer[1], Karina Krotova[1], Miriam Eisenstein[2], Gideon Schreiber[2], Patrycja Lech[3], Luis Blancas Mejia[3], Colin Caine[3], Thipparat Suwanmanee[3], Luke Breigenzer[3], Darren Phung[3], Tim Carey[1], Hamid Salimi[1], Emma Buck[1], Christian Kinney[1], Luke Russell[3], Kah-Whye Peng[3], Stephen J Russell[3], Menachem Rubinstein[2]

[1]Imanis Life Sciences, Rochester, MN,[2]Weizmann Institute of Science, Rehovot, Israel,[3]Vyriad, Rochester, MN

We have developed engager proteins that reversibly block VSV-G, directing VSV-G-pseudotyped lentiviral vectors (LVV) into resting CD3-positive T cells. Following selective binding of the engager-modified LVV particles to CD3, they are internalized into endosomes, where the engager is detached by the low pH and the absence of calcium ions, releasing unmodified LVV. Free LVV particles then fuse with the endosomal membrane and efficiently deliver their genetic cargo to the cytoplasm. These engager proteins are stable and easily produced in high yields, making them suitable for practical use. Reversible bi-specific engagers that bind to the homotrimeric VSV-G protein and redirect it to a targeted receptor were initially developed by genetically fusing a cell-targeting polypeptide to the VSV-G binding domains CR2 and CR3 of the LDL receptor (Israel Patent application No. 296547, 2022. Inventors: M. Rubinstein, G. Schreiber, D. Gataulin, Weizmann Institute). When pre-incubated with VSV and VSV-G-LVV, these engagers mediated selective vector entry into mammalian cells via the targeted receptor while preventing non-specific entry through LDLR. The monomeric engagers blocked binding of VSV-G to LDLR with an ED_{50} of 3 nM. Trimeric engager versions exhibited an ED_{50} of 20 pM. To increase the binding avidity of the engager to VSV-G, we engineered and produced trimeric engagers consisting of CD3-specific scFv fused through a trimerizing peptide to VSV-G binding domains of LDLR. When co-incubated with LVV, the engagers bound stably to LVV, preventing transduction through LDLR or its other family members, while mediating efficient transduction via the targeted CD3 receptor. CD3-directed engager-modified LVVs efficiently transduced and activated primary human T cells in PBMC cultures, exhibiting stable CD3 targeting even after prolonged storage at room temperature and freeze-thaw cycling. CD3-engager-modified LVV particles encoding an anti-BCMA CAR were administered intravenously to (human) PBMC-engrafted NSG-DKO mice bearing established BCMA-positive human myeloma xenografts. Rapid and complete tumor regressions were observed in all animals treated with the engager-modified LVVs. In summary, we have generated trimerizing bifunctional engagers that redirect the attachment and entry of VSV-G-pseudotyped lentiviral vectors into resting human T cells. Engager-modified LVVs encoding a CAR transgene were therapeutically effective when administered intravenously to tumor-bearing animals. Clinical translation is planned.

#0274 Overcoming recombination in semi-replicating retroviral vectors: A novel double suicide gene therapy for glioblastoma.

Soojin Kim[1], Moonkyung Kang[1], **Yeon-Soo Kim**[2]

[1]Articure, Yuseong, Daejeon, Korea, Republic of,[2]Chungnam National University, Yuseong, Daejeon, Korea, Republic of

One of the longstanding challenges in developing semi-replicating retroviral vector (sRRV) systems has been the loss of therapeutic genes due to non-homologous recombination during reverse transcription in dividing tumor cells. To address this, we developed a genetically stabilized sRRV platform capable of efficient combinatorial gene therapy, preserving the integrity of multiple therapeutic genes while replicating and spreading exclusively within tumors. Our system consists of two trans-complementing, replication-defective retroviral vectors: one encoding MuLV-Gag-Pol and cytosine deaminase (CD), and the other encoding GaLV-Env and HSV1-thymidine kinase (TK). These vectors co-infect tumor cells and propagate selectively within the tumor microenvironment. By eliminating homologous sequences between vectors, we achieved a recombination-resistant design, ensuring long-term genetic stability during serial replication. The antitumor efficacy of this platform was validated in two glioblastoma models. First, in a syngeneic rat orthotopic glioma model, C6 glioma cells were implanted intracranially into Wistar rats.The therapeutic vectors were directly injected into the tumor site, followed by systemic administration of prodrugs 5-fluorocytosine (5-FC) and ganciclovir (GCV). Histological analysis on day 98 revealed dose-dependent tumor regression, with complete tumor eradication in the high-dose, dual-prodrug cohort. Survival analysis confirmed significantly extended survival in treated groups. Second, in an intracranial xenograft model using athymic nude mice, human glioma cells were implanted in the brain parenchyma, followed by stereotactic delivery of the sRRV vectors and systemic prodrug treatment. Remarkably, complete tumor remission was again observed in the combination treatment group, despite the absence of adaptive immunity, highlighting the platform's intrinsic efficacy. Analysis of vector genomes recovered from tumor tissues revealed no evidence of recombination or gene loss, confirming the system’s robust genetic stability. The vectors maintained persistent coexpression of both therapeutic genes, which are essential for synergistic prodrug activation and tumor cell killing. In conclusion, this study presents a next-generation sRRV platform that resolves a major technical barrier—recombination-mediated gene loss—while enabling stable and tumor-selective delivery of multiple therapeutic genes. Its potent efficacy in both immunocompetent and immunodeficient brain tumor models, including intracranial xenografts, positions it as a promising candidate for clinical translation in glioblastoma and other refractory solid tumors.

#0275 Bioluminescent tools for quantification of *in vivo* CAR-T delivery systems.

Julia K. Gilden[1], Pete Stecha[2], Rich Moravec[2], Jun Wang[3], Rod Flemming[1], Jim Harnett[1], **Steven Edenson**[1], Kristin Riching[1], Jamison Grailer[1], Mei Cong[2]

[1]Promega, Madison, WI,[2]R&D, Promega, Madison, WI,[3]Promega, Fitchburg, WI

In vivo CAR-T engineering using mRNA-LNP, lentiviral (LV), or AAV vectors requires analytical methods that are rapid, scalable, and mechanistically informative across CMC and bioassay workflows. We assembled an integrated luminescent toolkit to quantify vector input, functional potency, and innate-immune risk. For mRNA-LNP, a Lumit® dsRNA detection assay uses a split luciferase system to quantify double-stranded RNA impurities that can trigger innate sensing and diminish transfection. For broader assessment of immunogenicity, cell-based TLR reporter assays profile vector- or formulation-induced pathway activation. For quantification of LV vectors, the homogeneous, no-wash Lumit® p24 Immunoassay measures the LV p24 capsid protein as a surrogate for viral particle count with a wide linear range in ~60 minutes. Functional potency can be measured using a cell-based reporter bioassay in which Jurkat T cells stably expressing an NFAT-Luc2 reporter are transduced with CAR LV and co-cultured with antigen-positive targets to generate an antigen-dependent luminescent signal that reflects LV identity and potency. Together, these assays streamline development, release, and comparability for in vivo CAR-T delivery systems.

#0276 Anti-tumor activity in humanized xenograft models and B-cell aplasia in non-human primates with a novel CD3-directed in vivo gene-modifying CAR (GCAR) lentivector encoding chimeric antigen receptors and a cellular fitness-enhancing co-stimulatory protein.

Michael Betts[1], Matilda Mostrom[2], Ewa A. Jaruga-Killeen[1], Frederic Vigant[1], Anirban Kunda[1], Michelle Andraza[1], Cody Gowan[1], Iryna Oliinyk[1], Gregory Wade[1], Gregory Schreiber[1], Carter Bir[1], Jason P. Dufour[2], Robert V. Blair[2], Nicholas J. Maness[2], H. Michael Shepard[3], **Gregory Ian Frost**[1]

[1]EXUMA Biotech Corp, West Palm Beach, FL,[2]Tulane National Biomedical Research Center, Covington, LA,[3]Shanghai- Jiaotong University Medical School, Ruijin Hospital, Shanghai, Shanghai, China

Introduction: An *in vivo* gene-modifying CAR (GCAR) platform has been developed to mitigate known clinical and logistical challenges with traditional ex-vivo manufactured CAR-T products. The GCAR platform incorporates an NHP/human reactive CD3-targeted lentivector (LVV) with complement resistant fusogen that encodes CD3zeta based CARs and a compact synthetic costimulatory protein (FD) optimized for proliferation, persistence, and cytotoxicity. The ability of GCAR LVVs to elicit potent, specific and persistent cytotoxicity towards target cells was evaluated *in vitro* and in humanized and non-human primate models. In *M. nemestrina*, GCAR CD20 CAR was evaluated for B-cell depletion compared to LVVs encoding conventional 41BB CARs without FD.

Methods: Anti-CD19 or anti-CD20 LVV's manufactured from 6L and 25L scales were characterized for CD3 reactivity in M. *nemestrina* and human PBMC *in vitro* and *in vivo*. Serum complement sensitivity and activation assays were used to characterize GCAR LVVs (encoding anti-CD20 CAR and FD) against human and NHP sera and CD3 positive lymphocytes. Escalating doses (IV or IN) of purified LVV's were evaluated in the NHPs. B-cells were quantified by flow cytometry and safety by clinical chemistry, hematology, and physical assessments.

Results: Exposure of human or *nemestrina* PBMC to GCAR LVVs resulted in dose and target-dependent cell lysis with rapid tumor clearance in Raji-Luc disseminated PBMC-humanized DKO NSG models. In CD34-humanized models, GCAR LVV generated CAR-T cells with durable B-cell depletion over >8 weeks of observation. Administration of GCAR CD20 LVV (IV or IN) was well tolerated in NHPs at all doses w/o severe CRS or neurologic toxicity. B-cell depletion kinetics post IV dosing of CD20 CARs with FD were dose dependent: minimally active doses demonstrated delayed onset of B cell depletion (from day 21 post dose) vs. B cell aplasia by day 7 at the most active doses. In contrast, a comparable GCAR LVV encoding 41BB CD20 CAR (w/o FD) by IV and IN injection elicited B cell depletion at 7 days post dose with reduced duration.

Conclusion: GCAR LVVs generated genetically modified lymphocytes resulting in durable CAR-dependent cell removal across mechanistic, murine, humanized, and NHP immune systems. The incorporation of FD may further improve cellular expansion and persistence, yielding *ex vivo*-like CAR-T activity profiles without lymphodepletion or cytokine support. The absence of acute and subacute safety signals, low off-target transduction, serum complement resistance, and deep B-cell depletion support the GCAR platform as a potential next-generation opportunity for clinical investigation as a novel gene modifying CAR approach.

#0277 IMV102, an *in vivo* BCMA-targeting CAR-T therapy, achieves durable tumor control in multiple myeloma models.

Yantao Li, Shuangshuang Zhang, Xiaojiang Fan, Zhenggang Jiang, Ruidong Hao, Minmin Sun

Shanghai Immunofoco Biotech Research Co., Ltd, shanghai, China

Introduction
Autologous CAR-T therapy has achieved marked success in hematologic malignancies, yet its widespread use remains challenging due to complex manufacturing and high costs. To overcome these limitations, we developed the iMagic platform, a lentiviral-based in vivo CAR-T system composed of a mutated MxV glycoprotein (MxV-G-mut) and a T cell targeting module (TCM3). This platform enables selectively activation and transduction of T cells in vivo. Here, we evaluated the specificity, efficacy, and safety of IMV102, a lentivirus carrying the BCMA-targeting CAR as the gene of interest based on the iMagic platform, for the treatment of multiple myeloma in preclinical models.
Methods
The transduction specificity and efficiency of IMV102 was assessed using tumor cell lines (Jurkat, H929, and Raji) and primary human cells (hepatocytes and PBMCs). In vitro cytotoxicity and IFN-γ secretion were measured following co-culture with target cells. In vivo efficacy was assessed in two separate models, H929-Luc or MM1.S-Luc xenografted MHC-I/II-DKO immunodeficient mice reconstituted with human PBMCs. Tumor burden, body weight, CAR-T expansion and plasma IFN-γ levels were monitored per schedule.
Results
After coincubation with IMV102, BCMA-CAR expression was detected on Jurkat T cells, while it showed significantly lower levels in Raji or NCI-H929 cells. Importantly, IMV102 coincubation resulted in negligible CAR expression on primary human hepatocytes. In PBMCs, IMV102 efficiently transduced T cells with similar transduction ratio on CD4 and CD8 cells and showed negligible off-target B cell transduction. IMV102-generated CAR-T cells displayed potent cytotoxicity against BCMA-positive tumor cells and secreted significant levels of IFN-γ. Furthermore, intravenous administration of IMV102 at dose of 5e6 TU/mice showed potent and durable tumor inhibition all through the over 50 days observation periods in both the NCI-H929 xenografted model and the MM1.S xenografted model. And the antitumor efficacy was accompanied by robust CAR-T generation and expansion, as well as IFN-γ release. Treatment was well tolerated, with no significant weight loss observed.
Conclusions
IMV102 enables efficient and selective in vivo generation of functional BCMA CAR-T cells, resulting in potent and durable antitumor activity in multiple myeloma models. These results pave the way for further clinical investigation.

#0278 *In vivo* adenine base editing of *STK11*^{Q37*} reprograms tumor for radiosensitizing effect.

Jiazhuo Yan[1], Yihan Xu[2], Qingxiao Fang[2], Jinpu Yu[2], Zhiyong Yuan[2]

[1]Department of Radiation Oncology, Tianjin Medical Univ. Cancer Inst. & Hospital, Tianjin, China,[2]Tianjin Medical Univ. Cancer Inst. & Hospital, Tianjin, China

In this study, we aim to investigate the therapeutic potential of in vivo genetic therapy using AAV-mediated adenine base editor (ABE) delivery for non-small cell lung cancer (NSCLC) carrying the *STK11* nonsense mutation *STK11*^{Q37*} (c.109C>T), and further explore the molecular mechanisms underlying its impact on radiosensitivity. Radiotherapy is a standard treatment for locally advanced or inoperable NSCLC patients, radiation resistance driven by tumor-promoting somatic mutations severely limits clinical efficacy, underscoring the urgent need for targeted strategies such as precise gene correction to overcome this barrier. Through CRISPR-based in vivo mutation library screening combined with whole-exome sequencing, we identified *STK11*^{Q37*} as a critical driver of radiation resistance. To restore *STK11* function, we engineered a panel of ABEs with distinct PAM/TAM compatibilities and further developed a high-fidelity variant, A8E-N108Q-R26G, which enables precise correction of the pathogenic adenine without bystander editing. Using HEK293T reporter cells stably harboring the *STK11*^{Q37*} locus, we found that spCas9-A8EQR (N108Q-R26G) achieved the highest overall correction efficiency, repairing up to 60% of mutant alleles with superior fidelity. The optimized editor was subsequently packaged into a dual-AAV system and delivered in vivo to humanized mice bearing subcutaneous patient-derived organoid xenografts. AAV-mediated base editing combined with radiotherapy produced synergistic antitumor effects and significantly suppressed tumor progression. Mechanistic studies revealed that precise correction of *STK11*^{Q37*} restores endogenous LKB1 protein expression and kinase activity, reactivating downstream signaling required for maintaining redox homeostasis. Restored LKB1 directly stabilizes the transcriptional regulator BACH1 by limiting its ubiquitination and proteasomal degradation, thereby preserving BACH1-mediated repression of antioxidant gene programs. Concurrently, LKB1 re-expression dampens *NRF2* nuclear accumulation and transcriptional activity, leading to reduced expression of *NRF2*-driven detoxification and antioxidant pathways. This coordinated regulation markedly elevates intracellular ROS levels following irradiation and reinstates radiation-induced cytotoxic stress, collectively enhancing tumor radiosensitivity. In summary, our study identifies *STK11*^{Q37*} as a therapeutically actionable driver of radiation resistance and demonstrates that precise ABE-mediated correction provides a promising gene-editing-based strategy to improve treatment outcomes in NSCLC.

#0279 Completion of IND-enabling studies for NRT-YHD_001, a macrophage checkpoint inhibitor in liver cancer.

Suk Woo Nam[1], In Seop Yoon[2], Sang Yean Kim[3], Minjeong Na[3], Jin Woong Ha[3], Soyoung Jeon[3], Hyunmin Lee[2], Seo Hyeon Mun[2], Chang Won Park[2]

[1]Catholic University of Korea, College of Medicine, Seoul, Korea, Republic of,[2]NEORNAT Inc, Seoul, Korea, Republic of,[3]The Catholic University of Korea, Seoul, Korea, Republic of

NRT-YHD_001 is a modified antisense microRNA targeting let-7i-5p, developed as a novel therapeutic candidate for hepatocellular carcinoma (HCC). This compound functions as a key regulator of macrophage activation within the tumor microenvironment. In in vitro phagocytosis assays, NRT-YHD_001 (GalNAc-conjugated form) demonstrated stronger macrophage activation than NRT-YHD (GalNAc-unconjugated form). Following a single intravenous injection in mice, NRT-YHD_001 selectively inhibited let-7i-5p without affecting other members of the let-7 family, confirming its high target specificity.To evaluate the in vivo efficacy of NRT-YHD_001 against advanced HCC, Ras-transgenic mice that spontaneously develop hepatic tumors at approximately 15-20 weeks of age, were used. After confirming tumor formation (~5 mm2) by ultrasonography, NRT-YHD_001 was administered intravenously once weekly at 5 mg/kg. Compared with the sorafenib-treated group, NRT-YHD_001-treated mice exhibited greater tumor suppression, demonstrating superior therapeutic efficacy.The NRT-YHD_001 formulation satisfied all CMC quality control criteria. After lyophilization, the formulation was reconstituted into a clear, colorless solution, with an assay value of 105.1% of the label claim (specification range: 90.0-110.0%). All other parameters, including impurity levels, pH (7.5), osmolality (324 mOsm/kg), endotoxin (<2.0 EU/mg), and sterility, met specification limits, confirming excellent quality attributes.Pharmacokinetic and ADME studies, metabolic stability assessments in serum and liver homogenates, and metabolite profiling were conducted in mice and cynomolgus monkeys. No treatment-related abnormalities were observed in the 4-week repeated-dose toxicity study. The drug substance (DS) and drug product (DP) were both manufactured and analytically validated by a global CDMO with FDA-approved manufacturing experience.Collectively, these results demonstrate that NRT-YHD_001 is a potent and selective let-7i-5p antisense therapeutic with macrophage-modulating activity and superior in vivo antitumor efficacy in an advanced HCC model. A complete nonclinical IND submission package has been finalized, with FTO clearance and full intellectual property protection secured. IND submissions to the MFDS (Korea) and FDA (U.S.) are planned for 2026.

: Innovative Therapeutic Modalities and Translational Platforms
Poster Session

#0283 Severe acidity in human tumors for pH-activatable cytokine therapy.

Qiang Feng[1], Jun Chen[1], William Hartnett[1], Raymundo Pantoja[1], Gang Huang[1], Isaac Chan[2], Baran Sumer[1], Jinming Gao[1]

[1]Simmons Comprehensive Cancer Center, University of Texas Southwestern Medical Center, Dallas, TX,[2]Internal Medicine, University of Texas Southwestern Medical Center, Dallas, TX

Introduction: Precise tumor targeting is essential for improving the therapeutic index of cancer immunotherapies. Systemic cytokine therapies, such as interleukin-2 (IL-2), suffer from narrow therapeutic windows due to dose-limiting toxicities. While receptor engineering and prodrug approaches have been widely investigated, their application is often limited to tumor subtypes that express the corresponding targets. In contrast, tumor acidity is a universal hallmark of the microenvironment, driven by elevated glycolysis, and offers a broadly applicable opportunity for tumor-specific therapy. However, the spatial heterogeneity of tumor acidity remains poorly understood, and its therapeutic application has not been fully demonstrated.
Methods: To systematically evaluate the heterogeneity of tumor acidity and its potential for targeted therapy, we employed ultra-pH-sensitive (UPS) nanoparticles that exhibit sharp ON/OFF transitions at defined pH thresholds. In 3D tumor cultures, we embedded UPS nanoprobes within extracellular matrix gels and assessed the spatial distribution of acidity at single-cell resolution. In human cancer patients, we evaluated the tumor-imaging properties of this acidity-targeting strategy and further investigated acidity patterns by analyzing UPS nanoparticle distribution in tumor tissues following intravenous injection. Building on these findings, we developed a formulation strategy to encapsulate IL-2-Fc into UPS micelles, enabling selective cytokine release in acidic microenvironments. This platform aims to provide a comprehensive understanding of spatial acidity and to test the therapeutic index of pH-activatable cytokine delivery.
Results: Through this work, we identified a severe acidity phenotype in cancer, where extracellular pH drops below 5.3 due to spatially polarized lactate export. Targeting acidity allows demarcation of tumor from surrounding tissue in intraoperative imaging, even when tumors are as small as 2 mm. Spatial transcriptomic analysis of human head and neck tumors after UPS nanoprobe injection revealed that these severely acidic regions co-localize with immune-infiltrated stromal zones. These regions serve as critical entry points for acid-targeting nanosystems, linking tumor metabolism, immune cell infiltration, and immune suppression in both preclinical models and human tissues. The UPS/IL-2-Fc formulation selectively releases IL-2-Fc within these regions and demonstrates potent antitumor efficacy with markedly reduced systemic toxicity, expanding the therapeutic window by over 10-fold compared to free IL-2-Fc in preclinical models.
Conclusion: This study identifies severe acidity as a spatially heterogeneous and translatable hallmark of the tumor microenvironment, enabling tumor-targeted imaging and immunotherapy.

#0284 From undruggable to actionable: Transcriptomic discovery of small-molecule modulators of oncogenic transcription factors.

Arianna Sabo, QUANTRO's Team

QUANTRO Therapeutics GmbH, Wien, Austria

Transcription factors (TFs) and their associated signaling networks remain among the most challenging and underexplored targets in oncology drug discovery. To address this gap, QUANTRO Therapeutics has developed a Transcriptomic Discovery Platform that measures cellular transcriptional activity by detecting changes in nascent RNA synthesis as early as one hour after cellular perturbation. Unlike conventional RNA-seq approaches, which capture only steady-state mRNA abundance with limited temporal resolution, this platform directly quantifies immediate transcriptional responses, providing a high-fidelity readout of TF activity.The QUANTRO platform currently comprises three complementary assays—QUANTROsens, QUANTROseq, and QUANTROslam—that together enable the identification, confirmation, and mechanistic characterization of transcriptional modulators. In particular, QUANTROseq enables high-throughput generation of dynamic transcriptional “fingerprints” induced by small molecules, which can be directly compared with signatures resulting from acute, controlled degradation of specific target proteins. By correlating these profiles, the platform precisely distinguishes compounds acting directly on TFs or cofactors from those exerting indirect effects through upstream pathways. As a demonstration of its capabilities, we present a systematic re-evaluation of published MYC inhibitors, revealing how traditional transcriptomic or reporter-based assays can misclassify indirect modulators as direct MYC inhibitors.Leveraging this technology, QUANTRO has initiated screening campaigns targeting key oncogenic drivers such as c-MYC and YAP/TEAD, leading to the identification of multiple high-quality hit clusters with clear on-target activity and minimal off-target effects. Collectively, these studies demonstrate the power of dynamic transcriptomic profiling to expand the druggable target space, accelerate discovery of first-in-class therapeutics, and illuminate transcriptional control mechanisms underlying cancer progression.

#0285 NEBNext UltraShear® Long Read: Enzymatic DNA fragmentation for long read sequencing of clinically relevant samples.

Keerthana Krishnan, Brittany S. Sexton, Matt Angel, Karen McKay, Jonathan Sanford, Ruby Moulton, Louise Williams, Bradley W. Langhorst, Pingfang Liu, V.K. Chaithanya Ponnaluri

New England Biolabs, Inc., Ipswich, MA

Advances in long read sequencing technologies have significantly improved accuracy and throughput, making them useful for clinical applications and personalized medicine. Ultra-long DNA molecules resulting from high quality extractions, if left intact, are generally inefficiently converted into libraries and sequenced on long-read platforms. Therefore, fragmentation is strongly recommended for high-throughput long read sequencing. DNA fragmentation upstream of long read sequencing typically also results in comparable fragment sizes across samples and experiments with higher and consistent N50 lengths as well as improved sequencing yields compared to ultra-long DNA. Current methods for DNA fragmentation include mechanical shearing and enzymatic fragmentation. Mechanical shearing (e.g., Covaris® g-TUBE and Megaruptor®) is the gold standard method for DNA fragmentation upstream of long read library preparation. Drawbacks to these methods include the use of expensive consumables and instruments that are not automation-friendly and result in sample loss. In contrast, enzymatic DNA fragmentation does not require expensive instruments and is automation friendly, however existing fragmentation parameters may not be optimal for long read sequencing.

To address these constraints, we developed a novel enzymatic fragmentation solution, NEBNext UltraShear® Long Read (UltraShear LR), that is quick, tunable, and automation friendly. Enzymatic fragmentation is time-dependent and can be used to generate a wide-range of DNA fragment sizes (2 to 30 kb) suitable for different applications and sequencing platforms. UltraShear LR is robust across a wide range of gDNA input amounts (250 to 5,000 ng) as well as different gDNA samples and species (e.g., animal, plant and human). Here we demonstrate that UltraShear LR fragmentation generates high quality libraries with tunable read lengths by sequencing on Oxford Nanopore™ Technologies and PacBio® platforms. UltraShear LR libraries retain base modifications (including CpG methylation) and identify more CpGs than mechanically sheared libraries at the same read count. Additionally, we applied the Twist cancer hotspot long read sequencing capture panel using matched normal and tumor samples to identify copy number variations and perform variant calling, demonstrating the applicability of UltraShear LR for clinically relevant samples.

The UltraShear LR system generates time-dependent DNA fragment sizes that are reproducible in a robust and cost-effective manner. UltraShear LR overcomes many limitations of mechanical shearing methods by simplifying sample processing, increasing throughput, and preserving base modifications. These advantages collectively improve usability and data quality in long read sequencing library preparation, making the approach well-suited for clinical applications and personalized medicine.

#0286 New approach methodologies for risk assessment and functional evaluation of immuno-oncology drug candidates.
Christoph Schifflers, Martijn Vlaming, Sofie Pattyn

IQVIA Laboratories, Gosselies, Belgium

Functional screening as well as safety and toxicity assessment of new drug candidates has routinely involved animal research. These models often involve time-consuming experiments and are associated with ethical concerns and high costs. New Approach Methodologies (NAM) are alternative methods for accelerated and cost-effective lead selection based on functionality and predictive risk assessment. Thereby, NAM further contribute to efforts to Replace, Reduce and Refine animal research. In this context, a variety of customized *in vitro* bioassays were developed to evaluate the risk of unwanted immunogenicity of immuno-oncology drug candidates as well as their potency. Drug candidates include biologics as well as small molecules and cell or gene therapy products. These *in vitro* assays are based on well-characterized high-quality primary immune cells from >1300 healthy donors. In addition, variants using non-lethal blood collections of animals such as cynomolgus monkeys, dogs, pigs etc. were established for functional and risk assessment screenings. These assays characterize the phenotype and function as well as secretions of a multitude of lymphoid and myeloid populations in cell type specific cultures or complex co-culture systems using multiplex Flow Cytometry, ELISA/Luminex Assays as well as Live-Cell Imaging.Thus, customized *in vitro* bioassays contribute to NAM, reducing animal requirement for drug development and promoting cost-effective lead selection.

#0287 Chemically ligated proteins enable quantitative ELISAs for p53 post-translational modifications.

Thomas Bailey

Abcam plc (UK), Cambridge, United Kingdom

Introductory Sentence: We developed chemically ligated protein standards to enable fully quantitative ELISAs for key post-translational modifications of p53, providing robust tools for cancer research.

Analysis of post translationally modified (PTM) proteins often relies on methods such as mass spectrometry or western blotting, which are non-quantitative, time consuming and costly. ELISAs offer a faster and more economical alternative; however, most PTM-targeted ELISAs are only semi-quantitative because they lack reference standards to generate a standard curve. To address this limitation, we developed chemically ligated proteins (CLPs) that serve as reference standards in ELISAs, enabling accurate detection and quantification of PTMs. This strategy was applied to quantify PTMs on the tumor suppressor p53 which is mutated or deleted in 50% of cancer tumors.[1] PTMs of p53 regulate its activity in the cell, making their precise measurement critical for understanding p53 function. Phosphorylation at serine 15 and serine 392 and acetylation at lysine 382 are well-characterized modifications associated with p53 activation. [2] To support oncology studies of this target, we developed ELISA kits to quantify these modifications. Development involved pair screening as well as biological validation. CLPs of modified, unmodified, and non-specifically modified p53 were used to select antibody pairs specific to each PTM site over unmodified or proximal modification sites of p53. Biological validation included detection of native signal, induction in cell extracts, and signal reduction following phosphatase treatment. Additional biological validation confirmed linearity of dilution, recovery, and precision across all sample types. Using this strategy, we generated three ELISA kits capable of accurately quantifying p53 pS15, pS392, and acK382, providing robust tools to advance research on p53 regulation and function.

1)Bailey, Matthew H et al. “Comprehensive Characterization of Cancer Driver Genes and Mutations.” *Cell* vol. 173,2 (2018): 371-385.e18. doi:10.1016/j.cell.2018.02.0602)Liu, Yanqing et al. “p53 modifications: exquisite decorations of the powerful guardian.” *Journal of molecular cell biology* vol. 11,7 (2019): 564-577. doi:10.1093/jmcb/mjz060

AB0578_v1.0_111725

#0288 Two-color bioluminescence analyses pairing NanoLuc® and red-shifted NanoPrism™ luciferases.

Juliano Alves, Karilyn Porter, Mike Killoran, Robin Hurst, Mark Klein, Debayan De Bakshi, Rahele Esmatpour, James J. Cali, Thomas Machleidt, Rachel F. Ohana, Hicham Zegzouti

Promega Corporation, Madison, WI

NanoLuc® luciferase (NLuc) and its complementation technologies, including the NanoBiT® LgBiT/HiBiT system, are widely applied in functional biology because of their exceptional brightness, broad dynamic range, and suitability for monitoring real-time cellular processes. Despite their versatility, NLuc-based reporters emit primarily at a single, blue-shifted wavelength (~460 nm), restricting their use in multiplexed assays where independent spectral channels are required. To overcome this limitation, we developed NanoPrism™ luciferases, engineered NLuc variants that employ highly efficient intramolecular energy transfer to red-shift the emission. Building on BRET-based strategies, we inserted circularly permuted NLuc or LgBiT into a surface loop of HaloTag®, enabling optimal positioning to covalently bound fluorophores and achieving exceptional BRET efficiency (~90%). By pairing these red-shifted NanoPrism™ reporters with unmodified NLuc® or NanoBiT®, we created a robust two-color bioluminescent platform with strong signal intensities and >100 nm spectral separation. This dual-channel system allows simultaneous monitoring of two proteins or cellular events, such as targeted protein degradation, signaling dynamics, or internal control measurements - in real time within a single experimental context.

#0289 Tracking APOBEC3A to overcome drug resistance in lung cancer.

Maria Vittoria Di Marco[1], Christopher Eggers[2], Aaron N. Hata[1]

[1]Massachusetts General Hospital, Charlestown, MA,[2]Promega Corp., Madison, WI

Targeted therapies have transformed treatment for advanced non-small cell lung cancer (NSCLC), but acquired resistance remains a challenge. We recently showed that the cytidine deaminase APOBEC3A (A3A) is induced by lung cancer targeted therapies and plays a crucial role in promoting acquired drug resistance by facilitating the evolution of drug-tolerant persister (DTP) cells. While A3A mutational signatures are found in 70-80% of tumors post-TKI treatment versus 20-25% in untreated samples, some resistant tumors lack these mutations. Similarly, while many lung cancer cell lines upregulate A3A expression upon TKI treatment, others do not. Our understanding of intra- and inter-tumoral heterogeneity of therapy-induced A3A expression and activity is limited. Most available methods for studying A3A expression and activity are endpoint assays performed on bulk populations. Because A3A activation is episodic and occurs before detectable genomic changes can be quantified, resolving the activity of A3A in single cells over time has not been possible. To overcome these barriers we adapted the HiBiT nano-luciferase reporter system to develop a method for real-time single-cell monitoring of A3A activity in drug-treated tumor cells.Leveraging the preference of A3A for mRNA hairpin substrates, we incorporated optimized A3A-substrate sequences into the HiBiT tag. In the unedited configuration, HiBiT is unable to complement with LgBiT. However when A3A creates a C>U edit within the mRNA hairpin loop, complementation occurs and the resulting luminescent signal reports that A3A is actively editing. We introduced the A3A-HiBiT reporter into patient-derived EGFR, ALK, and KRAS-mutant NSCLC cell lines. TKI treatment induced reporter editing, as detected by HiBiT luminescence and validated by allele-specific droplet digital PCR. No reporter activity was observed in the presence of catalytically inactive $A3A^{E72A}$ or in cell lines with deletion of A3A, confirming specificity for A3A-mediated editing. To investigate intra-tumoral heterogeneity of therapy-induced A3A activity in lung cancer cells treated with targeted therapies, we generated A3A-HiBiT cells stably expressing LgBiT. Experiments are underway to optimize ultra-sensitive bioluminescent microscopy to characterize and monitor the episodic nature of A3A editing in live single cells, as well as to correlate A3A-HiBiT editing with single cell transcriptional heterogeneity using single cell RNA-seq. In summary, our A3A-HiBiT reporter provides a sensitive, scalable, and quantifiable system for real-time monitoring of A3A activity, enabling new opportunities to study the role of A3A in tumor evolution and drug resistance.

#0290 Scientific justification for setting up an appropriate specification of residual solvent based on ICH guideline.

Zhanxiang Sun[1], Jianqiang Li[2], **Lynn Wang**[2], Xudong Wei[3]

[1]Payload-Linker Department, WuXi XDC, Cranbury, NJ,[2]Payload-linker Department, WuXi XDC, Cranbury, NJ,[3]WuXi XDC, Cranbury, NJ

Residual solvents present in payload-linkers, critical intermediates in antibody-drug conjugate (ADC) manufacturing, can be challenging to fully remove during process development. This may lead to levels exceeding ICH Q3 guidelines at the payload-linker stage. To address this, XDC conducted a comprehensive scientific assessment considering toxicological data from ICH Q3C(R8), process clearance capabilities, clinical safety requirements, and conjugation reaction conditions. Based on this evaluation, scientifically justified extensions of residual solvent limits were proposed to ensure both product safety and process feasibility. Assuming certain solvents cannot be completely eliminated during manufacturing and purification, a justification framework was developed to calculate appropriate specification limits for each residual solvent. This approach incorporates safety factors and regulatory guidance to establish scientifically sound limits. The outcome provides a practical solution for cases where complete removal is technically challenging, ensuring compliance with safety standards while supporting efficient ADC development.

#0291 Dual PHD2-HDAC inhibitor 31c prevents cisplatin-bevacizumab nephrotoxicity and preserves antitumor efficacy in cervical cancer.

Xi Chen[1], Dongyu Han[1], Xiaohua Kong[1], Wenfeng Gou[2], Yang Song[3], Huiqiang Wei[2], Yiliang Li[2], Yong Qin[1]

[1]The University of Texas at El Paso, El Paso, TX,[2]Peking Union Medical College & Chinese Academy of Medical Sciences, Tianjin, China,[3]The First Affiliated Hospital of Jinzhou Medical University, Jinzhou, China

Cisplatin-based chemotherapy combined with bevacizumab (CB) remains the standard first-line treatment for advanced or recurrent cervical cancer, integrating cytotoxic and anti-angiogenic mechanisms to improve clinical outcomes. However, treatment success is frequently undermined by dose-dependent nephrotoxicity caused by cisplatin and bevacizumab-induced vascular alterations. Thus, strategies capable of safeguarding renal function without attenuating antitumor activity are urgently needed to optimize treatment durability and patient survival. We previously developed 31c, a novel dual inhibitor of prolyl hydroxylase domain-containing protein 2 (PHD2) and histone deacetylases (HDACs), as a nephroprotective agent. Therefore, we evaluated the nephroprotective potential of 31c in a HeLa xenograft mouse model. Mice were treated with cisplatin, bevacizumab, or their combination, with or without 31c. Tumor growth kinetics and body weight were monitored to assess therapeutic response and systemic toxicity. Renal function was examined through blood urea nitrogen (BUN), serum creatinine (Scr), and erythropoietin (EPO) levels. Kidney tissues underwent histopathological evaluation using hematoxylin and eosin (H&E) and Masson's trichrome staining to quantify tubular injury and fibrosis. RNA sequencing (RNA-seq) of kidney samples identified transcriptomic alterations, and immunofluorescence staining validated renal injury markers lipocalin-2 (Lcn2/NGAL) and kidney injury molecule-1 (Havcr1/KIM-1). Co-administration with 31c preserved the antitumor efficacy of the CB regimen, yielding tumor inhibition comparable to CB alone. Notably, 31c markedly reduced renal toxicity. Mice receiving CB alone displayed significant increases in BUN and Scr levels, extensive tubular degeneration, and marked collagen accumulation, hallmarks of acute renal injury and fibrosis. In contrast, 31c significantly reduced these pathological changes and maintained normal tubular structure. Transcriptomic profiling revealed distinct clustering among treatment groups, with 31c partially reversing CB-induced transcriptional dysregulation. Among the most upregulated genes in CB group, Lcn2 and Havcr1 were significantly suppressed by31c, consistent with immunofluorescence validation. The dual PHD2-HDAC inhibitor 31c confers robust nephroprotection against cisplatin-bevacizumab-induced renal injury without compromising antitumor activity. This integrated protective strategy highlights a promising approach to enhance the safety, tolerability, and continuity of platinum-anti-angiogenic therapies. By preserving renal integrity, 31c may support sustained treatment intensity and prolonged therapeutic benefit in patients with advanced cervical cancer and potentially other malignancies treated with similar regimens.

#0292 AOH1996, a cancer-associated PCNA inhibitor, restores platinum sensitivity in urothelial carcinoma: *In vitro* and *in vivo* study.

Kuan-Lin Kuo[1], Kuo-How Huang[2], Yi Ju (Ellen) Kao[3], Chen-Hsun Hsu[1]

[1]Urology, National Taiwan University Hospital and National Taiwan University College of Medicine, Taipei, Taiwan,[2]National Taiwan University Hospital and National Taiwan University College of Medicine, Taipei, Taiwan,[3]National Taiwan University Hospital, Taipei, Taiwan

Urothelial carcinoma (UC) frequently develops resistance to platinum-based chemotherapy, resulting in limited treatment efficacy and dismal clinical outcomes. Proliferating cell nuclear antigen (PCNA) is a key regulator of DNA replication and repair, and cancer-associated PCNA (caPCNA), a structurally altered form selectively expressed in malignant cells, has emerged as a promising therapeutic target. AOH1996 is a first-in-class small-molecule inhibitor that selectively binds caPCNA and disrupts PCNA-dependent survival pathways. In this study, we investigated the antitumor activity of AOH1996 in UC and its ability to overcome resistance to cisplatin-based chemotherapy. Cisplatin-sensitive (T24, BFTC905) and cisplatin-resistant (T24/R) UC cell lines were treated with AOH1996 alone or in combination with cisplatin or gemcitabine. AOH1996 significantly reduced cell viability and clonogenic survival in both sensitive and resistant cells, induced apoptosis as evidenced by increased Annexin V-positive fractions and cleavage of caspase-3 and PARP, and caused cell-cycle arrest with accumulation of cells in the S/G2 phase. Mechanistically, AOH1996 downregulated PCNA-dependent DNA repair signaling and enhanced DNA damage, as shown by increased γH2AX expression. Combination index analysis demonstrated synergistic interactions between AOH1996 and cisplatin or gemcitabine, particularly in cisplatin-resistant T24/R cells. In a xenograft mouse model of UC, AOH1996 significantly inhibited tumor growth and further potentiated the antitumor effect of cisplatin without causing overt systemic toxicity or significant body weight loss. Together, these findings provide preclinical evidence that targeting caPCNA with AOH1996 exerts robust antitumor activity and restores chemosensitivity in UC, supporting caPCNA inhibition as a promising therapeutic strategy for patients with platinum-resistant disease.

#0293 Anti-cancer drug usage analysis among Korean patients with colorectal cancer.

Yu Jin Lim[1], Jeongseon Kim[2]

[1]The George Washington University, Washington, DC,[2]Department of Cancer Biomedical Science, Graduate School of Cancer Science and Policy, National Cancer Center, Goyang, Korea, Republic of

Combination chemotherapy has long been central to the management of colorectal cancer, and treatment patterns have evolved in response to emerging clinical evidence, changing guidelines, and the availability or withdrawal of specific agents. This study aims to characterize changes in medication utilization over time by providing a descriptive analysis of temporal changes in anticancer drug use among Korean colorectal cancer patients treated at the National Cancer Center (NCC) of Korea. Two patient cohorts were examined: individuals treated between 2000-2004 and those treated between 2010-2020. Sixteen anticancer agents administered to ≥10 patients in both cohorts were included. A total of 1,188 patients from the 2000-2004 cohort and 1,043 patients from the 2010-2020 cohort were analyzed using Stata/BE 18.0. In the 2000-2004 cohort, monotherapy was the most predominant treatment approach (55.89%), followed by two-drug combination therapy (17.68%). Among monotherapies, 5-fluorouracil (5-FU) was most frequently used (45.96%). The most common two-drug regimen during this period was capecitabine plus 5-FU (4.88%). By 2010-2020, treatment patterns shifted as two-drug combination chemotherapy became more common than monotherapy (38.73% vs. 32.02%). The 5-FU plus oxaliplatin combination emerged as the most frequently used regimen (25.98%). Capecitabine was the most common regimen for monotherapy (21%). Although the use of capecitabine monotherapy increased in 2010-2020 compared to 2000-2004 (21% vs. 5.56%), the difference in overall capecitabine usage was not statistically significant ($p = 0.872$), likely because capecitabine had frequently been used in combination regimens in earlier years. In contrast, use of 5-FU significantly declined ($p < 0.001$), while use of oxaliplatin and bevacizumab markedly increased (both $p < 0.001$). Meanwhile, tegafur/uracil and megestrol usage decreased significantly (both $p < 0.001$). This descriptive analysis highlights shifts in chemotherapy use among colorectal cancer patients treated at the NCC of Korea across two distinct periods. The earlier cohort (2000-2004) was characterized by predominant use of 5-FU-based monotherapy, whereas the later cohort (2010-2020) showed a marked transition toward two-drug combinations. These patterns mirror global changes in anticancer therapy drug usage. Further analyses should link treatment patterns to clinical outcomes, including evaluations of overall survival (OS) and disease-free survival (DFS), clarification of treatment lines, and resolution of overlapping-prescription or regimen-coding issues. This study was approved by the Institutional Review Board of the NCC (NCC2025-0115).

#0294 Comparative biochemical kinase activity analysis identifies lirafugratinib as a highly selective FGFR2 inhibitor.

Alison M. Schram[1], Grace Lee[2], Tracey Wei[2], Seong Jang[2], Kristin Ryan[2]

[1]Memorial Sloan Kettering Cancer Center, New York, NY,[2]Elevar Therapeutics, Fort Lee, NJ

Background: Genomic alterations in fibroblast growth factor receptor (FGFR) occur across tumor types and pan-FGFR inhibitors are standard-of-care in FGFR fusion positive cholangiocarcinoma (CCA). Recent efforts focused on designing more selective and covalent inhibitors to improve efficacy, safety, and tolerability. Lirafugratinib, a highly selective and irreversible FGFR2 inhibitor, was designed to target oncogenic *FGFR2* alterations to enhance efficacy outcomes without worsening toxicities due to inhibitions of other FGFR isoforms (e.g., hyperphosphatemia and diarrhea related to FGFR1 and FGFR4, respectively).
Methods: To understand and compare the relative selectivity of lirafugratinib kinase inhibition, we performed a head-to-head biochemical analysis against four pan-FGFR inhibitors. A KINOMEscan Profiling Service scanMAX and TREEspot™ interaction maps were used for evaluation and visualization of inhibition of kinases: a panel of 468 human target kinases and disease-relevant kinase mutant variants were tested at a concentration of 500 nM for lirafugratinib and four other pan-FGFR inhibitors (futibatinib, pemigatinib, erdafitinib, and AZD4547). The 90% and 75% inhibition thresholds were selected based on established and published research for methodologies related to kinome mapping.
Results: Among the 468 kinases and disease-relevant kinase mutants, lirafugratinib at 500 nM inhibited >90% of only two kinases (FGFR2 [94.1%] and MEK5 [92.4%]). The rest of kinases, including FGFR1, FGFR3 and FGFR4, were inhibited <75% except MKNK2 (89% inhibition). In contrast, futibatinib inhibited FGFR1, FRFR2, FRFR3, and FGFR4 by more than 90%, while showing minimal (<75%) inhibition of other kinases except MKK7 (83% inhibition). Similarly, pemigatinib, erdafitinib, and AZD4547 inhibited multiple kinases (including all FGFRs) - 11, 37, and 37 kinase targets, by more than 90%. Overall, lirafugratinib demonstrated the highest selectivity to inhibit FGFR2 without substantial inhibition of FGFR1, FGFR3 and FGFR4, compared to the FGFR inhibitors tested.
Conclusions: The head-to-head kinome analysis of lirafugratinib and four other FGFR inhibitors revealed that lirafugratinib inhibited FGFR2 with high selectivity, suggesting minimal off-target and off-isoform-related toxicities compared to pan-FGFR inhibitors used in clinical practice.

#0295 Antitumor effect of a new pyruvate kinase M2 (PKM2) inhibitor Acyclovir in experimental esophageal adenocarcinoma.

Md Sazzad Hassan[1], Mallory Turner[2], Elizabeth Heffernan[2], Katherine Millett[2], Oliver O'Reilly[2], Niranjan Awasthi[1], Usama Usama[2], Aktar Ali[2], Urs von Holzen[1]

[1]Indiana University School of Medicine (South Bend, IN), South Bend, IN,[2]University of Notre Dame, South Bend, IN

Background: Esophageal adenocarcinoma (EAC) is one of the most aggressive human cancers with poor prognosis even with modern combination therapies due to high resistance to chemotherapy. Therefore, new therapeutic approaches are urgently needed. Pyruvate kinase M2 (PKM2) is not only a key enzyme regulating cancer glycolysis but also translocate into the nucleus to regulate transcription. Although PKM2 is overexpressed in various tumor tissues including EAC, its functional role in esophageal EAC chemotherapy remains unexplored. The objective of this study was to determine whether acyclovir can act as an inhibitor of PKM2 and EAC tumor growth.
Methods: Virtual in silico screening using molecular docking was conducted to screen an FDA-approved chemical library for identification of potential PKM2 inhibitors. HER-2 overexpressing OE19, LPR-OE19 and OE33 EAC cell lines were used. The lapatinib-resistant OE19 (LPR-OE19) cell line was generated from parent OE19 cells through intermittent exposure to increasing concentrations of lapatinib for over six months. Acyclovir and nanoparticle albumin-bound paclitaxel (nab-paclitaxel), alone or in combination, were tested for effects on cell proliferation, lactate production, apoptosis, signaling pathways and tumor growth. Antiproliferative activities were measured by WST-1 assay. Western blotting was performed to evaluate expression of PKM2, apoptotic markers and cell signaling proteins. In-vivo antitumor efficacy was measured in a patient-derived xenograft (PDX) model of human EAC.
Results: Molecular docking identified acyclovir as a potential PKM2 inhibitor that showed lowest docking and glide scores, indicating a strong binding interaction with PKM2. Acyclovir inhibited both PKM2 expression and lactate production. It inhibited cell proliferation in 2D, 3D and organoid cultures of EAC in a dose dependent manner. Interestingly, addition of nab-paclitaxel enhanced the antiproliferative effect of acyclovir. Acyclovir increased expression of proapoptotic proteins and decreased expression of phospho AKT in EAC cells. In a subcutaneous PDX model, acyclovir induced a tumor regression compared to control as monotherapy, and acyclovir in combination with nab-paclitaxel showed a significant enhancement effect of tumor regression. The net change in tumor size in the control, acyclovir, nab-paclitaxel, and combination groups was 551.19 ± 99.69 mm^3, 347.33 ± 71.41 mm^3, 221.55 ± 43.73 mm^3, and 159.37 ± 39.29 mm^3. Reduction in PDX tumor growth corroborated decreased tumor cell proliferation results.
Conclusions: These data suggest that acyclovir, acting as a PKM2 inhibitor, in combination with nab-paclitaxel should be further investigated as a potential therapeutic strategy for HER2-positive EAC patients and could be a novel treatment strategy for EAC.

#0296 Evaluation of ingenane diterpenoids for BL2 triple-negative breast cancer.

Pamela R. Duarte, April L. Risinger

Pharmacology, UTHSA, San Antonio, TX

Breast cancers with high expression of estrogen receptor (ER), progesterone receptor (PR), or Human Epidermal Growth Factor Receptor 2 (HER2) have benefited dramatically from receptor-directed targeted therapies. In contrast, triple-negative breast cancers (TNBCs), which lack ER, PR, and HER2 expression, remain a significant therapeutic challenge. The basal-like 2 (BL2) molecular subtype of TNBC is of particular concern due to its extremely low rate of pathological response to standard chemotherapy. We found that BL2 TNBC cell lines are highly sensitive to protein kinase C (PKC)-activating diterpenes, including ingenol 3-angelate (I3A), tigilanol tiglate, and yuanhuacine, with potency in the nanomolar to picomolar range. Strikingly, these compounds demonstrate over a thousand-fold selectivity against BL2 cells as compared to other TNBC lines or normal breast cells, suggesting they could have a favorable therapeutic index for this indication. Preliminary evidence indicates that the vulnerability of BL2 TNBC lines is mediated by PKC, although it is unclear which isoform(s) and downstream signaling pathways are required for subtype-specific cytotoxicity. This project uses zebrafish tumor-bearing models as a strategy to establish the therapeutic index of these PKC agonists following systemic administration and to compare compounds that target distinct PKC isoforms. By integrating tumor response with pharmacologic profiling, this work aims to define the relationships between PKC activation, compound potency, and subtype-selective efficacy to identify the most promising candidate for preclinical development. Ultimately, this research aims to leverage PKC activation as a targeted therapeutic strategy for BL2 TNBC, expanding treatment options for this lethal breast cancer subtype.

#0297 Cymirafen: A protein-drug conjugate that delivers very intense short pulses of MMAE on a weekly schedule.

Maria Carmen Mulero Roig, Sukshala A. Jadhav, Willie Pi, Stephen B. Howell

UC San Diego-Moores Cancer Center, La Jolla, CA

INTRODUCTION: Cymirafen is a novel protein-MMAE conjugate that targets the LGR4/LGR5/LGR6 receptor whose pharmacokinetics suggest that it can address many of the limitations of existing ADCs that use MMAE as their warhead. The human doses of MMAE ADCs are very small (1.2 - 4.5 mg/kg/3 wk) because larger doses are simply not tolerated. At these doses the ADCs do not penetrate deeply into tumors, the plasma concentrations are too low to saturate all receptors on those cells the ADC can reach, and the very long duration exposure to high plasma free MMAE concentrations cause neurotoxicity. However, long exposures are not required for MMAE efficacy; intracellular MMAE kills with even short durations of exposure (days rather than weeks).
METHODS: PK studies used mice and Sprague-Dawley rats, and the SC OVCAR5 CDX model. Plasma and tumor lysate cymirafen was measured by ELISA using antibodies to different epitopes. Free MMAE was determined by LC-MS/MS.
RESULTS: Cymirafen is very potent. Across a panel of cell lines of mixed cancer types, IC_{50} was <10 nM in 70% and <5 nM in 34%. Nevertheless, very high doses are well tolerated in mice and rats. In nu/nu mice the MTD is 125 mg/kg and a dose of 85 mg/kg can be given weekly for 8 weeks without net weight loss. Single dose HNSTD of MMAE ADCs in the rat is 5 - 10 mg/kg whereas the HNSTD for cymirafen is 75 mg/kg, >10 times higher than MMAE ADCs. In both mouse and rat, the initial and terminal half-lives of cymirafen are ~ 4 h and 0.8 - 1.0 d whereas terminal half-lives for MMAE ADCs are 8.6 -14.6 d. In rats given 60 mg/kg, the peak total cymirafen was 3001 ± 813 nM. Free plasma MMAE peaked immediately after injection at 3.8 nM and declined with a half-life of 7 h to become undetectable after 48 h. Cymirafen was found to deliver MMAE to tumors very rapidly. Following an IP injection of cymirafen 85 mg/kg in nu/nu mice, free MMAE in the OVCAR5 tumor lysates rose very rapidly reaching 100 nM by 8 h and persisted for a prolonged period. The dose density of cymirafen (moles of MMAE per tolerated dose) is estimated to be ~2.5 times higher than that of MMAE ADCs because the MW of cymirafen is only half that of an ADC and very much larger doses are tolerated.
CONCLUSIONS: In contrast to MMAE ADCs, because of the much larger doses tolerated and the very much shorter half-life, cymirafen achieves very high plasma concentrations that load MMAE into tumors at a very high rate over just a few days. This favors deep penetration and complete saturation of receptors. The much higher payload dose means that many more moles of MMAE are delivered/dose, and since large doses of cymirafen can be given weekly, the rate and total amount of MMAE delivered over 3 weeks is far higher than what can be delivered by an MMAE ADC. Peak plasma free MMAE is only 0.09% of total cymirafen, and all free MMAE is cleared by 48 h. Low free MMAE plasma levels, and its short half-life, markedly reduce exposure of normal tissues to free MMAE and permits injection of very high doses.

#0298 An engineered human myeloid cell line with a UBA1 mutation frequently detected in VEXAS syndrome is sensitive to the proteasome inhibitor bortezomib.

Hina Yazawa[1], Youhei Sasaki[2], Norihiko Kawamata[3]

[1]Medical Technology, School of Health Sciences, Tokyo University of Technology, Tokyo, Japan,[2]Hematology, Showa Medical University, Tokyo, Japan,[3]Hematology, Sasaki Institute/Tojun Medical Plaza Hospital, Tokyo, Japan

VEXAS syndrome is a systemic inflammatory disorder caused by somatic point mutations ofthe UBA1 gene in hematopoietic progenitor cells. Myelodysplastic syndrome (MDS) is oneof hematologic malignancies, in which hematopoietic stem cells have genetic mutations,without curable drugs. The same types of point mutations of the UBA1 gene as detected inVEXAS syndrome are occasionally detected in MDS. Reagents targeting mutated UBA1proteins may be able to eradicate the abnormal cells with the UBA1 point mutations.To examine this hypothesis, we have established a model cell line with the UBA1 mutationand analyzed drug-sensitivity of the mutated cells. First, we employed AI-based predictionanalyses to find the most reliable target sites and enzymes for introduction of the mutationinto the UBA1 gene. Second, we introduced the point mutation into the second start codonof the UBA1 gene, which is often detected in VEXAS syndrome, using a modifiedCRISPR/Cas9 method, adenosine-base-editing (ABE) enzyme and a targeting sgRNAconstruct. Third, we introduced the mutation into 293T cells using polyethyleneimine andconfirmed the base-change of the target site and absence of non-specific base-changes aroundthe target site. Fourth, we also introduced the UBA1 mutation into a human myeloid cell line,K562, using electroporation and found massive cell death of the introduced cells afterbortezomib treatment (ED_{50} of wild-type cells was 15.7nM and ED_{50} of the introduced cellswas 3.8nM), which inhibits proteasome activity.UBA1 plays an important role in ubiquitin/proteasome pathway to destroy degraded proteins.The mutation of the UBA1 gene leads to accumulation of degraded proteins in the abnormalcells. Further accumulation of degraded proteins by inhibition of the ubiquitin/proteasomepathway with bortezomib may have killed the mutated cells.Of note, since only 30-40% of K562 cells had the base-change by this method, cells with thebase-conversion may have secreted cytotoxic cytokines/chemokines, killing neighboring cellswithout the base-conversion, causing the massive cell death.We successfully isolated single cells with the base-conversion and evaluated effects of a drug, bortezomib, which is frequently used at bedside for treatments of multiple myeloma, for thecells with the mutation of UBA1 gene.The engineered cell line we have established would help clinicians to find new drugs effectivefor MDS patients with the UBA1 mutations.

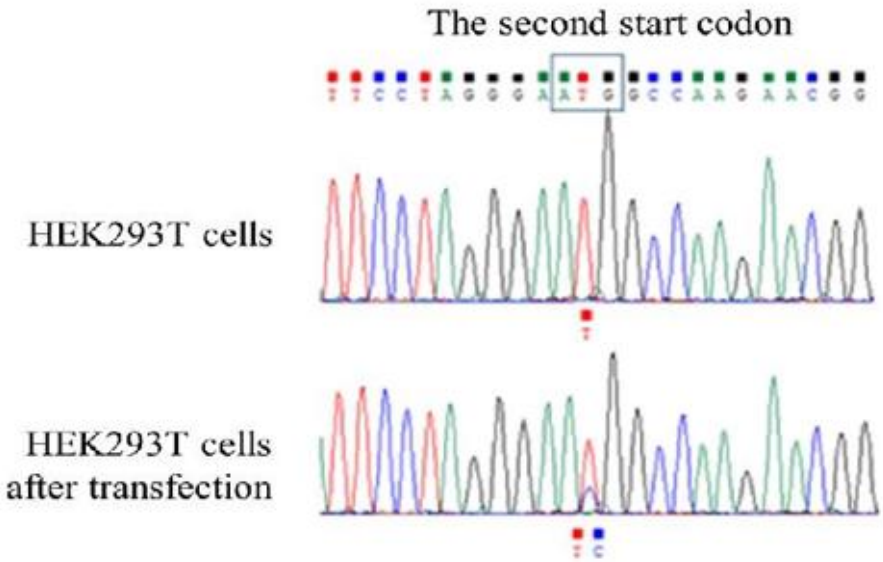

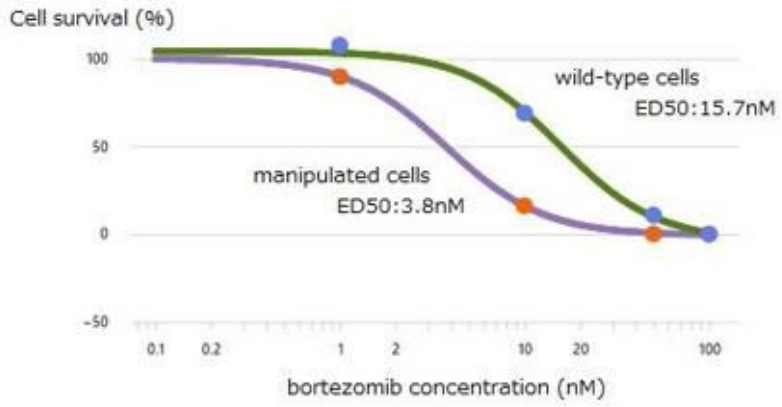

#0299 From factory to patient: *In vivo*-expressed biologics as a new paradigm for immunotherapy manufacturing.

Henry Leonard[1], Dan Rocca[1], Philipp Meyer[2], Ina Rohleff[2], Eva Oswald[2], Sarah L. Martin[3], Matthew Benson[3], Namrata Jayanth[4], Christian Cobaugh[5], Michael Shaw[5], Julia Schueler[2], Gemma Moiset[4], Roxana Redis[4], **Louise Brackenbury**[1], Justin Bryans[3]

[1]Charles River Laboratories, Bristol, United Kingdom,[2]Charles River Laboratories, Freiburg, Germany,[3]Charles River Laboratories, Cambridge, United Kingdom,[4]Charles River Laboratories, Leiden, Netherlands,[5]Vernal Biosciences, Colchester, VT

Advances in in vivo-expressed biologics are redefining how advanced modality therapeutics can be manufactured, delivered, and rapidly iterated for oncology and immune-modulating applications. Building on our existing mRNA-LNP platform for therapeutic antibody expression, we now extend this capability to mRNA-encoded chimeric antigen receptor (CAR) T cells, establishing an integrated, modular framework for generating functional biologics directly from modified RNA templates. Using clinically validated lipid nanoparticle (LNP) formulations, we have demonstrated efficient translation, secretion, and functional integrity of mRNA-encoded trastuzumab across in vitro, in vivo PK, and xenograft efficacy models. mRNA-derived antibody retained antigen specificity and ADCC potency equivalent to recombinant comparators, while in vivo studies showed sustained exposure and superior tumour growth control at reduced doses relative to protein-infused benchmarks. Additionally, we describe a complementary workflow enabling transient CAR expression in primary human T cells using SM-102-containing LNPs. Non-viral delivery of HER2-CAR mRNA resulted in >65% CAR-positive T cells following expansion, with robust surface expression and preserved viability. Functional cytotoxicity assays demonstrated potent, antigen-dependent killing of HER2-expressing tumour targets across a range of effector-to-target ratios, confirming that mRNA-encoded CAR T cells can be rapidly generated and evaluated using standard immunological assay infrastructure. Together, these datasets establish a unified platform for the rapid prototyping, optimisation, and functional validation of in vivo-expressed biologics. By combining antibody and cellular engineering workflows within a common mRNA-LNP framework, this approach enables scalable screening of candidate designs, supports mechanism-of-action studies, and lays a foundation for future in vivo investigations using targeted LNP technologies. The platform provides a flexible route to accelerate preclinical development of next-generation biologics, lowering dependency on complex manufacturing and enabling rapid iteration cycles aligned with the emerging field of mRNA-nanomedicine.

#0300 Mapping cellular fate: From metabolic dynamics to DNA damage responses.

Lorena Sueiro-Ballesteros, Henry Leonard, Dan Rocca, Lauren Schewitz-Bowers, **Louise Brackenbury**

Charles River Laboratories, Bristol, United Kingdom

Cellular homeostasis is maintained through a tightly regulated interplay of metabolic activity, cell cycle progression, programmed cell death, and genomic integrity. Perturbation of these pathways is a hallmark of oncogenesis. Analysis of these processes not only elucidates mechanisms of disease but also informs on therapeutic strategies. Here we present an integrated experimental framework designed to interrogate metabolism, cell cycle regulation, apoptosis, and DNA damage responses (DDR) in both immortalized cell lines and human primary cells. To assess cellular metabolic dependencies, we employed the SCENITH approach [1], which uses puromycin incorporation as a proxy for translational activity and, by extension, ATP production. This method enables quantification of reliance on glycolysis versus oxidative phosphorylation under defined conditions. Using metabolic inhibitors; 2-deoxyglucose to block glycolysis and oligomycin to inhibit mitochondrial ATP synthase, we observed distinct metabolic profiles. $CD8^+$ T cells exhibited pronounced dependence on oxidative phosphorylation, whereas HeLa cells maintained translational activity despite mitochondrial inhibition, indicating metabolic flexibility. Parallel to metabolic profiling, we implemented flow cytometric cell cycle analysis using FxCycle™ staining to determine DNA content and the proliferative state of cells. Cell lines, MOLT-4, were exposed to therapeutics with established antiproliferative activity. Cisplatin and palbociclib induced G_1-phase arrest, consistent with DNA crosslinking and CDK4/6 inhibition, respectively, while nocodazole, a microtubule disruptor, arrested cells in G_2/M. Apoptotic responses were concurrently evaluated via caspase 3 /DAPI staining, revealing cisplatin as the most potent inducer of early and late apoptosis compared to palbociclib and nocodazole. Finally, DDR was quantified by monitoring γH2AX and RAD51 foci formation following cisplatin treatment or exposure to irradiation. High-content imaging facilitated dose-response characterization and demonstrated that co-treatment with an ataxia-telangiectasia mutated (ATM) kinase inhibitor markedly amplified DNA damage accumulation, underscoring the therapeutic potential of DDR modulation. Collectively, these assays provide a customizable platform for dissecting cellular vulnerabilities and resilience under pharmacological stress. Such multidimensional profiling offers critical insights for precision oncology and immunotherapy, enabling the identification of context-specific targets and combinatorial strategies to overcome resistance. [1] Arguello 2020 https://pmc.ncbi.nlm.nih.gov/articles/PMC8407169/#ABS1

#0301 Population pharmacokinetics of nab-paclitaxel following administration of a nano-immunoconjugate with bevacizumab.

Mohd Beshr Chama[1], Matthew Stephen Block[1], Vera J. Suman[2], **Joel M. Reid**[1]

[1]Mayo Clinic College of Medicine and Science, Rochester, MN,[2]Mayo Clinic, Rochester, MN

Introduction. This study aimed to characterize the population pharmacokinetics (PopPK) of nab-paclitaxel following the administration of the nano-immunoconjugate nab-paclitaxel-bevacizumab to patients with unresectable stage IV melanoma or gynecological cancers (NCT02020707). The core objective was to characterize the population mean drug concentration-time profile, understand the variability in drug concentrations and identify factors that explain differences in paclitaxel plasma clearance. Also, we sought to explore the impact of the nano-immunoconjugate formulation on paclitaxel clearance.

Methods. Using Pumas AI - an advanced pharmacokinetic software program, integrating Machine Learning methods - a PopPK analysis was conducted using concentration-time data collected from 29 subjects, (681 concentration measurements). Patients received 75 - 175 mg/m^2 (total dose, 160 - 360 mg). Data were fitted to a 2-compartment model based biphasic decline observed in plasma concentration following intravenous administration. A critical requirement for the model was the inclusion of saturable elimination to accurately describe the drug's disposition. A comprehensive modeling workflow was implemented, starting with base models (mixed vs. non-linear clearance), followed by the sequential addition of covariates (Age, Sex, BSA, Tumor, Cycle). The Parsimony Principle was applied to select the most appropriate model.

Results. Population estimates for paclitaxel clearance and volume of distribution were 41.7 L/hr and 312 L, respectively. The analysis found paclitaxel clearance higher when compared with published data for nab-paclitaxel alone (21.1 or 25 L/h/m^2; Sparreboom et al, CCR 11:4136, 2005 and Ando et al, CCP 69:457, 2012). A covariate model incorporating BSA and Gender is the best. For every 2 m^2 increase in BSA, linear clearance (CL) increases by 6.9%. Females have 16.6% lower CL than males, which successfully characterized systematic differences in PK between subgroups of subjects.

Conclusion. The administration of nab-paclitaxel via the nano-immunoconjugate formulation led to increased clearance for paclitaxel consistent with known clearance mechanisms for therapeutic antibodies. The differences in drug clearance among patients were primarily attributable to covariates BSA and gender. These findings are crucial for identifying safe and effective dosing regimens and informing future clinical simulations.

#0302 Evaluating the influence of cholesterol content on the cellular uptake and formulation activity of nanoliposomal formulations against uveal melanoma.

Shrey Mehulkumar Patel, Francielle Mourisso, Bilal Habibeh, Anna Kleckerova, Robert B. Campbell

Massachusetts College of Pharmacy and Health Sciences, Worcester, MA

Introduction: Uveal melanoma (UM) is a rare but aggressive intraocular malignancy with limited responsiveness to current therapies. Nanoliposomal delivery systems can enhance intracellular drug transport, but their performance depends on lipid composition and the tumor's metabolic profile. UM exhibits dysregulated cholesterol metabolism driven by altered expression of enzymes such as SREBP2. Because cholesterol is a key structural membrane component that influences liposome properties, this study evaluated how cholesterol inclusion affects nanoliposome uptake and drug effects in UM cells.

Methodology: MP41 uveal melanoma cells (ATCC®) were cultured in RPMI supplemented with 25% FBS. Cells (2×10^4/mL) were seeded in vented centrifuge tubes and exposed to DPPE-rhodamine-labeled nanoliposomes containing 0, 5, 10, or 20 mol% cholesterol substituted for DOPC. Tubes were placed in an oscillating incubator at 37 °C for 60 minutes to promote liposome-cell interactions. Cellular uptake was quantified using a fluorescence microplate reader, and Quad Count™ was used for cell counting, viability, and growth-inhibition assessments.

Result: At 1 hour, the inclusion of cholesterol decreased the uptake of nanoliposomes by MP41 uveal melanoma cells. DOPC consistently demonstrated the highest cellular uptake values (≈2594-4543 RFU), while 95/5 and 90/10 formulations displayed lower values (≈800-3451 RFU) by comparison. These findings reveal a reproducible inverse relationship between cholesterol content and cellular uptake, suggesting that the inclusion of cholesterol in nanoliposome diminishes cellular uptake. Ongoing studies will evaluate additional time points and conditions, and whether the findings correlate with cytotoxicity studies.

Conclusion: Reduced cholesterol content in nanoliposomal formulations markedly enhanced cellular uptake by uveal melanoma cells. The consistently higher internalization observed with DOPC (100%) supports the use of relatively low-cholesterol (or cholesterol-free) preparations to enhance targeting. Cholesterol modulation could potentially enhance the effectiveness of therapeutics against uveal melanoma.

#0303 Turning tumors into therapeutic drug factories: Efficacy across oncology indications.

Moataz Reda, Blaine McCarthy, Sushil Lathwal, Evan Bishop, Priyanka Balasubrahmanyam, Robby Chandra, Nikki Kimura, Xiao Wu, Kim Tran, Jesse Simons, Ajda Rojc, Jayalakshmi Ramani, Dang Dang, David Rosen, Badri Ananthanarayanan, Nadege Morisot, David Suhy

Earli Inc., Redwood City, CA

Although DNA can be used to drive expression of cancer therapeutics, clinical use is often restricted to intratumoral injection due to lack of specificity. Earli's cancer-activated expression platform permits broad systemic DNA delivery to a multitude of cancers by using conditionally active promoters to drive potent anti-tumor activity while minimizing systemic toxicity. This is achieved via orthogonal levers of specificity: (1) lipid nanoparticles (LNP) for extrahepatic delivery of nucleic acids following intravenous (IV) injection to maximize tumor DNA delivery, and (2) highly engineered synthetic cancer-activated promoters (CAP) that restrict expression to malignant cells. As a result, the therapeutic protein production is concentrated within the diseased tissues while avoiding broad systemic exposure and corresponding dose-limiting toxicities.

Typically, IV-dosed LNPs are rapidly opsonized and cleared by the liver. Proprietary Earli LNPs were optimized for systemic delivery of DNA beyond the liver including solid tumors. Biodistribution and expression from different LNPs were assessed using a DNA with a CAG promoter driving luciferase in subcutaneous xenograft models. The lead LNP achieved more than a 6-fold higher tumor expression than the same DNA formulated in an LNP used in a commercial siRNA product. Importantly, tumor tropism confirmed a robust 88-fold difference in tumor-to-liver BLI ratio. Cancer-activated expression was initially tested in syngeneic subcutaneous models. An IV-dosed CAP-driven IL-12 DNA construct resulted in tumor regression in all treated animals, achieving a 100% cure rate at modest DNA levels. This response was accompanied by robust $CD8^+$ T cell activation. IL-12 was detected in the tumor but remained undetectable in the serum, confirming selective expression driven by the CAP element.

To demonstrate utility in clinically relevant models, the platform was tested in orthotopic models of lung cancer. In an aggressive lung metastases model, CAP-IL-12 significantly reduced lung tumor burden by over 7-fold compared to a non-expressing control construct, and significantly reduced metastatic nodules and lung weights. Immune-profiling revealed IL-12-driven immune activation, such as 2-fold increases in $Ki67^+$ cells and a 4-fold increase in cytotoxic $CD8^+$ T cells compared to control. Central and effector memory T cells were also elevated by 2-fold. Myeloid cells showed enhanced activation with a 3-fold increase in MHC II expression on dendritic cells, indicative of improved antigen presentation within the tumor microenvironment. Ongoing experiments are evaluating the efficacy of CAP-driven IL-12 delivered with newly developed LNPs in orthotopic bladder and liver models.

Overall, our findings demonstrate Earli's cancer-activated expression platform across cancer indications, supporting its development for broad application across oncologic indications.

#0304 A phase 1 study of intratumoral ultra-high concentration nitric oxide (UNO) gas injection in cutaneous and subcutaneous solid tumor metastases.

Amichay Meirovitz[1], Steve Lisi[2], Kim Sheva[1], David Greenberg[1], John Jett[2]

[1]Soroka Medical Center, Beer-Sheva, Israel,[2]Beyond Air, Inc., New York, NY

Background: Ultra-high concentration nitric oxide (UNO; >10,000 ppm) administered intratumorally has shown survival benefits in murine colon and breast cancer models. UNO modulates the tumor immune microenvironment, influencing M1 macrophages, Tregs, and $CD8^+$ T cells, and upregulates PD-1 expression, thereby enhancing the activity of immune checkpoint inhibitors (ICIs). In preclinical studies, UNO combined with anti-PD-1, anti-PD-L1, or anti-CTLA-4 improved tumor inhibition, and UNO alone surpassed anti-PD-1 efficacy in 4T1 breast tumor-bearing mice.

Methods: This phase 1 trial (NCT05351502) evaluated the safety, maximum tolerated dose (MTD), and recommended phase 1b dose of a single intratumoral UNO injection in patients with unresectable cutaneous or subcutaneous solid tumors (superficial axis 4.5-30 mm). UNO was administered at 25,000 or 50,000 ppm using a 23-gauge needle inserted horizontally through the tumor to create an exit portal, then retracted to the lesion center for treatment. Gas was delivered intratumorally at 0.2 L/min for 5 minutes.

Results: Ten heavily pretreated patients were enrolled: squamous cell carcinoma (n=2), melanoma (n=2), and breast cancer (n=6). Patients received a mean of 5.5 prior systemic therapies and 10.3 total cancer-directed treatments. Six patients were treated with 25,000 ppm UNO and four with 50,000 ppm. Overall, treatment was well tolerated; most treatment-related adverse events (AEs) were grade 1. One serious (S)AE (hypoxia) that occurred during a 25,000 ppm administration, was considered related but was not dose-limiting and resolved fully. No deaths occurred within 12 weeks post-treatment. As of October 1, 2025, seven of ten patients remain alive 19-37 months post-single UNO injection; one patient died of disease progression 25 months post-treatment. Two patients with triple negative breast are disease free.

Conclusions: Intratumoral administration of ultra-high-concentration UNO was feasible and well tolerated in patients with unresectable solid tumors. Durable long-term survival observed in this heavily pretreated population supports further evaluation of UNO, including in combination with ICIs.

#0305 Non-melanoma skin cancer treated with electrochemotherapy: Clinical outcomes and tolerability.

Felipe Horacio Maglietti[1], Raquel Lertora[2], Nazarena S. Martinez[1], Alexandre Da Rosa Silva[1], Marina Ribeiro Damasceno Silva[1], Sebastian D. Michinski[3]

[1]Instituto Barcelo de Investigacion Traslacional, Buenos Aires, Argentina,[2]Hospital Petrona V de Cordero, San Fernando, Argentina,[3]INFINA-CONICET, Buenos Aires, Argentina

Background: Electrochemotherapy (ECT) combines electroporation and chemotherapy to enhance cytotoxic drug uptake in tumor cells. This study evaluates the efficacy and safety of ECT using intravenous bleomycin in patients with non-melanoma skin cancer (NMSC).
Methods: Sixteen patients with histologically confirmed NMSC were treated under neuroleptoanalgesia in an outpatient setting. Intravenous bleomycin was administered at a dose of 15,000 IU/m² of body surface area. Electric pulses were delivered using the OncoPore device (BIOTEX SRL, Buenos Aires, Argentina). Each session lasted less than one hour, and all but one patient required a single treatment. Tumor response was assessed according to RECIST criteria, and adverse events were graded following CTCAE guidelines.
Results: Among the 16 treated patients, 11 had squamous cell carcinoma and 5 had basal cell carcinoma. Twelve patients (75%) achieved Complete Response, three (19%) had Partial Response, and one (6%) exhibited Stable Disease (SD), yielding an Objective Response rate of 94%. Notably, one patient with recessive dystrophic epidermolysis bullosa achieved a complete response without complications. Adverse events were mild to moderate and transient. The most frequent was pain (grade 2), effectively managed with nonsteroidal anti-inflammatory drugs. Erythema (grade 1) and swelling (grade 1-2) resolved spontaneously within one week. Infection (grade 2) occurred in four patients (25%) and was successfully treated with oral antibiotics. No severe or systemic adverse events were observed. Esthetic outcomes were excellent in all cases, with preservation of surrounding healthy tissue and minimal scarring.
Conclusions: ECT with intravenous bleomycin represents a safe, effective, and well-tolerated therapeutic option for patients with non-melanoma skin cancer. The high objective response rate, minimal toxicity, and favorable cosmetic results support its implementation in outpatient settings. Furthermore, its efficacy in a patient with epidermolysis bullosa suggests potential applicability in selected fragile-skin conditions. These results reinforce ECT as a valuable addition to the therapeutic armamentarium for NMSC management.

#0306 Integrative computational and functional genomic approach reveals UBE2Z-UBR2-Ecadherinaxis as a beta-catenin-specific vulnerability in colorectal cancer.

Chunhua Wan, Hugh Gao, Claire Sun, **Ron Firestein**

Hudson Institute of Medical Research, Clayton, Australia

Synthetic lethality provides a powerful framework for cancer therapy by targeting gene interactions that are selectively essential in tumor cells, but are non-essential in normal tissues.. This approach is particularly attractive in malignancies driven by oncogenes considered “undruggable”. Using a machine-learning multi-omics approach we identify UBE2Z/USE1, a key ubiquitin-conjugating enzyme of non-canonical E1 UBA6-charged ubiquitination cascade, as a synthetic lethal partner of oncogenic β-catenin. UBE2Z knockout markedly impairs nuclear β-catenin accumulation, suppresses Wnt target gene expression, and induces differentiation in cell lines, tumouroids and in vivo models. Strikingly, UBE2Z is exclusively necessary for oncogenic β-catenin activity and completely dispensable for physiological Wnt/β-catenin signaling, highlighting its tumor-specific role. Genome-wide CRISPR rescue screens identified E-Cadherin as a critical intermediate of UBE2Z activity. Integrative transcriptomic and proteomics analyses suggest that UBE2Z supports oncogenic β-catenin transcriptional activity by promoting the degradation of intracellular E-cadherin via UBRfamily N-end rule E3 ligases. Manipulating UBE2Z’s ubiquitin-conjugating activity recapitulates the potent inhibitory effect of E-cadherin overexpression on oncogenic β-catenin activity, underscoring its translational significance. These findings reveal the UBA6-UBE2Z non-canonical ubiquitination cascade as a druggable vulnerability in β-catenin-addicted cancers and underscore synthetic lethality as a rational strategy for targeting β-catenin-driven tumorigenesis.

#0307 Triple-negative breast cancer growth and metastasis suppression by CCN5 is mediated by Merlin/NF2 and Orai-1 molecular signatures.

Inamul Haque[1], Gargi Maity[2], Jamie L. Porter[2], Snigdha Banerjee[2], Sushanta K. Banerjee[2]

[1]Cancer Biology, University of Kansas Medical Center, Kansas City, KS,[2]Pathology and Laboratory Medicine, University of Kansas Medical Center, Kansas City, KS

Breast cancer (BC) is the second leading cause of cancer-related death among women, both in the United States and globally. This disease affects approximately one in eight women (around 12%), impacting nearly every family worldwide. The statistics are similarly relevant for female U.S. veterans. Current therapies for BC are thought to improve patient survival; however, one-third of patients with aggressive triple-negative breast cancer (TNBC) may experience more frequent relapses compared to those with hormone receptor-positive subtypes, and may eventually develop distant metastatic disease. Currently, there are no targeted therapies available for invasive and metastatic breast cancer, highlighting a critical need for improved treatment options. TNBC is a heterogeneous mix of cells, with significant variability both between and within tumors, which often makes therapeutic regimens less effective. A novel approach, diverging from existing treatment strategies, could positively influence both clinical study designs and future practices in BC, potentially increasing the number of TNBC survivors. Our previous studies examined CCN5 expression in a large cohort of primary BC samples and cell lines, finding that CCN5 expression is inversely correlated with disease in most samples. In this study, we demonstrated that CCN5 inhibits tumor growth and metastatic spread in genetically engineered mouse models (GEMMs) and human TNBC xenograft models, without causing any side effects. CCN5 may facilitate these critical processes by regulating the expression and activity of Merlin (a tumor suppressor gene) and Orai1 (a gene involved in metastasis) in TNBC cells. In addition, CCN5 suppresses the JunB/AP-1 transcription factor and VEGF-A, while protecting against ZO-1 loss (a downstream target of VEGF-A and a protein that acts as a barrier to metastasis), mirroring the blockade of permeability in endothelial cell (EC) monolayers. These collective findings suggest that CCN5 prevents or delays the growth, invasion, and metastasis of TNBC cells by regulating multiple gene signatures. Therefore, CCN5 treatment or restoration may represent a promising novel therapeutic intervention for breast cancer. (This work is supported by the VA Merit grants)

#0308 Melatonin activity in uterine leiomyoma and leiomyosarcoma cell lines: A preliminary study of its inhibitory potential in mesenchymal tumors.

Tatielly T. Miranda[1], Edmund C. Baracat[2], Roseli S. Soares[2], **Katia C. Carvalho**[1]

[1]Obstetrics and Gynecology, HCFMUSP, Sao Paulo, Brazil,[2]Sao Paulo University, Sao Paulo, Brazil

Background: Uterine smooth muscle tumors (USMT) encompass benign leiomyomas (LM) and highly aggressive leiomyosarcomas (LMS). Although melatonin has been reported to exert antiproliferative and oncostatic effects in several tumor models, its impact on the growth dynamics of LM and LMS cells remains poorly understood. Here, we evaluated the dose- and time-dependent effects of melatonin on the proliferation and migration of LM and LMS cell lines to investigate the responsiveness of both benign and malignant USMT cells.

Methods: LM and LMS cells were plated at a density of 1×10^4 cells per well in 96-well plates. Cell proliferation was assessed at 0, 24, 48, 72, and 96 hours following treatment with melatonin at 3 mM, 5 mM, or 10 mM. Each condition included six technical replicates and two experimental replicates. Control groups consisted of untreated cells (medium only) and vehicle controls (medium plus ethanol). Fluorescence-based viability/proliferation readings (Presto Blue reagent®) were used as a measure of cell growth over time. Scratch assays were used to assess the effects on the cell migration using the same time and doses of melatonin, followed by Image J® software analyses of the acquired pictures.

Results: Melatonin significantly inhibited proliferation in both LM and LMS cells in a dose-dependent manner. In LM cells, melatonin induced a marked and sustained reduction in proliferation at all-time points, with the strongest suppression observed at 10 mM, which maintained minimal proliferative activity throughout the experiment. LMS cells also exhibited reduced proliferation in response to melatonin, although the inhibitory effect was less pronounced than in LM cells, particularly at earlier time points. At 72 hours, control LMS groups displayed a sharp proliferative peak, whereas melatonin-treated cells - especially at 10 mM - showed substantial attenuation of this growth increase. Across both tumor types, 10 mM consistently showed the most robust antiproliferative effect. Very similar results were obtained for the migration analyses, both to LM and LMS cells.

Conclusion: Melatonin exerts clear inhibitory activity in USMT cells, with a stronger suppressive effect in LM cells compared with LMS cells. These findings suggest intrinsic differences in melatonin responsiveness between LM and LMS, potentially reflective of altered growth-regulatory pathways associated with malignant transformation. Melatonin may represent a biologically relevant modulator of uterine smooth muscle cells tumorigenesis, warranting further mechanistic studies and exploration as an adjunct therapeutic strategy.

#0309 Oncogenic cooperation of MUC13 and NDRG1 signaling in liver cancer.

Shabnam Malik[1], Mohammed Sikander[1], Daniel Zubieta[1], Mirza Sarwar Baig[2], Iris Enriquez[1], Murali M. Yallapu[1], Subhash C. Chauhan[1]

[1]The University of Texas Rio Grande Valley, Edinburg, TX,[2]School of Interdisciplinary Science and Technology, Jamia Hamdard, New Delhi, India

Background: Liver cancer is one of the leading causes of cancer-related mortality worldwide, highlighting the vital importance of understanding its molecular mechanism for the development of targeted therapies. Mucin 13 (MUC13), a transmembrane glycoprotein, has been associated with the oncogenic processes that cause liver cancer. Our previous studies have shown its significance in promoting cancer cell survival, proliferation, and metastasis. Emerging evidence indicates that NDRG1 (N-Myc downstream regulated gene 1), played a critical role in cell growth, development, stress response, invasion and migration, may also be implicated in the pathogenesis of liver cancer. The current study aims to investigate the influence of the co-expression of MUC13 and NDRG1 on liver cancer progression and determine if their co-expression is correlated with clinical outcomes.
Methodology: We employed liver cancer cell lines corresponding to different tumor grades characterized by MUC13 positivity. The expression levels of MUC13 and NDRG1 were evaluated in these cell lines. We performed confocal microscopy for immunofluorescence to examine co-localization of MUC13 and NDRG1. Furthermore, we conducted immunohistochemical analysis of MUC13-positive patient samples to evaluate NDRG1 expression levels. We additionally examined public databases to assess the correlation of NDRG1 and MUC13 expressions with patient survival.
Results: We identified a notable association between increased levels of MUC13 expression and elevated NDRG1 expression in MUC13-positive liver cancer cell lines, suggesting a potential interplay that may facilitate cancer progression. Immunofluorescence assays performed on these cell lines provided yields strong evidence of co-localization between MUC13 and NDRG1. Additionally, our studies demonstrated a direct molecular interaction between MUC13 and NDRG1 in liver cancer cells as evidenced by proximity ligation assay (PLA). We further confirmed NDRG1 expression in MUC13-positive and negative patient samples through immunohistochemical staining. To corroborate our findings, we conducted a correlational analysis using public clinical database, which revealed an association between NDRG1 and MUC13 expression levels, suggesting that higher co-expression of these two molecules is linked to poor overall survival (OS) rates.
Conclusion: The outcomes of this study indicate a notable co-expression of MUC13 and NDRG1 in liver cancer, potentially highlighting their cooperative involvement in tumor progression.

#0310 Translational development of NEU-002: Engineered therapeutic elastases demonstrate systemic anti-tumor activity via intraperitoneal and intravenous administration.

Maria Fumagalli, Chang Cui, Ravindra Gujar, Nicole Martinez, **Peter Haberz**, Court Turner, Lev Becker

Onchilles Pharma Inc, San Diego, CA

NEU-002 is a systemically deliverable engineered elastase targeting the ELANE pathway and is under development for solid tumors. To advance NEU-002 toward clinical translation, two optimized candidates, N17474 and N17482, were generated through rational sequence engineering. This optimization strategy focused on preserving elastase activity in blood by protection from serine protease inhibitors, as evaluated using a range of biochemical assays. Furthermore, we show that NEU-002 program compounds maintained robust anti-tumor efficacy in the CT26 colon cancer model following intravenous administration, demonstrating that essential functional properties were retained during optimization. In addition, we explored a new intraperitoneal route of administration to expand delivery options for NEU-002 and observed reductions in tumor burden in orthotopic colon cancer mouse models, supporting the feasibility of accessing tumors within visceral compartments. Collectively, these findings establish a strong translational foundation for NEU-002 and, together with planned pharmacokinetic studies in non-human primates, will directly inform the selection of the final development candidate for advancement toward clinical evaluation in solid tumor indications.
Generative artificial intelligence was used to assist in drafting text for this abstract.

#0311 Integrated strategies for producing functional recombinant proteins to advance autoimmune disease therapeutics.

Wenlin Ren[1], **Siwen Wang**[2], An Ouyang[2], Spencer Chiang[1], Yu Sun[1]

[1]ACROBiosystems Co., Ltd., Beijing, China,[2]ACROBiosystems Inc., Newark, DE

Autoimmune diseases result from immune dysregulation, characterized by loss of self-tolerance, chronic inflammation, and multiorgan pathology. However, the immune signaling pathway is a host of complex protein architectures, including polymeric cytokines, transmembrane receptors, and intracellular pathway mediators. Each are essential but challenging due to structural intricacies such as oligomerization, domain organization, and transmembrane regions. Herein, we present an integrated strategy to produce functional recombinant proteins to support research and therapeutic development in autoimmune disease. For soluble polymeric targets, structure-guided engineering is employed, encompassing linker optimization for IL-17A/IL-17F heterodimer stabilization. For other targets such as the assembly of IL-2 receptor subunits, the incorporation of protein tags is the optimal methodology for recombinant protein production. Finally, by utilizing targeted mutagenesis, oligomerization can be controlled for TL1A disulfide bonds to control oligomerization. With the incorporation of process optimization in culture and purification, the development of hard-to-express recombinant proteins helps preserve native conformation and bioactivity. These are encapsulated into three complementary platforms are implemented to ensure solubility and functional reconstitution: detergent micelles for structural studies, ELISA, and surface plasmon resonance; nanodiscs for detergent-free, cell-based assays; and virus-like particles providing a native membrane context and high immunogenicity. These proteins further enable antibody discovery, including epitope-focused immunogen design, for example, IL-23/IL-12 chimeras to reduce off-target responses. By adhering to Quality-by-Design principles, this closed-loop workflow from structural analysis through application validation ensures maintenance of native functionality, stability, and homogeneity. Collectively, these approaches accelerate drug discovery in autoimmune disease by generating high-quality reagents for mechanistic studies, screening, and therapeutic development, overcoming longstanding production bottlenecks in structurally complex targets.

#0312 Postbiotic based on sequential fermentation of *L.paracasei* NPB01 and *L.rhamnosus* GG exerts antitumor activities against breast cancer.

Roberto Berni Canani[1], Chiara Luongo[1], Laura Pisapia[1], Franca Oglio[1], Roberta Di Santillo[1], Alessia Gaeta[1], Chiara Scocco[1], Marco Michelini[1], Vittoria Mauriello[1], Alessia Cadavere[1], Camilla Messuri[1], Saranya Chumsri[2], Dawn Mussallem[1]

[1]University of Naples Federico II, Naples, Italy,[2]Mayo Clinic Florida, Jacksonville, FL

Backgroud. Breast cancer (BC) is the most common and deadly cancer in women worldwide. Emerging evidence highlights the role of gut microbiota in modulating breast cancer risk, treatment response, and recurrence through various mechanisms, including the production of biologically active compounds and metabolites. These non-viable microbial products and metabolic byproducts from probiotic fermentation, known as postbiotics, exert beneficial effects on the host without the need for live microorganisms. Postbiotics derived from *Lacticaseibacillus* species represent a novel class of therapeutics with potential anti-cancer properties. In this study, we investigated the therapeutic effects of an innovative postbiotic product (iPB), developed through sequential fermentation of *L.paracasei* NPB01 and *L.rhamnosus* GG, in BC experimental models.

Methods. The following cell lines were used to represent main BC subtypes: MCF7 cells (ER+/HER2), MDA-MB-231 (triple negative breast cancer), SKBR3 (HER2+). MCF-10A (normal breast epithelial cells), Caco-2 (enterocytes), and peripheral mononuclear blood cells (PBMC) were used as control. Cell viability was assessed by colony formation assay. Apoptosis was evaluated using Annexin V/7-AAD staining, HLA class I surface expression by flow cytometry, and cancer cells migration by wound healing assay.

Results. iPB exposure resulted in >50% colony formation reduction in MCF7, >30% in MDA-MB-231 and >40% in SKBR3 cells starting from 0.5 mg/ml for 72 h ($p<0.01$). iPB increased early and late apoptotic cell rate in all BC cell lines starting from 0.5 mg/ml for 72 h. On the contrary, iPB exposure up to 5 mg/ml for 120 h did not affect cell viability in control cells (MCF-10A, Caco-2, PBMC). 1.20 to 1.30 fold increase in HLA class I expression was observed in all BC cell lines after the exposure with iPB starting from the dose of 0.5 mg/ml for 72 h. A less intense HLA class I expression increase was observed in control cells after the iPB exposure. Cell migration process and inflammatory cytokines response were inhibited by the iPB exposure in all BC cell models.

Conclusions. iPB reduces cell viability and cell migration in all main BC phenotypes. These effects parallel with HLA class I surface expression increase in all BC cell phenotypes, potentially enhancing immunogenicity. These findings suggest that iPB may represent a promising novel agent in BC treatment and prevention.

: Kinase and Signaling Pathway Dependencies Driving Cancer Therapeutic Response
Poster Session

#0316 Subcellular localization of PARP1 by protein kinase D1 modulated cellular response to olaparib.

Sanjeev Shukla[1], Joseph McGrath[1], Robert Willis[2], Arjun Venkatesh[1], Jean-Pierre Kanumuambidi[1], Reynier Rodriguez-Rosales[1], Mario Mietzsch[3], Robert McKenna[3], K.C. Balaji[1]

[1]Urology, University of Florida Health, Jacksonville, FL,[2]Alabama College of Osteopathic Medicine, Dothan, AL,[3]University of Florida, Gainesville, FL

DNA damage and repair play a dual role in cancer: unrepaired lesions drive mutations and tumor growth, while repair pathways enable cancer cells to resist therapies like chemotherapy and radiation. PARP1 detects DNA breaks, adds poly(ADP-ribose) to target proteins, and recruits repair factors, with localization mainly in the nucleus but extending to other compartments under certain conditions. Inhibition of PARP1 prevents DNA repair, leading to cancer cell death, and FDA-approved PARP1 inhibitors show efficacy in metastatic castration-resistant prostate cancer, though dose-limiting toxicities reduce effectiveness. This study examines Protein kinase D1 (PrKD1) as a modulator of PARP1 and its impact on sensitivity to PARP inhibition. Using prostate cancer cell lines with altered PrKD1 expression (LNCaP, LNCaP ShPrKD1, C4-2, and C4-2 PrKD1), we found that PrKD1 overexpression increased sensitivity to Olaparib (PARP1 inhibitor), while downregulation conferred resistance. Pharmacological inhibition of PrKD1 with Compound-10 also enhanced Olaparib sensitivity. Co-immunoprecipitation studies suggest PrKD1-PARP1 interaction in subcellular fractionations, and PrKD1 transfection in C4-2 prostate cancer cells increased PARP1 membrane localization. Compound-10 treatment in prostate cancer cells and PDX models represented elevated PARP1 expression. *In-silico* modeling also identified a potential PrKD1 binding site adjacent to PARP1 WGR (tryptophan-glycine-arginine-rich) domain. Overall, PrKD1 emerges as a novel PARP1 regulator. Co-targeting PARP1 using Olaparib and Compound-10 may improve efficacy at lower doses, enhance tolerability, and expand therapeutic options. Based on the *in-vitro*, *in-vivo* and *in-silico* studies we may suggest the interaction between PrKD1 and PARP1 in subcellular membrane compartments. The discovery of PARP1 at the membrane opens new opportunities for theragnostic applications.

#0317 Glucose conditions influence CAMKK2-targeted therapy sensitivity in triple-negative breast cancer of different ancestry.

Elham Amini, Sree latha Aramgam, Kenisha Webb, Sean Kimbro

Morehouse School of Medicine, Atlanta, GA

Background: Triple-negative breast cancer (TNBC) is associated with a higher incidence and mortality in women with specific metabolic comorbidities, including obesity, diabetes, and dyslipidemia. Calcium/calmodulin-dependent protein kinase kinase 2 (CAMKK2) is a central kinase regulating cellular energy metabolism and stress adaptation in TNBC cells. This study examines how different glucose conditions affect the survival and response of TNBC cell lines to CAMKK2 inhibitors.
Methods: A panel of commonly used TNBC cell lines (MDA MB 231, MDA MB 468, MDA MB 157, HCC1806) were treated with STO 609 and SGC CAMKK2 1 at various glucose levels. Cells were incubated under four glucose conditions, 0.33 mM (severe hypoglycemia), 5 mM (physiological/normal), 17.5 mM (moderate hyperglycemia), and 50 mM (extreme hyperglycemia). IC_{50} values and cell viability were assessed following drug treatment across these conditions.
Results and Conclusion: In all cell lines, results indicated an overall increase in IC_{50} (reduced inhibitor sensitivity) as glucose levels changed from moderate (5, 17.5 mM) to either low (0.33 mM) or high (50 mM). For STO-609, IC_{50} values improved from 71-2533 µM at 0.33 mM to 32-91 µM at 17.5 mM but increased again to 92-894 µM at 50 mM. With SGC-CAMKK2-1, IC_{50} ranged from 112-619 µM at 0.33 mM to 48-148 µM at 17.5 mM and increased again to 154-520 µM at 50 mM. Notably, HCC1806 cells were the most sensitive to both CAMKK2 inhibitors, while MDA MB 157 was overall more resistant. Different glucose conditions have a significant impact on the efficacy of CAMKK2-targeted inhibitors in TNBC, with some cell lines displaying more metabolic sensitivity than others. These findings demonstrate that personalized therapeutic strategies, considering the metabolic background, may improve treatment outcomes in aggressive breast cancers.

#0318 The combination of STX-478 and lorlatinib for the treatment of *PIK3CA* mutant colorectal cancer.

Addison T. Zick[1], Alexa E. Schmitz[1], Cheri A. Pasch[1], Dustin A. Deming[2]

[1]Univ. of Wisconsin Madison Sch. of Med. & Public Health, Madison, WI,[2]University of Wisconsin Carbone Cancer Center, Madison, WI

Background: Over 15% of colorectal cancer (CRC) patients are *PIK3CA* mutant, making it a critical pathway for drug development. Recently, we performed a high throughput drug screen with STX-478, a mutant-selective *PIK3CA* inhibitor, and identified lorlatinib, an ALK inhibitor, as a potential means to enhance therapeutic efficacy. Here we confirm this efficacy and evaluate potential mechanisms of action, including the potential impact of lorlatinib on MYC protein abundance and target gene expression.

Methods: CRC cell lines SW48 and SW48PK (Horizon Discovery; SW48 with a *PIK3CA*^{H1047R} mutation) were used in a cell viability assay. Immunoblotting was performed on SW48, SW48PK and patient derived cancer organoids (PDCOs) with STX-478, lorlatinib, and combo treatment. ImageJ was used to quantify these blots to evaluate PI3K protein expression. *PIK3CA*^{H1047R} mutant PDCOs were treated, imaged, and the longest diameter of any organoid was measured. Glass's delta (GD) was used to determine effect size for each treatment group compared to control. Gene expressions for five MYC target genes were measured by quantitative PCR (qPCR).

Results: In SW48 and SW48PK cells, there were no significant differences in cell viability following lorlatinib single-agent treatment. However, combo treatment with STX-478 and lorlatinib significantly reduced cell viability in both cell lines (lorlatinib 500 nm, STX-478 500 nm; SW48 p=0.001, SW48PK p<0.001) In SW48PK, immunoblot analysis demonstrated a marked decrease in phosphorylation levels of ribosomal protein S6 (RPS6) and 4EBP1 under combo treatment, indicating suppression of downstream PI3K signaling (pRPS6: p=0.02, 4EBP1: p=0.03). There were no significant changes in protein expression of c-MYC and pAKT in any of the treatment groups. RT- qPCR analysis overall did not demonstrate a change in MYC target gene expression. The expression of LDHA, a key glycolytic gene upregulated under hypoxic conditions, was significantly decreased in SW48PK cells following treatment, indicating a potential reduction in glycolytic activity associated with the combined therapy (p=0.005). *PIK3CA*^{H1047R} mutant PDCOs treated with the combo of STX-478 and lorlatinib had a significant reduction in growth compared to control (relative change in diameter control versus combo = 42.9% vs 12.3%; GD=1.37).

Conclusion: The combination of STX-478 and lorlatinib was confirmed to have significant efficacy in PIK3CA mutant CRC models. This activity does not seem to be related to effects on MYC. Further studies look to determine the mechanism of action for the combo treatment, and confirm efficacy in vivo.

#0319 An analysis of orthosteric missense kinase mutations among a clinical sequencing cohort of over 90,000 cancer patients.

Jessica B. White[1], John D. Chodera[2], Wesley Tansey[3]

[1]Tri-Institutional PhD Program in Computational Biology and Medicine (Memorial Sloan Kettering Cancer Center), New York, NY,[2]Sloan Kettering Institute, Computational & Systems Biology Program, Memorial Sloan Kettering Cancer Center, New York, NY,[3]Computational Oncology, Memorial Sloan Kettering Cancer Center, New York, NY

Being among the most well-studied family in the human proteome, the approximately 500 kinases that constitute the human kinome possess ample sequence, structural, and functional annotations within both pan-proteome and kinase-specific resources. Analyzing mutations in homologous residues, particularly in the orthosteric binding pocket, can provide insights into recurrent mechanisms of pathogenicity and drug resistance. However, harmonizing these resources poses a non-trivial task: identifier disambiguation, mapping between disparate sequence representations, and even concordance between resources as to what constitutes a kinase enzyme all pose significant challenges. Here, we describe the creation of a Python package to reliably and reproducibly curate and harmonize kinase sequences. We use this toolkit to interrogate missense mutations within the orthosteric kinase binding site from Memorial Sloan Kettering Cancer Center's (MSKCC) clinical sequencing cohort. We mapped the 85-residue binding site from the Kinase-Ligand Interaction Fingerprints and Structures (KLIFS) database to the canonical UniProt sequence for a superset of kinases from various resources. Among the 126,930 samples from the 93,249 patients in MSKCC's clinical sequencing cohort as of mid-November 2025, we identified 99 kinase genes assessed for somatic mutations. Within the 87 kinases that mapped to the canonical UniProt sequence, we detected 6,198 unique single amino acid substitutions in the ATP-binding pocket in at least one sample in 11,071 (11.9%) of patients. KLIFS regions with significantly higher percentages of kinases containing one or more such alterations included the gatekeeper (median: 65.9%), linker (65.3%), catalytic loop (61.8%), activation loop/xDFG motif (61.2%), and glycine-rich loop (56.5%), while β-sheet regions (47.1%) had significantly lower percentages. Kinase families that possessed a significantly higher percentages of KLIFS residues containing one or more such alterations included tyrosine kinase (61.9%) and STE (59.5%), while tyrosine kinase-like (54.8%), AGC (51.8%), calcium/calmodulin-dependent protein kinase (51.2%), and atypical kinases (44.0%) had significantly lower percentages. Since our toolkit harmonizes sequences across the human kinome, it provides a multiple sequence alignment to evaluate species-level protein family conservation. We identified highly conserved, frequently mutated residues in the glycine residues of the glycine-rich loop, the arginine of the HRD motif, and the aspartic acid of the xDFG motif. Our analysis provides a unique pan-cancer assessment of missense mutations across the human kinome, suggesting shared functional mechanisms of pathogenicity for further characterization. Our tools can be used to interrogate missense kinase mutations in any cBioPortal cohort in a similar manner.

#0320 Targeting overexpressed TTK and NEK2 decreases early metastatic potential of triple-negative breast cancer cell lines.

Alexandra N. Aquino-Acevedo[1], Angel D. Colon-Burgos[1], Esther M. Irizarry-Quintana[2], Elliott Rodriguez-Lopez[1], Joel A. Orengo-Orengo[1], Marileana Rodriguez-Ruiz[3], Gretchen M. Albarran-Acosta[1], Melanie E. Cruz-Robles[1], Harold I. Saavedra[1]

[1]Basic Sciences, Ponce Health Sciences University, Ponce, PR,[2]U54 REC InterAmerican Undergraduate Program, Ponce Health Sciences University, Ponce, PR,[3]Moffitt U54 Summer Research Program, Ponce Health Sciences University, Ponce, PR

Triple-negative breast cancer (TNBC) is an aggressive form of breast cancer lacking estrogen, progesterone, and HER2 receptors, making it unresponsive to hormonal or anti-HER2 therapies. Non-Hispanic Black (NHB) and Hispanic/Latino (H/L) women have lower survival rates, partly due to later-stage tumor detection and higher TNBC prevalence. Higher African ancestry has been associated with increased expression of mitotic kinases, such as TTK and NEK2, which regulate cell division and tumor progression. Our research confirms that TTK overexpression is associated with TNBC growth and epithelial-to-mesenchymal transition (EMT). Preliminary analyses indicate that molecular functions and processes, such as β-catenin binding, are associated with TTK and NEK2 expression.Therefore, this study aims to investigate, via in vitro assays, the expression levels of EMT markers and transcription factors, as well as changes in the invasive capacity and motility of metastatic TNBC upon downregulation of TTK, NEK2, and β-catenin. To assess this, TNBC cell lines, MDA-MB-231 (NHW) or MDA-MB-157 (NHB), were cultured, followed by TTK/NEK2 or β-catenin siRNA-mediated knockdown. Western blotting was used to measure EMT-related proteins and transcription factors. Immunocytochemistry evaluated β-catenin co-localization. Invasion and migration assays used Matrigel-coated chambers and wound-healing models, respectively. In vitro assays showed a significant decrease in Vimentin protein levels in all TTK-, NEK2-, and double-knockdown treatment groups of the MDA-MB-231 cell line. TTK/NEK2 double knockdown, specifically, reduced N-cadherin, β-Catenin, and SNAIL transcription factor. In contrast, results from MDA-MB-157 cell lines showed a significant reduction in β-catenin protein levels upon NEK2 knockdown. Immunocytochemistry results also showed a decrease in cytoplasmic, nuclear, and membrane levels of β-catenin in the MDA-MB-157 cell line. Furthermore, downregulation of TTK, NEK2, and β-catenin reduces the invasive capacity and motility of both TNBC cell lines.These findings support a pivotal role for TTK and NEK2 in β-Catenin regulation, EMT, and the invasive behavior of TNBC cells. Dual targeting of these mitotic kinases may be a promising strategy to reduce the expression of key proteins involved in TNBC progression and metastasis.

#0321 PTPN1 activates neuroendocrine of treatment emergent prostate cancer by targeting the AR and REST complex.

Yu-An Chen, Mickey Glover, Rey-Chen Pong, Payal Kapur, Jer-Tsong Hsieh

UTSW, Dallas, TX

Treatment emergent neuroendocrine prostate cancer (t-NEPC) is a highly aggressive subtype of castration resistant prostate cancer (CRPC) with rapid progression and a very limited therapeutic arsenal. Clinical outcomes remain poor, and new treatment strategies with clear translational potential are urgently needed. Analyses of publicly available prostate cancer datasets showed that high PTPN1 expression is strongly associated with poor recurrence free survival in metastatic disease, suggesting that PTPN1 may serve as a clinically relevant molecular determinant of aggressive prostate cancer. We found that PTPN1 promotes t-NEPC progression and discovered a reciprocal interaction between PTPN1 and the androgen receptor and the RE1 silencing transcription factor (REST) repressor complex. This interaction represents a key regulatory mechanism driving the trans differentiation of androgen receptor positive CRPC into t-NEPC. Through CRISPR mediated PTPN1 knockout, PTPN1 cDNA overexpression, and pharmacologic inhibition in prostate cancer cells, we demonstrated that PTPN1 modulates neuroendocrine lineage plasticity. PTPN1 inhibition reduced neuroendocrine features and restored responses to anti androgen therapy in both in vitro and in vivo models. The therapeutic efficacy observed with PTPN1 inhibition highlights its translational potential as a druggable target for patients with t-NEPC, a population with urgent unmet clinical needs. These findings support further development of PTPN1 directed therapies and provide a strong rationale for future clinical investigation.

#0322 Differential effects of SRPK1 inhibition on HPV$^+$ and HPV$^-$ in cervical cancer: Transcriptome and splicing rewiring.

Afra Tsitsi Basera[1], Mohammed Alaouna[2], Janie Duvanhage[3], David Bates[4], **Zodwa Dlamini**[5], Rahaba Marima[5]

[1]Medical Oncology, University of Pretoria, Pretoria, South Africa,[2]SAMRC Precision Oncology Research Unit (PORU), DSI/NRF SARChI Chair in Precision Oncology and Cancer Prevention, Pan African Cancer Research Institute (PACRI), University of Pretoria, Pretoria, South Africa,[3]Nuclear Medicine Research Infrastructure NPC, Pretoria, South Africa,[4]Center for Cancer Sciences, BioDiscovery Institute, University Park, Nottingham, United Kingdom,[5]SAMRC Precision Oncology Research Unit (PORU), DSI/NRF SARChI Chair in Precision Oncology and Cancer Prevention, Pan African Cancer Research Institute (PACRI), University of Pretoria, Hatfield, Pretoria, South Africa

Background: Cervical cancer (CCa) remains a major cause of cancer-related mortality worldwide, largely driven by persistent infection with high-risk human papillomavirus (hrHPV) types such as HPV16 and HPV18. The viral E6 and E7 oncoproteins disrupt the p53 and Rb tumour suppressor pathways and reprogram host RNA processing, resulting in the production of tumour-promoting splice isoforms. Serine/arginine protein kinase 1 (SRPK1), a key regulator of splicing factor phosphorylation, has emerged as a potential therapeutic target. This study aimed to identify and evaluate splicing patterns in cervical cancer in response to SRPK1 inhibition.
Materials and Methods: HeLa (HPV18$^+$), SiHa (HPV16$^+$), and C33A (HPV$^-$) cervical cancer cell lines were treated with the SRPK1 inhibitor SPHINX31 (0.3-10 µM). Cell viability was assessed using the Alamar Blue assay, while cell cycle progression and apoptosis were evaluated by flow cytometry using fluorescence-activated cell sorting (FACS) and Annexin V/propidium iodide staining. Transcriptomic profiling was performed by RNA sequencing to identify differentially expressed genes and alternative splicing (AS) events, followed by pathway enrichment and protein-protein interaction (PPI)/MCODE network analyses. Molecular docking was used to assess the binding of SPHINX31 within the SRPK1 ATP pocket.
Results and Discussion: Treatment of cervical cancer cells with SPHINX31 resulted in a non-significant cellular response, with no effect on cell viability, cell cycle progression, or induction of apoptosis. In HPV-negative C33A cells, SRPK1 inhibition upregulated genes involved in translation, RNA processing, and glycosylation, which revealed ribosomal network hubs suggesting possible translational and metabolic adaptation. C33A also displayed skipped exon (SE) and retained intron (RI) events along with alternative 5' splice site (A5SS) alterations. In contrast, HPV16$^+$ SiHa cells exhibited downregulation of oncogenic signalling pathways, including Hippo, Wnt, PI3K-AKT, and ERK1/2. SiHa exhibited fewer overall AS events but with greater effect sizes. Molecular docking analyses supported a computationally predicted binding.
Conclusion: This study provides insight into the effects of SRPK1 inhibition on cellular response, splicing patterns, and the transcriptomic landscape. Overall, SRPK1 inhibition in CCa may induce changes that differ according to HPV status, with HPV$^+$ cells exhibiting vulnerability, while HPV$^-$ cells may display a possible metabolic adaptation.

#0323 Dual inhibition of SIK2/3 induces ER Stress and ER-phagy, enhancing the cytotoxicity of autophagy blockade in ovarian cancer.

Rumeysa Ozyurt, Gamze Bildik Elcik, Weiqun Mao, Robert C. Bast, Zhen Lu

Department of Experimental Therapeutics, UT MD Anderson Cancer Center, Houston, TX

Cancer cells rely heavily on protein quality control mechanisms to survive intrinsic stress from rapid proliferation and extrinsic stress from the tumor microenvironment. Among these mechanisms, endoplasmic reticulum (ER)-selective autophagy (ER-phagy) has emerged as a critical process that maintains ER homeostasis by removing damaged ER components and misfolded protein aggregates. When the protein-folding capacity of the ER is exceeded, misfolded proteins accumulate and trigger ER stress, activating the unfolded protein response (UPR) through three major branches: PERK-eIF2α-ATF4, IRE1-XBP1s, and ATF6. ER stress, in turn, can induce ER-phagy as an adaptive mechanism to alleviate proteotoxic stress. Salt-inducible kinases SIK2 and SIK3 (SIK2/3) are serine/threonine kinases that regulate cellular metabolism and stress responses. While SIK2 has been implicated in ER-associated degradation (ERAD) and in promoting ovarian cancer progression and survival, the roles of SIK2/3 in regulating ER stress and ER stress-mediated autophagy remain poorly understood in cancer. We hypothesized that inhibition of SIK2/3 induces ER stress, which subsequently activates ER-phagy to maintain proteostasis. Further, combining dual SIK2/3 inhibition with GRN-300 (a selective SIK2/3 inhibitor) and autophagy blockade using chloroquine (CQ, an autophagy inhibitor) should enhance proteotoxic stress and exert potent anti-tumor activity in ovarian cancer. Here we report that inhibition of SIK2/3 triggers ER stress and activates ER-phagy as an adaptive survival mechanism in ovarian cancer cells. Genetic or pharmacological inhibition of SIK2/3 activated all three UPR pathways (PERK-eIF2α-ATF4, IRE1-XBP1s, and ATF6), leading to accumulation of polyubiquitinated proteins and aggregates, as well as the induction of CHOP and apoptotic cell death. SIK2/3 inhibition also upregulated the ER-phagy receptor CCPG1 in an ATF4-dependent manner, enhancing autophagic flux. Notably, combination treatment with GRN-300 and CQ synergistically reduced cell viability (combination index, CI < 0.9), exacerbated proteotoxic stress, and triggered CHOP-dependent apoptosis in multiple ovarian cancer cell lines. In three ovarian cancer xenograft models (OVCAR8, OC316, and SKOv3), GRN-300 plus CQ markedly suppressed tumor growth, increased apoptotic markers, and significantly prolonged survival compared to either monotherapy. These findings reveal a previously unrecognized role of SIK2/3 inhibition in driving ER stress and CCPG1-mediated ER-phagy and provide strong rationale for combining GRN-300 with autophagy inhibition as a promising therapeutic strategy for ovarian cancer.

#0324 ASCL1-mediated transcriptional regulation of RET in neuroendocrine prostate cancer.

Sachi B. Tengse[1], Song Yi Bae[1], Hannah E. Bergom[1], Ella Boytim[1], Halena R. VanDeusen[1], Quynh Chau Dinh[1], Abderrahman Day[1], Rayhan Biswas[1], Farzana Kabir[1], Laura E. Hirsch[1], Yingtian Xie[2], Daniel A. Harki[1], Sylvan C. Baca[2], Henry Long[2], John K. Lee[3], Leigh Ellis[4], Justin Hwang[1], Justin M. Drake[1]

[1]University of Minnesota, Minneapolis, MN,[2]Dana-Farber Cancer Institute, Boston, MA,[3]University of California, Los Angeles, Los Angeles, CA,[4]Center for Prostate Disease Research, Bethesda, MD

Resistance to second-generation anti-androgen therapies can cause neuroendocrine prostate cancer (NEPC), an aggressive disease variant, in castration-resistant prostate cancer (CRPC) patients. With low survival outcomes and limited therapies, it is imperative to study the molecular basis of NEPC. We show that the receptor tyrosine kinase RET has elevated activity in aggressive variant prostate cancer cell lines. We also show that RET kinase is crucial for the growth and survival of NEPC cells. We aim to unravel the mechanism of RET activation in NEPC to develop novel approaches to target RET and identify additional drug targets. NEPC can be categorized into two subtypes based on the expression of ASCL1 or NEUROD1, two pro-neuronal transcription factors. We show that RET gene expression strongly correlates to ASCL1 gene expression, but not NEUROD1 gene expression in NEPC patient samples. This data is corroborated by single cell-RNA-sequencing data in NEPC patient samples. Informatics modeling of whole transcriptome sequencing data from patient samples shows that RET and ASCL1 have substantially similar gene network signatures in NEPC, implying that these genes share a gene ecosystem in NEPC. To investigate the relationship between RET and ASCL1, we analyzed publicly available ChIP-sequencing data from LuCaP NEPC PDX models and small cell lung cancer (SCLC) cell lines. NEPC and SCLC are known to have similarities, including disease aggressiveness, expression of neuroendocrine markers, and the presence of ASCL1-positive and NEUROD1-positive subtypes. Our analysis showed that ASCL1 directly regulates RET by binding to RET promoter regions. Hence, we note a similar relationship between RET and ASCL1 in SCLC where ASCL1 regulates RET expression. Using knockdown models, we show that the RET-ASCL1 axis is unidirectional with RET having no impact on ASCL1 expression. To drug this pathway, we aim to focus on cell surface targets such as RET. RET inhibitors are approved for non-small cell lung cancers or thyroid cancers with RET fusions, however, they may induce resistance via mutations. Additionally, they may be less effective in tumors with wild-type RET expression, which is typically seen in NEPC. PROTACs can bypass these drawbacks by degrading the entire protein instead of enzymatically inhibiting it, thus overcoming drug resistance. Additionally, PROTACs have a catalytic mechanism that can cause degradation of several target molecules with one PROTAC molecule, leading to longer elimination of target protein with lower doses. We are using RD-23, a published RET PROTAC based on the RET inhibitor selpercatinib, to investigate its effects on NEPC and SCLC cells. While further studies are needed to stratify patients and develop novel pharmacological interventions, these results highlight the crucial role of ASCL1 in mediating RET signaling in NEPC and SCLC.

#0325 Development of the pyridopyrimidine derivative KC12 as a selective dual Pim/Mnk inhibitor to inhibit leukemia cell growth.

Linxiang Zhao[1], Kun Xing[1], Jingyi Zhang[1], Shuwei Zuo[1], Fuyao Zhang[1], Samuel Waxman[2], Yongkui Jing[1]

[1]Shenyang Pharmaceutical University, Shenyang, China,[2]Samuel Waxman Institute for Aging and Cancer, New York, NY

Myeloid leukemia is an abnormal proliferative disease relying on fast cap-dependent protein translation. Both provirus integration in Maloney murine leukemia virus (Pim) kinases and mitogen-activated protein kinase-interacting kinases (Mnk) play key roles in activating cap-dependent translation, making them attractive targets for anticancer drug development. Although several selective Pim or Mnk inhibitors entered clinical trials, their efficacy was limited. We propose that concurrent inhibition of both Pim/Mnk kinases is necessary for effective treatment. Previously, we reported the first dual Pim and Mnk inhibitor 21o with a pyrido[3,2-*d*]pyrimidine core (IC_{50} Mnk1: 9 nM, Mnk2: 5 nM, Pim1: 120 nM), but suffered from poor solubility. We optimized 21o based on molecular docking and obtained a compound KC12 with enhanced kinase inhibitory activity (IC_{50} Mnk1:32 nM, Mnk2 3 nM; Pim 1 32 nM) and improved selectivity (only 4 out of 42 tested kinases showed >40% inhibition at 100 nM). KC12 exhibits increased aqueous solubility and superior anti-proliferative activity compared to 21o, as well as to the Pim inhibitor TP-3654 and the Mnk inhibitor eFT508. KC12 induced G0/G1 phase cell cycle arrest in K562 cells and apoptosis in MOLM-13 cells, correlated to the suppression of both eIF4E and 4EBP1 phosphorylation, and the cap-dependent translation products c-Myc and Mcl-1. Moreover, KC12 demonstrated a more favorable pharmacokinetic profile than 21o and exhibited enhanced antitumor efficacy in MOLM-13 xenograft models. These findings suggest that KC12 acts as a novel, potent, and selective dual Pim/Mnk inhibitor and is worthy of further development as a therapeutic agent.

#0326 Association of off targets of ALK inhibitors with their adverse reactions revealed by a novel comprehensive phosphorylation profiling platform.

Katsuhisa Horimoto[1], Satoshi Mikami[2], Lili Feng[3], Yu Zhang[3], Dongyin Chen[3], Feng Han[3], Satoshi Yamasaki[1], Shota Takei[1], Hiroshi Kagamu[1]

[1]Saitama Medical University International Medical Center, Hidaka, Japan,[2]SOCIUM Inc., Fujisawa, Japan,[3]Nanjing Medical University, Nanjing, China

Introduction: Five ALK inhibitors are currently approved for clinical use. Although all target ALK fusion proteins, their side-effect profiles differ markedly. These variations are suspected to result from off-target kinase interactions, but the molecular links remain unclear. We aimed to reveal this connection using a novel phosphorylation-based profiling system that comprehensively maps kinase-substrate relationships and pathway activations.

Materials and Methods: Using a recently developed cell-free phosphorylation array, we measured the overall phosphorylation activity within cells. This system does not focus on specific phosphorylation sites; instead, it identifies substrates that become phosphorylated under each experimental condition from a pool of 1,492 proteins (816 substrates for 190 kinases and 845 proteins constituting 273 pathways).Cell lysates treated with ALK inhibitors were applied to the array, enabling phosphorylation reactions that mimic intracellular kinase activity. Computational analyses extracted three layers of information, condition-specifically phosphorylated substrates, activated pathways and kinases, allowing simultaneous assessment of both on-target and off-target effects.

Results: Phosphorylation profiles induced by five ALK inhibitors were measured in EML4-ALK mutant cell line (NCI-H2228 [H2228]), and analyzed across substrates, kinases, and pathways. Each drug exhibited a distinct inhibition signature, indicating specific kinases and pathways selectively affected beyond ALK. Several off-target kinases and pathways associated with known clinical adverse reactions, providing mechanistic insight into drug-specific toxicities.

Conclusion: This comprehensive phosphorylation profiling platform enabled simultaneous evaluation of on-target and off-target effects of kinase inhibitors. By linking molecular signaling changes to clinical side effects, the system provides a powerful approach for understanding complex kinase networks and guiding the development of safer next-generation inhibitors.

#0327 MARK2/MARK3/MARK4 kinases are therapeutic targets for human head and neck squamous cell carcinoma with co-dependencies of YAP-TEAD pathway.

Se Eung Oh[1], Hwan Jung Lim[2], Seong Jun Park[2], Sang Uk Han[1], Jee Hung Kim[3], Seo Young Lee[3], Hei-Cheul Jeung[3]

[1]Medical Oncology, Yonsei University College of Medicine, Seoul, Korea, Republic of,[2]Drug Discovery, Korea Research Institute of Chemical Technology (KRICT), Daejeon, Korea, Republic of,[3]Medical Oncology, Gangnam Severance Hospital, Yonsei University College of Medicine, Seoul, Korea, Republic of

Background: Head and neck squamous cell carcinoma (HNSCC) requires the identification of new therapeutic targets to improve treatment outcomes. This study investigated the biological significance of Microtubule Affinity-Regulating Kinases (MARKs), a family of serine-threonine kinases that regulate microtubule-associated proteins (MAPs). Because MARK activity influences cell structure, intracellular transport, and proliferation, these kinases may represent promising therapeutic targets.
Materials and Methods: Protein expression levels of MARK family genes were evaluated in 20 human HNSCC cell lines. Cisplatin and docetaxel-resistant models were established by gradually escalating cisplatin and docetaxel concentrations up to 4 μM and 15 nM, respectively in CA9-22 and YD-8 cells. Cell viability was determined using WST assays. CRISPR/Cas9 genome editing was employed to generate MARK2/3/4 knockout cell lines. In addition, the anticancer efficacy of several newly developed MARK2/3/4 hits was assessed.
Results: MARK2/3/4-knock-out cells demonstrated significantly reduced proliferation and impaired matrigel invasion compared with wild-type controls. MARK kinase loss was associated with suppression of the MAPK- and PI3K-AKT signaling pathways. Because MARK proteins are known to interfere with MST/SAV and LATS complex formation through phosphorylation-dependent mechanisms, we further showed that MARK4 depletion reduced nuclear YAP/TAZ localization and decreased expression of YAP/TEAD transcriptional targets. Collaborative screening identified multiple candidate molecules for MARK-specific inhibition at the hit-compound stage; notably, one lead compound exhibited strong antiproliferative activity in HNSCC cells, including cisplatin-resistant models.
Conclusions: MARK proteins function as negative regulators of the HIPPO kinase cascade, thereby enhancing YAP/TAZ oncogenic activity in HNSCC. Loss of MARK function reduces tumorigenic phenotypes, supporting MARKs as promising therapeutic targets for future drug development.

#0328 Establishment of assay systems for drug development against the oncogenic phosphatase WIP1.

Daniel Feger[1], Daniel Muller[1], Lena Pilgermayer[1], Carolin Heidemann-Dinger[1], Sarah Ulrich[1], Michael Kubbutat[1], Holger Weber[1], Joe Lewis[2], Birgit Zech[2], **Jan E. Ehlert**[1]

[1]Reaction Biology Europe GmbH, Freiburg im Breisgau, Germany,[2]Anavo Therapeutics GmbH, Heidelberg, Germany

The serine/threonine phosphatase WIP1 (PPM1D) is a key negative regulator of the DNA damage response (DDR) and a recognized oncogene, frequently amplified or truncated in various cancers including breast, ovarian, neuroblastoma, and glioblastoma. Its inhibition restores DDR signaling, offering a promising therapeutic strategy. Despite initial efforts, including the development of the allosteric inhibitor GSK2830371, clinical translation has been limited. We report the establishment of a comprehensive assay platform to support drug development targeting WIP1. Biochemical assays were optimized using fluorescein diphosphate (FDP), malachite green with phosphopeptides (p53, H2AX, p38 MAPK), and TR-FRET formats, enabling robust activity profiling. Cellular mechanism-of-action assays were developed to monitor phosphorylation changes in WIP1 substrates, with pS15-p53 ELISA in U2OS cells selected for medium-throughput iterative compound profiling. Phenotypic assays demonstrated compound efficacy in 2D and 3D proliferation models, with leukemic cell lines showing pronounced sensitivity. Combination studies revealed strong synergy between WIP1 inhibitors and MDM2 antagonists (e.g., Nutlin3a), supporting a dual-targeting approach for p53 pathway reactivation. In vivo efficacy was confirmed in MV4-11 xenograft models, with dose-dependent tumor growth inhibition and favorable tolerability profiles. Our integrated assay suite enables iterative screening and lead optimization, culminating in the identification of a potent allosteric WIP1 inhibitor with nanomolar activity and promising preclinical efficacy. These findings support WIP1 as a viable target in oncology and provide a foundation for future clinical development.

#0329 PLK1 inhibitor onvansertib potentiates the antitumor efficacy of trastuzumab deruxtecan (T-DXd) and reverses its resistance in therapy-resistant HER2-low breast cancer models.

Sreeja Sreekumar[1], Elodie Montaudon[2], Zeena Eblimit[1], Migdalia Gonzalez[1], Davis Klein[1], Heloise Derrien[2], Ahmed Dahmani[2], Tod Smeal[1], Elisabetta Marangoni[2], Maya Ridinger[1]

[1]Cardiff Oncology, Inc., San Diego, CA,[2]Preclinical Investigation Laboratory, Translational Research Department, Institut Curie, Paris, France

HER2-low tumors represent 55-60% of all breast cancers, of which about 60-70% are hormone receptor-positive (HR+) and the rest triple-negative (TNBC). Most metastatic HER2-low breast cancers become resistant to standard therapies, underscoring the need for improved treatments. Trastuzumab deruxtecan (T-DXd) is a HER2-directed antibody-drug conjugate with a topoisomerase I inhibitor (TOP1i) payload approved for therapy-resistant metastatic HER2-low breast cancer. Combining T-DXd with agents that potentiate TOP1i activity may enhance its efficacy. Onvansertib, a selective polo-like kinase 1 inhibitor, has shown clinical benefit in combination with the TOP1i irinotecan in metastatic colorectal cancer. Here, we investigated the combination of onvansertib and T-DXd in HER2-low breast cancer models resistant to first-line therapies. The combination was evaluated in eight HER2-low breast cancer cell lines and six patient-derived xenograft (PDX) models, including one TNBC and five HR+ breast cancer models. The TNBC model was derived from a patient who had progressed on chemotherapy and immunotherapy. The HR+ PDXs originated from primary or metastatic tumors and were resistant to fulvestrant and/or CDK4/6 inhibitors. Tumor-bearing nude mice were treated with vehicle, onvansertib (45 mg/kg, orally, five times weekly), T-DXd (4 or 10 mg/kg, intravenously, every three weeks), or the combination and monitored for body-weight changes and tumor growth. The effects of the combination on cell viability, DNA damage and apoptosis were examined *in vitro*. The combination of onvansertib and T-DXd synergistically inhibited the viability of HER2-low breast cancer cell lines, including fulvestrant and CDK4/6i-resistant cells. *In vivo*, the combination was well tolerated and showed robust antitumor activity across all PDX models including five models resistant to T-DXd. In the resistant TNBC model and two HR+ models, the combination treatment induced tumor regression in nearly all mice, achieving complete response rates up to 62%. In the one T-DXd-sensitive model, the combination further increased tumor regression and complete responses compared with monotherapies. In the remaining resistant models, the combination enhanced tumor growth inhibition and extended event-free survival relative to single agents. Mechanistically, the combination induced increased and prolonged DNA damage, resulting in higher levels of apoptosis than either single agent alone in HER2-low breast cancer cell lines. Taken together, our data indicate that onvansertib enhances T-DXd's antitumor activity and overcomes resistance through synergistic induction of DNA damage and apoptosis. The findings support the clinical potential of this combination for advanced HER2-low breast cancer resistant to standard-of-care therapies.

#0330 EGFR suppression and drug-induced potentiation are widespread features of oncogenic RTK fusions.

Carol Gao[1], David Gonzalez Martinez[1], Sofia Wissert[1], Hana Bader[1], Nidhi Sahni[2], Anh T. Le[3], Robert C. Doebele[4], Lukasz Bugaj[1]

[1]University of Pennsylvania, Philadelphia, PA,[2]UT MD Anderson Cancer Center, Houston, TX,[3]University of Colorado, Denver, CO,[4]Rain Therapeutics, Aurora, CO

Regulation of cancer cells by their environment contributes to tumorigenesis and drug response, though the extent to which the oncogenic state can alter a cell's perception of its environment is not clear. Prior studies found that EML4-ALK, a receptor tyrosine kinase (RTK) fusion oncoprotein, suppresses transmembrane receptor signaling through EGFR. Moreover, suppression was reversed with targeted ALK inhibition, thereby promoting survival and drug tolerance. Here we tested whether such modulation of EGFR was common among other RTK fusions, which collectively are found in ~5% of all cancers. Using live- and fixed-cell microscopy in isogenic and patient-derived cell lines, we found that a wide variety of RTK fusions suppress transmembrane EGFR and sequester essential adaptor proteins in the cytoplasm, as evidenced by the localization of endogenous Grb2. Targeted therapies rapidly released Grb2 from sequestration and potentiated EGFR. Synthetic optogenetic analogs of RTK fusions confirmed that cytoplasmic sequestration of Grb2 was sufficient to suppress perception of extracellular EGF and could do so without driving signaling from the synthetic fusion itself, demonstrating that fusion signaling and suppression of EGFR could be functionally decoupled. Our study uncovers that a large number of RTK fusions simultaneously act as both activators and suppressors of signaling, the mechanisms of which could be exploited for new biomimetic therapies that enhance cell killing and suppress drug tolerance.

#0332 AKT1 mediated post translational modification of the glucocorticoid receptor drives resistance to prostate cancer therapy.

Surendra Gulla[1], Tej Sharma[1], Ephraim Gardner[1], Abbas Jawadala[1], Sasikumar Ponnusamy[1], Tobi Ogunbowale[1], Maddie Aust[1], Jonathan E. Bard[2], Remi Adelaiye-Ogala[1]

[1]Medicine, University at Buffalo, State University of New York, Buffalo, NY,[2]Genetics, Genomics and Bioinformatics Program, University at Buffalo, State University of New York, Buffalo, NY

Increasing evidence shows that resistance to androgen-deprivation therapy (ADT) and next-generation androgen receptor (AR) antagonists in advanced prostate cancers develops partly through compensatory activation of alternative nuclear hormone receptors. Notably, induction of the glucocorticoid receptor (GR) has been demonstrated in both preclinical and clinical studies to confer resistance to AR-targeted therapies. Although total GR is crucial for tissue homeostasis and normal inflammatory responses, our preliminary GR-phospho proteomics data reveal that, under enzalutamide resistance, GR undergoes increased phosphorylation, especially at serine-134 (p-GR(s134)), suggesting a post-translational mechanism driving a pro-oncogenic GR activation in therapy-resistant tumors. We have previously shown that inhibiting AKT signaling, GR expression, and its pro-oncogenic activity restores sensitivity to AR-directed therapy. Predictions from PhosphoNET.ca and functional studies identify AKT1 as the AKT isoform responsible for phosphorylating GR at S134. Importantly, both functional and pharmacologic inhibition of AKT1 reduced GR phosphorylation at s134 without affecting total GR protein levels. While GR can be activated by ligands such as dexamethasone, our data suggest that, in PCa cells that adopt GR compensatory signaling for survival, GR activation is mediated by AKT1 phosphorylation. Overall, our data show that suppression of pGR-s134 activity renders these cancer cells re-vulnerable to AR-targeted drugs such as enzalutamide and enhances their response to GR modulators.

#0333 Downregulation of AURKA and AURKB promotes a decrease in cell invasion in TNBC by modulating the expression of SNAIL1.

Joel Alexis Orengo Orengo[1], Elliott Rodriguez-Lopez[2], Selimar Alvarez Velazquez[3], William Frank Rodriguez[3], Alexandra N. Aquino-Acevedo[3], Melanie E. Cruz Robles[3], Harold Ivan Saavedra[4]

[1]Basic Sciences, Ponce Health Sciences University, Ponce, PR,[2]Ponce Health Sciences University, Ponce, PR,[3]Ponce Health Sciences University, Ponce, Puerto Rico,[4]Assistant Professor, Dept. of Rad. Oncology, Ponce Health Sciences University, Ponce, PR

Although chemotherapy is still the gold standard treatment in TNBC, patients often experience high levels of recurrence. Additionally, several studies have demonstrated that non-Hispanic Black (NHB) and Hispanic/Latino (H/L) women are more likely to be diagnosed and die from TNBC compared to non-Hispanic White women (NHW), indicating a significant health disparity in TNBC. While different molecular players can drive this aggressiveness and resistance in TNBC, mitotic kinases such as AURKA and AURKB are overexpressed in NHB diagnosed with TNBC. AURKA and AURKB play a pivotal role in regulating the cell cycle by promoting centrosome maturation, mitotic spindle formation, and proper chromosome alignment and segregation. However, when dysregulated, they can contribute to the epithelial-to-mesenchymal transition (EMT) by promoting the expression of EMT drivers. We hypothesize that the combined knockdown of AURKA and AURKB will significantly decrease the expression of EMT drivers and reduce the cells' ability to invade. TCGA data suggests a significant overexpression of AURKA and AURKB in breast cancer. Kaplan-Meier analysis indicates that overexpression of AURKA and AURKB is associated with a worse relapse-free survival rate compared to women who have normal expression. After performing the siRNA-mediated knockdown, MTT assay, immunoblotting, immunofluorescence, and invasion assays were performed. MTT data demonstrate that co-targeting AURKA and AURKB decrease cell viability; but most cells still proliferate. Immunoblotting data suggests that co-targeting AURKA and AURKB significantly decreases SNAIL expression in MDA-MB-157 (NHB), while immunofluorescence data indicate a decrease in Beta-catenin expression in both cell lines. Moreover, co-targeting AURKA and AURKB in both cell lines results in a significant reduction in the cells' ability to invade. Preliminary results in MDA-MB-231 (NHW) also suggest a decrease in the invasion capacity after a single knockdown of SNAIL1. Thus, this indicates that AURKA and AURKB can form a specific axis between beta-catenin and SNAIL1 in TNBC. As a future direction, we will use chemical inhibitors in combination to evaluate the expression of these EMT biomarkers. In addition, we will study tumour growth and metastasis rates in vivo models. In conclusion, since treatment options are limited in TNBC, our results suggest that combined targeting of AURKA and AURKB may be a potential approach to decrease the metastatic phenotype of TNBC while lowering the dose of each drug and thus the toxicity in patients.

#0334 A novel inhibitor of the atypical protein kinase C-ι decreases the proliferation of malignant gastric cancer cells and disrupts the Skp-2 pathway.

Abiral Hasib Shourav, Nuzhat Nowshin Oishee, Abigail Oluwafisayo Olatunji, Mahfuza Marzan, Khandker M. Khalid, Radwan Ebna Noor, Shreejana Rimal, Mildred Acevedo-Duncan

Chemistry, University of South Florida, Tampa, FL

Global data on Gastric Cancer (GC) exhibit that it is the fifth most common type of cancer and as far as mortality is concerned, it is the third most common type. Late-stage diagnosis of GC is an important cause for high mortality. Even though *Helicobacter pylori* are known to be the most common cause of gastric cancer, other notable risk factors also include high salt intake, age and diets lacking in fruits and vegetables. Endoscopic resection is considered as the major treatment procedure for early detected gastric cancer while those diagnosed in later stages are treated with surgeries such as D2 lymphadenectomy. Previously, the Atypical Protein Kinase C Iota (PKC-ι) has been documented to play significant roles in elevated cell proliferation in various cancer types. Here, we employed a novel inhibitor, ICA-1S (5-amino-1-((1R,2S,3S,4R)-2,3-dihydroxy-4-methylcyclopentyl)-1H-imidazole-4-carboxamide that specifically inhibits PKC-ι on a gastric cancer cell line (i.e., AGS) to observe its effects on cell proliferation. In separate trials, AGS cells were treated with ICA-1S for 96 hours (about 4 days). An assortment of drug concentrations for the inhibitor was tried and the analysis of the cell count demonstrated that the cell proliferation decreases were statistically significant. The highest decrease in cell proliferation was observed at 20 μM ($p < 0.0001$). Our previous research have revealed that this PKC inhibitor blocks PKC-ι and interferes with established cancer pathways to cause cell deaths. Based on that and the results from the preliminary data on this project, it can be hypothesized that this PKC inhibitor has the potential to lead to Gastric Cancer cell deaths by inducing apoptosis, which could potentially open a new door for Gastric Cancer therapeutics. Henceforth, the Western Blot analysis of AGS cells treated with ICA-1S has shown enhanced inhibition of PKC-ι, and increased apoptosis by the elevated cleavage of Caspase 3 and poly(ADP-ribose) polymerase (PARP). Moreover, we have seen an increased degradation in the S-phase kinase-associated protein 2 (Skp-2), an oncoprotein, suggesting that ICA-1S has the potential to be a drug candidate for the treatment of GC. Current investigations include examining how ICA-1S affects other proteins in the Skp-2 pathway to support our hypothesis that blocking PKC-ι disrupts the Skp-2 pathway, thereby killing GC cells.

#0335 Inhibition study of protein kinase C-iota mediated signaling pathways in diffuse midline glioma by ICA-1S inhibitor and temozolomide.

Radwan Ebna Noor[1], Nuzhat Nowshin Oishee[1], Abir Hasib Shourav[1], Mahfuza Marzan[1], Javad Nazarian[2], Michelle Monje[3], Mildred Acevedo-Duncan[1]

[1]Chemistry, University of South Florida, Tampa, FL,[2]DMG Research, George Washington University, Washington, DC,[3]Stanford Hospital, Stanford, CA

The Diffuse Midline Glioma (DMG) is a subtype of glial carcinoma that develops in the brain, primarily affecting the pons, midbrain, and thalamus. This malignant and fast-growing cancer affects both children and young adults. At present, pediatric DMG is an incurable childhood brain cancer. Interpreting the regulation of cell signaling pathways in pediatric DMG is crucial for targeting tumor cell migration and metastasis. These pathways must be understood comprehensively for effective treatment of this incurable primary brain tumor. Our goal is to investigate the role of atypical Protein Kinase C-iota (PKC-ι) expression levels in DMG cells, given that the kinase is over-expressed in most cancer cells. We aim to understand the PKC-ι-mediated cellular pathways involved in migration, invasion, and apoptosis in DMG (D1008) cells. Moreover, our study focuses on the inhibition of PKC-ι by the inhibitor ICA-1S (5-Amino-1-[(1R,2S,3R,4R)-2,3-dihydroxy-4[(phosphonooxy)methyl]cyclopentyl]-1H-imidazole-4-carboxamide) in combination with the FDA-approved glioblastoma treatment drug named temozolomide (TMZ) in the DMG D1008 cells. In this study, the effect of in vitro combination treatment with ICA-1S and TMZ on D-1008 cells is being investigated using cell viability assays, western blot analysis, scratch and wound healing assays, immunoprecipitation, flow cytometry, immunofluorescence, and small interfering RNA (siRNA) technology. The dose-response curve suggests that the ICA-1S and TMZ combination treatment is viable, as indicated by the half-maximal inhibitory concentrations (IC50). The Western blot analysis suggests that, in ICA-1S-treated DMG D-1008 cells, the expression of phosphorylated PKC-ι and total PKC-ι is reduced compared to untreated control cells. Moreover, our findings indicate that the inhibition of PKC-ι in D-1008 cells with ICA-1S leads to a significant increase in apoptotic markers, such as cleaved PARP and P53, compared to dual inhibition. The immunoprecipitation experiments in a previous study demonstrated that dual inhibition with ICA-1S and TMZ decreased the invasion of glioma cell lines by lowering the phosphorylation of Focal Adhesion Kinase (FAK) and paxillin in the PKC-ι/FAK/Paxillin pathway. In D-1008 cells, the complex between PKC-ι and FAK was not observed in immunoprecipitation, indicating a distinction in the cellular invasion pathway. The results from scratch & wound healing assays, immunoprecipitation, flow cytometry, immunofluorescence, and siRNA techniques will also be reported in this study. The objective is to establish the correlation between PKC-ι expression levels in D-1008 cells and the effects on PKC-ι-related cell signaling pathways when inhibited by the PKC-ι inhibitor ICA-1S and the drug TMZ as part of a new personalized treatment approach for this pediatric glioma.

#0336 Modular control of Pancreatic ductal adenocarcinoma (PDAC) progression by the substrate interaction domains of ERK2.

Monika Verma[1], Billy Truong[1], Sven Miller[2], Rachael Price[1], Dietmar Kappes[1], Paul Shapiro[3], Igor Astsaturov[2], David L. Wiest[1]

[1]Nuclear Dynamics and Cancer Program, Fox Chase Cancer Center, Philadelphia, PA,[2]Cancer Signaling and Microenvironment Program, Fox Chase Cancer Center, Philadelphia, PA,[3]Department of Pharmaceutical Sciences, University of Maryland School of Pharmacy, Baltimore, MD

Background: PDAC is a lethal disease with 5-year survival rate of just 13%, in desperate need of new therapeutic interventions. The primary driver of PDAC pathogenesis is the KRAS; however, current therapeutics targeting the activities of components of the KRAS/MAPK pathway fail to provide lasting benefit. We hypothesize that this results from active-site directed drugs attenuating the function of both substrate binding domains of ERK, which perform opposing roles in cancer pathogenesis. In myeloproliferative neoplasms, the ERK2-D domain promotes, and the ERK2-DBP domain impedes progression. Consequently, attenuating RAS/MAPK activity is akin to pressing both the gas and brake pedals on an automobile. Here we investigated the possibility that ERK signaling may also have cancer promoting and opposing roles in PDAC.
Methods: Here, we seek to determine which ERK family member (ERK1 or ERK2) is the primary driver of PDAC pathogenesis and if the ERK D and DBP substrate domains play opposing roles. To do so, we utilize the KPC-PDAC mouse model and cross it to mice deficient in ERK1, ERK2, or an ERK2-DBP mutant to assess the impact on PDAC pathogenesis. We also utilized an ERK2 allelic series of isogenic KPC mouse cell lines (FC1245) to study the impact of ERK2-D and DBP mutants on pathogenesis in vitro and upon transplantation into mice.
Results: We found that while ERK1 loss had no impact on PDAC pathogenesis, ablation of ERK2 markedly attenuated PDAC progression in KPC mice, indicating that ERK2 is primarily responsible for progression. Moreover, we found that inactivation of the ERK2-DBP domain was sufficient to delay PDAC progression to the same degree as ablation of ERK2. Attenuation of PDAC progression by ERK2-DBP mutation was associated with reduced expression and nuclear localization of c-Myc, a critical driver of PDAC progression. In addition to the cell autonomous effects of the ERK2-DBP mutation on PDAC, we also found differences in tumor-infiltrating immune cells, including fewer phenotypic myeloid derived suppressor cells and reduced expression of Tim3 on infiltrating T cells. The DBP mutation also attenuated colony formation in vitro, however, this was not observed for the ERK2-D domain, suggesting distinct functions in pathogenesis by the two ERK2 substrate domains. To investigate the therapeutic implications, we tested the efficacy of ERK2-DBP domain inhibitors to attenuate PDAC growth in vitro and in initial studies, determined that PDAC growth was substantially inhibited by DBP domain selective inhibitors.
Conclusion: ERK2 DBP is the domain responsible for PDAC progression and its inactivation delays tumor development. We are now using generative modeling to identify DBP inhibitors that have superior efficacy and ability to co-modulate the cell-autonomous effects on PDAC growth and the cell extrinsic effects on the immune system, alone and in combination with immune interventions.

#0337 Off-target activation of GCN2 by BRAF^{V600}inhibitors attenuates melanoma outgrowth.

C. Ryland III[1], Nasreen C. Marikar[1], Vu T. Nguyen[2], Brianna Fernandez[1], Varuna Nangia[1], Alicia M. Darnell[3], Matthew G. Vander Heiden[4], Philip Reigan[2], Sabrina L. Spencer[1]

[1]Biochemistry, University of Colorado, Boulder, CO,[2]Pharmacology, University of Colorado, Anschutz, CO,[3]Pharmacology & Cancer Biology, Duke University, Durham, NC,[4]Koch Institute for Integrative Cancer Research at MIT, Cambridge, MA

Clinical efficacy of small-molecule inhibitors can sometimes be attributed to multiple drug effects acting in concert. Herein, we define an off-target effect in which several clinical BRAF^{V600} inhibitors, including the widely used dabrafenib and encorafenib, interact directly with GCN2 to activate the Integrated Stress Response and ATF4. Blocking this off-target effect by co-drugging with a GCN2 inhibitor in A375 melanoma cells causes enhancement rather than suppression of cancer cell outgrowth, suggesting that the off-target activation of GCN2 is detrimental to these cells. This result is mirrored in PC9 lung cancer cells treated with erlotinib, an EGFR inhibitor, that shares the same off-target activation of GCN2. Using an *in silico* kinase inhibitor screen, we identified dozens of FDA-approved drugs that appear to share this off-target activation of GCN2 and ATF4. We further describe the activation of GCN2 signaling in melanoma patient-derived xenograft models treated with dabrafenib and trametinib, and observe a significant decrease in disease-free survival in a cohort of human melanoma patients with altered GCN2 pathway components. Finally, we describe the benefits of combining the next-generation “paradox breaker” RAF inhibitor naporafenib with a GCN2 activator, HC-7366, in A375 melanoma cells. Thus, GCN2 is emerging as a promising cotreatment candidate in melanoma and potentially beyond.

#0338 Discovery of novel pan-PI3K and mTOR dual inhibitors as first-in-class antibody-drug conjugate payloads.

Qi Liu[1], Lan Pham[1], Chin Pan[1], Jin Wang[2], Kamaldeep S. Dhami[1], Yingchun Li[2], Jeffrey Serrill[1], Ravi Kasiappan[1], Felix DeAnda[1], Screenivas Punna[1], Karl Haelsig[1], Apeksha Villath[1], Ketaki Gadkari[1], Geunbae Rha[2], Deanna Haasch[2], Albert Lai[1], James W. Purcell[1], Xueqing Wang[1]

[1]AbbVie Bay Area, South San Francisco, CA,[2]AbbVie Inc., North Chicago, IL

Despite the clinical success of microtubule inhibitor- and topoisomerase inhibitor-based ADCs, new classes of payloads with alternative mechanisms of action are needed to address clinical resistance and increase tumor responses. Constructing next-generation ADC payloads that target cancer-dependent pathways with a strong biological rationale for combination with other targeted agents, provides an opportunity to develop better-tolerated and more differentiated ADCs. The PI3K/AKT/mTOR signaling pathway is one of the most dysregulated in human cancers. Numerous small molecule efforts have targeted PI3K and mTOR, but these have achieved limited success. These agents are often associated with frequent dose interruptions and discontinuations due to undesirable on-target toxicities, as well as the emergence of drug resistance resulting from AKT reactivation.

Here, we present novel pan-PI3K and mTOR dual inhibitors developed as first-in-class ADC payloads. We hypothesize that this novel payload strategy will achieve more robust and durable inhibition of the PI3K/AKT/mTOR pathway. Delivery via an ADC approach is expected to provide meaningful improvements in efficacy and tolerability compared to systemic small molecule treatments.

Existing pan-PI3K and mTOR dual inhibitors often lack sufficient potency and present challenges for linker installation to enable an ADC approach. Guided by structure-based design, we have identified novel cores that significantly boost potency against various class I PI3K isoforms and mTOR enzymes, while maintaining excellent selectivity across a broad kinase panel. Additionally, we have explored multiple exit vectors to facilitate ADC linker installation, which is a critical component of ADC development.

The resulting PI3Ki/mTORi ADCs exhibited favorable drug-like properties and picomolar potency in cell-killing assays across a range of *in vitro* tumor models. Importantly, these ADCs also demonstrated a strong bystander effect, attributable to the highly efficient release of the cleavable linker within lysosomes and the permeable nature of the payloads being developed. These ADCs demonstrated significant *in vivo* efficacy by inducing tumor regressions across a variety of hematological and solid tumor models harboring PI3K genetic alterations, following administration of a single dose ranging from 3 to 10 mg/kg. Moreover, owing to their dual inhibitory activity against both PI3K and mTOR, our ADCs exhibited robust antitumor effects even in models with wild-type PI3K backgrounds, highlighting their broad therapeutic potential.

Taken together, the PI3K/mTOR dual-inhibitor modality, combined with an ADC platform, offers an opportunity to target various cancer indications with dependencies on the PI3K/mTOR pathway, and provides opportunities for combination treatment regimens with other anticancer agents.

: Mechanism-Guided Development of Targeted Cancer Therapies
Poster Session

#0342 LYW-105: A novel bispecific antibody-drug conjugate with enhanced antitumor efficacy and broader therapeutic index.

Qianqian Zhao, Zhangsheng Lu, Xun Cao, Xiaobing Tang, Liguo Wang, Peixiang Liu, Lu Wang, Jiajie Feng, Cexiong (Winston) Fu

LyncBio Therapeutics Co., Ltd., Shanghai, China

Introduction: Antibody-drug conjugates (ADCs) have made remarkable progress in cancer therapy; however, the development of ADCs with a wide therapeutic window that can effectively combat drug resistance and tumor recurrence remains a significant challenge. The fourth-generation ADC developed by LyncBio features homogeneous conjugation, a target-fit linker-payload design, and superior drug-like properties, aiming to break through the limitations of existing ADC therapeutic indices. LYW-105 is an innovative bispecific ADC designed to achieve more extensive and profound tumor regression through a dual-target approach. Its bispecific antibody components utilize a 1+1 format, with each arm demonstrating high affinity and efficient internalization, thereby enhancing therapeutic efficacy by addressing tumor heterogeneity and minimizing resistance. The linker design of LYW-105 allows for rapid lysosomal release and excellent buffer stability, resulting in reduced systemic toxicity and favorable pharmacokinetics. The payload is a topoisomerase I inhibitor with optimal potency and membrane permeability, effectively balancing tumor cytotoxicity with bystander effects.
Methods: We assessed the binding affinity of the bispecific antibody to its targets using ELISA, FACS, and BLI techniques. Internalization activity was measured using the pHrodo method, while developability was evaluated through methods such as SEC and HIC. The efficacy of LYW-105 was tested both in vitro and in vivo using established solid tumor models.
Results: In vitro studies showed that LYW-105 exhibited strong binding affinity to its targets and demonstrated approximately 2- to 30-fold greater internalization activity in tumor cell lines compared to reference monoclonal antibodies. Additionally, LYW-105 displayed 2- to 25-fold enhanced inhibition of tumor cell proliferation compared to in-house benchmark ADCs. Biophysical properties and stability assessments at 40°C indicated good developability, comparable to that of monoclonal antibodies. In vivo, LYW-105 demonstrated robust antitumor activity in mouse models, showing superior efficacy and prolonged tumor suppression compared to benchmark ADCs. Body weight changes remained stable across treatment groups, indicating that LYW-105 is well-tolerated.
Conclusions: In summary, LYW-105 has been thoroughly compared to benchmark single-target ADCs in preclinical settings. It demonstrated potent cytotoxicity in vitro and significant antitumor activity in vivo across various tumor cell lines, showcasing a broader therapeutic index than benchmark ADCs.

#0343 Role of BEN domain protein 4 (BEND4) in prostate cancer (PCa) and the effect of silencing BEND4 in PCa cell lines.

Janani Harikrishnan, Gnanasekar Munirathinam

Biomedical Sciences, University of Illinois College of Medicine (Rockford), Rockford, IL

Prostate cancer (PCa) is diagnosed in approximately 13% of men in their lifetime and is the second most diagnosed cancer in men. The existing treatments for PCa cause many severe side effects, including erectile dysfunction, hair loss, and anemia, while their effects may be reduced due to the development of treatment resistance. Due to these drawbacks associated with traditional treatments, research on targeted cancer therapy is conducted in the field of molecular oncology to develop efficient and safer treatment approaches for PCa. Many of the targets explored are involved in DNA Damage Response (DDR). One such potential cancer target is the BEN domain (BEND) protein, which is a chromatin boundary marker that recruits chromatin-modifying factors and regulates transcription. It has many functions in cancer cells related to DDR and cell proliferation. Recent studies have suggested that silencing BEND4 expression in pancreatic ductal adenocarcinoma (PDAC) promotes the accumulation of DNA damage and sensitizes cells to ATM/ATR inhibitors, thereby increasing cancer cell apoptosis. Moreover, it has been shown to be hypermethylation target in diffuse large B-cell carcinoma (DLBCL) and colorectal cancer. Therefore, these results demonstrate the potential of targeting BEND4 in the treatment and diagnosis of PCa. However, limited research has been conducted on BEND4 in PCa. The expression profile of BEND4 in PCa cell lines (androgen-dependent and androgen-independent) suggests, according to online prediction tools such as Betastasis and PCA tools, that androgen receptor-dependent (AR+) PCa cells express high levels of BEND4, indicating AR-dependent regulation of BEND4. They also imply that as the Gleason score increases, BEND4 expression decreases. To validate these findings in vitro, western blot and RT-qPCR were conducted, revealing that BEND4 expression is high in AR+ PCa cells, such as MDA-PCa-2b, LNCaP, and VCaP , and is lower in NCI-H660 and LASCPC (AR-negative and aggressive PCa cell lines). DepMap analysis assigned negative gene effect scores to AR+ cell lines such as VCaP and LNCaP, suggesting that BEND4 silencing has differential effects on PCa cells based on their androgen dependency. Follow-up studies of siRNA silencing of BEND4 reduced proliferation with an increase in siRNA concentration in AR+ cells, such as VCaP and MDA-PCa-2b. Taken together, our results suggest that BEND4 may have a role in promoting AR-driven PCa and may serve as a potential therapeutic target for AR-dependent PCa.

#0344 TIP60 mediates chemoresistance by reducing cisplatin-DNA adduct formation and enhancing their repair.

Madhavi P. Kadakia[1], Akshay Hira[1], Caroline McLaughlin[1], Michael Craig[1], Ramzi Nahhas[2], Jin Zhang[1], Mike Kemp[3]

[1]Biochemistry and Molecular Biology, Wright State University, Dayton, OH,[2]Population and Public Health Sciences, Wright State University, Dayton, OH,[3]Pharmacology and Toxicology, Wright State University, Dayton, OH

Cisplatin is a frontline chemotherapeutic agent for squamous cell carcinoma (SCC), yet resistance remains a major obstacle to effective treatment. Our previous work demonstrated that genetic knockdown or pharmacological inhibition of TIP60 sensitizes cisplatin-resistant SCC cells, induces cell cycle arrest and promotes cell death, suggesting a central role for TIP60 in mediating platinum resistance. Here, we demonstrate that TIP60 promotes cisplatin resistance by upregulating drug efflux transporter, suppressing intracellular drug accumulation, and enhancing DNA damage repair. Using both intrinsic and acquired cisplatin-resistant SCC cell line models, we show that elevated TIP60 levels correlate with reduced cisplatin-DNA adduct formation, accelerated repair kinetics, and increased cell survival. Mechanistically, we demonstrate that TIP60 plays a significant role in facilitating resistance to cisplatin through two key pathways. First, it increases the expression of ABCC1, which enhances the efflux of cisplatin and decreases its intracellular accumulation. Second, TIP60 promotes the expression of XPC, an essential element of the nucleotide excision repair (NER) pathway, facilitating the repair of DNA adducts. We show that TIP60 depletion decreases ABCC1 expression and increases cisplatin-DNA adduct accumulation, an effect also observed with the ABCC1 inhibitor, MK-571. Similarly, TIP60 knockdown impairs DNA repair and downregulates DNA damage response (DDR) genes, including XPC. Combining TIP60 inhibition with either ABCC1 inhibitor, MK-571 or spironolactone, which blocks NER further decreases cell survival and increases cell death. Together, these findings reveal a dual role for TIP60 in promoting cisplatin resistance through the coordinated regulation of drug efflux and DNA repair highlighting its potential as a therapeutic target to overcome platinum resistance in SCC.

#0345 Therapeutic restoration of p53 via engineered synthetic mRNA analogs in p53 mutant cancer.

Yong Ho Heo, Seung-Hyun Shin, Youngjin Han, Sol-Bi Shin, Innah Kim, Soye Jeon, Aran Park, Jooyun Byun, Daejin Kim, In Young Choi

Hanmi Pharm. Co., Ltd., Seoul, Korea, Republic of

TP53, which encodes the tumor suppressor protein p53, is a critical regulator of the cell cycle and apoptosis. Mutations in TP53 are among the most common oncogenic events across a wide range of cancers, contributing significantly to tumor development and poor clinical outcomes. Numerous therapeutic strategies have been investigated to restore wild-type p53 activity, including small molecules designed to reactivate specific mutant forms of p53, inhibition of p53 negative regulators to prevent its degradation, and gene delivery approaches using adenoviral vectors. However, these methods often face challenges due to the diverse spectrum of p53 mutations and limited therapeutic efficacy. In this study, we present an advanced synthetic mRNA-based therapeutic platform aimed at restoring p53 functionality in cancers characterized by high p53 mutation rates. Rather than relying on the wild-type p53 sequence, we engineered a more potent p53 analog with enhanced transcriptional activity to overcome the limitations posed by diverse mutation profiles. The Hanmi p53 mRNA construct was meticulously optimized—featuring customized 5′ and 3′ untranslated regions (UTRs), a refined open reading frame (ORF), and Hanmi's proprietary 5′ capping technology—to maximize expression and stability. The therapeutic efficacy of this analog mRNA was evaluated in both *in vitro* and *in vivo* models derived from p53 mutant cancers, including lung, ovarian, and other tumor types. Our study demonstrates that Hanmi's synthetic p53 mRNA analog therapy effectively suppresses the proliferation of p53 mutant cancer cells by inducing apoptosis and cell cycle arrest. Notably, the engineered p53 analog exhibited superior tetramerization capacity compared to the wild-type protein, resulting in enhanced transcriptional activity. *In vivo* ovarian xenograft model, p53 mRNA analog showed marked tumor growth inhibition without observable adverse effects on body weight. Moreover, in taxane-resistant cancer cell lines, the p53 mRNA analog demonstrated superior efficacy compared to wild-type p53 mRNA. These results highlight Hanmi's p53 mRNA analog as a promising therapeutic modality for p53 mutant cancers. Importantly, it also demonstrated the potential to overcome taxane resistance, offering a novel avenue for precision oncology.

#0346 TIP60 regulates PTEN expression, acetylation, and localization in cisplatin-resistant SCC.

Caroline McLaughlin, Akshay Hira, Madhavi Kadakia

Biochemistry and Molecular Biology, Wright State University, Dayton, OH

Non-melanoma skin cancers (NMSCs), including squamous cell carcinoma (SCC), remain highly prevalent, with global incidence rising each year. Cisplatin, a platinum-based chemotherapy drug, is commonly used to treat advanced SCC and several other cancers. Although many patients initially respond, intrinsic or acquired resistance frequently emerges, limiting its clinical efficacy. TIP60, a histone acetyltransferase that modifies both histone and non-histone substrates, plays key roles in DNA damage repair, cell-cycle progression, and apoptosis. Our research demonstrates that elevated TIP60 expression correlates with increased resistance to cisplatin in SCC cell lines. In contrast, the tumor-suppressor PTEN is essential for maintaining controlled cell growth and survival. Loss, decreased expression, or mislocalization of PTEN promotes drug resistance, proliferation, and enhanced cell survival across various cancer types. PTEN activity is regulated in part by acetylation and our lab has previously shown that ΔNp63α negatively regulates PTEN expression and activity. We hypothesize that TIP60 promotes resistance to cisplatin by suppressing PTEN expression, or modifying PTEN through acetylation, and altering its subcellular distribution. Consistent with this model, we found that PTEN levels were significantly reduced in cisplatin-resistant SCC cell lines compared with their cisplatin-sensitive counterparts. TIP60 knockdown in resistant cells increased PTEN transcript and protein levels, and enhanced PTEN promoter activity, supporting a transcriptional mechanism. TIP60 knockdown also reduced phosphorylated Akt levels, whereas TIP60 overexpression decreased PTEN and increased phosphorylated Akt. Subcellular fractionation demonstrated that TIP60 knockdown increased cytoplasmic PTEN in cisplatin-resistant cells. In addition, both TIP60 knockdown and pharmacological inhibition reduced PTEN acetylation, suggesting a post-translational mode of regulation. Together, these findings support a model in which TIP60 acetylates PTEN and negatively regulates its overall and cytoplasmic abundance, thereby enhancing pro-survival PI3K/Akt signaling and promoting cisplatin resistance. Defining the mechanisms underlying the TIP60-PTEN axis may uncover a novel therapeutic vulnerability to improve cisplatin effectiveness and support its continued use in SCC patients.

#0347 Dual dependency of large cell neuroendocrine carcinoma on Ras and ASCL1 oncogenic pathways.

Alyssa Cordes, Michael J. Peyton, Urooba Nadeem, Shreoshi Pal Choudhuri, Seth Hamilton, Shruti Raghavan, Kimberley Avila, Luc Girard, John D. Minna, Benjamin J. Drapkin

UT Southwestern Medical Center, Dallas, TX

Background: Large cell neuroendocrine carcinomas (LCNECs) harbor frequent activating alterations in Ras and Raf family members, which represent targetable oncogenes in non-small cell lung cancers (NSCLCs) lacking neuroendocrine (NE) gene expression. LCNECs also overexpress neurodevelopmental transcription factors such as Achaete-scute homolog 1 (ASCL1), which act as oncogenes in small cell lung cancers (SCLCs) and drive NE gene expression. We investigate whether these pathways represent dependencies in LCNEC that could be therapeutically targeted.
Methods: Most well-characterized lung cancer cell lines predate the introduction of LCNEC into the World Health Organization (WHO) Classification of Tumors in 2015. To address the scarcity of bona fide LCNEC models, candidate lung cancer cell lines were identified by genomic and transcriptomic features and credentialed rigorously through blinded review of cell line-derived xenografts by a multi-institutional panel of thoracic pathologists. In validated LCNEC lines, Ras pathway dependence was tested by comparing sensitivity to pharmacologic inhibitors with non-NE NSCLC lines harboring the same mutations, using rescue alleles to rule out off-target cytotoxicity. In parallel, ASCL1 dependence was assessed by survival after CRISPR-Cas9 gene deletion, and the therapeutic potential of targeting ASCL1-driven NE gene expression was explored with agents against Delta-like Ligand 3 (DLL3), a transcriptional target of ASCL1.
Results: LCNEC cell lines with Ras or Raf activation were sensitive to oncogene-targeted inhibitors. Among 20 lung cancer lines with oncogenic Ras alterations, efficacy of the pan-Ras inhibitor RMC-6236 did not differ between LCNEC (8) and non-NE NSCLC (12) models. In contrast, lines with alterations that bypass Ras, such as activating BRAF mutations, were comparably resistant to RMC-6236 regardless of NE expression. The first LCNEC lines to be re-credentialed (HCC1833, NCI-H1755, and NCI-H1385) expressed high ASCL1 and harbored activating Ras or Raf alterations. Each showed sensitivity to oncogene-targeted inhibitors comparable to non-NE models with the same alterations, and this sensitivity was rescued by on-target or bypass mutations. Proliferation of HCC1833 was greatly reduced by CRISPR-mediated ASCL1 loss, and its sensitivity to tarlatamab, a bispecific T-cell engager (BiTE) against DLL3, was comparable to the most responsive SCLC models.
Conclusions: Human LCNEC models demonstrate frequent dependence on both the Ras-activated kinase cascade and neurodevelopmental transcription factors such as ASCL1. This is unexpected, as forced Ras expression inhibits SCLC proliferation, and forced ASCL1 expression does the same in lung adenocarcinoma. Dual dependence on the Ras-activated kinase cascade and ASCL1 may be a defining feature of LCNEC, and we are now exploring therapeutic strategies to exploit this vulnerability.

#0348 GFH603: A molecular glue-like allosteric activator of the KEAP1-CUL3 E3 ligase complex for targeting NRF2-activated tumors.

Xiang Yu, Tao Jiang, Tao Liang, Feng Yan, Li Wang, Jingyang Zhang, Siyuan Le, Fusheng Zhou, Jiong Lan, Qiang Lu

GenFleet Therapeutics, Shanghai, China

Background:
Constitutive activation of NRF2, driven by *NFE2L2* gain-of-function or *KEAP1* or *CUL3* loss-of-function mutations, disrupts KEAP1-CUL3-mediated NRF2 degradation and contributes to resistance to chemotherapy, immunotherapy, and targeted therapies, including RAS inhibitors. This oncogenic pathway is frequently altered in squamous cell carcinomas — such as esophageal (ESCC) and lung squamous cell carcinoma (LUSC) — via *NFE2L2* hotspot mutations in the DLG/ETGE motifs. In lung adenocarcinoma (LUAD), *KEAP1* mutations are common and often co-occur with *KRAS* mutations. Although *KEAP1/NFE2L2* mutations are relatively uncommon in pancreatic ductal adenocarcinoma, more than half of tumors exhibit pronounced nuclear NRF2 accumulation, likely driven by activation of the RAS pathway. Despite the clinical relevance of this pathway, no approved therapies directly target *KEAP1/NRF2*-mutant tumors.
Methods:
GFH603 was developed as a molecular glue-like allosteric activator of KEAP1 to restore KEAP1-CUL3 E3 ligase function. Its ability to promote KEAP1-CUL3 complex formation, induce NRF2 degradation, and suppress proliferation of NRF2-driven cancer cells was evaluated *in vitro*. *In vivo* anti-tumor efficacy was assessed using xenograft models. Combination studies with pan-RAS inhibitors were conducted in KRAS/KEAP1 co-mutant cell lines. ADMET profiling was performed to assess drug-like properties.
Results:
GFH603 enhanced KEAP1-CUL3 complex assembly and promoted NRF2 degradation. *In vitro*, it induced NRF2 degradation in *NFE2L2 W24C*-mutant KYSE70 cells (IC_{50} = 1.7 nM) and inhibited proliferation of *NFE2L2*-amplified HCC95 cells (IC_{50} = 3.6 nM). In the HCC95 xenograft model, GFH603 (5 mg/kg once daily) achieved significant tumor growth inhibition (TGI = 114%) and robust NRF2 degradation in tumor tissues. In the LU6407 *NFE2L2*-mutant patient-derived xenograft model, GFH603 (10 mg/kg once daily) demonstrated strong tumor regression as a single agent, indicating its potential as an effective monotherapy. Furthermore, GFH603 demonstrated synergistic anti-proliferative activity when combined with pan-RAS inhibitors in *KRAS/KEAP1* co-mutant cell lines. ADMET profiling revealed favorable characteristics, including high oral bioavailability, low hERG liability, and negative Ames test results.
Conclusions:
GFH603 restores KEAP1-CUL3 E3 ligase activity through a molecular glue mechanism, enabling targeted degradation of NRF2 in *KEAP1/NFE2L2*-mutant tumors. It demonstrates potent efficacy as monotherapy in NRF2-activated squamous cancer models (e.g., ESCC, LUSC) and synergizes with pan-RAS inhibitors in *KRAS/KEAP1* co-mutant cells. These findings support GFH603 as a promising therapeutic candidate for overcoming NRF2-driven resistance and addressing a critical unmet need in oncology. Further preclinical and clinical development are warranted.

#0349 Next-generation sequencing and phospho-kinase analysis expose partner-specific profiles in CD74-ROS1 fusions.

Jasmine Vargas[1], Julia Olivieri[2], Georgios Pantouris[1]

[1]Chemistry, University of the Pacific, Stockton, CA,[2]Computer Science, University of the Pacific, Stockton, CA

The oncogenic fusion CD74-ROS1 is a genetic alteration found in a small subset of patients diagnosed with non-small cell lung cancer (NSCLC). This fusion can promote cancer progression in these individuals at both early and late stages, making it an attractive therapeutic target when the standard treatment plans fail. Currently, CD74-ROS1 is targeted with tyrosine kinase inhibitors (TKIs), which inhibit the activity of ROS1. Nevertheless, drug resistance often occurs leaving patients with no alternative therapeutic options. Because CD74-ROS1 is particularly aggressive, supporting the formation of metastatic lesions, dissecting the roles of each fusion partner is of great importance for understanding the biological mechanisms that drive its cancer-promoting properties. Our work focuses on the establishment and characterization of methodically designed CD74-ROS1 variants expressed in the A549 lung adenocarcinoma cell line. The goal is to advance our understanding of the individual and cooperative functions of CD74 and ROS1 in the context of the CD74-ROS1 fusion. Next-generation sequencing (NGS) analysis revealed distinct gene expression profiles across the different transfectants, while phospho-kinase analysis further supports the idea that each protein partner possesses unique functional features. This study aids the efforts in understanding the functionality of CD74-ROS1 positive NSCLC, providing at the same time new biological targets for future signaling studies and therapeutic targeting.

#0350 VHL loss-driven accumulation of GCN5L1 drives clear cell Renal Cell Carcinoma by regulating acetylation of mitochondrial proteins and metabolic reprogramming.

Bradley R. Webster[1], **Kumarkrishna Raychaudhuri**[2], Christopher Ricketts[1], W. Marston Linehan[1], Ramaprasad Srinivasan[1]

[1]Urologic Oncology Branch, National Cancer Institute, Bethesda, MD,[2]Urologic Oncology Branch, National Cancer Institute, NIH, Bethesda, MD

VHL loss-associated clear cell Renal Cell Carcinoma (ccRCC) is the most common renal malignancy. VHL is a component of an E3 ubiquitin ligase that targets hypoxia inducible factor (HIF) transcription factors to proteasomal degradation under normoxic conditions. VHL loss-driven stabilization of HIF1 and HIF2 results in numerous metabolic changes favoring tumorigenesis and cancer cell survival. Although the VHL-HIF pathway is well characterized, the role of HIF independent VHL targets in ccRCC is less clear and carries immense therapeutic interest. Using patient-derived tumor cell lines, we show that loss of VHL in ccRCC leads to an accumulation of GCN5L1, which mediates lysine hyperacetylation of mitochondrial proteins, thereby attenuating the activity of several enzymes in the β-oxidation pathway. Specifically, we show that HADHA, LCAD, and SCAD enzymes show hypoacetylation and increased activity upon downregulation of GCN5L1 protein. Downregulation of GCN5L1 protein levels results in an increase in lipid metabolism and limits cytoplasmic lipid accumulation. Mechanistically, VHL interacts with and regulates GCN5L1 in a HIF-independent manner and targets GCN5L1 to ubiquitination mediated proteasomal degradation. We also show that GCN5L1 attenuates CPT1A protein levels, a rate limiting enzyme in the β oxidation pathway. In vitro assays show that loss of GCN5L1 expression selectively inhibited cell proliferation, cell invasion and anchorage independent cell growth in ccRCC cell lines but not in RCC subtypes with intact VHL. Interestingly, using etomoxir, an irreversible CPT1a/ β-oxidation inhibitor, we show that the growth repression following GCN5L1 loss is dependent on increased CPT1A expression and activity, directly linking GCN5L1 activity to lipid metabolism and ccRCC growth. Mouse xenograft studies demonstrated diminished tumor-forming ability of ccRCC cells upon loss of GCN5L1 expression compared to wild-type cells. Analysis of TCGA data revealed worse overall survival in ccRCC patients with high GCN5L1 expression, further supporting our observations from in vitro and in vivo studies. The importance of lipid metabolism in ccRCC is only beginning to be appreciated and may offer unique therapeutic targets. Lipid accumulation confers a growth and survival advantage in ccRCC and may help protect tumor cells against oxidative and endoplasmic reticulum stress. Our results identify a novel oncogenic pathway in which unregulated GCN5L1 expression drives mitochondrial lysine hyperacetylation and limits activity of β oxidation pathway enzymes, leading to increased lipid accumulation in ccRCC. Therefore, GCN5L1 could be investigated further as a possible therapeutic target in ccRCC.

#0352 Long non coding RNA plasmacytoma variant translocation 1 alternative splicing in prostate carcinogenesis.

Seidu Adams[1], Dominique Weatherall[2], Rachel E. Bonacci[3], Chinedum Chukwuemeka Udekwu[4], Olorunseun O. Ogunwobi[4]

[1]Biochemistry and Molecular Biology, Michigan State University, East Lansing, MI,[2]Department of Biology,, Northeastern Illinois University, Illinois, IL,[3]Michigan State University, Howell, MI,[4]Michigan State University, East Lansing, MI

Prostate cancer remains a major global health concern and disproportionately affects Black men/men of African ancestry (MoAA). Compared to men of European ancestry (MoEA), MoAA experience both a higher incidence of prostate cancer and significantly elevated mortality rates. According to recent American Cancer Society reports, MoAA have a 67% higher incidence of prostate cancer and are more than twice as likely to die from the disease. While socioeconomic and healthcare access factors contribute to these disparities, growing evidence suggests that underlying molecular mechanisms also play a critical role. One emerging molecular factor is the long non-coding RNA Plasmacytoma Variant Translocation 1 (PVT1), which is consistently overexpressed in prostate tumors from MoAA. Prior studies have implicated PVT1 exon 9 in promoting tumor development and progression. Experimental overexpression of exon 9 in prostate cancer models increases tumor aggressiveness and enhances malignant cellular behavior, supporting a functional role in disease severity. In addition, PVT1 exon 9 induces malignant transformation of prostate epithelial cells. However, recent findings indicate that PVT1 is not expressed as a single transcript, but rather as a diverse set of alternatively spliced isoforms, raising the possibility that specific variants may contribute to the observed racial disparities. We hypothesize that a subset of these alternatively spliced PVT1 transcripts is differentially expressed in MoAA and contributes to the increased prostate cancer incidence and mortality observed in this population. To investigate this, we analyzed PVT1 splicing profiles using prostate cancer datasets from two independent studies, including TCGA. We identified ENST00000666076, an alternatively spliced PVT1 transcript located on Chromosome 8: 27,975,972-27,995,613, as being significantly overexpressed in MoAA compared to MoEA. This transcript includes five exons: ENSE00004271579, ENSE00004271636, ENSE00002081483, ENSE00002020395, and ENSE00004271500. In conclusion, our analysis supports the conclusion that distinct PVT1 splice variants may be involved in prostate carcinogenesis.

#0353 Pancreatic cancer modeling in germline *BRCA2* mutation carriers.

Yi Xu[1], Nur Yucer[2], Alyssa Okimoto[2], Bobbie J. Rimel[3], Kate Lawrenson[4], Pei Wang[1], **Simon A. Gayther**[4]

[1]UT San Antonio, San Antonio, TX,[2]Medicine, Center for Inherited Oncogenesis, San Antonio, TX,[3]UW Medicine, Seattle, WA,[4]Medicine, Center for Inherited Oncogenesis, UTHSA, San Antonio, TX

Background: Germline, pathogenic mutations in *BRCA2* (*BRCA2*^{mut}) are the strongest genetic risk factor for pancreatic cancer in men and women; pathogenic variants in this gene are implicated in about 5% of men and women with heritable risks of this cancer type. Moreover, *BRCA2*^{mut} are associated with increased risk of pancreatic cancer inHispanic/Latino populations specifically. Patient-specific induced pluripotent stem cell (iPSC) methods create opportunities to modelhuman diseases *in vitro*. iPSCs derived from patients with known genetic mutations carry thepatient's unique genetic background, to provide platforms for studying the functional effects ofspecific genes. Several inherited disease models created from iPSCs have successfully replicated high-risk cancers. This study aimed to utilize iPSC-based modeling to investigate thefunctional impact of pathogenic *BRCA2*^{mut} on early-stage pancreatic tissues (PT) and genomicalterations that contribute to pancreatic cancer (PC) progression.

Methods: We generated iPSC from *BRCA2*^{mut} positive and *BRCA widtype (BRCA*^{WT}) women and men. From these *BRCA2*^{mut} and *BRCA*^{WT} iPSCs we generated organoid models of pancreatic ductal and acinar precursors. In addition, we used lentiviral targeting to mimic thefunctional effects of specific genes involved in early stage pancreatic cancer pathogenesis, specifically *TP53* knockdown (using a *TP53* siRNA), and *TP53* and/or *KRAS* overexpression (*TP53* R175H and R273H; *KRAS* G12V) respectively.

Results: Following differentiation into PT organoids heterozygous for *BRCA2*^{mut} pancreatic ductal cells show specific cellular abnormalities - neoplastic transformation, ductal formation, expression of cancer-specific biomarkers - compared to *BRCA*^{WT} controls suggesting that *BRCA2* haploinsufficiency contributes to the observed phenotype. PC models from *BRCA2*^{mut} subjects exhibit abnormalities reminiscent of early-stage neoplastic development. Importantly, PC organoids with combinations of *BRCA2*^{mut}, *TP53* and *KRAS* alterations exhibited a moreaggressive PC phenotypes compared to *BRCA2*^{mut} and *BRCA*^{WT} organoids alone, and sharedgenomic signatures with primary PCs.

Conclusion and Impact: iPSC-derived organoids can accurately replicate *BRCA2*^{mut} and*BRCA*^{WT} pancreatic precursor tissues. This allows cancer to evolve in a dish, making it an ideal model for mechanistic studies and screening approaches to identify novel drug targets.

#0354 Distinct response profiles of TROP2-targeting ADCs Dato-DXd and sac-TMT across a large panel of cancer cell lines.

Janneke J. T. M. Melis, Eef F. P. Smits, Karsten P. F. van Doorn, Tsang W. Lam, Jeroen A. D. M. de Roos, Daphne J. F. Kluitmans, **Jeffrey J. Kooijman**, Guido J. R. Zaman, Jorg C. J. Benningshof

Oncolines B.V., Oss, Netherlands

Antibody-drug conjugates (ADCs) are targeted cancer therapies that deliver cytotoxic drugs directly to tumors by binding to receptors overexpressed on cancer cells. Following receptor binding, the receptor-bound ADC is internalized and the drug is released, triggering cell death.

Trophoblast cell surface antigen 2 (TROP2) is a cell surface receptor highly expressed in epithelial tumors, making it an attractive ADC target. Sacituzumab govitecan gained FDA approval in 2020 for triple-negative breast cancer (TNBC). However, its short plasma half-life motivated the development of more stable alternatives. Two newer ADCs, sacituzumab tirumotecan (sac-TMT) and datopotamab deruxtecan (Dato-DXd), have since been approved for clinical use. Both carry a topoisomerase-1 inhibitor payload but differ in antibody and linker design. Sac-TMT is approved for TNBC in China and has received FDA breakthrough designation for *EGFR*-mutated non-small cell lung cancer (NSCLC). Dato-DXd received FDA approval in 2025 for $HR^+/HER2^-$ breast cancer and *EGFR*-mutated NSCLC. Despite observed correlations between TROP2 expression and drug sensitivity, these ADCs are approved regardless of tumor TROP2 levels. This suggests that TROP2 expression alone may not predict therapeutic benefit, and alternative biomarkers may better explain clinical efficacy.

To explore this further, Dato-DXd and sac-TMT were profiled on a panel of approximately 270 cancer cell lines, representing diverse tumor types, including eight TNBC, three $HR^+/HER2^-$, and six EGFR-mutated NSCLC models. The TROP2 (*TACSTD2*) gene was widely expressed with over 2500-fold difference in basal expression levels across the panel. Surface TROP2 expression levels were quantified by flow cytometry in a subset of cell lines. Cells were exposed to a 9-point dose range of each ADC, and viability was assessed by intracellular ATP measurement. Half-maximum inhibitory concentrations (IC_{50}) were derived and integrated with genomic, transcriptomic and proteomic datasets to identify molecular predictors of drug response.

Dato-DXd exhibited a more selective inhibition profile than sac-TMT. When the IC_{50} “fingerprints” of the two ADCs were compared to a reference dataset of 248 anticancer agents, Dato-DXd clustered with EGFR inhibitors, whereas sac-TMT showed highest similarity to topoisomerase I inhibitors, indicating mechanistically distinct selectivity patterns. Moreover, correlation between drug sensitivity and TROP2 gene expression was stronger for Dato-DXd than for sac-TMT.

This large-scale cell panel profiling study underscores the power of integrative bioinformatic analyses to uncover biomarkers of ADC response, and identifies cell models suitable for investigating mechanisms of action, such as receptor internalization, payload processing, and bystander effects.

#0355 Co-expression of FIH1 and IL-12 in oncolytic HSV-1 blocks Notch signaling and enhances anti-tumor immunity.

Karina Vazquez-Arreguin, Balveen Kaur

Augusta University, Augusta, GA

Glioblastoma (GBM) is the most aggressive brain tumor in adults and remains a lethal disease with limited treatment options despite continuing worldwide efforts to develop new therapies. GBM cells often exhibit increased Notch signaling, whose activity contributes to tumor progression and therapy resistance. Previous clinical trials aimed to target Notch signaling using ɣ-secretase inhibitors (GSIs) but have not been fully successful due off-target effects, dose-limiting toxicity and eventual resistance. Here, we have generated an oncolytic herpes simplex virus (oHSV) that expresses the asparaginyl hydroxylase factor inhibiting HIF (FIH1) which efficiently targets Notch signaling locally and specifically in GBM and other solid tumors. Using this virus, OncoD-F, we have shown successful downregulation of Notch signaling *in vitro* and significant survival improvement in *in vivo* mouse models of GBM. Furthermore, scRNA sequencing analysis of mouse brain tumors treated with OncoD-F have shown a reduction in tumor associated macrophages and an enrichment in the T cell population. Based on these observations, and in order to enhance the cytotoxic activity of the recruited T cells, we combined OncoD-F treatment with intratumoral injections of the immunoregulatory cytokine IL-12 in a subcutaneous tumor model. Mice receiving the combination treatment had a delayed tumor growth and had a longer time to reach endpoint. Given the favorable response of the combination treatment, we have expressed IL-12 in OncoD-F to generate OncoD-F12. The findings from this study suggest the potential of multi-modality therapeutic strategies for GBM and other solid tumors that have oncogenic Notch activation.

#0356 Rezatapopt and KRAS inhibitors for the treatment of TP53 Y220C and *KRAS* mutant cancers.

Argun Akcakanat[1], Ecaterina E. Dumbrava[1], Kurt W. Evans[1], Ran Zhang[1], Ming Zhao[1], Amber Kennon[1], Xiaofeng Zheng[2], Stephen M. Scott[1], Erkan Yuca[1], Gabriela Raso[3], Elisabeth K. Kong[3], Yasmeen Rizvi[1], David Hong[1], Masha V. Poyurovsky[4], Guillermina Lozano[5], Anil Korkut[2], Funda Meric-Bernstam[1]

[1]Investigational Cancer Therapeutics, UT MD Anderson Cancer Center, Houston, TX,[2]Bioinformatics and Comp Biology, UT MD Anderson Cancer Center, Houston, TX,[3]Translational Molecular Pathology, UT MD Anderson Cancer Center, Houston, TX,[4]PMV Pharmaceuticals Inc., Princeton, NJ,[5]Genetics, UT MD Anderson Cancer Center, Houston, TX

Background: *TP53* and *KRAS* are two important genes involved in cancer development. *KRAS* is involved in cell growth and division, and *KRAS* mutant cancers often do not respond to treatments. P53 is a transcription factor that regulates cell cycle and prevents tumor formation. Cancer cells with *TP53* mutations can evade p53-mediated tumor suppression. Combined *TP53*/*KRAS* mutations are associated with drug resistance and worse prognosis. Rezatapopt is a small molecule reactivator of p53 Y220C protein. It binds the mutant protein and stabilizes p53 structure in the wild-type conformation restoring its functions. TP53 Y220C is present in approximately 1% of all solid tumors. We hypothesized that rezatapopt in combination with standard or targeted therapies enhances treatment response in TP53 Y220C/*KRAS* altered tumors.

Methods: We used three TP53 Y220C cell lines that also had KRAS G12D or Q61H mutations to analyze the effects of drug combinations. Following a high-throughput screening with 23 drugs using an ATP quantification-based cell viability assay, we selected 6 agents and confirmed the results using sulforhodamine B (SRB) assay. We used Chou-Talalay and Bliss methods to calculate IC50 and combination index. We analyzed the effect of rezatapopt in combination with pan-RAS inhibitors on long-term viability of treated cells by colony formation assay. *In vivo* antitumor activity was assessed by objective response and event-free survival (as defined by time to tumor doubling) per PDXNET metrics.

Results: Rezatapopt was synergistic with multiple chemotherapeutic and targeted therapy agents. SRB assay showed that both MRTX1133 (KRAS G12D inhibitor) or daraxonrasib (RMC-6236, pan-RAS inhibitor) were synergistic with rezatapopt in two TP53 Y220C and KRAS G12D cell lines. We generated a patient-derived xenograft model from a patient with colorectal cancer bearing TP53 Y220C and KRAS G12A mutations, and treated the model with rezatapopt (100 mg/kg, QD, PO), daraxonrasib (25 mg/kg, QD, PO), or the combination. Four out of 5 rezatapopt + daraxonrasib combination-treated tumors regressed greater than 30% from baseline by day 22 while only 1 out of 5 tumors treated with either single agent regressed by day 22. Event-free survival was significantly longer for combination-treated mice compared to mice treated with daraxonrasib alone ($p=0.013$) or rezatapopt alone ($p=0.016$).

Conclusion: Rezatapopt combined with KRAS inhibition increased antitumor activity. Further studies are needed to understand the mechanism of synergy.

#0357 DIRAS3 mimetic peptide achieves dual MAPK and PI3K pathway suppression across KRAS hotspot mutations.

Gamze Bildik[1], Junchen Liu[2], Weiqun Mao[1], Hailing Yang[1], John F. Hancock[2], Steven W. Millward[1], Robert C. Bast[1], Zhen Lu[1]

[1]The University of Texas MD Anderson Cancer Center, Houston, TX,[2]McGovern Medical School, The University of Texas Health Science Center, Houston, TX

Activating mutations in RAS occur in approximately 30% of human cancers, with hotspot alterations at codons G12, G13, and Q61 driving persistent downstream signaling through the MAPK and PI3K pathways. Although recent tricomplex RAS inhibitors have shown promise, their efficacy varies among different RAS mutants. Accumulating evidence indicates that the biochemical and signaling properties of G12X and Q61X mutants differ substantially, influencing their response to upstream and downstream modulation. G12X mutants depend on receptor tyrosine kinase activity for both MAPK and PI3K pathway activation, whereas Q61X mutants can independently activate MAPK signaling and maintain PI3K output even when RAS is inhibited. Consequently, Q61X tumors display intrinsic resistance to current RAS-targeted therapies, underscoring the need for agents capable of simultaneously suppressing both effector arms. DIRAS3 has emerged as a unique endogenous RAS inhibitor that disrupts RAS nanoclustering and effector engagement, while also modulating the PI3K/AKT axis in ovarian and pancreatic cancers, suggesting broader regulatory potential. To systematically define DIRAS3's inhibitory spectrum, we utilized RASless mouse embryonic fibroblasts (MEFs) reconstituted with individual KRAS hotspot alleles. DIRAS3 expression markedly reduced RAS-dependent clonogenic growth, inhibited MAPK and PI3K/AKT signaling in cells expressing oncogenic KRAS variants, with minimal effect on wild-type KRAS unless stimulated with EGF. Functional analysis demonstrated that both N- and C-terminal domains of DIRAS3 are essential for membrane localization and full inhibitory activity. Importantly, DIRAS3 disrupted KRAS nanoclustering in both G12X and Q61X mutant backgrounds, supporting its capacity to interfere directly with the KRAS-KRAS interface. To recapitulate DIRAS3's inhibitory effects, we designed a conformationally constrained cyclic DIRAS3 mimetic peptide based on the sequence spanning parts of α5 and the hypervariable regions critical for DIRAS3-KRAS binding. For translational comparison, we evaluated the tricomplex RAS inhibitor RMC-7977 alongside this DIRAS3-derived peptide. In G12X cells, both agents suppressed MAPK and PI3K outputs. However, in Q61X cells, RMC-7977 inhibited MAPK signaling but failed to suppress PI3K/AKT activity, whereas the DIRAS3 peptide effectively suppressed both pathways. Reduced PI3K activity correlated with enhanced sensitivity to the DIRAS3 peptide, and cells harboring Q61X mutations, which are less responsive to RMC-7977, remained equally responsive to the DIRAS3 peptide. Collectively, these results indicate that DIRAS3 provides a dual-pathway blockade of MAPK and PI3K signaling across diverse KRAS mutations, including Q61X variants that are refractory to existing agents, supporting its development as a broad-spectrum therapeutic for RAS-driven cancers.

#0358 EV-based delivery of chemically modified siRNA achieves MRTX1133-comparable efficacy in KRAS G12D-mutant pancreatic cancer.

Hyo Kyeong kim[1], Yujeong Choi[1], Kyoung Hwa Kim[1], Jae Hwan Kim[1], Shung Hyun An[1], Dae Ho Bae[1], Minyoung Lee[1], Jihwa Chung[1], Seok-Hyun Kim[1], **Kihwan Kwon**[2]

[1]Exollence Biotechnology Co. Ltd., Seoul, Korea, Republic of,[2]Ewha Womans University College of Medicine, Seoul, Korea, Republic of

Background: KRAS G12D-mutant pancreatic ductal adenocarcinoma (PDAC) remains largely incurable, with no clinically validated targeted therapies. RNA interference can selectively suppress mutant KRAS, yet current delivery technologies fail to achieve sustained, safe in vivo activity. We developed a shock wave-engineered extracellular vesicle (EV) platform (SWEET™) that enables efficient, stable encapsulation of KRAS G12D-targeting siRNA and overcomes key limitations of lipid nanoparticles (LNPs) and small-molecule inhibitors.

Methods: We designed and screened a 105-member panel of chemically modified siRNAs engineered for high stability and reduced innate immune activation to identify potent and allele-specific KRAS G12D silencers. Optimized shock-wave engineering achieved >90% encapsulation and >85% nuclease resistance. Lead candidates were evaluated across PDAC cell lines, patient-derived organoids (PDOs), xenografts, biodistribution studies, toxicity models, and GMP-aligned scale-up workflows.

Results: Five siRNAs exhibited single-digit nanomolar potency (IC50 < 10 nM). The lead, EV-siRNA #41, produced robust KRAS G12D knockdown and suppression of ERK/AKT signaling. In vivo, EV-siRNA #41 achieved markedly superior tumor accumulation relative to LNPs and induced significant tumor regression. Notably, a microdose of 25 μg EV-siRNA #41 produced antitumor efficacy comparable to or exceeding MRTX1133 at 30-60 mg/kg. PDO assays confirmed selective killing of KRAS G12D-mutant tumors with no effect on wild-type controls. Repeated-dose GLP toxicity studies established a high NOAEL without liver enzyme elevation or weight loss. GMP-aligned optimization increased EV yield from 1% to 7.5% with >80% loading efficiency.

Conclusions: Shock wave-engineered EV delivery overcomes the major barriers of RNA therapeutics in PDAC. EV-siRNA #41 demonstrates potent, selective, and durable antitumor activity at microdose levels and outperforms both LNPs and a leading KRAS G12D inhibitor. These data position EV-siRNA #41 as a first-in-class, mutation-specific RNA therapeutic ready for IND-enabling development.

Acknowledgments: This work was supported by the Korea Drug Development Fund (KDDF, Grant No. RS-2023-00282594), the Technology Development Program of the Ministry of Science and ICT (MSS, Grant No. RS-2023-00280797), and the Ultra-Gap Startup 1000+ Project for the promotion of ultra-gap startups, funded by the Ministry of SMEs and Startups of Korea in 2025 (Grant No. 20266766).

#0359 Development of a collection of cell lines from a genetically engineered mouse model of DICER1 syndrome-associated sarcoma for therapeutic assessment.

Lanlan Fang, Joyce Yu-Han Zhang, Shary Chen, Yannes Wai Yan Choi, Yemin Wang, David Huntsman

Department of Pathology and Laboratory Medicine, University of British Columbia, Vancouver, BC, Canada

Background: DICER1 syndrome, driven by loss-of-function germline variants in the *DICER1* gene, predisposes children and young adults to rare cancers in multiple organs such as the brain, thyroid, lung, kidney, and gynecologic tract. Most of these tumors are sarcomas, which share common histologic and molecular features regardless of their anatomic origins. A second hit impairing DICER1 RNase IIIb occurs in nearly all these cancers. We have recently developed two genetically engineered mouse models (GEMMs) of DICER1 syndrome-associated sarcomas, which fully recapitulates the human counterpart genetically and histologically. Here, we aim to develop a panel of cell lines from the GEMMs of DICER1 syndrome-associated sarcomas and utilize them for developing novel therapeutic strategies.

Methods: Mouse DICER1 syndrome-associated sarcoma cell lines are derived from tumors growing in $Hic1^{CreERT2};Dicer1^{fl/fl\text{-}D1693N};(Rosa26)^{LSL\text{-}tdTomato}$ (HDT) mice. Whole-exome sequencing was performed on HDT cell lines. IVADo regimen (ifosfamide/cyclophosphamide, vincristine, actinomycin-D, doxorubicin) and CDK4/6 inhibitor were selected to treat the cells. MTT assays were performed to assess cell viability. Metaphase chromosome analysis was used to detect chromosomal abnormalities.

Results: We validated that HDT tumors predominantly express the $Dicer1^{IIIb}$-mutant transcript and most tumors were quadriphasic (epithelial, undifferentiated blastema, stromal cells, and rhabdomyoblastic cells) with no to variable amounts of anaplastic sarcoma components. From these murine HDT tumors, we have successfully derived five HDT cell lines (HDT298, HDT340, HDT366, HDT546, and HDT1003 cell lines). Some of these cell lines have aberrant p53 expression (or p53 mutation) and *Kras* mutation, confirming their resemblance to human DICER1-sarcoma. Furthermore, we tested the response of HDT cell lines to the chemotherapeutic agents of the IVADo regimen and found that they are sensitive to vincristine, actinomycin-D, and doxorubicin. Next, we test potential therapeutic agents on these cell lines. Considering that the KRAS-mutant lung cancer cells have been reported to be hypersensitive to CDK4/6 inhibitor, we tested palbociclib sensitivity and found that only one out of two Kras-mutant cell lines was sensitive to palbociclib. Additionally, we identified that these HDT cell lines have an average chromosome number of 73, indicating the presence of chromosomal instability (CIN). Supporting this, our GEMM DICER1 sarcoma cohort has nearly ubiquitous CIN. We are currently investigating the underlying mechanism and testing whether it can be exploited for therapeutic targeting.

Relevance: Our DICER1-sarcoma GEMM and the derived tumor cell lines empower us to study the biology of DICER1 syndrome-associated sarcoma and inform future development of therapeutic strategies.

#0360 TM4SF1 as a promising ADC target for KRAS-mutated cancers.

Sewon Park[1], Youwon Lee[1], Jae-Sang Hwang[2], Ju-hyeon Lee[2], Mi Ran Yun[1], Byoung Chul Cho[3]

[1]Yonsei New Il Han Institute for Integrative Cancer Research, Seoul, Korea, Republic of,[2]Yonsei University College of Medicine SBSI, Seoul, Korea, Republic of,[3]Yonsei University College of Medicine, Seoul, Korea, Republic of

Transmembrane 4 L six family 1 (TM4SF1) is a protein with four transmembrane domains belonging to the transmembrane 4 L six family members. TM4SF1 interacts with tetraspanins, integrins, and various receptor tyrosine kinases. TM4SF1 promotes cancer cell migration and invasion and is overexpressed in many epithelial-derived malignancies, including prostate, breast, pancreatic, lung, colon, and gastric cancers, while found at low concentrations in normal human tissues like endothelium, skin, lung, and germ cells. In this study, we evaluated TM4SF1 as an ADC (antibody-drug conjugate) target and investigated its connection with KRAS-mutated cancer.To evaluate the potential of TM4SF1 as an ADC target, we employed both in silico analysis and in vitro assays. In silico analysis included data from TCGA/GTEx, single-cell RNA sequencing, and DEPMAP. In vitro assays comprised flow cytometry, internalization assays using IncuCyte, colony formation assays after gene knockdown, and cell viability assays using an ADC which was conjugated by ADC kit (CellMosaic, Inc., MA, USA).The key findings suggest that TM4SF1 is highly expressed in various solid tumors, particularly in KRAS-mutated tumors, indicating it is a promising ADC target. In silico analysis results revealed that TM4SF1 expression was significantly higher in lung cancer, pancreatic cancer, colorectal cancer, and bile duct cancer tumors compared to normal tissues; specifically, following our in-house scRNA sequencing data, expression was increased in EGFR wild-type and post-TKI treated lung tumors, and viability decreased upon gene knockout in many types of solid tumor. In vitro analysis confirmed TM4SF1 expression levels suitable for ADC targeting in 86% to 100% of various cancer cell lines (lung, pancreatic, colorectal, liver, gastric, etc.). Functional analysis demonstrated that TM4SF1 was internalized efficiently (comparable to or greater than the positive control CD71), and lung cancer cell line with high expression and KRAS mutation responded more sensitively to TM4SF1-targeting ADCs compare to low expression and without KRAS mutation or normal cell line. Our findings demonstrate that TM4SF1 is highly expressed in various solid tumors, particularly in specific genetic subsets such as those with KRAS mutated tumors. The observed high expression levels, efficient internalization kinetics (comparable to the positive control CD71), and robust in vitro efficacy of TM4SF1-targeting ADCs strongly suggest that TM4SF1 is a promising therapeutic target. These results provide a strong rationale for the clinical development of TM4SF1-targeting ADCs as a novel precision oncology treatment strategy across multiple cancer types.

#0362 Targeting RUNX transcriptional activity reduces tumor heterogeneity and aggressiveness in triple-negative breast cancer.

Natalia Brenda Fernandez[1], Facundo Luis Couto[2], Maria Sofia Sosa[1], Natalia Rubinstein[2]

[1]Instituto de Biociencias, Biotecnologia y Biologia traslacional (iB3); Facultad de Ciencias Exactas y Naturales (FCEN); Universidad de Buenos Aires (UBA), Buenos Aires, Argentina,[2]Instituto de Biociencias, Biotecnologia y Biologia traslacional (iB3); Facultad de Ciencias Exactas y Naturales (FCEN); Universidad de Buenos Aires (UBA). Consejo Nacional de Investigaciones Cientificas y Tecnicas (CONICET), Buenos Aires, Argentina

Triple-negative breast cancer (TNBC) is a highly aggressive disease, characterized by early relapse and enriched with cancer stem cells (CSCs), contributing to chemoresistance and metastasis. Our research focuses on RUNXs role in TNBC aggressiveness, cell migration promotion and regulation of gene expression. We reported that RUNX1 influences chemoresistance in androgen-responsive TNBC cell lines and Ferrari (2016) showed its correlation with poor prognosis in TNBC patients. Lv (2024) showed that RUNX2 is also implicated in chemoresistance, and Halperin (2022) established that RUNX1 is upregulated in cancer-associated fibroblasts of breast cancer patients and predicts poor disease outcomes. Our study explores how inhibiting RUNX transcriptional activity impacts TNBC cell lines aggressiveness and drug response. Using RUNX-CBFβ commercial inhibitors (AI-10-104 and AI-10-49) we observed significant reduction in viability and migration, and increased apoptosis in MDA-MB-231 and -468 cell lines. In a forced-suspended cell model, inhibiting RUNX transcriptional activity decreased mRNA levels of crucial genes for CSC maintenance. In MDA-MB-231 cells, RUNX inhibition completely hindered mammosphere formation. RUNX1 mRNA and protein expression increased in doxorubicin (Doxo) and paclitaxel (Px) treated cells. RUNX inhibition enhances drug toxicity, reducing viability and boosting apoptosis. Combined AI-10-104 and Doxo significantly reduced the number of mammospheres even more than Doxo alone, while AI-10-104 restored Px sensitivity in Px-resistant cells. By flow cytometry we observed that RUNX inhibition significantly downregulates PD-L1 expression, suggesting an important role in tumor immune escape. Furthermore, RUNX1 inhibition alters mitophagy-related gene expression and induces mitochondrial fragmentation in SUM-159PT cells. Finally, by transcriptomic analysis (cDNA-seq) using long-read oxford nanopore technology, we compare the expression profiles of adherent with forced-suspension growing MDA-MB-468 cells, treated with AI-10-104, and gain insights into the underlying mechanisms. Analyses have identified 10 genes including metabolic, stress, drug resistance' genes, among others, whose expression is differentially affected by RUNX transcriptional inhibition depending on the culture model. These findings point to potentially distinct RUNX-dependent regulatory mechanisms across tumor subpopulations, which are currently under our investigation. In summary, our results suggest that RUNXs play a critical role in generating chemoresistant TNBC cells by influencing intracellular heterogeneity and immune surveillance cancer hallmarks.

#0363 Targeting scaffold/matrix associated regions in pancreatic ductal adenocarcinoma: A novel carbazole-derived therapeutic.

Jack Prochnau[1], Daisy Medina[1], Jian Huang[2], Phat Do[1], Deepika Singh[3], Panneerdoss Subbarayallu[4], Stanton McHardy[5], Manjeet K. Rao[6]

[1]Cancer Biology, University of Texas San Antonio, San Antonio, TX,[2]University of Texas San Antonio, San Antonio, TX,[3]UT Health San Antonio Greehey Children's Cancer Res. Inst., San Antonio, TX,[4]UT Health San Antonio, San Antonio, TX,[5]UT San Antonio, San Antonio, TX,[6]Assistant Professor, Greehey Children's Cancer Research Institute, San Antonio, TX

Pancreatic cancer is the tenth most common cancer in the United States and is projected to become the second leading cause of cancer-related death by 2030. Most cases arise in exocrine cells and are driven by genetic mutations, such as *KRAS* and *CDKN2A*, as well as modifiable risk factors, including alcohol use, chronic pancreatitis, and obesity. The aggressive nature of pancreatic ductal adenocarcinoma (PDAC), coupled with its complex tumor microenvironment, leads to late-stage diagnoses and a five-year survival rate of 13%. Despite advances in treatment, which include surgical resection, radiotherapy, and chemotherapeutic regimens like gemcitabine and FOLFIRINOX, therapy-related toxicity and chemotherapy resistance remain significant barriers to improved outcomes. One promising therapeutic approach involves exploiting vulnerabilities in the DNA damage response (DDR) pathways unique to cancer cells. While cancer cells rely on an aberrant DDR to sustain unchecked replication, their increased mutational burden renders them particularly susceptible to DNA-targeting therapies. However, existing DNA-targeting treatments are limited by off-target effects, resulting in toxicity and the emergence of resistance. This underscores the need for novel, selective drugs capable of targeting DNA processes specific to cancer cells. We report on a novel carbazole-derived compound that represents a significant advancement in PDAC therapy. Carbazole, a nitrogen-containing heterocyclic molecule, serves as a pharmacophore in therapeutics with diverse applications, including antitumor, antiviral, and anti-inflammatory agents. Our compound demonstrates potent inhibition of PDAC growth and metastasis in both *in vitro* and *in vivo* models while sparing normal cells. Its mechanism of action involves selective targeting of Scaffold/Matrix Associated Regions (S/MARs), which play critical roles in chromatin organization and gene expression regulation. By disrupting S/MARs and their associated binding proteins, our compound downregulates essential genes involved in replication and DNA repair, including *CDK4*, *MCMs*, *GINS*, and *CDC6*. These findings suggest that our compound offers a unique therapeutic mechanism with high specificity and minimal toxicity. Furthermore, its potential to complement existing treatments and advance toward Investigational New Drug (IND) approval positions it as a promising candidate for PDAC therapy.

#0364 EMT-driven alterations promote dependency on nuclear kinase VRK1 activity to synergize with immune therapy in triple negative breast cancer.

Priyanka Sahu[1], Raymond Liu[1], Sergey Shmelkov[1], Uger Ozerdem[1], William C. Hahn[2], Jonathan So[1]

[1]NYU Langone Health Perlmutter Cancer Ctr., New York, NY,[2]Dana-Farber Cancer Institute, Boston, MA

Introduction: Triple-negative breast cancer (TNBC) is aggressive and often immune-cold, with ~12% 5-year survival and few targeted options. Cancer Dependency Map analyses identify the nuclear serine/threonine kinase VRK1 as broadly essential, with strongest dependency in EMT-high states. We propose that EMT-driven remodeling of the nuclear envelope (NE) creates a liability that heightens reliance on VRK1 to preserve NE integrity and genome stability. Pharmacologic or genetic VRK1 inhibition destabilizes the NE, generates micronuclei, and activates cGAS-STING/type I interferon signaling, offering a strategy to inflame refractory tumors and improve responses to immune checkpoint blockade.

Methods: Patient-derived TNBC lines (HCC1937, HCC1806, HCC1143) were treated with TGF-β for 72 h to induce EMT. EMT markers (E-cadherin, N-cadherin, Vimentin, SNAIL), NE proteins (LAMIN-B1, BANF1), and DNA damage (γH2AX) were quantified by immunoblotting and immunofluorescence. Functional dependency was assessed by CRISPR/Cas9 knockout of VRK1 or VRK2 with analyses of growth, cytoskeletal organization, and EMT dynamics. For in vivo studies, E0771 murine TNBC cells engineered to express a dTAG-degradable VRK1 were implanted into immunocompetent C57BL/6 mice and treated with the dTAG-V1 degrader, anti-PD-1, or both; tumor growth and immune modulation were evaluated.

Results: TGF-β induced EMT across TNBC lines, increasing Vimentin and N-cadherin and decreasing E-cadherin. EMT coincided with cytoskeletal remodeling, NE disruption, and elevated γH2AX. VRK1 and VRK2 expression increased during EMT. VRK1 knockout in epithelial-like TNBC cells heightened EMT marker expression and restricted growth under TGF-β, indicating a requirement for VRK1 to preserve NE integrity under EMT stress. In murine models, VRK1 depletion reduced tumor growth versus vehicle ($p<0.0001$); anti-PD-1 alone also reduced growth ($p<0.0001$). The combination of dTAG-V1 and anti-PD-1 produced the greatest reduction versus vehicle ($p<0.0001$) and outperformed either monotherapy, supporting synergy between VRK1 targeting and checkpoint blockade.

Conclusion: EMT-driven remodeling sensitizes TNBC to VRK1 inhibition, establishing VRK1 as a tractable vulnerability in mesenchymal-like disease. VRK1 sustains NE integrity; its inhibition destabilizes the NE, activates cGAS-STING, and converts immune-refractory TNBC toward an inflamed, therapy-responsive state. These findings support clinical exploration of VRK1 inhibition combined with anti-PD-1 to enhance antitumor immunity in aggressive TNBC.

: Mechanisms of Drug Resistance 1
Poster Session

#0368 CDC20 drives acquired resistance to CDK4/6 inhibitors in estrogen receptor positive breast cancer.

Kamal Pandey, SM Nashir Udden, Jamsey Mathew, Prasanna G. Alluri

Radiation Oncology, University of Texas Southwestern Medical Center, Dallas, TX

Purpose: Cyclin-dependent kinase (CDK) 4/6 inhibitors, such as palbociclib, in combination with endocrine therapy are the standard of care for patients with metastatic Estrogen Receptor-positive (ER+) breast cancer. Despite significant clinical benefit, acquired resistance to CDK4/6 inhibitors is nearly universal, and therapeutic strategies to overcome such resistance remain limited. To identify novel molecular mediators of resistance, we employed an unbiased integrative approach combining transcriptomic profiles with palbociclib sensitivity data to uncover molecular drivers of CDK4/6 inhibitor resistance.
Methods: We integrated RNA sequencing data from over 45 breast cancer cell lines with half-maximal inhibitory concentration (IC_{50}) values for palbociclib. We performed correlation analyses and identified candidate genes whose expression was associated with palbociclib response. Top correlated gene was validated using western blotting in parental MCF-7 cells and multiple genetically engineered palbociclib-resistant derivatives. Functional relevance was assessed through siRNA-mediated knockdown and overexpression experiments. *In vitro* cell survival assays and *in vivo* xenograft studies using athymic nude mice were performed to determine the impact of CDC20 modulation on palbociclib response.
Results: CDC20 expression showed a strong positive correlation with palbociclib IC_{50} values across multiple breast cancer cell lines, suggesting a potential role in mediating palbociclib response. Consistently, we observed a marked upregulation of CDC20 in palbociclib-resistant MCF-7 and T-47D derivative cells compared to their parental counterparts. Functional studies further supported this association; silencing CDC20 expression in resistant cells significantly restored their sensitivity to palbociclib. Conversely, overexpression of CDC20 in both MCF-7 and T-47D cells was sufficient to confer resistance to palbociclib. *In vitro* cell survival assays showed significantly reduced sensitivity to palbociclib in CDC20-overexpressing cells compared to parental controls ($p<0.001$, two-tailed t-test). *In vivo*, palbociclib treatment (100 mg/kg by oral gavage, daily) was completely ineffective in inhibiting the growth of MCF-7-CDC20 xenografts ($p>0.5$ for palbociclib vs. vehicle, unpaired two-tailed t-test).
Conclusion: Together, these findings identify CDC20 as a key functional mediator of palbociclib resistance and highlight its potential as a therapeutic target to overcome resistance to CDK4/6 inhibitors in ER-positive breast cancer.

#0369 Elucidation of intratumoral heterogeneity using patient-derived lung cancer cell line.

Tomoko Funazo[1], Hiroaki Ozasa[1], Takahiro Tsuji[2], Kazutaka Hosoya[1], Yusuke Shima[1], Masahiro Ooi[1], Keiichiro Suminaga[1], Kentaro Hashimoto[1], Hiroshi Yoshida[1], Hitomi Ajimizu[1], Takashi Nomizo[1], Hironori Yoshida[1], Toyohiro Hirai[1]

[1]Respiratory Medicine, Graduate School of Medicine Kyoto University, Kyoto, Japan,[2]Fred Hutch Cancer Center, Seattle, WA

Intratumoral heterogeneity has been reported to be associated with treatment resistance in various cancers, including lung cancer. Elucidating intratumoral heterogeneity is a critical issue that must be addressed to improve patient prognosis. Previous studies on intratumoral heterogeneity have primarily focused on collecting and analyzing patient-derived cancer cells, classifying them into subclones with distinct characteristics, and conducting comparative analyses. In contrast, few studies have focused on the early phase of intratumoral heterogeneity. We established a patient-derived cancer cell line (KTOR83) using pleural effusion collected from a lung cancer patient harboring a BRAF gene mutation. From KTOR83, we generated single-cell-derived clones and established five subclones (clones A, B, C, D, and E). In drug sensitivity assays using the BRAF inhibitor dabrafenib, clones A and B exhibited resistance, whereas clones C, D, and E were sensitive. In cell migration assays, clones D and E demonstrated high migratory capacity. In xenograft models, clones A, B, and C showed strong tumorigenic potential, while clones D and E exhibited low tumor-forming ability. Furthermore, flow cytometric analysis revealed that in clone C, the expression pattern of the cell surface marker EpCAM shifted from a unimodal to a bimodal distribution before and after dabrafenib exposure. To investigate whether this bimodal expression of EpCAM corresponds to two phenotypically distinct subclones, we plan to isolate EpCAM-high and EpCAM-low populations using flow cytometry and compare their phenotypic characteristics. Through cloning of patient-derived cancer cells, we confirmed the presence of subclones with distinct phenotypes. Moreover, in one of these clones, exposure to an anticancer drug induced a shift to bimodal expression of a cell surface marker, capturing an early event of intratumoral heterogeneity in which a single cell differentiates into phenotypically distinct populations. This study presents a novel approach to capturing the early phase of intratumoral heterogeneity and provides new insights into the mechanisms underlying tumor progression.

#0370 Low physiological pH drives P300 mediated acetylation of PARP1 and promotes PARP inhibitor resistance.

Hao Nie[1], Wei Zhou[2], Kaixin Cheng[1], Dajiang Guo[3], Liping Liao[1], Xu Zhang[1], Chen Wang[1], Rafal Zielinski[1], Janardan N. Gavade[1], Shruthi Sriramkumar[1], Yiming Fang[1], Shuai Wu[4], Hsin-Yao Tang[3], Andrew V. Kossenkov[3], Yuan Qi[1], Jinsong Liu[1], Kang Le[1], Dorothea C. Gruber[5], Michael Soth[6], Miriam D. Post[7], Anil K. Sood[1], Stefanie Fluckiger-Mangual[5], Timothy A. Yap[1], **Benjamin G. Bitler**[7], Rugang Zhang[1]

[1]MD Anderson Cancer Center, Houston, TX,[2]The University of Pennsylvania, Philadelphia, PA,[3]The Wistar Institute, Philadelphia, PA,[4]The Wistar Institute, Philadelpahia, PA,[5]Tolremo Therapeutics AG, Basel, Switzerland,[6]Institute for Applied Cancer Science, MD Anderson Cancer Center, Houston, TX,[7]University of Colorado Anschutz Medical Campus, Aurora, CO

Resistance to PARP inhibitors (PARPi) is a major clinical obstacle in epithelial ovarian carcinoma (EOC). Intrinsic and acquired PARPi resistance ultimately limit therapeutic efficacy and contribute to patient mortality. Despite multiple reported mechanisms of PARPi resistance, few studies have defined the contribution of the tumor microenvironment (TME) in modulating PARPi response. Here, we demonstrate that the acidic TME, commonly observed in EOC, drives a novel mechanism of PARPi resistance. In multiple in vitro and in vivo models, a physiologically low pH of 6.5 is sufficient to enhance DNA damage repair, reduce PARPi-mediated PARP trapping, and attenuate PARPi-mediated anti-tumor efficacy. Through three independent, epigenetically focused CRISPR/Cas9 screens conducted under low pH conditions, we identified p300 as a druggable target for overcoming pH-induced PARPi resistance. Mechanistically, in an unbiased functional proteomic evaluation, we identified an ERK1/2-p300-PARP1 signaling axis activated under low pH, which alleviates PARPi-induced PARP1 trapping and associated DNA damage by directly acetylating PARP1. In primary human tumors, elevated PARP1 acetylation significantly correlates with poorer overall survival and PARPi resistance. In multiple in vivo patient-derived and syngeneic EOC models, novel p300 bromodomain inhibitors, TT125-802 and IACS-16559, synergize with PARP inhibitors (olaparib or saruparib) to inhibit the growth of therapy-resistant tumors. Together, our findings establish p300 as a promising therapeutic target for overcoming acidosis-driven PARPi resistance.

#0371 Integrative analysis of capivasertib mediated AKT blockade with AR inhibition in mouse PTEN-deficient prostate cancer.

Marco A. De Velasco[1], Kazuko Sakai[1], Daiki Nakatsu[1], Takafumi Minami[1], Mamoru Hashimoto[1], Shingo Toyoda[1], Saizo Fujimoto[1], Kazuhiro Yoshimura[1], Simon T. Barry[2], Cath Eberlein[2], Claire Rooney[2], Kazuto Nishio[1], Hirotsugu Uemura[1], Kazutoshi Fujita[1]

[1]Kindai University Faculty of Medicine, Sakai City, Japan,[2]AstraZeneca, Cambridge, United Kingdom

Background: PTEN-deficient prostate tumors have poor prognosis and limited response to AR-targeted therapies. PI3K/AKT activation compensates for AR inhibition, reducing the efficacy of androgen deprivation therapy (ADT) and agents such as abiraterone (Abi). Capivasertib (Capiva, AZD5363), a potent pan-AKT inhibitor, is the first to demonstrate clinical benefit when combined with Abi and ADT in PTEN-deficient metastatic hormone-sensitive prostate cancer (HSPC), as shown in the Phase 3 CAPItello-281 trial.
Objective: To investigate biological responses and therapeutic outcomes of AKT inhibition with capivasertib plus AR-targeted therapy in HSPC using an integrative approach with a clinically relevant PTEN-deficient mouse model, enabling simultaneous assessment of cancer cell signaling and the tumor microenvironment.
Methods: Gene expression profiling, quantitative immunohistochemistry, and flow cytometry were combined with computational analysis to characterize molecular responses to ADT (A, n=13), ADT plus abiraterone (AA, n=14), and ADT plus Abi with Capiva (AAC, n=15) in an aged PTEN-deficient mouse model of locally invasive prostate adenocarcinoma. Treatment response was classified by tumor burden (TB) relative to the population median: ≥20%, high TB; <20% and >-20%, moderate TB; ≤-20%, low TB—serving as surrogates for progressive disease, stable disease, and partial response. Progressive disease was considered unfavorable; stable disease and partial response were favorable.
Results: Favorable outcomes occurred in 8/13 (61.5%), 7/14 (50%), and 12/15 (80%) of A, AA, and AAC groups. Approximately 70 markers related to signal transduction, AR signaling, DNA damage, epigenetic regulation, proliferation/apoptosis, angiogenesis, and immune composition were analyzed. Unfavorable AA outcomes correlated with high AKT signaling, PMN accumulation, and vascularization. AAC favorable responders showed sustained AKT inhibition, increased DNA damage, and reduced PMN infiltration; poor responders exhibited persistent AR signaling.
Conclusion: Capiva improved response to ADT and Abi in PTEN-deficient prostate cancer. Favorable outcomes were associated with sustained AKT inhibition, reduced pro-tumor immune infiltration, and decreased vascularization. These findings underscore the importance of targeting PI3K/AKT to overcome AR therapy resistance and highlight the value of integrative approaches for biomarker discovery and optimizing therapeutic outcomes.

#0372 ARNT2 and AhR promote resistance to HIF2a inhibitor belzutifan.

Dongkook Min, Sunil Poudel, Robert Morris, Irene Mitsiades, Monica Perez, Eric Zaniewski, Toshi Shioda, Esther Rheinbay, Mo Motamedi, Wilhelm Haas, Othon Iliopoulos

Krantz Family Center for Cancer Research, Massachusetts General Hospital, Boston, MA

Introduction: The von Hippel-Lindau (*VHL*) tumor suppressor gene is inactivated in all VHL disease-associated tumors and in more than 90% of sporadic renal cell carcinomas and central nervous system hemangioblastomas. VHL-depleted cells constitutively express high levels of the oncogenic transcription factors Hypoxia-Inducible Factors (HIF1a and HIF2a). HIF2a belongs to the family of bHLH-PAS proteins, it is a sensor of hypoxia and forms nuclear obligatory heterodimers with several adaptor bHLH-PAS protein. HIF-ARNT heterodimers bind HRE sequences in the promoters of hypoxia inducible genes. Belzutifan, a first in class oral medication, disrupt the interaction of HIF2a with ARNT (HIF1b) and suppresses HIF2a target genes expression that drive VHL tumor growth. De novo and acquired resistance to this medication has been detected.

Experimental procedures: Here we show that the nuclear levels of the bHLH-PAS protein ARNT2 contribute to the sensitivity or resistance of RCC to belzutifan. Knock down or knock out of ARNT2 in human cancer cell lines renders the cells resistant to belzutifan, while overexpression of exogenous ARNT2 increases the sensitivity of the cells to the anti-proliferative effect of belzutifan in vitro. Belzutifan disrupts preferentially the ARNT-HIF2a but not the ARNT2-HIF2a heterodimers and its effect depends on levels of ARNT-HIF2a. The global gene expression from bulk RNA sequencing in ARNT2 knock out cells clustered with HIF2a overexpression cells in PCA plot analysis and significantly induced detoxification signaling that functionally involved in AhR (Aryl hydrocarbon Receptor) sensor protein. Treatment of cells with belzutifan or an AhR ligand re-arranges these programs based on the nuclear levels of sensor and adaptor molecules. We show that belzutifan and/or AhR agonist, FICZ treatment increased AhR-Luc activity and CYP1A1 expression, which is a target gene of AhR, and affected to the sensitivity to belzutifan.

Summary: Our data suggest that strategies to increase ARNT2 cellular levels may help in combating de novo or acquired resistance to belzutifan.

#0373 Mitochondrial bioenergetics sustain ABCB1-driven temozolomide resistance in glioblastoma multiforme.

Ashutosh Shrivastava[1], Manendra Singh Tomar[1], Chirag Kulkarni[2], Sreyanko Sadhukhan[2], Priyanka Prajapati[3], Amit Lahiri[3], Naibedya Chattopadhyay[2]

[1]Center for Advance Research, King George's Medical University, Lucknow, India,[2]Division of Endocrinology, CSIR-Central Drug Research Institute, Lucknow, India,[3]Division of Toxicology and Experimental Medicine, CSIR-Central Drug Research Institute, Lucknow, India

Glioblastoma multiforme (GBM) is the most aggressive primary brain tumor and remains difficult to treat. Temozolomide (TMZ) is a cornerstone chemotherapeutic agent for GBM; however, the early development of TMZ resistance significantly limits its therapeutic benefit. ATP-binding cassette transporters such as ABCB1 reduce intracellular drug levels through active efflux. We hypothesized that ABCB1 mediates resistance to TMZ through metabolic rewiring. We investigated whether enhanced mitochondrial bioenergetics fuels ABCB1 function and promotes TMZ resistance. To test this, we generated LN-229 cells stably overexpressing ABCB1 and examined metabolic and bioenergetic changes using gas chromatography–mass spectrometry based metabolomics. We also conducted ATP and lactate assays, mitochondrial mass measurements, ROS profiling, and apoptosis analyses. ABCB1 overexpression caused marked metabolic shifts, including increased tricarboxylic acid (TCA) cycle intermediates, glycolytic activity, higher ATP levels, and increased mitochondrial mass. These findings indicate that metabolic alterations potentially fueled ABCB1drug efflux, as evidenced by reduced doxorubicin retention. We next inhibited mitochondrial complex I with metformin, which decreased ATP production, impaired efflux activity, and restored TMZ sensitivity. Combined metformin and TMZ treatment induced increased apoptotis, demonstrated by caspase-3 activation, PARP cleavage, and increased Annexin V-positive cells. Our findings identify mitochondrial metabolism as a key driver of ABCB1-mediated chemoresistance in GBM and suggest that targeting bioenergetic pathways may be an effective strategy to overcome TMZ resistance.

#0374 On-target WRN mutations drive resistance to WRN inhibitors in TA-repeat-expanded MSI cancers.

Gabriele Picco[1], Yanhua Rao[2], Angham Al Saedi[1], Samantha Walker[1], Shriram Bhosle[1], Yang Lee[3], Maria Garcia-Casado[1], Gilberto Valdes Garcia[2], Kieron May[4], Francesco Sassi[5], James P. Phelan[2], Philip Landis[2], Brian Jones[6], Diana Munoz[6], Jay Prakash Jain[6], Paul A. Barsanti[6], Joshua P. Taygerly[6], Michael P. DeMartino[2], Emanuel Goncalves[7], Andrea Bertotti[5], Livio Trusolino[5], Michael A. White[6], Geeta Sharma[3], Matthew A. Coelho[1], Jonathan Houseley[4], Benjamin Schwartz[3], Mathew J. Garnett[1]

[1]Wellcome Sanger Institute, Cambridge, United Kingdom,[2]GSK, Upper Providence, PA,[3]GSK, Cambridge, MA,[4]Babraham Institute, Cambridge, UK, United Kingdom,[5]Candiolo Cancer Institute, Candiolo, Torino, Italy, Italy,[6]IDEAYA Biosciences, South San Francisco, CA,[7]Instituto Superior Tecnico (IST), Lisboa, United Kingdom

Werner helicase inhibitors (WRNi) are in clinical development for microsatellite-unstable (MSI) tumours with defective DNA mismatch repair. A key genetic feature underlying this vulnerability is the expansion of TA dinucleotide repeats, which renders cells selectively reliant on WRN function. Despite this clear synthetic lethality, routes of tumour cell evolution under the selective pressure of WRN genetic loss or inhibition remain entirely unknown. Here, we investigate how cancer cell evolution shapes response to WRN inhibition and informs resistance mechanisms. Genome-wide CRISPR screens combined with complete WRN knockout revealed no bypass pathways, underscoring WRN's essential and non-redundant function in MSI cells. Pharmacogenomic profiling identified modulators of WRNi sensitivity, including the MRN complex, ATM, and SMARCAL1, but none rescued viability, confirming the robustness of the WRN-MSI synthetic-lethal interaction. WRN-MSI synthetic lethality remains robust across diverse models, including patient-derived organoids and immunotherapy-refractory tumours. Using semi-saturation mutagenesis, prolonged drug exposure across cell lines from diverse tissue lineages, and in vivo validation, we identified a spectrum of recurrent on-target WRN mutations driving acquired resistance to multiple WRNi. This was supported by in vivo evidence of acquired WRN mutations in both cell line-derived and patient-derived xenografts treated with HRO761, providing direct preclinical validation of this resistance mechanism. TA repeats, inferred by short-read sequencing and measured by long-read sequencing, remained stable under WRNi treatment and were unlinked to resistance. Resistant clones showed no evidence of MMR restoration or other bypass mechanisms. Some WRN mutations conferred broad cross-resistance, whereas others preserved sensitivity to alternative WRNi; for example, I852F retained sensitivity to VVD-133214 but not to HRO761, whereas F730L conferred pan-resistance to both yet remained vulnerable to GSK4418959. All three compounds are clinically advanced WRN inhibitors currently progressing through Phase I trials. Some differential sensitivity and resistance patterns were also validated in patient-derived organoids that acquired secondary resistance to HRO761 in vitro. Finally, resistant clones remained vulnerable to rational strategies: combining WRNi with irinotecan suppressed resistant outgrowth, while ATR inhibitors and orthogonal WRNi offer additional routes to extend response. These findings establish on-target WRN mutation as the dominant mechanism of resistance to WRN inhibitors and define a framework for resistance-informed clinical trial design. They also outline actionable strategies to detect and overcome resistance, including ctDNA-based molecular monitoring and rational combination therapies to extend clinical benefit.

#0377 Effects of aneuploidy associated RAD21 gain on therapeutic response to PARP inhibition in Ewing sarcoma and prostate cancer.

Chloe Springer[1], Elise DeArment[1], Ruoxi W. Wang[2], Thomas Janas[1], Xiaofeng A. Su[1]

[1]Center for Prostate Disease Research (CDPR), Bethesda, MD,[2]David H. Koch Institue for Integrative Cancer Research, Cambridge, MA

Chromosome 8 (chr8) gain, particularly the gain of its long arm 8q, represents one of the most frequent chromosomal abnormalities across multiple human cancers. In Ewing sarcoma, approximately 50% of cases exhibit chr8 gain while in prostate cancer, high level amplification of 8q occurs in about 24% of primary cases with much higher frequencies in metastatic cases. Across both diseases, the cohesin subunit gene *RAD21*, located on 8q24.11 region, has emerged as a key driver that facilitates chr8 gain by alleviating replication stress associated with oncogene activation. RAD21 is a highly conserved protein essential for establishing sister chromatid cohesin, chromatin looping, DNA replication, transcriptional regulation, and DNA damage repair. Our recent study demonstrated that elevated RAD21 expression correlates with increased cancer-specific mortality in prostate cancer, underscoring its potential role in tumor progression. However, how RAD21 mitigates replication-stress-associated DNA damage and modulates therapeutic response remains poorly understood. To address this gap, we investigated RAD21's role in the DNA damage response (DDR) and treatment resistance using Ewing sarcoma and prostate cancer cell models. Using TurboID-based protein proximity labeling and mass spectrometry, we have demonstrated that RAD21 interacts with several key DNA damage initiating factors upon oncogenic induction including PARP1 and MRE11, suggesting that RAD21 engages with DNA repair initiating and homologous recombination (HR)-associated machinery. Given the clinical use of DNA damage-inducing PARP inhibitors (PARPi) for targeting HR-deficient cancers, we evaluated FDA-approved PARPi in isogenic Ewing sarcoma and prostate cancer cell models engineered to express distinct levels of RAD21. Our data showed that RAD21 overexpression markedly altered the cellular response to PARP inhibition in both models and this effect appears to be independent from cell-cycle regulation, consistent with a potential role for RAD21 enhancing HR-mediated DNA repair. In summary, our findings reveal an often overlooked function of RAD21 in altering DNA repair and influencing the response to therapeutic drugs targeting DNA repair pathways. Dysregulation of cohesin could contribute to therapeutic resistance and a potential biomarker for stratifying patients for DDR-targeted treatments.

#0378 PGRMC1 induced lipid metabolic reprogramming leads to sorafenib resistance in hepatocellular carcinoma.

Poornima Devi Narayanan[1], Abigail Ramirez[2], Jazmin Lopez[2], Mahalakshmi Vijayaraghavan[2], Alfredo Roman[3], Kyle Nguyen[2], Mitchel Amador Rojo[2], Kariina Garcia[2], Kritika Soni[2], Grace Hua[2], Rajkumar Lakshmanaswamy[2], Ramadevi Subramani[2]

[1]Texas Tech University HSC El Paso, El Paso, TX,[2]Texas Tech Univ. Health Sciences Ctr. El Paso, El Paso, TX,[3]TTUHSC, EL PASO, TX

Background: Hepatocellular Carcinoma (HCC) is the most predominant type of liver cancer and are often diagnosed at advanced stage resulting in high rates of mortality. Sorafenib is a first-line medication which increases survival by an average of 10.7 months in patients with advanced patients. However, numerous studies have shown that after six months, patients develop resistance to sorafenib treatment. Therefore, understanding the molecular mechanisms of sorafenib resistance (SR) and determining the most promising therapeutic target for the treatment of HCC is of vital importance. Among the various pathways that lead to the development of SR are disruptions in the lipid homeostasis of HCC. PGRMC1, a protein that regulates lipid metabolism and heme stacking, has been recently identified as an onco-target in a number of malignancies. Thus, we have investigated PGRMC1's role in SR in HCC.
Methods: We established SR-HCC cell lines (Hep3B, HepG2, and Huh7) through a gradual rise in sorafenib dosage. PGRMC1 expression levels in THLE3 (normal liver cell line), parental HCC, and SR-HCC cell lines was assessed. Genetically modified HCC cell lines with PGRMC1 overexpression or silencing were evaluated for SR using cell viability, apoptosis, colony formation, migration, and invasion assays. To investigate the mechanism of PGRMC1-related SR, we conducted RTPCR using lipoprotein signaling and cholesterol synthesis pathway focused microarray. RT^2PCR, immunoblot, and immunofluorescence were utilized to validate the role of PGRMC1 in lipid metabolism associated with SR.
Results: PGRMC1 expression was higher in SR-HCC cell lines in comparison to HCC cells and normal liver cells. Furthermore, overexpression of PGRMC1 increased SR, but the silencing of PGRMC1 in HCC and SR-HCC led to the opposite effect. It is interesting to note that our studies revealed that SR-HCC and ovPGRMC1-GFP-Hep3B cells exhibited higher levels of membrane cholesterol and lipid peroxidation in comparison to parental HCC cells. Moreover, our findings indicate that PGRMC1alters lipid metabolism in HCC by upregulating APOC3, HMGCS2, NR0B2, STARD3, and SREBF2, and downregulating APOD. In addition, our data also demonstrates that inhibition of PGRMC1 effectively enhanced the anticancer effect of sorafenib by altering lipid metabolism in HCC.
Conclusions: We conclude that PGRMC1 is a feasible target for increasing sorafenib sensitivity through reprogramming lipid metabolism.

#0379 Cysteine-driven drug inactivation undermines covalent drug efficacy and drives resistance.

Maximilian Kobiesa, Jennifer A. Brain, Kelli J. Che, Leah G. Rector, Abby C. Jurasin, Sita Kugel, Lucas B. Sullivan

Fred Hutchinson Cancer Center, Seattle, WA

Background: Constitutive activation of ATF4 drives metabolic rewiring in cancer, enhancing tumorigenesis and therapy resistance. A key consequence is upregulation of the cystine/glutamate antiporter SLC7A11, leading to increased cystine import and excessive intracellular cysteine. Cyclin-dependent kinase 7 (CDK7) inhibitors, such as YKL-5-124, are emerging anticancer agents that target proteins essential for cell proliferation. These inhibitors can be subdivided into covalent and noncovalent classes. Covalent drugs, such as YKL-5-124, act via electrophilic warheads that irreversibly react with nucleophilic amino acids, whereas noncovalent drugs, such as SY-5609, inhibit through intramolecular interactions at the protein's active site. We hypothesized that excess intracellular nucleophiles, particularly cysteine, can sequester electrophilic drugs, reducing target engagement, and promoting resistance.
Methods: We quantified the efficacy of CDK7 inhibitors in pancreatic ductal adenocarcinoma (PDAC) cell lines upon treatment conditions that alter cysteine availability. Cell growth was quantified using Sulforhodamine B (SRB) assay following drug exposure. For studies of drug-thiol reactivity, both CDK7 inhibitors were preincubated with freshly prepared cysteine (10:1 ratio, thiol:drug) in degassed PBS on ice for 1 hour, then applied to cells. For LC-MS analysis, polar metabolites were extracted from cells with 80% methanol normalized to total cell volume. Drug metabolites were measured by untargeted LC-MS using a Q-Exactive HF-X Orbitrap.
Results: Pancreatic ductal adenocarcinoma (PDAC) cell lines with high SLC7A11 expression were resistant to the covalent CDK7 inhibitor YKL-5-124 compared to their low-SLC7A11 counterparts. Pharmacological inhibition of SLC7A11 with erastin sensitized high-SLC7A11 cells to YKL-5-124, whereas cotreatment of low-SLC7A11 cells with N-acetylcysteine, a cysteine prodrug, induced resistance. Sensitivity to SY-5609, a noncovalent CDK7 inhibitor, was unaffected by cysteine availability. These results suggested that cysteine may be directly acting upon covalent CDK7 inhibitors to prevent their efficacy. Indeed, pre-incubation with cysteine drastically decreased the efficacy of YKL-5-124, while SY-5609 was unaffected. LC-MS analysis detected YKL-cysteine conjugates in vitro and in cells grown under high-cystine conditions, supporting direct nucleophile-drug adduct formation.
Conclusion: Elevated intracellular cysteine can chemically sequester electrophilic drugs and drive resistance. Ongoing studies aim to determine if cysteine accumulation alone suffices to confer resistance to covalent CDK7 inhibition. These results highlight cysteine metabolism as a therapeutically actionable vulnerability, potentially guiding drug selection and combination regimens for patients receiving covalent inhibitors.

#0380 Chromatin rewiring and transcriptional plasticity drive a distinct dual-resistant state in ovarian cancer.

Won-Young Choi[1], Rachel Perkins[1], Jisun Kang[1], Haoxiang Lyu[1], Matthew S. Jung[1], Xiaoya Hou[1], Wei Li[2], Junming Yue[1], **Wenjing Zhang**[1]

[1]Pathology, University of Tennessee Health Science Center, Memphis, TN,[2]University of Tennessee Health Science Center, Memphis, TN

Background: Resistance to platinum-taxane combination therapy is a major clinical barrier in ovarian cancer (OC), yet the molecular determinants of dual resistance remain poorly defined. Single-agent cisplatin- or paclitaxel-resistant models are well characterized, but whether dual resistance represents an additive or fundamentally distinct state is unknown.
Methods: We performed paired RNA-seq and ATAC-seq on A2780 parental cells and isogenic cisplatin-resistant (CpR), paclitaxel-resistant (TxR), and dual-resistant (TxCpR) derivatives. Differential expression, chromatin accessibility, motif enrichment, and enhancer-promoter integration analyses were used to identify transcriptional and epigenomic features unique to each resistance state.
Results: CpR and TxR cells exhibited expected drug-specific adaptations, including upregulation of DNA repair genes (e.g., MLH1, LIG4) or cytoskeletal regulators and drug-efflux transporters (e.g., ABCB1, ALDH1A1). In contrast, TxCpR cells formed a distinct transcriptional and chromatin state, characterized by a hybrid epithelial-mesenchymal program, activation of developmental pathways, and selective retention of advantageous single-agent resistance traits. ATAC-seq revealed extensive remodeling of distal regulatory elements in TxCpR cells, with enrichment of MAFF, NFATC4, YY1, and ZNF549 motifs, implicating stress-response and chromatin-architectural regulators. Integrative analysis identified TxCpR-specific enhancers, including a CTCF-associated regulatory element near AIM2, suggesting emergent 3D chromatin restructuring that stabilizes dual-resistance transcriptional programs.
Conclusions: Dual resistance to cisplatin and paclitaxel is not a composite of single-agent responses but a reprogrammed regulatory state driven by enhancer remodeling and coordinated transcription factor networks. This dataset provides a unique paired RNA-seq/ATAC-seq resource and identifies candidate enhancer and architectural dependencies that may be therapeutically targetable in multidrug-resistant OC.

#0381 β-Hydroxybutyrate-mediated lysine butyrylation determines therapy response in liver cancer.

Minghe Zhang, Yunong Xie, Linglin Liu, Yimiao He, Carol Man Carol Tong

The Chinese University of Hong Kong, HONG KONG, Hong Kong

Hepatocellular carcinoma (HCC) has been a major public health concern worldwide for decades because of its high mortality rates and poor prognosis, which are attributable to frequent tumor relapse and limited treatment strategies. Lenvatinib is one of the tyrosine kinase inhibitors approved for first-line treatment of advanced HCC, but its efficacy remains modest. Growing evidence suggests that the unsatisfactory survival benefits of lenvatinib could be attributed to the acquired drug resistance developed in HCC patients. In this study, we aim to explore the intrinsic metabolic vulnerability which could be exploited to enhance the treatment efficacy of lenvatinib in HCC. Metabolomic profiling of lenvatinib-resistant HCC mouse models revealed significant alterations in the butanoate metabolism pathway, with β-hydroxybutyrate (BHB) identified as the most deregulated metabolite. Functional assays demonstrated that BHB treatment inhibited HCC cell proliferation and synergistically enhanced lenvatinib-induced apoptosis. Consistent with in vitro findings, BHB administration in HCC patient-derived xenograft models produced synergistic tumor-suppressive effects with lenvatinib. Combination treatment of lenvatinib and ketogenic diet which induces BHB level could drastically attenuate tumor development in mice bearing tumors. This study presents a potentially translatable combination treatment strategy to potentiate the therapeutic efficacy of lenvatinib in advanced HCC.

#0382 Exploring the role of LONP1 in lon-traditional mechanisms of glioblastoma resistance.

Shashi Jain[1], Dahlia A. Ordaz[2], Javier Lepe[2], Naomi Lomeli[2], James Pham[2], Bhaskar Das[3], Daniela A. Bota[4]

[1]Department of Neurology, School of Medicine, University of California Irvine, Irvine, CA,[2]UCI School of Medicine, Irvine, CA,[3]School of Pharmacy and Pharmaceutical Sciences,, SUNY, NY., NY,[4]Department of Neurology, University of California Irvine, Irvine, CA

Temozolomide (TMZ) continues to serve as the frontline chemotherapy for glioblastoma (GBM), yet its long-term efficacy remains critically compromised due to the emergence of treatment resistance. While the DNA repair enzyme O6-methylguanine-DNA methyltransferase (MGMT) is the well-known contributor to TMZ resistance, clinical observations have shown that even tumors with minimal or silenced MGMT expression eventually acquire resistance, indicating additional, MGMT-independent pathways are involved. To investigate these alternative resistance mechanisms, we established two distinct glioblastoma models: TMZ-resistant (TR) cells characterized by high MGMT expression, and O6-Benzylguanine and TMZ-resistant (OTR) cells exhibiting low MGMT levels relative to parental controls. Our extensive analyses reveal a key function of the mitochondrial protease LonP1 in promoting TMZ resistance through metabolic adaptation. Both TR and OTR cell lines demonstrated significantly upregulated LonP1 expressions compared to parent glioblastoma cells, implicating elevated LonP1 as a central mediator in resistance development.Functional studies underscore that increased LonP1 expression contributes to a metabolic shift within resistant glioblastoma cells, transitioning from glycolytic metabolism towards enhanced oxidative phosphorylation (OXPHOS). This metabolic reprogramming equips resistant cells with improved capacity to sustain energetic and biosynthetic demands under TMZ-induced therapeutic stress. To validate LonP1's causal role in resistance, we genetically overexpressed LonP1 in established glioma and patient-derived glioblastoma cell lines, resulting in robust acquisition of TMZ resistance. Conversely, downregulating LonP1 via targeted knockdown or pharmacologic inhibition restored sensitivity to TMZ, reducing cell viability and disrupting mitochondrial integrity. It is noteworthy that while our data firmly establish the necessity of LonP1 in maintaining TMZ resistance, the sufficiency of LonP1 overexpression to initiate resistance de novo in naïve tumor cells remains untested, as LonP1 knockout models were not leveraged for resistance induction.Collectively, our findings identify mitochondrial LonP1 protease as a promising target to overcome TMZ resistance in glioblastoma therapy. Inhibition of LonP1 activity could potentially reverse metabolic adaptations, thereby resensitizing resistant tumor cells to TMZ and improving treatment efficacy. This study provides a strong rationale for developing LonP1-targeted therapeutics as adjunctive agents in standard TMZ chemotherapy regimens, with the hope of delaying or reversing chemoresistance to improve clinical outcomes for glioblastoma patients.

#0383 Single-cell transcriptomic analysis of treatment-persistent residual disease in BRAF-mutant lung adenocarcinoma.

Constance Nicq[1], Etienne Vignaud[1], Alice Da Silva[2], Raphael Schneider[1], Genevieve De Souza[1], Ludovic Bigot[2], Aurelie Swalduz[1], Olivier Calvayrac[3], Pierre Saintigny[1], Luc Friboulet[4], **Sandra Ortiz-Cuaran**[1]

[1]Univ Lyon, Claude Bernard Lyon 1 University, INSERM 1052, CNRS 5286, Centre Leon Berard, Cancer Research Center of Lyon, Lyon, France,[2]Paris-Saclay University, Gustave Roussy, INSERM U981, Villejuif, France,[3]Centre de Recherches en Cancerologie de Toulouse,[4]Paris-Saclay University, Gustave Roussy, INSERM U981, Villejuif, France., Villejuif, France

Despite the encouraging results of BRAF-targeted therapies (BRAF-TT) in *BRAF*-mutant lung adenocarcinoma (LUAD), most tumor responses are only partial and limited in time, and ultimately all patients develop resistance to treatment. The limited number of pertinent preclinical models of *BRAF*-mutant LUAD has hindered the identification of molecular determinants of BRAF-TT response. In this context, treatment resistance may emerge from a subpopulation of drug-tolerant persister cells (DTP) that survive to treatment through early, non-genetic tumor cell adaptation, and might constitute the source of incomplete tumor responses and disease recurrence.

Here, we assessed the prevalence and dynamics of cell states associated with DTP in patient-derived LUAD models and established LUAD cell lines representing each of the three *BRAF* mutation classes.

Upon treatment with BRAF-TT (either with combined BRAF/MEK inhibitors or EGFR/MEK inhibitors), DTP exhibit different transcriptomic cell states, compared to treatment-naïve (TN) populations, in V600E, G469A and G466V-mutant cell lines and in a patient-derived organoid (PDO), generated from a G469A-mutant LUAD resected specimen. A small fraction of cycling DTP was observed in V600E and G469A cell lines. In both established cell lines and PDO, DTP systematically display features of phenotypic plasticity depicted by the enrichment of gene signatures related to epithelial-to-mesenchymal transition (EMT) and cell adhesion. Moreover, gene signatures associated with a dedifferentiation phenotype (i.e., alveolar and embryonic diapause) were increased in G469A treatment-residual organoids and cell lines but unchanged V600E-mutant cells.

In V600E-mutant cells and G469A-mutant PDO we identified a transition-like cluster, including subpopulations of DTP and TN cells, characterised by enriched EMT and cell migration signatures, down-regulation of G2/M checkpoint and intermediate “drug-tolerant_up” scores, suggesting that these constitute early events of BRAF-TT adaptation. Of note, in a BRAF-TT resistant patient-derived xenograft (PDX), scRNAseq revealed the presence of six different transcriptomic cell states, including a DTP-like cluster: increased “drug-tolerant_up” and embryonic diapause scores, and deregulation of G2/M checkpoint, denoting the dynamic nature of the DTP-like phenotype under treatment.

Trajectory and gene regulatory network bionformatic analyses are ongoing, together with functional experiments, to determine the role of phenotypic plasticity in treatment-persistent residual disease in BRAF-mutant LUAD.

Our results show evidence on how BRAF-mutant LUAD DTP remodel their molecular portraits at the single-cell level, and provide insights into the pertinence of these models to study treatment-residual disease in *BRAF*-mutant LUAD.

#0385 A genome derived non coding reporter of dynamic cancer cell state.

Noha Shendy[1], Yang Zhang[2], Stephanie Nance[2], Ha Won Lee[1], Shivendra Singh[1], Yousef Khashana[2], Vernon Ebegboni[2], Estevez Prado Daniel[2], Mohammad Ali Mohammad Nezhady[1], K. Elaine Ritter[2], Anoop Kavirayani[1], Bensheng Ju[2], Grace McKay-Corkum[1], Qi Liu[2], Yiping Fan[2], Gang Wu[3], Jun Qi[4], John B. Easton[5], Anand G. Patel[1], JUN YANG[2], Taosheng Chen[6], Brian Abraham[1], Adam D. Durbin[1]

[1]St. Jude Children's Research Hospital, Memphis, TN,[23]Computational Biology, St. Jude Children's Research Hospital, Memphis, TN,[4]Dana-Farber Cancer Institute, Boston, MA,[5]Staff Scientist, Dept. of Molec. Pharmacology, St. Jude Children's Research Hospital, Memphis, TN,[6]Associate Member, Chemical Bio. & Therapeutics, St. Jude Children's Research Hospital, Memphis, TN

Sequential changes in transcriptional cell state are essential for normal development and are coopted in cancer. Controlling these changes for therapeutic benefit has been limited due to a lack of tools that reflect different states in live cells. Here, we describe a new reporter method termed “TRECS” that integrates epigenomic and transcriptomic measurements to define endogenous genomic elements that label individual cells in different cell states. We use TRECS in the neural crest-derived, high-risk pediatric solid tumor neuroblastoma, where we demonstrate broad presence of cells with distinct transcriptomes, associated with functional chemoresistance and sensitivity. Experiments using neural crest stem cells and TRECS mouse knock-in model identified that TRECS-labelled cells reflect early developmental stages in the neural crest. These cells display real-time plasticity of transcriptional state and phenotype, in a manner unlinked to cell cycle control. Investigation of nominated loci demonstrates state-specific enrichment of elements marked by H3K27ac, H3K4me1 and open chromatin by ATAC-seq, which flexibly change as cells transition between these phenotypically divergent states. To investigate whether the primary nominated locus is a driver or reporter of cell state, we integrate micro-C, transcriptomics, truncation experiments and functional CRISPRi to identify that this region functions as a pure endogenous reporter of cell state. This, therefore, provides a mechanism to identify new, state-controlling transcription factors. Motif analysis demonstrated enrichment of AP1 transcription factor motifs in the chemoresistant state, and knockout of these AP1 transcription factors results in rewiring of cell state and enhanced chemosensitivity without effects on cell growth. To capitalize on the endogenous flexibility in this system and identify mechanisms to enforce cell state changes independent of cell growth and death, we performed high-content image-based small molecule screening to identify targets suitable to enhance chemosensitivity. These experiments identified EP300/CBP, master histone acetyltransferases, as crucial controllers of a primitive, chemoresistant cell state. Transient acetyltransferase and bromodomain-based inhibition of EP300/CBP results in transcriptional and epigenetic reprogramming *in vitro* and *in vivo*, leading to enhanced chemosensitivity and prolonged survival in murine models. These results demonstrate an unbiased method to identify non-coding genomic loci enriched in specific cell states, which can be harnessed to identify master transcription factors driving these cell states and similarly, mechanisms to enforce changes in cell state.

#0386 Targeting the YBX1-SREBP2 axis to overcome drug resistance in hepatocellular carcinoma.

Veerababu Nagati, Yamile Abuchard Anaya, Miguel Salazar, Kaylee Renteria, Ricardo Pequeno Bracho, Manish K Tripathi

Medicine and Oncology ISU, South Texas Center of Excellence in Cancer Research, The Univeristy of Texas Rio Grande Valley, McAllen, TX

Hepatocellular carcinoma (HCC) is a leading cause of cancer-related death worldwide, with limited treatment options and poor outcomes. Multikinase inhibitors remain the first-line therapy for advanced HCC. However, therapeutic resistance remains a significant challenge in HCC, and the molecular mechanisms underlying metabolic adaptation to drug resistance remain poorly understood. Here, we identify Y-box binding protein 1 (YBX1) as a key regulator of cholesterol metabolism that promotes tumor growth and drug resistance in HCC. Multi-omics and mechanistic analyses reveal that YBX1 transcriptionally activates Sterol Regulatory Element-Binding Protein 2 (SREBP2), a critical master regulator of cholesterol metabolism, and suppresses the cholesterol efflux transporter ABCA1, resulting in increased expression of cholesterol biosynthetic enzymes and intracellular cholesterol accumulation. Additionally, Cholesterol modulates TGFβ signaling and is implicated in drug resistance. This metabolic rewiring stabilizes membrane receptor tyrosine kinases (RTKs) and sustains downstream PI3K/Akt/mTORC1 and EMT signaling pathways, thereby fostering the development of drug resistance. Genetic silence or pharmacological inhibition of YBX1 or SREBP2 with SU056/Betulin restores sorafenib sensitivity and reduces tumor growth. Clinically, higher levels of YBX1 and SREBP2 expression are associated with poor therapeutic response and decreased overall survival in patients with HCC. These findings uncover a YBX1/SREBP2/Cholesterol metabolic axis that mediates adaptive resistance, offering a new therapeutic target to overcome drug resistance in HCC.

Keywords: Hepatocellular carcinoma, Drug resistance, YBX1, SREBP2, Cholesterol metabolism, Akt/mTOR signaling.

#0387 Precision combination therapy opportunities in colorectal cancer revealed by PDX drug screening.

Alexey Sorokin[1], Preeti Kanikarla Marie[1], Jay Saynonh[1], Christian Beke Onana[1], Fengqin Gao[1], Zhensheng Liu[1], Maya Ridinger[2], Scott Kopetz[1]

[1]UT MD Anderson Cancer Center, Houston, TX,[2]Cardiff Oncology, Inc., San Diego, CA

Colorectal cancer (CRC) exhibits extensive molecular heterogeneity driven by oncogenic alterations such as KRAS, NRAS, and BRAF mutations. Despite the promise of targeted therapies, clinical responses are variable and often limited by resistance, underscoring the need for improved molecular stratification and rational combination strategies. We conducted large-scale in vivo drug screening using 140 patient-derived xenograft (PDX) models representing key CRC molecular subtypes: KRAS G12C (n=40), RAS/RAF wild-type (n=40), and BRAF V600E (n=60). Models were treated with standard-of-care agents, including anti-EGFR, BRAF/EGFR, and KRAS G12C/EGFR inhibitors. Tumor responses were assessed alongside molecular profiling via whole-exome sequencing, RNA sequencing, and Reverse Phase Protein Array. Integrated multi-omics analyses identified biomarkers of response and resistance mechanisms. Resistant tumors frequently exhibited MAPK reactivation and RTK/PI3K-AKT pathway activation. BRAF V600E models showed heterogeneous responses to BRAF/EGFR inhibition (40% disease control), which improved with co-targeting of PI3K or downstream MAPK components. RAS/RAF wild-type models responded to anti-EGFR therapy (100% in treatment-naïve; 40% in pretreated), with resistance driven by RTK signaling mitigated via MAPK inhibition. KRAS G12C models demonstrated modest responses to KRAS/EGFR inhibitors (70% disease control), enhanced by SOS1, SHP2, or AKT inhibition. Additional genotype-specific vulnerabilities, including WEE1 and EZH2 sensitivity in KRAS G12C tumors, support rational combination strategies. This comprehensive PDX-based screen delineates actionable, genotype-specific vulnerabilities in CRC and provides a preclinical framework for precision combination therapies to guide future clinical trials.

#0388 DYRK1A-mediated quiescence establishes a therapeutically-resistant reservoir for glioblastoma recurrence.

Ameesha Paliwal[1], Kevin Faust[2], Okty Abbasi Borhani[2], Rifat S. Sajid[1], Evelyn R. Kamski-Hennekam[2], Ingrid Jin[1], Johnny L. McRae[2], Anzar Alvi[2], Parsa Babaei Zadeh[2], Dimitrios G. Oreopoulos[2], Lauren Omoto[1], Phedias Diamandis[2]

[1]Laboratory Medicine and Pathobiology, University of Toronto, Toronto, ON, Canada,[2]Princess Margaret Cancer Centre, Toronto, ON, Canada

Glioblastoma (GBM) is the most common and aggressive primary brain cancer in adults, owed to its extensive intratumoral heterogeneity and rapid disease progression. It is hypothesized that standard-of-care radio- and chemotherapy (temozolomide) treatments act as evolutionary pressures to select a minority subpopulation of temporally stable cells, which seed aggressive, therapeutically resistant recurrent tumors. This study aims to identify and target the therapeutic vulnerabilities of treatment-resistant GBM cells at diagnosis to proactively address disease progression.

We developed and applied a deep learning model to analyze whole patient-matched primary and recurrent GBM specimens to nominate temporally stable cell populations by conserved morphology, successfully identifying these cells in 31 of 40 analyzed cases. Morphologic feature analysis of nominated populations revealed irregular nuclear shape metrics consistent with mesenchymal histology, including reduced nucleus circularity (-8.6%; $p<0.0001$; $n=18$), increased nuclear axis length (+8.2%; $p<0.01$; $n=18$) , and increased cell area (+13.0%; $p<0.05$; $n=18$). Features of stable cells further correlated with a 38.6% reduction in overall survival in an external glioma cohort ($p<0.05$; $n=51$). To define molecular mechanisms underpinning stability, we performed mass spectrometry-based proteomic profiling of matched clinical specimens, which revealed the enrichment of DYRK1A-mediated cell quiescence programs via the DREAM complex as a potential mechanism for chemotherapy evasion ($p<0.01$; $n=36$). Consistent with a quiescence-driven resistance mechanism, Ki67 immunohistochemistry staining demonstrated a 47.5% reduction in the proliferative index of stable subpopulations in the primary tumor compared to the tumor bulk ($p<0.05$; $n=9$). To model these observations in vitro, we cultured CRISPR-Cas9 DYRK1A overexpressing GBM cells in an ex vivo mouse brain slice model and evaluated the effects of temozolomide administration. DYRK1A overexpression was found to ablate chemotherapy-induced GBM cell death in patient-derived cultures, compared to wildtype controls ($p<0.05$), confirming a functional role for DYRK1A in establishing therapeutic resistance in vitro.

Pre-clinical studies of DYRK1A/DREAM complex inhibition have been shown to reverse tumour cell quiescence and sensitize resistant cells to chemotherapy in extra-CNS cancers. These findings extend this concept to GBM and support strategies to target drivers of therapeutic resistance at diagnosis. Current therapeutic approaches in GBM are limited to reducing disease burden; this study informs interventions to proactively anticipate and interrupt disease progression.

#0389 GSDMB drives cGAS-STING-mediated immune evasion in HER2-amplified colorectal cancer.

Junyong Weng[1], Tianchen Xiong[2], Xinxiang Li[3], Ajay Goel[4]

[1]Beckman Research Institute of The City of Hope, Duarte, CA,[2]City of hope, DUARTE, CA,[3]Fudan shanghai cancer center, Shanghai, China,[4]City of Hope, Duarte, CA

Background: HER2-amplified metastatic colorectal cancer (CRC) represents an aggressive disease subtype with poor prognosis and limited response to standard therapies. The molecular mechanisms underlying its malignant behavior and immune evasion, particularly the contribution of specific genes and signaling pathways involved in tumor progression and immune regulation, remain insufficiently defined. This study investigated the biological mechanisms driving tumor progression and immune escape in HER2-amplified CRC.
Methods: We analyzed GSDMB and HER2 expression, copy number variations (CNVs), and patient survival in The Cancer Genome Atlas (TCGA) cohort, and compared expression across clinical stages, BRAF mutation status, and microsatellite status. Mechanistic studies, including RT-qPCR, western blotting, flow cytometry, and immunofluorescence, were conducted to evaluate the effects of GSDMB overexpression on mitochondrial integrity, activation of the cGAS-STING pathway, and immune-related molecule expression. Transcriptome analyses were conducted to identify pathways enriched in GSDMB-high tumors.
Results: GSDMB was the most significantly co-enriched gene in HER2-high CRC (FDR<0.001). Although overall GSDMB expression was not associated with survival (p=0.55), high expression predicted poorer survival in stage IV patients (p=0.005). GSDMB and HER2 are adjacent on the chromosome, and HER2 amplification was consistently accompanied by GSDMB co-amplification; all patients with GSDMB CNV gains (6.4%) or losses (0.3%) showed corresponding HER2 CNV changes. GSDMB expression was significantly elevated in BRAF-mutant (p<0.001) and MSI-H (p<0.001) tumors. Transcriptomic analyses revealed that GSDMB overexpression was associated with enrichment of HER2 signaling and IFNα Response pathways (FDR<0.001). Experimental validation demonstrated that GSDMB overexpression induced mitochondrial membrane pores, resulting in chronic, low-level leakage of mitochondrial double-stranded DNA into the cytoplasm, which activated the cGAS-STING pathway and induced chronic type I interferon responses. This, in turn, upregulated immune checkpoint molecules, impaired antigen presentation, and promoted T cell exhaustion/tolerance.
Conclusion: GSDMB is a recurrently co-amplified gene in HER2-amplified CRC and remodels the tumor immune microenvironment via mitochondrial dysfunction and chronic cGAS-STING/type I interferon signaling, driving immune evasion. Although GSDMB alone is not prognostically significant across all stages, it elevated expression predicts poor outcomes in advanced metastatic disease. These findings highlight GSDMB and its downstream immune pathways as promising therapeutic targets and prognostic biomarkers in HER2-amplified CRC.

#0390 Single cell multiomics reveals evolutionary and epigenomic trajectories of PARP inhibitor resistance in BRCA mutant TNBC.

Wei Hong[1], Pavan Kumar[1], Faiza Baameur Hancock[2], Helen M. Piwnica-Worms[3], **Mahinur Mattohti**[1]

[1]Houston Methodist Research Institute, Houston, TX,[2]UT MD Anderson Cancer Center, Houston, TX,[3]Vice Provost, Science, UT MD Anderson Cancer Center, Houston, TX

Poly (ADP-ribose) polymerase (PARP) inhibitors show marked efficacy in BRCA-mutant triple-negative breast cancer (TNBC), yet nearly half of patients treated with neoadjuvant PARP inhibition fail to achieve pathological complete response, revealing a major obstacle of intrinsic and therapy-induced resistance. To dissect the mechanisms enabling tumor persistence, we performed integrated single-cell transcriptomic and chromatin-accessibility profiling on paired pre- and post-treatment patient-derived xenograft (PDX) samples from a Phase II trial of single-agent talazoparib in germline BRCA1/2-mutant TNBC. This multi-omic framework resolved therapy driven remodeling of tumor ecosystems and gene regulatory circuitry at cellular resolution. We uncover that rare, pre-existing homologous-recombination proficient subclones selectively expand under PARP inhibition and act as reservoirs for residual disease. Network-level integration of expression and chromatin accessibility further revealed extensive epigenomic rewiring in therapy-induced resistant populations, characterized by elevated DNA-repair activity, metabolic reprogramming, and activation of survival pathways. We also identify candidate master transcription factors that likely orchestrate these resistance-associated regulatory states. Collectively, our findings delineate the evolutionary routes by which BRCA-mutant TNBC evades PARP inhibition and highlight how both baseline HRR-proficient subpopulations and transcription factor driven chromatin reprogramming shape therapeutic outcome. These insights nominate actionable vulnerabilities that may be exploited to prevent or overcome resistance and enhance the durability of PARP-inhibitor therapy.

#0391 TROP2 and PTEN are biomarkers of primary resistance to *TUSC2* gene therapy in non-small cell lung cancer (NSCLC).

Ismail M. Meraz[1], Renduo Song[1], Shuhong Wu[1], Yi Xu[1], Meng Feng[1], Lihui Gao[1], Chenghui Ren[1], Qi Wang[2], Jun Li[3], Mourad Majidi[1], Jing Wang[2], Mark Berger[4], Jack A. Roth[1]

[1]Thoracic and Cardiovascular Surgery, UT MD Anderson Cancer Center, Houston, TX,[2]Bioinformatics & Computational Biology, UT MD Anderson Cancer Center, Houston, TX,[3]School of Data Science and Society, University of North Carolina, Chapel Hill, NC,[4]Genprex Inc., Austin, TX

Primary resistance to targeted therapies, immunotherapies, and gene therapies in NSCLC continues to be a significant challenge. *TUSC2* tumor suppressor gene therapy has shown promising anti-tumor efficacy by overcoming resistance to targeted therapy and enhancing checkpoint blockade immunotherapy, including in a mutant *KRAS/LKB1*-driven immunotherapy-resistant NSCLC model. *TUSC2* protein expression is downregulated or absent in over 80% of NSCLC and 100% of SCLC cases., TUSC2 mediates cancer cell death through several mechanisms: inhibiting MAPK and mTOR signaling pathways, arresting cell growth, inducing programmed cell death, and activating immune responses. We established models primarily resistant to *TUSC2* gene therapy to find biomarkers indicative of *TUSC2* gene therapy resistance in NSCLC patient-derived xenografts (PDXs), PDX-derived organoids (PDXOs), and cell lines. A panel of 10 NSCLC cell lines screened for *TUSC2* sensitivity showed resistance in 50% of the cell lines, as assessed by annexin V staining and colony formation assays. We evaluated *TUSC2* sensitivity in 12 NSCLC PDXOs using ATP-based viability assays in 3D culture following TUSC2 or empty vector transfection. While some PDXOs were highly responsive to *TUSC2* within 72 hours post-transfection, 50% of PDXOs exhibited primary resistance. We developed TC314AR (Acquired Resistance) PDX tumors and xenograft models (A549, H1299, H23AR) in NSG mice and treated them with *TUSC2* gene therapy. 20-30% of tumors in every model showed resistance, with no significant reduction in size compared to the control tumors after treatment. Protein expression profiling using reverse-phase protein array (RPPA) analysis of 500 proteins showed distinct expression signatures, with several candidate biomarkers significantly altered in resistant cell lines and PDXOs. RPPA analysis of residual tumors from both the xenograft and PDX models revealed significant but model-specific alterations in protein expression between responders and non-responders. Comparative analyses across the three models showed low expression of TROP2 and high expression of PTEN as potential biomarkers of primary resistance. Overexpression of TROP2 in H1299 and H460 cells increased *TUSC2-induced* apoptosis. These findings suggest that TROP2 and PTEN may serve as biomarkers to predict *TUSC2* response and guide therapeutic strategies in NSCLC.

#0392 EMT-like reprogramming drives drug-tolerant persister cell plasticity in mantle cell lymphoma via ribosome biogenesis.

Wei Wang[1], Yang Liu[1], Heng-Huan Lee[1], Fangfang Yan[1], Yue Fei[1], Yijing Li[1], Chengtai Yu[1], Lin Tan[1], Lorenzi Phil[2], Qingsong Cai[1], Lei Nie[1], Michael Wang[1]

[1]UT MD Anderson Cancer Center, Houston, TX,[2]City of Hope, Los Angeles, CA

Epithelial-mesenchymal transition (EMT) is an evolutionarily conserved developmental program frequently co-opted in solid tumors to drive metastasis and therapy resistance. Whether analogous transcriptional and metabolic machinery operates in blood cancers has remained unexplored. Here, we demonstrate—for the first time—that drug-tolerant persister (DTP) cells in mantle cell lymphoma (MCL), a lethal non-Hodgkin's lymphoma, exploit an EMT-like program distinct from cancer stem cell pathways to establish stable resistance to BTK inhibitors (BTKi) and anti-CD19 CAR T-cell therapy. Using pirtobrutinib (a clinically approved non-covalent BTKi), we established a reproducible, non-stochastic DTP cell model in MCL. Integrated RNA sequencing and ultra-high-resolution metabolomics revealed that therapeutic pressure triggers a striking morphogenetic switch: proliferative lymphoma cells transform into enlarged, quiescent "Giant cells" characterized by profound dedifferentiation and loss of B-cell identity (including CD19). Upon drug withdrawal, Giant cells rapidly revert to proliferative, normal-sized progeny, exposing a previously unrecognized reversible plasticity in hematologic malignancies. Mechanistically, DTP cells rewire the TCA cycle by engaging the malate-aspartate shuttle, sustaining anabolic metabolism during drug exposure. Drug removal abruptly shifts the TCA cycle to catabolic mode, fueling re-entry into cell cycles. This metabolic switch orchestrates global transcriptomic reprogramming and elevates acetyl-CoA levels, which stabilize the core EMT transcription factor SNAI1 via non-histone protein acetylation. Remarkably, acetylated SNAI1 translocates to nucleoli, driving explosive ribosome biogenesis (marked by fibrillarin upregulation)—a hallmark less studied in conventional EMT of epithelial cancers. Perturbing ATP-citrate lyase (ACLi), SNAI1, or fibrillarin disrupts this axis: ACLi/SNAI1 blockade accelerates exit from the Giant cell state, whereas fibrillarin loss traps cells in quiescence, collectively ablating DTP plasticity and restoring therapy sensitivity. In therapy-refractory MCL patients, DTP/Giant cells can be dynamically abundant—far exceeding classic minimal residual disease—and detectable by immunohistochemistry, metabolic imaging, and single-cell RNA sequencing. Thus, unlike solid tumors where EMT primarily enables invasion, blood cancers repurpose this ancient developmental program for metabolic resilience and immune evasion. Our work establishes that an EMT-like network, orchestrated by metabolic reprogramming and nucleolar SNAI1-driven ribosome biogenesis, governs DTP cell fate in MCL. Targeting this axis—particularly ribosome biogenesis—offers a transformative strategy to eradicate persister cells and overcome resistance to BTKi and CAR T-cell therapy.

#0393 Uncovering mechanisms of PARP inhibitor resistance in IDH1-mutant cancers via serial tumor transplantation and genome wide CRISPR-Cas9 knockout screen.

Daniel Andres Colon-Rios[1], Jonathan Dow[1], Adam Krysztofiak[1], Yanfeng Liu[2], Faye A. Rogers[1], Peter M. Glazer[1]

[1]Department of Therapeutic Radiology, Yale School of Medicine, New Haven, CT,[2]Yale School of Medicine, New Haven, CT

Over the last two decades, novel cancer therapies have targeted genetic profiles identified through whole exome sequencing data, including mutations in the homology-directed repair (HDR) proteins breast cancer-associated genes 1 and 2 (BRCA1 and BRCA2), as well as cancer-linked mutations in isocitrate dehydrogenase (IDH), an essential tricarboxylic acid cycle enzyme. Our group and others recently reported that cancers harboring IDH1/2 mutations have defective recruitment of HDR factors to sites of DNA damage due to changes in chromatin dynamics and consequent sensitivity to poly(ADP-ribose) polymerase inhibitors (PARPi). These findings have led to multiple clinical trials exploiting this vulnerability to PARPi monotherapy and combinatorial therapy. To investigate potential mechanisms by which PARPi resistance might arise, we first modeled PARPi-resistance in IDH1-mutant tumors via serial transplantation of patient-derived xenografts in mice treated with the PARPi talazoparib. An analysis of candidate DNA repair factors in these resistant tumor populations revealed downregulation of end protection factors 53BP1, RIF1 and REV7—which are established negative regulators of HDR. Knockout of these factors by CRISPR/Cas9 in IDH1-mutant cancer cells conferred robust resistance to PARPi and restored HDR capacity, supporting the initial observation that mutations in IDH confer a fundamental HDR defect. To overcome this resistance, we found that treatment with the receptor tyrosine kinase inhibitor, cediranib, previously reported to suppress expression of downstream HDR factors, resensitizes these PARPi-resistant cells to PARPi treatment. As a next step, a genome wide CRISPR-Cas9 knockout screen is underway to uncover undescribed mechanisms PARPi resistance in IDH-mutant tumors. Our findings identify key pathways driving PARPi resistance in IDH1-mutant cancers and highlight potential therapeutic strategies to overcome this resistance.

#0394 Adaptive resistance mechanisms to mTOR inhibitor in lung squamous cell carcinoma.

Milica Momcilovic

UCLA David Geffen School of Medicine, Los Angeles, CA

Resistance to small molecule inhibitors targeting key metabolic pathways in lung tumors remains a significant challenge in personalized cancer therapy. In this study, we investigated the mechanisms of resistance to the small molecule mTOR inhibitor TAK228 across lung squamous cell carcinoma (LUSC) models, including cell lines, xenografts, and patient-derived xenografts (PDXs). Our findings reveal that LUSC cells adapt to mTOR inhibition by engaging macropinocytosis, a form of endocytosis that facilitates enhanced uptake of extracellular nutrients, thereby increasing amino acid availability. Co-inhibition of both mTOR and macropinocytosis using small molecule inhibitors effectively reduced tumor growth. Additionally, we identified angiogenesis as a key mechanism limiting the efficacy of mTOR inhibition in vivo. Notably, inhibiting angiogenesis in combination with inhibitors of mTOR and macropinocytosis reduced tumor growth in xenografts and PDXs. Moreover, prolonged treatment of LUSC PDXs with TAK228 and the glutaminase inhibitor CB-839 led to upregulation of vascularization, which coincided with a rebound in tumor growth despite continued therapeutic administration. These findings highlight adaptive resistance mechanisms to small molecule inhibitors that target key metabolic pathways, lending insight into potential future clinical strategies for the treatment of LUSC.

#0395 Identification of drug resistance factors in ALK-rearranged lung cancer using genome-wide CRISPR activation screening.

Mai Nagasaka, Marie Kawahara, Ken Uchibori, Makoto Nishio, Ryohei Katayama

Japanese Foundation for Cancer Research, Tokyo, Japan

Anaplastic lymphoma kinase (ALK)-rearrangements occur in approximately 2-5% of non-small cell lung cancers (NSCLC). Several ALK tyrosine kinase inhibitors (ALK-TKIs) have been developed, and six are currently approved for clinical use. Although these therapies have markedly improved clinical outcomes, most patients eventually relapse due to acquired drug resistance, which remains a significant clinical challenge and limits long-term survival. To date, numerous mechanisms of ALK-TKI resistance have been identified, including secondary mutations in the ALK kinase domain and activation of bypass signaling pathways, such as EGFR or MET. However, in a significant number of cases, the underlying mechanisms remain unknown, highlighting the need for unbiased approaches to identify novel drivers of ALK-TKI resistance. In this study, we first performed a genome-wide CRISPR activation (CRISPRa) gain-of-function screen in patient-derived ALK-positive NSCLC cell lines to identify genetic pathways conferring resistance to ALK-TKIs. The CRISPRa system enables sgRNA-directed activation of endogenous genes via dCas9-VP64, a nuclease-dead Cas9 fused to the transcriptional activator VP64. In JFCR-028-3 cells expressing dCas9-VP64, introduction of sgEGFR or sgMET led to upregulation of the targeted proteins and conferred resistance to ALK-TKIs. For the genome-wide CRISPRa screen, cells expressing dCas9-VP64 were transduced with a pooled sgRNA library targeting over 18,000 genes. The in vitro CRISPRa screen was performed by culturing the cells with alectinib, lorlatinib, or brigatinib for nine days, and sgRNAs enriched in the surviving drug-tolerant cells were analyzed by next-generation sequencing. The top-ranked hits in JFCR-028-3 included receptor tyrosine kinases (RTKs) such as EGFR, MET, and FGFR1, as well as the anti-apoptotic factor BCL2. Gene ontology analysis further revealed significant enrichment of pathways related to cell proliferation, RTK signaling, and regulation of apoptotic signaling among the hit genes. The screens with the three ALK-TKIs identified both shared and drug-specific hit genes, which may reflect differences in their off-target inhibitory profiles. Furthermore, the in vivo CRISPRa screen revealed top hits that differed from those in vitro, with enrichment of ligand-dependent factors, including EGFR and KIT, reflecting the influence of the physiological microenvironment. Together, these results reveal multiple novel factors responsible for ALK-TKI resistance, providing insight into previously unidentified mechanisms.

#0396 Nrf2 role in regulating kaempferol's inhibitory action on CDKs, PD-L-1, CCL2, and TGM2 in triple-negative breast cancer cells.

Sukhmandeep Kaur[1], Patricia Mendonca[1], Shubham D. Mishra[1], Karam F. a. Soliman[2]

[1]Pharmaceutical Sciences, Florida A&M University College of Pharmacy & Pharmaceutical Sciences, Tallahassee, FL,[2]Florida A&M University College of Pharmacy & Pharmaceutical Sciences, Tallahassee, FL

Triple-negative breast cancer (TNBC) is one of the most aggressive forms of breast cancer, marked by rapid progression, high recurrence, and limited treatment options. Emerging evidence suggests that both oxidative stress signaling and the tumor immune microenvironment (TIME) contribute to therapy resistance in TNBC. Kaempferol, a naturally occurring flavonoid found in fruits and vegetables, has shown promise as a multi-target anticancer compound, but its mechanisms of action remain incompletely understood. In this study, we explored how kaempferol regulates tumor growth, immune checkpoint activity, and inflammatory mediators in two genetically distinct TNBC cell lines, MDA-MB-231 (Caucasian) and MDA-MB-468 (African American). The results showed that kaempferol significantly reduced cell viability and proliferation, induced apoptosis, and caused S-phase cell cycle arrest by inhibiting the expression of CDK1, CDK4, CDK6, and CDK7. Under cytokine stimulation, kaempferol downregulated IFN-γ-induced PD-L1 via inhibition of the JAK1/STAT3 pathway and reduced TNF-α-induced CCL2 expression, indicating broad immunomodulatory activity. To understand the contribution of redox regulation, we silenced the transcription factor Nrf2 (NFE2L2) using Nrf2 siRNA. Interestingly, Nrf2 knockdown did not alter kaempferol's inhibition of PD-L1, suggesting that PD-L1 modulation occurs independently of Nrf2. In contrast, silencing Nrf2 markedly increased CCL2 and transglutaminase-2 (TGM2) expression, confirming Nrf2's repressive role in inflammatory signaling. Kaempferol treatment reversed these increases, bringing CCL2 and TGM2 levels back towards baseline. Together, these findings highlight kaempferol's dual ability to regulate both immune checkpoints and inflammatory mediators through distinct, Nrf2-dependent and independent pathways. In conclusion, this study describes the anticancer effects of kaempferol through various molecular mechanisms and targets, which may lead to the development of more effective adjuvant therapies against TNBC.

: Novel Antitumor Agents 1
Poster Session

#0398 NOVO-111: A macrocycle drug conjugate engineered for improved tumor targeting and tolerability.

Jonathan Felipe Aramubla[1], Guangan He[2], Gregory Thiabaud[3], Kathryn Shelton[4], Luke J. Segura[5], Jonathan L. Sessler[6], Rick A. Finch[7], Zahid H. Siddik[2]

[1]INNOVOTEX INC., Austin, TX,[2]UT MD Anderson Cancer Center, Houston, TX,[3]University of Texas at Austin, Austin, TX,[4]Texas Biomedical Research Institute, San Antonio, TX,[5]Comparative Medicine, UT MD Anderson Cancer Center, Bastrop, TX,[6]Chemistry, University of Texas at Austin, Austin, TX,[7]Associate Professor, Veterinary Sciences, UT MD Anderson Cancer Center, Bastrop, TX

Background: NOVO-111 is a novel gadolinium(III) texaphyrin-platinum(IV) complex designed as a tumor-affinic prodrug of oxaliplatin (1,2-diaminocyclohexane-platinum(II) oxalate). The texaphyrin moiety confers redox activity and tumor localization properties intended to improve platinum delivery and reduce systemic toxicity. Preclinical data suggest NOVO-111 is not only more effective as an antitumor agent but also better tolerated than oxaliplatin.
Methods: Pharmacokinetic (PK), biodistribution, and pharmacodynamic (PD) studies were performed in nude mice bearing HCT-116 colorectal xenografts (KRAS^G13D^). Animals received intravenous oxaliplatin (4 mg/kg, MTD) or equimolar (17 mg/kg) and three-fold higher (50 mg/kg; ≤MTD) doses of NOVO-111. Plasma and tissue samples were analyzed for platinum (Pt) levels and for activation of the p53/p21 pathway by immunoblotting.
Results: Following administration, ~97% of NOVO-111 became plasma bound over 2 hours. A small free Pt fraction (as NOVO-111) decayed slowly ($t_1/_2$ = 11.4 h), suggesting prolonged systemic exposure. Compared to oxaliplatin, NOVO-111 produced higher Pt accumulation (1.5-7-fold) in plasma, liver, kidney, heart, ovary, and testes, while tumor and ileum exposure were comparable at equimolar doses. At 50 mg/kg, Pt levels increased ~3-fold in normal tissues but >5-fold in tumor, consistent with selective texaphyrin-mediated accumulation. In vivo, NOVO-111 achieved greater HCT-116 tumor growth inhibition than an equi-tolerated dose of oxaliplatin, without increased systemic toxicity. Both agents, however, induced comparable tumor p53/p21 upregulation. indicating that PK features resulting in enhanced exposure and sustained Pt(II) release also likely drive NOVO-111's superior efficacy.
Conclusions: NOVO-111 displays unique PK and tumor-targeting characteristics that yield improved therapeutic performance relative to oxaliplatin. Prolonged Pt(II) persistence, enhanced tumor accumulation, and favorable tolerability together support its advancement as a next-generation platinum-based therapeutic for colorectal and other solid tumors. These findings underscore the translational potential of texaphyrin-guided delivery platforms to overcome long-standing limitations of traditional platinum chemotherapy.

#0399 Cyclopamine tartrate enhances antitumor immunity and suppresses triple-negative breast cancer growth.

Tianyuan Wang, Lorena Arango, **Li Liu**

UT Southwestern Medical Center, Dallas, TX

Introduction: Triple-negative breast cancer (TNBC) remains a clinical challenge due to limited therapeutic options and poor response to immune checkpoint inhibitors (ICIs). Tumor hypoxia and abnormal vasculature contribute to an immunosuppressive microenvironment that restricts T-cell infiltration. Cyclopamine tartrate (CycT), a heme-targeting small molecule, has been shown to inhibit tumor oxidative metabolism and improve oxygenation [1-2]. This study examined whether CycT suppresses tumor growth and modulates the immune microenvironment in TNBC.

Methods: Female BALB/c mice bearing orthotopic 4T1-Luc syngeneic tumors were treated with CycT (7.5 mg/kg Retro-Orbital Injection, twice weekly) or vehicle control. Digital calipers monitored tumor growth. Tumors were harvested for histology (H&E) and analyzed by multiparameter flow cytometry to quantify $CD8^+$ T-cell density and PD-1 expression on tumor-infiltrating lymphocytes. Statistical significance was determined using unpaired two-tailed t-tests.

Results: CycT significantly inhibited 4T1 tumor growth compared with control ($p < 0.001$), as shown by markedly smaller resected tumors and reduced volumes over 24 days of treatment. Flow cytometric analysis demonstrated that CycT increased intratumoral $CD8^+$ T-cell density ($p < 0.05$) and elevated PD-1 median fluorescence intensity on $CD8^+$ cells ($p = 0.016$), indicating a more active or antigen-experienced T-cell phenotype.

*Conclusion*s: These data indicate that CycT shows significant antitumor effects in a TNBC model while promoting $CD8^+$ T-cell infiltration and activation. The results suggest that CycT reprograms the tumor microenvironment to become immune-accessible, providing a mechanistic basis for future combination strategies with immune checkpoint blockade in TNBC.

References: 1. Sohoni, S. et al, Cancer Res (2019) 79 (10): 2511-2525. 2. Ghosh, P. et al., *Cancer* Res (2020) 80 (17): 3542-3555.

#0400 Combinatorial treatment of glioblastoma with temozolomide (TMZ) plus 5-ethynyl-2'-deoxyuridine (EdU).

Humeyra Kaanoglu, Yasemin Akyel, Adebimpe Adefolaju, Alain Valdivia, Dominique Higgins, Shawn D. Hingtgen, Andrew B. Satterlee, Aziz Sancar

University of North Carolina at Chapel Hill, Chapel Hill, NC

Background: Glioblastoma (GBM) remains highly lethal despite surgery, radiotherapy, and temozolomide (TMZ). We identified a therapeutic role for 5-ethynyl-2′-deoxyuridine (EdU), a thymidine analog whose incorporation is recognized and excised by nucleotide excision repair (NER). We hypothesized that combining TMZ (lesions processed by mismatch repair and base excision repair) with EdU (NER-triggered) would overload complementary DNA repair pathways and improve efficacy.
Methods: We tested TMZ+EdU across GBM cell lines (U87, GBM8), orthotopic mouse models (U87, GBM8), and living, passage-zero GBM patient tumor tissues on organotypic brain slice culture (OBSC). Viability was quantified by bioluminescence imaging; synergy via CompuSyn (cells) and ZIP scores (patient tissues). Short-course EdU dosing followed by histology assessed targeted localization of EdU to tumor cells.
Results: In vitro, TMZ+EdU produced strong synergy in U87 and GBM8 across TMZ doses. In mice bearing U87 orthotopic xenografts, median survivals, reported in days (d), were 29 d (PBS), 37 d with 200 mg/kg EdU (+~30% vs PBS, $p<0.001$), 43 d with 5 mg/kg TMZ (+~50% vs PBS, $p<0.001$), and 67 d with 5 mg/kg TMZ + 200 mg/kg EdU (+~131% vs PBS, $p<0.001$). Notably, the combination yielded a +~60-80% improvement over monotherapies ($p<0.001$). Approximately 13% of combination-treated mice survived to the study endpoint with no detectable tumor. In mice bearing orthotopic GBM8 xenografts, median survivals were 46 d (PBS), 51 d with 1 mg/kg TMZ (+~11% vs PBS, $p=0.004$), 135 d with 5 mg/kg TMZ (+~193% vs PBS, $p<0.001$), and 167.5 d with 200 mg/kg EdU (+~264% vs PBS, $p=0.001$). Median survival was not reached for either TMZ+EdU regimen (1 mg/kg TMZ + 200 mg/kg EdU or 5 mg/kg TMZ + 200 mg/kg EdU); all animals were alive with no detectable tumor at Day 170, significantly outperforming each monotherapy. Short-course dosing followed by histology in U87-bearing mice showed marked tumor-cell selectivity of EdU (~70-83-fold in tumor cells vs adjacent non-tumor cells). In living, passage-zero GBM patient tumor tissues on OBSC, TMZ+EdU was synergistic in 1/4 tumors (ZIP 14) and additive in the remainder (ZIP 2-3).
Conclusions: TMZ and EdU act through distinct DNA repair pathways to deliver synergistic antitumor activity across GBM cell lines, mouse models of GBM, and living, passage-zero GBM patient tumor tissues. Given EdU's brain penetration, the survival benefit observed preclinically, and the demonstration of synergy in a subset of GBM patient tumor tissues, TMZ+EdU represents a compelling strategy for translational development in GBM.

#0401 Targeting Hsp90β potentiates nab-paclitaxel-based chemotherapy response in pancreatic cancer models.

Mayra Garcia[1], Nicola Grimaldi[2], Nathan Tuchscherer[1], Md Sazzad Hassan[1], Urs von Holzen[3], Brain Blagg[4], **Niranjan Awasthi**[1]

[1]Indiana University School of Medicine, South Bend, IN,[2]Preprofessional Studies, University of Notre Dame, South Bend, IN,[3]Surgery, Indiana University School of Medicine, South Bend, IN,[4]Chemistry & Biochemistry, University of Notre Dame, South Bend, IN

Objective:
Pancreatic ductal adenocarcinoma (PDAC) is a highly aggressive malignancy with an extremely poor prognosis. Standard treatment with nab-paclitaxel and gemcitabine (NPT+GEM) yields a median survival of only 8.5 months. Heat shock protein 90 (Hsp90) client proteins—including EGFR, IGF-1R, Raf, PI3K, AKT, CXCR4, and MMP2/9—are implicated in proliferation, survival, angiogenesis, metastasis, and chemoresistance in multiple tumor types, including PDAC. Traditional Hsp90 inhibitors that bind to the N-terminal ATP-binding site exhibit pan-inhibitory activity against all four Hsp90 isoforms, leading to induction of the heat shock response, which causes chemoresistance and dose-limiting toxicities. Here, we evaluated the antitumor efficacy of novel Hsp90β-selective inhibitors in preclinical PDAC models.
Methods:
In vitro cell proliferation assays were performed using the colorimetric WST-1 method. Protein expression levels were analyzed by immunoblotting. Tumor growth studies were conducted using NOD/SCID mice bearing subcutaneous xenografts, and survival studies were carried out in PDAC peritoneal dissemination xenograft models.
Results:
Overexpression of Hsp90β and its client proteins—including EGFR, IGF-1Rβ, CXCR4, and AKT—was observed across PDAC-associated epithelial, endothelial, and stromal cells, whereas normal human pancreatic tissue showed negligible expression. The Hsp90β-selective inhibitors NDNB-25 and NDNB-21, synthesized through a structure-based approach, demonstrated dose-dependent antiproliferative activity and synergistic effects when combined with standard chemotherapy in Hsp90β-expressing PDAC epithelial and stromal cell lines. NDNB-25 reduced expression of key Hsp90 client proteins (EGFR, IGF-1R, HER2, p-MEK, p-ERK, p-S6, and c-Myc) without inducing HSP90 expression. Treatment also induced expression of apoptosis markers (cleaved caspase-3 and cleaved PARP-1) and the epithelial differentiation marker E-cadherin. In subcutaneous xenograft models using Hsp90β-overexpressing PDAC cell lines (AsPC-1 and Panc-1), NDNB-25 and NDNB-21 significantly inhibited tumor growth, with synergistic effects in combination with chemotherapy. In AsPC-1 xenografts, tumor growth inhibition ranged from 47-61% with NPT+GEM, 58-72% with NDNB-25 or NDNB-21 monotherapy, and 79-85% with combination treatment. In AsPC-1 peritoneal dissemination models, Hsp90β inhibitors provided limited survival benefit. In Capan-2 PDAC xenografts with low Hsp90β expression, the antitumor effects of NDNB-25 and NDNB-21 were less pronounced.
Conclusion:
Our preclinical data support the continued development of Hsp90β-selective inhibitors as next-generation agents capable of improving treatment outcomes in PDAC, particularly in tumors with high Hsp90β expression.

#0402 Discovery of JMKX005425, a potent WRN inhibitor highly efficacious in multiple MSI-H gastric cancer models.

Liyan Yue, Xiaoqin Lin, Xinfeng Liu, Yangyang Qiu, Shurong Yang, Dongdong Li, Wei Chen, Taylor B. Guo, Jianbiao Peng

Shanghai Jeyou Pharmaceutical Co., Ltd., Shanghai, China

The Werner Syndrome Helicase (WRN) plays an important role in DNA repair and the maintenance of genome integrity. Recent studies have validated WRN as a promising synthetic lethal target for microsatellite instability-high (MSI-H) tumors, which have the highest prevalence in colorectal (CRC), gastric (GC) and endometrial cancers (EC). While WRN inhibitors as monotherapy in MSI-H CRC have showed promising efficacy, their therapeutic potential in MSI-H GC needs to be further evaluated. JMKX005425 is a clinical-stage, oral WRN inhibitor developed by JeYou to treat MSI-H cancers. JMKX005425 potently inhibited WRN activity and showed selective anti-proliferative effects against various MSI-H CRC, GC and EC cells but not microsatellite stable cancer cells. JMKX005425 also caused DNA damage response as measured by γH2AX induction and WRN degradation in MSI-H cells. In vivo, JMKX005425 monotherapy was highly efficacious in multiple MSI-H Cell Line-Derived Xenografts (CDX) and Patient-Derived Xenografts (PDX) models, including those from heavily-treated, immunotherapy-refractory patients. Notably, in a panel of MSI-H GC PDX (n=14), daily oral administration of JMKX005425 led to significant tumor regression, defined as tumor growth inhibition (TGI) over 100%, in over 50% of the models after 4 weeks of treatment, and all but two of the models showed a TGI over 65% (range: 68.2% to 118.8%). Furthermore, low dose of JMKX005425 in combination with irinotecan completed suppressed tumor growth in an MSI-H CDX model. Last, whole-genome CRISPR screens in MSI-H cells identified several modifiers of sensitivity to JMKX005425 treatment, which may provide information for further studies of drug resistance or patient selection. In conclusion, JMKX005425 is a potent, selective WRN inhibitor and shows high efficacy in multiple MSI-H models, especially in GC PDX models, highlighting its potential as a promising treatment for MSI-H gastric cancer. JMKX005425 is current in a phase I dose escalation study in patients with advanced MSI-H/dMMR solid tumors in China (CTR20253477).

#0403 Synthesis and anti-cancer screening of benzopyran derivatives.

Razia Shaika[1], Brijesh Sharma[1], Mariappan Gurusamy[2]

[1]Pharmacy, Institute of Biomedical Education and Research, Manglayatan University, Aligarh, India,[2]Dept of Pharm Chemistry, St Mary's College of Pharmacy, Secunderabad, India

Introduction: Global cancer incidence continues to rise, with an estimated 20 million new cases and 10 million deaths reported in 2025. Despite significant advances in early detection and therapeutic strategies, cancer remains one of the leading causes of mortality worldwide. Current research efforts are directed toward the discovery and development of novel compounds that offer enhanced anticancer efficacy with minimal side effects.

Objectives of the Study: This study aims to synthesize and characterize a series of novel 2-(toluene sulfonamido)-3-cyano-7,7-dimethyl-4-substituted phenyl-5,6,7,8-tetrahydrobenzopyran-5-one derivatives and evaluate their anticancer potential against MCF-7 breast cancer cells. Cytotoxic activity is assessed using the MTT assay to determine IC_{50} values, with the objective of identifying a potent lead compound for the development of an effective breast cancer therapy.

Experimental Procedure: Substituted benzaldehyde and malononitrile were condensed in ethanol using sodium hydroxide to afford the arylidene-malononitrile intermediate which was subsequently refluxed with dimedone to yield the cyclized benzopyran compound, which was then treated with aryl sulfonyl chloride in the presence of triethylamine to furnish the final benzopyran derivatives. The reaction sequence proceeds through a Knoevenagel condensation followed by a Michael addition mechanism.

Spectroscopic Characterization: The synthesized compounds (THBP2 to THBP8) were characterized by melting point, UV, IR, ^1H NMR, and mass spectrometry. The spectral data obtained were in good agreement with the proposed molecular structures, confirming the successful synthesis and purity of the target compounds. MTT assay in MCF-7 cell line The cytotoxic activity of THBP2 to THBP8 was evaluated against MCF-7 breast cancer cells using the MTT assay at concentrations ranging from 6.25-100 µg/ml. Cell viability was determined from the reduction of MTT to formazan, and IC_{50} values were calculated from the dose response curves.

Research Outcome: A series of benzopyran derivatives were successfully synthesized and characterized using spectroscopic techniques. The MTT assay results demonstrated that THBP-6 exhibited the highest cytotoxic activity, with an IC_{50} value of 20.99 µg/mL, highlighting its potential as a promising anticancer lead compound. THBP6 exhibits low IC_{50} despite containing electron-donating groups, likely due to enhanced lipophilicity and optimal electronic or steric factors that promote stronger binding to the target in MCF-7 cells.

Conclusion: Five novel benzopyran derivatives were synthesized and screened for anticancer activity against MCF-7 cells. In future perspectives, the potent activity of THBP-6 suggests that sulphonamide and cyano substituted benzopyran scaffolds could be further optimized and explored as promising candidates for anticancer drug development.

#0404 The non-pungent N-AVAM capsaicin analog DOHEVANIL displays robust growth-suppressive activity in human endrometriod ovarian cancers *in vitro* and *in vivo*.

Kaitlyn Conley[1], Sarah L. Miles[2], Rama S. Gadepalli[3], John M. Rimoldi[4], Timothy E. Long[5], Yi Charlie Chen[6], Piyali Dasgupta[1]

[1]Marshall University, Joan C. Edwards School of Medicine, Huntington, WV,[2]Department of Biomedical Sciences, Joan C. Edwards School of Medicine, Marshall University, Huntington, WV,[3]Department of Biomolecular Sciences, School of Pharmacy, University of Mississippi, Oxford, MS,[4]University of Mississippi, Oxford, MS,[5]Department of Pharmaceutical Sciences, School of Pharmacy, Marshall University, Huntington, WV,[6]Department of Biology and Environmental Science, Bluefield State University, Bluefield, WV

Purpose of the Study: Endometrioid ovarian carcinomas (EOC) account for ~10% (range 8-15%) of all ovarian cancers. They are considered the second most common malignant ovarian neoplasm, after high-grade serous ovarian cancer (HGSOC). EOCs tumors are characterized by complex tubular and solid-cystic masses. The development of EOC may occur as a secondary event to an endometriosis lesion. The first line-treatment for EOC is surgery and combination chemotherapy involving platinum drugs and taxanes. However, most EOC patients become resistant to chemotherapy and the disease relapses within 12-36 months. Several lines of evidence show that nutritional compounds display robust anti-cancer activity in human cancers. Our laboratory observed that capsaicin (the spicy component of chili peppers) potently inhibited the growth of human EOCs. However, the clinical application of capsaicin as a viable anti-cancer drug is limited by its adverse side effect profile. Using SAR studies, we have identified a non-pungent analog of capsaicin, namely Dohevanil. The primary objective of this research project was to explore the growth-hindering activity of gemcitabine and Dohevanil in EOCs.
Experimental Procedures: MTT assays used to measure perform SAR studies in human EOC cell lines. The growth-suppressive activity of Dohevanil was tested in both human EOC cell lines and in normal human epithelial cells. The results obtained from the MTT assays were confirmed using the chicken chorioallantoic membrane (CAM) assay. Finally, the anti-cancer activity of Dohevanil was evaluated in SCID mouse tumor xenograft models of EOCs.
Results: Dohevanil displayed robust growth inhibitory activity in human EOC cell lines and in chicken CAM and mouse models
Conclusions: Non-pungent capsaicin analogs like Dohevanil may be useful adjunct therapies in human EOCs.
Support or Funding Information Funding for our study was supported by the NIH R15-AREA Grant (2R15CA161491-02 and 2R15CA161491-03), the Women's Health T3: 3P20GM103434-23W1 (PI: Dr. G Rankin) to PD and MAV and the NIAID-AI151970 grant to TEL. Furthermore, this study was supported in part by the West Virginia IDeA Network of Biomedical Research Excellence (WV-INBRE) grant (NIH grant P20GM103434; PI: Dr. G. Rankin), the National Institute of General Medical Sciences of the National Institutes of Health under the award number P30GM122733.

#0405 (Z)-endoxifen modulates estrogen receptor and cell-cycle signaling to induce synergistic antiproliferative effects with CDK4/6 inhibition in endometrial cancer models.

Grace Choong[1], Xiaonan Hou[1], Sandra Suarez Hammer[2], Scott M. Blackburn[2], John Weroha[1], Steven C. Quay[2]

[1]Department of Oncology, Mayo Clinic College of Medicine, Rochester, MN,[2]Atossa Therapeutics Inc, Seattle, WA

Background: Endometrial cancer (EC) remains a major gynecologic malignancy driven in part by aberrant estrogen receptor (ER) signaling. The active tamoxifen metabolite (Z)-endoxifen exhibits dual SERM/SERD-like activity, modulating ER function while exerting additional noncanonical antiproliferative effects. Understanding (Z)-endoxifen's mechanisms of action and its interaction with cell-cycle regulators is critical to optimizing targeted therapy in EC. This study investigated the molecular and functional effects of (Z)-endoxifen, alone and in combination with the CDK4/6 inhibitor abemaciclib, across diverse EC models to define mechanistic activity and translational potential.

Methods: ER+ (Ishikawa, HCI-EC23, patient derived organoid U1561.005) and ER-variable (ARK1, ARK2) EC models were treated with estrogen (0-10 nM), (Z)-endoxifen (125 nM-10 μM) or fulvestrant (0-2.5 μM), and abemaciclib (0-10 μM), as single agents or in combination. Cell viability was assessed using luminescence-based assays. Dose-response analyses and combinatorial synergy were evaluated to determine endocrine sensitivity, ER dependency, and downstream cell-cycle effects.

Results: Estrogen induced biphasic proliferative responses in ER+ models, confirming ligand-driven mitogenic signaling. (Z)-Endoxifen monotherapy suppressed viability across all cell lines, demonstrating superior potency to fulvestrant and activity independent of ER expression status. Mechanistically, (Z)-endoxifen abrogated estrogen-induced proliferative peaks, consistent with ER antagonism and potential receptor degradation, while also exerting ER-independent effects suggestive of cell-cycle modulation. Abemaciclib monotherapy inhibited viability in both ER+ and ER– models, and its combination with (Z)-endoxifen yielded strong synergistic activity (Chou-Talalay combination index < 1), including in ER-negative ARK2 and the ER+ U1561.005 organoid. This synergy likely arises from concurrent disruption of ER signaling and CDK4/6-cyclin D regulatory pathways.

Conclusions: (Z)-Endoxifen demonstrates dual ER-dependent and ER-independent activity in EC preclinical models. Synergy was observed in combination a CDK 4/6 inhibitor. These findings broaden the current understanding of (Z)-endoxifen's efficacy and support further exploration of its potential therapeutic role in ER-driven and mixed-phenotype EC, including evaluation of responses across ER expression levels.

#0406 Discovery of potent and selective TRIB2 inhibitors with therapeutic efficacy in therapy-resistant neuroendocrine prostate cancer<!--EndFragment-->.

Jitender Monga[1], Sang-Yoon Lee[2], Sharad K. Suthar[2], Sudha Sadasivan[3], Shirish Gadgeel[3], Craig Rogers[1]

[1]Department of Urology, Henry Ford Health + Michigan State University Health Sciences, Detroit, MI,[2]Department of Neuroscience, Neuroscience Research Institute, Gachon University, Incheon, Korea, Republic of,[3]Division of Hematology & Oncology, Henry Ford Health + Michigan State University Health Sciences, Detroit, MI

Background: Lineage plasticity and therapy resistance remain major challenges in advanced prostate cancer, where a subset of tumors evade androgen receptor (AR)-targeted therapy and acquire neuroendocrine (NE) features. Neuroendocrine prostate cancer (NEPC), whether arising de novo or following antiandrogen treatment, is highly aggressive and lacks effective targeted therapies. We previously identified the pseudokinase TRIB2 as a critical regulator of enzalutamide resistance, lineage plasticity, and tumor survival, establishing it as a potential therapeutic target. However, no TRIB2 inhibitors are currently available for clinical use, underscoring the need for therapeutic development.

Methods: Using structure-guided in-silico modeling, cell-based screening, and biochemical validation, we identified and optimized TRIB2-targeting small molecules. The lead compound, TBI-001, was evaluated for target engagement, specificity, and functional efficacy. Downstream signaling, phenotypic changes, viability, and apoptosis were evaluated in antiandrogen-resistant and NEPC cell models, as well as engineered cells with TRIB2 overexpression (e.g., LNCaP-TRIB2, RWPE1-TRIB2) using western blotting, IHC, and functional assays. Drug metabolism and pharmacokinetics were examined in preclinical models.

Results: TBI-001 is a potent and bioavailable TRIB2 inhibitor that directly binds TRIB2, induces its protein degradation, and suppresses downstream survival signaling, including pAKT and BCL2. TBI-001 broadly inhibited TRIB2-regulated NE and lineage-plasticity programs, including epigenetic and transcriptional regulators (EZH2, BRD4, SOX2, NMYC), canonical NE transcription factors (ASCL1, BRN2), the NE antigen DLL3, and the effector PEG10. Importantly, TBI-001 reduced CD56 (NCAM1), a NEPC surface marker linked to lineage plasticity, metastasis, and immune evasion, as well as the immune-modulatory molecule B7-H3 (CD276), indicating effects on both NE differentiation and immune-evasive signaling. Functionally, TBI-001 markedly reduced viability and induced apoptosis in antiandrogen-resistant prostate cancer cell lines and NEPC models (NCI-H660, LASCPC-01), while demonstrating limited effects in control epithelial cells. In vivo, TBI-001 treatment led to significant tumor regression in therapy-resistant NEPC xenograft models, decreased NE marker expression, and showed no observable toxicity. Metabolic profiling in human hepatocytes confirmed efficient hepatic metabolism and favorable stability.

Conclusions: These findings establish that pharmacologic targeting of TRIB2 with TBI-001 disrupts oncogenic signaling and neuroendocrine programs that drive aggressive prostate cancer behavior. TBI-001 demonstrates strong anti-tumor activity, favorable tolerability, and promising pharmacologic profile, supporting its advancement toward clinical development as TRIB2-targeted therapy for advanced, therapy-resistant prostate cancer.

#0407 Targeting AhR suppresses the generation of amivantamab-lazertinib-induced drug-tolerant persisters in EGFR-mutant lung cancer.

Joo Sung Shim[1], Mi Hyun Kim[2], Heekyung Han[2], Seongsu Jeong[2], Jae-Hwan Kim[1], Mi Ran Yun[3], Sun Min Lim[4], Byoung Chul Cho[5]

[1]Yonsei University Hospital Cancer Center, Seoul, Korea, Republic of,[2]Yonsei New Il Han Institute for Integrative Lung Cancer Research, Seoul, Korea, Republic of,[3]Yonsei University College of Medicine, Seoul, Korea, Republic of,[4]Yonsei Cancer Center, Yonsei University College of Medicine, Seoul, Korea, Republic of,[5]Yonsei University College of Medicine, Seoul

Introduction: In 2024, the U.S. FDA approved first-line amivantamab-lazertinib based on the MARIPOSA trial, which showed superior overall survival compared with osimertinib. However, mechanisms of resistance to this dual-target therapy remain poorly understood. Using multi-omics analyses of patient-derived and preclinical models, we identified the aryl hydrocarbon receptor (AhR) as a potential target to overcome amivantamab-lazertinib resistance.
Methods: Fresh tumor samples from a treatment-naïve EGFR exon 19 deletion patient were transplanted into athymic nude mice to establish patient-derived xenograft (PDX) models. Mice were treated with amivantamab-lazertinib for 10 days, followed by single-cell and bulk RNA sequencing, whole-exome sequencing, and immunohistochemistry to assess early-phase responses. In vitro, flow cytometry measured lazertinib-induced AhR expression, and HepG2 AhR-luciferase reporter assays evaluated lazertinib-AhR binding. In silico docking (SAMSON) assessed binding affinity. CellTiter-Glo and colony-formation assays tested combinatorial effects of amivantamab, lazertinib, and DA-4505, an investigational AhR antagonist.
Results: Single-cell RNA-seq identified AhR among the most upregulated genes in drug-tolerant persister (DTP) cells after amivantamab-lazertinib exposure. Docking analysis suggested lazertinib acts as an AhR agonist. FACS confirmed that the combination markedly increased AhR expression across NSCLC cell lines. Adding DA-4505 enhanced growth inhibition in H1975 and YU-1185 patient-derived cells, with colony assays confirming additive effects. Transcriptomic and phospho-flow analyses indicated that cell lines with activated Src signaling were most sensitive to triple-drug treatment. Early clinical data from a phase I trial showed DA-4505 monotherapy was well tolerated up to 400 mg.
Conclusion: Targeting AhR with DA-4505 augments the efficacy of amivantamab-lazertinib and may mitigate resistance in EGFR-mutant NSCLC. Ongoing clinical evaluation will determine its translational potential.

#0408 Discovery of a first-in-class dual microtubule- and RAF—targeting inhibitor.

Joshua W. Large, Yeni K. Romero, Kylie Luther, Molly M. Hood, Ranjan Preet, Cale L. Heiniger, Chase K. Crawley, Salim Javed, Yu Mi Ahn, Cynthia B. Leary, Forrrest A. Stanley, Justin T. Proto, Lakshminarayana Vogeti, Bertrand Le Bourdonnec, Bryan D. Smith, Daniel L. Flynn, Jeffery D. Zwicker, **Stacie L. Bulfer**

Deciphera Pharmaceuticals, LLC, Waltham, MA

Background: Microtubule-targeting agents (MTAs) are effective first-line cancer therapies, but novel agents are needed to overcome resistance mechanisms, minimize toxicities, improve delivery, and enhance outcomes with new combination strategies. Several kinase inhibitors have been shown to be MTAs, with some dual inhibitors demonstrating lower toxicities. However, no reported compounds have demonstrated dual RAF kinase-and microtubule-targeting activities. Given that mutations in the RAS/MAPK pathway drive 30% of all cancers, we sought to develop dual microtubule- and RAF—targeting inhibitors.

Methods: Tubulin polymerization inhibition and competition with a BODIPY-colchicine probe were measured using recombinant tubulin. RAF kinase inhibition and off-rate analysis were measured using recombinant enzymes. Structure-based drug design was enabled by X-ray crystallography. Cellular microtubule modulation was determined by a microtubule sedimentation assay, and cellular inhibition of pERK and pRSK was measured by AlphaLISA or ELISA. Cellular proliferation was monitored via resazurin. Spindle formation, cell cycle, and apoptosis were measured by immunofluorescence, flow cytometry, and Western blot. Pharmacokinetics (PK) in plasma, brain, and cerebrospinal fluid compartments were measured following oral dosing in rats. In vivo efficacy was assessed in *RAF*- and *RAS*-mutant mouse xenograft models.

Results: Compound D is an MTA that binds at the colchicine binding site and is also potent and selective for inhibition of RAF kinases. The dual-targeting mechanism was further validated via co-crystallization with the tubulin-stathmin-TTL complex and separately with BRAF. Inhibition of MAPK pathway signaling and cellular proliferation was observed in a wide range of *BRAF*- and *KRAS*-altered cell lines. In addition, compound D overcomes the tubulin-inhibitor resistant mechanism of MDR1 overexpression. Mechanistically, compound D disrupts normal spindle formation and induces G2/M arrest and apoptosis. Compound D has favorable ADME and PK properties, is orally available, and CNS-penetrant. Oral treatment as a single agent resulted in tumor regression or tumor growth inhibition in *BRAF*- and *KRAS*-mutant mouse xenograft models.

Conclusions: Compound D is the first reported microtubule destabilizing agent with dual RAF activity, leading to tumor regression or growth inhibition as a single agent in preclinical models. Our data provide proof of concept for designing orally available CNS-penetrant inhibitors targeting both microtubules and RAF kinases.

#0409 Subcellular targeted therapy using HMCD-artemisinin conjugates for metastatic castration-resistant prostate cancer.

Yan Ou[1], Adrian Lim[2], Mouad Edderkaoui[1], Ruoxiang Wang[1], Qiang Wang[1], Stephen J. Pandol[1], Yi Zhang[3]

[1]Department of Medicine, Cedars-Sinai Medical Center, Los Angeles, CA,[2]Department of Medicine and David Geffen School of Medicine, Cedars-Sinai Medical Center and University of California, Los Angeles, Los Angeles, CA,[3]Department of Biomedical Sciences, Cedars-Sinai Medical Center, Los Angeles, CA

Background: Resistance to androgen-deprivation therapy leads to metastatic castration-resistant prostate cancer (mCRPC), a lethal stage with limited treatment options. Artemisinin (ART) derivatives exert anti-tumor activity through reactive oxygen species (ROS) generation and mitochondrial disruption but lack tumor selectivity. Our laboratory identified a near-infrared (NIR) heptamethine carbocyanine dye (HMCD) that preferentially accumulates in tumors via organic anion-transporting polypeptides (OATPs) upregulated under hypoxia, enabling tumor-specific delivery.
Methods: To achieve subcellularly targeted chemotherapy, four HMCD-ART conjugates with distinct linkers were synthesized: HMCD-ART1 (artesunate linker), HMCD-ART2 (carbamate linker), HMCD-ART3 (ether linker), and HMCD-ART4 (ester linker). These were evaluated in androgen-independent prostate cancer models (22Rv1, PC-3, C4-2B, and resistant derivatives). Cytotoxicity, selectivity, and chemosensitization were analyzed in vitro, while subcellular localization, ROS generation, and cell-death mechanisms were examined by fluorescence microscopy, flow cytometry, and Western blotting. Tumor targeting and therapeutic efficacy were determined by NIR imaging and 22Rv1 xenograft models.
Results: Among the conjugates, HMCD-ART1 showed the greatest potency and selectivity, effectively killing taxane-, abiraterone-, and enzalutamide-resistant prostate cancer cells while sparing normal prostate epithelial cells. HMCD-ART1 enhanced sensitivity to chemotherapeutics, inhibited colony formation and migration, and demonstrated prolonged tumor retention for up to eight weeks. Mechanistic analyses revealed mitochondrial and lysosomal co-localization, ROS induction, cytochrome c release, DNA damage (pATM, γH2AX), and mitochondrial-fission-dependent necrotic death. In vivo, HMCD-ART1 significantly suppressed xenograft tumor growth without observable systemic toxicity.
Conclusion: HMCD-ART1 integrates NIR-guided tumor targeting with mitochondrial-specific cytotoxicity, providing a novel therapeutic platform to overcome drug resistance in mCRPC. This strategy represents a next-generation precision chemotherapeutic approach combining targeted delivery, subcellular selectivity, and enhanced safety.

#0410 Characterization of CGT1263, a KRAS (ON/OFF) inhibitor clinical candidate with selectivity for mutant KRAS over HRAS and NRAS.

John Fischer, Kim Alley, Karyn Bouhana, Richard Brizendine, Paul Carlson, Mark Chicarelli, Michelle Crow, Brad Fell, Jennifer Fulton, Anna Guarnieri, Jackie Harrison, Ravi Jalluri, Amber Johnson, Keith Koch, Cori Malinky, Macedonio J. Mejia, Brad Newhouse, Scott Niman, Rob Rieger, John Robinson, Mareli Rodriguez, Leah Salituro, Vinny Scarato, Aaron Smith, Francis Sullivan, Yang Wang, Shannon Winski, Silas Wood, Yeyun Zhou

Cogent Biosciences, Inc, Boulder, CO

Oncogenic KRAS mutations occur across multiple cancer types, including pancreatic, lung, and colorectal malignancies. While allele-specific KRAS inhibitors have demonstrated clinical benefit in patients, the majority of KRAS mutant cancers remain without effective therapies. Recent efforts to address this disparity have resulted in the identification of pan KRAS inhibitors that target clinically relevant mutations and alterations. Herein, we highlight the clinical candidate CGT1263, a novel pan KRAS inhibitor that engages both the active (ON) and inactive (OFF) states of KRAS while sparing HRAS and NRAS inhibition. CGT1263 demonstrates robust anti-proliferative activity across a tumor spheroid panel of KRAS altered cell lines. In vivo characterization of CGT1815, the prodrug of CGT1263, includes steady state pharmacokinetics across species, pharmacodynamics, and efficacy in KRAS altered mouse tumor models.

#0412 Tanshinone analog induces ER stress mediated growth suppression via inhibition of MYC and E2F pathways in prostate cancer cells.

Ching-Feng Cheng, Hui-Chen Ku, Guo-Zhou Cheng

Taipei Tzu Chi Hospital, Buddhist Tzu Chi Medical Foundation, New Taipei City, Taiwan

Prostate cancer (PCa) is the most common malignancy among men in developed countries, and its increasing incidence is closely associated with the rising prevalence of obesity and metabolic syndrome. Our previous studies demonstrated that the Tanshinone analog (TA) enhances *ATF3* expression, inhibits adipogenesis and lipogenesis, and promotes adipocyte browning. Although both native Tanshinones and their analogs have been reported to influence PCa cell growth, the underlying mechanisms remain incompletely understood. This study aimed to investigate whether TA regulates the growth of PCa cells through modulation of the endoplasmic reticulum (ER) stress/unfolded protein response (UPR) and E2F family-related pathways. Using androgen-dependent LNCaP cells and androgen-independent DU145 and PC3 cells as PCa models, we examined the effects of TA on cell growth and associated signaling pathways. TA treatment significantly reduced cell numbers in all three PCa cell lines in a dose-dependent manner, as determined by hemocytometer counting. Colony formation assays confirmed a marked decrease in both colony number and diameter, indicating strong anti-tumor activity. Gene Set Enrichment Analysis (GSEA) of RNA sequencing data revealed that TA markedly suppressed MYC- and E2F target-associated pathways in LNCaP and DU145 cells. In contrast, differential gene expression (DEG) enrichment analysis showed upregulation of ER stress-related pathways, which was further validated by qPCR and western blot analyses of ER stress markers including PERK, ATF6, IRE1α, ATF4, and CHOP. Additionally, TA reduced androgen receptor protein levels and its nuclear translocation in LNCaP cells. In vivo, TA treatment (10 mg/kg, i.p., twice weekly for six weeks) significantly reduced tumor growth in DU145 xenograft-bearing immunodeficient mice compared with controls (2.30 ± 0.23 g vs. 3.53 ± 0.43 g; $P < 0.05$). TA treatment also decreased lung weight relative to the control group (0.21 ± 0.03 g vs. 0.36 ± 0.06 g; $P < 0.05$), indicating effective inhibition of lung metastasis. Histological analysis further confirmed that both primary prostate tumors and metastatic lung tumors were smaller in the TA-treated group than in controls. Moreover, there was no biochemical evidence of hepatotoxicity or nephrotoxicity, as hepatic (ALT, AST) and renal (BUN, creatinine) biomarkers remained unchanged after six weeks of TA treatment. In conclusion, TA exerts multiple anti-tumor effects in PCa by activating ER stress and suppressing MYC- and E2F-related signaling. These findings highlight TA as a promising therapeutic candidate for prostate cancer treatment.

#0413 ADT-007: A mechanistically distinct Pan-RAS inhibitor with capacity to escape acquired resistance common to other RAS inhibitors.

Junwei Wang[1], Xi Chen[1], Sindhu Ramesh[1], Jeremy B. Foote[2], Chung-Hui Huang[1], Kristy L. Berry[1], Khalda Fadlalla[1], Dhana Sekhar Reddy Bandi[2], Purnachandra Ganji[2], Elmar Nurmemmedov[3], Ivan Babic[3], Donald Buchsbaum[2], Asfar S. Azmi[4], Yulia Y. Maxuitenko[1], Adam B Keeton[1], Bassel El-Rayes[2], Gary A. Piazza[1]

[1]Drug Discovery and Development, Auburn University, Auburn, AL,[2]University of Alabama at Birmingham, Birmingham, AL,[3]CellarisBio LLC, San Diego, CA,[4]Wayne State University School of Medicine, Detroit, MI

Gain-of-function mutations in RAS genes are the most prevalent oncogenic mutations responsible for about one-third of all human malignancies. Despite decades of research, direct targeting of RAS remains a major clinical challenge as RAS inhibitors recently FDA-approved or in clinical trials appear to have limited efficacy due to the emergence of acquired resistance. We recently described a mechanistically distinct pan-RAS inhibitor, ADT-007, that selectively kills cancer cells harboring activated RAS, whether driven by oncogenic mutations or activation by upstream receptor tyrosine kinase signaling. ADT-007 potently inhibited the growth of an array of cancer cell lines harboring various RAS mutations or activated RAS with low nM IC_{50} values. In contrast, cancer cells with downstream RAF mutations or cells of normal tissues were essentially insensitive. Cellular, biochemical, and biophysical studies demonstrated that ADT-007 binds nucleotide-free RAS to block GTP loading and activation of the MAPK/AKT signaling pathway, resulting in mitotic arrest and apoptosis. ADT-007's unique selectivity was attributed to metabolic detoxification by glucuronidation from UDP-glucuronosyltransferases (UGTs), which we found to be enriched in normal cells compared with RAS-mutant cancer cells. Notably, ADT-007 induced apoptosis and caused nearly complete inhibition of colony formation of Mia-PaCa-2 human pancreatic cell line, while the pan-KRAS inhibitor, BI-2865, and the pan-RAS inhibitor, RMC-6236, did not induce apoptosis, but only suppressed proliferation and marginally inhibited colony formation under the same conditions. Furthermore, RAS mutant colon and pancreatic cancer cells did not develop resistance to ADT-007 under chronic exposure, in contrast to sotorasib, BI-2865, and RMC-6236, which readily produced cultures that were essentially unresponsive to the inhibitor they were exposed to. Moreover, the resistant cell lines exhibited cross-resistance to mechanistically distinct classes of RAS inhibitors, including pan-KRAS, pan-RAS, and allele-specific KRAS inhibitors, but not to ADT-007 or a second-generation inhibitor, ADT-030. These observations suggest a shared mechanism of acquired resistance that may limit the efficacy of currently known RAS inhibitors (approved or in development). An orally bioavailable prodrug of ADT-007, ADT-1004, demonstrated favorable tolerability and suppressed tumor growth in orthotopic and patient-derived xenograft models of pancreatic cancer, accompanied by reductions in activated RAS and p-ERK levels. Consistent with resistance experiments, ADT-1004 displayed superior efficacy than sotorasib or adagrasib in a xenograft model using a resistant MIA-PaCa-2. These findings support further development of ADT-1004 that holds promise for broad and durable efficacy against RAS-driven cancers.

#0414 QED-203, a dual TRPV6 and AR small molecule preclinical candidate for advanced prostate cancer resistant to standard of care.

Kimberley Beaumont[1], Rebecca Pouwer[1], Mei Yeh[1], Melanie Robitaille[2], Rebecca Farrow[1], Matthew McLachlan[1], Therese Johnson[1], Akanksha Upadhyaya[1], Aaron Gregson[1], Raphael Rahmani[1], Claire Levrier[1], Hasanthi Wijesekera[1], Malika Kumasiri[1], Grant Stuchbury[1], Terrie-Anne Cock[1], Andrew Harvey[1], Gregory Monteith[2], Brian Dymock[1]

[1]QEDDI, UniQuest, University of Queensland, Brisbane, Australia,[2]School of Pharmacy, University of Queensland, Brisbane, Australia

TRPV6, a calcium channel, is an oncochannel that is overexpressed in epithelial cancers, especially prostate cancer. We have observed that concomitant TRPV6 and AR inhibition is synergistic in prostate cancer cells resulting in a strong anti-proliferative effect. Our preclinical candidate QED-203 inhibits TRPV6-mediated calcium influx (FLIPR and electrophysiology) and NFAT activity (NFAT luciferase reporter) with low nM potency and potently inhibits AR (AR ligand displacement, AR luciferase reporter and translocation assay). QED-203 maintains effectiveness in prostate cancer cell lines that are resistant to next generation AR inhibitors including enzalutamide with multiple resistance mechanisms. QED-203 has high oral bioavailability with a pharmacokinetic profile amenable to once-a-day dosing. QED-203 is well tolerated in rodents with excellent *in vivo* efficacy in castrated mouse models of prostate cancers, including a PDX model with resistance to first and second-generation AR inhibitors (HID-28). TRPV6 target engagement has been demonstrated for QED-203 in rodents through changes in urine calcium levels, and via gene expression changes consistent with TRPV6 and AR inhibition in xenograft tumours. QED-203 thus targets a novel dual axis pathway (AR/TRPV6) to supress prostate cancer growth. QED-203 may offer a new opportunity to treat prostate cancer patients who have developed resistance to next generation AR therapies, where there is a clear clinical need for new therapeutic approaches

#0415 Combination of VLS-1488 and taxanes induces anti-tumor synergistic effect in cancer cells.

Song Chen, Adriana Roopnariane, Arshi Arora, Samuel Bakhoum, Timothy Bowler, Sarah Bettigole, Scott Drutman, Celia Andreu-Agullo

Volastra Therapeutics, New York, NY

VLS-1488 is an oral small molecule inhibitor of kinesin family member 18 A (KIF18A) that has demonstrated a tolerable safety profile and preliminary efficacy in patients with advanced cancers such as high grade serous ovarian cancer (HGSOC). We and others have previously identified KIF18A, a mitotic kinesin, as a vulnerability specifically in chromosomally unstable cancer cells. VLS-1488 treatment in cancer cells results in defects in chromosome alignment and prolonged mitotic arrest. Taxanes are microtubule-stabilizing chemotherapy agents commonly used in many cancers including ovarian cancer, breast cancer, and non-small cell lung cancer (NSCLC). However, response rates vary widely and most resistance develops rapidly, resulting in limited treatment options thereafter. The similar mechanism of action of VLS-1488 and taxanes, which includes disruption of spindle dynamics and activation of the spindle assembly checkpoint, suggests a potential for synergistic anti-tumor activity when administered in combination. In this current study, we selected a panel of ovarian and NSCLC cell lines with different sensitivities to KIF18A inhibition and treated cells with a range of concentrations of VLS-1488 and taxanes, alone and in combination. Drug combination effects on cell growth inhibition were evaluated using Bliss synergy score. *In vitro*, combination of low doses of taxanes and VLS-1488 consistently resulted in synergistic growth inhibition in cell lines with low sensitivity or resistant to KIF18A inhibition, compared to that of VLS-1488 or taxanes alone. *In vivo*, xenograft studies using ovarian cancer cells resistant to VLS-1488 and paclitaxel single agent treatment, demonstrated that combination treatment of VLS-1488 and paclitaxel results in a synergistic anti-tumor activity, total prevention of tumor growth, and no significant loss in body weight. Further mechanistic studies revealed pronounced mitotic arrest with the combination treatment *in vivo*. We hypothesize that combination treatment of VLS-1488 and taxanes in cancer cells prolongs mitotic arrest and prevents mitotic slippage to an extent that induces cell death. Overall, our findings presented suggest that combination treatment of VLS-1488 and taxanes may offer benefit to patients with limited or no response to VLS-1488 monotherapy and/or taxanes.

#0416 HEC201625, a novel oral small molecule inhibitor of PD-L1, demonstrated potent anti-tumor activities both *in vitro* and *in vivo*.

Bing Liu, Mingyu Guan, Shaoyan Li, Ning Kang, Ming Li, Ying Zeng, Jing Li, Cliff Cheng, Yingjun Zhang, **Kai Lin**

Sunshine Lake Pharma Company, Ltd., Dongguan, China

Background: Despite the clinical success of PD-1 and PD-L1 antibodies, there remains a need for improvement, including the requirement for intravenous administration, suboptimal response rates, and immune-related toxicities. In contrast, orally bioavailable small molecule inhibitors of PD-L1 may address these issues by offering treatment convenience, better tissue distribution, and easier adverse events management in combination therapies. Herein, we report the discovery of HEC201625, a novel small molecule inhibitor of PD-L1, to enhance antitumor immune response by blocking the PD-1/PD-L1 pathway, providing an alternative for cancer immunotherapy.

Experimental Methods: *In vitro* efficacy was tested in HTRF binding and NFAT-driven reporter assays. Functional immune activation was evaluated in co-cultures of human primary T cells with tumor cells. *In vivo* efficacy was assessed in syngeneic MC38-hPDL1 models and PBMC humanized xenograft models with A375, NCI-H358, or MDA-MB-231 cells. Combination studies were performed with 5-FU, anti-VEGF, and KRAS G12C inhibitors. PK and toxicity profiles were evaluated both *in vitro* and in animal studies.

Results: HEC201625 binding induced PD-L1 dimerization and blocked PD-1/PD-L1 interaction potently and selectively with an IC_{50} of 2 nM. In the PD-1/PD-L1 NFAT blockade bioassay, HEC201625 effectively reversed PD-1/PD-L1 interaction and restored Jurkat T cell activity. In the co-culture assay with human primary T cells and tumor cells, HEC201625 enhanced human primary T cell activation in a dose-dependent manner. *In vivo*, HEC201625 showed antitumor activities comparable to those of the anti-PD-L1 antibody atezolizumab in the MC38-hPDL1 murine colon carcinoma model. HEC201625 also demonstrated equivalent or superior efficacy to atezolizumab across multiple humanized immune system tumor models, including A375, NCI-H358, and MDA-MB-231. Synergistic antitumor effects were observed when HEC201625 was combined with 5-FU, anti-VEGF, or KRAS G12C inhibitors. In contrast, no activity was detected in the immunodeficient NCG mice treated with HEC201625, confirming its immune-dependent mechanism. Moreover, HEC201625 demonstrated good bioavailability across multiple animal species, no significant inhibition against 87 off-target receptors, and a favorable safety profile in animal toxicology studies.

Conclusion: HEC201625 is a novel oral small molecule inhibitor of PD-L1 demonstrating potent and selective immune activation and favorable pharmacokinetics and preclinical safety profiles. These results support its further development as a clinical candidate, with IND-enabling studies ongoing and Phase I trials planned.

#0417 Structure-guided design of JZY3032, a dual-engaging DALTAC that miswires AR-p300 in prostate cancer.

Jianzhang Yang[1], Jie Luo[1], Mi Wang[1], Shicheng Jin[1], Arul M. Chinnaiyan[1], Shaomeng Wang[2]

[1]University of Michigan, Ann Arbor, MI,[2]Professor, University of Michigan, Rogel Cancer Center, Ann Arbor, MI

Chemical-induced proximity (CIP) strategies have expanded the therapeutic landscape by modulating protein-protein interactions, yet most current modalities, such as PROTACs and molecular glues—juxtapose non-physiological partners, often yielding variable or unpredictable outcomes. To address this limitation, we developed Domain-ALTeration Chimeras (DALTACs), a mechanistically distinct platform that selectively miswires endogenous protein complexes by enforcing *non-productive* domain-domain interactions between physiologic partners. Rather than degrading targets or stabilizing native interfaces, DALTACs reconfigure the topology of multi-domain complexes through rational ligand selection and linker engineering. As a proof of concept, we designed JZY3032, the first-in-class AR-p300 DALTAC, to disable the androgen receptor (AR)-p300 transcriptional complex, a critical regulatory node in prostate cancer. Guided by iterative medicinal-chemistry optimization, we conjugated an AR LBD inhibitor to a selective p300 bromodomain inhibitor using a tunable linker optimized for cooperative, simultaneous dual engagement. The resulting construct redirects the physiological AR-p300 interaction surface into a sterically misaligned, non-productive configuration, thereby preventing AR N-terminal domain communication with p300 and suppressing enhancer activation. Mechanistic specificity was confirmed using two negative-control analogs that selectively disrupt AR or p300 binding; both lacked biological activity, demonstrating that dual engagement and domain-reconfiguration are required for DALTAC function. SAR studies revealed that linker length, rigidity, and exit-vector orientation are key determinants of complex miswiring efficiency. Functionally, JZY3032 potently inhibits growth of AR- and p300-co-dependent prostate cancer models while sparing AR-negative lineages, establishing the lineage-selective therapeutic potential arising from engineered domain miswiring. Collectively, these data establish DALTACs as a new class of proximity-based therapeutics capable of disabling oncogenic transcriptional complexes through topology engineering. JZY3032 exemplifies a broadly extensible, modular chemistry platform for rationally designing future DALTAC molecules targeting diverse disease-relevant protein assemblies.

#0418 ETX-929, a potential best-In-class, oral, highly potent and selective dual ON / OFF state Pan-KRAS small molecule inhibitor for the treatment of KRAS mutant and wild-type amplified cancers.

Meghana M. Kulkarni, Lei Cui, Hongbo Deng, Tao Liu, Jingyan Gao, Fei Peng, Ying Lin, Yong Tang, Karan Kapoor, Minghong Hao, Robert F. Koncar, Robbie Chen, Eric Simone, Raj Nagaraja, Shengfang Jin, Jeffery Kutok

Ensem Therapeutics Inc., Waltham, MA

Oncogenic *KRAS* alterations occur in approximately 23% of all human cancers. The most common oncogenic *KRAS* alterations are G12D (~31%), G12V (~24%), and G12C (~15%) mutations. In addition, ~10% of KRAS-altered cancers have wild-type (WT) *KRAS* amplification or harbor multiple oncogenic *KRAS* alterations, including co-occurring *KRAS* mutations and amplifications. While there have been drug approvals for $KRAS^{G12C}$ targeting covalent inhibitors, there are currently no approved targeted therapies against other oncogenic *KRAS* alterations. Pan-KRAS inhibitors that target multiple oncogenic *KRAS* alterations while sparing other RAS isoforms have the potential to treat broad patient populations and address resistance to mutant selective KRAS inhibition while avoiding the on-target toxicities associated with pan-RAS inhibition. ETX-929 is an orally bioavailable, potent, dual GTP (ON)- and GDP (OFF)-state pan-KRAS inhibitor with excellent selectivity over other RAS isoforms. ETX-929 binds WT and mutant KRAS in active (ON) and inactive (OFF) conformations with high affinity [K_D(ON-state) = single digit nanomolar; K_D(OFF-state) = picomolar] and >100-fold selectivity over NRAS and HRAS. In the KRAS-RAF1 RAS-binding domain biochemical assay, ETX-929 potently inhibited complex formation when KRAS (WT / mutant) was either in the active GMPPNP-bound state (single digit nM IC_{50}) or inactive GDP-bound state (pM IC_{50}). In cells, ETX-929's dual ON / OFF-state inhibitory activity potently inhibits KRAS mutants that rapidly cycle between GTP- and GDP-bound states ($KRAS^{WTamp}$, $KRAS^{G12C}$) as well as slow cycling mutants ($KRAS^{G12V}$ and $KRAS^{Q61H}$) that predominantly reside in the ON state. In a broad panel of *KRAS* mutant (G12X, G13D, Q61H) and WT amplified cancer cell lines, ETX-929 potently inhibited the KRAS pathway (pERK median IC_{50} = 0.9 nM) and cell proliferation (median IC_{50} = 6.23 nM), while showing no viability effects on low copy number WT KRAS or mutant NRAS / HRAS cells. Oral ETX-929 showed dose-dependent exposures with concordant sustained tumor pERK reductions, inducing tumor stasis or regression in colorectal, stomach, and lung cancer cell line-derived xenograft models harboring *KRAS* alterations (G12D, G12V, G12C, and WT amplified). ETX-929 also shows good cross-species pharmacokinetics including higher species, excellent pre-clinical tolerability, and no meaningful off-target activity or *in vitro* safety signals, supporting its advancement toward clinical development. Overall, ETX-929 is a potential best-in-class, pan-KRAS inhibitor with superior potency, selectivity over NRAS / HRAS, excellent efficacy and favorable drug-like properties that could improve outcomes for KRAS-driven cancers that currently lack targeted therapeutic options.

#0419 Targeting NAMPT using Novel Inhibitor RPT-E-037 in Pancreatic Neuroendocrine Tumor.

Md Hafiz Uddin[1], Husain Yar Khan[2], Amro Aboukameel[3], Sahar F. Bannoura[3], Irfana Muqbil[4], Hugo Jimenez[1], Filza Khan[1], Rafic Beydoun[3], Gregory Dyson[3], Yang Shi[3], Mohammed N. Al Hallack[3], Nitin Vaishampayan[3], Ibrahim Azar[3], Steve Kim[3], Eliza W. Bael[3], Miguel Tobon[3], Khalil Choucair[3], Walid Sukkari[1], Hafsa Imtiaz[1], Herbert Chen[3], Muhammad W. Saif[3], Anthony Frank Shields[5], Ramzi M. Mohammad[3], Philip Philip[6], Bassel F. El Rayes[7], Min Wu[8], Michael Schelle[8], Boris Pasche[3], Asfar S. Azmi[3]

[1]Oncology, Barbara Ann Karmanos Cancer Institute, Wayne State University, Detroit, MI,[2]Barbara Ann Karmanos Cancer Institute, Detroit, MI,[3]Barbara Ann Karmanos Cancer Institute, Wayne State University, Detroit, MI,[4]Lawrence Technological University, Southfield, MI,[5]Associate Director for Clinical Research, Barbara Ann Karmanos Cancer Institute, Detroit, MI,[6]Henry Ford Cancer Institute, Henry Ford Health, Detroit, MI,[7]University of Alabama at Birmingham, Birmingham, AL,[8]Remedy Plan Therapeutics, Gaithersburg, MD

Background and Objective: Advanced pancreatic neuroendocrine tumors (pNETs) respond poorly to current FDA-approved therapies, emphasizing the urgent need to find new and effective treatment targets. Nicotinamide phosphoribosyltransferase (NAMPT), a key enzyme in the NAD biosynthesis pathway, has emerged as a crucial therapeutic target in pNETs. Despite its importance, specific inhibitors directly targeting NAMPT for pNET treatment are currently lacking. This study aimed to evaluate the efficacy of RPT-E-037, a novel NAMPT inhibitor, in preclinical models of pNETs. **Methods:** Growth inhibition was determined by MTT, colony formation and apoptosis assays. We also measured growth arrest using cell cycle analysis. Expression of gene or protein was determined using quantitative PCR, and western blotting techniques. The impact of NAMPT inhibitor RPT-E-037 was evaluated in pNET *in vitro* cultures and in *in vivo*. **Results:** RPT-E-037 demonstrated its growth inhibitory effect in BON-1 and QGP-1 pNET cell lines at pharmacologically relevant concentrations. The inhibitory concentration-50 (IC_{50}) were determined as 0.3 and 1.2 micromolar (μM) in BON-1 and QGP-1 cells respectively. Importantly, RPT-E-037 demonstrated selectivity, showing no adverse effects on normal islet cells (ABC-TC4286, AcceGen) at concentrations effective against tumor cells (reflected by its 40-folds higher IC_{50}). In addition, growth inhibitory effect of RPT-E-037 significantly rescued by nicotinic acid (niacin) treatment in BON-1 cells. Niacin also diminishes its colony reduction and apoptotic ability of RPT-E-037 in this cell line. The novel NAMPT inhibitor RPT-E-037 was shown to induce “DNA synthesis (S) phase” cell cycle arrest. However, niacin treatment switches “S phase” cell cycle arrest to “G0/G1 phase” cell cycle arrest. RPT-E-037 synergized with pNETs standard of care mTOR targeted agent everolimus in both BON-1 and QGP-1 cell lines leading to superior cell deaths (CI<1). The *in vivo* efficacy of RPT-E-037 in BON-1 and QGP-1 cell line derived xenografts (CDxs) are under way. **Conclusion:** For the first time, this study reveals the therapeutic potential of RPT-E-037, a new NAMPT inhibitor, for pNETs in preclinical models. RPT-E-037 shows promise as a novel NAMPT inhibitor and deserves further clinical investigation for pNETs.Generative AI was used for improving the language of the abstract.

#0420 Targeting proliferating cell nuclear antigen via a miRNA-CSC axis as a new therapeutic approach in multiple myeloma.

Jeffrey A. Zonder[1], **Bin Bao**[1], Amro Aboukameel[1], Sahar F. Bannoura[1], MD Hafiz Uddin[1], Husain Y. Khan[1], Rayyan Siddiqui[1], Yin Wan[1], Yang Shi[1], Ramzi Mohammad[1], Long Gu[2], Pouya Haratipour[2], Robert J. Hickey[2], Linda Malkas[2], Asfar Azmi[1]

[1]Oncology, Barbara Ann Karmanos Cancer Institute, Detroit, MI,[2]City of Hope National Medical Center, City of Hope, CA

Multiple myeloma (MM) is a plasma cell cancer, which is ranked as the second most common hematologic malignancy. Despite advances in treatment MM remains incurable. Proliferating cell nuclear antigen (PCNA) is an essential protein which plays a key role in regulation of cell growth and proliferation. A post-translationally modified isoform of PCNA plays a critical role in the pathogenesis of a wide variety of malignant diseases including MM. Increased expression of PCNA has been shown to be associated with an aggressive MM phenotype, making it an attractive therapeutic target. We tested the anti-tumor activity of the novel small molecule PCNA inhibitor AOH-1996 (alone and in combination with either bortezomib or venetoclax) against 5 different sub-types of MM cell lines. We assessed the cytotoxic anti-MM effects of varying doses AOH-1996 using standard viability assays and also 3D spheroid degradation assays. Changes in gene expression relevant to cell growth, cell-cycle progression, apoptosis, methylation status, and cytokine production following AOH-1996 exposure were analyzed using RT-qPCR and Western blotting, as appropriate. We also evaluated the impact of AOH-1996 exposure on miRNA levels. The anti-MM effect of AOH-1996 monotherapy and combinations versus the same cell lines was then further evaluated in xenograft animal model. AOH-1996 demonstrated dose-dependent reduction of cell growth (2D) and CSC-like sphere formation (3D) of different subtypes of MM cell lines. Cell cycle assay revealed that AOH1996 treatment resulted in the delayed mitosis in MM cells. AOH-1996 treatment also significantly down-regulated the gene expression of selected anti-apoptotic markers (PCNA, CDK4/6, BCL2), cancer stem cell markers (EZH2, Sox2), and inflammatory and pro-survival cytokines (IL-6, FGF2). AOH-1996 treatment down-regulated oncogenic miRNA (miR-21, miR-30a, miR-99a, miR-100, miR-142, miR-191 and miR-222) levels and up-regulated anti-oncogenic miR-145 along with the reduced cytokine production of VEGF. There was a synergic effect on cell growth and CSC-like sphere formation when either bortezomib or venetoclax was added to AOH-1996. AOH-1996 and its combination with venetoclax or velcade showed decreased the protein expressions of EZH2, c-Myc, and PARP in MM cells, and significantly inhibited MM.1S cell line-derived xenograft tumor growth. Re-expression of miR-145 by its mimic transfection decreased cell growth and increased the drug sensitivity of AOH-1996 along with the down-regulation of EZH2, CDK4, and CDK6 genes in MM cells, suggesting an important role of AOH1996-mediated miR-145 in MM cells. These findings clearly suggest that PCNA is a potential therapeutic target in MM. We have demonstrated for the first time that the PCNA inhibitor AOH-1996 shows potent anti-myeloma activity through its effects on several key tumor-associated genes/proteins and miRNAs.

#0421 Kirsten rat sarcoma virus (KRAS) oncoprotein as a new therapeutic target in multiple myeloma.

Jeffreay Zonder[1], **Bin Bao**[1], Amro AbouKameel[1], Sahar Bannoura[1], Husain Y. Khan[1], MD Hafiz Uddin[1], Walid M. Sukkari[1], Ramzi Mohammad[1], Long Gu[2], Pouya Haratipour[2], Robert J. Hickey[2], Linda Malkas[2], Asfar S. Azmi[1]

[1]Oncology, Barbara Ann Karmanos Cancer Institute, Detroit, MI,[2]Beckman Research Institute of The City of Hope, Duarte, CA

Kirsten rat sarcoma virus (KRAS) gene, a member of the well-known RAS oncogene family, has been identified in a wide variety of malignant diseases and plays a crucial role in oncogenesis and progression. KRAS mutations have been strongly associated with shorter overall and progression-free survival in many different malignant diseases, including multiple myeloma (MM). Multiple myeloma (MM) is a malignant plasma cell disorder ranked as the second most common blood cell malignancy. Clinically, it manifests as anemia, renal damage, skeletal lesions, and a high frequency of infections, often resulting in death. Despite significant progress in treatment such as immunotherapeutic drugs, proteasome inhibitors, and apoptosis inhibitors, MM remains incurable due to the development of drug resistance in patients. The overall survival rate is approximately 60% at 5 years, highlighting the urgent need for new and affective agents. At least 20% of MM patients have been reported to carry KRAS point mutations. Therefore, targeting the KRAS oncoprotein provides a potential therapeutic strategy in MM. Early evidence revealed that down-regulation of KRAS using siRNA inhibited MM tumor growth both in vitro and in vivo. Daraxonrasib (RMC6236), an FDA-approved small molecule pan-Ras (ON) state inhibitor, has shown anti-tumor activity in U.S. clinical trials. In this study, we evaluated the anti-myeloma activity of RMC6236 in MM cells. Our results showed that RMC6236 inhibited cell growth in a dose response manner across different MM cell subtypes, including both KRAS mutant and wild-type (WT) cells. Depending on the KRAS genotype mutational status, the IC50 of RMC6236 was estimated to range from 20 to 800 nM, Also, cell cycle assays revealed that RMC6236 treatment significantly decreased the number of cells in S phase (DNA synthesis), suggesting an inhibition of cell cycle progression in MM cells. Moreover, combining RMC6236 with anti-myeloma agent venetoclax or a novel anti-PCNA agent AOH1996 significantly reduced cell growth in KRAS mutant and WT MM cells. RT-qPCR assays revealed that RMC6236 treatment led to decreased gene expression of KRAS, CSC signature markers, anti-apoptotic markers, IL-6, STAT3, and mTOR in MM cells, along with the down-regulation of EZH2 and MEK/ERK signal pathways. These findings suggest that the inhibition of MM cell growth by RMC6236 may be linked to the down-regulation of these tumor-associated genes. Ongoing studies aim to further evaluate the anti-myeloma potential of RMC6236.

#0422 A novel potent tetrahydroisoquinoline analog: A cytostatic taxol-like agent.

Kinfe K. Redda[1], Madhavi Gangapuram[1], Suresh Eyunni[2], Elizabeth Mazzio[1], Karam F. A. Soliman[1]

[1]College of Pharmacy and Pharmaceutical Sciences, Florida A&M University, Tallahassee, FL,[2]College of Science and Technology, Florida A&M University, Tallahassee, FL

In 2024, according to the American Chemical Society, approximately 310,720 new cases of invasive breast cancer will be diagnosed among US women, and 42,250 women will die from breast cancer. Triple-negative breast cancer (TNBC) represents 10 to 15% of all breast cancers. TNBC has fewer treatment options than other types of invasive breast cancer, which limits the effectiveness of targeted hormonal or HER2-directed therapies and is heavily reliant on cytostatic agents such as taxanes and vinca alkaloids. The limited efficacy and increasing side effects of these agents highlight the urgent need for alternative small molecules that block proliferation through novel but less toxic mechanisms. We previously synthesized and characterized tetrahydroisoquinoline (THIQ) derivatives, identifying MG-KKR-4-53 as a highly soluble, non-toxic, and cytostatic agent that halts TNBC cell proliferation without functioning as a spindle poison. Instead, it arrests the cell cycle at G2/M phase. Continuing our research, we further developed a more potent analogue, MG-KRR-5-268, and performed comprehensive *in-silico* ADMET and cheminformatics analyses, comparing it with Taxol, vinblastine, and MG-KKR-4-53, which map directly to well-known predictive toxicology and metabolism databases/models powered by ADMETlab, SwissADME, and CYP/clearance data. The compounds of interest were synthesized in our lab using O-mesitylene sulfonylhydroxylamine as an aminating agent. Reaction of the Isoquinoliniumamino salt with substituted acid chlorides in anhydrous tetrahydrofuran gave stable ylides. Reduction of the ylides using sodium borohydride gave the target THIQ compounds, which were characterized by NMR and elemental analysis. Compound *3-fluoro-N-(7-hydroxy-3,4-dihydroisoquinolin-2(1H)-yl)-4-methylbenzamide* (MG-KKR-5-268) showed significant cytostatic activity with IC_{50} of 169 nM representing a 7.1-fold increase over MG-KKR-4-53 (IC_{50} = 1.2 µM). Paclitaxel (250 nM) solidified tumor spheroids at submicromolar concentrations, whereas vinblastine (123nM) caused their disassembly. MG-KRR-5-268 (257nM) exhibited strong prevention of spheroid compaction across submicromolar doses, phenocopying the disassembly of the vinblastine phenotype through a non-tubulin mechanism, compared to the other THIQ analogs. These findings highlighted MG-KRR-5-268 acted as the most potent compound with a novel capacity to prevent 3D tumor solidification through transcriptome reprogramming rather than microtubule binding.

#0423 ETX-880, a potential best-in-class, oral, highly potent and selective covalent inhibitor of Werner helicase for the treatment of microsatellite instability-high (MSI-H) cancers.

Robert F. Koncar, Daliya Banerjee, Mingzong Li, Tao Liu, Upul Bandarage, Alexandra Weinheimer, Jingyan Gao, Fei Peng, Ying Lin, Yong Tang, Karan Kapoor, Minghong Hao, Robbie Chen, Eric Simone, Raj Nagaraja, Shengfang Jin, Meghana M. Kulkarni, Jeffery Kutok

Ensem Therapeutics, Inc., Waltham, MA

DNA mismatch repair (dMMR) defects occur in a broad range of cancers and are characterized by genomic instability due to TA repeat expansion, a condition known as microsatellite instability-high (MSI-H). The use of immune checkpoint inhibitors (ICI) in MSI-H cancers has improved patient outcomes, but ~30-40% of patients do not respond and ~20-25% become refractory to ICI. Genetic ablation or pharmacological inhibition of Werner RecQ like, ATP-dependent helicase (WRN) activity has been shown to induce growth arrest and apoptosis in MSI-H cancer cells, but not in microsatellite stable (MSS) cells. Early clinical data with RO7589831 (covalent) and HRO761 (non-covalent) WRN inhibitors demonstrated clinical responses, validating WRN as an actionable target, but uncertainty remains on their ability to fully engage WRN. ETX-880 is a novel, potent and selective small molecule inhibitor of WRN for the treatment of MSI-H cancers. ETX-880 acts through an allosteric, ATP-cooperative binding mechanism and covalent ligation of WRN at cysteine 727 (C727). The preclinical activity of ETX-880 was characterized and compared to clinical stage WRN inhibitors, including RO7589831, HRO761, and GSK4418959 (non-covalent). ETX-880 demonstrated >2-fold tighter binding to WRN than RO7589831 (ETX-880 K_I = 0.44 µM versus RO7589831 K_I = 1.05 µM) with comparable reactivity for WRN C727. ETX-880 selectively inhibits the ATPase and DNA unwinding activities of WRN with 2-fold greater potency than RO7589831, excellent selectivity against other RecQ helicases, and no activity for the WRN^{C727A} mutant protein. ETX-880 shows strong anti-proliferative effects in a broad panel of MSI-H cancer cell lines with no measurable effects in MSS cells. In MSI-H cancer cells, ETX-880 shows 4-fold more potent anti-proliferative activity than RO7589831 and HRO761 and is ~30-fold more potent than GSK4418959. *In vivo*, ETX-880 depletes WRN protein and induces DNA damage markers in tumors and leads to deeper and more sustained tumor regressions than RO7589831 in an MSI-H colorectal cancer xenograft model. At the efficacious dose, ETX-880 achieves 100% target occupancy (TO) at 2 hours post dose and maintains ~85% TO at 24 hours, in contrast to RO7589831 which shows substantial loss (~40%) of TO by 24 hours. ETX-880 displays favorable drug-like properties, including good *in vitro* ADMET, excellent metabolic stability with low *in vivo* clearance and high oral bioavailability and exposures across animal species. Importantly, human PK predictions reveal low clearance, high oral bioavailability and long half-life, supporting a low once daily oral efficacious dose. Overall, ETX-880 is a potent, selective, covalent WRN inhibitor with excellent ADMET properties leading to deep and sustained target coverage, highlighting its best-in-class potential in MSI-H cancers.

#0424 Targeting tGLI1 in breast cancer brain metastases with a novel ketoconazole derivative.

Mariana Najjar[1], Daniel Doheny[2], Sara Manore[2], Joshua Cha[1], Phi-Long Tran[3], Elissa Bloom[1], Hui-Wen Lo[3]

[1]UT MD Anderson Cancer Center, Houston, TX,[2]Wake Forest University School of Medicine, Winston-Salem, NC,[3]Texas A&M University Health Science Center, Houston, TX

Metastasis is the major cause of mortality for breast cancer. Common metastatic sites include bones, lungs, brain, and liver; with breast cancer brain metastasis (BCBM) accounting for 20-40% of the metastatic cases. HER2-enriched and triple-negative breast cancer (TNBC) subtypes are more likely to develop BCBM compared to others. BCBM is associated with poor prognoses, with a median survival time of 7.9 months. The dismal outcomes are due to limited understanding of the molecular mechanisms driving BCBM and the lack of effective drugs capable of penetrating the blood-brain barrier (BBB). This underscores the critical need to identify new druggable targets and therapeutics for HER2 and TNBC BCBM. To address this urgent need, in earlier work our group identified a tumor-specific, alternatively spliced variant of the transcription factor GLI1 (glioma-associated oncogene homolog 1), termed truncated GLI1 (tGLI1). tGLI1 represents a novel therapeutic target for BCBM because of its selective overexpression in BCBM and the promotion of breast cancer stem cells (CSC), BCBM progression, and tumor microenvironment remodeling. In prior studies, screening of commercial drug libraries for tGLI1-selective agents revealed that the FDA-approved antifungal ketoconazole (KCZ) selectively inhibited tGLI1-positive breast cancer cells *in vitro* and suppressed tGLI1-driven brain metastases *in vivo*. However, KCZ's potent inhibition of the CYP3A4 enzyme raises safety concerns, including liver damage, adrenal insufficiency, and drug-drug interactions. To overcome these issues with toxicities, we modified the chemical structure of KCZ and identified the novel derivative KCZ-229A as a tGLI1 inhibitor candidate. We found that KCZ-229A retains selective inhibition of tGLI1-positive breast CSCs but loses the ability to inhibit CYP3A4 enzymatic activity *in vitro*. Additionally, KCZ-229A demonstrates no toxicity to normal brain, liver, or mammary epithelial cells *in vitro*, while *in vivo* studies confirmed no liver toxicity (normal serum ALT), no adrenal insufficiency (normal serum ACTH), no hematologic abnormalities, and no adverse effects on major organs. Moreover, mass spectrometry analysis of serum showed that KCZ-229A has enhanced bioavailability and BBB permeability. Mechanistic studies revealed that KCZ-229A binds directly and specifically to tGLI1 protein, induces apoptosis, suppresses the CD44+/CD24- stem cell population, and hampers migration and invasion of tGLI1-positive BCBM cells *in vitro*. An experimental mouse metastasis study using intracardiac inoculation demonstrated that systemic administration of KCZ-229A suppressed the progression of tGLI1-positive BCBM. These findings establish KCZ-229A as a brain-penetrant, and safe tGLI1-targeting compound, supporting its further preclinical development to optimize its pharmacological profile and assess its potential to both treat and prevent BCBM.

#0425 ISM6166, a novel oral pan-KRAS (ON/OFF) inhibitor discovered with generative AI shows robust anti-tumor activity in solid tumors with KRAS alterations.

Sujing Shi[1], Defeng Shen[1], Jianping Wu[1], Tingting Liu[1], Jinxin Liu[1], Qingshuo Meng[1], Zuoxiao Shi[1], **Suguna Rachakonda**[2], David Gennert[2], Luoheng Qin[1], Xin Cai[1], Man Zhang[1], Feng Ren[1], Alex Zhavoronkov[2]

[1]Insilico Medicine, Shanghai, China,[2]Insilico Medicine, Cambridge, MA

The small membrane-bound GTPase KRAS functions as an on/off switch for multiple important cellular signaling pathways, including RAF/MEK/ERK and PI3K/AKT. As one of the most prevalent cancer drivers, KRAS alterations occur in approximately 17% of all solid tumors, including pancreatic, colorectal, lung adenocarcinoma, and esophagogastric cancers. Despite recent advances, KRAS G12C-selective inhibitors face clinical challenges in achieving durable therapeutic efficacy due to acquired drug resistance, while the mutational diversity of KRAS-driven cancers restricts their utility across patient populations, representing a significant unmet medical need. On the other hand, targeting all RAS proteins, including HRAS and NRAS, might raise potential toxicity risk, as the RAS family is essential in normal cells. Here, we report an oral pan-KRAS (ON/OFF) inhibitor ISM6166 that selectively targets all major oncogenic KRAS variants in both inactive and active conformations across multiple solid tumors while sparing HRAS and NRAS.

Surface plasmon resonance revealed that ISM6166 binds to GDP-bound KRAS (inactive, or “off”) with picomolar affinity and to GTP-bound KRAS (active, or “on”) with sub-nanomolar affinity. Nucleotide exchange assays and RAS-cRAF binding assays further supported dual inhibitory function, together identifying sub-nanomolar IC50 values against KRAS variants (G12D, G12V, G12C, and WT). In cellular assays, ISM6166 suppressed cell growth with single-digit nanomolar IC50 values across cancer cell lines harboring major KRAS mutations or KRAS amplification, including GP2D (KRAS G12D), SW620 (KRAS G12V), NCI-H358 (KRAS G12C), and MKN1 (KRAS WT amplification).

Treatment *in vivo* at 10-30 mg/kg (BID) induced tumor regression in multiple CDX models driven by different KRAS alterations (KRAS G12D/V/C mutations or KRAS amplification), along with dose-dependent pharmacodynamic responses, including changes in ERK phosphorylation and DUSP6 transcription.

ISM6166 demonstrated reasonable solubility and permeability. *In vivo*, it exhibited good plasma clearance and bioavailability across mouse, rat, dog, and monkey. Additionally, mini-Ames and off-target safety panel profiling indicated no potential risk. Collectively, these findings highlight the potential of this novel molecule as a potent pan-KRAS (ON/OFF) inhibitor for the treatment of solid tumors with KRAS alterations.

#0426 Development of heptamethine carbocyanine based small molecule targeting platform for tumor specific drug delivery.

Paul Algate[1], Jeffrey A. Kern[2], Lyle Small[1], Ruizheng Wang[1], Ryan Westberry[1], Margaret Karow[1], Steve LaMond[1]

[1]Lahjavida, Colorado Springs, CO,[2]Medicine, National Jewish Health, Denver, CO

Improved tumor-targeting strategies are needed to enhance a cytotoxic drug's therapeutic efficacy while minimizing systemic toxicity. Antibody-drug conjugates (ADCs) have shown this potential but are limited by a restricted tumor-epitope diversity; Each ADC is designed for a single tumor type, with development, manufacturing, and cold-chain requirements adding complexity and cost. A targeting platform that is inexpensive, modular, and applicable across tumor types could address these gaps. Dye-drug conjugates (DDC) have the potential to overcome these limitations. DDCs are composed of heptamethine carbocyanine (HCC) compounds that selectively interact with Organic Anion-Transporting Polypeptides (OATPs), chemically conjugated to diverse cytotoxic payloads. DDCs target OATPs which are overexpressed across human tumor types and represent a novel class of tumor-selective transporter targets. Additionally, they possess near-infrared (NIR) fluorescence enabling both imaging and therapy delivery making them attractive as a single small molecule delivery framework. Novel HCC analogs were synthesized and characterized as tumor-targeting scaffolds. These compounds exhibited minimal intrinsic cytotoxicity in normal and tumor cell lines. In vitro imaging of tumor cell lines confirmed HCC uptake. In vivo and ex vivo imaging of tumor xenografts following HCC systemic administration confirmed HCC tumor accumulation with minimal accumulation in other organs. Two of the novel HCCs were synthesized with cytotoxic payloads including doxorubicin, SN38 and MMAE as pro-drugs, linked via a cathepsin B cleavable linker. Upon linker cleavage, the released drugs become active. These DDCs were assessed for solubility, thermodynamic stability and plasma stability (mouse, human) identifying promising candidates. Studying candidates further, in tumor cell lines HCC-MMAE was internalized, and cleaved to release MMAE, resulting in cell death. At 72H, IC50 of HCC-MMAE in A549 cells was 92.7±9.6nM, in MCF7 cells 59.3±4.6nM, and SW620 79.6±37.6nM. The IC50 for MMAE alone was 0.49±0.2nM, while HCC alone >1,000nM across all cell lines. In vivo and ex vivo imaging of tumor xenografts following systemic administration confirmed DCC tumor accumulation with minimal accumulation in other organs. In conclusion, novel HCC-based DDCs have been developed as tumor-selective targeting agents. Conjugation of cytotoxic payloads to the HCC scaffold allowed effective delivery of payload, with the potential ability to use compounds previously limited by their systemic toxicity. The HCC platform allows conjugation of diverse payloads, with broad tumor applicability through the OATP target, and is synthetically simple and cost-effective to produce.

#0427 PMR-116, a second-generation RNA polymerase I inhibitor displaying therapeutic efficacy in a broad spectrum of malignancies.

Nadine Hein[1], Rita Ferreira[2], Amee George[2], Katherine Hannan[1], Karagh Loring-White[3], Konstantin Panov[4], Eric Kusnadi[5], Richard Rebello[5], Alisee Huglo[5], Shelley Hedwards[5], Mitchell Lawrence[5], Mustapha Haddach[6], Denis Drygin[6], Ross D. Hannan[3], **Luc Furic**[5]

[1]Cancer Biology and Therapeutics, JCSMR, Acton, ACT, Australia,[2]ANU, Canberra, Australia,[3]ANU, Canberra City, Australia,[4]Queen's University, Belfast, United Kingdom,[5]Peter MacCallum Cancer Centre, Melbourne, Australia,[6]Pimera Inc, San Diego, CA

Ribosome biogenesis (RiBi) is a key driver of cell growth and is strongly elevated in cancers with high MYC activity. First-generation Pol I inhibitor CX-5461 showed clinical benefits but also triggered non-specific DNA damage. PMR-116 was developed to provide selective Pol I inhibition with improved tolerability, minimal off-target induced DNA damage and stronger on-target inhibition of rRNA synthesis.

PMR-116 anti-cancer activity was assessed across >100 cancer cell lines representing 20 major tumour types. It showed broad anti-proliferative activity, with GI50 values from 32-4500 nM and a median of approximately 300 nM. Normal tissue-derived cells were significantly less sensitive, with GI50 values between 6-33 µM. In vivo, PMR-116 significantly reduced tumour burden and improved survival in preclinical cancer models, including Vk*MYC multiple myeloma, CT26 colorectal cancer, MMTV-PyMT breast cancer and MLL-ENL+Nras AML (with and without TP53 mutation).

Given the strong dependence of MYC-driven cancers on elevated RiBi, PMR-116 produced marked responses in MYC-addicted cancer models, consistent with exploiting a core vulnerability in MYC-amplified disease. In the large MURAL cohort of advanced prostate cancer PDX, weekly PMR-116 monotherapy at 300 mg/kg produced complete responses in two models, including a neuroendocrine prostate cancer PDX, a subtype with limited therapeutic options. A targeted 3D culture screen identified synergy between PMR-116 and PARP inhibitors, and between PMR-116 and AR-targeting agents, both of which have clear clinical translation pathways.

In a phase I clinical trial, PMR-116 was well tolerated, demonstrated robust on-target activity producing approximately 50 percent reduction of rRNA synthesis in patient PBMCs within 24 hours. No global DNA damage signalling was detected at active dose levels.

Overall, PMR-116 shows potent anti-cancer activity across a wide range of malignancies, with particular strength in MYC-driven tumours. Its selectivity for Pol I and favourable safety profile support its progression into an MRFF-funded phase II basket trial commencing in 2026.

: Novel Therapeutics and Drug Targets 1
Poster Session

#0431 A new approach methodology (NAM) for specificity testing: ISTAND qualification of the membrane proteome array to evaluate off-target binding of MAb-based therapies.

Diana Norden, Jonathan T. Sullivan, Carmen Navia, **Jonathan Richards**, Alexander Hobby, Rachel Fong, Benjamin Doranz

Integral Molecular, Philadelphia, PA

Background: Scientifically validated New Approach Methodologies (NAMs) provide an opportunity to better predict drug safety in humans while also accelerating drug development and regulatory review. The FDA has established pathways to qualify NAMs as Drug Development Tools (DDTs) through various mechanisms that now include the Innovative Science and Technology Approaches for New Drugs (ISTAND) program.
Methods: We developed the Membrane Proteome Array (MPA) platform for specificity testing of antibody-based therapeutics. The MPA assesses binding interactions across ~6,000 membrane proteins, each individually expressed in their native structural configuration within live or unfixed cells. The screen uses high-throughput flow cytometry, allowing for quantitative and high-sensitivity detection, and any identified targets are validated by titration analysis. The MPA is being qualified as a novel DDT through FDA's ISTAND program.
Results: As part of our DDT qualification, we performed a comparison study of 35 antibody therapeutics evaluated for specificity using both our MPA and conventional tissue cross-reactivity (TCR) studies. We found that 17% of these drugs had an off-target that was not expected based on TCR results. Overall, the MPA and TCR results were consistent for only about half of the molecules tested. In numerous instances, TCR results were inconclusive based on technical variability, nonspecific or cytoplasmic staining, or false-positive staining. Such results highlight the difficulty of using TCR data for deciding actionable next steps. In contrast, off-targets from the MPA are de-risked by statistically quantifying relative affinity and binding levels, localizing binding to extracellular vs. intracellular epitopes, and determining tissue expression patterns in humans to assess the in vivo safety risk. Through the MPA qualification process, we have also quantified the sensitivity and reproducibility of the platform and implemented additional quality control procedures and data analyses.
Conclusions: MPA data is already routinely used in regulatory applications for antibody-based biotherapeutics and may be used to replace or complement other cross-reactivity studies. The MPA is currently in the last stages of review for DDT qualification through FDA's ISTAND program.

#0432 Targeting Brachyury with small molecules: A new therapeutic paradigm for chordoma and neuroendocrine carcinomas.

Gaelle Mercenne, Brian McEllin, Julia Robbins, Lindsay Pino, Gavin Hirst, Alexander Joel Federation

Talus Bio, Seattle, WA

Chordoma is a rare cancer arising from embryonic notochord remnants, most often in the sacrum and cervical spine. Although surgery and radiation are standard treatments, complete removal is frequently not possible and recurrence is common, leaving patients without effective targeted therapies. A defining molecular hallmark of chordoma is the aberrant reactivation of the transcription factor (TF) Brachyury (TBXT), a developmental regulator normally silenced in adult tissues. TBXT functions as a lineage-survival factor, driving tumor initiation and progression and establishing itself as both a diagnostic marker and compelling therapeutic target.However, TFs like TBXT are inherently difficult to drug due to their structural disorder and dependence on chromatin context. To overcome these barriers, we developed TF-Scan, a proteome-wide mass spectrometry platform that directly quantifies TF chromatin occupancy in live cells, enabling functional assessment and therapeutic targeting of TFs that were previously considered undruggable.Using TF-Scan, we discovered TAL61, a first-in-class covalent small-molecule hit that selectively binds TBXT and displaces it from chromatin. We initiated an iterative medicinal chemistry campaign, generating multiple analog series with improved covalent engagement, potency, and drug-like properties. Lead compounds strongly suppressed TBXT-dependent transcriptional programs and showed potent cytotoxicity in TBXT-expressing chordoma cell lines while sparing TBXT-negative controls. In vivo, optimized analogs produced robust tumor growth inhibition in UCH1 xenografts and the CF-365 patient-derived xenograft model, with excellent tolerability and durable pharmacodynamic activity.Transcriptomic analyses of TCGA, cBioPortal, and CRO datasets revealed aberrant TBXT expression in subsets of NECs, including Merkel Cell Carcinoma and Small Cell Lung Cancer. Ongoing work using cancer cell lines and patient-derived organoids is defining TBXT dependency in these diseases, suggesting that TBXT may serve as a broader lineage survival factor.Together, these results establish TF-Scan as a powerful TF drug discovery- platform and demonstrate the feasibility of pharmacologically targeting TBXT. Our covalent inhibitors show potent, selective antitumor activity in chordoma and point to new therapeutic opportunities in neuroendocrine cancers lacking targeted treatments.

#0433 A robust automated workflow for precise oncoprotein quantification to accelerate targeted degradation and oncology research.

Alex M. Strom[1], Quynh Nguyen[1], Qiuyan Ma[2]

[1]Protein, OriGene Technologies, Inc., Rockville, MD,[2]OriGene Technologies, Inc., Rockville, MD

Quantitative and reproducible measurement of oncoproteins is essential for evaluating signaling biology, validating biomarkers, and advancing targeted degradation strategies such as Proteolysis-Targeting Chimeras PROTACs. Traditional Western blotting is widely used but is limited by variable assay performance and poor reproducibility, hindering its ability to support rigorous protein quantification across diverse sample types.[1] Similarly, ELISA detection methods are often not sufficiently sensitive and do not confirm the molecular weight of the detected protein. We developed a fully automated, calibration-based workflow using the Jess™ automated Western system to enable sensitive and absolute quantification of endogenous and overexpressed proteins. KRAS was used as a representative oncogenic target. While historically KRAS has been regarded as an undruggable target, recent advances in the field have demonstrated that PROTAC strategies can effectively degrade this oncogenic protein, increasing the important of precise KRAS quantification tools.[2] A recombinant KRAS standard curve (0.012-1.5 ng/µL) demonstrated excellent linearity ($R^2 > 0.99$), broad dynamic range, and high sensitivity. Precision testing showed robust peak area agreement across capillaries and days, confirming stable performance suitable for quantitative protein profiling. Application of this workflow to HeLa lysates, transiently transfected HEK293 cells, and extracellular vesicle samples enabled reliable detection of both high- and low-abundance KRAS populations. Quantitative assessment of the constitutively active KRAS mutant G12D antibody further highlighted the platform's ability to resolve clinically relevant variants with high specificity and sensitivity.[3] Although demonstrated using KRAS, this automated workflow is broadly applicable to additional oncoproteins, signaling molecules, and degradation substrates. Its integration of automated capillary electrophoresis, defined calibration standards, and digital quantification supports key applications including PROTAC efficacy assessment, variant-specific analysis, and biomarker development. By coupling reproducible assay performance with absolute quantification, this method provides a powerful platform to accelerate oncology research and therapeutic discovery across multiple protein targets.

1. S. C. Taylor, L. K. Rosselli-Murai, B. Crobeddu, I. Plante, A critical path to producing high quality, reproducible data from quantitative western blot experiments. *Scientific Reports*. 12 (2022)

2. T. Kos, D. Saur, Breaking down KRAS: Small-molecule degraders for cancer therapy. *Signal Transduction and Targeted Therapy*. 10 (2025)

3. Y. Tang *et al*., Targeting KRASG12D mutation in non-small cell lung cancer: Molecular mechanisms and therapeutic potential. *Cancer Gene Therapy*. 31, 961-969 (2024)

#0434 Target agnostic phage display for nanobodies that alter immune cell function.

Peter Qian Leung[1], Todd A. Aguilera[2], Eslam A. Elghonaimy[2], Thillai Sekar[3], Mike Whitney[4], Isaac Gonzalez[2]

[1]UTSW, Dallas, TX,[2]University of Texas Southwestern Medical Center, Dallas, TX,[3]Pondicherry University, Puducherry, India,[4]UCSD, San Diego, CA

Introduction: The discovery of novel cancer immunotherapies is currently limited by a reliance on known antigens and screens that prioritize binding affinity over function. To overcome this, we developed INSPIRE-seq, a platform integrating NGS and phage display to unbiasedly select for nanobodies against cell subtypes within the tumor microenvironment (TME). Here, we advance this technology to address a critical unmet need: the direct isolation of nanobodies that functionally modulate immune cell behavior. Our objective is to move beyond simple binding and deploy a strictly target-agnostic strategy to identify therapeutic candidates based solely on their ability to enhance T cell efficacy, without prior knowledge of their molecular targets.

Experimental Procedures: To validate this functional selection strategy, we established an *ex vivo* model using bead-purified naïve CD8 T cells. Cells were activated with αCD3 and αCD28 antibodies in the presence of recombinant PD-L1 to mimic TME inhibitory signaling. Simultaneously, the cells were co-incubated with a library of nanobody-displaying bacteriophage. The top 10% of live T cells expressing the highest levels of the activation marker CD69 were sorted via flow cytometry to capture nanobodies capable of enhancing T cell activation, independent of their binding target. Enrichment dynamics were tracked via Oxford Nanopore sequencing. Individual phage clones were subsequently amplified and re-tested for both binding and functional modulation within the same assay.

New Data: We initiated the screen using a library with confirmed *in vivo* efficacy, verifying that this activity translated to detectable baseline modulation in our *ex vivo* model to ensure the presence of enrichable candidates. From this validated starting point, we performed four rounds of biopanning and sorting for increased CD69 expression. We isolated individual clones that, based on amplicon sequencing, collectively represented 25% of the starting library population. These dominant clones were individually tested for activity. Notably, clone 9-1-12 exhibited significant binding to CD8 T cells compared to controls. Critically, this binding was functionally linked to activation: the specific population of T cells bound by the nanobody displayed a significantly increased frequency of CD69 positivity despite the presence of PD-L1 inhibition. This demonstrates the feasibility of recovering a functional modulator solely through phenotypic selection.

Conclusions: Our findings provide evidence that INSPIRE-seq can select and enrich for nanobodies that alter cell function in a target-agnostic manner. This supports our central hypothesis that phenotypic screening can identify immunomodulators without prior antigen knowledge, offering a novel pipeline to uncover therapeutic candidates that overcome TME immunosuppression.

#0435 Novel anti-CD3 heavy chain-only antibodies for use in T-cell engaging therapeutics.

Noel Pauli, Hannah Watkins, Paul Khalife, Elizabeth Parker, Cameron Henkel, Todd Boland, Hailey Heston, Christin Strong, Jinfu Zhao, Irina Burnina, Michael Brown, Jessica Dawson, Garrett Rappazzo, Beth Sharkey, Morgan Morrill, Michael Battles, Robert Pejchal, Eric Krauland

Adimab, Lebanon, NH

Background: Multispecific T cell-engager (TCEs) antibodies have shown great promise as immunotherapeutic molecules. These therapies redirect T cells to recognize and kill cancer cells through co-engagement of tumor associated antigens and a T cell antigen, often CD3. Despite their clinical efficacy, the molecular complexity of current TCEs poses challenges for drug manufacturability, developability, and achieving desirable pharmacokinetic/pharmacodynamics. Currently, all approved TCE multispecifics rely on αCD3 binders derived from conventional IgG antibodies.Heavy chain-only antibodies (HCAbs) featuring a single-domain (VHH) binding moiety are attractive alternatives to conventional IgGs in immunotherapies. The absence of a light chain in HCAbs notably simplifies multispecific development. To-date, no αCD3 HCAbs with properties comparable to best-in-class clinically approved IgGs have been reported.

Methods: Functional αCD3 HCAbs were discovered by combining llama immunization and a novel yeast-based HCAb discovery technology. Following rounds of yeast-based HCAb selection, T cell stimulating αCD3 HCAbs were identified, humanized, and optimized to exhibit desirable drug profiles. We demonstrated the potency of these lead molecules in two bispecific formats: 1+1 αCD3 X αCD20 and as a VHH-TCR fusion using a TCR specific for the gp100 peptide HLA complex. CD3ε binding was confirmed by x-ray crystallography using one of the lead HCAbs.

Results: This study resulted in a panel of six functional αCD3 TCEs. These molecules predominantly competed with a known CD3 epitope, recognizing the CD3ε subunit of the human T cell receptor complex with weak to strong affinities and robust drug developability profiles. Crystallographic data and subsequent structural modelling show a unique angle of approach for our lead stimulating HCAb suggesting the interaction with the TCR complex is likely limited to only the CD3δε heterodimer, as CD3γε docking is modeled to produce significant steric clashes. The panel displayed a promising functional potency range as multispecifics; with two molecules displaying comparable *in vitro* tumor cell killing efficacy to clinically validated molecules such as the first-in-class TCR-αCD3 fusion TCE, tebentafusp.

Conclusions: We showcase the discovery and engineering of novel αCD3 HCAbs with functional potency comparable to other clinically validated molecules. This panel of highly-developable HCAbs provide new building blocks to expand the design space for TCE multispecifics and enable the next generation of multispecific immunotherapeutics.

#0436 Redox-DNA repair co-targeting with IP-DNQ and rucaparib induces oxidative DNA damage and GSDME-mediated pyroptosis in NQO1-positive tumors.

Soumya Tumbath[1], Hao Zhou[1], Jiangwei Wang[1], Lingxiang Jiang[1], Elin H. Chen[2], Celine Thormann[1], Xiumei Huang[1]

[1]Department of Radiation Oncology, Indiana University School of Medicine, Indianapolis, IN,[2]Benjamin Franklin High School, New Orleans, LA

Cancer remains a leading cause of mortality worldwide, with current therapies often failing to eradicate resistant tumor populations. This highlights the need for strategies that exploit tumor-specific metabolic and DNA repair vulnerabilities. NAD(P)H:quinone oxidoreductase 1 (NQO1), commonly overexpressed in solid tumors, enzymatically activates redox-cycling prodrugs, offering a selective tumor targeting strategy. Isopentyl-deoxynyboquinone (IP-DNQ), a potent NQO1-bioactivatable quinone, undergoes futile redox cycling to generate reactive oxygen species (ROS), induce oxidative DNA damage, and deplete NAD^+/ATP. Given that PARP activation is an early response to DNA damage, we investigated the mechanistic synergy between NQO1-dependent redox cycling and PARP inhibition using IP-DNQ combined with rucaparib, an FDA-approved PARP inhibitor. Rucaparib significantly enhanced IP-DNQ-induced ROS accumulation, DNA strand breaks, and metabolic collapse in an NQO1-dependent manner. This combination triggered caspase-3 activation and gasdermin E (GSDME) cleavage, leading to pyroptotic cell death characterized by LDH release and IL-1β secretion. Both pharmacologic inhibition and genetic knockout of NQO1 abolished these effects, confirming the essential role of IP-DNQ bioactivation. Importantly, the IP-DNQ/rucaparib combination suppressed tumor growth and prolonged survival in orthotopic pancreatic and lung cancer models without causing systemic toxicity. These findings uncover a novel redox-DNA repair co-targeting strategy that amplifies oxidative DNA damage and redirects apoptosis toward immunogenic GSDME-mediated pyroptosis. This approach broadens the therapeutic scope of PARP inhibitors and offers a promising platform for treating NQO1-overexpressing cancers.

#0437 Targeting RNA demethylase ALKBH5 with mefloquine enhances antitumor immunity and reduces osteosarcoma progression and metastasis.

Victoria Chen Mai[1], Daisy Medina[2], Manjeet K. Rao[3]

[1]UT Health Science Center San Antonio, San Antonio, TX,[2]UT Health Science Center at San Antonio, San Antonio, TX,[3]Assistant Professor, Greehey Children's Cancer Research Institute, San Antonio, TX

Background: Osteosarcoma (OS) is the most common form of bone cancer in youth, with a second incidence peak observed in adults over the age of 50. Current OS treatments rely on aggressive chemotherapy and surgery, which remain largely ineffective for patients with metastatic or relapsed disease. Approximately 20% of patients present with metastases at the time of diagnosis, with a five-year survival rate below 30%. This highlights an urgent need for a novel drug to treat OS. Recently, our group identified the RNA demethylase ALKBH5 as a key promoter of OS growth and metastasis. Using high throughput FDA approved drug library, we identified mefloquine as a small-molecule inhibitor of ALKBH5. Importantly, we discovered that mefloquine improves the efficacy of immunotherapy in OS. These findings indicate that mefloquine may serve as an effective therapeutic for treating osteosarcoma patients.

Methods: shRNA and CRISPR-Cas9 based knockout were used to assess the effects of ALKBH5 depletion on osteosarcoma growth and metastasis. Fluorescence-based high-throughput screening (HTS) of FDA-approved and LOPAC compound libraries identified mefloquine as a potential ALKBH5 inhibitor. RNA sequencing was performed to identify genes altered in mefloquine-treated OS cells. In vitro human and murine OS models were used to identify the inhibitory potency of mefloquine. Surface plasmon resonance (SPR) and m6A dot blot assays were used to validate mefloquine’s interaction with ALKBH5. In vivo orthotopic intratibial and tail vein mouse models were used to test the efficacy of mefloquine for reducing OS growth, metastasis, and improving immunotherapy response. Ongoing experiments aim to further elucidate the mechanisms of mefloquine-mediated OS suppression.

Results: Here, we demonstrate that mefloquine is a promising inhibitor of ALKBH5, suppressing OS growth and metastasis, and improving immunotherapy response. Loss of ALKBH5 in vitro and in vivo significantly reduced osteosarcoma cell growth and tumor burden. RNA sequencing revealed that mefloquine treatment led to upregulation of immune-related genes. In vivo mouse models showed reduction of tumor volume and metastatic burden in mice treated with mefloquine.

Conclusion: Our results establish mefloquine as a promising inhibitor of ALKBH5 in osteosarcoma, effectively suppressing tumor growth and metastasis while enhancing antitumor immune responses. As an FDA approved drug for malaria, mefloquine could be repurposed as a safe and effective therapy for OS.

#0438 The multibody drug conjugate (MDC) BD200 mediates anti-tumor activity through a novel dual-targeting mode.

Michael D. Oberst, Dror Luger, Micheal Kebede, Devi Gunasekera, Meital Gadrich, Yonit Ben David, Leah Asulin, Noam Grossman, Reut Fuchs, Hezi Sasson, Yael Diesendruck, Guy Nimrod, Tim Wyant, Ronald Herbst, Yanay Ofran, Inbar Amit

Biolojic Design, Rehovot, Israel

Purpose: The therapeutic efficacy of antibody drug conjugates (ADCs) relies on effective tumor targeting. However, intra-tumor and inter-lesional heterogeneity of target expression limit ADC efficacy. Moreover, treatment with an ADC exerts selective pressure favoring antigen-negative clones, thus enhancing drug resistance. To address this challenge, we introduce the Multibody technology, which allows for specific recognition of multiple tumor associated antigens through a simple symmetrical antibody.
Methods: Multibodies maintain the format of natural, symmetrical IgGs but can adjust their binding to different tumor surface-enriched antigens. This multi-specificity is designed to improve drug efficacy, reduce resistance and widen the responding patient population. BD200 is a multibody drug conjugate (MDC) whose fragment variable (Fv) domain is designed to bind alternatively to either TROP2 or Nectin-4 with high specificity. In its symmetrical human IgG1 format, two such identical Fv domains create an “OR" gate enabling the MDCs to bind bivalently to cells that express target A, cells that express target B or cells that express both A and B. BD200 incorporates a topoisomerase 1 inhibitor-based linker-payload. We tested BD200’s internalization and cell-killing on a wide array of tumor types, each expressing one or both antigens. In a series of in-vivo mouse studies using human cell line-derived xenograft (CDX) and patient-derived xenograft (PDX) models, we compared BD200’s efficacy to that of several approved anti-TROP-2 and anti-Nectin-4 ADCs. In these studies, we also tested BD200 in tumors that are refractory to approved ADCs. Finally, we assessed PK in NHPs to cross-compare with data from approved ADCs.
Results: BD200 demonstrated rapid internalization and strong cytotoxic potency across a wide range of tumor cells. While each approved monospecific ADC performed well on some tumor cell lines, BD200 was comparable or superior to approved ADC comparators with all cell lines tested in vitro. Assessing in vivo anti-tumor efficacy, BD200 showed deep and durable anti-tumor responses including in models refractory to approved ADCs. BD200 showed similar or superior serum stability and PK properties compared to approved ADCs.
Conclusion: The preclinical data suggest that a bivalent MDC addresses the challenge of tumor heterogeneity, while retaining the developability and the functional traits of a natural, simple, symmetrical human IgG. This may allow BD200 to drive deeper responses in more tumor types and more patients than existing ADCs.

#0439 Inhibition of extracellular matrix remodeling and metastatic activity by dichloroacetate and chloroquine in the presence of arsenite in 4nqo-induced oral squamous cell carcinoma.

Mounia Benbelkacem[1], Nabila Moulai[2], Eimen Kais Kadri[1], Lina Stamboul[1], Henni Chader[3], Wahiba Ouhaioune[2], Mehdi Bourouba[1]

[1]Laboratory of Cellular and Molecular Biology (LBCM), Team Biotechnology and System Biology, Faculty of Biological Sciences, University of Sciences and Technology Houari Boumediene (USTHB), Bab-Ezzouar, Algiers, Algeria,[2]Laboratory of Anatomopathology, Frantz Fanon Hospital, Blida: University of Blida, Faculty of Medicine, Blida, Algeria,[3]Laboratory of Pharmaco-toxicology, National Agency of Pharmaceutical Products, Faculty of Pharmacy, University of Algiers 1, Algiers, Algeria

Introduction: Oral squamous cell carcinoma (OSCC) is characterized by extracellular matrix (ECM) remodeling associated to a pro-inflammatory and protumoral metabolic activity that promote invasion and metastatic progression. This study assessed the effect of a triple therapy combining sodium arsenite (NaAsO2), chloroquine (CQ), and dichloroacetate (DCA) on inflammatory signaling and ECM remodeling in a 4-nitroquinoline-1-oxide (4NQO)-induced tongue OSCC mouse model.
Methods: Eight-week-old female BALB/c mice were exposed to chemical induction with the carcinogen (100 µg/ml) or treated with placebo (water control) for 16 weeks, then observed for up to 16 additional weeks. At 32 weeks post-treatment, mice were sacrificed, and their tongues were removed. The oral tumor tissues were then cultured for 24 hours in the presence of NaAsO2, CQ, and DCA. Tumor tissues and explants were analyzed for TNF-α, nitric oxide (NO), matrix metalloproteinase-9 (MMP-9), and collagen integrity.
Results: 4NQO carcinogenic activity on animal tongues led to a significant development of dysplasia and invasive SCC cases. OSCC explants culture showed in comparison to healthy tissues elevated levels of nitric oxide production, associated with increased expression of the pro-tumoral TNF-α, MMP-9 expression and collagen fiber disorganization were increased in such conditions. Surprisingly whereas NaAsO2 alone amplified inflammatory mediators, its combination with CQ and DCA significantly decreased NO and TNF-α levels. Strikingly this effect led to a significant downregulation of MMP-9, and preserved Type IV collagen architecture. Masson's trichrome staining revealed a restoration of dense, parallel collagen fibers resembling those found in an ECM architecture observed in low-grade dysplasic tongues in comparison with OSCC. These findings demonstrate that TNF-α/NO-driven MMP-9 activation is a central mechanism of ECM degradation in OSCC, and that a simultaneous modulation of aerobic glycolysis and autophagy may disrupt the metastatic signaling axis involved in extracellular matrix remodeling and metastatic activity in 4nqo-induced oral squamous cell carcinoma.
Conclusion: Altogether, our findings show that our combined treatment was able to reprogram the inflammatory process of tumor progression by inhibiting the molecular processes involved in extracellular matrix remodeling and invasion. This combined treatment represents a novel avenue for metabolic-inflammation-targeting strategy for OSCC in particular in view of the limited treatment options and the risk of chemoresistance.

#0440 Targeting oncogenic TBRI signaling inhibits androgen-independent prostate cancer growth and metastasis.

Per Flodbring Larsson[1], Alexej Schmidt[1], Yabing Mu[1], Guangxiang Zang[1], Jie Song[1], Vishnupriya Gajavilli[2], Junting Tao[2], Olena Rahkimova[1], Madelene Ericsson[1], Karthik Aripaka[1], Sofia Halin Bergstroem[1], Wei Yuan[3], Denisa Bogdan[4], Aaron Zhang[5], Jon Welti[5], Anders Bergh[1], Johann de Bono[6], Carl-Henrik Heldin[7], **Marene Landstroem**[1]

[1]Umea University, Umea, Sweden,[2]Department of Medical Biosciences, Umea University, Umea, Sweden,[3]The Institute of Cancer Research, London, London, United Kingdom,[4]The Institute of Cancer Research, Sutton, Sutton,[5]Institute of Cancer Research, London, United Kingdom,[6]Institute for Cancer Research, London, United Kingdom,[7]Uppsala University, Uppsala, Sweden

Metastatic castration-resistant prostate cancer (mCRPC) remains the primary cause of prostate cancer-related mortality. Despite available treatments, the molecular mechanisms underlying tumor invasion and metastasis are not fully understood, highlighting the need for novel therapeutic strategies. In this study, we developed fully human monoclonal antibodies (mAbs) that prevent the proteolytic cleavage of the transforming growth factor-beta (TGFβ) type I receptor (TβRI) by steric hindrance. This cleavage, mediated by the metalloprotease ADAM17 (a disintegrin and metalloprotease domain 17), also known as TACE, results in the generation of a soluble intracellular domain (TβRI-ICD) that translocates to the nucleus of castration-resistant prostate cancer (CRPC) cells and promotes epithelial-to-mesenchymal transition (EMT), invasion, and metastasis. High levels of *TGFBR1* were found to correlate with poor survival in two independent clinical cohorts of patients with mCRPC, and a strong positive association between *TGFBR1* and *ADAM17* expression was observed. In a preclinical human mCRPC mouse model, treatment with our therapeutic mAbs effectively prevented nuclear accumulation of TβRI-ICD, inhibited EMT, and suppressed tumor growth, invasion, and metastasis. Notably, the therapeutic effect was comparable to that of docetaxel, a current standard-of-care chemotherapy, and without noticeable side effects. These findings suggest that targeting TβRI cleavage using specific mAbs offers a novel precision medicine approach for mCRPC. By selectively blocking the pro-metastatic activity of TβRI-ICD without disrupting physiological TGFβ signaling, this strategy may provide a safer and more effective alternative to existing therapies for advanced prostate cancer.

#0441 Breaking the KRAS inhibitor induced resistance-wall: Targeting KRAS-SOS1 to disarm hypoxic survival.

Jooyun Byun[1], Heesun Moon[2], Jongmin Hong[3], Soye Jeon[3], Jaeyul Choi[3], Seung Hyun Jung[4], Yongjae Park[1], YoungGil Ahn[5], In Young Choi[6]

[1]Hanmi Pharmaceutical Co., Ltd., Seoul, Korea, Republic of,[2]Hanmi Pharmaceutical Co., Ltd., Hwaseong-si,[3]Hanmi Pharmaceutical, Hwaseung, Korea, Republic of,[4]Hanmi Pharmaceutical Co., Ltd., Seoul,[5]Hanmi Pharmaceutical Co., Ltd., Hwaseong-si, Korea, Republic of,[6]Hanmi Pharmaceuticals, Seoul, Korea, Republic of

Significant progress has been made in targeting KRAS, however, KRAS G12C inhibitors like sotorasib and adagrasib have shown only modest efficacy with ORR of 28-43% and PFS of around 6 months, highlighting unmet needs for overcoming the resistance compared to EGFR inhibitors like osimertinib with ORR of 77% and PFS of 18.9 months. Acquired resistance involves $KRAS^{G12C}$ amplifications, activating KRAS/NRAS mutations, and bypass activation of RTK, PI3K-AKT, YAP/TAZ-TEAD or JAK-STAT3 pathway. KRAS inhibitors also disrupt ERK-driven negative feedback, causing ERK reactivation and adaptive resistance. To address these limitations, vertical inhibition across the RTK-RAS-MAPK axis has gained attention[1)]. Here, to investigate mechanisms underlying acquired resistance and identify effective combination strategies, we established KRAS G12C inhibitor-resistant clones from NCI-H358 cells by performing ENU mutagenesis followed by single-cell selection, and then gradually exposing the selected clones to increasing concentrations of sotorasib and adagrasib for 6-9 months. In both sotorasib- and adagrasib-resistant clones, p-ERK was suppressed while elevation of p-AKT and YAP expression with enhanced nuclear localization was observed compared with parental cells. Surprisingly, SOS1 expression was significantly elevated over 3-fold in both sotorasib- and adagrasib-resistant clones without change in SOS2 levels, which is known to play a compensatory role, indicating that SOS1 co-inhibition is critical for overcoming KRAS inhibitor resistance. Our SOS1-panKRAS modulator, HM101207 exhibited strong synergy with KRAS G12C, RAS(ON) or MAPK pathway inhibitors in KRAS G12C-mutant NCI-H2122 and SNU-1411 cells. In NCI-H1373 and NCI-H2122 xenograft models, oral administration of HM101207 at 100 mg/kg produced a marked enhancement of antitumor activity when combined with adagrasib at low dose 20 mg/kg and high dose 100 mg/kg, or with RMC-6236 25 mg/kg. Notably, HM101207 restored tumor regression even after tumors relapsed under adagrasib or RMC-6236 monotherapy. To explore how SOS1 inhibitor modulates KRAS inhibitor-induced resistance, we performed RNA-seq on mouse xenograft tumors derived from KYSE-410 cell harboring the KRAS G12C mutation after HM101207 treatment. Differential expression analysis revealed that HM101207 significantly inhibited the expression of hallmark hypoxia genes including ALDOC, ENO2, HK2, MKNK2, PFKFB3, PGK1, SERPINE1, SLC2A1, VEGFA. Hypoxia is associated with the drug-tolerant persister state and eventually leads to drug-resistance. Therefore, HM101207 can overcome KRAS inhibitor resistance by strongly suppressing both MAPK and hypoxic pathways. As a combination therapy, it enables more durable pathway inhibition and enhanced antitumor efficacy. GLP toxicology studies are ongoing to support IND submission.

#0442 Crippling cancer's energy and escape: NAMPT and BCL2 as dual targets in T-ALL.

John Robert Sanchez[1], Daisy Diaz-Rohena[1], Valerio Ciaurro[1], Min Wu[2], Francis Roushar[2], Dennise A. De Jesus-Diaz[2], Gregory Crimmins[2], Pratibha Sharma[3], Vinay Puduvalli[3], Francisco Vega[4], Palaniraja Thandapani[1], Deepa Sampath[1]

[1]Hematopoietic Biology and Malignancy, UT MD Anderson Cancer Center, Houston, TX,[2]Remedy Plan Therapeutics, Gaithersburg, MD,[3]Neuro-Oncology, UT MD Anderson Cancer Center, Houston, TX,[4]Hematopathology, UT MD Anderson Cancer Center, Houston, TX

T-cell acute lymphoblastic leukemia (T-ALL) is a highly aggressive hematologic malignancy with limited targeted therapies. While chemotherapy induces remission, relapse remains a major challenge, with long-term event-free survival of only ~30%. Transcriptomic profiling of patient samples (GSE33469, GSE33470) revealed that T-ALL exhibits elevated oxidative phosphorylation (OXPHOS) activity and upregulation of NAMPT, the rate-limiting enzyme of NAD^+ salvage pathway. The salvage pathway is the main pathway utilized by eukaryotic cells to produce NAD+, a critical energy currency used for biological processes such as glycolysis, oxidative phosphorylation, and the DNA damage response. Previous targeting of NAMPT was unsuccessful because complete inhibition of NAMPT was associated with unacceptable toxicities. Here, we evaluate RPT1G, a novel hyperbolic NAMPT inhibitor designed to avoid toxicities associated with complete inhibition, as a therapeutic candidate for relapsed/refractory (R/R) T-ALL. RPT1G eliminates NAD+ in cancer cells while allowing NAD+ production in healthy tissues. This was linked to cytotoxicity in T-ALL whereas toxicity in normal PBMCs was mitigated sparing these cells. We hypothesized that hyperbolic inhibition of NAMPT with RPT1G would selectively impair T-ALL cell metabolism while sparing normal cells, and that combining RPT1G with agents targeting compensatory survival pathways could enhance therapeutic efficacy. RPT1G was evaluated in a Phase 1 healthy volunteer clinical study and showed a favorable safety and tolerability profile (NCT06667765). In T-ALL, RPT1G rapidly depleted intracellular NAD^+/NADH and ATP, with Seahorse assays confirming suppression of mitochondrial energy pathways such as glycolysis and OXPHOS compared to vehicle controls. Further, a CRISPR loss-of-function screen identified the antiapoptotic protein BCL2 as a synthetic lethal partner with RPT1G. Consistently, combining RPT1G with venetoclax, a clinically available BCL2 inhibitor, produced enhanced cytotoxicity across T-ALL cell lines and significantly enhanced ATP depletion compared to single agents. BH3 profiling, a functional assay used to determine BCL2 family dependencies, was used on several patient-derived xenograft (PDX) models. Using different concentrations of BH3 mimetics (BIM, BAD, MS1, and XXA1 0.01uM - 100uM) we demonstrated modest BCL2 dependency in these models, further supporting this strategy. In vivo, the RPT1G-venetoclax combination significantly extended survival in PDX-bearing mice compared to vehicle or monotherapy groups. These findings establish NAMPT inhibition with RPT1G plus BCL2 blockade with venetoclax as a promising therapeutic approach for R/R T-ALL, warranting further translational investigation.

#0443 LMTK2: A novel driver of endocrine resistance in ERα+ breast cancer.

Anna Detry[1], Sofia Marigliano[1], Jenna Heinen[1], Adam Bass[1], Calley Jones[1], Rajeev Muthyala[1], Matthew Goetz[2], John Hawse[1]

[1]Biochemistry and Molecular Biology, Mayo Clinic, Rochester, MN,[2]Oncology, Mayo Clinic, Rochester, MN

Breast cancer is the most common female malignancy in the U.S. and the leading cause of cancer-related deaths in women worldwide. Nearly 80% of breast tumors express estrogen receptor alpha (ERα) which drives tumor progression. While endocrine therapies and CDK4/6 inhibitors have increased overall survival, many patients experience recurrence of metastatic disease that is largely refractory to additional lines of endocrine therapy. Metastatic disease remains incurable, highlighting the need for alternative treatment approaches. Through a genome-wide CRISPR knockout screen, we identified Lemur Tail Kinase 2 (LMTK2) as the top hit exhibiting synthetic lethality in the presence of the endocrine therapy, endoxifen, in both endocrine-sensitive and -resistant cell line models. Using publicly available patient tumor databases we identified *LMTK2* copy number gain/amplification in 67% of ERα+ human metastatic breast tumors, while only 1% of primary tumors harbored these genomic alterations. Elevated LMTK2 expression in early-stage primary breast tumors was associated with worse recurrence-free survival and overall survival. We discovered that LMTK2 mRNA and protein levels were substantially elevated in nearly all cell-line and patient-derived models of endocrine and CDK4/6i resistance. Utilizing siRNAs and dox-inducible shRNA expressing cell lines, we found that knockdown of LMTK2 enhanced the efficacy of multiple endocrine therapies in treatment naïve models and resensitized resistant models to their respective treatment. LMTK2 overexpression was found to be sufficient for conferring resistance to all standard of care therapies tested including endocrine agents, CDK4/6i, and PI3K inhibitors. RNAseq and global proteomics of LMTK2 overexpressing and knockout models revealed the PI3K/AKT pathway and estrogen signaling as highly regulated pathways by LMTK2. Confirmatory western blot studies demonstrated that LMTK2 overexpression results in dramatic increases in AKT and ERα phosphorylation and activity, while knockout of LMTK2 diminishes these effects. Attempts to completely ablate LMTK2 in endocrine/CDK4/6i-resistant models via CRISPR were not successful, and continuous siRNA or shRNA-mediated knockdown was lethal in resistant cell lines, confirming its essentiality in this setting. In summary we have uncovered LMTK2 as a novel mediator of endocrine/CDK4/6i resistance that is mechanistically linked to the PI3K/AKT pathway among others. Genetic manipulation of LMTK2 has validated it as an ideal therapeutic target for both advanced and newly diagnosed forms of ERα+ breast cancer.

#0445 Evaluation of HERV-K as an unusual cancer therapeutic target.

Monica Gordon[1], James H. Torpey[2], Andy D. Martin[2], Benjamin R. Miller[2], Marica Speranza[3], Kenneth W. Hance[4]

[1]Oncology ETCT BU, GlaxoSmithKline plc, Stevenage, United Kingdom,[2]GlaxoSmithKline plc, Stevenage, United Kingdom,[3]Oncology ETCT BU, Glaxosmithkline, Boston, MA,[4]GlaxoSmithKline, Malvern, PA

Human endogenous retroviruses (HERVs) are abundant genomic elements, transcriptionally repressed under normal physiological conditions. However, epigenetic alterations during disease reactivate HERV expression. HERV-K, specifically, has been identified as prevalent in numerous tumor types, including prostate, lung, breast, colon, and ovarian cancers and its presence correlates with tumor progression and protumoral signalling. In addition, HERV-K's immunosuppressive role in the placenta, where it is usually expressed, points to a potential similar function within the tumor microenvironment, making it an attractive therapeutic target. We have comprehensively evaluated HERV-K as a potential target for T-cell Engagers (TCEs) and Antibody-Drug Conjugates (ADCs). This evaluation has been limited by the availability of tool antibodies. Employing flow cytometry and immunohistochemistry (IHC), HERV-K expression on the tumor cell surface was consistently low and unstable, often lost upon enzymatic cell detachment, indicating susceptibility to proteolytic cleavage. Receptor quantification on HERV-K+ tumor cell lines varied from 0-25,000 receptors per cell. IHC results confirmed low membranous staining across various tumor types, with a significant proportion of the protein detected in the cytoplasm, and thus, not available for antibody engagement. In vitro functional evaluation was performed by generating HERV-K tool TCEs and ADCs. While HERV-K TCEs demonstrated moderate and specific tumor cytotoxicity, HERV-K tool ADCs did not elicit HERV-K-dependent cytotoxic effects. In conclusion, while HERV-K presents an intriguing opportunity due to its tumor-selective expression, its inconsistent and labile surface presentation poses considerable challenges. Our findings suggest that HERV-K may be a viable target for TCE-based therapies, but less so for ADCs, primarily due to insufficient receptor density. Future efforts necessitate the development of high-quality specific antibodies to fully harness HERV-K's therapeutic potential in cancer. Note: Human biological samples were sourced ethically, and their research use was in accord with the terms of the informed consents. IHC experiments were done by DLS.

#0446 Pre-targeting with click chemistry facilitates selective MMAE activation in CEACAM5+ tumors: A first-in-class approach to enhance clinical benefit in targeted therapy.

Sangeetha Srinivasan, Masa Alečković, George Coricor, Stefanie Wagner, Jesse M. McFarland, Nathan A. Yee, Tri-Hung Nguyen, Michael Zacharian, Travis L. Biechele, Jose M. Mejia Oneto

Shasqi, Inc., San Francisco, CA

Targeted therapies such as antibody-drug conjugates (ADCs) have transformed the delivery of cytotoxic payloads to tumors, yet their clinical efficacy is often hampered by off-target toxicities. These toxicities arise when the antigen-binding component undergoes systemic catabolic elimination that leads to premature release of the cytotoxic payload in healthy tissues. A pre-targeting approach which separates the targeting binder from the cytotoxic payload and enables them to unite only at the tumor site, offers a promising solution. In this paradigm, the binder is allowed to concentrate at the tumor but clear systemically before the protodrug is administered, It ensures that the payload is activated predominantly where the binder has accumulated—at the tumor—thereby reducing off-target toxicity and increasing the therapeutic index. We present preclinical data on Shasqi's Click Activated Protodrugs Against Cancer (CAPAC®), a click chemistry-based pre-targeting technology that powers tumor-directed in vivo payload activation. The therapeutic candidate consists of a CEACAM5-targeted, clickable small format antibody binder and a chemically attenuated, clickable protodrug of monomethyl auristatin E (MMAE). Upon administration, the binder accumulates at the tumor, and a subsequent protodrug dose 'clicks' specifically with the binder, restoring cytotoxic activity. The CEACAM5 binder showed high affinity (KD 0.046 nM) and binding potency (EC50 3.06 nM) with minimal internalization while retaining its ability to activate protodrugs. The MMAE protodrug was attenuated ~700-fold in vitro and cleared rapidly in vivo (thalf, fast = 6 min, thalf, slow =19 min), minimizing systemic exposure. In multiple CEACAM5+ xenograft models, CAPAC enabled superior tumor control compared to a cognate ADC, including complete responses in highly sensitive tumors (pancreatic and lung) and durable stasis in minimally sensitive tumors (gastric). The treatment also induced marked tumor regression in large mouse tumors. It was well tolerated in naïve rodents. This first-in-class CEACAM5-directed pre-targeting strategy addresses key limitations of conventional targeted therapies by leveraging in vivo click chemistry to selectively concentrate cytotoxic payloads at the tumor. It illustrates robust anti-tumor efficacy in multiple tumor models, including large tumors, more representative of the disease in humans, and a favorable tolerability profile. By decoupling the targeting from the payload delivery, pre-targeting with CAPAC minimizes off-target toxicity, enables higher dosing and has the potential to enhance clinical benefit.

#0447 A M2-like tumor-associated macrophage-targeted nanoparticulate TLR7/8 agonist, UI-102, reprograms its phenotypes to induce potent anti-tumor immunity.

Yasuhiro Nagai, Ayaka Matsumoto, Nami Mizoguchi, Mina Tsukamoto, Junki Tashiro, Tadashi Inoue, Takatoshi Soga, Naozumi Harada

United Immunity Co., Ltd., Kobe, Japan

Background: Tumor-associated macrophages (TAMs) are a major component of the tumor microenvironment (TME) and exhibit functionally distinct phenotypes: anti-tumoral M1 and pro-tumoral M2 TAMs. The predominance of M2-like TAMs promotes tumor growth, angiogenesis, and immunosuppression, making them a promising target for cancer immunotherapy. M2-like TAMs frequently express the C-type lectin DC-SIGN/CD209, and we discovered that nanoparticles composed of pullulan polysaccharide are preferentially engulfed by DC-SIGN-expressing M2 macrophages. Leveraging this property, we developed UI-102, a novel nanoparticulate TLR7/8 agonist using pullulan nanoparticles as an M2 TAM-targeted drug delivery system. This study aimed to evaluate the anti-tumor efficacy and mechanism of action of UI-102, focusing on its ability to reprogram TAM phenotypes and activate anti-tumor immunity.
Methods: The anti-tumor activity of UI-102 was assessed in multiple murine syngeneic subcutaneous tumor models. Mechanistic studies included analysis of TAM phenotypic shifts and activation of the anti-tumor immune cascade. Biodistribution and TAM accumulation were examined in an orthotopic mouse model, comparing UI-102 with resiquimod sulfate and the naked TLR7/8 agonist used in the UI-102 formulation.
Results: UI-102 exhibited broad and potent anti-tumor activity across diverse cancer models, correlating with the degree of myeloid/macrophage infiltration in the TME. Despite a short plasma half-life (T1/2), UI-102 rapidly and selectively accumulated in TAMs in the orthotopic model. This targeted delivery induced a robust phenotypic switch from immunosuppressive TAMs to an M1-like state, triggering downstream anti-tumor immune cascades. These changes were associated with increased infiltration of T cells and NK cells and the induction of tumor antigen-specific CD8+ T cells. The anti-tumor effects of UI-102 were significantly superior to those of control agents, including resiquimod sulfate and the naked TLR7/8 agonist.
Conclusion: UI-102 effectively targets and reprograms immunosuppressive TAMs to an M1-like phenotype, thereby unleashing a strong anti-tumor immune response. This unique mechanism positions UI-102 as a promising novel immunotherapeutic agent for a wide range of solid tumors. A first-in-human clinical trial of UI-102 in solid tumors is planned for initiation in Q1 2026.

#0448 Intranodal chemokine therapy targeting the sentinel lymph node in head and neck squamous cell carcinoma.

Anais Aurelia Zourelidis[1], Jonathan Gunn[2], Tomoya Kurokawa[1], Sayuri Miyauchi[1], Kelsey Decker[1], Peter Vo[1], Pardis Mohammadzadeh[1], Jason Wu[2], Ester J. Kwon[2], Joseph A. Califano[1]

[1]Moores Cancer Center, University of California San Diego, La Jolla, CA,[2]Shu Chien-Gene Lay Department of Bioengineering, University of California San Diego, La Jolla, CA

Emerging evidence highlights the potential of lymphatic-sparing strategies in head and neck squamous cell carcinoma (HNSCC), as well as the sentinel lymph node (SLN) as a critical immunological niche [1-3]. Within this context, CCR7$^+$ dendritic cells (DCs) have been identified as an essential subpopulation for the response to immunoradiotherapy [4]. Here, we investigated the therapeutic effect of intranodal CCR7 agonists CCL19/21 into the SLN using a sustained-release fibrin gel-conjugate system in the syngeneic, orthotopic, partially programmed death-1 inhibitor (PD-1i) sensitive 4MOSC1 model of HNSCC [5], aiming to enhance DC function along the tumor-SLN axis. C57Bl/6 mice were injected with 4MOSC1 cells in the buccal space and underwent SLN mapping and injection of CCL19/21 conjugated (con.) to fibrinogen intranodal (i.n.), CCL19/21 unconjugated (uncon.) to fibrinogen i.n., PD-1i intraperitoneal (i.p.), CCL19/21 con. to fibrinogen i.n. + PD-1i i.p., or sham surgery following 6 days after tumor implantation. Animals were monitored for tumor volume and survival. Primary tumors were assayed by flow cytometry. Intranodal con. CCL19/21 led to a significantly reduced tumor growth (p= <0,0001 vs. sham) and complete response (CR) rate of 60%, whereas uncon. CCL19/21 i.n. (p=0,3354 vs. sham) and sham groups showed no CR. Combination of con. CCL19/21 + PD-1i significantly improved overall survival with 80% survival by day 34, compared to 60% for con. CCL19/21 i.n., and 0% for uncon. CCL19/21 i.n. and controls. Flow cytometric analysis 48 h following treatment shows enhanced DCs and enhanced activated DCs in tumors in con. CCL19/21 treated mice. Intranodal delivery of CCR7 agonists CCL19/21 significantly enhances DCs and activated DCs in tumors, reduces tumor growth and prolongs survival in the HNSCC 4MOSC1 mouse model.

1. Delclaux I et al. 2024;10(1):28-37.2. Saddawi-Konefka R et al. 2022;13(1):4298.3. Cochran AJ et al. 2006;6(9):659-670.4. Saddawi-Konefka R et al. 2025;16(1):6578.5. Wang Z et al. 2019;10(1):5546.

#0449 Albumin-based DLL3-targeted nano-immunoconjugates of SN38 preserve potency and demonstrate high-affinity DLL3 binding in small cell lung cancer.

Mohamed Shanshal[1], Lin Yang[2], Liyi Geng[3], Wendy Nevala[3], Aaron S. Mansfield[4], Bharath Wootla[5], Konstantinos Leventakos[1], Kyle Korshavn[1], Svetomir N. Markovic[3]

[1]Mayo Clinic Cancer Center Minnesota, Rochester, MN,[2]Research Associate, Dept. of Lab. Med. and Pathology, Mayo Clinic College of Medicine, Rochester, MN,[3]Mayo Clinic, Rochester, MN,[4]Mayo Clinic College of Medicine and Science, Rochester, MN,[5]Mayo Clinic Business Development, Mayo Clinic Cancer Center Minnesota, Rochester, MN

Background: Small cell lung cancer (SCLC) remains an aggressive malignancy with limited treatment options and a 5-year survival rate under 10%. Delta-like ligand 3 (DLL3), expressed in >85% of SCLC but absent from normal tissue, represents an attractive therapeutic target. Existing DLL3-directed antibody-drug conjugates suffer from poor payload stability and limited tumor penetration. To overcome these limitations, we engineered a DLL3-targeted nano-immunoconjugate (NIC) of SN38, the active metabolite of irinotecan, using an albumin-based nanoscaffold.

Methods: SN38 was encapsulated in a human serum albumin (HSA) matrix and non-covalently coated with a recombinant anti-DLL3 monoclonal antibody to yield DLL3-SN38-NIC. Stable conjugation was confirmed by HSA-IgG interactions and zeta-potential shift. Binding kinetics were evaluated using Biacore surface plasmon resonance (SPR) and Octet bio-layer interferometry (BLI) employing AHC biosensors to determine DLL3-antibody affinity and specificity. Cytotoxicity was assessed using IncuCyte live-cell imaging across five SCLC cell lines (DMS454, SHP77, NCI-H82, NCI-H889, and NCI-H211) with varying DLL3 expression.

Results: DLL3-SN38-NIC retained high-affinity DLL3 binding (KD ≈ 3×10^{-10} M) and demonstrated potent cytotoxicity in SCLC cell lines. NIC formation did not reduce cytotoxic activity compared with free SN38, confirming preserved potency. Cytotoxicity trends were consistent across lines with variable DLL3 expression, and DLL3 antibody alone exhibited negligible cytotoxicity. These findings confirm that nano-immunoconjugate formation maintains drug activity and DLL3 binding; additional in-vivo studies are underway to evaluate pharmacokinetics and tumor selectivity.

Conclusions: Albumin-based DLL3-SN38-NICs represent a novel nano-oncologic platform that preserves SN38 potency and achieves high-affinity DLL3 engagement. Ongoing studies will assess in-vivo selectivity, biodistribution, and therapeutic potential in DLL3-positive SCLC and other neuroendocrine malignancies.

Keywords: DLL3, nano-immunoconjugate, SN38, albumin nanocarrier, small cell lung cancer

#0450 JZY-2233: An antigen-targeted CBP/p300 degrader-antibody conjugate for advanced prostate cancer therapy.

Mi Wang[1], Jianzhang Yang[1], Brandon Bordeau[2], Shicheng Jin[1], Yu Wang[1], Shaomeng Wang[1]

[1]Department of Internal Medicine, University of Michigan, Ann Arbor, MI,[2]Department of Pharmaceutical Sciences, University of Michigan, Ann Arbor, MI

Background: CBP/p300 are essential transcriptional coactivators of the androgen receptor and play a critical role in prostate cancer pathogenesis. Small-molecule CBP/p300 degraders have demonstrated potent efficacy against prostate cancer but are limited by toxicity, impeding clinical translation.
Methods:To enhance tumor specificity and minimize systemic toxicity, we developed a Degrader-Antibody Conjugate (DAC) by linking a highly potent CBP/p300 degrader to a prostate-specific membrane antigen (PSMA) antibody, generating JZY-2233. In vitro antiproliferative activities were assessed using VCaP and LNCaP prostate cancer cell lines. In vivo efficacy, pharmacodynamics, and toxicity were evaluated in a LNCaP xenograft mouse model.
Results: JZY-2233 induced robust growth inhibition in VCaP and LNCaP cells, with picomolar IC50 values. In vivo, treatment with JZY-2233 led to sustained CBP/p300 degradation and suppression of c-Myc and PSA in tumor tissues, with effects persisting up to 168 hours post-dose. A single administration at 10 mg/kg resulted in complete tumor suppression for over 90 days in the LNCaP model, significantly exceeding the effect of the unconjugated parent degrader. Importantly, JZY-2233 markedly reduced systemic toxicity.
Conclusions: JZY-2233 is a highly potent, antigen-targeted CBP/p300-PSMA DAC, offering prolonged tumor suppression and reduced toxicity in models of advanced prostate cancer. This approach provides a strong rationale for further evaluation in clinical studies and may be adapted for targeting additional tumor antigens across diverse cancers.

#0451 Investigating SIX1 as a driver and target for a first in-class EMT degrader in head-and-neck squamous cell carcinoma.

Vic Scharfenberger, Asad Faili, Lucia Zoe Miehe, Ellen Weber, Samaneh Heydarzadeh, Reinhard Buettner, Tristan Lerbs

Pathology, University Hospital of Cologne, Cologne, Germany

Prognosis for head-and-neck squamous cell carcinoma (HNSCC) remains poor in advanced stages, and patients suffer from severe treatment-associated adverse effects. Here, we have preliminarily investigated whether the embryonic transcription factor SIX1 drives HNSCC and could serve as a target for a first-in-class EMT degrader. While SIX1 is required during embryonic development, it is no longer or only weakly expressed in adult tissue. However, many cancers show a reactivation of SIX1, leading to various pro-tumorigenic effects such as an increase in proliferation and an induction of epithelial-mesenchymal transition (EMT). This makes SIX1, particularly combined with its absent or low expression in normal tissue, a potentially therapeutic target. For this purpose, we developed a SIX1-specific PROTAC (ELX19) through a CRO. In this project, we have applied sequential immunofluorescence for the analysis of patient tissue, and in vitro assays to test the efficiency of the SIX1 degradation through ELX19 and detect associated phenotypic effects. The 36-marker immunofluorescence panel confirmed an increased SIX1 expression in cancer tissue and showed a correlation between SIX1 and an immunosuppressive immune infiltrate, highlighting potential mechanistic links between SIX1 and HNSC progression. Regarding the PROTAC, ELX19 led to an efficient SIX1 degradation in the nanomolar and low micromolar range (depending on the cell line) and induced therapeutically desirable effects, such as an increase in apoptosis under cisplatin. In conclusion, these preliminary results indicate the potential of SIX1 as a therapeutic option in HNSCC - an option that patients urgently need.

#0452 Therapeutic potential of AURKA inhibition in ER+ inflammatory breast cancer.

Tanu Sharma[1], Azadeh Nasrazadani[2], Ma Wencai[3], Jennifer Chen[4], Megumi Kai[2], Bora Lim[2], Michael Lewis[5], Lacey Dobrolecki[5], The MDACC IBC Team, Nikita Kotlov[6], Oleg Baranov[6], Disha Malani[6], Daria Goncharova[6], Anastasiya Evdokimova[6], Francesca Paradiso[6], Michael Hensley[6], Rachel Layman[2], Wendy Woodward[1]

[1]Breast Rad Onc - Research, UT MD Anderson Cancer Center, Houston, TX,[2]Breast Medical Oncology, UT MD Anderson Cancer Center, Houston, TX,[3]UT MD Anderson Cancer Center, Houston, TX,[4]Breast Surgical Oncology, UT MD Anderson Cancer Center, Houston, TX,[5]Baylor College of Medicine, Houston, TX,[6]BostonGene Corporation, Waltham, MA

Background: ER+ inflammatory breast cancer (IBC) is under-appreciated and under-investigated as an aggressive subset of ER+ breast cancer, despite having rates of metastasis comparable to triple negative (TN) IBC. Recent genome-wide profiling of tumors from patients with metastatic breast cancer has shown that IBC samples have a higher frequency of AURKA amplification than non-IBC samples. Our pilot studies in IBC validate these findings and suggest AURKA is amplified in TNIBC. We hypothesize that Aurora Kinase A (AURKA) is a viable therapeutic target in metastatic IBC and in particular ER+ IBC and may exhibit synthetic lethality with ARID1A and SMARCA4 in IBC.

Methods: We reviewed RNA and DNA data from clinically ordered BostonGene tumor assays for IBC versus non-IBC at MDACC. Using ER- IBC cell lines we examined the protein expression of AURKA and Alisertib efficacy was tested using WST assay in IBC cell lines. Senescence was examined using β-gal staining and ELISA assay. In vivo efficacy was studied in a novel ER+ IBC patient derived xenograft (PDX) MDA-BCM-IBC-102.

Results: We previously demonstrated using a large multi-institutional IBC data set including 137 IBC patient tissues analyzed using Affymetrix gene expression arrays, no clear clustering among ER response genes by ER+ subtypes and high AURKA expression in both ER+ and ER- cases. Comparing 23 ER+ IBC to 164 ER+ NON-IBC patient samples from Boston Gene, we find AURKA is amplified in 70% cases and a statistically significant inverse relationship between AURKA and SMARCA4 in IBC. Expression of AURKA by immunoblotting in IBC cell lines demonstrates AURKA expression in four IBC cell lines, including two HER2+ (IBC3 and KPL4) and two triple negative (A3250 and SUM149). Higher doses of Alisertib promote reversible senescence assayed by SA-βgal assay and high IL6 by ELISA validated senescence associated secretory phenotype. In collaboration with the PDX program at Baylor College of Medicine led by Dr. Lewis, our team has developed first novel ER+ PDX model from an ER+ IBC patient. *In vivo* study demonstrated combination treatment with Alisertib and fulvestrant significantly inhibited tumor growth in ER+ PDX models at 28 days compared to either monotherapy, indicating potential synergistic efficacy.

Conclusions: AURKA is commonly amplified in IBC and often associated with gene alterations that may predict synthetic lethality to AURKA targeting. In ER+ IBC AURKA amplification is inversely correlated with putative synthetic lethal partner SMARCA4. We have characterized IBC models with high AURKA expression and demonstrated sensitivity to AURKA inhibition with fulvestrant. Senescence at higher doses of Alisertib in TNIBC models may provide a direction for targeting resistance or escape. Further studies in ER+ organoids are ongoing.

#0453 Small molecule targeting of SERPINB3 as an anticancer strategy in cervical cancer.

Sarah Yu[1], Liyun Chen[1], Eric Liu[1], Ethan Memming[1], Clifford Luke[2], Gary Silverman[2], Stephanie Markovina[1]

[1]Department of Radiation Oncology, Washington University School of Medicine in St. Louis, St. Louis, MO,[2]Department of Pediatrics, Washington University School of Medicine in St. Louis, St. Louis, MO

SERPINB3, also known as squamous cell carcinoma antigen (SCCA) is a cysteine protease inhibitor and prognostic marker associated with poor outcomes in cervical cancer. SERPINB3 blocks lysosomal-mediated cell death by inhibiting lysosomal cysteine proteases such as Cathepsin L and S (CatL, CatS) promoting radioresistance, metastasis, and recurrence. Thus, SERPINB3 is a promising target for translational treatment. We hypothesize that SERPINB3-binding small molecules will sensitize tumor cells to radiation therapy (RT) by disrupting its protease inhibitor activity. Small molecule candidates were identified on a DNA-encoded library screen of 4.4 billion compounds. To test top candidates for cytotoxicity, cervical cancer cell lines CaSki vector control (CTRL) and SERPINB3-overexpressing (B3OE) cells were treated with SERPINB3-targeting small molecules for four hours, followed by increasing doses of RT. Cell death and viability were measured using LDH and CCK8 assays at 48 and 72 hours post-RT, respectively, and significance assessed with ANOVA analyses. Protease activity assays were performed using fluorogenic CatS substrate conversion following preincubation of recombinant SERPINB3 with candidate small molecules. One small molecule enhanced RT-induced cell death in CaSki cells in a concentration-dependent manner. SERPINB3-OE cells displayed even more radiosensitization by this compound compared to CTRL cells. Additionally, no cytotoxic effects were observed in non-malignant END1 cervical epithelial cells. Interestingly, none of the candidate small molecules blocked SERPINB3 function in in vitro protease assays, suggesting an alternative mechanism may be at play. Collectively, these results suggest that small molecule approaches may represent promising therapeutic avenues for targeting SERPINB3 to overcome radioresistance in cervical cancer, and further preclinical development is underway.

#0454 Overcoming PD-1 resistance with a first-in-class dual-mode agent that transforms ‘cold’ tumors to ‘hot’.

Tong Zhu[1], **Lixin Li**[2]

[1]Syntabio, San Diego, CA,[2]Birdiebio, Beijing, China

Background: Immune checkpoint blockade fails in most colorectal cancers (CRCs) because they are immunologically ‘cold’ and mismatch repair-proficient (pMMR). This stands in stark contrast to mismatch repair-deficient (dMMR) ‘hot’ tumors, which are highly responsive; neoadjuvant anti-PD-1 achieves a 100% clinical complete response in early-stage dMMR CRC. This profound disparity underscores the urgent need for a strategy to therapeutically convert pMMR tumors into a dMMR-like state. Current approaches lack the coordinated mechanism necessary to induce and sustain this conversion at the cellular level.

Methods: We have designed a panel of dual-mode agents to deliver two synergistic insults to individual tumor cells, directly and indirectly disrupting DNA mismatch repair (MMR) *MSH2/6* genes. Using a real-time microsatellite instability (MSI) reporter screen, we identified lead compounds that mechanistically induce a high MSI (MSI-H) phenotype. The most promising candidate was subsequently evaluated in murine models of pMMR CRC resistant to PD-1 blockade.

Results: We identified BDB025, a potent, first-in-class dual-mode agent that induces a robust MSI-H phenotype while simultaneously epigenetically silencing critical MMR genes. Crucially, this dMMR-like conversion is achieved at very low, sub-cytotoxic dosages, demonstrating a unique non-cell-death-mediated mechanism of action. This coordinated, two-pronged attack within the same cell overwhelms the DNA mismatch repair machinery, specifically *MSH2/MSH6*, increases tumor mutational burden and T cell influx. Consequently, BDB025 converts ‘cold’ pMMR tumors to ‘hot’, ablates established tumors, and overcomes resistance to anti-PD-1 therapy, significantly outperforming standard agents.

Conclusion: We demonstrate a paradigm-shifting therapeutic strategy: a single molecule that pharmacologically induces a synthetic dMMR state by co-opting two synergistic mechanisms of action. Our lead candidate, BDB025, effectively breaks PD-1 resistance, paving the way to extend the curative potential of immunotherapy to the vast population of patients with pMMR cancers.

Keywords: PD-1 resistance, colorectal cancer, MSI-H, DNA mismatch repair, MSH2, MSH6

#0455 MC001: A novel chemoimmunotherapy antibody drug conjugate for treating folate receptor alpha expressing pancreatic cancer.

Seah H. Lim[1], Hailiang Zheng[2], Peipei Zhong[2], Tawei Huang[2]

[1]Medicovestor, Inc., New York, NY,[2]Sanyou Biopharmaceuticals, Shanghai, China

Background: The prognosis for patients with advanced pancreatic ductal adenocarcinoma (PDAC) remains dismal, even with intensive multi-agent chemotherapy. Many patients are also unable to tolerate these regimens due to systemic toxicity. Folate receptor alpha (FRα), overexpressed in up to 80% of PDAC cases, is associated with poor clinical outcomes and represents a promising therapeutic target. MC001 is a novel chemoimmunotherapy antibody-drug conjugate (ADC) designed to target FRα and to harness both payload-mediated and antibody-mediated cytotoxic mechanisms. Here, we evaluated the preclinical efficacy and safety of MC001 in FRα-expressing PDAC models.

Methods: A high-affinity FRα-specific antibody was isolated from a human v-gene phage display library and engineered into a dimeric, tetravalent IgG1 antibody (ADoBind) through a disulfide bond generated by an S444C mutation. MC001 was synthesized by lysine-based conjugation of the ADoBind antibody to monomethyl auristatin E (MMAE) via an enzyme-cleavable linker, achieving an average drug-to-antibody ratio of 6.

Results: The tetravalent ADoBind antibody demonstrated higher avidity to FRα than its monomeric counterpart and mediated robust antibody-dependent cellular cytotoxicity (ADCC) against FRα-positive SU.86.86 human pancreatic cancer cells using human peripheral blood mononuclear cells (PBMCs), while complement-dependent cytotoxicity was not detected. In a SCID mouse xenograft model co-administered with human PBMCs, ADoBind antibodies induced potent ADCC in vivo and achieved significant tumor growth inhibition. In a single-dose PDAC xenograft study, ADoBind-MMAE ADC (MC001) produced approximately fivefold greater tumor inhibition than its monomeric ADC counterpart at equivalent molar dosing. Tumor suppression was durable, persisting beyond 30 days after a single injection, and resulted in improved overall survival. Single-dose toxicology studies in SD rats and cynomolgus monkeys showed that MC001 was well tolerated, with no significant systemic toxicities. Only transient, mild neutropenia was observed at the highest dose level (12 mg/kg). The serum half-life of MC001 was 5.4 days following a single 3 mg/kg dose, supporting favorable pharmacokinetics for intermittent dosing.

Conclusions: Up to 40% of ADC payloads may be released extracellularly before cellular internalization, revealing an opportunity to exploit the intrinsic antitumor activity of the antibody moiety. By combining antibody-mediated immune cytotoxicity with targeted delivery of a payload, MC001 represents a next-generation chemoimmunotherapy ADC capable of killing both proliferating and quiescent (G_0-phase) tumor cells. These results in preclinical models support advancement of MC001 and the ADoBind platform, which are currently progressing through IND-enabling development.

#0456 Discovery of KAT6A degrader enabled by structural proteomics and AI.

Yonatan Kedem[1], Nitzan Simchi[1], Anjana Shenoy[1], Andrew Morley[2], Alon Shtrikman[1], Michal Ran Shchory[1], Yaron Ben Shoshan-Galeczki[1], Dimitri Kovalerchik[1], Iris Alchanati[1], Galina Otonin[1], Noam Cohen[1], Gali Arad[1], **Eran Seger**[1], Kirill Pevzner[1]

[1]Protai, Ramat Gan, Israel,[2]O2H Discovery, Cambridge, United Kingdom

Lysine acetyltransferase 6 (KAT6A/B) is a MYST family member of histone acetyl transferases (HATs), with elevated activity across different cancer types. Due to its driving role in activation of hormonal signaling, KAT6 is a promising drug target specifically in estrogen receptor positive (ER+) breast cancer. Indeed, efficacy has been demonstrated in clinical trials investigating KAT6 inhibition in ER+ breast cancer. Proteolysis-targeted chimeras (PROTACs) are heterobifunctional molecules inducing the proximity between a target protein and an E3 ligase (e.g. CRBN), leading to target ubiquitination and subsequent degradation. KAT6 PROTAC can target both its enzymatic and scaffold functionalities, potentially leading to improved efficacy. In addition, selectivity towards KAT6A could increase drug tolerability and reduce adverse events.In the current work, we present a novel KAT6A-selective PROTAC, developed using the AIMS™ proteomics and AI platform. Using structural mass spectrometry (MS) data and AI modeling, we generated confident structures of the KAT6-E3-PROTAC ternary complex and identified PROTAC-dependent conformations, enabling accurate modeling of the complex for further optimization. The resulting PAI-PROTAC demonstrates efficient KAT6A degradation and growth inhibition in ER+ breast cancer cell lines, with high selectivity over KAT6B and over other KAT enzymes, as well as no degradation activity in CRBN neosubstrates. Altogether, these results illustrate how proteomics-aware-AI enables rational PROTAC design, leading to discovery of a potent and selective KAT6A degrader.

#0457 Nebivolol triggers apoptosis, ferroptosis and necroptosis in triple-negative breast cancer.

Wangjia Cao[1], Anh Vuong[1], Somik Chattertjee[1], Tagari Samanta[2], Radbod Darabi[1], Ashok Kumar[1], Benny A. Kaipparettu[2], Meghana Trivedi[1]

[1]University of Houston, College of Pharmacy, Houston, TX,[2]Baylor College of Medicine, Houston, TX

Background: Triple-negative breast cancer (TNBC) lacks effective targeted therapies and remains associated with poor outcomes. We are investigating nebivolol, an FDA-approved third-generation β-blocker, as a candidate for drug repurposing in TNBC. We have previously reported that nebivolol inhibits TNBC cell growth, proliferation, clonogenic potential and disrupts autophagic flux, leading to accumulation of autophagosomes and lysosomes. RNA-seq analysis further revealed enrichment of ferroptosis (FDR = 0.076), apoptosis (FDR = 0.111), and necroptosis (FDR = 0.133) pathways following nebivolol treatment. Here, we aimed to conduct deeper mechanistic investigation of nebivolol-induced cell death pathways.
Methods: Two TNBC cell lines (MDA-MB-231 and SUM159) were used for all the experiments. The effects of nebivolol (10 μM, 24h) on ferroptosis were assessed using the BODIPY C11 lipid peroxidation assay kit. Apoptosis and necroptosis were evaluated after treatment with 10 μM nebivolol for 24, 48, and 72h using FITC Annexin V Apoptosis Detection kit. Annexin V-positive cells were classified as apoptotic, whereas Annexin V-positive/PI-positive cells represented necroptotic and late-stage apoptotic populations. Nebivolol-induced apoptosis was confirmed using western blot analysis of cleaved/total PARP and caspase-3 and -7 at 24, 48, and 72h. Necroptosis-mediated membrane damage was measured by LDH release following 3-100 μM nebivolol treatment for 24h. All experiments included a minimum of three biological replicates, each with at least three technical replicates. Data were analyzed using GraphPad Prism 10.1, and statistical significance was determined by one-way ANOVA with multiple comparisons ($p < 0.05$).
Results: Consistent with RNA-seq results, nebivolol 10 μM significantly increased lipid peroxidation by 1.5- to 2-fold, confirming ferroptosis induction. Nebivolol 10 μM significantly increased Annexin V-positive/PI-positive but not Annexin V-positive/PI-negative populations in a time-dependent manner, suggesting its role in late-stage apoptosis and necroptosis. Nebivolol 10 μM treatment elevated cleaved PARP and caspase-7,but not caspase-3 levels, in a time-dependent manner, confirming apoptosis induction. Nebivolol 30 and 100 μM significantly increased LDH release indicating pronounced necroptosis-mediated membrane rupture.
Conclusion: Overall, nebivolol elicits multimodal programmed cell death in TNBC by activating both apoptotic and non-apoptotic pathways. These findings support nebivolol as a promising repurposed drug candidate for TNBC and identify ferroptosis and necroptosis as previously unrecognized components of its antitumor mechanism.

#1320 Interim results of clinical trial phase 1 of pan-mKARS or PTEN loss tumor targeting peptide drug conjugates (Maleimide-KGDEVD-Doxorubicin/Exatecan).

Byoungmo Kim[1], Ha Kyeoung Lee[1], Yun-Gun Ko[2], Kyu-pyo Kim[3], **Youngro Byun**[1], Sang Yoon Kim[4]

[1]Seoul National University College of Pharmacy, Seoul, Korea, Republic of,[2]Pharosgen Co, Seoul, Korea, Republic of,[3]Department of Oncology, University of Ulsan College of Medicine, Seoul, Korea, Republic of,[4]Professor, Otolaryngology, University of Ulsan College of Medicine, Seoul, Korea, Republic of

mKRAS and *PTEN* alterations are highly prevalent across multiple cancer types - occurring in approximately 45% of colorectal cancers (CRC) and up to 30-50% of non-small cell lung cancers (NSCLC) - yet they remain largely undruggable. These malignancies exhibit enhanced albumin metabolism and macropinocytosis to sustain their elevated metabolic demands, presenting a unique opportunity for selective, metabolism-guided drug delivery. We developed a next-generation platform of albumin-binding peptide drug conjugates (PDCs) to target *mKRAS* and/or *PTEN loss* tumors. The lead candidate, MPD-1 (Maleimide-KGDEVD-Doxorubicin), represents the first clinical-stage prototype in this series. MPD-1 couples a maleimide anchor for covalent albumin conjugation with a dual-cleavable KGDEVD linker that responds to both cathepsin B and caspase-3/7, enabling highly selective, apoptosis-responsive payload release within the tumor microenvironment. This dual-trigger mechanism ensures intracellular liberation of doxorubicin through lysosomal cathepsin B activity and secondary amplification via caspase-3/7 cleavage in neighboring apoptotic cells - sustaining cytotoxic activity through *in-situ* feedback amplification and a potent bystander effect. Preclinical studies demonstrated that MPD-1 exhibits strong antitumor efficacy in *mKRAS*-mutant colorectal and *PTEN*-loss NSCLC models, with approximately ten-fold lower systemic toxicity than free doxorubicin. Combination regimens with radiation, PARP inhibition, DNA-PK blockade, or immunotherapy yielded further synergistic effects. The ongoing Phase I clinical trial [NCT06944457] is open-label, single-center, dose-escalation and dose-finding trial to evaluate the MTD, RP2D and pharmacokinetics of MPD-1 in patients with advanced *mKRAS* and/or *PTEN loss* solid tumors. We are going to report the interim results of clinical study of MPD-1 as a first-in-class, caspase/cathepsin-responsive, albumin-binding peptide drug conjugate. We next engineered MPD-5 (Maleimide-KGDEVD-Exatecan) as a second-generation conjugate optimized for higher potency. MPD-5 extends the platform to topoisomerase I inhibition, and it showed superior efficacy in various mKRAS cancers and PTEN loss cancers.

Acknowledgments: This research was supported by the Korea Drug Development Fund (HN21C0264).

#5646 Fully human monoclonal antibodies for antibody drug conjugate development to a cell surface target expressed in cancers with unmet needs.

Ginette Serrero[1], Jorge Marquez[1], Jianping Dong[2], Jun Hayashi[3]

[1]A&G Pharmaceutical, Inc., Columbia, MD,[2]Target Discovery, A&G Pharmaceutical, Inc., Columbia, MD,[3]Precision Antibody, A&G Pharmaceutical, Inc., Columbia, MD

The development of Antibody drug conjugates (ADCs) has shown to provide a powerful approach for the development of targeted therapies in Oncology. The majority of approved ADCs are focused on a few targets using a limited number of antibodies conjugated to a large array of liners and payloads combinations. However, in spite of the availability of these approved ADCs, there are several cancer types with poor prognosis for which the availability of targeted therapies remains limited. Addressing this limitation would require the identification of cell surface targets overexpressed in these cancers, the determination whether these targets are internalized, thus enabling the development of internalizing monoclonal antibodies able to deliver cytotoxic payload within the cancer cells. We have recently identified by proteomics approach such a target named PTGFRN as an internalizing, cell surface protein overexpressed in several cancers in need of targeted therapies such as head and neck, lung, pancreatic cancers, medulloblastoma and mesothelioma. We have demonstrated that PTGFRN expression was associated with migration, proliferation and spheroid formation, key steps in the metastasis process making PTGFRN a target of interest for the development of novel anti-cancer therapy. PTGFRN expression was overexpressed in mesothelioma, head and neck and medulloblastoma while it remained negative in corresponding normal tissues. Using humanized transgenic mice, we have developed and characterized fully human monoclonal antibodies to PTGFRN. Several screening assays were used to select high affinity, internalizing fully human monoclonal antibodies. ADCs derived from these antibodies were efficacious in a dose dependent fashion at the nM range to inhibit proliferation in vitro and tumor formation in vivo. for several PTGFRN expressing human cancer cell lines while it had no effect on PTGFRN negative human cell line. These in vitro and in vivo data will be presented here. These results establish PTGFRN as a target for antibody-drug conjugate development for cancers with unmet needs.

#7455 The therapeutic potential of CCL5 and endoglin in ER-positive breast cancer.

Dominick Lomonaco, **Kideok Jin**

Albany College of Pharmacy and Health Sciences, Albany, NY

Estrogen receptor (ER) signaling drives approximately 75% of all breast cancers and remains the central target of endocrine therapies. However, therapeutic resistance—particularly in metastatic ER-positive tumors harboring activating ESR1 ligand-binding domain mutations such as Y537S and D538G—continues to pose a major clinical challenge. These mutations frequently arise under endocrine treatment pressure and are readily detected in metastatic lesions and circulating tumor DNA (ctDNA). Although CDK4/6 inhibitor-based combination therapies have improved patient outcomes, the mechanisms sustaining resistance in ESR1-mutant tumors and their associated therapeutic vulnerabilities are still not fully defined. To address this gap, we examined the crosstalk between endocrine-resistant breast cancer (ERBC) cells and the tumor microenvironment. Using co-culture systems comprising seven ERBC cell lines—including genome-edited ESR1 mutants—and four stromal cell types, we profiled 28 tumor-stroma secretome pairs using cytokine antibody arrays. This analysis identified CCL5 and endoglin as consistently upregulated in resistant tumor-stroma interactions. We hypothesized that CCL5 and endoglin promote endocrine resistance and metastatic progression through paracrine signaling within the microenvironment. To test this, we generated CCL5-knockout EO771 cells via CRISPR-Cas9 and validated CCL5 loss by qRT-PCR and ELISA. CCL5-deficient cells exhibited significantly reduced proliferation and migration in vitro. In orthotopic mouse models, CCL5 knockout tumors showed markedly diminished growth and metastatic spread. Furthermore, treatment with the CCR5 antagonist maraviroc and the anti-CD105 monoclonal antibody carotuximab selectively impaired the viability of wild-type but not CCL5-deficient cells. Together, these findings identify CCL5 and endoglin as key drivers of endocrine resistance and metastatic potential in ER-positive breast cancer, establishing them as actionable therapeutic targets. This work provides a foundation for future clinical strategies aimed at overcoming resistance in ESR1-mutant disease by disrupting CCL5-endoglin signaling.

: RNA, Gene and Cell Therapies, and Enabling Assay Technologies
Poster Session

#0459 CAR T cells engineered via mRNA exhibit enhanced targeting of colorectal cancer.

Walison Nunes da Silva[1], Pedro Henrique Dias Moura Prazeres[1], Marco Tullio Rodrigues Alves[1], Vivian Vasconcelos Costa[2], Mauro Martins Teixeira[3], **Pedro Pires Goulart Guimaraes**[1]

[1]Physiology and Biophysics, Universidade Federal de Minas Gerais (UFMG), Belo Horizonte, Brazil,[2]Morphology, Universidade Federal de Minas Gerais (UFMG), Belo Horizonte, Brazil,[3]Biochemistry and Immunology, Universidade Federal de Minas Gerais (UFMG), Belo Horizonte, Brazil

Chimeric antigen receptor (CAR) T-cell therapy has revolutionized the treatment of hematologic malignancies, achieving unprecedented remission rates in patients with refractory leukemias, lymphomas, and multiple myeloma. However, translating CAR T therapy to solid tumors remains challenging due to intratumoral heterogeneity, an immunosuppressive tumor microenvironment, and limited tumor-specific antigens. In this work, we employed a lipid nanoparticle (LNP)-based mRNA delivery platform to transiently generate CAR T cells targeting Claudin-6 (CLDN6), an oncofetal tight junction protein aberrantly expressed in multiple tumors, including colorectal cancers. To enhance antitumor efficacy, we combined CAR T cell therapy with localized LNP-mediated delivery of TRAIL mRNA (LNP-TRAIL). We evaluated this dual approach in a subcutaneous xenograft model using Colo 205-GFP+Luc+ human colorectal cancer cells in NSG mice. Tumor growth was monitored by quantitative bioluminescence imaging and caliper-based tumor volume measurements. Tumor-infiltrating lymphocytes (TILs) were profiled for activation markers, proliferation, cytotoxic mediators (IFN-y, Granzyme B), and immune checkpoint expression (PD-1, CTLA-4) to assess T cell exhaustion. To examine translational potential, we performed ex vivo assays using freshly resected human colorectal tumor fragments treated with CAR-T cells. The resulting CAR-T cells generated via LNP-mRNA exhibited robust activation, proliferation, and cytotoxicity against CLDN6+ colorectal cancer cells both in vitro and in vivo. Combined CAR-T and intratumoral LNP-TRAIL therapy significantly reduced tumor burden, enhanced T cell infiltration and effector function, and reversed markers of T cell exhaustion. Ex vivo co-culture with primary human tumor samples further confirmed the improved cytotoxic and immunostimulatory effects of the dual strategy. These results establish a modular mRNA nanoplatform that integrates transient CAR expression with LNP-TRAIL delivery to overcome major barriers to CAR-T efficacy in solid tumors, highlighting its translational potential for CLDN6+ malignancies.

#0460 A generic, high throughput unwinding assay for discovery of RNA helicase inhibitors.

Ha Pham[1], **Robert Lowery**[2]

[1]R&D, BellBrook Labs, LLC, Madison, WI,[2]BellBrook Labs, Madison, WI

DEAD-box (DDX) helicases catalyze ATP-dependent remodeling of RNA and nucleic acid-protein complexes. Because of their overlapping roles in RNA metabolism and innate immune signaling, they are emerging as important therapeutic targets in oncology, autoimmunity, and antiviral drug discovery. To enable discovery and mechanistic characterization of selective helicase inhibitors, we have developed a panel of high-throughput biochemical assays for measuring helicase enzymatic functions in homogenous (mix-and-read) format with far red fluorescent readouts. We previously demonstrated detection of RNA-dependent ATPase activity for a panel of DDX enzymes using the Transcreener® ADP[2] assay. Here, we describe the development and validation of the Heliscreener™ unwinding assay, which uses a fluorescence dequenching strategy to monitor separation of a labeled RNA duplex. We evaluated multiple reporter and capture RNA pairs and identified a single combination that supports robust, generic detection of unwinding by several helicases, including DDX3, DDX5, DHX9, and DDX17. Systematic optimization of ATP and RNA concentrations yielded conditions that provide strong signal-to-background with enzyme concentrations from 1.7 to 66 nM. Under these conditions, Heliscreener enables detection of unwinding activity in continuous or endpoint formats with Z′ factors >0.8, supporting its suitability for high-throughput screening. A pilot screen of 1,280 bioactive compounds identified 20 inhibitor hits and 6 apparent activators, ~50% of which were eliminated as fluorescent interference. Inhibitor selectivity profiles were generally concordant between ATPase and unwinding assays, but potencies often differed, with most compounds showing higher apparent potency in the unwinding assay, consistent with partial uncoupling of ATP hydrolysis from duplex separation. These results highlight the value of combining ATPase and unwinding readouts to obtain mechanistic insights that may impact the efficacy and selectivity of RNA helicase inhibitors.

#0461 Next-generation ERβ agonists with superior brain uptake suppress glioblastoma and enhance temozolomide response.

Uday Pratap[1], Karinel Nieves-Merced[2], Sridharan Jayamohan[3], Michael Tidwell[4], Annabel Maciolek[5], Khaled Mohamed Nassar[3], Henriette U. Balinda[6], Nicholas Clanton[7], Suryavathi Viswanadhapalli[1], Gangadhara R. Sareddy[3], Stanton McHardy[2], Andrew J. Brenner[3], Ratna K. Vadlamudi[1]

[1]UTHSA, San Antonio, TX,[2]Chemistry, UTSA, San Antonio, TX,[3]UT Health Science Center at San Antonio, San Antonio, TX,[4]Chemistry, UTSA, San ANtonio, TX,[5]Chemistry, UTSA, ntonio, TX,[6]Mays Cancer Center, UTHSA, San Antonio, TX,[7]Pharmacology, UTSA, San Antonio, TX

Background: Glioblastoma (GBM) is the most common and aggressive primary brain malignancy in adults, with a dismal 5-year overall survival rate. Epidemiologic studies suggest that estrogen receptor beta (ERβ) exerts tumor-suppressive effects in the brain, supporting its potential as a therapeutic target. However, the lack of potent, selective, and brain-penetrant ERβ ligands has hindered translational progress. We recently identified indanone- and tetralone-keto/hydroxyloxime derivatives (CIDD-0149897) as promising ERβ agonist. Here, we report the structure-guided design, synthesis, and preclinical validation of next-generation ERβ agonists with markedly improved potency, selectivity, safety, and blood-brain barrier permeability for GBM therapy.
Methods: To optimize the CIDD-0149897 scaffold and define key pharmacophores, we designed and synthesized 177 analogues using structure-based drug design incorporating ERβ-LBD X-ray data across multiple chemotypes. ERβ versus ERα selectivity was quantified using dual-luciferase reporter assays. Cytotoxicity and apoptosis were assessed in patient-derived and mouse glioblastoma stem cells (GSCs) via CellTiter-Glo and Annexin-V assays. Mechanistic studies employed Western blotting, RT-qPCR, comet assays, RNA-seq, and mass spectrometry. In vitro ADME and PK were performed through the UTSA Center for Innovative Drug Discovery. Therapeutic efficacy of lead ERβ agonists was evaluated in orthotopic syngeneic and patient-derived xenograft GBM models.
Results: Five optimized ERβ agonists displayed substantially improved potency and selectivity. ADME analyses demonstrated 20-50-fold higher aqueous solubility and excellent plasma stability relative to CIDD-0149897. Two analogues CIDD-0169124 and CIDD-0166596 showed ≥10-fold higher brain exposure than CIDD-0149897, with a peak brain/plasma ratio of 3.12 ± 0.84 at 15 minutes, indicating rapid brain uptake. Both lead molecules reduced human and mouse GSC viability with low-micromolar IC_{50} values and significantly enhanced temozolomide (TMZ) response, increasing DNA damage and suppressing neurosphere formation. Comet assays revealed marked increases in olive tail moment with combination treatment compared to monotherapy. In vivo, CIDD-0169124 and CIDD-0166596 significantly reduced tumor burden and prolonged survival in orthotopic xenograft GBM models. Combination with TMZ further extended survival. Immunohistochemistry of tumor sections showed decreased Ki-67 and increased cleaved caspase-3 in combination-treated tumors.
Conclusion: Two improved ERβ agonists outperformed CIDD-0149897 in potency, selectivity, safety, and brain penetration. These compounds show strong anti-GBM action and enhance TMZ efficacy, supporting their development as next-generation ERβ-targeted therapeutics for GBM. Supported by NIH RO1 CA269866.

#0462 Therapy and malignant progression reshape the splicing landscape to generate shared, tumor-wide neoantigens in IDH-mutant gliomas.

Tim Wu[1], Darwin Kwok[2], Joseph Costello[3], Hideho Okada[4]

[1]UCSF Helen Diller Family Comprehensive Cancer Ctr., San Francisco, CA,[2]UCSF - University of California San Francisco, San Francisco, CA,[3]University of California, San Francisco, San Francisco, CA,[4]UCSF - University of California San Francisco, Mill Valley, CA

Background: The low mutational burden and high heterogeneity of gliomas limit the efficacy of immunotherapy. Aberrant RNA splicing can generate targetable neojunctions (NJs) (Kwok et al., 2025), yet the impact of therapy and malignant transformation on this landscape remains unclear. We investigate these effects in IDH-mutant gliomas to identify conserved, upregulated, and potentially targetable splice-derived neoantigens.

Methods: Paired bulk RNA-seq data from primary and recurrent IDH-mutant gliomas were obtained from the UCSF Brain Tumor Center patient data and AG-120-treated glioma cell line data (Wu et al., Science 2025). NJs and their subsequent peptide sequences were characterized using the SSNIP pipeline (Kwok et al., Nature 2025). High confidence n-mer sequences were prioritized using HLAthena, MHCflurry, NetMHCpan, MUNIS, and HLApollo across five HLA-I alleles (A0101, A0201, A0301, A1101, A2402). Peptides scoring within the top first percentile on ≥ 3 platforms were filtered by FPKM × splice read frequency. DESeq2 and GSEA were used for differential gene expression analyses. Publicly available eCLIP sequencing near NJ sites identified potential cis-binding RNA-binding regulators.

Results: In patients treated with standard chemoradiation (n = 90), 1,806 of 57,400 NJs (3.1%) were significantly upregulated ($\log_2$[JPM] > 1; $p < 0.05$). In AG120-treated IDH-mutant glioma cell lines, 90 of 5,520 NJs (1.6%) were significantly upregulated versus non-treated controls. Across paired samples, NJ expression increased at recurrence ($p = 0.033$), a trend absent with AG120-treated cell lines ($p = 0.7$). NJ elevation was primarily associated with grade progression and differential gene expression analysis showed enrichment of intron-recognition/exclusion pathways. Further analysis of the chemoradiation cohort identified *BCAN, PTPRZ1* and *EEF1A1* NJ-derived targets as top HLA-A*11:01, HLA-A*24:02, HLA-A*11:01 candidates, respectively. Notably, the PTPRZ1 and EEF1A1 NJs were intratumorally conserved, and were more abundant than the immunogenic *GNAS* NJ reported by Kwok et al. Two upregulated AG120 NJs overlapped with those from the chemoradiation cohort and generated proteins. These two NJs generated distinct cancer 9-mers from *S100A13* and *RANBP2*, which were recurrently expressed and strongly predicted to bind HLA-A*02:01. Leading-edge analysis showed *IGF2BP3* upregulation, and eCLIP confirmed binding sites near the *S100A13* and *RANBP2* NJ sites. *IGF2BP3* knockdown in HepG2 cells caused distinct splicing alterations without global loss, while *S100A13* NJ expression decreased significantly post-KD.

Conclusion: We show that therapy and malignant progression remodel the splicing landscape of IDH-mutant gliomas via altered splicing regulator expression. Moreover, this remodeling produces conserved, tumor-wide, and putatively immunogenic NJs.

#0463 Inflammatory breast cancer patients derived explants: Autologous post-mastectomy wound fluid enhances the expression of adhesome and matrisome genes associated with recurrence and metastasis.

Mona Mostafa Mohamed[1], Hossam Taha Mohamed[2], Alshimaa Tarek[1], Shrouk Khalaf El-Sayed[3], Wendy A. Woodward[4], Jon Mark Hirshon[5]

[1]Cairo University Faculty of Science, Cairo, Egypt,[2]October University for Modern Sciences and Arts, Giza, Egypt,[3]Maadi Military Hospital, Cairo, Egypt,[4]Associate Professor, Radiation Oncology, UT MD Anderson Cancer Center, Houston, TX,[5]School of Medicine, University of Maryland, Baltimore, Maryland, MD

Inflammatory breast cancer (IBC) is an aggressive phenotype, cases diagnosed by IBC is increasing worldwide. Our previous study showed that cytokinome composing wound healing fluid contribute to the aggressive phenotype of inflammatory breast cancer (IBC) by inducing expression of genes associated with extracellular matrix remodelling, recurrence and metastasis. Indeed, studying whether wound drainage fluid, collected after modified radial mastectomy may contribute to IBC recurrence and activation of cancer stem cells is limited by the lack of models. Herein, we hypothesized that post-mastectomy wound fluid (WF) after neoadjuvant chemotherapy (NACT) contains biological mediators that induce recurrence.

Methods: Fifty patients (31 non-IBC; 19 IBC) who underwent mastectomy for breast cancer after neoadjuvant chemotherapy were enrolled in the present study. Patient-derived explants (PDEs) were generated from cancer and normal breast tissue of non-IBC and IBC to examine changes in the expression of matricellular- and stemness-related genes after exposing the PDEs to collected autologous postmastectomy-WF for each patient.

Results: Gene expression in non-IBC normal primary tissue was significantly different compared to IBC. The IBC cancer tissues showed a significant increase in E-cadherin gene (*CDH1*) a hall mark of IBC tumor emboli and Matrix metalloproteinases (*MMP*s). While the proteomic composition of IBC WF was significantly enriched for leptin, PDGF-BB, OSM, angiogenin, IL6, IL8, EGF, and others compared to non-IBC. Autologous IBC WF increased *SPARC*, *MMP2,*and *MMP3* in normal PDEs, and *CDH1*, *COL6A1*, *LAMA2*, *MMP1*, *MMP3*, *SELL*, and *THBS3* in cancer PDEs. We utilized different bioinformatics tools and applications such as Gene Ontology (GO) and Kyoto Encyclopedia of Genes and Genomes (KEGG) that bridges the gap between biological results and holistic approach to understand the difference between non-IBC and IBC disease biology. Findings provide a robust molecular framework for IBC, identifying candidate biomarkers for recurrence and potential therapeutic targets. The multi-layer validation of expression, interaction, survival, and mutation data strengthens the translational relevance of the detected candidate genes in IBC biology.

#0464 Assessment of tumor heterogeneity for Integrin beta-6 expression in non-squamous non-small cell lung cancer specimens using an investigational Integrin beta-6 IHC assay.

Stefanie Nicole Kapucija[1], Jim Christian[1], Dana Sprague[1], Nicole Medina[2], Laina Quinones[2], Maggie Hime[1], Kiera Borgert[1], Kevin Brown[1], Jason Berndt[3], Pauline Cronin[3], Emin Oroudjev[1], Juan Gutierrez[1], Juan Gutierrez[1]

[1]Agilent Technologies Inc., Carpinteria, CA,[2]Agilent Technologies, Inc., Carpinteria, CA,[3]Pfizer, Bothell, WA

Rapidly evolving investigational targeted therapies, such as antibody drug conjugates (ADCs), are introducing novel targets in oncology. An investigational ADC, sigvotatug vedotin (SV), is currently being studied in non-small cell lung cancer (NSCLC) and is directed to the novel target integrin beta-6 (IB6). IB6 is overexpressed in multiple solid tumor types and is a proposed negative prognostic indicator in many cancers, including NSCLC.

Integrin Beta-6 IHC 6.2A1 pharmDx is an immunohistochemistry assay developed for the detection of IB6 protein expression and is being used to assess IB6 expression in the ongoing Be6A-Lung-01 trial. Recent data showed this assay is sensitive, specific and precise at detecting IB6 protein expression in a large set of non-squamous NSCLC (nsqNSCLC) specimens. Tumor heterogeneity, originating from genomic instability, is a hallmark of cancer. Tumor heterogeneity in relation to changes in Integrin Beta-6 clinical diagnostic status needs to be understood. Here we present data on IB6 biomarker heterogeneity and further elaborate on the assay's reproducibility as it relates to clinically relevant assay parameters.

This assay uses Monoclonal Mouse Anti-Human Integrin Beta-6, Clone 6.2A1 on the Dako Omnis staining platform. IB6 expression in nsqNSCLC was evaluated by calculating the percentage of viable invasive tumor cells showing partial or complete IB6 membrane and/or cytoplasmic staining at ≥2+ staining intensity. The clinical diagnostic status of IB6 High or IB6 Low was determined using the cutoff ≥50%. Tumor heterogeneity was assessed by comparing staining across 200 µm of an FFPE block (intra-block, n=52), between blocks from the same tumor (intra-case, n=44), and between blocks from primary and metastatic tumor sites in the same patient (n=30 patients). Other clinically relevant assay parameters were also tested, including tissue section thickness, glass slide vs. digital whole slide image (WSI) scoring, and preanalytical variables.

Intra-block resulted in 96.3% overall agreement (OA) (n=52). Intra-case resulted in 95.5% OA (n=44). Primary vs. metastatic comparisons resulted in 83.3% OA (n=30). Tissue section thickness resulted in 99.1% OA. Evaluation of IB6 on glass slides compared to WSIs resulted in 98.9% OA. There was no significant difference in the detection of IB6 positivity across ischemia times of 0.5-72 hours and 10% NBF fixation times of 6-72 hours.

Integrin Beta-6 IHC 6.2A1 pharmDx demonstrates high reproducibility with respect to tissue heterogeneity around the ≥50% diagnostic cutoff, indicating there is uniformity in biomarker expression across and within tumor sites for nsqNSCLC. These preliminary findings may provide confidence that assessment of IB6 expression can be reliably performed across tumor sites and within tumor sites.

#0465 Targeted repression of UBTF inhibits growth and metastatic phenotypes of pancreatic cancer *via* inhibition of ribosome biogenesis.

Mudassier Ahmad[1], Sahir Sultan Alvi[2], Haider Ahsan[1], Rajasekhar Baru[1], Ayati Marzieh[3], Jose L. Gonzalez Hernandez[2], Genaro R. Corea[4], Dae Joon Kim[1], Mohammad Moshahid Khan[5], Subhash C. Chauhan[1], Bilal Bin Hafeez[2]

[1]Department of Medicine and Oncology-ISU, University of Texas Rio Grande Valley, Edinburg, TX,[2]Department of Pharmaceutical Sciences, College of Pharmacy and Allied Health Professions, South Dakota State University, Brookings, SD,[3]Department of Computer Science, College of Engineering and Computer Science, University of Texas Rio Grande Valley, Edinburg, TX,[4]Department of Human Genetics, University of Texas Rio Grande Valley, Edinburg, TX,[5]Department of Neurology, University of Tennessee Health Science Center, Memphis, TN

Pancreatic cancer (PanCa) is the third leading cause of cancer-related deaths in the United States due to lack of molecular understanding, diagnostic methods and effective therapeutic options. Emerging evidence suggests that cancer cells alter ribosome biogenesis machinery at genetic and epigenetic levels to meet high demand of protein synthesis. This study reveals a UBTF mediated novel ribosome biogenesis-associated molecular mechanism that might be crucial for pancreatic cancer progression. Our study suggests upregulation of UBTF, an upstream binding transcription factor (member of the HMG-box DNA-binding protein family) in pancreatic tumors. Its stable shRNA mediated knockdown in human PanCa cells (HPAF-II and MIA PaCa-2) showed remarkable decrease in tumorigenic and metastatic phenotypes of these cells in different functional assays (cell proliferations, colony formation, migration, invasion assays) along with altered expression of E-Cadherin (increase) and N-Cadherin (decrease). Additionally, ChIP assay showed that UBTF-knockdown decreased the occupancy of key components of RNA Polymerase I complex such as RPA194, RPA135, TAF1C and Rrn3 on rDNA which leads to the reduced transcription of rDNA products such as 5' ETS (a marker of pre-rRNA synthesis) and 18S rRNA in these cells. The UBTF repression also effectively inhibited tumor growth in ectopic xenograft mouse model and the growth inhibition was correlated with decreased expression of proliferative (PCNA and Ki67), and ribosome biogenesis (UBTF, RPA194) markers as compared to respective controls tumors. These findings suggest a critical role of UBTF in ribosome biogenesis in pancreatic cancer and that its strategic inhibition could be helpful for developing new therapeutic strategies for pancreatic cancer. In conclusion, this study elucidates a new molecular mechanism that can serve as a potential target for pancreatic cancer treatment.

#0466 Combinatorial screening reveals novel gene-drug synergies in breast cancer cells.

Jifeng Wang[1], Joshua A. Bauer[2], Jie Wu[1], Lili Xu[1], Regina Courtney[1], Guochong Damon Jia[1], Jirong Long[1], Wei Zheng[1], Qiuyin Cai[1]

[1]Vanderbilt University Medical Center, Nashville, TN,[2]Postdoctoral Fellow, Dept. of Biochemistry, Vanderbilt University, Nashville, TN

Background: Breast cancer is the most common malignancy among women in the United States. It is a molecularly heterogeneous disease with diverse therapeutic responses. Our previous transcriptome-wide association (TWAS) and fine-mapping studies identified candidate genes potentially involved in breast cancer susceptibility. To advance personalized chemo-preventive and therapeutic strategies, we conducted a gene-drug synergy study on selected candidate susceptibility genes.

Methods: Based on our previous multi-omics analyses, TWAS, and fine-mapping, we conducted a high-throughput siRNA screen to assess cell proliferation and prioritized 25 candidate genes for combinatorial screening. Using reverse transfection with ON-TARGETplus SMARTpool siRNAs (Dharmacon), these genes were silenced in three breast cancer cell lines (MCF-7, T47D, and MDA-MB-231). Following knockdown, cells were treated for 72 h with 18 clinically relevant agents for cancer therapy, including PARP inhibitors, CDK4/6 inhibitors, endocrine therapies, and chemotherapeutics, at clinically relevant concentrations. Cell viability and cytotoxicity were assessed by Hoechst 33342 and propidium iodide staining with automated image analysis. Gene-drug combinations showing >2-fold increase in cell death versus siRNA-silenced DMSO controls were considered synergistic. Statistical significance was determined using Student's t-test.

Results: This combinatorial screening approach revealed multiple gene-drug synergies. In MCF-7 cells, silencing *R3HDM2* markedly increased sensitivity to CDK4/6 inhibitors, with fold-changes >8 for abemaciclib and >4 for palbociclib, implicating a critical role in cell cycle regulation. *SUGP1* knockdown enhanced responsiveness to docetaxel (3.81-fold) and everolimus (3.37-fold). In T47D cells, knockdown of *SLC25A12*, *DNAJC27*, and *DYNC1I2* genes sensitized cells to everolimus, docetaxel, and lapatinib (fold-change >14, >6, and >5). In MDA-MB-231 cells, knockdown of *CEP192* and *SLC25A12* genes significantly enhanced sensitivity to anastrozole and docetaxel (fold-change >7 and >4).

Conclusions: Knockdown of several newly identified putative breast cancer susceptibility genes profoundly altered drug sensitivity in breast cancer cells, revealing mechanistic insights and potential drug targets for breast cancer. Genes such as *R3HDM2, SUGP1, CEP192*, and *SLC25A12* exhibited strong synergy with CDK4/6 inhibitors, taxanes, and mTOR-targeted agents, implicating roles in cell cycle regulation, microtubule dynamics, and metabolic signaling. These findings support using genetic information to guide treatment and personalized approaches in breast cancer care.

#0467 Profiling the effects of Peroxiredoxin 3 (PRX3) pharmacological inhibition and genetic deletion with the AVITI24™ multi-omic spatial biology platform.

Victoria Gibson[1], Seana Lymer[2], Trevor Wolf[2], Brian Cunniff[1]

[1]University of Vermont Cancer Center, Burlington, VT,[2]Element Biosciences, San Diego, CA

Targeting metabolic vulnerabilities of tumor cells, including tumor cell escape from oxidative stress, is an attractive therapeutic approach in oncology. Thiostrepton (TS), the active pharmaceutical ingredient of RSO-021, is a clinical stage peroxiredoxin 3 (PRX3) covalent inhibitor currently in phase 2 testing for the treatment of pleural mesothelioma (NCT05278975). PRX3 expression supports tumor cell escape from oxidative stress and genetic deletion via CRISPR/Cas9 or pharmacological targeting of PRX3 with TS inhibits mesothelioma tumor growth. To further profile cellular responses to PRX3 deletion and inhibition with TS we utilized the AVITI24™ multi-omic spatial biology platform to profile hundreds of thousands of cells in a single run. Using the Teton™ CytoProfiling assay, we analyzed high-dimensional morphology, targeted transcriptomic data, and multiplexed proteomic data, enabling direct linkage of molecular markers to pathway-level readouts. Differential expression was evaluated using two complementary approaches. Single-cell analyses used a Wilcoxon rank-sum test between conditions, while pseudobulk analyses aggregated replicate wells into pseudo-bulk groups and used DESeq for differential expression testing. Marker genes for each condition were identified using a $\log_2$FC threshold of 0.1, and results from both methods were compared to assess concordance. Deletion of PRX3 in the H-MESO-1 human mesothelioma cell line reduced expression of cell cycle and proliferation genes at the RNA level (ie. CDK1 and Kif11) and protein level (ie. phospho-p38, phospho-AKT1, phospho-CDK1). TS treatment of H-MESO-1 cells increased transcript and protein levels of genes related to Mitogen-activated protein kinase (MAPK) signaling (MAPK10, MAPK11), stress response (HSP70), and apoptosis (FASLG). TS treatment reduced expression of genes related to mitochondrial function, cell migration, and growth. TS treatment did not elicit the same effects on gene expression in PRX3 deleted cells as wild type treated cells with MAPK signaling being one common increased feature across PRX3 deletion and TS treatment (ie. MAPK13 and MAP3K5). Together the AVITI24™ multi-omic spatial biology platform provides a robust workflow that supported profiling genetic and pharmacological targeting of PRX3 in mesothelioma tumor cells, further supporting PRX3 as a novel and actionable therapeutic target in cancer.

#0468 Leveraging single-cell multiomics for a generalizable approach to differentiation therapy.

Scott C. Friedland[1], Tianli Ding[2], Gary Schweickart[2], Alice Mims[3], Katherine Miller[2], Adithe Rivaldi[2], Elizabeth Garfinkle[2], Sunkel Benjamin[2], Jaye Navarro[2], Michelle Wedemeyer[4], Ann-Kathrin Eisfeld[3], Elaine R. Mardis[5]

[1]Internal Medicine, Division of Medical Oncology, The Ohio State University James Cancer Hospital and Solove Research Institute, Columbus, OH,[2]Steve and Cindy Rasmussen Institute for Genomic Medicine, Nationwide Children's Hospital, Columbus, OH,[3]Division of Internal Medicine, Department of Hematology, Ohio State University College of Medicine, Columbus, OH,[4]Neurosurgery, Nationwide Children's Hospital, Columbus, OH,[5]Nationwide Children's Hospital, Columbus, OH

Among the different types of systemic therapies used in cancer treatment, differentiation therapy, perhaps the least frequently utilized but typically most tolerable form of treatment, aims to set cancer cells back on the developmental path from which they strayed, leading to cell death through multiple mechanisms. Acute promyelocytic leukemia (APL) is the exemplar for differentiation therapy wherein leukemic blasts arrested in a progenitor-like state are induced to continue their myeloid differentiation after treatment with all-trans retinoic acid (ATRA) and arsenic trioxide, resulting in >95% cure rates. In contrast to APL, other types of acute myeloid leukemia (AML) have only a 5-year survival of ~33%. However, recent advances in targeted therapies with novel, differentiation-inducing agents for AML with alterations in *IDH1/2 (isocitrate dehydrogenase 1* and *2)*, *NPM1 (nucleophosmin 1)*, and *KMT2A* (*lysine methyltransferase 2A*) have demonstrated efficacy in patients who are older, frail, or who have relapsed or refractory disease. However, the underlying mechanism of differentiation induction remains incompletely understood, limiting adoption for other AML subtypes or non-hematologic diseases. Establishing a rational means of discovering regulators of differentiation therapy could accelerate development of this class of drugs. Here, we present a platform for discovering the central regulators of differentiation as a means of identifying targets for downstream therapeutic development. Using single-cell multiomic (RNA- and ATAC-seq - scMultiome) data from clinical samples of *IDH1/2*-mutated (IDHm) AML as a test case, we utilized a software package called CellOracle to dissect the gene-regulatory networks (GRNs) underpinning the differentiation response throughout the course of IDH inhibition. With these analyses, we recapitulated a known pattern of “BRCAness” in IDHm AML with *in silico* knockout of *BRCA1 (breast cancer gene 1)* appearing to support the differentiation effect of IDH inhibition. We also discovered putative as-yet unidentified regulators of the differentiation phenotype including several Ikaros transcription factors. With this new platform, we also sought to identify targets for differentiation therapy in a solid tumor type, wherein examples of differentiation therapy are almost entirely lacking, with the noteworthy exception of ATRA for neuroblastoma. We utilized scMultiome data from H3K27M diffuse midline gliomas of the pons, which are known to have an epigenetically-based inhibition of terminal differentiation. These aggressive and devastating brain cancers affect exclusively school-aged children and have an approximately 95% 2-year mortality. Using the same pipeline we have identified several putative regulators of a malignant-to-normal transition, including several genes known to be important to normal glial development and maintenance of the cancer state.

#0469 Quaratusugene ozeplasmid mediated TUSC2 upregulation in EML4-ALK bearing non-small cell lung carcinoma induces apoptosis and is highly effective in preclinical studies.

Ananya Banerjee[1], Neeke Busette[1], Xu Cheng[1], Kerslee Kohagen[1], Liwei Bao[1], Lluis Lopez-Barcons[1], Mark S. Berger[2], Matthew B. Soellner[3], Angel Qin[1], Sofia Merajver[1], Nathan Merrill[1]

[1]Department of Internal Medicine, University of Michigan, Ann Arbor, MI,[2]Genprex, Inc., Austin, TX,[3]Medicinal Chemistry and Chemistry, University of Michigan, Ann Arbor, MI

Background: Non-Small Cell Lung Carcinoma (NSCLC) harboring the EML4-ALK fusion gene (Echinoderm Microtubule-Associated Protein-Like 4-Anaplastic Lymphoma Kinase) comprises about 5% of NSCLC cases. Tumors with this genetic alteration are initially responsive to ALK Tyrosine Kinase Inhibitors (TKIs), which constitute first- and second-line therapy. However, nearly all ALK-positive (ALK+) lung cancers ultimately develop resistance to ALK TKIs, highlighting the urgent need for alternative treatment options.
Methods and Results: Tumor Suppressor Candidate 2 (TUSC2) is a tumor suppressor gene with low endogenous expression in NSCLC. Quaratusugene ozeplasmid (QO), developed by Genprex, is a novel gene therapy that encapsulates the TUSC2 plasmid in non-viral lipid nanoparticles, effectively upregulating TUSC2 in cancer cells. We evaluated TUSC2 expression in a range of ALK+ cell lines and patient-derived organoids (PDOs), both prior to and following exposure to QO. Our findings show that QO-driven TUSC2 overexpression initiates a robust pro-apoptotic response in ALK+ models, not only in cells that are sensitive but also with acquired resistance (generated in the lab) to the ALK inhibitor, alectinib. This is evidenced by increased pro-apoptotic markers and lower cell viability when QO is used in combination with alectinib. To further assess the QO and alectinib combination, we tested it in two *in vivo* models: (1) an alectinib-sensitive model using subcutaneous injection of NCI-H2228 ALK+ cells into nude mice, and (2) an alectinib-resistant model using ALK167 PDX implants in NSG mice. Once tumors reached ~ 100 mm^3, mice were randomized into four groups: vehicle control; QO alone (25 µg/mouse, IV, every three days); alectinib alone (0.5 mg/kg for sensitive or 15 mg/kg for resistant, oral, daily); and QO plus alectinib at the same doses. In the sensitive model, tumors in the alectinib-treated group shrank by 60%. Notably, treatment with QO alone, and particularly QO combined with alectinib, resulted in 79% tumor shrinkage (p value 0.0135 versus control), demonstrating a 23% improved outcome than alectinib alone. This suggests that QO might serve as a valuable adjunct therapy, especially for patients who have advanced disease and/or experience resistance to TKIs.
Major new unpublished results: In the resistant model, the QO and alectinib combination produced a synergistic effect, achieving the greatest tumor reduction and improved overall survival (p value 0.0001 versus control), further supporting the clinical potential of this therapeutic strategy in ALK+ NSCLC. Altogether, our *in vitro* and *in vivo* studies indicate that QO-mediated TUSC2 overexpression in ALK+ NSCLC effectively curtails tumor growth and proliferation via activation of apoptotic pathways, providing a compelling rationale for progressing towards clinical trial.

#0470 JZP898, a conditionally activated interferon alpha, generates efficacy and robust TME engagement in syngeneic mouse models.

Ankur Karmokar[1], Emanuele Loro[2], Zhiling Zhang[3], Rao Mukavilli[3], Aparna Gupta[1], Kevin Trouba[4], Vian Amber[5], **Robin C. Humphreys**[1]

[1]Oncology Research, Jazz Pharmaceuticals, Palo Alto, CA,[2]Bioinformatics, Jazz Pharmaceuticals, Cambridge, United Kingdom,[3]DMPK Bioanalytical Science, Jazz Pharmaceuticals, Palo Alto, CA,[4]Toxicology, Jazz Pharmaceuticals, Palo Alto, CA,[5]Clinical Development, Jazz Pharmaceuticals, Oxford, United Kingdom

Interferon alpha (IFNα) is a cytokine belonging to type I IFNs that exert pleiotropic effects on cell functions. IFNα induces antitumor activity and has been extensively applied in clinical oncology. However, use of IFNα has historically been restricted in clinical practice largely due to systemic toxicity and limited clinical activity compared to currently approved immunotherapies. JZP898, a conditionally activated IFNα, has the potential to minimize the toxicity associated with systemic IFNα therapy, preferentially releasing IFNα to tumors and thereby expanding its clinical utility in treating cancer. Cleavage of a proprietary linker by tumor associated proteases controls the release of active IFNα into the tumor microenvironment. Here we describe the preclinical tumor activity, pharmacokinetic (PK) and pharmacodynamic (PD) profiles of JZP898 using a mouse specific analog of JZP898 (JZP898S). Targeted release of IFNα by JZP898S in syngeneic mouse tumor models increased tumor exposure relative to peripheral circulation, translating into greater achievable efficacy, both as a single agent and in combination with CPIs. JZP898S-induced antitumor activity correlated with immune cell activation in the TME and increased cytokine levels in the periphery; elevated peripheral cytokine levels correlated with increased JZP898S exposure. We observed increased number of activated cytotoxic T-cells and decreased number of regulatory cells within the TME. This effect on immune cells in the TME was extended a week beyond the last dose suggesting increased and sustained IFNα effects due to the conditional release of IFNα over time. Predictably, an IFNα gene expression profile was detected in treated tumors in a time and dose dependent manner and demonstrated a PK/PD relationship. From this data, we derived a JZP898-specific gene expression signature in tumors treated with JZP898S. These data support the utility and effectiveness of JZP898 as a novel mechanism to drive IFNα exposure in the TME and impact tumor growth while potentially attenuating IFNα associated tolerability and supports exploring the combinatorial effects with checkpoint inhibitors (CPIs).

#0471 DELs in cells: Small-molecule hits for transcription factor identified by intracellular DNA-encoded library screening.

Leif K. Larsen[1], Allan B. Christensen[1], Andrzej Taranta[1], Charlotte Andersen[1], Frank A. Slok[2], Lars K. Petersen[2], Ole Kristensen[1], Rico G. Petersen[2], Peter Blakskjar[2], Tobias N. Hansen[2], Nils J. V. Hansen[3]

[1]Biology, Vipergen Aps, Copenhagen, Denmark,[2]Chemistry, Vipergen Aps, Copenhagen, Denmark,[3]Vipergen Aps, Copenhagen, Denmark

Transcription factors (TFs) are high value yet challenging therapeutic targets in oncology. Most are considered “undruggable” due to the lack of well-defined small-molecule binding pockets, and the presence of extensive intrinsically disordered regions and shallow protein-protein interaction surfaces. Their active conformations further depend on post-translational modifications, cofactors, and the intracellular milieu - conditions difficult to recapitulate in vitro - therefore, strategies that interrogate TFs in their native cellular environment are preferable. DNA-Encoded Libraries (DELs) provide ultra-high-throughput access to small-molecule binders, but a complicating factor for screening DNA-binding proteins is false positives arising from barcode sequences that resemble native binding motifs. Mutant TF versions engineering to disrupt DNA-binding domains can reduce this issue but risks compromising TF structure and function. Therefore, screening full-length proteins appear highly desirable. Here, clusters of small-molecule hits were identified in an intracellular DEL screen against a full-length, cancer-relevant TF and positively validated in orthogonal assays. Importantly, in the screen, a duplex DNA containing the cognate binding motif was included and successfully suppressed barcode-mediated artifacts. A parallel screen including unrelated duplex DNA confirmed retention of sequence-specific TF-DNA interactions showing that the DNA-binding activity of the TF was intact during the screening. These findings demonstrate that intracellular DEL screening can overcome key mechanistic limitations in targeting transcription factors and enable robust discovery of small-molecule binders to functional, full-length TFs - expanding the druggable space for oncogenic transcriptional regulators previously inaccessible to small-molecule approaches.

#0472 Adapting a TR-FRET platform to decipher G protein-coupled receptor internalization and recycling kinetics.

Jie Gao[1], An Ouyang[2], Spencer Chiang[1], **Yu Sun**[1]

[1]ACROBiosystems Co., Ltd., Beijing, China,[2]ACROBiosystems Inc., Newark, DE

G protein-coupled receptors (GPCRs) represent one of the largest family of membrane receptors, mediating an extensive array of physiological responses through the activation of diverse intracellular signaling pathways. Due to their prominence as therapeutic targets, regulation of GPCR trafficking including internalization and recycling is a critical determinant of drug efficacy and signaling bias. Traditional biochemical and imaging approaches, while informative, often lack the throughput and temporal resolution required to systematically characterize receptor kinetics across large compound libraries. Herein, we describe the adaptation of a time-resolved Förster resonance energy transfer (TR-FRET)-based platform to quantitatively monitor GPCR internalization and recycling dynamics in living cells. By integrating donor-acceptor fluorophore pairs with receptor constructs labeled at extracellular epitopes, the assay enables real-time tracking of ligand-induced receptor trafficking with high sensitivity and minimal perturbation of cellular physiology. The TR-FRET readout allows precise kinetic profiling of receptor endocytosis and recycling across different ligand classes, facilitating the discrimination of biased agonists and the elucidation of pathway-specific trafficking signatures. As an example, an energy-donor tag-modified GLP-1R cell line was stimulated by energy-acceptor-modified agonists for comparison against activation by modified GLP-1. Before internalization, a high TR-FRET signal can be observed. As the receptor gets internalized, the increased distance between the membrane-bound donor with the acceptor agonists quenches the TR-FRET signal before resurfacing as the receptor gets recycled. Altogether, this mechanism helps researchers elucidate the signal duration, intensity, de/re-sensitization of the agonist on its receptor, impacting efficacy, potency and tolerance. Altogether, this optimized TR-FRET approach provides a scalable, high-throughput framework for assessing GPCR trafficking kinetics, bridging the gap between molecular pharmacology and system-level drug screening. By enabling rapid, quantitative evaluation of receptor dynamics, this platform holds significant potential to accelerate the discovery and optimization of therapeutics that leverage GPCR signaling for improved efficacy and safety profiles.

#0473 Accelerating integrated tumor profiling with QIAseq xHYB Pro: A fast, modular approach to CGP and HRD assessment.

Peter Hahn[1], Markus Storbeck[1], **Krishna Amin**[2], Jonathan Shaffer[2], Leif Schauser[3]

[1]QIAGEN GmbH, Hilden, Germany,[2]QIAGEN Sciences Inc., Frederick, MD,[3]QIAGEN, Aarhus A/S, Denmark

Comprehensive Genomic Profiling (CGP) and Homologous Recombination Deficiency (HRD) testing are critical components of precision oncology, guiding therapeutic decisions across a range of solid tumors. While CGP provides broad mutational insights, HRD status offers predictive value for PARP inhibitor response. However, integrating both assays into a streamlined workflow remains challenging due to reagent compatibility, workflow complexity, and sample limitations. QIAseq xHYB Pro is a next-generation hybrid-capture reagent chemistry designed to accelerate high-sensitivity, low-input genomic analysis for cancer research. Its optimized protocol enables a single-day hybrid capture workflow, with hybridization completed in minutes rather than hours, dramatically reducing turnaround time without compromising data quality. Among its key applications are HRD and CGP, two essential assays for therapeutic stratification and biomarker discovery. The HRD panel, developed in collaboration with Myriad Genetics, enables detection of genomic instability signatures including loss of heterozygosity (LOH), telomeric allelic imbalance (TAI), and large-scale state transitions (LST). Using QIAseq xHYB Pro, HRD can be deployed as a standalone assay (QIAseq xHYB HRD Panel) or integrated as a spike-in module within the QIAseq xHYB CGP Panel. This modularity allows researchers to flexibly configure assays based on study needs, enabling broad and deep tumor characterization from limited FFPE samples in a single, efficient workflow.

#0474 A comprehensive LinkLight platform for GPCR mechanistic profiling to support cancer drug discovery.

Yong Wan, Alisha D. Ianni, Haiching Ma, Jianghong Wu

Reaction Biology, Malvern, PA

Background: G protein-coupled receptors (GPCRs) are increasingly recognized as important targets in cancer therapy due to their roles in tumor growth, angiogenesis, and metastasis. LinkLight technology is a protein-protein interaction (PPI) detection platform that monitors β-arrestin recruitment to activated G protein-coupled receptors (GPCRs), complementing second messenger-based assays for ligand activity characterization. Here, we use LinkLight stable cell lines co-expressing TEV-protease-tagged GPCRs and permuted luciferase (pLuc)-tagged β-arrestin to study β-arrestin recruitment, cAMP signal, and calcium-influx within the same cellular context.
Methods: Cell-based functional assays were conducted in both agonist and antagonist modes across three GPCR LinkLight stable cell lines representing distinct G-protein couplings (Gs, Gi, and Gq). β-Arrestin-1/2 recruitment was quantified using the LinkLight PPI luminescence readout, while G-protein-mediated signaling was measured via cAMP or calcium-influx fluorescence, depending on receptor class.
Results: Ligands produced consistent, mechanism-appropriate responses across β-arrestin and second-messenger pathways. For Gq-coupled ADRA1A, the agonist Cirazoline induced robust β-arrestin-1/2 recruitment (EC_{50} = 2.51×10^{-8} M) and calcium influx (EC_{50} = 8.2×10^{-9} M), while the antagonist Prazosin inhibited both (β-arrestin EC_{50} = 2.51×10^{-8} M; calcium EC_{50} = 2.06×10^{-7} M). For Gi-coupled ADRA2A, the agonist Brimonidine stimulated β-arrestin-1/2 recruitment (EC_{50} = 2.64×10^{-8} M) and suppressed cAMP (EC_{50} = 8.88×10^{-10} M), whereas the antagonist Yohimbine blocked β-arrestin recruitment (EC_{50} = 1.78×10^{-8} M) and reversed cAMP inhibition (EC_{50} = 2.69×10^{-7} M). For Gs-coupled ADRB2, the agonist Fenoterol induced β-arrestin-2 recruitment (EC_{50} = 8.83×10^{-10} M) and cAMP signaling (EC_{50} = 1.52×10^{-9} M), while the antagonist Yohimbine (S)-Propranolol inhibited both (β-arrestin EC_{50} = 3.98×10^{-8} M; cAMP EC_{50} = 3.6×10^{-8} M). Across all receptors, β-arrestin recruitment aligned with G-protein-specific signaling in response to the same ligand, demonstrating the robustness of the comprehensive GPCR portfolio.
Summary: By enabling simultaneous assessment of β-arrestin recruitment and G-protein signaling in a unified cellular context, LinkLight technology offers a comprehensive, mechanistically informative platform for GPCR pharmacology. Integrated with G-protein activation data, LinkLight technology also supports high throughput profiling of ligand efficacy, bias, and receptor regulation for GPCR drug discovery against cancer.

#0475 A bioluminescent assay for detection of fatty acid oxidation.

Maggie Bach, Michael P. Valley, Hui Wang, Xavier Aguilar-Enriquez, Wenhui Zhou, Jolanta Vidugiriene

Promega Corp, Madison, WI

Research scientists measure fatty acid oxidation (FAO) to assess how efficiently cells and tissues convert fats into energy and how this process shifts under different physiological or pathological conditions. Because FAO is central to mitochondrial energy metabolism, its measurement reveals insights into metabolic flexibility, mitochondrial health, and substrate preference. Altered FAO is implicated in many diseases including diabetes, obesity, heart failure, and cancer, making it an important marker for both mechanistic studies and drug screening. Additionally, FAO measurements help evaluate the effects of exercise, diet, or pharmacological interventions on energy balance and cellular metabolism. Radiolabeled fatty acids and oxygen consumption assays are the most common methods for measuring fatty acid oxidation (FAO), but these approaches can be labor-intensive and technically demanding. To simplify FAO measurement, we developed a bioluminescent assay based on a fatty acid-linked pro-luciferin substrate. The substrate readily enters cells, where FAO enzymes remove the fatty acid moiety, releasing a modified luciferin precursor. Addition of a detection reagent converts this intermediate to luciferin, generating luminescence proportional to FAO activity. The signal scales with cell number and incubation time and is compatible with both cancer cell lines and primary cells. With just 20,000 cells and a 1-hour incubation, the assay generates strong signal-to-background ratios - about 200 in HEK293 cells and 100 in primary human hepatocytes. The assay is sensitive to inhibition by etomoxir, confirming dependence on carnitine palmitoyltransferase (CPT1) activity, a key regulatory step in mitochondrial FAO. After media removal, all steps are performed in an add-and-read format suitable for 96- or 384-well plates, enabling convenient, high-throughput quantification of FAO. AI was used to help construct this abstract.

#0476 A practical workflow for adaptive immune receptor profiling and screening of antigen-specific clonotypes with applications in cancer.

Alex Chenchik, Tianbing Liu, Dongfang Hu, Kitt Paraiso, Lester Kobzik, **Khadija Ghias**, Paul Diehl

Cellecta, Inc., Mountain View, CA

We developed a streamlined workflow linking adaptive immune receptor (AIR) profiling to antigen-specific functional screening for cancer-relevant T-cell receptor (TCR) and B-cell receptor (BCR) discovery. Bulk AIR sequencing of DNA and RNA from matched samples quantified clonal expansion while distinguishing transcriptionally activated tumor-infiltrating lymphocytes. Paired TCR chains were obtained using a 96-well plate-based, multiplex single-cell assay for TCR α β chain-pairs together with 36 T-cell marker genes, enabling simultaneous identification of full-length receptor sequences and functional phenotype.Reconstructed paired TCRs were cloned into GFP-reporter Jurkat cells, which were then screened using antigen-binding dextramers and co-cultured with K562 APCs expressing tumor-associated peptides. Reporter activation provided a sensitive readout of antigen recognition and allowed ranking of tumor-specific clonotypes. In proof-of-principle studies, the single-cell assay identified the most abundant TCR-α β clonotype in leukemic T cells (35 wells) and revealed co-expression of NKG7 and CCL5, markers associated with cytotoxic activation in cancer. Functional assays confirmed antigen-responsive signaling in the engineered Jurkat cells.This integrated workflow—from repertoire profiling to TCR-α β chain-pair reconstruction and antigen validation—will enable rapid discovery of tumor-associated clonotypes, characterization of cancer-specific immune responses, and the development of receptor-based cellular immunotherapies.

#0477 Lumit® hKi-67 immunoassay for cell proliferation with optimized performance for screening applications.

Kevin Kupcho[1], Jean Osterman[2], Hui Wang[2], Chao Gao[2], Wenhui Zhou[2], **Dan F. Lazar**[1]

[1]Promega Corporation, Madison, WI,[2]Promega Biosciences, LLC, San Luis Obispo, CA

Ki-67 is a well-established marker of cell proliferation and a valuable readout for evaluating anticancer agents across diverse biological models. Here, we describe an improved homogeneous luminescent immunoassay for detection of human Ki-67 using Lumit® technology. The assay incorporates optimized chemistry and a streamlined workflow and can be multiplexed with a same-well cytotoxicity readout. These features make the platform well suited for screening of proliferative and antiproliferative agents in primary immune cells, immortalized cell lines, and 3D cancer spheroids.

To enable use in automated and screening environments, we developed a robust detection reagent for room-temperature “on-deck” stability. This NanoBiT® substrate and buffer formulation yielded a detection reagent that retained ~90% brightness after a 4-h room temperature hold, with no loss in signal-to-background. The reagent also delivered stable glow kinetics, with a signal half-life of ~6 h. Assay robustness was demonstrated by treating Jurkat cells for 48 h with palbociclib (CDK4/6 inhibitor) or BAY-1895344 (ATR kinase inhibitor). Palbociclib reduced Ki-67 levels with an IC_{50} of 164 nM, while BAY-1895344 showed slightly more potent antiproliferative activity (IC_{50} = 94 nM). Normalized dose-response curves were unchanged whether the detection reagent was freshly prepared or held 4 h at room temperature, and results remained consistent when luminescence was measured between 5 min and 6 h after reagent addition. Same-well multiplexing with a cell-impermeant fluorogenic DNA dye revealed that palbociclib induced no cell death, whereas the ATR inhibitor was cytotoxic, enabling clear resolution of proliferative versus cytotoxic drug effects.

To increase ease of use and workflow flexibility, the assay protocol was optimized. Following the addition of an optimized lysis buffer, a brief shake and 10-min incubation produced maximal Ki-67 recovery in both adherent and suspension cell lines. Under these conditions, anti-CD3/CD28 stimulation of primary human $CD8^+$ T cells increased Ki-67 levels by 57-fold after 72 h, whereas total ATP levels increased by ~2-fold, highlighting the superior sensitivity of Ki-67 to changes in proliferative activity. The assay also performed robustly in 3D models: HCT116 spheroids generated over 3 days displayed >90% reductions in Ki-67 following 48-h treatment with BAY-1895344 or nutlin-3a (MDM2/p53 inhibitor), with the ATR kinase inhibitor demonstrating ~20-fold greater potency.

Together, these results demonstrate that the Lumit® hKi-67 immunoassay is a stable, scalable, and automation-friendly platform suitable for high-throughput screening and for profiling proliferative and antiproliferative mechanisms across 2D, 3D, and primary immune cell systems.

#0478 Implementation of single B-cell screening to select antibodies in one day based on affinity and multiple binding properties.

Marie-Claire Phelipot, Eric Chabrol, Julie Lichiere, Alice Aymard, alexandre Baagnolini, Nadjiba Mares, Cecile Lemoigne, Matthieu Tassa, Sophie Mesnard, Caroline Huber, Ester Morgado, Marion Seillier, **Jacques Fieschi**

Mimabs, Marseille, France

Purpose: The aim of this study was to establish a rapid and de-risked workflow enabling the selection and functional characterization of antibody-secreting plasma cells based on function, within a single day to streamline therapeutic antibody discovery.
Methods: BALB/c and transgenic mice carrying human VH/Vκ repertoires were immunized with the recombinant extracellular domain of a tumor-associated immunomodulatory protein. High-titer animals were screened on the Bruker Beacon microfluidic platform, which isolates single plasma cells in nanowells and enables multiplexed assessment of their secreted antibodies. First, beads coated with the ligand and a soluble target conjugated to a fluorochrome allowed simultaneous evaluation of binding affinity and neutralizing capacity. In a second step, beads coated with a structural analog of the target were used to assess the cross-reactivity. Plasma cells producing antibodies of interest were exported for VH/VL amplification, sequencing, and cloning into a mammalian expression vector. Recombinant antibodies were produced and purified for in-depth characterization. Binding affinity and functional blocking were confirmed by biolayer interferometry, while internalization kinetics were quantified using a lanthanide-based pH-sensitive probe. In-silico sequence analysis and structural modeling were applied to identify potential liabilities and exclude clones at risk of poor developability.
Results: The single-day screening workflow enabled high resolution discrimination of plasma cells based on fine differences in affinity and functional binding properties. 215 clones displayed high specificity for the target with no detectable cross-reactivity to analogs and effectively blocked target-ligand interactions. BLI confirmed the accuracy of the phenotypes identified on the microfluidic platform. Internalization assays identified a subset of antibodies with rapid uptake properties compatible with ADC development and computational filtering further refined the panel of antibodies of therapeutic interest by discarding clones with predicted structural liabilities or developability risks.
Conclusions: This integrated and accelerated workflow provides high-resolution functional screening of antibody-secreting plasma cells in a single experiment. By combining affinity ranking, specificity and cross-reactivity assessment, neutralization, internalization profiling, and developability evaluation, our antibody discovery process efficiently yields diverse and high-value therapeutic antibody leads with strong potential for development as immunomodulators or ADC candidates.

#0479 SONNET 5010, a novel proprietary peptide drug conjugate lock and load platform.

John K. Cini[1], Susan Dexter[1], Stephen McAndrew[1], Arron Hearn[2], Evert Bokma[2], Gavin Birch[2], Grant Harradence[2], Christopher Sayer[2], Rosa Gonzalez-Serrano[2], Joao Nunes[2]

[1]Sonnet Biotherapeutics, Inc., Princeton, NJ,[2]Abzena, Cambridge, United Kingdom

Background: Conventional IgG-based antibody-drug conjugates (ADCs) face major limitations, including heterogeneous drug-to-antibody ratios (DAR), variable pharmacokinetics, limited tumor penetration, and linker instability that can lead to off-target toxicity. To overcome these challenges, Sonnet has developed a non-IgG peptide drug conjugate (PDC) platform that enables precise drug loading and improved distribution. SON-5010 is the first proof-of-concept PDC generated using this approach and incorporates Sonnet's F_HAB® (Fully Human Albumin Binding) domain to enhance half-life, tumor accumulation, and overall pharmacokinetics.

Methods: SON-5010 consists of a dual anti-HER2 single-chain variable fragment (scFv) targeting domain flanking the F_HAB motif, combined with an 18-amino-acid Docking Peptide-Payload Domain (DPPD). The DPPD contains three lysine residues that enable deterministic DAR3 conjugation with MMAE. The scFv-F_HAB-scFv targeting domain was expressed in CHO cells, while the MMAE-loaded DPPD was chemically synthesized. The components were linked through standard conjugation chemistry to generate an ~88 kDa PDC. In vitro assessments included serum stability at 37°C and cytotoxicity testing in HER2-high (SKBR3) and HER2-negative (A549) cells. In vivo antitumor activity was evaluated in the HER2-positive BT-474 breast carcinoma xenograft model. SON-5010 was designed for direct comparison with trastuzumab, which contains the same anti-HER2 domain and Lys linker chemistry as MMAE (DAR3), except that it is attached to the DPPD rather than an IgG.

Results: SON-5010 demonstrated strong serum stability and potent cytotoxicity in HER2-expressing SKBR3 cells, with no activity in HER2-negative A549 cells. In vivo, SON-5010 produced tumor growth inhibition comparable to HER2-directed MMAE ADC control of trastuzumab. At 10 mg/kg, SON-5010 showed no detectable toxicity, with stable body weight and no adverse clinical signs. The smaller size of the PDC and the F_HAB-mediated albumin binding likely contributed to improved tumor penetration and favorable tolerability.

Conclusions: SON-5010 demonstrates the potential of Sonnet's modular PDC platform to address key limitations of IgG-based ADCs. The architecture enables full DAR control, enhanced penetration, and flexible engineering of targeting domains and payload chemistries. The platform also supports dual-payload and multispecific designs, offering opportunities to overcome resistance and improve therapeutic index. Early results indicate that SON-5010 is a promising next-generation targeted therapeutic candidate.

#0480 An HTS assay for detection of XRN1 exoribonuclease activity with unmodified RNA.

Mahbbat Ali, **Robert Lowery**

BellBrook Labs, Madison, WI

XRN1 is a 5' to 3' exoribonuclease that degrades both single- and double-stranded RNA to nucleotide 5' monophosphate products. It plays an important role in mRNA turnover and in innate immunity, by damping activation of cytosolic RNA sensors, e.g., PKR and MDA5. Loss of XRN1 has been linked to high interferon signaling in cancer cell culture models, making it an attractive target for cancer immunotherapy. Here we describe development of HTS-compatible assays for screening and profiling inhibitors using the Transcreener AMP^2/GMP^2 Assay. Existing assays for RNAses rely on fluorescently labeled RNAs, which impose limitations on the substrates that can be used and may affect enzyme binding or catalysis. WIth the Transcreener AMP^2/GMP^2 Assay, purine monophosphates produced by XRN1 are directly detected by a competitive immunoassay with a far-red, fluorescence polarization (FP) or time-resolved Förster-resonance-energy-transfer (TR-FRET) readout. This format is homogenous (mix-and-read), compatible with diverse RNA substrates, and resistant to interference from screening compounds. Using full length human XRN1 produced in BaV-infected insect cells, we tested a number of RNA substrates, including synthetic double and single strand oligos with different ends (blunt, overhang, etc.) as well as total yeast RNA. Rates of AMP/GMP formation ranging from 0.054 sec^{-1} to 0.52 sec^{-1} were observed, with single strand RNAs yielding higher activity than double strand substrates; polyA was used for more detailed studies. Though the K_m for poly-A was not length-dependent, the rate and extent of degradation was higher for a 100-mer than a 300-mer. A probe inhibitor, pAp, was tested in dose response experiments yielding an IC_{50} of 114.8 nM, which aligns well with the value measured using a fluorescently labeled DNA/RNA hybrid. The assays were validated for HTS by screening a collection of 1280 bio-actives, yielding a Z'> 0.9 and identification of hits that were confirmed in dose response experiments.

#0481 Drug sensitivity profiling of oncology drugs reveals candidate therapeutic targets in uterine leiomyoma subtypes.

Helmiina Jarvi[1], Simona Bramante[1], Juuli Raivola[1], Emilia Piki[2], Alice Dini[2], Maija Jantti[1], Emma Siili[3], Ralf Butzow[3], Oskari Heikinheimo[4], Annukka Pasanen[3], Niko Valimaki[1], Daniela Ungureanu[2], Kristiina Rajamaki[1], Lauri A. Aaltonen[1]

[1]Department of Medical and Clinical Genetics, University of Helsinki, Helsinki, Finland,[2]Disease Networks Unit, Faculty of Biochemistry and Molecular Medicine, University of Oulu, Oulu, Finland,[3]Department of Pathology, University of Helsinki and Helsinki University Hospital, Helsinki, Finland,[4]Department of Obstetrics and Gynecology, University of Helsinki and Helsinki University Hospital, Helsinki, Finland

Uterine leiomyomas (ULs) are benign smooth muscle tumors and the most common neoplasms in reproductive aged women affecting up to 80% globally. Although ULs rarely evolve into malignant leiomyosarcomas, they inflict a huge financial and social burden. ULs are known to emerge through a few distinct mutually exclusive genetic driver events, the most common being a hotspot mutation in *MED12* and genomic rearrangements of *HMGA2*.

Currently, ULs are often treated uniformly with surgery as the only curative option. Hormonal therapies can reduce tumor size and symptoms but are limited in efficacy and duration and do not consider the genetic subclass. Therefore, our aim was to characterize drug responses in UL-derived primary cell cultures representing the different tumor subtypes.

We established patient-derived primary cell cultures from 5 MED12 and 5 HMGA2 aberrated ULs and their matched normal myometrium. High-throughput drug sensitivity and resistance testing (DSRT) was performed using a comprehensive compound library with 526 clinically approved and investigational cancer drugs.

Preliminary results revealed clear differences in drug responses between ULs and matched myometrial cells, including distinct subclass-specific patterns. Principal component analysis and hierarchical clustering of drug response profiles separated ULs from normal tissue, as well as from epithelial ovarian cancer samples previously analyzed using the same compound library and DSRT workflow.

Among the 526 tested compounds for UL and myometrium, 280 were considered to have a substantial effect in at least one cell culture sample based on the drug sensitivity score (DSS) threshold set at 80th percentile of responses. Out of these compounds, 18% (N=50) induced stronger effects in tumor cell viability, while 82% (N=230) affected myometrial cells more. At the subclass level, 84% of drugs induced a stronger response in MED12 tumors compared to HMGA2. Notably, compounds inhibiting the insulin-like growth factor 1 receptor (IGF1R) and the phosphoinositide 3-kinase (PI3K), pathways recurrently activated across cancers, produced particularly strong effects in the UL cells with also responses varying between the two subtypes.

To date, broad drug discovery efforts for ULs have not been established. Despite their benign nature, ULs share dysregulated signaling pathways with cancers, making these pathways interesting drug targets. While we recognize that cancer drugs often have significant side effects and would not directly be suitable for UL treatment, integrating these cancer drug approaches could enable the development of effective personalized therapies for ULs. Moreover, comparison of drug responses in benign tumors and cancers could help to elucidate how alterations in the same pathways lead to different phenotypic characteristics.

#0482 Development of high-affinity human antibodies targeting POR006: A novel target in squamous cell carcinoma identified by spatial transcriptomics.

MinKyu Kim, Jinyeong Choi, Jae Eun Lee, Hongyoon Choi, Hyung-Jun Im

Portrai, Seoul, Korea, Republic of

Background: Squamous cell carcinoma (SQCC) is a malignant epithelial cancer that arises in various organs, including the lung and head and neck region. Spatial transcriptomics (ST) offers high-resolution mapping of gene expression while preserving spatial context within the tumor microenvironment, thereby facilitating the identification of tumor-specific targets for antibody drug conjugates (ADC) or radiopharmaceuticals. Through a data-driven discovery platform leveraging large-scale transcriptomic and ST datasets, POR006 was identified as a prioritized target associated with SQCC. Here, we generated and characterized human recombinant antibodies exhibiting high specificity and affinity toward POR006.
Methods: Phage display screening was performed to isolate hit antibodies with strong binding potential to POR006. ELISA was used to evaluate binding selectivity, confirming that the antibodies are preferentially bound to POR006 over control proteins. Surface Plasmon Resonance (SPR) was conducted to determine binding kinetics and affinity. Furthermore, flow cytometry and immunocytochemistry (ICC) were carried out to validate target-specific binding in POR006-positive and -negative cell lines.
Results: PortraiTARGET, a target prioritization platform based on human spatial transcriptomics data, identified POR006 as a novel therapeutic target exhibiting high tumor specificity and spatial homogeneity, suggesting potentially superior payload or radioisotope delivery to cancer cells compared to peer targets. Immunohistochemistry analyses confirmed that POR006 is highly expressed in lung and head and neck SqCC tissues, while its expression was minimal across a wide range of normal tissues. Two lead antibodies were isolated from a human phage display library and exhibited strong, selective binding to POR006. SPR analysis demonstrated sub-nanomolar affinities of 0.58 nM and 0.09 nM, respectively. Both antibodies showed selective binding to POR006-positive cells as determined by flow cytometry, with binding levels significantly higher than those of the IgG isotype control. Also, ICC confirmed target-specific staining patterns in agreement with the flow cytometry data.
Conclusion: Our study identified POR006 as a novel SQCC-specific therapeutic target and generated two fully human antibodies exhibiting high specificity and sub-nanomolar binding affinities. These antibodies selectively recognize POR006-expressing cells, supporting their potential for targeted therapeutic development. Based on these findings, ADC and radiopharmaceuticals formats are under development, and their therapeutic efficacy will be evaluated through comprehensive in vitro and in vivo studies. This work highlights the utility of spatial transcriptomics in uncovering novel, clinically relevant targets for precision oncology.

#0483 Organoids-based high-throughput drug screening identifies selective vulnerability of AR$^{-/lo}$ CRPC to inhibitors of neurotransmission signaling.

Shan Wu[1], Ruize Zhao[1], Xiaozhuo Liu[1], Wen (Jess) Li[1], Moyi Wang[1], Amanda Tracz[1], Henry Withers[2], Brian Buckley[3], Katerina Gurova[3], Prashant Singh[4], Eduardo Cortes[2], Jianmin Wang[2], Jason S. Kirk[1], Dean G. Tang[1]

[1]Department of Pharmacology & Therapeutics, Roswell Park Comprehensive Cancer Center, Buffalo, NY,[2]Department of Biostatistics & Bioinformatics, Roswell Park Comprehensive Cancer Center, Buffalo, NY,[3]Department of Cell Stress Biology, Roswell Park Comprehensive Cancer Center, Buffalo, NY,[4]Department of Cancer Genetics & Genomics, Roswell Park Comprehensive Cancer Center, Buffalo, NY

Introduction of the next generation of potent antiandrogens (abiraterone, enzalutamide, apalutamide, darolutamide) about a decade ago into the clinical management of advanced prostate cancer (PCa) patients has led to a substantial increase in a subtype of castration-resistant PCa (CRPC) that becomes independent of androgen receptor (AR) signaling and frequently lacks AR expression (i.e., AR$^{-/lo}$). The AR$^{-/lo}$ CRPC is *de novo* resistant to castration and enzalutamide (Enza), and there are currently no targeted therapies available for this subtype. To identify novel regulators and therapeutic targets in AR$^{-/lo}$ CRPC, we developed an organoids platform from the AR$^{-/lo}$ LAPC9-AI (androgen-independent, i.e., CRPC) xenograft model (Li and Deng et al., *Nat. Commun*. 2018) that recapitulates the AR$^{-/lo}$ CRPC phenotype and drug responsiveness. Using this platform, we conducted high-throughput screening (HTS) in a total of ~6,000 compounds and drugs (including 4,480 bioactive agents and 1,508 FDA-approved drugs). Secondary screening and validation experiments, surprisingly, uncovered 21 compounds effective in inhibiting the AR$^{-/lo}$ CRPC organoids, including JTC-801, Penfluridol and Terfenadine, which normally target the G protein-coupled receptors activated by neurotransmitters including dopamine receptor and opioid receptor. Notably, JTC-801 and Penfluridol specifically inhibited the growth of AR$^{-/lo}$ LAPC9-AI *in vivo*. Collectively, our study identifies novel therapeutic vulnerabilities in castration/Enza-resistant AR$^{-/lo}$ CRPC.

#0484 Hit finding and assay enablement for VRK1, a paralog synthetic lethal kinase target in VRK2-deficient cancers.

Katarzyna B. Handing, Kevin M. Cottrell, Mu-Sen Liu, Patrick McCarren, Brett Williams, Kiera M. Vassallo, Alvin Lu, Alice Tsai, Maria Dam Ferdinez, Sirimas Sudsakorn, Brian McMillan, Jannik N. Anderson, William D. Mallender, Wenhai Zhang, John Maxwell, Kimberly J. Briggs

Tango Therapeutics, Boston, MA

Vaccinia-related kinases (VRKs) are a family of serine/threonine kinases that regulate diverse cellular processes, including transcription factor activity, chromatin remodeling, nuclear envelope formation, and cell-cycle progression. Among them, VRK1 has emerged as a paralog-selective synthetic lethal target in cancers with low VRK2 expression, encompassing nearly all neuroblastomas and over 60% of glioblastomas, with potential for therapeutic expansion into additional tumor types.
Here, we describe the biochemical, biophysical, and cellular assays that enabled the discovery and optimization of novel inhibitors of VRK1 activity found through variety of binding screens, activity-based screens, and rational design. High-resolution crystal structures of both VRK1 and VRK2 in complex with inhibitors revealed their binding poses, identified key interactions, and confirmed orthosteric binding. Medicinal chemistry optimization yielded chemical series capable of achieving >4000X selectivity over the VRK1 paralog VRK2 in a biochemical assay conducted with a physiologically relevant ATP concentration, and >70X selectivity for VRK2-deficient cells in cellular viability assays. Notably, strong correlations between biochemical potency, cellular target engagement, pharmacodynamic response, and functional viability supported both the specificity of the chemical matter and the robustness of the assay platform.
Together, these findings establish VRK1 as a tractable and structurally enabled target and demonstrate that high paralog selectivity in cells can be achieved through orthosteric inhibition. This work provides the strong foundation necessary for structure-guided optimization of VRK1 inhibitors with potential therapeutic applications in cancers with low VRK2 expression, such as glioblastoma and neuroblastoma.

: Genomic Dissection to Define Novel Therapeutic Strategies
Poster Session

#0489 Multi-omic single-cell combinatorial indexing of gRNA, epitopes, and transcriptome uncovers modulators of drug sensitivity in K562 cells.

Sangwon Kang[1], Su-Hyeon Lee[2], Byungjin Hwang[2]

[1]Department of Biomedical Sciences, Graduate School of Medical Science, Brain Korea 21 Project, Yonsei University College of Medicine, Seoul, Korea, Republic of,[2]Department of Biomedical Sciences, Yonsei University College of Medicine, Seoul, Korea, Republic of

Identifying genes that modulate drug response is critical for understanding therapeutic resistance and discovering new targets to improve cancer therapy. Conventional pooled CRISPR screens, based on bulk measurements of guide RNA (gRNA) abundance, provide limited resolution and cannot capture transcriptomic or proteomic changes associated with gene perturbations. To overcome these limitations, we developed Single-cell combinatorial Guide RNA, Epitope, and Transcriptome Mapping Of Signals Across Integrated Cellular omics (scGET-MOSAIC) sequencing, a Cas13-based single-cell CRISPR screening platform that simultaneously captures gRNA identity, transcriptome, and surface protein expression from individual cells. This approach integrates the scalability of pooled screening with the molecular depth of single-cell multi-omics, enabling comprehensive functional interrogation of large druggable gene libraries. Compared to traditional bulk CRISPR screens, scGET-MOSAIC provides not only broader gRNA coverage but also multi-modal phenotypic profiles that reveal how each perturbation alters cellular states. Furthermore, the platform overcomes gene library size constraints found in other single-cell CRISPR methods, such as CROP-seq, allowing a substantially higher number of perturbations to be analyzed in a single experiment. We applied scGET-MOSAIC sequencing to the chronic myeloid leukemia cell line K562 treated with the tyrosine kinase inhibitor imatinib. Single-cell analysis across thousands of perturbed cells revealed distinct transcriptional and surface protein signatures associated with drug response. Through integrative analysis, we identified gene X as a critical modulator that enhances imatinib sensitivity, suggesting a potential combinatorial target for overcoming drug resistance. In summary, scGET-MOSAIC sequencing, powered by Cas13-mediated RNA targeting, establishes a versatile framework for large-scale, high-content CRISPR screening that connects genetic perturbations to transcriptomic and proteomic phenotypes. By directly perturbing RNA, this platform enables the exploration of both coding and non-coding gene functions, expanding the capacity of functional genomics to uncover novel therapeutic vulnerabilities in cancer.

#0490 High-throughput pooled CRISPR screening with high-capacity single cell analysis of the protein kinome using a dual inducible Cas9 system.

Clarence Mills[1], Anna Sheydina[2], Jesse Stombaugh[1], Emily Feldman[1], Josien Levenga[1], Kevin Taylor[2]

[1]Revvity, Lafayette, CO,[2]Revvity, San Diego, CA

Kinases are critical regulators of cellular processes such as proliferation, survival, and apoptosis. Dysregulation of kinase activity is implicated in a wide range of diseases, including autoimmune disorders, inflammatory conditions, and cancer, making kinases highly valuable therapeutic targets. Identifying clinically relevant drug targets is a foundational yet complex step in drug discovery. Genomic screening using CRISPR technology addresses this challenge by offering deep genetic insights. Traditional pooled CRISPR screens with phenotypic readouts are often limited to detecting changes that confer a fitness advantage or disadvantage or to sorting cells using proteins or intracellular components labeled with fluorescent dyes, reporters, or antibodies. Here we developed a unique, dual transcriptionally and post-translationally regulated inducible Cas9 system for rapid small-molecule induction of Cas9 with minimal background expression in the “OFF” state, allowing for precise temporal control of gene editing. We then transduced two cancer cell lines expressing the system with a guide RNA library targeting the protein kinome and employed a microfluidics-free, single cell workflow for unbiased analysis of transcriptional changes resulting from kinase-regulated signaling pathways and protein-protein interactions. This massively scalable approach facilitated the screening of 760 known protein kinases, with 99% of the guide RNA library recovered in the sequencing analysis and a median of >5000 transcribed genes detected per cell. Critically, it enabled the characterization of many kinases whose knockout do not elicit pronounced growth phenotypes. This proof of concept demonstrates the efficacy of high-throughput combinatorial CRISPR screening with high-capacity single cell analysis for kinase activity in cancer cell lines.

#0491 A 100 million cell single cell atlas enabling mechanistic and genotype-specific drug response discovery.

Aisling Sinclair, **Joey Pangallo**, Vuong Tran, Efthymia Papalexi, Simone Marrujo, Bryan Hariadi, Crina Curca, Olivia Kaplan, Sarah Schroeder, Ajay Sapre, Guillermo Gallareta Olivares, Maria Nigos, Oliver Sanderson, Hoai Hguyen, Alec Salvino, John Thompson, Ryan Koehler, Sam You, Gokhan Demirkan, Charles Roco, Alexander Rosenberg

Parse Biosciences, Inc., Seattle, WA

Machine learning promises major advances in drug discovery, but training effective models requires large, well-controlled datasets capturing how diverse compounds affect human cells. Traditional perturbation studies are limited by batch effects and experimental variability. Recent advances in combinatorial barcoding now allow tens of millions of transcriptomes to be profiled in unified workflows, greatly reducing technical noise.We created Tahoe-100M, a single cell atlas of more than 100 million cells spanning 50 human cell lines and 379 compounds. Mixed cell lines (Tahoe Therapeutics) were grown as 3D spheroids, treated for 24 hours across three doses, fixed, and processed in pooled batches of ~10 million cells using the Parse Biosciences GigaLab platform. Sequencing on the UG100 followed by Demuxlet assignment produced high quality transcriptomes at unprecedented scale.Tahoe-100M covers ~56,000 line-drug-dose combinations and reveals thousands of dose-dependent expression changes. Stratification by genotype uncovers lineage- and mutation-specific responses, including unexpected Dabrafenib sensitivity in additional cell lines not typically classified as BRAF-dependent. Cell cycle analysis exposes compound-specific effects, such as G1 or G2/M arrest by CDK inhibitors and G2/M accumulation after microtubule inhibition.The atlas also enables mechanistic discovery. For example, transcriptional similarity mapping shows that Saquinavir induces an adrenoceptor-agonist-like program, resembling Vilanterol and Norepinephrine, providing a molecular explanation for its known cardiovascular effects. Exploratory analyses further identify compounds that up-regulate MHC-I pathways, highlighting candidates that may enhance tumor immunogenicity.By processing fixed cells in massive pooled batches, we minimized batch effects and enabled direct comparison across the entire perturbation space. Tahoe-100M establishes a new benchmark for large scale drug response mapping and provides a foundation for AI-driven discovery across human cell models.

#0492 Uncovering therapeutically targetable mutations from The Cancer Genome Atlas (TCGA) whole-genome datasets.

Ryul Kim[1], Chunyang Bao[1], Hansol Park[1], Gang-Hee Lee[1], Won-Chul Lee[1], Jonghoon Lee[1], Yoonsuh Lee[1], Beomki Lee[2], David Lehotzky[3], Ron Solan[3], Antonia Kowalewski[3], Xavi Loinaz[3], Vasuki Narasimha Swamy[3], David I. Heiman[3], Samantha Van Seters[3], Saveliy Belkin[3], Sam Wiseman[3], Andrew D. Cherniack[3], Luis Antonio Corchete Sanchez[3], Brian P Danysh[3], Zachary Everton[3], Chip Stewart[3], Haruna Tomono[3], Gengchao Wang[3], Esther Rheinbay[3], Gad Getz[3], Young Seok Ju[1]

[1]Inocras, San Diego, CA,[2]Korea Advanced Institute of Science and Technology, Daejeon, Korea, Republic of,[3]Broad Institute of MIT and Harvard, Cambridge, MA

The systematic identification of therapeutically actionable genomic alterations across tumor types is essential to advance precision oncology. Using the CancerVision^{TM} whole-genome analysis platform, we analyzed >8,000 whole-genome sequencing (WGS) samples spanning more than 30 cancer types to characterize clinically actionable mutations. Actionability was defined according to the Cancer Knowledgebase evidence levels, where Level A denotes biomarkers linked to FDA-approved on-label therapies. Overall, 2903 patients (~32%) harbored at least one Level A actionable alteration encompassing ~20,100 events (median 2 per sample). Level A on-label targets were detected in more than half of THCA (thyroid cancer), KIRC (kidney clear-cell), SKCM (skin cutaneous melanoma), BRCA (breast cancer), and COAD (colon adenocarcinoma), underscoring their clinical relevance. The ten most frequent Level A targets were *PIK3CA, KRAS, BRAF, VHL, PTEN, ERBB2, BRCA1/2, NRAS,* and *EGFR*, showing variable frequencies among cancer types. Among *KRAS* alterations, p.G12C was the predominant actionable hotspot, mainly in lung adenocarcinoma with a few cases in colorectal and rectal cancers. A total of 950 fusion targets were identified across the cohort. BRCA exhibited the highest frequency (45 cases; 2.5%), including 40 *ESR1-CCDC170* fusions, followed by THCA (55 cases; 9.7%), dominated by *CCDC6-RET* (25 cases). *NRG1* fusions were found in 145 samples (1.7%), markedly higher than the historical pan-cancer frequency (~0.2%). Other recurrent targetable fusions included *NTRK* (0.7%; 60 samples), *RET* (0.7%), *ALK* (0.7%), *BRAF* (0.6%), and *FGFR* (2.5%; 210 samples), the latter largely involving *FGFR2* (~180 cases). Across all fusion classes, >80% retained the kinase domain, supporting oncogenic potential. Clinical-trial-matched targets were most commonly *TP53, PIK3CA*, and *CDKN2A*, reflecting their broad inclusion in precision-medicine studies. This comprehensive pan-cancer analysis defines the most extensive WGS-based landscape to date of actionable mutations and druggable fusions. The whole-genome approach enabled high-resolution detection of rare structural variants that are often missed by targeted sequencing panels, highlighting the potential of whole-genome profiling to uncover therapeutically relevant but under-recognized targets, supporting the integration of WGS into future tumor-agnostic clinical trial design.

#0493 Genomic landscape of targetable drivers in lung cancer.

Olivia Lee[1], Soo-Ryum Yang[2], Wei Zhao[1], Huu Phuc Hoang[1], Tongwu Zhang[1], Maria Teresa Landi[1]

[1]National Cancer Institute, Bethesda, MD,[2]Memorial Sloan Kettering Cancer Center, New York, NY

Lung cancer is the most commonly diagnosed cancer and the leading cause of cancer death worldwide. As global smoking rates decline, the incidence of lung cancer in never-smokers (LCINS) is rising, motivating more detailed investigation into its etiology. Non-small cell lung cancer (NSCLC) accounts for approximately 85% of lung cancers and is often driven by alterations in the MAPK pathway, including receptor tyrosine kinases (RTKs) and downstream RAS-RAF-MEK signaling, which are key targets of many current molecular therapies. However, 12-30% of NSCLC lack actionable driver alterations, and rare drivers (≤5%) remain poorly characterized, leaving many patients without targeted options. Currently, no large-scale study has systematically compared the distribution of genomic drivers by smoking history and ancestry, or comprehensively profiled rare oncogenic drivers in NSCLC. We analyzed whole-genome and RNA sequencing data from 799 treatment-naïve NSCLC from never-smokers (NS-NSCLC) and 336 NSCLC from smokers (S-NSCLC) in the Sherlock-Lung study. We integrated single-nucleotide variants (SNVs), structural variants, copy number alterations, and RNA-seq data with public cancer databases to identify canonical and potential drivers.

Overall, 98% of NSCLC harbored at least one genomic driver. More than half of both smokers and never-smokers carried at least one RTK/RAS/RAF (RPA)-positive driver. NS-NSCLC more frequently carried RPA-positive drivers than S-NSCLC ($p = 3.16 \times 10^{-19}$) and showed higher frequencies of fusions and tumor-suppressor deletions ($p < 7.10 \times 10^{-3}$). In contrast, S-NSCLC showed higher frequencies of *KRAS* mutations, oncogene amplifications, and rare drivers ($p < 2.10 \times 10^{-4}$). RPA-negative tumors were enriched in PI3K, NOTCH, and WNT signaling pathways, suggesting alternative oncogenic pathways may drive some NSCLC. We describe 60 novel rare driver genes in RPA-negative NSCLC.

Among NS-NSCLC, tumors from East Asians (EAS) showed significantly higher *EGFR* mutations ($p = 1.27 \times 10^{-13}$), while tumors from Europeans (EUR) exhibited heterogeneous SNV and fusion drivers. *EGFR* mutations from EAS tumors were enriched for classical activating variants, while EUR tumors had greater *EGFR* mutation heterogeneity. Furthermore, within RPA-positive NSCLC, EUR tumors showed a broader spectrum of RPA alterations, including *ERBB3, FGFR3/4,* and *ARAF*, whereas EAS tumors predominantly harbored canonical RTK/MAPK pathway oncogene mutations.

Together, these multi-omics analyses describe the genomic driver landscape of NSCLC in smokers and never-smokers, including rare molecular subtypes previously undetected in genomic landscapes. This study may help guide future molecular testing strategies and therapeutic management, particularly for patients with rare or currently non-targetable molecular alterations.

#0494 Multi-omics patient-derived organoid embeddings predict targeted therapy response and KRAS inhibitor sensitivity.

Lelia Polit, Nico Trummer, Rafal Pietrzak, Mateo Longarini, Alexis Finkbeiner, Anna-Rose Gryspeert, Jean Bouteiller, Jerome Caron, Fanny Jaulin, Gustave Ronteix

Orakl Oncology, Villejuif, France

Clinical trials remain a major bottleneck in contemporary drug development. Functional assays based on patient-derived organoids (PDOs) are a promising tool to derisk clinical trials, but their impact has been limited by small cohort sizes and a lack of systematic validation. Using the largest cohort of matched PDOs, longitudinal clinical data, transcriptomic data and WGS data, we generate multi-modal patient representations. We then evaluate how large collections of these representations can be used to characterize drug response phenotypes and to map how tumor-intrinsic features relate to sensitivity to targeted therapies, with a particular emphasis on KRAS inhibition.

Methods: We assembled 135 PDOs from colorectal (CRC) and pancreatic (PDAC) cancers, derived from primary tumors and metastatic biopsies. Patients were 31-89 years old and had received a mean of 2.6 prior lines of treatment at the time of tissue sampling. Each PDO underwent WES and bulk RNA-seq and was profiled in functional drug screens with a panel of targeted agents, including KRAS inhibitors. We generated embeddings from omics features for each PDO. These embeddings were used as inputs to machine-learning models trained to predict drug AUC values, enabling in silico estimation of PDO drug sensitivity from baseline molecular profiles. Within the same framework, we analysed KRAS inhibitor response by identifying molecular neighborhoods in the embedding space enriched for sensitive or resistant PDOs and stratifying samples accordingly.

Results: Embeddings captured major axes of biological variation across the PDO collection, including tumor type, key oncogenic alterations and clinically relevant subgroups, and enabled accurate prediction of AUC values for multiple targeted agents, including KRAS inhibitors. Predicted sensitivities were concordant with experimentally measured responses and reflected known dependencies associated with specific mutational backgrounds. We identified biomarkers and pathway-level signatures associated with response to different KRAS-targeted treatments. These signatures were reproducible across cross-validation procedures and aligned with reported mechanisms of KRAS inhibitor activity and escape.

Conclusions: Large, clinically annotated PDO collections coupled with multi-omics profiling support the construction of embeddings that both predict ex vivo drug response and highlight molecular contexts associated with sensitivity to targeted agents. Integrating these predictive models with systematic pathway interpretation provides a rigorous framework to uncover transcriptomic and genomic markers of response and resistance. For drug developers, this approach shows how PDO-based functional genomics combined with AI driven analysis can be used to derisk development of targeted therapies and inform patient stratification and trial design.

#0495 Single-cell multiomic drug response profiling of PRISM-multiplexed cancer cell lines sequenced with SBX.

Houlin Yu[1], Guoping Wang[1], Stephanie Yaung[2], Heejo Choi[1], Megan Rogers-Peckham[3], Michael Kartje[2], Matthew Rees[1], Paul Lund[4], Brian Haas[1], Charlotte Yang[3], Laura Doherty[1], Lacey McGee[3], Kendall Berg[3], Cynthia Cech[3], Salka Barrett[3], Anasha Arryman[3], Joanne Leadbetter[3], Taylor Lehmann[3], John Mannion[2], Chen Zhao[2], Marc Prindle[3], Melud Nabavi[3], Carolyn Morrison[4], Peter Smibert[4], Kit Nazor[5], Todd Golub[1], Catarina D. Campbell[1], Jennifer Roth[1], Niall Lennon[1], Victoria Popic[1], Dean Procter[1], Kokoris Mark[3], Aziz M. Al'Khafaji[1]

[1]Broad Institute of MIT and Harvard, Cambridge, MA,[2]Roche Sequencing Solutions, Inc, Santa Clara, CA,[3]Roche Sequencing Solutions, Inc, Seattle, WA,[4]10x Genomics, Pleasanton, CA,[5]Proteintech Genomics, San Diego, CA

Inter-individual variability in drug response is a key challenge in precision oncology. Despite recent breakthroughs in targeting RAS-mutant cancers, clinical responses remain heterogeneous. To systematically dissect the molecular determinants of drug sensitivity and resistance, we implemented a high-throughput single-cell multi-omic profiling framework using a PRISM pool: a barcoded co-culture platform of ~400 human cancer cell lines spanning diverse lineages and genetic backgrounds. We treated the PRISM pool with two RAS inhibitors (BI-2865 and RMC-6236), as well as a negative control (DMSO) and a positive control (Panobinostat), and collected cells at early time points (3h and 12h) to capture initial drug response dynamics. We employed a modified 10x Genomics Flex protocol enabling simultaneous capture of the whole transcriptome, a targeted proteome (~320-plex Proteintech panel), and PRISM identity via expressed DNA barcodes. The prototype Sequencing by Expansion (SBX) platform was leveraged to generate ~230 billion reads, enabling the analysis of 315,547 high-quality single cells.

Drug treatments induce diverse and cell line-specific shifts in transcriptional and proteomic states. Applying Non-negative Matrix Factorization (NMF) on each cell line's single-cell transcriptome data and then performing hierarchical clustering, we identified 20 drug-responsive, recurrently co-expressed gene meta-programs (MPs), condensing 1831 underlying programs related to cell cycle, growth, structure, and stress response. Multiple MP dynamics are associated with drug sensitivity and often stratified by genetic background. Notably, cell lines that exhibited a delayed stress-response MP (non-responsive at 3 hours but catching up at 12 hours) exhibited high drug sensitivity. To identify key protein players in drug response, we conducted differential expression (DE) analysis for each cell line comparing drug treatments and controls, identifying recurrently significant DE proteins whose altered expression was also significantly associated with cell viability. Importantly, these protein changes frequently lacked a corresponding significant change in the expression of their encoding RNA transcripts, underscoring the power of multi-modal profiling to more comprehensively illuminate functional mechanisms driving drug response.

Our study establishes a scalable paradigm for linking genotype, transcriptome, and proteome to pharmacologic phenotype at single-cell resolution across genetically diverse human models. These data, enabled with massively high-throughput sequencing using SBX, provide a rich resource for mechanistic discovery and rational design of combination therapies targeting the RAS pathway.

#0496 Oncolinkage: Discovery of tumor-selective surface targets for cancer therapy.

McKensie A. Collins, Benjamin T. Hallisey, Andrew Astley, Rick Nicoletti, **Murray O. Robinson**

Rubik Therapeutics, Cambridge, MA

Cancer therapeutics such as CAR T, Radioligand , ADC, and Bispecifics are all reliant on targeting cancer-selective surface proteins. A major limitation to these tethered killing strategies is the lack of targets that are exclusively expressed on tumor cells and not healthy tissues. Most cancer surface targets exhibit “lineage” expression properties, in which expression is shared by both the tumor and the normal tissue lineage from which the tumor developed. In many cases, expression in normal tissue leads to on-target off-tumor toxicity that can severely limit therapeutic benefit. To address this challenge, we developed Oncolinkage, a computational platform to identify novel tumor targets through their association with genomic changes that drive cancer development. Oncolinkage computationally identifies proteins whose expression is driven by an oncogenic event. While genomic lesions (e.g.amplification, epigenetic dysregulation) activate oncogenes in the developing tumor, many bystander genes are also dysregulated by the non-specific nature of these alterations. Oncolinkage screens for computational signals of cancer genomic lesions mathematically connecting the lesion to target upregulation. Because target expression is “linked” to the pro-tumorigenic lesion, Oncolinked targets are under positive selection, resulting in advantageous properties such as low tumor heterogeneity and resistance to loss. We show that the Cancer/Testis antigens of the MAGE family act as oncolinked targets. Normally restricted to male germ cells, MAGE genes are dysregulated in subsets of multiple solid tumors. Oncolinkage algorithms reveal a distinct set of tumor altered loci that correlate with this tumor-specific expression. We postulate that one or more transcription factors or epigenetic regulators in these loci drives tumor-selective dysregulation of these intracellular targets. Oncolinkage was further used to identify expression-disruptive lesions linked to germ cell restricted surface targets. Among more than a dozen identified oncolinked surface proteins, we found RT1, a protein with testis-restricted expression in normal tissue, but expression in 50% of TNBC and 70% of Ovarian Cancers. Tumor expression was linked to copy number gain on Chr10, the genomic locus of RT1. The known oncogene RET is also present on Chr10 providing a hypothesis that an amplification event targeting the RET oncogene also results in the dysregulation of CAR T target RT1 in subsets of breast and ovarian cancer. The oncolinkage platform is a promising computational approach to identify best-in-class targets for CAR T, RLT, and other tethered killing cancer therapies.

#0497 Transcriptomic predictors of therapy response across age groups in an omani breast cancer cohort.

Muna Al Dlali[1], Habiba El Keraby[1], Hamza Zaidom[1], Radiya Al ajmi[1], Cheryl Crozier[2], Jane Bayani[2], Sirin A. Adham[1]

[1]Sultan Qaboos University, Muscat, Oman,[2]Ontario Institute for Cancer Research, Toronto, ON, Canada

Breast cancer (BC) exhibits profound heterogeneity influenced by age, intrinsic subtypes, and treatment-induced molecular remodeling. We performed molecular analysis to identify transcriptomic biomarkers predictive of tumor biology, treatment response, and survival outcomes in Omani BC patients.

Methods: Archived FFPE tissues from 39 BC patients at Sultan Qaboos University Hospital were analyzed. Transcriptomic profiling using the NanoString Breast Cancer 360 assay was integrated with clinical and pathologic data. Spearman correlations were used to assess the relationships between age and biosignatures. Decision tree models were constructed to identify molecular determinants of (i) treatment allocation across age groups, (ii) pathologic complete response (pCR) versus partial response (pPR), and (iii) survival.

Results: Age showed a strong molecular pattern: older patients had higher ESR1, AR, PTEN, stromal, and Claudin-Low expression signatures, while younger patients exhibited higher $CD8^+$ T-cell, proliferation, HRD, p53, and BRCAness scores, consistent with a genomically unstable, immune-active phenotype. In early-onset disease, *ERBB2* was the dominant treatment classifier, with *CDK6* and macrophage signatures further stratifying endocrine versus TNBC chemotherapy; in late-onset tumors, IFN-γ and *SOX2* defined treatment branches, suggesting age-specific immune and stemness programs. Across response strata, pCR was driven by high*ERBB2* and $CD8^+$-rich immune signatures. In contrast, pPR was characterized by BRCAness and Cell Adhesion, indicating an overlap between HRD-like and adhesion-driven aggressiveness, as well as the impact of targeted therapies, such as trastuzumab, on response. Survival models mirrored this, linking long-term survival to HER2 modulation and immune activation and non-survival to AR and Claudin-Low-like states.

Conclusions: In this Omani cohort, age is associated with distinct, contextualized molecular programs. Younger patients exhibit HER2-driven, HRD-enriched, highly proliferative and immune-active biology, while older patients show hormone receptor-dominated, stromal and PTEN-preserved phenotypes. The data obtained indicate that integrating ERBB2 variations, immune metrics, and HRD-like signatures into future risk-adapted strategies in Middle East and North Africa (MENA) populations may be considered for diagnostic and treatment purposes.

#0498 The perturbation data gap: Accelerating discovery with CRISPR screening.

Elena Vialetto[1], Ronay Cetin[1], Sebastian Susser[2], Simran Rastogi[1], Angela Hinchie[1], **Jessica Martyn**[1], Martin Wegner[1], Manuel Kaulich[1]

[1]Vivlion GmbH, Frankfurt am Main, Germany,[2]IBCII, Goethe-Universitat Frankfurt am Main, Frankfurt am Main, Germany

At Vivlion, we continually strive to enhance CRISPR library and screening solutions. We introduce Alexandria, our flagship genome-wide PRCISR™ CRISPR knockout library, available in single-targeting and fixed-pair formats. The fixed-pair design delivers two sgRNAs per cell for the same gene (or predefined gene pairs), boosting editing efficiency and enabling combinatorial strategies. Alexandria broadens discovery by including ~1,800 newly annotated genes overlooked by previous reagents and covers 20,381 genes (~99.8% of ENSEMBL) with 4 sgRNAs per gene (2 pairs) to support confident hit calling across cell types and states.

All PRCISR™ libraries are produced with Vivlion's 3Cs technology, which utilizes the oligo pool directly and avoids PCR bias and cloning artefacts—yielding highly uniform gRNA distributions that preserve representation even in down-scaled screens (e.g., limited primary or iPSC material). Building on this, our library formats decouple sequence diversity from distribution, so users can deploy single-targeting, fixed-pair, or multiplex designs as their biology demands.

In practice, Alexandria enables researchers to identify context-dependent dependencies, explore pathway mechanisms, paralog buffering, and prioritise actionable targets that standard screens may miss. To streamline execution, Vivlion offers pooled and optical pooled screening, bioinformatics support, leveraging ReCo, our automated NGS read-counting pipeline for single and combinatorial CRISPR data that simplifies downstream analysis.

By combining advanced CRISPR screening with uniform, low-coverage reagents like Alexandria, researchers can accelerate discovery across disease and non-disease contexts alike.

#0499 Integrated genomic and spatial analyses elucidate the origins and vulnerabilities of urachal carcinoma.

Toru Imai[1], Tatsunori Shimoi[2], Akiko Maeshima[3], Jumpei Kashima[3], Ibuki Tsuru[1], Hisashi Hashimoto[1], Jun Takahashi[1], Eijiro Nakamura[4], Yoshiyuki Matsui[4], Hiroyuki Mano[1], Kan Yonemori[2], Yosuke Tanaka[1]

[1]Division of Cellular Signaling, National Cancer Center Research Institute, Tokyo, Japan,[2]Department of Medical Oncology, National Cancer Center Hospital, Tokyo, Japan,[3]Department of Diagnostic Pathology, National Cancer Center Hospital, Tokyo, Japan,[4]Department of Urology and Retroperitoneal Surgery, National Cancer Center Hospital, Tokyo, Japan

Introduction: Urachal carcinoma (UrC) is a rare and aggressive malignancy arising from the urachal remnant, an embryonic remnant located at the bladder dome. Despite its anatomic location, its pathological features—predominantly adenocarcinoma—resemble those of gastrointestinal adenocarcinomas. Due to its rarity, the molecular basis of UrC and the precise mechanisms underlying its carcinogenesis from the urachal remnant remain insufficiently understood, hindering the development of effective therapies. These gaps have limited therapeutic progress. To address this, we performed an integrated multi-omics and spatial analysis to delineate the molecular landscape, cellular origins, and evolutionary trajectory of UrC.

Methods: We conducted a comprehensive analysis of 53 UrC and 39 non-malignant urachal remnant samples. The multi-modal investigation included whole-exome sequencing (WES), RNA sequencing, spatial transcriptomics, and immunohistochemical analysis. To specifically investigate the pre-cancerous state, epithelial cells from urachal remnants were isolated using laser microdissection (LMD) for subsequent genomic analysis.

Results: Genomic analysis identified mutations in the RTK/RAS/MAPK pathway in approximately 60% of the tumor cases. The most frequent driver mutations were identified in *TP53*, *KRAS*, and *SMAD4*. The mutational profile was distinct from both colorectal and bladder cancers, establishing UrC as a unique molecular entity. While transcriptomic analyses clearly distinguished the pathological subtypes, investigation of cell clonality demonstrated shared ancestry among these different subtypes, implicating significant tumor plasticity. Importantly, our investigation into the tumor's origin revealed that urachal remnants undergo intestinal metaplasia, losing native urothelial characteristics while activating gastrointestinal-specific genes. We confirmed that UrC directly originates from these remnants through spatial trajectory analysis, and that genomic analysis of LMD-isolated epithelium identified shared clonal mutations between the precursor lesion and the adjacent tumor. Furthermore, spatial transcriptomics successfully characterized the unique tumor microenvironment (TME) of UrC.

Conclusion: We have elucidated key aspects of the molecular basis and origins of UrC, demonstrating that its diverse subtypes arise from a common ancestry within precursor lesions that undergo metaplasia and clonal expansion. Moreover, the characterization of the TME provides new insights into tumor biology. These findings may ultimately inform strategies for novel therapeutic intervention and the prevention of this lethal cancer.

#0500 Co-occurrence of gene fusions and microsatellite instability (MSI) defines a clinically distinct subtype of colorectal cancer.

Scott Kulm, Sebastia Franch-Exposito, Paul Fields, Catherine Igartua

Tempus, Chicago, IL

Background: Microsatellite instability (MSI) is a well-established biomarker in colorectal cancer. Gene fusions may also influence prognosis, but the clinical significance of their co-occurrence with MSI remains poorly understood.
Methods: We analyzed a cohort of colorectal (N = 29,099) cancer patients, all profiled with Tempus AIs xT platform. Fishers tests assessed the enrichment of pathogenic and likely pathogenic gene fusions within microsatellite stability groups. Cox models evaluated the independent and interaction effects of MSI status and gene fusions on real-world overall survival from at biopsy collection, adjusting for age, stage, line of therapy, tumor purity, tumor mutation burden, and PD-L1 combined positive score. We tested for enrichment of all fusions, kinase fusions (*NTRK1*, *NTRK3*, *RET*, *ALK*, *FGFR2*, *BRAF*), and NTRK fusions (*NTRK1*, *NTRK3*).
Results: The proportion of clinically relevant gene fusions was higher in MSI versus MSS colorectal cancer tumors (5.9% vs 1.8%): *NTRK1* (2.2% vs. 0.048%), *NTRK3* (1.2% vs. 0.14%), *RET* (0.87% vs. 0.096%), and *TPM3* (1.0% vs. 0.0074%). Survival analyses revealed that all fusions and kinase fusions were both associated with significantly worse overall survival (Table 1). These trends persisted in sub-cohorts. MSI was associated with increased overall survival in models including all fusions, kinase fusions, and *NTRK* fusions. We did not detect a significant interaction between MSI and gene fusions across any of the models, likely due to smaller sample sizes. However, we confirmed fusions remained associated with poor overall survival when restricting to MSS tumors for all gene fusions and kinase fusions. Additional models fit to patients treated with specific therapies, such as immunotherapy, did not converge.
Conclusion: Gene fusion rates differ between MSI and MSS colorectal tumors. While most fusions are generally associated with worse survival, this effect may be reversed in MSI cases.

Table 1: Overall Survival Association Results with fusions and MSI in Colorectal Cancer.

Restricted To	**Fusion Class**	**Fusion**			**MSI**		
		N	**Hazard Ratio**	**P**	**N**	**Hazard Ratio**	**P**
All	All	274	1.261	0.015	575	0.643	3.51E-05
Stage 3/4	All	234	1.253	0.025	426	0.677	0.002
Pre-Treatment	All	201	1.297	0.019	417	0.631	5.30E-04
MSS	All	226	1.260	0.015			
MSI	All	48	0.927	0.763			
All	NTRK	52	0.564	0.13	575	0.652	4.53E-05
Stage 3/4	NTRK	40	0.692	0.368	426	0.693	0.003
Pre-Treatment	NTRK	42	0.630	0.223	417	0.633	4.67E-04
MSS	NTRK	22	0.564	0.130			
MSI	NTRK	30	0.684	0.297			
All	Kinase	136	1.427	0.010	575	0.648	4.65E-05
Stage 3/4	Kinase	117	1.518	0.004	426	0.685	0.003
Pre-Treatment	Kinase	99	1.545	0.005	417	0.640	7.74E-04
MSI	Kinase	89	1.426	0.010			
MSS	Kinase	47	0.860	0.593			

#0501 Integrated multiomic profiling reveals SWI-SNF subunit-specific pathway alterations and targetable vulnerabilities.

Clemence Astier[1], Jorge Bretones Santamarina[2], Marlene Garrido[1], Leo Colmet-Daage[1], Thibault Delobel[2], Marcos Bolanos[2], Marianne Chasseriaud[1], Elodie Anthony[3], Daphne Morel[4], Roman M. Chabanon[1], Theo Roumeliotis[5], Mercedes Pardo[5], Elaine Del Nery[3], Jyoti Choudhary[5], Annabelle Ballesta[2], Sophie Postel-Vinay[6]

[1]Inserm U981, ATIP-Avenir, ERC StG, (Epi)genetic Vulnerabilities in Solid Tumors and Sarcoma Laboratory Institut Gustave Roussy, Villejuif, France,[2]Inserm U1331, Cancer Systems Pharmacology ATIP-Avenir team, Institut Curie, MINES ParisTech, CBIO, PSL Research University, Paris, France,[3]Biophenics, Institut Curie, PSL Research University, Department of Translational Research, Cell and Tissue Imaging Facility (PICT-IBiSA), Paris, France,[4]Universite Paris-Saclay, Kremlin-Bicetre, Institut Gustave Roussy, Villejuif, France,[5]Functional Proteomics group; The Institute of Cancer Research, London, United Kingdom,[6]Inserm U981, ATIP-Avenir, ERC StG, (Epi)genetic Vulnerabilities in Solid Tumors and Sarcoma Laboratory Institut Gustave Roussy, Drug Development Department (DITEP), Institut Gustave Roussy, University College of London, UK, Villejuif, France

Background: Mutations in subunits of SWI/SNF chromatin remodeling complex frequently occur in cancer and no targeted therapy is currently available for this patient population. To systematically characterize novel targetable vulnerabilities in SWI/SNF-deficient cancers, we integrated multiomics profiling and drug screening of tumor cell lines with publicly available molecular profiling and CRISPR screen, using newly developed bioinformatic methodologies.

Methods: We generated in-house transcriptome and proteome profiling with high-throughput drug screening on a panel of isogenic HAP1 cell lines knocked-out (KO) for genes encoding SWI/SNF subunits or other chromatin remodelers. We further acquired publicly available molecular profiling and CRISPR-screen datasets from the TCGA and DepMap projects, respectively, and integrated all results. Gene set enrichment analyses were performed using an optimized pipeline based on (i) a pruned version of the Reactome pathway database, (ii) combining ROntoTools and GSEA algorithms, which scored as top performant strategy. Synthetic lethal interactions (SLi) from the DepMap CRISPR screening were identified using a new benchmarked SLi algorithm, based on expression levels of genes on interest, to consider functional deficiencies.

Results: *Metabolism of proteins*, which had not previously been linked to SWI/SNF, was the most frequently dysregulated pathway category both in HAP1 SWI/SNF-KO mutant cell lines and in the DepMap analysis comparing models with low and high SWI/SNF subunit expression; it was the third most dysregulated in SWI/SNF-defective TCGA patient tumors (after *Signal transduction* and *Immune system*, potentially due to the presence of an immune microenvironment). High-throughput drug screen identified multiple pharmacological vulnerabilities, including inhibitors of the histone acetyltransferase CBP/EP300 or mitochondrial respiration, which were selectively cytotoxic in SWI/SNF-defective models. Our new SLi algorithm, also independently identified genetic synthetic lethality between SWI/SNF defects and *EP300* or mitochondrial respiration genes. These orthogonal genetic and chemical vulnerabilities were revalidated experimentally in histotype-relevant SMARCA4-isogenic models, using two highly selective EP300 inhibitors and the mitochondrial respiratory chain complex III inhibitor Antimycin A.

Conclusion: Integrating multi-omics profiling with high-throughput drug- and genetic- screening, respectively analyzed using an optimized enrichment pipeline and a newly developed SLi algorithm, enabled the identification of actionable genetic dependencies in SWI/SNF-defective cancers. These predicted synthetic lethal interactions were experimentally validated in relevant models, supporting their clinical relevance.

JBS and CA contributed equally. SPV and AB contributed equally.

#0502 Comparison of *MTAP* loss by immunohistochemistry (IHC) and *MTAP* homozygous deletion by next-generation sequencing (NGS) and DNA fluorescence in-situ hybridization (FISH).

Lisa Huang[1], Lauren Giampapa[1], Paige Montanaro[1], Ishwarya Krishna[1], Shannon Chilewski[1], Haeun Hwangbo[1], Wen-Chi Chou[1], Sarah Jamerson[1], Lynn Dong[1], Olufemi Adelakun[1], Juliana Coculo[1], John Rassa[1], Jonathan Baden[1], Travis Hollmann[1], **Igor Katsyv**[2]

[1]Bristol Myers Squibb, Princeton, NJ,[2]Bristol Myers Squibb, Cambridge, MA

Background: Methylthioadenosine phosphorylase (MTAP) deletion, resulting from genomic alteration, is observed in approximately 10%-15% of solid tumors, including NSCLC, PDAC, and others. Second-generation MTA-cooperative PRMT5 inhibitors have shown encouraging efficacy and safety in patients with advanced solid tumors, emphasizing the need for precise patient selection strategies. DNA NGS, DNA FISH, and IHC are the primary methods of MTAP loss detection in patient tumor samples. FISH is often considered the gold standard for confirming gene deletions due to its high spatial resolution and direct DNA-level detection; however, its limited scalability, longer turnaround, and operational complexity make it less practical for routine screening. NGS enables multiplexed, high-throughput detection of genomic alterations including MTAP deletions with strong analytical performance and broad molecular context. It supports treatment selection, prognostic assessment, and trial eligibility from a single tumor specimen. IHC offers rapid turnaround, preserves tumor morphology, and allows visualization of intratumoral heterogeneity. With the promising results that have been shown so far for MTA-cooperative PRMT5 inhibitors, flexibility in testing methods is important to meet the diverse needs of patients and physicians as the development of these agents moves forward. Here, we present the results of a study assessing the concordance of IHC, NGS, and FISH testing to assess the presence of MTAP loss.

Methods: We developed an MTAP IHC assay by screening, optimizing, and biophysically characterizing 13 commercially available antibody clones. We subsequently benchmarked our IHC assay using validated DNA NGS and/or FISH on > 160 solid tumor samples.

Results: IHC was highly concordant with NGS (> 90% agreement, Cohen's Kappa > 0.85) and with FISH (> 85% agreement, Cohen's Kappa > 0.70). Similarly, NGS and FISH showed strong concordance (> 90% agreement, Cohen's Kappa > 0.80). Through in-depth assessment of tumor morphology and review of FISH images, we attributed most discordance in the context of apparent MTAP loss on IHC without concomitant MTAP deletion detection on NGS and/or FISH to low/borderline tumor purity. When investigating preliminary patterns of exon-level MTAP homozygous deletion by NGS and FISH in our cohort, we observed some heterogeneity between methods in tumors with partial MTAP deletion.

Conclusions: These data demonstrate high overall agreement among IHC, NGS, and FISH for the detection of MTAP loss. IHC offers rapid screening with retained morphologic context, whereas NGS and FISH provide orthogonal molecular resolution. Our findings support IHC as a practical method for MTAP loss detection, along with NGS or FISH.

#0503 Assessing paralog dependency in ovarian cancer to drive target discovery.

Amy R. Lowe, Siobhan O'Brien, Marissa Fujimoto, Alice H. Berger

Fred Hutchinson Cancer Center, Seattle, WA

Ovarian cancer is the deadliest gynecologic cancer, and the fifth leading cause of cancer-related mortality in individuals assigned female at birth. Though some targeted therapies are available for the treatment of ovarian cancer, there is an unmet need especially for non-RAS or *BRCA1/2* mutant cases. Recent developments in CRISPR technology have allowed for high-throughput identification of genetic dependencies, accelerating the identification of new drug targets for cancer treatment. However, we and others have shown that many cellular dependencies are missed due to genetic redundancy within the human genome. Indeed, paralog genes can compensate for each other's functions and obscure gene-dependent phenotypes when using only single gene knockout tools. To assess paralog dependency, multiple genes must be knocked out at the same time. In this study, we developed the focused dual gene-targeting library pgMI, which is comprised of 3,800 paired-guide RNAs (pgRNAs) targeting 116 paralog pairs that have been identified as synthetic lethal in at least two published double knockout CRISPR screens. To aid in genetic interaction mapping, pgMI contains both single and double-targeting pgRNAs. In an initial analysis of six non-small cell lung cancer cell lines, we uncovered several cell line specific and pan-essential paralog dependencies. To assess paralog dependencies specific to ovarian cancer, we then performed pgMI CRISPR screens in three common ovarian cancer cell lines - SKOV3, JHOS4, and OVCAR8. These cell lines represent a diverse set of cancer driver genes, which include activating mutations in both the Wnt and RAS signaling pathways. pgMI screening uncovered paralog dependencies both unique and shared across ovarian cancer cell lines, providing a narrowed list of potential therapeutic targets for further study.

#0504 Interferon enriched gene expression signatures are associated with ADAR1 dependency in oral squamous cell carcinoma.

Pei San Yee[1], Jie Ying Teo[1], Shi Mun Yee[1], Shiyin Ooi[1], Yee Hua Tan[1], Mathew J Garnett[2], Siew Kit Ng[3], Annie Wai Yeeng Chai[1], Sok Ching Cheong[1]

[1]Cancer Research Malaysia, Subang Jaya, Malaysia,[2]Wellcome Sanger Institute, Cambridge, United Kingdom,[3]Universiti Sains Malaysia, Bertam, Malaysia

Oral squamous cell carcinoma (OSCC) is prevalent in Southeast Asia, and the 5-year survival rate remains poor due to limited effective treatments, underscoring the need for new therapeutic strategies. Our recent work shows that *adenosine deaminase acting on RNA 1* (*ADAR1*), particularly the p150 isoform, is essential for OSCC cell survival, making it a promising therapeutic target. However, determining which patients may respond from ADAR1 inhibition remains challenging because the basis of this dependency is not fully understood. This study aimed (1) to predict ADAR1 dependency in OSCC tumors and (2) to define the gene expression changes associated with ADAR1 loss. For Aim 1, differential gene expression (DEG) analysis was performed on OSCC cell lines with validated ADAR1 dependency status using RNA-sequencing data. ADAR1-dependency signature scores were generated from the average z-scores of these DEGs and applied to 313 OSCC tumors in The Cancer Genome Atlas (TCGA). For Aim 2, we selectively knocked down the p150 isoform using siRNA in multiple OSCC cell lines followed by RNA-sequencing. Gene Set Enrichment Analysis (GSEA) was used to identify pathways altered by ADAR1-p150 knockdown in both dependent and less-dependent lines. We found that ~93% of OSCC tumors were predicted to be ADAR1-dependent, consistent with our previous CRISPR screen findings. GSEA revealed enrichment of interferon (IFN)-alpha/beta signaling and keratinization pathways in ADAR1-dependent tumors. ADAR1-p150-dependent cell lines exhibited higher basal expression of numerous interferon-stimulated genes (ISGs). Upon ADAR1-p150 knockdown, these lines showed significant cell lethality accompanied by enrichment of IFN-related pathways, whereas less-dependent lines showed neither growth inhibition nor substantial upregulation in IFN signaling. Quantitative PCR and protein analyses confirmed upregulation of IFN-β and several ISGs including CXCL10 and ISG15 in dependent OSCC line upon ADAR1-p150 knockdown. Together, these findings show that ADAR1 dependency signatures can stratify OSCC tumors and identify patients likely to benefit from ADAR1-targeted therapies. OSCCs with enriched ISG expression are more susceptible to ADAR1-p150 loss, and the resulting upregulation of IFN-related gene signatures may serve as a biomarker of therapeutic response.

#0505 Molecular Standard of Care.

Sam Phillips, Eric Collisson

Fred Hutchinson Cancer Center, Seattle, WA

Background Molecular testing has transformed cancer care by enabling risk stratification, targeted therapy selection and improved patient outcomes. To evaluate the state of the field and ensure that molecular testing is consistently implemented in the appropriate clinical contexts, we developed a systematic framework—termed the *Molecular Standard of Care (MSoC)*—rooted in established guideline-based recommendations for molecular profiling.

Methods Assessment of the MSoC consisted of four components: (1) Establishment of Evaluation Criteria (EC), defining the molecular information required for guideline-concordant treatment; (2) Cohort Identification, including patients with (a) newly diagnosed metastatic disease and (b) receipt of treatment at Fred Hutch; (3) Data Abstraction, involving manual chart review of relevant disease-specific data elements and (4) Evaluation Synthesis, summarizing molecular testing data to determine adherence to the MSoC.

Results Four metastatic cancers (lung, colorectal, breast, and prostate) were evaluated using multiple cohort identification approaches. MSoCs were assembled. We reviewed 605 patients across 10 clinics over three months. 212 met inclusion criteria for MSoC assessment. The disease-specific MSoC criteria were met 89% across all four disease groups.

Conclusions MSoC can be quantitatively described with disease-specific criteria that will evolve with progress in the field. Fred Hutch Cancer Center demonstrated high adherence to guideline-based molecular testing standards across major metastatic cancers. Future work will focus on automating MSoC evaluation to reduce manual review burden and enable real-time assessment of molecular testing adherence across patient populations. This model may serve as a scalable approach to benchmarking molecular testing adherence in academic and community cancer centers.

#0506 High content CRISPR activation screens identified synthetically lethal RNA-based mechanisms to sensitize cancer cells to targeted T cell cytotoxicity.

Jeehyun Yoe, Reece V. Akana, Olivia Laveroni, Chang Sun, Young-Min Kim, Livnat Jerby

Department of Genetics, Stanford University, Stanford, CA

T cells recognize cancer (neo)antigens via T cell receptor (TCR) and selectively eliminate the target cancer cells, yet cancer cells often evolve evasion mechanisms or lack sensitizing cues that limit the efficacy of immunotherapy. While cancer CRISPR knockout screens have revealed genes whose loss drives immune evasion, far less is known about gain-of-function mechanisms capable of restoring tumor susceptibility to targeted T cell cytotoxicity. To address this gap, we developed an integrated framework combining CRISPR activation (CRISPRa), single-cell transcriptomics, and a new optical pooled high-content screening approach to uncover RNA-based mechanisms that sensitize cancer cells to TCR-specific cytotoxicity. In melanoma cells, CRISPRa screens uncovered functionally diverse regulators of T-cell killing, including the chromatin remodeler *SAFB* and additional sensitizing genes that restore susceptibility in cancer and virally infected cells. To decode how these regulators act within the native tumor context, we developed in situ Perturb-seq, a pooled optical genetic screening platform that enables single-molecule spatial transcriptomic readouts directly in intact tissues. In situ Perturb-seq, together with Perturb-seq, revealed that sensitizing perturbations converge on shared cell-autonomous and intercellular programs involving stemness-differentiation axes, cytokine networks, and ligand-receptor circuits. Notably, Wnt ligands that were found as sensitizing hits in cancer cells significantly enhanced T-cell effector functions, demonstrating how tumor-intrinsic gain-of-function perturbations can identify new modalities to reprogram and engineer T cells. Together, this work introduces a scalable platform to identify RNA-based immunomodulators and resolve their multicellular mechanisms across scales. By coupling CRISPRa screens with in situ Perturb-seq, we establish a broadly applicable framework for discovering and mechanistically defining gene activations that re-sensitize tumors to cytotoxic immune attack - including applicability beyond T cells to innate cytotoxic lymphocytes such as natural killer (NK) cells - and across distinct solid tumor types, thus opening avenues for RNA-based immunotherapies for disease treatment and prevention.

: Agentic AI in Cancer
Poster Session

#0016 DrBioRight: an AI research assistant for cancer data analysis.

Han Liang[1], Wei Liu[2]

[1]UT MD Anderson Cancer Center, Houston, TX,[2]UT MD Anderson Cancer Center

We present DrBioRight, a next-generation conversational AI platform that streamlines cancer omics analysis through a multi-agent large language model (LLM) architecture. Modern sequencing and imaging technologies generate vast and complex datasets, yet conventional analysis tools often require substantial computational expertise. DrBioRight overcomes this barrier by enabling researchers to engage in natural language dialogue with the system, transforming intricate analytical tasks into intuitive, conversational interactions. DrBioRight's chatbot-driven interface allows users to search and query datasets, execute multi-omics analyses, access interpretable insights, and generate publication-quality visualizations—all through simple questions or commands. This interaction model removes the need for programming, lowering the barrier to advanced bioinformatics and making omics research accessible to a broader scientific community. Key features include: (i) LLM-powered conversational analysis for RNA-seq, proteomics, single-cell, spatial, and clinical-genomic data ; (ii) A curated, high-performance cancer omics datastore drawing from TCGA, CPTAC, DepMap, and other public repositories; (iii) An extensible App Store integrating bioinformatics software packages, pipelines, and custom tools; (iv) Real-time task prediction, workflow guidance, and troubleshooting; (v) Collaborative workspace functionality for sharing analyses and results across research teams; (iv) Community-driven extensibility, enabling seamless integration of new datasets, modules, and analytical frameworks. By shifting from traditional technical interfaces to an interactive conversational paradigm, DrBioRight functions as an intelligent research assistant. It democratizes the use of complex omics analytics, enhances collaborative discovery, and accelerates translational research across the cancer research community.

#0017 A multicenter, prospective validation of an AI-based software (PanClaudinAI) for predicting claudin 18.2 expression via contrast-enhanced CT in pancreatic cancer.

Yaqi Zhang[1], Tianxing Zhou[2]

[1]Tianjin medical University Cancer Institute & Hospital, Tianjin, China,[2]Tianjin Medical Univ. Cancer Inst. & Hospital, Tianjin, China

Background: Claudin 18.2 (CLDN18.2) is a promising therapeutic target in pancreatic cancer. Current immunohistochemistry (IHC)-based assessment is invasive and limited by tumor heterogeneity. We developed a deep learning model using contrast-enhanced CT (CECT) to predict CLDN18.2 expression and validated it in a multicenter prospective cohort via a dedicated software application (PanClaudinAI).

Methods: We retrospectively collected CECT images and matched CLDN18.2 IHC data from 800 patients across three centers (Center A: n=400; Center B: n=230; Center C: n=170). CLDN18.2 positivity was defined as ≥75% moderate-to-strong staining. A Vision Transformer (ViT) model was trained using arterial-phase CT images. The model was integrated into a user-friendly software application (PanClaudinAI) for real-time inference. We subsequently conducted a prospective multicenter validation (Center D: n=100; Center E: n=120; Center F: n=140) to evaluate its clinical utility.

Results: The prevalence of CLDN18.2 positivity was 45.7% in the retrospective cohort and 50.2% in the prospective cohort. The AI model achieved an AUROC of 0.81 (95% CI: 0.76-0.86) with a sensitivity of 78.2% and specificity of 75.4% in center A; an AUROC of 0.84 (95% CI: 0.81-0.89) with a sensitivity of 81.5% and specificity of 79.3% in center B; and an AUROC of 0.86 (95% CI: 0.83-0.89) with a sensitivity of 82.7% and specificity of 80.1% in center C within the retrospective training set. In the prospective multicenter validation, the model maintained an AUROC of 0.79 (95% CI: 0.73-0.84) with a sensitivity of 76.5% and specificity of 74.2% in center D; an AUROC of 0.78 (95% CI: 0.74-0.82) with a sensitivity of 75.8% and specificity of 73.6% in center E; and an AUROC of 0.85 (95% CI: 0.82-0.91) with a sensitivity of 81.2% and specificity of 79.0% in center F. Moreover, the PanClaudinAI software demonstrated high usability and integration into clinical workflow, with an average processing time of <2 minutes per case.

Conclusions: We developed and prospectively validated a robust AI-based software (PanClaudinAI) that non-invasively predicts CLDN18.2 expression from routine CECT images across multiple centers. This tool facilitates rapid, reproducible, and accessible biomarker identification, potentially guiding patient selection for CLDN18.2-targeted therapies and reducing the need for invasive biopsies.

#0018 GP CoPilot: An AI-enhanced agent for cancer research.

Michael M. Reich, Thorin Tabor, Ted Liefeld, Anthony Castanza, Alexander T. Wenzel, Jill P. Mesirov

UCSD Medical Ctr., San Diego, CA

We have released GP CoPilot, a large language model (LLM)-based, chatbot-style interface allowing scientists to design and execute bioinformatic analyses and workflows conversationally. Agentic features range from basic operations such as managing files and finding and executing available analyses, to more complex behaviors such as designing workflows, monitoring running jobs, and executing bulk actions. The addition of a knowledgebase containing detailed information about the available analyses, use of the software tools, and a help forum with over 20 years of questions and answers, ensures that the recommendations that GP CoPilot provides are in general more accurate and specific than those provided by plain LLMs alone such as ChatGPT, Claude, Gemini, etc.GP CoPilot uses as its base the GenePattern platform for reproducible genomics research. First released in 2004, GenePattern provides non-computational scientists with a web-based, code-free user interface to hundreds of genomic analysis tools. These include preprocessing, expression analysis for bulk and single-cell RNA-Seq data, network and pathway analysis, proteomics, flow cytometry, as well as many general machine learning methods. Cancer-specific analyses include copy number alteration using GISTIC 2.0, significance of variants with MutSigCV, driver gene identification with MutPanning, ecDNA identification and structure elucidation with AmpliconArchitect, variant annotation with OpenCRAVAT, etc. A pipeline building tool allows for the creation of detailed workflows. When analyses are run, their inputs, parameters, and code version are recorded, ensuring reproducibility.The integration of large language models with the GenePattern platform enables a user interface that surpasses previous efforts at providing scientists with the power to design complex workflows without the learning curve required to become proficient with a tool. Even technical users can shorten the time it takes to perform analyses due to the ease with which an agent can perform low-level tasks such as retrieving data from web sites and reformatting datasets.

#0019 GenerAItive: An AI system for interpretation of gene expression analyses in cancer.

Muiz Khan, Alan Carbajo, Sorin Draghici

Computer Science, Wayne State University, Detroit, MI

High-throughput cancer studies are increasingly generating transcriptomic datasets of substantial size and complexity, prompting the adoption of systems biology approaches in medical research. Because transcriptomics analyses can yield thousands of differentially expressed genes (DEGs), enriched gene-sets, pathways, and associated regulators, pinpointing drivers of important biological processes is often time-consuming and challenging. To address this, we developed GenerAItive, an agent-based artificial intelligence (AI) that interprets gene expression analyses from iPathwayGuide, a widely used bioinformatics platform that reveals statistically significant downstream gene-sets, pathways, diseases, and upstream regulators. Our system retrieves iPathwayGuide output data and iteratively analyzes each result layer—including top DEGs, enriched gene sets (MSigDB, Gene Ontology), impacted pathways (KEGG), predicted upstream regulators (genes, miRNAs, chemicals), and associated diseases—using task-specific reasoning agents. These AI agents can investigate and interpret results that are most relevant in biological context, retrieving supporting evidence from literature and pathway analyses, and synthesizing them through large-language model reasoning to produce clear mechanistic explanations of how gene expression changes affect cancer-related processes. In testing, our system produced accurate, literature-supported interpretations of pathway activation, predicted regulators, and downstream effects. It also reproduced established findings in cancer datasets without prior exposure to those studies. These results suggest that generative AI can aid in interpretation of transcriptomic data, reduce overlooked relationships, and help researchers understand complex biological signals more quickly.

#0020 An agentic AI workflow for automated, high-fidelity curation of cancer diagnosis and staging from unstructured patient records.

Tian Kang, Elizabeth Dougherty, Shivam Mishra, Ryan Godart, Arpita Saha, Jonathan Wills, Victoria L. Chiou, Maria A. Berezina, Kunal Nagpal

Tempus AI, Inc., Chicago, IL

Purpose
Artificial intelligence (AI)-driven clinical document abstraction (CDA) using large language models (LLMs) is transforming oncology data management by extracting crucial data, such as staging and molecular profiles, from unstructured notes. We validated an agent that autonomously abstracts cancer diagnoses into structured, high-quality real-world evidence (RWE), accelerating research and supporting timely evidence-based treatment decisions with clinical-grade accuracy at scale and operational sustainability.
Methods
Our AI-CDA workflow uses a three-stage hybrid multi-agent AI design for high-accuracy, cost-efficient data abstraction:
1. Pre-screening: two specialized natural language processing (NLP) models fine-tuned on clinical notes scan the entire patient chart, classifying documents and identifying key cancer diagnosis events to select up to 100 relevant documents, reducing the LLM inference cost.
2. Extractor: a non-reasoning LLM (GPT-4.1) extracts all relevant diagnostic information from selected documents.
3. Structuring and normalization: a GPT-4.1 call synthesizes diagnosis summaries to produce structured clinical fields (e.g., diagnosis date, stage, histology) according to a predefined data model. Finally, structured fields are normalized to a fixed taxonomy by o3-mini.
System performance was benchmarked against manual abstraction on a cohort of 1497 patients (499 breast, 499 lung, 499 pan-cancer) sampled from the Tempus RW database.
Results
The automated workflow performed strongly against manual abstraction. Tissue of origin abstraction achieved a micro F1-score of 0.94, with excellent performance on common cancers (e.g., lung: 0.98, breast: 0.98, colon: 0.97). Metastasis status detection achieved 0.92 F1-score, histology 0.91, and overall stage 0.83. Initial diagnosis date accuracy was 0.90. A subsequent, adjudicated re-evaluation of discordance revealed an even higher real-world performance by correcting initial manual labeling errors. Histology F1-score rose to 0.96 (+0.05) and overall staging rose to > 0.91 (a lift of over 10%).
With regard to cost efficiency: pre-screening with two specialized NLP models reduced the average number of documents requiring LLM review >90% (from 266 to 24 per patient). This lowers LLM cost, mitigates performance degradation associated with longer context, and prioritizes only the most pertinent information.
Conclusions
This study demonstrates the feasibility and operational sustainability of an agentic AI-CDA workflow for highly accurate cancer data abstraction. This hybrid solution addresses three critical needs: scaling clinical research through automated, high-fidelity data abstraction; supporting timely evidence-based treatment decisions; and achieving operational sustainability by reducing inference cost and resourcing through a hybrid NLP/LLM workflow.

#0021 AI analysis agent to accelerate end-to-end spatial biology analysis for MERSCOPE.

Harihara Muralidharan[1], Cheng-Yi Chen[2], Friedrich Preusser[2], Ruben Cardenes[2], Kenny Workman[1], Hannah Le[1], Alfredo Andere[1], **Lorenz Rognoni**[2]

[1]LatchBio, San Francisco, CA,[2]Vizgen, Cambridge, MA

Background: Spatial biology assays on the MERSCOPE platform enable subcellular mapping of RNA transcripts and proteins within the tumor architecture. However, these assays generate terabyte-scale datasets that require complex computational workflows. Post-acquisition analysis including cell segmentation, cell typing, and spatial domain detection remains computationally intensive and requires specialized bioinformatics expertise. This can limit accessibility for many cancer biology laboratories. To overcome these barriers, Vizgen and LatchBio have developed an AI-driven workflow powered by large language model (LLM) agents, designed to streamline and simplify end-to-end spatial biology analysis for MERSCOPE in oncology research.
Methods: We implemented an LLM-driven agent tailored to the Vizgen data ecosystem. The agent (1) parses MERSCOPE outputs (multi-channel z-stack images, transcript coordinate files, metadata) and launches optimized GPU-accelerated workflows for image segmentation and transcript assignment; (2) presents an interactive notebook interface (Markdown, plots, widgets) so users can specify downstream questions in natural language (e.g., “Identify Cytotoxic T-Cells within tumor border regions”); (3) triggers bioinformatics pipelines for clustering, cell-type annotation, spatial domain detection, and differential expression/regulation; and (4) integrates with LatchBio’s scalable compute/storage infrastructure for large-scale runs (>1 TB per dataset). We validated performance on breast cancer and colorectal cancer samples processed on MERSCOPE.
Results: The agent successfully handled large-scale, multi-sample MERFISH spatial transcriptomics datasets. It performed end-to-end analysis (cell re-segmentation, unsupervised clustering, spatial domain detection, and differential expression in selected cell populations) within a single run. Outputs were delivered as interactive, reproducible notebooks for a rapid review of cell-type-annotated clusters, spatial domain maps, and differential expression summaries. Compared with a conventional manually scripted workflow, the agent completed full analyses in ~6 hours (vs ~72 h traditionally). In end-user testing, it reduced manual scripting and dependency management efforts by ~60 % and decreased downstream errors, improving pipeline reliability.
Conclusions: The Vizgen-LatchBio AI-agentic workflow provides a scalable, user-friendly solution for advanced MERSCOPE data analysis, enabling spatial biology labs to self-serve complex computational tasks. By abstracting computational complexity and embedding domain-specific logic, this system empowers biologists to focus on biological insights rather than technical tool-chaining. Consequently, it shortens time-to-insight and facilitates high-throughput workflows across drug discovery, disease research, and academic studies.

#0022 Multi-agent AI system for autonomous CAR-T development: Integrated target discovery, toxicity prediction, and rational molecular design for cancer immunotherapy.

Yi Ni, Liwei Zhu

Bio LIMS INC, Boston, MA

Background: Chimeric antigen receptor T-cell (CAR-T) therapy has achieved remarkable success in hematologic malignancies, yet only 6 products have gained FDA approval since 2017, with target selection and toxicity remaining critical bottlenecks. Conventional pipelines require 8-12 years with 40-60% failure rates due to inadequate validation or safety liabilities. Notable clinical setbacks underscore urgent need for autonomous systems predicting safety risks before costly trials.
Methods: We developed Bio AI Agent, a multi-agent AI system powered by large language models enabling autonomous CAR-T development. The architecture comprises six agents: (1) Target Selection for antigen prioritization, (2) Toxicity Prediction integrating tissue atlases and pharmacovigilance databases, (3) Molecular Design for modular CAR engineering, (4) Patent Intelligence for freedom-to-operate analysis, (5) Clinical Translation for regulatory guidance, and (6) Decision Orchestration for multi-agent coordination. Agents communicate through shared knowledge base with vector database and natural language interfaces.
Results: Retrospective validation demonstrated autonomous capabilities across key stages. Target assessment streamlined 3-4 month workflows to rapid processing. Toxicity prediction accurately identified problematic targets through expression profiling and adverse event analysis. Patent intelligence flagged infringement risks enabling compliant design strategies. Molecular design demonstrated systematic optimization with real-time prediction. Decision orchestration generated comprehensive roadmaps spanning validation, pathway development, and clinical translation.
Conclusions: Bio AI Agent addresses critical CAR-T development gaps through intelligent collaboration across target discovery, safety prediction, and molecular optimization. Autonomous identification of liability targets with mitigation strategies demonstrates potential for reducing attrition and improving safety. Multi-agent architecture enables parallel processing and specialized reasoning superior to monolithic systems. As CAR-T expands into solid tumors, autonomous platforms will be essential for accelerated precision oncology.

#0023 ImmunoVerse-Chat: A conversational agentic-AI engine for next-generation immunotherapeutic target discovery.

Aman Sharma[1], Guangyuan (Frank) Li[2], Xinya Liu[2], Mark Yarmarkovich[2]

[1]Perlmutter Cancer Center, Perlmutter Cancer Center, New York University Grossman School of Medicine, New York, NY,[2]Perlmutter Cancer Center, New York University Grossman School of Medicine, New York, NY

T-cell based immunotherapies such as CAR-T Cells, BiTEs and an expanding class of next-generation T-cell-engaging modalities, have revolutionized cancer treatment and dramatically improved outcomes for many patients. Yet, the success of these therapies fundamentally relies on identifying safe, tumor-specific targets. However, current practice relies on labor-intensive convoluted bioinformatics efforts that require deep domain expertise and extensive coordination between computational scientists and clinicians. These fragmented workflows slow the pace of discovery and significantly delay the transition of emerging targets into therapeutic development. To overcome these challenges and motivated by recent advances in large language models and agentic AI, we developed ImmunoVerse-Chat, an interactive agentic framework that integrates LLM-driven reasoning with high-performance immunogenomic pipelines to streamline and accelerate tumor-specific antigen discovery. Built upon our previously established ImmunoVerse, the most comprehensive pan-cancer therapeutic T cell targets to date, spanning over 21 tumors, 11 classes of molecular events. Together, these system-level innovations allow ImmunoVerse-Chat to uncover clinically meaningful antigen patterns that are often overlooked or inaccessible to conventional pipelines. ImmunoVerse-Chat streamlines the entire immunopeptidomic workflow from raw multi-omic data to pHLA identification and provides an interactive, reasoning-driven interface that enables rapid comparison of antigen landscapes, real-time target prioritization, and assessment of T-cell therapeutic potential. By leveraging the underlying pan-cancer antigen atlas, the system, through automated visualization modules, further contextualizes these findings across tissue types and molecular aberrations to distinguish shared and tumor-restricted pMHC candidates and uncover recurrent, population-relevant antigens, tumor-resident microbial epitopes, and molecular signatures linked to splicing, immune regulation, and endogenous retrovirus expression, including ERV-derived peptides. These integrated, multi-layered insights directly guide the selection of safe, immunogenic, and clinically meaningful T-cell targets. Overall, ImmunoVerse-Chat combines AI reasoning with multi-omic depth into a unified, interactive, and population-aware engine for T-cell target discovery, and we envision the broad adoption of this platform will democratize antigen discovery across oncology research and accelerate the development of next-generation immunotherapies.

#0024 CertisAI Assistant: An agentic AI platform for dynamic preclinical oncology model selection.

Luke Jervis, Warren Andrews, Yuan-Hung Chien, Raffaella Pippa, **Long Hoang Do**

Certis Oncology Solutions, San Diego, CA

Conventional tumor model selection often operates as a target-driven process, relying primarily on established biomarker strategies and prior treatment profiles to identify models aligned with a specific therapeutic goal. This methodology, rooted in static, retrospective datasets, frequently limits the scope of investigation and can result in selecting models that have reduced predictive power for complex clinical outcomes. To enhance the selection criteria for preclinical tumor models, we developed the CertisAI Assistant, an agentic AI platform that integrates real-time, on-demand therapeutic response prediction with deeply characterized tumor model datasets within a unified research environment.

The CertisAI Assistant functions as an interactive research tool, integrating models from the Cancer Cell Line Encyclopedia (CCLE) and Certis' proprietary patient-derived xenograft (PDX) data. Its core is CertisAI, an ensemble of machine learning models trained on extensive monotherapy and combination drug response data, leveraging gene expression and molecular fingerprints. We engineered a secure, self-service client that enables users to upload novel therapeutic compounds (via SMILES string) or sequencing data (via FASTQ files) for immediate, on-demand therapeutic predictions.

Prediction results are dynamically integrated into the generative AI assistant, allowing for natural language querying and comparative analysis. Key visualizations, including mono and combination therapy prediction results, are instantly available. The CertisAI Assistant moves beyond static data delivery, providing a dynamic, real-time analysis environment for therapeutic response prediction and model selection. This platform significantly accelerates preclinical oncology research by empowering users to rapidly test hypotheses, evaluate novel agents, and guide the development of effective combination strategies.

#0025 Agentic AI for RNA-Seq: From workflow automation to actionable insights.

Arthur Liberzon, Pablo Cingolani, Steven Wood Criscione, Etai Jacob

Oncology R&D, AstraZeneca, Waltham, MA

Automating bioinformatic analyses of RNA-seq data is challenging because each project requires unique combinations of analytical steps and frequent, case-specific adjustments. These project-specific processes limit the reusability of workflows to other analyses and require extensive manual coding. Large language model (LLM) agents are well-suited to address these challenges because they can interpret natural language instructions, dynamically plan workflows, and adapt to study-specific requirements without manual coding.We developed an agentic AI platform that uses LLMs to plan, execute, and interpret bulk RNA-Seq analyses via natural language instructions. The platform includes two implementations: an interactive Streamlit app where users can upload data and describe the project, and a non-interactive API for integration into larger agentic ecosystems to enable extension to single-cell RNA-Seq and mutation analyses. Our system leverages vetted, state-of-the-art methods to ensure reproducibility while performing analyses such as PCA, differential expression, and pathway enrichment in Python. The platform generates actionable reports that contextualize tables and figures in the project context. Key capabilities include automatic contrast generation, covariate handling, and accurate identification of differentially expressed genes and enriched pathways. Validation studies demonstrate that PCA clustering, differential expression and pathway scores align with expected biology and match manual pipeline accuracy.This agentic approach reduces coding effort, improves reproducibility, and democratizes the accessibility of RNA-Seq analysis, with the possibility of expanding multi-omics analyses.

#0026 Multi-agent AI orchestration for temporal-aware extraction of social determinants of health from unstructured clinical records in cancer populations.

Asim Waqas[1], Aakash Gireesh Tripathi[2], Kris Bowles[1], Brianna Miner[1], Jessica Yasmine Islam[3], Anna E. Coghill[1], Anastasia Jones[4], Matthew B. Schabath[3], Ghulam Rasool[5]

[1]Cancer Epidemiology, Moffitt Cancer Center, Tampa, FL,[2]H. Lee Moffitt Cancer Center,[3]Moffitt Cancer Center, Tampa, FL,[4]Anesthesiology, Moffitt Cancer Center, Tampa, FL,[5]Machine Learning, Moffitt Cancer Center, Tampa, FL

Purpose: Social determinants of health (SDOH) influence cancer outcomes, yet extraction of these variables from unstructured clinical documents in electronic health records remains challenging due to their temporal complexity and narrative dispersion across multiple document types. Single large language models (LLMs) frequently hallucinate, misidentify temporal context, and cannot reliably distinguish between current barriers and historical mentions. We developed a multi-agent artificial intelligence (AI) orchestration framework that employs specialized agents with defined roles to extract temporally-aware SDOH variables for cancer research and clinical decision support.

Experimental Design: We implemented coordinated agents with different roles, focused on specific social determinant domains, directing task allocation, verifying extracted information, and assembling temporally-ordered patient timelines. We assembled two retrospective cohorts including cancer patients with HIV (n=100) and peri-operative pain management (n=524), encompassing 81k words/patient (≈8.1M words in 3,460 documents) and 49k words/patient (≈25.8M words in 15,484 documents), respectively. The framework processed clinical data, nursing communications, social work assessments, pathology reports, and imaging reports.

Results: We successfully extracted temporal SDOH variables with >95% confidence across both cohorts, constructing comprehensive patient timelines that distinguished between current and historical barriers. The multi-agent architecture addressed single-model limitations by cross-validating extractions, grounding findings in specific document evidence, and maintaining temporal accuracy. For HIV cohort, the system processed 10.8M model tokens, automatically identifying financial difficulties, transportation barriers, and housing instability with dates and supporting documentation. The peri-operative pain cohort required 34.3M tokens, revealing temporal patterns in social support availability and medication access challenges. Beyond SDOH variables, system automatically extracted complementary clinical information, including diagnoses and care transitions, enabling researchers to contextualize SDOH within broader clinical narratives.

Conclusions: We demonstrated that orchestrated multi-agent AI can reliably extract temporally-aware SDOH from real-world clinical documentation, addressing critical limitations of single LLM approaches. By providing structured, time-stamped extraction with evidence provenance, the framework enables practical clinical applications including patient triage for social work intervention, standardized disparities reporting, and research cohort characterization, making it suitable for deployment across diverse cancer populations.

#0027 An MCP-enabled AI agent for automated multimodal genomics analysis in the Isabl Platform.

Juan E. Arango Ossa[1], Dylan Domenico[2], Asher Preska Steinberg[1], Eliyahu Havasov[2], Gunes Gundem[2], Konstantinos Liosis[2], Alessandro Grande[1], Jesus Gutierrez-Abril[3], Elli Papaemmanuil[2], Sohrab Shah[2], Andrew William McPherson[2]

[1]Computational Oncology, Memorial Sloan Kettering Cancer Center, New York, NY,[2]Memorial Sloan Kettering Cancer Center, New York, NY,[3]Memorial Sloan Kettering Cancer Center, New York

Background:
Modern precision oncology pipelines generate petabyte-scale multimodal genomics data requiring coordinated access to databases, APIs, and reproducible workflows. The Isabl Platform (Medina et al., BMC Bioinformatics 2020) is broadly adopted across multiple groups at Memorial Sloan Kettering Cancer Center (MSKCC) and external research institutions. In the Halvorsen Center for Computational Oncology at MSKCC, the platform manages 470 projects, 105k sequencing experiments from 70k individuals, and 580k analyses totaling more than 4.5 PB of data. Although powerful, its depth and schema complexity create a learning curve for analysts, clinicians, and computational researchers. Large Language Models (LLMs) reduce this barrier by translating natural-language questions into actionable queries, retrieving documentation, and safely interacting with evolving scientific tools.
Methods:
We developed the Isabl AI agent and an Isabl MCP, enabling any MCP client to access Isabl tools through a standardized interface. The agent integrates Retrieval-Augmented Generation (RAG), which retrieves relevant documentation to ground outputs, with the Model Context Protocol (MCP), a common standard for tool discovery and safe execution in LLM-based applications. GitBook documentation, the OpenAPI schema, CLI references, laboratory pipeline definitions, and core Isabl modules are indexed into a multi-vector semantic store. A ReAct-style agentic controller selects MCP tools such as call_isabl_api or run_isabl_app, supported by recursive chunking and modern embeddings.
Results:
The agent handles analytical tasks such as:
• Cohort discovery, e.g.: “Identify pediatric B-ALL tumors with IKZF1 deletions and available RNA-seq.” It retrieves samples, summarizes counts, and reports assay availability.
• Multi-step reasoning, e.g.: “How many high-risk neuroblastomas have 17q gain?” It finds eligible cases, locates CNV analyses, extracts 17q21-17q25 copy-number values, applies thresholds, and reports frequencies.
• Workflow execution, e.g.: “Launch the whole-genome variant-calling pipelines for newly added pediatric sarcoma patients with matched germline controls.” It identifies tumor-normal pairs, checks existing analyses, and submits pipelines. These tasks show reduced onboarding time, intuitive schema navigation, and improved execution through natural language.
Conclusions:
Isabl AI Agent + MCP demonstrates how RAG, MCP’s standardized interface, and agentic reasoning simplify access to complex genomic systems. As MCP adoption grows in AI for scientific discovery, an Isabl MCP enables domain-specific capabilities to integrate into general-purpose AI models, providing a sustainable path for AI copilots that accelerate translational genomics research.

#0028 PortrAIgent: Co-scientist agent for end-to-end spatial transcriptomics discovery.

Yuchang Seong, Dongjoo Lee, Chanho Park, Hongyoon Choi

Portrai, Inc., Seoul, Korea, Republic of

Background
Spatial transcriptomics (ST) technology maps gene expression within tissue structures, offering unprecedented insights into tissue organization and cellular interactions. Analyzing these complex datasets, however, remains a significant bottleneck. Current workflows demand specialized, multi-domain expertise and rely on heavy manual intervention, an expertise barrier that hinders the rapid translation of data into biological insights.
Method
To address this challenge, we developed 'PortrAIgent,' a co-scientist AI agent that autonomously manages complex analysis workflows. The system operates by having (1) a multimodal LLM for reasoning, planning, and code generation; (2) a LangGraph-based workflow manager control the execution order of analysis steps; and (3) specialized computational tools, including a code execution environment and a real-time literature retrieval tool. A core feature of the agent is its Retrieval-Augmented Generation (RAG) system, which leverages codebases from scanpy, squidpy, and scvi-tools to integrate diverse informatics tools for specialized objectives like cell typing, spatial profiling, or data integration.
Results
Two workflows were successfully validated: 1) Hypothesis-Driven Exploration: When a user presents a biological hypothesis, the agent proposes alternative hypotheses, refines them via literature search, and then passes the plan to a ‘Reviewer Agent’. Following this validated plan, the agent proceeds to execution. 2) Analysis-Driven Workflow: For simple requests (e.g., "group comparison"), the agent's Planner checks the AnnData object's state to determine the optimal analysis functions before generating and executing the code. We demonstrated PortrAIgent by applying it to analyzing TME by ST data. Autonomous reasoning capability of this framework was validated by testing the system on multiple ST datasets with varying preprocessing states. The agent consistently detected missing steps (e.g., normalization, HVG selection, batch correction), revised its own plan, and regenerated the appropriate code without manual intervention. It interpreted the biological meaning of the discovered patterns using real-time literature search and generated a comprehensive research report summarizing the entire discovery process.
Conclusion
PortrAIgent offers a novel approach to automated scientific discovery in spatial biology for oncology. Beyond the primary case study, the system was tested across multiple tissue contexts, where it reliably adjusted analysis plans, corrected missing preprocessing steps, and generated coherent biological interpretations comparable to expert feedback. By integrating dynamic RAG-based code generation, autonomous execution, and comprehensive report generation, PortrAIgent streamlines complex spatial data analysis and lowers the expertise barrier for understanding complex biological systems.

#0029 Reasoning-guided retrieval improves oncology trial eligibility matching from clinical notes.

Vivek Shetye, **Patrycja Nikol Krawczuk**, Ryan Godart, Arpita Saha, Gabriel Altay, Chelsea Osterman, Gena Rangel, Samantha Garrett, Victoria L. Chiou, Kunal Nagpal

Tempus AI, Inc., Chicago, IL

Purpose: Under-enrollment in oncology trials is exacerbated by the manual effort required to screen unstructured clinical records against complex eligibility criteria. Large language models (LLMs) augmented with retrieval mechanisms show promise for automating the process but often fail to capture dispersed evidence required for complex, multi-criterion eligibility decisions. We hypothesized that an agentic retrieval strategy, which empowers an LLM to autonomously and iteratively search, synthesize, and validate relevant information, would enhance evidence completeness and accuracy in eligibility classification.

Methods: Evaluation encompassed two task types: (i) complex eligibility reasoning and (ii) biomarker extraction. The complex tasks drew on two non-small cell lung cancer (NSCLC) studies with intricate eligibility criteria: stage III unresectable NSCLC and metastatic NSCLC. Each query represented a patient-level eligibility assessment (total n=618 queries) that required integrating multiple evidence types, including molecular findings, prior therapies, and clinical status. The biomarker task included 148 evaluations targeting key genomic alterations (EGFR, ESR1, RAS).We compared a retrieval-augmented generation (RAG) system that retrieved fixed, similarity-based text chunks with an agentic retrieval approach performing up to 8 adaptive searches. The agent autonomously assessed retrieved evidence, reformulated its queries, and iteratively expanded the search scope to assemble a comprehensive context. Both systems, using LLM (Gemini 2.5 Pro), reviewed up to 64 text chunks per query. Model outputs were benchmarked against expert-curated ground truth using F1-score, recall, and accuracy.

Results: Agentic retrieval improved performance across complex eligibility reasoning tasks. In the stage III NSCLC, accuracy rose from 68% to 80% (+12.7 pp; 95% CI: 7.9-17.7), driven by a 15% gain in recall (69% to 84%) and a 9% increase in F1-score from 79% to 88%. In metastatic NSCLC, accuracy improved from 77% to 84% (+6.3 pp; 95% CI: 1.3-11.6) and the F1-score from 86% to 90%. In contrast, the biomarker extraction task showed comparable performance (accuracy 95-96%, F1 96%) for both methods, indicating minimal benefit from agentic reasoning where retrieval complexity was low.

Conclusions: This study demonstrates the translational value of agentic retrieval for precise, scalable oncology trial screening. By enabling adaptive evidence synthesis rather than static retrieval, the system improves the completeness of eligibility assessment and minimizes manual review effort.

#0030 Automated cohort extraction from real-world oncology data using adaptive LLM-based agentic systems for clinical trial feasibility and patient selection.

Brandon Theodorou[1], Thomas Schmitt[2], Zifeng Wang[1], Venugopal Thati[1], Angela Watkins[2], Kimberly Banks[2], Jimeng Sun[1], Amar Das[2]

[1]Keiji AI, Seattle, WA,[2]Guardant Health, Palo Alto, CA

Clinical feasibility analysis and cohort identification have essential applications in precision oncology, including feasibility assessment for clinical trial and other study designs, cohort extraction for digital twin modeling and virtual trial simulation, and real-world evidence generation for regulatory submission and comparative effectiveness research. However, real-world oncology datasets pose significant challenges due to heterogeneous, nonstandard data formats and complex, interconnected inclusion criteria. These technical barriers are compounded by functional hurdles like technical understanding, data access, and code execution. Traditional approaches rely on slow, unscalable manual query construction, and even recent state-of-the-art large language models (LLMs) struggle with multi-step reasoning and adaptation to diverse data structures.

To address these issues, we developed an adaptive LLM-based agentic platform that autonomously learns data structures, generates and executes code, and iteratively refines analyses to extract patient cohorts meeting complex criteria. Unlike conventional LLMs that generate static code without execution capabilities or dataset adaptation, our platform's agentic architecture dynamically explores data schemas, validates intermediate outputs, and self-corrects errors. It also accepts expert guidance and allows fully auditable, editable, and exportable outputs at each step of the process. The system accepts natural language queries specifying complex criteria such as specific diagnoses, genomic profiles, treatment histories, and temporal relationships, then autonomously navigates real-world data (RWD) of any shape, size, and format to identify qualifying patients.

We evaluated performance by replicating 15 historical feasibility analyses from the GuardantINFORM™ database, which integrates genomic and epigenomic RWD from >550K patients with de-identified administrative claims data across multiple oncology indications and data tables. Our validation study found that the platform successfully extracted exact cohorts for 12 requests and delivered clinically acceptable approximations for 2 more. The final analysis failed due to a clinical misunderstanding but was correctable post hoc with improved guidance. In contrast, state-of-the-art LLMs without tuned agentic capabilities failed to adapt to dataset-specific structures and had low task completion rates, highlighting the critical importance of the task-based design, iterative execution, and self-correction. This performance democratizes access to sophisticated data analysis, addressing a critical bottleneck in translating RWD into actionable clinical insights and establishing a foundation for autonomous, adaptive AI systems that can accelerate oncology research.

#0031 Charles: A self-critical agentic AI drug discovery analyst for cancer.

Seyedmehdi Orouji, Ying Zhu, David Maxwell, Kaitlyn Russell, Bissan Al-Lazikani

UT MD Anderson Cancer Center, Houston, TX

Background: Agentic AI will be members of scientific teams of the future. AI hallucinations and unreliable and untraceable public data cast shadows on such a role. We developed what is to our knowledge the first self-critical, self-correcting agentic-AI drug discovery analyst: Charles. It supports information synthesis and hypothesis generation for cancer drug discovery while maintaining scientific robustness.

Methods: Charles is an agentic GPT-based LLM. Building Charles consisted of fact-constrained, imitation-based teaching exercise led by the human PI. A human supervisor carefully optimized the environment to constrain Charles to reliable sources and prevent retrieving external knowledge. An adversarial AI agent acts as the self-critical 'conscience' to test the veracity of Charles's answers against the true data. We further evaluated this by injecting decoy raw data, allowing quantitative evaluation of the models' veracity. The trained model was used to synthesize factual target summaries. We then developed a multi-agent LLM that leverages these data-grounded summaries to answer real-word drug discovery questions. A planner agent digests the user's questions and orchestrates a coordinated plan of action to direct the specialist agents (bio-/chemo-/systems etc). Finally, a critical AI agent fact-checks the responses from specialist agents, reporting them to the planner agent for further refinement of actions. Together, these modules form Charles.

Results: We demonstrate that Charles' responses are strictly grounded in the curated data. Initial evaluations show Charles reproduces all adversarial decoys indicating no outside leakage. To further evaluate the reasoning and factual accuracy of Charles, we utilized a question-answer dataset that Charles answers through interpretation of the >1000 protein summaries. Using the self-critical agent, we evaluated both the summaries and the answers to questions. The initial evaluation of the multi-agent framework shows 99% accuracy in Charles's responses. The planner successfully recruited the appropriate specialized agents while the critical agent showed promising behavior in detecting semantic and factual inconsistencies to the planner. The output summaries are publicly available via canSAR.ai.

Conclusions: Charles represents a self-critical, drug discovery-trained, AI analyst capable of synthesizing multimodal information, evaluating its own outputs, and refining the next steps based on that. By combining the reasoning power of LLM-based interactions with the assurance of verified curated data, Charles provides reliable access to complex oncological knowledge while minimizing hallucinations and enabling researchers to make data-driven decisions with more confidence in cancer research.

#0032 Agentic AI-enabled exploration of real-world immune-related adverse events.

Gabriela Fort[1], David Stone[1], Ching-Nung Lin[1], Arabella Young[2], Aik Choon Tan[1]

[1]Department of Oncological Sciences, University of Utah, Salt Lake City, UT,[2]Department of Pathology, University of Utah, Salt Lake City, UT

Immune checkpoint inhibitors (ICIs) have transformed cancer therapy, but their clinical benefit is often limited by the onset of immune-related adverse events (irAEs), which can be severe and lead to treatment interruption or discontinuation. A deeper understanding of irAEs is urgently needed to identify patients at highest risk of developing adverse events and to guide strategies for irAE prevention and risk management. The FDA's Adverse Event Reporting System (FAERS) database contains over 32 million adverse event reports submitted to the FDA to support drug safety surveillance. However, although a public dashboard exists to perform basic exploration of FAERS data, extracting immuno-oncology-related safety events or executing complex, multiparameter queries of this data still requires substantial technical expertise, programming skills, and a familiarity with the underlying database structure. To address this gap and to enhance the accessibility of this public resource, we downloaded all FAERS reports from 2012-2025 and systematically filtered for cancer cases treated with ICIs. We curated a high-quality, oncology-specific irAE dataset and generated a standardized flat-file resource for downstream data exploration and analysis. To further facilitate access and enable non-programmers to easily explore these data, we developed an agentic AI-driven interface and workflow that allows natural language querying of the dataset. Our system uses open-source large language models with specialized prompting to classify user intent and generate executable python code for complex analytical tasks including filtering, visualization, and statistical analyses, returning results in real time. This framework enables interactive and flexible exploration of irAE patterns across tumor types, drug classes, and other clinical features. Preliminary analyses recapitulate known irAE associations in cancer (e.g. elevated endocrine and cutaneous toxicities compared to other irAEs in anti-PD-1-treated patients) and reveal potential tumor and treatment-specific irAE profiles that warrant further investigation. In summary, this platform provides a transparent, scalable, and user-friendly approach for mining real-world immunotherapy safety data that may be leveraged to inform biomarker discovery, fuel hypothesis generation, and/or guide irAE risk mitigation strategies in immuno-oncology.

#0033 A healthcare system scale multimodal whole patient temporal foundation model.

Andrew Zhang[1], Tong Ding[1], Sophia J. Wagner[1], Caiwei Tian[1], Ming Yang Lu[1], Alexandre Misrahi[1], Joshua E. Lewis[1], Rowland Pettit[1], Long P. Le[2], Faisal Mahmood[1]

[1]Harvard Medical School/Brigham and Women's Hospital, Boston, MA,[2]Pathology, Harvard Medical School/Massachusetts General Hospital, Boston, MA

Healthcare data are fragmented across time and modalities, including clinical reports, imaging, and lab tests. While Electronic Health Records (EHRs) capture rich longitudinal health trajectories, current predictive modeling approaches typically model individual modalities in isolation, missing the context needed to understand complex diseases such as cancers. To bridge this gap, we aim to synthesize the entirety of a patient's medical history into a unified computable representation.

We curated a retrospective cohort from a major U.S. healthcare system, comprising 25 billion medical events from 7.2 million patients spanning 33 years. This dataset integrates 28 distinct clinical modalities, including structured data (diagnoses, medications, vital signs, flowsheet, and laboratory results), clinical notes, and imaging data. We developed a transformer-based multimodal temporal foundation model that tokenizes each modality with modality-specific encoders and fuses events over time into a unified patient embedding.

We evaluated frozen patient embeddings on 246 downstream prediction tasks, including new onset of 87 diseases, progression of 56 diseases, treatment response for 100 therapy-outcome pairs, and three short-term operational tasks. Across all tasks, the model achieved a mean AUROC of 0.77, outperforming age-sex, clinical text, and task-specific supervised baselines. On oncology-focused tasks spanning solid and hematologic malignancies and systemic therapies, the model outperformed the age-sex baseline by 9% for new neoplasm onset, 18% for neoplasm progression, and 16% for treatment response. Unsupervised clustering of patient embeddings recovered clinically coherent groupings of cancer types, comorbidities, and treatment patterns, forming a multiscale, data-driven atlas of medical phenotypes. The same embeddings enabled similarity search to identify patients with comparable trajectories, supporting automated cohort discovery and fine-grained clinical trial matching. Gradient-based interpretability analyses identified multimodal risk factors for disease onset and treatment response that aligned with clinical expectations, providing transparent attribution at both patient and population level.

A single multimodal, temporally aware EHR foundation model can learn general-purpose whole-patient representations that support accurate early prediction and phenotyping of cancer outcomes while remaining applicable across diverse diseases. By consolidating fragmented data into a continuously updated patient representation, this approach lays the groundwork for shifting oncology from reactive, episodic care to proactive, continuous risk management, and provides a scalable basis for risk stratification, trial optimization, and discovery of clinically interpretable multimodal biomarkers.

#0034 Attitudes and perception of artificial intelligence in healthcare: A cross-sectional survey among Arkansas-Louisiana-Texas (ArkLATX) veterans with cancer.

Philip A. Haddad[1], Sireesha Vutukuri[2], Philip Bouchette[2], Crystal Barmer[2], Ankita Gupta[2]

[1]LSUHSC-S/Overton Brooks VAMC, Shreveport, LA,[2]Overton Brooks VAMC, Shreveport, LA

Background: The attitudes about the use of Artificial Intelligence (AI) in healthcare are controversial. Unlike the perception of healthcare professionals, the attitudes of cancer patients, especially veterans, have hardly been explored. In this quality improvement study, we aimed at investigating veterans' perception of AI within the VA among this highly relevant group, along with digital affinity and sociodemographic factors.

Methods: We conducted a cross-sectional survey using a questionnaire-based interview with patients at Overton Brooks VA Medical Center Hematology-Oncology Clinics from December 2024 to February 2025. The questionnaire consisted of sections exploring demographics, participants' technical affinity, and their perception of the utility of AI in healthcare, the providers' AI competence, their concerns, and the need for oversight.

Results: A total of 250 participants were accrued with a median age of 72. Ninety-one percent were men, with 52% finishing high school and 44% feeling comfortable using technology. More than 78% read or heard about artificial intelligence, but only 8% reported knowing a lot. Asked about their general perception of AI utility in healthcare, 55% of the respondents rated the use of artificial intelligence as positive or very positive, 48% agreed to its incorporation in their own medical care, but only 11% held a negative or very negative perception. Forty percent of veterans expressed concerns about potential AI safety and security issues. Forty-five percent thought the providers knew enough about AI to use it properly. Ninety-five percent wanted artificial intelligence to be rigorously tested and deployed with a physician in the loop. Unlike age, sex, and educational level, only certain aspects of technical affinity statistically impacted the perception of AI healthcare utility, concerns, and AI oversight.

Conclusions: ArkLATX veterans with cancer are mostly open to the use of AI in healthcare. Although showing little to no knowledge about AI, a majority had a positive perception of its utility in healthcare. Nevertheless, veterans insist that a physician supervises AI and assumes ultimate responsibility for diagnosis and therapeutics.

#0035 Humans cannot live by artificial intelligence (AI) alone.

Kim Blenman, Ondrej Blaha, Sherry Qiu, Kelly Chen, Kiera Spall, Yiran Liu, Madsion Williams, Marissa Villa, Valeri Vankov, Kwabena Oteng Agyapong, Di Li, Holly Rushmeier

Yale University, New Haven, CT

INTRODUCTION: Differential expression (DE) analysis is the cornerstone of omics evaluation. It is used to identify biomarkers for cancer, therapeutic response, and drug-induced adverse events. DE methods use AI/ML (machine learning). If multiple DE methods could identify the same biomarkers, this would strongly support the biomarker's use as a robust candidate(s) for wet lab validation studies. It is unclear if the top DE methods identify the same biomarkers (i.e., shared). Therefore, we evaluated 4 DE methods for their ability to identify shared serum autoantibodies in cancer patients with and without immune-checkpoint inhibitor induced hypothyroidism (TEAE ThyDis).
METHODS: Patients with breast cancer (N=8) or melanoma (N=25) who were treated with durvalumab, ipilimumab, pembrolizumab, nivolumab, or combination who had TEAE ThyDis (N = 18) or No TEAE (N = 15) were included. Four DE methods (limma, DESeq2, edgeR, randomForest) were used in R. 15,500 pre-treatment autoantibodies with and without ComBat batch correction were evaluated for each patient.
RESULTS: In patients with breast cancer, limma, DESeq2, edgeR, and randomForest identified 201, 109, 158, and 472 biomarkers, respectively (Table 1). However, only up to 53 biomarkers were shared between the 4 DE methods. ComBat batch correction with limma or randomForest led to identification of 125 and 484 biomarkers respectively and up to 114 shared biomarkers between the 4 methods. In patients with melanoma, limma, DESeq2, edgeR, and randomForest identified 198, 244, 568, and 1042 biomarkers respectively with up to 183 biomarkers shared (Table 1). ComBat batch correction with limma or randomForest led to identification of 196 and 1088 biomarkers respectively and up to 257 shared. There was no biomarker that was shared in all methods.
CONCLUSIONS: Our data suggests that top AI/ML DE analysis methods identify different biomarkers. As a field, it is time to re-evaluate and re-vamp these tools as well as create new tools to ensure robust reproducible biomarker identifications.

: Mechanisms and Targets in DNA Damage Repair
Poster Session

#0510 Early metabolic and differentiation remodeling in *BRCA1/2* high-risk fallopian tube epithelium revealed by single-cell multi-omics.

Quentin Chartreux[1], Marcela Haro[1], Josh Brand[2], Andrew Li[3], Bobbie J. Rimel[4], Patrick Sung[5], Simon Gayther[1], Huy Dinh[2], Fabiola Medeiros[3], Kate Lawrenson[1]

[1]Center for Inherited Oncogenesis, University of Texas at San Antonio, San Antonio, TX,[2]School of Medicine and Public Health, University of Wisconsin-Madison, Madison, WI,[3]Cedars-Sinai Medical Center, Los Angeles, CA,[4]University of Washington, Seattle, WA,[5]Department of Biochemistry and Structural Biology, University of Texas at San Antonio, San Antonio, TX

Germline mutations in *BRCA1* and *BRCA2* greatly increase the risk of developing high-grade serous carcinoma (HGSC), yet the earliest molecular events driving malignant transformation in the fallopian tube epithelium, the likely site of origin, remain poorly understood. Defining these early alterations is essential for improving risk prediction and informing preventive strategies for *BRCA*-associated ovarian cancer.To investigate the initial cellular and molecular perturbations in high-risk individuals, we performed single-cell transcriptomic and multi-omic profiling on fallopian tube fimbrial samples obtained through exfoliative cytology brushings and conventional tissue specimens. Single-cell RNA sequencing was conducted on 14 brushings from BRCA1/2 mutation carriers, 3 brushings from average-risk individuals, and 12 tissue samples from average-risk controls. In parallel, single-cell multi-omic analysis was applied to short-term epithelial cultures derived from 4 high-risk and 2 average-risk individuals, enabling an integrated assessment of transcriptional states, chromatin accessibility, and gene regulatory programs.Brushings were enriched for epithelial and immune populations, facilitating high-resolution characterization of epithelial differentiation. Cells from *BRCA1/2* mutation carriers exhibited disrupted secretory-ciliated differentiation trajectories, accompanied by upregulation of mitochondrial respiration and oxidative phosphorylation genes, suggesting early mitochondrial and metabolic remodeling in high-risk epithelia. Multi-omic integration further identified a distinct epithelial cluster enriched in *BRCA1/2* carriers characterized by increased *RUNX3* transcription factor activity. Although these cells remain transcriptionally aligned with secretory epithelium, *RUNX3*-associated programs indicate a partial or intermediate differentiation state—potentially reflecting early lineage instability preceding malignant transformation. Subtle alterations in immune-related pathways were also observed, pointing to microenvironmental changes that may support a permissive niche for tumor initiation.Together, these data reveal early transcriptomic, metabolic, and gene-regulatory remodeling in the fallopian tube epithelium of *BRCA* mutation carriers. By defining epithelial states and pathways perturbed prior to neoplasia, this work provides new mechanistic insight into hereditary ovarian cancer predisposition and highlights potential biomarkers for early detection and prevention.

#0512 Wild-type IDH1 inhibition induces homologous recombination deficiency and enhances PARP inhibitor sensitivity in pancreatic cancer.

Mehrdad Zarei[1], Priyashree Sunita[2], Alexander Loftus[3], Faith Nakazzi[4], Semmer Ali[4], Om Prajapati[5], Soubhi Tahhan[6], Hallie J Graor[2], Shakti Prasad Pattanayak[2], Sami Abul-Khoudoud[7], Luke D. Rothermel[8], Rui Wang[4], Jonathan R. Brody[9], Jordan M. Winter[3]

[1]Surgery, Case Comprehensive Cancer Center, Cleveland, OH,[2]Case Western Reserve University School of Medicine, Cleveland, OH,[3]UH Cleveland Medical Center, Cleveland, OH,[4]Case Western Reserve University, Cleveland, OH,[5]Case Comprehensive Cancer Center, Cleveland, OH,[6]Tulane University, New Orleans, LA,[7]Surgery, University Hospitals, Cleveland, OH,[8]University Hospitals, Cleveland, OH,[9]Knight Cancer Institute, Oregon Health & Science University, Portland, OR

Objective: Pancreatic ductal adenocarcinoma (PDAC) remains one of the deadliest malignancies with limited therapeutic options. While PARP inhibitors benefit tumors with homologous recombination deficiency (HRD), fewer than 10-20% of PDAC cases harbor such mutations. The majority are homologous recombination proficient (HRP), representing a significant unmet need. Here, we identify wild-type isocitrate dehydrogenase 1 (wtIDH1) as a critical regulator of HR repair in HRP PDAC and propose a novel combinatorial strategy using IDH1 and PARP inhibition to induce synthetic lethality.

Methods: We assessed the role of wtIDH1 in DNA repair using HR and non-homologous end joining (NHEJ) reporter assays, Western blotting, and chromatin modification analyses. Effects of IDH1 inhibition (ivosidenib) and PARP inhibition (olaparib), alone and combined, were evaluated in vitro through cell viability, apoptosis, and DNA damage assays. In vivo efficacy was tested in xenograft and orthotopic PDAC mouse models, including survival studies. Additionally, tumor biopsies from patients in the ongoing phase Ib clinical trial (**NCT05209074**) receiving ivosidenib were analyzed for HR pathway activity and chromatin alterations.

Results: Pharmacologic wtIDH1 inhibition depleted α-ketoglutarate and induced histone hypermethylation, impairing HR repair and mimicking a BRCA-like phenotype in HRP PDAC cell lines (MiaPaCa-2, Panc-1). The combination of IDH1 and PARP inhibitors synergistically increased γ-H2AX accumulation and apoptosis, reducing cell viability. In vivo, dual therapy significantly suppressed tumor growth and extended survival compared to monotherapies. Importantly, tumor samples from **NCT05209074** patients treated with ivosidenib exhibited decreased expression of HR repair proteins and epigenetic changes consistent with a BRCAness phenotype, supporting translational relevance.

Conclusion: Our findings reveal a novel role for wtIDH1 in maintaining homologous recombination in PDAC. Inhibition of wtIDH1 functionally induces HR deficiency in HRP tumors, sensitizing them to PARP inhibition. This combination represents a promising therapeutic approach for the majority of PDAC patients lacking canonical HR mutations and warrants further translational development.

#0513 AZD5305, a PARP1 selective inhibitor, exhibits antitumor effects and stimulates immune response in homologous recombination (HR)-deficient gastric cancer cells.

Sujin Ham[1], Hae Min Hwang[1], Youlim Noh[1], Jiwon Koh[2], Chaeyoung Lee[1], Seohyeon Lim[1], Minyoung Jeong[1], Yu-Jin Kim[3], Minyoung Lee[4], Changhee Park[5], Dae-Won Lee[5], Kyung-Hun Lee[5], Seock-Ah Im[5]

[1]Cancer Biology, Graduate School of Interdisciplinary Graduate Program & Cancer Research Institute, Seoul National University, Seoul, Korea, Republic of,[2]Department of Pathology & Cancer Research Institute, Seoul National University Hospital & Seoul National University, Seoul, Korea, Republic of,[3]Cancer Research Institute, Seoul National University, Seoul, Korea, Republic of,[4]Cancer Biology, Graduate School of Interdisciplinary Graduate Program, Seoul National University, Seoul, Korea, Republic of,[5]Department of Internal Medicine & Cancer Research Institute, Seoul National University Hospital & Seoul National University, Seoul, Korea, Republic of

Background : Poly (ADP-ribose) polymerase (PARP) 1, a multifunctional protein, is widely recognized for its critical role in the HR-mediated DNA repair, and its inhibition has therefore been introduced into the treatment of various solid tumors. Besides DNA damage response (DDR), PARP1 has also emerged as a key regulator of immune modulation. This is attributed to the accumulation of cytosolic nucleic acids (NAs), such as dsDNA or dsRNA, which are sensed by innate immune pathways like cGAS-STING. However, the precise mechanisms by which PARP1 inhibition induces these cytosolic NAs and activates innate immune response remain to be elucidated. Thus, we investigated the anti-tumor and immune modulatory effects of AZD5305 in gastric cancer cells to explore the underlying mechanism.

Methods : To evaluate the *in vitro* antitumor effect, colony formation assay (CFA) was performed for 14 days with increasing concentrations of AZD5305 (dose range: 0-5nM). The *in vivo* antitumor activity was assessed using an SNU-601 xenograft model by monitoring tumor growth. Cell cycle distribution was analyzed by flow cytometry and apoptosis was assessed by annexin-V/PI staining. DNA damage was detected by comet assay and the cell immunofluorescence assay (IFA). To investigate immune modulation, the expression of immune-related molecules was quantified by qRT-PCR and western blot, while the formation of dsRNA was detected by cell IFA. RNAseq was performed using the cell lines for differentially expressed gene and gene set enrichment analyses.

Results : The RAD51C-deficient SNU-601 cells were highly sensitive to AZD5305 (IC_{50}: 0.25 nM), unlike the moderately sensitive SNU-668 (IC_{50}: 2.05 nM) or resistant KATOIII cells (IC_{50}>5 nM). Moreover, AZD5305 demonstrated potent antitumor activity in an SNU-601 xenograft model (52.4% TGI, p=0.003). After treatment, SNU-601 cells exhibited G2/M arrest and apoptosis, confirmed by an increased sub-G1 population, positive annexin-V staining, and cleavage of PARP and caspase-7, but not in KATOIII. This cytotoxicity was driven by the accumulation of DNA damage, as indicated by elevated p-RPA, γH2AX, and comet tail formation. Furthermore, AZD5305 increased cytosolic dsRNA and cGAS-STING signaling in SNU-601, triggering the innate immune response. Consistent with this, RNAseq confirmed enrichments of activated IFN-γ response pathways and corresponding increases in the expression of interferon-stimulated genes (ISGs) in SNU-601, but not in KATOIII.

Conclusion : AZD5305 exhibits potent cytotoxic effects in HR-deficient gastric cancer cell lines *in vitro* and *in vivo*, by inducing DNA damage and apoptotic cell death. Immune modulation by AZD5305 was characterized by innate immune activation with increased interferon signaling, and our findings suggest the formation of cytosolic dsRNA as a key mediator of this effect.

#0514 Potentiation ofPARP inhibitor activity in*BRCA*-wildtype breast cancer cell lines by 2-hydroxyflavanone.

Harshit Khosla[1], Sharda P. Singh[2], Chhanda Bose[2], Sharad S. Singhal[3], Sanjay Awasthi[4]

[1]UT Health Houston, Houston, TX,[2]Texas Tech University Health Sciences Center, Lubbock, TX,[3]Beckman Research Institute of The City of Hope, Duarte, CA,[4]Professor, Oncology & Diabetes, Texas Tech University Health Sciences Center, Lubbock, TX

Background: 2-hydroxyflavanone (2HF) is citrus derived compound which has demonstrated in vitro anticancer activity against multiple malignancies. Its presence inhibits RLIP, a protein encoded by RALBP1 gene which functions as an ATP dependent efflux pump for glutathione-electrophile conjugates, oxidative and alkylating intermediates and, mediates epidermal growth factor receptor endocytosis. Thus RLIP promotes oncogenesis with growth modulation and ability to resist chemotherapy with glutathione mediated xenobiotic efflux. Reduced RLIP expression by 2HF reduces spontaneous carcinogenesis in p53 null mouse models, indicating its utility in tumors with DNA repair-deficiency. BRCA1, BRCA2, and PALB2 are the pivotal genes involved in homologous recombination (HR) mutation which can be targeted by poly(ADP-ribose) polymerase pathway (PARP) inhibitors. Through this study we assessed the effects of PARP inhibitor AZD2461 alone and in combination with 2HF on cell viability of MDA-MB-231 and MCF-7 breast cancer cell lines.

Methods: Expression of mRNA of BRCA1, BRCA2 and PALB2 genes was assessed in MDA-MB-231 (triple negative) and MCF-7 (ER+) breast cancer cell lines after exposure to 2HF and LNA by using quantification cycle in Polymerase chain reaction. LDH release at 72 hours was measured and compared with controls in cells treated with 2HF or AZD2461 alone or in combination. Cytotoxicity was measured using absorbance of reduced WST-8 produced by the viable cells.

Results: RLIP depletion by 2HF reduced the expression of mRNA of HR genes BRCA1, BRCA2, and PALB2 to 2% - 20% of the level of untreated controls. PARP inhibitor induced LDH release with incremental dose of 2HF at 10, 20 and 40 µM, with greatest cytotoxic effects at 40 µM 2HF ($p < 0.001$). Addition of 2HF to PARP inhibitor AZD2461 increased cell lysis in MCF-7 and MDA-MB-231 cells, however only diminished cell viability in MCF-7 but not in MDA-MB-231.

Discussion: PARP inhibitors are very effective in tumors with HRD mutation, however their utility is limited in subjects with mutations involving non HRD pathways. RALBP1 inhibition with 2HF decreases the expression of gene involved in HR pathway thus stimulating a transcriptomic environment that is similar to HRD mutated cells. 2HF could thus sensitize BRCA-wildtype ER+ and possibly triple negative breast cancers to PARP inhibitors. This potentially has clinical application among patients who may benefit from PARP inhibitors outside of current indications such as BRCA or HRD deficient mutations. Through this work, we look forward to inspire more work on clinical exploration of 2HF with PARP inhibitors.

#0515 Substrate selectivity and RPA-mediated regulation of Topoisomerase3-Rmi1 decatenation.

Minyong Kim, Quan Wang, Hengyao Niu

Biochemistry, Indiana University, Bloomington, IN

Mutations in the RecQ helicase BLM, which cause the cancer-prone disorder Bloom syndrome, lead to a high frequency of sister chromatid exchanges (SCEs). This phenotype is attributed to defects in processing double Holliday Junctions (dHJs) formed during homologous recombination. The BLM-Topo IIIα-RMI1/2 complex (Sgs1-Top3-Rmi1 [STR] in *S. cerevisiae*) is critical for resolving dHJs into non-crossover products, thereby suppressing SCEs. This dissolution requires the Sgs1 helicase to drive convergent junction migration, creating a hemicatenane that is decatenated by the Topoisomerase III (Top3)-Rmi1 subcomplex in the model organism, *S. cerevisiae*.However, the precise molecular mechanism of this final strand passage is poorly understood. One of the key ambiguities is the role of Replication Protein A (RPA), the universal ssDNA-binding protein. Previous studies have shown contradictory findings, with some reporting that RPA *inhibits* TopoIIIα decatenation, while others—using different methodologies—suggest it *promotes* the reaction. Furthermore, the specific substrate requirements of Top3-Rmi1, such as sequence or polarity preference, remain uncharacterized.To elucidate the role of RPA and define the substrate requirements for Top3-Rmi1, we devised *in vitro* decatenation assay using a single-strand catenane substrate. This system allowed us to make two key discoveries: First, we reveal that Top3-Rmi1 activity has selectivity for both the sequence and polarity of the DNA substrate. Second, we propose that RPA plays a sophisticated regulatory role, acting to guide the strand passage activity of Top3. This model suggests RPA ensures that Top3 cleaves DNA only when the substrate is properly configured for productive strand passage and resealing.Furthermore, we used a key tool, Top3-W77A, a mutant we identified that exhibits an ~10-fold lower DNA binding affinity. We found that this mutant's decatenation activity is significantly diminished in the presence of RPA, suggesting its weakened DNA affinity makes its substrate more difficult to access when the DNA is coated by RPA. We used this mutant as an *in vivo* probe to determine the physiological involvement of RPA in two key STR-dependent pathways: double Holliday junction dissolution and replication fork template switching. Specifically, we are probing its function in defined genetic backgrounds: a rad18 deletion to assess its role in replication template switching, and an sgs1 deletion to determine the relative contributions of Sgs1.

#0516 Integrated genomic and transcriptional profiling of patient-derived ovarian cancers reveals HRD-associated features and *in vivo* response to PARP inhibition.

Kyle C. Strickland[1], Sheri Barnes[2], Zachary D. Wallen[1], Michelle F. Green[1], Laine V. Morris[1], Paul DePietro[1], Kobina A. Amoah[1], Jennifer B. Jackson[1], Pratheesh Sathyan[3], Taylor J. Jensen[1], Brian Caveney[4], Eric A. Severson[1], Rebecca A. Previs[1], Shakti Ramkissoon[1], Scott C. Wise[2]

[1]Labcorp, Durham, NC,[2]Labcorp, Ann Arbor, MI,[3]Illumina Inc., San Diego, CA,[4]Labcorp, Burlington, NC

Introduction

Homologous recombination deficiency (HRD) and BRCA1/2 alterations are key biomarkers for PARP inhibitor sensitivity in ovarian cancer. Transcriptional features such as RB1 expression may further refine biologic subgroups and therapeutic hypotheses. We performed integrated DNA/RNA profiling of FFPE ovarian tumors to characterize histologic distribution, genomic alterations, genomic instability score (GIS), RB1 expression, and in vivo olaparib response in selected HRD-positive models.

Methods

Thirty-two patient-derived FFPE ovarian tumor blocks were prepared, and H&E sections were reviewed by an anatomic pathologist (SR) to confirm sufficient tumor content prior to next-generation sequencing. Comprehensive genomic, immune profiling, and HRD assessment were performed. RNA-seq quantified RB1 expression, with “RB1-low” defined as TPM ≤ 6.26 (study 25th percentile). Two HRD-positive models were subjected to in vivo testing of olaparib response in female NSG mice following subcutaneous implantation.

Results

The cohort consisted predominantly of serous adenocarcinomas (71.9%), followed by ovarian adenocarcinoma NOS (21.9%), mucinous adenocarcinoma (3.1%), and carcinosarcoma (3.1%). TP53 mutations were present in 93.8% of cases. BRCA1 alterations were identified in 37.5% of tumors and BRCA2 alterations in 25.0%. HRD status was positive in 34.4% of cases, negative in 43.8%, and indeterminate in 21.9%. GIS scores varied across HRD categories, with HRD-positive tumors showing a range of 12-61 (median 29, mean 32.9), HRD-negative tumors ranging from 3-41 (median 11.5, mean 17.2), and indeterminate tumors ranging from 7-32 (median 19, mean 18.1). RB1-low expression was observed in 21.9% of tumors overall, with enrichment in HRD-positive cases (45.5%) compared to HRD-negative (7.1%) and indeterminate (14.3%) groups. To assess translatability of HRD findings, two HRD-positive serous adenocarcinomas were tested for olaparib response in vivo. One BRCA2-mutated tumor (LCOV-2089, GIS=32) demonstrated a robust therapeutic effect, with a median tumor volume reduction of 68.1% and durable complete responses in 33.3% of treated mice. In contrast, a second BRCA2-mutated tumor (LCOV-2118, GIS=17) did not exhibit tumor regression but showed an increased time to progression of >85% compared to untreated controls.

Conclusions

Overall, these findings suggest a meaningful correlation between genomic HRD status and in vivo therapeutic response, supporting the translational relevance of integrated profiling and the use of patient-derived models for preclinical investigations.

#0517 Comprehensive & precise structural variant detection with a single assay.

J. Zachary Sanborn, James Durbin, Mital Bhakta, Lisa Munding

Cantata Bio, LLC, Scotts Valley, CA

Structural variants (SVs) are increasingly recognized as key drivers of tumorigenesis, yet current technologies struggle to detect and accurately characterize them due to resolution limitations and sequencing constraints. As a result, attempts to produce complete somatic SV truth sets often suffer due to the gaps in detection performance of the sequencing technology utilized, impacting the truth sets' usefulness for benchmarking alternative technologies and/or SV callers. To this end, the National Institute of Standards & Technology (NIST) performed a deep benchmarking experiment for somatic SV detection, fully characterizing the structural changes of a pancreatic ductal carcinoma (PDAC, labeled HG008T) across 16 whole genome sequencing technologies and analyzing with multiple datatype-specific SV callers. NIST has published its Benchmark SV callset that is the result of integrating and manually curating calls from all analytes. With this benchmarking data, we tested the capability of Dovetail's LinkPrep chemistry alone to reproduce the NIST Benchmark callset using both open source and proprietary SV callers.

Dovetail LinkPrep libraries were generated for the HG008T cell line sample and sequenced to approximately 55x genomic coverage. Sequencing data was aligned to hg38 with bwa and SV calls generated by running a standard, HiC-based SV caller, HiC-Breakfinder, and Dovetail Precise (DP), a new SV caller developed by Dovetail Genomics. These callsets were separately compared to the NIST Benchmark callset to assess their performance in categories based on SV type and size.

Of the 109 total SVs in the NIST Benchmark callset, HiC-Breakfinder and DP detected 19 (18%) and 97 (92%) SVs, respectively. HiC-Breakfinder's ability to detect SVs was limited to translocations (8 of 12, 67%) and large intra-chromosomal SVs greater than 2 Mb in size (10 of 11, 91%), while unable to find any intra-chromosomal SV smaller than 2 Mb. In contrast, DP detected all translocations (12 of 12, 100%), the same number of large intra-chromosomal SVs (10 of 11, 91%), and the majority of smaller intra-chromosomal SVs (75 of 85, 88%) down to 47 bp in size. Furthermore, the difference in breakend locations between HiC-Breakfinder and the NIST Benchmark SVs ranged from 1,636 bp to 189 kb, while over 96% of DP calls (94 of 97) achieved base-level precision.

Dovetail's LinkPrep chemistry with the Dovetail Precise (DP) caller detected 92% of somatic structural variants (SVs) in the NIST Benchmark callset, including small variants down to 47 bp, strongly outperforming HiC-Breakfinder across all SV types and sizes. This high-resolution SV detection enables more comprehensive cancer genome characterization from a single assay and supports more accurate diagnostics and targeted therapy development.

#0518 Caspase-4 deficiency impairs nuclear actin-mediated DNA double-strand break repair and increases radiosensitivity in cancer cells.

Shohei Nagasaka[1], Tomomitsu Doi[2], Kunie Obayashi[3], Masaoki Kohzaki[4], Kazuhiro Sumida[3], Yosuke Chiba[3], Junkoh Yamamoto[5], Motoyoshi Endo[3]

[1]Neurosurgery and Molecular Biology, University of Occupational and Environmental Health, Kitakyushu, Japan,[2]Molecular Biology and Cellular Biology, University of Occupational and Environmental Health, Kitakyushu, Japan,[3]Molecular Biology, University of Occupational and Environmental Health, Kitakyushu, Japan,[4]Radiobiology and Hygiene Management, Institute of Industrial Ecological Sciences, University of Occupational and Environmental Health, Kitakyushu, Japan,[5]Neurosurgery, University of Occupational and Environmental Health, Kitakyushu, Japan

Background: Radiotherapy induces cytotoxicity primarily through DNA double-strand breaks (DSBs), and the efficiency of DSB repair is a key determinant of tumor radiosensitivity. Caspase-4 (CASP4), frequently overexpressed in human malignancies, has been implicated in actin cytoskeletal remodeling; however, its involvement in nuclear actin dynamics and DNA repair remains unclear.
Methods: We investigated the functional role of CASP4 in radioresponse using CASP4 knockout (KO) HepG2 and NCI-H292 cells. Colony formation assays, 53BP1 foci analysis, and a newly developed measurement system that enables the quantification of nuclear actin levels were used to assess DNA repair efficiency and actin distribution. Forced nuclear actin expression was used to evaluate its ability to rescue CASP4-dependent defects.
Results: CASP4 KO significantly sensitized tumor cells to ionizing radiation, associated with decreased colony formation and persistent 53BP1 foci, indicative of impaired DSB resolution. Although CASP4-deficient cells exhibited elevated cytoplasmic F-actin, nuclear actin translocation was reduced despite comparable total actin levels, suggesting defective actin shuttling. Quantitative imaging confirmed substantially diminished nuclear actin signals in CASP4 KO cells. Notably, enforced nuclear actin expression restored 53BP1 foci resolution in CASP4-deficient cells.
Conclusions: These findings identify a previously unrecognized role of CASP4 in promoting DNA DSB repair through regulation of nuclear actin dynamics. CASP4 facilitates the balance between cytoplasmic and nuclear actin to maintain efficient DNA repair and enhance radioresistance. Targeting CASP4 may therefore represent a promising strategy to overcome tumor resistance to ionizing radiation.

#0519 Decoding oncogene amplification structures from retinoblastoma aqueous humor cfDNA as a model for chromothripsis and ecDNA biology.

Yilin Chen, Liya Xu

Vision Center, Children's Hospital Los Angeles, Los Angeles, CA

Purpose: Complex oncogene amplifications—including MDM4 1q gains and MYCN high-level amplification—frequently arise through mechanisms such as chromothripsis, tandem-duplication cycles, and extrachromosomal DNA (ecDNA). These structural drivers shape tumor aggression and therapy resistance across cancers, yet they remain largely inaccessible in plasma ctDNA due to low tumor fraction and fragment constraints. Retinoblastoma aqueous humor (AH) contains predominantly tumor-derived cfDNA with a genomically simple background, providing a uniquely powerful human model system to benchmark the technical feasibility, data characteristics, and analytical requirements for cfDNA-based amplification profiling.

Methods: Deep whole-genome sequencing (>20×) was performed on AH cfDNA from four RB eyes having *MDM4* focal gain or *MYCN* high-level amplification. Matched long-read nanopore WGS was generated for canonical subtype cell lines: WERI-Rb1 (MDM4) and Y79 (MYCN) to serve as high-confidence reference amplification profiles. We evaluated copy-number resolution, breakpoint features, and junction-spanning fragment representation in cfDNA relative to long-read tumor DNA.

Results: All AH cfDNA samples achieved >20× genome-wide coverage with >90% inferred tumor fraction from Illumina PE150 NGS setting, enabling high-resolution focal amplification assessment. MDM4-positive AH samples demonstrated multi-segment focal 1q gain with moderate copy elevation (~3-8× over baseline) and sharp regional boundaries, while MYCN-amplified samples exhibited ultra-high amplification (>50× copies) with dense, localized breakpoint clustering. Long-read tumor DNA (>1.5× whole-genome coverage) provided a structural reference sufficient to confirm amplification topology and breakpoint positions. Junction-spanning cfDNA fragments aligned to predicted boundaries, supporting direct focal amplification recovery from liquid biopsy.

Conclusions: Aqueous humor cfDNA provides a high-performance testbed for characterizing focal amplification signatures and defining technical performance thresholds relevant to liquid biopsy assay development. These results establish analytical parameters—minimum sequencing depth, copy-number resolution limits, and junction-fragment detectability—that may inform future platform optimization for lower-tumor-fraction biofluids such as plasma and CSF.

#0520 Topoisomerase IIb binding delineates localized mutational processes and driver mutations in cancer genomes.

Liis Uuskula-Reimand[1], Christian A. Lee[2], Robin H. Oh[3], Zoe P. Klein[2], Nina Adler[4], Sana Akhtar Alvi[1], Ellen Langille[3], Elisa Pasini[5], Kevin C. Cheng[2], Evgenija Serafimova[3], Diala Abd Rabbo[2], Huayun Hou[1], Ricky Tsai[3], Mamatha Bhat[5], Daniel Schramek[3], Michael Wilson[1], Juri Reimand[2]

[1]The Hospital for Sick Children, Toronto, ON, Canada,[2]Ontario Institute for Cancer Research, Toronto, ON, Canada,[3]Lunenfeld-Tanenbaum Research Institute, Toronto, ON, Canada,[4]University of Toronto, Toronto, ON, Canada,[5]University Health Network, Toronto, ON, Canada

Type-II topoisomerases resolve topological stress in DNA by inducing and repairing double-strand breaks in a coordinated fashion. While topoisomerases are chemotherapy targets linked to therapy-related genotoxicity, TOP2B is uniquely positioned to influence mutagenesis through its activity in non-dividing cells and sensitivity to topoisomerase poisons. Here, to understand the role of TOP2B in mutagenesis and cancer driver mechanisms, we generated unique DNA-binding maps of TOP2B, CTCF, and RAD21 in human liver cancer samples using chromatin immunoprecipitation sequencing (ChIP-seq). Next, we conducted a systematic analysis of these genome-wide maps for cancer driver mutations and somatic mutational processes across a dataset of 6500 whole cancer genomes representing 18 major cancer types. We show that TOP2B-CTCF-RAD21 and TOP2B-RAD21 sites are enriched in somatic small mutations (SNVs, indels) as well as structural variants (SVs), particularly at sites with evolutionary conservation, high transcription and long-range chromatin interactions. When focusing on evolutionarily selected genes using a systematic driver analysis, TOP2B binding appears to underlie SVs and hotspot mutations in cancer-driving genes such as TP53, MYC, FOXA1, and VHL, and many frequently mutated non-coding regions. We show that the TOP2B-bound mutational hotspot at RMRP is a novel non-coding driver mutation that causes tumor initiation and growth in vivo and leads to transcriptional deregulation of migration and cell adhesion pathways. Together, these data highlights TOP2B as a safeguard of the genome integrity and a marker of mutational processes and hotspots in cancer, underscoring implications for cancer genomics research.

#0521 Impression of AKT inhibitor in chromatin accessibility in mCRPC.

Sasikumar Ponnusamy[1], Surendra Gulla[1], Tej Sharma[1], Ephraim Jeremiah Gardner[1], Abbas Jawadala[1], Adaora Amobi[1], Maddie Aust[1], Tobi Ogunbowale[1], Roberto Pili[2], Remi M. Adelaiye-Ogala[1]

[1]Department of Medicine, Jacobs School of Medicine and Biomedical Sciences, University at Buffalo, Buffalo, NY,[2]University at Buffalo, Buffalo, NY

The Androgen Receptor (AR) pathway is a primary target for metastatic castration-resistant prostate cancer (mCRPC) treatment, and AR blockade with enzalutamide is a well-established therapeutic option for targeting the AR pathway in mCRPC. However, prostate cancer cells can bypass AR blockades through induction of other pathways for survival, and recently numerous preclinical studies have made the PI3K-AKT pathway a target of interest for the treatment of drug-resistant mCRPC. The PI3K-AKT pathway has pleiotropic effects, and its inhibition has long been of interest in the management of prostate cancer. We previously reported that AKT inhibition (Ipatasertib) significantly decreases cell proliferation, increases canonical AR activity, and remodels the chromatin landscape *in vitro* and *in vivo*. However, the effects of AKT inhibition on chromatin accessibility remain poorly understood. This study aims to assess chromatin landscape modifications under PI3K-AKT pathway inhibition. In this study, LuCaP 167 patient-derived organoid (PDO) models were treated with AKT inhibitors (Ipatasertib and MK2206), and the chromatin landscape was studied using ATAC-seq. Preliminary results reveal that both Ipatasertib and MK2206 significantly altered chromatin accessibility in LuCaP 167 PDO compared with the non-treated control group. Interestingly, footprinting and motif analysis revealed several transcription factor motifs enriched by AKT inhibition, including KLF15, a tumor suppressor. While the results are preliminary, our data provide additional insights into AKT's influence on chromatin accessibility.

#0522 Oncometabolite D-2-hydroxyglutarate impairs homologous recombination by disrupting chromatin topology.

Fengchao Lang[1], Karambir Kaur[2], **Chunzhang Yang**[3]

[1]National Institutes of Health, Bethesda, MD,[2]NIH-NCI, Bethesda, MD,[3]NIH-NOB (Neuro-Oncology Branch), Bethesda, Maryland, MD

D-2-hydroxyglutarate (D-2-HG) is an abnormal metabolite produced in high concentrations in cancers with isocitrate dehydrogenase (IDH) mutations, such as glioma, acute myeloid leukemia, and chondrosarcoma. The IDH mutant enzyme exhibit neomorphic activity, driving the production of D-2-HG, which induces a unique oncogenic phenotype, characterized by genome-wide hypermethylation, reprogrammed metabolic landscape, and impaired DNA repair. Although these alterations contribute to tumor progression and increase therapeutic vulnerabilities, the exact molecular mechanisms linking D-2-HG to impaired DNA repair remain elusive. In the present study, we explore how D-2-HG affects chromatin structure to impair the DNA repair pathway, focusing specifically on homologous recombination (HR). We demonstrate that D-2-HG inhibits TET (ten-eleven translocation) methylcytosine dioxygenase activity, leading to widespread CpG island hypermethylation. This epigenetic modification dissociates the chromatin architectural protein CTCF (CCCTC-binding factor) from CpG-rich DNA regions. The loss of CTCF binding disrupts higher-order chromatin contacts critical for maintaining the structural integrity at the DNA damage sites. Consequently, key HR repair proteins, such as BRCA2 and RAD51, fail to be recruited to sites of DNA damage sites, significantly impairing HR efficiency. Our findings provide mechanistic insights into how the cancer metabolic signature leads to DNA repair deficiency, mediated by D-2-HG-induced chromatin alterations. The disruption of chromatin topology and loss of CTCF-mediated loops extrusion at DNA damage sites abolish effective DNA repair signaling, indicating a therapeutic vulnerability in IDH-mutant cells. Our study suggests that IDH-mutant tumors may be particularly susceptible to DNA repair inhibitors, such as PARP inhibitors, or other agents that further compromise HR repair.

#0523 Pan-cancer assessment of an RNA-based signature of HRD.

Stephanie N. Thiede, Hannah J. Glover, Matthew E. Berginski, Joshuah Kapilivsky, Andrew Sedgewick, Kyle A. Beauchamp, Chithra Sangli, Michelle M. Stein, Justin Guinney, Timothy Taxter

Tempus AI, Chicago, IL

Background. Pan-cancer biomarkers of homologous recombination deficiency (HRD) are an area of unmet clinical need due to efforts to develop second generation PARP inhibitors across solid tumor cancers. An RNA-based method has the potential to overcome limitations of DNA scar-based signatures, which are less robust across indications and represent historical, static measures of HRD.
Methods. We developed a 1660 gene expression-based logistic regression signature using Tempus xR to predict HRD status in solid tumors, including *BRCA*-cancers (pancreatic, prostate, ovarian, and breast) and 35 other cancers. Training labels were defined with DNA data (Tempus xT) with *BRCA1/2* biallelic loss as positive and wildtype (WT) in 14 homologous recombination repair (HRR) genes as negative. Data were split into training (N ~ 100k), evaluation for threshold selection (N~25k), and validation (N~25k).
Results. Sensitivity was 84% (ovarian), 82% (breast, pancreatic, prostate), and 54% for other cancers. Predicted HRD (HRD-RNA) prevalence was 27% in ovarian, 22% in breast, 14% in prostate, 8.9% in pancreatic and 5.4% in all other cancers. HRD-RNA prevalence was higher in HRR-biallelic altered tumors compared to HRR WT (31% vs. 11% in *BRCA*-cancers; 11% vs. 4.7% in other cancers). Among *CCNE1*-amplified ovarian tumors, thought to be mutually exclusive with HRD, HRD-RNA prevalence (12%) was lower than gwLOH-based calling (20%), highlighting improved specificity of this RNA-based approach. The model showed equivalent performance to cancer-specific models trained individually on pancreatic, ovarian, and prostate cancer, demonstrating generalizability.
Model gene features were positively enriched for hallmark pathways associated with DNA damage and repair including *E2F* family of transcription factors, G2/M checkpoint, *MYC* targets, mitotic spindle, HRR, and DNA damage response pathways. Negative enrichment was seen in the epithelial to mesenchymal transition pathway. The association of ssGSEA scores of these hallmark pathways with HRD-RNA status was consistent across most individual cancers. Similar associations of these pathways with other models of HRD have been shown in publicly available data (PMID: 39073402).
We also observed cancer-specific expression associated with HRD-RNA status. For example, *BRCA2* expression is positively associated with HRD-RNA in ovarian cancer and negatively associated in most other cancers, namely in prostate cancer. Notably, there is a strong positive relationship with the oxidative phosphorylation pathway ssGSEA scores in ovarian cancer, consistent with reports that HRD results in a shift from glycolytic to oxidative metabolism (PMID: 32400970).
Conclusion. The RNA signature detects HRD within and beyond *BRCA1/2* biallelic loss pan-cancer. Similar pathways were associated with HRD-RNA status as reported in DNA-based methods of HRD, highlighting the biological validity of an RNA-based HRD signal.

#0524 Characterizing PTEN:Ki67 interactions and contribution to radioresistance in glioblastoma.

Brandon Marshall Jones[1], Sejal Patel[2], Brett Taylor[3], Nidhi Nathwani[2], Takayuki Morimoto[2], Yashpreet Kaur[2], Frank Furnari[4]

[1]Biomedical Sciences, University of California San Diego, La Jolla, CA,[2]University of California San Diego, La Jolla, CA,[3]UC San Diego School of Medicine, La Jolla, CA,[4]Division of Regenerative Medicine, Department of Medicine, University of California San Diego, La Jolla, CA

Glioblastoma (GBM) is the most common and lethal primary brain tumor in adults, comprising approximately 50% of newly diagnosed solid brain tumors. Newly diagnosed GBM patients have a poor prognosis and median survival of only 12-15 months with current standard of care therapy. Precision oncology approaches that have worked in other cancers have largely failed to translate to GBM due to several unique GBM properties, including resistance to cell death caused by DNA damaging agents such as radiation therapy. One novel mechanism of radioresistance is through enhanced DNA damage response (DDR) mediated by nuclear-localized tyrosine-phosphorylated PTEN (pY240-PTEN) recruited to chromatin through interaction with the PP1 Binding Domain (PP1BD) of Ki67. While PTEN is known to play an important tumor-suppressive role and is found to be altered in approximately 40% of GBM, an analysis of an EGFR-positive, PTEN-positive patient cohort revealed that the presence of pY240-PTEN correlated with worse overall survival. As a more complete understanding of this interaction may provide valuable insight as to the role that Ki67 plays in GBM radioresistance, N-terminal biotinylated peptides were utilized to examine the contribution of each amino acid of the Ki67-PP1BD to PTEN binding. Through streptavidin pulldown assays, we uncovered a basic 5-amino acid patch critical for PTEN:Ki67 binding and through phosphorylation of these synthetic peptides, determined that Ki67 pT525 may play a role in determining occupancy of the Ki67-PP1BD. To further investigate the impact of PTEN:Ki67 interaction-dependent DDR, a Ki67 KO TS528 glioma stem-like cell line was established. Characterization of this line indicated that Ki67 loss had little impact on unperturbed cells but following radiation, resulted in decreased proliferation, decreased DDR, and a more significant G2 cell cycle arrest compared to WT TS528. Additionally, *in vivo* radiation treatment of mice harboring TS528 Ki67 KO tumors imparted a significant increase in overall survival, while TS528 parental cells had no benefit. To determine the contribution of PTEN to the observed Ki67 KO phenotype, Ki67 was knocked out in PTEN-null U87 glioma cells. In concordance with previous findings of PTEN:Ki67 interactions following radiation, I found that Rad51 foci formation was increased only in U87 cells expressing both Ki67 and PTEN. The impact of PTEN binding was also examined in TS528 Ki67 KO cells through lentiviral restoration of Ki67 with minigene constructs expressing WT Ki67-PP1BD, or harboring mutations disrupting PTEN binding, fused to the chromatin binding LR domain. Alanine substitution of critical PTEN binding residues disrupted interaction by CoIP and is currently being tested for radiosensitizing effects *in vivo*. This work characterizes a novel DNA damage repair pathway implicated in GBM radioresistance and proposes a new potential target for therapeutic intervention.

#0526 The role of ssDNA in alternative DNA DSB repair and the opportunity for therapeutic intervention.

Jessica Lynn Kersey[1], John J. Turchi[2]

[1]Biochemistry, Molecular Biology and Pharmacology, Indiana University School of Medicine, Indianapolis, IN,[2]Indiana University School of Medicine, Indianapolis, IN

DNA double-stranded breaks (DSBs) create genomic instability, a driving factor in cancer development. Targeting DNA repair is a pivotal strategy in cancer therapy by exploiting synthetic lethal interactions with PARP inhibitors in patients deficient in homologous recombination (HR) DSB repair. Despite these advances, the clinical outcomes and recurrence rate for these patients have remained relatively stagnant. Recurrence is a direct result of treatment resistance mechanisms which can include reactivation of HR or the use of alternative end-joining (alt-EJ) DSB repair pathways. Theta-Mediated End Joining (TMEJ) and Single-Strand Annealing (SSA) can be employed to maintain genome stability and elevated expression of proteins involved in these pathways, including PolQ and XPF, have been reported in ovarian and lung cancer. SSA and TMEJ repair pathways involve common steps of resection, homology searching/annealing, and DNA synthesis. However, protection and processing of the ssDNA intermediates has not been addressed. Replication Protein A (RPA) is the major single-stranded DNA (ssDNA) binding protein involved in replication and repair and has been implicated in both TMEJ and SSA repair pathways though definitive involvement and the putative mechanisms have not been elucidated. We propose that RPA impacts TMEJ and SSA dependent DNA DSB repair via binding to ssDNA intermediates. The impact of RPA activity on TMEJ and SSA was assessed via genetic knockdown (KD) of RPA using siRNA in HEK293T and H1299 cell lines. Following siRNA KD, TMEJ and SSA repair activity were measured using a repair pathway specific dual luciferase extrachromosomal reporter assay. Results demonstrate that RPA stimulates both TMEJ and SSA activity as loss of RPA activity resulted in a ≥50% reduction repair activity for both pathways. Furthermore, a qPCR based extrachromosomal reporter assay requiring an additional 25bp of synthesis for complete repair was also reliant on RPA. Interestingly, treatment of RPA KD cells with ART558, a PolQ inhibitor, had less of an impact compared the control cells suggesting that cells can use a PolQ-independent mechanism of TMEJ for repair under certain conditions. Additionally, the impact of XPF-ERCC1 activity on SSA repair was considered as XPF-ERCC1's major function is to cleave 3' ssDNA overhangs, a key intermediate that must be processed in SSA. The impact was assessed via SSA repair activity in H1299 XPF-ERCC1 genetic knockout cells compared to the H1299 Cas9 control cells. Loss of XPF-ERCC1 activity resulted in approximately a 6-fold decrease in SSA activity indicating that SSA repair heavily relies of XPF-ERCC1 for ssDNA processing. Collectively, these data establish that RPA and XPF have a stimulatory role in TMEJ and SSA repair. The insights gained from this research can be used to better understand how certain types of cancer modify their DNA repair mechanisms to enhance their chances of survival.

#0527 Development of novel Ku-targeted DNA-PK inhibitors for cancer therapy.

Katherine Pawelczak[1], Pamela S. VanderVere-Carozza[2], Maria Casiano[3], Lacey Dobrolecki[1], John J. Turchi[2]

[1]NERx Biosciences, Indianapolis, IN,[2]Indiana University School of Medicine, Indianapolis, IN,[3]Biochemistry, Indiana University School of Medicine, Indianapolis, IN

The DNA-dependent protein kinase (DNA-PK) is a clinically validated target for cancer therapy. It plays essential roles in the repair of DNA double-strand breaks (DSBs) via non-homologous end joining (NHEJ), and in the broader DNA damage response (DDR) signaling pathway. Given its pivotal roles in maintaining genomic stability, and its upregulation and hyperactivation in many cancers, DNA-PK is an attractive therapeutic target for single agent therapy and in combination with radiation or other DNA damaging chemotherapeutics. Existing DNA-PK inhibitors target the catalytic subunit (DNA-PKcs) but have suffered from poor selectivity, suboptimal pharmacokinetics, and dose-limiting toxicity. To overcome these limitations, we have developed a first-in-class series of small-molecule inhibitors that block Ku70/80 binding to DNA, the initial and essential step of DNA-PK activation. Our structure-based drug discovery program has led to the development of novel, drug-like Ku inhibitors that bind to unique pockets within the Ku interface, blocking DNA access and effectively shutting down DNA-PK activity. This novel, ATP-independent mechanism prevents assembly of NHEJ complexes, offering enhanced selectivity, reduced off-target toxicity, and a powerful new strategy for cancer therapy. Lead compounds potently inhibit DNA-PK catalytic activity at nanomolar concentrations, block Ku-dependent DNA binding, and sensitize cancer cells to ionizing radiation, etoposide, and bleomycin while sparing normal cells. Proof-of-concept studies confirm on-target mechanism, pharmacodynamic engagement, and enhancement of IR-induced antitumor activity in non-small cell lung cancer (NSCLC) xenograft models. Additionally, newly emerging and growing class of ADCs that induce DNA damage as their primary efficacious mechanism have been increasingly popular in the clinic. Ku inhibitors have strong mechanistic rationale as combination partners for ADCs, with the potential to overcome resistance and improve the therapeutic index of DNA damage inducing ADCs. Our results show significant increased efficacy in combination with the ADC topoisomerasel inhibitor, DXd, suggesting that Ku inhibition enhances DXd-induced cytotoxicity by impairing non-homologous end joining and sensitizing tumor cells to payload-mediated DNA damage. These results support the further development of Ku inhibitors as anticancer therapeutics.

#0528 Sun exposure shapes distinct mutational profiles in human skin cells.

Neda Bahrani, Aravind K. Bandari, Bishal Tandukar, Delahny Deivendran, Harsh Sharma, Alan Hunter Shain

UCSF Helen Diller Family Comprehensive Cancer Ctr., San Francisco, CA

Surprisingly little is known about how ultraviolet (UV) radiation exposure affects individual skin cell types. Prior studies relied on bulk sequencing of whole biopsies, masking cell type-specific mutational patterns, and often used narrow UV spectra, non-physiological doses, or focused only on immediate DNA damage rather than lasting mutations. To delineate the enduring genetic effects of UV-radiation, we measured somatic mutations and cellular viability in melanocytes, keratinocytes, and fibroblasts exposed to physiologically relevant simulated solar radiation.

We exposed primary neonatal melanocytes, keratinocytes, and fibroblasts to simulated solar radiation under three conditions: no irradiation (control), 5 minutes (~70.2 J/m^2), and 10 minutes (~129.9 J/m^2), corresponding to ~0, 0.42, and 0.83 Minimal Erythema Dose (MED). Cell counts were measured on days 1 (pre-irradiation), 3, and 5 (post-irradiation) to assess viability and proliferation. For mutational profiling, single cells from each condition were sorted, clonally expanded, and subjected to exome and transcriptome sequencing using G&T-seq. In total, we analyzed 9 fibroblast clones (n=4, 2, 3), 13 keratinocyte clones (n=5, 3, 5), and 12 melanocyte clones (n=4 per condition) to quantify UV-induced mutational burden.

All three cell types exhibited a dose-dependent reduction in cell counts following irradiation, though with differing magnitude. Keratinocytes showed the most pronounced decline, whereas melanocytes displayed a dose-dependent decrease but to a lesser extent. Fibroblasts were the most resilient, with the smallest reduction in cell count and the fastest post-irradiation recovery. Mutational profiling revealed a corresponding dose-dependent increase in mutation burden (mutations per megabase) and in the fraction of canonical UV-signature substitutions (C>T and CC>TT) across all cell types. After 10 minutes of simulated solar radiation, median mutation burdens reached 1.30 mut/Mb in keratinocytes, 0.52 mut/Mb in melanocytes, and 0.36 mut/Mb in fibroblasts. The cells also showed distinct mutation signature and gene expression profiles.

Together, these findings highlight both the physiological and genomic consequences of solar radiation in distinct skin cell types. The differences in mutational landscapes point to cell type-specific mutational processes and DNA repair mechanisms, providing a framework for understanding how UV exposure shapes the genomic architecture of human skin.

#0529 Interplay of circadian cryptochrome 1 (CRY1) and DNA repair in prostate cancer (PCa).

Arwa Fallatah[1], Stefan DiFazio[1], Lakshmi Ravindranath[1], Orly Richter[1], Christopher McNair[2], Ayesha Shafi[1]

[1]Center for Prostate Disease Research, Bethesda, MD,[2]Sidney Kimmel Cancer Center, Thomas Jefferson University, Philadelphia, PA

Background: Disruptions in circadian rhythm are linked to prostate cancer (PCa). Previous studies indicate that the core circadian clock factor cryptochrome 1 (CRY1) is pro-tumorigenic and associated with poor clinical outcomes in PCa. Beyond its transcriptional co-regulatory function, CRY1 was recently identified as a modulator of DNA damage repair (DDR) in advanced PCa. Molecular and pharmacological suppression of CRY1 impairs PCa cell growth, induces G2/M arrest, and disrupts homologous recombination (HR)-mediated DNA repair. However, the mechanistic role of CRY1 in disease progression from hormone therapy sensitive (HTS) to castration resistant prostate cancer (CRPC) remains incompletely defined.
Methods: We employed doxycycline-inducible CRY1 knockdown models of both HTS, using LNCaP cell line, and CRPC, using C4-2 cell line, along with pharmacological strategies to recapitulate physiologically relevant CRY1 modulation. Transcriptomic profiling, DDR-focused CRISPR knockout (KO) screening, and downstream functional assays were used to define CRY1-dependent transcriptional and repair programs across disease stages. This allows for the identification of potential novel targeted therapies as well as predicts patient response to DDR targeted therapy.
Results: Transcriptomic analyses revealed distinct CRY1-regulated gene networks in HTS versus CRPC models. In HTS, CRY1 activity was associated with pathways including base excision repair, mismatch repair, and G2/M checkpoint regulation, while in CRPC, CRY1 was specifically linked to HR-mediated DNA repair. DDR-targeted CRISPR screening further demonstrated that CRY1 promotes tumorigenesis via nucleotide excision repair in HTS and shifts to HR reliance in CRPC, suggesting stage-specific rewiring of repair pathway choice driven by CRY1. These findings identify a novel mechanism of DDR regulation across PCa progression.
Conclusions: In sum, our study reveals that CRY1 supports PCa progression via distinct DDR mechanisms in HTS and CRPC. Thus, targeting CRY1, alonge or in combination with DDR inhibitors, offers a promising therapeutic strategy tailored to disease stage in PCa.

#0531 Germline HRR alterations and ancestry-related outcomes in Brazilian triple-negative breast cancer patients: A comprehensive genomic and clinical study.

Rafael C. Brianese[1], Karina M. Santiago[1], Gabriel Bandeira do Carmo[1], Leticia S. Pimentel[1], Diego Ortunes[2], Rafaella Ormond[2], Marcos L. Santoro[2], Giovana T. Torrezan[1], Marcelo Moreno[3], Andrea R. dos Santos[4], Marina de Brot[5], Fabiana B. A. Makdissi[6], Solange M. Sanches[7], Jose C. C. Rocha[8], **Dirce Maria Carraro**[1]

[1]Clinical and Functional Genomics Group, A.C.Camargo Cancer Center, Sao Paulo, Brazil,[2]Department of Biochemistry, Federal University of Sao Paulo (UNIFESP), Sao Paulo, Brazil,[3]Medicine Course and Biomedical Sciences, Federal University of Fronteira Sul (UFFS), Chapeco, Brazil,[4]Laboratory of Human and Medical Genetics, Postgraduate Program of Genetics and Molecular Biology, In, Federal University of Para (UFPA), Belem, Brazil,[5]Department of Anatomic Pathology, A.C.Camargo Cancer Center, Sao Paulo, Brazil,[6]Department of Breast Surgery, A.C.Camargo Cancer Center, Sao Paulo, Brazil,[7]Department of Medical Oncology, A.C.Camargo Cancer Center, Sao Paulo, Brazil,[8]Department of Oncogenetics, A.C.Camargo Cancer Center, Sao Paulo, Brazil

Triple-negative breast cancer (TNBC) is an aggressive and heterogeneous breast cancer subtype frequently associated with early-onset, African ancestry, and germline pathogenic variants (GPVs), particularly in *BRCA1*. Loss of function germline mutation in homologous recombination repair (HRR) genes culminate in homologous recombination deficiency (HRD), a molecular phenotype that confers increased susceptibility to DNA-damaging agents such as platinum-based chemotherapy and PARP (poly ADP-ribose polymerase) inhibitors. While this mechanism is well-characterized in European and North American cohorts, studies in admixed populations remain limited. We conducted a comprehensive retrospective study of 320 unselected Brazilian TNBC patients, integrating multigene next-generation sequencing (NGS) panels, ancestry analysis, and clinical-pathological data. Germline variants were analyzed across cancer predisposition multi gene panels, and ancestry was determined in 248 patients using the Axiom Precision Medicine Diversity Array and ADMIXTURE (K=4). GPVs were detected in 29.1% of patients, with *BRCA1* being the most frequently altered gene (14.7%), followed by *BRCA2* (4.4%) and non-*BRCA* HRR genes (4.7%). Overall, 23.8% of patients harbored GPVs in HRR-related genes. *BRCA1* carriers were significantly younger at diagnosis, more likely to present bilateral tumors, and showed improved 3-year progression-free survival (3y-PFS) compared to non-carriers ($p = 0.0162$). Carriers of other HRR genes also had superior 3y-PFS ($p = 0.0398$). Combined, HRR-carriers exhibited better 3y-PFS ($p = 0.0025$) and 5-year overall survival (5y-OS, $p = 0.0260$) than non-carriers. Ancestry analysis revealed a predominance of European ancestry (87.1%) but also substantial African and Native American components (≥1% in 68.5% and 81.4%, respectively), confirming Brazil's complex admixture. Patients with predominant African ancestry had significantly worse 3y-PFS ($p = 0.0011$) and 5y-OS ($p = 0.0117$) compared to those with European ancestry. Self-reported race only partially correlated with molecular ancestry. Local ancestry analysis focused on the *BRCA1* locus showed that 25% of individuals carried African-derived haplotypes, but no significant associations were found between *BRCA1* local ancestry and cancer type ($p > 0.05$). This is the largest TNBC germline study conducted in a Latin American population to date, uniquely integrating genetic, clinical, and ancestry data. Our findings reinforce the central role of HRR genes, particularly *BRCA1*, in TNBC predisposition and prognosis, and reveal ancestry-related survival disparities that merit further investigation. Ongoing analyses of local ancestry components will provide additional insights into the genomic and clinical heterogeneity of TNBC in highly admixed populations.

#5134 *In vitro* and *in vivo* biology characterization of two novel inhibitors targeting the different domains of DNA polymerase theta (Polθ).

Omar Loss[1], Michael Bestwick[1], Tammy Ladduwahetty[1], Mark Andrews[1], Ju Wang[2], Jiangchuan He[2], Linli Ding[2], Tan Pang[2], Rui Yang[2], Hing Sham[3], Kui Lin[3]

[1]Pharmaron, Hoddesdon, United Kingdom,[2]Pharmaron, Beijing, China,[3]NewBay Pharma, Ningbo, China

DNA polymerase theta (Polθ) is a 290 kD specialized and error-prone Polymerase A family enzyme that executes microhomology-mediated end joining (MMEJ), possessing an N-terminal helicase-like domain and a C-terminal DNA polymerase domain, which are linked by a large, unstructured central region. Polθ is normally expressed at low levels but is frequently overexpressed in tumours and is critical for the survival of homologous recombination (HR)-deficient cancer cells. Accordingly, Polθ has been proposed as an attractive therapeutic target for the treatment of BRCA deficient and DNA repair pathway defective cancers. Several inhibitors targeting either the polymerase or the helicase domain of Polθ have been described and progressed to the clinic. However, it is not clear which axis of intervention is the most beneficial even though inhibition of either domain elicits synthetic lethality with BRCA genes preclinically. Here we compare the *in vitro* biological profile of two novel Polθ inhibitors, one targeting the C-terminal DNA polymerase (Pol) domain and the other targeting the N-terminal helicase-like domain (Hel). Both inhibitors exhibit similar potency in their respective biochemical assays (Hel inhibitor IC_{50} = 2.1 nM, Pol inhibitor IC_{50} = 4.2 nM). However, in a colony formation cellular assay the Hel inhibitor elicited significantly stronger synthetic lethality in BRCA2-mutant tumour cells (Hel inhibitor IC_{50} = 2.1 nM; Pol inhibitor IC_{50} 125.6 nM). Furthermore, this differentiation was evident mechanistically, where the Hel inhibitor inhibited MMEJ-mediated repair with a 3-fold higher potency and increased micronuclei formation in cells with a 200-fold higher potency when compared to the Pol inhibitor. When tested *in vitro*, in combination studies with the PARP inhibitor Niraparib, Hel showed a synergistic effect even at the lowest combination of concentrations tested (4 nM Hel, 15 nM Niraparib), whereas a 10-fold higher concentration of Pol inhibitor was needed to achieve the same synergistic effect. Based on its superior *in vitro* profile, the helicase inhibitor was progressed to BRCA1- and BRCA2-deficient xenograft models, where it evoked DNA damage and showed a dose-dependent sustained regression of tumour volume, in combination with a PARP inhibitor, even at the lowest dose tested of 3 mg/kg PO QD. The dose selection was based on the unbound exposure of the Hel inhibitor being in excess of the unbound cellular IC50 during the treatment period. Given the tumour regressive effects *in vivo* and favourable ADME profile in preclinical species and early human dose predictions, the helicase compound is currently undergoing evaluation in non-GLP toxicology studies.

: Metabolite Control of Chromatin, Redox, and Cellular Stress Responses
Poster Session

#0535 Acute sleep deprivation reprograms metabolic and mitochondrial pathways linked to cancer risk.
Behzad Varamini[1], Harrison Kim[1], Priscilla Kim[1], Madeline Lange[1], Stephanie Zeng[1], Jennifer Tudor[2]

[1]Biola University, La Mirada, CA,[2]Saint Joseph's University, Philadelphia, PA

Sleep deprivation is common and has been linked to elevated cancer risk, yet the immediate mammalian responses that connect acute sleep loss to cancer remain unclear. We asked whether a single 5-hour bout of acute sleep deprivation (ASD) reprograms metabolic and mitochondrial pathways across organs that govern whole-body energetics in a mouse model. Twelve-week C57BL/6 female mice underwent ASD or ad lib sleep; liver, hippocampus, prefrontal cortex, and gastrocnemius were collected immediately and profiled by RT-qPCR for energy sensing (AMPK), glucose transport (GLUT3), mitochondrial dynamics (DRP1/MFN1/OPA1), and hepatic lipid/cholesterol handling (ABCA1/SCARB1/apolipoproteins). ASD triggered rapid, tissue-selective remodeling: AMPK/GLUT3 and mitochondrial-dynamics transcripts rose in brain regions, while hepatic cholesterol transport and apolipoproteins were altered; however skeletal muscle showed minimal change. These coordinated shifts map to cancer-relevant processes—deregulated cellular energetics, mitochondrial quality control/redox, and sterol flux that shapes membrane signaling and tissue inflammation, positioning sleep state as a modifiable, system-wide determinant of cancer susceptibility and progression. Ongoing work will examine whether repeated ASD or sleep restoration tunes these pathways and related tumor-relevant endpoints.

#0536 A multiplexed LC-MS/MS metabolite assay to enable patient stratification and pharmacodynamic monitoring for MTA-cooperative PRMT5 inhibitors.

Ethan Stancliffe[1], Ashima Mehta[1], Douglas Guzior[1], Adam Richardson[1], Tom Cohen[1], Kevin Cho[2], Gary Patti[2]

[1]Panome Bio, St. Louis, MO,[2]Washington University in St. Louis, St. Louis, MO

The development of Protein Arginine Methyltransferase 5 (PRMT5) inhibitors, particularly MTA-cooperative agents that selectively target *MTAP*-deleted cancers, has created an urgent need for robust biomarkers to identify target patient populations and confirm pharmacodynamic (PD) target engagement. The purpose of this study was to develop and apply a highly sensitive, multiplexed liquid chromatography-mass spectrometry (LC-MS/MS) assay to quantify key PRMT5-related metabolites such as methylthioadenosine (MTA), symmetric dimethylarginine (SDMA), S-adenosylmethionine (SAM), and asymmetric dimethylarginine (ADMA), as well as interacting metabolites in the folate cycle, methionine cycle, and polyamine metabolism. The developed multiplexed LC-MS/MS method enables simultaneous quantification of MTA, SDMA, SAM, and SAH, and 12 other related metabolites from cell lysates, tumor tissue, and biofluids. The assay leverages isotopically labeled internal standards and fragment ion monitoring for robust quantitation and resolution of key PRMT biomarkers ADMA (Type I PRMTs, e.g., PRMT1) and SDMA (PRMT5). We then applied this assay to matched adenocarcinoma tumor and normal adjacent tissue (NAT) specimens from n=6 human patients. The results showed statistically significant ($p<0.05$) increases in SAM and MTA as well as S-adenosylhomocysteine (SAH) levels in the tumor. The elevated MTA levels was driven by a subset of patients, suggesting these individuals have *MTAP*-deleted tumors. SAM and SAH are reactants and products, respectively, of PRMT5 and Type I PRMTs like PRMT1. The elevation of SAM and SAH in the tumor suggests elevated PRMT activity. In examining SDMA and ADMA levels, we found that ADMA (PRMT1 biomarker) was elevated by 40% in the tumor, while SDMA (PRMT5 biomarker) showed less than 20% elevation. In total, these data demonstrate the utility of the developed metabolite assay for the development of PRMT5 therapies. The differences between tumor and NAT metabolite profiles are consistent with upregulated PRMT1 (or another Type I PRMT) in the tumor, leading to elevated ADMA, SAM, and SAH. PRMT5, on the other hand, is likely inhibited by elevated MTA levels in the *MTAP*-deleted tumors, making them more susceptible to MTA-cooperative PRMT5 inhibitors, despite not significantly increasing SDMA levels in the tumor.

#0537 Constitutive NRF2 activation drives excess cysteine stress.

Jennifer A. Brain[1], Anna-Lena B. G. Vigil[1], Kristian Davidsen[1], Ayaha Itokawa[1], Abby C. Jurasin[1], Hannah J. Kerbyson[1], Maximilian Kobiesa[1], Madeleine L. Hart[1], Sang Jun Yoon[2], Gina M. DeNicola[2], Lucas B. Sullivan[1]

[1]Fred Hutchinson Cancer Center, Seattle, WA,[2]H. Lee Moffitt Cancer Center, Tampa, FL

Constitutive NRF2 activation is prevalent in human cancers and drives increased cystine uptake via SLC7A11-mediated xCT antiporter activity, exceeding cysteine demands for conventional pathways including glutathione and protein synthesis. The metabolic fates and functional consequences of this excess cysteine remain incompletely understood. To identify potentially unknown cysteine fates, we developed RMA tracing, an untargeted isotope tracing/mass spectrometry approach using equimolar mixtures of labeled [$^{13}C_6$,$^{15}N_2$] and unlabeled cystine to identify cysteine metabolic fates based on characteristic isotopologue peak pairs. Our LC-MS tracing identified 29 cysteine fates, including 20 previously unknown metabolites enriched in NRF2-activated cells and tumors. Many derived from reactions between cysteine thiols and glucose-derived sugar metabolites, forming irreversible thioether conjugates with sugar phosphates and reversible hemithioacetal/thiazolidine products with carbonyl compounds. We were able to identify these novel fates in greater abundance in NRF2-activated cultured cells, mouse tumors, and human tumor samples. We then asked if there was a functional phenotype associated with excess intracellular cysteine. We grew cells in media with increased cystine and observed a dose-dependent proliferation impairment rescued by SLC7A11 inhibition with erastin. We note this proliferation defect was independent of glutamate depletion or NADPH consumption. Additionally, inhibiting glutathione synthesis with buthionine sulfoximine intensified cysteine accumulation and proliferation defects by preventing enzymatic cysteine consumption. Alternate cysteine delivery methods (beta-mercaptoethanol or N-acetylcysteine supplementation) similarly increased intracellular cysteine and conjugate accumulation, and impaired cell growth in an SLC7A11-independent manner. We define “excess cysteine stress” as both accumulation of novel cysteine-derived metabolites and a proliferation defect in high cystine conditions. Mechanistically, we attribute NRF2 activation with this cancer-associated metabolic vulnerability to excess cysteine through constitutive SLC7A11 expression. These findings delineate novel cysteine conjugates, validate their physiological relevance across models, and identify excess cysteine stress as a distinct metabolic vulnerability in NRF2-activated cancers that may inform future therapeutic strategies.

#0539 Cholesterol triggers chromatin stress to drive senescence and inflammation.

Yiqun Han[1], Yaobin Ouyang[2], Shouhai Zhu[2], Hangcheng Xu[2], Bin Chen[1], Ping Yin[2], Qin Zhou[1], Jinzhou Huang[2], Kuntian Luo[2], Zheming Wu[1], Huaping Xiao[1], Xinyi Tu[1], Jake A. Kloeber[2], Jiajun Jing[2], Xiaofeng Huang[2], Meng Xu Welliver[1], Zhenkun Lou[2], Robert Mutter[1]

[1]Radiation Oncology, Mayo Clinic, Rochester, MN,[2]Oncology, Mayo Clinic, Rochester, MN

Cholesterol has long been viewed as a structural component of cellular membranes, yet its role in DNA damage response remains poorly defined. Here, we show that ionizing radiation (IR) induces broad transcriptional upregulation of cholesterol biosynthesis, transport, and storage pathways, leading to sustained intracellular accumulation of cholesterol. BODIPY-cholesterol imaging, Filipin III staining, and quantitative subcellular fractionation confirmed selective nuclear enrichment of cholesterol following IR, coinciding with extensive chromatin remodeling. Proteomic profiling of cholesterol-interacting proteins revealed a strong enrichment of chromatin-associated factors, suggesting a previously unrecognized lipid-chromatin interface in irradiated cells. Functionally, cholesterol accumulation promoted chromatin compaction and repressive histone modification patterns, impairing DNA damage sensing and checkpoint activation despite increased underlying DNA lesions. These alterations facilitated aberrant mitotic entry, formation of cytoplasmic chromatin fragments (CCFs), and activation of cGAS-STING-NF-κB signaling. Cholesterol exposure ultimately diverted damaged cells toward a senescent fate, marked by Lamin B1 loss, p21 induction, and a robust senescence-associated secretory phenotype (SASP) enriched for IL-1 and TNF family cytokines. In vivo, dietary cholesterol exacerbated radiation-induced inflammation and weakened systemic anti-tumor immunity. Transcriptomic analyses of immunotherapy-treated patients revealed that tumors enriched for cholesterol import and senescence signatures were associated with poor response to PD-L1 blockade and worse survival. Together, these findings identify a cholesterol-chromatin-senescence axis that links metabolic remodeling to defective DNA damage signaling and immune suppression after radiation, highlighting cholesterol metabolism as a potential therapeutic vulnerability in cancer therapy.

#0540 Cancer cells are sensitive to methionine cycle perturbation in low-lipid environments.

Diya Lakshmi Ramesh[1], Keene L. Abbott[1], Ryan Elbashir[1], Edrees H. Rashan[2], Raphael Ferreira[3], Matthew G. Vander Heiden[4]

[1]Massachusetts Institute of Technology (MIT) Biology and Koch Institute for Integrative Cancer Research at MIT, Cambridge, MA,[2]Koch Institute for Integrative Cancer Research at MIT, Cambridge, MA,[3]Wyss Institute for Biologically Inspired Engineering and Harvard Medical School, Harvard University, Boston, MA,[4]Massachusetts Institute of Technology (MIT) Biology, Koch Institute for Integrative Cancer Research at MIT, and Dana-Farber Cancer Institute, Cambridge, MA

Nutrient availability varies across tissues and shapes how cancer cells use metabolism to proliferate and survive, creating context-specific vulnerabilities that might be targeted for improved therapy. Because access to lipids is constrained in some tissue environments, we sought to identify metabolic pathways required for proliferation under lipid-depleted conditions. Specifically, we performed a CRISPR/Cas9 loss-of-function screen targeting metabolic synthesis genes in human cancer cells cultured in lipid-replete versus lipid-depleted media. The screen identified methionine synthase (MTR), an enzyme linking the folate and methionine cycles, as a top hit required for proliferation in lipid-depleted conditions. Genetic validation confirmed that MTR knockout (KO) cell proliferation is impaired in lipid-depleted compared to lipid-replete conditions. Follow-up pharmacologic studies revealed that inhibition of methionine adenosyltransferase 2A (MAT2A), an enzyme in the methionine cycle that generates S-adenosylmethionine (SAM), also reduced proliferation in lipid-depleted conditions, suggesting that cells become broadly dependent on the methionine/folate cycle when lipids are scarce.To determine how methionine/folate cycle perturbations alter intracellular metabolism in lipid-depleted conditions, we performed LC-MS-based metabolomics. MTR KO in lipid-depleted media caused depletion of multiple nucleotide species, and supplementation with purine nucleotides or folinic acid fully rescued proliferation, consistent with impaired folate-dependent nucleotide synthesis. MTR KO cells also exhibited elevated markers of DNA damage, supporting a model in which MTR loss limits nucleotide availability under lipid-depleted conditions, leading to DNA damage. In contrast, MAT2A-inhibited cells were not rescued by nucleotides or folinic acid. Instead, supplementation with phosphatidylcholine, a major membrane phospholipid synthesized in a SAM-dependent manner, restored proliferation in lipid-depleted media. These results suggest that perturbing different nodes of the methionine cycle triggers distinct metabolic liabilities: MTR loss primarily limits nucleotide availability, whereas MAT2A inhibition restricts SAM-dependent phospholipid synthesis. Together, these findings reveal that cancer cells rely more heavily on methionine and folate metabolism when lipids are scarce and uncover two mechanistically distinct vulnerabilities that emerge in low-lipid environments with potential relevance for treating cancer.

#0541 102 Cancer studies including differentially expressed potassium channel (KCN) genes reveal pH sensitivity with stochastic preservation of a proposed K^+/H^+ initiated H^+ release strategy for pH reversal.

Marie E. Beckner

Brain Health Research Institute, Kent State University, Kent, OH

The potassium channel (KCN) family of proteins (≥90 members) is interactive and influenced by numerous factors including oncogenes. K^+ is the likely monovalent cation (versus Na^+) to shed its water with relative ease and replace protons on anions of cell membranes. H^+ is released for diffusion as H_3O^+, putatively into a Grotthuss water matrix for rapid transfer of protons to cell exits, including transporters of lactate with H^+, resulting in higher extracellular H^+ and lower intracellular H^+ to aid pH reversal (Beckner ME, Cell Settling, Migration, and Stochastic Cancer Gene Expression⋯, Biomolecules: 2025, 15,1177, https://doi.org/10.3390/biom15081177). 102 studies (new total), with no intent to include KCN genes, yielded results in 30 cancer types with ≥ 1 KCN differentially expressed gene (DEG) encoding a pH sensitive protein in 74.3% of studies, shown in heat maps, volcano plots etc. The most common cancers were breast, lung, and glioblastoma in 16, 14, and 12 studies, respectively, with 68.8%, 71.4%, and 83.3% containing ≥ 1 pH sensitive KCN DEG. 63 coding KCN genes found include 34 KCN(A-I,Q,S) encoding Kv proteins, 11 KCN (M,N,T) encoding KCa proteins, 8 KCNJ encoding Kir proteins, and 10 KCNK encoding K2P proteins. 3 non-coding KCNs were found. Among coding KCNs, 40 (63.5%) are pH sensitive. The most frequent KCN DEG (all pH sensitive), *KCNN4*, *KCNMA1, KCNN3,* and *KCNJ16*, were in 11, 9, 6, and 6 studies, respectively. With KCN DEG present, relatively intact non-KCN DEG were found that are needed in steps of H^+ release from cancer cells initiated by K^+/H^+ exchange on inner membranes. Na/K-ATPase and its regulators (*ATP1A2*,*B1*,*B2* and/or *FXYD1*,*D2* DEG in 9.8% of studies) that aid K+ intake, and for H+ exit with lactate (*LDHA* DEG in 2.9% of studies) and the monocarboxylate transporter complex (*CA2*, *CA9*, *SLC16A3* DEG in 1.0, 1.0, and 2.0% of studies, respectively). Also, lack of enhanced cytosolic H^+ transport by taurine is suspected (*SLC16A6* and *SLC36A1*(*PAT1*) taurine transporter DEG, 1% each) consistent with alternative cytosolic Grotthuss rapid proton transfer. Gap junction proteins are probably not at enhanced levels (*GJA1*, *GJB2*, *GJC3* DEG were 2.0, 1.0, and 1.0%, respectively). The most frequent oncogenic non KCN DEG were *BCL2* and *TGFB1*, 8 (100% pH sensitive) and 6 (83.3% pH sensitive) studies, respectively. Many pertinent non-KCN DEG were 0%. Stochastic findings are consistent with K^+/H^+ exchange on inner membranes initiating cytosolic proton diffusion via Grotthuss rapid water transfer to sites with release of H^+ along with lactate or alone to achieve pH reversal (pHe greater than pHi) in cancer cells. Without bias for KCN DEG, gene expression malignant landscapes stochastically suggest altered pH sensitive K^+ flux may promote K^+/H^+ exchange to initiate enhanced H^+ efflux underlying pH reversal in a subset of cancers.

#0542 A novel one carbon pathway generates nuclear SAM for chromatin methylation in cancer.

Tiziano Bernasocchi

Mass General Brigham, Boston, MA

Pancreatic Ductal Adenocarcinoma (PDAC) stands as the most common and one of the deadliest forms of pancreatic cancer, largely due to liver metastasis and the lack of effective targeted treatments 1,4. Emerging evidence comparing primary and metastatic cancer lesions suggests that key steps of metastasis are controlled by reversible epigenetic mechanisms, specifically DNA methylation and Histone Post Translational Modifications (PTMs) 10,11. These epigenetic changes are intricately linked to metabolic networks, which supply the essential substrates and cofactors for these modifications, thereby potentially playing a crucial role in metastasis adaptation 12. To explore this interplay between metabolism and epigenetics in PDAC, we leveraged the DepMap database to identify metabolic dependencies in pancreatic cancer cells. Our unbiased analysis revealed Methionine Adenosyltransferase 2A (MAT2A) as a specific vulnerability. MAT2A is a key enzyme in the One Carbon Metabolism (OCM), the pathway for transferring single-carbon units to various substrates. Crucially, the OCM is integral to DNA and histone methylation processes by generating S-adenosylmethionine (SAM), the universal methyl donor whose availability is tightly regulated by MAT2A itself 13. Strikingly, preliminary data reveal a specific nuclear localization of MAT2A in metastatic liver lesions, contrasting with its distribution in primary tumors. Additionally, untargeted metabolomic analysis of human liver metastases revealed that most one-carbon metabolism (OCM) intermediates, including SAM, are downregulated, indicating a high demand for these metabolites in metastatic cells. To mimic these conditions, we developed a Metastasis-like Media (MLM), and our in vitro experiments confirmed that under these conditions, MAT2A translocates to the nucleus, binds to chromatin and is required to sustain histone methyltransferases (HMTs) activity, forming a previously unrecognized OCM nuclear network. Targeting the nuclear activity of MAT2A—including its chromatin binding and interactions with chromatin-associated proteins—could represent a novel therapeutic strategy for metastatic PDAC. Furthermore, this proposal seeks to elucidate the specific mechanisms by which one-carbon metabolism influences DNA and histone methylation patterns, an area that remains unexplored in cancer treatment. Understanding these underlying mechanisms will enable the identification of potential metabolism-targeted therapies to improve the prognosis for PDAC patients. <!--EndFragment-->

#0543 Prevalence and significance of PSAT1 expression in human cancer.

Fiete Gehrisch[1], Hendrina Contreras[1], Maximilian Lennartz[1], Katharina Moller[1], Nathalia Gorbokon[1], Martina Kluth[1], Claudia Hube-Magg[1], Maria Christina Tsourlakis[1], Nina Schraps[1], Florian Viehweger[1], David Dum[1], Andrea Hinsch[1], Christoph Fraune[1], Christian Bernreuther[1], Patrick Lebok[1], Guido Sauter[1], Till S. Clauditz[1], Till Krech[1], Andreas H. Marx[2], Ronald Simon[1], Eike Burandt[1], Sarah Minner[1], Stefan Steurer[1], Ria Schlichter[1], Seyma Buyucek[1]

[1]Institute of Pathology, University Medical Center Hamburg-Eppendorf, Hamburg, Germany,[2]Department of Pathology, Academic Hospital Fuerth, Fuerth, Germany

Phosphoserine aminotransferase 1 (PSAT1) is an enzyme involved in de novo biosynthesis of L-serine by catalyzing the conversion of 3-phosphohydroxy-pyruvate to 3-phosphoserine. This reaction simultaneously produces α-ketoglutarate, thereby directly linking serine biosynthesis to glutamine metabolism, the tricarboxylic acid cycle and one carbon metabolism. L-serine is a vital substrate for numerous cellular processes such as the synthesis of proteins and neurotransmitters as well as nucleotide production and cell proliferation. Previous studies have linked PSAT1 upregulation to enhanced tumor cell proliferation, invasion and migration in various tumor entities, thereby suggesting a crucial role for PSAT1 in cancer development and progression. To learn more on the prevalence of PSAT1 expression and potential associations with phenotype across human malignancies, this study analyzed PSAT1 protein expression in a cohort of 14,966 tumor tissue samples from 134 different tumor entities in a tissue microarray format. PSAT1 staining was cytoplasmic and/or nuclear and occurred in various normal cell types and was seen in at least a fraction of cases in most tumor entities (124 of 134; 91.8%). Out of the 12,305 interpretable tumor samples, PSAT1 staining was found in 4,633 samples, including 3,168 (25.7%) with weak, 765 (6.2%) with moderate, and 700 (5.7%) with strong positivity. PSAT1 staining positivity was particularly frequent and high level in granular cell tumor (92.7%), urothelial carcinoma of the bladder (47.7-91.0%), embryonal carcinoma of the testis (88.4%), several subtypes of uterine cancer (65.1-87.5%), adrenal cortical adenoma and carcinoma (65.2-86.0%), ovarian cancer (15.4-84.6%), colorectal neuroendocrine carcinoma (63.3%), paraganglioma (63.3%), and in squamous cell carcinomas from different sites (50.6-62.2%). High PSAT1 expression was associated with unfavorable tumor phenotype in invasive breast carcinoma of no special type, clear cell renal cell carcinoma, papillary renal cell carcinoma, gastric adenocarcinoma, adenocarcinoma of the colon, and endometrioid endometrial carcinoma ($p \leq 0.05$ each). Low PSAT1 expression was associated with invasive tumor growth in urothelial carcinoma ($p \leq 0.05$ each). In conclusion, our data establish PSAT1 as a highly upregulated metabolic enzyme across a broad spectrum of human tumors. Its potential as both a prognostic biomarker and a therapeutic target is supported by an association with aggressive clinicopathological features in numerous tumor types.

#0544 Dissecting the biological functions of various isoforms of ferredoxin reductase for cell survival and DNA damage response.

Kenichi Nakajima, Shakur Mohibi, Kyle Kenji Hong, Xinbin Chen, Jin Zhang

UC Davis, Davis, CA

The ferredoxin reductase (FDXR) gene is expressed as seven isoforms: 1-6 by alternative splicing and 7 by alternative promoter. FDXR, primarily the reference mitochondrial isoform 1, is required for biosynthesis of sterols, heme and iron-sulfur clusters, but isoforms 2-7 are undefined. Here, we found that isoform 1 is the most abundant one, accounting for ~70% of total FDXR whereas isoforms 4 and 7 account for ~10% and ~7%, respectively. We found that isoforms 1 and 4 are mainly localized in the mitochondria whereas isoform 7, which lacks a mitochondria localization signal, is expressed in the cytosol. We also found that like the promoter for isoforms 1-6, the P2 promoter for isoform 7 can be induced by DNA damage in a p53-dependent manner. To determine isoform-specific activity, we generated multiple MCF7 cell lines in that one or more isoforms are knocked out. While total FDXR-KO MCF7 cells are non-viable, cells deficient in isoforms 1-6, isoforms 4 or 7 remain viable but are weak in cell proliferation, DNA damage response and repair. These data suggest that each FDXR isoform contributes to cell survival and that isoform 7 has an extra-mitochondrial activity sufficient for cell survival.

#0545 PFAS-mediated DRP1 deamidation couples mitochondrial dynamics to purine biosynthesis.

Xinchi Xie[1], Yongzhen Liu[1], Chao Qin[1], Jessica Carriere[2], Pinghui Feng[1]

[1]Herman Ostrow School of Dentistry, USC - University of Southern California, Los Angeles, CA,[2]Cedars-Sinai Health System, Los Angeles, CA

Cancer cells dynamically remodel mitochondrial networks to balance energy production and biosynthetic precursor generation, but how mitochondrial dynamics are coordinated with specific biosynthetic pathways during cell cycle progression remains unclear. Phosphoribosylformylglycinamidine synthase (PFAS) is a key enzyme in *de novo* purine synthesis. It forms purinosome with other purine synthetic enzymes to support rapid nucleotide synthesis. As the scaffold of this mitochondria-adjacent multienzyme complex, how PFAS links mitochondrial dynamics to purine synthesis remains unknown. We found that PFAS deletion markedly impaired cancer cell proliferation and depleted the nucleotide pool. Moreover, PFAS deletion led to reduced cellular energy production and disrupted redox balance. Interestingly, hypoxanthine supplementation in PFAS-deleted cells successfully restored nucleotide levels to control levels, but it did not rescue redox balance or cell proliferation, indicating a purine-independent function of PFAS. Moreover, [U-^{13}C]glucose isotope tracing experiments demonstrated that PFAS deletion reduced glucose-derived carbon entry into the TCA cycle, consistent with suppressed oxidative metabolism. In parallel, [U-^{13}C]glutamine tracing revealed that glutamine contribution to TCA intermediates and aspartate was increased upon PFAS depletion, indicating a shift toward glutamine-supported anaplerosis. Furthermore, mitochondrial proteomics showed that PFAS deletion caused a compensatory upregulation of enzymes in tricarboxylic acid (TCA) cycle and electron transport chain. PFAS-deletion-mediated metabolic defects suggested an impaired mitochondrial function. We therefore examined mitochondrial morphology in control and PFAS-deleted cells. Indeed, transmission electron microscopy revealed strikingly increased fragmentated mitochondria in PFAS-deficient cells. We then focus on the molecular mechanisms by which PFAS regulates mitochondrial morphology. LC-MS/MS and biochemical assays demonstrated that PFAS is a bona fide deamidase of DRP1. Deamidated DRP1 (N267D/N268D) completely lost GTPase activity and showed impaired GTP binding activity, further failing to drive mitochondrial fission. Interestingly, DRP1 deamidation increased during G1 phase and peaked in S phase, coinciding with mitochondrial elongation and the heightened nucleotide synthesis. Thus, PFAS-mediated DRP1 deamidation couples mitochondrial networks to the metabolic demand of proliferative cells. Collectively, the *de novo* purine synthetic enzyme PFAS deamidates DRP1 to regulate mitochondrial morphology, further promoting mitochondrial oxidative phosphorylation and nucleotide synthesis. These findings uncover a previously unrecognized link between nucleotide biosynthesis and mitochondrial dynamics, providing a framework for targeting the PFAS-DRP1 axis in cancer.

: Targeting Mitochondria and Metabolic Vulnerabilities for Cancer Therapy
Poster Session

#0549 BTM-3566 activation of the mitochondrial protease OMA1 increases sensitivity to venetoclax and azacitidine in acute myelogenous leukemia..

Matthew Kostura, Michael Luther, Todd Hembrough, Glen J. Weiss, Michael T. Stocum

Bantam Pharmaceutical, Durham, NC

Background: BTM-3566 is a member of the chemical class, 1-thiazol-2-yl-N-3-methyl-1H-pyrozole-5-carboxylic acids, which are potent, single agent anti-tumor agents in both B-cell lymphomas and select solid tumor malignancies. Therapeutic response is associated with activation of the mitochondrial metalloprotease OMA1. Drug induced activation of OMA1 leads to changes in mitochondria including alterations in cristae structure, morphology, and reduced expression of BH3 proteins such as MCL1. The therapeutic outcome is Bax-dependent apoptosis in B-cell lymphomas and regression or growth inhibition in solid tumors. We hypothesized that reductions in BH3 protein content and changes in mitochondrial cristae structure and function prime tumor cells for apoptosis. This may allow the use of BTM-3566 more broadly in conjunction with standard chemotherapy or targeted agents such as BH3 mimetics. Because venetoclax (a BH3 mimetic) and azacitidine are established standard-of-care (SOC) therapies for AML patients ineligible for intensive chemotherapy, we tested whether BTM-3566 enhances their activity. To test this hypothesis, BTM-3566 was evaluated in acute myelogenous leukemia (AML) cell lines to determine if synergy occurred in combination with venetoclax, azacytidine, or the ternary combination.
Methods: The activity of BTM-3566, venetoclax, and/or azacitidine was determined in AML cell lines (HL-60, Kasumi-1 and KG-1) using Cell-Titre Glo (CTG) which serves as a surrogate for cell numbers. Apoptosis was measured using Caspase 3/7 Glo. Drug activity interactions were quantified using Synergyfinder + software.
Results: BTM-3566 was active in all three AML cell lines (IC_{50} range 300-600 nM). BTM-3566 acted synergistically with venetoclax to inhibit cell growth in all cell lines, while synergy with azacitidine was observed only in HL-60 cells. The ternary combination of BTM-3566, venetoclax, and azacitidine resulted in increased cell killing with an apparent increase in the potency of venetoclax. Caspase 3/7 assays confirmed that BTM-3566 and venetoclax each induced a time-dependent increase in apoptosis in HL-60 and Kasumi-1, but not KG-1 cells. Binary drug treatment of venetoclax and BTM-3566 led to increased Caspase 3/7 activation and a BTM-3566 dose dependent increase in the activity of venetoclax in HL-60 and Kasumi-1 cells.
Conclusions: BTM-3566 targets a pathway important for mitochondrial integrity and control of apoptosis leading to reduced tumor cell growth and survival. Rational combinations of BTM-3566 with AML SOC agents demonstrate synergistic activity. Together, the findings support further evaluation of BTM-3566 to potentially broaden the utility of BH3-directed therapies in AML and potentially other difficult to treat malignancies. BTM-3566 is currently being evaluated in Phase I trials for DLBCL and select solid tumors.

#0550 Targeting heat shock factor 1 in pancreatic ductal adenocarcinoma autophagy and iron-sulfur cluster protein stability.

Rejina Shrestha, Shruti Ghai, Hannah Nam, Kuo-Hui Su

University of Toledo, Toledo, OH

Background: Pancreatic ductal adenocarcinoma (PDAC) cells exhibit elevated copper levels, an essential cofactor for cellular function, to support pancreatic tumor growth. Recent studies show that high levels of copper disrupt mitochondrial function by downregulating iron-sulfur (Fe-S) cluster proteins, leading to proteotoxic stress response and cell death; however, the detailed mechanism remains unclear. Heat shock factor 1 (HSF1), a key regulator of the proteotoxic stress response, is highly expressed in PDAC and supports protein stability, mitochondrial function, and tumor progression. This suggests HSF1 may help PDAC cells resist copper-induced cytotoxicity. The copper treatment also induces autophagy, yet whether copper-induced autophagy is regulated by HSF1 is not fully understood.
Objective: The objective of this study is to study the role of HSF1 in copper-mediated loss of mitochondrial Fe-S cluster proteins and autophagy in PDAC cells.
Methods and Results: In PDAC cell lines MIA PaCa-2 and PANC-1, treatment with copper ionophore elesclomol-copper (ES-Cu) led to reduced protein levels of mitochondrial Fe-S cluster proteins, including aconitase 2 (ACO2), ferredoxin 1 (FDX1), and lipoic acid synthase (LIAS), but not mRNA expression. Notably, HSF1 overexpression rescued the ES-Cu-decreased protein levels of ACO2, FDX1, and LIAS. Pharmacological inhibition of HSF1 led to increased lipidation of the autophagy marker microtubule-associated protein 1A/1B-light chain 3 (LC3). To investigate the mechanism of ES-Cu-mediated decrease of Fe-S cluster proteins, we pre-treated MIA PaCa-2 cells with hydroxychloroquine (CQ) along with ES-Cu. CQ did not rescue the ES-Cu-mediated decrease in Fe-S cluster proteins, suggesting that the degradation of Fe-S cluster proteins is not mediated by autophagy in copper-mediated cytotoxicity. Interestingly, inhibition of the mitochondrial-specific protease reversed the decrease in Fe-S cluster proteins under ES-Cu stress. Further, HSF1 inhibition with a small-molecule inhibitor significantly enhanced ES-Cu-reduced cell viability in PDAC cells.
Conclusion: Our findings suggest that HSF1 protects PDAC cells from mitochondrial toxicity by maintaining the stability of Fe-S proteins under copper stress. Targeting HSF1 in combination with copper-based therapies may enhance treatment efficacy by disrupting mitochondrial stress adaptation in PDAC.

#0551 Advancing cancer treatment through targeting dipeptidyl peptidase 8 an innovative strategy for overcoming resistance.

Paras Jawaid[1], Mati Ur Rehman[2], Azhar Hussain Rajabali[2], Ather Enam[3]

[1]Biological and Biomedical sciences, Centre of Oncological Research in Surgery, Aga Khan University Hospital, Karachi, Pakistan,[2]Biological and Biomedical Sciences, Aga Khan University Hospital, Karachi, Pakistan,[3]Neurosurgery, Centre for regenerative medicine and stem cell research, Aga Khan University, Karachi, Pakistan

Cancer remains one of the most complex and challenging diseases because of its heterogeneity and the ability of tumor cells to become resistant to the treatment. Among various cancers, glioblastoma and colon cancers are the most prevalent and deadliest cancer worldwide. It is responsible for significant burden on the healthcare system and affects millions of lives every year. Despite advancement in cancer treatment, including chemotherapy, radiotherapy, targeted therapies, and immunotherapy, achieving complete remission remains challenging that contributes to the poor prognosis of glioblastoma patients. One promising area of research involves a group of enzymes called dipeptidyl peptidases DPPs, a family of serine proteases which are known to regulate various biological processes, including immune function, metabolism, and cancer progression. Dipeptidyl peptidases DPPs, particularly DPP8, have emerged as promising molecular targets in cancer therapy. This study investigates the mechanistic role of DPP8 inhibition in glioblastoma and colorectal cancer cells. Cell viability was assessed using trypan blue and CCK8 assays, while apoptosis was evaluated via Giemsa staining, DNA fragmentation, Annexin V FITC PI, and cell cycle analysis. Flow cytometry revealed increased ROS production, loss of mitochondrial membrane potential and intracellular calcium level following treatment. Western blotting showed enhanced expression of apoptosis-related proteins 24 hr after treatment with DPP8 inhibitor. These findings suggest that DPP8 inhibition induce mitochondria mediated apoptotic pathways and may serve as a novel therapeutic strategy, offering potential for targeted and personalized cancer treatment approaches.

#0552 Functional effects of miPEP133 on mitochondrial integrity and treatment response in ovarian cancer.

Samantha Goncalves Novo, Miranda Mansolf, Tobias M. Hartwich, Jasmine Jathan, Viktoriia Kolesnyk, Yang Yang-Hartwich

Yale School of Medicine, New Haven, CT

Background: MiPEP133 is a microprotein encoded by the miR-34a precursor. In normal cells, it functions as a tumor suppressor and is expressed in colon, stomach, ovary, uterus, and pharynx, but its levels are markedly reduced in cancer. Localized in the mitochondria, miPEP133 regulates mitochondrial homeostasis through interactions with mitochondrial chaperones and has been reported to induce apoptosis and inhibit tumor cell migration in other cancer types. However, its functional role in ovarian cancer remains poorly defined. We investigated the biological impact of miPEP133 overexpression in patient-derived high grade serous ovarian cancer cell lines to further characterize its cellular effects and therapeutic relevance.

MethodsMiPEP133 was overexpressed in two patient-derived ovarian cancer cell lines using lentiviral vectors. Protein expression was confirmed by western blot. Cell growth kinetics were assessed using flow-cytometry-based proliferation assays. Mitochondrial morphology was evaluated by immunofluorescence staining. Sensitivity to chemotherapeutic agents (carboplatin and paclitaxel), MEK inhibitors, and mitochondrial modulators were measured using CellTiter-Glo assays. Apoptosis was quantified by Annexin V/PI staining and flow cytometry. Gene expression changes in treated and untreated miPEP133-overexpressing and control cells were evaluated by quantitative PCR (qPCR).

ResultsOverexpression of miPEP133 in the ovarian cancer cell lines led to a moderate reduction in cell proliferation, consistent with growth suppression. Immunofluorescence analysis revealed disruption of mitochondrial network structure and a decrease in mitochondrial mass. MiPEP133-overexpressing cells exhibited significantly increased sensitivity to MEK inhibitors and selected chemotherapeutic agents compared with control cells. Annexin V staining demonstrated increased apoptotic populations following chemotherapeutic treatment. qPCR analysis validated upregulation of genes involved in apoptosis, mitochondrial stress response, and oxidative stress pathways in miPEP133-overexpressing cells treated with MEK inhibitors and mitochondrial modulators.

ConclusionThese findings further characterize miPEP133 as a suppressor of ovarian cancer cell growth and a regulator of mitochondrial integrity in cancer cells. The restoration of miPEP133 function in ovarian cancer cells can enhance their sensitivity to chemotherapeutic and MEK-inhibitors. MiPEP133 represents a promising tumor suppressor with potential utility as both a therapeutic sensitizer and a biomarker in ovarian cancer.

#0553 Selective induction of cuproptosis in vivo by a soluble Elesclomol analog.

Piyush Mishra[1], Mainak Banerjee[2], Jian-Ren Lin[3], Shannon Coy[3], Jeffrey Hsiao[1], Jonah Lee[1], John Clohessey[1], Alexandre Detappe[4], Todd R. Golub[5], Loic Charbonniere[2], Sandro Santagata[3], Peter Tsvetkov[1]

[1]Beth Israel Deaconess Medical Center, Boston, MA,[2]Institut Pluridisciplinaire Hubert Curien, Universite de Strasbourg, Strasbourg, France,[3]Harvard Medical School, Boston, MA,[4]Strasbourg Drug Discovery and Development Institute (IMS), University of Strasbourg, Strasbourg, France,[5]Broad Institute, Cambridge, MA

Copper overload induced by specific ionophores can trigger cuproptosis, a newly defined form of regulated cell death that offers a novel strategy to target cancer. While this mechanism has been well characterized in cultured cells, its relevance in vivo and potential for therapeutic use remain unclear. The best-characterized ionophore, elesclomol (ES), had been previously tested in clinical trials with limited success; however, these studies were conducted without knowledge or consideration of its copper-binding mechanism or its ability to induce cuproptosis. Here, we define the biological and pharmacologic determinants of ES-induced cuproptosis in vivo, guiding the design of a more effective and tolerable ES analog. We first established that pre-bound ES (ES-Cu) is more potent and pharmacologically active than ES alone, maintaining on-target cuproptosis activity in culture and showing superior efficacy in a xenograft model. Although ES-Cu treatment produced marked tumor responses, complete regression was not achieved. To uncover mechanisms limiting response, we performed a genome-scale ORF overexpression screen and identified CYP11A1 and CYP27A1, mitochondrial partners of FDX1, as resistance factors. These findings indicate that FDX1 expression alone is not sufficient for sensitivity and that effective cuproptosis requires FDX1 activity uncoupled from CYP metabolism, a relationship that may also protect FDX1-high organs such as the adrenal gland and kidney from toxicity. To further overcome ES's poor solubility and pharmacokinetic limitations, we synthesized a new copper ES analog, which exhibits improved solubility, enhanced antitumor efficacy, and reduced systemic toxicity. Multiplexed imaging confirmed intratumoral aggregation of lipoylated proteins consistent with on-target cuproptosis induction. Together, these findings uncover a previously unrecognized role of FDX1-CYP coupling in regulating cuproptosis sensitivity and define a path toward biomarker-guided development of copper ionophore-based cancer therapies.

#0554 Asbestos exposure induces carcinogenesis via minority MOMP and displays characteristics of drug-tolerant persister cells.

Jaylon C. Aggison, Cristian G. Medina, Siqi Wu, Naren Li, Francisco A. Molina-Pelayo, Jessica B. Ji, Ritika Raj, Yuan Xu, Robert Taylor Ripley

Michael E. DeBakey Department of Surgery, Baylor College of Medicine, Houston, TX

Background Pleural mesothelioma (PM) occurs many years after asbestos fiber exposure; yet the mechanism that converts chronic damage into malignancy remains unclear. Asbestos fibers induce persistent oxidative and genomic stress that should activate apoptosis via mitochondrial outer membrane permeabilization (MOMP); however, these cells do not undergo apoptosis and instead develop into malignancy. MOMP normally triggers cytochrome c (cyt c) release as well as mitochondrially derived damage-associated molecular patterns (DAMPs), resulting in caspase activation and cell death. Sublethal activation of MOMP can lead to a phenomenon known as Incomplete or Minority mMOMP, in which cells survive and develop somatic mutations which contribute to carcinogenesis. In this study, we evaluated whether minority MOMP induced carcinogenesis in PM cells.

Methods We investigated whether prolonged exposure to asbestos fibers drives mMOMP in non-transformed, pleural mesothelial cells (MeT-5A). Cells were cultured for six months with chrysotile (Chry-Asb) or crocidolite (Croc-Asb) asbestos fibers. Cellular phenotypes were assessed by clonogenicity, migration, and invasion assays to evaluate malignant transformation. Reactive oxygen species (ROS) production, cytochrome (cyt) c release, γH2AX phosphorylation, and caspase 3 activation were measured to evaluate mitochondrial and apoptotic responses.

Results Chronic asbestos exposure increased clonogenicity, migration, and invasion of MeT-5A cells, suggesting transformation toward a malignant phenotype. Additionally, we observed the phenotypic characteristics of minority MOMP, including elevated ROS, cyt c release, an increase in the MOMP effector proteins (Bax/Bak), caspase activation, and γH2AX phosphorylation while lacking induction of apoptosis. Furthermore, the anti-apoptotic mitochondrial protein Myeloid Cell Leukemia-1 (MCL-1) was upregulated by asbestos, facilitating minority MOMP by preventing a shift to complete MOMP. Metabolomic analysis revealed a Warburg effect. Consistent with the Warburg effect, both Seahorse analysis and Gene Set Enrichment Analysis showed increased glycolysis in both cell lines. Additionally, asbestos-induced minority MOMP was associated with characteristics of drug-tolerant persister cells (DTPs) including slower proliferation, change in cell phenotype, and resistance to cisplatin.

Conclusion Minority MOMP promotes malignant transformation of mesothelial cells while enabling resistance to apoptosis. Our findings suggest that minority MOMP contributes to carcinogenesis by altering mitochondrial dynamics and metabolic reprogramming, reprogramming cells to a DTP phenotype. Targeting mitochondrial pathways to convert Minority MOMP into complete MOMP may represent a novel therapeutic strategy to overcome treatment resistance in pleural mesothelioma.

#0555 Prostaglandin E2 increases lipid droplet accumulation and peri-droplet mitochondria population in acute lymphoblastic leukemia.

Byourak Shabane, Cristiane Beninca, Michael Cohen, Nikole Scillitani, Ugochukwu Ihenacho, Orian Shirihai, Steven D. Mittelman

University of California, Los Angeles, Los Angeles, CA

Acute lymphoblastic leukemia (ALL) is the most prevalent childhood cancer, representing approximately 70% of all pediatric malignancies. While some patients attain remission following intensive chemotherapy regimens, multiple demographical and biological factors have been identified that worsen treatment outcomes. Obesity, clinically defined by body mass index (BMI), has been strongly associated with reduced survival rates, increased toxicity from chemotherapy, and increased risk of relapse. Our laboratory has previously demonstrated that adipose tissue supplies free unsaturated fatty acids and amino acids to ALL cells and protects the cells from chemotherapy. To identify the mechanisms by which adipose tissue alters the metabolism of ALL, we previously performed a single-cell RNA sequencing experiment on mice to compare the gene expression profiles of ALL cells between adipose tissue and bone marrow. This experiment uncovered a potential link between adipose tissue prostaglandin E2 (PGE2) synthesis and ALL cell lipid droplet maturation. To explore this, we cocultured human BV173 and RS4-11 ALL cells in transwell inserts above human visceral adipose tissue explants obtained from UCLA's Translational Pathology Core. Coculture with adipose tissue increased ALL cell lipid droplet-associated proteins perilipin (PLIN) 2 and 5 gene and protein expression (n=4-8). We next treated ALL cells with PGE2 (200ng/mL) and observed increased gene and protein expression in PLIN2 and PLIN5 (n=3-4). Confocal imaging confirmed that PGE2 induced lipid droplets in human ALL cell lines, along with peri-droplet mitochondria, a specialized subset of mitochondria known to promote lipid droplet synthesis. We hypothesize that adipose tissue PGE2 induces ALL cell lipid droplet accumulation and peri-droplet mitochondria formation and that these may contribute to protecting ALL cells from cytotoxicity.

PLIN5 and PLIN2 gene and protein expression in human ALL cells cocultured w human adipose explants

	BV173	BV173	BV173	RS4;11	RS4;11	RS4;11
	mean +/- SD	P-value	n	mean +/- SD	P-value	n
PLIN5 gene	3.6±2.0	<0.0001	6	3.6±2.8	0.03	4
PLIN2 gene	1.2±0.3	n.s	6	1.9±0.8	n.s	4
PLIN5 protein	1.3±0.2	0.01	7	1.5±0.5	0.02	8
PLIN2 protein	2.3±0.6	0.002	6	2.0±0.8	0.02	8

#0556 Inhibition of mitochondrial protein MAGMAS increases sensitivity to standard of care treatment.

Javier J. Lepe[1], Shashi Jain[2], Naomi Lomeli[1], Claire Chen[3], Bhaskar C. Das[4], Daniela A. Bota[1]

[1]UCI School of Medicine, Irvine, CA,[2]UCI School of Medicine,, Irvine, CA,[3]UCI, Irvine, CA,[4]Weill Cornell Medical College, New York, NY

Glioblastoma is a highly aggressive CNS cancer that affects 3 in 100,000 people every year in the U.S. The majority of patients experience tumor recurrence within the first year after initial diagnosis and after receiving standard of care treatment. GBM is characterized by its high mitotic index, capacity to invade other regions of the brain and modulate the tumor microenvironment (TME). Options are extremely limited for patients suffering from recurrent GBM as tumors become increasingly resistant to chemotherapy. Resistance to chemotherapy can be attributed to several factors that include DNA damage response (DDR), glioma stem cells (GSCs), TME, senescence mechanisms, and metabolic reprogramming. Mitochondria-associated granulocyte macrophage colony-stimulating factor molecule (MAGMAS), a mitochondria protein and subunit of the translocase of the inner membrane 23 (TIM23) complex, regulates protein trafficking into the mitochondria by recruiting DNAJC19 to the TIM23 complex. The present work was to investigate the role of MAGMAS in GBM tumor biology and mechanisms of resistance to TMZ. Computational analysis of MAGMAS/PAM16 expression levels from publicly available databases revealed that MAGMAS levels are significantly elevated in recurrent tumors and is positively correlated with the DNA repair enzyme O(6)-methylguanine-DNA methyltransferase (MGMT) expression in primary patient tissues. We generated genetically modified glioma cells expressing shpam16 constructs and found that MAGMAS deficient glioma cells were sensitized to standard of care treatment that include TMZ, radiation and tumor treating fields (TTFs). Additionally, we discovered that silencing PAM16/MAGMAS reduced MGMT expression and reduced extracellular excretion of lactic acid. Interestingly, we also discovered that the cytokine IL7 and IL15 were significantly upregulated in MAGMAS KD cells. Taken together, our results demonstrate that MAGMAS plays an important role in chemotherapy resistance, metabolic reprogramming and potentially modulating the TME. By targeting MAGMAS, we can promote favorable conditions to enhance anti-tumor response using immunotherapy strategies in the future.

#0557 TRAP1 represents a mitochondrial target and biomarker of dedifferentiated liposarcoma.

Roma Karna[1], Esin Ulker[2], Sydney Rentsch[1], Marina Capece[1], Sayumi Tahara[1], Qi Zhang[1], Patricia Sarchet[1], Giovanni Nigita[1], Paolo Fadda[1], Fernanda Costas Casal de Faria[1], Valerie Grignol[1], Nicholas C. Denko[2], Carlo M. Croce[3], Raphael E. Pollock[1], Federica Calore[1]

[1]The Ohio State University, Columbus, OH,[2]Dept. of Rad. Onc., OSU Comprehensive Cancer Center, Columbus, OH,[3]OSUCCC - James, Columbus, OH

Dedifferentiated liposarcoma (DDLPS) is a rare and aggressive adipocytic malignancy with a nearly 85% local recurrence rate, exceptionally high compared to other tumors, and a 10-year survival rate of only 10%. No reliable biomarkers currently predict recurrence or therapeutic response. Current management relies primarily on radical surgery, often combined with non-specific chemotherapy, which yields poor outcomes and severely compromises patients' quality of life. The aggressiveness of DDLPS and the lack of effective systemic therapies highlight an urgent need for novel molecular targets and treatment approaches.

We identified the mitochondrial chaperone TRAP1 (TNF Receptor-Associated Protein 1) as a potential oncogenic driver and therapeutic target in DDLPS. TRAP1 is a master regulator of mitochondrial metabolism, oxidative stress, and apoptosis, yet its role in DDLPS remains unknown. Our preliminary data show that TRAP1 protein and mRNA levels are significantly overexpressed in DDLPS compared to low grade well-differentiated liposarcoma (WDLPS) and Normal Adjacent Tissue (NAT), suggesting a contribution to tumor progression.

To explore its therapeutic potential, we silenced TRAP1 using siRNA and inhibited its activity with MitoQuinone (MitoQ), a TRAP1 inhibitor currently evaluated in non-cancer clinical trials. TRAP1 silencing significantly reduced DDLPS cell proliferation and increased cell death, as shown by MTS assays and Annexin V/PI assays. MitoQ treatment led to significant, dose- and time-dependent cytotoxicity in DDLPS cells compared to their WDLPS counterpart, and impaired spheroid growth in 3D models. Moreover, TRAP1 knockdown significantly decreased mitochondrial membrane potential compared to control conditions, and triggered G1/S cell-cycle arrest, indicating disruption of mitochondrial function.

Ongoing studies are investigating how TRAP1 modulation affects ROS production, mitochondrial dynamics and energy metabolism using Seahorse metabolic flux analysis, to define its contribution to metabolic reprogramming and redox balance in DDLPS. Finally, to establish TRAP1's clinical relevance, we will assess TRAP1 mRNA expression in a larger cohort of liposarcoma patient samples to correlate its levels with recurrence rates and survival outcomes. This work positions TRAP1 as a mitochondrial therapeutic target and potential biomarker, offering novel mechanistic insight and paving the way for innovative DDLPS treatment strategies.

#0558 Benzyl isothiocyanate induced mitochondrial dysfunction via ROS generation sensitizes head and neck squamous cell carcinoma to cisplatin and radiation.

Imani Aliah Kirven[1], Francesca Spirito[2], Patrice Penfornis[3], Kristin S. Edwards[1], Gary R. Bishoop[1], Linda L. Eastham[1], Chunli Yang[4], Rojymond Jacob[4], Pier Paolo Claudio[1]

[1]Pharmacology & Toxicology, University of Mississippi Medical Center, Jackson, MS,[2]Clinical and Experimental Medicine, University of Foggia, Foggia, Italy,[3]Cancer Institute, University of Mississippi Medical Center, Jackson, MS,[4]Radiation and Oncology, University of Mississippi Medical Center, Jackson, MS

Accounting for nearly 4% of all cancer diagnoses and 2% of all cancer-related mortality in the United States, head and neck squamous cell carcinoma (HNSCC) originates from the squamous epithelial cells lining the mucosal surfaces of the oral cavity, pharynx, larynx, lips, and sinonasal tract. HNSCC is notable for its resistance to conventional therapy, with mitochondria serving as central mediators through multifaceted contributions, including the regulation of cellular signaling pathways, modulation of energy metabolism, and control of apoptotic responses. Although modulation of mitochondrial pathways has emerged as a potential therapeutic target, its role in HNSCC progression and treatment response remains incompletely understood. Benzyl isothiocyanate (BITC), a naturally derived bioactive compound found in cruciferous vegetables, selectively induces excessive reactive oxygen species (ROS) and depletes glutathione in cancer cells, leading to mitochondrial dysfunction and impaired bioenergetic flexibility. Building on the role of mitochondria in therapeutic resistance, we explored the effects of BITC in sensitizing paired primary and metastatic HNSCC cell lines isolated from two patients to cisplatin (CDDP) and radiotherapy (RT). Cell viability and caspase-3/7 activity were assessed at 72 hours on HNSCC cells pretreated for 1 hour with BITC, followed by 24 hours of cisplatin with or without the addition of 4 or 8 Gy radiation. Electron Paramagnetic Resonance (EPR) and glutathione (GSH) rescue assays were used to measure oxidative stress, identify different types of ROS produced, and investigate resistance mechanisms to therapy after up to 24 hours of BITC exposure. Real-time fluororespirometry was employed to evaluate the overall mitochondrial bioenergetic status, also following up to 24 hours of BITC exposure. In all four HNSCC lines, BITC treatment significantly increased sensitivity to both CDDP and RT by inducing apoptosis through Caspase-3/7 activation. BITC treatment effectively induced ROS, which was rescued by the addition of GSH. Within one hour, BITC exposure induced a pronounced decline in mitochondrial respiration and Bioenergetic Health Index (BHI), followed by a transient increase in respiration at 3-5 hours, suggesting metabolic reprogramming. However, by 24 hours, metabolic exhaustion culminated in cell death. Our findings demonstrate that BITC disrupts mitochondrial bioenergetics, limits metabolic adaptability, and increases the efficacy of standard-of-care therapies through excessive ROS production, supporting its potential as a novel adjuvant therapeutic strategy for HNSCC.

#0559 Combination of PRMT5 and Mcl-1 inhibitors overcomes immune checkpoint inhibitor resistance in pleural mesothelioma.

Siqi Wu, Jaylon Aggison, Cristian Medina, Naren Li, Francisco Molina-Pelayo, Ritika Raj, Yuan Xu, Robert T. Ripley

Baylor College of Medicine, Houston, TX

Introduction: Pleural mesothelioma (PM) is an aggressive cancer with a poor prognosis. Primary resistance to chemotherapy and immune checkpoint inhibitors (ICI) is common, demanding new therapeutic strategies. Our previous work showed the anti-apoptotic protein, Myeloid Cell Leukemia 1(MCL-1) drives chemoresistance. What is unknown is whether targeting MCL-1 will sensitize PM to ICIs. Our multi-omic data linked Mcl-1 to ICI resistance through the methionine metabolic pathway, in which PRMT5 is a critical enzyme. This study evaluates whether targeting the PRMT5/MCL-1 axis will overcome ICI resistance in PM to increase response rates.
Methods: Inhibition of PRMT5 and Mcl-1 was assessed in PM cell lines (H28 and H2452) and Patient-Derived Xenograft (PDX) models. Transcriptomics, metabolomics and reverse-phase protein array were performed on PDX model comparing treatment arms of PRMT5 inhibition, MCL-1 inhibition, and the combination (Cmb) versus vehicle control (Cnt). Additionally, ICI treatment response was evaluated by in *vitro* T-cell co-culture assays. The synergistic effects of PRMT5 and Mcl-1 inhibition were investigated in PM lines by Western Blot with both shRNA-mediated gene knockdown or inhibitor treatment. Annexin V/propidium Iodide staining and flow cytometry analysis were performed.
Results: In vitro, the combination of PRMT5 and Mcl-1 inhibition significantly increased apoptosis compared to either single agent alone and control (Cnt vs Cmb, H28: 8.1% vs 34.1%; H2452: 7.2% vs 25.1%). These cells also displayed synergistic lack of proliferation (Cnt vs Cmb: H28: ~1.6-fold; H2452: ~2-fold). In the PDX model, PRMT5 and Mcl-1 inhibition showed a significant decrease of tumor growth (Cnt vs Cmb: ~1.8-fold). Multi-omic analyses implicated the PI3K/Akt signaling pathway in tumor growth suppression with the combined treatment. Western blot analysis confirmed this mechanism based on phosphorylation of proteins in PI3K/Akt and mTOR signaling pathway, including GSK-3a/b, PRAS40, mTOR, TSC2, P70S6K and AKT1. The combination of PRMT5 and Mcl-1 inhibitors also showed a significant improvement of ICI (anti-PD-L1) response in *vitro* (Cnt vs Cmb: ~1.4-fold).
Conclusion: Co-targeting PRMT5 and Mcl-1 synergistically enhance apoptosis and proliferation via PI3K/Akt/mTOR pathway in PM. Inhibition of PRMT5/Mcl-1 axis may improve treatment response and overcome primary resistance. Our findings provide a novel strategy to translate into clinical trials.

: Tumor Cell Plasticity, Microenvironment, and Stress-Response Pathways
Poster Session

#0563 WEE1 reinforces C-MYC driven oncogenic programs through GSK3ß inhibition.

Krishnapriya Thangaretnam[1], Islam MD Obaidul[2], Jialun Lyu[2], Zhenzhen Zhang[1], Lei Chen[2], Farah Ballout[1], Heng Lu[1], Dunfa Peng[3], Alexander I. Zaika[4], Wael El-Rifai[5], Zheng Chen[6]

[1]University of Miami Miller School of Medicine, Miami, FL,[2]Surgery, University of Miami Miller School of Medicine, Miami, FL,[3]University of Miami, Miami, FL,[4]Professor of Surgery & Cancer Biology, University of Miami, Miami, FL,[5]Director, Surgical Oncology Research, University of Miami, Miami, FL,[6]Surgery, University of Miami, Miami, FL

Background: Esophageal adenocarcinoma (EAC) remains a lethal malignancy with a 5-year survival rate below 20%. The nuclear kinase WEE1 is a key regulator of the G2/M checkpoint, whereas the oncogenic transcription factor c-MYC, dysregulated in ~70% of human cancers, is challenging to target directly. Identifying upstream regulators that control MYC stability offers an alternative therapeutic strategy. Here, we discovered that WEE1 reinforces MYC-driven oncogenic programs by inhibiting GSK3β, and that inhibition of WEE1 promotes proteasome-mediated MYC degradation.
Methods and Results: Gene set enrichment analysis across TCGA and GEO datasets showed consistent enrichment of MYC target gene signatures in WEE1-high EAC tumors. Immunofluorescence in normal esophagus and EAC tissues demonstrated strong overexpression and positive correlation between WEE1 and C-MYC, which was also validated in EAC cell lines compared to non-cancerous and Barrett's esophagus cells. Genetic knockdown or pharmacologic inhibition of WEE1 reduced MYC protein levels, transcriptional activity, and downstream gene expression, as confirmed by reporter assays, qRT-PCR, and RNA sequencing. Cycloheximide chase assays revealed a shortened MYC half-life upon WEE1 inhibition, whereas the proteasome inhibitor MG132 rescued MYC degradation.
Mechanistically, WEE1 inhibition activated GSK3β, a kinase required for MYC ubiquitination and proteasomal turnover. Conversely, WEE1 overexpression stabilized MYC by elevating inhibitory GSK3β-S9 phosphorylation. A kinase-dead WEE1 mutant failed to stabilize MYC, indicating a catalytic-activity-dependent mechanism. Proximity ligation assays further demonstrated increased GSK3β-MYC interaction following WEE1 inhibition. A high-throughput screen of 892 FDA-approved drugs identified Panobinostat as a synergistic partner of the WEE1 inhibitor MK1775. The combination significantly
suppressed the growth of human EAC PDX-derived organoids and inhibited tumor progression in EAC PDX models in vivo.
Conclusion: These findings define a WEE1-GSK3β-MYC signaling axis in which WEE1 stabilizes MYC and sustains MYC-driven oncogenic programs. WEE1 inhibition activates GSK3β, promoting proteasome-mediated MYC degradation. The combination of WEE1 inhibition and Panobinostat represents a promising therapeutic approach for MYC-driven EAC.

#0564 Clonal diversity drives cooperative growth in lung cancer.

Yan Jennifer Gu[1], Salil Garg[2]

[1]Laboratory Medicine, Yale School of Medicine, New Haven, CT,[2]Laboratory Medicine, Genetics, Pathology, Yale University, New Haven, CT

Cell-cell communication within the tumor microenvironment is critical for cancer growth and therapy resistance. While many studies have focused on interactions between tumor cells and the surrounding microenvironment, this study investigates how interactions between distinct tumor cell states contribute to tumor growth. We constructed an in vitro system using the H1975-Clonebow lung cancer cell line, which allows for stochastic recombination of distinct fluorescent proteins to yield unique color signatures for lineage tracing. From the parental H1975-Clonebow line, we derived and expanded 218 single-cell clones and compared each clone's growth rate to the heterogeneous parental population. The parental line grew faster than 86% of clones, suggesting a cooperative advantage of clonal diversity. Systematic "mixing" at fixed total cell numbers showed that mixed-clone populations consistently outperformed single clones, which we interpret as evidence for adaptive heterogeneity. Across 4-clone mixes, quantification during unmixing revealed that both fast- and slow-growing clones proliferated better in mixtures than in isolation, indicating non-random cooperation that promotes collective growth. To capture cooperation-associated programs, we performed bulk RNA-seq on clones fluorescently sorted after 4-clone mixing, with identically sorted single-clone cultures grown alone as controls. Transcriptomes clustered primarily by clone identity but converged on shared signaling modules in mixes, consistent with the observed growth boost. Mix-induced gene programs were more strongly enriched in malignant cells from patient-derived NSCLC tumors than programs from individually grown clones. Ligand-receptor (LR) analysis highlighted an integrin-centered adhesion program: multiple integrin LR pairs consistently ranked among the top tumor cell-cell interactions in vitro and in patient tumors, with β1-integrin (ITGB1) recurring as a hub. Consistent with this, β1-integrin blockade preferentially reduced the mix-specific growth advantage. Future experiments will involve longitudinal live-cell imaging to directly test whether the cooperative growth phenotype requires sustained inter-clone contact. Together, these data suggest that emergent cooperation between tumor cells promotes growth and may be targetable for therapeutics. Targeting β1-integrin-mediated adhesion at the tumor cell-cell interface represents a feasible strategy to disrupt cooperative growth in EGFR-mutant lung cancer.

#0565 Establishing the mechanistic link between chemotherapy response and Hippo-YAP signaling in ovarian cancer.

Jonathan C. Vose, Elizabeth I. Harper, Sheetal Kooduvalli, Joanne Kotelawala, Ashani Weeraratna, Jennifer M. Kavran

Biochemistry and Molecular Biology, Johns Hopkins Bloomberg School of Public Health, Baltimore, MD

Ovarian cancer is one of the leading causes of cancer related deaths for women. First-line treatment includes surgical resection followed by a regimen of cisplatin. More than 70% of tumors, however, acquire chemoresistance. Our understanding of the molecular mechanisms mediating this resistance remains limited. Increased expression of YAP, a transcriptional co-factor inhibited by the Hippo pathway, correlates with poor prognosis, and is a biomarker of poor response to metal-based chemotherapies; yet the mechanistic link between chemotherapy treatment, regulation and changes of YAP driven transcription, and tumor cell response remains unclear. Using a combination of biochemistry, biophysics, and cell-based assays we sought to determine the molecular mechanism and consequences of cisplatin induced YAP activation in ovarian cancer. To determine whether and how cisplatin alters YAP activity in ovarian cancer, we monitored YAP localization, using immunofluorescence, and YAP target-gene transcription, using qPCR, in two ovarian cancer cell lines in the presence or absence of treatment. We find that cisplatin increased YAP nuclear localization and target gene transcription. To identify the step in Hippo signal transduction inhibited by cisplatin, we monitored known phosphorylation events in the Hippo core kinase cassette, via Western blot, in both ovarian cancer cells and in a recombinant system using purified proteins in the presence or absence of cisplatin. In both scenarios, we find that cisplatin prevented activation of the Hippo kinase LATS1/2 but did not alter the activity of the upstream Hippo kinase MST1/2. To determine the mechanism by which cisplatin inhibits LATS1/2, we monitored the solution behavior of LATS1 and its allosteric activator MOB1A; using mass photometry we find that the addition of cisplatin disrupts complex formation between LATS1 and MOB1A. Together, our data provides the first insights into the molecular mechanism by which cisplatin inhibits signal transduction in the Hippo pathway driving YAP activation in ovarian cancer. Future work aims to identify the YAP driven transcriptional changes that mediate chemoresistance to identify potential therapeutic strategies.

#0566 UVRAG-ITCH-ESCRT axis mediates a lysosomal off-switch dampening NOTCH1 signaling in cancer.

Behzad Mansoori[1], Zihan Zheng[1], Chintan Parekh[2], Chengyu Liang[1]

[1]The Wistar Institute, Philadelphia, PA,[2]Children's Hospital Los Angeles, Los Angeles, CA

NOTCH1 signaling is a conserved pathway essential for cell fate decisions, and its dysregulation drives multiple cancers such as T-cell acute lymphoblastic leukemia (T-ALL). Precise control of NOTCH1 signal strength and duration is critical, yet mechanisms fine-tune NOTCH1 signaling remains poorly understood. Here we identify a previously unrecognized endo-lysosomal “off-switch” for NOTCH1 mediated by the UVRAG-ITCH axis. We demonstrate that UVRAG (UV radiation resistance-associated gene), traditionally known for its role in autophagy, acts independently of autophagy to negatively regulate NOTCH1 signaling. UVRAG physically engages the membrane-tethered NOTCH1 extracellular truncation (NOTCH1ΔE), the activated intermediate generated after ligand-induced or mutational S2 cleavage, and recruits the E3 ubiquitin ligase ITCH. The UVRAG-ITCH complex catalyzes non-canonical Lys27-linked ubiquitination of NOTCH1ΔE at a conserved lysine (K1795) in its RAM domain, thereby tagging this intermediate for recognition by endosomal sorting complexes (ESCRT) and routing to lysosomes for degradation. Consequently, UVRAG-ITCH-mediated degradation of NOTCH1ΔE limits its availability for γ-secretase (S3) cleavage, reducing the generation of the NOTCH1 intracellular domain (NICD) and attenuating downstream transcriptional activity. Disruption of this UVRAG-ITCH-ESCRT checkpoint leads to accumulation of NOTCH1ΔE and excessive NICD production. In T-ALL cells harboring hyperactive NOTCH1 mutations, we found that UVRAG expression is often suppressed. Restoration of UVRAG in T-ALL models reinstated the lysosomal off-switch: it promoted NOTCH1ΔE ubiquitination and degradation, lowered NICD levels, and dampened oncogenic NOTCH1 signaling. UVRAG re-expression in these cells significantly impaired leukemia cell proliferation and self-renewal, reduced the population of leukemia-initiating cells, and even enabled partial differentiation of malignant T-cell blasts. Notably, reinstating UVRAG also sensitized T-ALL cells to γ-secretase inhibitors (GSIs). The combination of UVRAG reactivation with GSI treatment synergistically induced apoptosis and tumor regression. In xenograft and patient-derived T-ALL models, enforced UVRAG expression combined with GSI therapy dramatically reduced leukemic burden and prolonged survival, underscoring the therapeutic potential of co-targeting this pathway. In conclusion, our study reveals that the UVRAG-ITCH axis functions as a lysosomal off-switch to terminate aberrant NOTCH1 signaling at the membrane intermediate stage. This degradation-based checkpoint offers a novel therapeutic target to restrain NOTCH1-driven malignancies and potentially enhance the efficacy of NOTCH1 pathway inhibitors.

#0567 SGK1 may represent a therapeutic target in BRAF-mutant melanoma.

Boyd Griffiths[1], Camden VanTassell[1], Joshua Knight[1], Madison Hawkins[1], Landen Barnett[1], Katie Culver[2], Ashley Thompson-Chadwick[2], Sheri L. Holmen[3], Gennie Lynne Parkman[1]

[1]Dept of Zoology, Weber State University, Ogden, UT,[2]University of Utah, Salt Lake City, UT,[3]University of Utah Huntsman Cancer Institute, Salt Lake City, UT

Despite advancements in treatment, the five-year survival rate for Stage IV melanoma remains low, around 30%, highlighting the urgent need for new therapies. Two key signaling pathways, RAS>RAF>MEK>ERK (MAPK) and PI3K>AKT, are often co-activated in melanoma and play a central role in its initiation and progression. About 50% of melanomas have a BRAF mutation, but many patients develop resistance to therapies targeting this pathway. Additionally, disruptions in the PI3K>AKT pathway, such as loss of the tumor suppressor PTEN or activation of PI3K or AKT, are common in BRAF-mutant melanomas. Despite promising preclinical studies, no PI3K or AKT inhibitors have been approved for advanced melanoma treatment. The serine/threonine kinase SGK1 (serum and glucocorticoid-regulated kinase 1) plays a pivotal role in cellular processes such as survival, proliferation, and migration, and has been implicated in various cancers, including melanoma. Our previous work has shown that AKT was inhibited, SGK1 was upregulated, potentially rescuing cell survival and acting as an inherent resistance mechanism for AKT inhibition. SGK1 was also found to be higher in primary melanoma tumors compared to normal skin lesions. *In vivo* experiments in a mouse melanoma model demonstrate that overexpressing SGK1 promotes tumor growth and reduces survival, and these experiments are currently ongoing to examine the impact on metastasis in this mice. These findings position SGK1 as a promising therapeutic target for melanoma, particularly in combination with existing treatment strategies. This body of work underscores the importance of further investigating SGK1's molecular mechanisms and its potential to improve melanoma treatment outcomes.

#0568 The YAP1-IGFBP2 axis as a predictive biomarker and therapeutic target in gastric cancer metastasis.

Emily Hancin[1], Hyun-Kyung Ko[2], Madeline B. Torres[1], Xiaodan Yao[3], Yibo Fan[4], Melissa Pool Pizzi[4], Shilpa S. Dhar[5], Francis Spitz[1], Generosa Grana[2], Jaffer A. Ajani[5], Shumei Song[3]

[1]Department of Surgery, Cooper University Hospital, Camden, NJ,[2]MD Anderson Cancer Center at Cooper, Camden, NJ,[3]Coriell Institute for Medical Research, Camden, NJ,[4]Department of GI Medical Oncology, The University of Texas MD Anderson Cancer Center, Houston, TX,[5]The University of Texas MD Anderson Cancer Center, Houston, TX

Background: Gastric cancer (GC) with peritoneal metastasis (PM) carries a poor prognosis, with a five-year survival rate of only 5%. Insulin-like growth factor binding protein 2 (IGFBP2) has been implicated in tumor proliferation, invasion, and metastasis through both IGF-dependent and independent mechanisms in various cancers. However, its role in GC progression and PM remains undefined. This study investigates the functional significance of the IGFBP2-YAP1 axis in GC tumorigenesis and metastasis, particularly to the peritoneum.

Methods: Single-cell RNA sequencing (scRNA-seq) of GC primary tumors, matched normal tissues, and PM was performed to characterize IGFBP2 expression across cellular compartments. Bulk RNA sequencing of Yes-associated protein 1 (YAP1) knockout (KO) vs control GC cell lines, followed by quantitative PCR (qPCR) and enzyme-linked immunosorbent assay (ELISA), evaluated YAP1-dependent regulation of IGFBP2 transcription and secretion. Protein expression of IGFBP2 and YAP1 was assessed by Western blotting (WB) in multiple GC cell lines. IGFBP2 knockdown (KD) was achieved by short-hairpin RNA (shRNA) vectors in HGC27 and MKN7 cells. ELISA, migration, and invasion assays were conducted to determine the functional impact upon depletion of IGFBP2.

Results: scRNA-seq revealed that both YAP1 and IGFBP2 are highly enriched in PM of GC compared to primary and normal gastric tissues, and their elevated expression correlates with poor prognosis. Among nine GC cell lines, AGS, GA0518, SNU16, HGC27, and MKN7 cells exhibited high expression of both YAP1 and IGFBP2 proteins. RNAseq of YAP1 KO vs control cells revealed significant downregulation of IGFBP2 upon YAP1 depletion, implicating YAP1 as an upstream regulator. Consistently, qPCR and ELISA confirmed reduced IGFBP2 transcription and secreted protein levels in YAP1 KO cells. Functionally, recombinant IGFBP2 (rIGFBP2) rescued the impaired invasiveness of YAP1 KO patient-derived GC PM cells (GA0518). IGFBP2 KD in HGC27 and MKN7 cells was validated by qPCR and WB, and these cell lines demonstrated reduced extracellular IGFBP2 levels along with diminished migration and invasion compared with controls.

Conclusions: Our findings define the YAP1-IGFBP2 axis as a key driver of GC and PM. Elevated co-expression of IGFBP2 and YAP1 in PM, combined with loss of function studies demonstrating reduced migration and invasion upon IGFBP2 deletion, underscores their cooperative role in metastatic adaptation. These findings identify IGFBP2 as a YAP1-regulated effector that promotes tumor aggressiveness, highlighting the clinical potential of targeting the YAP1-IGFBP2 axis. Collectively, the YAP1-IGFBP2 axis may serve as both a predictive and prognostic biomarker and a promising therapeutic target for advanced GC patients with PM.

#0569 Acetylcholine-induced YAP stabilization enhances HIF-1 signaling under hypoxia via the nAchR-α7/PI3K/PDPK1 pathway in pancreatic cancer cells.

Yunmi Cho, Ha Hyeong Kim, Eun-Taex Oh

Department of Biomedical Sciences, Inha University College of Medicine, Incheon, Korea, Republic of

The pancreas is highly innervated by the autonomic nervous system. Recent studies have extensively addressed the potential role of the autonomic nervous system in the development of pancreatic ductal adenocarcinoma (PDAC).Hypoxia-inducible factor-1α (HIF-1α) regulates tumor adaptation to hypoxia by controlling genes linked to angiogenesis, metastasis, and therapy resistance. We previously showed that neurotransmitter acetylcholine (Ach) enhances HIF-1α expression in pancreatic cancer cells via the nAchR-α7/PDPK1/YAP pathway under hypoxia, but the underlying molecular mechanisms remained unclear. Following our previous findings, this study aims to elucidate the molecular signaling mechanism by which Ach regulates HIF-1α expression under hypoxic conditions in pancreatic cancer cells. Here, we treated human pancreatic cancer cells with Ach under 0.5% oxygen. Protein levels, phosphorylation, and interactions were assessed using Western blot, qRT-PCR, and co-immunoprecipitation. PI3K, PDPK1, and YAP expression were silenced by siRNA. In vivo, the effect of Ach was tested using tail-vein Ach injections in a subcutaneous xenograft mouse model. We found that Ach activated PI3K downstream of nAchR-α7, increasing PDPK1 phosphorylation. This reduced YAP phosphorylation at serine 397, stabilizing YAP and promoting its nuclear translocation. In the nucleus, YAP bound to HIF-1α, enhancing its stability and transcriptional activity. Knockdown of PI3K, PDPK1, or YAP suppressed Ach-induced HIF-1α upregulation. *In vivo*, Ach significantly promoted tumor growth in mice implanted with control pancreatic cancer cells, but had no effect in mice bearing tumors derived from nAchR-α7-silenced cells. Analysis of clinical datasets revealed that high nAchR-α7 expression correlates with poor prognosis in PDAC patients. Collectively, these findings reveal that Ach promotes pancreatic tumor progression under hypoxia via the nAchR-α7/PI3K/PDPK1/YAP pathway, which stabilizes HIF-1α. This signaling axis represents a promising therapeutic target in acetylcholine-associated pancreatic cancer.

#0570 Soft extracellular matrix orchestrates gastric cancer progression by triggering RNF146-mediated AMOT degradation and YAP/TAZ-driven senescence in macrophages.

Guofei Deng[1], Yusheng Luo[1], Yuxi Pan[1], Xiaorong Lin[1], Yuzhi Zhang[1], Yuqing Lin[1], Fuhui Wang[2], Jiancheng Wang[1], Shuo Fang[1]

[1]The Seventh Affiliated Hospital of Sun Yat-sen University, Shenzhen, China,[2]University of South Florida, Tampa, FL

The mechanical properties of the tumor microenvironment (TME) are critical regulators of cancer progression. While the role of a stiff extracellular matrix (ECM) is well-established, how soft ECM—common in early or remodeled tumors—modulates immune function in gastric cancer remains elusive. This study unveils a complete mechano-immunological pathway wherein soft ECM drives tumorigenesis by inducing pro-tumorigenic senescence in tumor-associated macrophages (TAMs). We demonstrate that soft ECM initiates this cascade through cytoskeletal remodeling and F-actin depolymerization, which displaces Angiomotin (AMOT) from the actin network, increasing its cytoplasmic pool. The liberated AMOT is then specifically targeted by the E3 ubiquitin ligase RNF146, which is upregulated in TAMs in response to soft mechanical cues, leading to AMOT ubiquitination and proteasomal degradation. This degradation relieves the cytoplasmic sequestration of YAP/TAZ, enabling their nuclear translocation and transcriptional activation within TAMs. This mechanochemical reprogramming initiates a distinct senescence-associated secretory phenotype (SASP), characterized by elevated secretion of CCL2, IL-8, MMP-12, and TGF-β, which collectively promote tumor cell invasion, angiogenesis, and immunosuppression. Functional validation using co-culture assays and orthotopic gastric cancer models confirmed that RNF146-mediated AMOT loss is sufficient to induce senescence and accelerate tumor growth and metastasis. Conversely, myeloid-specific RNF146 knockout stabilized AMOT, suppressed the SASP, and potently inhibited tumor progression. Our findings thereby delineate a complete pathological axis in gastric cancer: from soft ECM sensing and cytoskeletal remodeling to RNF146-mediated degradation of displaced AMOT, YAP/TAZ-driven macrophage senescence, and ultimately tumor progression. This work resolves the long-standing paradox of soft ECM in cancer by mechanistically linking it to pro-tumorigenic immune senescence, and nominates the RNF146-AMOT axis as a novel and promising stromal target for therapeutic intervention.

#0571 WNT and Notch crosstalk in pregnancy-associated breast cancer.

Charles Moore, Wen-Cheng Chung, Shifa Khan, Keli Xu

UMMC Cancer Center and Research Institute, Jackson, MS

Introduction Pregnancy-Associated Breast Cancer (PABC) is defined as breast cancer diagnosed during pregnancy, lactation, or throughout the post-partum period. Approximately 1 in 3000 pregnant women will be diagnosed with this condition. The purpose of this study was to identify cell-of-origin and relevant signaling pathways implicated in the development and progression of PABC.
Methods Immunohistochemistry was used for lineage tracing and protein expression patterns. Tumor-free survival calculations were made to asses tumor onset phenotypes in transgenic mice. Western blot was used to determine protein expression differences in comparative genotypes.
Unpublished Data We have generated a PABC mouse model by crossing oncogenic $Kras^{G12D}$ with WAP-Cre mice. These mice develop tumors in a pregnancy-dependent manner that are histologically heterogeneous as well as estrogen and progesterone receptor negative. Our model recapitulates many features of PABC, including aggressive biological nature and frequent lung metastasis. Indeed, nearly all mice developed distant lung tumors during the lactational period. Preliminary studies using this model suggest that alveolar progenitor cell populations may represent the primary cell-of-origin in PABC. Lineage tracing in virgin mammary glands revealed very few cells labeled by WAP-Cre. Interestingly, mice that express $Kras^{G12D}$ exhibited drastic expansion of WAP-labeled cells, along with the development of precancerous lesions, even before pregnancy. WNT and Notch, two evolutionarily conserved pathways, regulate the fate of alveolar progenitors in normal mice, where dysregulation of these pathways facilitates oncogenic transformation and rapid tumor formation. Deletion of Notch3 significantly delayed Kras-driven tumor onset. Surprisingly, deletion of Jagged1, a Notch ligand, accelerated tumor onset. Further lineage tracing shows that deletion of Notch3 reduced the number of WAP-labeled progenitor population. Contrastingly, Jagged1 deletion leads to an expansion of WAP-labeled cells. Interestingly, despite accelerated tumor onset, deletion of Jagged1 significantly reduced the incidence of lung metastasis. In all mice, some percentage of tumor histology demonstrated a squamous phenotype. Deletion of Jagged1 resulted in 100% of these tumors developing a squamous phenotype. Overexpression of beta-catenin, the signaling effector of WNT, has been shown to promote squamous transdifferentiation. We show an increase in beta-catenin associated with the deletion of Jagged1. Additionally, strong positive immunostaining for non-phosphorylated, active, beta-catenin in Kras;WAP-Cre tumors was seen.
Conclusions These findings suggest a crosstalk between Notch and WNT signaling. We propose that WAP-labeled alveolar progenitor cells serve as the cell-of-origin in PABC and that Notch and WNT signaling are key factors in tumor initiation, progression, and metastasis.

#0572 Defining a DLG5-NUAK2-LATS1 complex that regulates Hippo signaling output.

Youchen Song[1], Abiodun Ogunjimi[2], Siyuan Song[3], Jeffrey L. Wrana[2], Liliana Attisano[3]

[1]Medical Biophysics, Univ. of Toronto Faculty of Medicine, Toronto, ON, Canada,[2]Lunenfeld-Tanenbaum Research Institute, Toronto, ON, Canada,[3]Biochemistry, Univ. of Toronto Faculty of Medicine, Toronto, ON, Canada

Introduction: The Hippo signaling pathway is a critical regulator of cell growth and organ size, and its dysregulation, leading to activation of the transcriptional effectors YAP/TAZ, is common in solid cancers. The AMPK-related kinase NUAK2 is an established positive regulator of Hippo signaling through its interaction with LATS1, yet the precise mechanisms governing this interaction remain undefined. Our research aimed to identify novel proximal interactors of NUAK2 to uncover new regulatory complexes that control Hippo pathway output.

Methods: We utilized a BioID-mass spectrometry screen to identify NUAK2 proximal interactors. Validation of protein-protein interactions was performed using co-immunoprecipitation and GST pull-down assays. The potential structure interface was predicted using AlphaFold, and the physical assembly of the complex was validated via Ni-NTA affinity purification. The effect of DLG5 loss on Hippo signaling was assessed in both 2D cancer cell lines and 3D colorectal cancer organoids by RT-qPCR of Hippo target genes, immunofluorescence microscope for YAP/TAZ localization, and cell growth assays.

Results: Our proteomic screen identified the scaffolding protein DLG5 as a prominent and novel NUAK2 interactor. We subsequently validated that DLG5 scaffolds a trimeric complex, co-eluting with both NUAK2 and the core Hippo kinase LATS1 in affinity purification assays. Functionally, knockdown of DLG5 disrupted Hippo signaling, leading to YAP/TAZ cytoplasmic localization and a corresponding decrease in the transcription of canonical YAP/TAZ target genes (e.g., *ANKRD1, CTGF*) in cell lines and CRC patient-derived organoids. The loss of DLG5 also suppressed cell growth in cancer cells, consistent with NUAK2 inhibition.

Conclusion: Our findings reveal a previously unknown regulatory axis where DLG5 acts as a scaffold to assemble the DLG5-NUAK2-LATS1 complex. This scaffolding allows NUAK2 to interact with LATS1, thereby regulating Hippo signaling. Our work identifies a novel role of DLG5 in the Hippo pathway, and future structural studies will further define the molecular architecture of this complex to guide therapeutic targeting.

#0573 Cooperative mechanisms driving prostate cancer progression.

Runhua Liu, Chao Zhang, Haiyan Yui, Lizhong Wang

UAB Heersink School of Medicine, Birmingham, AL

Signal transducer 24 (CD24) is a GPI-anchored cell surface molecule expressed in hematopoietic and immature neuronal cells, but at very low levels in normal differentiated cells. Although commonly used as a stem cell marker, CD24 is also linked to poor prognosis in many cancers, including prostate cancer (PCa). PCa poses major clinical challenges due to its diverse progression mechanisms and pronounced heterogeneity. Recent studies have identified overexpression of Regulator of Chromosome Condensation 2 (RCC2), a multifunctional protein involved in mitosis and cell motility, which contributes to cancer development across tumor types. This study reveals a novel interaction between CD24 and RCC2 in PCa, highlighting their cooperative roles in tumor growth and metastasis. Functionally, RCC2 knockout inhibited proliferation but enhanced migration, while CD24 knockout suppressed both processes; dual knockout synergistically reduced proliferation. In mouse models, RCC2 loss increased lung metastasis, whereas CD24 loss reduced both tumor growth and metastatic spread. Mechanistically, RCC2 regulates motility through vimentin ubiquitination, whereas CD24 promotes RCC2 degradation to modulate β-catenin signaling. Overall, CD24 regulates RCC2 stability and function, influencing key pathways that control proliferation, migration, and epithelial-mesenchymal transition (EMT). This CD24-RCC2-vimentin-β-catenin axis provides new insight into prostate cancer progression and represents a potential therapeutic target to limit metastasis.

#0574 Exploring the therapeutic vulnerability of castration-resistant prostate cancer via Hippo-YAP/TAZ-TEAD signaling.

Vandana Mohan, Sweaty Koul, Mousa Vatanmakanian, Santosh Lamichhane, Praveen K. Jaiswal, **Hari K. Koul**

LSU-LCMC Cancer Center, LSUHSC, School of Medicine, New Orleans, LA

Background: The Hippo-YAP/TAZ-TEAD signaling axis is frequently upregulated in many cancers, including subsets of prostate cancer (PCa). However, its role in therapy resistance remains incompletely understood. In this study, we investigated the therapeutic potential of targeting YAP/TAZ-TEAD signaling in PCa, with an emphasis on androgen-independent and enzalutamide-resistant disease.
Methods: LNCaP, PC3, and DU145 cells were obtained from ATCC. Enzalutamide-resistant lines (LNCaP-ENZR/PCaNO1 and C4-2-ENZR/PCaNO2) were generated by culturing LNCaP and C4-2 cells with 5 μM enzalutamide for >6 months. mRNA expression was quantified by qRT-PCR, and protein levels were examined by western blotting. Anti-tumor effects of YAP/TAZ-TEAD inhibitors (GNE-7883, K-975) were assessed using IncuCyte live-cell imaging for proliferation; long-term survival was measured by colony formation assays. Cell migration and invasion were evaluated using scratch-wound healing and Matrigel transwell assays, respectively.
Results: Androgen-independent PCa cells (PC3 and DU145) exhibited marked upregulation of YAP/TAZ-TEAD transcriptional targets compared to LNCaP cells. Enzalutamide-resistant PCaNO1 and PCaNO2 cells displayed strong induction of YAP/TAZ-TEAD target genes and increased YAP1, TAZ, and TEAD protein levels relative to parental controls. Enzalutamide resistance was also associated with elevated PD-L1 expression. Pharmacologic inhibition of YAP/TAZ-TEAD signaling significantly suppressed cell growth and proliferation, and reduced colony formation, migration, and invasion across PCa models. Ongoing experiments are assessing the impact of YAP/TAZ-TEAD inhibition on PD-L1 regulation.
Conclusion: YAP/TAZ-TEAD inhibitors effectively block proliferation and invasiveness of prostate cancer cells, including enzalutamide-resistant models. These findings support YAP/TAZ-TEAD signaling as a promising therapeutic vulnerability and potential strategy to overcome therapy resistance in subsets of advanced prostate cancer.

#0575 Cooperative regulation of YAP activity by STK40 and CDK7 in cancer progression.

Pei Yi Li, Yi Chin Chen, Feng Chiao Tsai

National Taiwan University, Taipei, Taiwan

Yes-associated protein (YAP) is a mechanosensitive transcriptional co-activatorthat drives cell proliferation and tumorigenesis. We previously identified thepseudokinase STK40 as a scaffold that directly binds and post-translationallyregulates YAP, with STK40 knockdown reducing YAP abundance and nuclearlocalization. In hormone receptor positive breast cancer, resistance to CDK4/6inhibitors remains a major challenge, and emerging evidence from ourcollaborative studies suggests that CDK7 transcriptionally regulates YAPthrough a CDK7-RNAPII-YAP-CDK6 axis contributing to therapeutic resistance.Whether STK40 and CDK7 function independently or converge on a sharedmechanism remains unknown. Using SAS cells, we found that CDK7knockdown reduced YAP protein levels in both cytosol and nucleus anddecreased the nuclear-to-cytosolic ratio, whereas dual CDK7 and STK40knockdown phenocopied CDK7 loss alone. CDK7 overexpression partiallyrescued YAP depletion caused by STK40 knockdown, indicating that CDK7acts downstream of STK40 in the same regulatory pathway. Proximity ligationassays confirmed a direct STK40 and YAP interaction. Reducing actomyosintension caused YAP to relocalize to the plasma membrane, but thisredistribution was abolished by STK40 knockdown. ROCK inhibition enhancedYAP Y357 phosphorylation at the plasma membrane, a modification requiredfor nuclear entry, yet this phosphorylation was completely lost in STK40-depleted cells, indicating that STK40 is required for positioning YAP at themembrane to initiate mechanotransduction driven nuclear import. In contrast,CDK7 knockdown did not prevent YAP membrane recruitment but caused YAPto accumulate at the nuclear envelope without entering the nucleus, suggestingthat CDK7 regulates a downstream step essential for nuclear translocation.Together, these data reveal a previously unrecognized STK40 and CDK7regulatory mechanism that cooperatively controls YAP abundance andsubcellular distribution. STK40 directs YAP to the plasma membrane for Y357phosphorylation, whereas CDK7 acts as a critical checkpoint enabling tension-dependent nuclear import. This mechanism represents a potential therapeuticvulnerability in YAP-driven cancers, including CDK4/6 inhibitor-resistant HR+breast cancer.

#0576 Investigating BMP signaling as a therapeutic vulnerability in endometrial cancer.

Purva Vinayak Gade, Craig Ceol

University of Massachusetts Medical School, Worcester, MA

Introduction: Endometrial cancer (EC) is the sixth most common malignancy in women worldwide, with nearly 400,000 new cases annually. Aggressive EC subtypes are associated with poor prognosis, highlighting the urgent need for mechanism-based therapies. Emerging evidence implicates Bone Morphogenetic Protein (BMP) signaling as a driver of EC progression. Approximately 5% of EC tumors harbor ACVR1(R206H) gain-of-function mutations, which overactivate BMP signaling. Our goal is to define the prevalence, sources, and functional consequences of BMP activation in EC and assess whether pharmacologic inhibition suppresses tumor growth.
Methods: Phospho-SMAD1/5/8 (pSMAD) levels were quantified in EC tumors and normal endometrium to assess BMP pathway activation. Genomic and transcriptomic datasets were analyzed to identify ACVR1 mutations and BMP ligand expression associated with patient survival. Functional studies were conducted in multiple EC cell lines using the pan-BMP inhibitor DMH1. pSMAD was measured by western blot, downstream BMP target gene transcription (ID1/ID3) was assessed by qPCR, and cell viability was evaluated to determine the effect of BMP inhibition on tumor cell survival and proliferation.
Results: pSMAD levels were elevated in over half of EC tumors compared with low-to-moderate levels in normal endometrium. High expression of BMP ligands GDF6 and BMP7 correlated with poor overall survival. DMH1 selectively reduced pSMAD without affecting total SMAD, downregulated ID1 and ID3, and decreased viability in Ishikawa, HEC1A, and AN3CA cells within 24 hours, demonstrating that BMP signaling is required to sustain tumor growth and proliferation.
Conclusions: BMP signaling is recurrently activated in EC through receptor mutation and ligand overexpression, promoting aggressive tumor behavior. Pharmacologic inhibition reverses downstream transcriptional activity and suppresses tumor cell viability, establishing BMP signaling as an actionable therapeutic vulnerability. These findings support the development of BMP-directed strategies to improve clinical outcomes in patients with endometrial cancer.

#0577 Defects in junctional localization of desmosomal proteins in cancer cells triggered by loss of Septin-9.

Cate G. Lyerly, Zach N. Pierce, Adi Dara Dubash

Furman Univ., Greenville, SC

Desmosomes are specialized adhesive junctions that link adjacent cells and provide structural integrity in tissues exposed to significant mechanical stress, such as the skin and heart. Disruption of the desmosome adhesion complex is observed in a range of different cutaneous syndromes and during tumor progression. Dysregulation of desmosomal proteins has been associated with enhanced cancer motility, invasion and metastatic potential. Diverse mechanisms for the disruption of desmosome dynamics have been reported, but the specific signaling pathways regulating the expression and localization of desmosome proteins remain elusive. Prior studies have shown that Septin family proteins play an important role in the maintenance and function of adherens junctions and tight junctions. Referred to as the fourth component of the cytoskeleton, Septins are GTP-binding proteins that form oligomeric filamentous structures that associate with cellular membranes and act as scaffolding proteins for a variety of different cellular functions. In particular, Septin-2 has been found adjacent to VE-cadherin containing cell-cell junctions, and loss of Septin-2 disrupts adherens junction structure and barrier integrity in endothelial cells. Septin-9 has also been shown to control adherens junction structure, apico-basal polarity and lumen formation in polarized MDCK cells. In our study, we sought to investigate the importance of Septins in the formation of desmosomal cell-cell adhesions by performing knockdown experiments for Septin-9 in squamous cell carcinoma 9 (SCC9) cells and T47D breast cancer cells. Our experiments show a significant disruption of desmosomal cell-cell junctions in both cancer cell types expressing siRNA specific for Septin-9 (siSept9), in comparison to control siRNA-expressing cells. In particular, border localization of the desmosomal cadherin Desmoglein-2 (Dsg2) and the desmosomal plaque protein Plakophilin-2 were dramatically perturbed in siSept9 cells (determined via immunofluorescence), while the localization of other desmosomal proteins (such as Plakoglobin) remained unaffected. Loss of Dsg2 and PKP2 border staining was not accompanied by changes in total protein expression, suggesting that these changes are predominantly an effect of protein localization. This study has therefore uncovered an important role for Sept9 in maintenance of desmosomal structure in cancer cells, providing insight into mechanisms which may perturb junction structure during cancer progression.

#0578 Emerging roles of Cyclin F in Non-small lung cell carcinoma during metabolic stress.

Rohini Tamang[1], Sanjeev Das[2], Sangeeta Choudhury[1]

[1]Department of Biotechnology and Research, Sir Ganga Ram Hospital, New Delhi, India,[2]Molecular Oncology Laboratory, National Institute of Immunolgy, New Delhi, India

Introduction: Cyclin F, the orphan Cyclin, is unique from other Cyclins- 1) it does not bind to any cyclin dependent kinase (cdk) and 2) It has a domain which categorizes Cyclin F as a member of a distinct class of proteins the F-box proteins. Proteins such as Cyclin F, thereby facilitates the recognition of substrate proteins and mediates the ubiquitylation and degradation of the protein by the Skp1-Cul1- F box (SCF) complex. Role of Cyclin F in tumorigenesis is obscure but owing to its role as a genome guardian and nutrient sensing molecule, we explored its role in tumor in a lung cancer model

Aim: To delineate the unique function of Cyclin F driven ubiquitylation and regulation of cellular proteins which alters the tumorigenic capacity of cancers.

Methodology: Identification of Cyclin F interactome- ectopic expression of Cyclin F using adenoviral system; immunoprecipitation of Cyclin F and its putative interacting proteins, detection of proteins with LC-MS/MS. Investigate the dynamics of the interaction under physiological conditions. Understanding the effect of Cyclin F mediated regulation of proteins in cellular pathways in cancer cells (Non-small lung cell carcinoma**;** NSCLC).

Results: We developed an adenoviral vector expressing Cyclin F along with HA and FLAG tags (Ad-CCNFHF-GFP). Adenovirus expressing Cyclin F and the tags were produced from HEK293A cells. The viral titer was used to ectopically express Cyclin F in H1299 cells, followed by immunoprecipitation of Cyclin F and identification of the proteome associated with Cyclin F. We identified an RNA binding protein in our screen, called PTBP1. PTBP1, is associated with aberrant splicing activity in tumor cells and its expression is associated with poor prognosis. We verified that Cyclin F upregulation during a period of starvation led to concomitant decrease in PTBP1 protein levels. PTBP1 downregulation led to exclusion of exon 10 of PKM mRNA and altered the PKM2/PKM1 ratio. We observed that Cyclin F mediated depletion of PTBP1 and PKM2, lowering the glycolytic capacity in tumor cells. It further led to decrease in proliferation and invasion and migration rates of cancer cells upon starvation. Mice data also corroborate similar results.

Conclusion: Our study provides clues on how protein interaction during metabolic stress can shift the fate of cancer cells. It establishes that Cyclin F negatively regulates PTBP1/PKM2 levels and reduces the tumorigenic potential of NSCLC cells in in-vitro/in-vivo models. Elucidating molecular interactions will provide insight into NSCLC progression and therapeutic resistance, which is the first step towards designing targets.

Key words: Non-small lung cell carcinoma, Cyclin F, tumorigenic capacity, adenoviral expression, RNA binding proteins

#0579 Effects of arylsulfatase B and pembrolizumab on the progression of syngeneic B16F10 metastatic pulmonary melanomas.

Joanne Kramer Tobacman[1], Insug O-Sullivan[2], Sumit Bhattacharyya[3]

[1]Medicine, University of Illinois at Chicago and Jesse Brown VA Medical Center, Chicago, IL,[2]Research, Jesse Brown VA Medical Center and University of Illinois Chicago, Chicago, IL,[3]Research, Jesse Brown VA Medical Center, Chicago, IL

The chondroitin 4-sulfate (C4S) sulfatase Arylsulfatase B (ARSB; N-acetylgalactosamine-4-sulfatase) inhibits the growth and improves survival of C57BL/6J mice with B16F10 subcutaneous melanomas, inhibits the growth of A375 human melanomas in humanized mice with PBMC implants, and reduces the progression of metastatic pulmonary melanomas in the B16F10 syngeneic mouse model. Cleaved caspase-3 is enhanced by treatment with rhARSB and is mediated by increased expression of the E3 ubiquitin ligase constitutive photomorphogenic (COP)1, which reduces nuclear ETS-1 and thereby BCL2 expression. Combined treatment of B16F10 pulmonary melanomas by rhARSB and Pembrolizumab leads to greater increase in cleaved caspase-3 and greater decline in Bcl2, but no further increase in COP1 than by rhARSB alone. Similarly, in cultured A375 cells, cleaved caspase-3 is increased and BCL2 is reduced further by combined treatment of rhARSB and Pembrolizumab in the presence of PBMC, without further increase in COP1. The greater decline in Bcl2 is attributable to effects of rhARSB and Pembrolizumab in the presence of PBMC on Granzyme B. In contrast to no effect of Pembrolizumab, rhARSB reduces expression of the matrix metalloproteinases MMP2 and MMP9 in A375 melanoma cells and in B16F10 pulmonary melanomas, leading to decline in invasiveness. The mechanism by which ARSB regulates MMP expression is attributable to rhARSB-mediated decline in chondroitin 4-sulfate binding with SHP2, leading to declines in ERK1/2 phosphorylation, nuclear c-Myc-DNA-binding, and MMP2 and MMP9 promoter activation. In the B16F10 pulmonary melanomas, the combination of Pembrolizumab and rhARSB increased the mRNA expression of MCP1 and IL-10 and reduced the expression of KC and IL-6, more than either treatment alone. ARSB alone increased IL-17α and TNFα, which was reduced by Pembrolizumab and overall by their combination. The combined effects of rhARSB and Pembrolizumab demonstrate synergism which may be of significant clinical benefit. Enhanced apoptosis mediated by different Bcl2 regulatory mechanisms, decline in matrix metalloproteinases and associated invasiveness of tumor cells due to signaling effects of rhARSB, as well as combined effects on cytokine expression are anticipated to inhibit melanoma progression.

#0580 TPM4 overexpression modifies differentiated colon epithelial cell barrier integrity.

Brenna Backus[1], **Michael Papetti**[2]

[1]Touro University, New York City, NY,[2]High Point University, High Point, NC

Colon epithelial cell migration out of the stem cell compartment in colon crypts is essential for normal differentiation and growth arrest. Altered expression of contractility- and migration-specific genes may disrupt these processes and contribute to early stages of colon tumorigenesis. One such gene, tropomyosin-4 (*TPM4*), is overexpressed in early and late stages of colorectal cancer. Determining how *TPM4* overexpression contributes to colon cell tumorigenesis may identify novel therapeutic targets. We hypothesized that *TPM4* overexpression may promote colon tumorigenesis by disrupting cell-cell junctions and reducing epithelial barrier integrity in differentiating colon epithelial cells. To test this, we utilized Caco2 cells, an *in vitro* model of colon epithelial cell differentiation derived from a human colon adenocarcinoma. Our approach was to determine whether artificially increasing *TPM4* expression by stable transfection in differentiating Caco2 cells, when *TPM4* is normally suppressed, will decrease integrity of the Caco-2 cell monolayer. To assess this, we measured transepithelial electrical resistance (TEER), an indicator of cell-cell junction integrity, in differentiating *TPM4*-overexpressing Caco-2 monolayers relative to control transfectants. 100,000 Caco2 cells were seeded in 6 well filter inserts in wells of a 6-well plate at day 0. TEER measurements were recorded in triplicate every other day from day 6 to 24 using the Millicell ERS 3.0 Digital Voltohmmeter. We observed significant differences between TEER measurements in two clones of *TPM4*-overexpressing Caco2 cells and control transfectants. TEER values in control empty vector stable transfectants plateaued between 1237-1445 ohm-sq. cm, while those in two *TPM4*-overexpressing stable clones plateaued between 464-898 ohm-sq. cm (clone 1) and 1743-1868 ohm-sq. cm (clone 7). Clone 1 TEER values plateaued at a similar time point (day 12) as empty vector control, whereas clone 7 TEER values plateaued later (day 16). In addition, we observed alterations in expression of genes encoding junctional complex proteins in TPM4-overexpressing cells relative to controls. These results indicate that *TPM4* overexpression modulates the integrity of cell-cell junctions in an *in vitro* model of differentiating colon epithelial cells. Future experiments will determine whether differences observed between the two distinct clones may be due to the extent of *TPM4* overexpression in each clone. Our study suggests that sustained *TPM4* overexpression may disrupt colon epithelial cell differentiation and promote tumorigenesis by altering normal epithelial barrier formation and junctional integrity. Therefore, we identify a potential mechanism that may link *TPM4* overexpression to early colorectal tumorigenesis and elucidate possible novel approaches to prevent and treat colon cancer, particularly at early stages.

#0581 FUT8-mediated fucosylation promotes colorectal cancer growth and metastatic potential via tumor-fibroblast interactions.

Zimo Huang[1], Sree K. Kondapuram[1], Xiang Y. Zheng[1], Praveen Agrawal[1], Chaoyuan Kuang[2]

[1]Albert Einstein College of Medicine, Bronx, NY,[2]MonteFiore Einstein Comprehensive Cancer Center, Albert Einstein College of Medicine, Bronx, NY

Colorectal cancer (CRC) remains a major clinical burden despite advances in targeted therapies. Aberrant glycosylation, including fucosylation, is increasingly recognized as a key regulator of tumor progression. Analysis of TCGA COAD/READ datasets identified FUT8, the sole enzyme mediating core fucosylation, as significantly elevated in CRC tumors. Its expression pattern and functional activity position FUT8 as a key driver of CRC growth and metastatic traits, including cancer-associated fibroblast (CAF)-mediated tumor-stroma interactions.

Transcriptomic and survival analyses were performed using TCGA COAD/READ and the Montefiore-Einstein Comprehensive Cancer Center (MECCC) CRC biobank datasets. FUT8 protein expression was evaluated in paired tumor and normal tissues from MECCC TMAs. Functional characterization was carried out using FUT8 overexpression (OE) and knockdown (KD) CRC cell models, followed by proliferation assays, colony-forming assays, and transwell invasion assays under baseline and CAF-conditioned medium conditions.

FUT8 was consistently upregulated in CRC tumors compared with matched normal tissues across TCGA COAD/READ and MECCC transcriptomic cohorts. Stage I/II CRC patients with high FUT8 expression (Q4) exhibited significantly reduced 5-year overall survival compared with the lowest quartile (Q1) (log-rank $p = 0.03$). In sixteen paired samples from MECCC TMAs, FUT8 protein levels were markedly elevated (about 2-fold) in tumors compared with normal tissues ($p < 0.001$). Functionally, FUT8 modulation did not alter CRC cell proliferation but robustly regulated aggressive properties: FUT8 OE increased colony size and markedly enhanced transwell invasion, whereas FUT8 KD suppressed both colony formation and invasion. These effects were further amplified in CAF-conditioned medium, suggesting that FUT8 enhances CRC-CAF crosstalk and drives an invasive phenotype.

Across transcriptomic analyses and functional assays, FUT8 emerges as a clinically relevant regulator of CRC progression. FUT8 enhances colony formation and invasion independent of proliferation, with its pro-invasive effects strengthened by CAF signaling, establishing FUT8-mediated fucosylation as a driver of CRC aggressiveness.

#0582 Disruption of *Cenpj,* a centriole biogenesis regulator, diminishes oral cancer susceptibility through p53-dependent DNA-damage repair and apoptosis pathways.

Mousumi Bhattacharjee, Heena Dave, Rekha Jalandra, Radhika R. Gudi, Chenthamarakshan Vasu

The Medical University of South Carolina, Charleston, SC

Mutations in centrosomal P4.1-associated protein (CPAP; Gene: CENPJ), a microtubule-bindingcentriolar protein, can lead to microcephaly (MCP) in humans. While CPAP dysfunction is knownto cause centrosome aberrations and genomic instability, its impact on tumor initiation andprogression is largely unknown. Our recent reports showed that CPAP regulates endocyticvesicular transport function and epidermal growth factor receptor (EGFR) homeostasis andsignaling dynamics. CPAP depletion endows human oral squamous cell carcinoma (OSCC) celllines with epithelial-mesenchymal transition (EMT) phenotype, and enhanced EGFR-dependentinvasive and tumorigenic properties in vitro and in a xenotransplant model, respectively. Here, weemployed a mouse model with hypomorphic allele of *Cenpj*, which shows dwarfism andmicrocephaly phenotype (MCP mice), to determine the impact of CPAP function on EGFR levelsand chemical carcinogen-induced oral tumorigenesis. Similar to human OSCC cell lines,fibroblasts, and tongue epithelium organoids from MCP mice exhibited defective vesiculartransport function and markedly increased EGFR protein levels. However, to our surprise, MCPmice exhibited diminished susceptibility to 4-Nitroquinoline 1-oxide (4NQO) -induced oraltumorigenesis as compared to their wild-type counterparts. Epithelial cell proliferation at all stagesof tumor progression and the eventual tumor burden were profoundly lower in MCP mice. Tonguefibroblasts and epithelial organoids treated with DNA damage-inducing agents were used todetermine the molecular mechanism(s) of reduced tumor susceptibility of *Cenpj* hypomorphicmice. These cells from MCP mice were highly susceptible to DNA damage and showed higheractivation of p53 and DNA-damage repair (DDR)- and apoptotic- pathways. For instance, gamma-H2AX and cleaved caspase-3 levels, and apoptotic death were significantly higher in cells withhypomorphic allele of *Cenpj* as compared to cells with WT allele. Our ongoing studies are focusedon determining how CPAP-mediated EGFR homeostasis and centriolar function impactgenotoxicity and epithelial cell transformation at different stages of oral tumorigenesis. Overall,our findings, for the first time, show a role for critical centriole biogenesis and microcephaly-associated protein in tumor initiation and progression under genotoxic stress and are expected tohelp design novel targeted therapies for OSCC.

#0583 Septin-9 binds to Desmoglein-2 and controls cell-cell junction strength in cancer cells.

Michael W. Jaber, Emily G. Bernier, Adi Dara Dubash

Furman Univ., Greenville, SC

Septins are a conserved family of GTP-binding cytoskeletal proteins which form oligomeric filamentous structures that play important roles in a wide variety of dynamic cellular processes, including cytokinesis, membrane remodeling and cell migration. Expression of Septins is dysregulated in different tumors, with some isoforms being either upregulated or downregulated, and prior evidence has highlighted a role for several Septins in controlling malignant phenotypes. In particular, Septin-9 is frequently dysregulated in cancer, with genomic amplification at the SEPT9 locus being commonly detected in high-grade carcinomas. Several different mechanisms have been put forth to explain a role for Septin-9 in cancer progression, including control of cell-matrix adhesion, migration and invasion. For example, overexpression of Septin-9 has been shown to enhance extracellular matrix degradation and invasion in breast cancer via recruitment of matrix metalloproteinases. In contrast, less is known about how Septin-9 affects cell-cell junctions, which are also frequently perturbed during cancer progression and metastasis. In our study, we provide evidence that Septin-9 localizes to desmosomal cell-cell junctions in the T47D cancer cell line. Desmosomes have a tripartite organizational structure wherein transmembrane cadherins (Desmoglein and Desmocollin) link adjacent cells, plaque proteins (Plakoglobin and Plakophilin) stabilize arrays of desmosomes on the intracellular face, and a cytoskeletal linker proteins (Desmoplakin) anchors desmosomes to the intermediate filament cytoskeleton. Importantly, we show an interaction between the cadherin Desmoglein-2 and Septin-9 via immunoprecipitation experiments. Loss of Septin-9 does not dramatically perturb mRNA or protein levels of different desmosomal components in T47D cells. Nevertheless, Septin-9 knockdown does result in a statistically significant loss of cell-cell junction strength in squamous cell carcinoma (SCC9) cells (measured via dispase assays), likely as an effect of disrupted localization of desmosomal proteins to cell-cell junctions. Taken together, these studies highlight an important role for Septin-9 in maintenance of desmosome-mediated adhesion in cancer cells.

#0584 Context-dependent roles of sFRP1 in melanoma.

Cierra Perron[1], Douglas Quilty[1], Farzaneh Afzali[1], Bianca Dauber[1], Tyler Cooper[2], Krista M. Vincent[3], Ivan Topisirovic[4], Lynne-Marie Postovit[1]

[1]Biomedical and Molecular Science, Queen's Univ. Cancer Research Inst., Kingston, ON, Canada,[2]Department of Obstetrics and Gynecology, Centre de recherche du Centre hospitalier de l'Universite de Montreal, Montreal, QC, Canada,[3]Anatomy and Cell Biology, Western University, London, ON, Canada,[4]Department of Oncology, McGill University, Montreal, QC, Canada

Elevated levels of secreted Frizzled-Related Protein 1 (sFRP1) in melanoma patient datasets correlate with reduced overall and distant metastasis-free survival, suggesting a clinically significant role in disease progression. To explore the mechanisms underlying this association, we compared melanoma cell lines with differing basal sFRP1 levels and assessed proliferation, migration, and invasion following sFRP1 overexpression or knockdown. Proliferation was measured with standard assays, while migration and invasion were quantified using scratch and Boyden chamber assays.

Across cell lines, sFRP1 produced divergent phenotypic outcomes, indicating that its activity is highly context-specific. Preliminary mechanistic analyses suggest that sFRP1 does not act through a single canonical pathway; instead, it appears to influence components of the tumor microenvironment, including markers linked to immune-regulatory pathways. These context-dependent changes highlight a broader role for sFRP1 in shaping interactions between melanoma cells and their surrounding microenvironment. Overall, these findings support a model in which sFRP1 modulates melanoma progression through multifactorial, microenvironment-dependent mechanisms rather than exerting uniformly oncogenic or suppressive effects. The impact of sFRP1 on melanoma appears shaped by intrinsic features of individual tumors. Ongoing studies aim to define the mechanisms, extracellular pathways, and tumor contexts that determine sFRP1-driven phenotypes and their potential clinical relevance.

#0585 Effects of bisphenols on gene expression and cellular outcomes in MDA-MB-231 breast cancer cells mediated via G protein-coupled estrogen receptor.

Norman R. Estes, Cameron Sheeler

University of Alabama at Birmingham, Birmingham, AL

Bisphenol A (BPA) is used in the manufacturing of consumer products such as plastic bottles, food-can epoxy resins, thermal printing paper, and dental sealants. BPA functions as an endocrine disruptor and can mimic estrogen through activation of estrogen receptor signaling pathways and can regulate estrogen-responsive genes through classical estrogen receptor-mediated mechanisms. BPA exposure is linked to several health risks, including hormone-dependent cancers, metabolic diseases, and developmental defects. However, the effects of BPA and its alternatives on gene expression and cellular behavior through the membrane-bound G-protein-coupled estrogen receptor (GPER) remain unclear. MDA-MB-231 triple-negative breast cancer (TNBC) cells express GPER but lack the classical estrogen receptor (ER), progesterone receptor (PR), and human epidermal growth factor receptor 2 (HER2). These studies aim to determine whether BPA and BPA alternatives, acting through GPER, differentially affect gene expression, cell proliferation, and cell migration. Preliminary RNA sequencing data show distinct gene expression changes in cells treated with BPA or 17β-estradiol, including alterations in cancer-related pathways, CREB signaling, and G-protein-coupled receptor mediated pathways. Cell migration assays performed on MDA-MB-231 cells treated with BPA, BPB, BPC, or 17β-estradiol further suggest differential effects on migration, with BPC inducing the highest degree of cell migration. These findings indicate that BPA and its alternatives influence both gene expression and cell migration in TNBC cells and may impact therapeutic outcomes in TNBC patients. Current studies focus on validating key pathways identified through RNA sequencing and clarifying the role of GPER-mediated signaling in TNBC cells exposed to BPA and BPA alternatives.

#0586 Pdcd4/mTORC2 axis regulates glycolysis via PFKFB3 in NSCLC.

Elham Zokaei[1], Hsin-Sheng Yang[2], Qing Wang[2], Yanquan Zhang[2]

[1]Toxicology and cancer biology, University of Kentucky, Lexington, KY,[2]University of Kentucky, Lexington, KY

Programmed cell death 4 (PDCD4) is a tumor suppressor frequently downregulated in non-small cell lung cancer (NSCLC), yet its role in metabolic regulation remains poorly understood. Using reverse-phase protein array analysis, we found that loss of PDCD4 significantly upregulates the glycolytic enzyme PFKFB3, which produces fructose-2,6-bisphosphate to activate the rate-limiting enzyme PFK1. PFKFB3 is highly expressed in NSCLC and correlates with advanced tumor stage. Because PDCD4 suppresses mTORC2 activity, we investigated whether mTORC2 regulates PFKFB3. Co-immunoprecipitation and in vitro kinase assays showed that mTORC2 directly interacts with and phosphorylates PFKFB3, and mapping analysis identified Ser461 as the targeted phosphorylation site. To determine its functional significance, we generated phosphorylation-deficient (S461A) and phospho-mimetic (S461D) PFKFB3 mutants. Protein stability assays revealed that S461A undergoes rapid proteasomal degradation, whereas S461D exhibits enhanced stability compared with wild-type (WT) PFKFB3. Seahorse XF glycolysis stress tests demonstrated that WT and S461D significantly increased basal and maximal glycolytic activity, while S461A markedly impaired glycolysis and metabolic capacity. Consistent with these effects, WT and S461D promoted proliferation and colony formation, whereas S461A suppressed cell growth. These findings identify mTORC2-mediated phosphorylation of PFKFB3 at Ser461 as a critical regulator of PFKFB3 stability and glycolytic function and show that PDCD4 loss enhances mTORC2 activity to drive glycolytic reprogramming in NSCLC. Targeting the PDCD4-mTORC2-PFKFB3 axis may offer a promising therapeutic approach to disrupt tumor metabolism in lung cancer.

#0587 Choline Acetyltransferase: A novel drug target in lung adenocarcinoma patients who are exposed to tobacco smoke.

Piyali Dasgupta[1], Eric W. Bow[2], Krista Denning[3], Rama S. Gadepalli[2], John M. Rimoldi[2], Yi Charlie Chen[4], Sarah L. Miles[5]

[1]Marshall University, Joan C. Edwards School of Medicine, Huntington, WV,[2]Department of Biomolecular Sciences, University of Mississippi, University, MS,[3]Department of Pathology, Marshall University, Joan C. Edwards School of Medicine, Huntington, WV,[4]Department of Biology and Environmental Sciences, Bluefield State University, Bluefield, WV,[5]Department of Biomedical Sciences, Marshall University, Joan C. Edwards School of Medicine, Huntington, WV

Purpose of the study: Lung cancer is not a single disease entity; it represents a spectrum of malignancies. Out of these lung adenocarcinoma (LUAD) accounts for about 65% of all lung cancers and shows a strong etiological correlation with smoking. Clinical studies show that about 30% of LUAD patients continue to smoke after being diagnosed with lung cancer. In addition, many others are exposed to nicotine via secondhand smoke and smoking cessation devices. Nicotine, the addictive component of tobacco smoke, accelerates the growth of human LUADs via the by nicotinic acetylcholine receptors (nAChRs) on target cells. The first-line therapy for LUAD patients involves the administration of tyrosine kinase inhibitors (TKIs) targeting EGFR, ALK, MET kinases. Such targeted therapies show potent anti-cancer activity in non-smokers and never smokers but show poor efficacy in patients who continue to smoke after their diagnosis. The primary objective of our research is to evaluate the potential of choline acetyltransferase (ChAT, the enzyme which synthesizes acetylcholine) as a drug target for LUAD in smokers. We evaluated the anti-neoplastic activity of BW813U (small molecule inhibitor of ChAT) in LUADs associated with moderate-heavy smoking history. We also investigated the anti-angiogeneic activity of BW813U (as a molecular mechanism underlying its growth-inhibitory effects) LUAD.
Experimental procedures. Primary human microvascular endothelial cells from the lung (HMEC-L) were used for all the experiments. These cells were used between passage 3-7. The anti-angiogenic activity of BW813U was measured in cell culture models by using the “MATRIGEL ASSAY”. The results obtained from the “MATRIGEL ASSAY” were confirmed using chicken chorioallantoic membrane (CAM) angiogenesis experiments. Finally, the anti-tumor activity of BW813U was measured *in vivo* by using xenograft model systems in SCID mice. Our studies also investigated the signaling pathways underlying the anti-angiogenic activity of BW813U, using chemical inhibitors and siRNA methodology.
Results: BW813U robustly suppressed angiogenesis in Matrigel assays and CAM model systems. The administration of BW813U potently decreased the growth rate of H838 tumors xenotransplanted in SCID mice. Immunohistochemical staining experiments revealed that the anti-tumor activity of BW813U was correlated with decrease of CD31 angiogenic biomarker in H838 tumor sections. The anti-angiogenic activity of BW813U was mediated by the alpha7-nAChR pathway and involved the nitric oxide pathway. Taken together, our studies show that ChAT may be a valuable drug target for the therapy of LUAD.
Conclusions: ChAT antagonists like BW813U decrease the growth of LUAD by suppressing tumor angiogenesis.

#0588 Enhancing the efficacy of 5-fluorouracil in targeting thymidylate synthase (TYMS) for breast cancer treatment using honokiol.

Santosh K. Singh, Rajesh Singh

Morehouse School of Medicine, Atlanta, GA

Breast cancer (BrCa), in particular, triple-negative breast cancer (TNBC), is a complex disease to treat and respond to conventional chemotherapy. Recently, thymidylate synthase (TYMS), has gained attention as important enzyme whose inhibition has been reported to be effective in the inhibition of the de novo production of 2 2-deoxythymidine-5-monophosphate (dTMP), involved in DNA synthesis in cancer cells. TYMS is a known target of 5-fluorouracil (5-FU), a widely used antimetabolite chemotherapeutic agent, effective against various tumors. Nevertheless, clinical application is commonly compromised by serious side effects, resistance to drugs, and upregulation of TYMS. Additionally, drug-induced activation of NF-κB contributes to the overexpression of TYMS, thereby promoting tumor cell proliferation and chemotherapeutic resistance. Therefore, identifying new anti-cancer agents that can be used alongside 5-FU to target cancer cells while sparing healthy cells is crucial. Recently, honokiol (HNK), a natural biphenolic compound from *Magnolia officinalis*, has shown promise as an anti-inflammatory, antioxidant, and anti-tumor agent. HNK is known to inhibit NF-κB activation in response to various stimuli. In this study, we investigated the synergistic effects of HNK and 5-FU in TNBC cells (MDA-MB-468 and MDA-MB-231), with a focus on the suppression of NF-κB-mediated TYMS expression. To determine the optimal IC50 values and synergy, TNBC cells were treated with HNK, 5-FU, or a combination of both at various time points and dosages, followed by a cell viability assay (MTT assay). Our results, which include cell cytotoxicity assays, apoptosis assays, cell cycle assays, RT-qPCR analysis, and Western blots, demonstrate that the combined treatment is most effective in inhibiting TYMS, reducing cell proliferation, and inducing apoptosis. The combination inhibits NF-κB p65 activation, thereby disrupting the transcriptional regulation of target genes associated with cell survival and communication with TYMS. This dual inhibition causes a cell cycle arrest at the G_0/G_1 phase, and upregulates the cell cycle inhibitors, including p21, which, in turn, downregulates the expression of the cyclin D1/CDK2 and CDK4 complexes. These findings suggest that NF-κB may stimulate TYMS transcription under inflammatory conditions. Additionally, the combinatorial treatment increased the number of apoptotic cells compared to the individual or control groups. These results suggest that the combination of HNK and 5-FU may alter DNA synthesis and repair, predisposing TNBC cells to apoptosis. This dual-targeting strategy, which involves direct inhibition of TYMS by 5-FU and suppression of its NF-κB-mediated upregulation by HNK, presents a promising approach to overcoming chemoresistance and improving therapeutic outcomes in patients with BrCa.

#0589 Ubiquitin specific peptidase 37 (USP37) facilitate Replication stress tolerance to promote prostate cancer oncogenesis.

Suraja Kumar Das[1], Lakshay Malhotra[2], Gunjan Dagar[1], Teena Haritwal[3], Atul Batra[4], Ajaz A. Bhat[5], **Mayank Singh**[3]

[1]Medical Oncology Lab, All India Institute of Medical Sciences (AIIMS) New Delhi, New Delhi, India,[2]Sri Venkateswara College University of Delhi, New Delhi, India,[3]All India Institute of Medical Sciences (AIIMS) New Delhi, New Delhi, India,[4]Medical Oncology, All India Institute of Medical Sciences (AIIMS) New Delhi, New Delhi, India,[5]Translational Medicine, Sidra Medicine, Doha, Qatar

Several reports have suggested that the DUBs (Deubiquitinating enzymes) are highly-elevated in various cancers, Reverses the process of ubiquitination and are responsible for stabilization of oncoproteins. Among DUBs, Ubiquitin-specific peptidase 37 (USP37) is one of the least studied member of the Ubiquitin specific protease family. USP37 controls numerous aspects of oncogenesis, including stabilizing many oncoproteins as reported in our recent studies. Prostate cancer (PC) is the most common cancer diagnosis made in men remains the leading cause of cancer death in men. However, the biological functions of USP37 in prostate cancer remain unclear. Analysis of TCGA data indicated that overexpression of USP37 correlated with reduced progression free survival (PFS) in prostate cancer patients. Mass spectrometry (MS) analysis of Prostate cancer cells (DU145) indicated that distinct set of genes were altered on knockdown of USP37. Survival Data indicate that USP37 overexpression confers survival advantage while its depletion enhances sensitivity for cell killing in PC cells. USP37 overexpressing cells were able to resolve DNA damage foci much more rapidly than the control cells or cells in which USP37 was depleted in response to genotoxic stress. USP37 depletion results in reduced resolution of γ H2AX and 53BP1 DNA damage foci which indicates the reduced ability of cells to carry out constitutive DNA replication. USP37 was found to interact with different replication factors as also seen in our MS analysis including many previously reported partners. We further correlated our data with archived tissue blocks of PC patients by analyzing if USP37 overexpression correlated with disease progression. Present data suggests that USP37 is required for tolerance of replication stress in PC and is required to dock additional replication factors and stabilize DNA replication fork. The current data provides novel pathways regulated by USP37 in PC cells which reinforce development of targeting strategies against USP37 in context of Prostate Cancer.

#0590 Role of cellular prion protein in breast cancer through Wnt signaling.

Parul Dubey, Manoj Kumar Mishra

Department of Biological Sciences, Alabama State University, Montgomery, AL

Cellular prion protein (PrP^C) is a GPI-anchored surface glycoprotein encoded by the *PRNP* gene. While PrP^C is widely studied in neurodegenerative diseases, recent evidence has revealed its involvement in various aspects of cancer biology. Although PrP^C contributes to tumor progression, its mechanistic role in breast cancer aggressiveness remains elusive. In this study, we investigate the role of PrP^C on key properties of tumors and on WNT/β-catenin signaling in triple-negative breast cancer (TNBC) cells. Using *PRNP*-targeted siRNA, the *PRNP* was transiently silenced, resulting in a significant reduction in migration and invasion, as demonstrated by the scratch and transwell invasion assays. This data was consistent with a shift in epithelial-mesenchymal transition (EMT) markers, characterized by increased E-cadherin and decreased N-cadherin expression. The metabolic activity, assessed by Alamar-blue assay, was significantly alleviated in the siPRNP group, accompanied by reduced proliferative activity, consistent with decreased PCNA levels. Additionally, flow-cytometric cell-cycle profiling demonstrated a significant accumulation of cells in the G0 phase, indicating growth arrest, consistent with reduced proliferation and metabolic quiescence. Furthermore, to determine whether WNT signaling mediated these effects, we examined the key pathway components. Silencing *PRNP* decreased GSK3β phosphorylation and increased its active form, promoting β-catenin phosphorylation at Ser (33/37) and its subsequent degradation. These changes indicate effective attenuation of canonical WNT signaling. Collectively, our findings suggest that PrP^C promotes TNBC cell migration, invasion, and proliferation through activation of WNT/β-catenin signaling and maintenance of EMT characteristics. Therefore, targeting PrP^C may offer a promising therapeutic strategy to limit TNBC aggressiveness.

#0591 The ubiquitin ligase HUWE1 controls the balance between β-catenin functions in WNT signaling and cell adhesion.

Caleb Kwame Sinclear, Joseph McKenna, Yalan Wu, Praveen Sonkusre, Andres M. Lebensohn

Laboratory of Cellular and Molecular Biology, Center for Cancer Research, NIH-NCI, Bethesda, MD

β-catenin plays two major roles in the cell, one as the key mediator of transcriptional responses to WNT signaling in the cytoplasm and nucleus, and the other as a structural component of adherens junctions, cell-cell adhesion complexes at the plasma membrane. How the balance between these spatially separate and functionally distinct pools of β-catenin is controlled is not well understood. WNT/β-catenin signaling is a fundamental signaling pathway, dysregulation of which can drive many types of cancer. Disassembly of adherens junctions, often caused by reduced β-catenin, is a hallmark of epithelial-mesenchymal transition (EMT), a process that promotes cancer metastasis. The goal of this study was to investigate the mechanisms that regulate the balance between the two spatially and functionally distinct pools of β-catenin. During WNT/β-catenin signaling, the main regulated step is β-catenin phosphorylation and degradation mediated by the destruction complex, composed of the scaffold proteins APC and AXIN1/2, and the kinases casein kinase 1α and GSK3α/β. Using CRISPR, we created two disease model cell lines from haploid human (HAP1) cells: 1. casein kinase 1α knock-out cells, and 2. β-catenin ST-A cells, containing mutations in β-catenin that render it insensitive to phosphorylation and degradation by the destruction complex. In both cell lines, we observed by confocal microscopy that β-catenin accumulates in the cytoplasm and the nucleus, and promotes hyperactive WNT signaling. Importantly, we found that loss of the E3 ubiquitin ligase HUWE1 in casein kinase 1α knock-out cells induced a marked change in the localization of β-catenin from the nucleus to the plasma membrane, which was accompanied by a substantial reduction in WNT/β-catenin signaling. Through proximity ligation assays and a new adherens junction-dependent cell adhesion assay that we developed, we found that localization of β-catenin to the plasma membrane caused by HUWE1 loss promotes β-catenin incorporation into adherens junctions and increases its functional contribution to cell-cell adhesion. In β-catenin ST-A cells that contain non-degradable β-catenin, regulation of β-catenin subcellular localization by HUWE1 was also observed. Taken together, these results demonstrate that HUWE1 regulates the balance between β-catenin transcriptional activity in WNT signaling and its cell adhesion functions. Therefore, regulation of β-catenin functions through HUWE1 may open new therapeutic avenues for cancers caused by hyperactive WNT signaling, and/or in metastasis driven by EMTs.

#0592 NSD2 regulates cell growth and oncogenic signaling pathways in laryngeal carcinoma.

Ahmed Ismail[1], Iuliia Topchu[2], Amr Ismail[1], Tingting Zhang[1], Xu Jia[1], Peter Makhov[3], Yanis Boumber[1]

[1]Section of Hematology and Oncology, Department of Medicine, University of Alabama at Birmingham & O'Neal Comprehensive Cancer Center, Birmingham, AL,[2]Kazan Federal University, Kazan, Russian Federation,[3]Fox Chase Cancer Center, Philadelphia, PA

Head and neck squamous cell carcinoma (HNSCC) is the sixth most common cancer worldwide. Despite the current advances in management, the 5-year survival rate for HNSCC remains around 66%. HPV-negative HNSCC accounts for approximately 70% of all diagnosed HNSCC cases. Therefore, a better understanding of the HPV-negative HNSCC drivers and targetable points may lead to significant clinical advances. NSD2 is a histone methyltransferase that catalyzes histone H3 lysine 36 di-methylation ($H3K36me^2$). Mutations leading to NSD2 loss-of-function are associated with improved outcomes in about 5% of HNSCC, including about 15% of laryngeal carcinoma (LC) patients. In our study, we demonstrate that NSD2 shRNA depletion in JHU-011 and JHU-022 LC cell lines results in a reduction of H3K36me2 levels and reduced cell growth in these cells in vitro. To evaluate downstream cancer signaling regulated by NSD, we performed a reverse-phase protein array (RPPA) upon NSD2 depletion in LC cell lines. Validation of RPPA using Western blot analysis suggests that NSD2 may regulate the expression of critical proteins responsible for the DNA damage response (DDR), including ATM kinase, PTEN, Akt/mTORC1 signaling pathway, and the cell cycle-related protein CDC2/p-CDC2 Y15 (CDK1/p-CDK1 Y15). Taken together, these data identify NSD2 as a likely regulator of the DNA damage response, Akt/mTORC1 signaling, cell cycle transition, and cell growth in HNSCC, suggesting that NSD2 may be a valuable therapeutic target in LC.

: Tumor Suppressors
Poster Session

#0596 DDX3 modulates mitochondrial function to inhibit HCC progression.

Jun-Huan Huang[1], Heng-Yu Lin[2], Yi-Yuan Su[3], **RU-TSUN MAI**[3]

[1]Institute of Molecular Medicine and Bioengineering, National Yang Ming Chiao Tung University, Hsinchu, Taiwan,[2]Center for Intelligent Drug Systems and Smart Bio-devices (IDS2B), National Yang Ming Chiao Tung University, Hsinchu, Taiwan,[3]Department of Biological Science and Technology, National Yang Ming Chiao Tung University, Hsinchu, Taiwan

Background: Mitochondria are essential organelles responsible for ATP generation and play pivotal roles in diverse cellular processes. Mitochondrial dysfunction contributes to various pathological conditions, including cancer development. As the central organ for nutrient metabolism, the liver contains a particularly high density of mitochondria. Impaired mitochondrial function leads to excessive generation of reactive oxygen species (ROS) and oxidative stress, resulting in cellular damage closely associated with hepatocellular carcinoma (HCC). Cancer cells frequently undergo metabolic reprogramming to sustain their high energy demands during rapid proliferation. Given our previous findings identifying DDX3 as a tumor suppressor in HCC, this study aims to elucidate the effects of DDX3 on mitochondrial function and redox regulation, as well as its implications for HCC tumorigenesis.
Methods: Mitochondrial morphology in DDX3-deregulated HCC cells was analyzed using super-resolution confocal microscopy. The expression of mitochondrial dynamics-related proteins was assessed by immunoblotting and quantitative real-time PCR. Metabolic activity was examined by MitoTracker Red/Green staining and Seahorse extracellular flux analysis. Redox homeostasis was evaluated by MitoSOX and DCFH-DA staining, along with measurements of the GSH/GSSG ratio and NADPH/$NADP^+$ levels. DDX3-regulated cellular functions were investigated through proliferation, colony formation, and transwell migration/invasion assays, with or without metabolic inhibitors. Cancer stemness was assessed using sphere-formation, chemoresistance, and flow cytometry-based assays.
Results: Reduced DDX3 expression in HCC cells led to marked alterations in mitochondrial morphology and increased mitochondrial oxidative phosphorylation (OXPHOS), resulting in elevated mitochondrial superoxide accumulation. Unexpectedly, the total cellular ROS levels were decreased in DDX3-knockdown cells. Further analyses revealed that low DDX3 expression enhances the cellular capacity to maintain redox balance, conferring a more robust antioxidant defense. Additionally, HCC cells with reduced DDX3 expression exhibited greater proliferation and self-renewal potential under varying nutrient conditions, effects that were attenuated upon treatment with metabolic inhibitors.
Conclusion: Our results suggested that DDX3 may suppress HCC progression by inhibiting mitochondrial activity, thereby reinforcing its role as a tumor suppressor in HCC.

#0597 CREBBP mutation promotes tumor growth by impairing HDAC3 acetylation-dependent expression of PTEN.

Xiang Wang, Wenquan Hu, **Qing Robert Miao**

NYU Langone Hospital - Long Island, Mineola, NY

Somatic mutations in CREB binding protein (CREBBP or CBP), which encodes a histone acetyltransferase, are frequently observed in cancers such as lymphoma and non-small cell lung cancer. Here, we report that CREBBP loss-of-function (LOF) mutations lead to the deacetylation of histone deacetylase 3 (HDAC3) and promote cancer cell growth by transcriptional silencing of the tumor suppressor gene phosphatase and tensin homolog (PTEN). Mechanistically, we found that CBP specifically binds to HDAC3 and acetylates it at a previously unknown residue, which is necessary for reducing HDAC3 activity and increasing histone acetylation. Additionally, our data show that HDAC3 acetylation is crucial for maintaining PTEN expression via acetylated histone-regulated transcription. The loss of HDAC3 acetylation in cancers with CBP LOF mutations results in PTEN deficiency, thereby promoting tumor development and resistance to chemotherapy. Our findings reveal a novel epigenetic mechanism regulating PTEN expression and suggest that HDAC3 could be a potential alternative target for cancers with CBP LOF mutations.To our knowledge, this is the first report of the previously unrecognized acetylation of HDAC3, a critical deacetylase involved in cancer. This discovery is significant because our data show that HDAC3 acetylation is essential for regulating its activity by disrupting the CK2a-mediated phosphorylation of HDAC3. We clarify that HDAC3 acetylation is controlled by the acetyltransferase CBP and the deacetylase Sirt1. The key finding is the connection between HDAC3 acetylation and PTEN loss in CBP mutant cancers. Our data also link HDAC3 acetylation to cancer patient survival and suggest that targeting HDAC3 could help restore the tumor suppressor PTEN in cancers with CBP LOF mutations. Our results provide a new understanding of the epigenetic regulation of PTEN in tumor development.

#0598 CRISPR Cas9 Screens in Mice to Identify Tumor Suppressors of Aggressive Human Lymphoma.

Vivian Morris[1], Julius Enssle[1], Ashok Kumar[1], Arnold Bolomsky[1], Moyi Li[1], Yandan Yang[1], Da Wei Huang[1], George Wright[2], Weihong Xu[1], Hong Zhao[1], James Phelan[1], Jagan Muppidi[1], Louis Staudt[1]

[1]Lymphoid Malignancies Branch, NIH NCI, Bethesda, MD,[2]Biometric Research Branch, Division of Cancer Treatment and Diagnosis, NIH NCI, Bethesda, MD

Diffuse Large B Cell Lymphoma (DLBCL), the most common form of aggressive Non-Hodgkin's Lymphoma, has been subdivided into genetic subtypes that respond differentially to therapy. The MCD subtype, characterized by MYD88L265P and CD79B mutations, is a subtype of DLBCL with some of the worst clinical outcomes. Patients have the lowest response rates to the standard of care - R-CHOP immunochemotherapy. To study MCD biology, we have developed a mouse model harboring four MCD-associated genetic alterations. With age, these mice develop DLBCL that arises in the spleen following an accumulation of spontaneous germinal center B Cells (GC Bs) suggesting they play a role in the transformation to malignancy. These MCD mice develop DLBCL with age which suggests additional genetic events are necessary to accelerate tumor development. The MCD genetic subclass of DLBCL is enriched for mutations in many genes that could potentially function as tumor suppressors. Thus, we conditionally expressed Cas9 in the MCD murine model enabling loss-of-function assays to study putative tumor suppressors in a premalignant setting. We screened candidate tumor suppressor genes using CIRSPR/Cas9 mediated knockout, which revealed that loss of Setd1b, a histone methyltransferase, and Tbl1xr1, a subunit of a transcriptional repressor complex, caused the largest increase in premalignant splenic GC Bs, suggesting they play a key role in driving MCD pathogenesis. Furthermore, the combined loss of these genes causes an even larger increase in this premalignant subpopulation, indicating a functional relationship between these two genes. Single cell RNA sequencing data showed that loss of Setd1b and Tbl1xr1 alters the phenotype of splenic GC B, resulting in a neomorphic cell state with features of both GC Bs and memory B cells. The combinatorial loss of these genes also induced gene expression signatures characteristic of the oncogenic signaling pathways that human MCD tumors depend upon. These data point towards a cooperative functional relationship between these genes, a discovery that is further supported by analysis of human MCD tumors, in which SETD1B and TBL1XR1 are genetically inactivated in the same tumors significantly more often than expected by chance. Thus, we aged MCD-Cas9 mice transduced with either guide-RNAs against both Setd1b and Tbl1xr1 or a non-targeting control and found the double knockout mice had accelerated tumorigenesis. As we continue to investigate the role of these now validated tumor suppressors in the development of MCD-DLBCL, we hope to shed valuable light on their contribution to lymphomagenesis, which may reveal new therapeutic vulnerabilities in this aggressive cancer.

#0599 AKT2 loss inhibits mixed lineage liver malignancy induced by PTEN loss involving TGFb-Notch-SOX9 signal.

Qi Tang, Yiwei Gu, Jingyu chen, Lina He, Ni Zeng, Shunan Hu, Slarve Ielyzaveta, Diala Alhousari, Guo Zhang, Zifei Xu, Phillip Nguyen, Gray Kanel, Shefali Chopra, Liyun Yuan, Bangyan L. Stiles

University of Southern California, Los Angeles, CA

Primary liver malignancies—including hepatocellular carcinoma (HCC) and cholangiocarcinoma (CCA)—originate from the oncogenic conversion of hepatocytes and cholangiocytes, respectively. Loss or attenuation of phosphatase and tensin homolog (PTEN), a critical negative regulator of the PI3K-AKT signaling axis, is frequently observed in roughly 70% of CCA and 50% of HCC cases. Intriguingly, the incidence of PTEN mutations is approximately doubled in tumors manifesting a combined HCC-CCA phenotype relative to tumors classified as either HCC or CCA alone. Using lineage-specific liver-specific PTEN-deficient mouse models, we show that PTEN loss drives cellular dedifferentiation and oncogenic progression, a process that exhibits strict dependence on AKT2. Mechanistically, we show that PTEN deficiency induces upregulation of NOTCH and SOX9 signal, with SOX9 playing important roles in tumor cell transformation. Furthermore, PTEN loss deficiency enhances the susceptibility of tumor cells to TGFβ, with TGFβ treatment repressing the expression of SOX9 in the absence of PTEN. Together, our study identifies PTEN-AKT2 signaling as a key regulator of hepatocyte lineage fidelity and reveals how its disruption enables the reprogramming of mature hepatocytes or cholangiocytes into liver cancer stem cells (LCSCs). We further delineate the cooperative interplay between NOTCH and TGFβ pathways in PTEN loss-driven liver tumorigenesis.

#0600 ZNF865 as a novel molecular target for cancer treatment.

Cansu Umran Tunc[1], Hamid Ghandehari[1], Robert Bowles[2]

[1]Molecular Pharmaceutics, University of Utah College of Pharmacy, Salt Lake City, UT,[2]Biomedical Engineering, University of Utah College of Engineering, Salt Lake City, UT

Despite the advancements and increased availability of conventional cancer therapies, there is a need for strategies to enhance treatment, prolong survival, and prevent recurrence and resistance. Gene therapies can address the limitations of traditional anti-cancer therapies to improve outcomes. Modulation of cancer-related genes has shown promising results. Identifying specific proteins and pathways that drive cancer cell proliferation and survival as molecular targets is fundamental for cancer gene therapy. ZNF865 is a 1056 amino acid-long protein with 20 unique ZNF and two transactivation domains identified by our team [1]. Even though ZNF865 is widely expressed in all cell types, the function of this protein is not fully known. We have demonstrated that the expression of ZNF865 affects the viability and proliferation of multiple cell types, and that upregulation of ZNF865 leads to the repair of DNA damage, while downregulation leads to rapid DNA damage accumulation, which pushes cells into and out of senescence. DNA damage/cellular senescence is recognized as a key tumor-suppressor mechanism in cancer. A dramatic decrease in cell proliferation capacity in ZNF865 downregulated cells suggests that this protein may be a molecular target for cancer. Survival analysis of lung and esophageal cancers showed a correlation between ZNF865 expression and survival probability. The purpose of this study is to investigate the role of ZNF865 in cancer cell proliferation and invasion. For this, ZNF865 was knocked down in lung adenocarcinoma cells (A549) with CRISPRi using the lentivirus system. The ZNF865 downregulated cells were sorted with flow cytometry. The proliferation of the cells was assessed using colony formation assay. The cells were allowed to proliferate for 14 days. The changes in the invasive potential of the cells were assessed using scratch assay for 48 h. Apoptosis rates of the cells were determined using Annexin-V/PI analysis, and the cell cycle phase distributions of the cells were analyzed by flow cytometry. The toxicity of cisplatin was tested using CCK8 viability assay. The ZNF865 knockdown resulted in approximately 90% decrease in clonogenic survival of the lung cancer cells ($p<0.001$). The gap closure in scratch assay was inhibited by 35% in the ZNF865 downregulated cells compared to the non-target control at 24 h ($p<0.001$). Apoptosis rates, cell cycle phase distributions, and cisplatin toxicity were not significantly affected by inhibition of ZNF865 expression, indicating alternate molecular mechanisms of action. Our findings suggest that silencing ZNF865 gene inhibited proliferation and decreased the invasion rate of the A549 cells, indicating ZNF865 may be a therapeutic target for lung cancer treatment. Future studies include validating the effect of ZNF865 downregulation on cancer proliferation and invasion in additional cancer cell types. 1. Lewis, C., et al., ZNF865 (BLST) Regulates Human Cell Senescence and DNA Damage. 2025.

#0601 Translational reprogramming disrupts mitosis to drive SMAD4-deficient esophageal adenocarcinoma.

Julia V. Milne, Ka Meng Wu, Sasha Witts, Eric Kusnadi, Kenji Fujihara, Katherine Papastratos, Maree Pechlivanis, Anna Trigos, Metta Jana, Luc Furic, Kaylene Simpson, David Liu, Cuong Duong, Wayne Phillips, Nicholas Clemons

Peter MacCallum Cancer Centre, Melbourne, Australia

Esophageal adenocarcinoma (EAC) develops from a precursor lesion named Barrett's esophagus; a progression that can be mapped by increasing genomic instability. We have previously shown that SMAD4 loss induces tumorigenesis and increased copy number alterations (CNA) in Barrett's esophagus cells with an existing *TP53* mutation. The observed CNA increase was especially pronounced in the resultant SMAD4-deficient tumor cells, suggesting that accumulation of mitotic errors occurs in these cells throughout their oncogenic progression. However, such an effect cannot be explained by our current understanding of canonical SMAD4 signalling. Thus, in this study, we aimed to delineate the role of SMAD4 in maintaining chromosomal stability in EAC. Our multi-omics (RNA-sequencing, proteomics and reverse-phase protein array) approach detected both deregulated translation and mitosis signatures in SMAD4-deficient cells. Using live cell imaging, we demonstrated that *TP53*-mutant SMAD4-deficient cells exhibit significantly more mitotic errors than *TP53*-mutant only cells, particularly chromosome segregation defects, which frequently result in chromosomal instability (CIN). Consistent with this, analysis of TCGA data demonstrated that CIN was more prevalent in tumours with both *SMAD4* and *TP53* mutation than either mutation alone. Further biochemical analyses revealed an increase in cap-dependent translation in these cells, and a decrease in internal ribosome entry site (IRES)-mediated translation. IRES-mediated translation is essential for synthesis of many important mitotic proteins, including a mitosis-specific isoform of a cell cycle kinase. Polysome sequencing showed decreased translation (but not transcription) of this kinase in SMAD4-deficient cells. Ectopic expression of mitosis-specific isoform of this kinase rescued the mitotic errors that arose as a consequence of SMAD4 loss. In sum, we present a model where translational reprogramming disrupts mitosis, inducing CIN and potentially driving EAC tumorigenesis in response to loss of SMAD4. This represents a novel mechanism of tumorigenesis in EAC and a previously unknown role of SMAD4 in maintaining chromosomal integrity.

#0602 Primary site specific distribution and prognostic significance of p53 immunohistochemistry patterns in 1,515 patients with head and neck squamous cell carcinoma.

Takane Watanabe[1], Yoshitaka Honma[2], Toshihide Ueno[3], Yukiko Nakamura[2], Eijitsu Ryo[4], Hideaki Takahashi[2], Akiko Mori[5], Yuko Kubo[6], Mitsuhiko Katoh[7], Kohtaro Eguchi[7], Azusa Sakai[7], Toshihiko Sakai[7], Chihiro Fushimi[7], Go Omura[7], Kenji Okami[1], Yasushi Yatabe[8], Hiroyuki Mano[3], Seiichi Yoshimoto[7], Taisuke Mori[8]

[1]Otorhinolaryngology/Head and Neck Surgery, Tokai University Hospital, Isehara, Japan,[2]Head and Neck, Esophageal Medical Oncology, National Cancer Center Hospital, Tokyo, Japan,[3]Cellular Signaling, National Cancer Center Research Institute, Tokyo, Japan,[4]Molecular Pathology, National Cancer Center Research Institute, Tokyo, Japan,[5]Dental Surgery, National Cancer Center Hospital, Tokyo, Japan,[6]Diagnostic Radiology, National Cancer Center Hospital, Tokyo, Japan,[7]Head and Neck Surgery, National Cancer Center Hospital, Tokyo, Japan,[8]Diagnostic Pathology, National Cancer Center Hospital, Tokyo, Japan

Background: Head and neck squamous cell carcinoma (HNSCC) is characterized by a high prevalence of TP53 mutations, reported in approximately 70% of cases in The Cancer Genome Atlas (TCGA). Although primary site-specific variation in TP53 mutation prevalence and related clinical behavior has been suggested, the TCGA cohort is biased toward certain primary sites—particularly the oral cavity and larynx—with limited representation of oropharyngeal and hypopharyngeal tumors. To address this sampling bias, we aimed to clarify the prevalence and anatomical distribution of HNSCC, as well as its prognostic implications, using comprehensive p53 immunohistochemistry (IHC) in a large institutional cohort.

Methods: We retrospectively analyzed 1,515 patients with HNSCC who underwent biopsy or surgery at the National Cancer Center Hospital between 2013 and 2023. TP53 status was inferred from p53-IHC patterns (wild-type, lost-type, or accumulation-type), and p16-IHC was performed to assess HPV association. Primary site-specific and subsite-specific prevalence patterns were evaluated using Fisher's exact test and odds ratios (ORs). Overall survival (OS) and disease-specific survival (DSS) were assessed in 1,364 patients after excluding carcinoma in situ, best supportive care, and outside-treated cases.

Results: Among 1,515 HNSCC cases, 409 (27.0%) were classified as p53 wild-type, 736 (48.6%) as accumulation-type, and 370 (24.4%) as lost-type. The prevalence of p53 mutated-type tumors varied markedly across anatomical sites. Mutation-enriched primary sites included the hypopharynx/cervical esophagus (OR = 5.10, 95% CI: 3.49-7.46, $p < 0.01$), larynx (OR = 1.88, 95% CI: 1.22-2.88, $p < 0.01$), and oral cavity (OR = 1.54, 95% CI: 1.19-2.00, $p < 0.01$). In contrast, p53 wild-type tumors were significantly frequent in the oropharynx (OR = 0.25, 95% CI: 0.19-0.33, $p < 0.01$) and nasopharynx (OR = 0.24, 95% CI: 0.13-0.47, $p < 0.01$). Survival analysis revealed significantly improved outcomes in the p53 IHC wild-type group compared with the mutated-type group (median OS: not reached vs. 110 months; HR = 0.59, 95% CI: 0.46-0.76, $p < 0.01$; median DSS: both not reached; HR = 0.65, 95% CI: 0.47-0.89, $p = 0.01$).

Conclusion: This large cohort study demonstrates substantial primary site-specific variation in p53 alteration patterns across HNSCC, with notable enrichment of IHC p53-mutated tumors in the hypopharynx and larynx, and enrichment of p53 IHC wild-type tumors in oropharyngeal, nasopharyngeal, and gingival cancers. The p53 IHC wild-type pattern was consistently associated with significantly better survival. These findings highlight the importance of anatomical subsite context when interpreting TP53 status and suggest that p53 IHC serves as a robust, clinically relevant biomarker in HNSCC.

#0603 Variation at the R181 residue of p53 confers loss of p53 DNA binding cooperativity with the retention of mitochondrial-associated apoptosis.

Renyta Moses[1], Alexandra Indeglia[2], Alison Schwartz-Levine[3], Ryan Hausler[1], Gregory Kelly[1], Sven Miller[4], Isabel Anez[3], Melissa Heller[1], Rosella Delgado[1], Caitlin Orr[1], Wendy Kohlmann[5], Anne Naumer[5], Jennie Vagher[5], Sophie H. Cahill[3], Luke D. Maese[5], John Karanicolas[4], Judy E. Garber[6], Maureen E. Murphy[7], Kara N. Maxwell[8]

[1]University of Pennsylvania, Philadelphia, PA,[2]Brigham and Women's Hospital, Boston, MA,[3]Dana-Farber Cancer Institute, Boston, MA,[4]Fox Chase Cancer Center, Philadelphia, PA,[5]University of Utah Huntsman Cancer Institute, Salt Lake City, UT,[6]Director, Center for Cancer Genetics and Prevention, Dana-Farber Cancer Institute, Boston, MA,[7]Professor, The Wistar Institute, Philadelphia, PA,[8]Perelman School of Med. Univ. of Pennsylvania, Philadelphia, PA

TP53 is the most frequently mutated gene in cancer, and its encoded protein p53 has many tumor-suppressive functions. p53 primarily acts as a transcription factor and binds to target sites on DNA cooperatively as a tetramer. This cooperative binding is mediated by salt-bridge interactions between p53 residues E180 and R181 from two different p53 monomers. Variants at the R181 residue are one of the most identified *TP53* pathogenic variants by germline genetic testing, however the mechanism by which these variants disrupt p53 tumor suppression is not understood. We show that families with *TP53* p.R181H and p.R181C variants have an attenuated cancer risk phenotype compared to patients with hotspot loss of function *TP53* variants. Despite this clinical phenotype, we find that p53 R181H and R181C variants have significantly diminished ability to transactivate a set of ~300 known p53 target genes in CRISPR knock-in colorectal and breast cancer cell lines. This loss of transactivation ability does not occur through defects in p53 structure or oligomerization, but through reduced cooperative binding to p53 target sites on DNA as determined using fluorescence polarization assays on purified p53 proteins and using chromatin immunoprecipitation sequencing in R181-mutant cancer cells.
Despite the complete loss of p53's transcriptional function, R181 mutants retain some tumor suppressive function. Colony formation assays show efficient colony suppression by R181H and R181C, and injecting R181 knock-in cancer cells into the subcutaneous tissue of mice results in comparable tumor progression levels between R181H, R181C, and wild-type p53. Interestingly, we observe residual apoptotic activity in R181H and R181C mutant cells when treated with DNA-damaging agent 5-fluorouracil, despite the poor transactivation of p53's proapoptotic targets. This suggests that the R181 mutants retain the p53 transcription-independent mechanism of apoptosis, where p53 goes to the mitochondria to induce apoptosis. Indeed, proximity ligation assays between p53 and mitochondrial BAK show that R181 mutants traffic to the mitochondria upon genotoxic stress. Our study elucidates p53 tumor suppressive activities that are lost versus retained by R181 variants, which is estimated to account for 0.5% of all p53 missense mutations.

#0604 Second site rescue mutants as tools to uncover reactivation mechanisms of p53 cancer mutants.

Fiona Law, Zane Norman, Mark Villamil, Peter Kaiser

Uc-Irvine, Irvine, CA

TP53 is an important tumor suppressor and is the most frequently mutated gene in human cancer. A large fraction of cancers with mutated p53 carry missense mutations, so they express full-length but nonfunctional p53. Therefore, reactivating mutated p53 to a wildtype-like conformation has long been a major therapeutic goal. However, the mechanisms underlying p53 reactivation are still poorly understood. To dissect this mechanism, this study employs a genetic strategy in which a second amino acid is mutated in addition to the G245S mutation found in cancer. This second mutation induces structural changes to compensate for the defect caused by p53 cancer mutations. Two second site rescue mutations were used in this study: N239Y, known to stabilize p53, and T123P, located within the transient L1/S3 pocket implicated in small molecule binding. When expressed alongside the cancer mutation G245S, both second site rescue mutations restored tumor suppressive properties, including suppressed growth, activated canonical p53 downstream targets, and restored DNA binding both in vitro and in cells. Differential scanning fluorimetry confirmed that N239Y increased folding stability of the G245S mutant. However, despite rescuing p53 activity, T123P further destabilized the structural stability of the G245S mutant. These findings demonstrate that p53 reactivation can occur through distinct and mechanistically divergent pathways, including those independent of global thermostabilization.Our results provide a genetic framework to classify reactivation mechanisms of p53 cancer mutants and define gene-expression signatures associated with each mechanism. Rather than being a direct treatment, this framework can help guide the identification and development of future small molecule p53 reactivators.

#0605 Mapping loss of heterozygosity in Li-Fraumeni Syndrome to uncover early molecular drivers of tumorigenesis.

Hailey Stack[1], Ashby Kissoondoyal[1], David Malkin[2]

[1]Genetics and Genome Biology, The Hospital for Sick Children, Toronto, ON, Canada,[2]The Hospital for Sick Children, Toronto, ON, Canada

Li-Fraumeni syndrome (LFS) is a cancer predisposition syndrome caused by germline mutations in TP53. Mutant p53 impairs DNA damage repair, causing dysregulation in cell growth and division. LFS patients have a 40% chance of developing cancer during childhood/early adolescence, and an almost 100% lifetime risk of developing a variety of cancers. A recent study found that 86% of tumors in LFS patients exhibit loss of the wild-type (WT) allele (loss of heterozygosity (LOH)), which was absent in healthy tissue, indicating specificity to pre-malignant and malignant cells. LOH appeared to occur many years before tumor diagnosis, likely in utero or early life, suggesting it plays an early role in LFS precancer development and later tumorigenesis. In cancers with somatic TP53 mutations, LOH is an early event in tumor evolution, leading to detrimental genomic events and accelerated tumor development. While the aftermath of TP53 LOH has been explored in sporadic cancers, the extent and contribution of LOH to cancer evolution and development in LFS remains poorly understood. We leveraged LFS patient-derived skin fibroblasts, collected either pre- or post-cancer diagnosis, to map LOH in cell culture over time. Droplet digital PCR was used to determine the allelic ratio between the WT and mutated copy of TP53. Interestingly, a significant increase in the mutated TP53 allele was seen in fibroblasts collected from patients years after diagnosis, suggesting loss of the WT allele, which was not observed in fibroblasts collected prior to cancer diagnosis. Single-cell RNA sequencing (scRNA-seq) will be used to identify gene expression at an individual cell level to distinguish between cells which have undergone allelic change and those which have not. This method will help identify transcriptomic changes, with subsequent GO analysis revealing biological pathway changes before, during, and after loss of WT TP53, generating specific LOH signatures in vitro. This signature identified will be mapped back to an in vivo LFS mouse model ($Trp53^{R172H/WT}$), probing for these in vitro transcriptomic signatures in scRNA-seq data across embryonic, post-natal and post-cancer development. LOH of WT TP53 precedes tumorigenesis, many years before tumor diagnosis in LFS. Knowing this, it is important to better understand mechanisms influencing, contributing, and responding to LOH in LFS. This is critical for cell evolution and precancer development in LFS, offering insight into opportunities for tumor prevention or interception. This project is generating the first map of LOH in LFS patient-derived fibroblasts, integrating allelic analyses and transcriptomic data, providing critical insights into the earliest stages of precancer evolution. By uncovering pathways that are differently regulated across distinct LOH states, the mechanisms of precancer development and potential therapeutic targets will be revealed.

#0606 DACH1 conveys isoform specific tumor suppressor functions.

Kenneth A. Iczkowski[1], Zhiping Li[2], HIdetoshi Mori[3], Danni Li[2], Samiha Nasser[4], Csaba Kerepesi[5], Andras Benczur[5], Hallgeir Rui[6], Ritika Harish[2], Xuanmao Jiao[2], Fred Saad[7], **Richard G. Pestell**[2]

[1]Pathology and Laboratory Medicine, University of California- Davis, Sacramento, CA,[2]Pennsylvania Cancer and Regenerative Medicine Research Center, Baruch S. Blumberg Institute, Wynnewood, PA,[3]University of California-Davis, Davis, CA,[4]The Ohio State University Wexner Medical Center, Columbus, OH,[5]Institute for Computer Science and Control (SZTAKI), Hungarian Research Network (HUN-REN), Budapest, Hungary,[6]Thomas Jefferson University, Philadelphia, PA,[7]University of Montreal, Montreal, ON, Canada

Introduction. DACH1 is expressed in renal glomerular podocytes and distal tubules. DACH1 has been described as either a tumor suppressor or oncogene, with increased or decreased abundance depending upon the tissue type. Recent studies showed that poor outcome of prostate cancer was correlated with the deletion of the DACH1 gene, within the 13q21 region, and prostate-specific deletion promoted prostatic intraepithelial neoplasia in prostate onco-mice. DACH1 generates several splice variant isoforms with a common carboxyl (C) terminus that cross-reacts with commercially available antibodies.

Methods. We characterized the function of three DACH1 isoforms. We developed a DACH1a isoform-specific antibody. We assessed DACH1a variant vs. DACH1 common C terminal immune reactivity in prostate cancer. Analysis included patient gene expression, tumor histology, tissue culture, and tissue-specific gene knockout transgenic mice.

Findings. Expression of DACH1a inhibited AR activity. DACH1a inhibited DNA synthesis and indicators of EMT, contrasting with the effects of DACH1b and DACH1c.

Compared to normal tissue, DACH1 expression was reduced in urogenital cancer (kidney cancer (chromophobe, clear cell, papillary) and testicular germ cell), sarcomas, and lung cancer, but increased in acute leukemia, lymphoma, colon and ovarian tumors. The relative levels of expression of the three isoforms of DACH1 (DACH1a, 1b, 1c), however, varied substantially between cancer types. The C terminal antibody cross-reacted with each isoform-generated DACH1 protein.

Monoclonal DACH1a specific antibody, which detected DACH1a in the kidney glomerular podocyte and distal tubule, showed a substantially different subcellular distribution to C terminal antibody immune reactivity in benign prostate vs. cancer. We conducted quantitative immunofluorescence at a single cell level using the opal multi-fluorophore technology, using the DACH1a specific antibody and additional DACH1a candidate interactors. Immunofluorescent staining of DACH1a showed reduced staining in prostate cancer compared to adjacent benign tissue.

Conclusions. Functional analysis shows DACH1 conveys isoform-specific tumor suppressor functions. Since the DACH1a isoform conveys specific and distinct functions, compared to other DACH1 isoforms, DACH1a isoform specific analysis may be required to predict patient outcome.

#0607 Quantitative analysis of microtubule lattice damage in NF1-deficient HER2-positive breast cancer under mitotic and pharmacological stress.

Eleonora Messuti[1], **Alessia Castiglioni**[1], Simona Rodighiero[1], Ambra Dondi[1], Bruno Achutti Duso[2], Luca Mazzarella[1]

[1]Department of Experimental Oncology, IEO - European Institute of Oncology, Milan, Italy,[2]Department of Cancer Medicine, Gustave Roussy Cancer Campus Grand Paris, Paris, France

Our understanding of microtubule (MT) dynamics has recently expanded to include remodeling events within the lattice, where mechanical stress generates discontinuities repaired through intra-lattice tubulin incorporation and EB1 redistribution. Only two factors, CLASP1 and SSNA1, are known to recognize and modulate this form of MT damage. Methods to reliably estimate MT damage and repair are not established, leaving their contribution to tumorigenesis and anticancer drug activity unclear. In our previous work, we demonstrated that loss of the tumor suppressor NF1, a new MT-associated protein (MAP), leads to increased MT damage in HER2-positive breast cancer cells. This in turn causes mitotic defects (potentially contributing to tumorigenesis) but also sensitization to maytansinoids like DM1, a drug class frequently used in Antibody-Drug Conjugates (ADC, T-DM1 and Mirvetuximab Soravtansine). To investigate MT damage and repair upon pharmacological and mechanical stress, we analyzed the distribution of EB1, normally confined to growing MT tips but known to redistribute along the MT body upon structural disruption or when repair factors like CLASP are ablated. We developed a novel method to systematically quantify EB1 and tubulin signal along single MTs. To achieve the spatial precision required to resolve EB1 we combined DeepSIM and expansion microscopy (ExM) with two complementary analytical strategies: manual 3D MT tracing using SNT ImageJ plugin (designed for neurite tracing) and an automated pipeline for MT segmentation and EB1 signal extraction. Upon DM1 treatment, EB1 showed progressive re-localization from the tip to the MT body, consistent with partial intra-lattice disruption in addition to its established de-polymerizing activity at the tip. In NF1 deficient cells, an initial increase in intra-lattice EB1 was followed by a sharp reduction in overall EB1 signal and pronounced MT fragmentation, indicating faster DM1-induced MT fracturing and depolymerization; this was abolished by NF1 re-expression. These results directly show how failed MT repair, more prominent in NF1 deficient cells, creates further intra-lattice DM1 binding sites explaining increased sensitivity. In mitosis, NF1 deficient cells showed strongly increased EB1 signal on the MT shaft, consistent with failure of repair under strong mechanical stress. EB1 shaft localization and mitotic defects (chromosome missegregation, aneuploidy) were rescued by NF1 re-expression.By establishing a quantitative framework to measure EB1 redistribution at single MT resolution, our study provides a previously unavailable strategy to monitor intra-lattice damage in cancer cells. These findings establish for the first time a direct causative link between unrepaired MT damage and chromosomal instability, providing a new model to understand maytansinoid mechanism of action.

#0608 Ccn6 loss cooperates with EZH2 overexpression to induce sarcomatoid differentiation in metaplastic breast carcinoma.

Maria E. Gonzalez[1], Ahmad Eido[1], Kendall Miller[1], Celina G. Kleer[2]

[1]University of Michigan, Ann Arbor, MI,[2]Harold A. Oberman Collegiate Professor, Dept. of Pathology, University of Michigan Medical School, Ann Arbor, MI

Background: Triple negative breast cancers (TNBC) have proven resistant to conventional and immune therapies with 5-year survival rates of 50%. Among the most aggressive of these is metaplastic breast carcinoma (mBrCA), a unique histopathology with spindle or sarcomatoid (chondroid/osseous) components and low immune cell infiltration with poor responses to immunotherapy. We have reported that mammary epithelial cell-specific *Ccn6* knockout mice (MMTV-Cre;*Ccn6*$^{fl/fl}$) develop mBrCAs like human spindle mBrCAs, defining *CCN6 as a tumor suppressor for spindle mBrCA*. Lately we showed CCN6 antagonizes the pro-invasive effects of Wnt/ β-catenin/EZH2 signaling. Here, we tested the hypothesis that CCN6 genetically interacts with EZH2 to induce a phenotypic switch from spindle to sarcomatoid cancer cell phenotype and limits CD8$^+$T cell infiltration.

Methods: MDA-MB-231 (TNBC) and Ccn6-KO cells derived from MMTV-Cre;Ccn6$^{fl/fl}$ (Ccn6-KO) TNBC mouse model were transduced with vector or EZH2 shRNA knockdown (KD). Ccn6-KO EZH2 KD cells were rescued with lentivirus containing EZH2-wild-type (WT). To overexpress EZH2 we infected cancer cells with adenovirus with vector or EZH2-MYC construct. We investigated how Ccn6 loss and EZH2 affect mBrCA sarcomatoid by differentiation assays of the breast cancer cells in chondrogenic and osteogenic specialized media compared to controls. In vivo, to recapitulate the bone microenvironment, we injected Ccn6-KO cells into the tibia of FVB mice and treat them with the EZH2 inhibitor EPZ-6438. Flow cytometry analyses of tumors derived from Ccn6-KOshC, shEZH2 and EZH2-wild type rescue cells and IHC of Ccn6-KO tumors treated with EZH2i were used to measure the percentage of CD8$^+$gzmb$^+$IFNg$^+$ T cells. ChIP-sequencing studies in dominant negative (dn)TCF4 mutant vs. controls were used to study regulation of bivalent genes in Ccn6-KO cells.

Results: EZH2 overexpression in Ccn6-KO spindle mBrCA cells induces chondrogenic and osteogenic differentiation in cells grown in specialized media and EZH2 inhibition rescues the sarcomatoid phenotype in vivo. We found that EZH2 shRNA KD or pharmacological inhibition increases CD8+T cell infiltration in Ccn6-KO tumors, which is rescued by EZH2 overexpression. WNT/β-catenin signaling blockade in Ccn6-KO cells using dnTCF4 downregulates EZH2 and H3K27me3 mark at the promoter regions of 19 bivalent gene targets with roles in development.

Conclusion: These data provide a clear link between CCN6 defects and EZH2 overexpression as inducers of sarcomatoid immune cell-low mBrCAs. We demonstrate the effectiveness of pharmacological inhibition of EZH2 methyltransferase activity in reversing these aggressive phenotypes. These data reveal a novel oncogenic cooperation and provide evidence to support the potential therapeutic value of CCN6 restoration, Wnt pathway and EZH2 inhibition as promising strategies for mBrCA patients

#0609 Investigating tumor suppressor function and regulatory control of NISCH in breast cancer.

Abigail E. Rink[1], Suresh K. Alahari[2]

[1]Louisiana State University Health Sciences Center, New Orleans, LA,[2]Brazda Professor, Biochem. & Molec. Bio., Louisiana State University Health Sciences Center - New Orleans, LA, New Orleans, LA

Purpose: This study aimed to characterize the role of Nischarin (NISCH) in breast cancer by examining its expression patterns in relation to clinical outcomes and exploring potential regulatory mechanisms—specifically promoter methylation and copy number alterations—that may underlie its dysregulation.

Methods: Data were acquired for NISCH from the Molecular Taxonomy of Breast Cancer International Consortium (METABRIC) and The Cancer Genome Atlas (TCGA) via UCSC Xena and cBioPortal, including expression levels of NISCH and several DNA methyltransferases (DNMTs), promoter methylation beta values, copy-number values, demographic variables, and clinical data. All retrospective analyses were performed using GraphPad Prism.

Results: High expression of NISCH was significantly associated with improved overall survival in breast cancer, as well as longer distant metastasis-free survival and relapse-free survival. When comparing demographics, a lower expression of NISCH was observed in patients diagnosed at younger ages, within the Basal PAM-50 subtype, and among the Asian race. Several CpG islands proximal to the promoter region showed both a negative correlation with NISCH expression and elevated methylation in tumor samples. Co-expression studies revealed inverse correlations between three DNMTs and NISCH, indicating possible involvement in the silencing of the gene. Furthermore, shallow deletions at the NISCH locus correlated with reduced mRNA expression and were linked to poorer survival outcomes.

Conclusions: Together these findings support NISCH's profile as a tumor suppressor in breast cancer, with high mRNA expression consistently linked to better survival outcomes across multiple clinical metrics. Moreover, identifying lower NISCH expression in biologically aggressive subsets of breast cancer—the Basal PAM-50 subtype and younger age at diagnosis—enhances NISCH as a putative marker for poor prognosis. Both promoter methylation and shallow deletions reduced expression of NISCH, indicating that the locus may be regulated through several genomic and epigenetic mechanisms. Inverse expression patterns between NISCH and three DNMTs across similar demographic subsets provides additional evidence that promoter-methylation may drive the silencing process. Collectively, these findings strengthen the rationale for future functional studies to investigate the mechanisms controlling NISCH expression, and to evaluate its potential as a biomarker or therapeutic target in breast cancer.

#0610 Lack of circadian regulator PER2 enhances breast cancer susceptibility and progression via immunosuppression.

Yixin Duan[1], **Helen Zhang**[1], Hongyong Zhang[2], Jie Huang[3], Xiong Zhang[1], Aris Alexandro[4], Dake Hao[5], Jonathan I. Berg[1], Ming Fan[1], Yili Wang[6], Loning Fu[7], Hong-Wu Chen[8], Jian Jian Li[1]

[1]UC Davis Medical Center, Sacramento, CA,[2]UC Davis, Davis, CA,[3]Hangzhou Cancer Hospital, Hangzhou, China,[4]Holy Cross College, Notre Dame, IN,[5]UC Davis, Sacramento, CA,[6]Jiaotong University, Xian, China,[7]Asst. Professor, Dept. of Pediatrics, Baylor College of Medicine, Houston, TX,[8]Associate Professor, UC Davis Comp. Cancer Center, Sacramento, CA

Circadian rhythm (CR) orchestrates the physiological functions of nearly all organs in the human body. Disruption of circadian rhythm (CRD), caused by environmental factors such as shift work or by loss of core clock genes, is associated with heightened susceptibility to malignancies of the female reproductive system, particularly breast cancer (BC). However, whether deficiency of a specific clock gene directly confers breast cancer susceptibility and systemic immune suppression remains largely unresolved. Here, we investigated the role of the circadian regulator Period 2 (PER2) in breast tumorigenesis and immune evasion.

Combined the data from TCGA datasets and a DMBA-induced mammary tumor model established in $Per2^{def}$ and $Per2^{wt}$ mice we analyzed the tumor immune profiles assessed by IHC and flow cytometry. The effects of PER2 loss on breast cancer malignancy were tested using proliferation, invasion, and clonogenic assays. Mechanistic studies (Western blot, qRT-PCR, and luciferase assays) defined the PER2-dependent pathway regulating tumor immune escape. PER2 expression was markedly reduced in BC and correlated with poor prognosis in female patients. Per2^def mice exhibited significantly increased susceptibility to DMBA-induced mammary tumor formation, indicating an intrinsic tumor-protective role for PER2. Immune profiling revealed a profoundly immunosuppressed microenvironment in Per2^def tumors, characterized by reduced cytotoxic $CD8^+$ T cells and $CD80^+$ M1 macrophages, accompanied by elevated pro-tumor $FOXP3^+$ regulatory T cells and $CD206^+$ M2 macrophages.

In human breast cancer cells, PER2 knockdown induced aggressive and clonogenic phenotypes, whereas PER2 reconstitution reversed these effects. Loss of PER2 led to increased expression of HER2 and CD47, two oncogenic drivers of proliferation and immune evasion, respectively. Consistent with this, PER2 overexpression suppressed, whereas PER2 silencing enhanced, the transcriptional activities of HER2 and CD47 promoters. JASPAR predictions identified CLOCK-binding motifs within both promoters, and mutation of these motifs markedly diminished transcriptional activation in MCF7 and SKBR3 cells. Luciferase reporter assays further demonstrated that PER2 represses HER2 and CD47 expression by inhibiting CLOCK-mediated transactivation.

Collectively, these findings reveal that PER2 deficiency triggers CLOCK-dependent upregulation of HER2 and CD47, promoting both tumor aggressiveness and immune escape. This study uncovers a dual mechanism by which clock gene loss enhances breast cancer susceptibility with systemic immunosuppression, highlighting $PER2^{def}$-CLOCK-HER2/CD47 signaling as a potential integrated therapeutic axis to mitigate CRD-associated breast cancer risk and tumor aggressiveness.

#0611 NSD1-AURKA-SETD2 axis creates novel mitotic vulnerabilities in clear cell renal cell carcinoma.

Manga Motrapu, Ashley Boice, Richard Han, Xiaoli Wang, Pratim Chowdhury, Sung Jung, **Ruhee Dere**

Baylor College of Medicine, Houston, TX

Background: Chromothripsis-driven 3p deletion and 5q amplification are early, clonal events in clear cell renal cell carcinoma (ccRCC). These lesions respectively target the epigenetic regulators SETD2 and NSD1. Paradoxically, although NSD1 is amplified on 5q, it is frequently hypermethylated and transcriptionally silenced, suggesting functional inactivation is selected for. The mechanistic implications of *NSD1* and *SETD2* loss in mitotic control remain poorly understood.

Methods: We integrated multi-pronged approaches using in vitro kinase and methyltransferase assays, mass spectrometry, molecular modeling, and CRISPR-engineered models to dissect the regulatory relationship between NSD1, AURKA, and SETD2. Protein-protein interactions and post-translational modifications were characterized via co-immunoprecipitation, immunoblotting, fluorescence microscopy, and quantitative proteomics.

Results: We identified NSD1 as a methyltransferase that directly methylates AURKA, serving as a negative regulator of its kinase activity and subcellular dynamics during mitosis. Loss of *NSD1*, through genetic deletion or pharmacologic inhibition, led to AURKA hyperactivation, defective spindle architecture, chromosome mis-segregation, and increased micronuclei formation. Unexpectedly, we found that AURKA phosphorylates SETD2, functionally linking these two epigenetic regulators. This phosphorylation selectively regulated SETD2's cytoskeletal activity without affecting its chromatin-associated roles. Disruption of this modification—via AURKA inhibition or mutation of the phosphorylation site—compromised mitotic fidelity and enhanced genomic instability.

Conclusions: Our findings reveal a novel regulatory pathway in which NSD1-mediated methylation suppresses AURKA, while AURKA phosphorylation regulates SETD2 activity on the cytoskeleton, linking these two tumor suppressors altered in renal cell carcinoma (RCC). Disruption of this NSD1-AURKA-SETD2 axis creates a state of mitotic vulnerability, opening the door for therapeutic intervention using AURKA inhibitors in genetically defined subsets of ccRCC. Our data present a rationale for loss of *NSD1* and *SETD2* in the setting of RCC aimed at dismantling this regulatory axis to drive tumor evolution. This dual loss creates a state of dependency on AURKA activity, providing a rationale for AURKA-based inhibition in a subset of RCC patients with dual loss of *NSD1* and *SETD2*.

#0612 A novel regulatory pathway as a driver of malignant transformation in mesothelioma..

Flavia Novelli[1], Lydia Giannakou[1], Jin Hee Kim[1], Joelle S. Suarez[1], Cristina Favaron[1], Qian Wang[2], Angela Bononi[1], Michele Carbone[1], Haining Yang[1]

[1]University of Hawaii Cancer Center, Honolulu, HI,[2]University of Science and Technology of China, Hefei, China

Mesothelioma is a highly aggressive malignancy of the serosal membranes. Alterations in regulatory mechanisms controlling tumor suppressor gene expression play a critical role in Mesothelioma and other malignancies. Although tumor suppressor genes are central to cancer biology, the upstream regulation networks governing their activity remain poorly defined. Here, we identify a novel molecular pathway that directly regulates BAP1 tumor suppressor gene transcription and drives oncogenic phenotypes in Mesothelioma. Using patient-derived fibroblasts harboring germline mutations, mesothelioma cell lines, and a genetic knockout mouse model, we demonstrate that disruption of this pathway markedly decreases tumor suppressor expression, whereas its activation restores gene transcription and promotes cell proliferation, migration, and invasion. These findings reveal a novel regulatory loop mechanism in which tumor suppressor gene inactivation facilitates malignant transformation, while its activation sustains tumor progression. Similar regulatory dynamics were observed across additional cancer types, including lung, colon, and cholangiocarcinoma, indicating a conserved process. This work defines a novel transcriptional axis integrating tumor suppressive and oncogenic signaling in Mesothelioma and other cancers, offering new therapeutic opportunities.

#0613 Bap1 driven soft tissue sarcomas: Mouse modeling and therapeutic strategies.

Xingliang Liu, William Haugh, Bryan R. Bell, **Jianguo Huang**

Earle A. Chiles Research Institute, Portland, OR

Objective: Soft tissue sarcomas (STS) are rare in both pediatric and adult cancer patients, yet they remain highly lethal and understudied. Many STS subtypes, including undifferentiated pleomorphic sarcoma (UPS) and embryonal rhabdomyosarcoma (eRMS), exhibit significant genetic heterogeneity and lack recurrent oncogenic driver mutations, complicating the development of broadly effective therapies. A promising strategy is to design targeted treatments for subsets of STS driven by specific tumor suppressor alterations. However, the molecular pathogenesis of UPS and eRMS remains poorly understood, limiting therapeutic progress. Germline and somatic mutations in BRCA1-associated protein 1 (BAP1), an epigenetic regulator, have been linked to multiple STS subtypes, yet its role in suppressing sarcoma development is unclear. Using a murine model, we recently identified BAP1 deletion as a driver event in STS development. This model provides a platform to dissect BAP1's functional role and to explore novel therapeutic strategies.

Methods: We established well-characterized Bap1-deficient sarcoma cell lines derived from mouse models of STS driven by somatic deletion of Bap1 and Trp53. A high-throughput epigenetic inhibitor screen using the CellCyte proliferation assay was performed to identify the most effective inhibitors. Additional approaches included syngeneic and primary sarcoma mouse models, CRISPR/Cas genetic tools, flow cytometry, multiplex immunohistochemistry (IHC), single-cell RNA sequencing, and bulk RNA sequencing to evaluate the impact of epigenetic inhibitors on Bap1-driven STS and its immune-suppressive microenvironment.

Results: Bap1-deficient sarcoma cells exhibited marked sensitivity to several potent epigenetic inhibitors, including histone deacetylase inhibitors (HDACi), bromodomain and extra-terminal domain inhibitors (BETi), and histone demethylase inhibitors. Studies assessing their effects on the immune-suppressive microenvironment are ongoing.

Conclusion: Our findings establish Bap1 deficiency as a driver of STS development and reveal that Bap1-deficient sarcomas are highly susceptible to epigenetic inhibition. These results lay the foundation for translating epigenetic therapies into effective treatment strategies for patients with Bap1-driven STS, a population currently lacking targeted options.

#0615 AMBRA1-mediated nucleocytoplasmic control promotes early onset of liver cancer.

Yimiao He[1], Linglin Liu[2], Yunong Xie[1], Minghe Zhang[1], Yan Liu[1], **Man Tong**[3]

[1]The Chinese University of Hong Kong, Shatin, Hong Kong,[2]The Chinese University of Hong Kong, Hong Kong SAR, China,[3]The Chinese University of Hong Kong, Hong Kong, Hong Kong

Hepatocellular carcinoma (HCC) is one of the leading causes of cancer-related mortality worldwide, largely driven by uncontrolled cell proliferation and the loss of tumor suppressor activity in the liver. By analyzing publicly available genome-wide CRISPR screening datasets, we identified AMBRA1 as a strong anti-proliferative candidate. Analysis of a clinical HCC patient cohort revealed that AMBRA1 expression was significantly reduced in tumor tissues, and its downregulation was tightly associated with poor patient outcomes. The downregulation of AMBRA1 was consistently validated in multiple HCC mouse models established through somatic mutations and high-fat diet challenge at early stages. Functionally, CRISPR-mediated knockout of AMBRA1 accelerated early spontaneous liver tumor initiation in vivo. AMBRA1 co-immunoprecipitated with key proteins involved in nucleocytoplasmic transport, suggesting a novel function for AMBRA1 in modulating nucleocytoplasmic trafficking in HCC. Collectively, our findings establish AMBRA1 as a bona fide tumor suppressor with clinical and functional importance in HCC.

#0616 Making sense of mis-sense and non-sense: Tumor cells hijack mutation-induced mis-localization of tumor suppressors.

Murali Dharan Bashyam[1], Sanjana Sarkar[2], Jimlee Saikia[1]

[1]Laboratory of Molecular Oncology, BRIC-Centre for DNA Fingerprinting and Diagnostics (BRIC-CDFD), Hyderabad, India,[2]BRIC-Centre for DNA fingerprinting and Diagnostics (BRIC-CDFD), Hyderabad, India

The SWI/SNF chromatin remodeler utilizes energy of ATP hydrolysis to slide or evict nucleosomes or histones, thus enabling nuclear processes by driving an 'open' chromatin architecture. The mammalian SWI/SNF, also termed the BrG1/Brm associated factor (BAF) complex, is the major chromatin remodeler in ontogeny and adult life. Three biochemically distinct BAF complexes namely canonical (cBAF), polybromo (PBAF), and non-canonical (ncBAF) have been characterized. BAF components, classified as canonical nuclear tumor suppressors, exhibit frequent inactivating mutations in cancers. Though, several studies have evaluated the functioning of BAF subunits, very few have attempted to characterize the role of BAF component mutation identified across cancer types. In our previous studies, we identified early-onset rectal cancer specific truncation mutations in the gene encoding the PBAF component 'A-T rich interaction domain containing 2' (*ARID2*), precluding its nucleal localization signal (NLS). These truncations were also identified across cancer types based on analysis of cancer mutation databases. NLS-inactivated ARID2 exhibited cytoplasmic localization (cARID2) and promoted tumorigenesis in colorectal, breast and lung cancer cell lines. Here, we present detailed mechanistic characterization of ARID2 truncations, presumed to be inactivating in nature, but exhibiting a gain of oncogenic function. We show that the glutamine rich GLN domain (amino acids 793-1128) is essential for the oncogenic function of cARID2. Tandem affinity purification mass spectrometry identified PBAF components in the interactome of wild-type but not of cARID2, as expected. More importantly, a novel interaction between cARID2 (but not wild type ARID2) and AKAP8L, validated using biochemical approaches. cARID2 devoid of the GLN domain, did not interact with AKAP8L. AKAP8L belongs to the AKAP95 domain containing family of proteins that interact with and activate protein kinase A (PKA) leading to oncogenic activation of CREB signalling. Further, cARID2 effected an increase in the phosphorylated (active) form of CREB and in transcript levels of canonical CREB targets including ATF3, ATF4, and CREM, indicators of activation of the CREB signalling axis. AKAP8L itself was shown to activate oncogenesis in CRC cells. Analysis of RNA Sequencing is currently underway to confirm the activation of the PKA/CREB oncogenic signalling by cARID2. Nude mice xenograft assays are also underway to confirm the oncogenic potential of cARID2. Overall, the findings reveal a Yin-Yang tumor suppressor/oncogenic role for ARID2 in cancer, similar to our previous discovery for ARID1B, an ARID2 paralogue. More importantly, our study has revealed novel therapeutic options for tumors exhibiting cytoplasmic ARID2.

#0617 OSTM1 is a ubiquitin E3 ligase that suppresses B-cell malignancy by activating the cAMP/PKA pathway.

Muhammad Usama Tariq[1], Namratha Sheshadri[1], Julia Shen[1], Jaeyong Jung[1], Rongrong Li[1], Kevin Lu[2], Junrong Yan[1], Mark Koch[3], Hassan Sajjad[1], Barbara Rosati[3], Giuseppe Caso[3], Richard LIN[3], Brinda Vallat[1], Stephen Burley[1], Tong Liu[4], Hong Li[4], Christian Hinrichs[1], Jun Wang[1], Lynn Wang[5], Jean Vacher[6], Ping Xie[7], Wei-Xing Zong[1]

[1]Rutgers University - New Brunswick, New Brunswick, NJ,[2]Rutgers Graduate School of Biomedical Sciences, Paramus, NJ,[3]Stony Brook, Stony Brook, NY,[4]New Jersey Medical School, Newark, NJ,[5]Fox Chase Cancer Center, Philadelphia, PA,[6]Montreal clinical research institute, Montreal, QC, Canada,[7]Rutgers University - New Brunswick, Piscataway, NJ

Osteoclastogenesis-associated transmembrane protein 1 (OSTM1) is a membrane-integral glycosylated protein that regulates lysosomal homeostasis and osteoclast maturation. Its loss-of-function mutations cause autosomal recessive osteopetrosis (ARO). In addition, OSTM1 was described as a putative ubiquitin E3 ligase yet with ill-defined substrates and biological functions. Using a whole-genome CRISPR/Cas9 screening in the interleukin-3 (IL3)-dependent Ba/F3 murine pro-B cell line, we identified OSTM1 whose silencing confers IL3-independent growth and in vivo transformation of Ba/F3 cells. In humans, OSTM1 is frequently deleted or downregulated across a wide range of B cell malignancies. In mice, B cell-specific monoallelic and biallelic ablations of Ostm1 cooperates with Cdkn2a ablation to drive lymphomagenesis with a near 100% penetrance. Mechanistically, a fraction of OSTM1, non-glycosylated and cytosol located, acts as an E3 ligase and interacts with phosphodiesterase 3B (PDE3B) to promote its proteasomal degradation. As PDE3B catalyzes the conversion of cAMP to AMP hence negatively regulates the cAMP-dependent PKA/CREB/CREBBP tumor suppressive pathway, loss of OSTM1 leads to PDE3B stabilization and increased cell growth. Together, our findings uncover OSTM1 as a tumor-suppressive E3 ligase by promoting the proteasomal degradation of PDE3B and activating the cAMP-dependent PKA pathway.

#0618 Evaluating the role of choline acetyltransferase (ChAT) in T cell malignancies.

Arwa Hilal[1], Maureen A. Cox[2], Michael St. Paul[3], Tak W. Mak[4]

[1]Immunology, University of Toronto, Toronto, ON, Canada,[2]University of Oklahoma Health Sciences Center, Oklahoma City, OK, Canada,[3]University of Toronto, Toronto, ON, Canada,[4]UHN Princess Margaret Cancer Centre, Toronto, ON, Canada

Acetylcholine (ACh) is a classical neurotransmitter increasingly recognized for its immunoregulatory roles. Beyond neural tissues, activated T cells express choline acetyltransferase (ChAT), enabling the local synthesis and release of ACh, which acts through nicotinic and muscarinic receptors to modulate activation, cytokine production, and vascular tone. While this pathway can dampen inflammation and sustain immune homeostasis, its function within malignant T cells remains poorly understood. PTEN loss, a hallmark of aggressive T cell malignancies, constitutively activates the PI3K-Akt pathway to promote unchecked growth and survival. We hypothesized that tumour-intrinsic ChAT restrains these Akt-dependent stress responses, serving as an intrinsic brake on malignant progression. Using a conditional T cell PTEN-deficient mouse model, we found that ChAT is upregulated at specific thymocyte developmental stages that coincide with PI3K Akt hyperactivation, and that ChAT-positive thymocytes in the pre-malignant PTEN-deficient setting display higher activation marker expression and a more activated developmental phenotype compared to ChAT-negative cells. Loss of ChAT in the PTEN-null background further increases pAkt levels and alters early activation markers, which is consistent with a shift toward heightened oncogenic stress. Functionally, deleting T cell-specific ChAT in this model shortens lymphoma survival in an allele dosage-dependent manner, indicating that endogenous cholinergic activity provides a measurable constraint on tumour aggressiveness. Together, these findings support a model in which cholinergic signalling intersects with oncogenic PI3K Akt activity in T cell malignancy. This proposal will define the cellular, molecular, and therapeutic relevance of this interaction, with the overall goal of identifying cholinergic pathways as new entry points for modifying tumour evolution in PTEN-deficient T cell cancers.

: Developmental Origins, Drivers, and Heterogeneity in Pediatric Cancer
Poster Session

#0622 Infant *KMT2A::AFF1* acute lymphoblastic leukemia stem cell model reveals early impact on the proteome.

Alexandra Prosser-Dombrowski[1], Irina Pushel[1], Priyanka Prem Kumar[1], Thomas Gremminger[2], Michaella Rekowski[2], Midhat S. Farooqi[3], Michael Washburn[2], Jay L. Vivian[1], John M. Perry[1]

[1]Children's Mercy Kansas City, Kansas City, MO,[2]The University of Kansas Medical Center, Kansas City, MO,[3]Children's Mercy Research Institute, Kansas City, MO

Infants with acute lymphoblastic leukemia (iALL) are at high risk of early relapse, rapid progression, and poor survival despite intensive therapies. Rearrangement of *KMT2A* (*KMT2A*-r) is an established feature of these cases, creating a fusion oncogene that leads to epigenomic dysregulation. Genomic studies have failed to find collaborating oncogenic drivers that would explain why infants have such a high risk of relapse compared to older patients with the same rearrangement. To expand our understanding of *KMT2A*- driven leukemogenesis, we applied global proteomic profiling to identify potential nongenomic drivers that could provide novel therapeutic targets.For this study, we performed proteomics with our human inducible pluripotent stem cell model (iPSC) of *KMT2A*-r iALL. We have engineered this model with a human *KMT2A*-r transgene construct (rearranged with the most common partner *AFF1*) incorporated with an established doxycycline (dox) regulated platform. These cells tightly express the *KMT2A::AFF1* transgene only in response to dox treatment. We have developed functional hematopoietic stem cells (HSPC) that we have induced with dox to express *KMT2A*-r and represent the preleukemic state. With replicates of dox-induced *KMT2A::AFF1* HSPC and of non-dox control, we generated proteomic profiles via data independent acquisition (DIA) using the timsTOF HT (Bruker). Data were searched in DIA-NN using the Bruker spectral library and human protein database downloaded from Uniprot on 05-05-2024. Data analysis was performed in R 4.3.3 including differential expression analysis using limma 3.58.1, pathway enrichment using gProfiler 0.2.3, and network analysis using STRING 12.0.Differential expression analysis identified 149 proteins with higher and 381 proteins with lower expression in *KMT2A*-r HSPC as compared to the control ($p < 0.05$, $|log2FC| > 1$). Histone binding is a top upregulated pathway of proteins with the most significance (adjusted $p < 0.05$), which is what we would expect with induction of a epigenomic regulator. Pathways downregulated in *KMT2A*-r HSPC largely involve the extracellular environment (for example, cell adhesion mediator activity, collagen binding, extracellular matrix organization). STRING analysis of the downregulated proteins also demonstrates a prominence of extracellular factors (i.e. MFAP4, L1CAM, COL5A1). Comparison to bulk RNA sequencing on the model at the same timepoint reveals protein expression correlates with gene expression about half of the time. Phosphoproteomics has been performed and is currently being analyzed for further comparison. Preleukemic *KMT2A*-r HSPC demonstrate early changes in the proteome that suggest the extracellular environment may play a key role in leukemogenesis. With further validation and testing of these factors, we will aim to identify essential drivers that may provide new therapeutic targets for this devastating disease.

#0623 Targeting PAX3::FOXO1 condensates in fusion-positive alveolar rhabdomyosarcoma via disordered-region mimetic peptides.

Michael Di Martino, Yanghao Zhong, Shasha Chong

Division of Chemistry and Chemical Engineering, California Institute of Technology, Pasadena, CA

Background: PAX3::FOXO1 (P3F1) is a fusion oncoprotein that drives fusion-positive alveolar rhabdomyosarcoma (aRMS), a highly lethal pediatric cancer with <30% 5-year survival in high-risk patients. Targeted therapy development has been limited by P3F1's largely disordered structure and poorly understood interaction mechanisms. Recent work has shown that short peptides targeting intrinsically disordered regions (IDRs) can disrupt transcriptional hubs and impair tumor growth, but this strategy requires identifying key interaction partners that often regulate other signaling pathways. We previously discovered that P3F1 demonstrates a neomorphic hub formation propensity that corresponds with its transcriptional activity, suggesting that disrupting these hubs can hinder said activity.
Purpose: To design short peptides modelled from the P3F1 IDR itself that disrupt P3F1 hubs and suppress P3F1-mediated transcription and aRMS cell proliferation.
Experimental Procedures and Results: Using the LacO array assay, an established in-cellulo method that quantifies IDR interaction strength, we discovered that truncating the P3F1 392-510 region significantly decreased IDR interaction strength. Further, the same truncation significantly altered its interaction strength with p300, a key transcriptional coactivator known to promote P3F1's function. Finally, dual luciferase assay results showed that a 392-510 deletion significantly decreased P3F1's transactivation ability. Taken together, this suggested that P3F1 392-510 is a key interaction hotspot that influences its transcriptional capability. Sequence analysis revealed that P3F1 392-510 is enriched in cationic and aromatic residues, consistent with cation-π and π-π interactions common in IDRs. FINCHES interaction mapping showed that mutating either all cationic or all aromatic residues in this region reduces P3F1 homotypic interactions, with aromatic-to-alanine mutations producing the stronger effect. Ongoing experiments utilizing the LacO array assay are probing these interaction modes to guide the design of optimized P3F1 392-510 peptide mimics.
Conclusions: P3F1 392-510 is critical for P3F1's IDR-mediated interactions and transcriptional activity. Its cationic and aromatic composition suggests cation-π and/or π-π interactions as key interaction modes. Future work will experimentally dissect these interaction modes and develop peptide inhibitors informed by this mechanistic insight.

#0625 Early tumor priming in Li-Fraumeni Syndrome muscle using a rhabdomyosarcoma model.

Ashby Kissoondoyal, Paula Rosanna Quaglietta, Brianne Laverty, David Malkin

The Hospital for Sick Children, Toronto, ON, Canada

Li-Fraumeni Syndrome (LFS), caused by germline *TP53* mutations, markedly increases the risk of developing rhabdomyosarcoma (RMS) and other childhood cancers, often emerging during early neonatal life. This early onset, in conjunction with findings that genomic alterations occur well before cancer onset in LFS, strongly suggests malignant transformation in LFS begins during embryogenesis, within developmental windows where differentiation is normally tightly regulated. Despite the developmental connection to LFS tumorigenesis, mechanisms through which inherited *TP53* dysfunction perturbs embryonic muscle development to create tumor-permissive states are not well understood. Using LFS-associated RMS (LFS-RMS) as a model, we examined how germline *Trp53* mutations alter myogenesis and predispose LFS muscle to tumorigenesis. We performed single-nuclei RNA sequencing (snRNA-seq) across LFS-RMS tumors, matched distal muscle, and healthy embryonic, postnatal muscle tissue from *Trp53*$^{R172H/+}$ (R172H) and wild-type (WT) littermates. To map accompanying genomic changes, we also generated deep (800x) whole-exome sequencing (WES) from these samples. The two datasets were integrated to identify genomic alterations that aligned with developmental transcriptional shifts observed in LFS. We identified a reproducible myogenic LFS-RMS signature enriched for WNT signaling, RNA metabolic pathways, and glycolytic reprogramming. This signature was present in LFS-RMS tumors and elevated in R172H embryos during the peak of myogenesis (E12-E14). Further analyses revealed delayed myogenic maturation in LFS embryos and the presence of progenitor-like cell states that become enriched in LFS-RMS, indicating that tumor-relevant states arise during LFS embryogenesis. By integrating WES with snRNA-seq, we found that transcriptionally unstable developmental periods in LFS embryos overlap with early genomic alterations, suggesting that transcriptional and genomic disruptions emerge in parallel. By defining these molecular patterns, our work identifies early transcriptomic and genomic predictors of LFS-RMS and how germline *Trp53* mutations reshape developmental programs. Ongoing efforts include incorporating extra-embryonic tissues such as placenta and amniotic fluid to evaluate their potential as accessible prenatal cancer risk indicators. Ultimately, characterizing developmental progression in a germline *Trp53* mutant model will reveal the sequence of events that drive LFS-RMS. From these findings we can better and define windows of vulnerability and work towards a prenatal screening tool for LFS.

#0626 *TLX3* represses IKZF2 to activate PI3K/AKT signaling: A novel transcriptional axis driving leukemia initiation.

Gisele Rodrigues, Julie Hixon, Hila Winer, Timothy Gower, Francisco Lobo, Nathan Wong, Erica Matich, Steven Hsu, Emma Wachter, Elijah Edmondson, Maggie Cam, Caroline Andrews, Sarah Cramer, Wenqing Li, Scott Durum

NIH-NCI, Frederick, MD

Background/Methods: Despite major therapeutic advances, current treatment protocols for acute lymphoblastic leukemia (ALL) remain limited by toxicity and relapse, driving efforts to develop safer and more selective therapeutic strategies. We have shown that oncogenic IL7Rα mutations (mutIL7R) occur in approximately 10 percent of ALL cases but require cooperating lesions to induce transformation. In a related context, IL-7R signaling pathway components are also recurrent in mixed phenotype acute leukemia (MPAL), where they frequently coincide with TLX3 dysregulation. However, the mechanism by which TLX3 cooperates with mutIL7R remains unknown.

Results: In this study, we first show that co-expression of TLX3 and mutIL7R in murine double-negative thymocytes induces aggressive mixed-lineage leukemia within three weeks following transplantation into Rag1 knockout mice. We then integrated single-cell RNA-seq, CITE-seq, and TCR beta repertoire analysis and observed that Helios (IKZF2) is specifically downregulated by TLX3. Mechanistically, TLX3-mediated repression of IKZF2 amplifies PI3K/AKT signaling. Enforced IKZF2 expression suppressed AKT phosphorylation, whereas IKZF2 knockdown enhanced it, establishing IKZF2 as a key regulator that limits PI3K/AKT signaling downstream of TLX3 and mutant IL7R. Leukemia serial transplantation further demonstrated increasing disease aggressiveness and a lineage shift from mixed T or myeloid to B-like phenotypes, recapitulating the plasticity observed in patient MPAL.

Conclusions: Our data identify TLX3 and mutant IL7R as cooperative drivers that reprogram transcriptional and signaling landscapes, linking lineage plasticity with oncogenic PI3K/AKT activation. Taken together, our results define the IL7R-TLX3 leukemogenic program, revealing a targetable vulnerability in TLX3-positive and mutIL7R-positive leukemias and providing a strong rationale for PI3K pathway-directed therapeutic intervention.

#0627 Investigating ATRT cell of origin and tumor heterogeneity via hiPSC-derived models.

Clark G. Wang[1], Qi Wang[2], Nidhi Nathwani[3], Bryan K. Li[4], Takayuki Morimoto[3], Alison D. Parisian[1], G. Praveen Raju[5], Frank B. Furnari[3]

[1]Biomedical Sciences Program, Division of Regenerative Medicine, Department of Medicine, University of California San Diego, La Jolla, CA,[2]Department of Bioengineering, University of California San Diego, La Jolla, CA,[3]Division of Regenerative Medicine, Department of Medicine, University of California San Diego, La Jolla, CA,[4]Department of Pediatrics, University of California San Diego, La Jolla, CA, Division of Pediatric Hematology/Oncology, Rady Children's Hospital, San Diego, CA,[5]Department of Neurosciences, University of California San Diego, La Jolla, CA, Rady Children's Health, San Diego, CA

Atypical teratoid rhabdoid tumors (ATRTs) are rare, highly malignant pediatric brain cancers that almost always result from biallelic inactivation of *SMARCB1*, a core subunit of the SWI/SNF chromatin remodeling complex. Despite presenting a remarkably simple genome defined by SMARCB1 loss, ATRTs are molecularly diverse, consisting of three subgroups with distinct DNA methylation profiles, transcriptomes, and clinical outcomes, suggesting differences in cells of origin and unique mechanisms of oncogenesis. Neural progenitor cells (NPCs) and neural crest cells (NCCs) have been proposed as potential cells of origin, with NPCs aligning more with the ATRT-SHH subgroup. On the other hand, NCCs may account for the molecularly identical extracranial malignant rhabdoid tumors as well as the remaining intracranial subgroups, ATRT-TYR and ATRT-MYC, which have suspected extra-CNS origins. To study SMARCB1 loss in a genetically defined neural progenitor cellular context, our lab previously engineered human induced pluripotent stem cells (hiPSCs) with doxycycline (DOX)-inducible *SMARCB1* knockdown. NPCs derived from these hiPSCs, that were differentiated without *SMARCB1* expression, exhibited an ATRT-SHH subgroup transcriptome and formed orthotopic tumors. Building upon these findings, these engineered hiPSCs were differentiated into neural crest cells. In comparison with isogenic controls, neural crest cells differentiated without *SMARCB1* expression acquired a proliferative phenotype, enhanced clonogenic potential, and became arrested in a “progenitor” state by maintaining expression of neural crest differentiation pathway genes. Furthermore, *SMARCB1* knockdown during neural crest differentiation upregulated target genes of REST, a transcription factor that is enriched in ATRT-MYC. In contrast, REST target genes were found to be downregulated in SMARCB1-depleted NPCs, highlighting the impact of cell identity upon phenotypes and the utility of hiPSC-derived models for investigating mutations within different clinically relevant cellular contexts. Future work aims to orthotopically engraft SMARCB1-depleted NCCs and characterize chromatin accessibility of SMARCB1 loss within NPCs versus NCCs via ATACseq. Furthermore, since recent findings suggest that the p53 pathway is often suppressed in rhabdoid tumors via MDM2 overexpression, MDM2 and a dominant-negative p53 mutant will be introduced individually into this model to determine whether p53 pathway inactivation cooperates with SMARCB1 loss within these cellular contexts.

#0628 Investigating the role of *BRCA2* in the development of pediatric rhabdomyosarcoma.

Phillip Adam Weinstein[1], Elif Asik[1], Pagna Sok[1], Cem Ozdemir[2], Wei-Che Tseng[2], Ryan Zabriskie[1], Aniko Sabo[1], Philip J. Lupo[2], Alison A. Bertuch[1], Kyle Miller[2], Sharon E. Plon[1]

[1]Baylor College of Medicine, Houston, TX,[2]Emory University School of Medicine, Atlanta, GA

Introduction: In a large-scale exome sequencing study of pediatric rhabdomyosarcoma (RMS) patients (n=615), we identified a statistical enrichment of patients with germline pathogenic variants in *BRCA2 (Li et al., JNCI, 2020)*. However, paired tumor-normal investigations of pediatric cancers have demonstrated that pediatric tumors do not typically exhibit somatic loss of *BRCA2*, a departure from what is typical of adult cancers which result in profound homologous recombination (HR) deficiency. These findings prompted our multi-pronged study to assess the role of heterozygous *BRCA2* variants in the development of pediatric RMS.

Methods: All patient samples were obtained from ongoing Children's Oncology Group protocols. As part of the Gabriella Miller Kids First Program, paired tumor-normal whole genome sequencing and somatic RNA sequencing of RMS patients was conducted at HudsonAlpha. This included a subset of the initially detected six patients with germline *BRCA2* variants. As a potential precursor model for RMS, we engineered *BRCA2* loss-of-function (LOF) variants in immortalized mesenchymal stem cell (MSC) lines. We used CRISPR to induce frameshift alleles in exons 10 and 11 (c.1345dup and c.5680del) and prime editing to create two RMS patient-specific LOF variants in exons 5 and 17 (c.7857G>A and c.462_463del), followed by DNA repair and genomic stability assays of the recombinant cell lines.

Results: Evaluation of three RMS tumors from patients with germline *BRCA2* variants was negative for loss-of-heterozygosity at *BRCA2*, additional somatic *BRCA2* mutations, or decrease in *BRCA2* expression. However, these tumors showed evidence of modest decrease in homologous recombination (HR) relative to other age-matched RMS tumors (n=21), measured via the DirectHRD pipeline. The *BRCA2* heterozygous MSC cell lines demonstrate equivalent overall DNA double-strand break repair capacity but significantly diminished HR activity when assayed by integrating larger (700bp) repair cassettes, and increased micronucleus formation after treatment with ionizing radiation. Despite these functional impairments, we found no change in response to targeted therapies, including the PARP inhibitor olaparib and newer generation polymerase theta inhibitors.

Conclusions: Through RMS tumor analysis and *in vitro* assays, we observed modest HR impairment resulting from heterozygous *BRCA2* mutations, but to a lesser extent than seen in adult cancers with complete loss of *BRCA2* and PARP sensitivity. These findings support a model where heterozygous germline variants in *BRCA2* modestly increase genomic instability, leading to an increased risk of pediatric RMS and may explain other pediatric tumors where enrichment of *BRCA2* germline variants has been described.

#0629 SMARCD3-regulated Purkinje cell migration underlies cerebellar development and group 3 medulloblastoma metastasis.

Yash Patel[1], Han Zou[1], Allen Zheng[2], Anjali Talluru[2], Nirja Divekar[2], Chaim Sneiderman[1], Meghana Dodda[2], Katie Dietrich[2], Siheng Chao[2], Sameer Agnihotri[3], Gary Kohanbash[3], Antony Michealraj[3], Ian Pollack[3], Baoli Hu[3]

[1]University of Pittsburgh School of Medicine, Pittsburgh, PA,[2]University of Pittsburgh, Pittsburgh, PA,[3]Department of Neurological Surgery, University of Pittsburgh, Pittsburgh, PA

Medulloblastoma (MB) is a heterogeneous brain tumor arising in the cerebellum and is the most common malignant pediatric brain tumor. Group 3, one of four molecular MB subgroups (WNT, SHH, Group 3, and Group 4), is the most aggressive and malignant type in children, usually characterized by metastasis at diagnosis. In this study, we identify that SMARCD3/BAF60c (SMARCD3 hereafter), a core component of the SWI/SNF chromatin-remodeling complexes, is highly expressed in Group 3 MB and Purkinje cells (PCs) of the developing cerebellum. Elevated SMARCD3 expression is associated with poorer patient outcomes, MB metastasis, and activation of the Disabled1 (DAB1)-Reelin signaling pathway that is required for PC migration and positioning during cerebellar development. Conditional SMARCD3 deletion in early PCs results in embryonic and early postnatal lethality in mice, and the surviving animals exhibit significant deficits in motor coordination and balance. Immunostaining of SMARCD3 deleted murine cerebellar tissue shows disorganized PC alignment and reduced dendritic branching, confirming the critical role of the SMARCD3-Reelin pathway function in PC migration, positioning, and maturation. These data demonstrate that the SMARCD3-associated SWI/SNF chromatin-remodeling complex regulates Reelin signaling pathway in PC migration and positioning during cerebellar development; however, this neurodevelopmental program is hijacked to promote MB metastatic dissemination. To further understand this mechanism, we analyzed spatiotemporal gene expression and chromatin accessibility data of the human and mouse cerebellum, noting the SMARCD3/Reelin signaling decreased in the mature cerebellum, but is highly upregulated in metastatic medulloblastoma. The study provides compelling functional evidence of SMARCD3 and the associated SWI/SNF complexes' involvement in cerebellar development, tumor metastasis, and the molecular connections between early brain development and tumorigenesis, offering new rationales for the development of innovative therapies for patients with MB.

#0630 Elucidation of PAX3::FOXO1 tumor initiation mechanisms in human induced pluripotent stem cell models.

Bradley T. Stevens, Yang Zhang, Brian J. Abraham, Mark E. Hatley

St. Jude Children's Research Hospital, Memphis, TN

Rhabdomyosarcoma (RMS) is the most common pediatric soft tissue sarcoma. Alveolar RMS (ARMS) is driven by either t(2;13)(q35;q14) or t(1;13)(p36;q14) resulting in the PAX3-FOXO1 (P3F) and PAX7-FOXO1 (P7F) fusion oncoproteins, respectively and has a poor prognosis. A deeper understanding of P3F mediated tumorigenesis is needed to discover novel targets. Current model systems fail to recapitulate the human disease in terms of timing, location, and the formation of other tumor types. Previously, our lab generated an ARMS model system derived from human induced pluripotent stem cells (iPSCs), in which forced P3F expression during endothelial directed differentiation blocked endothelial maturation instead reprogramming cells to skeletal muscle-like that form ARMS tumors in mice. Building off this model, we generated a doxycycline inducible iARMS model driven by degradable P3F-FKBP12^{F36V} (ddP3F cells) allowing for fine control over P3F expression. Degradation of P3F did not significantly reduce viability or proliferation but reduced the ability of ddP3F cells to undergo myogenic differentiation. P3F-negative ddP3F cells continued to proliferate for multiple passages and retained the ability to form foci. Transcriptional analyses revealed ARMS cell states remained stable upon P3F loss. Taken together, this data shows that P3F is important for ARMS fate initiation but not maintenance, indicating further examination of the initiation event was needed for insight into ARMS biology. To elucidate the P3F-mediated initiation mechanism, I turned to our previously established iARMS model. I utilized CUT&RUN for P3F and H3K27ac to assess P3F occupancy and enhancer landscape and RNA-seq to assess gene expression changes at timepoints throughout the transformation event. Analysis of this data revealed that ARMS fate commitment occurred within two days of P3F expression that was reinforced throughout the time course. Mechanistically, P3F established a novel enhancer landscape resulting in the early expression of one myogenic and a few neural transcription factors (core TFs). Single cell multiome profiling confirmed early fate commitment and revealed heterogeneous expression of the core TFs. Taken together, these data show that P3F initially establishes cell fate through enhancer landscape alterations with both myogenic and neural transcription factors but not necessarily in the same cells. Overall, our novel cellular models revealed insights into P3F independent maintenance of ARMS cell fate, uncovered a mechanism of P3F-mediated establishment of ARMS cell state, and provides a platform to dissect the specific dependencies required for ARMS cell state. Understanding the fundamental mechanism of ARMS tumorigenesis provides greater resolution into the key disease determinants to generate better model systems, focus pre-clinical efforts, and identify novel targets.

#0631 Trans-species analysis of central nervous system developmental-specific replication repair deficiency reveals differential patterns of gliomagenesis and response to immunotherapy.

Zoya Aamir, Melissa A. Galati, Emma Gattoni, Owen Crump, Nemanja Ilic, Anirban Das, Nicholas R. Fernandez, Angel K. Q. Wong, Lucie Stengs, Jose R. Dimayacyac, Yuan Chang, Vanessa Bianchi, Melissa Edwards, David Malkin, Cynthia Hawkins, Nuno M. Nunes, Uri Tabori

Sick Children's Hospital, Toronto, ON, Canada

Introduction: Replication repair deficiency (RRD) is a pan-cancer mechanism caused by germline and/or somatically acquired mutations in the replication repair machinery - DNA polymerase proofreading and the mismatch repair (MMR) system. Germline monoallelic (Lynch Syndrome, LS) or biallelic (Constitutional Mismatch Repair Deficiency, CMMRD) mutations in MMR genes are present in 5-10% of glioblastomas in children, adolescents, and young adults. RRD gliomas are lethal, chemoradiation-resistant cancers, characterized by universal hypermutation and variable susceptibility to immune-checkpoint inhibition (ICI). These tumors exhibit variability in patient age of onset, type, location, and response to ICI.

Methods: To understand the clinical and biological differences associated with RRD central nervous system (CNS) tumors, we used germline mutations and brain development-specific *Cre*-drivers to generate murine models that recapitulate the phenotypic and genomic characteristics of each human RRD subgroup: **1) MMRD+PPD** (*Nestin*- and *Olig2-Cre*$^{+}$*/ Msh2*$^{LoxP/LoxP}$*/Pole*$^{S459F/+}$ and *LSL-Pole*$^{P286R/+}$): MMR-deficiency (MMRD) in combination with polymerase proofreading deficiency (PPD). **2) MMRD-only** (*Nestin-Cre*$^{+}$*/Trp53*$^{LoxP/LoxP}$ and *Msh2*$^{LoxP/LoxP}$ or *Mlh1*$^{-/-}$): MMRD lacking PPD associated with *TP53* mutations.

Results: Using trans-species comparative approach, we elucidated a mechanistic model of RRD-driven brain tumorigenesis. We revealed that the cell-of-origin significantly contributes to determining brain tumor type, location, and age of tumor onset, suggesting a strong impact of early- or late-RRD mutational onset in shaping tumor biology ($p<0.0001$). Importantly, using murine neural stem cells, we discovered that germline mutagenesis onset directly influences timeline of brain tumor formation and survival between CMMRD and LS patients ($p<0.05$). We further demonstrate the interplay between *POLE* mutations and MMRD status in modulating the likelihood of brain tumorigenesis in both species. To understand the interaction between hypermutation and the immune system, we characterized the tumor immune microenvironment in spontaneously forming tumors. We uncovered subgroup-specific immune landscapes, with $CD8^{+}$ T cell activity emerging as a key modulator in controlling brain tumor growth ($p<0.0001$), suggesting an underlying mechanism that may inform therapeutic strategies in RRD patients.

Significance: Altogether, our models accurately mimic the human condition, providing a mechanistic framework of RRD-driven brain tumorigenesis, optimization of subgroup-tailored immunotherapy approaches, and putative surveillance protocols.

#0632 Dynamic characterization of tumor-microenvironment factors that drive pediatric low-grade gliomas.

Jenna Robinson[1], Joohee Lee[1], Sarah Reel[2], Shriya Rangaswamy[1], Michelle Boisvert[1], John Doench[3], David TW Jones[4], Timothy Phoenix[2], Pratiti Bandopadhayay[1]

[1]Dana-Farber Cancer Institute, Boston, MA,[2]University of Cincinnati, Cincinnati, OH,[3]Broad Institute, Cambridge, MA,[4]DKFZ, Heidelberg, Germany

Pediatric low-grade gliomas (pLGGs) are the most common brain cancers diagnosed in children, often leading to life-long neurological impairments. Whilst targeted inhibitors exist, their effects are often short-lived, highlighting the urgent need for innovative treatments. Notably, some pLGG tumors spontaneously regress with age, suggesting that changes in the tumor microenvironment can arrest tumor growth. In this work, we aim to characterize which signaling interactions promote the growth of pLGG cells and how these interactions change dynamically with time. To achieve this, we have optimized a protocol for introducing pLGG mutations into developing mouse brains via in utero electroporation. This study revealed that brains harboring the common *KIAA1549::BRAF* fusion mutation have a striking phenotype characterized by increased astrocyte reactivity and myeloid cell infiltration. To better understand how signals derived from immune cells may impact pLGG cell fitness, we are additionally performing a high-throughput cytokine screen. We are developing barcoded cytokine constructs tethered to the cell membrane to comprehensively screen the impact of cytokine signaling on the growth of neural stem cells engineered to overexpress common pLGG mutations. Together this work aims to unravel which signaling factors govern the age-dependent growth of pLGG tumors, which may reveal targetable aspects of the tumor microenvironment amenable to therapeutic intervention.

#0633 AVIL's dependency on YAP as a key mediator of oncogenic activity offers a therapeutic opportunity in rhabdomyosarcoma.

Martyna Glowczyk-Gluc, Robert Cornelison, Zhongqiu Xie, Julie Fanburg-Smith, Robin D. LeGallo, Eyas Alzayadneh, Hui Li

University of Virginia, Charlottesville, VA

Rhabdomyosarcoma (RMS) is a prevalent pediatric soft-tissue cancer with a survival rate below 27% for high-risk patients. Despite significant genetic differences among RMS subtypes, frontline therapy remains largely uniform and ineffective for metastatic and recurrent cases. After decades of research, targeted therapies are currently unavailable, underscoring the urgent need for novel targets and effective treatment strategies. Our previous published studies identified *AVIL* as a novel, *bona fide* RMS oncogene. *AVIL* encodes a calcium-regulated, actin-binding protein critical for actin cytoskeleton organization. While its expression in healthy adult tissue is limited, *AVIL* is aberrantly upregulated in RMS and correlates with poor patient prognosis. *AVIL* silencing significantly reduces cell proliferation and migration, induces cell death *in vitro*, and prevents tumor formation *in vivo*. Our recent studies reveal that AVIL functions upstream of the transcriptional coactivator YAP, a key regulator of proliferation, survival, and stemness that is frequently hyperactivated in RMS. Through integrated transcriptomic, biochemical, and imaging analyses, we discovered that AVIL promotes YAP nuclear translocation, enhances its transcriptional activity, and increases cellular sensitivity to YAP pathway blockade. Conversely, genetic silencing of *AVIL* disrupts YAP signaling and restores the expression of myogenic differentiation markers, implicating AVIL's role in maintaining the undifferentiated, proliferative state of RMS cells. Functionally, AVIL-high RMS cells exhibit enhanced response to pharmacologic YAP inhibition, while AVIL depletion diminishes this effect, underscoring a mechanistic dependency of AVIL-driven oncogenic programs on YAP signaling. *In vivo*, administration of a YAP inhibitor to patient-derived RMS xenografts with high AVIL expression significantly reduces tumor incidence compared with vehicle-treated controls. Together, these findings uncover a previously unrecognized mechanism by which AVIL modulates YAP activity in RMS, revealing a therapeutically actionable axis that sustains tumor growth and impedes myogenic differentiation.

#0634 Subpopulations of CAF contribute to chemotherapy resistance in tumors through different MYCN-dependent and independent mechanisms.

Kevin Louault[1], Laurence Sarte[1], Liron D. Grossmann[2], Bruce Pawel[1], John M. Maris[3], Shahab Asgharzadeh[1], Yves Albert DeClerck[1]

[1]Children's Hospital Los Angeles, Los Angeles, CA,[2]Edmond and Lily Safra Children's Hospital, Tel-Hashomer, Israel,[3]Children's Hospital of Philadelphia, Philadelphia, PA

Cancer-associated fibroblasts (CAF) are among the most prevalent non-malignant cell subtypes in the tumor microenvironment (TME) of neuroblastoma (NB). CAF cooperate with tumor-associated macrophages to promote therapeutic escape in many cancers including NB. CAF are heterogeneous and several subpopulations have been described based on specific transcriptomic signatures. In recent work, we show by single cell (sc)RNA sequencing the presence of different subpopulations of CAF in human NB tumors, including myofibroblasts (myCAF), inflammatory (i)CAF, dividing (d)CAF and vascular (v)CAF. However, the specific functions of these sub-populations are not entirely known because of difficulties in isolating CAF subpopulations. Here, we have isolated by flow cytometry and characterized two subpopulations of CAF from human NB tumors based on their expression of the receptor for platelet-derived growth factor-beta (PDGF-Rβ) and CD29 (Integrin β1). We show that these sub-populations maintain a stable phenotype *in vitro* (for at least 31 days) allowing to study their specific function. According to their gene and protein expression, PDGF-Rβ+/CD29- cells were identified as myCAF and CD29+/PDGF-Rβ- cells as iCAF. myCAF secreted TGF-β1 and activated a TAK1/NF-κB signalling pathway in NB cells, whereas iCAF secreted interleukin (IL)-6 and IL-8 and activated STAT3 in NB. We discovered that both subpopulations enhanced resistance to doxorubicin and etoposide but through different paracrine mechanisms. myCAF increased the expression of multi-drug resistance proteins MRP1 and MDR1 via a TGF-β/TAK1/NF-κB signalling pathway, and iCAF increased the expression of anti-apoptotic proteins BCL-xL and BCL2 via an IL-6/STAT3 signalling pathway. Furthermore, myCAF also activated an autocrine IL-6/STAT3 pathway in NB cells in a MYCN-dependent mechanism. A multiplex immunochemistry analysis of human NB revealed the presence of myCAF expressing PDGF-Rβ and iCAF expressing CD29 in TME-rich tumors but an absence of myCAF in TME-poor tumors. Our data highlights differences in the contribution of CAF subtypes to drug resistance and points to a potentially critical role of CAF in the emergence of therapeutic resistance.

#0635 Defining the intertumoral and intratumoral transcriptional heterogeneity of EWS::FLI1 in Ewing sarcoma.

Rachael Hinshaw[1], Zachary P. Tolstyka[1], Susan M. Kitchen-Goosen[2], Seneca Kinn-Gurzo[3], Rebecca Kaufman[3], Maggie Chasse[3], Elizabeth Wilson[3], Gretchen Lam[1], Stephanie The[1], Elissa Boguslawski[1], Patrick J. Grohar[1]

[1]Pediatrics, University of Michigan, Ann Arbor, MI,[2]Van Andel Institute (VAI), Grand Rapids, MI,[3]Children's Hospital of Philadelphia, Philadelphia, PA

Introduction: Ewing sarcoma (ES) is an aggressive pediatric bone and soft tissue cancer that is absolutely dependent on the EWS::FLI1 fusion transcription factor. Despite this dependency, ES tumors demonstrate substantial variability in EWS::FLI1 transcriptional activity both across tumors and within individual tumors. Here, we investigate the inter- and intra-tumoral heterogeneity of EWS::FLI1 and its functional importance.
Methods: We established a highly optimized siRNA knockdown protocol for EWS::FLI1 in 6 preclinical ES cell line models to achieve equal levels of suppression and evaluate differences in induced and repressed transcriptional targets and DNA binding events of EWS::FLI1. In order to investigate underlying mechanisms driving resistance, we employed state-of-the-art techniques including Cleavage Under Target (CUT&Tag), single nuclei RNA sequencing, and spatial transcriptomics of preclinical cell line models and ES patient samples to characterize the inter- and intra-tumoral heterogeneity of EWS::FLI1.
Results: Differential expression analysis of 6 cell lines with knockdown of EWS::FLI1, revealed that each cell line exhibited as many unique induced targets as shared ones, and repressed targets were even more cell line specific. The heterogeneity was functionally important as cell migration and migration signatures varied among the 6 models. Knockdown of EWS::FLI1 resulted in increased migration in one cell line and impaired migration in other cell lines. Intratumoral heterogeneity was also evident in single cell data with multiple transcriptional clusters evident in different proportions across the models. These different clusters also appear to be functionally important as at least two clusters resisted suppression by the EWS::FLI1 targeted agent, trabectedin, in patient samples collected on a recent trial. The heterogeneity was rooted in a combination of cell line specific EWS::FLI1 DNA binding events determined by CUT&Tag, cell specific copy number variants (CNV), and cofactor expression.
Conclusion: Our data suggests that EWS::FLI1 exhibits highly unique transcriptional activity between models which leads to a heterogeneous representation of target genes. In patients, EWS::FLI1 heterogeneity leads to the expression of a high-risk population of cells resistant to EWS::FLI1 targeting. We are working to understand mechanisms driving the high-risk population of ES cells and identify new druggable targets for these transcriptionally distinct tumor cell populations.

#0636 Dissecting the complex ecosystem of intracranial germ cell tumors by spatial RNA and protein analysis.

Torsten Pietsch[1], Verena Dreschmann[1], Pia Zapka[1], Evelyn Dorner[1], Christian Vokuhl[2]

[1]Institute of Neuropathology, University of Bonn Medical Center, Bonn, Germany,[2]Department of Pathology, University of Bonn Medical Center, Bonn, Germany

Background and Objectives: Central nervous system germinomas are characterized by a massive immune cell infiltrate. This inflammatory component can be so extensive that tumor diagnostics is challenging because of masking of the malignant germ cell tumor (GCT) component. Similarely, it is often difficult to detect other malignant components in mixed germ cell tumors that dictate the biology and treatment stratification. In this study we employed recent comprehensive technologies to study the composition and spatial distribution of malignant as well as inflammatory components of the tumor microenvironment (TME).
Methods: We systematically characterized immune cells in a cohort of germinomas by immunophenotyping and image analysis of formalin-fixed, paraffin-embedded (FFPE) tumor samples. Bulk mRNA expression data was generated by Nanostring technology and high-resolution spatial RNA expression data by Visium-HD technology. With the latter method we studied 10 germinomas and 3 mixed germ cell tumors. Individual candidate transcripts and proteins were validated by in-situ RNA hybridization and immunohistochemistry.
Results: Spatial transcriptomics by Visium-HD allowed the sensitive detection of different malignant germ cell tumor components including germinoma, yolk sac tumor, embryonal carcinoma and choriocarcinoma components, as well as the spatial distribution of immune cells. Tumor infiltrating lymphocytes in germinomas were abundant and predominated by CD3-positive T cells, including CD4-positive T-helper cells, CD8-positive cytotoxic T cells and interspersed FoxP3-positive regulatory T cells. B lymphocytes outnumbered plasma cells. Some germinomas and mixed GCT showed tertiary lymphoid structures. Tumor-associated macrophages (TAM) consisted of clusters of activated PD-L1-positive macrophages and interspersed anti-inflammatory macrophages expressing CD163. While germinoma cells did not express PD-L1 on both the RNA and protein level, a high expression of *BIRC5* (survivin) as anti-apoptotic gene was identified. Spatial mRNA expression analysis indicated specific ligand-receptor interactions between malignant GCT cells and TME components. In particular, germinoma cells produced high levels of macrophage migration inhibitory factor (MIF), and its receptor CD74 was found expressed in adjacent inflammatory cells.
Conclusions: In conclusion, spatial high resolution transcriptomics was able to sensitively identify different malignant germ cell tumor components by their signature. The strong immune reaction observed in germinomas involved various inflammatory as well as suppressive mechanisms. Interaction analysis between GCT and TME cells indicated paracrine mechanisms in the control of growth and survival of intracranial GCT cells.

#0637 CyTOF analysis of heterogeneity between Ewing sarcoma cell lines in vitro and in vivo.

Piper Harrell, Lily Golzar, Kenzie Wells, Poornima Gourabathini, Kimberly Q. McKinney, Erin M. Trovillion, Javier Oesterheld, **Kaitlyn H. Smith**

Atrium Health Wake Forest Baptist Comprehensive Cancer Center, Charlotte, NC

Introduction: Ewing sarcoma (ES) is the second most common bone cancer in children and is known to be driven by an oncogenic fusion, most commonly EWS:FLI1. Recent work has identified that ES tumors are heterogenous and there are populations of cells within tumors with varying levels of the EWS:FLI1 fusion. These populations have differences in morphology, proliferation, drug sensitivities, and invasiveness. Further, it is known that cancer stem cell populations are also found within ES tumors and these cells also have differences in morphology and drug sensitivity. The purpose of this study was to use CyTOF to assess differences in EWS:FLI1 fusion and cancer stem cell heterogeneity and immune infiltration between various ES cell lines in vitro and in vivo.
Methods: In vitro, A673, TC71, RDES, and SL00015 cells were seeded separately at equal numbers and stained for CyTOF the following day. In vivo, A673, RDES, or SL00015 cells were injected subcutaneously into Nude mice. Once tumors reached 1500-2000mm^3, they were harvested and dissociated for CyTOF analysis. The CyTOF panel used was designed to assess EWS:FLI1 fusion heterogeneity, the cancer stem cell population, and immune cell infiltration. OMIQ was used for data analysis which included phenograph clustering with UMAP visualization, heatmap of expression patterns, and changes in tumor and immune cell populations.
Results: In vitro, each of the 4 cell lines have varying morphologies and their growth ranges from adherent to clusters of cells in suspension. Phenograph clustering revealed different expression patterns among the cell lines. Interestingly, the expression patterns of different cell lines grown in vivo clustered together more than the in vivo grown cells did with their in vitro counterpart. Overall, the cells grown in vivo had a higher percentage of the EWS:FLI1^{low} population compared to the respective cell line grown in vitro. The amount of cancer stem cells varied among cell lines and sample types, though the percentage was generally higher in the in vitro samples compared to in vivo. Further, immune infiltration also varied across tumors formed from different cell lines with the RDES tumors having the most overall infiltration.
Conclusions: The CyTOF panel used in this study can identify distinct expression patterns among cell lines and sample types. The differences in expression patterns identified between a cell line grown in vitro or in vivo could be an important consideration in drug efficacy or mechanism studies in the context of Ewing sarcoma.

#0638 Spatial organization of epithelial- and neural-like tumor phenotypes and their cellular neighborhoods in desmoplastic small round cell tumors.

Jiaqian Fan, Kevin Murgas, Diana Shamsutdinova, Davis Ingram, Alexander Lazar, Danh Truong, Joseph A. Ludwig

UT MD Anderson Cancer Center, Houston, TX

Desmoplastic small round cell tumor (DSRCT) is a rare and aggressive sarcoma driven by the EWSR1::WT1. Histologically, DSRCT is characterized by distinct spatial heterogeneity of tumor nests surrounded by a desmoplastic stroma. Our previous study showed that DSRCT exhibits heterogeneous expression of androgen receptor (AR)-associated and neuron-specific enolase (NSE)-associated markers, highlighting these as important lineage features of the disease. However, how these AR (Epithelial-like)- and NSE (Neural-like)- associated phenotypes are organized at the single-cell level and contribute to tumor biology remains poorly understood. This study aims to define these phenotypes and delineate their spatial and neighborhood patterns within the DSRCT microenvironment. We used the Lunaphore COMET system to evaluate 12 DSRCT patient specimens, comprising a 20-marker panel on nine slides and a separate 24-marker panel on three slides, which collectively covered epithelial, neural, fibroblast, endothelial, and immune cell types. Using Visiopharm, we applied deep-learning algorithms to identify individual cells and quantify protein expression data. Four custom RNAscope probes targeting EWSR1::WT1-associated neogenes were used to detect tumor cells and identify EWSR1::WT1 activity. Tumor cells were distributed along an AR-NSE expression spectrum, including AR-high, AR-low, double-negative (AR-NSE-), NSE-positive, top 1% NSE-strong, and hybrid phenotype (AR+NSE+). Among AR-associated phenotypes,gradient analysis revealed that AR-high tumor cells were enriched at the tumor nest center and gradually decreased in abundance toward the tumor-stroma interface, where AR-low tumor cells were more prevalent and in closer proximity to fibroblast-rich stromal regions. Among NSE-associated phenotypes, NSE-positive tumor cells were positioned closer to fibroblast-rich stromal regions. In contrast, both the top 1% NSE-strong and AR+NSE+ hybrid phenotypes localized deeper within the tumor region and were farther from fibroblasts. Our work identified novel conserved neighborhoods across samples: tumor-centered, transitional, and fibroblast-enriched neighborhoods. AR-high phenotypes predominantly mapped to tumor-centered neighborhoods, whereas AR-low phenotypes were enriched in transitional and stromal-interacting neighborhoods. These spatial distributions suggest distinct microenvironmental contexts at the center and periphery of the tumor nests, where stromal interactions are more pronounced. Future work will elucidate how stromal cues mediate phenotypic changes in DSRCT.

#0639 Distinct microenvironments define subtypes of neuroblastoma.

Joseph Seamus Toker[1], Katherine Elizabeth Masih[2], Noemi Kedei[2], Zahin Islam[2], Ben J. Somerville[2], Amir Jassim[1], Michail Mamalakis[1], Aysen Yuksel[3], Daniel R. Catchpoole[3], Li Zhou[3], Paul Aiyetan[4], Yong Yean Kim[5], David Milewski[2], Shaoli Das[2], Xinyu Wen[2], Yong Song[2], Jun Wei[2], Richard J. Gilbertson[1], Javed Khan[2]

[1]University of Cambridge, Cambridge, United Kingdom,[2]National Cancer Institute, Bethesda, MD,[3]Tumour Bank, Children's Cancer Research Unit, The Children's Hospital at Westmead, Westmead, NSW, Australia,[4]Neopathology Corp, Frederick, MD,[5]Pediatrics, Stanford University, Stanford, CA

Originating from the neural crest, neuroblastoma is the most common extracranial solid tumor in children. Infiltrating immune cells contribute to the tumor's growth and treatment response, as patients with high-risk disease, associated with *MYCN* amplification, benefit from anti-GD2 antibody immunotherapy. However, *MYCN*-amplified disease remains lethal in more than half of cases and has been associated with immunosuppression in bulk RNA studies. We thus hypothesize that *MYCN* activation, in conjunction with other molecular and clinical traits, influences the tumor microenvironment (TME), which can either support or suppress the disease. To comprehensively characterize the neuroblastoma TME, we performed CO-Detection by indEXing (CODEX), a multiplex immunohistochemistry technique, on 5 clinically annotated tissue microarrays containing 371 neuroblastic tumors from 179 patients representing all major disease subgroups and treatment protocols. In a subset of specimens, we also applied Visium HD spatial transcriptomics to identify regional malignant programs and their associated immune infiltrates. In parallel, we developed a novel natural language processing approach to detect generalizable spatial cell networks across these tissues. Interrogating more than 40 tumor-, immune-, and stroma-associated proteins revealed that neuroblastomas, despite downregulating MHC class I (MHC-I), harbor rich TMEs composed of about 20 phenotypically distinct cell populations, including multiple lymphoid- and myeloid-derived subsets. *MYCN*-amplified tumors are profoundly deficient in infiltrating helper, memory, and cytotoxic T cell lineages, whereas they form prominent tertiary structures in non-amplified disease. By contrast, antigen-presenting suppressor-like myeloid cells dominate the *MYCN*-amplified microenvironment, where they persist in chemotherapy-resistant tumors. These subtype-specific differences prompted functional studies of intrinsic immune and cytokine programs. RNA-seq of multiple human *MYCN*-amplified cell lines revealed that the differentiation therapy retinoic acid, while suppressing *MYCN*, drastically upregulated class I antigen presentation and pro-inflammatory cytokines. To further understand *MYCN*- and treatment-related changes in the inflammatory secretome, we are currently performing extracellular proteomics on these cell lines. Integrative spatial profiling by CODEX and Visium HD reveals that MYCN amplification fosters a T cell-poor, myeloid-rich microenvironment, in contrast to the organized lymphoid structures characteristic of non-amplified neuroblastoma. Together with the finding that retinoic acid restores MHC-I and pro-inflammatory programs in MYCN-amplified tumors, these results suggest that combining retinoic acid with cellular immunotherapies and myeloid-targeting approaches may significantly improve survival in patients with high-risk neuroblastoma.

#0640 Multiomic profiling reveals endothelial cell plasticity in metastatic osteosarcoma.

Ying Wu, Julian Burks, Demond Williams, Carly Sayers, Vidhur Daulatabad, Neeraja Syed, John F. Shern, **Troy A. McEachron**

Pediatric Oncology Branch, National Cancer Institute, Bethesda, MD

Metastatic osteosarcoma is an aggressive malignant bone tumor that primarily affects pediatric, adolescent, and young adult populations and represents an understudied disease with significant unmet medical need. Recent research has increasingly focused on understanding the complex biology of the osteosarcoma microenvironment. While prior studies have primarily examined the roles of macrophages, lymphocytes, and, to a lesser extent, fibroblasts, the tumor vasculature has received comparatively little attention.
To address this critical gap, we performed single-nuclei multiome (RNA+ATAC) sequencing on a cohort of 24 human metastatic osteosarcoma specimens. Our data reveal that endothelial cells within the metastatic microenvironment adopt a hybrid transcriptional state indicative of endothelial-to-mesenchymal transition (EndMT). Leveraging our multimodal dataset, joint copy number analysis identified a subset of tumor cells that cluster with endothelial cells, demonstrating that osteosarcoma cells engage in vascular mimicry. Further investigation of gene regulatory networks revealed a subset of endothelial cells undergoing endothelial-to-osteoblastic conversion and confirmed endothelial-specific regulatory programs in the osteosarcoma vascular mimics. Analysis of immunosuppressive gene expression suggests that endothelial cells in metastatic osteosarcoma also function in an immunoregulatory capacity.
Both *in vitro* and *in vivo* functional assays were employed to validate these findings. Modified transwell co-culture assays demonstrated that osteosarcoma-derived factors induce osteoblastic gene expression programs in lung microvascular endothelial cells. Additionally, using endothelial lineage-tracing mice in combination with GFP^+ syngeneic murine osteosarcoma cells, we provide *in vivo* evidence that endothelial cells can be reprogrammed into osteoblast-like cells that integrate into malignant osteoid, while osteosarcoma cells themselves are capable of vascular mimicry.
Collectively, these findings highlight the remarkable plasticity and lineage infidelity of both endothelial and tumor cells, provide novel insights into the functional role of endothelial cells in the metastatic osteosarcoma microenvironment, and challenge current understanding of osteosarcoma biology.

#0641 Identifying vulnerabilities through an elucidation of the tumor-host interplay that drives osteosarcoma lung colonization.

Fatemeh Yazarlou, Matthew Cannon, Yogesh Budhathoki, Amy C. Gross, Leyre Jimenez Garcia, James Reinecke, **Ryan D. Roberts**

Nationwide Children's Hospital, Columbus, OH

Metastasis is the single most critical determinant of outcome in many solid tumors. In pediatric osteosarcoma, the development of lung metastases is associated with more aggressive and treatment-resistant tumor behavior. While many have assumed that metastasis is a consequence of this more aggressive behavior, emerging evidence suggests that interactions driving colonization reshape the behavior of both tumor and stromal compartments, reinforcing the resilience of metastatic lesions.

Our recent work has shown that colonization induces changes in lung epithelial cells, infiltrating macrophages, and tumor cells, forming a microenvironment dominated by a dense, scar-like matrix that promotes tumor survival and proliferation. While we have shown that this aberrant niche can be disrupted by several multireceptor tyrosine kinase inhibitors (TKIs), each agent appears to affect lesions through distinct mechanisms. Identifying the specific pathways responsible for these anti-tumor effects has proved challenging.

To address this, we developed an algorithm that identifies aberrantly activated, kinase-dependent signaling pathways within each individual cell type. This approach revealed that several distinct, self-reinforcing microenvironments can emerge during lung colonization, and that each of these emergent networks activates a characteristic subset of kinase-dependent pathways. Importantly, these pathway signatures can be matched against the known activity profiles of available TKIs to predict which agents may be most effective for a given tumor.

To improve the effectiveness of this algorithm, we refined this predictive process by using CROP-seq to generate a purpose-built database for the accurate identification of kinase-driven transcriptional programs within each relevant cell type. The incorporation of spatial transcriptomics further refines predictions by resolving cellular neighborhoods to identify the most meaningful interactions occurring within a metastatic lesion.

Through this process, we aim to make every patient an exceptional responder by elucidating the targetable pathways driving the formation and maintenance of individual metastatic lesions and matching these vulnerabilities to the most effective available drug.

#0642 Extracellular viscosity modulates spheroid formation in SMARCB1-deficient brain tumor cells.

Yihsuan Chen[1], Long-Sheng Lu[2], Yu-Chun Lin[1]

[1]Graduate School of Advanced Technology, National Taiwan University, Taipei, Taiwan,[2]Graduate Institute of Biomedical Materials and Tissue Engineering, Taipei Medical University, Taipei City, Taiwan

Background In the developing pediatric brain, the viscosity of the tissue microenvironment changes dynamically with tissue maturation, providing a unique mechanical microenvironment that may influence cellular behavior through mechanotransduction. SMARCB1 deficiency causes the most aggressive pediatric central nervous system malignancies, which have high tissue specificity, extremely early onset, epigenetic dysregulation, and altered metabolic states. Despite this unique biological context, whether extracellular viscosity interacts with SMARCB1 loss to alter tumor cell behavior has never been explored.

Methods To investigate how extracellular viscosity affects SMARCB1-deficient brain tumor cells, gellan gum (GG), a biocompatible viscosity modifier, was incorporated into culture medium to generate viscosities of 2.2 (0%), 10 (0.01%), and 34 (0.03%) mPa·s at 37 °C. SMARCB1-deficient Re1P6 cells (c.157>T mutation and established from a patient-derived xenograft) were compared with SMARCB1-proficient glioma cell lines (T98G). Single-cell suspensions were seeded on ultra-low attachment plates and cultured in media of increasing viscosities to monitor cell growth and spheroid formation. Pre-formed spheroids were also transferred into media with varying viscosities to evaluate spheroid stability and dispersion. Changes in stemness markers and other cellular phenotypes were further examined under each condition.

Results We found that elevated extracellular viscosity selectively modulates spheroid formation in SMARCB1-deficient Re1P6 cells but not in SMARCB1-proficient glioma cells. Re1P6 exhibited a nonlinear response to viscosity, forming the most uniform spheroids (~200 μm in diameter) with increased cell growth (~30-fold) at 10 mPa·s, whereas spheroid formation was almost suppressed and proliferation remained unchanged at 34 mPa·s. SMARCB1-proficient glioma cells showed minimal changes in spheroid formation or cell growth across the same viscosity conditions. Pre-formed Re1P6 spheroids developed irregular boundaries at higher viscosity, suggesting viscosity-dependent disruption of spheroid cohesion. High-viscosity conditions also appeared tp decrease SOX2 and increase vimentin expression. Overall, Re1P6 cells exhibited greater phenotypic modulation in response to viscosity-dependent microenvironments than SMARCB1-proficient controls.

Conclusion Our early findings suggest a potential link between extracellular viscosity and the malignant behavior of pediatric SMARCB1-deficient tumors. Future work will investigate whether the viscosity-dependent response is linked to mechanosensing signaling pathway and metabolic-epigenetic changes, providing new insights into their tissue-specificity.

#0643 The Sean Karl Cohort: An international single-cell RNAseq study of paired patient Ewing sarcoma specimens.

Abbe Pannucci[1], Elina Mukherjee[1], Jessica D. Daley[2], Shireen Sita Ganapathi[3], Elissa Boguslawski[4], Lea Surrey[5], Lauren Gutstein[5], Patrick Azar[6], Emily Stockfisch[7], Azfar Neyaz[2], Ivy John[8], Jennifer Picarsic[8], Yutaro Tanaka[9], Byron Butaney[9], Riaz Gillani[9], Brian D. Crompton[9], Katherine A. Janeway[9], Jaclyln Taroni[10], Jessica Davis[6], Damon Reed[7], Adam Shlien[11], Theodore W. Laetsch[5], Rajen Mody[4], Clemence Henon[12], Thomas G. Grunewald[12], Elizabeth R. Lawlor[3], Filemon Dela Cruz[7], Patrick J. Grohar[13], Jovana Pavisic[14], Ally Hawkins[10], Anthony R. Cillo[1], **Kelly M. Bailey**[15]

[1]University of Pittsburgh, Pittsburgh, PA,[2]UPMC, Pittsburgh, PA,[3]Seattle Children's Research Institute, Seattle, WA,[4]University of Michigan, Ann Arbor, MI,[5]Children's Hospital of Philadelphia, Philadelphia, PA,[6]Indiana University, Indianapolis, IN,[7]Memorial Sloan Kettering Cancer Center, New York, NY,[8]The University of Pittsburgh School of Medicine, Pittsburgh, PA,[9]Dana-Farber Cancer Institute, Boston, MA,[10]The Childhood Cancer Data Lab, Wynnewood, PA,[11]Graduate Student, Dept. of Genetics & Genome Bio., The Hospital for Sick Children, Toronto, ON, Canada,[12]Hopp Children's Cancer Center Heidelberg (KiTZ), Heidelberg, Germany,[13]University of Michigan Medicine, Ann Arbor, MI,[14]Memorial Sloan Kettering, New York, NY,[15]Mayo Clinic, Rochester, MN

Introduction: Ewing sarcoma (EwS) is a FET::ETS family member-driven primary bone cancer demonstrating vast heterogeneity. Between a patient's primary diagnosis and disease progression, tumor cell state adaptation, microenvironment changes, and the landscape of evolving therapeutic vulnerabilities remain poorly understood. To address these gaps, the Sean Karl Cohort was established in 2025 to conduct the largest single-cell transcriptomic analysis of retrospective paired tumor samples from patients with EwS. Here, we present data from the five analytic teams, and through shared SOPs now expand this cohort to Europe.
Methods: Common sample processing SOPs were established to isolate cells from FFPE material from paired patient EwS samples. Single-cell (sc) RNAseq was generated using the GEM-X Flex Gene Expression protocol (10x Genomics). Alex's Lemonade Stand Foundation (ALSF) Data Lab established a common data processing and integration pipeline with an EwS-specific cell annotation workflow to create a harmonized dataset for downstream analyses. Analytic teams were created to define tumor cell subpopulations and their therapeutic vulnerabilities and to characterize the tumor microenvironment.
Data: We demonstrate the feasibility of generating high-quality scRNAseq profiles from retrospective FFPE-preserved EwS tumors. To date, 116 samples have yielded ~800,000 cells. Integrated analysis reveals reproducible EwS tumor cell states shared across patients with regulatory network analyses nominating candidate therapeutic vulnerabilities. The scale of this international cohort enables saturation analysis for rare cell populations. Paired and longitudinal samples further allow correlation of emergent cell states with therapy resistance and metastatic progression. For example, immune-focused analyses show increases in T cell and macrophage populations in post-therapy samples. A novel, standardized EwS-specific cell annotation workflow has been developed to harmonize analyses and findings. These data will be openly shared with the community through the ALSF Single-cell Pediatric Cancer Atlas Portal.
Conclusion: Large-scale international collaborative sample sharing, standardized processing pipelines, and harmonized EwS-specific annotations now enable deep single-cell analyses to characterize tumor heterogeneity in this rare pediatric and adolescent cancer. An in vivo expansion of the Sean Karl Cohort is underway to assess conservation of EwS tumor cell states and regulatory vulnerabilities identified in human tumors pre- and post-therapy in preclinical models, further supporting translation of these findings toward therapeutic strategies.

#0644 Evaluating GD2-targeting antibody-drug conjugates for DIPG using human organoid-based preclinical platforms.

Zhikun Wang, Emily Miller, Wei Huang, Satoru Kawakita, Lauren Vanderpool, Francisco Bustamante, Uijin Kim, Zhaohui Wang

Terasaki Institute for Biomedical Innovation, Los Angeles, CA

Diffuse intrinsic pontine glioma (DIPG) is a universally fatal pediatric brain tumor with a median survival of less than 12 months. Although the recent FDA accelerated approval of ONC201 offers a long-awaited sense of progress for the DIPG/DMG community, the central therapeutic problem remains far from solved. The frequent presence of H3K27M mutations in DIPG is associated with elevated expression of GD2, a clinically actionable surface antigen. GD2-directed CAR-T therapies have shown encouraging early activity in DIPG. However, challenges such as antigen heterogeneity, inherent manufacturing lead time, and risks of neurotoxicity remain. Antibody-drug conjugates (ADCs) offer a more controllable, off-the-shelf therapeutic approach that could overcome these limitations, yet their potential in DIPG remains unexplored. To evaluate the efficacy, resistance, and safety of GD2-targeting ADCs, we employed two complementary human-derived organoid platforms. First, DIPG models were generated using NanoGlio, a high-throughput nanoliter-volume droplet 3D organoid system. Second, we established a co-culture model with DIPG NanoGlio and iPSC-derived brain organoids to assess neurotoxicity. We successfully generated NanoGlio derived from 9 DIPG models reflecting the key genetic alterations typically identified in DIPG, including mutations in *H3.3 (H3F3A)* or *H3.1 (HIST1H3B).* We assessed the expression of GD2 by flow cytometry and 3D-Fluorescence Antibody Cell Tracking (3D-FACT) and observed widely variable GD2 expression across DIPG models. We tested M3554, a first-in-class clinical-stage anti-GD2 ADC conjugated to exatecan, a topoisomerase I inhibitor, in these models. M3554 exhibited potent cytotoxicity across DIPG NanoGlios. Resistance profiling using its unconjugated payload, Exatecan, revealed that reduced ADC response was primarily driven by intrinsic payload resistance rather than low GD2 expression. DIPG models with very low GD2 expression, including SF7761 and SU-DIPG-IV, also responded strongly to M3554, consistent with a bystander killing effect. iPSC-derived brain organoids (GD2-negative) showed minimal toxicity with M3554, whereas equivalent doses of Exatecan induced extensive cell death. Future work will systematically evaluate GD2 ADC bystander effect via co-encapsulation of GD2+ and GD2- DIPG cells, and assess the efficacy and neurotoxicity of M3554 using our DIPG-brain co-culture model. Successful completion of this study will provide critical preclinical evidence supporting the assessment and use of GD2-targeting ADCs in DIPG treatment.

#0645 Enhancement of antigen presentation restores immune recognition in rhabdomyosarcoma.

Maya Groff[1], David Milewski[1], Hsien-Chao Chou[1], Vineela Gangalapudi[1], Alexandra Urbanek[2], Young Song[1], Meijie Tian[1], Yong Yean Kim[1], Jun Wei[1], Javed Khan[1]

[1]Center for Cancer Research, NIH-National Cancer Institute, Bethesda, MD,[2]NIH-National Eye Institute, Bethesda, MD

Background: Immunotherapy offers a promising therapeutic option against pediatric tumors, but it is limited by suppression of the antigen processing machinery (APM), including major histocompatibility complex class I (MHC-I). In this study, we quantify antigen presentation in pediatric tumors and explore the role of transcriptional regulators and epigenetic-targeted therapies to restore antigen presentation and immune recognition in rhabdomyosarcoma (RMS).
Methods: Expression of HLA-A/B/C was quantified by RNA sequencing (RNA-seq) in adult tumors (n=657) and pediatric cell lines (n=131). Surface MHC-I expression was quantified by flow cytometry in pediatric cell lines (n=76). RMS cell lines (n=9) were treated with IFN-γ and clinically relevant drugs, decitabine (DAC), mocetinostat, and tazemetostat. Changes in MHC-I and APM gene expression were measured by RNA-seq and flow cytometry. NLR family CARD domain-containing 5 (NLRC5) was induced in RMS cell line and patient derived xenograft (PDX) models using lentiviral overexpression or CRISPR activation. MHC-I and APM expression were measured by RNA-seq, flow cytometry, and western blot. T cell cytotoxicity assays were performed with T cells expressing a PRAME-specific HLA-A*02:01 T cell receptor (TCR).
Results: Pediatric tumors exhibited variable MHC-I expression, as determined by flow cytometry, and this expression was significantly lower than adult tumors, with RMS displaying low or absent expression. IFN-γ and pharmacologic treatment increased MHC-I surface expression and immune gene signatures in RMS. NLRC5, a key immune regulator, was found to be most significantly correlated with MHC-I expression and induced by treatment with DAC. Epigenetic priming with DAC and upregulation of NLRC5 was sufficient to restore MHC-I expression and sensitized an RMS PDX to killing by engineered TCR-T cells targeting PRAME.
Conclusions: Pediatric tumors show distinct patterns of antigen presentation, such as high MHC-I in alveolar soft part sarcoma and low expression in RMS, though individual tumor subtypes exhibit internal variability. IFN-γ and epigenetic agents restore antigen presentation, including increased NLRC5 expression. Pharmacological treatment and NLRC5 restoration enhanced antigen presentation and sensitized RMS PDX to TCR mediated T-cell cytotoxicity. Compounds that reverse APM silencing will be systematically evaluated for their ability to enhance adoptive TCR therapies. This work will establish a foundation for overcoming immune resistance and expanding the impact of MHC-I dependent cancer immunotherapies.

#0646 Exploring actionable therapeutic targets associated with SMARCB1 deficiency in Epithelioid sarcoma.

Jiyeon Park[1], Ryo Miyamoto[2], David G. Kirsch[1]

[1]Department of Medical Biophysics, University of Toronto, Toronto, ON, Canada,[2]Princess Margaret Cancer Centre, University Health Network, Toronto, ON, Canada

Epithelioid sarcoma (EPS) is a rare, slow-growing yet highly metastatic mesenchymal neoplasm characterized by inactivation of SMARCB1. Although the EZH2 inhibitor Tazemetostat has been approved for EPS patients, clinical outcomes remain poor. In this study, we performed functional genomic studies to identify therapeutic vulnerabilities of EPS and to elucidate their underlying mechanisms.CRISPR screening using an sgRNA library targeting ~2,700 druggable genes identified dependencies of EPS cells on; BAF complex subunits (SMARCA4, SMARCC2 and SMARCD1), integrin pathway genes (ITGAV, PTK2, PTPN11) and the cyclin-dependent kinases (CDK4 and CDK6). A clinically available CDK4/6 dual inhibitor Palbociclib effectively inhibited EPS cell proliferation *in vitro* and significantly delayed tumor growth in human EPS cell line-derived xenograft models. Moreover, the CDK4-selective inhibitor Atirmociclib showed profound cytotoxicity in cell lines with low CDK6 expression, suggesting the feasibility of tailoring CDK4/6-targeted therapy based on CDK6 expression levels.Re-expression of SMARCB1 using a Tet-ON conditional expression system induced growth arrest, accompanied by reduced RB phosphorylation and decreased cyclin A2 (CCNA2) expression. SMARCB1 re-expression also upregulated the CDK inhibitors, p21 and p27, indicating compromised cell cycle control. The strong dependency of EPS on p21/p27-CDK4/6 axis supports CDK4/6 inhibition as a therapeutic strategy. Our CRISPR screen and *in vitro* viability assays demonstrated that EPS cell lines are intrinsically resistant to Tazemetostat, with genetic and epigenetic silencing of p16 emerging as a potential mechanism underlying this resistance.Together, functional genomic screens define key therapeutic vulnerabilities in EPS, suggesting CDK4/6 inhibitors as a promising treatment option for EPS patients. We propose that expression levels of CDK6 and p16 may serve as predictive biomarkers for response to EZH2 and CDK4/6 inhibitors, thereby informing patient stratification and improving clinical outcomes.

#0647 EWSR1::FLI1 suppresses ribosome biogenesis and creates a targetable vulnerability in Ewing sarcoma.

Matteo Colombo[1], Jason Sims[1], Christoph Dotter[1], Hana Bernhardova[1], Sanskriti Balaji[2], Jonathan Levi[2], Aleksandra S. Anisimova[3], Anja Wagner-Schrittwieser[4], Tamina Stelzer[1], Aikaterini M. Formouzi[1], Bernadette Liegl-Atzwanger[5], Marita Koelz[6], Anke Scharrer[6], Markus Schosserer[4], Peter Schlogelhofer[3], Thomas G. P. Grunewald[7], G. Elif Karagoz[3], Alice Soragni[2], Eleni M. Tomazou[1]

[1]St. Anna Children?s Cancer Research Institute, Vienna, Austria,[2]Department of Orthopaedic Surgery, David Geffen School of Medicine, University of California Los Angeles, Los Angeles, CA,[3]Max Perutz Labs, Vienna BioCenter Campus (VBC), Vienna, Austria,[4]Center for Pathobiochemistry and Genetics, Medical University of Vienna, Vienna, Austria,[5]Diagnostic and Research Institute for Pathology, Medical University of Graz, Graz, Austria,[6]Department of Pathology, Medical University of Vienna, Vienna, Austria,[7]Division of Translational Pediatric Sarcoma Research, German Cancer Research Center (DKFZ), Heidelberg, Germany

Enhanced ribosome biogenesis has long been regarded as a defining feature of malignant growth, sustaining the elevated biosynthetic and translational demands of cancer cells. However, emerging evidence suggests that the relationship between ribosome production and cancer biology is more complex, with alterations in ribosome biogenesis exerting diverse cellular effects. This complexity is particularly evident in Ewing sarcoma (EwS), a malignancy affecting children and young adults, and is driven by the EWSR1::FLI1 fusion oncoprotein. Intriguingly, its histological hallmark of inconspicuous nucleoli suggests profoundly altered ribosome biogenesis. Given its low mutational burden and reliance on non-genetic mechanisms, we reasoned that dissecting the rewiring of post-transcriptional regulation and ribosome biogenesis could reveal previously unexplored therapeutic vulnerabilities. Using super-resolution imaging (STED), we found that EwS cells display pronounced nucleolar disorganization, characterized by aberrant clustering of the rDNA transcription factor UBF1 and loss of canonical nucleolar compartmentalization. Mechanistically, the EWSR1::FLI1 fusion protein sequesters endogenous EWSR1, leading to R-loop accumulation at rDNA loci and suppression of rDNA transcription. As a result, EwS cells exhibit reduced ribosome biogenesis and global protein synthesis - an unexpected deviation from the hyperactive state typical of most tumors. Despite this reduction, polysome sequencing revealed a compensatory translational program with selective enhancement of 5′TOP mRNAs translation, sustaining a minimal yet efficient ribosome output. This compensatory mechanism, while sufficient to sustain baseline survival, operates at the edge of translational capacity, creating a therapeutically exploitable vulnerability to agents that further compromise ribosome biogenesis. Indeed, pharmacologic inhibition of RNA polymerase I with CX-5461 disrupts this fragile balance, inducing rapid translational shutdown and apoptosis specifically in EwS cells, an effect that is reversed by EWSR1::FLI1 depletion. Moreover, etoposide treatment selectively triggers SLFN11-dependent translational shutdown in EwS cells, in addition to inducing DNA damage, highlighting its dual impact on both the genome and the already fragile translational machinery. Finally, CX-5461 demonstrated potent therapeutic activity with evidence of synergistic effects when combined with the PARP inhibitor Olaparib selectively in EwS, warranting further investigation of rational combination strategies. Together, our findings reveal that reduced ribosome biogenesis - rather than its hyperactivation - is an important feature of EwS and creates a distinct therapeutic vulnerability. Targeting this constraint offers a promising new strategy for a disease that currently lacks effective targeted therapies.

#0648 PP2A reactivation upregulates *FGA* gene in neuroblastoma.

Nazia Nazam[1], Shamza Manzoor[1], Maryam Ghufran[1], Morgan L. Brown[1], Ali M. Eakes[1], Pranava Nande[1], Joel C. Opara[1], Abdulraheem Kaimari[1], Michael Ohlmeyer[2], Elizabeth A. Beierle[1]

[1]University of Alabama at Birmingham, Birmingham, AL,[2]Atux Iskay, LLC, Plainsboro, NJ

Background: High-risk neuroblastoma (NBL), driven by *MYCN* amplification, remains fatal for many children. Our previous work demonstrated that pharmacologic PP2A reactivation decreases NBL in vivo tumor growth through suppression of MYCN expression and stability by reducing MYCN phosphorylation and promoter acetylation, concurrent with BRD4 and RNA Pol II dephosphorylation. The current study is an extension of this previous work, in that we performed loss-of function tests validating the previous findings, and identified a downstream target regulated by *MYCN* within this PP2A-controlled network.

Methods: The *MYCN* amplified human NBL cell line SK-N-BE(2) was treated with the PP2A activator, ATUX-1215, or the PP2A inhibitor, okadaic acid (OA). Immunoblotting quantified phospho-BRD4, BRD4, MYCN, PP2Aαβ-C subunit, acetylated histones (H3K27ac, H3ac), total H3, and GAPDH. PP2A activity was measured enzymatically. Bulk RNA sequencing identified transcriptional alterations, and qRT-PCR confirmed the findings. Public NBL datasets (TARGET and Capasso) were analyzed.

Results: OA treatment increased phospho-BRD4, MYCN, H3K27ac, and H3ac while decreasing PP2A expression and activation. Densitometric analysis of immunoblots validated these transcriptional and epigenetic marker changes. Bulk RNA-seq revealed fibrinogen alpha chain (*FGA*) as a significantly upregulated gene following PP2A activation with ATUX-1215. Gene Set Enrichment Analysis (GSEA) identified enrichment of MYCN associated pathways, specifically the WEI_MYCN_TARGETS_WITH_E_BOX gene set, with *FGA* among upregulated targets. Increased *FGA* mRNA abundance was confirmed with qRT-PCR in ATUX-1215 treated NBL cells (24 h - 72 h). Public dataset analysis demonstrated that elevated *FGA* expression correlated with improved overall survival in *MYCN* amplified and stage 4 NBL patients.

Conclusion: We have found that PP2A reactivation involves BRD4-mediated epigenetic regulation and histone acetylation, upregulates *FGA* gene, and that increased *FGA* is associated with improved NBL survival. These findings suggest that PP2A reactivation may restore beneficial MYCN-linked transcriptional programs, offering potential therapeutic strategy for high-risk NBL.

#0649 Site-specific phospho-regulatory collapse of PML governs RTK hyperactivation in high-risk pediatric malignancy..

Sreenidhi Mohanvelu, Poorvi Subramanian, Natarajan Aravindan

Oklahoma State University, Stillwater, OK

High-risk neuroblastoma (HR-NBL), a deadly pediatric malignancy of neural crest origin is characterized by persistent hyperactivation of receptor tyrosine kinases (RTKs) such as ALK, EGFR that orchestrates oncogenic trajectory and perpetuates aggressive, treatment refractory phenotype. Despite extensive characterization of the RTK signaling, the upstream regulatory mechanism that constrain RTK activity and restore lineage commitment remain elusive, limiting the efficacies of differentiation-based therapies. Stability and functional integrity of promyelocytic leukemia protein (PML) and its nuclear body architecture are essential for sustaining differentiation and therapeutic sensitivity. Our recent studies identified a mechanism that derange PML stability, defining a site-specific (serine 518, S^{518}) post-translational modification that dictates PML functional integrity. Herein, we delineate a S^{518} phosphorylation-centric signaling architecture driving oncogenic RTK signaling. To this end, we employed a dual modality framework integrating RD3 expression modulation (knockout, $RD3^{-/-}$ or overexpression, $RD3^{+/+}$) that dictates S518 phosphorylation, and stable site-specific mutagenesis of PML S^{518} to phospho-dead (A^{518}) or phosphomimic (E^{518}), in patient-derived NBL cells representing distinct clinical stages, diagnostic (Dx) and progressive disease (PD). Functionally, RD3-loss dependent PML destabilization ($RD3^{-/-}$ and $RD3^{+/+}$PML E^{518}) led to a hyperphosphorylated cellular state, disrupting post-translational signaling control and reinforcing an aggressive, therapy defiant phenotype. Quantitative profiling of RTKs phosphorylation (curated panel of 71 human RTKs, phospho-RTK array) was performed to assess pro-oncogenic transformation signaling. $RD3^{-/-}$ and $RD3^{+/+}$PML E^{518} clones exhibited a pronounced increase in phospho-RTK signals, consistent with hyperactivated receptor landscape. Notably, RD3 loss driven PML S^{518} site specific phosphorylation included robust activation of tightly integrated oncogenic RTKs (e.g., Lyn, SYK, Tie-1), that are decisively documented in HR-NBL pathogenesis. In contrast, RD3 overexpression and PML S^{518} phospho-dead mutants attenuated RTK phosphorylation profiles, with minimal activation of canonical oncogenic RTKs. These findings critically demonstrate that RD3 loss driven S^{518} site-specific phosphorylation of PML reprograms the cellular signaling landscape towards a programmed RTK hyperactivation, mechanistically bridging nuclear architectural disruption with membrane-proximal oncogenic signaling. Targeting the RD3-PML-RTK axis offers a mechanistically anchored strategy restoring differentiation competence and attenuate the malignant trajectory of HR-NBL. Funding: Department of Defense CA-210339; OCAST-HR19-04; NIH-P20GM103639; and supported by P30CA225520 and P30GM154635.

: Ex Vivo Systems: Patient-Derived, Patient-Specific Tumor Cultures
Poster Session

#0653 Rapid drug sensitivity testing of passage-zero patient brain tumor tissues to inform preclinical and clinical decisions: results from a clinical feasibility study.

Breanna Mann[1], Nichole Artz[1], Adebimpe Adefolaju[1], Alain Valdivia[1], Xiaopei Zhang[1], Rajaneekar Dasari[1], Caroline Stockwell[1], Morrent Thang[1], Allison Murray[1], Noah Bell[1], Andrew Buckley[1], Rami Darawsheh[1], Kerry Fitzgerald[2], Jonathan Williams[2], Hardik Parikh[3], Shuang Gao[3], Jie An[3], Yvette Rodriguez[3], Daniel Metzger[3], Collin Parrow[3], Dylan Riley[3], Robert Seager[3], Stephanie B. Hastings[4], Taylor Jensen[4], Shakti Ramkissoon[4], Dominique Higgins[1], Yasmeen Rauf[1], Scott Elton[1], Kimberly Hamilton[1], Jeremy Wang[1], Albert Baldwin[1], Shawn Hingtgen[1], David Kram[1], Andrew Satterlee[1]

[1]University of North Carolina at Chapel Hill, Chapel Hill, NC,[2]Labcorp, San Diego, CA,[3]Labcorp, Buffalo, NY,[4]Labcorp, Durham, NC

Functional precision medicine (FPM) offers a promising path forward in neuro-oncology, where genomic profiling alone often fails to predict therapeutic response. To bridge this gap, we developed the Screening Live Cancer Explants (SLiCE) platform, a rapid *ex vivo* drug screening assay that functionally tests passage-zero patient brain tumor tissues engrafted atop living organotypic brain slice cultures (OBSCs). With an assay time of just four days, SLiCE preserves key tumor characteristics not maintained *in vitro*, including genomic fidelity, growth, invasion, and treatment response, with higher engraftment rates and faster assay speeds than *in vivo* models. Our standard cryopreservation workflow enables reproducible, iterative, and on-demand testing of a single zero-passage specimen banked in multiple replicate aliquots, setting SLiCE apart from organoid and precision-cut tumor explant models. Here, we describe results from our actively accruing clinical feasibility study (NCT05978557), where we successfully engrafted and tested 35 of 36 diverse brain tumor specimens on SLiCE, achieving our study's primary endpoint ahead of schedule. SLiCE produced multi-parametric drug sensitivity scores (DSSs), each normalized to off-target toxicity, for all samples within a clinically actionable 28-day window. Across 530 experiments, we generated 142 DSSs from unique drug-tumor combinations, forming a reference library for future benchmarking. We then further analyzed a subset of IDH-WT glioblastoma tumor specimens in which SLiCE DSSs correlated with patient response to temozolomide (AUC = 0.875, p = 0.0175) and overall survival (R^2 = 0.73). Additionally, this study validated surgically aspirated tumor tissue as a genomically, transcriptomically, and functionally similar tumor source compared to the standard, manually excised remnant tumor sample approved by clinical pathology. Collecting this often-discarded tumor source increased the mass of tumors accrued by nearly 5-fold and enabled collection from 11 additional patients, significantly increasing tumor tissue for downstream testing on SLiCE. These findings establish SLiCE as a scalable, clinically relevant platform for FPM in brain cancer, with potential to guide individualized treatment decisions and accelerate preclinical drug development.

#0654 A modular positioning platform for standardized ex vivo specimen analysis in preclinical optical imaging.

Max Harlacher, Jeffrey D. Peterson, James Tseng, **Jessica Pesner**, Bincy John

Revvity, Waltham, MA

Efficient and organized handling of ex vivo specimens is critical for advancing preclinical imaging workflows, particularly in studies requiring high-throughput analysis of tumors, organs, and bone tissues. We developed a novel modular ex vivo sample holder, specifically designed to integrate seamlessly with Revvity's IVIS optical imaging systems for bioluminescence, fluorescence, or x-ray imaging applications. This innovative accessory addresses key challenges in specimen organization, imaging throughput, and experimental reproducibility. In this study, we designed two ex-vivo sample holders with 16-25 separate non-reflective chambers that enable researchers to image multiple samples simultaneously and efficiently. Each chamber has light-blocking walls to prevent crosstalk of signal emission and sample. A wide range of ex vivo specimens including brain, heart, lung, kidneys, liver, spleen, bladder, and gastrointestinal tract were placed on the sample holder with a unique optically dark sheet and imaged using Revvity's IVIS optical systems. We tested multiple types of black sheets and the ideal optically dark sheet was selected based on minimum background effects, reproducibility, and ease-of-operation. The sample holder is designed to incorporate the disposable optically dark paper and minimizes cross-contamination of ex-vivo samples. This paper provides a clean, non-reflective surface that is easily replaceable between experiments, ensuring optimal imaging conditions. Furthermore, the holder's design enhances workflow efficiency by reducing setup time and facilitating rapid specimen arrangement, making it ideal for high-throughput imaging studies. Additionally, IVIS software tools support region of interest (ROI) template creation, allowing for precise and consistent quantitative analysis. The holder's modular compartments allow for different configurations that can be customized to accommodate varying specimen sizes, offering flexibility across diverse experimental needs. This accessory represents a significant advancement for ex vivo optical imaging, providing researchers with a practical solution for improving imaging efficiency, reproducibility, and data quality. By combining ergonomic design, modularity, and software integration, the novel ex vivo sample holder empowers laboratories to achieve greater throughput and precision in preclinical imaging applications.

#0655 Clinical validation of pembro response predictions from TNBC patient biopsies using E slices.

Kyuson Yun[1], Viridiana L. Leyva-Aranda[2], Claire Yun[2], Nourhan ABDELFATTAH[1], Clinton Yam[3], Fransisca Leonard[1], Reece Kang[1], Jangsoon Lee[4], Naoto Ueno[4]

[1]Houston Methodist Research Institute & Weill Cornell Medical College, Houston, TX,[2]EMPIRI, Houston, TX,[3]UT MD Anderson Cancer Center, Houston, TX,[4]U Hawaii Cancer Center, Honolulu, HI

The efficacy of immunotherapies depends on complex and dynamic interactions among immune cells, stromal cells, and cancer cells. Currently, no functional precision medicine assays can accurately predict individual patient responses to immunotherapies in a clinically actionable timeframe. The E-slice platform is a proprietary 3D human tumor tissue culture system that enables rapid, personalized drug sensitivity testing in 8-12 days from the time of tumor biopsies or surgical resections.E-slices are distinct from other 3D human model systems in multiple, critical ways. E-slices are:
1) never dissociated or reconstituted or expanded ex vivo; therefore, the platform maintains individual patient tumors' histoarchitecture, cellular composition including tumor-infiltrating immune cells, and the spatial relationships among different cell types, enabling evaluation of immunotherapies (antibody drugs, ADCs, cell therapies, oncolytic virus, etc.) in intact human tumor tissues;
2) cultured in serum-free, chemically defined medium, preventing artificial activation or altering of immune and cancer cell states;
3) validated at single-cell RNA-sequencing level to maintain tumor associated immune cells ex vivo for at least 8 days, not only in numbers but also in their activation states;
4) scalable and can be generated from needle biopsy cores to inform clinical trials or patient care as well as surgical samples for multi-dimensional analyses; 5) compatible with all major solid tumor types in human, and 6) compatible with all anti-cancer treatment modalities, including biologics, small molecules, cell based therapies, and virotherapies.Here, we report two retrospective and one prospective clinical studies that demonstrate that E-slices are highly accurate in predicting patient responses to anti-cancer agents. Two small retrospective studies, using colorectal cancer patient PDX tumors, demonstrated that E-slices can accurately predict patients' responses to chemo + targeted therapy combinations with 100 percent Specificity and sensitivity. An interim analysis of an ongoing prospective clinical study using TNBC patient biopsy cores (n=10) shows that E-slice can accurately predict patient responses to the KEYNOTE-522 regimen, which includes pembrolizumab plus chemotherapies with Specificity at 100 percent and Sensitivity at 87.5 percent. Furthermore, this platform enables treatment response to Pembo alone ex vivo, which showed 14 percent response rate from the first 14 patients, which is remarkably similar to the benefit reported in the KEYNOTE-522 study (13.6%). In summary, we report a novel 3D human tumor culture system that can accurately predict patient responses to immunotherapy in a clinically actionable time frame and can provide deep molecular and cellular insights to accelerate immunotherapy testing and development.

#0656 A patient-derived *ex vivo* platform for personalized evaluation of both direct and immune-mediated drug responses.

Jie Wen, Hao Cheng, Nan Yang

PharmaLegacy Laboratories, Shanghai, China

Patient-derived xenograft (PDX) models represent a milestone of preclinical oncology research, serving as a valuable *in vivo* system for evaluating drug efficacy in mice and informing potential personalized therapeutic strategies. However, widespread application of PDX models has been limited by prolonged and variable engraftment timelines, relatively low success rates, and substantial operational costs. Moreover, the gradual replacement of human tumor microenvironment (TME) with murine stromal components compromises the fidelity of PDX models, particularly for evaluating immunomodulatory agents, which requires an intact human immune context. While patient-derived organoids (PDOs) offer a faster and more efficient modeling alternative, their utility is limited by absence of a representative TME, difficulties in assay standardization, and inherent selection bias towards specific cancer cell clones. These limitations raise concerns regarding their ability to provide reliable prediction on efficacy to complex treatment regimens, thereby motivating the development of more holistic *ex vivo* approaches.

In the current study, we established an *ex vivo* tissue culture platform utilizing freshly resected patient tumors to evaluate anti-tumor efficacy of test articles across a panel of patient tumors. Tumor samples obtained from surgery were processed immediately into uniform sections by tissue slicing and cultured in a trans-well system exposed to various stimulants and/or test articles. Post incubation, the cultured tumor tissues were subjected to multiple downstream analyses, including tumor killing assessment, immune cell profiling, biomarker analysis, immunohistochemistry (IHC) and immunofluorescence (IF). The culture medium was analyzed to profile secreted cytokines and chemokines. An illustrative application: tumor tissues collected from lung cancer patients were evaluated on this platform to compare anti-PD1 responses. Tumor collected from anti-PD1 responsive patient revealed pronounced tumor suppression characterized by a 25% increase in $CD8^+CD103^+$ T cells and a 22% reduction in $CD163^+$ macrophages by flow cytometry, enhanced caspase-3 staining, decreased Ki-67 and TGF-β signals via IF, and elevated expression levels of cytokines associated with immune suppression and TAM recruitment as measured by Luminex, collectively distinguishing this profile from that of non-responders.

This *ex vivo* tissue culture system dramatically expands the utility of clinical specimens while maintaining native architecture and cellular heterogeneity. It enables rapid and direct assessment of therapeutic responses and shows strong correlation with *in vivo* outcomes, bridging a critical gap between traditional *in vitro* assays and subsequent *in vivo* studies. This approach may accelerate the pipeline for anti-cancer drug discovery and development.

#0657 The era of NAMS, incorporating tumor heterogeneity and immune context into human-relevant patient avatar cancer models.

W. Gregory Sawyer, Ryan Smolchek, Duy Nguyen, Alfonso Pepe, Diego Pedro, Erin George, Roger Li

Moffitt Cancer Center, Tampa, FL

Patient-derived microtumor avatars are at the forefront of NAMs (New Approach Methodologies) that recapitulate intratumoral heterogeneity and incorporate the full immune cell tumor microenvironment. To address ongoing challenges in translational cancer modeling, we developed a platform enabling secondary addition of tumor-infiltrating lymphocytes (TILs), CAR T-cells, PBMCs, checkpoint blockade agents (aPD1), antibody-drug conjugates, and conventional chemotherapies to these microtumor systems. Using validated models from ovarian, pancreatic, bladder, colorectal, and endometrial cancers, we have demonstrated high-fidelity assessment of therapeutic response and immune dynamics. High-resolution time-lapse imaging reveals spatiotemporal kinetics of tumor clearance by immune effectors at single-cell resolution, and additional movies demonstrate mechanisms of immune-mediated tumor eradication. These findings benchmark the robustness and translational potential of microtumor avatars for preclinical immuno-oncology research and mechanistic testing.

Purpose: To evaluate the use of microtumor avatars in cancer research, focusing on the integration of tumor heterogeneity and immune context for faithful translational models in NAMs.

Methods: NAMs viability was regularly assessed via immunofluorescence imaging using LIVE/DEAD cell imaging and a Nikon AXR and Multiphoton confocal microscope outfitted with the NSPARC super-resolution detector. Characterization of the patient microtumors was performed using a variety of stains for nuclei, Ki67 activity, Collagen Type I, EpCAM, E-Cadherin, N-Cadherin, VE-Cadherin, Vimentin, CD45, CD3, Trop-2, Nectin-4, and others. Following long duration time-lapse experiments, super-resolution microscopy was performed using our typical fixation and permeabilization protocols.

Results: Patient-derived microtissues were maintained in culture for extended periods and exhibited sustained viability and diverse cellular composition, as confirmed by the above imaging techniques. Proliferative activity, dynamic tissue architecture, and variable marker expression were revealed using immunofluorescence across all microtumors. Drug response studies using targeted agents, immune checkpoint inhibitors, and broad-spectrum cytotoxics demonstrated in vitro outcomes concordant with patient therapies, including both sensitivity and resistance patterns in solid tumor models. Furthermore, functional assays with engineered immune cells such as CAR T-cells and TILs confirmed robust immune-mediated tumor killing within these microtumor platforms.

Conclusions: These results support that advanced patient-derived microtissue NAMs now enable robust opportunities for increased precision in translational cancer research and therapeutic discovery.

#0658 Establishment of a novel ex vivo bone metastasis culture platform for triple-negative breast cancer.

Tiina E. Kahkonen[1], Saif Wahid[2], Sangita Kushary[2], Debabani Roy Chowdhury[2], Arnab Roy Chowdhury[2], Jussi M. Halleen[1]

[1]OncoBone Ltd, Kiviniemi, Finland,[2]Mestastop Solutions Pvt Ltd, Bangalore, India

Drug development for bone metastasis has been hindered by the lack of appropriate in vitro models in early testing. Typical in vitro models lack the crucial bone microenvironment, leading to wrong conclusions about efficacy on bone metastases in vivo. We have established a novel bone metastasis ex vivo culture platform including bone discs from tibiae of mice with 4T1 triple-negative breast cancer (TNBC) tumors.

Female Balb/c mice were injected intratibially with 10,000 (10k) or 20,000 (20k) 4T1 mouse TNBC cells or PBS (control). Tumor-induced bone changes were monitored by X-ray imaging. 4T1 tumor and control bones were collected and cut into 2-3 mm thick discs, rinsed with antibiotic-containing medium, and cultured in basal medium (RPMI-1640 medium supplemented with 10% FBS) in a humidified incubator. Osteoblastic medium included ascorbic acid and beta-glycerophosphate, and osteoclastic medium included M-CSF and RANKL supplements. The culture medium was partially replenished every 72 hours. Culture lengths from 7-21 days were tested and analyzed for cell viability (trypan blue), proliferation (CCK-8 assay), bone resorption (TRACP5b ELISA) and bone formation (PINP EIA and Alizarin S Red staining).

Intratibial inoculation of 10k and 20k 4T1 cells induced progressive osteolytic lesions that were monitored for 13 days by X-ray imaging. Based on the extent of osteolytic lesions, days 3-5 were selected to model early bone metastasis growth with visible tumor-induced effects on bone, and 20k 4T1 cells were selected for future studies due to more uniform tumor growth. In ex vivo cultures of tibia bone discs in basic medium, cell viability remained high at days 7 and 10 (88 and 91%, respectively) but dropped to 47% at day 14. Therefore, 10 days was considered maximum culture length. In discs with 4T1 tumors, cell doubling time was higher than in control discs. Addition of osteoblastic supplements increased PINP levels in control discs and in discs including 4T1 tumors at day 10, after which the values decreased. Increased Alizarin Red staining was observed at day 10. Addition of osteoclastic supplements increased TRACP5b levels at days 10 and 14, after which the values decreased. Similar increase was not observed when adding both osteoblastic and osteoclastic supplements. Discs with 4T1 tumors had higher baseline TRACP5b levels than control discs, and the values were further increased with osteoclastic and both osteoclastic and osteoblastic supplements.

We have established a novel ex vivo bone metastasis culture platform where cancer cell, osteoclast and osteoblast activities were maintained after in vivo extraction of bone discs, indicating that the ex vivo cultures were able to maintain in vivo properties of the tumor and its bone microenvironment. We conclude that this platform provides a miniaturized, labor and cost-effective way for preliminary testing of effects of experimental therapies on bone metastases.

#0659 Ex vivo evaluation of a MUC1-targeted bispecific T-cell engager in ovarian tumoroids using Nilogen's 3D-EXpress platform.

Vanessa Garrido, Janine DeBlasi, Andrea Mockabee, Seth Currlin, Justin Silberman, Jessica Linkous, Alliyah Humphrey, Jared Ehrhart

Nilogen Oncosystems, Tampa, FL

BACKGROUND: Mucin 1 (MUC1) is a relevant target for bispecific T-cell engagers due to its expression in epithelial malignancies. Nilogen Oncosystems' 3D-EXpress ex vivo tumoroid platform enables direct assessment of patient-specific responses to immunotherapies in a physiologically preserved tumor-immune microenvironment. This study evaluated the activity of a commercially available recombinant Anti-CD3 x Anti-MUC1 bispecific T cell engager antibody (MUC1-TCE) in cryopreserved ovarian tumor-derived tumoroids to characterize immune activation using Nilogen's integrated platform combining flow cytometry, cytokine profiling, and RNA transcriptomic analysis.

METHODS: Pathology reports were reviewed for all tissues and confirmed characteristic histological features consistent with high-grade ovarian carcinoma. Tissues were evaluated for MUC1 expression, showing high to low levels. Tumoroids were generated by mechanical dissociation without enzymatic digestion or in vitro propagation. After thawing, tumoroids were treated with MUC1-TCE, isotype control, or positive control. Multiparametric flow cytometry measured T-cell activation. Parallel supernatants were collected for multiplex cytokine profiling, and RNA was isolated for downstream transcriptional analysis.

RESULTS: MUC1-TCE treatment induced clear immune activation across multiple tissues. CD4+ T cells upregulated 4-1BB, CD25, CD69, OX40, and PD-1, while CD8+ T cells upregulated 4-1BB, CD25, ICOS, and OX40. Cytokine profiling showed strong induction of inflammatory mediators, with IFN-γ and TNF displaying the greatest response. Preliminary RNA analysis revealed enrichment of immune-activated, inflammatory, and cytokine-driven pathways consistent with effector engagement.

CONCLUSIONS: These findings demonstrate the feasibility of using cryopreserved patient-derived tumoroids for ex vivo testing of bispecific T-cell engagers while preserving the native tumor-immune microenvironment. Integration of cytokine measurements, transcriptomic readouts, and immune phenotyping provides a scalable approach for characterizing mechanisms of action of MUC1-targeted agents and supports continued development of bispecific immunotherapies for solid tumors.

#0660 Integrating passage-zero patient tumor tissues from distant institutions into a rapid, ex vivo drug screening platform.

Adebimpe Adefolaju[1], Breanna Mann[1], Rajaneekar Dasari[1], Emma Livne[1], Caroline Stockwell[1], Alain Valdivia[1], Sonia Lipp[2], Angel Augst[2], Kerry Fitzgerald[3], Jonathan Williams[3], Hardik Parikh[4], Shuang Gao[4], Jie An[4], Taylor Jensen[5], Shakti Ramkissoon[5], Dominique Higgins[1], Yasmeen Rauf[1], Scott Elton[1], Kimberly Hamilton[1], Yair Gozal[2], Vincent DiNapoli[2], Albert Baldwin[1], Shawn Hingtgen[1], David Kram[1], **Andrew Satterlee**[1]

[1]University of North Carolina at Chapel Hill, Chapel Hill, NC,[2]Mayfield Clinic, Cincinnati, OH,[3]Labcorp, San Diego, CA,[4]Labcorp, Buffalo, NY,[5]Labcorp, Durham, NC

Access to living patient tumor tissue remains a major barrier to accelerating preclinical drug development and informing clinical care. Over the last decade, we have developed a “New Approach Methodology” platform called Screening Live Cancer Explants (SLiCE), which reproducibly engrafts living, passage-zero patient tumors atop substrates of living tissue. Our streamlined four-day drug screening workflow enables tumor engraftment within one day of resection, drug addition one day post-engraftment, and quantification of tumor survival three days later. This procedure is fast enough to accelerate preclinical workflows and inform clinical decisions while minimizing genetic drift. As we expand use of SLiCE in the preclinical setting, our established protocols for collecting and cryopreserving passage-zero tumor tissue have thus far enabled us to cryopreserve over 150 grams of viable brain tumor tissue in over 700 cryovials from 41 patients for personalized drug sensitivity profiling and preclinical testing. Through an active collaboration between UNC and Labcorp, we have shown that replicate cryopreserved aliquots of tumor samples post-thaw are equivalent by whole-exome sequencing (WES), RNA sequencing, and functional drug response. Still, availability of living, passage-zero patient tumor tissue remains our limiting component to further scaling this assay for broad adoption and impact. To overcome this hurdle, our SLiCE Team at UNC is expanding collection of viable tumor tissue to other groups and institutions. A new collaboration with the Mayfield Clinic has successfully yielded shipment of tumor tissues freshly resected from patients at partnering hospitals to UNC. These tumor specimens were viably maintained throughout overnight shipping at 4C, quantified by live tumor cell metabolism via Presto Blue assay, and have been successfully engrafted on SLiCE, quantified by live tumor cell bioluminescence on Day 4 after seeding, the length of our standard drug screening assay. These data provide our first proof-of-concept evidence that tumors resected from patients at distant institutions can be shipped fresh to UNC for testing on SLiCE. Our goal is to continue receiving 3-4 tumors per month from Mayfield to optimize and refine this process. These efforts position SLiCE as a leading New Approach Methodology to test promising experimental agents and one day guide clinical care using passage-zero patient tumor tissues, including fresh, living tumors shipped from other sites.

#0661 Rapid CAR T testing in an ex vivo platform that maintains passage-zero patient tumor tissues and their native immunosuppressive microenvironment.

Xiaopei Zhang[1], Breanna Mann[1], Adebimpe Adefolaju[1], Alain Valdivia[1], Rajaneekar Dasari[1], Caroline Stockwell[1], Noah Bell[1], Ashley Geiger[1], Tracy A. Withers[1], Xin Zhou[1], Alexa Rodriguez[1], Kerry Fitzgerald[2], Jon Williams[2], Hardik Parikh[3], Shuang Gao[3], Jie An[3], Taylor Jensen[4], Shakti Ramkissoon[4], Dominique Higgins[1], Yasmeen Rauf[1], Scott Elton[1], Kimberly Hamilton[1], Albert Baldwin[1], Barbara Savoldo[1], Shawn Hingtgen[1], David Kram[1], **Andrew Satterlee**[1]

[1]University of North Carolina at Chapel Hill, Chapel Hill, NC,[2]Labcorp, San Diego, CA,[3]Labcorp, Buffalo, NY,[4]Labcorp, Durham, NC

Adoptive T cell therapies, including chimeric antigen receptor (CAR) T cells, have shown limited success in solid tumors, largely due to widespread preclinical models that fail to capture patient tumor heterogeneity and the immunosuppressive tumor microenvironment (TME). Conventional systems, including cell lines, xenografts, and organoids, often lack critical TME features, leading to overestimation of therapeutic potency. Progress in next-generation CAR T therapies requires more biologically representative models. We have therefore developed Screening Live Cancer Explants (SLiCE), a New Approach Methodology platform that engrafts living, passage-zero patient tumors onto substrates of living tissue. This design preserves tumor heterogeneity better than in vitro culture and enables investigation of how patient tumor-associated cells influence T cell activity. As proof of concept, we tested B7-H3-targeted CAR T cells from three healthy donors against cell lines and passage-zero adult and pediatric brain tumors (n = 3 GBM, 2 medulloblastoma, 1 ATRT). B7-H3 expression was quantified by IHC (H-score) and flow cytometry. CAR T or control T cells were added to SLiCE-engrafted tumors at effector-to-target ratios from 1:3 to 3:1. Tumor kill was measured by live tumor cell bioluminescence within four days of seeding. Killing of B7H3+ tumors occurred only in the presence of CAR+ T cells and not non-transduced T cells; killing among multiple tumor specimens collected from the same patient positively correlated with B7H3 expression (assessed by flow cytometry). Notably, the ATRT tumor showed minimal killing despite high B7-H3 expression (H-score = 152). Flow/CyTOF analyses revealed inhibitory myeloid cells, regulatory T cells (~30% CD4+CD25+FoxP3+), and >60% PD-L1+ tumor cells, features likely suppressing CAR T activity. These findings indicate SLiCE maintains key immunosuppressive TME elements and can dissect mechanisms of immune evasion. Ongoing studies aim to overcome these barriers. Together, these data highlight SLiCE as a model that can uniquely leverage passage-zero patient tumor and tumor-associated cells to rapidly predict outcomes and potential challenges for CAR T cells and other cell-based therapies.

#0662 Non-animal platforms using ex-vivo human tissue and live-cell biosensors enable functional drug testing in renal cell carcinoma.

Shuchi Gulati[1], Madhura Patankar[2], Elijah Kofke[3], Michael Pargett[3], Daniel Oberbauer[3], Ching-Hsien Chen[4], John G. Albeck[3]

[1]UC Davis Comprehensive Cancer Center, Sacramento, CA,[2]UC Davis Comprehensive Cancer Center, Davis, CA,[3]University of California Davis, Davis, CA,[4]UC Davis, Sacramento, CA

Background: Animal models frequently fail to recapitulate the immune and metabolic complexity of renal cell carcinoma (RCC). To address this, we developed two complementary non-animal platforms, a patient-derived ex vivo tissue system and a biosensor platform to enable rapid, mechanistic, and clinically relevant drug testing.
Experiments: i) Fresh RCC specimens were sectioned into precision-cut tissue slices (PCTS) and co-cultured with autologous peripheral blood mononuclear cells (PBMCs) (5x10^5 co-cultured with one PCTS) for six days. Treatment groups included: a) cabozantinib (cabo) alone, b) cabo with cemiplimab (cemi, a PD-1 inhibitor), c) cemi with fianlimab (fin, a LAG-3 inhibitor). The co-cultured PCTS were analyzed using H&E staining and a Live-Dead stain to assess cell viability. ii) Using RCC cell line 786O, which recapitulates the canonical metabolic phenotype of clear cell RCC (high glycolytic flux and HIF1A stabilization), we performed time-course experiments to assess dynamic changes in biosensor signal. Cells were plated on biosensor-compatible microplates and treated with metabolic inhibitors (2-DG, oligomycin) and pharmacological targeted drugs relevant to RCC [(PI103- PI3K/mTOR inhibitor), sunitinib and cabozantinib (tyrosine kinase inhibitors), and linsitinib (IGF1R inhibitor)]. Biosensor output was recorded at 30-minute intervals over 12 hours to generate high-resolution kinetic profiles.
Results: i) Viability assessment of co-cultured PCTS indicated a significantly higher proportion of dead cells in the cabo+cemi compared with either a single agent or cemi+fin doublet strategy. Additionally, the number of viable PBMCs, assessed six days post-co-culture, was also highest in the cabo+cemi-treated tumors. MxIF analysis is ongoing.
ii) In the biosensor experiment, 786O RCC cells showed minimal AMPK response to oligomycin, suggesting reliance on glycolysis. Further, these cells, upon treatment with Linsitinib and PI103, induced a rapid and sustained reduction in HYLIGHT (glycolysis) signal intensity. A more gradual decrease was observed with cabozantinib, whereas sunitinib showed almost no effect, suggesting partial metabolic inhibition or pathway compensation. Ongoing work is using a modified protocol, SCENITH (Single-Cell ENergetic metabolism by profiling Translation Inhibition), which allows evaluation of cellular energy metabolism at single-cell resolution using puromycin-based labeling to quantify protein synthesis in the presence of metabolic inhibitors.
Conclusion: This integrated, fully non-animal strategy overcomes key limitations of animal models by combining preserved human tumor microenvironments with high-resolution metabolic biosensing. Together, these platforms enable rapid and mechanism-based profiling of therapeutic vulnerabilities in RCC.

#0663 TOP1i-ADC demonstrates immune-stimulating activity in colorectal cancer explants.

Irene I. Lee, Durga B. Dandamudi, Yoshiko Hashikawa, Marion L. Refici, Michelle Belmont, Iraz Aydin, Rhyannon Spangler, Steven Chirieleison, David Sharon, PK Epling-Burnette, Athan Vasilopoulos, Tamar Uziel, Jack Chen, Lloyd Lam

AbbVie Inc., North Chicago, IL

Topoisomerase 1 (TOP1) is a ubiquitous enzyme that primarily regulates the topology of DNA by governing the relaxation of DNA supercoiling. When TOP1 is inhibited by camptothecin and its analogs, re-ligation of TOP1 cleavage complexes (TOP1cc) is prevented, leading to the accumulation of TOP1cc-associated DNA damage, inhibition of cellular proliferation, and eventual cell death. Antibody drug conjugates (ADCs) are a class of cancer therapeutics in which a potent cytotoxic payload is linked to a tumor-targeting antibody. ADCs allow direct delivery of a drug to tumor cells, thus enhancing tumor cell-specific killing. Several TOP1 inhibitor-ADCs (TOP1i-ADCs) have been approved, and others are under clinical investigation, showing efficacy in solid tumors. Beyond direct cytotoxicity, recent evidence suggests that TOP1i and TOP1i-ADCs trigger immunogenic changes in cancer cells, fostering immune activation. In studies using colorectal (CRC) cell lines treated with adizutecan, a proprietary AbbVie TOP1 inhibitor, we observed upregulation of gene pathways involved in the Type I Interferon response. Notably, adizutecan increased surface expression of immunogenic markers including MHC-I, MHC-II, CALR, and PD-L1 in CRC lines. To evaluate TOP1i-ADC-induced immune activation within a native tumor microenvironment, organotypic tumor slices from fresh human metastatic colorectal carcinoma were utilized for this study. We treated these fresh human metastatic colorectal carcinoma tissue slices with TOP1i-ADC and evaluated changes in both the tumor and immune cells by flow cytometry and spatial transcriptomics. TOP1i-ADC treatment led to reduced tumor cell proliferation and viability, and consistent activation of dendritic cells as well as CD4 T cells. CD8 T cell activation was observed in 3 out of 5 explant samples. The flow cytometry data was further supported by the secretome profile, which shows elevated levels of pro-inflammatory chemokines and cytokines such as CCL3, CXCL10, G-CSF and granzyme B (GZMB). Spatial transcriptomics analysis revealed TOP1i-ADC treatment reduced DNA replication and cell cycle gene signatures consistent with TOP1i payload release within the tumor explant. Consistent with the flow cytometry data, immune cell responses displayed dendritic cell maturation in both proximal and distal regions to the tumor cells. CD8 T cell activation, evidenced by higher granzyme B (*GZMB*) expression, was especially prominent in distal areas consistent with spatially distinct regional activation. Collectively, these findings support that TOP1i-ADC therapy drives potent immune activation and immunogenicity, complementing its direct antitumor effects and highlighting its promise for enhancing cancer treatment efficacy.

#0664 Bulk cancer spheroid preservation and post-thaw viability for high-throughput screening applications.

Hilary Sherman[1], Rock Pulak[2]

[1]Corning Incorporated, Tewksbury, MA,[2]Union Biometrica, Holliston, MA

Three-dimensional cancer spheroids provide physiologically relevant models that closely mimic in vivo tumor architecture, making them valuable tools for drug screening and tumor biology research. Despite their advantages, integration into high-throughput workflows is often hindered by labor-intensive and time-sensitive culture processes. In this study, we investigated the feasibility of bulk cryopreservation of cancer spheroid lines using Corning's 12K Flask format, followed by assessment of post-thaw viability and performance in downstream assays. Our findings demonstrate that bulk freezing effectively preserves spheroid morphology and cellular viability across multiple cancer cell types. Post-thaw spheroids retained structural integrity and metabolic activity, supporting their use in screening applications. This scalable approach enhances experimental reproducibility and workflow flexibility, enabling broader adoption of 3D models in preclinical research. These results support the incorporation of cryopreserved spheroids into high-throughput platforms, advancing the utility of 3D culture systems in cancer drug discovery.

#0665 Bridging tumor heterogeneity and drug response: A patient-derived immune-competent 3D spheroid model for translational oncology.

Charlotte Veser, Zuzanna Kotkowska, Irina Agarkova, Sue Grepper, Madhu Nag-LAL, Laure-Anne Ligeon

Insphero, Schlieren, Switzerland

The tumor microenvironment (TME) and immune context are critical determinants of therapeutic outcome. Further, inter-patient variability in cellular composition and immune activity drive differential responses to therapy. However, the majority of preclinical models depend on epithelial monocultures and lack stromal and immune components. This failure to capture multicellular interactions limits their translational relevance for drug development and patient stratification.To address these limitations, we established a patient-derived immune-competent 3D tumor spheroid platform. This platform preserves patient-specific cellular diversity and microenvironmental interactions while maintaining compatibility with high-throughput applications. We demonstrate the pipeline's capabilities using patient samples from cases of breast, colorectal, and non-small cell lung cancer.Patient tumor resections were dissociated into single-cell suspensions and subsequently re-aggregated under defined conditions to form uniform3D tumor spheroids. The single-cell suspensions are analyzed to identify different cell types, such as epithelial, stromal, endothelial, and immune cells, and to assess patient-specific tumor and stromal marker expression. Flow cytometry and high-content imaging confirmed retention and self-organization of diverse cell populations within aggregated spheroids. Functional assays revealed patient-specific responses to standard-of-care and targeted therapies, reflecting patient heterogeneity observed in the clinic. Parallel isolation of autologous peripheral blood mononuclear cells (PBMCs) enabled immune co-culture assays reflecting autologous tumor-immune interactions and cytokine secretion.This platform offers a robust and scalable approach to modelling the complex tumor- immune microenvironment across multiple solid cancers in a patient-specific manner. This approach enables more predictive preclinical testing and supports precision oncology.

#0666 Developing an ascitic fluid-derived organoid model for transcriptomic and therapeutic investigations in ovarian cancer.

Md Mynul Hassan[1], Zulfikar Azam[2], Taslim A. Al-Hilal[2], Sourav Roy[3]

[1]The University of Texas at El Paso, El Paso, TX,[2]Department of Molecular Pharmaceutics, University of Utah, Salt Lake City, UT,[3]Biological Sciences, The University of Texas at El Paso, El Paso, TX

Introduction: Epithelial ovarian cancer (EOC) spreads freely within the intraperitoneal cavity, enabling tumor dissemination, abdominal organ adhesion, and ascites formation through lymphatic obstruction. Because solid-tumor samples are scarce after debulking surgery, ascites provide a crucial window into disease evolution. Its rich cellular and acellular components fuel tumor survival, immune evasion, and chemoresistance but remain underused in preclinical models. We therefore aim to establish and characterize an ascites-derived organoid (AsO) platform that captures this heterogeneous tumor microenvironment (TME) and improves drug-response profiling.
Methods: Malignant ascites and tumor tissues were collected from consenting Hispanic patients under an approved IRB protocol. Ascitic fluid was centrifuged and repeatedly lysed to remove red blood cells. The whole ascitic cells (WhAs) were divided for organoid culture and biobanking. Part of WhAs was embedded in extracellular matrix and overlaid with optimized organoid culture media. Organoids were passaged every 8-13 days and cryopreserved in freezing media. We documented morphology with brightfield imaging, stained FFPE sections with H&E, and immuno-stained whole-mount organoids. Bulk RNA-seq was performed on matched primary tumors (WhTu), WhAs and AsO, and we quantified expression using standard bioinformatics pipelines followed by correlation and pathway analyses. Drug sensitivity in organoids was measured by live/dead assay (CC50) and luminescence assay (IC50).
Results: Organoid culture media optimization markedly improved organoid formation, passaging efficiency, and long-term expansion. A major achievement was the successful cryopreservation of both WhAs and AsO, which resumed growth after resuscitation in nearly all cases. H&E staining revealed nuclear atypia, a hallmark of EOC, and immunofluorescence confirmed expression of key biomarkers including PAX8, p53, CK8, and Ki67. Pearson correlation coefficients demonstrated strong global transcriptional similarity ($R^2 = 0.87$) between AsO and WhAs. To identify ascites-specific genes within the ovarian cancer (OC) TME, we also examined transcriptional differences (DEGs) between AsO and WhTu. We identified 22 overlapping genes when comparing between the top 50 highly expressed genes from AsO and OC tumor-derived organoid datasets from Gene Expression Omnibus (GEO). Patient-specific drug responses to Carboplatin, Paclitaxel, Lenvatinib, and Saruparib have been observed.
Conclusion: The comprehensive characterization of ascites-derived organoids at histological, protein marker, and transcriptomic levels, along with systematic drug sensitivity comparisons across multiple experimental platforms, will significantly enhance their clinical and translational relevance.

#0667 Mapping and targeting spatial heterogeneity in CRC through patient-derived organoids.

Maxim Norkin[1], Jonathan Bac[1], Louis McConnel[1], Sylvie Andre[1], Marina Alexandra Gaveta[1], Joerg Huelsken[2], Marianna Rapsomaniki[1], Raphael Gottardo[1], Krisztian Homicsko[1]

[1]Oncology, CHUV, Centre hospitalier universitaire vaudois, Lausanne, Switzerland,[2]EPFL, Lausanne, Switzerland

Inter- and intra-patient heterogeneity, as well as spatial heterogeneity of cancer cells and the tumor microenvironment (TME), is a formidable barrier for cancer therapies. Ex vivo, patient-derived organoids (PDOs) hold promise as better platforms for drug development and can be applied in personalized medicine. Previous work has shown that genomic and clonal heterogeneity of tumors, as well as expression heterogeneity, can be maintained in PDOs. However, it remains unclear whether PDOs preserve the same degree of spatial expression heterogeneity observed in the original tumors. We propose an analytical pipeline combining spatial transcriptomic and phenotypic analysis of PDOs that can capture and track spatial heterogeneity across multiple assays, including during drug treatment.We have developed an organoid multi-embedding platform that allows parallel analysis of multiplex organoid cultures using imaging-based spatial transcriptomics. We validate the platform by comparison to non-spatial single-cell transcriptomic and donor tumor spatial transcriptomic analyses. With that, we have analyzed 40 CRC (colorectal cancer) PDOs and 16 CRC PDO-tumor pairs by spatial transcriptomics (Xenium 10x), including drug treatments, organoid developmental trajectories, and co-culture experiments. We have discovered intra- and inter-patient heterogeneity in tumors and PDOs and linked gene expression to organoid shapes. We further distinguished different expression programs in CRC and linked them to the spatial positioning of malignant cells in tumors. Finally, we have identified and analyzed dormant organoids in heterogeneous PDO cultures and compared them to the original tumors.The combination of ex vivo PDOs and spatial transcriptomics could open novel avenues for drug development selectively targeting spatial subsets of cancer cells and the TME.

#0668 Establishment of a patient-derived organoid-immune cell co-culture platform for evaluating the efficacy of immuno-oncology therapies.

Yuhui Wang, Pengyu Li, Chuyue Yu, Mingshuo Zhang, Pengwei Pan, Fang He

Pharmaron Beijing Co., Ltd., Beijing, China

Introduction: Tumor immunotherapy, known for its high specificity and favorable safety profile, inhibits tumor progression and prolongs patient survival by activating the immune system. However, the full potential of many immuno-oncology agents and the underlying mechanisms of therapeutic resistance remain incompletely understood. The emergence of organoid technology has not only improved the accuracy of tumor modeling but also enabled co-culture with immune cells, thereby advancing the study of tumor-immune interactions and immunotherapy evaluation. Here, we established a human tumor organoid-immune co-culture platform for assessing responses to multiple immunotherapies.

Methods: We established human tumor-immune co-culture models by introducing immune components-including allogeneic PBMCs with PDX-derived organoids (PDXOs) across several cancer types. For drug efficacy assessment, above co-culture models were treated with monoclonal antibodies (mAb) to evaluate antibody-dependent cellular cytotoxicity (ADCC). Additionally, ovarian cancer (OVC) PDXOs were co-cultured with PBMCs to assess T-cell engager (TCE)-mediated, TROP2-targeted T-cell-dependent cytotoxicity (TDCC). To mitigate graft-versus-host effects associated with allogeneic PBMCs, we further developed a PDO-autologous tumor-infiltrating lymphocytes (TILs) co-culture system and used it to modeling the patient responses to immune checkpoint inhibitors (ICIs).

Results: In the PDXO-PBMC co-culture system, live-cell and high-content imaging revealed that in the presence of Trastuzumab, HER2-high CRC PDXOs were effectively targeted and infiltrated by immune cells, whereas these results were not observed in HER2-low PDXO models. Similarly, Sacituzumab only induced significant ADCC in TROP2-high PDXO models. The co-culture platform also proved effective for evaluating TCEs: a TROP2xCD3 bispecific TCE significantly mediated TDCC in TROP2-high OVC PDXOs. Furthermore, screening of ICIs across multiple PDO-TILs co-culture models demonstrated that this co-culture system accurately predicted clinical treatment efficacy.

Summary: We have established a versatile tumor organoid-immune co-culture platform that recapitulates key features of the tumor immune microenvironment. This platform enables efficient evaluation and validation of diverse immunotherapies, including mAbs-mediated ADCC, TCE-mediated TDCC, and the efficacy of ICIs. This biomimetic in vitro model provides a powerful tool for immuno-oncology drug screening, accelerates drug development, and offers a human-relevant alternative that circumvents species-specific limitations and animal welfare concerns associated with preclinical animal models.

#0669 Development and characterization of a patient-derived liver organoid biobank for toxicology and functional studies.

Rudra Bhowmick[1], Benjamen O'Donnell[1], Fong Cheng Pan[1], Mahi Rahman[1], Sameena Wani[1], Willem Kools[2], Vi Chu[1]

[1]MilliporeSigma, Temecula, CA,[2]MilliporeSigma, Burlington, MA

Liver is the largest solid internal organ and performs numerous critical functions. Annually, liver diseases claim about 2 million lives globally (1). Traditional models for investigating liver biology, including 2D cultured cell lines, primary cells, and 3D spheroids, fail to accurately represent the in vivo metabolic and structural complexities. Additionally, animal models are expensive, time-consuming, ineffective, and may pose ethical dilemmas. Therefore, there is an urgent need for advanced liver models that can accurately mimic tissue characteristics.Organoids are self-organizing 3D structures that replicate the architecture and functionality of the original tissue (2). Patient-derived organoids (PDOs) closely resemble the source tissue and may reflect individual responses to therapy. In this study, we present the development and characterization of a biobank consisting of 11 individual liver PDO lines, which capture donor variability and enhance the applicability of these models for toxicology studies.Liver tissues were collected with donor consent. PDOs were created by adapting a previously published protocol (3). Briefly, tissue samples were minced, digested, filtered, combined with Matrigel (Corning), and cultured in liver PDO-specific growth media. When suitable, undifferentiated PDOs were matured using tailored media.PDO lines were effectively expanded and cryopreserved, demonstrating their robustness. All lines expressed liver-specific biomarkers, verified by qPCR and confocal microscopy. Each line was confirmed to be free of infectious agents and validated as unique via short tandem repeat analysis. Upon maturation, these lines exhibited increased albumin and urea production, along with inducible cytochrome P450 (CYP) activity, confirming their functional maturity. Donor-dependent variability in these phenotypes indicated that the biobank may represent the patient population. Four liver PDO lines were also evaluated for their response to 3 DILI drugs. Based on these results, the liver biobank was concluded to be a robust in vitro model for testing drug responses.Our liver PDO biobank reflects the patient population and will be a valuable tool for pharmaceutical clients. We have successfully established and characterized 11 liver PDO lines, with further characterization efforts ongoing. These PDOs will significantly advance our understanding of liver biology and disease mechanisms, offering applications in drug testing, including DMPK and ADME/ Tox studies. Future initiatives will focus on scaling up, developing specific assays, and creating PDOs from patients with liver conditions, such as hepatocellular carcinoma.

References:1.Asrani et al., 2019. J. Hepatol.2.Zhao et al., 2022. STAR Protocols3.Broutier et al., 2016. Nature Protocols

#0670 Understanding the role of the tumor suppressor gene *ARID1A* in gastric cancer initiation.

Alexa Morales Arana, Nicole Britney Halmai, Jasmine Diaz, Hongyong Zhang, Paul Lott, UCaMP consortium, UCaTS consortium, Luis Carvajal-Carmona

UC Davis, Davis, CA

Introduction: Gastric cancer remains a major cause of global cancer mortality and disproportionately affects underserved racial and ethnic minority populations in the United States. Latino patients experience a higher incidence and worse outcomes, yet genomic data and patient-derived models remain underrepresented. Whole-exome sequencing (WES) of our Latino GC cohort showed that 30% of tumors harbor pathogenic ARID1A mutations, paralleling TCGA frequencies. ARID1A, a core subunit of the SWI/SNF chromatin-remodeling complex, regulates enhancer activity and transcriptional accessibility. Its loss is linked to poor prognosis and metastasis. We hypothesized that ARID1A loss establishes an early premalignant state through chromatin dysregulation and transcriptional reprogramming. To test this, we developed long-term gastric organoid models derived from Latino patients to define the earliest cellular and molecular consequences of ARID1A loss.

Methods: We generated multiple isogenic gastric organoid lines using CRISPR/Cas9 editing in Latino patient-derived normal gastric organoids, including ARID1A/TP53 double-knockout (dKO) organoids and TP53 knockout controls. Organoids were cultured long-term for up to 350 days, with early (~150-day) and late (~350-day) time points analyzed. Multi-omic characterization included H&E histology, RNA sequencing, whole exome sequencing, and CUT&RUN profiling. Comparisons across dKO, TP53 KO, and wild-type controls were used to define the effects of ARID1A loss on early tumorigenesis.

Results: Genome editing generated ARID1A and TP53 loss, and dKO organoids developed progressive morphological abnormalities, including increased proliferation and distinct architectural changes compared to controls. RNA-seq analyses showed genotype-specific and time-dependent transcriptional reprogramming. Differential expression analysis revealed downregulation of digestion and iron transport pathways and upregulation of cilium movement and ciliogenesis. Whole exome sequencing analysis showed fourteen variants were shared across long-term dKO clones, while each clone independently acquired 1-6 additional unique mutations. Affected genes were involved in transcriptional regulation, extracellular matrix remodeling, vesicle trafficking, and receptor tyrosine kinase signaling. The presence of shared and clone-specific variants suggests progressive genomic instability and supports early neoplastic evolution driven by dual ARID1A/TP53 loss.

Conclusion: Latino-derived gastric organoid models demonstrate that ARID1A and TP53 loss cooperatively drive transcriptional reprogramming, genomic instability, and early dysplastic progression. Ongoing CUT&RUN profiling will define chromatin accessibility changes. This work provides a mechanistic foundation for drivers of gastric cancer and a platform for precision prevention strategies.

#0672 Mapping tumor heterogeneity: Ex-Vivo drug responses in synchronous matched primary and metastatic tumors using a 3D functional precision platform.

Rajeshwar Nitiyanandan, Ivan Trus, Chiara Maestri, Ricardo J. Parker, Chris Apfel

SageMedic Corp., Redwood City, CA

Background: Tumor heterogeneity remains a major driver of therapeutic resistance and determining how metastatic dissemination affects functional drug response is critical for clinical decision making. We have developed a 3D microtumor functional profiling assay that preserves native tumor architecture and produces reliable drug response profiles within 7 to 10 days in a CLIA lab environment. This update expands our earlier dataset with additional synchronous pairs of cancer specimen.
Methods: Matched synchronous tumors were obtained from primary ovary, colon, and breast cancers with metastases into the omentum, liver, peritoneum, lung, and axilla. All samples were cooled and shipped overnight, processed within 24 hours, and exposed to NCCN recommended and mechanistically relevant chemo or targeted therapies. Viability was assessed after 72 h to generate cytotoxicity dose responses and concordance was measured using coefficient of determination (R2).
Results: We are reporting on 162 drug comparisons from seven patients with matched primary and metastatic tumors. Drug-response concordance varied substantially by metastatic route. Local metastases showed the highest correlation. A lymphogenic metastasis (breast to axilla) showed moderate correlation. Hematogenic metastases exhibited the weakest correlation, with colon-lung and ovarian soft-tissue/colon pairs showing only modest similarity. However, one ovarian local spread to the omentum demonstrated only moderately strong correlation.
Conclusions: The data suggest that sensitivity and resistance spectra from local metastases tend to correlate well with those from the primary tumors. Furthermore, for metastases from lymphogenic or hematogenic spread, while the correlation tends to be only modest, functional profiling may still be useful to significantly reduce the risk for receiving ineffective treatment.

Correlation of synchronously matched tumor samples

Tumor Type	**Metastasis**	**Relationship**	**R^2**
Ovarian	Omentum	Local	0.98
Ovarian	Liver Capsule	Local	0.93
Colon	Peritoneum	Local	0.93
Ovarian	Omentum	Local	0.47
Breast	Axilla	Lymphogenic	0.77
Colon	Lung	Hematogenic	0.51
Ovarian	Soft Tissue and Colon	Hematogenic	0.42

#0673 Longitudinal mapping of immune activation to tumor response in anti-PD1-treated patient-derived organotypic tumor spheroids (PDOTS).

Jun Yang[1], Julia Vail[2], Eunju Shin[1], Kyungjin Boo[1], Kirti Khardenavis[2], Sinal Patel[2], Kyoung Wan Yoon[1], **Michael A. Perricone**[2]

[1]NEX-I, Inc, Seoul, Korea, Republic of,[2]Xsphera Biosciences, Inc., Cambridge, MA

Nivolumab is an anti-PD-1 immune checkpoint inhibitor approved for colorectal cancer (CRC) with an Microsatellite Instability-High (MSI-Hi) profile, yet patient-to-patient variability and the short-term dynamics of immune and tumor signaling is not well characterized. Patient-derived organotypic tumor spheroids (PDOTS) preserve the multicellular architecture and immune microenvironment of individual tumors, providing an ex vivo platform to monitor these dynamics under controlled conditions. In this study, we used CRC PDOTS from eight patients to characterize day-scale effects of nivolumab on tumor burden and transcriptional programs over a 72 hour peroid. Freshly resected tumors were processed into PDOTS, loaded into microfluidic devices, and treated with nivolumab (100 µg/mL) or a media control. The tumor response to nivolumab was quantified on days 1, 2, and 3 using Hoechst/propidium iodide imaging and automated analysis of live tumor area and the percent tumor killing relative to matched controls. In parallel, RNA was isolated from treated and control PDOTS at each timepoint and profiled using the NanoString IO360 panel to capture coordinated changes in tumor-associated transcripts and immune- and signaling-related gene sets. Across the cohort, nivolumab induced distinct temporal patterns of transcriptional change rather than a uniform on/off signature. A subset of PDOTS showed rapid day-1 increases in immune- and inflammation-related transcriptional programs that remained elevated through 72 hours. A second subset appeared transcriptionally cold at day 1 but developed coordinated shifts in immune and signaling pathways on days 2-3, with preferential upregulation of genes associated with interferon signaling, T-cell engagement, and leukocyte trafficking. A third group displayed minimal changes in these programs over the full 72-hour window. Notably, many PDOTS with strong day-3 pathway modulation showed little or no change from day 1, underscoring the risk of underestimating drug-associated biology from single early timepoints. These temporal patterns of immune activation loosely preceded tumor response. These findings demonstrate that longitudinal profiling in CRC PDOTS reveals discrete patterns of nivolumab-induced immune and tumor signaling dynamics that are not apparent from single terminal measurements, and support the use of time-resolved ex vivo platforms to refine mechanistic studies and biomarker development for immune checkpoint blockade.

#0674 Expansion of multilineage prostate organoids derived from human tissue in ProstaCult™ organoid medium.

Angela Tsai, Allen C. Eaves, Sharon A. Louis, John Stingl

STEMCELL Technologies Inc., Vancouver, BC, Canada

Organoids have emerged as a powerful model for studying normal and tumour cell biology; however, the application of organoid technology for culturing human prostate epithelial cells has been challenging due to the difficulty in maintaining multilineage organoids with androgen receptor (AR)-expressing cells in culture for extended periods of time. To address this, we developed serum-free ProstaCult™ Organoid Medium (Human) to robustly expand human prostate epithelial cells long-term as organoids. Benign human prostate tissue was dissociated and seeded either directly into Matrigel® dome cultures or pre-cultured up to 4 passages in adherent culture in EpiCult™ Plus medium prior to seeding. The resulting organoids were passaged as small fragments every 10 - 12 days. Cultures were analyzed by flow cytometry and immunocytochemistry for the expression of pan epithelial marker EpCAM, luminal markers CD26, keratin 8 (K8), and androgen receptor (AR) protein, and basal markers CD271 and K14. Our results demonstrate that prostate epithelial cells can generate multilineage organoids consisting of a polarized epithelium with both basal ($EpCAM^+$, $K14^+$, $CD271^{high}/CD26^{low}$) and luminal cells ($EpCAM^+$, AR^+, $K8^+$, $CD271^{low}/CD26^{high}$) in 10 - 12 days. These human prostate organoids can be expanded for at least 7 passages while maintaining appropriate marker expression (n = 5) and can be cryopreserved without losing long-term expansion potential. The organoids were responsive to dihydrotestosterone (DHT) removal from the culture medium, with a 43 ± 7% decrease in the total number of luminal cells generated over 3 passages (mean ± SEM; n = 4; $p \leq 0.01$, paired t-test) and a downregulation of AR expression (n = 4). Similarly, enzalutamide treatment resulted in a 24 ± 9% decrease in the total number of luminal cells generated over 3 passages (mean ± SEM; n = 4). These results demonstrate that ProstaCult™ Organoid Medium (Human) enables robust long-term maintenance of multilineage organoids containing AR+ luminal cells *in vitro*, providing an optimized and standardized model system for prostate cancer research.

#0675 B7-H3 targeting ADC GSK5764227 demonstrates broad and varied anti-tumor activity across solid tumor translational models.

Michael Adam[1], Miriam Doepner[1], Ning Sun[1], Chris Hopson[1], Derek Poore[1], Prajna Behera[2], Jenny Laraio[1], Anthony Mazurek[1], Andrew Gehman[1], Shannon McKearnan[1], Jacob Parsons[1], Bjoern-Philipp Kloke[1], Shoba Shetty[1], Ken Hance[1], Jeremy Waight[1], Klaas Bakker[1]

[1]GSK, Collegeville, PA,[2]GSK, Waltham, MA

B7-H3 (B7 homolog 3 protein), also known as CD276 (cluster of differentiation 276), is a cell surface protein that is over-expressed across multiple solid tumors. B7-H3 suppresses T-cell function (e.g. proliferation, activation, and cytokine release) to promote tumorigenesis. Due to its tumor-promoting functions and broad expression profile on a range of malignancies, B7-H3 is an attractive therapeutic target for antibody-drug conjugates (ADCs). GSK5764227 is a B7-H3 targeting ADC conjugated to a topoisomerase I (TOPO1) inhibitor payload, with a DAR of 4. Here we demonstrate in vitro and in vivo efficacy data of GSK5764227 in different preclinical models - including cell lines, *in vitro* patient-derived organoids (PDOs), and *in vivo* patient-derived xenografts (PDX) - across multiple tumor indications including lung, bladder, pancreatic, colorectal (CRC), uterine, prostate, and gastric cancers, supporting the broad therapeutic potential of GSK'227 across different malignancies. Activity was highly varied across tumor histologies in cell lines and PDO models. Similarly, responses were observed across a wide range of PDX indications, but depth of response varied among models within indications. These findings underscore the promise of B7-H3 targeting ADCs with topoisomerase payloads for treating a broad range of cancers, while highlighting the need for further exploration of patient population and/or predictive biomarkers to elucidate determinants of response. Together, this work supports GSK5764227 ongoing clinical development as an innovative therapeutic strategy to address unmet patient needs.

#0676 Modeling patient-specific therapeutic outcomes in cervical cancer using organoid technology.

Shalmoli Bhattacharyya[1], Surbhi Singla[1], Reena Sharma[2], Bhavana Rai[2], Rashmi Bagga[3], Radhika Srinivasan[4], Prateek Bhatia[5]

[1]Biophysics, PGIMER, Chandigarh, India,[2]Radiotherapy and Oncology, PGIMER, Chandigarh, India,[3]Obstetrics and Gynecology, PGIMER, Chandigarh, India,[4]Cytology and Gynecological Pathology, PGIMER, Chandigarh, India,[5]Pediatrics, PGIMER, Chandigarh, India

Organoids have emerged as good preclinical models of human tumors, facilitating translation from basic research to clinical practice. Patient derived organoids recapitulate the heterogeneity and pathophysiology of the cancer and represent the complex tissue environment of clinical tumors more closely than *in vitro* cell lines and animal models. In the present study, we established patient-derived cervical cancer organoids (CC-PDOs) using a modified culture protocol. Tumor specimens were obtained from treatment-naive patients diagnosed with different histological subtypes of cervical cancer (squamous cell carcinoma and adenocarcinoma). The tissues were enzymatically dissociated to generate single-cell suspensions. The cells were embedded in Matrigel and cultured in DMEM media containing defined growth factors to initiate organoid formation. Comprehensive characterization of the established PDOs (n=12) demonstrated that they retained the HPV status and histopathological features of the corresponding primary tumors. The key somatic mutations in cervical cancer-associated genes like *PIK3CA, LRP1B, KMT2A, NF1, TTN,* and *FGFR2* were consistent in both the PDOs and the corresponding patient tumor tissue. Base variant analysis further confirmed that the organoids preserved the mutational landscape of the parent tissue, with C>T transitions representing the predominant base substitution type. The organoids directly derived from patients represent the heterogeneity of cervical cancer patients. To investigate organoids' potential for clinical translation, the correlation between the sensitivity of *ex vivo* tumor organoids and clinical outcomes were recorded. The *ex vivo* chemo-radiation responses of the PDOs showed strong concordance with the clinical outcomes of the respective patients during a six-month follow-up period, thus demonstrating their ability to capture patient radiation heterogeneity. Collectively, these findings demonstrate the feasibility of generating cervical cancer PDOs that faithfully mirror patient-specific tumor characteristics and therapeutic responses, thereby establishing a robust *in vitro* platform for drug screening and the advancement of personalized therapeutic strategies.

#0677 Development of an in vitro exhaustion assay for functional screening of CAR T cell enhancements.

Carla N. Castro[1], Veronica Bergo[1], Marina Zintchenko[2], Susana Minguet[2], Philipp Metzger[1], Cynthia Obodozie[1], **Holger Weber**[1]

[1]Reaction Biology Europe GmbH, Freiburg, Germany,[2]Signaling Research Centres BIOSS and CIBSS; Department of Synthetic Immunology, Faculty of Biology, University of Freiburg, Freiburg, Germany

Chimeric antigen receptor (CAR) T cells have emerged as a powerful tool in cancer immunotherapy, particularly in hematologic malignancies such as B-cell leukemia and lymphoma. CAR T cell therapy involves genetically engineering patient-derived T cells to express synthetic receptors that target tumor-associated antigens, enabling precise and potent immune responses against cancer cells. Despite remarkable clinical successes, especially with CD19-targeted CAR T cells, the therapy has limitations that hinder broader application and long-term efficacy. A significant challenge is T cell exhaustion, a dysfunctional state involving reduced proliferation, diminished cytokine production, and impaired cytotoxicity. Exhaustion often arises in the tumor microenvironment, where persistent antigen stimulation, immunosuppressive signals, and metabolic stress collectively impair CAR T cell function. This limits durability and contributes to relapse in many patients. Overcoming CAR T cell exhaustion is essential to improving efficacy and durability of cellular therapies. Strategies under investigation include optimizing CAR architecture by using alternative co-stimulatory domains, transiently modulating inhibitory pathways, and refining manufacturing protocols to preserve T cell fitness.

An in vitro assay that reliably mimics exhaustion is essential for identifying and validating improvements. In this study, we present several approaches to inducing exhaustion-like phenotypes in CAR T cells. Chronic, antigen-agnostic stimulation and repeated co-culture with antigen-expressing target cells are used to model persistent activation, and to compare various functional readouts. We discuss the advantages and limitations of different assay setups to help identify the most suitable approach depending on the specific experimental needs. A robust and reproducible assay system is key to reliably screening novel CAR T cell designs and therapeutic interventions aimed at mitigating T cell exhaustion. We compare T cell functionality using multiple readout technologies, including impedance-based measurements using xCelligence for adherent and selected suspension cells and luminescence assays with luciferase-expressing target cells as well as flow cytometry. This allows us to highlight the strengths and constraints of each method in capturing functional decline and exhaustion phenotypes.

Our findings support the use of standardized in vitro exhaustion models as valuable tools for the preclinical evaluation of next-generation CAR T cell therapies and combination strategies. Furthermore, our antigen-agnostic model enables evaluation of the impact of any T cell modulation approach on exhaustion dynamics. These models enable more predictive and efficient development of strategies to enhance therapeutic performance.

#0679 BRAF-defined canine urothelial carcinoma organoids as a comparative oncology platform for drug response evaluation.

Kieun Bae[1], Kyong-Ah Yoon[1], Doyoung Jeon[1], Jimin Park[1], Aryung Nam[2], Jung-Hyun Kim[2], Hyun-Jung Han[3], Hun-Young Yoon[4]

[1]Department of Veterinary Biochemistry, College of Veterinary Medicine, Konkuk University, Seoul, Korea, Republic of,[2]Department of Veterinary Internal Medicine, College of Veterinary Medicine, Konkuk University, Seoul, Korea, Republic of,[3]Department of Veterinary Emergency and Critical Care, College of Veterinary Medicine, Konkuk University, Seoul, Korea, Republic of,[4]Department of Veterinary Surgery, College of Veterinary Medicine, Konkuk University, Seoul, Korea, Republic of

Canine urothelial carcinoma, also referred to as transitional cell carcinoma (TCC), is the most common malignancy of the canine urinary tract, with the BRAF V595E mutation reported in approximately 70-85% of cases. This mutation is the canine homolog of the human oncogenic BRAF mutation, which is frequently detected in melanoma and papillary thyroid carcinoma. However, whereas BRAF mutation is a potent therapeutic target in human cancers, clinical efficacy in canine TCCs remains unclear, highlighting the need for additional research. In this study, cancer organoids were established from surgically resected tissues of canine patients six BRAF V595E-mutated TCCs, two BRAF wildtype TCCs, and two cystitis samples. The organoids expressed urothelial markers (cytokeratin-7, uroplakin-3A) and retained BRAF status identical to the parental tumors. Organoids harboring BRAF mutation showed enhanced proliferation and motility, consistent with Ki-67 and vimentin expression. To validate these in vitro results, canine TCC organoids were injected into mice via the tail vein. After seven weeks, all injected mice developed multiple pulmonary nodules, confirming strong metastatic capacity. Tumors were re-cultured as organoids, which retained aggressive phenotypes ex vivo alongside sustained ERK phosphorylation and the BRAF V595E mutation. Organoid-based in vitro assays demonstrated that six targeted inhibitors commonly used in human cancers effectively reduced phosphorylated-ERK expression. Among these agents, sorafenib showed the strongest cytotoxic activity. In xenografted mice, six weeks of oral administration of sorafenib or vemurafenib, markedly reduced tumor formation. Mice treated with BRAF inhibitors also showed decreased p-ERK expression in metastatic lesions and lower BRAF mutant allele fractions in circulating tumor DNA, indicating suppression of metastatic progression through inhibition of the BRAF/MAPK pathway. Collectively, our findings demonstrate that canine TCC organoids function as a comparative model bridging human and canine cancers, enabling us to dissect BRAF-dependent oncogenic mechanisms, evaluate anti-metastatic drug efficacy, and monitor treatment response via ctDNA.

#0680 Clinically predictive patient-derived cells and organoids platforms for precision therapeutic evaluation in NSCLC.

Jiwoo Hwang[1], **Min Hak Lee**[2], Gang-Taik Lee[1], So Young Park[1], Byoung Chul Cho[3]

[1]Department of Research Support, Yonsei Biomedical Research Institute, Yonsei University College of Medicine, Seoul, Korea., Seoul, Korea, Republic of,[2]JEUK Institute for Cancer Research, Gumi-City, Korea, Republic of,[3]Division of Medical Oncology, Department of Internal Medicine and Yonsei Cancer Center, Severance Hospital, Yonsei University College of Medicine, Seoul, Korea., Seoul, Korea, Republic of

Purpose: Patient-derived cells (PDCs) and organoids (PDOs) are established from pleural effusion or ascites to recapitulate the biological features of individual patients. In cancer research, PDC/PDOs serve as valuable preclinical tools because they preserve tumor-specific mutations. Conventional cell lines often fail to capture resistance mechanisms to modern targeted therapies. Consequently, PDC/PDOs offer robust systems for predicting the efficacy of next-generation anticancer treatments. This study aims to demonstrate that PDC/PDO lines serve as suitable platforms for evaluating the efficacy of investigational therapeutics and screening novel therapies for non-small cell lung cancer (NSCLC).

Experimental design: PDC/PDO models were generated from malignant pleural effusions or ascites, using only cytologically confirmed specimens that formed tumor colonies. Genomic alterations were profiled by Sanger sequencing, Whole-exome sequencing (WES), or RNA sequencing. Drug responses were evaluated according to each patient's treatment history to directly compare clinical outcomes with ex vivo sensitivity.

Results: A total of 60 PDCs and 181 PDOs were established from NSCLC patients, including models harboring sensitizing EGFR mutations, KRAS mutations, uncommon mutations, ALK fusions, ROS1 fusions, EGFR exon 20 insertion, and BRAF V600E. Whole-exome sequencing (WES) was performed on 41 newly established NSCLC PDO lines to characterize their genomic alterations. The analysis revealed that EGFR alterations in the PDO cohort comprised 29 amplifications, 20 missense mutations (including L858R, T790M, G719X, C797S, and other mutations), 9 in-frame deletions (E19del), and 1 in-frame insertion (E20ins). Furthermore, MET alterations included 16 amplifications and 1 loss, while ERBB2 exhibited 6 amplifications and 1 in-frame insertion. In three newly established BRAF V600E-mutant PDC models (YU-1171, YU-1172, and YU-1195), exposure to the targeted agents dabrafenib and trametinib revealed distinct patterns of drug sensitivity. The IC_{50} values for dabrafenib and trametinib in YU-1171 were 31.2 nM and 2.96 nM, respectively. In YU-1172, the IC_{50} for dabrafenib exceeded 1 μM, whereas that for trametinib was 14.2 nM. In YU-1195, the corresponding IC_{50} values were 438.4 nM and 10.9 nM. These in vitro trends were concordant with clinical outcomes, as the duration of dabrafenib and trametinib treatment in the corresponding patients was significantly associated with the respective IC_{50} profiles.

Conclusions: Clinically matched patient-derived cells and organoids reliably recapitulate tumor characteristics, providing a robust ex vivo platform for precision therapeutic evaluation in NSCLC.

#0681 C3PO: complex 3D patient organoids for preclinical drug testing in brain tumors.

Antonino Cucinotta, Maria Rosaria Battista, Francesco Scalabri, Anastasiya Kraynyeva, Chiara Soldati, Cristina Alli, Carlo Toniatti, **Alessandro Carugo**, Francesca Puca

IRBM Spa, Pomezia, Italy

Background. Glioblastoma (GBM) remains one of the most aggressive and therapeutically challenging brain tumors, with current treatments offering limited survival benefits. One of the major obstacles in developing effective therapies is the lack of physiologically relevant preclinical models that can accurately recapitulate the structural, molecular, and cellular complexity of the human tumor microenvironment. Conventional 2D cultures and animal models often fail to predict clinical efficacy and are associated with high variability and limited translational value.

Methods. To overcome these limitations, we have developed advanced *ex vivo* 3D glioblastoma models, termed Complex 3D Patient Organoids (C3POs), designed to reproduce the architecture, multicellular composition, and microenvironmental gradients of GBM. Each C3PO integrates patient-derived glioma stem-like cells (PD-GSCs) with astrocytes and microglia in defined ratios, generating self-assembled spheroids that mimic the tumor-stroma interactions observed *in vivo*. To ensure biological relevance, all patient-derived GSCs were also profiled for key genomic alterations commonly associated with GBM. Distinct models representing different molecular GBM subtypes were established and characterized using high-content imaging and fluorescent tracking of individual cell populations. These models have been used to evaluate both proprietary compounds and clinically used agents such as temozolomide, under conditions that more faithfully reproduce the pathophysiological features of GBM.

Results. Preliminary findings revealed subtype-specific responses to treatment, with C3POs of mesenchymal background displaying higher drug resistance and C3POs of proneural background showing higher sensitivity, consistent with a subtype-specific clinical outcome. Furthermore, 3D co-culture systems exhibited reduced drug sensitivity compared to monocultures, underscoring their higher biological fidelity. Current studies are focused on correlating *in vitro* efficacy and pharmacokinetic (PK) data from C3PO models with results previously obtained in orthotopic GBM mouse models, to quantitatively assess their predictive potential.

Conclusions. The C3PO platform provides a robust and scalable tool for *ex vivo* pharmacological testing of anti-GBM agents. By improving translational predictivity and reducing reliance on animal models, these complex 3D systems represent a promising advancement toward more ethical, cost-effective, and clinically relevant preclinical strategies for the development of new therapies targeting brain tumors.

: Methods to Measure Tumor Evolution and Heterogeneity
Poster Session

#0685 eTRACER illuminates the spatiotemporal landscape of immune escape in EGFR-mutant lung adenocarcinoma.

Hongbin Ji[1], Zheng Hu[2], Jinhua Yang[3], Liangzhen Hou[4], Xue Wang[3]

[1]Westlake University, Hangzhou, China,[2]Shenzhen Institute of Advanced Technology, Chinese Academy of Sciences, Shenzhen, China,[3]Center for Excellence in Molecular Cell Science, Shanghai, China,[4]Shenzhen Institutes of Advanced Technology, Shenzhen, China

EGFR-mutant lung adenocarcinoma (LUAD), prevalent among East Asian non-smoking women, typically exhibits a strong initial response to tyrosine kinase inhibitors. However, resistance inevitably develops and these tumors often show poor responsiveness to immune checkpoint blockade. Deciphering the mechanisms of cellular evolution underlying immune evasion in EGFR-mutant LUAD could provide critical insights for developing effective immunotherapies. Here we developed eTRACER, an endogenous gene 3'UTR-based CRISPR-Cas9 lineage tracer that avoids lineage information-disruptive large deletions of traditional techniques and enables the reconstruction of high-fidelity spatiotemporal phylogeny through integration of single-cell RNA-seq, chromatin accessibility and/or spatial transcriptome. We applied eTRACER to systematically decode clonal and phenotypic fate maps of EGFR-mutant LUAD under $CD8^+$ T cell-mediated cytotoxicity in mice. Quantitative analyses of temporally-resolved single-cell lineages across baseline, early- and late-immune escape stages revealed the dynamics of cell-state transitions from the Hypoxic and Proliferative states to the epithelial-mesenchymal transition (EMT) state leading to immune evasion. Spatially-resolved lineage tracing unveiled evident stratification of distinct tumor cell states and location-primed transitions to the EMT state. Multiomic study uncovers the cooperation between the intrinsic role of the activator protein 1 (AP-1) in cancer cells and the spatially stratified interactions between macrophages and tumor cells in promoting the transition to the EMT state. Collectively, we have developed a powerful lineage tracing system eTRACER and uncovered the spatiotemporal cell-fate dynamics underlying immune evasion in EGFR-mutant LUAD. These findings hold important implication for future design of effective immunotherapy.

#0686 Dissecting colorectal cancer heterogeneity and microbiota interactions using murine and patient-derived organoids.

Markus Tschurtschenthaler[1], Valentina Brunner[1], Nicholas Bodenstein[1], Expedito M. Diogenes[1], Lisa Niedermeier[2], Nicole A. Schmid[1], Miguel G. Silva[1], Moritz Jesinghaus[3], Roland Rad[1], Barbel Stecher[2], Julius Fischer[1], Dieter Saur[1]

[1]TUM Universitatsklinikum, TranslaTUM, Technical University of Munich, Munich, Germany,[2]Chair of Intestinal Microbiome, ZIEL - Institute for Food and Health, Technical University of Munich, Freising, Germany,[3]Institute of Pathology, University Hospital Marburg, Marburg, Germany

Alterations in gut microbiota composition and metabolism are tightly linked to colorectal cancer (CRC) initiation, progression, and therapy response, yet underlying mechanisms remain unclear. We established an integrated platform combining organoid biobanks, germ-free orthotopic models, and microbial communities to dissect the interplay between oncogenic signaling, microbiota composition, microbial metabolism, and therapy response in CRC. We generated a comprehensive murine CRC organoid biobank encompassing distinct genotypes, histological subtypes, and tumor stages, together with a complementary collection of patient-derived organoids (PDOs). To probe microbial influence *in vivo*, we developed the first germ-free orthotopic CRC model enabling colonoscopy-guided engraftment of tumor organoids under germ-free (GF) conditions. Parallel transplantation into specific pathogen-free (SPF) and GF mice allows direct assessment of microbiota-dependent effects on tumor progression. We also established stool-derived *in vitro* communities (SDICs) from oncogenic and wild-type backgrounds. Cultured anaerobically in physiologically relevant media, SDICs preserve their native metabolic output, enabling functional assessment of microbiota-derived metabolites on organoid viability and therapy response without artifacts from direct bacteria-organoid co-cultures. Comparative analyses of SPF and GF mice revealed comparable survival after carcinoma organoid transplantation, whereas GF mice showed significantly prolonged survival after adenoma transplantation, indicating tumor growth and progression are slowed without microbiota. To dissect this host-microbiota interplay, we analyzed SDIC-derived metabolites and found that supernatants from wild-type SDICs were more effective than those from oncogenic SDICs in reducing tumor organoid viability. Notably, wild-type SDIC metabolites also sensitized tumor organoids to radiation therapy, highlighting microbiota-mediated modulation of therapeutic response. These findings demonstrate that epithelial oncogenic mutations not only drive tumorigenesis but also remodel the gut microbiota, depleting protective taxa and enriching tumor-promoting species. Consistent with this, 16S rRNA and metagenomic analyses confirmed host genotype dictates gut microbiota composition. To provide a translational bridge to murine models, we transplanted PDOs orthotopically and showed that both PDOs and their xenografts faithfully recapitulated patient-specific histology, molecular features, and therapy responses, establishing robust preclinical models to target colorectal cancer heterogeneity. Together, these findings identify microbiota-derived metabolites as critical regulators of CRC evolution and therapy response, and establish a modular framework for microbiota-informed precision oncology.

#0687 *In situ KRAS*-mapping and spatial -omics characterization in lung premalignancy.

Amanda Lindberg[1], Bartosz Sobocki[2], Patrick Micke[1], Carina Strell[1]

[1]Immunology, genetics and pathology, Uppsala University, Uppsala, Sweden,[2]Department of Oncology and Radiotherapy, Medical University of Gdańsk, Gdańsk, Poland

Introduction: Lung cancer symptoms typically do not appear until advanced stages, leading to late diagnoses. This delay is a major contributor to its poor prognosis, resulting in lung cancer being the leading cause of all cancer-related deaths worldwide. Essential biological understanding of how lung cancers arise and progress is still lacking. Studying premalignant lesions that eventually develop into invasive carcinomas helps to bridge this knowledge gap. We are focusing on adenocarcinomas (ACs), the most common subtype of lung cancer, and especially, activating mutations in the *Kirsten rat sarcoma virus oncogene (KRAS),* which is among the most common oncogenic mutations and has previously been reported in premalignant lung lesions. Given that *KRAS* signaling is growth-promoting, it is reasonable to assume that *KRAS*^{mut} promotes tumor formation and progression. However, the extent of its influence, the timing of when it arises, and particularly its connection to histologic and phenotypic changes driving tumor evolution, remain unclear.

Methods: We have collected a cohort from biopsy material, initially collected for diagnostic purposes from AC patients at varying stages of tumor evolution, with some matched 'normal-histology' samples when available. In total, tissue from 38 patients with AC premalignancies is available for investigation. To map *KRAS* mutations *in situ,* we employed a BaseScope assay with commercial detection probes against the different *KRAS*^{mut} transcripts. To map *KRAS* statuses to cellular phenotypes in the microenvironment, we are running a 6K panel on the CosMx platform (Bruker) on a subset of patients, which is a highly sensitive spatial transcriptomics technique at single-cell resolution. Spatial Mass Spectrometry (MS) tracking metabolic features on the timsTOF flex MALDI-2 (Bruker) is also being performed on a subset of patients.

Results: Initial tests of the BaseScope assay have revealed specific, yet not sensitive, signals of *KRAS*^{mut} transcripts in premalignant lesions. While advanced cancers display distinct signals, premalignant lesions have fewer, if any, signals. This might be due to the lower expression levels of *KRAS* at the earlier stages. To address this, we are now applying a BaseScope assay with signal amplification to be able to track *KRAS* expressed at lower levels. Preliminary analyses of the Spatial MS matrix have revealed highly individual metabolomics features, with great inter-patient heterogeneity. This pattern is also reflected in bulk RNA-seq data, revealing expression profiles more similar across, e.g., Adenocarcinoma *in Situ* (AiS) and invasive AC from the same patient, than between the AiSs from different patients.

Conclusions: By applying this state-of-the-art multi-omics approach to premalignant adenocarcinomas, we hope to identify key regulators of early lung cancer progression and to translate these findings to clinically relevant basic molecular diagnostics.

#0688 Pan-cancer mapping of genetic immune escape evolutionary trajectories.

Shengqing Gu, Wenjie Chen, Toby Baker, Zhihui Zhang, Huw A. Ogilvie, Peter Van Loo

UT MD Anderson Cancer Center, Houston, TX

Immune escape is a fundamental hallmark of cancer, facilitating disease progression and resistance to therapy. The temporal dynamics and genetic evolution underlying immune escape across diverse cancers remain incompletely characterized. Here we developed an integrative framework that systematically identifies immunomodulatory genes from functional genomic screens and reconstructs tumor evolutionary history using whole-genome sequencing data to infer mutation timing. Applying this approach to 2,658 tumors across 38 cancer types, we generated the first pan-cancer atlas of immune escape evolution, revealing distinct trajectories such as late amino acid metabolism mutations in pancreatic adenocarcinoma, early neuroactive ligand-receptor and IFNγ pathway mutations in esophageal adenocarcinoma, and late protein methylation mutations in breast adenocarcinoma. These findings provide a comprehensive map of genetic immune evasion evolution, offering insights that may inform early detection strategies, immunoprevention, and therapeutic interventions across cancers. To facilitate easy access to the results, we further built a user-friendly website to interactively interrogate the evolution of immune escape.

#0689 Significance of prostaglandin E_2 signaling in the carcinogenesis of ulcerative colitis.

Tatsunari Fukuoka[1], Masakazu Yashiro[2], Hiroaki Kasashima[3], Nobuhiro Naito[4], Iguru Omori[4], Yasuhiro Fukui[4], Yuki Seki[4], Kenji Kuroda[4], Yuichiro Miki[4], Mami Yoshii[4], Tatsuro Tamura[4], Masatsune Shibutani[4], Takahiro Toyokawa[4], Kiyoshi Maeda[4]

[1]Gastroenterological surgery, Osaka City General Hospital, Osaka, Japan,[2]Molecular Oncology and Therapeutics, Osaka Metropolitan University Graduate School of Medicine, Osaka, Japan,[3]Department of Gastroenterological Surgery, Graduate School of Medicine, Osaka Metropolitan University, Osaka, Japan,[4]Department of Gastroenterological Surgery, Osaka Metropolitan University Graduate School of Medicine, Osaka, Japan

Background The incidence of colorectal cancer arising in the setting of long-standing inflammatory bowel disease (IBD) has been increasing with the rising prevalence of ulcerative colitis (UC). Patients with long-standing UC have an approximately five-fold higher risk of colorectal cancer (CRC) compared with the general population. However, the molecular mechanisms underlying UC-associated carcinogenesis remain poorly defined. Prostaglandin E_2 (PGE_2) signaling is one of a key mediators of inflammation, and elevated PGE_2 levels have been observed in inflamed colonic tissue of UC patients. PGE_2 signaling also promotes tumor proliferation and metastasis in several cancer types.

Objective To clarify the involvement of PGE_2 signaling in UC-associated carcinogenesis by examining the expression of PGE_2 receptors EP2 and EP4 in UC-related neoplastic lesions.

Methods Forty-one patients who underwent the surgical operation for UC-associated neoplasia (16 dysplasia, 25 carcinoma) at our institution were included. Paraffin-embedded sections of dysplastic and cancerous lesions were subjected to immunohistochemical staining for EP2 and EP4. Expression intensity and proportion of EP2/EP4 were scored, and correlations between EP2/EP4receptor expression and clinicopathological parameters were analyzed.

Results Cancer tissues showed higher expression of EP2 and EP4 than dysplastic tissues in UC-associated neoplasia. Expression of either receptor (EP2 or EP4) was more frequent ($p = 0.0678$) in cancer lesions (81.5%, 22/27) compared with dysplastic lesions (50.0%, 7/14). EP2 positivity was observed in 66.7% of cancer lesions (18/27) and 42.9% of dysplastic lesions (6/14) ($p = 0.189$). EP4 expression tended to be higher ($p = 0.0516$) in cancer lesions (63.0%, 17/27) than in dysplastic lesions (28.6%, 4/14) ($p = 0.0516$) while EP2 positivity was not ($p = 0.189$;observed in 66.7% of cancer lesions (18/27) and 42.9% of dysplastic lesions) (6/14) ($p = 0.189$). Expression of either receptor (EP2 or EP4) was more frequent in cancer lesions (81.5%, 22/27) compared with dysplastic lesions (50.0%, 7/14) ($p = 0.0678$). In contrast, EP2 or EP4 Receptor expression was not significantly associated with cancer tumor stage, depth of invasion, or prognosis.

Conclusion These findings suggest that PGE_2 signaling, particularly through the EP4 receptor, may might contribute to the carcinogenesis in UC ulcerative colitis. EP4-mediated pathways may represent potential therapeutic or preventive targets in UC-associated CRC colorectal cancer.

#0690 Hierarchical mixed effects cubic spline modeling of methylation-based tumor fraction dynamics for pan-cancer assessment of treatment response and outcomes in immunotherapy patients.

Christopher Pretz[1], Amar Das[1], Carin Espenschied[2], Sara Wienke[3], Samantha I. Liang[4], Christopher Cabanski[4]

[1]Real World Evidence, Guardant Health Laboratory, Redwood City, CA,[2]Guardant Health, Spokane, WA,[3]Guardant Health, Charleston, SC,[4]Parker Institute for Cancer Immunotherapy, San Francisco, CA

Background: Methylation-based tumor fraction (TF) dynamics are a promising surrogate marker for monitoring disease, but their evolution varies widely across patients and cancer types. To characterize these patterns, we developed a hierarchical mixed-effects cubic spline model that captures non-linear longitudinal TF trends while accounting for patient-level heterogeneity and clinical covariates. Compared with traditional approaches, this framework supports multiple cancer types, baseline factors, and generates outcome-stratified trajectories (e.g., disease progression and survival). By enabling trajectory bifurcation by outcome, the model simultaneously reflects treatment response and prognosis, improving our understanding of how TF dynamics relate to therapeutic efficacy across diverse cancer types.

Methods: We analyzed 519 patients from the RADIOHEAD study consisting of 1,070 immunotherapy-naive patients receiving standard-of-care immune checkpoint inhibitor (ICI) regimens. Included patients had ≥2 plasma samples beyond baseline. TF was measured using Guardant Reveal, a clinically validated methylation-based assay. Model selection using Akaike information criterion compared linear, non-linear, and spline models; a natural cubic spline with five knots best fit the data. Covariates included age, smoking status, stage (III vs IV), and gender. Cancer types analyzed were lung, bladder, melanoma, renal cell carcinoma, and head and neck carcinoma. Binary outcomes were 15-month survival (alive/deceased) and disease progression (yes/no).

Results: Because spline coefficients are not interpretable, findings were presented graphically. After adjusting for covariates, TF trajectories diverged beyond 95% confidence bands and exhibited distinct patterns by cancer type and outcome. An interactive R Shiny application was developed to display these trajectories, along with velocity plots providing the instantaneous rate of TF change to aid interpretation.

Conclusions: This analysis provides a framework for characterizing TF evolution during immunotherapy and how these dynamics differentiate clinical outcomes across cancer types. Outcome-stratified trajectories and TF velocity may help identify early indicators of treatment response, supporting more informed therapeutic decisions. Additionally, since TF dynamics vary by disease indication, future studies could integrate TF dynamics with genomic and other clinical indicators to better understand response mechanisms, resistance factors, and other biological drivers that may underly a heterogeneous response to ICIs.

#0691 Visualizing differential prostate cancer lesion growth in longitudinal MRIs of patients on active surveillance: Quantitative mapping by Habitat Risk Score and digital pathology.

Sandra M. Gaston[1], Yuwei Zhang[2], Veronica M. Wallaengen[1], Amanda Galvez[1], Leonard Salcedo[1], Adrian L. Breto[1], Ahmad Algohary[1], Noah C. Lowry[1], Jakub Karczmarzyk[2], Gupta R. Rajarsi[2], Erich Bremer[2], Tahsin Kurc[2], Benjamin O. Spieler[1], Oleksandr N. Kryvenko[1], Alan Pollack[1], Sanoj Punnen[1], Joel Saltz[2], Radka Stoyanova[1]

[1]University of Miami Miller School of Medicine, Miami, FL,[2]Stony Brook University, Stony Brook, NY

Introduction: Active surveillance (AS) is now incorporated into many prostate cancer (PCa) management guidelines to reduce overtreatment, but it requires frequent monitoring because of the risk of disease progression. Improved risk-stratification tools are needed to distinguish indolent from aggressive disease early in surveillance so that the window for curative treatment is not missed. At many institutions, multiparametric MRI (mpMRI) and MRI-ultrasound (MRI-US) fusion biopsies are standard of care for interval monitoring of patients on AS. Here, we show that a quantitative mpMRI system, the Habitat Risk Score (HRS), identifies differential lesion growth on longitudinal mpMRI and correlates strongly with quantitative analysis of digital pathology from radical prostatectomy (RP) specimens.

Study Methods: Patients from “MRI-Guided Biopsy Selection of PCa Patients for Active Surveillance versus Treatment: The Miami MAST Trial” (ClinicalTrials.gov: NCT02242773; total accrual = 208) with confirmed PCa underwent 12-36 months of AS prior to RP. The mpMRI exams consisted of T2-weighted (T2W), Dynamic Contrast Enhanced (DCE)-MRI, and Diffusion Weighted Imaging (DWI) acquired according to PI-RADSv2 recommendations. The HRS approach automatically identifies suspicious prostate lesions on mpMRI by assigning a 10-point pixel-by-pixel risk score presented as a heat map, overlaid on the T2W. Longitudinal mpMRI images, biopsy pathology at 12, 24 or 36-months of surveillance and RP specimen pathology were analyzed. The temporal changes in HRS mpMRI volumes were tracked and HRS maps from the last time point (prior to RP) were examined for correlation with H&E and digital pathology.

Results: Detailed HRS mpMRI review of 34 MAST participants with biopsy progression followed shortly (within six months) by RP showed that 55% exhibited mpMRI evidence of histopathological progression that was not detected on their last surveillance biopsy. Standard-of-care prostate mpMRI, including that used in MAST, is limited by subjective interpretation, and even expert radiologists may miss significant lesions. In contrast, HRS provides an objective, quantitative assessment of prostate mpMRI images. Findings on HRS correlated closely with both expert pathology review and quantitative digital pathology, with the strongest spatial concordance observed between HRS maps and digital pathology.

Conclusion: Our results indicate the utility of HRS mpMRI to detect tumor growth in AS patients. The differential growth in the lesions can be used to guide tissue selection for genomic testing. The study found excellent correlation between HRS and H&E and digital pathology from RP specimens. HRS volumes may serve as quantitative biomarkers for early detection of progression.

#0692 Novel single cell and bulk NGS assays for improved assessment of MRD (measurable residual disease) and clonal dynamics in acute myeloid leukemia (AML).

Crystal Zhou[1], Ruwan Gunaratne[1], Emily Yang[1], Rachel Agoglia[2], Diwash Jangam[3], Charu Tiwari[1], Kailee Tanaka[4], Tsoyu Chiang[3], Chandler Ho[3], Sydney Lu[1], James L. Zehnder[3], Bing Melody Zhang[3], Henning Stehr[3], Tian Yi Zhang[1]

[1]Hematology, Stanford University School of Medicine, Stanford, CA,[2]Mission Bio, South San Francisco, CA,[3]Pathology, Stanford University School of Medicine, Stanford, CA,[4]Stanford Cancer Institute, Stanford, CA

Background: The genomic heterogeneity of AML and high rates of relapsed/refractory (R/R) disease necessitate improved tools for detecting MRD and studying clonal evolution. Standard-of-care (SOC) MRD methods, namely multiparametric flow cytometry (MFC) or single-variant molecular assays, are limited in sensitivity, applicability across diverse AML genomes, and ability to resolve clonal dynamics. We evaluated the Tapestri single-cell multiomics AML assay (Mission Bio) and HemeSTAMP-MRD, a novel high-sensitivity bulk NGS assay, as alternative platforms for MRD detection and clonal profiling.

Methods: We analyzed 72 bone marrow or peripheral blood mononuclear cell samples from 24 AML patients at diagnosis (n=18), remission (n=35), or R/R disease (n=19). Tapestri single-cell genotypic and immunophenotypic analysis was performed after CD34+/CD117+ enrichment using a 41-gene panel and 17-cell surface marker panel. HemeSTAMP-MRD, a bioinformatically optimized version of an in-house 203-gene error-corrected clinical NGS panel (Kim et al. 2022), was performed on paired whole blood samples in the CLIA-certified Stanford Molecular Pathology Laboratory. Each patient had ≥ 1 trackable diagnostic variant(s). MRD results were compared with SOC MFC.

Results: 87% (21/24) of patients achieved initial clinical remission (CR1), of whom 62.5% (15/21) relapsed. MFC detected MRD in only 33% (5/15) of patients with pre-relapse CR1 samples, while Tapestri and HemeSTAMP each identified MRD in 67% (10/15), including 8 patients with positive concordance. Among MFC-negative cases (n=10/15), 4 had detectable MRD by Tapestri and/or HemeSTAMP at variant allele frequencies < 1%, including one with actionable *IDH2*-mutant disease who relapsed and died before receiving targeted therapy. The 3 patients who relapsed despite negative MRD by all assays either had exclusively extramedullary relapse, loss of trackable variants, or inadequate sampling prior to relapse. Among patients yet to relapse, Tapestri and HemeSTAMP-MRD detected residual variants during CR1 in 5 of 6 patients, although 4 of whom later received allogenic transplant as a confounding factor.
During active disease (diagnosis or R/R timepoints), Tapestri identified a median of 4 clones per sample (range 1-9). In paired samples, 8/9 (88%) patients showed clonal evolution between diagnosis and R/R disease: 3/8 (37.5%) gained at least one emergent clone and 5/8 (62.5%) lost at least one. The most dynamic genes were *NRAS*, *NF1*, *PTPN11* and *TET2*, while *TP53* and *DNMT3A* were most stable.

Conclusion: Tapestri and HemeSTAMP-MRD both demonstrated improved MRD level detection, relapse prediction, and greater capacity to identify actionable mutations compared to MFC, with Tapestri uniquely enabling single-cell resolution of clonal dynamics to interrogate drivers of R/R disease. Larger cohort validation is ongoing.

#0693 ET-resistant cell populations in ER positive breast cancer: From profiling to therapeutic targeting.

Svetlana Semina[1], Rosemary Huggins J. Huggins[2], Huiping Zhao[3], Virgilia Macias[4], Leo Feferman[5], Andre A. Kajdacsy-Balla[6], Debra A. Tonetti[7], Kent F. Hoskins[8], Geoffrey L. Greene[9], Jonna M. Frasor[3], Jonathan Coloff[3]

[1]Physiology and Biophysics, University of Illinois Chicago, Chicago, IL,[2]Office of Education and Career Development, Comprehensive Cancer Center, University of Chicago Medicine, Chicago, IL, USA, Chicago, IL,[3]University of Illinois Chicago, Chicago, IL,[4]Department of Pathology, University of Illinois Chicago, Chicago, IL,[5]Research Informatics Core, Research Resourced Center, University of Illinois Chicago, Chicago, IL,[6]Director of Transdisciplinary Path., University of Illinois Medical Center, Chicago, IL,[7]Associate Professor of Pharmacology, Biopharmceutical Sci., University of Illinois at Chicago, Chicago, IL,[8]University of Illinois College of Med. at Chicago, Chicago, IL,[9]University of Chicago, Chicago, IL

Even though most women with estrogen receptor positive (ER+) breast tumors can benefit from endocrine therapy (ET), up to 40% of these patients will eventually experience relapse. Moreover, when these tumors recur, they tend to be more metastatic and therapy-resistant, resulting in disease progression and fatalities. One contributing factor to ET failure and recurrence is intratumoral heterogeneity, where tumors have distinct populations of cells with different sensitivity to ET. Here, we developed an integrated framework that combines clinical and experimental data with cutting edge bioinformatics tools to systematically identify and target ET-resistant cell populations. Leveraging single cell RNA sequencing data from the FELINE clinical trial, we profiled tumors from nine ER+ breast cancer patients treated with letrozole at baseline and after 14 days of therapy. We found that ET-sensitive populations are conserved across patients, whereas ET-resistant populations are more heterogeneous and not defined by ER expression, signaling activity, or molecular subtype. Moreover, gene signatures from ET-resistant clusters are predictive of poor patient survival and adverse pathological features in METABRIC dataset. To functionally validate these findings and target ET-resistant cell populations, we build a panel of patient-derived xenograft organoid (PDxO) models that retain key features of the original tumors and mirror findings from the clinical trial. Using a novel predictive therapeutic pipeline that integrates transcriptional profiling with drug response modeling on PDxOs, we identified and validated candidate drugs targeting both shared and patient-specific ET-resistant populations, including known drugs already used in clinic, such as dasatinib, as well as novel compounds such as pluripotin and AZD8055. These findings demonstrate that ET-resistant cell states emerge early under therapeutic pressure and persist despite treatment, representing a major barrier to ET response. Our integrated framework allowed us to uncover both patient-specific and shared ET-resistant cell populations, and to test personalized therapeutic strategies for targeting ET resistance. Together, our findings reveal a complex and heterogeneous landscape of endocrine therapy response, highlighting the critical importance of single-cell resolution to inform therapeutic strategies aimed at overcoming resistance and improving patient outcomes.

#0694 Spatially resolved genomics reveals evolutionary modes and imaging correlates in glioblastoma.

You Jin Song[1], Yelyzaveta Miller-Michlits[2], Karl-Heinz Nenning[3], Christoph Bock[4], Ji Yoon Lee[1], Jiwon Kim[1], Jisoo Hong[1], Dayoung Lee[1], Namsung Moon[1], Harim Koo[5], Jason K. Sa[1], Adelheid Woehrer[2]

[1]Korea University College of Medicine, Seoul, Korea, Republic of,[2]Medical University of Innsbruck, Innsbruck, Austria,[3]The Nathan S. Kline Institute for Psychiatric Research, New York, NY,[4]Austrian Academy of Sciences, Vienna, Austria,[5]Graduate School of Medical Science, University of Ulsan, Ulsan, Korea, Republic of

The spatial evolutionary dynamics of glioblastoma remain poorly understood. Here, we performed spatially resolved molecular profiling of 78 multi-regional tumor specimens from 24 GBM patients by integrating neuro-navigation-guided intraoperative sampling with deep whole-exome sequencing. This dataset represents one of the most spatially detailed genomic resources for GBM to date. By coupling spatial coordinates with genomic complexity, we delineated two distinct evolutionary trajectories: an “Expansive” model, in which three-dimensional growth and molecular diversification proceed in parallel, and a “Stochastic” model, where genomic diversification occurs independently of spatial expansion. These models were supported by phylogenetic reconstruction and radiogenomic analyses, revealing how spatial architecture constrains clonal dynamics. Quantitative integration of molecular and physical distances uncovered that tumors with greater spatially correlated genomic diversity exhibited worse clinical outcomes. Patients harboring “Stochastic” tumors demonstrated inferior survival probabilities compared to those with “Expansive” tumors, suggesting that spatially derived molecular metrics may serve as prognostic indicators of tumor aggressiveness. Furthermore, MRI-derived radiomic features, particularly texture-based metrics from T1-contrast enhanced images, mirrored underlying genomic complexity and aligned with evolutionary modes, establishing a link between intratumoral heterogeneity and noninvasive imaging phenotypes. While prior genomic studies have characterized GBM evolution at the molecular level, most lacked spatial resolution and failed to capture the three-dimensional architecture of tumor growth within the human brain. Our study overcomes this limitation through an international collaboration between the Medical University of Innsbruck and Korea University College of Medicine. Together, these results define anatomically distinct evolutionary trajectories of GBM and underscore how spatial context shapes molecular diversity, clinical behavior, and imaging manifestations. This spatially integrated framework provides a foundation for precision oncology approaches that incorporate spatial evolutionary constraints into therapeutic stratification.

#0696 In vivo clonal lineage tracing using methylation barcodes in the protocadherin gene cluster.

Christopher T. Boniface[1], Samuel Hackett[2], Adriana V. A. Fonseca[2], Akemi Ramos-Yamasaki[2], Caroline Watson[2], Joanna Baxter[2], Jyoti Nangalia[3], Sadik Esener[1], Hisham Mohammed[1], Jamie Blundell[2]

[1]Division of Oncological Sciences, OHSU Knight Cancer Institute, Portland, OR,[2]University of Cambridge, Cambridge, United Kingdom,[3]Wellcome Sanger Institute, Hinxton, United Kingdom

Resolving the lineage history of cells is crucial for understanding tissue development, stem cell dynamics, and cancer, but is hampered by methods that are invasive, low-resolution, or prohibitively expensive for human studies. Clonal expansion of a single stem cell lineage is a hallmark of pre-cancer in both solid tissue tumors and hematological malignancies. Here, we describe a native, in vivo lineage tracing system that utilizes the stochastic (de)methylation of CpGs in the protocadherin (PCDH) gene cluster. By phasing these CpGs in bulk methylation sequencing we construct in situ evolvable methylation “barcodes” that uniquely mark stem cell clones. We longitudinally tracked these barcodes in annual blood samples from 50 individuals and age-matched controls up to a decade prior to acute myeloid leukemia (AML) diagnosis. We show that polyclonal tissues have high barcode diversity—reflecting a broad stem-cell pool—which then collapses during a clonal sweep. The fractional abundance of dominant barcodes provides a quantitative measure of clone size that precisely tracks genetic estimates from somatic mutations. However, 10% of pre-AML donors harbored expanded barcodes but lacked detectable somatic driver mutations, suggesting the presence of clonal expansions with cryptic drivers years before diagnosis. Barcode trajectories also reveal subclonal competition and interference. Because these barcodes evolve by stochastic (de)methylation at approximately 1% per CpG per year, heritable diversity is generated in clonal populations enabling the tracking and quantification of subclonal growth dynamics. We then demonstrate that barcodes containing dozens to hundreds of PCDH CpGs produced from long-read sequencing allow for deep phylogenetic reconstruction from a single time point. Finally, we observed expanded barcodes in solid tumor tissues, including prostate and kidney. PCDH methylation barcodes therefore represent a scalable, cost-effective, and pan-tissue tool for high-resolution lineage tracing in humans, opening new avenues for studying somatic evolution in health and disease.

#0697 Label-free spatial profiling of the melanoma tumor microenvironment using metasurface-enhanced Raman spectroscopy.

Kai Chang[1], Mamatha Serasanambati[1], Feven Naba[1], Priyanuj Bordoloi[1], Antony Georgiadis[1], Emma Wagner[1], Hamish Carr Delgado[1], Chih-Yi Chen[1], Varun Dolia[1], Baba Ogunlade[1], Remi Dado[1], Ariel Stiber[1], Jack Hu[2], Amanda R. Kirane[3], Jennifer Dionne[1]

[1]Stanford University, Stanford, CA,[2]Pumpkinsed Technologies, Inc., Palo Alto, CA,[3]Stanford University School of Medicine, Stanford, CA

The spatial organization of the tumor immune microenvironment (TIME) is a critical determinant of cancer progression and response to precision therapies. Understanding this complex ecosystem holds immense potential for developing diagnostics and immunotherapies. Current spatial omics methods, including transcriptomics and proteomics, however, have limited translational and clinical adoption. These methods require invasive or destructive, time-intensive protocols, are expensive, and may not always capture structural or post-translational modifications driving tumor behavior. Here, we propose a high-throughput, label-free spatial profiling method combining metasurface-driven surface-enhanced Raman spectroscopy (mSERS) and machine learning (ML) that enables holistic cell phenotyping in melanoma TIME.

Our metasurfaces are composed of dielectric (high-index silicon nitride) nanoresonators on microscope slides optimized for 785 nm laser excitation. These slides localize Raman scattering in uniform and discretized sub-wavelength “hot-spots” that can span full tissue surface areas, all while minimizing cell heating damage. On these slides, we collect subcellular SERS maps across monoculture of TIME-relevant melanoma and immune cell lines and simplified TIME cocultures of two cell types (YUMM1.7, RAW264.7). We compare Raman spectral features against brightfield and fluorescence imaging and develop cell segmentation algorithms to isolate single-cell spectral maps. For a small cohort of FFPE patient tumors with complete, partial, and non-responses to immune checkpoint inhibitor PD-1 (nivolumab), we image and construct a melanoma tumor atlas with co-registered Raman, spatial transcriptomics, and multiplex immunofluorescence (mIF) data.

We show enhancements of $>10^5$ over non-SERS at 10 nm above the surface and across the cell membrane. We achieve >96% differentiation accuracy across cell types and confirm spectral features associated with subcellular features (e.g. nucleus, membrane). Our segmentation algorithm correctly labels coculture cells in agreement with co-registered mIF. In our patient tumor data, we show unique nivolumab-relevant biomarkers identifiable by mSERS and not by other modalities in isolation. By extending our findings to tumor FFPE and historical clinical specimens, the implications of our all-optical approach have the potential to advance cancer knowledge, clinical biomarker efforts, and impact precision treatment decisions for cancer patients.

#0699 Dynamic adaptation and heterogeneity in tumor patient-derived organoids: Insights into cancer evolution and drug resistance.

Javier Frias Aldeguer, Jasmin Pourfarzad, Alessandro Gregory, Farzin Pourfarzad, Rene Overmeer, Robert G. J. Vries, Sylvia F. Boj

HUB Organoids B.V., Utrecht, Netherlands

Tumor plasticity and cellular heterogeneity have long been recognized as major contributors to the limited success of cancer therapies, underscoring the need for more physiologically relevant preclinical models. Patient-derived organoids (PDOs) offer a three-dimensional, heterogeneous platform that better reflects tumor complexity compared to traditional cell lines or animal models. Their adoption in drug development pipelines and avatar clinical trials has grown significantly in recent years. In this study, tumor PDOs were characterized using single-cell RNA sequencing, whole-exome sequencing, and sub-lethal therapeutic exposure to assess intra- and inter-patient heterogeneity and adaptive dynamics. PDOs from different donors exhibited patient-specific transcriptional signatures while retaining stem-like features. Mutational landscapes evolved over time, with variants being retained, lost, or acquired relative to the original tissue. Notably, subpopulations persisted through treatment and gave rise to distinct clonal cultures with unique transcriptional profiles upon drug withdrawal. These findings confirm that tumor PDOs preserve cellular heterogeneity and exhibit dynamic adaptability, making them powerful tools for investigating cancer evolution, drug resistance, and mutation dynamics. Inter-patient variability highlights the need for personalized therapeutic strategies, while intra-patient heterogeneity positions PDOs as ideal models for studying complex cellular interactions and mechanisms of pharmacological persistence.

#0700 Feasibility to detect genomic loss of HLA alleles by One Lambda LABType products combined with novel data analysis algorithm.

Svetlana Argounova, Bernabe Valdez, Kevin Lam, Hanna Bennett, **Anna Chikova**

One Lambda Inc., Thermo Fisher Scientific, West Hills, CA

Loss of heterozygosity in human leukocyte antigens (HLA) is a phenomenon frequently observed in relapses of myeloid leukemia treated by allogeneic hematopoietic stem cell transplantation. Loss of HLA was also described in multiple studies of solid tumors (Montesion et al. 2021, Zhang et al. 2022) where loss of HLA may be particularly important for patients treated by HLA restrictive immunotherapy. Identifying loss of heterozygosity (LOH) during relapses may provide information critical for treatment selection in affected patients. One Lambda LABType products utilize reverse-sequence-specific oligonucleotide (rSSO) typing method with the LABScan 100 or LABScan3D instruments, to provide HLA typing in up to 11 HLA loci. Though this product is used for HLA genotyping in transplant diagnostic practices, we explored potential feasibility to use LABType kits to detect complete or partial loss of HLA alleles in human genome. We used homozygous DNA samples well characterized for all 11 HLA loci and tested different ratios of DNAs in each mixture to mimic LOH characteristics and analyzed all samples with One Lambda LABType products for several loci. Our new loss of HLA analysis algorithm was able to clearly distinguish between homozygous DNA and DNA mix containing only 10% of minor allele. Assay allowed clearly distinguish 1:1 DNA mix from 30, 20 and 10% of minor allele and comparing different SSO products showed that LABType CWD kits were quantifying residual allele with higher level of confidence. To challenge our algorithm further, we tested mixture of 3 DNAs imitating haplo-matched stem cell transplant, when donor is sharing one set of HLA alleles with the patient while other donor's allele is different. We mimicked different levels of chimerism and different levels of HLA loss by mixing these 3 DNAs representing heterozygous donor and two patients alleles in different ratios. Experiment demonstrated ability of LABType CWD test to detect as little as 1% of minor allele present in 20 ng of total DNA per reaction. Further evaluation of new data analysis approach using LABType technology for complete or partial loss of HLA may be beneficial for both transplant medicine related research and oncology fields. New algorithm is intended for research use only and is not commercially available at this time.

#0701 Patient-derived organoid biobanks preserve tumor heterogeneity and molecular signatures.

Rene Overmeer, Farzin Pourfarzad, Alejandra Hernandez Segura, Merel Derksen, Carla Verissimo, Robert G. J. Vries, Sylvia F. Boj

HUB Organoids B.V., Utrecht, Netherlands

Tumor heterogeneity—both within individual tumors and among different patients—poses a significant challenge for effective cancer treatment. To advance precision oncology, preclinical models that capture this complexity are essential. Patient-derived organoids (PDOs) provide a physiologically relevant platform that maintains the architecture and diversity of the original tumor, making them ideal for studying heterogeneity and patient-specific biology. In this study, we established and characterized PDO biobanks from colorectal and bladder cancers to evaluate their ability to represent intra-tumor heterogeneity and patient-specific molecular signatures. We profiled organoids using whole-exome sequencing and bulk RNA sequencing to assess their genomic and transcriptomic fidelity. Our analyses revealed that PDOs retain key mutational profiles and transcriptional programs of the original tumors, including subtype-specific signatures. Importantly, we observed distinct cellular subpopulations within individual PDO cultures that reflect intra-tumor diversity, including stem-like and differentiated phenotypes. These features persisted over time, confirming the stability of heterogeneity in vitro. Across the biobank, PDOs captured the spectrum of molecular subtypes present in colorectal and bladder cancers, enabling subtype-specific drug testing and biomarker discovery. This diversity highlights the potential of PDO platforms to model patient variability and inform personalized therapeutic strategies. Our findings demonstrate that PDOs are not only accurate representations of patient tumors but also dynamic systems that preserve heterogeneity at multiple levels. By integrating genomic and transcriptomic profiling with functional assays, PDO biobanks provide a powerful resource for studying tumor complexity and accelerating precision medicine.

#0702 Harnessing clonal dynamics to overcome resistance: An adaptive therapy framework in colorectal cancer.

Harley I. Richker[1], Bailey Sierra Kane[1], Gissel Marquez Alcaraz[1], Ellie Pahl[1], Ryan Carr[2], Nagarajan Kannan[2], Carlo C. Maley[3]

[1]Arizona State University Biodesign Institute, Tempe, AZ,[2]Mayo Clinic, Rochester, MN,[3]Arizona State Univ. Biodesign Institute, Tempe, AZ

Therapeutic resistance to chemotherapy is frequently the proximate cause of increased tumor burden, cancer treatment failure, and ultimately, patient mortality. The most successful therapy strategy derived from evolutionary practices to date, Adaptive Therapy (AT), leverages the fitness cost of developing therapeutic resistance. AT avoids treating cancer cells with the Maximum Tolerated Dose (MTD) of therapeutic drugs and instead incorporates a series of adaptive dosing schedules. Treatment-sensitive cells are bolstered by modulating or pausing treatment to out-compete and suppress treatment-resistant cell growth. We are evaluating AT for the first time in colorectal cancer, using a syngeneic orthotopic xenograft model. This work represents several key advances: it is the first to longitudinally and non-invasively track sensitive and resistant clones in vivo, to evaluate adaptive therapy in an immunocompetent mouse model, to incorporate multi-drug treatment regimens, and to integrate a targeted therapeutic agent. The dual-bioluminescent sensitive and resistant CT26 cell lines developed for this study allow real-time visualization and quantification of each population throughout tumor progression and treatment. Together, these advances establish a robust and clinically relevant platform for characterizing resistance dynamics and refining adaptive therapy strategies aimed at improving treatment outcomes in colorectal cancer.

#0703 Tracking tumor evolution and heterogeneity in fusion-driven sarcomas through cell-free DNA analysis.

Tom T. Fischer[1], Panna Lajer[2], Konstantin Okonechnikov[1], Anke King[1], Karla Catacora[1], Katharina Bauer[2], Iris Oezen[1], Tanja Jutzi[2], Katherine Kelly[1], Calvin Hans Setiadi[2], Waqar Hussain[3], Kendra K. Maass[1], Roland Imle[1], Anja Speicher[4], Kamelia Soleiman-Masihi[4], Nadine Volk[4], Birgit Besenbeck[4], Robert Kuechler[4], Anu Mathews[4], Editha Gnutzmann[4], Julia Ketzer[5], Daniela Richter[3], Daniel Huebschmann[4], Ana Banito[1], Claudia Ball[3], Kathrin Schramm[1], David T. W. Jones[1], Jan-Philipp Mallm[2], Uta Dirksen[5], Sabine Stegmaier[6], Monika Sparber-Sauer[6], Richard F. Schlenk[4], Hanno Glimm[3], Stefan Froehling[2], Stefan M. Pfister[1], Supat Thongjuea[1], Kristian W. Pajtler[1], Daniel B. Lipka[2]

[1]Hopp Children's Cancer Center (KiTZ), Heidelberg, Germany,[2]German Cancer Research Center (DKFZ), Heidelberg, Germany,[3]National Center for Tumor Diseases Dresden (NCT/UCC), Dresden, Germany,[4]National Center for Tumor Diseases Heidelberg (NCT), Heidelberg, Germany,[5]University Hospital Essen, Essen, Germany,[6]Zentrum fur Kinder-, Jugend- und Frauenmedizin (Olgahospital), Klinikum der Landeshauptstadt Stuttgart, Stuttgart, Germany

Background: Tumor evolution and intra-tumoral heterogeneity drive therapy resistance and relapse, yet remain poorly understood and difficult to track in real time. HEROES-AYA, a German multi-center consortium funded by the National Decade Against Cancer, leverages fusion-driven bone and soft tissue sarcomas in children, adolescents, and young adults as a model system to dissect these processes. Defined by diverse oncogenic fusions, these aggressive tumors frequently evade therapy, leading to poor outcomes. In parallel with bulk and single-cell multi-omics profiling of tumor tissue, we employ plasma liquid biopsies as a minimally invasive, serially collectable source of circulating tumor DNA (ctDNA) to map spatiotemporal tumor dynamics.

Methods: 112 plasma samples from 60 patients (12 alveolar rhabdomyosarcoma, 11 synovial sarcoma, 8 myxoid liposarcoma, and 29 other fusion-driven sarcomas) were collected retro- and prospectively in several German sarcoma trials (1-15 samples per patient). Plasma from healthy donors served as control. Cell-free DNA (cfDNA) was profiled using an ultra-sensitive enzymatic methylation sequencing assay optimized for pico- to nanogram inputs and sequenced at 10-20x. A multi-layered bioinformatics framework integrated copy number variations (CNVs), single-nucleotide variants (SNVs), and methylation profiles of cfDNA, benchmarked against matched tumor profiles. For 30 patients (58 tumor samples), single-cell multi-omics profiling (RNA, ATAC, and DNA sequencing) of paired tumor tissue was used to decode cfDNA clonal composition.

Results: Despite low cfDNA input amounts (median: 3ng; range: below detection limit - 17ng), genome-wide cfDNA profiles were successfully generated for all samples. ctDNA signals showed strong concordance with matched tumor tissue across CNV, SNV, and methylation layers. Longitudinal plasma sampling added molecular time points unavailable from tissue biopsies, revealing newly acquired broad copy number alterations and focal amplifications (affecting, e.g., *CDK6*) at progression. Integration with single-cell data enabled deconstruction of bulk cfDNA profiles, revealing distinct compositions in the plasma with dominant, multiple, or divergent clones relative to tumor tissue. For example, in a case of pediatric alveolar rhabdomyosarcoma, ctDNA at relapse more closely resembled the profiles of the primary tumor rather than those in a concurrent lymph node metastasis, demonstrating how liquid biopsies capture tumor dynamics across anatomical sites.

Conclusions: The integration of a multi-layered cfDNA assay with single-cell tumor sequencing provides an improved understanding of clonal dynamics and tumor evolution. By identifying cfDNA markers of heterogeneity and emerging resistance, this approach may establish a translational path for their longitudinal assessment via liquid biopsies in precision oncology.

#0704 Full-range genomic analysis at single-cell resolution reveals genetic, epigenetic, and parallel evolution of melanoma subclones.

Chi-Ping Day[1], Yuelin Liu[1], Anton Goretsky[1], Ayse Keskus[1], Salem Malikic[1], Eva Perez-Guijarro[2], Glenn Merlino[3], Eytan Ruppin[1], Suleyman Cenk Sahinalp[1], Mikhail Kolmogorov[1]

[1]National Cancer Institute, Cancer Data Science Laboratory, NIH, Bethesda, MD,[2]Institute for Biomedical Research Sols-Morreale, Universidad Autonoma de Madrid, Madrid, Spain,[3]National Cancer Institute, Laboratory of Cancer Biology and Genetics, NIH, Bethesda, MD

Tumor evolution is driven by various mutational processes, ranging from single nucleotide variants (SNVs) to large structural variants (SVs) to dynamic shifts in DNA methylation. Current short-read sequencing methods struggle to accurately capture the full spectrum of these genomic and epigenomic alterations, as well as their relations, due to inherent technical limitations. Here we used Nanopore long-read sequencing to profile 23 subclones, each derived from a single cell of a mouse melanoma cell line, for precise detection and evolutionary ordering of SNVs, SVs, copy number alterations (CNAs), and DNA methylation changes at subclonal level. Through phylogenetic analysis of these subclones, we reconstruct the timing of mutational processes and their contributions to diverse clonal phenotypes. The analysis reveals recurrent amplifications of putative driver genes, generated by independent SVs across different lineages, suggesting parallel evolution. Additionally, we described lineage-specific methylation changes associated with aggressive tumor subclones, highlighting epigenetic trajectories linked to tumor progression. Overall, we demonstrate that our long-read approach enables a uniquely comprehensive view of melanoma progression, highlighting that SVs and methylation played an important role in initiation, clonal diversification, and development of therapeutic resistance in this tumor, in consistence with recent clinical findings. We will release the sequencing data and curated variant calls to encourage developments of new computational methods.

#0706 Beyond a single core biopsy: Spatial genomic profiling improves therapeutic target detection in glioblastoma.

Enmar Harfoush[1], Taylor Weiskittel[1], Mylan Blomquist[2], Dustin Grief[3], Aadel A. Chaudhuri[1], Leland S. Hu[3], Nhan L. Tran[3], Shannon Fortin-Ensign[3]

[1]Mayo Clinic, Rochester, MN,[2]University of California San Francisco, San Francisco, CA,[3]Mayo Clinic Arizona, Scottsdale, AZ

Purpose: Despite advances in molecular diagnostics, glioblastoma (GBM) remains incurable, with recurrence driven by residual invasive tumor cells that escape surgical resection and therapy. Current genomic profiling to guide therapy for recurrent disease typically relies on a single-site clinical biopsy (SSCB) obtained from the contrasting-enhancing (CE) tumor core - the region targeted for maximal resection and most visible on Magnetic Resonance Imaging (MRI). However, this region poorly represents the non-enhancing (NE) invasive tumor margins, which harbor treatment-resistant and genetically distinct cell populations responsible for disease recurrence. GBM exhibits extensive spatial heterogeneity, raising concerns that a single tissue may underrepresent the true actionable landscape of the tumor.

Experimental Procedures: We analyzed 302 biopsies from 66 GBM patients who underwent multiregional whole exome and RNA sequencing across CE and NE tumor regions. Of these, 17 patients also had standard-of-care SSCB molecular profiling utilizing clinically available genomic sequencing panels outside of the multiregional protocol. Variants that have been targeted in ongoing or successful human clinical trials were annotated as actionable. We compared actionability profiles between SSCB and multiregional sampling, to determine the gain of actionable variant detection across the two sampling strategies. We performed an in-silico biopsy simulation to model the coverage of these alterations across the tumor landscape with increasing sampling frequency in the multiregional protocol, versus the coverage from clinical sequencing panels on SSCBs.

Results: Clinical sampling identified a median of one actionable mutation per patient (range 0-3). In contrast, multiregional profiling revealed additional potentially actionable variants in over 70% of patients, particularly within NE infiltrative regions that are not captured by conventional resection. Notably, nine potentially actionable copy-number variants, including *PDGFRA* amplification, were consistently absent from SSCB results and underrepresented in most clinical panels. In silico biopsy simulations demonstrated that actionable variant detection continues to rise even after sampling five additional regions, reflecting spatial segregation of therapeutic targets.

Conclusions: These findings demonstrate that a single sample from the CE tumor core fails to capture the biologically diverse invasive tumor populations responsible for GBM recurrence. Multiregional sequencing uncovers clinically meaningful alterations that would otherwise remain undetected with conventional sampling, highlighting the risk of incomplete molecular characterization in current clinical biopsy workflows.

#0707 Phylogenetic and machine learning analyses of simulated ancestral sequences reveals heterogeneous ccRCC evolution.

Nic Fisk[1], Christopher Cross[2], Brian M. Shuch[3], Jeffrey Peter Townsend[2]

[1]University of Rhode Island, Kingston, RI,[2]Yale University, New Haven, CT,[3]UCLA Medical Center, Santa Monica, CA

Clear-cell renal-cell carcinoma (ccRCC) accounts for 70-80% of kidney cancers, with increasing incidence driven by improved imaging, aging populations, and rising obesity rates. No routine diagnostic tests currently predict which small renal masses will progress to large, aggressive tumors, leaving a fundamental clinical question unresolved: do lethal tumors arise with inherently aggressive molecular characteristics, or do they gradually evolve from indolent precursors?

To investigate size-specific evolutionary trajectories, we integrated cancer effect size quantification, mutational signature analysis, phylogenetic reconstruction, and machine learning classification. We calculated cancer effect sizes stratified by tumor size (≤3 cm vs >3 cm) using single-nucleotide variant data from TCGA-KIRC (n=339) combined with five additional studies (total n=656). We additionally leveraged multi-region tumor sequencing data from 20 patients to investigate the evolutionary history of these tumors by performing Bayesian phylogenetic reconstruction to generate chronograms. To characterize ancestral tumor states, we developed a novel binomial sampling simulation parameterized by variant allele frequencies to generate mid-branch sequence states representing likely ancestral tumor configurations, which were then classified as "small" or "large" using a neural network trained on mutational matrices incorporating recurrent cancer effect sizes and de novo mutational signature weights.

Our neural network classified ccRCC size with 86.48% accuracy and an F1 score of 0.86. Among the patient subset with large tumors, half showed small-like ancestral midpoints while half showed large-like midpoints; in contrast, small tumors overwhelmingly classified as having small ancestral states, supporting model reliability. We also found that VHL mutations clustering around the binding pocket exhibited the highest cancer effects, supporting observations from the literature. Interestingly, while feature importance analysis identified approximately 1000 variants contributing discriminatory power, only one VHL mutation (a truncation mutation) was in the 100 most informative variants, despite VHL's overall importance in ccRCC and may be especially influential on evolutionary trajectory.

These results suggest that ccRCC tumors follow heterogeneous evolutionary paths—some large tumors pass through small-like feature states while others do not. This framework demonstrates the utility of evolutionary embeddings for machine learning classifiers and offers a generalizable approach for investigating ancestral tumor characteristics.

: Molecular Pathology
Poster Session

#0711 Single-cell and spatial profiling identifies tumor features and actionable surface targets in primary breast angiosarcoma.

Asumi Iesato, Masashi Akiya, Kazutaka Otsuji, Sumito Saeki, Natsue Uehiro, Tetsuo Noda, Tomo Osako, Takayuki Ueno, Reo Maruyama

Japanese Foundation for Cancer Research, Tokyo, Japan

Background: Primary breast angiosarcoma (PBA) is an extremely rare and aggressive vascular malignancy with limited therapeutic options. Genomic studies have identified recurrent alterations such as KDR, PIK3CA, TP53, and FLT4, but gene-expression patterns have been scarcely reported, and their spatial context remains poorly defined. Only two spatial transcriptomic studies have been published, both from a single institution and focused mainly on immune-cell distribution while analyzing breast and non-breast angiosarcomas together. These two studies identified tumor regions based on endothelial markers (ERG/CD31); yet these markers can be diminished in dedifferentiated angiosarcoma, and reliable tumor-specific markers remain unavailable. Whether PBA shares molecular features with angiosarcomas from other anatomical sites also remains unclear. **Objective**: To delineate transcriptional programs of primary and metastatic PBA and validate them using integrated spatial analysis, and to identify candidate tumor cell markers with therapeutic applicability.
Methods: We integrated single-cell RNA sequencing (scRNA-seq) and spatial transcriptomics from matched PBA specimens. Fresh tumors (361T, 256T) were profiled using BD Rhapsody scRNA-seq and integrated with normal breast tissue (388D). CNVs were inferred by InferCNV. Visium spatial transcriptomics were performed on FFPE samples from two cases, with ovarian and liver metastases available from one (256T). CD276 expression was evaluated by immunohistochemistry in 3 PBA cases.
Results: Integrated scRNA-seq from the three samples identified three endothelial clusters: c5 (normal ECs), c7 (tumor ECs), and c11 (lymphatic ECs). Cluster 7 expressed PECAM1/CDH5 and angiogenic/lymphangiogenic regulators, and InferCNV confirmed its tumor identity. Differential expression between c7 and c5 yielded a tumor-specific gene set (AS_signature) enriched for extracellular-matrix organization, receptor tyrosine-kinase signaling, and basement-membrane remodeling. Spatial InferCNV reproduced tumor-associated CNVs in Visium tumor regions. Joint analysis of ovarian and liver metastases of 256T showed complete UMAP separation and divergent CNV architectures; primary-tumor subclusters localized preferentially to ovarian or hepatic lesions, suggesting organ-selective subclonal dissemination. Twelve membrane-localized candidates were identified, and CD276 (B7-H3) showed strong membranous staining.
Conclusions: Integrated single-cell and spatial profiling delineated tumor-derived endothelial features in PBA and validated their spatial and CNV context. The AS_signature robustly distinguished tumor from normal endothelium. Divergent metastatic CNV profiles suggest subclonal evolution with organ-specific tropism. CD276 emerged as a clinically actionable membrane antigen for ADC development.

#0713 Quantitative 3D histology: Million-cell-scale spatial multi-omics in intact FFPE specimens.

Lichun Zhang[1], William C. S. Cho[2], Li Joshua[3], Molly Li[4], Tony S. Mok[4], **Hei Ming Lai**[1]

[1]Chemical Pathology, The Chinese University of Hong Kong, Hong Kong, Hong Kong,[2]Clinical Oncology, Queen Elizabeth Hospital, Hong Kong, Hong Kong,[3]Pathology, University of Hong Kong, Hong Kong, Hong Kong,[4]Chinese University of Hong Kong, Hong Kong, Hong Kong

Cancer exhibits profound heterogeneity both within and between patients, spanning from individual cell phenotypes to complex microenvironmental niches. Current technologies fail to capture this multiscale complexity while preserving native tissue architecture holistically. Here we present a quantitative 3D histology platform that enables spatially resolved, million-cell-scale multi-omic profiling of intact formalin-fixed paraffin-embedded (FFPE) specimens. It eliminates sampling error and subjectivity in histopathology, and facilitates quantitative phenotyping to guide patient selection in treatments.

We applied this platform to profile diverse cancer specimens, uncovering cancer-nerve interactions, cancer-immune cell interactions, and generating quantitative continuous scores for actionable targets, including TROP2 and HER2, through normalised membrane ratios (NMRs) in >0.5 million cells per sample. We also identified missed cancers, pre-cancerous lesions, and lymphovascular invasion in designated normal tissue blocks, as well as decision dilemmas and errors in 2D quantitative digital pathology efforts, due to the fundamental limitations offered by a random specimen cut.

In developing this platform, we devised novel chemistry for low-temperature FFPE retrieval to prevent biomolecular damage, followed by custom supramolecular reaction systems that enable deep antibody penetration for up to 28-plex multiplexed immunostaining in > 1,000 µm-thick specimens. Non-destructive tissue clearing, coupled with light-sheet microscopy, then captures the entire specimen in 3D with optical sectioning. We then trained a family of neural networks to segment individual cells in their native 3D positions with precise cellular geometry, allowing computation of distances to tissue boundaries and features (vessels, nerves), as well as spatial relationships between cell types. These 3D masks quantify marker expression across major subcellular compartments, generating continuous molecular scores for each cell.

Crucially, tissues remain structurally and molecularly intact throughout processing. Comparative analyses pre- and post-3D profiling show indistinguishable results for H&E, immunohistochemistry, whole-genome sequencing, bulk RNA-seq, laser-capture mass spectrometry proteomics, and 2D spatial transcriptomics. We demonstrate the feasibility of integrating 2D spatial transcriptomic data into the 3D volume for comprehensive single-cell molecular profiling. Moreover, the 3D histology pipeline requires no specialized equipment, is fully automatable, and generalizes across tissue types, enabling rapid clinical deployment for precision oncology applications where spatial context drives therapeutic decisions.

Our technology addresses the fundamental limitations of current 2D pathology methods, with broad applicability across multiple cancers.

#0714 Enhanced in vivo and ex vivo analysis enables deeper characterization of humanized mouse models for immuno-oncology research.

Maria Stecklum[1], Joshua Alcaniz[1], Lea Bornemann[2], Jens Hoffmann[1]

[1]EPO GmbH, Berlin, Germany,[2]Miltenyi Biotec B.V. & Co. KG, Bergisch Gladbach, Germany

Background
We previously demonstrated that humanized mouse models can be generated using peripheral blood mononuclear cells (PBMCs), PBMC subpopulations such as T and NK cells, or $CD34^+$ hematopoietic stem cells (HSCs), depending on the research objective. As next-generation immunotherapies advance—including checkpoint inhibitors (CPIs), engineered immune cells, and immune-cell engagers—establishing suitable in vivo and ex vivo analytical platforms becomes essential. Fully humanized mouse models containing both a human immune system and human tumors provide a more physiologically relevant setting for evaluating these therapies.
Methods
Humanized mice were established through intravenous transplantation of $CD34^+$ cells, PBMCs, or purified NK or T cells into immunodeficient mice. Cell-derived xenograft (CDX) and patient-derived xenograft (PDX) tumors were engrafted either subcutaneously (s.c.) or orthotopically (intravenously or into the mammary fat pad). Tumor progression was assessed using caliper measurements (s.c.) or bioluminescence imaging (BLI) for orthotopic models.
Quantitative immune cell composition in blood, bone marrow, spleen, and tumor tissue was analyzed by flow cytometry. 3D-Light-sheet fluorescence microscopy with the Ultramicroscope Blaze was established to enable spatial analysis and localization of immune-cell infiltration in tumors and spleen.
Results
Both CDX and PDX tumors from multiple cancer types successfully engrafted in humanized mice, with >70% engraftment success and no significant differences in tumor growth kinetics compared to non-humanized controls. Immunotherapy treatment revealed distinct responder and non-responder profiles, characterized by differential immune-cell infiltration patterns.
Flow cytometry reliably monitored human immune reconstitution and quantified immune and tumor cell populations over time. Flow cytometry has also been used to follow therapeutic treatment effects. BLI provided a non-invasive method for longitudinal tumor assessment in orthotopic models.
3D-Light-sheet imaging with the Ultramicroscope Blaze enables the confirmation of FACS-based findings and visualized tumor-infiltrating lymphocytes (TILs), unlocking spatial mapping of immune-cell localization within tumors and lymphoid organs.
Conclusions
Continuous refinement of our humanized mouse models enables robust preclinical evaluation of emerging immunotherapies. Integration of spatial biology enhances mechanistic insight by providing high-resolution visualization of immune-cell behavior within the tumor microenvironment, strengthening the translational value of these platforms.

#0715 Robust segmentation-free stain quality concordance metrics in the SpaceIQ™ multi-omic analysis platform.

Brian Falkenstein[1], Raymond Yan[1], A. Burak Tosun[1], S. Chakra Chennubhotla[2], Filippo Pullara[1]

[1]Computational and Systems Biology, PredxBio, Inc., Pittsburgh, PA,[2]Computational and Systems Biology, PredxBio, Inc. / University of Pittsburgh, Pittsburgh, PA

Background: Spatial imaging outputs continue to grow in scale and complexity. While brightfield IHC and H&E remain the qualitative gold standard for antibody-based assessment, mIF offers quantitative protein measurement on a single slide. However, challenges such as non-specific binding, imaging artifacts, and variability across sites and operators limit confidence in mIF reproducibility. A quantitative, robust method is needed to assess concordance between IHC and mIF stains.
Methods: Using a pan-cancer dataset with a 4-plex mIF panel and matched IHC sections from consecutive slides, we first co-registered images into a shared coordinate space with Valis, applying global rigid and non-rigid transformations from feature matches. IHC stain channels were isolated via stain-matrix-based deconvolution. A tissue mask was generated on the mIF image using Otsu thresholding and morphology operations and then projected onto the IHC slide.Tissue was divided into tiles whose size accounted for section-to-section distance, registration error, and biological variability. Within each tile, random windows were sampled to perform two tests: (1) identify whether the tile contains high stain intensity and (2) determine whether the corresponding IHC and mIF tiles exhibit statistically concordant staining. This approach yields both a DICE score for high-stain region overlap and a stain concordance metric capturing agreement across high- and low-stain regions. Tile-level results and heatmaps are visualized in SpaceIQ™.
Results: Concordance between mIF and IHC varied substantially across markers, with CD8 showing the highest and FoxP3 the lowest agreement, a trend consistent across samples. Concordance heatmaps also revealed strong spatial effects, with some tissue regions highly concordant and others clearly discordant. Expert visual review matched these quantitative findings.
Conclusions: This segmentation-free framework identifies substantial marker- and region-specific variation in concordance between mIF and IHC staining. Because the method is marker-agnostic and compensates for registration error and inter-section biological differences, it provides a generalized, quantitative approach for evaluating agreement between paired mIF and IHC slides across platforms.

#0716 AI-driven live 3D/4D spatial multimodal evaluation of a HER2-targeting ADC: delivery, lysosomal cleavage, payload action, and bystander effects resolved by holotomography and fluorescence.

Seock-Jin Chung[1], Eric Sha[2], Minji Kim[3], Youngwon Cho[3], Seunghyi Kook[3], Soonyoung Lee[4], Jongseong Jang[4], Eunyoung Choi[3], Tae Hyun Hwang[3]

[1]Surgery Department, Vanderbilt University Medical Center, Nashville, TN,[2]Vanderbilt University, Nashville, TN,[3]Vanderbilt University Medical Center, Nashville, TN,[4]LG AI Research, Seoul, Korea, Republic of

Background: Enhertu (trastuzumab-deruxtecan) is a HER2-targeting antibody-drug conjugate (ADC) that has demonstrated remarkable efficacy in HER2-positive cancers. Its design features a GGFG tetrapeptide linker that is selectively cleaved by lysosomal enzymes such as cathepsins to release the potent cytotoxic payload, deruxtecan (DXd). However, the precise intracellular trafficking, timing of linker cleavage, and kinetics of payload release remain poorly understood. This study aimed to elucidate these mechanisms using advanced 3D imaging platforms.

Methods: HER2-positive NCI-N87 and HER2-negative AGS gastric cancer cell lines were used for comparative analysis. Enhertu was labeled with Alexa 647 dye using a commercial labeling kit. Cells were stained with LysoTracker and treated with fluorescence labeled Enhertu, followed by 3D correlative imaging with holotomography (HT) and multichannel fluorescence imaging machine (HT-X1 Plus; Tomocube). The target specificity of Enhertu was confirmed by pretreating cells with an excess of trastuzumab before Enhertu treatment. HER2-positive gastric cancer organoids (SC128) were cultured in both 2D and 3D conditions. After Enhertu treatment, 3D HT and fluorescence imaging were taken, followed by HER2 immunofluorescence staining after fixation.

Results: Enhertu selectively bound to the plasma membrane of NCI-N87 cells, followed by internalization and subsequent merging with lysosomes, as visualized by LysoTracker staining. Blocking experiments validated the HER2 specific binding of Enhertu. Enhertu demonstrated higher cytotoxicity in HER2-positivie NCI-N87 cells compared to HER2-negative AGS cells and induced a bystander effect in co-culture, highlighting its potential to overcome tumor heterogeneity. In SC128 organoids, Enhertu bound to apical regions with strong HER2 expression and gradually internalized into the organoid interior. Prolonged exposure disrupted the organoid membrane and led to cell death, consistent with DXd-mediated cytotoxic effects.

Conclusions: This study provides a comprehensive analysis of Enhertu's intracellular trafficking and functional mechanisms. Using 3D holotomography and multichannel fluorescence imaging, we visualized the processes of HER2-specific binding, cleavage by lysosome, and DXd release. These findings will enhance our understanding of ADC mechanisms and offer valuable insights for optimizing future ADC designs to improve therapeutic efficacy.

#0717 Advancing spatial oncology research with open-panel multiplex IHC/IF using a novel heat-free antibody stripping reagent.

Shuhui Chen, **Erika Leonard**, Shamali Roy

Vector Laboratories, Inc., Newark, CA

Purpose: Spatially resolved multiplex immunohistochemistry (IHC) and immunofluorescence (IF) assays are essential for profiling the tumor microenvironment and identifying biomarkers that predict response to cancer immunotherapies, yet many platforms rely on proprietary closed antibody panels and harsh, heat-based stripping that damage FFPE tissue and reduce antigenicity, limiting target choice and rapid adoption of new markers. We developed a heat-free stripping reagent that removes primary and secondary antibodies and other non-covalently bound detection reagents between staining cycles while preserving tissue architecture and antigen integrity. This abstract summarizes its performance in multiplex IHC, IF, and tyramide-based workflows and its compatibility with common autostainers.

Experimental Procedures: FFPE tumor and normal tissues were stained using sequential multiplex IHC, IF and TSA workflows in both manual and automated staining, with panels targeting immune, stromal, and tumor markers. After each staining round, slides were treated with the heat-free reagent before the next cycle. Residual signal was assessed by imaging previously used channels after stripping and by chase experiments to detect previously applied antibodies. Antigen preservation was evaluated by comparing staining intensity and distribution for the same targets across early and late cycles, and morphology by H&E.

Summary of New Data: The stripping reagent consistently removed bound antibodies and associated detection reagents, with no detectable residual signal in previously used channels. Across multiple sequential rounds, key tumor and immune markers maintained expected expression patterns and subcellular localization, with no appreciable loss of antigen detectability. Tissue morphology remained intact after repeated stain-strip cycles. The reagent performed robustly in chromogenic IHC, IF, and TSA multiplex workflows, enabling multi-marker panels on a single section without cross-reactivity or signal carryover. Protocols were easily adapted to autostainers, integrating into translational and biomarker pipelines.

Conclusions: This heat-free stripping reagent enables robust multiplex IHC, IF, and TSA staining on FFPE tissue while preserving morphology and antigenicity across multiple sequential cycles and is readily adaptable to autostainers. It simplifies adoption of multiplex panels in oncology research, conserves clinical specimens, and enables deeper characterization of the tumor immune microenvironment and biomarkers for precision oncology. Unlike closed multiplex platforms, it is compatible with investigator-selected antibodies and detection reagents, supporting flexible panels that keep pace with evolving oncology targets.

#0718 Novel characterization of tumor transport dynamics using Cross-Voxel eXchange Model and DCE-MRI.

Janny Kim[1], Noha Sinno[2], Michael Milosevic[2], Catherine Coolens[2]

[1]University of Toronto, Toronto, ON, Canada,[2]Princess Margaret Cancer Centre, Toronto, ON, Canada

Despite significant advances in oncology, tumor heterogeneity continues to drive inconsistent responses to emerging therapeutics. Biophysical features of the tumor microenvironment (TME) - particularly elevated interstitial fluid pressure (IFP) and reduced hydraulic conductivity (K) generate outward convective flow that limits drug and tracer transport, contributing to resistance. Improved characterization of these parameters is essential for understanding TME-mediated barriers across tumor sites. In this work, the diverse ME180 tumor microenvironments were evaluated to test the ability of the Cross-Voxel eXchange Model (CVXM) to quantify transport properties and elucidate dynamic interactions between the TME and pharmacokinetics.ME180 cervical carcinoma xenografts were established in orthotopic, intramuscular, and subcutaneous sites in immunodeficient NRG mice. CVXM applied to 7T DCE-MRI (Biospec, Bruker) yielded voxel-wise estimates of extravasation, convection (velocity), diffusion, and hydraulic conductivity. Direct IFP measured with a solid-state transducer and ex vivo hydraulic conductivity measurements were used to validate CVXM-derived K. A subset of orthotopic tumors received fractionated radiotherapy (RT): 5×5 Gy (SmART+, Precision), and DCE-MRI acquired five days post-RT was used to assess CVXM sensitivity to RT-induced TME changes.CVXM produced spatial maps of key transport parameters (extravasation, tracer velocity, diffusion, and hydraulic conductivity) across tumor models. Extravasation ranged from 0.002-0.084min^{-1}, peripheral velocity from 0.91-6.8μm/s and mean diffusion from 168-250$μm^2/s$, all within reported physiological ranges. CVXM-derived K strongly correlated with convection-derived velocity (R^2 = 0.49-0.65, $p < 0.001$), with mean values ranging from $9.96×10^{-8}$ to $3.88×10^{-7}cm^2/(mmHg·s)$, consistent with previously published ME180 measurements. Following RT, orthotopic tumors exhibited a 12% reduction in IFP, accompanied by a 49% decrease in tracer velocity and a 29% decrease in CVXM-derived K at five days post-RT. These data indicate that CVXM provides a non-invasive means to characterize transport behavior within tumors and to detect biophysical changes resulting from treatment.These findings demonstrate that CVXM provides a non-invasive, imaging-based platform for quantifying tumor transport properties and detecting treatment-induced shifts in TME biophysics. By linking radiologic transport metrics with underlying physiology, CVXM offers a translational tool for monitoring therapy response and identifying biophysical biomarkers relevant to drug delivery and radiation efficacy.

#0719 A multi-scale imaging pipeline identifies regions of NMII activation in colorectal cancer which promote tumor survival.

Derek H. Abbott[1], Bassel Dawod[2], Arely Perez Rodriguez[2], Tai Ngo[1], Gaudenz Danuser[3], Kevin M. Dean[1], Todd A. Aguilera[2]

[1]Lyda Hill Department of Bioinformatics, UT Southwestern Medical Center, Dallas, TX,[2]UTSW, Dallas, TX,[3]UT Southwestern Medical Center, Dallas, TX

The aim of this study is to define the spatial activation of non-muscle myosin II (NMII) in colorectal cancer (CRC) and determine how it promotes tumor survival. Our lab has identified curvature-sensing, pro-survival signaling hubs that form at the base of ROCK1/NMII-driven blebs in low-adhesion environments. Adoption of this weakly adherent, highly contractile amoeboid phenotype is associated with metabolic shifts and immunosuppression that worsen prognosis. However, these observations come largely from mouse models and have yet to be validated in human disease. We hypothesize that, in human CRC, elevated actomyosin contractility sustains tumor survival in poorly adherent regions by activating ROCK1/NMII signaling and reducing tumor-immune cell engagement. To test this hypothesis, we developed a cyclic multiplexed immunofluorescence panel (CODEX) and applied it to a CRC tissue microarray and whole-slide CRC specimens. The panel included markers of cell identity, metabolism, proliferation, and immune activation. Spatial analysis was performed using SPACEMAP, a consensus machine-learning platform that integrates multiple phenotyping algorithms to improve cell-type classification accuracy. To characterize nanoscale architecture, a 30-µm section adjacent to each CODEX-imaged slide was embedded in a hydrogel, expanded, and imaged using Axially Swept Light-Sheet Microscopy (ASLM). Expanded volumes were registered to the multiplexed immunofluorescence dataset, enabling subcellular analysis with ~80-nm isotropic resolution. 3D segmentation and morphological quantification were performed using u-Segment3D. Active NMII (pMLC2) signal in the tumor epithelium was observed in 25% of CRC cases, localizing to discrete regions with reduced cell-cell adhesion, including necrotic zones, mucin pools, luminal surfaces, and isolated tumor cells. pMLC2-high tumor cells exhibited decreased proliferation and increased mitochondrial abundance. Strikingly, both granulocytes and cytotoxic T cells also demonstrated elevated pMLC2 expression, and these pMLC2-high immune cells showed increased markers of immunosuppression. Registration of CODEX and ExASLM datasets enabled high-resolution assessment of membrane architecture, revealing distinct alterations in tumor cell morphology and cell-cell interfaces within pMLC2-high niches. Together, these findings demonstrate that CRC tumors upregulate pMLC2 within low-adhesion microenvironments, supporting tumor survival through coordinated changes in proliferation, metabolism, membrane architecture, and immune engagement. This work identifies spatially regulated actomyosin contractility as a critical survival program in CRC and highlights it as a potential therapeutic vulnerability.

#0720 Nerve innervation in solid tumors.

Hui Yu[1], Aglaia Schiza[1], Victor Ponten[1], Viktoria Thurfjell[1], Amanda Lindberg[1], Julia Sidenius Johansen[2], Ulrike Segersten[3], Anca Dragomir[1], Bengt Glimelius[1], Artur Mezheyeuski[4], Astrid Borretzen[5], Yun-Fan Sun[6], Lars A. Akslen[5], Patrick Micke[1], Carina Strell[5]

[1]Department of Immunology, Genetics and Pathology, Uppsala University, Uppsala, Sweden,[2]Herlev Hospital, Herlev, Denmark,[3]Department of Surgical Sciences, Uppsala University, Uppsala, Sweden,[4]Molecular Oncology Group, Vall d'Hebron Institute of Oncology, Barcelona, Spain,[5]CCBIO, Department of Clinical Medicine, University of Bergen, Bergen, Norway,[6]Liver Surgery & Transplantation, Zhongshan Hospital, Shanghai, China

The role of nerve innervation in cancer progression remains highly debated. While various in vitro and in vivo models suggest that tumor cells can actively induce neoneurogenesis, tissue-based evidence remains sparse. In this project, we critically examine the hypothesis of tumor-associated nerve innervation by seeking direct, tissue-based evidence of nerve innervation and sprouting in relation to histopathological tumor features.Our study cohort comprises diagnostic FFPE whole-tissue samples from six solid tumor types: breast cancer (Luminal A/B, HER2+, TNBC), non-small cell lung cancer (adenocarcinoma, squamous cell carcinoma), colorectal cancer, pancreatic cancer (PDAC and periampullary adenocarcinoma), prostate cancer, and urinary bladder cancer.Nerve structures are identified via multiplexed immunofluorescence and multispectral imaging, targeting neurofilament light chain (NFL, 70 kDa) and growth-associated protein 43 (GAP43). To delineate the tumor microenvironment, additional markers include CD34 (perineural sheath), CD31 (endothelial cells), CD3 (T-cells), and pan-cytokeratin (tumor cells). We developed both a deep-learning-based algorithm and a thresholding approach to segment nerve fibers and characterize their spatial organization. A custom Python script quantifies nerve density (nerves/tumor area), nerve size (μm²), and the integrity of the perineural sheath via CD34 staining. In parallel, we are constructing 3D nerve reconstructions by aligning and analyzing 30 consecutive 4 μm sections using tailored Python tools.Perineural invasion, as defined as direct contact between tumor cells and nerves, is most frequently observed in tumors from highly innervated organs such as PDAC and prostate cancer, while appearing only sporadically in the other tumor types.In subsequent analyses, nerve features will be systematically correlated with histopathological tumor characteristics, microenvironmental profiles, and clinical data. Ultimately, this study aims to generate a comprehensive atlas of nerve-tumor interactions in human cancer and to delineate both shared and tumor-type-specific patterns of innervation and perineural invasion.

#0721 High-plex 3D imaging of the tumor-immune microenvironment.

Peter Karl Sorger[1], Clarence Yapp[2], Alex Wong[2], Yi Daniel Lu[2]

[1]Dept. of Systems Biology, Harvard Medical School, Boston, MA,[2]Laboratory of Systems Pharmacology, Harvard Medical School, Boston, MA

Solid tumors evolve in competition with the immune system and must attract resources such as nutrients and oxygen to proliferate and invade normal tissue. This results in complex spatial distribution of tumor, immune, and stromal cell types within the tumor microenvironment (TME). Regulatory interactions among these cells involved in tumor progression and response to therapy are found on a wide range of length scales from subcellular membrane domains (involved in autocrine signaling between PD1 and PDL1 for example) to extended structures spanning thousands of cell diameters such as lymphoid aggregates and tumor invasive boundaries. Highly multiplexed tissue imaging (spatial proteomics), in combination with other single cell methods, promises to reveal the composition and regulation of these TME features in molecular detail but the great majority of data collected to date, including all classical histopathology based on hematoxylin and eosin (H&E) and immunohistochemistry (IHC), involves thin 2D tissue slices. We have recently demonstrated that no cells in such 5 micron tissue section are intact and that this substantially impacts cell type identification and interaction analysis (Yapp...Sorger et al (2025) *NatMeth,* PMID: 41023436). We will now describe the development of a suite of computational and experimental methods for performing 3D image-based profiling of human tumor sections at different resolutions and spatial scales ranging from ~50 micron thick (with confocal imaging) to 1 mm thick (with cyclic light sheet microscopy). Thick section 3D cyclic immunofluorescence (CyCIF) makes it possible to map cell-cell interactions based on the proximity of cell membranes rather than simply the location of nuclei, as commonly done in spatial tissue analysis. Moreover, by performing 50-plus marker, high resolution (below 200 nm), thick section CyCIF we are able to infer dynamic biological processes using fixed time data and trajectory analysis. Chief among these processes is T-cell mediated cytotoxicity as assayed by formation of immune synapses and polarized secretion of granzyme and/or granulysin containing vesicles toward tumor cells. To date, light sheet fluorescence microscopy (LSFM) has been applied primarily to the analysis of tissues in model organisms (particularly mice and fish) with structures of interest labelled either by fusion to fluorescence proteins or by injecting dyes. We have now developed methods to perform cyclic LSFM on human FFPE tissue, enabling large multi-cellular assemblies to be studied in detail. We will describe an analysis of secondary and tertiary lymphoid structures and their roles in programming B and T cells for anti-tumor immunity. Finally, we will describe how different types of 3D profiling can be combined to span the diversity of spatial scales and regulatory interactions within the human TME.

#0722 Discovery of an evolutionarily conserved GPCR-like protein shaping glioblastoma cell networks.

Jennifer Arcuri[1], Bruno Colon[2], Shraddha ChandThakuri[3], Daniel Isom[1]

[1]University of Miami Sylvester Comprehensive Cancer Center, Miami, FL,[2]3Molecular and Cellular Pharmacology Graduate Program, University of Miami, Miami, FL,[3]University of Miami Miller School of Medicine, Miami, FL

Glioblastoma multiforme (GBM) is among the most aggressive and lethal brain cancers, and despite advances in surgery, radiation, and chemotherapy, median survival remains approximately 20 months. A defining morphological feature of GBM is the formation of tumor microtubules (TMs), thin cytoplasmic extensions that create open-ended channels between tumor cells. These structures transform isolated GBM cells into a coordinated multicellular network capable of rapidly transferring cytoplasmic components across distance, reshaping tumor behavior and promoting therapy resistance. Using AI-driven structural approaches, our lab identified TM184C, an ancient GPCR-like protein that regulates autophagy and the formation of intercellular connections and transcellular material and organelle transfer. Notably, HEK293A cells overexpressing TM184C generate intercellular connections that phenocopy the TM184C-positive structures and vesicle distributions observed in patient-derived GBM cells. Given these findings, and the observation that TM184C expression correlates with poor prognosis in GBM, we will report on our efforts to define how TM184C contributes to GBM projections, intercellular connectivity, and tumor progression.

#0723 Geometry and orientation influences beam hardening in a new high-throughput bone imaging cassette system for microCT.

James Tseng, Max Harlacher, Alex Allphin, Jeffrey D. Peterson, Jeroen Hostens, Tomasz J. Czernuszewicz, Wendy Harrop, **Zachary H. Houston**

Revvity, Waltham, MA

Primary and metastatically derived bone cancers can significantly change bone structure and composition. Visualization and quantification of changes in bone morphology and bone mineral density using high-resolution microCT is a key diagnostic measurement of disease progression and treatment efficacy. The scan quality needed to measure small changes within internal bone structures of mice requires a smaller field of view and longer imaging times across high quantities of samples. Bones are also individually scanned to ensure data quality is not corrupted by beam hardening, a well-known microCT artifact that can reduce the accuracy of calibrated density measurements. In this study, we found that the geometry and corresponding orientation of multiple bones within the field of view are crucial to ensure accurate quantification of cortical bone. By combining the fast-scan rates of the Quantum GX3 microCT (Revvity, Inc.) and a high-capacity (18) bone holder, we report a high-resolution/high-throughput (6 µm, 40 s/bone) microCT imaging methodology, without sacrificing statistical significance in quantification of cortical bone due to beam hardening. To confirm the optimal configuration, healthy bones harvested from age-matched mice with similar mean HU values for cortical bone were arranged in different patterns (2/3/6 bones) in a customized, 3D printed bone holder using low a density plastic scaffold. As a reference, the same bones were scanned individually to compare the effect of beam hardening attenuation in cortical bone (defined as >3000 HU). The mean HU values for each bone's cortical tissue were used to assess the effect of the geometry of one (control), two, three and six bones. Each configuration was scanned in the same field of view (18 mm), time (4 mins) and resolution (6 µm) at soft (70kV, 160 µA,1.0 mm Al filter) and hard (85 kV, 140 µA, 0.5/0.06 mm Al/Cu) x-ray conditions. Calculated HU values (Analyze 15) and the dimensions of the stage and bore were used to design and 3D-print three interlocking cassettes, each with a capacity of six bones for a total of 18 per image. In both hard and soft x-ray images measurable differences in mean HU values were observed, confirming the influence of beam hardening is directly influenced by the geometry of the bones in the holder; however, when compared to the control, a maximum of 4% or 5% difference was observed for any bone in hard and soft x-ray conditions, respectively. Our results show potential for high-throughput and accurate quantification of high-resolution bone scans in the Quantum GX3 microCT. Future work will focus on refining the cassette's design to improve sample loading, evaluating time savings, increasing flexibility in sample type, and providing seamless software integration with AI-enabled segmentation tools.

#0724 Engineered synthetic nano-composite hydrogels as tunable SERS substrates for biomolecule detection.

Harlie G. Rios[1], Cason M. Hancock[2], Swarna Ganesh[2]

[1]Biomedical Engineering, University of Arizona, Tucson, AZ,[2]University of Arizona Cancer Center, Tucson, AZ

The development of reproducible and sensitive plasmonic materials is essential foradvancing single-molecule detection using surface-enhanced Raman spectroscopy (SERS),specially for label-free biomedical sensing and cancer diagnostics. We fabricated silvernanoparticle–embedded hydrogels that are stable, active SERS substrates enabling highlysensitive, label-free molecular analysis. SERS enhances Raman scattering by placing targetmolecules in close proximity to a roughened metallic surface, generating localized surfaceplasmon resonances that amplify the Raman signal. Silver, which induces strong and consistentplasmonic enhancement compared to other metals, and methylene blue, a model analyte forwell-defined Raman peaks, provide a reliable standard for measuring enhancement performance.Silver nanoparticles were synthesized by chemical reduction of silver nitrate ($AgNO_3$),combination of PVP K90 and L-ascorbic acid and the addition of heat to promote nucleation andgrowth before purification into concentrated pellets. Nanoparticle size will be measured usingdynamic light scattering (DLS),and SERS performance was evaluated using methylene blue,which produced characteristic peaks at 770, 1389, and 1620 cm^{-1}. Comparative analysis showedthat the nanoparticle-embedded hydrogels produced stronger signal than conventional Ramanmeasurements, confirming effective SERS amplification for low-concentration biomoleculardetection.Hydrogel matrices made from poly(ethyleneglycol)diacrylate (PEGDA)provided ahydrated, tunable backbone that uniformly dispersed and stabilized the nanoparticles.Optimization efforts targeted UV curing time, PEGDA concentration, and nanoparticle loadingto maintain structural integrity and maximize signal enhancement. By varying nanoparticle sizeand comparing reducing agents such as L-ascorbic acid and sodium borohydride, we found thathigher particle concentrations did not always improve SERS intensity, underscoring the need tooptimize particle size and distribution for effective plasmonic coupling.In conclusion, the PEGDA–silver composite hydrogels functioned as robust,reproducible, and tunable SERS substrates for label-free molecular sensing with clear potentialfor cancer diagnostics. Optimizing nanoparticle synthesis, reduction chemistry, and hydrogelformulation improved both sensitivity and structural stability. Demonstrating a promisingpotential for future SERS-based chemical and diagnostic applications.

#0725 *In-vivo* fluorescence lifetime tomography for detection and quantification of programmed death ligand-1.

Rahul Pal[1], Murali Krishnamoorthy[2], Xin Liu[3], Satoru Morita[3], Atsuyo Morita[4], Hak Soo Choi[3], Dan Duda[5], Anand T. N. Kumar[1]

[1]Otolaryngology - Head and Neck Surgery, Mass Eye and Ear, Boston, MA,[2]Biomedical Engineering, Indian Institute of technology, Madras, India,[3]Massachusetts General Hospital, Boston, MA,[4]MGH, Boston, MA,[5]Houston Methodist Academic Institute, Houston, TX

Programmed death ligand-1 (PD-L1) is the only clinically approved predictive biomarker for cancer immunotherapy; however, its expression is highly heterogeneous and routinely assessed by *ex vivo* immunohistochemistry. To enable spatially resolved, noninvasive PD-L1 quantification, we employed fluorescence lifetime (FLT) tomography with a normalization strategy designed to account for nonspecific probe uptake. C57BL/6 mice bearing orthotopic RIL-175 liver tumors (n=10) were injected with αPDL1-800 (anti-PD-L1 antibody conjugated to IRDye 800CW). 48 hours post-injection, we performed *in vivo* time-domain FLT imaging with co-registered CT, followed by *in situ* FLT imaging and western blotting to validate PD-L1 expression. Bi-exponential fitting of the time-resolved fluorescence data yielded spatial maps of FLT (τ) and amplitude (*a*). The top 10% of FLTs within the tumor were averaged to define the bound lifetime component (τ_b), while the mean FLT in the normal liver was considered as the FLT of the unbound component (τ_u). Amplitudes of bound (a_b) and unbound (a_u) probes were extracted and segmented into tumor (a_b,T; a_u,T) and normal (a_b,N; a_u,N) ROIs. Among four normalization strategies tested, one correcting for background cross-talk (a_b,T - a_u,T) and normalizing by total uptake (a_b,N - a_u,N) showed the strongest correlation with PD-L1 expression (R^2 = 0.77). 3D reconstructions using asymptotic time-domain analysis confirmed accurate tumor localization and size. FLT tomography distinguished bound from unbound αPDL1-800 and enabled quantitative assessment of PD-L1 expression in deep-seated tumors. The normalization method enabled accurate quantification of PD-L1 expression across tumors, supporting the utility of FLT imaging for preclinical immunotherapy evaluation and biomarker-guided therapy monitoring.

#0726 Engineered multiplexed optical sensors to detect inflammatory cytokines in the tumor microenvironment.

Ryan M. Williams[1], Amelia Ryan[2], Syeda Rahman[2], Atara Israel[2]

[1]Medicine, Stony Brook University, Stony Brook, NY,[2]Biomedical Engineering, City College of New York, New York, NY

Inflammation is a hallmark of cancer development as well as a consequence of cancer progression. Chronic inflammatory pathways promote solid tumor growth, metastasis, and immune evasion. Indeed, chronic signaling of several inflammatory cytokines that lead to tumor formation include TNF-alpha, while persistent IL-6 signaling drives cell survival and proliferation as well as angiogenesis. IL-12, however, is a powerful anti-tumor cytokine, which promotes macrophage and T-cell cytotoxicity in addition to inhibiting angiogenesis. Despite their importance, it is difficult to model and monitor real-time inflammatory cytokine signaling in the tumor microenvironment during cancer initiation and progression. The ability to do so non-invasively in animal tumor models would allow for a better understanding of the key drivers of this important cancer hallmark, while the ability to do so in a patient could be a diagnostic and prognostic tool.

To this end, we have engineered a multiplexed optical sensor platform for inflammatory cytokines TNF-alpha, IL-6, and IL-12. Individual sensors are synthesized from species-sorted single-walled carbon nanotubes (SWCNT), which exhibit tissue-transparent near-infrared fluorescence. For each cytokine, we non-covalently attached an antibody or ssDNA aptamer to SWCNT, allowing for molecularly-specific detection and a change in emission spectra upon biomarker binding. We found that sensor performance was quantitative with a limit of detection in the clinical range following inhibition of non-specific surface adsorption with passivation agent polymers and proteins. Further, we demonstrated the ability to detect IL-6 and IL-12, key pro-tumor and anti-tumor cytokines respectively, simultaneously in solution, as well as IL-6 excreted by macrophages in response to pro-inflammatory stimuli. Together, we anticipate further deployment of these inflammatory cytokine monitoring sensors in vivo and translation to patient diagnostic and prognostic profiling.

#0727 Tumor specific induction of surface calreticulin by doxorubicin in pancreatic ductal adenocarcinoma.

Jasmine A. Watts[1], Ronald Watts[1], Chloe La Prairie[2], John B. Rose[3], Rachael Guenter[1]

[1]Surgery, University of Alabama at Birmingham, Birmingham, AL,[2]Pediatric Dentistry, University of Alabama at Birmingham, Birmingham, AL,[3]Surgery, Birmingham VA Medical Center, Birmingham, AL

BackgroundPancreatic ductal adenocarcinoma (PDAC) accounts for most pancreatic cancer cases. Despite advances in surgery and chemotherapy, the 5-year survival rate is only 13%. The aggressive nature of PDAC combined with delayed diagnosis highlights the need for new targeted diagnostic and treatment strategies. Calreticulin (CALR) is an endoplasmic reticular chaperone protein that can translocate to the cell surface under stress conditions such as chemotherapy. We hypothesized that systemic doxorubicin induces tumor specific surface translocation of CALR in PDAC.

MethodsMouse 2838c3 PDAC cells were injected subcutaneously into mice. Once the tumors were palpable, the mice were treated with two intraperitoneal injections of doxorubicin (10 mg/kg) or saline, spaced 48 hours apart and then sacrificed. Tumors and major organs (heart, lung, kidney, pancreas, colon, small intestine, liver, and spleen) were harvested and prepared for either flow cytometry or immunofluorescence analyses. For flow cytometry, tumors and organs were dissociated into non-permeabilized, fixed single cell suspensions and stained with a fixable live/dead dye and an anti-CALR antibody. Immunofluorescence staining was performed under non-permeabilized conditions using an anti-CALR antibody and wheat germ agglutinin (WGA) membrane mask. Signal intensity was quantified in Fiji as integrated density/area. Unpaired t-test with Welch's correction was utilized for comparison.

ResultsDoxorubicin treatment significantly increased surface CALR expression in PDAC tumors compared to saline-treated controls as measured by flow cytometry (3.0-fold increase; $p < 0.05$) and immunofluorescence (1.3-fold increase; 9623 AU ± 522.6 vs. 7341 AU ± 485.9, mean ± SEM, $p = 0.0021$). Increases in surface CALR were consistent across biological replicates. Importantly, there were no significant differences in CALR expression after doxorubicin induction in non-tumor tissues such as liver, spleen, heart, lung, kidney, pancreas, colon, or small intestine via flow cytometry or immunofluorescence analyses.

: Noninvasive Imaging and Analysis of Animal and Tissue Models
Poster Session

#0731 From hours to seconds: a new tool for accelerating in vivo rodent imaging data analysis using AI algorithms.
Hannah Sweezo[1], Juan Rojas[1], Thomas Kierski[1], Adam Aji[1], Jessica Pesner[1], Joseph Betthauser[1], Zachary Houston[1], Kyle Kloepping[1], James Tseng[1], Craig McMannus[1], Bincy John[1], Jeffrey Peterson[1], Julia B. Schueler[2], **Ryan Gessner**[1], Tomasz Czernuszewicz[1]

[1]Revvity, Waltham, MA,[2]Charles River Labs, Freiburg, Germany

Background: Advances in noninvasive imaging for cancer research have increased the demand for larger animal cohorts to achieve statistical power. However, in vivo image analysis remains challenging, often requiring skilled users to manually process organs or tumors in 2D and 3D images—a time-intensive task that can take hours to weeks depending on study size. The need to master multiple software platforms for different imaging modalities further extends analysis time, often surpassing image acquisition time.
Methods: To address these challenges, we developed a Python-based multimodal software application designed to accelerate data processing through AI-assisted segmentation and batch analysis across multiple timepoints. Here, we report the performance of the software and multiple integrated AI segmentation models for ultrasound and optical imaging.
Results: Analysis throughput improved by 9x for 3D ultrasound and up to 60x for 2D optical imaging compared to manual workflows. The software demonstrated strong agreement compared to human ground truth segmentations and ex vivo validation standards.
BLI Imaging: Deep learning-based masking showed near-perfect agreement with standard quantification methods ($R^2 = 0.995$ vs circular ROI; $R^2 = 0.996$ vs bounding boxes) while reducing analysis time from 15-20 seconds to ~2 seconds per study.
Ultrasound Imaging: AI-measured spleen size correlated strongly with postmortem spleen weights ($R^2 = 0.93$) and MRI volumes ($R^2 = 0.90$). AI segmentations achieved an average Dice score of 0.89 against ground truth human segmentations with predicted volumes correlating at $R^2 = 0.95$. For subcutaneous tumors, agreement was lower, but still strong when comparing AI versus human segmentations (Dice = 0.82; $R^2 = 0.78$) despite a more challenging heterogeneous echotexture profile.
Conclusions: AI-driven automation significantly accelerates multimodal image analysis without compromising accuracy. These advances highlight the potential of integrated automation to streamline preclinical imaging workflows and enhance research efficiency.

#0732 Enhanced antitumor efficacy of combination therapy via intravesical perfusion in an orthotopic muscle-invasive bladder cancer model.

Balaji Ramachandran, Satheeshkumar Rajendiran, Girish Joshi, Krishnappa Haladasappa

In vivo Pharmacology, Adgyl Lifesciences Private Limited, Bangalore, India

Bladder cancer is a prevalent and aggressive disease with serious health risks if not properly treated. Muscle-invasive orthotopic animal models closely replicate the pathophysiology of human bladder cancer. Orthotopic muscle-invasive bladder cancer model is more technically demanding but essential for translational research. In these models, IVIS-based optical imaging provides a non-invasive and dynamic method to monitor tumor progression in real time. Given the disease's heterogeneity and resistance to therapy, combination treatments are essential to enhance efficacy by targeting multiple oncogenic pathways. In this study, a muscle-invasive orthotopic bladder cancer model was developed in athymic nude rats by injecting T24-Luc cells directly into the bladder wall. A minor abdominal incision exposed the bladder for catheter placement, which was secured with a purse-string suture and tunnelled to the neck, connected to a harness. After recovery, T24-Luc cells were accurately delivered into the bladder wall without leakage. Tumor progression was monitored twice weekly using IVIS optical imaging. Rats were grouped by total flux intensity, then treated via bladder cannulation with Erdafitinib (5µg/mL), Doxorubicin (400µg/mL), Gemcitabine (90µg/mL) as standalone and combination with Erlotinib, delivered through continuous perfusion over a 7-day period. Total flux (photons/second), changes in body weight, clinicals signs, mortality were monitored twice weekly up to 2 weeks. At end of the study, bladder was excised for assessment of treatment efficacy through multiple parameters, including ex-vivo bioluminescence imaging, bladder weight measurement, photographed, and histopathological and IHC analysis. In the current orthotopic muscle-invasive bladder cancer (MIBC) model, treatment with standalone Erdafitinib, Doxorubicin, or Gemcitabine led to moderate tumor regression. Whereas combination of Doxorubicin and Gemcitabine with Erdafitinib demonstrated the highest anti-tumor efficacy, as evidenced by marked reductions in bioluminescence signal intensity, bladder weight. Histopathological analysis revealed no signs of tumor formation or invasion into deeper bladder layers, and the combination therapy significantly prolonged survival compared to individual treatments. Overall, the findings from this study indicate that combination therapy integrating conventional chemotherapeutic agents with targeted FGFR inhibitors significantly enhances anti-tumor efficacy than monotherapies. Continuous intravesical perfusion via bladder cannulation enables localized drug delivery, effectively minimizing systemic toxicity while maximizing tumor exposure and therapeutic impact

#0733 Targeting HCC tumor microenvironment interactions using an advanced HCC patient-derived on-chip model.

Orsola Mocellin[1], Stephane Treillard[1], Abbie Robinson[1], Aleksandra Olczyk[1], Thomas Olivier[1], Chee P. Ng[1], Arthur Stok[1], Giles van Tienderen[2], Monique Verstegen[2], Jeroen Heijmans[1], Dorota Kurek[1], Sebastian J. Trietsch[1], Henriette Lanz[1], Paul Vulto[1], Jos Joore[1], **Karla Queiroz**[1]

[1]MIMETAS B.V, Oegstgeest, Netherlands,[2]Department of Surgery, Erasmus MC-University Medical Center Rotterdam, Rotterdam, Netherlands

Hepatocellular carcinoma (HCC) is the most common type of liver cancer, with rising incidence closely linked to advanced liver disease. Interactions within the HCC tumor microenvironment (TME)—between tumor cells and associated stroma—actively regulate tumor initiation, progression, metastasis, and therapy response. Current in vitro systems often fail to replicate this complex microenvironment, including vascular structures, limiting accurate efficacy evaluation and the translational value of preclinical studies. To address these gaps, we developed a scalable, vascularized 3D HCC patient-derived Organ-on-a-Chip (PDChip) model using the OrganoPlate Graft platform. This advanced system incorporates relevant cellular players of the HCC microenvironment and enables medium- to high-throughput phenotypic drug screening. Approximately 1,200 patient-derived cultures from 8 primary HCC tumors and 2 cell lines were grown under perfusion flow, exposed to 28 treatment conditions—including standard of care (SoC), single agents, and combinations—and assessed for viability, vascular bed responses, and chemokine/cytokine changes. The screen revealed that SoC drugs sorafenib and lenvatinib reduced culture viability and induced profound changes in vascular bed organization, while atorvastatin decreased viability without affecting vascular structures. All three compounds also altered chemokine and cytokine profiles. Tocilizumab, galunisertib, and vactosertib lowered IL6 levels, whereas halofuginone increased IL6. These findings highlight the utility of the PDChip model in visualizing drug-induced responses at both molecular and morphological levels, providing detailed insights into drug effects on specific cellular compartments within the HCC TME. This platform enabled a detailed evaluation of drug-induced responses in the tumor and associated microenvironment, highlighting their importance in preclinical research for understanding diseases and developing new drugs.

#0734 High-content image analysis of colorectal cancer patient-derived tumroids identifies high intra- and inter-patient heterogeneity associated with drug activity and mode-of-action.

Peter W. Eide[1], Nicolas Pasquir[1], Christer A. Andreassen[1], Anne Hansen Ree[2], Knut M Augestad[2], Sebastian Meltzer[2], **Jarle Bruun**[1]

[1]Oncosyne AS, Oslo, Norway,[2]Akershus University Hospital, Lorenskog, Norway

Background: Ex vivo culture of colorectal cancer (CRC) patient-derived tumoroids reveals a rich heterogenous pool of growth morphologies, within and among models. Quantitative analysis of tumoroid morphologies can uncover new biology and predictive relationships. Studies have shown that compact vs. cystic morphology reflects drug sensitivity, with cystic tumoroids being sensitive to Wnt inhibitors and resistant to MEK inhibitors as compared to compact tumoroids.
Methods: Individual tumoroids (n=4049) were annotated based on visual assessment of brightfield, nuclear and nuclear dead stain multi-channel images. ConvNeXt v2 classifiers were trained on the resulting dataset, using brightfield or all three channels as inputs.
Results: We developed a phenotyper algorithm (iCANdy) stratifying CRC tumoroids into 10 classes: compact, budding, acinar, cystic (thick-walled), cystic (thin-walled), invasive, fibroblastic, monolayer, single/apoptotic and mixed/other. Performance was similar for brightfield and multi-channel inputs. Classifying all tumoroids according to the nearest morphology yielded an F1-score of 0.80 and balanced accuracy of 0.75, the most ambiguous class being mixed/other as expected. iCANdy was applied on brightfield images of 10.2 million tumoroids from a total of 22k drug treatment/control wells from 57 tumoroid models, using 37 drugs or drug combinations. For untreated controls, the dominant morphology in terms of total area varied across models with compact (39%), invasive (32%), single/apoptotic (12%), budding (9%), and cystic (thick-walled) (7%) being most common. We observed high intra-patient heterogeneity, the proportion of the dominant morphology ranging from 20% to 54% with a median of 36% (excluding single/apoptotic structures). Inter-patient heterogeneity was also associated with the activity of several drugs. While atorvastatin showed a similar single-oriented shift for both compact (82%) and invasive (100%) structures, other drugs such as 5-FU exhibited strong differences (68% and 18% respectively). Other compounds with limited impact on cell viability induced morphological phenotypes indicating mode-of-actions such as cytostasis or senescence. Interestingly, methotrexate caused an invasive-oriented shift for 80% of the cystic (thick-walled) structures but only 14% of the compact clusters.
Conclusions: Quantitative phenotyping of tumoroids can identify novel predictive morphological relationships, drug mode-of-action and more accurately predict drug activity.

#0735 Establishing diffuse gastric cancer patient-derived organoids for drug response analysis.

Carolina Bizama[1], Patricia Garcia[1], Franz Villarroel[2], Marcelo Garrido[3], Arnoldo Riquelme[4], Nicole Babbitt[5], Gareth-I Owen[5], Enrique Norero[6], Ignacio Carrasco[1], Adolfo Rojas[7], Vinicius Maracaja-Coutinho[7], Yareni Avalos-Guajardo[1], Angel Castillo[1], Juan Carlos Roa[1]

[1]Department of Pathology, Faculty of Medicine, Pontificia Universidad Catolica de Chile, Santiago, Chile,[2]Fundacion Arturo Lopez Perez (FALP), Santiago, Chile,[3]Centro de Oncologia de Precision, Universidad Mayor, Santiago, Chile,[4]Department of Gastroenterology, Faculty of Medicine, Pontificia Universidad Catolica de Chile, Santiago, Chile,[5]Department of Physiology, Faculty of Biological Sciences, Pontificia Universidad Catolica de Chile, Santiago, Chile,[6]Complejo Asistencial Hospital Dr. Sotero del Rio, Santiago, Chile,[7]Facultad de Ciencias Quimicas y Farmaceuticas & Facultad de Medicina, Universidad de Chile, Santiago, Chile

Introduction: Gastric cancer (GC) is a major health problem in Chile, with high incidence and mortality rates, particularly among younger populations. Diffuse GC is the most aggressive subtype, characterized by a poorly cohesive and signet-ring cell features, matching the genomically stable molecular subtype. These tumors are frequently linked to advanced nodal metastasis and peritoneal dissemination. Response to chemotherapy is generally limited, although a subset of GC patients can achieve significant clinical efficacy from first-line immunotherapy (PD-1/PDL-1 inhibitors plus chemotherapy). Patient-derived organoids (PDOs), three-dimensional cultured generated from stem cells, can recapitulate tumor heterogeneity and have emerged as a powerful preclinical model for studying tumor biology and predicting response to anticancer treatments. The aim of this study was to characterize GC PDOs and evaluate their responses to drug treatment.

Material and Methods: Fresh tumor tissues and ascites samples obtained from GC patients were enzymatically dissociated using collagenase/dispase solution and cultured following a modified protocol previously described. PDOs and their corresponding original tissues were characterized using H&E staining, immunohistochemistry, immunofluorescence, and flow cytometry. GC PDOs were then subjected to chemotherapy dose-response assays using oxaliplatin, 5-fluorouracil and irinotecan, and additionally screened against 103 FDA-approved anticancer drugs. After 72 hours of treatment, cell viability was assessed using the CellTiter-Glo 3D assay.

Results: Eight GC PDOs were successfully established from endoscopic biopsies or ascites fluid samples. The PDOs preserved the histopathological features and epithelial polarity of their tumors of origin and retained key mutations, including *TP53* and *CDH1*. The EPCAM-positive organoid population displayed membranous PD-L1 expression ranging from 0.28-75% by flow cytometry. Based on normalized AUC analysis, the PDOs showed heterogeneous responses to standard chemotherapies, and several specific drugs reduced the organoid viability.

Conclusions: The GC-PDOs effectively recapitulated the histological and molecular characteristics of their epithelium tumor of origin and demonstrated differential sensitivity to chemotherapeutic and targeted agents. These findings support the use of GC PDOs as a valuable tool for investigating tumor biology and provide a promising platform for precision medicine approaches in the treatment of diffuse gastric cancer.

Funding: ANID-FONDECYT 1221253, 1221345. ANID-FONDAP-CECAN 152220002, ANID-FONDAP-ACCDIS 15130011.

#0737 Single cell stiffness analysis using a ferrohydrodynamic-microfluidic platform.

Yuhao Zhang, Yang Liu

CMBE, University of Georgia, Athens, GA

Accurate measurement of cell stiffness is essential for understanding how cells adapt to changes in their physical and biological environment, including those associated with cancer progression, immune activity, and tissue remodeling. Conventional techniques such as atomic force microscopy (AFM), optical tweezers, and micropipette aspiration are widely used, but they are limited by low throughput and cannot be readily integrated with molecular analysis. To overcome these constraints, we developed a ferrohydrodynamic microfluidic platform capable of quantifying single-cell stiffness in a high-throughput and label-free manner, while also enabling direct assessment of cytoskeletal protein expression.

In this platform, the magnetic force acting on each cell varies with cell size, ferrofluid concentration, and magnetic field strength. Stiffness is quantified by estimating the forces acting on the cell at its measured position within the channel, including magnetic buoyancy and hydrodynamic drag. To ensure consistent and comparable measurements, cell size was incorporated into numerical simulations used to optimize the channel-width gradient and the resulting force distribution. Simulated magnetic fields and deformation patterns matched experimental results, confirming the mechanical reliability of the system. The device was further calibrated with polyacrylamide gel beads of known elastic moduli to examine how bead stiffness, ferrofluid concentration, and magnetic force distribution affect measurement accuracy.

We evaluated the platform using human cancer cell lines and generated stiffness maps that revealed substantial mechanical heterogeneity within phenotypically similar populations. To explore the relationship between mechanics and behavior, we incorporated a single-cell migration module and compared the stiffness of cells before and after migration. Cells that successfully migrated consistently exhibited lower stiffness, suggesting that increased deformability may facilitate motility. To identify potential molecular contributors, we used immunofluorescence staining and single-cell western blotting (scWB) to quantify vimentin and lamin A/C. Their expression levels varied in patterns that aligned with stiffness differences across individual cells.

#0738 Organoids from primary human prostate cancer exhibit heterogeneity in the states of tumor-associated epithelial cells.

Nilton J. Santos, Larissa C. R. Caldeira da Costa, Fabiana O. Buono, Fabiano P. Saggioro, Antonio A. Rodrigues Junior, Rafael Neuppmann Feres, Rodolfo Borges dos Reis, Jeremy A. Squire, Leticia Frohlich Archangelo

Ribeirao Preto Medical School, University of Sao Paulo (USP), Ribeirao Preto, Brazil

Prostate cancer (PCa) is the most commonly diagnosed malignant tumour in men and the second leading cause of cancer-related mortality worldwide. Despite the high long-term survival rates in localised PCa, metastatic disease remains largely incurable even after intensive multimodal therapy. Our limited understanding of the drivers of aggressive behaviour in advanced PCa and the molecular pathways that underlie their failure to respond to various drug therapies underscores the need to study tumours in vitro so that more effective therapies can be evaluated. Tumour-derived organoids represent an advanced in vitro model for studying cancer and are increasingly being used in the development of new therapeutic strategies, serving as valuable tools for advancing precision medicine in oncology. Our goal was to characterise patient-derived organoids from our prostate samples cohort of the FMRP-USP, which accurately model the original patient tumours. Our approach involved establishing longer-term organoid cultures from biopsy samples in Matrigel. For this, we used 9 fresh prostatectomy tissue samples that were processed by mechanical dissection and enzymatic digestion, then filtered and cultured in advanced DMEM/F12 medium with supplements (GlutaMAX, B27, N-acetylcysteine, recombinant EGF, FGF-10 and FGF-2, A-83-01, SB202190, nicotinamide, DHT, PGE2, Y-27632, Noggin, and R-spondin). Nine patients were aged between 50 and 75 years and diagnosed with high-risk PCa with ISUP grade of 4 or 5 (Ethics Committee Number 88216025.3.0000.5440). The organoids were characterized using morphological 3D imaging and histological (H&E staining, IHC and IF) approaches and compared to the primary sample of the same tumor to confirm their cancer-modelling capacity and suitability for the downstream assays. We successfully established long-term organoid culture for up to 2 months. We verified through characterisation that the organoids presented a morphology and tumour immune profile similar to the tissues of origin. In summary, we have successfully established and characterised long-term patient-derived PCa organoids, which closely recapitulate the original tumours, providing a robust platform for future pre-clinical studies and precision oncology applications.

#0739 Tissue-engineered organ-specific cancer metastasis model for cancer research.

Yi Yin[1], Andrew Z. Wang[2]

[1]Radiation Oncology, University of Texas Southwestern Medical Center, Dallas, TX,[2]University of Texas Southwestern Medical Center, Dallas, TX

Understanding the biology of cancer metastasis is crucial for developing more effective treatments in oncology. A significant challenge in this area has been the lack of cancer models that accurately reflect the biology of metastasis, especially regarding organ-specificity, which is a key feature of cancer spread. This creates a strong unmet need for new models that can mimic the organ-specific dynamics of tumor spread. Our research group has been utilizing tissue engineering techniques to develop in vitro models of cancer metastasis. We hypothesize that decellularized tissues can effectively replicate the organ microenvironment associated with metastatic processes, serving as platforms for tumor cell growth. We had previously reported the use of decellularized liver and lung tissue as strata for tumor metastasis modeling. In this study, we have expanded the model using a panel of decellularized tissues to study the “good soils” and “bad soils” of metastasis. In experiments using several cancer cell lines, we found that tumor cells can spontaneously cluster and form colonies on biomatrices derived from common metastatic sites, such as the liver and lungs, often referred to as “good soil.” Decellularized biomatrices from the upper and lower gastrointestinal tract, and pancreas can also recapitulate the “bad soil” of cancer metastasis. These findings underscore that our proposed model of cancer metastasis is a powerful tool for cancer biology research and has great potential for precision oncology.

#0741 Illuminate your targets: Endogenous HiBiT knock-in monoclones—inventory + rapid custom.

Xiaomeng Gou, Yue Huang, Yu Wang, jinying Ning, **Feng Hao**

Kyinno Biotechnology Co., LTD, Beijing, China

Background & significance — applications HiBiT is an 11-aa tag that complements LgBiT to reconstitute NanoLuc, delivering a bright, linear bioluminescent readout that scales with target protein abundance. Compared with Western blot-centric workflows, endogenous HiBiT knock-ins enable real-time, quantitative kinetics under native regulation, accelerating mechanism confirmation, potency ranking, SAR, and combination design across modalities—PROTACs, molecular glues, LYTACs, and AbTACs.

Kyinno case series — what's in the panel (representative scope) Kyinno has established a broad, ready-to-run portfolio of HiBiT-KI monoclonal cell lines covering more than 30 endogenously tagged genes across diverse biological categories—oncogenic signaling, kinases, transcription factors, and E3-amenable targets. These include representative nodes such as KRAS, CDK family members, PRMT5, EGFR, AR, BRD family proteins, EZH2, STATs, and so on. The panel thus provides comprehensive coverage of major target classes relevant to targeted protein degradation, signal transduction, and transcriptional regulation. Rapid custom knock-in (N- or C-terminal) further extends the platform to program-specific targets and variants, allowing teams to start immediately with inventory models or quickly obtain bespoke constructs.

Methods & deployment — how it works now We implement a dual-stable system: (i) genome-integrated LgBiT to minimize signal drift, and (ii) CRISPR-Cas9 HDR to precisely insert HiBiT at endogenous loci while preserving gene dosage and protein function. Single-cell clones are sequence-verified, STR-authenticated, and mycoplasma-free. Standardized NanoLuc assays (10-point curves, 72-96 h or live kinetic) output quantitative degradation/turnover trajectories with plate-to-plate comparability. This platform compresses assay setup from weeks to days, unifies readouts across targets and hosts, and provides a scalable path from hit triage to translational method transfer—bringing HiBiT quantitation everywhere you need it.

#0742 Unlocking 3D: TumorMACS media as a dual-purpose solution for primary 2D and 3D tumor organoid cultures.

Lea Eich, Marla Schneider, Olaf Hardt, David Agorku, **Benjamin Theek**

Miltenyi Biotec B.V. & Co. KG, Bergisch Gladbach, Germany

Background: 3D cell culture models are gaining more and more interest in cancer research by more accurately mimicking the in vivo tumor environment compared to traditional 2D cultures. These models provide critical insights into tumor biology, including cell-cell interactions, drug resistance, and gene expression profiles. By offering a more physiologically relevant context, 3D cultures enhance the predictive power of preclinical studies, facilitating the development of more effective cancer therapies. As such, the demand for versatile, reproducible, and efficient media that support both 2D and 3D growth is increasingly important in advancing cancer research and drug discovery. Traditional media often lack the versatility required for seamless transitions between 2D and 3D cultures, posing challenges in workflow efficiency.
Methods: We initially cultivated primary colon, lung and breast cancer cells in 2D using the respective TumorMACS media. These cells were transferred into 3D cultures by generating 4x10^5 cells/ml growth factor reduced Matrigel domes (embedded culture) or using 2x10^4 cells/ml TumorMACS medium with 2%(v/v) Matrigel (suspension culture). For each cell line the entity specific TumorMACS media was supplemented with StemMACS Y-27632 and used for bi-weekly media changes, for up to 14 days of culture. Mature tumoroids were dissociated into single cells for doubling time calculations and surface marker analysis using the MACSQuant Analyzer.
Results: The transition from 2D to 3D cultures was successful across all cell cultures evaluated. Embedded cultures showed doubling times of approximately 3 days for colon and breast cells, and 4 days for lung cells. Although static suspension cultures exhibited similar doubling times, they presented greater variability. The higher uniformity in size of tumoroids grown in embedded cultures suggest improved consistency, which is critical for reliable assay results. However, next to the expansion of cells in 2D, suspension cultures can be an attractive alternative to scale cell numbers more efficiently before the assay start.
Conclusion: TumorMACS media's dual-purpose capability enables seamless transitions between 2D and 3D cultures, enhancing research efficiency and accelerating the development of cancer therapies. Its use simplifies experimental workflows and offers a cost-effective alternative to specialized tumoroid media.

#0743 Characterizing organoid maturation and disease progression through recombinant monoclonal antibodies.

Mark Machak[1], Nicole Schultz[1], Rudra Bhowmick[2], Joseph Boyd[1], Fong-Cheng Pan[1], John Larsen[3], Vi Chu[4], Mary Mills[3], Chandra Mohan[1], I-Fang Ling[1], Arazo Saadat[5], **Mark A. Santos**[1]

[1]R&D, MilliporeSigma, Temecula, CA,[2]MilliporeSigma, Burlington, MA,[3]R&D, MilliporeSigma, St. Louis, MO,[4]MilliporeSigma, Milwaukee, WI,[5]MilliporeSigma, Temecula, CA

Organoids are three-dimensional structures derived from either pluripotent stem cells or adult stem cells, consisting of multiple cell types that interact with one another. They are highly sought after for research in organ development, disease modeling, and drug testing. Organoids can be engineered to replicate specific disease conditions, enabling researchers to study disease progression and design therapeutic modalities. We have used recombinant monoclonal antibodies, produced using a proprietary B-cell immortalization technique and a high-yield expression system, for characterizing organoids. These antibodies provide consistent performance across various experimental conditions and exhibit high specificity and sensitivity, allowing for precise detection of target proteins in biological samples. They can be utilized to identify specific cell types during organoid development, study the time-dependent expression of proteins, and analyze the interactions among multiple cell types during development. We have examined organoid development and maturation through immunohistochemistry using selected recombinant antibodies. Immunohistochemistry analysis conducted on normal liver tissue sections, as well as progenitor and mature organoid sections, revealed remarkable staining patterns for targets such as FOXA2, HNF4alpha, and Keratin 7. These applications may significantly enhance our understanding of the mechanisms involved in tissue development and disease progression.

#0744 In vitro and in vivo evaluation of the bystander-killing effect of ADCs.

Chong Wang, Mengya Tong, **Tan Pang**, Jingqi Huang

Pharmacology, Pharmaron, Ningbo, China

Antibody-drug conjugates (ADCs) represent a promising class of therapeutics with a broader therapeutic window than conventional chemotherapeutic agents, owing to their efficient and specific drug delivery. In addition, some ADCs produce a bystander-killing effect through mechanisms such as soluble toxic mediators, gap junction intercellular communication, immune-mediated killing, or Fc-mediated effector functions. This effect benefits not only antigen-expressing tumor cells, but also adjacent antigen-negative cells. Trophoblast cell-surface antigen 2 (Trop-2) is a transmembrane glycoprotein highly expressed in many epithelial cancers and serves as an attractive target for ADC development. In this study, we assessed the bystander-killing effect of two Trop-2-targeted ADCs—sacituzumab govitecan (SG) and datopotamab deruxtecan (Dato-DXd). To evaluate this effect, we used both in vitro co-culture assays and in vivo mixed-cell xenograft tumor models. Three cell line pairs (BxPC-3/UM-UC-3, HCC1806/UM-UC-3, NCI-N87/UM-UC-3) were selected for the in vitro assay based on Trop-2 expression. Dato-DXd exhibited higher payload release in both the BxPC-3 group and the BxPC-3/UM-UC-3 co-culture group compared to UM-UC-3 alone, which showed minimal payload release. In contrast, SG demonstrated similar payload release across all groups. Cell proliferation assays revealed that Dato-DXd had potent cytotoxicity against Trop-2-positive cells (BxPC-3, HCC1806, NCI-N87) but was ineffective in UM-UC-3 cells. Conversely, SG exhibited comparable cytotoxicity across all four cell lines. Notably, Dato-DXd reduced the viability of UM-UC-3 cells in all co-culture groups, with the BxPC-3/UM-UC-3 group showing the strongest bystander effect (80% inhibition of UM-UC-3 cells). Unlike Dato-DXd, SG exhibited strong cytotoxicity in both co-culture and UM-UC-3 groups. A similar observation was made in vivo using a mixture of BxPC-3 and UM-UC-3-Luc cell line-derived xenograft model, with tumor volume monitored via imaging. These results demonstrate that co-culture systems and in vivo imaging are valuable tools for ADC drug discovery. Both in vitro and in vivo assays are essential for understanding bystander-killing mechanisms and predicting clinical success.

#0745 Immunopeptidomic profiling of OncoPro tumoroid models enables MHC-I enrichment and neoantigen target discovery.

Pradip Shahi Thakuri[1], Logan Wilson[1], Colin D. Paul[1], Chris Yankaskas[1], Shyanne Salen[1], Anastasia Klenke[2], Fernanda Salvato[2], Tonya Pekar Hart[2], Joanna S. Geddes[2], Dominique Figueroa[3], Kevin Yen-Yu Yang[3], Bhavin B. Patel[2], Matthew R. Dallas[1], David Kuninger[1]

[1]Cell Biology, Thermo Fisher Scientific, Frederick, MD,[2]Thermo Fisher Scientific, Rockford, IL,[3]Thermo Fisher Scientific, San Jose, CA

Cancer immunotherapy leverages the immune system's capacity to recognize and eliminate tumor cells through peptides presented by major histocompatibility complexes (MHCs). Immunopeptidomics, the large-scale identification of MHC-bound peptides, provides critical insights into tumor antigen presentation and supports the discovery of targets for personalized immunotherapies. Here, we describe a reproducible workflow for enrichment and profiling of MHC-I peptides from patient-derived tumoroid (also known as cancer organoid) models that recapitulate the complexity and heterogeneity of primary tumors. A panel of OncoPro™ Tumoroid Cell Lines was analyzed using LC-MS–based global proteomics. MHC-I profiling demonstrated high enrichment of HLA-A, HLA-B, and HLA-C proteins in the endometrial donor line HuEn033122, which was selected for immunopeptidome characterization. Tumoroids were cultured in OncoPro™ Tumoroid Culture Medium, pre-treated with 10 ng/mL interferon-γ for 18 hours prior to sample collection to enhance expression of MHC-I expression and antigen presentation capacity, and collected as frozen cell pellets. Pellets of ten million cells were processed per the manufacturer's instructions for the different lysis buffers: Thermo Scientific™ Mem-PER™ Plus Membrane Solubilization Buffer, Thermo Scientific™ Pierce™ IP Lysis Buffer, Thermo Scientific™ T-PER Tissue Protein Extraction Reagent, and Thermo Scientific™ Pierce™ GPCR Extraction and Solubilization Buffer. MHC peptide complexes were immunoprecipitated with W6/32 antibody–coupled supports, eluted with 1% TFA, and analyzed by nanoLC-MS/MS on Thermo Scientific ™ Orbitrap™ instruments. Data was analyzed using PEAKS® Studio 12.5 using the DeepNovo Peptidome workflow (6–30 mers, 1% FDR, DeepNovo score ≥ 70%). Immunopeptidomic profiling revealed a dominant 9-mer peptide population (~53%), consistent with canonical MHC-I binding and confirming high-quality enrichment. This 9-mer dominance serves as a robust quality control indicator of workflow specificity and reproducibility. Integration of immunopeptidomic data with whole-exome and RNA sequencing, and bulk proteomics will enable identification of expressed, mutation-derived neoantigens unique to each tumoroid model. Collectively, this platform establishes a physiologically relevant and reproducible approach for neoantigen discovery, advancing precision cancer immunotherapies.

#0746 Modeling micro- and nanoplastics-induced colon aging in organoids to unravel pathways leading to early-onset colorectal cancer.

Zahra Heydari, Gobinda Sarkar, Lisa A. Boardman

Mayo Clinic, Rochester, MN

Background: Early-onset colorectal cancer (EOCRC) is rapidly increasing, with projections that by 2030, one in ten colon cancers will occur in individuals under 50. Unlike hereditary syndromes, most EOCRC cases are sporadic, implicating environmental and aging-related mechanisms. Accelerated biological aging, characterized by telomere attrition, oxidative stress, and senescence-associated inflammation, is a defining feature of EOCRC. Micro- and nanoplastics (MNPs) can accumulate in the gut, induce oxidative stress, and damage DNA. These processes mirror hallmarks of aging, suggesting that chronic MNP exposure may accelerate colonic epithelial aging and promote EOCRC initiation. Methods: To test this hypothesis, we used patient-derived human colon organoids from normal and polyp tissues. Apical-out organoids, which expose the luminal surface to the environment, were treated with defined polyethylene-derived microplastics (1.7-2.2 µm) and nanoplastics (0.04-0.06 µm) at 0, 1 and10 µg/mL for up to 72 hours. We assessed viability, oxidative stress, senescence markers, and inflammatory cytokines. Telomere length will be quantified by qPCR, and cytokine profiling was performed using Olink proteomics. Results: Live/Dead assays revealed minimal cytotoxicity at 1 µg/mL, while nanoplastics induced greater cell death and oxidative stress at 10 µg/mL. Preliminary data suggest that nanoplastic exposure leads to telomere shortening. Moreover, gene expression analyses showed that nanoplastics triggered stronger mitochondrial and redox stress responses than microplastics, consistent with higher reactivity of smaller particles. Additional experimental groups will be included to validate and expand upon these preliminary findings. Conclusions: Although preliminary, these data point to potential links between MNP exposure and early aging-associated stress pathways in the colon epithelium. Continued refinement of this organoid model, together with expanded sample sizes and multiomic analyses, will be essential for determining whether these early signals represent meaningful contributors to EOCRC risk.
Funding: Individualizing colorectal cancer patient care using the host and tumor telomere phenotype (RO1 CA204013), Curtiss Fund (92541775), C-SiG Core(s): Epigenomics & Spatial Biology Core, and Clinical Core of the Mayo Clinic Center for Cell Signaling in Gastroenterology (P30DK084567)

#0749 Modulating cancer stemness in commercial OCSCC spheroid cultures through microenvironmental stress.

Anuleka Elapavaluru[1], Stephen Keysar[2], Herman Li[1], Antonio Jimeno[2], Minsoo Kim[1], **Farshad N. Chowdhury**[1]

[1]Univ. of Rochester School of Medicine & Dentistry, Rochester, NY,[2]University of Colorado School of Medicine, Aurora, CO

Oral cavity squamous cell cancer (OCSCC) recurrence is linked to cancer stem cells (CSCs), which persist despite treatment. To enable reproducible CSC studies, we established a scalable system using the commercially available ATCC SCC-9 cell line subjected to physical and metabolic stress gradients—standard monolayer, AggreWell spheroids (moderate stress), and ultra-low attachment (ULA) spheroids (maximal stress)—in both nutrient-rich (RMk media) and nutrient-deficient (CSC media) conditions.
SCC-9 cells were expanded in standard tissue culture flasks and seeded at defined concentrations into five experimental conditions: (1) standard attachment monolayer, (2) 24-well AggreWell 400 plates in RMk media, (3) 24-well AggreWell 400 plates in CSC media, (4) ULA plates in RMk media, and (5) ULA plates in CSC media. After four days, spheroids were imaged, dissociated with Accutase, and analyzed for CSC enrichment by flow cytometry. CD44 expression was quantified by median fluorescence intensity (MFI), and increased aldehyde dehydrogenase activity was detected using the Aldefluor assay. MFI for CD44 rose progressively with microenvironmental stress, from 18,340 (monolayer) to 42,924 (ULA plate in CSC media), representing a 2.3-fold increase. The double-positive CSC-like population (CD44high/Aldefluor+) was nearly absent in low-stress monolayer and moderate-stress AggreWell cultures, but increased to 0.12% in ULA RMk and tripled to 0.42% in ULA CSC media. These results demonstrate that both CSC prevalence and marker intensity can be systematically tuned by adjusting physical and metabolic stress.
This protocol allows researchers to enhance CSC-like enrichment in a stepwise manner using a widely available OCSCC cell line. The methodology supports applications in drug testing, differentiation studies, and immune interaction assays, leveraging commercial plates and reagents for reproducibility across laboratories. The dynamic range of CSC induction provides a practical tool for studying OCSCC recurrence and therapeutic resistance.

#0750 Optimization of cancer-associated fibroblast expansion and co-culture with patient-derived tumoroids.

Shyanne Salen, Colin D. Paul, Pradip Shahi Thakuri, Matt Dallas, David Kuninger

Thermo Fisher Scientific, Frederick, MD

Patient-derived 3D cancer models (tumoroids or cancer organoids) maintain key patient-specific mutations and gene expression profiles during in vitro culture. Gibco™ OncoPro™ Tumoroid Culture Medium Kit was developed as an easy-to-use tumoroid culture system for the expansion of tumoroid lines. Consequently, single cell RNA sequencing of established tumoroid models shows decreases in immune, stromal, and endothelial cells compared to the initial tumor samples from which they were derived. The tumor microenvironment (TME), specifically cancer-associated fibroblasts (CAFs), has been shown to contribute to poor prognosis and therapy resistance. Therefore, there is interest in reliably expanding and culturing CAFs from donor cells for integration with tumoroid cultures and in vitro reconstruction of the TME. Here, we optimized culture conditions for CAF generation from donor cancer samples and explored methods for CAF and tumoroid co-culture. We aimed to create a robust workflow to obtain CAFs from dissociated tumor cells procured from Discovery Life Sciences and, when available, fresh tissue resections. Dissociated cells were plated in Gibco™ Human Fibroblast Expansion (HFE) Medium supplemented with 2% Gibco™ Low Serum Growth Supplement in Thermo Scientific™ Nunc™ Multidishes with Nunclon™ Supra Surface. CAFs were passaged when they reached 80-90% confluency and continuously expanded in Thermo Scientific™ Nunc™ EasYFlask™ Flasks with Nunclon™ Supra Surface for up to 8 passages until a bank was established. Flow cytometry was performed on the CAF cultures, and CAFs were identified as being negative for EpCAM, CD45, and CD31. CAFs were considered a line based on morphology, having less than 15% epithelial, endothelial, and immune populations, and obtaining more than 3 cumulative population doublings. We successfully created CAF lines from 5 out of a total of 6 samples, which included lung, breast, and colorectal DTCs or resected tissue. A colorectal tumoroid line was previously engineered with an eGFP lentivirus and used in co-culture studies. CAFs from this same donor tissue were labeled with Invitrogen™ CellTracker™ Red CMTPX and mixed with the engineered tumoroid line. When cultured in suspension in a 50:50 mixture of HFE medium and OncoPro with 2% Gibco™ Geltrex Flex, the stromal cells and tumoroids self-organized with the stromal cells invading around and into the tumoroids, creating large lobular structures after 7 days in culture. In summary, this method can be leveraged for preclinical studies to develop critical new therapies and further explore the role of CAFs in the TME, enabling the investigation of tumor-stroma crosstalk. We anticipate that CAF-integrated models will be valuable for studies exploring mechanisms of drug resistance, metabolic reprogramming, ECM remodeling, and immunomodulation, as well as for evaluating the efficacy of anti-fibrotic or stroma-targeting agents.

#0751 A workflow integrating multi-omics with patient-specific 3D cell models for interrogating precision medicine approaches in clinically-relevant timeframes.

Elahe Minaei[1], Stella Davy[1], **Ali McCorkindale**[1], Peilin Tian[2], Joanna Wasielewska[1], Sean Porazinski[1]

[1]Inventia Life Science, Alexandria, Australia,[2]School of Chemistry and Australian Centre of NanoMedicine, Sydney, Australia

The complexity and heterogeneity of cancers within and between patients has led to the precision medicine paradigm of cancer therapy where treatment should be personalized to individual patients to achieve maximal outcomes. Large scale endeavours such as the NCI-MATCH study [1] have investigated the benefits of tumor DNA sequencing, in order to best match the patient to a targeted therapy for their cancer. These studies demonstrate improved outcomes with matching approaches, but raise questions about genetic influences on drug resistance, suggesting sequencing alone may not be sufficient to guide molecular targeted therapies.

New Approach Methodologies (NAMs) such as tumoroids are patient-derived cancer cells that grow as 3D self-organized, multicellular structures that maintain key characteristics of the patient tumor of origin including genotype and transcriptomic profiles, as well as biological behaviors. These NAMs serve as valuable tools for studying tumor biology and patient-specific responses to various anti-cancer therapies.

Here, we utilize the RASTRUM^{TM} Allegro platform from Inventia Life Science and Gibco^{TM} OncoPro^{TM} colorectal cancer (CRC) Tumoroid Cell Lines (ThermoFisher Scientific [2]) to easily create plug and play patient-derived 3D cell models within synthetic PEG-based hydrogel matrices, which were tuned to mimic the stiffness and ECM composition of CRC tumors. Coupling these biologically-relevant tumoroid models with molecular insights from comprehensive proteomics and transcriptomics characterization, we demonstrate the utility of this workflow for throughput drug screening and determining personalized therapy responses in clinically-relevant timeframes.

Our approach provides a scalable framework for evaluating precision medicine approaches using biologically-relevant patient-derived tumoroids. Future work will focus on the development of processes to support direct dissociation and generation of patient-derived models from specimens from a variety of cancer types. Utilization of the RASTRUM platform in these precision medicine workflows to generate real-time drug sensitivity data, could be leveraged to inform clinical treatment decision making.

References

1. O'Dwyer P.J. et al. The NCI-MATCH trial: Lessons for precision oncology. Nature Medicine 2024, 29(6):1349-1357.

2. Paul, C.D. et al. Long-term maintenance of patient-specific characteristics in tumoroids from six cancer indications. Scientific Reports 2025, 15(1):3933.

#0752 Bioluminescent intestinal reporter organoids as in vitro tools to monitor inflammatory effects of compounds.

Subhashree Kumaravel[1], Carolina J. Sierra[1], Trish T. Hoang[2], Kevin Su[1], Vi Chu[1], Jeong-Hee Lee[2], Helena Borges[2], Thomas Machleidt[2]

[1]MilliporeSigma, Temecula, CA,[2]Promega Corporation, Madison, WI

Intestinal cancer ranks as the second leading cause of cancer-related deaths in the United States, with an anticipated toll of 52,900 fatalities in 2025. Chronic inflammation is a recognized contributor to carcinogenesis. Patients with inflammatory bowel disease, face a 1.7-fold increased risk of developing cancer. Identifying compounds that either induce or mitigate inflammation is crucial for cancer prevention and treatment. Organoids, as in vitro 3D cell culture mimetics of specific organs, provide a more physiologically relevant and reliable human-based model for testing drug efficacy and toxicity compared to traditional 2D cell cultures or animal models. This study focuses on the development and application of bioluminescent intestinal inflammatory reporter organoids to screen and monitor the effects of various inflammatory and anti-inflammatory agents. Healthy intestinal organoids from induced pluripotent stem cells (iPSCs) or patient-derived tissues were transduced with the NF-kB nanoLuc® reporter plasmid, enabling luminescence-based monitoring of NF-kB activity. We employed lentiviral (LV) and adeno-associated viral (AAV) delivery systems to create stable and assay-ready NF-kB reporter organoids respectively. The successfully transduced organoids were assessed in both 3D and 2.5D formats to evaluate the impact of different inflammatory and anti-inflammatory compounds. To measure the activation of NF-kB, we utilized the Lumit® immunoassay to detect phosphorylated p65 levels. Protein and mRNA levels of various secreted and intracellular cytokines and chemokines were quantified through immunoassays and RT-qPCR. Stable NF-kB NanoLuc reporter organoids were established via LV transduction at a multiplicity of infection of 1000, followed by puromycin selection. Additionally, we generated transient, assay-ready reporter organoids using AAV serotype 3. Among the cytokines analyzed, the highest reporter activity was observed following treatment with a cocktail of TNFα, IL-1β, and flagellin at 3- and 6- hours post-treatment. The increase in intracellular phospho-p65 levels correlated with the observed reporter activity. Furthermore, NF-kB activation resulted in significant upregulation of other intracellular and secreted cytokines, including CXCL8, IL-1β, and TNFα. Importantly, treatment with established anti-inflammatory agents, such as Tofacitinib, led to a reduction in elevated reporter activity and downstream cytokine levels. In conclusion, the bioluminescent intestinal NF-kB reporter organoids developed through our optimized protocol represent a high-throughput platform for effectively monitoring the inflammatory effects of potential drug candidates.

: Application of Bioinformatics to Cancer Biology 1
Poster Session

#0039 Single-cell dissection of ESCC identifies targetable cells-of-origin and therapeutic vulnerabilities in early tumorigenesis.

Kyung Pil Ko[1], Jie Zhang[1], Sohee Jun[1], Jae-Il Park[2]

[1]UT MD Anderson Cancer Ctr., Houston, TX,[2]Asst. Professor, Exp. Radiation Oncology, UT MD Anderson Cancer Ctr., Houston, TX

Identifying the cells of origin is critical for overcoming therapy resistance and improving early intervention strategies in esophageal squamous cell carcinoma (ESCC). Despite advances in genomic profiling and lineage-trajectory studies, the cellular hierarchies and molecular programs that initiate ESCC remain poorly defined. To address this gap, we applied machine-learning-guided single-cell trajectory analysis to carcinogen (4NQO)-induced ESCC, genetically engineered organoid models, and their normal esophageal counterparts, enabling reconstruction of lineage relationships during early tumorigenesis. Integrating these data with gene regulatory network analysis allowed us to pinpoint transcriptional drivers of tumor initiation, and a transcriptome-based drug repurposing strategy identified candidate compounds capable of targeting these early malignant populations. Our multimodal analyses revealed several distinct epithelial clusters that likely act as cells of origin for ESCC, each exhibiting unique stem- or progenitor-like transcriptional states. Regulatory network analysis highlighted activation of key programs, including PRRX2 and CEBPβ, across these initiating populations. In parallel, the drug repurposing screen identified five candidate compounds, four of which were potent cyclin-dependent kinase (CDK) inhibitors. Correspondingly, CDK inhibitors robustly suppressed ESCC cell proliferation, underscoring their therapeutic potential. Together, these findings define the putative cells of origin in ESCC and their core regulatory networks, establishing a single-cell-driven framework that exposes actionable vulnerabilities in tumor-initiating populations.

#0040 Integrated transcriptomic and immune-clonal evolution defines stepwise molecular progression in lung adenocarcinoma.

Kang Qin[1], An Qin[2], John V. Heymach[3]

[1]University of TEXAS, MD Anderson Cancer Center, Houston, TX,[2]Loyola University of Chicago, Chicago, IL,[3]UT MD Anderson Cancer Center, Houston, TX

Background: Progressive immune remodeling is a hallmark of early lung adenocarcinoma (LUAD) evolution, yet the integrated transcriptional and clonal trajectories underlying this process remain poorly defined.

Methods: Single-cell RNA sequencing (scRNA-seq) data from *GSE189357* and *HDAC000630* were analyzed across 33 lung samples, spanning normal to invasive adenocarcinoma. After quality control (200 < genes < 5,000; mitochondrial < 10%), 187,880 high-quality cells were processed in *Seurat* with Harmony integration, PCA, and clustering (resolution = 0.3). Cell types were annotated using canonical markers and *CellMarker 2.0*. Matched single-cell and bulk T-cell receptor (TCR) repertoires (87 samples from *GSE164789*) were analyzed in *scRepertoire* to quantify clonal expansion, diversity (Shannon, Simpson, D50), overlap, CDR3 length, rare-clone contribution, and TRBV/TRBJ gene usage.

Results: Single-cell transcriptomics resolved 15 major cell types and revealed progressive microenvironmental remodeling. Epithelial, fibroblast, and endothelial lineages expanded from atypical adenomatous hyperplasia (AAH) to invasive adenocarcinoma (IAC), whereas cytotoxic, NK, and dendritic cells declined, indicating immune attenuation and fibrovascular dominance. Stage-specific transcriptional programs showed sequential activation of extracellular-matrix organization, angiogenesis, immune suppression, and oxidative metabolism, capturing the molecular evolution of invasion. Integrated single-cell TCR analysis revealed stage-specific immune compartmentalization and progressive loss of repertoire diversity. UMAP visualization highlighted enrichment of $CD8^+$ cytotoxic and $FOXP3^+$ regulatory T-cell clones with hyperexpanded clonotypes in advanced lesions. Clonal distributions shifted from polyclonal equilibrium in normal tissue to oligoclonal dominance in IAC. Bulk TCR profiling confirmed reduced Shannon and inverse Simpson diversity indices and expansion of high-frequency clonotypes. Clonal overlap analysis demonstrated minimal sharing across lesions, suggesting localized antigen-driven responses. Progressive CDR3 shortening and biased V-J recombination indicated convergent clonal selection along the LUAD continuum.

Conclusions: Integrated single-cell transcriptomic and TCR analyses define a unified trajectory of LUAD evolution driven by transcriptional reprogramming, stromal expansion, and progressive immune restriction. The convergence of epithelial remodeling with oligoclonal T-cell expansion delineates early immunologic bottlenecks and highlights potential therapeutic windows for immune interception.

#0041 Integrative analysis of genomic and transcriptomic data informs precancer progression in the pancreas.

Kathleen Noller[1], Jiaying Lai[2], Daniel Lesperance[3], Ricky S. Adkins[3], Ahmed M. Elhossiny[4], Paola A. Guerrera[5], Kimal Rajapakshe[5], Anirban Maitra[6], Anup Mahurkar[1], Owen White[3], Marina Pasca Di Magliano[7], Michael Ochs[3], Luciane Tsukamoto Kagohara[2], Laura Wood[2], Rachel Karchin[8], Elana Judith Fertig[1]

[1]University of Maryland School of Medicine, Baltimore, MD,[2]Johns Hopkins University, Baltimore, MD,[3]University of Maryland, Baltimore, MD,[4]University of Michigan, Ann Arbor, MI,[5]University of Texas MD Anderson Cancer Center, Houston, TX,[6]NYU Langone, New York, NY,[7]University of Michigan Medical School, Ann Arbor, MI,[8]Johns Hopkins Univ., Baltimore, MD

Pancreatic ductal adenocarcinoma (PDAC) arises from heterogeneous precursor lesions, including intraductal papillary mucinous neoplasms (IPMNs), but the features distinguishing indolent from progressive lesions remain unclear. We performed an integrative analysis of transcriptomic, genomic, and microenvironmental profiles of IPMNs to define multi-omic phenotypes. Using transfer learning, we projected IPMN-derived transcriptional programs onto spatial transcriptomic datasets from IPMNs and pancreatic intraepithelial neoplasias (PanINs). We identified two major phenotypes: one associated with cancer-associated fibroblasts and epithelial-to-mesenchymal transition, shared across IPMN, PanIN, and PDAC; and a second, glycolysis-enriched phenotype with a unique somatic variant profile specific to IPMN. Spatial mapping further revealed grade-specific enrichment of transcriptional programs and distinct interactions with stromal and immune subtypes, underscoring the role of the precancer microenvironment in progression. These findings establish multi-omic phenotypes that unify genetic, transcriptional, and microenvironmental heterogeneity, providing a framework for distinguishing progressive from indolent precancers and a web-based public atlas for future exploration of these data and transcriptional phenotypes.

#0042 Engineering antigen-dependent stability in nanobodies: A bioinformatics tool for tuning intracellular nanobody stability.

Alvin Fu[1], Rohith Leeladharan[2], Junhee Park[3], Shriya Kapila[4], Liuhan Ke[1], Amina Mohamed[5], Cynthia Zhao[6], Radha Manohar Kapgate[1], Anh Leith[1], Jonathan Tang[1]

[1]Center for Integrative Brain Research, Seattle Children's Research Institute, Seattle, WA,[2]Paul G. Allen School of Computer Science & Engineering, University of Washington, Seattle, WA,[3]Information School, University of Washington, Seattle, WA,[4]Nikola Tesla STEM High School, Seattle, WA,[5]University of Washington School of Medicine, University of Washington, Seattle, WA,[6]Department of Statistics, University of Washington, Seattle, WA

Nanobodies, derived from camelid antibodies, are highly prized reagents due to their ability to bind their antigen with high affinity, specificity and due to their ease of genetic expression inside cells. Conditionally stable nanobodies, nanobody variants containing mutations in their sequence, are stable only upon antigen binding, making them ideal biosensors. However, the generalizability of conditionally stable nanobodies depends on contextual interactions between nanobody sequences as well as with their fusion protein sequences. To account for contextual effects and thereby creating an individualized way of engineering nanobody for desired stability modulations, we developed a novel bioinformatics tool based on large language model (LLM) that takes an input nanobody sequence and makes predictions about its intracellular stability. The predictions integrate information about nanobody binding to avoid disruptive mutations, guided by a dataset of 389 nanobody-target interfaces. The LLM was first pre-trained on 1.4 million camelid antibody sequences, then fine-tuned to perform binary classification of intracellular stability, producing an F1 score of 0.8. Generative models were developed using a form of Masked Language Modeling (MLM). Models' predictions were validated using reporter assays and western blot in human cell culture. The tool integrates concepts from LLM, nanobody bidirectional stability modulation, nanobody interface classifications, and web integration of modalities to create a tool that can facilitate biomedical and cancer endeavors in the creation of biosensors against any target intracellular proteins for which nanobodies can be selected. This tool has the potential to greatly speed up biosensor engineering, promoting diverse applications in biomedicine and cancer research.

#0043 Epigenetic-neurotransmitter crosstalk between EZH2 and dopamine D1 receptor signaling in triple-negative breast cancer.

Maciej Pietrzak[1], Xilal Y. Rima[2], Gautam Sarathy[3], Shivani Dhekne[3], Lara Rizotto[4], Dario Palmieri[4], Sanjay Gupta[5], Daniel G. Stover[6], Giovanni Nigita[7], Eduardo Reategui[2], Pierre Giglio[8], Christian Rolfo[7], Eswar Shankar[3]

[1]Department of Biomedical Informatics, College of Medicine, The Ohio State University, Columbus, OH,[2]Department of Chemical and Biomolecular Engineering, The Ohio State University,, Columbus, OH,[3]Division of Medical Oncology, Department of Internal Medicine, Wexner Medical Center, The Ohio State University, Columbus, OH,[4]Department of Cancer Biology and Genetics, The Ohio State University College of Medicine, The Ohio State University, Columbus, OH,[5]Department of Urology, School of Medicine, Case Western Reserve University, Cleveland, OH,[6]OSUCCC - James, Columbus, OH,[7]Division of Medical Oncology, Department of Internal Medicine, Wexner Medical Center, The Ohio State University, Columbus, OH,[8]Department of Neurology, School of Medicine, Wexner Medical Center, The Ohio State University, Columbus, OH

Triple-negative breast cancer (TNBC) remains a clinically intractable subtype defined by the absence of ER, PR, and HER2 and characterized by aggressive progression and limited therapeutic vulnerabilities. EZH2, the catalytic subunit of PRC2, is a known oncogenic driver in TNBC through deposition of H3K27me3 and repression of tumor-suppressive programs. In contrast, dopamine D1 receptor (DRD1) signaling has recently emerged as an unexpected tumor-suppressive axis. However, the mechanistic interplay between EZH2-mediated epigenetic repression and DRD1-mediated neurotransmitter signaling is unknown, representing a critical gap in understanding neuro-epigenetic integration in cancer. We hypothesized that coordinated dysregulation of EZH2 and DRD1 reprograms are transcriptional states that govern TNBC aggressiveness. CRISPR-engineered EZH2 and DRD1 knockouts (KO) were generated in MDA-MB-231 cells and validated by immunoblotting. DRD1 KO significantly increased proliferation and migration, whereas EZH2 KO diminished growth and disrupted cytoskeletal architecture. Notably, DRD1 ablation enhanced EZH2 activity, indicating a previously unrecognized feedback loop linking dopaminergic signaling to epigenetic repression. RNA-seq profiling (n=4/group) revealed extensive remodeling of transcriptional networks with discrete EZH2- and DRD1-dependent signatures (FDR < 0.05, |log2FC| > 2). EZH2 KO selectively induced cytokine activity, calcium ion binding, MHC class II interactions, and biological processes regulating adhesion, cell-cell communication, leukocyte activation, and axon/projection guidance, collectively reflecting cytoskeletal restructuring and immune-modulatory reprogramming. In contrast, DRD1 KO enriched signaling receptor binding, regulator/activator activity, receptor-ligand interactions, and pathways governing adhesion, migration, and IL-10-mediated inflammatory signaling, consistent with a pro-invasive, pro-inflammatory phenotype. Together, these data delineate a coordinated epigenetic-dopaminergic axis in TNBC. DRD1 loss potentiates EZH2-driven inflammatory and migratory programs, while EZH2 depletion activates adhesion and immune-regulatory pathways that constrain tumor aggressiveness. Targeting this dual regulatory node may represent a novel strategy to disrupt pro-tumor transcriptional circuitry and improve therapeutic outcomes in TNBC (Supported by DOD: W81XWH2010065, Eswar Shankar).

#0044 scSubtype2.0: Predictor of breast cancer molecular subtypes at single cell resolution.

Alexander V. Lobanov[1], Hani Jieun Kim[2], Sehrish Kanwal[3], Kate Harvey[2], John Reeves[2], Marcel Batten[2], Beata Kiedik[2], Daniel L. Roden[2], Mun N. Hui[4], Kym Pham Stewart[3], Oliver Hofmann[3], Sandra O'Toole[2], Elgene Lim[2], Sean M. Grimmond[3], Alexander Swarbrick[2], Charles M. Perou[1]

[1]UNC Lineberger Comprehensive Cancer Center, Chapel Hill, NC,[2]Garvan Institute of Medical Research, Darlinghurst, Australia,[3]Collaborative Centre for Genomic Cancer Medicine, Parkville, Australia,[4]Chris O'Brien Lifehouse, Camperdown, Australia

Breast cancer is a heterogeneous disease with distinct clinical and molecular biomarkers used to determine treatment options. The three main clinical subtypes of the disease are Estrogen Receptor (ER+)/HER2-negative, Human Epidermal Growth Receptor 2 positive (HER2+), and Triple Negative Breast Cancer (TNBC). Breast cancer can also be stratified based upon gene expression into four distinct molecular subtypes: Basal-like, HER2-enriched, Luminal A, and Luminal B. These phenotypes are typically assigned using the PAM50 molecular subtyping predictor using bulk-tumor gene expression data. Advances in single cell sequencing now allow researchers to distinguish cell types within tumors and focus on cancerous cells. While PAM50 remains an important biomarker, the algorithm is optimized for bulk-tumor gene expression and performance drops precipitously when applied to individual scRNA-seq cells. An accurate predictor of molecular subtypes of cancer cells at single cell resolution could allow for further exploration into the heterogeneity of breast cancers and their microenvironments.

Previously, we developed a single-cell version of PAM50 called scSubtype, however, it was trained using only 2-3 samples per molecular subtype. Here, we build upon this foundation by greatly expanding our training sample set to 151 breast cancer tumors with matched bulk and single cell RNA-seq. We leveraged this new large-scale dataset to develop scSubtype2.0, an updated cancer cell intrinsic molecular subtype predictor at single cell resolution. We filtered for robust samples of each molecular subtype that have matching bulk and single cell derived pseudo-bulk PAM50 calls, high silhouette width, and high cancer cell content. The final training data is made up of 53 tumors encompassing 118,188 tumor cells and at least 10 tumors per molecular subtype. We performed differential expression analyses to identify single-cell subtype-defining genes (LumA: 60 genes, LumB: 129 genes, HER2-enriched: 231 genes, Basal-like: 271 genes) and used them as a signature to assign each tumor cell to the highest scoring subtype. All training set tumors had 80%+ of their cell calls match their corresponding bulk PAM50 subtype, suggesting our lists encapsulate the full breadth of each molecular subtype. To objectively evaluate the new model's performance and our gene lists, we crafted synthetic, homogenous tumors of each subtype from previously annotated test data set. We show that scSubtype2.0 outputs the correct subtype of the crafted tumors with a 91% accuracy and outperforms its predecessor's classifications. The algorithm continues to be improved and will soon include predictors of additional tumor cell states including the claudin-low/mesenchymal subtype, and a hypoxic state. Overall, we believe scSubtype2.0 is a robust and accurate predictor of molecular subtypes to individual cancer cells and a novel measure of intra-tumor heterogeneity.

#0045 Identification of germline *AEN* polymorphisms as risk factors in cervical cancer.

Golya Shahrokhi[1], Mari Kylleso Halle[2], Vinodh Srinivasasaina-gendra[3], Jianqing Zhang[4], Aishwarya Sundaresan[5], Roshan Kumar[1], Shafiq Shaikh[1], Nichol He[1], Camilla Krakstad[2], Sadeep Shrestha[6], Paul Auer[7], Janet Rader[1], Hemant Tiwari[3], Akinyemi I. Ojesina[1]

[1]Department of Obstetrics and Gynecology, Medical College of Wisconsin, Wauwatosa, WI,[2]Department of Obstetrics and Gynecology, University of Bergen, Bergen, Norway,[3]Department of Biostatistics, University of Alabama at Birmingham, Birmingham, AL,[4]Department of Epidemiology, University of Alabama at Birmingham, Birmingham, AL,[5]Department of Biostatistics, University of Alabama, Birmingham, AL,[6]University of Alabama at Birmingham, Birmingham, AL,[7]Division of Biostatistics, Medical College of Wisconsin, Wauwatosa, WI

Background: Inherited genetic variation contributes 27-36% of cervical cancer risk. While genome-wide association studies (GWAS) and candidate gene approaches have identified both risk and protective alleles, mostly associated with immune and DNA repair pathways, much remains unknown about the role of rare or low-frequency germline variants across the exome.

Methods: We performed gene-based association testing on whole-exome sequencing from blood-derived DNA of 105 Norwegian cervical cancer patients and 263 cancer-free European female controls (1000 Genomes). High-quality and high-confidence variants were identified following GATK best practices for variant calling, and a gene-based sequence kernel association test (SKAT) was performed to identify significant gene-level associations. The presence and linkage of significant variants were further examined in a cohort of 9,286 Norwegian newborn genotypes. To assess the potential functional impact and the effects on cancer risk of the identified variants, vector constructs containing wild-type and variants introduced into C4I cervical cancer cells and cell proliferation rates were measured.

Results: The Apoptosis Enhancing Nuclease (*AEN*), a *TP53*-related gene, showed significant germline association with cervical cancer (SKAT-RC $p = 3.69\times10^{-9}$). The signal was driven by two low-frequency variants, rs61752779 and rs118097475, which were about 9-fold more common in cases than controls. Linkage analysis showed that these two variants were strongly correlated ($r^2 = 0.996$) in cervical cancer patients and similarly linked in the Norwegian newborns ($r^2 = 0.948$). Functional validation revealed that overexpression of the wildtype *AEN* construct in the C4I cervical cancer cell resulted in reduced cellular proliferation. However, overexpression of an *AEN* construct with both variants resulted in increased cell proliferation compared with the wildtype AEN construct.

Conclusions: This study provides both statistical and experimental evidence supporting the role of *AEN* as a tumor suppressor gene and suggests that two highly linked germline variants may contribute to cervical cancer risk.

#0046 High-definition signatures of single-base substitutions in human cancer.

Jessica N. Au[1], Marcos Diaz-Gay[2], Raviteja Vangara[3], Pilar Gallego-Garcia[2], Mousumy Kundu[3], S.M Ashiqul Islam[4], Maria Zhivagui[5], Zichen Jiang[3], Christopher Steele[3], Sarah Moody[6], Michael R. Stratton[7], Paul J. Brennan[8], Ludmil B. Alexandrov[3]

[1]Departments of Bioengineering, Cellular and Molecular Medicine, Moores Cancer Center and BISB, University of California, San Diego (UCSD), La Jolla, CA,[2]Digital Genomics Group, Cancer Genomics Program, Spanish National Cancer Research Center, Madrid, Spain,[3]Departments of Cellular and Molecular Medicine, Bioengineering, and Moores Cancer Center, University of California, San Diego (UCSD), La Jolla, CA,[4]Department of Epidemiology and Biostatistics, College of Integrated Health Sciences, University at Albany- State University of New York, Albany, NY,[5]University of Nevada, Las Vegas (UNLV), Las Vegas, NV,[6]Wellcome Sanger Institute, Cambridge,[7]Wellcome Sanger Institute, Cambridge, United Kingdom,[8]International Agency for Research on Cancer, Lyon, France

Cancer genomes accumulate mutations through diverse biological processes, including defective DNA repair, exposure to carcinogens, and normal aging. These processes leave characteristic patterns known as mutational signatures. Identifying these signatures in patient tumors enables researchers to understand disease mechanisms and infer past exposures.The current standard resource, COSMIC v3.5, catalogs over 90 single base substitution (SBS) signatures using the SBS-96 mutational context, which characterizes each mutation by the substituted base and one flanking nucleotide on each side. This reference is widely used across cancer genomics studies to decode the mutational processes active in tumors. However, challenges have emerged where signatures overlap and can be misassigned, leading to incorrect interpretations of the mutational processes driving individual cancers. While we showed that higher-resolution methods using extended sequence contexts can differentiate these overlapping signatures and reveal novel processes, these findings were limited to specific cancer types such as colorectal, esophageal, renal, and head and neck. Additionally, no comprehensive high-resolution reference currently exists.To address this, we developed a high-definition (HD) mutational signature SBS reference set using over 40,000 whole-genome sequences from 14 cohorts spanning diverse cancer types and non-cancer tissues, including both primary and metastatic tumors. We analyzed mutations at SBS-4608 resolution, combining extended pentanucleotide sequence contexts with strand orientation information. This represents the practical limit of current sequencing technology. Our analysis clarifies several ambiguous signatures from the existing reference, improving accuracy when identifying mutational processes in individual tumors. We also discovered novel signatures that were previously undetectable at standard resolution, revealing new insights into the mutational landscape of human cancers.This HD reference set addresses critical limitations in current mutational signature analysis, enabling more accurate interpretation of mutational processes in cancer genomes and improving the reliability of downstream biological and clinical insights. By providing a comprehensive resource that resolves signature overlaps and reveals previously hidden mutational processes, this work will enhance precision in understanding cancer biology and tumor mutagenesis. The reference will be made publicly available to the research community upon publication.

#0047 Identifying noncanonical sources of cancer neoepitopes using PEPMatch and CEDAR.

Daniel Marrama[1], Ibel Carri[1], Nina Blazeska[1], Randi Vita[1], Hannah K. Carter[2], Morten Nielsen[3], Alessandro Sette[1], Zeynep Kosaloglu-Yalcin[4], Bjoern Peters[1]

[1]La Jolla Institute for Immunology, La Jolla, CA,[2]UC San Diego, La Jolla, CA,[3]Technical University of Denmark, Lyngby, Denmark,[4]La Jolla Institute for Immunology, San Diego, CA

Emerging evidence suggests that immunogenic cancer antigens may originate from the "dark genome", which comprises non-coding regions, alternative open reading frames (ORF), and untranslated regions (UTR), traditionally excluded from most neoepitope prediction pipelines. Consequently, systematic identification and validation of these noncanonical antigens has been technically challenging. To address this gap, we leveraged PEPMatch, a high-throughput peptide search tool, integrated with the Cancer Epitope Database and Analysis Resource (CEDAR) to systematically identify noncanonical sources of experimentally validated neoepitopes. We compiled seven comprehensive human databases encompassing both canonical and noncanonical protein sources: UniProtKB (human reference proteome with isoforms), UniParc (UniProt protein archive), Ensembl canonical proteins (ENSP), validated non-canonical ORFs (ncORF), and three-frame translations of complementary DNAs (cDNA) and non-coding RNAs (ncRNA), and six-frame translations of full gene sequences, including UTRs and introns (ENSG). Using PEPMatch's exact matching algorithm, we performed searches of 28,601 CEDAR neopeptides tested in 40,800 T cell assays against all seven databases.

To validate our pipeline, we first analyzed 840 MHC class I cryptic neopeptides found by mass spectrometry, achieving a total mapping success of 98.33% using a sequential attribution search that revealed an enrichment in noncanonical sources (ncORF: 14.76%, cDNA: 41.55%, ncRNA: 4.76%, ENSG: 1.67%). Out of these cryptic neoepitopes, 5.60% were found in the human reference proteome and 28.93% in the UniParc database prior to the noncanonical sources. Applying this methodology to all 28,601 CEDAR's neopeptides revealed that 1.91% originated from noncanonical sources. We then focused on the relevant subset of 6,394 positive neoepitopes with confirmed immunogenicity from T cell assays. Notably, a significant percentage of these immunogenic positive neoepitopes mapped to noncanonical databases compared with the negative peptides (ncORF: 0.1% vs 0.0%, cDNA: 8.8% vs 2.6%, ncRNA: 1.4% vs 0.6%, ENSG: 3.4% vs 1.5%), suggesting that the 'dark genome' is a source of targetable neoepitopes. The specificity of this mapping approach was validated using randomly shuffled peptide controls, which yielded <1% spurious matches.

These findings demonstrate that PEPMatch successfully identifies noncanonical genomic origins of cancer neoepitopes at scale given the appropriately curated database sources. CEDAR is implementing this annotation pipeline to provide researchers with mappings for dark genome antigens, enabling validation and discovery of unconventional targets for immunotherapy development. This work expands the targetable landscape of cancer immunotherapy by systematically cataloging epitopes from previously overlooked genomic regions.

#0048 Somatic *NFKBIZ v*ariant modulates inflammation at single-cell resolution.

Catherine H. Feng[1], Andrew R. D'Avino[2], Anders W. Rasmussen[2], Dan Landau[3]

[1]Harvard University, Cambridge, MA,[2]New York Genome Center, New York City, NY,[3]Weill Cornell Medical College, New York, NY

The human body is a somatic mosaic, with normal tissue colonized by cell populations carrying distinct mutations. Intriguingly, in tissues affected by chronic disease, such as inflammatory bowel disease (IBD), disease-specific drivers of clonal expansion emerge. IBD is characterized by chronic intestinal inflammation and increased cancer risk. This inflammatory environment exerts selective pressure promoting the growth of clones carrying somatic mutations in IL-17 inflammatory pathway genes. While many such mutations have been implicated in downregulating inflammation and protecting against colitis-associated colorectal cancer, their presence has yet to be characterized at single-cell resolution in solid human tissue. We used SComatic to identify somatic single nucleotide variants in single-cell RNA-sequenced colorectal samples from IBD patients (*n*=204). Among them, we found a novel missense mutation predicted to be highly pathogenic in the ankyrin repeat domain of *NFKBIZ*, which is critical for promoter binding in the IL-17 pathway. *NFKBIZ* is a key regulator of intestinal inflammation and a known driver of clonal expansion in IBD. Notably, while *NFKBIZ* variants are highly prevalent in IBD, they are rarely found in colitis-associated cancer, suggesting this adaptation in chronically inflamed tissue is protective against cancer. Strikingly, we found that the variant appears exclusively in epithelial cells. In this compartment, it exhibited a high variant allele frequency of 0.727, suggesting substantial remodeling of colonic epithelium during chronic inflammation. Functionally, the variant appeared to disrupt IL-17-mediated signaling, as its presence was associated with reduced expression of *DUOX2*, a known IL-17 target gene that causes DNA damage and is frequently upregulated in colonic inflammation in IBD. This shows, for the first time at single-cell resolution in native human tissue, previously hypothesized protective mechanisms driven by somatic *NFKBIZ* mutations. Our work reveals how protective clones emerge in specific cell types in response to chronic inflammation, highlighting how epithelial remodeling can influence IBD disease progression and treatment response.

#0049 The PER3-RORB axis defines a tumor-suppressive circadian state associated with improved survival in head and neck squamous cell carcinoma.

Harold Nathan Tan, Oriol Mirallas, Paul Selvadurai, Michael Wotman, Luana Sousa, Neal Akhave, Khaled Sanber, Renata Ferrarotto, George R. Blumenschein, Maura L. Gillison, Faye M. Johnson, Timothy A. Yap

The University of Texas MD Anderson Cancer Center, Houston, TX

Background: The circadian clock governs DNA repair, cell-cycle progression, metabolism, and stress responses. Circadian disruption has been linked to tumor progression and therapy resistance, yet the clock components influencing prognosis in head and neck squamous cell carcinoma (HNSCC) remain undefined. We sought to characterize circadian dysregulation in HNSCC and identify circadian signatures that predict overall survival (OS).
Methods: RNA-seq, clinical, and survival data from TCGA-HNSCC (n=565) were analyzed using a circadian gene panel comprising core positive regulators (BMAL1, CLOCK, NPAS2, RORA, RORB, RORC) and negative regulators (PER1/2/3, CRY1/2, NR1D1/2). Log_2-normalized expression was z-standardized per gene, and composite positive- and negative-arm scores were generated as mean standardized expression within each panel. Prognostic performance was evaluated using time-dependent ROC curves and multivariable Cox models. Circadian network integrity was assessed using the clock coherence disruption (ΔCCD) metric, comparing clock-gene correlation structure in tumors against a GTEx esophageal mucosa reference across 1,000 permutations. Differential expression between circadian-defined subgroups was evaluated with limma's empirical Bayes-moderated models.
Results: Circadian gene expression was heterogeneous across primary sites and AJCC stages, indicating circadian disruption independent of clinical factors. High RORB (HR= 0.75, p=0.015), and PER3 (HR=0.88, p=0.05) were associated with reduced mortality. In ROC analysis, PER3 and RORB showed modest prognostic discrimination individually (AUC 0.39/0.43 and 0.41/0.47 at 3/5 years, respectively). In contrast, the PER3-RORB composite score (0.52/0.56) outperformed all other circadian metrics. Clock coherence analysis demonstrated preserved circadian correlation structure in PER3-RORB-High tumors (CCD = 0.44) and marked disruption in PER3-RORB-Low tumors (CCD = 0.74), yielding a ΔCCD of 0.31. No permutation replicate exceeded this value (empirical $p < 0.001$), indicating highly non-random network breakdown associated with PER3-RORB loss. PER3-RORB-high tumors showed coordinated upregulation of NPAS2, metabolic and stress-response genes (DHCR24, ABCA1, LRP1, ATP6V1A) and modulation of mitochondrial components (NDUFB6), linking this axis to metabolic and stress adaptation programs.
Conclusion: PER3-RORB defines a biologically coherent circadian state linked to improved survival in HNSCC. While these findings support a tumor-suppressive role for PER3-RORB, independent external validation is required to confirm robustness and clinical generalizability. This work highlights circadian regulation as a mechanistic modifier of tumor behavior and a promising avenue for biomarker development.

#0050 Spatial transcriptomics uncovers patterns of transcriptional reprogramming and immune evasion in small cell lung cancer.

Emmanuel S. Spanos[1], Meng Wang[2], Amin Sabet[2], Esther Redin[2], Charles M. Rudin[2], Joseph Chan[2]

[1]Physiology, Biophysics, and Systems Biology, Weill Cornell Grad. School of Medical Sci., New York, NY,[2]Memorial Sloan Kettering Cancer Center, New York, NY

Histologic transformation from non-small cell lung cancer (NSCLC) to small cell lung cancer (SCLC) is a major mechanism of therapeutic resistance, yet the spatial and molecular programs governing this phenotypic switch remain poorly defined. 10X Xenium In Situ spatial transcriptomics was used to generate subcellular-resolution transcriptomic maps of 22 primary and metastatic lung tumors across 16 patients with SCLC transformation, totaling >10 million cells. Matched single-cell RNA sequencing enabled integrated analysis of transcriptional states and served as a complementary modality to support spatial findings. Spatial profiling with a 389-gene panel encompassing neuroendocrine (NE), epithelial, stemness, immune, and stromal programs revealed 30 distinct cell types and marked inter- and intra-tumoral heterogeneity across lung adenocarcinoma (LUAD), squamous cell carcinoma (LUSC), and small cell lung cancer subtypes (ASCL1+: SCLC-A and NEUROD1+: SCLC-N). Tumors organized into several canonical structural patterns: (1) discrete subtype compartmentalization, (2) speckled NE transformation, and (3) self-contained, multilayered subtype organization.A representative resection of a lymph-node metastasis with SCLC transformation displayed two separate tumor regions, each with a striking radial arrangement. In the first region, admixed LUAD and NOTCH1- SCLC-A formed the tumor core, followed by concentric layers of NOTCH1+ SCLC-A and SCLC-N, with immune cells at the periphery. Given the established role of Notch signaling in SCLC subtype switching, and our observation of inhibitory DLL3-NOTCH1 interactions across neighboring tumor subtypes, these regulatory relationships may contribute to the spatial compartmentalization of tumor subtypes. The second tumor region lacks the LUAD and NOTCH1+ SCLC-A populations, instead composed of a NOTCH1- SCLC-A core encased by SCLC-N, again surrounded by immune zones. Pseudotime analysis of the Xenium data across both regions also recapitulated a trajectory from LUAD to SCLC-A to SCLC-N. These two findings, combined with previous studies characterizing SCLC-N as an “immune-cold” tumor devoid of immune infiltrate, suggest that this spatial patterning and interplay between subtypes may be an important mechanism for immune evasion and progression in a hostile environment.Due to imbalance in cell number and sample area within the cohort, spatial comparisons were constrained to smaller regions of interest (ROIs). Clustering ROI cell-cell adjacency matrices uncovered recurring spatial interaction patterns associated with specific tumor subtypes and microenvironmental states, such as necrosis or immune infiltration. These analyses highlight distinct architectural modes of neuroendocrine transformation and underscore the role of spatial context in shaping phenotypic evolution during resistance.

#0051 RAS(ON) multi-selective inhibition remodels cancer-associated fibroblast subtypes and extracellular matrix in pancreatic cancer.

Lorenzo Tomassoni[1], Allison C. Hess[1], Kevin Munoz Forti[2], Hun Jin Jeong[3], Deanna J. Besart[1], Tanner C. Dalton[1], Urszula N. Wasko[1], Carmine F. Palermo[1], Stephen A. Sastra[1], Chang H. Lee[4], Andrea Califano[1], Simon Schworer[2], Marie C. Hasselluhn[1], Kenneth P. Olive[1]

[1]Columbia University Irving Medical Center, New York, NY,[2]University of Chicago, Chicago, IL,[3]University of Maryland Eastern Shore, Princess Anne, MD,[4]Columbia University, New York, NY

Oncogenic KRAS mutations occur in >90% of pancreatic ductal adenocarcinomas (PDACs) and are the principal drivers of malignant transformation and tumor progression. Sustained KRAS signaling in malignant epithelial cells orchestrates a network of paracrine interactions that define the cellular and extracellular composition of the tumor microenvironment (TME). In the TME, cancer-associated fibroblasts (CAFs) are particularly responsive to KRAS-dependent paracrine signals, including Sonic Hedgehog (SHH), a ligand that is overexpressed and secreted from malignant epithelial cells, thereby driving the proliferation of cancer-associated myofibroblasts. RMC-7977 is a RAS(ON) multi-selective inhibitor that inhibits GTP-bound RAS proteins, including wild type and mutant variants of KRAS, NRAS, and HRAS. It showed broad anti-tumor activity in PDAC preclinical models, extending overall survival of the KrasLSL.G12D/+;Trp53LSL.R172H/+;Pdx1-cretg/+ (KPC) mouse model by more than 3-fold. The KPC mouse model recapitulates the desmoplasia observed in patients, allowing the assessment of KRAS inhibition on stromal composition and function. To study the impact of RAS inhibition in PDAC, we did single cell RNA sequencing (scRNA-seq) on KPC tumors treated with RMC-7977 at multiple timepoints. After a week of RMC-7977 treatment, the dominant CAF subtype in KPC tumors shifted from myofibroblastic CAFs (myCAFs) to inflammatory CAFs (iCAFs). This observation was validated by co-immunofluorescence on tumor sections, which indicated that (PDPN+, αSMA+) myCAFs showed decreased abundance and proliferation whereas (PDPN+, IL6+) iCAF abundance increased. Similar effects were observed ex vivo in human and murine PDAC explants. Mechanistic studies showed that this phenotype was mediated by a downregulation of SHH ligand expression in response to RAS inhibition. We also used the scRNA-seq data to assess the contribution of CAF subtypes to the generation, regulation, and degradation of the extracellular matrix (ECM) in PDAC. We found that myCAFs and iCAFs have both overlapping and distinct roles in the regulation of the ECM and that these were differentially impacted by RMC-7977 treatment. Thus, pan-RAS-GTP inhibition indirectly remodeled ECM composition both by impact CAF subtype distribution and by altering matrix composition and regulation by CAFs. Accordingly, nanoindentation measurements on KPC tumors and human explants confirmed a significant decrease in modulus (a measurement for tumor stiffness) after RMC-7977 treatment. In summary, we report that RMC-7977 switches the myCAF-dominant CAF landscape towards an iCAF-enriched TME through the KRAS-SHH axis and this alters TME composition and reduces tumor stiffness through ECM remodeling. Future studies will examine the impact of these finding on drug delivery, tumor invasiveness, tumor differentiation state.

#0052 Quantifying the selective advantage of copy number amplifications to reveal therapeutic targets in ovarian cancer.

Meng Liu[1], Jeff Mandell[2], Jeffrey Peter Townsend[2]

[1]Yale School of Public Health, Biostatistics, Yale University, New Haven, CT,[2]Yale University, New Haven, CT

Ovarian cancer (OV) remains one of the most lethal malignancies, and target discovery is hindered by limited oncogenic somatic single-nucleotide mutations and extensive chromosomal instability. Conventional strategies prioritize targeting of amplified genes based on frequency and amplitude of copy number amplification. However, these metrics are confounded by regional genomic architecture and abundant passenger events, rendering it difficult to identify the amplifications that truly increase cell proliferation and survival during tumor evolution. To address this problem, we developed an evolutionary model that quantifies the cancer effect size (CES) of amplifications, directly estimating the selective advantage conferred by each event, mirroring methodologies developed for single-nucleotide variants. By integrating observed amplification patterns with regional background copy number alteration (CNA) rates to quantify fitness contributions, we distinguished amplifications that genuinely drive tumor evolution from passengers elevated by genomic instability. Using segmented copy number profiles from a cohort of 554 ovarian cancer tumor sequences, we quantified cancer effects of amplifications across the genome. Known oncogenes like MYC and CCNE1 exhibit high CES. Some oft-reported recurrent amplifications exhibited low CES, consistent with a passenger status, whereas several moderately high-frequency focal amplifications exhibited strong selective advantage, representing key CNA drivers that are obscured by conventional copy-number metrics. This stratification is critical for therapeutic development because high-CES amplifications mark loci where tumors are both dosage-increased and selectively dependent. Dosage-increased, selectively dependent loci have direct translational relevance for triplex-forming oligonucleotide (TFO) therapies, which trigger DNA damage at triplex-forming motifs, with amplified loci providing increased target dosage. High-CES loci simultaneously provide abundant TFO-binding sites and represent core cancer dependencies, embodying a mechanism for durable therapeutic impact. Quantification of selection for amplifications provides a rigorous, evolutionarily grounded basis for cancer effect, identifying true amplification drivers of oncogenesis and precisely positioning therapeutically actionable targets in cancers dominated by chromosomal instability.

#0053 RNA fusions: An untapped source of neoantigens for immune based breast cancer prevention and treatment across all subtypes of breast cancers.

Anjana Bhardwaj[1], Chathurani Ranathunge[2], Shiyanth Thevasagayampillai[2], Aaranyah Kandasamy[2], Brandon H. Than[2], Constance T. Albarracin[3], Isabelle Bedrosian[1]

[1]Department of Breast Surgical Oncology, UT MD Anderson Cancer Center, Houston, TX,[2]University of Houston, Houston, TX,[3]Department of Pathology, UT MD Anderson Cancer Center, Houston, TX

Background: Breast tumors are considered immunologically cold with an overall low to moderate mutation burden resulting in limited neoantigen repertoire that can be used for discovering a breast cancer vaccine. RNA fusions lead to the generation of neoantigens that are more immunogenic than insertion or deletion mutations. Identification of such targets in high risk mammary tissue and tumors represent novel opportunities for breast cancer prevention and treatment. The objective of this study was to characterize the prevalence of chimeric RNAs in precancerous breast tissue and breast tumors from sporadic breast cancer patients.
Methodology: Fusions were identified by RNA sequencing 225 breast tissues from breast tumors and paired adjacent- and distant-tissues of 25 Her2 positive, 25 hormone receptor positive (HR) and 25 triple negative (TN) patients. The RNA sequencing reads were processed through modified ARRIBA fusion discovery pipeline for fusion calling. Breast samples obtained from cancer-free women undergoing breast reduction surgery were obtained from Komen Tissue Bank and used as controls to exclude normal mammary tissue associated chimeric RNAs from analysis.
Results: All major subtypes of breast tumors (TNBC, Her2+ and HR+) express RNA fusions. TNBC and Her2+ tumors expressed substantially larger number of unique RNA fusions than HR+ breast tumors. Every tumor sample possessed at least 2 novel RNA fusions. In line with high genomic instability of TNBC subtype of breast cancer, about 1/3 of the TN breast tumors expressed greater than 15 RNA fusions. We found non-coding RNAs to be also implicated in the biogenesis of RNA fusions in addition to coding genes. Approximately 1/5th of RNA fusions identified in sporadic breast tumors were driven from at least one oncogene partner. Interestingly, we found a substantial number of RNA fusions to possess multiple break points suggesting multiple areas within a gene that are prone to break and fuse with another gene partner. In line with patient tumor heterogeneity, RNA fusions in breast tumors were overwhelming private. In order to identify RNA fusions that are relevant for breast cancer prevention, we investigated the presence of RNA fusions in the paired adjacent samples as compared to the index tumor. Although, we found preneoplastic breast tissue to possess a rich repertoire of RNA fusions, majority of these were different from those identified in paired breast tumors.
Conclusions: RNA fusions are frequently present in breast tumors as well as at risk breast tissue and may provide novel opportunities for developing vaccines for breast cancer prevention and treatment.

#0054 Integrating connectivity mapping resources to prioritize and personalize drug candidates for individual triple negative breast cancer patients.

Lily D. Taub[1], Anna Byrd[1], Daniel J. Clarke[1], Ido Diamant[1], Criseyda Martinez[2], Elisa Port[2], Hanna Y. Irie[2], Avi Maayan[1]

[1]Pharmacological Sciences, Icahn School of Medicine at Mount Sinai, New York, NY,[2]Medicine, Icahn School of Medicine at Mount Sinai, New York, NY

Triple negative breast cancer (TNBC) is the most aggressive type of breast cancer with the least therapeutic options. While some patients respond to aggressive standard treatments, many others do not, and recurrence risk for many patients diagnosed with TNBC remains high. With the aim of furthering our understanding of mechanisms of TNBC tumorigenesis and treatment resistance, and to accelerate the development of novel personalized therapeutics on an individual patient level, we analyzed RNA-seq samples collected from eight primary TNBC tumors and their matched PDX models created from patients treated at the Dubin Breast Center. First, we identified differentially expressed up-regulated genes that are uniquely highly expressed in the primary tumors and their matching PDX models while lowly expressed across hundreds of normal human tissues and cell types profiled and harmonized from GTEx, ARCHS4, and Tabula Sapiens. We then examined the effect of knocking out these up-regulated genes in TNBC by querying the DepMap resource. From each patient's up-regulated genes, we selected those that were most essential to the viability of TNBC cell lines in CCLE and DepMap. To identify small molecule compounds that may down-regulate the expression of individual patient-specific targets, and in turn specifically reduce the viability of the cells within the TNBC tumors, we integrated five Connectivity Mapping resources that measured transcriptomics responses of human cell lines to thousands of approved drugs and other compounds. The Connectivity Mapping resources integrated are the LINCS L1000 dataset (33,571 compounds), Novartis Institutes for BioMedical Research (NIBR) DRUG-seq U2OS MoA Box (4,343 compounds), Gingko Bioworks GDPx1 and GDPx2 (1,353 compounds), and Tahoe-100M (379 compounds). We queried these resources to find consensus FDA approved and pre-clinical compounds that would maximally reduce the expression of the patient-specific identified target genes. This approach is encoded into an online tool called Dr. Gene Budger 2.0 (DGB2), which integrates the Connectivity Mapping resources for the purpose of identifying drugs that maximally increase or decrease the mRNA expression of a single target or a set of genes. With DGB2, we identified candidate therapeutic compounds, individualized for each patient TNBC tumor/PDX model, that are predicted to inhibit tumor growth. Once validated, this approach can be translated to individualize treatment for patients with TNBC, particularly those with disease that is resistant to current standard-of-care treatments. DGB2 is freely available at https://appyters.maayanlab.cloud/#/Drug_Gene_Budger2.

#0055 Differentiation state and immune interaction contribute to drug response in AML.

Natasha R. A. Black[1], Dharani Thirumalaisamy[2], Mira Rajagopalan[3], Trevor Enright[1], Melissa Stewart[1], Evan Lind[1], Elie A. Traer[4], Jeffrey W. Tyner[5], Olga H. Nikolova[1]

[1]Oregon Health & Science University, Portland, OR,[2]Department of Biomedical Engineering, Oregon Health & Science University, Portland, OR,[3]The University of Texas at Austin, Austin, TX,[4]Instructor, Ctr. for Hematologic Malignancies, Oregon Health & Science University, Portland, OR,[5]OHSU Knight Cancer Institute, Portland, OR

Introduction: We and others have linked efficacy of targeted therapies to cellular differentiation state in acute myeloid leukemia (AML). In this study, we refine this link by integrating ex vivo drug response, joint single-cell transcriptomic and proteomic, and cell-surface proteomics data that measures both myeloid differentiation and immune markers.
Methods: A total of 90 AML patient samples were profiled by CyTOF (cytometry by time-of flight) with ~100 immune and myeloid differentiation makers to characterize the landscape of cell-surface protein expression. Matched drug response data was used from the largest assembled AML patient cohort BeatAML. Concurrently, five AML patient samples were profiled following ex vivo drug treatment using CITE-seq (cellular indexing of transcriptomes and epitopes by sequencing) with a total of 6 treatments (3 single agent, 2 pairwise and 1 triple combination treatment) and compared to DMSO treated cells. Custom computational pipelines were developed to enable data analysis. Topic modeling using the latent Dirichlet allocation (LDA) model was used to identify topics emerging in the space of both myeloid differentiation and immune markers. Topics were then stratified by matched drug response. Single-cell drug response prediction methods were trained on sc-RNA-seq to identify cell type-specific drug response signatures.
Results: Our results recapitulate known biomarkers of response to single agents BCL2 inhibitor venetoclax (ven) and menin inhibitor revumenib. Further, we observe known and novel gene expression and cell population shifts when combined with hypomethylating azacytidine. For example, venetoclax eliminates primitive and B-cell populations. When ven is used in combination with revumenib, intermediate populations such as pro-monocytes mature into monocytes, yielding predominantly differentiated cells. Adding azacytidine to ven+revumenib further depletes intermediate populations, including pro-monocytes. Our topic modeling identified 5 (out of 10) topics that have a stark opposing pattern in drugs targeting primitive vs differentiated cells. We further identified the most prominent immune markers associated with each of these topics.
Conclusion: Our results recapitulate previously established links between myeloid differentiation state and selective efficacy to targeted compounds in AML. Notably, our recent findings informed by topics compromised of immune signatures further deconvolute these trends, pointing to new immune programs associated with cell state driven drug response.

#0056 COSMIC: Advancing the cancer genomics knowledgebase of somatic mutations.

Madhumita Madhumita, Madiha Ahmed, Joanna Argasinska, David Armstrong, Nidhi Bindal Dhir, Denise Carvalho-Silva, Lucie Chadelle, Patrick Dao, Stephen Duke, Giovanna Fasanella, Muhammad Fouzan, Abishekraj Gnanasambandam, Avirup Guha Neogi, Susan Haller, Bhavana Harsha, Balazs Hetenyi, Leonie Hodges, Steven Jupe, Rachel Lyne, Thomas Maurel, Karen McLaren, Thomas Mutimer, Sumodh Nair, Hanna Najgebauer, Helder Pedro, Sophie Poole, Amaia Sangrador-Vegas, Zoe Sheard, Manpreet Singh Chawla, Michael Starkey, Rebecca Steele, Sari Ward, Ellen Wiedemann, Jennifer Wilding, Siew Yit Yong, Jon Teague

COSMIC, Wellcome Sanger Institute, Cambridge, United Kingdom

COSMIC (Catalogue Of Somatic Mutations in Cancer) has evolved from an initial catalogue to the world's most comprehensive knowledgebase of somatic variants in cancer, built upon a foundation of continuous, expert curation. COSMIC currently aggregates over 29 million unique somatic variants carefully curated from 1.5 million samples, establishing an essential resource for studying the cancer genome. This rich dataset is the result of extensive, dedicated work, drawing on insights from more than 30,000 scientific publications and major studies.

COSMIC is structured into a suite of specialized modules that collectively transform raw genomic variants into biologically and clinically meaningful insight. These include the Cancer Gene Census (CGC), which systematically classifies causal cancer genes; the Cancer Mutation Census (CMC), which distinguishes driver from passenger mutations through computational and evidence-based annotation; Mutational Signatures, which captures genome-wide mutagenic processes; COSMIC 3D, which contextualizes variants within protein structures; and the Actionability and Resistance resources, which map genomic alterations to therapeutic response and resistance mechanisms. Together, these modules provide a framework essential for interpreting somatic variant landscapes in precision oncology.

We highlight ongoing research on the next iteration of the Cancer Mutation Census (CMC v2), designed to enhance COSMIC’s ability to extract biologically meaningful signals from large-scale somatic datasets. CMC v2 applies refined background models to identify mutation hotspots at the amino acid level across cancer genes in a pan-cancer context, focusing on positions exhibiting statistically significant enrichment of somatic variants. This approach isolates non-random, spatially coherent clusters of mutations that represent strong candidates for driver activity. Although currently under development, these analyses demonstrate the potential of CMC v2 to provide higher-resolution insights into cancer gene dysregulation and support more nuanced interpretation of tumor evolution.

The development of CMC v2 marks a key step in COSMIC’s evolution toward more data-driven, biologically grounded interpretation of cancer variants. By integrating statistical modeling with expert insight, CMC v2 refines our capacity to distinguish meaningful mutational patterns from background noise across diverse tumor contexts. These advances exemplify COSMIC’s ongoing commitment to translating large-scale genomics into actionable biological knowledge. As the knowledgebase continues to expand and engage with the global cancer research community, COSMIC remains an indispensable foundation for understanding cancer gene function, refining biomarker discovery, and supporting precision oncology.

#0057 Functional pathway analysis reveals discordance between clinical HER2 status and downstream effector activation in breast cancer.

Salim Arslan[1], Julian Schmidt[1], Cher Bass[1], Foivos Ntelemis[1], J Carl Barrett[2], Oscar Maiques[3], Jakob Nikolas Kather[4], **Pahini Pandya**[1]

[1]Panakeia Technologies, Cambridge, United Kingdom,[2]University of North Carolina at Chapel Hill, Chapel Hill, NC,[3]Barts Cancer Institute, Queen Mary University of London, London, United Kingdom,[4]Technische Universitat Dresden, Dresden, Germany

Background: HER2-targeted therapies are guided by HER2 protein overexpression or ERBB2 amplification. However, these biomarkers may imperfectly reflect functional dependence on HER2 signaling. We performed an integrative multi-omic analysis to quantify the discordance between clinical HER2 status and its corresponding functional biology, assessing both downstream pathway activation in HER2-positive (HER2+) tumors and inactivity in HER2-negative (HER2−) cases.
Methods: Analysis was performed on the TCGA breast cancer dataset. HER2+ (n=106) and HER2− (n=595) cohorts were defined using clinical HER2 status. Transcriptomic and proteomic over-/under-expression states were derived for clinically relevant driver genes by thresholding RNA/protein expression values. For each tumor, we assessed activation of HER2-associated pathways (e.g., direct HER2 targets, PI3K-AKT-mTOR, MAPK, RTK crosstalk) by comparing expression states against the expected direction of activation. A pathway was considered 'validated' when at least half of the tested states aligned with expected activation patterns. Samples with no available data were excluded from the analysis, reducing the evaluable cases to 85 and 457 for HER2+ and HER2−, respectively.
Results: Among HER2+ tumors, proximal HER2 signaling showed strong concordance with clinical status, with direct targets being active in 80.0% of cases. In contrast, canonical downstream pathways were often inactive, with PI3K-AKT-mTOR and MAPK activity validated in only 29.4% and 15.3% of tumors, respectively. This heterogeneity suggests that many HER2+ tumors may rely less on canonical HER2-driven signaling than expected. In HER2− tumors, proximal HER2 signaling and MAPK pathway activity were appropriately low as validated in >96% cases. However, the PI3K-AKT-mTOR pathway was active in 132/457 (28.9%) HER2− tumors, revealing a sizable subset with HER2-independent PI3K activation.
Conclusions: Our findings highlight biological mechanisms that may underlie therapeutic resistance and reveal alternative targets for expanding precision treatment strategies across breast cancer subtypes. The limited canonical signaling in most HER2+ tumors suggests pathway-independent drivers, feedback inhibition, or gaps in transcriptomic/proteomic measurements that miss critical phosphorylation events. In contrast, activation signatures in a subset of HER2− tumors indicate therapeutically relevant HER2-low biology. The results support complementing standard testing with biology-aware signatures to (i) flag HER2+ tumors unlikely to respond to combination therapies and (ii) stratify HER2− patients into actionable groups, including those who may benefit from PI3K/mTOR inhibitors. Future work will incorporate phospho-proteomic data and link pathway signatures to treatment response to refine patient selection.

#0058 Characterizing tumor-stroma interfaces in chemotherapy-treated ovarian cancer via spatial transcriptomics.

Po-Yuan Chen[1], Tyler M. Yasaka[1], Tzu-Hung Hsiao[2], Tai-Ming Ko[3], Yu-Chiao Chiu[1]

[1]University of Pittsburgh School of Medicine, Pittsburgh, PA,[2]Department of Medical Research, Taichung Veterans General Hospital, Taichung, Taiwan,[3]Department of Biological Science and Technology, College of Engineering Bioscience, National Yang Ming Chiao Tung University, Hsinchu, Taiwan

The tumor-stroma interface (TSI) is a key microenvironmental region where malignant and non-malignant cells interact and influence therapeutic resistance and disease progression. Despite its importance, this area remains insufficiently characterized at the transcriptomic level, and the cellular features that connect its organization to treatment outcomes are not well defined. This gap limits the translational interpretation of spatial microenvironmental structure in the context of patient response. To address this need, we developed an integrative framework that identifies and characterizes the TSI using spatial transcriptomics. The approach combines spot-level tumor detection with a neighborhood analysis that delineates interface regions surrounding cancer spots. We applied this framework to a post-chemotherapy high-grade serous ovarian cancer dataset generated by Elena Denisenko et al. (n = 8; three good responders, two partial responders, and three poor responders) and defined tumor, TSI, and normal regions across all samples. Linear mixed-effects modeling identified significantly different proportions of EIF4A3+ cancer associated fibroblasts, endothelial cells, and myofibroblasts between outcome groups within the TSI. Among them, myofibroblasts were elevated specifically within the TSI of poor responders, but not in tumor or normal regions, indicating a localized rather than tissue-wide shift. Although T-cell proportions were not significantly different between outcome groups, bivariate Moran's I analysis showed strong spatial co-localization between T cells and tumor cells in good responders, whereas this spatial coupling was largely absent in poor responders. These findings suggest that both immune cell organization and abundance may contribute to more effective post-treatment activity in favorable outcomes. Pathway analysis further revealed distinct functional programs within the TSI. Good responders showed enrichment of immune activation and antigen-presentation pathways, whereas poor responders displayed increased extracellular matrix remodeling and stromal signaling. Regression analysis confirmed that myofibroblast proportion was tightly linked to these pro-resistance pathways and negatively correlated with humoral immune response activity, connecting stromal remodeling with reduced immune pathway engagement in poor responders. Collectively, these findings highlight the functional heterogeneity of the TSI and its potential role in modulating treatment response. By integrating tumor detection, interface mapping, and pathway-level analysis, our framework offers a scalable strategy to dissect interface biology and bridge spatial transcriptomics with treatment-related mechanisms. This framework may enable the discovery of spatially informed biomarkers for predicting therapeutic outcomes in ovarian cancer and beyond.

#0059 Mutational signatures in cancer genomes alter short linear protein motifs involved in cellular signaling networks.

Jigyansa Mishra[1], Masroor Bayati[1], Nina Adler[2], Zoe P. Klein[1], Kevin C. L. Cheng[1], Juri Reimand[1]

[1]Ontario Institute for Cancer Research, Toronto, ON, Canada,[2]University of Toronto, Toronto, ON, Canada

Cancer genomes accumulate somatic mutations from diverse mutational processes, driven by extrinsic carcinogen exposures and intrinsic DNA repair deficiencies, leaving distinct genomic imprints referred to as mutational signatures. Mutational signatures are inferred computationally from large cancer genomics datasets and validated in experiments, however their functional impacts on protein-coding sequences and protein function remain largely unexplored. Leveraging machine learning and statistics, we aimed to discern the impact of single base substitution (SBS) mutational signatures in rewiring conserved short linear protein motifs (SLiMs). These are peptide sequences that mediate key protein-protein interactions and post-translational modifications. We performed a proteogenomic analysis of 1.1 million missense single-nucleotide variants (msSNVs) in 12,000 genomes across 19 cancer types. We assessed the impact of msSNVs on 150 classes of SLiMs recognized by kinases and other enzymes involved in cellular signaling networks. Distinct signatures were significantly associated with msSNVs that disrupted, created or switched between specific SLiMs. For example, UV light-associated signature SBS7b disrupted proline-directed kinase motifs, while signatures arising from aberrant APOBEC cytidine deaminase activity, SBS2 and SBS13, disrupted caspase-cleavage motifs, vital for apoptosis, as well as motifs involved in the DNA damage response. These differential signature impacts stem from their trinucleotide-context biases, which steer specific codon changes, inducing amino acid substitutions in distinct SLiMs. At the gene level, recurrent SLiM-rewiring variants clustered in 22 canonical cancer drivers such as *BRAF*, *CTNNB1* and *U2AF1*, and 35 candidate genes revealing mechanistic connections between mutational processes and oncogenic signaling pathways. UV light-induced V600E substitutions in BRAF create a novel polo-like kinase (PLK1)-binding motif, putatively contributing to vemurafenib resistance in melanoma patients. Recurrent S34F substitutions in the splicing factor U2AF1 are driven by APOBEC activity and disrupt a regulatory phosphorylation site critical in splice-site fidelity, suggesting a link between APOBEC-driven mutagenesis and RNA splicing dysregulation in lung cancer. Lastly, motif-rewiring alterations in cellular signaling networks strongly correlated with patient attributes such as smoking status and functional characteristics such as APOBEC gene expression, revealing how lifestyle variables and intrinsic mutagenic programs can potentially reconfigure cellular signaling and protein-protein interactions. Together, our results uncover process-specific proteomic consequences of mutational processes, offering mechanistic insights into cancer etiology and exposing potential therapeutic vulnerabilities.

#0060 CpGene: a DNA methylation-based biomarker discovery platform.

Konstantinos Lazaros[1], Vasiliki Tzelepi[2], Christopher J. Logothetis[3], Aristidis G. Vrahatis[1], **Susan (Souzana) Logotheti**[4]

[1]Informatics, University of Ionion, Corfu, Greece,[2]Pathology, School of Medicine, University of Patras, Patras, Greece,[3]Chairman/Professor, Gu Med. Onc., UT MD Anderson Cancer Center, Houston, TX,[4]Pathology, School of Medicine, Univeristy of Patras, Patras, Greece

Background: DNA methylation (DNAme) has been established as the key player in the epigenetic regulation of the gene expression. While high throughput techniques are essential in rigorous research, data analysis requires in dept bioinformatic knowledge to provide a comprehensive approach to biomarker identification. Recognising this challenge, we developed CpGene, a web application that prioritises accessibility and usability, allowing users to perform robust DNA methylation microarray data analysis (e.g., Illumina 450K, EPIC v1.0, EPIC v2.0) and derive biologically relevant conclusions for biomarker discovery.
Methods: The backbone of CpGene is built upon the integration of well-established and widely known packages, ensuring reliability, transparency and repeatability. Data preprocessing including beta value generation and quality control is conducted using minfi R package, while limma package and machine learning-based feature selection approaches are performed for differential methylation analysis. Functional enrichment analysis is obtained using Enrichr API and result visualization is performed using multiple R and python packages (e.g. ggplot2, lattice, matplotlib).
Conclusions: CpGene offers an accessible, interactive and user-friendly workspace to perform DNA methylation analysis from microarray data. The platform caters not only to experienced bioinformaticians, but also to basic scientists and clinicians who possess foundational bioinformatics knowledge. The intuitive interface and streamlined workspace enable users from various backgrounds to effectively utilise the platform, regardless of their level of computational expertise. As a result, CpGene empowers both scientific and clinical communities seeking to characterize disease-linked epigenetic alterations and pinpoint actionable DNA methylation biomarkers, even in the absence of advanced bioinformatics training.

#0061 Defining spatial biomarkers of survival across solid tumors using a pan-cancer proteomics atlas.

Khoa Huynh[1], Joaquin Reyna[1], Bruno Matuck[2], KEVIN BYRD[3], Jinze Liu[4]

[1]VCU Massey Comprehensive Cancer Center, Richmond, VA,[2]VCU School of Dentistry, Richmond, VA,[3]Philips Institute for Oral Health Research, Richmond, VA,[4]Massey Comprehensive Cancer Center, Richmond, VA

The spatial architecture of the tumor microenvironment (TME) governs cancer progression and therapeutic response, yet pan-cancer analyses linking multicellular organization to patient survival remain unclear. As part of the PROSPECTS (Pancancer Reconstruction Of Spatial Profiles and Therapeutic TargETs) Initiative, we assembled a large-scale spatial proteomic atlas comprising 415 patients across six major malignancies: Head and Neck Squamous Cell Carcinoma (HPV-positive and HPV-negative), Lung Cancer (NSCLC and LUAD), Triple-Negative Breast Cancer, High-Grade Serous Ovarian Cancer, Colorectal Adenocarcinoma, and Hepatocellular Carcinoma (HCC). Our dataset includes over 1,000 tissue cores and over 4.4 million single cells with balanced representation across indications: HNSCC (1,218,385 cells, 145 patients), Lung (906,537 cells; 63 patients), Breast (765,232 cells; 60 patients), Ovarian (590,945 cells; 53 patients), Colorectal (511,610 cells; 37 patients), and Liver (474,237 cells; 57 patients). Using a 30-plex antibody Phenocycler, we spatially mapped 15 major cell types at single-cell resolution. We developed a next-generation multi-scale computational pipeline within AstroSuite (Stratica Biosciences), integrating TACIT and Constellation algorithms to quantify TME architecture at the levels of cell state, intercellular distance, and higher-order motifs including pairwise, triplet, and quartet cellular neighborhoods. These deep spatial metrics were linked to overall survival with adjustment for clinical covariates. We identified marked heterogeneity in TME structure, with each cancer type exhibiting distinct prognostic architectures. In TNBC, Tumor Cell-Neutrophil interactions emerged as one of the strongest adverse prognostic features (P=0.00001). In Lung cancers, vascular-immune and stromal-tumor interfaces were key, particularly vascular endothelial cell-Macrophage adjacency (P=0.0003) and Fibroblast-Tumor Cell interactions (P=0.002). Despite these cancer-specific patterns, PROSPECTS uncovered conserved spatial signatures. A recurrent fibroblast-tumor cell interface motif appeared across malignancies, though stromal drivers varied: Myofibroblast-Treg interactions were prognostic in Colorectal cancer (P=0.002), while Fibroblast-Treg interactions predicted outcome in Ovarian cancer (P=0.002). In HCC, immune-to-immune interactions such as Treg-B Cell crosstalk (P=0.002) were significantly associated with survival. Complex spatial syntax proved superior to simple pairwise interactions for prognosis, highlighting the value of higher-order TME modeling. This work establishes the first pan-cancer spatial proteomic comparison linking TME organization to clinical outcome, revealing that spatially resolved cellular interaction networks constitute a new class of clinically actionable biomarkers.

#0062 Comprehensive characterization of m^{6}A RNA methylation across human cancers.

Yining Zhao[1], Ke Chen[1], Hu Chen[2], Yizhe Song[3], Kamalika Mojumdar[1], Wei Liu[1], Stephanie H Ting[4], Ayush Semwal[5], Hui Shen[6], Li Ding[7], Genomic Data Analysis Network, Katherine Hoadley[4], Han Liang[1]

[1]UT MD Anderson Cancer Center, Houston, TX,[2]Baylor College of Medicine, Houston, TX,[3]Washington University School of Medicine in St. Louis, Saint Louis, MO,[4]University of North Carolina, Chapel Hill, NC,[5]Department of Epigenetics, Van Andel Research Institute, Grand Rapids, MI,[6]Graduate Student, Van Andel Research Institute, Grand Rapids, MI,[7]Washington University School of Medicine in St. Louis, St. Louis, MO

N6-methyladenosine (m^{6}A) is the most abundant internal mRNA modification and plays essential roles in gene regulation, tumor progression, and therapeutic response. However, the biomedical and clinical significance of m^{6}A RNA methylation in human cancer remains incompletely understood. Here, using m^{6}A-seq profiling, we generated a comprehensive transcriptome-wide atlas of m^{6}A modifications across 15,812 sites from 226 tumor samples spanning 23 cancer types in The Cancer Genome Atlas (TCGA). To elucidate the regulatory determinants and downstream consequences of m^{6}A variation, we integrated these data with a broad spectrum of multi-omics features. We found that global m^{6}A patterns segregate into five major clusters largely driven by cancer lineages. Somatic mutations exert widespread yet diverse effects on local m^{6}A levels through alteration of DRACH motifs. Approximately 10% of protein-coding genes showed consistent positive or negative associations between m^{6}A abundance and mRNA or protein expression. These genes are enriched for transcription factors, and their m^{6}A levels strongly influence key tumor cell states such as epithelial-mesenchymal transition (EMT) and hypoxia. We further characterized the protein expression landscape of 15 m^{6}A regulators in 7482 TCGA samples and uncovered frequent dysregulation across cancers arising from multiple distinct genetic and epigenetic mechanisms. Finally, we developed a deep-learning model that integrates local DNA sequence context, gene-level features, m^{6}A regulator states, and tumor-specific context to predict m^{6}A intensity. The model achieved high accuracy for a substantial fraction of m^{6}A sites, enabling large-scale inference of m^{6}A variation and facilitating biomarker discovery in extensive patient cohorts. Together, this study provides a key resource for understanding the genomic landscape and regulatory architecture of m^{6}A methylation in cancer and establishes a foundation for leveraging m^{6}A as a new class of biomarkers and therapeutic targets.

#0063 Intratumoral *Candida albicans* associates with hypoxia and poor outcomes in non small cell lung cancer (NSCLC).

Dipankor Chatterjee[1], Dennis J. Grencewicz[2], Alexander Loncar[3], Ruohan Wu[4], Alex Samouilov[2], Sylvain Ferrandon[5], McKenzie Kreamer[6], Yogita Mehra[7], Aspen Carson[8], Rebecca Hoyd[8], Shiva Jahanbakhshi[8], Fouad Choueiry[6], Matthew Anderson[9], Martin Benej[10], Dustin Bosch[11], Jiangjiang (Chris) Zhu[3], Jinghai Wu[12], Therese Bocklage[13], Martin McCarter[14], Ahmad Tarhini[15], Bodour Salhia[16], Christopher A. Moskaluk[17], Gregory Riedlinger[18], Song Yao[19], Ashiq Masood[20], Sheetal Hardikar[21], Mmadili N. Ilozumba[22], Cornelia M. Ulrich[21], Abdul Rafeh Naqash[23], Carlos H.F. Chan[24], Craig D. Shriver[25], Dinesh Pal Mudaranthakam[26], Aaditya Pallerla[27], Michelle Churchman[28], Robert J. Rounbehler[29], Laura Chambers[7], Matthew F. Kalady[5], Nicholas C. Denko[30], David P. Carbone[31], Dan Spakowicz[8]

[1]Molecular Genetics, The Ohio State University, Columbus, OH,[2]College of Medicine, The Ohio State University, Columbus, OH,[3]The Ohio State University, Columbus, OH,[4]The Ohio State University Wexner Medical Center, Hilliard, OH,[5]Department of Surgery, The Ohio State University College of Medicine, Columbus, OH,[6]Department of Radiation Oncology, The Ohio State University Comprehensive Cancer Center, Columbus, OH,[7]Department of Gynecologic Oncology, The Ohio State University Comprehensive Cancer Center, Columbus, OH,[8]Pelotonia Institute for Immuno-Oncology, The Ohio State University Comprehensive Cancer Center, Columbus, OH,[9]Department of Medical Genetics, University of Wisconsin-Madison, Columbus, OH,[10]Molecular Medicine and Therapeutics, The Ohio State University College of Medicine, Columbus, OH,[11]Department of Pathology, University of Iowa, Iowa City, IA,[12]The Ohio State University Comprehensive Cancer Center, Department of Radiation Oncology, OH,[13]Markey Cancer Center, Lexington, KY,[14]University of Colorado Anschutz Medical Campus, Aurora, CO,[15]Moffitt Cancer Center, Tampa, FL,[16]USC Norris Comprehensive Cancer Center, Los Angeles, CA,[17]Assoc. Professor, Dept. of Pathology, University of Virginia Health System, Charlottesville, VA,[18]Rutgers Cancer Institute of New Jersey, New Brunswick, NJ,[19]Postdoctoral Res. Associate, Dept. of Cancer Prev. & Control, Roswell Park Cancer Institute, Buffalo, NY,[20]Indiana University Simon Cancer Center, Indianapolis, IN,[21]University of Utah Huntsman Cancer Institute, Salt Lake City, UT,[22]Huntsman Cancer Institute, Salt Lake, UT,[23]College of Medicine, University of Oklahoma, Oklahoma, OK,[24]Carver College of Medicine, University of Iowa, Iowa City, IA,[25]Uniformed Services University, Bethesda, MD,[26]University of Kansas Medical Center, Kansas, KS,[27]College of Medicine, University of Cincinnati, Cincinnati, OH,[28]Aster Insights, Hudson, FL,[29]Aster Insights, Tampa, FL,[30]Assistant Professor, Dept. of Rad. Onc., The Ohio State University Comprehensive Cancer Center, Columbus, OH,[31]The Ohio State University College of Medicine, Columbus, OH

Resistance to radiation, chemotherapy, and immunotherapy remains a major challenge in non-small cell lung cancer (NSCLC), and emerging evidence suggests tumor-resident microbes may influence therapeutic response. To address this, we combined patient-level modeling with mechanistic studies in preclinical models. We first analyzed RNA-sequencing data from 2,156 NSCLC tumors collected under the Total Cancer Care Protocol (NCT03977402) within the ORIEN network using a contamination-aware pipeline to quantify intratumoral *Candida albicans* (CA) and assess its impact on treatment outcomes. We developed MEC-TX (Mechanistic Clustering Treatment), a digital-twin framework that compares patients receiving similar treatment regimens differing only by CA burden. CA was detected in ~55% of tumors; high CA burden was associated with significantly shorter overall survival (hazard ratio 1.6, $p < 0.01$), and similar trends were observed in radiation- and chemotherapy-treated cohorts defined by MEC-TX. After adjusting for clinical covariates (age, sex, stage, BMI), CA remained an independent predictor of poor survival, underscoring MEC-TX's ability to isolate biologically meaningful signals. Transcriptomic profiling revealed CA-high tumors had elevated hypoxia-related gene expression ($p = 0.0045$), suggesting a link between fungal infiltration and tumor microenvironment. To test this, we implanted Lewis lung carcinoma cells into syngeneic C57BL/6 mice and gavaged them with CA, *Blautia obeum* (commensal control), or saline (vehicle control). CA-gavaged tumors were significantly larger ($p = 0.0108$) and exhibited lower pH ($p = 0.024$) and reduced intratumoral pO_2 ($p = 0.051$) compared to controls, as measured by EPR oximetry, after adjusting for tumor size, supporting CA's role in creating a hypoxic, therapy-resistant niche. *In vitro*, CA-conditioned media conferred radioresistance across multiple cell lines ($p = 0.001$), implicating secreted molecules as drivers of this phenotype. Collectively, these findings reveal a novel mechanism by which intratumoral fungi promote hypoxia and treatment resistance, providing a strong rationale for microbiome-informed strategies to overcome hypoxia-driven resistance and improve precision oncology.

#0064 Mechanisms of resistance to CDK4/6 inhibitors: Insights from single-cell nucleus sequencing and spatial transcriptomics.

Seung-eun Bang[1], EunChae Kim[1], Won-Ji Ryu[2], Hyein Jung[2], Yoonjin Cha[3], Joohyuk Sohn[4], Gun Min Kim[4], Kyoo Hyun Kim[4], Byungjin Hwang[1], Min Hwan Kim[5]

[1]Department of Biomedical Sciences, Graduate School of Medical Science, Brain Korea 21 Project, Yonsei University College of Medicine, Seoul, Korea, Republic of,[2]Avison Biomedical Research Center, Yonsei University College of Medicine, Seoul, Republic of Korea, Seoul, Korea, Republic of,[3]Department of Pathology, GangNam Severance Hospital, Yonsei University College of Medicine, Seoul, South Korea, Seoul, Korea, Republic of,[4]Division of Medical Oncology, Department of Internal Medicine, Yonsei cancer center, Yonsei University College of Medicine, Seoul, Republic of Korea, Seoul, Korea, Republic of,[5]Department of Internal Medicine, Division of Medical Oncology, Yonsei University College of Medicine, Severance Hospital, Seoul, Korea, Republic of

Breast cancer incidence is increasing worldwide and represents the second most common malignancy in women after lung cancer. Among its subtypes, luminal B accounts for 10-20% of cases and shows a faster proliferation rate. Also, a poorer prognosis than luminal A, with a 5-year survival rate of only 32% at stage 4. Luminal B tumors are characterized by active estrogen receptor signaling and high expression of proliferation-associated genes such as *Ki-67* and *E2F*, leading to enhanced estrogen-driven cell cycle progression. Consequently, CDK4/6 inhibitors, which block the G1 to S phase transition, have shown favorable therapeutic outcomes. However, in a subset of patients, treatment with CDK4/6 inhibitors induces a luminal-to-basal-like phenotypic conversion, which is associated with poor clinical prognosis. To elucidate the mechanism underlying this phenotype, we performed single-nucleus RNA sequencing and spatial transcriptomic analyses on paired pre- and post-treatment tumor biopsies from three patients who exhibited poor responses to CDK4/6 inhibition. After UMAP projection and batch correction, cell type annotation revealed no major changes in the overall cellular composition, with epithelial/tumor cells remaining dominant. Differential expression analysis showed minimal transcriptional changes in endothelial and fibroblast cells but substantial alterations in tumor/epithelial and immune cell populations. Focusing on immune cells, which displayed the largest number of DEGs, subclustering analysis revealed a marked post-treatment increase in innate lymphoid cells (ILCs), while overall immune cell numbers decreased following treatment. Cell-type-specific DEG analysis further identified substantial transcriptional reprogramming within plasma cells, $CD4^+$, and $CD8^+$ T cells. In parallel, tumor/epithelial cells exhibited distinct subtype redistribution after CDK4/6 inhibition, which is currently under detailed characterization. Spatial transcriptomic mapping based on nucleus-seq-derived cell type signatures is underway to visualize cell-type distribution and microenvironmental remodeling before and after treatment. Collectively, our integrative analyses aim to uncover the mechanisms of CDK4/6 inhibitor resistance, highlighting the potential roles of ILC expansion, immune remodeling, and epithelial plasticity in luminal-to-basal transition, and to identify biomarkers predictive of therapeutic response.

#0065 Integrating spatial transcriptomics and digital pathology with whole-genome data from Genomics England to characterise the tumour and it's microenvironment in colorectal cancer.

Luke McNickle[1], Assya Legrini[1], Yoana Doncheva[1], Mari-Claire McGuigan[1], Ghazal Latifi[1], Claire Kennedy Dietrich[1], Molly McKenzie[1], Phimmada Hatthakarnkul[1], Tom Wright[1], Leonor Patricia Schubert Santana[1], Emma McCargow[2], Cong Chen[2], Henry M. Wood[3], Jon Laye[3], Gemma Hemmings[3], Caroline Cartlidge[3], Derek Magee[4], Phil Quirke[3], Joanne Edwards[1], Nigel Jamieson[1]

[1]School of Cancer Sciences, University of Glasgow, Glasgow, United Kingdom,[2]Genomics England Limited, London, United Kingdom,[3]Division of Pathology and Data Analytics, University of Leeds, Leeds, United Kingdom,[4]School of Computer Science, University of Leeds, Leeds, United Kingdom

Introductory Sentence:
By combining spatial transcriptomics and digital pathology with whole-genome-sequenced samples from Genomics England's 100,000 Genomes Project, we can directly link spatial gene expression patterns to genetic alterations and morphological features.
Brief Description of Pertinent Experimental Procedures:
We applied Bruker Spatial Biology's CosMx™ High Plex (6K) spatial transcriptomics platform to tissue microarray (TMA) cores derived from Genomics England colorectal cancer samples. H&E-stained sections were reviewed by pathologists for morphological assessment and AI-based detection of lymphocytes and stroma. Across 65 TMA cores on three slides, we performed cell segmentation, gene expression quantification, and multi-step quality control. A total of 966,500 cells were detected pre-QC, with 935,262 high-quality cells retained post-QC for downstream analyses, including cell typing, pathway enrichment, spatial neighbourhood, and regulatory network inference. Integrative comparisons were made across MMR status, Klintrup inflammation, SARIFA (Stroma AReactive Invasion Front Areas) scoring, and the underlying mutational landscape from matched whole-genome sequencing data.
Summary of New Unpublished Data:
Our results demonstrate successful implementation of high-plex spatial transcriptomics on Genomics England tissue samples with high-quality pathology input. We observed distinct spatial and transcriptional signatures—at both gene and module levels—between MMR-proficient and MMR-deficient tumours, and across gradients of histopathological inflammation and SARIFA metrics. Integration of genomic variants revealed transcriptional programmes associated with cellular activity and phenotypic divergence. These data highlight the ability of spatially resolved transcriptomics to contextualise genomic alterations within the complex cellular landscape of the tumour microenvironment.
Statement of the Conclusions:
This study establishes the feasibility and analytical power of applying spatial transcriptomics to Genomics England's whole-genome-characterised samples. Integrating spatial, histological, and genomic data provides new insight into immune-stromal dynamics and tumour heterogeneity. This approach demonstrates the potential for large-scale spatial multi-omic profiling across Genomics England cohorts, enabling deeper functional interpretation of genomic data and advancing the next generation of precision oncology research.

#0066 Gene co-amplification and structural patterns reveal principles of extrachromosomal DNA in cancer.

Jens Luebeck[1], Ted Liefeld[1], Edwin Huang[1], Forrest Kim[1], Bhargavi Dameracharla[1], Michael A. Chan[1], Dhruv Khatri[1], Kyra Fetter[1], Kaiyuan Zhu[1], Thorin Tabor[1], Soyeon Kim[2], Hoon Kim[2], Roel Verhaak[3], Michael M. Reich[4], Paul S. Mischel[5], Jill P. Mesirov[1], Vineet Bafna[1]

[1]UC San Diego, La Jolla, CA,[2]Sungkyunkwan University, Suwon, Korea, Republic of,[3]Yale School of Medicine, New Haven, CT,[4]UCSD Medical Ctr., San Diego, CA,[5]Stanford University School of Medicine, Stanford, CA

The amplification of oncogenes on extrachromosomal DNA (ecDNA) enables aggressive, rapidly evolving tumors. Its defiance of Mendelian segregation enables extreme copy number amplifications that escape chromosomal regulatory constraints. Our AmpliconSuite toolset is the most widely used tool for ecDNA analysis in whole genome sequencing data, now deployed on over 43,000 tumor samples. Here, we present novel insights into ecDNA biology enabled through large-scale integrative analysis with these methods.

We analyzed 6,366 whole-genome sequenced tumors from combined ICGC and Hartwig Medical Foundation datasets, identifying 2,366 distinct ecDNA capturing >11,000 different genes. Our systematic gene co-amplification analysis revealed striking patterns of gene selection on ecDNA. CDK4-MDM2 co-amplification occurred predominantly via ecDNA (75% of co-amplifications). These loci, normally separated by >11Mbp on chromosome 12, preferentially assembled onto the same ecDNA molecule 93% of the time as revealed by structural analysis of the ecDNA. This suggests selective pressure for maintaining cell cycle and p53 pathway regulators on the same inheritable unit. Our analysis of frequent co-amplifications also revealed that ecDNA preferentially packages chromatin remodelers (NSD3, RSF1) alongside driver oncogenes, as well as including genes that support transcription and translation (INTS4, BRF2), creating self-contained oncogene “support” hubs. Structural analysis revealed cancer type-specific patterns to ecDNA structures, with EGFR ecDNA showing simple architectures in glioblastoma versus complex rearrangements in lung and breast cancers, suggesting distinct formation histories in different cancers.

Through AmpliconRepository.org, we provide public access to these ecDNA predictions and co-amplification analysis across major cancer cohorts, currently hosting 16,000+ analyzed samples and 5,000+ characterized ecDNA amplifications. Uniquely open to community contributions, this resource enables researchers to explore patterns across datasets and validate findings. These findings reveal fundamental principles governing ecDNA formation and selection, with implications for understanding tumor heterogeneity, therapeutic resistance, and dependencies which underlie ecDNA-targeted therapies.

#0067 Validation of a gene pair-based machine learning model for treatment prioritization in breast cancer.

Rishi Nair[1], Nicholas R. Mistry[1], Roy Khalife[2], Anthony M. Magliocco[2]

[1]University of Central Florida, Orlando, FL,[2]Protean BioDiagnostics Inc, Orlando, FL

Introduction: Drug resistance in breast cancer (BC) can arise from synergistic genetic alterations. We previously developed a machine learning (ML) model that ranks treatment categories by 5-year predicted overall survival (POS) based on altered gene pairs. Here, we perform the first retrospective validation of this model using an independent BC patient cohort that received next-generation sequencing (NGS)-directed therapy.

Methods: Thirty metastatic BC patients who received NGS-directed therapy with FoundationOne Companion Diagnostic (CDx) profiling were analyzed (PMID: 34572791). For each patient, logits scores (representing the probability of death at 5 years) were generated across 8 treatment categories combined with altered gene pair combinations from the CDx gene-set. Inverse logits, representing POS, were computed using a virtual clinical trial where a decoder model received patient data and output probability distributions for each gene pair. Synthetic patient populations were then randomly generated from these probabilities and used to calculate POS rates for each treatment category per patient. Mean inverse logits were analyzed per patient using repeated-measures ANOVA, Friedman tests and pairwise Holm t-tests. The Shapiro-Wilk test and η^2 values assessed model normality and strength of association.

Results: Across all patients, the POS rate was 70.0%, compared to the actual rate of 62.9%. A one-sample z-test indicated a significant difference ($Z=6.82$, $p<0.001$), although the model's predictions were directionally aligned with actual outcomes. Shapiro-Wilk testing indicated that 79.2% of treatment categories across all patients had $W>0.9$, suggesting an approximately normal distribution of logits. Repeated-measures ANOVA confirmed significant treatment-dependent differences in logits for all 30 patients ($p<0.001$, $\eta^2_{avg}=0.72$). This indicates that 72% of the variance in POS is explained by the treatment category, after accounting for differences in gene pair alterations across patients. Radiation and tyrosine kinase inhibitors were the treatment categories that consistently ranked highest across patients, while PI3K inhibitors and DNA damage agents consistently ranked lowest. Pairwise Holm t-tests indicated that metabolic agents and receptor tyrosine kinase inhibitors consistently showed no significant difference in POS among patients who received either treatment in real life ($p>0.05$).

Conclusion: Our findings demonstrate strong internal consistency with a ML-based approach to predict survival using gene pair and treatment data. Promising external validity is shown by POS within 8% of observed outcomes. Further calibration and validation of this model with subtype-stratified cohorts is warranted to improve validity, enhance clinical utility and maintain predictive stability.

#0068 YAP-TEAD-dependent VASP expression increases cell stiffness and migration in TNBC cells under high extracellular glucose conditions.

Wonkyung Lee[1], Seeun Oh[2], Tae-Hyung Kim[3]

[1]Yeungnam University College of Medicine, Daegu, Korea, Republic of,[2]Department of Molecular Genetics & Microbiology, University of New Mexico, School of Medicine, Albuquerque, NM,[3]University of New Mexico, Albuquerque, NM

Triple negative breast cancer (TNBC) is an aggressive subtype lacking targeted therapies, highlighting the urgent need for novel treatment strategies. Clinical observations indicate that TNBC patients with obesity or diabetes have a worse prognosis, underscoring the impact of metabolic dysregulation on disease progression. We previously demonstrated that extracellular glucose regulates F-actin assembly and non-muscle myosin activity via the cAMP-RhoA-ROCK pathway in TNBC cells, linking glucose metabolism to cytoskeletal remodeling and cell invasion. In this study, we aimed to further elucidate the molecular mechanisms by which extracellular glucose regulates cell mechanics and motility. We hypothesized that the Hippo pathway, particularly YAP, regulates expression of a cytoskeletal remodeling gene, VASP in response to glucose metabolic signaling. To test the hypothesis, we utilized public ChIP-seq datasets, to identify four YAP-TEAD binding domains (CBDs) within the human VASP gene enhancer region. TEAD motif analysis using FIMO revealed predicted TEAD-binding sites in each region. We then experimentally validated those identified CBDs. These enhancer fragments were subcloned into luciferase reporters. For exogenous validation, we measured luciferase activity after TEAD inhibitor treatment and performed site-directed mutagenesis to determine whether TEAD binding is required for VASP gene regulation. To determine which TEAD isoforms contribute most to VASP regulation, we performed siRNA-mediated knockdown of TEAD1-4 and found that TEAD1 and TEAD4 were the most significant regulators of VASP expression. For endogenous validation, we conducted Western Blotting after 24hours of TEAD inhibitor treatment. To test whether this regulatory axis is responsive to glucose levels, we performed glucose-dependent luciferase assays for exogenous validation, and RNA sequencing and Western Blotting to evaluate endogenous VASP expression under different glucose conditions. These analyses demonstrated that the YAP-TEAD-VASP axis is upregulated in high-glucose settings. Finally, to explore the translational implications of these findings, we assessed whether TEAD inhibitors could suppress migration in a hyperglycemic context. Since VASP promotes F-actin polymerization, we hypothesized that TEAD inhibition would reduce F-actin rearrangement and thereby decrease cell contracility, which in turn suppress cell migration. In scratch wound healing assays, TEAD inhibitors significantly reduced cell migration across glucose concentrations tested. In summary, we identify VASP as a novel YAP-TEAD target gene regulated under hyperglycemic conditions and demonstrate that TEAD inhibition alters contracility and suppresses migration in TNBC cells.

: Physicochemical Modulation of Cancer Ecosystems: Mechanical Forces, Hypoxia, and Acidosis
Poster Session

#0756 Matrix stiffness induces Ca^{2+}-DCLK1-PIP5K1A mechanotransduction as a biomechanical checkpoint in pancreatic cancer progression and chemotherapy resistance.

Haoxiang Zhang[1], Chuanbin Zhao[2], Jiaoshun Chen[2], Xiaoqing Hu[3], Jianwei Bai[4], Long He[2], Zanglong Deng[2], Tao Yin[2]

[1]Department of Hepatopancreatobiliary Surgery, Fuzhou University Affiliated Provincial Hospital, Fuzhou, China,[2]Department of Pancreatic Surgery, Union Hospital, Tongji Medical College, Huazhong University of Science and Technology, Wuhan, China,[3]Department of Ultrasound Medicine, Union Hospital, Tongji Medical College, Huazhong University of Science and Technology, Wuhan, China,[4]Department of Biliary-Pancreatic Surgery, Xiangyang Central Hospital, Xiangyang, China

Background: Alterations in extracellular matrix (ECM) architecture and stiffness are hallmarks of rapid pancreatic cancer progression. However, the mechanisms by which ECM biomechanical properties influence malignant biological behavior remain largely unknown. Calmodulin-dependent protein kinase DCLK1 has been implicated in cancer progression, but its role in integrating biomechanical signals in pancreatic cancer has not been elucidated.
Methods: We investigated the relationship between ECM stiffness and DCLK1 activation in pancreatic cancer using in vitro biomechanical stress models and in vivo solid tumor experiments. DCLK1 expression and activity were manipulated via overexpression or knockdown, and calcium signaling was modulated using specific inhibitors. Single-cell RNA sequencing was performed to identify potential pathways by which calcium inhibition sensitizes tumors to chemotherapy. Multicolor immunofluorescence staining of clinical tumor samples was used to examine the correlation between the PIEZO1-DCLK1-PIP5K1A-AKT signaling axis and ECM stiffness in situ. Mechanistic studies included protein interaction assays and phosphorylation analyses to define the DCLK1-PIP5K1A-PI3K-AKT signaling cascade.
Results: DCLK1 expression and activation were selectively induced under high biomechanical stress mediated by the PIEZO1/calcium/HPCAL1 axis. Overexpression of DCLK1 under low stiffness conditions accelerated tumor progression and chemoresistance, which could be partially reversed by calcium inhibitors. Conversely, under high stiffness conditions, DCLK1 knockdown inhibited tumor growth and increased chemosensitivity, but attenuated the sensitizing effect of combined calcium inhibitor treatment. Single-cell RNA sequencing identified calcium-related pathways contributing to chemotherapy sensitization. Mechanistically, DCLK1 interacted with PIP5K1A by inhibiting its threonine phosphorylation, promoting membrane localization of PIP5K1A and activating the downstream PI3K-AKT pathway. Multicolor immunofluorescence confirmed the correlation of PIEZO1-DCLK1-PIP5K1A-AKT activation with ECM stiffness in clinical samples.
Conclusions: DCLK1 functions as a biomechanical checkpoint in pancreatic cancer, integrating ECM-derived mechanical cues to exacerbate tumor progression and chemotherapy resistance. Targeting the calcium/DCLK1 signaling axis may enhance the efficacy of adjuvant therapy in pancreatic cancer patients

#0757 Matrix stiffness encoded mechanical memory maintains proliferative dominance in tumor metastasis.

Yusheng Luo[1], Yuxi Pan[2], Xiaorong Lin[2], Shuo Fang[2]

[1]Digestive Medicine Center, The Seventh Affiliated Hospital, Sun Yat-Sen University, Shenzhen, China,[2]Department of Oncology, The Seventh Affiliated Hospital, Sun Yat-sen University, Shenzhen, China

Clinical observations revealed that the progression of newly developed pulmonary metastasis during systemic therapy reflected resistance in primary lesions and suggested that metastatic foci may retain biological characteristics similar to those of the primary tumor. However, how tumor cells in pulmonary metastatic lesions retained the biological characteristics of the primary tumor in different microenvironments remained unclear. We reported that mechanical memory enabled tumor cells to resist biomechanical stress and sustain malignant traits. Stiff matrix activated the RhoA-ROCK1 signaling pathway, leading to actin cytoskeletal remodeling and the suppression of mitochondrial fission. This dysregulation of mitochondrial dynamics enhanced fatty acid β-oxidation, accumulating acetyl-CoA and subsequent histone hyperacetylation. This epigenetic reprogramming was mitotically heritable, allowing progeny cells to retain a proliferative advantage after detachment from stiff environments. Inhibiting RhoA-ROCK1 disrupted mechanical memory, reducing HCC pulmonary metastasis. Our findings proposed targeting mechanical memory as a novel metastasis prevention strategy.

#0758 ECM mimicking tunable 3D hydrogels to model Ewing sarcoma.

Aakanksha Jha[1], Cole DeForest[2], Elizabeth Lawlor[1]

[1]Ben Towne Center for Childhood Cancer and Blood Disorders Research, Seattle Children's Research Institute, Seattle, WA,[2]Chemical Engineering, University of Washington, Seattle, WA

The extracellular matrix (ECM) is increasingly recognized as a critical regulator of tumor progression and metastasis. Despite its strong influence on tumor fate, the ECM remains poorly characterized within the solid tumor microenvironment. Ewing sarcoma (EwS), an aggressive bone and soft tissue malignancy affecting adolescents and young adults, may be particularly dependent on ECM-mediated cues for progression. Here, we present a synthetic three-dimensional (3D) hydrogel model designed to recapitulate key biochemical features of the EwS tumor microenvironment. Using a polyethylene glycol (PEG) backbone functionalized with ECM-derived integrin-binding peptides, we engineered hydrogels incorporating motifs from collagen I, fibronectin, and the tumor-associated glycoprotein tenascin-C (TNC). Incorporation of TNC-derived peptides, which are heterogeneously distributed in EwS tumors, enabled controlled ECM heterogeneity within the platform. CHLA10 human EwS cells encapsulated in these hydrogels exhibited peptide-dependent proliferation and altered expression of ECM-related and matrix-remodeling genes, highlighting the role of ECM proteins including TNC in influencing cell state. Importantly, the hydrogels were designed with sortase-degradable crosslinkers, enabling gentle and bioorthogonal retrieval of viable cells for transcriptomic and functional analyses—an advance over traditional biomaterial-based systems. This modular 3D system provides a physiologically relevant, animal-free model to study sarcoma–ECM interactions and identify ECM-regulated mechanisms of tumor adaptation and metastasis. Our findings demonstrate that ECM heterogeneity, particularly TNC enrichment, may be a key driver of EwS progression and highlight the potential of biomaterial platforms in uncovering therapeutic targets within the tumor microenvironment.

#0759 Mechanical remodeling of the tumor microenvironment promotes breast cancer and neutrophil-ssociated immunosuppression through ERG3-ALOX5 signaling.

Lingpeng Tang[1], Liangyu Wei[2], Jinpeng Lu[3], Haoxiang Zhang[4], Songsong Wu[1]

[1]Fujian Medical University, Fuzhou, China,[2]Fuzhou University School of Medicine, Fuzhou, China,[3]Shengli Clinical Medical College of Fujian Medical University, Fuzhou, China,[4]University of Kentucky, Lexington, KY

Background: Tumor extracellular matrix (ECM) stiffness is linked to breast cancer progression and immune evasion. The mechanisms by which mechanical signals influence tumor immune evasion through the immune microenvironment remain unclear. This study explores how ECM stiffness impacts the immune landscape and tumor progression via the “mechanical signal-matrix-neutrophil reprogramming-tumor immune escape” axis.

Methods: ECM stiffness in breast cancer patients was assessed using ultrasound elastography, with correlation to prognosis. In preclinical models, a mouse xenograft and 3D cell cultures were used to investigate the effects of ECM stiffness on tumor growth and immune cell infiltration. Single-cell RNA sequencing (scRNA-seq) and multicolor immunofluorescence analyzed immune cell composition in varying stiffness microenvironments. The role of stromal mechanical signals in neutrophil chemotaxis was studied using Piezo1-Ca^{2+}-EGR3 pathway modulation through gene interference, Ca^{2+} signaling blockade, and ChIP-seq. The efficacy of combined EGR3 inhibition and PD-L1 therapy was evaluated in a mouse model.

Results: Single-cell RNA sequencing revealed significant enrichment of tumor-associated neutrophils (TANs) and regulatory T cells (Tregs) in high-stiffness microenvironments, with a reduction in $CD8^+$ T cells. This remodeling was linked to upregulation of PD-L1, Arg1, and TGF-β, suggesting immune escape. TANs in high-stiffness environments exhibited enhanced immunosuppressive traits, correlating with tumor immune evasion. Increased ECM stiffness elevated tumor cell histone acetylation via Piezo1-mediated Ca^{2+} influx, promoting EGR3 transcription. ChIP-seq analysis showed that EGR3 activates ALOX5, driving LTB4 synthesis and enhancing tumor cell chemotaxis toward TANs. The study reveals that ECM stiffness regulates neutrophil chemotaxis via the Piezo1-Ca^{2+}-EGR3-ALOX5-LTB4 pathway, promoting immune evasion. Functional assays demonstrated that inhibiting EGR3 or ALOX5/LTB4 impaired neutrophil chemotaxis and immune evasion. In a mouse model, combining PD-L1 therapy with inhibition of the EGR3 or ALOX5/LTB4 pathways significantly suppressed tumor growth.

Conclusion: ECM stiffness promotes immune evasion in breast cancer via the Piezo1-Ca^{2+}-EGR3-ALOX5-LTB4 axis, creating an immunosuppressive microenvironment that drives tumor progression. These findings suggest new therapeutic targets for breast cancer immunotherapy.

#0761 Collagen turnover is dominated by fibrogenesis in lung adenocarcinoma and fibrolysis in lung squamous cell carcinomas.

Victoria Batto[1], Marselina Arshakyan[1], Rasmus Sund Pedersen[2], Neel Ingemann Nissen[2], Enrico Almici[3], Noemi Reguart[4], Morten Karsdal[5], Nicholas Willumsen[6], Jordi Alcaraz[1]

[1]Universitat de Barcelona, Barcelona, Spain,[2]Nordic Bioscience, Herlev, Denmark,[3]Institut de Bioenginyeria de Catalunya, Barcelona, Spain,[4]Medical Oncology Department, Hospital Clinic i Provincial de Barcelona, Barcelona, Spain,[5]Nordic Biosciences, Herlev, Denmark,[6]Nordic Bioscience

The tumor stroma in non-small cell lung cancer (NSCLC) is highly desmoplastic/fibrotic and is emerging as a key regulator of tumor progression, immune evasion and therapy resistance. Tumor fibrosis is characterized by the aberrant accumulation of collagen. However, our understanding of collagen turnover and its potential dependence on the histologic subtype is very limited. Here, we combined transcriptional profiling and ELISA-based assays for neoepitope collagen fragments to analyze collagen production (fibrogenesis) and degradation (fibrolysis) in tumor-associated fibroblasts (TAFs) and in tumor samples from the major NSCLC histologic subtypes: lung adenocarcinoma (LUAD) and lung squamous cell carcinoma (LUSC). In culture, LUSC-TAFs exhibited enhanced collagen turnover with increased markers of both production (exPRO-C1, PRO-C3 and PRO-C6) and degradation (C1M, C3M, C6M). Consistently, LUSC-TAFs exhibited higher RNA levels of both fibrillar collagens and collagenolytic MMPs, whereas TIMP-1 (a natural inhibitor of major collagenolytic MMPs) showed opposite patterns at the RNA and secreted protein levels. Consistent hystotype-dependent collagen-turnover signatures were observed in bulk RNA-seq data (TCGA) and in histologic analyses of TMAs from surgical specimens. Our results indicate that fibrogenesis is favored in LUAD through increased production of TIMP-1 and lower levels of collagenolytic MMPs, whereas fibrolysis is dominant in LUSC through increased production of collagenolytic MMPs (notably MMP1) and reduced production of TIMP-1. Mechanistically, TGF-β1 is a major driver of tumor fibrosis, and knocking-down SMAD2 or SMAD3 in normal fibroblasts —to mimic previously reported histotype-specific SMAD2/3 expression patterns in lung TAFs (Ikemori et al, Cancer Res 2020) — was sufficient to recapitulate key differential features of collagen turnover between LUAD and LUSC. Together, these data reveal opposite collagen-turnover programs in NSCLC, in which LUAD are predominantly fibrogenic, whereas LUSC are largely fibrolytic through histotype-dependent regulatory processes. Targeting these divergent programs may help revert pathologic fibrosis and improve responses to chemotherapy and/or immunotherapy in NSCLC.

#0762 A tunable 3D organoid model reveals stiffness-dependent stromal activation and cytokine signaling in pancreatic cancer.

Carolyn M. Ruiz-Rivera[1], Ba Xuan Hoang[1], Jamel Ali[2], Thomas D. Schmittgen[3], Bo Han[1]

[1]Keck School of Medicine of USC - University of Southern California, Los Angeles, CA,[2]FAMU-FSU College of Engineering, Tallahassee, FL,[3]Department of Pharmaceutics, University of Florida, Gainesville, FL

Pancreatic ductal adenocarcinoma (PDAC) is characterized by a dense fibrotic stroma and stiff extracellular matrix (ECM) that together shape the tumor microenvironment (TME) driving disease progression. Mechanical stiffness regulates fibroblast activation and inflammatory signaling through mechanotransduction, yet its contribution to tumor-stroma crosstalk remains incompletely understood. To investigate this, we developed a tunable 3D co-culture organoid model by embedding PDAC cells alone or in combination with stromal cells within soft or stiff collagen-based matrices. Conditioned media were collected one week post-seeding and analyzed via ELISA for TNF-α, IL-1β, and IL-6. Cell viability was assessed using CellTiter-Glo, and fibroblast activation markers (α-SMA, IL-6) were quantified by RT-PCR. Finally, immunostaining was performed to evaluate organoid morphology. Our results show that PDAC cells secreted elevated TNF-α in soft matrices, suggesting early cytokine-driven remodeling. Fibroblasts in stiff matrices exhibited a CAF-like phenotype with strong IL-1β secretion, while both fibroblasts and MSCs produced significantly higher IL-6 under stiff conditions, further amplified in PDAC co-cultures. Stiff ECM enhanced stromal viability and induced α-SMA and IL-6 upregulation, confirming mechanotransductive activation. Morphological analysis revealed that PDAC organoids formed larger, well-organized 3D structures under stiff conditions, indicating matrix-dependent growth and adaptation. We conclude that ECM stiffness acts as a potent regulator of stromal activation and inflammatory cytokine signaling in PDAC, establishing a tumor-promoting feedback loop that sustains fibrosis and inflammation. Future studies will incorporate mechanotransduction inhibitors (e.g., TGF-β or integrin blockers) and extended time courses to further define the dynamics of stiffness-driven inflammation and remodeling in the PDAC microenvironment.

#0763 Bridging the translational gap: Critical TME differences between human PDAC and mouse models.

Rachael Guenter[1], Libby A. Boykin[1], Khidr Kishan K. Budhwani[1], Brahma Mubarak K. Budhwani[1], Chelsea L. Crawford[1], J. Bart Rose[2], **Karim I. Budhwani**[1]

[1]CerFlux, Birmingham, AL,[2]Department of Surgery, University of Alabama at Birmingham, Birmingham, AL

Background: Pancreatic ductal adenocarcinoma (PDAC) develops within a dense, heterogeneous tumor microenvironment (TME) in which collagen and hyaluronic acid (HA) shape tissue architecture, biomechanics, and therapeutic response. Although mouse PDAC models are widely used, their ability to recapitulate human extracellular matrix (ECM) organization remains uncertain. This study aimed to quantitatively compare ECM composition and spatial topology in human PDAC versus a commonly used mouse model.
Methods: Tissue sections from primary human PDAC (n=6) and a syngeneic PDAC mouse model (n=3) were stained with H&E and a dual Picrosirius Red (collagen) and Alcian Blue (HA) protocol. The mouse model was generated by subcutaneous implantation of 2838c3 cells into C57BL/6 mice under approved protocols, with tumors resected at ~100 mm^3. High-resolution brightfield images were acquired under identical conditions using Agilent Lionheart. Quantitative analyses across 63 histomorphometric and spatial parameters, including area fractions, edge-to-core localization, and texture, were performed using the CerFlux PEER AI/ML imaging and analytics platform and cross-validated in Fiji. Texture and spatial order were quantified using gray-level co-occurrence matrix features and Moran's I.
Results: Human PDAC exhibited balanced ECM composition (collagen=0.16±0.04; HA=0.18±0.04), whereas mouse tumors showed HA enrichment and collagen depletion (collagen=0.04±0.002; HA=0.26±0.09). Edge mapping revealed proportionate collagen and HA in human samples (edge ratio=0.9±0.46) but 4-fold peripheral collagen enrichment in mouse tumors (edge ratio=4.3±1.3). Human tumors demonstrated higher entropy (collagen=8.1±0.2; HA=7.9±0.2) and substantial HA autocorrelation (Moran's I=0.58±0.22; 0.60±0.42), reflecting heterogeneous, regionally clustered desmoplasia. Mouse tumors displayed reduced entropy (~7.8) and lower Moran's I (0.32±0.05; 0.17±0.01), indicative of ordered, capsule-like ECM organization. Principal component analysis distinctly segregated species: PC1 (42%) collagen-HA balance, with human samples scoring positive and mouse samples negative; PC2 (21%) textural heterogeneity versus edge-localized order.
Conclusions: These findings show that the murine PDAC model fails to reproduce the balanced collagen-HA composition and spatially disordered desmoplasia of human PDAC, instead forming an HA-rich, collagen-depleted core encased in an ordered collagen capsule with markedly lower stromal entropy and autocorrelation. These findings highlight the limitations of mouse models, particularly subcutaneous tumor models, and underscores the need for human-relevant new approach methods (NAMs) for translational therapeutic studies.

#0764 *Mig-6* deficiency accelerates fibrotic tumor microenvironment formation in *Pten*-deficient endometrial tumors.

Shamsun Nahar[1], Kyeong A So[1], Keun Chen Kim[1], Jung Yoon Yoo[2], Jiyoung Yu[3], Kyunggon Kim[3], Eunhee M Jeong[1], Da-Hye Kang[1], Tae Hoon Kim[1], Jae-Wook Jeong[1]

[1]Department of Obstetrics, Gynecology and Women's Health, University of Missouri, Columbia, MO,[2]Yonsei University Mirae Campus, Wonju, Korea, Republic of,[3]Convergence Medicine Research Center, Asan Institute for Life Sciences, Asan Medical Center, Seoul, Korea, Republic of

Endometrial cancer (EC) is the most common gynecological malignancy, and metastatic or recurrent EC remains largely incurable with current therapies. Emerging evidence shows that alterations in the tumor microenvironment play a critical role in driving therapeutic resistance and poor outcomes in EC. Here, we investigated the molecular pathways that drive aggressive tumor behavior in EC using genetically engineered mouse models. Uterine specific conditional *Pten* and *Pten*/*Mig-6* knockout mice were generated using the Pgr^{cre} system. Quantitative proteomic profiling of uterine tissues using the ASTRAL platform identified 862 differentially expressed proteins (DEPs) (fold change > ±2, FDR < 0.05) between double mutant ($Mig\text{-}6^{d/d}Pten^{d/d}$) and single mutant ($Pten^{d/d}$) uteri at 4-months of age. Ingenuity pathway analysis revealed significant enrichment of fibrosis-related signaling, collagen organization, cellular invasion, and proliferative pathways. Consistent with these results, immunohistochemistry demonstrated increased expression of collagen alpha-1(I) chain, MMP3, and phospho-ERK1/2 in double mutant uteri compared to single mutants, correlating with enhanced fibrotic remodeling. Masson’s trichrome staining further confirmed extensive collagen deposition and fibrosis accompanying tumor progression in the double mutant mice. Collectively, these findings suggest that loss of *Mig-6* in a *Pten*-deficient uterus activates ERK signaling and MMP-mediated extracellular matrix remodeling, promoting a fibrotic and invasive tumor microenvironment that contributes to metastasis and therapeutic resistance in endometrial cancer. This work was supported by NCI R01CA264944.

#0765 Tumor extracellular matrix drivesEMT and cellular reprogrammingin Wilms tumor.

Wilson Yeung[1], Matthew E. Thornton[2], Hripsime Chomoyan[1], David Koos[1], Justin Sunwoo[1], Brendan H. Grubbs[2], Roger E. De Filippo[3], Stefano Da Sacco[3], Laura Perin[3], Astgik Petrosyan[3]

[1]Children's Hospital Los Angeles, Los Angeles, CA,[2]Keck School of Medicine of USC, Los Angeles, CA,[3]Children's Hospital Los Angeles/Keck School of Medicine of USC, Los Angeles, CA

Introduction: The extracellular matrix (ECM) is a dynamic component of the tumor microenvironment (TME) that orchestrates cancer progression, invasion, metastasis, and therapy resistance. Wilms tumor (WT), a pediatric renal malignancy, presents an altered ECM architecture. We investigated how WT ECM influences cellular behavior and transcriptional programs compared to normal kidney ECM.
Methods: Spatial transcriptomics and immunohistochemistry mapped ECM localization in WT and normal kidneys. Decellularization protocols were established to completely remove cellular materials while preserving the fibrillar ECM architecture and embedded soluble matrix proteins, as validated by second-harmonic generation imaging and ECM-associated proteins profiling using a cancer biomarker antibody array. Moreover, cancer and normal cells were cultured on decellularized ECM (dECM) scaffolds of WT and normal kidney for 21 days. Cellular dynamics were monitored via two-photon microscopy, and transcriptional changes were assessed by bulk RNA sequencing.
Results: WT ECM exhibited disorganized collagen networks and elevated levels of inflammatory markers, cytoskeletal proteins, and epithelial-mesenchymal transition (EMT) regulators. Cancer cells cultured on WT dECM upregulated EMT-related genes (e.g., FOXC2, TGFB2) and ECM remodeling enzymes (e.g., ADAMTS5), while downregulating cell cycle and integrin-associated genes. Normal cells seeded on WT dECM also adopted cancer-like transcriptional profiles, including increased expression of survival and proliferation genes (e.g., AKT3, BCL2) and decreased integrin-related gene expression.
Conclusion: WT ECM is structurally and molecularly distinct from normal kidney ECM and actively promotes EMT, stemness, and tumor-supportive reprogramming. These findings underscore the ECM as a crucial driver of cancer progression and highlight ECM-targeted strategies as a promising therapeutic approach for combating aggressive cancers.

#0766 Physically driven chromosome instabilities spur macrophages to attack cooperatively.

Dennis Discher, Markus Sprenger, Joanna Georgiou, Tristan Marchena, Jude Khatib

University of Pennsylvania, Philadelphia, PA

Extracellular matrix often accumulates in and around solid tumors, and such tumors also evolve diverse mutations that drive cancers, confound therapies, and modulate immune interactions. Across cancer types, we observe chromosome number changes associate with collagen-I levels, and our experiments show rare heritable chromosome losses are induced by a stiff 3D matrix around spheroids. Chromosome reporters (ChReporters) reveal losses in as few as ~0.1% of cells, with a mechanism in spheroids based on distortion of mitotic spindles - which increases with knockdown of the candidate tumor suppressor myosin-II. Chromosomes mis-segregate into micronuclei that increase with matrix stiffness despite suppressed cell division. Drugs that increase micronuclei in 2D and that rely on an unperturbed spindle show no effect in 3D where the spindle is perturbed. Tumors *in vivo* that are surrounded by stiff collagen likewise show more but varied chromosome loss and slower growth than 2D cultures. High variance of ChReporter-negative colonies further illustrate increased heterogeneity with 3D matrix stiffness and heritable mutations per Luria-Delbruck theory. Physical learning models of evolving chromosome numbers in proliferating cells are developed and fit key statistical trends.Temperature is another physical stressor - as solid tumors tend to be warm - and we show it has similar outcomes as matrix physical properties. Heating is also now part of various therapies as are immune-engineering approaches. We take advantage of Macrophages that often pervade solid tumors where clusters of macrophages are sometimes seen and associate with longer survival of patients. However, clustering mechanisms, responses to stressor above, and impacts on key functions such as phagocytosis remain obscure. Under conditions that maximize cancer cell phagocytosis within cohesive tumors, we uncover pathways that favor dynamic clusters and find a colocalization of tumor-intrusive pseudopodia which we term “intrudopodia.” Cluster formation is favored by M1 macrophages after exposure to interferons and T cell-derived cytokines. M1 macrophages upregulate specific cell-cell adhesion receptors but suppress actomyosin contractility, with both pathways contributing to cluster formation and unleashing pseudopodia. Macrophage neighbors in tumor spheroids indeed coextend intrudopodia between cancer cell junctions—at least when phagocytosis conditions are maximized by checkpoint disruption and other strategies. Intrudopodia from neighbors help detach and individualize cancer cells for rapid engulfment. Cooperative phagocytosis thus overcomes solid tumor cohesion—and might explain why the macrophage clustering factor *ITGAL* associates with patient survival.

#0767 Tumor stiffness as a functional biomarker of KRAS-mutant NSCLC: Insights from the ARTIDIS prospective clinical cohort.

Jordi Alcaraz[1], Elba Marin[1], Hector Sanz-Fraile[1], Marina Querol[2], Paula Gausa[2], Keat Neal[1], Marselina Arshakyan[1], Marc Rico-Pasto[1], Marc Boada[3], David Sanchez[3], Carolina Ortiz Velez[4], Reinier Oropesa Nunez[4], Gitika Srivastava[4], Ahmed Jizawi[4], Sara Nizzero[4], Tobias Appenzeller[4], Philipp Oertle[4], Marko Loparic[4], Marija Plodinec[4], Noemi Reguart[5]

[1]Biomedicine, Universitat de Barcelona, Barcelona, Spain,[2]Thoracic Oncology Unit, Hospital Clinic i Provincial de Barcelona, Barcelona, Spain,[3]Thoracic Surgery, Hospital Clinic i Provincial de Barcelona, Barcelona, Spain,[4]ARTIDIS AG, Basel, Switzerland,[5]Medical Oncology Department, Hospital Clinic i Provincial de Barcelona, Barcelona, Spain

Background: Nanomechanical properties of tumors are emerging biomarkers reflecting extracellular matrix (ECM) remodeling, immune exclusion, and aggressiveness. The AFM-based ARTIDIS platform measures nanomechanical signatures (NS) from fresh biopsies within hours, providing rapid diagnostic and prognostic information while preserving tissue for conventional analyses. Prior work showed that ARTIDIS NS distinguishes malignant from uninvolved lung tissue and predicts early postoperative recurrence. However, the relationship between NS and oncogenic drivers such as *KRAS* remains unclear. As *KRAS* influences ECM composition, matrix remodeling, and stromal activation, we evaluated the preliminary nanomechanical and microenvironmental features of *KRAS*-mutant NSCLC in our prospective cohort.

Methods: Fresh tumor and paired uninvolved lung tissue were collected from 70 early-stage NSCLC patients undergoing curative resection. NS were measured on the ARTIDIS platform. Samples were formalin-fixed for quantitative immunohistochemistry (IHC) of α-SMA, picrosirius red, Ki-67, CD31, CD4, CD8, FOXP3, CD68, and PD-1. Clinical characteristics, driver mutations, and outcomes were recorded with a 36-month follow-up. A focused analysis was performed in KRAS-mutant cases.

Results: Preliminary analyses showed that ARTIDIS NS distinguished malignant from uninvolved tissue with 88% sensitivity, 86% specificity, and 87% accuracy (n=52 paired samples). Eleven patients carried *KRAS* mutations (G12A/D/F/S, G13D, Q16H). Median age was 68.5 years; 63.4% were former smokers. Most tumors were early-stage (IA-IIB), and 45.5% were poorly differentiated. Across the full cohort, 17 patients recurred, including 3 patients (27.3%) with *KRAS* mutations. ARTIDIS NS predicted progression within 10 months after surgery with 100% sensitivity and 93% specificity, including predictions derived from uninvolved tissue. *KRAS*-mutant tumors showed higher stiffness than *KRAS*-wild-type or driver-negative tumors. Quantitative IHC demonstrated a higher percentage of proliferating cancer cells together with increased Treg infiltration and PD-1 expression in *KRAS*-mutant samples compared with uninvolved lung tissue, suggesting immune exhaustion.

Conclusions: This study provides the first evidence that *KRAS*-mutant NSCLC displays a distinct, stiffer nanomechanical phenotype. These findings support tumor stiffness as a functional characteristic of *KRAS*-driven biology and highlight ARTIDIS NS as a rapid biomarker complementing histopathology and molecular profiling. A 200-patient prospective validation study is underway to confirm the clinical utility of NS for risk stratification and personalized treatment planning.

#0768 Modeling the triple-negative breast cancer extracellular matrix in a 3d tumor scaffold.

Katherine Hebert[1], Thomas Cheng[1], Sophie Dietrich[1], Mackenzie Hawes[1], W. Todd Monroe[2], Jorge Belgodere[1], Elizabeth Martin[3]

[1]Tulane University School of Medicine, New Orleans, LA,[2]Louisiana State University, Baton Rouge, LA,[3]Tulane University, New Orleans, LA

Breast Cancer is the second leading cause of cancer death in women and incidence rates are increasing 0.5% per year. Triple negative breast cancer (TNBC), which is classified by negative hormone receptors (HR-), progesterone and estrogen, and human epidermal growth factor receptor 2 (HER2) negative, is the most aggressive subtype and occurs more often in younger Black and Hispanic women. TNBC, compared to other subtypes, is difficult to treat due to the treatment response rate of 30%. Neoadjuvant chemotherapy is the standard treatment for TNBC. This is attributed to the lack of preclinical models that allow multi-cellular interactions in the highly heterogenous nature of TNBC. Due to this, there is a critical need for 3D TNBC tumor models that recapitulate the complex extracellular matrix (ECM). Most ECM-cancer studies focus on collagen I (COL1); however, COL1 is not a prognostic marker for TNBC and is often not observed to be elevated in TNBC. Evaluation of ECMs overexpressed in a primary TNBC tumor compared to adjacent adipose demonstrated elevated ECM protein expression. To determine the impact of distinct ECMs in TNBC breast cancer progression, we explored changes in ECM protein expression (MFAP5, FN1, and POSTN) in TNBC cell lines and fabricated matrix for *in vitro* systems. qRT-PCR and RNA sequencing, genes associated with epithelial-to-mesenchymal transition and inflammation were significantly upregulated in ECM-OE expressing cells in 2D culture. Next, we created 3D models of TNBC ECM through the fabrication of ECM matrix coated cell culture plates (COL1, FN1, and POSTN) and 3D scaffolds using bioinert fish gelatin methacrylol (fgelMA). Taken together, this work identifies ECM proteins - MFAP5, FN1, and POSTN - attribute to TNBC proliferation and survival through epithelial to mesenchymal transition. Overall, our results establish an extracellular signature for the triple-negative tumor type while also demonstrating fabricated 3D ECM models can be used to advancing the development of potential treatments for TNBC.

#0769 Matrix mechanics modulate cancer cell plasticity and drug responses.

Chantal Kopecky[1], Elvis Pandzic[2], **Morgan Hamon**[3], Sean Porazinski[3], Justin Gooding[1], Kristopher A. Kilian[1]

[1]School of Chemistry, Australian Centre for NanoMedicine, Faculty of Science, UNSW, Sydney, Australia,[2]Katharina Gaus Light Microscopy Facility, Mark Wainwright Analytical Centre, UNSW, Sydney, Australia,[3]Inventia Life Science, Alexandria, Australia

The ability of cancer to adapt and evolve within its microenvironment drives metastasis and therapy resistance, with cancer cell plasticity playing a central role in these processes. To uncover how the tumour microenvironment (TME) shapes cancer cell behaviour to influence drug responses, we built next-generation in vitro models that recapitulate the key biophysical and biochemical cues of in vivo tumours.

Using precision-engineered 2D hydrogel micropatterning techniques and 3D bioprinted matrices, generated with the RASTRUM™ platform, we created spatially controlled “tumour environments" where cancer cells experienced defined stiffness, confinement, and extracellular matrix (ECM) architecture and composition. These mechanically tunable systems enabled interrogation of how substrate-cancer cell interactions and matrix mechanics orchestrate cellular transitions, organisation, and standard-of-care drug responses across cancer models.

Our results reveal that subtle changes in stiffness and confinement dramatically reorganise cancer cell populations, mimicking spatial hierarchies observed in vivo. In 3D, softer matrices enriched stem-like cancer subpopulations with increased invasiveness potential and chemoresistance, underscoring the powerful influence of matrix mechanics on tumour evolution.

Together, these bioengineered platforms offer an accessible, high-throughput approach for investigating the mechanical underpinnings of cancer cell plasticity. By merging bioprinting precision with biological complexity, this work lays the foundation for more predictive models of tumour progression and opens new avenues for developing approaches targeting resistant cancer cell states.

#0771 ECM stiffness and glutamine availability rewire metabolic and immune phenotypes in 3D Co-culture models of pancreatic cancer and cancer-associated fibroblasts.

Jonathan Barajas[1], Carolyn Ruiz[1], Zhi Yang[1], Bo Han[1], Edward Agyare[2], Xueyou Zhu[2], Saun-Joo Yoon[3]

[1]USC - University of Southern California, Los Angeles, CA,[2]Florida A&M University, Tallahassee, FL,[3]University of Florida, Gainsville, FL

Pancreatic ductal adenocarcinoma (PDAC) develops within a dense, tumor microenvironment (TME) enriched with extracellular matrix (ECM) and cancer-associated fibroblasts (CAFs). PDAC tumors also rely heavily on glutamine metabolism. While ECM stiffness and nutrient availability each influence tumor behavior, their combined effects on CAF and PDAC phenotypes in 3D contexts are not well defined. We investigated how matrix stiffness and glutamine supplementation modulate oxidative stress, lipid metabolism, mitochondria, cellular architecture, and PD-L1 expression in CAFs and patient-derived PDAC cells. Soft (3A) and stiff (6A) collagen-based ECM gels were generated in-house. Primary human CAFs or PDAC lines (G43, G46) were embedded in 3D and assessed at 48 hr and 7 days. CAFs were analyzed using CellROX, JC-1, BODIPY, phalloidin, and PD-L1 staining. PDAC cells were cultured in basal DMEM, glutamine-supplemented DMEM, or organoid-like media. Mitochondria were detected using an anti-mitochondrial antibody with AF488 secondary. All samples were imaged in 3D at 20× magnification. ECM stiffness significantly altered CAF oxidative stress responses. At 48 hr, CAFs in soft and stiff ECM showed comparable but detectable CellROX signal, whereas by 7 days, stiff ECM produced a marked increase in oxidative stress with a higher number of strongly CellROX-positive nuclei. Quantification of fluorescence intensity confirmed a time-dependent rise in oxidative stress that was amplified under stiff ECM conditions. This increase aligned with elevated JC-1 J-aggregate formation at 7 days, indicating enhanced mitochondrial polarization. CAFs in stiff ECM also exhibited greater F-actin alignment, cell spreading, and lipid accumulation, suggesting coordinated metabolic and cytoskeletal adaptation to mechanical stress. PD-L1 expression likewise increased over time and remained higher in stiff ECM, supporting a role for mechanosensing in promoting immune-evasive CAF phenotypes. In PDAC cells, ECM stiffness and nutrient environment jointly controlled metabolic outputs. BODIPY staining revealed stiffness-dependent lipid droplet patterns, which were further amplified by organoid-like media. Glutamine supplementation increased mitochondrial signal intensity and reorganized mitochondrial networks in both G43 and G46, consistent with glutamine-driven metabolic activation. ECM stiffness also shaped F-actin architecture and mitochondrial localization, indicating a biomechanical-metabolic interaction. Together, these results show that ECM stiffness and glutamine availability reprogram CAF and PDAC metabolic and immune features. This work underscores the need to incorporate both mechanical and metabolic cues when modeling PDAC and identifies metabolic-immune pathways as potential therapeutic vulnerabilities within the TME.

#0773 Single-cell and spatial transcriptomic profiling reveal fibrosis-related tumor states in lung squamous cell carcinoma associated with idiopathic pulmonary fibrosis.

KENTA MANABE[1], Atsushi Matsuoka[1], Kazuhiko Shien[1], Shuta Tomida[2], Hidejiro Torigoe[1], Kazuya Hisamatsu[1], Ryota Fujiwara[1], Kosei Ishimura[1], Shunsuke Mori[1], Ryunosuke Fujii[1], Asuka Mimata[1], Kazuhiro Okada[1], Ryo Yoshichika[1], Mao Yoshikawa[1], Yuma Fukumoto[1], Haruchika Yamamoto[1], Kumi Nakajima[1], Shin Tanaka[1], Ken Suzawa[1], Kentaroh Miyoshi[1], Mikio Okazaki[1], Seiichiro Sugimoto[1], Shinichi Toyooka[1]

[1]Thoracic, Breast and Endocrinological Surgery, Okayama Univ. Graduate School of Med., Dentistry & Pharm. Sci., Okayama, Japan,[2]Center for Comprehensive Genomic Medicine, Okayama University Hospital, Okayama, Japan

Background: Patients with idiopathic pulmonary fibrosis (IPF) have an elevated risk of lung cancer, particularly lung squamous cell carcinoma (LUSC), which is associated with limited treatment options and poor outcomes. Although LUSC occurring in IPF patients is collectively referred to as LUSC associated with IPF regardless of location, tumors arising within usual interstitial pneumonia (UIP) lesions may harbor distinct molecular traits shaped by the local fibrotic microenvironment compared with those arising outside UIP.
Methods: We performed integrated single-cell RNA sequencing (scRNA-seq) and Digital Spatial Profiling (GeoMx DSP) to characterize tumors and adjacent lung tissue from LUSC patients with UIP patterns. scRNA-seq was performed on paired tumor and adjacent lung tissue from an In-UIP case and an Out-UIP case, while GeoMx profiling was conducted in an independent cohort (In-UIP n=3, Out-UIP n=3). scRNA-seq data were processed using Scanpy (v1.10.4) and spatial transcriptomics data were processed using GeomxTools (v3.8.0). Cellular trajectories were analyzed using scTour (v1.0.0). Spatial deconvolution was performed using Cell2location (v0.9.6), with validation in an external fibrosing ILD spatial dataset.
Results: To infer lineage relationships from the scRNA-seq data, we applied partition-based graph abstraction (PAGA), which demonstrated a connection between basal cells and malignant cells, suggesting basal cells as a cellular origin of LUSC. Tumor cells were further resolved into four transcriptionally distinct malignant states, one of which was characterized by upregulation of oxidative stress-response and detoxification programs, including induction of multiple WNT ligand genes. scTour vector-field and pseudotime modeling showed expansion of this state at late phase exclusively in the In-UIP tumor. Spatial profiling by GeoMx DSP followed by Cell2location deconvolution confirmed significant enrichment of this stress-tolerant malignant state in In-UIP tumors compared with Out-UIP tumors. In adjacent non-malignant regions, UIP lungs exhibited marked expansion of basal and club populations, reflecting UIP-specific epithelial remodeling. Analysis of an independent spatial ILD cohort validated this epithelial shift specifically in IPF.
Conclusions: Single-cell and spatial analyses demonstrate that UIP lesions create a selective niche that reshapes local epithelial composition and promotes regional enrichment of a stress-tolerant malignant cell state. These data indicate that the fibrotic lung microenvironment of IPF conditions malignant cell states and their spatial organization, nominating microenvironment-driven programs as potential therapeutic targets in LUSC associated with IPF.

#0774 Aligned ECM influences neuroblastoma cell plasticity via YAP-WT1 association.

Vic Zamloot[1], Chandra Kaladhar Vemula[1], Antonios Chronopoulos[2], JinSeok Park[1]

[1]Children's Hospital Los Angeles, Los Angeles, CA,[2]Stanford University, Stanford, CA

Introduction

Neuroblastoma (NB) is the most common extracranial pediatric solid tumor and is comprised of two interconvertible cell states: the less-aggressive adrenergic (ADRN) and the aggressive, therapy-resistant mesenchymal (MES) subtypes. Through an ADRN-to-MES transition (AMT), NB cells become more refractory to existing therapeutics, as is often observed in high-risk (HR) and relapsed NB. We previously identified that aligned extracellular matrix (ECM) proteins, featured in HR and relapsed NB, drive AMT in NB by facilitating epigenetic silencing of ADRN signatures. Our study aims to further characterize the underlying mechanisms driving AMT in NB, specifically how aligned ECM increases MES signatures through activation of yes-associated protein (YAP), which interacts with Wilm's Tumor 1 (WT1) to regulate activity of the MES driver, paired related homeobox 1 (PRRX1).

Experimental Procedures

To interrogate how aligned ECM influences MES signatures, we employ a nanogrooved collagen-coated array (NGCA) that models the aligned collagen observed in HR and relapsed NB. Cells plated on this *in vitro* platform are assessed for differences in MES signatures and expression of YAP, WT1, and PRRX1 via biochemical analyses including Western blot, immunofluorescent (IF) staining, and chromatin immunoprecipitation sequencing (ChIP-seq). We also use cells with knockdown and overexpression of YAP as well as knockdown of WT1 to determine their roles in our proposed AMT mechanism. The association of YAP and WT1 is physically evaluated using proximity ligation assay (PLA) and co-immunoprecipitation (co-IP).

Results

Our data demonstrate that aligned ECM modeled *in vitro* with NGCA increases MES signatures and YAP expression in NB. NGCA additionally promotes expression of the MES driver PRRX1 in a YAP-dependent manner, suggesting its recruitment by YAP to increase MES signatures. Furthermore, ChIP-seq highlights an association between YAP and WT1 that promotes PRRX1 expression. Computational analysis identifies WT1 as a transcription factor interacting with PRRX1, an association we confirm through reduction of PRRX1 expression following WT1 knockdown. We show that WT1 expression and nuclear localization are associated with YAP activity; indeed, PLA and co-IP analyses reveal that YAP and WT1 form a complex in response to NGCA, which then translocates to the nucleus.

Conclusions

Together our data support a mechanism by which YAP and WT1 interact in response to aligned ECM to promote PRRX1 expression, thereby increasing MES signatures. Identification of this process uncovers pharmacological and therapeutic targets for re-sensitization of HR and relapsed NB to existing treatments to improve clinical outcomes.

#0775 Matrix stiffness remodels the immunosuppressive tumor microenvironment via the PIEZO1-DCLK1-STAT5B pathway.

Liangyu Wei[1], Lingpeng Tang[2], Jinpeng Lu[2], Ting Hu[2], Shi Chen[2], Zuwei Wang[2], **Haoxiang Zhang**[1]

[1]School of Medecine, Fuzhou University, Fuzhou, China,[2]Shengli Clinical Medical College, Fujian Medical University, Fuzhou, China

Background Pancreatic ductal adenocarcinoma (PDAC) has an abysmal 5-year survival rate (8%), largely attributed to its dense fibrotic stroma that forms a high-stiffness microenvironment. This biomechanical feature exacerbates immunosuppression and promotes immune escape, but the molecular mechanism by which matrix stiffness-derived mechanical signals convert into immunosuppressive cues remains undefined. This study aims to uncover the key mechanotransduction-immunity crosstalk pathway in PDAC and provide novel therapeutic targets.

Methods We utilized our established adjustable extracellular matrix (ECM) stiffness models (in vitro 3D culture and in vivo orthotopic transplantation) as core research platforms. Integrated approaches including CRISPR-Cas9 gene editing, multi-omics (protein modification omics, CUT&Tag-seq), single-cell RNA sequencing, and spectral flow cytometry were employed to dissect the mechanotransduction pathway and its regulatory effect on the tumor microenvironment.

Results We identified a novel PIEZO1-Ca^{2+}-DCLK1-STAT5B axis mediating stiffness-induced immunosuppression. High matrix stiffness specifically activated the mechanosensitive ion channel PIEZO1, triggering Ca^{2+} influx. Intracellular Ca^{2+} upregulated and activated DCLK1 via dual mechanisms: inhibiting ANAPC5/PSMA7-mediated ubiquitination and promoting HPCAL1-dependent serine phosphorylation. Activated DCLK1 bound to STAT5B through its serine/proline-rich linker domain (DCLK1) and SH2 domain (STAT5B), inducing STAT5B phosphorylation and nuclear translocation. Nuclear STAT5B, under the regulation of super-enhancers (marked by H3K27ac/H3K4me1), transcriptionally activated immunosuppressive genes (TGF-β, PD-L1, KRAS), ultimately shaping an immunosuppressive microenvironment characterized by increased infiltration of Tregs, MDSCs, and M2 macrophages, and impaired effector T cell function. Preliminary data confirmed that high stiffness upregulated all components of this axis, and STAT5B inhibition significantly reduced TGF-β/PD-L1/KRAS expression and immunosuppressive cell infiltration.

Conclusion This study is the first to uncover a biomechanics-driven immunosuppression pathway in PDAC, establishing a direct link between matrix stiffness and immune escape. The PIEZO1-Ca^{2+}-DCLK1-STAT5B axis provides a novel therapeutic target for reversing immunosuppression and improving PDAC therapeutic efficacy.

#0776 A cancer cell intrinsic program for matrix remodeling and CAF recruitment in slow growing, poor prognosis colorectal cancers.

Claudio Isella[1], Anna Cassisa[1], Consalvo Petti[2], Alexandra Ambra Ulla[1], Jie Zhou[3], Carlo Leonardi[1], Roberta Porporato[1], Daniela Cantarella[1], Letizia Franco[2], Cinzia Benetti[1], Jill Carol Rubinstein[4], Jessica Erriquez[2], Mariangela Russo[5], Francesco Sassi[2], Elena Grassi[2], Ymera Pignochino[6], Alberto Puliafito[2], Ivan Molineris[1], Rebecca Senetta[7], Andrea Bertotti[8], Livio Trusolino[9], Jeffrey H. Chuang[10], Alberto Bardelli[11], Enzo Medico[12]

[1]Universita degli Studi di Torino, Torino, Italy,[2]Institute for Cancer Research and Treatment, Candiolo, Italy,[3]The Jackson Laboratory for Genomic Medicine, Farmington, CT,[4]The Jackson Laboratory for Genomic Medicine, Bridgeport, CT,[5]IRCC - Institute for Cancer Research and Treatment, Institute for Cancer Research and Treatment, Candiolo, Italy,[6]Junior Group Leader, Dept of Oncology, Institute for Cancer Research and Treatment, Candiolo, Italy,[7]University of Turin, Turin, Italy,[8]Asst. Professor, Dept. of Oncological Sci., University of Turin, Candiolo (TO), Italy,[9]Fondazione del Piemonte per l'Oncologia, Candiolo, Italy,[10]The Jackson Laboratory, Farmington, CT,[11]IFOM Istituto Fondazione di Oncologia Molecolare ETS, Milan, Italy,[12]Candiolo Cancer Institute, FPO-IRCCS, Candiolo, Italy

To investigate how the molecular programs of cancer cells shape their crosstalk with the tumor microenvironment, we generated mouse xenografts from 19 human colorectal cancer (CRC) cell lines and performed RNA sequencing, separately profiling human (cancer) and murine (stromal) transcriptomes. Xenograft growth rates varied markedly across lines and correlated with stromal abundance: slower-growing tumors accumulated more stroma. Cancer cells from these stroma-rich, slow tumors displayed a coordinated transcriptional program involving epithelial-mesenchymal transition (EMT) and extracellular matrix (ECM) remodeling, which we termed the *EMT-Matrix Remodeling* (EMR) signature. The corresponding stromal fibroblasts exhibited matrix-remodeling activity defined by a *matrix-remodeling cancer-associated fibroblast* (mrCAF) signature. Integration of human CRC bulk, single-cell, and spatial transcriptomics confirmed the co-occurrence and spatial proximity of EMR cancer cells and mrCAFs, both associated with adverse clinical outcome. A pan-cancer analysis revealed that EMR and mrCAF signatures recur across multiple tumor types, where they similarly mark aggressive disease. Collectively, these findings uncover a conserved mechanism of ECM remodeling driven by reciprocal cancer-stromal interactions: cancer cells with an EMT-like, matrix-remodeling phenotype recruit and instruct CAFs to reshape the tumor microenvironment, thereby promoting tumor progression.

#0777 An ATP-grasp superfamily enzyme induced under serum starvation and hypoxia as a potential biomarker for pancreatic cancer diagnosis.

Katsuya Takenaka[1], Yukako Komori[2], Yoshiyasu Nakamura[2], Shiro Koizume[2], Yohei Miyagi[2]

[1]Fundamental Research Unit, TR Business Division, Shin Nippon Biomedical Laboratories, Ltd., Kagoshima, Japan,[2]Molecular Pathology and Genetics Division, Kanagawa Cancer Center Research Institute, Yokohama, Japan

Pancreatic cancer is one of the most prognostically unfavorable cancers worldwide. On the other hand, favorable outcomes have been reported when treatment is initiated at an early stage, and there is great expectation for the development of early diagnostic technologies. Most solid tumors, including pancreatic cancer, contain areas of hypoxia where the dominant cells show increased resistance to both chemo- and radiotherapy. We hypothesized that tumor cells proliferate under the ischemic environment, which is generally unfavorable for cell survival, through specific gene expression. Genes exhibiting such expression changes may serve as candidates for early detection or therapeutic targeting. To identify such candidates, we cultured human pancreatic cancer cell lines under serum starvation and hypoxic conditions to mimic the ischemic tumor microenvironment. Genes synergistically induced by these combined conditions were identified by DNA microarray analysis. One of the candidates was an ATP-grasp superfamily enzyme, RIMKLA, which is involved in glutamine family amino acid metabolic process, and its inducible expression was presented by qRT-PCR for at least four pancreatic cancer cell lines. We raised antibodies against peptides corresponding to specific regions of the polypeptide and showed that the protein synthesis is also induced. In mouse xenograft models, RIMKLA expression was seen in hypoxic regions where HIF-1α was induced, and the product of this enzyme was quantitatively detected by mass spectrometry. Tumorigenicity of the gene knockout cells was significantly reduced compared to that of wild-type cells, and necrotic regions were observed within hypoxic areas even in small xenografts. Immunohistochemical staining and mRNA *in situ* hybridization performed on surgical specimens from pancreatic cancer patients demonstrated that this enzyme is specifically expressed in pancreatic cancer tissues. These observations support the potential application of this protein as a clinical biomarker for pancreatic cancer diagnosis. In addition to detecting and targeting the enzyme molecule in tissue samples, minimally invasive diagnostic methods could be developed based on detecting this relatively small product in peripheral blood. Since the genetic disruption of the enzyme impairs tumor formation, its enzymatic activity appears to play an important role in tumor cell survival. These findings support the potential development of molecular targeted therapies based on gene disruption or enzymatic activity inhibition.

#0778 Hypoxia shapes tumor immune microenvironment through cell-type dependent responses in diffuse astrocytomas.

Aliisa Tiihonen[1], **Iida Salonen**[2], Iina Koivisto[2], Anni Ritamaki[2], Serafiina Jaatinen[2], Tanja Hyvarinen[2], Johanna Tilvis[2], Joose Kreutzer[2], Masi Valkonen[2], Goktug Karabiyik[1], Sonja Mantyla[2], Maryam Mohammadlou[2], Miina Hoikka[2], Jurgen Beck[3], Roland Rolz[3], Mikael Marttinen[1], Matti Nykter[1], Joonas Haapasalo[4], Pekka Ruusuvuori[2], Seppo Parkkila[1], Pasi Kallio[1], Sanna Hagman[2], Juha Kesseli[1], Vidhya Madapusi Ravi[3], Hannu Haapasalo[1], Arja Jukkola[1], Kevin Joseph[3], Kirsi Rautajoki[1]

[1]Tampere University, Tampere, Finland,[2]Tampere University, Faculty of Medicine and Health Technology, Tampere, Finland,[3]Department of Neurosurgery, Medical Center - University of Freiburg, Faculty of Medicine, Freiburg, Germany,[4]Tampere University, Faculty of Medicine and Health Technology and Tampere University Hospital, Department of Neurosurgery, TAYS Cancer Centre, Tampere, Finland

Background
Hypoxia is a critical driver of tumor aggressiveness in high-grade gliomas, yet its cell-type-specific effects on immune cell populations within the tumor microenvironment (TME) remain poorly understood.
Materials and methods
We have investigated how hypoxia shapes the spatial distribution and functional states of monocyte-derived macrophages (MDMs) and brain-resident microglia (MG) in diffuse astrocytomas and glioblastomas (GB) by using cyclic immunohistochemistry (cIHC), single-cell RNA sequencing, spatial transcriptomics, and in vitro cell culture models in controlled oxygen and pH conditions.
Results
Hypoxia induces divergent responses in these myeloid subsets, driving spatial immune patterning. In GB, $CD163^-$ MDMs dominate hypoxic niches, while MG populations are excluded from these regions, correlating with hypoxia-induced TNF upregulation, stress response signatures, and dampened interferon responses. Conversely, MDMs exhibit a shift towards hypoxia-associated immunosuppressive traits, altered metabolism and upregulated cell survival. GBs display elevated hypoxic intensity compared to diffuse astrocytomas, as supported by hypoxia-response gene expression in the TCGA dataset. In vitro, MG are characterized by heightened sensitivity to hypoxia-associated acidity compared to MDMs, suggesting that their exclusion from hypoxic zones results from intrinsic vulnerability.
Conclusion
Our findings reveal that hypoxia and hypoxia-associated acidity remodel the TME by promoting immunosuppressive MDM accumulation and depletion of MG, creating spatially distinct immune landscapes that may underlie GB progression. These results highlight hypoxia-driven immune dysregulation as a therapeutic target and underscore the importance of cell-type-specific strategies to counteract TME-driven immunosuppression in malignant gliomas.

#0779 Hypoxia-driven epithelial reprogramming elevates CD46 and promotes vasculogenic mimicry in immune-desert NSCLC.

Minyeop Kim[1], Youwon Lee[1], Seung Yeon Oh[1], Eun Ji Lee[1], Ji Hyung Moon[1], Ji Ae Ko[1], Ji Woo Lim[1], Sujin Choi[1], Jae-Hwan Kim[2], Jii Bum Lee[1], Min Hee Hong[3], Sun Min Lim[1], Byoung Chul Cho[1], Mi Ran Yun[1]

[1]Yonsei University College of Medicine, Seoul, Korea, Republic of,[2]Yonsei University Hospital Cancer Center, Seoul, Korea, Republic of,[3]Yonsei University College of Medicine SBSI, Seoul, Korea, Republic of

Introduction: Immune-desert non-small cell lung cancer (NSCLC) presents a major challenge for immunotherapy due to poor T-cell infiltration despite the presence of tumor antigens. While immune suppression in these tumors is well recognized, the contributions of epithelial and stromal compartments to shaping the tumor microenvironment (TME) remain poorly defined.
Methods: We analyzed bulk RNA-seq profiles from 60 lung adenocarcinoma (LUAD) tumors and classified them as immune-desert or inflamed using a T-cell inflammed signature. Matched tumors were further characterized using single-cell RNA sequencing (scRNA-seq) to dissect epithelial, stromal, and immune compartments within the TME. Key findings were validated using public datasets, immunohistochemistry (IHC) of patient specimens, and functional assays in CRISPR/Cas9-edited cell lines.
Results: Compared with immune-infiltrated epithelial cells, desert epithelial cells were enriched in complement cascade, hypoxia, cholesterol homeostasis, and EMT pathways, while OXPHOS and antigen-processing programs were downregulated. Regulon analysis identified XBP1 as a key transcription factor in desert epithelial cells, which targeted other genes driving desert-enriched pathways, including CD46, complement-regulatory modules, and cytokines/chemokines involved in myeloid recruitment and immune evasion. These results suggest that desert epithelial cells are in an stress-adapted, plastic state. In the endothelial lineage, Desert tumors exhibited reduced PCV scores, a metric associated with T-cell infiltration, alongside an increased proportion of Epi-like endothelial cells expressing cancer stemness-related genes. Among regulators of this program, ELF3, a hypoxia-inducible transcription factor, was strongly upregulated in vascular mimicry (VM)-associated cells. IHC confirmed robust CD46 expression on epithelial surfaces of Desert tumors. Notably, CD46-high NSCLC lines formed significantly more VM networks than CD46-low lines. Analyses of public datasets further corroborated inverse relationships among CD46 expression, hypoxia signaling, VM enrichment, immune infiltration, and immunotherapy response, consistent with a role for these programs in mediating immune exclusion.
Conclusions These findings indicate that hypoxia-linked epithelial stress programs, driven in part by XBP1, elevate CD46 and support VM-related plasticity, forming both immunologic and structural barriers characteristic of the immune-desert state. Together, these results outline how hypoxia-adapted epithelial and endothelial transitions reorganize the architecture of Desert tumors and help explain their persistent resistance to T-cell infiltration, highlighting the value of considering structural remodeling alongside immune suppression when interpreting the desert phenotype.

#0780 Tumor cell adaptation to nutrient stress via metabolic change due to fibronectin/integrin internalization.

Arin Nam, Tasha Nguyen, Tami von Schalscha, Sara M. Weis, David A. Cheresh

UC San Diego Health, San Diego, CA

Tumor cells that adapt to stressors in the microenvironment gain a stem-like, aggressive phenotype, promoting cancer progression and drug resistance. We previously showed that integrin αvβ3 induced by stress could promote tumor cell adaptation to nutrient stress. Here, we show that tumor cell-derived fibronectin (FN), a ligand for αvβ3, was also upregulated in response to stress and that FN specifically bound to αvβ3 could be internalized providing a survival benefit under nutrient-limited conditions. Nutrient-starved cells either lacking FN or αvβ3 expression displayed decreased intracellular glutamine and TCA cycle metabolites leading to cell death. Surprisingly, while integrin α5β1 is the predominant FN receptor on these cells and is critical for cell surface FN localization, it did not promote FN internalization that protected cells from nutrient stress. These findings highlight a novel mechanism by which αvβ3-mediated uptake of FN mitigate nutrient stress thereby representing a critical property of cancer stem cells.

#0782 Tolerance to extracellular acidic pH facilitates tumor plasticity.

Manami Hasegawa[1], Bo Xu[1], FeiFei Cai[1], Runmei Cui[2], Ritsuko Ando[1], Ken Matsumoto[1], Chisato Iwabuchi-Yoshida[1], Kazuyuki Yamagata[1], Rika Tsuchida[1], Tsuyoshi Osawa[1]

[1]Division of Nutriomics and Oncology, RCAST, The University of Tokyo, Tokyo, Japan,[2]Department of Biological Sciences, Graduate School of Science, The University of Tokyo, Tokyo, Japan

Cancer cells maintain glycolytic metabolism despite oxygen availability, resulting in an acidic microenvironment mediated by enhanced proton and lactate secretion. We have previously reported that this acidic tumor microenvironment induces the activation of the cholesterol biosynthesis pathway and polyamine pathway. Although these metabolic adaptations have been well documented, the mechanisms governing cell survival under acidic conditions are poorly understood. We first demonstrated that severe acidification (pH 5.6) triggered necroptotic cell death, whereas moderate acidification (pH 6.8) prevented necroptosis and allowed anchorage-independent survival and tumor initiation. At pH 5.6, PANC1 and MIA-PaCa2 pancreatic cancer cells exhibited phosphorylation of RIP1 and MLKL, and Calcein-AM live imaging confirmed membrane-rupturing cell death; these features were not observed at pH 6.8. In addition, when PANC1 floating cells (pH 7.4 or pH 6.8) were subcutaneously injected into SCID/SCID mice, tumor initiation was observed only in the mice implanted with pH 6.8 floating cells by day 7. RNA sequencing comparing adherent and floating cells at pH 6.8 and pH 7.4 revealed activation of the complement pathway specifically in pH 6.8 floating cells, suggesting that complement inhibition may selectively eliminate acid-tolerant cancer cells. A genome-wide CRISPR-Cas9 knockout screen in chronically acid-exposed PANC1 cells identified FAM129C as a critical regulator of acid tolerance and cell survival. In xenograft models, FAM129C overexpression led to downregulation of PIGR. Conversely, in murine pancreatic Pan02 cells overexpressing PIGR, immune profiling showed enhanced immune cell infiltration, particularly increased macrophage infiltration. Finally, we evaluated the therapeutic efficacy of combining an anti-PD-L1 antibody (αPD-L1) with PMX53, a complement inhibitor. This synergistic treatment markedly suppressed tumor growth in PIGR-overexpressing Pan02 tumors. Immunohistochemistry revealed that the combination therapy increased IFN-γ^+ $CD8^+$ T cells and reduced macrophage infiltration within the tumor microenvironment. Our findings reveal a previously uncharacterized pathway that evades necroptotic cell death and enhances cellular plasticity under acidic stress, offering new therapeutic approaches for cancer treatment through pH-dependent cell death modulation.

#0783 Exploring landscapes of T cell activation in acidic environment for tumor immunotherapy.

Minkyeong Ro, Youngjun Park

College of pharmacy, Jeju national University, Jeju, Korea, Republic of

Effector T cells are central to anti-cancer immunity but, within the nutrient-poor, hypoxic, and acidic tumor microenvironment (TME) sculpted by dysregulated tumor metabolism, they become dysfunctional. Tumor cell-derived lactic acid accumulates in the tumor microenvironment as lactate and protons; while lactate's immunosuppressive effects are well established, the contribution of the accompanying protons remains largely unknown. We hypothesized that extracellular acidity per se programs T cell activation. Here we show that lactate-independent extracellular acidity—achieved by titrating media with hydrochloric acid or sodium carbonate to tumor-relevant pH—impairs acquisition of inflammatory effector signatures and curtails clonal expansion in T cells. Collectively, the results indicate that protons may underlie the TME-driven limitation on T-cell antitumor activity. Thus, defining the molecular sensors and signaling nodes that transduce proton stress should reveal druggable targets and rational combination strategies for microenvironmental reconditioning to enhance tumor immunotherapy.

#0785 Elucidating the molecular regulation of superdark transmembrane protein 184C (TM184C).

Shraddha ChandThakuri[1], Jennifer Arcuri[2], Daniel Isom[2]

[1]Cancer Biology, University of Miami Miller School of Medicine, Miami, FL,[2]Molecular And Cellular Pharmacology, University of Miami Miller School of Medicine, Miami, FL

Using structure-to-sequence predictions, our lab recently identified TM184C as a previously uncharacterized ‘superdark’ GPCR-like protein. We have shown that this protein is highly enriched in cellular projections and facilitates cargo transfer through microtubule-based intercellular connections. Alongside, we have also shown that TM184C controls the formation and activity of autophagosomes leading to constrained autophagy. Furthermore, our results provide preliminary insights into why TM184C is a poor prognosticator in cancers such as glioblastoma, pancreatic cancer, and ovarian cancer. As such, we are now trying to understand the different modes of TM184C regulation and how they relate to cancer biology.We have shown that TM184C functions primarily in vesicles with acidified lumen, including autophagosomes, late endosomes, and lysosomes. This led us to hypothesize its spatiotemporal function may be partly regulated by pH. To address this question, we performed a structural analysis to identify residues that may confer pH regulation of TM184C. We stably expressed these mutant residues in HEK293A cells as the non-cancerous model, and Panc-1 cells, as the pancreatic cancer model. With the use of live cell confocal fluorescence microscopy, we observed that these mutants produce striking cellular phenotypes, including abnormal nucleus and vesicles, consistent with hyperactivation or loss of function, supporting a model in which TM184C responds directly to vesicular acidity. Our mutational studies thus strongly indicate that TM184C is indeed regulated by vesicular pH, suggesting that any diseases or drugs that alter vesicular pH may modulate TM184C function. Our research has important implications in cancer biology since disrupted pH and autophagy are two of the key components that tumor cells exploit to resist therapy and adapt to the tumor microenvironment.

: Spatial Protein Profiling and Multi-Modal Mapping of Tumor and Circulating Ecosystems
Poster Session

#0789 PaintScape™ enables in situ, single cell spatial multiomic visualization of 3D genome organization in fresh frozen colorectal carcinoma tissue in spatially resolved tissue microenvironments.

Shyamtanu Chattoraj, Pamela Flatley, Stacy Elliott, David Castillo, Kenny Chung, Doug Werner, Jude Dunne, Huy Nguyen

Research and Development, Bruker Spatial Genomics, San Jose, CA

Intratumoral heterogeneity (ITH) continues to be one of the major challenges in successful cancer treatments causing poor prognosis, therapeutic resistance, metastasis and relapses across many human cancer types. This heterogeneity largely originates from the complex tumor immune microenvironment, where cancer and immune cells engage in intricate signaling crosstalk, shaped by clonal and sub-clonal variations in genomic, transcriptomic, and proteomic networks across cancer and immune cells. In recent years, disruptions in 3D genome architecture, including CNVs, SVs, and topological changes, have been shown to drive oncogene activation, tumor suppressor silencing, and gene expression dysregulation in many different cancers. While methods like WGS and Hi-C offer bulk-level insights into genomic dysregulation, they disrupt native tissue architecture and lack the single cell nuclear examination, limiting the ability to analyze spatial relationships and organizational features essential for understanding cellular context and heterogeneity. Given its emerging role in therapeutic resistance and poor prognosis, understanding the molecular mechanism behind high ITH demands advanced single-cell and spatial technologies for early detection and disease monitoring. Here, we present a novel multiomic jebFISH™ protocol on the PaintScape™ platform that can be used to characterize ITH of 3D chromatin architecture of fresh frozen normal human colon tissue and colorectal cancer (CRC) samples in different tissue microenvironments at single cell, sub-population and population level. Using the ChromoPaint™ PanChromo MPX Panel, which visualizes over 400 genomic loci across all chromosomes per nucleus, we show chromosomal instability including CNVs such as gain in Chr20q, loss in Chr17p, copy loss of Chr 14, SVs such as Chr13-Chr20q translocation and complex rearrangement of Chr13 in different colon cancer cell sub-populations *in situ* within the tissue. These genomic aberrations were specific to histologically cancerous sections and were not detected in the normal region of the tissue. By combining the jebFISH protocol with multiplexed immunofluorescence, we characterize 3D genome organization of cancer cell sub-populations with unique cell states along with associated proteomic signatures e.g. Pan-CK+ CDH1- and Pan-CK+ CDH1+ subpopulations in different tissue microenvironments. We also visualized genome structure in different tumor-immune microenvironments, e.g. M2 macrophage rich vs CD3+ T-cells rich regions within the same CRC tissue section. In-situ multiomic capability of the PaintScape platform enhances understanding of colon cancer progression and reveals 3D genomic heterogeneity of single cells and sub-populations in their spatial context in native tissue microenvironments.

#0790 Cellular decomposition and metabolic profiling of the tumor microenvironment tumor-stroma interface using high-dimensional spatial proteomics and image analytics.

Arutha Kulasinghe[1], Felicia Roland[2], Michelle Poulin[2], Ritu Mihani[2], Katherine Hales[3], Daniel Winkowski[3]

[1]Frazer Institute, University of Queensland, Woolloongabba, Australia,[2]Quanterix, Marlborough, MA,[3]Visiopharm Corp, Broomfield, CO

Introduction There is an urgent need for the development of better prognostic and predictive biomarkers for cancer immunotherapy across a number of solid cancers. Here we sought to characterise the tumour microevironment (TME) using high-dimensional spatial proteomics paired with advance image analytics to define tumour, stomal and interface regions. We developed custom functional and metabolic content to profile these interface regions to determine activity across transitional zones.

Methods Using high dimensional spatial proteomic profiling (Phenocycler Fusion, Quanterix) with a custom immuno-metabolic panel targeting over 68 proteins, including markers for tumor, stroma, structural components, immune cell types, functional states, and metabolic activity, we characterized cell types, sub-types and metabolic activity across the tumor-stromal interface regions. Custom image analytics, utilizing Visiopharm's analytic pipeline and workflow, enabled precise identification and mapping of spatially distinct tumor and stromal interface regions associated with TME composition. Characterization of cellularity and metabolic activity was further performed through the Phenoplex™ guided workflow.

Results We found intra-tumor and intra-stromal regions were distinct from tumor-interface and stromal-interface regions in terms of TME composition and metabolic activity. Moreover, whilst cell proportions alone were not predictive of clinical benefit, the nuances were in the tumor and immune cell sub-types which were functionally and metabolically characterized. We found a tumor metabolic signature predictive of poorer clinical outcomes and reciprocally high metabolic activity in immune cells at the TME interface associated with benefit from immunotherapy.

Conclusion Taken together, this study highlights the value of high-dimensional spatial proteomics covering functional and metabolic profiling of the TME and the advanced image analytics providing insights into the TME.

#0791 Novel tools for spatial profiling of protein glycosylation in cancer biology.

Shuhui Chen, Erika Leonard, Shamali Roy

Vector Laboratories, Inc., Newark, CA

Glycan modifications play critical roles in cell function in both healthy and diseased states, from controlling proliferation to modulating the immune response. Lectins are glycan-binding proteins that recognize specific glycan structures. Their glycan-specific nature makes them important tools to profile, characterize, and capture the complexity of glycans in biological systems. To explore the complexity of glycan modifications, Vector Laboratories provides Glysite™ Scout Glycan Screening Kits, which are fully integrated kits for the detection of glycan expression in tissue sections. Our curated lectin selection enables the detection of the major glycan motifs including sialylation, fucosylation and galactosylation, for the evaluation of glycan distribution in a target specimen. Here, we established a standard workflow of lectin-integrated tissue immunoassays. Formalin-fixed, paraffin-embedded (FFPE) tissue sections were prepared from a selected panel of normal and cancerous tissues including colon, pancreas, breast, kidney, brain, and lung. Our lectin histochemical analysis revealed tissue-dependent glycopatterns, and our result was aligned with morphological changes observed in disease progression. We then utilized Glysite Explorer in situ PLA Glycan Detection Kit, a novel proximity-based detection technology, to investigate protein-specific glycosylation changes from healthy to diseased tissues. Our findings highlight distinct glycosylation patterns associated with pathological conditions, including cancer, underscoring the relevance of glycosylation in disease mechanisms. In summary, Glysite™ Scout Glycan Screening Kits are easily plugged into day-to-day tissue immunoassays that allow comprehensive screening of N- and O-glycan profiles in various tissue sections. Then Glysite Explorer Kit can be used to explore the glycosylation changes of specific biomarkers in cancer tissues. Altogether, this new data will add to the growing understanding of the impact of protein glycosylation on cancer biology, enriching biomarker discovery and therapeutic targeting.

#0792 A standardized pan-cancer framework for spatial profiling of the tumor microenvironment using multiplex immunofluorescence.

Sidney van der Zande[1], Outi H. J. Hasu[1], Zhiying He[1], Katja E. Valimaki[1], Tuomas Mirtti[2], Antti S. Rannikko[3], Heini J. Lassus[4], Ari P. Ristimaki[2], Pia Osterlund[5], Tero A. Aittokallio[1], Lassi Paavolainen[1], Mikko J. Loukovaara[4], Olli P. Kallioniemi[1], Ralf C. Butzow[4], Teijo S. Pellinen[1]

[1]Institute for Molecular Medicine Finland (FIMM), University of Helsinki, Helsinki, Finland,[2]Department of Pathology, Helsinki University Hospital, Helsinki, Finland,[3]Department of Urology, University of Helsinki, Helsinki, Finland,[4]Department of Obstetrics and Gynecology, University of Helsinki, Helsinki, Finland,[5]Faculty of Medicine and Health Technology, Tampere University Hospital, Tampere, Finland

A growing number of studies have shown the key role of the spatial layout and interactions between cells in the TME in determining patient prognosis and therapy response. While substantial effort has been invested in profiling individual cancers, differences in staining methods and analysis pipelines make it increasingly difficult to study spatial TME patterns in a pan-cancer setting. To address this issue, we developed standardized multiplex immunofluorescence (mIF) staining protocols and computational pipelines to profile TME architecture across tissue microarrays from endometrial, ovarian, breast, prostate, and colorectal carcinomas. Our mIF panels include up to 50 protein targets capturing major immune and stromal populations, epithelial states, and markers of stemness, allowing us to profile the TME in great detail. To achieve high-confidence cell classification, we integrated classical thresholding with pixel-based models and unsupervised clustering to produce a consensus cell-type annotation. Our analyses show that pixel-based and unsupervised clustering methods outperform thresholding by enhanced separation of ambiguous signal and improving reproducibility. Incorporating cellular shape parameters further enhanced the identification of morphologically distinct populations such as fibroblasts and macrophages. We first applied this framework to a gynecological discovery set comprising endometrial and ovarian carcinomas (n > 1600 patients, multifocal sampling). Preliminary analyses indicate that endometrial and endometrioid ovarian carcinomas, both derived from Müllerian epithelium, share similar immune and stromal profiles, whereas ovarian clear cell carcinoma shows a distinct TME composition. In addition, reduced fractions of B cells and increased fractions of dedifferentiated epithelial cells were both strongly associated with recurrence in endometrial carcinoma (two-sided t-test with FDR; both $p < 0.001$). Endometrioid ovarian carcinoma showed similar trends for these features, but no statistically significant associations with recurrence were found ($p = 0.453$ and $p = 0.055$, same order). Neither B-cell fraction nor dedifferentiated epithelial cells showed any association with recurrence in ovarian clear cell carcinoma ($p = 0.339$ and $p = 0.339$, respectively). These findings suggest that the cancer cell of origin may exert a stronger influence on TME composition than the anatomical site of disease. Together, our work will establish a harmonized pan-cancer mIF framework and reveal conserved TME features with clinical relevance. These standardized tools enable cross-cancer comparisons, improve the interpretability of spatial biomarkers, and may guide the development of broadly applicable therapeutic strategies.

#0793 Multiplexed spatial profiling of the tumor microenvironment in syngeneic mouse models using Cell DIVE imaging.

Jeremy Fisher[1], Emily Quann Alonzo[1], Vasundhara Agrawal[2], Sophie Struble[2], Richard A. Heil-Chapdelaine[2], Natasha F. Diaz Granados[2], **Arindam Bose**[2]

[1]Cell Signaling Technology, Danvers, MA,[2]Leica Microsystems, Waltham, MA

Comprehensive spatial and phenotypic characterization of the tumor immune microenvironment (TIME) in preclinical models is essential for understanding mechanisms of immune modulation and resistance. In this study, we employed the Cell DIVE™ multiplex immunofluorescence platform to spatially profile formalin-fixed paraffin-embedded (FFPE) sections from syngeneic mouse tumor models—MC38 (colorectal) and LL/2 (lung)—using a panel of antibodies from Cell Signaling Technology (CST), targeting epithelial, stromal, immune, and checkpoint markers. Multiplexed imaging data were analyzed using Aivia software to enable cell-level segmentation, phenotype classification, and spatial context analysis. We conducted a comprehensive comparison of the TME between the two tumor types, revealing distinct immune and stromal cell compositions, including differential infiltration of cytotoxic cells, regulatory T cells, and macrophage subsets. AI-powered spatial analyses uncovered unique patterns of immune cell localization and checkpoint molecule expression, highlighting potential mechanisms of immune exclusion and exhaustion. Co-localization and proximity analyses further elucidated interactions between immune and tumor cells, offering insights into the immunogenicity of each model. This study demonstrates the utility of multiplexed, spatially resolved immunofluorescence to dissect the complex tumor immune microenvironment in syngeneic mouse models. This approach enables a deeper understanding of tumor immunobiology in preclinical models and provides a foundation for identifying spatial biomarker patterns associated with therapeutic response. The combination of highly validated monoclonal antibody conjugates, Cell DIVE™ multiplexing, and advanced AI-powered image analysis, creates a more powerful and comprehensive tool for preclinical evaluation of immune-oncology (IO) therapeutics.

#0794 Spatial analysis of the DLBCL tumor microenvironment via the novel SignalStar® multiplex immunohistochemistry assay.

Jennifer Ziello[1], Jason Weirather[2], Derek Papalegis[1], Lily Vu[1], Gabriella Spang[1], Sizun Jiang[3], Giorgio Ga. Inghirami[4]

[1]Cell Signaling Technology, Danvers, MA,[2]Elucidate Bio, Inc., Boston, MA,[3]Harvard Medical School, Boston, MA,[4]Weill Cornell Medical College, New York-Presbyterian, New York, NY

The complexity of the immune landscape in Diffuse Large B Cell Lymphoma (DLBCL) tumors underscores the necessity of understanding the interplay between T cell activation and immunosuppression within the tumor microenvironment (TME). Given the heterogeneity of these tumors and the importance of cellular interactions within the TME, there is a pressing need for advanced technologies capable of visualizing multiple biomarkers and cell phenotypes simultaneously. Multiplex immunohistochemistry (mIHC) offers an effective solution for this detailed spatial analysis.

Here, we developed a 20-plex SignalStar multiplex immunohistochemistry (mIHC) panel aimed at profiling T cell activation and suppression states, as well as spatially characterizing tumor, myeloid, and vascular cells within the TME. The resulting images underwent processing using the Elucidate Bio Spatial Analysis pipeline. The images were co-registered and segmented based on DAPI staining and marker-specific classifiers were employed to label cells as either positive or negative for each respective stain. Expression intensities were subsequently normalized and clustered using the Leiden algorithm to assign predominant lineage phenotypes. Through graph-based community detection, higher-order cellular neighborhoods were identified. We also correlate the Signalstar spatial proteomics data to an orthogonal single cell RNA sequencing data. Our analysis revealed six distinct cell neighborhoods with unique spatial organization and cellular composition, consisting of those that were rich in either CD4+ T cells, CD8+ T cells, M2-like macrophages, dendritic cells, tumor cells with immune cell infiltration or tumor cells without immune cell infiltration. Substantial heterogeneity was observed with respect to the cell phenotypes and cell neighborhoods that were present, both inter- and intra-tumorally. While there were no statistically significant differences in the numbers of the various cell neighborhoods that were present, the overall number of M1-like macrophages was found to be significantly higher in complete responders vs. progressors. DLBCL tumors are composed of microenvironments filled with diverse cells of various types, all arranged into distinct neighborhoods. Our findings indicate that the SignalStar mIHC assay, when paired with the Elucidate Bio Spatial Analysis pipeline, serves as an effective means to explore the intricate composition and spatial layout of this complex tumor microenvironment.

#0795 Integrating spatial transcriptomics and Imaging Mass Cytometry™ for multi-omic mapping of hepatocellular carcinoma.

Atefeh Khakpoor[1], **Qanber Raza**[2], Merrin Mary Eapen[1], Dina Kazemi[1], Erin Coll[3], Liang Lim[2], Christina Loh[2], Nick Zabinyakov[2], Ling Qiao[4], Anna Di Bartolomeo[4], Helen McGuire[5], Jacob George[3], Ankur Sharma[1]

[1]Garvan Institute, Sydney, Australia,[2]Standard BioTools, Markham, ON, Canada,[3]University of Sydney, Sydney, Australia,[4]Storr Liver Centre, Sydney, Australia,[5]The University of Sydney, Sydney, Australia

Hepatocellular carcinoma (HCC) is a heterogeneous malignancy, requiring spatially resolved multi-omic approaches to advance therapeutic strategies. Spatial transcriptomics using the Xenium™ platform enables high-throughput mapping of hundreds to thousands of RNA targets within intact tissue architecture. While transcript-level insights provide critical context for understanding gene expression patterns, integrating proteomic data adds a complementary layer that enables direct validation of biomarker expression. Spatial proteomics technologies, such as Imaging Mass Cytometry™ (IMC™), complement transcriptomics by providing high-dimensional protein expression data at subcellular resolution. IMC leverages metal-tagged antibodies and laser ablation to simultaneously quantify over 40 protein markers with 5 orders of magnitude linear dynamic range, surpassing traditional immunohistochemistry and immunofluorescence. We demonstrate the feasibility and biological insights gained from applying IMC to same tissue sections previously processed with Xenium, integrating transcriptomic and proteomic data through computational co-registration. Formalin-fixed, paraffin-embedded HCC tissue sections were profiled using a custom Xenium v1 transcriptomic panel, followed by IMC with a 43-marker immuno-oncology themed antibody panel on the same section. IMC was also performed on serial sections without prior Xenium processing for performance comparison. Data integration was achieved using Xenium Explorer software, which employs a computational co-registration algorithm to align nuclei across modalities, enabling overlay of transcriptomic and proteomic biomarkers for spatial correlation analysis. IMC performed post-Xenium processing generated high-quality data comparable to IMC alone, preserving tumor and immune cell phenotyping capabilities. Both techniques localized macrophages, neutrophils, B cells, cytotoxic T cells, and T helper cells and their activation states within distinct tissue regions. Computational integration of transcriptomic and proteomic datasets revealed subpopulations of immune cells and activation states, as well as discrepancies between RNA and protein localization for several markers, underscoring the importance of multi-modal validation. This integrated approach provided a more nuanced view of HCC microenvironmental complexity. Overall, we demonstrate concurrent application of spatial transcriptomics and proteomics at the cellular level on the same tissue section. This integrated workflow, enabled by computational co-registration, delivers a multidimensional perspective of tumor biology and uncovers spatial relationships between unique cell populations with varying activation states offering novel insights into HCC heterogeneity and informing the development of precision therapeutic strategies.

#0796 Digital spatial profiling reveals immune heterogeneity across tumor and stromal compartments in hepatocellular carcinoma.

Min Qing[1], Qibiao Wu[1], Xuesong Lyu[1], Tao Chen[1], Mingxuan Xia[1], Joshua J. Rusbuldt[2], Denis Smirnov[2], Flora Berisha[2], Longen Zhou[1], Chia-Jui Yen[3]

[1]Johnson & Johnson, Shanghai, China,[2]Johnson & Johnson, Spring House, PA,[3]National Cheng Kung University Hospital, Taiwan, China

Introduction: Hepatocellular Carcinoma (HCC) is one of the most devastating malignancies around the world, especially in East Asia. Despite significant advances in immune checkpoint inhibitors in the past decade, many patients show poor response, highlighting the need to better understand tumor heterogeneity, especially at the spatial level. GeoMx™ Digital Spatial Profiler (DSP) is a spatial biology platform that enables high-plex, in situ profiling of FFPE samples, allowing molecular characterization within distinct tissue compartments while preserving spatial context. In this study, DSP was exploited for immune profiling utilizing FFPE samples from HCC patients.

Methods: A total of 4 immune-related panels were used for DSP protein profiling. Thirty HCC FFPE slides were used, and 341 regions of interest were identified from tumor and tumor stroma tissue for DSP analysis. Four morphology markers (CD45/Vimentin/CK8/18/SYTO83) were selected for Immunofluorescence (IF) staining to guide the regions of interest (ROI) selection for tissue structure and distinct cell types.

Results: DSP analysis revealed distinct immune patterns within HCC tissues. Principal component analysis of immune-related markers stratified regions of samples distinctly by tumor and stroma, highlighting the spatial heterogeneity of immune engagement. Notably, stromal compartments exhibited stronger differential expression of immune activation markers (e.g, CD45), particularly T cell-associated proteins such as CD3, CD4, and CD8 compared to tumor regions. Quantitative analysis demonstrated a strong correlation of CD45 expression measured by IF and DSP regardless of tissue compartments. IF staining confirmed low CD45 expression (<2%) within tumor regions in majority of HCC samples, indicating limited immune cell infiltration. However, a subset of samples still showed relatively higher CD45 expression in either the stroma, tumor, or both compartments, suggesting variable immune engagement across patients. Collectively, these results illustrate diverse patterns of immune infiltration in HCC.

Conclusions: This study highlights the spatial heterogeneity of immune cell infiltration within the tumor microenvironment of HCC. Stratification of samples by tissue origin and the distinct expression of immune activation markers in stromal regions underscore the importance of compartment-specific analysis. The strong concordance between DSP and IF quantification for CD45 expressions supports the robustness of spatial profiling approaches. These findings may inform the development of spatially guided immunotherapeutic strategies.

#0797 Integrating hematoxylin & eosin histology with multiplexed imaging mass cytometry for spatial proteomic profiling of antibody-drug conjugate targeted biomarkers.

Nick Zabinyakov, Qanber Raza, Liang Lim, James Mansfield, Christina Loh

Standard BioTools, Markham, ON, Canada

Hematoxylin and Eosin (H&E) staining remains the cornerstone of histopathology, providing essential morphological context for tissue architecture and disease characterization. However, traditional H&E lacks the ability to deliver comprehensive molecular insights required for precision medicine application. Imaging Mass Cytometry (IMC) addresses this gap by enabling simultaneous detection of 40+ biomarkers at subcellular resolution using metal-tagged antibodies. Unlike fluorescence-based multiplexing, IMC is a quantitative, high-throughput spatial proteomics methodology with a huge (5 orders of magnitude) linear dynamic range, making it a perfect match for ADC work. Applying IMC directly to H&E-processed slides and aligning the resulting images combines the familiarity of histology with the power of spatial proteomics, allowing researchers and pathologists to overlay molecular data on conventional morphology without compromising tissue integrity. We implemented a workflow integrating H&E-stained sections with IMC antibody panels targeting biomarkers relevant to antibody-drug conjugate (ADCs) development. Regions of interest were selected based on histological features, followed by IMC acquisition and computational analysis for cell phenotyping and spatial mapping. Alignment of images and integration of H&E morphology with IMC data enabled spatially resolved correlation of histopathological features with multiplexed protein expression on the same tissue section. Using a computational pipeline, H&E-derived regions of interest were aligned with IMC segmentation maps, achieving high registration accuracy across diverse tissue architectures. IMC uses metal-labeled primary antibodies without amplification and maintains the sensitivity to quantitate the intensity of biomarkers. Quantitative analysis demonstrated the ability to identify and enumerate cells expressing ADC targets (HER2, TROP2, EGFR, etc.) within specific histological contexts, providing insights into spatial patterns of biomarker distribution. Overall, this integrated workflow improved cell-type annotation and spatial interpretation, uncovering clinically relevant microenvironmental heterogeneity not apparent from morphology alone. Integrating IMC with H&E histology provides a powerful platform for ADC development, offering unparalleled capability to link tissue architecture, biomarker expression, and immune contexture and enables the use of archival material for spatial proteomic studies. Clinically, this approach could inform patient stratification, guide ADC selection, and predict therapeutic response by correlating immune infiltration with target expression, ultimately supporting personalized oncology strategies. *For Research Use Only. Not for use in diagnostic procedures.*

#0798 Tumor-associated neutrophil density and cancer cell interaction in microsatellite stable and unstable gastric cancer using multiplex immunofluorescence.

Soo Kyung Nam[1], Seo Hwan Yu[2], Sun Young Ahn[3], Yujun Park[4], Yoonjin Kwak[3], Sujin Oh[5], Kyoung Un Park[5], Hye Seung Lee[1]

[1]Interdisciplinary Program in Cancer Biology, Seoul National University College of Medicine, Seoul, Korea, Republic of,[2]Seoul National University College of Medicine, Seoul, Korea, Republic of,[3]Pathology, Seoul National University Hospital, Seoul, Korea, Republic of,[4]Pathology, CHA Bundang Medical Center, Seongnam, Korea, Republic of,[5]Laboratory Medicine, Seoul National University College of Medicine, Seoul, Korea, Republic of

Purpose: Tumor-associated neutrophils (TANs) play diverse roles in the tumor microenvironment, yet their clinicopathologic and prognostic significance in gastric cancer (GC), particularly the relevance of activated TAN subsets and their spatial interactions with tumor cells, remains unclear. This study aimed to characterize TAN density, activation status, and spatial proximity to tumor cells, with focus on microsatellite instability-high (MSI-H) GC.
Methods: Single immunohistochemistry (sIHC) for CD66b, CD8, HER2, p53 and E-cadherin was performed in 1,060 GCs, together with MSI testing and Epstein-Barr virus (EBV) in situ hybridization. To explore potential sex-related differences in TAN-associated survival, ER sIHC was additionally performed. To define functional TAN subsets, Opal multiplex immunofluorescence (mIF) for cytokeratin (CK), CD66b, and CD177 was conducted in 59 microsatellite-stable (MSS) and 60 MSI-H cases. Immune cell densities were quantified using QuPath (sIHC) and InForm (mIF). Spatial proximity between TANs and CK+ tumor cells was calculated. Survival was assessed by Kaplan-Meier analysis.
Results: A high density of CD66b+ TANs on sIHC was more frequently observed in intestinal-type GC and at lower pT stages (P<0.001). A higher TAN density was correlated with HER2 positivity, membranous E-cadherin expression, EBV positivity, and the MSI-H phenotype (P<0.001). A moderate correlation was found in TAN densities between the tumor center and invasive margin. Patients with a high density of CD66b+ TANs tended to have better overall survival (OS), and combined analysis of central and invasive margin TAN densities indicated an independent prognostic factor (P=0.036). In subgroup analysis, higher TAN density was associated with improved OS in female patients (p<0.001). By mIF, the densities of CD66b+ TANs and CD66b+/CD177+ activated TANs were significantly higher in MSI-H than MSS GC (p<0.01). The distance from GC cell to the nearest CD66b+ TAN or CD66b+/CD177+ activated TAN was significantly shorter in MSI-H GC (p<0.001). TAN density was higher in
areas adjacent to tumor cells and lower in distant regions, with a more pronounced gradient in MSI-H GC. A shorter TAN-tumor distance was associated with better survival. In particular, closer proximity of activated CD66b+/CD177+ TANs to tumor cells was independently associated with improved OS (p=0.041).
Conclusions: The distance between TANs and GC cells was significantly shorter in MSI-H tumors, and a shorter TAN-tumor distance-especially for activated CD66b+/CD177+ TANs-was associated with better overall survival. These findings highlight TAN-tumor spatial proximity as a key prognostic factor and a potential target for future therapeutic strategies in GC.

#0799 Integrated spatial multiomics pipeline for visualizing protein interactions in the tumor microenvironment.

Anushka Dikshit[1], Josh Brownlee[1], Ge-Ah Kim[1], Sonali Deshpande[1], Diane Robirds[2], Anne Hellebust[3]

[1]ACD, a Bio-Techne brand, Newark, CA,[2]Leica Biosystems, Deer Park, IL,[3]ACD, a Bio-Techne brand, Albuquerque, NM

Protein-protein interaction is one of the many mechanisms where individual cells communicate with nearby cells or extracellular matrix to modulate the tissue environment. Visualizing these interactions using a spatial platform can validate known interactions implicated in disease pathology within relevant spatial domains, especially in cancer. We developed the ProximityScope™ assay that can be used with the RNAscope™ Multiomic LS assay to detect protein interactions and their impact on molecular pathways by simultaneously visualizing proteins and RNA on a single tissue section. This workflow is fully automated on Leica Biosystems' BOND RX staining platform. The assay detects one protein-protein interaction and can be combined with five RNA/protein targets simultaneously on the same section. Here, we demonstrate a complete end-to-end workflow by staining FFPE human tonsil tissue samples to detect PD1-PDL1 interactions along with immune cell markers such as PDCD1 RNA, CD68 RNA, CD4 protein, CD8 protein, and PanCK protein. Images were acquired using the Aperio FL 120 by Leica Biosystems.[AD1] Using the HALO® image analysis software from Indica Labs, we performed RNA and protein quantification as well as cell phenotyping. PD-1/PD-L1 interactions were successfully visualized between immune cells and tumor cells. T cells were identified by either CD8 or CD4 protein detection, macrophages were identified with *CD68* RNA, while tumor cells were identified by PanCK protein staining. Interactions appear as punctate dots or dot clusters between two cells or on the cell surface. HALO software identified the PD-1/PD-L1 interaction between adjacent cells. This study demonstrates the importance of having an end-to-end spatial solution for staining, imaging, and quantification of target protein interactions to evaluate protein function. The ProximityScope assay has the potential to study a broad range of protein interactions to evaluate signaling pathways and gain biological insights, assess therapeutic success, or detect PD-1/PD-L1 and related interactions that can serve as biomarkers for patient stratification.For Research Use Only. Not for use in diagnostic procedures.

#0801 Genomic and spatial single-cell profiling reveals BRCA-linked tumor microenvironment signatures in high-grade serous ovarian carcinoma.

Jue young Kim, Hayeon Shin, Yoon Joo Kim, Yookyung Lee, Jae-Hoon Kim

Department of Obstetrics and Gynecology, Gangnam Severance Hospital, Yonsei University College of Medicine, Seoul, Korea, Republic of

Background: High-grade serous ovarian carcinoma (HGSOC) is the most aggressive and lethal subtype of ovarian cancer, accounting for more than 70% of ovarian cancer-related deaths. Because most cases are diagnosed at advanced stages with distant metastasis, early detection and effective treatment strategies remain a major challenge. Although PARP inhibitors benefit patients with BRCA mutations or homologous recombination deficiency (HRD), many still develop therapeutic resistance. This study investigates how BRCA-associated immune activation and tumor microenvironment (TME) features influence treatment outcomes using spatial single-cell transcriptomic profiling.
Methods: A total of 89 HGSOC samples were obtained from the Korea Gynecologic Cancer Bank (KGCB) with comprehensive clinicopathological annotation. Whole genome sequencing (WGS) was performed using tumor samples matched with peripheral blood mononuclear cells (PBMCs) to identify somatic and germline genomic alterations. Tissue microarrays (TMAs) were constructed and analyzed using NanoString's spatial single-cell RNA sequencing platform (Human Discovery Panel, 6,000 genes) to characterize spatial heterogeneity within the TME.
Results: WGS profiling revealed distinct genomic alteration patterns associated with BRCA mutation status, highlighting differences in key cancer-related pathways. Spatial single-cell analysis demonstrated heterogeneous tumor-immune-stromal interactions and identified BRCA-linked TME remodeling patterns. BRCA-mutated patients showed higher chemosensitivity ($p=0.045$) and significantly longer progression-free interval (PFI, $p=0.018$), recurrence-free survival (RFS, $p=0.022$), and overall survival (OS, $p=0.032$) compared with BRCA wild-type patients. Kaplan-Meier analysis confirmed significant OS differences according to BRCA mutation status ($p=0.009$), and chemotherapy resistance strongly affected both RFS and OS ($p=0.000$).
Conclusion: BRCA mutations in HGSOC are strongly associated with enhanced chemosensitivity and improved survival outcomes. Integrated WGS and spatial single-cell analysis revealed BRCA-related genomic features and TME remodeling patterns that shape therapeutic response. These findings highlight the potential of combining BRCA status, genomic profiling, and spatial TME analysis as predictive biomarkers for prognosis and personalized treatment strategies in HGSOC.

#0802 Multi-omic profiling maps the immune multicellular environment of renal cell carcinoma.

Thao Tran[1], Maikel L. Colli[1], Nathan H. Patterson[1], Qanber Raza[2], Liang Lim[2], Lauren Tracey[2], Alice Ly[1], Sanja Bajovic[1], James Mansfield[2], Christina Loh[2], Marc Claesen[1]

[1]Aspect Analytics NV, Genk, Belgium,[2]Standard BioTools, Markham, ON, Canada

Clear cell renal cell carcinoma (ccRCC) is a biologically heterogeneous malignancy shaped by complex tumor–immune–stromal interactions that drive progression and influence therapeutic response. Despite advances in immunotherapy and combination regimens, many patients exhibit intrinsic or acquired resistance, underscoring the need for spatially resolved, multimodal profiling of the tumor microenvironment to elucidate mechanisms of treatment failure and discovery of therapeutic targets.

To this end, we integrate Imaging Mass Cytometry (IMC) with Spatial Transcriptomics (ST) to enable simultaneous *in situ* phenotyping of protein and transcript expression within intact tissue architecture. IMC using the Hyperion XTi delivers high-resolution protein mapping across lymphoid, myeloid, and stromal compartments, including extracellular matrix components such as collagen, fibronectin, and αSMA that define desmoplastic barriers and immune-excluded niches. Complementary ST with the Xenium immune-enriched 5000-gene panel reveals transcriptional programs related to T-cell exhaustion, cytotoxicity, antigen presentation, interferon signaling, and stress responses, capturing functional states not readily discernible at the protein level.

The combination of per-cell spatial proteomic and transcriptomic data improves the understanding of the tumor-immune microenvironment. A central advance of this study is the direct correspondence established between protein-defined multicellular embeddings and transcriptomics-derived cellular states. IMC protein markers delineate the structural organization of cell neighborhoods consistently across tissue sections, while spatial transcriptomics assigns the functional programs operating within each niche and show how variable those states are. This integration reveals how specific transcriptional states concentrate within distinct structured microenvironments, including CD8+ T-cell rich inflammatory zones and tumor-stromal cells interface, co-localized with macrophage subpopulations. By anchoring gene expression states to well-resolved protein architectures, the analysis exposes the spatially organized mechanisms through which ccRCC shapes immune responses and promotes therapeutic resistance. This multimodal framework yields a more mechanistic understanding of tumor–immune interactions and enables the identification of spatially grounded biomarkers and intervention points that are not apparent from single-modality profiling.

Combining ST and IMC unlocks a powerful framework for deciphering tumor complexity. By linking molecular expression to spatial context through integrative computational analysis, this strategy has the potential to identify novel biomarkers, refine therapeutic targets, and transform precision oncology.

For Research Use Only. Not for use in diagnostic procedures.

#0803 A spatial profiling approach to evaluating the prognostic impact of heterogeneity in the triple-negative breast cancer immune microenvironment.

Prerana Sensharma[1], Huidan Zuo[2], Melanie Dawe[3], Megan Hopkins[4], Zeynep Baskurt[5], Osvaldo Espin-Garcia[5], Philippe L. Bedard[6], Melanie Spears[4], Susan J. Done[2]

[1]Medical Biophysics, University of Toronto, Toronto, ON, Canada,[2]Laboratory Medicine and Pathobiology, University of Toronto, Toronto, ON, Canada,[3]Princess Margaret Cancer Center, Toronto, ON, Canada,[4]Ontario Institute for Cancer Research, Toronto, ON, Canada,[5]Department of Biostatistics, Princess Margaret Cancer Center, Toronto, ON, Canada,[6]UHN-Toronto General Hospital, Toronto, ON, Canada

Triple-negative breast cancer (TNBC), the breast cancer subtype defined by the absence of hormone receptors and no amplified HER2 receptors, is the most aggressive breast cancer subtype. Targeted treatment remains a challenge with TNBC. Non-targeted chemotherapy regimens have been the longstanding treatment modality, recently supplemented by immune checkpoint inhibitors (ICIs) targeting the PD-1/PDL1 pathway. TNBC's high tumor mutational burden, PD-1 expression, and immunogenicity make it a good candidate for immunotherapy. However, further studies are needed to determine the individuals that benefit most from this treatment. Factors like the spatial patterns of immune cell infiltration, immune-tumour cell and immune-immune cell relationships impact the immune microenvironment's anti-tumour response and ICI response. The high-plex spatial analysis of archival patient tissue samples—an abundant but underutilised resource for tumor characterization—has remained a challenge. However, using the GeoMx Digital Spatial Profiler (DSP), the spatial immune heterogeneity of 40 immune markers were quantified in a cohort of archival treatment-naïve TNBC tumours
(n=140). The heterogeneity of 40 immune markers identifying immune cell lineages and sub lineages, activation and exhaustion states was quantified across separate stromal spatial regions of immune infiltration (n=486 from 140 patients). Tumours with overall low immune cell infiltration were significantly associated with higher spatial immune heterogeneity. Notably, low immune infiltration was also associated with a significantly higher spatial immune heterogeneity and total expression of multiple immunosuppressive markers, some of which are ICI targets This suggests that immunosuppression is spatially localized in stromal niches, which would impact immunotherapy response. High spatial immune heterogeneity was also associated with a trend of poorer patient survival.

#0804 Distinct cellular phenotypes and spatial neighborhoods constitute the heterogeneous microenvironment of desmoplastic small round cell tumor.

Kevin A. Murgas[1], Jiaqian Fan[1], Diana Shamsutdinova[2], Khalida Wani[2], Davis R. Ingram[2], Alexander J. Lazar[2], Danh D. Truong[1], Joseph A. Ludwig[1]

[1]Sarcoma Medical Oncology, MD Anderson Cancer Center, Houston, TX,[2]Anatomical Pathology, MD Anderson Cancer Center, Houston, TX

Desmoplastic Small Round Cell Tumor (DSRCT) is an ultra-rare, aggressive sarcoma primarily affecting young adults. Characterized by a pathognomonic *EWSR1::WT1* gene fusion, DSRCT typically presents with extensive peritoneal metastasis and has a 5-year overall survival rate of 15-25%. Histologically, these tumors exhibit marked peritumoral desmoplasia and minimal immune infiltrate ("immune-cold"). However, substantial heterogeneity among and within tumors has hindered the identification of secondary molecular mechanisms and the discovery of novel therapeutic targets.

We constructed a first-of-its-kind DSRCT tissue microarray (TMA), comprising over 260 specimens from 63 patients spanning 13 years. We applied sequential multiplexed immunofluorescence imaging using a 20-antibody panel (selected based on prior studies) to map tumor, stroma, and immune cell components simultaneously. Our image analysis pipeline utilized tissue and cell segmentation to extract proteomic expression data from nuclear and cytoplasmic compartments of each cell. We applied Harmony batch correction and Leiden clustering to assign putative cell identities based on multi-marker expression.

Our analysis of over 800,000 cells revealed significant inter- and intra-tumoral heterogeneity. We observed a variety of tumor nest morphologies, including well-circumscribed and trabecular architectures, as well as a range of stromal densities. We observed distinct marker expression phenotypes, with some cores dominated by AR-positive, epithelial-like (Pan-Keratin+) cells, while others display prominent neural markers (NSE+/SYP+). Estimated TMA core compositions quantitatively confirmed a range of tumor phenotypes and highlighted variable stromal predominance and a sparse immune infiltrate. Spatial analysis revealed distinct cellular neighborhood patterns and spatial arrangements among the tumor, stromal, and immune components. Finally, we correlated spatial signatures with clinical outcomes.

Our work provides the first comprehensive spatial proteomic atlas of DSRCT at a single-cell resolution using a TMA. This foundational resource aims to elucidate the complex cellular environment of DSRCT, uncover novel biological insights into tumor-driving mechanisms, and ultimately identify new therapeutic vulnerabilities in DSRCT. Ongoing work will incorporate spatial transcriptomics to augment cell phenotyping and identify signalling pathways implicated in the tumor and microenvironment.

#0805 Fluorescence-guided multi-sampling and spatial multi-omics reveal functional lipid vulnerabilities in glioblastoma.

Adele-Asia Ponzoni[1], Evangelos Liapis[1], Lea Anne T. Maristela[1], Elizabeth E. Ginalis[2], Linda Szymanski[3], Kar Fai Chow[4], Kangmin Lee[5], George J. Kaptain[5], Claire L. Carter[6]

[1]Center for Discovery and Innovation, Hackensack Meridian Health, Nutley, NJ,[2]Department of Neurosurgery, Rutgers New Jersey Medical School, Newark, NJ,[3]Department of Pathology, Hackensack University Medical Center, Hackensack, NJ,[4]Biorepository, Hackensack University Medical Center, Hackensack, NJ,[5]Department of Neurosurgery, Hackensack University Medical Center, Hackensack, NJ,[6]Department of Pathology, Hackensack Meridian School of Medicine, Nutley, NJ

Background: Glioblastoma (GB) is the most common and aggressive primary brain tumor in adults. Tumor recurrence occurs in most cases, typically within 2 cm of the resection margin, despite chemo and radiotherapy. This highly invasive nature and the marked heterogeneity of the tumor microenvironment make it challenging to treat. Fluorescence-guided multiple sampling of patient samples is being used to study intra-tumor heterogeneity. In this study we combined mass spectrometry imaging (MSI) with multiplex immunofluorescence (mIF) and histology to identify new therapeutic vulnerabilities based on spatial tumor biology. We developed a same slide workflow applying all 3 technologies to the same section to identify functional lipids that can be manipulated as less toxic therapeutic options.
Methods: Twenty GB patients underwent craniotomies and tumor tissue was surgically resected from multiple different fluorescing and non-fluorescing brain locations. MSI was carried out using a Bruker Solarix FTICR mass spectrometer, the same section then underwent mIF for cell and organelle phenotyping, followed by H&E-staining for histopathology. The Leica Stellaris 5 and GT 450 slide scanner were used for confocal and histological image acquisition, respectively. Data analysis was carried out using the SciLs lab, Leica LAS X and Imaris software. Processed mIF, H&E and MSI data were integrated in SciLS Lab for multimodal analysis on the same section.
Results: Integration of spatial lipidomic, proteomics and histopathology identified functional lipids that correlated with different pathological presentations and cellular neighborhoods within each sample. We focused on two multifunctional lipids: cardiolipins (CLs) and gangliosides (GGs). CLs are unique mitochondrial lipids that contain four acyl chains, whose structure is known to regulate mitochondrial function. In GB, we detected differential accumulation based upon fatty acid residue composition, which correlated with mitochondrial numbers and phenotype. Peritumoral regions showed interconnected mitochondria, while tumor regions with vascular proliferations displayed abundant fragmented mitochondria, indicative of altered metabolism and dynamics. GGs are involved in cell-cell interaction, immune modulation, and tumor growth. Anti-GD2 immunotherapy is FDA-approved for neuroblastoma and in clinical trials for other solid tumors. In GB, we identified over 30 GGs species across the GM1-3, GD1-3 and GT1,3 series, which segmented with different pathological regions based on acyl chain and sialic acid composition.
Conclusions: We optimized a same section spatial multi-omics workflow that identified tumor-specific lipid pathways as therapeutic vulnerabilities in glioblastoma.
Ongoing studies are using patient-matched 3D models to determine the functional relevance of these findings and for drug screening studies.

#0806 Tumor microenvironment of ampulla of Vater cancer reveals distinct spatial niche of CAF, TIL, and TAM and their correlation with clinicopathologic features.

Yesul Jeong[1], Se Jun Park[2], Sung Hak Lee*[3], Younghoon Kim*[3]

[1]Department of Hospital Pathology, St. Vincent's Hospital, College of Medicine, The Catholic University of Korea, Seoul, Korea, Republic of,[2]Division of Medical Oncology, Department of Internal Medicine, Seoul St. Mary's Hospital, Seoul, Korea, Republic of,[3]Department of Hospital Pathology, Seoul St. Mary's Hospital, Seoul, Korea, Republic of

Background:
While the individual roles of cancer-associated fibroblasts (CAFs), tumor-infiltrating lymphocytes (TILs), and tumor-associated macrophages (TAMs) in the tumor microenvironment (TME) of ampulla of Vater (AoV) carcinomas are recognized, a detailed understanding of their collective interplay and its correlation with clinicopathologic features and patient survival is still lacking.
Methods:
A retrospective cohort of 87 patients with resected stage IB-III AoV adenocarcinoma (Seoul St. Mary's Hospital between 2007 and 2021) was selected. TMAs (2-mm cores) were constructed and immunostained for tumor cell markers (EGFR, HER2, and c-MET), TME markers (CD3, CD8, FOXP3, CD68, CD163, alpha-SMA, FAP, PDPN, and POSTN), and Masson's Trichrome (MT) staining for fibrosis. Multiplex IF was performed for high-plex spatial proteomic analysis (CellScape). All slides were digitized and analyzed to quantify the immune cell densities (cells/mm2), mesenchymal marker H-scores, and spatial relationships (cell-cell distance) to define the TME niches. The primary endpoints analyzed using R were disease-free survival (DFS) and overall survival (OS). A two-sided p-value of <0.05 was considered to be statistically significant.
Results:
TAM markers showed a significant positive correlation with T-cell markers but a negative association with CAF markers. FAP and POSTN were positively correlated with each other but negatively correlated with PDPN and IL6. ACTA2 and IL6 were negatively correlated with most other markers, while being positively correlated with each other. Univariate Cox regression for DFS identified high EGFR (HR=6.89, 95% CI: 2.94-16.20, p=0.026), FAP (HR=2.21, 95% CI: 1.27-3.86, p=0.027), and high fibrosis (MT) (HR=2.49, 95% CI: 1.42-4.37, p=0.008) as unfavorable prognostic factors. CD3 and POSTN showed a trend towards prognostic significance for OS (p=0.07 and p=0.06, respectively). In multiplex IF, spatial analysis revealed that TAMs (CD68 and CD163) were located closest to the tumor cells, followed sequentially by CAF markers (vimentin and SMA), Collagen IV, and TIL markers, which were the most distant.
Conclusions:
Our findings demonstrate that TME components in AoV carcinoma form distinct spatial niches, characterized by TAMs proximal to tumor cells and TILs in the distal region. This specific architecture, especially when dominated by high FAP and fibrosis, is significantly associated with poor survival, highlighting the importance of spatial TME analysis as a critical prognostic tool.

#0807 Integrated transcriptomic and proteomic characterization of the lung tumor microenvironment using BD®OMICS-One-Protein-Panels for CITE-seq.

Samuel X. Shi[1], Cynthia Sakofsky[2], Hye-won Song[1], Manish Thakran[2], Tamiyo Kobayashi[3], Aruna Ayer[2]

[1]BD Biosciences, San Diego, CA,[2]BD Biosciences, Milpitas, CA,[3]BD Biosciences, Chiba, Japan

The tumor microenvironment (TME) is a heterogeneous and continuously evolving system. It is composed of malignant cells, numerous infiltrating immune cells, stromal cells, blood vessels, and extracellular matrix. The interactions of tumor and non-tumor cells produce an immune-reactive milieu, altering cellular phenotypes and function, thus contributing to tumor growth and progression or antitumor immunity. Profiling the components and alterations in the TME at high resolution is crucial to identify factors influencing cancer progression or evaluating the efficacy of immunotherapies. Advancements of single cell multiomics techniques provide powerful means to scrutinize the tumor and TME at high resolution, shedding light on discrete cell subsets and their potential functions. Cellular Indexing of Transcriptomes and Epitopes by Sequencing (CITE-seq) enables concurrent single-cell RNA sequencing alongside surface protein profiling by using oligonucleotide-tagged antibodies. By combining proteomic and transcriptomic data from the same cell, CITE-seq is an especially powerful approach for phenotyping discrete cell populations, especially suitable for the TME.
Here we applied CITE-seq to clinically relevant human lung cancer samples. A single cel suspension was obtained with BD Horizon™ Dri Tumor & Tissue Dissociation Reagent and then frozen with BD®OG-Cryopreservation Buffer, a non-cross-linking buffer. At another location, CITE-seq was conducted on the samples with the BD OMICS-One™ WTA Next Assay as well as the BD®OMICS-One-Protein-Panels, which are lyophilized and pre-titrated oligonucleotide-tagged antibody panels. Non-supervised clustering of transcriptomic and proteomic data revealed 12 major cell clusters, including infiltrating lymphocytes (TILs), resident and infiltrating immune cells, as well as non-immune intrinsic tumor cells. Over 50 protein epitopes were detected and used to identify tumor intrinsic cells with their expression of well published protein signatures of non-small cell lung cancer. Differential gene and protein expression profiles distinguish distinct tissue-resident alveolar-macrophages from infiltrating hematogenous macrophages. Moreover, T cell gene sets of naive, activation/stimulation, and exhaustion states were used to identify the functional heterogeneity of TILs. We successfully detected over fifty epitopes in this sample, enabling the identification of cancer specific cellular states, varied immune functions and potential interactions with other cells, when integrated with transcriptomic data. We demonstrate an end-to-end workflow from sample collection, storage, single-cell capture, sequencing, and analysis to characterize TME heterogeneity and further understand tumor biology.

#0808 Single cell spatial multiomics of TCR and BCR repertoires using CosMx® SMI to characterize immune cell dynamics in PBMCs and tumors.

Margaret L. Hoang, Rachel Liu, Dan McGuire, Ashley Heck, Kimberly Young, Megan Vandenberg, Claire Williams, Martin Shelton, Prajan Divakar, Patrick Danaher, Erin Piazza, Joseph M. Beechem

Research and Development, Bruker Spatial Biology, Seattle, WA

Immune cell dynamics shape tumor responses to therapy. Peripheral blood mononuclear cells (PBMCs) offer a systemic view of adaptive immunity, yet conventional immune sequencing lacks the spatial resolution to contextualize these findings within tissue architecture. High resolution spatial mapping of tumor-infiltrating lymphocyte (TILs) reveals cell-to-cell interactions, illustrating how immune cells engage with tumor cells and the tumor microenvironment (TME) to influence immunotherapeutic outcomes.We present a spatial multiomics strategy using the CosMx Spatial Molecular Imaging (SMI) platform to simultaneously profile T-cell receptor (TCR) and B-cell receptor (BCR) repertoires within PBMCs and tumor tissues. Immune profiling incorporated the CosMx TCR Add-on panel covering V, J, and constant segments of α, β, γ, and δ chains, along with BCR heavy chain V and constant region. These assays were integrated with CosMx Whole Transcriptome (WTX) and the Human Immuno-Oncology 64-plex protein panel for comprehensive immune cell characterization in PBMCs. High-resolution subcellular CosMx SMI imaging of tumor FFPE sections, combined with advanced computational pipelines, enabled single cell spatial mapping of TILs, capturing TCR/BCR clonotype distributions and immune cell interactions with tumor cells and the extracellular matrix (ECM) components including cancer-associated fibroblasts (CAFs), fibronectin (FN1), α-smooth muscle actin (α-SMA).We uncovered distinct patterns of T- and B-cell phenotypes across PBMCs and tumors, including multiomics signatures of activation, exhaustion, and cytokine signaling. Spatial context revealed immune niches enriched for T and B cells, as well as regions of TIL exclusion associated with immunosuppressive ECM signals. By combining spatial multiomics with immune repertoire profiling, this approach uncovers critical immune dynamics across systemic and tumor compartments, informing biomarker discovery and immunotherapy strategies.

#0809 Spatially resolved multiomics profiling of glioblastoma reveals molecular signatures of neuropathology and immuno-oncology architecture using CosMx SMI.

Yi Cui, Claire Williams, Chia-Ying Lee, Chi Phan, Sierra Mckinzie, Shanshan He, Ashley Heck, Kimberley Young, Lidan Wu, John Lyssand, PRAJAN DIVAKAR, Joseph M. Beechem

Bruker Spatial Biology, Seattle, WA

Glioblastoma (GBM) is a highly heterogeneous and aggressive brain tumor with limited therapeutic success, underscoring the need for advanced approaches to decode its complex molecular landscape. Here, we employed the CosMx® Spatial Molecular Imager to perform same-cell spatial multiomics profiling on serial sections from a human GBM tissue block, integrating the whole-transcriptome RNA panel (~19,000 genes) with two high-plex protein panels encompassing 64 neuropathology or immuno-oncology markers. This comprehensive dataset enables correlative mapping of transcriptomic and proteomic features across tumor and peri-tumoral regions. We identified five GBM tumor cell subtypes - astrocyte-like, OPC-like, mesenchymal-like, stem-like, and proliferating cells - each exhibiting distinct spatial localization and transcriptional signatures. Concurrent protein profiling uncovered regionally enriched phospho-Tau variants (e.g., p-Tau S214, S396, S404), whose accumulation marked hypoxic and epithelial-mesenchymal transition (EMT) active tumor microenvironments. Spatial regression analyses linked elevated neighborhood p-Tau scores to coordinated upregulation of hypoxia-responsive genes (e.g., HIF1A, VEGFA) and metabolic stress pathways, revealing a localized molecular response to cellular stress. Integration of the immuno-oncology protein panel highlighted spatially restricted immune checkpoint expression, including PD-L1, B7-H3, and TIM-3, delineating immune-evasive niches within distinct tumor neighborhoods. Tumor niches driven by divergent subtype GBM cells adopted unique immune evasion strategies, suggesting microenvironment-specific mechanisms of immune suppression. Overall, this study demonstrates the power of spatially resolved, same-cell multiomics to dissect GBM's transcriptional and proteomic heterogeneity at unprecedented resolution. The findings establish a mechanistic link between phospho-Tau-associated stress adaptation, metabolic remodeling, and immune modulation in GBM. This scalable framework offers a blueprint for future multi-sample spatial oncology studies aimed at uncovering therapeutic vulnerabilities, stratifying tumors by microenvironmental features, and identifying biomarkers predictive of treatment response.

#0810 Multi-omic spatial analysis reveals a distinct pattern of cellular neighborhood in gastric cancer.

Takashi Semba, Huaitao Wang, Atsuko Yonemura, Yilin Tong, Takatsugu Ishimoto

Japanese Foundation for Cancer Research, Tokyo, Japan

The tumor microenvironment (TME) consists of diverse cells, and recent studies suggest that their spatial relationships may be crucial for cellular function. However, the spatial organization of the gastric cancer (GC) TME remains poorly understood. In this study, we performed spatial analysis of the GC TME using multiplex immunohistochemistry (IHC) and spatial transcriptomics on paraffin blocks from 10 advanced gastric cancer cases. From more than 30-plex IHC images obtained using the RePROBE method, which we recently developed, we annotated each cell as fibroblasts, immune cells, etc., based on marker expression levels. We then performed cellular neighborhood (CN) analysis based on the annotated cell location information. This resulted in the identification of eight distinct CN meta-clusters. Furthermore, spatial transcriptomics analysis revealed the intercellular interactions occurring within spots. For example, an intercellular communication analysis based on a ligand-receptor database showed that within the CN primarily composed of fibroblasts, signals related to collagen and the extracellular matrix were intensely active. We also identified the transforming growth factor beta (TGF-β) and mitogen-activated protein kinase (MAPK) pathways as the driving pathways for this activity. Moreover, when we scored gastric cancer cases from The Cancer Genome Atlas cohort using gene signatures derived from differentially expressed genes in each CN, we found that cases with high scores for the fibroblast-dominant CN showed significantly poorer prognosis. In addition, graph-based cell network analysis revealed that poor lymphocyte network formation was associated with fewer progenitor-like exhausted CD8 T cells, and fibrotic TME may inhibit the formation of lymphocyte networks. These results highlight the immunosuppressive role of fibrotic TME and its potential as a therapeutic target.

#0811 Novel tyramide signal amplification dyes optimized for the detection of IO markers and four-plex detection of heterogeneously expressed targets.

Marco T. Pinheiro[1], Paul Wood[1], Sean Goggins[1], Henry Lamparski[2], John Donaldson[2], Grant Esomonu[2], Renzo Adilardi[2], Emerald Doolittle[2], Rose Delvillar[2], Hannah Maple[1]

[1]Bio-Techne Corporation, Bristol, United Kingdom,[2]Advanced Cell Diagnostics, Newark, CA

Spatial biology techniques such as RNAscope™ and multi-omics in situ hybridization (ISH) offer critical insights into tumor biology and the tumor microenvironment by enabling spatially resolved gene expression analysis. However, conventional ISH methods often lack the sensitivity required to detect low-abundance transcripts, which can hold key mechanistic, prognostic, and therapeutic significance. In this study, we present an enhanced and optimised ISH approach that integrates a new specifically designed range of fluorophores for tyramide signal amplification (TSA) with RNAscope™ Multiplex Assay probes to improve the detection of immuno-oncology (IO)-related targets. These two new reagents targeted at 620nm and 690nm wavelengths increase the number of assessable targets and enable robust four-plex detection of heterogeneously expressed transcripts. Our findings demonstrate that the new bright TSA reagents significantly increase the sensitivity and dynamic range of transcript and protein detection, facilitating the reliable identification of targets across a spectrum of expression levels. The newly developed four-plex dye system further expands upon multiplexing capabilities, supporting comprehensive spatial profiling in complex tumor tissues.

#0812 Spatial architecture of head and neck squamous cell carcinoma (SCCHN): An IMMUcan/EORTC analysis.

Lucas Michon[1], Athenais van der Elst[2], Daniel Herrero-Saboya[3], Marie Morfouace[4], Preethi Devanand[5], Robin Liechti[6], Daniel Schulz[7], Maya Persoons[1], Sylvie Rusakiewicz[5], Nils Eling[8], Paul-Antoine Nicolas[3], Stephanie Renaud-Tissot[5], Bernd Bodenmiller[9], Henoch Hong[10], Rachel Galot[11], Paolo bossi[12], Julio Oliveira[13], Florian Estrade[14], Caroline Even[15], Sophie E. Lucas[16], Loredana Martignetti[3], Celine Lefebvre[17], jean-pascal Machiels[11], Pierre Saintigny[1]

[1]Ctr. Leon Berard, Lyon, France,[2]Institut de Recherche Clinique et Experimentale, Universite catholique de Louvain (UCLouvain), Brussels, Belgium,[3]Institut Curie, Paris, France,[4]Marie Morfouace (Individual), Villejuif, France,[5]Centre Hospitalier Universitaire Vaudois, Lausanne, Switzerland,[6]SIB Swiss Institute of Bioinformatics, Lausanne, Switzerland,[7]ETH Zurich, Switzerland,[8]Department of Quantitative Biomedicine, University of Zurich, Zurich, Switzerland,[9]University of Zurich, Zurich, Switzerland,[10]Merck KGaA, Darmstadt, Germany,[11]Universite catholique de Louvain, Brussels, Belgium,[12]Humanitas University,[13]Instituto Portugues de Oncologia de Porto Franscisco Gentil, Porto, Portugal,[14]Centre Eugene Marquis, Rennes, France,[15]Gustave Roussy, Villejuif, France,[16]Catholic University of Louvain, Brussels, Belgium,[17]Servier Research & Development, Saclay, France

Background: The association of spatial architecture of SCCHN with clinical and molecular characteristics is poorly understood.
Methods: 253 recurrent/metastatic (R/M) SCCHN, including 77 pre-immunotherapy (IO) samples, were analyzed by imaging mass cytometry to study cancer cells and 13 immune cell types (PMID **40930089)**. Global cell densities (cellD, n/mm^2) and cellular neighborhoods (CN) were analyzed. Local cellD (degree of immune infiltration/exclusion within cancer cells) and cell interaction coefficients between pair-wise phenotypes, both independent of global cellD, were computed. Weighted correlation network analysis was used to detect modules of cell interaction coefficients. TLS and cancer cells states [hypoxic, cell cycling, EMT, β2-microglobulin (β2m) loss] were explored. Data were correlated with IO primary vs. secondary resistance (R), HPV status, survival, DNA and RNA profiles.
Results: 8 CN were identified (pure cancer cells, internal and external (cancer/stroma) interfaces, aggregation of plasma cells, neutrophils (PMN), macrophages/mural cells, T-cells and macrophages/mural/T-cells). HPV+ tumors had decreased external interface. Refractory HNSCC had decreased interfaces and lower DC infiltration. Cancer cells were increasingly hypoxic or had decreasing β2m expression and decreasing EMT in external interface vs. internal interface vs. pure cancer cells CNs. Overall, cancer cell states had profound impact by either increasing (cycling cancer cells) or decreasing (hypoxic cancer cells) immune cells infiltration. We identified 3 clusters of SCCHN: C1 (45%) had high global immune cellD but low local cellD; C2 (40%) was desertic; C3 (15%) was highly infiltrated (high local cellD) and had the best survival in IO-treated pts. RNA-based 'Classical' SCCHN were almost exclusively C2. C3 was enriched in extracellular matrix organization, immune cell and migration. Specific TLS CN included B compartment, germinal center and plasma aggregation. HPV+ tumors had increased B compartment but decreased plasma aggregation. All 3 TLS CN were decreased in refractory SCCHN and in primary vs. secondary R. In IO-treated pts, TLS presence improved outcome and the closer TLS were to cancer cells, the better was the outcome. While the interaction between PMN and immune cells was associated with worse outcome, PMN infiltrating cancer cells was associated with improved survival together with T-cells interacting with cancer cells or with HLADR, MacCD163 and mural cells. Finally, mutations were generally associated with more exclusion of immune to cancer cells e.g. T-CD8 and PMN were more excluded in SCCHN mutated for RB1 and FAT4-PTPRT respectively; and BAP1 and HRAS mutations had exclusion of MacCD163-NK-mural-HLADR-plasma and B cells respectively.
Conclusion: we provide a comprehensive description and clinical/molecular correlatives of the spatial architecture of SCCHN.

#0813 Linking tumor-infiltrating immune cells from tissue and peritoneal cytology to molecular markers in endometrial cancer.

Seungmee Lee[1], Jin-Young Kim[2], Shin-Wha Lee[3], Eun Ji Nam[4], Ji Hae Seo[5], Sojin Shin[1]

[1]Gynecologic Oncology, Keimyung University School of Medicine, Daegu, Korea, Republic of,[2]Division of Hematology/Oncology, Department of Internal Medicine, Keimyung University School of Medicine, Daegu, Korea, Republic of,[3]Asan Medical Center, University of Ulsan, Seoul, Korea, Republic of,[4]Yonsei University College of Medicine, Seoul, Korea, Republic of,[5]Department of Biochemistry, Keimyung University School of Medicine, Daegu, Korea, Republic of

Background

The composition of tumor-infiltrating lymphocytes (TILs) in endometrial cancer may be linked to both clinicopathologic factors and underlying molecular alterations. We sought to characterize TIL subsets recovered from fresh tumor tissue and peritoneal washing cytology and to determine how these immune profiles relate to routinely used immunohistochemical markers.

Methods

Fresh surgical specimens and peritoneal washings were obtained from patients with endometrial cancer who provided informed consent. Mononuclear cells were isolated and analyzed by flow cytometry to quantify $CD3^{-}CD19^{+}$ B cells, $CD3^{-}CD16^{+}CD56^{+}$ natural killer (NK) cells, $CD4^{+}CD25^{+}$ regulatory T cells (Tregs), and $CD3^{+}CD8^{+}$ cytotoxic T cells. These populations were compared according to histopathologic features and immunohistochemical results, including lymphovascular space invasion (LVSI), PD-L1, estrogen receptor (ER), p53, HER2, mismatch repair proteins (MLH1, MSH2, MSH6, PMS2), and microsatellite instability (MSI) status.

Results

Sixty immune profiles derived from endometrial cancer specimens were evaluable. Higher proportions of $CD3^{-}CD19^{+}$ B cells were observed in LVSI-positive tumors, whereas ER-positive tumors showed lower levels of this subset (both $p<0.05$). $CD3^{-}CD16^{+}CD56^{+}$ NK cells were more prevalent in cases with deficient mismatch repair (dMMR). $CD4^{+}CD25^{+}$ Tregs were reduced in ER-positive tumors ($p<0.05$). $CD3^{+}CD8^{+}$ cytotoxic T cells were less frequent in HER2-positive tumors but increased in dMMR cases. No additional significant associations were detected between immune subsets and the other immunohistochemical markers examined.

Conclusions

Immune cell profiles obtained from endometrial tumor tissue and peritoneal washing cytology appear to capture key clinicopathologic and molecular features, particularly LVSI, ER, HER2, and mismatch repair status. Validation in larger cohorts with integrated oncologic outcome data is needed to clarify the prognostic and potential predictive relevance of these immune signatures.

#0814 Lymphatic exudate is a novel source of tumor-associated immune cells.

Seka Lazare[1], Michael A. Harmon[1], Ashley Tellis[1], Zachary Costliow[1], Zhuosheng Gu[1], Adam Benson[1], Samuel Espinoza[1], Abbey Crittenden[1], Megan Rivera[1], Michael Abern[2], Sunil Patel[3], Kamal Pohar[4], Gautum Agarwal[5], Rohann Correa[6], Wendy Winckler[1]

[1]Droplet Biosciences, Inc., Cambridge, MA,[2]Duke University Department of Urology and Duke Cancer Institute, Durham, NC,[3]Johns Hopkins, Caltimore, MD,[4]Ohio State University, Columbus, OH,[5]Mercy Clinic, St. Louis, MO,[6]London Health Sciences Centre, London, ON, Canada

Autologous tumor-infiltrating lymphocyte (TIL) therapy has demonstrated efficacy in multiple solid tumor types, but therapy requires surgery and extensive manufacturing. Lymphatic exudate (“lymph”) is routinely collected from surgical drains following tumor resection. Although usually discarded, we have shown that this novel proximal biofluid is rich in ctDNA and prognostic of recurrence in head and neck squamous carcinoma (HNSCC) patients. Here, we investigate lymph as a novel, accessible source of tumor-associated lymphocytes.

Lymph was collected 24 hours post-surgery from 11 HPV- HNSCC and 14 bladder cancer (BLC) patients in K_2EDTA blood collection tubes. Cells were isolated from lymph and immune populations were characterized by flow cytometry. Bulk T-cell receptor b (TCR-b) sequencing was performed on 17 patient sets with matched tumor (11 HNSCC, 6 BLC). Two BLC patients failed sequencing QC. TCR repertoires were compared between tumor and lymph and Simpsons clonality was used to assess clonal diversity.

Lymph cells displayed high viability (>85%). Immune subpopulations are described in Table 1. Both $CD4^+$ and $CD8^+$ T cells were detected with variable CD4/CD8 ratios (1.05-4.9 [HNSCC] and 0.11-8.869 [BLC]). Bulk TCR-b analysis showed substantial clonal overlap between lymph and tumor (HNSCC mean 13.1% [0-33.1%] and BLC 9.1% [0.3-23.8%]), exceeding typical overlap described for peripheral blood. Lymph TCRs exhibited clonal expansion (Simpsons clonality means: HNSCC = 0.58% and BLC = 0.64%). Based on surgical drainage rates (median 1-3.5 mL/hour) and median number of CD3+ cells per mL, an estimated 4.8×10^6 - 1.68×10^7 T cells could be recovered daily from drains.

Table 1. Mean cell frequencies by indication measured by FACS; immune subsets expressed as % of CD45

	HNSCC	**BLC**
CD45+	95.36%	85.85%
T cells	3.92%	15.08%
NKT cells	0.78%	2.63%
B cells	0.55%	3.60%
Monocytes	0.37%	7.90%

Post-surgical lymph contains viable immune populations with substantial TCR overlap with tumor infiltrating lymphocytes. Lymph could enable the isolation of tumor-associated T cells without the challenges around metastasectomy. Lymph T cells may represent a novel, abundant, low cost, and easily accessible source for adoptive cell therapy.

#0815 Simultaneous spatial transcriptome and epigenome profiling in fresh frozen and FFPE tissues with spatial CoPro.

Katelyn Noronha, Molly Wetzel, Abigail Chang, Jennifer M. Garbarino, Jiaying Chen, Jeffrey Sabina, Colin Ng

AtlasXomics Inc., New Haven, CT

Understanding how gene regulation drives tumor evolution and therapeutic response requires spatially resolved, multi-omic data from clinically relevant samples. Current approaches for mapping gene expression dynamics rely on pairing spatial ATAC-seq with separate spatial or single-cell transcriptomic assays performed on adjacent sections. This consumes precious tissue, requires cross-slide computational integration, and makes it difficult to capture the state of the same cells—often obscuring key regulatory relationships and cell states. Here we introduce Spatial CoPro, a multi-omics assay that captures open chromatin and unbiased whole-transcriptome states within the same section, preserving morphology and spatial context in both fresh frozen and FFPE tissues. Built on the Deterministic Barcoding in Tissue for Spatial Omics Sequencing (DBiT-seq) platform, the innovation centers on a random hexamer priming strategy for unbiased capture of coding and noncoding transcripts. Unlike poly(A)-based approaches that capture only polyadenylated transcripts and are not suitable for fragmented or degraded RNA, random priming recovers RNA fragments across the gene body, making it particularly effective for both Fresh Frozen and FFPE samples. This provides a more complete and less biased view of transcriptional states while directly pairing with high-resolution chromatin accessibility data. Our Spatial CoPro assay achieves >2,000 fragments (FRiP >20%) for chromatin accessibility and >500 UMIs with >300 detected genes for RNA capture per 10 µm × 10 µm spot, approaching single-nucleus resolution across a 5.5 mm × 5.5 mm region in mouse hippocampus and human prostate cancer. Transcriptome performance matches industry standard spatial transcriptomics assays, while chromatin accessibility matches single-modality spatial ATAC-seq. Matched fresh frozen and FFPE sections correlate strongly across modalities (R >0.7), ensuring robustness across clinical specimens. This unified and FFPE-compatible workflow enables analysis of spatially distinct regulatory programs, enhancer-gene interactions, and tumor cell states not detectable with single-omic assays. By extending multi-omic spatial profiling to clinical specimens, Spatial CoPro establishes a new standard for spatial epigenome-transcriptome integration, advancing studies of tumor heterogeneity, therapeutic resistance, and disease progression to accelerate precision oncology and biomarker discovery.

#0816 Spatial metabolic gradients drive epigenetic reprogramming in human glioblastoma.

Sankha Subhra Chakrabarty[1], Yilin Xu[1], Shannon Coy[1], Jia-Ren Lin[2], Dimitrius Tansini Pramio[3], Pilar Baldominos[4], Clement Bodineau[5], Nathalie Y. R. Agar[6], Judith Agudo[7], Marcos Simoes-Costa[8], Keith L. Ligon[9], Peter Karl Sorger[2], Sandro Santagata[1]

[1]Laboratory of Systems Pharmacology/Pathology, Harvard Medical School/Brigham and Women's Hospital, Boston, MA,[2]Harvard Medical School, Boston, MA,[3]Harvard Medical School/Boston Children's Hospital, Boston, MA,[4]Harvard Medical School/Dana-Farber Cancer Institute, Boston, MA,[5]Harvard Medical School/Brigham and Women's Hospital, Boston, MA,[6]Department of Neurosurgery, Harvard Medical School/Brigham and Women's Hospital, Boston, MA,[7]Dana-Farber Cancer Institute, Boston, MA,[8]Systems Biology/Pathology, Harvard Medical School/Boston Children's Hospital, Boston, MA,[9]Assistant Professor of Path., Dept. of Med. Onc., Dana-Farber Cancer Institute, Boston, MA

Human glioblastoma (GBM) contains sharp spatial transitions in oxygen tension, metabolism, and lineage organization, yet how these microenvironmental cues become epigenetically encoded at the chromatin level remains poorly understood. Using cyclic immunofluorescence (CyCIF) on human IDH-wildtype GBM specimens enriched for necrosis, we mapped tumor cell lineages and histone H3K18 lactylation (H3K18la) at single-cell resolution. Necrotic and hypoxic regions displayed distinct lineage organization and elevated H3K18la, consistent with increased glycolytic flux and lactate accumulation under oxygen deprivation. In patient-derived GBM cell lines, hypoxia-mimetic treatment with deferoxamine (DFX) recapitulated this epigenetic response. RNA-sequencing and CUT&RUN profiling revealed that H3K18la associates with activation of hypoxia and epithelial-to-mesenchymal transition-related transcriptional programs, along with repression of cell-cycle and mitotic regulators. Together, these findings demonstrate how spatial metabolic gradients shape chromatin states and transcriptional networks in GBM, highlighting lactylation as a mechanism by which microenvironmental stress becomes epigenetically encoded and manifested as lineage-specific transcriptional adaptation.

#0817 Spatial characterization, of T-cell receptors at subcellular resolution using in situ sequencing-by-synthesis and spatial protein detection on the same tissue section.

Hansueli Meyer[1], Robert Pinard[1], Ryan Hindman[2], Emily Neil[1], Chris Nehme[1], Sameh Soliman[1], Dongju Park[1], Rebecca C. Hennessey[1], Jinling Wang[1], Alex Makrigiorgos[1], John Lee[1], Seiyu Hosono[1], Matthias Wahl[3], Dominic Mangiardi[1], Mong Marma[1], Hsu-yi Lee[1], Andreas Bosio[3]

[1]Miltenyi Biotec, Waltham, MA,[2]Miltenyi Biotec, Gaithersburg, MD,[3]Miltenyi Biotec, Bergisch-Gladbach, Germany

Abstract: Analyzing the tumor microenvironment (TME) and its immune context based on protein and RNA expression, alongside RNA sequencing, offers a powerful approach to understand tumor biology, predict treatment response, and guide the development of personalized therapies. It provides a more comprehensive understanding of tumor biology and the interplay between genetic alterations, cellular environment, and immune response. Currently, commercially available spatial transcriptomics methods require cDNA barcoding on tissue and ex situ cDNA sequencing on a separate instrument which limits the ability to directly sequence known or unknown regions in situ, such as T-cell or B-cell receptor (TCR/BCR) complementarity determining regions. This limitation can impact the detailed analysis of immune responses within tissue. Advances in technology are needed to enable direct in situ sequencing for more comprehensive insights.

Here, we present a novel approach combining in situ sequencing-by-synthesis with high-plex protein detection (30+), H&E, and DAPI — all performed on the same formalin-fixed, paraffin-embedded section. The technology is based on iterative detection of rolling circle amplified RNAs detection probes, proteins with directly conjugated antibodies and is also capable of in situ four color-based sequencing-by-synthesis (SBS) analysis of known and unknown RNA sequences. The detection of known RNA transcripts and unknown RNA sequences can be combined with existing pre-tested, ready to use MICS antibodies by Miltenyi Biotec, to identify proteins on the same FFPE tissue section.

Using this novel approach we generated data that enabled detailed characterization of TCRs in their spatial context. Five to ten µm thick tumor FFPE sections were transferred to glass slides, followed by deparaffinization and antigen retrieval. In situ sequencing was concurrently combined with an extensive panel of Miltenyi Biotec's MICS antibodies and DAPI imaging, followed by H&E staining on the same FFPE tissue section**.**

We observed high diversity of clonotypes which were assigned to T-cell subtypes and used to generate clonotype maps. Co-localized alpha and beta chain receptors within the same cell were identified as well. We also further applied immune cell protein markers for segmentation and mapping in the complex tissue environment. Our approach enables researchers to identify and analyze the diversity of T-Cell populations based on their unique receptor sequences, while spatially mapping immune cell clonality directly on tissue. This nondestructive method preserves the tissue in its original context.

#0818 Simultaneous spatial transcriptome and methylation profiling in fresh frozen and FFPE tissues.

Katelyn Noronha, Molly Wetzel, Jennifer M. Garbarino, Jiaying Chen, Jeffrey Sabina, Colin Ng

AtlasXomics Inc., New Haven, CT

Epigenetic regulation via DNA cytosine methylation is a key determinant of transcriptional programs, lineage specification, and cancer evolution as well as a prognostic indicator for certain cancer types at well characterized loci. Although spatial transcriptomics and chromatin profiling have expanded our understanding of gene-regulatory microenvironments, direct spatial mapping of the methylome in intact tissues has remained elusive. Spatial co-profiling of the transcriptome and DNA methylome bridges this gap by directly linking transcriptional output to epigenetic regulation within the tissue microenvironment. The AtlasXomics platform, built on the Deterministic Barcoding in Tissue for Spatial Omics Sequencing (DBiT-seq) assay, enables simultaneous capture of the whole transcriptome and genomic DNA fragments within defined spatial pixels, termed Spatial-DMT. RNA is reverse-transcribed with barcoded primers, while genomic DNA is processed by an enzymatic methyl-seq workflow that detects native cytosine methylation without bisulfite degradation. The paired libraries yielded co-registered maps of gene expression and DNA methylation in human medullablastoma and glioblastoma at 10µm resolution. Integration of methylome and transcriptome data delineated tissue architecture, lineage trajectories, and region-specific epigenetic states undetectable by transcriptomics alone. Implemented on the commercial AtlasXomics spatial barcoding platform, Spatial-DMT offers a standardized, scalable workflow compatible with frozen and FFPE specimens. This adaptability positions the method for translational studies of tumor heterogeneity, epigenetic reprogramming, and therapy response. By integrating methylation and gene expression within intact tissue architecture, Spatial-DMT bridges discovery-stage research and clinical pathology. Spatial DNA methylation and whole transcriptome profiling establish a powerful tool for spatial cancer epigenomics, enabling discovery of spatial epigenetic biomarkers, tumor-stroma interactions, and therapeutic response patterns. By uniting spatial methylome and transcriptome in clinical specimens, this technology advances precision oncology and bridges molecular profiling with clinical pathology.

: Stem Cell Plasticity and Lineage Reprogramming in Cancer
Poster Session

#0822 Netrin-1/UNC5B-TFF3 axis modulates cancer stem cells self-renewal and chemoresistance in metastatic colorectal cancer.

Morgan Brisset[1], Kristina Radkova[1], Andrea Paradisi[1], Lea Stephan[1], Robin Wagner[2], Cyril Degletagne[1], Fabien Luiggi[1], Lisa Frydman[1], Alexander Heriot[3], Corina Behrenbruch[4], Tamara Vu[4], Frederic Hollande[4], Patrick Mehlen[1]

[1]Cancer Research Center of Lyon (CRCL), Lyon, France,[2]The University of Melbourne Department of Clinical Pathology, Melbourne, Australia,[3]Department of Surgical Oncology, Peter MacCallum Cancer Centre, Melbourne, Australia,[4]The University of Melbourne, Melbourne, Australia

Purpose: Metastatic colorectal cancer (mCRC) exhibits poor outcomes due to recurrence and resistance to chemotherapy driven by cancer stem cells (CSCs). We investigated the role of the dependence receptor ligand netrin-1 and its receptor UNC5B in CSC self-renewal and evaluated therapeutic inhibition of netrin-1 using the anti-netrin-1 antibody NP137.
Experimental Procedures: Patient-derived organoids (PDOs) from colorectal liver metastases were treated with recombinant netrin-1, NP137, or controls. Self-renewal was quantified by extreme limiting dilution assays. UNC5B was silenced by CRISPR/Cas9 to determine receptor the implication of this Netrin-1 receptor. Single-cell RNA-sequencing elucidated signaling pathways affected by NP137. In vivo efficacy of NP137 alone or combined with FOLFOX chemotherapy was tested in PDO-xenografted mice, and paired tumor biopsies from an mCRC patient enrolled in an NP137 clinical trial were analyzed by RNA-seq.
Results: Netrin-1 enhanced CSC self-renewal and survival, effects abolished by NP137 or UNC5B knockout. NP137 treatment triggered CSC apoptosis, an effect reversed by caspase inhibition. Single-cell transcriptomics revealed that UNC5B-positive cells secreted trefoil factor 3 (TFF3), which acted paracrinally to maintain stemness gene expression (LGR5, SOX4, SMOC2, PROM1). NP137 suppressed TFF3 and stemness transcripts in both PDOs and a treated patient's tumor. Blocking TFF3 dimerization phenocopied NP137 activity, confirming TFF3 as a critical downstream effector. FOLFOX exposure upregulated netrin-1 and UNC5B, and combination therapy (FOLFOX + NP137) significantly reduced self-renewal and tumor growth in mice while decreasing intratumoral TFF3.
Conclusions: Netrin-1 sustains mCRC CSC self-renewal through an UNC5B-dependent, TFF3-mediated paracrine survival mechanism. Pharmacologic inhibition of netrin-1 with NP137 induces CSC apoptosis and enhances chemotherapy efficacy, identifying the netrin-1/UNC5B/TFF3 axis as a promising therapeutic target to overcome stemness-driven resistance in metastatic colorectal cancer.

#0824 PPARδ overexpression drives transformation of multiple gastric progenitor and stem cells and tumorigenesis in mice.

Xiangsheng Zuo[1], Yi Liu[1], DAOYAN WEI[1], James C. Yao[2], Imad Shureiqi[3]

[1]UT MD Anderson Cancer Center, Houston, TX,[2]Assistant Professor, Dept. of Gastrointestinal Medical Oncology, UT MD Anderson Cancer Ctr., Houston, TX,[3]University of Michigan, Ann Arbor, MI

Background Peroxisome proliferator-activated receptor delta (PPARδ) is upregulated in many types of human cancers, including gastric adenocarcinoma (GAC). Elevated PPARδ expression correlates positively with GAC grade and stage, and negatively with patient survival. Overexpression of PPARδ in villin-positive gastric progenitor cells (VGPCs) has been shown to spontaneously induce GAC in villin-PPARδ mice through CCR20/CCR6 axis-mediated remodeling of the gastric tumor microenvironment. Lgr5-positive gastric stem cells (LGSCs), located in the gastric antrum and corpus glands, have also been widely studied for their role in GAC initiation and progression. However, whether this PPARδ-driven GAC is specific to particular cell types or models remains largely unknown.

Methods A new conditional transgenic PPARδ overexpression mouse line (CAG-LSL-PPARδ) was generated and subsequently crossed with villin-Cre or Lgr5-EGFP-IRES-CreERT2 mice (Lgr5-CreERT2) to generate CAG-LSL-PPARδ; villin-Cre ($PPAR\delta^{villin\text{-}cre}$) or CAG-LSL-PPARδ; Lgr5-CreERT2 ($PPAR\delta^{lgr5\text{-}creERT2}$) mice, in which PPARδ was overexpressed in VGPCs or LGSCs following tamoxifen induction. $PPAR\delta^{villin\text{-}cre}$ mice (n=15) and their controls (villin-Cre, n=12) were followed up until 45 weeks of age, whereas $PPAR\delta^{lgr5\text{-}creERT2}$ (n=16) and their controls (Lgr5-CreERT2, n=14) were observed for 45 weeks post-tamoxifen induction. Additionally, villin-PPARδ mice were bred with CCR6 knockout (CCR6-KO) mice to generate villin-PPARδ; CCR6-KO mice, which along with villin-PPARδ mice, were monitored until 35 weeks of age. All mice were evaluated for tumor multiplicity and subjected to histopathological examination.

Results Gastric hyperplasia and/or low-grade dysplasia occurred in the corpus of 100% of $PPAR\delta^{villin\text{-}cre}$ and $PPAR\delta^{lgr5\text{-}creERT}$ mice. High-grade dysplasia and/or locally invasive GAC were found in the corpus of 27% (4/15) of $PPAR\delta^{villin\text{-}cre}$, in both the corpus and antrum of 13% (2/16), and in the corpus of 19% (3/16) of $PPAR\delta^{lgr5\text{-}creERT2}$, whereas none of the control mice developed these lesions. Chronic inflammation was present in gastric lesions and positively correlated with tumor progression from hyperplasia to locally invasive GAC. CCR6 KO markedly suppressed PPARδ overexpression in VGPCs-induced gastric inflammation and tumorigenesis.

Conclusions PPARδ overexpression in both VGPCs and LGSCs induces chronic gastric inflammation and tumor formation. PPARδ, CCR6, VGPCs, and LGSCs may represent potential therapeutic targets for GAC.

#0825 Bone marrow from acute myeloid leukemia (AML) and multiple myeloma (MM) patients can be used to evaluate target expression and on-target efficacy for novel antibody drug conjugates (ADCs).

Aisha Mergaert, **Coranna Akdemirbey**, Mariah Suchan, Tara Murray, Emer Clarke

Discovery Life Sciences, Seattle, WA

The clinical efficacy of an ADC is heavily influenced by its ability to selectively target its designated epitope, however ADCs exhibit high off-target toxicity to tissues without epitope expression, thus limiting clinical efficacy. We evaluated an *in-vitro* platform to characterize potential hematological toxicity (neutropenia) associated with ADCs in patients with AML and MM. ADCs may still cause hematotoxicity, for example Trastuzumab vedotin, which targets human epidermal growth factor receptor 2 (HER2) which is not present on hematopoietic cells. Gemtuzumab ozogamicin (Mylotarg), Belantamab Mofodotin (Blenrep) and Trastuzumab vedotin were evaluated for toxicity to hematopoietic progenitor cells using the colony forming cell assay (CFC) in diseased (on-target efficacy) and normal bone marrow (NBM) (off-target toxicity). Mylotarg, an ADC targeting CD33, was evaluated for on-target efficacy on AML bone marrow and for off-target toxicity on NBM. Blenrep, an ADC targeting B-cell maturation antigen (BCMA) in MM, was evaluated on MM and NBM. Trastuzumab vedotin was evaluated on AML, MM and NBM. Cells were pretreated with ADCs for 72 hours, and then transferred to methylcellulose containing appropriate cytokines (AML, NBM) or conditioned medium (MM) and placed in a humidified incubator for 14 days. CFU-GM, AML-blast CFC or MM-blast CFC were assessed microscopically and colony numbers enumerated. Additionally, flow cytometric analyses of CD33 and BCMA expression were performed on the relevant diseased and NBM. Mylotarg significantly inhibited AML- blast CFC with an average IC_{50} value of 0.008 µg/mL (on-target efficacy). The IC_{50} values for AML-blast inhibition were not associated with CD33 expression. Mylotarg additionally significantly inhibited NBM progenitors with an average IC_{50} value of 0.01 µg/mL (off-target toxicity) and once again, was not associated with the CD33 expression. There was no significant difference between the IC_{50} values on AML versus NBM clonal growth. Trastuzumab vedotin also demonstrated toxicity to NBM progenitors with a mean IC_{50} value of 3.8 µg/mL demonstrating off-target toxicity. Blenrep exhibited different effects to the disease progenitors as compared to the healthy donor progenitors. Blenrap in MM patient bone marrow had IC_{50} values which ranged from 4.4 to 46 µg/mL with an average IC_{50} value of 21 µg/mL, compared to evaluation in NBM which resulted in IC_{50} values > 30 µg/mL (highest tested concentration) and rarely had any impact on colony growth. These data suggest that the CFC assays with primary normal and diseased bone marrow cells may provide insight as to relative potency of an ADC on a disease-specific target as well as potential off-target toxicity to normal hematopoietic progenitors.

#0826 Investigating TWEAK-mediated regulation of ovarian cancer cell survival.

Harshada Sapre, Mikella Robinson, Carrie House

San Diego State University, San Diego, CA

High-Grade Serous Ovarian Cancer (HGSOC) remains a salient concern in women's health, with 90% of patients eventually experiencing resistance to standard-of-care chemotherapies. Research implicates a subpopulation of quiescent, multipotent cells termed Cancer Stem-like Cells (CSCs) in contributing to resistance and relapse. We previously identified Tumor Necrosis Factor-Like Weak Inducer of Apoptosis (TWEAK), a pro-inflammatory cytokine, as highly enriched in the tumor microenvironment following chemotherapy and a critical mediator of CSCs by activating NFkB signaling to increase survival. We also found that a subpopulation of cells without CSC features were more sensitized to chemotherapy in the presence of TWEAK, suggesting a dual role for TWEAK. Canonically, TWEAK influences cell differentiation; however, this role is ill-defined in ovarian cancer. We hypothesize that TWEAK induces chemosensitivity in non-CSCs and chemoresistance in CSCs in ovarian cancer. To study this signaling in an immunocompetent mouse model recapitulating the tumor microenvironment, the murine ovarian surface epithelial cell line ID8 (p53-mutant and p53-wild type) were used. Combination IC50 of Carboplatin and Paclitaxel was studied in both cell lines for accurate drug dosing. A panel of surface markers was assessed for baseline expression by flow cytometry, including the TWEAK receptor Fn14 (27%), and CSC markers LGR5 (3.19%), GRP78 (29%), CD117 (70%), and αVβ3(0.27%). GRP78 was identified as a promising CSC marker in the p53-mutant ID8 cell line, with baseline expression of 29% increasing significantly to 53% post-chemotherapy. FACS sorting of GRP78+ enriched fractions to have high baseline expression of stem genes SOX2,OCT4, and NANOG. To assess TWEAK induction of CSC features, pre-treatment of TWEAK in GRP78 + and GRP78- factions showed an overall increase in viability after chemotherapy treatment, suggesting TWEAK treatment before chemotherapy may provide an advantage in survival. Current work is investigating GRP78+ ID8 cells using in vitro assays for spheroid formation, extreme limiting dilution, and chemoresistance in response to TWEAK stimulation. An in vivo murine relapse model will be used to test the role of TWEAK in maintaining GRP78+ cells and relapse potential. Future studies will elucidate the role of TRAF proteins in directing the downstream effects of TWEAK-Fn14 activity. Together, these investigations provide valuable insights into the mechanisms underlying chemoresistance.

#0827 Actin cytoskeleton modulation reprograms resistant GBM spheroids and GSCs, enhancing response to IR and temozolomide in vitro and in vivo.

Yuli Thamires Magalhaes[1], Viktor Kalbermatter Boell[2], Leticia Ramos Molica[1], Donna Joe[1], Fabio Luis Forti[3]

[1]Biochemistry, University of Sao Paulo - Institute of Chemistry, Sao Paulo, Brazil,[2]IQ USP, Sao Paulo, Brazil,[3]University of Sao Paulo, Sao Paulo, Brazil

Actin cytoskeleton regulate essential processes in cancer progression, including cell division, migration, invasion, and genomic stability. Nuclear F-actin has emerged as a critical regulator of DNA repair, chromatin organization, and transcription, representing a potential therapeutic target. Glioblastoma (GBM), a highly aggressive tumor with strong resistance to ionizing radiation (IR) and temozolomide (TMZ), frequently relies on GBM stem-like cells (GSCs) to sustain recurrence. GSCs exhibit enhanced DNA repair, and their stemness is influenced by pathways linked to actin dynamics. We investigated whether targeting actin polymerization sensitizes GBM to therapy by modulating DNA damage response (DDR) and GSC phenotypes. IR- and TMZ-resistant U87-MG cells generated through cyclic treatments were grown as 3D spheroids. Resistant spheroids showed increased proliferation, faster cell-cycle progression, elevated cell death within the core, and markedly enhanced self-renewal, supporting a stem-like tumorigenic profile. Interestingly, resistant cells exhibited distinct invasion patterns: IR-resistant were more invasive, whereas TMZ-resistant were more migratory, consistent with pFAK and vimentin immunoblotting, indicating distinct GSC-like subtypes within each resistant population. Strikingly, spheroid assembly in the presence of F-actin-disrupting drugs (cytochalasin D/B or latrunculin B) reduced therapy resistance and diminished tumorigenicity. Zebrafish xenotransplantation confirmed the aggressive proliferation, mortality rates, and metastatic dissemination of resistant cells, all of which were significantly reduced upon actin-targeting treatments, resulting in increased animal survival. RNA-seq, qPCR, immunoblotting, and immunofluorescence revealed upregulation of GSC markers in resistant spheroids, while actin disruption markedly reduced their expression. We propose that nuclear F-actin regulates transcriptional circuits that maintain stemness and therapy resistance. Consistently, resistant cells exhibited elevated nuclear actin which was dynamically modulated by genotoxic stress or pharmacological actin disruption. Ongoing chromatin-fraction proteomics aim to identify nuclear F-actin-associated proteins under damage conditions. Finally, in PDX GSC23 cells, inhibition of F-actin polymerization reduced stemness markers under self-renewal conditions and prevented serum-induced differentiation. Cytochalasin D enhanced sensitivity of GSC23 to IR and TMZ, reducing proliferation, viability, and tumorigenicity. Collectively, these findings reveal actin cytoskeleton regulation, particularly nuclear F-actin, as a vulnerability that can be therapeutically exploited to overcome GBM resistance, supporting actin-modulating compounds as promising adjuvants for GBM therapy.

#0828 Investigation of developmental LIN28/*let-7*/SOX2/SOX9 feedback loop during cell migration and metastasis.

Indhujah Thevarajan, Maria Osuna, Bareun Kim, Jihan K. Osborne

Pharmacology, University of Texas Southwestern Medical Center, Dallas, TX

The RNA binding protein LIN28, and the microRNA (miRNA) *let-7* family represent an evolutionarily conserved developmental feedback loop that acts as a regulator of developmental timing in metazoans. We have recently published data demonstrating that in the developing lung and brain, Sox2 and Sox9 transcriptionally regulate *Lin28a/b*. Moreover, previous work from our lab show that Lin28a binds *Sox2* and *Sox9* mRNAs and regulates their stability and translation. Our hypothesis is that reactivation of an early developmental pathway governed by SOX9 and SOX2 lead to transcriptional upregulation of LIN28A/B at various times during tumorigenesis. Our goal is to understand why developmental pathways are re-expressed during tumorigenesis as well as find ways to specifically target these pathways to inhibit metastasis. We established transient SOX9 knockdown (KD) using siRNA and stable SOX9 KD using lenti-viral shRNA construct in normal and cancer cell lines of lung and pancreas. We performed migration assays in control and SOX9 KD cells to test protein expression of SOX9, SOX2, LIN28A, and LIN28B using immunoblot and immunofluorescence experiments at different migratory stages. We performed migration/invasion assays using the Incucyte SX5 live-cell imager via high throughput migration assays to test migratory potential of control and SOX9 KD cells. We have found that SOX9 expression becomes nuclear during migratory stages in normal and cancer cells indicating a potential transcriptional activation during cell migration. We noticed that SOX9 expression is increased at different migratory stages but decreased after wound closure. Interestingly, SOX2 expression is higher in cancer cell lines after wound closure when SOX9 expression is lower. LIN28A and LIN28B expression is increased at different migratory stages in lung and pancreatic cancer cell lines, but not in the normal cell lines. Importantly, we observed that in lung and pancreatic cancer cells migration, invasion and proliferation are slow after SOX9 KD. We will now investigate whether LIN28A/B are functional downstream targets of the SOX9/SOX2 axis during the pathophysiology of non-small cell lung cancer (NSCLC) and pancreatic cancer with specific focus on migration/invasion and metastasis.

#0829 Infiltration of hematopoietic stem cells (HSC) is associated inversely with cell proliferation, with better patient survival, and its reduction by neoadjuvant chemotherapy relates with poor survival in breast cancer.

Masanori Oshi[1], Rongrong Wu[1], Li Yan[1], Takashi Ishikawa[2], Itaru Endo[3], Kazuaki Takabe[1]

[1]Roswell Park Comprehensive Cancer Center, Buffalo, NY,[2]Breast Surgery, Tokyo Medical University, Tokyo, Japan,[3]Yokohama City University, Yokohama, Japan

Background: Hematopoietic stem cell (HSCs), also known as blood stem cells, are self-renewable cells that can develop into all types of blood cells. They are found in bone marrow and peripheral blood. However, the clinical relevance of HSCs in breast cancer (BC) tumor microenvironment (TME) remains unknown. The aim of this study was to elucidate the clinical significance of HSC infiltration in the TME of BC.

Methods: In silico analyses were conducted on 5,176 BC patients, including large independent cohorts; The Sweden Cancerome Analysis Network-Breast (SCAN-B) and the Molecular Taxonomy of Breast Cancer International Consortium (METABRIC), as well as multiple single-cell sequenced cohorts. HSC were identified through the xCell algorithm, and patients with high HSC levels were defined as those with HSC expression above the median in each cohort.

Results: Fraction of HSCs ranged from 0.04-0.50% of all cells in BC TME by single cell transcriptome analyses. HSC infiltration was not correlated with its lineage cells, common myeloid progenitor cells and common lymphoid progenitor cells, but was associated with high infiltration of dendritic cells and stromal-related cells and low infiltration of Myeloid-related cells; M1-macrophages, and eosinophils, and lymphoid-related cells; Th1 cells, Tregs, NK T cells, and memory B cells. HSC high BC enriched TGF-β signaling, myogenesis, coagulation, and angiogenesis gene sets. On the other hand, all the cell proliferation-related gene sets in Hallmark collection; E2F targets, G2M checkpoint, MYC targets-v2, and mitotic spindle, enriched to low HSC BC, and HSC infiltration was significantly lower in high histological grade BC and in Ki67 high expression BC. HSC high patients were significantly associated with better overall survival compared to low patients in ER+/HER2- (both $p<0.02$), but not in TNBC in both cohorts. Interestingly, there was no survival difference by HSC infiltration in ER+/HER2- when neoadjuvant chemotherapy (NAC) was used. Together with our finding that HSC in the TME markedly reduced by NAC, we cannot help but speculate that the loss of HSCs by NAC may have contributed to loss of their benefit in patient prognosis. Lastly, high levels of HSC were associated with significantly lower risk of lung metastasis and better survival, but not with brain and bone metastases.

Conclusions: This is the first report that quantified HSCs in TME using transcriptome and demonstrated that they are rare, associated inversely with cell proliferation and with better survival in ER+/HER2- BC patients. Survival benefit of HSC infiltration was lost with NAC that reduce its infiltration. HSC high BC was associated with lower risk of lung metastasis and with better survival, but not with brain nor bone metastasis.

#0831 The functional crosstalk between tissue transglutaminase (TG2) and CD24 enhances cancer stem cell traits and therapy resistance in high grade serous ovarian cancer.

Rohit Pravin Nagare[1], Habeebunnisa Begum[1], Ben Wamba[2], Jogender Tushir-Singh[2], Fabrizio Pin[3], Salvatore Condello[1]

[1]Indiana University School of Medicine, Indianapolis, IN,[2]Department of Medical Microbiology and Immunology, University of California Davis, California, CA,[3]Department of Cell Biology and Physiology, Indiana University School of Medicine, Indianapolis, IN

High-grade serous ovarian cancer (HGSOC) remains one of the most lethal gynecologic malignancies, largely due to persistent cancer stem cells (CSCs) that drive disease progression. Our data revealed that tissue transglutaminase 2 (TG2) is a central mediator of OCSC biology through its interaction with fibronectin (FN) and integrins, activating oncogenic pathways, including Wnt signaling, that promote stemness and platinum resistance. We further identified that TG2 cooperates with the immune-regulatory receptor CD24 to anchor OCSCs to peritoneal organs, facilitating early metastatic implantation and ascites formation. To therapeutically disrupt this axis, we synthesized a selective peptide inhibitor (BP) that blocks the TG2-FN interaction and developed a CD24-neutralizing antibody (CD24-Ab), each of which suppresses CSC function in preclinical models. We then combined these modalities into a single first-in-class antibody-peptide conjugate, APC (CD24-Ab-TG2-BP), designed to simultaneously disrupt CD24 signaling and TG2-mediated CSC-tumor microenvironment (TME) interactions. TCGA analysis of HGSOC revealed TG2 and CD24 *m*RNA amplification in 3% and 2% of cases, respectively. Flow cytometry confirmed robust TG2 (58%, 51%) and CD24 (98%, 100%) expression, with substantial co-expression (55%, 45%) in OVCAR4 and OVCAR5 cells, respectively. APC treatment significantly downregulated CSC-associated markers (NANOG, OCT4, SOX2, ALDH1A1) and disrupted spheroid architecture. Co-immunoprecipitation demonstrated a specific TG2-CD24 interaction in SKOV3 and OVCAR4 cells, while biochemical fractionation localized the complex to lipid raft microdomains, signaling platforms that integrate receptors and downstream oncogenic effectors. In OC xenograft models, treatment with APC significantly reduced tumor volume (0.22 ± 0.11 mm^3 vs. 1.7 ± 1.1 mm^3; N =5, $P < 0.001$), tumor weight (0.64 ± 0.21 gm vs. 1.53 ± 0.46 gm; N =5, $P < 0.01$), and metastasis (5.3 ± 3.6 vs. 10 ± 3.6; N =5, $P < 0.001$) when compared with IgG controls, thus demonstrating potent anti-tumor efficacy. Collectively, these findings identify a lipid raft-restricted TG2-CD24 complex as a novel driver of OCSC maintenance and chemoresistance in HGSOC. Targeting this interaction with APC effectively disrupts CSC-TME crosstalk and suppresses tumor progression, establishing TG2/CD24 axis as a novel therapeutic vulnerability for overcoming resistance and recurrence in HGSOC.

#0833 Desmoglein-2 carrying cancer stem cell-derived extracellular vesicles promote lung cancer aggressiveness.

Prita Pandya, Aamena Ahmed, Nayya Murray, Dania S. Al-Qasrawi, Anaya Y. Clarke, Reagan Carris, Verline Justilien

Mayo Clinic Florida, Jacksonville, FL

Lung cancer remains the leading cause of cancer-related deaths worldwide, with non-small cell lung cancer (NSCLC) accounting for approximately 85% of all cases. Despite advances in targeted and immuno-therapies, overall survival for NSCLC remains below 25%, due to late-stage detection and therapeutic resistance. Cancer stem cells (CSCs), a highly tumorigenic subpopulation within NSCLC, drive relapse, metastasis, and treatment failure. Understanding the mechanisms by which CSCs promote the aggressiveness of NSCLC may reveal new diagnostic and therapeutic opportunities. CSCs establish an intercellular communication network through the secretion of extracellular vesicles (EVs), membrane-bound nanoparticles that transport proteins, lipids, and nucleic acids that can influence recipient cell behavior. Our previous work demonstrated that CSCs secrete significantly more EVs compared to bulk cancer cells (BCCs) and induce an enhanced tumorigenic phenotype in BCCs. However, the EV protein cargo that mediates these CSC-driven phenotypes and the signaling they promote remain poorly understood. This study aimed to identify and characterize CSC-derived EV protein cargo that contributes to NSCLC growth and metastasis. CSC- and BCC-derived EVs were isolated using tangential flow filtration and characterized according to MISEV guidelines. Mass spectrometry and pathway analysis were performed to compare the proteome of CSC- and BCC-derived EVs, followed by functional characterization *in vitro* and *in vivo.* Our results showed that EVs exhibited expected morphological, biochemical, and physical properties. Pathway analyses showed that CSC-derived EVs were enriched in proteins that localize to exosomes and associate with metabolism and cell adhesion. Comparison of BCC and CSC-derived EVs revealed Desmoglein-2 (DSG2) as one of the proteins exclusively detected in CSC-derived EVs. shRNA-mediated knockdown of DSG2 significantly reduced invasion, clonal expansion, and transformed growth *in vitro* and decreased tumor growth and metastasis *in vivo*. Furthermore, DSG2-competent EVs partially rescued the effects of DSG2 knockdown on CSC tumor growth *in vivo*. Together, these findings identify DSG2 as a key CSC-specific EV protein cargo that promotes an enhanced tumorigenic phenotype and NSCLC tumor growth. This work highlights the role of CSC-derived EV proteins as mediators of NSCLC aggressiveness and as candidates for biomarker and therapeutic development.

#0834 Unveiling the association of cancer stem cell markers with survival in follicular lymphoma patients.

Xin Zhang[1], Olivia White[1], Daniel Ashley[2], Betty Chung[3], Li Li[4]

[1]Institute of Translational Research, Ochsner Health System, New Orleans, LA,[2]University of Queensland-Ochsner Clinical School, New Orleans, LA,[3]Department of Pathology, Ochsner Health System, New Orleans, LA,[4]Ochsner Health System, New Orleans, LA

Background: Follicular lymphoma (FL) is the second most prevalent subtype of non-Hodgkin's lymphoma characterized by a protracted waxing and waning clinical course. Despite advances in treatments, about half of FL patients experience relapse within five years and become refractory to treatment. Clinical risk factors such as FL International Prognostic Index (FLIP) have not been used to guide the selection of treatment strategies. So far there are no prognostic markers for FL patients or physicians to select their treatment or understand their treatment resistance as well as relapse courses. Here we identified the cancer stem cell (CSC) markers in tissue microarray slides (TMA) and determined their association with FL patient survival.

Methods: Total 105 FL pts with available lymph node biopsy blocks were identified by AI software Deep6 and Slicer Dicer for query building in EPIC (ICD-10 code: C82.9). Demographic and clinicopathological characteristics of these FL pts were collected. FL patients were divided in two groups: FL pts with short-term survival (less than 5 years) and long-term survival (more than 20 years). FFPE blocks from 59 FL pts lymph node biopsies were collected and used to create tissue microarray slides (TMA). H&E staining and IHC staining of FL cells (CD20) and CSCs (ABCG2, Ki67, and OCT3/4) were performed. Frequency of CSCs was analyzed using HALO® software. statistical analyses were performed using GraphPad prism 9. Two-sided p values <0.05 were considered statistically significance.

Results: Among 59 FL patients, 26 (44.1%) pts were short-term survival, and 33 (55.9%) FL pts were long-term survival. Although no difference in the frequencies of CD20+ cells between the short-term and long-term survival groups, significant increases in the frequencies of single CSC markers (ABCG2, Ki67, or OCT3/4) as well as CSC combination markers (ABCG2+, Ki67+, OCT3/4+) were found in the short-term survival group compared to the long-term group (p values <0.05).

Conclusion: Our results unveil phenotypically distinct CSC markers that are independence of existing prognostic markers and associated with short-term survival in FL pts, indicating their prognostic value in predicting FL patients' outcome. Evaluation of CSC markers may aid in identifying high-risk individuals and guiding personalized treatment in FL patients.

#0835 Modeling endometrial cancer using iPSC-derived endometrial organoids integrating genetic determinants of ethnicity.

Sueanne Chear[1], Simon Gayther[2], Kate Lawrenson[2]

[1]University of Texas Health Science Center San Antonio, San Antonio, TX,[2]Center for Inherited Oncogenesis, University of Texas Health Science Center at San Antonio, San Antonio, TX

BACKGROUND: Endometrial cancer is the most common gynecologic cancer in developed countries with an increasing incidence of 28.3 per 100,000 women per year in the United States alone. The cancer arises from the glandular epithelium of the endometrium and typically progresses by invading the stroma and myometrium. Development of endometrial cancer is influenced by genetic mutations (PTEN, TP53, mismatch repair genes), as well as ethnic, environmental, and hormonal factors. A scalable, physiologically relevant human model of endometrial cancer that captures these complex factors remains lacking.
METHODS & RESULTS: We have established human induced pluripotent stem cell **(**iPSC)-derived endometrial organoids as a platform for studying the early mechanisms of endometrial cancer, including cancer initiation and progression. We first used different protocols to create endometrial-like epithelium and stroma. Human iPSCs from a healthy individual were differentiated into epithelial organoids consisting of early-stage Müllerian duct-like cells (MDLCs) with an epithelial-mesenchymal hybrid phenotype (Pan-CK+/VIM+). To promote endometrial identity, epithelial organoids were co-cultured with endometrial stromal cells and treated with a single cycle of steroid hormones mimicking the human menstrual cycle. Immunofluorescence staining showed the organoids developed luminal epithelial and glandular-like structure (KRT8+/PAX8+/CDH1+), surrounded by VIM+ mesenchymal cells. Endometrial organoids are hormone responsive and express functional markers of uterine endometrium, including the secreted proteins, PRL and IGFBP1. By incorporating iPSCs from individuals of diverse ethnic backgrounds and introducing pathogenic genetic variants, we aim to uncover how genetic variation and population-specific factors contribute to endometrial cancer development and progression.
CONCLUSIONS: We anticipate this model will enable us to study the multifactorial contributors to endometrial cancer and support the identification of early disease events and therapeutic targets.

#0837 IDH mutations disable the tumor suppressive activity of GSX2 to promote gliomagenesis.

Yi Xiao[1], Diana D. Shi[2], Lei Guo[1], Ethan Neumann[1], Michael M. Levitt[1], Pranita Kaphle[1], Tracey Shipman[1], Haocheng Li[1], Feng Cai[1], Denise M. O. Ramirez[1], Lauren G. Zacharias[1], Zhenkang Chen[1], Mathew Lin[2], Vinesh T. Puliyappadamba[1], Tao Chen[1], Milan R. Savani[1], Salvador Pena[1], Janaka Wansapura[1], Thomas P. Mathews[1], Prashant Mishra[1], Yoon Jung Kim[1], Prithvi Raj[1], Timothy E. Richardson[3], Jian Xu[4], Stephen C. Mack[4], Gilbert J. Rahme[5], Bradley E. Bernstein[2], Ralph J. DeBerardinis[1], Itay Tirosh[6], Mario L. Suva[2], Lin Xu[1], Kalil G. Abdullah[7], Samuel K. McBrayer[1]

[1]UT Southwestern Medical Center, Dallas, TX,[2]Harvard Medical School, Boston, MA,[3]Icahn School of Medicine at Mount Sinai, New York, NY,[4]St. Jude Children's Research Hospital, Memphis, TN,[5]Renaissance School of Medicine at Stony Brook University, Stony Brook, NY,[6]Weizmann Institute of Science, Rehovot, Israel,[7]University of Pittsburgh Medical Center, Pittsburgh, PA

Isocitrate dehydrogenase (*IDH*) mutations arise early in glioma development and are associated with a defined neurodevelopmental cancer cell hierarchy. However, how mutant IDH contributes to this hierarchy and whether this interaction promotes gliomagenesis remain unclear. Progress in addressing these questions has been hindered by technical limitations. Patient-derived models rarely capture the biology of tumor initiation, as surgical specimens are obtained only after these phases of cancer evolution have passed. Moreover, the lack of faithful preclinical models of mutant IDH has constrained mechanistic investigation. To overcome these challenges, we developed a genetic mouse model of mutant IDH-driven gliomagenesis and IDH-wildtype companion models to enable direct testing of causal genotype-phenotype relationships involving the *Idh1-R132H* oncogene. We leveraged these models to survey IDH-mutant glioma initiation by performing time-resolved, joint single-cell RNA and ATAC sequencing analysis of engineered neural cells. Mutant IDH activates neural progenitor cells (NPCs) and drives NPC lineage switching. These actions expand oligodendrocyte precursor cells, the predominant cell-of-origin for these tumors, at the expense of interneurons, a lineage incompatible with mutant IDH-induced transformation. We further find that lineage switching is mediated by promoter hypermethylation and silencing of *Gsx2*, a homeobox gene required for neurogenesis. Critically, *Gsx2* ablation recapitulates NPC fate reprogramming by mutant IDH while restoring *Gsx2* expression in IDH-mutant neurosphere lines impairs their self-renewal and tumorigenic potential. Our work uncovers the molecular mechanisms by which mutant IDH reprograms neural lineage specification to promote cancer initiation, providing a new model of neural cell fate control by IDH oncogenes and insights into the developmental origins of glioma.

#0838 Single cell multiomic profiling of heterogenousPROCR+ cells in mouse mammary gland and its implication for breast cancer.

Jose Silva[1], Koon-Kiu Yan[2], Erin Nekritz[1], Jiyang Yu[2]

[1]Icahn School of Medicine at Mount Sinai, New York, NY,[2]St. Jude Children's Research Hospital, Memphis, TN

Introduction: The mammary gland is a dynamic organ that undergoes extensive tissue remodeling during the female lifetime. In all these stages, epithelial enlargement is supported by a population of adult mammary epithelial stem cells (MaSCs) residing at the apex of the hierarchy. MaSC homeostasis needs to be tightly regulated in time and space to ensure proper organ function and avoid pathological consequences. Thus, dysregulation of stem cell activity has been linked to tumor initiation, and aggressive breast cancers are frequently enriched in cells exhibiting stem cell like properties. Although MaSCs are fundamental to mammary gland development, their precise identity and defining characteristics remain poorly understood. Notably, protein C receptor (PROCR) marks a rare subset of mammary epithelial cells with stem-like properties, but their low abundance has hindered their characterization.
Methods: Here, we combine targeted FACS enrichment with single-cell RNA sequencing and chromatin accessibility profiling to generate a multimodal atlas of $PROCR^{+}$ mammary epithelial cells across developmental stages.
Summary of results: We uncover heterogeneity within this compartment and identify a previously unrecognized $Procr^{+}$, $Cdh5^{-}$, $Col1a1^{+}$ population that exhibits the highest developmental potency, strongest EMT-like signature, and earliest pseudotime position, consistent with a bona fide mammary stem cell (MaSC) state. Integration of scRNA-seq and scATAC-seq reveals the transcriptional regulatory architecture governing MaSC identity and basal versus luminal lineage commitment, including direct master regulators whose motif accessibility and activity shift along differentiation trajectories. Comparative analyses with human mammary epithelium identify analogous $PROCR^{+}$ subpopulations, and interrogation of breast cancer datasets demonstrates that the $Procr^{+}$, $Cdh5^{-}$, $Col1a1^{+}$ MaSC signature is selectively enriched in triple-negative and claudin-low tumors.
Conclusions: These findings refine the cellular hierarchy of the mammary epithelium, define regulatory programs underlying stemness and lineage bifurcation, and establish a molecular link between a distinct MaSC state and the biology of aggressive breast cancer subtypes.

#0839 Single cell cloning iPSCs with the Pala single cell sorter preserves colony stemness and cell viability for high-throughput cell line engineering workflows.

Bhamini Purandare, Francisco Ramirez, **Ryan McComb**, Chris Heger

Bio-Techne, San Jose, CA

Stable cell line development is a critical process for developing and manufacturing biologics, generating disease relevant cellular models, and creating the next generation of cell & gene therapies. The utility of new cell models (patient derived iPSCs), the development of new genome editing technologies (CRISPR) and the deployment of automation and AI for high-throughput screening are creating a greater demand for scaling cell line development capabilities and workflows. Bio-Techne has developed the Pala single cell sorter and dispenser that incorporates microfluidics, flow cytometry, and liquid dispensing in a portable, easy to use, and gentle device for generating high rates of single cell derived clones for enhancing cell line engineering workflows. Here, Pala is compared to traditional limiting dilution (LD) to dispense induced Pluripotent Stem Cells (iPSCs) for single cell cloning and colony outgrowth. Single dissociated iPSCs from two different lineages were dispensed in matrix coated 96-well plates or hand pipetted at 0.4 cells/well using LD. Colony health and stemness are compared between each method using clone area and TRA-1-60 immunofluorescence staining. Pala, on average, generated ~3-fold greater numbers of single cells deposited and colonies generated than LD. Additionally, colony health showed equivalence between the two methods demonstrating that Pala derived clones are as healthy as clones derived with LD. This work demonstrates the gentleness and efficiency of Pala for use in stem cell/gene editing workflows for enhancing throughput of single cell cloning.

#0840 Multi-tissue modeling of *BRCA* cancers using iPSC-derived organoids platform.

Nur Yucer[1], Alyssa Okimoto[2], Subash Dhungana[1], Dean Bacich[1], Rebecca Webster[1], Beatriz German Falcon[3], Michelle Jones[4], Sarah Parker[4], Bobbie Jo Rimel[5], Beth Y. Karlan[6], Leigh Ellis[3], Matthew Freedman[7], Robin J. Leach[8], Xiaojiang Cui[4], Kate Lawrenson[1], Simon Gayther[1]

[1]Medicine, Center for Inherited Oncogenesis, UT Health San Antonio, Long School of Medicine,, San Antonio, TX,[2]Center for Inherited Oncogenesis, UT Health San Antonio, Long School of Medicine,, San Antonio, TX,[3]Department of Surgery, Center for Prostate Disease Research, Murtha Cancer Center Research Program, Uniformed Services University of the Health Sciences,, Bethesda, MD,[4]Cedars-Sinai Medical Center, Los Angeles, CA,[5]University of Washington Department of Obstetrics and Gynecology, Seattle, WA,[6]UCLA David Geffen School of Medicine, Los Angeles, CA,[7]Department of Medical Oncology, Dana-Farber Cancer Institute, Harvard Medical School, Boston, MA,[8]UT Health Science Ctr. at San Antonio, San Antonio, TX

Germline pathogenic mutations in the BRCA1 and BRCA2 genes (BRCA1/2mut) are the strongest genetic risk factors for high-grade serous ovarian cancer, and estrogen receptor-positive (ER+) and triple-negative breast cancer (TNBC). Pathogenic variants in these genes are implicated in about 15% of women with heritable risks of these cancers. Moreover, BRCA2^{mut} are associated with increased risk of ER+ breast cancer and aggressive prostate cancer in men. Precise risk estimates for BRCA1/2^{mut} that affect different cancer types are crucial to evaluate treatments and enhance drug sensitivity. Patient-specific induced pluripotent stem cell (iPSC) methods create opportunities to model human diseases in vitro. iPSCs derived from patients with known genetic mutations carry the patient's unique genetic background, to provide platforms for studying the functional effects of specific genes. Several inherited disease models created from iPSCs have successfully replicated high-risk cancers. This study aimed to utilize iPSC-based modeling to investigate the functional impact of pathogenic BRCA1/2^{mut} on early-stage phenotypes and genomic alterations that contribute to cancer progression.

Methods: We generated iPSC from both BRCA1/2^{mut} carriers' women and BRCA2^{mut} carrier male. From female BRCA1/2^{mut}, we have established iPSC-derived organoid models of ovarian cancer -OC-(fallopian tube epithelium, FTE) and breast cancer -BC-(mammary gland epithelium, MGE) and from male BRCA2^{mut} prostate cancer-PC.

Results: Following differentiation into FT organoids, both heterozygous BRCA1/2^{mut} models show specific cellular abnormalities - neoplastic transformation, expression of cancer-specific biomarkers - compared to BRCA^{WT} controls. ER+ BC and TNBC models revealed that following differentiation into MG organoids: models from heterozygous BRCA1/2^{mut} carriers conferred a neoplastic phenotype reminiscent of a ductal carcinoma in situ (DCIS) compared to BRCA^{WT} controls. Notably, the development of DCIS in BRCA2^{mut} carriers was dependent on estrogen (E2) exposure, while in BRCA1^{mut} carriers, it was independent of hormonal influences; this may suggest that BRCA haploinsufficiency contributes to the observed phenotype. PC models from BRCA2^{mut} subjects exhibit abnormalities reminiscent of early-stage neoplastic development. Importantly, prostate organoids with combinations of BRCA2^{mut} and PTEN alterations exhibited more aggressive PC phenotypes compared to BRCA2^{mut} and BRCA^{WT} organoids alone, and shared genomic signatures with primary aggressive PC.

Conclusion and Impact. iPSC-derived multi-tissue organoid platform can accurately replicate BRCA1/2^{mut} and BRCA^{WT} precursor tissues. This allows cancer to evolve in a dish, making it an ideal model for mechanistic studies and screening approaches to identify novel drug targets.

#0841 Maternal obesity reprograms intestinal stem cells to elevate colorectal cancer risk in offspring.

Gourab Lahiri[1], Karla Mullen[1], Yesenia B. Millan[1], Swathi Sankar[1], Dominic R. Saiz[1], Thomas H. McDermott[1], Madeline Blatt[1], Abhigyan Shukla[1], Khashayarsha Khazaie[2], Miyeko D. Mana[1]

[1]School of Life Sciences, Arizona State University, Tempe, AZ,[2]Mayo Clinic, Phoenix, AZ

Maternal obesity has been epidemiologically linked to an increased risk of sporadic colorectal cancer (CRC) in offspring, the third most prevalent cancer worldwide. This association underscores the lasting influence of early-life exposures on long-term health and disease susceptibility. Intestinal stem cells (ISCs), the long-lived cells that sustain epithelial renewal and often serve as the origin of intestinal cancers, are thought to play a central role in mediating this elevated cancer risk. However, how maternal obesity shapes the early-life programming and maturation of ISCs in their offspring remains poorly understood. Using mouse models of diet-induced obesity, we show that offspring exposed to a maternal high-fat Western diet (HFD) during pre- and postnatal development exhibit increased colonic proliferation, enhanced stem cell self-renewal, and a hypermetabolic state that persists into adulthood, even after dietary normalization. Alongside changes in stem cell properties, we observe a significant shift in epithelial cell composition, characterized by an increase in cells of secretory lineage at the expense of absorptive enterocytes, and these changes endure into adult life. Additionally, these changes are accompanied by an increased tumor burden in the loss of Apc heterozygosity model. Our data indicate that IL-17a, a pro-inflammatory cytokine, is critical in mediating these changes. Specifically, receptor IL-17RA/C expression is significantly upregulated in ISCs and secretory cells in maternal HFD-exposed offspring. Administration of IL-17a to intestinal organoids demonstrates sufficiency by mimicking the maternal obesogenic phenotype, indicating that immune-epithelial interactions influence ISC function and may be a driver of durable molecular patterning. These findings emphasize the long-term consequences of maternal HFD exposure on intestinal stem cell activity and epithelial composition, and possibly contribute to a higher risk of CRC in offspring later in life.

#0843 Protection of human bone marrow MSC from room air oxygen during isolation accelerates cell growth.

Alicia D. Henn, Shannon L. Darou, Collins E. Gbegbeawu, Syed A. Mustafa

BioSpherix, LLC, Parish, NY

The role of mesenchymal stromal/stem cells (MSC) in the cancer microenvironment is of great interest, not only for the fundamental roles that MSC play in inflammation, organoids, and regenerative medicine, but also as producers of exosomes. These extracellular vesicles, which can deliver cargo to other cells, are gaining interest as tumor-homing vehicles for therapeutic agents. However, the solid tumor environment is hypoxic, and even normal tissues reside at oxygen levels far below that of room air, where MSC are grown for exosome production. Exposure to supraphysioxic room air changes MSC, modulating HIF-1a which is upstream of signaling pathways related to cell proliferation, differentiation, and cell death. We previously showed that eliminating exposure of human bone marrow MSC to room air during cell culture and handling can prevent HIF-1a modulation, improve cell division rates, and reduce cell senescence in later passages. Here we extend those findings, isolating cells from cadaver bones that were sourced from a licensed organ procurement agency, under constant physioxia (5%O2/ 5%CO2) in an Xvivo System. Flow cytometric analyses and differentiation of the plastic-adherent bone marrow cells into adipocytes, chondrocytes, and osteocytes confirmed the bone marrow MSC phenotype. Having never experienced room air, these MSC exhibited faster cell growth at passage 8 (mean doubling time 43.2 +/- 1.2 hrs, n = 3 separate cultures) than commercially sourced MSC that had been isolated, expanded, and cryopreserved under traditional laboratory conditions (mean doubling time 128 +/- 15.2 hrs, n = 2 separate cultures). We concluded that protecting MSC from room air exposure, even during isolation, can improve human bone marrow MSC growth kinetics for studies of the tumor microenvironment, inflammation, and tumor-homing exosomes.

#0844 Investigating the ability of *foxo1* to maintain stem cells.

Stella Aime Rios, Megan E. Keniry

College of Sciences, University of Texas Rio Grande Valley, Edinburg, TX

Background: Our group discovered that FOXO transcription factors drive stem gene expression in cancer to promote aggressiveness. Work by our group and others demonstrated that FOXO factors universally maintain stem cells including in cancer, embryonic, hematogenic and neuronal contents. Our current efforts are delineating the molecular underpinnings by which FOXO factors halt differentiation to maintain stem cells. In this project, we are employing myoblasts as a valuable model to examine how Foxo1 maintains stem cells. Foxo1-regulated genes in myoblasts closely parallel its targets in glioblastoma and basal breast cancer stem cells, including targets such as *Leukemia Inhibitory Factor*, *Lif,* encoding a cytokine that prevents differentiation. Understanding how Foxo1 maintains stem cells is crucial, as it holds the potential to uncover new therapeutic options that could target the fundamental biological processes involved in cancer progression and chemotherapeutic resistance.

Methods: RNAi was performed on C2C12 myoblasts cells to create *Foxo1* knockdown and control lines, followed by assessment of target genes involved in differentiation, proliferation, and muscle fiber types using qRT-PCR. Fluorescent microscopy was utilized to investigate the structural differences in actin filaments and nuclei between *Foxo1* knockout cells and the control group. Our initial work, including investigating candidate genes using qRT-PCR. We are currently taking genomics approaches to investigate the role of Foxo1 in myoblast/stem cell differentiation.

Results: In *Foxo1* knockout cells, there was a notable decrease in *Lif* expression, suggesting differentiation. Downregulation of genes like *Igfbp1*, *Socs1*, and *Socs2* indicates possible direct or indirect activation by *Foxo1*, with implications for cell growth and cytokine signaling. Additionally, downregulation of *Pepck* and the modulation of energy metabolism pathways suggest altered metabolic states. The downregulation of *Stat1* and *Wnt3* implies disruptions in pathways that promote proliferation to favor differentiation. This aligns with observations of increased nuclei and actin filament abundance in *Foxo1* knockout cells, reflecting enhanced muscle differentiation and myotube formation.

Conclusion: *Foxo1's* involvement in regulating cellular dynamics through gene expression is complex and dynamic, impacting differentiation and proliferation, with notable changes in the cytoskeleton facilitating myoblast fusion and differentiation. Gaining insights into the relationship between *Foxo1* and target genes will clarify potentially conserved roles that determine the differentiation status of stem and progenitor cells. We are anticipate that this model system will allow us to glean fundamental mechanisms that maintain stems cells to ultimately target cancer stem cells, which are known to trigger recurrence and chemotherapeutic resistance.

#0845 Tumor-associated mesenchymal stem cells accumulate in high oxidative phosphorylation regions of peritoneal dissemination in gastrointestinal cancers.

Nobuhiko Kanaya, Yu Mikane, Shinji Kuroda, Eri Takeda, Makoto Matsumoto, Kosuke Yunoki, Yudai Mimata, Hitoshi Minagi, Tetsuya Katayama, Daisuke Kadowaki, Masashi Hashimoto, Yoshihiko Kakiuchi, Shunsuke Kagawa, Hiroshi Tazawa, Toshiyoushi Fujiwara

Department of Gastroenterological Surgery, Okayama University Graduate School of Medicine, Dentistry and Pharmaceutical Sciences, Okayama, Japan

Peritoneal dissemination represents a lethal metastasis in gastrointestinal malignancies; however, cellular constituents that sculpt the metastatic niche remain poorly resolved. Recent studies reveal tumor associate mesenchymal stem/stromal cells (TA-MSCs) induce tumor migration and immune suppression in several tumors such as ovarian cancer. In this study, we focused on TA-MSCs as potential stromal drivers of metabolic adaptation within the peritoneal dissemination from gastrointestinal malignancies, especially colorectal cancer. First, public multi-omics datasets revealed tumor type-dependent variation in canonical MSC transcripts. Next, in surgical specimens of the peritoneal dissemination from patients with colorectal, gastric, and pancreatic cancer, the immunohistochemistry demonstrated marked elevation of CD90 and CD73 compared with non-tumor peritoneum, indicating robust stromal expansion. Single-cell transcriptomes from peritoneal lesions further identified a distinct MSC-like cluster enriched for THY1 (CD90) high cells, supporting an MSC-dominated stromal architecture in the peritoneal dissemination. To model this interaction in vivo, murine colorectal cancer bearing peritoneal dissemination mouse models exhibited a similar amplification of MSC markers compared to primary tumor controls. Notably, Oxidative Phosphorylation (OXPHOS) dominant metabolic signatures were prominent both in human metastatic peritoneum and in peritoneally adapted MC38 derivatives isolated from mice. Then, the correction between OXPHOS specific metabolism and localization of MSCs was assessed. Interestingly, the area of high OXPHOS expression into colorectal cancer derived peritoneal dissemination contained the higher MSCs infiltration using immunohistochemistry. These data proposes that MSC directed metabolic status, specifically toward oxidative phosphorylation constitutes a tractable vulnerability in peritoneal dissemination.

#0846 Evidence of functional cytotoxic T-cell responses to induced pluripotent stem cells (IPSCs): Paving the way for IPSC-derived cancer vaccines.

Valentine Feyants[1], Catherine Martel[2], Christophe Desterke[1], Mequa Maatoug[1], Diana Chaker[2], **Ali G. Turhan**[2], Annelise Bennaceur Griscelli[2], Frank Griscelli[3]

[1]INSERM U1310, Universite Paris-Saclay, Villejuif, France,[2]INSERM U1310, Universite Paris-Saclay CITHERA, Villejuif, France,[3]INSERM U1310, Gustave Roussy Cancer Center, Villejuif, France

Background: Recent studies have demonstrated that both allogeneic or autologous iPSC-based vaccines represent a promising new approach to preventive or curative cancer immunotherapy strategies particularly against aggressive tumors harboring stemness features with high risk of metastatic spread. We have previously demonstrated the in vivo efficacy of this cancer vaccine strategy in mice models (Kishi et al, Front Med, 2021) but the immunogenicity of iPSCs in the context of human cells remains unknown. Methods:To address this issue in human cells, we developed a Mixed Lymphocyte Reaction (MLR) bioassay from collected batches of peripheral blood mononuclear cells (PBMC) from HLA-A2+ donors. The assay was standardized by co-culturing CD8+ naïve T Cells and Dendritic Cells (DCs) derived from CD14+ monocytes which were loaded with iPSCs derived-lysates generated from several iPSCs lines. The primed CD8+ T cells with the lysates were assessed using proliferation assays, phenotypic profiling, and cytokine secretion. Cytotoxic function of the primed CD8+ T cells was assessed after co-culture with several HLA A2+ human cancer cell lines, including melanoma (SK-MEL5), triple negative breast carcinoma (MAD-MB-231) and human colorectal adenocarcinoma (SW-620). Results: After differentiation and maturation, DCs loaded with iPSC-derived lysates highly expressed CD80, CD11c, CD86, MHC class I and II. After co-culture with these DCs, in all tested conditions, primed CD8+T cells exhibited significantly enhanced lysis of the cancer cell lines as compared to control T lymphocytes. These activated T cells displayed an effector phenotype marked by CD137, CD107a, IFN-γ, and TNF-α expression suggesting that iPSCs were able to transmit a a broad array of immunogenic epitopes. We further analyzed the clonal diversity of the α/β TCR repertoire in CD8+T cells primed with different iPSCs using single-cell RNA sequencing. Sixteen distinct T cell clusters were identified, including a minor population of CD8+ Flt3+T cells and a dominant cluster of CD83+ CD8+T cells comprising over 1,000 unique α/β TCR clones. Single cell RNA sequence analyses of these T cells are in progress. Conclusions: Our results provide strong evidence that iPSCs can effectively activate DCs and induce the generation of phenotypically activated and functionally competent cytotoxic T cells. This strategy holds great potential for the development of off-the-shelf, IPSC-based cancer vaccines leveraging the broad antigenic repertoire of iPSC-derived cells able to generate immune response against cancer stem cell genes expressed in the most aggressive cancers such as non-small cell lung cancer, pancreas cancer and glioblastoma.

#0847 The role of tissue renewal in early-onset colorectal cancer.

Bruce M. Boman, Anh Nguyen, Chi Zhang

Helen F. Graham Cancer Center & Research Institute, Newark, DE

A genetic etiology hasn't been discovered yet for early-onset CRC (EOCRC). An essential question is why do somatic *APC* mutations occur at a relatively young age in EOCRC patients? Indeed, *APC* mutations are the initiating event in both EOCRC and later-onset CRC (LOCRC). Moreover, most other cancer types frequently have inactivated *APC* due to promoter hypermethylation. However, we didn't find that other early onset cancer types (age <50) have increased *APC* hypermethylation. So, for EOCRC, we surmise that something is retarding tissue renewal such that cells with acquired *APC* mutations are retained instead of being extruded during tissue turnover. We conjectured that EOCRC involves an essential nutrient required for tissue renewal. Accordingly, we investigated the seven essential vitamins that require adequate dietary intake. Indeed, these vitamins are essential for tissue homeostasis because germline mutations in their receptors cause birth defects. Our bioinformatics analysis shows a high frequency of somatic mutations (2x-fold) in receptors for vitamin A *(STRA6*), and retinoic acid (*RARG*, *PPARG*) in EOCRCs (<45) *vs*. LOCRCs. We also found *RARG* hypermethylation occurs frequently in EOCRCs ($p<0.05$). Moreover, population-based studies report relatively frequent vitamin A deficiency in pre-school-aged children. Consequently, young-aged individuals might be prone to any cancer-initiating effects of vitamin A deficient diets. Indeed, vitamin A plays a crucial role in cell differentiation, particularly in the differentiation of stem cells and during tissue regeneration. Thus, incomplete differentiation of crypt cells due to reduced retinoic acid signaling may provide a mechanism that explains how delayed tissue renewal causes retention of somatic *APC* mutations in colonic epithelium. Thus, we put forth the hypothesis that aberrant vitamin A (retinol) metabolism and *APC* mutation-induced activation of WNT signaling are co-factors in promoting EOCRC.

#0848 Redox regulation of breast cancer metastasis via phenotypic and metabolic adaptation.

Rachel Hazan[1], Viney Kumar[1], Outhiriaradjou Benard[1], premprashant chaudhary[2], mahaldeep kaur[2], Ian Myles , Bethesda[2], Larry Norton[3]

[1]Albert Einstein College of Medicine, Bronx, NY,[2]National Institutes of Health, Bethesda, MD,[3]Dep. Physician-In-Chief For Breast Cancer Prog., Memorial Sloan Kettering Cancer Center, New York, NY

Background: Tumor heterogeneity fuels breast cancer metastasis by selecting subpopulations withepithelial-mesenchymal (EMT) plasticity and stemness. Loss of the antioxidant enzyme glutathione peroxidase 2 (GPx2) in the PyMT mouse model promotes phenotypic and metabolic reprogramming through ΔNp63-regulated hybrid EMT and fatty acidoxidation (FAO)-driven metabolism.
Results: Using our newly engineered PyMT/GPx2 knockout (KO) transgenic mouse model, we observed a striking increase in reactive oxygen species (ROS), HIF1α stabilization, vascular malformation, proliferation (Ki67), stemness (organoid formation), and lung metastasis compared with control tumors. GPx2-deficient tumors were markedly enrichedfor hybrid EMT cells co-expressing p63, KRT8, and KRT14. Flow cytometry confirmed that ~85% of GPx2-KO tumor cells were hybrid ($CD104^+/CD44^+$), with only minor epithelial ($CD104^+/CD44^-$, ~4%) and mesenchymal ($CD104^-/CD44^+$, ~0.8%) fractions. Metabolic profiling revealed FAO as the dominant energy source in GPx2-KO tumors, supported by Seahorse assays showing elevated mitochondrial ATP production, a higherOCR/ECAR ratio, and enhanced palmitate oxidation. GPx2 loss increased p-AMPK,indicative of AMPK-mediated OXPHOS activation, and upregulated GLUT1 whilesuppressing de novo lipogenesis. These changes indicate dependence on exogenousfatty acids through CD36/CPT1-mediated β-oxidation. Notably, lung metastases derivedfrom GPx2-KO tumors showed a shift toward glycolytic metabolism, highlightingmetabolic plasticity during dissemination.
Conclusion: GPx2 loss integrates redox dysregulation with EMT and metabolic reprogramming, fostering hybrid E/M cells endowed with high metastatic potential and adaptive energymetabolism.
Clinical implications: Targeting ΔNp63 signaling or FAO pathways may selectively eliminate metabolically flexible, aggressive hybrid tumor populations, offering a potential strategy to mitigate breast cancer metastasis.

#0850 SOX9 and SEMA7A regulate epithelial cell plasticity in the postpartum mammary gland with implications for postpartum breast cancer.

Lauren M. Cozzens[1], Brendan Hinckley[1], Sonali Jindal[2], Virginia F. Borges[3], Pepper Schedin[4], **Traci Renae Lyons**[5]

[1]University of Colorado Anschutz Medical Campus, Aurora, CO,[2]UT MD Anderson Cancer Center, Houston, TX,[3]Associate Professor, Dept. of Medical Oncology, University of Colorado Denver, Denver, CO,[4]OHSU, Portland, OR,[5]Medicine/Medical Oncology, University of Colorado Anschutz, Aurora, CO

Postpartum breast cancers (PPBCs), defined as breast cancers diagnosed within ten years of childbirth, carry a significantly higher risk of metastasis and mortality compared to breast cancers diagnosed in nulliparous women. Preclinical studies implicate postpartum mammary gland involution, a period marked by extensive epithelial cell death, tissue remodeling, and inflammation, as a driver of this poor prognosis. However, the epithelial programs that govern cell survival, plasticity, and transformation susceptibility during the postpartum window remain incompletely understood. We have previously published that SEMA7A, which is linked to PPBC progression, is involved in the survival of luminal progenitor cells (LPCs) during postpartum involution. Thus, we utilized single-cell RNA sequencing to further define SEMA7A-expressing cells in mouse mammary glands during both lactation and involution to show that SEMA7A is primarily expressed on cells of the endothelium, including pericytes, but less so on mammary epithelial cells. We also revealed that Sox9, a transcription factor that is known to be expressed on mammary epithelial cells, is expressed on LPCs in the mammary gland during involution. Notably, LPCs have been suggested as key cells-of-origin for several mammary tumors. We describe the expression pattern of SOX9 throughout lactation and involution, showing that SOX9 expression changes over the course of involution in both mouse and human samples. Functional *in vitro* models of lactogenic differentiation and involution with immortalized mammary epithelial cells were utilized to define the relationship between SOX9 and SEMA7A in these epithelial states. We found that SEMA7A is low in these epithelial cells across the differentiation and involution process and that SOX9 knockdown in mammary epithelial cells results in increased SEMA7A expression and drives mesenchymal cell phenotypes, uncovering a regulatory axis in which SOX9 restrains SEMA7A-mediated cellular plasticity. Analysis of breast cancer datasets shows that dysregulation of this axis, resulting in co-expression of SOX9 and SEMA7A, correlates with metastatic risk. Together, these findings reveal a previously unrecognized SOX9-SEMA7A signaling axis in the postpartum mammary gland and highlight how studies of normal development can uncover mechanisms of PPBC progression and point toward new avenues for prevention.

#0851 BMP inhibition is an effective treatment for targeting stem-like glioblastoma cell states.

Davey (Cheng Zhe) Li, Michael Luo, Phuong U. Le, Maryam Safisamghabadi, Tuong V. Kieu, Andy Nkili, Paul Wambo, Rozica Bolovan, Javad Nadaf, Kevin Petrecca

Department of Neurology and Neurosurgery, Montreal Neurological Insitute-Hospital, McGill University, Montreal, QC, Canada

Glioblastomas are an aggressive and incurable type of brain cancer with an estimated 250,000 people around the world receiving this devastating diagnosis every year. With a median survival of 14.6 months, standard of care (surgery, radiation, and chemotherapy) is ineffective as it fails to eliminate residual glioblastoma stem cells (GSCs), which cause cancer recurrence.
Previous work suggests that GSCs arise from aberrantly activated neural stem cells (NSCs) from the subventricular zone (SVZ). This unique brain region supports NSC growth and potentially subsequent glioblastomagenesis. Single-cell RNA sequencing (scRNA-seq) and MERFISH spatial transcriptomics of glioblastoma tumors and SVZ tissue from patients have allowed us to generate an atlas of 2 million cells to identify and spatially validate primordial developmental pathways that drive the malignant transformation of SVZ-NSCs and promote GSC survival. Cell-cell interaction, consensus non-negative matrix factorization (cNMF), spatial domain, and neighborhood enrichment analysis revealed bone morphogenetic protein (BMP) signaling as a key pathway maintaining stem-like glioblastoma cells. Thus, we tested LDN193189, a potent BMP signaling inhibitor that selectively blocks the BMP type I receptors ALK2/3.
Using patient-derived GSCs treated with LDN193189, we observe a robust reduction of cell viability at 24 and 48 hour timepoints. Daily treatment for 7 days with LDN193189 on GSCs in vitro displayed reduction in cell cycling, decreased astrocytic stemness markers and BMP downstream signaling, while ablating the oligodendrocytic lineage. Assessment of LDN193189 in a patient-derived ex vivo explant organoid model demonstrated a reduction of cycling cells and reduced BMP signaling. Multiplexed spatial proteomics were performed to further interrogate the glioblastoma explant microenvironment and characterize the treatment response to LDN193189. These results suggest that disrupting key developmental pathways exploited by GSCs can halt highly proliferative GSC stem cell states, thus allowing us to target glioblastoma at its origin to prevent recurrence. Based on these promising pre-clinical results, we are currently exploring launching a Phase 1/2 open-label clinical trial for treating glioblastoma patients with BMP inhibitors.

: Survivorship Research
Poster Session

#0855 A systematic analysis on patients with NSCLC transformation to SCLC.

Duo Xu[1], Xiaomei Wu[2], Bo Zhu[1]

[1]Liaoning Cancer Hospital & Institute, Shenyang, Liaoning, China,[2]The First Hospital of China Medical University, Shenyang, Liaoning, China

Background: Lung cancer is a leading cause of global cancer mortality. Histologic transformation to small-cell lung cancer (SCLC) is a clinically significant yet under-recognized resistance mechanism in non-small cell lung cancer (NSCLC). However, a systematic review encompassing all NSCLC subtypes is lacking. To address this gap, this study integrates published cases to define the clinicopathological features and prognosis of this transformation, thereby guiding clinical management.
Method: We systematically reviewed the published literatures from 2015 to the present using PubMed database to summarize the characteristics and prognosis of cases with transformation from NSCLC to SCLC, included keywords like "transition from NSCLC to SCLC" and "NSCLC conversion to SCLC."
Results: Analysis of 72 publications identified 82 T-SCLC patients (54.9% male; median age 61 (IQR: 52-68). Available data showed 53.97% were never-smokers (34/63) and 53.66% had stage IV disease (44/65). Initial histology was adenocarcinoma (87.80%). The EGFR mutation rate was 58.54% (48/53) pre-transformation, mostly exon 19 Del (40.24%), rising notably to 84.6% (11/13) post-transformation.For pre-transformation, the first-line treatment was targeted therapy (35.37%), combination therapy (29.3%), and chemotherapy (28.0%), with a median progression-free survival (PFS) of 12.1 months (7.0-24.0); the first-generation EGFR-TKIs (18.3%) were most common. Targeted agents were also the most frequent choice in second-line (50.9%). Post-transformation, the mPFS was 8.0 months (5.0-13.0) and platinum-etoposide was the backbone (70.8%). Subsequent lines saw increased targeted therapy use but a sharp patient decline beyond third-line.Survival data post-SCLC diagnosis was accessible for 53 patients. The median overall survival (mOS) was 47.0 months (95% CI, 30.0-66.0 months) . Longer survival was associated with male, adenocarcinoma, smoker, non-metastatic disease, and early-stage disease at initial diagnosis. The median time from the first diagnosis of NSCLC transforming to SCLC was 29.0 months(20.0-46.0). The mOS after the diagnosis of SCLC was 12.0 months (7.0-19.0). The mOS of never smoker was 36.0 months (20.0-78.0). In comparison to male, female had a shorter mOS after converting to SCLC (11 vs 12).
Conclusion:This review systematically summarizes the pathological features of the transformation from NSCLC to SCLC, which primarily occurs in adenocarcinomas harboring EGFR mutations. Despite the availability of platinum-based combination chemotherapy with etoposide tailored for SCLC, patient prognosis remains poor, highlighting a critical therapeutic challenge. This underscores the urgent need for prospective clinical trials and investigations into the mechanisms of resistance to improve patient outcomes.

#0856 Lymphedema symptom burden patterns and cancer recurrence worry among Hispanic breast cancer survivors: Latent profile analysis.

Eunkyung Lee[1], Brian D. Sukhu[1], Jaeyoung Park[2], Jennifer Crook[3], Jongik Chung[4], Victoria Loerzel[3]

[1]Health Sciences, University of Central Florida, Orlando, FL,[2]School of Global Health Management and Informatics, University of Central Florida, Orlando, FL,[3]Nursing Practice, University of Central Florida, Orlando, FL,[4]Statistics and Data Science, University of Central Florida, Orlando, FL

Background: Breast cancer survivors often experience persistent physical and psychosocial challenges, including lymphedema symptoms and unmet supportive care needs. Previous studies have noted that the simultaneous occurring of these burdens may compound their effects on psychological stress, such as recurrence worry. Hispanic populations may face unique survivorship challenges that limit access to healthcare and support.
Objective: This study examined latent profiles of burden from lymphedema symptoms and unmet support needs, and differences in recurrence worry across these profiles within Hispanic women with breast cancer.
Methods: Hispanic women aged 20 and older, previously diagnosed with breast cancer in Central Florida, were for a population-based study examining health-related quality of life from September 2023 to October 2025. Five lymphedema symptoms (pain, swelling, movement, numbness, stiffness) were assessed using the FACT-B+4 scale. The strength of 5 unmet need domains (information needs, care needs, quality of life needs, psychological needs, and practical needs) was assessed using the 35-item Cancer Survivors' Unmet Needs questionnaire. Latent profile analysis was conducted to identify the distinct latent burden patterns, and model performance was evaluated with BIC, AIC, and entropy. Multivariable linear regression compared differences in recurrence worry (frequency, mood impact, daily function interference), measured by the 3-item Lerman Breast Cancer Worry Scale, across the identified profiles.
Results: A total of 564 breast cancer survivors (mean age: 58.9 ± 11.9 years; mean time since diagnosis: 4.1 ± 2.0 years) were included in the latent profile analysis. The five-profile model was selected as the optimal model. The five distinct profiles include low symptoms and moderate needs (Profile 1: n = 72, 12.8%), high symptoms and moderate needs (Profile 2: n = 52, 9.2%), high symptoms and strong needs (Profile 3: n = 34, 6.0%), low symptom and low needs (Profile 4: n = 303, 53.7%), and moderate symptoms but low needs (Profile 5: n = 103, 18.3%). Profiles differed significantly in recurrence worry frequency, mood impact, daily activity interference (all $p < 0.001$). Survivors in Profiles 1, 2, and 3 reported more frequent worry, higher impact on mood, and higher interference with daily functioning than those in Profiles 4 and 5.
Conclusions: Distinct burden profiles highlight heterogeneity in the survivorship experience of Hispanic women with breast cancer. Particularly, survivors with moderate or strong unmet needs reported elevated recurrence worry. Investigating the barriers to symptom management and the strategies to address unmet support needs is crucial to reducing psychological stress and enhancing the quality of life among breast cancer survivors.
Funding: Florida Breast Cancer Foundation.

#0857 Impact of delayed screening/care and frequent mental distress during COVID-19 among SGM cancer survivors.

John A. Fuller, Jessica Wells

Nell Hodgson Woodruff School of Nursing, Emory University, Atlanta, GA

Purpose: Sexual and gender minority (SGM) survivors have a significantly higher risk of late-stage cancer diagnosis compared with cisgender-heterosexual survivors, possibly due to historical exclusion from screening and higher engagement in risk behaviors like smoking, binge drinking, and risky sexual practices. Discrimination, stigma, and minority stress in healthcare settings limit access to screening, care, and treatment and contribute to increasing mental distress. The link between delays and mental health is unclear. This study examines the association between delayed screening/care and frequent mental distress (FMD) during COVID-19 among SGM survivors.

Methods: We utilized secondary data from OUT: The National Cancer Survey, an online questionnaire administered to U.S. adult SGM cancer survivors from September 2020 to March 2021. Participants self-reported delayed screening/care (coded as “Yes,” “No,” or “No, not applicable”) and the number of poor mental health days (free-text response) in the past month. FMD was analyzed as a binary outcome using a Centers for Disease Control and Prevention (CDC)-validated cutoff (i.e., 14 or more PMHD in the last 30 days). Age was included as a covariate, given its established impact on mental health outcomes. Descriptive statistics, bivariate correlations, and logistic regression with sensitivity analyses were performed.

Results: On average, participants (N = 2,073) were aged 58.69 years (SD = 11.12). The number of poor mental health days reported ranged from 0 to 30, with an average of 9.88 days (SD = 10.75). Delayed screening/care was significantly associated with FMD. 37.5% of participants reported delayed screening/care experienced FMD, compared to 49.6% of those who did not ($p < 0.001$). Multivariable regression analysis revealed that delayed screening/care and age were significant predictors of FMD. Participants who reported delayed screening/care were 84% more likely to experience FMD compared to those who did not report delayed screening/care (OR = 1.84, 95% CI: 1.41-2.41, $p < 0.001$). Age was inversely associated with FMD, with each additional year of age reducing the odds of experiencing FMD by 4% (OR = 0.96, 95% CI: 0.95-0.97, $p < 0.001$).

Conclusion: This study highlights the social determinants of health contributing to delays in cancer screening, care, and treatment among SGM cancer survivors. Future research should focus on guiding oncology providers in developing targeted strategies to improve mental health outcomes among marginalized communities, especially during periods of increased healthcare disruption like the COVID-19 pandemic.

#0858 Patient navigation as an equity intervention in head and neck cancer: Perspectives from a geocoded EMR cohort and qualitative insights from frontline navigators.

Alexandra L. Lindgren, Diana L. Morales, Trista A. Beard, Alyssa F. Harlow, Chanita Hughes Halbert

Department of Population and Public Health Sciences, Keck School of Medicine of USC, Los Angeles, CA

Background: In head and neck cancer (HNC), shorter time from surgery to post-operative radiation therapy (PORT) is associated with survival and improved local control. However, delays are common and distributed unevenly, reflecting social determinants of health (SDOH) such as insurance, transportation, language, and housing and food instability. Patient Navigation has been demonstrated to improve screening, follow up, and appointment adherence in breast, lung, and colorectal cancers; however, rigorous evaluations specific to HNC patient navigation and PORT timelines remain extremely limited. This mixed methods study explores the lived experiences and perceived impact of navigators working within a tertiary academic Head and Neck surgical center.
Methods: This concurrent mixed method study includes a quantitative arm and a quantitative interview arm. The quantitative arm utilizes a curated dataset with prespecified inclusion/exclusion criteria with the primary aim of describing baseline disparities in PORT timeliness pre-and-post initiation of the Patient Navigation HNC program and the secondary aims assessing 90-day post-operative emergency room visits and one year survival. Multivariable regression and time-to-event analysis will adjust for clinical factors and SDOH covariates. The qualitative arm comprises semi-structured interviews with all employed Head and Neck Cancer Patient Navigators (PNs). Analysis was conducted utilizing an inductive thematic approach. Interviews were then appraised using a structured three-domain evaluation framework.
Results: Four overarching themes emerged from the conversations: (1) Relational coordination and patient advocacy (2) Incremental process improvement (3) Systematic Barriers and Resource Constraints (4) Vision for program growth. Navigator composite scores ranged from 6-8 of 9, reflecting strong engagement in patient-centered interventions and iterative workflow improvements. For the quantitative arm we will report (1) distributions of time to PORT across SDOH strata (2) adjusted effect estimates for PN on timeliness and adherence, and (3) themes mapping structural and process barriers to delays. Mixed methods integration will yield targets for intervention and measurable Patient Navigator performance indicators.
Conclusions: By pairing robust analytics with Patient Navigator perspectives, this study will clarify if and how patient navigation reduces PORT delays in HNC, define SDOH-responsive metrics for quality improvement of Patient Navigation programs, and inform scalable implementation to improve both oncologic and equity outcomes.

#0860 Development of and consensus building towards shared metrics, measures and benchmarks for the connecting patient populations to clinical trials (CP2CT).

Folakemi T. Odedina[1], Jennifer Le-Rademacher[2], Robert Freimuth[2], Cristina Orozco[1], Laura Lectora[1], Timethia Bonner[1], Holly Thorson[2], Connecting Patient Populations to Clinical Trials(CP2CT) Program Evaluation Work Group, Connecting Patient Populations to Clinical Trials(CP2CT) Steering Committee

[1]Mayo Clinic Florida, Jacksonville, FL,[2]Mayo Clinic Rochester, Rochester, MN

Background: Multidisciplinary research networks often face challenges in harmonizing metrics and measures across participating sites, limiting the ability to aggregate data and generate generalizable insights. To address this barrier within the Connecting Patient Populations to Clinical Trials (CP2CT) Network, the Data, Evaluation, and Coordinating Center (DECC) coordinated the establishment of a unified framework that supports comparable evaluation and enhances the scientific impact of network-wide activities.
Methods: Consensus was developed through a structured, iterative, and collaborative process: (1) drafting initial constructs, metrics, measures, and benchmarks informed by Network site materials and relevant literature; (2) soliciting qualitative and quantitative feedback from Network sites via Basecamp, an innovative online collaborative workspace for construct development; (3) conducting open dialogue sessions followed by systematic review and integration of site feedback; and (4) refining all elements through repeated feedback cycles until no further modifications were requested. Each iteration strengthened the clarity, coherence, and scientific precision of the final constructs.
Results: A total of seven constructs were incorporated into the consensus-development process: clinical trials referral, clinical trials accrual, participants' awareness of clinical trials, participants' knowledge of clinical trials, providers' awareness of NCI-supported clinical trials, providers' engagement with NCI-supported clinical trials, and providers' referral to NCI-supported clinical trials. For each construct, the Network established a conceptual definition (broad description of the construct), an operational definition (specification of how the construct is measured or observed), benchmarks (standards for assessing performance), metrics (quantitative indicators of performance), and measures (tools used to quantify inputs, processes, or outcomes). Common measures were developed for two constructs—clinical trials accrual and participants' knowledge of clinical trials. Although full consensus was not achieved across all four Network sites for every construct, at least three sites reached consensus for the remaining five constructs.
Conclusion: This consensus-building initiative resulted in the development of a unified, scientifically grounded framework. By harmonizing key elements related to clinical trial referral, accrual, awareness, knowledge, and provider engagement, the Network has established foundational tools that enable cross-site data comparability and facilitate more rigorous assessment of efforts to connect diverse patient populations to clinical trials. This framework positions the Network to inform strategies that improve equitable clinical trial participation.

#0861 Examining social determinants of health and clinical trial participation among cancer survivors: A multi-state cross-sectional study.

Amrita S. Mukunda[1], Hui Xie[2], Priyanka N. Srinivasan[1], Qian Wang[3]

[1]Case Western Reserve University School of Medicine, Cleveland, OH,[2]Joseph J. Zilber School of Public Health, University of Wisconsin-Milwaukee, Milwaukee, WI,[3]Seidman Cancer Center University Hospitals, Cleveland, OH

Introduction: Clinical trials are essential for advancing cancer treatment options and providing patients access to novel therapies, yet recruitment and participation among cancer patients remain low. This study examined whether social determinants of health (SDOH) were associated with clinical trial participation among cancer survivors.

Methods: This cross-sectional study analyzed Behavioral Risk Factor Surveillance System data from 2022 to 2024. The sample included cancer survivors aged 18 years or older from 15 states and 2 U.S. territories. An SDOH composite score (range 0-9) was calculated by summing binary responses across nine domains: life satisfaction, social/emotional support, loneliness/isolation, employment disruption, SNAP benefits, food insecurity, housing/utility payment difficulty, threats of utility service shut-off, and transportation barriers. A higher composite score indicated greater social disadvantage. Adjusted logistic regression models identified factors associated with clinical trial participation. All analyses were weighted.

Results: Of the 6,929 cancer survivors, 370 (5.34%) reported clinical trial participation as part of their treatment. Cancer survivors who participated in a clinical trial as part of their treatment were younger, more likely to be female, and from racial/ethnic minority groups compared to non-participants (all p-values <0.05). After adjusting for age, sex, race/ethnicity, marital status, income, comorbidity burden, and health insurance type, SDOH composite score was not associated with clinical trial participation.When examining individual SDOH factors, cancer survivors who had experienced threats of utility service shut-offs (electric, gas, oil, and/or water) in the past 12 months were less likely to have participated in clinical trials (aOR: 0.504, 95% CI: 0.257-0.989, p=0.046). Additionally, cancer survivors with private insurance (aOR: 1.62, 95% CI: 1.14-2.30, p=0.007) and Medicare beneficiaries (aOR: 1.69, 95% CI: 1.22-2.33, p=0.001) were more likely to participate in clinical trials compared to those with Medicaid.

Conclusion: Overall SDOH burden was not associated with clinical trial participation among cancer survivors; however, insurance type and individual determinants of financial vulnerability did have a significant impact. While privately insured survivors and Medicare beneficiaries showed higher participation, those experiencing utility shut-off threats had significantly reduced participation. These findings highlight the importance of addressing financial stressors to improve clinical trial access for patients with cancer.

#0862 Trends in disability among US adult cancer survivors, 2016-2024.

Junlan Pu, Hermine Poghosyan

Yale University, New Haven, CT

Background Cancer and its treatments often lead to physical and functional limitations, placing cancer survivors at increased risk for disability. Yet, there is a limited understanding of how the prevalence of disability has shifted in recent years. Thus, we estimated the trends in disability prevalence of cancer survivors aged ≥18 years overall and by age, sex, race and ethnicity groups.

Methods We used nationally representative data from 2016-2024 Behavioral Risk Factor Surveillance System, a series of cross-sectional and telephone-based surveys of the US noninstitutionalized adults (≥18 years). Adults with self-reported cancer history (except non-melanoma skin cancer) were included. Disability was defined as having difficulty in any of the six domains: hearing, vision, cognition, mobility, self-care, and independent living. We analyzed combined disability and each disability type separately. We used a multivariable logistic regression model to estimate disability prevalence over the years, adjusting for survey year and socio-demographic and health-related factors. Subgroup analyses were performed based on age, sex, race and ethnicity. Analyses accounted for sampling weights and complex survey design.

Results We included 311143 cancer survivors, representing an estimated 124.78 million survivors. Overall, 53.67% of survivors were aged ≥65 years, 57.44% were female and 35.6% had ≤high school education. The adjusted prevalence of disabilities among cancer survivors increased by 5.67% (95% CI: 4.20-7.12; *P* for trend<0.001), from 40.12% in 2016 to 45.78% in 2024. The steepest increase occurred between 2020 and 2021 (by 4.04%, 95% CI: 2.28-5.80). All six disability domains increased (*P* for trend<0.001), with mobility disability showing the most pronounced growth. In 2024, mobility issues were the most prevalent disability (28.73%, 95% CI: 27.77-29.69), followed by the cognition impairment (16.08%, 95% CI: 15.19-16.97), hearing disability (14.68%, 95% CI: 13.92-15.43), difficulty in independent living (13.64%, 95% CI: 12.85-14.42), vision disability (8.87%, 95% CI: 8.11-9.62) and self-care disability (7.56%, 95% CI: 6.90-8.23). The largest increase in disability occurred in 18-34-year age group (10.04%, 95% CI: 1.62-18.45), males (6.06%, 95% CI: 3.96-8.16), and other races and ethnicities (12.78%, 95% CI: 3.70-21.85). Cancer survivors with disability were more likely to be male, Non-Hispanic Black or Hispanic, less educated, unemployed, unmarried, have lower income, report poorer health, and delay medical care (*P*<0.05) than those without disability.

Conclusion Disability among cancer survivors increased steadily, particularly for mobility disability, yet this burden is not equally distributed across age, sex, and racial and ethnic groups. Early identification of disability and the integration of tailored care into survivorship plans are essential, especially for subgroups who experience an unequal burden.

#0863 Internal, external and structural barriers in cancer care faced by survivors from the caribcares study.

Nancy Raquel Cardona-Cordero[1], Ana Patricia Ortiz-Martinez[1], Claudia Boneu[1], Polaris Torres-Rodriguez[1], Marievelisse Soto-Salgado[2]

[1]University of Puerto Rico Comprehensive Cancer Center, San Juan, PR,[2]University of Puerto Rico - Medical Sciences Campus, San Juan, PR

Introduction. Timely diagnosis is a public health priority. However, a great proportion of the population is often diagnosed with advanced disease or as an emergency. The study aimed at examining factors contributing to diagnostic delays and inequalities in cancer care among a subset of cancer survivors in Puerto Rico.
Methods. The Caribbean Cancer Research Center on Environmental and Natural Hazards (CARIBCARES) has been recruiting cancer patients who are or have been in active treatment over the past 12 months since August 20, 2025, to assess the impact of extreme weather events on the quality of life of this population. We conducted a cross-sectional study among participants (n=135) from the ongoing research project of CARIBCARES. Trained research assistants interviewed eligible participants who completed the 60-minute survey. A with a $20.00 incentive was provided to each participant.
Results. Participants' median age was 60 years, and 41% were living below poverty level. Females were willing to participate than males accounting for 66.4% and 33.6% of the sample, respectively. Over half (53%) of participants had a localized stage at cancer diagnosis, while 35% had regional or distant cancer. Around 49.6% of participants reported delays in their diagnosis. The top reported challenges were problems with their health insurance (24%), financial problems (20%) and Lack of communication with health care providers (14%). Smaller groups of participants were affected due to absence of confirmatory or genetic tests (4.4%), while 3% were unable to attend a medical appointment due to damage to their home or neighborhood caused by an extreme weather event.
Discussion. This study highlights critical barriers in the cancer diagnostic and care continuum among survivors participating in the CARIBCARES study, revealing important inequities that disproportionately affect populations in Puerto Rico. These findings underscore systemic weaknesses in healthcare access and navigation that must be addressed to improve early detection and survival outcomes.

#0864 Association between emergency department (ED) involvement in cancer diagnosis and survival across cancer types in the Medicare population.

Shannon Heitkamp[1], Eric Olsen[2], Ali Tafazzoli[3], Bethany Houpt[1], Olivia Hunt[1], **Anuraag R. Kansal**[3], A. Mark Fendrick[4], Eric Klein[3]

[1]Avalere Health, Washington, DC,[2]Department of Emergency Medicine, UCHealth Poudre Valley Hospital, Fort Collins, CO,[3]GRAIL, Inc., Menlo Park, CA,[4]Department of Internal Medicine; Center for Value-Based Insurance Design, University of Michigan, Ann Arbor, MI

Background: A substantial proportion of cancers are diagnosed following an emergency presentation, a pathway consistently associated with advanced stage at diagnosis, poorer survival, and worse patient experience. We aimed to quantify the association between ED involvement in the diagnosis of cancer and overall survival across different cancer types in the Medicare population.
Methods: We conducted a retrospective cohort study of SEER-Medicare beneficiaries diagnosed with invasive cancer between 2010 and 2020 and followed for mortality until 12/31/2020, defining the earliest cancer-related claim as the index date. We excluded beneficiaries without at least 12 months of continuous Medicare Parts A/B/D enrollment before and 1 month after the index date or with a prior cancer diagnosis within one year. Patients with an ED visit within 30 days before the index date were classified as having ED involvement in their diagnosis. Overall survival was evaluated using 17 independent multivariate Cox proportional hazards models, each corresponding to a cancer grouping defined according to SEER major cancer sites with available AJCC staging data (breast, prostate, lung, colorectal, bladder/urothelial tract, uterine, kidney, lymphoma, pancreatic, oral, liver, stomach, ovarian, esophageal, cervical, anal). Covariates included age, sex, race/ethnicity, dual eligibility status, Charlson Comorbidity Index, year of diagnosis, and tumor stage. This analysis did not adjust for some potential confounders including differences in duration of symptoms, performance status, and therapy access or initiation which were not captured in the dataset.
Results: Among 818,120 beneficiaries newly diagnosed with cancer (mean age 74.4 years), 26.4% had ED involvement in their diagnosis. The proportion with ED involvement increased with advancing stage across all cancer types (stage I: 13.8%, II: 26.3%, III: 23.7%, IV: 47.3%) and varied across cancer types, ranging from 6.1% for breast cancer to 53.4% for pancreatic cancer. Mortality during the study period was 44.4% among patients with ED involvement versus 19% among those without, with 46% of cancer deaths following ED involvement. ED involvement was associated with significantly higher mortality across nearly all cancer types, except cervical cancer (HR 0.81; 95% CI 0.28-2.37), ranging from pancreatic (1.61; 1.54-1.67) and colorectal (1.88; 1.84-1.93) to esophageal (3.86; 2.25-6.62) and bladder (4.08; 3.23-5.18).
Conclusion: ED involvement was associated with a significant fraction of overall mortality in patients with cancer and was a strong independent predictor of mortality after adjustment for patient factors including socioeconomics, comorbidities, and cancer stage at diagnosis. These findings highlight the need for strategies that promote earlier, non-emergency diagnostic pathways and structured follow-up.

#0866 Chronic stressors, biological age and deficit accumulation frailty in black breast cancer survivors.

Jeanne S. Mandelblatt[1], Iwalola Awoyinka[2], Jamaica R. Robinson[3], Xingtao Zhou[1], Julie Ruterbusch[4], Jaeil Ahn[1], Lucile L. Adams-Campbell[5], Steven Cole[6], Ann G. Schwartz[3], Brent Small[7], Zhaoming Wang[8], Kelly Rentscher[9], Judith E. Carroll[6]

[1]Oncology, Lombardi Comprehensive Cancer Center, Georgetown University, Washington, DC,[2]Medical College of Wisconsin, Wauwatosa, WI,[3]Karmanos Cancer Institute, Detroit, MI,[4]Wayne State University, Detroit, MI,[5]Georgetown Lombardi Comprehensive Cancer Ctr., Washington, DC,[6]UCLA, Los Angeles, CA,[7]University of North Carolina, Chapel Hill, Chapel Hill, VA,[8]St. Jude Children's Research Hospital, Memphis, TN,[9]Oncology, Medical College of Wisconsin, Milwaukee, WI

Introduction: Chronic social stressors contribute to disparities in population morbidity and mortality. One putative mechanism for these patterns is that stressors, which are differentially experienced by population sub-groups, result in cumulative wear and tear that increases biological aging via sustained release of stress hormones. However, these relationships have not been well studied in cancer survivors.

Methods: This cross-sectional study included 258 Black women from the Detroit Research on Cancer Survivors study. Survivors were 12-60 months post-diagnosis of stage 1-3 breast cancer and had germline DNA available for methylation analyses. Biological age was assessed using the Illumina Infinium Methylation EPIC Array for GrimAge, PhenoAge, Extrinsic Age and Dunedin Pace of Aging. Social stressors included life stress (financial, housing and food insecurity, lack of transportation to medical care, area safety; 0-5 composite score), racial discrimination and neighborhood area deprivation. The outcome was a deficit accumulation frailty index score (0-1; <0.20=robust, 0.20-0.35=pre-frail and >0.35=frail; differences of 0.02-0.06 points are clinically meaningful). Separate linear regression models tested associations of each stressor and deficit accumulation, considering age, time from diagnosis and cytotoxic treatment (chemotherapy, radiotherapy). Mediation models explored whether the relationships between stressors and deficit accumulation were statistically mediated by biological age.

Results: Survivors were an average of 58.8 years (range 30-83), were 21.1 (SD 14.6) months from diagnosis and 69.6% were pre-frail or frail. Between 55-78% had biological age greater than chronological age on one or more epigenetic clock and 88% had a faster pace of aging than expected based on chronological age. For each 1-point increase in life stress there was a 0.06 point increase in adjusted deficit accumulation ($p<0.001$) and life stress accounted for 67% of the explained variance in deficit accumulation. Biological age measured by GrimAge mediated 11.8% of the association between life stress and deficit accumulation ($p<0.05$) and there was similar but non-significant mediation by other epigenetic measures. Living in the most vs. least deprived area was also associated a large clinically meaningful increase in adjusted deficit accumulation ($p=0.007$), but discrimination had a smaller, non-significant effect.

Conclusions: These findings demonstrate an association between experiencing social stressors and deficit accumulation frailty among Black breast cancer survivors and this association was partially driven by biological aging. Future studies are needed to identify aging pathways and possible modifiable factors that could be targeted by policy, behavioral and pharmacological interventions to reduce disparities and improve outcomes among cancer survivors.

#0867 Cancer treatment-related cardiotoxicity among survivors of childhood cancer: A comparative and integrated view of multiple measures of biological age acceleration.

Xiaoxi Meng[1], Tiffany Eulalio[1], Kwangyeon Oh[1], Noel-Marie Plonski[1], Kyla Shelton[1], Heather L. Mulder[1], John B. Easton[1], Jinghui Zhang[1], Emily Walker[1], Geoffrey A. Neale[1], Deo Kumar Srivastava[1], Rebecca M. Howell[2], Jeanne S. Mandelblatt[3], Bonnie Ky[4], Stephanie B. Dixon[1], Gregory T. Armstrong[1], Melissa Maria Hudson[1], Kirsten K. Ness[1], Zhaoming Wang[1]

[1]St. Jude Children's Research Hospital, Memphis, TN,[2]The University of Texas MD Anderson Cancer Center, Houston, TX,[3]Georgetown University, Washington, DC,[4]University of Pennsylvania, Philadelphia, PA

Introduction: Mounting evidence suggests that childhood cancer survivors experience biological age acceleration (BioAgeAccel) and are at increased risk for cardiovascular disease. We performed an integrated analysis of multiple BioAgeAccel measures to examine how aging relates to treatment-related toxicity and cardiovascular risk, and how biomarkers developed under different methodological schemes capture this pathway.

Methods: Cardiovascular disease (CVD) was defined as either cardiomyopathy or myocardial infarction (MI). DNA methylation (DNAm) profiles of peripheral-blood-mononuclear-cells from 2,941 St. Jude Lifetime Cohort participants were generated using Illumina EPIC BeadChips. Biological age was assessed using 43 DNAm-based biomarkers, including epigenetic clocks such as GrimAge, PhenoAge, and DunedinPACE, as well as molecular biomarkers such as C-reactive protein (DNAmCRP). BioAgeAccel was defined as residuals from regressing biological age on chronological age at DNAm blood draw (except DunedinPACE). Cardiotoxic treatment exposures included radiation potentially exposing the heart (heart-RT; mean dose >15 Gy considered high-dose) and anthracycline chemotherapy (cumulative dose ≥250 mg/m^2 doxorubicin equivalents considered high-dose). Multivariable logistic regression models evaluated the associations of each biomarker with CVD. BioAgeAccel was also evaluated as a mediator between heart-RT or anthracycline exposure and CVD to examine its role in the causal pathway. Mediation analyses were conducted for each biomarker individually and for a composite measure derived from principal component analysis.

Results: Median age at cancer diagnosis was 6.1 years (range 0-23.6; Q1-Q3: 2.8-12.6), and at DNAm blood draw was 30.1 years (range 0.2-66.6; Q1-Q3: 21.7-38.0). Overall, 9.4% developed cardiomyopathy (median onset 34.7 years), and 2.3% developed MI (median onset 40.7 years). Most BioAgeAccel measures were elevated after high-dose heart-RT, with fewer associations for high-dose anthracyclines. PC version of GrimAge showed the strongest association with MI (OR=1.85, 95%CI: 1.45-2.36; Bonferroni *P*=4.06E-05), and DNAmCRP showed the strongest association with cardiomyopathy (OR=1.31, 95%CI: 1.14-1.50; Bonferroni *P*=5.17E-03). Mediation estimates varied across biomarkers. A composite BioAgeAccel measure accounted for 31.6% of the heart-RT-MI association, 35.9% of the heart-RT-cardiomyopathy association, and 7.7% of the anthracycline-cardiomyopathy association.

Conclusions: BioAgeAccel measures vary in their associations with cardiotoxicities and treatment-related aging pathways. These findings support further refinement and validation of DNAm-based aging biomarkers to advance future risk stratification and targeted prevention of long-term CVD in survivors.

#0868 Survival outcomes associated with hypothyroidism following cancer therapies.

Harry D. Momo[1], Megan R. Haymart[2], Xu Shi[3], Alison M. Mondul[1]

[1]Department of Epidemiology, University of Michigan, Ann Arbor, MI,[2]Department of Internal Medicine, University of Michigan, Ann Arbor, MI,[3]Department of Biostatistics, University of Michigan, Ann Arbor, MI

Background: Hypothyroidism is a recognized adverse effect of cancer therapies such as immunotherapy (immune checkpoint inhibitors, ICIs), chemotherapy (tyrosine kinase inhibitors, TKIs), and radiotherapy. Although proposed as an indicator of treatment response, its prognostic significance across cancer types and therapies remains under-explored. This study evaluated survival outcomes associated with treatment-induced hypothyroidism.

Methods: We conducted a retrospective cohort study using de-identified electronic health record data from the University of Michigan between 2006 and 2023. Adults (≥18 years) receiving ICIs, TKIs, or radiotherapy, without prior thyroid disease or malignancy were included. We defined hypothyroidism by institutional laboratory criteria or thyroid hormone initiation. Time-dependent Cox models estimated hazard ratios (HRs) and 95% confidence intervals (CIs) for overall and cancer-specific survival, adjusting for demographic, clinical, and lifestyle factors. Analyses were stratified by treatment class and cancer site; sensitivity analyses assessed robustness.

Results: Among 9,909 patients (57,772 person-years; median follow-up 4.64 years), 2,177 (22.0%) developed hypothyroidism (median onset time: 5.04 months). Treatment-induced hypothyroidism was associated with improved overall (HR = 0.86 [0.79-0.93], $p < 0.001$) and cancer-specific survival (HR = 0.76 [0.70-0.84], $p < 0.001$). Stratified analyses showed significant survival benefits with hypothyroidism following immunotherapy (overall HR = 0.75 [0.61-0.92], $p = 0.01$; cancer-specific HR = 0.75 [0.66-0.94], $p = 0.01$) and radiotherapy (HR = 0.88 [0.81-0.96], $p = 0.01$; cancer-specific HR = 0.76 [0.68-0.84], $p <0.001$), but not for chemotherapy. Site specific survival benefits were observed in brain/CNS (HR = 0.39 [0.26-0.61], $p < 0.001$), lip/oral cavity/pharyngeal (HR = 0.77 [0.61-0.97], $p = 0.03$) and lung/bronchus cancers (HR = 0.80 [0.66-0.97], $p = 0.03$) but higher mortality in colon cancer (HR = 1.82 [1.10-3.02], $p = 0.02$). Results were consistent across sensitivity analyses.

Conclusion: Hypothyroidism after immunotherapy and radiotherapy was associated with improved survival, supporting its potential as a prognostic biomarker of therapeutic benefit. Future studies should investigate the underlying mechanisms and clinical implications.

#0869 Sleep duration predicts quality of life during colorectal cancer survivorship across age groups: Results from the ColoCare Study.

Victoria Damerell[1], Sheetal Hardikar[2], Apurva S. Medhe[3], Nathalie Nguyen[4], Christoph Kahlert[1], Christopher I. Li[5], David Shibata[6], Doratha A. Byrd[7], Cornelia M. Ulrich[2], Jane C. Figueiredo[4], Adetunji T. Toriola[3], Anita R. Peoples[8], Biljana Gigic[1]

[1]Department of General, Visceral and Transplantation Surgery, Heidelberg University Hospital, Heidelberg, Germany,[2]Huntsman Cancer Institute, Salt Lake City, UT,[3]Department of Surgery, Washington University St. Louis, St. Louis, MO,[4]Department of Medicine, Samuel Oschin Comprehensive Cancer Institute, Cedars-Sinai Medical Center, Los Angeles, CA,[5]Fred Hutchinson Cancer Center, Seattle, WA,[6]Department of Surgery, University of Tennessee Health Science Center, Memphis, TN,[7]Department of Cancer Epidemiology, Moffitt Cancer Center, Tampa, FL,[8]Department of Population Science, American Cancer Society, Atlanta, GA

Background Early-onset colorectal cancer (EO-CRC, <50 years) survivors often face unique quality of life (QoL) challenges compared with late-onset (LO-CRC, ≥50 years) patients. Sleep disturbances are common during and after cancer treatment and sleep duration of <7 hours may worsen physical and emotional symptoms, however, longitudinal evidence on QoL is limited. This study examined the influence of sleep duration on QoL trajectories over 24 months after primary tumor resection across EO- and LO-CRC patients.
Methods We used mixed-effects models to assess changes in functional and symptom-related QoL domains by age group and sleep duration in 905 CRC patients from three sites of international ColoCare Study: Heidelberg University Hospital, Washington University St. Louis and Cedars-Sinai Medical Center. We assessed sleep duration by the Pittsburgh Sleep Quality Index and QoL scales using the EORTC-QLQ-C30 at enrolment (baseline), and at 6, 12, and 24 months. Time (baseline, 6, 12, 24 months), age group (EO-CRC vs. LO-CRC), and sleep duration (<7 vs. ≥7 hours/night) were included as fixed effects, while QoL scores were used as random effects. Interactions between time, age group, and sleep duration were tested.
Results Functional QoL scores improved over time, with higher global and emotional functioning at 12 and 24 months ($p < 0.01$), while cognitive and role functioning remained stable. Symptom-related QoL fluctuated, with higher dyspnea at 6 months that generally improved by 12 and 24 months. Sleeping fewer than seven hours per night was consistently associated with lower global, social, role, and cognitive functioning as well as greater fatigue, insomnia, nausea, pain, constipation, and appetite loss at baseline ($p < 0.01$). EO-CRC patients reported higher physical but lower social and role functioning as well as higher fatigue, nausea and financial difficulties at baseline ($p < 0.01$) with improvements across most domains over time. EO-CRC patients with short sleep duration experienced lower insomnia at 12 months compared to LO-CRC patients sleeping ≥7 hours ($p < 0.05$). Three-way interactions were limited, suggesting the effects of insufficient sleep on QoL were broadly similar across age groups.
Discussion Sleep duration is a predictor of QoL in CRC survivors, independent of age. EO-CRC patients exhibited distinct baseline deficits in social and role functioning, yet short sleep adversely affected all groups. These findings highlight the potential benefit of interventions targeting sleep to improve both functional and symptom-specific QoL throughout CRC survivorship. Integrating sleep screening and management into routine follow-up could further enhance QoL.

#0870 Neighborhood disparities and treatment outcomes in pediatric acute lymphoblastic leukemia (ALL): A report from the REDIAL Consortium.

Rutu Rathod[1], Amy E. Hughes[2], Pagna Sok[3], Karen Rabin[4], Sandi L. Pruitt[5], Philip J. Lupo[6], Michael E. Scheurer[6], Jeremy M. Schraw[7]

[1]Epidemiology, University of Arkansas for Medical Sciences, Little Rock, AR,[2]University of Texas Southwestern Medical Center, Dallas, TX,[3]Baylor College of Medicine, Houston, TX,[4]Pediatrics, University of California, San Francisco, CA,[5]UT Southwestern Medical Center, Dallas, TX,[6]Pediatrics, Emory University School of Medicine, Atlanta, GA,[7]Pediatrics, Baylor College of Medicine, Houston, TX

Introduction- Acute lymphoblastic leukemia (ALL), the most common pediatric cancer, shows persistent outcomes disparities among socioeconomically disadvantaged and Hispanic children. Structural factors such as neighborhood socioeconomic status (nSES) and residence in Hispanic enclaves - culturally distinct neighborhoods with high concentrations of Hispanic residents, linguistically isolated households, and ethnic resources - may influence cancer outcomes, yet their impact on pediatric ALL remains unclear. We examined associations of nSES and Hispanic enclave residence with treatment outcomes in children with ALL.

Methods- The REducing Disparities in Acute Leukemia (REDIAL) Consortium includes six pediatric cancer centers across Texas. We included children (0-24 years) diagnosed with ALL between 2005-2017 and treated at centers in Houston, Fort Worth, and McAllen. Census tract Hispanic enclave and nSES (Yost) indices were computed from U.S. Census and American Community Survey data. We defined Hispanic enclaves as tracts in the highest quintile (Q5) or Q4 adjacent to Q5 with >250 Hispanic residents, and low nSES as tracts in the lowest two quintiles of statewide distribution, using patient addresses at the time of diagnosis. Outcomes included end-of-induction (EOI) minimal residual disease (MRD) positivity (≥0.01%), relapse, event-free survival (EFS), and overall survival (OS). Associations were evaluated using logistic and Cox regression models adjusted for sex, age at diagnosis, race/ethnicity, NCI risk group, ALL immunophenotype, cytogenetic subtype, and treating institution.

Results- Among 1,348 patients, 41% resided in low nSES tracts and 42% in Hispanic enclaves; 59% were Hispanic and 90% had B-ALL. Median follow-up was 5.6 years for EFS and 5.2 years for OS. In adjusted analyses, neither enclave residence (aOR= 1.22; 95% CI= 0.82, 1.80) nor low nSES (aOR= 1.06; 95% CI= 0.73, 1.55) were associated with EOI MRD positivity; similar null associations were observed for relapse (enclave: aOR= 0.88; 95% CI= 0.52, 1.49; low nSES: aOR= 1.04; 95% CI= 0.66, 1.64), EFS (enclave: aHR= 0.81; 95% CI= 0.52, 1.26; low nSES: aHR= 1.04; 95% CI= 0.71, 1.54), and OS (enclave: aHR= 1.07; 95% CI= 0.59, 1.94; low nSES: aHR= 0.89, 95% CI= 0.53, 1.51). Although unadjusted analyses indicated slightly poorer 5-year EFS for low nSES areas (81% vs. 85%, p=0.04), this difference attenuated after adjustment.

Conclusions- In this large, multi-center, and diverse cohort of children with ALL, neighborhood socioeconomic disadvantage and residence in Hispanic enclaves were not independently associated with treatment outcomes after accounting for clinical and cytogenetic features. Future studies should examine other social determinants and the influence of neighborhood context on disease characteristics, survivorship, and late effects.

#0871 Surgical approach and five year survival in early stage cervical cancer: A national cancer database analysis.

Vishruti Pandya[1], Marguerite R. Irvin[2], Sharad Ghamande[3], Charles A. Leath[1], Chenguang Wang[4], Steve Coughlin[5], Warner K. Huh[1], **Sejong Bae**[5]

[1]Obstetrics and Gynecology, University of Alabama at Birmingham, Birmingham, AL,[2]Epidemiology, University of Alabama at Birmingham, Birmingham, AL,[3]Obstetrics and Gynecology, Augusta University, Augusta, GA,[4]Statistical Innovation Biostatistics and Data Management, Regeneron, Basking Ridge, NJ,[5]Biostatistics, Data Science, and Epidemiology, Augusta University, Augusta, GA

Background: The optimal surgical approach for early-stage cervical cancer remains debated, especially after the Laparoscopic Approach to Cervical Cancer (LACC) trial raised concerns about minimally invasive surgery (MIS). This study evaluates the association between surgical approach (robotic/MIS vs. open surgery) and five-year survival, accounting for demographic, facility, and clinical factors.

Methods: We analyzed data from the National Cancer Database (NCDB) for patients diagnosed with AJCC stage I-IIA cervical cancer from 2004-2022 who underwent surgery. Patients were classified as cases (died within five years) or controls (alive at five years). Multivariable logistic regression assessed the association between surgical approach and five-year mortality, adjusting for age, race, insurance, facility type, geographic region, distance traveled, tumor grade, comorbidity, adjuvant therapy, length of stay, and 30-day readmission.

Results: Among 18,849 patients, 2,263 (12.0%) died within five years. Robotic/MIS was associated with lower five-year mortality compared to open surgery (adjusted OR: 0.86; 95% CI: 0.76-0.99). Higher mortality was independently associated with receipt of adjuvant therapy (aOR: 1.79), older age (aOR per year: 1.05), Black race (aOR: 1.40), public insurance (aOR: 1.41), treatment at comprehensive community cancer centers (aOR: 1.38), travel >50 miles (aOR: 1.35), higher tumor grade (aOR: 2.66), and greater comorbidity burden (aOR: 2.30). Readmission rates did not differ significantly by surgical approach.

Conclusions: Robotic/MIS was significantly associated with improved five-year survival compared to open surgery in early-stage cervical cancer. However, demographic, facility, and clinical factors, including race, insurance, facility type, and comorbidities, were also strong predictors of mortality, highlighting persistent disparities. These findings underscore the need to address healthcare inequities and optimize care delivery. Future research should further explore how patient and systemic factors modify survival outcomes.

#0872 Trajectories of body image distress among diverse young adult cancer survivors.

Mariah Bianca Echeverria[1], Dayanara Ruiz[1], Julia Stla[2], Maureen Cairns[1], Priscilla Marin[1], Jonathan Kaslander[1], Kimberly A. Miller[1]

[1]Department of Population and Public Health Science, Keck School of Medicine of USC, Los Angeles, CA,[2]Department of Medical Oncology, Division of Population Sciences, Dana-Farber Cancer Institute, Boston, MA

Introduction: Body image distress (BID) is a psychological stressor for young adult cancer survivors (YACS), but its trajectory over time remains underexplored due to limited longitudinal data among this population. We examined how BID trajectories evolve as YACS progress throughout survivorship and assessed differences by Hispanic/Latino (H/L) ethnicity.

Methods: YACS aged 18-39 years were recruited within 3 months of a de novo cancer diagnosis from two comprehensive cancer centers and a safety-net hospital, across all cancer stages. The 9-item Body Image Scale (BIS) assesses cancer-specific BID on a 5-point Likert scale, ranging from “not at all” to “very much”. The BIS was administered at three time points (baseline, 3 months, and 12 months); mean scores ≥ 10 were considered clinically meaningful. Latent Growth Curve Modeling (LGCM) was used to model and estimate longitudinal BID trajectories, with an unconditional model (model 1) for the overall trajectory and a conditional model (model 2) for ethnicity that included covariates of gender, socioeconomic status (SES), age at diagnosis, and education. Model fit indices evaluated the models.

Results: Among the sample of 119 YACS, 56.3% were of H/L origin, 67.2% female, 44.5% were of low SES (<$40k), and 47.9% were college graduates or higher; participants had a mean age at diagnosis of 32.0 (*SD*: 5.45). BID trajectories were slightly above the clinical threshold at all timepoints (baseline = 10.7; 3-month = 10.9; 12-month = 10.6; $p > .10$), suggesting that BID did not improve over time. Model 1 fit well (CFI = 1.00), the slope was non-significant ($p = .89$), and the intercept showed significant variability ($p < .001$), indicating individual differences in BID severity. Model 2 also fit well (CFI = 1.00); gender predicted higher BID, as females had significantly greater BID across all time points ($p < .001$). By ethnicity, non-H/L YACS showed a gradual rise in BID over time, while H/L YACS had a slight decrease in BID over time, suggesting a protective trend; however, this trend was not significant ($p = .87$). No relationship was found between SES, education, and age at diagnosis.

Conclusion: Among YACS in this cohort, clinically significant BID persisted throughout the first year of survivorship and did not improve over time. Findings reveal a need for longitudinal monitoring of BID and the need for gender-specific interventions to mitigate BID throughout survivorship. Though non-significant, divergent directional trends by ethnicity suggest possible culturally informed protective factors that warrant further evaluation in larger samples.

#0873 Factors associated with functional status among older women with ovarian cancer.

Minh Tung Phung[1], Lisa M. Barroilhet[2], Neil Binkley[3], Ronald E. Gangnon[4], Janelle Sobecki[2], Britton Trabert[5], Amy Trentham-Dietz[1]

[1]Department of Population Health Sciences & Carbone Cancer Center, University of Wisconsin-Madison, Madison, WI,[2]Department of Obstetrics and Gynecology & Carbon Cancer Center, University of Wisconsin-Madison, Madison, WI,[3]Department of Geriatrics and Endocrinology, University of Wisconsin-Madison, Madison, WI,[4]Department of Biostatistics and Medical Informatics, University of Wisconsin-Madison, Madison, WI,[5]Department of Obstetrics and Gynecology & Huntsman Cancer Institute, University of Utah, Salt Lake, UT

Background: Women aged 65+ account for nearly half of new ovarian cancer diagnoses. This patient group faces a substantial risk of declining functional status, i.e., the capability to carry out essential daily activities necessary for basic needs and health, such as dressing, bathing, toilet use, and eating. For this patient group, maintaining functional independence is a top priority. However, factors influencing functional status in older women with ovarian cancer remain poorly understood. This study aimed to identify demographic and clinical factors associated with functional status in this vulnerable population.

Methods: We utilized data from the Minimum Data Set (MDS), which provides standardized functional assessments for U.S. nursing home residents. MDS data were linked with SEER-Medicare to capture cancer diagnoses and medical histories. The cohort included 6,257 women with primary invasive epithelial ovarian cancer diagnosed at age 65+ between 2000-2019. Functional status was quantified using a validated Activities of Daily Living (ADL) scale ranging from 0-28, with higher scores indicating greater dependency. A linear mixed-effect model was fit to identify factors associated with functional status during the first year after diagnosis, while accounting for repeated measures. Variables included age at diagnosis, Charlson Comorbidity Index, tumor stage, histotype, race/ethnicity, and Medicaid enrollment (as a proxy for socioeconomic status).

Results: Median age at diagnosis was 79 years (interquartile range 74-84 years) with most diagnosed at distant stage (74%). Older age was associated with higher ADL scores (mean difference [MD]=0.07 per one year increase in age, 95% confidence interval [CI] 0.05-0.09, $p<0.01$). Other factors associated with higher ADL scores included: higher comorbidity (MD=0.41 per unit increase in Charlson Comorbidity Index, 95% CI 0.33-0.50, $p<0.01$), later tumor stage (distant vs. localized stages: MD=1.38, 95% CI 0.80-1.95, $p<0.01$) and non-serous histotype (non-serous vs. serous: MD=0.90, 95% CI 0.63-1.18, $p<0.01$). Higher ADL scores were also observed for non-White vs. White women (MD=1.95, 1.45, 1.14 for Black, Hispanic, and Asian/Pacific Islander, respectively, all $p<0.01$) and Medicaid-enrolled patients vs. non-enrolled (MD=0.65, 95% CI 0.11-1.18, $p=0.02$).

Conclusions: Older age, higher comorbidity, later tumor stage, non-serous histotype, non-White race/ethnicity, and Medicaid enrollment are independently associated with increased functional dependency in older women with ovarian cancer. These findings suggest both biological and socioeconomic drivers of functional decline. Targeted supportive care is needed to mitigate functional decline, particularly for women with advanced disease, comorbidities, minority backgrounds, and low socioeconomic status.

#0874 Maintenance therapy in first remission for advanced fibrolamellar carcinoma.

Laura Golian[1], Paul M. Kent[2], Tom Stockwell[1]

[1]FibroFighters Foundation, Temecula, CA,[2]FibroFighters Foundation, River Forest, IL

Background: Fibrolamellar carcinoma (FLC) is a rare primary liver malignancy affecting predominantly adolescents and young adults, with high recurrence rates even after complete macroscopic resection. Traditionally, surgical intervention alone was largely considered the only curative strategy. Research in recent years suggests the role of systemic therapy, however no consensus guidelines currently exist. This study evaluates progression-free survival (PFS) and overall survival (OS) after surgery, while incorporating stage, type of therapy, and resection margin status as prognostic factors. This is the first study to evaluate outcomes associated with maintenance/adjuvant therapy following surgical resection in a real-world FLC cohort.

Methods: We analyzed 207 patients with FLC who underwent surgical resection in a retrospective multicenter dataset. Adjuvant systemic therapy was categorized as “none,” “chemotherapy,” or “immunotherapy.” Endpoints included PFS and OS calculated from date of surgery. Kaplan-Meier estimates and log-rank tests assessed unadjusted differences. Multivariable Cox proportional hazards models evaluated the independent effects of therapy type, stage (Localized = Stage 1, Regional = Stages 2 & 3, Metastatic = Stage 4), and margin status (R0 = NED, R1 =Microscopic Disease, R2 = Gross Disease Remains).

Results: A total of 200 patients were evaluable for PFS (163 progression events) and 199 for OS (75 deaths). Stage was the strongest predictor of outcome: metastatic disease was associated with an 8.6-fold higher hazard of progression and a 47.7-fold higher hazard of death relative to localized disease. Margin status was prognostic, with R2 resections conferring a significantly increased hazard of death (HR 2.87, 95% CI 1.50-5.47).Adjuvant systemic therapy was independently associated with prolonged PFS after adjusting for stage and margin. Compared with no therapy, chemotherapy (HR 0.44, 95% CI 0.25-0.75) and immunotherapy (HR 0.41, 95% CI 0.26-0.66) both benefitted metastatic patients. Although there was no statistical significance in OS for chemotherapy or immunotherapy, this is likely the result of other factors and suggests need for additional study.

Conclusions: In this large real-world surgical cohort of FLC patients, postoperative chemotherapy and immunotherapy were independently associated with reduced risk of progression, with the most pronounced benefit in metastatic disease. OS was driven primarily by disease stage and margin status. These findings suggest a potential role for postoperative systemic therapy in patients with advanced FLC and highlight the critical importance of achieving negative surgical margins. Prospective studies are needed to validate these results and define evidence-based guidelines.

#0875 Identifying novel therapeutic targets for cancer-related fatigue in colorectal cancer patients using lipidomics: Results from the ColoCare Study.

Nicole C. Lorona[1], Mary C. Playdon[2], James E. Cox[3], Alan Maschek[4], Xiaoyin Li[5], Aasha I. Hoogland[5], Maria F. Gomez[5], Patricia A. Erickson[2], Mmadili N. Ilozumba[2], Victoria Damerell[6], Ildiko Strehli[2], Megan Mclaws[2], Lyen C. Huang[2], Paul Stewart[2], Sheetal Hardikar[2], Jennifer Ose[7], Anita R. Peoples[2], Brent Small[8], David Shibata[9], Doratha A. Byrd[5], Adetunji T. Toriola[10], Christopher I. Li[11], Cornelia M. Ulrich[2], Biljana Gigic[6], Heather S. L. Jim[5], Jane C. Figueiredo[1]

[1]Department of Medicine, Samuel Oschin Comprehensive Cancer Institute, Cedars-Sinai Medical Center, Los Angeles, CA,[2]Huntsman Cancer Institute, University of Utah, Salt Lake City, UT,[3]Department of Biochemistry, University of Utah, Salt Lake City,, UT,[4]Department of Nutrition and Integrative Physiology and the Diabetes and Metabolism Research Center, University of Utah, Salt Lake City, UT,[5]Department of Health Outcomes and Behavior, H. Lee Moffitt Cancer Center and Research Institute, Tampa, FL,[6]Heidelberg University Hospital (UKHD), Heidelberg, Germany,[7]Department of Information and Communication, University of Applied Sciences and Arts, Hanover, Germany,[8]School of Nursing, The University of North Carolina at Chapel Hill, Chapel Hill, NC,[9]University of Tennessee Health Science Center - Memphis, Memphis, TN,[10]Washington University School of Medicine in St. Louis, Saint Louis, MO,[11]Fred Hutchinson Cancer Center, Seattle, WA

Background: Cancer-related fatigue (CRF) is the most frequently reported symptom among patients with colorectal cancer (CRC), with limited therapeutic options. Alterations in metabolic pathways related to lipid metabolism have been shown to play a role in non-cancer fatigue-associated diseases, and are hypothesized to influence CRF. The purpose of the present study was to investigate serum lipidomic biomarkers to identify longitudinal predictors of CRF in a prospective cohort of patients with CRC.
Methods: The ColoCare Study enrolled men and women ages 18 to 89 with newly diagnosed primary stage I-IV CRC at six U.S. sites and one German site. CRF was measured using the fatigue subscale of the European Organization for Research and Treatment of Cancer Quality of Life Questionnaire C30 (EORTC QLQ-C30) at T0 (CRC surgery/baseline), T1 (6 months post-surgery), T2 (12 months), and T3 (24 months). Using blood collected at each time point, we performed targeted lipidomics following comprehensive protocols for measurement and quality control. For the present study, participants with stage I-III disease and at least one measurement of CRF and lipidomic profiling (N=863) were included. Using linear mixed effects models with an interaction term with time point and subject-specific random intercepts, we assessed associations between individual lipids and CRF at each time point. We adjusted for multiple testing using the Benjamini-Hochberg correction for false-discovery rate. Models also adjusted for age, sex, tumor site, stage, body mass index, chemotherapy, radiation, and study site. We used elastic net regression on a training subset (n=176) to identify lipids at T1 (when first-line treatment was nearing completion) that were predictive of fatigue at T2. Further analyses validating prediction models and using metabolic pathway analyses are ongoing.
Results: Mean age was 61.6 years (SD: 12.7). N=305 total lipids were identified. In linear mixed effects models, no lipids were associated with CRF at T0 or T1. At T2 and T3, higher levels of ceramides (20), monohexosylceramides (11), gangliosides (4), trihexosylceramides (1), and sphingomyelins (16) were associated with lower CRF after adjustment for multiple testing. Predictive modeling identified higher levels of three sphingolipids at T1 associated with lower CRF at T2 and higher levels of two lipids (one diglyceride and one ceramide) at T1 associated with higher CRF at T2.
Conclusions: Specific sphingolipids, including ceramides, monohexosylceramides, and sphingomyelins, were inversely associated with CRF, suggesting a protective role. Predictive modeling supports their potential as targetable biomarkers of fatigue. These findings highlight lipid metabolism as a promising target for understanding and mitigating fatigue in cancer survivors, warranting external validation and mechanistic research.

#0876 Medication adherence and contributing factors among cancer survivors with cardiovascular disease.

Hyunjung Lee, Lynda Waku Kouomou, Farhad Islami

Surveillance & Health Equity Science Department, American Cancer Society, Atlanta, GA

Background Cardiovascular disease (CVD) is the leading cause of non-cancer mortality among cancer survivors. CVD incidence is about twice as high in cancer survivors as in the general population, likely driven by cardiotoxic cancer therapies and shared risk factors like smoking and obesity. Among those with known CVD, adherence to CVD medications often declines following a cancer diagnosis. Previous studies found higher non-adherence in younger ages, females, and those with high copayment insurance but reported mixed findings for other sociodemographic factors and comorbidity burden. This study investigates determinants of suboptimal adherence to CVD medications among cancer survivors with CVD.

Method We used nationally representative data from the pooled 2010-2022 Medical Expenditure Panel Survey. The primary outcome was CVD medication adherence, defined as the proportion of days covered ([total days supplied ÷365]×100) of ≥80%. Logistic regression was used to estimate associations between medication adherence and individual sociodemographic, access to medication, and health-related factors, adjusting for potential confounders.

Results Approximately 70% of cancer survivors aged ≥18 years had CVD (N=18,461). In adjusted models, CVD medication adherence among cancer survivors was lower in ages 18-44 (adjusted OR [AOR]=0.51, 95%CI=0.37,0.71) and 45-64 (AOR=0.79, 95%CI=0.70,0.90) than ages ≥65 years; females (AOR=0.79, 95%CI=0.70,0.88) than males; and those with a high school diploma (AOR=0.80, 95%CI=0.70,0.92), some college education (AOR=0.78, 95%CI=0.67,0.90), or a bachelor's or higher degree (AOR=0.72, 95%CI=0.62,0.84) than those with less than high school education. Adherence was also lower among cancer survivors who only used community pharmacies (AOR=0.82, 95%CI=0.69,0.98) than those who have ever used mail order or online pharmacies. Adherence was higher among cancer survivors in the Midwest (AOR=1.27, 95%CI=1.10,1.47) and South (AOR=1.23, 95%CI=1.08,1.40) than West; those with comorbidity score of 3 (AOR=1.23, 95%CI=1.02,1.48) than comorbidity score of zero; and those taking ≥5 medications (AOR=2.32, 95%CI=2.07,2.59) than taking <5 medications. Other factors including race and ethnicity, marital status, income, employment status, health insurance, activity limitation, self-reported health status, and type of cancer were not associated with adherence in adjusted models.

Conclusions CVD medication adherence among cancer survivors was lower among young adults; women; individuals with higher education, multiple chronic conditions, limited access to mail-order or online pharmacies, or managing multiple medications; and in the Midwest and South regions. Targeted interventions are needed to improve cardiovascular medication adherence and long-term health outcomes in cancer survivors.

#0877 Optimal post-diagnostic dietary patterns for prevention of frailty among men with prostate cancer.

Chaoran Ma[1], Yuanyuan Deng[1], Li-Wei Wu[2], Jane Bailey Vaselkiv[3], Colleen B. McGrath[3], Caroline Himbert[4], Lorelei A. Mucci[3], Edward L. Giovannucci[5]

[1]University of Massachusetts - Amherst, Amherst, MA,[2]National Defense Medical Center Taipei Taiwan, Taipei, Taiwan,[3]Harvard T.H. Chan School of Public Health, Boston, MA,[4]University of Utah, Salt Lake, UT,[5]Professor of Nutrition & Epidem., Harvard TH Chan School of Public Health, Boston, MA

Background. Frailty has been associated with poor prognosis in prostate cancer patients. Diets with a focus on plant-based foods associated with a lower risk of frailty, but few studies have examined these diets on frailty among prostate cancer survivors. We thus prospectively assessed various dietary patterns after prostate cancer diagnosis in relation to risk of frailty in a large U.S. prospective cohort.

Methods. We included 5,191 males who were not frail prior to their prostate cancer diagnosis between 1986 and 2018 from the Health Professional Follow-up Study and assessed post-diagnostic dietary patterns based on general dietary recommendations. Incident frailty was defined as having ≥3 out of five criteria (fatigue, reduced resistance, reduced aerobic capacity, having several illnesses, and a significant weight loss during the previous year) in the FRAIL scale through 2020. We used left-truncated Cox proportional hazards regression models to estimate hazard ratios and 95% confidence intervals for frailty across quartiles of dietary scores adjusting for potential confounders.

Results. During a median follow-up of 12 years, we observed 1,433 events of frailty among 5,191 men with prostate cancer. Participants with better adherence to the post-diagnostic diets were more likely to have a lower BMI, be more physically active, to use multivitamins, and less likely to smoke. In models adjusting for age, lifestyle factors, clinical characteristics, treatments, and other health conditions, comparing extreme quartiles, adherence to the Diabetes Risk Reduction Diet (DRRD, HR = 0.81, 95% CI = 0.76, 0.86), Dietary Approaches to Stop Hypertension score (HR = 0.84, 0.79, 0.90), Alternative Healthy Eating Index-2010 (HR = 0.85, 0.79, 0.91), and Alternate Mediterranean Diet (HR=0.92, 0.87, 0.98) were associated with a lower risk of frailty (P for trend < 0.01 for all), while no association was found for the World Cancer Research Fund/American Institute for Cancer Research diet, healthful plant-based diet, empirical dietary index for hyperinsulinemia (EDIH), and empirical dietary inflammation pattern. The inverse associations between dietary patterns and frailty persisted in subgroups, and were generally stronger in men who were younger, overweight or obese, engaged in vigorous physical activity, never smoked, with lower alcohol consumption, with higher Gleason score, and ever received androgen deprivation therapy. The associations between dietary patterns and frailty were similar in the 4-year lagged analysis. When excluding prostate cancer cases diagnosed before 2008, a more pronounced trend was observed for the DRRD (HR=0.62, 0.42, 0.91) and reversed EDIH (HR=0.51, 0.34, 0.78).

Conclusions. Adherence to healthy dietary patterns after prostate cancer diagnosis were associated with lower risk of frailty, which may inform on future dietary guidelines for prostate cancer survivors.

#0878 Long-term physical quality of life in survivors of adolescent and young adult Hodgkin lymphoma: Risk factors and associations with adverse health outcomes.

Carlos Cruz[1], Amanda Warner[1], Adiya Rahman[1], Bryce West[1], Mia Brumlow[1], Qian Xiao[2], Karen Albritton[3], Gregory Aune[4], Karen Eshelman-Kent[4], Sairah Ahmed[1], Kelly Merriman[1], Susan Peterson[1], Michael Roth[1], Michelle A. T. Hildebrandt[1]

[1]UT MD Anderson Cancer Center, Houston, TX,[2]UTHealth School of Public Health, Houston, TX,[3]Cook Children's Medical Center, Fort Worth, TX,[4]UTHealth San Antonio/Mays Cancer Center, San Antonio, TX

Purpose: Few studies characterize patient-reported outcomes in long-term survivors of adolescent and young adult (AYA, age 15-39 years at diagnosis) Hodgkin Lymphoma (HL). The present study aims to describe long-term health outcomes of survivors and identify the impact of cancer diagnosis and treatment exposures on health and quality of life (QoL).

Methods: This study included AYA HL survivors (N=264) previously treated at MD Anderson Cancer Center who were at least 5 years post diagnosis. At time of study enrollment, participants completed a comprehensive health questionnaire, which included the SF-36 QoL questionnaire. The SF-36 was used to calculate Physical Component Summary (PCS) and Mental Component Summary (MCS) scores. A subset of HL patients (N=44) had also previously completed the SF-12 questionnaire within 6 weeks of diagnosis. In parallel, 67 siblings of cancer survivors completed the same health questionnaire. Clinical characteristics and treatment information were obtained from the medical record. Area deprivation index (ADI) was calculated based on zip code at time of questionnaire completion.

Results: The median age at HL diagnosis and questionnaire completion of 26.0 and 41.8 years, respectively. Survivors had a significantly poorer PCS compared to siblings (45.3 vs 47.5, p=0.03), as well as a greater proportion of individuals with extremely poor PCS scores (scores ≤40; 16% vs 10%). Among HL survivors, no difference in PCS was observed by race/ethnicity (p=0.82). However, survivors who resided in neighborhoods with increased deprivation had significantly lower PCS compared to those in the highest resource neighborhoods (p=0.003). Treatment exposures and clinical characteristics were also related to PCS, in which survivors who received radiation treatment and had HL relapse were linked to lower PCS scores compared to survivors who did not (44.5 vs 46.7, p=0.03 and 43.5 vs 45.9, p=0.04). Survivors with extremely poor PCS reported increased prevalence of adverse health outcomes, such as diagnoses impacting cardiovascular, respiratory, and nervous systems (p<0.001 for each) compared to survivors with a PCS >40. These patients also reported increased cholesterol, pain, and depression medication use (p<0.001 for each). No differences in mental QoL defined by the MCS were observed between survivors and siblings.

Conclusion: HL is characterized by long-term survival, making health outcomes and QoL integral aspects of their cancer experience. This study showed that long-term survivors of HL experience reduced physical QoL. Moreover, this reduction is related to adverse health outcomes, underscoring the necessity of long-term support and clinical interventions to improve physical health for HL survivors.

#0879 Utilization of pelvic floor therapy after a colorectal cancer diagnosis in a universal-access health system.

Kimberly R. Robins[1], Yvonne Eaglehouse[2], Craig D. Shriver[3], Kangmin Zhu[4]

[1]Murtha Cancer Center Research Program, Uniformed Services University, Henry M. Jackson Foundation, Bethesda, MD,[2]Murtha Cancer Center Research Program, Uniformed Services University Walter Reed Surgery, Henry M. J, Bethesda, MD,[3]Uniformed Services University, Bethesda, MD,[4]Professor, Walter Reed National Military Medical Center, Rockville, MD

Background: About 70-90% of patients with colorectal cancer experience declined bowel function after treatment. Pelvic floor therapy (PFT) can improve bowel function and quality of life, yet access to PFT remains limited and factors associated with its use are understudied. Conducting this research within the U.S. Military Health System, a universal healthcare system, allows a clearer assessment of demographic, clinical, and system-level factors associated with receiving PFT while minimizing the effects of affordability and access on the results.

Methods: We conducted a nested case-control study of adults (≥18 years) with stage I-III colorectal cancer who had surgery within 6 months of diagnosis (2001-2014) in the MilCanEpi database. PFT recipients (cases) and non-recipients (controls) were matched by diagnosis month/year with a 1:1 ratio. Patients with non-TRICARE insurance (except Medicare which is part of coverage for all patients aged ≥65 years with TRICRE for Life) were excluded. Stepwise multivariable logistic regression was used to calculate adjusted odds ratios (aORs) with 95% confidence intervals (CIs) and identify factors associated with PFT use. To assess potential effect modification by sex, results from the overall adjusted model were compared with a men-only analysis.

Results: PFT recipients (n=679) were older (median [min-max]: 60 [21-94] vs 55 [23-88]) and more likely to be male (64% vs 58%), unmarried (24% vs 19%), have ≥1 comorbidity (43% vs 32%), and receive care at a military treatment facility (MTF; 37% vs 29%) than non-recipients (n=679). In the fully adjusted model, the use of PFT was more likely among patients with increased age (aOR=1.03, 95% CI: 1.01, 1.04), males (aOR=1.34, 95% CI: 1.02, 1.77), ≥3 comorbidities (aOR=2.13, 95% CI: 1.34, 3.38), active-duty status (aOR=1.67, 95% CI: 1.09, 2.55), and among those receiving care at a MTF compared to the private-sector (aOR=1.91, 95% CI: 1.39, 2.61). Among men, older age (aOR=1.04, 95% CI: 1.02, 1.06), total (vs partial) colectomy and/or proctectomy (aOR=4.97, 95% CI: 1.52, 16.27) and receiving care at a MTF compared to the private-sector (aOR=3.08, 95% CI: 1.60, 5.91) were associated with higher PFT use.

Conclusion: Within the MHS, fully adjusted analyses showed that PFT utilization after colorectal cancer surgery was higher among older patients, males, those with ≥3 comorbidities, active-duty service members, and patients receiving care at a MTF compared to the private-sector, highlighting the influence of demographic, clinical, and healthcare system factors on PFT use. In men, total (vs partial) surgery was the only factor additionally associated with higher PFT use. These findings suggest that targeted strategies may be needed to increase PFT utilization among groups of patients with a lower likelihood of use in the MHS, such as among younger patients and females.

#0881 Association of social support patterns on health-related quality of life among Hispanic breast cancer survivors .

Brian D. Sukhu[1], Jongik Chung[2], Leslie Palomino[1], B'Ellana Schlosser[1], Angello Pena[1], Eunkyung Lee[1]

[1]Health Sciences, University of Central Florida, Orlando, FL,[2]Statistics and Data Science, University of Central Florida, Orlando, FL

Objectives: Social support influences health-related quality of life (HRQoL) among Hispanic breast cancer survivors, but prior research has not examined which combination of dimensions of social support shapes HRQoL. Thus, we examined the association of social support profiles with HRQoL among Hispanic breast cancer survivors.
Methods: Hispanic women aged 20 and older, diagnosed with breast cancer at least six months earlier, residing in Central Florida, and able to read or speak English or Spanish were recruited via the Florida Cancer Registry's recruitment procedure for a population-based study examining intra-Hispanic disparities in HRQoL. Social support was assessed using the 19-item Medical Outcomes Study questionnaire. Latent Profile Analysis was conducted to explore distinct social support patterns with the four (emotional, tangible, affective, social network) domains as profile indicators. Model fit was determined using AIC and BIC. Functional Assessment of Cancer Therapy - Breast (FACT-B) assessed HRQoL. A multivariable regression model compared FACT-B scores across the identified profiles.
Results: Among 583 women recruited during September 2023 to October 2025, 560 women who completed the social support and HRQoL assessments were included in the analysis. Mean age was 58.9 ±11.9 years, and mean time since diagnosis was 4.1 ±2.0 years. Five support profiles emerged: low support across domains (8.0%), average support (16.6%), above average support (18.4%), high in affection/social support but low tangible support (7.1%), and moderately high support (49.8%). After controlling for age at diagnosis, Hispanic origin, BMI, race, multimorbidity, income, education, functionality, years living in the USA, and current age, we found that women in Profile 4 ($\beta = 15.34$, $p = 0.001$) and Profile 5 ($\beta = 19.19$, $p < 0.001$) had significantly higher FACT-B scores compared to those in Profile 1. Profiles 2 and 3 did not differ significantly from Profile 1.
Conclusions: This study identified five distinct social support profiles among Hispanic women with breast cancer and demonstrated that higher levels of affective and social support are associated with better HRQoL, underscoring the critical role of social resources in survivorship outcomes. These findings highlight the need for culturally tailored interventions that strengthen emotional and social networks to improve quality of life. Funding: Florida Breast Cancer Foundation Scientific Research Grant.

#0882 Cardiovascular disease mortality among breast cancer survivors in Puerto Rico: A population-based competing risk analysis.

Genesis Rodriguez-Ortiz[1], Barbara Segarra-Vasquez, DHSc[2], Francisco Cordova-Perez[3], Vivian Colon-Lopez[1], Cynthia M. Perez[4], Carola T. Sanchez-Diaz[1]

[1]Division of Cancer Control and Population Sciences, University of Puerto Rico Comprehensive Cancer Center, San Juan, PR,[2]School of Health Professions - Clinical Laboratory Science Program, University of Puerto Rico Medical Sciences Campus, San Juan, PR,[3]Section of Cardiology, Veterans Affairs Medical Center, San Juan, PR,[4]Professor/Biostatistics and Epidemiology, University of Puerto Rico Med. Sciences Campus, San Juan, PR

Purpose: Cardiovascular disease (CVD) is an increasingly important cause of death among breast cancer (BC) survivors, yet competing mortality risks remain understudied in Puerto Rico. This study estimated the cumulative incidence of BC-specific and CVD-specific mortality and identified associated risk factors among Puerto Rican BC survivors using competing risk methodology.
Methods: Data were analyzed from 17,430 female BC patients recorded in the Puerto Rico Central Cancer Registry (2004-2019) who survived at least 1 year post-diagnosis and were followed through 2021. Deaths were categorized as BC- or CVD-related. Fine-Gray competing risk models estimated subdistribution hazard ratios (HRs) with 95% confidence intervals, stratified by age group (18-64, 65-79, 80+), to evaluate demographic and clinical correlates of BC and CVD mortality at 5, 10, and 15 years post-diagnosis.
Results: Among 17,430 survivors, 6,881 (39.5%) died during follow-up. BC was the leading cause of death (3,636 deaths; 52.8%), while 470 (6.8%) were due to CVD. Median survival was longer among those who died from CVD (5.5 years (IQR: 3.1, 8.7)) than from BC (3.6 years (IQR: 2.2, 5.9)). By 15 years post-diagnosis, CVD had become a major competing risk: among women aged 80+, the cumulative incidence of CVD mortality reached 14.5% (95% CI: 9.3, 19.4), approaching the BC mortality risk of 16.6% (95% CI: 12.4, 20.6). In younger survivors (ages 18-64), comorbidity significantly increased CVD mortality risk (HR=2.7, 95% CI: 1.5, 4.8) but was not associated with BC mortality (HR=1.0, 95% CI: 0.9, 1.2). Advanced stage and aggressive treatment modalities were consistently associated with greater BC mortality across age groups, while comorbidity and older age were key drivers of CVD mortality.
Conclusions: While BC remains the primary cause of death among survivors, CVD emerges as a substantial competing risk, especially in older women with extended survivorship. Distinct risk profiles, such as the strong influence of comorbidities on CVD mortality in younger survivors and the narrowing difference between BC and CVD mortality in the 80+ age group, underscore the need for survivorship care models that integrate cancer surveillance and cardiovascular management.

#0883 Parental concerns about hereditary risk in adolescent and young adult cancer survivors.

Dayanara Ruiz[1], Kimberly A. Miller[1], Jonathan Kaslander[1], Julia Stal[2], Mariah Bianca Echeverria[1], Charite N. Ricker[1], Andrea C. Betts[3], David Freyer[4], Michael Roth[5], Jessica L. Corredor[6]

[1]Keck School of Medicine of USC, Los Angeles, CA,[2]Dana Farber Cancer-Institute, Boston, CA,[3]UTHealth Houston, Houston, TX,[4]Children's Hospital Los Angeles, Los Angeles, CA,[5]The University of Texas MD Anderson Cancer Center,[6]UT MD Anderson Cancer Center, Houston, TX

Background: Adolescent and young adult cancer survivors (AYAs; diagnosed between ages 15-39) report worries regarding the health of their children, particularly regarding their chance of developing cancer. This study describes the frequency of reproductive health concerns among ethnically diverse survivors of AYA cancer and examines how genetic counseling impacts these concerns.
Methods: AYAs between 18-39 years at diagnosis were recruited from two NCI-designated comprehensive cancer centers and a safety-net hospital. Concerns regarding the health of future children were evaluated using the three-item Child's Health Subscale (CHS), a subset of the Reproductive Concerns after Cancer Scale. Receipt of genetic counseling was self-reported. Descriptive statistics and mean overall score comparisons were examined, stratified by ethnicity and receipt of counseling.
Results: The sample included 58 AYAs (48% Hispanic, 79% female) diagnosed at a mean age of 36 years (SD=5). The most common cancer types were breast (22%) and brain/spinal cord (19%). Additional cancer types included in our sample were cervical, uterine, ovarian, Hodgkin lymphoma, non-Hodgkin lymphoma, colorectal, melanoma, sarcoma, and ovarian. Overall, 56% (n=32) of AYAs reported they did not receive any form of counseling. AYAs had a mean CHS score of 2.11 (SD=0.8; range 1-3, where higher scores reflect greater concern), indicating moderate concern about their future child's health. Mean CHS scores did not differ significantly for those who had received counseling versus those who had not (2.3 [SD=.7] vs 2.1 [SD=.9], p=.2, respectively). No significant differences were found between mean overall CHS scores and ethnicity.
Conclusion: In this study, AYAs expressed moderate concerns about their future child's health regardless of whether they received genetic counseling, suggesting that current counseling practices may not fully address the factors driving these concerns. Moreover, high concern levels among AYAs who did not receive counseling (presumably those not identified as having an indication for it) highlight potential gaps in how risk information and reassurance are conveyed within survivorship care. These findings indicate the need to strengthen reproductive health and genetic risk discussions across the survivorship continuum, ensuring both indicated and non-indicated survivors receive appropriate guidance, reassurance, and support.

#0884 Waist-hip ratio (WHR) defined obesity phenotype and risk of diabetes in cancer survivor women from Sister Study.

Mahfuja Luna[1], Hazel B. Nichols[2], Katie M. O'Brien[3], Michael G. Fradley[4], Mario Schootman[5], Michael R. Thomsen[6], Benjamin C. Amick III[1], Clarice R. Weinberg[7], Dale P. Sandler[8], Yong-Moon (Mark) Park[1]

[1]Department of Epidemiology, Fay W. Boozman College of Public Health, University of Arkansas for Medical Sciences, Little Rock, AR,[2]Department of Epidemiology, University of North Carolina, Chapel Hill, NC,[3]Epidemiology Branch, National Institute of Environmental Health Sciences,, Research Triangle Park, NC, NC,[4]Cardio-Oncology Program, Division of Cardiology, Department of Internal Medicine, University of Pennsylvania, Philadelphia, PA,[5]Department of Internal Medicine, College of Medicine, University of Arkansas for Medical Sciences Northwest, Springdale, AR,[6]Department of Health Policy and Management, Fay W. Boozman College of Public Health, University of Arkansas for Medical Sciences, Little Rock, AR,[7]Biostatistics and Computational Biology Branch, National Institute of Environmental Health Sciences, Research Triangle Park, NC, NC,[8]Epidemiology Branch, National Institute of Environmental Health Sciences, Research Triangle Park, NC, NC

Introduction: Cancer survivors are at elevated risk of developing diabetes and often experience treatment-related changes in body composition and insulin sensitivity. However, few studies have evaluated whether general and central obesity, independently and jointly, are associated with diabetes risk in long-term cancer survivors. We examined whether obesity phenotype (general, central, or combined) is associated with incident diabetes among women cancer survivors.

Methods: We included 1,924 women (aged 35 to 74 years) from the Sister Study (enrolled 2003-2009) who reported a history of cancer other than breast or non-melanoma skin cancer and had no diabetes at baseline. We excluded participants diagnosed <1 year before enrollment (median time since diagnosis: 11.6 years). Participants were followed through September 2021. General obesity was defined as examiner-measured body mass index (BMI)≥30 kg/m^2, and central obesity as waist-hip ratio (WHR)≥0.85. Participants were categorized as: no obesity (BMI<30, WHR<0.85), central-only (WHR≥ 0.85, BMI<30), general-only (BMI ≥30, WHR<0.85), and combined obesity (BMI≥30 and WHR ≥0.85). Incident diabetes was identified by self-reported new physician diagnosis during follow-up. Multivariable Cox proportional hazards models were used to estimate hazard ratios (HRs) and 95% confidence intervals (CIs) for incident diabetes across obesity phenotypes.

Results: At baseline 16.5% of participants had central-only obesity, 14.0% had general-only obesity, and 13.3% had combined obesity. Over a median follow-up of 12.9 years, 157 women (8.2%) developed incident diabetes. After adjusting for potential confounders, central obesity alone was associated with more than 2-fold higher diabetes incidence (HR 2.14, 95% CI 1.25-3.68), and general obesity alone showed a similar >2-fold association (HR 2.33, 95% CI 1.38-3.92), each compared with no obesity. The combined obesity phenotype was associated with the highest incidence, showing a more than 6-fold risk (HR 6.48, 95% CI 4.13-10.19) with a significant multiplicative interaction between general and central obesity (p for interaction <0.0001). Alternative central obesity parameters (waist circumference ≥88 cm and waist-height ratio ≥0.50) showed similar associations. Associations were generally consistent across categories of time since cancer diagnosis (<5 years, 5-<15 years, and ≥15 years). These associations also were seen among women with prevalent hypertension, dyslipidemia, or cardiovascular disease.

Conclusion: Our findings suggest that central and general obesity, especially in combination, are strongly positively associated with diabetes incidence in cancer survivors. Incorporating WHR-based obesity assessment into survivorship care may help identify women cancer survivors who would benefit from targeted diabetes prevention and monitoring.

: Survivorship Research Addressing Cancer Disparities
Poster Session

#0888 Impact of neighborhood disadvantage, travel distance, and travel time on clinical outcomes of multiple myeloma patients treated with idecabtagene vicleucel.

Alicia R. Richards, Jessica Y. Islam, Yu Chen Lin, Ariel F. Grajales-Cruz, Guillermo Gonzalez-Calderon, Melanie Buhlmann, Gabe DeAvila, David Scheiber-Camoretti, Vivien Yin, Brandon Blue, Laura B. Oswald, Brandon Kale, David Kaldas, Ken Harada, Rebecca Gonzalez, Ciara L. Freeman, Hien Liu, Fabiana Perna, Taiga Nishihori, Rachid Baz, Kenneth H. Shain, Melissa Alsina, Frederick L. Locke, Omar Castaneda Puglianini, Doris K. Hansen, Lauren C. Peres

Moffitt Cancer Center, Tampa, FL

Purpose: To examine the association of neighborhood disadvantage and travel distance (TD)/time (TT) with clinical outcomes in multiple myeloma (MM) patients treated with the first chimeric antigen receptor T-cell therapy (CAR T) for MM, idecabtagene vicleucel (ide-cel).
Methods: MM patients who received ide-cel at Moffitt Cancer Center by July 2024 were included. Neighborhood disadvantage was defined using the Area Deprivation Index (ADI), Social Deprivation Index (SDI), and Social Vulnerability Index (SVI), with higher values indicating more disadvantaged neighborhoods (DN). TD/TT from patients' residence to Moffitt were calculated via Google Directions API. Chi-squared, log-rank tests, and Kaplan-Meier curves were used to compare patient characteristics, safety, and efficacy by each index and TD/TT using the upper quartile as the cut-point. Multivariable logistic and Cox regression were used to examine the association of each index and TD/TT with ide-cel response and survival, respectively, adjusting for relevant covariates.
Results: Among 173 MM patients treated with ide-cel, most were male (54%), non-Hispanic White (73%), and >60 years (75%). Median follow-up was 12.6 months (range 0.1-38.4). Median ADI was 42 (range 1-96), SDI was 38 (range 1-100), and SVI was 0.7 (range 0.1-1.0). Patients living in more vs less DN were younger (all indices, $p<0.05$), more likely to be Black (SDI: 37% vs 10%, $p<0.001$), had a prior autologous stem cell transplant (ADI: 80% vs 61%, $p=0.02$), and extramedullary disease (ADI: 32% vs 14%, $p=0.01$). Patients with higher SVI were more likely to develop infections (44% vs 25%, $p=0.02$) and less likely to achieve a complete response (CR) or better (44% vs 63%, $p=0.03$). Patients living in more vs less DN had inferior overall survival (OS; SDI: median 27 months vs not reached, $p=0.04$; SVI: median 18 months vs not reached, $p=0.01$). In multivariable models, patients living in more vs less DN were less likely to have a CR or better response (SDI: odds ratio [OR]=0.39, 95% confidence interval [CI]=0.16-0.91; SVI: OR=0.40, 95% CI=0.17-0.90) and had worse OS (SDI: hazard ratio [HR]=1.78, 95% CI=0.97-3.28; SVI: HR=2.14, 95% CI=1.16-3.95). No other differences in outcomes were observed by DN. Median TD and TT were 76.5 miles (range 2.5-1079.6) and 90 minutes (range 10-1022), respectively. No differences in patient characteristics or clinical outcomes by TD/TT were noted except patients with a longer TD/TT were more likely to have high-risk cytogenetics (58% vs 28%, $p<0.001$). Patients from more DN had shorter TD/TT (all indices, $p<0.05$).
Conclusion: In MM patients treated with ide-cel, most lived in less DN yet faced significant TD/TT. The marked travel burden overall and the worse responses and inferior OS in patients living in more DN highlight the need to address systemic barriers to improve CAR T access and outcomes.

#0889 Assessment of disparities in breast reconstruction following breast cancer surgery at a Central Illinois Breast Cancer Program.

Hajar Amina El Amri[1], Kathy Robinson[2], Shreya Arikati[3], Kristin Delfino[4], Ricardo Cossyleon[5], Krishna A. Rao[6]

[1]Internal Medicine, Southern Illinois University School of Medicine, Springfield, IL,[2]Hematology and Oncology, Simmons Cancer Institute at Southern Illinois University School of Medicine, Springfield, IL,[3]University of Illinois Urbana-Champaign, Champaign, IL,[4]Department of Surgery, Southern Illinois University School of Medicine, Springfield, IL,[5]Simmons Cancer Institute at Southern Illinois University School of Medicine, Springfield, IL,[6]Assistant Professor, Internal Med., Southern Illinois University School of Medicine, Springfield, IL

Introduction: Despite increases in reconstruction rates and legislative efforts to improve access, disparities in post-mastectomy breast reconstruction persist. Prior studies have shown lower reconstruction rates among racial and ethnic minorities, patients with lower socioeconomic status, those insured with Medicare/Medicaid, older patients, and individuals living in rural areas.
Methods: We performed a retrospective cohort study of 99 patients (>18 years) who underwent total/simple, skin-sparing, nipple-sparing, or modified radical mastectomy for breast cancer between January 2020 and December 2022 at our institution. Patients who underwent partial mastectomy/lumpectomy were excluded. Clinical, demographic, socioeconomic, and operative data were extracted from the electronic medical record and managed in REDCap. Rural vs. urban residence was determined using RUCC codes (1-3 urban; 4-9 non-urban).The primary outcome was receipt of post-mastectomy breast reconstruction.
Results: The majority of patients in the cohort were Caucasian (87%), with racial and ethnic minority groups representing a smaller proportion. Race was not significantly associated with receipt of breast reconstruction. Patients who underwent reconstruction were significantly younger than those who did not (50.4 ± 11.7 vs. 61.6 ± 12.3 years, $p < 0.0001$). Geographic residence(urban vs. non-urban), smoking status, and comorbidities, including type 2 diabetes, congestive heart failure, and COPD were not associated with reconstruction. Cancer stage and receipt of adjuvant chemotherapy or radiation therapy also did not significantly influence reconstruction rates. Patients who underwent contralateral prophylactic mastectomy were significantly more likely to receive reconstruction ($p = 0.00005$); of these, only 3 patients had a BRCA mutation, while the remainder opted for the procedure by personal choice.
Conclusion: In our cohort, younger age and undergoing contralateral prophylactic mastectomy were the strongest predictors of post-mastectomy reconstruction. Other demographic and clinical factors, including race, geographic residence, and adjuvant treatment, did not affect reconstruction. Standardizing patient education and early referral to plastic surgery may help reduce variation and support more equitable care.

#0890 Addressing heterogeneity in breast cancer outcomes and patterns of care among Asian Americans in Los Angeles: the AMBER-LA Study..

Junrui Lyu[1], Kelsey Lam[1], Grace Guo[1], Andrei Mikhael Galura[2], Emily Kumagai[1], Bodour Salhia[1], Evanthia T. Roussos Torres[1], Chanita Hughes-Halbert[1], Veronica Wendy Setiawan[1], Jennifer Tsui[1]

[1]Keck School of Medicine of USC, Los Angeles, CA,[2]Dornsife College of Letters, Arts and Sciences, University of Southern California, Los Angeles, CA

Background: Breast cancer (BC) is the most diagnosed cancer among Asian American (AA) women, and its incidence continues to rise rapidly. Although emerging evidence suggests variation in cancer outcomes across AA groups, most studies have aggregated Asians into one category. To address this gap, we aimed to build a cohort of diverse AA BC patients to characterize ethnic group-specific patterns of care and cancer outcomes.
Methods: The Asian American Breast Cancer Research in Los Angeles (AMBER-LA) is an exploratory study assessing the feasibility of recruiting AA BC patients to identify multilevel factors associated with care and disease prognosis. Chinese, Korean, and Filipino women aged 21-75 years, residing in Los Angeles County, and diagnosed with invasive BC since January 2021, were recruited from a large academic health center and community outreach events. Data on demographics, cancer diagnosis, and patterns of care were collected through surveys and medical record abstractions. Differences across AA groups were examined using Fisher's exact test.
Findings: Among the 51 participants enrolled to date, including 19 Chinese, 11 Filipino and 21 Korean women, most (94.1%) were recruited from telephone and in-person outreach within clinic settings, and 88.2% were born outside the US. Although 72.5% completed the survey in English, only 17.6% prefer English in their daily life. The mean age at diagnosis was 53.0 years (SD: 10.8). Although not statistically significant, Filipino participants in this sample were more likely to be diagnosed before the age 50, compared with other groups. Modes of diagnosis were similar across groups, with half being detected through routine screening and half after seeking care for symptoms. The median time from abnormal results to seeing a specialist was 21 days (IQR: 10-32). Compared with other groups, Korean participants were more likely to be referred within two weeks, although the differences were not significant. Although 98.0% of participants reported being insured, 15.7% of them reported delaying or not receiving care due to cost in the past year. Alarmingly, experience of discrimination during care was reported by 68.4% of Chinese, 36.4% of Filipino and 42.9% of Korean participants. The most frequently reported experience differed by AA groups: Chinese participants reported not being listened to, Filipino participants reported being treated with less courtesy, and Korean participants described feeling inferior.
Conclusion: Recruiting AA BC patients was challenging, however, engagement with healthcare providers made it feasible. Preliminary evidence of younger age at diagnosis, variation in referral interval, and differential experience of discrimination highlight the need for culturally relevant, group-specific care strategies to improve patient experience and quality of care for AA women.

#0891 A comparison of black and white women with breast cancer in the Deep South and their experiences utilizing theAoUdataset.

Lauren K. Evans[1], Ivan T. Jubilee[2], Layja J. L. Grant[3], Nelson R. Lemieux[4], KiTani Parker Lemieux[5]

[1]Basic Pharmaceutical Sciences, Xavier University of Louisiana, College of Pharmacy, New Orleans, LA,[2]Division of Basic Pharmaceutical Sciences, Xavier University of Louisiana - College of Pharmacy, New Orleans, LA,[3]Public Health, Xavier University of Louisiana, New Orleans, LA,[4]Seven Star Academy, Inc, New Orleans, LA,[5]Xavier University of Louisiana - College of Pharmacy, New Orleans, LA

Purpose: In 2024, Black women had a 38% higher breast cancer mortality rate than their white counterparts, despite a lower incidence. The impact of the social determinants of health (SDoH) within this disparity remains unclear. The Deep South, an area associated with poorer health outcomes, hosts the highest cancer-related death rates nationwide. As such, evaluation of women with breast cancer in this region may influence the understanding of socioeconomic burden. This research examines and compares perceptions of healthcare interactions, access to infrastructure, and community dynamics to contribute to the understanding of social determinants in a black, southern population living with breast cancer.

Methods: Participant and survey data were derived from the All of Us Research Program (AoURP) workbench and SDOH survey. The AoURP is an initiative focused on improving health outcomes through a diverse research database. Inclusion criteria consisted of adult women with breast cancer who self-identified as White or Black/African American and lived in the Deep South (Alabama, Georgia, Louisiana, and Mississippi). Selected survey questions addressed neighborhood perspectives, access to neighborhood resources, and discriminatory experiences in healthcare settings. Black and white participants were identified via the cohort selection tool and further subdivided based on 3-digit zip code values. Using Python in Jupyter Notebook, participant responses were extracted and quantified to allow comparison.

Results: Inclusion criteria were met by 457 black women and 587 white women. Response counts per survey question varied. Black women were significantly more likely to express that their neighborhoods were noisy, unsafe, and unclean. Additionally, black women felt less listened to during health care experiences ($p = 0.0068$) and as if they were treated with less courtesy ($p = 0.0001$). Most questions addressing infrastructure did not result in statistically significant differences. Low-cost recreational facilities and shops were not within walking distance for the majority of both black and white respondents.

Conclusion: These results indicate that black women with breast cancer are impacted by aspects of the SDoH more than their white counterparts. Negative neighborhood dynamics, as well as feelings of less respect and courtesy, may impact prognosis and rates of early diagnosis. Additionally, both cohorts indicated a disparity in infrastructure, which aligns with the predominantly rural composition of the Deep South.

#0892 Distance and deprivation: geographic and contextual influences on pediatric cancer outcomes.

Emma Hymel[1], Kendra L. Ratnapradipa[1], Cheng Zheng[2], Edward S. Peters[1], Jenna Allison[3], Sarah H. Nash[4], Mei-Chin Hsieh[5], Shinobu Watanabe-Galloway[1]

[1]Epidemiology, University of Nebraska Medical Center, Omaha, NE,[2]Biostatistics, University of Nebraska Medical Center, Omaha, NE,[3]Pediatrics, University of Nebraska Medical Center, Omaha, NE,[4]Epidemiology, University of Iowa, Iowa City, IA,[5]Epidemiology and Population Health, LSU Health Sciences Center, New Orleans, LA

Introduction: Cancer is the number one cause of death by disease in children in the US and while survival rates have improved significantly, differences persist in pediatric cancer outcomes by a number of factors. The objective of this study was to demonstrate how cancer registry data can be used to assess social and geospatial predictors of pediatric cancer mortality and their combined effects.

Methods: This population-based longitudinal study used data from the Louisiana Tumor Registry and Iowa Cancer Registry and included all individuals aged 0-19 at primary cancer diagnosis from 2000 to 2020. Travel distance was estimated using the great-circle distance method in ArcGIS Pro, neighborhood deprivation was characterized with the Area Deprivation Index, and rurality was measured at the census tract level with Rural Urban Commuting Area codes. Cox regression models were used to assess the association between social and geospatial predictors and pediatric cancer mortality, adjusting for confounding variables identified through a directed acyclic graph.

Results: Of the 6,982 children with cancer identified from the two states, 4,871 had complete information on home addresses at diagnosis and treatment facilities and were included in the final analysis. Of the cases from Iowa, 40.31% resided in rural census tracts, compared to 15.00% of cases from Louisiana. Five-year survival was higher for children in Iowa (86.63%, 95% CI: 85.19-88.14%) than Louisiana (83.41%, 95% CI: 82.00-84.88%). Compared to children with low travel distances and low neighborhood deprivation, those experiencing both high travel distance (distance in the fourth quartile) and high neighborhood deprivation (ADI in top 50%) have an 82% high hazard of cancer mortality (95% CI: 1.43-2.32). When looking at the combined effects of rurality and travel distance, mortality differences appeared to be driven more by distance than rurality. Interestingly, compared to children in urban areas with a low travel distance to treatment, the hazard of death was highest for children with high travel distances residing in urban areas (aHR=1.41, 95% CI: 1.17-1.71), followed by children with high travel distances in rural areas (aHR=1.28, 95% CI: 1.01-1.62).

Conclusions: By integrating cancer registry data with geospatial and neighborhood social and economic indicators, we identified that children facing both long travel distances and high neighborhood deprivation experience significantly elevated hazards of mortality. Importantly, geography and context are not just a backdrop, but a determinant of survival. These findings highlight the need for multilevel interventions that target individual, hospital, neighborhood, and policy drivers of differences in cancer outcomes for children.

#0893 Real-world bladder cancer survival across the immunotherapy era: Persistent age-, stage-, and race-ethnicity disparities demand precision oncology strategies..

Maria Ivette Lopez Martinez, Bharat Peddinani, Aura Calderon, Everardo Cobos, Diane NGUYEN

The University of Texas Rio Grande Valley, Edinburg, TX

Background: Bladder cancer represents 5% of U.S. malignancies, with 82,000 new cases and 17,000 deaths annually. Most tumors are non-muscle invasive, yet recurrence is common and requires long-term surveillance. Five-year survival is high for non-invasive and localized disease (96% and 70%) but drops sharply for regional (34%) and metastatic stages (5%). Despite advances with platinum regimens and, more recently, immune checkpoint inhibitors (ICIs), mortality gaps persist, especially among older adults, Black patients, and those with advanced diseases.

Methods: We assessed relative survival for invasive and in situ bladder cancer using SEER-21 data (2000-2021), stratified by race/ethnicity, age, and SEER summary stage. Hispanic origin followed the NAACCR Hispanic Algorithm; AI/AN estimates were limited to PRCDA regions. Survival from 1-10 years after diagnosis was calculated using expected-survival life tables.

Results: Overall five-year survival was 78%. Persistent disparities were noted: • Non-Hispanic White: 79.1%• Hispanic: 74.0% • Asian/Pacific Islander: 77.0% • AI/AN: 70.7% • Non-Hispanic Black: 65.0% Age and stage influenced outcomes, with survival ranging from 86.8% (<50 yrs) to 75.3% (≥65 yrs), and from 71.3% (localized) to 7.5% (distant). Since 2016, ICIs—including atezolizumab, pembrolizumab, nivolumab, durvalumab, and avelumab—have improved response durability, achieving complete responses in ~6% and a median OS of ~15 months in selected patients.

Conclusions: Although immunotherapy has expanded options for metastatic urothelial carcinoma, its real-world impact remains uneven. Survival gains are modest, and demographic inequities persist across age, race/ethnicity, and stage. Black and AI/AN patients continue to face the highest mortality, and older adults—who represent most cases—often benefit less due to cisplatin ineligibility, comorbidities, and variable ICI responsiveness. These patterns show that therapeutic advances alone are insufficient; strategies integrating biomarker-based selection, optimized sequencing, and multimodal approaches are urgently needed. Without targeted action, current progress risks widening long-standing disparities in bladder cancer survival.

Impact: Closing these gaps requires precision-guided care and equitable access to emerging therapies to ensure survival gains are shared by all patient groups.

#0894 Prostate cancer outcomes in Hispanic/Latino ethnic enclaves: Results from the California Cancer Registry and American Community Survey.

Diego Alvarez-Lopez, Joel Sanchez Mendez, Michelle Tran, Laura Thompson, Lihua Liu, Myles Cockburn, Mariana C. Stern

Department of Population and Public Health Sciences, Keck School of Medicine, USC - University of Southern California, Los Angeles, CA

Introduction: Prostate cancer (PCa) is the most commonly diagnosed cancer among Hispanic/Latino (H/L) men and the fourth leading cause of cancer-related death. We and others have shown that nativity influences patterns of PCa treatment and survival among H/L men. Here, we examined whether these associations were modified by residence in H/L ethnic enclaves.
Methods: We conducted a retrospective, population-based study of primary PCa cases diagnosed from 2005-2021 in the California Cancer Registry, linked to census tract characteristics from the American Community Survey (2010, 2015, 2020). A composite H/L Enclave Index (HEI) was created using the proportions of H/L residents, non-US-born H/L residents, H/L individuals with limited English proficiency, and linguistically isolated households, with principal components analysis applied to all census tracts to derive the first component. Enclave residence was defined as living in a census tract in the 5th quintile of HEI with ≥ 250 H/L residents or in an adjacent 4th-quintile tract meeting the same threshold. We examined enclave residence as a main exposure in the full cohort and, among H/L patients, as a potential modifier of nativity-outcome associations. Multivariable mixed-effects logistic regression models estimated associations with high-grade disease (Gleason ≥ 8), treatment receipt and treatment delay (≥3 months), including nativity-enclave interaction terms. Prostate-specific survival was evaluated using a covariate-adjusted mixed-effects Weibull model. All models included random intercepts to account for census tract clustering.
Results: A total of 249,860 prostate cancer cases were included (29,159 H/L), of which 75,496 (30.2%) had ever resided in an H/L ethnic enclave: 17.1% NHW men, 50.1% US-born and 71.8% of non-US-born H/L men (pairwise $p<0.01$). Living in an H/L ethnic enclave was associated with 4% higher odds of presenting with high-grade disease (OR= 1.04; 95% CI: 1.02-1.07) and 15% higher hazard of mortality (HR= 1.15; 95% CI: 1.08-1.22). Among H/L men living outside enclaves, non-US-born men had lower odds of high-grade disease compared with US-born men (OR=0.90; 95% CI: 0.83, 0.97); however, we found no evidence of effect modification (interaction $p = 0.17$). Similarly, we found no evidence that enclave residence modified nativity differences in treatment receipt (interaction $p = 0.22$), treatment delay (interaction $p = 0.66$), or survival (interaction $p = 0.08$).
Conclusions: Our analyses show that residence in an H/L ethnic enclave is associated with higher risk of high-grade PCa and mortality. Ethnic enclave residence had limited influence on differences in prostate cancer stage, treatment, or survival among H/L patients by nativity. Our findings suggest that neighborhood ethnic composition alone may not drive our previously observed disparities in prostate cancer outcomes by nativity.

#0895 Impact of immigration and acculturation on mortality in Asian American women with breast cancer.

Alfredo V. Chua[1], Rabsa Sikder[1], Luna Gao[2], Julie Von Behren[2], Janise M. Roh[3], Esperanza Castillo[2], Isaac J. Ergas[3], Iona Cheng[2], Marilyn L. Kwan[3], Salma Shariff-Marco[2], Mi-Ok Kim[2], Katherine Lin[2], Brittany N. Morey[4], Anna H. Wu[5], Esther M. John[6], Lenora W. M. Loo[7], Allison W. Kurian[6], Christine B. Ambrosone[1], Lawrence H. Kushi[3], Scarlett L. Gomez[2], Song Yao[1]

[1]Department of Cancer Prevention & Control, Roswell Park Comprehensive Cancer Center, Buffalo, NY,[2]Department of Epidemiology & Biostatistics, University of California, San Francisco, CA,[3]Division of Research, Kaiser Permanente Northern California, Pleasanton, CA,[4]Department of Health, Society & Behavior, Wen School of Population & Public Health, University of California, Irvine, CA,[5]Division of Epidemiology, Keck School of Medicine, University of Southern California, Los Angeles, CA,[6]Department of Epidemiology & Population Health, Stanford University School of Medicine, Stanford, CA,[7]Department of Epidemiology, University of Hawai'i Cancer Center, Honolulu, HI

Purpose: Immigration/acculturation may affect breast cancer outcomes among minoritized racial and ethnic populations. Limited data exist on how these factors influence survival in Asian American women with breast cancer. We investigated associations of immigration/acculturation with all-cause (ACM) and breast cancer-specific mortality (BCSM) in this population.
Methods: 3971 Asian American women with breast cancer were included from the Asian American Resiliency and Cancer Disparities (ARC) Study. Measures of immigration/acculturation included nativity (born in the US vs. outside the US), number of years (y) and percent (%) of life lived in the US, age at immigration, Asian country of birth, and preferred language at interview. Primary outcomes were ACM and BCSM. Cox proportional hazards were used to estimate hazard ratios (HRs) for ACM and Fine and Gray competing risk models for BSCM, adjusted for clinical, demographic, socioeconomic, reproductive, and lifestyle factors. Analyses were stratified by follow-up duration (≤10 y and >10 y).
Results: Women born outside the US had lower ACM compared with women born in the US at 10 y (HR 0.72, 95% CI 0.61-0.85, p<0.001) and beyond 10 y (HR 0.72, 95% CI 0.63-0.82, p<0.001) follow-up. No statistically significant differences by nativity in BCSM were observed overall; however, higher BCSM in women born outside the US after 15 y of follow-up was suggested. Among women born outside the US, living longer in the US was associated with higher ACM, particularly beyond 40 and 50 y (HR 1.49, 95% CI 1.05-2.10, p=0.02; HR 1.94, 95% CI 1.34-2.81, p<0.001, respectively), which became non-significant after adjustment. Earlier age at immigration was associated with lower ACM and BCSM, and immigration in late adulthood (≥55 y) with higher ACM (<10-y HR 2.04, 95% CI 1.09-3.80, p=0.02; >10-y HR 2.05, 95% CI 1.23-3.41, p=0.006). However, after adjustment, associations with ACM remained significant only for immigration in adolescence (13-17 y) (<10-y HR 0.56, 95% CI: 0.36-0.88, p=0.01) and early adulthood (25-34 y) (>10-y HR 0.75, 95% CI: 0.59-0.96, p=0.02). For BCSM, associations were seen for immigration in adolescence (<10-y HR 0.56, 95% CI: 0.34-0.92, p=0.02), adult transition (18-24 y) (>10-y HR 0.71, 95% CI: 0.52-0.97, p=0.03) and middle adulthood (35-54 y) (<10-y HR 0.62, 95% CI: 0.39-0.97, p=0.04; >10-y HR 0.60, 95% CI: 0.40-0.88, p=0.01). No significant associations were observed between % of life in the US, Asian country of birth, or preferred language at interview, and ACM or BCSM.
Conclusions: Immigration factors may influence long-term mortality in Asian American women with breast cancer. Women born outside the US demonstrated lower ACM, but the length of stay in the US and age at immigration may have influenced this association. This highlights the need for culturally tailored survivorship and public health interventions that promote native cultural behaviors in this population.

#0896 Age-based left-digit bias in the treatment of pancreatic adenocarcinoma.

Qianyun Luo, Bethel Ozed-Williams, David Brauer, Bryan Trottier, Todd Tuttle, Jane Hui, Eric H. Jensen, Jacob Ankeny, Christopher J. LaRocca, Schelomo Marmor

University of Minnesota, Minneapolis, MN

Purpose: Left digit bias, where the left-most digit disproportionately influences decision-making, can impact treatment decisions and patient outcomes. This study examines how such bias may affect treatment decisions for patients with pancreatic adenocarcinoma (PDAC), focusing on differences between patients aged 79 and 80.

Method: A retrospective cohort study using the National Cancer Database (2004-2020) analyzed patients with PDAC aged 79 and 80. The primary exposure was age-based left-digit bias. The main outcomes measured included differences in treatment received and overall survival. Statistical analyses included chi-square tests, multivariate analysis, Kaplan-Meier survival curves, and Cox proportional hazards models.

Results: Among 5,304 patients (2,718 aged 79, 2,586 aged 80), chemotherapy use was higher in 79-year-olds (50.3%) than 80-year-olds (45.1%) (OR 0.79, 95% CI 0.70-0.89, $p<0.01$). No significant differences were found in surgery or radiation. Chemotherapy was associated with lower mortality risk (HR 0.85, 95% CI 0.79-0.92, $p<0.01$). Adjusted overall survival was similar between groups (HR 1.00, 95% CI 0.93-1.07, $p=0.91$).

Conclusion: Left digit bias was observed in the treatment of PDAC, with a tendency to favor chemotherapy for patients aged 79 over 80. This highlights the need for age-neutral decision-making in treatment planning to avoid biases that could impact patient care and outcomes.

#0897 Missed opportunity or standard of care.

Lilia Olsen, Antonio Logan, Paul Kent

FibroFighters, Temecula, CA

Fibrolamellar Carcinoma (FLC) is a rare cancer that primarily affects children and young adults and is easily confused with the common Focal Nodular Hyperplasia (FNH) on imaging. Often, a biopsy is not performed at initial presentation and the opportunity for an early diagnosis of FLC can be missed. Our study aims to evaluate the effects of delayed diagnosis, and based on those results propose an addendum to the current HCC liver biopsy guidelines. We reviewed all FLC patients diagnosed in the last 10 years that had complete records in our database. This was a retrospective observation study that initially looked at 216 patients. We excluded patients who did not have a reference to benign tumors or FNH, or who did not have a pathological diagnosis of FLC. After exclusion we had a cohort of 35 patients. We compared this cohort to 95 patients who had complete records and were not assumed to have FNH at time of diagnosis. A Mann-Whitney U test was performed to compare the time delay between first images and pathological diagnosis between females and males. The analysis shows a significant result between delay and sex, U=59.00, Z= -2.189 p= 0.028. The average diagnostic delay in females was 347.85 days SD= 571.686 and the average diagnostic delay was 41.22 days SD= 31.630 in males. A Mann-Whitney U test showed a significant result between delay in those assumed to have FNH and delay in those who did not, U = 647.500, Z= -5.591, p= <0.001. Based on these results we are suggesting an addendum to the current recommendations. 1. Give FLC its own section separate from HCC 2. Biopsy should be used to confirm diagnosis of FLC or FNH 3. Recommend that a biopsy should be considered when a unique patient population is identified. 4. Close and reliable follow-up for all patients 5. If the neoplasm is in a surgically complicated area, where tumor growth could significantly affect prognosis or possibility of resection, a biopsy should be considered 6. Acquire B12 levels, if they are >2000pg/mL a biopsy should be recommended. 7.A chest x-ray should be acquired to assess possible lung nodules. Due to the gap in guidelines, 70% of our patients experienced a delay in diagnosis. We believe that adding a separate section in the current liver biopsy guidelines for FLC with seven stipulations could help amend this gap in care.

#0898 HER2 as a therapeutic target in prostate cancer: Multi-omic and spatial insights across genetic ancestries.

Nicole Mavingire[1], **Abdulrahman M. Dwead**[1], Joy Solomon[2], Janelle Moore[1], Moyinoluwa Adeniyi[2], Odunayo Oluokun[2], Jabril R. Johnson[1], Estefania Labanca[3], Peter Shepherd[3], Mya Walker[4], Isaiah Sailors[4], Serene Dowiri[4], Greisha L. Ortiz Hernandez[4], Jillian C. McDonough[4], Diana LeVasseur[1], Jazlyn Farlough[1], Justin Tran[4], Frank Myers[4], Fornati Bedell[4], Zhirong Yin[4], Rachel Martini[1], Melissa B. Davis[1], Clayton C. Yates[5], K. Sean Kimbro[1], Rick A. Kittles[1], Tanya Dorff[4], Cristina Magi-Galluzzi[6], Soroush Rais-Bahrami[7], Firas Kobeissy[1], Yehia Mechref[2], Leanne Woods-Burnham[1]

[1]Morehouse School of Medicine, Atlanta, GA,[2]Texas Tech University, Lubbock, TX,[3]UT MD Anderson Cancer Center, Houston, TX,[4]City of Hope National Medical Center, Duarte, CA,[5]Sidney Kimmel Comprehensive Cancer Center, Baltimore, MD,[6]The University of Alabama at Birmingham, Birmingham, AL,[7]Wake Forest University School of Medicine, Winston-Salem, NC

INTRODUCTION: Patients with prostate cancer (PC) initially respond to androgen deprivation therapy. However, relapse is lethal. For this reason, inhibiting androgen-independent signaling pathways—such as human epidermal growth factor receptor 2 (HER2)—is a promising area of investigation. HER2 overexpression in PC tumors correlates with worse prognosis, but has not been sufficiently evaluated in Black men. We hypothesize that unique ancestry-associated multi-omic molecular signatures are modulated with anti-HER2 drug targeting.

METHODS: Using RNA sequencing, we quantified *HER2/ERBB2* in primary patient tissue and correlated with quantified ancestry estimates. IHC staining was used to detect HER2 expression in primary prostate tissue. We quantified transcript and protein levels of HER levels in PC cell lines by qPCR and ELISA. CellTiter-Glo® assessed cell viability in PC cells treated with anti-HER2 drug. We performed multi-omic analyses using LC-tandem mass spectrometry and LC-PRM mass spectrometry. Biological pathway and network analysis was performed using Qiagen's Ingenuity Pathway Analysis. We validated significantly modulated genes with qPCR. We performed immunofluorescence staining of HER2 and androgen receptor (AR) in treated vs. untreated PC cell lines. To resolve the spatial dynamics of *ERBB2* and *AR* in ancestry genotyped patient-derived xenografts (PDXs), we utilized the 10x Genomics Xenium *In Situ* spatial transcriptomics platform.

RESULTS: We detected moderate correlation with *HER2/ERBB2* and West African genetic ancestry (WAA) in primary prostate tissue in a cohort of Black men (n=36). We detected HER2-positive scores in 70% of primary PC tissue in a separate cohort of Black men (n=10). Transcript and protein levels of HER2 were confirmed in PC cells. We observed significantly reduced viability only in HER2-targeted PC cells from Black patients. Systems biology revealed differential pathway and network expression in HER2-targeted PC cells derived from Black men compared with white men. Common significantly modulated genes *ERBB2, MYC, MYCN,* and *TP63* were validated. HER2 and AR immunofluorescence staining diminished with HER2 drug targeting. Spatial transcriptomic analysis revealed that the *ERBB2* and *AR* transcript burden per tumor area were significantly higher in a PDX developed from a Black patient (58% WAA) compared to a PDX developed from a white patient (0% WAA).

CONCLUSIONS: Thorough evaluation of the molecular mechanisms by which HER2 overexpression confers tumor progression and treatment-resistance will provide the foundation to address high-risk PC with precision medicine. By leveraging the unique characteristics of HER2-positive tumors, an additional oncogenic pathway can be therapeutically targeted which will have a major impact in reducing progression to metastasis and reducing mortality.

#0899 Building a national network coordination center for clinical trials: Early implementation outcomes from the CP2CT DECC.

Laura E. Lectora[1], Cristina J. Orozco[1], Holly A. Thorson[2], Timethia Bonner[1], Robert R. Freimuth[2], Jennifer G. Le-Rademacher[2], Folakemi T. Odedina[1]

[1]Mayo Clinic, Jacksonville, FL,[2]Mayo Clinic, Rochester, MN

Background: Despite the decline in overall mortality and incidence of cancer in the US population, the burden of cancer is still high, especially in underserved and under-researched populations. A major contributor to poor cancer outcomes is the absence of dedicated efforts utilizing scientifically rigorous approaches and implementation strategies to optimize participant enrollment and accrual in clinical trials. The Connecting Patient Populations to Clinical Trials (CP2CT) program implements innovative multilevel interventions to enhance clinical trial awareness and optimize referral pathways that facilitate patient enrollment. The CP2CT Data, Evaluation, and Coordinating Center (DECC) supports its data and evaluation activities, and coordinates a learning collaborative towards mitigating the key barriers of cancer burden in all populations.
Methods: Using an implementation science-informed approach, the DECC deployed coordinated strategies over three years: (1) administrative structuring through streamlined governance, centralized reporting, and stakeholder integration; (2) data standardization via Common Data Elements (CDEs), a cross-network REDCap system, and a multi-institution Data Transfer Agreement (DTA); (3) evaluation infrastructure through a Network Logic Model, evaluation plan, standardized constructs, and a Process Evaluation Plan with tools; (4) learning supports through an internal website and expanded Speaker Series; and (5) site-level implementation facilitation through structured visits.
Results: In collaboration with the CP2CT Network and NCI, the DECC's achievements span four domains: (1) Administrative: built infrastructure, deployed centralized reporting platforms, coordinated key meetings, and strengthened community integration. (2) Data: standardized collection, secured network-wide data sharing through the DTA, enabled harmonized multi-site reporting, and advanced groundwork for interoperability and scientific value. (3) Program Evaluation: linked CP2CT activities to measurable outcomes through a Network-wide Logic Model, guided evaluation, established shared evaluation language, and launched a transferable Process Evaluation framework. (4) Learning Collaborative: developed a centralized resource hub, expanded the Speaker Series, and advanced authorship transparency with the CP2CT Publication Policy. <
Conclusion: The CP2CT DECC has established a sustainable, scalable infrastructure that integrates administrative coordination, standardized data collection, robust program evaluation, and a collaborative learning environment. These efforts enhance clinical trial awareness, optimize referral pathways, and provide a transferable model for improving participant enrollment and scientific rigor across national research networks, ultimately addressing disparities in cancer outcomes.

#0900 Risk of second cancer in survivors of early-onset colorectal cancer: racial and ethnic differences in a population-based study.

Aniruddha B. Rathod[1], Caitlin C. Murphy[2], Sandi L. Pruitt[3]

[1]Epidemiology, University of Arkansas for Medical Sciences, Little Rock, AR,[2]Pediatrics, University of Chicago, Chicago, IL,[3]UT Southwestern Medical Center, Dallas, TX

Introduction: Early-onset colorectal cancer (EOCRC) incidence is rising sharply in the US, yet the long-term survivorship experience of this population remains poorly defined particularly among groups experiencing unequal cancer burden. Because racial and ethnic disparities persist in cancer-related exposures, treatment experiences, and survivorship care, the long-term probability of developing a second primary cancer (SPC) after EOCRC may also vary across population groups. We estimated risk of SPC by race and ethnicity to improve understanding of long-term survivorship following EOCRC.
Methods: We used SEER 12 registry data to identify adults aged 18-49 years with stage 0-III EOCRC between 1992-2021. SPC was defined as any new primary cancer diagnosed ≥6 months after EOCRC. Accounting for competing risk of death, we estimated cumulative incidence of 1) any SPC and 2) second CRC by calendar time and attained age. Standardized incidence ratios (SIRs) compared risk to the general population. Analyses were stratified by sex and racial/ethnic groups.
Results: Among 29,115 EOCRC survivors, 53.5% were male, and the racial/ethnic distribution was non-Hispanic White (NHW: 54%), non-Hispanic Black (NHB: 10.9%), Hispanic White (HW: 16.7%), Asian/Pacific Islander (API: 15%), and other (3.4%). Overall, 8.4% developed any SPC and 2.8% developed a second CRC. Cumulative incidence of any SPC did not differ significantly by race/ethnicity for men and women. Among men, SIRs for any SPC were 1.4 (95% CI: 1.3-1.5) for NHW, 1.4 (1.2-1.6) for NHB, 1.8 (1.5-2.1) for HW, and 2.4 (2.0-2.8) for API. Among women, SIRs were 1.3 (1.2-1.4) for NHW, 1.6 (1.3-1.9) for NHB, 1.6 (1.4-1.9) for HW, and 1.8 (1.6-2.1) for API. Cumulative incidence of second CRC differed significantly by race/ethnicity for men and women. At 25 years after diagnosis, cumulative incidence of second CRC was 2.8% (95% CI: 2.3-3.5) for NHW women; 4.6% (3.9-5.4) for NHW men; 5.5% (4.0-7.4) for NHB women; 4.0% (2.8-5.5) for NHB men; 5.9% (4.2-8.0) for HW women; 7.0% (5.3-9.1) for HW men; 4.0% (2.9-5.5) for API women; and 6.6% (4.8-8.9) for API men. By age 70, estimates were 2.9% (2.3-3.6) for NHW women, 4.7% (4.0-5.5) for NHW men, 5.6% (3.9-7.8) for NHB women, 4.6% (3.1-6.4) for NHB men, 4.9% (3.6-6.5) HW women, 6.7% (5.1-8.6) for HW men, 4.5% (3.1-6.3) for API women, and 6.1% (4.5-8.1) for API men. Second CRC SIRs showed similar patterns, with highest risks in HW men (SIR: 8.0; 95% CI: 6.3-10.0) and HW women (SIR: 7.1; 95% CI: 5.2-9.5).
Conclusion: Despite no statistical differences in risk of any SPC, second CRC risk differed significantly by racial and ethnicity. HW men and women showed higher cumulative incidence over time, partly reflecting younger age at diagnosis and longer time at risk. Additional genetic, lifestyle, and care-related factors may contribute and warrant study to guide prevention and early detection in EOCRC survivors.

#0901 Disparities in gastric cancer treatment and related adverse events in older adults.

Nana Owusu[1], Jennifer Ferris[2], Ji Yoon Yoon[3], Jeong Yun Yang[2], Josephine Soddano[2], Sophie Wagner[2], Chin Hur[2]

[1]Columbia Univ. Vagelos College of Physicians & Surgeons, New York, NY,[2]Department of Medicine, Columbia University Irving Medical Center, New York, NY,[3]Department of Gastroenterology, Icahn School of Medicine at Mount Sinai, New York, NY

Background: Disparities in treatment-related adverse events (AEs) may contribute to racial differences in cancer outcomes. In this study, we performed a comprehensive analysis of treatment patterns and related AEs between non-Hispanic White (NHW) and non-Hispanic Black (NHB) gastric cancer (GC) patients.

Methods: We queried SEER-Medicare (2000-2017) for NHW and NHB patients aged ≥66 years with histologically confirmed GC. Inpatient and outpatient claims within 1 year of diagnosis were collected for chemotherapy, surgery, and radiation treatments. Chemotherapy treatments were classified as 'NCCN' if consistent with first/second-line regimens per 2025 NCCN GC guidelines, and 'non-NCCN' otherwise. Chemotherapy-related AEs were identified using hospitalization claims for hematologic, gastrointestinal, infectious, and metabolic toxicities within 21 days of treatment consistent with prior SEER-Medicare studies. Cohort differences were tested with χ^2 or t-tests. To control for repeated observations (e.g., treatment cycles) per patient, we used multivariable Generalized Estimating Equations to measure associations between race and AEs.

Results: The cohort included 18,089 patients (15,824 NHW; 2,265 NHB). SEER stage distribution was consistent across both NHW and NHB cohorts (33% vs. 34% metastatic disease, P=0.32). NHW patients were more often male (64% vs. 55%, P<0.01) and had more cardia primaries (59.9% vs. 37.0%, P<0.01), while NHBs had higher comorbidities (mean NCI Index 0.64 vs. 0.50, P<0.01). NHBs were less likely to receive chemotherapy (aOR 0.80, 95% CI 0.71-0.89) or radiation (aOR 0.76, 95% CI 0.66-0.86), and had longer mean time to treatment initiation (chemotherapy: 82 vs. 73 days; radiation: 100 vs. 85 days; both P<0.01) than NHWs. Among 5,748 chemotherapy recipients (5,147 NHW; 601 NHB), mean treatment cycles did not differ between NHWs and NHBs (5.0 vs. 5.2, P=0.19). However, NHBs had higher AE risk (aOR 1.15, 95% CI 1.02-1.30) per treatment than NHWs. Metastatic disease (aOR 1.49, 95% CI 1.39-1.59) and non-NCCN regimens (aOR 1.31, 95% CI 1.22-1.40) were also associated with elevated AE risk. Further sub-group analyses showed higher AE risk for NHBs relative to NHWs in the non-NCCN cohort (aOR 1.35, 95% CI 1.10-1.65) but not in the NCCN cohort (aOR 1.11, 95% CI 0.95-1.28).

Conclusions: NHB patients with GC were less likely to receive chemotherapy or radiotherapy and experienced longer treatment delays than NHW patients. NHB patients also had greater risk of chemotherapy-related AEs, particularly when using non-NCCN regimens. These findings highlight persistent inequities in GC care and support further investigation into structural and biological drivers of AE disparities.

#0902 Characterizing barriers and facilitators to healthcare access among female breast cancer patients in The Gambia.

Anjali Gupta[1], Jen Gathings[2], Ami Mejia[2], Ramatoulie Jobe[3], Anna Korrea[3], Abdul K. Fye[3], Joseph W. Jatta[3], Ashwini Joshi[4], Ousman Sanyang[3], Alagie Manneh[3], Charles A. P. Roberts[3], Lamin Jaiteh[3], Gabriel O. Ogun[3], Tomi F. Akinyemiju[4]

[1]School of Medicine, Stanford University, Stanford, CA,[2]ETR Services, LLC, Durham, CA,[3]School of Medicine & Allied Health Sciences, University of The Gambia, Banjul, Gambia,[4]School of Medicine, Duke University, Durham, NC

Background: The Gambia, the smallest country within mainland Africa, is estimated to have one of the lowest cancer survival rates of countries in Africa, Asia, and Central America. Although poor access to healthcare contributes to low breast cancer survival rates in The Gambia, little is known about patient experiences across multiple healthcare access domains. The purpose of this study was to characterize healthcare access barriers and facilitators to breast cancer care.
Methods: Twenty-three breast cancer patients from the Edward Francis Small Teaching Hospital (EFSTH; largest referral center in the country) in Banjul, The Gambia participated in semi-structured interviews from June-December 2023. Interviews were conducted in Wolof, Mandinka and/or English as appropriate. Topics included patient experiences and pathways to diagnosis, prior knowledge and beliefs about breast cancer, barriers to accessing care, and cultural factors impacting the treatment journey. Analysis coupling an inductive approach with an initial deductive approach following Penchansky and Thomas's (1981) theoretical framework of healthcare access resulted in a final set of codes.
Results: Of the 21 participants with available age data, the mean (SD) age was 44 (10) years. Most participants had little to no knowledge of breast cancer prior to their diagnosis. The time from symptom onset to diagnosis ranged widely from a few weeks to months or years. Seven participants (30%) reported using traditional medicine prior to visiting a healthcare professional. Affordability of diagnostic procedures and treatments was the most frequently mentioned barrier (91% of participants), followed by availability of services (e.g., providers, working equipment, facilities' capacities to perform procedures, medications, etc.; 83%), accessibility (distance and travel) of providers (74%), accommodation (health system organization) in relation to the preferences of the patients (43%), and acceptability (quality of patient-provider interaction; 9%). Family, peers, and faith were important sources of support and comfort during the cancer journey.
Conclusions: Our results highlight major barriers to healthcare access among breast cancer patients in The Gambia, leading to delays in diagnosis and treatment. Multi-level initiatives to address these barriers will be crucial to reducing the breast cancer burden within the country.

#0903 Socioeconomic and system-level factors influencing receipt of advanced NSCLC surgery..

Nimish Valvi[1], Francesca Kowalik[1], Dejana Braithwaite[2], Mihika Shinde[2], Hiren Mehta[3], **Shama Karanth**[2]

[1]Ball State Univ., Muncie, IN,[2]Department of Surgery, University of Florida, Gainesville, FL,[3]Department of Medicine, University of Florida, Gainesville, FL

Background: Lung cancer is a major contributor to cancer-related morbidity and mortality in the United States. Although advances in medical and surgical treatment have improved outcomes, economically disadvantaged patients, particularly those living in rural areas or lacking health insurance, continue to experience substantial treatment disparities. These disparities are exacerbated by the introduction of newer surgical technologies, as underserved patients often have limited access to these modern treatments.
Objective: To evaluate the association between area-level socioeconomic status (SES) and type of surgery received, robotic-assisted thoracic surgery (RATS), video-assisted thoracic surgery (VATS), and open lobectomy among patients with non-small-cell lung cancer (NSCLC).
Methods: Data were drawn from the 2015-2022 National Cancer Database and included patients diagnosed with Stage 0-IIIa NSCLC. The primary exposure was area-level income, defined by quartiles of median household income in the patient's zip code. Multinomial logistic regression was used to estimate adjusted odds ratios (aORs) and 95% confidence intervals (CIs) for the association between income quartiles and surgical approach, using open surgery as the reference group. Models were adjusted for patient, clinical, hospital, and socioeconomic characteristics. All comparisons were considered statistically significant with $p < .05$.
Results: The study included 84,931 patients with NSCLC, with a mean age of 67.8 ±8.5 years. Patients were identified as having undergone either an open lobectomy (38.4%), VATS (33.3%), or RATS (28.2%) during the study period. Most patients were older, White, and Medicare-insured, with care predominantly at academic metropolitan centers. In the adjusted models, low-income (<$46,277) patients were less likely to undergo RATS (aOR: 0.81, 95% CI: 0.76-0.87) or VATS (aOR: 0.82, 95% CI: 0.77-0.87) versus open lobectomy compared to patients from high-income (≥$74,063) areas. Compared to academic hospitals, community centers were 67% less likely to receive RATS (aOR: 0.33, 95% CI: 0.30-0.37) and 39% less likely to receive VATS (aOR: 0.61, 95% CI: 0.57-0.67). Additionally, males were less likely than females to receive RATS or VATS.
Conclusions: The findings indicate that patients with NSCLC from low SES areas have reduced access to advanced, minimally invasive surgical techniques (RATS and VATS). Targeted efforts to ensure access to modern surgical care are warranted to reduce and mitigate treatment disparities and improve patient outcomes.

#0904 Developing a polysocial risk score for prostate cancer patients treated with radical prostatectomy.

Kelsie Campbell, Dayoung Bae, Chanita Hughes-Halbert

Population and Public Health Sciences, USC Keck School of Medicine, Los Angeles, CA

Introduction: Prostate cancer is the leading cause of cancer morbidity and mortality among men in the United States, with stark racial disparities. Black men experience both higher incidence and worse outcomes compared to White men, even after accounting for clinical stage and treatment. Social determinants of health (SDOH) are increasingly recognized as critical drivers of these disparities, influencing care across the prostate cancer continuum—from screening to survivorship. We developed a novel polysocial risk score that integrates multiple psychosocial and socioeconomic factors to quantify cumulative SDOH burden, and evaluated its associations with race, clinical characteristics, and neighborhood context in a prostate cancer cohort.

Methods: We retrospectively identified 126 prostate cancer patients who underwent radical prostatectomy between 2011 and 2019 at a single academic cancer center. Eleven candidate variables—capturing perceived stress, loneliness, financial strain, and socioeconomic status (education, income, employment)—were included in an exploratory factor analysis. A 7-item unidimensional composite (1 stress item, 3 loneliness items, 1 financial strain item, 2 SES items) was retained based on factor loadings and showed acceptable internal consistency (Cronbach's $\alpha = 0.74$). We compared polysocial risk scores by self-reported race (Black vs. White) and examined associations with tumor stage, prostate-specific antigen (PSA), the Social Deprivation Index (SDI), and neighborhood collective efficacy.

Results: The final score accounted for 39.6% of variance in the item set, reflecting a cohesive social risk construct. Black patients had significantly higher scores than White patients (mean 2.79 vs. -1.08, $p < .001$), indicating greater cumulative social adversity. The score was not associated with tumor stage ($p = .89$), suggesting social risk burden was independent of disease severity. However, higher scores were correlated with neighborhood disadvantage (SDI, $r = 0.52$, $p < .001$) and lower collective efficacy (trust; $r = -0.20$, $p = .03$).

Conclusion: This composite measure of psychosocial and socioeconomic adversity revealed markedly higher cumulative social risk among Black prostate cancer patients, despite similar clinical profiles. The polysocial risk score may aid in identifying patients with unmet social needs who could benefit from targeted supportive interventions. Integrating social risk assessment into prostate cancer care may promote health equity by addressing upstream determinants of disparate outcomes.

#0905 Racial disparities in geographic access to uterine cancer clinical trials across U.S. counties.

Caitlin E. Meade[1], Jennifer A. Sinnott[2], Simran A. Kanal[1], Laura M. Chambers[3], **Ashley S. Felix**[1]

[1]College of Public Health, Ohio State University, Columbus, OH,[2]College of Arts and Sciences, Ohio State University, Columbus, OH,[3]College of Medicine, Ohio State University, Columbus, OH

Purpose: Uterine cancer mortality is rising, disproportionately affecting racially and socioeconomically marginalized populations. Clinical trials improve access to novel therapies and outcomes, yet racial disparities in trial enrollment persist. Because the geographic distribution of trials shapes opportunities for enrollment, we examined associations between race and county-level availability of interventional uterine cancer trials, and whether this relationship varies by neighborhood vulnerability.

Methods: We identified US-based uterine cancer interventional trials from the Aggregate Analysis of ClinicalTrials.gov database (2008-2021) and aggregated site ZIP codes to counties, counting multiple sites per county as one trial. County-level trial availability was linked to the CDC Social Vulnerability Index (SVI; range 0-1, higher scores = greater vulnerability) and uterine cancer cases in SEER (2008-2021). Multivariable logistic regression estimated associations between race/ethnicity (American Indian/Alaska Native, Asian, Black, Hispanic, Native Hawaiian/Pacific Islander, and White) and county-level trial availability, adjusting for clinical characteristics and county size. Effect modification by SVI [high (≥90th percentile) vs. low (<90th percentile) was assessed.

Results: We included 151,610 uterine cancer cases (mean [SD] age at diagnosis, 61.7 [11.7] years) diagnosed between 2008 and 2021. Two-hundred and twenty-five unique interventional uterine cancer clinical trials were open in the year of diagnosis and county of residence for these cases; 78% lived in a county with at least one open interventional trial. Compared to White women, Asian, Black, and Native Hawaiian/Pacific Islander women had higher odds of trial availability, whereas American Indian/Alaska Native and Hispanic women had lower odds. We observed effect modification by SVI (p-interaction <0.001): in areas of high vulnerability, Black compared to White women had higher odds of trial availability (OR=1.31, 95% CI=1.08-1.60).

Conclusions: Our findings highlight racial disparities in geographic access to uterine cancer clinical trials - an essential prerequisite for enrollment. Among residents of more socially vulnerable areas, trial availability was higher for Black than White women, contrasting with prior research showing lower enrollment among Black patients. This suggests structural barriers beyond proximity continue to limit equitable participation, even where trials are accessible.

#0906 Sex-based differences in lung cancer survival: A competing risks model using the PLCO trial.

Veer N. Shah[1], Grace Mhango[1], Darshi Shah[2], Paolo Boffetta[3], Juan P. Wisnivesky[1]

[1]Icahn School of Medicine at Mount Sinai, New York, NY,[2]Stony Brook University, Renaissance School of Medicine, Stony Brook, NY,[3]Stony Brook University, Stony Brook, NY

Purpose:Lung cancer causes more than 130,000 deaths each year in the United States. Although females with non-small cell lung cancer (NSCLC) appear to have better survival than males, many prior studies did not fully account for key confounders, including smoking history and competing causes of mortality. Moreover, large cohort analyses often relied on Cox models, which may overestimate cause-specific risks when competing mortality is substantial. Hence, in this study, we assessed whether sex-based survival differences in NSCLC persist after adjusting for these confounders and applied competing risk regression to adequately account for competing causes of death and more accurately quantify lung cancer-specific mortality.
Methods:Using data from the Prostate, Lung, Colorectal, and Ovarian (PLCO) trial, we selected patients whose first-ever malignancy was primary NSCLC, excluding anyone with a prior other cancer diagnosis or secondary/metastatic lung tumors. Lung cancer-specific survival for females versus males was evaluated using Fine and Gray competing risk models, adjusting for sociodemographic factors, cancer location, histology, treatment, smoking status, and comorbidities. Because patients with NSCLC experience substantial mortality from non-cancer-related causes, we applied a competing risk model to accurately account for this. This approach avoids the more than twofold (2.25-fold) overestimation of cause-specific risk that can occur when Cox models are used in elderly populations. All analyses were performed using SAS 9.4.
Results:Among 2,793 patients (59% male, 41% female), 2,006 (72%) experienced lung cancer-related death, 531 (19%) died from other causes, and 256 (9%) were alive at last follow-up. Female patients were more likely to be never smokers (14% vs 5%, $p<0.0001$), have adenocarcinoma (55% vs 42%, $p<0.0001$), and less likely to have cardiovascular disease (heart failure: 7% vs 18%, $p<0.0001$). Unadjusted Fine and Gray models showed (hazard ratio [HR]: 0.81, 95% confidence interval [CI]: 0.74-0.88) lower lung cancer-specific mortality among women. Adjusted analyses demonstrated that female sex (HR: 0.85, 95% CI: 0.74-0.98) was associated with decreased risk of lung cancer-specific death. A significant interaction between female sex and stage IV disease (b coefficient: 0.18, 95% CI: 0.99-1.45) showed that lung cancer-specific survival of women and men was similar among patients with advanced disease.
Conclusions:Females with NSCLC demonstrate reduced lung cancer-specific mortality after adjustment for competing risks and confounders. These results could be suggestive of sex-based disparities in inherent biological differences in tumor biology, natural disease progression, or overall increased life expectancy in females, further supporting investigating molecular pathways including hormonal signaling and immune responses to guide optimal treatment strategies.

#0907 Impact of socioeconomic status and travel distance on treatment outcomes in soft tissue sarcoma: A retrospective analysis from a high volume tertiary care center.

Cordero Lee McCall[1], Janelle Cordero[2], Meena Bedi[1], David King[3]

[1]Medical College of Wisconsin, Wauwatosa, WI,[2]Fordham University, Bronx, NY,[3]Orthopedic Surgery, Medical College of Wisconsin, Milwaukee, WI

Introduction: Soft tissue sarcomas (STS) are rare mesenchymal tumors with substantial clinical complexity. Although tumor size, grade, and histology are established prognostic factors, socioeconomic status (SES) and geographic access to specialized care may also influence outcomes. Prior studies in multiple cancers show that socioeconomic disadvantage and longer travel distances can delay treatment and worsen prognosis. High-volume sarcoma centers offer multidisciplinary management that improves survival, yet SES-related barriers may still affect access. This study evaluates the impact of SES, travel distance, treatment patterns, and survival outcomes among STS patients treated at a high-volume tertiary center.

Methods: A retrospective cohort of 364 patients with primary STS treated over 20 years at a single tertiary center was analyzed. Patients with metastatic disease at diagnosis, incomplete treatment data, or inadequate follow-up were excluded, leaving 357 eligible patients. SES was measured using the Area Deprivation Index (ADI) and classified as high (ADI 8-10) or low (0-7) deprivation. Travel distance was calculated using the Haversine formula. Kaplan-Meier analyses assessed overall survival (OS), progression-free survival (PFS), and distant metastasis-free survival (DMFS). Logistic regression evaluated factors associated with wound complications.

Results: No significant differences were found in OS (p=0.2), PFS (p=0.3), DMFS, or wound complications (p=0.1) between high- and low-ADI groups. Treatment patterns were similar, including adjuvant chemotherapy (8.9% vs. 8.7%, p=1.000) and radiation (10.7% vs. 11.8%, p=1.000). High-ADI patients traveled slightly farther (median 24.8 vs. 18.5 miles), but this modest increase was not associated with differences in treatment delivery or outcomes. On multivariate analysis, tumor grade, age, and Karnofsky Performance Status predicted OS.

Conclusion: Despite marginally longer travel distances, socioeconomically disadvantaged patients had comparable treatment patterns and survival outcomes to more advantaged patients. The small travel difference did not impede access to multidisciplinary sarcoma care. High-volume tertiary centers may help mitigate SES-related disparities by providing equitable, standardized treatment across diverse populations.

#0908 An intersectional analysis of physical and mental health-related quality of life among LGBTQ+ patients with cancer.

Rolando F. Trejos, Shahrzad Zamani, Matthew B. Schabath

Department of Cancer Epidemiology, Moffitt Cancer Center, Tampa, FL

Background: Prior studies report that LGBTQ+ patients with cancer report poorer health-related quality of life (HRQOL), but very little is known about how their LGBTQ+ identity intersects with their race and ethnicity. Guided by Intersectionality and Minorities' Diminished Returns theories, this study sought to explore the impact of the intersection of these identities on cancer patients' HRQOL. We hypothesize that ethnoracially diverse LGBTQ+ cancer patients will have poorer HRQOL.
Methods: Self-reported data were obtained from 97,346 patients, of whom 3,353 self-identified as LGBTQ+, who completed a standard-of-care electronic questionnaire including demographics, psychosocial measures, and the validated Short Form Health Survey-12. Sexual orientation (SO) and gender identity (GI) were used to identify sexual minorities, gender minorities, and cisgender heterosexual persons. SF-12 scores were used to calculate the Physical Component Summary (PCS) and Mental Component Summary (MCS). Age-adjusted generalized linear models estimate mean MCS and PCS for intersectional identities using SAS (version 9.4). For the SO analyses, the reference group was non-Hispanic White heterosexual patients; while for GI analyses, it was non-Hispanic White cisgender male patients.
Results: For the intersectional analyses by SO, 39 identities were analyzed. Twenty identities were associated with lower MCS, of which White Heterosexual and Hispanic multiracial lesbian/gay patients had statistically significantly lower scores. For PCS, 23 identities were associated with lower scores, but only while multiracial non-Hispanics with unspecified SO had significantly lower PCS. PCS was significantly higher among Black Hispanic patients who did not disclose their sexual orientation. For the intersectional analyses by GI, 26 of 43 identities were associated with lower MCS, of which White Hispanic transgender, White cisgender females, and Non-Hispanic Asian patients had significantly lower scores. For PCS, 26 identities were associated with lower scores, but only Hispanic Native Hawaiian or other PI Cisgender males had significantly lower PCS. When SO+GI were combined with non-Hispanic White straight cisgender males as the reference, 20 identities had significantly lower MCS, including non-Hispanic Asian straight transgender males and non-Hispanic multiracial genderqueer patients. For PCS, 24 groups had significantly lower scores, including Hispanic American Indian/AN cisgender males and non-Hispanic multiracial bisexuals with other GI.
Conclusions: This analysis of intersectional identities by LGBTQ+ status, race, and ethnicity highlights the importance of collecting detailed demographics to reveal cancer-related disparities and underscores the need for personalized care and the delivery of supportive services to populations disproportionately experiencing worse HRQOL.

#0909 Disparate access and outcomes of immunotherapy treatment in patients with head and neck cancer.

Morgan C. Byrd[1], Tariq M. Omer[2], Alexandra Hunter[2], Rong Jiang[3], Aleksandr R. Bukatko[4], Oyomoare L. Osazuwa-Peters[3], Tammara L. Watts[3], Nosa Osazuwa-Peters[2]

[1]Head and Neck Surgery & Communication Sciences, Duke University School of Medicine, Durham, NC,[2]Duke University School of Medicine, Durham, NC,[3]Duke Cancer Institute, Durham, NC,[4]St. Louis University School of Medicine, St. Louis, MO

Introduction: Head and neck cancers (HNC) are often treated with surgery, radiation, and chemotherapy which can cause significant morbidity. Immune checkpoint inhibitors activate the immune system to target cancer cells and may reduce treatment-related complications. We examined clinical and sociodemographic factors associated with first-line immunotherapy receipt and timing, and assessed survival impacts in a hospital-based cohort.

Methods: Adults with advanced stage (III-IV) HNC (n=414,380) from the National Cancer Database (2004-2022) were analyzed. Multivariable regression estimated differences in time to immunotherapy and adjusted odds ratios (aORs) for receipt, adjusting for age, sex, race, tumor site, insurance, Charlson-Deyo comorbidity (CDCC), income, and education. Overall survival was evaluated using Cox models comparing immunotherapy timing relative to surgery (immunotherapy only, neoadjuvant, or adjuvant) versus no immunotherapy, adjusting for the same covariates plus radiation and chemotherapy. A secondary model among immunotherapy recipients evaluated survival by sociodemographic factors.

Results: The cohort was 74.2% male, mean age 62.5 years, 85.6% White; 4.7% had immunotherapy. Black patients (ß 11.06, 95% CI 5.12-16.99), females (ß 6.24, 95% CI 1.99-10.50), and tumors in the mouth/oral cavity (ß 10.95, 95% CI 6.42-15.49) or nasopharynx/nasal cavity/sinus (ß 13.96, 95% CI 5.75-22.18) had longer times to immunotherapy compared to oropharynx. Areas with higher low-education also had delays. Older age was associated with shorter delays; insurance and income showed no differences. Females (aOR 0.83, 95% CI 0.80-0.86) and tumors in the mouth/oral cavity (aOR 0.78, 95% CI 0.75-0.81), larynx/hypopharynx (aOR 0.73, 95% CI 0.70-0.77), and nasopharynx/nasal cavity/sinus (aOR 0.6, 95% CI 0.63-0.73) had lower odds of receipt than oropharynx. Higher comorbidity, Medicaid/Medicare, and higher income were associated with increased odds of receipt. Adjuvant immunotherapy improved survival (aHR 0.95, 95% CI 0.90-0.99), while immunotherapy alone (aHR 1.25, 95% CI 1.22-1.29) and neoadjuvant therapy (aHR 1.12, 95% CI 1.04-1.20) were linked to worse survival compared to no immunotherapy. Older age, Black race, non-oropharynx tumors, higher comorbidity burden, lower income, and residence in areas with lower educational attainment were each independently associated with higher mortality. Among immunotherapy recipients only, Black race (aHR 1.23, 95% CI 1.14-1.31) and increasing CDCC scores predicted worse survival, while private insurance was protective (aHR 0.64, 95% CI 0.57-0.72).

Conclusion: Differential access to immunotherapy and survival outcomes in HNC disproportionately affects racial minorities and socioeconomically disadvantaged populations, underscoring multifactorial determinants of survival and the need for equitable cancer care interventions.

#0910 Disparities in 5-year relative survival rates of cervical cancer by age and stage at diagnosis between African Americans and Whites, in the USA, from 2016 to 2022.

Milahni Wilkerson[1], John Heath[2], **Ehsan Abdalla**[1]

[1]Tuskegee University College of Veterinary Medicine (TUCVM), Tuskegee, AL,[2]CBR/RCMI, Tuskegee University, Tuskegee, AL

BACKGROUND: The overall five-year relative survival rates (RSRs) for cervical cancer in the USA are about 67%, varying significantly by stage at diagnosis. Localized cervical cancer has a higher survival rate, approximately 91%, while later stages (regional or distant) have lower rates, with the regional stage it is 62% and the distant stage it is 19%.
OBJECTIVE: To compare differences in cervical cancer RSRs by age and stage at diagnosis between African Americans and Whites in the U.S.
METHODS: Using data from the 2016 to 2022 SEER (Surveillance, Epidemiology, and End Results) database, we analyzed 356 African Americans and 4,612 Whites diagnosed with cervical cancer. RSRs compared African Americans and Whites by age and stage at diagnosis using SEER*Stat software.
RESULTS: At the localized stage, Whites aged 15-44 had an RSR of 97.1% (95% CI, 95.5-98.2), consistently higher than African Americans, except those aged 45-54 and 55-64, who had slightly higher RSRs at 94.6% and 91.6% (95% CIs: 77.0-98.8 and 65.2-98.2), respectively. At the regional stage, Whites had better survival overall, with an RSR of 60.7% (95% CI, 50.3-69.5). The exception was African Americans aged 75 and older, who had a higher RSR of 56.2% (95% CI, 0.2-94.9) than Whites in the same age group. At the distant stage, both African Americans and Whites aged 15-44 had similar lower RSRs of 31.5% (95% CI, 19.8-30.1). African Americans aged 55-64 and 65-74 had higher RSRs of 22.6% and 25.3% (95% CIs: 9.10-39.7 and 6.2-50.6) than their White counterparts. Among those aged 75 and older, Whites had a higher RSR (7.4%, 95% CI: 1.9-17.9). For cases with an unknown stage, Whites aged 15-44 had an RSR of 91% (95% CI, 73.5-97.2), again higher than African Americans. However, African Americans aged 45-54 had a higher RSR of 67.3% (95% CI, 5.1-94.9) compared to Whites in the same age group.
DISCUSSION/CONCLUSION: Significant disparities in cervical cancer RSRs exist by race, age, and stage. Overall, African Americans had lower RSRs than Whites, underscoring persistent disparities in cervical cancer outcomes among these two groups.

#0911 Racial and ethnic differences in cardiovascular disease mortality among women diagnosed with ductal carcinoma *in situ* in the United States.

Yancen Pan[1], Ziad Zakaria[1], Jessica Li[1], Lene HS Viega[2], Amy Berrington de Gonzalez[3], Geetanjali Datta[1], Jacqueline B. Vo[2], Cody Ramin[1]

[1]Samuel Oschin Comprehensive Cancer Institute, Cedars-Sinai Medical Center, Los Angeles, CA,[2]Division of Cancer Epidemiology and Genetics, National Cancer Institute, Bethesda, MD,[3]Division of Genetics and Epidemiology, The Institute of Cancer Research, London, United Kingdom

Background: Ductal carcinoma *in situ* (DCIS) is associated with an elevated risk of cardiovascular disease (CVD) mortality, which may be due to comorbidities or cancer treatment, yet prior studies examining racial and ethnic differences are limited. The aim of this study is to investigate the association between race, ethnicity and CVD mortality among women diagnosed with DCIS in the United States.
Methods: We included women diagnosed with a first primary DCIS aged 20-84 between 2000 to 2017 in the U.S. Surveillance, Epidemiology, and End Results, and followed for more than one year. Fine and Gray regression was used to estimate sub-distribution hazard ratios (HRs) for CVD mortality by race and ethnicity (Hispanic, non-Hispanic Asian American (NH-AA), NH-Black, NH-Native Hawaiian and other Pacific Islander (NH-NHPI), and NH-White), adjusting for age at diagnosis, year of diagnosis, surgery type, and radiotherapy, and accounting for competing risks of non-CVD death. Models were further stratified by DCIS diagnosis age (<50 and ≥ 50) and year (2000-2004, 2005-2009, and 2010-2017). Cumulative incidence of CVD mortality was also assessed by race and ethnicity, accounting for competing risks.
Results: Among 158,072 women diagnosed with DCIS (median follow-up=6.80 years; mean age=58.47 years), 4,504 CVD deaths were identified (3,190 heart disease, 964 cerebrovascular disease, and 350 other CVD deaths). Compared to NH-White women, NH-Black and NH-NHPI women had a higher risk of CVD mortality ($HR_{NH\text{-}Black}$ = 1.61, 95%CI=1.48-1.76; $HR_{NH\text{-}NHPI}$ = 1.80, 95%CI=1.22-2.65) while NH-AA women had a lower risk of CVD mortality ($HR_{NH\text{-}AA}$ = 0.68, 95%CI=0.60-0.79). There was no significant association of CVD mortality for Hispanic women compared NH-White women ($HR_{Hispanic}$ = 0.91, 95%CI=0.80-1.03). Although the increased risk of CVD mortality remained higher in NH-Black and NH-NHPI women regardless of age at DCIS diagnosis, younger women (<50 years) had greater relative risk compared to older women (≥50 years) in stratified analyses ($HR_{NH\text{-}Black,\ <50}$ = 3.93, 95%CI=2.62-5.90, $HR_{NH\text{-}Black,\ \geq 50}$ = 1.56, 95%CI=1.43-1.71; $HR_{NH\text{-}NHPI,<50}$ = 4.19, 95%CI=1.04-16.97, $HR_{NH\text{-}NHPI,\ \geq 50}$ = 1.73, 95%CI=1.16-2.59). Risk of CVD mortality increased by year of diagnosis, especially among NH-Black and NH-NHPI women. NH-Black and NH-NHPI women had the highest cumulative incidence of CVD mortality at 5-years (1.51%, 95%CI=1.33%-1.72% and 1.53% 95%CI=0.81%-2.66% respectively) and 10-years (4.29%, 95%CI=3.90%-4.70% and 4.17% 95%CI=2.62%-6.26% respectively) post DCIS diagnosis.
Conclusions: NH-Black and NH-NHPI women diagnosed with DCIS had higher CVD mortality compared to NH-White women, especially among younger women and those diagnosed in recent years. Further studies are needed to understand multi-level factors driving the increased risk of CVD mortality in NH-Black and NH-NHPI women with DCIS.

#0912 Non-Hodgkin's lymphoma survival by neighborhood disinvestment and socioeconomic composition.

Jesse J. Plascak, Elizabeth Ghias, Daniel C. Trotier, James L. Fisher, Kami J. Maddocks, Jennifer A. Woyach

The Ohio State University Comprehensive Cancer Center, Columbus, OH

Background: Socioeconomic factors have been associated with adverse survival from non-Hodgkin's Lymphoma (NHL), but few studies have considered the role of neighborhood disinvestment. This study investigated associations among neighborhood socioeconomic composition, disinvestment (e.g., disrepair and deterioration), stage at diagnosis, and NHL survival.
Methods: Age, sex, marital status, race-ethnicity, diagnosis date, residence at diagnosis, health insurance, stage at diagnosis (localized, regional, distant), and histologic subtype (Diffuse large B-Cell lymphoma, follicular, Chronic lymphocytic leukemia / small lymphocytic lymphoma, other B-cell, and T-cell) were from 1209 Franklin County, Ohio residents diagnosed with non-Hodgkins lymphoma between 2010 and 2019 as recorded in the Ohio Cancer Incidence Surveillance System. Neighborhood disinvestment was from a virtual neighborhood audit of 6 indicators - garbage, graffiti, dumpsters, building conditions, yard conditions, abandoned buildings - within 5,000+ Franklin County Google Streetview location-dates estimated at residential addresses and diagnosis dates using spatio-temporal models. Census tract-level, neighborhood socioeconomic composition was measured by the Yost index - a validated composite of seven socioeconomic factors annually assessed from the US American Community Survey - and linked to each NHL case by residential census tract and year of diagnosis. We fitted accelerated failure time models of all-cause and NHL-specific survival time as functions of neighborhood socioeconomics, disinvestment, and stage, adjusted for covariates. Survival time was right-censored at the earliest of death from other causes, loss to follow-up, or end of follow-up (12/31/2020).
Results: Across 5308 person years, there were 362 all-cause and 163 NHL-specific deaths. Disinvestment and stage statistically interacted in models of all-cause but not NHL-specific deaths. Among those diagnosed regional stage, all-cause survival time decreased by 35% (95% CI: 7%, 55%), with each standard deviation increase in disinvestment after adjustment for covariates. There was no evidence of associations between disinvestment and all-cause survival among localized and distant stages, disinvestment and NHL-specific survival, and socioeconomic composition and NHL-specific survival.
Conclusion: Both neighborhood socioeconomic composition and disinvestment among those diagnosed at regional stage are independently associated with shorter all-cause, but not NHL-specific, survival among NHL cases within a Midwestern Metropolis.

#0913 Acuity circles policy and persistent socioeconomic disparities in liver transplantation.

Sungsu Park[1], Junho Song[2], Hyungjune Ku[3], Tehyun Phillip Eom[4], Sunghan Kim[4], Changmin Jo[5], Minkwan Kim[6], Amy Choi[7], Dongyeol Lee[8], Sangsoo Lee[3], Jihyun Park[9], Hyewon Kim[10], Seoyeong Ku[11], Heekyoo Kim[3]

[1]Daegu Catholic University School of Medicine, Daegu, Korea, Republic of,[2]Northwestern University - Chicago, Hershey, PA,[3]Kosin University College of Medicine, Busan, Korea, Republic of,[4]CHA University School of Medicine, Seongnam-si, Korea, Republic of,[5]Chung-Ang University College of Medicine, Seoul, Korea, Republic of,[6]Independent researcher, Gwangmyeong-si, Korea, Republic of,[7]Department of Medicine, Penn State College of Medicine, Hershey, PA,[8]Department of Medicine, Penn State College of Medicine, Chicago, IL,[9]Montini Catholic High School, Lombard, IL,[10]Hanyang University College of Natural Sciences, Seoul, Korea, Republic of,[11]Seoul Women's University, Seoul, Korea, Republic of

Background: The Acuity Circles policy, implemented by UNOS on April 2, 2020, aimed to improve geographic equity in liver transplantation by prioritizing local candidates with high medical acuity. However, concerns remain about whether this policy adequately addresses persistent socioeconomic disparities in transplant access. We evaluated the impact of Acuity Circles on disparities in deceased donor liver transplant (DDLT) rates across socioeconomic factors including race/ethnicity, insurance status, education, employment, citizenship, and geographic region.

Methods: Using UNOS data from adult HCC patients listed for liver transplant, we analyzed 13,589 patients in the 21-month periods before (n=7,380) and after (n=6,209) Acuity Circles implementation. We employed competing risks analysis with Aalen-Johansen cumulative incidence functions to estimate DDLT rates, accounting for death/deterioration as competing events. Socioeconomic disparities were assessed using Gray's test for equality of cumulative incidence functions. Time origin was listing date with era-specific censoring.

Results: Overall DDLT rates were comparable between the pre- and post-policy eras: 49.5% at 12 months pre-policy vs. 48.1% post-policy (Gray's test p=0.93). Regarding race/ethnicity, pre-policy, Asian patients had DDLT rates of 44.0% vs. 50.0% for White patients (reference) and 54.9% for Black patients. Post-policy, Asian rates remained lower at 44.9% vs. 49.0% for White patients, with Black patients at 52.7% (Gray's test: pre $p<0.001$, post $p<0.001$). By insurance status, private insurance patients maintained higher DDLT access compared to public insurance patients in both eras (Gray's test: pre p=0.002, post p=0.012). For education, patients with less than college education had slightly different DDLT rates compared to college graduates in both periods (49.4% vs. 48.0% pre-policy, 47.3% vs. 47.5% post-policy; Gray's test $p<0.001$ both eras). Additionally, US citizens had higher access than non-US citizens (p=0.001 pre, p=0.009 post), employed patients had better access than unemployed ($p<0.001$ both eras), and significant regional variation remained ($p<0.001$ both eras). Gender differences were not significant.

Conclusions: The Acuity Circles policy did not significantly alter overall DDLT rates or reduce existing socioeconomic disparities in liver transplantation. Despite its goal of improving geographic equity, race/ethnicity, insurance, employment, citizenship, and regional disparities persisted at similar magnitudes before and after implementation. These findings highlight the need for complementary policy interventions that directly address socioeconomic determinants of transplant access beyond geographic redistribution of organs.

#0914 Racial disparities in immune-related adverse events with immune checkpoint inhibitors: A systematic review and meta-analysis.

Toshiaki Takahashi[1], Yu Fujiwara[2], Ahmad Bouhuwaish[3], Kohei Chida[2], Rodrigo Paredes[4], Sarbajit Mukherjee[5]

[1]Department of Medicine, John A. Burns Sch. of Med. Univ. of Hawaii at Manoa, Honolulu, HI,[2]Department of Medicine, Roswell Park Comprehensive Cancer Center, Buffalo, NY,[3]Department of Public Health, Sechenov University, Moscow, Russian Federation,[4]Department of Medicine, Icahn School of Medicine at Mount Sinai, Mount Sinai West/Morningside, New York, NY,[5]Miami Cancer Institute | Baptist Health South Florida, Miami, FL

Background: There is insufficient data on whether immune-related adverse events (irAEs) from immune checkpoint inhibitors (ICIs) differ by race/ethnicity. The objective of our study was to systematically evaluate the incidence of irAEs by race to inform equitable treatment approaches.

Methods: We searched PubMed/MEDLINE and Embase from inception through December 16, 2024 for randomized trials and cohort studies in adults receiving ICIs. Race-specific incidence was pooled using a generalized linear mixed-effects proportional meta-analysis. Within-study odds ratios (ORs) versus White were pooled with random-effects inverse-variance models; heterogeneity was summarized with I^2 and inspected with leave-one-out analyses. Subgroup analyses were conducted based on ICI class (PD-1 monotherapy and dual PD-1/CTLA-4 therapy), tumor type (lung cancer), and study design (excluding organ-specific irAE reports and excluding registry-based database studies).

Results: Of the 3,397 records screened, 510 full-text articles were assessed for eligibility, and 24 studies comprising 109,902 patients were included in the analysis. In the overall population, the pooled incidence of irAEs was 13.7% (95% CI, 2.7-47.5) in Asian, 20.6% (8.6-41.7) in Black, 16.0% (5.1-40.5) in Hispanic, and 20.5% (11.1-34.8) in White patients, with substantial heterogeneity (I^2=85.7-99.8%). Pooled ORs versus White were not statistically significant: non-White 1.28 (95% CI 0.82-1.98), Asian 1.67 (0.76-3.70), Black 1.37 (0.83-2.27), and Hispanic 0.89 (0.55-1.42); all p>0.05. Findings showed a consistent trend across the ICI-class subgroups, the lung-cancer subgroup, and the subgroup excluding registry-based studies.

Conclusion: No significant differences in irAEs were observed among races. These findings support equitable access to ICI therapy and culturally competent toxicity monitoring.

Pooled incidence of irAEs and odds ratios (ORs) by race. Abbreviation: NA, not applicable

	Overall population					**Sensitivity analysis, excluding studies reporting only organ-specific irAEs**				
Race	**Incidence % (95% CI)**	**I^2 (%)**	**OR vs White (95% CI)**	**p**	**I^2 (%)**	**Incidence % (95% CI)**	**I^2 (%)**	**OR vs White (95% CI)**	**p**	**I^2 (%)**
Asian (n=3516)	13.7 (2.7-47.5)	98.1	1.67 (0.76-3.70)	0.20	80.7	63.0 (57.6-68.3)	0.0	0.97 (0.40-2.37)	0.95	75.4
Black (n=8864)	20.6 (8.6-41.7)	98.3	1.37 (0.83-2.27)	0.45	94.8	43.4 (34.0-53.3)	94.0	1.37 (0.57-3.30)	0.47	94.8
Hispanic (n=638)	16.0 (5.1-40.5)	85.7	0.89 (0.55-1.42)	0.61	66.5	43.5 (39.1-47.9)	33.2	0.41 (0.18-0.93)	0.03	NA
White (n=86676)	20.5 (11.1-34.8)	99.8	NA	NA	NA	40.0 (29.8-51.2)	98.7	NA	NA	NA
Non-White (n=14565)	NA	NA	1.28 (0.82-1.98)	0.27	94.6	NA	NA	1.15 (0.66-2.01)	0.62	93.1

#0915 Disparities and underutilization of MyChart among patients with pancreatic ductal adenocarcinoma.

Anjani D. Kapadia[1], Yijia He[2], Samantha Kwock[3], Bradford Chong[4]

[1]Internal Medicine and Pediatrics, University of Chicago, Chicago, IL,[2]Center for Health and the Social Sciences, University of Chicago, Chicago, IL,[3]Pritzker School of Medicine, University of Chicago, Chicago, IL,[4]SectionSection of Gastroenterology, Hepatology, and Nutrition, Department of Medicine, University of Chicago, Chicago, IL

Background: Electronic health record portals such as MyChart support patient engagement, communication, and access to medical information. Although engagement may vary across demographic and socioeconomic groups, the relationship between portal utilization and clinical characteristics in oncology populations is poorly understood. In pancreatic ductal adenocarcinoma (PDAC), where timely diagnosis and treatment are critical, it is essential to understand how portal engagement relates to health outcomes.
Objective: We aimed to determine predictors of MyChart utilization among patients with PDAC and associations between portal engagement and stage at diagnosis. We hypothesized that greater portal use is protective against advanced stage diagnosis.
Methods: We conducted a retrospective cohort study of patients diagnosed with PDAC at the University of Chicago between 2012-2022. MyChart activity was abstracted and categorized into appointment/scheduling, health maintenance/test results, clinical messaging/document viewing, eCheck-in/eVisit, medication-related actions, and other categories. Demographic variables included age, sex, race, ethnicity, and Area Deprivation Index (ADI). Clinical variables included stage at diagnosis. We used multivariable logistic models for MyChart use and for pre-diagnosis use predicting stage, and multivariable linear regression for post-diagnosis engagement, modeling log-transformed session counts by stage.
Results: Among 1,463 patients with PDAC, 478 used MyChart after diagnosis. Black patients had lower odds of MyChart use compared with white patients (OR 0.66, p = 0.014), and those in the highest-deprivation neighborhoods (ADI 75-100) had substantially lower engagement (OR 0.52, p = 0.006). Age, sex, and ethnicity were not significant predictors of utilization. Higher MyChart utilization after diagnosis was associated with lower odds of advanced-stage disease (OR = 0.82, p = 0.007), and each category of activity showed significant or near-significant inverse associations with advanced stage. High clinic-hours use showed a stronger inverse association with advanced stage (OR 0.78, p = 0.001) than after-hours use (OR 0.86, p = 0.033). Pre-diagnosis MyChart use (n = 101) was also associated with lower odds of advanced-stage presentation (OR 0.59, p = 0.026), though intensity of pre-diagnosis activity was not significantly associated with stage.
Conclusions: Our findings highlight clear disparities in MyChart engagement among vulnerable populations. MyChart is underutilized in patients with advanced stage PDAC, both before and after diagnosis. These patterns suggest that patients who interact more frequently with digital health tools may enter the care pathway earlier or maintain stronger connectivity to healthcare services. Addressing disparities in digital engagement may support earlier diagnosis and streamlined cancer care.

#0916 Prevalence of screen-detectable cancers among adults aged 18-49 years: Findings from HINTS-SEER.

Gaurav Y. Kulkarni[1], Matthew Untalan[1], Wayne R. Lawrence[2], Ami E. Sedani[3], Subhankar Chakraborty[4], Dede K. Teteh-Brooks[5], **Aldenise P. Ewing**[6]

[1]The Ohio State University, Columbus, OH,[2]National Institutes of Health, Betheseda, MD,[3]School of Public Health, UT Health Houston, Houston, TX,[4]College of Medicine, The Ohio State University, Columbus, OH,[5]MD Anderson Cancer Center, Houston, TX,[6]College of Public Health, The Ohio State University, Columbus, OH

Background/Purpose: Over the past two decades, the incidence of cancers diagnosed among adults younger than age 50 (e.g., early-onset cancer) has risen globally. Emerging evidence indicates these trends span multiple cancer types, disproportionately burdening women, and racially and ethnically minoritized populations. However, population-level estimates of the burden of screen-detectable cancers among younger adults remain poorly characterized, limiting efforts to inform public health strategies. This study aims to quantify the prevalence and distribution of screen-detectable cancers among adults diagnosed before age 50.
Methods: We utilized 2022 data from Health Information National Trends Survey-Surveillance, Epidemiology, and End Results (HINTS-SEER), a registry-linked national survey of cancer survivors. Weighted prevalence estimates of cancers survivors among adults aged 18-49 were calculated to describe screen-detectable cancers among adults diagnosed before age 50. Cancer sites were categorized as breast, colorectal, cervical, lung, prostate, and non-melanoma skin. Weighted estimates accounted for complex survey design. Findings were stratified by birth sex, race and ethnicity.
Results: The analytic sample included 298 respondents (weighted N ≈ 119,131). Screen-detectable cancers accounted for 60.0% of diagnoses. By site, prevalence estimates were breast (29.0%), non-melanoma skin (16.1%), colorectal (7.2%), prostate (4.3%), lung (2.3%), and cervical (1.0%). Mean age varied by site, from 28.2 years for cervical cancer to 43.0 years for colorectal cancer. The sample was predominantly female (67.6%) and included respondents who were non-Hispanic White (73.6%), Hispanic (13.4%), non-Hispanic Asian (7.6%), non-Hispanic Black (3.2%), and non-Hispanic other (2.2%). Most participants (87.3%) reported at least one first- or second-degree relative with cancer, and one-third (31.6%) reported undergoing genetic testing.
Conclusions (Interpretation/Implications): Screen-detectable cancers represent a substantial proportion of early-onset cancers, driven primarily by breast and non-melanoma skin cancers, with meaningful contributions from colorectal, prostate, lung, and cervical cancers. These findings highlight critical opportunities to refine screening initiation ages, improve awareness, and implement risk-based screening strategies for younger populations. Although subgroup estimates were limited by small sample sizes, overall patterns underscore the urgency of targeted prevention and early detection efforts. Registry-linked national surveys such as HINTS-SEER provide essential context to guide policy and resource allocation tin response to the growing burden of early-onset cancers.

: Cancer in the Community: Epidemiology, Experimental Knowledge, Action, and Communication
Poster Session

#0919 Provider communication strategies that promote HPV vaccination in adults 27-45 years for oropharyngeal cancer prevention: A call to action.

Lauryn Trisha Kibugi[1], Yaeli Greenblum[1], Isabella Banan[1], Iris Chang[1], Edward Rego[1], Samantha Kaplan[2], Vincent D'Anniballe[3], Nosa Osazuwa-Peters[4]

[1]Duke University, Durham, NC,[2]Medical Center Library & Archives, Duke University, Durham, NC,[3]Medical Scientist Training Program, Duke University, Durham, NC,[4]Duke University School of Medicine, Durham, NC

Background: At least 21,000 oropharyngeal cancer (OPC) cases are diagnosed annually, with an estimated 70% attributable to Human papillomavirus (HPV) infection. Unlike cervical cancer, there are no established screening tools for early OPC detection, making vaccination the only proven method of prevention. In 2018, the FDA expanded HPV vaccine eligibility to adults up to age 45. This expansion heightens the need for effective shared decision-making between providers and patients. We conducted a scoping review to examine the landscape of provider communication strategies aimed at promoting HPV vaccine uptake in adults aged 27-45, with a focus on OPC prevention.
Methods: A medical librarian with expertise in systematic searching developed a comprehensive strategy using keywords to capture the concepts of HPV vaccination, patient-provider communication, vaccine uptake, and OPC. The databases MEDLINE, Embase, and the Web of Science were searched from inception to September 4, 2025. All results were compiled in EndNote and imported into Covidence for deduplication and screening.
Results: Of the 325 studies reviewed, 43 met the criteria for full-text screening and 9 were included in the analysis. Concerningly, only one study included otolaryngologists, who are critical in managing OPC. Eight studies consisted primarily of cross-sectional studies, surveys, and interviews with dental providers. Few evidence-based communication strategies specific to head and neck cancer prevention were identified. One promising approach was a dialogue tool that facilitated conversations about the HPV vaccine between dental providers and patients. However, significant barriers to uptake were identified: only half of dental providers believed it was their role to recommend the HPV vaccine, and only 18% of providers actually made recommendations. Only 16% of referred patients received their first dose within 6 weeks. Additional barriers included limited time, hesitancy, inadequate training, and cost. Limitations: Many dental providers indicated that they lacked sufficient training to counsel patients about HPV vaccination and oropharyngeal cancer prevention.
Conclusions: Across the literature, one study evaluated communication strategies among otolaryngologists—despite their direct involvement in the management of HPV-related OPC. This near-total absence of ENT-focused communication research signals a missed opportunity for specialty engagement. Given the expanded adult HPV vaccine indication and the rising incidence of HPV-related OPC, the field urgently needs targeted provider-facing communication tools to promote vaccination in adults aged 27-45. This review serves as a call to action for otolaryngology, dentistry, and primary care alike to fill this gap develop evidence-based communication strategies that support mid-adult HPV vaccine promotion.

#0922 Expanding HPV-related cancer awareness through multichannel communication among youth and young adults living in Los Angeles.

Samantha B. Verganza[1], Patricia Escobedo[2], Rosa Barahona[3], Letech Caldera-Huerta[3], Lourdes Baezconde-Garbanati[2]

[1]USC Norris Comprehensive Cancer Center, Los Angeles, CA,[2]Keck School of Medicine of USC, Los Angeles, CA,[3]USC, Los Angeles, Los Angeles, CA

Background: In Los Angeles County, HPV prevention remains challenging due to social media misinformation and limited audience-segmented materials. Most campaigns target parents of adolescents rather than youth and young adults, who face the highest risk for new infections. HPV communication has also focused primarily on women and cervical cancer, overlooking other HPV-related cancers that affect people of all genders. Using a community-driven audience segmentation approach, we developed multi-media HPV informational materials to raise awareness among youth and young adults across Los Angeles County.
Methods: From 2024-2025, seven listening sessions and three focus groups with LA County youth and young adults identified preferred communication channels, messaging, and information gaps. From July 2024-November 2025, the USC MICEO campaign disseminated tailored materials through social media, community partners, and cancer wellness hubs. The USC Norris Cancer Center Office of Community Outreach and Engagement and other partners supported distribution. Community health worker trainings on HPV-related cancers and prevention strategies were also conducted.
Results: Youth and young adults were reached through Instagram, YouTube, billboards, and community outreach. The campaign produced seven informational videos, eleven educational posts, and five billboard variations in Spanish, English, and Simplified Chinese. Two informational handouts on cervical cancer and HPV-related cancers supported outreach efforts. Thirty-six community health workers were trained and received two toolkits to guide dissemination. Messaging improved visibility of HPV, affected populations, HPV-related cancers, and recommended protective behaviors. Preliminary analytics show more than 8,162 social media views and over 926 in-person interactions during community outreach.
Conclusion: MICEO delivered audience-segmented HPV-related cancer information through diverse communication channels to address persistent information gaps among youth and young adults. Ongoing pre- and post-surveys are assessing changes in knowledge, attitudes, behaviors, and beliefs to inform future HPV prevention campaigns aimed at reducing cancer burden in LA County communities.

#0923 Preliminary results of a community-based randomized controlled trial to raise colorectal cancer awareness: The Community Genetic Navigation Engagement Specialist (CoGENES) Program.

Bianca Rosales[1], **Diego Alvarez-Lopez**[2], Janet Rodriguez[3], Joel Sanchez Mendez[2], Charite N. Ricker[4], Rosa Barahona[2], Heinz Josef Lenz[4], Lourdes Baezconde-Garbanati[4], Mariana C. Stern[5]

[1]USC Norris Westside Cancer Ctr., Inglewood, CA,[2]USC - University of Southern California, Los Angeles, CA,[3]USC Norris Comprehensive Cancer Center, Los Angeles, CA,[4]Keck School of Medicine of USC, Los Angeles, CA,[5]Associate Professor, Dept. of Prev. Medicine, USC Norris Comprehensive Cancer Center, Los Angeles, CA

Introduction: Knowledge and awareness of colorectal cancer (CRC) prevention and genetic testing remain limited in many Los Angeles County (LAC) communities. To address this, we trained 42 CRC-specialized community health workers (CoGENES) through a train-the-trainer program. We present preliminary results of a community-based randomized controlled trial (RCT) to evaluate the impact of materials and training delivered by CoGENES as part of an NCI funded PE-CGS network program at USC.
Methods: A two-armed, single blinded RCT was launched in August 2024. Participants are ≥ 18 years of age and residents of LAC. The intervention included the delivery of an educational session by CoGENES and an *a priori* developed educational handbook. The control group received standard CRC and genetic testing materials. Data on demographics, acculturation, cultural values and fatalism, health literacy, numeracy, generalized self-efficacy (GSE), genomic knowledge, cancer prevention behaviors and attitudes, were collected at baseline with validated or team-developed surveys. Follow-up surveys at 6-12 weeks and 6-8 months after intervention receipt evaluate changes in GSE, genomic knowledge, and cancer prevention behaviors. Paired dietary changes were evaluated using McNemar's test. Paired t-tests and independent t-tests were used to compare baseline and follow-up results within and between arms, respectively.
Results: A total of 138 participants (mean age = 48.8 years, SD = 13.6) were randomized to the intervention (n = 72) or control (n = 66) arm, with no baseline differences. All were Hispanic/Latine, most were female (83%), Mexican (64%), Catholic (61%), married (50%), completed ≤11th grade education (51%), and spoke primarily Spanish (69%). Interim analyses showed that by 6-8 weeks, participants in the intervention arm demonstrated improved dietary behaviors, with a higher proportion limiting processed food intake (rarely or never: 48.6% at baseline vs 69.8% at follow-up; $p < 0.05$). We observed significant improvements in cancer genetic knowledge within the intervention arm at 6-12 weeks, with more correct answers (mean difference = 4.32; $p < 0.01$), and fewer "don't know" responses (mean difference = -5.40; $p<0.01$). These improvements were greater than in the control arm: 2.7 more correct answers ($p<0.01$) and 3.25 fewer "don't know" responses ($p<0.01$). Genetic literacy and comprehension scores also improved (mean difference = 11.38; $p < 0.01$), though not significantly more than in the control group (difference-in-differences = 2.20; $p = 0.43$).
Conclusion: We present preliminary evidence that deploying CRC prevention trained educators in a community setting, may improve CRC genetic knowledge, and highlights opportunities and willingness to improve lifestyle and dietary patterns to reduce CRC incidence.

#0924 Association between proxy markers of insulin resistance and colorectal cancer risk: results from a large scale prospective cohort of Korean adults.

Sukhong Min[1], Hyobin Lee[1], Sinyoung Cho[2], So-Yoon Lee[1], Jeongheon Kim[1], Ji-Yeob Choi[3], Daehee Kang[1]

[1]Department of Preventive Medicine, Seoul National University College of Medicine, Seoul, Korea, Republic of,[2]Department of Family Medicine, Seoul National University Hospital, Seoul, Korea, Republic of,[3]Department of Biomedical Sciences, Seoul National University College of Medicine, Seoul, Korea, Republic of

Background: Colorectal cancer (CRC) remains one of the most common cancers in Korea, underscoring the importance of identifying modifiable risk factors. Although insulin resistance has been implicated in CRC development, existing evidence remains inconsistent, and direct measures of insulin resistance are not routinely collected in clinical practice. This limitation highlights the potential utility of simple proxy markers of insulin resistance in epidemiologic and clinical settings. In this study, we investigated the associations between several proxy insulin resistance markers and CRC risk among Korean adults.

Methods: Using data from the Korean Genome and Epidemiology Study Health Examinee cohort, we evaluated the associations between several proxy markers of insulin resistance, including the TG/HDL ratio, triglyceride-glucose index (TyG), TyG-BMI index, TyG-waist circumference index (TyG-WC), TyG-waist-to-height ratio index (TyG-WHTR), and the metabolic score for insulin resistance (METS-IR), and CRC risk using Cox regression models. Subgroup analyses were stratified by sex, age, diabetes status, and prior screening experience, and sensitivity analyses were conducted based on varying follow-up durations.

Results: During a median follow-up period of 9.3 years, 795 new CRC cases were observed among 106,965 Koreans aged 40-69 years (36,899 men and 70,066 women). For the TG/HDL ratio, individuals in the highest quartile had a significantly elevated CRC risk compared with the lowest quartile (HR: 1.23, 95% CI: 1.00-1.53). A similar pattern was observed for the TyG and TyG-WC indices, where quartile 4 was associated with increased CRC incidence (TyG Q4 HR: 1.30, 95% CI: 1.04-1.63; TyG-WC Q4 HR: 1.36, 95% CI: 1.01-1.83). Finally, the METS-IR index showed a graded association, and the highest quartile was significantly associated with CRC incidence (Q4 HR: 1.26, 95% CI: 1.02-1.57).

Conclusions: In this large population-based cohort, multiple surrogate markers of insulin resistance were independently associated with an increased risk of colorectal cancer, with the strongest effects observed in the highest quartiles. These findings indicate that metabolic dysregulation related to insulin resistance contributes to colorectal carcinogenesis and that simple lipid-glucose-anthropometric markers may help identify individuals at elevated risk.

#0925 Examining trends of public interest in fasting and cancer-fasting clinical trials in the U.S..

Alanna Burwell[1], Maria Mogollon[2], Alexander Hernandez[2], Nadine Friedrich[2], Pao-hwa Lin[3], Stephen J. Freedland[2]

[1]North Carolina Institute for Medical Research, Durham, NC,[2]Department of Urology, Samuel Oschin Comprehensive Cancer Institute, Cedars-Sinai Medical Center, Los Angeles, CA,[3]Department of Medicine, Duke University School of Medicine, Durham, NC

Background: Interest in fasting related to cancer has increased as evidence suggests fasting may have anti-cancer benefits. Fasting has been shown to deprive cancer cells of nutrients, thereby inhibiting their growth and proliferation and making them more sensitive to chemotherapy in preclinical studies. Clinical trials incorporating fasting have grown over the years; however, recruiting participants remains challenging due to eligibility criteria, protocol complexities, and public interest. Identifying public interest in fasting and cancer, as well as in cancer-fasting clinical trials could help improve methods to raise awareness of the importance of fasting clinical trials and increase the number of trials to improve cancer.
Objective: To determine if public interest in fasting and cancer corresponds with cancer fasting clinical trials.
Methods: U.S. Google Trends data were queried by region from January 2004 to October 2025 to identify public interest in fasting overall (across all categories) and by cancer. Data are presented using relative search interest (RSI) ranging from 0 to 100, with 100 indicating the most searched, 50 representing half as many searches, and zero or null indicating insufficient data. Data from clinicaltrials.gov and Surveillance, Epidemiology, and End Results (SEER) Program were queried and used for trend analysis.
Results: Public interest in fasting in general, not restricted to cancer, across all categories was low prior to 2011 (RSI generally <20). RSI began to increase slightly after 2011 and grew to 30 by 2016. There was a sharper increase after 2016 with interest peaking in November 2019 (RSI=100) but has remained consistently high since (RSI range 50-80 since 2019). When examining only cancer interest, fasting related to cancer remained low with occasional spikes, but began to increase after 2016, in-line with the increased interest in fasting not limited to cancer. Indeed, interest in fasting and cancer largely mirrored general interest in fasting trends. Among all states with data, most had an RSI of 75 or higher for fasting across all categories. From 1991 to the present, 255 clinical trials have been initiated on fasting and cancer. The number of new trials per year slightly rose from 2000 to 2008, then dipped a bit, and then grew again slightly from 2013 (15 new trials in 2013) to 2025 (18 new cancer-fasting trials in 2025).
Conclusions: Public interest in fasting and cancer in the past ~12 years has grown 2-3-fold and been sustained at a high level over the past ~8 years. In contrast, the number of new trials started per year has barely changed over this time. While the reasons fasting trial numbers have lagged public interest are unknown, we speculate challenges enrolling and receiving funding for dietary trials may play a role. Given promising preclinical data coupled with public health interest, there should be increased funding and support for fasting trials in patients with cancer.

#0926 Prolonged high fat dietary intake increases pancreatic intraepithelial neoplasia to cancer progression.

Urvinder Kaur Sardarni[1], Erika Y. Faraoni[2], Alyssa Waller[1], Lincoln Strickland[1], Baylee O'Brien[3], Jesse Cox[1], Florencia McAllister[2], Jennifer Bailey-Lundberg[1]

[1]University of Nebraska Medical Center, Omaha, NE,[2]UT MD Anderson Cancer Center, Houston, TX,[3]Texas A&M Medical School, College Station, TX

Background: Emerging evidence implicates dietary macronutrient composition as a key modulator of pancreatic tumorigenesis. While the high-fat diet (HFD) drives acinar-to-ductal metaplasia (ADM) and pancreatic intraepithelial neoplasia (PanIN) progression in *Kras*^{G12D} mice, the impact of ketogenic diet (KD) remains controversial. To determine how KD affects early *Kras*-driven neoplasia, we investigated the effects of KD, HFD, and low-fat diet (LFD) on pancreatic disease initiation and progression using the *Ptf1a*^{CreERT2} *Kras*^{G12V} *(KC*^{Acinar}*)* mouse model.

Methods: Six- to eight-week-old *KC*^{Acinar} and wild-type (WT) mice were maintained on standard chow (SD) or switched to LFD, HFD, or KD for four weeks before tamoxifen-induced *Kras*^{G12V} activation. Mice were monitored for survival, body weight, and glucose tolerance. Pancreatic tissues were collected for histopathological evaluation, trichrome staining, and immunohistochemistry. Reverse-phase protein array (RPPA) of pancreatic lysates and serum cytokine profiling were performed to assess signaling and systemic changes.

Results: KD-fed *KC*^{Acinar} mice showed the shortest survival (median 26 ± 7 days) compared with SD (87 ± 29; p = 0.02) and LFD (57 ± 27; p = 0.02), while HFD also reduced survival compared with SD (35 ± 25; p = 0.05). KD feeding induced glucose intolerance in both WT and *KC*^{Acinar} mice. Histological analysis revealed that both KD- and HFD-fed *KC*^{Acinar} mice developed a higher incidence of invasive PDAC with fibrosis, accompanied by reduced CD8^{+} T-cell infiltration and increased stromal CD39 expression relative to tumor compartments. Proteomic profiling showed increased Akt, phospho-S6, Paxillin, and YTHDF2, and decreased PUMA, STAT5A, PHGDH, FASN, and ASNS expression in KD- and HFD-fed *KC*^{Acinar} mice. Pathway enrichment analysis identified upregulation of EGFR tyrosine kinase inhibitor resistance, chemokine, PI3K-Akt-mTOR, Rap1, and VEGF signaling pathways. Serum cytokine profiling further revealed elevated systemic levels of Ang-2, CCL6, LDLR MMP-9, PAI-1, PTX3, TNFSF13B, and OPG in KD-fed *KC*^{Acinar} mice.

Conclusions: Dietary lipid content before oncogenic *Kras* activation critically shapes pancreatic cancer development. Both ketogenic and high-fat diets accelerated progression from PanIN to invasive PDAC, accompanied by fibrosis, immune suppression, and activation of PI3K-Akt-mTOR and EGFR signaling. These findings reveal that lipid-rich diets can potentiate oncogenic and inflammatory pathways in the pancreas and caution against the use of ketogenic diets in prevention settings or early stages of pancreatic cancer.

#0927 Impact of loneliness on dietary habits of individuals with or without cancer history.

Sayantani Sarkar

Center for Information Technology Research in the Interest of Society and the Banatao Institute, University of California Berkeley, Berkeley, CA

Introduction Loneliness is a widespread health concern that affects health behaviors, lifestyle, physical health, psychological well-being, and overall quality of life of individuals. Limited literature exists about how loneliness impacts healthy dietary habits among individuals with and without a cancer history. Hence, the purpose of our study is to investigate the association between self-reported loneliness and daily dietary consumption habits.

Method Secondary analysis of the cross-sectional data collected via the Health Information National Trends Survey-HINTS-7 (2024), comprising US adults with or without a cancer history. Final analysis includes 5,597 individuals with (n=844) and without (n=4,753) cancer history. The predictor was loneliness, measured with four items on a 5-point scale, with a total score ranging from 4 to 20 (Never=4, Mild=5-8, Moderate=9-12, Severe=13- 20). The outcome variables were the amounts of daily fruit and vegetable consumption (<2 or≥2 cups per day). Descriptive statistics and multivariable logistic regression were conducted using statistical software STATA.

ResultsAmong cancer survivors, the majority were white (75.4%), male (55.7%), aged ≥75 years (32.16%), and college-educated (79.4%). Of those without a history of cancer, 60.7% were white, 51.4% were male, 5.0% were aged ≥75 years, and 73.6% were college educated. About 37% of cancer survivors and 35% of those without cancer reported obesity. Among cancer survivors, 30.8% reported consuming ≥2 cups of vegetables and 23.6% consuming ≥2 cups of fruits per day. Among individuals without a history of cancer, 27.5% reported consuming ≥2 cups of vegetables and 19.4% consuming ≥2 cups of fruits per day. More than 62% cancer survivors suffer from some degree of loneliness, including 10.7% reporting severe loneliness. Among those without cancer, 64.8% reported loneliness, including 13.7% stating severe loneliness. In the regression model, a one-unit increase in loneliness score is associated with 3% lower odds of consuming vegetables (OR = 0.97, 95% CI = 0.95-0.99, p = 0.007). There was no statistically significant association between loneliness and fruit intake (OR=0.98, 95% CI 0.95-1.02, p=0.271). After incorporating the interaction term into the model, we found that the relationship between loneliness and vegetable or fruit intake does not differ significantly between the two groups.

Conclusion Loneliness impacts vegetable consumption, highlighting the importance of screening for loneliness, regardless of oncologic status, to maintain a healthy dietary intake.

#0928 Variability in anthocyanin content among commercial blueberries and implications for dietary cancer prevention.

Noemi Y. Li, Lane Firestone, William W. Li, Vincent W. Li

The Angiogenesis Foundation, Cambridge, MA

Early intervention through dietary cancer prevention may reduce tumor risk, as supported by experimental models and epidemiologic studies linking diet to lower cancer incidence. Mechanisms of cancer prevention for many edible fruits are mediated by bioactive phytonutrients. For example, consumption of two servings of blueberries per week was associated with a 25% lower cancer mortality among breast cancer patients in the Nurses' Health Study, and anthocyanin consumption was linked to a 22% reduced risk of colorectal cancer in a meta-analysis. Anthocyanins, a major class of bioactive flavonoids in blueberries, modulate endothelial growth and inhibit VEGF-driven angiogenesis in preclinical models, suggesting that differences in anthocyanin concentration across blueberry cultivars may influence their anticancer potential. Commercially grown blueberries are available in a variety of cultivars and regions, potentially resulting in substantial variability in anthocyanin content and bioactivity. To investigate this and identify candidates for mechanistic studies, blueberries were collected from 11 commercially available sources. Samples were frozen at -20°C, pulverized, solvent-extracted, and analyzed by high-performance liquid chromatography (HPLC) in triplicate, using cyanidin-3-0-glucoside (C3G) as a validated standard. Anthocyanin concentrations ranged from 0.204 to 4.244mg/g wet weight (C3G equivalents). Wild lowbush Maine blueberries contained the highest anthocyanin concentrations and had a distinct chromatographic profile, while highbush cultivars, which dominate U.S. commercial blueberry production, showed more variable levels, with several also ranking relatively high. Overall, these findings demonstrate that anthocyanin content differs significantly among blueberry types and provide a rationale for selecting specific cultivars for mechanistic studies of dietary angioprevention. Based on these results, representative extracts (high and low anthocyanin content) were selected for subsequent in vitro studies of endothelial tube formation. Such comparative biochemical characterization is essential to optimize the design of future investigations into the cancer-preventive potential of blueberry-derived anthocyanins.

#0929 High red meat diet promotes colorectal tumorigenesis via gut microbiota mediated Th17/Treg imbalance.

Yamei Hu[1], Yating Wei[2], Runjie Song[3], Yilin Tang[2], Dongli Pei[2], Zigang Dong[2]

[1]Department of Pathology, The Third Affiliated Hospital of Zhengzhou University, Zhengzhou University, Zhengzhou, China,[2]Department of Pathophysiology, School of Basic Medical Sciences, Zhengzhou University, Zhengzhou, China,[3]School of Life Sciences, Zhengzhou University, Zhengzhou, China

Background: Excess red and processed meat consumption is a known risk factor for colorectal cancer (CRC), but the underlying mechanisms remain unclear. Given that dietary components reshape gut microbial ecology and mucosal immunity, we hypothesized that high red meat consumption promotes CRC by disrupting microbiota-immune crosstalk that maintains intestinal homeostasis.
Methods: The C57BL/6 mice were fed isocaloric diets with increasing proportions of red meat-derived protein (20%, 50%, 100%) compared with a 20% casein control. Tumorigenesis was assessed in azoxymethane (AOM)/dextran sulfate sodium (DSS)-induced mouse and $Apc^{Min/+}$ mouse models, complemented by orthotopic MC38-Luc-implantated mouse models as well as AOM/DSS-induced $Lgr5^{GFP\text{-}Slp\text{-}mCherry}$ transgenic mouse engineered to trace intestinal stem cells ($GFP^{+}mCherry^{-}$) and tumor microenvironmental cells ($GFP^{-}mCherry^{+}$). Colonic tumors were subjected to single-cell RNA sequencing to delineate immune landscape shifts, while fecal samples were analyzed by metagenomics and metabolomics to profile microbiota and microbial metabolites.
Results: Higher dietary red meat led to significantly increased colonic tumor burden in a dose-dependent manner. scRNA-seq revealed a progressive shift toward a pro-inflammatory T cell milieu with escalating Th17/Treg ratios: 0.26 (control diet), 0.44 (20% red meat diet), 0.61 (50% red meat diet) and 0.71 (100% red meat diet). Th17 transcriptional signature including IL17A and RORγt as well as IL-6/STAT3 signaling was enhanced in tumors from red meat-fed mouse, consistent with amplified Th17 responses. Metagenomic profiling identified the depletion of a commensal consortium “PFIO” comprising *Parasutterella excrementihominis*, *Faecalibaculum rodentium*, *Ileibacterium valens* and *Oscillospiraceae* species linked to short-chain fatty acid synthesis and bile acid homeostasis. Metabolomic data confirmed reduced SCFA and secondary bile acids levels, consistent with an inflammatory gut environment conducive to Th17 polarization.
Conclusions: These findings define a microbiota-Th17/Treg axis that mechanistically links red meat consumption to colorectal tumorigenesis. Disruption of SCFA-producing commensals amplifies Th17 dominance, driving tumor-promoting inflammation. Therapeutically restoring microbiota composition or Th17/Treg balance may offer preventive strategies for red meat diet associated CRC.

#0930 Mediterranean versus Western diet - preventative and interventional effects of dietary lipids on colorectal tumor growth and biology.

Cara C. Wallingford[1], Anindita Mahanty[1], Revan Hammontree[1], Alexa Magstadt[2], Jennifer Davis[1]

[1]Cancer Biology, University of Kansas Medical Center, Kansas City, KS,[2]University of Kansas, Lawrence, KS

The purpose of this study was to examine the preventative and interventional effects of different fat sources (lard verses olive oil) and their respective lipid components in a Western-style high-fat diet and Mediterranean-style high-fat diet on tumor biology *in vivo* in a Cre-lox mouse model called iKAP (inducible Kras, Apc, p53) of colorectal cancer (Boutin et al, *Genes & Development* 2017, 31:370).
Experimental Procedures: At 8-11 weeks of age, mice are randomized to a control lard-based 10% fat diet with high fiber (low-fat diet, LFD), a lard-based 45% fat diet with low fiber (high-fat diet, HFD) or olive oil-based 43% fat Mediterranean diet (MD) with the fiber matched to the LFD control. To measure diet-induced metabolic dysfunction, body composition and glucose tolerance are measured with EchoMRI and glucose tolerance tests (GTT) every three and six weeks, respectively. After 12 weeks post-randomization on diet, mice undergo a submucosal induction with 4-hydroxytamoxifen (4-OHT), which deletes loxP conditional *Apc* and *Trp53* in intestinal cells expressing the Villain promoter, thus causing tumorigenesis. Endoscopies are done every two weeks and tumor growth is measured by percent luminal occlusion - or the percent of the lumen taken up by the tumor over time - until end-of-study (one year or mortality due to tumor burden). In addition to understanding how the two diets affect tumor growth when given before tumor development, an arm of the study aims to understand the effects of an interventional diet post-tumor initiation. To accomplish this, a proportion of mice on LFD or HFD will be assigned to MD two weeks after induction with tamoxifen.
Results: At 12 weeks post-randomization with diet, mice on both HFD and MD show evidence of metabolic dysfunction (higher body weight, high fat mass and glucose intolerance) compared to LFD. In addition, mice on HFD and MD consume more chow. Interestingly, preliminary data suggests that systemic cholesterol levels in MD and LFD mice are at similar levels and significantly lower than that of HFD mice. Orthogonal *in vitro* studies using immunofluorescence, fatty acid oxidation assays and molecular profiling of protein pathways involved in lipogenesis (SREBP1/2, FASN, ABCA1) and cancer cell growth/metabolism (AKT, PI3K, mTOR) are ongoing to understand the influence of different dietary fatty acids (oleic and palmitic acids) and cholesterol/phytosterols in the context of tumorigenesis.
Conclusion: Based on preliminary findings, both the Western HFD and MD effectively induce metabolic dysfunction in an iKAP murine model. However, the lipid components of the diets are significantly different; thus, differences in tumor metabolism and growth remain a pertinent question.

#0931 Air pollutants remodel mutant epithelia toward a convergent lung adenocarcinoma progenitor state.

Michelle M. Leung[1], Maria Zagorulya[2], Tej Pandya[2], Marcellus Augustine[2], Anthony J. Griffen[3], Alix Le Marois[2], Sophia Ward[2], Hubert Slawinski[2], Alejandro Suarez-Bonnet[4], Simon L. Priestnall[4], Alexandros Hardas[4], Erik Sahai[2], Lindsay M. LaFave[3], Eva Gronroos[2], Nicholas McGranahan[1], William Hill[2], Clare Weeden[2], Charles Swanton[2]

[1]University College London (UCL) Cancer Institute, London, United Kingdom,[2]The Francis Crick Institute, London, United Kingdom,[3]Albert Einstein College of Medicine, New York, NY,[4]Royal Veterinary College, London, United Kingdom

The lung epithelium harbours progenitor populations, including basal, club, neuroendocrine, and alveolar type I/II (AT1/AT2) cells. A highly plastic Krt8+ alveolar intermediate cell state (KAC) arises in *Kras*-driven tumorigenesis and in lung injury models. Environmental particulate matter (PM) exposure promotes lung tumorigenesis through macrophage-derived interleukin-1β (IL-1β). How *EGFR* mutations (EGFRm), the most common genomic driver of lung cancer in never-smokers, and tumour promotion drive lung adenocarcinoma (LUAD) at the single cell level from diverse lung epithelial lineages remains unclear. Understanding this will aid development of molecularly targeted prevention approaches, particularly in never-smokers.

We generated mouse models of lineage-specific activation of *EGFR-L858R* within basal, club, neuroendocrine, and AT2 lineages. LUAD development and lineage convergence were assessed using histology and snRNA-seq across 37,627 cells from 100 mice. For PM effects, *EGFR-L858R* induction in AT2 cells was achieved via Ad5-Spc-Cre intratracheal instillation, followed by PM or PBS exposure. 10X multiome snRNA-seq (34,459 AT2-lineage cells) and snATAC-seq were used to profile transcriptional and epigenetic changes. EGFRm precision-cut lung slices (PCLS) were exposed to PM *ex vivo* in presence of IgG or anti- IL-1β blocking antibodies.

Our analysis revealed that LUAD arises from basal, club, neuroendocrine, and AT2 lineages — all converging on an alveolar-like state, mirroring the trajectory observed in KRAS-driven LUAD. Notably, alveolar KACs were detected in EGFRm cells derived from basal, club, and AT2 lineages, indicating a conserved transitional state during early tumorigenesis. EGFRm activation also induced KAC-signature genes while preserving lineage-specific markers, reflecting a dual programme of lineage convergence and memory. Upon PM exposure, EGFRm KACs exhibited pronounced upregulation of stress-responsive and inflammation-induced epithelial genes. Compared with wild-type AT2 controls, PM-exposed EGFRm KACs exhibited strong enrichment of LUAD-associated transcripts, with over 30% overlap encompassing 1,298 genes. This highlights the synergy between EGFRm and environment-induced injury. Furthermore, we identified epigenetic rewiring of KACs, marked by activation of transcription factors linked to the IL-1β pathway upon PM. Functionally, blocking IL-1β in PCLS effectively inhibited KAC formation, establishing a mechanistic link between inflammatory signalling and early tumour cell fate.

In conclusion, we showed that epithelial lineages converge on KACs en-route to *EGFR*-driven LUAD, which expands and undergoes transcriptional and epigenetic remodelling upon PM-exposure. Future studies defining key regulators of KAC expansion and its IL-1β dependency could inform novel therapeutic avenues for molecular cancer prevention.

#0932 High sucrose intake amplifies and independently promotes anthracycline-induced cardiac dysfunction and senescence in juvenile mouse models.

Alaina L. Poche[1], Huaxian Ma[1], Prince Jeyabal[1], Fei Wang[1], Efstratios Koutroumpakis[2], Eugenie S. Kleinerman[1], Joya Chandra[1]

[1]Department of Pediatrics Research, The University of Texas MD Anderson Cancer Center, Houston, TX,[2]Department of Cardiology, The University of Texas MD Anderson Cancer Center, Houston, TX

Anthracyclines such as doxorubicin (dox) are effective chemotherapeutic agents frequently used in adolescents and young adults (AYAs) with cancer but are associated with cardiotoxicity. Mitigation of cardiac late effects through modifiable behaviors has global and cost-effective benefits, but parameters influencing potential benefit remain unclear. Here, we investigated the impact of sucrose consumption on dox-induced cardiotoxicity and senescence in vivo. Male and female p16/3MR transgenic mice were provided normal (NSW, 0%) or high (HSW, 45%) sucrose water and treated with dox (2.5 mg/kg, tail vein ×4 doses). Cardiac function was assessed by echocardiography to measure ejection fraction (EF) and fractional shortening (FS). Cardiac miR-1a and miR-499 expression were quantified by qRT-PCR, and senescent cell accumulation was visualized in heart tissue by red fluorescent protein (RFP) signal. High sucrose intake worsened dox-associated reductions in ejection fraction, with the HSW + dox group showing the greatest functional decline, a pattern that was statistically significant at 4 weeks ($p = 0.0187$) and 6 weeks ($p = 0.0353$) post-treatment. Notably, high sucrose alone reduced EF relative to NSW controls, indicating diet-induced impairment of cardiac function. Dox treatment elevated biomarkers of myocardial stress (miR-1a and miR-499) in cardiac tissue, and high sucrose alone produced comparable upregulation. Senescence, as measured by RFP fluorescence, increased in both dox- and sucrose-exposed hearts. Interestingly, the HSW + dox group demonstrated the highest RFP signal, compared to both dox and diet controls, indicating a synergistic enhancement of senescence, suggesting that molecular senescence markers may capture early injury preceding functional decline. High dietary sucrose both amplifies and independently impairs cardiac function and increases senescence, with combined sucrose and dox exposure promoting the strongest EF reduction and senescence elevation. These findings underscore the contribution of sucrose consumption to anthracycline-associated cardiac injury and support the investigation of dietary modulation as a potential strategy to mitigate long-term cardiac damage.

#0933 PHGG supplementation modulates gut microbiome metabolites and breast cancer progression.

Sercan Kenanoglu, Fabia de Oliveira Andrade, Leena Hilakivi-Clarke

The Hormel Institute, University of Minnesota, Austin, MN

Short-chain fatty acids (SCFAs) are linked to improved anti-tumor immune responses and reduced breast cancer risk. Isoflavones in soybean-based (SB) high fiber diets may block fiber's advantages by triggering immunosuppression. We investigated the effect of SB diet, combined with partially hydrolyzed guar gum (PHGG) supplementation, on triple negative E0771 mammary tumor growth in mice fed AIN93G control or SB diet. Some SB-fed mice received PHGG or maltodextrin (MDX) control in drinking water. We found that SB diet increased tumor burden, and both MDX and PHGG revered the increase. Fecal microbiota transplants (FMTs) were prepared from the AIN93G, SB, SB+PHGG, and SB+MDX fed mice, and transferred to antibiotic-treated hosts fed AIN93G diet. Tumor burden was similar in hosts receiving FMT from AIN93G, SB, or SB+MDX donors, suggesting that SB diet did not increase mammary tumorigenesis through changes in the gut microbiome but perhaps directly by affecting immune cells in the tumor microenvironment. Mice receiving FMT from SB+PHGG fed donors exhibited significantly reduced tumor burden. To further investigate whether cellulose in AIN93G diet affected PHGG's ability to reduce mammary tumorigenesis, compared with MDX, we fed mice cellulose-free AIN93G diet. In this setting, PHGG reduced tumorigenesis compared with MDX. However, PHGG increased fecal SCFAs both in cellulose containing and cellulose-free AIN93G diet fed mice. Further, PHGG-supplemented mice exhibited significantly increased FFAR3 expression in CD4+ T cells in the spleen. Our findings indicate that PHGG reduces mammary tumorigenesis in mice fed fiber-deficient diet, and the effect is likely mediated through the gut microbiome.

#0934 Comparison of colonoscopy using a multipurpose rigid endoscope with postmortem detection of polyp in Pirc rat model of familial adenomatous polyposis.

Ishan T. Narkar[1], Vesna Tumbas Saponjac[2], Ming Hu[2], Rashim Singh[2]

[1]Michael E. DeBakey High School for Health Professions, Houston, TX,[2]University of Houston, College of Pharmacy, Houston, TX

Background: Familial adenomatous polyposis (FAP) is a rare disease affecting ~1 in 10,000 individuals and accounts for <1% of colorectal cancer cases. Untreated FAP carries a nearly 100% lifetime risk of colorectal cancer, typically manifesting by age 40 and is treated by colon resection between 15-25 of age. The Pirc (polyposis in rat colon) model of FAP harbors an *Apc* gene mutation analogous to that in humans. This model develops multiple polyps in the colon and duodenum with age and is widely used to test preventive interventions and in mechanistic studies. Longitudinal monitoring of polyp number, size, and grade is essential for preclinical testing of efficacy of preventive interventions and can be achieved through colonoscopy. In this study, we compared rigid endoscope-enabled colonoscopy with postmortem analysis of polyps in Pirc rats.

Methods: Colons of 16-week-old male and female Pirc rats (n=8) were examined using a rigid endoscope (Small Coloview scope, 10 cm, Karl Storz, Tuttingen, Germany). Before colonoscopy, rats were anesthetized with isoflurane, colons were flushed with warm water to remove fecal matter. In the video review, polyps were graded based on the degree of lumen obstruction: G1: barely detectable; G2: ≥ barely detectable to <1/8th of lumen; G3: ≥1/8 to <1/4 of lumen; G4: ≥1/4 to <1/2 of lumen; and G5: ≥1/2 of lumen to complete blockade. Animals were then euthanized, and colons were excised to determine polyp number and diameter measured with digital caliper (General® Ultratech, CA, USA). Total and detectable polyp counts were compared between the two methods using Wilcoxon matched-pairs signed rank test. Mean ± standard deviation (SD) of polyp diameter for each polyp grade was reported. Statistical analyses were performed using GraphPad Prism v.10.

Results: The median total polyps count was 2 (range: 0-5) using the endoscope and 3 (range: 1-12) postmortem, with no statistically significant difference (p= 0.09). Because the rigid endoscope visualizes only the distal 10 cm of rat colon, detectable polyps were compared. The median detectable polyps count was 2.5 (range: 0-7) postmortem and was not significantly different from colonoscopy (p= 0.5). The mean ± SD of the polyp diameter was as follows: G2: 2.9±0.7 mm, G3: 3.4±0.5 mm, G4: 3.6±0.6 mm, and G5: 3.6±0.7. Limitations of colonoscopy included incomplete visualization of the entire colon, difficulty distinguishing adjacent polyps, and challenges in detecting rectal polyps.

Conclusion: Polyp detection using a rigid endoscope is feasible and comparable to postmortem evaluation, supporting its use for longitudinal monitoring in preclinical prevention studies. Flexible and extendable endoscopes may enhance polyp detection and monitoring. **Acknowledgements:** This research was funded by CPRIT RP240401. Dr. Rashim Singh is supported by the NCATS/NIH under award number K12TR004522.

#0935 Nutritional disruption of folate homeostasis triggers an endogenous genotoxic carcinogen.

Christopher Mellor[1], Saeideh Azad[1], Nicholas Cheng[1], Brandon James[1], Vicky A. Simon[1], Olga V. Malysheva[1], Guillermo Burgos Barragan[2], John Blenis[3], Martha S. Field[1], **Meng Wang**[1]

[1]Division of Nutritional Sciences, Cornell University, Ithaca, NY,[2]Weill Cornell Medical College, New York, NY,[3]Professor of Pharmacology, Weill Cornell Medical College, New York, NY

Background: Formaldehyde, a human carcinogen found in industrial chemicals, is also produced by mammalian metabolism. The toxicity of endogenous formaldehyde is most severe in children with inborn errors in formaldehyde detoxification enzymes (ALDH2/ADH5), causing early-onset bone marrow failure and leukemia through formaldehyde-DNA damage. While endogenous formaldehyde exists in all healthy tissues, the nutritional and metabolic factors controlling its production remain unknown. Prior in vitro studies showed folate can spontaneously decompose to release formaldehyde. However, folate metabolism's contribution to endogenous formaldehyde in vivo has never been studied. Given widespread folate supplementation and the 2 billion people with folate insufficiency worldwide, we investigated how folate excess and deficiency affect endogenous formaldehyde in mouse models.

Methods: For folate excess, wildtype and *Adh5*$^{-/-}$ mice received high-folate diet (10x recommended daily allowance) for 8 weeks. For deficiency: 1) SLC46A1 deletion causing folate malabsorption, and 2) folate-depleted diet for 8-12 weeks. We developed ultra-sensitive mass spectrometry to quantify formaldehyde-DNA adducts as biomarkers of tissue formaldehyde exposure.

Results: Contrary to in vitro predictions, tissue folate accumulation did not elevate endogenous formaldehyde. Strikingly, folate deficiency significantly increased formaldehyde in liver, spleen, and bone marrow. In folate-deficient *Adh5*$^{-/-}$ mice with impaired formaldehyde clearance, hepatic formaldehyde increased 35-fold with elevated DNA damage, severe anemia (50% reduction in red cells), and hematopoietic stem cell loss. Metabolomics revealed folate-deficient livers upregulated choline oxidation to generate one-carbon units, a pathway that produces formaldehyde as a toxic byproduct.

Conclusions: We establish folate metabolism as a critical safeguard against endogenous formaldehyde accumulation, with deficiency triggering formaldehyde production through compensatory choline oxidation. Our findings have three major implications: First, they validate the safety of folate supplementation, used by millions for prenatal care and cancer treatment, by proving excess folate does not generate formaldehyde. Second, we hypothesize a mechanism underlying cancer risk in folate-deficient individuals worldwide, particularly the 500 million with ALDH2 deficiency who cannot detoxify formaldehyde. Third, we identify choline as an unexpected endogenous formaldehyde source, highlighting the need for caution with choline supplementation during low-folate status. These findings support targeted folate supplementation as a cancer prevention strategy for high-risk populations with ALDH2 deficiency

#0936 Temporal dependency of STAT3 signaling dictates hepatocarcinogenesis in metabolic dysfunction-associated steatohepatitis.

Jie Qing Eu[1], Nur Afiqah Binte Mohamed Salleh[2], Ming Yee Sim[2], Zi Swan Tan[2], Daniel Q. Huang[3], Tuan Zea Tan[4], Boon Cher Goh[4], **Li Ren Kong**[1]

[1]Nanyang Technological University Singapore, Singapore, Singapore,[2]National University of Singapore, Singapore, Singapore,[3]Dept. of Medicine, NUS Yong Loo Lin School of Medicine, Singapore,[4]Cancer Science Institute of Singapore, Singapore, Singapore

Background: Metabolic dysfunction-associated steatohepatitis (MASH) is rapidly surpassing viral and alcoholic etiologies as the leading cause of hepatocellular carcinoma (HCC). Despite so, the molecular checkpoints governing the transition from metabolic injury to malignancy remain poorly understood. Hyperactivated STAT3 has been implicated in lipid dysregulation, inflammation, fibrosis, and oncogenic signaling. However, its dynamic regulation during MASH-to-HCC progression remains undefined.
Methods: We performed longitudinal profiling of diseased mouse and human liver tissues to map STAT3 signaling dynamics across disease stages. Using the STAM model, we administered a hepatocyte-targeting, GalNAc-conjugated Dicer-substrate siRNA (GalNAc-STAT3) to selectively silence STAT3 at distinct disease phases: (i) early MASH and (ii) post-tumor initiation. Disease outcomes were evaluated using histopathology and serum proteomics. Spatial transcriptomics and immune phenotyping were used to resolve microenvironment- and subtype-specific responses.
Results: STAT3 suppression exhibited striking stage-specific effects. Early intervention prior to malignant transformation substantially reduced HCC initiation and tumor burden despite persistent steatosis, demonstrating that lipid accumulation alone is insufficient to drive carcinogenesis. Multi-omics analyses identified a STAT3-dependent, TGF-β1-associated fibrogenic and inflammatory program in peritumoral regions that acted as a key molecular driver for malignant progression. In contrast, late intervention failed to reduce tumor nodule formation despite effect STAT3 inhibition, indicating loss of STAT3 dependency following malignant transformation. Spatial interrogation further revealed subtype-specific adaptive remodeling through metabolic re-differentiation in glutamine synthetase (GS)-positive nodule, and activated stress tolerance transcriptional programs in GS-negative tumors.
Conclusions: This work uncovers a previously unrecognized temporal dependency of STAT3 during MASH-associated hepatocarcinogenesis. STAT3 is essential as an early driver in establishing pro-tumorigenic niche, but is dispensable once malignant cell states emerge. These discoveries redefine the therapeutic window for STAT3 inhibition, positioning it as an early stage interception strategy rather that treatment for advanced tumors.

#0937 Breast cancer risk prediction model for racially diverse women with benign breast disease.

Alzina Koric, Yikyung Park, Shu Jiang, Fouad Boulos, Debbie L. Bennett, Graham A. Colditz

Washington University School of Medicine in St. Louis, St. Louis, MO

Purpose: Existing breast cancer risk prediction models are ineffective for women with benign breast disease (BBD) and do not stratify risk by key histologic subtypes, especially in racially and ethnically diverse populations. Although BBD and breast cancer share several risk factors, women with BBD have a higher underlying risk due to accumulated changes in benign breast tissue compared to the general population. The magnitude of risk varies by morphologic subtype—modestly increased for proliferative disease without atypia (PDWA), and highest for atypical hyperplasia (AH). We aimed to refine a prediction model for breast cancer through risk stratification by PDWA and AH subtypes, using data from a contemporary and racially diverse cohort of women.
Methods: 8,870 women diagnosed with histologically confirmed benign lesions were identified at the Siteman Cancer Center in St. Louis from 2010-2023 (followed until June 10, 2025). Risk modeling was performed with Cox regression and internally validated through a bootstrap resampling method (i.e., corrected for overfitting). Model discrimination was estimated with Harrell's C-index. Model calibration was assessed by the 5-year observed-to-expected (O/E) ratio. Positive and negative predictive values (PPV/NPV) were estimated for a 3% 5-year risk threshold per national guidelines to define increased risk.
Results: Among the 8,870 women with BBD, there were 362 subsequent breast cancers at least 6 months following a benign biopsy. 11.2% were triple negative tumors (ER-PR-HER2-); 73.8% were invasive breast cancers. The cohort is 64.3% White, 32.5% Black, and 3.2% Asian. On average, women were 50 (SD=13) years of age at biopsy. Average age at menarche was 13 (SD=1.8) and average BMI 29.6 kg/m2 (SD=7.7). Harrell’s C-index was 0.68 (95% CI: 0.65-0.71) in the original sample and 0.67 (95% CI: 0.65-0.70) in the bootstrap sample. At 5 years, the overall model calibration was 0.99 (95% CI: 0.86-1.13). Women predicted to be in the high-risk group (≥3%, 5y) included those with atypia and half of those with proliferative disease without atypia. Of these women, 7.0% developed breast cancer, and in the average-risk group, 97.5% did not in the 5 years following a benign biopsy.
Conclusion: Our model demonstrates sound discriminatory ability in the internal validation within a racially diverse cohort of women followed after benign biopsy. With a 5-year PPV of 7%, the model effectively flags women at high-risk (≥3%, 5y), providing a meaningful basis for intensified surveillance or preventive measures for early detection after benign biopsy showing proliferative disease with or without atypia.

#0939 Patient and oncologist factors associated with trastuzumab drug choice and administration route.

Derek Hsu[1], Liam Schmitt[2], Austin Wesevich[3]

[1]University of Chicago, Chicago, IL,[2]Center for Personalized Therapeutics, University of Chicago, Chicago, IL,[3]Section of Hematology/Oncology, University of Chicago, Chicago, IL

Background: As biosimilars and subcutaneous (SQ) formulations of intravenous (IV) biologics enter the market, it is unclear how prescribers determine which formulation to give a patient. While patients may generally prefer SQ administration, IV biosimilars may be less expensive than newer SQ formulations. We focused on trastuzumab, which has name-brand SQ, name-brand IV, and biosimilar IV formulations, to assess potential association of patient and oncologist factors with drug choice and administration route.
Methods: This cross-sectional study included patients with HER2+ breast or gastrointestinal (GI) cancer who received trastuzumab at the UChicago from 1/1/2021 to 12/31/2024. Patient factors, trastuzumab formulation and administration route, and prescriber were extracted from the electronic medical record. Prescriber demographics were obtained using public data from the Centers for Medicare & Medicaid Services. Multilevel multivariable logistic regression models assessed associations of patient and oncologist factors with IV vs SQ trastuzumab and brand-name IV vs biosimilar, nesting doses within patients and patients within oncologists. Models adjusted for patient insurance, age, race, sex, SVM quartile, ECOG score, BMI, cancer stage, and oncologist sex and years since graduation. The name-brand IV vs biosimilar model also adjusted for cancer type. The SQ vs IV model only included those with breast cancer as SQ trastuzumab is not approved for GI cancer, and it also accounted for concurrent IV chemotherapy administration.
Results: A total of 35 oncologists and 368 patients were included, of which 319 (87%) had HER2+ breast cancer and 49 (13%) had HER2+ GI cancer. Most patients had private (47%) or Medicare (41%) primary insurance, and oncologists had a mean of 22 years of experience. IV biosimilars were given to 89% of patients. Patients with Medicaid had lower odds of receiving a biosimilar than patients with private insurance (aOR 0.11, 95% CI 0.04-0.34). No patients with GI cancer and 69 (22%) of patients with breast cancer received SQ. Patients with Medicare had lower odds of receiving SQ than those with private insurance (aOR 0.18, 95% CI 0.04-0.75). Except for concurrent IV chemotherapy administration in the SQ vs. IV model, no other patient factors beyond insurance and no oncologist factors were significantly associated with drug formulation or administration route.
Conclusions: Drug choice and administration route were significantly associated with patient insurance. While administration route may be driven by the logistics of giving IV trastuzumab along with concurrent IV chemotherapy, no patient or oncologist factors were identified in prescribers' decision-making about drug choice or administration route beyond insurance. It may be difficult to incorporate patient preferences or cost-saving measures into prescribing patterns if insurance does not allow for drug choice.

: Experimental Chemoprevention and Interception: Data and Tools
Poster Session

#0942 Target validation and high-throughput screening assay development for natural product discovery for cancer prevention and interception.

Yurong Song[1], Brandon Somerville[1], Kajal Biswas[2], Karim Baktiar[1], Liankun Song[3], Sara Sanders[4], Tanja Grkovic[5], Ligia A. Pinto[1], Ana Catarina Menezes[6], Paul P. Liu[6], Matthew J. Hart[7], Chinthalapally V. Rao[7], Shugeng Cao[8], Xin Chen[8], Xu Wu[9], Xiaolin Zi[3], Mark J. Henderson[4], Barry R. O'Keefe[5], Altaf Mohammed[2], Robert H. Shoemaker[2]

[1]Frederick National Laboratory for Cancer Research, Frederick, MD,[2]Division of Cancer Prevention, National Cancer Institute, Bethesda, MD,[3]Department of Urology, University of California, Irvine, CA,[4]National Center for Advancing Translational Science, Rockville, MD,[5]National Cancer Institute at Frederick, Frederick, MD,[6]National Human Genome Research Institute, Bethesda, MD,[7]University of Oklahoma Health Sciences Center, Oklahoma City, OK,[8]University of Hawai'i at Hilo, Hilo, HI,[9]Massachusetts General Hospital and Harvard Medical School, Charlestown, MA

Background Natural products (NPs) represent a rich source of bioactive compounds with cancer prevention/interception potential. NPs offer unique chemical diversity and a history of safe human use, making them attractive candidates for long-term use. High-throughput screening and mechanistic studies are key to discovering promising leads and translating them into effective and safe cancer prevention and interception strategies. To support the Discovery and Development of Natural Products for Cancer Interception and Prevention (DDNP-CIP) Initiative, we aimed to validate potentially clinically relevant molecular targets (SKP2, TEAD2, 5-LOX and RUNX1) and establish and optimize assays to enable high-throughput NPs library screening for cancer prevention.
Methods Target validation was performed using tissue microarrays. SKP2, a component of the SKP2-SCF E3 ligase complex, and TEAD2, a DNA-binding transcription factor, were evaluated for their expression levels in TMAs of prostate and liver cancer, respectively. In addition, cell-based platforms were developed or adapted to identify NPs exhibiting immune-modulating activity or targeting either 5-LOX, a lipid-peroxidizing enzyme, or RUNX1, a transcription factor critical for hematopoietic differentiation and frequently mutated in hematologic malignancies. These assays utilized stably expressing reporter cell lines.
Results SKP2 was significantly over expressed in 68.6% of prostate hyperplasia, 97.6% of prostate intraepithelial neoplasia, and 81.9% of adenocarcinoma compared with normal tissue. TEAD2 was highly expressed in liver hyperplasia and significantly upregulated in hepatitis ($p = 0.0041$), hepatocellular carcinoma ($p = 0.0012$), and intrahepatic cholangiocarcinoma ($p < 0.0001$). To identify NPs with immune-modulating activity, an assay using the THP-1 ISRE FRET reporter cell line was adapted and optimized. Reference compounds and initial challenge plates were tested, with several samples eliciting positive responses. A cell line expressing 5-LOX was generated and validated. An inhibition assay using a positive compound nordihydroguaiaretic acid demonstrated dose-dependent inhibition (29% at 0.1uM to 92% at 1uM) upon arachidonic acid treatment without toxicity. To screen NPs for splicing modulating activity, nano-luciferase reporter cell lines with RUNX1 mutations identified in patients with familial platelet disorder with associated myeloid malignancy were generated. Several reference compounds showed positive responses in selected mutations.
Summary Validated targets and assay platforms establish a foundation for high-throughput NPs screening. These efforts advance the DDNP-CIP's mission to identify and develop NPs for cancer prevention and interception. Funded partly by the National Cancer Institute under Contract No. HHSN261201500003I

#0943 Chemoprevention of hepatocellular carcinoma by next-generation antipsychotic aripiprazole.

Nevena Slović[1], Sumit Mishra[2], Subhojit Paul[2], Marine A. Oudot[1], Frank Juhling[1], Hiroaki Kanzaki[2], Julien Moehlin[1], Margaux Denos[1], Anouk Charlot[1], Sarah C. Durand[1], Courtney Katz[2], Cloe Gadenne[1], Emanuele Felli[3], Joachim Lupberger[1], **Emilie Crouchet**[1], Yujin Hoshida[2], Thomas F. Baumert[1]

[1]Institute for Translational Medicine and Liver Disease (ITM), University of Strasbourg/Inserm U1110, Strasbourg, France,[2]Department of Internal Medicine, University of Texas Southwestern Medical Center, Dallas, TX,[3]Hospital Group Saint Vincent, Strasbourg, France

Hepatocellular carcinoma (HCC) is the most common form of liver cancer and is a major global health burden, ranking sixth in incidence and third in cancer-related mortality. Despite therapeutic advances, treatment options for advanced liver disease and HCC are limited and strategies to prevent HCC development are lacking. To address the urgent need for chemopreventive strategies, we identified Aripiprazole, an oral atypical antipsychotic, as a candidate for HCC chemoprevention. Transcriptomic analyses of clinical liver tissues showed an association of Aripiprazole target gene expression with fibrotic liver diseases severity. In a rat model of MASH-induced HCC induced by choline-deficient L-amino acid-defined and high-fat diet, Aripiprazole prevented liver disease progression toward HCC development by modulating fibrogenesis, inflammation, and immunity-related pathways. Moreover, Aripiprazole exhibits an antifibrotic effect and reverses the high-risk status of the prognosis liver signature (PLS), a signature associated with disease progression and HCC risk in patients, in multiple human liver cell-based models. Mechanistic studies demonstrated that Aripiprazole exerts antifibrogenic, and anti-proliferative effects via suppression of TGF-β, NF-kB, cMet-ERK, and PI3K/AKT signaling in liver epithelial cells and myofibroblasts. Finaly, perturbation studies in patient-derived cell lines and patient-derived tumorspheroid system showed that Aripiprazole has a direct anticancer effect, by modulating the tumor microenvironment and suppressing tumor cell survival and invasion. Collectively, these findings suggest that treatment with aripiprazole is a clinically relevant approach for HCC chemoprevention.

#0944 The combination of EPA and Naproxen prevents iCAF polarization and attenuates inflammation associated with Pirc tumor development.

Niti Jani[1], Ryan Beach[1], Michael Martinez[1], Shizuko Sei[2], Vignesh Gunasekharan[2], Daniel W. Rosenberg[3]

[1]University of Connecticut Health Center, Farmington, CT,[2]Division of Cancer Prevention, National Cancer Institute, Rockville, MD,[3]Professor of Med. & Co-Director, Colon Cancer Prev. Prog., University of Connecticut Health Center, Farmington, CT

We recently reported that eicosapentaenoic free fatty acid (EPA-FFA) or a chemically stable EPA analog (TP-252), when combined in the diet with naproxen, reduces colon tumor development by up to 98% in the highly penetrant Pirc rat model. Cancer suppression is dependent, in part, upon modifications of eicosanoid biosynthesis. The following study expands upon these initial findings using genome-wide RNA-sequencing (RNA-seq) analysis to identify specific molecular pathways in Pirc tumors affected by drug treatment. Colon tumors isolated from untreated control Pirc rats maintained on AIN93G diet exhibited gene expression profiles associated with the presence of inflammatory cancer-associated fibroblasts (iCAFs). Following a twenty-week treatment with a combination diet of EPA-FFA (2% w/w) and naproxen (200 ppm), there was a marked reduction in inflammatory and proliferative gene signatures. Further analysis of these drug combination-treated tumors showed expression profiles resembling a less inflammatory fibroblast phenotype, suggesting the presence of myofibroblasts (myCAFs). To further establish potential mechanisms, we isolated CAFs from colon tumors of untreated Pirc rats. CAFs were then stimulated for 12 hours with individual cytokines (TNF-a, IL-1β or IL-6) to promote iCAF activation. The secretion of a panel of inflammatory cytokines (IL-6, Cxcl2, Csf3 and Nos2) determined in IL-1β activated CAFs were similar to those found by RNA-seq analysis of colon tumors from untreated Pirc diet controls. In addition, the combination treatment of EPA-FFA and naproxen attenuated polarization of CAFs towards an iCAF phenotype upon IL-1β stimulation. The present work contributes further to our understanding of intestinal tumor protection afforded by a combination of dietary EPA and naproxen. These findings further uncover potential mechanisms that can be exploited in future clinical chemoprevention studies.

#0945 Chemoprevention of triple-negative breast cancer originating from cancer stem cells using OXPHOS inhibitors.

Esra Akkus[1], Cemile Uslu[2], Mert Gungor[1], Beyza Şimbil[3], Elif Uzun[4], Etna Abad[5], Alex Lyakhovich[6]

[1]Molecular Biology, Genetics and Bioengineering, Sabanci Universitesi, Istanbul (Anatolia), Turkey,[2]Sabanci Universitesi, Istanbul,[3]Molecular and Cellular Biology, Heidelberg University, Heidelberg, Germany,[4]Regenerative Biology and Medicine, Technical University of Dresden, Dresden, Germany,[5]Vall d'Hebron Institute of Oncology (VHIO), Barcelona, Spain,[6]Molecular Biology, Genetics and Bioengineering, Sabanci Universitesi, İstanbul, Turkey

We and other researchers have recently demonstrated in vitro that chemoresistant and stem-like triple-negative breast cancer cells preferentially obtain energy through mitochondrial oxidative phosphorylation (OXPHOS) compared to their chemosensitive counterparts, which undergo glycolysis. Proteomic profiling revealed several possible survival mechanisms for the resistant phenotype, including OXPHOS-associated pathways. Since metastasis and poor clinical prognosis are often associated with the dormant subset of slow-growing cancer stem cells (CSCs), we treated tumor models derived from mammospheres with pre-selected bactericidal antibiotics—OXPHOS inhibitors - AMX, FSS and others. Our results demonstrate significant inhibition of tumor growth in the inhibitor-treated groups compared to the placebo-treated group. Furthermore, this inhibition was more pronounced in tumors derived from CSCs than in tumors derived from chemosensitive cancer cells prone to glycolysis, further emphasizing the role of OXPHOS in CSCs. Since CSCs are often associated with a pool of chemoresistant OXPHOS-dependent cells, we conducted a chemoprevention experiment in which nude mice were given the above-mentioned inhibitors for several weeks, followed by injection with CSC-like cells (mammospheres) to create tumors. Our results showed a slowdown in tumor growth in the group of mice that had previously received these inhibitors, compared to mice that received a placebo. Thus, our experiments may be of interest for modeling the prevention of OXPHOS-dependent breast tumors.

#0946 Liposomes encapsulated chloroform fraction of *Cassia fistula* L. bark enhances anticancer efficacy in ehrlich ascites carcinoma mice model.

Satwinderjeet Kaur, Rasdeep Kour

Department of Botanical and Environmental Sciences, Guru Nanak Dev University, Amritsar, India

Cancer remains one of the eminent causes of mortality and a major health concern profoundly influencing life expectancy worldwide. *Cassia fistula* L. commonly known as 'Golden shower' finds its application in the Ayurveda and Chinese traditional medicines. The phytoconstituents from the bark powder were obtained using organic solvents in the increasing order of polarity viz. *CaMH* (hexane fraction), *CaMC* (chloroform fraction), *CaME* (ethyl acetate fraction) and *CaMM* (methanol fraction). These bark fractions were tested for their cytotoxic potential in HeLa (cervical cancer), MCF-7 (breast cancer), LN-18 (brain glioblastoma), MG-63 (osteosarcoma), A431 (skin cancer), MIA PaCa-2 (pancreatic cancer) and normal cell line L929 (human fibroblast cells) using MTT assay. Among all the tested fractions, *CaMC* fraction shows highest selective cytotoxicity against HeLa cells with GI_{50} value of 41.53 µg/mL. Silica gel column chromatography of *CaMC* fraction yielded *Cf-1* fraction spectroscopically deciphered as Piperine. It showed significant cytotoxicity against HeLa, MG-63 and MCF-7 cell line with GI_{50} of 0.10 mM, 0.37mM, 0.56 mM respectively. *CaMC* and *Cf-1* fractions treated HeLa cells showed significant manifestations of apoptosis in morphological and flow cytometric investigations. These induced cell cycle arrest at G_0/G_1 phase in concentration-dependent manner. Molecular mechanistic studies of *CaMC* and *Cf-1* fraction depicted upregulation of apoptotic markers including p53, caspase 3 and 9, and downregulation of Bcl-2. Furthermore, the *in-vivo* studies evaluated in Ehrlich Ascites Carcinoma-bearing Swiss albino mice showed that liposomal encapsulated *CaMC* fraction (*CaMC-LP*) resulted in 82.23% tumor growth inhibition in contrast to *CaMC* fraction with 60.81% tumor inhibition, comparable to 86.39% inhibition by 5-Fluorouracil. The use of liposomal encapsulation enhanced the anticancer efficacy *in vitro,* and *in vivo* showing significant tumor inhibition in EAC- bearing mice without inducing toxicity. These findings suggest that *C. fistula* L. bark constituents have cancer chemopreventive and chemotherapeutic potential which can further be exploited for the benefit of mankind.

#0947 Mammary gland architectural modulation with a natural galactagogue *Asparagus racemosus* (Shatavari root extract) and its impact against triple negative breast cancer (TNBC) tumorigenesis.

Md. Imtiazul Kabir, Robin Kumar, Lakshmi Sai Pratyusha Bugata, **Komal Raina**

Dept. of Pharmaceutical Sciences, South Dakota State University, Brookings, SD

The roots of *Asparagus Racemosus Willd.* (Shatavari) are known for its galactagogue properties and often used as a traditional/ alternative way to increase milk production during lactation and for breast size augmentation. There is also supporting evidence that it has anti-cancer properties against various cancers including carcinogen-induced breast cancer in pre-clinical *in vivo* studies and against ER positive breast cancer cell lines. In the present study we investigated the anti-cancer potential of standard extract of roots of *Asparagus Racemosus* (AR^{RE}) against triple negative breast cancer (TNBC). We conducted orthotopic tumorigenesis studies in C57Bl/6 female mice. Five weeks old C57Bl/6 female mice (Jackson Labs), were maintained on control AIN-76A diet from Envigo diets, Inc. After 1 week of acclimatization mammary tumors were induced by orthotopic injection of $2x10^6$ PY230 breast cancer cells in the 4^{th} mammary fat pad (either left or right) on day 0. n=7 mice per group were treated with or without AR^{RE} as an oral intervention agent (including with and without tumor inoculation). The dose of AR^{RE} was 250 mg/kg body weight/day (volume 200µl sterile distilled water)-prepared fresh daily. Study end point was 8 weeks following cell inoculations. At study end, tumor tissues, tumor adjacent breast fat pad was harvested from mice and processed for pathological/ molecular analysis. AR^{RE} treatment caused an increase in latency time (time taken for appearance of palpable TNBC tumors) indicating its preventive benefits. AR^{RE} treatment did not have any significant impact on TNBC tumorigenesis; however, tumors had the appearance of differentiated lobular/glandular formation in AR^{RE} - fed groups compared to undifferentiated tumor cells in the controls. Proteomic profiling of mammary gland tissues indicated there were 43 differentially expressed biomarkers after AR^{RE} intervention. Out of the 43 differentially expressed biomarkers, there were 2 molecules [Methylenetetrahydrofolate dehydrogenase 1 (MTHFD1) and Mitogen-activated protein kinase kinase kinase kinase 4 (MAP4K4) that were significantly decreased in the AR^{RE} control (treated tissue). Importantly, these two molecules are reported to be overexpressed in breast cancer and implicated in the growth and progression of breast cancer. Overall, the results indicated that AR^{RE} intervention results in modulation of signaling pathways (that are associated with breast cancer growth and progression) and had the potential to induce differentiation in TNBC tumors, which could possibly be a novel approach to target TNBC malignancy. Taken together, the study outcomes favor the use of AR^{RE} as a preventive or therapeutic modality against TNBC but warrants further investigation.

#0948 TRAIL inducing drug, ONC201 prevents adenocarcinoma in transgenic KRAS^{G12V} mouse lung cancer model.

Karthikkumar Venkatachalam[1], Gopal Pathuri[1], Nicole Stratton[1], Anil Singh[1], Nandini Kumar[1], Shizuko Sei[2], Vignesh Gunasekharan[2], Chinthalapally V. Rao[1], Venkateshwar Madka[1]

[1]Center for Cancer Prevention and Drug Development, Stephenson Cancer Center, Department of Medicine, University of Oklahoma HSC, Oklahoma City, OK,[2]Division of Cancer Prevention, National Cancer Institue, Rockville, MD

Lung cancer is one of the leading cancers worldwide. Around 226,000 people will be diagnosed with lung cancer in the US during 2025. Almost one-fourth of all lung cancers are KRAS-mutated tumors, which are very challenging to treat and have poor prognosis. Interception of lung cancer is of utmost importance to reduce the burden and mortality. However, there are currently no interception agents approved by FDA. TCGA database revealed that the apoptosis mediating TRAIL expression is lost during the progression of lung tumor stages. ONC201 (Dordaviprone) is an orally active TRAIL inducing small molecule compound with proven preclinical efficacy and is being clinically evaluated against multiple cancers. Previously we reported the cancer prevention potential of ONC201 in an NNK-induced lung cancer model in A/J mice. Here, we evaluated the efficacy of ONC201 in an aggressive KRAS^{G12V} lung tumor mouse model. Male and female KRAS^{G12V} mice were generated by inhouse breeding. Six-week aged mice were randomized (n=20/sex) into placebo and interception groups. Beginning at 8 weeks of age (early adenoma stage) mice were gavaged one of the doses of ONC201 (0, 25, 50, 100mg/kg in PBS vehicle) twice weekly for 28 weeks. All mice were euthanized at 36 weeks of age, and lungs were evaluated to determine tumor incidence and multiplicity. Both the male and female KRAS^{G12V} mice in placebo group developed lung tumors (~100% incidence) with average tumor multiplicity of 12.2±1.5 (male) and 11.7±0.8 (female) per mouse. ONC201 treatment resulted in significant reduction in total lung tumors multiplicity in both male (34%-63% less; $p<0.05$-$p<0.0001$) and female (33%-55% less; $p<0.001$-$p<0.0001$) mice in a dose dependent-manner as compared to their control group. H&E stained lung tumor sections were histologically classified as adenomas (AD), and adenocarcinomas (ADCA). Placebo mice showed multiplicity of 9.3±1.3 ADCA, and 12±1.2 AD+ADCA in male; 8.3±0.6 ADCA, and 11.61±0.87 AD+ADCA in female mice. Histopathology results indicated dose-dependent reduction in ADCA multiplicity in ONC201 treated mice in male (53%-86%; $p<0.001$ - $p<0.0001$) and female mice (54%-79%; $p<0.0001$) when compared to their respective control mice. There was no clinical sign of toxicities observed in all three doses tested in both male and female mice. Immunoblotting and IHC results revealed that TRAIL inducing ONC201 triggering the downstream signaling molecules (TRAIL, DR5, FADD, Apaf1), elevated apoptosis markers (Caspases), concurrently reduces the proliferation markers (PCNA, Cyclin D1, EGFR, Ki67). In conclusion, ONC201 demonstrated strong efficacy in preventing lung cancer in two preclinical mouse models and warrants further clinical development for the prevention of lung tumor in high risk populations.
(Project funded 100% with Federal funds from NCI, NIH, DHHS, under Contract 75N91019D00020_75N91022F00003)

#0949 Prevention of insulin receptor isoform A formation inhibits MASH-driven hepatocellular carcinoma.

Yanting Wang, Manasi Das, Panyisha Wu, Yunpeng Yang, Isabella Maranan, Liping Zeng, Yichun Ji, Deepak Kumar, Nicholas Webster

University of California San Diego, San Diego, CA

Introduction: Metabolic dysfunction-associated steatohepatitis (MASH) has emerged as a leading driver of hepatocellular carcinoma (HCC). Our previous work identified that the loss of the RNA splicing factor SRSF3 is an early event in chronic liver disease. This loss leads to the aberrant skipping of exon 11 in the insulin receptor (*INSR*) gene, shifting the isoform expression from the normal hepatic IR-B to the fetal IR-A isoform. Unlike IR-B, IR-A binds insulin-like growth factor 2 (IGF2) with high affinity, potentially establishing a mitogenic autocrine loop. We hypothesized that this specific splicing switch is a critical driver of hepatocarcinogenesis and that preventing it could inhibit tumor formation.

Methods: To test this hypothesis, we generated a novel "Exon 11+" mouse model in which *Insr* exon 11 inclusion is genetically enforced, thereby preventing the production of the IR-A isoform. We subjected Exon 11+ mice and wild-type (WT) littermates to a chemical-dietary carcinogenesis protocol. Mice received a single injection of diethylnitrosamine (DEN) at 2 weeks of age, followed by chronic administration of thioacetamide (TAA) and a Western diet (MASH conditions) for 24 weeks to induce HCC. Tumor burden was assessed by surface counting and measuring. Liver tissues were analyzed via histology (H&E, Sirius Red, Reticulin), immunohistochemistry (Ki67, CD45), and qPCR.

Results: WT mice developed extensive liver tumors accompanied by severe fibrosis and inflammation. In striking contrast, Exon 11+ mice were significantly protected against tumorigenesis, exhibiting a profound reduction in both the number (decrease >80%, $p<0.001$) and size ($p<0.05$) of surface tumors. Histological analysis confirmed that Exon 11+ mice had significantly reduced liver fibrosis (Sirius Red, $p<0.001$) and immune cell infiltration (CD45, $p<0.01$) compared to WT controls. Notably, Reticulin staining revealed that Exon 11+ livers maintained normal hepatic plate architecture (1-2 cell thickness), whereas WT livers displayed disorganization and thickening characteristic of HCC. Furthermore, enforcing IR-B expression significantly suppressed hepatocyte proliferation (Ki67, $p<0.0001$) and downregulated the expression of key proinflammatory (Tnf, Il6, Ccl2) and profibrogenic (Col1a1, Col3a1) genes (all $p<0.05$).

Conclusions: Our data provide the first *in vivo* genetic evidence that the alternative splicing switch of the insulin receptor from IR-B to IR-A is a necessary event for MASH-driven HCC progression. Blocking this specific splicing error is sufficient to suppress inflammation, fibrosis, and tumor development in a harsh carcinogenic environment. These findings suggest that targeting the IGF2/IR-A signaling axis or correcting *INSR* splicing represents a potent therapeutic strategy for preventing MASH-associated liver cancer.

#0950 Efficacy of androgen receptor inhibitor, Apalutamide, in intercepting bladder cancer in a BBN-induced rat bladder tumor model.

Venkateshwar Madka[1], Gopal Pathuri[1], Anil Singh[1], Surya P. Singh[1], Anh Bao[1], Nicole Stratton[1], Shizuko Sei[2], John Clifford[2], Chinthalapally V. Rao[1]

[1]Center for Cancer Prevention and Drug Development, Stephenson Cancer Center, Department of Medicine, University of Oklahoma HSC, Oklahoma City, OK,[2]Division of Cancer Prevention, National Cancer Institute, Rockville, MD

Bladder cancer (BC) is the second-most diagnosed genitourinary cancer. Most tumors are detected at the non-muscle invasive (NMIBC) stage and treated; however high recurrence rate, treatment resistance, tumor progression and metastasis contribute to significant mortality annually. Many studies have indicated significantly higher incidence rates and BC progression to be more predominant in men. Experimental data have also showed strong association of BC tumorigenesis with androgen receptor (AR) signaling , making AR a promising target for cancer interception. In this study, AR antagonist, apalutamide (APA) was evaluated for BC preventive efficacy in a N-butyl-N-(4-hydroxyl)-nitrosamine (BBN)-rat BC model. Male and female Fischer rats were randomized into placebo and intervention groups (30 rats/group/sex: 24 BBN+6 Saline). At 8 weeks of age, rats in carcinogen groups received BBN by oral gavage (150mg/dose; 2x/week for 8 weeks) to induce BC. APA was given to rats in intervention groups at 7.5, 15, or 30mg/kg body weight by oral gavage (5x/week) until termination. Early intervention with APA started at carcinogenesis stage i.e., a week after last BBN, while delayed intervention began at papilloma stage i.e., ~10 weeks after last BBN. Bladder tumors were assessed at 40 and 50 weeks of age in male and female rats respectively. APA did not cause any overt-toxicities. BBN treatment induced bladder tumors in all rats, resulting in significantly larger bladders in placebo group compared to normal bladders in saline group. Importantly, APA significantly reduced bladder weights suggesting tumor growth inhibition in intervention groups compared to placebo. With early intervention, bladder weights were reduced by 60%-65% in male rats ($p<0.05$) and by 54%-63% in female rats ($p<0.05$) when compared to the placebo group. Incidence of large bladder tumors was also significantly decreased with APA treatment by 30%-47% in males ($p<0.05$-$p<0.01$) and by 32%-50% in females ($p<0.05$) in a dose dependent manner. Delayed intervention also resulted in 21%-53% ($p<0.01$) reduction of bladder weights and 28%-66% less incidence of large tumors in male rats only. Histopathological analysis of the tumor sections demonstrated suppression of tumor progression in APA treated rats as indicated by the significant decrease in multiplicity of papillomas, NMIBC, and MIBC when compared to placebo. Biomarker and gene expression analysis suggested modulation of critical tumor promoting pathways with APA treatment. In summary, this preclinical study demonstrated that an AR antagonist, apalutamide, can intercept bladder tumor growth and progression and warrants further investigation in clinical trials. (Project funded in whole with Federal funds from the NCI-NIH, DHHS, under Contract No. 75N91019D00020 - 75N91022F00002).

#0951 STAT3 inhibitor TTI-101 effectively intercepts bladder cancer in a carcinogen-induced rat bladder tumor model.

Venkateshwar Madka[1], Gopal Pathuri[1], Anil Singh[1], Nicole Stratton[1], Anh Bao[1], David J. Tweardy[2], Shizuko Sei[3], Vignesh Gunasekharan[3], Chinthalapally V. Rao[1]

[1]Center for Cancer Prevention and Drug Development, Stephenson Cancer Center, Department of Medicine, University of Oklahoma HSC, Oklahoma City, OK,[2]Division of Internal Medicine, The University of Texas MD Anderson Cancer Center, Houston, TX,[3]Division of Cancer Prevention, National Cancer Institute, Rockville, MD

Bladder cancer (BC) is the 9th most common cancer worldwide. Most bladder tumors are detected and treated at the non-muscle invasive (NMIBC) stage. However, tumors recur frequently, many progress to MIBC and metastasize contributing to significant mortality. Rising incidence and mortality in BC underscore the need to develop new regimen for its management. Transcriptional factor Signal transducer and activator of transcription 3 (STAT3) regulates cell proliferation through inflammation and immune responses. Its activation is highly regulated in normal cells but in cancers including BC, it is constitutively active. Expression of dominant-negative STAT3 was shown to inhibit tumor formation in nude mice. Earlier we and others reported that STAT3 inhibitors reduces BC cell survival and proliferation. In the present study, we determined pharmacodynamic pSTAT3 inhibitory effect of STAT3 inhibiting small molecules (GLG-302, SH5-07, TTI-101) *in-vitro* BC cells and *in-vivo* rat tumors. TTI-101 was further evaluated for its potential to intercept BC in a N-butyl-N-(4-hydroxyl)-nitrosamine (BBN)-rat BC model. Female F344 rats were randomized into a placebo, STAT3 (n=24) and Sulindac (n=18) intervention groups. Eight-weeks of age, rats were given BBN by oral gavage (150mg/dose; 2x/week for 8 weeks). Drug treatment was initiated at papilloma stage i.e., ~10 weeks after last BBN. Rats in intervention groups received TTI-101 at 25 or 75mg/kg body weight by oral gavage (5x/week) for 20 weeks. Sulindac was administered at 10mg/kg BW as a comparator. All drugs were formulated using 60% labrasol:40% PEG400. Bladder tumors were assessed at ~45 weeks of age. TTI-101 did not cause any overt-toxicities. BBN-induced bladder tumors in all rats, resulting in larger bladders in placebo group (0.31±0.06g; Mean±SEM). Importantly, bladder weights in TT1-101 25mg/kg and 75mg/kg groups were 0.21±0.06mg (32% inhibition; $p>0.05$) and 0.13±0.01g (58% inhibition; $p<0.01$) when compared to the placebo. Sulindac treatment had non-significant 46% inhibition (0.17±0.02g; $p=0.07$). In the placebo group, about half of all rats developed large bladder tumors (>200mg; 50% incidence). Interestingly, significantly fewer rats developed such tumors with TTI-101 25-mg/kg (17% incidence; $p<0.05$) and at 75mg/kg BW dose (8% incidence; $p<0.005$) in a dose dependent manner (67%-83% less respectively). Thus, STAT3 inhibition with TTI-101 resulted in a dose dependent inhibition of bladder tumors growth. Biomarker and gene expression analysis suggested modulation of critical tumor promoting pathways with decrease in pSTAT3 expression. Collectively, our study demonstrated that STAT3 inhibition using TTI-101 can intercept bladder tumor growth and warrants further investigation in clinical trials. (Project funded in whole with Federal funds from the NCI-NIH, DHHS, under Contract No. 75N91019D00020-75N91020F00005).

#0952 Silibinin induced mast cell regulation: Potential immunomodulation via ODC1 in pancreatic cancer prevention and therapy.

Neha Mishra[1], Sandeep Paudel[1], Komal Raina[2], Chapla Agarwal[1], **Rajesh Agarwal**[1]

[1]University of Colorado Anschutz Medical Campus, Aurora, CO,[2]San Diego State University, San Diego, CA

It has been estimated by the American Cancer Society that in the US in 2025, ~67,440 people (34,950 men; 32,490 women) will be diagnosed with, and ~51,980 people (27,050 men; 24,930 women) will die of pancreatic cancer (PC). Additionally, the average lifetime risk of developing PC has been estimated to be ~1 in 56 in men and ~1 in 60 in women. PC has been reported to be the 4th leading cause of cancer deaths in the US with a <5% overall 5-year survival rate. The role of immune system, particularly the primary cellular responders, the mast cells (MCs), in PC remains obscure. The natural flavonolignan silibinin (SB), has been effective in preclinical models of PC; however, its role in the immune modulation in PC has not been reported, to our knowledge, particularly with respect to MCs. We previously reported immunomodulation by SB in basal cell carcinoma, prostate cancer, colon cancer, and hepatocellular carcinoma. Thus, mechanistic aspects of SB treatment on MCs in PC were determined, leveraging bone marrow MCs (BMMCs) derived from C57BL/6 mice, in the presence of IL-3 and SCF (confirmed using flow cytometry [cKit/Fc€RI dual staining]). BMMCs were exposed to different doses of SB (25-100 μM) and two concentrations (25 μM; SB 25 and 100 μM; SB 100) were selected for further experiments. BMMCs treated with SB 25, SB 100, and untreated (control) were subjected to proteomics (LCMS on Fusion Lumos mass spectrometer); 3575 proteins were identified using the annotated mouse proteome. Statistical analysis (ANOVA followed by Fisher's posthoc analysis; $p<0.05$, FDR<0.01) and 166 proteins were found to have statistically significant differential expressions amongst the three groups (n=4/group). These 166 proteins were selected for further pathway analysis using Ingenuity Pathway Analysis (IPA; Qiagen). Only pathways specifically demonstrated experimentally in immune cells/cell lines in PC were selected for further analysis. Top canonical pathways associated with SB treatment of immune cell regulation via MCs were found to be folate signaling pathway, senescence-associated secretory phenotype, cyclins and cell cycle regulation, transcriptional regulation by RUNX2, as senescence pathway. Important upstream regulators were found to be ODC1, CDKN1A, SMAD2, PLAC8, TP53. Important nodes determined were KRAS, GLI1, and ODC1, with the main causal network implicated being polyamine synthesis, hinged on ornithine decarboxylase 1 (ODC1). ODC1 inhibition is proposed to be a potential therapeutic strategy, as pancreatic tumors particularly those resistant to conventional treatments are highly dependent on this enzyme for tumor progression. Thus, SB may play an important immunomodulatory role in PC via regulation of MCs and ODC1. Further studies are warranted to delineate these mechanisms leveraging SB in the form of a preventive or treatment option (supported by R01 CA140368).

#0953 Chemopreventive effects of *Rheum webbianum* against colorectal cancer via modulation of Wnt/β-catenin and TGF-β signaling: Insights from in-vitro and in-vivo studies.

Umer Majeed Khaja[1], Reena Singh[1], Showkat Ahmad Ganie[2]

[1]Bioengineering and Biosciences, Lovely Professional University, Phagwara, Punjab, India,[2]Department of Clinical Biochemistry, University of Kashmir, Srinagar, Jammu and Kashmir, India

Background: Colorectal cancer (CRC) is one of the most prevalent malignancies worldwide, largely influenced by lifestyle and environmental factors. The search for safe, natural chemopreventive agents remains a key research priority. *Rheum webbianum* Royle (RW), a Himalayan medicinal plant with notable ethnopharmacological significance, has shown promising anticarcinogenic activity in prior studies. Building on our earlier findings demonstrating its protective effects against DMH-induced colon carcinogenesis, the present study further explores the anticancer potential of RW ethanolic extract, focusing on its influence on molecular pathways and rectal tissue morphology.

Methods: The ethanolic extract of RW was assessed using both *in-vitro* and *in-vivo* approaches. In HT-29 colorectal adenocarcinoma cells, cytotoxicity and wound-healing assays were used to examine antiproliferative and antimigratory effects. Western blotting analyzed alterations in β-catenin and TGF-β1 expression. In-vivo evaluation was performed using a 1,2-dimethylhydrazine (DMH)-induced CRC rat model to investigate molecular modulation and histopathological alterations in rectal tissues.

Results: *In-vitro*, RW extract markedly reduced HT-29 cell viability in a dose- and time-dependent manner, reaching approximately 80% inhibition at 200 µg/mL, and significantly impaired cancer cell migration. *In-vivo*, RW treatment downregulated β-catenin and TGF-β1 expression, indicating inhibition of oncogenic and pro-metastatic signaling.Histopathology: Microscopic examination revealed marked restoration of rectal tissue architecture in RW-treated groups compared to DMH-only rats. RW-treated animals showed reduced epithelial disruption, congestion, inflammatory infiltration, crypt abscesses, and dysplasia, while DMH-only groups exhibited severe mucosal damage, irregular glandular organization, and extensive inflammatory lesions with crypt abscesses and dysplasia. These findings suggest the protective efficacy of RW extracts in preventing DMH-induced colorectal tissue degeneration.

Conclusion: The ethanolic extract of *Rheum webbianum* demonstrates strong chemopreventive potential against colorectal carcinogenesis by suppressing tumor cell proliferation, migration, and aberrant activation of Wnt/β-catenin and TGF-β signaling pathways, along with restoring rectal tissue integrity. These outcomes support RW as a promising natural candidate for colorectal cancer prevention and integrative therapeutic development.

#0954 Dabigatran etexilate potentiates the anti-tumor effects of anti-CTLA4 antibody through remodeling the immune microenvironment in a syngeneic mouse model of MyC-CaP cells.

Liankun Song, Matthew Gozon, Andrewtrung Le, Jun Xie, Xiaolin Zi

UC Irvine, Irvine, CA

Dabigatran etexilate, an FDA approved thrombin inhibitor, has been used for treatment of venous thromboembolism for many years in cancer patients, including prostate cancer patients. Beyond its anticoagulant properties, the anti-prostate cancer properties and immunomodulatory capacity of dabigatran etexilate remain largely uncharacterized. Therefore, this study aims to determine the anti-tumor effects of dabigatran etexilate alone and its combination with anti-CTLA4 antibody in a syngeneic mouse model of MyC-CaP cells. Mice bearing MyC-CaP xenograft tumors received dabigatran etexilate daily via oral gavage and/or anti-CTLA4 antibody treatments every other day through intraperitoneal injection for 14 days. Tumor volumes were monitored throughout the treatments, after which fresh tumor tissues were dissected for flow cytometric characterization of tumor-infiltrating lymphocytes (TILs). The combination of dabigatran etexilate and murine anti-CTLA4 blocking antibody resulted in significantly enhanced anti-tumor efficacy, achieving 18% greater tumor growth inhibition compared to anti-CTLA4 monotherapy alone, and markedly prolonged overall survival of tumor bearing mice. Flow cytometry analysis revealed that dabigatran etexilate in combination with anti-CTLA4 antibody significantly increased effector T cell (Teff) populations while reducing regulatory T cells (Tregs). Notably, granzyme B-positive cytotoxic CD8+ T cells increased by 1.6 folds in the combination group compared to anti-CTLA4 monotherapy. In addition, granulocytic myeloid-derived suppressor cells (Gr-MDSCs) were significantly reduced in the combination group. Furthermore, single-cell analysis of tumor-infiltrating lymphocytes revealed that dabigatran etexilate and anti-CTLA4 combination therapy markedly increased cytotoxic natural killer (NK) cell infiltration while decreasing suppressive and exhausted NK cell populations. Taken together, our data has shown that dabigatran etexilate potentiates anti-CTLA4 therapy by activating cytotoxic T and NK cells while suppressing immunosuppressive Tregs and Gr-MDSCs. These results suggest that dabigatran etexilate deserves further investigation as a new immunomodulatory agent for prostate cancer prevention and treatment.

#0955 Development of HiBiT tagged high-throughput screening assay for the discovery of SKP2 targeting degraders in prostate cancer.

Liankun Song, Merry Chai, Matthew Gozon, Jun Xie, Saiyang Zhang, Xiaolin Zi

University of California, Irvine, Irvine, CA

S-phase kinase associated protein 2 (SKP2), an E3 ubiquitin ligase for protein degradation and regulating the cell cycle, is overexpressed in high-grade prostatic intraepithelial neoplasia and prostate adenocarcinoma compared to normal prostate tissues, and its higher mRNA levels in prostate tumor tissues are significantly associated with poorer survival of prostate cancer patients. Therefore, identifying novel molecules that promote SKP2 degradation represents a promising strategy for intercepting prostate cancer. We have generated the CRISPR/Cas9 knock-in (KI) of the HiBiT tag at the endogenous *SKP2* locus in the 22Rv1 prostate cancer cell line with *SKP2* gene amplification to enable high-throughput screening of SKP2 protein degraders. Sanger sequencing, western blot and luminescence imaging were performed to confirm the successful expression of the endogenous SKP2-HiBiT in 22Rv1 cells. Screening conditions adapted with nano-Glo® HiBiT lytic detection assay were well established in a 384 well plate format, yielding a high signal-to-background ratio of 69. We have further validated the screening assay with SKP2 C1 inhibitor and Flavokawain A, a naturally occurring chalcone from the Kava plants. Flavokawain A (degrading SKP2 protein) but not C1 (a SKP2 enzyme inhibitor) inhibited the HiBiT luminescence signal, confirming the specificity of the assay. In addition, we have synthesized a small library of chalcone derivatives and by screening them in SKP2-HiBiT-KI 22Rv1 cells, three new SKP2 degraders with improved efficacy have been identified. To avoid false positives due to assay artifacts, compounds that significantly inhibit luminescence within 5 minutes of treatment are excluded from the hits list. The screening assay exhibited robust performance with Z′ factors exceeding 0.6. These three SKP2 degraders significantly reduced the HiBiT luminescent signal at low micromolar concentrations after 8 hours of treatment compared to vehicle control treatment, with minimal effects on cell viability. Western blot analyses further confirmed that these three hits downregulated the protein levels of SKP2 in a dose and time dependent manner. In addition, PC3 cells overexpressing SKP2 are more sensitive to the growth inhibitory effects of these three degraders than SKP2 non-overexpressing PC3 control cells, suggesting the specificity of these degraders for targeting SKP2 overexpressing prostate cancer cells. In conclusion, we successfully established and validated the SKP2-HiBiT-KI 22Rv1screening platform that enables the identification of highly potent, low-toxicity SKP2 degraders for prostate cancer interception.

#0956 The repurpose of dabigatran etexilate for improving prostate cancer prevention and treatment through down-regulating Myc and E2F target genes and inducing autophagic apoptosis.

Guanxing Zhai, Vinh Le, **Liankun Song**, Yixi "Michael" Wu, Xiaolin Zi

UC Irvine, Irvine, CA

Dabigatran etexilate (DAB), an FDA-approved oral anticoagulant drug, has been safely used in cancer patients. While it has been concurrently administered with anti-androgens like enzalutamide in some prostate cancer patients, the potential interactions between DAB and enzalutamide and their effects on prostate cancer cells remain unknown. In this study, we have shown that DAB selectively inhibited prostate cancer cell growth with minimal growth inhibitory effects on normal prostate epithelial cells. Dabigatran induced autophagic apoptosis as evidenced by LC3B/Caspase 3 cleavages and increased autophagic vesicles. Oral administration of DAB significantly inhibited in vivo tumor growth in a xenograft model of 22Rv1 cells and reduced AR and Ki67 expression levels in tumor tissues. A systematic transcriptome analysis of gene expression regulation in DAB treated 22Rv1 cells revealed that the DAB regulated genes were significantly enriched in c-Myc and E2F targets and apoptosis and G2M checkpoint related genes. In addition, DAB acted synergistically with enzalutamide to reduce cell viabilities of prostate cancer cell lines: 22Rv1 and MyC-CaP. Our results indicate that DAB deserves further investigation as a novel anti-cancer agent, for prostate cancer prevention and for treatment of prostate cancer in combination with the main clinically used drug enzalutamide.

#0958 Novel syngeneic models for evaluating therapies targeting $EGFR^{L858R/T790M}$ and $EGFR^{L858R/T790M/C979S}$ resistance mutations in NSCLC.

Lei Ci, Kai Zhou, Jiangyan Liu, Ruilin Sun

GenoBioTX LLC, Suger Land, TX

Both the first and second-generation EGFR-TKIs drugs have markedly improved the survival of NSCLC patients with activating EGFR mutations. However a secondary T790M mutation rapidly drives resistance towards these drugs. Third-generation EGFR-TKIs potently suppress the T790M mutant, but the subsequent C797S mutation abolishes their covalent binding, leaving no currently approved targeted options. Therefore, our laboratory generated conditional knock-in C57BL/6 mice harboring human $EGFR^{L858R/T790M}$ or $EGFR^{L858R/T790M/C979S}$, which quickly develop spontaneous NSCLC and yield primary tumor cell lines.In syngeneic, immune-competent C57BL/6 hosts, the fourth-generation TKI under research, BLU-945, markedly inhibited both $EGFR^{L858R/T790M}$ and $EGFR^{L858R/T790M/C979S}$ tumor growth. In contrast, osimertinib was effective only against $EGFR^{L858R/T790M}$, but failing against the $EGFR^{L858R/T790M/C979S}$ mutation. This demonstrates how our novel mouse models faithfully recapitulate and allow the reversal of osimertinib resistance *in vivo*.

#0959 Harnessing Id1 as a Biomarker in a Plasmid Reporter System for Cervical Cancer.

Abbigael V. Eli, Benjamin B. Kasten, Yolanda Hartman, Rebecca C. Arend, Jason M. Warram

University of Alabama at Birmingham (UAB), Birmingham, AL

Introduction: Ten-year cervical cancer (CC) incidence in the U.S. has remained stable despite screening advancements such as HPV testing, suggesting that new CC screening technologies are needed to address stagnant rates. We proposed a diagnostic plasmid for screening that induces expression of a reporter enzyme (secreted embryonic alkaline phosphatase, SEAP) through the control of the cancer-specific inhibitor of differentiation 1 (Id1) promoter sequence. The resulting plasmid (pId1-SEAP) was used to transfect CC cells in vitro and characterize reporter SEAP production based on Id1 expression. Methods and Results: Western Blot and immunohistochemistry were used to establish Id1 expression in cell models and human tissues. Timed transfections in various conditions were used to correlate Id1 and SEAP expression. CC cell lines (HeLa 3.0±0.13, SiHa 2.9±0.27, CaSki 3.1±0.19, all $P<0.0001$) expressed increased normalized baseline Id1 compared to non-cancer 3T3 fibroblasts (1.0±0.0). In a microarray of CC tissues, normal samples had mean Id1 staining value of 3E4±3E4, while early- and late-stage cancers had increased mean Id1 staining (3E5±1E5 $P<0.0001$ and 2E5±1E5 $P=0.0002$, respectively). HeLa and SiHa lines produced increased normalized SEAP amounts with pId1-SEAP (0.63±0.25 and 0.50±0.10, $P<0.05$) compared to 3T3 cells with pId1-SEAP (0.16±0.058). Id1 and SEAP expression were strongly correlated (Pearson's $r=0.99$, $P=0.012$). As few as 12,500 pId1-SEAP plasmid-exposed HeLa cells co-cultured with naïve cells resulted in an increased SEAP value (3E4±3E3 $P=0.004$) compared to background level (1E4±4E2). Conclusions and Future Directions: pId1-SEAP can transfect CC cells to produce SEAP proportionally to endogenous Id1 expression, demonstrating its potential for future diagnostic tests for CC. These data support further studies to characterize pId1-SEAP function in 3-D tissue models and in vivo animal models, towards the development of a home-based approach to screen for cervical cancer using Id1 expression as a biomarker.

#0960 Dysregulation of the islet hormone cholecystokinin drives obesity-associated pancreatic cancer.

Daniel C. McQuaid[1], Cathy C. Garcia[1], Aarthi Venkat[1], Christian F. Ruiz[1], Christy Zheng[1], Smita Krishnaswamy[2], Mandar Deepak Muzumdar[3]

[1]Yale School of Medicine, New Haven, CT,[2]Yale University, New Haven, CT,[3]Fellow, Medical Oncology, Yale University, New Haven, CT

Pancreatic ductal adenocarcinoma (PDAC) is the third-leading cause of cancer death in the United States with a 5-year survival rate of ~13%. Obesity is a key PDAC risk factor associated with increased incidence and decreased survival, but the mechanisms by which obesity promotes PDAC development and progression remain unclear. To study how obesity drives PDAC, our lab developed a novel genetically engineered mouse model of obesity-associated PDAC and found that obese mice had significantly increased disease burden relative to lean controls, a phenotype which was abrogated by early induced weight loss. Molecular analyses of the pancreata from obese mice showed marked upregulation of the peptide hormone cholecystokinin (CCK) in β cells of the endocrine pancreas due to stress-responsive JNK/cJun signaling. CCK canonically promotes digestive enzyme release in exocrine acinar cells, the putative PDAC cell-of-origin, and acts as a survival factor in endocrine β cells under conditions of increased insulin demand, such as obesity. Exogenous CCK stimulates acinar cell proliferation and ductal metaplasia, early prerequisite steps in PDAC development. Strikingly, we found that β cell CCK overexpression was sufficient to enhance exocrine tumorigenesis in lean mice, phenocopying the effects of obesity and validating β cell CCK as an independent driver of PDAC development. Conversely, pancreas-specific CCK knockout significantly abrogated exocrine tumorigenesis in obese mice similar to levels seen in lean mice. Critically, tumor burden was significantly positively associated with pancreatic CCK expression and negatively correlated with endogenous insulin production, suggesting that CCK, rather than insulin, drives obesity-associated tumorigenesis. Finally, treatment of obese mice with GLP-1 receptor agonists (GLP-1RAs), which augment glucose-stimulated insulin secretion and improve β cell health, enhanced β cell function and significantly decreased pancreatic CCK expression. Together, this work has established endocrine-exocrine CCK - rather than insulin - as a critical previously unappreciated mediator of obesity-driven PDAC and enabled the identification of novel translational approaches, including GLP-1RAs, to intercept obesity-associated PDAC development.

#0961 HSC-humanized mouse model: Invivo CAR-T mediated B-cell depletion and application in targeted drug screening.

Xiaolei Qiu, Lei Ci, Ruilin Sun

GenoBioTX LLC, Sugar Land, TX

Background: In the research of targeted therapy for B-cell related malignant tumors and autoimmune diseases, traditional animal models have limitations such as significant species differences and inadequate mimicry of human immune function, which hinder the efficiency of drug development. Hematopoietic Stem Cell (HSC)-humanized mice can reconstitute a functional human immune system, providing an ideal in vivo research platform to address these issues. Their application value in the evaluation of in vivo CAR-T (Invivo CAR-T) therapy and screening of innovative drugs urgently needs to be verified.

Methods: A standardized protocol was used to construct the HSC-humanized mouse model: Severe immunodeficient NMG mice were preconditioned with sublethal dose irradiation (1.2 Gy) to disrupt the endogenous hematopoietic system and create space for human HSC engraftment. Subsequently, 1.5×10^5 sorted and purified human umbilical cord blood-derived $CD34^+$ HSCs per mouse were transplanted via tail vein injection. After stable model reconstitution (peripheral blood $hCD45^+$ cell ratio ≥25%), the CD19-targeted Invivo CAR-T system was used for intervention. CAR gene/mRNA was delivered via viral vectors (e.g., lentivirus, adeno-associated virus) or targeted lipid nanoparticles (tLNP). Following a single administration, the B-cell depletion efficiency in peripheral blood and spleen, as well as the CAR transfection positive rates in $CD4^+$ T cells and $CD8^+$ T cells, were detected simultaneously.

Results: After transplantation, $CD34^+$ HSCs successfully engrafted in the bone marrow of HSC-humanized mice and achieved multi-lineage differentiation, forming a stable population of human immune cells. The immune reconstitution exhibited a time-dependent characteristic: T cells accounted for 40%-50% at 14-20 weeks, B cells were the dominant population in the early stage, accompanied by low-proportion reconstitution of myeloid cells such as NK cells (average proportion ~2%) and monocytes. Human immune checkpoint molecules were expressed on the surface of immune cells. After Invivo CAR-T intervention, autologous B cells in the peripheral blood and spleen of mice were significantly depleted with a near-complete clearance efficiency, and positive CAR expression was detected in both $CD4^+$ T cells and $CD8^+$ T cells. Further analysis showed that B-cell reconstitution was dominated by naive B cells after depletion, suggesting functional resetting of the immune system. By synchronously monitoring CAR transfection efficiency and target cell clearance effect, it provides crucial technical support for the efficacy screening, dosage optimization, and safety evaluation of innovative drugs targeting B cells.

#0962 Phenylacetaldehyde induces apoptosis through endoplasmic reticulum stress and potentiates the effect of 5-FU treatment in colorectal cancer.

Sylvain Ferrandon[1], Cheng Kong[2], sara soltani tehrani[1], Joseph Fedro[1], Rami-James Aoun[1], Zeneng Wang[3], Chureeporn Chitchumroonchokchai[1], Huanlong Qin[4], Steve Clinton[1], Matthew F. Kalady[1]

[1]The Ohio State University College of Medicine, Columbus, OH,[2]Fudan University Shanghai Cancer Center, Shanghai, China,[3]The Lerner Research Institute - Cleveland Clinic, Cleveland, OH,[4]Shanghai Tenth People's Hospital, Shanghai, China

Introduction: Phenylacetaldehyde (PAA), a product of phenylalanine metabolism, is generated by microbiota and has demonstrated anticancer properties in breast cancer. As intestinal homeostasis is influenced by the gut microbiome, we investigated the effect of PAA on colorectal cancer (CRC).

Methods: Serum PAA levels and feces microbiota from a test cohort of 30 CRC patients and 30 healthy control patients were analyzed by targeted GC-MS/MS and metagenomic sequencing. A validation cohort of 75 CRC patients and 53 healthy control patients was analyzed for PAA levels in serum. CRC cell lines and CRC-patient-derived organoids were cultured and treated with PAA alone or in combination with 5-fluorouracil (5-FU), then evaluated for viability, proliferation, , and cell death *in vitro*. The effect of PAA alone or in combination with 5-FU on tumor growth was also tested *in vivo*. We identified the mechanisms induced by PAA treatment using RNA sequencing, western blot, immunostaining, ROS quantification assay, cysteine and glutathione quantification.

Results: PAA levels were significantly decreased in the circulation of CRC patients compared to healthy controls in our study population and the validation cohort. Metagenomic sequencing indicated the bacteria that positively correlated with PAA levels were significantly more abundant in healthy controls; while bacteria that negatively correlated with PAA were more abundant in CRC. *In vitro*, PAA inhibited the viability and colony formation of CRC cell lines as well as human-derived organoids in a concentration-dependent manner. Mechanistically, PAA treatment induced generation of ROS leading to cysteine and reduced glutathione depletion. An investigation by RNA sequencing and immunoblotting showed that PAA inhibits CRC by inducing endoplasmic reticulum stress-induced autophagy accompanied by downregulation in PI3K/AKT/mTOR and ERK pathways. When combined with 5-FU, PAA enhanced the potency of 5-FU on viability, cell death, DNA damage and tumor growth.

Conclusions: The bacteria metabolite PAA increased CRC cell death by endoplasmic reticulum stress-induced autophagy and downregulation of the PI3K/AKT/mTOR and ERK pathways. PAA also potentiated the chemotherapeutic efficacy of 5-FU through induction of DNA damages. These findings warrant further exploration of PAA as a potential CRC biomarker and novel therapeutic agent.

#0963 Preclinical testing of A_{2B} adenosine receptor inhibitor PSB1115 for pancreatic cancer immunoprevention.

Alyssa M. Waller[1], Lincoln Strickland[1], MacKenzie Demmel[1], Erika Y. Faraoni[2], Michelle I. Savage[3], Shizuko Sei[4], John L. Clifford[4], Powel H. Brown[5], Eduardo Vilar-Sanchez[5], Florencia McAllister[5], Jennifer Bailey-Lundberg[1]

[1]University of Nebraska Medical Center, Omaha, NE,[2]Department of Genetics, The University of Texas MD Anderson Cancer Center, Houston, TX,[3]Department of Clinical Cancer Prevention, The University of Texas MD Anderson Cancer Center, Houston, TX,[4]Division of Cancer Prevention, Chemopreventative Agent Development Research Group, National Cancer Institute, Rockville, MD,[5]UT MD Anderson Cancer Center, Houston, TX

Introduction: Pancreatic ductal adenocarcinoma (PDAC) is an aggressive malignancy with very poor prognosis due to low efficacy of current treatments and late-stage diagnosis. PDAC is characterized by a profoundly immunosuppressive tumor microenvironment (TME), with the adenosine signaling pathway acting as an important mediator of immune suppression. In this pathway, adenosine (an immunosuppressive metabolite) signals via adenosine receptors, including the A_{2B} receptor. The goal of this study is to test immunopreventative strategies that target the A_{2B} adenosine receptor to reduce intratumoral adenosine and prevent immune suppression. We hypothesize that the use of small molecule A_{2B} inhibitors will prevent the progression of PDAC by shifting the immune microenvironment and promoting anti-tumor immunity.

Methods: A syngeneic model of PDAC was used with tumor cells derived from $Kras^{G12D}$; $Trp53^{R172H}$/+; Pdx1:Cre (KPC) mice. Tumor cells were implanted subcutaneously in the flanks of immunocompetent C57BL/6 mice. Oral gavage delivery of PSB1115 (small molecule A_{2B} inhibitor) began 14 days after KPC implantation, when tumors were palpable. Mice were treated either three days/week or seven days/week at 0.7mg/kg, and tumor sizes were measured twice weekly. After two weeks of treatment, mice were euthanized. Blood and tumors were collected at the time of euthanasia. Histology was analyzed and 10 fields per mouse were quantified using ImageJ.

Results: Oral gavage delivery of PSB1115 reduced the growth rate of KPC subcutaneous tumors in the syngeneic model. While mice treated with PSB1115 trended to have smaller final tumor volumes when compared to vehicle controls in both the 3 and 7 days a week treatment groups, these changes were more pronounced in the 7 days/week group (three-fold reduction; $p=0.07$) as compared to the 3 days/week group (two-fold reduction; $p=0.1$). Immunohistochemical staining of tumors showed that treatment with PSB1115 induced significant $CD8^+$ T-cell infiltration ($p=0.0174$) and increased Granzyme B expression ($p<0.0001$), indicating an activated cytotoxic immune response. There was no significant increase in the amount of NIMPR14+ cells when comparing the vehicle control and PSB1115 treated tumors ($p=0.1565$). When compared to vehicle controls, tumors treated with PSB1115 had significantly increased levels of CD68 ($p<0.0001$), with no significant increase in CD163 levels ($p=0.1174$), indicating infiltration of anti-tumor M1-like macrophages.

Conclusions: Oral gavage delivery of PSB1115 and targeting of the adenosine A_{2B} receptor alters the immune landscape in subcutaneous PDAC tumors, promoting $CD8^+$ T-cell and M1-like macrophage infiltration through reduced A_{2B} receptor signaling. Small molecule inhibitors targeting the A_{2B} adenosine receptor are promising candidates for immunoprevention in PDAC. [Supported by NCI 75N91019D00021/75N91023F00003]

#0964 Accelerated Pirc rat model for animal efficacy trials for prevention and treatment of colorectal cancer.

Rashim Singh, Vesna Tumbas Saponjac, Trang Le Nu Huyen, Jie Yang, Jie Chen, Taijun Yin, Songpol Srinual, Ming Hu

Pharmacological and Pharmaceutical Sciences, University of Houston, College of Pharmacy, Houston, TX

PURPOSE: The Pirc rat (F344/NTac-Apc^{am1137}) model has played a critical role in advancing our understanding of colorectal cancer (CRC) pathogenesis and in evaluating preventive/therapeutic strategies. The objective of this study was to establish an inflammation-driven accelerated model of colon polyp growth in Pirc rats. This model replicates chronic epithelial barrier disruption and low-grade gut inflammation, thereby reflecting real-world scenarios of lifestyle and environmental factors combined with genetic predisposition towards CRC development.

METHODS: Dextran sodium sulfate/DSS (in drinking water) and/or high-fat diet/HFD (60 kcal% as fat) treatment was given to Pirc rats, whereas control rats received a regular rodent diet with no DSS. Two cycles (5 days ON, 9 days OFF, and 3 days ON) of DSS treatment (1-2% w/v) were administered starting at 6.5 weeks of age to accelerate colon polyp development without causing colitis. The effects of HFD treatment alone (6.5-16.5 weeks) and in combination with 2%DSS treatment were established. 2%DSS+HFD-treated rats received Celecoxib (70 mg/Kg/day, p.o. from 10.5-16.5 weeks) to confirm the response of the model to the anti-inflammatory agent. The colon polyp burden was determined after euthanizing rats at Week 16.5.

RESULTS: No colitis was observed in animals during 1% or 2%DSS treatment, whereas consumption of HFD caused constipation. Minor body weight loss (<5%) was observed during DSS treatment. Administration of 2%DSS but not 1%DSS or HFD alone increased the polyp burden (n=2/group). However, the addition of HFD to 2%DSS treatment dramatically increased colon polyp number (9.7-fold, $p<0.001$) and volume (12.7-fold, $p<0.01$) in treated female rats (n=10) as compared to control rats (n=10), with larger size (>6 mm in diameter) polyps observed in the treated group only. In male rats, 2% DSS alone (n=4) or in combination with HFD (n=7) led to higher polyp numbers (2.6-2.8-fold), volumes (1.8-3.5-fold), and larger size compared to control (n=7). Celecoxib treatment reduced the polyp growth in male and female rats treated with 2%DSS+HFD (n=7), though statistical significance was not achieved.

CONCLUSION: We successfully established an accelerated polyp development Pirc rat model, providing a better platform for high-throughput screening of pharmacological and dietary interventions for CRC chemoprevention in FAP and other high-risk populations, with greater translational potential. A single anti-inflammatory agent was ineffective at preventing aggressive polyp growth in this model, suggesting that combination therapies targeting multiple targets may be required. The mechanism of action underlying CRC development in this model is being investigated to identify new pharmacological targets and combinations.

ACKNOWLEDGEMENTS: This research was funded by CPRIT RP240401. Rashim Singh is supported by the NCATS under award number K12TR004522.

#0965 A novel agonist of CD137, SA-4-1BBL, as a single agent halts spontaneous breast cancer progression.

Yongyong Li[1], Sarita Rani[1], Feyza Nur Arguc[1], Yichen Wang[1], Daniel Davis[2], Esma S. Yolcu[3], Haval Shirwan[4]

[1]Molecular Microbiology and Immunology, NextGen Precision Health, University of Missouri-Columbia, Columbia, MO,[2]Pathobiology and Integrative Biomedical Sciences, University of Missouri-Columbia, Columbia, MO,[3]Molecular Microbiology and Immunology, Pediatrics, NextGen Precision Health, University of Missouri-Columbia, Columbia, MO,[4]Molecular Microbiology and Immunology, NextGen Precision Health, School of Medicine, University of Missouri-Columbia, Columbia, MO

Introduction: Breast cancer is the most commonly diagnosed cancer among women globally, and early immunologic intervention could reduce disease burden and improve long-term outcomes. Immunotherapy has demonstrated encouraging efficacy and an acceptable safety profile in both early-stage and metastatic triple-negative breast cancer. However, currently approved immunotherapies such as PD-1/PD-L1 blockade, HER2-targeted antibodies, and tumor vaccines exhibit highly variable responses due to tumor-intrinsic factors and the immunosuppressive tumor microenvironment. A novel CD137 agonist, SA-4-1BBL, as a single agent, prevents the development of various transplantable tumor types as well as a tobacco carcinogen, NNK, induced spontaneous lung cancer in preclinical models with an excellent safety profile. Here, we evaluated the immunoprevention efficacy of SA-4-1BBL in a mouse model of spontaneous breast cancer, MMTV-PyMT, which recapitulates the progression of human breast cancer.
Study design: Female MMTV-PyMT C57BL/6J mice, aged 5 (n=12) or 8 (n=17) weeks, were assigned to either the SA-4-1BBL or saline (n=19) treatment groups. SA-4-1BBL was administered every two weeks for a total of four doses. Tumor growth was monitored twice weekly for 120 days, at which time animals were euthanized to collect tumors, tumor-draining lymph nodes, and spleen for tumor weight measurement, histology, and deep immunophenotyping.
Results: SA-4-1BBL significantly delayed the onset of tumors and inhibited their progression in both the 5-week and 8-week treatment cohorts. Median tumor appearance was observed at 13 weeks in PBS controls, compared to 16.5 weeks for the 5-week cohort and 15 weeks for the 8-week cohort. Tumor growth was markedly reduced in both SA-4-1BBL-treated groups ($p < 0.0001$). As compared to saline controls, both SA-4-1BBL treatment groups showed a significant reduction in tumor weight by ~76% and a decrease in the number of tumor-bearing mammary glands by ~50%. Deep immunophenotyping of tumor-draining lymph nodes showed substantial increases in multiple immune cell subsets, including NK cells, $CD4^+$ T cells, and $CD8^+$ T cells, demonstrating enhanced antitumor immunity.
Conclusion: SA-4-1BBL, as a single agent, effectively suppresses spontaneous breast tumor development and progression in the MMTV-PyMT model. These findings support its potential as a promising biologic for breast cancer immunoprevention. Elucidation of the underlying mechanisms will further guide the optimization and clinical translation of this protocol for immunoprevention of cancer in high-risk individuals.
Acknowledgment: Supported in part by the Paula and Rodger Riney Foundation and NCI (5UG3CA290305-02).

#0966 Development of a humanized IL-17A/IL-17F mouse model for preclinical efficacy studies of IL-17-related diseases.

Huacheng He, Ailin Yang, Shuang Li, Qingqing Qi, Yi Li, Ruilin Sun

GenoBioTX LLC, Sugar Land, TX

Background: IL-17 cytokine family members exert diverse biological functions, promoting protective immunity against many pathogens while also driving inflammatory pathology in infection and autoimmunity. The IL-17 pathway has therefore become a major therapeutic target in autoimmune and chronic inflammatory disorders such as rheumatoid arthritis, multiple sclerosis, and psoriasis. Therapeutic monoclonal antibodies targeting IL-17A, IL-17A/IL-17F, the IL-17 receptor, or IL-23 have demonstrated substantial clinical efficacy in several of these conditions. In this study, we developed a novel humanized IL-17A/IL-17F mouse model and established an imiquimod (IMQ) -induced psoriasis model to evaluate the preclinical efficacy of bimekizumab and other test articles.
Methods: The hIL-17A/hIL-17F dual knockin mice were generated by homologous recombination, replacing the entire coding sequences of mouse *Il-17a* and *Il-17f* with their human counterparts while preserving the endogenous murine signal peptides. Human IL-17A and IL-17F mRNA transcription was validated by qRT-PCR, and corresponding serum protein levels were quantified by ELISA. Finally, topical IMQ application was used to trigger psoriasiform dermatitis on the back and ear skin of the hIL-17A/hIL-17F dual knockin mice. Bimekizumab and additional test agents were administered, and in vivo efficacy was assessed by H&E staining, pathological scoring, and cytokine profiling.
Results and Conclusion: IMQ treatment induced a psoriasis-like phenotype in hIL-17A/hIL-17F mice and resulted in high expression of human IL-17F. Bimekizumab and the test articles markedly improved histopathological features and reduced the levels of IL-17F in our mice. Overall, these findings demonstrate that the hIL-17A/hIL-17F dual humanized mouse provides an advanced tool for preclinical efficacy studies of IL-17-related therapeutics.

#0967 Prevention and interception of triple-negative breast cancer and its metastasis to the brain with brain-permeant L024.

Atieh Hajirahimkhan[1], Alexander D. Eremin[1], Elizabeth Bartom[2], Saktimayee M. Roy[1], Daniel M. Watterson[1], Susan E. Clare[3], Seema A. Khan[4]

[1]Northwestern University - Chicago, Chicago, IL,[2]Northwestern University, Evansville, IL,[3]Associate Professor, Surgery, Northwestern University Feinberg School of Medicine, Chicago, IL,[4]Professor of Surgery & Bluhm Family Professor of Cancer Research, Robert H. Lurie Comp. Cancer Center of Northwestern University, Chicago, IL

Introduction: Estrogen receptor-negative (ER-neg) breast cancer (BC) disproportionatelyaffects younger women, women of African descent, and underserved populations. Nopreventive agents are approved for this subtype. ER-neg BCs, including triple-negative (TNBC)and HER2+ tumors, often metastasize to the brain early, yet remain undetected until neurologicsymptoms emerge, when prognosis is poor. Current therapies, including ER-neg adjuvantagents, offer limited brain efficacy due to poor blood-brain barrier penetration. Radio-surgicalinterventions for brain metastases have severe side effects with no survival benefit. There is acritical need for safe, risk-reducing therapies that prevent both ER-neg BC and braindissemination.We identified L024, a first-in-class agent with efficacy against ER-neg BC. Mechanistically, L024inhibits SREBP1-driven lipogenesis, suppresses the PI3K-AKT axis, and downregulates NF-κB-mediated inflammation, key pathways in ER-neg progression. We have demonstrated that L024suppresses tumor growth and we hypothesize that it will intercept early brain metastasis, offering a novel preventive and interceptive approach.
Methods: We assessed L024's antiproliferative activity in six ER-neg BC lines: MDA-MB-231,HCC-1937, HCC-3153, 4T1, 4T1-BM2, and MDA-MB-231-Br using IncuCyte live cell imaging. Xenografts were developed using MDA-MB-231 cells in nude mice; L024 (80 mg/kg/day) was administered when tumors reached threshold size. Tumor growth was monitored over 28 days;RNA-seq was performed on excised tumors. Transwell assays with/without matrix assessedinvasion/migration of brain-tropic cells after a sublethal L024 dose (2.5-5 μM). Western blotswere performed after 24 h L024 (5 μM) exposure to assess downstream effectors. ADMEproperties were evaluated in silico (ACD Lab). PK was analyzed in female CD-1 mice dosed with L024 (50 mg/kg), with drug levels in plasma, mammary, and brain measured with LC-MS/MS, and modeled using SAAM II.
Results: L024 significantly inhibited TNBC proliferation in a dose-dependent manner, with sustained effects six days post-treatment. It reduced tumor growth and epithelial-to-mesenchymal transition in the xenografts. Sublethal doses impaired invasion and migration ofbrain-tropic cells. Western blots showed reduced PI3K, AKT, and pAKT (Ser473). In silicoprofiling predicted CNS permeability: molecular weight <400 Da, LogP = 3.9, TPSA = 66.76 Å^2,and no P-gp/BCRP efflux. In vivo PK confirmed high brain exposure (Kp >1 between 1-8 h),cleared by 24 h, supporting prevention/therapy potential.
Conclusions: L024 reprograms metabolic pathways essential for ER-neg BC progression,specifically targeting multiple steps of the metastatic cascade. CNS PK supports furtherevaluation in immunocompetent TNBC models with brain metastatic potential.

#0968 Fully human anti-PD-L1 antibodies with tumor cytotoxicity: Screening in SmocMab mice.

Ningning Ge, Huacheng He, Lei Ci, Ruilin Sun, Dongxiao Feng

GenoBioTX LLC, Sugar Land, TX

PD-L1 is highly expressed across a broad spectrum of tumor cells and negatively regulates the tumor cytotoxicity of T cells. Herein, we generated multiple fully human anti-PD-L1 antibodies with high binding affinity through single B cell screening, utilizing SmocMab mice humanized for the variable regions of immunoglobulin heavy and light chains. These antibodies effectively blocked the PD-1/PD-L1 interaction *in vitro* and exhibited potent endocytic activity. In *in vivo* studies, monotherapy with the anti-PD-L1 antibodies demonstrated significant tumor-suppressive effects in hPD1 C57BL/6 mice. Furthermore, PD-L1 antibody-drug conjugates (ADCs) constructed based on these anti-PD-L1 antibodies substantially enhanced tumor-killing efficacy. Collectively, these findings validate that SmocMab mice serve as a robust platform for the screening of fully human antibodies with promising therapeutic potential.

#0969 Humanized TFR1 knock-in mice: A powerful platform for evaluating TFR1-targeting brain shuttles.

Liping Feng, Shuang Li, Zixuan Cao, Yi Li, Dongxiao Feng, Ruilin Sun

GenoBioTX LLC, Sugar Land, TX

Background: The development of therapeutic antibodies and antibody-based diagnostics for the neurological disorders and gliomas is largely hampered by the presence of blood-brain barrier (BBB). While the BBB restricts most large molecules, it permits the transport of essential nutrients through selective transport mechanisms, creating opportunities to delivery drugs into the central nervous system using brain shuttle technologies. Transferrin receptor 1 (TFR1), which is expressed on brain endothelial cells (BECs), is one of the most extensively studied targets for receptor-mediated transcytosis (RMT) and has been validated as a gateway for brain drug delivery. To support the development of TFR1-targeting antibody or peptide-based brain shuttles, we generated a humanized TFR1 knock-in mouse model (hTFR1), serving as a robust preclinical platform for evaluating the efficacy, safety, and PK/PD profiles of TFR1-targeted therapeutics.

Methods: The hTFR1 knock-in mouse model was generated by inserting the full-length human TFR1 coding sequence plus WPRE/polyA stop cassette into mouse *Cd71* gene locus in C57BL/6 background via ES cell-based gene targeting, in which full-length human TFR1 proteins are expressed on the surface of targeted cells. To characterize the human TFR1 expression in the hTFR1 knockin mice, we assessed its localization on the brain endothelial cells by immunofluorescence (IF) staining and performed flow cytometry analysis to characterize its expression on activated T cells. Finally, we administered Trontinemab and the anti-human TFR1 antibodies generated via our SmocMab platform to hTFR1 mice through *i.v.* injection to evaluate th PK characteristics and brain uptake capability across the BBB.

Results: Human TFR1 expression in hTFR1 mice was confirmed in brain microvessels and was upregulated on activated T lymphocytes. For PK analysis, brain tissues and serum samples were collected 24 hours after a single intravenous dose (10 mg/kg) of the human-specific TFR1 antibodies or a control antibody. Antibody concentrations were quantified by ELISA. The human-specific TFR1-binding antibody showed accelerated serum clearance and increased brain uptake compared with the control antibody, demonstrating its enhanced ability to penetrate the BBB.

Conclusions: Our humanized TFR1 knockin mice provides a powerful tool for preclinical evaluation of TFR1-targeting therapeutic antibodies.

#0970 A Jak2-V617F knock-in mouse model for assessing therapeutic efficacy in myeloproliferative neoplasms.

Ailin Yang, Shuang Li, Qingqing Qi, Yi Li, Ruilin Sun

GenoBioTX LLC, Sugar Land, TX

Background: Myeloproliferative neoplasms (MPN) are a group of malignant hematological disorders characterized by excessive proliferation of blood cells and are often accompanied by splenomegaly, thrombosis, and bleeding tendencies. The main subtypes of MPN include polycythemia vera (PV), essential thrombocythemia (ET), and primary myelofibrosis (PMF). The acquired somatic JAK2-V617F mutation occurs in approximately 95% of PV cases and in about 50% of ET or PMF patients. This mutation results in constitutive activation of the JAK2 kinase signaling pathway, establishing it as a critical therapeutic target in MPNs. Therefore, to enable preclinical evaluation of therapies targeting this mutation, we developed a novel Jak2-V617F knock-in mouse model.
Method: Firstly, we generated Jak2-Flox-V617F mice by inserting the inverted exon 14 cassette (carrying the c.1849 G>T, p. V617F mutation) flanked by antiparallel loxp sites into the endogenous *Jak2* exon14 locus via ES cell-based gene targeting. These mice were then crossed with Vav1-Cre mice to obtain heterozygous Jak2-Flox-V617F/Vav1-Cre offspring (Jak2-V617F mice), in which Cre-mediated recombination induces Jak2-V617F expression specifically in the hematopoietic cells. The mutant mice were phenotyped using blood routine analysis, flow cytometry, H&E staining and pathology analysis. Finally, we tested the JAK inhibitor Ruxolitinib, a clinical agent for myelofibrosis, for its efficacy in this model.
Results: Compared with wild-type mice, Jak2-V617F mice exhibited significantly elevated hemoglobin and hematocrit levels, marked thrombocytosis, increased neutrophils, alopecia and splenomegaly at 8 weeks. By 28 weeks, pathology analysis revealed megakaryocyte hyperplasia and extramedullary hematopoiesis in bone marrow, spleen, and liver in Jak2-V617F mice. Notably, these hematological abnormalities and splenomegaly were significantly mitigated by oral administration of Ruxolitinib.
Conclusion: Taken together, our Jak2-V617F mouse model provides a unique platform for studying the mutation of Jak2 in the hematopoietic cells and evaluating the efficacy of potential therapeutic targets in preclinical studies.

: Computational, Technological, and Mechanistic Advances
Poster Session

#0974 AI-driven- structure-based drug discovery and validation of novel compounds as CTLA-4/B7 inhibitors.

Poonam Kalhotra[1], Tzayhri Gallardo-Velazquez[2], Guillermo Osorio-Revilla[3], Veera Chandra Sekhar Reddy Chittepu[4]

[1]Medical Oncology, Jerome Lipper Multiple Myeloma Disease Center, Dana-Farber Cancer Institute, Harvard Medical School, Boston,, MA,[2]Departamento de Biofisica, Escuela Nacional de Ciencias Biologicas, Instituto Politecnico Nacional, Mexico City, Mexico,[3]Departamento de Ingenieria Bioquimica, Escuela Nacional de Ciencias Biologicas, Instituto Politecnico Nacional,, Mexico City, Mexico,[4]Harvard Medical School/Brigham and Women's Hospital, Boston, MA

In recent years, CTLA-4/B7 immune checkpoints have been well known to suppress T-cell activation, with implications for patient survival under targeted therapeutics. Monoclonal antibodies targeting this immune checkpoint pathway have proven effective, and the use of recently FDA-approved antibodies clearly demonstrates their clinical and therapeutic value, showing promise across solid and hematologic cancers. However, the potential of small molecules derived from nature as future CTLA-4/B7 inhibitors remains largely unexplored. Naturally occurring compounds, as sources of chemical diversity, could yield novel leads for immune checkpoint inhibition. This approach may serve as one of the core strategies in modern immuno-oncology, complementing antibody-based therapies to improve patient outcomes in clinical settings.
In this study, we developed CTLA-4/B7-specific machine learning (ML) and artificial intelligence (AI) models, along with 3D-QSAR models, to assist in ligand discovery as CTLA-4/B7 inhibitors. Structure-based virtual screening of compounds arising from natural sources was performed. Any compound predicted by our AI models as positive served as a candidate for subsequent structural biology studies. Protein-ligand interactions were investigated using molecular docking simulations, and the stability of resulting CTLA-4-inhibitor-B7 complexes was assessed using molecular dynamics simulations.To study biological relevance, we employed a PBMC-based functional assay and a tumor-relevant co-culture model (PBMC-B7 + tumor cells) to determine whether discovered leads could restore T-cell cytokine responses suppressed through CTLA-4/B7 engagement, complementing binding studies.
Our ML/AI models prioritized flavones as new potential CTLA-4/B7 inhibitors, predicting binding affinity and favorable IC_{50} values. Molecular dynamics simulations further confirmed the stability of protein-flavone interactions. Experimentally, we selected chrysin, naringenin, and morin as representative molecules to validate that our workflow has potential to aid in the discovery of CTLA-4/B7 inhibitors. Functional assays revealed that flavones restored cytokine production suppressed as a result of CTLA-4/B7 engagement, thereby validating their immunological activity.Overall, our approach broadens therapeutic possibilities beyond antibody-based blockade, offering benefits in combination with existing therapeutics. The leads discovered may serve as starting points to develop derivatives that could advance next-generation immuno-oncology therapeutics to improve cancer care.

#0975 Deep learning-based screening and design of novel therapeutics that reverse cancer-associated transcriptional phenotypes.

Jing Xing[1], Mingdian Tan[2], Dmitry Leshchiner[1], Mengying Sun[3], Shreya Paithankar[1], Rama Shankar[1], Erika Lisabeth[3], Bilal Aleiwi[3], Ruoqiao Chen[3], Matthew Giletto[3], Richard Neubig[3], Samuel So[2], Edmund Ellsworth[3], Mei-Sze Chua[2], Jiayu Zhou[4], **Bin Chen**[1]

[1]Michigan State University, Grand Rapids, MI,[2]Stanford University, Palo Alto, CA,[3]Michigan State University, East Lansing, MI,[4]University of Michigan, Ann Arbor, MI

Identifying drugs that reverse expression of disease-associated transcriptomic features has been widely explored as a strategy for discovering drug repurposing candidates, but its potential for novel compound discovery and optimization remains largely underexplored. Here, we present a deep learning-based drug discovery platform, guided by transcriptomic features, that screens large compound libraries and optimizes lead compounds. We first develop a model that predicts gene expression changes solely from chemical structures and deploy it to infer the expression changes induced by compounds in large screening libraries. We then refine compound scoring and employ a Monte Carlo Tree Search method for multi-objective optimization. By incorporating Structure-Gene-Activity Relationships, we uncover drug mechanisms directly from transcriptomic data. To demonstrate the utility of the system, we identify and validate compounds for hepatocellular carcinoma (HCC). In HCC, we design a novel compound that improves the IC_{50} from 4 μM to 0.5 μM, with increased *in vitro* selectivity, favorable pharmacokinetics and *in vivo* activity.

#0976 FGFR3-TACC3 fusion: multi-omics and machine learning characterization across tumor types.

Manuel Pedregal[1], Esther Cabanas Morafraile[2], Balazs Győrffy[3], Ester Garcia[4], Miriam Dorta[4], Bernard Gaston Doger de Speville[4], Emiliano Calvo[5], Alberto Ocana[6], Victor Moreno Garcia[4]

[1]START - Madrid, Madrid, Spain,[2]Center for Biological Research Margarita Salas (CIB-CSIC), Spanish National Research Council, Madrid, Spain,[3]Institute of Transdisciplinary Discoveries, Medical School, University of Pecs, H-7624, Pecs, Hungary, Budapest, Hungary,[4]START - Madrid - FJD, Madrid, Spain,[5]START Madrid CIOCC - Catedra Intheos-START-CEU, Madrid, Spain,[6]Catedra INTHEOS-START-CEU, Madrid, Spain

Background: The FGFR3-TACC3 (FGFR3-TACC3) fusion is a recurrent oncogenic alteration observed in gliomas, urothelial, and head and neck cancers. This fusion drives constitutive FGFR3 kinase activation and disrupts mitotic spindle organization through TACC3, leading to uncontrolled proliferation and transcriptional reprogramming. To elucidate the molecular landscape and therapeutic vulnerabilities of FGFR3-TACC3-positive tumors, we integrated genomic, transcriptomic, and computational analyses.
Methods: Transcriptomic data from TCGA cohorts were analyzed to compare FGFR3-TACC3-positive and wild-type tumors. Differentially expressed genes (fold change > 2 or < -2) were intersected with druggability databases to identify actionable targets. In parallel, we analyzed 58 FGFR3-TACC3 fusion samples and 9,642 non-fusion cases to determine recurrently mutated genes and enriched Gene Ontology (GO) terms. A combined neural network and random forest classifier was trained on mutational and functional features to discriminate fusion from non-fusion profiles.
Results: FGFR3-TACC3 fusion tumors exhibited a distinct transcriptional and mutational signature, including 1,984 upregulated and 2,504 downregulated genes, with enrichment in RTK/MAPK signaling, mitotic spindle assembly, and vesicle transport pathways. Integration with pharmacologic databases revealed 48 co-expressed druggable genes, encompassing oncogenic kinases (FGFR3, EGFR, CDK4, PDGFRA, NTRK3) and neurotransmission-associated receptors (OXTR, ADORA1, GRIA3/4). Machine-learning analysis identified 9 recurrently mutated genes and 69 informative GO terms, achieving an AUC of 0.85 and accuracy of 0.79, highlighting a robust functional signature of FGFR3-TACC3 fusion tumors.
Conclusions: This integrated multi-omics and machine-learning study suggests a functional, transcriptional, and pharmacologic landscape of FGFR3-TACC3 fusion-driven cancers. The combined mutation-GO-transcriptome framework uncovers potential druggable co-dependencies and provides hypotheses for rational combination strategies and precision therapies for FGFR3-TACC3-positive tumors that warrant experimental validation.

#0977 VINI: A multimodal *in silico* platform for discovering rational drug combinations in KRAS-mutant pancreatic cancer.
Drasko Tomic

Ruđer Bosković Institute, Zagreb, Croatia

Rational combination therapies are urgently needed for aggressive KRAS-mutant cancers such as pancreatic ductal adenocarcinoma (PDAC), which has a 5-year survival rate below 10%. VINI is a multimodal *in silico* platform that integrates AI, quantum-informed algorithms, pathway modeling, and structural data to accelerate the discovery of effective drug combinations. Its foundation is based on KEGG cancer pathways, with gene expression and mutation data from the Cancer Cell Line Encyclopedia (CCLE), molecular structures from PubChem and DrugBank, three-dimensional protein structures from RCSB PDB or AlphaFold predictions, and protein sequences from UniProt and DrugBank (for monoclonal antibodies), capturing disease-specific biology.
VINI uses AI and semi-empirical quantum-informed virtual screening (planned for implementation in the upcoming Horizon project) to predict intracellular drug efficacy and multi-drug synergy. Classical computational chemistry tools, including Rosetta, AutoDock Vina, UCSF Chimera, and Scripps MGLTools, are used by VINI to generate high-quality predictions, with high-performance computing enabling rapid evaluation.
Proof-of-concept studies demonstrated VINI's ability to predict novel triple-drug combinations targeting ALK, BCL-2, mTOR, DNA repair, and androgen pathways in hormone-sensitive prostate cancer, achieving 79.3% agreement with clinical outcomes across 16 cancer types and 100% for DU-145 and PC3 lines. VINI has also been applied to SARS-CoV-2 drug combinations, illustrating its broad applicability.
In the upcoming EU Horizon project, VINI will be instrumental in identifying effective three-drug combinations against KRAS-mutant PDAC: (1) novel KRAS inhibitors developed at the University of Toronto, (2) DNMT1 inhibitors discovered at RBI, and (3) targeted monoclonal antibodies against PDAC hallmarks, also identified at RBI using VINI. Through this multinational consortium - including the University of Toronto, Lund University, Fraunhofer, EPFL, and seven other leading institutions - VINI will integrate AI, structural modeling, and computational chemistry to provide actionable insights for treatment-resistant cancers and guide future preclinical validation.

#0978 Deep learning frameworks for translating cancer drug response from cell-level to patient-level by modeling transcriptome.

Sun Kim[1], Bonil Koo[1], Dongmin Bang[2], Inyoung Sung[1], Changyun Cho[2], Sangseon Lee[3], Kyoung Jae Won[4]

[1]Seoul National University, Seoul, Korea, Republic of,[2]AIGENDRUG Co. Ltd., Seoul, Korea, Republic of,[3]Inha University, Incheon,[4]Cedars-Sinai Medical Center, Los Angeles, CA

Introduction: Measuring perturbations of the transcriptome upon drug treatment can be highly informative, yet perturbed transcriptome profiles are often unavailable at both the cell-level and the patient-level. A key challenge, therefore, is how to infer such unobserved drug responses. Because drug treatment perturbs not only individual gene expression levels but also the underlying gene-gene interactions, the major challenge is how to model perturbations of these gene-gene interactions at the gene-level in LINCS so that unobserved drug responses of cancer cells and patients can be inferred.
Methods: To predict unobserved perturbation of transcriptome after drug treatment, we have developed a deep learning model that captures perturbations of gene-gene interactions in LINCS, Condition-Specific Gene-Gene Attention (CSG2A, *Bioinformatics/ISMB* 2024). CSG2A models dosage- and time-dependent transcriptome perturbation and serves as as *perturbation-based* pretrained model. As change in transcriptome can be also seen as transcriptomic cellular state change, we used an existing pre-trained *rank-based* model (Geneformer, *Nature* 2024). Given these models of transcriptomic changes, we model the cancer patient in two different approaches in terms of transcriptome profiles. In the first approach, a deep learning model, called THERAPI, embeds a tumor by combining arbitrary sets of cancer cells in GDSC, after which perturbations of gene-gene interactions are predicted with the *perturbation-based* and *rank-based* models. In the second approach, we proposed PREDIKTOR, which uses a network-based representation of the patient transcriptome with DysRegNet (*British Journal of Pharmacology* 2024), and then predicts drug-induced perturbations of gene-gene interactions using the *perturbation-based* pre-trained model.
Results: We developed two computational frameworks for predicting patient-level drug response from cell-line response, THERAPI and PREDIKTOR. Both THERAPI and PREDIKTOR outperformed existing deep learning models with significant margin up to 8.5% improvement in experiment with TCGA data and the I-SPY2 patient cohort.
Conclusion: These two frameworks are being deployed on the Amazon cloud as “DrugVLAB^{TM} response” so that any researchers around the world can utilize for drug response prediction. Our systems can evolve with upcoming deep learning models, propriety or public, for more accurate drug response prediction.

#0979 DrugVLAB for oncogenic kinase inhibitor generation.

Sun Kim[1], hyerin kim[2], Bokyung Park[2], Joonho Seong[2], kim youngkuk[1], Seokchol Hong[2], Changyun Cho[2], Heejoon Chae[3], Kyoung Jae Won[4]

[1]Seoul National University, Seoul, Korea, Republic of,[2]AIGENDRUG Co. Ltd.,, Seoul, Korea, Republic of,[3]Sookmyung Women's University, Seoul, Korea, Republic of,[4]Cedars-Sinai Medical Center

Introduction: The dysregulation of kinases is a major mechanism for cancer development and progression. Rapid advances in generative deep learning technologies now allow models to generate candidate kinase inhibitors. However, with over 500 human kinases, the major challenge is to design inhibitors that are highly selective for the oncogenic kinase without blocking other essential ones. Thus, all generated molecules need to be tested rigorously for interactions with specific residues and overall affinity to pockets of both target and off-target kinases. This task requires orchestrating multiple AI tools in a well-defined workflow, which is not trivial to researchers.

Methods: To address the challenges, we developed DrugVLAB for Kinase Inhibitor Generation, a comprehensive Amazon cloud-based workflow, built through our collaboration, that enables human-in-the-loop search.*Workflow*: The workflow consists of more than 20 cutting edge AI tools. It begins with in-house fragment-based molecule generations (ICLR 2025). Users can specify requirements such as residue-atom interactions and drug-likeness filters using in-house tools (JCIM 2025, ICML 2025, ISMB 2025). Candidate molecules then undergo docking simulations with Autodock Vina, followed by additional filtering based on residue-atom interactions while considering docking pose. Finally, drug target affinity (DTA) can be rigorously checked using in-house tools (ICLR 2025, ISMB 2025). At this stage, molecules are ranked by DTA values for synthesis and evaluation. As molecules are generated with fragments, most of them are synthesizable. This will conclude the execution of one round of DrugVLAB^{TM} for Kinase. A unique and notable feature of our cloud system is to incorporate assay results of newly synthesized and evaluated molecules. Our system identifies fragments or substructures enriched in active and inactive molecules. With these new fragment sets, itinitiates the next round of assay-guided molecule generation. Our experience is that better, more active molecules are generated as the round goes on.

Results: DrugVLAB can generate 3000 molecules on Amazon cloud in 2.5 hours and a complete round of evaluation can be done in 2.5 hours for a target kinase and five off-targets.

Conclusion: Our system is implemented on Amazon cloud, enabling researchers around the world to generate and evaluate molecules as kinase inhibitors. DrugVLAB for kinase is designed in a modular way so that any newly developed AI tools can be incorporated easily and timely.

#0980 Multimodal chemogenomic modeling-based drug repurposing for targeted therapy of PDAC.

Adil Ibrahim Mohammed[1], Zhaowei Han[2], Yuanhao Huang[2], Zihe Meng[3], Jie Liu[2], Shuibing Chen[3]

[1]Cornell University/Weill Cornell Medicine, Ithaca, NY,[2]University of Michigan, Ann Arbor, MI,[3]Weill Cornell Medicine, New York, NY

Pancreatic Ductal Adenocarcinoma (PDAC) is a disease with a high mortality rate primarily due to its aggressive nature, late-stage prognosis, and limited effective treatment regimens. Current standard-of-care drugs for treatment include Gemcitabine and the combination drug FOLFIRINOX. However, precision and personalized treatment for PDAC is still missing. Mutations of *KRAS*, *TP53*, and *SMAD4* are the most common and highly effective genetic mutations in PDAC, resulting in the initiation, proliferation, and therapy resistance of tumor cells. Though drug candidates and inhibitors of $KRAS^{G12D}$, the most prevalent *KRAS* mutation, are being tested in clinical trials but mutations of $TP53^{R172H}$ and *SMAD4*, seen in 70% and 50% of PDAC cases respectively, remain to be effectively targeted because precision therapy is restricted. To address this challenge, we propose a precision medicine-based drug repurposing strategy to identify and prioritize mutation-specific drug candidates and their combinations for PDAC treatment. Using an isogenic murine organoid platform developed by our lab, we integrate multimodality data, including in house Whole Genome Sequencing (WGS), single cell RNA-seq (scRNAseq) and a preliminary drug screening library. We first compute Differentially Expressed Genes (DEGs) from scRNAseq data and a list of acquired gene mutations from WES data for each of the isogenic organoids lines and then query these gene signatures to computationally screen for potential drug compounds against the Connectivity Map touchstone dataset by computing a similarity based enrichment score. Next, using the chemical screening library of ~5000 compounds, we perform molecular docking simulations against the target proteins associated with the three driver mutations and run a Quantitative Structure Activity Relationship (QSAR) analysis to pinpoint chemical scaffolds and functional groups associated with stronger activity, thereby refining candidate hits from the Connectivity Map analysis. We also use the docking scores to perform an in-silico perturbation screen to capture downstream shifts in order to synergize target identification and engagement. We finally present high confidence drug candidates to target $KRAS^{G12D}$, $TP53^{R172H}$ and *SMAD4* identified through an integrated chemo-omics analysis. Ongoing work includes computational validation to top hits using Cancer Drug Response models and in vitro validation of selected drugs and combinations.

#0981 MTA-DTA: A multi-token attention framework for drug-target binding affinity prediction.

Il-san Jeong, Seung-Woo Baek, Jee-Woo Seo, Yeo-Gyeong Yoon, Jae-Yoon Kim, Seon-Young Kim, Seon-Kyu Kim

Genomic Medicine Research Center, Korea Research Institute of Bioscience and Biotechnology, Daejeon-city, Korea, Republic of

Backgrounds: Accurate prediction of drug-target affinity (DTA) is a key step in drug discovery, but experimental measurement remains costly and time-consuming. Deep learning-based approaches have recently shown strong performance using sequence- or graph-level representations of drugs and proteins, and attention mechanisms provide interpretability by highlighting key molecular subsequences. However, conventional attention computes dependencies between single token pairs, which cannot fully capture the cooperative and multi-residue binding behaviors that characterize real protein-ligand interactions.
Methods: We propose a Multi-Token Attention (MTA)-based DTA model that models both global and local interaction contexts between drug and target proteins. The model was trained and evaluated on the widely used Davis and KIBA benchmark datasets for binding affinity prediction. Protein sequences and drug SMILES were both embedded using pretrained models - ESM2 (esm2_t33_650M_UR50D) for proteins and ChemBERTA (ChemBERTAa-77M-MTR) for compounds. The MTA module incorporates key-wise convolution to aggregate local token neighborhoods before attention calculation and head-mixing convolution to fuse inter head information, allowing multi-token contextual dependencies.
Results: Across two benchmark datasets, MTA-DTA consistently outperformed prior methods. On Davis, it achieved an MSE of 0.225, R^2 of 0.7155, and CI of 0.8796. On KIBA, it reached an MSE of 0.1612, R^2 of 0.7661, and CI of 0.8781, exceeding the performance of existing DTA models. In addition, qualitative analyses of the attention maps revealed that MTA captured biologically meaningful binding regions, highlighting continuous residue segments and sub-structural motifs rather than isolated token pairs. This indicates that the model effectively integrates both local chemical context and global interaction patterns, leading to improved accuracy and interpretability in drug-target affinity prediction.
Conclusion: In summary, the MTA-DTA model enhances conventional attention by extending it from single-token to multi-token interaction modeling, thereby bridging the gap between sequence-based learning and the true cooperative nature of molecular binding. By incorporating key-wise and head-mixing convolutions, the model gains the ability to represent local interaction motifs while maintaining global dependency awareness, resulting in more biologically realistic affinity predictions.

#0982 Pharmacophore profiling highlights diverging binding modes of nemtabrutinib and ibrutinib across tyrosine kinases.

Charly Empereur-mot[1], Giulio Sartori[2], Luca Pesce[1], Filippo Spriano[2], Chiara Tarantelli[2], Luciano Cascione[2], Alberto J. Arribas[3], Luca Aresu[4], Davide Rossi[2], Giovanna L.M. Damia[5], Massimo Broggini[5], Daniela Polino[1], Francesco Bertoni[2]

[1]Department of Innovative Technologies, University of Applied Sciences and Arts of Southern Switzerland, Lugano, Switzerland,[2]Institute of Oncology Research, Bellinzona, Switzerland,[3]Universita della Svizzera italiana, Lugano, Switzerland,[4]Department of Veterinary Science, Grugliasco (TO), Italy,[5]Istituto di Ricerche Farmacologiche Mario Negri IRCCS, Milan, Italy

Background. Commanding kinase selectivity remains a major bottleneck in the discovery of targeted anticancer drugs, with homologous ATP-binding pockets leading to off-target inhibition, toxicity, and reduced clinical effectiveness. Addressing these difficulties, we present a streamlined computational workflow allowing rationalizing selective compound activity by capturing subtle, transient structural differences across many homologous kinases. We demonstrate our approach by characterizing the diverging mechanisms of action of nemtabrutinib and ibrutinib in cell lines derived from two specific B-cell lymphoma subtypes (activated B-cell like [ABC] and germinal-center B-cell like [GCB] DLBCL), correlating *in vitro* anti-tumor activity with *in silico* selectivity scores computed across 20 tyrosine kinases.

Methods. To enable high-throughput, cost-efficient parallel processing of ATP-binding pocket variants, as a preliminary step we compiled a subset of metastable pocket conformations adopted by tyrosine kinases (DFG motif and associated dihedral) with and without generic compound binding (templating with AlphaFold2 and publicly available data). The structural alignment of this conformational dictionary and its processing via structure-based pharmacophore methods (CDP:Kit) produced rich maps of kinase pocket interactomes. Fitting compounds into these maps then enabled scoring matching pharmacophore features and computing a relative selectivity score between kinases for each compound (CDP:Kit and lightweight binding energy estimations) using BTK as baseline for confirmed targeting.

Results. We deciphered the synergistic interplay of 10 residue locations within the extended ATP-binding pocket, responsible for the selective binding of nemtabrutinib and ibrutinib across tyrosine kinases. As aligned to human BTK sequence and specifying potential for modified interactions, we highlight reference locations: Q412 (loop-mediated covalent binding, none), V416 (hydrophobic, H-bond), F442 and M449 (hydrophobic, sulfur-aromatic, cation-pi), L460 and I472 (hydrophobic, sulfur-aromatic, pi-stacking), T474 (hydrophobic, halogen-bond, H-bond, sulfur-aromatic, pi-stacking), C481 (covalent binding, H-bond, none), N484 (H-bond, none) and L542 (hydrophobic, sulfur-aromatic, none).

Conclusions. We demonstrate a general strategy for rational, structure-guided characterization of selective compound activity across conserved kinase families. Our approach enabled characterizing the diverging binding modes of nemtabrutinib and ibrutinib across 20 kinases, in agreement with anti-tumor activity data and expression levels in cell lines derived from two B-cell lymphoma subtypes. We identified FYN, FRK and MAST1 as likely targets of nemtabrutinib and not of Ibrutinib, responsible for GCB DLBCL non-proliferation.

#0983 Beyond the active site: Discovery of novel PYCR1 allosteric binding sites via structure-oriented fragment crystallographic screening.

Olha Tarkhanova[1], Kaylen R. Meeks[2], Juan Ji[3], Caitlin J. Mattingly[3], Jay C. Nix[4], Mykola Protopopov[1], John J. Tanner[3]

[1]Chemspace LLC, Charlotte, NC,[2]Brookhaven National Laboratory, Upton, NY,[3]University of Missouri, Columbia, MO,[4]Lawrence Berkeley National Laboratory, Berkeley, CA

Pyrroline-5-carboxylate reductase 1 (PYCR1), a member of the PYCR enzyme family, plays a pivotal role in the proline biosynthesis pathway. Enzymes involved in proline metabolism have been increasingly recognized as key regulators of cancer cell metabolic reprogramming, contributing to enhanced proliferation, survival, metastasis, and resistance to stress. Overexpression of PYCR1 has been consistently reported across multiple malignancies, including hepatocellular carcinoma, breast cancer, gastric cancer, bladder cancer, and lung cancer, as well as in fibrotic disorders. These observations highlight PYCR1 as an attractive therapeutic target for oncology drug discovery.

Despite its therapeutic potential, PYCR1 remains an understudied target, with limited data available on active small-molecule ligands and binding site characterization. Consequently, the discovery of novel chemical probes is critical both for validating PYCR1's role in disease pathology and for initiating structure-based drug design campaigns.

To this end, a fragment-based screening campaign was initiated using a focused subset of carboxylic acid-containing fragments from the Enamine fragment library. The subset was rationally designed through molecular docking of fragment-like, carboxylic acid-containing compounds from Enamine's in-stock collection, targeting the active site of PYCR1. A total of 37 fragments were selected and screened via X-ray crystallography. This screen yielded eight fragments with confirmed binding to the PYCR1 active site, as determined by co-crystal structures. Among these, three compounds demonstrated inhibitory activity in biochemical assays, with IC_{50} values ranging from 29 µM to 5.4 mM.

Encouraged by these results, a follow-up screen was conducted using 22 fragment-like compounds containing bioisosteres of the carboxylic acid functional group (e.g., tetrazoles, oxadiazoles) and sulfonic acid groups, to explore alternative chemical scaffolds. This second crystallographic screen identified one additional active-site binder. Importantly, at least two previously uncharacterized allosteric binding sites were discovered, both of which showed a measurable inhibitory effect on PYCR1 enzymatic activity. These findings open promising new avenues for the development of non-classical inhibitors targeting PYCR1.

#0984 MHC-associated peptide proteomics for immunogenicity risk assessment of immuno-oncology drug candidates.

Chloe Ackaert[1], Jana Schockaert[1], Aurelie Mazy[1], **Christoph Schifflers**[1], Martijn Vlaming[1], Elise Pepermans[2], Sofie Pattyn[1]

[1]IQVIA Laboratories, Gosselies, Belgium,[2]ImmuneSpec, Niel, Belgium

Traditional monoclonal antibodies and bispecifics have shown great promise for the treatment of various tumor entities. However, managing unwanted immunogenicity has become a challenge in the development of these promising therapeutics as there is a trend towards higher unwanted immune responses compared to classical monoclonal antibodies. Thorough assessment of their immunogenic potential is a crucial step in the development of safe biotherapeutics with high treatment efficacy. MHC-associated peptide proteomics (MAPPS Assay) enables the precise identification of all the regions of a protein that may evoke an immune response. High-sensitive MAPPS workflow in combination with high quality primary cells leads to higher numbers of identified self + non-self peptides and provides the analysis depth required for confident immunogenicity derisking and modulation. Here, we report the importance of peptides presented by HLA-DP and HLA-DQ (next to the standard HLA-DR presented peptides). Next, we also showed the first ever comparison of presented peptides by true immune cells: myeloid dendritic cells *versus* monocyte derived dendritic cells.

#0985 Anticancer efficacy of tricarbonylperrhenato(bathophen)rhenium(I) organometallic compound in pancreatic ductal adenocarcinoma.

Ishita Saha[1], Cecilia Parpinelli[2], Birsen Varisli[3], Santosh Mandal[3], **Santanu Bhattacharya**[1]

[1]Mayo Clinic Florida, Jacksonville, FL,[2]University of Central Florida, Orlando, FL,[3]Morgan State University, Baltimore, MD

Organometallic rhenium compounds have become powerful anticancer agents that show possibilities as a substitute for traditional platinum-based medications. While platinum-based chemotherapeutics like FOLFIRINOX and cisplatin are frequently used to treat pancreatic ductal adenocarcinoma (PDAC), they have a number of side effects, such as ototoxicity, neurotoxicity, nephrotoxicity, and peripheral neuropathy. Hepatotoxicity, cardiotoxicity, gastrointestinal toxicity, cytopenias, anaphylaxis, pain, alopecia, anorexia, cachexia, and asthenia are other commonly reported adverse effects.
However, ligands based on rhenium have been shown to preferentially cause cytotoxicity in cancer cells while avoiding harm to healthy cells. This suggests that rhenium could be a safer and more effective cancer treatment option. Different rhenium compounds with different ligands have been produced by Mandal et al. for a range of medicinal uses. In this work, we assessed the therapeutic potential of tricarbonylperrhenato(bathophen)rhenium(I) (PR-6) in PDAC. The cytotoxic effects and IC_{50} value of PR-6 were assessed in the metastatic pancreatic cancer cell line AsPC-1 using the MTS assay. The IC_{50} value for PR-6 in AsPC-1 cells was determined to be 5.85 µM. PR-6 treatment significantly inhibited cell growth, migration, and survival at the IC_{50} concentration, with a post-treatment survival rate of 2.3 ± 3.97%. Furthermore, PR-6 treatment led to the downregulation of phosphorylated MEK (pMEK) and phosphorylated P38 (pP38) protein expression, indicating its modulatory effect on the MAPK signaling pathway. According to our research, PR-6 has a great therapeutic promise for treating pancreatic cancer and efficiently alters the tumor microenvironment in PDAC cells.

#0986 Silyl ethers analogs of SN-38 with unique blue-fluorescent properties exhibit potent anti-cancer activity through topoisomerase I inhibition.

Sanika Vaidya[1], Ashley Mo[1], Alyssa Yee-Xin Chia[1], Katelyn Li[1], Shreya Somani[1], Isabella Lo[1], Lekhya Menta[1], Gary Johanning[2], Feng Wang-Johanning[2], **Edward Njoo**[1]

[1]Chemistry, Aspiring Scholars Directed Research Program (ASDRP), Fremont, CA,[2]SunnyBay Biotech, Fremont, CA

Topoisomerase I inhibitors, such as deruxtecan and irinotecan, represent an important class of cell cycle inhibitors in the treatment of cancers. Among these, silylated topoisomerase inhibitors, including DB-67 and karenitecin, have exhibited increased antiproliferative potency. In this study, we prepared and evaluated the biological activity of four synthetic SN-38 analogs bearing the tert-butyldimethyl, tert-butyldiphenyl, triisopropyl, and dimethylthexyl siloxy groups, blocking a key metabolic site and imbuing bright blue-fluorescent properties in such compounds. When evaluated against colorectal, TN breast cancer, and ovarian, non-small cell lung, and liver cancer models, we observed comparable or greater antiproliferative activity. Our dimethylthexyl siloxytecan demonstrated the greatest potency among the four analogs, with a 96 hour IC50 of 6 nM in HCT-116 cells. Correspondingly, analysis by flow cytometry indicates that the siloxytecans, compared to their parent compounds, display comparable apoptotic activity and increased cell cycle G2 arrest. Uniquely, we demonstrate that the enhanced fluorescence of these compounds enables real-time, quantitative visualization of the dynamics and selectivity of intracellular uptake through fluorescence microscopy without the need for extensive sample preparation or installation of auxiliary fluorophores, with the dimethylthexyl siloxytecan displaying the greatest rate of cellular uptake. Additionally, quantification of relaxed and nicked DNA levels via cell-free biochemical studies suggests that these siloxytecans largely exhibit increased topoisomerase inhibition from SN-38. Further computer modeling studies validated that differences in potency and permeability were not attributed to the siloxytecans' positioning within the Topoisomerase I-DNA binding pocket. This initial SAR is further supplemented by an evaluation of these compounds' DMPK properties and metabolic stability, with an assessment of different in-vivo delivery strategies. Moreover, direct tissue injection of the siloxytecans has demonstrated exceptional tissue retention and durability, establishing the dimethylthexyl siloxytecan as a preclinical lead for in vivo evaluation. Collectively, these studies demonstrate improved intracellular delivery of topoisomerase inhibitors with the introduction of silicon-containing motifs and highlight the utility of these compounds for enhanced anticancer activity with unique lipophilicity and fluorescent properties that enable quantitative tracking of compound distribution in cancer cells, which is currently being investigated for in vivo activity in triple negative breast cancer studies.

#0987 Optimization of bioinformatics parameters for DIA-based proteomics in targeted protein degradation.

Hui Zhou, Yi Liu, Aijuan Yu, Naizhong Zheng

DeepKinase Biotechnologies Ltd., Beijing, China

Targeted Protein Degradation (TPD) is a transformative strategy for targeting oncoproteins previously considered undruggable. A central challenge in translating TPD compounds into viable cancer therapeutics is the accurate delineation of on-target efficacy from off-target toxicities, which is critical for patient safety and therapeutic efficacy. Data-Independent Acquisition (DIA) mass spectrometry provides the profound sensitivity and comprehensive proteome coverage necessary for systematically mapping protein abundance changes induced by TPD compounds. However, the accurate assessment of on-target efficacy and off-target effects critically depends on the selection of appropriate bioinformatic parameters in DIA proteomics data analysis. To address this, we conducted a systematic evaluation of key bioinformatic parameters. Our findings identify Unique Peptide filtering and Imputation as the most influential factors in precisely defining both on-target efficacy and off-target effects. Specifically, applying a UniquePep threshold ≥2 effectively minimized off-target misidentification. For imputation methods: when data was completely missing in treatment groups, row_min imputation yielded non-significant p-values; when data was partially missing, min imputation resulted in high intra-group variance with non-significant p-values. Therefore, we recommend row_min_half as a general-purpose imputation approach. Furthermore, we investigated the impact of peptide-level bioinformatic parameters on on-target efficacy and off-target effects. Our analysis revealed that high-abundance outlier peptides in control groups, low peptide detection rates in samples, and the selection of specific peptides to represent protein abundance significantly influence result accuracy. These confounding factors can be mitigated by filtering high-abundance outlier peptides, improving peptide detection rates, and implementing appropriate peptide-level missing value imputation, thereby optimizing the reliability of TPD outcomes. This study provides a critical, optimized framework for DIA proteomics analysis specifically tailored to TPD research. By ensuring accurate assessment of degrader specificity, this pipeline will accelerate the prioritization of lead compounds and de-risk the development of safer, more effective targeted protein degraders for cancer therapy.

#0988 Synthesis, characterization, and biological evaluation of polyisoprenylated phosphonyl ester inhibitors on triple-negative breast cancer.

Joshua Kofi Ablordeppey, Kweku Ofosu-Asante, Amarender Burra, Jahnissi Odoom, Desmond Kwakye, Nazarius S. Lamango

Florida A&M University College of Pharmacy & Pharmaceutical Sciences, Tallahassee, FL

Triple-negative breast cancer (TNBC) is an aggressive subtype lacking molecular targets and resistant to conventional therapy. Small GTPases such as RAS, RHO, and RAC regulate proliferation and cytoskeletal organization through prenylation and subsequent methylation-demethylation cycles. The methylation of prenylated cysteine residues by prenylated protein methyltransferase (PPMTase) and demethylation by polyisoprenylated methylated protein methyl esterase (PMPMEase) maintains GTPase turnover, activation and membrane localization. Overexpression of PMPMEase in cancers accelerates this cycle, disrupting the balance between methylated and demethylated states and sustaining aberrant MAPK and PI3K/AKT signaling that drives malignant growth. To selectively disrupt this process, polyisoprenylated phosphonyl ester inhibitors (PPEIs) were designed as irreversible, mechanism-based inhibitors that exploits PMPMEase's substrate recognition. Each PPEI incorporates a farnesyl tail that mimics the prenylated cysteine terminus of native substrates, promoting high-affinity binding and covalent modification of the catalytic serine. PPEIs were synthesized from farnesylated cysteine precursors and characterized by NMR and ion-trap mass spectrometry. Treatment of MDA-MB-231 and MDA-MB-468 cells with PPEIs produced dose-dependent reductions in viability and actin cytoskeletal integrity. NSL-AB-01 exhibited EC_{50} values of 4.1 µM (MDA-MB-231) and 3.3 µM (MDA-MB-468), while NSL-AJ-01 showed higher potency (3.2 µM and 2.7 µM, respectively). Actin-staining analysis revealed ~90% reduction in mean cell area, indicating impaired Rho-family GTPase signaling. Western blotting showed decreased p-AKT (-25% in MDA-MB-231; -50% in MDA-MB-468) and increased p-ERK (≈2.8-fold in MDA-MB-231; +70% in MDA-MB-468). To determine whether PPEI-induced cytotoxicity was associated with oxidative stress, intracellular ROS generation was quantified using DCFDA fluorescence. NSL-AJ-01 and NSL-AB-01 induced strong, concentration-dependent ROS production in TNBC cells. NSL-AJ-01 increased ROS levels approximately 25-fold in MDA-MB-231 and 24-fold in MDA-MB-468 at 3 µM ($p < 0.001$). NSL-AB-01 induced even greater oxidative responses, causing an approximately 32-fold increase of ROS in MDA-MB-231 and 30-fold increase in MDA-MB-468 at 3 µM ($p < 0.0001$). Together, these findings demonstrate that PPEIs induce oxidative damage to breast cancer cells, suppress pro-survival AKT signaling, and activate ERK-mediated stress pathways, driving cytoskeletal disassembly and reduced TNBC cell viability.

#0989 PTBP1-targeted siRNA reprograms cellular metabolism and induces apoptosis in human gastric cancer cells.

Hirokatsu Hayashi, Keita Matsumoto, Masashi Kuno, Masahiro Fukada, Ryuichi Asai, Yuta Sato, Itaru Yasufuku, Tajima Jesse Yu, Yoshihiro Tanaka, Manabu Futamura, Nobuhisa Matsuhashi

Gifu University, Gifu, Japan

Background: The prognosis of advanced gastric cancer remains poor despite recent therapeutic progress, underscoring the need for novel strategies. Cancer cells commonly rely on aerobic glycolysis (the Warburg effect). PTBP1 contributes to this metabolic phenotype by regulating the alternative splicing of the *PKM* gene, suppressing PKM1 and promoting the PKM2 isoform, which supports glycolytic metabolism. We hypothesized that PTBP1 inhibition would suppress tumor growth by shifting metabolic flux toward oxidative phosphorylation.
Methods: Thirteen chemically modified siR-PTBP1 derivatives were synthesized and tested in the gastric cancer cell line MKN1. Cell viability was measured by crystal violet staining. PTBP1 expression, PKM1/PKM2 isoform switching, ATP production, and apoptosis (cleaved PARP) were evaluated by Western blotting and ATP assay.
Results: Optimized siR-PTBP1 selectively reduced PTBP1 expression and increased the PKM1/PKM2 ratio, indicating metabolic reprogramming. ATP assay demonstrated that siR-PTBP1 treatment increased intracellular ATP production, supporting a metabolic shift from glycolysis toward oxidative phosphorylation. These metabolic changes were accompanied by elevated cleaved PARP levels, consistent with apoptosis induction. Consequently, siR-PTBP1 significantly inhibited MKN1 cell proliferation.
Conclusion: PTBP1 inhibition reprograms tumor metabolic pathways and triggers apoptosis in gastric cancer cells. siR-PTBP1 represents a promising metabolism-targeted nucleic acid therapeutic candidate, warranting further evaluation in in vivo xenograft models.

#0990 SR-B1 gene variants, inhibitors and the effect of glucose on IC50s in breast cancer.

Nandini Bhattacharya[1], Sree Aramgam[1], K. Sean Kimbro[2]

[1]Microbiology, Biochemistry, and Immunology, Morehouse School of Medicine, Atlanta, GA,[2]Morehouse School of Medicine, Atlanta, GA

Background: Ancestry-related genetic variations have been observed to influence the risk of certain cancers and diabetes through inherited genetic variations and their interaction with lifestyle and environment. Type 2 diabetes has been considered a risk factor for breast cancer, thus suggesting metabolism may drive cancer progression. The reverse cholesterol transporter and membrane receptor Scavenger receptor B1 (SR-B1), which is involved in insulin resistance and lipid metabolism, with its ancestry enriched variants, is evaluated in breast cancer as a novel target.
Methods: The triple negative breast cancer cell lines MDA.MB 231 and MDA.MB 468 were employed for this study. SNP genotyping to determine the genotype of each cell line was performed using the TaqMan SNP Genotyping assays for the SR-B1 missense SNP variant rs2293440. Cells were grown in media with varying glucose levels of 5.5 mM, 17.5 mM and 25 mM, representative of the blood glucose level indicator HbA1C. The cells were then treated with different concentrations of the SR-B1 inhibitor drug, Block lipid transport 1 (BLT-1), for total of 48 hours. After 48 hours, cell survivability assay was used to determine percent survival for each cell line under the conditions mentioned.
Results: The SNP genotyping results indicated that MDA.MB 231 contained the wild-type allele while MDA.MB 468 contained the variant allele. Results of the cell survivability assay showed that sensitivity of both the cell lines to BLT-1 was increased by 3-fold and 5-fold at 5.5 mM glucose concentration in media for MDA.MB 231 and 468 respectively, as was confirmed by the IC50 values. Both cell lines displayed resistance to BLT-1 at the higher media glucose concentrations of 17.5 and 25 mM with their IC50 values exhibiting up to a 5-fold increase. Further, MDA.MB 468 displayed almost 2-fold higher sensitivity to BLT-1 at both 5.5 mM and 17.5 mM media glucose concentration in comparison to MDA.MB 231.
Conclusions: These results indicate that there is a correlation between the blood glucose levels and the drug sensitivity or drug response in cancer. Further, our results suggest that the response to metabolism inhibitor drugs in cancer and glucose metabolism may also be impacted by the ancestry and genetic variation of an individual.

#0991 Synergistic effects of antineoplastic drugs and gap junction enhancer in heterogenous colorectal cancer.

Tomas Lugo[1], Annelise Nguyen[2]

[1]Texas Tech University, Lubbock, TX,[2]Texas Tech University, Amarillo, TX

Fibroblast tumor cell crosstalk, particularly through gap junction mediated signaling, is increasingly recognized as a modifier of colorectal cancer drug response. To test whether restoring gap junction function can enhance chemotherapy, we used co-culture spheroids composed of CCD-112 CoN fibroblasts and colorectal cancer cells (SW620, SW480, HT-29, or Caco-2) in a 1:1 ratio in 96-well plates. Doxorubicin, erlotinib, nilotinib, and cediranib were tested across multiple concentrations, alone and in combination with the gap junction enhancer, PQ, and drug interactions were quantified using the ZIP model, analytic tool and visualized using gigamap approach. For the combination treatment of doxorubicin and PQ, ZIP analysis revealed both antagonistic and synergistic regions. PQ alone and low concentrations of doxorubicin were predominantly antagonistic, with ZIP scores ranging from approximately 0.2 to −17.19. In contrast, high concentrations of both chemicals produced marked synergy, with a maximal ZIP score of 44.05 and an overall global ZIP synergy score of 4.53. On the 2D heatmap, this appears as largely additive to mild antagonistic effects at low to intermediate doses, with a distinct red hot spot of synergy in the upper-right corner (high [PQ]/high [Doxorubicin]). Consistently, the 3D surface plot shows a ridge of positive zip scores that increases with rising concentrations of both drugs. Together, these findings indicate that PQ enhances doxorubicin efficacy in a concentration dependent manner, with synergy restricted to a specific high-dose window rather than across all dose combinations. Similarly, the BCR-ABL targeted therapy nilotinib displayed a biphasic response in combination with PQ, characterized by two synergistic peaks at low and high concentrations separated by an antagonistic valley at intermediate doses. In conclusion, these results highlight both the synergistic and antagonistic properties of PQ with commonly used antineoplastic agents and support the approach of combinational treatment for colorectal cancer.

#0992 A novel targeted protein degradation platform based on internalization-enhancing peptide for lysosomal degradation of cell-surface proteins.

Dae Young Kim, Dahye Sim, Daeho Park, Yujin Park, Hee Young Kang, Hoil Choi

Peptron, Inc., Daeieon, Korea, Republic of

Targeted protein degradation (TPD) is an emerging therapeutic approach that enables the selective elimination of undesirable proteins with high specificity. Although TPD holds great promise for targeting traditionally undruggable proteins and overcoming resistance often seen with inhibition-based therapies, several challenges remain, including suboptimal pharmacokinetics, limited internalization, and the dependency on E3 ligases or lysosome-targeting receptors. Here, we present a novel TPD platform based on internalization-enhancing peptide (IEP). IEP binds tightly yet non-covalently to antibodies (Abs) without altering their structure and enhances Ab internalization. We hypothesized that IEP could promote lysosomal degradation of cell-surface proteins by facilitating internalization. To demonstrate its potential, Atezolizumab (ATZ), an FDA-approved monoclonal antibody targeting PD-L1, was used as a model. Since ATZ alone does not strongly induce PD-L1 internalization, it provides an ideal system to test IEP-mediated degradation. Indeed, PD-L1 protein levels were markedly reduced in MDA-MB-231 (TNBC) cells treated with ATZ-IEP (a non-covalent ATZ/IEP complex), whereas no reduction was observed with ATZ or IEP alone. The decrease in PD-L1 was blocked by BafA1, a lysosomal proteolysis inhibitor, but not by MG132, a proteasome inhibitor—indicating that ATZ-IEP mediates lysosomal, rather than proteasomal, degradation. To assess the generality of this effect, Durvalumab (DUR), another FDA-approved anti-PD-L1 antibody, and HCC827 (NSCLC) cells were tested. PD-L1 levels were reduced with DUR-IEP (a non-covalent DUR/IEP complex) to a similar extent as with ATZ-IEP, and ATZ-IEP also decreased PD-L1 expression in HCC827 cells, comparable to the effect observed in MDA-MB-231 cells. These results indicate that IEP functions broadly across different antibodies and tumor types. Intriguingly, using transgenic CHO cell lines with varying PD-L1 expression, we found that the extent of PD-L1 reduction increased as baseline PD-L1 expression decreased (~70 % in PD-L1^{Low} vs. ~20 % in PD-L1^{High}). This finding suggests that IEP may help overcome anti-PD-L1 resistance in tumors with low PD-L1 expression. In summary, ATZ-IEP mediates lysosomal degradation of PD-L1 and demonstrates broad applicability across antibodies and tumor types. Ongoing in vivo studies aim to confirm the efficacy of ATZ-IEP, further supporting the versatility of IEP as a novel TPD platform.

#0993 From phenotypic screening to mechanistic insight: Rational discovery of chemosensitizers for glioblastoma.

Lukas Gorecki, Lubica Muckova, Michaela Sadibolova, Ondrej Soukup

Biomedical Research Center, University Hospital Hradec Kralove, Hradec kralove, Czech Republic

Glioblastoma multiforme (GBM) represents the most aggressive form of primary brain tumor, characterized by rapid progression, therapeutic resistance, and near-universal recurrence. Despite multimodal treatment strategies—comprising maximal surgical resection followed by radiotherapy and temozolomide (TMZ)-based chemotherapy—median survival remains dismal, with most patients succumbing within one-year post-diagnosis. TMZ and ionizing radiation exert their cytotoxic effects primarily through the induction of DNA lesions, including single- and double-strand breaks. The cellular DNA damage response (DDR), encompassing a complex signaling network of kinases, repair enzymes, and checkpoint regulators, orchestrates the detection and repair of these lesions. Dysregulation or hyperactivation of DDR pathways—including those mediated by ATR/ATM signaling, PARP-dependent repair, and cell cycle checkpoints (e.g., WEE1, CDK1)—has been implicated in the pronounced therapeutic resistance of GBM. In this study, we pursued the rational design and synthesis of novel small molecules aimed at potentiating TMZ- and radiation-induced cytotoxicity in GBM. Over seventy compounds were generated across five focused series using structure-based design principles. Phenotypic screening was conducted in the TMZ-resistant T98G line and patient-derived GBM cultures to evaluate both intrinsic cytotoxicity and TMZ sensitization. Several lead candidates demonstrated superior chemosensitization efficacy compared to clinical DDR inhibitors. Interestingly, broad kinase profiling revealed an absence of canonical DDR kinase inhibition, indicating a potential non-classical mechanism of action. To delineate this mechanism, comprehensive quantitative proteomic analyses were performed, revealing modulation of pathways associated with DNA repair, stress response, and cell cycle control. The most promising candidates exhibited favorable pharmacokinetic and toxicological properties, along with effective blood-brain barrier penetration in vivo.

This work has been supported by the grant from the Ministry of Health of the Czech Republic (NW24J-03-00005); and by the Long-term development plan Military Faculty of Medicine, Healthcare Challenges of WMD II (DZRO-VLF22-ZHN II).

#0994 Selective oncolysis via oncomiR-driven DNA self assembly.

Akimitsu Okamoto[1], Kunihiko Morihiro[1], Makoto Yamamoto[2]

[1]University of Tokyo, Tokyo, Japan,[2]TKG Therapeutics, Inc., Tokyo, Japan

Introduction: Artificial nucleic acids attract significant attention as cancer immunotherapy materials because they can be recognized by various extracellular and intracellular nucleic acid sensors and stimulate innate immune responses. However, their low selectivity for cancer cells causes severe systemic immunotoxicity, hindering the realization of immune cancer therapy using artificial nucleic acid molecules. To address this challenge, we propose a hairpin DNA self-assembly technology that induces cytotoxicity through cancer-selective immune activation. Here, we discuss cancer growth suppression via DNA self-assembly triggered by overexpressed oncomiRs.

Experimental Design: Two hairpin DNA sequences were designed based on predictions of nucleic acid structural thermal stability (oHP-1 and oHP-2). This pair of hairpin DNAs (oHPs) triggered binding with one oncomiR, miR-21, forming a double-stranded DNA over 500 bp in length as a DNA aggregate. This structure is sufficiently large to induce innate immune activation. We examined the immune response induced by oHPs using cancer cells and tumor-bearing mice.

Results: DNA aggregates formed by oHPs bound to cGAS within cancer cells that abundantly express miR-21. Consequently, IFN-β was produced through the cGAS-STING pathway, resulting in selective cell killing. When oHPs were administered into tumors of cancer-bearing mice using an appropriate DDS, tumor growth was strongly suppressed. $CD8^+$ T cells and $CD4^+$ T cells were observed to accumulate at the periphery of the tumor tissue. While sufficient tumor growth suppression was observed with oHPs alone, higher efficacy was observed when combined with anti-PD-1 antibody.

Conclusions: This approach represents the first technology enabling selective tumor lysis derived from intracellular DNA self-assembly, providing a potent therapeutic modality for cancer treatment. The engineered oHPs assemble into long double-stranded DNA via cancer-associated miR-21, functioning as a selective immune amplifier and booster circuit for targeted tumor lysis. This design exhibits non-responsiveness in miR-21-deficient cells and immunodeficient cells, demonstrating significant potential as an efficient targeted cancer therapy.

#0996 Novel sulfonamide-aromatic amine hybrids: Synthesis, cytotoxic screening, and transcriptomic insights into anticancer activity.

Mohamed A. Eltokhy[1], Eman A. Fayed[2], Moustafa S. Abusaif[3], Ahmed Ragab[3], Yousry A. Ammar[3], Sahar Radwan[4], Sanjay K. Srivastava[1]

[1]Immunotherapeutics and Biotechnology, Texas Tech University Health Sciences Center, Abilene, TX,[2]Pharmaceutical Organic Chemistry, Al-Azhar University, Cairo, Egypt,[3]Chemistry, Al-Azhar University, Cairo, Egypt,[4]Microbiology and Immunology, Al-Azhar University, Cairo, Egypt

Cancer remains one of the causes of mortality worldwide and a major global health challenge. These challenges are attributed to factors such as medication resistance, tumor complexity, and heterogeneity. Targeted therapy with small molecules has emerged as a promising approach due to its ability to selectively inhibit cancer cell growth while minimizing off-target effects. In this study, a series of derivatives synthesized from 3-formyl-4-hydroxy benzene sulfonyl chloride (FHS) were evaluated for their cytotoxic effects on various cancer cells. The objective was to identify compounds with potent anticancer activity and favorable selectivity profiles for further development. The synthesis process began with FHS as the starting material, subjected to a series of chemical reactions to generate a library of compounds labeled C3 through C10. These compounds were characterized by using a combination of analytical techniques, including melting point determination, Proton Nuclear Magnetic Resonance (^{1}H NMR), Carbon-13 Nuclear Magnetic Resonance (^{13}C NMR), and Infrared (IR) spectroscopy to confirm their structural integrity. Cytotoxic effects were evaluated using Sulforhodamine B (SRB) assay for cytotoxicity was applied to an extensive panel of cancer cell lines, categorized into such as colorectal cancer (HT-29, MC38, CT26and COLO 205), hepatic (C3a and PLC/PRF), pancreatic (Suit-2, MiaPaca2, As-PC1 and Panc 02.03, CI66), breast (MDA-MB-468, MDA-MB-231, BT20, MCF7, 4T1, 4T1 paclitaxel resistant, JIMT-1, ZR-75-1, E0771, T47D, and HCC1806) and ovarian (OVCAR-5) cell lines. Normal breast epithelial cell line MCF10a was tested to analyze safety. Based on the SRB assay, 7 compounds exhibited variable but significant cytotoxicity in various cancer models. The most effective compound, C5, was chosen for further analysis to identify mechanism of its cytotoxic effect by transcriptomic analysis. The transcriptomic results showed ten genes with log2 fold change between control and treatment. These genes were related to DNA damage inducible transcript 4, FXYD domain containing ion transport regulator 4 and CHAC1 (glutathione-specific gamma-glutamylcyclotransferase 1). Further in vivo experiments and validation experiments are in progress to determine the most significant pathway for cytotoxicity.

#0997 Development of polyHis-targeting chimeras (HisTACs) for targeted protein degradation.

Annan Sun[1], Dong Zhu[2], Hui Chen[1], Monica Billitti[2], Lingtao Jin[3], Dongwen Lyu[2], Guangrong Zheng[1]

[1]Department of Medicinal Chemistry, University of Florida, Gainesville, FL,[2]Department of Cellular Biology and Anatomy, Augusta University, Augusta, GA,[3]Department of Molecular Medicine, University of Texas Health San Antonio, San Antonio, TX

Induced-proximity degraders hold great promise for oncology, yet their utility remains constrained by the need for high-affinity ligands for each protein of interest. Tag-based degrader systems provide ligand-independent surrogates but are limited by large tag size, risk of tag-driven ubiquitination, and difficulty of engineering substantial tags into endogenous genes. To address these challenges, we developed a polyhistidine-directed degrader platform (HisTAC) that uses Ni^{2+}-nitrilotriacetic acid (Ni^{2+}-NTA) to engage His-tagged proteins and recruit CRBN or VHL E3 ligases.Cellular uptake was first confirmed with a fluorescent His_6-CPP/Ni-NTA probe, which exhibited rapid entry and widespread intracellular distribution. We then generated a HeLa cell line with endogenously His_6-HiBiT-tagged BRD4 and screened a panel of Ni^{2+}-NTA-based degraders. Constructs containing two Ni^{2+}-NTA groups displayed the highest potency, yielding >50% BRD4 loss at micromolar levels. MG-132 co-treatment fully blocked BRD4 depletion, confirming proteasome dependence. Immunoblotting further revealed preferential degradation of BRD4 long isoform, with moderate reduction of the short isoform. VHL-recruiting HisTACs also induced potent, isoform-selective BRD4 degradation with sub-micromolar efficacy toward the long isoform.To test the generalizability of this platform, we engineered a polyHis-HiBiT-tagged PSPC1 cell line—an RNA-binding protein lacking tractable ligands. Both CRBN- and VHL-based HisTAC degraders induced rapid, dose-dependent PSPC1 degradation, demonstrating the applicability of Ni^{2+}-NTA-guided proximity to traditionally “undruggable” targets.
Together, these results establish HisTAC degraders as a versatile, ligand-independent strategy for probing challenging cancer targets and accelerating degrader discovery and mechanistic studies in cancer research.

#0998 The NVL inhibitor benzothiazepinone targets colorectal cancer by blocking ribosome biogenesis.

Ye Tao[1], Holly Guo[1], Min Fang[1], VIshal Khivansara[1], Shanhai Xie[1], Ashley Leach[1], Divya Reddy[1], Noelle S. Williams[2], Arin B. Aurora[1], Deepak Nijhawan[1], Jef K. De Brabander[1]

[1]Radiation Oncology, Section in Molecular Medicine, UT Southwestern Medical Center, Dallas, TX,[2]Dept. of Biochemistry, UT Southwestern Medical Center, Dallas, TX

The identification of new cancer-relevant protein targets is a major bottleneck in the discovery of small molecule therapies for the treatment of cancer. To meet this challenge, our team developed a platform that combines cell-based, high throughput phenotypic screens with forward genetics to identify new cancer targets and accompanying small molecule leads. By combining this approach with biochemical reconstitution and structural biology, we identified MM017 (benzothiazepinone scaffold) as a novel small molecule with anti-proliferative activity in colorectal cancer cells and its target nuclear valosin-containing protein-like (NVL), a hexameric AAA+ translocase required for large ribosomal subunit (60S) assembly. Simultaneously, an advanced medicinal chemistry campaign was launched to establish the SAR and to evaluate how continual modification balances the chemical-physical properties of candidate small molecules. Compounds that meet minimal criteria for in vitro ADME properties are progressed through the funnel and further evaluated through preclinical models to assess pharmacokinetics, toxicity, and efficacy.

#0999 N/C-terminus modification: enhanced TROP2-targeting cyclic peptide for PET imaging.

JONGMIN AN[1], Nisi Zhang[2], Marian Awadalla[1], SPENCER TUMBALE[3], Marina Raie[3], Basit Jan[3], Katherine W. Ferrara[4]

[1]Stanford University School of Medicine, Stanford, CA,[2]Stanford University School of Medicine, Palo Alto, CA,[3]Stanford University School of Medicine, Stanford, Palo Alto, CA,[4]Stanford University, Palo Alto, CA

Trophoblast cell surface antigen 2 (TROP2) has emerged as a compelling target in cancer therapy because it is highly overexpressed in many epithelial-derived malignancies while showing relatively low expression in normal tissues. To exploit this target, several modalities have been developed, including small molecules (e.g., Bruceine D) and antibody-based therapeutics (e.g., Sacituzumab govitecan). Despite these advances, challenges related to cost, specificity, and selectivity remain. In this flow, cyclic peptides have gained attention as attractive alternatives to conventional approaches due to their reduced conformational entropy and favorable biocompatibility.In this study, we report a chemically modified cyclic peptide designed for the visualization of TROP2 overexpression in cancer via PET/CT imaging. The peptide was modified at the N/C-terminus to promote π-π or cation-π interactions, thereby enhancing key biological properties such as binding affinity and stability. Each cyclic peptide was synthesized through Fmoc-based solid-phase peptide synthesis using HBTU/collidine-mediated amide coupling, and the final products were validated by mass spectrometry. The impact of the chemical modifications was assessed using circular dichroism (CD) spectroscopy, bio-layer interferometry (BLI), LogP analysis, and serum/glutathione stability assays. Radiolabeling with ^{68}Ga and ^{64}Cu demonstrated the preclinical capacity of this cyclic peptide. This strategy provides a versatile framework for the rational modification of cyclic peptides and supports the development of clinically relevant theragnostic agents.

#1000 Stereocontrolled synthesis and evaluation of functionalized lactams as potential anti-triple-negative breast cancer agents.

Leila Rahimian[1], Tolulope Omolekan[1], Ojasvi Dutta[1], Konstantin G. Kousoulas[1], Timothy K. Beng[2], Jean C. Chamcheu[3]

[1]Louisiana State University, Baton Rouge, LA,[2]Department of Chemistry, Central Washington University, Ellensburg, WA,[3]Department of Biological Sciences and Chemistry, Southern University and A&M College, Baton Rouge, LA

Triple-negative breast cancer (TNBC) is an aggressive subtype compromising ~ 10-15% of cases and defined by loss of ER, PR, and HER2, leading to limited therapies. Chemoresistance and tumor heterogeneity underscore the need for new small-molecule agents. Medicinal chemists note that stereocenters enhance drug potential; thus, chiral N-based cyclic compounds like lactams are valued. Here, we report the synthesis and anticancer evaluation of functionalized lactams bearing four contiguous stereocenters against TNBC models.A diversity-oriented synthesis strategy generated 40 structurally varied lactams. Compounds were screened for cytotoxicity against three TNBC (MDA-MB-231, BT-549, and 4T1) and one normal breast epithelial (MCF10A) cell lines using MTT assay. Clonogenic, wound-closure, ROS and Boyden chamber assays assessed growth and migration. Compounds with strong cancer-cell cytotoxicity and low MCF10A toxicity were selected for further analysis. Mechanistic data were obtained via immunoblotting and immunofluorescence for apoptosis markers. SwissADME was used for pharmacokinetic and drug-like predictions.Multiple lactams showed potent antiproliferative activity with sub-micromolar IC_{50} values, identifying W11, W12, and W23 as the most active, with IC_{50} values of (28.8, 40.8, and 28.4) μM in 4T1; (40.7, 38.7, and 21.6) μM in MDA-MB-231; and (22.2, 28.7, and 28.6) μM in BT-549. Lead compounds W11, W12, and W23 with cisplatin as control, significantly and dose-dependently reduced ROS, clonogenicity and migration, indicating anti-metastatic potential. W11 had the lowest EC_{50} (~23 μM), while W12, W23, and cisplatin showed EC_{50} values around 30-34 μM. These results indicate that the lead compounds reduce viability and impair TNBC cell motility. Mechanistic studies revealed robust activation of apoptosis pathways. SwissADME predicted high GI absorption, optimal lipophilicity (LogP<5), Lipinski compliance, and favorable biodegradability.This study identifies lactams W011, W012, and W023 as promising small-molecule candidates for TNBC. Their modulation of apoptotic and other pathways such as ROS-induction, along with favorable predicted pharmacokinetics, supports further preclinical optimization and development toward targeted TNBC therapy.

#1001 Targeting regulation of F-actin in cutaneous T-cell lymphoma: Synergistic inhibition of p38β with p38γ inhibitors.

Xu Hannah Zhang, Jack Hsiang, Markus Kalkum, Jun Wu, Steven T. Rosen

Beckman Research Institute of The City of Hope, Duarte, CA

Cutaneous T-cell lymphoma (CTCL) is an incurable T-cell malignancy characterized by dysregulated p38 MAPK signaling. Our recent studies identify p38β as an F-actin-binding kinase that regulates T-cell receptor (TCR) polarization and cytoskeletal organization. Loss or pharmacologic inhibition of p38β triggers compensatory activation of p38γ, promoting epithelial-to-mesenchymal transition (EMT) and potentially accelerating disease progression. To counter this effect, we evaluated a dual-targeting strategy combining the p38β inhibitor Nilotinib with p38γ inhibitors F7 (ATP-site) and CSH71 (ligand-binding-domain site). In Hut78 CTCL cells, combined F7 + CSH71 treatment significantly reduced cell viability with strong synergy (31.25 nM F7 + 1.25 μM CSH71; CI = 0.69). This dual inhibition markedly decreased F-actin polymerization, disrupted cellular polarization, and enhanced apoptosis compared with either single agent. Similarly, Nilotinib synergized with CSH71 in CTCL cells but not in healthy PBMCs, demonstrating tumor-selective cytotoxicity. Mechanistic analyses revealed that Nilotinib reduced γ-actin and ribosome-biogenesis-related proteins such as MDN1, as determined by LC-MS/MS, whereas CSH71 suppressed F-actin formation. These convergent effects destabilized the actin cytoskeleton and impaired TCR-dependent survival signaling. To extend these findings in vivo, ongoing studies using Hut78 xenograft mice are evaluating tumor reduction, apoptosis, survival benefit, and systemic safety following triple-drug combination (Nilotinib + F7 + CSH71). Collectively, these results support dual p38β/p38γ inhibition as a promising therapeutic approach for CTCL and other hematologic malignancies driven by cytoskeletal and stress-kinase dysregulation, while providing mechanistic insight into how targeted therapies remodel the F-actin network in vivo.

#1002 Parallel drug development strategies for fibrolamellar hepatocellular carcinoma and proteasome-dependent multiple myeloma.

Shalini Rawat, Najmeh Rahimi, Jared Alderman, Celeste Villasenor, Rodolfo Tello-Aburto, Barbara Lyons

Chemistry and Biochemistry, New Mexico State University, Las Cruces, New Mexico, NM

Fibrolamellar Hepatocellular carcinoma (FLC) is a rare liver cancer which occurs primarily in young adults and children under the age of 40. In FLC, a deletion of 400,000 base pairs occurs in one chromosome 19 copy, leading to the formation of a fusion protein comprised of a domain of the heat shock protein DNAJB1 and the catalytic subunit of Protein Kinase A (DNAJB1-PRKACA). Patients are typically asymptomatic at early stages, and 5-year survival remains below 50%. With surgery as the only partially effective treatment and no approved systemic therapies, there is a critical need for new therapeutics. The primary model compound of this project, Napabucasin, is a naphthoquinone natural product that has shown wide spectrum anti-cancer activities. Napabucasin was found to be a top hit in drug screening showing potency against FLC patient derived xenografts (PDX) models and direct-from-patient FLC tumor cells. Napabucasin is known to work in multiple signaling pathways including protein translation, the generation of reactive oxygen species, suppression of tumor cell stemness, and blocking tumor cell apoptotic escape. We anticipate the organic synthesis and development of optimized Napabucasin analogues, along with the evaluation of their cytotoxicity and proliferation effectiveness compared to the parent compound, Napabucasin, will result in compounds with improved bioavailability and efficacy, particularly in FLC model cell lines (Huh7-Chimera). In an additional approach to cancer drug development, we are evaluating the efficacy of promising next generation proteasome inhibitors. In eukaryotic cells, protein homeostasis is maintained through controlled synthesis and degradation, with the Ubiquitin Proteasome System (UPS) serving as the major pathway for regulated proteolysis. Cancer cells increase UPS activity to manage proteotoxic stress from rapid proliferation, leading to degradation of tumor-suppressive proteins and activation of oncogenic pathways. Targeted inhibition of UPS function causes accumulation of ubiquitinated proteins, G2/M arrest, and apoptosis, establishing the proteasome as a validated anticancer target. The 20S core of proteasome contains three catalytic β subunits (β1, β2, β5). Among all three, the chymotrypsin-like β5 activity remains the primary driver of cytotoxicity for clinically approved inhibitors such as bortezomib, carfilzomib; however, their therapeutic use is limited by toxicity. Peptidic β-lactones (the cystargolide family), are promising next-generation proteasome inhibitors. This project evaluates newly synthesized cystargolide analogs for cytotoxicity, bioavailability, and proteasome inhibition in RPMI-8226 myeloma cells. Using cell-based assays and IC_{50} determination, we aim to establish structure activity relationships and advance optimized β-lactone inhibitors with improved therapeutic potential.

#1003 Targeted co-delivery of gemcitabine and atRA via a GSH-responsive mutual prodrug enhances cytotoxicity through redox imbalance and Pin1 inhibition.

Nanhee Song[1], Ilseob Kim[1], Chnagjin Lim[1], Dongwon Lee[1], Sun Il Choi[2], Yun-Hee Kim[3]

[1]Jeonbuk National University, Jeonju-si, Korea, Republic of,[2]Research Institute of National Cancer Center, Goyang-si, Korea, Republic of,[3]National Cancer Center - Korea, Goyang-si, Korea, Republic of

Combination therapy offers strong potential to enhance anticancer efficacy, yet its success depends on the concurrent and targeted delivery of multiple agents. To address this challenge, we designed a self-assembling trimeric mutual prodrug, RqGem, which covalently links gemcitabine (GEM) and all-trans retinoic acid (atRA) through a glutathione (GSH)-depleting linker. This architecture enables excipients-free nanoassembly, achieving 100% drug loading and ensuring simultaneous delivery of both agents. RqGem nanoassemblies remained stable under physiological conditions and underwent esterase-mediated activation, releasing GEM and atRA along with a quinone methide intermediate that rapidly depletes intracellular GSH. This GSH depletion-driven redox modulation potentiated the cytotoxic mechanisms of both drugs by elevating oxidative stress and sensitizing cells to DNA damage and differentiation cues.The multiple and synergistic therapeutic actions of RqGem nanoassemblies were evaluated using cell culture and mouse models. RqGem nanoassemblies demonstrated significantly greater cytotoxicity, enhanced cellular uptake, and stronger apoptosis induction than the equivalent mixture of free GEM and atRA, reflecting robust synergy between atRA-mediated signaling modulation and GEM-induced DNA damage. The combined actions of self-assembly, 100% drug loading, concurrent drug release, and redox-dependent sensitization collectively contributed to the high potency of RqGem. Given that the role of atRA in targeting Pin1, a peptidyl-prolyl isomerase overexpressed in cancers and associated with poor prognosis, we further evaluated the impact of RqGem on Pin1 expression. Western blot analyses in AsPC-1 and CFPAC-1 pancreatic cancer cells showed marked Pin1 downregulation following RqGem treatment, supporting its dual mechanism of GEM delivery and atRA-mediated oncogenic pathway inhibition. Ongoing studies in orthotopic pancreatic tumor models aim to define the signaling pathways underlying RqGem-driven Pin1 suppression and its contribution to treatment synergy. Collectively, these findings establish RqGem as a rationally engineered, self-synergistic mutual prodrug that integrates drug self-delivery, controlled activation, and redox regulation to achieve potent and targeted anticancer activity. This platform holds strong translational promise for combination therapy in pancreatic cancer and beyond.

: Biomarkers Predictive of Therapeutic Benefit 1
Poster Session

#1008 Effect of the KRAS G12C inhibitor MK-1084 on circulating tumor DNA levels in participants with KRAS G12-mutated tumors.

Carlos Rojas[1], Matteo Simonelli[2], Adrian Sacher[3], Mehmet Ali Sendur[4], Rafal Dziadziuszko[5], Joon Oh Park[6], Victor Moreno Garcia[7], Jair Bar[8], Yun Fan[9], Mustafa Erman[10], Shun Lu[11], Jenny H. Lee[12], Rosalyn A. Juergens[13], Bangwei Cao[14], Cai Chen[15], Razvan Cristescu[15], Thomas Jemielita[15], Yewon Sofia Choi[15], Mark D. Ayers[15], Iwona Lugowska[16]

[1]Bradford Hill Clinical Cancer Research Center, Santiago, Chile,[2]IRCCS Humanitas Research Hospital, Rozzano MI and Humanitas University, Pieve Emanuele MI, Italy,[3]Princess Margaret Cancer Centre and University of Toronto, Toronto, ON, Canada,[4]Ankara Yıldırım Beyazıt University and Ankara Bilkent City Hospital, Ankara, Turkey,[5]Medical University of Gdansk, Gdansk, Poland,[6]Associate Professor, Dept. of Hem./Onc., Samsung Medical Center, Sungkyunkwan University, School of Medicine, Seoul, Korea, Republic of,[7]START Madrid, Madrid, Spain,[8]Jusidman Cancer Center, Sheba Medical Center, Tel Hashomer, Ramat Gan, Israel,[9]Zhejiang Cancer Hospital, Hangzhou, China,[10]Hacettepe University Cancer Institute, Ankara, Turkey,[11]Shanghai Chest Hospital, Shanghai Jiao Tong University, School of Medicine, Shanghai, China,[12]Chris O'Brien Lifehouse Research Institute, Camperdown, Australia,[13]Hamilton Health Sciences-Juravinski Cancer Centre, Hamilton, ON, Canada,[14]Beijing Friendship Hospital, Capital Medical University, Beijing, China,[15]Merck & Co., Inc., Rahway, NJ,[16]Maria Sklodowska-Curie National Research Institute and Oncology Centre, Warsaw, Poland

Background: Preliminary data from the phase 1 KANDLELIT-001 trial (NCT05067283) showed a manageable safety profile and preliminary antitumor activity for MK-1084, a next-generation, selective KRAS G12C-GDP covalent inhibitor, in participants (pts) with previously treated, *KRAS* G12C-mutant solid tumors. Here, we examine the effect of MK-1084 monotherapy on KRAS G12C variant allele frequency (VAF) and maximum somatic allele frequency (MSAF) ctDNA levels in pts with advanced KRAS G12C-mutant solid tumors during the monotherapy dose escalation phase of KANDLELIT-001.
Methods: KANDLELIT-001 enrolled pts with any KRAS G12C-mutated advanced solid tumor to receive MK-1084 alone or in various combination therapies. Pts with any advanced solid tumor and ≥1 prior systemic therapy received MK-1084 monotherapy PO QD or BID in Arm 1 (total daily dose, 25-800 mg). Serial blood samples collected from pts enrolled in Arm 1 were evaluated for changes in ctDNA KRAS-G12C VAF and MSAF levels at baseline, and before beginning cycle 1 and cycle 3 using the Guardant Health OMNI panel. Differences in ctDNA levels were assessed using descriptive statistics.
Results: In Arm 1, 22 of 23 pts were evaluable for changes in ctDNA levels. Median KRAS G12C VAF and MSAF ctDNA levels decreased ≥90% each from 14% to 0.9% and from 25% to 2%, respectively, from cycle 1 (pre-dose, day 0) to cycle 3 (day 42 on treatment); 6 (26%) pts achieved complete clearance of KRAS G12C VAF ctDNA. Greater reductions in tumor size were observed in pts who achieved complete clearance of KRAS G12C ctDNA. Larger reductions in ctDNA levels were seen in pts with a complete or partial response (responders) vs those with no response. Co-occurring mutations in PI3KCA, KEAP1, and KRAS G12D, Q61H, and BRAF were detected at baseline.
Conclusions: In a cohort of 23 patients with KRAS G12C mutations receiving MK-1084 monotherapy, tumor response was associated with reductions in KRAS G12C VAF and MSAF ctDNA levels. This potentially reflects the molecular activity and therapeutic effect of MK-1084 in KRAS G12C-mutated tumors. The small sample size of this analysis limits interpretation of these findings.

#1009 Landscape of homozygous copy number (CN) losses with established and emerging clinical actionability across 430,467 pan-tumor tissue samples.

Timothy A. Yap[1], Jessica K. Lee[2], Xin Liu[2], Erica Gornstein[2], Amaya Gasco[2], Richard S. P. Huang[2], Alexa B. Schrock[2]

[1]UT MD Anderson Cancer Center, Houston, TX,[2]Foundation Medicine, Inc., Boston, MA

Background: Loss-of-function (LOF) alterations (alts) in *BRCA1/2* and *PTEN* are associated with approved therapies in multiple tumor types, *RB1* and *STK11* are established prognostic biomarkers, and LOF of a growing number of additional genes (e.g. *MTAP, NF1*) have emerging actionability and are under investigation in clinical trials. LOF alts include inactivating mutations, rearrangements, and homozygous CN losses, which can be analytically challenging to detect. With the growing clinical importance of CN losses, we assessed their prevalence in a cohort of pan-tumor samples submitted for tissue comprehensive genomic profiling (CGP).
Methods: 430,467 pan-tumor tissue samples underwent NGS-based CGP on FoundationOne®CDx. A genome-wide CN model for each sample was generated, segmented and combined with variant allele frequencies of heterozygous SNPs to estimate tumor purity (TP), ploidy and CN for each segment; the presence of homozygous CN losses was assessed for 310 genes.
Results: CN losses were detected in 31% of pan-tumor samples and were most prevalent in glioma (53%), pancreas (50%), and gallbladder (50%). The most prevalent pan-tumor homozygous losses were in *CDKN2A/*B (15/17%), *MTAP* (11%), *PTEN* (4.2%), *SMAD4* (2.2%), and *RB1* (1.5%). Disease-specific CN loss enrichments were observed, including *PTEN* in prostate (22%), *SMAD4* in GI tumors (12% pancreas, 8.2% gallbladder, 8% small intestine, 4.9% CRC), *RB1* in SCLC (12%), *STK11* in cervix (5.0%) and NSCLC (2.9%), *NF1* in ovarian (4.2%), and *KEAP1* in NSCLC (0.6%). HRD associated losses were also detected in *BRCA2* (2.8%, 0.5%, and 0.3%), *BRCA1* (0.06%, 0.3%, and 0.6%), and *PALB2* (0.02%, 0.03%, and 0.02%) in prostate, breast, and ovarian cancers, respectively. CN losses comprised >98% of LOF alts in *CDKN2B* and *MTAP*, and >20% of LOF alts in many genes including *CDKN2A*, *PTEN, RB1*, and *STK11*. 27% of samples harbored a CN loss associated with a clinical trial enrolling based on LOF alts (across 63 genes), and 22% harbored a CN loss (across 16 genes) associated with trials specifically requiring a CN loss or deletion vs. any LOF alt. The median TP of a sample with a CN loss detected was 50% (IQR 33-68%). The pan-tumor prevalence was 16% in samples with TP < 20% (n=65,881), increased to 34% in samples with 20-30% TP, and remained relatively stable at higher TPs: 36% at 30-40% TP and 33% at >40% TP.
Conclusions: CN losses were detected in >30% of pan-tumor tissue samples and included losses associated with approved or investigational therapies such as *BRCA1/2, PTEN, MTAP*, and *NF1*, and losses with prognostic implications such as *RB1* and *STK11*. Prevalence trended with increasing TP and reached the prevalence of the overall cohort in samples with TP ≥ 20%. CN losses are a diverse class of analytically challenging but increasingly clinically relevant biomarkers, and reliable detection of these events will be important for optimal therapy selection.

#1010 DNA-level complex fusions show high discordance with RNA expression: A validation study of 115 Chinese cases.

Xinyue Wang[1], Lu Zhang[2], Xinyan Li[1], He Jiang[1], Jiayi Zhao[1], Richeng Jiang[1]

[1]Center for Precision Cancer Medicine & Translational Research, National Clinical Research Center for Cancer, Tianjin Medical University Cancer Institute & Hospital, Tianjin, China,[2]Center for Precision Cancer Medicine & Translational Research, Tianjin Cancer Hospital Airport Hospital, Tianjin, China

Background:
Gene fusions identified by DNA-based next-generation sequencing (DNA-NGS) play a crucial role in guiding targeted therapy for solid tumors. However, complex fusion structures may not always transcribe into functional chimeric RNAs or proteins, due to disrupted open reading frames, opposing transcriptional directions, or absence of promoter elements. Such discrepancies can lead to false-positive DNA-NGS findings and subsequent inappropriate treatment decisions.
Methods:
We analyzed 115 tumor samples from the Chinese population with DNA-NGS-identified complex fusions using simultaneous DNA and RNA-based NGS (DR-NGS) for validation. Seven samples with inadequate pathology quality control were excluded.
Results:
Lung cancer accounted for the majority of the 115 samples (89, 77.4%). Complex fusion patterns included 5′-5′ fusions, 3′-3′ fusions, primary/reciprocal fusions, non-canonical breakpoints or partners, co-occurrence of multiple fusion drivers, UTR-region fusions, and intergenic fusions. The involved genes were *ALK* (32), *ROS1* (10), *NTRK* (6), *EGFR* (9), RET (28), *HER2/3* (2), *MET* (4), *FGFR1-4* (15), *NRG1* (1), *BRAF* (4), and multiple co-existing fusion genes (3).
Among the 108 successfully tested cases, 45 showed no fusions by DR-NGS testing but revealed other driver mutations in 57.78% of cases, including *EGFR* (22, 48.89%), *FGFR2* (1), *BRAF* (1), and *KRAS* (2). In the remaining 63 cases, DR-NGS testing confirmed the presence of fusions, with only one case showing a co-existing *EGFR* mutation (1.59%, $p < 0.001$). Among these, 55 exhibited classic single fusions at the RNA level after transcriptional splicing, while 8 cases with rare fusion partners in DNA-level were validated as true partners by DR-NGS testing.
RNA fusion-positive and -negative groups showed male-to-female ratios of 21:42 and 23:22 ($p = 0.064$), and age distributions (≥65 vs. <65 years) of 9:54 and 20:25 ($p < 0.001$), respectively.
Conclusion:
This study reveals a substantial discordance between DNA-level complex fusions and their RNA expression. Nearly half of the DNA-identified complex fusions were not transcribed, with many instead harboring other driver mutations—most commonly EGFR. By contrast, RNA-verified fusions predominantly presented as classic single transcripts, with rare co-occurrence of other driver mutations. RNA fusion status was also significantly associated with patient age. These findings underscore the necessity of RNA-based confirmation for DNA-detected complex fusions, especially those coexisting with other driver gene mutations, to prevent false-positive interpretations and to optimize targeted therapy selection.

#1011 Correlation of mitophagy related genes expression and clinical outcome in metastatic colorectal cancer patients enrolled in CALGB (Alliance)/SWOG 80405.

Shivani Soni[1], Yan Yang[2], Michela Bartolini[1], Pooja Mittal[3], Fang-Shu Ou[4], Lesly Torres-Gonzalez[5], Unnati Hemant Shah[5], Jae Ho Lo[1], Steve Soto Trujillo[1], Yitzhar Goretsky[5], Wu Zhang[5], Alan P. Venook[6], Sandra Algaze[1], Joshua Millstein[7], Heinz-Josef Lenz[5]

[1]Medical Oncology, USC Norris Comprehensive Cancer Center, Los Angeles, CA,[2]Population and Public Health, USC Norris Comprehensive Cancer Center, Los Angeles, CA,[3]Keck School of Medicine of USC, Los Angeles, CA,[4]Alliance Statistics and Data Management Center, Mayo Clinic, Rochester, MN,[5]USC Norris Comprehensive Cancer Center, Los Angeles, CA,[6]University of California, San Francisco, CA,[7]Population and Public Health Sciences, USC Norris Comprehensive Cancer Center, Los Angeles, CA

Background. Mitophagy plays a crucial role in removing dysfunctional mitochondria to maintain cellular homeostasis but also has been implicated in cancer tumorigenesis. Previously, we showed that genetic variation in mitophagy pathway genes holds a predictive value in metastatic CRC (mCRC) patients (pts) treated with bevacizumab-based chemotherapy. In this study, we analyzed the correlation between tumor expression profiles of genes associated with PINK1/Parkin and BNIP3/NIX/FUNDC1 mitophagy pathways with clinical outcome in a large phase III randomized clinical trial CALGB SWOG 80405.

Method. We analyzed 433 pts with mCRC treated with first-line chemotherapy in combination with the targeted agents bevacizumab (Bev, $n = 226$) or cetuximab (Cet, $n = 207$). Tumor RNA isolated from FFPE samples was sequenced using the HiSeq 2500 platform (Illumina). Median Overall survival (mOS) and median progression-free survival (mPFS) were compared across pts groups divided into high, medium, and low tertiles based on mitophagy-related gene (*BNIP3*, *BNIP3L*, *PINK1*, *PRKN*) expression levels. Likelihood ratio tests, hazard ratios (HRs), and 95% confidence intervals (CIs) were calculated using multivariable Cox proportional hazards models, adjusting for age, sex, ECOG performance status, tumor location, number of metastatic sites, *KRAS* status, Consensus Molecular Subtypes, and treatment arm.

Results: Overall, *BNIP3L* demonstrated significant prognostic value for both PFS and OS after adjustment for multiple testing (false discovery rate [FDR] < 0.05). Tumors with low *BNIP3L* expression showed longer PFS and OS compared to those with medium or high expression levels (mPFS 14.8 vs. 10.0 vs. 9.2 months, HR 1.16, 95% CI 1.04 - 1.29$p = 0.0182$; mOS: 37.4 vs. 30.2 vs. 24.4 months, HR 1.22, 95% CI 1.09 - 1.38, $p = 0.0036$), independent of treatment. In pts treated with Cet, high *PRKN* expression was associated with improved PFS and OS (mPFS: 8.9 vs. 10.3 vs. 14.6 months, HR 0.79; 95% CI 0.69 - 0.91, $p = 7.3e-05$; mOS: 21.2 vs. 27.7 vs. 41.1 months, HR 0.87; 95% CI 0.75 - 1.01, $p = 0.00084$), whereas low *PINK1* expression was significantly associated with longer OS (mOS: 24.9 vs. 30.9 vs. 39.2 months, HR 1.23; 95% CI 1.04 -1.46, $p = 0.013$). No significant associations were observed in Bev-treated patients for *PRKN* or *PINK1*. No significant results were found for *BNIP3* expression analysis.

Conclusion. Mitophagy is a crucial player in CRC biology due to its tumor-intrinsic (mitochondrial bioenergetics) and microenvironment (interacts with immune components) effects. Our study highlights the prognostic value of *BNIP3L* and predictive potential of *PINK1* and *PRKN*, suggesting a potential combinatorial therapeutic approach using mitochondrial targeting drugs and targeted agents e.g Cet, which warrants further investigation.

Support: Genentech; Clinicaltrials.gov Identifier: NCT00265850

#1012 Multi-omic method to detect MTAP homozygous deletions enables high sensitivity detection from blood samples.

Geethika Yalamanchili, Sean Gordon, Evan Warner, Shile Zhang, Keelia Clemens, Matthew Ellis, Vishnu Ramani, Marisa Juntilla, Martina Lefterova, Justin Odegaard, Darya Chudova

Guardant Health, Palo Alto, CA

Introduction: The methylthioadenosine phosphorylase (*MTAP*) gene encodes a tumor suppressor and component of the methionine salvage pathway. *MTAP* homozygous deletion (HomDel) can induce synthetic lethality when either PRMT5, MAT2A, or both are inhibited. Successful detection of *MTAP* HomDel can, therefore, offer novel options for targeted therapy. Unfortunately, tumor tissue is often unavailable for genomic profiling and detection of *MTAP* HomDel. While cfDNA testing is available for CGP, detection of *MTAP* HomDel in plasma cfDNA is challenging, as detection by conventional coverage-based methods is masked by non-tumor DNA coverage, especially in low-tumor fraction samples, thus limiting sensitivity in these settings.

Methods: We developed a multi-omic approach that integrates genomic and tumor-specific methylation features to enhance detection sensitivity for *MTAP* HomDel in circulating tumor DNA (ctDNA). Tumor-specific methylation features were identified by analyzing methylation profiles from 100,089 plasma samples spanning diverse solid tumor types and used to train a classifier optimized to detect *MTAP* HomDel using the Guardant360 Liquid test. The resulting tumor-specific methylation classifier was then combined with genomic copy-number calling to maximize sensitivity and specificity for *MTAP* HomDel detection in plasma. Analytical accuracy was assessed in 87 matched cfDNA and tissue samples (NSCLC = 40%, pancreatic = 9%, melanoma = 9%, breast = 7%, other = 35%) from patients with advanced cancer. *MTAP* HomDel and single copy number loss were treated as distinct categories. Consecutive samples tested in routine clinical care were used to determine detection rates. Limit of blank (LoB) specificity was established using 120 cancer-free donor cfDNA samples (30 ng input), and the 95% Limit of Detection (LoD) was determined via *in silico* dilutions of 50 high confidence *MTAP* HomDel samples.

Results: Our multi-omic methodology achieved a positive predictive value (PPV) of 100% and negative percent agreement (NPA) of 100% above LoD (90.9% and 96.6% overall) against a tissue-based reference. No false positives were observed among 120 cancer-free donors. Assessment of cfDNA samples from patients with advanced cancer demonstrated that multi-omic *MTAP* HomDel detection was over 2.4 fold as sensitive as genomic-only methods.

Conclusion: Augmenting genomic information with tumor-specific methylation significantly enhances the detection of *MTAP* HomDel in plasma cfDNA, especially in low-tumor-fraction samples. Future work may leverage similar methylation coverage on the Guardant360 Tissue test to enhance *MTAP* HomDel detection in low input and low tumor purity tissue samples. This approach has potential to not only improve patient access to PRMT5- and MAT2A-targeted therapies but also to other therapies that are guided by gene deletions.

#1013 Immune microenvironment driven immunotherapy resistance in 11q13-amplified hepatocellular carcinoma.

Weiping Zhu

Fudan University Shanghai Cancer Center, Shanghai, China

Background: Immune checkpoint inhibitors (ICIs) have provided new therapeutic opportunities for patients with liver hepatocellular carcinoma (LIHC); however, only a subset of patients achieve meaningful benefit. Previous studies have suggested that co-amplification of the chromosome 11q13 region—which includes CCND1, FGF3, FGF4, and FGF19—is associated with poor immunotherapy response and unfavorable prognosis. Nonetheless, whether the immune microenvironment contributes to ICI resistance in 11q13-amplified LIHC remains unclear. This study aimed to elucidate the genomic and immunologic correlates of 11q13 amplification in LIHC.

Methods: Tumor samples from 890 LIHC patients were analyzed using a 733-gene next-generation sequencing (NGS) panel to characterize genomic alterations, including DNA damage repair (DDR) pathway genes, tumor mutation burden (TMB), and intratumor heterogeneity (ITH). Multiplex immunofluorescence (mIF) was performed to evaluate the immune microenvironment, focusing on stromal and intratumoral immune cell populations. Comparative analyses were conducted between patients with and without 11q13 amplification to determine differences in genomic alterations and immune cell infiltration patterns.

Results: Among the 890 LIHC patients, 8.9% (79/890) harbored chromosome 11q13 amplification. Genomic profiling revealed no significant differences in DDR pathway mutations, TMB, or ITH between 11q13-amplified and non-amplified patients, suggesting that 11q13-associated immunotherapy resistance is unlikely to stem from genomic instability. In contrast, immune microenvironment analysis revealed substantial alterations associated with 11q13 amplification: patients with amplification demonstrated increased stromal $CD8^+$ T-cell positivity (P=0.04), as well as significantly elevated intratumoral infiltration of $CD68^+CD163^+$ M2-TAMs (higher density, P=0.03; higher positivity, P=0.03) and increased positivity of $CD68^+HLA\text{-}DR^+$ M1-TAMs (P=0.03). These findings indicate that 11q13-amplified tumors may harbor a more complex immunosuppressive and inflammatory microenvironment, potentially contributing to ICI resistance.

Conclusion: Chromosome 11q13 amplification in LIHC is not associated with distinct genomic instability features but is strongly correlated with alterations in the tumor immune microenvironment, including increased $CD8^+$ T-cell presence and enrichment of both M1 and M2 tumor-associated macrophages. These results suggest that immune microenvironment dysregulation, rather than genomic variation, may underlie immunotherapy resistance in 11q13-amplified LIHC, underscoring the need for tailored immunotherapeutic strategies for this molecularly defined subgroup.

#1014 Multimodal AI predicts immune checkpoint inhibitor response from clinically available inputs and whole-slide images with explainable tumor biology and combination therapy insights.

Felicia Kuperwaser, Sunil Kumar, Sepideh Foroutan, Dillon Tracy, Kevin Freisen, Taylor Wood, Zong Miao, Nathaniel Tann, Fahad Khan, Jean Michel Rouly, Anshu Jain, Jeff Sherman, Emily Vucic, **Maayan Baron**

Zephyr AI, McLean, VA

Background: Immune checkpoint inhibitors (ICIs) provide durable benefit for a subset of patients, yet most do not respond and current biomarkers (PD-L1, TMB, MSI) have limited predictive value. We developed AIM-io, a multimodal, biologically interpretable AI model that predicts ICI response using routine clinical inputs including liquid biopsy, tissue NGS and, for proof-of-concept, whole-slide images (WSI) processed with publicly available research-only foundation-model embeddings. AIM-io integrates reconstructed gene-expression and TME programs with predicted small-molecule sensitivities, enabling biological interpretation of each prediction.
Methods: A pan-cancer real-world cohort (~3,000 patients, 13 tumor types) treated with anti-PD-(L)1 or anti-CTLA-4 therapy was assembled with linked rwOS/rwPFS. Inputs included liquid-biopsy, tissue NGS, or WSIs encoded embeddings (e.g., GigaPath, UNI). AIM-io incorporated clinical variables, genomic alterations from commercial LDTs, reconstructed expression/TME signatures (AIM-Ex), ICI drug/target embeddings, and AIM-Bx-derived small-molecule sensitivity profiles (~100 agents). Performance was assessed using C-index, hazard ratios, KM stratification, and comparisons to available biomarkers.
Results: AIM-io showed robust cross-modality performance. In held-out LDT data, AIM-io significantly separated responders vs. non-responders ($p < 10^{-7}$, HR = 0.23, 95% CI 0.14-0.41), outperforming PD-L1 ($p = 0.26$, HR = 0.77, 95% CI 0.48-1.22) and TMB ($p < 10^{-3}$, HR = 0.39, 95% CI 0.24-0.65). Using liquid-biopsy DNA, AIM-io significantly stratified outcomes ($p < 0.05$, HR = 0.63, 95% CI 0.39-1.01). Results were consistent across cancer types and NGS platforms. With WSI-only inputs, AIM-io achieved significant outcome separation (HR = 0.46, $p < 0.05$; 95% CI 0.22-0.97) and outperformed models using WSI embeddings alone (HR = 0.62, $p = 0.12$), demonstrating feasibility in settings lacking molecular assays. Predicted responders showed enrichment for reconstructed TME programs (e.g., lymphocyte infiltration), whereas non-responders showed immunosuppressive signatures (e.g., TGF-β, wound healing). Small-molecule sensitivity predictions differed, with responders showing greater predicted PARPi sensitivity and non-responders enriched for VEGFi sensitivity.
Conclusions: AIM-io provides an explainable multimodal framework for ICI-response prediction using diverse, clinically accessible inputs—including liquid biopsy DNA and WSI embeddings. By integrating reconstructed expression, TME biology, and predicted therapeutic vulnerabilities, AIM-io offers an assay-agnostic approach for retrospective evaluation of immunotherapy response and hypothesis generation for rational combinations. Prospective validation is warranted.

#1015 Quantitative c-MET immunohistochemistry reveals prognostic subgroups in papillary renal cell carcinoma.

Yong Il Lee[1], Jamin Park[1], Sun Young Yoon[1], Yong Mee Cho[1], Inkeun Park[2], **Bokyung Ahn**[1]

[1]Department of Pathology, Asan Medical Center, University of Ulsan College of Medicine, Seoul, Korea, Republic of,[2]Department of Oncology, Asan Medical Center, University of Ulsan College of Medicine, Seoul, Korea, Republic of

Background: MET is a key driver gene in papillary renal cell carcinoma (PRCC), yet the prognostic significance of c-MET immunohistochemical (IHC) expression remains unclear. Previous studies have been limited by heterogeneous cohorts containing mixed renal tumor entities and by subjective variability inherent to manual IHC assessment. As c-MET targeted antibody-drug conjugates (e.g., Telisotuzumab vedotin) show therapeutic promise in several cancers, we aimed to quantitatively evaluate c-MET expression in a strictly defined PRCC cohort and to clarify its prognostic value using an image analysis platform.
Methods: A total of 505 surgically resected PRCC cases (1989-2023, Asan Medical Center) were reclassified according to the 2022 WHO system after excluding non-PRCC entities using a 19-marker IHC panel. c-MET IHC (SP44, Ventana) was performed in the final 415 PRCC cases and scored both manually (H-score) and by HALO image analysis. Expression levels were dichotomized into high and low by the median value. Statistical analyses included Spearman correlation, and survival analyses for 5-year recurrence-free (RFS) and disease-specific survival (DSS).
Results: HALO-based c-MET quantification showed a strong correlation with manual scoring ($R = 0.88$, $P < 0.001$), supporting the validity of automated evaluation. HALO scoring demonstrated significantly higher c-MET expression in type 1 compared to type 2 PRCC (median 64.03 vs. 33.26, $P < 0.001$). Type 2 PRCC exhibited worse RFS and DSS than type 1 (both $P < 0.001$). In subgroup analyses, type 2 PRCC with low c-MET expression had significantly poorer DSS than type 1 PRCC with either low ($P = 0.022$) or high ($P = 0.029$) expression, however type 2 PRCC with low c-MET expression did not show statistical significance compared to type 1 PRCC. For RFS, type 2 PRCC showed consistently worse outcomes than type 1 PRCC regardless of c-MET level. However, c-MET expression was not an independent prognostic factor in univariate or multivariate Cox models.
Conclusions: This study's strength lies in its large, rigorously reclassified PRCC cohort and the combined use of manual and automated scoring methods. Importantly, automated HALO scoring provided an objective, reproducible measure of c-MET expression while maintaining excellent concordance with manual evaluation, supporting its utility in standardizing biomarker assessment. Although PRCC subtyping is no longer recommended in the current WHO classification, we found that low c-MET expression strongly correlated with type 2 morphology and poorer DSS, reflecting the fundamentally different underlying molecular pathways between type-specific phenotypes. Also, since type 2 PRCC with high c-MET expression showed survival patterns similar to type 1, quantitative assessment of c-MET expression may refine risk stratification in PRCC and furhter guide patient selection for emerging MET-targeted therapies.

#1016 PHIT score integrates tumor biology to predict PDAC prognosis and therapy response.

Derek Erstad[1], Alejandro Zulbaran y Rojas[1], Christy Chai[1], Eugene Choi[1], George Van Buren[1], E. Ramsay Camp[1], William E. Fisher[1], Natalie Vokes[2]

[1]Baylor College of Medicine, Houston, TX,[2]University of Texas MD Anderson Cancer Center, Houston, TX

Background: Pancreatic ductal adenocarcinoma (PDAC) exhibits wide variation in tumor plasticity (P), heterogeneity (H), immune suppression (I), and treatment resistance (T). Existing clinical and molecular classifiers capture only part of this biology. We developed PHIT, a 12-gene transcriptomic score integrating these four axes, and evaluated its prognostic and therapeutic relevance across resected and metastatic PDAC.

Methods: RNA-seq from TCGA, PACA-CA/ICGC, and CPTAC (n=419) was batch-corrected and analyzed with weighted Cox models to generate gene-level survival coefficients. These were integrated with chemotherapy-response metrics from the metastatic COMPASS cohort (n=188; continuous tumor-volume change and PR/SD/PD categories across all patients and within FOLFIRINOX and gemcitabine/nab-paclitaxel subgroups) to build a joint survival-chemo composite. Bootstrap selection yielded a 12-gene PHIT signature. PHIT scores were computed using training-cohort means/SDs and Cox logHR weights. Prognostic performance was tested using Kaplan-Meier, Cox models, and c-index. Validation included PACA-AU, Chen, Nones, and Moffitt cohorts (n=339). Hallmark analyses compared PHIT-high vs PHIT-low tumors within molecular subtypes.

Results: PHIT significantly stratified overall survival (OS) in the 419-patient training cohort (median 32.7 vs 10.4 months for PHIT Q1 vs Q4; HR 3.49, $p=7\times10^{-14}$), improved a tumor grade/stage model (c-index 0.590→0.685), and remained independently prognostic after adjustment for Moffitt, Collisson, and Bailey molecular subtypes (HR 2.36, $p<0.001$). In COMPASS, PHIT correlated with chemotherapy resistance (tumor-volume change $r=0.40$ overall; 0.45 FOLFIRINOX; 0.34 GA) and stratified metastatic OS (12.6 vs 5.6 months; HR 2.92, $p=1.4\times10^{-5}$). In validation cohorts, PHIT consistently separated risk: PACA-AU (50.4 vs 10.9 months; HR 4.90, $p=0.008$), Chen (31.5 vs 15.6; HR 3.09, $p=0.01$), Nones (24.5 vs 15.1; HR 3.47, $p=0.01$), and combined arrays (30.1 vs 15.1; HR 2.45, $p=6.45\times10^{-5}$). Mechanistically, PHIT-high Classical tumors showed selective enrichment of EMT, ECM remodeling, and inflammatory NF-κB pathways, whereas PHIT-high Basal-like tumors showed glycolytic and metabolic plasticity with hypoxia, mTORC1, and proliferative G2M/E2F programs. These subtype-specific patterns were reproducible across Collisson and Bailey frameworks.

Conclusions: PHIT is a concise transcriptomic score that integrates four dimensions of aggressive PDAC biology. It predicts survival across seven cohorts (n=946), correlates with chemotherapy response, and reveals distinct EMT- and glycolysis-associated high-PHIT phenotypes, supporting its utility for biological risk stratification and treatment selection.

#1017 STAT5A promoter hypermethylation as a biomarker of immune checkpoint inhibitor response in squamous cell carcinoma in cfDNA liquid biopsies.

Janice Patterson, Brooke Overstreet, Jiemin Liao

Guardant Health, Palo Alto, CA

Background: STAT5A is a downstream transcription factor in the JAK-STAT pathway that regulates immune- and tumor-related gene expression. Hypermethylation of the STAT5A promoter is linked to immune cell depletion and reduced antitumor immune activity in head and neck squamous cell carcinoma (HNSCC) and lung squamous cell carcinoma (LSCC) (Liang et al. 2023). We hypothesized that STAT5A promoter hypermethylation (PM) detectable in cfDNA is a predictive biomarker of immune checkpoint inhibitor (ICPI) response in squamous cell carcinomas (SCC).
Methods: Guardant360 Liquid (Guardant Health, Palo Alto, CA) was used to detect hypermethylated STAT5A promoter region, defined initially as 5kb upstream from the transcription start sites (TSS). Correlation between methylation and expression for PM regions was determined using The Cancer Genome Atlas (TCGA) data to identify loci where PM was associated with transcriptional silencing. Candidate loci were evaluated in a large cohort of cancer-free samples (n=32k) to ensure analytical specificity. PM status is distinguished relative to constitutively hypermethylated control regions, measuring methylation level relative to total cfDNA. Clinical outcomes analyses used the GuardantINFORM real-world clinico-genomics database.
Results: STAT5A PM prevalence as measured by Guardant360 Liquid was concordant with published datasets across tumor types. The assay demonstrated high analytical specificity (negative percent agreement > 98%). STAT5A PM was associated with a shorter time to next treatment (TTNT) among ICPI-treated patients with SCC (n=815, 91% LSCC, 9% HNSCC, unadjusted log-rank p=0.01). Median TTNT for STAT5A PM+ patients (n=16) was 8.6 mo (95% CI, 4.6-10.4) versus 30.7 mo (95% CI, 25.6-38.1) for PM- patients (n=799). In a multivariable Cox proportional hazards model, adjusting for clinical covariates (age, gender, and line of therapy), PM+ remained independently associated with shorter TTNT (HR=2.10; p=0.03). When analyzed by cancer type, the association between STAT5A PM and TTNT was primarily driven by LSCC (HR=2.33; p=0.01). The limited number of PM+ HNSCC cases (n=3) precluded statistical significance in that subgroup.
Conclusion: Non-invasive detection of STAT5A PM using Guardant360 Liquid is inversely correlated with real-world ICPI benefit in patients with LSCC, adding to a growing list of biomarkers demonstrated to have predictive significance in ICPI and broadening the role of methylation-based profiling in precision oncology.

#1018 Longitudinal peripheral blood TCR tracking predicts response to immune checkpoint inhibitors.

Dingyuan Wang[1], Kaiyan Xu[2], Parker J. Li[3], David J. H. Shih[3], Matthew K. L. Chiu[1], Jason W. H. Wong[3], Wei Dai[1], Aya El Helali[1]

[1]Department of Clinical Oncology, School of Clinical Medicine, LKS Faculty of Medicine, The University of Hong Kong, Hong Kong, Hong Kong,[2]Centre for Oncology and Immunology, Hong Kong Science Park, Hong Kong, Hong Kong,[3]School of Biomedical Science, The University of Hong Kong, Hong Kong, Hong Kong

Background: While immune checkpoint inhibitor (ICI) therapy has revolutionized oncology, reliable biomarkers to predict clinical response are critically needed. Static, single-time-point analysis of the T-cell receptor (TCR) repertoire has proven inadequate. We hypothesized that the longitudinal tracking of TCR clonal dynamics would provide a more powerful and predictive biomarker of clinical outcome.

Methods: To test this hypothesis, we employed a two-stage strategy. First, we performed an exploratory analysis on the public longitudinal TCR-seq dataset GSE212217 to investigate whether dynamic changes in TCR clones could distinguish responders from non-responders. Based on the observed temporal expansion patterns, we developed a novel classification model that categorizes TCR clones algorithmically by quantifying the direction and magnitude of change in their relative abundance over time. Clones are assigned to distinct behavioral types, Response, Super-response, Transient, and Quiescent, based on specific, quantitative criteria applied to their longitudinal trajectories. Second, we validated this model in an independent, prospective pilot cohort of advanced melanoma patients using TCR sequencing from serial blood samples.

Results: Analysis of the public dataset confirmed that baseline TCR diversity metrics were unable to differentiate between clinical responders and non-responders. In contrast, our longitudinal model identified distinct clonal expansion trajectories. This novel response score was significantly elevated in responders compared to non-responders in the discovery cohort (Wilcoxon test, $P = 0.011$). Critically, patients with a high score exhibited a marked survival advantage (Log-rank $P = 0.040$), confirming the clinical prognostic value of our dynamic metric. Validation in our independent melanoma cohort confirmed the clinical utility of our model. Strikingly, the patient with disease progression exhibited a low proportion of active, expanding clones (5.5%), whereas the patient achieving a deep clinical response demonstrated a markedly higher proportion of active, expanding clones (10.5%).

Conclusion: We have developed and validated a novel biomarker based on the dynamic expansion of T-cell clones that effectively predicts ICI response and survival. This work definitively moves beyond the limitations of static TCR metrics, establishing longitudinal clonal tracking as a crucial strategy for liquid biopsy. This approach provides a critical tool for real-time response monitoring and precision stratification of cancer immunotherapy.

#1020 Characterization of functional estrogen receptor (ER) dependence via comprehensive epigenomic liquid biopsy stratifies endocrine therapy (ET) responders with metastatic breast cancer (MBC).

Stefania Morganti[1], Jonathan Beagan[2], Ningxuan (Shirley) Zhou[1], Khoi Nguyen[2], Kalie Smith[1], Ashka Patel[1], Catherine Stever[1], Katheryn Santos[1], Molly Skeffington[1], Olivia D'Amico[1], Travis Clark[2], Justin Finkle[2], Anthony D'Ippolito[2], Mike Zhong[2], Jamey Guess[2], Kristian Cibulskis[2], Aparna Gorthi[2], Tyrone Tamakloe[2], Charlene O'Brien[2], Baovy Tran[2], Mary McGillicuddy[2], Nabihah Tayob[1], Sara M. Tolaney[1], Nancy U. Lin[1], Hillary Heiling[1], Corrie A. Painter[2], Matthew L. Eaton[2], J. Carl Barrett[2], Heather A. Parsons[3]

[1]Dana-Farber Cancer Institute, Boston, MA,[2]Precede Biosciences, Boston, MA,[3]Fred Hutch Cancer Center, Seattle, WA

Background: Endocrine therapy (ET) is standard of care for ER+ MBC, but virtually all patients (pts) develop ET resistance over their disease course. Biomarkers predictive of loss of ER dependence to guide therapy (tx) are lacking.
Methods: We identified 122 pts with ER+/HER2- MBC enrolled in the EMBRACE study at Dana Farber Cancer Institute who received 1-2 lines (L) of ET and had a blood drawn within +/- 30 days of switch from 1L to 2L (n=77) or from 2L to 3L (n=53). Using 1mL plasma, we profiled genome-wide enhancers, promoters and DNA hypermethylation to infer pathway activation and gene expression levels. Samples that did not meet quality thresholds (n=16) or had tumor fraction <0.5% (n=48) were excluded. We applied the Precede ER dependence index (PERDI) that quantifies relative activities of ER-driven vs estrogen-starvation-induced enhancers and classified samples as PERDI-high or -low using a predefined threshold. We investigated the association between PERDI and time-to-next-treatment (TTNT). A conditional landmark approach defined TTNT beginning from 30 days after the start of tx of interest (ET or non-ET) until the start of the next tx line, considering only tx switch for tumor progression as events. Time-dependent ROC curves were used in the prespecified primary analysis investigating the association between PERDI and early progression on ET. Kaplan Meier methods and Cox proportional hazard models were used in additional analyses.
Results: A total of 71 pts (79 samples) were included: 57 pts had draws collected before ET (40 switch from 1L to 2L ET, 17 from 2L to 3L ET); 22 pts had samples collected from 2L ET to 3L non-ET. Most common next-line ET regimens were SERD (n=17), SERD + CDK4/6 inhibitors (i) (n=14), aromatase inhibitors (AI) + mTORi (n=9), SERD + other targeted therapy (n=6). Among 57 pts starting next-line ET, PERDI was associated with landmark TTNT (median TTNT 2.4 months (mo) with low vs 4.1 mo with high PERDI, HR 2.65, 95% confidence interval [CI] 1.24-5.66, p=0.012). However, PERDI did not reliably identify early progressors to next-line ET (time-dependent AUC at 2 mo c = 0.51). Among 22 pts who switched from ET to non-ET (primarily chemotherapy), PERDI was not associated with TTNT (HR 0.66, 95% CI 0.23-1.85, p=0.426), suggesting a potential predictive role specifically for ET. Among pts with high PERDI but poor response to next-line ET, preliminary analyses identified 6 outliers for activity of known resistance pathways (e.g. *FGFR1*, *ERBB2*).
Conclusions: We observed a significant association between PERDI and benefit from ET. Our exploratory analysis integrating resistance pathways beyond ER further identified pts with high PERDI but ET resistance. Upon further clinical validation, this blood based comprehensive epigenomic assay could become a valuable tool to guide tx for pts with ER+/HER2- MBC.

#1021 Detection of rare genomic fusions revealed through comprehensive genomic profiling of atypical tumors.

Jennifer B. Jackson[1], Stanislav Fridland[2], Behtash G. Nezami[2], Gunja Pathak[1], Jennifer Dickey[1], Lawrence Jennings[2]

[1]Labcorp, Baltimore, MD,[2]Department of Pathology, Northwestern University Feinberg School of Medicine, Chicago, IL

Next-generation sequencing (NGS) of tumor tissue is the gold standard for genomic profiling of most solid cancer types, facilitating the identification of treatment options and patient management strategies by uncovering clinically actionable variants that can be targeted with biomarker-specific FDA-approved drugs. Validation of NGS assays requires large numbers of patient samples to evaluate the performance of each variant class, including single nucleotide variants, insertions and deletions, structural variants like copy number amplifications and translocations, as well as genomic signatures (microsatellite instability and tumor mutation burden). Sourcing clinical samples, however, is often a challenge due to limited number of patient samples available and more so by the biological prevalence of rare biomarkers, such as *NTRK3* and *RET* fusions. An often-overlooked source of patient samples is those where genomic profiling is not regularly employed due to the early stage of the cancer that can be treated with curative surgical resection rather than requiring targeted precision oncology drugs. Furthermore, uncommon tumor types rarely receive comprehensive genomic profiling as it is not considered standard of care or medically necessary and therefore are not well-characterized for genomic alterations. Using the PGDx elio™ tissue complete, a 505-gene FDA-cleared NGS solid tumor profiling assay, several tumor types not traditionally profiled were assessed under investigator-initiated studies and were unexpectedly found to have an enrichment of *NTRK3* and *RET* fusions. *NTRK3* fusions, occurring in less than 1% of most adult cancers, were observed at a higher-than-expected frequency in atypical Spitz tumor, an uncommon melanocytic skin lesion normally treated through surgical resection. Other tumor types positive for this fusion were ganglioglioma and secretory carcinoma. *RET* fusions, with prevalence highest in papillary thyroid carcinoma at 2-5%, were also identified in atypical Spitz tumor, glioblastoma, and lung adenocarcinoma. To confirm these findings, samples were also run on a validated, modified Archer FusionPlex® solid tumor RNA-based panel targeting 142 genes. Of the 13 *NTRK3* and 10 *RET* fusions detected by the PGDx elio tissue complete, all fusions were confirmed by the RNA-based fusion panel. These findings demonstrate the performance of PGDx elio tissue complete for rare fusion detection and also identify a unique source for these variants that are critical to biomarker validation. Additional work is warranted to establish the prevalence of these rare, targetable fusions in these tumor types which may represent a potential opportunity for targeted therapy.

#1022 NFKBIA amplification attenuates B2M expression in NKX2.1-amplified lung adenocarcinoma, indicating immune evasion potential.

Ka Yee Li, Anthony J. Iafrate

Molecular Pathology, Massachusetts General Hospital, Boston, MA

Introduction: Lung adenocarcinoma (LUAD) is the predominant subtype of non-small cell lung cancer, accounting for approximately 40% of cases. With growing insights into tumor immunology and the advancement of immunotherapy, LUAD has shown remarkable therapeutic benefits in clinical trials. *NKX2.1* is located in the 14q13.3 amplification interval and is the most frequently amplified genes in LUAD. *NFKBIA*, also resides in this region, is frequently co-amplified with *NKX2.1*. *NFKBIA* encodes IκBα, an inhibitor of NF-κB transcription factors that prevents their activation. A major challenge in lung cancer immunotherapy is the loss of major histocompatibility complex (MHC) class I expression. β2-microglobulin (B2M) is an essential subunit of MHC class I molecules and is crucial for presenting tumor antigens to T cells. Loss of B2M expression contributes to immune evasion and is regulated by the NF-κB signaling pathway. We hypothesize that NFKBIA amplification suppresses B2M, impairing immune responses and reducing immunotherapy efficacy. This study investigates whether reducing *NFKBIA* can restore B2M and enhance immunotherapy in *NKX2.1* amplified LUAD.

Methods: Multiple LUAD cell lines were treated with TNF-α to activate NF-κB. Stable cell lines with CRISPR-mediated NFKBIA knockout or overexpression were generated to assess effects on NF-κB activity and B2M expression.

Results: Western blot analysis revealed that cell lines with high IκBα expression showed low B2M expression, suggesting that elevated IκBα inhibits NF-κB activation and reduces transcription of its target genes. TNF-α treatment significantly increased B2M expression within 12 h, with variable duration across cell lines. H3122 and HCC827 maintained elevated B2M levels for more than 5 days, while H23 and H661 showed transient induction returning to baseline within 3 days. These differences may serve as potential biomarkers predicting immunotherapy response. H3122 and H23 cells with *NFKBIA* knockout exhibited increased baseline B2M levels and enhanced induction after TNF-α treatment. Conversely, MGH006 and H2228 cells with NFKBIA overexpression showed reduced baseline B2M and diminished induction following TNF-α stimulation. Further studies on NFKBIA's role in NF-κB signaling and validation using clinical LUAD samples are ongoing.

Conclusion: TNF-α-mediated NF-κB activation enhances B2M expression in LUAD, with duration varying by cell line. *NFKBIA* knockout increases, and overexpression decreases, B2M and NF-κB activation. *NFKBIA* may serve as a prognostic biomarker and therapeutic target to improve immunotherapy efficacy.

#1023 Ki67-kinetics and tumor biology shifts during neoadjuvant letrozole and ribociclib in ER-pos./HER2-neg. breast cancer: Insights from the NEOLETRIB-trial.

Julius Johannes Grindahl Hettich[1], Kamilla Fjermeros[1], Stephanie Beate Geisler[1], Manouchehr Seyedzadeh[2], Xavier Tekpli[3], Vessela N. Kristensen[4], Elin Edda Seland Agustsdottir[5], Unn-Cathrin Edvardsen Buvarp[1], Marie Fongaard[3], Tatiana Bosnjak-Olsen[6], Oeyvind Sundby[7], Alina Carmen Porojnicu[8], Helle Kristine Skjerven[9], Tone Hovda[10], Kristine Kleivi Sahlberg[11], Andliena Tahiri[12], Torben Luders[13], Lilly Anne Torland[14], Silje Mathiassen[15], Sofie Flovik Ranestad[15], John Christopher Noone[15], Elma Bahonjic Honigsperger[15], Clara Hammarstrom[15], Jurgen Geisler[16]

[1]Department of Oncology, Akershus Univ. Hospital, Lorenskog, Norway,[2]Department of Radiology, Akershus Univ. Hospital, Lorenskog, Norway,[3]Department of Medical Genetics & Department of Pathology, Oslo University Hospital, Oslo, Norway,[4]Department of Medical Genetics & Institute of Clinical Medicine, Faculty of Medicine, Oslo University Hospital, Oslo, Norway,[5]Department of Breast & Endocrine Surgery, Akershus Univ. Hospital, Lorenskog, Norway,[6]Novartis Pharma AG, Basel, Switzerland,[7]Novartis AS, Oslo, Norway,[8]Department of Oncology, Drammen Hospital, Drammen, Norway,[9]Department of Breast- and Endocrine Surgery, Radiumhospitalet, Oslo University Hospital, Oslo, Norway,[10]Department of Radiology, Drammen Hospital, Drammen, Norway,[11]Department of Research & Innovation, Drammen Hospital, Drammen, Norway,[12]Department of Clinical Molecular Biology (EPIGEN), Akershus Univ. Hospital, Lorenskog, Norway,[13]Institute of Clinical Medicine, Faculty of Medicine, Oslo University Hospital, Oslo, Norway,[14]Department of Research & Innovation, Vestre Viken Hospital Trust, Drammen, Norway,[15]Department of Pathology, Akershus Univ. Hospital, Lorenskog, Norway,[16]Department of Oncology & Institute of Clinical Medicine, Faculty of Medicine, Akershus Univ. Hospital/Oslo University Hospital, Lorenskog/Oslo, Norway

Background:
Cyclin-dependent kinase 4 and 6 (CDK4/6) inhibitors have recently transformed the treatment algorithms for hormone receptor-positive (HR+), human epidermal growth factor receptor 2 negative (HER2-) breast cancer. This has led to approval in combination with antihormonal therapies for first- and second-line therapy in the metastatic setting as well as in the adjuvant setting. The NEOLETRIB trial investigated the combination of the CDK4/6 inhibitor ribociclib with the aromatase inhibitor letrozole as neoadjuvant therapy in patients will locally advanced HR+/HER2- breast cancer characterized by cT3-cT4 tumors and/or cN2-3 lymph node involvement. This analysis focused on a comprehensive exploration of Ki67 kinetics and biology shifts to improve patient selection.
Patients and Methods:
NEOLETRIB was a single-arm, multicenter, open-label, phase II neoadjuvant trial enrolling 85 patients who received six cycles of ribociclib (starting dose: 600 mg once daily, 21 days on / 7 days off) combined with continuous letrozole prior to surgery. Ki67 was evaluated on tumor-biopsies obtained at baseline, day 21 of cycles 1 and 6, and at surgery. Thirty one patients from the Akershus cohort were randomly selected for additional Prosigna® testing in order to assess molecular subtype shifts between baseline and surgery.
Results:
Of 85 patients enrolled in this trial, 4 withdrew consent or were excluded due to screening failure. Complete tumor biopsy sets at all four time points were available from 71 patients. Patients were grouped in mutually exclusive groups based on Ki-67 profiles: Group 1 (Ki67 <20% at any timepoint) included 43 patients; Group 2 (Ki67 ≥20% at baseline and <20% later) included 21 patients. Four patients maintained Ki67 ≥20% at both baseline and surgery (Group 3) and 3 patients experienced Ki67 ≥30% at both baseline and surgery (Group 4). A total of 8 patients had Ki67 ≥50% at any given timepoint (Group 5).
Among 31 patients analyzed by Prosigna, 9 were classified as Luminal B at baseline, out of whom 8 converted to Luminal A after treatment. Three patients were classified as HER2-enriched at both time points despite having HER2 negative disease by immunohistochemistry routine staining. All three belonged to the high-proliferation (Ki67 >50%) subgroup 5.
Conclusions:
Neoadjuvant treatment with ribociclib in combination with letrozole appears to induce antiproliferative effects and a shift of molecular subtype from Luminal B to Luminal A in the majority of HR-positive, HER2-negative breast cancer patients in this trial. Improved understanding of the Ki67 dynamics and Prosigna-signatures may help identify subgroups of patients who may benefit from neoadjuvant letrozole/ribociclib combination and may potentially inform postneoadjuvant treatment decisions in the long run.

#1024 CIN signatures as biomarkers of drug sensitivity: Real-world evidence from DNA targeted sequencing data.

David Gomez-Sanchez[1], Adam Price[1], Max Schmidt[1], Sharafudeen Abubakar[1], Farheen Shah[1], Christina Lee[1], Chin-Tung Chen[1], Barbara Hernando[2], Daniel Muldoon[1], Areej Alsaafin[1], Evan Seffar[1], George Li[1], Subhiksha Nandakumar[1], Wassim Abida[1], Stephen Graves[1], Mackenzie Sullivan[1], Rachel N. Grisham[1], Britta Weigelt[1], Luc GT Morris[1], Nadeem Riaz[1], Pedram Razavi[1], Allison L. Richards[1], Mark Donoghue[1], Walid Khaled Chatila[1], Chaitanya Bandlamudi[1], Nikolaus Schultz[1], Michael F. Berger[1], Sohrab Shah[1], Geoff Macintyre[2], Julio Garcia-Aguilar[1], Francisco Sanchez-Vega[1]

[1]Memorial Sloan Kettering Cancer Center, New York, NY,[2]Spanish National Cancer Research Ctr. (CNIO), Madrid, Spain

Chromosomal instability (CIN) signatures are DNA copy number-based genomic biomarkers with emerging evidence for predicting treatment sensitivity across multiple drugs and cancer types. Modern computational approaches enable the quantification of CIN signatures from clinically validated targeted DNA sequencing panels such as MSK-IMPACT.

In this study, we derived copy number profiles from 63,630 tumor-normal MSK-IMPACT pairs using FACETS and computed pan-cancer CIN signatures across 73 cancer types. Analyses were restricted to pre-treatment samples, and CIN signature exposures were used to build three therapy-specific biomarkers: (i) a new biomarker of sensitivity for PARP inhibitors (PARPi) trained on progression-free survival (PFS) data from BRCA wild-type (BRCAwt) high-grade serous ovarian cancer (HGSOC) (ii) a new biomarker of sensitivity to platinum-based chemotherapies trained on disease-free survival (DFS) data from locally advanced rectal cancer (LARC) and (iii) an existing biomarker for resistance to anthracycline-based chemotherapies, now derived from targeted sequencing data for the first time. Each biomarker was validated in at least one independent MSK-IMPACT cohort of a different cancer type, using PFS calculated from treatment initiation and assessed at 12 months.

The PARPi biomarker performed similarly to the Myriad MyChoice Genomic Instability Score (GIS) in identifying BRCAwt HGSOC patients with longer PFS after treatment (CIN signatures: n=84, HR=0.38, p=0.005; GIS: n=84, HR=0.41, p=0.004) and fully identified responders in an independent BRCAwt prostate adenocarcinoma (PRAD) cohort (Sensitivity 100%, Specificity 60%, AUC=0.73). The platinum biomarker predicted longer PFS in primary head and neck squamous cell carcinoma (HNSCC) (n=82, HR=0.43, p=0.007). The anthracycline biomarker predicted shorter PFS in hormone-receptor positive HER2 negative (HR+/HER2-) breast cancer - both primary (n=191, HR=1.72, p=0.015) and metastatic (n=216, HR=1.72, p=0.003) - and in primary soft-tissue sarcoma (n=251, HR = 1.81, p=0.006).

These results highlight the feasibility and clinical potential of CIN signatures at a pan-cancer level, illustrating how the frequently overlooked complexity of genome-wide copy number alterations contained in routine targeted panels can be transformed into interpretable biomarkers to guide therapy selection. This proof-of-concept establishes that CIN signatures can be extracted from regulatory-approved assays such as MSK-IMPACT, although further validation is needed to facilitate clinical adoption.

#1025 Monitoring PD-L1 in tumor macrophage fusion cells in blood correlates to PD-L1 checkpoint inhibitor responses in metastatic breast cancer.

Sonia Muthuraj[1], Massimo Cristofanilli[2], Carolina Reduzzi[2], Giuseppe Del Priore[3], William V. Williams[3], Cha-Mei Tang[4], Daniel L. Adams[5]

[1]Rutgers University, New Brunswick, NJ,[2]Weill Cornell Medicine, New York, NY,[3]BriaCell Therapeutics, Philadelphia, PA,[4]Creatv MicroTech, Inc., Rockville, MD,[5]Creatv MicroTech, South Brunswick, NJ

In metastatic breast cancer (mBC), anti-PD-L1/PD-1 immune checkpoint inhibitors (ICIs), e.g. pembrolizumab, are approved in a subpopulation of mBC patients (pts) with a PD-L1 combined positive score (CPS) ≥10, median progression-free survival (mPFS) of 9.7 months and median overall survival (mOS) of >24 months. However, 62% of pts have CPS <10, and may also benefit from ICIs (i.e. ≥1 CPS have mPFS=7.6 months vs 5.6 for chemotherapy). One hypothesis to why low PD-L1 pts respond to ICIs is dynamic PD-L1 upregulation after starting a new therapy, requiring a biomarker to monitor PD-L1 and subsequent ICI benefit. Recent studies have identified PD-L1 expressing myeloid cells that disseminate into the blood from primary tumors, tumor-macrophage fusion cells (TMFCs), which may predict ICI response. However, dynamic changes in TMFC PD-L1 during ICI and their relationship to patient response is unknown. In this study, we monitored PD-L1 expression in TMFCs during ICI treatment, compared to tumor CPS, in mBC pts to evaluate PFS & OS at 24 months. We conducted a prospective pilot study of n=43 pts with pathologically confirmed mBC prior to receiving anti-PD-L1 ICIs. CellSieve microfilters isolated TMFCs from 7.5ml peripheral blood samples at 4 time points, prior to start of PD-L1 ICI (T0) and at monthly timepoints (T1-T3) for 4 months after ICI induction. TMFCs were identified by enlarged cell size (>30 μm) and polyploid nucleus. Average PD-L1 expressions in TMFCs were categorized as negative/low or high. Pearson's correlation compared average TMFC PD-L1 to CPS PD-L1 from tissue. TMFC PD-L1 expression and CPS were compared to pts' PFS and OS by Cox proportional univariate/multivariate analysis at 24 months. 95.3% (n=41/43) of pts provided a T0 sample. 90.7% (n=39/43) of pts provided a T1 sample (~28 days after ICI). 67.4% (n=29/43) of pts provided a T2 sample (~71 days), and 41.9% (n=18/43) of pts provided a T3 sample (~117 days). mPFS of pts with CPS ≥10, 1-10, <1 was 8.5, 7.0, 2.0 months, respectively (≥10 CPS vs <10 CPS HR=1.5, p=0.9180), and mOS was 12.1, 9.0, 18.9 months (≥10 CPS vs <10 CPS HR=0.6, p=0.9981). No correlations were identified between CPS and T0 TMFC PD-L1 (p=0.6109). Further, pts with high TMFC PD-L1 at T2 (HR=3.1, p=0.0475) had significantly better PFS, while T1 (HR=1.8, p=0.1843) and T3 (HR=4.0, p=0.0686) trended toward better PFS, but not for OS. Pts with high TMFC PD-L1 at any time point had significantly improved PFS (HR=2.8, 95% CI=1.4-5.5, p=0.0052), but not OS, compared to pts with consistently low TMFC PD-L1. In this pilot study, tumor PD-L1 CPS was not found to be correlated with clinical outcomes. However, high TMFC PD-L1 expression at any timepoint correlated with improved PFS, suggesting that monitoring PD-L1 in TMFCs may serve as a real-time biomarker to better indicate ICI response. Further studies into the role of TMFC PD-L1 in predicting therapeutic response are ongoing.

#1026 The copy number amplification of MYCL indicated activation of angiogenesis in small cell lung cancer.

Zihang Yuan, Jingwei Zhang, Yan Ju, Xingyuan Wu, Mantang Qiu, Xiao Li

Department of Thoracic Surgery, Peking University People's Hospital, Beijing, China

Background: Amplification of MYC family genes (MYC/MYCN/MYCL), a common phenomenon in small cell lung cancer (SCLC), has been widely reported to promote tumor angiogenesis. However, previous studies mainly focused on MYC and MYCN, while the role of MYCL amplification remains largely unexplored due to relatively low frequency. Here we aim to characterize the distribution of MYCL amplification in SCLC and elucidate the potential mechanism related to angiogenesis.
Methods: A total of 135 surgically resected SCLC patients with stage IA to IIIB were recruited from Peking University People's Hospital. A triple-color MYC-paralogs FISH probe was used to assess amplification patterns of MYC family genes. The amplification status were defined in the samples with ≥ 4 signals of each MYC-paralogs per cell in average. Immunohistochemistry (IHC, CD31/PAS) and multiplex IHC (mIHC, CD31/CD3/CD68/CD11b/PanCK/Ki67) were performed on tissue microarrays (TMA, n = 96) to quantify microvessel density (MVD) and endothelial cell proportion. Paired whole genome sequencing (WGS) and single-cell RNA sequencing (scRNA-seq) of SCLC patients (n = 20) were performed to define MYCL amplification status and cell proportion for functional analysis.
Results: Among the 135 SCLC samples, a total of 9 samples were identified as MYCL-amplified samples (6.7%). A higher proportion of endothelial cells in MYCL-amplified samples (n = 7) were observed compared to non-amplified samples (n = 89, Mann-Whitney U test, $p = 9.5\times10^{-3}$), as well as higher MVD in MYCL-amplified SCLC ($p = 5.7\times10^{-3}$). To further explore potential mechanism, we performed scRNA-seq in MYCL-amplified (n = 6) and non-amplified (n = 14) SCLC samples based on WGS results. A total of 199,644 cells were clustered and annotated into 28 cell subtypes, and elevated vascular endothelial cell proportion were further confirmed in MYCL-amplified samples. Additionally, MYCL-amplified samples exhibited the activation of cell adhesion, endothelial cell migration and angiogenesis pathways, indicating the highly activated vasculature morphogenesis process associated with MYCL amplification. Meanwhile, we also found higher hypoxia signature scores in MYCL-amplified samples using AddModuleScore, as well as enhanced VEGF signaling-mediated communication from MYCL+ tumor cells to endothelial cells by CellChat, indicating that MYCL+ tumor cells may drive angiogenesis through the activated VEGF pathway in hypoxic tumor microenvironment.
Conclusions: The amplification of MYCL exhibited higher endothelial proportion and elevated vascular density, potentially through activated interaction between hypoxic tumor and VEGF-induced angiogenesis, which may serve as potential biomarkers for anti-angiogenic therapy in SCLC.

#1027 A robust predictive marker of clinical outcomes to immune-checkpoint inhibition in advanced squamous head-and-neck cancer calculated from histopathological slides.

Yaron Kinar[1], Tien-Hua Chen[2], **Gal Dinstag**[3], Ranit Aharonov[1], Tuvik Beker[3], Johnathan Arnon[4], Anna Elia[4], Aron Popovtzer[5], Changsu Lawrence Park[6], Carlos Diego H. Lopes[6], Muh-Hwa Yang[2]

[1]Pangea Biomed, Tel Aviv, Israel,[2]Taipei Veterans General Hospital, Taipei City, Taiwan,[3]Pangea Biomed, TEL AVIV-JAFFA, Israel,[4]Hadassah-Hebrew University Medical Center, Jerusalem, Israel,[5]Sharett Institute of Oncology, Jerusalem, Israel,[6]Division of Medical Oncology and Hematology, Princess Margaret Cancer Centre, Toronto, ON, Canada

Background: Immune checkpoint inhibitors, namely programmed death-1 (PD-1) inhibitors, prolong survival in advanced head and neck squamous cell carcinoma (HNSCC). The combined positive score (CPS) guides treatment selection but has limited predictive value, underscoring the need for development of accurate and practical biomarkers in this space. ENLIGHT-DP predicts clinical outcomes to targeted and immune therapies directly from hematoxylin and eosin (H&E) slide scans. We previously showed that ENLIGHT-DP is predictive of outcomes in HNSCC treated with PD-1 inhibitors and in other indications. Here, we train and test an ENLIGHT-DP biomarker on a cohort of HNSCC cases using cross-validation (CV), and further validate it on two independent cohorts.
Methods: We obtained high resolution scans of pre-treatment tumor H&E slides of 89 advanced HNSCC patients from National Yang Ming Chiao Tung University (NYCU) treated with first-line PD-1 inhibitors +/- chemotherapy. Response (RECIST v1.1) was available for all cases, and long-term follow up for 65 of them. Using this dataset, we trained a model to predict response, in leave-4-out-CV. The model consists of (1) splitting the slides into tiles of 256x256 pixels, (2) extracting tile features using a deep learning model, (3) predicting tile states using a multi-layered perceptron, (4) pooling the tile states into a whole slide state using attention-based multiple instance learning, and (5) Predicting the response from the pooled state using a linear layer. We report the CV results on this dataset, as well as the performance of the same model on two previously reported cohorts from Hadassah Medical Center (Hadassah, n=25, Oral Oncology 2025) and Princess Margaret Cancer Centre (BIO2, n=14, JITC 2019, ASCO 2025).
Results: The model is predictive of ORR in the NYCU cohort with ROC AUC of 0.67 and was able to stratify progression free survival (PFS, HR: 0.943, p=0.017). Applying the model to the Hadassah cohort resulted in ROC AUC of 0.76, and stratification of PFS (HR: 0.89, p=0.023), while CPS, which was available for that cohort, exhibited no predictive power (AUC=0.47, insignificant PFS association). Applying the model to the BIO2 cohort also resulted in ROC AUC of 0.76 and showed an insignificant trend for PFS prediction. CPS exhibited a much weaker effect for response prediction, with an AUC of 0.56, and insignificant association with PFS.
Conclusion: The ENLIGHT-DP IO biomarker predicts response to immunotherapy directly from whole H&E slide image scans and demonstrates high predictive power for ORR to PD-1 inhibitors +/- chemo in HNSCC. Although the model was trained on a relatively small cohort and using only response labels, it achieves significant results in terms of both response and PFS and generalizes well to two independent cohorts, on which it outperforms the commonly used PD-L1 IHC marker.

#1028 A tumor-agnostic YAP/TAZ score predicts TEAD inhibitor sensitivity independent of Hippo alterations.

Michael Wegert-Verhoeven[1], Mathea Fransisca[1], Sylvia Martin[1], Attila Jady[2], Daniela Richter[3], Malgorzata Oles[4], Timon A. Blindauer[5], Jan-Philipp Mallm[6], Jasmina Paluncic[2], Claudia Dagostino[2], Olga Ermakova[7], Annika Schneider[8], Matthew The[8], Annika Baude-Muller[9], Katja Beck[10], Maximilian Bullemer[1], Victor Didier Perez Meza[11], Vivek Venkataramani[12], Ralf C. Bargou[12], Heiko Becker[13], Melanie Boerries[14], Armin Tuchscherer[15], DKFZ/NCT/DKTK MASTER consortium[16], Martin Wermke[17], Andreas Brunschweiger[18], Mohammed Al-Saeedi[19], Dirk Jager[20], Olaf Witt[21], Denis Schapiro[5], Bernhard Kuster[22], Andreas Hartig[23], Michael Allgaeuer[24], Alexander Brobeil[25], Christoph E. Heilig[10], Maria Veronica Teleanu[10], Simon Kreutzfeldt[10], Peter Horak[10], Daniel Hubschmann[26], Wolfgang Hartmann[27], Marcel Trautmann[27], Ina Oehme[28], Claudia R. Ball[29], Stefan Frohling[30], Stefan M. Pfister[31], Hanno Glimm[32], Sebastian M. Dieter[33]

[1]Section Translational Precision Oncology, Division of Translational Medical Oncology, National Center for Tumor Diseases (NCT) Heidelberg and German Cancer Research Center (DKFZ), Translational Functional Cancer Genomics, NCT Heidelberg and DKFZ, Heidelberg, Germany,[2]Department for Translational Medical Oncology, NCT/UCC Dresden, a partnership between DKFZ, Faculty of Medicine and University Hospital Carl Gustav Carus, TUD Dresden and Helmholtz-Zentrum Dresden-Rossendorf (HZDR), Dresden, Germany,[3]Department for Translational Medical Oncology, NCT/UCC Dresden, a partnership between DKFZ, Faculty of Medicine and University Hospital Carl Gustav Carus, TUD Dresden and Helmholtz-Zentrum Dresden-Rossendorf (HZDR); German Cancer Consortium (DKTK), Partner Site Dresden, Dresden, Germany,[4]Computational Oncology Group (CO), Molecular Precision Oncology Program (MPOP), NCT Heidelberg and DKFZ, Heidelberg Germany, Heidelberg, Germany,[5]Institute for Computational Biomedicine, Faculty of Medicine, University Hospital Heidelberg, Heidelberg University; Translational Spatial Profiling Center (TSPC), Heidelberg; Institute of Pathology, University Hospital Heidelberg, Heidelberg, Germany,[6]Single-cell Open Lab, DKFZ, Heidelberg, Center for Quantitative Analysis of Molecular and Cellular Biosystems (BioQuant), Heidelberg University, Heidelberg, Germany,[7]Division of Pediatric Neurooncology, DKFZ, Hopp Children's Cancer Center Heidelberg (KiTZ), Heidelberg, Germany,[8]School of Life Sciences, Technical University of Munich, Freising, Germany,[9]Division of Translational Medical Oncology, DKFZ, Heidelberg, National Center for Tumor Diseases (NCT), NCT Heidelberg, A Partnership Between DKFZ, The University Hospital Heidelberg (UKHD), The Heidelberg Medical Faculty of the Heidelberg University, and The Thorax Clinic Heidelberg, Heidelberg, Germany,[10]Division of Translational Medical Oncology, DKFZ, Heidelberg, National Center for Tumor Diseases (NCT), NCT Heidelberg, A Partnership Between DKFZ, The University Hospital Heidelberg (UKHD), The Heidelberg Medical Faculty of the Heidelberg University, and The Thorax Clinic Heidelberg; DKTK, Core Center Heidelberg,, Heidelberg, Germany,[11]Institute for Computational Biomedicine, Faculty of Medicine, University Hospital Heidelberg, Heidelberg University, Heidelberg, Germany,[12]Comprehensive Cancer Center Mainfranken, NCT WERA, University Hospital Wurzburg, Wurzburg, Germany,[13]Department of Medicine I, Medical Center, University of Freiburg, Faculty of Medicine, University of Freiburg, Freiburg, Germany,[14]Institute of Medical Bioinformatics and Systems Medicine, Medical Center - University of Freiburg, Faculty of Medicine, University of Freiburg; DKTK, Partner site Freiburg, a partnership between DKFZ and Medical Center - University of Freiburg, Freiburg, Germany,[15]Department I of Internal Medicine, Center for Integrated Oncology Aachen Bonn Cologne Duesseldorf, University of Cologne, Faculty of Medicine and University Hospital, Cologne, Heidelberg, Germany,[16]Molecularly Aided Stratification for Tumor Eradication Research Program, NCT Berlin, NCT Dresden, NCT Heidelberg, NCT SudWest, NCT WERA, NCT West, DKFZ; DKTK sites: Berlin, Dresden, Essen/Dusseldorf, Frankfurt/Mainz, Freiburg, Heidelberg, Munchen, Tubingen, One NCT, Germany,[17]TU Dresden, NCT/UCC Early Clinical Trial Unit and Medical Clinic and Poliklinik I, University of Technology Dresden (TUD), Dresden, Germany,[18]Institute of Pharmacy and Food Chemistry, Julius-Maximilians-Universitat Wurzburg, Am Hubland, Wurzburg, Germany,[19]Department of General, Visceral and Transplantation Surgery, Heidelberg University Hospital, Heidelberg, Germany,[20]Department of Medical Oncology, NCT Heidelberg and Heidelberg University Hospital, Heidelberg, Germany,[21]Clinical Cooperation Unit Pediatric Oncology, DKFZ and DKTK, Hopp Children's Cancer Center Heidelberg (KiTZ); Department of Pediatric Oncology, Hematology and Immunology, Heidelberg University Hospital, Heidelberg, Germany,[22]School of Life Sciences, Technical University of Munich, German Cancer Consortium (DKTK), partner site Munich a partnership between DKFZ and Technical University of Munich (TUM), Munich, Germany,[23]Institute of Pathology, Carl Gustav Carus University Hospital, Dresden, Germany,[24]Institute of Pathology, University Hospital Heidelberg, Heidelberg, Germany,[25]Institute of Pathology, University Hospital Heidelberg, Tissue Bank of the NCT, Heidelberg, Heidelberg, Germany,[26]Computational Oncology Group (CO), Molecular Precision Oncology Program (MPOP), NCT Heidelberg and DKFZ; DKTK, Core Center Heidelberg, Heidelberg, Germany,[27]West German Cancer Center, University Hospital Munster, Munster, Germany,[28]Clinical Cooperation Unit Pediatric Oncology, NCT and DKFZ Heidelberg and DKTK Heidelberg, Department of Pediatric Oncology, Hematology and Immunology, Heidelberg University Hospital; Hopp Children's Cancer Center Heidelberg (KiTZ), Heidelberg, Germany,[29]Department for Translational Medical Oncology, NCT/UCC Dresden, a partnership between DKFZ, Faculty of Medicine and University Hospital Carl Gustav Carus, TUD Dresden and Helmholtz-Zentrum Dresden-Rossendorf (HZDR); TUD Dresden University of Technology, Faculty of Biology, Dresden, Germany,[30]Division of Translational Medical Oncology, DKFZ, Heidelberg, National Center for Tumor Diseases (NCT), NCT Heidelberg, A Partnership Between DKFZ, The University Hospital Heidelberg (UKHD), The Heidelberg Medical Faculty of the Heidelberg University, and The Thorax Clinic Heidelberg; DKTK, Core Center Heidelberg, Heidelberg, Germany,[31]Division of Pediatric Neurooncology, DKFZ, Heidelberg, Hopp Children's Cancer Center Heidelberg (KiTZ); Department of Pediatric Oncology, Hematology and Immunology, Heidelberg University Hospital, Heidelberg, Germany,[32]Department for Translational Medical Oncology, NCT/UCC Dresden, Translational Functional Cancer Genomics, NCT Heidelberg and DKFZ; German Cancer Consortium (DKTK), Partner Site Dresden, Dresden, Germany,[33]Section Translational Precision Oncology, Division of Translational Medical Oncology, NCT and DKFZ Heidelberg; Department of Medical Oncology, NCT Heidelberg and Heidelberg University Hospital, Heidelberg, Germany

YAP and TAZ are Hippo pathway effectors that bind TEAD transcription factors to drive oncogenic programs. First-in-human trials of TEAD inhibitors (TEADis) showed activity and tolerability in pretreated mesothelioma patients, yet current trials focus on mesotheliomas and rare Hippo-altered tumors, despite the broad oncogenic role of YAP/TAZ in various solid cancers. Whether YAP/TAZ target gene signatures can identify tumors with high YAP/TAZ activity and potential TEADi sensitivity beyond these indications remains unclear.

We profiled YAP/TAZ activity using a 22-gene signature across 2390 advanced pediatric and 3746 advanced rare cancers or cancers from young adults (<51y) from the INFORM and DKFZ/NCT/DKTK MASTER (MASTER) trials. Benchmarking against mesothelioma

and YAP fusion-driven ependymoma revealed subsets of cancers across entity baskets with equal or higher YAP/TAZ activity independent of Hippo alterations.
To dissect tumor-intrinsic versus stromal contributions, we performed spatial transcriptomics on MASTER samples using microarrays and the Xenium platform (n=106 cores from 89 tumors representing >70 histological subtypes). Tumor-cell YAP/TAZ scores correlated strongly with bulk scores (r=0.61), whereas fibroblast (r=0.23) and immune-cell (r=0.35) correlations were weak, indicating that bulk scores largely reflect tumor-cell activity.
We highlight a MASTER patient with MET-amplified carcinoma in whom progression on the MET inhibitor capmatinib coincided with a marked YAP/TAZ-score increase. In MET-amplified HS746T gastric cancer cells, genetic YAP/TAZ activation reduced capmatinib sensitivity, partially reversed by TEAD inhibition, supporting an unrecognized YAP/TAZ-linked resistance mechanism.
To evaluate predictive capacity of the YAP/TAZ signature, 23 cancer cell lines and 30 patient-derived spheroid cultures (PDSCs) were treated with IAG933 (Ω-loop-binding TEADi) or VT107 (TEAD autopalmitoylation inhibitor). Across compounds and models, expression of genes most strongly associated with TEADi response were enriched for YAP/TAZ targets, enabling refinement of a TEADi response signature. This refined signature correlated with area-under-the-drug-response-curve (AUC) values (IAG933: Pearson r=0.81 for cell lines, r=0.60 for PDSCs; VT107: r=0.46 and r=0.45).
Notably, the refined signature derived from INFORM/MASTER tumors predicted TEADi response in matched PDSCs (n=13; r=0.70 for IAG933, r=0.72 for VT107), with IC50 values as low as 30 nM. Sensitive PDSCs included atypical rhabdoid tumor, colorectal, and pancreatic carcinoma - all lacking Hippo alterations and representing entities not typically considered YAP/TAZ-driven.
In summary, these data provide a strong rationale for a transcription-based stratified clinical trial evaluating TEAD inhibition across pediatric and adult advanced cancers irrespective of Hippo alterations.

: Biomarkers Predictive of Therapeutic Benefit 2
Poster Session

#1033 Leronlimab induces PD-L1 expression and is associated with long-term survival with an ICI in PD-L1 low metastatic TNBC.

Richard G. Pestell[1], Ritika Harish[1], Zhiping Li[1], Danni Li[1], Xuanmao Jiao[1], Hallgeir Rui[2], Massimo Cristofanilli[3], Daniel L. Adams[4], Neil E. Buss[5], Jonah B. Sacha[6], Jacob P. Lalezari[7]

[1]Pennsylvania Cancer and Regenerative Medicine Research Center, Baruch S. Blumberg Institute, Wynnewood, PA,[2]Thomas Jefferson University, Philadelphia, PA,[3]Cornell University, New York, NY,[4]Creatv MicroTech, Inc., Monmouth Junction, NJ,[5]Nucleus Global, Buren, Switzerland,[6]Vaccine and Gene Therapy Institute, Oregon Health and Science University, Portland, OR,[7]CytoDyn Inc, Vancouver, WA

Introduction. Patients with metastatic triple-negative breast cancer (mTNBC) have poor survival but may be eligible for immune check point inhibitor (ICIs). CCR5 is overexpressed in ~95% of TNBC. Data suggest that combining the CCR5 inhibitor leronlimab with an ICI may improve survival in mTNBC.
Methods. Analysis of patient gene expression, tumor histology, cancer-associated macrophage-like cells/circulating tumor cells (CAML/CTC) from clinical studies and tissue cultures of TNBC were conducted.
Findings. In breast cancer cohorts (N=1,096) CCR5 expression correlated with gene signatures of T cell immune exhaustion. Across public TNBC cohorts (N=73; after deduplication), CCR5 expression correlated with both GSEA and gene signatures of T cell infiltration and T cell immune exhaustion. TNBC subtype analysis showed CCR5 enrichment in epithelial cells of MLIA (Mesenchymal-like Immune-Altered, Jézéquel subtype) and IM (immune modulatory, Lehmann subtype). TNBC Subtype analyses showed higher CCR5-related signals in tumors classified as MLIA and IM subtypes. In cultured MDA-MB-231 TNBC cells, CCR5 expression suppressed glycosylated PDL1; CCR5 inhibition increased the abundance of PDL1 (18 kDa, 35 kDa, and glycosylated 55 kDa forms). To understand the mechanisms by which CCR5 may promote immune exhaustion, we investigated a heterotypic signal between TNBC cultured cells and the tumor microenvironment (TME) using a proteomic approach. CCR5 activity induced sB7-H3 (CD276), sTyro3 and the Tyro3 ligand Pros1. Both CD276 and Tyro3 are associated with ICI resistance; and abundance of both were attenuated by CCR5 blockade with leronlimab.
In Vivo. Leronlimab induced PD-1 expression in $CD8^+$ T cells in lymph node of rhesus macaques and had variable modulation on expression of several T cell exhaustion markers. In a retrospective analysis of data pooled from 28 patients with mTNBC leronlimab induced PD-L1 in CTC/CAMLs. Leronlimab was generally well tolerated. Higher leronlimab dose (550-700 mg once weekly), induction of PD-L1, and the formation of CCR5 dots in CTC/CAMLs, and treatment with leronlimab in combination, or subsequently, with an ICI were associated with improved survival. The median age of the 28 patients was 48.5 years (range 32-83), patients had a median of 2 prior lines of therapy in the metastatic setting (range 0-5), 18 patients had visceral metastases (64%), of which 8 had brain metastases, and 10 had non-visceral metastases, 17.9% of heavily pretreated mTNBC patients are currently alive after median >60 months of follow-up.
Conclusions. Leronlimab is well tolerated, inducing PDL1 expression on CTC/CAMLs, which may prime tumors for PDL1 blockade. CCR5 may promote ICI resistance in TNBC by upregulating immune checkpoints (sB7-H3) and sTyro3. Overall, 17.9% (5/28) of patients with mTNBC treated with leronlimab are currently alive after a median of >60 months follow-up.

#1034 Transcriptomic and genomic signatures associated with response or resistance to immunotherapy(IO) in locally advanced/metastatic (LA/M) head and neck squamous cell carcinoma (HNSCC) patients.

Elodie Girard[1], Sonia Canjura-Rodriguez[2], Bastien Cabarrou[3], Constance Lamy[1], Anne Schnitzler[1], Frederique Penault-Llorca[4], Emmanuel Bouilhol[5], Roger Sun[6], Eric Deutsch[7], Francois Legrand[8], Severine Tabone-Eglinger[9], Valery Attignon[2], Caroline Even[10], **Christophe Le Tourneau**[1], Ellen Van Obberghen-Schilling[5], Marta Jimenez[11], Nicolas Servant[1], Thomas Filleron[3], Edith Borcoman[1], Pierre Saintigny[12], Ivan Bieche[13]

[1]Institut Curie, Paris, France,[2]Centre Leon Berard, Lyon, France,[3]Oncopole Claudius Regaud - IUCT-O, Toulouse, France,[4]Centre Jean Perrin, Clermont Ferrand, France,[5]Institut de Biologie Valrose, Nice, France,[6]Radiotherapy, Institute Gustave Roussy, Villejuif, France,[7]Full Professor, Dept. of Radiation Onc., Institute Gustave Roussy, Villejuif, France,[8]R&D, Unicancer, Paris, France,[9]Cancer Research Center of Lyon, Lyon, France,[10]Gustave Roussy, Villejuif, France,[11]Unicancer, Paris, France,[12]Ctr. Leon Berard, Lyon, France,[13]Genetics Department, Inst. Curie, Paris, France

Background: IO efficacy in LA/M HNSCC patients is limited. Identifying biomarkers of resistance and response is crucial to better stratify patients. We characterized the genomic and transcriptomic landscape of IO-naive HNSCC patients to identify specific genomic and transcriptomic signatures of response to IO.
Methods: We analyzed baseline FFPE samples of 176 LA/M HNSCC patients treated with IO from CHECK'UP (NCT03412058) and TOPNIVO (NCT03226756) trials, for whom baseline RNAseq data were available. A penalized Cox model with Elastic Net procedure was used to identify gene signatures associated with PFS and OS. Using a resampling procedure, a bootstrap selection stability (BSS) index was computed for each gene and only those with a BSS > 30% were included in the final model to determine a score for both PFS and OS. In addition, 149 paired tumor and germline DNA were sequenced using whole exome. For biostatistics analysis using genomic alterations, only variants (SNVs, Indels, CNVs) in oncogenes, tumor suppressor genes with a variant allele frequency (VAF) of at least 10% and altered signaling pathways were considered.
Results: The cohort (median age 62.5 yo) included a majority of oropharynx (39.8%) and oral cavity (29.8%) tumors, 77.8% males, 62.3% with alcohol and 81.7% with tobacco use history and 60.0% of them were metastatic. Objective response rate was 17.4%, median PFS and OS were 1.9 months (mo) (95%CI=[1.8-2.5]) and 8.1 mo (95%CI=[6.1-9.7]), respectively (median follow-up of 33.3 mo, 95%CI=[28.7-36.5]). The most frequent genomic alterations affected *CCND1*, *CDKN2A*, *FAT1*, *TERT*, *TP53* genes and a gain of 3q26-q28. In univariable analyses, the presence of *TERT* or *FAT1* alteration were significantly associated with worse PFS. After adjustment for clinical variable, the presence of *FAT1* alteration and the upregulation of Hippo signalling pathway remained associated with worse PFS. The presence of *TERT* mutation was also associated with worse OS whereas the PI3K/AKT/mTOR pathway was associated with
improved OS in univariable and multivariable analysis, respectively. Among the 500 most differentially expressed transcripts, 21- and 18-gene expression signatures were selected to assess their association with PFS and OS, respectively. C-Index was 0.72 and 0.71 (0.58 and 0.57 after internal bootstrap validation) for PFS and OS, respectively. Scores were dichotomized using time-dependent ROC Curve (Low vs High) and HR adjusted for clinical factors were 3.62 (95%CI = [2.42; 5.43]) and 3.86 (95%CI = [2.52; 5.91]; p<0.0001) for PFS and OS, respectively.
Conclusions: We identified robust transcriptomic signatures and genomic alterations strongly associated with IO resistance, offering potential biomarkers for patient stratification. *TERT* or *FAT1* alteration were associated with worse prognosis.

#1035 Ultrasensitive cfDNA fragmentomics assay for early treatment response assessment in solid tumors.

Atul Bharde[1], Kiran Kirdat[1], Amol Chaudhari[1], Ajay Pandita[2], Gowhar Shafi[3], Mohan Uttarwar[2], Sudhir K. Sinha[4], Hiromi Brown[4], Bill Haack[5]

[1]1Cell.Ai, Pune, India,[2]1Cell.Ai, Foster City, CA,[3]1Cell.Ai, Mumbai, India,[4]InnoGenomics Technologies, New Orleans, LA,[5]Cadex genomics, New Orleans, LA

Introduction: Early identification of treatment response remains a major clinical challenge, as imaging lacks the spatial and temporal resolution required to measure the therapy response. Liquid biopsy (Lbx)-based fragmentomics offer a minimally invasive, tumor-agnostic approach to capture dynamic changes in tumor burden and can serve as an early surrogate marker for response. Here, we present the analytical validation of OncoAlibrex, a highly sensitive, NGS independent cfDNA fragmentomics assay for therapy response monitoring (TRM), and demonstrate its clinical utility in patient samples.

Methods: Analytical validation was conducted to evaluate various assay parameter using cfDNA extracted from healthy plasma and cancer patient samples (n =140). cfDNA fragments were quantified using multiplexed qPCR on ABI 7500 thermal cycler. Primers and probes were designed based on high copy number Alu and SVA retrotransposon represented across the genome. cfDNA fragment distributions at >80 bp, >105 bp, and >265 bp to detect tumor relevant shifts linking to tumor burden was detected using fragment-specific primer pairs. Therapy response was predicted using an integrated algorithm developed to interpret cfDNA fragments distribution.

Results: Standard cfDNA samples, and cfDNA isolated from healthy volunteers (n = 10) and cancer patients, were analyzed in triplicate across multiple days, operators, and reagent lots. Intra-assay variability was ≤1 % for ct value and ≤13 % for the ratiometric quantity, while inter-assay precision showed <2.0% ct variability. Excellent linearity ($R^2 \geq 0.99$) and qPCR efficiencies (>98%) were demonstrated across 0.6 pg to 20 ng/µL of ccfDNA. Analytical sensitivity parameters per CLSI were: limit of blank = 0. 37 pg/µL (>80 bp, ctDNA specific), 0. 01 pg/µL (>105 bp, ctDNA specific), 0.021 pg/µL (>265 bp, non-tumor specific); limit of detection = 0. 85 pg/µL (>80 bp), 0.17 pg/µL (>105 bp), and 0.074 pg/µL (>265 bp). Fragmentation pattern of patient-derived ccfDNA was enriched with shorter fragments (80-105 bp) compared to healthy individuals. The cfDNA specific fragmentation pattern of cancer patients showed high progression score with 100 % specificity to indicate therapy non-response.

Conclusions: OncoAlibrex assay detected tumor-specific cfDNA fragmentation pattern indicative of therapy resistance with very high sensitivity, specificity, and accuracy. This assay can be used for TRM during the early phase of the treatment and MRD detection post-treatment independent of the sequencing-based Lbx assays.

#1036 An integrated clinicopathologic and genomic analysis of *PPP2R1A* alterations reveals distinct patterns in uterine and ovarian cancers.

Kai Wang, Bo Yang, Chengyi Wang, Yannan Zhu, Jinmei Wang, Kunxu Xu, Zanmei Xu

OrigiMed, Shanghai, China

Purpose: *PPP2R1A* (encoding the PP2A Aα subunit) mutations are increasingly associated with immune checkpoint blockade (ICB) response in gynecologic cancers. However, their distinct patterns across histologies remain unclear. We bridged this gap via a comprehensive clinicogenomic analysis of *PPP2R1A*-mutant tumors.

Methods: We retrospectively profiled 159 Chinese patients with *PPP2R1A*-mutant gynecologic cancers using next-generation sequencing (NGS) in a CAP/CLIA-certified laboratory. Variant classes interrogated included single nucleotide variants (SNVs), indels, copy number alterations, and fusions. Tumors were categorized by primary site (uterine vs. ovarian) and histology. We assessed features including co-mutation patterns, pathways, tumor mutational burden (TMB), and PD-L1 expression.

Results: We identified 182 *PPP2R1A* genomic alterations across 159 patients (SNVs/indels 95.1%; amplifications 3.8%; rearrangements 1.1%). Uterine primaries predominated (109/159, 68.6%), most commonly with endometrioid histology (48.1%). Three hotspot SNVs (R183W, P179R, and S256F) accounted for 39% of all alterations. R183W was significantly enriched in ovarian clear cell carcinoma (OCCC) compared with endometrioid carcinoma (42.1% vs 20.0%; $P<0.05$). Overall PD-L1 positivity (CPS ≥1) was 66.4% (73/110) and was strongly associated with TMB-H in uterine tumors. Notably, 11.9% of patients (19/159) carried ≥2 *PPP2R1A* alterations (“multi-hit”). These multi-hit cases were almost exclusively uterine endometrioid cancers, demonstrated 81.2% dual positivity (TMB-H and PD-L1+). Mean TMB was markedly higher in uterine versus ovarian tumors (118.7 vs 14.9; $P<0.001$). *POLE* co-mutations (25.8%) are all TMB-H, and consistently conferred hypermutation. Frequent *PPP2R1A* co-mutations included *TP53* (61.6%), *PIK3CA* (57.9%), *ARID1A* (49.1%), and *PTEN* (44.7%). *PTEN* co-mutation was strongly enriched in uterine tumors (60.6% vs 9.8%; $P<0.001$).

Conclusions: *PPP2R1A* alterations show distinct clinicogenomic patterns that vary by primary site and histology. Uterine *PPP2R1A*-mutant tumors differ clearly from ovarian tumors, with higher TMB and frequent *PTEN* co-mutations. In contrast, ovarian tumors, especially OCCC, tend to have low TMB and rarely show combined TMB-H/PD-L1 positivity, suggesting different underlying biological pathways. For the first time to our knowledge, we also identified a “multi-hit” *PPP2R1A* subgroup (11.9%), observed almost exclusively in uterine cancers that were enriched for TMB-H/PD-L1 positivity and diagnosed at early stage. These findings reinforce that *PPP2R1A* alterations are highly context-dependent and support the need for integrated clinicogenomic assessment when selecting patients for future immunotherapy and ICB trials.

#1037 Single cell and spatially resolved determinants of the clinical outcome of patients (pts) treated with locally advanced/metastatic head and neck squamous cell carcinoma (LA/M SCCHN) treated with immunotherapy (IO).

Mehdi Lamkhioued[1], Thimothee Casini[1], Elodie Girard[2], Karene Mahtouk[1], Sonia Canjura-Rodriguez[1], Valery Attignon[1], Bastien Cabarrou[3], Constance Lamy[2], Anne Schnitzler[2], Frederique Penault-Llorca[1], Caroline Even[4], Christophe Le Tourneau[4], Ellen Van Obberghen-Schilling[5], Nicolas Servant[2], Fayette Jerome[1], Nathalie Bendriss-Vermare[1], Ivan Bieche[6], Pierre Saintigny[1]

[1]Ctr. Leon Berard, Lyon, France,[2]Inst. Curie, Paris, France,[3]IUCT Oncopole, Toulouse, France,[4]Gustave Roussy, Paris, France,[5]Universite cote d'Azur, Nice, France,[6]Genetics Department, Inst. Curie, Paris, France

Background: We developed a composite Gene Expression Signature (cGES) comprising 22 protective (P) and 19 adverse (A) genes, agnostic of the tumor type, stratifying IO-treated pts in 3 risk groups : low (L-), intermediate (I-) and high-risk (H-) (abstract#6360 AACR2025). Herein, we validate its predictive value for progression free (PFS) and overall survival (OS) in a prospective cohort and uncover the single-cell and spatial determinants underlying clinical outcomes.
Methods: (1) The cGES was computed in 170 pts with LA/M SCCHN from 2 trials (NCT03226756; NCT03412058). (2) Next, we built a scRNAseq SCCHN atlas (scAt) of 219,138 cells from 77 independant pts including 19 and 21 pts classified as H-risk and L-risk respectively, and studied the distribution and functional states of cell populations between the 2 groups of pts. Cell-type-specific enrichments of A & P genes werequantified and intercellular communication networks were inferred to identify ligand-receptor (L-R) interactions. (3) Deconvoluted Visium data from 12 of the 77 SCCHN including 3 H-risk and 3 L-risk pts were used to map the spatial organization of cGES and to localize specific L-R interactions.
Results: (1) Multivariate analysis adjusted for ECOG, age, gender, and alcohol/tobacco use showed that I- and L-risk pts had significantly better outcomes. For PFS, hazard ratios were 0.64 ($p=0.04$) and 0.51 ($p=0.005$), and for OS 0.81 ($p>0.05$) and 0.54 ($p=0.015$), respectively. (2) Analysis of the scAt revealed that A genes from cGES were mainly expressed by epithelial and stromal cells. Conversely, P genes were mainly expressed by immune cells. H-risk tumors exhibited an altered communication landscape marked by strengthened epithelial junctions, developmental signaling, and universally increased EGFR L-R activity, whereas L-risk tumors showed an immune-enriched network dominated by extracellular remodeling, adaptive immune activation and immune cell recruitment. (3) Visium deconvolution identified 5 major cell-composition clusters (C), with epithelial-enriched C2 showing the highest A genes expression, while T cell-enriched C4/C5 displayed the strongest P genes expression. H-risk tumors exhibited prominent EGFR ligand expression, consistent with the results from the scAt data. In contrast, L-risk tumors displayed increased antigen-presentation, T-cell chemotaxis, and complement signaling.
Conclusion: cGES reliably stratified prognosis and reflects tumor ecosystem biology. H-risk tumors were dominated by epithelial-driven, EGFR-centered signaling, whereas L-risk tumors showed coordinated inflammatory T-cell-oriented programs. These findings suggest cGES as a prognostic and mechanistic biomarker, and provides a rational for EGFR-IO combination strategies to improve outcomes in LA/M SCCHN.

#1038 Integrating genomics and real-world data to predict fam-trastuzumab deruxtecan response in metastatic breast cancer across HER2 subtypes.

Abraham Apfel[1], Alka A. Potdar[1], Yuanqing Ye[1], Viswanath Devanarayan[1], Evvie Jagoda[2], Shelley MacNeil[2], Yan Zhang[1], Pallavi Sachdev[1]

[1]Eisai Inc., Nutley, NJ,[2]Tempus, Chicago, IL

Background: Metastatic breast cancer (MBC) is a major clinical challenge. Fam-trastuzumab deruxtecan-nxki (T-DXd), an antibody-drug conjugate targeting HER2, has shown efficacy across HER2+ and HER2-low subtypes. However, predictive biomarkers beyond HER2 status are underexplored in real-world settings. We leveraged real-world data from the Tempus database[1] to evaluate associations between somatic mutations and clinical outcomes in a clinically annotated cohort of patients with MBC treated with T-DXd, aiming to identify genomic correlates of response and survival to inform patient selection and therapeutic strategies.

Methods: We analyzed 124 patients with MBC with baseline tumor-normal matched sequencing data (Tempus xT [2]). Endpoints included real-world best overall response (rwBOR), progression-free survival (rwPFS), time to next treatment (rwTTNT), and overall survival (rwOS). Patients were classified as responders (CR/PR) or nonresponders (SD/PD) based on curated rwBOR. Oncoplots identified frequently mutated genes by rwBOR and HER2 status. Logistic regression assessed rwBOR (nonresponder as reference); Cox proportional hazard models evaluated rwPFS, rwTTNT, and rwOS, adjusting for age at T-DXd initiation, ER/PR status, care plan, sampling time, and tissue location. Models were run for all variants and for pathogenic-only subsets, stratified by HER2 status. Genes with >4% mutation frequency were included (50-60 genes for all-variant models; 11-13 genes for pathogenic-only models).

Results: The most frequently mutated genes were *TP53* (48%), *PIK3CA* (31%), and *GATA3* (17%). In all-variant models, *DYNC2H1* was associated with worse rwBOR (HER2+: P= 0.006; HER2-low: P=0.049), rwOS (HER2-low: P=0.014), and rwTTNT (HER2-low: P=0.004). *PIK3CA* mutations correlated with improved rwBOR (HER2+: P=0.016), rwPFS (all: P=0.01; HER2-low: P=0.007), and rwOS (HER2-low: P=0.002). Additional genes with consistent associations included *SPEN*, *POLQ*, *MED12*, *MAP2K4*, *ARID1B*, *SYNE1*, *KMT2C*, and *RB1*. Pathogenic-only analyses confirmed *PIK3CA* as a key predictor across multiple endpoints. While most models yielded FDR-adjusted P values >0.2, we prioritized genes with nominal P<0.1 and consistent prognostic direction across endpoints as indicative of potential signal.

Conclusions: Mutations such as *PIK3CA* were consistently correlated with improved outcome across HER2 subtypes, suggesting potential as predictive/prognostic biomarkers. Conversely, *DYNC2H1* mutations correlated with poorer outcomes, particularly in HER2-low patients, implicating potential resistance mechanisms. These findings support integrating genomic data into real-world evidence frameworks to enhance patient stratification, personalize treatment, and guide biomarker-driven clinical trials in MBC.

References: 1. www.tempus.com 2. Tempus-xT.v4_Validation

#1040 Blinded clinical validation of LiquidTME, a cell-free DNA assay for predicting response to immunotherapy by noninvasively profiling the tumor microenvironment.

Aadel A. Chaudhuri[1], David Y. Chen[2], Tucker Hansen[2], Mirna Jarosz[3], Vincent A. Miller[3], Aaron M. Newman[4]

[1]Mayo Clinic, Rochester, MN,[2]Washington University in St. Louis, St. Louis, MO,[3]LiquidCell Dx, San Carlos, CA,[4]Stanford University, Stanford, CA

Background: Combination immune checkpoint inhibitor (ICI) therapy represents a standard-of-care for patients with metastatic melanoma. However, >40% of patients do not respond to treatment and severe immune-related toxicity affects up to 60% of patients. Accordingly, we need more precise ways to select patients for combination ICIs. To address this, we developed LiquidTME, a liquid biopsy method based on Spatial EcoTyper (*Cancer Res* (2025) 85 (8_Supplement_1): 153) that leverages a deep learning approach to noninvasively assess the tumor microenvironment from cell-free DNA (cfDNA) methylation data. LiquidTME was previously trained to predict ICI response using 78 patients with advanced melanoma treated at Yale University. Here we performed a blinded validation of LiquidTME in coordination with clinicians at Washington University (WashU).

Methods: The WashU cohort consisted of pre-ICI plasma from 34 patients with advanced melanoma, each treated with ipilimumab and nivolumab (n=27) or relatlimab and nivolumab (n=7). ICI response was classified as durable clinical benefit (DCB) or no durable benefit (NDB) by a board-certified oncologist. Tumor mutational burden (TMB) was determined for 27 patients using commercial CLIA assays and analyzed as nonsynonymous mutations (mt) per megabase (Mb), using the FDA-approved 10 mt/Mb cutpoint for TMB-high and -low groups.

The WashU cohort was sent to a scientific team that was blinded to all clinical and TMB data. Cell-free DNA was extracted from 2 mL plasma per patient and subjected to enzymatic methyl-seq (EM-seq) at a median depth of 15x. LiquidTME was performed on the resulting profiles, yielding a binary response prediction and a continuous response score for each sample. Test results were locked down and returned. Both assays were compared by AUC and two-sided Wilcoxon rank-sum tests for response classification, and Kaplan-Meier analysis for progression-free survival (PFS).

Results: Median follow-up time of the cohort was 21.6 months. LiquidTME performed on cycle 1 day 1 pre-ICI plasma significantly stratified PFS with a hazard ratio (HR) of 0.27 ($P = 0.005$), with LiquidTME(+) patients achieving a median PFS of 1.7 years longer than LiquidTME(-) patients. LiquidTME distinguished DCB from NDB with an AUC of 0.77 ($P = 0.007$). Similar performance was seen across distinct combination ICI regimens. In patients with TMB data, LiquidTME maintained whole-cohort performance with a PFS HR of 0.30 ($P < 0.03$; AUC = 0.77). In contrast, TMB high vs. low subsets failed to stratify PFS (HR = 0.49; $P = 0.17$) or response (AUC = 0.53; $P = 0.8$).

Conclusion: LiquidTME identified durable responders to combination ICI from pretreatment plasma in this blinded validation cohort of melanoma patients. Given its favorable performance, LiquidTME shows promise as a clinical tool to guide personalized immunotherapy decision-making.

#1041 Extracellular vesicle-associated noncanonical ORFs as biomarkers of surgical outcome and chemoresistance in ovarian cancer.

Tatiana V. Karpinets[1], Xiaogang Wu[1], Sara Corvigno[2], Amma Asare[2], Joseph Celestino[2], Jeffry J. Cutrera[2], Pamela T. Soliman[2], Shannon N. Westin[2], Amir A. Jazaeri[2], P. Andrew Futreal[1], Anil K. Sood[2], **Sanghoon Lee**[2]

[1]Genomic Medicine, UT MD Anderson Cancer Center, Houston, TX,[2]Gynecologic Oncology and Reproductive Medicine, UT MD Anderson Cancer Center, Houston, TX

Background: High-grade serous ovarian cancer (HGSOC) is the deadliest gynecologic malignancy, with recurrence and chemoresistance driving poor survival outcomes. Beyond canonical resistance mechanisms, large portions of the genome encode non-canonical open reading frames (ncORFs) that produce short, intrinsically disordered proteins/peptides (ncPRs), largely undetectable by standard proteomics (“dark proteome”). Emerging evidence implicates ncPRs in tumor plasticity, stress adaptation, intercellular communication, and drug resistance. Their role in HGSOC chemoresistance and packaging into extracellular vesicles (EVs) remain unexplored.

Methods: We analyzed RNA-seq datasets from primary tumors of 30 patients and matched EV RNA-seq from 28 patients. Cohorts included patients with complete gross resection (CGR, n = 10) and neoadjuvant chemotherapy (NACT) with excellent (NACT-ER, n = 9) or poor response (NACT-PR, n = 9). ncORF abundances were quantified using a non-canonical ORF database and associations with clinical outcomes were assessed.

Results: Primary tumors and EVs showed distinct ncORF biotype distributions. exhibited a 17% decrease in coding and 10% decrease in intronic ncORFs ($p < 0.0001$), with 64% and 53% increases in pseudogene- and ncRNA-derived ncORFs and 3′UTR-derived ncORFs, respectively ($p < 0.0001$). Although fewer in number, pseudogene-derived ncORFs showed higher mean abundance than coding-derived ncORFs in EVs. Their abundance patterns trended toward discriminating CGR versus NACT patients (Fishers’ exact test $p = 0.004$) and NACT-ER vs NACT-PR ($P = 0.08$).

Conclusions: ncORFs, particularly pseudogene and ncRNA-derived, are selectively enriched in EVs from HGSOC patients, suggesting roles in intercellular communication and therapy response. These findings highlight EV-associated ncORFs as potential biomarkers and therapeutic targets in ovarian cancer.

#1042 Clinical and immune correlates of response to neoadjuvant chemoimmunotherapy in dMMR/MSI-H gastric cancer.

Pengfei Yu[1], Xingmao Huang[2], Xiangliu Chen[1], Hang Chen[1], Song Wang[3], Di Wang[3], Junrong Yan[3], Jiahui Chen[1], Qing Wei[1], Zequan Wu[1], Shengxin Fang[1], Han Chen[1], Hongtao Wang[1], Chengkang Zhu[1], Ling Huang[1], Yian Du[1], Hua Bao[3], **Haimeng Tang**[3], Xue Wu[3], Xiangdong Cheng[1]

[1]Zhejiang Cancer Hospital, Hangzhou, China,[2]The First Affiliated Hospital of Ningbo University, Ningbo, China,[3]Nanjing Geneseeq Technology Inc., Nanjing, China

Background: Neoadjuvant chemoimmunotherapy (NCIT) has shown promising efficacy in resectable deficient DNA mismatch repair/microsatellite instability-high (dMMR/MSI-H) gastric or gastroesophageal junction adenocarcinoma (GAC/GEJAC), yet predictive biomarkers of response remain unclear.
Methods: We analyzed 22 patients with resectable dMMR/MSI-H GAC/GEJAC treated with perioperative sintilimab plus oxaliplatin and S-1 (SOX). Clinical response, pathological regression, genomic alterations, and tumor microenvironment (TME) features were characterized by imaging, histopathology, multi-omics profiling, and multiplex immunohistochemistry. Patients were classified as responders or non-responders based on radiological and pathological evaluations.
Results: Radiological partial response was achieved in 10 of 22 patients (45.5%). Seventeen underwent R0 resection, with Becker tumor regression grades 1a, 1b, and 2 in 10, 1, and 6 cases, yielding a pathological complete response rate of 58.8%. Two-year event-free and overall survival were 81.8% and 80.7%. Non-responders exhibited poorer survival and greater baseline intratumor heterogeneity, with enriched mutations in *NF1*, *KDR*, *CDKN2A*, and *PLK1*. Transcriptomic profiling revealed upregulation of *GYLTL1B*, *PHLDA1*, *IGFN1*, and *SH2D5* in responders, alongside activation of proliferative (E2F, MYC targets) and immune-stimulatory (TNFA-NFKB, interferon) pathways. In contrast, non-responders lacked these signatures and showed immunosuppressive TME features, including elevated methylated tumor-infiltrating lymphocytes, Th17 signature expression, and M1 macrophage infiltration. Post-treatment analysis indicated favorable immune remodeling in responders, marked by increased dendritic and NK cells and decreased M1 macrophages, while non-responders maintained an M1-dominant state. Predictive biomarkers such as *CDKN2A* mutation, Fanconi anemia pathway alteration, and specific transcriptomic signatures correlated with both response and prognosis.
Conclusions: NCIT yielded high pathological response and survival rates in dMMR/MSI-H GAC/GEJAC. Integrated molecular and immune profiling identified genomic and transcriptomic determinants of response, supporting biomarker-guided therapeutic strategies in this molecularly defined cohort.

#1043 MUC5AC expression defines an immune-inflamed but functionally restrained tumor microenvironment in pancreatic ductal adenocarcinoma.

Ashish Manne[1], Wancai Yang[1], Yongchen Guo[1], Vaibhav Sahai[2], Prachi Bajpai[3], Yonghua Bao[1], M Khalid Khan Niazi[1], Alejandro Leyva[1], Upender Manne[3]

[1]The Ohio State University, Columbus, OH,[2]Fellow, Univ. of Michigan, Ann Arbor, MI,[3]University of Alabama at Birmingham, Birmingham, AL

Pancreatic ductal adenocarcinoma (PDAC) is highly resistant to immune checkpoint inhibitors (ICIs), largely due to an immune-excluded and stromal-dense microenvironment. MUC5AC, a gel-forming mucin aberrantly expressed in PDAC, is implicated in tumor progression and immune evasion. To define its role in shaping the tumor immune landscape, we investigated transcriptomic pathway, and immune infiltration features of MUC5AC-high versus MUC5AC-low PDACs. Transcriptomic data from TCGA, ICGC, and GEO PDAC cohorts (N=1047) were analyzed. Differential expression and pathway enrichment were assessed using Gene Ontology and KEGG. To ensure cross-platform robustness, immune cell infiltration was inferred using multiple transcriptomic deconvolution algorithms, including CIBERSORT, CIBERSORT-Abs, EPIC, MCPcounter, quanTIseq, xCell, ESTIMATE, and TIMER. Expression of immunomodulator and immune inhibitory genes was correlated with MUC5AC levels using median cut-offs, with cross-cohort validation. MUC5AC-high tumors showed enrichment of lipid and glycan metabolism, glycosyltransferase activity, extracellular vesicle secretion, and cytoskeletal/adhesion pathways, consistent with metabolic rewiring and stromal remodeling. Although KEGG immune pathways (T cell receptor, B cell receptor, NK cytotoxicity, chemokine signaling) were transcriptionally activated, functional signature evidence indicated immune suppression. Immune infiltration analysis revealed that MUC5AC-high tumors had significant associations ($p<0.05$) with higher Tregs, resting memory $CD4^+$ T cells, M0 macrophages, resting natural killer (NK) cells, memory B cells, plasma cells, and resting dendritic cells, and lower $CD8^+$ T cells, activated NK cells, follicular helper T cells, activated memory $CD4^+$ T cells, M1 macrophages, naïve B cells, γδ T cells, and M2 macrophages . Importantly, immunomodulator profiling demonstrated significant differences ($p<0.05$) in inhibitory molecules, with positive associations with PD-L1, LGALS9, IL10/IL10RB, TGFB1/TGFBR1, and IDO1, and negative associations with PD-1, PD-L2, CTLA4, LAG3, and TIM-3.Thus, MUC5AC-high PDAC exhibits an “immune-inflamed but functionally restrained” phenotype, characterized by immune signaling engagement but dominance of stromal, metabolic, and ligand-driven suppressive programs. MUC5AC may serve as a biomarker of immune exclusion, guiding patient stratification for ICI-based therapies.

#1044 Class II HLA supertype diversity predicts poor outcomes with immune checkpoint inhibitors in a pan-cancer cohort.

Luke Xiyu Zhao[1], Franshisca Hayek[2], Howard Liu Li[2], Mark Yarchoan[2], Mari Nakazawa[2]

[1]The Johns Hopkins Hospital, Baltimore, MD,[2]Sidney Kimmel Comprehensive Cancer Center, Baltimore, MD

Background: HLA diversity shapes the T-cell repertoire and antigen presentation, with potential effects on immune checkpoint inhibitor (ICI) outcomes. Several diversity metrics have been proposed, including zygosity, HLA evolutionary divergence (HED), and HLA supertype diversity (functional peptide-binding groups). Their relative value in pan-cancer cohorts remains unclear.
Methods: We examined the relationship between HLA diversity and clinical outcomes in a pan-tumor cohort of 140 patients treated with ICIs at Johns Hopkins. DNA was extracted from peripheral blood mononuclear cells and genotyped using the Illumina Infinium Global Screening Array v3.0. Class I and Class II HLA alleles were imputed from SNP genotype data using standard reference panels, and from these we derived Class I and Class II zygosity, HLA epitope diversity (Grantham distance matrix-based HED), and Class I and Class II supertype diversity (9 Class I and 7 Class II functional groups from IMGT/HLA). High versus low diversity was defined by cohort median splits. Treatment response was defined as complete or partial response. Multivariate logistic regression adjusted for age, gender, race, BMI, cancer type, MSI/TMB status, line of therapy, therapy class, and all HLA diversity metrics simultaneously.
Results: In the fully adjusted model, only Class II supertype diversity remained significant. Patients with at least four distinct supertypes had lower response rates than those with fewer than four (23.2% vs 36.9%, OR 0.199 [0.060-0.608], p=0.006). The effect was unchanged in models without cancer type terms (OR 0.199, p=0.005) and in models conditioning on DR4 and DPmain (OR 0.235, p=0.019). Spline analyses supported the four-supertype cutoff (LR test p=0.274), and no interactions were observed with line of therapy, MSI/TMB, or treatment class. Cox models showed worse OS (HR 1.834 [1.017-3.304], p=0.044) and PFS (HR 1.981 [1.067-3.678], p=0.030), with similar HR in cancer type-stratified and DR4 or DPmain-conditioned analyses. Individual Class II supertypes were consistent with the composite index: DR4 carriers had worse OS (HR 2.062, p=0.007) and PFS (HR 1.872, p=0.025), and DPmain carriers had worse OS (HR 1.524, p=0.043). Alternative constructs including Class I/II zygosity and HED were less informative or nonsignificant.
Conclusions: Class II HLA diversity emerged as an unexpected negative predictor of response and survival with ICI therapy. These findings differ from results reported in other ICI-treated cohorts. Although increased HLA diversity can broaden antigen recognition in some settings, prior studies also show that greater Class II diversity can increase thymic deletion of self-reactive T cells. This process reduces the breadth of the peripheral T-cell repertoire and limits tumor neoantigen recognition, providing a biologically plausible explanation for the pattern observed here.

#1045 A novel epithelial tumor signature predicts survival and response to PD-1 blockade in non-small cell lung cancer.

Muaath Alsufi[1], Jehad Yasin[1], Muthafar Alsufi[1], Osama Younis[1], Amro Assayed[2], Fawzi Abu Rous[3]

[1]Faculty of Medicine, University of Jordan, Amman, Jordan,[2]University of Central Florida, Orlando, FL,[3]Henry Ford Health System, Detroit, MI

Introduction: Immune checkpoint inhibitors (ICIs) are the standard of care for NSCLC lacking driver alterations, yet many patients do not derive clinical benefit. Current biomarkers, such as PD-L1, are imperfect in predicting response. Identifying tumor epithelial gene markers linked to immunotherapy response could improve prediction of patient outcomes.
Methods: A single-cell RNA (scRNA) dataset (GSE205335, n=12,975 cells) of NSCLC patients treated with anti-PD1 therapy was analysed to identify DEGs between responders (CR/PR) and non-responders (SD/PD). A bulk RNA-seq cohort (SU2C-MARK, n=142) was used to build a prognostic model. Genes associated with overall survival (OS) were identified using univariate Cox regression, followed by Least Absolute Shrinkage and Selection Operator (LASSO) and a multivariate Cox model to identify independent predictors of survival. A signature-based risk score was calculated, stratifying patients into High and Low-Risk groups based on median risk score. Associations with response and survival were assessed using Wilcoxon, Kaplan-Meier, and log-rank tests. Multivariate Cox analysis was performed to adjust for clinical covariates. The signature was validated using combined, batch-corrected datasets (GSE13522, GSE126044, GSE190265, GSE274975; n=129). xCELL was used to perform computational immune deconvolution.
Results: scRNA-seq analysis revealed 816 epithelial genes linked to treatment response. Univariate Cox regression of the bulk RNA-seq cohort identified 36 OS-associated genes, which were reduced to 17 genes by LASSO-Cox. Multivariate Cox regression resulted in a 4-gene signature of independent predictors of survival: CXCL8 (HR: 1.27, p=0.008), C11orf58 (HR: 0.59, p=0.010), SERF2 (HR: 2.11, p=0.015), and MT-CO1 (HR: 1.27, p=0.045). The 4-gene risk score was used to split patients into High (n=71) and Low (n=71) risk groups. High-Risk patients exhibited shorter OS and PFS (HR=3.49, $p = 4\times10^{-7}$; HR=2.029, p = 0.0007), and non-responders were associated with higher risk scores (p=0.0175). The 4-gene risk score was an independent predictor of OS (HR=2.785, p=0.0082) and PFS (HR=1.650, p=0.028) after adjusting for age, sex, stage, smoking, and PD-L1 TPS. TME deconvolution revealed that the High-Risk group featured higher Macrophages (M0, M1) and Neutrophils, while the Low-Risk group featured higher CD4+ T-cells and naive B-cells. In the combined validation dataset (n=129), the High-Risk group experienced worse PFS compared to the Low-Risk group (HR=1.58, p=0.036).
Conclusion: We present a novel signature of 4 tumor-intrinsic epithelial genes (CXCL8, C11orf58, SERF2, MT-CO1) that predict response and survival in NSCLC patients treated with anti-PD-1 therapy. The link between these genes and the immune microenvironment highlights a key tumor-TME axis, and represents promising potential for translational biomarker studies.

#1046 Leveraging transcriptomic profiles and deep learning to detect homologous recombination deficiency in breast cancer with softHRD.

Yashwin Madakamutil, Leo Joseph, Daniyal Rahman, Ammal Abbasi, Ludmil Alexandrov

Bioengineering, UCSD Medical Ctr., San Diego, CA

The homologous recombination (HR) pathway is the canonical repair mechanism by which cells repair DNA double-strand breaks. Defects in this pathway, known as homologous recombination deficiency (HRD), can lead to genomic instability and are observed in approximately 13% of breast cancers. HRD is often driven by somatic or germline mutations in *BRCA1/2*, which render tumors sensitive to PARP inhibitors and platinum-based therapies through synthetic lethality. However, many HRD-positive cancers lack *BRCA1/2* mutations, underscoring the need for more reliable approaches to identify tumors likely to benefit from these treatments. To address this, we developed softHRD, a transcriptomics-based framework for detecting HRD in breast cancer. softHRD was trained on RNA-seq profiles from 857 breast cancer patients in The Cancer Genome Atlas (TCGA), filtered for protein-coding genes. A variational autoencoder was first used to reconstruct these transcriptomic profiles, generating latent representations that capture the underlying structure of gene expression patterns. A sparse autoencoder was then applied to these latent features to derive mechanistically interpretable components and identify an HRD-associated gene set. These genes were subsequently leveraged to train a downstream Elastic Net regression model, yielding a robust 111-gene transcriptional signature indicative of HRD. We validated softHRD in 80 breast cancer patients from the I-SPY 2 clinical trial treated with neoadjuvant chemotherapy and olaparib. The model identified a statistically significant difference in pathologic complete response between HRD-predicted and HR-proficient tumors ($p = 0.00676$). Unlike whole-genome sequencing, which provides a static view of mutational alterations, transcriptomic profiling captures the dynamic state of gene expression, revealing biological changes that genomic methods may overlook. softHRD demonstrated robust performance across all PAM50 breast cancer subtypes, highlighting its generalizability. With the growing integration of transcriptomics into clinical research and diagnostics, softHRD represents a scalable and adaptable framework for accurate, efficient HRD characterization, with potential applications across multiple cancer types.

#1047 MORPHEUS-lung: Biomarkers and clinical response to atezolizumab + bevacizumab + stereotactic body radiotherapy in patients with metastatic non-small cell lung cancer.

Byoung Chul Cho[1], Sun Min Lim[2], Sang Hoon Lee[3], **Dong Kwon Kim**[3], Nuria Pardo[4], Hen Prizant[5], Yaacov R. Lawrence[6], Nedal Al-Sakaff[7], Hans-Joachim Helms[7], Gayevskiy Velimir[8], Barzin Nabet[8], Jan Pintoffl[7], Francois Ghiringhelli[9]

[1]Yonsei University College of Medicine, Seoul,[2]Department of Internal Medicine and Yonsei Cancer Center, Division of Medical Oncology, Seoul, Korea, Republic of,[3]Severance Biomedical Science Institute, Seoul, Korea, Republic of,[4]Vall d'Hebron University Hospital, Vall d'Hebron Institute of Oncology (VHIO), Barcelona, Spain,[5]Genentech, Inc., South San Francisco, CA,[6]Sheba Medical Center, Jerusalem, Israel,[7]F. Hoffmann-La Roche Ltd, Basel, Switzerland,[8]Genentech, South San Francisco, CA,[9]Department of Medical Oncology, Centre le Cancer G.-F. Leclerc, INSERM, Dijon, France

Purpose: Results from the MORPHEUS-Lung (NCT03337698) study suggest that atezolizumab+bevacizumab+stereotactic body radiotherapy (SBRT) was associated with numerically improved efficacy outcomes vs docetaxel (control) in immune checkpoint inhibitor-exposed patients with metastatic non-small cell lung cancer. We report exploratory analyses to identify potential biomarkers associated with this clinical response.
Experimental Design: Tumor samples were analyzed for differential gene expression and pathway/immune subset gene signatures by single cell RNA-sequencing and further validated with bulk RNA-sequencing.
Results: A total of 58 patients were included in the biomarker-evaluable population (atezolizumab + bevacizumab + SBRT (Atezo+Bev+Radio), n = 26; docetaxel control, n = 32). In the discovery analysis comparing patients with clinical benefit (CB) versus non-clinical benefit (non-CB) at baseline, tumor-resident memory $CD8^+$ T cells (CD8 T_{RM}) were significantly enriched in the CB group (P = 0.027) accompanied by an increased T-cell receptor clonality, indicating clonal expansion of tumor-reactive T cells (Gini index P = 0.018). PDCD1, the target molecule of immune checkpoint therapy, was highly expressed in CD8 T_{EX}, supporting their responsiveness to atezolizumab treatment. Furthermore, the CB group showed increased abundance of $CXCL10^+$ and $FOLR2^+$ macrophages, suggesting enhanced myeloid-T cell crosstalk. CD8 T_{RM} with high tumor-recognition potential exhibited strengthened antitumor activity through CXCL-mediated interactions with $CXCL10^+$ macrophages, which expressed PD-L1 at the highest level. Following Atezo+Bev+Radio treatment, CD8 T_{RM}—identified as predictive biomarkers—maintained a persistent tumor-reactive state, whereas CD8 TEMRA cells showed increased cytotoxic function likely driven by radiation exposure. Atezo+Bev+Radio treatment also induced a marked increase in $FOLR2^+$ and $FABP4^+$ macrophages in the post-treatment group. $FOLR2^+$ macrophages interacted with CD8 T cells expressing ICOS via the ICOS-ICOSL signaling pathway, promoting T cell-mediated antitumor immunity. In contrast, $FABP4^+$ macrophages engaged Treg cells expressing TIGIT through the PVR-TIGIT signaling axis, thereby contributing to immune suppression. Integration of the data revealed T cell- and macrophage-related gene signatures validated in an independent cohort, correlating with survival benefit after atezolizumab + bevacizumab + SBRT treatment.
Conclusions: These results suggest that activation of T cells and macrophages are associated with a favorable clinical response Atezo+Bev+Radio. Moreover, CD8 T_{RM}, CD8 T_{EX}, and $CXCL10^+$ macrophages may serve as potential biomarkers of response to Atezo+Bev+Radio treatment and potentially aid in tailored, precision medicine for individual patients.

#1048 Smad deficiency impacts chemotherapeutic responses through alterations in immuno-stromal microenvironment of pancreatic adenocarcinoma.

Chih Chieh Yen[1], Ying Jui Chao[2], Ping Jui Su[2], Ting Kai Liao[2], Wei Hsun Lu[2], Zhe Wei Hsu[3], Chien Jui Huang[4], I Ting Liu[1], Wen Yen Huang[5], Yan Shen Shan[2], Chia Jui Yen[1]

[1]Department of Oncology, National Cheng Kung University Hospital, Tainan, Taiwan,[2]Department of Surgery, National Cheng Kung University Hospital, Tainan, Taiwan,[3]Department of Pathology, National Cheng Kung University Hospital, Tainan, Taiwan,[4]Division of Gastroenterology and Hepatology, Department of Internal Medicine, National Cheng Kung University Hospital, Tainan, Taiwan,[5]Institute of Clinical Medicine, National Cheng Kung University, Tainan, Taiwan

Background: Pancreatic adenocarcinoma (PDAC) is a devastating cancer with a dismal prognosis. Preoperative chemotherapy (PreOP_CT) has reshaped the treatment paradigm. However, factors influencing therapeutic responses and immune/stromal alterations have not been established. Smad family exerts pivotal biological actions through transforming growth factor-β (TGFβ) axis and affects tumor microenvironment (TME), yet the correlation with therapeutic responses has not been fully explored.
Methods: We explored a prospective cohort of patients with resectable PDAC who received PreOP_CT. Genomic aberrations of the Smad family in the TGFβ axis were assessed and compared for clinical outcomes. Single-cell RNA sequencing delineated the immuno-stromal alterations in Smad-deficient vs. -proficient tumors.
Results: Fifteen of 106 patients had Smad-deficient tumors and showed reduced tumor regression, higher metastatic progression and adverse survival as compared with -proficient ones. *SMAD4* or *TGFBR2/3* mutations were observed in Smad-deficient tumors. Smad deficiency correlated with different enrichments of tumor-infiltrating immune cells (TIMCs) and cancer-associated fibroblasts (CAFs). Collectively, inflammatory and antigen-presenting CAFs were distinctive in the deficient tumors and presented with immune evasive actions.
Conclusion: Smad deficiency influences therapeutic and surgical outcomes in PreOP_CT-treated PDAC. The Smad family potentially affects TIMCs and CAFs, potentiating an immune evasive and profibrotic TME. The results provide insight into a putative biomarker for PreOP therapies in PDAC.

#1049 DNA repair phenotypes inform carboplatin and PARP inhibitor response.

Ionut-Gabriel Funingana[1], John Ambrose[2], Luca Porcu[1], Philip Smith[1], Bradley Thomas[1], Ines Prata Machado[3], Patrick Tarpey[4], Mireia Crispin-Ortuzar[3], Marc Tischkowitz[5], Florian M. Markowetz[1], Alona Sosinsky[2], James D. Brenton[1]

[1]CRUK Cambridge Institute, University of Cambridge, Cambridge, United Kingdom,[2]Bioinformatics Department, Genomics England, London, United Kingdom,[3]Early Cancer Institute, University of Cambridge, Cambridge, United Kingdom,[4]East Genomic Laboratory Hub, Cambridge, United Kingdom,[5]Department of Genomic Medicine, University of Cambridge, Cambridge, United Kingdom

High-grade ovarian carcinoma (HGOC) is characterized by multilayered genomic complexity driven by early disruption of the p53 pathway which enables diverse mutational processes and chromosomal instability (CIN). The molecular consequences of defective DNA repair and replication have been used to derive mutational signatures to predict mutational processes operative in each HGOC. Clinical testing for homologous recombination deficiency (HRD) signatures does not reliably guide the use of platinum-based therapy or poly(ADP-ribose) polymerase inhibitors (PARPi) for women with HGOC. Previous studies have shown that multiple HRD signatures are operative at the single-base substitution, indel, and structural variant levels in the same tumors. However, separate signatures do not capture the continuum of erroneous repair programs active in *BRCA1*- and *BRCA2*-deficient tumors. Here, we propose a new integrative mathematical approach to recover all naturally occurring genomic features associated with operational DNA repair pathways. We established a national healthcare outcome study of 466 HGOC patients, integrating tumor-normal deep whole-genome sequencing (WGS) with real-world treatment and outcomes. We demonstrated that seven integrative genomic features (IGFs) capture the mutational programs operative in HGOC tumors. We validated the clinical relevance of these IGFs using causal-inference methods. IGF2 captured microhomology-flanked deletions, templated insertions (TINs), and interstitial deletions. IGF5 captured 1 kilobase (kb) to multi-megabase (Mb) tandem duplications (TDs) and blunt deletions. IGF8 was rich in inversions and multi-Mb TDs, whereas IGF10 linked CpG transversions with TINs. IGF2 reflects polymerase theta-mediated end joining, associated with *BRCA2* inactivation, favorable prognosis after first-line platinum, and reduced benefit from maintenance PARP inhibitors. IGF5, marked by tandem duplications and non-homologous end joining, is enriched in *BRCA1*-inactivated tumors and predicts earlier relapse but increased benefit from maintenance PARPi. In Cox models (per 1 standard deviation unit), IGF2 improved overall survival (OS) (HR 0.81, 95% CI 0.71-0.92) and IGF8 was adverse (HR 1.25, 1.08-1.46), and IGF10 predicted benefit at second-line relapse when half of patients received maintenance PARPi (progression-free survival HR 0.75, 0.62-0.89). IGF2 modified second-line PARPi benefit (IGF2-binary x PAPRi interaction P=0.042), with benefit confined to IGF2-low. This WGS-based taxonomy reframes HRD as a continuum of DNA double-strand break repair choices. The mechanism-specific, WGS-derived phenotypes can be replicated in clinical practice, providing a basis for biomarker-stratified trials of PARP inhibitors and emerging polymerase theta (POLQ) inhibitors in ovarian cancer and in other tumors with DNA-repair defects.

#1050 Assessment of spectral overlap and crosstalk in multiplex digital PCR for effective monitoring of next-generation CAR T-cells in cancer clinical trials.

Sarah Johnson, Yogita Raj, Nathan Riccitelli

Navigate BioPharma Services, Inc., Carlsbad, CA

Introduction: As new chimeric antigen receptor (CAR) T cells emerge as secondary therapies in patients already treated with an approved CAR, clinical trial investigation of next generation constructs requires monitoring for the presence of residual first generation CAR-T therapies, often from limited patient samples. Multiplex digital PCR (dPCR) enabling absolute quantification without standard curves and supporting detection of as few as 10 copies, is an ideal approach to monitor multiple approved CAR-Ts in a limited clinical trial specimen (Morley, 2014; QIAGEN, n.d.). While multiplexing improves efficiency, it introduces challenges such as spectral overlap, potentially causing crosstalk and misinterpretation. Herein, we investigate how bleed-through affects signal interpretation in multiplex dPCR and evaluate the effectiveness of threshold adjustments and software updates in mitigating crosstalk and preserving monitoring accuracy of multiple CAR-Ts on the QIAcuity platform.

Method: A multiplexed dPCR assay targeting three CAR domains, a viral safety marker, and one reference gene was tested using probes labeled with FAM, TxRED, VIC, TAMRA, and Cy5 across five optical channels. Two formats were run on QIAcuity: singleplex reactions to confirm specificity and baseline crosstalk, and multiplexed reactions to assess cumulative interference. Analysis was performed using Software Suite (SS) versions 2.5 and 3.1. Fluorescence plots assessed signal clarity, crosstalk, and the impact of optical and threshold settings on droplet classification and quantification.

Result : Singleplex reactions showed no bleed-through in FAM, VIC, TAMRA, or Cy5 channels. TxRed bled into Cy5. TxRED bled into Cy5, and TAMRA into VIC, confirmed by 2D plots showing double-positive patterns and unexpected VIC-positive droplets in TAMRA-only samples. VIC-to-TAMRA crosstalk was concentration-dependent, decreasing at lower input levels, while TxRED-to-Cy5 remained constant. Signal clarity for TAMRA improved with optical or threshold adjustments. Despite visible bleed-through, multiplex quantification remained accurate. Cy5-labed targets were correctly identified, with software ignoring TxRED bleed-through. No differences in crosstalk or quantification accuracy were observed between SS versions 2.5 and 3.1, confirming consistency across updates.

Conclusion: Spectral bleed-through, especially from TxRED into Cy5, was a key source of signal misclassification. Manual thresholding and optical adjustments in both software versions effectively reduced crosstalk and improved quantification of all CAR domains. These findings highlight the importance of optimized assay design and analysis tools for reliable quantification of residual CAR-T therapies, which are critical for safe advancement of next generation CAR-T therapies.

#1051 CXCR4/LITAF as predictive biomarkers for nimotuzumab plus AG therapy in pancreatic cancer with liver metastasis: Integrative single-cell and spatial analysis.

Linze Xu[1], Yang Liu[1], Linlin Fu[2], Dandan Wu[1], Jin Zhang[1], Hao Wang[1], Huikai Li[2], Jihui Hao[3]

[1]Department of Hepatobiliary Cancer, Liver Cancer Center, Tianjin Medical University Cancer Institute & Hospital, National Clinical Research Center for Cancer, Key Laboratory of Cancer Prevention and Therapy, Tianjin's Clinical Research Center for Cancer, TianJin, China,[2]Department of Hepatobiliary and Pancreatic Oncology, Tianjin Cancer Hospital Airport Hospital, TianJin, China,[3]The Pancreas Center, Tianjin Medical University Cancer Institute & Hospital, National Clinical Research Center for Cancer, Tianjin Key Laboratory of Digestive Cancer, Tianjin's Clinical Research Center for Cancer, Tianjin, China

Background: Pancreatic cancer with liver metastasis (PCLM) accounts for most advanced pancreatic cancer cases and carries poor prognosis. While Gemcitabine plus Nab-paclitaxel (AG) remains the NCCN-recommended regimen for fit patients, outcomes remain suboptimal. Previous studies suggested that adding Nimotuzumab may improve conversion to resection, but the molecular determinants of response are unclear (2025 AACR# CT167, NCT06405685) . This study integrates clinical and correlative analyses to identify predictive biomarkers for Nimotuzumab + AG therapy.
Methods: Treatment-naïve PCLM patients received Nimotuzumab (400 mg iv, qw) plus AG (Gemcitabine 1000 mg/m² and Nab-paclitaxel 125 mg/m², d1, d8, q3w). Primary endpoints were objective response rate (ORR) and disease control rate (DCR); secondary endpoints included conversion and R0 resection rates. In parallel, single-cell RNA-seq data from paired primary and metastatic lesions (GEO) were analyzed to identify PCLM-specific subpopulations via hdWGCNA and machine-learning algorithms (SVM, LASSO, random forest). For clinical validation, immunofluorescence staining of CXCR4 and LITAF was performed on PCLM tumor tissues. Spatial quantification was performed using an automated CK-pan-guided epithelial segmentation. Intensities were normalized and a hotspot-weighted aggregation produced a combined CXCR4/LITAF score per patient, reflecting co-activation.
Results: Among 23 evaluable PCLM patients, the ORR was 17.4%, DCR 78.3%, and 43.5% achieved conversion surgery, consistent with previous findings. Single-cell analysis identified 22 cell clusters, including a distinct PCLM-specific subpopulation enriched in hepatic metastases. CXCR4 and LITAF emerged as central hub genes positively correlated with the abundance of these metastatic-specific cells and with poorer clinical outcomes. Imaging-based spatial quantification showed that patients with higher CXCR4/LITAF combined scores exhibited significantly worse treatment responses (progressive disease, PD). The automated pipeline—from epithelial segmentation (CK-pan-guided) to combined molecular scoring—achieved robust reproducibility across samples and accurately stratified responders versus non-responders. Preliminary analyses suggest that KRAS-mutant tumors may exhibit enhanced CXCR4/LITAF co-activation, contributing to therapeutic heterogeneity.
Conclusions: Nimotuzumab plus AG demonstrates favorable disease control and conversion potential in PCLM. Integrative single-cell and spatial analyses identify CXCR4 and LITAF as candidate biomarkers linked to treatment response. The CXCR4/LITAF combined spatial score offers a quantitative imaging tool for predicting response to Nimotuzumab + AG in metastatic pancreatic cancer.

#1052 Real-world treatment patterns and outcomes reveal distinct clinical trajectories of patients with Cyclin E1-positive ovarian cancer.

Jinkil Jeong[1], Mona Abed[1], Catherine Lee[1], Heekyung Chung[1], Alexandra Levy[1], Nandini Molden[1], Divya Rajendran[1], Joyce F. Liu[2], Leslie M. Randall[3], Fiona Simpkins[4], Funda Meric-Bernstam[5], Danielle D. Jandial[1], Doris Kim[1], Olivier Harismendy[1]

[1]Zentalis Pharmaceuticals, San Diego, CA,[2]Dana-Farber Cancer Institute, Boston, MA,[3]Inova Health, Fairfax, VA,[4]University of Pennsylvania, Philadelphia, PA,[5]University of Texas MD Anderson Cancer Center, Houston, TX

Background: The success of novel therapies as they progress in later phases of clinical development requires accurate benchmarking of the benefit provided by the standard of care (SOC) at the time of clinical study completion. Information collected from published investigational studies or retrospective registries can be outdated or may not reflect the most current SOC. Furthermore, the development of novel agents, especially for patients on later lines of treatment, may be restricted to select populations, not previously characterized in the literature, perhaps defined by criteria such as a novel biomarker (e.g. Cyclin E1 positive tumors) or narrow indication sub-types (e.g., platinum resistant ovarian cancer with less than N prior therapy lines). Here, we demonstrate how the analysis of Real-World Data (RWD), as well as screening data — collected in the context of recent early phase clinical studies — is guiding development of the WEE1 inhibitor azenosertib in Cyclin E1 positive high grade serous ovarian cancer (HGSOC). Methods: The records of medications and lines of therapy were curated from Tempus Lens (TLOv) or Zentalis Retrospective Study of Early Treatment (ReSET) cohorts. Outcomes such as best response, progression free survival and treatment free survival were evaluated for patient subsets defined by treatment history or Cyclin E1 expression status from RNA sequencing (for TLOv) or protein immunohistochemistry (IHC for ReSET) after benchmarking RNA-based classification using independent HGSOC tissues (N=92). Results: Compared to IHC, RNA-based Cyclin E1 classification was > 70% accurate, with higher rates of False Negative than False Positives, providing an acceptable surrogate to stratify patients in the TLOv cohort. The treatment regimens used in early lines were consistent between TLOv and ReSET cohorts and reflected current SOC, including partial use of PARPi in 1L maintenance and a preference for doxorubicin-based regimens in 2L for platinum-resistant patients. The data confirmed previous observations that BRCA-mutated patients had better prognosis, likely due to PARPi treatment eligibility after 1L. Patients with Cyclin E1 positive tumors were observed in both platinum-resistant and platinum-sensitive settings, with a higher prevalence in platinum-resistant setting. Patients with Cyclin E1 positive tumors had worse outcomes in 1L, or with selected treatment regimens in subsequent lines, highlighting their consistent unmet need throughout the entire treatment journey. Conclusions: RWD represents a reliable and up-to-date source of treatment and outcomes information for HGSOC patients. Clean identification of lines and intent of treatment as well as availability of direct or surrogate Cyclin E1 expression status were key to highlighting the unmet need of patients with Cyclin E1 positive tumors, informing azenosertib’s development.

#1053 Single-cell immune profiling reveals biomarkers of pembrolizumab response in early triple-negative breast cancer.

Inaki Comino-Mendez[1], Maria Rosario Chica-Parrado[1], Maria Elena Quiros-Ortega[1], Ana Godoy-Ortiz[1], Maria Emilia Dominguez-Recio[1], Esperanza Lopez-Lopez[1], Maria Victori Ortega-Jimenez[2], Martina Alvarez[1], Javier Pascual[1], Enrique de Alava[3], Emilio Alba[1]

[1]Institute of Biomedical Research of Malaga (IBIMA), Malaga, Spain,[2]Hospital Universitario Virgen de la Victoria, Malaga, Spain,[3]Department of Normal and Pathological Cytology and Histology, Institute of Biomedicine of Sevilla (IBiS), Sevilla, Spain

Background: Triple-negative breast cancer (TNBC) is an aggressive subtype representing 15-20% of all breast cancers, characterized by early recurrence and lack of targeted therapies. The addition of pembrolizumab to standard neoadjuvant chemotherapy significantly improves outcomes; however, clinical benefit remains heterogeneous and predictive biomarkers of response or resistance are still lacking.
Objectives: To characterize peripheral immune cell states associated with response and resistance to pembrolizumab-based neoadjuvant therapy in early TNBC.
Methods: Patients with early TNBC treated with neoadjuvant pembrolizumab plus chemotherapy were included. Serial blood samples were obtained at baseline, during treatment, before surgery, and one month after surgery. Peripheral blood mononuclear cells (PBMCs) were analyzed by single-cell RNA sequencing and paired TCR/BCR sequencing using the 10x Chromium platform. Cellular composition, transcriptional states, checkpoint expression, and clonal architecture were compared between responders, defined as patients with Residual Cancer Burden (RCB 0) and non-responders (RCB I-III).
Results: Single-cell analysis revealed distinct systemic immune profiles between responders and non-responders at baseline. Responders displayed an immune-prepared state characterized by enriched cytotoxic NK cells and effector T cells, together with reduced naïve CD4+ T cells and regulatory T cells. In contrast, non-responders showed dominance of naïve and suppressive populations. At the transcriptional level, CD4+ T cells from responders exhibited lower basal activation (↓AP-1, ↓TNF) but higher antigen presentation and proliferation signatures. NK and monocyte compartments were more inflammatory and metabolically active, while B cells showed increased antigen-presenting capacity (↑MHC-II, ↑CD86). Checkpoint expression analysis revealed higher mean and frequency of *TIGIT*, *TIM3*, and *PD-1* across multiple immune lineages in responders. TCR-seq data showed oligoclonal expansions in responders, contrasting with the polyclonal, unexpanded repertoires of non-responders.
Conclusions: Peripheral immune profiling reveals distinct systemic immune programs associated with response and resistance to pembrolizumab in early TNBC. Responders display features of antigen-experienced, cytotoxic, and clonally expanded immune populations, whereas resistant cases show quiescent and regulatory-dominant profiles. These findings highlight the potential of immune-based liquid biopsy as a minimally invasive tool to identify predictive biomarkers of immunotherapy efficacy and resistance in breast cancer.

#1054 Plasma metabolomic profiling predicts response to neoadjuvant immunochemotherapy in locally advanced NSCLC.

Yan Wang[1], Hui Yang Shi[1], Haonan Gu[2], Wenxin Jiang[1], Linyan Tian[1], Fang Wei[1], Danru Zheng[1], Haiyan Xu[3], Ting Xiao[2]

[1]Department of Medical Oncology, National Cancer Center/ National Clinical Research Center for Cancer/ Cancer Hospital, Chinese Academy of Medical Sciences and Peking Union Medical College, Beijing, China,[2]State Key Laboratory of Molecular Oncology, Department of Etiology and Carcinogenesis, National Cancer Center/ National Clinical Research Center for Cancer/ Cancer Hospital, Chinese Academy of Medical Sciences and Peking Union Medical College, Beijing, China,[3]Department of Comprehensive Oncology, National Cancer Center/ National Clinical Research Center for Cancer/ Cancer Hospital, Chinese Academy of Medical Sciences and Peking Union Medical College, Beijing, China

Background: While immune checkpoint inhibitors (ICIs) have demonstrated significant benefit in non-small cell lung cancer (NSCLC), the efficacy varies substantially among individuals. Established biomarkers like PD-L1 expression and tumor mutational burden (TMB) offer limited predictive value, underscoring the critical unmet need for more reliable predictive biomarkers. To address this, our study aimed to discover predictive plasma metabolomic biomarkers for treatment response to neoadjuvant immunochemotherapy in patients with locally advanced NSCLC.

Methods: Between November 2023 and July 2025, 71 patients with locally advanced NSCLC receiving neoadjuvant immunochemotherapy were prospectively enrolled. According to best overall response (BOR), patients were classified into the good response (GR) group (n=38, partial response) and the limited response (LR) group (n=33, stable or progressive disease). Plasma sampling included 71 baseline samples, 50 samples after cycle one and 39 samples after cycle two. The association between clinicopathological features and clinical response was assessed using multivariate logistic analysis. Untargeted metabolomic profiling of all plasma samples was conducted using liquid chromatography-tandem mass spectrometry (LC-MS/MS) to identify predictive metabolic biomarkers.

Results: After neoadjuvant therapy, surgical resection in 22 patients revealed a pathological complete response (pCR) rate of 36.4% (8/22). Multivariate analysis identified squamous cell carcinoma histology and tumor cell PD-L1 expression >50% as predictors of good response to neoadjuvant immunochemotherapy. Plasma metabolomic profiling detected 3,756 metabolites. The GR group exhibited significantly higher levels of glycerol ester of acylcarnitine and hydroxypropionylcarnitine, whereas the LR group was enriched in glycocholic acid, phosphatidylcholine and taurocholic acid. KEGG pathway analysis indicated that the differential metabolites were involved in primary bile acid biosynthesis and cholesterol metabolism. Using machine learning, we integrated the baseline, post-cycle one and post-cycle two plasma metabolomic profiles to develop a 15-signature GLMNet model for pCR prediction, which achieved an area under curve (AUC) of 0.906.

Conclusion: Dynamic plasma metabolomic signatures are promising non-invasive biomarkers for predicting outcomes to neoadjuvant immunochemotherapy in NSCLC. These findings provide a rationale for leveraging metabolomics to stratify patients and optimize personalized treatment strategies.

#1055 Assessing biomarker reproducibility for glioblastoma patient response stratification.

Christopher M. Jannotta[1], **C. Zoe Linke**[1], Charles A. Whittaker[2], Vikas Patil[3], Accelerating GBM Therapies TeamLab, Farshad Nassiri[4], Gelareh Zadeh[5], E. Antonio Chiocca[1], Alexander L. Ling[1]

[1]Department of Neurosurgery, Brigham and Women's Hospital, Boston, MA,[2]Bioinformatics & Computing Core Facility, Massachusetts Institute of Technology, Cambridge, MA,[3]Princess Margaret Cancer Center, University Health Network, Toronto, ON, Canada,[4]Division of Neurosurgery, University Health Network, Toronto, ON, Canada,[5]Department of Neurosurgery, Mayo Clinic, Rochester, MN

Purpose: Glioblastoma (GBM) is the most common and aggressive primary malignant brain tumor, with a median survival of only 15 months. Effective therapeutic advances remain limited, with few clinical trial patients exhibiting robust responses to experimental therapies. This has led to efforts to identify molecular biomarker signatures capable of stratifying patient responses either prognostically (pre-treatment) or diagnostically (post-treatment). This study aims to assess the robustness and reproducibility of published transcriptional GBM biomarker signatures for predicting clinical outcomes in GBM trials.

Methods: We analyzed published RNA-seq data from 4 clinical trials involving oncolytic virotherapy and immune checkpoint inhibitors, as well as multiple cohorts of patients treated via the Stupp protocol. The performance of reported immune gene signatures was evaluated across all datasets using both grouped and continuous survival modeling. Intra-patient signature variation between different biopsy sites and timepoints was assessed using longitudinal, multi-site sampling collected by the Break Through Cancer Accelerating GBM Therapies TeamLab. LASSO, multivariate Cox regression, and risk scoring with FDR adjustment were used to identify novel signatures with cross-cohort utility.

Key Findings: No single published signature consistently predicted survival across all analyzed trials. A post-treatment ssGSEA antitumor cytokine signature that was associated with survival in the CAN-3110 OV trial ($R = 0.74$, $p < 0.01$) was also significantly associated with improved survival in an adjuvant anti-PD1 trial ($R = 0.75$, $p = 0.03$) and neoadjuvant anti-PD1 trial ($R = 0.30$, $p = 0.05$), but not in standard-of-care controls. PAM clustering of MCP immune signatures, as reported for the DNX-2401 OV+Anti-PD1 trial, also stratified post-treatment survival in the CAN-3110 OV trial ($p < 0.01$), with the coldest TME subtype consistently predicting worse survival. However, the prognostic value of the most immune enriched TME subtype was inconsistent and did not extend to the Anti-PD1 trials. Furthermore, multi-site, longitudinal biopsy samples revealed marked heterogeneity in biomarker signatures between biopsies from individual patients, even when assessed at the same timepoint. We've identified several candidate transcriptomic signatures that show promise for generalizable prognostic value in GBM patient cohorts and are characterizing their spatiotemporal variability.

Conclusions: While no individual immune signature is universally predictive in GBM immunotherapy, certain post-treatment cytokine signatures and TME stratifications are significant in multiple immunotherapy contexts, though not in standard-of-care patient cohorts. Marked spatiotemporal heterogeneity in these signatures underscores the need for composite prognostic markers resilient to sampling variance.

#1056 Integrative multi-omics characterization and AI-driven biomarker discovery for NSCLC stage III outcomes.

Katherina C. Chua, Yun-Ching Chen, Ariel Chen, Stewart Bates, Mehdi Pirooznia, Assieh Saadatpour

Johnson & Johnson, New Brunswick, NJ

Background: The PACIFIC trial established consolidation durvalumab as standard of care for unresectable stage III non-small cell lung cancer (NSCLC) following concurrent chemoradiotherapy (CRT). Real-world studies such as PACIFIC-R confirmed these benefits; however, comprehensive characterization of molecular features in this setting remains limited. Advances in AI enable integration of heterogeneous genomic and transcriptomic data, opening new opportunities for biomarker discovery. Our study applies a multimodal AI framework combining contrastive learning and foundational-model representations to identify distinct molecular features associated with survival outcomes from pre-treatment tumor data.

Methods: Stage III NSCLC *EGFR*/*ALK*-negative patients with unresectable disease who received CRT with subsequent durvalumab (CRT+D, N=281) or CRT alone (N=72) were identified from the Tempus AI multimodal real-world database. Molecular characterization included assessment of radiation and immunotherapy (IO)-related biomarkers to evaluate the impact on real-world progression-free survival (rwPFS). To identify potential DNA and RNA biomarkers, a multimodal AI framework was developed via integration of two recently published models: 1) COMPASS, a foundation model encoding RNA profiles into 43 interpretable immune-related concept scores, and 2) Predictive Biomarker Mapping Framework, a deep learning model mapping molecular features to treatment outcomes in CRT+D when compared to CRT-alone.

Results: In the CRT+D group, patients with high levels of biomarkers linked to IO response, such as PD-L1 ≥50% (p-value = 0.01) and a high tumor mutational burden (p-value = 0.02), showed improved survival rates. Patients exhibiting low *STK11* gene expression signature had shortened rwPFS (p-value=0.03). Tumors classified as radioresistant using the radiosensitivity index also showed diminished rwPFS benefit (p-value=0.02). Our multimodal AI framework revealed additional markers associated with improved rwPFS to CRT+D therapy, including tumors with adenocarcinoma histology, mutations in *LRP1B*, *NF1*, *KRAS*, and *CDKN2A*, and enrichment in expression of immune activation pathways (cytotoxic T-cell, IFN-γ, tertiary lymphoid structure, and immune-checkpoint signatures). In contrast, tumors with mutations in *TP53*, *RB1*, *NOTCH1*, *CUX1*, and *STK11* as well as those with elevated expression of regulatory and stromal signals (Tregs, exhaustion, stroma) were linked to worsened outcomes in patients treated with CRT+D. Cross-validation confirmed model reproducibility and feature stability.

Conclusions: Our study demonstrates the utility of a multi-omics approach to characterize molecular landscape of tumors treated with consolidation durvalumab and to drive biomarker discovery using an AI-driven, foundational-model-based framework.

: Digital Pathology 1
Poster Session

#0070 SPOT-Met: Spatially decoding organotropism and immunotherapy response in colorectal cancer from 1,000 multi-omic tumors.

Jiwoon Park[1], Ryan Shultzaberger[2], Braulio Banuelos[2], McKenzie Pavlich[2], Sabrina Shore[2], Daan Witters[2], Kyung-A Kim[3], Taeyul K. Kim[3], Minsun Jung[3], Han Sang Kim[1], Christopher E. Mason[1]

[1]Weill Cornell Medicine, New York, NY,[2]Singular Genomics, San Diego, CA,[3]Yonsei University, Seoul, Korea, Republic of

Metastasis accounts for over 90% of mortality in colorectal cancer (CRC), yet predicting whether, when, and where it will occur remains a major clinical challenge. Existing tools, including TNM staging, ctDNA, and mutational profiling, cannot anticipate metastatic tropism or guide site-specific surveillance and therapy decisions. Consequently, many patients with stage II-III CRC receive suboptimal postoperative treatment. To address this gap, we established SPOT-Met (Spatial Predictors Of Tropism and Metastasis), a foundation-scale initiative that integrates subcellular-resolution spatial multi-omics with AI-driven modeling to infer the molecular and architectural rules governing organ-specific metastasis. We spatially profiled 1,000 CRC primary tumors and ~100 matched metastatic and adjacent normal tissues using the Singular Genomics G4X platform, generating >300 million same-sample transcriptomic, proteomic, and morphologic cell profiles at submicron resolution. Each case is linked to bulk RNA-seq, qPCR-based mutational data, and detailed clinical metadata encompassing metastasis site, timing, therapy response, and survival. SPOT-Met also incorporates a focused cohort of patients treated with pembrolizumab, enabling the spatial dissection of immunotherapy responses. Comparative analyses of responders and non-responders are underway, revealing emerging spatial differences in immune and stromal architecture. Preliminary data suggest that immune organization and cell-cell topology, rather than total immune content, may distinguish therapeutic outcomes, highlighting the potential of spatial context as a predictive biomarker beyond PD-L1 expression or tumor mutational burden. Early findings further indicate that liver-tropic tumors preferentially form perivascular stromal hubs enriched for metabolic and extracellular matrix signatures, whereas non-metastatic tumors retain compact, immune-regulated crypt structures. Integrating these spatial and molecular features enhances the retrospective classification of metastatic organotropism compared to histopathology alone. SPOT-Met is being developed as a biopsy-compatible diagnostic assay to predict metastatic potential and organotropism at the time of diagnosis, aiming to double current prognostic precision for stage II-III CRC. By uniting spatial multi-omics and AI at unprecedented scale, SPOT-Met transitions metastasis research from retrospective observation to prospective prediction, advancing precision oncology and immunotherapy stratification.

#0071 Bridging histopathology and spatial transcriptomics for comprehensive tumor microenvironment profiling.

Xiaohan Xing, Lei Xing

Stanford University, Palo Alto, CA

Purpose: The tumor microenvironment (TME) critically influences cancer progression, treatment response, and patient outcomes. Histopathology reflects morphological features of TME states but lacks molecular specificity, whereas spatial transcriptomics (ST) provides spatial gene expression yet is costly and impractical for large-scale use. To bridge this gap, we develop a multimodal AI framework that transfers spatial molecular information from ST into histopathology-derived representations, enabling reconstruction of molecular programs, TME phenotypes, and spatial biology directly from routine H&E slides. This sequencing-free approach supports biomarker discovery and advances precision oncology through scalable molecular profiling.

Methods: We introduce a multi-scale multimodal learning strategy that aligns two large-scale foundation models: UNI (trained on 100,000 pathology slides) [1] and Visiumformer (trained on 3.94 million ST profiles) [2]. Rather than training a unified model from scratch, we integrate the two modalities through multi-scale contrastive alignment. We curated 355 samples from the HEST-1K dataset [3], comprising 801,157 paired H&E patches and ST spots across 16 tissue types. At the patch level, we enforce consistency between paired histology and ST embeddings. At the region level—where each region is defined as a cluster of nine neighboring patches—we further constrain cross-modal agreement. To maintain hierarchical coherence, we additionally encourage alignment between each patch and its corresponding parent region. This multi-scale contrastive alignment effectively transfers spatial molecular knowledge from ST into histopathology-based representations, enhancing various downstream tasks.

Results: We evaluated our framework on two downstream tasks. (1) Gene expression status prediction: On the BCNB dataset (n=1,058 WSIs), our model improved ER/PR/HER2 prediction over pretrained UNI. ER AUC/BACC increased from 0.882/0.780 to 0.891/0.771; PR from 0.792/0.712 to 0.812/0.715; and HER2 from 0.662/0.602 to 0.696/0.634. (2) Spatial spot classification: On the DLPFC dataset (n=12 WSIs), linear probing achieved 71.75% balanced accuracy and 78.15% weighted F1, compared with 55.19% and 63.61% for UNI—improvements of 16.56% and 14.54%.

Conclusions: Our multi-scale contrastive alignment framework transfers spatial molecular signals from ST into histopathology-derived representations, improving gene expression prediction, mutation inference, and spatial TME characterization. By enabling sequencing-free reconstruction of molecular and microenvironmental features, this approach offers a scalable solution for large-cohort cancer profiling and may facilitate biomarker discovery, patient stratification, and biologically informed precision oncology.

#0072 Unbiased AI detection of tertiary lymphoid structures from H&E whole-slide images using mRNA-derived labels predicts survival in NSCLC.

Anthony J. Wong[1], **Jessica Kim**[2], Shinkyo Yoon[3], Young Kwang Chae[1]

[1]Northwestern Univ. Feinberg School of Medicine, Chicago, IL,[2]Northwestern University, Evanston, IL,[3]Department of Oncology, Asan Medical Center, College of Medicine, University of Ulsan, Seoul, Korea, Republic of

Tertiary lymphoid structures (TLS) are recognized prognostic markers in non-small cell lung cancer (NSCLC), yet manual detection from H&E whole-slide images (WSI) remains subjective and labor-intensive, limiting clinical adoption.
We conducted an integrative analysis combining transcriptomic and histopathologic approaches. TCGA NSCLC mRNA expression data (n = 922) were analyzed using xCell to compute enrichment scores for B cells, T cells (CD4+ and CD8+), and dendritic cells. TLS enrichment score was calculated by averaging z-standardized xCell aggregate enrichment scores for B cells, T cells, and dendritic cells. Samples in the upper quartile were labeled 'TLS enriched' and those in the lower quartile were labeled 'TLS non-enriched.' These quartile-derived labels were then used to train a machine learning model for TLS detection from TCGA H&E whole-slide images using Imagene's OI Suite platform with a 3:1 train-test split. Univariable and multivariable cox proportional hazards regression analysis evaluated whether AI-predicted TLS enrichment independently predicted overall survival (OS).
The AI model demonstrated robust performance for TLS detection, achieving an AUC of 0.84 in the training set and a test AUC of 0.92. Kaplan-Meier analysis showed that patients in the AI-predicted TLS-enriched group (n = 366, 366/922=39.7%) demonstrated improved OS compared with the AI-predicted TLS-non-enriched group (n = 556, 556/922=60.3%; HR 0.76; 95% CI 0.61-0.94; log-rank p = 0.014). Adjusting for age, sex, and histology, AI-predicted TLS enrichment remained independently associated with favorable OS (HR 0.77; 95% CI, 0.61-0.97; p = 0.025). Among the covariates, older age (greater than the cohort median) was associated with worse survival (HR 1.25; 95% CI, 1.01-1.55; p = 0.039), while sex and histologic subtype (LUSC vs LUAD) were not significant predictors (HR 1.12; 95% CI, 0.89-1.41; p = 0.337 and HR 0.99; 95% CI, 0.79-1.25; p = 0.957, respectively). These findings indicate that the model's TLS-enrichment prediction captures clinically meaningful tumor microenvironment features that stratify OS beyond standard clinicopathologic factors.
AI-assisted H&E WSI analysis helps identify TLS enrichment as a potential independent predictor of overall survival in NSCLC. This unbiased computational approach provides a reproducible and objective methodology for TLS assessment and survival prediction in a resource-limited context using H&E WSI only, and may support downstream treatment selection in the context of precision immunotherapy.

#0073 Accurate prediction of microsatellite instability-high gastric cancer from H&E-stained whole slide images.

Shima Nofallah[1], Jake Conway[1], Jacqueline Brosnan-Cashman[2], Syed Ashar Javed[1], Bahar Rahsepar[2]

[1]PathAI, Boston, MA,[2]PathAI, Inc., Boston, MA

Background: While prognosis is poor for patients with gastric cancer (GC), those with microsatellite instability-high disease (MSI-H) respond well to checkpoint inhibition. Next-generation sequencing approaches for MSI-H detection are complicated by cost, turnaround time, and accessibility. Artificial intelligence (AI)-powered pathology has the potential to improve MSI-H detection.
Methods: Hematoxylin and eosin (H&E)-stained GC whole slide images (WSIs; N=316) from TCGA were used, and ground truth MSI-H status was determined as described [1]. A model, utilizing an additive multiple instance learning (aMIL) framework [2] and embeddings from PLUTO v3.1* [3] (PathAI, Boston, MA), a pathology foundation model, was trained to predict slide-level MSI-H status using 5-fold cross-validation. Model predictions were compared to ground truth labels using area under the receiver operating curve (AUROC) analysis.
Results: Model performance results are summarized in Table 1. The aMIL model achieved a mean AUROC of 0.86 (range: 0.81-0.89). These model predictions were highly accurate and consistent across folds, suggesting that the model is highly robust for predicting MSI-H status.
Conclusions: Here, we describe an AI pathology model that consistently and accurately identifies MSI-H GC from H&E-stained WSIs. The application of such models to routine GC biopsies has the potential to streamline the detection of MSI-H and other molecular biomarkers. Future studies will assess histologic features associated with model attention and extend this work to other MSI-H cancer types, including colorectal and endometrial cancer.
References:

1) JCO Precis Oncol. 2017;1:PO.17.00073.

2) arXiv:2206.01794

3) arXiv:2405.07905

*For Research Use Only. Not for use in diagnostic procedures.

Table 1. Performance of aMIL model for prediction of MSI-H in gastric cancer.

Fold	aMIL Model AUROC
1 (N_{MSI-H}=11; N_{total}=64)	0.87
2 (N_{MSI-H}=9; N_{total}=63)	0.88
3 (N_{MSI-H}=11; N_{total}=63)	0.89
4 (N_{MSI-H}=14; N_{total}=63)	0.85
5 (N_{MSI-H}=14; Nt_{otal}=63)	0.81

#0074 Improving histopathological diagnostic turnaround time through the GLORIA Telepathology Network in complex oncological cases.

Rafael Parra-Medina[1], Andres Mosquera-Zamudio[1], Rita Paez[2], Manuel Lopez[3], Maria Alejandra Espinosa[4], Yeison Carlosama Rosero[5], Yesid Poveda[6], Katherine Redondo-De Oro[7], Marcela Gomez-Suarez[8]

[1]Research Institute, FUCS, Bogota, Colombia,[2]Laboratorio Rita Paez, Armenia, Colombia,[3]Research Institute, Laboratorio Lopez Correa, Pereira, Colombia,[4]Laboratorio de Patologia, Clinica IMAT Oncomedica Auna S.A.S., Monteria, Colombia,[5]Laboratorio de patologia, Patologos asociados, Bogota, Colombia,[6]Laboratorio de patologia, Medical Duarte, Cucuta, Colombia,[7]Laboratorio de Patologia, CENDIPAT, Cartagena, Colombia,[8]Research Institute, FUCS, FUCS, Colombia

Introduction: In Latin American countries, disparities in access to timely and accurate oncological diagnoses contribute to differences in survival outcomes between urban and rural populations. Colombia exemplifies this situation, with only 0.88 pathologists per 100,000 inhabitants and a very limited number of oncopathologists, most of whom are concentrated in major cities.The GLORIA Telepathology Network was developed to address these inequities by implementing a digital diagnostic platform that connects peripheral hospitals with expert centers. Through whole-slide imaging (WSI) and real-time remote consultations, GLORIA enhances diagnostic accuracy, reduces turnaround time for histopathological reports, and supports clinical decision-making in oncological care across the country. The aim of this study is to describe the most frequently consulted tumor types and to evaluate the diagnostic turnaround times since the implementation of Telepathology Network.

Methdology: Six WSI scanners (Roche DP200) were installed in different regions of Colombia (Armenia, Pereira, Pasto, Cartagena, Cúcuta, and Montería) to enable the digitalization of oncological cases that present diagnostic challenges. These digital slides are remotely reviewed and discussed with specialized oncopathologists

Results: During the first 10 months of implementation, including the progressive integration of the digitalization centers, a total of 363 oncological cases were interconsulted. The most frequently interconsulted tumor types were: Skin tumors (14.0%), Gynecologic tumors (10.7%), Breast tumors (9.6%) and Soft tissue tumors (9.4%). The average diagnostic turnaround time (from case upload to expert report) was 18 hours.

Discussion: This reduction in turnaround time reflects a substantial improvement compared to traditional consultation methods (20 days). The implementation of the GLORIA Telepathology Network demonstrates the critical role of telepathology in reducing diagnostic delays, particularly in regions lacking access to oncopathologists. By enabling rapid expert review and fostering nationwide collaboration, GLORIA contributes to more equitable and timely oncological care across Colombia.

#0075 From single H&E to virtual immunohistochemical biomarker staining in the lung tumor microenvironment.

Kenneth To[1], Christopher Jackson[1], Louis Vaickus[2], Lawrence Schobs[1], Rohan Kamra Lyons[1], Rafay Azhar[1]

[1]ViewsML, Vancouver, BC, Canada,[2]Darthmouth-Hitchcock Medical Center, Lebanon, NH

Profiling the tumor microenvironment (TME) is fundamental to understanding immune, stromal, and tumor interactions influencing cancer diagnosis, progression, and therapeutic response. Physical immunohistochemistry (IHC) remains essential but is limited by reagent dependency, labor-intensive workflows, and tissue exhaustion. This study aimed to develop and validate a virtual IHC platform to reproduce biomarker staining directly from hematoxylin and eosin (H&E) slides, enabling high-fidelity TME characterization while conserving tissue. Using the ViewsML deep learning platform, a virtual TME panel was trained to predict five key biomarkers: CD31 (endothelial/vasculature), CD45 (pan-leukocyte), CD68 (macrophage), smooth muscle actin/SMA (activated fibroblasts and pericytes), and cytokeratin AE1/3 (tumor epithelium). 316 digitized lung cancer biopsy slides (Aperio GT450) encompassing over 150 million annotated cells were used. Data were split into training (70%), validation (15%), and test (15%) sets. Neural networks were optimized for biomarker-specific predictions, and model performance was evaluated using ROC AUC metrics and blinded pathologist review. Virtual biomarkers showed strong concordance with physical IHC, achieving AUCs of CD31=0.91, CD45=0.90, CD68=0.93, SMA=0.91, and CK AE1/3=0.90. Pearson's correlations were 0.73, 0.72, 0.76, 0.73, and 0.76 ($p<0.0001$). Virtual stains preserved spatial and morphological features, including CD31-positive vascular frameworks at tumor-stroma boundaries, CD45-positive immune infiltration, CD68-positive macrophage aggregates, SMA-positive stromal reaction patterns, and CK-positive tumor epithelium. Quantitative per-cell biomarker expression enabled automated precise cell fraction, cell ratio, spatial proximity, and immune and macrophage clustering analysis. These findings demonstrate that ViewsML's virtual IHC technology can reproduce physical staining from standard H&E slides, offering a scalable solution for digital TME profiling and conserving tissue. This approach supports translational research, virtual biomarker screening in drug development, and clinical application by enabling immune versus stroma-dominant tumor stratification to guide immunotherapy. Future work will extend this platform to more tumor types and incorporate multiplex virtual staining for broader digital pathology integration.

#0076 IHCExplore: An AI-driven computational pathology platform for accurate and scalable immunohistochemistry scoring.

Kelsey Luu[1], Ciyue Shen[2], Chintan Shah[3], John Shamshoian[3], Blake Martin[1], Daniel Shenker[1], Jackson nyman[1], Nhat Le[1], Zahil Shanis[1], Syed Ashar Javed[3], Matthew Bronnimann[3], Robert Egger[4], Harsha Pokolla[1], Andrew H. Beck[5], Benjamin Glass[2], Jennifer Hipp[3], Ryan Leung[6], Jacqueline Brosnan-Cashman[1], Santhosh Balasubramanian[1], Bahar Rahsepar[1], Emma Krause[7]

[1]PathAI, Inc., Boston, MA,[2]PathAI, Boston, MA,[34]PathAI, Inc.,[5]PathAI, Inc., Cambridge, MA,[6]Pathai, Boston, MA,[7]PathAI, boston, MA

Precise scoring of biomarker expression using immunohistochemistry (IHC) influences the success of precision therapeutics in oncology, such as antibody-drug conjugates (ADCs). However, manual IHC scoring by pathologists is limited by inter- and intra-pathologist variability, poor scalability, and limitations in visually accessible (e.g., spatial) information.

IHCExplore* is an artificial intelligence (AI)-enabled tool that provides comprehensive and reproducible characterization of protein expression from an IHC specimen. IHCExplore leverages PLUTO, a pathology foundation model,1 and was trained on a dataset of 24,390 whole slide images (WSIs) from 123 distinct staining assays. The model identifies cell types (cancer cells and lymphocytes) and segments tissue regions into cancer epithelium, cancer-associated stroma, and necrosis. It further segments the nucleus, cytoplasm, and membrane of individual cells to quantify protein expression at subcellular resolution.

Model-derived features quantify expression at the slide-level and classify cancer cells into unstained, low-, medium-, and high-intensity categories. Spatial features describe the distribution of these cells within the tumor microenvironment. Additional quantitative readouts include continuous H-score, membrane: cytoplasm intensity ratio, expression heterogeneity score, and spatial proximity score (to assess bystander activity).As a proof of concept, IHCExplore features were used to calculate PD-L1 tumor proportion score (TPSIHCExplore) as follows: total cancer cells with membrane staining above a threshold/total cancer cells. In a cohort of non-small cell lung cancer WSIs (N=597) stained with multiple PD-L1 clones (SP263, SP142, 28-8, 22C3), TPSIHCExplore was compared to manual consensus TPS from N=5 pathologists using intraclass correlation coefficient (ICC). After adjusting the staining threshold from a preset cutoff (4) to a calibrated cutoff (7), the ICC of TPSIHCExplore compared to consensus increased from 0.73 to 0.91, a value on par with the ICC of the average annotator compared to consensus (0.90). Therefore, outputs from routine IHCExplore deployments can recapitulate existing biomarker scoring with simple threshold optimization.Thus, IHCExplore is a scalable and accurate AI-driven solution for IHC scoring. The model's ability to generalize across tumor types and staining modalities, along with its fine-grained cell compartment segmentation, positions it as a powerful tool for biomarker discovery, assay optimization, and potential deployment as a companion diagnostic or scoring-assist system for precision oncology.

*IHCExplore is For Research Use Only. Not for use in diagnostic procedures.

1Juyal, D. et al. (2024) PLUTO: Pathology Universal Transformer. arXiv:2405.07905

#0077 AI-driven 3D spatial transcriptomics for 3D tumor microenvironment mapping in prostate adenocarcinoma.

Cristina Almagro-Perez[1], Andrew Song[1], Luca Weishaupt[1], Ahrong Kim[2], Guillaume Jaume[1], Konstantin Hemker[1], Drew F.K. Williamson[3], Stephanie Pei Tung Yiu[4], Qinghua Han[5], Renao Yan[5], Elena Baraznenok[5], Long Phi Le[1], Alexander S. Baras[6], Ali Bashashati[7], Sizun Jiang[4], Jonathan T.C. Liu[5], Faisal Mahmood[4]

[1]Brigham and Women's Hospital, Boston, MA,[2]Pusan National University, Busan, Korea, Republic of,[3]Emory University, Atlanta, GA,[4]Harvard Medical School, Boston, MA,[5]Stanford University, Palo Alto, CA,[6]Johns Hopkins Medicine, Baltimore, MD,[7]University of British Columbia, Vancouver, BC, Canada

Prostate adenocarcinoma (PRAD) is a multifocal and highly heterogeneous malignancy, marked by the coexistence of multiple Gleason grade glands within the same tumor microenvironment (TME). Spatial Transcriptomics (ST) has recently emerged as a powerful technology for characterizing the TME, yet its application is largely limited to two-dimensional (2D) histological sections, which typically capture less than 0.1% of the three-dimensional (3D) tumor context available upon resection. While promising, recently proposed in-situ approaches for 3D ST remain confined to reduced patient cohorts due to lengthy processing times and substantial costs.

To enable scalable 3D morphomolecular analysis of PRAD TME, we devise an AI framework that obtains 3D spatial molecular maps in a cost-effective and efficient manner. Our framework, VORTEX (Volumetrically Resolved Transcriptomics EXpression), leverages 3D high-resolution tissue morphology from 3D pathology imaging modalities, and minimal 2D ST to predict 3D ST. By pretraining on diverse 3D morphology-transcriptomic pairs from heterogeneous tissue samples and then fine-tuning on minimal 2D ST data from a specific volume of interest, VORTEX captures both generic tissue-related and sample-specific morphological correlates of gene expression. Our framework leverages pathology and single-cell foundation models, and integrates a cross-modal registration pipeline for accurate learning of morphomolecular links.

To evaluate our approach, we apply VORTEX to a cohort of 23 3D pathology volumetric images of PRAD specimens across 17 patients, acquired with micro computed tomography (microCT, 11 volumes) and open-top light-sheet microscopy (OTLS, 12 volumes). We additionally collect 88 sections of Visium ST across these samples and public cohorts, resulting in 243,682 spots with corresponding morphology. We demonstrate that VORTEX accurately predicts 3D ST and we identify two major trends: incorporating 3D morphology enhances the ability to learn morphomolecular links compared to 2D morphology alone, and including 2D ST data from the volume of interest further improves the performance by accounting for inter-patient heterogeneity. We observe that VORTEX captures intra-tumoral and inter-tumoral heterogeneity, with genes such as AZGP1 or GLO1 showing different expression profiles across patients and Gleason Grades. Furthermore, by analyzing 3D ST from multiple genes through Hallmark's pathways, we identify hidden structures in 2D views, including the 3D invasive tumor front.

In summary, VORTEX, by leveraging AI, 3D tissue morphology and 2D ST, generates 3D spatial molecular maps in a reliable, efficient and scalable manner. The combined morphomolecular analysis of the 3D tumor context can provide a novel perspective of the TME for improved characterization of PRAD heterogeneity.

#0078 OncoPredikt: A deep-learning framework for tumor detection and biomarker quantification in breast cancer IHC whole-slide images.

Gowhar Shafi[1], PM Shivamurthy[1], Aditya Satpute[1], Hrishita Kothavade[1], Aarthi Ramesh[2], Mohan Uttarwar[3], Nandini Ramchandani[1]

[1]OneCell Diagnostics India Private Limited, Pune, India,[2]1Cell.Ai, Mumbai, India,[3]1Cell.Ai, Foster city, CA

Background: Biomarker quantification in breast cancer remains challenging despite standardized protocols. Manual pathologist assessment introduces variability and misses subtle HER2 patterns, with inter-pathologist concordance for HER2 0 vs. 1+ distinction at only 26%. Second-generation antibody-drug conjugates now target HER2-low and HER2-ultralow tumors, but traditional visual assessment fails to reliably identify patients with barely detectable HER2 (faint staining in ≤10% of cells). We present an AI-driven approach for objective tumor detection and automated biomarker quantification of ER, PR, HER2 and Ki67 in Breast Cancer.
Methods: AI-based OncoPredikt model was designed and trained on H&E images (130 training, 53 validations from TCGA/in-house cohorts), tested on IHC WSIs for cross-stain generalization for automated Tumor detection. Further, automated biomarker quantification was performed within the detected tumor regions. The workflows were all validated against pathologist annotations.
Results: Tumor masks achieved Dice Similarity Coefficient >0.8 on H&E and better results with IHC WSIs. The ER/PR prediction using our AI-based approach shows a weak positive for a negative sample. For 2 pathologist-analyzed IHC 0 (Neg) HER2 samples tested through the AI-based approach yielded Ultra-Low (0+) and (1+) predictions indicating subtle positivity. The algorithm demonstrated promising performance in discriminating 0+ ultra-low (faint staining ≤10% cells) from 0 (no staining), addressing the critical diagnostic gap where HER2-ultralow patients were previously inaccessible for ADC selection. Automated assessments showed strong concordance with pathologist scoring across ER/PR Allred classification and Ki67 proliferation indices.
Conclusion: The HER2 ultra-low detection capability directly addresses a recognized bottleneck: visual inspection of faint, incomplete membrane staining in <10% of cells fall below reliable human detection, yet clinical trials confirm ADC efficacy in HER2-low/ultralow disease. The 26% inter-pathologist concordance for 0 vs. 1+ distinction underscores the clinical value of objective quantification. The shift from manual annotation to algorithm-derived tumor masks eliminates observer variability and saves the time of pathologists with heavy workload and reduces subjectivity in reporting. Thus, AI-driven tumor detection coupled with objective biomarker quantification constitutes a meaningful advancement for precision oncology in breast cancer, enabling identification of biomarkers previously invisible to standard pathology assessment. Further validation on large sample sets is still warranted.

#0079 From pixels to spatial microenvironments: AI-powered CAF-Epi niche prediction on H&E slides.

Zhixuan You[1], Qiankun Li[2], Jiaying Zhu[3], Guoyu Cheng[1], Yanrong Shen[1], Jiang Chang[2], Chen Wu[1]

[1]Department of Etiology and Carcinogenesis, National Cancer Center/National Clinical Research Center/Cancer Hospital, Chinese Academy of Medical Sciences (CAMS) and Peking Union Medical College (PUMC), Beijing, China,[2]Huazhong University of Science and Technology, Wuhan, China,[3]College of Computing and Data Science, Nanyang Technological University, Singapore, Singapore

Routine H&E slides remain the most accessible and rapid diagnostic material in clinical practice, particularly for gastrointestinal cancers. However, although H&E effectively distinguishes cancer from non-cancer, it provides insufficient information to predict treatment response. Spatial niches can be conceptualized as multicellular microanatomical units—defined by characteristic patterns of cellular adjacency, interaction and coordinated signaling. Using spatial transcriptomics across multistage esophageal squamous cell carcinoma (ESCC), we identified a CAF-epithelial (CAF-Epi) niche in which cancer-associated fibroblasts and epithelial cells cooperatively shield tumor cells from immune surveillance. In a neoadjuvant immunotherapy cohort, we found CAF-Epi score derived from this niche robustly discriminated responders from non-responders and stratified long-term survival, indicating that this functional niche, rather than subtle changes in cell proportions or morphology, more directly governs treatment outcome. To enable scalable CAF-Epi assessment on routine histopathology, we developed SHEEN-CAF (Spatial H&E-based CAF-Epi niche model), a deep-learning model that identifies ST-defined CAF-Epi niches directly from H&E slides. We assembled a paired H&E-ST atlas of 198 multistage ESCC specimens, totaling 9.6 million cell annotations and 275,753 CAF-Epi-labeled FOVs. SHEEN-CAF learns multi-scale morphological representations and reconstructs whole-slide CAF-Epi distributions. In the test set, it achieved an AUC of 0.91 with cross-center accuracies of 87-94%. In an independent external validation cohort with paired H&E and multiplex immunofluorescence, SHEEN-CAF-derived CAF-Epi scores correlated with immunofluorescence-defined CAF-Epi signals ($r = 0.81$, $P < 0.01$) and discriminated high- versus low-CAF-Epi burden lesions (AUC = 0.89). In an ESCC cohort treated with immune checkpoint blockade, non-responders exhibited significantly higher CAF-Epi scores than responders ($P < 0.05$), linking CAF-Epi burden on routine H&E to immunotherapy resistance. In summary, SHEEN-CAF converts CAF-Epi niche burden—previously measurable only with advanced spatial-omics—into an automated, quantitative biomarker derived solely from routine diagnostic H&E slides. By requiring no additional tissue or sequencing, it provides an efficient and scalable measure of the spatial microenvironment, with potential to refine immunotherapy response assessment and risk stratification in ESCC.

#0080 Quantitative assessment of tumor-infiltrating lymphocytes using AI in non-small cell lung cancer and association with immunotherapy response.

Mona Tuysserkani[1], Siraj Ali[2], Yoojoo Lim[2], Ken Nesmith[2], Sanghoon Song[2], Sanja Dacic[1], David Rimm[1]

[1]Pathology, Yale School of Medicine, New Haven, CT,[2]Lunit, Seoul, Korea, Republic of

Tumor-infiltrating lymphocytes (TILs) have been associated with treatment outcomes in non-small cell lung cancer (NSCLC), but challenges in visual and digital assessment have limited their clinical use. In this study, we used a quantitative AI-based approach on digitized H&E-stained sections to quantify intratumoral (iTIL) and stromal (sTIL) TILs and to evaluate optimal digital cutoff points associated with clinical outcomes across NSCLC cohorts treated with non-neoadjuvant and neoadjuvant immunotherapy. Two independently collected, annotated retrospective NSCLC cohorts from surgical resections treated with immune checkpoint inhibitors (ICIs) were included: the Yale 471 cohort (training set, n=42) and the Yale 592 cohort (validation set, n=41). Quantification of iTIL and sTIL was performed on whole-tissue H&E sections using the SCOPE IO™ platform developed by Lunit. A cutoff associated with clinical outcome was identified in the training cohort and applied to the validation cohort to assess associations with progression-free survival (PFS) and overall survival (OS). The two cohorts were then combined into a larger non-neoadjuvant training set (n=83). An optimal cutoff point was applied to the neoadjuvant validation set collected from pretreatment transbronchial and needle-core biopsies of patients with surgical resection after neoadjuvant therapy (n=76). This neoadjuvant cohort provided a clinically enriched population for assessing associations with PFS and OS. In the Yale 471 training cohort, higher sTIL scores were significantly associated with longer progression-free survival (PFS) at an optimal cutoff point of 2.4% (HR = 2.7). This cutoff remained significant in Yale 592 (HR = 5.8; $P < 0.0001$). No significance was found when assessing iTIL in this manner. In the non-neoadjuvant training set, higher iTIL scores were linked to longer PFS with an optimal cutoff point of 0.28%, dividing patients into equal groups (HR = 0.36). The neoadjuvant cohort showed significance (HR = 0.28; $P = 0.0045$). Higher sTIL scores were also associated with improved PFS in the non-neoadjuvant training cohort using the same 2.4% cutoff point, splitting patients into 70% high and 30% low groups (HR = 0.21). The neoadjuvant validation set showed significance (HR = 0.34; $P = 0.0066$). Although higher iTIL and sTIL values showed consistent trends for overall survival (OS) in the training sets, these associations did not reach statistical significance. Quantitative assessment of tumor-infiltrating lymphocytes (TILs) may provide an objective biomarker for immunotherapy response in NSCLC, particularly for intratumoral TILs (iTIL), which are not assessable by pathologists. Future work is planned to include additional analyses of neoadjuvant and prospective NSCLC cohorts to further validate associations between TIL assessment and clinical outcomes.

#0081 Clinical-grade quality control and stain harmonization enhancement in whole-slide images of lung cancer using deep learning.

Meghdad Sabouri Rad[1], Mohammad Mehdi Hosseini[1], Rakesh Choudhary[1], Harmen Siezen[2], Saverio J. Carello[1], Ola El-Zammar[1], Michel R. Nasr[1], **Bardia Rodd**[1]

[1]SUNY Upstate Medical University, Syracuse, NY,[2]University of Maryland at College Park, College Park, MD

Background: Deep learning models trained on hematoxylin-eosin (H&E) whole-slide images (WSIs) increasingly support prognostic and therapeutic-response biomarkers in lung cancer. However, their reliability is often compromised by image blur, scanner and pen artifacts, and inter-slide stain variability that obscure tissue morphology and introduce spurious predictive signals. To mitigate these issues, we developed a comprehensive, quantitative WSI quality-control (QC) and stain-harmonization pipeline tailored to single-pattern lung adenocarcinoma and assessed its downstream impact on clinical outcome prediction.
Methods: We analyzed 143 H&E WSIs (20×, 0.5 µm/pixel) from a Dartmouth lung adenocarcinoma cohort. QC incorporated multiple slide-level metrics, including tissue masks excluding artifacts, quantification of local blur using variance of the Laplacian across ≤600 tissue-centered crops, thumbnail-derived brightness statistics, and hematoxylin optical-density medians. Slides were retained only if they satisfied strict thresholds: tissue coverage ≥40%, artifact fraction ≤1%, blurry-tissue fraction ≤5%, brightness 140-210, and hematoxylin median 0.10-0.35. Among QC-cleared slides, an automated procedure selected a cohort-representative reference slide based on proximity to median brightness and hematoxylin metrics; its Macenko stain vectors and 99th-percentile concentration parameters were used for harmonization. All accepted WSIs were normalized to this reference. From normalized slides, 256×256 tiles (stride 256) with tissue fraction ≥70% and artifact fraction ≤2% were extracted to train a slide-level binary outcome model.
Results: Of 143 WSIs, 140 (97.9%) passed QC; three were excluded. Retained slides had a median resolution of 33,792 × 46,080 pixels. From 128 QC-passing cases, we obtained 215,220 analysis-ready tiles (median 1,590 per slide). By comparison, a simpler Otsu-based pipeline produced 249,073 tiles; thus, QC-aware masking removed 13.6% of candidates—primarily low-tissue or artifact-laden regions—without diminishing tumor or stromal coverage. Stain-normalized previews demonstrated highly consistent H&E appearance. Classifier performance improved from 90.63% ± 9.36 without QC/harmonization to 95.32% ± 4.05 following implementation.
Conclusions: This standardized QC and stain-harmonization framework effectively excludes low-quality slides and artifact-heavy regions while substantially improving the stability and accuracy of deep learning-based clinical outcome prediction in lung adenocarcinoma. By reducing technical confounders and enforcing stain consistency, the workflow enhances the robustness, reproducibility, and translational readiness of WSI-derived biomarkers and supports multi-institutional harmonization efforts in computational pathology.

#0082 Artificial intelligence derived spatial transcriptomic signatures from H&E slides predict survival in primary melanoma.

Amritpal Singh[1], Merin George[2], Tilak Pathak[1], Ujjwal Baid[1], Douglas Parker[3], Michael C. Lowe[4], Anant Madabhushi[1], **Bhakti Baheti**[1]

[1]Department of Biomedical Engineering, Emory University, Atlanta, GA,[2]Mercer University School of Medicine, Macon, GA,[3]Department of Pathology and Laboratory Medicine, Emory University, Atlanta, GA,[4]Department of Surgery, Emory University, Atlanta, GA

Introduction: Melanoma exhibits pronounced spatial and molecular heterogeneity, which drives tumor progression and clinical outcomes. While spatial transcriptomics (ST) assays can capture this complexity, their high cost and limited tissue availability hinder widespread use. Recent advances in computational pathology enable prediction of spatial gene expression directly from routine Hematoxylin and Eosin (H&E) whole slide images (WSIs), providing a scalable virtual alternative for true spatial profiling. This work investigates whether artificial intelligence (AI) derived ST features extracted from TCGA-SKCM H&E slides can serve as prognostic biomarkers of overall survival (OS) in primary melanoma.

Methods: We analyzed formalin-fixed paraffin-embedded H&E WSI of primary melanoma from TCGA-SKCM with available survival data (N=292 patients). Dataset was randomly split in a 30:70 ratio to generate training (N=87) and testing (N=205) cohorts. WSI were divided into patches of 290x290 pixels, and spatial expression of 5000 genes was predicted using the pretrained DeepSpot model. Downstream analyses were limited to 18 melanoma-relevant genes shortlisted from prior literature. AI predicted spatial gene expression values of these genes were summarized into per-spot and per-gene descriptors, producing 269 quantitative features encompassing statistical metrics, spatial autocorrelation indices, and Ripley's K derived spatial clustering measures. After removing highly correlated and low-variance features, bootstrapped LASSO regression was used to select the top 5 survival-informative features. A Cox proportional hazards model was used to create an integrated AI signature. Model performance for 10-year OS was evaluated using hazard ratios (HR), concordance indices, log-rank tests, and Kaplan Meier analyses on training and holdout testing cohorts.

Results: Survival times were right-censored at 10 years, resulting in 116 observed deaths and 176 censored patients. AI derived ST signature consisted of spatial features for KRT6B, UBE2L6, and PFKFB3 genes, along with average gene expression, and significantly stratified patients by OS. In the training set, the high-risk group had significantly poorer survival (HR = 3.39; 95% CI: 1.67-6.88; $p < 0.001$, C-index = 0.654). Independent validation in the testing cohort confirmed prognostic utility (HR = 2.17; 95% CI: 1.37-3.44; $p = 0.001$; C-index = 0.615), demonstrating generalizability.

Conclusion: AI inferred ST features derived from standard H&E slides capture biologically meaningful patterns associated with outcomes in primary melanoma. This virtual-omics pipeline provides a scalable and non-destructive approach for prognostication and may complement or substitute traditional molecular assays in settings where ST is not feasible.

#0083 AI-powered analysis of pancreatic ductal adenocarcinoma tissues to study the tumor immune ecosystem and identify novel classifiers.

Rebecca Polidori[1], Marika Viatore[1], Anna Rita Putignano[2], Greta Donisi[2], Capretti Giovanni[2], Arturo Bonometti[2], Silvia Uccella[2], Silvia Bozzarelli[2], Jakob Nikolas Kather[3], Massimo Locati[1], Federica Marchesi[1]

[1]University of Milan, Milan, Italy,[2]IRCCS Humanitas Research Hospital, Rozzano, Italy,[3]Technische Universitat Dresden, Dresden, Germany

Background: Digital pathology and artificial intelligence (AI) are emerging as powerful tools in immuno-oncology, enabling enhanced diagnostic and prognostic workflows. The current trend regards the application of AI on histopathological images to extract relevant features beyond human visual perception. Pancreatic ductal adenocarcinoma (PDAC) is one of the deadliest cancers worldwide, for which lack of efficient biomarkers to stratify patients and grade the response to therapy may play a significant impact. *Aim*: This project presents a computational pipeline integrating machine and deep learning approaches to characterize the PDAC tumor immune ecosystem and extract features with potential clinical relevance.

Methods: Whole-slide images from 53 PDAC patients, including those treated and untreated with neoadjuvant chemotherapy (NAT), were analyzed. Slides were stained with H&E, picrosirius red to detect fibrosis, and a CD68 antibody to detect macrophages. On H&E slides, a deep learning tissue classifier pretrained on colorectal cancer quantified Tumor and Stroma areas and their Spatial Entropy. QuPath-based pixel classifiers segmented CD68+ regions to compute macrophage abundance and spatial aggregation measured by the Morisita Index, and quantified picrosirius red+ areas to assess fibrosis and collagen maturity. Tissue and immune metrics were correlated, and slide-level embeddings extracted with the foundation model CTransPath were projected onto UMAP to explore clustering patterns.

Results: The deep learning tissue classifier achieved a global F1-score of 0.79 on PDAC slides. High macrophage abundance and Stroma Entropy were associated with worse overall survival. Integrating immune with tumor or stromal features improved patient stratification. NAT-treated patients showed increased fibrosis and reduced macrophage infiltration, with Stroma Entropy being predictive only in this group. Moreover, CTransPath-derived embeddings of CD68 and picrosirius red-stained slides clustered according to NAT regimen.

Conclusions: This AI-driven pipeline enables quantitative spatial profiling of the PDAC immune microenvironment, revealing interpretable features with prognostic and predictive value. Our findings highlight the potential of computational pathology to derive clinically meaningful biomarkers and support therapy response evaluation.

#0084 Deep-learning prediction of progression-free survival to EGFR inhibitors from H&E tissue slides in advanced *EGFR*-mutated non-small cell lung cancer.

Lodovica Zullo[1], Elin Samuelsson[2], Fabrizio Citarella[3], Mina Farag[2], Francesco Cortiula[4], Andrea De Giglio[5], Frank Aboubakar[6], Katharina von Loga[2], Etienne Hatton[2], Lorenzo Nibid[3], Giovanna De Maglio[4], Francesca Ambrosi[7], Beatrice Ramella Pollone[8], Melanie Janson[9], Alessandro Russo[10], Andrew Whittum[1], Ingrid Garberis[1], Victor Aubert[2], Hortense Deslandes[2], David Planchard[1], Fabrice Andre[1], Cecile Badoual[1], Benjamin Besse[1], Maria Rosa Ghigna[1], Mihaela Aldea[1]

[1]Gustave Roussy, Villejuif, France,[2]Owkin France, Paris, France,[3]Campus Bio-Medico, Rome, Italy,[4]University Hospital of Udine, Udine, Italy,[5]University of Bologna, Bologna, Italy,[6]Cliniques Universitaires Saint-Luc, Bruxelles, Belgium,[7]Maggiore Hospital-AUSL Bologna, Bologna, Italy,[8]IRCCS Ospedale Policlinico San Martino, Genova, Italy,[9]Francois BACLESSE, Comprehensive Cancer Center, Caen, France,[10]Ospedale Papardo, Messina, Italy

Background: Third-generation tyrosine kinase inhibitors (TKIs) like osimertinib are standard for untreated advanced non-small cell lung cancer (aNSCLC) with common *EGFR* mutations (exon 19 deletion/L858R). Combination with chemotherapy, bispecific antibodies or anti-angiogenic agents prolong survival but raises toxicity. No biomarker identifies patients benefiting from combinations versus osimertinib alone, yet.

Methods: We trained a multiple-instance model to predict progression-free survival (PFS) to first line EGFR-TKIs from hematoxylin-eosin (H&E) tissue slides, adjusting to the TKI type. Diagnostic slides from primary tumors of aNSCLC with common *EGFR* mutations were digitized at 20× at three independent institutions, and retrospectively included with clinical data. Performance was evaluated with C-index for continuous PFS and AUC for 1-year PFS, using bootstrapping.

Results: In total, 141 patients were included (n=73 osimertinib; n=68 erlotinib/gefitinib). We trained on Gustave Roussy (GR, France) and inferred on Campus Bio-Medico (CBM, Italy) and University Hospital of Udine (U, Italy). Patients were mostly female (65%, 62%, 72%), with no smoking habit (63%, 59%, 55%), had adenocarcinoma (92%, 94%, 100%) and exon 19 deletions (56%, 56%, 55%) across GR, CBM, U cohorts. Median (IQR) age was 65 (56-74), 71 (62-78), 68 (63-73) years in GR, CBM, U, respectively. Median true PFS and model performances are presented in the table.

Conclusion: This is the first study to predict PFS to EGFR-TKIs from H&E slides. Despite limited sample size, these findings support further investigation of digital pathology for PFS prediction in *EGFR*-mutated NSCLC. Results on additional cohorts, combination of the model with clinical variables, and interpretability will be presented at the congress.

Model's performance across cohorts

Cohort	Subset	#Patients	True PFS median (95%CI)	C-index continous PFS Mean (95%CI)	AUC 1-year PFS Mean (95%CI)
	All TKIs	78	11.9 (9.5, 15.4)	NA-Training cohort	NA-Training cohort
GR	Osimertinib	42	12.6 (9.8, 16.9)	NA-Training cohort	NA-Training cohort
	Erlotinib/gefitinib	36	9.9 (7.0, 15.4)	NA-Training cohort	NA-Training cohort
	All TKIs	34	9.5 (6.4, 16.3)	0.63 (0.53, 0.73)	0.73 (0.57, 0.86)
CBM	Osimertinib	16	13.6 (5.5, 23.3)	0.63 (0.49, 0.77)	0.62 (0.40, 0.86)
	Erlotinib/gefitinib	18	7.4 (2.1, 9.5)	0.59 (0.44, 0.74)	0.77 (0.57, 0.94)
	All TKIs	29	13.0 (9.4, 17.9)	0.78 (0.70, 0.84)	0.83 (0.69, 0.95)
U	Osimertinib	15	23.0 (6.7, 50.1)	0.84 (0.70, 0.94)	0.90 (0.72, 1.00)
	Erlotinib/gefitinib	14	12.7 (8.0, 17.5)	0.74 (0.61, 0.85)	0.73 (0.46, 0.93)

#0085 Path2Marker: Cell-level prediction of multiplex protein expression from routine H&E slides.

Amos Stemmer[1], Tiangen Chang[1], Thomas Cantore[1], Saugato Rahman Dhruba[1], Sumona Biswas[1], Sumeet Patiyal[1], Eldad David Shulman[1], Emma M. Campagnolo[2], Aagam Shah[3], Simon Knott[3], Chi-Ping Day[2], Danh-Tai Hoang[1], Eytan Ruppin[3]

[1]National Cancer Institute - Cancer Data Science Laboratory (CDSL), Bethesda, MD,[2]National Cancer Institute - Cancer Data Science Laboratory (CDSL), Bathesda, MD,[3]Cedars-Sinai Medical Center, Los Angeles, CA

Background: High-plex spatial proteomics platforms (e.g., PhenoCycler) have transformed our ability to map the tumor microenvironment (TME) at single-cell resolution, but their cost constrains cohort sizes for biomarker discovery and validation. Recently, ROSIE (Wu et al., Nat Commun 2025) aimed to tackle this problem by predicting protein markers directly from H&E stained slides. However, the number of robustly predicted markers obtained by it has been fairly limited, with only 5 markers reaching a Pearson r correlation of above 0.4 between measured and predicted marker intensity. Here, we present Path2Marker, a cell-level deep learning framework that substantially expands the panel of robustly predicted protein markers in multiple tumor types.**Methods:** We analyzed three new cancer-specific PhenoCycler (CODEX) cohorts with paired H&E and multiplex immunofluorescence, including lung cancer (88 samples, 660791 cells), colorectal cancer (106 samples, 624919 cells) and breast cancer (115 samples, 901684 cells), each stained with a 55 proteomic marker panel. For each disease, we trained a cancer-specific model to predict per-cell marker intensities from the H&E slides, and additionally evaluated an ensemble model that averages predictions from all three cancer-specific models. Model performance was evaluated on 60 held-out samples (all three diseases; 396,995 cells), using Pearson correlation between the measured and predicted marker intensities.**Results**: We robustly predict (Pearson r > 0.4 for measured vs. predicted intensity) 23, 26, and 44 markers in the breast, lung and colorectal cohorts, respectively, markedly outperforming the published state of the art. When benchmarked on the same samples, ROSIE achieved fewer robustly predicted markers, with only 3 markers in colon, 2 in lung and 0 in breast. The ensemble model significantly improved mean marker-level correlation in lung and was comparable to the indication-specific models in breast and colorectal cancer. Top-performing markers included EpCAM in colon (r=0.79), PanCK in lung (r=0.73), and PanCK in breast (r=0.64). Notably, they include not only lineage markers (e.g., PanCK, CD3e) but also functional markers (e.g., PD-L1, Ki-67), enabling downstream cell-state and cell-type annotation, laying the basis for robust annotation of 25, 16, and 17 different cell-types in colon, lung, and breast, respectively.**Conclusion**: Path2Marker enables robust prediction of more than 20 multiplex protein markers at single-cell, spatial resolution directly from standard H&E slides across three major solid tumors. It markedly improves upon the predictive accuracy of extant tools, opening up the possibility of fast and low-cost annotation of large cancer patients cohorts directly from the histopathology slides.

#0087 *Path2Prot* offers a new way for breast tumor subtyping and treatment response prediction from AI-inferred proteomic biomarkers.

Saugato Rahman Dhruba[1], Danh-Tai Hoang[1], Sumit Mukherjee[1], Amos Stemmer[1], Eldad Shulman[1], Ranjan Kumar Barman[2], Sanna Madan[2], Sanju Sinha[3], Kenneth D. Aldape[4], Eytan Ruppin[5]

[1]National Cancer Institute - Cancer Data Science Laboratory (CDSL), Bethesda, MD,[2]National Cancer Institute - Cancer Data Science Laboratory (CDSL), Rockville, MD,[3]Sanford Bernham Prebys, La Jolla, CA,[4]Professor, Dept. of Pathology, Chair, NCI-CCR, Bethesda, MD,[5]Cedars-Sinai Medical Center, Los Angeles, CA

Background: The advent of AI is revolutionizing precision medicine, including digital pathology where large foundation models (FMs) are applied to readily extract genomic/transcriptomic patterns from tumor whole-slide histopathology images (WSIs). In contrast, fewer studies have attempted to derive direct functional insights *via* proteomics from tumor morphology in WSIs, partly due to data scarcity. Henceforth, we propose a weakly-supervised deep learning model called *Path2Prot* to infer the relative abundance of 413 clinically relevant proteomic biomarkers in breast cancer (BC) from tumor H&E slide images. We show the clinical utility of such models in tumor subtyping and treatment response prediction by leveraging the inferred proteomic markers.

Methods: *Path2Prot* is composed of two stages: *First*, each WSI is preprocessed *via* a standard pipeline to a set of 512 x 512 tile images at 20x magnification, which are fed to a transformer-based FM to extract morphological features; *Next*, using these features with matched patient-level proteomics, a multilayer perceptron is trained to infer the proteomic marker levels. To train, we used 2,074 WSIs from 841 TCGA-BRCA patients and the matched reverse-phase protein array (RPPA) data for 413 proteins (total + post-translationally modified). We leveraged both WSI types available *via* building three distinct models: *FFPE model*, trained on 893 formalin-fixed paraffin embedded WSIs (used for diagnosis); *FF model*, trained on 1,181 fresh-frozen WSIs (better RNA quality); and *Combo model*, combining the predictions of both models.

Results: We assessed model performance with Pearson correlation (R) between inferred and measured proteomics, where proteins with $R \geq 0.4$ are referred as the *well-predicted proteins* (WPPs). The Combo model performed the best with 23.7% WPPs (mean R = 0.31) in cross-validation and successfully generalized to cross-platform mass spectrometry proteomics in external validation with CPTAC-BRCA with 27.1% WPPs (mean R = 0.28; Overlap-in-WPPs = 71.8%). We further dichotomized the inferred HER2 and ER levels to identify their immunohistochemistry status and assigned patient tumors to clinically actionable subtypes (HER2+, ER+ & TNBC) across TCGA-BRCA (n = 733), CPTAC-BRCA (n = 89), TransNEO (n = 160) and IMPRESS (n = 126). This task can be done fairly well, yielding area under the curve (AUC) values of HER2+ = 0.69-0.72, ER+ = 0.72-0.77 and TNBC = 0.83-0.88. Finally, the inferred protein targets successfully estimated anti-HER2 response in TransNEO (n = 60, AUC = 0.71) and CSHS-BRCA (n = 20, AUC = 1.0) cohorts, and anti-PD1 response in CSHS-BRCA (n = 16, AUC = 0.78).

Conclusion: Our analysis reveals a clinically important subset of proteins in breast cancer can be robustly predicted from routine WSIs for clinical application. One may expect to significantly improve upon these results with the advent of larger proteomics datasets.

#0088 Multiscale characterization of early morphologic radiation response in rectal cancer via digital pathology.

Sriya Veerapaneni[1], Paul Acosta[2], Bassel Dawod[3], Sebastian Diegeler[4], Mengxi Yu[1], Eslam Elghonaimy[3], Megan Wachsmann[5], Purva Gopal[5], Todd Aguilera[3], Satwik Rajaram[1]

[1]Lyda Hill Department of Bioinformatics, The University of Texas Southwestern Medical Center, Dallas, TX,[2]The University of Texas MD Anderson Cancer Center, Houston, TX,[3]Department of Radiation Oncology, The University of Texas Southwestern Medical Center, Dallas, TX,[4]University of Cambridge, Cambridge, United Kingdom,[5]Department of Pathology, The University of Texas Southwestern Medical Center, Dallas, TX

With effective neoadjuvant chemotherapy and radiotherapy (RT), some patients with locoregional rectal cancer may avoid surgery. However, patient responses are highly heterogeneous and poorly understood. Although morphological assessment remains the clinical gold standard, it is often dominated by tumor abundance, potentially overlooking complex biological adaptations to treatment. To address this, we sought to gain insights through a multiscale characterization of early histologic changes following RT. We leveraged matched pre- and post-RT histology slides from the INNATE trial dataset, using adjacent tissue as a control, to develop a dual-pipeline framework: (1) C-MorphQuant, for analysis of predefined classical features such as tissue composition, spatial organization, and nuclear morphology based on a finetuned cell classifier and a trained region classifier; and (2) DL-RadScore, a novel deep learning metric that learns de novo morphological features by distinguishing irradiated from non-irradiated tissue. Our C-MorphQuant analysis revealed: (1) compositionally, a clear reduction in tumor and normal epithelium with a commensurate increase in stroma; (2) spatially, the disruption of glands into fragmented small clusters (<30 nuclei); and (3) nuclearly, alterations in size and shape that were evident but patient-specific. Notably, while the overall radiation impact was generally stronger in tumor, C-MorphQuant phenotypes were more heterogeneous than the stereotypical adaptations observed in adjacent normal tissue. The DL-RadScore accurately distinguished unseen pre- and post-radiation samples. We established biological relevance by comparing with tumor epithelial Ki67 proliferation and found strong negative correlations at both the patient ($r = -0.59$, $p = 2.08*10^{-2}$) and intra-slide ($r = -0.43$, $p = 2.17*10^{-78}$) levels. While DL-RadScore maintained strong concordance with C-MorphQuant composition metrics, it outperformed measures of tumor cellularity in capturing proliferative status. Most intriguingly, our results demonstrated that rather than a gradual accumulation of morphological changes, some tumors appeared to initially "shrug off" early radiation doses, preserving a pre-treatment-like morphology, yet ultimately collapsed by the time of surgery. In summary, this study underscores the value of characterizing treatment-induced phenotypes beyond mere tumor cell abundance and highlights the complex non-linear spatiotemporal dynamics in which early morphological persistence does not preclude long-term cure.

#0089 TissueTrek: An interactive multimodal web-based platform for exploring spatial morphology-molecular relationships in cancer.

Vibha R. Rao[1], Marvin Escobar Barajas[2], Candice C. Black[1], Madhumala K. Sadanandappa[1], Scott M. Palisoul[1], Adrienne A. Workman[1], Todd A. MacKenzie[2], Louis J. Vaickus[1], Mary D. Chamberlin[1], George J. Zanazzi[1], **Shrey S. Sukhadia**[1]

[1]Pathology and Laboratory Medicine, Dartmouth Health, Lebanon, NH,[2]Dartmouth College, Hanover, NH

Background: The spatial organization of epithelial, stromal, and immune compartments plays a fundamental role in shaping tumor behavior, yet researchers and clinicians lack accessible tools to concurrently explore morphology, pathomic features, and spatial molecular measurements. Existing methods typically examine a single modality at a time, require specialized expertise, or offer limited interpretability. To address this gap, we developed TissueTrek, an interactive web-based platform that integrates H&E morphology, quantitative pathomics, spatial gene and protein expression, and explainable Machine Learning(ML) outputs into a unified environment that can be easily used by researchers, clinicians, trainees, and patients alike.

Methods: The platform was built using a GeoMx DSP cohort of 57 FFPE triple-negative breast cancer (TNBC) tissue cores. Board-certified pathologists annotated tumor regions of interest (ROIs). Three ROI-matched modalities were extracted: 77 pathomic features from H&E images, 91 spatially profiled and biologically relevant genes, and 570 spatially profiled proteins. The results from several ML pipelines developed upstream were incorporated to aid interpretability. Several web-based technologies enabled dynamic linking of ROIs with their molecular, pathomic, and model-derived representations for real-time exploration.

Results: TissueTrek provides the first ROI-resolved interface enabling simultaneous visualization of (i) spatially measured gene and protein expression, (ii) quantitative pathomic features, and (iii) interpretable deep-learning and pathomics-ML outputs within the same tissue context. Users can interactively conduct exploration of results through multiple features to decipher the biology underlying the tissue ROIs. The Model Output panel displays interpretable maps of these ROIs, enabling the study of spatial morphology-molecular relationships in TNBC that are otherwise difficult to discern.

Conclusions: TissueTrek represents a first-of-its-kind, fully interpretable spatial pathology interface that unifies morphologic, molecular, and deep-learning-derived insights into the same ROI-resolved environment. Although demonstrated in TNBC, the framework is generalizable and is capable of seamlessly incorporating additional biomarkers, diseases, or spatial-omics technologies, making it widely accessible, from expert computational scientists to clinicians, trainees, and patients seeking to understand their tissue biology. By enabling broad, user-friendly access to multimodal spatial biology, the platform advances computational pathology toward more transparent, clinically translatable, and educationally usable digital tissue ecosystem. This platform will be updated with the data and results constantly to serve the community better.

#0090 Histologic stratification of hepatocellular carcinoma using deep learning informed by spatial transcriptomics.

Tyler M. Yasaka[1], Chang Kyung (Joanna) Kim[1], Po-Yuan Chen[1], Rebekah E. Dadey[1], Riyue Bao[1], Satdarshan Pal S. Monga[2], Yu-Chiao Chiu[3]

[1]University of Pittsburgh, Pittsburgh, PA,[2]Associate Professor of Pathology & Med., University of Pittsburgh, Pittsburgh, PA,[3]UPMC Hillman Cancer Center, Pittsburgh, PA

Introduction: Hepatocellular carcinoma (HCC) is a leading cause of cancer-related mortality. Although multiple classification systems have been developed, their clinical utility remains limited. With the increasing use of tissue biopsies in targeted therapy trials, there is an opportunity to advance both molecular and histologic approaches for HCC stratification.
Methods: Publicly available spatial transcriptomics data with paired hematoxylin and eosin (H&E) images from 10 HCC slides were used to train deep learning models to predict Hoshida subtype (S1, S2, S3) signatures within spatial transcriptomics spots from corresponding H&E tiles. Models were evaluated using an 80/20 training/test split and subsequently applied to H&E whole-slide images from The Cancer Genome Atlas (TCGA; n=340) as well as an in-house validation cohort (n=48). Tile-level predictions were aggregated to generate patient-level histologic scores, which were then clustered into three subclasses (A, B, and C), which were then assessed for unique clinical and molecular characteristics.
Results: Models achieved holdout AUROCs of 0.93 (S1), 0.92 (S2), and 0.94 (S3). In TCGA, subclasses predicted overall survival (A vs B, $p<0.0001$; A vs C, $p<0.0001$), disease-free interval (A vs B, $p<0.001$; A vs C, $p<0.0001$), and progression-free interval (A vs B, $p<0.01$; A vs C, $p<0.0001$). Histologic subtypes were independently prognostic when considered alongside clinical variables via stepwise Cox proportional hazards (A vs B, $p=0.008$; A vs C, $p=0.001$). Each cluster associated with distinct clinical features (e.g. cluster A with early pathologic stage and HBV etiology, and cluster B with late stage), mutations, and enriched pathways (cluster A with metabolic pathways, cluster B with cell cycle pathways, and cluster C with immune pathways). Cluster C was also enriched for a signature of anti-PD-1 response in HCC ($p<1x10-10$). In the validation cohort, overall survival trends were maintained (A vs B, $p=0.121$, A vs C, $p=0.005$).
Conclusions: Using a deep learning model which predicts spatial subtype signatures from H&E whole slide images, we developed a histology-based stratification with improved prognostic power compared to existing HCC subtypes. The associated clinical and molecular features suggest that these subtypes exhibit not only distinct phenotypes (metabolic, proliferative, and immune) but also potentially pathogenesis, supporting the potential of H&E to guide patient stratification in clinical trials and inform personalized therapeutic strategies.

: Circulating Tumor Cells, Metastasis, and Dissemination Biology 1
Poster Session

#1061 Tumor-informed circulating tumor DNA identifies high-grade serous ovarian cancer patients at highest risk for recurrence despite optimal first-line treatment with primary macroscopic complete resection.

Magdalena Postl[1], Christina Victoria Tauber[2], Valentina Glueck[3], Mira Maria Gliga[2], Nuria Segui[4], Karen Howarth[4], Miguel Alcaide[4], Lucia Oton[4], Gerda Hofstetter[5], Isabelle Maurer[2], Alexander Burges[2], Sven Mahner[2], Mirjana Kessler[2], Melina Danisch[1], Stephan Polterauer[1], Nicole Concin[1], Christoph Grimm[1], Fabian Trillsch[2]

[1]Department of Obstetrics and Gynecology, Gynecologic Cancer Unit, Comprehensive Cancer Center, Medical University of Vienna, Vienna, Austria,[2]Department of Obstetrics and Gynecology and Comprehensive Cancer Center Munich, LMU University Hospital, LMU Munich, Munich, Germany,[3]Department of Obstetrics and Gynecology, Klinikum Starnberg, Starnberg, Germany,[4]SAGA Dx, Morrisville, NC,[5]Department of Pathology, Medical University of Vienna, Vienna, Austria

Background: Complete macroscopic tumor resection estimation as visualized by the surgeon is the foremost prognostic factor in high-grade serous ovarian cancer (HGSOC). Objective measures of postoperative molecular residual disease (MRD) are lacking, including serologic and radiologic evaluation. Tumor-informed circulating tumor DNA (ctDNA) has shown promise as a new approach to identify patients at higher risk for relapse.
Methods: This prospective bicentric study included advanced HGSOC patients (pts) undergoing primary debulking surgery (PDS), six cycles of chemotherapy and maintenance therapy (07/2021 - 09/2024). Whole-genome sequencing of tumor tissue identified structural variants, used to design personalized multiplex dPCR assays to detect MRD. Plasma samples were collected: perioperatively (preop, postop day[d]2 and d10), during chemotherapy (C1, C3, C6) and every 3 months (mo) until progression or 24 mo of follow up (FU). CA-125 was analyzed accordingly (cutoff 35 kU/L). Statistics included chi-square and log-rank tests, multivariate Cox model and Kaplan-Meier estimates for progression-free survival (PFS).
Results: 33/84 pts (39%) experienced relapse with a median PFS of 12.0 mo during a median FU time of 15.4 mo. ctDNA was detected in 77/82 pts (94%) at baseline and in 63/74 pts (85%) postoperatively. At postop d10, pts with complete tumor resection had significantly lower ctDNA levels than pts with postop residual disease (p=0.0018). Median ctDNA level decreased by 94% between preop and postop d10 in pts with complete tumor resection (p=0.0247), but not in pts with postop tumor residuals (p=0.891). Within the pt subgroup with complete tumor resection, ctDNA clearance at C1 (20%) and C6 (70%) was associated with significantly lower recurrence risk compared to persistent ctDNA levels (C1: 80%, C6: 30%) with a stronger association at C6 (C1: HR=3.39, p=0.0470, C6: HR= 52.21, p<0.0001). Median time to recurrence in the C6 ctDNA positive group was 10.7 mo compared to 21.3 mo in the ctDNA negative group. This effect was not observed at postop d10 (p=0.273) or for pts with residual tumor. ctDNA outperformed CA-125 for prognosis, as CA-125 levels at C1 or C6 failed to predict recurrence (C1: p=0.189; C6: p=0.165). In a multivariate analysis, ctDNA persistence at C6 (HR=14.58, p<0.0001) and postoperative residual tumor were confirmed as independent prognostic markers.
Conclusion: Tumor-informed ctDNA analysis can further accurately stratify HGSOC pts at high risk of recurrence despite primary surgery with complete macroscopic resection. ctDNA assessment at C6 may provide an opportunity window for risk-stratified treatment adjustments directly after chemotherapy, enabling new personalized maintenance strategies.

#1062 Longitudinal monitoring of circulating tumor cells (CTC) reveals dynamic CTC behaviors associated with disease progression and survival in ALK-positive NSCLC.

Yuru Chen[1], Shamileh Fouladdel[1], Leah Kidder[1], Yuehang Tang[1], Harrison Ball[1], Habib Serhan[1], Zhaoping Qin[1], Albert Liu[1], Xu Cheng[1], Liwei Bao[1], Varun Kathawate[1], Larua Goo[1], Mary Horn[1], Stacy Fry[1], Aaron N. Hata[2], Justin Gainor[3], Jessica J. Lin[4], Stuart Hinton[5], Chao H. Huang[6], Nathan Merrill[1], Aaron M. Udager[1], Peter J. Ulintz[1], Angel Qin[1], Sofia Merajver[1], Sunitha Nagrath[1]

[1]University of Michigan, Ann Arbor, MI,[2]Massachusetts General Hospital, Charlestown, MA,[3]Harvard Medical School, Boston, MA,[4]Mass General Brigham Cancer Institute, Boston, MA,[5]Hematology Oncology, University of Kansas Hospital Authority, Kansas City, KS,[6]Internal Medicine / Division Hem & Oncology, University of Kansas Medical Center, Westwood, KS

Introduction: Heterogeneous mutation profiles are common in anaplastic lymphoma kinase-positive non-small cell lung cancer (ALK+ NSCLC), especially upon progression, supporting that robust longitudinal monitoring to detect these changes early can play a role in disease management. Circulating tumor cells (CTCs) provide a minimally invasive modality for real-time monitoring. We longitudinally analyze CTC counts and sc-transcriptomes to assess their reflection of clinical responses and correlation with progression risk in ALK+ patients.

Methods: Following informed consent, we collected 61 samples from 12 ALK patients (2-10 timepoints/patient; 11 Stage IV, 1 Stage III). Serial peripheral blood samples were processed using the in house developed microfluidic Labyrinth device for CTC enrichment. CTC subgroups were identified by immunofluorescence staining for Cytokeratin (CK), EpCAM, and Vimentin. At each sampling point, clinical response was assessed by a treating physician. Sc-RNA sequencing was performed on enriched CTCs, characterizing differentially expressed gene (DEG), survival, trajectory states, immune interactions, and inferred CNV profiles.

Results: Patients receiving a single TKI treatment (Alectinib) with clinically stable disease showed decreasing CTC burden. Patients with prior exposure to multiple TKIs and progressive disease showed fluctuating dynamics. Kaplan-Meier analysis showed a decrease in total CTCs (77%, p=0.016) and a decrease in CK+ CTCs (6.05%, p=0.049) significantly correlated with lower progression risk. scRNA-seq on three Stage IV patient's CTC collected at multiple time points revealed dynamic immune populations changed between the visits. DEGs in CTC compared to the rest of immune cells in all 3 visits displayed EMT-associated upregulation (TUBB1, PPBP, ITGA2B); and downregulation of GATA2, consistent with its reported reduction in lung cancer. A composite of 45 consistently downregulated genes was correlated with reduced survival, using a TCGA cohort (n=500; p=0.039). Notably, downregulated genes obtained after the patient started progressing showed increasingly more significant associations with poor survival (p=0.21, p=0.019, p=0.0067). Trajectory analysis identified two CTC clusters, with later visits mapping to higher pseudotime states. CNV analysis revealed a CDK4 copy-gain specifically at progression. Intercellular communication analysis showed decreased CTC-B-cell and increased CTC-monocyte interactions at progression, which may suggest reduced anti-tumor surveillance and enhanced myeloid support.

Conclusion: Longitudinal monitoring integrating CTC burden and scRNA analysis provides insights into tumor evolution and immune interactions in ALK+ NSCLC, potentially signaling imminent progression and may help guide personalized treatment strategies.

#1063 Serum neuron-specific enolase (NSE) as a biomarker of central nervous system (CNS) metastases: Updated results from the BrainStorm program (Oncodistinct 006).

Soraia Lobo-Martins[1], Diogo Martins-Branco[1], Luca Arecco[1], Guilherme Nader-Marta[2], Andrea Gombos[3], Anthony Goncalves[4], Eleonora Stephane de Maio D'Esposito[5], Philippe Barthelemy[6], Vincent Vanhaudenarde[7], Florian Clatot[8], Stephane Holbrechts[9], Francois P. Duhoux[10], Edith Borcoman[11], Elisabeth Pop[12], Damien Parlier[12], Claire Cheymol[13], Joseph Gligorov[14], Hannelore Denys[15], Paul Clement[16], Caroline Duhem[17], Lore Decoster[18], Jean-Luc Canon[19], Nadege Kindt[20], Francoise Rothe[21], Ahmad H. Awada[22], **Nuria Kotecki**[3]

[1]Academic Trials Promoting Team (ATPT), Universite libre de Bruxelles (ULB), Hopital Universitaire de Bruxelles (H.U.B), Institut Jules Bordet, Brussels, Belgium,[2]Medical Oncology Department, Dana-Farber Cancer Institute, Boston, MA,[3]Medical Oncology Department, Universite libre de Bruxelles (ULB), Hopital Universitaire de Bruxelles (H.U.B), Institut Jules Bordet, Brussels, Belgium,[4]Medical Oncology, Institut Paoli-Calmettes, Marseille, France,[5]IUCT Oncopole-Institut Claudius Regaud, Toulouse, France,[6]Hopitaux Universitaires de Strasbourg, Strasbourg, France,[7]Medical Oncology Department, CHU UCL Namur, site Ste-Elisabeth, Namur, Belgium,[8]Medical Oncology Department, Centre Henri Becquerel, Rouen, France,[9]CHU HELORA Hopital de Mons site Kennedy, Mons, Belgium,[10]Medical Oncology Department, Cliniques Universitaires Saint-Luc, Brussels, Belgium,[11]Department of Drug Development and Innovation (D3i), Institut Curie, Paris, France,[12]Clinical Trials Center (CTC), Universite libre de Bruxelles (ULB), Hopital Universitaire de Bruxelles (H.U.B), Institut Jules Bordet, Brussels, Belgium,[13]Centre Oscar Lambret, Lille, France,[14]APHP Tenon, IUC-UPMC, Sorbonne University, Paris, France,[15]Ghent University Hospital, Gent, Belgium,[16]UZ Leuven Gasthuisberg, Leuven, Belgium,[17]Centre Hospitalier de Luxembourg, Luxembourg, Luxembourg,[18]UZ Brussel, Brussels, Belgium,[19]Oncologie Medicale, Grand Hopital de Charleroi, Charleroi, Belgium,[20]Laboratory of Clinical and Experimental Oncology, Universite libre de Bruxelles (ULB), Hopital Universitaire de Bruxelles (H.U.B), Institut Jules Bordet, Brussels, Belgium,[21]Breast Cancer Translational Research Laboratory, Universite libre de Bruxelles (ULB), Hopital Universitaire de Bruxelles (H.U.B), Institut Jules Bordet, Brussels, Belgium,[22]Medical Oncology Department, Chirec Cancer Institute, Brussels, Belgium

Background: Serum NSE, a marker of neuronal injury, may serve as a non-invasive indicator of early CNS involvement in solid tumors. Here, we explore the role of NSE for predicting development of CNS metastases.
Methods: The BrainStorm program, is an ongoing international, multicenter prospective initiative, allowing the constitution of a large clinicopathological database and biobank to study CNS metastases. The program is recruiting patients (pts) with newly diagnosed non-CNS metastatic solid tumors at high risk of (Part A) or with CNS metastases (Part B and C). All pts undergo serologic NSE testing at baseline and at regular intervals pre- and post-CNS metastases. Main objective of the present analysis was to assess the role of baseline NSE as a predictive biomarker of CSN development from pts tested in Part A vs B, using Mann-Whitney test for group comparisons and logistic regression models to estimate OR.
Results: 124 pts with available NSE results were included in the program from Nov/2020 to Jun/2025 (Part A, n=73; Part B, n=51) - Table 1. NSE levels were significatively higher in Part B than Part A (median 15.0 (IQR 12.8-24.3) vs 13.6 (IQR 11.4-16.4) ng/mL; p=0.017). In Part A, baseline NSE, as a continuous variable, was significantly associated with CNS metastases development (OR per ng/mL increase 1.12; 95% CI 1.02-1.22). Using the upper limit of normal as a categorical cut-off, baseline NSE showed a trend toward higher odds of CNS metastases (OR 2.84; 95%CI 0.60-13.39; 8 CNS events).
Conclusions: These findings support a potential role for NSE as a non-invasive predictive biomarkers for the development of CNS metastases although confirmation in the fully accrued BrainStorm program is required.

Table 1 - Baseline characteristics

	Part A (N=73)	**Part B** (N=51)
Age in years, median (IQR)	58 (48-66)	62 (56-68)
Female, n (%)	65 (89)	40 (78)
ECOG-PS, n (%)		
0	40 (55)	10 (20)
1	27 (37)	28 (55)
2	4 (5)	9 (18)
Cancer type, n (%)		
TNBC	12 (16)	8 (16)
HER2+ BC	45 (62)	11 (22)
ER+/HER2- BC	-	11 (22)
NSCLC	10 (14)	13 (25)
SCLC	4 (5)	3 (6)
Melanoma	2 (3)	0 (0)
Other	-	5 (10)
No. metastatic sites, median (IQR)	2 (1-2)	2 (1-3)
Months from non-CNS metastases to NSE, median (IQR)	206 (76-495)	178 (26-972)
Weeks from CNS metastases to NSE, median (IQR)	-	15 (10-26)
Baseline serum NSE in ng/mL, median (IQR)	13.6 (11.4-16.4)	15.0 (12.8-24.3)

#1064 Novel approach of single-cell RNAseq analysis to assess cancer cells in prostate core biopsy specimens.

Dai Takamatsu[1], Kelly K. Chong[1], Gianna Jimenez[2], David Krasne[3], Jennifer A. Linehan[2], Timothy G. Wilson[2], Dave S. B. Hoon[1]

[1]Translational Molecular Medicine, Providence St. John's Cancer Institute, Providence Health System (PHS), Santa Monica, CA,[2]Urology and Urologic Oncology, Providence St. John's Health Center (PSJHC), PHS, Santa Monica, CA,[3]Surgical Pathology, PSJHC, PHS, Santa Monica, CA

Background: The core biopsy of prostate for detection of prostate cancer (PCa) remain heavily reliant on histopathology, varying by both surgeon and pathologist but carries the risk of misdiagnosis. This can result in missed opportunities for timely intervention or unnecessary treatment strategies. Our study leverages single-cell RNA (scRNA) seq analysis to enhance diagnostic accuracy, aiming to identify PCa cells by a novel precision oncology approach at the cellular and molecular level. **Methods**: We investigated 23 biopsy cases from patients with potential PCa. Core fine needle biopsies were performed on patients undergoing MRI-fusion image-guided prostate biopsy prior to decision to perform robotic-assisted radical prostatectomy if biopsy is diagnosed PCa positive. We used the pico-well-based HIVE™ (HoneyComb Biotech, MA) to isolate barcoded sc from the cell suspension of prostate tissue biopsy. This method allows specific physical single-cell analysis followed by in-depth scRNAseq. Each sample underwent traditional pathology diagnosis at post biopsy and prostatectomy. Initially, cell type markers were used to classify each clusters cell type from the scRNA seq data. For known PCa gene markers, we assessed KLK3, FOLH1, PCA3, KRT34, AMACR, and TP63. To improve the accuracy of the subset identified as PCa cells, Single Cell Variational Aneuploidy analysis (SCEVAN) classification was used to categorize subsets of cells based on calculated aneuploidy level. This algorithm accurately performs a variational deconvolution to unravel the clonal substructure of tumors using the scRNAseq data. It employs a multichannel segmentation approach based on the premise that cells within a particular copy number clone have similar breakpoints. **Results**: Our study included 23 patients categorized into 5 benign cases versus specific PCa Gleason grades: 4 GG1, 5 GG2, 3 GG3, 3 GG4, and 3 GG5 based on standard histopathology. The subsets of tumors classified using 2 approaches; deconvolution with cell mRNA markers and deconvolution of marker expression profiles with SCEVAN classification, were consistent. These tumor subsets analysis by the 2 analytic approaches identified PCa cells. Notably, in cases initially diagnosed as benign, scRNAseq data showed variability; some cases were benign with no detectable PCa cells, while others displayed PCa cells through SCEVAN classification, highlighting the potential of the approach uncovering hidden molecular malignant profiles. **Conclusion**: Our study demonstrates the efficiency of scRNAseq data in detecting PCa cells, which can improve and further validate conventional histopathology diagnosis. This novel approach allows one to uncover occult PCa cells by molecular profiling, enhancing diagnostic status prior to therapy, and potentially triaging patients for surgery, radiation, or observation.

#1065 Mitosis in circulating tumor cells correlates with highly aggressive disease in metastatic breast cancer.

Alexis B. Duffy[1], Massimo Cristofanilli[2], Carolina Reduzzi[2], WIliam V. Williams[3], Giuseppe Del Priore[3], Saranya Chumsri[4], Cha-Mei Tang[5], Toshiaki Iwase[6], Naoto Ueno[6], Daniel L. Adams[1]

[1]Creatv MicroTech, Inc., Monmouth Junction, NJ,[2]Weill Cornell Medicine, New York, NY,[3]Briacell Therapeutics Corp., Philadelphia, PA,[4]Mayo Cancer Clinic, Jacksonville, FL,[5]Creatv MicroTech, Inc., Rockville, MD,[6]University of Hawai'i Cancer Center, Honolulu, HI

Background: Circulating tumor cells (CTCs) are a well-known non-invasive blood biomarker which can stratify metastatic breast cancer (mBC) patients, especially those with highly aggressive subtypes. Initial pilot studies have characterized a distinct subtype of CTCs undergoing mitosis, whose presence correlates with worse survival outcomes than CTCs alone. However, their prognostic value and their influence in different therapeutic regimes remains unknown. In a multi-institutional prospective study, we isolated CTCs from n=138 mBC patients to categorize mitotic CTCs, evaluate their association with progression-free survival (PFS) & overall survival (OS) over 2 years, and how their response rates effect different therapeutic strategies.

Methods: Peripheral blood samples (7.5ml) were collected from n=138 mBC patients progressing on systemic therapies but prior to new systemic therapies (i.e. chemotherapy n=48, hormone therapy n=17, immunotherapy n=64, targeted therapy n=22). CellSieve microfilters isolated CTCs via size exclusion and cells fluorescently stained for CD45, Cytokeratin, and DAPI. CTCs were imaged, enumerated, and subtyped based on the presence of ≥1 mitotic CTC, using previously established visual indicators. PFS and OS were assessed over 2 years by censored univariate and multivariate analyses. Therapy efficacy was assessed by comparing median PFS (mPFS) and median OS (mOS) in the therapy categories.

Results:

CTC Type	Treatment	mPFS (months)	mOS (months)
No CTCs (n=77/138)	All Pts (n=77)	5.0	16.6
	Chemotherapy (n=23)	4.0	9.2
	Hormone Therapy (n=9)	>24.0	>24.0
	Immunotherapy (n=39)	4.3	13.1
	Targeted Therapy (n=11)	13.1	>24.0
Non-mitotic CTCs (n=30/138)	All Pts (n=30)	4.0	14.2
	Chemotherapy (n=9)	3.1	13.0
	Hormone Therapy (n=4)	6.7	>24.0
	Immunotherapy (n=14)	3.3	7.4
	Targeted Therapy (n=5)	14.1	20.0
Mitotic CTCs (n=31/138)	All Pts (n=31)	2.4	4.1
	Chemotherapy (n=12)	2.4	4.3
	Hormone Therapy (n=4)	1.3	7.1
	Immunotherapy (n=11)	2.0	4.7
	Targeted Therapy (n=6)	3.5	18.6

Conclusion: In this study, patients with CTCs had poorer outcomes than patients with no CTCs, while patients with mitotic CTCs had the worst outcomes. Further, patients with no CTCs or non-mitotic CTCs showed similar PFS & OS in some treatment types, while patients with no CTCs treated with hormone therapy had better PFS and patients with mitotic CTCs had better OS if treated with targeted therapy. This study highlights the need for larger more comprehensive studies to expand on these prognostic findings and correlations to therapy types.

#1066 Early detection of prostate carcinoma using trajectories of circulating epithelial tumor cell (CETCs/CTCs) numbers.

Dorothea Schott[1], Monika Pizon[2], Joachim Fluhrer[1], Ulrich Pachmann[1], Katharina Pachmann[3], Peter Eng[4]

[1]Laboratory Dr. Pachmann, Bayreuth, Germany,[2]Simfo GmbH, Bayreuth, Germany,[3]Pachmann (Individual), Bayreuth, Germany,[4]Eng Medical Centre, Melbourne, Australia

Background: Prostate cancer is a leading cause of mortality in elderly men, underscoring the need for early and effective detection strategies. PSA-based screening remains controversial due to uncertain benefits in reducing mortality and associated risks, such as invasiveness, comorbidities, and overdiagnosis. Overdiagnosis can lead to unnecessary treatments and complications for indolent disease. In clinical practice, patients often retain limited information after consultations, and inconsistent risk communication by physicians can hinder informed shared decision-making. Therefore, a minimally invasive screening approach using serial circulating epithelial tumor cells (CETCs/CTCs) in patients at increased risk of prostate cancer may enhance informed decision-making.
Methods: CETCs/CTCs were quantified in peripheral blood from men aged 50-85 years in a screening cohort (n=35) and in patients undergoing PSMA-PET for suspected prostate cancer (n=49). PSA levels were measured at the time of PSMA-PET, and serial CETC/CTC counts were correlated with PSMA-PET findings.
Results: Serum PSA levels did not differ significantly between patients with positive (n=27) and negative (n=24) PSMA-PET scans ($p=0.94$). However, CETC/CTC counts were significantly higher in PSMA-PET-positive patients compared to those in the screening cohort ($p<0.001$). ROC analysis identified an optimal threshold of 450 CETCs/CTCs per mL blood, with a specificity of 0.7 and a sensitivity of 0.6. Serial monitoring revealed distinct trajectories: increasing CETC/CTC counts were observed in 11 of 13 (90%) patients who later developed PSMA-PET-positive findings, while only 2 of 21 (8%) patients with decreasing CETC/CTC counts were PSMA-PET positive. Kaplan-Meier analysis demonstrated a highly significant difference in PSMA-PET-free survival between the two groups ($p<0.001$; hazard ratio 9.48).
Conclusions: Serial monitoring of CETCs/CTCs provides dynamic, non-invasive insights into prostate cancer activity. Rising CETC/CTC counts were strongly associated with PSMA-PET positivity, suggesting their potential as early biomarkers for prostate cancer progression and treatment monitoring.

#1067 Whole genome sequencing of multiple myeloma genomes with a novel clinical assay enables identification of genetic alterations underlying immunotherapy resistance.

Bruno Paiva[1], Peter Voorhees[2], Patricia T. Greipp[3], Danielle Sookiasian[4], Julian Hess[4], Marisa DeMeo[4], Vicki Pounder[4], Sarah Calkins[4], Reid Meyer[3], Linda B. Baughn[3], Christine-Ivy Liacos[5], Meletios-Athanasios Dimopoulos[5], Alexandra Papadimou[5], Taouxi Konstantina[5], Efstathios Kastritis[5], Jesus Berdeja[6], Daniel Auclair[4], Valentina Nardi[4], Thomas Mullen[4], Francois Aguet[4], Shaji Kunnathu Kumar[3]

[1]Univ. de Navarra, Pamplona, Spain,[2]Levine Cancer Institute, Atrium Health Wake Forest University School of Medicine, Charlotte, NC,[3]Mayo Clinic, Rochester, MN,[4]Predicta Biosciences, Cambridge, MA,[5]National and Kapodistrian University of Athens School of Medicine, Athens, Greece,[6]Greco-Hainsworth Centers for Research at Tennessee Oncology, Nashville, TN

The detection of genetic abnormalities is required during diagnostic workup and for potential individualization of therapy selection in multiple myeloma (MM) and its precursor conditions. At present, this relies on invasive bone marrow (BM) biopsies, severely limiting early detection, frequent longitudinal monitoring, and the precise selection of therapy. The current standard for detecting genetic alterations in MM is fluorescence in situ hybridization (FISH), which cannot detect point mutations and other clinically relevant alterations. Consequently, the IMS-IMWG guidelines were recently updated to require next-generation sequencing for the classification of high-risk MM. To address these needs, we recently launched GenoPredicta, a CLIA-approved LDT that enables routine monitoring, informing diagnosis, and treatment selection by comprehensively characterizing MM genomes with whole genome sequencing (WGS) from as few as 50 circulating tumor cells (CTCs) isolated from peripheral blood (PB) or tumor cells from BM. Briefly, tumor cells are isolated from samples using fluorescence-activated cell sorting and subjected to WGS, from which copy number alterations, structural variants, and short variants (SNVs/indels) are identified using a fully automated pipeline generating physician-ready clinical reports from raw sequencing data in ~6h. Analytical validation of GenoPredicta showed complete concordance with FISH results.
Identifying alterations in therapeutic targets (e.g., BCMA, GPRC5D) for guiding MM immunotherapies is becoming increasingly important. Here, we describe GenoPredicta results from relapsed/refractory MM patients, highlighting resistance-conferring alterations that can only be detected by WGS, such as deletions in the kilo- to megabase scales that are observed in conjunction with SNVs and indels, leading to biallelic loss/inactivation of the gene, including at subclonal levels. In addition to biallelic loss of BCMA and GPRC5D in response to CAR T or T cell engager therapies, we observed similar resistance mechanisms for targets of immunomodulatory drugs, e.g., CRBN. The observation of these resistance mechanisms was consistent with patients' clinical histories.
In summary, we demonstrate that low input WGS-based characterization of MM from BM or CTCs is a viable replacement for FISH for clinical diagnosis and monitoring, with CTC-based measurements enabling comprehensive profiling of the MM genome. Crucially, this includes genetic alterations that confer resistance to therapy, allowing for both early detection of such alterations and more precise selection and guidance of therapy. The dramatically improved variant calling ability from WGS, especially in low-input CTC applications, extends to other malignancies and will gain wider adoption as sequencing costs continue to decrease.

#1068 Combining circulating tumor cells and cancer associated macrophage-like cells enhances risk stratification models in pan-cancer metastatic disease.

Daniel L. Adams[1], Steven H. Lin[2], Massimo Cristofanilli[3], Carolina Reduzzi[4], Saranya Chumsri[5], Martin J. Edelman[6], Susan Tsai[7], Raymond C. Bergan[8], Mohammed Aldakkak[9], Thai H. Ho[10], Cha-Mei Tang[11]

[1]R&D, Creatv Microtech, Inc, Monmouth Junction, NJ,[2]Asst. Professor, Dept. of Radiation Onc., UT MD Anderson Cancer Center, Houston, TX,[3]Weill Cornell University, New York, NY,[4]Weill Cornell Medicine, New York, NY,[5]Mayo Clinic Florida, Jacksonville, FL,[6]Fox Chase Cancer Center, Philadelphia, PA,[7]Ohio State University, Columbus, OH,[8]Stony Brook University, Stony Brook, NY,[9]The Medical College of Wisconsin, Milwaukee, WI,[10]Medical University of South Carolina, Charleston, SC,[11]Creatv MicroTech, Inc., Rockville, MD

Background: In metastatic cancer, Circulating Tumor cells (CTCs) are established prognostic indictors of patients (pts) less likely to respond to new lines of systemic therapy, with poor clinical outcomes, such as shorter progression free survival (PFS) and overall survival (OS). However, CTCs are typically found in specific malignancies (breast, prostate & colon), often in <20% of pts with metastatic disease, and pts without CTCs may also rapidly progress. Recently, an inflammatory pro-tumorigenic macrophage emanating from tumor stroma (i.e. Cancer associated macrophage-like cell [CAML]) was found in >90% of metastatic cancer pts, and whose phagocytic engorgement appears to correlate with poor outcomes, independent of CTCs. As CTCs and CAMLs are isolated in conjunction from a single blood sample, and both are prognostic for outcomes, we evaluated their utilization prior to induction of new systemic therapy in 6 types of metastatic cancer to model pt risk stratification based on 2 year outcomes.
Methods: A prospective 2 year blind multi-institutional study was undertaken to model CTCs and CAMLs in prognosticating outcomes prior to induction of a new line of systemic therapy (n=233) in metastatic: Breast (n=60), Prostate (n=40), Pancreas (n=25), Colon (n=28), Renal Cell Carcinoma (RCC) (n=39), and Lung (n=40). Blood was filtered by CellSieve^{TM} filters with subtypes of CTCs & hyper-enlarged CAMLs (≥100µm) enumerated. A machine learning algorithm was trained on this initial data set to develop predictive models which could stratify pt populations by risk for likelihood of PFS & OS over 2 years, including known clinical variables.
Results: CTCs were absent in 80% (n=185/233) of pts, and their absence was prognostic for better PFS (HR=1.6, p=0.046), but not OS (HR=1.3, p=0.2045). In parallel, enlarged CAMLs (≥100µm) were found in 28% (n=51/185) of pts without CTCs, and were also prognostic for worse PFS (HR=2.0, p=0.0082) and OS (HR=1.9, p=0.0412). Specifically, CTCs were found in 55% (n=33) breast, 20% (n=8) prostate, 12% (n=3) pancreas, 11% (n=3) colon, 0% (n=0) RCC, and 0% (n=0) lung pts. Enlarged CAMLs were found in 45% (n=27) breast, 20% (n=8) prostate, 44% (n=11) pancreas, 44% (n=17) colon, 18% (n=7) RCC and 20% (n=8) lung pts. Overall, models indicated that ≥1 CTC (n=47) had mPFS=3.9 & mOS=14.9, while pts with 0 CTCs and ≥100µm CAMLs (n=51) had a mPFS=6.9 & mOS=13.8, and pts with 0 CTCs and <100µm CAMLs (n=134) had a mPFS=10.7 & mOS>24 months.
Conclusions: These initial models confirm that both CTCs and enlarged CAMLs are prognostic indicators of worse PFS & OS. The simultaneous quantification both CTCs and CAMLs allows for more accurate pan-cancer risk stratification in an array of cancer pt populations. Additional clinical variables incorporated into the models may allow better risk subtyping and possibly forecast optimal treatment regimens.

#1069 Clinical significance of viable circulating tumor cells (v-CTCs) and PD-L1 expression in pancreatic cancer patients using a novel oncolytic virus system.

Masahiro Tanemura[1], Hisataka Ogawa[1], Yoshiaki Ohmura[1], Tadafumi Asaoka[2], Yasuo Urata[3], Daisaku Yamada[4], Hirofumi Akita[4], Hidetoshi Eguchi[4]

[1]Department of Surgery, Rinku General Medical Center, Izumisano, Japan,[2]Department of Surgery, Osaka Police Hospital, Osaka, Japan,[3]Oncolys BioPharma Inc., Tokyo, Japan,[4]Department of Gastroenterological Surgery, University of Osaka Graduate School of Medicine, Osaka, Japan

Background: Detecting circulating tumor cells (CTCs) as a peripheral blood liquid biopsy is a promising approach. We previously succeeded in visualizing viable-CTCs (v-CTCs) with high biological activity from the peripheral blood of resectable and borderline resectable pancreatic cancer (PC) patients using a novel telomerase-specific oncolytic virus (TelomeScan F35). This study aimed to analyze the clinical significance of v-CTC detection and the expression of PD-L1 on v-CTCs in PC patients to explore potential therapeutic selection strategies.
Methods: Thirty-nine PC patients were analyzed. CTCs were analyzed at pre-/post-operative time points in the Upfront Surgery (S) group, and at pre-NACRT, post-NACRT, and post-operative time points in the Neoadjuvant Chemoradiotherapy (NACRT) group (RT + GEM + S-1). PD-L1 expression was also assessed in v-CTCs, primary tumors and metastatic lymphnodes.
Results: [S Group] (n=24; M/F=12/12; median age 73). All patients underwent curative resection. Six patients were consistently v-CTC negative (pre- and post-op); five of these patients remained disease-free, with only one case of peritoneal recurrence. In contrast, 18 patients were v-CTC positive at either or both time points; 13 of these developed early distant metastatic recurrence post-surgery. [NACRT Group] (n=15; M/F=4/11; median age 67). All patients underwent curative resection. Five patients were consistently v-CTC negative at all three time points and all remain disease-free. In six patients who were v-CTC positive pre-NACRT, the v-CTC count significantly increased post-NACRT in five cases, and three of them developed early liver metastasis, suggesting that RT might induce v-CTC intravasation/dissemination. [PD-L1 Expression] PD-L1 analysis was performed on 18 patients in the S group and 3 in the NACRT group. In primary tumors of the S group, PD-L1 expression was observed in 0%/10%/20%/40% of tumor cells in 6/6/4/2 cases, respectively. The expression rate on v-CTCs was 97% pre-operation and 81% post-operation. Among 12 patients with lymph node metastasis, PD-L1 expression was positive in only 4 cases (33%). In the NACRT group, primary tumors were all PD-L1 negative. The expression rate on v-CTCs was 50% pre-NACRT, 96% post-NACRT, and 50% post-operation. Two cases showed lymph node metastasis, both PD-L1 negative.
Conclusion: The presence of v-CTC dissemination suggests a risk of metastasis development following NACRT, advocating for upfront surgery or neoadjuvant chemotherapy (NAC) without RT in v-CTC positive patients. Given the high rate of PD-L1 expression on v-CTCs, immune checkpoint inhibitors are expected to be effective for targeting v-CTCs and controlling distant metastasis. Detection of v-CTC dissemination may be utilized for therapeutic selection in PC patients.

#1070 Molecular profiling of diffuse gliomas via liquid biopsy: Insights from circulating tumor cells and ctDNA analysis.

Josef Srovnal[1], Pavel Stejskal[1], Ondrej Kalita[2], Marek Slachta[2], Lumir Hrabalek[2], Alona Rehulkova[1], Monika Vidlarova[1], Marian Hajduch[1]

[1]Institute of Molecular and Translational Medicine, Palacky Univ. Faculty of Medicine, Olomouc, Czech Republic,[2]Department of Neurosurgery, University Hospital Olomouc, Olomouc, Czech Republic

Introduction: Diffuse gliomas are the aggressive primary brain tumor, characterized by poor prognosis and pronounced molecular heterogeneity. Although systemic spread is uncommon due to the blood-brain barrier, tumor cells and nucleic acids can still reach the peripheral circulation. Liquid biopsy, including circulating tumor cells (CTCs) and circulating tumor DNA (ctDNA), provides a minimally invasive approach for tumor characterization and monitoring in diffuse gliomas.
Methods: After validating our CTC detection workflow using spiking experiments with the U87-MG cell line, we analyzed peripheral blood samples from patients undergoing curative resection for diffuse gliomas. Samples were collected prior to surgery in Cell-Free DNA BCT® tubes (Streck, Inc.). CTCs were identified using the CytoTrack CT11™ (2/C) semi-automated immunofluorescence microscopy platform, with immunostaining for GFAP, vimentin, and CD45, and DAPI nuclear counterstaining. For ctDNA analysis, cfDNA was isolated from 2 ml of plasma using the QIAamp Circulating Nucleic Acid Kit (Qiagen), and the IDH1 R132H mutation was assessed by digital droplet PCR (Bio-Rad Laboratories, Inc.).
Results: CTCs were detected in 29.1% of 110 blood samples collected from patients at the time of their first surgery. Among 19 samples from relapsing patients, CTC positivity increased to 54.5%. Kaplan-Meier survival analysis in a cohort of 67 patients with IDH wildtype glioblastoma and at least two years of follow-up revealed no significant association between CTC status and overall survival.Analysis of cfDNA identified IDH1 R132H mutations in 14% of patients with diffuse gliomas, including cases with both tumor-informed positive and negative status.
Conclusion: Our results demonstrate that both CTCs and ctDNA can be reliably detected in patients with diffuse gliomas, underscoring the potential of liquid biopsy to complement traditional tissue-based diagnostics. Detection of IDH1 R132H mutations in plasma— even in tumor-informed negative cases—may indicate intratumoral heterogeneity, compartmentalized tumor biology, or sampling limitations. The lack of survival association may reflect the overall short life expectancy in GBM and/or restricted tumor proliferation outside the CNS. Patient recruitment and data collection remain ongoing. Acknowledgment: This study was supported by European Union - Next Generation EU (LX22NPO5102), Palacky University Olomouc (IGA LF 2025_006), and SALVAGE - CZ.02.01.01/00/22_008/0004644.

#1071 Delta-like ligand 3 (DLL3)-based enrichment enables sensitive and specific detection of circulating tumor cells during immunotherapy in small-cell lung cancer.

Hyung-Joo Oh[1], Hyun-Ju Cho[1], Seung-Hee Song[1], Yoo-Duk Choi[2], Woo-Jae Son[3], Jin-Han Bae[3], In-Jae Oh[1], Young-Chul Kim[1], Hae Ung Lee[3], Cheol-Kyu Park[1]

[1]Internal Medicine, Chonnam National University Medical School and Hwasun Hospital, Hwasun, Jeollanam-do, Korea, Republic of,[2]Pathology, Chonnam National University Medical School, Gwangju, Korea, Republic of,[3]CTCELLS, Inc., Seoul, Korea, Republic of

Background: Delta-like Ligand 3 (DLL3), a Notch receptor ligand, is highly expressed in small cell lung cancer (SCLC) and has emerged as a promising therapeutic target. Circulating tumor cells (CTCs), abundant in SCLC, interact with diverse immune cell populations in peripheral blood. This study investigates the potential of DLL3 as a biomarker to enhance CTC detection and monitor immunotherapy response in SCLC.

Methods: We enrolled 17 patients with extensive-stage (ES) SCLC and 5 with stage IV non-small cell lung cancer (NSCLC; as controls), all scheduled for an immune checkpoint inhibitor or a bispecific T-cell engager. Whole blood (6 mL) was collected before and during treatment. CTCs were enriched using CTCeptor^{TM}, a fully automated, negative depletion-based continuous centrifugal microfluidic system, and classified into three phenotypes: pan-cytokeratin (CK)$^+$/DLL3$^-$/CD45$^-$, CK$^-$/DLL3$^+$/CD45$^-$, or CK$^+$/DLL3$^+$/CD45$^-$. Baseline tumor samples were analyzed by immunohistochemistry for SCLC molecular subtypes and DLL3.

Results: DLL3$^+$/CD45$^-$ CTCs were detected in all ES-SCLC patients (100%) prior to treatment with atezolizumab plus chemotherapy or tarlatamab, with a median count of 23 (range 7-121) and a median size of 9.71 μm (7.33-12.18). In contrast, no DLL3$^+$/CD45$^-$ CTCs were detected in NSCLC patients, where only CK$^+$/DLL3$^-$/CD45$^-$ CTCs were observed (1-4 cells). Among ES-SCLC patients, CK$^-$/DLL3$^+$/CD45$^-$ cells were the predominant subtype (63.3%, 522/825), while CK$^+$/DLL3$^+$/CD45$^-$ CTCs accounted for 27.7% (228/825) of all detected CTCs, representing additional CTCs not captured by CK-based detection alone. ASCL1 was the most prevalent molecular subtype (12/17), with DLL3 exhibiting the highest H-score (median, 185; range, 20-300). Notably, no correlation was observed between the number or proportion of DLL3$^+$CTC and the DLL3 H-score (r = -0.163, p = 0.578), while DLL3$^+$CTCs remained prevalent in NERUDO1 and POU2F3 subtypes. Furthermore, both total and DLL3$^+$CTC counts markedly decreased within 2 cycles of atezolizumab chemotherapy or 1 week after tarlatamab treatment.

Conclusion: DLL3$^+$CTCs can be efficiently and specifically detected in ES-SCLC patients using CTCeptor^{TM}, serving as a complementary marker to CK for CTC identification. DLL3 appears more frequently in CTCs than in tumor tissue. These findings support DLL3 as a potential biomarker for CTC-based monitoring in ES-SCLC and warrant further validation in larger cohorts, including analyses of immunologic features.

#1072 Parallel microfluidic platform enables efficient label-free capture of p16+ circulating tumor cells in oropharyngeal cancer.

Chameera E. Weeramange[1], Jian Zhou[2], Sreedevi Damodaran[1], Chiara F. Ghera[3], Lizbeth Kenny[4], Brett Hughes[4], Sarju Vasani[5], Omar Breik[6], Rahul Ladwa[7], **Ian Papautsky**[3], Chamindie Punyadeera[1]

[1]Institute for Biomedicine and Glycomics, Griffith University, Nathan, Australia,[2]Rush University Medical Center, Chicago, IL,[3]University of Illinois Chicago, Chicago, IL,[4]Cancer Care Services, Royal Brisbane and Women's Hospital, Herston, Australia,[5]Otolaryngology, Royal Brisbane and Women's Hospital, Herston, Australia,[6]Oral and Maxillofacial Surgery, Royal Brisbane and Women's Hospital, Herston, Australia,[7]Cancer Care Services, Princess Alexandra Hospital, Woolloongabba, Australia

Circulating tumor cells (CTCs) are clinically significant biomarkers for cancer detection and monitoring due to their role in metastasis. However, their extreme rarity in peripheral blood and phenotypic heterogeneity, particularly following epithelial-to-mesenchymal transition (EMT), pose challenges for reliable isolation. Conventional epitope-dependent capture methods often fail to detect mesenchymal-like CTCs. Label-free microfluidic platforms offer a promising alternative by exploiting biophysical properties such as size and deformability. Building on our prior work, we developed a high-throughput multi-flow microfluidic (MFM) device to isolate diverse CTCs from clinically relevant blood volumes, with a focus on oropharyngeal cancer (OPC), where CTCs exhibit favorable size characteristics for inertial separation. A parallel microfluidic device comprising six inertial separation channels was fabricated using dry film photolithography and PDMS molding. Two versions were constructed: Chip A (20 mm in length) and Chip B (25 mm in length), both with a 150 µm x 50 µm cross-section. Device performance was evaluated using fluorescent microparticles (10.3, 15.5, and 18.7 µm) and head and neck cancer cell lines CAL27, SCC9, and HPV16-positive SCC2. Samples were processed at 600 µL/min with a buffer flow of 1.2 mL/min. Cell recovery and purity were assessed by high-content imaging and immunofluorescence. SCC2 DNA enrichment was quantified by qPCR. Clinical validation involved 20 p16+ oropharyngeal cancer patients. The MFM device achieved a 5-fold increase in throughput compared to the earlier single-channel design, while maintaining high separation efficiency. Chip A (~14 µm cutoff) recovered 90-94% of CAL27 and SCC9 cells with <17% WBC contamination. Chip B (~12 µm cutoff) improved recovery to 92%-97%, but with slightly higher WBC carryover. PCR analysis of HPV16-positive SCC2 cells confirmed >35-fold enrichment of tumor DNA in the CTC fraction. In clinical samples, CTCs were detected in 60% of OPC patients, including epithelial, mesenchymal-like, and dual CK/CSV-positive phenotypes. Notably, dual CK/CSV-positive CTCs, indicative of partial EMT, were observed in 25% of patients. p16 expression was observed in CTCs from 4 of 14 patients, suggesting potential concordance with tumor HPV status. The device preserved cell integrity, enabling downstream molecular analysis. The parallel MFM platform enables robust, label-free isolation of phenotypically diverse CTCs from clinically relevant blood volumes. Its ability to detect EMT-associated phenotypes and HPV16/p16 expression supports its utility in head and neck oncology. Compatibility with molecular workflows such as qPCR and successful clinical validation in OPC patients highlight its translational potential for liquid biopsy applications, including disease monitoring and precision oncology.

#1073 Monitoring androgen receptor and neuroendocrine marker expression dynamics in CTCs in patients with mCRPC.

Nobuaki Matsubara[1], Kentaro Shirai[2], Hiroyuki Obinata[2], Hiromichi Nakajima[1], Chikako Funasaka[1], Chihiro Kondoh[1], Kana Kawasaki[2], Eri Katsumata[2], Taiga Ajiri[2], Maharjan Bishnu[2], Fumie Kato[2], Masatoshi Yanagida[2], Reiko Watanabe[1], Toru Mukohara[1]

[1]National Cancer Center Hospital East, Kashiwa, Japan,[2]Sysmex Corporation, KOBE, Japan

Androgen receptor (AR) remains important treatment target for prostate cancer and androgen receptor signaling inhibitor (ARSI), such as abiraterone acetate (AA) or enzalutamide have already been widely used in daily practice. However, approximately 30% of patients show primary refractory and almost all patients eventually resist ARSI within several years. One of the resistant mechanisms is *AR* amplification and/or mutation which is detected by ctDNA after ARSI treatment. Another one is phenotypic transformation from adenocarcinoma to neuroendocrine prostate cancer (NEPC) by treatment pressure with ARSI. This study investigated dynamic changes of AR and neuroendocrine markers expression during abiraterone treatment by longitudinal Circulating Tumor Cells (CTCs) collection. We have developed a method using molecular imaging flow cytometry to detect CTCs and their AR and Synaptophysin (SYP) expression. For CTC enrichment from whole blood, cell size-based approach using microfluidics technology was adapted. Our focus was on AR nuclear localization status of CTCs in patients with metastatic castration resistant prostate cancer (mCRPC). To validate the analytical performance of our method, the AR and SYP expression of detected CTCs was compared with the pathological results of tissue biopsy obtained within 28 days before or after blood sampling. One or more CTCs were detected in 89.4% (17/19) of patients, and 13 of 17 patients had available pathological results. The sensitivity and specificity of CTC detection for the pathological results were 67% and 100% in AR, and 75% and 89% in SYP, respectively. Additionally, SYP showed relatively high positive predictive value of 75% and negative predictive value of 89%. Furthermore, we have studied the change in AR nuclear localization of AR-positive CTCs before and one month after the start of AA treatment. The degree of AR nuclear localization of each CTC was quantified by calculating the similarity between the nucleus staining and AR immunofluorescent image. Our results demonstrated the tendency with lower degree of AR nuclear localization in patients who responded to AA. In the AA-treated cohort, PSA responders showed a decrease in AR nuclear localization in average and non-responders did not (AR nuclear localization positive rate one month after treatment (0% vs 33.0%, p=0.206, Fisher’s exact tests). In contrast, in the control cohort (non-AA-treated group), AR nuclear localization scores remained unchanged or increased in both PSA responders and non-responders (33.0% vs 33.3%, p=1.0). Our observations suggest that CTC SYP may guide indication for tissue re-biopsy to detect NEPC and the AR nuclear localization in CTCs may serve as a pharmacodynamic marker of AA for mCRPC. It represents an important finding for clinical applications such as predicting treatment efficacy, monitoring treatment and selection for anti-prostate cancer drug.

#1074 Pre-treatment circulating tumor cells are a significant predictor of progression in patients with metastatic breast cancer undergoing abemaciclib therapy.

Qiang Zhang[1], Justin Zhang[2], Andrew A. Davis[3], Natalie Heater[4], Diana Jaber[5], Paolo D'Amico[6], Jianhua Jiao[7], Weijun Qin[8], Pan Du[9], Shading Jia[9], Akhil Chawla[10], Janice Lu[11], Lisa Flaum[4], William J. Gradishar[1]

[1]Department of Medicine, Division of Hematology and Oncology, Robert H. Lurie Cancer Center, Northwestern University - Evanston, Chicago, IL,[2]Department of Surgery, Division of Surgical Oncology, Northwestern University and Whitney High School, Chicago, IL,[3]Washington University School of Medicine in St. Louis, St. Louis, MO,[4]Department of Medicine, Division of Hematology and Oncology, Robert H. Lurie Cancer Center, Northwestern University, Chicago, IL,[5]Department of Medicine, Division of Hematology and Oncology, Northwestern University, Chicago, IL,[6]Northwestern University, Chicago, IL,[7]Fourth Military Medical University, Xi'an, China,[8]Department of Urology, Fourth Military Medical University, Xi'an, China,[9]Predicine Inc, San Francisco, CA,[10]Department of Surgery, Division of Surgical Oncology, Northwestern University, Chicago, IL,[11]Department of Medicine, Division of Hematology and Oncology, Stanford University, Stanford, CA

Background: Abemaciclib, a CDK4/6 inhibitor widely used in the treatment of metastatic breast cancer (MBC), has significantly improved progression-free survival. However, despite these therapeutic benefits, a substantial proportion of patients still experience recurrence. This ongoing clinical challenge highlights the urgent need for reliable biomarkers that can identify high-risk individuals *before* treatment initiation which remains insufficiently explored. Our previous work showed that monitoring circulating tumor cells (CTCs) and ctDNA mutations can serve as a predictive tool for poor prognosis in MBC (ASCO 2025 #1042; AACR 2025 #3613; CCR 2024). Here, we report new findings demonstrating that baseline CTC levels provide important predictive value for identifying recurrence risk in patients receiving abemaciclib.

Methods: A total of 66 $ER^{+}/HER2^{-}$ MBC patients were enrolled, and due to treatment discontinuation and re-initiation among some individuals, 76 courses of abemaciclib therapy were administered at Northwestern Memorial Hospital (2016-2024, IRB: NU16B06). The median follow-up period was 36.3 months. Blood samples (7.5 mL) were collected from patients prior to initiating abemaciclib therapy. CTC enumeration (classified as CK+/DAPI+/CD45–) was performed in FDA-approved CELLTRACKS System. Statistical analyses were conducted using causal inference with ensemble learning approaches.

Results: Of the 76 treatment courses, 28 patients had CTC counts ≥5, while 48 patients had CTC counts <5. All patients were categorized into two cohorts based on progression after abemaciclib treatment. First analysis (cut-off: 6 months): Cohort 1 (early progression <6 months): 29 patients (range: 0.5-5.5 months; median: 2.75 months); Cohort 2 (late progression ≥6 months): 36 patients (range: 6.5-45 months; median: 17.5 months), plus 11 patients with no progression at the end of the study (follow-up: >12 to >70 months). The mean CTC count in Cohort 1 was 9.2, significantly higher than 6.1 in Cohort 2 ($P < 0.01$). Second analysis (cut-off: 12 months): Cohort 1 (early progression <12 months): 41 patients (range: 0.5-11 months; median: 3.75 months). Cohort 2 (late progression ≥12 months): 24 patients, plus the same 11 patients with no progress. The mean CTC count in Cohort 1 was 11.2, significantly higher than 2.8 in Cohort 2 ($P < 0.01$). There was no significant difference in CTC levels between the late-progression group (mean 2.3) and the no-progression group (mean 3.1).

Conclusions: These findings demonstrate, for the first time, that pre-treatment CTC levels serve as a strong predictor of progress following abemaciclib therapy. Early identification of elevated CTCs in patients with MBC may therefore be critical for optimizing CDK4/6 inhibitor treatment strategies and identifying patients who may benefit from alternative therapeutic approaches.

#1075 Comparison of tissue and liquid biopsy CGP in advanced solid tumors: Insights from a community cancer center.

Padmapriya Swaminathan[1], McKenna Perrin[1], Crystal Hattum[1], Stephanie B. Hastings[2], Shakeel Mir[3], Zachary Wallen[2], Lucia Speroni[3], Michelle F. Green[2], Emily Teslow[3], Heidi Ko[2], Rebecca A. Previs[2], Kalpesh Patel[2], Shakti Ramkissoon[2], David Starks[1], Benjamin Solomon[1], William Spanos[1], Tobias Meissner[1], Rachel Elsey[1]

[1]Avera Cancer Institute, Sioux Falls, SD,[2]Labcorp, Durham, NC,[3]Tempus AI, Chicago, IL

Introduction: Next-generation sequencing (NGS) tumor profiling is a mainstay for guiding therapy in oncology. Circulating tumor DNA (ctDNA) testing offers an additional, minimally invasive approach of detecting actionable alterations. We evaluated the concordance between solid tissue and liquid biopsy comprehensive genomic profiling (CGP) results in a largely rural cohort within the Great Plains.
Methods: Participants were enrolled in the Avera Cancer Sequencing and Analytics Protocol (ASAP; NCT05142033). Inclusion required an advanced unresectable or metastatic solid tumor and concurrent tumor and liquid biopsy CGP collected within 90 days. Concordance was calculated based on reported alterations after excluding those not covered by both panels (liquid biopsy panel: Tempus xF+; solid tissue panel: Labcorp OmniSeq INSIGHT®; analyzed alterations: 388 SNV, 7 CNV, 10 Fusions) and variants of unknown significance (VUS).
Results: Eighty-six patients met criteria (mean age +/- SD: 65 +/-10y; 52% female). Seventeen tumor types were represented; lung cancer (26%) and head-and-neck cancer (16%) were most frequent, and 20% had ≥ 2 cancer diagnoses. Patient-level full concordance, defined as identical sets of biologically relevant identified in both tissue and liquid biopsy, was 59%. Variant-level concordance across all alteration types was 31% (CNV [n=23]: 22%, Fusion [n=6]: 50%, SNV [n=365]: 30%). Among unique variants, most SNVs (54%) and CNVs (89%) were detected only in tissue. After filtering 17 genes related to clonal hematopoiesis (CH) from liquid biopsy, variant-level concordance across all alteration types was 35% (CNV [n=23]: 22%, fusion [n=6]: 50%, SNV [n=296]: 38%). OncoKB levels of therapeutic evidence (1-4 and R1-2) were applied to the variants and tumor types in which they were identified. Of the 112 variants with an annotated level of evidence in the data set, 42 were concordant variants, 45 unique to tissue, and 25 to liquid biopsy. MSI status was 100% concordant (2 MSI-high / 84 MSI-stable). High tumor mutational burden (TMB-H) showed 90% concordance (72/80 concordant, 8/80 discordant, 6 non-evaluable). Additional analyses will assess concordance by tumor type, tissue sampled, metastatic sites, treatment, time between liquid and tissue sample collection, and time from diagnosis to sample collection.
Conclusions: Tissue and liquid biopsy CGP each provide complementary, actionable information for therapy selection. Forty percent of patients had unique findings in liquid or tissue-based testing. These results support the value of a comprehensive CGP strategy in advanced solid tumors.

#1076 Cancer-neuron interaction initiates neural mimicry and brain colonization in EGFR-mutant NSCLC.

Sam Song[1], Tomohiro Takehara[2], Yan Yang[1], Monique B. Nilsson[1], Alissa Poteete[2], Sherise Desiree Ferguson[1], Xiuning Le[1], John V. Heymach[1]

[1]UT MD Anderson Cancer Center, Houston, TX,[2]MD Anderson Cancer Center, Houston, TX

Brain metastasis is a major clinical challenge for patients with non-small cell lung cancer (NSCLC), and NSCLC patients with tumors harboring EGFR mutations have an increased risk of central nervous system (CNS) involvement, with up to 50-60% of patients developing CNS metastasis. The process of metastasizing to the brain is a complex multistep process in which tumor cells must cross the blood-brain barrier and adapt to the unique CNS environment. Recent studies in small cell lung cancer (SCLC) suggested that lung cancer cells residing in the brain acquired neural-like transcriptomic programs as compared to primary tumors in the lung. Given that EGFR mutant NSCLC tumor cells can exhibit lineage plasticity through processes including epithelial to mesenchymal transition (EMT) and SCLC or neuroendocrine transformation as part of acquired therapeutic resistance to EGFR inhibitors, we hypothesized that EGFR mutant NSCLC cells may interact with neuronal cells to facilitate CNS metastasis and lineage change. Here, we used in vitro and in vivo models to evaluate the impact of neuronal interaction on EGFR mutant NSCLC cells. We isolated primary murine neurons and co-cultured them with HCC827, HCC4006, and H1975 EGFR mutant NSCLC cells. After two days, immunofluorescent staining for neuronal markers, NeuN and MAP2, showed that EGFR mutant tumor cells co-cultured with neurons upregulated expression of these neuronal markers whereas tumor cells grown alone did not. Our in vivo models of EGFR mutant NSCLC brain tumors supported the enrichment of neuronal, synaptic, and axonal genes in cancer cells exposed to neuronal interaction. Moreover, we performed spatial transcriptomic analysis of human EGFR mutant NSCLC brain tumors paired with primary lung tumors to evaluate alteration of tumor microenvironment (TME) compartments associated with brain metastasis. Together, we propose neural mimicry as a potential mechanism exploited by EGFR-mutant NSCLC cells growing in the brain microenvironment. Our study further sheds light on novel targets for disrupting cancer-neuron interaction to inhibit the growth of brain metastasis in EGFR mutant NSCLC.

#1077 Discordance in molecular classification of primary and metastatic endometrial cancer: Implications for precision treatment.

Mari Kylleso Halle[1], Janka Babickova[1], Hege Fredriksen Berg[1], Erling Andre Hoivik[2], Rose M. Gold[1], Kadri Madissoo[1], Marta Hjelmeland[1], Hilde Eide Lien[1], Jone Trovik[3], Ingfrid S. Haldorsen[4], Kathrine Woie[5], Gema Moreno-Bueno[6], Rameen Beroukhim[7], Camilla Krakstad[1]

[1]Department of Clinical Science, Centre for Cancer Biomarkers, University of Bergen, Bergen, Norway,[2]Gynecology & Obstretics, Haukeland University Hospital, Bergen, Norway,[3]Department of Obstetrics and Gynecology, Haukeland University Hospital, Bergen, Norway,[4]Department of Radiology, Haukeland University Hospital, Bergen, Norway,[5]Department of Obstetrics and Gynecology, Haukeland Univesity Hospital, Bergen, Norway,[6]Biochemistry Department, Universidad Autonoma de Madrid, Madrid, Spain,[7]Department of Cancer Biology and Department of Medical Oncology, Dana-Farber Cancer Institute, Boston, MA

Background: Endometrial cancer is the most prevalent gynecological cancer in high-income countries, and the incidence rate is increasing. Molecular classification with *POLE* sequencing and immunohistochemistry (IHC) for mismatch-repair (MMR) proteins and p53, refines prognostic accuracy when integrated with existing risk models. This study investigates whether molecular classification derived from primary tumor biopsies (PBs) is retained in matched metastatic biopsies (MBs), as reclassification may influence treatment strategies for advanced and recurrent disease.

Material and methods: We analyzed 155 patients with matched PBs and MBs. *POLE* mutations were identified via Sanger sequencing of exons 9, 11, 13, and 14. IHC was used to assess expression of MSH2, MSH6, PMS2, MLH1, and p53. For 75 patients, whole-exome sequencing (WES) data provided mutational profiles for *POLE* and *TP53* in both PBs and MBs. Molecular classification was assigned using the ProMisE algorithm to separately classify PBs and MBs in four molecular groups.

Results: Molecular classification was discordant between PBs and MBs in 19% of cases. The most frequent discrepancy involved MMR status, with 10% (n = 16) showing MMR proficiency in PBs and deficiency in MBs. For p53, 9% (n = 20) had aberrant expression in PBs but wildtype in MBs. Notably, inter-MB heterogeneity was observed in both IHC-detected p53 expression and WES-derived *TP53* mutations. All *POLE* mutations were conserved across PB-MB pairs. Molecular classification based on MBs was significantly associated with prognosis ($p = 0.01$), whereas classification from PBs was not ($p = 0.31$).

Conclusions: This comprehensive molecular profiling reveals substantial shifts in molecular classification between primary and metastatic lesions, particularly in MMR and p53 status. These changes have prognostic implications and underscore the importance of reassessing molecular features in metastatic biopsies to guide precision treatment strategies for advanced endometrial cancer.

#1078 From protocol to practice: The gap in obtaining progression disease biopsies across 182 oncology trials.

Anjali Vinocha, Kanwal Pratap Singh Raghav, David S. Hong, Christine Parseghian, Joshua P. Hein, Jyotsna Pera, Funda Meric-Bernstam, Scott Kopetz, Alda L. Tam, Michael J. Overman

UT MD Anderson Cancer Center, Houston, TX

Background: Post-progression (PD) biopsies provide critical insights into treatment resistance and tumor evolution. Despite their growing inclusion in clinical trial designs, the extent to which PD biopsies are successfully obtained and the factors that influence said acquisition are unknown.
Methods: Protocols from consecutive oncology clinical trials that integrated at least one research biopsy [at either pre-treatment, on-treatment and/or post-progression timepoint(s)] from 1/2021 to 12/2022 were reviewed and categorized according to tumor type, trial phase, study type, planned biopsy timepoints, mandatory/optional biopsy status, biopsy rationale and endpoint inclusion. All enrolled patients at the University of Texas MD Anderson Cancer Center were reviewed for research biopsy execution. Statistical associations were tested using Fisher's exact or chi-square analyses, with $p<0.05$ considered significant.
Results: A total of 182 clinical trial protocols were analyzed, of which 119 (65%) included a PD research biopsy. Of these 119 protocols, 81% involved solid tumors, 87% were multicenter, 59% were phase 1 trials, 27% specified PD biopsy as mandatory, and 7% included use of PD biopsy as a study endpoint. Incorporating a PD biopsy in a protocol was significantly associated with cancer type (hematologic (81%) vs solid tumors (19%), $p = 0.042$) and study type (multicenter (87%) vs. single center (13%), $p = 0.003$). In these 119 protocols a total of 797 patients were enrolled at MDACC (median 3, range 0-66), of whom 465 (58%) were treated (median 2, range 0-25). At least one research biopsy [screening (n=263), on-treatment (n=126), or PD (n=48)] was performed in 74 trials (62%), with a median of 2 biopsies per trial (range 1-46). PD biopsies were obtained in 24 of 119 protocols (20%) with a median of 1 PD biopsy per trial (range 1-12). Phase 1 trial type was the only protocol factor significantly associated with obtaining any research biopsy ($p = 0.01$). No protocol factors were statistically associated with a patient undergoing a PD biopsy. Among protocols where PD biopsy was mandated, 9/32 (28%) executed a PD biopsy versus 15/87 (17%) in optional protocols ($p = 0.204$). Similarly, 3/8 (38%) of protocols listing PD biopsy as a study endpoint
executed a PD biopsy versus 21/111 (19%) of those without endpoint incorporation ($p = 0.201$).
Conclusions: Despite widespread protocol inclusion, PD biopsies were successfully obtained in only one-fifth of eligible trials, underscoring the gap between design intent and clinical feasibility, which limits the ability to study mechanisms of resistance and tumor evolution. These findings highlight the need for pragmatic trial designs (PD biopsies at time of tumor marker rise or increasing RECIST percentage) and institutional infrastructure that support consistent tissue collection at progression.

#1079 Over expressing PD-L1 circulating tumor cells with clusters in prostate cancer patients.

Jayant Khandare[1], Bharat Bhosale[2], Gourishankar Aland[3], Sreeja Jayant[3], Amrut Ashturkar[3], Vikas Jadhav[3], Ashish Joshi[4], Sourav Mishra[5], Pradip Kendre[6], Aravindan Vasudevan[3], Vashishth Maniar[7], Jagdeesh Kulkarni[8]

[1]Research, Actorius Innovations and Research, Pune, India,[2]Research, Bombay Hospital, Mumbai, India,[3]Actorius, Pune, India,[4]Mumbai Oncocare Center, Mumabi, India,[5]Research, AIIMS Bhubaneswar, Bhubaneswar, India,[6]Oncology, Mumbai Oncocare Centre, Mumbai, India,[7]Medical Oncology, Mumbai Oncocare Center, Mumbai, India,[8]Surgery, Bombay Hospital, Mumbai, India

Background:
Prostate cancer (PC) detection remains challenging due to the limited specificity and sensitivity of current screening methods, including PSA testing. However doesn't distinguish aggressiveness from indolent disease, leading to overdiagnosis and overtreatment. Circulating Tumor Cells (CTCs), however, offer greater clinical value as they provide real-time insights into tumor biology, disease progression, and treatment response. Unlike PSA, CTCs represents a dynamic biomarker implicating minimal cellular residual disease (MCRD) systemically, helpful for monitoring and guiding the personalized prostate cancer management. In addition, the over-expression of PD-L1 on CTCs provides insights into immune evasion mechanisms and may have predictive and prognostic value in PC. We report CTC capture, having PD-L1 positivity and clusters, in PC patients.
Methods:
Retrospectively, 239 prostate cancer patients were analysed for presence of CTC-PD-L1 and CTC clusters, including 216 (90.4%) baseline and 23 (9.6%) follow-up samples. CTCs were isolated using the CDSCO-approved (India) *OncoDiscover Test* employing anti EpCAM antibody-based immunomagnetic enrichment / 1.5 ml of blood. CTCs were identified as $CK18^{+}/DAPI^{+}/CD45^{-}$, PD-L1 $expression^{+}$ cells with distinct morphology. Automated fluorescence imaging quantified signal intensities to correlate with clinicopathological parameters. Patients were stratified for age, and quantitative analysis of CTC positivity, PD-L1 expression, and cluster frequency was performed.
Results:
CTCs were detected in 173 (72.4%) patients, while 66 (27.6%) were negative. Amongst 157 evaluable samples for PD-L1, 131 (54.8%) were PD-L1 positive and 26 (10.9%) were negative. CTC clusters were observed in 19 (11%) patients, while 154 patients (89%) had only single CTCs. At baseline, CTCs were detectable in 70.4% of patients, increased to 91.3% at follow-up patients. While, CTC-PD-L1 positivity was observed in 52.3% patients at baseline and 85.7% in follow-up. Additionally, PD-L1-positive CTC clusters increased from 10.5% at baseline to 13.1% at follow-up. The predominant age groups were 61-70 years (39.0%) and 71-80 years (39.9%), together comprising nearly 80% of the cohort. The mean distribution of CTC counts per patient were 1.14, 0.95 for CTCs with PD-L1, and 0.12 for CTC clusters.
Conclusion:
A high prevalence of CTCs and PD-L1 expression was observed among prostate cancer patients, particularly in older age groups. The detection of PD-L1 +ve CTCs highlights the presence of confirmative MCRD, and presence of disease in circulation. The relatively low incidence of CTC clusters suggests limited collective migration, although their presence may signify more aggressive disease phenotypes.

#1080 Development of a murine leptomeningeal disease model for a point-of-care cerebrospinal fluid liquid biopsy assay.

Eileen Shiuan[1], Jorge Salcedo-Sifuentes[2], Leilani Pradis[2], Trinh Phan[2], Sonia Su[3], Martin Shum[3], Daniel T. Kamei[3], Won Kim[2], Robert M. Prins[2]

[1]Hematology/Oncology, UCLA Health, Los Angeles, CA,[2]Neurosurgery, UCLA Health, Los Angeles, CA,[3]Bioengineering, UCLA Samueli School of Engineering, Los Angeles, CA

Background: Leptomeningeal disease (LMD), the metastatic dissemination of cancer cells to the leptomeninges and cerebrospinal fluid (CSF), is a devastating complication of cancer. LMD occurs most commonly in advanced melanoma, lung, and breast cancers, and typically portends a poor prognosis that is accompanied by rapid neurological decline. Diagnosis and disease monitoring has been historically challenging. Prior work by our colleagues has led to the development of a barcode-style rapid, semi-quantitative lateral flow assay (LFA) able to detect MCF-7 breast cancer cells in artificial CSF using an epithelial marker. Here, we present murine models of LMD developed to further refine the assay and test its detection limit in an *in vivo* setting.

Methods: Two brain-tropic murine cancer lines previously generated by serial *in vivo* intracarotid injections, B16-BrM melanoma and LLC-LeptoM lung carcinoma, were engineered to stably express mCherry and secreted Gaussia luciferase (sGluc) via lentiviral transduction. Pure populations were isolated by fluorescence-activated cell sorting, and bioluminescence signal was evaluated *in vitro* using cultured supernatant at various cell concentrations. For *in vivo* studies, 1000 parental or mCherry-sGluc cells were stereotaxically injected into the right lateral ventricle of syngeneic C57BL/6 mice at 8-10 weeks of age. CSF was collected terminally via cisterna magna puncture on days 1, 5, 9, and 13 post-implantation. Tumor burden was assessed using bioluminescence and flow cytometry on CSF. Murine brains were collected and processed for histological analyses.

Results: Bioluminescence signal was detectable in cultured supernatant from both B16-BrM and LLC-LeptoM cells, even in concentrations less than 10 cells per ml. When adopted into the *in vivo* LMD model, mice began to display clinical decline starting around day 12 post-implantation. Histological analysis demonstrated tumor cell clusters sequestered in the ventricular space. Bioluminescence signal was detectable from just 1 ul of mouse CSF in animals injected with mCherry-sGluc cells, compared to those injected with parental cells or with no injection. On day 13 post-implantation, bioluminescence signal was saturated in about half of the experimental cohort. In most cases, bioluminescence was detected in CSF even when mCherry+ cells were not detected on flow cytometry.

Conclusion: We have established a murine LMD model that allows for highly sensitive detection of tumor burden via liquid biopsy of CSF. Further studies evaluating tumor burden kinetics and the performance of the point-of-care LFA on mouse and human CSF are ongoing. The success of this work may revolutionize the diagnosis and management of LMD.

#1081 Development and validation of a standardized CELLSEARCH® assay for real-time monitoring of prostate-specific membrane antigen (PSMA) expression on circulating tumor cells.

Steven M. Jones, Thai Bui, Damodara Gullipalli, Shemeeakah Powell, Margaret LaCava, **Zoltan Simandi**

Menarini Silicon Biosystems, Huntingdon Valley, PA, PA

BACKGROUND:
Prostate-Specific Membrane Antigen (PSMA) is a critical biomarker whose dynamic expression dictates the clinical utility of emerging PSMA-targeted radioligand therapies. A major clinical challenge remains the lack of a standardized, highly sensitive, and minimally invasive method for PSMA expression monitoring. We addressed this by developing and validating a novel PSMA-specific assay integrated into the CELLSEARCH® platform, the only FDA-cleared system for CTC enumeration.
METHODS:
The PSMA assay utilizes the CELLSEARCH® platform's immunomagnetic enrichment of EpCAM+ CTCs, followed by staining with fluorescently labeled anti-cytokeratin, anti-CD45, DAPI, and a high-affinity anti-PSMA antibody. Analytical validation was conducted using PSMA-positive (LNCaP, 22Rv1) and PSMA-negative (PC-3.9) cell lines spiked into healthy donor blood, assessing assay sensitivity, specificity, and recovery over a 96-hour sample preservation time in CellSave™ tubes. Captured CTCs are suitable for both platform imaging and subsequent molecular analysis.
RESULTS:
The customized PSMA assay demonstrated exceptional analytical performance, meeting all pre-defined criteria. The linear relationship between spiked and recovered PSMA-positive LNCaP cells was robust, achieving R^2 values >0.999 across all tested donors. High accuracy was confirmed by mean percent recovery for PSMA-positive cells, which ranged from 83.3% to 93.3% for spike levels of 10 to 1000 cells. Assay precision was also confirmed, with a Coefficient of Variation (CV) of 6.97% at the 10-cell spike level. In a preliminary clinical cohort (N=20) of PCa patients, the assay successfully detected PSMA+ CTCs. Enriched patient samples were then subjected to orthogonal flow cytometry analysis and cell sorting to provide independent confirmation of PSMA protein expression. Downstream molecular analysis of the sorted cells confirmed the presence of PCa-specific genomic alterations, providing molecular verification of the PSMA-positive CTC population.
CONCLUSIONS:
This novel, fully validated PSMA CTC assay provides a highly specific, and standardized liquid biopsy tool for PSMA detection. Its robust analytical performance establishes the utility of the platform in monitoring PSMA expression dynamics to inform therapeutic decisions in metastatic prostate cancer patients.

#1082 Development of a novel CDH17 CTC assay to monitor colorectal patient blood and cerebrospinal fluid.

Jennifer C. Chow[1], Casey E. Helmicki[1], Rachel Ponting[1], Arturo B. Ramirez[1], **Pashtoon Murtaza Kasi**[2]

[1]RareCyte, Inc., Seattle, WA,[2]City of Hope Comprehensive Cancer Ctr., Duarte, CA

CDH17 is a cell adhesion molecule typically expressed in intestinal epithelial cells and pancreatic ducts. CDH17 overexpression is linked to tumor progression, metastasis and poorer prognosis and is being investigated as a target of CAR-T therapies currently in clinical development. Circulating tumor cells (CTCs) are intact cells shed from the tumor into blood or other biological fluids and can serve as a liquid biopsy for dynamic assessment of tumor protein expression. In this study we developed and validated an immunofluorescent assay to measure CDH17 expression in CTCs, and enable longitudinal monitoring of tumor CDH17 expression in patient blood and cerebrospinal fluid (CSF) samples. To optimize the CDH17 CTC assay, multiple clones were screened using positive and negative cell lines spiked into healthy donor blood. Clone E5J8Z (Cell Signaling Technologies) applied using the Leica BOND RX autostainer, provided the highest signal-to-background (S:B) ratio between positive negative cell lines. Final assay had S:B of 138 and 99.9% accuracy in distinguishing positive from negative cells.The verified assay was applied to 4 longitudinal blood and CSF samples collected from a stage IV colorectal cancer patient with brain metastasis undergoing CAR-T therapy targeting CDH17 (see table). CDH17(+) CTCs were detected in both blood and CSF, with higher CTC numbers and CDH17 expression observed in CSF samples compared to blood from the same timepoint. CTC numbers and CDH17 expression in blood and CSF decreased upon anti-CDH17 CAR-T therapy and reached undetectable levels in later samples.

This study demonstrates the feasiblity and robust performance of the CDH17 CTC assay in blood and CSF of a CRC patient. Changes in CTC number and CDH17 expression can be harbingers of response to therapy and offer a minimally invasive method to longitudinally monitor biomarker expression. This approach may offer predictive and prognostic insights for patients on CDH17-targeted therapies.

Longitudinal CTC and CDH17 monitoring

Draw #	Sample	Collection Date	Volume (mL)	CTC #	CTC#/mL	CDH17 MFI	% positive CDH17
1	Blood	27NOV2024	3.8	0	0	not performed	not performed
2	Blood	20MAY2025	6.6	0	0	not performed	not performed
2	CSF	20MAY2025	3	11	1.7	not performed	not performed
3	Blood	30JUN2025	6.1	1	0.2	9	0
3	CSF	30JUN2025	2	4	2	3969	100
4	Blood	28JUL2025	6.6	4	0.6	47	0
4	CSF	28JUL2025	2.9	1	0.3	84	100
5	Blood	22AUG2025	3	0	0	-	-
5	CSF	22AUG2025	2	0	0	-	-
6	CSF	2SEP2025	1	0	0	-	-

#1083 Kras activity-linked glycolysis and immunosuppression in metastatic pancreatic cancer.

Shuichi Mitsunaga[1], Mari Masuda[2], Kota Kato[1], Hidetaka Suzuki[1], Mitsuhito Sasaki[3], Hiroki Yoshimatsu[4], Yoichi Kamei[4], Masafumi Ikeda[3]

[1]Division of Biomarker Discovery, National Cancer Center, Exploratory Oncology Research & Clinical Trial Center, Kashiwa, Japan,[2]Staff Scientist, National Cancer Ctr. Research Inst., Tokyo, Japan,[3]Department of Hepatobiliary and Pancreatic Oncology, National Cancer Center Hospital East, Kashiwa, Japan,[4]Pfizer R&D Japan G.K., Tokyo, Japan

Background: KRAS mutations act as a driver of pancreatic ductal adenocarcinoma (PDAC), involving ERK-dependent gene transcription. Inhibition of mutated KRAS activity suppresses glycolysis and reshapes the poor immune profile in murine PDAC. Identification of these relationships in human PDAC is useful for realizing pivotal drivers of metabolic and immune dependency. Recently identified PDAC siKRAS KRASi iKras gene sets enable the creation of a precise KRAS signature score for KRAS activity. Using liver metastasis (LM)-derived transcriptome data, we evaluated the effect of KRAS signature score on clinical outcomes and the molecular features of metastatic PDAC.
Methods: Comprehensive mRNA expression on cDNA microarray and 435 protein expressions on reverse-phased protein array (RPPA) were measured using needle-biopsied samples from treatment-naïve LM of PDAC. KRAS signature score was calculated in each sample. A KRAS-related gene module was determined based on the relationship between KRAS signature score and module eigengene from weighted co-expression network analysis. Hierarchical clustering of RPPA data generated KRAS-related subtypes, in which a KRAS-related protein was selected from the molecule encoded by the genes of KRAS-related gene modules.
Results: KRAS signature score in LMs was calculated in 77 patients (Male: 65%; median age: 66 years). Patients with high KRAS signature score tumors (n=38) showed poor overall survival as compared to those with low KRAS signature score tumors (n=39; hazard ratio: 1.895 [95% confidential interval: 1.123 to 3.198]). KRAS mutated LMs (90.9%) were related to high KRAS signature scores (P=0.004). *DUSP4* mRNA expression, an ERK-dependent negative feedback gene for ERK dephosphorylation, increased in tumors with high KRAS signature scores (P=0.017) and with KRAS mutation (P<0.001). Thirty-seven proteins were identified as KRAS-related UP proteins, including those involved in the glycolysis pathway and a lactate transporter, MCT4. The gene up-regulation of glycolysis and lactate-efflux pathway was found in *HK2* (P=0.132), *Eno1, 2* (P<0.001, P=0.016), *PKM* (P<0.001), *LDHA* (P<0.001), and *MCT4* (P<0.001). ZAP-70, a cytosolic tyrosine kinase essential for T cell receptor signaling, was present in nine KRAS-related DOWN proteins. The gene down-regulation of the immune profile was found in *CD4* (P<0.001), *CD8A* (P<0.001), *CD8B* (P=0.013), and *ZAP-70* (P<0.001).
Conclusion: KRAS up-regulated tumors showed elevation of glycolytic molecules and immunosuppression in LM of pancreatic cancer. KRAS activity might drive metabolic and immunological aggravation, leading to a poor prognosis.

#1084 Serum proteomic profiling reveals metastasis-associated molecular signatures and early systemic remodeling in triple-negative breast cancer.

Jina Kim[1], Hyoyoung Kim[1], Sunao Tanaka[1], Takeo Fujii[2], Sungyong You[1], **Hideki Furuya**[1]

[1]Cedars-Sinai Medical Center, Los Angeles, CA,[2]National Cancer Institute, Bethesda, MD

Background and Objectives: Triple-negative breast cancer (TNBC) is an aggressive subtype with high risk of distant metastasis and limited biomarkers for early detection of recurrence. Clinical surveillance relies on imaging, which often identifies metastasis only after systemic progression. This study evaluated whether serum proteomic profiling can identify molecular changes associated with metastatic transition in TNBC. **Methods:** Serum samples were collected from 29 patients with TNBC and 10 healthy donors. Among TNBC cases, 12 and 9 samples were obtained at the time of initial diagnosis from patients who never developed distant recurrence (NR-DIG) and those who developed distant recurrence (DR-DIG), respectively. Eight samples were collected at recurrence (DR-REC). All samples were analyzed using the SomaScan® 11K proteomic platform. Differential protein expression ($|\log_2[\text{Fold Change}]| > 0.35$, False Discovery Rate (FDR) < 0.10), pathway enrichment, and immune deconvolution analyses were performed. **Results:** Comparison between DR-REC and DR-DIG identified 299 differentially expressed proteins (DEPs; 260 upregulated, 39 downregulated). Inflammation, coagulation, angiogenesis, and extracellular matrix remodeling were significantly enriched by the DEPs. Unsupervised hierarchical clustering distinguished DR-REC from DR-DIG, and one serum sample clinically classified as DR-DIG clustered with DR-REC, suggesting that metastasis-associated proteomic changes may precede clinical detection. Immune deconvolution revealed increased monocyte and neutrophil signatures in DR-REC compared with NR-DIG and DR-DIG, indicating systemic immune remodeling during metastatic progression. **Conclusions:** Serum proteomic profiling can detect molecular alterations associated with metastatic transition in TNBC, even before radiographic evidence of recurrence. These findings support the feasibility of a proteomics-based liquid biopsy as a minimally invasive approach for early detection and monitoring of metastatic progression in TNBC.

#1085 PHF8 is a major upstream regulator of RIPK2 in prostate cancer cells.

Jaceline Pires Sanches, Ahmed Elgehama, Lili Guerra, Wei Yang

Stony Brook University, Stony Brook, NY

Background: Despite significant progress, prostate cancer (PC) remains a leading cause of cancer-related death in men, underscoring the urgent need for new therapeutic strategies. Our previous study demonstrated that RIPK2 is overexpressed in advanced PC and promotes disease progression and metastasis by activating a noncanonical RIPK2/MKK7/c-Myc signaling pathway (*Nature Communications*, 2022). However, beyond gene amplification, the mechanisms underlying RIPK2 upregulation in PC cells remain elusive. The present study aims to identify the key transcription factor regulating RIPK2 expression in PC cells.
Methods: PC 22Rv1 and PC3 cells were treated with three NF-κB modulators, and RIPK2 and NF-κB target gene expression was measured by RT-qPCR. Candidate RIPK2 transcription factors were identified by integrating CHEA, ENCODE, JASPAR, and EoRothEA databases, and ranked using PCTA and TCGA correlations plus ENCODE ChIP-Seq data. PHF8 expression and its correlation with RIPK2 were assessed by RT-qPCR and western blotting in eight prostate cell lines. PHF8 was knocked out in two PHF8-high lines (22Rv1, PC3) via CRISPR/Cas9, and re-expressed using lentiviral wild-type (WT), demethylase-inactive (H283A. A dual-luciferase reporter assay was performed to evaluate the effect of PHF8 and its enzymatic activity on *RIPK2* promoter activity. A multiplexed fluorescence immunohistochemistry assay was developed to assess the correlation between PHF8 and RIPK2 in tumor cells within clinical tissue specimens.
Results: NF-κB decreased RIPK2 mRNA levels, indicating that NF-κB acts as a transcriptional repressor rather than a transcriptional activator of RIPK2 in PC cells. Integrative analysis identified 156 candidate RIPK2 transcription factors, with seven consistently correlated with RIPK2 mRNA (average rho > 0.25) in both PCTA and TCGA cohorts. Among these, PHF8 showed strong RIPK2 promoter binding in ENCODE ChIP-Seq data. Western blotting confirmed a strong PHF8-RIPK2 protein correlation across eight PC cell lines, with PHF8 most abundant in 22Rv1 and PC3. Genetic or pharmacologic PHF8 inhibition in these cells markedly reduced RIPK2 pre-mRNA, mRNA, and protein levels, whereas PHF8 overexpression in RWPE-2 and LNCaP increased RIPK2 in an enzymatic activity- and dose-dependent manner. In clinical tissue specimens, PHF8 and RIPK2 protein levels were significantly correlated in prostate tumor cells.
Conclusion: Our findings identify PHF8, rather than NF-κB, as a major transcriptional regulator of RIPK2 in PC cells and demonstrate that PHF8's demethylase activity is essential for its transcriptional regulation of RIPK2.

#1086 HER2 expression in circulating tumor cells as a minimally invasive biomarker of therapeutic response to trastuzumab deruxutecan in breast cancer.

Toru Mukohara[1], Nobuaki Matsubara[1], Yusuke Takahashi[2], Kentaro Shirai[2], Hiromichi Nakajima[1], Chikako Funasaka[1], Chihiro Kondoh[1], Kana Kawasaki[2], Maharjan Bishnu Devi[2], Fumie Kato[2], Hiroyuki Obinata[2], Taiga Ajiri[2], Masatoshi Yanagida[2], Reiko Watanabe[3]

[1]Department of Medical Oncology, National Cancer Center Hospital East, Kashiwa, Japan,[2]Central Research Laboratories, Sysmex Corporation, Kobe, Japan,[3]Department of Pathology and Clinical Laboratories, National Cancer Center Hospital East, Kashiwa, Japan

Over the last decade, a variety of antibody-drug conjugates (ADCs) have entered clinical practice. The antitumor activity of some ADCs is correlated with the level of target proteins. Trastuzumab deruxutecan (T-DXd), an anti-HER2 ADC, is presently indicated for breast cancer with a wide range of HER2 expression, from ultralow to overexpresssion. However, evaluation of HER2 status in a tumor poses significant clinical challenges. First, although HER2 expression levels have been shown to change during treatment, it is not always feasible to obtain tumor samples immediately before administration of T-DXd. Second, heterogeneity of HER2 has been reported in breast cancer, both between and within tumors. Therefore, there is a need for a noninvasive method that can evaluate HER2 expression across the entire tumor, thereby ensuring that T-DXd is delivered to patients most likely to benefit from this agent. Circulating tumor cells (CTCs) can be measured by blood sampling, providing a minimally invasive approach that allows molecular information to be obtained in a timely manner and is valuable for guiding therapeutic decisions. Single-cell analysis allows for precise detection of tumor heterogeneity, offering insights into the diverse characteristics of cancer cells. We have developed a method for detecting CTCs and evaluating their HER2 expression by combining size-based CTC isolation with molecular imaging flow cytometry. In this study, we compared HER2 expression in CTCs from whole blood samples drawn from 17 patients with breast cancer who had pathological results available from biopsy tissue specimens collected within 28 days before or after blood sampling. CTC-based evaluation of HER2 expression in tissue demonstrated a sensitivity of 71% and a specificity of 33%. The positive predictive value was 83%. We also evaluated the relationship between HER2 expression in CTCs and the therapeutic effect of T-DXd in a separate cohort. CTC measurements were performed up to three times, namely, before T-DXd, one month after initiation of T-DXd, and at the time of disease progression whilst receiving T-DXd. One month after initiation of T-DXd, the number of HER2-expressing CTCs decreased in all five patients who achieved stable disease or a partial response and increased in four of five patients with progressive disease. These findings suggest that HER2 expression in CTCs may reflect that in tumors. This CTC detection method may help to address the challenges faced during treatment, such as intratumoral molecular heterogeneity and dynamic changes in molecular expression. Ultimately, this detection method could replace tissue biopsies and improve the outcomes of cancer therapy.

#1087 Patient-derived breast and melanoma circulating tumor cell (CTC) *in vitro* models as encouraging new tools for cancer research.

Paul Lovell, Karlie Wysong, Fafali Deegbe, **Fang Tian**

American Type Culture Collection (ATCC), Manassas, VA

Circulating Tumor Cells (CTCs) have emerged as powerful tools for understanding the mechanisms behind cancer biology, particularly in context of metastatic disease. Although rare, CTCs are increasingly recognized for their potential in the early diagnosis, monitoring, and progression of tumors. These cells can detach from a primary cancer tumor and enter the bloodstream, facilitating metastasis at distant tissue sites. As research into CTCs advances, new opportunities will continue to emerge to better manage therapeutic targets, especially for metastatic disease. Despite progress in CTC isolation techniques, detecting CTCs remains challenging due to their rarity in the bloodstream. Furthermore, long-term and scalable in vitro culture of CTCs has not been previously achieved. As a result, there is a significant lack of widely available CTC models for studying cancer biology, metastatic progression and development of new treatment strategies. ATCC is actively collaborating with various institutions to make CTCs widely available for cancer research, focusing on the development of standardized expansion and characterization protocols for CTCs isolated from clinical patient samples. In this study, we present the successful propagation and characterization of six well-established breast and melanoma CTC models originating from metastatic breast and melanoma disease: Brx50 (ATCC® CRL-3648™), Brx61 (ATCC® CRL-3649™), Brx142 (ATCC® CRL-3650™), MEL167 (ATCC® CRL-3651™), MEL182 (ATCC® CRL-3652™) and PEM78 (ATCC® CRL-3653™). We evaluated the genomic, proteomic, and functional characteristics of both the breast cancer and melanoma CTC models. Genetic profiling via sequencing revealed key oncogenic drivers potentially linked to metastatic behavior. Gene expression profiles were compared with commonly used breast and melanoma cell lines to highlight distinct molecular signatures. Immunofluorescence staining was performed to assess the distinct presence of breast cancer or melanoma molecular biomarker panels. Drug response assays were conducted to evaluate the sensitivity of the breast models to estrogen receptor (ER) inhibitors and melanoma models to BRAF inhibitors. Additionally, drug response profiles of the breast CTC models were compared to those of commonly used triple-positive and triple-negative breast cancer cell lines, while melanoma CTC models were compared to the A375 melanoma cell line and CRISPR-engineered drug-resistant variants. In conclusion, metastatic disease remains difficult to treat due to reduced therapeutic response rates and increased disease relapse potential. The six new widely available CTC lines—Brx50, Brx61, Brx142, MEL167, MEL182 and PEM78—represent robust and versatile models for investigating the role of CTCs in pre-clinical diagnostics, disease monitoring, and the progression of metastatic breast cancer and melanoma.

#1092 Multi-analyte blood-based screening early detection of HPV-associated oropharyngeal and anal cancer within the PLCO cohort.

Krystle A. Kuhs[1], Hilary Robbins[2], Li Chen[3], Xiaoshuang Feng[4], Yana Al-Inaya[5], Gjystina Lumaj[6], Samuli Eldorfs[5], Qin Wang[5], Tim Waterboer[7], Dipon Das[5], **Daniel Faden**[8]

[1]Department of Epidemiology and Environmental Health, University of Kentucky, Lexington, KY,[2]International Agency for Research on Cancer, World Health Organization, Lyon, France,[3]University of Kentucky, Lexington, KY,[4]World Health Organization,[5]Otolaryngology-Head and Neck Surgery, Massachusetts Eye and Ear, Boston, MA,[6]Massachusetts Eye and Ear, Otolaryngology-Head and Neck Surgery, MA,[7]DFKZ-German Cancer Research Center, Heidelberg, Germany,[8]Mass General Brigham, Boston, MA

Background: Despite rising incidence, there are no early detection methods for HPV+ oropharyngeal (HPV+OPC) and anal (HPV+AC) cancers. HPV16 E6 antibody (E6 Ab) positivity is a promising early biomarker, appearing in most patients at diagnosis and years before symptoms, but the long interval between seroconversion and cancer limits clinical utility. Additional tumor-indicative biomarkers are needed. Circulating tumor HPV DNA (ctHPVDNA) is highly sensitive and specific for detecting HPV+ cancers at diagnosis. Ultrasensitive HPV whole genome sequencing (WGS) assays such as HPV-DeepSeek have shown strong performance for HPV+OPC early detection in a single institution cohort.
Methods: ctHPVDNA testing was performed on serial pre-diagnostic plasma samples from 73 OPC and 19 AC cases and 183 matched PLCO controls with available E6 Ab results. Samples were blinded, underwent cfDNA extraction, and were analyzed using HPV-DeepSeek as previously described.
Results: ctHPVDNA detection was strongly associated with future OPC and AC development (OR 20.52 [95% CI 4.80-87.59], P<0.0001; OR 33.63 [95% CI 7.05-Infinity], P<0.0001). Among E6 Ab positive cases (N=31, surrogate marker to HPV+), ctHPVDNA sensitivity was 61.3% (95% CI 42.2-78.2) for OPC and 71.4% (95% CI 29-96.3) for AC. Sensitivity was highest near diagnosis (100% for OPC within 2 years; 100% for AC within 5 years) and declined with longer lead time. ctHPVDNA read counts increased as the lead time to diagnosis decreased. Eighteen OPC and nine AC cases positive for ctHPVDNA had serial samples. 10 OPC (56%) were positive in all serial samples (median time between first positive ctHPVDNA test to diagnosis: 3.5 years) and 8 (44%) converted from ctHPVDNA negative to positive over follow-up (median time from conversion to diagnosis: 4.7 years, range 0.6 to 8.9 years). 2 AC (22%) were positive in all serial samples (median time between first positive ctHPVDNA test to diagnosis: 6.6 years) and 6 (67%) converted from ctHPVDNA negative to positive over follow-up (median time from conversion to diagnosis: 2.4 years, range 1.2 to 15.4 years).
Conclusions: ctHPVDNA, measured using an ultrasensitive WGS assay, HPV-DeepSeek, was strongly associated with future HPV cancer risk. Among E6 Ab positive cases, ctHPVDNA achieved 100% sensitivity in the years immediately preceding diagnosis in both OPC and AC. Serial sampling showed increasing detection rates and read counts as diagnosis neared, supporting ctHPVDNA as a time-dependent marker of emerging disease. Combining E6 Ab testing with ultrasensitive ctHPVDNA detection provides complementary information for blood-based early detection of HPV+ cancers which should be tested in prospective early detection trials.

#1093 Validation of a blood test for multi-cancer risk stratification in a lung cancer screening cohort.

Ehsan Irajizad[1], Johannes Fahrmann[2], Hamid Rudsari[1], Jody V. Vykoukal[2], Iakovos Toumazis[2], Sara Khoramisarvestani[1], Sara Ansari[3], Jane Yang[3], Nicole M. Kettner[2], Jennifer B. Dennison[4], Edwin Justin Ostrin[5], Samir M. Hanash[5]

[1]The University of Texas MD Anderson Cancer Center, Houston, TX,[2]University of Texas MD Anderson Cancer Center, Houston, TX,[3]Quest Diagnostics, San Juan, CA,[4]Postdoctoral Fellow, UT MD Anderson Cancer Center, Houston, TX,[5]UT MD Anderson Cancer Center, Houston, TX

Purpose: We report a blinded validation study of a ten-protein marker blood test for assessing risk of developing or harboring nine common cancers in a prospective lung cancer screening cohort. **Patients and Methods:** The foundation of the multi-cancer risk stratification test (MCaST), test is a 4-marker protein panel consisting of ProSFTPB, CEA, CA125, and CYFRA-21 which has been extensively validated for risk of lung cancer and which has been expanded to include six additional markers to encompass, in addition to lung cancer, prostate, colorectal, breast, ovarian, pancreatic, liver, esophageal, and stomach cancers. Blinded validation samples consisted of 1,235 plasmas collected prior to diagnosis from 171 cancer cases and 526 randomly selected non-case controls. Fixed individualized combination rules as well as cancer-specific risk thresholds predefined based on established clinical guidelines were applied. **Results:** At the subject level, the MCaST tested positive for imminent risk of lung cancer in 65 of 73 lung cancer cases, including 45 of 51 early-stage cases, with a median time of 12.7 months (interquartile range [IQR]: 1.7 - 27.8 months) between the first positive MCaST and diagnosis of lung cancer. The positive rate of MCaST for other cancers was 88.9% for prostate, 63.6% for invasive breast, 85.7% for CRC, 50% for ovarian, 50% for pancreatic, and 67% for esophagus plus stomach cancers with a median (IQR) time of 20.7 months (10.2 - 42.8 months) from the first positive MCaST to a clinical diagnosis across the cancer types. Overall accuracy for tissue-of-origin (TOO) signal was 94.6%, and as high as 98.1% for lung cancer. **Conclusion:** MCaST has utility for assessing cancer risk for common and lethal solid cancers in this smoker population.

#1094 Circulating tumor DNA (ctDNA) for molecular residual disease (MRD) detection and recurrence monitoring in hepatocellular carcinoma (HCC); COSMOS-HCC01.

Masashi Kudo[1], Mitsuhito Sasaki[2], Shinji Itoh[3], Teiichi Sugiura[4], Tsuyoshi Kobayashi[5], Keishi Sugimachi[6], Shinichi Nakanuma[7], Yuta Abe[8], Hisashi Kosaka[9], Nobuhiro Nakamoto[10], Naoto Yamamoto[11], Makoto Ueno[12], Takuji Okusaka[13], Atsushi Takebe[14], Minoru Esaki[15], Kazuyoshi Ohkawa[16], Hisateru Komatsu[17], Yu Takahashi[18], Masatake Tanaka[19], Takeshi Aramaki[20], Tomokazu Kawaoka[21], Rie Sugimoto[22], Taro Yamashita[23], Takashi Yamaguchi[24], Masatoshi Kudo[25], Masato Ozaka[26], Chiemi Notake[27], Hiroshi Uchigata[27], Masafumi Ikeda[2], Naoto Gotohda[1], Yoshiaki Nakamura[27]

[1]Department of Hepatobiliary and Pancreatic Surgery, National Cancer Center Hospital East, Chiba, Japan,[2]Department of Hepatobiliary & Pancreatic Oncology, National Cancer Center Hospital East, Chiba, Japan,[3]Department of Surgery and Science, Graduate School of Medical Sciences, Kyushu University, Fukuoka, Japan,[4]Division of Hepato-Biliary-Pancreatic Surgery, Shizuoka Cancer Center, Shizuoka, Japan,[5]Department of Gastroenterological and Transplant Surgery, Graduate School of Biomedical and Health Science, Hiroshima University, Hiroshima, Japan,[6]Department of Hepatobiliary and Pancreatic Surgery, NHO Kyushu Cancer Center, Fukuoka, Japan,[7]Department of Hepato-Biliary-Pancreatic Surgery and Transplantation, Kanazawa University, Ishikawa, Japan,[8]Department of Surgery, Keio University School of Medicine, Tokyo, Japan,[9]Department of Hepatobiliary Surgery, Kansai Medical University, Osaka, Japan,[10]Division of Gastroenterology and Hepatology, Department of Internal Medicine, Keio University School of Medicine, Tokyo, Japan,[11]Department of Gastrointestinal Surgery, Kanagawa Cancer Center, Kanagawa, Japan,[12]Department of Gastroenterology and Hepatology, Kanagawa Cancer Center, Kanagawa, Japan,[13]Department of Hepatobiliary and Pancreatic Oncology, National Cancer Center Hospital, Tokyo, Japan,[14]Department of Surgery, Kindai University Faculty of Medicine, Osaka, Japan,[15]Department of Hepatobiliary and Pancreatic Surgery, National Cancer Center Hospital, Tokyo, Japan,[16]Department of Hepatobiliary and Pancreatic Oncology, Osaka International Cancer Institute, Osaka, Japan,[17]Department of Gastroenterological Surgery, Osaka International Cancer Institute, Osaka, Japan,[18]Division of Hepatobiliary and Pancreatic Surgery, Cancer Institute Hospital, Japanese Foundation for Cancer Research, Tokyo, Japan,[19]Department of Medicine and Bioregulatory Science, Graduate School of Medical Sciences, Kyushu University, Fukuoka, Japan,[20]Division of Interventional Radiology, Shizuoka Cancer Center, Shizuoka, Japan,[21]Department of Gastroenterology, Hiroshima University Hospital, Hiroshima, Japan,[22]Department of Hepato-Biliary-Pancreatology, NHO Kyushu Cancer Center, Fukuoka, Japan,[23]Department of Gastroenterology, Kanazawa University Graduate School of Medical Science, Ishikawa, Japan,[24]Department of Gastroenterology and Hepatology, Kansai Medical University, Osaka, Japan,[25]Department of Gastroenterology and Hepatology, Kindai University Faculty of Medicine, Osaka, Japan,[26]Department of Hepato-Biliary-Pancreatic Medicine, Cancer Institute Hospital, Japanese Foundation for Cancer Research, Tokyo, Japan,[27]Translational Research Support Office, National Cancer Center Hospital East, Chiba, Japan

Background:
Surgery and ablation can be curative for early-stage HCC, but up to 70% recur or develop new primary HCC. ctDNA-based MRD assessment may improve risk assessment and identify recurrence earlier than current tools. Because HCC is often diagnosed radiologically and ablation yields no tissue, tumor-informed assays may be infeasible and unable to detect new primaries.
Methods:
Patients with completely resected or ablated stage I-III HCC were prospectively enrolled across 13 Japanese sites (Mar 2021-May 2022). Plasma was collected pre- and 4 weeks post-procedure and every 3-6 months with standard imaging and biomarker assessment. ctDNA was analyzed retrospectively using a tissue-free epigenomic assay (Guardant Reveal) evaluating ~20,000 differentially methylated/control regions. Samples are classified as ctDNA detected/not detected based on a pre-defined threshold. Associations between ctDNA status and recurrence were analyzed.
Results:
Among 95 patients eligible for this interim analysis, (87% resected, 57% stage I, median age 74), 610/611 samples were successfully analyzed. At 36.9 months median follow-up, 42 recurred. Pre-procedure ctDNA was detected in 75% (70/94) and correlated with shorter time to recurrence (HR 4.4; 95% CI 1.7-14.6; $p < 0.001$). Post-surgery ctDNA detection at 4 weeks also correlated (HR 3.8; 95% CI 1.7-7.8; $p = 0.002$) and was the only variable that remained statistically associated with recurrence on multivariate analysis at this timepoint. Surveillance ctDNA sensitivity was 60% (25/42), specificity was 98% (52/53), and median lead time was 63 days. ctDNA outperformed other biomarkers evaluated in this cohort (Table 1).
Conclusions:
Epigenomic ctDNA analysis enabled tissue-free MRD detection with high accuracy and superior performance vs conventional biomarkers, supporting its use for individualized recurrence risk assessment and surveillance.

Table 1. Performance of biomarkers (ever/never detected) to predict HCC recurrence during post-treat

	ctDNA	AFP (>10ng/mL)	AFP-L3 (>9.9%)	PIVKA-II (>39mAU/mL)
Sensitivity (positive/recurrence)	60% (25/42)	33% (14/42)	54% (13/24)	44% (18/41)
Specificity (negative/no recurrence)	98% (52/53)	87% (46/53)	68% (15/22)	87% (45/52)
Median lead time	63 days	55 days	12 days	32 days
HR (95% CI)	10.1 (5.3-20.3), P < 0.001	2.2 (1.1-4.1), P = 0.024	1.7 (0.7-3.9), P = 0.213	3.6 (1.9-6.7), P < 0.001

#1095 ARID1A protein expression enhances risk stratification in colorectal polyp surveillance.

Aula Ammar[1], Amna Matly[1], Kimiya Kabiri Arani[1], Scott Murray[1], Mayuri Hendricks[1], Alexander Winton[1], Natalie Fisher[2], Gerard Lynch[1], Mark Johnstone[1], Colin Steele[1], Noori Maka[3], Jennifer Hay[4], Philip Dunne[2], Stephen McSorley[1], **Joanne Edwards**[1]

[1]University of Glasgow, Glasgow, United Kingdom,[2]Queen's University Blefast, Glasgow, United Kingdom,[3]NHS Greater Glasgow & Clyde, Glasgow, United Kingdom,[4]Francis Crick Institute, London, United Kingdom

Background: Polyps detected during bowel cancer screening indicate an increased risk of developing metachronous colorectal lesions. Current British Society of Gastroenterology (BSG 2020) surveillance guidelines use polyp size, number, histology, and dysplasia grade to assess this risk but do not include molecular markers limiting accurate risk stratification. To address this gap, we investigated ARID1A expression as a potential predictive biomarker for metachronous colorectal lesions.
Methods: A total of n=1184 archival colorectal polyp samples assembled into tissue microarrays (TMAs) were stained for ARID1A protein expression using immunohistochemistry (IHC) and epithelial ARID1A histoscores were assessed using Qupath. Data were divided into training (n=819) and test (n=365) datasets. Molecular profiling included somatic mutation sequencing (n=623) and bulk RNA Temp-O-seq comparing low vs high ARID1A expression (n=117 for each group). Pathway analyses incorporated Hallmark gene sets using GSEA and ssGSEA as well as Reactome pathway enrichment and Dorothea transcription factor activity scoring.
Results: High ARID1A expression was identified as a predictor of metachronous disease independent of number of polyps, location of index polyp, dysplasia grade and sex (training HR=1.372, p=0.014; test HR=1.893, p=0.003). ARID1A predictive value was particularly strongest in patients with 1-4 polyps and in left-sided lesion and the rectum. ARID1A was among the most frequently mutated genes in precancerous polyps. ARID1A protein expression was decreased in presence of *ARID1A* and *KMT2D* mutations ($p<0.001$ and $p=0.021$, respectively). The most common type of base alteration in *ARID1A* mutations was C>T (47.96%) followed by G>A (16.33%). Truncation mutations accounted for 48% of ARID1A gene mutations and significantly correlated with reduced protein expression ($p<0.001$). Transcriptomic analysis showed a significant enrichment of proliferative Myc-targets_V2 pathway in ARID1A-high polyps, whereas inflammatory and differentiation pathways were enriched in ARID1A-low polyps. Transcription factor activity suggested a shift toward regenerative stem-cell signatures in ARID1A-high lesions, whereas ARID1A-low lesions showed TFs linked to suppression of transcription.
Conclusion: ARID1A expression is a promising molecular biomarker that improves prediction of metachronous colorectal lesions beyond current guideline criteria, particularly among patients currently classified as low risk. The associated biological programs highlight increased proliferation and activation of regenerative stem-cell pathways in ARID1A-high polyp, supporting ARID1A's potential utility in personalised surveillance strategies.

#1096 OncoSeek 2.0: An advanced multi-cancer blood test enhancing early detection and aiding cancer diagnosis.

Mao Mao[1], Yong Shen[2], Shiyong Li[1], Wei Wu[1], Yinyin Chang[3], PingPing Xing[3], Chenyu Ding[3], Dandan Zhu[3], Qingxia Xu[2], Wei Cui[2]

[1]SeekIn, Shenzhen, Guangdong, China,[2]The Affiliated Cancer Hospital of Zhengzhou University and Henan Cancer Hospital, Zhengzhou, Henan, China,[3]Shenyou Bio, Zhengzhou, Henan, China

Background: Early cancer detection and timely diagnosis are critical for improving patient outcomes and reducing healthcare costs. OncoSeek is an AI-driven, low-cost multi-cancer early detection (MCED) assay integrating seven protein tumor markers (PTMs) with clinical data, previously demonstrating 58.4% sensitivity, 92.0% specificity, and 70.6% tissue-of-origin accuracy in over 15,000 participants. Here, we present OncoSeek 2.0, an upgraded version that incorporates three additional PTMs to enhance the detection of prostate, lung, and squamous cell carcinomas, and evaluate its performance in validation cohorts and its expanded use for assisting cancer diagnosis in patients with tissue masses.

Methods: OncoSeek 2.0 retained the original machine learning framework with expanded biomarker inputs. MCED performance was assessed in a retrospective cohort including 722 cancer and 355 non-cancer subjects. To further evaluate clinical utility, a prospective cohort of 732 patients with tissue masses, clinically deemed likely malignant and scheduled for surgery, was analyzed to assess the assay's effectiveness in aiding cancer diagnosis.

Results: Compared with OncoSeek 1.0, OncoSeek 2.0 achieved a higher AUC (0.934 vs. 0.888) and improved sensitivity from 70.4% to 83.5% at 90.1% specificity across 15 prespecified cancer types collectively accounting for 76.5% of global cancer mortality. Sensitivity gains were notable in lung (79.9% → 89.6%), prostate (58.8% → 94.1%), cervical (44.4% → 72.2%), and esophageal (41.6% → 64.4%) cancers. In the prospective tissue-mass cohort, OncoSeek 2.0 correctly identified 573 of 682 confirmed cancers (84.0% sensitivity). Across the same 15 cancer types, sensitivities exceeded 80% in 12, with slightly lower values observed in ovary (76.9%), breast (72.3%), and lymphoma (63.6%). Among the remaining 50 patients with pathologically confirmed benign lesions, 28 (56.0%) were correctly classified as non-cancer, potentially sparing them from unnecessary surgical procedures.

Conclusion: OncoSeek 2.0 significantly improves sensitivity while maintaining high specificity and affordability (~$30 reagent cost per test). The upgraded assay strengthens its utility for multi-cancer early detection and demonstrates validated diagnostic value in clinically suspected cancer cases. Its ability to correctly identify 84% of confirmed cancer cases in a tissue-mass cohort demonstrates meaningful diagnostic support to help prioritize patients needing confirmatory procedures. These findings position OncoSeek 2.0 as a practical and scalable solution for both population-level cancer early detection and real-world diagnostic support, particularly for cancers without USPSTF-recommended screening modalities or established non-invasive diagnostic pathways, where surgical procedures are commonly needed for definitive diagnosis.

#1097 Performance of a blood-based screening test for the early detection of advanced precancerous lesions.

Prashanthi Natarajan, Preethi Srinivasan, Hsiao-Yun Huang, Alan Selewa, Rebecca Panitch, Caitlin Guccione, Fatemeh Almodaresi, Jayashree Joshi, Su Maw, Misagh Kordi, Yunshu Song, Yu Lin, Osama Khan, Breeana L. Mitchell, Adham Jurdi, Minetta C. Liu, Johannes G. Reiter, Trupti Kawli, Matthew Rabinowitz, Alexey Aleshin

Natera, Inc., Austin, TX

Current colorectal cancer (CRC) screening methodologies, such as colonoscopy and stool-based tests, have shown substantial efficacy but are often constrained by low patient compliance. A minimally-invasive blood-based test can enhance screening adherence. Previous studies evaluating the performance of our blood-based CRC screening test demonstrated high sensitivity and specificity; however these studies did not include precursor or early cancer lesions, the identification of which is critical for cancer prevention. Here, we evaluate the performance of a blood-based early cancer detection (ECD) screening test for advanced colorectal neoplasia (ACN) with a focus on advanced precancerous lesion (APL) performance in an average-risk population. A targeted panel for CRC screening composed of differentially methylated genomic regions was developed, and a machine-learning model was trained to classify patient samples into cancer-free and ACN based on observed differential methylation patterns in circulating cell-free DNA. This ECD screening blood test was applied to plasma samples from 92 sequentially collected subjects with APL and a representative cohort of 366 healthy individuals. These participants were drawn from the first 1400 cases of the ongoing, prospective, PROCEED-CRC clinical study (NCT06620627), designed for the collection of clinically annotated biospecimens from participants ≥40 years old who underwent asymptomatic colonoscopy screening. Performance of the blood-based ECD test was assessed based on its sensitivity to detect APL and specificity across different APL types and age groups. Based on colonoscopy findings from the 458 PROCEED-CRC study participants included in the study (median age: 57 years, range: 43-75 years), 79.9% (n=366) were cancer-free and 20.1% (n=92) had APL. Among those with APL, 6.5% (n=6) had polyps with high-grade dysplasia. Mean sensitivity across all subtypes of APL was 22.5% (CI: 15.4%-32.4%). Median size of APL lesions was 12 mm and 99% of APL were <30mm in size. Sensitivity of APL at 5-9 mm was 20% and sensitivity increased with increasing size. Overall specificity was 91.5% (CI: 88.2%-94%). We did not observe deterioration of specificity with increasing age (p-value n.s., $p > 0.05$). APL detection is critical for intercepting CRC before it develops. The performance reported here highlights the strong potential of minimally invasive, blood-based early detection assays in identifying ACNs, including APLs, with robust performance across the screening participant ages. Notably, most APLs included in this study were <30 mm, representing a challenging set of lesion sizes to detect. Detection of CRC and APL will be further evaluated in the ongoing FIND clinical study (NCT07046585).

#1098 Discrete precancer subtypes and biomarkers of cancer progression identified with spatiotemporal analysis of CDH1-driven diffuse gastric cancer.

Jeremy L. Davis[1], Amber Famiglietti[2], Yunhe Liu[3], Rachael Belcher[1], Sun A Kim[4], Baktiar O. Karim[5], Donna Butcher[5], Linghua Wang[3]

[1]University of Maryland School of Medicine, Baltimore, MD,[2]Department of Surgery, Georgetown University, Washington, DC,[3]UT MD Anderson Cancer Center, Houston, TX,[4]Laboratory of Pathology, National Cancer Institute, Baltimore, MD,[5]Frederick National Laboratory for Cancer Research, Frederick, MD

Introduction: Diffuse gastric cancer (DGC) is a sub-type of gastric adenocarcinoma for which early detection is uncommon. Early-stage gastric signet ring cell (SRC) lesions are ubiquitous in patients with germline CDH1 variants. Though SRC lesions appear to be non-obligate precursors of DGC, the drivers of SRC progression to DGC remain unknown. We sought to derive transcriptomic gene signatures associated with gastric SRC and advanced DGC.

Methods: We employed a single-cell spatial transcriptomic analysis (10X Genomics Xenium) of both early SRC (pT1a) and advanced DGC (≥T2) from 18 patients with germline *CDH1* variants. Spatially resolved analyses were conducted on 42 fields of view derived from gastric biopsies and total gastrectomy specimens that were analyzed according to depth of cancer cell invasion. Biomarkers of SRC precancer progression were identified within discrete epithelial cell subpopulations according to differentially expressed gene profiles. Immunohistochemistry was performed to correlate protein expression with mRNA markers of interest.

Results: Advanced DGC exhibited three distinct transcriptomic clusters based on depth of tumor invasion into the mucosa, submucosa and muscularis propria layers and clustered distinctly from early SRC precursor lesions. SRC phenotype varied based on depth of invasion of the gastric mucosa; SRC1 (superficial) and SRC2 (deep). Multi-modal segmentation of SRC1 and SRC2 subtypes within the SRC precancer cluster demonstrated distinct, spatially resolved transcriptomic profiles. Pathway analysis showed potential functional divergence between SRC1 and SRC2, such that SRC2 possessed a migratory and proliferative phenotype whereas SRC1 displayed loss of cell adhesion and epithelial architecture. We observed three differentially expressed genes with increased expression according to depth of tumor invasion: clusterin (CLU*)*, eukaryotic translation initiation factor 3 (EIF3E), and annexin A2 (ANXA2). CLU, a known regulator of epithelial-to-mesenchymal transition and apoptosis, was over-expressed both in advanced SRC lesions ($p<0.05$) compared to early SRC lesions and within SRC lesions compared to gastric epithelium ($p=0.03$). Clusterin protein expression was quantitatively greater in SRC lesions compared to unaffected gastric epithelium, with more intense staining associated with depth of tumor cell invasion in advanced DGC.

Conclusions: Signet ring cell precancers that originate due to *CDH1* loss-of-function mutations have discrete subtypes based on cell phenotype, depth of mucosal invasion, and spatial transcriptomic profile. Clusterin appears to be a biomarker of early SRC lesions and correlates with depth of gastric cancer invasion. These results may support novel strategies for cancer interception and increase our knowledge of diffuse gastric precancers.

#1099 The RNA editing enzyme ADAR1 is involved in carcinogenesis associated with intraductal papillary mucinous neoplasm.

Masashi Kayano, Kunitoshi Shigeyasu, Kazuya Moriwake, Toshiaki Takahashi, Eiki Miyake, Yuhei Kondo, Yuya Sakurai, Shunsuke Nakamura, Masafumi Takahashi, Kaori Nitta, Kazuya Yasui, Tomokazu Fuji, Kosei Takagi, Hiroshi Tazawa, Toshiyoshi Fujiwara

Okayama University Graduate School of Medicine, Dentistry, and Pharmaceutical Sciences, Okayama, Japan

Background: Intraductal papillary mucinous neoplasm (IPMN) is a mucin-producing subtype of the pancreatic cyst lesions arising from the pancreatic duct system. IPMN is a potential precursor of pancreatic cancer and surgical decision-making is guided by “high-risk stigmata” and “worrisome features” according to international evidence-based Kyoto guidelines for the management of IPMN. However, these criteria can be insufficient for the prediction of invasive intraductal papillary mucinous carcinoma (IPMC). Adenosine-to-inosine (A-to-I) RNA editing, which is regulated by adenosine deaminase acting on RNA (ADAR) was reported to induce the posttranscriptional modification of oncogenes. However, the significance of RNA editing in IPMN remains unclear. We investigated whether ADAR1 expression increases with pathological progression in IPMN and whether higher expression is associated with adverse clinical outcomes.
Methods: We analyzed gene profiling dataset from IPMN tissue samples in silico discovery from GEO (Gene Expression Omnibus). AS a clinical validation analysis, we analyzed 102 IPMN patients who received surgical resection in our institution. Functional analysis was evaluated in ASAN-PaCa cell lines using small interfering RNA (siRNA) transfection.
Results: The mRNA expression data were obtained from a publicly available GEO dataset, comprising samples from 7 normal main pancreatic ducts, 6 low-grade intraductal papillary mucinous neoplasms (LGD-IPMNs), 7 high-grade IPMNs (HGD-IPMNs), and 3 invasive intraductal papillary mucinous carcinomas (IPMCs). Compared to normal epithelial cells, the expression of ADAR1 were elevated in LGD-IPMNs, HGD-IPMNs, and invasive IPMC samples ($p=0.0383$, 0.0383, and 0.0227, respectively). Among the participants in our hospital, 44 had LGD-IPMNs, 29 had HGD-IPMNs, and 29 had invasive IPMC. ADAR1 expression was significantly higher in the HGD-IPMNs and invasive IPMCs than in the LGD-IPMNs ($p<0.01$ for both). We observed a shorter OS and DFS in the high ADAR1 group (OS: $p = 0.0279$, DFS: $p = 0.0163$). In univariate Cox regression, high ADAR1 expression was significantly associated with shorter OS and DFS (OS HR=2.63, $p=0.034$; DFS HR=2.83, $p=0.021$). In multivariate analysis, ADAR1 remained an independent prognostic factor for both OS and DFS (OS HR=2.45, $p=0.042$; DFS HR=2.66, $p=0.033$). In comparison with control cells, ADAR1 knockdown cells exhibited significantly reduced proliferative activity ($p<0.01$) and decreased invasion potential, indicating that ADAR1 contributes to both cell growth and invasiveness in vitro.
Conclusion: IPMC showed frequent ADAR1 overexpression, and higher ADAR1 expression was associated with poorer prognosis. These findings suggest that elevated ADAR1 expression may be involved in IPMN carcinogenesis and could potentially serve as a biomarker for clinical application.

#1100 Epigenetic profiling identifies markers of aggressive cancer subtype using a targeted methylation-based multi-cancer early detection (MCED) blood test.

Kezhong Chen[1], Jian Huang[2], Dahong Zhang[3], Shu Wang[4], Hongxu Liu[5], Wenzhao Zhong[6], Xiangnan Li[7], Qiang Zhang[5], Zhigao Li[8], Jiaqi Liu[9], Ziqing Tian[10], Fei Zhou[11], Gongsheng Jin[12], Xudong Xiang[13], Zhigang Li[14], Hui Xie[15], Ya Wei[16], Guochun Zhang[17], Guolin Ye[18], Ming Cai[19], Junfeng Wang[8], Yan Zhang[20], Chao Cheng[21], Hefei Li[22], Desong Yang[23], Jianhong Lian[24], Sheng Huang[25], Tao Xu[26], Zengjun Wang[27], Xi Guo[28], Zhuowei Liu[29], Minfeng Chen[30], Yang Wang[31], **Yue An**[31], Yanzhan Yang[31], Min Li[31], Jing Liu[31], Baoliang Zhu[31], Yonghui Li[31], Xiaohui Wu[31], Fan Yang[1], Jun Wang[1]

[1]Thoracic Oncology Institute and Department of Thoracic Surgery, Peking University People's Hospital, Beijing, China,[2]The Department of Breast Surgery, Second Affiliated Hospital, Zhejiang University School of Medicine, Hangzhou, China,[3]Urology & Nephrology Center, Department of Urology, Zhejiang Provincial People's Hospital (Affiliated People's Hospital), Hangzhou Medical College, Hangzhou, China,[4]Breast Disease Center, Peking University People's Hospital, Beijing, China,[5]Liaoning Provincial Cancer Hospital, Shenyang, China,[6]Guangdong Lung Cancer Institute, Guangdong Provincial People's Hospital (Guangdong Academy of Medical Sciences), Southern Medical University, Guangzhou, China,[7]The First Affiliated Hospital of Zhengzhou University, Zhengzhou, China,[8]Harbin Medical University Cancer Hospital, Harbin, China,[9]Department of Breast Surgical Oncology, National Cancer Center/National Clinical Research Center for Cancer/Cancer Hospital, Chinese Academy of Medical Sciences and Peking Union Medical College, Beijing, China,[10]Department of Thoracic Surgery, The Fourth Hospital of Hebei Medical University, Shijiazhuang, China,[11]Shanghai Pulmonary Hospital, Shanghai, China,[12]The First Affiliated Hospital of Bengbu Medical College, Bengbu, China,[13]Department of Thoracic Surgery, Yunnan Cancer Hospital, Kunming, China,[14]Department of Thoracic Surgery, Shanghai Chest Hospital, Shanghai Jiao Tong University School of medicine, Shanghai, China,[15]Department of Breast Cancer Research Center, Jiangsu Cancer Hospital & Jiangsu Institute of Cancer Research & Affiliated Cancer Hospital of Nanjing Medical University, Nanjing, China,[16]Anyang Tumor Hospital, Anyang, China,[17]Department of Breast Surgery, Guangdong Provincial People's Hospital, Guangzhou, China,[18]Department of Breast Cancer, The First People's Hospital of Foshan, Foshan, China,[19]Department of Urology, The Second Affiliated Hospital, School of Medicine, Zhejiang University, Hangzhou, China,[20]Department of Oncology, Shijiazhuang People's Hospital, Shijiazhuang, China,[21]Department of Thoracic Surgery, The First Affiliated Hospital of Sun Yat-Sen University, Guangzhou, China,[22]Department of Thoracic Surgery, Affiliated Hospital of Hebei University, Baoding, China,[23]Hunan Cancer Hospital & The Affiliated Cancer Hospital of Xiangya School of Medicine, Central South University, Changsha, China,[24]Department of General Surgery,Shanxi Cancer Hospital, Taiyuan, China,[25]Department of Breast Surgical Oncology,Yunnan Cancer Hospital, Kunming, China,[26]Peking University People's Hospital, Beijing, China,[27]Department of Urology, The First Affiliated Hospital of Nanjing Medical University, Nanjing, China,[28]Department of Urology, Hunan Provincial People's Hospital, the First Affiliated Hospital of Hunan Normal University, Changsha, China,[29]Sun Yat-sen University Cancer Center, Guangzhou, China,[30]Department of urology, National Clinical Research Center for Geriatric Disorders, Xiangya Hospital, Changsha, China,[31]Shanghai Xiaohe Medical Laboratory Co. Ltd., Shanghai, China

Background: Previous MCED studies have shown differences in detection performance across different aggressiveness cancer subtypes. However, the methylation profiles and ctDNA shedding patterns across different aggressiveness subtypes have not been analyzed. We systematically compared cell-free DNA (cfDNA) tumor fraction and methylation profiles across aggressiveness subtypes in three cancers to identify epigenetic biomarkers that differentiate tumor aggressiveness.
Methods: Blood samples from a case-control study (NCT06217900) including 757 cancer cases were analyzed using a targeted methylation-based MCED test. We compared cfDNA tumor fraction and methylation profiles between aggressiveness subtypes, stage-matched small cell lung cancer (SCLC) (n=137) versus (vs) non-small cell lung cancer (NSCLC) (n=137), stage I invasive lung adenocarcinoma (IAC) (n=81) vs minimally invasive adenocarcinoma (MIA) (n=81), triple-negative breast cancer (TNBC) (n=151) vs non-TNBC (n=151), and intermediate/high-grade prostate cancer (Gleason Grade Group[GG] 2-5)(n=14) vs low-grade prostate cancer(GG1)(n=6). Tumor fraction was estimated using zero-inflated Negative Binomial model based on the distribution of methylation signals, and methylation profiles were assessed by calculating methylated/unmethylated (M/U) ratios between different aggressiveness subtypes. Marker comparisons were conducted using the Mann-Whitney U test with multiple testing corrections.
Results: The sensitivity is higher in more aggressive subtypes (lung cancer 93.73% vs SCLC 99.27%; breast cancer 70.76% vs TNBC 81.46%; prostate cancer 40% vs intermediate and high-grad prostate cancer 42.86%). In lung cancer, SCLC exhibited a significantly higher cfDNA tumor fraction than NSCLC (Wilcoxon $p = 2.24\times10^{-24}$), with 41,136 markers (79.18% hypomethylated) showing elevated M/U ratios. In stage I lung adenocarcinoma, IAC demonstrated a higher cfDNA tumor fraction (Wilcoxon $p = 2.55\times10^{-6}$) and systematic methylation differences compared to MIA. In breast cancer, TNBC had a significantly higher cfDNA tumor fraction than non-TNBC (Wilcoxon $p = 2.55\times10^{-6}$), with 25,717 markers (80.32% hypomethylated) displaying increased M/U ratios. Among prostate cancers of the same stage, GG2-5 cases exhibited higher cfDNA tumor fraction (Wilcoxon $p = 0.038$) and systematic methylation alterations compared to GG1.
Conclusion: Aggressive tumor subtypes consistently display elevated cfDNA tumor fraction and characteristic methylation profiles marked by increased M/U ratios. These findings suggest cfDNA methylation patterns are promising epigenetic biomarkers for distinguishing tumor aggressiveness, potentially improving cancer screening precision and reducing overdiagnosis.

#1101 A novel method for tumor fraction estimation using methylation sequencing data.

Daokun Sun, Yu Sun, Alex Robertson, Lee A. Albacker, Chang Xu

Computational Biology, Foundation Medicine, Cambridge, MA

Introduction: Accurate estimation of tumor fraction in cell-free DNA (cfDNA) is critical for molecular residual disease monitoring and early cancer detection. Current approaches, such as maximum somatic allele frequency, i.e., MSAF, rely on the presence of detectable somatic mutations, limiting their sensitivity in samples with low tumor burden or shallow sequencing depth. Moreover, these approaches are susceptible to bias from clonal hematopoiesis and uneven mutation distribution, which can compromise the accuracy of tumor fraction (TF) estimation. DNA methylation signatures offer a promising avenue due to their abundance, consistency, and robustness. However, current methods to harness this information for tumor fraction estimation remain suboptimal.

Methods: We developed a new and tumor-naive computational framework that leverages DNA methylation signatures to quantify tumor-derived DNA with markedly high analytical sensitivity. The approach integrates pre-selected methylation markers and weighted linear regression to quantify tumor-derived DNA to a minimal detection threshold. Our machine learning-based method combines tumor- and normal-specific prior methylation frequencies and target coverage information to achieve a more reproducible and reliable estimation of tumor fraction. The method was developed using in-house clinical samples, and its performance was benchmarked against mutation-based ctDNA tumor fraction from FoundationOne Liquid CDx (F1LCDx). Besides, *in silico* and *in vitro* dilutions were used to assess accuracy and sensitivity at low tumor fractions.

Results: Our method demonstrated a limit of detection reaching the 0.01% TF, with strong accuracy maintained down to 0.1% in both *in vitro* and *in silico* dilution series. *In vitro* dilution experiments demonstrated a Spearman correlation of 0.86 and a Pearson correlation of 0.88 on $\log_{10}$-transformed data, with median fold changes of 0.84 at 0.1% TF and 3.76 at 0.01% TF. Performance was further supported by *in silico* dilution analyses, yielding a Spearman correlation of 0.98 and Pearson correlation of 0.97 on $\log_{10}$-transformed data. Additionally, when benchmarked against ctDNA TF estimates from F1LCDx, our method achieved a Spearman correlation of 0.88, a Pearson correlation of 0.90, and a median fold change of 0.91.

Conclusions: We present a novel methylation-based approach for TF estimation in cfDNA. This approach enables highly sensitive and accurate TF estimation, particularly at low TFs, highlighting its potential utility in molecular residual disease detection, early cancer detection or treatment response monitoring. This approach offers a powerful tool for advancing liquid biopsy applications in cancer diagnostics and clinical management, with validation in larger cohorts ongoing.

#1102 Uncovering early transcriptional alterations in lung cancer: Preliminary insights from the Boston Lung Trans-omics (BOLT) Initiative.

Yu Chen Zhao[1], Li Su[2], Lorelei A. Mucci[1], Timothy R. Rebbeck[3], Yi Li[4], David C. Christiani[5]

[1]Department of Epidemiology, Harvard T.H. Chan School of Public Health, Boston, MA,[2]Department of Environmental Health, Harvard T.H. Chan School of Public Health, Boston, MA,[3]Division of Population Sciences, Dana-Farber Cancer Institute, Boston, MA,[4]Department of Biostatistics, University of Michigan Medical School, Ann Arbor, MI,[5]Department of Medicine, Harvard Medical School, Boston, MA

Lung cancer's high mortality is driven by advanced-stage diagnoses and high recurrence rates. Existing genomic markers lack sensitivity for early detection and predicting recurrence, presenting ongoing clinical challenges. We introduce the Boston Lung Trans-omics (BOLT) Initiative, an early-stage sub-cohort of the Boston Lung Cancer Study with 1446 paired tumor/adjacent-normal bulk RNA-sequenced tissues from 723 NSCLC patients. We performed paired differential gene expression analysis between tumor and adjacent normal tissues using limma-voom, adjusting for batch effects and patient ID to account for inter-individual confounding. Statistically significant differentially expressed genes were defined as genes with FDR-adjusted $p<0.05$ and log2 change $|LFC|>2$. To emphasize biological relevance and minimize false positives, we performed pathway enrichment analysis with the Gene-set Enrichment Analysis software using curated pathway data retrieved from the Molecular Signature Database, Broad Institute. We then applied weighted gene co-expression network analysis (WGCNA) to the top 5000 most variable genes across all samples to identify gene modules and assessed module-trait associations. We identified 738 significant DEGs in the paired tumor/normal comparison. Among these, 387 (52%) were upregulated in tumor compared to normal lung tissues. *AGER* of the receptor for advanced glycation end-products (RAGE) pathway was the top downregulated gene in tumor compared to adjacent normal tissues ($FDR=3.3*10^{-156}$; LFC=-4.4) while *SPP1* of the PI3K/mTORC1 signaling and glycolysis pathways was the top upregulated gene in tumor compare to normal lung tissues ($FDR=3.6*10^{-134}$; LFC=4.8). Pathway enrichment analysis revealed that genes upregulated in tumors compared to normal tissues were most strongly associated with MYC target activation, MTORC1 signaling, glycolysis, and inflammatory responses. Modules defined by WGCNA recapitulated tumor/normal distinctions, suggesting system-level gene programs underlying early tumorigenesis.These preliminary insights from BOLT reveal consistent early transcriptional differences between NSCLC tumors and adjacent normal tissues characterized by upregulation of both novel and known oncogenic pathways and immune/inflammatory responses. Co-expression networks support the tumor/normal status as the principal driver of gene modules at early stages of NSCLC. Modeling time to recurrence remains a critical yet understudied area in lung cancer research. We will develop and validate predictive gene expression signatures and co-expression networks in BOLT to stratify early-stage NSCLC patients by recurrence risk and anticipated time to recurrence following primary treatment or neoadjuvant therapies.

#1103 The genomic landscape of melanoma-prone skin.

Katie Lee[1], Yung-Ching Kao[1], Darren Smit[1], Marietta K. Saldias Montivero[2], Joshua Jay Levy[3], Brock C. Christensen[2], Quan Nguyen[4], H. Peter Soyer[1], **Mitchell S. Stark**[1]

[1]Frazer Institute, University of Queensland, Brisbane, Australia,[2]Dartmouth Geisel School of Medicine, Lebanon, NH,[3]Cedars-Sinai Medical Center, Los Angeles, CA,[4]QIMR Berghofer Medical Research Institute, Herston, Australia

Normal skin carries a high burden of somatic mutations, yet this does not explain where a melanoma will form. From 3D total body photography studies of high-risk individuals, we have observed a trend toward melanoma excisions clustered in regions on the back. This posed the question - are these melanoma-prone skin regions? The PhotoMelanoma Study aimed to determine the genomic architecture of the microenvironment that favours melanoma formation. We assessed photodamaged skin adjacent to an invasive melanoma excision, photodamaged skin 5cm away, and photoprotected skin from the same individual. To address this, we invited 19 study participants from our high-risk melanoma cohort (n=300+) to donate three biopsies for genomic analysis. Firstly, we derived a single-cell whole transcriptome library to determine cell types present at each biopsy site. Next, each biopsy was evaluated for hotspot mutations via the ultra-sensitive droplet digital PCR system; somatic mutation burden, mutation signature, and copy number aberrations via deep panel sequencing of 300+ cancer-related genes (PanelSeq), and global methylation profiling of 900K loci. In brief - as expected, PanelSeq showed UV-related mutation signatures (SBS7) with levels similar the across sun-exposed sites, whereas signature SBS2 (APOBEC activity) was enriched (67%) at the scar-adjacent site, with the number of mutations associated with SBS2 reaching significance (Wilcoxon matched-pair; p=0.015). *BRAF* V600E mutations were significantly enriched near prior melanoma and were present in all sites including sun-protected. Global DNA methylation profiling identified 2000+ loci differentially methylated between photodamaged and photoprotected sites, including HOX family members, and 70 loci were differentially methyated between prior melanoma vs 5cm away, indicating that even with the same level of UV damage, skin sites may be more melanoma-prone. These data are part of a comprehensive genomic and transcriptomic profile to characterise melanocytes, naevi, and the microenvironment to identify the molecular triggers for melanoma formation. In sum, we have uncovered enrichment of somatic events at melanoma excision sites that may provide the soil for de novo melanoma development.

#1104 Detection of bladder cancer via urinary DNA mutation and methylation using modified qPCR.

Di Jin[1], **Roy Tan**[2], Ruiyun Zhang[1], Haige Chen[1]

[1]Ren Ji Hospital, School of Medicine, Shanghai Jiao Tong University, Shanghai, China,[2]Biovuetech Co Ltd, Shanghai, China

Background: Cystoscopy is the gold standard for diagnosing and monitoring bladder cancer (BC), but it is invasive and painful. Previous studies on urine biopsy have shown that urinary DNA mutation and methylation markers are promising auxiliary diagnostic methods; however, current PCR-based methods for detecting gene mutations or methylations are not accurate enough. This shortcoming highlights the urgent need for a more precise DNA marker detection technology and an auxiliary diagnostic method for bladder cancer.
Methods: We developed MTPD-PCR, a highly specific PCR-based detection method that uses dideoxyribonucleic acid (ddNA)-blocking PCR primers and pyrophosphorolysis-activated polymerization to prevent artificially erroneous amplification products that may be introduced by conventional PCR primers, achieving stable detection of mutations with an abundance of 0.01%. We used this method to integrate bladder cancer DNA mutation and methylation biomarkers for non-invasive detection of bladder cancer in urine samples. We conducted a prospective study in a two-center cohort from two tertiary hospitals in China, including 302 patients with histologically confirmed bladder cancer and 200 non-bladder cancer controls. Using cystoscopy combined with histopathological examination as the reference standard, diagnostic accuracy parameters (sensitivity, specificity, and accuracy) were calculated.
Results: The study cohort included 302 patients with bladder cancer, of which 114 (37.8%) were low-grade, 175 (58.0%) were high-grade, and 13 (4.2%) were ungraded. Evaluation of 489 analyzable samples showed an overall sensitivity of 85.9%, a specificity of 95.8% (100% in the healthy control group), and a diagnostic accuracy of 89.8%. The positive predictive value and negative predictive value were 97.0% and 81.3%, respectively. For different non-bladder cancer controls, the sensitivity was 85.95%, and the specificity ranged from 90% to 100%. Clinically significant, the method achieved a sensitivity of 70.3% in 91 early-stage tumors and maintained a sensitivity of 81.7% in a validation set of 191 T1/Tis/Ta stage tumors, indicating good performance across different disease stages.
Conclusion: This method demonstrated good performance in a cohort of 489 patients, exhibiting high sensitivity and accuracy. This non-invasive molecular detection method can detect bladder cancer at an early stage and serve as a treatment reference, especially suitable for cases with low DNA content, potentially reducing the burden of cystoscopy and avoiding unnecessary secondary transurethral resection of bladder tumors.

#1105 Nestin expression is prevalent but highly variable in human cancer: A tissue microarray study involving 5,917 cancers from 107 tumor entities.

Clara von Bargen[1], Muriel Torzewski[1], Fiete Gehrisch[1], Anne Menz[1], Florian Lutz[1], Viktoria Chirico[1], Florian Viehweger[1], David Dum[1], Ria Schlichter[1], Andrea Hinsch[1], Christoph Fraune[1], Chrisitan Bernreuther[1], Seyma Buyucek[1], Martina Kluth[1], Claudia Hube-Magg[1], Georgia Makrypidi-Fraune[1], Nina Schraps[1], Katharina Moller[1], Andreas M Luebke[1], Patrick Lekok[1], Guido Sauter[1], Maximilian Lennartz[1], Till Clauditz[1], Andreas H Marx[2], Ronald Simon[1], Eike Burandt[1], Natalia Gorbokon[1], Maria Chrisitna Tsourlakis[1], Sarah Minner[1], Till Krech[1], Morton Freytag[1], Viktor Reiswich[1], Stefan Steurer[1]

[1]University Medical Center Hamburg-Eppendorf, Hamburg, Germany,[2]Academic Hospital Fuerth, Furth, Germany

Nestin (neuroepithelial stem cell protein) is a class VI intermediate filament protein which is transiently expressed in subsets of precursor cells of the peripheral and the central nervous system, muscle cells and other tissues during development. Upon differentiation, nestin expression becomes replaced by tissue-specific intermediate filament but it can be reinduced in the adult during pathological situations. In cancer, nestin was shown to promote tumor cell proliferation, migration, invasion, and angiogenesis. To determine the prevalence of nestin in cancer, nestin expression was analyzed by immunohistochemistry on tissue microarrays containing 5,917 samples from 107 different tumor types. Nestin positivity occurred in 749 (15.7%) of the 4,775 analyzable tumors, and was considered weak in 8.7%, moderate in 4.3%, and strong in 2.7% of cases. Of 107 tumor entities, 70 (65.4%) showed nestin expression in at least one case, and 22 (20.6%) included at least one case with strong nestin positivity. Highest rates tumors with nestin positivity occurred in pleomorphic adenoma of the parotid gland (100%), gastrointestinal stromal tumor (GIST; 93.8%), metastatic malignant melanoma (75.0%), pheochromocytoma (69.8%), leiomyosarcoma (47.4%), cholangiocarcinoma (40.6%), leiomyoma(40.0%), yolk sac tumor (34.1%), squamous cell carcinoma of the vagina (31.0%), the pharynx (27.3%), vulva (25.6%), anal canal (25.5%), oral cavity (24.7%), penis (19.4%), skin (14.7%), larynx (14.5%), cervix (10.8%), esophagus (9.5%), and the urinary bladder (9.5%), serous carcinoma of the ovary (26.7%), embryonal carcinoma of the testis (26.3%), adenocarcinoma of the cervix (26.1%), endometrioid endometrial carcinoma (22.1%), carcinosarcoma of the uterus(20.8%), pancreatic neuroendocrine tumor (20.7%), muscle-invasive urothelial carcinoma (18.3%), prostatic adenocarcinoma (17.2%), gastric adenocarcinoma of the intestinal type (16.2%), adenocarcinoma of the esophagus(15.1%), urothelial carcinoma of the kidney pelvis (14.3%), and in mucinous carcinoma of the ovary (14.3%). The largest cohort of tumors from one entity included 1,186 evaluable invasive breast cancers of no special type (NST). In these tumors, nestin staining was negative in 94.1%, weak in 3.9%, moderate in 1.3%, and strong in 0.8% of cases. A comparison with tumor phenotype revealed that detectable nestin expression was associated with advanced pT stage ($p=0.0103$), high grade of malignancy ($p<0.0001$), absence of estrogen ($p=0.0054$) and progesterone ($p=0.0051$) receptor expression as well as with “triple negativity” ($p=0.0028$). The data from this study provide an overview of nestin expression in human cancer and demonstrate that increased nestin levels can occur in many different tumor entities. At least in breast cancer NST, nestin positivity goes along with increased cancer aggressiveness.

#1106 Rapid identification of comprehensive multi-omic protein and RNA biomarkers on a single FFPE tissue section using a novel integrated nCounter® workflow.

Lakshmi Chandramohan[1], Kirsteen Maclean[1], Quratul Ain[1], Brigitte Lovell[1], Lisa Duncan[1], Sergio Hernandez[1], Christina Bailey[2], Michael Bailey[2], Patrick Danaher[2], Wei Yang[2], Shanshen He[2], Joseph M. Beechem[2]

[1]NeoGenomics, Fort Myers, FL,[2]Bruker Spatial Biology, Bothell, WA

Background: Biomarker detection approaches capable of rapid identification and quantification of both transcriptomic and proteomic datasets from the same tissue section have become increasingly valuable for investigating the highly complex biology of tumors. Unfortunately, today, the main challenges of true multi-omic analysis of protein and RNA on e.g. FFPE slides are the degradation and cross-linking of molecules from formalin fixation and storage, leading to variable and low-quality nucleic acids and proteins. This degradation, combined with inherent sample heterogeneity, makes it difficult to extract high yields of molecules and requires sophisticated bioinformatic methods to integrate resulting complex and often noisy multi-omics data. To address this need, we have developed and validated a novel workflow using the nCounter® Analysis System that enables simultaneous quantification of mRNA and protein targets from the same slide. This 'multiomics made simple' approach is uniquely enabled by Bruker Spatial Biology's streamlined workflow and direct hybridization chemistry, now accessible and validated through NeoGenomics.
Methods: The core innovation of this workflow lies in its ability to measure both mRNA and protein signal from a single FFPE slide as part of a simple 3-step protocol. Specifically, the assay leverages the harmonization of traditional nCounter mRNA Panels such as the PanCancer IO 360™ panel that measures up to 800 gene expression targets alongside newly designed and optimized Protein Panels capable of analyzing up to 800 proteins within a unified protocol. To validate performance specifications, NeoGenomics, a leading clinical research organization, evaluated this multi-omics application across diverse FFPE sample types, including breast, lung, colorectal, bladder, and urothelial tumors.
Results: Across all tissue types, the streamlined assay demonstrated high specificity, strong correlation between replicate runs, and excellent dynamic range for both mRNA and protein analytes. These results confirm the platform's utility across a wide range of tumor biology contexts and support its adoption for biomarker discovery, target validation, and mechanism-of-action studies. By delivering combined mRNA and protein profiling from a single tissue section, the nCounter platform enables rapid identification of tumor-specific signatures, strengthening biological interpretation and simplifying translational workflow complexity.
Conclusions: This newly validated application, now available through NeoGenomics, empowers research teams to unlock the synergistic power of true tissue multiomics through a simple, scalable, and reproducible workflow—making same-slide mRNA+Protein analysis from FFPE tissue a practical reality for pharma and translational research.

#1107 Development and performance of a multiomics lung cancer screening blood test.

Ofer Shapira, Alexander F. Lovejoy, Alvaro Gonzalez, Urvee Desai, Thomas Royce, Gurnit Atwal, Ian Bast, Eric Beraut, Alexandra Buckley, Austin Cauwels, Peter Combs, Nicholas Eisele, G Parker Flowers, Lourdes Gomez, Rebecca Gupte, Johnnie Hahm, Teng-Kuei Hsu, Saiful Islam, Poorval Joshi, Amanda Kahn-Kirby, Phuong Thuy Menchavez, Erene Mina, Jinesh Niroula, Cameron Pospisil, Sodany Son, Rashmi Sriram, Peter Ulz, Russell Williams, Rui Yang, Wilson Zhang, Marian Navratil, C Jimmy Lin, Tanya Moreno, Richard Bourgon

Freenome Holdings, Inc., South San Francisco, CA

Lung cancer is the leading cause of cancer death in the US. Early detection is crucial for improving survival rates, yet only 18% of eligible high-risk adults (aged 50-80 with ≥20 pack-years of cigarette smoking history) are up to date with recommended annual low-dose computed tomography screening. Non-invasive blood tests could increase screening participation. Here, we evaluate a multiomics approach for lung cancer detection in patients in the intended use population (IUP). Our test uses base-resolution methylation sequencing of circulating cell-free DNA (cfDNA), as previously described, and plasma protein immunoassays. An artificial intelligence/machine learning classifier was trained on tissue (n = 136) and plasma (n = 6,716) samples. Accuracy was evaluated in a cohort of 673 plasma samples, including lung cancer cases (n = 363) and cancer-negative controls (n = 310) from the IUP. This cohort encompassed all cancer stages and three major subtypes — adenocarcinoma, squamous cell carcinoma and small-cell lung cancer (SCLC) — and its age and pack-year smoking history distributions reflected the IUP. Two specificities were considered: 50% (prioritizing sensitivity) and 75% (prioritizing specificity). Reported sensitivities were adjusted for stage and subtype to address differences between the evaluation cohort and literature-reported distributions for the IUP. (Adenocarcinoma and squamous data were weighted per stage and subtype; due to small sample size, SCLC data were weighted only per subtype.) 95% confidence intervals (CIs) were computed via Wilson's method. The multiomics test had an IUP-adjusted sensitivity of 90.7% (CI: 86.8 - 93.7%) at 50% specificity and 80.4% (75.4 - 84.7%) at 75% specificity. Results for a methylation-only test were 85.8% (81.3 - 89.5%) and 78.2% (73.1 - 82.8%), respectively. The multiomics test showed higher sensitivity at both specificities but the differences were not statistically significant. At 50% specificity, the multiomics test had adjusted sensitivity for stages I through IV of 77.7% (73.3 - 89.0%), 95.2% (85.0 - 98.1%), 98.8% (93.6 - 99.7%) and 97.1% (90.7 - 98.9%), respectively. Corresponding results at 75% specificity were 63.5% (51.9 - 71.6%), 89.8% (76.6 - 94.1%), 90.9% (85.0 - 96.3%) and 95.9% (89.8 - 98.6%). At 50% specificity, the multiomics test's adjusted sensitivity for adenocarcinoma and squamous cell carcinoma was 88.7% (81.4 - 92.0%) and 91.1% (84.3 - 96.1%), respectively; nominal sensitivity for SCLC was 97.1% (85.1 - 99.5%). Corresponding results at 75% specificity were 73.0% (63.1 - 77.6%), 88.6% (81.6 - 94.6%) and 91.2% (77.0 - 97.0%). Our multiomics platform demonstrated promising initial performance for blood-based lung cancer detection. The complementary nature of cfDNA methylation and plasma protein may enhance performance relative to a methylation-only approach, and this will be further assessed in a future study with a previously unseen evaluation cohort.

#1108 Performance of an optimized methylation-protein multi-cancer early detection (MCED) test classifier.

Vladimir G. Gainullin[1], Melissa Gray[1], Madhav Kumar[1], Stephen Luebker[1], Amy Lehman[1], Darl D. Flake[1], Avinash Shanmugam[1], Kevin Cortes[1], Emily Chang[1], Philip J. Uren[2], Amin Mazloom[2], Jorge Garces[1], Gerard A. Silvestri[3], David W. Chesla[4], Robert W. Given[5], Tomasz M. Beer[1], **Frank Diehl**[2]

[1]Exact Sciences Corp., Madison, WI,[2]Exact Sciences Corp., La Jolla, CA,[3]Medical University of South Carolina, Charleston, SC,[4]Corewell Health, Grand Rapids, MI,[5]Urology of Virginia, Virginia Beach, VA

Background: Multi-cancer early detection (MCED) tests can detect several cancer types and stages. We previously developed a methylation and protein (MP V1) MCED classifier with a target specificity of ≥98.0% (Gainullin, medRxiv, 2025.08.24.25334244). Herein, we describe a refined MP V2 classifier that was identified based on the evaluation of classifier model architectures that improved performance.

Methods: Compared to MP V1, the MP V2 classifier was trained to achieve increased early-stage sensitivity at a case-control target specificity of ≥97.0%. MP V2 classifier architecture was developed using a training set (654 cancer; 2,373 non-cancer) partitioned into 5-fold cross validation and mini-holdout sets. Locked candidate models were compared using an independent mini-holdout test set (110 cancer; 509 non-cancer). MP V1 and MP V2 classifier performance were compared using a previously described test set (729 cancer; 2,434 non-cancer), and MP V2 performance was also evaluated in an independent clinical validation test set (324 cancer; 800 non-cancer) that was designed to more closely mimic the intended use population.

Results: Compared to MP V1, MP V2 (specificity of 97.4%) demonstrated a 7.3% increase in overall sensitivity, with sensitivity increases of 7.6%, 9.2%, 8.3%, 8.0%, 3.8%, and 13.3% for stages I, II, stages I/II, III, IV, and unknown, respectively, in the test set (Table 1). In the independent validation set, MP V2 (specificity 97.4%; 95% CI: 96.0-98.3%) overall sensitivity was 41.4%, with sensitivities of 16.0%, 31.3%, 22.8%, 52.9%, and 83.1% for stages I, II, stages I/II, III and IV, respectively. Excluding breast and prostate cancers, MP V2 overall sensitivity was 55.6%, with sensitivities of 26.8%, 42.9%, 34.8%, 63.6%, and 89.3% for stages I, II, stages I/II, III, and IV, respectively, in the validation set.

Conclusion: In a case-control setting, the MP V2 classifier offered improved sensitivity for early-stage cancers at a lower specificity target.

Table 1. MP V1 and MP V2 classifier performance in the test set. a breast and prostate excluded.

	MP V1 Classifier Performance (95% CI)	**MP V2 Classifier Performance (95% CI)**
Measured Specificity (N=2,434)	98.5% (97.9-98.9)	97.4% (96.7-97.9)
Overall Sensitivity, all cancers (N=729)	50.9% (47.3-54.5)	57.8% (54.1-61.3)
Stage I (n=182)	15.4% (10.9-21.3)	21.4% (16.1-27.9)
Stage II (n=163)	38.0% (30.9-45.7)	46.0% (38.5-53.7)
Stage III (n=180)	67.8% (60.6-74.2)	76.1% (69.4-81.8)
Stage IV (n=172)	85.5% (79.4-90.0)	89.5% (84.1-93.3)
Unknown Stage (n=32)	37.5% (22.9-54.7)	50.0% (33.6-66.4)
Stages I/II (n=345)	26.1% (21.7-31.0)	33.0% (28.3-38.2)
Overall Sensitivity, (N=590)[a]	56.8% (52.8-60.7)	64.1% (60.1-67.8)
Stage I (n=145)	17.2% (12.0-24.2)	24.8% (18.5-32.4)
Stage II (n=109)	48.6% (39.4-57.9)	57.8% (48.4-66.6)
Stage III (n=151)	73.5% (66.0-79.9)	81.5% (74.5-86.8)
Stage IV (n=155)	86.5% (80.2-91.0)	90.3% (84.6-94.0)
Unknown Stage (n=30)	40.0% (24.6-57.7)	53.3% (36.1-69.8)
Stages I/II (n=254)	30.7% (25.4-36.6)	39.0% (33.2-45.1)

#1109 The complementary contributions of methylation and protein biomarker classes in a multi-cancer early detection (MCED) test.

Vladimir G. Gainullin[1], Melissa Gray[1], Madhav Kumar[1], Stephen Luebker[1], Avinash Shanmugam[1], Kevin Cortes[1], Emily Chang[1], Philip J. Uren[2], Amin Mazloom[2], Jorge Garces[1], Tomasz M. Beer[1], **Frank Diehl**[2]

[1]Exact Sciences Corp., Madison, WI,[2]Exact Sciences Corp., La Jolla, CA

Background: Cancer is a complex disease driven by a multitude of molecular alterations. Multi-cancer early detection (MCED) tests rely on highly sensitive technologies to measure these diverse tumor-associated biomarker classes in blood. A multi-biomarker MCED testing approach may have the potential to detect more cancers than a single biomarker approach, as release of biomarkers into the circulation is driven by different mechanisms. We previously developed a multi-biomarker class (methylation and protein; MP V1) MCED classifier (Gainullin, medRxiv, 2025.08.24.25334244). Herein, we describe the contributions attributable to protein (P) and methylation (M) using a newly developed (MP V2) classifier.

Methods: A prospectively collected case-control study (N=3,163; 729 cancers, 2,434 non-cancers) was used to develop a refined MP V2 classifier. MP V2 was trained to achieve robust early-stage sensitivity at a target specificity of ≥97.0%. M and P classifiers were trained individually; results were combined using a logical OR overarching classifier to generate the final call. MP V2 calls were deemed positive when either the M or P assay provided a positive call. We assessed the percentage of MP V2 positive calls due to P-only, M-only, and M+P (logical AND) positive calls.

Results: Of the 378/590 positive MP V2 calls in the intended use (breast and prostate cancers excluded) cohort, M+P-positive calls were observed in 45.5%, P-only in 7.4%, and M-only in 47.1%. A P-only positive call was observed in 13.9%, 9.5%, 11.1%,6.5%, 5.7%, and 6.3% of stage I (N=36), II (N=63), stages I and II combined (N=99), III (N=123), IV (N=140), and unknown stage (N=16) MP V2 positive calls, respectively. An M-only positive call was observed in 63.9%, 65.1%, 64.6%, 52.0%, 28.6%, and 62.5% of stage I, II, stages I and II combined, III, IV, and unknown stage MP V2 positive calls, respectively. An M+P positive call was observed in 22.2%, 25.4%, 24.2%, 41.5%, 65.7%, and 31.1% of stage I, II, stages I and II combined, III, IV, and unknown stage MP V2 positive calls, respectively. Of the 64/2,434 (2.6%) false positive calls, none were positive for M+P; all false positives were a result of P-only or M-only positive calls.

Conclusions: M and P biomarker classes provide independent contributions for MP V2 classifier positive calls, especially in early-stage (I and II) cases, demonstrating the potential value of adding proteins to methylation analysis in MCED testing. Prospective, real-world evaluation of the MP V2 classifier is currently underway.

#1110 Promote biomarker identification for early detection of head and neck cancers through AHEAD and EDRN programs under the leadership and collaboration between NIDCR and NCI.

Zhong Chen[1], Wendy Wang[2], Guillermo Marquez[2], Jason Wan[3], Sudhir Srivastava[2]

[1]Oral Mucosa & Cancer Biology Program, Chronic Dental, Oral and Craniofacial Conditions Branch, National Institute of Dental & Craniofacial Research, National Institutes of Health, Bethesda, MD,[2]Cancer Biomarkers Branch, Division of Cancer Prevention, National Cancer Institute, National Institutes of Health, Bethesda, MD,[3]Odontogenic Diseases Program, Chronic Dental, Oral and Craniofacial Conditions Branch, National Institute of Dental and Craniofacial Research, National Institutes of Health, Bethesda, MD

The Oral Mucosa & Cancer Biology Program at National Institute of Dental and Craniofacial Research (NIDCR) supports research activities that improve early detection and treatment of cancers of the oral cavity, pharynx, and salivary glands. National Cancer Institute (NCI)'s Early Detection Research Network (EDRN) supports discovery, development, and validation of biomarkers and imaging methods for early detection and risk assessment of cancer, translating these discoveries into clinical tests. NIDCR and NCI have a long-standing collaborative relationship and jointly launched the AHEAD Program (Advancing Head and Neck Cancer Early Detection) in 2023. The AHEAD program co-funds seven research projects aimed at discovering and developing molecular signatures of early detection and diagnosis of HPV positive and negative head and neck cancer (HNC). The AHEAD leadership team and investigators actively participated in the EDRN Lung and Upper Aerodigestive Cancers Collaborative Group and have shared their work widely through national and international conference presentations and publications in high-impact journals. AHEAD investigators have also organized and led symposia and workshops at major scientific meetings to raise awareness of early detection and diagnosis of HNC. Ongoing AHEAD activities include identifying and validating biomarkers for early detection, creating a virtual tumor bank of oral potentially malignant disorders, conducting spatial transcriptomics analyses to identify high priority biomarkers, and publishing papers to describe AHEAD activities and progress. At the 2026 AACR Annual Meeting, NIDCR and NCI program directors will present an overview of the AHEAD program, highlighting collaborative efforts and funding opportunities between the two institutes, with an emphasis on early cancer detection and biomarker discovery and validation. This collaboration between NIDCR and NCI provides a unique and powerful platform to advance basic, translational, and clinical research aimed at improving early detection of head and neck cancer and ultimately benefiting patients.

#1111 Promoting awareness and enhancing access to low-dose computed tomography screening for early detection of lung cancer in underrepresented minority communities in Northern Illinois.

Subaranjana Saravanaguru Vasanthi[1], Georgia Kapetaneas[2], Rose Bahari[2], Shylendra B Sreenivasappa[3], Nameer Mardini[4], Sandra Martell[5], Joseph Ross[6], Yamile Molina[7], Neelu Puri[1]

[1]Department of Biomedical Sciences, University of Illinois College of Medicine (Rockford), Rockford, IL,[2]College of Medicine, University of Illinois College of Medicine (Rockford), Rockford, IL,[3]Department of Hematology Oncology, OSF Saint Anthony Medical Center, Rockford, IL,[4]Department of Oncology, UW Health Swedish American Carbone Cancer Center, Rockford, IL,[5]Public Health Administrator, Winnebago County Health Department, Rockford, IL,[6]Clinical Family and Community Medicine, University of Illinois College of Medicine (Rockford), Rockford, IL,[7]Associate Director, Community Outreach and Engagement, University of Illinois College of Medicine (Rockford), Rockford, IL

Background: Lung cancer remains one of the leading causes of cancer-related deaths in the United States, posing a persistent and inequitable public health challenge. In 2025, an estimated 226,650 new cases and 124,730 deaths are expected, disproportionately affecting racially and ethnically underrepresented minority communities. It's high mortality rate is partially due to the fact that ~75% of new cases are diagnosed in late stages. As of 2022, the age-adjusted mortality rates of Winnebago County and Ogle County are 22% and 30% higher than the national rate respectively. In the National Lung Screening trial (NLST), 90.9% of participants were white, 4.5% were African American, and 1.8% were Hispanic, highlighting the need for more widespread implementation of early-stage lung cancer screening. Low dose computed tomography (LDCT) is a valuable screening tool that utilizes ~90% less ionizing radiation than conventional chest CT scans.
Hypothesis/Aims: Increased awareness of LDCT in clinical and community settings will lead to higher rates of lung cancer detection at early-stages, reduce mortality and improve prognosis.
Study Design: We implemented a multifaceted approach to promote Low-Dose Computed Tomography (LDCT) screenings in four Illinois counties - Winnebago, Boone, Ogle, and Stephenson. We conducted community outreach through booths at minority-centered events, educating community members and physicians on the US Preventive Services Task Force (USPSTF) and ACS set LDCT guidelines. Participant ethnicity and their zip codes were recorded. To evaluate the impact of our efforts, hospital data from June 2015 to December 2025 were analyzed for LDCT screenings and lung cancer cases.
Results: From June 2015 to April 2026, 28 seminars and 76 public awareness booths targeting 3,055 people, with an estimated 335 physicians and 2,720 smokers were conducted to promote LDCT screening. Our outreach work reached 21.5% of Hispanics and 36.5% of African Americans out of 13,997 total LDCT screenings. There were 13,997 total LDCT screenings conducted, detecting 181 lung cancer cases, with 110 cases being diagnosed at early stages in our partnered local hospitals. Among all individuals who underwent LDCT screenings, ~86% were White, 8% were African American, 2% were Hispanic, and 1% were Asian and the rest 3% were other populations.
Conclusion: Rural and minority communities remain underrepresented in LDCT screenings for lung cancer. Thus, continued efforts to promote lung cancer screening and awareness in rural and minority communities may increase the rate of early detection of lung cancer among smokers, which is the primary goal of our study.

#1112 Circulating early myeloid-derived suppressor cells as indicators of tumor-driven myelopoiesis and disease progression in lung cancer.

Anna Zanichelli, Orazio Fortunato, Mara Lecchi, Paolo Verderio, Luigi Rolli, Ugo Pastorino, Gabriella Sozzi, Claudia Chiodoni, Sabina Sangaletti

Fondazione IRCCS Istituto Nazionale dei Tumori, Milan, Italy

Background: Lung cancer (LC) remains the leading cause of cancer-related mortality worldwide. Despite major therapeutic advances, LC patients still experience poor prognosis. Increasing evidence indicates that tumor-driven hematopoietic remodeling and systemic inflammation actively sustain immune suppression and disease progression. The expansion of immature myeloid populations, particularly myeloid-derived suppressor cells (MDSCs), represents a hallmark of tumor-induced emergency myelopoiesis. However, the composition and developmental hierarchy of circulating MDSC subsets remain unclear. Here, we identify a previously unrecognized subset of circulating early MDSCs (eMDSCs) that mirrors tumor-driven myelopoietic activation and lung cancer progression.
Methods: In a prospective discovery cohort including LC patients (n=63) and heavy smokers without cancer (HS, n=52), circulating myeloid subsets were characterized from fresh peripheral blood. Multiparametric flow cytometry enabled comprehensive profiling of peripheral blood mononuclear cells (PBMCs). eMDSCs were defined as $CD11b^{+}CD33^{+}CD15^{-}$ within the $Lineage^{-}HLA\text{-}DR^{-}$ compartment. A retrospective validation cohort (LC, n=58; HS, n=58), matched for sex, age, and smoking status, confirmed the findings and explored associations with tumor stage and COPD-related inflammation. FACS-sorted eMDSCs from representative LC and HS samples underwent qPCR analysis for PD-L1 and ARG1 expression. Statistical analyses were performed using the Kruskal-Wallis (KW) and Wilcoxon (WILC) tests.
Results: In both discovery and validation cohorts (total n=231), LC patients displayed an increased enrichment of circulating $CD11b^{+}$ myeloid populations (WILC test p-value: non-significant p=0.052, p=0.001), particularly $Lin^{-}HLA\text{-}DR^{-}CD33^{+}CD11b^{+}$ MDSCs (WILC test p-value: p<0.0001, p=0.009). Within this population, a distinct immature subset of $CD15^{-}$ early MDSCs was identified (WILC test p-value: p<0.0001, p=0.014) and found to be specifically increased in stage II-III LC, but not further expanded at stage IV (KW test p-value: p=0.015). No association emerged between eMDSC levels and COPD-related inflammation, supporting a tumor-specific expansion. Moreover, NK cell frequencies increased in parallel with eMDSCs, suggesting a functional interplay, as eMDSCs may suppress NK activity (KW test p-value: p=0.002). Consistently, qPCR analysis revealed higher PD-L1 and ARG1 expression in LC-derived eMDSCs compared with HS, indicating their immunoregulatory polarization.
Conclusion: Our findings identify circulating early MDSCs as a hallmark of lung cancer-associated emergency myelopoiesis. Their selective expansion in stage II-III disease supports their potential as circulating biomarkers to identify and monitor tumor-driven myelopoietic activation and lung cancer progression.

#1113 Clinical validation of a targeted multi-cancer early detection (MCED) test using cfDNA mutation and integrated genomic signatures analysis.

Chee-Onn Leong[1], Boon Shing Tan[1], Hiu Ching Toh[1], Ee Mun Loo[1], Anand Mohan[1], Teryna Thu[1], Zhi Win Ng[2], Xin Yi Chew[1], Chin King Looi[2], Felicia Fei Lei Chung[3], Chun Wai Mai[2]

[1]AGTC Genomics, Kuala Lumpur, Malaysia,[2]International Medical University, Kuala Lumpur, Malaysia,[3]Sunway University, Kuala Lumpur, Malaysia

Early cancer detection significantly improves survival, particularly for high-burden cancers across Asia that are often diagnosed late. Plasma-derived cell-free DNA (cfDNA) is a promising non-invasive biomarker for identifying cancer earlier than conventional methods. This study evaluated the performance of a targeted multi-cancer early detection (MCED) test that analyzes tumour-associated mutations in cfDNA to detect 20 cancer types commonly seen in Asian populations. In this retrospective, multicentre validation study, participants aged ≥20 years with either confirmed cancer or cancer-free status were recruited. Plasma cfDNA was sequenced using a targeted panel constructed from large genomic datasets. Machine learning models were trained and validated in a blinded manner to assess diagnostic performance. Among 2342 cancer cases and 1646 controls, the MCED test achieved a sensitivity of 83.1% (95% CI: 81.5-84.6%) and specificity of 95.4% (95% CI: 94.4-96.4%), with a false-positive rate of 4.6%. Performance surpassed that of traditional biomarkers such as CEA. Notably, high sensitivity was observed in cancers of major concern in Asia—liver, gastric, pancreatic, bile duct, and nasopharyngeal cancers—with early-stage detection ranging from 75.0-91.3% and late-stage detection from 95.5-100%. These findings support the potential of cfDNA-based MCED testing as a non-invasive, complementary screening approach for populations in Asia. Its strong performance across multiple high-mortality cancers underscores its value for early detection, risk stratification, and integration into regional cancer control strategies.

#1114 Informatics-Driven Integration of OpenMRS and iBreastCheck to Strengthen Community-Based Cancer Screening in Ethiopia.

Tsedey Michele Tsegaye, Mukesh kumar Patel, Tulay Soylu

Collage of public health, Temple University, Philadelphia, PA

Background: Ethiopia faces a rising and disproportionate cancer burden, particularly among women, with breast, cervical, and colorectal cancers representing majority of cases. Limited healthcare infrastructure, fragmented data systems, and late-stage detection contribute to high mortality rates, especially in rural areas where access to oncology services is constrained. These systemic gaps highlight the urgent need for integrated, scalable, and data-driven solutions to improve early detection, care coordination, and health information management across all levels of the healthcare system. Objective: This study aims to design and propose an informatics-enhanced model that will integrate a customized OpenMRS electronic medical record platform with the mHealth application iBreastCheck to strengthen cancer screening, data interoperability, and referral pathways in Ethiopia. The model will be tailored to leverage existing community health structures specifically Health Extension Workers (HEWs) and designed to function in low-connectivity settings, with the goal of improving early cancer detection and standardizing oncology data capture. Methods: A multi-phase implementation approach will be employed, beginning with stakeholder interviews and training of HEWs on iBreastCheck for community-based breast cancer education and risk assessment. In parallel, OpenMRS will be customized and deployed with oncology-specific modules to support interoperability, using HL7 and XML standards for data exchange, and configured for offline functionality. The system design will emphasize open-source technologies, SQL-based data querying, and integration with national digital health infrastructure, supported by partnerships with the Ethiopian Ministry of Health, WHO, and NGOs. Results: The integrated OpenMRS and iBreastCheck model is projected to enhance cancer data completeness, improve screening participation through community health workers, and reduce diagnostic delays. By enabling standardized digital workflows and facilitating communication between community and clinical levels, the system will support more timely referrals and consistent protocol adherence. The use of offline-capable, interoperable tools will ensure functionality even in settings with limited internet connectivity, broadening accessibility across rural and underserved regions. Conclusion: The combination of OpenMRS and mHealth technologies offers a feasible and Scalable, model for improving cancer screening and care coordination in low-resource settings like Ethiopia. By aligning technology design with local infrastructure and human resource capacities, this approach addresses critical gaps in the oncology care continuum and provides a replicable framework for other low- and middle-income countries implementing digital health solutions for cancer control.

#1115 Expression of annexin A4 in cancer: A tissue microarray study involving 6,058 cancers from 105 tumor entities.

Cosima Volkel[1], Nayma Malas[1], Fiete Gehrisch[1], Nina Schraps[1], Anne Menz[1], Florian Lutz[1], Viktoria Chirico[1], Florian Viehweger[1], David Dum[1], Ria Schlichter[1], Andrea Hinsch[1], Christoph Fraune[1], Christian Bernreuther[1], Seyma Buyucek[1], Martina Kluth[1], Claudia Hube-Magg[1], Georgia Makrypidi-Fraune[1], Katharina Moller[1], Andreas M. Luebke[1], Patrick Lebok[1], Guido Sauter[1], Maximilian Lennartz[1], Till S. Clauditz[1], Andreas H. Marx[2], Ronald Simon[1], Eike Burandt[1], Natalia Gorbokon[1], Maria C. Tsourlakis[1], Sarah Minner[1], Till Krech[1], Morton Freytag[1], Viktor Reiswich[1], Stefan Steurer[1]

[1]Institute of Pathology, University Medical Center Hamburg-Eppendorf, Hamburg, Germany,[2]Department of Pathology, Academic Hospital Fuerth, Fuerth, Germany

Annexin A4 (ANXA4) is a member of the annexin family of calcium-dependent phospholipid-binding proteins. In line with its capability to bind to phospholipid membranes, it has roles in processes related to membrane dynamics such as membrane trafficking, vesicle aggregation, membrane organization, and ion channel regulation. ANXA4 dysregulation can contribute to abnormal cell migration, proliferation, and resistance to apoptosis. ANXA4 overexpression has been described in several cancer types and has been linked to tumor aggressiveness and treatment resistance. Due to its differential expression in tumors versus normal tissues, ANXA4 is being investigated as a diagnostic biomarker. To learn more on the role of ANXA4 in cancer, ANXA4 expression was analyzed by immunohistochemistry (IHC) on tissue microarrays (TMAs) containing 6,058 samples from 105 different tumor types. ANXA4 staining was seen in 3,649 (75.4%) of the 4,839 analyzable tumors, and was considered weak in 11.3%, moderate in 17.5%, and strong in 46.6% of cases. Of 105 tumor categories, 100 (95.2%) showed ANXA4 expression in at least one case, 92 (87.6%) showed ANXA4 staining in more than 50% of cases, and 90 (85.7%) included at least one case with strong ANXA4 positivity. Highest rates of strong ANXA4 positivity occurred in adenocarcinoma of the ampulla Vateri (100%) and ductal adenocarcinoma of the pancreas (96.0%), gallbladder adenocarcinoma (100%), gastric adenocarcinoma (93.0-99.1%), clear cell (97.7%), papillary (97.4%) and chromophobe (94.9%) renal cell carcinoma (RCC), Brenner tumor (96.4%), colorectal adenocarcinoma (95.0%), clear cell carcinoma of the ovary (94.7%), adenocarcinoma of the esophagus (94.7%), oncocytoma od the kidney (94.6%), hepatocellular carcinoma (91.8%), mucinous carcinoma of the ovary (90.9%), cholangiocarcinoma of the liver (88.6%), adenocarcinoma of the cervix uteri (87.0%), endometrioid endometrial carcinoma (76.1%), endometrioid carcinoma of the ovary (66.7%), and in urothelial carcinoma of the kidney pelvis (66.7%). The 1,219 evaluable breast cancers of no specific type (NST) represented the largest subset of tumors from one entity. In these tumors, ANXA4 staining was negative in 642 (52.7%), weak in 84 (6.9%), moderate in 169 (13.9%), and strong in 324 (26.6%) cases. A comparison with tumor phenotype revealed that low ANXA4 expression was linked to advanced pT-stage ($p<0.0001$), high grade of malignancy ($p=0.0018$), and nodal metastasis ($p=0.0247$). In summary, our data provide a comprehensive overview on ANXA4 expression in cancer. They demonstrate, that ANXA4 is often expressed at high levels in a broad range of different tumor entities. At least in breast cancer NST, a low level of ANXA4 expression is a feature of high cancer aggressiveness.

#1116 A scalable multimodal framework for unbiased risk biomarker discovery across multiple cancer types.

Constantin Petrescu, Lisa Schmunk, Jack Monahan, Abbas Salami, **Thomas M. Stubbs**

Hurdle.bio/Chronomics Ltd., London, UK, United Kingdom

Background: Most existing cancer risk models are built on single modalities and hand-selected features. Systematic, unbiased integration of germline genetics, plasma proteomics, and deep clinical phenotyping holds promise for revealing novel risk biomarkers across diverse cancer types.
Methods: We developed a multi-modal biomarker discovery engine that can be used for discovering risk, diagnostic, prognostic, predictive and monitoring biomarkers. Currently the framework handles:

- Germline genetics and polygenic risk scores
- High-dimensional plasma proteomics (Olink)
- Longitudinal primary-care records, hospital episodes, laboratory results, lifestyle questionnaires, and cancer registry linkages

Key design features include modular cohort handling, automated data preprocessing, and machine-learning models (including: gradient boosting and neural networks).
Application: The platform is currently deployed on the UK Biobank (n = 502,505 participants; >46,000 incident cancers across 22 cancer types) with active model training and biomarker discovery in progress. The architecture is cohort-agnostic and ready for direct application to emerging large-scale resources including Our Future Health and the All of Us Research Program.
Poster presentation: We will demonstrate the platform's configurability through examples of cancer-risk modelling in the UK Biobank, showcasing: (i) comparative performance of individual modalities versus multimodal ensembles, (ii) cancer-specific patterns of modality contribution, and (iii) the effect of time-window filtering on separating true predictive signals from prevalent disease effects.
Conclusions: By eliminating bias in feature engineering and supporting seamless integration of diverse health data streams, this scalable framework provides a robust foundation for data-driven discovery of multimodal cancer risk biomarkers, paving the way for next-generation precision prevention strategies.

: Liquid Biopsies: Circulating Nucleic Acids 1
Poster Session

#1121 Detection of postoperative minimal residual disease in colorectal cancer using a novel ultrasensitive whole-genome sequencing-based ctDNA test.

Maria Honholt[1], Tenna V. Henriksen[1], Mads H. Rasmussen[1], Christina Demuth[1], Thomas Kolbro[2], Peter Bondeven[3], Jeppe Kildsig[4], Per V. Andersen[5], Anders Tottrup[6], Nis H. Schlesinger[7], Claudia Jaensch[8], Ole Thorlacius-Ussing[9], Christensen Peter[10], Alessio Monti[11], Yingyu Wang[12], Tam Berntsen[12], George Yeung[12], Paul Tang[12], Tobias Wittkop[12], Malek Faham[12], Li Weng[12], Lene Hjerrild Iversen[13], Kare A. Gotschalck[14], Claus L. Andersen[1]

[1]Department of Molecular Medicine, Aarhus University and Aarhus University Hospital, Aarhus, Denmark,[2]Odense University Hospital, Odense, Denmark,[3]Aarhus University Hospital, Aarhus, Denmark,[4]Department of Surgery, Copenhagen University Hospital, Herlev, Denmark,[5]Department of Surgery, Odense University Hospital, Odense, Denmark,[6]Department of Surgery, Regional Hospital Viborg, Viborg, Denmark,[7]Department of Surgery, Copenhagen University Hospital, Bispebjerg, Denmark,[8]Department of Surgery, Regional Hospital Godstrup, Herning, Denmark,[9]Department of Gastrointestinal Surgery, Aalborg University Hospital, Aalborg, Denmark,[10]Department of Surgery, Aarhus University Hospital, Aarhus, Denmark,[11]Department of Surgery, North Denmark Regional Hospital Hjorring, Hjorring, Denmark,[12]AccuraGen, Inc., San Jose, CA,[13]Department of Surgical Oncology, Aalborg University Hospital, Aalborg, Denmark,[14]Department of Surgery, Regional Hospital Horsens, Horsens, Denmark

Introduction:
Accurate detection of minimal residual disease (MRD) after curative intent surgery remains a major limitation in colorectal cancer (CRC) management. Current ctDNA assays identify only 30-50% of patients who later develop clinical recurrence, restricting their utility for both escalation and safe de-escalation of adjuvant therapy. We evaluated a novel, ultrasensitive, tumor-informed, whole-genome sequencing (WGS)-based ctDNA test engineered to maximize detection sensitivity while simplifying clinical implementation by eliminating the need for bespoke patient-specific capture panels, reducing turnaround time, and requiring only 1mL of plasma.
Methods:
Pre- and postoperative plasma samples (drawn 14 and 30 days after operation) from 300 stage II-III CRC patients (median follow-up 35.7 months) were collected. At the time of abstract submission, 161 patients have been analyzed, but complete cohort results (n = 300) will be presented at AACR 2026. The test (*AccuScan*) utilizes rolling-circle amplification to convert single-stranded cfDNA into concatemers, enabling >1000-fold error suppression at modest sequencing depth (median 28×). Tumor-informed variant tracking was derived from paired tumor/germline WGS. ctDNA detection was done blinded to clinical information. Performance was evaluated against recurrence outcomes.
Results:
Among the 161 analyzed patients, 43 (26.7%) recurred. A median of 11,822 tumor-derived variants per patient were tracked with a mean error rate of 4.97×10^{-7}. Preoperatively, the novel WGS test detected ctDNA in 98.1% of samples. Postoperatively, ctDNA was detected in at least one sample (day 14 or 30) in 69.8% of recurrence patients with a specificity of 91.5%. Sensitivity and specificity were 55.8% and 96.6% at day 14 and 62.8% and 94.1% at day 30. ctDNA levels in recurrence patients reached as low as 2.7 ppm (median 162 ppm). Extrapolating the performance to an unselected stage III population indicates a ~10% 3-year recurrence rate for postoperative ctDNA-negative individuals, comparable to low-risk stage II disease, for which adjuvant therapy is generally not recommended. Postoperative ctDNA status was a strong predictor of recurrence-free survival (HR 11.9; 95% CI, 6.2-23.1; p<0.001). In a head-to-head comparison, tumor-informed digital PCR using 8mL plasma aliquots achieved substantially lower sensitivity both preoperative (75.4%) and postoperative (33.3% day 14; 51.5% day 30).
Conclusion:
The novel WGS-based test delivers exceptional sensitivity in both preoperative and postoperative settings while requiring minimal plasma. The streamlined workflow is compatible with real-world clinical implementation. Sensitive detection at day 14 offers an opportunity for earlier therapeutic intervention, and the assay's performance supports its use in future therapy de-escalation trials.

#1122 Methylation-based tumor fraction monitoring identifies patients with putative molecular progression who may benefit from comprehensive genomic profiling.

Jun Zhao[1], Rihao Qu[1], Katie Quinn[1], Tingting Jiang[1], Jack Tung[1], Carin R. Espenschied[2], Samantha I. Liang[3], Vishnu Ramani[1], Jing Wang[1], Sean Gordon[1], Martina Lefterova[1], Darya Chudova[1]

[1]Guardant Health, Palo Alto, CA,[2]Guardant Health, Spokane, WA,[3]Parker Institute for Cancer Immunotherapy, San Francisco, CA

Background: Longitudinal monitoring of circulating tumor DNA (ctDNA) using methylation-based tumor fraction (TF) provides sensitive detection of disease dynamics in cancer patients over time. Patients with increasing TF may be undergoing molecular progression (MP) preceding clinical progression. They may have developed clinically relevant variants (CRVs, associated with response or resistance to targeted therapies) detectable by comprehensive genomic profiling (CGP) that can guide treatment options. Here, we describe a workflow that applies TF change thresholds to identify patients with putative MP, maximizing detection of CRVs.
Methods: To establish the thresholds for significant TF change, we used in-silico dilutions (ISD) from clinical samples to train an input-dependent model targeting 90% analytical specificity. We also determined an absolute TF threshold to maximize detection of CRVs. These thresholds were analytically evaluated by comparing two aliquots from the same blood draw (n=1061, simulating “no TF change” between consecutive samples), as well as longitudinal pan-cancer samples from patients undergoing treatment (n=2103, representing real-world TF changes). The model was also clinically evaluated in the RADIOHEAD cohort[1] (n=116) in which patients with advanced solid tumors received standard-of-care immune checkpoint inhibitors (ICI). Adjusted hazard ratios (aHR) and p-values (p) were determined via Cox proportional hazards with sex, age, and baseline TF as covariates.
Results: Significant TF change between consecutive timepoints of >50% increase, along with an absolute TF of >0.1% were yielded from simulation and optimization approach as thresholds for putative MP assessment. When evaluated in replicate plasma samples that simulate no biological change, these thresholds demonstrated empirical specificity of 97%. In serial samples from advanced cancer patients undergoing treatment, 29.5% met the criteria for MP. Critically, 55% of patients with putative MP harbored CRVs not detected at baseline. In the RADIOHEAD cohort, patients with putative MP had significantly worse real-world progression-free survival (rwPFS) compared to those with stable/decreasing TF (HR=4.30, 95% CI: 2.93-6.33, p<0.001). Among patients with putative MP, 65.1% had new CRVs, compared to 26.2% in patients with TF decrease.
Conclusions: We developed criteria for putative MP that achieve 97% specificity and are associated with shorter rwPFS in patients receiving ICI. CGP in patients meeting these criteria detects new actionable variants in 55-65% of cases, supporting its utility for guiding therapeutic decision-making upon MP during longitudinal ctDNA monitoring.

References

1. Liang S, *et al. Cancer Res Commun.* 2025;5(8):1384.

#1123 Machine learning classifier for cancer type identification via multi-feature genome-wide cfDNA profiling.

Yunjian Zhang[1], Liang Liu[2], Hua Bao[3], **Haimeng Tang**[3], Ke Xu[3], Hao Zhang[4], Song Wang[3], Shuang Chang[3], Dongqin Zhu[3], Zongyao Huang[5], Zheng Wang[2], Liu Yang[6], Bingzhong Zhang[7], Ji Tao[8], Wenhua Liang[9], Jierong Chen[10], Shanshan Yang[3], Xue Wu[3], Yang Shao[3], Wenquan Wang[2], Dongyuan Zhu[11]

[1]First Affiliated Hospital of Sun Yat-sen University, Guangzhou, China,[2]Zhongshan Hospital, Fudan University, Shanghai, China,[3]Geneseeq Techonolgy Inc., Toronto, ON, Canada,[4]Xuzhou Medical University, Affiliated Hospital of Xuzhou Medical University, Xuzhou, China,[5]University of Electronic Science and Technology of China, Sichuan Cancer Hospital & Institute, Chengdu, China,[6]Colorectal Center, Jiangsu Cancer Hospital, Nanjing, China,[7]Sun Yat-sen Memorial Hospital, Sun Yat-sen University, Guangzhou, China,[8]Harbin Medical University Cancer Hospital, Harbin, China,[9]The First Affiliated Hospital of Guangzhou Medical University, Guangzhou, China,[10]Guangdong Provincial People's Hospital, Guangzhou, China,[11]Shandong First Medical University and Shandong Academy of Medical Sciences, Jinan, China

Background: Determination of the tissue of origin (TOO) of cancer is essential for appropriate clinical management and treatment selection. Liquid biopsy using circulating cell-free DNA (cfDNA) offers a non-invasive approach for cancer detection and TOO prediction. Circulating tumor DNA (ctDNA), a tumor-derived fraction of cfDNA, carries genomic and epigenomic signatures reflective of its origin. Recent advances in machine learning have enable the development of models to predict TOO from cfDNA profiles. However, current methods show variable performance, particularly in samples with low ctDNA fractions (ctDNA < 3%), and accuracy remains inconsistent across different cancer types.

Methods: We developed a TOO classifier using whole genome cfDNA profiles from 1814 patients across 17 cancer types. Multiple distinct cfDNA features were extracted to reveal diverse cancer-associated alterations, including copy number variations, repeat elements, fragment end motifs associated with DNA methylation, fragment size distribution and coverage, microsatellite instability, mutational signatures, nucleosome occupancy, tissue-specific fragmentation patterns, and the presence of cancer-associated viral DNA. Model performance was evaluated in an independent external cohort of 1221 patients. Additional tests were conducted in cohorts of patients with cancers of unknown primary (CUP) and multiple primary cancers (MPC).

Results: Our cancer classifier achieved an overall top 1 accuracy of 78% and top 2 accuracy of 89% in the training cohort, with consistently high accuracy across all cancer types. In the independent validation cohort, the model maintained robust performance, with top 1 and top 2 accuracies of 80% and 90%, respectively. Sensitivity increased with the advancing cancer stage, improving from 66.8% in stage I to 86.2% in stage IV. Among 612 low-ctDNA samples, 435 cases (71.1%) were correctly classified. The classifier also showed strong potential in CUP, with 11 of 15 cases (73.3%) aligning with the clinically suspected primary site. Furthermore, among 20 MPC cases with two primary sites, both were correctly identified within the top three predictions in 9 cases. In 3 MPC patients with three primary sites, two of the three sites were accurately captured among the top three predictions.

Conclusion: Our cfDNA-based machine learning classifier provides a robust, non-invasive approach for accurate cancer tissue-of-origin identification. Integrating 11 distinct cfDNA-derived fragmentomic, genomic, epigenomic, and microbiomic features, the model achieved high accuracy across multiple cancer types and maintained strong performance in low-ctDNA samples. Its promising results in CUP and MPC further highlight its potential clinical utility in resolving diagnostically challenging cases and guiding precision oncology applications.

#1124 cfDNA fragmentomics enables sensitive early detection and tissue-of-origin prediction in gynecologic cancers.

Jin Li[1], Xun Zhang[2], Song Wang[3], Xiaoying Wu[3], Jinpeng Zhang[3], Hua Bao[3], Shanhui Liang[1], Xiaotian Han[1], Jiangchun Wu[1], Hao Wen[1], Hairong Bao[3], **Haimeng Tang**[3], Xue Wu[3], Xiaohua Wu[1], Zhao Wu[2], Xiaoqiu Li[4]

[1]Department of Gynecologic Oncology, Fudan University Shanghai Cancer Center, Shanghai, China,[2]Department of Obstetrics and Gynecology, Sichuan Provincial People's Hospital, Chengdu, China,[3]Nanjing Geneseeq Technology Inc., Nanjing, China,[4]Department of Pathology, Fudan University Shanghai Cancer Center, Shanghai, China

Background: Early detection of gynecologic cancers remains challenging due to nonspecific symptoms and limited sensitivity of conventional biomarkers. We aimed to develop and validate cfDNA-based models for cancer detection and tissue-of-origin (TOO) classification.

Methods: We prospectively enrolled 1,007 participants from two hospitals, of whom 763 passed eligibility and quality control. The training set (N=363; 173 cancer, 190 non-cancer) was used to develop models integrating four cfDNA features reflecting fragmentation, chromatin architecture, and epigenetic regulation via machine learning. The internal test set (N=158; 86 cancer, 72 non-cancer) and an independent external test set (N=242; 127 cancer, 115 non-cancer) were used for validation.

Results: The diagnostic model achieved area under the curve (AUC) values of 0.974 (95% confidence interval [CI]: 0.954-0.994) and 0.975 (95% CI: 0.959-0.992) in the internal and external cohorts, with sensitivities of 83.7% and 82.7% at 98% specificity. High performance was observed across ovarian (AUC: 0.992 and 0.999), cervical (AUC: 0.972 and 0.989), and endometrial (AUC: 0.948 and 0.937) cancers, including stage I disease (AUC: 0.955 and 0.961). The model detected over 77% of cancers that were missed by CA125. Interception modeling projected a 26.4-68.9% increase in stage I diagnoses and 11.6-37.8% 5-year survival gains. The TOO model achieved >73% overall accuracy, with the highest accuracy for ovarian (81.3-86.7%), followed by cervical (70.7-73.3%) and endometrial (59.1-62.7%) cancers. Analytical validation demonstrated robust performance even at ultra-low sequencing depths of 1x, supporting scalability for population screening.

Conclusions: cfDNA fragmentomics enables sensitive detection and tissue-of-origin classification of gynecologic cancers, complementing conventional biomarkers. These models hold promise for cost-effective, population-level early detection and risk stratification.

#1125 Characterizing the cfDNA fragmentome in patients with hepatocellular carcinoma.

Hope Orjuela[1], Carter Norton[1], Shashikant Koul[1], Daniel C. Bruhm[1], Akshaya V. Annapragada[1], Sarah Short[1], Keerti Boyapati[1], Adrianna Bartolomucci[1], Vilmos Adleff[1], Nicholas A. Vulpescu[1], Kaui Lebarbenchon[1], Jacob Carey[2], Carter Portwood[2], Andrei Sorop[3], Razvan Iacob[3], Speranta Iacob[3], Liana Gheorghe[3], Simoni Dima[3], Katherine A. McGlynn[4], Manuel Ramirez-Zea[5], Jillian Phallen[1], Robert B. Scharpf[1], John Groopman[1], Victor E. Velculescu[1], Zachariah Foda[1]

[1]The Sidney Kimmel Comprehensive Cancer Center, Johns Hopkins University School of Medicine, Baltimore, MD,[2]DELFI Diagnostics, Baltimore, MD,[3]Center of Digestive Diseases and Liver Transplantation, Fundeni Clinical Institute, Bucharest, Romania,[4]Division of Cancer Epidemiology and Genetics, National Cancer Institute, Rockville, MD,[5]Research Center for the Prevention of Chronic Diseases, Institute of Nutrition of Central American and Panama (INCAP), Guatemala City, Guatemala

Hepatocellular carcinoma (HCC) is the third leading cause of cancer death globally and is one of the most rapidly increasing causes of cancer mortality in North America and Europe due to metabolic and emerging risk factors. Here, we show that cell-free DNA (cfDNA) fragmentation profiles reflected underlying disease biology and that a machine learning classifier detected HCC across diverse populations and was enhanced by incorporating patient clinical risk and protein concentrations. Characteristics of the cfDNA fragmentome, including genome-wide chromatin, repeat elements, methylome, and mutational profiles, were altered in patients with HCC, including those with metabolic risk factors and aflatoxin exposure. Novel whole-genome tissue-of-origin deconvolution analyses identified increased representation of cfDNA originating from hepatocytes ($p=2.4x10^{-10}$) and CD8+ T cells ($p=5.8x10^{-7}$) and decreased contribution of NK cells ($p=3.0x10^{-6}$) in patients with cancer. Using a previously locked fragmentome classifier for liver cancer detection, we analyzed 377 individuals with and without HCC from two distinct geographic cohorts. We found that the cfDNA fragmentome classifier detected HCC across all stages and diverse etiologies with a sensitivity of 70% (95% CI=65%-75%) and specificity of 94% (95% CI=90%-97%), outperforming the commonly used alpha-fetoprotein (AFP) biomarker which had a sensitivity of 62% (95% CI=57%-67%) and specificity of 93% (95% CI=88%-96%). A combined approach using cfDNA fragmentomes, AFP, and clinical risk achieved a sensitivity of 74% (95% CI=66%-80%) at a specificity of 85% (95% CI=78%-89%) in transplant curable disease (Milan criteria) in both cohorts and was more sensitive than standard-of-care AFP and ultrasound performance for early-stage disease (reported 63% sensitivity at 84% specificity). This study provides insights into the origins of altered cfDNA and circulating proteins for populations at risk of liver cancer and supports the use of a genome-wide fragmentome approach for non-invasive detection of HCC.

#1126 Pervasive early dissemination in pancreatic cancer uncovered by tissue-paired plasma whole-genomes.

Yuanchang Fang[1], Michelle Chan-Seng-Yue[2], Karen Ng[3], Amy Zhang[2], Tuan Hoang[1], Gun Ho Jang[2], Sabiq Chaudhary[2], Catia Gaspar[3], Eugenia Flores-Figueroa[3], Daniela Bevacqua[3], Stephanie Ramotar[3], Ayelet Borgida[3], Shawn Hutchinson[3], Anna Dodd[3], Barbara Grunwald[4], Julie Wilson[2], Robert Grant[3], Erica Tsang[3], George Zogopoulos[5], Masoom Haider[1], Jennifer Knox[3], Steven Gallinger[3], Faiyaz Notta[1]

[1]University of Toronto, Toronto, ON, Canada,[2]Ontario Institute for Cancer Research, Toronto, ON, Canada,[3]University Health Network, Toronto, ON, Canada,[4]University Hospital Essen, Essen, Germany,[5]McGill University, Montreal, QC, Canada

In pancreatic cancer, 50% of the patients are diagnosed at the metastatic stage due to a lack of symptoms. The overall survival rate dramatically reduces from 44% in early-stage resectable patients to 3% in metastatic cases. However, even in early-stage patients, >75% of them still recur after resection and adjuvant therapies. Therefore, there is an urgent need to develop a sensitive strategy to detect this disease earlier before it spreads. Characterizing circulating tumor DNA (ctDNA) in plasma is an effective approach to detect and monitor cancer. Whole-genome sequencing (WGS) tracks all the tumor mutations simultaneously, and has a higher sensitivity than targeted approaches, especially in samples with extremely low tumor burden. In this study, to investigate the ctDNA dynamics and early dissemination in pancreatic cancer, we established a cohort of 1,013 samples from 277 donors, including plasma WGS at 20-60x, alongside germline DNA WGS, tissue WGS and transcriptomic sequencing. Using a tumor-guided approach, we found that the early-stage resectable cases shed very little ctDNA (<1% tumor fraction, TFx). Plasma TFx levels were elevated at the metastatic stage, but were also dependent on metastatic tissue site, where patients with liver metastases had higher TFx than the ones with only non-hepatic lesions. We further discovered the tumor-intrinsic features that were related to increasing ctDNA shedding, such as whole-genome duplication (WGD), high cell cycle activity and non-glandular morphology, as well as extrinsic features related to reduced shedding, including a reactive microenvironment and B cell immunity. Our analysis on tumor clonal architecture revealed that subclonal mutations were more frequently detected than the clonal ones in plasma samples with low ctDNA levels or from early-stage patients, which strongly suggests that dissemination from early-stage primary tumors mostly derived from subclones. In the longitudinal plasma, we observed that subclones seeded metastasis years before imaging diagnosis. This study with a unique large cohort of paired tumor and plasma sequencing data provided a comprehensive insight on ctDNA dynamics, disease monitoring and early detection in pancreatic cancer.

#1127 Interim analysis of tumor-informed ctDNA detection in head and neck squamous cell carcinoma: The PECAN trial.

Paul van der Leest[1], Joris Elbers[2], Amy Greer[3], Sten Cornelissen[1], Theodora C. Linders[1], Mirthe Lanfermeijer[1], Kalpana Ramkisoensing[1], Ellen Verner[3], Laura Smit[1], Mark Sausen[3], Abrahim Al-Mamgani[4], Daan van den Broek[1]

[1]Netherlands Cancer Institute, Amsterdam, Netherlands,[2]Erasmus MC Cancer Institute, Rotterdam, Netherlands,[3]Labcorp, Baltimore, MD,[4]Amsterdam University Medical Center, Amsterdam, Netherlands

Background: Head and neck squamous cell carcinomas (HNSCC) are a heterogeneous group of malignancies of the upper aerodigestive tract, encompassing multiple tumor (sub)sites and entities. Current treatment often relies on radiotherapy, with or without concurrent chemotherapy. Clinical surveillance remains the sole indicator of recurrent disease, despite relapse rates of 25-40%. There is a clear unmet clinical need for biomarkers that can predict treatment efficacy prior to and during (chemo)radiotherapy and that can identify residual disease and cancer recurrence early during surveillance.
Methods: Seventy-two HNSCC patients were enrolled in the PECAN trial. Plasma and saliva samples were collected at baseline; during (chemo)radiotherapy; and at 2 weeks, 3 months, 6 months, 1 year, and 2 years after treatment. Tumor-informed whole-genome sequencing (WGS) was performed on circulating cell-free DNA (ccfDNA) extracted from plasma for 57 evaluable patients. Molecular findings were correlated with treatment response and clinical outcome. Analysis of the remaining patients, saliva samples, human papilloma virus (HPV) abundance, and imaging are ongoing.
Results: At baseline, circulating tumor (ctDNA) was detectable in 92% HNSCC patients based on tumor-informed molecular fingerprinting. All patients with undetectable baseline ctDNA remained negative throughout the monitoring period, and none experienced disease recurrence. Among patients with detectable ctDNA, 84% cleared ctDNA during (chemo)radiotherapy; however, ctDNA clearance during treatment was not predictive of recurrence. In landmark analysis at 3 months after treatment, ctDNA was detected in 6% of patients, all of whom subsequently developed recurrence. During the entire 2-year surveillance period, no ctDNA was detected in patients who remained relapse-free. In case ctDNA was detected recurrence was always diagnosed, resulting in a positive predictive value of 100%. ctDNA detection at end of follow-up (EoF), whether due to recurrence or completion of surveillance, was associated with reduced progression-free survival (hazard ratio [HR] = 5.9) and overall survival (HR = 7.1).
Conclusion: This interim analysis of the PECAN trial demonstrates the clinical relevance of ctDNA monitoring following (chemo)radiotherapy, showing substantially reduced survival in patients with detectable ctDNA during surveillance. These data suggest that ctDNA serves as a robust biomarker for recurrence detection and could guide initiation of follow-up treatment. Sensitivity of ctDNA detection in the heterogeneous disease spectrum of HNSCC may be improved by complementary analysis of saliva samples and alternative biomarkers (e.g., HPV). For this cohort, the added value of incorporating additional time points, saliva-based detection, HPV abundance, and imaging correlations for all evaluable cases will be presented at AACR.

#1128 Personalized cell-free DNA fragmentation dynamics in early-stage NSCLC in TRACERx.

Jonathan C. M. Wan[1], Wing Kin Liu[2], James R. M. Black[2], Alexander Mark Frankell[3], Alexander Azizi[1], Olivia Lucas[1], Woody Z. Zhang[3], Chris Bailey[1], Nnennaya Kanu[2], Mariam Jamal-Hanjani[2], Charles Swanton[1]

[1]The Francis Crick Institute, London, United Kingdom,[2]University College London (UCL) Cancer Institute, London, United Kingdom,[3]University of Cambridge, Early Cancer Institute, Cambridge, United Kingdom

Background: Plasma cell-free DNA (cfDNA) fragmentation reflects underlying chromatin organization and can be disrupted in cancer. Circulating tumor DNA (ctDNA) fragments differ from non-tumor cfDNA in size, genomic distribution, and end-motif characteristics. Recent studies have shown that fragmentomic profiles can distinguish individuals with and without lung cancer, and fragment sizes from targeted sequencing can be leveraged for cancer detection.
In the TRACERx study, personalized ctDNA sequencing has previously been used to monitor individuals with stage I-III non-small cell lung cancer (NSCLC) who underwent curative-intent surgery, enabling prognostication at baseline and post-operative landmark timepoints. Here, we investigate the dynamics of ctDNA and cfDNA fragmentation in response to surgery, relapse and systemic therapies.
Methods: We characterised cell-free DNA (cfDNA) fragmentation in 1,069 longitudinal plasma samples from 197 individuals using Anchored multiplex PCR and targeted sequencing. We developed a computational pipeline to extract fragment size distributions and end-motif features from tumor-derived and non-tumor cfDNA fragments.
Results: Distinct cfDNA fragmentation dynamics were observed across clinical timepoints, and mutant fragments were shorter than non-mutant fragments. Treatment effects on fragmentation were observed: a transient release of non-tumor cfDNA was observed post-surgery, plus systemic therapies were associated with alterations in fragmentation pattern. Associations between fragmentation metrics, clinicopathologic features, and biological variables such as extrachromosomal DNA, were explored.
Conclusion: Targeted plasma sequencing within TRACERx enables integrated evaluation of tumor- and non-tumor-derived cfDNA. Fragmentation dynamics reflect treatment and disease status, suggesting their potential as a complementary non-invasive marker for monitoring and mechanistic insights in early-stage NSCLC.

#1129 Analytical and clinical sensitivity of tumor-informed and tumor-naïve ctDNA residual disease detection during neoadjuvant immune checkpoint inhibition in resectable cancers.

Paul K. Lee[1], Blair V. Landon[1], Ezgi Oner[1], Jaime Wehr[1], Qiong Meng[1], Amna Jamali[1], Mimi Najjar[2], Gavin Pereira[1], Samira Hosseini-Nami[1], Rachel Keogh[1], Chen Hu[1], Ronan J. Kelly[3], Joshua E. Reuss[4], Patrick M. Forde[5], Mark Sausen[6], Vincent K. Lam[1], Robert B. Scharpf[1], Noushin Niknafs[1], Valsamo (Elsa) Anagnostou[1]

[1]Sidney Kimmel Comprehensive Cancer Center, Johns Hopkins University, Baltimore, MD,[2]Cleveland Clinic, Cleveland, OH,[3]Charles A. Sammons Cancer Center, Baylor University Medical Center, Dallas, TX,[4]Department of Hematology/Oncology, Georgetown University, Washington, DC,[5]Trinity St. James's Cancer Institute, Trinity College Dublin, Dublin, Ireland,[6]Labcorp, Baltimore, MD

Background: Circulating tumor DNA (ctDNA) has become a key biomarker for minimally invasive detection of residual disease during neoadjuvant immunotherapy. However, its integration into routine clinical decision-making remains limited by modest sensitivity and the practical constraints of current assays. **Methods:** We performed multi-modality matched tumor, white blood cell (WBC), and cell-free DNA (cfDNA) next-generation sequencing (NGS) of 520 biospecimens (56 tumor, 105 WBC, 359 plasma) from 32 patients with operable gastroesophageal (GE) cancer (NCT03044613) and 30 patients with resectable pleural mesothelioma (PM; NCT03918252). ctDNA residual disease analyses were performed at baseline, before each cycle of neoadjuvant immunotherapy, and preoperatively. For the tumor-informed approach, whole genome sequencing (WGS) data of matched tumor, WBC, and cfDNA (80x, 40x, and 30x coverage) were integrated through a random forest machine learning model and calibrated using a reference set of noncancerous cfDNA to determine cfDNA tumor fraction (TF). In parallel, we performed orthogonal tumor-naïve, fixed-gene-panel targeted error-correction NGS of cfDNA and WBC (30,000x), filtering germline and clonal hematopoiesis variants. **Results:** Overall, the tumor-informed assay showed significantly higher sensitivity, evidenced by a higher ctDNA detection rate at all evaluated timepoints compared to the tumor-naïve assay. In the GE cohort, the tumor-informed assay detected ctDNA for 22 of 25 (88%), 20 of 25 (80%), 18 of 26 (69%), and 5 of 21 (24%) patients at baseline, cycle 2, cycle 3, and preoperatively, respectively. By contrast, 13 of 30 (43%), 12 of 30 (40%), 11 of 30 (37%), and 5 of 25 (20%) had detectable ctDNA by the tumor-naïve assay at corresponding timepoints. In detectable cases, cfDNA TFs were highly concordant between approaches ($R = 0.85$, $p < 0.001$). In the PM cohort, 12 of 26 (46%), 11 of 25 (44%), 7 of 21 (33%), and 13 of 25 (52%) had ctDNA detected by the tumor-informed assay at baseline, cycle 2, cycle 3, and preoperatively, respectively. Having demonstrated higher analytical sensitivity with the tumor-informed approach in the GE cohort, we applied the tumor-naïve approach only in cases with detectable ctDNA by the tumor-informed assay. Of these, 6 of 14 (43%), 6 of 13 (46%), 5 of 8 (63%), and 7 of 15 (47%) had ctDNA detected at corresponding timepoints. cfDNA TFs were concordant at timepoints when ctDNA was detectable by both approaches ($R = 0.63$, $p = 0.002$). Tumor-informed ctDNA residual disease preoperatively was associated with shorter progression-free survival (log-rank, $p = 0.0059$). **Conclusion:** Tumor-informed WGS-based liquid biopsies reliably measure ctDNA residual disease during neoadjuvant immunotherapy, demonstrating greater sensitivity compared to a tumor-naïve approach, supporting their clinical value.

#1130 Tracing tumor-specific EV-miRNA signatures via patient-derived explant models to advance liquid biopsy in non-small cell lung cancer.

Miranda Burdiel[1], Carlos Rodriguez-Antolin[1], Ana Arauzo-Cabrera[1], Olga Pernia[1], Rocio Moreno-Velasco[2], Laura Gutierrez-Sainz[1], Oliver Higuera[1], Olga Vera[1], **Javier de Castro**[1]

[1]Hospital Universitario La Paz, Madrid, Spain,[2]CIBERONC, Madrid, Spain

Background: Non-small cell lung cancer (NSCLC) remains a leading cause of cancer mortality, largely due to late diagnosis and limited early-stage biomarkers. Liquid biopsy offers noninvasive monitoring, but most circulating markers lack clear tissue origin, limiting clinical interpretation.
Methods: We developed a patient-derived explant workflow to trace the origin of extracellular vesicle-associated microRNAs (EV-miRNAs) and evaluate their clinical utility in plasma. Fifteen resected lung adenocarcinoma specimens and matched normal tissues were cultured ex vivo to collect tissue and secreted small EVs. Small-RNA sequencing of 60 samples (30 EV, 30 tissue) and RNA-seq of 30 tissues identified neuro-metabolic mRNA targets potentially regulated by miRNA shifts. 77 miRNAs were differentially sorted into tumor versus control EVs; 25 candidates were selected for validation. A custom TaqMan OpenArray™ panel demonstrated high concordance with qPCR, enabling high-throughput profiling.
Results: We quantified these 25 EV-miRNAs in three cohorts: (1) 38 resectable patients with paired baseline and recurrence plasma; (2) 292 treatment-naïve patients across stages I-IV; and (3) 50 healthy controls. Six miRNAs - three “tumor-high” (miR-21-3p, miR-409-3p, miR-503-5p) and three “tumor-low” (miR-486-5p, miR-486-3p, miR-451a) - tracked recurrence in >50% of relapsing patients but remained stable in non-relapsers. Cross-sectional analysis showed stage IV patients recapitulated EV dysregulation (miR-21-3p high, miR-486-5p low), while localized disease mirrored controls. Prognostic modeling revealed stage-specific patterns: in stage III, low EV-miR-21-3p, miR-503-5p, and miR-486-3p predicted shorter progression-free survival; in stage IV, high EV-miR-21-3p correlated with worse overall survival, whereas high EV-miR-486-5p trended favorably. Exploratory Kaplan-Meier curves combining miR-503-5p/miR-486-5p for PFS and miR-21-3p/miR-486-5p for OS suggested risk stratification potential.
Conclusions: Our explant-to-liquid biopsy approach identifies EV-miRNA signatures that reflect tumor biology, monitor recurrence, and stratify prognosis across NSCLC stages. These findings support clinical validation of miR-21-3p, miR-486-5p, and miR-503-5p as prognostic biomarkers and highlight patient-derived explants as a powerful platform for biomarker discovery.

#1131 A novel detection strategy for an emerging biomarker: *MTAP* loss detection with circulating tumor DNA (ctDNA).

Lauren S. Welch[1], Radhika Gutta[2], Fawzi Abu Rous[2], Bindu R. Potugari[2], Sudha Sadasivan[2], **Shirish M. Gadgeel**[2]

[1]Guardant Health, Inc, Palo Alto, CA,[2]Henry Ford Cancer Center, Henry Ford Health System, Detroit, MI

Background: Methylthioadenosine Phosphorylase (*MTAP*) is a tumor suppressor gene frequently deleted in cancer, most often through loss of the 9p21 locus (*MTAP*, *CDKN2A*, *CDKN2B*). *MTAP* loss is an emerging biomarker with investigational therapies, yet detection has relied on tissue analysis, with prevalence estimates of 10-18% in advanced (adv) non-small cell lung cancer (NSCLC). Detection of large gene deletions by ctDNA is technically difficult and *MTAP* loss is not reported on most commercial ctDNA panels. Given the convenience of liquid biopsy and potential to expand trial eligibility, we analyzed the prevalence and genomic landscape of *MTAP* loss in lung cancer using a commercial ctDNA assay.

Methods: Patients (pts) with adv lung cancer who had Guardant360® Liquid testing between 7/2024-6/2025 were identified from the Guardant Health database. The start date aligned with assay expansion (>740 genes/epigenomics) and inclusion of *MTAP* loss reporting. *MTAP* loss was defined as bi-allelic loss by homozygous deletion (HomDel) or single copy deletion (del) with a co-occurring loss of function variant; prevalence and co-alterations (co-alt) were assessed by histology and tumor fraction (TF). Co-alt comparisons used two-sided Fisher's Exact Test ($p<0.05$ significant).

Results: *MTAP* loss was detected in 1.9% (330/17,333) of all lung cancer pts, 2.1% (55/2591) squamous, and 1.8% (244/13,745) non-squamous (nsq), regardless of TF; 94% (310/330) were NSCLC. Median (m) age was 69; 54.2% were male. For adv NSCLC, prevalence increased with TF, reaching 10.9% (294/2706) in pts with TF ≥10%, consistent with tissue-based rates. In nsqNSCLC, frequently co-altered genes included *CDKN2A* (96%), *TP53* (73%), *EGFR* (43%), *KRAS* (28%), *KEAP1* (27%), *STK11* (26%), *RB1* (25%), and *CCNE1* (24%). Compared to nsqNSCLC without *MTAP* loss, *CDKN2A (*mostly HomDel), *CCNE1*, *EGFR*, *BRCA2*, *KEAP1*, *STK11*, *RB1*, and *FGFR1* were enriched ($p<1\times10^{-}10$). mTF and bTMB were higher in the *MTAP* loss cohort (30.9% vs 0.7%; 15.1 vs 12.5 mut/Mb). Oncogenic *EGFR* mutations (muts) occurred in 16.4% (54/330), including exon 19 del (46%), L858R (23%), exon 20 insertion (11%), and other muts (20%); mTF was 28.1% (range 7.7-90%). Oncogenic *KRAS* muts were present in 19.1% (63/330), most commonly G12X (70%), with mTF of 26.3% (range 1.6-80.7%). Overall prevalence of *MTAP* loss in *EGFR* and *KRAS* mutated NSCLC was 2.3% (54/2304) and 2.0% (63/3172), respectively.

Conclusion: This first ctDNA analysis of *MTAP* loss prevalence and co-mutational landscape in NSCLC demonstrates that *MTAP* loss can be detected by ctDNA across histologies when TF is sufficient, offering a practical alternative when tissue is unavailable or rapid results are needed. ctDNA detection of *MTAP* loss may be further enhanced by methylation approaches for low-shed cases. Broader use of ctDNA testing could expand *MTAP* loss detection, increasing clinical trial eligibility and access to new therapies.

#1132 Malignant effusions for cfDNA/RNA genotyping and drug testing: Turning malignant fluids into personalized cancer models.

Elba Marin[1], Silvia Garcia-Roman[1], Cristina Aguado[1], Marta Vives[1], Sonia Rodriguez[1], Susana Munoz[1], Noelia Armiger[1], Alejandro Martinez-Bueno[2], Maria Gonzalez-Cao[2], Ana Velasco[3], Serafin Morales[4], Reyes Roxana[5], Ekaterina Meshoulam[2], Andres Aguilar[2], Clara Mayo de las Casas[1], Miguel Angel Molina-Vila[1]

[1]Pangaea Oncology, Hospital Universitari Dexeus, Barcelona, Spain,[2]Instituto Oncologico Dr. Rosell, Hospital Universitari Dexeus, Barcelona, Spain,[3]Institut de Recerca Biomedica de Lleida (IRBLleida), Lleida, Spain,[4]Hospital Universitari Arnau de Vilanova, Lleida, Spain,[5]Instituto Oncologico Dr. Rosell, Hospital Teknon, Barcelona, Spain

Introduction and objectives: Malignant effusions (MEs), including pleural, ascitic and pericardiac fluids, occur in 33% of patients with solids tumors, either at diagnosis and/or at progression to therapy. These fluids are very valuable when tumor tissue samples are inaccessible, as circulating free DNA/RNA (cfDNA/RNA) obtained from MEs enable accurate molecular diagnosis. Primary cultures can be established from tumor cells present in MEs, allowing for the *in vitro* testing of antitumor drugs and being of help in treatment selection due to their similarity with the patient's tumor. In this study, we aimed to incorporate MEs analysis into the routine clinical practice to determine clinically relevant alterations and to establish 2D and 3D primary culture models to be used in drug testing.
Materials and methods: MEs from patients with solid tumors were prospectively collected, with volumes ranging from 5-5,000 mL. cfDNA/RNA was extracted from all fluid samples and subjected to genotyping using a 30-gene DNA next generation sequencing (NGS) panel and a commercial mRNA nCounter panel containing 770 mRNA hybridization probes. In parallel, tumor cells contained in the MEs were isolated by centrifugation of the entire volume, cultured in complete culture media to establish 2D and 3D in vitro models, and molecularly characterized by NGS and nCounter. In successfully established pure tumor primary cultures (PTPC), cell viability assays were performed with chemotherapeutic agents and/or targeted therapies based on the detected alterations. Clinical follow-up data were collected to evaluate prognostic associations. Results We collected 382 MEs from 314 solid tumor patients. Of them, 49.7% (n=190) were collected at therapy progression, 28.3% (n=108) at baseline and 8.4% (n=32) while the patient was still on treatment. In 13.6% (n=52) cases, no data regarding collection time was available. Genotyping of cfDNA/RNA from 334 samples identified clinically relevant alterations in 77.3% (n=258), including mutations, amplifications, and/or fusions at variant allele frequencies (VAF) ranging from 0.33 to 93%. Among these, 35.3% (n=91) were considered targetable. Information on paired cytology samples was available in 11.6% (n=93) cases, showing a concordance rate of 80% with cfDNA/RNA genotyping. PTPCs could be successfully established from 61 MEs, mainly from pleural effusions (70.5%, n=43) and lung cancer cases (54.1%, n=33). Drug sensitivity assays were performed in 47 PTPCs (77%), including chemotherapy and targeted therapies. In 14 cases (29.7%) correlation between treatment received and sensitivity results could be analyzed, showing a 93% agreement.
Conclusions: MEs can be prospective collected in the clinical setting and used for a dual purpose. cfDNA and cfRNA can be isolated from the fluid fraction and employed for genotyping, while cells can be cultured and antitumor drugs tested.

#1133 Urine cell-free RNA captures tumor-reflective long intergenic noncoding and circular RNA programs in bladder cancer.

Pradeep Chauhan[1], Li Lin[2], Irfan Alahi[1], Jessica Linford[1], Lilli J. Greiner[1], Ayesha Hashmi[1], Anushka Viswanathan[1], Nathan Colon[3], Faridi Qaium[1], Peter K. Harris[2], John Sheng[2], Jacob J. Orme[1], Eric H. Kim[4], Zachary L. Smith[5], Woodson Smelser[2], Christopher A. Maher[2], Aadel A. Chaudhuri[1]

[1]Mayo Clinic, Rochester, MN,[2]Washington University School of Medicine, Saint Louis, MO,[3]Hoag Foundation, Newport Beach, CA,[4]University of Nevada Reno, Reno, NV, Reno, NV,[5]Advent Health, Orlando, FL

Introduction: Long intergenic noncoding RNAs (lincRNAs) and circular (circ) RNAs have been shown to play key roles in carcinogenesis and tumor progression. Urine represents a promising source of tumor-reflective signals shed directly from the urothelial microenvironment in bladder cancer (BC) patients. Here, we evaluate the urine cell-free (cf) RNA transcriptome in a cohort of 50 patients with localized BC.
Methods: A total of 50 localized BC patients and 24 healthy adults were enrolled. Pre-operative urine (collected on the day of radical cystectomy) was processed to isolate cfRNA from urine supernatant. Libraries were prepared using an Illumina tagmentation-based RNA enrichment workflow and sequenced to 100M paired-end reads per sample on a NovaSeq X. FASTQ files were concatenated per sample and QC-checked with RNA-SeQC and Samtools. Reads were aligned to GRCh38/hg38 with STAR, and gene counts were generated using Feature Counts. Linear differential expression analysis (DEA) was performed with DESeq2. For discovery we used random halves of TCGA-BLCA and healthy urine cfRNA samples, alongside a second DEA with random halves of urine BC cfRNA vs. controls; overlapping upregulated genes were validated in the remaining samples. For circular (circ) RNAs, annotations from MiOncoCirc were used; junctions with ≥5 supporting reads were retained, and DEA was conducted with edgeR.
Results: In this study, the median age was 68 years, and 80% (40/50) were male. Among the cohort, 66% (33/50) had muscle-invasive bladder cancer (MIBC), of whom 54% received neoadjuvant chemotherapy. Differential expression analysis of TCGA-BLCA tumors and BC urine cfRNA, identified 27 genes commonly upregulated, with 23 of the 27 shared genes strikingly being long intergenic noncoding RNAs (lincRNAs). These BC/urine-specific lincRNAs—including LINC00930, LINC01004, DLG5-AS1, APTR, PSORS1C3, and SERPINB9P1—have known roles in proliferation, EMT, metabolism, and immune signaling. Outside of lincRNAs, tumor-reflective coding transcripts in BC/urine were enriched for autophagy, driven by MAP1LC3B2.TCGA-BLCA survival analysis showed that LINC00930 and PSORS1C3 were associated with worse overall survival. Expanding beyond linear RNA sequences, analysis of urine circRNAs from BC patients revealed a strong cancer-specific dysregulation pattern, with 77 circRNAs significantly upregulated compared with healthy controls. Upregulated urine circRNAs arose from host genes involved in BC-relevant pathways, including invasion (*DOCK1*, *ARHGAP5*), autophagy/ER stress (*VMP1*, *ERN1*), and luminal differentiation (*GRHL2*, *ESRP1*).
Conclusion: Cell-free RNA profiling reveals a distinct transcriptomic signature including differential lincRNA- and circRNA-driven autophagy, EMT, proliferation, metabolic, differentiation, and immune signaling programs in the urine of bladder cancer patients.

#1134 Cell-free DNA fragmentomes capture response to immuno-radiotherapy in metastatic non-small cell lung cancer.

Noushin Niknafs[1], Lavanya Sivapalan[1], Bahar Alipanahi[2], Gavin Pereira[1], Amna Jamali[1], Jaime Wehr[1], Daniel Rabizadeh[1], Christopher Cherry[1], Bryan Chesnick[2], Nicholas C. Dracopoli[2], Jamie Medina[2], Stephen Cristiano[2], Willemijn S. Theelen[3], Robert Scharpf[1], Lorenzo Rinaldi[2], Victor E. Velculescu[1], **Valsamo (Elsa) Anagnostou**[1]

[1]Johns Hopkins School of Medicine, Baltimore, MD,[2]Delfi Diagnostics, Baltimore, MD,[3]Netherlands Cancer Institute, Amsterdam, Netherlands

Background: Timely assessment of response to immune checkpoint inhibition (ICI) is critical but often limited by the heterogeneity of radiographic responses. Mutation-based analyses of cell-free DNA (cfDNA) circumvent these challenges, but are, in turn, prone to artifacts arising from clonal hematopoiesis. Plasma cfDNA fragmentome analyses using low-pass whole genome sequencing (WGS) may enable a scalable approach to evaluate systemic tumor burden in a tumor- and mutation-naïve manner.
Methods: cfDNA fragmentome analyses were performed following low-pass WGS of 244 plasma samples from 62 patients treated with pembrolizumab +/- radiotherapy (NCT02492568). A locked instance of the DELFI-TF, a random forest regression model based on genome-wide fragmentation patterns and aneuploidy, was applied to determine cfDNA fragmentome-based estimates of tumor fraction. The 95th percentile of tumor fraction in a non-cancer reference set established the limit of blank (LOB). Fragmentome-based landmark molecular response was defined as ctDNA below LOB at 6 weeks. Baseline tumor samples (n=24) patients were analyzed by RNA sequencing to characterize transcriptomic profiles stratified by cfDNA fragmentome profiles. Clinical outcomes were evaluated by RECIST 1.1 (at 6 and 12 weeks), progression-free survival (PFS), and overall survival (OS).
Results: At baseline, DELFI-TF values were correlated with radiographic tumor burden (R=0.32, P=0.017). Notably, tumors from patients with high DELFI-TF showed an enrichment in gene sets related to cell cycle, DNA replication and repair (adjusted P<0.05), suggesting that fragmentome TF accurately captured cellular turnover. At 6 weeks, 73% (8 out of 11) of patients with radiographic response attained fragmentome molecular response, while the subset of patients with radiographically stable or progressive disease was more heterogeneous in their fragmentome molecular response (24 out of 50, 48%). Fragmentome molecular response was more concordant with best overall response (BOR) at 12 weeks (Fisher's exact P=0.018). Analysis of baseline tumors from patients achieving fragmentome molecular response revealed an inflamed tumor microenvironment (adjusted P-value <0.001). Among patients with stable or progressive disease at the first radiographic evaluation, fragmentome response predicted longer PFS (logrank P=0.0096) and OS (logrank P=0.012). Similarly, fragmentome molecular response predicted PFS (logrank P=7.4e-5) and OS (logrank P=0.00028) across the entire cohort.
Conclusions: Plasma cfDNA fragmentome-derived tumor fraction reflects cellular turnover and lung cancer biology within the context of immunotherapy, while also enabling reliable, cost-effective, and scalable molecular response evaluations.

#1135 Lung cancer subtyping using cell-free DNA fragmentomes and protein biomarkers.

Stephen Cristiano[1], Paul van der Leest[2], **Jamie Medina**[1], Zachary Skidmore[1], Milou M. Schuurbiers[3], Garrett Graham[1], Alessandro Leal[4], Bryan Chesnick[1], Kim Monkhors[2], Nicholas C. Dracopoli[1], Robert Scharpf[5], Peter B. Bach[1], Daan van den Broek[2], Amoolya Singh[1], Victor E. Velculescu[5], Sian Jones[1], Michel M. van den Heuvel[3], Lorenzo Rinaldi[1]

[1]Delfi Diagnostics, Palo Alto, CA,[2]Netherlands Cancer Institute, Amsterdam, Netherlands,[3]Department of Pulmonary Diseases, Radboud University Medical Center, Nijmegen, Netherlands,[4]NYU Langone Health Perlmutter Comprehensive Cancer Center, New York, NY,[5]Sidney Kimmel Comprehensive Cancer Ctr., Baltimore, MD

Introduction: Lung cancer is the leading cause of cancer-related mortality worldwide. Accurate histological subtyping to differentiate between lung adenocarcinoma (LUAD), lung squamous cell carcinoma (LUSC), and small cell lung cancer (SCLC) is critical for guiding optimal therapeutic strategies. However, up to 20% of patients lack sufficient tissue for conventional histopathological classification. Liquid biopsies using cell-free DNA (cfDNA) fragmentomics offer a promising non-invasive alternative for cancer characterization when tissue is not available.

Methods: We examined 761 patients with newly diagnosed, treatment-naive lung cancer of all stages, including lung adenocarcinoma (n=468), squamous cell carcinoma (n=156), small cell carcinoma (n=42), large cell carcinoma (n=15) and other subtypes (n=80) from the prospective Lung Cancer Early Molecular Assessment trial (LEMA, NCT02894853). Low-coverage whole genome sequencing of cfDNA plasma samples was performed to derive genome-wide fragmentation features. Circulating tumor DNA (ctDNA) burden was estimated from fragmentation using the DELFI-TF method. We developed a machine learning classifier trained exclusively on the tissue-based copy number signatures from the Clinical Lung Cancer Genome Project (CLCGP) and applied it to patient cfDNA samples to predict lung cancer subtypes.

Results: This tissue-trained subtyping algorithm was evaluated on all available plasma samples, achieving an AUC of 0.99 (95% CI = 0.98-1.00) for distinguishing NSCLC from SCLC and an AUC of 0.91 (95% CI=0.87-0.95) for differentiating LUAD from LUSC. The model correctly classified 88% of SCLC, 80% of LUAD and 87% of LUSC cases where the tumor fraction was ≥0.3% (n=276). Among a subset of 361 NSCLC patients, integration of five blood protein biomarkers resulted in a multimodal model that differentiated LUAD from LUSC across all tumor fractions with high performance (AUC=0.85, 95% CI=0.80-0.90), an improvement over cfDNA ($p<0.01$; AUC=0.78, 95% CI=0.74-0.82) or protein-only classifiers ($p<0.001$; AUC=0.70, 95% CI=0.62-0.78).

Conclusions: These findings establish cfDNA fragmentation and protein biomarkers as a viable non-invasive approach for lung cancer subtyping when tissue is unavailable, with potential to expedite subtype-specific treatment selection and improve clinical outcomes

#1136 Analytical evaluation of a whole genome tumor-informed molecular residual disease detection assay with high sensitivity and specificity.

Weida Gong[1], Sung Kim[2], Guidantonio Malagoli Tagliazucchi[3], Tevfik Umut Dincer[1], Megha Ghildiyal[2], Magdalena Gantuz[2], Grace Kim[2], Quyen Bui[2], Yuan Ding[2], Jacob Gibson[2], Leland Mencik[2], Ambrose Vuong[2], Marcus Valancius[2], Kimberly Gietzen[2], Jennifer Becq[3], Carey Davis[2], Josh Bernd[2], Martin Chian[1], Dan Schmidt[2], Eileen de Feo[1]

[1]Illumina, Inc., Foster City, CA,[2]Illumina, Inc., San Diego, CA,[3]Illumina, Inc., Cambridge, United Kingdom

Introduction: Molecular residual disease (MRD) testing involves the detection of circulating tumor DNA (ctDNA) in plasma after cancer treatment. Tumor-informed Whole Genome Sequencing (WGS) workflows for the qualitative detection of MRD have been shown to be highly sensitive. We present an automated and scalable solution for patients with bladder, breast, melanoma, non-small cell lung (NSCLC), and colorectal (CRC) cancers with turnaround as fast as 8 to 9 days. This includes automation of DNA extraction, library preparation, sequencing, data analyses, and reporting. Here, we summarize the analytical performance of a research use only workflow intended as a service for research and clinical partners, such as pharmaceutical companies.
Methods: The workflow requires 3 different sample types: formalin-fixed, paraffin-embedded (FFPE), Buffy Coat, and 2 to 4ml plasma aliquots. The optimal inputs are: i) 5ng (minimum 2ng) cell-free DNA (cfDNA) from plasma, ii) 100ng (minimum 50ng) tumor tissue DNA, and iii) 50ng DNA from Buffy Coat. DNA is extracted from different sample types with WGS libraries preparation and sequencing on NovaSeq™ 6000. Sequencing analyses, fingerprint generation, and MRD detection are performed using DRAGEN™. The assay uses a patient's tumor and germline sample to generate a patient-specific somatic variant list, *i.e.* fingerprint. Subsequently, the cfDNA sequence data is evaluated against the fingerprint to determine the presence or absence of tumor DNA indicative of MRD. Both clinical and contrived samples were used to evaluate accuracy, analytical sensitivity, analytical specificity and precision.
Results: Twenty-five clinical samples (5 samples for each cancer type) resulted in 100% overall percent agreement (OPA) in MRD status relative to a reference method, with ctDNA concentration as low as 0.035%. A panel of 20 healthy plasma samples assessed against 25 fingerprints across multiple cancer types resulted in a 100% negative percent agreement. Sensitivity analysis demonstrated 100% detection rate at variant allele frequency of 0.003% for NSCLC, 0.005% for bladder and CRC, and 0.006% for melanoma and breast samples. Precision was evaluated using all specimen types across multiple operators, instruments, and library preparation start days. There was 100% OPA in MRD status across intra-run and inter-run replicates at ctDNA concentrations of 0.009% to 0.018%.
Conclusions: We present a whole genome fully automated workflow capable of generating tumor- informed MRD status with high analytical sensitivity and specificity. The assay requires low DNA input from plasma samples and enables a sample-to-report turnaround time as fast as 8 to 9 days. The results demonstrate that the WGS MRD detection platform is a scalable, robust, and highly sensitive assay for multiple cancer types.

#1137 Validation of a sensitive, tissue-free blood test for biomarker discovery and tumor burden assessment.

Zeliang Deng, Xiaoling Li, Xinyue Kang, Jiayue Xu, Jing Su, Xianrong Chen, Qiancheng You, Xingyu Yang, **Zhihong Zhang**, Bingsi Li

Research and Development, Burning Rock Biotech, Shanghai, China

Background: Rapid progress in molecular and computational technologies for circulating tumor DNA (ctDNA) analysis is transforming precision oncology, allowing tumor detection, relapse surveillance, and treatment selection without invasive tissue sampling. Among these approaches, methylation profiling of ctDNA offers a sensitive and quantitative measure of tumor burden. However, signal-to-noise ratios varies across cancer types and technologies, underscoring the need for tumor-specific assay optimization and rigorous validation. We previously developed a tissue-free, methylation-based assay and demonstrated its clinical validity in lung, colorectal, and liver cancers. Here we report expanded, larger scale validation across additional tumor types, including pancreatic cancer (PDAC) and bile tract cancer (BTC).

Methods: The CanCatch® Surf classifier was trained and subsequently locked, as previously described. The total analytical performance testing dataset comprises >1,000 contrived and clinical samples (10-30 ng input). In this study, we constructed dilution series of PDAC- and BTC-derived cell-line and cfDNA mixtures spanning 0.001-0.5% tumor allele fraction (TAF). The *in-silico* titration dataset was generated by digitally blending sequencing reads from PDAC and BTC patients with those from cancer-free donors at defined proportions (0.001-0.5%). Probit regression identified the limit of detection (LoD) as the lowest TAF detected with ≥95% probability; the limit of blank (LoB) was the per-sample positivity rate in age-matched cancer-free donors.

Results: The analytical sensitivity for PDAC and BTC reached 0.02% for *in silico* mixtures, cell-line dilutions and cfDNA titrations, with no false positives among 72 age-matched cancer-free donors (0 %; 95% CI 0-5.0%). Evaluation of 176 pre-treatment plasmas (57 PDAC, 50 BTC, 69 controls) demonstrated a sensitivity of 84.2% for PDAC (stage I 75.0 %, II 86.7%, III 83.3%, IV 100%) and 82.0% for BTC (stage I 71.4%, II 66.7%, III 93.3%, IV 92.3%), both at 98.6 % specificity; larger cohorts are in progress, and updated results will be presented as available.

Conclusions: CanCatch® Surf's non-invasive approach to ctDNA detection in solid tumors has demonstrated performance comparable to traditional tissue-based methods, thus holding promise for broader clinical use in monitoring disease recurrence and assessing treatment effectiveness.

#1138 Clinical grade circulating tumor DNA methylation predicts outcome to brigatinib plus local consolidative therapy in patients with ALK rearranged NSCLC - Liquid biopsy correlates from the BRIGHTSTAR trial.

Simon Heeke[1], Saumil Gandhi[1], Hai T. Tran[2], Lauren Averett Byers[1], Don Gibbons[3], Carl M. Gay[1], Mehmet Altan[3], Mara B. Antonoff[3], Xiuning Le[1], Janet Tu[3], Anne S. Tsao[4], Tina Cascone[1], Marcelo V. Negrao[1], George R. Blumenschein[5], John V. Heymach[1], Yasir Y. Elamin[1]

[1]UT MD Anderson Cancer Center, Houston, TX,[2]Associate Professor, Dept. of Cancer Medicine, UT MD Anderson Cancer Center, Houston, TX,[3]MD Anderson Cancer Center, Houston, TX,[4]Associate Professor, Div. of Cancer Medicine, UT MD Anderson Cancer Center, Houston, TX,[5]Associate Professor of Medicine, Dept. of Thoracic/Head & Neck Med. Oncology, UT MD Anderson Cancer Center, Houston, TX

Background: The phase II BRIGHTSTAR trial assessing the combination of brigatinib with local consolidative therapy in patients with ALK rearranged non-small cell lung cancer demonstrated promising clinical activity with a 5-year progression-free survival rate of 51% (Elamin et al. WCLC. 2025). To better characterize patients that would benefit of this treatment regimen, we performed clinical grade ctDNA methylation analysis for the detection of residual disease and prognostic.

Methods: We profiled 84 samples from 29 patients with stage IV or recurrent non-small cell lung cancer (NSCLC) and confirmed *ALK* rearrangement that were treated with local consolidative therapy (LCT) and brigatinib (BRIGHTSTAR; NCT03707938). Sample timepoints included baseline prior to therapy, at 8 weeks of brigatinib induction prior to local consolidative therapy (Pre-LCT) as well as after local consolidative therapy (Post-LCT) and at progression. Samples were profiled using the Guardant INFINITY platform for the detection of ctDNA using DNA methylation. Data was correlated to progression-free survival on treatment using Kaplan-Meier analysis and cox proportional hazard ratio.

Results: Circulating tumor DNA was persistently detected across timepoints with detection rates of 72% (N = 21/29) at baseline, 39% Pre-LCT (N = 11/28), 29% Post-LCT (N = 7/24) and 80% at progression (N = 4/5) demonstrating insufficient ctDNA clearing by brigatinib plus LCT treatment regimen. However, patients without detectable ctDNA at baseline using the DNA methylation classifier ($ctDNA^{METH}$) had significantly longer progression-free survival compared to patients with detectable ctDNA (38.2 months versus not reached; log-rank p = 0.04; HR = 0.16 (95% CI: 0.02-1.19)). No statistically significant difference in outcome was reported for patients who clear ctDNA Pre- or Post-LCT and patients with persistently detected ctDNA compared to pretreatment timepoint.

Conclusions: Clinical grade ctDNA methylation analysis allows the sensitive detection of ctDNA in patients with ALK rearranged NSCLC and is prognostic of outcome to brigatinib plus LCT therapy.

#1139 Early detection of treatment failure and disease dissemination inBCG-treated NMIBC using liquid biopsies and urine proteomics.

Trine Strandgaard[1], Tine Ginnerup Andreasen[1], **Iver Nordentoft**[1], Nathalie Demuth Fryd[2], Philippe Lamy[3], Julie Pedersen Harrits[1], Boris Oklander[4], Danielle Afterman[4], Tal Katz-Ezov[4], Imane Bourzgui[4], Jorn Jakobsen[5], Kristian Juul[5], Jorgen Bjerggaard Jensen[1], Lars Dyrskjot[1]

[1]Department of Clinical Medicine, Aarhus University, Aarhus, Denmark,[2]Department of Urology, Aarhus University Hospital, Aarhus N, Denmark,[3]Department of Molecular Medicine,, Aarhus University Hospital, Aarhus, Denmark,[4]Veracyte, Inc., Haifa, Israel,[5]Ferring Pharmaceuticals, A/S, Kastrup, Denmark

Only about 40% of patients with non-muscle invasive bladder cancer (NMIBC) respond to Bacillus Calmette-Guérin (BCG) therapy. While immune cell exhaustion has been linked to BCG resistance, early disease dissemination (i.e., occult muscle-invasive disease) may also contribute to BCG failure. We assessed whether serial analysis of urine and plasma samples could reveal signs of immune exhaustion, residual disease, and early dissemination, predictive of BCG outcome. In a prospective cohort of 102 BCG-treated NMIBC patients (median follow-up 28 months; inclusion ended April 2024), whole-genome DNA sequencing (WGS) was used to generate patient-specific genomic-wide tumor-based signatures (Veracyte) from paired buffy coat and tumor or urine pellet (UPEL) DNA. These were applied to cfDNA WGS data from 271 urine and 329 plasma samples collected before, during, and after treatment to detect urinary tumor (ut)DNA and circulating tumor (ct)DNA. In parallel,344 urine supernatants were profiled using Olink immuno-oncology panels, and total RNA sequencing was performed on 55 tumors. Updated follow-up will be presented at the meeting. Plasma ctDNA was detected pre-BCG in 5 (6%) patients; three later developed high grade (HG) recurrence or progressed. Pre-treatment ctDNA positivity was associated with higher recurrencerisk (HR = 6.88) but not with tumor stage ($p > 0.42$) or grade ($p = 0.91$). Urine utDNA was detected in 58%, 51% and 27% of patients before, during, and after BCG, respectively. utDNA-positivity during or after BCG correlated with shorter recurrence-free survival. Recurrence was observed in 10/22 (45%) patients with detectable post-BCG utDNA and in 11/49 (22%) patients without measurable utDNA ($p=0.022$). On average, utDNA preceeded clinical detection with 133 days (range: 4-405). UPEL DNA enabled patient-specific model generation and ctDNA/utDNA detection in cases with limited tumor material (CIS only). BCG therapy induced increased urinary immuno-oncology proteins. Tumor-associated proteins (MMP-12, IL6, IL8) were elevated pre-BCG, while eight immunemodulatory proteins - including HO-1, GZMA, GZMB, LAP TGF-beta-1 and TRAIL were upregulated early during treatment in HG-recurrent versus non-HG-recurrent cases. Pre-treatment ctDNA identified patients at high risk of HG recurrence or progression, supporting a role as a potential restaging tool. UPEL DNA was a reliable tumor proxy and useful when tissue was limited (e.g., CIS). utDNA detection identified patients at high risk of recurrence and earlier than cystoscopy. Urine proteomics mirrored BCG-induced immune responses, with distinct early on-treatment profiles in recurrent versus non-recurrent patients. Together, ctDNA/utDNA and proteomic monitoring may enable early detection of treatment failure and guide timely therapeutic interventions.

#1140 Longitudinal tumor-informed cell-free DNA whole genome sequencing coupled with transcriptomic analysis captures tumor burden dynamics in resectable gastroesophageal cancer.

Blair V. Landon[1], Jaime Wehr[1], Rachel Keogh[1], Noushin Niknafs[1], Christopher Cherry[1], Nisha Rao[1], Gavin Pereira[1], Mark Sausen[2], Richard J. Battafarano[3], Stephen C. Yang[3], Stephen Broderick[3], Jinny Ha[3], Russell K. Hales[4], K. Ranh Voong[4], Kristen A. Marrone[1], Chen Hu[1], Josephine L. Feliciano[1], Ali H. Zaidi[5], Ronan J. Kelly[6], Vincent K. Lam[1], Valsamo (Elsa) K. Anagnostou[1]

[1]The Sidney Kimmel Comprehensive Cancer Center, Johns Hopkins University School of Medicine, Baltimore, MD,[2]Labcorp, Baltimore, MD,[3]Department of Surgery, Johns Hopkins University School of Medicine, Baltimore, MD,[4]Department of Radiation Oncology, Johns Hopkins University School of Medicine, Baltimore, MD,[5]Allegheny Health Network Cancer Institute, Allegheny Health Network, Pittsburgh, PA,[6]The Charles A. Sammons Cancer Center, Baylor University Medical Center, Dallas, TX

Introduction: Circulating tumor DNA (ctDNA) has been established as a promising biomarker for detecting residual disease and monitoring therapy response across the cancer care continuum, however its utility to assess response to neoadjuvant immune checkpoint inhibition (ICI) is still being investigated. We utilized a tumor-informed cell-free DNA (cfDNA) whole genome sequencing (WGS) approach to molecularly monitor tumor burden dynamics and link clinical outcomes with transcriptomic assessment of baseline tumors based on ctDNA status in gastroesophageal cancer treated with neoadjuvant ICI.
Methods: We performed WGS on tumor (n=28), matched white blood cell (WBC, n=28), and serial plasma samples (n=97) from patients with resectable gastroesophageal cancer treated with neoadjuvant ICI and chemoradiation prior to surgical resection (NCT03044613). Tumor and WBC sequence data was used to identify tumor-specific single nucleotide variants (SNVs). High quality SNVs were utilized to determine the presence of ctDNA in plasma through a random forest machine learning model. ctDNA status and tumor fraction (TF) were assessed across four timepoints (baseline, post-ICI cycle 1, post-ICI cycle 2, and pre-operatively). Results were compared with tumor-naïve gene panel ctDNA targeted NGS (n=32 patients, n=152 samples) and correlated with clinical outcomes. Additionally, bulk RNA sequencing (RNAseq) was performed on baseline tumor samples (n=28) and utilized for gene set enrichment analyses (GSEA).
Results: Patients with pre-operative ctDNA TF above the median had a significantly shorter overall survival (OS) compared to those with ctDNA TF below the median or undetectable ctDNA (logrank $p < 0.0001$). Among patients who were undetectable pre-operatively via the tumor-naïve targeted NGS panel, individuals with detectable ctDNA via the tumor-informed WGS approach attained a numerically shorter OS compared to individuals with undetectable ctDNA (logrank p=0.1). Similarly, patients with ≥95% reduction in cfDNA TF pre-operatively had longer recurrence-free (logrank p=0.002) and OS (logrank p= 0.0001). GSEA of RNAseq data from baseline tumors revealed enrichment of G2/M cell cycle checkpoint and E2F targets in tumors from individuals with detectable baseline ctDNA via the tumor-informed WGS approach (FDR-adjusted p=2.31e-12), suggesting that cfDNA TF detection captures cellular turnover in the blood stream. The upregulation of proliferation and cell cycle progression-associated gene sets was not observed in stratified analyses by ctDNA detection utilizing the tumor-naïve approach.
Conclusions: Tumor-informed cfDNA WGS analyses accurately capture tumor burden dynamics and cellular turnover during neoadjuvant immunotherapy, opening a window of opportunity for further therapeutic intervention and optimization.

#1141 A liquid biopsy-based predictive model identifies potential candidates for bladder preservation after neoadjuvant chemotherapy in muscle-invasive bladder cancer.

Randi Istrup Juul[1], Iver Nordentoft[1], Sia Viborg Lindskrog[1], Abhijit Dasgupta[2], Diana Merino Vega[2], Gitte Lam[3], Line Hammer Dohn[4], Knud Fabrin[5], Andreas Carus[6], Astrid C. Petersen[7], Ulla N. Joensen[8], Helle Pappot[9], Per Sondergaard Holt[10], Niels Viggo Jensen[11], Boris Oklander[12], Danielle Afterman[12], Mads Agerbak[13], Jorgen B. Jensen[14], Lars Dyrskjot[1]

[1]Department of Molecular Medicine, Aarhus University Hospital, Aarhus N, Denmark,[2]AstraZeneca US, Gaithersburg, MD,[3]Department of Urology, Herlev Hospital, Herlev, Denmark,[4]Department of Oncology, Herlev Hospital, Herlev, Denmark,[5]Department of Urology, Aalborg University Hospital, Aalborg, Denmark,[6]Department of Oncology & Clinical Cancer Research Center, Aalborg University Hospital, Aalborg, Denmark,[7]Department of Pathology, Aalborg University Hospital, Aalborg, Denmark,[8]Department of Urology, Copenhagen University Hospital, Rigshospitalet, Copenhagen, Denmark,[9]Department of Oncology, Copenhagen University Hospital, Rigshospitalet, Copenhagen, Denmark,[10]Department of Urology, Odense University Hospital, Odense, Denmark,[11]Department of Oncology, Odense University Hospital, Odense, Denmark,[12]Veracyte, Haifa, Israel,[13]Department of Oncology, Aarhus University Hospital, Aarhus N, Denmark,[14]Department of Urology, Aarhus University Hospital, Aarhus N, Denmark

Detection of circulating tumor DNA (ctDNA) and urinary tumor DNA (utDNA) after neoadjuvant chemotherapy (NAC) has been shown to predict treatment response and outcome in muscle-invasive bladder cancer. Pathological complete response (pCR) is associated with improved survival outcomes and serves as a proxy for treatment response. We hypothesize that combining ctDNA, utDNA, and clinical variables in a predictive model could improve prediction of treatment response and outcome and potentially be used to identify candidates for bladder preservation.

We analyzed a unique dataset of urine and plasma samples together with detailed clinical measures and outcomes from 167 patients with localized muscle-invasive bladder cancer treated with at least three cycles of cisplatin-based NAC followed by radical cystectomy. ctDNA and utDNA measurements were performed using a tumor informed whole genome sequencing approach (TrueMRD, Veracyte) before (at baseline) and after NAC. pCR was defined as ypT0N0M0 at the time of radical cystectomy. Gradient boosting models were trained on 70% of the data using clinical variables alone and in combination with utDNA status and/or ctDNA dynamics and baseline ctDNA levels as well as imaging results from CT scans during NAC. Testing was done on the remaining 30% of data. Model performance was evaluated using the area under the precision-recall curve (AUCPR), and associations with ctDNA-free survival were investigated using Kaplan-Meier analyses.

For prediction of pCR, a model including baseline clinical variables as well as utDNA status, ctDNA dynamics, baseline ctDNA levels and imaging results gave an AUCPR of 0.93 and a negative predictive value (NPV) of 0.80. Using this model, patients with predicted pCR had a significantly better 1-year ctDNA-free survival (HR = 0.2, p = 0.03). A model including clinical variables, utDNA status, ctDNA dynamics and baseline ctDNA levels had a similar performance (AUCPR = 0.90; NPV = 0.82). A model including only the baseline clinical variables performed poorly (AUCPR = 0.54; NPV = 0.50). Adding either imaging results (AUCPR = 0.52; NPV = 0.48), utDNA status (AUCPR = 0.81; NPV = 0.65), or ctDNA dynamics and baseline ctDNA levels (AUCPR = 0.73; NPV = 0.62) did only make minor improvements.

Our findings demonstrate that integration of ctDNA dynamics and utDNA status, as well as imaging results into predictive models significantly enhances prediction of response to NAC and enables a clinically meaningful stratification of patients. Future independent testing in clinical trials is required, but our results support the development of liquid biopsy-guided bladder-sparing strategies in muscle-invasive bladder cancer.

#1142 Ultra-sensitive CRISPR-based NGS (MUTE-Seq) of pancreatic cyst fluid: KRAS variant allele fraction as an early marker of malignant potential.

Min Kyu Sung[1], Jungmin Kim[2], Yoon-Ho Won[3], Sung Sun Koo[3], In Seon Lee[3], Woohyung Lee[1], Ki Byung Song[1], Jae Hoon Lee[1], Dae Wook Hwang[1], Jin-Soo Kim[4], Seong Hyeok Ye[3], Junseok W. Hur[5], Song Cheol Kim[1]

[1]Department of Surgery, Asan Medical Center, Seoul, Korea, Republic of,[2]Genomic R&D Center, Korea Univ. College of Medicine, Seoul, Korea, Republic of,[3]GeneCker Co., Ltd., Seoul, Korea, Republic of,[4]Department of Oncology, Seoul National University Boramae Medical Center, Seoul, Korea, Republic of,[5]Department of Neurosurgery, Korea Univ. College of Medicine, Seoul, Korea, Republic of

Background: Conventional cytology of pancreatic cystic fluid from endoscopic ultrasound-guided fine-needle aspiration offers limited sensitivity for malignant potential of pancreatic cystic neoplasm. This proof-of-concept study aims to explore the clinical utility of cyst fluid next generation sequencing (NGS) using the ultra-sensitive MUTE-Seq assay.
Methods: Twenty-two patients who underwent surgical resection for pancreatic cystic lesions at Asan Medical Center, Korea, between November 2019 and July 2025 were prospectively enrolled. Approximately 1 mL of pancreatic cyst fluid was obtained intraoperatively from the resected specimens, from which cell-free DNA (cfDNA) was isolated and subjected to targeted NGS using the MUTE-Seq assay, a CRISPR-based technology that enhances cancer-associated variant detection by selectively suppressing cfDNA from normal cells. Custom primers amplified genomic regions of interest across 14 cancer-associated genes (AKT1, APC, BRAF, EGFR, KRAS, PDGFRA, PIK3CA, TP53, BRCA1, CTNNB1, ERBB2, IDH1, MYCN, and NRAS).
Results: Twenty-two patients with a median age of 60.5 years were analyzed. Initial pathologic diagnoses included serous cystic neoplasm (SCN, n = 4), mucinous cystic neoplasm (MCN, n = 4), intraductal papillary mucinous neoplasm-low grade (IPMN-LG, n = 7), IPMN-high grade (IPMN-HG, n = 4), pancreatic adenocarcinoma (PDAC, n = 2), and MCN with invasive carcinoma (n =1). Across the 14-gene panel, mutations in ERBB2, IDH1, PIK3CA, and AKT1 were sporadically detected in low-grade lesions without a discernible relationship to neoplastic grade. One PDAC case harbored a high TP53 variant allele fraction (VAF) of 47.475%.
In contrast to these sporadic findings, KRAS VAFs measured by MUTE-Seq demonstrated the strongest pathologic correlation. SCN had a median VAF of 0.14% (IQR 0-0.64), and MCN demonstrated a median VAF of 0% (IQR 0-0.12). High-grade lesions showed consistently elevated values, with IPMN-HG exhibiting a median of 41.04% (IQR 37.35-43.19) and PDAC a median of 31.545%. The case of MCN with invasive carcinoma showed a high KRAS VAF of 29.67%. KRAS VAFs in IPMN-LG were heterogeneous: three cases had low values (median 0.35%, IQR 0.3-0.75), while four cases showed high values (median 41.73%, IQR 36.56-42.63). Notably, one IPMN-LG case with a high KRAS VAF progressed to pancreatic carcinoma within three years, suggesting potential prognostic value.
Conclusions: Quantitative assessment of KRAS VAF using MUTE-Seq reliably distinguishes benign from neoplastic pancreatic cystic lesions, sensitively detects lesions with mixed invasive pathology, and may offer early molecular clues to malignant transformation, even in cases with borderline histology. Further study with additional specimens is underway to refine performance metrics and establish a clinically meaningful cutoff value for KRAS VAF.

#1143 Enspyre: A novel enrichment technology enables ultra-sensitive ctDNA detection with 98% reduction in sequencing requirements.

Paul Labrousse[1], Sophie Hackinger[2], Hugh Russell[1], Daniel Stetson[1], David Shera[3], Paulina Powalowska-Picton[2], Katarzyna Anton[2], Maria Litovchenko[2], Ernesto Lowy-Gallego[2], Amy Lovell[2], Magdalena Stolarek-Januszkiewicz[2], Barnaby Balmforth[2], James Hadfield[4]

[1]AstraZeneca, Waltham, MA,[2]Biofidelity, Cambridge, United Kingdom,[3]AstraZeneca, Philadelphia, PA,[4]AstraZeneca, Cambridge, United Kingdom

Background: Circulating tumor DNA (ctDNA) liquid biopsies show promise for minimal residual disease (MRD) detection, but clinical implementation is limited by high sequencing costs and the need for ultra-deep coverage to detect ctDNA at levels ≤100 parts per million (ppm). Current tumor-informed assays require >500 million reads per sample, necessitating sample batching and high-throughput platforms, which limits accessibility and increases turnaround times.

Methods: We evaluated Enspyre (Enrichment by selective pyrophosphorolysis and release), a novel enrichment technology that enables selective enrichment of specific variant molecules rather than just target regions. Eight lung cancer patients underwent whole genome sequencing of FFPE tumor tissue (median coverage 118x) for personalized probe design targeting a median of 1,995 somatic variants. Patient plasma samples were diluted to create a concentration series (5-1000 ppm) using healthy donor plasma. Enspyre enrichment was performed on low-input cfDNA samples (median 7.67 ng) followed by sequencing on NextSeq 550 with only 9.6 million read pairs per sample. ctDNA detection and quantification were performed using a Bayesian MRD estimation model, with analyses conducted blinded to ground truth concentrations.

Results: Enspyre demonstrated exceptional analytical performance across 72 patient samples and 8 controls. The assay achieved 100% sensitivity at 10 ppm (6/6 samples detected) and 20% sensitivity at 5 ppm (1/5 samples detected) without molecular barcodes. 100% specificity was maintained with no false positives in control samples (10/10 correctly called negative). Quantitative ctDNA estimates showed strong linear correlation with expected values ($r=0.90$, $p<2.2\times10^{-16}$), with estimates averaging 1.22-fold of target concentrations. Performance was maintained despite low DNA inputs, with successful detection from as little as 0.84 ng cfDNA. Compared to standard hybrid capture methods, Enspyre achieved equivalent sensitivity with a 98% reduction in sequencing depth (10M vs 500M reads per sample).

Conclusions: Enspyre enables ultra-sensitive ctDNA detection at 10 ppm with dramatically reduced sequencing requirements, addressing key barriers to clinical implementation. The technology's ability to maintain performance with low DNA inputs and simplified workflows makes ctDNA testing accessible on benchtop sequencers, potentially enabling broader adoption in clinical trials and community oncology. Sample throughput increases from 1 to 40 samples per NextSeq run represent a 40-fold improvement in accessibility. These results support Enspyre's potential to democratize ctDNA-based MRD detection while maintaining the analytical rigor required for clinical decision-making.

#1144 Tumor genomic features and postsurgical ctDNA status in patients with stage I-IV uterine cancer.

Tara Berman[1], Bhakti Dwivedi[2], Carly B. Scalise[3], Punashi Dutta[2], Adam ElNaggar[2], Minetta Liu[2], Casey Cosgrove[4]

[1]Dana-Farber Cancer Institute, Boston, MA,[2]Natera, Austin, TX,[3]Natera, Autin, TX,[4]James Cancer Hospital Solove Research Institute, Columbus, OH

Introduction: Molecular residual disease (MRD) detection using personalized, tumor-informed circulating tumor DNA (ctDNA) is a promising biomarker for early detection of recurrence and treatment response in uterine cancer (UC). However, the biological and genomic correlates of ctDNA positivity remain poorly understood in this setting. This study aimed to evaluate the prevalence and dynamics of ctDNA in UC patients, and associations with key genomic alterations derived from Altera™ comprehensive genomic profiling.

Methods: A retrospective cohort of 200 UC patients with available post-surgical ctDNA testing (Signatera™, Natera, Inc.) and Altera™ profiling from the same primary tumor tissue were analyzed. Inclusion criteria required blood collection within 2 months of surgery, and availability of at least one additional timepoint during adjuvant or surveillance period. Associations between ctDNA status/dynamics and Altera-reported genomic results were assessed.

Results: Among 200 evaluable UC patients, 43% (86/200) were ctDNA-positive (+) and 57% (114/200) were ctDNA-negative (-) within the MRD window. When stratified by stage, 15% (12/82) of early-stage (ES, stages I-II) and 63% (74/118) of late-stage (LS, stages III-IV) patients were ctDNA(+), indicating a higher MRD burden in advanced/aggressive disease. Genomic correlation analyses demonstrated that during the MRD window, ctDNA status was significantly associated with MSI-H/MSS status (chi-square test, $p<0.05$). ctDNA positivity rate was 78% (66/85) and 22% (19/85) among MSS and MSI patients, respectively. *POLE* exonuclease mutations (N=11; ctDNA(+): 18% [2/11]; ctDNA(-): 82% [9/11]) were seen in 55% (6/11) of MSS and 45% (5/11) of MSI-H patients. Among MSS patients with *POLE* mutations (N=6), 17% (1/6) were ctDNA(+) and 83% (5/6) were ctDNA(-). Similarly, among MSI-H patients with *POLE* mutations (N=5), 20% (1/5) were ctDNA(+) and 80% (4/5) were ctDNA(-). Notably, all MSS patients without an MMR alteration were ctDNA(+). When analyzed longitudinally, 93% (14/15) of MMR-altered ctDNA(-) patients remained serially ctDNA(-) throughout adjuvant/surveillance period, while 50% (4/8) of MMR-altered ctDNA(+) patients cleared ctDNA. Conversely, in the non-altered MMR group, 81% (18/95) of ctDNA(-) patients remained serially ctDNA(-), and 27% (21/77) of ctDNA(+) patients cleared ctDNA.

Conclusions: Post-surgical ctDNA status and dynamics are associated with disease stage and genomic features. Overall, ctDNA status within the MRD window was associated with MSI status. Post-surgical lack of ctDNA positivity and sustained clearance of ctDNA in the adjuvant period were associated with POLE alterations and/or MMR-altered phenotype, consistent with better prognosis. Given high prognostic value of ctDNA status and dynamics, integrating ctDNA-based MRD monitoring may aid in recurrence risk assessment and guide adjuvant therapy decisions.

#1145 Genome-wide cell-free DNA fragmentomes from blood and saliva enable early detection of head and neck cancers.

Akshaya Vijaya Annapragada[1], Shanaya Patel[2], Sarah Short[1], Keerti Boyapati[1], Shashi Koul[1], Hope Orjuela[1], Alice Eastman[1], Aditi Patel[2], Shreya Lotia[2], Vaishnavi Patel[2], Jason Zavras[1], Adrianna Bartolomucci[1], Dushyant Mandlik[3], Kaustubh Patel[3], Vivek Tanavde[2], David Sidransky[1], Mariana Brait[1], Rob Scharpf[1], Victor Velculescu[1], Jillian Phallen[1]

[1]Johns Hopkins University School of Medicine, Baltimore, MD,[2]Ahmedabad University, Ahmedabad, India,[3]HCG Cancer Centre, Ahmedabad, India

INTRODUCTION: Over a billion people globally are impacted by risk factors for head and neck squamous cell carcinoma (HNSCC) - primarily smoking and smokeless tobacco, alcohol and human papillomavirus (HPV) - and may benefit from screening programs if they were available (five-year survival more than doubles for early-stage compared to metastatic disease across tumor sites but currently only 30% of cancers are diagnosed in early stages). We previously developed non-invasive blood tests for multiple cancer types using cell-free DNA (cfDNA) fragmentation profiles (DELFI) and repeat landscapes (ARTEMIS). These tests use cost-effective low-coverage whole-genome sequencing (WGS) to analyze millions of cfDNA fragments whose length, composition, and genome-wide distribution reflect cancer-related genetic and epigenetic changes. Here, we expand these analyses to another non-invasively sampled biofluid, saliva, and demonstrate their use for HNSCC detection.

METHODS: We established a prospective single-center collection of blood and saliva samples from individuals with and without HNSCC (n=329). These include 68 healthy individuals without high-risk exposures, 62 healthy individuals who use chewing tobacco, 17 individuals with high-risk leukoplakia, and 182 individuals with cancer, including 39, 37, 27, and 79 with stages I-IV of HNSCC respectively. We extracted cfDNA from blood (all, n=329) and saliva (subset, n=96), performed low-coverage WGS, and split individuals into Discovery (n=244) and Validation (n=85) cohorts. We evaluated genome-wide fragmentation profiles (DELFI) and repeat landscapes (ARTEMIS) in blood and saliva. We cross-validated three ARTEMIS-DELFI classifiers using blood, saliva, or features from both biofluids when available in the Discovery Cohort, and evaluated the locked models in the held-out Validation Cohort.

RESULTS: Genome-wide fragmentomes were concordant between blood and saliva samples from the same patients (median correlation coefficient r=0.76, IQR 0.64 - 0.87), and reflected cancer-related alterations including chromosomal changes such as 8q gain and 3p and 9p loss. In the Discovery Cohort, individuals with HNSCC were detected with high performance (AUC=0.87, 95% CI=0.83-0.91 and AUC=0.85, 95% CI=0.76-0.94 for plasma and saliva, respectively), and a combined model using features from both biofluids achieved an AUC of 0.89 (95% CI 0.82-0.97). In the Validation Cohort, at locked thresholds corresponding to 90% specificity, 65%, 71%, and 71% of cancers were detected by the blood, saliva and combined models, respectively. Across cohorts, sensitivity for Stage I tumors was >= 50% for all models.

CONCLUSIONS: We demonstrated that cfDNA fragmentation profiles and repeat landscapes can be obtained from both blood and saliva. These approaches may enable accessible, high-performance screening for HNSCC in global high-risk populations.

: Mechanistic Insights for Targeted Therapies in Pediatric Cancer
Poster Session

#1149 Multimodal liquid biopsy of Ewing sarcoma reveals high sensitivity prior to radiotherapy.

Roman O. Kowalchuk, Lilli J. Greiner, Yohan Kim, Rubia Noori, Jeffrey Szymanski, William S. Harmsen, Pradeep S. Chauhan, Adam C. Amundson, Andrea M. McMahon, Peter J. Schoettler, Wendy A. Allen-Rhoades, Stephanie F. Polites, Peter S. Rose, Kelly M. Bailey, Linda M. McAllister-Lucas, Anita Mahajan, Fabrice Lucien-Matteoni, Nadia N. Laack, Aadel A. Chaudhuri

Mayo Clinic Cancer Center Minnesota, Rochester, MN

Introduction: Detectable circulating tumor DNA (ctDNA) is associated with inferior outcomes in Ewing sarcoma (ES); however, ctDNA clears in nearly all patients within 2 of the 6 chemotherapy cycles before radiotherapy (RT) or surgery. Given a 3-year EFS of 37% on AEWS 1221 (metastatic) and 5-year EFS of 78% on AEWS 1031 (localized), current ctDNA testing fails to predict most relapses. Extracellular vesicles (EVs) are microscopic particles studied as a biomarker in multiple cancer types. We hope to improve the sensitivity of ctDNA in ES and provide the first application of EVs in ES.
Methods: cfDNA was isolated from 1mL plasma, quantified by Qubit, and sequenced as NEBNext Enzymatic Methyl-seq v2 libraries. We performed a systematic unsupervised clustering analysis of 27 ES plasma cfDNA profiles using 4 differentially methylated regions (DMR) subsets (63 strong DMRs, top 30, top 15, and 10 promoter-proximal loci), 3 clustering algorithms (k-means, Ward hierarchical, PAM), and k=2-5 clusters, testing associations with tumor burden and progression. EV analysis involved antibody detection against ES surface markers, including LINGO1, ENPP1, CDH11, and CD99. Concentrations of EVs were determined by standardized and calibrated high-resolution flow cytometry then analyzed with custom-built software to automatically determine and apply gates. Samples were de-identified, randomly coded, and run in triplicates. The senior research technologist responsible for EV analysis was blinded to patient information and clinical data.
Results: EV analysis included 36 pre-RT samples from 16 metastatic and 20 localized ES patients from a prospectively maintained biobank, with 27 pre-RT samples in the cfDNA analysis and 19 healthy donor (HD) samples. 35 of 36 patients had chemotherapy before sample collection. cfDNA concentrations were markedly elevated in ES patients compared with HD (24.4 vs 4.6 ng/mL, $p<0.0001$), and 74% of ES samples exceeded the HD 95th-percentile detectability threshold (7.0 ng/mL). Across clustering configurations, ES cfDNA profiles consistently exhibited reproducible methylation substructure. One configuration (PAM clustering, k = 5, 63 strong DMRs) showed a modest but permutation-supported association with primary tumor size (nominal $p \approx 0.04$; empirical $p \approx 0.03$-0.04). ES samples had increased EV concentration compared to HD ($p<0.001$), with AUC 0.988 for distinguishing between ES and HD ENPP1 ($p<0.0001$). The highest ENPP1 EV values were in patients with large primary tumors (>8 cm vs. ≤ 8cm) and metastatic disease ($p=0.066$).
Conclusions: cfDNA- and EV-based liquid biopsy provide encouraging signals for high ES detectability pre-RT. We also show the first study of EVs as a novel biomarker in ES, which may provide complementary information to ctDNA. Multimodal liquid biopsy in ES may identify candidate patients for systemic or local therapy escalation and facilitate personalized care.

#1150 Combining CDK4/6 inhibitor with TMZ and radiation alters cell states for synergistic responses in orthotopic DIPG models.

Zilu Huang[1], Tongchao Jiang[2], Milagros M. Suarez Palacios[2], Tommy Ouyang[2], Aalaa Abdallah[2], Long Niu[2], Jinnan Chen[2], Xin Zhai[2], Emily Ciolak[2], Wenan Qiang[2], Runxin Wu[3], Nitin Wadhwani[4], Alicia Lenzen[4], Michael DeCuypere[4], Sandi Lam[3], Shi-Yuan Cheng[5], Ching Man Wai[6], Brian Wray[6], Matthew John Schipma[6], Xinkun Wang[4], Wan-Yee Teo[7], Daniel J. Brat[8], Yuchen Du[4], Yunfei Xia[1], Xiao-Nan Li[4], John Kalapurakal[9]

[1]Department of Radiation Oncology, Sun Yat-Sen University Cancer Center, Guangzhou, China,[2]Pediatrics, Northwestern Univ. Feinberg School of Medicine, Chicago, IL,[3]Northwestern Univ. Feinberg School of Medicine, Chicago, IL,[4]Ann & Robert H. Lurie Children's Hosp. of Chicago, Chicago, IL,[5]Professor, Northwestern University, Chicago, IL,[6]NUSeq Core Facility, Center for Genetic Medicine, Northwestern Univ. Feinberg School of Medicine, Chicago, IL,[7]National Cancer Center, Singapore, Singapore,[8]Professor, Dept. of Path. & Lab Med., Northwestern University, Chicago, IL,[9]Department of Radiation Oncology, Northwestern Univ. Feinberg School of Medicine, Chicago, IL

Background: To develop effective therapies for DIPG at different clinical stages, we examined efficacy and mechanisms of action of a combination therapy—abemaciclib (a CDK4/6 inhibitor), temozolomide (TMZ), and radiation (XRT)—in two patient-derived orthotopic xenograft (PDOX) models derived from treatment-naïve (IBs-9119DIPG) and autopsied (IBs-A0317DIPG) tumors.
Methods: In vitro synergistic anti-tumor activities were examined in tumor organoids, and in vivo efficacy in the PDOX models treated with abemaciclib (75 mg/Kg × 14 days), TMZ (50 mg/Kg × 5 days) and XRT (2 Gy/day × 5 days) alone and in combination (n=10/group, 60 mice/model). Changes of animal survival times were analyzed with log-rank analysis. Mechanisms of treatment response and resistance were elucidated by immunohistochemistry and scRNA-seq analysis.
Results: The triple therapy generated synergistic anti-tumor effects in organoids and significantly extended survival times in both PDOX models ($P<0.05$) despite their strong cellular state differences. scRNAseq identified reduction of oligodendrocyte-progenitor-like (OPC-like) cells in both models and astrocyte-like (AC-like) cells in IBs-A0317DIPG as response mediators; and revealed expansion of neural progenitor-like (NPC-like) cells in IBs-A0317DIPG and of mesenchymal-like (MES-like) and mitotic-like cells in IBs-9119DIPG as resistance contributors. Pseudotime trajectory analysis uncovered the exit of stemness into differentiation in oligodendrocyte-progenitor-like (OPC-like) cells as a novel mechanism of resistance in the treatment-naïve IBs-9119DIPG, in contrast to the enrichment of stem-like cells in the recurrent model IBs-A0317DIPG. A radiation-resistant subpopulation with novel candidate targets (*NPAS3, TBC1D5, INPP4B*) was also discovered.
Conclusions: This study demonstrated strong anti-DIPG capacities of the triple therapy in both untreated and recurrent DIPG tumors by acting on distinct cellular and molecular targets, and identifies previously unrecognized mechanisms underlying DIPG therapy response and resistance.

#1151 Targeting high risk osteosarcoma: MYC modulation alters metastasis.

Emily Seiden[1], Scott Sauer[2], Emma Hiscock[1], Nha Nhu Le[1], Ainsley Hellens[1], Monica Inda[1], Andrew Fuller[1], Sridhar M. Veluvolu[3], Rachael Hinshaw[1], Zachary P. Tolstyka[1], Elissa Levine[1], Rashmi Chugh[1], Theodore W. Laetsch[3], Nouri Neamati[4], Heather Wilson-Robles[5], Chand Khanna[6], David Warshawsky[2], Patrick J. Grohar[1]

[1]University of Michigan Medical School, Ann Arbor, MI,[2]Healx USA, Inc, Hoboken, NJ,[3]Children's Hospital of Philadelphia, Philadelphia, PA,[4]Univ. of Michigan College of Pharmacy, Ann Arbor, MI,[5]Ethos Discovery, Washington D.C, DC,[6]Ethos Discovery, Washington D.C., DC

Osteosarcoma (OS) is a bone tumor that affects human and canine patients. Standard of care is neoadjuvant chemotherapy and surgery resulting in a 5 year survival rate for patients with localized disease of ~70%. However, patients with metastatic disease and relapsed disease have a 5 year overall survival of less than 30%. Therefore, there is a critical need for improved therapies and a better understanding of the biological underpinnings of high risk disease. A subset of patients with particularly poor outcomes are known to have copy number amplification of MYC. However, it is not known if MYC contributes to the high risk phenotype by driving metastatic progression or drug resistance. Importantly, 20 compounds have been described as MYC inhibitors and perturb different steps of MYC driven transcription. In this report, we found that MYC drives cell migration and outgrowth but does not appear to contribute to drug resistance in OS cells. More precisely, MYC silencing reversed the metastatic phenotypes of migration and outgrowth of OS cells. Further, MYC downstream targets play an important role in metastatic progression. Silencing of MYC in 5 different cell lines revealed 45 common induced targets, many of which are known to modulate different steps in the metastatic cascade. We screened all 20 compounds previously shown to interfere with MYC transcription using an approach designed to capture the compound that modulates both MYC activity and the metastatic phenotype. Fourteen compounds modulated expression of MYC and/or downstream targets in 4 different OS models. Of those,10 compounds had a profound impact in cell viability in both 2D and 3D assays. Five of these showed selective toxicity in 3D relative to 2D; a phenotype linked to metastatic progression. Importantly, not all compounds that modulated MYC showed therapeutically favorable effects on migration or metastatic organization and outgrowth with at least 2 compounds driving a dramatic increase in migration despite suppressing expression of MYC. Nevertheless, 2 compounds, samuraciclib and THZ531, blocked MYC expression, downstream target expression, cell migration, metastatic organization and outgrowth. We confirmed these results and showed reversal of metastatic competence and complete reversal of metastatic outgrowth using the in vivo/ex vivo pulmonary metastasis assay (PuMA). We are now working to integrate CUT&Tag with BRUseq, an assay of nascent transcription, to determine if modulation of different steps in MYC transcription drives diverse cellular phenotypes as we hypothesized. Nevertheless, the top hit of the screen, samuraciclib, convincingly reverses MYC activity and the associated metastatic phenotype and is undergoing additional testing in metastatic OS mouse models and a canine clinical trial is under development. Correlative biology such as spatial transcriptomics will be used to guide the translation of samuraciclib to patients with high risk osteosarcoma.

#1152 Targeting *Yap1*-B7-H3 signaling stimulates CD8$^+$ anti-tumor response preferentially in male SHH medulloblastoma.

Nourhan Abdelfattah*[1], **Maryam Faisal***[1], Han Nhat Tran[1], Thomas Wong[1], Freddys Rodriguez[2], Carston R. Wagner[2], Kyuson Yun[1]

[1]Neurology, Houston Methodist Research Institute, Houston, TX,[2]Medicinal Chemistry, University of Minnesota, Minneapolis, MN

Sex-biased mechanisms in cancer remain poorly understood. We recently reported an unexpected sex-biased function of *Yap1*, an oncogene dysregulated in many human cancers, in murine models of SHH medulloblastoma (MB). *Yap1* deletion significantly extends survival preferentially in male animals and enhances immune infiltration, in part by attenuating the expression of the immune checkpoint molecule *Cd276* (B7-H3) in MB cells. These findings are clinically relevant because male patients with MB, the most common pediatric brain malignancy, exhibit worse survival and a higher incidence.

Here, we investigate the sex-specific consequences of *Yap1* loss and evaluate therapeutic targeting of CD276 using systemically administered CD276-targeting chemically self-assembled nanorings (CD276-CSANs).

Extensive characterization of the immune microenvironment in *Yap1*-deleted male and female tumors, conducted via single-cell RNA sequencing and high-parameter flow cytometry, revealed a significant increase in CD8+ T cells exhibiting cytotoxic properties in males, but not in females. In contrast, *Yap1*-deleted females had higher numbers of exhausted CD8+ T cells and regulatory T cells. Further, *in vivo* CD8 T cell depletion abolished the survival advantage seen in *Yap1*-deleted male MB, confirming the functional importance of these cells.

T-cell proliferation assays demonstrated that in male MB cells, targeting either *Yap1* or CD276 restored T-cell activation. In contrast, females, which have higher baseline CD276 expression, required both *Yap1* deletion and CD276 blockade/deletion to achieve similar activation. Consistently, CD276 blockade with CD276-CSANs phenocopied the male-biased survival advantage of *Yap1* deletion and increased CD8+ T-cell infiltration *in vivo*.

Overall, these findings reveal that *Yap1* promotes male-biased MB progression via *Cd276*-mediated CD8+ T cell suppression, resulting in immune evasion and highlighting CD276 as a promising therapeutic target for improving male MB prognosis.

*contributed equally

#1153 Genome-driven molecular stratification and clinical impact in pediatric solid tumors: Results from the STREAM program.

Ji Won Lee[1], **June-Young Koh**[2], Chang Yeon Kim[2], Joo Whan Kim[3], Jung Yoon Choi[3], Seung Ah Choi[3], Seung-Ki Kim[3], Se Hoon Kim[4], Ji Hoon Phi[3], STREAM Consortium

[1]Samsung Medical Center, Seoul, Korea, Republic of,[2]Inocras Inc., San Diego, CA,[3]Seoul National University Hospital, Seoul, Korea, Republic of,[4]Yonsei University College of Medicine, Seoul, Korea, Republic of

The STREAM (Strategic TREatment And Magic for pediatric cancers) program, launched in March 2023, is a nation-wide precision-medicine platform for paediatric solid tumours and, unlike prior WGS studies centred on relapsed or high-risk disease, predominantly captures newly diagnosed patients. The programme integrates tumour-germline whole-genome sequencing, transcriptome and methylome profiling, in-vitro drug-response testing, centralised pathology review and multidisciplinary interpretation. Among 308 patients, somatic drivers were identified in 253 (82.1%), totalling 1,082 events across 404 genes. Pathogenic germline variants occurred in 32 of 303 evaluable patients (10.4%). Genomic profiling refined diagnosis in 85 cases, informed prognostic stratification in 20 and revealed 117 actionable targets across 99 patients. In-vitro drug screening from 58 patients yielded 496 sensitive and 1,376 resistant drug-tumour interactions. The genomic landscape showed lower mutational burden than adult cancers and was dominated by key pathways in cell-fate commitment, organ development and cell-cycle control. Using driver-gene alterations mapped to curated signalling programmes, we performed unsupervised clustering, identifying ten molecular sub-clusters. Several represented biologically coherent groups not captured by morphology: MAPK-driven pilocytic astrocytoma, Langerhans-cell histiocytosis and PLNTY formed one cluster; atypical teratoid/rhabdoid tumour and supratentorial ependymoma aligned through shared cell-cycle and epigenetic dysregulation; and medulloblastoma segregated into WNT, SHH and heterogeneous Group 3-4, the latter marked by SBS39 exposure linked to homologous-recombination deficiency. For prognostic evaluation, we analysed primary-diagnosis solid tumours (n=185), excluding relapse samples and haematologic malignancies. Survival differed significantly across clusters (OS p=0.0071). Cluster 6, composed mainly of Ewing sarcoma and rhabdomyosarcoma with growth-factor-receptor and secondary-signalling alterations, showed the highest mortality and relapse frequency and was the only group with a reached median OS. Clusters 2, 7 and 9 showed no deaths; Cluster 2 comprised Hedgehog-dominant medulloblastoma and related fibro-osseous tumours; Cluster 7 consisted of Group 3-leaning medulloblastoma and DNA-repair-altered tumours; and Cluster 9 included proliferative-signal-driven sarcomas and neuroblastoma, with no relapses observed. These molecular subgroups also showed strong concordance with in-vitro drug-response patterns. In this nation-wide cohort, molecular sub-clustering enhances diagnostic resolution, reveals pathway-defined biology missed by morphology and provides clinically meaningful prognostic stratification.

#1154 Multi-omic profiling of cellular heterogeneity and microenvironmental remodeling underlying treatment resistance in neuroblastoma.

Eun Seop Seo[1], JI WON LEE[1], In Woo Hwang[1], Woong-Yang Park[2], Jun Sun Kim[1], Ki Woong Sung[1]

[1]Samsung Medical Center, Seoul, Korea, Republic of,[2]Geninus, Seoul, Korea, Republic of

Background: Relapse and therapy resistance in high-risk neuroblastoma (NBL) remain major clinical challenges. The dynamic evolution of neuroblasts and their tumor microenvironment (TME) during treatment is not fully characterized. We established a multi-omic, longitudinal cohort to dissect the cellular and molecular mechanisms driving therapeutic failure.
Methods: We established a multi-omic longitudinal cohort of high-risk neuroblastoma. This included single-cell RNA sequencing (scRNA-seq) on 18 tumors (7 pre-treatment, 5 post-treatment, 6 relapsed), complemented by matched Xenium spatial transcriptomics for spatial mapping. Parallel Nanopore sequencing was conducted on a longitudinal NBL cohort to define the genomic and epigenomic landscape. A validation cohort of 76 bulk RNA-seq samples was used to correlate findings with clinical outcomes.
Results: Our scRNA-seq analysis identified a distinct ADRN_proliferating neuroblast subtype. In our validation cohort (n=76), the signature of this subtype was significantly associated with poor prognosis and correlated with the poorest response to induction chemotherapy. Longitudinal sampling showed that induction chemotherapy drives a predominant ADRN to MES shift in neuroblasts, while relapsed tumors exhibit the re-emergence of ADRN-like cells. However, this re-emergence was accompanied by markedly increased spatial heterogeneity.
Methylation profiling revealed an epigenetically post-imprinted ADRN program at relapse; these cells retained post-treatment-like methylation patterns in key TFs, such as GATA3, distinct from their treatment-naïve state. The TME underwent progressive remodeling from pre- to post-chemotherapy toward a more unfavorable, immunosuppressive state characterized by enrichment of $SPP1^{+}$ macrophages and other myeloid populations. This unfavorable TME was largely maintained at relapse, even as MES-like tumor cells reverted toward an ADRN phenotype, creating a highly treatment-refractory ecosystem. Ligand-receptor analysis implicated monocyte- and neutrophil-derived RTN4R signaling to neuroblasts and NOTCH signaling from Schwann cells as potential mediators of this relapse-prone niche.
Conclusion: Our multi-omic analysis demonstrates that NBL relapse is not a simple reversion but the emergence of a novel, epigenetically primed ADRN state co-evolving with a sustained, immunosuppressive TME.

#1155 High-throughput screening identifies synergistic drug interactions between CDK8/19 and DHFR inhibitors in rhabdomyosarcoma.

Ukhyun Jo[1], Ying Wu[2], Lisa M Jenkins[3], Tapan Kumar Maity[4], Seth P Zimmerman[5], Chris M. Counter[6], Assil Fahs[7], Corinne Linardic[5], Craig J. Thomas[3], John F. Shern[8]

[1]National Cancer Institue, Bethesda, MD,[2]Frederick National Laboratory for Cancer Research, Frederick, MD,[3]National Cancer Institute, Bethesda, MD,[4]Senior Research Fellow, Medical Oncology Branch, NCI-CCR, Bethesda, MD,[5]Duke University, Chapel Hill, NC,[6]Professor, Duke University Medical Center, Durham, NC,[7]Duke University, Durham, NC,[8]Clinical Fellow, Pediatric Oncology, NCI-CCR, Bethesda, MD

Rhabdomyosarcoma (RMS) is an aggressive pediatric soft-tissue sarcoma marked by substantial treatment-related morbidity and poor outcomes, particularly in metastatic or recurrent disease. Although diagnostic and therapeutic approaches have improved, survival remains low for patients with high-risk molecular features, including tumors harboring the PAX3::FOXO1 fusion. This fusion protein drives an aberrant transcriptional program that promotes tumor progression and resistance to therapy, underscoring the need for new treatment strategies. In this work, we investigated therapeutic vulnerabilities created by inhibiting the transcription-regulatory kinases CDK8/19. Using a high-throughput drug combination screen, we tested several CDK8/19 inhibitors against a library of 2,803 preclinical, investigational, and approved small molecules. The screen identified a strong synergistic interaction between CDK8/19 inhibitors and dihydrofolate reductase (DHFR) inhibitors. Unsupervised hierarchical clustering showed that multiple DHFR inhibitors formed a distinct cluster with highly similar patterns of synergy, supporting the robustness of this interaction. Follow-up viability assays confirmed synergy in both PAX3::FOXO1-positive and fusion-negative RMS cell lines. To define the biological basis of this synergy, we examined effects on transcriptional regulation, cell-cycle dynamics, and apoptosis. Annexin-V/DAPI staining demonstrated that combined treatment produced significantly higher apoptosis and G1 arrest than either drug alone. EdU incorporation assays showed a strong decrease in DNA replication, indicating impaired nucleotide synthesis. Transcriptomic profiling, including gene set enrichment analysis, revealed that CDK8/19 inhibitors upregulated PAX3::FOXO1 fusion targets, MYC-regulated genes, and oxidative phosphorylation pathways, whereas DHFR inhibitors primarily induced immune-related and KRAS signaling programs. The transcriptional responses to each drug class were largely distinct, and combination treatment reversed expression patterns driven by single agents. Importantly, DHFR inhibition triggered compensatory activation of pyrimidine biosynthesis genes, a response that was suppressed by CDK8/19 inhibition, providing a mechanistic basis for the observed synergy. ChIP-seq and proteomic data further supported these findings. Additionally, CDK8/19 inhibition amplified DHFR inhibitor-induced DNA damage, reflected by elevated γH2AX accumulation. Overall, these results highlight a therapeutic strategy that concurrently disrupts PAX3::FOXO1-driven transcriptional programs and nucleotide-dependent DNA repair. The combination of CDK8/19 and DHFR inhibitors may therefore overcome resistance mechanisms and enhance treatment efficacy in RMS.

#1157 Preclinical evaluation of PEG-[SN22]$_4$ (PEEL-224), a multivalent polymeric camptothecin prodrug, in pediatric solid tumor patient-derived xenograft models.

Filemon S. Dela Cruz[1], Kristina C. Guillan[1], Samantha Brosius[1], Armaan H. Siddiquee[1], Glorife Ibanez Sanchez[1], Daoqi You[1], Kristen Victor[1], Paul Calder[1], Trent Fowler[2], Joshua D. Schiffman[2], Andrew L. Kung[3]

[1]Memorial Sloan Kettering Cancer Center, New York, NY,[2]Peel Therapeutics, Salt Lake City, UT,[3]Chair, Division of Pediatric Hematology/Oncology, Memorial Sloan Kettering Cancer Center, New York, NY

Background:
PEEL-224 is a multivalent polymeric prodrug of the topoisomerase I inhibitor SN22 designed to sustain intratumoral exposure and reduce transporter-mediated efflux. Desmoplastic small round cell tumor (DSRCT) and osteosarcoma (OS) are high-risk sarcomas of children and adolescents/young adults where irinotecan+temozolomide (I/T) provides modest, short-lived benefit. Early-phase clinical evaluation of PEEL-224 is ongoing (NCT06709495, NCT06721689, NCT05329103). However, the comparative activity of PEEL-224±TMZ versus irinotecan-based therapy has not been defined in disease-relevant models, prompting evaluation in DSRCT and OS patient-derived xenografts (PDXs).
Methods:
PDX-bearing NSG mice were randomized to vehicle, irinotecan, I/T, PEEL-224, or PEEL-224+TMZ. Tumor growth was assessed using Vardi's test for area-under-the-curve comparisons. Event-free survival (EFS) was defined as time to progression (≥100% relative tumor volume [RTV] increase from baseline) or euthanasia for tumor burden and analyzed by Kaplan-Meier with log-rank tests. Response criteria: PD = ≥100% RTV increase or euthanasia; SD = <100% increase and ≤50% reduction; PR = >50% reduction; CR = >95% reduction. Objective response rate (ORR) was the proportion achieving PR or CR. Treatment arms were expanded in an adaptive manner based on disease control to increase cohort size for key comparisons.
Results:
In DSRCT, tumor volume comparisons showed significantly greater control with PEEL-224 monotherapy vs irinotecan (p=0.04), while PEEL-224+TMZ and I/T showed similar control at this stage; cohort expansion is ongoing. EFS analysis showed PEEL-224 significantly prolonged EFS vs irinotecan (p=0.01) and PEEL-224+TMZ vs I/T (p=0.02). At end of therapy (Day 29), ORR was 0% (vehicle), 20% (irinotecan, 1/5 PR), 20% (I/T, 1/5 PR), 100% (PEEL-224, 5/5 PR), and 100% (PEEL-224+TMZ, 5/5 PR). At end of study (Day 113), irinotecan and I/T had 0% ORR, while PEEL-224 maintained 60% (3/5 PR, 2/5 SD) and PEEL-224+TMZ 100% (5/5 PR). Regimens were well tolerated. In OS, PEEL-224±TMZ produced disease stabilization and early regression, though statistical significance has not yet emerged (n=3/arm); expansion is ongoing.
Conclusions:
PEEL-224 demonstrated superior disease control as monotherapy and in combination over irinotecan-based therapy in DSRCT and early activity in OS. These preclinical data, alongside ongoing clinical evaluation, support advancement of PEEL-224 for high-risk pediatric and AYA sarcomas.

#1158 Hypermutation patterns shape tumorigenesis and immunotherapy response in mismatch repair deficient glioma.

Nicholas R. Fernandez[1], Yuan Chang[1], Nuno M. Nunes[1], Jose R. Dimayacyac[1], Adrian Levine[1], Amit Ringel[1], Logine Negm[1], Ayse B. Ercan[1], Julian Hess[2], Olfat Ahmad[3], Caitlin Lee[1], Lucie Stengs[1], Vanessa Bianchi[1], Melissa Edwards[1], Sheradan Doherty[1], Jiil Chung[1], Liana Nobre[4], Julie Bennett[1], Andrew J. Dodgshun[5], David TW Jones[3], Stefan M. Pfister[6], Anita Villani[1], David Malkin[1], Vijay Ramaswamy[1], Annie Huang[1], Eric Bouffet[1], Melyssa Aronson[7], Peter B. Dirks[1], Adam Shlien[1], Gad Getz[2], Yosef E. Maruvka[8], Birgit Ertl-Wagner[1], Cynthia Hawkins[1], Anirban Das[1], Uri Tabori[1]

[1]Hospital for Sick Children, Toronto, ON, Canada,[2]Broad Institute of MIT and Harvard, Cambridge, MA,[3]Hopp Children's Cancer Center (KiTZ), Heidelberg, Germany,[4]Stollery Children Hospital, Edmonton, AB, Canada,[5]Christchurch Hospital, Christchurch, New Zealand,[6]Pediatric Neurooncology, Hopp Children's Cancer Center Heidelberg (KiTZ), Heidelberg, Germany,[7]Zane Cohen Centre for Digestive Diseases, Toronto, ON, Canada,[8]Technion-Israel Institute of Technology, Tel Aviv, Israel

Primary mismatch repair deficient (priMMRD) glioma are deadly cancers comprising 5-10% of gliomas in children and young adults. PriMMRD glioma are characterized by universal hypermutation, resistance to chemo-irradation, and striking, but hetergeonous, responses to anti-PD1 immunotherapy. To elucidate the impact of replication-error driven mutagenesis on priMMRD glioma evolution and their heterogenous clinical courses, we analyzed genomic, methylomic, immune, and clinical data on a large cohort of priMMRD glioma (n=162) from the the International Replication Repair Deficiency Consortium. MMRD contributed to high microsatellite instability and hypermutation resulting in global DNA hypomethylation compared to non-MMRD gliomas and potentially affecting their classification. Recurrent somatic driver mutations in replicative polymerases and *IDH1* stratified priMMRD gliomas into 3 distinct genetic and clinical subgroups: priMMRD1 (MMRD+*POLE/POLD1*, 56%), priMMRD2 (MMRD-only, 27%), and priMMRD3 (MMRD+*IDH1*, 17%). PriMMRD1 gliomas, which harbor complete replication repair deficiency, originated from germline biallelic MMRD (CMMRD), occurred at young ages, and exhibited ultrahypermutation. PriMMRD2 gliomas were enriched for monoallelic germline MMRD (Lynch syndrome) and older ages. Finally, *IDH1*-driven priMMRD3 gliomas harboured germline mutations in MutSα (*MSH2*/*MSH6*), lower mutation burden, and distinct imaging patterns. Subgroups also utilized different mechanisms of genomic instability: while priMMRD1 gliomas harboured frequent point mutations in glioma drivers, priMMRD2 and priMMRD3 gliomas had higher rates of copy alteration in the same genes, including *CDKN2A* ($P<0.0001$) and *PTEN* ($P<0.0001$). Driver mutations observed in MMRD-driven gliomagenesis could be explained by the specific trinucleotide contexts that compose MMRD mutational signatures. Hotspot mutations in *TP53* and *IDH1* occurred in contexts commonly mutated by MMRD, while pediatric glioma drivers (*BRAF*/*H3-3A)*, which do not arise from frequently mutated contexts, were rare. Using mutational signatures and variant allele fractions, we built a model of MMRD gliomagenesis where TP53 mutations occur early, followed by secondary mutations in *POLE/POLD1*, *IDH1*, and other glioma drivers. PriMMRD glioma subgroups differed in their immune microenvironment and response to immunotherapy: priMMRD1 gliomas were associated with the highest 2-year overall survival on anti-PD1 monotherapy (75%), exhibited pro-immune expression signatures, and high CD8+ T-cell infiltration, contrasting priMMRD2 (24%) and priMMRD3 gliomas (0%). These findings suggest that MMRD mutagenesis shapes the unique landscape of priMMRD glioma through driver mutation acquisition and responses to immunotherapy, providing a rational approach for the refinement of subgroup-specific immunotherapy combinations.

#1159 Trans-species analysis of replication repair deficient medulloblastoma and response to immune checkpoint inhibition: An IRRDC report.

Nicholas R. Fernandez[1], Anirban Das[2], Adrian Levine[2], Kyle Smith[3], Evan Wang[2], Melissa Galati[2], Zoya Aamir[2], Jiil Chung[2], Logine Negm[2], Hope Friedman[2], Katharine O'Flaherty[2], Owen Crump[2], Quang M. Trinh[4], Nuno M. Nunes[2], Vanessa Bianchi[2], Lucie Stengs[2], Melissa Edwards[2], Lincoln Stein[4], Eric Bouffet[2], Michael D. Taylor[5], Paul Northcott[3], Vijay Ramaswamy[2], Cynthia Hawkins[2], Uri Tabori[2]

[1]Sick Children's Hospital, Toronto, ON, Canada,[2]Hospital for Sick Children, Toronto, ON, Canada,[3]St. Jude Children's Research Hospital, Memphis, TN,[4]Ontario Institute for Cancer Research, Toronto, ON, Canada,[5]Baylor College of Medicine, Houston, TX

Replication repair deficiency (RRD), caused by germline biallelic mutations in mismatch repair, leads to hypermutant brain tumour development in children and adolescents. RRD medulloblastoma have been reported but how RRD driven mutagenesis contributes to their clinical, genomic, and immune profiles is unknown. Through the International RRD Consortium, we enrolled 43 RRD medulloblastoma, analysed their exomes, methylomes, transcriptomes, and clinical outcomes. To better understand the mechanisms underlying their development and to assess preclinical responses to immunotherapy, we analyzed the histology and exomes of embryonal brain tumours developed in RRD mouse models (Nestin-Cre^{+}/*MSH2*$^{LoxP/LoxP}$/*POLE*$^{S459F/+}$). RRD medulloblastoma were enriched for anaplasia (61%), localised disease (77%), and harboured hypermutation and microsatellite instability, contrasting with “quiet” genomic profiles of non-RRD medulloblastoma ($p<0.0001$). Point mutations were frequent in *POLE/POLD1* (80%), *TP53* (48%), SHH pathway genes (56%) and, notably, glioma driver genes (*ATRX*, *NF1*, *RB1*: 50%). *TP53* hotspot mutations were distinct from non-RRD medulloblastoma and occurred in trinucleotide sequence contexts which were highly mutated by RRD mutational signatures, suggesting that replication errors shape their genetic evolution. Copy-number changes were infrequent (<20%) and inversely correlated with tumour mutation burden. While most did not classify with high confidence (>0.9) on DNA methylation subtyping tools, RRD medulloblastoma shared methylation programs with SHH medulloblastoma. Non-promoter genomic regions were hypomethylated relative to non-RRD medulloblastoma, partially explaining their failure to perform in DNA methylation classifiers. Transcriptomics reflected shared expression programs between RRD and SHH medulloblastomas. RRD medulloblastoma demonstrated high CD8^{+} T-cell infiltration and response to anti-PD1 monotherapy, with 60% three-year progression-free survival. Outcome was worse for tumours with *TP53*-mutation ($p=0.04$). Recurrent/progressive RRD medulloblastoma treated with anti-PD1 monotherapy had prolonged survival compared those which were not ($p = 0.02$), including responses in *TP53*-mutant tumours. RRD mouse models developed tumours that mirrored histological and genetic profiles of human disease and responded to anti-PD1 monotherapy, highlighting their relevance for future preclinical studies. Human RRD medulloblastoma are distinguished by their unique spectrum of driver mutations and hypomethylation profiles, shaped by RRD mutagenesis. Mouse models recapitulate human features and offer a mechanistic model for tumorigenesis and immunotherapy responses. Importantly, immune-hot microenvironments in RRD medulloblastoma contribute to successful salvage therapy for tumours failing chemo-radiation.

#1160 Characterizing neddylation as a potential vulnerability in MYC-amplified medulloblastoma.

Qiyun (Rachel) Shao, Vijay Ramaswamy

The Hospital for Sick Children, Toronto, ON, Canada

Background: Medulloblastoma (MB) is the most common malignant pediatric brain tumor. Children with MYC-amplified MB almost universally fail current treatments, highlighting a critical need for targeted therapeutic strategies. Our previous data revealed an enrichment of protein synthesis pathways in MYC-amplified MB, pointing toward protein turnover as a potential target. Neddylation is a post-translational modification process that plays a role in protein turnover through proteasomal degradation. We hypothesize that characterizing neddylation in MYC-amplified MB will identify novel therapeutic vulnerabilities, and that targeting neddylation is a rational therapeutic strategy for MYC-amplified MB.
Methods: Cell viability assay was conducted in four MYC-amplified MB cell lines and normal human astrocyte (NHA) control after 96hr treatment of neddylation inhibitor MLN4924 or TAS4464. Western blot was performed in TAS4464-treated MYC-amplified MB cell lines to evaluate MYC protein dynamics. To characterize neddylation proteome in MB, Co-Immunoprecipitations (Co-IP) were performed using lysates from MB or NHA models with NEDD8 or IgG (negative control) antibodies. Protein identification and quantification were carried out via mass spectrometry (MS), and the resulting dataset was subjected to STRING-based pathway enrichment analysis.
Results: All MYC-amplified MB cell lines exhibited significant sensitivity to TAS4464 compared to NHA. Western blot analysis revealed a transient accumulation of MYC followed by a sustained depletion, consistent with the disruption of neddylation-dependent turnover mechanisms. Nearly 1,000 conserved neddylation substrates were identified across MB cell lines, with the majority representing previously unidentified targets. MB-specific high-confidence targets are enriched in components comprising the mRNA splicing pathway and spliceosome complex. Further functional validation using distinct RNA splicing inhibitors induced potent, dose-dependent cytotoxicity in MYC-amplified MB, with markedly reduced sensitivity observed in NHA.
Conclusion: These findings establish neddylation as a critical dependency in MYC-amplified MB, essential for maintaining MYC protein stability and tumor cell survival. The potency of TAS4464 provides preclinical validation for targeting neddylation pathway. Our proteomics data unveiled a previously unrecognized dimension of neddylation in MB, identifying mRNA splicing machinery as a targetable vulnerability. This study represents the first link between neddylation driving splicing in MYC-amplified MB, suggesting a previously undescribed critical and actionable vulnerability that provides a mechanistic rationale for clinical investigation of neddylation inhibitors in very high-risk MYC-amplified MB.

#1161 Comprehensive pediatric biobanking and model development in the Beat Childhood Cancer Research Consortium.

Divya Gandra[1], Katherine McClain[1], Meenakshi Shukla[1], Laura Vazquez[1], Mohammad Haque[1], Jonathan Lerch[1], Muhammad Younis[1], Thussenthan Walter Angelo[1], Jeremy Hengst[1], Giselle Saulnier Sholler[2]

[1]Penn State College of Medicine, Hershey, PA,[2]Penn State Health Children's Hospital, Hershey, PA

The Pediatric Oncology Translational Research Lab (POTRL) at Penn State University (PSU) provides a critical centralized, LIMS-tracked repository of over 70,000 pediatric cancer specimens and patient-derived models, enabling validated resources for innovative translational research in precision-oncology through the Beat Childhood Cancer (BCC) Research Consortium.

Background:

Reliable translational research depends on high quality, well characterized patient materials. BCC operates a centralized repository managed through the POTRL at PSU. POTRL receives, processes, and stores biospecimens from multiple BCC clinical trials representing children with neuroblastoma, CNS tumors, sarcomas, and other solid malignancies. The repository includes tumor tissue, tissue slides, paraffin-embedded blocks, and blood/plasma that are processed for ctDNA, buffy coats, immune cells, cytokines, and biomarker analyses.

Methods:

All specimens are accessioned and tracked in Freezerworks LIMS to ensure accurate labeling and storage. Patients are consented to the BCC-BIO-001 study (NCT04715178) which collects whole exome and whole transcriptome sequencing of tumors, clinical diagnosis, pathology, treatment and outcomes of patients. Upon receipt, samples are inspected for integrity and temperature compliance. Cell lines, organoids and xenografts are generated from tumor tissue and bone cores/aspirates each of which undergo authentication at IDEXX BioAnalytics using short tandem repeat profiling with concurrent mycoplasma testing and matched patient references. Tumor line validation is performed by flow cytometric analysis using tumor-specific marker panels such as Ewings sarcoma (CD99); neuroblastoma (GD2, CD56, Synaptophysin); or medulloblastoma (CD56, Synaptophysin).

Results:

The repository currently houses more than 70,000 specimens from over 5,000 pediatric patients. Over 750 patient-derived cell lines and 150 patient-derived xenograft models have been established. Implementation of LIMS-based tracking has improved specimen organization and data consistency allowing for tracking of sequential patient samples. Each sample is correlated to timepoints in treatments and outcomes stored in the REDCap database. Development of patient-derived organoid models has recently begun and is ongoing across multiple tumor types, maintaining marker profiles consistent with primary tumors.

Conclusions:

POTRL provides an integrated platform for the collection, validation, and model generation of pediatric cancer specimens. These well characterized resources support translational research projects at Penn State and are shared throughout the BCC research centers nationally and internationally to accelerate biomarker discovery, preclinical testing, and precision-oncology studies for pediatric cancers.

#1162 Revealing the transformative role of METTL13 in human hematopoietic stem cells and progression of pediatric leukemia.

Sabina Enlund[1], Chae-Eun Lim[2], Isabella Hoang[2], Sonali Joshi[2], Amanda Ramilo Amor[1], Cecilia Thomsson[1], Maria Rivera[2], **Adena Pepich**[2], Indranil Sinha[1], Shahrzad S. Fard[1], Anna Nilsson[1], Ola Hermanson[1], Qingfei Jiang[2], Frida Holm[1]

[1]Karolinska Institutet, Stockholm, Sweden,[2]UC San Diego, La Jolla, CA

Childhood leukemia's five year survival rate has been improving over the last 40 years, but still only reaches 86.3% relative survival in the United States according to the Surveillance, Epidemiology, and End Results (SEER) program in 2025. Aberrant post-transcriptional RNA modifications, specifically N6-methyladenosine (m6A) methylation and adenosine to inosine (A-to-I) editing have previously been shown to push malignant transformations of hematopoietic stem cells (HSC). In order to unravel the mechanism behind these RNA modifiers and decipher whether methyltransferases (METTLs, such as METTL3 and METTL14) catalyzing m6A methylation work in concert with the A-to-I editing enzymes, adenosine deaminase acting on RNA 1 (ADAR1) to drive malignant transformation of HSCs. By first exploring differentially expressed genes in lentiviral over-expressed ADAR1 hematopoietic cells and progenitor cells we observed downregulation in the m6A complex (i.e. METTL3, METTL14, and other METTLs), except METTL13. While METTL13 knockdown converged with the other m6A complex knockdown results in immune signaling and survival, METTL13 knockdown uniquely affected cancer related pathways compared to other METTLs. Using publicly available RNA sequencing data from TARGET, we determined that increased METTL13 expression, in both T cell ALL and B cell ALL correlated to poor patient prognosis. Additionally, functional studies for cell proliferation and survival, both in vitro and in vivo, demonstrated METTL13's role in T-ALL when it is removed or lost. Overall these findings display the oncogenic role of METTL13 in T-ALL pathogenesis and pre-leukemic transformations, while revealing a continued research into this potential novel target for new therapies.

#1163 Combined AKT and XPO1 inhibition to target chimeric transcription factor-driven pediatric sarcoma pathogenesis.

Cameron Bumbleburg, Suprina Neupane, Henry Schrecker, Megan VanGarven, Janaia Jackson, Allison Reno, Emma Saunders, Jacob Lenski, Reid Barker, Hannah Gulbronson, Jamie Silverman, Kajol Patel, Elizabeth Maahs, C. A. Colvert, Abasi-ama Udeme, Moriah Heifetz, Jenna Schwesig, Margaret Taquey, Abbigayle Szcinski, Abigail Miller, Benjamin Caiello, Joshua Monts, B. J. Kendrick, Evan Bagley, **Casey G. Langdon**

The Medical University of South Carolina, Charleston, SC

Ewing sarcoma (EwS) is the most common chimeric transcription factor-driven pediatric bone cancer. One third of EwS patients are refractory to multimodal therapy (combination chemotherapy, surgery, radiation), especially those with recurrent or metastatic disease. New targeted therapies for EwS are urgently needed. We posit targeted combination therapies will be most effective at thwarting sarcoma pathogenesis. Examining reverse phase protein array data from the Cancer Dependency Map (DEPMAP), we found elevated expression or phosphorylation of phosphatidylinositol-3-kinase (PI3K) pathway members in EwS cell lines, highlighting the importance of PI3K pathway activity for EwS. We identified a subset PTEN-deficient EwS cell lines which was associated with increased sensitivity to AKT inhibition. Lower *PTEN* gene expression in EwS tumors is associated with poorer overall survival. Modulating PTEN levels or enhancing AKT activity altered PI3K pathway inhibition response, with AKT inhibitors showing a distinct effect compared to other pathway-targeting agents. Specifically, PTEN loss or increasing AKT phosphorylation heightened sensitivity to AKT blockade, whereas restoring PTEN expression conferred resistance. For EwS cells with high PTEN protein expression, PTEN was both cytoplasmic- and nuclear-localized. We hypothesized treating EwS cells with a nuclear export inhibitor could block PTEN trafficking out of the nucleus, reactivate the PI3K pathway, and synergize with AKT inhibition to thwart EwS pathogenesis. Indeed, we showed treating EwS cells with selinexor, an FDA-approved exportin 1 (XPO1) inhibitor, increased nuclear PTEN protein levels. Additionally, treating EwS cells with selinexor further activated the PI3K pathway. Dual AKT and XPO1 inhibition also synergized to limit EwS cell viability, induced cytotoxicity, and decreased xenografted tumor volume. Furthermore, combined AKT and XPO1 inhibition was also effective against other pediatric sarcomas driven by chimeric transcription factors, including desmoplastic small round cell tumors (EWSR1::WT1), PAX3::FOXO1-positive rhabdomyosarcomas, and clear cell sarcomas (EWSR1::ATF1). In conclusion, we demonstrated that PI3K pathway signaling is elevated in EwS cells and that low *PTEN* gene expression correlates with poor survival outcomes. Nuclear export inhibition altered PTEN subcellular localization and increased PI3K activity, contributing to the synergy between AKT and XPO1 inhibition. This combination therapy displayed efficacy across multiple fusion-driven childhood sarcomas, supporting its potential as an effective combination targeted therapeutic strategy for chimeric transcription-factor driven pediatric sarcomas.

#1164 Pacritinib mitigates doxorubicin resistance in osteosarcoma by inhibiting WNT/β-catenin, efflux proteins and receptor tyrosine kinase network.

Marina Curcic, **Sanjay Kumar Srivastava**

Texas Tech University Health Sciences Center, Abilene, TX

Chemoresistance remains the major obstacle to desirable responses in osteosarcoma (OS). We have previously identified pacritinib (PCT), an FDA-approved JAK2 inhibitor, as a modulator of the AXL/β-catenin axis. In parental osteosarcoma cells, pacritinib treatment reduced proliferation, induced apoptosis, and suppressed β-catenin-dependent transcription. Our docking studies, using Seam Dock server, supported direct engagement of both AXL and β-catenin with pacritinib. In vivo experiments showed growth inhibition of K7M3 tumors by pacritinib treatment in mice without any toxicity. Here, we evaluated the effect of pacritinib in sensitizing doxorubicin-resistant (DXR) osteosarcoma cells to doxorubicin.To determine key players in causing resistance, we first performed RNASeq analysis in doxorubicin-resistant (DXR) MG63 osteosarcoma cells and compared with parental MG63 sensitive -cells, with or without 1.5 μM pacritinib treatment for 24 hours. Gene-set enrichment from transcriptome data revealed significant activation of WNT/β-catenin programs in DXR cells compared to sensitive counterparts, with increased expression of canonical targets and receptors (e.g., WNT ligands, FZD receptors, TCF/LEF targets) and reciprocal loss of antagonists (DKK/SFRP/WIF1). Notably, drug-efflux machinery mainly ABCB1/MDR1 was elevated in MG63-DXR cells. In addition, receptor tyrosine kinase (RTK) network including AXL was also enhanced in DXR cells. The signature proteins identified by RNASeq analysis were further confirmed in MG63-DXR cells. Western blots confirmed the overexpression of AXL, β-catenin, and MDR1 in MG63-DXR cells relative to sensitive MG63 cells. Sulforhodamine-B cell viability assay showed that pacritinib reduced the growth of MG63-DXR cells in a dose-dependent manner. Growth suppressive effects were more pronounced in MG63-DXR cells when treated with pacrinitib in combination with doxorubicin, as compared to any individual treatments, showing synergism. Pacritinib treatment decreased AXL and β-catenin protein levels, attenuated downstream β-catenin targets, as well as reduced MDR1 in MG63-DXR cells. Notably, RNA-seq data of pacritinib-treated MG63-DXR cells showed a “reversal” trend: transcripts that were elevated in DXR (including β-catenin and efflux genes) were reduced by pacritinib treatment, whereas WNT antagonists increased, supporting pathway-level inhibition. An in vivo experiment is currently underway to validate that pacritinib exhibits synergistic effect with doxorubicin in suppressing MG63-DXR tumors in mice.Taken together, our data indicates that pacritinib synergistically enhances the effects of doxorubicin in suppressing the growth of MG63-DXR osteosarcoma tumors through a well-defined mechanism.

#1165 Vps34 inhibition enhances immunogenicity and immune-mediated killing in MYCN-amplified neuroblastoma.

Elisabetta Bartolini[1], Teresa L. Ramos[2], Ruize Gao[2], Bassam Janji[2]

[1]University of Luxembourg, Luxembourg, Luxembourg,[2]Luxembourg Institute of Health, Luxembourg, Luxembourg

Neuroblastoma is the most common extracranial solid tumor in children, accounting for approximately 10% of all pediatric cancers and 15% of cancer-related deaths in children under 15 years of age (1). High-risk neuroblastoma, often characterized by MYCN amplification, remains a major therapeutic challenge due to its aggressive behavior and an immunosuppressive tumor microenvironment (TME), which limits the efficacy of current immunotherapies.

Based on our previous findings (2), we assessed the therapeutic potential of targeting the autophagy regulator class III phosphatidylinositol 3-kinase (PIK3C3, also known as Vps34) to enhance anti-tumor immunity in high-risk neuroblastoma cells.

Transcriptomic analysis on murine MYCN-amplified neuroblastoma cells (NHO2A) treated with two distinct Vps34 inhibitors revealed marked upregulation of the pro-inflammatory chemokines CCL5 and CXCL10, both of which are critical for the recruitment of cytotoxic immune cells into the TME. Gene set enrichment analysis (GSEA) further demonstrated significant enrichment of immune activation, cytokine production pathways and biological oxidations, indicating increased tumor immunogenicity upon Vps34 inhibition.

Our preliminary results further suggest that Vps34 inhibition may trigger features consistent with immunogenic cell death (ICD), as treatment with Vps34 inhibitors significantly increased ATP release. Additional ICD markers are currently being investigated.

At the functional levels, in vitro co-culture assays demonstrated that Vps34 inhibition enhances CD8+ T cell-mediated cytotoxicity against MYCN-amplified neuroblastoma cells, confirming the immunostimulatory potential of Vps34 targeting.

Collectively, our findings underscore the potential of Vps34 inhibition as a promising strategy to render high-risk neuroblastoma cells more susceptible to immune-mediated killing. In vivo studies are currently ongoing to evaluate the therapeutic efficacy of combining Vps34 inhibitors with anti-PD-1 therapy which may pave the way for novel immunotherapeutic approaches for aggressive neuroblastoma.

References

1. Colon, N. C., Chung, D. H. (2011). Neuroblastoma. Advances in pediatrics.

2. Noman, M. Z., Parpal, S., Van Moer, K., Xiao, M., Yu, Y., Viklund, J., De Milito, A., Hasmim, M., Andersson, M., Amaravadi, R. K., Martinsson, J., Berchem, G., Janji, B. (2020). Inhibition of Vps34 reprograms cold into hot inflamed tumors and improves anti-PD-1_PD-L1 immunotherapy. Science advances.

#1166 Genetic and pharmacologic suppression of pink1 prolongs survival in sonic hedgehog driven medulloblastoma and related mouse model.

Bahauddeen M. Alrfaei[1], Amani Almuaysib[1], Ahmed Aloraidi[2], Ali Assiri[3]

[1]Blood and Cancer Research, King Abdullah International Medical Research Center, Riyadh, Saudi Arabia,[2]Neurosurgery, King Abdulaziz Medical City, Riyadh, Saudi Arabia,[3]Pathology and Laboratory Medicine, King Abduaziz Medical City, Riyadh, Saudi Arabia

Mitochondrial quality control plays a key role in helping cancer cells survive, but its impact on medulloblastoma is still not well understood. Here, we examined how the mitochondrial kinase PINK1 contributes to medulloblastoma growth by blocking its activity pharmacologically and by genetic loss-of-function approaches in mouse brain tumor models. Human medulloblastoma cells, MB004 and D425, were pretreated with a PINK1 inhibitor prior to orthotopic implantation. Kaplan-Meier analysis demonstrated significantly prolonged survival in mice receiving PINK1-inhibited tumor cells compared with controls (MB004: $p = 0.0288$; D425: $p = 0.0284$), indicating that disruption of PINK1 enhances therapeutic vulnerability. To further assess the role of Pink1 in vivo, we generated a genetically engineered mouse model without Pink1 in a Trp53-/-; Ptch1+/- background. This is a spontaneous tumor formation model at 90% rate. Pink1 deletion significantly increased survival compared with Pink1-active Trp53-/-; Ptch1+/- mice ($p = 0.0491$), supporting a tumor-promoting role for Pink1 in Sonic Hedgehog-driven medulloblastoma. Histopathological analysis of hematoxylin and eosin stained brain sections presented normal brain structure in the control animals, while Trp53-/-; Ptch1+/- mice developed high-grade tumors. Interestingly, Trp53-/-; Ptch1+/-; Pink1-/- brains showed reduced tumor burden and retained more tissue structure, consistent with the observed survival advantage. Together, these findings demonstrate that PINK1 is required for efficient medulloblastoma growth and that its inhibition—either through acute pharmacologic targeting or permanent genetic disruption—improves survival and reduces tumor pathology. Targeting mitophagy pathways such as disruption of PINK1 activity may therefore represent a promising therapeutic strategy for medulloblastoma, particularly in resistant or high-risk disease.

#1167 The pan-CLK DYRK inhibitor SM09419 prolongs animal survival times in a subset of pediatric medulloblastoma patient-derived orthotopic xenograft mouse models.

Xin (Alice) Zhai[1], Zilu Huang[1], Milagros Suarez Palacios[2], Tongchao Jiang[2], Aalaa Abdallah[3], Jinnan Chen[4], Yiming Mei[1], Emily Ciolak[1], Nitin Wadhwani[5], Alicia Lenzen[5], Yuchen Du[6], Xiao-Nan Li[6]

[1]Northwestern University - Chicago, Chicago, IL,[2]Northwestern University, Chicago, IL,[3]Northwestern Univ. Feinberg School of Medicine, Chicago, IL,[4]Ann & Robert H. Lurie Children's Hosp. of Chicago,[5]Lurie Childrens Medical Group, Inc., Chicago, IL,[6]Ann & Robert H. Lurie Children's Hosp. of Chicago, Chicago, IL

Background: Aberrant RNA splicing contributes to oncogenic transcriptional dysregulation in pediatric brain tumors. SM09419 is a potent pan-CLK/DYRK inhibitor that modulates alternative splicing and Wnt-related signaling pathways. SM09419 is a closely structurally related analog of Cirtuvivint (SM08502), another CLK/DYRK inhibitor from Biosplice Therapeutics, TenaRx, Inc., which has been studied in two completed Phase I clinical trials for treatment in adult solid tumors (NCT03355066 and NCT05084859), and is currently being studied in adults with AML or MDS (NCT06484062), Soft tissue sarcomas (NCT07032285), Ovarian cancer (NCT06856499) and Small cell lung cancer (NCT07155200).. The objective of this study is to evaluate antitumor efficacy as a single CLK/DYRK targeting agent in different molecular subtypes of medulloblastoma (MB) in a panel of patient-derived orthotopic xenograft (PDOX) models.
Methods: Eleven MB PDOX models including G3 (ICb-1572MB, ICb-1595MB, ICb-2555MB, ICb-5301MB), SHH (ICb-5610MB, ICb-3854MB, ICb-984MB, ICb-4989MB) and WNT (ICb-1192MB, ICb-1140MB, ICb-S1218MB) were treated with SM09419 (25 mg/kg, oral, once daily for 21 days). Changes of animal survival times were assessed by Gehan-Breslow-Wilcoxon tests. Cell proliferation (Ki-67) and (apoptosis cleaved-PARP1, cleaved-Caspase-3) was quantitatively evaluated by Visiopharm-aided immunohistochemistry.
Results: Significant extension of survival times were generated by SM09419 in three MB models, increasing median survival times from 27 days (control) to 36 days (treated) (33.3%) ($P = 0.0143$) in ICb-1572MB (G3); from 38.0 to 46.0 days (21.1%) ($P = 0.0029$) in ICb-5610MB (SHH) and from 154.0 days to 219.0 Days (42.2%) ($P = 0.0359$) in ICb-3854MB (SHH), accompanied by a significant reduction of Ki-67 ($P < 0.05$) and increased trends in cleaved-PARP1 and cleaved-Caspase-3 levels ($P > 0.05$) in ICb-1572MB and ICb-5610MB. No significant changes of animal survival times were detected in 7 models ($P > 0.05$), while the last model exhibited decreased survival times ($P < 0.05$) following drug treatment.
Conclusions: SM09419 produced significant therapeutic efficacy a subset of MB PDOX models characterized by decreased proliferative activity. Our findings highlight the biological heterogeneity among MB subtypes and support continued investigation of splicing-modulatory CLK/DYRK inhibitors as potential targeted therapies for pediatric brain tumors.

#1168 Development of RT-dPCR-based functional release assays for the *RPS19* gene therapy for Diamond-Blackfan anemia.

Neshat Masud, Sabina Ranjit, Nana Liu, Madhuri Kalathur, Senthil Bhoopalan, Catherine Willis

St. Jude Children's Research Hospital, Memphis, TN

Diamond-Blackfan Anemia (DBA) is a congenital ribosomopathy primarily caused by heterozygous loss-of-function mutations in *RPS19*, a key component of the 40S ribosomal subunit. RPS19 haploinsufficiency disrupts ribosome biogenesis, triggers p53-dependent cellular stress, and impairs the survival of erythroid progenitor cells. Beyond severe anemia, DBA patients exhibit a slightly elevated risk of hematologic and solid malignancies, highlighting a direct link between ribosomal dysfunction and cancer predisposition. Currently, the only curative approach for DBA is allogeneic bone marrow transplantation which is associated with risk of graft failure and graft-versus-host disease. Gene addition using a third-generation self-inactivating lentiviral vector encoding RPS19 (SJEFS-S19 LV) offers a promising strategy to restore functional RPS19 expression in patient hematopoietic stem and progenitor cells (HSPCs) while maintaining genomic safety and avoiding immune toxicities. Preclinical studies demonstrate that SJEFS-S19 LV effectively corrects erythropoietic defects, restores pre-rRNA processing, and generates a polyclonal, genomically stable population of HSPCs. LVs predominantly integrate into open chromatin regions associated with active transcription. To ensure product quality and functional integrity, we developed a reverse transcription digital PCR (RT-dPCR)-based release assay designed to detect and quantify *RPS19* transcript originating specifically from the integrated lentiviral vector following transduction. This approach partitions nucleic acid samples into thousands of micro-reactions, enabling absolute quantification with minimal amplification bias. For determining the RPS19 LV functionality, HEK293 *RPS19*-heterozygous knockout cells were transduced at varying multiplicities of infection (MOI), and total RNA was extracted for one-step RT-dPCR targeting the LV-derived codon-optimized *RPS19* sequence. Increasing MOI correlated with higher normalized *RPS19* transcript copies per ng genomic DNA, confirming successful vector integration and expression. This assay provides a robust, quantitative measure of functional gene expression, supporting critical quality attribute assessment of SJEFS-S19 LV. This functional assay concept is being translated into a critical release assay for the RPS19 Gene Therapy Drug Product in transduced CD34+ cells. Overall, this assay platform enables precise assessment of vector performance and provides a framework for translating LV gene therapy toward clinical applications in DBA patients, with potential implications for understanding how restoration of ribosomal protein function may impact oncogenic susceptibility.

#1169 Global proteomic analysis of pediatric T-cell acute lymphoblastic leukemia patient samples reveals distinct protein upregulation signature.

Irina Pushel[1], Thomas Gremminger[2], Lisa Lansdon[1], Michaella Rekowski[2], Midhat S. Farooqi[1], Michael Washburn[2], Keith August[1]

[1]Children's Mercy Kansas City, Kansas City, MO,[2]University of Kansas Medical Center, Kansas City, KS

Acute lymphoblastic leukemia (ALL) is one of the most frequently diagnosed pediatric cancers. Despite significant improvements in overall survival rates, children with T-cell ALL (T-ALL), accounting for approximately 15% of pediatric ALL cases, have worse outcomes than children with B-cell ALL, particularly upon relapse. Although T-ALL cases have been extensively profiled at the genomic and transcriptomic levels, the molecular mechanisms underlying poor therapeutic response remain unclear. To address this gap and identify novel putative therapies, we utilized mass spectrometry-based global proteomic profiling to reveal potential targetable features unique to this leukemia. In this study, we identified eight pediatric T-ALL patients treated at Children's Mercy with bone marrow aspirate samples collected at both diagnosis and remission banked in the Children's Mercy Biorepository. We generated global proteomic profiles for paired diagnosis and remission samples via data independent acquisition (DIA) using the timsTOF HT (Bruker). Data were searched in DIA-NN using the Bruker spectral library and human protein database downloaded from Uniprot on 05-05-2024. Downstream data analysis was performed in R 4.3.3 including differential expression analysis using limma 3.58.1 and pathway enrichment using gProfiler 0.2.3. Differential expression analysis identified 374 proteins more highly expressed at diagnosis and 434 proteins more highly expressed at remission ($p < 0.05$, $|\log2FC| > 1$). Pathways upregulated at diagnosis include cell cycle processes, cellular senescence, and nucleoside triphosphate diphosphatase activity. A number of proteins including CD7, CD38, HDAC1, HDAC2, and IL3RA (CD123) show elevated expression at diagnosis compared to remission, consistent with prior flow cytometry and/or gene expression studies of T-ALL. Surprisingly, several tumor suppressors including PTEN and BRCA2 also show elevated expression at diagnosis. While constitutive expression of PTEN has previously been reported in leukemias, it has typically been associated with mutations in the *PTEN* gene, which were not observed in these patients. This cohort of T-ALL patients shows upregulation of several proteins at diagnosis which are not seen in our analyses of other leukemias including B-cell ALL and acute myeloid leukemia. Global proteomic analysis comparing paired T-ALL samples from diagnosis and remission recapitulates increased expression of known proliferation and T-cell specific markers at diagnosis, as well as unexpected elevation of tumor suppressor protein expression. Further investigation of kinase activity and validation of these findings may reveal novel therapeutic targets to improve outcomes for pediatric T-ALL patients.

#1170 Proton-induced exosomal signatures reveal radiation response pathways in pediatric diffuse midline glioma.

Ann Morcos[1], Yeonkyu Jung[1], Nathan R. Wall[2]

[1]James M. Slater, MD Proton Treatment & Research Center Department of Radiation Medicine, Loma Linda University, Loma Linda, CA,[2]Assistant Professor of Basic Sciences, Pediatrics & Rad. Med., Loma Linda University, Loma Linda, CA

Diffuse intrinsic pontine glioma (DIPG) primarily affects children between five and ten years of age and carries a poor prognosis, with median survival of nine to twelve months. Standard treatment options are limited and typically include radiation therapy, which provides only temporary improvement, while chemotherapy and targeted therapy trials remain ongoing. DIPG remains one of the most lethal pediatric brain tumors, and emerging evidence suggests that extracellular vesicles such as exosomes may contribute to treatment resistance by carrying cargo that regulates apoptosis, DNA damage signaling, and intercellular survival pathways. Despite growing interest in exosome-mediated communication, the radiation-dependent dynamics of exosome release in DIPG remain understudied and poorly defined. This study aims to characterize radiation response features in DIPG1 and DIPG16A by comparing proliferation behavior, cell cycle distribution, and apoptosis and necrosis patterns after proton exposure, while establishing early and late exosomal dynamics through quantification of exosome release and size distribution. Here, we provide early evidence that proton radiation induces distinct cellular stress phenotypes accompanied by measurable and time-dependent exosomal output, suggesting an active radiation-responsive vesicle program. DIPG16A was derived from a treatment-naïve pretreatment biopsy specimen, whereas DIPG1 was obtained from a post-treatment autopsy specimen following exposure to radiation and multiple chemotherapeutic regimens. Both cell lines were cultured under standard conditions, exposed to graded proton doses, and exosomes were isolated and analyzed using nanoparticle tracking. A summary analysis of global treatment response revealed model-specific differences that may reflect prior therapeutic exposure and intrinsic tumor biology. Proliferation assays demonstrated that DIPG16A was more sensitive to radiation than DIPG1. DIPG16A showed a higher apoptotic population after irradiation, while both models displayed minimal necrosis and neither line showed detectable cell cycle arrest. Nanoparticle tracking analysis confirmed measurable exosome release at both early and late intervals in each line, establishing the foundation for future work investigating how apoptosis inhibitor proteins within exosomes may contribute to exosome-mediated radiation resistance in diffuse midline glioma. Collectively, these findings highlight proton-induced exosomal signaling as a potentially important and previously underappreciated component of treatment response in pediatric diffuse midline glioma and support further mechanistic exploration of exosome-carried survival factors. Generative artificial intelligence was used only for text editing and clarity, and all scientific content was produced and verified by the authors.

#1171 Copy number variation in Sonic hedgehog-medulloblastoma with unique p53 mutations: Inhibition of PI3K/AKT/mTOR pathways with HDAC inhibitors can serve as therapeutic options.

Austin Carpenter[1], Mohan Das[1], Raphael Salles S Medeiros[2], Sidnei Epelman, Epelman,[3], Nelci Zanon[4], Chirag D. Gandhi[1], **Meena Jhanwar-Uniyal**[1]

[1]Department of Neurosurgery, New York Medical College/Westchester Medical Center, Valhalla, NY,[2]Divisao de Anatomia Patologica, Hospital das Clinicas HCFMUSP, Faculdade de Medicina, Universidade de Sao Paulo, Sao Paulo, Brazil,[3]Department of Pediatric Oncology, Hospital Santa Marcelina, Sao Paulo, Brazil,[4]Department of Neurology and Neurosurgery,, Sao Paulo, Brazil, Brazil

The Sonic hedgehog subgroup of medulloblastoma (SHH-MB) originates from the cerebellar granule neuron progenitor (CGNP) population that relies on SHH pathway signaling for its perinatal expansion. Copy number variation (CNV) is a genomic structural variation that causes abnormal gene copy numbers including gene amplifications, gains, and losses. It is a vital factor regulating the expression of both protein-coding and non-coding genes, affecting various signaling pathways. Based on p53 mutations, the WHO has classified SHH-MB into two distinct prognostic categories. Here, we decipher the genomic patterns of SHH-MB tumors and evaluate the use of PI3K and HDAC inhibitors as therapeutic options. We utilized SHH-MB tumors (IRB-approved) from the Brazilian population to evaluate the genomic abnormalities using OncoScan CNV Plus-Assay and ChAS 4.2 software. Presence of isochromosome 17q [i(17q)] was determined by FISH. Effects of small molecule inhibitors targeting PI3K (Buparlisib; BKM-120) and HDAC (LBH-589) in SHH-MB cells (Daoy), were assessed via functional assays, such as cell proliferation, migration, cell cycle, and drug resistance. Results demonstrated: 1. Approximately 30% of patients exhibited i(17q) with multiple p53 mutations in the hotspot zone of the gene; 2. Other frequent genetic aberrations in IDH2:p.R140Q:c.419G>A (40%); PTEN:p.P248fs*5:c.741_742insA (60%); and KRAS:p.Q61H:c.183A>C (60%); 3. Some patients display aberrant chromosome 9; 4. Treatments with BKM-120 or LBH-589 or combined treatments inhibited cell proliferation, migration, cell cycle entry, and tumor formation of SHH-MB cells; 5. SHH-MB cells displayed resistance to BKM-120 treatments; 6. Western blotting analysis revealed that BKM-120 suppressed the activation of Akt and downstream target of mTOR, S6K, as evident by reduced levels of phosphorylation. In conclusion, we observed discrete genetic alterations in SHH-MB in a specialized population. The presence of i(17q) may define a poor prognosis and aberrant p53 is possibly an essential criterion for disease progression leading to therapy resistance. Furthermore, small molecule PI3K and HDAC inhibitors suppressed PI3K/AKT/mTOR pathways inhibiting cell proliferation, migration, and tumor formation. These studies provide evidence of genomic anomalies as well as treatment options for SHH-MB.

#1172 Inhibition of GSK3B signaling in pediatric brain tumors.

Mohammad Haque[1], Elizabeth Wert[1], Jeremey Hengst[1], Muhammad Younis[1], Katherine McClain[1], Tarlan Arjmandi[2], Meenakshi Shukla[2], Jonathan Lerch[2], Thussenthan Walter Angelo[2], Giselle L. Saulnier Sholler[2]

[1]Penn State University, Hershey, PA,[2]Penn State College of Medicine, Hershey, PA

Advances in genomic profiling have enabled increasingly precise molecular classification of pediatric embryonal brain tumors. However, the five-year overall survival rate for atypical teratoid/rhabdoid tumors (ATRT) and embryonal tumors with multilayered rosettes (ETMR) remains below 30%, despite intensive multimodal therapies. 9-ING-41 is a potent GSK3B inhibitor that has been shown to cross the blood-brain barrier and have biological activity against patient-derived intracranial xenograft models of other brain tumors, as well as good tolerability in recent Phase I human clinical trials. Previously we demonstrated that 9-ING-41 decreases ETMR and ATRT cell viability through apoptosis and increases p53 signaling, however the exact mechanism is unknown. The primary objective of this study was to determine whether GSK3B inhibition using 9-ING-41 could effectively suppress ATRT and ETMR growth by modulating p53 signaling pathway. ATRT and ETMR cell lines were grown for 24 hours prior to 9-ING-41 treatment in DMEM and Neurocult medium, respectively. Cell viability was assessed after 72hrs of treatment using Cell Titer Glo 2.0. Cells treated with IC50 determined dosing for 24-72 hours were collected for Western blot analysis of key proteins responsible for apoptosis and p53 signaling molecules. Cells were harvested for RNA isolation using Qiagen RNeasy kit. Transcriptomic profiles were established by RNA seq. Neurosphere assays were done by seeding two cells per well in a 96-well plate followed by treatment with 9-ING-41. In vivo xenograft models were established by orthotopic injection of ATRT 2141 cells into the mice brain through intra cranial stereotaxic system followed by treatment with either vehicle or 70mg/Kg 9-ING-41 by I/P injection for 9 weeks. In vitro analyses using multiple ATRT and ETMR cell lines revealed a significant therapeutic response to GSK3B inhibitor within clinically relevant dosing ranges. The IC50 of 9-ING-41 in BT183, CHLA02-ATRT, ATRT-2187, ATRT 2141 are 145.5, 481.2, 503.1, and 528.3nM respectively. Whole-exome and RNA sequencing of treated cells demonstrated upregulation of p53 tumor suppressor genes and downregulation of Shh pathway genes, supporting a tumor-suppressive mechanism. Protein expression analyses of p53 negative regulator further confirmed that 9-ING-41 treatment enhanced the activation of apoptotic pathways through p53 signaling pathway. In vivo studies showed a significant improvement in overall survival in mice treated with 9-ING-41 increased survival from 35 days to 55 days ($P < 0.0001$). Mechanistic evaluation of tumor tissues revealed increased p53 expression and marked downregulation of Ki-67, indicating reduced proliferative activity.

#1173 Trans-species analysis of mismatch repair deficient IDH1 mutant gliomas reveals a unique genomic and immune landscape resulting in favorable response to combination immune and targeted therapy.

Vienna Mazzoli[1], Nicholas R. Fernandez[1], Zoya Aamir[1], Olha Kos[1], Emma Gattoni[1], Owen Crump[1], Lucie Stengs[1], Nuno M. Nunes[1], Katharine O'Flaherty[1], Hope Friedman[1], Olfat Ahmad[2], Abigail Suwala[2], Kevin Bielamowicz[3], Gadi Abebe-Campino[4], Shani Caspi[4], Per Nyman[5], Richard Graham[6], John Y. H. Kim[7], Mari Wilhelmsson[8], Mette Jorgensen[9], Orli Michaeli[10], Maria Baro[11], Alyssa Reddy[12], Nicolas Jose Llosa[13], Amanda Li[1], Adrian Levine[1], Logine Negm[1], Melissa Edwards[1], Vanessa Bianchi[1], Birgit Ertl-Wagner[1], Julie Bennett[1], Stefan M. Pfister[2], Peter B. Dirks[1], Eric Bouffet[1], Cynthia E. Hawkins[1], Anirban Das[1], Uri Y. Tabori[1]

[1]The Hospital for Sick Children, Toronto, ON, Canada,[2]German Cancer Research Centre, Heidelberg, Germany,[3]Arkansas Children's Hospital, Little Rock, AR, Canada,[4]Chaim Sheba Medical Center, Ramat Gan, Israel,[5]Crown Princess Victoria Children's Hospital, Linkoping, Sweden,[6]Cincinnati Children's Hospital Medical Center, Cincinnati, OH,[7]Kaiser Permanente, Oakland, CA,[8]Karolinska Universitetssjukhuset, Stockholm, Sweden,[9]Great Ormond Street Hospital, London, United Kingdom,[10]Schneider Children's Medical Center of Israel, Petah Tikva, Israel,[11]University Hospital 12 de Octubre, Madrid, Spain,[12]University of California San Francisco, San Francisco, CA,[13]Johns Hopkins University School of Medicine, Baltimore, MD

High-grade gliomas are deadly tumors in children and young adults (CAYA). Mismatch Repair Deficiency (MMRD) is present in 5-10% of CAYA gliomas and is typically associated with favorable response to immune checkpoint inhibitors (ICI). Interestingly, a subset of MMRD-CAYA gliomas harboring *IDH1* mutations fails to respond to ICI. At the molecular level, the interaction of MMRD with mutant IDH (mIDH) and the causes of ICI resistance are not well understood.

To tackle this challenge and develop effective therapeutic strategies for these cancers, we performed trans-species clinical, multi-omic, and immune analysis of human and murine tumors.

Molecularly, MMRD-mIDH gliomas displayed a profile resembling mismatch repair proficient (MMRP) astrocytomas, characterized by frequent *TP53* (83%) and *ATRX* (76%) mutations and absence of oligodendroglioma-associated alterations (1p/19q codeletion). Nevertheless, in contrast to MMRP-mIDH gliomas, which more commonly present as low-grade tumors, >91% of MMRD-mIDH gliomas were high-grade, exhibiting significantly worse outcomes ($p<0.001$). Compared with MMRD-IDH wildtype gliomas, MMRD-mIDH gliomas exhibited reduced tumor mutation burden (TMB, 113 vs 28 mutations/Mb, $p<0.05$) and immune infiltration, quantified by Tumor Inflammation Signature and CD8+ T cell density, partially explaining their inferior survival under ICI treatment.

In order to study tumor development, metabolic and immune profiles, as well as response to combination therapy, we developed a novel MMRD-mIDH glioma mouse model (*Olig2-Cre*$^{+}$*/Msh2*$^{LoxP/LoxP}$*/Trp53*$^{LoxP/LoxP}$*/LSL-Idh1*$^{R132H/+}$). Mouse MMRD-mIDH gliomas displayed characteristic features of human gliomas, including TMB (20 mutations/Mb), altered glioma driver genes (*ATRX, NF1)*, diffuse cerebral involvement, and low immune infiltrates ($p<0.05$) as compared with MMRD-IDH wildtype models. Preliminary data reveals that mIDH inhibition does not impact proliferative and stemness capacity of MMRD-mIDH mouse glioma cells *in vitro,* while detailed analysis of the effect of mIDH inhibition on genomic, transcriptomic, and immune profiles are ongoing.

Strikingly, informed by our trans-species analysis, an initial trial using the addition of IDH inhibitor to ICI (n=13 patients) led to objective radiological responses and prolonged survival at 12-months compared to ICI monotherapy ($p=0.01$).

MMRD-mIDH gliomas are a genetically and biologically distinct group of tumors with limited therapeutic options. Molecular and immune profiling of MMRD-mIDH gliomas, from both patients and a novel mouse model, enables investigation of the biology underlying glioma development and testing of improved therapeutic approaches.

: Prognostic Biomarkers 1
Poster Session

#1177 Prognostic implications of circulating Hepsin in prostate cancer.

Taylor Wadley[1], Adam Cole[2], Blake P. Johnson[3]

[1]Navaux, Inc., Little Rock, AR,[2]TruCore Pathology, Little Rock, AR,[3]Navuax, Inc., Little Rock, AR

Introduction and Objective: Hepsin, a type II transmembrane serine protease, has been implicated in prostate tumor progression and metastasis. Recent studies have uncovered its proteolytic auto-activation and ectodomain shedding, supporting its potential as a circulating serum biomarker. We developed a quantitative sandwich ELISA to detect non-membrane-associated (circulating) Hepsin and evaluated its clinical relevance across benign prostatic hyperplasia (BPH), primary prostate cancer, and biochemical recurrence (BCR) following radical laparoscopic prostatectomy (RALP).
Methods: A proprietary ELISA was established using two monoclonal antibodies screened against ovarian ascites to identify native circulating Hepsin. Antibodies were further validated using recombinant extracellular Hepsin containing a thrombin cleavage site, mimicking auto-activation and shedding. The detection antibody was characterized via High-Mass MALDI mapping to the poorly conserved non-catalytic domain of Hepsin. Retrospective analyses were performed on data from an IRB-approved prospective study (2018-present) including 543 patients undergoing prostate evaluation, stratified by Hepsin status. Clinicopathologic variables (BPH, tumor stage, metastasis) were compared between Hepsin-positive and -negative groups using Chi-square or Fisher's Exact tests. Among 200 RALP patients, BCR-free survival was analyzed by Kaplan-Meier and Cox regression.
Results: Hepsin positivity occurred in 109 of the 543 (20%) patients. Compared to Hepsin-negative patients, positive patients showed higher cancer incidence vs BPH ($p<0.05$), advanced stage (≥pT3a) ($p<0.05$), and metastasis ($p<0.05$). Kaplan-Meier analysis demonstrated significantly reduced recurrence-free survival in Hepsin-positive patients (log-rank $p < 0.001$), with a Cox hazard ratio of 4.2 (95% CI 2.3-7.8). Notably, circulating Hepsin was determined to be an independent predictor of BCR ($p = 0.0001$). Furthermore, in comparison to CAPRA-S low-risk with concurrent Hepsin-negativity, Hepsin-positivity rendered an additive prognostic potential in patients with concurrent high CAPRA-S scores ($p = 0.0003$) compared to CAPRA-S high alone ($p = 0.0007$).
Conclusions: This study provides early evidence regarding Hepsin's ability to identify prostate cancer patients harboring a significantly elevated risk of BCR and adverse pathology post-RALP. These data highlight a novel role for non-invasive, longitudinal evaluation of circulating Hepsin levels in the prostate cancer setting.

#1178 STING-induced cytokine profiles in tumor fragments correlate with recurrence in head and neck cancer patients.

Animesha Krishnamurthy, Shuyue Ye, Vijay Basava, Oreoluwa Onabolu, Baran Sumer, Qiang Feng, Jinming Gao

UT Southwestern Medical Center, Dallas, TX

Only about 20% of head and neck squamous cell carcinoma (HNSCC) patients respond to immune checkpoint blockade (ICB), underscoring the need for alternative immunotherapeutic strategies and functional assays to assess patient-specific immune function. Activation of the stimulator of interferon genes (STING) pathway has emerged as a promising, tumor-agnostic approach capable of enhancing cytotoxic immune activity and overcoming ICB resistance. Our lab previously developed PolySTING, a polymeric STING agonist whose efficacy is mediated by cDC1-driven myeloid activation. To assess interpatient heterogeneity in STING responsiveness, we established an ex vivo patient-derived tumor fragment (PDTF) platform using resected HNSCC specimens that preserves native tumor architecture and resident immune populations. Cytokine profiling of tumor fragments following PolySTING treatment revealed distinct immune response phenotypes across patients, associated with *innate immune signaling, adaptive immune activation, or acute inflammatory states*. These immune response phenotypes correlated with the baseline immune composition of each tumor and, notably, with clinical outcomes, particularly post-surgical recurrence in the source patients. Our findings suggest that ex vivo STING perturbation of HNSCC tumor fragments captures clinically relevant immunosuppressive states and provide a functional biomarker to identify patients at risk of post-surgical recurrence.

-

References:

Wang J, Li S, Wang M, et al. STING licensing of type I dendritic cells potentiates antitumor immunity. Science Immunology. 2024;9(92).
Voabil P, De Bruijn M, Roelofsen LM, et al. An ex vivo tumor fragment platform to dissect response to PD-1 blockade in cancer. Nature Medicine. 2021;27(7):1250-1261.
Chen S, Pyne JM, Liu Y, et al. Nodal Yield From Neck Dissection Predicts the Anti-Tumor Immune Response in Head and Neck Cancers. Head & Neck. 2025;47(4):1199-1208.

#1179 *BRAF* copy number alterations and ultralow *BRAF* mRNA expression are prognostic for poor overall survival in prostate cancer.

Jesenia Marie Perez[1], David R. Moline[2], Hedyeh Ebrahimi[3], Ella Boytim[2], Eamon Toye[4], Stamatina Fragkogianni[5], Emmanuel S. Antonaraki[2], Alexander Chehrazi-Raffle[3], Justin Hwang[2]

[1]Department of Pharmacology, University of Minnesota, Minneapolis, MN,[2]Department of Medicine, University of Minnesota, Minneapolis, MN,[3]Department of Medical Oncology, City of Hope Comprehensive Cancer Center, Duarte, CA,[4]Perelman School of Medicine, University of Pennsylvania, Philadelphia, PA,[5]Tempus AI, Inc, Chicago, IL

Background. Prostate cancer (PC) is the second most common cancer among men in the US, with adenocarcinomas being the most prevalent histologic subtype (≥99%). Emerging evidence suggests that *BRAF* alterations, mostly annotated by protein altering mutations, may be drivers of prostate cancer progression in up to 6% of patients. Here we characterized, to our knowledge, the largest cohort of whole-exome and -transcriptome sequenced *BRAF*-altered PCs. We aimed to interrogate molecular features and clinical outcomes in *BRAF*-altered PCs.

Methods. The Tempus Lens Platform (Tempus AI, Inc., Chicago, IL) was used to query the Tempus multimodal de-identified database and establish a cohort of 485 patients with prostate adenocarcinoma with xT (DNA) and xR (RNA) testing. Of those, 137 had *BRAF* alterations while the remaining 348 were considered *BRAF* wildtype (wt). *BRAF* alterations were defined as including a copy number alteration (CNA) or a single nucleotide variant (SNV) resulting in a short variant mutation. Of the *BRAF*-wt group, 94 were primary-tumor biopsies while 43 were metastatic biopsies. Within the *BRAF-wt* group, there were 210 primary tumors and 138 metastatic biopsies. RNA expression data was normalized and quantified as transcripts per million (TPM). *BRAF* mRNA expression from metastatic tissue were grouped as ultra-low (10th percentile), low (25th percentile), mid (50th percentile), and high (75th percentile). Overall survival (OS) was defined as the time from biopsy collection to death or loss to follow up and conducted using risk set adjustment through Cox proportional hazard analysis and reported by hazard ratios (HR).

Results. We confirmed prior studies in that Class 2 *BRAF* mutations (p.K601) were the predominant form of alteration in PC (46%, 63 of 137). CN gains were the second most common *BRAF* alteration (15%, 21 of 137). Patients with *BRAF* Class 1, 2, 3 mutations demonstrated no significant difference in OS. However, metastatic PC patients with *BRAF* CN gain had worse OS relative to *BRAF-wt* (HR: 2.4, CI 95% 1.18-4.85, p=0.01). Among *BRAF*-wt PCs from metastatic tissues, those with ultra-low *BRAF* mRNA expression (bottom 10% within metastatic patients) exhibited worse OS compared to mid *BRAF* expression (HR:2.43, CI 95% 1.22-4.84, p=0.01). The median OS for PC patients with CN gain and ultralow *BRAF* gene expression were at 9.4 and 6.6 months, as compared to the wt group of metastatic patients at 15.6 months.

Conclusions. The current paradigm for reporting *BRAF* status in PC patients requires revision. In addition to SNVs (class 1,2,3), we recommend reporting *BRAF* CN gain and *BRAF* mRNA ultralow expression - both may be indicative of a subset of prostatic adenocarcinomas with very poor OS. Future studies should examine the functional consequences of these *BRAF* perturbations in larger cohorts of PC patients as well as their therapeutic implications.

#1180 Integrating methylation-based circulating tumor DNA analysis with PSMA-PET/CT primary staging for enhanced risk stratification in *de novo* metastatic prostate cancer.

Karoline Kondrup[1], Mads Ryo Jochumsen[2], Laura Iisager[1], Paul V. Salachan[1], Maibritt Norgaard[1], Philippe Lamy[1], Bodil G. Pedersen[3], Michael Borre[4], Karina D. Sorensen[1]

[1]Department of Molecular Medicine, Aarhus University Hospital, Aarhus, Denmark,[2]Department of Nuclear Medicine, Aarhus University Hospital, Aarhus, Denmark,[3]Department of Radiology, Aarhus University Hospital, Aarhus, Denmark,[4]Department of Urology, Aarhus University Hospital, Aarhus, Denmark

Background: Metastatic prostate cancer (mPC) is associated with high mortality. Newly diagnosed PC patients suspected of metastasis can undergo imaging-based primary tumor staging by PSMA PET/CT. Accurate staging is crucial for treatment selection, as localized PC may be cured by surgery or radiation therapy, while de novo mPC is treated systemically and with intensification for high-volume disease. However, the prognostic value of PSMA PET/CT remains unclear and novel biomarkers are needed to improve risk stratification and inform treatment selection. To this end, analysis of plasma cell-free DNA (cfDNA) offers promising biomarker potential, as detection of tumor-derived cfDNA (ctDNA) has demonstrated prognostic value in multiple cancer types. In this study, we aimed to establish a methylation-based approach for detecting ctDNA in plasma from mPC patients and evaluate its utility as a prognostic biomarker.

Methods: We generated cfDNA methylome profiles for 68 castration-resistant mPC (mCRPC) patients and 62 controls using methylated cfDNA immunoprecipitation and sequencing. From a subset of the cohort (27 mCRPCs, 10 controls), we established an mPC-associated multi-region methylation signature (cfMeCaP). A ctDNA detection cutoff was defined using mean cfMeCaP methylation of controls, yielding 93% sensitivity and 96% specificity in the remaining cohort (41 mCRPCs, 52 controls). Next, to test cfMeCaP ctDNA detection in mPC at diagnosis, we generated cfDNA methylome profiles for another cohort of 117 PC patients who had undergone PSMA PET/CT for primary tumor staging upon suspicion of de novo mPC. Based on PSMA PET/CT findings, patients were grouped into localized PC (n=24), low-volume mPC (n=61), and high-volume mPC (n=28).

Results: Using cfMeCaP, ctDNA was detectable in 32/117 (27%) PC patients at primary tumor staging. Highest sensitivity was observed in patients with high-volume mPC (15/28, 54%) relative to low-volume mPC (14/61, 23%) and localized PC (2/24, 8.0%). Mean cfMeCaP methylation was positively correlated with the total tumor volume, as estimated from the PSMA PET/CT scans (ρ=0.47, $p<0.01$). This correlation was largely driven by the total metastatic tumor volume (ρ=0.52, $p<0.01$) rather than the total primary tumor volume (ρ=0.16, p=0.08). In mPC patients, ctDNA detection at primary tumor staging was associated with significantly shorter time to mCRPC progression as compared to ctDNA negative patients (median PFS of 25.6 months vs median PFS not reached, p=0.01), suggesting ctDNA positive low-volume mPC patients represent a high-risk subgroup that may benefit from treatment intensification.

Conclusion: These findings highlight the promising potential of plasma ctDNA as a minimally invasive biomarker to improve risk stratification in patients with de novo mPC, warranting large-scale clinical validation.

#1181 Transcriptomic analysis of NDRG1 amplification in aggressive breast cancer.

Emilly S. Villodre[1], Ganiraju Manyam[2], Xiaoding Hu[1], Isabella L. Rizzo[1], Lan H. L. Phi[1], Kiros H. Tesfamariam[1], Azadeh Nasrazadani[3], Rachel M. Layman[3], Bora Lim[3], Vicente Valero[3], Savitri Krishnamurthy[4], The MDACC IBC Team, MDACC Rare Tumor Initiative Team, Jing Wang[2], Xiaoping Wang[5], Naoto Ueno[5], Wendy A. Woodward[6], Bisrat G. Debeb[1]

[1]Breast Medical Oncology, MDA Morgan Welch Inflammatory Breast Cancer Clinic and Research Program, UT MD Anderson Cancer Center, Houston, TX,[2]Bioinformatics & Computational Biology, UT MD Anderson Cancer Center, Houston, TX,[3]Breast Medical Oncology, UT MD Anderson Cancer Center, Houston, TX,[4]Pathology, MDA Morgan Welch Inflammatory Breast Cancer Clinic and Research Program, UT MD Anderson Cancer Center, Houston, TX,[5]University of Hawai'i Cancer Center, Honolulu, HI,[6]Experimental Radiation Oncology, MDA Morgan Welch Inflammatory Breast Cancer Clinic and Rsch Program, UT MD Anderson Cancer Center, Houston, TX

Background: Inflammatory breast cancer (IBC) is a rare but highly aggressive variant of breast cancer, accounting for 10% of breast cancer-related deaths. We have identified NDRG1, located on chromosome 8q24.3 near MYC within a commonly amplified region, as a key promoter of tumor growth and progression in IBC models and is associated with poor survival outcomes. Unlike many oncogenes, NDRG1 is rarely deleted or silenced and is more frequently expressed in IBC compared to non-IBC tumors. A recent study reported NDRG1 amplification in 42% of triple-negative IBC cases. We hypothesize that NDRG1 amplification in triple-negative IBC is associated with distinct gene expression profiles and enrichment of oncogenic pathways that contribute to the aggressive phenotype of the disease.

Methods: RNA sequencing data from 19 triple-negative IBC tumors (8 NDRG1 amplified, 11 non-amplified) were analyzed using DEseq2 package. Heatmaps were generated to visualize clustering and expression differences. Gene Set Enrichment Analysis (GSEA) was performed using Hallmark and KEGG pathway databases. Publicly available TCGA and METABRIC breast cancer datasets were used to assess NDRG1 amplification and its association with mRNA/protein expression and survival outcomes.

Results. Among the 19 triple-negative tumors analyzed, 8 (42%) exhibited *NDRG1* amplification, which was significantly correlated with increased RNA expression ($p = 0.05$). Differential expression analysis identified *CALCA*, *RHO*, *DPYSL5*, *GPR101*, *ZIC3*, and *IRS4* as the most upregulated, and *SERPINA6*, *SCGB3A1*, *PI3*, *LRG1*, *DAPL1*, *MYEOV* as the most downregulated in *NDRG1*-amplified tumors. GSEA revealed enrichment of DNA repair, cell cycle, mTOR signaling, and MYC target pathways, and downregulated pathways included interferon gamma response, estrogen response and NFkB pathway. TCGA and METABRIC analyses confirmed that NDRG1 amplification correlates with elevated mRNA expression ($p<0.0001$) and elevate protein levels ($p<0.0001$) and poorer overall survival ($p=0.013$, TCGA; $p=0.0002$, METABRIC).

Conclusions: *NDRG1* amplification marks a transcriptionally distinct subset of triple-negative IBC, enriched in proliferative and DNA repair pathways. These molecular features highlight its potential as a biomarker of aggressive disease biology and potential target for further mechanistic investigation and therapeutic intervention.

#1182 A unified clinical and molecular framework to standardize chromosomal instability assessment in gastric, GEJ, and esophageal cancer (GEC).

Jierui Xu, Charlton Tsai, Henry Walch, Patrick Evans, Jessica Posada, Samuel Cytryn, Steven Maron, Adam Bass, Kevin M. Boehm, Francisco Sanchez-Vega, Nikolaus Schultz, Walid K. Chatila, Yelena Y. Janjigian

Memorial Sloan Kettering Cancer Center, New York, NY

Background:
Chromosomal instability (CIN) is a dominant molecular feature of gastroesophageal adenocarcinomas and is associated with poor outcomes to standard chemotherapy and chemo-immunotherapy. Given its high prevalence and the absence of standardized, clinically deployable methods to identify CIN, we sought to develop a unified clinical and molecular framework to quantify CIN across real-world and phase III datasets and to build NGS- and histopathology-based tools for routine CIN classification.
Methods:
We analyzed 3,822 tumors across complementary platforms: 2,613 patients profiled with MSK-IMPACT, 587 RNA-seq and whole-exome sequencing samples from patients treated on Phase III CheckMate-649 (CM649) trial, and 622 TCGA samples. CIN was defined by fraction of genome altered (absolute $\log_2$ deviation >0.2) and complemented by arm-level and focal copy-number metrics using FACETS. Clinicopathologic, molecular, and outcome associations were evaluated across CIN strata. CIN will be integrated with CM649 transcriptomic programs and survival to assess predictive value for chemotherapy with and without nivolumab.
Results:
CIN was present in 63% of tumors within the MSK-IMPACT cohort, including 76% in esophageal, 68% in GEJ, and 47% in gastric cancers. Among 2,445 microsatellite-stable tumors, CIN tumors were enriched for TP53 mutations (79% vs 64%), CDKN2A loss (24% vs 10%), and focal amplifications in CCND1, MYC, EGFR, ERBB2, VEGFA, and CCNE1 (FDR <0.001), whereas CDH1 and RHOA mutations were enriched in non-CIN tumors. CIN exhibited a graded spectrum, with higher FGA associated with increased aneuploidy and a greater number of unique metastatic sites. Deep-learning models trained on H&E whole-slide images are being developed to infer CIN, with validation alongside CM649 clinical outcomes ongoing. Matched primary-metastatic and longitudinal samples are additionally being analyzed to define CIN evolutionary trajectories.
Conclusions:
We provide a unified genomic and histologic framework to standardize CIN assessment across clinical and phase III esophagogastric cancer samples. By linking CIN to reproducible molecular features and treatment outcomes—and by developing NGS- and H&E-based tools compatible with routine pathology workflows—this work lays the foundation for integrating CIN as a practical biomarker for patient stratification, risk enrichment, and future trial design targeting chromosomal instability.

#1183 Early ctDNA quantification by ctFE outperforms Max VAF for survival stratification across locally advanced and oligometastatic NSCLC treated with radiotherapy.

Ayesha Hashmi[1], Jessica Linford[1], Pradeep S. Chauhan[1], Kaushal Parikh[1], Rotem Ben-Shachar[2], John Guittar[2], Malvika Pillai[2], Jyoti Patel[2], Matteo Bergsagel[1], Nicholas P. Semenkovich[3], Kenneth R. Olivier[1], Sean S. Park[1], Dawn Owen[1], David M. Routman[1], Katie N. Lee[1], Alex D. Sherry[1], Aaron S. Mansfield[1], Daniel Morgensztern[4], Ramaswamy Govindan[4], Clifford G. Robinson[4], Carmen Bergom[4], Saiama N. Waqar[4], Bruna Pellini Ferreira[5], Gregory R. Vlacich[4], Aadel A. Chaudhuri[1]

[1]Mayo Clinic, Rochester, MN,[2]Tempus AI Inc, San Francisco, CA,[3]Medical College of Wisconsin, Milwaukee, WI,[4]Washington University, Division of Oncology, Washington University, MO,[5]H. Lee Moffitt Cancer Center and Research Institute, Tampa, FL

Background: Personalizing chemoradiotherapy (chemoRT) for locally advanced non-small cell lung cancer (LA-NSCLC) is limited by the lack of early biomarkers that inform response during treatment. Current circulating tumor DNA (ctDNA) molecular residual disease assays predict post-treatment outcomes but lack mid-treatment utility. ctDNA burden estimation has traditionally relied on variant-centric metrics such as maximum variant allele fraction (Max VAF), which rely on mutation-specific signals and may be confounded by histology-dependent shedding variability, allelic imbalance, and clonal hematopoiesis. Here we present circulating tumor fraction estimate (ctFE), a machine-learning composite score that integrates VAF distributions, copy-number alterations, and germline B-allele frequency deviations to approximate global tumor burden using a widely available, tumor-naïve clinical platform.

Methods: A burden-based ctFE threshold was derived using pre-treatment plasma from a prospective phase II clinical trial of MR-guided hypofractionated chemoRT (LA-WU, n=26), locked, and applied unchanged to early mid-treatment samples (day 10-14). To test scalability and generalizability, its prognostic performance was validated in two real-world cohorts: 94 LA-NSCLC patients receiving definitive chemoRT (LA-RW) and 309 oligometastatic NSCLC patients receiving consolidative RT (OM-RW). ctFE and Max VAF were compared as continuous predictors across cohorts.

Results: ctFE consistently outperformed Max VAF. In LA-WU, pre-treatment ctFE was associated with overall survival (OS HR=1.15, p=0.04) and progression-free survival (PFS HR=1.84, p=0.009), whereas Max VAF was not. Mid-treatment ctFE remained prognostic for PFS (HR=1.14, p=0.026). Early ctFE dynamics defined three molecular response groups with marked OS separation: consistently low, responder, and nonresponder groups (median OS 60.8 vs 13.0 vs 2.9 months, respectively; p<0.001). In multivariable models including both biomarkers, higher ctFE remained independently associated with worse survival in LA-RW (OS HR=1.88, p=0.010) and OM-RW (OS HR=1.37, p=0.040; PFS HR=1.45, p=0.008), whereas Max VAF did not. The locked ctFE threshold stratified OS across all cohorts (LA-WU HR=5.93; LA-RW HR=9.08; OM-RW HR=2.26; all p<0.001).

Conclusion: ctFE provides clinically meaningful pre- and mid-treatment risk stratification and consistently outperforms Max VAF across locally advanced and oligometastatic NSCLC cohorts. We show that ctFE is a biologically informative, clinically generalizable and scalable ctDNA burden metric measurable using a tumor-naïve, off-the-shelf assay, supporting its practical utility in biomarker-adapted radiotherapy strategies.

#1184 IHC-based prognostic sub-stratification of ovarian endometrioid carcinoma.

Gamaliel Taengwa[1], Hunter J. Atkinson[1], Bryan M. McCauley[1], Sebastian M. Armasu[1], Chen Wang[1], Jennifer A. Doherty[2], Holly R. Harris[3], Ellen L. Goode[1], Martin Koebel[4], Stacey J. Winham[1]

[1]Quantitative Health Sciences, Mayo Clinic, Rochester, MN,[2]University of Utah Huntsman Cancer Institute, Salt Lake City, UT,[3]Public Health Sciences Division, Fred Hutchinson Cancer Center, Seattle, WA,[4]University of Calgary, Calgary, AB, Canada

Ovarian endometrioid carcinoma (OEC) is the second most common histotype associated with the most favorable prognosis among ovarian carcinomas. Similar to endometrial carcinoma, OEC exhibit significant molecular diversity. We aimed to develop a practical immunohistochemical (IHC) prognosticator by integrating IHC biomarkers with clinical substage, and surgical outcomes. This multi-institutional study included participants with primary invasive OEC from the Alberta Cancer Registry (AOVT), Mayo Clinic, and Disease of the Ovary and their Evaluation Study (DOVE). Pathology review excluded misclassified high-grade serous and mesonephric carcinomas leaving 422 OEC cases (AOVT N=158; DOVE N=143; Mayo N=121) with available tumor biospecimens who did not receive neoadjuvant treatment. Clinical characteristics included age, stage, grade, residual disease and 5-year survival. Clinical risk group was defined by combining stage and residual disease: Low (FIGO stage IA/IB & no macroscopic disease), Intermediate (stage IC-II& no macroscopic disease), High (stage III/IV or macroscopic disease). Tissue microarrays were stained for TP53, PMS2, MSH6, PGR, and CTNNB1 using IHC and were scored by a single pathologist. Tumors were hierarchically categorized as TP53-abnormal (TP53abn)/PGR-loss, mismatch-repair deficient (MMRd, via PMS2 and MSH6), nuclear-CTNNB1 (nCTNNB1), or no-specific-immunohistochemical-profile (NSIP). Overall survival (OS) at 5 years was compared across clinical risk and biomarker groups using Cox regression, adjusted for age and site to generate hazard ratios (HR), and 5-year survival rates (5-YSR). High clinical risk group was associated with worse 5-year OS compared to low & intermediate risk ($p<0.0001$). Hierarchical IHC biomarker groups were also associated with 5-year OS, adjusted for age and study site ($p<0.0001$), with consistently worse survival for combined TP53abn/PGR-loss (n=17, HR=6.07, 95% CI 2.78-13.26), PGR-loss only (n=55, HR=4.17, 95% CI 2.19-7.94), TP53abn only (n=29, HR=2.04, 95% CI 0.85-4.90), and better survival for nuclear-CTNNB1 (n=146, HR=0.22, 95% CI 0.07-0.65) compared to NSIP (n=132). Within the low-risk group, MMRd, nCTNNB1, or NSIP had greater than 97% 5-YSR, while OEC with TP53abn/PGR-loss or PR-loss only had less than 75% 5-YSR. Within the intermediate group, only nCTNNB1 exceeded a 5-YSR of greater than 97%. Within the high-risk group, 5YSR for nCTNNB1 OEC was 90.9%, compared to only 16.7% for TP53abn/PGR-loss. This IHC-based algorithm refines prognosis beyond clinical substage. It identifies low-risk patients with unfavorable prognosis (TP53abn/PGRloss, PGR loss only) who may benefit from adjuvant therapy, and also patients with favorable prognosis within the intermediate group for whom adjuvant therapy could be de-escalated. Further patient selection for chemo vs. hormone therapy in the high-risk group may be improved by biomarkers.

#1185 Radiographic thymic health as host-intrinsic determinant of immunotherapy outcomes across cancer types.

Simon Bernatz[1], **Vasco Prudente**[1], Suraj Pai[1], Asbjorn Kjar[2], Alessandro Di Federico[3], Andrew Rowan[4], Selvaraju Veeriah[5], Lars Dyrskjot[6], Leonard Nurnberg[1], Joao Victor M. Alessi[3], Patrick Ott[3], Elad Sharon[3], Allan Hackshaw[7], Nicholas McGranahan[8], Christopher Abbosh[9], Raymond H. Mak[1], Danielle S. Bitterman[10], Mark M. Awad[3], Biagio Ricciuti[3], Charles Swanton[4], Mariam Jamal-Hanjani[11], Nicolai Juul Birkbak[2], Hugo JWL Aerts[1]

[1]Mass General Brigham, Boston, MA,[2]Aarhus University, Aarhus, Denmark,[3]Dana-Farber Cancer Institute, Boston, MA,[4]The Francis Crick Institute, London, United Kingdom,[5]University College London, London, United Kingdom,[6]Aarhus University, Aarhus N, Denmark,[7]Cancer Research UK & UCL Cancer Trials Centre, London, United Kingdom,[8]UCL London Cancer Institute, London, United Kingdom,[9]Christopher Abbosh (Individual), London,[10]Brigham and Women's Hospital, Boston, MA,[11]University College London (UCL) Cancer Institute, London, United Kingdom

Background: Immune checkpoint inhibitors (ICIs) depend on effective T-cell priming and renewal, yet current biomarkers focus primarily on tumor-intrinsic features (PD-L1, TMB). Because the thymus maintains naïve T-cell output and repertoire diversity, we hypothesized that an individual's thymic health represents a host-intrinsic determinant of ICI benefit.
Methods: We developed a self-supervised deep learning model to quantify thymic function, here termed thymic health, from routine CT scans. Thymic health was independently evaluated in 3,476 patients treated with ICI for tumors of various entities. Associations with PFS and OS were assessed using multivariable Cox models adjusting for key epidemiological and clinical factors. Sensitivity analyses evaluated the incremental contribution of thymic health. Biological validation was performed in treatment-naïve NSCLC patients from TRACERx (n=464) using T-cell receptor (TCR) sequencing and plasma proteomics.
Results: In patients with NSCLC (n=1,218), high thymic health was associated with significantly reduced risk of progression (HR 0.65; 95% CI, 0.54-0.77) and death (HR 0.56; 95% CI, 0.46-0.68); preserved after full multivariate adjustments for sex, age, PD-L1, TMB, ECOG, histology, treatment line and stratification by treatment type ($P<0.001$). Adding thymic health improved model fit beyond demographic, clinical, and tumor-intrinsic variables (likelihood ratio $P<0.001$). Importantly, including thymic health did not attenuate PD-L1 or TMB effects, indicating complementary, non-redundant prognostic information. Across PD-L1 and TMB strata, higher thymic health was consistently associated with improved PFS and OS ($P<0.03$). In TRACERx, thymic health was positively associated with T cell receptor excision circles, i.e., T cell output, and correlated with greater peripheral and intratumoral TCR diversity and with proteomic signatures of adaptive immune activation, biologically supporting its role as a radiographic proxy for immune competence. Pan-cancer analyses across 2,258 ICI-treated patients (melanoma, renal, breast, and others) showed consistent positive associations between thymic health and improved outcomes.
Conclusions: Thymic health was consistently associated with improved immunotherapy outcomes across cancer types and added independent information beyond PD-L1, TMB, and standard clinical variables. These findings support thymic health as a possible non-invasive, host-intrinsic biomarker with potential to refine patient stratification and advance precision immuno-oncology.
Clinical trial identification: ClinicalTrials.gov: TRACERx, NCT01888601

#1186 Plasma proteomic profiling of lung cancer blood samples reveals immune-related inflammatory signatures as prognostic biomarkers.

Akila Wijerathna-Yapa[1], Aaron Kilgallon[1], Clara Lawler[1], James Monkman[2], Nathaniel Robichaud[3], Alyssa Rosebloom[4], William Mullaly[5], Ken O'Byrne[6], **Arutha Kulasinghe**[1]

[1]Frazer Institute, University of Queensland, Brisbane, Australia,[2]The University of Queensland, Woolloongabba, Australia,[3]Nomic Bioscience, Quebec, Australia,[4]Nomic Biosciences, Quebec, QC, Canada,[5]Cancer Care Services, Princess Alexandra Hospital, Brisbane, Australia,[6]Princess Alexandra Hospital, Brisbane, Australia

Background. Lung cancer presents a significant global burden of mortality. Predictive biomarkers are urgently needed to help stratify patient populations for targeted and systemic therapies. Here, we performed comprehensive proteomic profiling using the nELISA technology to identify baseline and post treatment proteomic signatures associated with clinical outcomes to immune checkpoint immunotherapy (ICI).

Methods. Plasma were prepared from 66 patients who underwent ICI (63 pre-treatment samples, 19 post-treatment samples). The nELISA assay (Nomic Bio, Canada) was used to detect the abundance of 969 proteins. Data QC, Differential expression, survival modelling, and pathway enrichment was performed to understand associations with clinical endpoints.

Results. Baseline blood samples from patients who experienced disease progression demonstrated coordinated activation of three interconnected pathways: coagulation, complement cascade, and IL-6/JAK/STAT3 signalling. This pattern was consistent across PFS events ($p<0.001$), OS events ($p<0.001$), and progressive disease comparisons (RECIST, PR vs PD: $p=0.002$). In contrast, baseline samples from patients with better clinical outcomes exhibited enrichment of type I/II interferon responses, DNA damage response and intact apoptotic machinery. Notably, patient responders maintained balanced inflammation with high interferon signalling, while patient non-responders showed high inflammatory markers paradoxically paired with low interferon activity, suggesting dysfunctional, immunosuppressive inflammation. Analysis of paired PRE/POST samples (n=19) revealed that patients who progressed exhibited marked treatment-induced increases in TNFα/NFκB signaling, inflammatory responses, combined with decreases in IL-2/STAT5-mediated T cell signalling. This pattern, consistent across OS ($p=0.001$), PFS ($p=0.002$) suggests treatment-related immune dysregulation or failed immune reconstitution despite checkpoint blockade. Importantly, the coagulation signature present at baseline decreased post-treatment in poor-outcome patients, possibly reflecting consumption coagulopathy during systemic inflammatory states. Post-treatment proteomic changes in deceased patients included shifts from fatty acid oxidation toward adipogenesis with concurrent decreases in myogenesis, collectively indicating cancer cachexia-associated metabolic reprogramming that may contribute to treatment intolerance and mortality.

Conclusion. We identified two distinct baseline immunophenotypes predictive of immunotherapy outcomes including an “immune inflammed” and “thrombo-inflammatory.” The protein signatures warrant prospective validation as predictive biomarkers for immunotherapy patient selection and response monitoring, with potential to guide precision medicine approaches.

#1187 Serological detection of Type XVII collagen shedding suggests prognostic relevance in esophageal adenocarcinoma.

Eleonora Moroncini[1], Andrea Ponzetta[2], Rene Thieme[3], Stefan Niebisch[3], Ines Gockel[4], Magnus Nilsson[5], Fredrik Klevebro[5], Rebecca Maltez de Sousa[2], Nora Noren[5], Nicholas Willumsen[1], Morten Karsdal[1]

[1]Nordic Bioscience, Copenhagen, Denmark,[2]Karolinska Insitutet, Stockholm, Sweden,[3]University Hospital Leipzig, Leipzig, Germany,[4]St Clara Hospital Basel, Basel, Switzerland,[5]Karolinska Institutet, Stockholm, Sweden

Esophageal adenocarcinoma (EAC) is an aggressive malignancy with poor prognosis and rising incidence in Western countries. Identifying reliable, non-invasive biomarkers for prognostic stratification and disease monitoring remains a clinical challenge. Type XVII collagen is a transmembrane protein mediating epithelial-basement membrane adhesion. Its aberrant expression and ectodomain shedding have been linked to epithelial damage and tumor progression. Interestingly, COL17A1 has been reported to be downregulated in EAC compared to Barrett's esophagus and healthy tissue, suggesting loss of epithelial integrity during malignant transformation. In this study, we evaluated the serological biomarker potential of PRO-C17, which quantifies the shed ectodomain of type XVII collagen, in two independent cohorts of treatment-naïve EAC patients.

PRO-C17 levels were measured by competitive ELISA in EDTA plasma from 57 treatment-naïve EAC patients (Cohort I, Karolinska University Hospital). A second cohort (Cohort II, University of Leipzig) included 64 serum samples from treatment-naïve EAC patients. All samples were collected at diagnostic endoscopy prior to oncologic treatment. For both cohorts, 20 healthy controls were included, matched for sample matrix, age, and gender.

Prognostic associations with overall survival (OS) were assessed in resectable patients (n=54 in Cohort I; n=44 in Cohort II) using Kaplan-Meier and multivariate Cox models. Cohort-specific median PRO-C17 levels were used as cut-offs.

In Cohort I, PRO-C17 levels were significantly lower in EAC patients compared to controls ($p<0.001$); in Cohort II, no significant difference was observed, though a similar trend was noted. In both cohorts, high baseline PRO-C17 levels were independently associated with poorer OS (Cohort I: $p=0.01$, HR=2.63, 95% CI: 1.20-5.56; Cohort II: $p=0.013$, HR=2.85, 95% CI: 1.22-6.71). Among early-stage patients, elevated PRO-C17 identified individuals with significantly worse OS, suggesting that PRO-C17 may reflect tumor aggressiveness even in clinically early-stage disease. No significant differences were seen in late-stage subgroups. In Cohort II, lower baseline PRO-C17 was also associated with better tumor regression grades (TRG), suggesting potential predictive value for treatment response.

PRO-C17 shows consistent prognostic value across two independent EAC cohorts with different sample matrices. Elevated levels were associated with poorer OS, particularly in early-stage disease, supporting its use as a non-invasive biomarker for risk stratification. Increased ectodomain shedding may reflect tumor aggressiveness, while the overall lower PRO-C17 levels in EAC vs. healthy controls may reflect COL17A1 downregulation during tumor progression. These findings support prospective validation of PRO-C17 as a clinically relevant biomarker in EAC.

#1188 Associations between Breast Cancer Index and MSK-IMPACT genomic and transcriptomic profiles in HR+ breast cancer.

Hong Zhang[1], Niloufar Khojandi[2], Natalia Siuliukina[2], Julia Ah-Reum An[1], Darya Dahi[1], Luca Boscolo Bielo[1], Subhiksha Nandakumar[1], Enrico Moiso[1], Edaise M. da Silva[1], Mehnaj Ahmed[1], Lisa Loudon[1], Konner Nelson[1], Kevin Murphy[1], Jade Oghoanina[1], Mark E. Robson[1], Sarat Chandarlapaty[1], George Plitas[1], Amanda K. L. Anderson[2], Yi Zhang[2], Pedram Razavi[1], Kai Treuner[2]

[1]Memorial Sloan Kettering Cancer Center, New York, NY,[2]Biotheranostics, Inc. A Hologic Company, San Diego, CA

Background: The Breast Cancer Index (BCI) is a gene expression-based assay that stratifies patients based on their risk of overall (0-10 years) and late (beyond 5 years) distant recurrence. In addition , BCI can also predict the benefit of extended endocrine therapy in early-stage, HR+ breast cancer. In this study, we assessed the relationships between BCI and risk of distant recurrence and explored associations between BCI classification and the tumor genomic and transcriptomic profiles of HR+ patients who experienced metastatic relapse.

Methods: Primary tumors from patients with metastatic or recurrent HR+ breast cancer underwent BCI testing, MSK-IMPACT targeted sequencing (up to 505 cancer genes), and mRNA sequencing. Time to DR (TTDR) was defined as the time from surgery to first distant recurrence. A 5-year cutoff was used to distinguish early versus late DR groups. Kaplan-Meier and Cox proportional hazards analyses were used to assess BCI's prognostic value. Wilcoxon tests were applied for pairwise comparisons of BCI scores between early and late DR groups, and Fisher's exact tests were used to identify genomic alterations differing by BCI groups as well as DR groups. Given the limited cohort size, multiple testing correction was not applied. Transcriptomic data (N=91) were analyzed for differentially expressed genes by comparing BCI high-risk vs. low-risk tumors and early vs. late DR groups ($|\log_2 FC|>1$, adjusted $p<0.05$).

Results: The study included 180 HR+ patients (47% post-menopausal, 61% N+, 65.3% grade 3). Most tumors were classified as BCI high risk (86.7%), and patients classified as high risk by BCI had earlier recurrence than those classified as low risk (median TTDR: 3.0 years vs. 4.7 years; HR = 1.89, 95% CI: 1.20-2.96; p = 0.0053). BCI scores differ significantly between early and late DR groups (p = 0.005). The genomic landscape was consistent with high-risk luminal tumors and showed frequent *TP53* mutations (38%). *PIK3CA* and *TBX3* mutations were more common in BCI low-risk tumors (71% vs. 41%, p=0.007; 21% vs. 5%, p=0.01). *CDKN2A* deletions and *MCL1* amplifications were enriched in early DR, whereas *ERBB2* and *SPOP* amplifications as well as *NOTCH3*, and *MAP2K4* mutations were more frequent in late DR ($p<0.05$). Transcriptomic analysis revealed downregulation of cell cycle, p53 signaling, senescence, and progesterone-mediated oocyte maturation pathways in BCI high-risk tumors. The cell cycle pathway was also downregulated in late recurrences, suggesting reduced proliferative activity associated with delayed relapse.

Conclusion: BCI remained a strong prognostic indicator in this HR+ metastatic cohort, with higher scores predicting shorter TTDR. Integrated genomic and transcriptomic profiling highlighted distinct molecular programs associated with BCI classification providing insight into biological mechanisms underlying early versus late relapse in HR+ breast cancer.

#1190 Decoding the multiomic signatures of oral cancer progression.

Maple Lei[1], Kelly Yi Ping Liu[2], Steven John Jones[3], Catherine FY Poh[4]

[1]Canada's Michael Smith Genome Sciences Centre, Vancouver, BC, Canada,[2]University of British Columbia, Vancouver, BC, Canada,[3]BC Cancer Agency, Vancouver, BC, Canada,[4]Associate Professor, University of British Columbia Faculty of Dentistry, Vancouver, BC, Canada

Oral cavity squamous cell carcinoma (OCSCC) is frequently preceded by oral epithelial dysplasias (OEDs), yet current clinical tools provide limited ability to identify which OPMLs will progress. This study applied an integrated multiomics approach to identify molecular features of progression and define biomarkers that may improve risk assessment.

We analyzed well-annotated flash-frozen oral tissues collected at surgery, with concurrent blood samples for germline DNA. Tissue samples were pathologically reviewed and microdissected to be labelled as “premalignant” or “malignant”. Short-read whole-genome sequencing (≥80× tumor, ≥30× germline) and RNA sequencing (≥200 million reads per library) were used to characterize somatic mutations, copy number alterations, and transcriptional differences. A subset of samples underwent long-read nanopore sequencing (20× coverage) to refine methylation patterns and their relationship to expression. Data were integrated using established pipelines, and candidate features were evaluated through machine learning-based classification. AI was used to enhance abstract clarity.

A total of 305 patient samples were submitted of which 96% (138 OED, 154 OSCC) were successfully sequenced. Mutational landscapes were similar across premalignant and malignant groups, sharing alterations in *TP53*, *CDKN2A*, *FAT1*, *NOTCH1*, and *CASP8*. *HLA-A* emerged as the top differentially mutated gene, pointing to altered immune-related pathways. Differential expression analysis showed clear separation of sample types, with broad increases in expression in OSCC. TPM values from 961 genes were used to train a proof-of-concept random forest classifier after iterative feature elimination, yielding a model with 92% confidence and 96% AUC. The most informative features aligned with top differentially expressed genes, and pathway analysis indicated enrichment in signaling, adhesion, and structural organization. Differential methylation analysis (75 OED, 40 OSCC) showed higher CpG island methylation in OSCC samples. Top differentially methylated genes included *ARHGEF17* and *PHLDB1*, which participate in cell cycle regulation and signaling, and *MIR27B*, previously described as a regulator of cellular growth and movement in oral epithelial models.

Using one of the largest, most comprehensively profiled OED cohorts to date, this work shows that lesions harbor distinct genomic, epigenomic, and transcriptional changes detectable before malignant transformation. Convergent key markers identified support development and validation of clinically actionable tests to be applied to formalin-fixed paraffin embedded samples for early identification of higher-risk lesions. Ongoing efforts integrate these molecular signatures with longitudinal clinical outcomes and map them to biological pathways and molecular oral cancer subtypes to advance screening, early intervention, and individualized patient management.

#1191 Depth of immunoparesis predicts time to first therapy in newly diagnosed monoclonal B-cell lymphocytosis and chronic lymphocytic leukemia.

Yuan Yao[1], Kari G. Rabe[2], Eli Muchtar[1], Paul Hampel[1], Yucai Wang[1], Lindsey Roeker[1], Saad Kenderian[1], Amber Koehler[1], Catherine Wagner[1], Amy Behnken[1], Jose F. Leis[3], Mazie Tsang[3], Talal Hilal[3], Ricardo Daniel Parrondo[4], Susan M. Schwager[1], Min Shi[5], Curtis A. Hanson[5], Celine M. Vachon[6], Shaji Kunnathu Kumar[1], Esteban Braggio[7], Neil E. Kay[1], Susan Slager[8], Sameer A. Parikh[1]

[1]Division of Hematology, Mayo Clinic, Rochester, MN,[2]Division of Clinical Trials and Biostatistics, Mayo Clinic, Rochester, MN,[3]Division of Hematology and Medical Oncology, Mayo Clinic, Phoenix, AZ,[4]Division of Hematology-Oncology, Mayo Clinic, Jacksonville, FL,[5]Department of Laboratory Medicine and Pathology, Mayo Clinic, Rochester, MN,[6]Division of Epidemiology, Mayo Clinic, Rochester, MN,[7]Division of Hematology and Medical Oncology, Mayo Clinic, Phoenix, MN,[8]Division of Hematology; Division of Computational Biology, Mayo Clinic, Rochester, MN

Background: Hypogammaglobulinemia at the time of CLL diagnosis predicts shorter time to first therapy (TTFT). However, the depth of immunoparesis and its impact on TTFT in newly diagnosed MBL/CLL remains unexplored.
Methods: We identified previously untreated MBL/CLL patients from Mayo Clinic CLL Database (2000-2024) who had serum immunoglobulin (Ig; IgG, IgM and IgA) and monoclonal protein assessed within 1 year of diagnosis. Immunoparesis was evaluated: a) qualitatively by classifying patients into preserved, partial and full Ig suppression, based on the number of suppressed Igs; and b) quantitatively by calculating the average relative difference (ARD), defined as the mean percentage below normal for all Igs. For both methods, only uninvolved Igs were considered for those with monoclonal protein. TTFT was estimated by Kaplan-Meier with competing risk of death. Cox models estimated hazard ratios (HR) and 95% confidence intervals (CI).
Results: Among 1420 patients, median age at diagnosis was 65 (range 28-96); 954 (67%) were male; 493 (44.8%) had unmutated *IGHV*, and 86 (6.8%) had *TP53* disruption. The median [range, mg/dL] serum IgG, IgA, and IgM were 889 [111-5290], 132 [1-4880], and 49 [4-9480]. Low IgG was present in 472 (33.2%), low IgA in 223 (16.4%), and low IgM in 530 (37.3%) patients. An M-spike was detected in 122 (8.6%) patients; distribution was: IgG (73), IgM (30), IgA (6), or multiple (13). By qualitative assessment, preserved Ig were seen in 664 (46.8%), partial Ig suppression in 604 (42.5%), and full suppression in 152 (10.7%) patients. By quantitative assessment, median ARD was 0.6 (-0.8 to 11.3); 280 (19.7%) patients had negative ARD, and 1140 (80.3%) had positive ARD. In those with negative ARD, 128 (9%) had partial Ig suppression and 152 (10.7%) had full Ig suppression; in those with positive ARD, 664 (46.8%) had preserved Ig and 476 (33.5%) had partial Ig suppression. Median follow-up was 14.7 years; 510 patients progressed requiring therapy. Median TTFT was 9.6 years. Median TTFT for patients with preserved Ig was 12.6 years, 8.0 years for partial Ig suppression (HR 1.4, 95%CI 1.1-1.7), and 1.8 years for full Ig suppression (HR 3.1, 95%CI 2.4-4.0). The median TTFT was 2.3 and 12.1 years for patients with negative vs positive ARD; negative ARD was associated with shorter TTFT (HR 2.4, 95%CI 2.0-2.9). After adjusting for sex and CLL-International Prognostic Index (CLL-IPI) score, full Ig suppression (HR 2.9, 95%CI 2.2-3.9) and partial Ig suppression (HR 1.6, 95% CI 1.3-2.0) were associated with shorter TTFT (model 1, c-stat 0.77); and negative ARD (HR 2.4, 95%CI 2.0-2.9) was associated with shorter TTFT (model 2, c-stat 0.76). Negative ARD identified an additional 9% of patients at higher risk for shorter TTFT beyond full Ig suppression.
Conclusions: The depth of immunoparesis at diagnosis predicts TTFT and enhances risk stratification in newly diagnosed MBL/CLL.

#1192 Survival trends in the management of carcinoid heart disease among patients with neuroendocrine tumors.

Sarah Gyojin Jung[1], Rebecca Steinberg[2], Angel Xi[3], Jeffrey Switchenko[3], Olatunji Alese[4]

[1]Emory University School of Medicine, Atlanta, GA,[2]Department of Medicine, Division of Cardiology, Duke University, Durham, NC,[3]Biostatistics Shared Resource, Winship Cancer Institute of Emory University, Atlanta, GA,[4]Department of Hematology/Medical Oncology, Winship Cancer Institute of Emory University, Atlanta, GA

Background: Nearly 20% of patients diagnosed with neuroendocrine tumors (NET) will develop carcinoid syndrome (CS), with 20-25% of CS patients developing carcinoid heart disease (CHD). The risk factors for developing CHD and prognostic variables in the current day of NET management are lacking.
Objectives: The main objectives of this study were to describe the clinical, laboratory, and imaging risk factors for developing CHD in CS patients, and to identify predictors of survival in NET patients.
Methods: A single-institution, retrospective analysis of patients with well-differentiated NET from January 2010 to December 2024 was conducted. Cox proportional hazard regression assessed the association between baseline covariates and CHD development (primary endpoint), and overall survival (OS; secondary endpoint). CHD was defined as moderate or severe tricuspid regurgitation on echocardiogram, consistent with prior studies. Survival curves for OS and CHD development were estimated using the Kaplan-Meier method. A p-value of 0.05 was considered statistically significant.
Results: We identified and included 270 patients with NET in the study. Median age was 64.5 years, 52% were male and 5.6% were diagnosed with CHD. CS was present in 10% of patients (n=27), and 41% of those with CS developed CHD. The most common primary tumor sites were
lung (26%), pancreas (17.4%), and small intestine (16.2%). On multivariable analysis, right ventricular (RV) dilation was also associated with shorter time to CHD diagnosis (hazard ratio [HR] 7.65, 95% CI: 1.03-56.78, p=0.047). The diagnosis of CHD was associated with a higher number of hospitalizations overall and the use of systemic or multimodal therapies.For the secondary endpoint of OS, median OS for patients with CHD was 90.8 months, while median OS was not reached for the full NET cohort. CHD development was independently associated with worse OS in extended Cox models (HR 7.09; 95% CI 1.84-27.40, p=0.004), highlighting its strong prognostic impact beyond baseline tumor factors. The use of systemic therapy (HR 8.97; 95% CI: 1.78-45.25, p=0.0101) and high-grade (G3) tumors were associated with worse OS (HR 6.92; 95% CI: 2.40-19.92, p<0.001).
Conclusion: Among patients with NET, the diagnosis of CHD, use of systemic/multimodal therapy, and high-grade tumors were associated with worse overall survival. Although the incidence of CHD is low, close monitoring for early diagnosis and intervention remain critical in the management of these patients.

#1193 Breast cancer recurrence risk stratification using rapid, cost-effective TempO-Seq profiling and an XGBoost classifier outperforms Oncotype DX.

Juan Barrasa[1], Salvatore Camiolo[1], Hanna Ha[1], Zhoutao Chen[2], Joanne M. Yeakley[2], Joel McComb[2], **Bruce Seligmann**[2]

[1]BioClavis, LTD., Glasgow, United Kingdom,[2]BioSpyder Technologies, Inc., Carlsbad, CA

Introduction: The market standard Oncotype DX 21 gene Recurrence Score predicts risk of distant recurrence in HR+/HER2- breast cancer, has a 7-14 day turnaround (TAT), requires 50-300 ng total RNA from FFPE sections with ≥5 mm² tumour, and costs ~$4,000. The low-cost extraction free targeted sequencing TempO-Seq® assay uses lysates of FFPE without RNA extraction or reverse transcription, has a 2 day TAT, and measures the whole transcriptome or any actionable subset of genes. We evaluated if TempO-Seq profiling of lysates from a single 1 mm^2 tissue microarray (TMA) core could match or surpass the clinical performance of Oncotype DX.
Methods: A TempO-Seq panel of the 21 Oncotype DX signature genes was implemented which incorporated attenuation of highly expressed gene signals. Sample processing and reaction conditions were optimized to deliver robust data from a single 5 µm thick, 1 mm diameter TMA core.
Results: Biological reproducibility of the TempO-Seq workflow was robust, with a median intercore correlation r>0.80. We developed a Support Vector Machine (SVM) learning model using 70% of the samples from a cohort of 86 patients, for which we had 10-year recurrence data and Oncotype DX scores from matched sections. Testing the other 30% of patients, this model accurately identified 100% of the patients with recurrence and 71% of the patients without recurrence. In comparison, Oncotype DX identified 65% of the patients with recurrence as high/intermediate risk and 52% of the patients without recurrence as low risk. Recognizing that TempO-Seq's performance could have been biased by training and testing on the same dataset, we trained an XGBoost algorithm, which is more reliable for handling independent cohorts with potential batch effects, using 70% of an independent cohort of 245 samples for which we only had 10-year recurrence data. Testing with the remaining samples, the XGBoost model correctly identified 80% of the patients with recurrence and 48.7% of the patients with no recurrence. Additionally, the model maintained its consistency when classifying all the samples in the 86 sample cohort, correctly identifying 76.8% of the patients with recurrence and 48.9% of the patients with no recurrence. We also trained the model to classify 90% of patients with recurrence as high risk, and 31% of patients with no recurrence as low risk.
Conclusions: TempO-Seq outperformed Oncotype DX results from the 86 patient cohort in classifying patients with recurrence, and models classifying patients from multiple cohorts could be built that were equivalent to or outperformed published Oncotype DX data. Thus, TempO-Seq enables accurate and reproducible prediction of recurrence from a minimal FFPE input, suggesting its potential as a fast TAT, lower cost alternative for risk stratification in $HR^+/HER2^-$ breast cancer.

#1194 A novel ferroptosis-related lncRNA-miRNA-mRNA genes signature for predicting prognosis and tumor immune microenvironment in endometrial cancer.

Hikaru Murakami, Junlong Wang, Herbert Yu

Cancer Molecular Epidemiology, University of Hawai'i Cancer Center, Honolulu, HI

Ferroptosis, an iron-dependent form of cell death, is known to be involved in cancer process and tumor immunity, and to be regulated by not only coding (mRNA) but also non-coding genes such as long non-coding RNA (lncRNA) and microRNA (miRNA). However, little is known about the involvement of ferroptosis in endometrial cancer (EC). The aim of this study is to identify comprehensive ferroptosis-related lncRNA-miRNA-mRNA interactions and to construct a ferroptosis-related lncRNA-miRNA-mRNA model for predicting overall survival (OS) and tumor immune microenvironment in EC. Tumor transcriptomes and corresponding clinical data of 544 EC patients were extracted from TCGA, and the ferroptosis database, FerrDb, was used to identify ferroptosis-related coding genes (FRGs) (mRNAs). Ferroptosis-related lncRNAs and miRNAs were selected based on their correlations with FRGs. Univariate, multivariate, and Lasso Cox regression analyses were conducted to construct a prognostic model based on ferroptosis-related lncRNA-miRNA-mRNA genes. EC patients were grouped into high- and low-risk categories based on the risk score which is constructed using the expression levels of ferroptosis-related transcripts. Kaplan-Meier (K-M) analysis and receiver operating characteristic (ROC) curves were used to evaluate the prognostic value. Gene Set Enrichment Analysis (GSEA) was conducted to explore biological pathways between the high- and low-risk groups. Besides, the proportion of infiltrating immune cells and the expression level of immune checkpoints between the risk groups were compared. All signature RNAs were validated using an independent CPTAC cohort (n = 213). Sixteen ferroptosis-related RNAs (10 lncRNAs, 2 miRNAs, and 4 mRNAs) were identified as prognostic markers. A ferroptosis-related lncRNA-miRNA-mRNA co-expression network was constructed. K-M analysis demonstrated that patients in the high-risk group had a worse OS ($P < 0.001$). ROC curves showed that the area under curve (AUC) values of the model were 0.731, 0.749, and 0.768 for 1, 3, and 5 years of survival, respectively, and the model had a better ability to predict the prognosis of EC patients than other clinical factors (age, grade, and stage). Moreover, the predictive nomogram suggested that our model could offer an independent prognostic evaluation with high accuracy. GSEA revealed that patients in the high-risk group had an enrichment of cancer-related pathways. Tumors in high-risk patients had lower levels of antitumor immunity, and there were several differences in the expression of immune checkpoints between the groups. In the CPTAC dataset, these RNAs were confirmed to be similarly associated with EC prognosis. This study provides new insight into ferroptosis-related molecular mechanisms and novel directions for prognostic assessments, immunotherapies, and targeted treatments of EC.

#1195 Prognostic value of circulating CD11b$^+$CD33$^+$myeloid cells in localized prostate cancer.

Viola Moscarda[1], Sara Merler[1], Daniele Braga[1], Bianca Cali[1], Federica Cetti[1], Giuseppe Reitano[2], Filippo Carletti[2], Gianmarco Randazzo[2], Davide Minardi[2], Sara Zumerle[3], Mirko Minini[4], Anna Sordo[5], Giovanna Pecoraro[6], Nicola Fossati[7], Andrea Gallina[7], Ricardo Pereira Mestre[6], Silke Gillessen[6], Alessandro Morlacco[2], Fabrizio Dal Moro[2], Andrea Alimonti[1]

[1]IOR - Institute of Oncology Research, Bellinzona, Switzerland,[2]Department of Surgery, Oncology and Gastroenterology; Urologic Unit, University of Padova, Padova, Italy,[3]IOV - Istituto Oncologico Veneto, Padova, Italy,[4]Sorbonne Universite, Inserm, Centre de Recherche Saint-Antoine (CRSA), Paris, France,[5]CRC - Centro ricerche cliniche, Verona, Italy,[6]Oncology Institute of Southern Switzerland (IOSI), Ente Ospedaliero Cantonale (EOC), Bellinzona, Switzerland,[7]Urology Service, Department of Surgery, Ente Ospedaliero Cantonale (EOC), Lugano, Switzerland

Risk stratification in localized prostate cancer (PCa) relies on clinical and pathological parameters, as well as molecular assays that are often limited in accessibility. While circulating myeloid cells are associated with poor prognosis in advanced disease, their role in primary PCa remains unclear. This study aimed to determine whether circulating CD11b$^+$CD33$^+$ myeloid cells could serve as a minimally invasive, cost effective prognostic biomarker in localized PCa.

We analyzed a prospective cohort of 79 patients with localized PCa undergoing radical prostatectomy. Circulating CD11b$^+$CD33$^+$ myeloid cells were quantified by flow cytometry. Associations between CD11b$^+$CD33$^+$ frequency and clinical parameters were evaluated, including EAU risk group, postoperative pathological features and biochemical recurrence (BCR). RNA sequencing was performed on FACS sorted circulating CD11b$^+$CD33$^+$ cells from 39 patients, including 15 from this prostatectomy cohort and 24 from an independent biopsy cohort.

Circulating CD11b$^+$CD33$^+$ cell frequency was significantly higher in patients classified as high risk at diagnosis, versus intermediate ($p = 0.0419$) and low risk ($p = 0.0087$), and associated with adverse pathological features such as ISUP grade 4 and 5 ($p = 0.0034$) and perineural invasion ($p = 0.0303$). Transcriptomic profiling of these cells revealed distinct transcriptional programs in high risk versus intermediate risk patients, with enrichment of tumor promoting and immunosuppressive gene signatures. Higher circulating CD11b$^+$CD33$^+$ frequency associated with shorter BCR free survival ($p = 0.028$), particularly in high risk patients, after a median follow up of 31.8 months. Notably, the frequency of these cells outperformed the EAU risk classification, identifying a subset of high risk PCa patients at highest risk of early recurrence.To validate these findings, we analyzed the TCGA cohort of localized PCa patients ($n = 329$); although only tumor transcriptomic data were available, high intratumoral CD11b$^+$CD33$^+$ gene expression was associated with shorter disease free survival, especially in high risk patients. A custom four gene myeloid signature derived from genes upregulated in our cohort further refined risk stratification, predicting early relapse in high risk cases.

Higher frequencies of circulating CD11b$^+$CD33$^+$ myeloid cells are observed in high risk localized PCa and associate with shorter BCR free survival. Remarkably, this myeloid expansion occurs even in organ confined disease, revealing an early systemic immune response previously unrecognized in localized PCa. Transcriptomic profiling confirmed enrichment of immunosuppressive and tumor promoting programs in these cells. Circulating CD11b$^+$CD33$^+$ frequency and associated gene signatures represent a novel prognostic biomarker, with potential to improve risk stratification in localized PCa, warranting validation in larger cohorts.

#1196 A pre-treatment cfDNA methylation signature linking prognosis and drug-resistance biology in pancreatic ductal adenocarcinoma.

Ashish Manne[1], Lianbo Yu[1], Wancai Yang[1], M Khalid Khan Niazi[1], Ravi Paluri[2], Anup Kasi[3], Prachi Bajpai[4], Alejandro Leyva[1], Upender Manne[4]

[1]The Ohio State University, Columbus, OH,[2]Atrium Health Wake Forest Baptist, Winston Salem, NC,[3]University of Kansas Medical Center, Kansas City, MO,[4]University of Alabama at Birmingham, Birmingham, AL

Pre-treatment risk-stratification of pancreatic ductal adenocarcinoma (PDAC) can individualize response monitoring and streamline trial triage. We refined the previously reported treatment resistance-associated, literature-curated protein-informed cell-free DNA (cfDNA) methylation signature for baseline prognostication. Notably, the panel includes genes whose protein products are implicated in resistance to commonly used PDAC therapies. The goal was to identify high-risk PDAC populations before administration of the current standard of care first-line chemotherapy (FLC) combinations, such as FOLFIRINOX (FFX) or gemcitabine and nab-paclitaxel (G-NP). The study included PDAC patients treated at The Ohio State University between 2010 and 2022 who had plasma samples available before initiation of first-line chemotherapy. Targeted enzymatic methylation sequencing was performed for cfDNA methylation profiling. In our 45-patient retrospective cohort the distribution was as follows, Stage at diagnosis (StD): 18 early stage (ES = borderline/resectable), 13 metastatic (met), and 14 locally advanced (LA); Ultimately, 18 had surgery (SR) (9 upfront surgery (UpS) and 9 had neoadjuvant therapy (NAT)) and 27 had palliative therapy (PT, 2 LA had surgery and 2 ES progressed to met); FLC in PT-group, 10 FFX, 15 GA, 2 others; Most of the patients who received NAT (7/9) or adjuvant (AT) after UpS (5/9) received FFX. A fixed 16-gene signature (cfMeth-OS16) was scored per patient (continuous z-score) and dichotomized at the study median into high-risk (HR) and low-risk (LR) groups; overall survival (OS) was modeled with Cox regression, discrimination summarized by Harrell's C-index, and survival compared by log-rank. cfMeth-OS16 separated the population significantly (HR vs. LR: 11 vs. 39 months (m); hazard ratio (HR) of 7; C-index of 0.8, p-value -<0.01). Adding StD improved the cfMeth-OS's performance (7 vs. 39m; 12; 0.87; <0.01) while FLC (FFX vs. G-NP vs. other) in any setting (PT, NAT, or AT in UpS) did not substantially improve it (10 vs. 39m, 12, 0.83; <0.01). A comprehensive model (cfMeth-OS + FLC + age + gender + RS (yes/no) + radiation received (yes/no)) achieved a higher C-index with a large, adjusted HR (7 vs. 39; 34; 0.89, <0.01). Compared to our previous signature derived from a cohort that included some post-treatment samples, cfMeth-OS showed modestly increased discrimination and extended long-survival estimates (vs. 10 vs. 33m; 8.7; 0.78). cfMeth-OS16 provides independent risk stratification for PDAC beyond FLC selection and routine clinical factors. The study's limitations include its modest sample size, single-center retrospective design, and heterogeneity in treatments and stages, which may constrain generalizability. Prospective, multi-institutional validation will be critical to confirm the robustness and potential predictive value of cfMeth-OS16

#1198 Stage-dependent expression of Fanconi anemia pathway genes in HPV-negative head and neck squamous cell carcinoma.

Olivia A. Swaim, Alexander Straughan, Beverly Wuertz, Frank Ondrey

University of Minnesota Medical School, Minneapolis, MN

The Fanconi Anemia/BRCA DNA repair pathway plays a critical role in genomic stability and treatment response in head and neck squamous cell carcinoma (HNSCC). However, whether FA pathway gene expression changes with tumor stage in sporadic HNSCC is insufficiently understood. We examined stage-dependent expression patterns of 23 FA pathway genes in HPV-negative HNSCC. We analyzed mRNA expression data (RNA-seq Z-scores) from 415 HPV-negative HNSCC tumors in The Cancer Genome Atlas via cBioPortal. Twenty-three FA pathway genes were examined across core complex, ID2 complex, homologous recombination, nuclease, and associated components. Tumors were stratified by AJCC stage into early-stage (I/II, n=84) and late-stage (III/IV, n=292) groups, eliminating 39 unstaged patients. Lymph node staging data was available for 402 patients (96.9%), with late-stage tumors showing significantly higher rates of lymph node involvement compared to early-stage disease (67.1% vs 1.2% N+, $p<0.001$). We performed differential expression analysis using two-sample t-tests with Benjamini-Hochberg FDR correction for multiple testing ($\alpha=0.05$). Effect sizes were calculated using Cohen's d. Late-stage tumors demonstrated more aggressive clinical features with increased lymph node metastases. After FDR correction, only RAD51C showed significant differential expression ($q=0.046$), with higher expression in late-stage disease (mean±SD: 7.86±0.62 vs 7.65±0.51, log2 FC=-0.21, $p=0.002$, $d=-0.37$). Six additional genes showed nominal significance ($p<0.05$) but did not survive FDR correction. Four genes were elevated in early-stage tumors: BRCA2 (log2 FC=0.33, $p=0.006$), ERCC4 (log2 FC=0.16, $p=0.022$), SLX4 (log2 FC=0.12, $p=0.023$), and BRIP1 (log2 FC=0.24, $p=0.042$). Two genes were elevated in late-stage tumors: FANCE (log2 FC=-0.20, $p=0.009$) and UBE2T (log2 FC=-0.21, $p=0.025$). All effect sizes were small ($|d|=0.24$-0.37). Most FA pathway genes in the RNA-seq dataset (16/23, 70%) showed no stage-dependent differences, including BRCA1, PALB2, RAD51, and most core complex members. RAD51C is uniquely upregulated in late-stage HPV-negative HNSCC after correction for multiple testing, distinguishing it from other FA pathway genes. This finding suggests that RAD51C could be a targetable weakness specifically in advanced HNSCC, which deserves further investigation for stage-directed therapies. Because the six additional genes which showed nominal significance did not survive FDR correction, this suggests that aside from RAD51C, the FA pathway appears to be preserved during HNSCC progression. For both Fanconi Anemia cancers and sporadic non-Fanconi HNSCC, the next step would be examining mutations in these genes to see how they affect function in stage-dependent pathophysiology.

: Spatial Proteomics and Transcriptomics 1
Poster Session

#1200 Spatially resolved tumor-cell MHC class II shapes adaptive immunity and therapeutic response in triple-negative breast cancer.

Yi Liu[1], Sachin Kumar Deshmukh[2], Thiti Susiriwatananont[1], Panuch Eiamprapaporn[1], Bogang Wu[3], Heikki Joensuu[4], Roberto A. Leon-Ferre[5], David Zahrieh[6], Judy C. Boughey[7], James Newell Ingle[8], Fergus J. Couch[9], Sharon Wu[2], Shipra Gandhi[10], Maryam Lustberg[11], George W. Sledge[2], Matthew P. Goetz[9], Keith L. Knutson[1], E Aubrey Thompson[1], Jodi Carter[12], **Saranya Chumsri**[1]

[1]Mayo Clinic Florida, Jacksonville, FL,[2]Caris Life Sciences, Phoenix, AZ,[3]Mayo Clinic Phoenix, Phoenix, AZ,[4]University of Helsinki, Helsinki, Finland,[5]Mayo Clinic, Rochester, MN,[6]Health Sciences Research, Mayo Clinic, Rochester, MN,[7]Radiation Oncology, Mayo Clinic, Rochester, MN,[8]Professor, Dept. of Oncology, Mayo Clinic College of Medicine, Rochester, MN,[9]Mayo Clinic College of Medicine and Science, Rochester, MN,[10]Emory University School of Medicine, Atlanta, GA,[11]Yale School of Medicine, New Haven, CT,[12]University of Alberta, Edmonton, AB, Canada

Background: MHC class II molecules are normally restricted to professional antigen-presenting cells. Prior TNBC studies have focused on immune-compartment MHC-II. Using spatial transcriptomics, we recently identified aberrant tumor-cell MHC-II expression. Here, we characterized the immune architecture surrounding HLA-DRA-expressing tumor cells.
Methods: High-plex single-cell spatial transcriptomics (CosMx^{TM} SMI) was performed on treatment-naïve TNBC (Mayo TMA, n=65) and two neoadjuvant pembrolizumab cohorts (Mayo n=8; Emory n=4). Spatial neighborhoods were mapped relative to HLA-DRA-high tumor cells. Differential expression and adaptive immune gene-set scores were evaluated. Clinical relevance was assessed using FinXX (n=114), I-SPY2 (n=364), and Caris CODEai (n=3,662).
Results: HLA-DRA-high tumor regions showed significant enrichment of adaptive immune subsets within ≤50 μm, including B cells, CD8$^+$ T cells, NK cells, macrophages, and plasmacytoid dendritic cells. In pembrolizumab-treated cohorts, responders exhibited higher proportions of HLA-DRA-high tumor cells and greater numbers of B cells, plasmablasts, CD4$^+$ and CD8$^+$ T cells, and macrophages near tumor cells. Responders' tumors showed upregulation of antigen-presentation machinery, B-cell/plasma-cell programs, CXCL13, and NOTCH3/DLL1. Across I-SPY2 and FinXX, higher HLA-DRA correlated with pathologic complete response and improved survival. In CODEai TNBC, high HLA-DRA expression correlated with higher CXCL13 (median TPM 7.5 vs. 1.1, $q<0.05$) and longer overall survival (24.2 vs. 18.5 months, HR 0.77, 95% CI 0.71-0.83, $p<0.0001$). This association was TNBC-specific. High CXCL13 also predicted improved survival (26.6 vs. 16.5 months, HR 0.64, 95% CI 0.59-0.69, $p<0.0001$).
Conclusions: Tumor-cell HLA-DRA expression defines a highly organized adaptive immune niche enriched with B cells and activated T-cell populations in close proximity. Adaptive immune programs—including enhanced antigen presentation and CXCL13-mediated B-cell/plasma-cell pathways—consistently associate with improved outcomes across TNBC cohorts treated with chemotherapy and immune checkpoint blockade. Aberrant tumor-cell MHC-II expression may contribute to antitumor immunity and warrants further investigation as a potential therapeutic target.

#1201 Spatial 3D and multi-omics mapping of diffuse gastric cancer evolution from preinvasive to invasive lesions in CDH1 mutation carriers.

Yunhe Liu[1], Idania Carolina Lubo Julio[2], Wei Lu[2], Alejandra G. Serrano[2], Jean R. Clemenceau[3], Amber Famiglietti[4], Karen Colbert[5], Yibo Dai[1], Yang Liu[1], Jun Wang[1], Jeremy L. Davis[6], Mingyao Li[7], Paul F. Mansfield[8], Tae Hyun Hwang[3], Luisa M. Solis-Soto[9], Linghua Wang[1]

[1]Department of Genomic Medicine, The University of Texas MD Anderson Cancer Center, Houston, TX,[2]Department of Translational and Molecular Pathology, The University of Texas MD Anderson Cancer Center, Houston, TX,[3]Department of Surgery, Vanderbilt University Medical Center, Nashville, TN,[4]National Institute of Dental and Craniofacial Research, National Institutes of Health, Bethesda, MD,[5]Department of Clinical Cancer Prevention, The University of Texas MD Anderson Cancer Center, Houston, TX,[6]BioChemistry&Molecular Biology, University of Maryland School of Medicine, Baltimore, MD,[7]University of Pennsylvania, Philadelphia, PA,[8]Vice President, Acute Care Services, UT MD Anderson Cancer Ctr., Houston, TX,[9]Department of Translational Molecular Pathology, the university of MD Anderson cancer center, Houston, TX

Background: Hereditary diffuse-type gastric cancer (DGC) lacks a defined precursor sequence. Germline CDH1 loss-of-function mutations confer a high lifetime risk, and prophylactic gastrectomies in asymptomatic carriers frequently reveal numerous occult intramucosal signet-ring cell (SRC) foci that can remain indolent for years. The biological mechanisms underlying the progression from these indolent SRC foci to invasive DGC remain largely unknown.
Methods: We profiled primary DGCs from 26 patients, sampling the full histologic continuum from SRC foci to invasive lesions and overtly invasive fronts. Whole-slide sections were pathologist-annotated for tumor subtype and key microenvironmental features. Serial sections were assayed with complementary spatial multi-omics platforms: GeoMx DSP, Visium, Xenium Prime 5K with post hoc Codex (IO60), and CosMx (WTX). Selected specimens also underwent high-plex spatial multi-omics sequencing (transcriptome/protein/TCR/BCR) using Singular G4X, as well as 3D modeling with both Singular G4X and holotomography (HT-X1). Cross-platform datasets were co-registered to common coordinates; cell segmentation, phenotype annotation, and neighborhood/niche mapping quantified transcriptomic dynamics and tumor-microenvironment interactions across regions spanning preinvasive to invasive lesions. Integration of Singular G4X and Label-free holotomography provided 3D context.
Results: Spatial transcriptomic profiling revealed invasion-associated transcriptional programs along the SRC-to-invasive continuum. The meta-programs (MPs) associated with discrete stages of progression were defined. Histology-integrated analyses highlighted invasion-depth-dependent shifts in cell-cycle, EMT, and stress-metabolism pathways, and trajectory/differentiation analyses supported a continuous invasion axis. Copy-number inference indicated two evolution trajectories, linear and branched. Single-cell-resolution spatial multi-omics refined tumor cell-state signatures and their spatial neighborhoods, revealing lymphocyte-dominant microenvironmental states at early lesions and stromal/myeloid remodeling with deeper invasion, corroborated by multiplex proteomics (IO60). Cross-section registration with label-free 3D holotomography generated volumetric reconstructions mapping coherent clonal sectors and concordant TME remodeling along the invasion axis.
Conclusions: We present a spatial multi-omic atlas of DGC progression. The work delineates subtype- and region-specific gene programs, clonal architectures, and TME remodeling at high spatial and molecular resolution, modeling disease progression in 3D. Our findings identify candidate biomarkers of progression, risk stratification, and potential therapeutic interception of SRC tumorigenesis in CDH1 mutation carriers.

#1202 Spatially-resolved transcriptome analysis of renal tumors with sarcomatoid/rhabdoid dedifferentiation uncovers underlying biology and new biomarkers relevant to these tumors.

Minjun Kim[1], Mustafa Soytas[1], Burge Ulukan[2], Tamiko Nishimura[1], Senthilkumar Kailasam[1], Ariel Madrigal[1], Zohreh Mehrjoo[1], Kate Glennon[1], Eleonora Scarlata[3], Madeleine Arseneault[1], Morag Park[4], Hamed Najafabadi[1], Fadi Brimo[5], Ozgur Sahin[2], Simon Tanguay[3], Yasser Riazalhosseini[1]

[1]Victor Phillip Dahdaleh Institute of Genomic Medicine, McGill University, Montreal, QC, Canada,[2]Department of Biochemistry and Molecular Biology, Hollings Cancer Center, Medical University of of South Carolina, Charleston, SC,[3]Division of Urology, Department of Surgery, McGill University, Montreal, QC, Canada,[4]Goodman Cancer Institute, McGill University, Montreal, QC, Canada,[5]Department of Pathology, McGill University, Montreal, QC, Canada

The presence of sarcomatoid (Sarc) and rhabdoid (Rhab) dedifferentiation in renal cell carcinoma (RCC) is linked to poor clinical outcomes and higher risk of metastatic disease. Previous molecular studies on renal tumors with these dedifferentiated features lacked spatial resolution to distinguish these aggressive regions from classical RCC histology, leaving the biology underlying these aggressive phenotypes poorly understood. We applied spatial whole transcriptome profiling (GeoMx DSP) to 370 regions exhibiting Sarc, Rhab, clear cell, papillary, or benign kidney from 54 RCC tumors. We combined these spatial transcriptome profiles with our single-cell RNA-sequencing atlas consisting of different RCC subtypes to investigate Sarc/Rhab biology and verified clinical significance of our findings using public databases such as The Cancer Genome Atlas (TCGA) and Clinical Proteomic Tumor Analysis Consortium (CPTAC). Deconvolution of the spatially resolved transcriptome data revealed substantial gene expression reprogramming in Sarc/Rhab regions. Notably, Sarc/Rhab areas featured a high fibroblast-like gene expression pattern and a loss of cytokeratin expression as a defining hallmark of Sarc and Rhab dedifferentiation, reflecting their histological nature. We established cancer cell-intrinsic gene expression signatures of Sarc and Rhab tumors and found they are highly correlated with higher tumor grade in the ccRCC cohorts from both TCGA (n=485) and CPTAC (n=103). Importantly, these signatures significantly predicted poor disease-free survival in clinically low-risk (Stage 1-2) ccRCC patients. In the ccRCC cohort of TCGA, tumors with high Sarc gene signature levels were enriched for mutations in *SETD2*, *PTEN*, *MTOR*, and *KDM5C*, as well as specific copy-number variations, notably loss of 14q, 9, 18, and 6p and gain of 20, 12, and 8q, compared to other tumors. Pathway enrichment analyses suggested that genes related to extracellular matrix organization, coagulation, and epithelial-mesenchymal transition were highly enriched in Sarc/Rhab regions compared to classical ccRCC regions, while pathways for oxidative phosphorylation, adipogenesis, and amino acid metabolism were decreased.These findings provide novel insights into the biology of Sarc/Rhab dedifferentiation in RCC, paving the way for the development of improved prognostic markers and targeted therapeutic strategies.

#1203 Spatial archetypes of conserved and cancer-specific immune-stromal niches.

Tian Chu[1], Jimin Min[2], Yunhe Liu[1], Yang Liu[1], Yibo Dai[3], Kyung Serk Cho[3], Xueshuai Han[3], Kai Yu[3], Fuduan Peng[3], Anirban Maitra[4], Humam Kadara[3], Linghua Wang[3]

[1]Genomic Medicine, UT MD Anderson Cancer Center, Houston, TX,[2]Medicine, New York University Grossman School of Medicine, New York, NY,[3]UT MD Anderson Cancer Center, Houston, TX,[4]Department of Pathology, New York University Grossman School of Medicine, New York, NY

Background: Spatially organized immune-stromal interactions critically shape tumor progression, yet a systematic characterization of conserved and cancer-specific microenvironmental architectures across human tumors remains limited. Recent advances in high-resolution spatial transcriptomics provide an exceptional opportunity to define these spatial niches, characterize cellular neighborhoods in situ, and delineate their clinical relevance as potential diagnostic or prognostic biomarkers.

Methods: We performed single-cell spatial profiling using the Xenium 5K platform on 40 cancer tissues across eight cancer types and paired uninvolved normal tissues, generating a spatial atlas of over ten million cells. By integrating transcriptional similarity, spatial proximity, and cellular composition, we defined spatial niches using an unsupervised framework. We then dissected the structural and functional characteristics of tumor microenvironments (TME). Association between transcriptional signatures and TME were further validated using public spatial-omics datasets.

Results: We identified 31 spatial niches (SNs), including both tumor-associated and tissue-specific niches. Some SNs were conserved across multiple cancer types, whereas others were enriched in organ-specific tissues and cancers, suggesting both universal and context-dependent TME programs. Spatial heterogeneity was most pronounced at tumor-stroma interfaces, where niche diversity markedly increased. Several niches were enriched for distinct CAF subsets or myeloid populations such as macrophages and neutrophils, indicating diverse stromal remodeling dynamics across tumors. $CD8^+$ T cell-enriched niches exhibited distinct spatial localization and transcriptional features, with $CD8^+$ T cell states ranging from activated to terminally exhausted, illustrating how cytotoxic responses are shaped by local context. These immune niches differed not only in $CD8^+$ T cell states but also in their surrounding cellular ecosystems, such as co-enrichment with regulatory T cells or chemotactic myeloid cells. Notably, in two immunotherapy cohorts, higher baseline abundance of SN11—a niche characterized by strong CD8-tumor interactions—was associated with better response to immune checkpoint blockade.

Conclusions: This study presents a large-scale spatial framework to characterize immune and stromal compartments across tumors. We define conserved and cancer-specific microenvironmental architectures, including spatially distinct immune niches with potential clinical relevance. The distinct spatial and cellular compositions of these niches highlight their potential as spatially resolved biomarkers of immune state, tumor progression, and therapeutic response, with implications for early detection and patient stratification in oncology.

#1204 Spatial multiomic characterization of spontaneous lung tumors in aged mice.

Adam Thiesen[1], Sema Akkurt[1], Javad Noorbakhsh[1], Te-Chia Wu[2], Andrew Salner[3], Peter Yu[3], Susan Airhart[4], Olga Anczukow[1], Ron Korstanje[4], Karolina Palucka[5], Jeffrey H. Chuang[5]

[1]The Jackson Laboratory for Genomic Medicine, Farmington, CT,[2]Jackson Laboratory, Farmington, CT,[3]Hartford Hospital, Hartford, CT,[4]The Jackson Laboratory, Bar Harbor, ME,[5]The Jackson Laboratory, Farmington, CT

Introduction: Lung cancer is one of the most common malignancies and is the leading cause of cancer related deaths worldwide. While lung cancer incidence has decreased over time with the success of smoking and tobacco cessation campaigns, a significant burden of disease remains among non or never-smokers. Advancing age is a key risk factor for lung cancer, with incidence escalating most steeply in the fifth decade. Here we show that laboratory mice also spontaneously develop lung tumors with age. Additionally, we show that these tumors are often malignant adenocarcinomas as opposed to the adenomas traditionally described. Using spatial transcriptomic and proteomic approaches we aimed to study whether the adenocarcinomas that develop spontaneously in aged mice were similar to human never-smoking tumors.

Methods: Diversity Outbred (DO) and UM-HET3 mice were housed and aged to 24 months. At 24 months, necropsies were performed on more than 600 mice, and all tissues were examined for the presence of tumors. The identified lung lesions were annotated by pathologists on hematoxylin and eosin (H&E)-stained sections to assess tumor type. Those annotated as adenocarcinomas were assessed for 2mm diameter regions of interest (ROIs) to be incorporated into Tissue Microarrays for downstream Xenium spatial transcriptomics and Codex spatial proteomic profiling. The Spacec package was used for codex and Scanpy was generally used for Xenium analysis. These data were compared against publicly available TCGA bulk RNA-seq as well as Xenium data collected from patients at local hospitals.

Results: About 40% of mice developed lung lesions, with 30% of those being adenocarcinomas. Unsupervised leiden clustering of the Xenium single cell data revealed a common signature between mouse epithelial tumors defined by inflammatory markers (*Chil1*). Other clusters associated more aggressive tumor progressions. Codex analysis revealed tumors with pockets of high P21 protein expression distributed throughout the tumor but found closer to the stromal boundary compared to the interior ($p < 0.05$). When we compared aggressive mouse tumor signatures to TCGA bulk RNA-seq signatures these patients have worse survival outcomes. *CD2AP* was a shared transcript significantly up-regulated in both mouse and human tumors ($P < 0.05$). Additionally, the microenvironment of these aggressive tumors often contained p21 positive potentially senescent dendritic cells, which colocalize with T cells.

Conclusion: Genetically diverse mice develop spontaneous lung adenocarcinomas that can develop into higher grade states. Multimodal analysis has revealed common pathways between spontaneously occurring mouse and human adenocarcinomas.

#1205 Trajectory-aware spatial transcriptomics deconvolution *via* image representation of RNA-seq data.

Junyan Liu, Md Tauhidul Islam, Lei Xing

Stanford University, Palo Alto, CA

Introduction: Intra-tumor heterogeneity across malignant clones, immune infiltrates and hypoxic niches drives spatially variable radiosensitivity within the same lesion. Spot-based spatial transcriptomics (ST) affords location-resolved gene expression across whole sections, yet each spot aggregates multiple cell types and states, obscuring the micro-ecologies that define the tumour microenvironment (TME). Although single-cell-resolution ST (e.g., imaging-based transcriptomics) can localize transcripts at sub-cellular scales, its cost, assay time and specialized infrastructure currently limit routine deployment in clinical settings. Accurate deconvolution of spot profiles into cell-type/state proportions is therefore essential to derive mechanistic biomarkers such as subtype-specific radiosensitivity scores or hypoxia indices that can guide biologically adaptive radiotherapy. However, existing deconvolution approaches that directly match ST expression to pre-measured reference profiles are vulnerable to technical variation, including batch effects and gene dropouts, particularly when references and ST are generated on different platforms. In this study, we present an optimal transport (OT) framework for ST deconvolution that leverages the geometry of the gene-expression manifold to stabilize estimates, yielding robust quantification of spot composition.

Methods: We represent each spot's gene expression profile as a "genomap" image, ensuring a consistent 2D arrangement of genes across samples. From these per-spot genomap embeddings, we learn a graph using our previously developed "genoTrajectory" method to capture the manifold of spots. To estimate cell-type compositions, we align the graph to a single-cell reference atlas using optimal transport that integrates both gene-expression similarity and manifold geometry, where the loss function consists of transcriptomic dissimilarity between spots and reference cells, and the geodesic distances between the graphs.

Preliminary Results: We applied the geometry-aware deconvolution to a breast cancer dataset with paired single-cell-resolution ST (Xenium) and spot-based Visium measurements. Using Xenium as the reference ground truth, our method achieved a mean Pearson correlation of r = 0.68 between predicted per-spot cell-type proportions and the Xenium-derived proportions.

Conclusion: Current results demonstrate promising performance for characterizing tumor microenvironment. Future work will expand validation to additional datasets, benchmarking against state-of-the-art methods, and extend analysis to the immune landscape and hypoxia status, with the goal of linking these features to radiotherapy response.

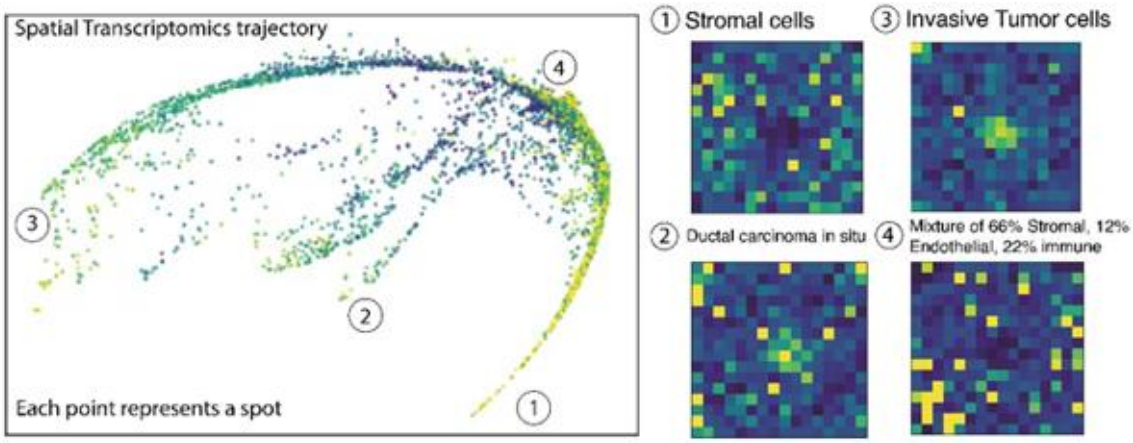

Figure 1. Genomaps and genoTrajectory derived from spot-based ST.

#1206 Large-scale spatial molecular profiling uncovers distinct macrophage activation states across meningioma methylation classes.

Domenico Calafato[1], Yiheng Tang[1], Gleb Rukhovich[1], Elyas Heidari[1], Leonille Schweizer[2], Michael Weller[3], Christine Haberler[4], Till Acker[5], Bhuvic Patel[6], Abigail Suwala[7], Felix Sahm[7], Felix Hartmann[8], Moritz Gerstung[1]

[1]Division of Artificial Intelligence in Oncology, DKFZ German Cancer Research Center, Heidelberg, Germany,[2]Institute of Neurology (Edinger Institute), University Hospital Frankfurt, Goethe University, Frankfurt am Main, Germany,[3]Department of Neurology, Clinical Neuroscience Center, University Hospital and University of Zurich, Zurich, Switzerland,[4]Division of Neuropathology and Neurochemistry, Department of Neurology, Medical University of Vienna, Vienna, Austria,[5]Institute of Neuropathology, University hospital Giessen, Giessen, Germany,[6]Department of Neurosurgery, Washington University School of Medicine, St. Louis, MO,[7]Department of Neuropathology, University Hospital Heidelberg, Heidelberg, Germany,[8]Division of Systems Immunology and Single cell Biology, DKFZ German Cancer Research Center, Heidelberg, Germany

Recent advances in neuro-oncology have highlighted the meninges as a key immunological hub at the interface between systemic immunity and the central nervous system (CNS). While meningiomas are primarily benign, ~20% exhibit high-grade features including brain invasion, recurrence, and treatment resistance. Macrophages in the tumor microenvironment are of particular interest due to their high abundance and phenotypic plasticity. While many studies have investigated macrophage diversity in cancer, this study spatially resolves myeloid activation programs in their native tissue context, exploring correlates with clinical parameters including meningioma molecular subtypes and recurrence. We combine spatial transcriptomics (Xenium) with multiplexed ion beam imaging (MIBI), integrating gene expression and high-dimensional protein data at single-cell resolution. Our large multi-center retrospective cohort of 368 FFPE samples includes cases with detailed molecular and clinical annotations. To enable scalable spatial analysis, we sampled pathologist-annotated regions and imaged tissue-micro-arrays (TMAs). Myeloid activation programs were discovered using cNMF. Delaunay algorithms delineated niches in Xenium data, while CellCharter discovered tissue niches in MIBI data. Spatial protein and transcriptomic data from consecutive sections reveal spatially segregated biological processes. The myeloid compartment in meningioma makes up a significant part of the tumor bulk, especially in low-grade tumors. Protein-level analysis shows clear tissue zonation marked by specific metabolic marker expression such as MCT1 and differential infiltration by microglia-like macrophage subsets. Spatial transcriptomics revealed at least 5 nuanced transcriptional myeloid activation programs that differ across methylation classes of over 320 cases. These differential enrichments were accompanied by distinct infiltration patterns and cell-type co-localization suggesting interaction-driven activation of myeloid programs. Overall, tumor-associated macrophages (TAMs) exhibit context-dependent prognostic significance across cancer types, most evidence supports their association with poor prognosis. In meningiomas, dense TAM infiltration is a key feature of benign subtypes. This study provides spatial context to meningioma methylation classes and addresses critical questions regarding the microenvironmental cues that shape TAM diversity and whether specific TAM activation programs have prognostic value, potentially revealing novel therapeutic avenues.

#1207 Multimodal profiling of STIC lesions identifies precursor states with genomic features of high grade serous ovarian cancer.

Duaa Hassan Al-Rawi[1], Nataly Naser Al Deen[1], Cristina Sotomayor-Vivas[1], Kerstin Thol[1], Herman Chui[1], Aveline Filliol[1], Areej Alsaafin[1], Hunter Green[1], Danguole Norkunaite[1], Mercedes Duran[1], Nicholas Ceglia[1], Kara Long-Roche[1], Britta Weigelt[2], Andrew McPherson[1], Scott W. Lowe[1], Sohrab Shah[1]

[1]Memorial Sloan Kettering Cancer Center, New York, NY,[2]Assistant Member (Level 1), Dept. of Pathology, Memorial Sloan Kettering Cancer Center, New York, NY

High-grade serous ovarian cancer (HGSC) is a lethal malignancy marked by near-universal *TP53* mutation and chromosomal instability (CIN) due late stage diagnosis. Surgical removal of fallopian tubes (FT) is the only effective prevention strategy. Even after surgery, a subset of individuals develops primary peritoneal carcinoma (PPC). When serous tubal intraepithelial carcinoma (STIC) is identified in the FT, PPC risk exceeds 30-fold. To study the steps required for HGSC initiation and identify features of high risk STICs, we assembled a 201-patient cohort spanning HGSC development from normal FT, p53 signatures, STIC, early and advanced-stage HGSC. All specimens underwent multiplexed immunofluorescence (mpIF), and 45 samples from 36 patients were profiled by Visium HD spatial transcriptomics generating >20million 8μM bins of data. We analyzed epithelial state transitions and inferred copy number variation (CNV) using inferCNV. In one case we validated CNV calls with matched FFPE single-cell whole-genome sequencing. mpIF revealed variable emergence of cGAS staining in STIC lesions, indicating evolving tolerance to CIN prior to invasion. Using unsupervised clustering of the epithelial bins, we found that STIC lesions formed distinct transcriptional clusters that faithfully mapped to STIC histologic features. Trajectory analyses suggests a putative precursor state bridging ciliated and secretory lineages. STIC clusters were enriched for NFκB and TGF-β signaling but lacked evidence of JAK/STAT signaling observed in advanced HGSC. inferCNV showed that normal fallopian tube/p53 signature lesions were largely chromosomally stable, whereas STICs displayed broad, genome-wide alterations, reminiscent of advanced HGSC, including losses affecting *TP53*, *BRCA1*, and *BRCA2* and amplifications of *MYC* and *CCNE1*. In a germline *BRCA2* patient, we identified polyclonal STICs with distinct CNV profiles. Pseudotime trajectory analysis in this case suggested early copy number changes within an expanded secretory population, followed by loss of chromosome 17 (*TP53*), loss of chromosome 13 (*BRCA2*), and subsequent oncogene amplifications (e.g., *MYC*). As STIC lesions become invasive, we observed spatial bins with unique inferred copy number profiles, indicating the emergence of neighborhoods of clonally related invasive cells. These tumor neighborhoods exhibit different microenvironments, including differences in fibroblast phenotypes and vascularization. This multimodal map of fallopian tube transformation supports a model in which *TP53* loss precedes *BRCA1/2* inactivation and indicates that STICs are genomically similar to advanced HGSC. Together, these data provide a framework for studying early HGSC evolution and may inform strategies for risk reduction and early interception.

#1208 The MONSTAR-SCREEN-3 Spatial Atlas: Pan-cancer TME archetypes and clinically relevant tumor-immune ecosystems.

Mitsuho Imai[1], Eun Seop Seo[2], Jiyeon Hyeon[3], Shingo Sakashita[4], Yuka Nakamura[4], Tadayoshi Hashimoto[4], Shin Kobayashi[4], Jun Yuda[1], Riu Yamashita[4], Taro Shibuki[4], Takao Fujisawa[4], Masataka Amisaki[4], Kensuke Matsuda[1], Shun-ichiro Kageyama[5], Michiko Nagamine[5], Takeshi Kuwata[6], Hideaki Bando[7], Woong-Yang Park[3], Takayuki Yoshino[7]

[1]National Cancer Center Hospital East, Kahsiwashi, Japan,[2]GxD Inc, Seoul, Korea, Republic of,[3]GxD Inc, Kashiwashi, Japan,[4]National Cancer Center Hospital East, Kashiwashi, Japan,[5]National Cancer Center Hospital East, Kashiwanoha, Japan,[6]Pathology, NCCHE, Kashiwa, Japan,[7]National Cancer Center Hospital East, Kashiwa, Japan

Background: The SCRUM-Japan MONSTAR-SCREEN consortium is a nationwide molecular profiling initiative spanning all solid tumors except lung cancer and hematologic malignancies. The next-generation MONSTAR-SCREEN-3 (M3) project incorporates spatial transcriptomics to achieve a "quantum leap" by integrating novel modalities to decode the tumor microenvironment (TME) architecture governing therapeutic response. This study presents the foundational pan-cancer spatial atlas from the initial M3 dataset.
Methods: MONSTAR-3 enrolls ~3,200 cases, and spatial analysis is being performed on eligible specimens. Among these, 331 FFPE tumors across 21 solid types were analyzed. Spatial profiling used the Xenium 5K platform within a standardized NCCE-GxD workflow (NCCE tissue preparation, GxD Xenium processing; ~10-week pipeline). Cell types were annotated using a consensus framework across four pipelines. Malignant epithelial cells were distinguished from benign epithelium through integrated spatial context, transcriptional features, and pathologist-guided review. We quantified malignant program heterogeneity and identified shared and distinct spatial niches linked to clinical variables.
Results: We generated a high-confidence spatial atlas comprising ~20 million cells. Across 21 tumor types, TME was organized into conserved, pan-cancer spatial ecosystem archetypes that stratified prognosis and therapeutic response. Spatial heterogeneity in malignant programs correlated with advanced disease. We also defined 15 conserved pan-cancer cellular niches (metaclusters), each with distinct compositions and spatial architectures. Among these, two tumor-stromal interface archetypes emerged: MC9, an innate-immune-rich interface, and MC5, a lymphocyte-dominant interface. The MC9 niche was significantly enriched in the advanced-stage tumors, showed increasing prevalence with higher TNM stages, and its derived signatures were associated with poor prognosis in legacy cohorts (e.g., TCGA). Conversely, B-cell-dominant (MC10) and B-cell/CD4+ T-cell-rich (MC14) niches were associated with favorable outcomes. These lymphocyte-dominant structures were further resolved into simple aggregates, primary follicles, and secondary follicles indicative of TLS formation. Secondary follicle signatures correlated with improved prognosis and response in an independent immunotherapy-treated cohort.
Conclusions: This study presents one of the largest pan-cancer spatial transcriptomic atlases and establishes a foundational component of the M3. We provide a robust framework for analyzing spatial transcriptomics and conserved, clinically actionable spatial ecosystems. This resource paves the way for spatially-driven patient stratification, next-generation biomarker development, and accelerated precision oncology within the SCRUM-Japan framework.

#1209 *FGFR2* translocated sinonasal adenocarcinoma: A biphasic seromucinous adenocarcinoma with a distinctive and targetable molecular phenotype.

Diana Bell[1], Randal S. Weber[2], Miao Zhang[2], Michelle Afkhami[3], Raja R. Seethala[1]

[1]University of Pittsburgh, Pittsburgh, PA,[2]University of Texas MD Anderson Cancer Center, Houston, TX,[3]City of Hope, Duarte, CA

Sinonasal adenocarcinomas (SNACs) are the second most common carcinoma category in the sinonasal tract after squamous cell carcinomas and include intestinal type adenocarcinoma, non-intestinal type adenocarcinomas and salivary-type adenocarcinomas. Surgery with postoperative radiation therapy is standard treatment for SNAC. Molecular characterization lists provisional subtypes (*BRAF V600E*-mutated sinonasal ductal-like tumors, *MAPK / PI3-K* altered SNAC, *CTNNB1*-mutated sinonasal carcinoma, fusion-kinase associated SNAC e.g. *ETV6::NTRK3*, *FGFR*-rearranged biphasic SNAC).We report a biphasic/basaloid SNAC (maxillary sinus epicenter, extending into nasal cavity; pT4N0M0) with a novel *FGFR2::SORB3* fusion. Targeted NGS was performed with a solid tumor comprehensive assay including DNA sequencing and RNA sequencing. RNA expression profiles of 1392 genes, related to tumor-immune interaction was generated. Representative SNAC region was subjected to 10X Genomics Visium Spatial Gene Expression analysis. NGS showed 9 clinically significant variants: *BMPR1A* loss; *DICER1* loss, *FGFR2* amplification, *GATA4* loss, p*MITF*, p*NF2*, *PIK3R1*, *PTEN* loss, p*PTEN*; TMB low, MSI stable; a novel *FGFR2::SORBS3* fusion was noted on RNAseq. *FGFR2* breakapart FISH showed a complex rearrangement with loss of the 3' signal and concurrent amplification of the 5' signal. The HTG panel showed the top upregulated IL DEGs(*IL12A*, *SPP1*, *IL12RAP*), with *SOX2* most downregulated.ST analysis of the annotated spots demonstrated 5 distinct clusters corresponding to histologically distinct compartments (biphasic-2 clusters; monophasic/ solid/ clear-1 cluster; stroma-1 cluster; tumor-stroma interface-1 cluster). Top shared upregulated DEG were *OLFM4*, *LTF* and *KRT14* while the top downregulated DEG were *BPIFA1*, *ALOX15*, and *C20orf85*. GSEA across several MSigDB collections showed muscle cell differentiation pathway upregulation. Phosphorylation and intracellular signaling cascade pathways PI3K-AKT, JAK, STAT3, IL6, IFNɣ response was identified in most clusters. Stromal/ tumor-stromal interface clusters were enriched for EMT pathways, followed by inflammatory response, angiogenesis, K-Ras signaling up. *FGFR2* translocated SNAC may represent a distinct basaloid biphasic tumor with a seromucinous phenotype. Morphology and muscle cell differentiation enrichment suggests homology with salivary epithelial-myoepithelial carcinoma, but the 'hotter' immune microenvironment sets it somewhat apart from most salivary type carcinomas. *FGFR2::SORBS3* is rare even among the 150+ identified partners in other tumor types (i.e. cholangiocarcinoma) but appear to function similarly, upregulating phosphorylation pathways. Recognition of this tumor subtype could help select patients potentially amenable to FDA- approved oral FGFR2 inhibitors (pemigatinib, futibatinib).

#1210 Integrated spatial and single-cell profiling uncovers a pre-existing, treatment-resistant subclone that drives early local relapse in luminal breast cancer.

Kazutaka Otsuji[1], Tomo Osako[2], Yoko Takahashi[3], Chikako Shibata[4], Sumito Saeki[4], Asumi Iesato[1], Tetsuo Noda[5], Kengo Takeuchi[2], Takayuki Ueno[3], Reo Maruyama[4]

[1]NEXT-Ganken Program, Japanese Foundation for Cancer Research, Koto-ku, Tokyo, Japan,[2]Division of Pathology, Cancer Institute, Japanese Foundation for Cancer Research, Koto-ku, Tokyo, Japan,[3]Breast Oncology Center, Cancer Institute Hospital of JFCR, Japanese Foundation for Cancer Research, Koto-ku, Tokyo, Japan,[4]Division of Cancer Epigenomics, Cancer Institute, Japanese Foundation for Cancer Research, Koto-ku, Tokyo, Japan,[5]Director's room, Japanese Foundation for Cancer Research, Koto-ku, Tokyo, Japan

Background
Early local relapse during adjuvant endocrine therapy in hormone receptor (HR)-positive breast cancer, although uncommon, may reflect selection of pre-existing subclonal populations with intrinsic resistance. While endocrine resistance has been linked to aberrant cell-cycle activation and attenuated estrogen signaling, the spatial organization and transcriptional evolution of resistant subclones within tumors remain insufficiently resolved.
Methods
We performed multimodal profiling of paired primary and early local-relapse tumor specimens using the 10x Visium and Xenium spatial transcriptomics platforms. Additionally, a diagnostic core-needle biopsy obtained from the relapse lesion before resection underwent single-cell (sc) RNA sequencing. Spatial inferCNV was applied to Visium data to delineate clonal architecture and identify putative malignant subclones in an unbiased manner. Clone-specific transcriptional programs were characterized through differential expression and pathway enrichment analyses. Gene signatures derived from relapse scRNA-seq clusters were computationally projected onto the matched spatial transcriptomics data to map subclone-specific transcriptional phenotypes with high spatial resolution. Xenium profiling of the primary tumor was used to evaluate local microenvironmental features associated with resistant and responsive clones.
Results
Spatial inferCNV revealed marked clonal remodeling between the primary and relapse tumors: a minor primary-tumor subclone with distinct copy-number features expanded disproportionately and became the dominant malignant population at relapse. scRNA-seq demonstrated that transcriptional clusters corresponding to this conserved clone exhibited increased E2F target and G2/M checkpoint activity, concomitant with reduced estrogen-responsive signaling, consistent with an estrogen-independent proliferative phenotype. Single-cell resolution analysis of Xenium data from the primary tumor revealed that regions enriched for the resistant clone exhibited lower T-lymphocyte density compared to areas dominated by treatment-responsive subclones, suggesting early spatial segregation and microenvironmental differences that may have facilitated selective survival under endocrine therapy.
Conclusions
This integrated spatial and single-cell analysis of a rare rapid-relapse HR-positive breast cancer case demonstrates that a transcriptionally distinct, estrogen-independent, E2F-driven subclone was already embedded within the primary tumor and later seeded early local recurrence. These findings highlight the power of multimodal transcriptomics to uncover clinically occult resistant subclones and provide a framework for identifying patients at risk of early relapse despite standard adjuvant endocrine therapy.

#1211 Spatial transcriptomics uncovers pharmacokinetic barriers and tumor-intrinsic determinants of resistance to trastuzumab deruxtecan in breast cancer.

Changhee Park[1], Minki Choi[2], Jiwon Koh[3], Sungwoo Bae[4], Hongyoon Choi[4], Kwon Joong Na[4], Dae-Won Lee[1], Kyung-Hun Lee[1], Han Suk Ryu[3], Seock-Ah Im[1]

[1]Seoul National University Hospital, Seoul, Korea, Republic of,[2]Pathology, Asan Medical Center, Seoul, Korea, Republic of,[3]Pathology, Seoul National University Hospital, Seoul, Korea, Republic of,[4]Portrai Inc., Seoul, Korea, Republic of

Introduction: Trastuzumab deruxtecan (T-DXd) is an antibody-drug conjugate (ADC) that is effective for both HER2-positive and HER2-low metastatic breast cancers (MBC). While correlation between HER2 expression levels and response to T-DXd was identified, effective biomarkers and mechanisms of sensitivity or resistance remain elusive, partly due to complex pharmacokinetics of T-DXd. Our goal is to delineate spatial transcriptomic (ST) features which is associated with therapeutic response and resistance to T-DXd.
Methods: We performed ST with the 10x Genomics Visium HD on formalin-fixed paraffin-embedded tumor tissues from patients with MBC treated with T-DXd. Responders to T-DXd were defined as patients who experienced objective response or stable disease for more than 6 months, and non-responders were defined as otherwise. Fragments of pre-treatment biopsy samples from patients classified as responders were designated as "sensitive fragment" while that of pre-treatment biopsy samples from non-responders or post-progression biopsy samples from responders were defined as "resistant fragment". Various transcriptome analyses were performed including the compartment modeling-based methods for estimating antibody and payload concentrations from T-DXd pharmacokinetic profiles.
Results: A total of 20 tumor tissues from 13 patients were available including matched pre- and post-treatment biopsied in 5 patients. After quality check, 11 T-DXd-sensitive (19 fragments) and 7 resistant tissue samples (27 fragments) were included for analysis. Utilizing autocorrelation-related indices, spatial heterogeneity of *ERBB2* gene expression influenced outcomes, with more dispersed *ERBB2* gene expression distributions by cancer cells correlating with improved response. In HER2-positive tumors, resistant fragments showed downregulation of *ERBB2* gene expression and activation of PI3K and EGFR pathways, with autocrine amphiregulin-EGFR signaling emerging as a candidate resistance mechanism. In HER2-low tumors, resistance was notably associated with pharmacokinetic barriers: resistant fragments exhibited increased cancer-vessel distance, reduced colocalization of *ERBB2* expression with cathepsin linker-cleaving enzymes and diminished predicted tumor-to-non-tumor payload concentration ratio. Exploratory longitudinal analyses of paired pre- and post-treatment samples revealed temporal increases in vessel-cancer distance at resistance.
Conclusion: These findings highlight potential determinants of T-DXd efficacy. Our study demonstrates the utility of ST for uncovering ADC response mechanisms in clinical samples and potential novel therapeutic strategies.

#1212 Spatial transcriptomics reveals distinct SPP1-CD44 signaling networks in neoadjuvant osimertinib treated EGFR mutant non-small cell lung cancer.

Whitney Tamaki[1], Daniel L. Kerr[2], Wei Wu[1], Grant Eilers[3], Anatoly Urisman[3], Yu-Ting Chou[1], Philippe Gui[1], Shigeki Nanjo[4], Johannes Ruediger Kratz[1], David Jablons[1], Trever G. Bivona[1], Collin M. Blakely[5]

[1]UCSF, San Francisco, CA,[2]University of Washington, Seattle, WA,[3]Anatomic Pathology, UCSF, San Francisco, CA,[4]Kanazawa Univ. Hospital, Kanazawa, Japan,[5]Clinical Fellow, Medical Oncology, UCSF, San Francisco, CA

Background: Lung cancer is the leading cause of cancer mortality, and despite improvements in treatment, tumors typically respond incompletely and resume growth after acquisition of drug resistance. Recent completion of a neoadjuvant osimertinib Phase II trial treating patients with surgically resectable stage I-IIIA EGFR-mutated non-small cell lung cancer (EGFRm NSCLC) (NCT03433469) has highlighted the importance of further identifying non-genomic, transcriptionally adapted mechanisms of persistence and resistance to targeted therapy.

Methods: We analyzed these patient samples to identify transcriptionally regulated signaling patterns enriched at Residual Disease (RD) after neoadjuvant osimertinib treatment compared to treatment naïve samples (TN. Spatially resolved transcriptomic sequencing was performed, using the 10X Genomics Visium platform, on 36 tissue sections (n=9 TN, n=19 RD, n=4 Progressive Disease (PD), n=4 Tumor Adjacent Normal), from 25 patients. TN and PD samples were from standard-of-care surgical resections. 18 of 19 RD samples were from NCT03433469. After quality control, 91,582 array spots remained for downstream analysis.

Results: We identified high confidence tumor array spots annotated both as “Cancer” by a board-certified pathologist and with tumor characteristic copy number variations. We applied disease-matched single-cell RNA-sequencing reference profiles to deconvolute the spatial transcriptomic data and estimate cell-type abundances. Analysis of cell-cell signaling networks identified significantly enriched or abundant SPP1-CD44 interactions between macrophage subtypes and tumor cells at the RD state. Specifically, PDPN+ Macrophages were identified as a primary source of SPP1 expression. Additional differential gene analysis identified significant upregulation of TM4SF4 and SERPINA3, known genes up and downstream, respectively, of SPP1, in the RD tumor nest, as compared to TN. SERPINA3 has previously been shown to positively regulate PI3K/AKT signaling pathway.

Conclusion: The interaction between macrophages and tumor cells through SPP1-CD44 signaling significantly contributes to EGFRm targeted therapy-induced tolerance and resistance. Future studies will focus on elucidating the regulatory mechanisms governing the TM4SF4/SPP1/SERPINA3 axis and evaluating its contribution to therapy resistance, as well as its potential as a therapeutic target, using preclinical models.

#1213 Mitochondrial transcriptome profiles associated with clinical responses to CAR-T therapy in aggressive lymphoma.

Jacqueline Turner[1], Panwen Wang[2], Patrizia Mondello[1], Melinda Tan[3], Christoph Schaefers[1], Chen Wu[4], Andre de Menezes Silva Corraes[4], Kevin Regan[4], Zuoyi Shao[4], Ma Audrey[4], Arushi Khurana[4], Nora N. Benanni[4], Yucai Wang[4], Paul Hampel[4], Saad J. Kenderian[4], Jonas Paludo[4], Urshila Durani[4], Patrick B. Johnston[5], Jose Caetano Villasboas[4], Stephen M. Ansell[6], Haidong Dong[1], Ying Li[4], Zeng Hu[4], Yi Lin[7]

[1]Mayo Clinic College of Medicine and Science, Rochester, MN,[2]Mayo Clinic, Scottsdale, AZ,[3]Mayo Clinic Cancer Center Minnesota, Rochester, MN,[4]Mayo Clinic, Rochester, MN,[5]Hematology, Mayo Clinic College of Medicine, Rochester, MN,[6]Assistant Professor, Div. of Hematology, Mayo Clinic College of Medicine, Rochester, MN,[7]Asst. Professor, Div. of Hemat., Mayo Clinic, Rochester, MN

Introduction: Therapeutic outcomes in B-cell non-Hodgkin's lymphoma (B-NHL) have substantially improved with the introduction of chimeric antigen receptor T-cell (CAR-T) therapy. Yet, persistent immune dysfunction and underlying metabolic dysregulation remain major obstacles to achieving durable clinical responses in B-NHL. We hypothesize that mitochondrial pathways play a critical role in mediating anti-tumor immunity during CAR-T therapy.
Methods: Peripheral blood mononuclear cells were collected from healthy controls (CNTRL, n=5) and patients with advanced stage lymphoma (LYM) who received FDA approved CAR-T (n=32). Samples were collected before lymphodepletion (BL), at peak CAR-T expansion (PK) and one-month post-infusion (M1). Single-cell RNA sequencing was used to interrogate differential mitochondrial gene expression. Samples were obtained from LYM patients with complete remission for ≥6 months (CR), primary refractory (PD1), or relapsed (PD2) disease.
Results: Compared to CNTRLs, LYM patients exhibited reduced expression of cytochrome c oxidase. At BL, CR patients demonstrated broader mitochondrial differential gene expression across all T-cell subsets relative to PD1 and PD2 and showed higher expression of *MT-ATP-6*, *MT-ATP-8*, and *MT-CO3*. Following CAR-T infusion, global mitochondrial gene expression increased across patients corresponding with expansion of CD8 effector T cells (Tem tumor circulating) and activated peripheral memory T cells (Tpm). Certain mitochondrial genes, such as *MT-CO1*, were durably expressed across LYM patients at BL, PK, and M1 in peripheral and central memory T cells (Tpm, Tcm). At PK, cytochrome c oxidase and ATP synthase genes were upregulated in CR Tpm and Tcm. At M1, *MT-ATP-6*, *MT-ATP-8*, *MT-CO3* were significantly upregulated in CD8 memory precursor effector T-cells (MPECs) of CR patients compared to both PD1 and PD2. While CR and PD2 patients appeared clinically responsive at M1, CR samples maintained significantly higher *MT-ATP-8* expression across T cell subsets (CD8 MPECS, Tpm, Tcm) compared to PD2 (p values 0.008; <0.0001; <0.0001).
Conclusions: We report a temporal shift in immunometabolism with CAR-T therapy in LYM. Clinical responders exhibited sustained mitochondrial activity characterized by persistent expression of ATP synthase in CD8 MPECs and cytochrome c oxidase in Tpm and Tcm. In sum, mitochondrial programming may distinguish effective versus dysfunctional T cells and identify targets for therapeutic development.

#1214 SPACE: Spatially resolved multiomic analysis for high-throughput CRISPR screening in 3D models.

Mengwei Hu[1], Yi Cui[2], Qianhui Huang[1], Khoi Chu[1], Sierra McKinzie[2], Michael Patrick[2], Sharanya Iyengar[1], Maerjianghan Abuduli[1], Marianne Spatz[1], Nandita Joshi[1], Brendan Miller[1], Shams Vellarikkal[1], Timothy Riordan[2], Danny Bitton[3], Jan Lubojacky[3], Iya Khalil[1], Federica Piccioni[1], Michael Rhodes[2], Alex Tamburino[1], Shanshan He[2], Joseph Beechem[2], Vanessa Peterson[1]

[1]Merck & Co., Inc, Cambridge, MA,[2]Bruker Spatial Biology, Seattle, WA,[3]MSD, Prague, Czech Republic

High-content single-cell perturbation screens are pivotal for elucidating gene functions and uncovering novel biology, yet conventional methods necessitate cell dissociation, forfeiting critical spatial information essential for dissecting cell-cell interactions and tissue architecture in complex microenvironments. While spatial CRISPR screening mitigates this partially, existing technologies are constrained by hypothesis-driven phenotyping panels limited to sparse RNA or protein coverage, curtailing comprehensive gene function assessment and discovery breadth.To overcome these barriers, we developed SPACE (SPAtial Cell Exploration), a pioneering platform that fuses whole-transcriptome profiling, CRISPR perturbations, and multiplexed protein detection at single-cell resolution within intact 3D tissue contexts. SPACE delivers unbiased, transcriptome-wide readouts alongside compatibility for up to 76 protein markers, vastly expanding phenotypic landscapes in spatial screens. As the highest-plex multimodal spatial CRISPR assay to date, SPACE achieves this at unprecedented scale and affordability and largely outperforms sequencing-based alternatives in efficiency.We applied SPACE across 42 gene perturbations in cancer-associated fibroblasts (CAFs) co-cultured with tumor cells in 3D spheroids, yielding multidimensional multiomic datasets from hundreds of spheroids. High-confidence guide RNA detection was coupled with robust endogenous mRNA characterization. Unbiased analyses uncovered new insights on CAF-tumor dynamics: extracellular matrix (ECM) remodeling, spatially resolved ligand-receptor interactions, and perturbation-specific gene variability.Notably, *ISG20* knockout in CAFs profoundly suppressed multiple matrix metalloproteinases - an unreported link validated orthogonally - implicating *ISG20* in novel ECM regulation and tumor progression. Some perturbations were further revealed to reshape intercellular signaling, revealing knockout-dependent spatial ligand-receptor shifts and coordinated expression signatures that underscore microenvironmental crosstalk in tumor phenotypes.Culminating in a landmark demonstration, SPACE simultaneously captured whole transcriptomes, CRISPR identities, and 68 protein markers on one slide, enabling holistic perturbation phenotyping. This transformative technology propels spatial CRISPR screening into translational realms, facilitating target and biomarker identification in multicellular models mirroring human tissue intricacy. By merging high-throughput perturbations with spatially resolved multiomics at transcriptome scale, SPACE catalyzes discovery in heterogeneous tissues. SPACE datasets will fuel generative AI models for causal biology inference, accelerating drug discovery and precision medicine.

#1215 Spatial transcriptomic analysis of primary melanomas with extreme clinical outcomes.

Prachi Bhave[1], Marie Trussart[2], Anthony T. Papenfuss[2], Grant A. McArthur[3]

[1]The Sir Peter MacCallum Department of Oncology, University of Melbourne, Melbourne, Australia,[2]Walter & Eliza Hall Institute of Medical Research, Melbourne, Australia,[3]Peter MacCallum Cancer Centre, Melbourne, Australia

Introduction: Most patients that die from melanoma do so after recurrence of early stage disease. There is, therefore, an urgent need to improve the identification and management of patients with early stage melanoma at high risk of recurrence. The tumour microenvironment (TME), subclonal tumour cell intrinsic features and cellular interactions likely play key roles in melanoma recurrence. Spatial transcriptomics (ST) is optimally positioned to characterize these factors and may provide novel insights and strategies to overcome early stage melanoma recurrence.

Methods: We examined 12 early stage (thick, T4b) FFPE primary melanoma samples with extreme clinical outcomes, identified from the prospectively collected Melanoma Research Victoria database. Of these, 7 patients had T4b melanoma with an unexpectedly good outcome of no recurrence ≤5 years of diagnosis and 5 patients had T4b melanoma with an expectedly poor outcome of recurrence ≤5 years of diagnosis (late and early recurrence groups, respectively). Samples were interrogated using 10X CytAssist Visium with comparisons between the two groups. Comprehensive bioinformatics analyses were performed including Bayespace and Harmony for initial spot clustering; SingleR for cluster annotation; RCTD deconvolution to refine cluster identification; edgeR on pseudo-bulk counts and gene set testing of differentially expressed genes (DEG); sscomp for differential cellular composition; SPIAT for spatial immune-tumor architecture analysis and non-negative matrix factorization (NMF) and SpaceMarkers for exploration of gene expression patterns and interacting regions.

Results: Key cell types were revealed within each sample, including tumor cells, diverse immune cell subsets, fibroblasts, macrophages and keratinocytes. Tissue architecture including dermis, epidermis and invasive tumour front were well characterised. DEG identified downregulation of SLC5A10, PFKFB2, FBXO32, GABRB3, SMIM38 and CDH7 in the late group relative to the early group. Gene set analysis revealed upregulation of the hallmark hypoxia, angiogenesis, EMT, glycolysis, IL2, TNFa and TGFb pathways in the late relative to the early group. Cellular compositions varied across the two groups, with the late group having significantly lower tumour purity and higher abundance of immune cells than the early group. NMF revealed specific patterns associated with tumor and immune cells, with significant downregulation of IGHA2, CYP4X1, RBMXL3 and AIRE at the interacting region between tumor and immune cells in the late relative to the early group.

Conclusion: This study is one of the first to analyze primary melanoma samples with extreme clinical outcomes using ST. Our results reveal that differences in cellular composition of primary melanomas as well as differential expression of key genes involved in immune activation, inflammation and metabolism may be associated with melanoma recurrence.

#1216 Profiling colon cancer architecture with spatial transcriptomics identifies clinically relevant stromal ecotypes.

Antoine Cazelles[1], Camilla Pilati[1], Delphine Le Corre[1], Gadea Cabrejas[1], Marine Sroussi[1], Claire Mulot[1], Claire Gallois[1], Gilles Manceau[1], Mehdi Karoui[1], Isaias Hernandez-Verdin[1], Antoine Bougouin[1], Wolf-Herman Fridman[1], Aurelien de Reynies[1], Come Lepage[2], Thierry Andre[3], Jean-Francois Emile[4], Theo Z. Hirsch[1], Julien Taieb[1], Pierre Laurent-Puig[1], **Sophie Mouillet-Richard**[1]

[1]Centre de Recherche des Cordeliers, Paris, France,[2]University of Burgundy and Franche Comte, Dijon, France,[3]Hopital Saint-Antoine, Paris, France,[4]Ambroise-Pare Hospital, Boulogne, France

Despite progress in the understanding of intra-tumor heterogeneity in colon cancer, the spatial organization of the cell types and states that compose colon tumors remains to be fully delineated. We constructed a large spatial transcriptomic atlas of 48 stage III colon cancers and identified recurrent, biologically relevant spatial ecosystems, including tumor and stromal ecotypes. Analysis of recurrence-associated profiles revealed a stromal-specific upregulation of a set of genes that includes the regenerative/revival-stem cell (REC/RSC) marker *ANXA1*. Disease recurrence was accompanied by stromal-specific enrichment of REC/RSC and YAP activation signatures, together with increased associations between levels of *ANXA1* and those of collagen-expressing genes. Dissection of the stromal compartment uncovered hidden heterogeneity and sub-cluster-specific enrichment in *ANXA1* and related markers in patients with relapse. Further profiling at single cell resolution with Visium HD allowed spotting *ANXA1*-expressing tumor cells within an environment marked by abundant collagen-producing cancer-associated fibroblasts (CAFs). Finally, we translated these findings to bulk transcriptomics by performing univariate and multivariate analyses and demonstrated the prognostic value of gene signatures derived from the spatial ecotypes and stromal sub-clusters across three independent cohorts comprising >3,500 stage II and stage III colon cancer patients. By mapping cellular ecosystems in localized colon cancer, this work lays the foundation to elucidate mechanisms of disease recurrence and inform therapeutic strategies. The validation of the spatially-derived prognostic signatures in bulk transcriptomic data paves the way for their potential integration into clinical practice to improve patient stratification.

#1217 Multi-omics integration of bulk, single-cell, and spatial transcriptomics identifies robust prognostic biomarkers in head and neck salivary adenoid cystic carcinoma.

Gopikrishnan Bijukumar[1], Kathryn J. Brayer[2], David Lee[2], Scott A. Ness[3], Jeremy S. Edwards[1], **Viswanathan Palanisamy**[4]

[1]Chemistry and Chemical Biology / Cancer Research Facility, University of New Mexico, Albuquerque, NM,[2]University of New Mexico, Albuquerque, NM,[3]Professor, Dept. of Molec. Genetics & Microbiol., University of New Mexico School of Medicine - Albuquerque, Albuquerque, NM,[4]Internal Medicine / Comprehensive Cancer Center, University of New Mexico Health Sciences, Albuquerque, NM

Adenoid Cystic Carcinoma (ACC) of the head and neck is a rare malignancy with a paradoxical clinical course, slow-growing yet highly invasive, with limited therapeutic options and no validated molecular prognostic biomarkers. To address this unmet need, we implemented a comprehensive multi-omics strategy integrating bulk RNA sequencing (n=20), single-cell RNA sequencing (n=24), and high-resolution spatial transcriptomics (4 Visium HD samples) from ACC tumors spanning eight distinct anatomical subsites. Clinical metadata enabled stratification into “poor” (<2-year survival) and “good” (>5-year survival) prognosis groups. In the absence of definitive cause-of-death data, we developed a machine learning-based classifier to define transcriptomic prognosis subgroups, revealing biologically coherent clusters aligned with clinical outcomes.Our biomarker discovery pipeline encompassed three key phases:

1.Cross-Modality Differential Expression and Pathway Profiling: We identified conserved gene expression signatures and dysregulated pathways distinguishing poor from good prognosis tumors across bulk, single-cell, and spatial modalities. High-risk tumors exhibited consistent enrichment of oncogenic signaling (e.g., MYC, NOTCH), immune suppression, and stromal activation programs across shared cell types and anatomical regions.

2. Spatially Resolved Cellular Ecosystem Mapping: Integration of single-cell and spatial transcriptomics enabled precise localization of malignant cell states and immune niches associated with poor prognosis. Spatial analyses revealed intratumoral “hotspots” characterized by elevated oncogenic activity, immune exclusion, and stromal remodeling. Ligand-receptor interaction networks, validated by spatial proximity, uncovered key signaling axes (e.g., CXCL12-CXCR4, TGFB1-TGFBR2) driving tumor progression.

3. Development of a Prognostic Biomarker Panel: We constructed a machine learning-derived multi-gene signature reproducible across all modalities. This panel demonstrated superior risk-stratification performance compared with existing ACC gene sets, with prognostic accuracy independent of clinical features. Importantly, the biomarker panel is amenable to clinical translation via bulk RNA profiling, offering immediate utility for patient stratification and therapeutic decision-making. In summary, our integrative multi-omics approach reveals robust molecular programs and spatially defined cellular ecosystems underlying poor prognosis in ACC. The resulting biomarker panel offers a powerful tool for precision prognostication and lays the foundation for targeted therapeutic development in this challenging malignancy.

#1218 Development of a proximity ligation-imaging mass cytometry platform for spatially resolved immune checkpoint analysis.

Ghazal Lessan Toussi[1], Lars Muhl[2], Anna Gorbunova[1], Austin James Rayford[3], Amanda Lindberg[4], Neda Hekmati[4], Viktoria Thurfjell[4], Aglaia Schiza[4], Agata Zieba Wicher[5], Patrick Micke[4], **Carina Strell**[4]

[1]Department of Clinical Medicine, University of Bergen, Bergen, Norway,[2]Department of Medicine, Huddinge, Karolinska Institutet, Stockholm, Sweden,[3]Department of Biomedicine, University of Bergen, Bergen, Norway,[4]Department of Immunology, Genetics and Pathology, Uppsala University, Uppsala, Sweden,[5]Navinci Diagnostics AB, Uppsala, Sweden

Introduction: Immune checkpoint inhibitors (ICIs) have transformed cancer therapy, yet durable clinical benefit remains limited to a subset of patients. Current biomarkers, such as PD-L1 immunohistochemistry (IHC), reflect protein abundance rather than functional receptor-ligand engagement and therefore provide only modest predictive value. To address this, we previously demonstrated that mapping PD1-PD-L1 interactions using a proximity ligation assay (PLA) outperforms PD-L1 IHC in predicting immunotherapy response in non-small cell lung cancer (NSCLC) [1].

Methods: Building on these findings, we developed a triplex PLA detecting PD1-PD-L1, PD1-PD-L2, and CD8-MHC I interactions and integrated it with Imaging Mass Cytometry (IMC). This approach enables high-plex (≈40 markers) spatial quantification of active immune signaling pathways alongside detailed immune phenotyping. The platform was applied to human tonsil tissue as a biological control and to pre-treatment NSCLC and triple-negative breast cancer (TNBC) biopsies to map checkpoint engagement, antigen recognition, and T-cell functional states within the tumor microenvironment.

Results: In tonsil, PD1-PD-L1 and PD1-PD-L2 interactions were observed primarily between $CD8^+$ T cells and follicular B cells, while additional PD1-PD-L1 interactions occurred between $CD8^+$ T cells and $CD68^+$ macrophages. These patterns suggest partly distinct cellular contexts for PD-L1 and PD-L2 engagement in lymphoid tissue. Consistent with this, preliminary tumor data indicate that PD1-PD-L2 interactions are relatively rare in TNBC compared with NSCLC, suggesting that PD-L2 involvement varies across tissue types and immune environments.

Conclusion: PLA-IMC provides a functional, spatially resolved platform for screening and quantifying active immune checkpoint signaling directly in tissue. This approach holds promise to identify functional biomarkers for refined patient stratification and mapping of context-specific checkpoint activity to guide rational immunotherapy combinations in solid tumors.

References: [1] Lindberg A, Muhl L, Yu H, et al. In situ detection of programmed cell death protein 1 and programmed death ligand 1 interactions as a functional predictor for response to immune checkpoint inhibition in NSCLC. J Thorac Oncol. 2025; 20:625-640.

#1219 Spatial multi-omic profiling to capture functional signatures in HER2-heterogeneous FFPE breast cancer tissue.

Dongyoon Shin[1], Sumin Lee[2], **Young June Jeon**[3], Jeongwoo Hong[4], Sohyun Yang[5], Amos Chungwon Lee[4], Han Suk Ryu[5], Youngsoo Kim[1], Sungwoo Cho[6], Song-A Park[6], Sihun Cho[7], Sungho Ko[6], Junho Park[8]

[1]CHA Research Institute, CHA Bundang Medical Center, Seongnam-si, Korea, Republic of,[2]Meteor Biotech Co., Ltd., Seoul,[3]Department of Life Sciences, CHA University, Seongnam-si, Korea, Republic of,[4]Meteor Biotech, Seoul, Korea, Republic of,[5]Seoul National University Hospital, Seoul, Korea, Republic of,[6]Humanase Co, Seongnam, Korea, Republic of,[7]CHA University, Department of Biotechnology, Seongnam-si, Korea, Republic of,[8]School of Medicine, CHA University, Seongnam-si, Korea, Republic of

Intratumoral heterogeneity in human epidermal growth factor receptor 2 (HER2)-positive breast cancer can lead to variable therapeutic responses, but its spatially resolved molecular characteristics in formalin-fixed, paraffin-embedded (FFPE) tissue are not fully characterized. In this study, we applied spatial multi-omic profiling to investigate how regional differences in HER2 expression within the same HER2-positive breast cancer tissue are reflected at the proteome and transcriptome levels. Using hematoxylin and eosin (H&E) and HER2 immunohistochemistry (IHC)-guided spatially resolved laser-activated cell sorting (SLACS), we isolated 200 μm × 200 μm × 10 μm regions of interest (ROIs) corresponding to HER2-high and HER2-low areas from FFPE tumor sections and analyzed them with an optimized trace-level LC-MS workflow. To extend the analysis to the multi-omics level, we additionally performed RNA sequencing on adjacent ROIs from the same tissue sections. This approach consistently quantified an average of more than 4,400 proteins per ROI (approximately 60-80 cells), yielding a total of 6,116 identified proteins and revealing 1,188 differentially expressed proteins (DEPs) between HER2-high and HER2-low regions. Protein-protein interaction network analysis of DEPs upregulated in HER2-high regions revealed tightly connected functional modules mainly related to protein synthesis, metabolism, intracellular trafficking, and cellular stress responses, whereas DEPs upregulated in HER2-low regions were enriched in modules associated with mitochondrial and energy metabolism, extracellular matrix organization, and cellular differentiation and cytoskeletal regulation. Canonical pathway analysis further showed that hallmark HER2 signaling in breast cancer, together with PI3K/AKT and mTOR-related pathways, were predicted to be activated in HER2-high regions, while several tumor microenvironment-associated pathways and sirtuin signaling pathways were predicted to be inhibited, indicating region-specific rewiring of oncogenic and microenvironmental signaling networks. Although HER2-related pathways were enriched in both transcriptomic and proteomic data, pathway activation was more clearly resolved in the proteome, suggesting post-transcriptional regulation and highlighting the added functional information obtained from proteomics. Collectively, these results indicate that spatial multi-omic profiling of HER2-heterogeneous FFPE breast cancer tissue captures region-specific pathway activities and biological functions associated with varying HER2 expression.

#1220 Spatial transcriptomics revealed potential resistance and response factors of sacituzumab govitecan in metastatic breast cancer.

Mengni He[1], Charles J. Robbins[2], Julia Benanto[2], Thazin Nwe Aung[2], Yalai Bai[2], Ian E. Krop[2], David L. Rimm[2]

[1]Yale University, New Haven, CT,[2]Yale School of Medicine, New Haven, CT

Background: Sacituzumab govitecan (SG) is a TROP2-targeting antibody-drug conjugated that is approved in metastatic and locally advanced hormone-receptor positive HER2 negative and triple negative breast cancer. Its clinical trials showed significant improvement in clinical benefits, but the reported objective response rates were about 30%. Biomarkers associated with response or resistance to SG are poorly understood.

Methods: GeoMx® DSP was performed on tissue transfer arrays generated from 17 biopsies of SG-treated metastatic breast cancer patients. Patients with long time-on-treatment (≥ 10 cycles) were considered responders (N = 7) whereas patients with short time-on-treatment (≤ 4 cycles) were considered non-responders (N = 10). Expression of the whole human transcriptome represented by over 18,000 genes were profiled within the cytokeratin labeled tumor segments and stroma segments. Differentially expressed genes between responders and non-responders were calculated using the linear mixed model with Benjamini-Hochberg procedure. Gene set enrichment analysis (GSEA) was performed using the Reactome pathway database.

Results: Over 10,000 gene targets in 117 segments passed the quality control pipeline and therefore used for analysis. In the tumor segments, 7 genes were upregulated in responders including immunoglobin heavy chain genes IGHG2, IGHG3, and IGHG4. 25 genes were upregulated in non-responders, including genes encoding for extracellular matrix (ECM) proteins (TNC, MMP11, MMP14, COL1A, FKBP10, and POSTN). GSEA indicated that ECM organization and proteoglycan regulating pathways are highly expressed in non-responders whereas eukaryotic translation termination pathways, regulation of ornithine decarboxylase, and mitotic G1 phase and G1/S phase transition pathways are upregulated in responders. In the stroma segments, 6 genes were upregulated in the responders including immune related genes (C7, IGHG2, IGHG3, and IGHG4) and lipid metabolism regulating gene APOC1. 11 genes were upregulated in the non-responders, including ECM protein encoding genes (MMP11, COL11A1, COL12A1, and CA2) and immune related genes (HLA-DQA1, PIP, and TSPAN1). GSEA also showed that ECM organization pathways and elastic fiber formation pathways are upregulated in non-responders whereas eukaryotic translation termination, interferon α/β signaling, B cell related signaling, and plasma lipoprotein assembly, remodeling and clearance pathways are upregulated in responders in the stroma segments.

Conclusions: Our study identified differential expressed genes between SG-responding and -resistance tumors. Specifically, the upregulation of immune-related genes is associated with response and upregulation of ECM organizations and remodeling are associated with resistance. Validation of these observations is underway.

#1221 Imaging mass cytometry of pelareorep treated early breast cancer samples reveals developing tertiary lymphoid structures.

Julian P. Olea[1], Homa Dadrastoussi[1], Kaijin Wu[1], Harley Wu[1], Paniz Zarand[1], Claudia Villa Celi[1], Jennifer S. Carew[2], Steffan T. Nawrocki[2], Xuelian Chen[1], Richard Trauger[3], Thomas C. Heineman[3], Kevin R. Kelly[1]

[1]Hematology, Keck School of Medicine of USC, Los Angeles, CA,[2]Hematology and Oncology, University of Arizona Cancer Center, Tucson, AZ,[3]Oncolytics Biotech, Inc., Calgary, AB, Canada

AWARE-1 is a window-of-opportunity study evaluating the effects of the oncolytic virus (OV) pelareorep in early-stage breast cancer patients. This analysis focuses on Cohort 2 (n = 8), consisting of HR+ HER2- patients who received pelareorep on days 1, 2, 8, 9; letrozole on days 1-21; and atezolizumab on day 3. Biopsies were collected pre-treatment, on day 3, and on day 21. Tissue was stained using an imaging mass cytometry (IMC) antibody cocktail targeting a variety of immune cell subsets to characterize changes over time in the tumor immune microenvironment (TiME) and the subsequent development of tertiary lymphoid structures (TLS) in select subjects. Unsupervised PhenoGraph clustering identified 18 distinct phenotypes, including T helper (Th), activated T helper (ATh), cytotoxic T cells (CTC), B cells (BC), differentiated B cells (DBC), and dendritic cells (DC). CTC's were significantly increased from screening to day 21 samples ($p = 0.04$) and from day 3 to day 21 samples ($p = 0.04$). Further analysis of these cell types and how they interact is performed using cellular neighborhood analysis, which identifies common arrangements of certain cell types throughout the samples. Cellular neighborhood analysis yielded an interesting neighborhood cluster comprising CTC, DC, TH, BC, DBC, and M2 Mac cells - defined as the TLS neighborhood. Visualization of the TLS neighborhood showed progressing stages of T cell and B cell organization, with T cells and B cells being largely diffuse and unstructured at screening and concentrating into zones of BC - BC aggregates surrounded by CTC, TH, and ATH cells at day 21. Pairwise permutation-based interaction analysis was applied to the cells comprising the TLS neighborhood to validate significant biological organization. At day 21 BC - TH, DBC - BC, and DBC - DBC interactions were significantly more likely to occur than at screening. Other interactions of note were between tumor - ATH, tumor - CTC, tumor - DC, CTC - ATH, and CTC - CTC interactions were significantly increased at surgery. This study is the first of its kind to identify and spatially validate the unique cell-cell interactions in the TiME of early breast cancer patients treated with the OV pelareorep as developing TLS's, highlighting coordinated TiME reorganization and novel cell-cell interaction dynamics associated with TLS formation.

#1222 Spatial transcriptomics of trastuzumab deruxtecan-treated metastatic breast cancer identifies candidate response and resistance factors.

Charles J. Robbins, Mengni He, Julia Benanto, Thazin Nwe Aung, Yalai Bai, Ian E. Krop, David L. Rimm

Yale School of Medicine, New Haven, CT

Background: Trastuzumab deruxtecan (T-DXd) is a HER2-targeting antibody-drug conjugate approved for metastatic breast cancer (mBC) with HER2-positive, low, and “ultralow” expression. However, reliable tissue biomarkers for predicting response or resistance are poorly understood. We applied GeoMx® digital spatial profiling to 41 T-DXd-treated mBC samples from Yale New Haven Hospital to identify spatially-informed gene expression markers linked to therapy outcomes.
Methods: Biopsies from 41 mBC patients treated with T-DXd (5 HER2+, 28 HER2-/HR+, 8 TNBC) were collected. Patients were classified as responders (time-on-treatment >6 months, N=26) or non-responders (≤6 months, N=15). Tissue transfer arrays from these samples were prepared for digital spatial profiling. Spatial profiling was performed on tumor (CK+), immune (CD45+), and stroma (CK- and CD45-) segments using the GeoMx® human whole transcriptome atlas RNA assay. Sequencing data was processed on the Nanostring platform. For each segment, differentially expressed genes (DEGs) between responders and non-responders were identified using a linear mixed model with Benjamini-Hochberg correction. Over-representation analysis used Enrichr gene sets; gene set enrichment analysis (GSEA) used KEGG and Reactome pathways.
Results: Over 10,000 genes in 511 segments from 41 patient biopsies passed quality control. In tumor segments, 20 genes upregulated in responders included early estrogen response (MUC1, MLPH, MAST4), extracellular matrix (ECM1), and integrin signaling pathways (COL4A5, NTN4). Non-responders showed upregulation of 37 genes enriched for ubiquitin-specific proteases (ADRM1, PSMB1, PSMA7, UBA52). GSEA indicated increased APC/Cdc20 mediated degradation pathways in non-responder tumor segments. In immune and stroma segments, 12 upregulated genes in responders included negative regulators of immune cell trafficking (RGS1, RGS5). Non-responders upregulated 53 genes, including markers of tumor-associated macrophages (APOE, APOC1, SPARC, SERPINA1) and cancer-associated fibroblasts (FN1, POSTN, COL1A1/2). GSEA showed enrichment for immunoglobulin-mediated immune response, antigen processing, and ECM organization pathways in responder immune and stroma segments.
Conclusions: Spatial transcriptomics revealed DEGs associated with T-DXd response and resistance in mBC. Responders were enriched for early estrogen response and ECM/integrin signaling pathways, whereas non-responders showed upregulation of ubiquitin-proteasome pathways and tumor-associated macrophage/cancer-associated fibroblast gene signatures. Validation of these findings is underway with the goal of finding biomarkers that provide predictive value beyond measurement of ADC target.

#1223 Spatial transcriptomics identifies a suppressive T-cell excluded tumour microenvironment in extramedullary multiple myeloma.

Nicholas E. Bingham[1], Julie R. Boiko[2], Daniel C. Jones[3], Daniel Wong[1], Tiffany Khong[1], Sridurga Mithraprabhu[1], Kathleen S. Ensbey[2], Anna E. Elz[3], Evan W. Newell[4], Andrew Spencer[1], Geoffrey R. Hill[2]

[1]Australian Centre for Blood Diseases, Alfred Health - Monash University, Melbourne, Australia,[2]Translational Science and Therapeutics Division, Fred Hutchison Cancer Centre, Seattle, WA,[3]Vaccine and Infectious Diseases Division, Fred Hutchison Cancer Centre, Seattle, WA,[4]Vaccine and Infectious Diseases Division, Fred Hutchinson Cancer Centre, Seattle, WA

Introduction: Extramedullary disease (EMD) in multiple myeloma (MM) is associated with poor prognosis due to aggressive disease kinetics and therapy resistance. Bone marrow (BM) restricted MM is highly dependent on the BM microenvironment for survival, putatively contributing to drug-resistance. In EMD, the biology and particularly the role of the tumor microenvironment (TME) is unknown.

Methods: Eight biopsies from 8 patients with hematogenous EMD were analyzed using 10x Xenium In Situ Prime 5K. Subsequent analysis utilized the recently described high resolution ProSeg cell segmentation algorithm.

Results: A total of 500,102 cells from 8 samples were included. Plasma cells (PC) in EMD maintain a PC transcriptome with expression of *XBP1*, *IRF4* and *PRDM1* without significant expression of *PAX5*, *FOXP1*. After dimensionality reduction, like BM-restricted MM, PC clustering was driven primarily by inter-patient variability. The TME was assessed. The most numerous immune cells were macrophages, specifically those with an immune-suppressive 'M2' phenotype, demonstrated by expression of markers such as *CD163* and *MRC1*. Infiltrating CD8+ T-cells co-expressed cytotoxicity and exhaustion genes. Cancer associated fibroblasts were the most common non-immune cell in the TME. Spatial analysis was performed with recurrent microenvironments identified: immune suppressed (IS), immune excluded (IE) and immune permissive (IP). The IS niches, characterised by macrophages, fibroblasts and endothelial cells, were enriched for immune cells and more proliferative PC subsets. The bulk of tumors (>70%) comprised the IE niche, with a very high proportion of PC (>90% cells) with the lowest proportion of T-cells. Rarer areas with increased T-cells and interferon-reactive macrophages, presumed IP regions, were present in two samples.

Predicted cell-cell interactions identified a complex, bidirectional network. PC interactions with the TME via signals including *TGFB1/3*, PGE2 and *THBS1* were evident, predicted to drive a suppressive macrophage phenotype and a fibrotic extracellular matrix. Conversely, macrophages in the TME expressing *APRIL* and *BAFF* are predicted to promote PC survival via canonical ligands including BCMA, *CXCR4* and *CD38*. This bidirectional signalling between suppressive myeloid cells in the TME and PC thus putatively promote myeloma growth directly whilst concurrently constraining anti-myeloma immunity. The presence of the suppressive and excluded niches in all samples suggests an important role in EMD biology.

Conclusions: Our findings provide new insights into the spatial organisation of MM EMD and identify prominent suppressive macrophage rich niches in the context of T cell exclusion within the TME, together with proliferative signalling networks in PC, that represent new clinically tractable targets.

#1224 Antibody-drug conjugate immuno-oncology panel for comprehensive characterization of the tumor and associated microenvironment.

Sandra F. Lam, Kevin Gallagher, Maryam Rohafza, Courtney Todorov, Harry Nunns, Marianne Thio, Flora Sahafi, Kathy Pham, Victoria Gomez, Erinn A. Parnell, Qingyan Au

NeoGenomics Laboratories, Aliso Viejo, CA

Antibody-drug conjugates (ADCs) represent a rapidly advancing class of targeted therapeutics that integrate the specificity of monoclonal antibodies with the potent cytotoxicity of small-molecule drugs. By coupling antibodies to highly active payloads through linkers, ADCs enable selective delivery of cytotoxic agents to tumor cells while minimizing systemic toxicity. Pivotal studies have shown compelling evidence that this strategy of anti-cancer therapeutics can dramatically improve outcomes for patients. Despite notable success, challenges such as tumor heterogeneity and predicting clinical efficacy have been difficult to overcome. Because ADCs rely on precise spatial localization of target antigens to optimize treatment efficacy, subcellular resolution of protein expression is required. To provide insight into spatial patterns and heterogeneity within a tumor, we used the Paletrra™ (NeoGenomics Laboratories, Inc) platform. Paletrra™ is a proprietary multiplex immunofluorescence (mIF) platform for the visualization and characterization of up to 60 protein biomarkers in a single FFPE section and offers high-resolution spatial and quantitative analysis of protein expression in tissue samples. Herein we report the design and use of a novel panel of commercially available antibodies to support ADC development in lung and breast cancer samples. The panel can measure common ADC targets such as B7-H3, B7-H4, c-MET, EGFR, HER2, HER3, and TROP2 combined with a membrane marker to enable subcellular differentiation between membrane and cytoplasmic expression. Quantitative image analysis enables normalization of protein expression and computation of membrane-to-cytoplasmic expression ratio, providing enhanced biological context. Moreover, because ADCs have been shown to modulate the tumor immune microenvironment, additional markers in the panel provide insight into immunogenicity, cellular relationships, and overall structural biology within the tumor samples. Application of this assay supports translational research and clinical development of ADCs, facilitating identification of patients with optimal target expression and localization.

#1225 3D spatial multiomics characterization of ovarian cancer tissue samples.

Lena Nolte[1], Diogo Bessa-Neto[1], Salpy Baghdo[1], Bernadett Szabo[1], Fabio El Yassouri[1], Emily Neil[2], Robert Pinard[2], Werner Muller[1], Dominik Eckardt[1], Christoph Herbel[1], Andreas Bosio[1]

[1]Miltenyi Biotec, Bergisch Gladbach, Germany,[2]Miltenyi Biotec, Waltham, MA

The complex interplay between genetic alterations, cellular environments, and immune responses in ovarian cancer demands advanced analytical approaches to inform personalized therapies. Conventional two-dimensional analyses fail to capture the tumor's complex three-dimensional (3D) architecture and cellular organization, limiting insight into immune dynamics and the tumor microenvironment. To overcome this, we developed a fully automated spatial biology workflow integrating 3D multiomics. This workflow combines RNAsky® technology for precise RNA detection with multiplexed protein profiling using recombinant REAfinity™ and REAdye_lease™ antibody conjugates, analyzed via the MACS® iQ View - Spatial Biology Image Analysis Software for accurate 3D segmentation. The inclusion of multiple layers in the z-dimension allows precise annotation of individual cells, and thus precise RNA and protein localization at the single-cell level. By analyzing ovarian cancer tissues with an immuno-oncology antibody panel and a complementary RNA panel, we characterized primary, untreated ovarian cancer tissues and their microenvironment. This enabled spatial mapping of diverse lymphoid cell populations including T-cells, B-cells, and NK cells, as well as cells of myeloid lineage such as dendritic cells and macrophages. Additionally, cancer cells were characterized and the stromal compartment encompassing fibroblasts, endothelial and neuronal cells were identified. These aspects revealed structural and immunological features which may influence tumor progression and treatment response. The 3D analysis uncovered spatial relationships among various cell types, in particular, 3D analysis resolved key anatomical features of tissue architecture, which play crucial roles in tumor growth and metastasis. By correlating these 3D spatial data with clinical outcomes, the workflow may provide insights into resistance mechanisms, potential biomarkers, and therapeutic targets. This integrated 3D multiomics workflow offers a holistic, high-resolution view of tumor organization and immune contexture, advancing the understanding of ovarian cancer biology and supporting precision medicine across cancer types.

: Survivorship, Supportive Care, and Quality of Life in Oncology
Poster Session

#1227 Enhancing individualized interventions with machine learning: A better approach?.

Wonshik Chee[1], Jiwon Baek[2], Dongmi Kim[2], Seulgi Ryu[2], **Yeeun Kim**[2], Eun-Ok Im[2]

[1]Department of Kinesiology and Health Education, College of Education, University of Texas at Austin, Austin, TX,[2]School of Nursing, University of Texas at Austin, Austin, TX

Background: Asian American breast cancer survivors face additional cultural, linguistic, and access barriers that impede optimal pain self-management and timely mental-health care. These challenges underscore the need for culturally responsive, scalable interventions. Building on preliminary Cancer Pain Management Program (CAPA) work, we developed the Cancer Pain Management: A Technology-Based Intervention Program (CAI) that augments CAPA with depression-focused components for survivors reporting depressive symptoms and a machine learning feature for individualized support.
Methods: As part of an ongoing randomized controlled trial, 106 Asian American women with a history of breast cancer were randomized: 58 to the intervention group and 48 to the active control group. The intervention group used the CAI and the active control group used the CAPA. CAI and CAPA were culturally tailored, multi-component, web-based interventions identical in structure, except CAI included depression-focused content and machine learning-driven personalization. Primary outcomes included pain (Cancer Pain Management [CPM], Brief Pain Inventory-short form [BPI-SF]), symptom burden (Memorial Symptom Assessment Scale-Short Form: MSAS-SF), depression (Center for Epidemiologic Studies Depression Scale: CES-D), and quality of life (Functional Assessment of Cancer Therapy Scale-Breast Cancer: FACT-B). Assessments occurred at baseline (T0), 1 month (T1), and 3 months (T2). Mixed-effects growth models tested group, time, and interaction effects.
Results: At baseline, groups were well balanced; no significant differences were observed in sociodemographic variables, breast cancer-related characteristics, or primary outcome measures (all $p > 0.05$). Significant improvements over time were observed for pain (BPI-SF, $p < 0.001$), depression (CES-D, $p < 0.001$), and quality of life (FACT-B, $p < 0.001$). However, no significant group or group-by-time interaction effects emerged (all $p > 0.05$), indicating that CAI did not outperform CAPA despite its machine learning component.
Conclusion: Both interventions improved outcomes over time; however, CAI, which incorporated machine learning-driven individualization, showed greater improvements than CAPA, although these differences were not statistically significant. These findings highlight the need for further research to evaluate and optimize personalization strategies using machine learning.

#1228 Disparities in post-survivorship psychiatric diagnoses among adult cancer patients in a multi-center academic health system.

Suraj Manohar Rajan[1], Vivian Tran[1], Carol Y. Ochoa[2], Joshua Demb[1], Melody Schiaffino[1], James Murphy[1], Brent S. Rose[2], Matthew P. Banegas[3]

[1]UCSD Moores Cancer Center, La Jolla, CA,[2]UC San DIego Moores Cancer Center, La Jolla, CA,[3]Cancer Prevention Fellow, UC San Diego, San Diego, CA

Background: Cancer patients experience substantial psychological burden, yet mental health conditions often remain unrecognized and untreated. Disparities in psychiatric care may exist across demographic groups, though comprehensive multi-cancer analyses examining these patterns are limited.

Methods: We conducted a retrospective cohort study of 1,161,370 adult patients diagnosed with ten common cancers between January 2015 and September 2025 within the University of California Health system. Patients with pre-existing psychiatric diagnoses (12 months prior) or palliative-intent treatment were excluded. Primary outcomes were new-onset depression and anxiety diagnoses following cancer diagnosis. Multivariable logistic regression identified predictors of psychiatric diagnosis, adjusting for age, sex, race, ethnicity, insurance type, cancer type, and diagnosis year.

Results: Of 1,161,370 patients (mean age 66.1 years, 52.9% female), 258,076 (22.2%) received new psychiatric diagnoses: 8.4% anxiety only, 5.7% depression only, and 8.2% both conditions. While 22.5% of patients with both conditions were diagnosed within one month of cancer diagnosis, 32-43% received diagnoses beyond 12 months, indicating delayed recognition. Significant demographic disparities emerged. Female patients had higher odds of depression (aOR=1.35, 95%CI:1.32-1.38) and anxiety (aOR=1.57, 95%CI:1.54-1.61) diagnoses than males. Asian patients had substantially lower odds of depression (aOR=0.58, 95%CI:0.56-0.59) and anxiety (aOR=0.56, 95%CI:0.55-0.58) compared to White patients. Hispanic/Latino patients had 51% lower odds of depression diagnosis (aOR=0.49, 95%CI:0.37-0.56). Patients with Medicaid had elevated odds of both depression (aOR=1.40, 95%CI:1.37-1.44) and anxiety (aOR=1.12, 95%CI:1.09-1.14) compared to privately insured patients. Breast cancer patients had the highest psychiatric diagnosis rates across cancer types, while prostate cancer patients had substantially lower odds (depression aOR=0.79, anxiety aOR=0.63).

Conclusions: Nearly one-quarter of cancer patients receive new psychiatric diagnoses, yet substantial disparities exist by sex, race, ethnicity, insurance status, and cancer type. Delayed recognition with most diagnoses occurring beyond 12 months post-cancer highlights missed opportunities for early intervention. These findings suggest inequitable mental health recognition and care delivery in oncology. Systematic implementation of culturally appropriate screening, enhanced provider training, improved behavioral health integration throughout the cancer continuum, and policy reforms ensuring equitable mental health access are essential to address these disparities.

#1229 Suicidal ideation endorsed by long-term survivors of blood or marrow transplantation: A BMTSS report.

Ritika R. Samant[1], Devika Bhatia[2], Qingrui Meng[1], Yanjun Chen[1], Lindsey Hageman[1], Liton Francisco[1], Sarah Palmer[1], Eunice Choe[1], Nora Balas[1], Alysia Bosworth[3], Ravi Bhatia[1], Lennie Wong[3], Daniel Weisdorf[4], Wendy Landier[1], Saro Armenian[3], Smita Bhatia[1]

[1]University of Alabama at Birmingham, Birmingham, AL,[2]University of Colorado, Denver, CO,[3]City of Hope, Duarte, CA,[4]University of Minnesota, Minneapolis, MN

Background: High intensity therapeutic exposures and prolonged immune suppression place blood or marrow transplant (BMT) survivors at a higher risk of long-term physical and psychological morbidity that could lead to suicidal ideation endorsed by survivors.
Methods: We examined suicidal ideation in BMT survivors who received autologous or allogeneic BMT between 1974 and 2014 at one of three transplant programs (City of Hope, University of Minnesota, or University of Alabama at Birmingham) and survived ≥2y after BMT. Overall, 3,841 BMT survivors and 1,261 siblings completed a 255-item survey at age ≥18y were included in this analysis. The survey assesses sociodemographics, chronic health conditions, and psychological health.
Results: Overall, 5.7% of the BMT survivors and 3.1% of the siblings reported suicidal ideation. BMT survivors were at a 1.9-fold greater odds of endorsing suicidal ideation compared with siblings (95%CI=1.34-2.68, p-value=0.003). Multivariable analysis adjusting for age at survey, sex, income, and insurance, severe/life-threatening chronic health conditions, pain, and depression to the model, mitigated the difference in suicidal ideation between BMT survivors and siblings (OR=1.04; 95%CI=0.71-1.53, p=0.84). Restricting the analysis to BMT survivors, we found that younger age at study (18-34y: OR=2.2, 95%CI=1.4-3.6, p=0.002; reference: age >65y), lower income (<$75,000: OR=1.43, 95%CI=1.0-2.0; reference: ≥$75,000, p=0.04), depression (OR=9.81, 95%CI=7.2-13.4), and pain (OR=1.65, 95%CI=1.2-2.3, p=0.002) were associated with suicidal ideation.
Conclusions: The higher prevalence of pain, depression, and chronic health conditions explain the higher odds of suicidal ideation endorsed by BMT survivors compared with siblings. BMT survivors with lower income, depression and pain are at the highest risk of endorsing suicidal ideation. These findings suggest a need for increased surveillance and intervention for suicidal ideation among at-risk BMT survivors.

#1230 Surviving to thriving: Empowering breast cancer survivors through community-based health coaching.

Cameron J. Arriaga[1], Emily L. Cauble[1], Uloma S. Nwogu[1], Mitchell Rodenbaugh[2], Madisen Novelo[1], David Gorman[3], Jessica Clague DeHart[1]

[1]Claremont Graduate University, Claremont, CA,[2]Pitzer College, Claremont, CA,[3]Columbia Vagelos College of Physicians and Surgeons, New York, NY

Background: Breast cancer survival rates are improving, yet the collateral damage of successful treatment is often overlooked. Over 4 million survivors are left in silence asking “now what?”— many facing ongoing struggles with their physical abilities, emotional well-being, quality of life, and adverse health outcomes that often go unaddressed in a traditional survivorship care plan.
Objective: LYTE (Living Your Truth Empowered) Foundation with Claremont Graduate University piloted a novel approach to address this gap: a personalized health coaching program designed to empower survivors to reclaim their health, rebuild their confidence, improve their quality of life, and thrive, not just survive.
Methods: This one-arm quasi-experimental pilot study was designed to evaluate the program’s feasibility and effectiveness on the quality of life, physical health, and well-being of breast cancer survivors. Female, adult breast cancer survivors (N=9) completed a 9-week health coaching program consisting of weekly, live virtual coaching sessions. Participants completed pre and post in-person assessments (body composition, metabolic health, and physical ability) and online surveys (physical activity/function, nutrition, quality of life and self-confidence).
Results: The coaching program demonstrated strong feasibility, with all 9 participants completing the intervention and high approval of Zoom utilization (89% participants reported ‘very much’ easy to use). Post-intervention, participants reported improvements in functional physical activity and reduced difficulty of everyday tasks, including climbing stairs, walking and shopping. Participants engaged in more frequent and longer sessions of vigorous and moderate physical activity, accompanied by an increase in self-reported walking pace. Psychological and environmental barriers to physical activity improved, and confidence in daily movement and physical activity increased. A few challenges (time constraints and financial limitations) persisted or slightly increased. In-person assessment data supported self-reported survey data. Participants showed gains in right-hand grip strength and high-density lipoprotein (HDL) levels and decreases in weight, BMI, and blood pressure. There was also a statistically significant increase in the participants post-intervention walking distance ($p=0.0005$).
Conclusion: LYTE’s health coaching program offers an innovative, survivor-centered approach to improving quality of life, physical health, and well-being. The findings from this pilot study demonstrate feasibility and effectiveness of a health coaching program and lays the groundwork for a larger, randomized control trial. Most importantly, the study highlights the potential of personalized health coaching to help breast cancer survivors illuminate their brightest path forward.

#1231 Breaking the ice: Prostate cancer advocacy and awareness programs in Nigeria and their role in changing men's health narratives.

Catherine Adebukola Oladoyinbo, African Behavioral Research Center

Nutrition and Dietetics/ABeR, Federal University of Agriculture Abeokuta, Abeokuta, Ogun, Nigeria

Prostate cancer (CaP) stands among the leading cancers responsible for male mortality worldwide. Statistics reveal that approximately 397,430 men across the globe have lost their lives to this disease in 2022. Research further confirms that CaP tends to be more aggressive in Black men coupled with late presentation, making it a major cause of death within this group. With this reality, it becomes paramount that advocacy and awareness efforts be intensified. The African Behavioural Research (ABeR) center set up three channels for CaP advocacy in order to increase awareness, knowledge and screening uptake. The first initiative was the CaP advocacy training program which was conducted using the Mayo Clinic Advocacy Training Manual. The training was specifically designed to equip men especially CaP survivors with skills for CaP advocacy. Seven (7) CaP survivors from across West Africa received training in the science of advocacy. Following this, they were supported with pilot grants to implement CaP awareness projects within their respective communities. The second initiative was the development and validation of a CaP awareness video among three hundred and twenty-two (322) men. This was translated into four (4) indigenous Nigerian languages. The third initiative was the creation of a platform to educate men aged 40years and above on the signs, symptoms, regular screening CaP (Nutrition Rx)Results from the CaP survivors pilot projects showed that 420 men were reached by three of the survivors and one hundred and seventy (170) men were screened for CaP. The CaP awareness video after validation, showed a significant increase in CaP knowledge (P=0.0001) among the participants(https://drive.google.com/file/d/1mE857ZHr7dUA97vtvmEmwxgzdQhnj3Ey/view?usp=sharing). The translated video have been deployed for use at the urology clinic of the Federal Medical Center Abeokuta. The Nutrition Rx program has successfully reached over 2000 men across Nigeria and West Africa. The platform has been used to distribute healthy food items and also to educate men on prostate health. The advocacy initiatives by the center has proven to be effective in improving CaP knowledge and raise awareness on the importance of screen for early detection.

#1232 The impact of a culturally tailored technology-based cancer pain management program on the quality of life by psychosocial factors among Asian American breast cancer survivors.

Yeeun Kim, Jiwon Baek, Dongmi Kim, Seulgi Ryu, Wonshik Chee, Eun-Ok Im

The University of Texas at Austin, Austin, TX

Background: Breast cancer survivors face challenges in maintaining their quality of life during their treatment and survivorship process. Especially, Asian American breast cancer survivors frequently encounter constrained social supports and difficulties in accessing adequate emotional and practical support. Cultural barriers are often the major cause of the difficulties. This study aimed to explore the impact of a culturally tailored technology-based cancer pain management program on the quality of life (QoL) by psychosocial factors among Asian American breast cancer survivors.

Methods: This is a part of an ongoing randomized controlled trial among Asian American women breast cancer survivors. Data was collected at T0 (baseline), T1 (after 1 month; during intervention), and T2 (after 3 months; post intervention) during the 3-month intervention process. Only the data from 57 participants who completed the intervention were included in this analysis. The instruments included the Perceived Isolation Scale, (PIS) and the Questions on Attitudes, Self-Efficacy, Perceived Barriers, and Social Influences (QASPS), and the Functional Assessment of Cancer Therapy Scale-Breast Cancer (FACT-B). K-means cluster analysis was conducted using baseline data. The optimal number of clusters (k=2) was selected using NbClust package in R. The participants were classified into two clusters, which were then crossed with the interventions form a total of four groups. Longitudinal trajectories were examined using linear mixed model (LMM) to test interaction effects between Time, Cluster, and Intervention

Results: Two clusters emerged from the K-means analysis. Cluster 1 (n=18; CAI=9, CAPA=9) showed higher loneliness, lower social support, less positive attitude and self-efficacy, and more perceived barriers, whereas Cluster 2 (n=39; CAI=26, CAPA=13) showed the opposite pattern. LMM analysis revealed significant effects of Time and Cluster on the QoL. In both groups, the QoL improved over time (T1 vs T0: p=.003, T2 vs T0: p<.001). Cluster 2 reported higher QoL (Cluster 2 vs Cluster 1: p=.002) than Cluster 1. Except Time 2 x Cluster 2 interaction (p=.040), no other significant interaction effects were found.

Conclusion: This study demonstrated that technology-based interventions can positively impact QoL for breast cancer survivors, regardless of participants' level of psychosocial factors. However, caution is required when interpreting the results due to the small sample size and imbalance between clusters. Future studies should include a large enough sample size to confirm the long-term effects of Intervention CAI.

#1233 Exploring the spiritual detriments of the quality of life among patients with advanced cancers undergoing palliative chemotherapy.

Jiyeon Son[1], Jieun Lee[2], **Suhyeon Hwang**[2], Junglyun Kim[2]

[1]Dankook Univ. Hospital, Cheonan-si, Korea, Republic of,[2]Chungnam National University, Daejeon, Korea, Republic of

Background: Cancers account for 28.7% of total deaths, with the leading cause of death, and this trend is steadily increasing. In South Korea, cancer survival rates have also consistently improved, from 45.2% to 72.9% between 1991 and 2022. As 7 out of 10 cancer patients now survive more than five years, the interest of healthcare providers has shifted beyond merely improving survival rates to enhancing quality of life (QoL). QoL is recognized as an essential indicator in cancer treatment and recovery processes. Especially in patients with advanced cancer, improving QoL during their remaining life span becomes a key therapeutic goal, requiring continuous assessment and interventions. Although existing cumulative evidence for QoL in the cancer population, understanding the spiritual determinants of QoL among patients with advanced cancers undergoing palliative chemotherapy is still limited. This study aimed to explore the spiritual detriments of the QoL among patients with advanced cancers undergoing palliative chemotherapy.
Methods: This cross-sectional, descriptive study utilized convenience sampling to recruit participants undergoing palliative chemotherapy at a university hospital between September 2023 and March 2025. Uncertainty, Cancer coping, Spiritual well-being, and QoL were measured by the Korean version of the Mishel Uncertainty in Illness Scale - Adult Form, the Cancer Coping Questionnaire, the Functional Assessment of Chronic Illness Therapy-Spiritual Well-being Scale, and the Cancer-Specific Quality of Life scale, respectively. Demographic and Clinical data were obtained from electronic health records or demographic questionnaires. Multiple regression analysis was performed using SPSS version 30.0.
Results: Among a total of 165 participants, 88 (53.3%) were males; the mean age was 54.86 (SD = 8.34) years; 62(37.6%) were diagnosed with colorectal cancers. The average number of chemotherapy sessions was 17.16 (SD =17.03). Pain (β=-.221, p=.001), uncertainty (β=-.250, p=<.001), and spiritual well-being (β=.316, p=<.001), Colorectal cancer (β=.250, p=.002) explained 37.2% of the variance (adjusted R^2 of .372) in QoL.
Conclusion: To improve the QoL of patients with advanced cancers undergoing palliative chemotherapy, maintaining spiritual well-being is crucial. Holistic assessment of QoL, including spiritual components and management of pain, providing treatment information in a timely manner to reduce uncertainty, should be included in the intervention strategy to improve QoL in patients with advanced cancers.

#1234 Bioelectrical impedance analysis-derived body composition metrics as prognostic biomarkers in lung cancer.

Jeongung Cha[1], Yeong Hak Bang[2], Narin Kim[3], Juwon Jung[2], Hyunsu Kim[2], Jinyong Kim[2], Sungyoon Cho[3], Aekyeong Jin[3], HeeHwan Kim[3], Sehhoon Park[2]

[1]Department of Health Sciences and Technology, Samsung Advanced Institute of Health Sciences and Technology, Sungkyunkwan University, Seoul, Korea, Republic of,[2]Division of Hematology-Oncology, Department of Medicine, Samsung Medical Center, Sungkyunkwan University School of Medicine, Seoul, Korea, Republic of,[3]InBody Co., Seoul, Korea, Republic of

Background: Body composition changes are common in lung cancer and relate to poor outcomes, but their treatment-related changes and prognostic value are not well defined. This study serially evaluated body composition metrics in patients with lung cancer receiving palliative treatment.

Methods: In this study, we prospectively and serially evaluated body composition metrics in patients with lung cancer receiving palliative treatment, using bioelectrical impedance analyzer (InBody 770 and S10, InBody Co., Seoul, Korea). The patients were scheduled for a minimum of 12 weeks of treatment, and the analysis was conducted every 3 weeks, in addition to collecting clinical data. The optimal thresholds of the death and progression prediction model were identified based on area under curve (AUC) and F1 score.

Results: A total of 141 patients were enrolled in the study. The median follow-up duration was 21.3 months (range, 13.2-24.9 months). Nearly half of the cohort was aged ≥65 years (N=75, 53.2%). The majority of patients had non-small cell lung cancer (N=127, 90.1%), with a smaller subset having small cell lung cancer (N=14, 9.9%). Among the enrolled patients, 92 (65.2%) received palliative cytotoxic chemotherapy (CTx group), and 49 (34.8%) received palliative tyrosine kinase inhibitor therapy (TKI group). From baseline to the end of treatment, CTx group showed a decrease in phase angle (from 4.7 ± 0.78 to 4.48 ± 0.71; $p < 0.001$) and an increase in extracellular water (ECW) ratio (from 0.392 ± 0.008 to 0.395 ± 0.008; $p < 0.001$). Whereas no significant changes of metrics were observed in TKI group. For death prediction using time-point-specific body composition metrics, the CTx group showed the highest performance for events occurring within 1 year, whereas the TKI group performed best for events within 2 years. For progression prediction, the CTx group performed best for 6-month events, while the TKI group showed the best performance for 18-month events. In the CTx group, the prediction models achieved AUCs of 0.899 for death and 0.831 for progression, with corresponding F1 scores of 0.708 and 0.790. In the TKI group, the AUCs were 0.961 for death and 0.829 for progression, with F1 scores of 0.640 and 0.817, respectively. Shapley Additive exPlanations (SHAP) analysis identified percent body fat (PBF) and skeletal muscle index (SMI) as the most influential predictors for both outcomes.

Conclusions: Serial body composition metrics assessments captured treatment-related body composition changes in lung cancer, and models based on these metrics showed prognostic performance. These findings support the use of longitudinal body composition monitoring in personalized patient management.

#1235 Exercise volume, skeletal muscle maintenance, and plasma IL-6/IL-6R in patients with PDAC.

Guanshu Liu[1], Sumedha Pareek[1], Truong Lam[1], Nathan Parker[2], Naveen Garg[3], Matthew HG Katz[4], Laura Prakash[4], Jian Wang[5], An Ngo-Huang[6], Keri Schadler[1]

[1]Department of Pediatrics Research, The University of Texas MD Anderson Cancer Center, Houston, TX,[2]Health Outcomes & Behavior Program, Moffitt Cancer Center, Tampa, FL,[3]Department of Abdominal Imaging, The University of Texas MD Anderson Cancer Center, Houston, TX,[4]Department of Surgical Oncology, The University of Texas MD Anderson Cancer Center, Houston, TX,[5]Department of Biostatistics, The University of Texas MD Anderson Cancer Center, Houston, TX,[6]Department of Palliative, Rehabilitation, and Integrative Medicine, The University of Texas MD Anderson Cancer Center, Houston, TX

Pancreatic ductal adenocarcinoma (PDAC) is often accompanied by debilitating muscle wasting, which is associated with reduced treatment tolerance and survival. IL-6 and IL-6 receptor (IL-6R) have been implicated in cancer-associated muscle loss and as exercise-responsive myokines, though variable results have made the roles of IL-6 and IL-6R in muscle wasting unclear. This study investigated the relationship between skeletal muscle, plasma IL-6/IL-6R levels, and exercise in PDAC patients undergoing neoadjuvant therapy. The PancFit randomized controlled trial (NCT03187951) included a usual care and an exercise intervention arm in which patients with borderline resectable PDAC were asked to perform ≥ 150 minutes/week of moderate intensity aerobic exercise and ≥ 2 strength training sessions per week during the time of neoadjuvant treatment. Physical activity was monitored by Fitbits and self-reported by Godin-Leisure Questionnaire. Skeletal Muscle Index (SMI) was measured by CT images obtained at study enrollment (baseline) and at pre-operative re-staging (end of neoadjuvant therapy and intervention) in 112 patients. Plasma IL-6 and IL-6R were measured by ELISA at the same timepoints in 26 patients. Due to variability in quantity of exercise in both arms, we performed post hoc analysis in which all patients were pooled, then regrouped based on average weekly strength sessions (≥2 vs. <2 sessions/week) or average very active minutes (VAM, by Fitbit/ week). Spearman rank correlations or student's t-test were used for analysis. Patients who completed <2 strength training sessions / week had an average SMI loss of -3.9% ± 8.9 SD from enrollment to pre-operative staging, while those who performed ≥ 2 strength training sessions per week had an average SMI maintenance of +0.35% ± 9.5 SD ($p = 0.03$). There was no correlation between VAM and SMI. There were no significant correlations between the change in SMI from baseline to pre-op and plasma IL-6 at baseline, IL-6 at pre-operative restaging, or in the change in IL-6 between timepoints. However, there was a significant negative correlation between the change in SMI and plasma IL-6R at baseline ($p=0.002$, $r = -0.5$), pre-operative restaging ($p <0.0001$, $r = -0.67$), and in the change in IL-6R over time ($p=0.03$, $r = -0.38$), and between SMI and IL-6R at pre-operative restaging ($p=0.02$, $r =-0.41$). No correlations were observed between VAM and plasma IL-6 or IL-6R at any timepoint. Strength training may be one method to maintain SMI for patients with PDAC undergoing neoadjuvant therapy. Plasma IL-6R, but not IL-6, may be a blood biomarker of SMI. A future randomized controlled trial focusing on strength training is needed to further understand these relationships.

#1236 FOLFIRINOX represents the preferred therapeutic option for patients with pancreatic acinar cell carcinoma: A multi-center study.

Guoliang Qiao

The First Affiliated Hospital of Zhejiang University School of Medicine, Hangzhou, China

Background: Pancreatic acinar cell carcinoma (PACC) is a rare pancreatic malignancy, and evidence guiding systemic therapy remains limited. To address this unmet need, we conducted a multi center study to characterize real world treatment patterns and clinical outcomes, with the goal of informing evidence-based therapeutic recommendations for PACC.
Methods: Clinical and treatment data were collected from 156 patients with PACC across eight pancreatic centers in China. Analyses focused on systemic therapy regimens and survival outcomes. Additional stratified analyses were performed among patients who underwent surgical resection to assess the therapeutic value of FOLFIRINOX in neoadjuvant and adjuvant settings.
Results: A total of 156 patients were identified. The median age at diagnosis was 65.3 years, and 48.6% of patients underwent surgical resection. Most patients presented with abdominal pain or pancreatitis (69%). Laboratory parameters showed no correlation with tumor size, metastatic status, or survival. The median overall survival (OS) was 18.9 months from diagnosis, with significant differences based on metastatic status (15.6 vs. 31.8 months). Both surgical resection and FOLFIRINOX were associated with improved OS. Among surgically treated patients, neoadjuvant or adjuvant FOLFIRINOX conferred a significant OS advantage compared with gemcitabine- or capecitabine-based regimens ($p = 0.001$). In a multivariable Cox regression model, both surgical resection and FOLFIRINOX remained independent predictors of superior OS.
Conclusions: This multi center study provides the largest real-world evidence to date supporting FOLFIRINOX as the preferred systemic therapy for PACC. Ongoing incorporation of international cohorts and expanded stratified analyses will further refine treatment recommendations. The overarching objective of this project is to establish standardized, evidence-based guidelines for the management of PACC.

#1237 Effects of a home-based walking intervention on serum metabolomic profiles in men with prostate cancer on active surveillance.

Rebecca E. Graff[1], Ritu Roy[1], Oliver Fiehn[2], Adam Olshen[1], Erin Van Blarigan[1], Stacey Kenfield[1], Jeffry P. Simko[1], Anthony Luke[1], Lee Jones[3], Matthew R. Cooperberg[1], Peter R. Carroll[1], **June M. Chan**[1]

[1]University of California, San Francisco, San Francisco, CA,[2]University of California, Davis, Davis, CA,[3]City of Hope, Duarte, CA

Introduction: The potential for long-term exercise to affect the metabolome in healthy individuals is well established. Given the metabolic underpinnings of prostate cancer, it is important to investigate whether long-term exercise similarly alters the metabolome in disease-affected men. This study is among the first to characterize metabolic changes in individuals with prostate cancer, comparing those assigned to a home-based walking program to those assigned to printed materials with physical activity recommendations.
Methods: Fifty-one men with prostate cancer on active surveillance were randomly allocated to the exercise or control intervention. Metabolomic profiling of primary metabolism, complex lipids, and biogenic amines was performed at the West Coast Metabolomics Center on serum samples collected at baseline and after the 16-week interventions; data were successfully generated for 22 participants in the exercise arm and 23 participants in the control arm. To identify intervention-related differences in metabolic changes, we performed hierarchical clustering and fit mixed-effects models including an arm x time interaction.
Results: Hierarchical clustering indicated limited separation in metabolic profiles between the exercise and control groups at 16 weeks. Although none of the 1,220 named metabolites exhibited statistically significant differences in change between the two groups (q<0.10), 85 (7.0%) demonstrated nominal significance (p<0.05). Among the 15 metabolites with the smallest p-values, six (40%) were sphingolipids - specifically sphingomyelins - though sphingolipids comprised only 11% of all named metabolites. All six sphingomyelins decreased more over time in the exercise group than in the control group.
Conclusions: Although metabolic profiles were not significantly altered overall, a walking intervention may promote the reduction of sphingomyelins, thereby shifting lipid signaling toward pathways that enhance mitochondrial function and reduce inflammation. Such changes are consistent with biologically plausible mechanisms through which exercise could favorably influence prostate cancer biology, even in the absence of broad metabolomic shifts.

#1238 Ketamir-2, a novel oral ketamine analogue for chemotherapy-induced peripheral neuropathy.

Itzchak Angel[1], caraco Yoseph[2], **Erez Aminov**[1]

[1]MIRA Pharmaceuticals Inc., Miami, FL,[2]Clinical Pharmacology Unit, Hadassah Medical Center, Jerusalem, Israel

Background: Ketamir-2 is a next-generation ketamine analogue designed to improve oral bioavailability and safety relative to existing ketamine-based pain therapies. It acts as a low-affinity N-methyl-D-aspartate (NMDA) receptor antagonist with selective binding to the phencyclidine (PCP) site, a mechanism believed to underlie its analgesic potential while reducing dissociative effects.
Methods and Results: In preclinical studies, oral administration of Ketamir-2 (pamoate salt) produced significant analgesic activity across established rodent models of neuropathic pain, including the Chung spinal nerve ligation model in rats and the paclitaxel-induced mechanical allodynia model in mice. In both models, Ketamir-2 demonstrated superior efficacy compared with oral ketamine and the standard neuropathic pain agents pregabalin and gabapentin, which served as positive controls. Pharmacological profiling confirmed robust oral bioavailability and lack of P-glycoprotein (P-gp) substrate activity, supporting its efficient penetration across the blood-brain barrier—an essential property for central nervous system (CNS) therapeutics. Notably, Ketamir-2 exhibited a favorable safety profile with no evidence of dissociative or psychedelic side effects typically observed with ketamine.
Clinical Development: Results from the first-in-human (FIH) study will be presented. This randomized, double-blind, placebo-controlled Phase 1 trial, conducted at the Clinical Pharmacology Unit of Hadassah Medical Center, evaluated the safety, tolerability, and pharmacokinetics of Ketamir-2 in healthy adult volunteers. A total of 56 participants were enrolled across single-ascending-dose (SAD) and multiple-ascending-dose (MAD) cohorts.
Conclusions: These findings support Ketamir-2 as a promising oral NMDA-receptor modulator for the treatment of chemotherapy-induced peripheral neuropathy (CIPN) and other neuropathic pain disorders, offering a differentiated profile combining efficacy, safety, and oral convenience.

#1239 Clinical outcomes of Ayurveda Rasayana therapy (ART) in advanced pancreatic cancer patients: A retrospective study.

Yogesh Bendale[1], Priyanka Shirole[1], Poonam Birari-Gawande[1], Avinash Kadam[1], **Mukta Marathe**[2]

[1]Rasayu Cancer Clinic, Pune, India,[2]AatharvaN Ayurved & Yog, LLC, Phoenix, AZ

Purpose: A significant proportion, 25-60%, of pancreatic cancer patients cannot receive standard chemotherapy or surgery, usually due to poor performance status, advanced disease, or significant comorbidities. The median survival of these patients is only 3-6 months, and the primary therapeutic goals are improvement of Quality of Life (QoL) and extension of survival. This study evaluates the role of Ayurveda Rasayana Therapy (ART) in this category of patients.

Method: We retrospectively analyzed data from 17 patients with advanced, inoperable pancreatic cancer who were ineligible for chemotherapy. Patients were treated exclusively with Ayurvedic Rasayana preparations primarily containing preparations like *Heeraka Bhasma (diamond)*, *Suvarna Bhasma (gold)*, and *Tamra Bhasma (copper)*, *Shankha Bhasma (Conch)*, *Moutika Bhasma (Pearl)*. Health-related QoL was assessed by the FACT-G questionnaire, and performance status was measured by the ECOG scale at baseline and on day 90. The patient's anorexia was measured by the Anorexia-Cachexia Scale (ACS).

Results: The patients mean age was 62.75±9.14. Treatment significantly improved FACT-G overall quality of life scores (48±14.71 vs 56.35±10.85; $p < 0.05$). ECOG performance status showed significant improvement as compared to baseline (2.29±0.84 vs 1.85±0.79; $p < 0.05$). A significant reduction in anorexia was also noted (19±35 vs 28.35±8.20; $p < 0.05$). Partial tumour response was recorded for two patients. The average survival seen in this group was 316±248.76, days which surpassed the expected range of 3 to 6 months.

Conclusions: This preliminary data indicates that Ayurveda Rasayana Therapy may be a beneficial intervention to improve quality of life, reduce disease-related distress, and extend survival in pancreatic cancer patients with no standard treatment options. As these results are based on observations from a small sample size, they should be interpreted with caution and need further rigorous investigation.

#1240 Pain severity is related to molecular pathways underlying aggressive disease and poor survival in OSCC.

Minh Phuong Dong[1], Gary Yu[2], Michele Arambula[1], Bac An Luong[1], Paul Walker[1], Traeden Wilson[1], Khanh Nguyen[1], Carissa M. Thomas[3], Yi Ye[4], Bradley Aouizerat[4], Chi Viet[5]

[1]Loma Linda University, Loma Linda, CA,[2]Columbia University, New York, NY,[3]University of Colorado, Aurora, CO,[4]New York University, New York, NY,[5]Loma Linda University, Loma Linda, NY

Pain is one of the worst symptoms experienced by patients with oral squamous cell carcinoma (OSCC), which impairs patients' function and quality of life. Yet its clinical and molecular determinants remain poorly defined. The objective of this study was to investigate how pain, quality of life (QoL), and tumor biology intersect to improve prognostication and patient-centered care. This prospective multi-institutional study enrolled 196 OSCC patients from Loma Linda University (LLU) and the University of Alabama at Birmingham (UAB). Pain was assessed using the UCSF Oral Cancer Pain Questionnaire and, Brief Pain Inventory (BPI). Functional and symptom disturbance (QoL) were characterized using EORTC QLQ-C30/H&N35. Flash frozen tumors were collected at surgery for RNA-Seq. Data were analyzed using Spearman correlation, Wilcoxon, Kruskal-Wallis tests, ANCOVA, Kaplan-Meier log-rank test, and Cox hazard regression. Our results revealed that patients reporting high pain demonstrated significantly lower overall QoL, including reduced functional scores (physical, role, emotional, cognitive, and social functioning) and higher symptom burden ($p<0.05$), entirely independent of their cancer stage at diagnosis. Additionally, morphine milligram equivalents (MME/day) were strongly correlated with pain severity and worse QoL metrics ($p<0.05$). Kaplan-Meier analysis showed that high pain (UCSF and BPI), higher symptom score, and higher H&N35 score, lower global health status score and functional score, and opioid use were associated with worse survival ($p<0.05$). After adjustment for confounders (age, sex, race, pathologic stage, PNI, LVI, smoking status), Cox hazard regression analysis revealed functional score (HR = 0.5, CI 95% [0.287-0.873]), symptom score (HR = 2.144, CI 95% [1.169-3.934]), HN35 scores (HR = 2.192, CI 95% [1.195-4.023]) and opioid use (HR = 2.665, CI 95% [1.510-4.706]) as independent predictors of survival. RNAseq analysis of 128 patients comparing high- and low-pain tumors identified significant enrichment in GO pathways related to axonogenesis, neuron to neuron synapse, and in KEGG involved pathways of neurodegeneration-multiple disease, Alzheimer's, and Huntington's disease pathways. In addition, the top dysregulated GO pathways in patients with low function (low functional score) were cytoplasmic translation, ribosome biogenesis, and regulator of signal transduction by p53 class mediator. In conclusion, these findings demonstrated that pain severity, opioid requirement, and diminished quality of life are tightly linked to aggressive tumor features and poorer survival in OSCC. Molecular analyses highlight the potential of neural-associated dysregulation in OSCC pain.

#1241 Early outcomes of an AI-driven chatbot application for symptom management in patients with cancer: Interim analysis of a prospective digital health study.

Hyun Woo Lee[1], Tae Jun Park[1], Seok Yun Kang[2], Jang Hee Kim[2]

[1]Ajou University School of Medicine, Suwon, Korea, Republic of,[2]Ajou university school of medicine, suwon, Korea, Republic of

Background:Cancer patients frequently experience persistent symptoms such as pain, fatigue, and treatment-related distress. Despite guideline-based recommendations, real-time symptom monitoring and supportive care delivery remain suboptimal. We developed an AI-based chatbot application designed to provide personalized symptom management education, self-management guidance, and interactive support. This study evaluates user experience, self-efficacy, psychological distress, and early clinical impact.
Methods:A prospective digital-health intervention study was conducted using an AI chatbot delivering education aligned with NCCN supportive-care guidance. A total of 192 participants were enrolled, including both solid tumor and hematologic malignancy patients. Validated instruments included UMUX-Lite for usability, SEMCD-6 for self-management self-efficacy, DT for psychological distress, perceived usefulness (PU), engagement frequency, and e-health literacy measures (instrument details in slide deck). Outcomes were assessed at baseline and follow-up. Group × time effects were analyzed using mixed-effects models.
Results: User experience remained consistently high throughout the study period, with favorable UMUX and PU scores. Although short-term and mid-term objective improvements were modest, the intervention group demonstrated significantly greater improvements in key patient-reported outcomes, including:- Reduced psychological distress (P = 0.013)- Improved self-efficacy domains (multiple SEMCD items showing significant change; P = 0.008 in primary domains) Higher e-health literacy was associated with larger improvements in self-efficacy and perceived usefulness. Subgroup analyses suggested heterogeneous treatment effects, with males, lung-cancer patients, and individuals with lower educational attainment showing greater unmet needs and requiring tailored support. Engagement (days of chatbot use per week) showed a positive dose-response trend with outcome improvement.
Conclusions: The AI chatbot application demonstrated high sustained user satisfaction and early signals of benefit in psychological distress reduction and self-management confidence among cancer patients. While objective clinical markers showed limited short-term changes, differential effects across demographic and diagnostic subgroups highlight the need for targeted personalization. Ongoing analyses will evaluate mediators such as digital literacy, therapeutic alliance, intervention usability, and long-term clinical outcomes.

#1242 Cannabis use during cancer treatment: Patterns and perceptions of cannabis use among cancer survivors at a Wisconsin cancer center.

Apoorva C. Reddy[1], Jennifer Dykema[2], Betty Chewning[3], Kristine Kwekkeboom[4], Heather Neuman[1]

[1]Department of Surgery, Univ. of Wisconsin Madison Sch. of Med. & Public Health, Madison, WI,[2]Survey Center, University of Wisconsin-Madison, Madison, WI,[3]University of Wisconsin-Madison School of Pharmacy, Madison, WI,[4]University of Wisconsin-Madison School of Nursing, Madison, WI

Background:Cancer survivors increasingly use cannabis products to manage treatment-related symptoms. Yet, little is known about their perceptions of the helpfulness of cannabis products for symptom relief or what barriers shape their use. We aimed to characterize cannabis product use and perceptions among cancer patients.
Methods:We administered a cross-sectional survey to 650 adult patients at UW Health/Carbone Cancer Center clinics who had received treatment within the last 3 months, with a response rate of 54% (54 patients died, 320 responded). Patients who reported using cannabis products after being diagnosed with cancer (n=92) were eligible for this analysis. The survey captured demographics, perceived symptom change with cannabis product use, and barriers to use. Descriptive analyses and Kendall-Wei Rank were completed using STATA and R.
Results: Patients who responded had a median age of 62 (IQR: 53-67) years; 51% were women, 89% were White, 34% had an annual income of $100,000 or more, 50% had completed college or technical school, and 35% used tobacco in the past year. Half the patients had metastatic cancer (48%). Most patients received chemotherapy (55%) and/or radiation (54%) within the prior 3 months. Patients were most likely to report that cannabis products improved their pain (76%) and nausea/vomiting (76%) (Table 1). Patients' most-reported barriers to cannabis product use were cost (35%) and concern about legal risk (32%). Most patients were in favor of legalizing the medicinal use of THC (94%) and CBD (96%). Most patients were very or extremely likely to use cannabis products in the future (66%).
Conclusion:In this cohort of Wisconsin patients with cancer who used cannabis products after diagnosis, the majority perceived cannabis products to be beneficial in managing cancer symptoms, particularly pain. Despite the reported benefits, cost and legality are barriers to cannabis use among Wisconsinites.

Table 1. Patient self-report of receiving benefit (i.e., symptoms or side effects improved) from can

Symptom	**Number of patients reporting this symptom**	**Benefit n (%)**
Pain	72	55 (76%)
Lack of appetite	67	48 (72%)
Sleep loss	78	53 (68%)
Irritability	67	46 (69%)
Anxiety	70	42 (60%)
Nausea/vomiting	58	44 (76%)
Depression	61	30 (49%)
Fatigue or low energy	78	31 (40%)
Headache	51	22 (43%)
Neuropathy	57	13 (23%)
Lack of sexual interest or activity	61	12 (20%)
Sweating, including hot flashes or night sweats	56	6 (11%)

#1243 Cancer survivors' acceptance of technology-based tools for stress management and effective communication.

Ana C. Sala[1], Liliana Castro Jimenez[2], Brenda Torres[2], Zaydelis Tamarit[3], Marievelisse Soto-Salgado[3], Vivian Colon-Lopez[3]

[1]Department of Cancer Medicine, Comprehensive Cancer Center University of Puerto Rico, San Juan, PR,[2]Biostatistics and Bioinformatics Core, Comprehensive Cancer Center University of Puerto Rico, San Juan, PR,[3]Division of Cancer Control and Population Sciences, Comprehensive Cancer Center University of Puerto Rico, San Juan, PR

Cancer survivors process complex diagnosis and treatment information making medical appointments a source of stress. Uncertainty about medical decisions heightens stress limiting quality of communication during appointments. Artificial intelligence (AI) tools are emerging as approaches to enhance patient support yet use with Spanish-speaking cancer survivors is limited. This study sought to characterize stress levels of Puerto Rican cancer survivors and assess preparedness before meeting with physicians. We also assessed openness to use technology for stress management and communication with physicians. We hypothesized survivors would report high stress levels, low preparedness, and acceptance of technology. In this cross-sectional study, 169 cancer survivors aged ≥21 were recruited prior to their appointment in oncology waiting rooms. Upon consenting, they completed a survey to assess stress, preparedness, and openness to technology. Stress levels in the past 30 days, prior to appointments, and regarding the current visit were measured. Preparedness for the visit was assessed with a 1-10 scale and asking if they had prepared a list of questions for their physicians. Openness to technology was assessed with questions about willingness to: *use a phone/tablet for a relaxation exercise and submit questions electronically for physicians to read before appointments.* Statistical analyses were performed using R. Descriptive statistics were used to assess variables of interest. Most study participants (68.6%) were women; mean age 57.8 (SD=14.5). Average age at cancer diagnosis was 55 (SD=14.7). Reasons for visit included routine follow-up (61.7%), test results discussion (9%), first appointment (9%), and follow-up for new symptoms (4.2%). More than a third (36.3%) reported usually/always feeling stress in the past 30 days, 55.6% reported stress prior to appointments, and 53% about their current visit. Despite an average self-reported preparation score of 8.4 (out of 10) and 92% indicating they felt prepared for the visit, only 27% had written a list of questions to guide the conversation with their physician. As for acceptance to technology-based tools, 68% indicated they would benefit from a stress management exercise before appointments and 66% were willing to send questions electronically to their physicians. Among those unwilling, the most common reason was preference for in-person discussion (27.2%). Stress may impair memory interfering with survivors' intentions to ask questions during visits. Findings confirm high pre-appointment stress among cancer survivors and a low tendency to write questions to aid communication. This highlights a need for strategies to enhance emotional readiness and preparedness. Results suggest openness to AI-assisted tools for stress management and improved patient-physician communication, supporting its integration into standard cancer care.

#1244 Health-related quality of life in EGFR-mutant lung cancer survivors: SEER-MHOS analysis.

Shuyan Qiu, Yiwey Shieh, Christine Garcia, Eunji Choi

Weill Cornell Medicine, Cornell University, New York, NY

Introduction: The proportion of lung cancer among never-smokers is rising, with EGFR mutations observed in approximately 40-60% of these cases. Given that EGFR-mutated (EGFRmt) lung cancer is more prevalent in non-smokers, females, and individuals of Asian ancestry, their survivorship needs likely differ from the typical lung cancer cohort, which primarily consists of older males with a history of heavy smoking. This study examined the mental and physical health outcomes, including perceived changes in health status, among three distinct groups: EGFRmt lung cancer patients, non-EGFRmt lung cancer patients and non-cancer controls.

Methods: We utilized linked data from SEER registries, the Medicare Health Outcomes Survey (MHOS), and Medicare Part D prescription records to identify adults aged ≥65 years with lung cancer and receipt of EGFR tyrosine kinase inhibitors (TKIs) between 2007 and 2020. We identified non-EGFRmt lung cancer patients matched to EGFRmt cases by diagnosis year and cancer stage. Non-cancer controls were selected by matching to all lung cancer patients on survey age and survey year. Primary outcomes included (1) mental and physical health, assessed using the Veterans RAND instrument, and (2) perceived changes in mental and physical health compared with the previous year. Primary outcome information was derived from the MHOS survey nearest to the initial lung cancer diagnosis. Multinomial logistic regression models were applied to identify survivorship needs among EGFRmt and other lung cancer patients relative to non-cancer controls, adjusting for sex, race, and smoking status.

Results: A total of 130 EGFRmt lung cancer patients, 520 non-EGFRmt patients, and 650 non-cancer controls were identified. EGFRmt patients were more frequently female (65% vs. 49% of non-EGFRmt patients and 62% of non-cancer controls), of Asian ancestry (18% vs. 4.8% and 4.5%), and less likely to be active smokers (13% vs. 25% and 7.4%). In adjusted multinomial logistic models, EGFRmt patients had a 1.20-fold higher likelihood of poor mental health (odds ratio [OR] = 1.20, 95% CI 1.02-1.39), while non-EGFRmt patients had a 1.14-fold higher likelihood (OR = 1.14, 95% CI 1.04-1.26), relative to non-cancer controls. Similarly, EGFRmt patients were most likely to report worsened mental health compared with non-cancer controls (OR = 2.81, 95% CI 1.66-4.76), whereas non-EGFRmt patients also demonstrated an elevated risk, though to a lesser degree (OR = 1.86, 95% CI 1.30-2.67). Across all lung cancer patients, poor outcomes in social and physical functioning, vitality, bodily pain, and general health were more prevalent than among non-cancer controls.

Conclusion: Patients with EGFRmt lung cancer experience more deterioration of mental health than other lung cancer patients and non-cancer individuals. Targeted mental health interventions may improve long-term survivorship outcomes in this growing patient population.

#1245 Suicide Risk in Oncology: Sex and Cancer Type Differences in a Case-Control Study.

Brandy M. Byrwa-Hill[1], Eric T. Monson[1], Emily DiBlasi[1], Hilary Coon[1], Danli Chen[1], Michael J. Staley[2], Amanda V. Bakian[1]

[1]Department of Psychiatry, Spencer Fox Eccles School of Medicine and Huntsman Mental Health Institute, University of Utah, Salt Lake City, UT,[2]Utah State Office of the Medical Examiner, Utah Department of Health and Human Services, Salt Lake City, UT

Background: Suicide risk among people with cancer may vary by sex and cancer site, reflecting different biological, psychosocial, and care-system pathways. We used statewide linked mortality and clinical data to examine whether cancer history and sex-specific cancer types differentially relate to pre-death suicidality and suicide mortality.
Methods: We conducted a two-step study using population-level data from Utah linking suicide mortality, cancer, and electronic health records. First, we compared suicide decedents with versus without a prior cancer diagnosis (n=14,644) on suicidal ideation (SI), self-injurious behavior (SI), prior suicide attempts (SA), psychiatric and medical comorbidities. Second, we performed an age-and sex-matched case-control analysis of suicide decedents (cases; n=1,015) and living controls (n=9,173) to estimate adjusted odds of suicide death associated with any cancer history and specific cancer types, stratified by sex. Logistic regression models adjusted for prior suicidality, diagnosed mental and substance use disorders (SUD), and chronic medical morbidity. We also characterized the temporal sequencing of first-recorded encounter types (mental health, SUD, chronic medical, or cancer-related).
Results: Among suicide decedents, those with any history of a cancer diagnosis had higher odds of pre-death SA (OR=1.27, 95% CI 1.09-1.49), SII (OR=1.34, 1.12-1.60), and SI (OR=1.29, 1.07-1.56) than decedents without cancer. Mental-health burden was substantially greater among female than male decedents (OR=7.90 vs 2.07). In case-control analyses, a history of any cancer was associated with lower overall odds of suicide death, but this aggregate effect masked heterogeneity by sex and cancer type. Among women, cervical cancer/dysplasia was over-represented in cases compared to controls (OR=1.53, 1.13-2.06), suggesting elevated risk in sex-specific, identity-salient cancers. Among men, prostate cancer was inversely associated with suicide death (OR=0.73, 0.59-0.91). First encounters for mental health and substance use were over-represented among cases of both sexes, while chronic-condition encounters suggest additional risk in men.
Conclusions: In this study, any history of a cancer diagnosis was linked to greater pre-death suicidality but lower overall odds of suicide death, with important sex-and cancer-type specific differences. Patterns may support a dual-pathway model in which psychosocial/identity-related mechanisms may predominate among women with sex-specific cancers, whereas functional or disease-burden pathways may predominate among men with high-burden cancers. Tailored, sex-and cancer-type-specific suicide risk screening that leverages mental health and substance use encounter history may improve prevention in oncology settings.

#1246 The comprehensive outcomes for after cancer health (COACH) study: Interim analysis of baseline demographic and patient reported outcome data for individuals with advanced cancer.

Kelly J. Brassil[1], Trudy Buckingham[2], Anneliese Gonzalez[3], Michael Harrison[4], Kaukab Jafry[3], Abbey Kaler[5], Hilda H. Lewis[6], Jennifer Loftis[4], Kathrin Milbury[7], Darcy Ponce[8], Michelle Schumacher[6], Meagan Whisenant[8], Cosmina Hogea[2]

[1]Medical Affairs, Quest Diagnostics, Houston, TX,[2]Gilead Sciences, Foster City, CA,[3]UT Health Houston, Houston, TX,[4]Medical Affairs, Quest Diagnostics, Secaucus, NJ,[5]Breast Medical Oncology, The University of Texas MD Anderson Cancer Center, Houston, TX,[6]Radiation Oncology, Montefiore Medical Center, Bronx, NY,[7]Behavioral Science, The University of Texas MD Anderson Cancer Center, Houston, TX,[8]UT Health Houston Cizik School of Nursing, Houston, TX

Background: Patients with metastatic cancer face complex self-management challenges requiring symptom monitoring, care coordination, and psychosocial support. Digital tools, including electronic patient-reported outcomes (ePROs), wearables, and health coaching (DHC), have demonstrated improvement outcomes, including overall survival for individuals with cancer, yet less is known about their effect for individuals with advanced breast (aBC) or lung(aLC) cancer. The COACH trial (NCT05349227) evaluates a comprehensive DHC program combining clinical, ePRO, wearable, and gut microbiome data to address survivorship needs in these unique groups.

Methods: This multicenter, randomized, wait-list controlled trial enrolls 675 adults (≥18 years) within one year of completing primary therapy or with metastatic disease, across 8 sites. Subpopulations include aBC (n=150) and aLC (n=100). Participants are randomized to 6 months of DHC or control, with crossover at month 6. All participants are provided with activity trackers (Fitbit), complete ePROs over the course of 12 months, and provide fecal microbiome specimens and dietary data at baseline and month 6.

Interim Outcomes: As of November 2025, 91 aBC participants have been enrolled, of whom 75 have completed baseline ePRO assessments, and 41.5% have connected their Fitbit device to the cloud for data collection. Baseline PROMIS scores for 61 participants with data available for analysis are presented in the Table.

Conclusion: Interim data suggest that individuals with metastatic cancer have numerically higher anxiety and lower cognitive and physical functioning compared to population mean scores. Outcomes from this study will evaluate if and how DHC can be used to address these challenges. Multimodal data derived from this study is intended to enhance understanding of the potentially unique survivorship needs of individuals with advanced cancer.

Table. Consented Participant Demographic Data and Mean Baseline Scores for The National Institutes o

Demographic Data (n=75)	**Mean (SD)/n(%)**
Age	57.09 (12.65)
Sex	Female: 75 (100%)
Race and Ethnicity (Participants could select >/= 1 response)	
Asian	3 (4.0%)
Black or African American	17 (22.7%)
White	43 (57.3%)
Hispanic or Latino	17 (22.7%)
Not Hispanic/Latino	58 (77.3%)
Multiethnic/Other	6 (8%)
Prefer not to answer	6 (8%)
Employment Status	
Full time	26 (34.7%)
Part time	4 (5.3%)
Homemaker	5 (6.7%)
Retired	19 (25.3%)
Medical leave of absence	2 (2.7%)
Disabled due to illness	12 (16%)
Unemployed	4 (5.3%)
Unknown	3 (4%)
Patient Reported Outcomes Measurement Information System (PROMIS) Tool Baseline Scores (n)*	Mean Score (SD; Range; *Population average for individuals with cancer*)
Anxiety (60)	53.1 (9.1; 37.1-75.1; *50.6*)
Cognitive Function (61)	46.8 (9.4; 24.4-63.9; *49.9*)
Depression (61)	49.8 (8.5; 38.2-74.3; *50-53*)
Physical Function (61)	43.6 (8.7; 25.2-61.9; *46.1*)

#1247 Efficacy of pain neuroscience education compared to conventional therapy in managing oncologic pain: A controlled clinical trial.

Leidy T Ordonez-Mora[1], Rocio Guil[2], Ilem D. Rosero[3], Marco Morales-Osorio[4], Juan M Henao-Bermudez[5], Giovanna Rivas-Tafurt[6], Juan Avila-Valencia[7], Julian Agudelo[8]

[1]Universidad Santiago de Cali, Valle del Cauca, Colombia,[2]Universidad de Cadiz, Cadiz, Spain,[3]Universidad Santiago de Cali, Cali, Colombia,[4]Universidad San Sebastian, Concepcion, Chile,[5]Instituto departamental de Bellas Artes, Valle del Cauca, Colombia,[6]Clinica de occidente, Cali, Colombia,[7]Clinica de Occiente, Valle del Cauca, Colombia,[8]Clinica de occidente, Valle del Cauca, Colombia

Background: Pain is a multifaceted sensory and emotional experience that may arise even without evident tissue injury. Among individuals undergoing cancer treatment, it represents one of the most prevalent and burdensome symptoms, frequently resulting from surgical interventions, radiotherapy, or treatment-related toxicity. Oncologic pain profoundly impacts functional capacity, emotional well-being, and overall quality of life. Given its multidimensional nature, it involves complex interactions between cognitive, affective, and neurophysiological mechanisms, including processes of central sensitization and altered pain modulation. These complexities highlight the need for integrative approaches that move beyond traditional biomedical management. Educational strategies such as Pain Neuroscience Education (PNE) have emerged as promising interventions aimed at reshaping maladaptive pain beliefs, reducing fear and catastrophizing, and fostering more effective self-management.
In this context, the present study aimed to determine the efficacy of Pain Neuroscience Education compared to conventional therapy in managing oncologic pain.
Methods: A randomized controlled clinical trial with a parallel-group design and blinded outcome assessment was performed following the CONSORT recommendations (ClinicalTrials.gov ID: NCT05581784). The intervention comprised a structured nine-session program centered on the application of neuroscience principles to pain education, based on a previously published manual. All outcome measures were collected after a 10-week period. The primary endpoint was the variation in pain intensity, assessed using the Visual Analog Scale (VAS), comparing baseline and post-intervention scores between groups.
Results: A total of eighty-two patients with oncologic pain were included in the study. The most common cancer diagnosis was breast cancer. Regarding disease stage, 63% of participants were classified as stage III, 31.8% as stage IV, and 4.5% as stage V. In the intervention group (PNE), mean pain intensity decreased from 5.32 ± 2.12 at baseline (T1) to 3.85 ± 1.98 after the intervention (T2), reflecting a statistically significant reduction of 1.47 points ($p < 0.001$). Conversely, in the control group, pain intensity values were 5.57 ± 2.29 at T1 and 5.39 ± 2.15 at T2, showing no significant change ($p = 0.46$). The reduction in pain intensity observed in the PNE group represents a clinically meaningful improvement compared with the control condition.
Conclusion: The intervention grounded in Pain Neuroscience Education (PNE) led to a statistically and clinically meaningful decrease in pain intensity. These findings support the inclusion of individualized educational approaches as a complementary component of oncologic pain management.

#1248 Perspectives on cancer survivorship: Voices of family caregivers.

Opeyemi Oreoluwa Bolajoko[1], Jada Melton[1], Mary Ellen Young[2], Folakemi T. Odedina[1]

[1]Mayo Clinic Florida, Jacksonville, FL,[2]Inclusive Cancer Care Research Equity, Jacksonville, FL

Background: Cancer survivorship requires significant contributions from family caregivers at home. This role can be burdensome because family members play a vital role in the physical, functional, and emotional well-being of patients diagnosed with cancer. Although optimum care throughout the care continuum requires significant caregiver support at home, family caregivers' contribution to survivorship care is usually neglected. We provide the preliminary outcomes of caregivers' challenges and experiences in providing care and survivorship support to Black cancer survivors. We also identified ways to provide support for family caregivers.
Methods: This qualitative study obtained information from 8 caregivers who care for Black cancer survivors who have completed treatment in the United States. The study used a phenomenological design to obtain data from participants. In-depth interviews focused on participants' lived experiences caring for Black patients with cancer. The study captured caregivers' personal stories of how they dealt with diagnosis, feelings, emotions, reactions, understanding of the disease, prognosis, and treatment options and decision process, as well as survivorship of their care recipients. All interviews were video recorded and transcribed verbatim. The transcript of each participant's interview was reviewed, analyzed, and coded, with emerging themes interpreted.
Results: The major cahllenges identified were (1) lack of knowledge of cancer, the disease and treatment course before the diagnoses; (2) home care burden, which include the challenges of combining care for a sick person at home with caring for other members of the family and taking care of domestic chores; (3) patient care navigation, including identifying healthcare professional for specialist care, adequate health insurances, scheduling doctors' appointment, transportation, insurance and treatment paperwork; (4) financial challenges, especially keeping up with job, family income reduction, increase out of pocket spendings, as well as expensive drugs and treatment co-pays. Most of the caregivers agreed that they neglected their personal health while caring for their care recipient. All caregivers wished they received more information and training on how to care for a patient with cancer. Possible solutions identified were care packets providing information on cancer and how to provide care at home, patient care navigation to social determinants of health and financial support programs, counselling for mental health and emotional support, peer support groups for caregivers, health checks, and a contact to call for support.
Conclusion: Caring for cancer patients at home is very challenging; having a care packet and caregiving training is important to support survivorship and reduce the caregiving burden experienced by family caregivers.

#1249 The inverse association between non-melanoma skin cancer and alopecia areata: A systematic review and meta-analysis.

Simonetta I. Gaumond[1], Alireza Abdshah[2], Isabella Kamholtz[2], Peyton V. Warp[2], Keyvan Nouri[3], Antonella Tosti[3], Joaquin Jimenez[4]

[1]Department of Biochemistry and Molecular Biology, Department of Biochemistry and Molecular Biology, University of Miami Miller School of Medicine, Miami, FL,[2]Dr Phillip Frost Department of Dermatology and Cutaneous Surgery, University of Miami Miller School of Medicine, Miami, FL,[3]Dr Phillip Frost Department of Dermatology and Cutaneous Surgery, Dr Phillip Frost Department of Dermatology and Cutaneous Surgery, University of Miami Miller School of Medicine, Miami, FL,[4]Department of Biochemistry and Molecular Biology, University of Miami Miller School of Medicine, Miami, FL

Non-melanoma skin cancers (NMSC), including basal cell carcinoma (BCC) and squamous cell carcinoma (SCC), are the most common malignancies worldwide and remain clinically relevant in survivorship care. While many autoimmune diseases carry increased cancer risk, alopecia areata (AA), a T cell-mediated autoimmune disease, may instead confer enhanced cutaneous tumor immunosurveillance. We conducted a systematic review and meta-analysis to evaluate NMSC risk in AA and assess its potential as a human model of immune-mediated cancer protection. PubMed, Embase, Scopus, and ClinicalTrials.gov were searched through July 2025 for observational studies reporting BCC or SCC incidence in AA versus controls. Effect estimates were pooled using random-effects models with REML and Hartung-Knapp adjustment. Heterogeneity was assessed with I^2 and leave-one-out sensitivity analyses. Eight retrospective cohorts (n = 854,000 AA patients) met inclusion criteria, four reported BCC and five SCC outcomes. Across studies, AA patients consistently demonstrated lower skin cancer incidence compared with controls (OR 0.58; 95% CI, 0.27-1.22). Pooled estimates suggested reduced risk for BCC (OR 0.43; 95% CI, 0.11-1.75) and SCC (OR 0.66; 95% CI, 0.28-1.57), though neither reached statistical significance. Between-study heterogeneity was high (I^2 > 80%), reflecting differences in study design, case ascertainment, and adjustment for UV exposure, phototype, and treatment history. Sensitivity analyses confirmed stability of the protective direction, with no evidence of publication bias detected. These findings support a possible inverse association between AA and NMSC, contrasting with malignancy patterns seen in other autoimmune conditions. AA may represent a natural model of heightened cutaneous immune surveillance, with relevance to understanding cancer risk in the context of JAK inhibition and immune signaling. Further prospective studies with standardized outcome definitions, including diverse patient populations, are warranted to validate this association and explore translational implications for cancer prevention and survivorship care.

#1250 N-acetylcysteine pharmacokinetics and neuroprotection in a translational ovarian cancer model of cancer-related cognitive impairment.

Naomi Lomeli[1], Diana C. Pearre[2], Javier J. Lepe[1], Thomas H. Taylor[1], Daniela A. Bota[1]

[1]Neurology, UCI School of Medicine, Irvine, CA,[2]Gynecologic Oncology, Providence Cancer Institute, Burbank, CA

Background: Platinum-based chemotherapy is part of the standard of care for ovarian cancer treatment, yet more than 70% of patients develop cancer-related cognitive impairment (CRCI) during and after treatment. Cisplatin-induced CRCI is associated with alterations in plasma cytokines, mitochondrial dysfunction, and glutathione depletion. In an ovarian cancer xenograft rat model, the antioxidant N-acetylcysteine (NAC; 250 mg/kg, i.p.) prevented cisplatin-induced CRCI. To inform a Phase 1 study of oral NAC for CRCI prevention in ovarian cancer patients, we compared oral and i.p. NAC administration on brain and blood glutathione, plasma cytokines, circulating NAC levels, and cognition in female rats with or without ovarian cancer.
Methods: Female RNU rats bearing SKOV3.ip1 xenografts received cisplatin (5 mg/kg, i.p.) biweekly for four cycles with or without NAC (250 mg/kg/day, i.p.) administered for five days during each cycle, 10 hours after cisplatin. Cognitive testing (novel object recognition, NOR) was performed 6-7 weeks after treatment completion. For NAC pharmacokinetic studies, 70 female non-tumor-bearing Sprague Dawley rats were randomized to vehicle, 250 mg/kg NAC i.p., and 159, 212, 265, 370, 476 mg/kg oral NAC, with or without cisplatin. Plasma, whole blood, and brain tissue were collected 2 hours after one cycle, and plasma NAC levels were quantified by mass spectrometry.
Results: Ovarian tumor-bearing rats treated with or without cisplatin (OvT+VEH, OvT+CDDP) showed reduced NOR discrimination ratios (≤0.5) compared with non-tumor-bearing controls (NT+VEH, P=0.0207). NAC prevented cisplatin-induced impairments in the NOR task (OvT+CDDP vs. OvT+CDDP+NAC, P=0.0343). Cisplatin significantly reduced hippocampal and frontal cortex glutathione levels within 48 h, which was prevented by 250 mg/kg NAC, i.p. administration. NAC did not alter cisplatin's anti-cancer activity or survival. Comparative analysis of plasma NAC levels after oral vs. i.p. administration is ongoing.
Conclusions: NAC prevents cisplatin-induced CRCI in a clinically relevant ovarian cancer rodent model. Ongoing pharmacokinetic analyses will guide the design of a Phase 1 study of oral NAC in patients with ovarian cancer.

#1251 Real-world evaluation of multimodal AI: Foundation model-driven multimodal AI for GBM, NSCLC, and PDAC.

Aakash Gireesh Tripathi[1], Asim Waqas[2], Evan W. Davis[3], Jennifer B. Permuth[4], Jack Farinhas[5], Yasin Yilmaz[6], Matthew B. Schabath[4], Ghulam Rasool[7]

[1]Machine Learning, H. Lee Moffitt Cancer Center, Tampa, FL,[2]Cancer Epidemiology, Moffitt Cancer Center, Tampa, FL,[3]H. Lee Moffitt Cancer Center, Tampa, FL,[4]Moffitt Cancer Center, Tampa, FL,[5]Diagnostic Imaging and Interventional Radiology, Moffitt Cancer Center, Tampa, FL,[6]University of South Florida, Tampa, FL,[7]Machine Learning, Moffitt Cancer Center, Tampa, FL

Purpose: Translating multimodal AI from curated research datasets to real-world clinical practice remains a critical challenge in precision oncology. In this study, we adapted HONeYBEE, a foundation model-driven multimodal AI platform, for real-world oncology workflows. We focused on three cancers, glioblastoma (GBM), non-small cell lung cancer (NSCLC), and pancreatic ductal adenocarcinoma (PDAC), using routine clinical documentation, radiology/ pathology reports, and imaging studies to improve survival prediction and cohort stratification.

Methods: We curated 3 cohorts (GBM n=160, NSCLC n=580, PDAC n=171), spanning 911 patients from single NCI-designated Cancer Center. The framework processed multimodal embeddings generated via HONeYBEE. Unlike curated research datasets, these cohorts had incomplete available data (8.2-47% missing), heterogeneous documentation and imaging protocols. We employed cross-modal attention mechanisms to dynamically learn hierarchical relationships between modalities while incorporating 99.96% dimensionality reduction. Cross-validation was used to evaluate concordance index (C-index), risk stratification for survival outcomes, and three attribution methods that quantify per-modality contributions.

Results: The framework achieved C-indices of 0.637±0.087 for GBM, 0.598±0.021 for NSCLC, and 0.679±0.029 for PDAC, demonstrating consistent performance across cancer types despite substantial missing data. Risk stratification for survival outcomes identified clinically meaningful groups with four-fold (GBM: low 28 months vs. high-risk 6 months), five-fold (NSCLC: low 60 months vs. high-risk 12 months), and three-fold (PDAC: low 100 months vs. high-risk 35 months) differences in median survival. Attribution analysis revealed disease-specific patterns reflecting clinical reality. Text reports dominated GBM predictions (43.7%), capturing critical clinical information, imaging data drove NSCLC predictions (49%), reflecting central role of CT in staging, and balanced contributions characterized PDAC (31-35% per modality), aligning with guidelines emphasizing comprehensive assessment. Patient-level attribution demonstrated that high-risk individuals relied heavily on adverse imaging features, while low-risk patients showed balanced modality contributions, providing actionable insights for clinical review.

Conclusions: This work successfully extends research from datasets to real-world clinical environments, demonstrating practical utility for treatment stratification and prognostic assessment across three challenging malignancies. Framework's modular architecture enables seamless integration with existing systems. By generating standardized patient embeddings with incomplete and heterogeneous data, we provide a scalable infrastructure for deploying multimodal AI in routine oncology care.

: Targeting DNA Repair, Cell Cycle, and Tumor Metabolism
Poster Session

#1256 A novel therapeutic approach to overcome metabolic reprogramming in lung cancer.

Nicholas Blazanin, Xiaobing Liang, **Yonathan Lissanu**

University of Texas MD Anderson Cancer Center, Houston, TX

Lung cancer remains the leading cause of cancer-related deaths. Genomic studies have identified frequent mutations in subunits of the SWI/SNF chromatin remodeling complex, particularly in *SMARCA4* and *ARID1A*, in non-small cell lung cancer, with mutations occurring in up to 33% of advanced cases. Previously we have shown that *SMARCA4*-mutant lung cancers are highly dependent on oxidative phosphorylation (OXPHOS). However, OXPHOS inhibitors as single agents have failed to show substantial efficacy in clinical trials. Thus, like other therapeutics aimed at cancer metabolism, the most feasible route for further development of OXPHOS inhibitors is through rational combination strategies. To this end, we undertook a functional genomics screen to identify combination strategies by utilizing a CRISPR-Cas9 library targeting genes with FDA approved therapeutics in genetically defined lung cancer models. Importantly, we utilized very low doses of the OXPHOS inhibitor IACS-10759 that are known to be well-tolerated in patients. Among our top hits was ROCK1/2. We show that Belumosudil, a clinically-utilized ROCK inhibitor known for its robust safety and tolerability profile, exhibits profound synergistic anti-tumor activity when combined with IACS-10759 in cell lines as well as in multiple mouse xenograft and human PDX models. Mechanistically, metabolic profiling reveals that the combination of ROCK and OXPHOS inhibition triggers bioenergetic stress and cell cycle arrest. This is primarily attributed to the inhibition of the adaptive increase in glycolysis that occurs following OXPHOS inhibition by ROCK, via suppression of GLUT1-mediated glucose uptake. Through quantitative proteomics, phospho-proteomics and kinase motif analysis, we identified several direct ROCK substrates including PPP1R12A and PPP1R12C that play critical roles in actin cytoskeleton regulation and glucose transport. Taken together, we identified the mechanistic underpinnings of a highly synergistic combination strategy that overcomes adaptive metabolic reprograming which has been a central challenge in the successful development of therapeutics targeting cancer metabolism.

#1257 Synergistic inhibition of PARP and ATM leads to unresolved DNA damage and cohesin-mediated collapse in pediatric osteosarcoma.

Janeala Morsby[1], Sona Kocinsky[2], Estevez Prado Daniel[3], John Harper[4], Charlie Wright[3], Monika Weirdl[3], Caroline Wechsler[5], Gabriela Alexe[6], Kimberly Stegmaier[6], Paul Geeleher[7], Lillian Guenther[1]

[1]Molecular Oncology, St. Jude Children's Research Hospital, Memphis, TN,[2]Tufts University, Trumbull, CT,[3]Molecular Oncology, St. Jude Childrens Research Hospital, Memphis, TN,[4]St. Jude Childrens Research Hospital, Memphis, TN,[5]University of Pennsylvannia, Philadelphia, PA,[6]Dana Farber Cancer Institue, Boston, MA,[7]Computational Biology, St. Jude Childrens Research Hospital, Memphis, TN

Osteosarcoma (OS) is the most common malignant bone tumor in children. Currently, metastatic and relapsed patients with OS have long-term survival of less than 30% with available therapies. Due to high levels of genomic instability and tumor heterogeneity, novel therapeutic development has been challenging in OS. Recently, homologous recombination deficiency (HRD) has been observed using computational signatures in OS, which has led to investigations of efficacy of PARP inhibitors (PARPi) in this disease. PARPi are FDA approved for use in other HRD-marked cancers; however, in pre-clinical models, single agent PARPi has had mixed efficacy in OS. Thus, we aimed to investigate synergistic targets with PARPi in OS, with the hypothesis that we could increase the utility of this drug class, deepen understanding of the biology of DNA damage repair (DDR) in OS, and circumvent drug resistance which is seen with many targeted therapies, including PARPi. To explore rational combinations with PARPi in OS, we performed a genome-scale CRISPR-Cas9 screen in the presence of the PARPi olaparib in two OS cell lines. *ATM* emerged as a top druggable sensitizer to PARPi across both models. We first performed lentiviral CRISPR knockout (KO) of *ATM* in OS cell lines and treated with a range of PARPi doses and observed a signal of increased efficacy to PARPi, validating our screen. Next, we tested a small molecule ATM inhibitor (ATMi), AZD1390, combined with multiple PARPi, using a novel drug synergy platform in a panel of OS including low-passage patient-derived cell lines, observing profound synergy across OS models compared to non-OS cell lines using ATP-based assays and live cell imaging. Dual ATMi/PARPi demonstrated significantly increased DNA damage by immunofluorescence, G2/M cell cycle arrest by flow cytometry, and DNA replication stress by immunoblotting (IB), which led to increased apoptosis measured by increased caspase 3/7 and annexin V dyes. Given the known contribution of ATM to regulation of the cohesin complex, we next investigated modulation of the cohesin complex by ATMi/PARPi by IB. In combination-treated cells, we observed a marked reduction in the cohesin release factor WAPL across cell lines at early time points. Bortezomib therapy rescued dual-treated cells from WAPL depletion and partially rescued apoptosis in dual treated cells, confirming proteasomal degradation in this context. Based on our data, we propose that the combination reduces cohesin unloading, thereby changing chromatin accessibility and increasing DDR, leading to unresolved DNA damage and, ultimately, apoptosis. *In vivo* work has confirmed an increase in survival in mice bearing OS tumors treated with the combination compared to control. We are repeating these experiments to confirm the clinical relevance for OS patients using synergistic low doses to achieve efficacy without toxicity.

#1258 Harnessing combinatorial nanomedicine for simultaneous BRD4 degradation and stromal disruption against pancreatic ductal adenocarcinoma.

Drishti Rathod, Ketankumar Patel

St. John's University, Queens, NY

Pancreatic ductal adenocarcinoma (PDAC) will become the second leading cause of cancer death by 2030 yet remains largely untreatable. Limited therapeutic options and desmoplastic microenvironment collectively result in poor clinical outcome. This necessitates dual targeting strategies that can simultaneously disrupt the microenvironment barrier and eliminate oncogenic protein drivers. Focal adhesion kinase inhibitor: PND 1186 was selected to compromise the tumor stromal barrier while BRD4 degrading PROTAC was explored to inhibit the proliferation. To overcome pharmacokinetic barriers, we designed a dual-route nanomedicine platform: oral self-nanoemulsifying PND-1186 (PNDnano, FAK inhibitor) and intravenous albumin-anchored ARV-825 nanoliposomes (AAnano, BRD4 PROTAC). This study aims to: (a) develop and characterize PND and ARV nanoformulations, (b) evaluate anticancer efficacy in 2D/3D PDAC models, and (c) assess therapeutic efficacy in xenograft studies. PNDnano was developed by screening different excipients and ones exhibiting superior solubility of PND were selected for developing SNEDDS. AAnano was formulated via modified hydration method using DGS-NTA-Ni for surface conjugation of histidine-tagged human serum albumin. Both nanoformulations showed 2-3-fold higher *in-vitro* cytotoxic effect in PDAC cells compared to individual drugs alone. Combenefit analysis revealed robust synergistic cytotoxicity between ARV and PND in MIA PaCa-2, achieving maximum synergy (score = 28) at 0.5 µM ARV and 2 µM PND with a combination index of 0.8. Scratch assay revealed potent anti-migratory effects, with ARV+PND achieving superior inhibition (1.9-fold in MIA PaCa-2; 2.7-fold in BxPC-3) versus monotherapies. Clonogenic assays demonstrated >90% reduction in the number and area of colonies in PDAC cells, with complete eradication in MIA PaCa-2, following ARV+PND treatment. Combination treatment showed 4.4-fold decrease in invadopodia length, enhancing inhibition in invasiveness of spheroids. 3D spheroid assays revealed significant growth inhibition with the monotherapies and ~63% reduction with combination therapy by day 8, demonstrating superior clinical relevance in PDAC. The anticancer effect of AAnano+PNDnano in the mice bearing subcutaneous tumor (MIA PaCa-2) xenograft model achieved 56.9% tumor suppression surpassing monotherapies. All treatment groups maintained stable body weights, indicating excellent tolerability with no systemic toxicity. This dual-targeting approach provides robust antitumor efficacy without systemic toxicity, addressing a critical unmet need in PDAC treatment. This strategy that simultaneously disrupts stromal barriers and eliminates oncogenic drivers, transcending conventional chemotherapy limitations and providing a translational framework for treating desmoplastic malignancies.

#1260 LIPA inhibition enhances the therapeutic efficacy of DNA-damaging agents in ovarian cancer through induction of ER stress and enhancing DNA damage.

Durga Meenakshi Panneerdoss[1], Tae-Kyung Lee[2], Khaled Mohamed Nassar[1], Gaurav Sharma[1], Scott Terry Elmore[2], Henry Neal[2], William Cole Arnold[1], Edward Kost[1], Suryavathi Viswanadhapalli[1], Jung-Mo Ahn[2], Ganesh V. Raj[3], Ratna K. Vadlamudi[1]

[1]UTHSA, San Antonio, TX,[2]UT Dallas, Dallas, TX,[3]EtiraRx, Dallas, TX

Background: Ovarian cancer (OCa) is the most lethal gynecologic malignancy in the United States, largely due to the lack of effective early detection strategies and the development of chemoresistance following initial treatment. These challenges emphasize the urgent need for improved therapeutic approaches. Recently, our team identified ERX-208, a potent tris-benzamide molecule (IC_{50}-100 nM) with strong activity against OCa cells. ERX-208 targets lysosomal acid lipase A (LIPA), inducing endoplasmic reticulum (ER) stress, disrupting protein synthesis, and promoting apoptosis. The objective of this study is to evaluate the potential of ERX-208 in enhancing the efficacy of FDA-approved chemotherapeutics.

Methods: In our study, we performed in vitro screening of 147 FDA-approved chemotherapy drugs in combination with ERX-208 to assess their effects on the viability of OCa model cells. The drug combination dose-response data were analyzed using the SynergyFinder Plus software. To validate the synergistic effects, we conducted several in vitro assays, including tests for cell proliferation, colony formation, cell cycle progression, DNA damage, comet assays, apoptosis, and invasion. Furthermore, preclinical studies were carried out using patient-derived organoids (PDO) and xenograft (PDX) models to evaluate the combination's efficacy in a more clinically relevant setting.

Results: Combination therapy screening of 147 FDA-approved chemotherapeutic agents with the LIPA inhibitor ERX-208 identified multiple synergistic drug pairs in OCa models. SynergyFinder analysis revealed strong combination sensitivity and synergy scores for several DNA-damaging agents. ERX-208 monotherapy inhibited OCa cell growth in vitro and in vivo, consistent with its mechanism of inducing LIPA-dependent ER stress. Combination treatments with paclitaxel or cisplatin further amplified these effects, significantly reducing cell viability across OCa cell lines compared to monotherapy. Mechanistic studies demonstrated enhanced gamma-H2AX accumulation, increased DNA damage, robust induction of ER stress markers, and reduced invasion following combination therapy. In PDO and PDX models, ERX-208 combined with DNA-damaging agents produced marked tumor growth suppression beyond monotherapies, confirming the translational relevance of the synergy. Furthermore, ERX-208 effectively reduced the viability of therapy-resistant OCa models in vitro and inhibited xenograft growth in vivo. These findings support ERX-208 as a potent ER stress-inducing agent that enhances the therapeutic efficacy of standard chemotherapies in OCa models.

Conclusions: Our findings demonstrate that combining ERX-208 with DNA-damaging agents significantly enhances therapeutic efficacy, highlighting the potential of ERX-208-based combination therapy for treating OCa.

#1261 Mutation-dependent sensitivity to the dual TTK/PLK1 inhibitor BAL0891 in patient-derived gastric cancer organoids.

Chan Hee Park[1], Jinsoo Jang[2], Woo Sun Kwon[1], Tae Soo Kim[3], Seunghyun Ma[4], Minkyung Kang[5], Sun Young Rha[1]

[1]Yonsei University College of Medicine, Seoul, Korea, Republic of,[2]Song-Dang Institute for Cancer Research,, Seoul, Korea, Republic of,[3]Song-Dang Institute for Cancer Research, Seoul, Korea, Republic of,[4]Sillagen Biotherapeutics, San Francisco, CA,[5]Sillajen Biotherapeutics, Inc., Jung District

Background: BAL0891 is a first-in-class dual inhibitor of threonine tyrosine kinase (TTK, Mps1) and polo-like kinase 1 (PLK1), which cooperatively regulate the spindle assembly checkpoint (SAC) to maintain mitotic fidelity. Dysregulated SAC signaling contributes to chromosomal instability and tumor progression, particularly in gastric cancer. Targeting the SAC through dual kinase inhibition has emerged as a promising approach to exploit mitotic vulnerabilities in solid tumors.
Methods: The pharmacologic effects of BAL0891 were evaluated across 40 patient-derived gastric cancer organoids representing distinct molecular subtypes. Cytotoxicity (IC_{50}) was analyzed in relation to TTK and PLK1 protein expression and compared across mutation-defined subgroups, including *KRAS*, *SMAD4*, *PTEN*, *PIK3CA*, and *BRAF* alterations identified by WGS. LC/MS-MS was additionally performed to characterize SAC-associated signaling and mitotic regulatory networks linked to BAL0891 response.
Results: Among the 40 patient-derived gastric cancer organoids analyzed, six harbored KRAS alterations, while the remaining samples were wild-type. In the KRAS-mutant, TTK expression was significantly higher in drug-sensitive organoids than in resistant ones. In contrast, PLK1 expression showed no significant association with drug response, suggesting that KRAS-driven mitotic signaling preferentially relies on TTK-mediated regulation. Excluding KRAS-mutant cases, additional alterations were detected in PTEN (n = 3), PIK3CA (n = 2), and BRAF (n = 1). In these mutation contexts, both TTK and PLK1 expression tended to be higher in resistant samples ($p = 0.078$ and $p = 0.087$, respectively), implying that enhanced PLK1/TTK activity stabilizes the SAC and promotes survival through PI3K-AKT or MAPK signaling, thereby conferring relative resistance. Overall, these findings demonstrate that the relationship between mitotic kinase expression and drug response is context-dependent: KRAS-altered tumors with high TTK expression exhibit increased sensitivity due to heightened SAC dependency, whereas PTEN, PIK3CA, and BRAF mutant tumors with elevated kinase activity maintain checkpoint stability and survival signaling, resulting in reduced responsiveness to BAL0891.
Conclusion: BAL0891 effectively disrupts mitotic checkpoint signaling through simultaneous inhibition of TTK and PLK1. The therapeutic outcome is genotype-dependent: KRAS-mutant tumors exhibit TTK-driven SAC dependency and higher sensitivity, whereas PTEN, PIK3CA, and BRAF mutants show relative resistance due to compensatory survival signaling. These findings identify SAC dysregulation as a predictive biomarker for BAL0891 responsiveness in gastric cancer.

#1262 Depletion of dominant-negative mutant p53 improves the efficacy of mutant p53 reactivators.

Allison St. John, Mrinalini Bhosale, Alejandro Parrales, Atul Ranjan, Tomoo Iwakuma

Children's Mercy Research Institute, Kansas City, KS

TP53 (p53) forms a tetramer and functions as a transcription factor to upregulate mRNA expression of genes involved in cell cycle progression and apoptosis, thereby functioning as a tumor suppressor. P53 is the most commonly mutated gene in human cancers, and approximately 75% of p53 mutations are missense mutations. When p53 is mutated, the mutant p53 (mutp53) is no longer able to bind DNA, losing its transcriptional and tumor suppressor activities. Missense mutp53 is roughly classified as DNA contact mutants with a relatively intact p53 structure and conformation or structural mutants with a misfolded p53 structure. This cancer-specific missense mutp53 represents a critical target for the development of innovative precision therapies. Mutp53-targeting reagents include “depleters” that suppress mutp53-addicted tumors by reducing mutp53 protein levels and “reactivators” or “stabilizers” that restore the transcriptional activity of p53. Depleters include HSP90 inhibitors that induce degradation of both DNA contact and conformational mutp53, as well as statins or HSP40/DNAJA1 inhibitors that primarily deplete conformational mutp53. Reactivators include APR-246 ($PRIMA1^{met}$) and arsenic trioxide (ATO). While APR-246 and ATO have been in several clinical trials, successful outcomes have not yet been reported, despite the evidence that these reactivators efficiently restore the intact conformation of p53 in culture. Thus, it remains unclear how to efficiently reactivate p53 in mutp53-expressing cancers and why the reactivated p53 cannot efficiently induce tumor suppression. We hypothesize that reactivated p53 (R-p53) is dominant-negatively bound by non-reactivated mutp53 (NR-mutp53), making the reactivator not fully effective; hence, the combination of reactivators with depleters to eliminate NR-mutp53 would improve the treatment efficacy of reactivators, leading to improved tumor suppression. To test this hypothesis, we used conformation-specific antibodies detecting NR-mutp53 and R-p53 to confirm their interactions in multiple cancer cell lines with conformational and DNA contact mutp53. Our study revealed that NR-mutp53 interacted with R-p53 in cells treated with the reactivator alone, while this interaction was eliminated when reactivators were combined with depleters. Moreover, our RT-PCR studies demonstrated that the combination of reactivator with depleters significantly increased mRNA expression of p53 downstream targets, as compared to that of the reactivator treatment alone. These results strongly suggest that the combination of reactivator drugs with depleter drugs could improve the treatment efficacy of reactivators to suppress mutp53-carrying tumors.

#1263 Development of a novel selective CDK4 inhibitor for HR+/HER2- breast cancer.

Apeng Liang #,*, Meihua Li #,*, Kai Wang, Yi Long, Hui Xu, Haoyun Li, Jian Zhu, Guangbin Liu, Ling Fang, Xi Wang, Yiming Cai, Xiang Zhang, Shengli Dong, Yu Yu, Xinlong Yang, Chao Zhou, Teng Zhou, Wei Wu, Chengshan Niu, Shaoqing Chen, Jun Li*, Yusheng Wu

TYK Medicines, Inc., Changxing, Zhejiang, China

Targeting cell cycle-dependent kinases 4 and 6 (CDK4/6) has been proven to be a successful strategy for blocking oncogenic cell cycle progression in breast cancer cells. FDA-approved CDK4/6 inhibitors have delivered significant clinical benefits in patients with HR+/HER2- breast cancer. However, despite remarkable clinical and commercial success, dual CDK4/6 inhibitors are associated with severe on-target toxicity, leading to serious adverse events (SAEs), such as neutropenia in clinical settings. The mechanism underlying these hematologic adverse events was attributed to CDK6, rather than CDK4, for its direct mediation of myeloid cell differentiation when CDK6 expression is upregulated. To avoid CDK6 toxicity, we sought to develop selective and potent CDK4 inhibitors that in ideal cases only inhibit CDK4 activity with no impact on CDK6 or other CDKs in HR+/HER2- breast cancer cells to improve the hematologic safety of the therapeutic approach targeting the cancer cell cycle. TYK Medicines has been making continuous efforts to develop better CDK4 inhibitors with higher selectivity, potency, and lower hematologic toxicity. The candidate CDK4 inhibitor discussed in this abstract exhibits strong selectivity for CDK4 over CDK6 compared to palbociclib, confirming its identity as a selective CDK4 inhibitor rather than a dual CDK4/6 inhibitor. The compound confers a dose-dependent reduction in phosphorylated RB (Ser780) in HR+/HER2-breast cancer cell lines following a 48-hour treatment with the cells. The antiproliferative effects of the candidate compounds were evaluated via CTG cell viability assays after 5-day incubation in three cell lines: MCF7, JEKO-1, and MOLM13. Palbociclib potently inhibited MCF7/T47D cells because of its dual CDK4/6 kinase activity. In contrast, the selective CDK4 inhibitor strongly inhibited JEKO-1 cells and had no inhibitory effect on MOLM13 cells expressing high levels of CDK6. In a MCF7-xenograft mouse model, the compound significantly suppressed tumor growth in a dose-dependent manner. It also exhibited synergistic antitumor effects when combined with fulvestrant, with good tolerability evidenced by stable animal body weight throughout the study. Given the genetic diversity of HR+/HER2-breast cancer patients, targeting CDK4 may present a keystone strategy in a spectrum of combinatorial therapies. Preliminary in vitro combination studies revealed that pairing the selective CDK4 inhibitor with a CDK2 inhibitor or a PI3K inhibitor produced significant synergistic inhibitory effects on MCF7 and palbociclib-resistant MCF7 cells. Optimization of the lead compound is ongoing with the goal of identifying a preclinical candidate (PCC) for IND-enabling studies.

# Apeng Liang and Meihua Li contributed equally to this work.
* Correspondence authors.

#1264 Limited apoptotic response in RBM10 wild type/deficient EGFR-mutant lung cancer patient-derived models overcome by combined EGFR and BCL-2/BCL-xL inhibition.

Jonathan Wesley Riess, Hongyong Zhang, Jasmine Diaz Sezati, Peyton Apruzzese, Dongguang Wei, Tiffany Le, Luis G. Carvajal-Carmona

University of California, Davis, CA

Background: Loss of RBM10, an RNA splicing regulator, occurs in ~8-10% of *EGFR*-mutant NSCLC and has been associated with reduced apoptosis and a poor response to EGFR-TKIs. RBM10 deficiency decreases the pro-apoptotic Bcl-xS/Bcl-xL ratio, thereby limiting osimertinib-induced cell death. We investigated whether combined inhibition of EGFR and BCL-2/BCL-xL overcomes this apoptotic defect using lung cancer organoids and PDXs harboring EGFR mutations with or without RBM10 deficiency.
Methods: Patient-derived organoids from two EGFR-mutant PDX models—LG-0591 (RBM10-deficient/RBM10 wild type) and LG-0807 (RBM10-intact)—were treated with osimertinib, ABT-263 (navitoclax), or the combination—dose-response assays (CellTiter-Glo) quantified viability. Parallel in vivo studies were performed in NSG mice bearing LG-0591 PDXs treated for 28 days. Tumors harvested on treatment days 5 and 28 were analyzed by immunoblotting for EGFR, AKT, ERK, mTOR, 4EBP1, RBM10, Bcl-2 family proteins, Ki-67, cleaved PARP, and cleaved caspase-3.
Results: RBM10-deficient, EGFR mutant organoids (LG-0591) showed reduced sensitivity to osimertinib monotherapy and minimal induction of cleaved PARP and caspase-3 relative to RBM10-normal organoids (LG-0807). RBM10 deficiency was associated with elevated Bcl-2/Bcl-xL and reduced Bcl-xS expression. ABT-263 alone showed modest activity; however, osimertinib + ABT-263 produced strong synergistic killing, restoring apoptosis and significantly lowering IC50 values in RBM10-deficient organoids. In vivo, osimertinib treatment suppressed EGFR/AKT/ERK signaling at day 5, but apoptosis remained limited in RBM10-deficient tumors, leading to tumor regrowth by day 28. ABT-263 alone modestly affected growth. The combination therapy achieved sustained suppression of downstream signaling, markedly increased cleaved PARP and cleaved caspase-3, and produced the most significant tumor regression with no observed toxicity. These effects were durable through day 28.
Conclusions: RBM10 deficiency mediates intrinsic resistance to osimertinib by impairing mitochondrial apoptosis. Combined EGFR and BCL-2/BCL-xL inhibition fully restores
apoptotic signaling and provides superior and durable antitumor activity in RBM10-deficient EGFR-mutant lung cancer, even if not RBM10 mutant. These findings support the clinical actionability of cotargeting EGFR and BCL-2/BCL-xL in patients with EGFR-mutant/RBM10-deficient NSCLC.
Keywords: EGFR, RBM10, NSCLC, osimertinib, ABT-263, BCL-xL, apoptosis, organoids, PDX

#1265 PRKDC regulates CDK2 expression and pancreatic neuroendocrine cancer sensitivity to chemotherapy.

Subin Kim[1], Mahnaz Norouzi[1], Courtney M. Townsend[2], B. Mark Evers[3], Piotr Rychahou[1]

[1]University of Kentucky, Lexington, KY,[2]University of Texas Medical Branch, Galveston, TX,[3]UK Markey Cancer Center, Lexington, KY

Background: Pancreatic neuroendocrine tumors (pNETs) frequently present with extensive inoperable metastases that develop resistance to DNA-damaging chemotherapy. This study evaluated DNA-PK inhibition as a strategy to enhance doxorubicin efficacy against metastatic tumors and examined the DNA-PK-CDK2 axis, with PRKDC identified as a regulator of CDK2 expression.
Methods: DNA double-strand breaks were induced using the topoisomerase II inhibitor doxorubicin. DNA-PK activity was inhibited with peposertib or via siRNA-mediated DNA-PK knockdown in BON and QGP-1 neuroendocrine cell lines. Transcriptomic data from DNA-PK knockdown cell lines were analyzed to identify gene expression relationships. Dose-dependent effects of doxorubicin on CDK2 levels were evaluated by western blot and confocal microscopy. The effect of DNA-PK inhibition and knockdown on doxorubicin-induced CDK2 expression was assessed by western blot. Therapeutic efficacy of combined low-dose doxorubicin (2 mg/kg, i.p.) and peposertib (100 mg/kg, oral gavage) was evaluated in a BON metastatic lung colonization mouse model using bioluminescence imaging to quantify metastatic burden.
Results: In BON and QGP-1 cells, doxorubicin consistently induced CDK2 upregulation, and both Western blotting and confocal microscopy showed a dose-dependent increase in CDK2 protein levels, implicating a chemotherapy-activated program of adaptive resistance. Transcriptomic analyses revealed a positive correlation between PRKDC (encoding the DNA-PK catalytic subunit) and CDK2 expression. Importantly, PRKDC knockdown or pharmacologic DNA-PK inhibition prevented this CDK2 induction, establishing a PRKDC-dependent mechanism of CDK2-mediated chemoresistance and identifying DNA-PK as a therapeutic target to block the adaptive response. Consistent with these in vitro findings, two cycles of low-dose doxorubicin combined with peposertib markedly suppressed pulmonary metastatic growth and limited extrathoracic dissemination in a BON lung metastasis model.
Conclusions: These findings support a role for DNA-PK in mediating CDK2 upregulation in response to chemotherapy and highlight the clinical relevance of low PRKDC and CDK2 expression with improved survival in NET patients. Collectively, these findings identify a PRKDC-CDK2 survival axis as a driver of chemoresistance and demonstrate that sustained, low-intensity DNA damage, when coupled with selective DNA-PK inhibition, disrupts this adaptive program, substantially reduces metastatic burden, and delivers more durable responses in pNETs.
AI use disclosure: Portions of this abstract were revised with the assistance of generative AI and were fully reviewed and verified by the authors.

#1268 Targeting PRMT5 enhances ferroptosis in B-cell lymphomas.

Yunxia Liu[1], Ruoyu Chen[1], Xiaoyue Gao[1], Fen Zhu[1], Qinyu Ni[1], Zhuoyan Zai[1], Paul D Bates[1], Victoria Ann Obernberger[1], Christian Capitini[1], Lixin Rui[2]

[1]Univ. of Wisconsin Madison Sch. of Med. & Public Health, Madison, WI,[2]University of Wisconsin School of Medicine, Madison, WI

Protein arginine methyltransferase 5 (PRMT5) catalyzes the symmetric arginine dimethylation of proteins to regulate gene expression. PRMT5 expression is upregulated in B-cell non-Hodgkin lymphomas, including the most common diffuse large B-cell lymphoma (DLBCL) and the currently incurable mantle cell lymphoma (MCL). Ferroptosis is a form of regulated cell death driven by the accumulation of iron-dependent lipid reactive oxygen species (ROS) on cellular membranes, distinguishing it from other types of cell death. This process is initially triggered by the inhibition of system Xc^- or GPX4 activity, which ultimately leads to cell death. Lymphoma-related pathways, such as the p53 pathway, MYC, and the PI3K-AKT-mTOR signaling pathway, are involved in the regulation of ferroptosis. We and others have shown that upregulated PRMT5 enhances cell proliferation and survival in lymphoma cells by activating various mechanisms, including the PI3K-AKT signaling pathway and MYC target genes. However, whether PRMT5 is involved in ferroptosis in B-cell lymphoma remains unknown. Therefore, understanding and targeting ferroptosis in B-cell lymphoma is an urgent clinical need. Our lab previously performed PRMT5 knockout RNA sequencing. Re-analysis of the RNA-seq data revealed several metabolic-related pathways affected by PRMT5 knockout in both OCI-Ly7 and TMD8 cells, including the fatty acid metabolism pathway. Treatment of DLBCL and MCL cells with various PRMT5 inhibitors or genetic knockdown alone did not induce lipid peroxidation but enhanced DMF-induced lipid peroxide accumulation. Interestingly, PRMT5 knockout or inhibition in DLBCL and MCL cells increased sensitivity to DMF treatment. Moreover, the combination of DMF and GSK3326595 exhibited a significant synergistic effect. Mechanistically, PRMT5 inhibition reduced system Xc^- expression by targeting the PI3K-AKT-MYC signaling pathway. To determine whether PRMT5 inhibition promotes lipid peroxidation in various cell lines in response to DMF and other ferroptosis-inducing agents (FINs), we treated multiple DLBCL and MCL cell lines with different concentrations of the GPX4 inhibitor RSL3 and the SLC7A11 inhibitor Erastin, both alone and in combination with the PRMT5 inhibitor GSK3326595. Both RSL3 and Erastin demonstrated significant synergistic effects across different DLBCL and MCL cell lines. More importantly, a combination of GSK3326695 and DMF achieved a greater anti-tumor effect compared with either drug alone in patient-derived xenograft MCL models. In summary, we demonstrate that targeting PRMT5 through pharmacological inhibition and genetic knockdown sensitizes DLBCL and MCL cells to DMF-induced lipid peroxidation and ferroptosis. These findings provide a rationale for developing a new therapeutic strategy that induces ferroptotic cell death to treat lymphoma patients with relapsed or refractory disease.

#1269 Silencing of ACACA sensitizes acute myeloid leukemia cells to venetoclax.

Akansha Jalota[1], Anna Skwarska[1], Yen Bao Huynh[2], Fumiaki Sato[3], Christina Glytsou[4], Iannis Aifantis[5], Yoko Tabe[3], Stefano Tiziani[6], Marina Konopleva[1]

[1]Department of Oncology, Albert Einstein College of Medicine, Bronx, NY,[2]Department of Nutritional Sciences, College of Natural Sciences, The University of Texas at Austin, TX,[3]Laboratory of Pathophysiology, Faculty of Pharmacy, Juntendo University, Chiba, Japan,[4]Department of Chemical Biology, Ernest Mario School of Pharmacy, Rutgers, The State University of New Jersey, Piscataway, NJ,[5]Department of Pathology, New York University Grossman School of Medicine, New York, NY,[6]Department of Nutritional Sciences, Dell Pediatric Research Institute, College of Natural Sciences & Dell Medical School, The University of Texas at Austin, Austin, TX

Introduction: Acute myeloid leukemia (AML) is an aggressive blood cancer marked by malignant myeloid stem/progenitor cell proliferation in the bone marrow, with a long-term survival rate below 30%. The FDA-approved BCL-2 inhibitor venetoclax (VEN), combined with Azacitidine, is a standard-of-care therapy in older, unfit for chemotherapy AML patients, but this treatment achieves only about 50% clearance of minimal residual disease. AML cells rely on oxidative phosphorylation and fatty acid oxidation, along with other amino acids metabolism for survival. Acetyl-CoA-carboxylases are known to regulate fatty acid metabolism. While ACACA is involved in fatty acid synthesis, ACACB governs fatty acid oxidation. Thus, we hypothesize that fatty acid oxidation (FAO) inhibition by ACACA knockdown might sensitize AML cells to BCL-2 inhibitors (Venetoclax).
Methods: Knockout of ACACA was performed using CRISPR Cas9 system in AML cell lines and patient samples. Cell viability was assessed by CTG assay and colony assay was performed using methylcellulose-enriched media. Medium and long-chain fatty acid profiling was conducted via a gas chromatography mass spectrometry approach. Seahorse assay was performed to measure fatty acid oxidation.
Results: Genome-wide CRISPR screen in human AML cells treated with BH3 mimetics combinations (Glytsou et al., Cancer Discovery, 2023), demonstrated enrichment of fatty acid metabolism. We found that genes involved in both FAO, such as CPT1b, and fatty acid synthesis, such as Acetyl-CoA Carboxylase Alpha (ACACA), are top significant synthetic lethal targets with VEN/AZA. We first tested the efficacy of ND-630, known to inhibit ACC carboxylases (ACACA and ACACB) in combination with VEN. The combination was found to be effective in VEN-resistant THP-1, OCI-3 and SKM-1 cell lines in 1% FBS media. In THP-1 cell line, ND-630 reduces colony formation by 35±8%, VEN by 29±6% and the combination yielded 62±3% reduction. VEN-resistant patient samples (n=2) responded well to the combination as compared to VEN-sensitive primary AML samples (n=1). Ablating ACACA through CRISPR Cas9 system led to a reduction in colony formation in THP-1 and SKM-1 cells (36±8% and 28±4%, respectively). There was 26±4% reduction in cell viability in ACACA KO VEN-resistant primary AML cells treated with lower doses of Ven (100nM) as compared to the control. Additional primary samples are being tested and will be reported. Knockdown of ACACA resulted in a reduction of fatty acid synthesis in primary AML sample. Seahorse fatty acid oxidation assay was performed in THP-1 cell line after ACACA knockdown. We found that maximal respiration in ACACA knockdown cells was reduced compared to control cells, suggesting limited fatty acid oxidation.
Conclusion: These findings suggest that VEN-resistant AML rewire metabolism through ACACA-driven fatty acid synthesis and that inhibition of Acetyl-CoA-carboxylase restores VEN sensitivity in AML.

#1270 Immunotoxin GB13 Targets GBM and H3.3K27M DIPG with the activation of Golgi-to-ER retrograde transport pathways.

Nanyun Tang[1], Yue Hao[2], Valerie DeLuca[2], Charles Caleb Shaffer[3], Randy Schrecengost[4], Michael E. Berens[2]

[1]Clinical Genomics and Therapeutics Division, Translational Genomics Research Institute, Phoenix, AZ,[2]TGen (The Translational Genomics Research Institute), Phoenix, AZ,[3]Beckman Research Institute, City of Hope, Duarte, CA,[4]Targepeutics, Inc, Hummelstown, PA

GB13, an IL13Ra2-targeted immunotoxin, shows potent therapeutic potential against Glioblastoma (GBM) and H3.3K27M mutant Diffuse Midline Glioma (DIPG). The toxin, comprising Pseudomonas exotoxin A and IL-13 mutein, binds to IL13Ra2, which is frequently overexpressed on the surface of GBM and DIPG with histone 3.3 (H3.3) K27M mutation. GB13 is internalized through this binding and processed via Golgi-to-ER pathway. The active domain of the toxin is translocated to ADP-ribosylating eukaryotic elongation factor 2 (eEF-2) and halts protein synthesis, inducing apoptosis. *In vitro* drug dose-response assays demonstrated a 280-300 fold differential response in patient-derived GBM and DIPG models. Sensitivity correlated with IL13RA2 abundance and the H3.3K27M mutation. Gene Set Enrichment Analysis confirmed that sensitivity is linked to activated Golgi-to-ER retrograde transport pathways, the required trafficking route for GB13's cytotoxic release. Furthermore, these transport pathway scores negatively correlate with patient age in the TCGA-GBM dataset, suggesting demographic dependence. PBT29, the most sensitive H3.3K27M mutant DIPG line, showed the highest transport pathway enrichment. GB13's selective activity and its association with a Golgi-to-ER retrograde transport, as a predictive signature make it a highly promising candidate for these devastating diseases. The presence of these molecular signatures of vulnerability (mSov) could serve as an inclusion criterion for patient enrollment in clinical trials.

#1272 Targeting autophagy sensitizes cancer cells to proteasome inhibitors.

Jing Li[1], Yi Bao[1], Ava Cardenas[2], Ariba Saoda[2], Fengyu Su[1], Yuanyuan Qiao[1], Xuhong Cao[1], Arul M. Chinnaiyan[1]

[1]Michigan Center for Translational Pathology, University of Michigan, Ann Arbor, MI,[2]University of Michigan, Ann Arbor, MI

Eukaryotic cells preserve proteostasis and organelle integrity through two interconnected degradation machineries: the ubiquitin-proteasome system (UPS) and autophagy. Together, these pathways constitute a coordinated quality control network that orchestrates the selective turnover of misfolded proteins and damaged organelles. Proteasome inhibitors have achieved clinical success in hematologic malignancies, but their activity is limited by intrinsic and acquired resistance, which varies substantially across cancer types. In this study, we hypothesize that autophagy inhibition can overcome resistance to proteasome inhibition. Mechanistically, proteasome inhibition induces endoplasmic reticulum (ER) stress in sensitive cancer cells but fails to elicit this response in resistant ones. Co-treatment with autophagy inhibitors restore ER stress induction and synergistically enhances cytotoxicity in the resistant cells. In multiple in vivo cancer models including pancreatic and triple-negative breast cancers, combined inhibition of autophagy and UPS synergistically inhibited tumor growth and improved survival outcomes. At the molecular level, this dual blockade activates the PERK-pEIF2α-ATF4 signaling axis effectively, leading to apoptotic cell death. Collectively, our findings identify a mechanistic basis for overcoming resistance to proteasome inhibitors and provide a rationale for future clinical evaluation of autophagy-UPS combinatorial therapy across diverse malignancies.

#1273 Antitumor activity of PARPi and POLQi combination therapy in a BRCA-mutated PDAC model.

Chani Stossel[1], Dikla Atias[1], Yulia Glick-Gorman[1], Josep Forment[2], Lee Mulderrig[2], Gali Altman[1], Hanita Ovadia[1], Liora Chouchan[1], Elina Haimov-Talmoud[1], Tamar Beller[1], Talia Golan[1]

[1]Sheba Medical Center, Tel Hashomer, Israel,[2]Oncology Targeted Discovery Bioscience, AstraZeneca, Cambridge, United Kingdom

Pancreatic ductal adenocarcinoma (PDAC) is one of the deadliest cancers. BRCA1/2-mutated PDAC is a unique subgroup with exceptional responses to platinum chemotherapy/PARP inhibition (PARPi). A spectrum of responses is observed, from refractory to long term-remission Despite this promising strategy, most patients develop resistance. Inhibition of DNA-polymerase theta (POLQ), a key component in DNA-repair, may further sensitize cancer cells to platinum/PARPi in combination with a PARP1-selective (AZD5305/saruparib) or non-selective PARP inhibitor (olaparib). We conducted a long-term *in vivo* experiment testing PARPi and POLQi combination utilizing a platinum-sensitive, BRCA2 mutated PDAC PDX model to investigated the potential to prolong response and reduce resistance. Simultaneously, this combination was tested in accordance to the maintenance approach in clinical setting: a cisplatin induction followed by maintenance PARPi, POLQi and their combinations. A total of 159 tumor-bearing mice were randomized to: vehicle control; olaparib; saruparib; POLQi; saruparib+POLQi; olaparib+POLQi, and maintenance treatment groups by cisplatin induction for four weeks followed by switch to: vehicle control; POLQi, saruparib and saruparib+POLQi (n=8-19/group). POLQi alone had no effect on tumor growth. Both PARPi (olaparib/saruparib) monotherapies significantly delayed tumor growth, with saruparib displaying a trend towards prolonged effect vs olaparib (saruparib 69% complete responders (CR) vs control p=0.0014; olaparib 47% CR vs control p=0.0052). Combination therapy of olaparib and POLQi also showed a trend towards extended duration of response compared to olaparib monotherapy (olaparib vs control p=0.005; olaparib+POLQi vs control p=0.00017). Acquired resistance developed in seven mice (22%) with PARPi monotherapy (olaparib n=4, saruparib n=3) and was only seen in five (13%) mice in combination therapy with POLQi (saruparib+POLQi n=3; olaparib+POLQi n=2). In the maintenance study, cisplatin induction initiated a strong anti-tumor effect that was not maintained after switching to vehicle (22% CR by end of study). Addition of saruparib maintenance alone or in combination with POLQi significantly extended the duration of responses (60-70% CR by end of study). Our pre-clinical *in vivo* data indicate that 1) saruparib displayed a trend towards increased efficacy vs olaparib; 2) combined PARPi and POLQi therapy showed a trend towards extending the duration of response and delaying resistance; 3) cisplatin induction produced a strong antitumor effect which remained with maintenance PARPi±POLQi. Tumors with acquired resistance are undergoing extensive molecular analyses to determine the mechanisms of resistance.This preclinical study enables further understanding and investigation of this unique subtype with the aim to develop alternative treatments to prevent acquisition of resistance.

#1274 Integrated multiomics analysis identifies defective CoQ10 interactome in human kidney cancers.

Gregory M. Miller[1], Nischal Mahaveer Chaud[1], Catarina M. Quinzi[2], Brian Berman[1], **Vivek K. Vishnudas**[1], Vijay Modur[1], Vlatcheslav Akmaev[1], Niven R. Narain[1], Stephane Gesta[1], Michael A. Kiebish[1]

[1]BPGbio, Waltham, MA,[2]Columbia University, New York, NY

Defective energy metabolism has been established as a hallmark of cancer; however, the specific genetic basis underlying this relationship across cancers remains unclear. Ubiquinone (CoQ10) plays an essential role in regulating efficient generation of mitochondrial ATP and reactive oxygen species levels. Multi-omics assessment of the CoQ10 biosynthesis pathway genes in The Cancer Genome Atlas Program (TCGA) revealed Kidney Clear Cell Carcinoma (KIRC) and Kidney Papillary renal cell carcinoma (KIRP) as cancers that demonstrated a significant relationship between poor prognosis and low expression or copy number deletions in the CoQ10 biosynthesis genes. However, the link between deletions and low expression in CoQ10 biosynthesis genes and poor outcomes remains unknown. Towards this aim, we defined the CoQ10 interactome as a set of 37 protein encoding genes that bind with CoQ10, along with enzymes involved in downstream pathways impacted by CoQ10 homeostasis, based on literature review. We then investigated this CoQ10 interactome for their association with outcomes for KIRC and KIRP patients in TCGA datasets. First, patients were grouped into low/high expression groups based on median gene expression levels for the indication. We then investigated the association of outcome measures Overall Survival (OS) and Progression Free Interval (PFI) with expression groups in KIRC (n=530) and KIRP (n=288) patients. Our results found that low gene expression in 21 of 37 CoQ10 interactome genes in KIRC, and 3 of 37 CoQ10 interactome genes in KIRP were associated with significantly worse OS and PFI. Next, we analyzed copy number deletions and their association with patient outcomes. Patients were grouped as having a deletion in the gene or not. In line with the prior analysis, we observed that deletions in 9 of 37 CoQ10 interactome genes, and 12 of 37 CoQ10 interactome genes were associated with significantly worse OS and PFI in KIRC and KIPR, respectively. Notably, we observed that deletions in ETHDH (KIRC OS HR = 1.95, *q-value* = 0.0045, n deletion = 75; KIRP OS HR = 5.42, *q-value* = 0.00008, n deletion = 28) and PRODH (KIRC OS HR = 2.06, *q-value* = 0.0144, n deletion = 41; KIRP OS HR = 2.71, *q-value* = 0.01866, n deletion = 60) were associated with significantly poorer OS and PFI in both KIRC and KIRP. These results demonstrate that CoQ10 and its interactome are significantly impacted in kidney cancer subtypes and deletions or low expression in these key genes are associated with poorer survival outcomes for patients. This data indicates potential for therapeutic intervention with BPM31510, a nanoparticle formulation of oxidized CoQ10, which is currently in Phase 2 clinical trials for oncology indications.

#1275 Phospholipase D1 overexpression drives metabolic survival and stress resistance in cervical cancer.

Sung Wan Kang[1], Dong Woo Kang[1], Yu-na Noh[1], Young-Jae Lee[1], Min-Seo Lee[1], Yong-Man Kim[2], Shin-Wha Lee[1]

[1]Asan Medical Center, University of Ulsan College of Medicine, Seoul, Korea, Republic of,[2]CHA Bundang Medical Center, CHA University School of Medicine, Seoul, Korea, Republic of

Background: Cervical squamous cell carcinoma (SCC) and adenocarcinoma (ADC) are clinically and biologically distinct subtypes, yet the metabolic drivers of SCC aggressiveness remain poorly understood. Phospholipase D1 (PLD1), a lipid-modifying enzyme involved in oncogenic signaling and cancer metabolism, has been reported to be elevated in various malignancies. However, its subtype-specific expression pattern and functional relevance in cervical cancer have not been clearly delineated.
Methods: PLD1 expression was evaluated using TCGA datasets and validated in primary cervical tumors by qRT-PCR, PLD activity assays, and immunohistochemistry. Functional studies were performed in primary SCC and ADC cells using shRNA-mediated PLD1 knockdown or a PLD1-selective inhibitor. Apoptosis, ATP levels, glycolytic activity, clonogenic survival, and invasion were measured under basal and metabolic stress conditions.
Results: PLD1 was significantly overexpressed in SCC compared with ADC at the mRNA, protein, and enzymatic activity levels. PLD1 inhibition markedly decreased SCC cell survival, whereas ADC cells exhibited minimal sensitivity. PLD1 blockade reduced glycolytic flux and ATP production and increased apoptosis under serum starvation, glucose restriction, and hypoxia. PLD1 knockdown also impaired clonogenic survival and suppressed invasion. These effects were further enhanced by co-treatment with the glycolysis inhibitor 2-deoxy-D-glucose, highlighting a strong dependency of SCC cells on PLD1-mediated metabolic regulation.
Conclusions: PLD1 is selectively upregulated in cervical SCC and serves as a key regulator of glycolysis, energy homeostasis, and adaptation to metabolic stress. The pronounced metabolic dependence on PLD1 identifies it as a promising therapeutic target in SCC, and PLD1 inhibition may effectively exploit metabolic vulnerabilities unique to this tumor subtype.

#1276 Dual epigenetic-kinase targeting to overcome resistance and immune evasion in hepatocellular carcinoma.

Kyounghyun Kim[1], HongDuck Yun[2], Gabin Kwon[2]

[1]University of Arkansas for Medical Sciences, Little Rock, AR,[2]Pharmacology & Toxicology, University of Arkansas for Medical Sciences, Little Rock, AR

Hepatocellular carcinoma (HCC) incidence and mortality continue to rise in the United States, largely driven by increasing rates of chronic liver disease, viral hepatitis, and metabolic dysfunction. Despite progress in immunotherapy, first-line immune checkpoint inhibitor (ICI)-based combinations benefit only a subset of patients, and many individuals with HCC are ineligible due to contraindications such as varices, autoimmune disorders, or immunosuppression. Second-line agents, including the multi-kinase inhibitor lenvatinib, provide only modest and short-lived clinical responses. These persistent challenges—tumor heterogeneity, rapid development of therapeutic resistance, and limited options for patients with hepatic dysfunction—underscore the urgent need for innovative, durable, and widely accessible treatment strategies for HCC. Epigenetic dysregulation mediated by the histone demethylase LSD1 (KDM1A) is a key driver of HCC stemness, plasticity, and immune evasion. LSD1 is frequently overexpressed in HCC and strongly associated with poor survival. Notably, high LSD1 expression correlates with adverse clinical outcomes in both $CD8^+$ T cell-enriched and $CD8^+$ T cell-exhausted tumors, highlighting its role in establishing a cold or immunosuppressed tumor microenvironment. Thus, we hypothesize that LSD1 inhibition will suppress aggressive tumor phenotypes, limit intratumoral heterogeneity, delay therapeutic resistance, and enhance anti-tumor immunity, with enhanced efficacy when combined with lenvatinib. Our preliminary data support this hypothesis. Pharmacologic inhibition or genetic depletion of LSD1 with or without Lenvatinib treatment significantly reduces HCC cell proliferation and aggressive tumor behaviors—including migration, invasion, tumor sphere formation, and xenograft tumor growth. Importantly, the combination of LSD1 inhibition and lenvatinib further enhances $CD8^+$ T cell-mediated immune surveillance and restores immune killing capacity against HepG2 cells, which are typically resistant to immune-mediated cytotoxicity. These findings provide a strong mechanistic and translational rationale for advancing LSD1-targeted epigenetic therapy, alone or in combination with lenvatinib, as a promising therapeutic strategy for patients with advanced HCC who are underserved by current ICI-based treatments. By directly targeting LSD1-driven epigenetic reprogramming and overcoming key resistance mechanisms, this project addresses a critical unmet medical need and establishes a robust foundation for future clinical evaluation of combined LSD1-Lenvatinib therapy.

#1277 Overcoming glioblastoma resistance by targeting its heterogeneity with a synergistic approach: TTFields stimulation and tmCLIC1 impairment.

Francesca Cianci[1], Elisa Meraviglia[1], Guido Rey[2], Stefania Castiglione[1], Antonio M. Polito[1], Sara Torabi[3], CHIARA MERCURIO[3], Dietmar Krex[3], Tatiana Vorobyov[4], Kerem Wainer-Katsir[5], Martin Gabay[3], YAARA PORAT[3], Roni Blatt[3], Ori Braten[6], Tullio Florio[3], Itai Tzchori[3], **Michele Mazzanti**[1]

[1]University of Milan, Milan, Italy,[2]University of Milan, Milano, Italy,[34]Novocure, Baar, Switzerland,[5]Israel,[6]Novocure, Haifa, Israel

Glioblastoma (GB) is the most malignant and aggressive primary brain tumor in adults, characterized by rapid growth, diffuse infiltration, and strong resistance to treatments. As a result, most patients inevitably experience tumor recurrence, and median survival remains around 15 months. In this context, Tumor Treating Fields (TTFields) have emerged as an innovative and noninvasive therapy. Although clinical use of TTFields has shown survival benefits, most patients relapse, highlighting adaptive mechanisms that enable GB cells to survive prolonged treatment. To better understand the molecular basis of TTFields resistance, we created an experimental model that mimics clinical exposure by applying long-term TTFields stimulation to patient-derived GB cultures representing different molecular subtypes. Initial responses to therapy varied among cell lines; however, after extended exposure, all resistant groups developed a typical mesenchymal-like phenotype, indicating a shared adaptive response. Transcriptomic analysis of paired patient samples before and after treatment further showed that TTFields-treated tumors tend to upregulate pathways related to myelin formation, consistent with a mesenchymal-like phenotype. While these pathways reflect a shift toward a more invasive and therapy-resistant state, they offer limited options for direct drug targeting. We identified the transmembrane form of Chloride Intracellular Channel 1 (tmCLIC1) as a potential target. tmCLIC1 has been linked to GB stem cell metabolism, regulation of oxidative stress, and tumor growth, suggesting it plays a critical role in maintaining resistance to TTFields. Based on these findings, we tested the therapeutic benefit of concomitant treatment of TTFields and metformin, a well-known antidiabetic drug that inhibits tmCLIC1 in GB. Remarkably, this combination produced a strong synergistic effect, significantly reducing GB cell viability in vitro and slowing tumor growth in vivo. These results show that prolonged TTFields exposure pushes GB cells toward a mesenchymal-like, therapy-resistant phenotype and highlight tmCLIC1 as a key player in this adaptive process. Targeting tmCLIC1 with metformin offers a promising strategy to sensitize resistant cells and improve the effectiveness of TTFields. This work provides a mechanistic framework for developing combination therapies to overcome treatment resistance and enhance long-term outcomes for GB patients.

#1279 Exploiting Wnt-induced DNA damage repair vulnerability with PARP inhibitors to overcome chemoresistance in multiple myeloma.

Kaushlendra Tripathi, Gabriella Santos, Camila Pacocha, Shadika Panta, Emma Younger,, Trevor Stepanyan,, Lauren Fowler,, Brandon Smith,, Ryan O'Hare,, Xavier Noel Pin Harry,, Daniel Ross,, Bidyut Mohanty,, David Eagerton,

Microbiology and Immunology, Edward Via College of Osteopathic Medicine-Carolinas Campus, 350 Howard St. Spartanburg, SC 29303, Spartanburg, SC

Multiple Myeloma (MM) is a plasma cell malignancy characterized by the clonal proliferation of malignant plasma cells in the bone marrow, leading to the excessive production of monoclonal immunoglobulin. This proliferation and the subsequent interaction with the bone microenvironment result in significant end-organ damage, classically represented by the CRAB criteria: Calcium elevation (hypercalcemia), Renal failure, Anemia, and Bone lesions (lytic lesions, pain, and fractures). It is a highly aggressive and lethal cancer, notorious for high recurrence rates and a lack of effective targeted therapies. While PARP inhibitors (PARPi) are potent agents, their clinical benefit is narrowly restricted to the small patient subset harboring BRCA mutations. We present a strategy to expand PARPi efficacy in MM. We discovered that the Wnt signaling transcription factor, beta-catenin, controls the expression of the critical Fanconi Anemia DNA repair protein, FANCD2 and cohesion protein CTCF in MM cells. Crucially, inhibiting beta-catenin in initially resistant MM cells (those that are homologous recombination, or HR, proficient) induces a BRCA-like deficiency known as BRCAness and severe replication stress. This combination—beta-catenin inhibition paired with PARPi—shows enhanced DNA damage, striking synergistic lethality in cell models, and powerful anticancer activity in organoid models. This dual-targeting approach offers a novel and effective strategy to overcome resistance in MM.

#1280 Pathway-based radiosensitivity and therapeutic targeting in triple-negative breast cancer subtypes.

Jaitri Joshi[1], Jenna Jacoby[2], Shan Xu[2], Noelle Francois[2], Tiziana DeAngelis[2], Anuradha Shastri[2], Adeseye Adekeye[2], Nicole L. Simone[2]

[1]University of Minnesota Medical School, Minneapolis, MN,[2]Sidney Kimmel Cancer Center, Thomas Jefferson University, Philadelphia, PA

Triple-negative breast cancer (TNBC) is an aggressive and heterogeneous disease with subtypes that differ in therapy response and radiosensitivity. Experimental models suggest that pathway-level modulation may provide more actionable insights into resistance mechanisms. Using syngeneic, aggressive murine models of breast cancer (4T1), 60 female Balb/c mice were randomized after palpable tumor formation to six treatment arms: ad libitum feeding (AL), radiation alone (8 Gy), caloric restriction (CR, 30% reduction in intake), CR+RT, curcumin alone, and curcumin+RT. CR evoked a marked delay in tumor growth, with AL mice reaching a 1 cm^3 tumor volume at ~24 days post-injection, while CR mice reached this threshold at ~37 days. CR also increased overall survival and markedly reduced pulmonary metastases: at 35 days post-injection, the total metastatic burden was 1360 mm^3 in AL-fed mice compared to 150 mm^3 in CR mice. Transcriptome profiling of CR-treated tumors revealed 18 dysregulated pathways, including downregulation of c-MYC, PIK3CA, and androgen receptor, suggesting a mechanistic basis for radiosensitization. Tumor volume trajectories in curcumin-treated groups revealed non-monotonic growth patterns, while curcumin combined with a 3-dose 2 Gy radiation regimen between days 6-10 resulted in a flatter post-radiation trajectory. During the radiation window, curcumin alone tumors expanded by +815 mm^3, whereas curcumin + RT increased by +568 mm^3, representing a ~30% smaller rise. Over the full 20-day study, curcumin + RT showed a 28% lower cumulative volume increase (1026 vs 1434 mm^3) and a reduced daily growth rate (51 vs 72 mm^3/day). These trends suggest that curcumin may modulate stress adaptation and survival signaling under radiation exposure. Mouse weights remained stable across all arms, supporting tolerability. In conclusion, pathway-level interventions such as caloric restriction and curcumin demonstrate potential to enhance radiosensitivity in preclinical TNBC models. Therefore, interventions such as caloric restriction and curcumin may enhance radiosensitivity by modulating pathways relevant to established radioresistant BL2 and M TNBC subtypes. Ongoing cell line studies in HCC1806 (BL2) and MDA-MB-231 (Mesenchymal) can test whether these mechanisms observed in vivo are recapitulated in defined subtype models. By refining these strategies and integrating pathway biology into subtype classification, translational radiosensitization approaches may be improved.

: Liquid Biopsy: Multi-Analyte and Multi-Omic
Poster Session

#0094 Liquid biopsy profiling of the tumor microenvironment to determine response to immunotherapy regimens across solid tumors.

Erin L. Brown[1], Wubing Zhang[1], Abul Usmani[2], Noah Earland[2], Ayesha Hashmi[3], Chibuzor Olelewe[3], Anushka Viswanathan[3], Pradeep S. Chauhan[3], Minji Kang[1], Chloe B. Steen[4], Hyun Soo Jeon[1], Susanna Avagyan[1], Irfan Alahi[3], Nicholas P. Semenkovich[5], Matteo Bergsagel[3], Janella C. Schwab[1], Chloe M. Sachs[2], Kaushal Parikh[3], Faridi Qaium[3], Peter K. Harris[2], Antonella Bacchiocchi[6], Qingyuan Cai[7], Andrew J. Gentles[1], Rondell P. Graham[3], Peter C. Lucas[3], Ryan C. Fields[8], Jacob J. Orme[3], Aaron S. Mansfield[3], Mario Sznol[6], Ruth Halaban[6], David Y. Chen[2], Aaron M. Newman[1], Aadel A. Chaudhuri[3]

[1]Stanford University School of Medicine, Stanford, CA,[2]Washington University in St. Louis, St. Louis, MO,[3]Mayo Clinic, Rochester, MN,[4]Oslo University Hospital and University of Oslo, Oslo, Norway,[5]Medical College of Wisconsin, Milwaukee, WI,[6]Yale University School of Medicine, New Haven, CT,[7]Columbia University, New York, NY,[8]University of Rochester School of Medicine, Rochester, NY

Background: Spatial cellular ecosystems in the tumor microenvironment (TME) form dynamic signaling hubs that critically influence cancer disease progression and response to therapy, including response to immune checkpoint inhibitors (ICIs). However, tumor sampling bias and the impracticality of acquiring serial tumor biopsies have made it challenging to profile the TME clinically. To address this challenge, we developed Liquid EcoTyper, a multi-analyte AI framework to quantify TME spatial cellular ecosystems—termed spatial ecotypes (SEs)—noninvasively from cell-free DNA (cfDNA) methylation data.
Methods: In previous work, we discovered nine spatial ecotypes, including SEs associated with ICI response (e.g., SE7 with benefit, SE4 with resistance), and quantified them from 1,249 bulk tumor RNA-seq profiles of melanoma, non-small cell lung cancer (NSCLC), and bladder cancer (BC) patients (*Cancer Res* (2025) 85 (8_Supplement_1): 153). Here we trained Liquid EcoTyper, an interpretable deep learning model, to transfer SE profiling to cell-free DNA using CpG methylation profiles. Performance was quantified using simulated and real data, including methylation profiles (EM-seq) of plasma cfDNA paired with tumor biopsy-derived SE levels determined by EM-seq (n=20 pairs) or 10x Visium (n=15 pairs). Clinical outcome prediction was evaluated using pretreatment plasma from patients treated with ICI alone (n=78 melanoma pts), chemotherapy and ICI (n=25 NSCLC pts), and enfortumab vedotin and ICI (n=10 localized muscle-invasive BC (MIBC) pts). Tumor mutational burden (TMB), tumor PD-L1, or circulating tumor DNA (ctDNA) were profiled as a comparator where possible.
Results: We observed striking concordance between plasma-derived SE levels and tumor biopsy-confirmed SE levels from the same patients, demonstrating that liquid biopsy analysis of cfDNA methylomes can recapitulate TME spatial biology. Underscoring specificity, no reliable SE signal was detectable from peripheral blood mononuclear cells. In pre-ICI plasma, liquid SE levels were significantly associated with ICI-based response (SE7) versus resistance (SE4) in patients with melanoma, NSCLC, and MIBC, with a mean cross-cancer area under the curve (AUC) of 0.87 for SE7 (range 0.8-0.97) and 0.81 for SE4 (range 0.76-0.85)—far surpassing TMB, tumor PD-L1, and ctDNA in evaluable patients, both in binary analyses of response and multivariable models of survival. Our results also showed potential to predict pathologic complete response in the neoadjuvant setting.
Conclusion: Liquid EcoTyper is a scalable noninvasive AI-based framework for spatiotemporal assessment of the TME. By enabling TME-informed risk stratification without surgical biopsies, Liquid EcoTyper has potential to enable more precise and actionable decision making in patients with solid tumors.

#0095 PlasmaCHORD- A machine learning method for identifying clonal hematopoiesis variants in liquid biopsies.

Daniel J. Rabizadeh[1], Jenna VanLiere Canzoniero[1], Ilias Ziakas[1], Jaime Wehr[1], Archana Balan[1], Amna Jamali[2], Blair V. Landon[1], Susan Combs Scott[1], Gavin Pereira[1], Vincent K. Lam[1], Christine L. Hann[1], Christine M. Lovly[3], Jessica Tao[1], Patrick M. Forde[1], Joseph C. Murray[1], Mark Sausen[4], Gerrit A. Meijer[5], Geraldine Vink[6], Remond J. A. Fijneman[5], Victor E. Velculescu[1], Jillian Ayn Phallen[1], Robert Scharpf[1], Valsamo Anagnostou[1]

[1]Johns Hopkins University School of Medicine, Baltimore, MD,[2]Sidney Kimmel Comprehensive Cancer Center, Baltimore, MD,[3]Vanderbilt University Medical Center, Nashville, TN,[4]LabCorp, Baltimore, MD,[5]Department of Pathology, Netherlands Cancer Institute, Amsterdam, Netherlands,[6]Research, Netherlands Comprehensive Cancer Organisation, Urecht, Netherlands

Introduction: Genomic profiling of circulating tumor DNA (ctDNA) through liquid biopsies has become an important diagnostic method in clinical oncology. However, detection of variants related to clonal hematopoiesis (CH) is a major confounder that impairs the clinical utility of liquid biopsies. Strategies that reduce biological noise from CH in plasma NGS include deep sequencing of matched WBC DNA and/or tumor tissue sequencing. While these methods effectively distinguish most CH variants, the need for extra biospecimens and sequencing raises costs and limits feasibility.

Methods: Using a training cohort of 426 variants identified in ctDNA NGS from 225 patients with stage I-IV solid tumors, we developed plasmaCHORD, a machine learning model (MLM) that includes fragmentomic, variant, and patient-level features to distinguish between tumor- and CH-origin for mutations detected by fixed gene panel hybrid capture NGS. Model performance was assessed by comparison to the reference origin of each plasma variant determined from matched WBC and tumor NGS. Following locking the model parameters, we applied plasmaCHORD to an independent validation cohort of 1,412 plasma variants detected in 114 patients with metastatic cancers, as well as to cfDNA NGS from patients enrolled in a prospective liquid biopsy-informed clinical trial (NCT05585684).

Results: PlasmaCHORD predicted tumor versus CH-origin in the training set with high accuracy (cross-validated AUC=0.94), outperforming individual features such as variant allele frequency and canonical CH genes. Model performance remained robust when restricted to mutant DNA fragments supported by 3-5 mutant reads (AUC = 0.84). plasmaCHORD was locked for evaluation using a score of 0.5 as cutoff for distinguishing tumor- versus CH-origin variants. In the independent validation cohort, the locked model maintained similar overall accuracy (AUC=0.9) with a sensitivity of 82%, specificity 80.3% and accuracy of 80.2%. Our approach was shown to be highly reliable in classifying variant origin in clinically actionable genes not canonically associated with CH, including *AKT1, ATM, BRCA1, BRCA2,* and *EGFR,* as well as adjudicating cellular origin for *TP53* mutations that are encountered in both solid and hematologic malignancies. Performance was consistent across cancer types, sequencing platforms, mutation classes, and a wide range of allele fractions. When applied to clinically challenging cases in the context of a precision oncology clinical trial, plasmaCHORD precisely determined variant origin, preventing mismatches with genotype-targeted therapies.

Conclusions: plasmaCHORD, a multi-feature machine-learning classifier, can significantly enhance the ability to identify *bona fide* tumor variants in routine plasma-only NGS, addressing a critical need in implementing liquid biopsy-guided therapy by minimizing misinterpretation caused by CH.

#0096 Real time multimodal ctDNA and imaging assessment enables adaptive treatment in HPV related oropharyngeal cancer.

Bill H. Diplas[1], David N. Brown[1], Xin Pei[1], Yingjie Zhu[1], Achraf Shamseddine[1], Chiharu Graybill[2], W. Michael Korn[3], Emily Westheimer[2], Luc GT Morris[1], Richard J. Wong[1], Sean M. McBride[1], Alan L. Ho[1], Heiko Schoder[1], Eric Sherman[4], Robert Daber[2], Nora Katabi[1], Jorge Reis-Filho[1], Britta Weigelt[1], Nancy Lee[1], Nadeem Riaz[1]

[1]Memorial Sloan Kettering Cancer Center, New York, NY,[2]Labcorp, San Francisco, CA,[3]Biocartis, Itasca, IL,[4]Memorial Sloan-Kettering Cancer Center, New York, NY

Purpose: Circulating tumor DNA (ctDNA) has emerged as a sensitive biomarker for minimal residual disease detection, but its potential for real-time adaptation during curative therapy remains unexplored. Integrating ctDNA dynamics with imaging could enable more precise, risk-adapted treatment modifications beyond current radiological monitoring alone. HPV-associated oropharyngeal cancer (OPC) presents an ideal context given high cure rates, active treatment de-escalation efforts, and protracted chemoradiation courses allowing mid-treatment adaptation. We sought to determine whether longitudinal ctDNA profiling integrated with multimodal MRI could inform response-adapted treatment strategies.

Methods: A total of 158 patients with HPV OPC were enrolled on a personalized de-escalation trial (NCT03323463). Blood samples for ctDNA analysis were collected pre-treatment and weekly during therapy, with 980 longitudinal samples obtained from 119 patients over up to 126 weeks (mean 8.2 samples/patient). We developed a dual Personalized Cancer Monitoring (PCM)-HPV ctDNA assay combining patient-specific tumor-informed variant detection (average 47 variants/patient) with probes targeting high-risk HPV subtypes, especially E6 and E7 genes of HPV-16 and HPV-18, both using anchored multiplex PCR (AMP) followed by high-throughput sequencing with Invitae (now Labcorp, San Francisco, CA). Weekly MRIs (T2-weighted) were performed concurrently to determine tumor volume.

Results: Integrating somatic mutations with viral ctDNA detection increased baseline ctDNA detection from 80.3% (HPV ctDNA only) and 89.4% (PCM ctDNA only) to 93.9%. Baseline circulating HPV levels correlated with tumor volume, apoptotic signaling, necrosis, and primary tumor viral load (combined R^2=0.54). During treatment, ctDNA showed broader dynamic range and faster kinetics than volumetric imaging. Critically, absolute ctDNA fraction at week 2 of treatment predicted patients requiring treatment intensification (p=0.0003). A multimodal model integrating on-treatment ctDNA assessment and imaging improved identification of patients with high-risk disease, surpassing either modality alone.

Conclusions: Early on-treatment ctDNA dynamics capture aggressive disease biology during a critical window for adaptation. Multimodal integration of molecular and imaging assessments provides superior risk stratification, demonstrating that they capture complementary biology early in therapy and establishing a framework for real-time treatment personalization.

#0098 Surveillance for recurrent bladder cancer using Oncuria-Monitor, a urine-based multiplex immunoassay.

Sunao Tanaka[1], Charles Rosser[1], Yair Lotan[2], Menghan Liu[3], Takashi Kobayashi[4], Sima P. Porten[5], Yuki Kita[6], Yingye Zheng[7], Zhen Zhang[8], Hideki Furuya[1]

[1]Cedars-Sinai Medical Center, Los Angeles, CA,[2]Associate Professor of Urology, UT Southwestern Medical Ctr., Dallas, TX,[3]Fred Hutchinson Cancer Center, Seattle, WA,[4]Postdoctral Research Fellow, Dept. of Urology, Kyoto University Graduate School of Medicine, Kyoto, Japan,[5]UCSF, San Francisco, CA,[6]Institute for Virus Research, Kyoto Univ., Kyoto, Japan,[7]Fred Hutchinson Cancer Research Ctr., Seattle, WA,[8]Associate Professor, Dept. of Pathology & Oncology, Johns Hopkins University School of Medicine, Baltimore, MD

Introduction - Over 50% of patients with non-muscle invasive bladder cancer (NMIBC) will have a recurrence, necessitating a rigorous surveillance schedule. As urinary cytology's performance is poor, cystoscopy is standard of care in surveilling these patients. Oncuria-Monitor, a liquid biopsy to detect recurrent bladder cancer from a single voided urine sample demonstrated favorable performance.
Methods- To investigate whether Oncuria-Monitor, a multiplex immunoassay that detects a bladder cancer associated diagnostic signature composed of 10 proteins in voided urine could improve bladder cancer detection while surveilling patients with a history of bladder cancer. From February 2017 through August 2020, 7 academic, private practice, and hospital facilities in the US and Japan prospectively enrolled 300 consecutive patients with a history of bladder cancer into this longitudinal study, which followed patients for two years. Diagnosis of bladder cancer recurrence, based on cystoscopy with biopsy, was accepted as the reference standard. At each cystoscopic clinic visit during the two years, patients provided a urine sample for analysis of Oncuria-Monitor (analyzed in a blinded manner), BladderChek and urine cytology. The performance of Oncuria-Monitor was compared with BladderChek and urine cytology as an aid to cystoscopy to detect recurrent bladder cancer.
Results - Recurrent bladder cancer was diagnosed in 93 of the 300 patients (31%) by histopathological evaluation. Oncuria-Monitor detected 61 of 92 cancers with a sensitivity 74.2% (95% CI, 67.5-81.8%), specificity of 39.2% (95% CI, 34.6-43.1%) and negative predictive value (NPV) of 73.9% (95% CI, 68.6-79.9%), while sensitivity, specificity and NPV of BladderChek were 12.9%% (95% CI, 7.9-17.8%), 99.1% (95% CI, 98.1-99.8%) and 66.1% (95% CI, 63.9%-70.8%), respectively and sensitivity, specificity and NPV of urinary cytology were 28.8% (95% CI, 21.1-36.7%), 97.0% (95% CI, 95.3-98.4%) and 71.1% (95% CI, 62.7%-83.8%), respectively.
Conclusions - In this large prospective trial, Oncuria-Monitor, had a substantially superior sensitivity compared to both BladderChek and urinary cytology in detecting recurrent bladder cancers.

#0099 Enhanced detection of EML4-ALK fusions through integration of complex genomic rearrangements in DNA-based assays.

Aidan C. Manning, Sante Gnerre, Jamie Hutchins

Guardant Health Laboratory, Redwood City, CA

Introduction: *ALK* fusions, particularly *EML4-ALK*, are well-established therapeutic biomarkers in non-small cell lung cancer (NSCLC) and other malignancies. In DNA-based fusion detection, genomic rearrangements at *ALK* loci can be complex, often involving non-canonical or fragmented configurations. These include events where *EML4* and *ALK* breakpoints are both detected, but occur at separated genomic positions, sometimes bridged by intergenic sequences or intervening genes. Such configurations may still yield functional *EML4-ALK* transcripts yet fall outside canonical DNA-based fusion-calling rules. In this study, we explore the potential impact of broadening reporting criteria to include these distanced non-canonical *EML4-ALK* rearrangements and assess their clinical relevance.

Methods: We analyzed paired DNA and RNA sequencing data from 7,810 tissue samples (Guardant360 Tissue; Guardant Health, Inc. Palo Alto, CA) and DNA sequencing data from 151,517 liquid samples (Guardant 360 Liquid; Guardant Health, Inc. Palo Alto, CA) from advanced stage patients across cancer types to determine the prevalence of *EML4-ALK* fusions. DNA-based fusions were classified as canonical (*EML4-ALK* with direct adjacency) or non-canonical (*EML4-ALK* with separated intra-chromosomal breakpoints). For tissue samples with paired RNA data, we compared results across the two assays to evaluate concordance and to determine whether RNA evidence supported transcriptionally active *EML4-ALK* fusions from these complex, non-canonical DNA events.

Results: Among pan-cancer tissue samples, 45 (0.57%) harbored canonical *EML4-ALK* fusions, while 5 (0.06%) contained non-canonical EML4-*ALK* rearrangements with preserved *ALK* kinase domains. All five were confirmed by RNA and found exclusively in lung cancers. In liquid, 612 (0.40%) cases with a canonical event and 55 (0.04%) with non-canonical events were observed; 91% retained a complete kinase domain, and 73% were found in lung cancer patients. The genomic distance between *EML4* and *ALK* breakpoints typically fell within a few kilobases to several megabases but within the same chromosomal context, suggesting structural complexity. Including non-canonical events improved fusion detection sensitivity by ~13% in tissue and ~8% in liquid while maintaining high cancer-type specificity.

Conclusions: A subset of *EML4-ALK* fusions exhibit non-canonical, intra-chromosomal breakpoints detectable at the DNA level yet yield functional, targetable, *EML4-ALK* fusion products at the RNA level. These rearrangements preserve the *ALK* kinase domain and are highly enriched in NSCLC, supporting their biological and therapeutic relevance. Expanding DNA fusion criteria to capture these complex, functional events could enable the identification of additional *ALK*-positive NSCLC patients eligible for targeted therapies by NGS, improving precision oncology outcomes.

#0100 Blood-based integration of epigenomic profiles, TMB, and MSI to predict immune checkpoint inhibitor response in advanced non-small cell lung cancer (aNSCLC).

Sean Gordon, Jing Wang, Shile Zhang, Marisa Juntilla, Tingting Jiang, Matthew Ellis, Vishnu Ramani, Reagan Barnett, Bernard Herrman, Justin Odegaard, Darya Chudova

Guardant Health, Palo Alto, CA

Introduction. Immune checkpoint inhibitors (ICIs) have transformed cancer treatment, yet identifying patients most likely to benefit remains challenging. Established biomarkers such as tumor mutational burden (TMB) and microsatellite instability (MSI) have performance limitations. We hypothesized that combining MSI and TMB with epigenomic features of tumor-intrinsic immune regulation and the tumor microenvironment from pretreatment plasma would improve prediction. We developed and validated a multimodal immunotherapy response score (MIRS-Score) that integrates MSI, TMB, and epigenomic signatures (Guardant360 Liquid) to identify patients likely to respond to ICI alone or in combination with chemotherapy.

Methods. From the de-identified GuardantINFORM database we identified 695 advanced NSCLC (aNSCLC) patients treated with first- or second-line ICI monotherapy or ICI+chemotherapy and randomly split them into training (n=483) and test (n=212) sets. A literature-curated, data-driven epigenomic signature associated with real-world time to treatment discontinuation (rwTTD) was combined with MSI and TMB to train the multimodal model. Patients ≥80th MIRS percentile were labeled MIRS-High. Cox proportional hazards models adjusted for sex, age, therapy type (mono vs combo), line of therapy, and baseline tumor fraction provided adjusted hazard ratios (aHR); median rwTTD was estimated by Kaplan-Meier.

Results. In the independent test set (n=212), MIRS-High patients had longer rwTTD (median 8.7 vs 5.1 months; aHR 0.61, 95% CI 0.41-0.93, p=0.02) and improved overall survival (OS) (aHR 0.33, 95% CI 0.16-0.68, p<0.005). In the ICI monotherapy subgroup (n=69), MIRS-High showed median rwTTD 11.0 vs 4.9 months (aHR 0.31, 95% CI 0.13-0.75, p=0.01) and longer OS (aHR 0.18, 95% CI 0.04-0.79, p=0.023). MIRS-High was not associated with rwTTD in patients treated with chemotherapy alone (aHR 1.16, 95% CI 0.94-1.44, p=0.18).

Conclusions. A pretreatment plasma-based score combining MSI, TMB, and epigenomic signatures identifies aNSCLC patients with superior outcomes on ICI and outperforms MSI or TMB alone. The ICI treatment-specific stratification and strong association with both rwTTD and OS support the clinical utility of this multimodal approach, warranting further evaluation to assess the potential for guiding ICI treatment decisions.

#0101 Fragmentomics-based cancer type and subtype classification in 60,000 cell-free DNA samples.

Zhenjia Wang, Kevin Cabrera, Yanmei Huang, Daniel S. Lieber, Justin Y. Newberg, Ethan S. Sokol, Zoe Fleischmann

Foundation Medicine Inc., Boston, MA

Purpose: Tissue-of-origin prediction and tumor subtyping enable more precise treatment selection, especially for cancers of unknown primary (CUP) or without a defined subtype, though these remain a challenge in liquid biopsy applications. Current genomic approaches include methylation profiling or whole-genome sequencing, which require additional laboratory workflows on top of comprehensive genomic profiling, or may utilize multiple detected somatic alterations, which may not be present in low tumor fraction liquid biopsy samples. Cell-free DNA fragmentation patterns reflect tissue-specific chromatin architecture and gene expression programs. We evaluated whether fragmentomic features could enable cancer type and subtype classification on our comprehensive genomic profiling platform.

Methods: We analyzed 60,000 FoundationOne® Liquid CDx samples and extracted fragmentomic features for research use only across 10,510 genomic target regions. Disease classification was performed in lung, breast, prostate, and colorectal cancer using a feedforward neural network classifier with an 80/20 training-test split using cross-entropy loss. Subtype classifiers were developed in lung cancer for histological subtype and in breast cancer for hormone receptor status.

Results: We developed a 4-disease classifier using fragmentomic features in samples with circulating tumor DNA (ctDNA) fraction of 1% or greater. A high AUC was achieved across diseases (lung: 0.95, breast: 0.97, prostate: 0.97, colorectal: 0.97), with performance maintained even at low shed level (ctDNA fraction of 1-2%, AUCs 0.94-0.98). The lung histological subtype classifier achieved >90% accuracy in distinguishing between adenocarcinoma, squamous cell carcinoma, and small cell carcinoma. A breast cancer hormone receptor status classifier achieved >95% accuracy using inferred status from genomic data.

Conclusions: Fragmentomic features in liquid biopsy samples enable accurate cancer type and histological subtype classification at ≥1% tumor fraction without requiring somatic variant detection. This approach has promise to address unmet needs in precision oncology.

#0102 TAPS+ enables direct 5mC/5hmC-resolved genomic and methylation profiling of CNS tumors in CSF-derived ctDNA and FFPE.

Johnathan Rafailov[1], Eloise Freitag[1], Aditya Deshpande[1], Kevin Hadi[1], Camila Fang[1], Alexa Oviedo[1], Emma Hanley[1], August Kolb[1], Neha Dhasmana[1], Hannah Weiss[1], Chanel Schroff[1], Yiying Yang[1], Jonathan Serrano[1], Kazimierz Wrzeszczynski[1], Stergios Zacharoulis[2], Daniel Orringer[1], Alexandra M. Miller[1], Marcin Imielinski[1], Matija Snuderl[1]

[1]NYU Langone Health, New York, NY,[2]Columbia University Irving Medical Center, New York, NY

DNA methylation profiling has become a critical tool in the classification of CNS tumors, helping to refine diagnoses when histology or imaging are inconclusive. In parallel, liquid biopsy approaches analyzing circulating tumor DNA (ctDNA) from cerebrospinal fluid (CSF) offer minimally invasive windows into tumor biology, with applications in diagnosis, treatment monitoring, and relapse detection. A unified method that profiles both methylation and somatic alterations from low-input DNA—such as CSF-ctDNA and FFPE—would provide substantial clinical value. TET-Assisted Pyridine-Borane Sequencing (TAPS+) enables such integrated profiling through a bisulfite-free workflow that preserves DNA integrity while detecting CpG methylation, mutations, indels, copy-number changes, and gene fusions from a single library. We applied TAPS+ to 139 CSF samples and 61 FFPE CNS tumors to evaluate analytical performance and clinical utility.

Methods: CSF samples were collected through the Perlmutter Cancer Center liquid biopsy program and FFPE CNS tumors from archival tissue. TAPS+ libraries were prepared from 1-100 ng DNA using the Watchmaker Genomics kit and sequenced to 10-80× depth. Somatic variants were called using the nf-gOS pipeline. The Rastair methylation framework was extended to incorporate strand-discordance logic and probabilistic CpG scoring to distinguish true variants from methylation-derived C>T transitions.

Results: Across six matched FFPE tumors, Heidelberg classifier confidence improved after applying our CpG-probability and strand-discordance model, increasing from a mean of 0.20 to 0.81, with all samples gaining 0.50-0.79 and low-confidence calls converted to high-confidence predictions. CpG methylation sensitivity improved from 0.78 to 0.99 while maintaining high specificity (0.998→0.991), enabling accurate discrimination of methylation-derived artifacts from true variants. In CSF-derived ctDNA, excluding 11 QC failures, TAPS+ detected ≥1 tissue-confirmed variant in 43 of 67 evaluable samples (64%), while 24 (36%) were ctDNA-negative despite adequate coverage. TAPS+ also recovered canonical CNS tumor drivers across tissue and CSF, including 1p/19q codeletion, trisomy 7, chromosome 10 loss, EGFR and MET amplification in GBM, ERBB2 amplification, IDH pathway mutations, MN1::CXXC5 and EGFRvIII fusions, and MGMT promoter methylation concordant with array-based calls.

Conclusions: TAPS+ enables accurate, bisulfite-free profiling of methylation and somatic alterations from low-input and degraded DNA. Improved classifier performance in FFPE tumors and reliable variant recovery in CSF support TAPS+ as a unified genomic-epigenomic assay.

#0103 A multiomic ensemble-based approach for high-specificity detection of clonal hematopoiesis in cfDNA liquid biopsy.

Patrick C. Fiaux, Mingyang Cai, Jeffrey L. Werbin, Andrew Gross, Che-Yu Lee, Marisa Juntilla, Tingtin Jiang, Reagan Barnett, Errin Lagow, Shile Zhang, Martina Lefterova, Darya Chudova

Guardant Health, Palo Alto, CA

Introduction: Variants arising from clonal hematopoiesis (CH, or CHIP) can be misclassified as tumor-derived in liquid biopsy, and are a challenge especially in expanded gene panels. Sequencing both buffy coat and plasma samples can help adjudicate CH but is costly and limited by the sensitivity of buffy coat sequencing at low allele fractions and its inability to capture somatic variants of non-tumor and non-peripheral blood origin. To address this we developed a high-specificity plasma-only CH classifier for late-stage cancer patients and applied it to clinical data for insights into CH prevalence and potential clinical impact.
Methods: This multiomic classifier categorizes non-germline variants as CH- or tumor-derived and is an ensemble model leveraging fragmentomics, methylation tumor fraction (mTF), variant allele frequency (VAF) and variant- and sample-level metadata from over 250,000 Guardant Health samples and public data bases (GnomAD, COSMIC). A total of 1033 samples consisting of paired buffy coat and plasma (N=686) or paired tissue-plasma (N=305) from patients with cancer, and samples from cancer-free individuals (N=42) were used for training and testing, reflecting the age (median: 65) and cancer type distribution of the intended use population. Population-level CH characteristics were evaluated in 30,000 late-stage cancer samples (median age: 67).
Results: Feasibility results of 185 testing samples showed panel-wide sensitivity and specificity over 90% in genes with recurrent CH variants (N≥6). In nearly 30,000 late-stage cancer samples, CH variant rates were elevated in prostate cancer relative to other cancer types. Somatic variant counts increased with rising mTF, whereas CH variant counts remained relatively stable. In samples with mTF of 1% or higher, our approach revealed that for 16.9% of samples the maximum variant allele frequency (VAF) corresponded to a CH variant. Finally, we recapitulated previously reported findings that lymphoid-associated CH variants increase less rapidly with age compared to myeloid-associated CH variants.
Conclusion: We present a plasma-only CH classifier, applied on cancer patients run on the Guardant360 Liquid test (GuardantHealth, Palo Alto, CA). Feasibility data shows panel-wide sensitivity and specificity above 90%, enabling population-scale characterization of CH. Notably, in almost 17% of samples with mTF of 1% or greater the lead variant was determined to be non-tumor-derived, highlighting that this approach allows for disambiguation of CH variants that contribute to total VAF in cfDNA (maxMAF).

#0104 A machine learning approach to predict and mitigate artifact variants for molecular residual disease detection.

Violeta B. Guthrie, Aamir Shahpurwalla, Daryanaz Dargahi, Onur Sakarya, Spenser Alexander, Tina Wang, Fei Lu, Alexander Hsieh, Ryan Ptashkin, Matthew Rabinowitz, Eser Kirkizlar, Ahmet Zehir

Natera, Inc., Austin, TX

Tumor-informed molecular residual disease (MRD) detection requires removal of artifacts from tissue whole-genome sequencing (WGS), which can cause false positive calls in plasma, even in healthy donors (HDs). To address this, we developed a machine-learning framework to score the reliability of tissue variants, thereby improving the specificity and sensitivity of tissue-informed MRD detection. We used retrospective WGS data from 47 tumor and matched normal (T&MN) samples across a diverse set of cancer types. Somatic single nucleotide variants (SNV) were identified via a consensus calling strategy from multiple variant callers. We extracted variant features from each caller relating to signal amount and quality, and subsequently engineered additional features to qualify strand bias, variant- and locus-specific characteristics. To generate training labels, SNV were evaluated in matched patient plasma and 107 HD plasmas. Variants with high mean VAF across the HD plasma samples were labeled as likely artifacts (~16k), while those with high VAF in the matched patient plasma were labeled as true tumor variants (~187k). An extremely randomized trees model was then trained using 17 informative, uncorrelated features. Model performance was measured by calculating the area under the curve (AUC) from a receiver operating characteristic (ROC) analysis. Our model distinguished true tumor variants from likely artifacts with a cross-validated ROC AUC of 0.94 and an average precision of 0.99. Key predictive features from the tissue included tumor VAF, mutant allele count, and a read orientation quality metric. In each patient, the model-derived confidence score demonstrated a strong and negative correlation with the mean VAF in the HD plasma samples (median Spearman $\rho = -0.30$), outperforming a previous method (median $\rho = -0.17$). This work provides a data-driven framework that systematically ranks and filters tissue variants by their likelihood of being artifacts. By enhancing the reliability of mutation calls from the tissue sample, this method can improve the accuracy of tissue-informed MRD detection.

#0105 Quantification of circulating tumor DNA (ctDNA) in patients using cancer-specific, methylation-based, tissue-free tests for the detection of molecular residual disease (MRD).

Princy Parsana, Tzu-Chun Chen, Nathan Liang, Amanda Kennedy, Veronica Rodriguez, Jie Zhang, Boris Gutman, Ehsan Haghshenas, **Garima Kushwaha**, Breeana L. Mitchell, Minetta Liu, Ehsan Tabari, Joshua Babiarz, Trupti Kawli, Johannes G. Reiter, Matthew Rabinowitz, Alexey Aleshin

Natera, Inc., Austin, TX

While MRD detection by differential methylation patterns has been shown to predict disease recurrence, clinical decision-making and disease management are increasingly dependent on the exact level of the measured biomarker. We assessed quantitative results by methylation-based MRD assays designed for colorectal (CRC), breast, lung, and muscle-invasive bladder cancer (MIBC). Each cancer-specific, methylation-based, tissue-free ctDNA assay uses next-generation sequencing to query regions of the human genome that are differentially methylated in patients with colorectal, breast, lung, or MIBC cancer compared to cancer-free individuals. Plasma samples from Signatera-tested cancer patients with stage I-IV disease (CRC N=105, breast N=112, lung N=113, MIBC N=60) and from cancer-free individuals (N=223, sex-matched for breast cancer) were analyzed in a cross-validation setup. We compared ctDNA levels measured by the methylation-based assay (estimated by the fraction of differentially methylated alleles for circulating cell-free DNA targets across regions, DMAF) with those from a bespoke, tumor-informed ctDNA assay (SignateraTM, measured as variant allele fraction, VAF), which served as the reference, by calculating the mean squared error (MSE) and Pearson's Correlation Coefficient (ρ). For each comparison of the cancer-specific, tissue-free, methylation-based assay with the personalized tumor-informed assay, DMAF and VAF were strongly correlated for patients with CRC (VAF median [range]: 1.43% [0.003-8.26%], MSE: 0.064, ρ: 0.955), breast cancer (VAF median [range]: 1.08% [0.002-7.80%], MSE: 0.161, ρ: 0.863), lung cancer (VAF median [range]: 0.93% [0.005-12.9%], MSE: 0.179, ρ: 0.829), and MIBC (VAF median [range]: 2.33% [0.005-9.26%], MSE: 0.079, ρ: 0.954). Among patients with breast cancer, the correlation between DMAF and VAF was maintained across subtypes, including HR+ (MSE: 0.132, ρ: 0.888), HER2+ (MSE: 0.272, ρ: 0.815), and triple-negative (MSE: 0.109, ρ: 0.897). Similarly, the correlation between DMAF and VAF was strong across lung cancer subtypes, non-small cell lung cancer (MSE: 0.207, ρ: 0.802) and small cell lung cancer (MSE: 0.069, ρ: 0.941). For all cancer-specific, tissue-free, methylation-based assays, DMAF levels were independent of patient characteristics such as sex (excluding breast), age, and stage (I-III), as well as cell-free DNA input. These data demonstrate that the abundance of differential methylation in patients with CRC, breast, lung, or MIBC cancer correlates with tumor-informed ctDNA levels, supporting each tissue-free methylation-based assay as a promising tool for informing prognosis and patient management. Future studies will investigate the quantitative abilities of the tissue-free assay in different patients with specific clinicopathological features.

#0106 Integrated plasma multi-omics profiling identifies circulating predictive biomarkers and biological pathways associated with treatment response in NSCLC.

Laura Heeb[1], Polina Shichkova[2], Sandra Schar[2], Luca Rass[2], Arthur Viode[2], Martin Mehnert[2], Tobias Treiber[2], Esther Wortmann[3], Gordian Adam[3], Alice Limonciel[3], Markus Joerger[4], Jana Musilova[4], Stefanie Hayoz[4], Anurag Gupta[1], **Yuehan Feng**[2], Alessandra Curioni-Fontecedro[5]

[1]Faculty of Science and Medicine, University of Fribourg, Fribourg, Switzerland,[2]Biognosys AG, Schlieren, Switzerland,[3]Biocrates Life Sciences GmbH, Innsbruck, Austria,[4]Swiss Group for Clinical Cancer Research (SAKK), Bern, Switzerland,[5]Clinic of Oncology, HFR Hospital Fribourg, Fribourg, Switzerland

In non-small cell lung cancer (NSCLC), identifying circulating predictive biomarkers is critical to optimize patient selection and improve therapeutic outcomes. Plasma-based biomarkers offer a minimally invasive and serially accessible approach for monitoring treatment response; however, the low abundance of disease-relevant analytes within a background of highly abundant plasma proteins presents significant analytical challenges. Highly sensitive and reproducible multi-omics assays are therefore required to detect subtle but biologically relevant changes associated with therapy.

To address this, we implemented a plasma multi-omics workflow integrating unbiased mass spectrometry (P2 DIA-MS), the NULISA inflammation panel, and targeted metabolomics using the Biocrates MxP Quant 1000 kit. This workflow was applied to longitudinal plasma samples from patients with NSCLC enrolled in the multicenter phase II clinical trial SAKK 17/18. Parallel profiling quantified approximately 6,000 plasma proteins, 250 inflammation-related markers, and more than 1,200 metabolites and lipids, enabling cross-platform integration of proteomic, cytokine, and metabolic signatures.

For predictive biomarker discovery, we applied a machine learning framework to integrate proteomic, inflammatory, and metabolic data. Incorporation of multi-omics features improved the stratification of responders versus non-responders compared with single-omic models, underscoring the complementary nature of each dataset. To further investigate biological relationships among omics layers, we evaluated several data integration methods, including Multi-Omics Factor Analysis (MOFA), to identify shared sources of variation and linked biological pathways. This analysis revealed coordinated processes connecting plasma proteomic changes with inflammatory and metabolic networks. For example, immune activation signatures arising from the integration of unbiased proteomics with inflammation markers, and metabolic stress adaptation reflected in proteomic-metabolomic associations.

In conclusion, this plasma multi-omics approach demonstrates the potential of integrated proteomic, inflammatory, and metabolic profiling to identify predictive circulating biomarkers and to elucidate biological mechanisms of treatment response in NSCLC. The workflow provides a scalable and clinically applicable strategy for biomarker discovery and response monitoring in oncology.

#0107 An expanded negative prediction algorithm for actionable mutations utilizing genomic and epigenomic profiling in cfDNA.

Andrew M. Gross, Hao Wang, Brandy Freschi, Keelia Clemens, Marisa Juntilla, Martina Lefterova, Justin Odegaard, Darya Chudova

Guardant Health Laboratory, Redwood City, CA

Introduction: When using cell-free DNA (cfDNA) for comprehensive genomic profiling, it is important to differentiate between true biomarker-negative status and absence of the biomarker due to low tumor shed. This could inform whether treatment decisions can be made in the absence of tissue testing, potentially impacting time to treatment and cost of diagnostic workup. Here we expand our 'negative prediction' algorithm to eleven tumor types, leveraging both epigenomic and genomic signals to provide a posterior confidence of a sample being truly negative for specific clinically actionable biomarkers.

Methods: The algorithm utilizes population prevalence of specific alterations, locus-specific sequencing coverage, sample-level epigenomic tumor fraction, and sub-detection level genomic evidence to inform the estimate of an alteration and posterior probability for the absence of clonal, somatic FDA-approved biomarkers. Leveraging a clinical cohort of >80,000 cfDNA samples (Guardant360 Liquid, Guardant Health, Palo Alto, CA) across 11 tumor types, we compiled prior likelihood tables for actionable variants spanning diverse classes. This builds on the previous release on colorectal carcinoma and non-small lung cancer to include breast, prostate, pancreatic, bladder, endometrial, ovarian, gastric/gastroesophageal, cholangiocarcinoma, and melanoma tumor types. We expanded our probabilistic approach to model the likelihood of homozygous deletions, and refined our approach towards assessing microsatellite instability, fusions, and focal amplifications.

Results: Positivity rates for clinically actionable biomarkers varied across tumor types from 5% in pancreatic cancer to 47% in breast cancer. Among negative samples, at least 49% of samples were associated with either a biomarker-positive or a 'confident negative' status (confidence >90%). Variability in confidence of negative samples was associated with tumor shedding profiles, as well as biomarker prevalence and composition, with more complex variants, such as homozygous deletions and gene fusions, reducing confidence levels. As an initial accuracy assessment, we compiled a cohort of >350 subjects with matched tissue and plasma genotyping results, among which 81/84 (96%) of confident negative samples were confirmed as negative in tissue. Finally we assessed discordances between plasma and tissue, which highlighted clonal/resistance dynamics as the major source of discrepancies.

Conclusion: Here we demonstrate our ability to assess the confidence of biomarker negative samples across diverse cancer types. This helps address a known potential limitation for liquid biopsy and may be able to assist in therapy making decisions and accelerate time to treatment initiation, particularly in cases where tissue NGS is not available.

#0108 Fragmentomics powers improved classification of somatic mutations in liquid biopsy.

Mouses Stamboulian, Anton Valouev, Tingtin Jiang, Jamie Hutchins

Bioinformatics, Guardant Health, Palo Alto, CA

Introduction: Accurate discrimination between somatic and germline variants in cell-free DNA (cfDNA) is critical for precision oncology. Somatic variant calling in liquid biopsy can be challenging, particularly for variants with high mutant allele frequency (MAF) in high tumor fraction samples. We developed a fragmentomics-based machine learning model to improve somatic variant classification in liquid biopsy.

Methods: We benchmarked our model on 4,250 clinical samples from 3,313 unique patients processed on Guardant360 Liquid (Guardant Health, Palo Alto, CA), where variant germline status could be confidently derived from longitudinal data. Training data comprised 5,253 unique variants; independent test data included 11,612 variants. We engineered 55 fragmentomics features and multiple classifiers were evaluated; optimal performance was demonstrated with logistic regression with L2 penalty using fragment length and relative VAF features. We chose a cutoff threshold for classification scores to maintain less than 10% false positives by the model. The model was integrated as an additional correction step to re-evaluate variants classified as germline by a baseline calling algorithm.

Results: Starting with a truth set of 26,900 variants from 2,874 unique samples whose somatic or germline origin were known from longitudinal data, 22,687 had a truly somatic origin and 4,213 were germline. Our baseline calling algorithm assigned germline status to 770/22,678 somatic variants and likelihood of mis-assignment was associated with a high ctDNA tumor fraction. The fragmentome-assisted approach was able to 'rescue' 558 of the mis-assigned variants including 226 with direct clinical actionability. In terms of sensitivity (true somatic variant/true somatic variant+somatic variant called germline) and specificity (true germline variant/true germline variant+germline variant called somatic), our approach improved sensitivity compared to the baseline calling algorithm from 96.61% to 99.07%, while specificity decreased from 99.00% to 93.38%. Despite the drop in specificity, accuracy and F1 score increased by 1.18% and 0.76%, respectively. The logistic regression model demonstrated robustness across cancer types and varying fragment profiles, with the most predictive features being di-nucleosome fragment lengths and relative allele frequencies over fragments ranging between 180 to 220 bases.

Conclusions: Inclusion of model-based fragmentomics signals in a cfDNA germline-somatic discrimination caller significantly improves somatic variant detection sensitivity while maintaining high accuracy, enabling confident reporting of additional clinically actionable alterations. The boost in sensitivity at the expense of specificity is clinically acceptable given the intended use of the test for detection of targetable somatic alterations.

#0109 Integrative analyses of the cfDNA fragmentome and TCR repertoires capture chemo-immunotherapy response in diffuse pleural mesothelioma.

Jinny Huang[1], Jennifer Li[1], James R. White[1], Shashikant Koul[1], Gavin Pereira[1], Nisha Rao[1], Jennie Yao[1], Julie R. Brahmer[1], Robert B. Scharpf[1], Rachel Karchin[1], Victor E. Velculescu[1], Zhouxin Sun[2], Suresh S. Ramalingam[3], Patrick M. Forde[1], Noushin Niknafs[1], Valsamo (Elsa) K. Anagnostou[1]

[1]Sidney Kimmel Comprehensive Cancer Center, Johns Hopkins University School of Medicine, Baltimore, MD,[2]Dana-Farber Cancer Institute, Boston, MA,[3]Winship Cancer Institute of Emory University, Atlanta, GA

Background: Immunotherapy-containing therapies have shown promise for patients with unresectable diffuse pleural mesothelioma (DPM), yet there are no reliable strategies to monitor therapy response. By expanding the compendium of cancer-associated alterations profiled, including genome-wide fragmentation patterns, cell-free DNA (cfDNA) whole genome sequencing (WGS) enables tracking of tumor dynamics. In tandem, while understudied, T cell clone dynamics may be informative in capturing early immunotherapy response.

Methods: Using 314 tumor and peripheral blood biospecimes, we analyzed serial plasma cfDNA samples (n=135) from 55 patients with unresectable DPM, who received durvalumab with platinum-based chemotherapy (NCT02899195). Following cfDNA extraction and genomic library preparation, cfDNA at baseline (C1D1), Cycle 2 Day 1 (C2D1), and Cycle 5 Day 1 (C5D1) underwent low-coverage (1-2x) whole genome sequencing. Tumor- and mutation-naive estimates of tumor fraction were derived by applying the DELFI tumor score (DELFI-TS) model, which integrates genome-wide fragmentation patterns and chromosomal arm aneuploidy. In parallel, we performed TCR Vβ CDR3 next-generation sequencing on tumor (n=43) and peripheral serial blood (n=136) samples. The TCR repertoire was characterized using clonality, TCR clonotype/cluster dynamics, and the Morisita-Horn similarity index to assess repertoire similarity across samples. Clinical outcomes were assessed by radiographic response, progression-free (PFS), and overall survival (OS).

Results: Patients with distant metastasis (M1) had higher DELFI-TS levels (p=0.038). At baseline, DELFI-TS levels were numerically higher for radiographic non-responders (SD/PD) vs responders (CR/PR). Using the 92th percentile of DELFI-TS in non-cancer cfDNA control samples to determine the limit of blank, patients with detectable baseline DELFI-TS (ctDNA^{+}) had shorter PFS and OS (log-rank p<0.001). Patients that attained a radiographic response had more clonal peripheral TCR repertoires at both baseline and on-therapy timepoints compared to non-responders (p=0.037 at C1D1; p=0.007 at C2D1; p=0.042 at C5D1). Morisita-Horn similarity between C1D1 and on-therapy was lower in non-responders than responders (p=0.019 for C1D1 vs C2D1; p=0.036 for C1D1 vs C5D1). In contrast, a more diverse intra-tumoral TCR repertoire was noted for patients with an OS of 12 or more months (p=0.018).

Conclusions: Our findings provide proof-of-concept that cfDNA fragmentomic analyses can quantify pre-treatment cfDNA tumor fraction that may capture clinical outcomes with chemo-immunotherapy response for patients with DPM. Longitudinal analyses of peripheral TCR
repertoires can further differentiate responding from non-responding DPM, supporting the notion that joint analyses may more accurately capture immunotherapy response.

#0110 Clinical utility of landmark ctDNA molecular response as an early indicator of immunotherapy outcomes in lung cancer.

Jaime Wehr[1], Noushin Niknafs[1], Lavanya Sivapalan[1], Archana Balan[1], Gavin Pereira[1], Samira Hosseini-Nami[1], Iiasha Beadles[1], Aliyah Pabani[1], Kristen Marrone[1], Qing K. Li[1], Joseph Christopher Murray[1], Mark Sausen[2], Bryan Chesnick[3], Lorenzo Rinaldi[3], Christine L. Hann[1], Susan Combs Scott[1], Josephine Feliciano[1], Vincent K. Lam[1], Benjamin Levy[1], Patrick M. Forde[1], Julie R. Brahmer[1], Valsamo (Elsa) Anagnostou[1]

[1]Johns Hopkins University, Baltimore, MD,[2]LabCorp, Baltimore, MD,[3]Delfi Diagnostics, Inc., Baltimore, MD

Background: Circulating tumor DNA (ctDNA) analyses are informative as an early indicator of immunotherapy response in advanced non-small cell lung cancer (NSCLC), however the clinical role of ctDNA molecular response requires further validation.
Methods: As part of a prospective clinical protocol (NCT05995821), we performed ctDNA (n=328) and matched white blood cell DNA (WBC; n=109) targeted 521 fixed gene panel next-generation sequencing (Elio Plasma Complete) from 109 patients with advanced/metastatic NSCLC who received anti-PD-(L)1 as monotherapy or in combination with chemotherapy. Following variant cellular origin resolution, landmark molecular response (mR) was defined as undetectable ctDNA within 3-9 weeks of treatment initiation. For a subset of patients (n=34), whole-exome sequencing of baseline tumors was performed and used in benchmarking ctDNA detection and therapy response assessment.
Results: Among 2,818 plasma variants, 23% were clonal haematopoiesis-related, which confounded the interpretation of driver gene associations with clinical outcomes and assessment of molecular responses. Implementing a tumor-naïve WBC DNA-informed approach increased the number of evaluable cases while maintaining the overall accuracy of landmark ctDNA molecular responses. Pre-treatment ctDNA burden but not blood tumor mutation burden, predicted survival. Overall, 77 patients were evaluable for landmark molecular response assessment; of these, 29 patients (38%) attained a mR. Landmark evaluation of molecular response enabled evaluation of all cases, was highly specific (92%), and achieved a higher sensitivity (66%) compared to clearance or ctDNA reduction from baseline (sensitivity 59%). In predicting landmark progression-free survival (PFS) at 6 months (durable clinical benefit, DCB), the tumor-agnostic WBC-informed approach strikes a balance between sensitivity (71.4%) and specificity (100%) compared to plasma-only (sensitivity=14.3%, specificity=100%) or tumor-informed (sensitivity=78.6%, specificity=71.4%) approaches. A significant enrichment in landmark ctDNA mR was noted among patients with DCB with immunotherapy (p=2.5e-05) and chemo-immunotherapy (p=0.02). Patients in the landmark mR group attained longer PFS (p=1.6e-06) and overall survival (p=2.5e-05) compared to those with molecular progression. The association between landmark molecular response and survival remained significant (PFS and OS, $P < 0.001$) after accounting for clinical covariates, line of therapy, and baseline ctDNA levels.
Conclusions: Our findings indicate that landmark ctDNA molecular response at 3-9 weeks on treatment provides a real-time and accurate approach for monitoring immunotherapy clinical outcomes. Although not currently validated for regulatory use, these findings demonstrate the potential utility of ctDNA as an early endpoint in clinical trials.

#0111 Integrated, base-resolution profiling of genetic and epigenetic signatures in cell-free DNA.

Xingyu Yang, Jing Su, Chen Yang, Xiaoling Li, Si Zhang, Xianrong Chen, **Zhihong Zhang**, Bingsi Li

Research and Development, Burning Rock Biotech, Shanghai, China

Background: Epigenetic and genetic alterations synergistically drive cancer initiation and progression, yet one blood draw rarely yields enough cell-free DNA (cfDNA) to profile both modalities. Current co-detection strategies either demand high tumor burden or custom chemistry and cannot be retro-applied to existing datasets. We present MMcall, a computational tool that reconstructs the original four-base genome from conventional bisulfite-sequencing reads and simultaneously detects mutations and methylation variants without new benchwork, delivering fully integrated genomic/epigenomic signatures from one single library.
Methods: MMcall reconstructs the original four-base genome from standard bisulfite-converted reads by jointly modeling complementary top- and bottom-strand base counts. Because the G nucleotide on the strand opposing a C is unaffected by bisulfite conversion, the strand-specificity principle is used to restore pre-conversion sequence. A machine-learning error-suppression module is then applied to suppress the high technical noise inherent to bisulfite treatment. The algorithm simultaneously outputs methylation-variant allele frequency (MVAF) and somatic-variant allele frequency (SVAF) from the same library, enabling epigenetic and genetic profiling without additional wet-lab steps.
Results: Benchmarked against 0 -1% tumor-fraction serial dilutions of Seraseq® ctDNA Reference Material and an in-house standard (OverC Monitor panel; 1000X methylation depth, 20000X mutation depth), MMcall demonstrated near-perfect concordance with expected methylation levels (R^2>0.99) and detected mutations down to 0.25%. At 0.5-1% VAF, SVAF measurements by MMcall closely matched those obtained by ultra-deep sequencing (HS-UMI, 35000X), yielding > 99.7% NPA (95% CI: 99.3-99.9%) and > 86.9 % PPA (95 % CI: 77.8-93.3%). No false-positive calls were observed across predefined hotspot loci in any negative control, confirming robust suppression of technical noise.
Conclusion: MMcall jointly calls mutations and methylation variants at single-base resolution without additional bench steps. The method offers a cost-effective route to richer molecular information for early cancer detection and minimal residual disease monitoring.

#0112 Analytical performance of an enhanced variant (EV) pipeline for improved circulating tumor DNA (ctDNA) detection in samples with low tumor burden.

Dina Hafez, Bin Dong, Aamir Shahpurwalla, Bharat Sridhar, Alexander Hsieh, Jordan Feeney, Vu Ngo, Noura Tbeileh, Alexey Aleshin, Matthew Rabinowitz, Himanshu Sethi, Chenlu Hou, Ryan Ptashkin, Eser Kirkizlar, Ahmet Zehir

Natera, Inc., Austin, TX

EVs represent a distinct class of genomic events, offering opportunities in cancer diagnostics. Tumor-informed ctDNA detection, a sensitive and specific approach for monitoring molecular residual disease (MRD) in plasma, continues to evolve with the discovery of novel biomarkers. Developing methodologies for unbiased EV detection could enhance assay performance. Here, we report on the performance of a novel EV caller. EV caller performance was evaluated using 2 cancer cell lines and their matched normal cell lines. EV truth sets were established based on the pure cell lines (100%; no dilution). Contrived genomic DNA samples were prepared to emulate 3 different tumor purity levels relative to normal (50%, 25%, 10%) and analyzed using whole genome sequencing. The results from the titrations were compared to the 100% tumor cell line (“truth set”) to estimate the EV caller’s performance. Finally, to assess the performance of the EV caller in detecting ctDNA, a custom cfDNA-based mPCR primer design strategy was developed and applied to EVs in a tumor:normal cell line dilution series (range, 1:500 - 1:200,000), with 2-5 replicates for each condition. Each cancer cell line had approximately 700 EVs detected. Across all emulated tumor purity levels, the EV caller demonstrated a positive predictive value (PPV) of 90-95% at 5-10% variant allele frequency (VAF) and >99% PPV at >10% VAF. A positive percent agreement of >95% at >10% VAF was observed. For cell line ctDNA titrations, the EV caller showed target-level detection down to 0.0006% VAF. The target-level specificity was 99.99%. At the sample level, EVs were detected at the lowest tested dilution level (1:200,000). These analytical results demonstrate the exceptional performance of the EV caller algorithm to detect targets with high precision and specificity. EVs represent promising biomarkers that could enhance ctDNA assay sensitivity and specificity, particularly in samples with low tumor burden.

#0113 Assessment of sequencing error rates in healthy plasma samples across two whole genome sequencing platforms.

Aamir Shahpurwalla, Zach Montague, Fei Lu, Spenser Alexander, Garima Goyal, Dina Hafez, Matthew Rabinowitz, Eser Kirkizlar, Ahmet Zehir

Natera, Inc., Austin, TX

Accurate detection of error signals in healthy samples is critical for improving assay specificity and sensitivity in ctDNA analysis. Sequencing artifacts and biological noise, arising from PCR, oxidative damage, or clonal hematopoiesis variants, can obscure low-frequency tumor somatic mutations. This study aims to systematically characterize error profiles in healthy plasma samples and develop context-aware filtering and models to distinguish true variants from background noise. Whole-genome sequencing data were generated from 80 healthy plasma samples (pWGS) using two sequencing platforms (sequencer A: N=52; sequencer B: N=28). Mutation-specific features were computed across sequencing fragments using a custom pWGS analysis module that incorporated information both at the fragment- and the position-level. We compared a probabilistic classifier (Model 1) and an advanced deep learning based model (Model 2) trained on the same feature set, incorporating features that we identified as key predictors of sequencing error. Error rates within the plasma samples were quantified at genomic positions corresponding to tumor mutation target sets identified from 26 tissue samples (breast N=4, lung N=5, ovarian N=10, N=7 bladder). Using sequencing platform A, error rates showed strong dependence on fragment-level and sequence-context features. Error rates were not evenly distributed among variant types. Error rates were elevated near fragment ends and within GC-rich regions (>55% GC). Median raw error rates across cancer indications ranged from 19 to 59 parts per million (ppm). Application of Model 1 reduced background error rates by up to 65%, while Model 2 achieved up to a 90% reduction, with minimum error rates approaching ~5 ppm. Sequencing data from platform B that were processed with a base quality > 50 filter achieved comparable coverage (~65×) and similar error rates (~5 ppm). Across both sequencing platforms, further reductions are possible by incorporating additional fragment-level features and leveraging more advanced modeling approaches. This work establishes a foundational framework for pWGS error characterization and demonstrates the effectiveness of fragment- and context-based modeling in reducing sequencing noise.

#0114 Unraveling tumor- and tissue-specific gene expression patterns from plasma-derived cfRNA.

Maria Savchenko, Tatiana Nemchaninova, Alexey Dudakov, Aleksandr Serdiukov, Daria Shafranskaya, Artemiy Nikitin, Anastasia Tarabarova, Desiree Schenk, Alexandr Zaitsev, Anastasia Yudina, **Michael F. Goldberg**, Alexander Bagaev

BostonGene Corporation, Waltham, MA

Minimally invasive plasma-derived cell-free RNA (cfRNA) profiling captures blood-derived clinical markers when white blood cells (WBCs) are unavailable, harboring potential for molecular diagnostics and disease monitoring. Our study explored cfRNA analysis as a promising method for deconvolving signals from tumors and various tissues from a single blood draw, expanding its utility to include functional genomics that reveals gene expression patterns and their impact on disease status.

Plasma cfRNA was obtained from 207 healthy donors and 214 cancer patients. For comparison, 96 paired tumor whole exome sequencing (WES) and 208 paired WBC RNA-seq samples were used. Gene expression was quantified using pseudo-alignment with *Kallisto* and signature scores were computed by single-sample gene set enrichment analysis. Statistical significance was assessed with the Mann-Whitney *U* test. Somatic single nucleotide variants (SNVs) identified by tumor WES were cross-checked for detection in matched plasma cfRNA.

Extracellular matrix organization, cell proliferation, and T- and B-cell recruitment signatures were significantly elevated in cfRNA compared with WBCs (p values 1.1×10^{-55}, 3.8×10^{-63}, and 2.8×10^{-62}, respectively). These cfRNA (but not WBC) signatures effectively distinguished cancer patients from healthy donors (p value 6.5×10^{-11}, 1.1×10^{-4}, and 2.3×10^{-5}, respectively). The epithelial signature was enriched in carcinoma cfRNA, with higher scores corresponding to larger numbers of metastatic sites (p value 1.5×10^{-7}). Conversely, this score remained low in sarcomas originating from non-epithelial tissues.

SNVs identified by tumor WES were detected in cfRNA in 20/29 (68.9%) of breast, 8/14 (57.1%) of colorectal, 7/13 (53.8%) of lung, and 5/11 (45.4%) of pancreatic cancer cases. The number of variants detected per patient trended positively with cancer stage. In colorectal cancer, samples with detected variants had higher epithelial and colon tissue signature scores, which aligns with reported cfDNA shedding levels for the diagnosis . Fisher's exact test showed the cfRNA-tumor variant overlap to occur significantly more often (p-value = 9×10^{-129}) in matched pairs than in random sample comparisons, indicative of the reliability of our approach for detecting tumor-related signals.

This proof-of-concept study shows that cfRNA harbors tumor- and tissue-specific expression patterns that complement blood cell-based RNA-seq, providing additional biological and clinical information. Our framework integrates genomic and transcriptomic data to deconvolve tumor-related and systemic tissue signals from plasma, supporting cfRNA signatures as a clinically relevant resource for patient stratification, discovery of novel drug targets and plasma-based biomarkers, and disease progression and treatment response monitoring, with prospects for better trial design and treatment optimization.

#0116 Comprehensive ctDNA profiling reveals molecular and prognostic landscapes in Korean pan-cancer patients.

Jiwon Kim[1], Kyong Hwa Park[2], Soohyeon Lee[2], Jwa Hoon Kim[2], Ju Won Kim[2], Ji Won Lee[2], Ji Yoon Lee[1], You Jin Song[1], Dayoung Lee[1], Hyeonmin Jeong[1], Wooseok Lee[1], Yoon Ji Choi[2], Jason K. Sa[1]

[1]Korea University, Seoul, Korea, Republic of,[2]Korea Univ. Medical Center, Seoul, Korea, Republic of

Liquid biopsy offers a non-invasive approach for capturing essential molecular profiles to make informed decisions within a clinical framework. However, large-scale, population-specific studies evaluating its clinical utility remain scarce. To address this unmet need, we established a Korean advanced pan-cancer circulating tumor DNA (ctDNA) atlas and systematically evaluated its clinical feasibility. We also assessed concordance with tissue-based sequencing, explored East Asian-specific molecular disparities, and quantified the prognostic impact of genomic alterations using a newly developed prognostic framework. We analyzed 1,243 ctDNA samples across 17 tumor types, integrating genomic alterations with long-term clinical follow-up. Somatic mutations were identified and clinically interpreted using the OncoKB database, and compared with the MSK-ACCESS cohort to identify population-level genomic differences. To quantify the degree of prognostic significance, we developed the Molecular-Prognostic Index (MPI), a unified metric capturing the magnitude and significance of survival effects for individual genomic alterations at both pan-cancer and individual tumor levels. Using this framework, we identified key alterations and pathways shaping patient survival and therapeutic sensitivities. East Asian cancer patients demonstrated distinctive mutational profiles compared with MSK-ACCESS, including a higher prevalence of *MTOR*, and *FGFR3* mutations in NSCLC and enriched *BRCA2* alteration in breast cancer. Comparison with tissue-based sequencing revealed higher *TP53* mutations detected in tissue, whereas clinically actionable *ESR1* E380Q and Y537S (OncoKB Level 1), were more prevalent in ctDNA. Pathway-level enrichment analysis exhibited strong concordance between tissue and ctDNA profiles in intestinal and prostate cancers, but marked discrepancies in lung and breast cancers, underscoring tumor type-specific biological and shedding differences. Across multiple tumor types, increased tumor mutation burden (>= 3) was significantly associated with poor clinical outcomes. *BRAF* V600E predicted an unfavorable prognosis in patients diagnosed with NSCLC and colorectal cancer. MPI analysis further identified *PIK3R1* alterations as high-risk predictors in breast cancer and *TP53* Y220C as a poor prognostic marker in prostate cancer, while *NOTCH1* mutations emerged as a favorable biomarker in intestinal tumors. This large-scale ctDNA-based analysis in parallel with long-term clinical follow-up of East Asian solid tumors provides a comprehensive reference for understanding tumor propagation and therapeutic vulnerabilities. We demonstrated that ctDNA recapitulates key tumor characteristics and reveals prognostic insights. The newly developed MPI framework stratifies patient risk based on ctDNA features, and supports liquid biopsy for precision oncology.

#0117 Single-cell transcriptomic and CNV profiling reveal distinct circulating tumor cell signatures in pancreatic ductal adenocarcinoma.

Se-Eun Choi[1], **Jihyun Lee**[2], Hyunjung Kee[3], Moon Jae Chung[4], Jungwon Kim[2], Semin Lee[1]

[1]Department of Biomedical Engineering, Ulsan National Institute of Science and Technology, Ulsan, Korea, Republic of,[2]CytoGen, Inc., Seoul, Korea, Republic of,[3]Institute of Gastroenterology Research, Yonsei University College of Medicine, Seoul, Korea, Republic of,[4]Department of Internal Medicine, Yonsei University College of Medicine, Seoul, Korea, Republic of

Pancreatic ductal adenocarcinoma (PDAC) is an aggressive malignancy with poor prognosis and limited early detection methods. Circulating tumor cells (CTCs) provide a minimally invasive opportunity to investigate tumor heterogeneity and disease progression, yet their reliable identification among peripheral blood cells remains challenging. In this study, peripheral blood samples were collected from PDAC patients and healthy controls. CTCs were enriched using CytoGen's Smart Biopsy™ Platform, and the CTC-enriched fractions were analyzed using single-cell RNA sequencing (Cell Ranger 8.0.1). Low-quality and doublet cells were filtered (nFeature_RNA > 500, percent.mt < 10, doublet score < 0.25). Dimensional reduction and clustering (resolution 0.8) enabled cell type annotation, and copy number variation (CNV) profiles were inferred at the subcluster level (k=5) to assess potential malignant characteristics. Consequently, Distinct cell clusters exhibiting PDAC-associated transcriptional signatures were identified. CNV pattern analyses revealed that certain clusters displayed genomic variability distinct from typical immune and blood cell populations. Comparison with TCGA-PAAD reference data indicated partial resemblance to tumor-like CNV profiles. Moreover, CNV-based stratification tended to distinguish PDAC-derived CTC-enriched clusters from those observed in healthy blood, suggesting potential diagnostic utility. Overall, these integrative single-cell transcriptomic and CNV analyses provide valuable insights into CTC heterogeneity in PDAC and suggest that CNV-informed profiling may enhance the identification of putative CTC populations and facilitate future biomarker development for liquid biopsy-based cancer monitoring.

Acknowledgement: This work is supported by the National Research Foundation of Korea (NRF) funded by the Ministry of Science and ICT (RS-2023-00261820).

#0118 Detecting early cancer using cfDNA methylation signatures with nanopore sequencing.

Yi Yang Hou[1], Nicholas Cheng[1], Jared T. Simpson[2], Philip Awadalla[3]

[1]Molecular Genetics, University of Toronto, Toronto, ON, Canada,[2]Ontario Institute for Cancer Research, Toronto, ON, Canada,[3]Oxford University, Oxford, United Kingdom

Early cancer screening improves survival by enabling timely treatment before the disease progresses. However, current population-wide screening tools are limited to a few cancer types, highlighting the need for novel detection methods that can be routinely used to detect multiple cancers. Plasma tumour-derived cell-free DNA (cfDNA) carries the tumour's genetic and epigenetic alterations and can be used to develop new screening methods. Here, we aim to identify precancerous and early tumour-associated cfDNA methylation signatures. We analyzed nanopore sequencing data performed on plasma collected up to 10 years before clinical diagnosis from patients with breast or prostate cancer, and stage II diagnostic plasma from breast cancer patients. Preliminary data revealed global hypomethylation and increased inter-patient variability in the diagnostics breast cancer samples, both of which were more pronounced in younger patients. Notably, global hypomethylation was found in Triple Negative Breast Cancer (TNBC) and ER+/HER2- Breast Cancer, but not in other subtypes. These global alterations were not observed in precancerous lesions in both cancer types, suggesting such epigenetic alterations may arise or become detectable during malignant transformation rather than early tumour initiation. To identify loci that are associated with precancerous epigenetic alterations, differentially methylated regions (DMRs) were selected across different functional elements in the genome. Using these DMRs, an ensemble random forest model was built in the discovery cohort (pre-breast: n = 33; pre-prostate: n = 35) for each cancer type. The trained model showed moderate discriminability for both breast (AUC = 0.76, pre-breast: n = 12; stage II breast: n = 12) and prostate (AUC = 0.83, n = 5) cancer in the validation set, and both models performed better in the older age group. In addition, promoter methylation signatures are also capable of stratifying patients into high-risk and low-risk of developing breast cancer. Pathway enrichment analysis will be performed to investigate the oncogenic relevance of selected features. Success in this project will define how early cancer can be detected through liquid biopsy and advance the timeline of early detection. This project has the potential to develop a single blood test for multi-cancer detection and monitoring.

#0119 A lightweight self-supervised deep learning framework for automated detection of circulating tumor cells and cancer-associated fibroblasts.

Hyeongjung Woo[1], Seonghwan Park[2], Jungmin Lee[3], Inkyu Moon[2], Minseok S. Kim[1]

[1]Department of New Biology, Daegu Gyeongbuk Institute of Science and Technology (DGIST), Daegu, Korea, Republic of,[2]Department of Robotics & Mechatronics Engineering, Daegu Gyeongbuk Institute of Science and Technology (DGIST), Daegu, Korea, Republic of,[3]CTCELLS Inc., Seoul, Korea, Republic of

Circulating rare cells (CRCs), including circulating tumor cells (CTCs) and circulating cancer-associated fibroblasts (cCAFs), serve as valuable liquid biopsy biomarkers, yet their detection remains challenging due to extreme rarity and morphological heterogeneity. Current identification methods predominantly rely on fluorescence-based imaging and manual, time-consuming assessments by trained experts, which limit high-throughput analysis, reproducibility, and clinical implementation. Moreover, the strong dependence on subjective visual judgment makes CRC calling highly operator-dependent, introducing substantial inter- and intra-observer variability and complicating assay standardization across centers. To overcome these constraints, we developed a self-supervised deep learning framework that enables robust and interpretable detection of CRCs using minimal labeled data and with reduced dependence on fluorescence signals. Our approach employs a two-stage training strategy in which a model is first pretrained on large-scale white blood cell (WBC) datasets using contrastive learning, allowing it to learn generalizable morphological representations from abundant, morphologically similar cells. In the next step, knowledge distillation is used to transfer this learned knowledge into a lightweight student model that is subsequently fine-tuned on limited CRC data. This distillation process significantly reduces model complexity while preserving detection accuracy, thereby enabling real-time inference that is suitable for clinical workflows. In our experiments using samples from 27 patients with early-stage breast cancer, conventional fluorescence-based analyses manually identified both CTCs and cCAFs. When applied to the same dataset, the proposed framework achieved CRC detection sensitivity and specificity exceeding 90% while operating with minimal computational burden and showed high concordance with manual expert assessment. Compared with conventional fluorescence-based manual annotation, our approach offers substantial gains in speed, consistency, and scalability, while eliminating inter-observer variability inherent to expert-dependent assessments. These results suggest that self-supervised representation learning combined with knowledge distillation provides a practical and clinically viable strategy for automated CRC detection, with potential applications in early cancer diagnosis, longitudinal disease monitoring, and treatment response assessment.

#0120 Two integrative molecular subtypes of hepatocellular carcinoma with predictive therapeutic potential: Toward liquid biopsy-guided precision medicine.

Jiyon Lyu[1], **Woo Young Kwon**[2], Sung Hwan Lee[3]

[1]CHA University School of Medicine, Pocheon, Korea, Republic of,[2]CHA Bundang Medical Center, CHA Universit, Seongnam, Korea, Republic of,[3]Department of Surgery, CHA Bundang Medical Center, Seongnam, Korea, Republic of

Hepatocellular carcinoma (HCC) is the third leading cause of cancer mortality worldwide, with a variety of therapeutic options in the advanced stage. Although immune checkpoint inhibitors (ICIs) and targeted therapies have transformed treatment paradigms, clinical decision-making regarding first-line therapy and subsequent lines remains challenging. Existing molecular classifications provide biological insights but often lack direct clinical translation. We aimed to identify robust, reproducible molecular subtypes of HCC that not only reflect tumor biology but also predict differential therapeutic responses, thereby advancing the potential for liquid biopsy-guided precision medicine.

Transcriptomic data from the CCLE served as a discovery set and were validated with six cohorts, including TCGA. We identified two distinct molecular subtypes—METabolic and Immune—from the HCC cell line transcriptome using non-negative matrix factorization (NMF) at the REACTOME pathway level. Subtype-specific features were characterized by drug sensitivity, signaling pathway, cross-omics integration, and tumor microenvironment (TME) analyses. Therapeutic benefits from current first lines were validated across IMbrave150 and BIOSTORM. Serum proteomic and somatic mutation data from 35 patients were analyzed to identify predictive biomarkers.

The METabolic subtype was characterized by elevated MET expression and enrichment of signaling pathways associated with cell survival, growth, and differentiation. In contrast, the Immune subtype exhibited prominent immune infiltration—particularly macrophages/monocytes, regulatory T cells, and $CD8^+$ T cells—along with activation of PD-1/CTLA-4 pathways and poorer overall survival (OS). In the IMbrave150 cohort, the Immune subtype showed superior survival outcomes to atezolizumab-bevacizumab ($p < 0.0001$). Conversely, the METabolic subtype was associated with 100% recurrence after sorafenib treatment, suggesting potential benefit from MET inhibitors after sorafenib failure. A machine learning model using mutations and serum biomarkers (myoglobin, IL-6R beta, *TP53*, *CTNNB1*) achieved robust performance (AUC = 0.88; accuracy = 87.1%) for subtype prediction.

This study establishes clinically relevant HCC subtypes associated with distinct responses to currently recommended therapies and proposes a liquid biopsy-based approach using four predictive biomarkers. We provide rationale for the early use of MET inhibitors such as cabozantinib in the first-line setting, given its potential resistance to both sorafenib and ICI-based therapies. Additionally, our study suggests the Immune subtype is an optimal candidate for immunotherapy combined with anti-VEGF(R) agents. Further validation in larger, prospective cohorts is warranted to translate these findings into clinical practice.

#0121 Single stranded ligation enhances the performance of the duet evoC 6-base assay, enhancing value in low DNA input applications including liquid biopsy.

Tom Charlesworth, Audrey Vandomme, Jens Fullgrabe, Ermira Lleshi, Lidia Prieto-Lafuente, Edyta Bocian-Canepa, Elena Pahiti, Rebecca Ellwood, Mengjie Li, Marjana Lila, Robert Crawford, Robert J. Osborne, **Brett Evans**

biomodal Ltd, Cambridge, United Kingdom

The 6-base genome, provided by duet evoC, provides the canonical 4-base genome whilst simultaneously distinguishing 5-methylcytosine from 5-hydroxymethylcytosine to provide the 5th and 6th, epigenetic, bases. The 6-base genome has been shown to be a powerful tool for the discovery of biomarkers of early biological change and provides mechanistic insight across important applications including oncology, liquid biopsy and neurology. In these applications it is important to maximise the information derived from precious DNA samples, both in terms of multiomic data and material recovery. [RO1] Here we present the next evolution of the duet product portfolio. Through implementation of a novel single-stranded ligation approach, we demonstrate marked improvements[RC2] in assay performance including material recovery and DNA methylation calling sensitivity, whilst maintaining high genetic and epigenetic accuracy. These improvements derive from the ability of single-stranded ligation to maintain the original cfDNA strands. In contrast, end-repair can fill-in 5' overhangs with unmodified cytosines (reducing methylation detection sensitivity) and can introduce errors at 5' overhangs in addition to nicks and gaps. In addition, end-repair can remove information by degrading 3' overhangs. The single-stranded ligation method also captures both single and double stranded cfDNA, maximizing recovery of unique molecules. This is a critical parameter for liquid biopsy applications, where it is important to assay as many circulating-tumor (ctDNA) molecules as possible. We anticipate that these improvements will further enhance the power of the duet portfolio to reveal powerful novel biomarkers and provide mechanistic insight in sample-constrained liquid biopsy applications.

#0122 Using the 6-base genome for full multiomic analysis of cfDNA through combined methylation and fragmentomic analysis to enhance classification of clinical cancer cfDNA samples.

Tom Charlesworth, Fabio Puddu, Luke Sarre, Elena Pahiti, Lidia Prieto-Lafuente, Aurelie Modat, Robert Crawford, Simeone Angela, Robert J. Osborne, **Steven Ciaramaglia**

biomodal Ltd, Cambridge, United Kingdom

Sensitive detection of circulating tumour DNA (ctDNA) within the total pool of cell-free DNA (cfDNA) is crucial for the early diagnosis of cancer via liquid biopsy, and for monitoring ctDNA levels during treatment and remission. This enables earlier monitoring of treatment response, identification of minimal residual disease, and early detection of cancer. However, ctDNA typically represents only a minor fraction of overall cfDNA, posing significant challenges for conventional biomarker-based detection methods. Recently, fragmentomics-based approaches have shown promising results for ctDNA detection in liquid biopsy samples, with studies demonstrating that analysis of fragment size distributions across genomic regions, the frequency of 5' end motifs, and nucleosome positioning patterns near functional genomic sites can substantially enhance sensitivity and specificity. The advent of advanced methylomic profiling methods, such as 6-base sequencing with duet evoC, which distinguishes 5-methylcytosine (5mC) from 5-hydroxymethylcytosine (5hmC), has further expanded the analytical landscape. Integrating 5mC and 5hmC profiling with ctDNA detection strategies extends the spectrum of discernible fragment end motifs and provides orthogonal data layers to fragment size and nucleosome positioning analysis. These multidimensional epigenetic signatures hold the potential to markedly improve the resolution and accuracy of ctDNA detection. Here, we evaluate the impact of these additional epigenetic layers on ctDNA detection in liquid biopsy samples from a cohort of healthy volunteers and patients with different stages of colorectal cancer. We show that as well as different 5mC and 5hmC profiles between healthy, and early or late stage CRC, there are distinct differences in fragmentomics metrics when comparing across these groups. We identify regulatory regions displaying differences in nucleosome positioning in cfDNA derived from healthy individuals and CRC patients. Finally, we compare the ability of fragmentomics and epigenetic modalities (individually and in combination) to classify CRC patients. These classifiers evidence the utility of full multiomic datasets in cfDNA applications.

#0123 The importance of high analytical sensitivity and specificity of 5 and 6-base assays to enhance the detection of ctDNA in liquid biopsy applications.

Tom Charlesworth, Luke Sarre, Cillian Nolan, Fabio Puddu, Annelie Johansson, Aurelie Modat, Ermira Lleshi, Simeone Angela, Robert Crawford, Robert J. Osborne, **Thao Huynh**

biomodal Ltd, Cambridge, United Kingdom

Sensitive detection of cancer-derived DNA fragments (ctDNA) within cell-free DNA (cfDNA) in liquid biopsy is essential for identifying early-stage cancers, monitoring treatment response and minimal residual disease. A major challenge in these applications is detecting ctDNA, indicative of disease state, when this represents a small fraction of the total cfDNA. Advances in methylomic profiling, including 6-base sequencing with duet evoC which distinguishes 5-methylcytosine (5mC) and 5-hydroxymethylcytosine (5hmC), have enabled high-sensitivity ctDNA detection by analyzing methylation patterns across individual sequencing fragments (fragment level analysis) as opposed to more traditional analyses that average methylation levels at individual CpG loci. We present a comparative analysis of the background error rates in fragment-level methylation analysis between the duet suite of methylation assays from biomodal and alternative methylation sequencing technologies, showing error rates below 10^{-5} for both biomodal assays compared to error rates above 10^{-4} for alternative technologies. We further show how this lower error rate can enable more sensitive detection of ctDNA, and present the application of these technologies to detecting ctDNA in cfDNA from patients diagnosed with stages I-IV colorectal cancer. Our findings further emphasize the power of fragment-level analyses in cfDNA-based applications. They illustrate that it is critical to carefully consider analytical performance to achieve maximum clinical sensitivity and specificity from limited cfDNA samples.

: Alternative Cell Type and in Situ Cell Therapies
Poster Session

#0127 Riboflavin biosynthesis byproducts increase the vulnerability of cancer to adoptive MAIT TCR-engineered T-cell transfer.

Ying Zheng[1], Pakhi Birla[2], Wanting Shan[1], Samuel Huang[1], Franck Housseau[1], Drew Pardoll[1]

[1]Oncology, Johns Hopkins University School of Medicine, Baltimore, MD,[2]Immunity, Transplantation and Infection, Stanford University School of Medicine, Stanford, CA

Introduction: Mucosal-associated invariant T (MAIT) cells are innate-like T lymphocytes expressing a semi-invariant T-cell receptor (TCR) α-chain (TRAV1-2 joined to TRAJ33/12/20) paired with a restricted TCR β repertoire. Unlike conventional T cells that respond to peptide antigens, MAIT cells recognize and kill infected or transformed cells presenting non-polymorphic MHC class-I (MR1) molecule covalently loaded with microbial riboflavin (vitamin B2) biosynthetic intermediates. A key riboflavin precursor, 5-amino-6-D-ribitylaminouracil (5-A-RU), undergoes non-enzymatic condensation to form potent MR1 ligands such as 5-OP-RU, which can prime tumor cells to express MR1. These features make MAIT TCRs an attractive platform for adoptive T-cell therapy across cancer types, independent of HLA molecules or tumor genetics.
Methods: Human CD3+ T cells isolated from healthy donor peripheral blood mononuclear cells (PBMC) were engineered to express MAIT TCRs (TRAV1-2/TRAJ12 or TRAV1-2/TRAJ33) using a CRISPR-Cas12-mediated homology-directed repair (HDR) strategy. TCR knockout (*TRAC*/*TRBC* double-knockout) T cells lacking any introduced TCR served as controls. Antitumor activity was assessed in vitro and in vivo. Cytotoxicity against the human B-cell acute lymphoblastic leukemia line NALM6 was measured by flow cytometry. For in vivo evaluation, luciferase-expressing NALM6 cells were injected intravenously into *NOD/SCID/ Il2rg–/–* (NSG) mice, followed by infusion of engineered T cells. A 5-A-RU prodrug was administered intraperitoneally. Tumor burden was monitored by bioluminescent imaging.
Results: In vitro, MAIT TCR-engineered human T cells exhibited distinct baseline cytotoxicity against NALM6 cells (approximately 60-70% for J12 and ~10% for J33 in the absence of ligand). Addition of 5-A-RU resulted in near-complete tumor cell elimination for both MAIT TCR variants. In xenograft models, neither J12 nor J33 MAIT TCR T cells showed significant antitumor activity without exogenous 5-A-RU. However, intraperitoneal delivery of the 5-A-RU prodrug had no effect in TCR-knockout controls but markedly enhanced the antitumor activity of both MAIT TCR-engineered T-cell products. Mice receiving MAIT TCR T cells plus 5-A-RU showed delayed tumor progression and significantly improved survival compared with controls.
Conclusion: MAIT TCR engineering confers potent antitumor activity to human T cells, which is strongly augmented by riboflavin pathway metabolites such as 5-A-RU. These findings support a model in which metabolite supplementation prime tumor cells to express MR1 and redirect MAIT TCR-engineered T cells cytotoxic activity towards tumor. Further studies are underway to define the therapeutic window, evaluate potential toxicities, and identify the breadth of tumor types responsive to MAIT TCR-based adoptive cell therapy.

#0128 Synthetic reprogramming of γδ CAR T cells with the LTBR gene optimizes function in the TME and overcomes effector limitations.

Mitchell S. Wang, Ivan Reyes-Torres, Kristen C. Vogt, Caroline K. Hanlon, Ashley N. Thornal, Maria Guarino, Eric M. Johnson, Mark P. Roberto, Navamallika G. Reddy, Miao Chen, **Theodore Giavridis**, Mateusz Legut

OverT Bio, New York, NY

Cell therapies have transformed outcomes in hematologic cancers, yet their efficacy in solid tumors remains limited by the profoundly immunosuppressive tumor microenvironment (TME), which employs multiple, overlapping mechanisms to suppress immune activity. Current armoring strategies address these barriers individually, leaving key vulnerabilities, while autologous approaches remain costly and difficult to scale. Allogeneic γδ CAR T cells represent an attractive, off-the-shelf platform, but their persistence and potency within the solid tumor TME require enhancement.

To advance scalable and effective solid tumor therapies, we pursued a data-driven strategy to optimize γδ T cell biology while increasing TME resilience. Owing to limited knowledge of γδ T cell functional states in antitumor response, we implemented an empirical approach integrating genome-scale discovery and AI-driven analytics to uncover pathways governing γδ CAR T function. We conducted a genome-wide overexpression screen to identify reprogramming genes that protect CAR T cells from adenosine, TGF-β, immunosuppressive macrophages, and regulatory T cells while improving persistence. Among 12,000 genes screened, 51 candidates conferred protection against three or more suppressive mechanisms. Lymphotoxin beta receptor (LTβR)—a TNF superfamily receptor not normally expressed in T cells—emerged as the top hit, reprogramming T cells into highly proliferative, persistent, and multifunctional states, as confirmed by bulk and single-cell RNA-seq.

In high-stress assays, LTβR expression conferred broad resistance to immunosuppression, including complete abrogation of Treg-mediated inhibition. In γδ CAR T cells, LTβR induced an αβ-like effector program characterized by enhanced cytotoxicity, persistence, and cytokine modulation. scRNA-seq revealed new mechanisms of γδ CAR T exhaustion and effector differentiation distinct from αβ CAR T cells. In vivo, LTβR-armored αβ and γδ CAR T cells targeting CLDN6 mediated complete, durable regressions in an aggressive ovarian cancer model where controls were ineffective.

Finally, we established a GMP-compatible manufacturing process tailored to γδ T cell biology, producing highly pure, potent cells suitable for multi-patient allogeneic use. Together, this work defines a comprehensive next-generation engineering and manufacturing framework that overcomes γδ CAR T cell limitations and enables durable activity in solid tumors.

#0130 Expanding the ACT paradigm: B cell engineering via spherical nucleic acids for cancer immunotherapy.

Maryam Balibegloo[1], Yingying Li[1], Abu Baker[1], Jie Fan[1], Ping Xie[1], Mi Ran Choi[1], Catalina Lee Chang[2], Vinzenz Mayer[3], Michael Evangelopoulos[3], Chad A. Mirkin[3], Bin Zhang[4]

[1]Northwestern Univ. Feinberg School of Medicine, Chicago, IL,[2]Northwestern Univsity, Chicago, IL,[3]Northwestern University, Evanston, IL,[4]Northwestern University - Chicago, Chicago, IL

Adoptive cellular therapy (ACT) has revolutionized cancer immunotherapy, yet its focus remains largely on T cells. B cells, despite their potent antigen-presenting capacity and role in adaptive immunity, have been underutilized due to inefficient antigen delivery and activation. We developed an ex vivo strategy leveraging spherical nucleic acids (SNAs) to license B cells for ACT. This platform synchronizes pH-controlled co-delivery of tumor antigen peptides and TLR9 agonists into shared endosomal compartments, enabling sustained antigen presentation and robust cross-priming of tumor-specific $CD8^+$ T cells, resulting in epitope spreading and durable antitumor immunity.SNA-trained B cells exhibited lymphoid homing and secreted CCL3/CCL4, establishing a CCR5-dependent chemotactic axis that recruited effector $CD8^+$ T cells and cDC1, creating spatial immune hubs within tumors. Multiplex immunohistochemistry analysis revealed clustering of transferred B cells, $CD8^+$ T cells, and cDC1 in draining lymph nodes, facilitating antigen handoff and reciprocal activation. Mechanistic studies confirmed that CCR5 blockade or $CD8^+$ T-cell depletion abrogated efficacy. Across multiple murine and humanized tumor models, SNA-trained B cells outperformed controls, reduced metastasis, and synergized with PD-1 blockade to improve survival. Single-cell transcriptomics and BCR-seq demonstrated progression toward plasma cell differentiation, oligoclonal expansion, and IgG2 class switching.This work introduces a nanomaterial-based platform to reprogram B cells for ACT, overcoming limitations in immunologically “cold” and checkpoint-refractory tumors. SNA-trained B cells broaden the ACT paradigm beyond T cells, offering a versatile and well-tolerated strategy for durable antitumor immunity.

#0131 Enhanced feeder-free expansion, survival, potency and post manufacture stability of NK cells for CAR-NK therapies using human platelet lysate.

Vanesa Alonso-Camino, Andrew Sullivan

Mill Creek Life Sciences, Rochester, MN

Natural killer (NK) cells have emerged as a promising platform for chimeric antigen receptor (CAR) engineering, offering inherent anti-tumor activity and a favorable safety profile compared to CAR-T cells. Unlike T cells, NK cells belong to the innate immune system and do not require prior antigen sensitization, making them attractive for “off-the-shelf” allogeneic therapies. Clinical interest in CAR-NK cells has surged, with over 50 trials registered globally, driven by their reduced risk of cytokine release syndrome and graft-versus-host disease. Despite these advantages, the widespread adoption of CAR-NK therapies faces two major challenges: achieving clinically relevant NK cell numbers and ensuring post-manufacturing stability. NK cells are less abundant than T cells, exhibit limited in vitro expansion capacity, and have a short lifespan. Traditional methods rely on feeder cell co-culture, often using tumor-derived lines, which introduces technical and regulatory hurdles and yields inconsistent results. To address these limitations, we developed a feeder-free expansion protocol using human platelet lysate (hPL), enabling robust NK cell proliferation while preserving phenotype and cytotoxic function. Beyond expansion, we focused on a critical bottleneck in CAR-NK manufacturing—cryopreservation. Using proprietary cryopreservation solutions and protocols following hPL-based culture, we achieved significantly improved NK cell survival, maintenance of activating receptor expression, and retention of anti-tumor potency post-thaw. This advancement mitigates the logistical challenges of CAR-NK production, supporting scalable, ready-to-use cell therapy products. Our integrated approach—combining efficient feeder-free expansion with optimized cryopreservation—represents a major step toward reliable, high-quality CAR-NK therapies for clinical application.

#0132 Improving effector cells for CAR-NK immunotherapy against colorectal cancer.

Marco Cortese, Alice D'Andrea, Alfonso Navarro Zapata, Sahar Taebi, Consalvo Petti, **Enzo Medico**

Candiolo Cancer Institute, FPO-IRCCS, Candiolo, Italy

Chimeric Antigen Receptor (CAR)-based immunotherapy targeting carcinoembryonic antigen (CEA) represents a promising strategy for the treatment of colorectal cancer (CRC), a leading cause of cancer-related mortality worldwide. With respect to CAR-T cells, whose activity against solid tumors is limited by significant side effects, CAR-NK cells represent a potentially safer alternative, offering reduced toxicity while maintaining effective anti-tumor activity. We therefore worked at developing and optimizing CEA-specific CAR-NK cells against CRC, along three research lines: (i) selection and validation of a reference CEA CAR in the NK-92 model; (ii) further engineering of CEA.CAR-NK-92 cells with interleukins, and (iii) exploration of additional NK effector types. To select the reference CEA CAR construct, second generation CARs based on two scFvs with different affinities (hMN-14 and BW431/26, respectively higher and lower affinity) were constructed. Stable NK-92 clones were generated for each construct (higher affinity: NK-92.F3 clone; lower affinity: NK-92.G8 clone) and functionally characterized. *In vitro*, the NK-92.F3 clone exhibited stronger killing activity against CEA-positive CRC cells. *In vivo*, in NOD/Scid mice bearing CEA+ CRC xenografts, the two clones displayed comparable activity, both significantly reducing tumor progression and confirming their therapeutic potential. Considering the higher affinity and the better *in vitro* performances, the hMN-14-based CAR was selected as the reference CAR for subsequent evolutions of the NK platform. To enhance CAR-NK-92 performances, wild-type NK-92 and NK-92.F3 cells were engineered to constitutively express different interleukins. Functional assays demonstrated that specific interleukin expression markedly increased cytotoxicity and activation, highlighting cytokine engineering as an effective strategy to potentiate CAR-NK activity. To overcome the major intrinsic limitation of NK-92 cells, i.e. the need for irradiation before infusion, we investigated induced pluripotent stem cell (iPSC)-derived NK cells (iNKs) as a renewable and clinically scalable alternative NK source. Four iPSC-to-NK differentiation protocols were compared, three based on 3D embryoid body intermediates and one on 2D monolayer. Of these, one 3D and the 2D protocol proved more reliable. iPSC cells were then transduced with the reference CEA CAR, cloned, differentiated into NK and validated for functionality and cytotoxic performances. In conclusion, this work identified a robust reference CEA-CAR construct and established two complementary strategies, cytokine engineering to enhance effector function and iPSC-derived NK cell generation to overcome NK-92 limitations, providing a foundation for the development of safer, scalable, and next-generation CAR-NK therapies for colorectal cancer.

#0133 NEO-201-recognized truncated Core 1 O-glycans represent a new target for CAR-NK therapy in AML.

Joseph A. Clara[1], Nile Liu[1], Mala Chakraborty[2], Kwong Y. Tsang[3], Massimo Fanitni[3], Philip M. Arlen[3], Richard W. Childs[2]

[1]Division of Hematology and Oncology, University of Virginia, Charlottesville, VA,[2]National Heart, Lung, and Blood Institute, National Institutes of Health, Bethesda, MD,[3]Precision Biologics, Inc, Bethesda, MD

Introduction: Acute myeloid leukemia (AML) continues to have poor long-term outcomes, particularly in high-risk and relapsed/refractory disease. Progress in AML immunotherapy has been hindered by the scarcity of antigens selectively expressed on leukemic cells while sparing hematopoietic stem/progenitor cells (HSPCs). AML-restricted surface glycans represent an underexplored class of targets. NEO-201 is a humanized IgG1 monoclonal antibody that binds truncated Core 1 O-glycans expressed by several solid tumors, circulating neutrophils, and select leukemia cell lines, with limited reactivity to most normal tissues and an acceptable safety profile in a phase I solid tumor trial (NCT03476681). We evaluated the NEO-201-recognized truncated O-glycan antigen as an AML-associated antigen, characterized its expression across AML subtypes, and developed a CAR NK cell therapy directed against this target.

Methods: Ten AML cell lines representing diverse molecular subtypes were analyzed for NEO-201 binding by flow cytometry. NK cells from healthy donors were expanded ex vivo using lymphoblastoid feeder cells and IL-2. CAR NK cells were generated via retroviral transduction with a second-generation CAR, incorporating a NEO-201-binding domain, CD8α transmembrane region, 4-1BB co-stimulation and CD3ζ signaling domains, and a truncated CD34 (tCD34) marker. Cytotoxicity was assessed in co-culture assays using calcein-AM-labeled AML targets at varying effector-to-target ratios. Antigen expression across hematopoietic maturation stages was evaluated by flow cytometry in G-CSF-mobilized peripheral blood to assess potential on-target/off-tumor toxicity.

Results: The NEO-201-recognized antigen was expressed at >40% in 6 of 10 AML cell lines, spanning FLT3-ITD-mutated, MLL-rearranged, biphenotypic, and core-binding factor leukemias. Expression ranged from 41-100% in positive lines: THP-1 (100%), MOLM-14 (88%), MV4-11 (60%), U-937 (45%), HL-60 (44%), and ME-1 (41%). NEO-201-based CAR NK cells demonstrated potent antigen-dependent cytotoxicity, including against lines with lower antigen density. At a 10:1 E:T ratio, CAR NK cells lysed 61% of THP-1, 45% of HL-60, and 40% of MOLM-14 targets. Antigen expression was minimal or absent on $CD34^+$ HSCs (0-1%), low on early myeloid progenitors (10-15%), and enriched in mature neutrophils (~99%), consistent with restricted expression during late myeloid maturation.

Conclusion: This study identifies Core 1 O-glycans recognized by NEO-201 as a novel AML-associated antigen present across multiple subtypes and largely absent from early hematopoietic progenitors. The potent antileukemic activity of NEO-201CAR NK cells in preclinical systems highlights the promise of this approach and sets the stage for advancing O-glycan-directed CAR NK therapy into translational and clinical development.

#0134 Anti-tumor activity of engineered iPSC-derived NK cells against metastatic uveal melanoma cells.

Nadia Anikeeva[1], Tong Zhang[1], Sota Deguchi[1], Sergei Koshkin[1], Masashi Yamada[2], Kouichi Tamura[2], Hironobu Kimura[2], Vitali Alexeev[3], Yuri Sykulev[1], Takami Sato[3], Mizue Terai[3]

[1]Medical Oncology, Sidney Kimmel Medical College, Thomas Jefferson University, Philadelphia, PA,[2]Kobe Research institute, HEALIOS K.K, Kobe, Japan,[3]Medical Oncology, Sidney Kimmel Comprehensive Cancer Center, Thomas Jefferson University, Philadelphia, PA

Background:Uveal melanoma (UM) preferentially metastasizes to the liver, leading to a poor prognosis. The immunosuppressive microenvironment of the liver and the low mutation burden of metastatic UM (MUM) contribute to the limited efficacy of immunotherapies, including immune checkpoint inhibitors and adoptive T-cell transfers. Existing evidences highlight the crucial role of Natural Killer (NK) cells in monitoring and targeting circulating MUM cells, suggesting that therapeutic strategies that enhance NK cell activity may offer clinical benefits. Donor variability and limited expansion capacity restricted clinical application of primary NK cells. NK cells derived from induced pluripotent stem cells (iPSCs) present distinct benefits, especially in their ability to be genetically modified to produce cells with improved antitumor characteristics. Therefore, we investigated the antitumor activity of iPSC-NK cells against MUM.
Methods:The functions of iPS-NK cells were enhanced by gene editing, resulting in the production of engineered iPS-NK cells (eNK) that express NKG2D, CD16, CCR2, and secrete CCL19 and IL-15. eNK is being developed as AKT-01/HLCN061 through a collaboration between Akatsuki Therapeutics Inc. and Healios K.K.. The functional properties of eNK cells against UM cell lines, UM001 and UM004, were evaluated in comparison with the intact highly cytotoxic NK92 cell line or with NK92 cells genetically modified with CD16 (NK92-CD16). The activities of the NK cells were assessed using (i) cytotoxic assay; (ii) ADCC assay with anti-GD2 antibodies; (iii) CD107a degranulation assay; and (iv) intracellular cytokine staining. The migration of eNK cells toward UM was evaluated using a transwell migration assay.
Results:The eNK and NK92 cells exhibit a comparable effectiveness in targeting UM001 cells, killing up to 50% of the tumor cells and showing similar frequency of the cells that produce detectable levels of cytolytic granules and IFNγ (5-10%). The cytolytic activity of NK92 cells against UM004 cells was negligible, as was the frequency of cells releasing cytolytic granules and expressing IFNγ. In contrast, eNK cells killed approximately 25% of the UM004 cells, upregulating CD107a membrane expression and intracellular IFNγ production to a similar extent as in the case of UM001 cells. ADCC against UM004 cell lines in the presence of anti-GD2 antibodies was similar (~15%) for both eNK and NK92-CD16 cells. The TNFα intracellular staining in response to UM cells targets was observed only for eNK cells. Importantly, TNFα treatment increased CCL2 production by the UM cell lines. In accordance with this, eNK cells exhibited enhanced migration into chambers containing supernatants from TNFα-stimulated UM001 or UM004 cells.
Conclusions:The data indicated that eNK cells have anti-tumor activity and potential as improved adoptive cell therapeutics in the treatment of MUM.

#0135 Memory-like NK cell targeting to CD123 and CD33 improves killing of acute myeloid leukemia.

Emily Phillips[1], Lyra Morina[1], Lynne Marsala[1], Wilbur Song[1], Michelle Becker-Hapak[1], Yoojin Ahn[1], Sushanth Pureti[1], Elizabeth Juarez Diaz[1], Sadia Afrin[1], Pamela Wong[1], Jennifer Tran[1], Joseph Rueve[1], Allison Burdi[1], Nancy Marin[1], Melissa Marie Berrien-Elliott[1], Martin Felices[2], Jeffrey S. Miller[3], Todd A. Fehniger[1]

[1]Washington University School of Medicine in St. Louis, St. Louis, MO,[2]Masonic Cancer Center, Minneapolis, MN,[3]University of Minnesota, Minneapolis, MN

Background: Memory-like natural killer (ML NK) cells are NK cells which upon stimulation with IL12/15/18 undergo a differentiation process to develop improved metabolic fitness and enhanced killing capabilities of different types of malignant cells. They are a promising cellular therapeutic against acute myeloid leukemia (AML), for which the prognosis remains dismal for both pediatric and adult patients who experience relapse of their AML. Phase I studies of adoptive ML NK cell therapy in adult and pediatric patients showed promising results with several patients achieving complete responses, but many go on to relapse after a few months. We investigate two strategies to improve recognition of AML by memory like NK cells by targeting them to AML surface antigens CD33 and CD123.

Objective: We target ML NK cells to CD123 by engineering ML NK cells to express a chimeric antigen receptor (CD123 CAR ML NK). We target ML NK cells to CD33 via a trispecific killer engager (CD33 TriKE) that enhances the immune synapse by engaging CD16 on the ML NK cell and CD33 on AML. The CD33 TriKE also contains IL-15 to enhance ML NK activation and survival. We also explore whether both technologies function synergistically to prevent immune escape.

Methods: Treatment of AML with ML NK cells vs CD123 CAR ML NK cells, ML NK cells plus CD33 TriKE, or the combination, was compared in series of short and long-term assays. AML targets include MOLM13, THP-1, and Primary AML blasts. Interferon gamma production was assessed in a 6-hour co-incubation. In-vitro killing was assessed at 4-hours using a flow-based killing assay, and at 24 hours using a luciferase-based assay. Tumor control was assessed over 5 days using Incucyte (live cell imaging). Tumor control and survival *in vivo* was assessed using an THP-1 Xenograft model in NSG mice. Primary AML xenografts using NSG-S mice is under development. Results: Both targeting strategies demonstrate an antigen-specific killing response. Both strategies significantly increase interferon gamma production compared to ML NK cells (CAR vs MOLM13: +16.57%, p=0.0002, Primary AML #34: IFNg +9.1% p=0.0092; CD33 TriKE vs MOLM13: +24.42%, p=.0015, AML34: +9.1% p=0.0092). Both strategies also demonstrated increased AML killing at various E:T ratios (CAR vs MOLM13: p=.0011; AML34: p=.0006; CD33 TriKE vs MOLM13: p<.0001; AML34 p=.0026). Both CD123 CAR and CD33 TriKE improved THP-1 control in vivo (bioluminescence at 23 days-CD123 CAR: p=0.004, CD33 TriKE: p<.0001). Both therapies improved median survival by about 3 weeks (CD123 CAR: p<.0001, CD33 TriKE: p=.0001).

Conclusion: CD123 CAR ML NK cells and ML NK cells treated with CD33 TriKE both enhance the abilities of ML NK cells to kill AML *in vitro* and *in vivo*, and prolong time of survival of THP-1 bearing mice. Treatment of CD123 CAR ML NK cells with CD33 TriKE may prevent antigen escape. Either of these targeting strategies are highly translatable to the clinical setting.

#0136 Surface engineered-NK/trastuzumab cells as a novel immunotherapy for HER2-low breast cancer.

Maria Jose Godoy Calderon[1], Manali Patwardhan[1], Shruti Rodrigues[2], Saanvi Sethi[1], Eric Gauchat[3], Vk Gadi[1]

[1]University of Illinois at Chicago, Chicago, IL,[2]University of Illinois College of Med. at Chicago, Chicago, IL,[3]University of Illinois Chicago, Chicago, IL

Purpose: HER2-low breast cancers, which account for most metastatic cases, remain challenging to treat. Although trastuzumab-deruxtecan has shown clinical benefit, its use is limited by high toxicity and disease progression, underscoring the need for safer, more effective, and more accessible targeted options. These tumors disproportionately affect underserved populations, amplifying disparities in care. Building upon our previous development of a murine HER2-low model and NK/Trastuzumab (Tz) surface-engineering platform, we now evaluated the therapeutic potential and selectivity of SE-NK/Tz cells against HER2-low human and murine tumors, including 3D tumor spheroids.

Methods: SE-NK cells were generated by embedding 25 µg of Tz onto the mouse-derived LNK cells or human NK92 cells using a hydrophobic linker, and conjugation efficiency was verified by flow cytometry and confocal imaging. HER2-specific cytotoxicity was evaluated by luciferase-based killing assays in 2D and 3D cultures of 4T1-HER2-low murine cells (generated in our lab) and HER2-low MDA-MB-175 human breast cancer cells. HER2-negative cells were used to assess specificity.

Results: SE-LNK/Tz cells exhibited significantly enhanced cytotoxicity against 4T1-HER2-low targets (86 ± 1 % vs 55 ± 2 %, $p < 0.0001$ at E:T 10:1), consistent across multiple effector-to-target ratios (20:1-2.5:1), compared with unmodified NK cells. SE-NK92/Tz cells similarly increased cytotoxicity against MDA-MB-175 targets (57 ± 1% vs 42 ± 3 %, $p < 0.01$ at E:T 1:1). Importantly, SE-NK/Tz cells showed markedly lower killing of HER2-negative cells (mouse 6 ± 5% vs 69 ± 2%; human 42± 1% vs 57± 1 %, $p < 0.0001$), confirming HER2-specific targeting. SE-LNK/Tz cells maintained activity in 3D spheroid assays, indicating effective tumor penetration.

Conclusions: This study advances our surface-engineering NK platform from proof-of-concept to functional validation in both murine and human HER2-low systems, including 3D culture models. SE-NK/Tz cells display potent and selective cytotoxicity against HER2-low breast cancer, supporting their potential as a next-generation, low-toxicity immunotherapy for this underserved patient population. Ongoing work focuses on exploring mechanisms of immune activation and therapeutic efficacy in diverse in vivo HER2-low models.

#0137 Harnessing allogeneic CAR-iNKT cells for next-generation treatments in oncology and autoimmunity.

Yuhua Wan[1], Dexian Quan[1], Feng Xu[2], Yuzhu Cui[2], Jian Hua[1], Jingyu Li[2], **Hua Zhang**[2]

[1]SPH Biotherapeutics (Shanghai) Limited, Shanghai, China,[2]SPH Biotherapeutics (HK) Limited, Hong Kong, Hong Kong

Background: Chimeric antigen receptor (CAR)-engineered invariant natural killer T (iNKT) cells have demonstrated promising outcomes in clinical studies for both cancer and autoimmune disorders. Their distinctive ability to recognize and eliminate tumor cells, coupled with efficient infiltration into solid tumors and modulation of the tumor microenvironment (TME), positions them as a compelling therapeutic strategy for solid malignancies. Moreover, because iNKT cells do not trigger graft-versus-host disease (GvHD), they are particularly well-suited for allogeneic, off-the-shelf cell therapy approaches.
Methods: Two CAR constructs targeting CD19 and GPC3 were independently generated to evaluate therapeutic efficacy. For CD19 CAR-iNKT cells, NSG mice were intravenously inoculated with 1×10^6 Nalm6 cells per mouse, allowed to engraft for two days, and subsequently treated with either a single dose or three sequential doses of 1×10^6 CAR^+ iNKT cells per mouse administered on days 2, 4, and 6. In parallel, the activity of GPC3 CAR-iNKT cells engineered with PD-1 deletion was assessed in NOG-hIL15Tg mice. Each mouse was implanted with 1×10^6 Hep3B cells three days prior to treatment and then received three tail-vein injections of 18×10^6 GPC3 CAR-iNKT cells (50% CAR^+) or untransduced iNKT cells on days 3, 6, and 9.
Results: In bioluminescent imaging, three sequential doses of CD19 CAR-iNKT cells achieved marked clearance of CD19-positive Nalm6 cells compared with unmodified iNKT cells or a single CD19 CAR-iNKT injection, underscoring their therapeutic potential in B-cell malignancies and autoimmune disorders such as ALL, CLL, and SLE. In contrast, within the Hep3B xenograft model, only GPC3 CAR-iNKT cells engineered with PD-1 deletion,rather than conventional GPC3 CAR-iNKT cells induced tumor regression beginning on day 10, ultimately achieving complete elimination by days 24 and 31 without evidence of graft-versus-host disease.
Conclusions: These findings highlight iNKT cells as a potent allogeneic platform for CAR-based immunotherapy, with broad applicability across cancer and autoimmune diseases, thereby establishing a robust basis for continued clinical investigation.
Ethics Approval: The study was approved by Medicilon's Ethics Board, approval number SWSH(YF)2025-034.

#0138 Generation of scalable off-the-shelf iNKT therapies.

John J. Swain[1], Eoin C. Whelan[2], Chiquita Hanindya[3], Peter Keller[3], **Antonia Rotolo**[4]

[1]Pathobiology, University of Pennsylvania, Philadelphia, PA,[2]Biomedical Sciences, University of Pennsylvania, Philadelphia, PA,[3]BlueWhale Bio, Philadelphia, PA,[4]Pathobiology, Penn Vet Cancer Center, University of Pennsylvania, Philadelphia, PA

Invariant natural killer T cells (iNKTs) are rare T lymphocytes, emerging as an off-the-shelf platform for the treatment of blood and solid tumors, severe viral infections, and graft-versus-host disease. These features hold promise for improving global and equitable access to advanced cellular immunotherapies. However, limited scalability and persistence of donor-derived iNKT products hinder worldwide impact. We set out to establish large-scale iNKT off-the-shelf products capable of extended *in vivo* persistence, including enhanced tumor-redirected iNKTs engineered with chimeric antigen receptors (CAR-iNKT).

Methods. To investigate clinically relevant methods to expand large-scale off-the-shelf products, we tested: 1) activating beads coated with αCD3/αCD28 antibodies; 2) α-galactosylceramide (αGC)-loaded artificial antigen-presenting cells (aAPCs), generated by engineering K562 cells expressing CD80/CD83/CD86/41BBL with the iNKT-specific antigen CD1d; and 3) cell-derived nanoparticles (CDNPs, Synecta T1), a feeder-free platform engineered to display membrane-bound OKT3, co-stimulatory ligands, and IL-7/IL-15 cytokines in a scalable, closed-system format, providing key aAPC-like stimulation cues without using live cell lines. To determine the resulting therapeutic potential, we assessed iNKT purity, yield, memory/exhaustion phenotype, and anti-tumor efficacy via *in vitro* 4h killing and cytokine assays and *in vivo* NSG xenografts.

Results. All activation systems produced pure iNKT products. aAPCs induced the highest iNKT yield, as expected from antigen-specific CD1d-αGC stimulation. CDNPs were as effective as αCD3/αCD28 beads in sustaining proliferation after repeated stimulations. Phenotypically, aAPCs induced the highest CD62L levels, a known predictor of persistence, whereas CDNPs exhibited the most favorable effector profile, including the lowest LAG-3 and TIM-3 expression. CDNPs also showed the strongest *in vitro* cytotoxicity against tumor targets, with up to 60% killing as compared to aAPCs 25% and αCD3/αCD28 beads 35%. *In vivo*, aAPC-manufactured CAR-iNKTs persisted in osteosarcoma-bearing NSG xenografts for 90 days after a single infusion — the longest persistence reported in such a model — associated with complete and durable tumor eradication. Bead-expanded CAR-iNKTs eradicated tumors but were not detected at comparable late time points.

Conclusions. We established clinically scalable iNKT/CAR-iNKT manufacturing workflows yielding high-purity cells. All products exhibited potent anti-tumor activity, but aAPC-expanded CAR-iNKTs resulted in exceptional persistence *in vivo*, superior to bead-expanded cells. The CDNP platform provides a clinically translatable, feeder-free activator that achieves superior functional potency, reduced exhaustion, and regulatory readiness (FDA-reviewed DMF), enabling scalable off-the-shelf iNKT/CAR-iNKT therapy for a broad range of applications.

#0139 Functional profiling of an allogeneic NK cell therapy product in NSCLC patient-derived organotypic tumor spheroids.

Chunxiao Cui[1], Anthony Attardo[1], Mei Rosa Ng[2], Yana Wang[2], **Michael A. Perricone**[3]

[1]XSphera Biosciences, Inc., Cambridge, MA,[2]Takeda Pharmaceuticals International Company, Cambridge, MA,[3]Xsphera Biosciences, Inc., Cambridge, MA

Allogeneic natural killer (NK) cell therapies offer an off-the-shelf strategy for targeting solid tumors, but their functional activity within complex human tumor microenvironments remains poorly defined. We evaluated an allogeneic NK-cell therapy product design (NK cells) and tested its performance using the Xsphera platform, which incorporates patient-derived organotypic tumor spheroids (PDOTS) embedded in extracellular matrix (ECM) and cultured in microfluidic devices that preserve tumor-immune-stromal architecture ex vivo. Assay conditions were first optimized using LS1034 tumor cell spheroids as target cells and cryopreserved NK cells to identify parameters that maximized NK cell activity, including ECM concentration, effector-to-target (E:T) ratio, exposure duration, and media composition. Under optimal conditions, NK cells induced up to 40% tumor spheroid killing, as quantified by live/dead imaging using Hoechst and propidium iodide staining. We next applied these conditions to PDOTS generated from five non-small cell lung cancer (NSCLC) patients. NK cells were introduced at an estimated 2:1 E:T ratio and cultured for 96 hours. Live/dead imaging revealed significant cytotoxic responses in 2 of 5 PDOTS, with live tumor area reductions of up to 50%. The NK cells expressed activation markers (NKG2D, CD69) and secreted elevated levels of interferon-γ, tumor necrosis factor, and granzyme B. Transcriptomic profiling of the media revealed enrichment of interferon-stimulated genes and cytotoxic effectors. Notably, these molecular features did not correlate with tumor responsiveness. These findings demonstrate the utility of the PDOTS platform for functionally profiling NK cell potency in physiologically relevant tumor models and support its use in the rational development of next-generation NK cell therapy products for solid tumors.

#0140 Allogeneic CAR-iNKT cell therapy targeting CLDN18.2-positive gastric and pancreatic cancers.

Clinton M. Heinze[1], Elisa Landoni[2], Michelle Ferguson[1], Nicole van der Weerden[1], **Robson Dossa**[1], Simon Poon[1], Kelvin Yip[1], Jacqui Cumming[1], Alfie Baker[1], Sandford Sarah[1], Michael J. Baker[1], Barbara Savoldo[2], Gianpietro Dotti[2]

[1]Arovella Therapeutics, Melbourne, Australia,[2]University of North Carolina, Chapel Hill, NC

Allogeneic cell therapy offers the advantage of immediate and scalable access to healthy and potent effector cells for the treatment of solid tumors, overcoming patient immune dysfunction and potential manufacturing delays, while enabling durable anti-tumor responses. Invariant natural killer T (iNKT) cells are a rare, specialized subset of unconventional T cells that represent an ideal allogeneic cell therapy platform. They express a semi-invariant T cell receptor (iTCR) that recognizes glycolipid antigens presented by the monomorphic, MHC-like molecule, CD1d. Previous studies have shown that iNKT cells do not induce acute graft-versus-host disease, and iNKT cells engineered to express chimeric antigen receptors (CARs) have demonstrated therapeutic potential. In addition to tumor recognition via the CAR, iNKT cells can engage tumors via the endogenous iTCR binding to glycolipid-bound CD1d and via the NKG2D receptor. CAR-iNKT cells offer distinct advantages in the treatment of solid tumors due to their natural ability to home to tissues, infiltrate tumors, and modulate the tumor microenvironment.

Claudin 18.2 (CLDN18.2) has emerged as a high-priority target for novel cancer therapies. Under normal physiological conditions, its expression is limited to tight junctions between epithelial cells and remains inaccessible on the cell surface. However, in several malignancies, including gastric, esophageal, and pancreatic cancers, CLDN18.2 becomes surface-exposed as tumor cells lose normal tissue architecture during growth and invasion. This aberrant presentation in malignant tissue makes CLDN18.2 an attractive target for CAR-directed cell therapies.

Here, we present the first PBMC-derived CAR-iNKT cell therapy product targeting CLDN18.2. This second-generation CAR features a short chain variable fragment (scFv) derived from SPX-101, a novel monoclonal antibody engineered for enhanced affinity and selectivity for CLDN18.2. To support iNKT cell function, membrane-bound IL-12 (IL-12-TM) was incorporated to provide cytokine armouring, which has been shown to enhance CAR-iNKT cell activity. In this work, iNKT cells were isolated from healthy donor PBMCs, activated, transduced to express the CLDN18.2 CAR with and without IL-12-TM co-expression, and expanded in culture. Cytotoxic activity and effector expansion were evaluated using a serial tumor re-challenge assay against CLDN18.2-positive gastric and pancreatic cancer cell lines. CLDN18.2 CAR-iNKT cells exhibited potent and sustained cytotoxic activity against CLDN18.2-positive tumor cells, and co-expression of IL-12-TM improved the persistence and durability of response under repeated high tumour burden. These findings support the potential of cytokine-armoured CLDN18.2-directed CAR-iNKT cells as an allogeneic cell therapy for the treatment of gastric and pancreatic cancers.

#0141 Selecting cord blood-derived NK cells enriched in mature subsets optimizes CAR-NK cell-based anti-tumor therapy.

Ye Ethan Li, Huihui Fan, Rafet Basar, Wilson Jeffrey, Patrick Zhang, Katayoun Rezvani

UT MD Anderson Cancer Center, Houston, TX

Background: CAR-modified natural killer (CAR NK) cell therapy offers a promising "off-the-shelf" cell therapy, with promising clinical activity with a favorable safety profile. Clinical efficacy, however, varies between umbilical cord blood (CB) donors. A deeper understanding of the cellular and molecular factors driving this variability is essential to improve the manufacturing and performance of CAR NK therapies.

Methods: We analyzed products from our first-in-human clinical study of CB-derived CAR19/IL-15 NK cells in B cell malignancies (NCT03056339). We had shown that donor selection affected clinical outcome, with some donors linked to better responses and longer progression free and overall survival, and others to poorer outcomes. To define the cellular basis for this effect, we returned to those specific donors and performed integrated single-cell RNA and antibody-derived tag (ADT) sequencing on their NK cells both before manipulation and after *ex vivo* expansion using the same protocol used for the trial. We then related donor intrinsic states and specific cellular subsets with clinical responses.

Results: Unsupervised clustering identified two distinct NK cell subsets based on their expression of CD16 and CD161. A double-negative (DN) subset ($CD56^{bright}CD16^{-}CD161^{-}$) and its expanded progeny showed reduced expression of key activating receptors and adaptor molecules, consistent with limited effector function signatures after expansion. Conversely, the double-positive (DP) subset ($CD56^{dim}CD16^{+}CD161^{+}$) maintained a robust adaptive-like cytotoxic profile, characterized by stronger membrane-proximal activation signaling and high effector-gene expression that persisted through expansion. Notably, trial CAR-NK cell products generated from CB donors enriched for the DP subset were associated with superior clinical benefits, whereas enrichment for the DN subset was associated with worse outcomes.

Conclusions: Our single-cell multiomic analysis reveals previously underappreciated donor-intrinsic diversity within CB-NK cells, which may explain the functional heterogeneity among CAR NK cell products. These results provide a mechanistic foundation for donor selection strategies and for targeted genetic improvements that can raise the consistency and potency of future allogeneic CAR NK cell therapies.

#0142 A universal multi-receptor NK cell platform engineered for synergistic combination with antibody and T-cell engager therapies.

Rafet Basar[1], Bin Liu[1], Nadima Uprety[1], Francia Reyes Silva[1], Rejeena Shrestha[1], Sunil Acharya[2], May Daher[1], Ana K. Nunez Cortes[1], Deqiang Zhang[1], Bingqian Hu[1], Silvia Tiberti[1], Madison Moore[1], Ye Ethan Li[1], Pinghua Liu[1], Hila Shaim[1], Jeong-Min Park[1], Mecit Kaplan[1], Xingliang Guo[1], Mayra Shanley[1], Ping Li[1], Paul Lin[1], Pinaki Banerjee[1], Huihui Fan[1], Patrick Zhang[1], Enli Liu[1], Seema Rawal[3], Elizabeth Joan Shpall[4], Katayoun Rezvani[1]

[1]UT MD Anderson Cancer Center, Houston, TX,[2]Molecular and Cellular Oncology, UT MD Anderson Cancer Center, Houston, TX,[3]Postdoctoral Fellow, UT MD Anderson Cancer Center, Houston, TX,[4]Professor of Medicine, Dept. of Stem Cell Transplant & Cell Therapy, UT MD Anderson Cancer Center, Houston, TX

Background: Monoclonal antibodies (mAbs) and T-cell engagers (TCEs) redirect immune effector cells toward malignant targets, yet their efficacy is often limited by patient T- and NK-cell dysfunction. Conventional CAR strategies target a single antigen, requiring new construct design, GMP production, and separate regulatory pathways for each target. To combine the strengths of engager- and cell-based approaches, we developed PluraliNK cells, a universal multireceptor NK-cell platform activated through CD3/TCR- and Fc-dependent pathways. This enables redirection by any approved mAb or TCE without additional engineering, creating a flexible plug-and-play NK therapy.

Methods: NK cells were engineered using two polycistronic vectors to express the full CD3 complex, IL-15 for cytokine support, high-affinity CD16A (F158V) for enhanced Fc engagement, and an invariant TCR α/β (iTCR) to stabilize CD3 and permit CD1d-restricted recognition. This dual-activation system allows PluraliNK cells to respond to CD3- or CD16-mediated signals and to pair with diverse mAbs or TCEs without further modification.

Results: PluraliNK cells showed potent cytotoxicity across hematologic and solid tumor models when combined with approved mAbs (rituximab, trastuzumab) or TCEs (blinatumomab, glofitamab, elranatamab), consistently outperforming mAb/TCE monotherapy or unmodified NK cells. The platform supports simultaneous engagement by multiple antibodies or TCEs, enabling clearance of heterogeneous tumor populations and reducing antigen escape. Dual-input signaling enhanced activation, serial killing, and resistance to exhaustion, an advantage in solid tumors with spatial heterogeneity and lineage plasticity. Because PluraliNK activation depends on an external mAb or TCE, the system provides an additional safety layer compared with constitutively active CAR constructs. In NSG xenograft models, PluraliNK cells combined with mAbs or TCEs achieved superior tumor clearance, improved infiltration, and enhanced in vivo persistence without off-target toxicity.

Conclusions: This universal NK-cell platform enables multiantigen targeting and integration with existing mAbs and TCEs, addressing tumor heterogeneity and immune escape without requiring antigen-specific CAR redesign. A first-in-human clinical trial of PluraliNK cells with antibody therapy has been initiated.

#0143 Enhancing γδ CAR T cell function through alternative CD3 cytoplasmic domains.

Philipp Metzger[1], Marina Zintchenko[2], Susana Minguet[2], Cynthia Obodozie[1], **Holger Weber**[1]

[1]Reaction Biology Europe GmbH, Freiburg, Germany,[2]Signaling Research Centres BIOSS and CIBSS; Department of Synthetic Immunology, Faculty of Biology, University of Freiburg, Freiburg, Germany

Gamma delta (γδ) T cells are a unique subset of lymphocytes that possess innate and adaptive immune functions. Unlike conventional αβ T cells, γδ T cells recognize antigens in an MHC-independent manner. This allows them to detect a wide range of stress-induced ligands that are commonly expressed on tumor cells. This property makes γδ T cells particularly attractive for cancer immunotherapy, especially in cases where tumors evade immune surveillance by downregulating MHC molecules. Recent advances in cellular engineering have made it possible to generate γδ T cells that express chimeric antigen receptors (CARs), which combines their natural tumor-recognition capabilities with the targeted specificity of CARs. γδ CAR T cells offer several advantages over αβ CAR T cells, including lower graft-versus-host disease risk, suitability for allogeneic applications (“out-of-the-shelf”), and enhanced solid tumor infiltration due to tissue-homing properties. These properties provide a strong rationale for investigating γδ CAR T cells as a novel cancer therapy approach and underscore the importance of continued optimization to realize their full therapeutic potential.

This study explores strategies to improve the intracellular signaling domain of CAR constructs with a focus on γδ T cells. The CD3ζ domain has traditionally been used as the primary activation motif in CAR design. However, emerging evidence suggests that it may not be optimal for all T cell subsets. Therefore, we investigated alternative CD3 subunits, specifically, CD3δ, CD3ε, and CD3γ, as intracellular signaling domains in CAR constructs. Our in vitro data show that CARs with these alternative CD3 cytoplasmic tails are more effective than conventional CD3ζ-based CARs in terms of activation and cytotoxicity. In vivo validation of αβ CAR T cells incorporating alternative CD3 subunits has demonstrated enhanced antitumor efficacy. To extend these findings, in vivo experiments are currently underway using the NALM-6_luc (luciferase expressing) xenograft model, a well-established system for evaluating next-generation cellular therapies. These experiments aim to explore whether similar benefits apply to γδ CAR T cells. If confirmed, these results would underscore the potential of leveraging alternative CD3 signaling domains to optimize CAR T cell performance, particularly in γδ T cell-based therapies.

Our findings provide a compelling rationale for reevaluating CAR construct design, suggesting that alternative CD3 subunits could significantly enhance the therapeutic potential of γδ CAR T cells in cancer treatment.

#0144 *In vivo* CAR mRNA engineering of both adaptive and myeloid cells enables potent anti-tumor control of solid cancers.

Junming Tong[1], Moore Chen[2], Kevin Sek[1], Meghan Harris[3], Jerome Chal[3], Colin Pouton[2], Angus Johnston[2], Daniel Getts[3], Robert Hofmeister[3], Phil Darcy[1], **Jian Ding**[3]

[1]Sir Peter MacCallum Department of Oncology, University of Melbourne, Peter MacCallum Cancer Centre, Melbourne, Australia,[2]Drug Delivery, Disposition and Dynamics, Monash Institute of Pharmaceutical Sciences, Monash University, Parkville, Australia,[3]CREATE Medicines, Cambridge, MA

Background: In solid tumors, chimeric antigen receptor (CAR) T cell therapies are limited by their inability to overcome poor trafficking, antigen heterogeneity and the immunosuppressive myeloid cells in the tumor microenvironment (TME). Here, we introduce in vivo multi-immune cell programming designed to precisely and simultaneously program multiple immune cell types using a single engineered product. This approach builds on the clinical experience with in vivo CAR-mRNA engineered CAR myeloid cells that created a pro-inflammatory tumor environment. Combining non-targeted and targeted LNP delivery, optimized mRNA, and cell-specific CAR architecture, we endow myeloid cells, NK cells and T cells with tailored effector functions.
Methods: Anti-HER2 CAR mRNAs optimised for myeloid, NK or T cell signalling were encapsulated in LNPs and delivered intravenously. Anti-tumor efficacy was evaluated in immunocompetent hHER2 transgenic mice bearing syngeneic hHER2-MC38 colon adenocarcinoma tumors.
Results: In a colorectal tumor model, myeloid- and NK-cell reprogramming with CAR mRNA/LNPs drove tumor regression, prolonged survival, remodeling of the tumor microenvironment, greater antigen presentation, and enhanced T-cell infiltration and activation. Likewise, T cell engineered with CAR mRNA/tLNPs elicited robust anti-tumor activity. Notably, co-delivery of cell-specific CAR mRNA/LNPs to both myeloid and T-cell compartments produced even stronger tumor control, highlighting the power of coordinated multi-lineage immune engineering.
Conclusions: This work demonstrates that simultaneous In vivo engineering of myeloid cells, T cells, and NK cells with CARs can orchestrate the coordinated actions of both innate and adaptive immunity for potent anti-tumor activity. This strategy offers a scalable and off-the-shelf approach for cell therapy and establishes a new therapeutic paradigm for overcoming the complexity of solid tumors.

#0145 CD8 nanobody-targeted lipid nanoparticles encapsulating CD13 nanoCAR circular RNAs for in situ CAR-T cell eradication of acute myeloid leukemia.

Wilson Huang[1], Diva Chen[1], Yun-Chin Chou[1], Tsung-Chih Chen[1], Chia-Jen Wu[2]

[1]Citil Pharma, Cambridge, MA,[2]Academia Sinica, Taipei, Taiwan

Acute myeloid leukemia (AML) is an aggressive and recurrent cancer with a high mortality rate. Chimeric antigen receptor (CAR)-T cell therapy is an FDA approved therapy for acute lymphoblastic leukemia (ALL) but not for AML mainly due to hematopoietic stem and progenitor cell side effects. This is driven by persistent CD13, CD33, CD123 targeting from lentivirus-transduced CAR-T cells. Yet, CD13, a prognostic marker for AML, identifies 95% of the AML blasts and most leukemic stem cells (LSCs). AML is also a heterogenous cancer with diverse antigen profiles, posing treatment challenges. Finally, current CAR-T cell therapies are immensely costly due to cumbersome ex vivo T cell and viral procedures, restricting patient access.

We aim to overcome these technical challenges by leveraging the low tonic signaling of VHH-based nanobodies, transient expression of circular RNAs (circRNAs), and non-viral properties of lipid nanoparticles for effective eradication of AML while minimizing negative hematopoietic effects. Specifically, we attached CD8 nanobodies to lipid nanoparticles, constructed CD13 nanoCARs on circRNA backbones, and assembled the targeted circRNA lipid nanoparticle complexes. These complexes enable in situ, cell-specific engineering of splenic human CD8+ T cells and generate cytotoxic CD13 nanoCAR-T cells that target the prevalent AML population. We demonstrated the feasibility of this approach by generating a CD8 nanobody with 86% reactivity toward human CD8+ T cells. We then customized the CD8 nanobody with a negatively charged polyglutamic acid tail to form strong electrostatic associations with our positively charged, proprietary lipid nanoparticles. We produced CD13 nanoCAR circRNAs with undetectable levels of double-stranded RNA impurities through cellulose purification and encapsulated them in the lipid nanoparticles by microfluidic mixing. The entire targeted circRNA lipid nanoparticle complex selectively transfected 24% of the human CD3+ lymphoid T cells in the spleen of NPG mice previously reconstituted with human PBMCs. We then assayed and selected the THP-1 human AML cell line showing high CD13 expression and low nonspecific T cell killing in vitro. In an immunodeficient NPG CDX mouse model, CD8 nanobody-targeted lipid nanoparticles encapsulating CD13 nanoCAR circRNAs exhibit specific and effective in vivo killing of a subcutaneously engrafted THP-1 tumor.

#0146 *In vivo* lentiviral CAR-T gene delivery demonstrates high specificity and potent anti-tumor activity in a humanized B cell lymphoma model.

Ilian Radichev[1], Devin Stranford[2], Hailey Edelstein[2], Oanh Pham[1], Destanie Rose[1], Jiwon Yang[1], Mahdy Yassine[2], Henry Schirmer[2], Teresa Nikolich[2], Joshua Leonard[2], James Keck[1], Matteo Stoppato[2]

[1]Innovation and Product Development, The Jackson Laboratory-West, Sacramento, CA,[2]Syenex, Inc, Evanston, IL

Introduction: Chimeric Antigen Receptor T (CAR-T) cell therapies have revolutionized treatment for hematologic malignancies, particularly B cell cancers, and show promise in autoimmune diseases and solid tumors. Despite this success, the conventional approach to CAR-T manufacturing presents several limitations: it requires leukapheresis, PBMC isolation, ex vivo genetic modification and expansion, and reinfusion back into the patient. These steps are time-consuming, costly, and logistically complex, limiting scalability and patient accessibility. Furthermore, current CAR-T therapies have shown limited efficacy against solid tumors due to poor trafficking, immunosuppressive microenvironments, and antigen heterogeneity.

Methods: To improve the cost-inefficient and time-consuming challenges of the standard CAR-T therapy, Syenex developed Vivo-T, a novel T cell-specific lentiviral vector (LVV) platform enabling in vivo delivery of CAR constructs, eliminating the need for ex vivo manipulation and personalized CAR-T manufacturing. This system was evaluated in JAX PBMC-humanized B cell lymphoma mouse model. NSG-MHC I/II double knockout mice were irradiated and injected intravenously with 2.5×10^5 Raji-Luc cells. Five days later, mice were engrafted with 1×10^7 human PBMCs. Between 4-24 hours post-engraftment, mice received intravenous doses of T cell-targeted LVVs encoding anti-CD19 CARs. Tumor burden was monitored via IVIS imaging for 3 weeks. Toxicity was assessed through body weight, clinical observations, and serum cytokine analysis. CAR-T engraftment and expansion were evaluated by flow cytometry of peripheral blood.

Results: In vivo delivery of the CAR construct resulted in efficient T cell transduction, with rapid and robust CAR-T expansion surpassing that of ex vivo-engineered CAR-T control. Notably, significant anti-tumor activity was observed as early as 7 days post-LVV administration. Initial signs of toxicity were primarily attributed to high viral titers; however, these effects were mitigated by reducing the viral load, without compromising the antitumor efficacy of the treatment. These findings validate the efficacy of the in vivo CAR-T system and support its potential for clinical translation.

Conclusion: The Vivo-T system represents a transformative approach to CAR-T therapy by simplifying manufacturing, reducing costs, and enabling scalable, off-the-shelf immunotherapy.

#0147 A multipronged approach to improve gene delivery efficiency for *in vivo* CAR-T using CD3 and CD7 retargeted LVVs.

Longshan Liu[1], Cheng Luo[1], Yangyang Tang[1], Lianqu Li[1], Hai Huang[1], Mangmang Li[1], **Yu Liang**[2]

[1]Probio Inc, Nanjing, China,[2]Probio Inc, Pennington, NJ

Chimeric antigen receptor (CAR)-T therapies have advanced cancer treatment; however, for conventional *ex vivo* CAR-T therapies, patient access is often hindered by high costs, long manufacturing times, lymphodepleting chemotherapy needed to precondition the patient, and the inconvenience to travel to specialized treatment centers. To address these limitations, strategies have recently emerged to generate CAR-T cells *in situ*. These approaches, comprising the field of *in vivo* CAR-T, are based on delivering the CAR construct to T cells *in situ* typically using either lentiviral vectors (LVV) or lipid nanoparticles (LNP) decorated with T cell-specific antibodies. *In vivo* CAR-T approaches have demonstrated encouraging efficacy in preclinical and early clinical studies, but still face challenges in terms of efficiency, specificity, durability, and scalability. CD3 and CD7 are well-established T cell targets used in current *in vivo* CAR-T delivery vehicles, and such LVV and LNP-based approaches are showing encouraging efficacy in CAR gene delivery to T cells *in situ*; however, the efficiency of current approaches based on monospecific CD3 or CD7 antibodies for *in vivo* gene delivery still remains low, thereby limiting their therapeutic potency. By using internally developed CD3 and CD7 VHH antibodies, we implemented a multipronged approach to improve the gene delivery efficiency *in vivo*, including 1) incorporation of a CD3+CD7 bispecific antibody in the LVV particle; 2) inclusion of a HIV component in the LVV particles that counteracts host antiviral defense mechanisms to enhance transgene expression; 3) co-administration of an approved cardiovascular drug that enhances CD7 expression in T cells. *In vitro* assays in a T cell line and primary T cells and in vivo studies with mice and non-human primates demonstrated that these novel approaches and their combinations substantially improved CAR gene expression compared with CD3 or CD7 monospecific-targeted LVVs.

#0148 *In vivo* CAR-T T-LNP system (GT801) drives potent B cell depletion and clinical feasibility in hematologic and autoimmune conditions.

Jingwei Sun[1], Xi Zhu[2], Jiahui Jin[1], Yiyang Tan[1], Liang Lin[1], Zhao Xu[1], Jingman Wang[1], Dalang Li[2], Hong Chen[2], Jiaming Ren[2], Jun Cui[1], Jing Yu[1], **Pin Wang**[3], Yarong Liu[4]

[1]Grit Biotechnology, Shanghai, China,[2]Shanghai Vitalgen Biopharma, Shanghai, China,[3]University of southern california, Los Angeles, CA,[4]Vivacta Biotechnology (Shanghai) Co., Ltd., Shanghai, China

Background: CAR-T therapies have revolutionized hematologic malignancies treatment but remain constrained by complex autologous manufacturing, high cost, and lymphodepletion toxicity. In vivo CAR-T approaches aim to overcome these barriers by engineering T cells directly in patients, which requires targeted delivery, durable CAR expression, potent cytotoxicity, and re-dosing potential. Toward this goal, we present the development, preclinical data, and preliminary clinical results for GT801, a novel anti-CD19 in vivo CAR-T candidate.

Methods: GT801 uses T cell-targeted lipid nanoparticles (T-LNPs) encapsulating chemically modified linear mRNA encoding an anti-CD19 CAR. T-LNPs were surface-engineered with a VHH antibody using the CLAMP platform, enabling site-specific antibody attachment, controlled ligand density, and efficient, selective T-cell uptake. Formulation and mRNA design were optimized for targeting specificity, robust CAR expression, and functionality. B-cell depletion, PK, and preliminary toxicology of GT801 were assessed in vitro and in humanized NOG mouse models.

Results: With optimized mRNA chemistry, the T-LNP platform achieves robust and durable CAR expression in human PBMCs for >14 days in vitro. Targeted delivery at 0.1 mpk reached receptor-saturating levels across multiple lymphoid tissues, while off-target uptake remained <1%. In human PBMC-engrafted NOG mice, a single i.v. dose as low as 0.01 mpk achieved >95% B-cell depletion, and 0.1 mpk achieved near-complete clearance (<0.1%) across multiple lymphoid tissues. CDX models demonstrated potent antitumor activity and enhanced CAR-T expansion upon repeat dosing, suggesting good in vivo fitness post-transfection and expansion driven by B cell depletion. Primary B-cell killing was robust in PBMCs from healthy donors and autoimmune patients at only 0.1 μg within 24 hours. Serial-dose toxicology elicited minimal cytokine release (IL-6, TNF-α) and no organ toxicity in any tested organs, supporting the platform's good safety profile. Preliminary clinical data with B-cell hematological malignancies and autoimmune diseases demonstrated high in vivo CAR expression and confirmed repeat-dosing feasibility.

Conclusion: These findings demonstrate that our T-LNP platform enables efficient, targeted, and sustained in vivo CAR expression with a favorable safety profile and scalable manufacturing. The platform's robust preclinical B cell depletion efficacy, validated by preliminary clinical data confirming high in vivo CAR expression and repeat dosing feasibility, successfully validates the system for clinical use. Ongoing patient accrual will further inform clinical outcomes.

#0149 Erythrocyte-mediated mRNA delivery enables *in vivo* generation of CAR-myeloid cells for cancer immunotherapy.

Xiaoqian Nie, Yuehua Liu, Xiaofei Gao

Westlake University, Hangzhou, China

Background: Engineering myeloid cells with chimeric antigen receptors (CARs) holds great therapeutic promise, yet their generation *in vivo* remains challenging. Despite the success of COVID-19 vaccines, targeted mRNA delivery to immune cells remains inefficient. Conventional lipid nanoparticles (LNPs) primarily target the liver upon systemic administration, limiting their utility for lymphoid organs. Moreover, LNPs suffer from low endosomal escape rate and may induce off-target toxicities. Here, we developed an erythrocyte-mediated mRNA delivery system in which mRNA-loaded LNPs are covalently conjugated to erythrocyte membrane proteins in a “plug-and-play” manner, termed mRNA-LNP-Ery. Leveraging erythrocytes’ natural splenic homing, mRNA-LNP-Ery enables selective spleen-specific targeting and efficient mRNA delivery to immune cells for cancer immunotherapy.
Method: We characterized the biodistribution of mRNA-LNP-Ery across multiple mRNA cargoes. To elucidate internalization mechanisms, time-course confocal imaging was performed. Anti-HER2 and anti-CD19 CAR mRNAs were delivered via erythrocytes, and the therapeutic efficacy was assessed in corresponding syngeneic tumor models.
Result: Exploiting erythrocytes’ intrinsic splenic homing capacity, mRNA-LNP-Ery achieved highly selective and efficient mRNA delivery to the spleen while minimizing hepatic uptake. Cellular characterization showed preferential targeting of splenic $CD11b^+$ myeloid cells. Mechanistically, mRNA-LNP-Ery was internalized through phagocytosis while escaping lysosomal degradation, resulting in markedly enhanced mRNA translation and protein expression. To evaluate the therapeutic potential of this platform, we delivered mRNAs encoding CARs targeting HER2 or CD19, which generated functional CAR-myeloid cells *in vivo*, which adopted a pro-inflammatory, antigen-presenting phenotype. These cells migrated to tumors, eliminated cancer cells, and remodeled the tumor microenvironment, leading to increased infiltration of effector T and NK cells. Functionally, mRNA-LNP-Ery induced stronger and more durable tumor regression than conventional mRNA-LNPs across multiple tumor models, including immune-cold tumors, despite using only one-tenth the mRNA dose. The antitumor effect was abolished in splenectomized mice and partially diminished in nude mice, indicating dependence on both CAR-myeloid formation in the spleen and crosstalk with adaptive immunity. Moreover, mRNA-LNP-Ery induced minimal systemic toxicity, underscoring the safety and translational potential of this spleen-targeted delivery approach.
Conclusion: Together, our findings establish a clinically translatable erythrocyte-based mRNA platform that integrates with existing LNP technology to enable direct *in vivo* immune cell programming and advance CAR-immune cell therapies for solid tumors.

#0150 T-cell specific transcriptional control eliminates CAR-mediated off-target transduction by CD3-retargeted lentiviral vectors, enabling safe *in vivo* generation of potent αBCMA-CAR T cells.

Karina Krotova[1], Nandakumar Packiriswamy[1], MD Yeashin Gazi[1], Collin Gwilt[1], Chia-Hsuan Chin[1], Ajay Kumar[1], Aaron Hawkes[1], Gopal Naik Nenavath[1], Thipparat Suwanmanee[2], Darren Phung[2], Luke W. Breigenzer[2], Timothy Carey[1], Christian Kinney[1], Hamid Salimi[1], Patrycja Lech[2], Kah-Whye Peng[2], Stephen Russell[2]

[1]Imanis Life Sciences, Rochester, MN,[2]Vyriad, Rochester, MN

CAR T-cell therapy is a transformative treatment for hematologic malignancies. A key milestone to expand access to this technology is to enable CAR-T generation directly within the patient. For in vivo therapy, the CAR delivery vehicle must resist serum neutralization, target T cells and exhibit minimal or no off-target effects. We recently developed the CD3-targeted lentiviral vector LV-169 which delivers a BCMA CAR transgene to lymph node-resident primary T cells in vivo. LV169 incorporates a VSV-G protein that has been detargeted (blinded) from its natural LDL receptor and re-targeted to T cells via a displayed CD3-specific scFv. However, CAR proteins incorporated into the LV-169 envelope during packaging can induce off-target transduction of malignant plasma cells. Here, we reversed the orientation of the CAR transgene and placed it downstream of the human distal Lck promoter. In contrast to the EF1α promoter, the Lck promoter was transcriptionally silenced in 293 suspension cells but was insufficiently active in Jurkat cells and primary T cells. We therefore inserted a TATA box and a CMV enhancer into the Lck promoter (Lck1.3). The reverse-orientation Lck1.3-driven CAR construct (R-Lck1.3) did not express the BCMA-CAR protein in transfected 293 LV producer cells but was highly active in LV-transduced Jurkat cells and primary human T cells. Western blotting confirmed the high abundance of CAR protein in EF1a-driven vector particles and its absence in R-Lck1.3 particles. Therapeutic efficacy of LV169-R-Lck1.3 vectors encoding the BCMA-CAR was evaluated in human PBMC-engrafted NSG-DKO mice with advanced, disseminated human multiple myeloma. Mice were engrafted with OPM-2-FLuc cells and humanized with PBMCs one week prior to vector infusion. Tumor burden was monitored weekly via luciferase imaging. A single intravenous dose of LV169 (1×10^9 LVP) resulted in complete tumor clearance within 14 days. Circulating anti-BCMA CAR-T cells were detectable 14 days after LV injection but became undetectable once the tumor was eliminated. No severe toxicity was observed, based on stable body weight and cytokine levels in the blood. No tumor growth was observed in treated mice that were re-challenged with OPM-2 on days 22 and 30. In summary, our newly developed LV169-R-Lck1.3 platform encoding the BCMA-CAR demonstrates potent therapeutic activity, and its further clinical translation is underway.

#0151 Combination of cytokines, PM21-particle stimulation, and TGF-β conditioning results in Natural Killer cells with enhanced cytotoxicity and infiltration of solid tumors.

Jeremiah L. Oyer[1], Tayler J. Croom-Perez[1], Javier A. Rivera-Huertas[1], Brian P. Tullius[2], Alicja J. Copik[1]

[1]Burnett School of Biomedical Sciences, University of Central Florida, College of Medicine, Orlando, FL,[2]Pediatric Cellular Therapies, Advent Health for Children, Orlando, FL

In this study, feeder cell-free PM21 particle activation of Natural Killer (NK) cells was combined with cytokine activation and TGF-β conditioning to produce highly proliferative and cytotoxic NK cells that can infiltrate solid tumors. Development of NK cell therapeutics is a promising anti-cancer therapy. For clinical applications, NK cells are typically either *ex vivo* activated with cytokines or expanded with feeder cells or by feeder cell-free methods. One such method for feeder cell-free expansion of highly cytotoxic NK cells uses plasma membrane particles containing surface IL-21 and 41BBL (PM21). Additionally, NK cells expanded with IL-12, IL-15, and IL-18 in combination with PM21 stimulation (CAP-NK cells) exhibit robust proliferation, potent cytotoxicity, and memory-like features. To further improve their activity against solid tumors—a setting often resistant to NK cells—we introduced TGF-β conditioning. Previous studies have shown that ex vivo TGF-β conditioning induces IFNγ hypersecretion. To assess whether this could enhance anti-tumor function, PM21- and CAP-NK cells were expanded in the presence of TGF-β. The CAP-based expansion method still resulted in enhanced NK-cell expansion, even with TGF-β conditioning. CAP-based expansion remained highly effective even with TGF-β conditioning, achieving an average 4000±700-fold expansion by day 14 compared to 1800±60-fold for PM21-NK cells. TGF-β conditioned NK cells retained high viability after cryopreservation (>80% immediately and at 16 h post-thaw) and 99±1% expressed CD25 by day 7. These cells produced significantly more IFNγ upon stimulation than unconditioned CAP-NK cells. Moreover, TGF-β conditioned CAP-NK cells acquired a tissue-resident-like phenotype (CD103+, CD49a+, CD300a–) not observed in PM21- or CAP-NK cells, which would be expected to enhance their ability to infiltrate tumors. To test this, labeled TGF-β conditioned CAP-NK and PM21-NK cells were co-cultured with large lung tumor spheroids and monitored via live-cell imaging. TGF-β conditioned NK cells penetrated tumors faster and deeper than PM21-NK cells, which remained mostly at the periphery, resulting in greater spheroid killing—even in tumors overexpressing TGF-β.TGF-β conditioning also enhanced cytotoxicity against multiple solid tumor cell line spheroids, including lung, pancreatic, and neuroblastoma. Overall, these findings support TGF-β conditioned CAP-NK cells as a potent cellular therapy candidate for solid tumors.

#0152 Toward an *in vivo* anti-BCMA/CD19 CAR-T cell treatment of B cell-mediated autoimmune diseases.

Alexander J. Najibi, Denise Wong, Jeff Wood, Tharani Sivanandam, Han K. Lee, Josue Figueroa, Kelly Nichols, Yao Wei, Emily T. Beura, Shannon Grande Contrastano

Kelonia Therapeutics, Boston, MA

B cell-mediated autoimmune disorders, including systemic lupus erythematosus (SLE), can represent lifelong inflammatory conditions with limited therapeutic options. Autologous CD19-specific CAR-T cells have been demonstrated as an effective treatment option. However, access to CAR-T cell therapies and the use of preparative chemotherapy will ultimately limit the reach of this powerful modality. Moreover, recent data suggest that CD19-negative pathogenic plasma cells can emerge and contribute to SLE disease etiology, suggesting that development of CAR-T cells addressing both CD19-positive and CD19-negative pathogenic B cells is warranted. Here, we describe the preclinical development of an engineered lentiviral vector (LVV) previously shown to specifically modify T cells in vivo (in vivo gene placement system (iGPS®)), encoding a chimeric antigen receptor (CAR) that recognizes both CD19 and B-cell maturation antigen (BCMA) antigens ("tandem CAR"). The operative arms of the tandem CAR were identified by screening a panel of human anti-BCMA and anti-CD19 antibodies incorporating a variety of design features. Candidate tandem CAR constructs were expressed in T cells from healthy donors and SLE patients using iGPS particles. The constructs that caused antigen-specific in vitro T cell activity, assayed by cytotoxicity and cytokine release to cell lines expressing BCMA and/or CD19, were tested in several animal models. First, an SLE mouse model was established using immunocompromised mice humanized with peripheral blood mononuclear cells from SLE patients. After a single dose of the lead tandem CAR iGPS particle, CAR-T cells were generated and expanded in vivo resulting in complete elimination of SLE B cells in the blood, spleen, and bone marrow. In a second mouse model treating an aggressive B cell lymphoma, the iGPS particle delivering the lead tandem CAR caused effective tumor control after a single treatment. These data demonstrated the potential of a tandem anti-BCMA/CD19 CAR-T cell generated in vivo with iGPS particles as an effective treatment of autoimmune disorders. Moreover, persistent CAR-T cells generated using an LVV may provide a single, off-the-shelf treatment capable of eliminating both pathogenic CD19-positive B cells and emergent CD19-negative plasma cells and provide a needed therapy for patients.

#0153 Improvement of monoclonal antibody therapy against cancer through engineering stem cell-derived CD16-enhanced universal NKT cells.

Yan-Ruide Li, Yichen Zhu, Yanqi Yu, Lili Yang

Department of Microbiology, Immunology & Molecular Genetics, University of California, Los Angeles, Los Angeles, CA

Monoclonal antibody (mAb)-based immunotherapies have revolutionized cancer treatment, yet their efficacy remains limited in many solid and hematologic malignancies due to insufficient effector cell engagement, tumor antigen loss, and immunosuppressive tumor microenvironments. To overcome these limitations and enhance the therapeutic potential of mAb therapy, we developed an allogeneic invariant natural killer T (NKT) cell platform through hematopoietic stem cell (HSC) engineering and feeder-free in vitro differentiation. Specifically, we introduced an invariant NKT T cell receptor (TCR) and a high-affinity, non-cleavable CD16a (FcγRIIIa) receptor into HSCs, enabling the generation of CD16-enhanced HSC-engineered NKT (^{CD16}HSC-NKT) cells. These cells can be produced at high yield and purity in a scalable, feeder-free culture system. The resulting ^{CD16}HSC-NKT cells preserve the hallmark NKT phenotype and exhibit robust cytokine secretion, cytotoxicity, and tumor infiltration capacity. Functionally, ^{CD16}HSC-NKT cells mediate potent antibody-dependent cellular cytotoxicity (ADCC) both in vitro and in vivo when combined with tumor-specific monoclonal antibodies, leading to synergistic tumor regression. Beyond direct cytotoxicity, ^{CD16}HSC-NKT cells also display multi-targeted antitumor mechanisms, including recognition of CD1d-presented glycolipid antigens and engagement of stress-induced NK ligands. In preclinical tumor models, ^{CD16}HSC-NKT cells demonstrated superior persistence and metabolic fitness compared with conventional peripheral blood-derived NKT cells. Importantly, ^{CD16}HSC-NKT cells were found to reshape the tumor microenvironment by selectively depleting immunosuppressive tumor-associated macrophages (TAMs) and myeloid-derived suppressor cells (MDSCs), thereby promoting a more pro-inflammatory and immune-permissive milieu. No evidence of graft-versus-host disease, cytokine release syndrome, or long-term organ toxicity was observed, supporting a favorable safety profile. Collectively, our study establishes ^{CD16}HSC-NKT cells as a universal, off-the-shelf cellular immunotherapy that can be flexibly paired with diverse monoclonal antibodies to enhance their efficacy, overcome resistance, and expand the therapeutic reach of antibody-based cancer treatment.

#0154 Robust engraftment of human γδ T cells in humanized NSG™-SGM3-IL-15 × MHC I/II double knockout mice for the evaluation of γδ T cell-based therapeutics.

Kevin Tsai, Beau Parry, Destanie Rose, James G. Keck, Li-Chin Yao

Innovation and Product Development, The Jackson Laboratory, Sacramento, CA

Background Gamma delta (γδ) T cells represent a minor subset of T lymphocytes capable of recognizing a wide range of universally conserved antigens expressed by cancer cells. Unlike conventional T cells, their recognition is independent of MHC, making them strong candidates for next-generation universal cancer therapeutics targeting various malignancies. Our preliminary donor screening results demonstrated that engrafting human peripheral blood mononuclear cells (PBMCs) into irradiated NSG™-SGM3-IL-15 × MHC I/II DKO (SDKO) mice could lead to the expansion of circulating γδ T cells to a concentration comparable to those in human and robust γδ T cell recovery from tissues. To demonstrate our PBMC-SDKO mice platform for *in vivo* evaluation of γδ T cell related therapeutics, we conducted γδ T cell engraftment experiments using irradiated SDKO mice and PBMC from 9 donors. We also assessed the anti-cancer functionality of these isolated γδ T cells from PBMC engrafted mice using *in vitro* co-culture experiments with human lymphoma or triple-negative breast cancer cell lines.

Methods Irradiated SDKO mice were engrafted with PBMCs from 9 different human donors. Leukocyte engraftment in the periphery was monitored weekly post PBMC injection using flow cytometry to enumerate the frequency and numbers of αβ T cells, γδ T cells and their subpopulations Vδ1, and Vδ2. γδ T cells engrafted in spleen and lungs were isolated using antibody conjugated magnetic beads and then co-cultured *in vitro* with Raji or MDA-MB-231 cells to assess their anti-tumor functionality.

Results We found that circulating γδ T cells expanded greatly in engrafted SDKO mice. In some of the donors, the concentration of γδ T cells reached up to 4×10^2 cells/μL - a level comparable to that of circulating human B cells, which is a major population in peripheral blood. Among the γδ T cell subsets, the Vδ2 subset exhibited the most robust and consistent expansion, while other γδ T cell subsets such as the Vδ1 were donor dependent. In addition to peripheral blood, we also observed robust engraftment and recovery of γδ T cells from the lungs and spleens of engrafted SDKO mice. Our *in* vitro co-culture experiments demonstrated that the γδ T cells isolated from the spleens and lungs of SDKO mice showed elevated cell surface expression of CD69, granzyme B secretion in response to cancer cells and reduced the number of Raji or MDA-MB-231 cell numbers at effector to target ratios of 1:1 and 3:1. Our results suggest that γδ T cells can be robustly expanded and recovered from the SDKO mice and that the recovered cells possess potent cytolytic activity against tumor cells.

: Immune Cell Biology and Tumor-Immune Crosstalk
Poster Session

#0158 PI3Kδ in CD4⁺ T cells protects against lung metastases through IFNγ-induced tumor senescence.

Leqi Tang[1], Grace Cooper[1], Linsey Porter[2], Seung joon Kim[3], Erick Armingol[4], Oliver Burton[1], James E. Thaventhiran[5], Walid T. Khaled[6], Roser Vento-tormo[4], Rahul Roychoudhuri[1], Klaus Okkenhaug[1]

[1]Department of Pathology, University of Cambridge, Cambridge, United Kingdom,[2]Cambridge Stem Cell Institute, Cambridge, United Kingdom,[3]University of Oxford, Oxford, United Kingdom,[4]Wellcome Sanger Institute, Cambridge, United Kingdom,[5]MRC Toxicology Unit, Cambridge, United Kingdom,[6]Department of Pharmacology, University of Cambridge, Cambridge, United Kingdom

PI3Kδ is a key lymphocyte signaling hub for manipulating antitumor immunity. In cancer, most work has centered on inhibiting PI3Kδ, particularly in regulatory T cells, to relieve immunosuppression and enhance effector T cell control of established tumors. Yet lung metastasis remains a leading cause of cancer mortality, and the impact of PI3Kδ modulation on metastatic outgrowth remains incompletely understood. Inspired by gain-of-function PIK3CD mutations that cause activated PI3Kδ syndrome (APDS), we ask whether enhancing PI3Kδ signaling can be harnessed to prevent melanoma lung metastases. Here, we demonstrate that hyperactivation of PI3Kδ confers robust protection against pulmonary melanoma metastases in a CD4⁺ T cell - dependent manner that drives IFNγ-mediated tumor cell senescence.

We employed mice with germline or conditional hyperactive PI3Kδ, challenged intravenously with B16F10 melanoma to establish lung metastasis. Cell-specific Cre systems identified critical immune populations mediating metastasis rejection. Single-cell RNA-seq and spectral cytometry defined immune remodeling, while depleting and neutralizing antibodies as well as CRISPR-edited melanoma lines revealed underlying mechanism.

Germline hyperactive-PI3Kδ mice developed markedly fewer lung metastases than wild-type controls, and inducible activation of hyperactive PI3Kδ in the hematopoietic compartment was sufficient to confer protection. Protection was dependent on CD4⁺ T cells - CD4⁺ T cell specific PI3Kδ hyperactivation recapitulated germline protection, while B cell, NK cell and CD8⁺ T cell specific PI3Kδ hyperactivation did not. Antibody depletions confirmed that CD4⁺ depletion abolished protection while CD8⁺ depletion had no effect. Hyperactive PI3Kδ CD4⁺ T cells showed enhanced Th1 differentiation with increased IFNγ and IFNγ-neutralization eliminated the protection against metastasis. Mechanistically, tumor control required IFNGR1/JAK1 signaling in cancer cells but not TNFR1, and operated independent of tumor MHC-I or MHC-II expression. The protective mechanism converged on IFNγ-induced tumor senescence, as lung metastases from hyperactive-PI3Kδ mice displayed increased SA-β-gal activity, indicating that CD4⁺ T cells halt metastatic progression by enforcing tumor cell senescence.

Our findings reveal a novel protective axis where hyperactive PI3Kδ signaling in CD4⁺ T cells drives a type 1-skewed pulmonary anti-metastasis microenvironment. This elevates CD4⁺ T cells from "helpers" to anti-metastatic effectors using IFNγ-dependent tumor-intrinsic senescence to achieve durable immune control. These results reveal hyperactive PI3Kδ as a double-edged sword: while pathogenic in APDS, it reinforces immune surveillance of metastasis, offering new therapeutic avenues for preventing metastatic progression by enhancing PI3Kδ signaling.

#0159 Itaconate promotes memory CD8$^+$ T cell development by epigenetic modification and glucose flux redirection in viral infection and cancer.

Xiao Yang, Mengyao Su, Jiacheng Wang, Yue Deng, Lingyi Kong, Kunyu Yang, Chao Wan

Huazhong University of Science and Technology, Wuhan, China

Background: Coordinated metabolic alterations and epigenetic remodeling are known to critically influence T cell fate decisions and functional states. However, the specific extrinsic metabolic signals that guide CD8$^+$ T cell memory differentiation remain to be fully elucidated.

Methods: Naïve CD45.1$^+$ OT-I CD8$^+$ T cells were adoptively transferred into Listeria monocytogenes-infected CD45.2 mice to track in vivo differentiation trajectories. Tumor-infiltrating CD8$^+$ T cells were analyzed by single-cell RNA sequencing to delineate T cell subclusters. Mechanistically, we profiled global chromatin accessibility of CD8$^+$ T cells under itaconate treatment using ATAC-seq, revealing its epigenetic remodeling effects. Through a combination of surface plasmon resonance (SPR) and complementary biochemical assays, we demonstrated that itaconate directly binds to lysine demethylase 5B (KDM5B) and functionally antagonizes α-ketoglutarate (α-KG). Furthermore, metabolic flux analyses, along with direct measurements of NADPH and GSH levels, confirmed that itaconate drives metabolic reprogramming in CD8$^+$ T cells to sustain redox balance and memory differentiation capacity.

Results: We found that itaconate, induced during immune responses, is a critical promoter of memory T cell (T_M) differentiation. Mechanistically, itaconate directly binds to KDM5B and acts as an α-KG antagonist, competitively inhibiting KDM5B-dependent demethylation of H3K4me3. This inhibition leads to increased chromatin accessibility at genes essential for T_M cell differentiation. Furthermore, itaconate redirects glucose flux from glycolysis to the PPP, thereby ensuring high levels of NADPH and glutathione in TM cells to alleviate oxidative stress.

Conclusions: Our results identify itaconate as a key immunometabolic regulator that promotes durable immune memory in viral infections and cancer by concurrently modulating epigenetic programming and metabolic fitness. This machinery presents a potential therapeutic target to enhance the stem-like phenotype and persistence of CAR T cells.

#0160 FGFR3 impairs DC1s/CD8$^+$ T cell clustering in bladder cancer preventing the PD-1/PD-L1 blockade-induced CD8$^+$ T cell phenotypes associated with immunotherapy efficacy.

Andrea Ziblat, Ken Hatogai, Anthony A. Fernald, Danny E. Kim, Hyunsik Lee, Alexander T. Pearson, Madeleine S. Torcasso, Randy F. Sweis

Medicine, University of Chicago, Chicago, IL

Background: Despite advances in immunotherapy, median survival for advanced bladder cancer remains under 3 years, and mechanisms governing PD-1/PD-L1 blockade efficacy remain ill defined. Activation of fibroblast growth factor receptor-3 (FGFR3) has been shown to be linked to a non-T cell-inflamed tumor microenvironment (TME) and with resistance to checkpoint blockade. Using human bladder tumors and murine models, we investigated mediators of immunotherapy response and how FGFR3 shapes the immune landscape affecting PD-1/PD-L1 treatment efficacy.
Methods: Multiplex immunofluorescence (mIF) and RNAscope were performed on 47 human bladder tumors to assess immune infiltrates and FGFR3 expression. A second cohort of 21 bladder tumors collected before anti-PD-1/PD-L1 therapy was analyzed by mIF and spatial transcriptomics (ST). CD8+ T cell and DC1 clustering was evaluated using an unbiased computational analysis (K-cross, a modified Ripley's K function). ST was used to investigate the effect of FGFR3 expression on immune cells spatial distribution and transcripts. In vivo, subcutaneous and orthotopic MB49 models expressing FGFR3 G370C activating mutation, FGFR3 kinase-dead mutant (K508M), or control vector were used with/without anti-PD-L1. FTY720 was used to assess the requirement for new T cell entry into the TME for anti-PD-L1 efficacy. Tumor growth and immune phenotypes were analyzed by spectral flow cytometry.
Results: FGFR3-activated tumors showed reduced CD86+ DC1s in tumor-draining lymph nodes (tdLN), impaired CD8+ T cell activation, greater exhaustion, and fewer TCF-1+ progenitor-exhausted CD8+ T cell (TPE) in the TME after anti-PD-L1 treatment. Blockade of new T cell entry to the TME abrogated the anti-PD-L1-induced accumulation of TPE in control tumors. FGFR3-kinase-dead mutation resulted in higher TPE frequencies in tumors, tdLN, and spleen, and reduced CD8+ T cell exhaustion. In human tumors, clinical response to PD-1/PD-L1 blockade was associated with CD8+/DC1 clustering rather than absolute cell numbers. FGFR3 expression inversely correlated with CD8+ and DC1 abundance and co-localization. Within tumors, FGFR3+ regions showed fewer DC1s, CD8+ T cells, reduced co-localization, and diminished expression of chemokines that recruit these cells. CD8+ T cells in FGFR3+ areas exhibited lower activation/effector and TPE gene expression and higher exhaustion/inhibitory-related transcripts, compared to those in FGFR3 negative areas.
Conclusions: Our results indicate that DC1/CD8+ T cell clustering is essential for PD-1/PD-L1 efficacy in bladder cancer, and FGFR3 activation drives resistance by disrupting this interaction, preventing CD8+ T cells from acquiring phenotypes required for effective immunotherapy.

#0161 Adenosine signaling promotes double-negative t-cell anticancer responses in conditions of CD8 t-cell lymphopenia.

Brionna King[1], Zhi Huang[1], Laura Naldi[1], Lucio Miele[2], Giulia Monticone[2]

[1]Genetics, LSU Health New Orleans, New Orleans, LA,[2]LSU Health New Orleans, New Orleans, LA

CD8 T-cells lymphopenia is a feature of several pathological conditions and is associated with decreased survival and increased risk of developing cancer and infections. Increase in Double-Negative T-cells (DNTs), a subset of T-cells which lack CD8 and CD4 receptors, has been found in both human patients and mice with lymphopenia. DNTs could be either suppressive or immunoprotective. Generating immunoprotective DNTs could be useful to compensate for the lack of CD8 T-cells, but how to stimulate them remains unclear. Forodesine (Foro) is a nucleoside analog which has known antileukemic activity. Foro can also stimulate T-cell function, but the mechanism behind this effect and what type of T-cells is targeted by the drug is still unclear. In this study, we investigated strategies to promote immunoprotective antitumor DNTs in conditions of CD8 T-cells lymphopenia using the antileukemic drug Foro. To determine whether and how Foro stimulates T-cells, we tested Foro in an orthotopic syngeneic triple-negative breast cancer model (C0321-FVB mice). Foro significantly reduced tumor growth and stimulated tumor-infiltrating CD8 T-cells, suggesting that CD8 T-cells modulation mediates its effect. However, when CD8 T-cells were depleted to mimic CD8 T-cells lymphopenia, Foro showed an even stronger anticancer effect. Interestingly, Foro increased CD69+ DNTs in tumors and in circulation, in blood, and this increase correlated with smaller tumors, suggesting that Foro stimulates anticancer DNTs responses when there is a lack of CD8 T-cells. We next studied how Foro could promote antitumor DNTs. Our previous work showed that nucleoside analogs, like Foro, can modulate immunity by blocking the A2A receptor (A2AR). Consistently, blocking A2AR with the antagonist ZM-241385 (ZM) also increased CD69+ DNTs in immunocompetent mice, mimicking Foro treatment. To confirm whether the immunomodulatory effect of Foro in DNTs is based on its capacity to modulate A2AR, we: (i) predicted the interaction between A2AR and Foro using our validated molecular docking modeling; (ii) found that Foro reduced adenosine-induced cyclic AMP (cAMP), the second mediator of A2AR, in A2AR-expressing cells, like ZM; (iii) observed increased Notch1 activation, which is downstream of A2AR, in CD69+ DNTs in Foro-treated mice. Finally, we found that CRISPR-KO of Notch1 significantly reduced CD69+ DNTs, suggesting that Notch1 is critical for the generation and function of DNTs, in response to Foro. Our results indicate that blocking the A2AR signaling promotes Notch1 activation leading to the generation of anticancer CD69+ DNTs, a T-cell subpopulation which could compensate for the lack of CD8 T-cells when lymphopenia occurs. This can be achieved pharmacologically using compounds with A2AR antagonistic properties like Foro. Our work put forward a new rationale for the treatment of cancer patients affected by lymphopenia.

#0162 Early CD8⁺T and NK cell interactions orchestrate preemptive immunosurveillance to potentiate optimal cytotoxicity that blocks tumor antigen-escape variants.

Thanigaivelan Kanagasabai[1], Salvador Gonzalez Ochoa[1], Roman V. Uzhachenko[1], Maria Teresa P. de Aquino[1], Harshana Rajakaruna[2], Muna A. Mohammed[3], Jane Tonello[1], Maria Johnson Irudayam[2], Alla V. Ivanova[1], Anil Shanker[1]

[1]Department of Biochemistry, Cancer Biology, Neuroscience and Pharmacology, Meharry Medical College, Nashville, TN,[2]The Office for Research and Innovation, Meharry Medical College, Nashville, TN,[3]Department of Biomedical Sciences, Meharry Medical College, Nashville, TN

Background: Tumor antigen-escape variants pose a major barrier to immunotherapy by disrupting lymphocyte effector pathways and reconfiguring tumor-immune landscapes. A deeper understanding of immune networks during tumor development is required. We assessed whether homeostatic CD8⁺ T cell-NK cell interactions can preemptively block tumor antigen escape.

Methods: Adoptive CD8⁺ T cell transfers were performed either before tumor implantation (D_{-7}, homeostatic pre-priming) or after tumor establishment (D_{+1}) in $Rag1^{-/-}$ and $Rag1^{-/-}\gamma c^{-/-}$ mice. Antigen presentation, immune activation, proliferation, cytotoxicity, and memory differentiation were quantified using multiparameter flow cytometry, live bioluminescence imaging, and high-resolution confocal microscopy. Intercellular interactions were modeled through monoculture, co-culture, and a 3D silica nanofiber carpet that recapitulates basement-membrane-like architecture. Phospho-signaling arrays and cellular motion metrics (Speed-Distance Index, deceleration) were employed to assess activation dynamics and coordination. Human ligand-receptor pairs implicated in CD8⁺ T-NK cell crosstalk were identified through in silico analyses.

Results and Discussion: Our study shows that pre-tumor (D_{-7}) CD8⁺ T cell transfer establishes a preemptive immune surveillance network by orchestrating NK cell activation and effector function. These early T cells enhance NK cytotoxicity (CD25, CD69, CD107a, T-bet, GzmB) and promote $CD62L^{+}CD44^{+}$ central-memory CD8⁺ T (T_{CM}) precursors, providing immediate and long-term protection. Spatial analyses reveal that early T cells reposition NK cells toward tumors, increasing synapse formation and infiltration effects absent in post-tumor (D_{+1}) transfers that allow antigen-loss variants despite potent T cell cytotoxicity. Mechanistically, CD8⁺ T-NK interactions via pseudopodial nanotubes enable bidirectional membrane/vesicle exchange and coordinated STAT, Akt, AMPK, and mTOR signaling, enhancing NK metabolic fitness, mitochondrial potential, and T_{CM} differentiation. In silico analyses identify conserved human adhesion and co-signaling networks (CD200-CD200R, PD-L1-PD-1, CD18/CD11a-DNAM-1, TIGIT-PVR, NTB-A/SLAM) regulating adhesion, activation thresholds, and cooperative effector functions, with translational relevance. Precise molecular signaling remains under investigation.

Conclusion: Early CD8⁺ T-NK crosstalk establishes preemptive immunosurveillance by integrating metabolic, cytokine, and adhesion signals to potentiate optimal cytotoxicity blocking tumor antigen escape. This axis represents a targetable checkpoint and a framework for next-generation preventive immunotherapies against antigen-loss tumors.

#0163 Allogeneic double-negative T cells induce an innate-like cytotoxic function in CD8$^+$T cells against acute myeloid leukemia.

Leanne Palichuk[1], **Enoch Tin**[1], Pauline Douglas[1], Ruzena Filandrova[1], David Schriemer[1], Juan Arteaga[1], Michele Nawata[1], Sandeep Kaur[2], Sonia Cerquozzi[2], Michelle Geddes[2], Lynn Savoie[2], Jongbok Lee[1]

[1]Arnie Charbonneau Cancer Institute, University of Calgary, Calgary, AB, Canada,[2]Department of Medicine, University of Calgary, Calgary, AB, Canada

Background: Acute myeloid leukemia (AML) is characterized by malignant cells of myeloid origin and poor long-term survival due to relapse following conventional therapies. $CD3^+CD4^-CD8^-$ double-negative T cells (DNTs) are a rare T-cell subset that can kill AML cells without causing graft-vs-host disease in preclinical models. A prior phase I trial demonstrated the feasibility, safety, and potential efficacy of healthy donor-derived allogeneic DNT therapy among patients with relapsed AML. However, the interaction between allogeneic DNTs and host immune cells remains unclear.

Purpose: This study aims to investigate how allogeneic DNTs invigorate $CD8^+$ T cells to better target AML.

Methods: $CD8^+$ T cells were collected from patient samples or healthy peripheral blood mononuclear cells after incubation with DNTs or various activation factors (anti-CD3/CD28 beads, AML cells, or AML cells with DNTs), respectively, followed by CD8 positive selection. Proteomic and single-cell RNA-sequencing (scRNA-seq) techniques were performed to identify unique immune pathways in DNT-activated $CD8^+$ ($CD8^{DA}$) T cells to kill AML cells. Findings of $CD8^{DA}$ T cells were verified through cytotoxic co-culture assays, immunophenotyping, genetic knockouts (KOs), and inhibition assays.

Results: $CD8^+$ T cells from AML patient samples co-cultured with DNTs were highly activated and exhibited potent cytotoxicity against autologous AML blasts, compared to those cultured in the absence of DNTs. Mass spectrometry identified a unique proteomic profile in $CD8^{DA}$ T cells, which were enriched for innate immune response markers relative to the other forms of activation. Interestingly, a higher $CD8^{DA}$ T-cell signature score in patients' $CD8^+$ T cells correlated with a response to anti-CTLA4 and decitabine treatment. Furthermore, $CD8^{DA}$ T cells can target MHC^{KO} AML cells, while anti-DNAM-1 antibodies reduce $CD8^{DA}$ T-cell potency, indicating an innate-like immune mechanism. ScRNA-seq conducted on co-cultures of $CD8^+$ T cells with AML, in the presence of DNTs or anti-CD3/CD28 beads, revealed an enrichment of ferroptosis-related genes in AML cells in the group cultured with DNTs. Using various cell-death inhibitors, only ferroptosis inhibitor Liproxstatin-1 significantly reduced the cytotoxic function of $CD8^{DA}$ T cells. Clinically, lower expression of *GPX4* or *AIFM2* (FSP1), negative regulators of ferroptosis, resulted in better survival among two AML cohorts.

Conclusion: DNTs stimulate an innate-like ability in $CD8^+$ T cells to kill AML in an MHC-independent, DNAM-1-dependent manner through ferroptosis, yielding a potential clinical benefit for patients with AML.

#0164 Restoring TUSC2 function boosts NK cell cytotoxicity and antitumor immunity in vivoand in vitro.

Muna Ahmed Eltayeb A. Mohammed[1], Salvador Gonzalez Ochoa[1], Jane Tonello[1], Thanigaivelan Kanagasabai[1], Mark S. Berger[2], Alla Ivanova[3], Anil Shanker[4]

[1]Meharry Medical College, Nashville, TN,[2]Genprex, Austin, TX,[3]Alla Ivanova (Individual),[4]Biochemistry and Cancer Biology, Meharry Medical College, Nashville, TN

Background: Tumor Suppressor Candidate 2 (TUSC2), located on chromosome 3p21.3, is frequently deleted in multiple human cancers, including non-small cell lung carcinoma (NSCLC), small cell lung carcinoma (SCLC), mesothelioma, breast cancer, and head-and-neck cancers. Loss of TUSC2 is associated with reduced survival and increased tumor aggressiveness. Although TUSC2 is known to suppress tumor cell proliferation and induce apoptosis, its regulatory role in the immune system—particularly in innate lymphoid populations—remains insufficiently defined. Building on our prior work identifying TUSC2 as a mitochondrial protein involved in calcium regulation and immune modulation, we hypothesized that TUSC2 exerts antitumor effects in part by enhancing NK cell cytotoxicity.

Methods Tusc2 knockout (Tusc2 KO) and wild-type (Tusc2 WT) mice were challenged with syngeneic tumor cells (344SQ) and treated with TUSC2-expressing lipoparticles (quaratusugene ozeplasmid, Quar Oze). The therapeutic group received Quar Oze after tumor establishment starting at day 8 from cell line injection, while prophylaxis group received Quar Oze before tumor establishment, starting 2 days before injection of cell lines. Control groups received empty lipoparticles. After three weeks from cell line injection, tumor volumes were assessed, and mice were euthanized for collection of tumors, spleens, and tumor-draining lymph nodes (TDLN). Immune cell phenotypes and cytotoxic markers were analyzed using flow cytometry. *In vitro* studies evaluated NK cell cytotoxic function following Quar Oze treatment by measuring CD107a degranulation and CellTrace Violet-based proliferation

Results In the therapeutic treatment group, 67% of Tusc2 KO mice and 33% of Tusc2 WT mice achieved complete tumor regression, with all remaining mice showing significant tumor reduction compared with controls. Prophylactic administration did not induce complete tumor clearance but consistently reduced tumor growth across all mice. Immune profiling of the tumor microenvironment revealed that Quar Oze robustly enhanced NK cell cytotoxicity, particularly increasing granzyme B and perforin expression. *In vitro* assays confirmed that TUSC2 restoration significantly increased NK cell degranulation and proliferation, supporting the *in vivo* findings.

Conclusion TUSC2 acts as a critical enhancer of innate antitumor immunity by boosting NK cell cytotoxic function. Therapeutic delivery of TUSC2 *via* Quar Oze suppresses tumor progression and, in many cases, drives complete tumor elimination. These results highlight TUSC2 as a potent immunomodulatory tumor suppressor and support its development as a dual-function therapeutic that directly targets tumor cells while also activating NK cell-mediated immunity

#0165 Role of SRC-3 in regulatory T cells as a modulator of activation and immunological memory.

Davis A. Graham, Yan Xia, Subhashree Pradhan, Amrit Koirala, Xiaobin Yu, Adam M. Dean, Bryan C. Nikolai, Aiden L. Moser, Jianming Xu, Cristian Coarfa, Bert W. O'Malley, David M. Lonard

Molecular and Cellular Biology, Baylor College of Medicine, Houston, TX

While Steroid Receptor Coactivator 3 (SRC-3) is best known for its role in promoting proliferation of breast cancer cells, our group has recently identified a key role for SRC-3 in regulatory T cells (Tregs). Treg specific knockout (KO) of SRC-3 results in the long-term eradication of primary tumors in a syngeneic model of triple negative breast cancer. SRC-3 KO Treg mice also can resist rechallenge with a second dose of tumor cells. This long-term anti-tumor immunity points to the potential that SRC-3 KO Treg cells are differentiating into T memory cells. Our data shows that SRC-3 KO Tregs express higher levels of the T memory cell markers CD44 and CD62L than wild type Tregs and that SRC-3 KO Tregs downregulate inducible T-cell co-stimulator (ICOS), c-MAF, and interleukin 10 (IL-10). Utilizing single cell multiome sequencing and subsequent functional assays, we aim to further delineate the role of SRC-3 in Tregs and the impact of SRC-3 KO Tregs on the broader effector immune system. Through these assays we will gain insight into the role that SRC-3 has on T memory cell formation and function and the impact of SRC-3 KO Tregs on other immune cells. This work aims to provide a mechanistic delineation of the long term anti-tumor effects of SRC-3 KO Tregs.

#0166 Rewiring the dendritic cell: Regulatory T cell axis sensitizes prostate cancer to immunotherapy.

Jessica C. Hill, Kade R. Copple, Collin Jugler, Phuong Nguyen, Nilika Bhattacharya, Jessica N. Lancaster, **Casey R. Ager**

Mayo Clinic Arizona, Phoenix, AZ

Introduction: The prostate cancer (PCa) tumor microenvironment (TME) is immunosuppressive and resistant to immune checkpoint blockade (ICB). Based on multi-omic single cell correlatives of response to neoadjuvant Fc-enhanced (FcE) αCTLA-4 in high-risk localized PCa (NCT04301414), we explored how modulating the balance between regulatory T cells (Tregs) and dendritic cells (DCs) in the PCa TME affects sensitivity to ICB.

Methods: We leveraged three single cell transcriptomic atlases of PCa to assess how Tregs and DC frequencies are dynamically regulated during PCa progression. To investigate responses to Treg depletion (via FcE-αCTLA-4) alongside DC expansion (via Flt3L-Ig) and stimulation (via STING agonist ADU-S100) in PCa, we employed the castration-sensitive MycCaP PCa model and 45-parameter spectral flow cytometry. To investigate novel direct mechanisms of DC stimulation by FcE-αCTLA-4 via Fcγ receptor (FcγR) engagement, we optimized reductionist *in vitro* assays involving bone marrow-derived DCs (BMDCs) from wild-type (WT) mice or mice deficient in activating FcγRs (*Fcer1g*$^{-/-}$) or inhibitory FcγRIIb (*Fcgr2b*$^{-/-}$). To validate this effect *in vivo* we established a tumor antigen-specific T cell priming assay with both flow cytometry and *ex vivo* 2-photon live cell imaging readouts.

Results: In three independent single cell transcriptomic PCa atlases, we find cDC2 frequencies are significantly decreased in advanced PCa while effector Tregs (*TNFRSF9*$^{+}$) increase in proportion. Hypothesizing that excessive Treg function and DC insufficiency drive ICB resistance in PCa, we find *in vivo* DC expansion (Flt3L-Ig) prior to hormonal therapy, Treg depletion (FcE-αCTLA-4), and *in situ* DC stimulation (ADU-S100) drives robust control of established MycCaP tumors, with 87% of animals tumor-free 40-days post-treatment (27/31). Using 45-parameter spectral flow cytometry we find FcE-αCTLA-4 drives DC activation prior to Treg depletion in the TME, supporting a novel direct mechanism of DC modulation by FcE-αCTLA-4. *In vitro*, we find cell-associated FcE-αCTLA-4 is sufficient to drive BMDC maturation in an FcγR-dependent manner. *In vivo*, FcE-αCTLA-4 augments DC-mediated T cell priming in an FcγR-dependent manner. Ongoing experiments are investigating how FcE-αCTLA-4 shapes DC-T cell interactions via FcγR engagement and how DC/Treg axis modulation can be optimized to improve long-term curative response rates in the MycCaP model.

Conclusions: DC insufficiency and effector Treg differentiation are hallmarks of advanced PCa. Enhancing DC number and function concomitant with Treg depletion can drive effective antitumor immunity in a pre-clinical PCa model. Direct DC modulation via FcγR engagement represents a novel mechanism of response to CTLA-4-targeted ICB. These findings will inform ongoing translation of FcE-αCTLA-4 agents and development of novel immunotherapy strategies for PCa.

#0167 Preclinic study of src3-ko regulatory T cells in mouse breast cancer model.

Yan Xia[1], Yosef Gilad[1], Davis Graham[1], Bert W. O'Malley[2], David M. Lonard[1]

[1]Baylor College of Medicine, Houston, TX,[2]Professor & Chairman, Dept. of Cell Biology, Baylor College of Medicine, Houston, TX

Introduction: Regulatory T cells (Tregs) play a critical role in balancing immune responses to prevent autoimmune disease through their immunosuppressive activities. However, the suppressive activity of Tregs can be coopted by cancers to evade immune surveillance, leading to tumor progression. Steroid receptor coactivator 3 (SRC-3) is highly expressed in Tregs and we have discovered that genentically engineered mice with SRC-3 specifically knocked out in Tregs are resistant to breast cancer growth, suggesting SRC-3-KO Tregs are a potential therapy for breast cancer patients. In this study, we explored the therapeutic effect of SRC-3 KO Tregs in a mouse model of triple negative breast cancer (TNBC).

Method: A mouse syngeneic, immune-intact breast cancer model was produced by injecting luciferase expressing E0771 TNBC cells into the fourth mammary pad. To closely mimic a clinical scenario, Treg cells were isolated from the spleens of tumor-bearing C57BL/6J donor mice. After disrupting the SRC-3 gene by CRISPR/Cas9 targeting, Tregs were allowed to recover and proliferate in vitro for 4 days before collecting them for adoptive cell therapy (ACT) into C57BL/6J recipient mice with established breast cancer. Wild type Treg cells without gene editing were used as control. Tumor growth was monitored by bioluminescence imaging twice a week for 3 weeks. By the end of experiment, mice were sacrificed and spleen, blood, and tumors were collected for flow cytometry analysis as well as immunofluorescence staining.

Results: ACT of SRC-3 KO Tregs significantly reduced tumor growth or cleared tumosr in all treated mice. SRC-3KO Treg treatment also prolonged mice overall survival. Both ACTed WT and SRC-3KO Tregs were detected in the spleen, blood, and tumors of recipient mice. Moreover, many more cytotoxic T cells, including CD8 and granzyme B+ cells were found in SRC-3-KO Treg treated tumor-bearing mice, compared to WT Treg treated controls.

Conclusion: Deleting the SRC-3 gene in Tregs derived from tumor-bearing donors possess potent anti-tumor effects in an immune-intact mouse breast cancer model. These SRC-3 KO Tregs exert their effects by enhancing the cytotoxicity of effector CD8+ T cells in the tumor microenvironment. Our results reinforce the clinical potential of using SRC-3 KO Treg cells as an effective immunotherapy for TNBCs.

#0168 Harnessing TLS-derived B cells through STING and LTβR activation reveals a novel opportunity to antibody-mediated immunotherapy in pancreatic cancer.

Maxwell Duah[1], Yasuhiro Kikuchi[2], Fumiaki Kanamori[2], Tomoko Stansel[3], Gabrielle Brown[2], Masanobu Komatsu[2]

[1]Johns Hopkins School of Medicine/ All Children's Hospital, Saint Petersburg, FL,[2]Cancer and Blood Disorders Institute, Johns Hopkins School of Medicine/ All Children's Hospital, Saint Petersburg, FL,[3]Shared Resources, Johns Hopkins All Children Hospital, Saint Petersburg, FL

B cells are increasingly recognized as key orchestrators of anti-tumor immunity, yet their therapeutic potential remains far less developed than T cell-based strategies. Tumor-infiltrating B cells often assemble into tertiary lymphoid structures (TLS), which associate with improved immune activation and favorable clinical outcomes across multiple malignancies. However, whether TLS-resident B cells directly mediate tumor control has remained unresolved. We recently demonstrated that concurrent activation of STING and lymphotoxin β receptor (LTβR) signaling reliably induces mature, germinal center-like B cell-rich TLS across diverse tumor models. Here, we investigated the functional requirement for TLS formation using CD79a-deficient mice, which lack B cells and therefore cannot generate TLS. In parallel, we used hybridoma technology to isolate monoclonal antibodies secreted by TLS-derived B cells. In wild-type pancreatic tumor models, dual STING+LTβR activation induced high endothelial venules, promoted robust TLS maturation, and drove the development of class-switched IgG+ memory B cells and long-lived plasma cells. This intervention constrained tumor growth, improved responsiveness to anti-PD-1 therapy, and when deployed as neoadjuvant treatment, prevented recurrence and conferred complete protection upon tumor rechallenge. TLS induction was observed across distinct tumor types and anatomical locations. Hybridoma clones derived from intratumoral TLS-B cells secreted tumor-reactive IgG that activated NK cells and stimulated the release of cytotoxic effector molecules, including Granzyme B, TNF-α, IFN-γ, and Perforin, consistent with potent antibody-dependent cellular cytotoxicity. In contrast, CD79a-deficient mice, despite maintaining T cell infiltration and forming high endothelial venules, failed to develop TLS and exhibited significantly reduced survival following rechallenge, underscoring the essential contribution of B cells and TLS-derived humoral immunity to durable anti-tumor effect. We are now leveraging the TLS-derived IgG for antibody therapy and antigen discovery. Using immunoprecipitation pull-down assays followed by mass spectrometry, we aim to identify novel tumor-associated antigens in pancreatic cancer as candidate therapeutic targets. Together, these findings show that therapeutically induced TLS function as in situ factories for generating potent, tumor-specific antibodies and reveal a promising B cell-centered strategy to overcome the resistance of immune-cold pancreatic tumors.

#0169 A TNF-producing neutrophil subset drives age-dependent hepatotoxicity.

Jin Lee[1], Yiming Gao[1], Yufei Zhang[1], Aaron Havas[2], Peter Adams[2], Gerald S. Shadel[3], Susan M. Kaech[3], Gen-Sheng Feng[1]

[1]University of California San Diego - UCSD, La Jolla, CA,[2]Sanford Burnham Prebys Medical Discovery Institute, La Jolla, CA,[3]Salk Institute for Biological Studies, La Jolla, CA

The mechanisms by which aging contributes to the detrimental effect of cancer therapy remain poorly understood. Herein we show that while a synthetic dsRNA (polyIC) effectively suppresses liver tumors in young mice, it induces lethal liver necrosis in aged mice. Single-cell and functional analyses unearthed a $CD14^+$ neutrophil subset featured by robust TNFα induction by polyIC exclusively in the aged liver. Impaired NR3C1 expression and elevated NF-κB and AP-1 signaling drive a skewing toward Tnf^+ over $Saa1^+$ neutrophils in the aged liver. TNF neutralization rescued polyIC-induced mortality, while also enhancing its antitumor effect in aged mice. Bioinformatic analysis revealed significant association of a Tnf^+Saa1^- neutrophil gene signature with reduced survival in liver cancer patients over 60. This study uncovers a previously unknown detrimental mechanism in the aged liver, which is undetectable under basal conditions. We provide a new strategy to improve therapeutic outcomes in elderly patients by mitigating treatment-associated toxicity.

#0170 Biphasic, time-dependent neutrophil biology in glioblastoma revealed by *in vivo* survival and flow cytometry with single-cell transcriptomic corroboration.

Matthew Alexander Abikenari[1], John Choi[1], Justin Liu[2], Adam Sjoholm[2], George Nageeb[1], James Poe[1], Brandon Hwa-Lin Bergsneider[3], Andrew Tran[1], David Bakalov[4], Ravi Medikonda[1], Lily Kim[1], Rohit Verma[3], Caren Wu[1], Kwang Bog Cho[1], Matei Banu[2], Michael Lim[2]

[1]Neurosurgery, Stanford University School of Medicine, Stanford, CA,[2]Neurosurgery, Stanford University School of Medicine, Stanford, CA, United States, Stanford, CA,[3]Stanford University School of Medicine, Stanford, CA,[4]Physician Scientist Training Program, University of Utah, Salt Lake City, UT, United States, Salt Lake City, UT

Introduction: Tumor-associated neutrophils (TANs) are abundant in glioblastoma (GBM), yet their functions are phase-dependent. We investigated whether TANs are differentially transcribed from peripheral blood neutrophils (PBNs), if they acquire antigen-presenting functions in situ, and if neutrophil depletion timing influences survival and intratumoral immunity
Methods: Transcriptomics: Integrated analysis of publicly deposited recent human GBM data sets (bulk RNA-seq and scRNA-seq; Seurat standard pipeline, stringent QC, integration/UMAP, Wilcoxon DE). Prespecified modules: co-stimulation (CD83/CD86/CD40/ICOSLG), MHC-II (HLA-DRB3/A, DPA1/DPB1), and antigen-processing/chaperones (CD74, CALR, PSME2, HLA-DMA/DMB).
In vivo survival: Orthotopic CT2A and GL261; anti-Ly6G (1A8) or isotype on two schedules, (day −1 pre-implantation through ≥day 14) and delayed (start day +8). Kaplan-Meier/log-rank; Cox models (HR, 95% CI).
Ex vivo flow (day 8): Bead-normalized spectral cytometry; CD45+ leukocytes; CD11b+ myeloids (Ly6G+ neutrophils; Ly6C^hi monocytes), F4/80+ TAMs with MHC-II, CD3+/CD8+ T cells. Two-sided Mann-Whitney; FDR where indicated. Ly6G epitope masking identified; depletion confirmed by CD11b+SSC^hi back-gating and weekly blood counts.
Results: Transcriptomics: TANs vs PBNs showed coherent upregulation of APC/co-stimulatory programs (CD83/CD86/CD40/ICOSLG; HLA-DR/DP; CD74/CALR/PSME2/HLA-DMA/DMB), in line with dendritic-like, non-cytotoxic TAN states.
Survival (biphasic): Previous anti-Ly6G impaired outcomes, CT2A (n=9/arm) median 17 vs 23 days; HR 1.95 (1.10-3.46), p=0.018. Subsequent depletion abrogated this penalty, CT2A HR 1.23 (0.68-2.22), p=0.49;
Flow (day 8): Early-depleted tumors contained more Ly6C^hi monocytes (of CD45+: 29% vs 18%, p=0.006), fewer CD8+ T cells (3.2% vs 6.1%, p=0.011), and lower CD8:Ly6C^hi ratio (0.11 vs 0.36, p=0.004). Directional but non-significant aggregates: CD11b+ myeloids (68% vs 55%, p=0.07), CD3+T cells (9% vs 14%, p=0.09), reduced MHC-II on F4/80+ TAMs (p=0.08), reduced CD11c^{+}MHC-II^hi APCs (q≈0.12).
Conclusion: Human TANs take up APC/co-stimulatory programs, and timing is critical: pre-implantation neutrophil depletion imposes a myeloid-skewed, antigen-poor, T-cell-depleted setting, augments survival, while late targeting diminishes this. These observations favor phase-specific TAN modulation. maintenance or re-education of early TANs and suppression of late suppressive programs selectively, to regulate biomarker-based GBM immunotherapies.

#0171 KEAP1 loss-of-function suppresses immunogenic ferroptosis and limits PD-1 blockade efficacy through an NRF2-FSP1 pathway.

Xinfeng Wang[1], Yuxin Yao[1], Tomi Jun[2], Kuan-lin Huang[2], Nan Sun[1], Jie He[1]

[1]Department of Thoracic Surgery, Chinese Academy of Medical Sciences Cancer Hospital, Beijing, China,[2]Department of Genetics and Genomic Sciences, Center for Transformative Disease Modeling, Icahn School of Medicine at Mount Sinai, New York, NY

Background Loss-of-function mutations in KEAP1 frequently occur in lung adenocarcinoma and are associated with poor prognosis and limited benefit from immunotherapy. However, the mechanisms linking KEAP1 deficiency to immune evasion remain elusive.
Methods We combined patient data analysis, in vivo tumor models, and in vitro co-culture systems to investigate how KEAP1 deficiency shapes dendritic cell (DC) biology and response to PD-1 blockade. Ferroptosis induction assays, damage-associated molecular patterns (DAMPs) quantification, cytokine profiling, and mechanistic interrogation of the FSP1-CoQ10 axis were performed to delineate underlying pathways.
Results Clinically, KEAP1 mutations correlated with poor response to PD-1 blockade and reduced DC infiltration. In murine models, KEAP1-deficient tumors exhibited marked resistance to anti-PD-1 therapy. Mechanistically, KEAP1 loss impaired DC function in vitro, as evidenced by reduced maturation, phagocytosis, and naïve $CD8^+$ T-cell priming capacity. This defect was linked to two complementary mechanisms. First, KEAP1-deficient tumor cells resisted ferroptosis and failed to release immunogenic DAMPs, including extracellular ATP, HMGB1, and calreticulin. Second, KEAP1 deficiency reprogrammed the cytokine secretion profile, with downregulation of CCL2, IL-6, CXCL1, and CXCL2, thereby diminishing DC recruitment and inflammatory signaling. Notably, inhibition of the FSP1-CoQ10 antioxidant axis restored ferroptosis-associated immunogenic cell death.
Conclusions Our study identifies KEAP1 deficiency as a driver of immune-cold tumor microenvironments and resistance to PD-1 blockade, acting through impaired ferroptosis-induced immunogenic cell death and disrupted DC function. Targeting the FSP1-CoQ10 pathway may restore DC function and sensitize KEAP1-mutant lung cancers to immunotherapy.

#0172 Investigating how host TLR5 signaling modulates FLT3 ligand therapeutic efficacy for ovarian cancer.

Cara Hatzinger, Mitchell McGinty, Simona Bajgai, Mika Poblete, Akshita Mirani, Audrey Putelo, Mirna Perusina Lanfranca, Una Miagkov, Melanie Rutkowski

Microbiology, Immunology, and Cancer Biology, University of Virginia School of Medicine, Charlottesville, VA

Ovarian cancer continues to be the most fatal gynecological malignancy, and survival rates of individuals with this disease have remained relatively unchanged for the past 30 years. Though immunotherapies such as immune checkpoint blockades have drastically improved survival outcomes for other cancers, they rarely induce a therapeutic response for ovarian cancer. We have identified toll-like receptor 5 (TLR5) signaling, the only known ligand of which is bacterial flagellin, as a host- intrinsic factor that orchestrates the failure of checkpoint therapy for ovarian cancer. Mechanistically, ovarian tumors induce chronic gut leakage, enabling dissemination of flagellin into the ovarian tumor microenvironment (TME). Chronic TLR5 signaling disrupts the accumulation of IL-12+ anti-tumorigenic dendritic cells (DCs) in the ovarian TME and promotes expansion of PD-L1 expressing immature myeloid populations, culminating in failure of immune checkpoint blockade. One strategy to overcome this deficit is to promote further expansion of DCs via administration of the DC growth factor fms-like tyrosine kinase receptor 3 ligand (FLT3L). Although no benefit was observed for wild type (WT) mice with intact TLR5 signaling, an observation consistent with poor clinical efficacy of FLT3L therapy, FLT3L administration in TLR5-deficient (TLR5KO) mice resulted in prolonged and durable survival for over 80% of animals when combined with PD-L1 blockade. These data suggest that in the absence of TLR5 signaling, the ovarian TME becomes more responsive to immunotherapy, and justifies further investigation into how TLR5 signaling is disrupting FLT3L expanded DCs. High dimensional flow cytometry data show that in the absence of ovarian tumors, FLT3L significantly expands the proportion of DCs in multiple tissues, including the peritoneal cavity, in both TLR5KO and WT mice. Phenotypic profiling of tumor nodules and the peritoneal cavity in ovarian tumor- bearing TLR5KO and WT animals 24 hours after FLT3L treatment ceases shows significantly higher frequencies of DCs in the peritoneal cavity of TLR5KO mice as compared to WT. Analysis of tumor nodules also reflects a significant increase in the frequency of dendritic cells infiltrating tumors as compared to WT mice. These preliminary results suggest TLR5 signaling is impacting the expansion and/or recruitment of dendritic cells into the ovarian tumor microenvironment. Ongoing and future experiments will assess chemokines and cytokines the periphery, peritoneal washes, and tumor lysates to define TLR5-mediated signaling pathways that inhibit DC maturation and recruitment. Our results aim to mechanistically define how chronic TLR5 signaling is impacting FLT3L efficacy, and further elucidate how TLR5 signaling is a host intrinsic process whereby the microbiome is driving resistance to immune therapies.

#0173 Targeting tumoral GLI1 in triple-negative breast cancer: A novel strategy to reverse the immunosuppressive microenvironment.

Qiang Shen

University Health Network, Toronto, ON, Canada

Triple-negative breast cancer (TNBC) comprises 15-20% of breast cancer cases, is highly aggressive, lacks effective treatment options and represents a disproportionately high number of BC-related deaths. Despite the clinical success of immune checkpoint blockade (ICB) in many malignancies, ICB has failed to demonstrate a similar response in TNBC, where most cases are highly infiltrated by tumor-associated macrophages (TAMs), which can dampen CD8+ cytotoxic T-lymphocyte (CTL) function and promote resistance to ICB. The hedgehog (HH) signaling pathway is highly activated in TNBC and higher expression of GLI1 is associated with worse overall survival. Recent pan-cancer analyses highlight a significant correlation between activated HH signaling and characteristics of immune evasion.

Results: To examine how activated HH signaling regulates the tumor immune microenvironment (TIME) in TNBC, murine KBP (K14-*cre*; Brca1*fl/fl*; P53*fl/fl*) TNBC cells were transfected with CRISPR/Cas9 + sgRNA targeting GLI1 or GLI2 (GLI1/2). KBP and KBP-GLI1/2-KO cells were orthotopically injected into the mammary fat pads of FVB mice and allowed to grow for 6-8 weeks. Compared to wild-type KBP tumors, KBP-GLI1-KO tumors, but not KBP-GLI2-KO tumors, were smaller. Flow cytometric analyses showed that KBP GLI1-KO tumors were infiltrated with fewer F4/80+ CD11b+ TAMs, particularly the CD206+ pro-tumoral M2-like subtype. This was accompanied by increased CD8+ and CD4+ T cells. Similar results were observed in the modified murine TNBC KBP transgenic mouse model where either GLI1 or GLI2 was genetically deleted in tumor cells. In GLI1 (but not GLI2) KBP mice reduced delayed tumor onset and growth were accompanied by reduced M2-like TAM and increased CD8+ and CD4+ T cells infiltration in TIME. Moreover, compared with the low responsiveness of KBP tumors to anti-PD1, the therapeutic benefit of anti-PD1 in KBP-GLI1-KO tumors was markedly improved and was accompanied by increased activated, anti-tumoral CD8+GrB+ T cell infiltration.

Conclusion: here we demonstrate that tumoral GLI1, but not GLI2, promotes tumor growth and supports an immunosuppressive TIME in TNBC. Targeted deletion of GLI1 reduces TAMs, increases CTLs, and re-shapes TIME towards a pro-inflammatory ‘hot’ tumor phenotype, potentiating anti-PD1 ICB in immunocompetent mouse models of TNBC. Overall, these preliminary findings identify GLI1 as a potential therapeutic target to improve ICB response in TNBC.

#0174 Tumor-reactive CD8 lymphocyte isolated from melanoma brain metastasis show that a subset of the total population is better at controlling tumor growth after adoptive transfer into a xenograft model.

Jeffrey Wu[1], Mike Beymer[1], Rebekka Duhen[2], Venkatesh Rajamanickam[1], Colin Thalhofer[3], Prakash Ambady[1], Andrew D. Weinberg[1]

[1]Earle A. Chiles Research Institute, Portland, OR,[2]Oregon Health and Science University, Portland, OR,[3]Agonox, Portland, OR

Previously, we demonstrated that the vast majority of CD8 T cell tumor reactivity was found within the CD39+ CD103+ (Double Positive, DP) population when isolated from the tumor microenvironment. These cells can be sorted and expanded from thousands to billions in defined culture conditions. After adoptive cell transfer, they can cause tumor regression in vivo in a human melanoma xenograft model that constitutively secrete human IL-2 (NOGhIL-2). In the current study, we found that DP CD8 tumor infiltrating lymphocytes (TILs) isolated from a melanoma brain metastasis could not regress autologous tumor in the NOGhIL-2 mice. After adoptive transfer tumors progressed in mice that received DP TIL and grew at a similar rate compared to CD8 T cells that had little to no tumor reactivity. Co-culture experiments with the total CD8 DP TIL population and autologous tumor showed that there was a subset of T cells that greatly upregulated 4-1BB+ CD25+ over an extended period of time (~5-10% of total population). We sorted this subset away from the total DP TIL population and expanded them in culture. When the sorted population was compared to the parental CD8 DP TIL population in tumor co-culture experiments there was an increase in 4-1BB expression and 3 to 8-fold higher interferon gamma levels. Upon adoptive transfer into the tumor xenograft model, the sorted subset completely regressed autologous tumor, whereas the tumors grew progressively in mice receiving the unsorted population. Single cell TCRseq and RNA profiling revealed interesting differences between these two populations. Our findings suggest that specific subsets within the CD8 DP TIL total population might play an important role in controlling brain metastases in cancer patients with recurrent disease.

#0176 Intrinsic failure of immune activation in *NRAS*-mutant melanoma reveals a targetable mechanism of checkpoint resistance.

Inyoung Cho[1], Sung Eun Kim[2], Joong-Bae Ahn[3], Sang Joon Shin[3]

[1]Department of Clinical Drug Discovery and Development, Yonsei University College of Medicine, Seoul, Korea, Republic of,[2]Department of Medicine, Yonsei University College of Medicine, Seoul, Korea, Republic of,[3]Division of Medical Oncology, Department of Internal Medicine, Yonsei Cancer Center, Seoul, Korea, Republic of

Background: Melanoma is frequently driven by MAPK pathway mutations, most prominently BRAF (~50%) and NRAS (20-30%). Unlike *BRAF*-mutant melanoma, which benefits from effective targeted therapies, *NRAS*-mutant melanoma responds poorly to MEK inhibition and lacks approved targeted options, contributing to poorer outcomes. This limitation has encouraged immunotherapy-based combinations, yet responses to immune checkpoint blockade (ICB) remain variable. We found that *NRAS*-mutant melanoma exhibits high immune-gene activity in cancer cells alone but shows suppressed inducibility upon immune stimulation, indicating an intrinsic failure to activate immune programs that may limit ICB responsiveness.

Methods: DEG and pathway analyses were performed using DESeq2 and GSEA with TCGA-SKCM (tumor biopsy) and CCLE/DepMap (cell line RNA-seq) datasets. “Shift genes” were defined by comparing relative expression between cell line-intrinsic and tumor datasets, selecting genes with the largest directional changes and significant adjusted p-values (FDR < 0.05, moderated t-tests). Anti-PD-1-resistant cell lines were generated through serial in vivo selection involving repeated implantation and anti-PD-1 treatment of *NRAS*-mutant melanoma until tumor growth matched untreated controls.

Results: RNA expression analysis of *NRAS*-mutant melanoma cell lines revealed strong intrinsic immune-gene activity; however, this activity was markedly reduced in TCGA tumors, indicating suppressed inducibility in the tumor setting. Among the T cell-inflamed GEP genes—an established immune signature highly expressed in tumors responding to anti-PD-1 therapy—MHC class II-related genes and CCL5 showed the most pronounced reduction (≈1.3-1.4-fold), while most others remained stable. Consistent with these findings, *NRAS*-mutant murine melanoma cell lines exhibited high basal immune-gene expression but nearly 200-fold weaker induction following Interferon-γ stimulation—used to evaluate inducible immune-gene responses—compared with wild-type cells. Anti-PD-1-resistant models mirrored this pattern, suggesting that such immune non-responsiveness reflects an inherent characteristic of *NRAS*-mutant melanoma.

Conclusion: The immunotherapy responsiveness of *NRAS*-mutant melanoma remains uncertain, underscoring the need to define its immune features. Our findings indicate that the immune unresponsiveness in this subtype reflects a fundamental, cell-intrinsic limitation rather than an acquired consequence, suggesting a targetable mechanism to improve ICB outcomes.

#0177 In vivo CRISPR screening uncovers Folr1-mediated metabolic remodeling that sensitizes colorectal cancer to PD-1 blockade.

Boping Jing[1], Feng Guo[2], Tadahito Yasuda[2], Mayu Yasuda[2], Hudie Li[3], Fabio Mello[3], Jay Paul Overholser[1], Pravin Kaumaya[1], Yaoqi Alan Wang[2]

[1]IUPUI, Indianapolis, IN,[2]Indiana University School of Medicine, Indianapolis, IN,[3]Indiana University, Indianapolis, IN

Introduction: Colorectal cancer (CRC) is a leading cause of cancer-related mortality worldwide. KRAS mutations are present in approximately 40-50% of CRCs, with G12D being the most prevalent subtype. Accumulating evidence indicates that $KRAS^{G12D}$ CRC responds poorly to immune checkpoint blockade (ICB) therapy, reflecting intrinsic resistance to immunotherapy. To identify key regulators capable of overcoming this resistance, we conducted an in vivo CRISPR/Cas9 genetic screen in a $KRAS^{G12D}$-driven CRC model. Furthermore, we investigated the underlying mechanisms contributing to immune resistance.

Methods: $KRAS^{G12D}$ colorectal cancer cell lines, MC38K and Caco2K were generated. An immune-related sgRNA library was designed using PD-1/PD-L1/MHC-I and ESTIMATE data, and MC38K cells carrying the library were tested under anti-PD1 treatment in vivo. RNA sequencing and metabolic profiling were performed to elucidate immune-related mechanisms, and Seahorse assays were used to validate metabolic alterations. Multiple CRC models were used to evaluate Folr1 inhibition combined with anti-PD1 therapy, and a Folr1-based peptide vaccine was developed to overcome resistance.

Results: $KRAS^{G12D}$ overexpression accelerated tumor growth and conferred anti-PD1 resistance in MC38K models. Through the in vivo CRISPR/Cas9 screen, Folr1 emerged as the top depleted gene, ranking first among all candidates associated with immunotherapy resistance. Notably, Folr1 is a clinically actionable target with existing therapeutic antibody currently approved by FDA. RNA-seq analysis of Folr1-knockout MC38K and Caco2K cells revealed profound metabolic remodeling, particularly involving glycolysis. GSEA demonstrated that hallmark pathways including glycolysis, hypoxia, and mTORC1 signaling were downregulated, validated by qRT-PCR, OCR/ECAR assays, and L-lactate measurements. In multiple in vivo models, Folr1 knockout combined with anti-PD1 therapy significantly delayed tumor growth and extended overall survival. Furthermore, the Folr1-based peptide vaccine also markedly suppressed tumor progression.

Conclusions: Our study identifies Folr1 as the top-ranked gene mediating immunotherapy resistance in $KRAS^{G12D}$-driven colorectal cancer. Targeting Folr1 reprograms tumor metabolism, enhances antigen presentation, and restores responsiveness to anti-PD1 therapy. These findings establish Folr1 as a translationally relevant therapeutic target to overcome immune resistance in $Kras^{G12D}$ CRC.

#0178 Exploring the role of catecholamine signaling in CD8+ T cell immunity to neuroblastoma.

Mark B. Chudnovsky, Daniela Vega-Mendoza, Elinor L. DeCleene, Jose Almeida-Santos, Naomei Lidman, Mingkee Achom, Jared H. Rowe

Pediatric Oncology, Dana-Farber Cancer Institute, Boston, MA

Neuroblastoma (NBL) is the most common extracranial solid tumor in children. NBL tumors arise from the malignant transformation of sympathoadrenal precursor cells in the developing neural crest. The origin of NBL cells leads to their retention of the ability to synthesize catecholamines, which normally regulate our stress response. Recent studies have demonstrated that immune responses are also modulated by catecholamine signaling through beta-adrenergic receptors expressed on T cells. Particularly, catecholamines derived from sympathetic neurons can signal CD8+ T cells via the beta-adrenergic receptor (ADRB1). In tumors this signaling is associated with the progressive loss of CD8+ T cell function, a process known as “exhaustion.” We hypothesized that in catecholamine producing tumors, like NBL, the excessive ADRB1 signaling T cells will suppress antitumor immunity. To investigate the cell-intrinsic role of beta-adrenergic signaling in CD8+ T cell function in protection from NBL we selectively ablated the ADRB1 (*Adrb1*) gene in murine T cells using an *in vivo* immune competent NBL model. A syngeneic NBL cell line was engineered to express ovalbumin (OVA) as a surrogate tumor-specific antigen. Cas9-expressing T cell receptor transgenic (TCR) T cells for OVA (Cas9-OT-I) were transduced with *Adrb1*-gRNA and adoptively transferred into recipient mice prior to implantation of 9464D-OVA. Surprisingly, we found that *Adrb1*-deficient CD8+ T cells had inferior tumor control compared to T cells transduced with non-gene targeting control gRNA. Despite this observation, *Adrb1*-deficient CD8+ displayed a competitive advantage in the tumor microenvironment compared to control T cells. This suggests that the loss of ADRB1 is impacting the function of anti-NBL T cells. These findings directly contrasted the robust protection of *Adrb1*-deficient CD8+ T cells in a model of melanoma (B16-OVA). Interestingly, we found that pharmacologic treatment of melanoma bearing mice with the selective ADRB1 antagonist atenolol was sufficient to control some tumors and promote animal survival. NBL bearing mice receiving atenolol had no effect on tumor growth or animal survival. Ongoing experiments are addressing how the timing (i.e. pre-activation, post-exhaustion) and context (whole body, T cell-intrinsic, tumor microenvironment) of ADRB1 blockade impacts the function of T cells in NBL. These preclinical studies will support ongoing efforts to target catecholamine signaling to reduce exhaustion and support the function of cellular therapies against NBL.

: Inflammation and Cancer Progression
Poster Session

#0182 Systemic immune reprogramming by extracranial melanoma reshapes the melanoma brain metastasis microenvironment.

Prabhjeet Singh, Saurabh Sharma, Jay Chadokiya, Amanda Kirane

Surgery, Stanford University, Stanford, CA

Introduction: Melanoma brain metastases (MBM) remain a critical unmet need, with median survival of only ~6 weeks after immune checkpoint blockade (ICB) failure. This lethality is driven by an immunosuppressive tumor immune microenvironment enriched for tumor-associated macrophages (TAMs) and dysfunctional dendritic cells (DCs). Emerging evidence suggests bidirectional crosstalk between extracranial and intracranial tumors may reshape systemic immunity and influence therapeutic outcomes, yet the mechanisms remain unclear. We therefore investigated how an extracranial melanoma alters the cranial tumor-immune microenvironment and modulates ICB efficacy.
Methodology: A multi-site murine MBM model was established using YUMM1.7 melanoma cells. Subcutaneous (extracranial) tumors were implanted 48 h prior to stereotactic intracranial injection. Tumor progression was monitored by bioluminescence imaging (BLI). At day 21, blood and major tissues (skin, brain, and organs) were excised and analyzed using flow cytometry (tumor and TAMs, DC, T-cell profiling) and Lunaphore COMET™ multiplex immunofluorescence (mIF) imaging for PD-1/PD-L1, and LRP-1 expression on TAMs/DCs/T-cells, to better understand the tumor-immune microenvironment modulation in both intracranial and extracranial site. Kaplan-Meier survival was plotted to determine the tumor growth dynamics.
Results: The multi-site MBM model was successfully generated and validated by BLI and histologic immune cell infiltration at both tumor sites. Mice bearing both intracranial and extracranial tumors showed significantly delayed intracranial tumor growth compared with mice bearing intracranial tumors alone ($p<0.05$), indicating systemic immune reprogramming driven by the extracranial tumor. mIF further revealed differential expression of PD-1/PD-L1 interactions and LRP-1 on TAMs, DCs, and T cells in multi-tumor mice relative to intracranial-only controls ($p<0.05$), highlighting dynamic modulation of the intracranial TiME.
Conclusion: Extracranial melanoma reshapes the cranial immune landscape and attenuates intracranial tumor progression through systemic tumor-immune microenvironment reprogramming. PD-1/PD-L1 and LRP-1 emerge as key regulators of immunosuppression in MBM, supporting combinatorial ICB strategies targeting these axes. Ongoing studies leveraging LRP-1 knockout models aim to refine mechanistic understanding and improve immunotherapeutic efficacy in MBM, addressing a major gap in neuro-oncology.

#0183 NOX2-driven macrophage reprogramming enhances breast cancer metastasis.

Mustafa Kaya[1], Olivia Johnsson[1], Nuttida Issdisai[1], Hugo Soderberg[1], Ilayda Altinonder[2], Roberta Kiffin[1], Xavier Tekpli[2], Kristoffer Hellstrand[1], **Anna Martner**[1]

[1]University of Gothenburg, Gothenburg, Sweden,[2]Oslo University Hospital and University of Oslo, Oslo, Norway

Tumor-associated macrophages (TAMs) are considered key determinants of breast cancer progression, yet the molecular mechanisms shaping their immunosuppressive phenotypes remain incompletely understood. The NOX2 enzyme of myeloid cells generates antimicrobial reactive oxygen species (ROS) in myeloid cells, but its potential contribution to macrophage programming within the tumor microenvironment is largely unknown. This study aimed at identifying the potential role of NOX2 in regulating M2-like macrophage polarization for breast cancer growth and dissemination. Analysis of single-cell RNA sequencing data from 100 human breast tumors revealed selective upregulation of NOX2 in M2-like TAM clusters, associated with an immunosuppressive transcriptional profile. Consistently, transcriptional data showed that macrophages from *Nox2*-deficient mice displayed a shift toward a pro-inflammatory, M1-like state, marked by altered transcription factor networks and enrichment of inflammatory gene signatures. *In vitro*, pharmacologic or genetic inhibition of NOX2 blocked M2 polarization induced by colony-stimulating factor-1 (CSF-1) (P=0.0006, n=4-11/group, one-way ANOVA) or breast cancer-derived conditioned media (P=0.02, n=4/group, Mann-Whitney test), implying that NOX2 activity is required for tumor-driven macrophage reprogramming. Mechanistically, our results suggested that NOX2-derived ROS activated NRF2-dependent transcriptional pathways that stabilized the M2-like phenotype. In two distinct murine breast cancer *in vivo* models, *i.e.* orthotopic EO771 implantation and the genetically engineered MMTV-PyMT model, genetic deletion of *Nox2* entailed reduced abundance of M2-like TAMs (P=0.006, n=4-7/group), enhanced intratumoral T cell infiltration (P=0.04, n=4-7/group), and markedly suppressed primary tumor growth (P=0.01, n=4-7/group) and metastatic spread (P=0.02, n=6-8/group, Mann-Whitney test for all). Mining of public datasets revealed that high expression of M2-associated markers and NRF2 target genes correlated with inferior survival in human breast cancer (P=0.02 for CD206 and P=0.04 for HO-1, n=65, log-rank test). These findings position NOX2 as a key driver of immunosuppressive macrophage plasticity in breast cancer and highlight the NOX2-NRF2 axis as a potential therapeutic target to counteract metastasis-promoting myeloid programming.

#0184 TNF-alpha plays pleiotropic role in innate immune activation and blood-brain barrier disruption driving brain metastasis.

Neva Celiker[1], Fulya Koksalar Alkan[1], Hilmi K. Alkan[1], Ahmet Caglayan[2], Aminal Lawal[1], Morhaf Al Achkar[1], Wicha S. Max[3], Hasan Korkaya[1]

[1]Oncology, Wayne State University, Detroit, MI,[2]University of Michigan, Ann Arbor, MI,[3]Department of Internal Medicine, University of Michigan, Ann Arbor, MI

Tumor necrosis factor-α (TNFα) is a central inflammatory cytokine with paradoxical functions in cancer, capable of promoting robust innate immune activation while simultaneously inducing tissue damage that facilitates metastatic dissemination. Our preliminary data show that TNFα triggers membrane localization and secretion of HSP70 in murine EMT6 breast cancer cells, enabling HSP70 to function as a potent tumor-associated antigen that activates innate immunity and mediates clearance of disseminated tumor cells. To extend these in vivo, we investigated the pleiotropic effects of TNFα in EMT6 orthotopic models, where TNFα-treated EMT6-conditioned medium (EMT6-CM) unexpectedly induced both early systemic immunization and late development of brain metastases.Our preliminary data reveal that EMT6-CM derived from TNFα-treated cells contains high concentrations of soluble TNFα that compromise blood-brain barrier (BBB) integrity, generating a permissive niche for metastatic colonization. Besides, the same CM harbors HSP70-rich extracellular vesicles that promote anti-tumor immune priming in peripheral tissues. Thus, TNFα exerts a paradoxical influence: beneficial through HSP70-mediated innate immune activation, yet detrimental through TNFα-driven BBB disruption that facilitates brain metastatic outgrowth.To mechanistically separate these opposing functions in our ongoing studies, we are selectively depleting TNFα from EMT6-CM using immunoabsorption approaches while preserving HSP70-containing vesicles and soluble fractions. TNFα-depleted CM will be used to immunize BALB/c mice for 1-2 weeks, followed by orthotopic challenge with EMT6-Luc cells. We hypothesize that mice receiving TNFα-depleted, HSP70-enriched CM will reject EMT6-Luc tumors, demonstrating that HSP70-driven immunogenicity is sufficient for tumor protection in the absence of TNFα-induced BBB damage. Successful rejection will validate our model in which TNFα is necessary for BBB disruption but dispensable for HSP70-mediated anti-tumor immunity.Collectively, our findings reveal a previously unrecognized dichotomy in TNFα biology, with significant implications for cytokine-based immunotherapies and mechanisms underlying breast cancer brain metastasis. Understanding how to uncouple TNFα's immunostimulatory and pathological effects may guide development of safer and more effective immune-modulating strategies.

#0185 Thyroid hormones modulate the lung immune microenvironment to regulate breast cancer metastasis.

Gonzalo Gonzalez, Florencia Menay, Johanna Diaz Albuja, Maria M. Debernardi, Lucero Alvarado, Maria A. Paulazo, Cinthia Rosemblit, Florencia Cayrol, Graciela A. Cremaschi, **Helena A. Sterle**

Instituto de Investigaciones Biomedicas (BIOMED-UCA-CONICET), Buenos Aires, Argentina

Thyroid disorders and breast cancer (BC) are both more prevalent in women, yet the influence of thyroid hormones (THs) on BC progression and metastasis remains poorly understood. We previously showed that hyperthyroid mice bearing 4T1 BC tumors display accelerated primary tumor growth, whereas hypothyroid mice develop slower-growing tumors but a higher number of lung metastases. To elucidate the mechanisms underlying these effects, we first evaluated the direct influence of THs on 4T1 cell migration using wound-healing assays. We then examined the impact of thyroid status on the immune subpopulations and cytokine milieu in the lungs. For this, female Balb/c mice were induced to a hyperthyroid state by daily thyroxine (T4) administration for 4 weeks, to a hypothyroid state by propylthiouracil (PTU) for 2 weeks, or to a reverted euthyroid condition by supplementing triiodothyronine (T3) after PTU treatment. Mice were subsequently inoculated with 4T1 cells orthotopically or intravenously. In vitro, T3 and T4 did not modify 4T1 cell migration, indicating that THs regulate metastasis indirectly through host mechanisms. In vivo, thyroid status profoundly altered the pulmonary immune landscape. Lungs from hyperthyroid mice exhibited increased proportions of cytotoxic T lymphocytes, natural killer (NK) cells, and B cells, accompanied by higher IFN-γ and IL-2 levels ($p < 0.05$), consistent with a more cytotoxic microenvironment. In contrast, lungs from hypothyroid mice displayed increased myeloid-derived suppressor cells (MDSCs) and elevated CCL5, CCL17, and CCL22 levels ($p < 0.05$), which are associated with heightened immunosuppression, cell recruitment, and metastasis formation. These alterations were reverted by short-term T3 treatment. Moreover, hyperthyroid mice intravenously inoculated with 4T1 cells also showed increased NK cell levels, whereas hypothyroid mice exhibited higher MDSCs, suggesting that this effect is independent of the primary tumor. Collectively, our findings demonstrate that thyroid hormones do not directly affect BC cell migration but critically modulate the immune microenvironment in metastatic target organs. Hyperthyroidism promotes cytotoxic and humoral immune responses that may restrain metastasis, while hypothyroidism drives an immunosuppressive cytokine network that favors lung colonization. Understanding how thyroid hormones influence immune responses is key to developing more effective therapeutic strategies for breast cancer.

#0186 Thyroid hormones as systemic regulators of melanoma progression and dissemination.

Helena Andrea Sterle, Maria M. Debernardi, Gonzalo Gonzalez, Lucero Alvarado, Florencia Menay, Maria A. Paulazo, Graciela A. Cremaschi, Florencia Cayrol

Instituto de Investigaciones Biomedicas (BIOMED-UCA-CONICET), Buenos Aires, Argentina

Melanoma (ME) is the most lethal form of skin cancer, and resistance to immune checkpoint inhibitors remains a major clinical challenge. Thyroid hormones (THs) are master regulators of metabolism, proliferation, and differentiation, yet their role in melanoma biology remains poorly defined. This study aimed to elucidate both the direct and systemic effects of THs on melanoma progression.
We first assessed the expression of nuclear (TR) and membrane (integrin αVβ3) TH receptors in human (A375, WM35) and murine (B16F10, B16F1) melanoma cell lines. Both receptor types were detected at mRNA and protein levels in all cell lines analyzed. Functional assays demonstrated that physiological and supraphysiological TH concentrations increased ME cell proliferation by 20-40% ($p<0.01$), an effect prevented by the αVβ3 inhibitor cilengitide ($p<0.05$), indicating that THs promote melanoma growth predominantly through αVβ3-mediated signaling. Consistently, TCGA-SKCM data showed co-expression of αV and β3 integrins in patient melanoma samples, supporting αVβ3 as a potential therapeutic target.
To evaluate systemic effects of THs, syngeneic B16F1 and B16F10 melanoma models were established in euthyroid, hypothyroid, and hyperthyroid mice. In both models, hyperthyroid mice exhibited significantly increased tumor growth rates compared with euthyroid controls ($p<0.05$), whereas hypothyroidism did not markedly affect primary tumor expansion. In contrast, in experimental metastasis assays using B16F10 cells, hypothyroid mice developed a significantly higher number and larger size of lung metastatic foci ($p<0.01$), indicating that TH deficiency facilitates metastatic dissemination.
Immune profiling of tumor-infiltrating cells did not reveal significant differences among experimental groups. However, tumor-draining lymph nodes from hyperthyroid mice showed reduced cytotoxic $CD8^+$ T lymphocytes ($p<0.05$), while spleens from hypothyroid mice exhibited increased B lymphocytes ($p<0.01$) and myeloid-derived suppressor cells ($p<0.05$), suggesting that TH status modulates systemic immune cell distribution.
Overall, these findings demonstrate that thyroid hormones exert dual and context-dependent effects on melanoma: TH excess enhances primary tumor growth through integrin αVβ3 signaling, whereas TH deficiency promotes metastatic dissemination, likely through modulation of systemic antitumor immunity. The thyroid axis emerges as a novel systemic regulator and potential therapeutic target in melanoma.

#0188 Commensal dysbiosis mediates changes in mammary tissue mast cells and fibroblasts to promote HR$^+$breast tumor dissemination.

Simona Bajgai[1], Alkaid Feng[1], Audrey Putelo[1], Mika Poblete[1], Scott Dunn[2], Mirna Perusina Lanfranca[1], Cara Hatzinger[1], Akshita Mirani[1], Una Miagkov[1], Melanie R. Rutkowski[3]

[1]Microbiology, Immunology, and Cancer Biology, University of Virginia School of Medicine, Charlottesville, VA,[2]Chemistry, University of Virginia, Charlottesville, VA,[3]University of Virginia School of Medicine, Charlottesville, VA

We aim to uncover host-intrinsic factors influencing HR$^+$ breast cancer metastasis by focusing on interactions between mast cells and fibroblasts, two mammary tissue-associated cell types involved in the orchestration of metastatic breast cancer. Metastatic dissemination remains a significant barrier to reducing mortality associated with HR$^+$ Her2$^-$ breast cancer. Dissemination occurs early and is driven by immune-mediated crosstalk between the tumor microenvironment and the adjacent tissue. We have demonstrated that commensal dysbiosis, an inflammatory gut microbiome with low biodiversity, promotes long-term cellular and molecular changes in normal (non-tumor-bearing) mammary tissues. When commensal dysbiosis is established in a mouse model before tumor initiation, dissemination of HR$^+$ breast tumor cells is significantly increased, whereas primary tumor growth remains unaffected. Gut microbiome changes have been associated with relapse and metastatic disease in women with breast cancer, highlighting the importance of defining how the gut microbiome regulates breast cancer through modulation of the mammary tissue environment. Our preliminary data suggest that dysbiosis activates a mast cell/fibroblast axis in the normal mammary tissue that enhances HR$^+$ tumor dissemination. We are using a combination of methods including but not limited to untargeted proteomics, spatial profiling, high-dimensional flow cytometry, scRNAseq, coupled with various *in vivo* and *in vitro* assays to define the contribution of this axis to early metastasis. Flow cytometry analysis and experiments using mast cell-deficient sash mice have demonstrated that dysbiosis increases the number of mammary tissue mast cells and causes changes in their phenotype. We have also observed that dysbiosis increases mammary tissue fibroblast activation in a mast cell-dependent mechanism. Supporting the role of mast cells in programming fibroblasts to promote breast tumor metastasis, spatial transcriptomic analysis has revealed a correlation between fibroblast activation and proximity to mast cells. Orthotopic transfer of fibroblasts from dysbiotic and non-dysbiotic mice has demonstrated that fibroblasts from the mammary tissues of dysbiotic mice are sufficient to increase early tumor dissemination. By uncovering mechanisms of mast cell-fibroblast crosstalk, our findings have the potential to inform the development of therapeutic and diagnostic strategies aimed at targeting tissue remodeling in patients at risk for metastatic disease. Ultimately, this work lays the foundation for repurposing clinically available drugs that target mast cell function or tissue fibrosis to prevent HR$^+$ breast cancer metastasis.

#0190 Breast cancer liver metastasis: Primary tumor predictors and histopathologic characteristics of metastatic lesions.

Hatun Duran Cete, Alexandra Bartlett, Michelle Kayoko Ozaki, Jackie Phipps, Pepper Schedin

Knight Cancer Institute, OHSU, Portland, OR

Background: Breast cancer metastasis to the liver (BCLM) has poor outcomes because predicting patients at risk for liver metastasis remains elusive as does effective targeting of metastatic lesions. Known risk factors for BCLM include young patient age and primary breast cancer diagnoses of high grade, late stage and triple negative or HER2+ subtypes. Prognostic sensitivity is currently low. Further, lack of histopathologic characterization of BCLM tumors in the literature limits development of targeted therapeutics.
Methods: We collected retrospective and prospective BCLM tissues from forty-seven breast cancer patients who underwent liver biopsy (87%) or surgical resection (13%) for clinical indications of BCLM at OHSU Portland, Oregon. Patients were enrolled regardless of age or breast cancer subtype. Patient clinicopathological characteristics at time of primary breast cancer diagnosis were used to identify breast cancer attributes associated with liver metastasis. Histological and immunohistology analyses of formalin fixed paraffin (FFPE) embedded BCLM tissues were employed to assess metastatic tumor and tumor niche characteristics within the liver.
Results: At primary breast cancer diagnosis, 38% of cases were ≤45 years of age, with 72% of these young cases diagnosed within 10 years of childbirth. Regardless of patient age, 85% of the primary cancers were ER+, 60% luminal A, 57% low grade, and 73% early stage. The majority of the BCLM lesions were also ER+, while ~10% of the ER+ primary lesions converted to ER- in metastasis. Progesterone receptor switching from ER+PR+ primary to ER+PR- BCLM occurred in ~50% of ER+PR+ cases. High GATA3 staining was observed in 86% of the BCLM tumors, supporting luminal breast cell origin. Replacement growth pattern was dominant, observed in 87% of cases, with immunohistology and immunofluorescence evidence that breast tumor cells utilize existing sinusoidal architecture to establish and maintain metastatic outgrowth.
Conclusions: In our single institution cohort, we find that recent pregnancy, young age and proximity to recent childbirth are associated with breast cancer metastasis to the liver. We found most primary cancers that progressed to liver metastasis were ER positive, luminal A, low-grade and early-stage, suggesting these classically-good prognostic indicators in breast cancer may not remain good indicators when accompanied by metastasis to the liver. Finally, improved understanding of the dominant replacement growth pattern and the relation between tumor cells and the liver sinusoids may lead to new drug targets and precision therapies.

#0191 Pulmonary tuberculosis as a modifier of molecular features and survival in lung cancer patients.

Cristina Torres-Mallma[1], Ronald Calle Valdez[2], Yomali Aroa Ferreyra[3], Natalia Valdiviezo[1], Rossana Ruiz[1], Ofelia Coanqui[4], Marco Galvez-Nino[5], Enriqueta Felip[6], Luis Mas[1]

[1]AUNA - Oncosalud, Lima, Peru,[2]Hospital Nacional Alberto Sabogal Sologuren, Lima, Peru,[3]Health Innovation Laboratory, Institute of Tropical Medicine "Alexander von Humboldt", Universidad Cayetano Heredia, Lima, Peru,[4]Medical Oncology Department, Instituto Nacional de Enfermedades Neoplasicas, Lima, Peru, Lima, Peru,[5]Inst. Nacional de Enfermedades Neoplasicas, Lima, Peru,[6]VHIO Vall D'Hebron Institute of Oncology, Barcelona, Spain

Pulmonary tuberculosis (TB) may influence lung tumor biology through chronic inflammation and immune dysregulation, but its clinical and molecular implications remain poorly understood in high TB-burden regions. This study aimed to evaluate the impact of active and prior TB on molecular characteristics and survival outcomes in patients with non-small cell lung cancer (NSCLC). We conducted a retrospective observational study including 219 patients diagnosed with NSCLC at the Instituto Nacional de Enfermedades Neoplásicas (INEN), Lima, Peru, between 2010 and 2023. Patients were classified as having active TB (a-TB, n=45) or prior TB (p-TB, n=174) according to clinical and radiologic data. Clinical, pathological, and molecular variables were collected. The primary endpoint was overall survival (OS); secondary endpoints included molecular profile distribution and progression-free survival (PFS). The median age was 57 years in a-TB and 64 years in p-TB. Adenocarcinoma was the predominant histology (94%). EGFR mutations and ALK rearrangements were found in 10.5% and 4.1% of the overall cohort, respectively. PD-L1 expression <1% was frequent (82.3%) and significantly associated with prior TB (p=0.004). In multivariable analysis, the absence of a driver mutation was independently associated with inferior OS in both a-TB (HR 2.94; p=0.046) and p-TB (HR 1.78; p=0.040) groups. Among patients with p-TB, longer TB exposure (>30 years) was associated with poorer OS (HR 1.47; p=0.039). In conclusion, pulmonary tuberculosis, particularly remote infection, was linked to immunosuppressive tumor profiles and decreased survival in NSCLC. These findings suggest that TB history may act as a biological modifier of tumor behavior and should be considered in the prognostic assessment and therapeutic planning of lung cancer patients in endemic regions.

#0192 Chronological evolution of immune tumor microenvironment (TME) from esophageal dysplasia (ED) to esophageal squamous cell carcinoma (ESCC).

Jhe-Cyuan Guo[1], Yen-Lin Huang[2], Chia-Lang Hsu[3], Tsung-Che (Nathan) Wu[3], Chien-Huai Chuang[3], Ta-Chen Huang[3], Wen-Lun Wang[4], Chih-Hung Hsu[3]

[1]National Taiwan University Cancer Center (NTUCC), Taipei City, Taiwan,[2]National Chung Hsing University, Taichung, Taiwan,[3]National Taiwan University Hospital, Taipei, Taiwan,[4]Department of Internal Medicine,E-Da Hospital/I-Shou University, Kaohsiung, Taiwan, Institute of Clinical Medicine,National Cheng Kung University Hospital, College of Medicine, Nationa, Kaohsiung City, Taiwan

Background: Previous studies have shown that ED, a precancerous stage of ESCC, exhibits genetic alterations and genomic instability similar to those observed in ESCC. Other factors—such as alterations in immune surveillance—may also contribute to the progression from dysplasia to invasive cancer.
Methods: Patients with a history of ED prior to the diagnosis of ESCC were enrolled for gene expression profiling (GEP) study of esophageal lesions and patients with early stage ESCC treated with endoscopic submucosal dissection (ESD) were enrolled for immunohistochemistry (IHC) study. Formalin-fixed paraffin-embedded tissues (FFPEs) from ED diagnosed more than 6 months prior to the diagnosis of ESCC (denoted as dysplasia-1), ED diagnosed within 6 months prior to the diagnosis of ESCC (denoted as dysplasia-2), and ESCC were retrieved. Transcriptomic data were generated by NanoString nCounter platform with Human PanCancer Immune Profiling panel and were further analyzed for the expression levels of infiltrating immune cells by CIBERSORT. FFPEs from another cohort of patients with early stage ESCC treated with ESD were stained with anti-CD68 (Rabbit polyclonal, abcam, UK) and anti-CD163 (Rabbit polyclonal, Synaptic Systems GmbH, Göttingen, Germany). Their expression levels were semi-quantitatively determined in the stroma and intratumoral fields and were compared among the areas of normal mucosa, dysplasia, and ESCC in the same patient.
Results: Seventeen ESCC patients were enrolled for GEP study. The median time periods from the diagnosis of dysplasia-1 to that of ESCC and from the diagnosis of dysplasia-2 to that of ESCC were 8.6 months and 3.0 months, respectively. The analysis of immune cell signatures defined by NanoString platform revealed that multiple cell types were significantly increased in ESCC compared with dysplasia-1 (mast cell, macrophage, and dendritic cell, all $P < 0.05$) and in ESCC compared with dysplasia-2 (macrophage, mast cell, CD8 T cell, dendritic cell, total TIL, T cell, and regulatory T cell, all $P < 0.05$). No significant difference was found between dysplasia-1 and dysplasia-2. Immune cells classified by CIBERSORT showed an increase of M2 macrophage and a decrease of M1/M2 ratio in ESCC compared with dysplasia-1 or dysplasia-2 (both $P < 0.05$). Eighty-two early ESCC patients were enrolled for IHC study. A progressive increase in the expression levels of CD68 and CD163 was found from mucosa to dysplasia then to ESCC (all $P < 0.001$)
Conclusions: The increased expression of M2 macrophages in the ESCC TME compared with precancerous dysplasia supports the hypothesis that immune TME alterations may drive the progression from dysplasia to ESCC. (Funded by MOST 107-2314-B-002-199-, MOST 109-2314-B-002-231-, MOHW114-TDU-B-221-144006, NSTC 114-2314-B-002 -206 -MY3, NTUCCS-110-10, and NTUCCS-111-05)

#0193 Tumor-agnostic analysis identified pan-cancer immune archetypes and CD8⁺FoxP3⁺ cells as novel in situ predictors of survival.

Artur Mezheyeuski[1], Emma Sandberg[2], Max Backman[3], Ali Teymur Kahraman[3], Amanda Lindberg[3], Carina Strell[2], Hans Brunnstrom[4], Jutta Huvila[5], Malin Sund[6], Fredrik Warnberg[7], Bengt Glimelius[3], Ina Hrynchyk[8], Siarhei Mauchanski[9], Salome Khelashvili[10], Klara Hammarstrom[3], Margret Agnarsdottir[3], Gemma Garcia-Vicien[11], DAVID G. MOLLEVI[12], Aine O?Reilly[13], Sara Corvigno[14], Hanna Dahlstrand[3], Johan Botling[15], Ulrika Segersten[4], Agnieszka Krzyzanowska[16], Anders Bjartell[4], Jacob Elebro[4], Margareta Heby[4], Sebastian Lundgren[4], Charlotta Hedner[4], David Borg[4], Jenny Brandstedt[4], Hanna Sartor[4], Per-Uno Malmstrom[3], Martin Johansson[15], Anna Portyanko[10], Bjorn Nodin[4], Cecilia Lindskog[3], Karin Leandersson[4], Karin Jirstrom[4], Tobias Sjoblom[3], Patrick Micke[3]

[1]Vall d'Hebron Institute of Research, Barcelona, Spain,[2]Uppsala University, Dept of Immunology, Genetics and Pathology, Uppsala, Sweden,[3]Uppsala University, Uppsala, Sweden,[4]Lund University, Lund, Sweden,[5]University of Turku, Turku, Finland,[6]Umea University, Umea, Sweden,[7]Sahlgrenska University Hospital Goteborg, Goteborg, Sweden,[8]City Clinical Pathologoanatomic Bureautitute (VHIR), Minsk, Belarus,[9]Vall d'Hebron Institute of Oncology (VHIO), Barcelona, Spain,[10]N.N. Alexandrov National Cancer Centre of Belarus, Minsk, Belarus,[11]IDIBELL L'Hospitalet de Llobregat Barcelona, Barcelona, Spain,[12]LABORATORI DE RECERCA TRANSLACIONAL, INSTITUT CATALA D'ONCOLOGIA, BARCELONA, Spain,[13]Karolinska Institutet, Stockholm, Sweden,[14]UT MD Anderson Cancer Center, Houston, TX,[15]Sahlgrenska Universitety Hospital Goteborg, Goteborg, Sweden,[16]Lund University, Malmo, Sweden

Immune infiltration shapes anti-tumor responses and is associated with patient outcomes. Yet, comprehensive studies comparing infiltration patterns and their clinical impact across cancer types are scarce.We profiled the tumor immune microenvironment across 16 solid tumor types from more than 2,700 patients using multiplex immunofluorescence with pathologist-curated image analysis to quantify major lymphoid and myeloid subsets and their spatial organization in situ.Across all cancer types, lung, endometrial, and high-grade serous ovarian cancers were highly infiltrated, whereas prostate and ER-positive breast cancers were comparatively “immune cold”. Cancer-agnostic consensus clustering resolved four reproducible immune archetypes with distinct outcomes, including an immune-hot group enriched for CD4, CD8, and B cells that associated with the best survival ($p<0.001$). Notably, the tumor type accounted for only a part of the immune contexture, as most cancers spanned multiple immune signature groups. Nevertheless, a machine-learning classifier trained on immune compositions distinguished tumor types with high accuracy (AUC = 0.96), confirming that each cancer maintains a recognizable immune imprint even among pan-cancer archetypes.Analysis of survival associations of individual cell classes revealed a rare CD8⁺FOXP3⁺ T-cell phenotype that emerged as a strongest positive prognostic factor across cancers (HR=0.79, 95%CI:[0.70-0.89], p=0.002). Single-cell RNA sequencing data indicated that CD8⁺FoxP3⁺ cells exhibit two distinct gene programs, with regulatory and cytotoxic capacities. Spatial mapping suggested context-dependency in the function of CD8⁺FoxP3⁺ cells, as their proximity to CD8 T cells was linked to better survival (enrichment at 10um: HR=0.76, 95%CI:[0.67-0.90], p=0.0006), whereas proximity to tumor cells was associated with worse prognosis (enrichment at 10um: HR=1.29, 95%CI:[1.12-1.49], p=0.0005).Together, our findings define pan-cancer immune archetypes that are both shared and disease-specific, explaining why “immune hot” and “cold” states are not synonymous with pure infiltration quantities. We identified CD8⁺FoxP3⁺ immune cells as a cell type with strong biomarker potential independent of cancer type.

#0194 Lung adenocarcinoma promotion by chemokine CXCL13.

Xiao-Liang Jie, Yang-Tong Liu, Yi-Shuai Tan, San-Hui Gao, Zheng Wang, Gui-Zhen Wang, **Guang-Biao Zhou**

Cancer Hospital Chinese Academy of Medical Sciences, Beijing, China

Chemokine C-X-C motif ligand 13 (CXCL13) is a B lymphocyte chemoattractant that plays an important role in immune system and is involved in the pathogenesis of a number of benign and malignant diseases. Previously, we reported that deficiency in Cxcl13 significantly attenuated air pollutant-induced lung cancer in mice. In this study, we established Cxcl13-overexpressing mouse models to investigate its cancer initiating activity. We found that 15 (51.7%) of 29 mice that received an intratracheal injection of Cxcl13-encoding lentivirus developed lung adenocarcinoma (LUAD), as detected by hematoxylin-eosin (H&E) staining and confirmed by immunohistochemistry for TTF1 in the lung tumor tissues. Of the 21 surfactant protein C (SPC) promoter-driven Cxcl13 transgenic mice, 7 (33.3%) developed LUAD. By single-cell RNA sequencing, we identified a fraction of Ecm1-expressing M2 type macrophages and Itga2^{+} cancer cells that expressed high level of wnt/β-catenin carcinogenic pathway. Overexpression of CXCL13 in cancer cells promoted CD47 accumulation on the surface of tumor cells to shield themselves from macrophage phagocytosis. Targeting CXCL13 combined with CD47 pathway blockade exerted synergistic anti-tumor efficacy in patient-derived xenograft models of NSCLC. Collectively, our findings indicated that the up-regulation of CXCL13 in lung epithelial cells promotes tumorigenesis, and targeting CXCL13 may provide a potential therapeutic approach for NSCLC.

#0195 IL-33/JAK2/RAB21/PLD4-Sphingolipid network drives gastric carcinogenesis.

Hui Liu, Yunxiao Ge, Yubing Zhou, Hangrui Liu, Zigang Dong

Department of Pathophysiology, Zhengzhou University, Zhengzhou, China

Gastric cancer (GC), the fifth most prevalent malignancy and fourth leading cause of cancer mortality globally, is synergistically promoted by *Helicobacter pylori* infection and alcohol consumption through exacerbated gastric mucosal inflammation. To delineate key biomarkers in the gastritis-to-cancer transition and identify actionable targets for primary prevention and therapy, we integrated proteomic and metabolomic analyses of *Helicobacter pylori* plus alcohol induced GC mouse model and human gastritis/GC tissues. It revealed that significant Ras-related protein RAB21 is upregulated in gastritis and gastric cancer tissues, and metabolomics identified sphingolipid metabolism reprogramming is a key signature in GC tumorigenesis. *In vitro* experiments showed that RAB21 downregulation suppressed GC cell proliferation, and *in vivo* studies including RAB21 conditional knockout mice further demonstrated that RAB21 depletion inhibited GC tumorigenesis. Mechanistically, RAB21 binds to tyrosine-protein kinase JAK2 and is phosphorylated at tyrosine 88 by JAK2, regulating expression and phospholipase activity of 5'-3' exonuclease PLD4. *Helicobacter pylori* plus alcohol induced upregulated interleukin-33 (IL-33) promotes JAK2 and RAB21 expression via forkhead box protein P3 (FOXP3), promoting RAB21 nuclear translocation to regulate PLD4 expression, and converged with the phosphatidic acid-sphingosine kinase-sphingosine-sphingosine 1-phosphate (PA-SPHK-SPHG-S1P) metabolic flux to drive GC tumorigenesis and progression. This study elucidates the protein-metabolic network in gastric carcinogenesis and provides experimental rationale for targeting IL-33/JAK2/RAB21/PLD4-sphingolipid metabolism axis for GC prevention and treatment.

#0196 Lung inflammation accelerates tumor progression in a mouse model of oncogenic KRAS driven lung adenocarcinoma.

Samantha A. Nelson, Jacob Kassama, Christina M. Cabana, Alexandria M. Jefferson, Tyler E. Jacks

Biology, Massachusetts Institute of Technology (MIT), Cambridge, MA

Recent studies of human tissue samples in various organs including the lung have revealed the presence of canonical oncogenic mutations at rates higher than known incidence rates of cancers associated with these tissues. Other work has linked diverse inflammatory diseases to increased incidence rates of cancers associated with the involved organs. In the context of lung adenocarcinoma (LUAD), inflammatory lung diseases may produce a favorable environment for the outgrowth of tumors, and characterizing how this may occur could uncover avenues for LUAD prevention. Using a transgenic mouse model where LUAD is initiated by inducing expression of oncogenic KRAS and the fluorophore tdTomato in normal alveolar type II cells via delivery of Cre-expressing virus into the lung, we demonstrated that a range of inflammatory insults accelerated early tumor growth. Modelling of idiopathic pulmonary fibrosis and bacterial or viral lung infections in these tumor bearing mice each resulted in an increase in average tumor size and total tumor burden at both early and late timepoints of tumor progression, despite showing many divergent impacts on lung immune populations and signaling factors as characterized through flow cytometry, RNA sequencing, and ELISAs. Immunofluorescence staining of early lesions allowed us to quantify the increase in lesion size under inflammatory conditions and to investigate the association of immune cells with these small lesions, revealing that KI-67+ F4/80+ macrophages showed increased density proximal to lesions under all inflammatory conditions. We are actively working to uncover the points of communication between immune populations and early cancer cells that result in this accelerated tumor growth under these conditions. We have observed that in our LUAD mouse model tumor growth is accelerated by exposure to lung inflammation, and through characterization of the inflamed immune microenvironment and communication between immune and cancer cells during inflammation that mediate accelerated growth, this project aims to identify molecular targets for LUAD prevention.

#0197 LPS-induced superoxide anion-dependent macrophage extracellular traps by store-operated calcium entry.

Ngoc Thang Nguyen, Wen-Tai Qiu

Department of Biomedical Engineering, National Cheng Kung University, Tainan City, Taiwan

Macrophage extracellular traps (METs) contribute to chronic inflammation in the tumor microenvironment, promoting cancer progression via necroptosis-induced extracellular matrix degradation. This study investigates the role of store-operated calcium entry (SOCE) in calcium-induced MET formation, a process that amplifies pro-tumorigenic inflammatory responses in macrophages. Mouse macrophage RAW264.7 and human monocyte U937 cells were stimulated with lipopolysaccharide (LPS) or phorbol myristate acetate (PMA), with or without pretreatment using Ca^{2+} chelator BAPTA-AM, mechanical Ca^{2+} channel inhibitor $GdCl_3$, SOCE inhibitors SKF96365 or YM58483, or superoxide anion scavenger thymoquinone (TQ). METotic cells were identified via immunofluorescence staining for Lamin B after digitonin permeabilization. LPS and PMA triggered SOCE-mediated Ca^{2+} influx, leading to elevated cytoplasmic Ca^{2+} levels that activated NADPH oxidase (NOX) to produce superoxide anions, culminating in MET formation. Pharmacological inhibition of SOCE attenuated Ca^{2+} influx and superoxide anion, whereas superoxide scavenging significantly inhibited METosis without altering NOX1/2 protein levels, indicating Ca^{2+}-dependent NOX activation. These results reveal a SOCE-NOX-superoxide axis driving LPS-induced METosis, highlighting its potential in tumor progression. Targeting SOCE could disrupt macrophage-mediated inflammatory circuits in cancer initiation and progression

#0198 The IL-33/ST2 signaling reshapes the immune landscape and promotes leukemia transformation in acute myeloid leukemia.

Yu-Hsuan Fu, Man Li, Ying-Chieh Chen, Lianjun Zhang, Wancheng Guo, David E. Frankhouser, Denis O'Meally, Jihyun Irizarry, Jennifer Rangel Ambriz, Ziang Chen, Bin Zhang, Sergio Branciamore, Guido Marcucci, Russell Rockne, Ya-Huei Kuo

City of Hope National Medical Center, Duarte, CA

Acute myeloid leukemia (AML) is an aggressive malignancy with a 5-year survival rate of ~30%, largely due to relapse and immune evasion. Using a state-transition modeling framework on time-series RNA-seq from a *Cbfb::MYH11* (CM) knock-in AML mouse model, we identified *IL1RL1* (ST2), the receptor for IL-33, as a leukemia-promoting gene upregulated early in leukemogenesis. Similarly, ST2 expression is elevated in AML patients —particularly in inv(16) and t(8;21) subtypes— and correlates with poor prognosis (TCGA, n = 139, $p < 0.001$). ST2 regulates inflammatory responses, including Th2 immune response and mast cell activation. The $ST2^+$ regulatory T cells (Treg) have been shown to exert immune suppression function in AML, whereas ST2's impact on the other immune cells and the molecular mechanisms remain largely unexplored. We first generated CM mice with ST2 knockout (CM-ST2-KO), which showed delayed leukemia onset, reduced circulating blasts, and extended survival compared to CM mice (median survival 192 days vs. 103 days; $p < 0.0001$). The scRNA-seq of leukemic stage bone marrow from CM mice revealed high ST2 expression in leukemia-enriched cell types (stem cells, erythrocytes, and mast cells). Further cell-cell communication analysis via CellChat discovered enhanced crosstalk between leukemic cells and immune cells in CM mice, which was reduced in CM-ST2-KO mice. Dysregulation of immunosuppressive pathways were identified, including PD-L1 and ALOX5, both elevated in CM and reversed in CM-ST2-KO mice. Experimental validation by ectopically overexpressing ST2 enhanced PD-L1 and ALOX5 expression, upon IL-33 stimulation. By flow cytometry, enhanced PD-L1 level was found in hematopoietic stem and progenitor cells (HSPCs) and myeloid populations, which were skewed toward immunosuppressive subsets [i.e, M2 macrophages, $PD\text{-}L1^{high}$ Ly6C+ myeloid-derived suppressor cells (MDSCs)] with reduced $PD\text{-}L1^{low}$ Ly6G+ MDSCs in CM mice. Moreover, increased expression of T cell checkpoint markers was shown, including PD-1 and TIGIT on CD8+ T cells and CD160 on CD4+ T cells. These immunosuppressive phenotypes were all reversed in CM-ST2-KO mice. Furthermore, direct co-culturing T cells from healthy mice with the Lin^-cKit^+ cells (LK cells) from CM mice suppressed T cell proliferation compared to LK cells from WT, which can be rescued in CM-ST2-KO co-culture. In summary, we identified ST2 as a key regulator of leukemia progression and immune suppression in AML. Our data indicates that ST2 promotes leukemic transformation and reshapes the bone marrow immune landscape by upregulating ALOX5 and PD-L1, expanding immunosuppressive myeloid populations, and enhancing T cell exhaustion. Genetic knockout of ST2 reverses these immunosuppressive phenotypes and prolongs survival, supporting the therapeutic potential of targeting ST2 to improve immune-based therapies in AML.

#0199 Identification of oncohistone-dependent changes in chromatin accessibility and the tumor microenvironment in a new inducible and reversible H3.3K27M mouse model of diffuse midline glioma (DMG).

Mostafa M. H. Ibrahim[1], Niloofar Khairkhah[1], Sienna L. Galban[2], Megan Faunce[1], Yue Zhao[3], Stefanie Galban[1]

[1]Department of Radiology, University of Michigan Medical School, Ann Arbor, MI,[2]Davidson School of Chemical Engineering, Purdue University, West Lafayette, IN,[3]Gilbert S. Omenn Department of Computational Medicine and Bioinformatics, University of Michigan Medical School, Ann Arbor, MI

Tumor recurrence remains a major obstacle to the successful clinical management of H3K27M-altered diffuse midline glioma (DMG), a pediatric high-grade tumor arising in the brain stem. Currently available therapies do not prevent tumor recurrence, observed in nearly all treated patients. A desperate need remains to understand epigenetically, H3K27M-driven gene expression and the remodeling of the tumor immune/stromal microenvironment to prevent tumor recurrence.

Here, we introduce new inducible and reversible H3.3 and H3.1K27M cell and mouse models of DMG that enable the evaluation of the biological effects on tumor growth and recurrence of oncohistone expression, and at the same time, the characterization of changes in the microenvironment and epigenome upon H3K27M activation, inactivation and re-activation. Tetracycline-inducible and reversible PiggyBac-based expression vectors for H3.3K27M and H3.1K27M were utilized to engineer patient- and murine-derived DMG cell and *in vivo* models. Inducibility and reversibility of H3K27M in cells and tumors was validated by live cell flow cytometry for fluorescent marker expression and intracellular flow cytometry and western blotting for expression of the oncohistone. We detected characteristic morphological changes and repression of astrocytic markers upon H3K27M re-expression in KO cells. Furthermore, decrease in tumor growth upon oncohistone expression was observed in DMG *in vivo* models using bioluminescence imaging, providing proof-of-concept for inhibiting oncohistone expression in progressing tumors. In addition, we demonstrated changes in chromatin accessibility between ON, OFF and OFF-ON cells and importantly, identified mechanisms of immunosuppression through regulation of PD1 in the ON and OFF-ON groups, providing rationale for future targeted therapies. Single-cell RNA sequencing (scRNA-seq) of tumors in ON and OFF groups showed a complex TME that is modulated by expression of the oncohistone.

In conclusion, these newly developed iH3.3 and H3.1K27M cell and mouse models are ideal to study oncohistone dependent pathobiological consequences, as they allow controlled expression of the oncohistone in physiologically relevant and immune proficient settings. Furthermore, they lend themselves to comparative studies between H3.3 and H3.1 expression in DMG. Our studies will provide future strategies for targeting immune and stromal compartments with the potential to prevent tumor recurrence and inform the feasibility of future CRISPR editing strategies for targeting the oncohistone directly.

#0200 Spatiotemporal analysis reveals tsMHC-I downregulation-induced neutrophil extracellular traps as a driver of lung adenocarcinoma neoplastic evolution.

Yanhua Tian[1], Jian-Rong Li[2], Bo Zhu[1], Jared Fradette[1], Hong Chen[1], Zhubo Wei[1], Jie Ye[1], Shao-Wei Lu[1], Andrew Y. Liu[1], Samrat T. Kundu[1], Haoyi Wu[1], Shucheng Miao[1], Xiuning Le[1], Linghua Wang[1], Jia Wu[1], Alexandre Reuben[1], John V. Heymach[1], Andy Futreal[1], Honami Naora[3], Chao Cheng[2], Don L. Gibbons[1], Jianjun Zhang[1]

[1]UT MD Anderson Cancer Center, Houston, TX,[2]Baylor College of Medicine, Houston, TX,[3]Associate Professor, Dept. of Systems Biology, UT MD Anderson Cancer Center, Houston, TX

Background: Loss of tumor-specific MHC class I (tsMHC-I) is a recurrent feature of lung adenocarcinoma (LUAD) progression and is associated with immune escape and poor outcomes. However, how tsMHC-I downregulation shapes tumor evolution and remodels the immune microenvironment remains unclear.
Methods: We integrated single-cell RNA sequencing, spatial transcriptomics, and multiplex imaging from human LUAD samples spanning precancerous lesions to advanced tumors, together with longitudinal genetically engineered mouse models (GEMMs). Functional assays—including neutrophil co-culture, assessment of neutrophil extracellular traps (NETs), and in vivo tumor studies—were performed to define mechanistic consequences of tsMHC-I loss.
Results: Progressive tsMHC-I downregulation was observed across LUAD evolution and validated in GEMMs. Single-cell trajectory analysis showed that reduced tsMHC-I is linked to loss of alveolar type II identity, increased chromosomal instability, heightened tumor plasticity, and acquisition of epithelial-mesenchymal transition (EMT) programs. Functionally, tsMHC-I^{Low} malignant cells displayed increased invasiveness and metastatic capacity. Spatial and immunophenotypic profiling revealed that tsMHC-I downregulation reshapes the tumor microenvironment toward a neutrophil-enriched, cytotoxic cell-excluded niche. tsMHC-I^{Low} regions exhibited dense tumor-associated neutrophil aggregates and depletion of CD8^{+} T cells, NK cells, and other effector populations. Mechanistic studies showed that tsMHC-I^{Low} malignant cells induce robust NET formation. In vitro assays identified Annexin A2, a tumor-secreted protein, as a key driver of NET induction. Annexin A2 expression and secretion were consistently elevated in tsMHC-I^{Low} cells across human and mouse models, and Anxa2 knockdown markedly reduced NET formation. Targeting NETs in vivo with DNase I selectively suppressed growth and metastatic spread of tsMHC-I^{Low} tumors, restored cytotoxic immune infiltration, and reversed the immune-excluded phenotype. In tsMHC-I heterogeneous tumors, combining NET inhibition with anti-PD-1 enhanced tumor control and survival.
Conclusions: Our integrated analyses reveal that tsMHC-I downregulation drives neutrophil recruitment and NET formation through Annexin A2 secretion, creating an immunosuppressive barrier that promotes LUAD progression and limits immunotherapy response. These findings identify a previously unrecognized tsMHC-I-NET axis as a therapeutic vulnerability in LUAD.

#0201 Development of an immunocompetent orthotopic mouse model recapitulating metastatic endometrial cancer.

Keun Cheon Kim, Cassandra Schmidt, Eunhee M Jeong, Tae Hoon Kim, Jae-Wook Jeong

University of Missouri, Columbia, MO

Endometrial cancer (EC) is the most common gynecologic malignancy. However, progress in developing new therapeutic strategies has been limited by the lack of immunocompetent animal models that faithfully recapitulate human EC, including intact immune responses and the ability to form distant metastases. To address this gap, we developed an orthotopic, immunocompetent EC mouse model using the GFP-labeled mouse endometrial cancer cell line MECPK (Pten-deleted, Kras-activated). Following uterine abrasion, 50,000 MECPK cells were injected into the uterine lumen of recipient mice. Uterus tissues with EC were collected from mice at 4, 5, 6, and 8 weeks post-induction using a fluorescence-guided dissecting microscope. Samples were processed for hematoxylin and eosin (H&E) staining and immunohistochemistry for E-cadherin, followed by AI-based image analysis. Tumor initiation was first detectable at 5 weeks after induction, and 66.7% of mice (6/9) developed distant lung metastases by 8 weeks. All tumor-bearing mice succumbed to disease before 10 weeks post-transplantation. We performed quantitative IHC analysis of PD-L1, MLH1, and MSH2 to evaluate biomarkers associated with immunotherapy response. PD-L1 was highly expressed at all stages of tumor progression. While MLH1 expression did not differ significantly between EC and normal regions, MSH2 expression was remarkably reduced during cancer progression. MSH2 expression in primary cancer at 5 weeks (246.55 ±6.39) was not significantly different from that in normal epithelium (256.15 ±10.96). However, MSH2 levels were significantly decreased in primary cancer at 6 weeks (95.65 ±17.88, $p<0.001$) and 8 weeks (133.16 ±12.98, $p<0.001$), as well as in metastasis endometrial cancer in lung at 8 weeks (110.89 ±19.26, $p<0.001$). These findings establish a robust immunocompetent orthotopic EC model that recapitulates primary tumor progression and distant metastasis, providing a valuable platform for mechanistic studies and preclinical evaluation of emerging therapies, including immunotherapy.

This work was supported by NCI R01 CA264944

#0202 The early immune landscape of breast cancer and the role of tertiary lymphoid structures.

Thila Vanhulst[1], Soizic Garaud[2], Alexandre De Wind[3], Anais Boisson[1], Pauline Delvaux[1], Doina Sofronii[1], Mireille Langouo Fontsa[1], Karen Willard-Gallo[1]

[1]Molecular Immunology Unit, Institut Jules Bordet, Brussels, Belgium,[2]Universite Brest, Inserm, Brest, France,[3]Departement of Pathology, Institut Jules Bordet, Brussels, Belgium

Ductal carcinoma *in situ* (DCIS), stage 0 breast cancer (BC), is defined by tumor cells confined to the duct. Tumor infiltrating lymphocytes (TIL) are prognostic for invasive ductal carcinoma (IDC) of the breast; however, their role in DCIS remains unknown. Some DCIS studies have analyzed TIL subpopulation balances with a few identifying tertiary lymphoid structures (TLS) but their roles in progression and recurrence remains unclear due to contradictory findings. The aim of this study is to investigate the functionality and organization of TIL into TLS in pre-invasive BC lesions. Fresh tumor samples were obtained at surgery from patients with DCIS (n=19), IDC (n=19) and mammary reductions (MR; n=8 controls) for the prospective cohort. Tissues were dissociated without enzymes and immunophenotyped by flow cytometry. A retrospective cohort of FFPE tissue blocks (DCIS n=30, IDC n=30) were dual-stained by chromogenic immunohistochemistry (cIHC) for CD3+CD20 and PD-1+Ki67 and scored for TILs and TLS, with selected patients (DCIS n=10, IDC n=10) also stained by multiplex IHC (mIHC). We extended our analyses by re-analyzing public scRNA-seq datasets (DCIS n=6, IDC n=6) to further explore the immune landscape. Patients were matched by BC molecular subtypes to control variation between subtypes. In the prospective cohort, a higher proportion of B cell and T follicular helper (Tfh) TIL were detected in DCIS vs. MR, with the former paralleling IDC levels and potentially signaling a TLS presence. In the retrospective cohort, TLS were detected by dual cIHC in 75% of DCIS compared to 58% of IDC, the latter consistent with our previous analysis of >300 IDC patients. Spatial mIHC analysis of CD3, CD20, AID and CD23 revealed that while AID^+ B cells were less frequent in DCIS-TLS the number of $CD23^+$ mature FDC were comparable with IDC. Thus, DCIS-TLS have a mature stroma but limited Ig diversification, suggesting these structures are at an earlier stage of differentiation. Tfh cells play a crucial role in B cell maturation and antibody production. Flow cytometric data from the prospective cohort detected lower frequencies of functional $CXCR5^+PD1^{hi}ICOS^{int}$ Tfh cells in DCIS vs IDC. scRNA-seq analysis revealed that DCIS Tfh were more naïve, whereas IDC Tfh had enhanced effector signatures. In the prospective cohort, CXCL13-producing $CXCR5^-PD1^{hi}ICOS^{int}$ Tfh cells, known for their critical role in IDC-TLS formation, were also reduced in DCIS with CXCL13 expression primarily detected in podoplanin$^+$ stromal cells within DCIS-TLS. Our data show that while high densities of TIL and TLS are observed in DCIS, adaptive immunity responses are less mature and therefore less functional than in IDC. This may partly explain why dense TIL and TLS in DCIS are not consistently associated with a good prognosis, unlike IDC. Our findings highlight the need to further dissect, beyond simple quantification, the immune composition and spatial organization across BC stages.

: Virology and Cancer
Poster Session

#0206 Dependencies of diffuse large B-cell lymphoma on EBV oncoproteins.

Lily Catherine Foreman Wenger[1], Quincy Rosemarie[2], Eric C. Johannsen[2]

[1]McArdle Laboratory for Cancer Research, University of Wisconsin-Madison, Madison, WI,[2]University of Wisconsin - Madison, Madison, WI

Background: Up to 14% of diffuse large B-cell lymphomas (DLBCL) are Epstein-Barr virus-positive (EBV+), and their growth and survival are dependent on EBV latency gene products. DLBCL is a heterogeneous group of aggressive lymphomas, and we previously found that EBV is associated with the BN2 LymphGen subtype. Additionally, multiple genes were mutated at lower frequencies in EBV+ tumors relative to EBV-, suggesting viral oncogenes functionally replace host driver mutations. To identify the EBV oncogenes essential for EBV+ DLBCL and the functional consequences of their inactivation, we are conducting CRISPR/Cas13d screens in EBV+ DLBCL cell lines.
Methods: EBV+ DLBCL cell lines (Farage, BCKN1, IBL1, and IBL4) were characterized using whole-exome sequencing (WES), RNA sequencing (RNA-seq), and immunoblotting. We compared the mutational and transcriptomic profiles of EBV+ tumors and cell lines to inform CRISPR/Cas13d functional screens. These screens aim to identify EBV gene product dependencies in EBV+ DLBCL and the impact on cell growth and survival.
Results: WES analysis revealed the genetic subtype of each EBV+ DLBCL cell line: Farage was classified as ST2, and the rest were classified as “Other”. RNA-seq and immunoblotting revealed that all expressed an atypical latency III program, characterized by the absence of LMP2A expression. This novel latent gene program was also observed in the EBV+ DLBCL tumors. All cell lines were infected with EBV1, except IBL1, which, to our knowledge, is the only known cell line infected with an EBV1/EBV2 intertypic recombinant. By employing Cas13d for our knockdown screen, we can determine the specific transcripts within the complex EBV latent transcriptome that are essential for the growth and survival of EBV+ DLBCL. Targeting RNA also avoids excessive DNA damage and low sensitivity that arises from targeting 10-20 copies of EBV DNA per cell with Cas9. We have stably expressed two different Cas13d orthologs in each cell line and are optimizing their RNA knockdown efficiency using a FACS-based transient knockdown strategy. Use of clones achieving the most efficient knockdown will allow us to identify essential EBV latent genes and determine the phenotypic consequences (growth arrest, apoptosis, etc.) of inactivating each essential viral oncogene.
Conclusions: EBV+ DLBCL exhibits distinct host mutation and gene expression profiles, including the replacement of several subtype-defining mutations with EBV oncogenes. The available EBV+ DLBCL cell lines faithfully model the ST2 or “Other” LymphGen subtypes and exhibit the same atypical EBV latent gene expression pattern as tumors. By determining EBV oncogene dependencies and the effects of their inactivation, we aim to uncover how EBV cooperates with host driver mutations in the pathogenesis of EBV+ DLBCL. Understanding these therapeutic vulnerabilities will provide a foundation for precision therapy.

#0207 Decoding the circRNA-miRNA-mRNA regulatory network in hepatitis B Virus-driven hepatocellular carcinoma.

Kainat Ahmed[1], Anwaruddin Mohammad[2], Nan Chaiyariti[3], Danya Sankaranarayanan[1], Pankaj Kumar[2], Sudhakar Jha[1]

[1]Oklahoma State University, Stillwater, OK,[2]University of Virginia, Charlottesville, OK,[3]Mahidol University, Bangkok, Thailand

Integration of the hepatitis B virus (HBV) genome into the host chromosome of infected patients poses a threat to those with HBV-associated hepatocellular carcinoma (HCC) due to challenges in early diagnosis and poor prognosis. CircRNAs are known for their oncogenic and biomarker potential in various cancers, including HBV-HCC, by sequestering tumor suppressive miRNAs, which, when free, can silence the expression of oncogenic mRNAs. Therefore, we aimed to identify the circRNA-miRNA-mRNA axis in HBV-integrated HCC cell lines to find prognostic biomarkers specific to HBV-HCC patients. We identified dysregulated host circRNA and mRNA from HBV-negative and HBV-integrated cells using RNA-seq followed by differential gene expression analysis with DESeq and performed pathway analysis using GSEA. Junctional sequences of the circRNAs were validated by Sanger sequencing of the amplified products. RT-qPCR further confirmed the dysregulation of 9 randomly selected circRNAs chosen from those with the highest fold-change and adjusted p-values. The miRNA partners for each of the circRNA idenfied using mirDB. miRNA expression validation was performed using the publicly available GEO database of same cells and cumulative distribution plots were generated to assess the fold change of mRNAs in potential binding miRNA partners. The mRNA targets for 10 miRNA ECDF plots were subjected to GO and KEGG pathway analysis, and hub genes were identified using STRING cytohubba protein-protein interaction (PPI) analysis. Survival analysis of hub genes was plotted, and a competitive endogenous RNA (ceRNA) network was constructed using Cytoscape.We identified 494 dysregulated circRNAs, 311 dysregulated miRNAs and 10,419 dysregulated mRNA in HBV-integrated cells. circADGRL2 (~25-fold) showed the highest upregulation and miR-361-5p acted as a central node of multiple circRNAs: circADGRL2, circPROX1 and circPALS2. BDNF, a target mRNA of miR-361-5p, was identified as the highest risk ratio in HBV-HCC patients, suggesting a possible circADGRL2-miR-361-5p-BDNF axis. The target mRNAs of miRNAs were found to be associated with several cancer pathways, such as MAPK and RAS. Our data indicate that HBV integration reprograms the circRNA-miRNA-mRNA axis, leading to a poor prognosis for HBV-HCC patients.

#0208 HERV-K env gene promotes tumorigenicity and metastasis through multiple signal pathways, including the Ras/ERK signaling pathway and epithelial-mesenchymal transition (EMT), in breast cancer cells.

Feng Wang-Johanning[1], Gary Johanning[1], Fuling Zhou[2], Edward Njoo[3]

[1]SunnyBay Biotech, Fremont, CA,[2]Zhongnan Hospital of Wuhan University, Wuhan, China,[3]Aspiring Scholars Directed Research Program (ASDRP), Fremont, CA

Background: Overexpression of the human endogenous retrovirus type K (HERV-K) envelope (*env*) gene was demonstrated in various cancers. However, its precise role as a "driver" (initiating tumor development) or "passenger" (simply a consequence of the cancerous state) is still a subject of ongoing research and debate within the scientific community.

Methods: The role(s) of HERV-K expression was investigated in multiple cell lines by stably transfecting with the full length HERV-K *env* gene.

Results: Enhanced expression of K-Ras and its activity were detected in normal breast cells after expressing the HERV-K *env* gene. Enhanced expression of multiple oncogenes was also observed in cancer cells that expressed HERV-K *env*. Upregulation of expression of EMT markers and β-Catenin accompanied upregulation of HERV-K expression. Importantly, metastasis to multiple organs was discovered *in vivo*. Of interest, cancer prevention was demonstrated in mice immunized with HERV-K surface (SU) to a greater extent than with transmembrane protein (TM), due to increased CD8 T cells, decreased Treg cells, and increased Th1 cytokine secretion.

Conclusion: The HERV-K *env* gene is an oncogene that promotes tumorigenesis and metastasis through upregulated expression of the Ras/Raf/MEK/ERK, EMT, and PI3K/AKT pathways. In addition, the HERV-K SU domain but not the TM domain is a tumor-associated antigen (TAA) that can trigger immune responses.

#0209 Unexpected identification of tumor-infiltrating H. pylori or human papillomavirus (HPV) 16 in three exceptional responders in immunochemotherapy-treated esophageal cancer.

Sabrina A. James[1], Hannah S. Fuchs[1], Thomas M. Carroll[1], Phil F. Xie[1], Joseph A. Chadwick[1], Brittany-Amber Jacobs[1], Tim Waterboer[2], Michal Bassani-Sternberg[3], Florian Huber[3], Duncan Parkes[1], Simon Lord[4], Lucinda Bones[5], Tim Underwood[6], Ioannis Karydis[6], Russell D. Petty[7], Benjamin Schuster-Boeckler[1], Richard P. Owen[1], Mark R. Middleton[4], Xin Lu[1]

[1]Ludwig Institute for Cancer Research, University of Oxford, Oxford, United Kingdom,[2]German Cancer Research Center, Heidelberg, Germany,[3]Ludwig Institute for Cancer Research, University of Lausanne, Lausanne, Switzerland,[4]Department of Oncology, University of Oxford, Oxford, United Kingdom,[5]Oncology Clinical Trial Office (OCTO), Department of Oncology, University of Oxford, Oxford, United Kingdom,[6]University of Southampton, Southampton, United Kingdom,[7]University of Dundee, Dundee, United Kingdom

Background: Understanding why only few patients achieve durable responses to therapy remains challenging. Of 38 metastatic esophageal cancer (EC) patients treated on the LUD2015-005 trial (NCT02735239), three achieved >7 year ongoing survival following anti-PDL1/CTLA4 immunochemotherapy, in contrast to the median survival of 9-12 months under then standard of care. While microbial pathogens are increasingly recognized for their role in modulating tumor immunogenicity, their role in EC remains controversial.

Methods: Bulk and single-cell RNA sequencing, including B and T cell receptor (TCR) analysis, were performed on serial tumor biopsies. Humoral responses to HPV16 were assessed via multiplex serology, using patient plasma and recombinantly expressed tumor-infiltrating antibodies. ELISpot assays were performed against HPV16-derived peptides. Subsequent TCR sequencing of peptide-stimulated immune cells was used to identify antigen-specific clones for recombinant expression and validation.

Results: Transcriptomic profiling of all three long-term survivors unexpectedly revealed intratumoral presence of H. pylori (n=1) and HPV16 (n=2), alongside a highly pro-inflammatory tumor microenvironment. Based on available material, the contribution of HPV16 in one patient's durable response was further investigated. Upon 4 weeks of immunotherapy, complete tumor clearance was accompanied by an HPV-targeted host response: serological analysis identified a systemic response against the E6 oncoprotein as well as an intratumoral B cell clone targeting E2. ELISpot assays revealed broad virus-specific T cell reactivity and led to the identification of nine novel HLA-A*02:01-restricted TCRs specific for E2 (2 epitopes) and E6 (1 epitope), each demonstrating high avidity (nM EC_{50}). Notably, clonally expanded T cells expressing these TCRs were also identified within the tumor where they exhibited a tissue-resident memory phenotype, consistent with antigen-driven activation and long-term immune surveillance.

Conclusions: Our findings demonstrate that H. pylori and HPV16 can be detected in EC. We show that HPV16-derived antigens are targeted by both peripheral and tumor-resident immune cells and, alongside the striking response to immunotherapy, suggest that virus-specific immunity may play a role in tumor clearance and long-term disease control. The naturally derived, HPV16-specific TCRs identified here represent promising candidates for adoptive immunotherapy across a range of HPV-driven cancers. More broadly, detection of microbial signatures alongside a robustly activated tumor microenvironment in all three exceptional responders supports the exploration of pathogen-directed therapies in cancers not typically linked to infection, opening new avenues to enhance immunotherapy outcomes.

#0210 Bivalent nanoparticle vaccine elicits cross-protective antibody against oncogenic herpesviruses.

Mu-Sheng Zeng[1], Chu Xie[1], Cong Sun[1], Pei-Huang Wu[1], Peng-Lin Li[1], Bing-Zhen Cheng[2], Ge-Xin Zhao[3], Guo-Long Bu[1], Wen-Ting Du[1], Zi-Ying Jiang[1], Hang Zhou[1], Xin-Yan Fang[2], Xian-Shu Tian[1], Yan-Lin Yang[1], Sen-fang Sui[2], Zheng Liu[2]

[1]Sun Yat-sen University Cancer Center (SYSUCC), Guangzhou, China,[2]Southern University of Science and Technology, Shenzhen, China,[3]Columbia University, New York, NY

Background: Epstein-Barr virus (EBV) and Kaposi's sarcoma-associated herpesvirus (KSHV) are oncogenic γ-herpesviruses causally linked to multiple malignancies but lack approved vaccines. As virus-associated cancers represent a substantial global tumor burden, preventive vaccination offers a rational approach to cancer prevention. Both viruses depend on the conserved gHgL heterodimer for receptor engagement and entry, suggesting gHgL as a shared vaccine target for broad γ-herpesvirus protection.
Methods: We developed a bivalent nanoparticle vaccine (bi-NP) that co-displays EBV and KSHV gHgL on the self-assembling I53-50 scaffold and compared its immunogenicity and protecting efficacy with single-antigen and soluble counterparts. Structural and antigenic integrity of immunogens were validated by size-exclusion chromatography, negative-stain electron microscopy and binding to specific monoclonal antibodies. Immunogenicity was evaluated in mice, rabbits, and non-human primates (NHPs), while in vivo protection was evaluated using heterologous (murine γ-herpesvirus 68, MHV-68) and homologous (EBV/KSHV co-infection in humanized mice) challenge models.
Results: The bivalent gHgL nanoparticle elicited consistently higher and more balanced antibody responses against both EBV and KSHV across species, effectively blocking viral infection of their respective susceptible cell types. Bi-NP immunization induced cross-reactive antibodies recognizing conserved gHgL epitopes, increasing the frequency of B cells cross-binding both EBV and KSHV gHgL in rabbits, eliciting antibodies cross-neutralizing MHV-68, and conferring in vivo cross-protection against MHV-68 mice challenge. Moreover, passive transfer of IgG purified from bi-NP-immunized macaques protected humanized mice from EBV/KSHV co-infection, markedly reducing viral DNA copies, preventing weight loss, and diminishing $EBER^+$ and $LANA^+$ pathology.
Conclusions: This study establishes gHgL as a rational bivalent vaccine target and demonstrates that nanoparticle co-display of EBV and KSHV antigens elicits cross-reactive, broadly protective antibodies across divergent γ-herpesviruses. The findings highlight a promising platform for preventive strategies against γ-herpesvirus-associated cancers and potential zoonotic infections.

#0211 Association between prior smoking and the time between HPV16-E6 seroconversion and development of oropharyngeal squamous cell carcinoma.

Stale Nygard[1], Lea Schroeder[2], Marie Gulla[1], Aida Ferreiro-Iglesias[3], Paul Brennan[3], Hilde Langseth[1], Giske Ursin[1], Aimee R. Kreimer[4], Mattias Johansson[3], Hilary Robbins[3], Tim Waterboer[2], Mari Kiens Nygard[1]

[1]Cancer Registry of Norway, Norwegian Institute of Public Health, Oslo, Norway,[2]Infections and Cancer Epidemiology, German Cancer Research Center (DKFZ), Heidelberg, Germany,[3]Genomic Epidemiology Branch, International Agency for Research on Cancer, Lyon, France,[4]NCI Div. of Cancer Epidemiology & Genetics, Bethesda, MD

Background and aims: Human papillomavirus (HPV) type 16 E6 oncoprotein antibodies in peripheral blood are a strong marker of oropharyngeal squamous cell carcinoma (OPSCC). In a previous study, HPV16-E6 seroconversion was observed from 6 to 28 years before cancer diagnosis. In the present study, the serology measurements were complemented with DNA and RNA genotyping of HPV from cancer tissue from the same OPSCC patients. We aimed to refine estimates of timing of and age at HPV16-E6 seroconversion before HPV-driven OPSCC and to investigate their dependence on notable covariates such as tobacco use.
Patients and methods: 307 OPSCC cases were identified from the prospective Janus Serum Bank Cohort in Norway enrolled from 1972 to 2004. Pre-diagnostic samples were analyzed for antibodies against proteins of HPV16 and other oncogenic HPV types by multiplex serology. Diagnostic formalin-fixed paraffin-embedded tumor blocks were obtained from different hospitals and HPV DNA and RNA genotyped by Multiplex Papillomavirus Genotyping and HPV type-specific E6*I RNA assays. Cancers positive for DNA *and* RNA of the same HPV type were regarded as *HPV-driven*. Information about smoking status was available from questionnaires. For every HPV16-driven cancer, an age and time interval for HPV16-E6 seroconversion was inferred and the Turnbull estimator for interval-censored data was applied.
Results: Out of 242 OPSCC cases with a retrieved and successfully sectioned tumor block, 221 (83.7%) had a valid HPV DNA/RNA cancer tissue test. The proportion of OPSCC driven by HPV increased rapidly from 1990 (0%) to 2010 (over 60%). The majority of the HPV-driven OPSCC cases were caused by HPV16 (55.2% of all OPSCC cases), followed by HPV33 (5.4%). All patients developing HPV16-driven cancer within 10 years from blood draw were HPV16-E6 seropositive at blood draw. The estimated median age of HPV16-E6 seroconversion for HPV16 driven cancers was 43 years with an interquartile range (IQR) of 41-46, and the median time from seroconversion to HPV16-driven cancer was 16 years (IQR: 12-22). Current smokers had a much shorter time from seroconversion to cancer than former and never smokers (median of 14 vs 18 and 21 years).
Conclusions: The high sensitivity and specificity of HPV16-E6 seropositivity makes it a promising early biomarker for HPV-driven OPSCC. HPV16-E6 seropositive individuals that were smokers at the time of blood draw developed HPV16-driven OPSCC 8 years earlier than seropositive individuals that never smoked, suggesting intensified follow-up of HPV16-E6 seropositive smokers. The age at HPV16-E6 seroconversion indicates that many cancer-causing HPV infections are acquired after mid-20s, with the implication that young adults would benefit from HPV vaccination for prevention against oropharyngeal cancer.

#0212 Targeting STAT3 promotes cell death and enhances T-cell activity in HPV-associated cancer.

Ruben Prins, Daniel Fernandez, W. Martin Kast

Immunology and Immune Therapeutics, University of Southern California, Los Angeles, CA

Human papillomavirus oncoproteins early (E)6 and E7 are crucial for sustaining chronic infection and driving malignant transformation in stratified epithelia when the immune system fails to clear the virus. In addition to impairing the cellular surveillance systems that maintain genomic integrity and promoting cell cycle progression, these oncoproteins increase interleukin-23 (IL-23) production by tumor-associated macrophages in HPV$^+$ cancers, leading to suppression of local tumor-specific T-cell immunity. IL-23 signaling through the IL-23 receptor (IL-23R) on HPV-specific CD8$^+$ T cells reduces their cytotoxicity and proliferative capacity. Downstream, IL-23R activates signal transducer and activator of transcription 3 (STAT3), a transcription factor known to drive multiple cancer hallmarks. To investigate how STAT3 signaling affects both the progression of HPV+ tumors and specifically the T-cell response against its E6 and E7 proteins, we employed the C3.43 syngeneic murine tumor model, which expresses the full length HPV16 genome under its native promoters, and used the cisplatin derived small molecule inhibitor CPA-7 to inhibit STAT3. IL-23R signaling induces phosphorylation of STAT3 monomers (pSTAT3), leading to their dimerization and subsequent nuclear translocation, where they bind DNA. CPA-7 prevents dimerized STAT3 from binding DNA and functionally reduces overall pSTAT3 levels. In vitro treatment of HPV$^+$ C3.43 tumor cells with CPA-7 revealed that STAT3 inhibition induces tumor cell death. In vivo, mice challenged with C3.43 tumor cells and treated with CPA-7 completely eradicated their tumors, with 4 of 10 mice demonstrating durable immune memory upon tumor re-challenge. Remarkably, even established, late-stage HPV$^+$ tumors were fully eradicated upon CPA-7 treatment. Full eradication required an intact adaptive immune system, as CPA-7 treatment failed to eliminate HPV$^+$ tumors in mice lacking both CD4$^+$ and CD8$^+$ T cells. Together, these data demonstrate that STAT3 promotes HPV$^+$ tumor cell survival and suppresses the adaptive, tumor-specific T-cell immune response. Targeting STAT3 may therefore represent a promising strategy to induce tumor cell death and counteract IL-23-induced, STAT3-mediated immune suppression in HPV-associated cancers.

#0213 Targeting lytic cycle with ciclopirox derivative in Epstein-Barr Virus+ gastric cancer.

YUXIN ZHUANG[1], Srishti Chakravorty[2], Shrinidhi Annadka[3], Marwa G. M. Elnaggar[4], Luopin Wang[3], Subhransu S. Sahoo[1], Abigail H. Lee[1], Shyaman Jayasundara[5], My An Nguyen[3], Steven Chang[6], Jason A. Hanna[3], Behdad Afzali[7], Matthew Olson[3], Bo Zhao[8], Daniel P. Flaherty[3], Yoon Yeo[9], Majid Kazemian[3]

[1]Biochemistry, Purdue University, West Lafayette, IN,[2]Merck, South San Francisco, CA,[3]Purdue University, West Lafayette, IN,[4]Industrial pharmacy, Purdue University, West Lafayette, IN,[5]Computational Science, Purdue University, West Lafayette, IN,[6]Computer Science, Purdue University, West Lafayette, IN,[7]National Institute of Diabetes and Digestive and Kidney Diseases, Bethesda, MD,[8]Brigham and Women's Hospital, Boston, MA,[9]Industrial and Molecular Pharmaceutics, Purdue University, West Lafayette, IN

Epstein-Barr Virus (EBV) is a ubiquitous human herpesvirus that infects around 90% of the global adult population. Upon infection, the virus typically establishes latency within the host cell, expressing viral genes that promote tumorigenesis, inhibit apoptosis, and suppress immune recognition of infected cells. Induction therapy was introduced to counter these effects by driving the switch from latent to lytic phase, which is a process called lytic reactivation. This transition results in cell lysis with viral particle release and the expression of viral proteins that can be targeted by antiviral agents and the immune system. Here, we developed a novel in-silico drug prediction method to identify compounds capable of inducing the EBV lytic cycle in various EBV+ epithelial malignancies. In vitro treatment of top candidates has successfully triggered lytic reactivation on EBV+ gastric cancer cell lines, namely, SNU719 and AGSBX1. Among these candidates, Ciclopirox (CPX), a clinically used antimycotic agent that has a fungistatic and iron chelation capability, showed strong activity in inducing the EBV lytic cycle, inhibiting proliferation and survival of EBV+ gastric cancer cells by blocking the cell cycle. RNA sequencing revealed that CPX-mediated lytic induction acts primarily through the hypoxia pathway, specifically via hypoxia-inducible factor 1-alpha (HIF1α). CPX treatment increased HIF1α binding to chromatin regions associated with genes involved in gastric cancer proliferation and migration. Co-treatment with a HIF1α inhibitor abolished both the cytotoxic and lytic-inducing effects of CPX, confirming the pathway's central role. Despite its efficacy, a major limitation of CPX is its instability. During CPX administration, excess iron from both intracellular and extracellular environments will lead to degradation and inactivation of CPX. Co-treatment with equal molarity of ferric ion has completely abolished the lytic-inducing ability of CPX. To address this, we adopt the pro-drug strategy by adding a protective group on CPX, creating a protected derivative mCPX. mCPX has shown comparable activity in lytic induction, while significantly improved resistance toward iron-mediated inactivation compared to CPX or another published pro-drug fosciclopirox. Finally, in an SNU719 xenograft, mCPX demonstrated superior in vivo anti-tumor activity relative to CPX. Altogether, using in-sillico drug prediction platform, we have successfully repurposed CPX as a lytic-induction-based anti-tumor agent against EBV+ gastric cancer, and developed the pro-drug mCPX to enhance its in vivo stability.

#0215 Primary cardiac lymphoma and HIV: A nationwide analysis of hospitalizations.

Omar Hozayen[1], Jay Hozayen[1], Benjamin Behers[1], Christoph Stephenson-Moe[1], Maha Hameed[1], Matthew Miller[1], Laura De Jesus Herrera[1], Anas Abu Jad[1], Rheiner Kammer[1], Mohab Idriss[1], Ahmed Aboutaleb[1], Bashar Roumia[1], Patricia Riano[1], Nicolas Riveros Neira[1], Brooke Hartenstein[1], Robert Taylor[1], Manuel Rosario Espinal[1], Brett M. Behers[2], Alya Hozayen[3], Mohamed Ibrahim[4], Karen Hamad[1]

[1]Florida State University - Sarasota Memorial Hospital, Sarasota, FL,[2]Mountain Area Health Education Center, Asheville, NC,[3]American University of Integrated Sciences, Tucker, GA,[4]Mayo Clinic, Jacksonville, FL

Background: Primary Cardiac Lymphoma (PCL) is an exceptionally rare malignancy. While clinical case reports have postulated an association with human immunodeficiency virus (HIV), large-scale epidemiological data corroborating this link are limited.
Objective: To determine whether HIV is associated with increased prevalence of PCL in a large, nationally representative sample of US hospitalizations.
Methods: We performed a retrospective, cross-sectional analysis using the Healthcare Cost and Utilization Project National Inpatient Sample from 2016 to 2019, representing approximately 35 million unweighted hospitalizations. Hospitalizations were identified using a proxy definition for PCL, requiring ICD-10-CM codes for both cardiomyopathy (I42.*) and extranodal non-Hodgkin lymphoma (i.e., C83.39, C85.99). HIV status was identified using codes B20-B24 and Z21. We compared the prevalence of PCL in hospitalizations with versus without HIV and calculated odds ratios using Fisher's Exact Test, reporting corresponding 95% confidence intervals (CI) and p-values.
Results: We identified 569 hospitalizations meeting our operational definition for PCL out of 34,955,252 total discharges. The prevalence of PCL was significantly higher among hospitalizations with HIV (6.2 per 100,000) compared with those without HIV (1.6 per 100,000; $p < 0.0001$). HIV was associated with a 3.86-fold increased odds of PCL (OR: 3.86; 95% CI: 2.23-6.70; $p < 0.0001$).
Conclusion: In this nationwide analysis of 35 million hospitalizations, HIV was strongly associated with a higher prevalence of PCL. Hospitalizations with HIV had nearly 4-fold higher odds of PCL, as defined by co-occurrence of cardiomyopathy and extranodal lymphoma, compared with hospitalizations without HIV. This population-level finding evinces the association previously suggested in clinical case reports.

#0216 Exploring viral influence on susceptibility to retinoblastoma in northern Tanzania, The ENVISION-Tanzania study.
Atukuzwe Kanyandekwe Kahakwa

Kilimanjaro Christian Medical Centre, Moshi, Tanzania, United Republic of

Background Retinoblastoma (RB) is the most common intraocular malignancy in children, with survival rates exceeding 90% in high-income countries but remaining unacceptably low in many low- and middle-income settings. While RB arises primarily from bi-allelic inactivation of the RB1 tumour suppressor gene, emerging evidence suggests that viral oncogenesis particularly from high-risk human papillomavirus (HR-HPV) may also contribute to tumour initiation and progression. The E6 and E7 oncoproteins of HR-HPV disrupt the p53 and pRb pathways, molecular mechanisms central to both HPV-driven malignancies and RB pathogenesis. However, the potential role of HR-HPV in RB remains poorly explored, especially in African populations where both HR-HPV prevalence and RB incidence are high. Generating region specific evidence could reshape understanding of RB biology and inform new preventive strategies
Objective To investigate the association between maternal and tumour HR-HPV infection and the development of retinoblastoma in children in Northern Tanzania
Methods This cross-sectional, hospital-based study will be conducted at Kilimanjaro Christian Medical Centre (KCMC), the principal paediatric oncology referral centre in Northern Tanzania. We aim to recruit 215 children diagnosed with RB and their 215 biological mothers. Enucleated tumour specimens will be processed into formalin-fixed, paraffin-embedded (FFPE) blocks for DNA extraction and HPV genotyping using PCR-based assays. Maternal cervical swabs will be collected and analysed for HR-HPV detection and genotyping. Quantitative RT-PCR will be used to assess E6 and E7 oncogene expression, while immunohistochemistry will localize viral proteins and evaluate the expression of key tumour suppressor proteins (pRb, p53, p16). Logistic regression models, adjusted for clinical and demographic variables, will be used to estimate the association between maternal HR-HPV infection and RB occurrence in offspring.
Status The study is currently in the preparatory phase. Ethical approvals have been obtained, and logistical arrangements for molecular analysis are underway at KCMC's pathology and molecular oncology units.
Expected Impact The ENVISION Tanzania study will generate the first molecular data examining viral contributions to RB in Sub-Saharan Africa. Identifying HR-HPV as a potential co-factor in RB pathogenesis could fundamentally shift paradigms in paediatric oncology by linking viral prevention strategies to childhood cancer control. Beyond its scientific contribution, the project aims to strengthen local molecular oncology capacity, foster North South research collaborations, and build a sustainable platform for infection-related cancer research in Tanzania.

#0217 Advanced OnePCR HPV panel: Fast POCT platform covering complete high, medium & low-risk genotypes.

Bahadur Singh Gurjar, **Giulliana Tessarin**, Nishant Kumar, Namrata Erande

Research & Development, Genes2Me Pvt. Ltd., Gurugram, India

Human Papillomavirus (HPV) is a major global health concern due to its strong association with cervical cancer in women and oropharyngeal cancer in men. With 200+ related viruses, persistent infection with high-risk genotypes can drive malignant transformation. Cervical cancer remains the 4th most common cancer in women, with around 660,000 new cases and 350,000 deaths in 2022 94% occurring in low- and middle-income countries. Early screening, vaccination, and timely treatment are key to reducing this burden.Innovative Diagnostic Platforms Genes2Me delivers advanced HPV detection through two powerful systems: OnePCR System - A fully automated *Sample-IN Result OUT* platform that integrates extraction and real-time PCR in one cartridge. It detects up to 20 targets per sample with zero pipetting steps and provides results in around 100 minutes. Rapi-Q and Rapi-X16 System - A semi-POCT high-throughput solution enabling extraction of up to 16 samples simultaneously and multiplex PCR in 8 tube format, offering scalability and precision for busy laboratories. Comprehensive HPV Genotyping Panels Genes2Me HPV assays use multiplex real-time PCR with fluorescent probes for accurate genotype differentiation. High-Risk Panel (Tube 1): HPV16 (HEX), HPV18 (FAM), 12 pooled HR genotypes (Texas Red); beta-Actin internal control. Low & Medium-Risk Panel (Tube 2): HPV6, 11, 44 and others using FAM/HEX/Texas Red; Cy5 internal control. Expanded Low/Medium Panel (Tube 3): 14 genotypes categorized into FAM / HEX / Texas Red groups with Cy5 internal control.

#0218 Zika virus demonstrates oncolytic efficacy against high-risk rhabdomyosarcoma in both in vitro cultures and in vivo murine xenograft models.

Emily Gearhart, Caroline Finn, Catherine Collins, Rajarajeshwari Venkataraman, Peter Phelan, Kenneth Alexander

Biomedical Research, Nemours Children's Hospital, Lake Nona, FL

High-risk rhabdomyosarcoma (RMS) carries a poor prognosis, with 5-year survival rates of ~30%, emphasizing the urgent need for novel therapeutic strategies. Zika virus (ZIKV), which causes asymptomatic or mild infection in children and adults, has emerged as a promising oncolytic agent. Previous work from our group and others has demonstrated ZIKV's antitumor activity in a variety of tumor models, including ovarian cancer, neuroblastoma, and glioblastoma multiforme. ZIKV exhibits a natural tropism for cells expressing AXL and CD24 making these markers potential indicators of ZIKV susceptibility. Because RMS cells lines (RH30, RH41, RD) express AXL and CD24 observed by both transcript and surface marker expression, we investigated the efficacy of two FDA-approved replication-competent ZIKV strains (ZIKV-A1, ZIKV-A2). In vitro plaque assay demonstrates both ZIKV strains replicated efficiently and induced cell lysis in all 3 RMS cell lines. In vivo, NOD-SCID-IL2Rγ^{null} (NSG) mice bearing subcutaneous RD or RH30 cell-derived tumors were given intratumor injections of ZIKV-A1 or ZIKV-A2. Both strains dramatically reduced tumor volume within 11 days post-viral injection compared to control mice. ZIKV infection was confirmed in tumor tissue by qPCR, immunoblot, and histological detection of the ZIKV non-structural (NS1 and NS2B) and envelope proteins. In a dual-tumor xenograft model, intratumor ZIKV-A1 injection reduced the growth and size of both the injected and contralateral untreated tumors, suggesting that systemic viral dissemination by lymphatic and/or hematogenous spread is sufficient to treat widespread tumors. These findings open the door to clinical trials of subcutaneously administered ZIKV for the treatment of pediatric and adult RMS cancers.

#0219 Spondweni virus is highly oncolytic in endometrial carcinoma-derived HEC-1-A cells.

Catherine Collins, Emily Gearhart, Caroline Finn, Rajarajeshwari Venkataraman, Peter Phelan, Kenneth Alexander

Nemours Children's Health, Orlando, FL

Endometrial adenocarcinoma accounts for approximately 80% of all endometrial cancers, affecting more than 400,000 women per year. With advanced disease, the 5-year survival rate drops from 81% to 15%. Previously, our laboratory found that Zika virus (ZKV) has promising oncolytic and anti-tumor activities, reducing tumor volume in murine xenograft models of ovarian and endometrial cancer. Spondweni (SPN) is a flavivirus phylogenetically related to but immunologically distinct from ZKV. Like ZKV infection, most human SPN infections are asymptomatic. We hypothesized that SPN would exhibit oncolytic activity like that of ZKV. The endometrial adenocarcinoma cell line HEC-1-A, which was derived from a stage IA endometrial tumor, was selected for infection with three ZKV strains (MR766, ZIKV-A1, and ZIKV A-2) and one SPN strain (SPN A-1). Using viral plaque assays, AlamarBlue™ cell viability assays, and western blots, we examined viral replication in ZKV- and SPN-infected HEC-1-A cells, measuring NS-1 and viral envelope protein expression, and comparing rates of cell death following viral infection. Our data indicated that HEC-1-A cells are more susceptible to SPN than to ZKV. This discovery provides insight into SPN as an oncolytic therapy and opens the door to exploring its use in other cancer types.

#0220 Investigating nonsense-mediated decay (NMD) as a restriction factor for EBV-reactivation.

Emilie Greene[1], Eric C. Johannsen[2]

[1]Oncology, McArdle Laboratory for Cancer Research, University of Wisconsin-Madison, Madison, WI,[2]Department of Medicine, Division of Infectious Disease, University of Wisconsin, Madison, Madison, WI

Approximately 0.01% of adults infected with Epstein-Barr virus (EBV) will develop an EBV-associated cancer which equates to 200,000 annual cases globally. EBV malignancies are dependent on EBV latency gene products for continued growth and survival, making the disruption of latency a promising therapeutic approach. Despite this vulnerability, EBV-targeting strategies have yet to be successfully translated into therapy for EBV-associated cancers. “Lytic induction therapy” combines small molecules capable of reactivating EBV from latency with antiviral drugs to increase toxicity to tumor cells and prevent EBV particle production. Although this therapeutic strategy has been well tolerated in clinical trials, current induction agents display low efficacy. The full potential of this approach will require the development of second-generation induction agents, necessitating a greater understanding of EBV biology and host-pathogen interactions. Recent studies have identified nonsense-mediated decay (NMD), a host regulatory pathway, is a key restriction factor for EBV reactivation. The EBV transcript encoding Rta, one of the two viral transcription factors responsible for entry into the lytic cycle, contains multiple splice junctions downstream of its stop codon. Consequently, the Rta transcript is rapidly degraded by NMD. This previously unrecognized post-transcriptional regulation revealed that strategies inducing the lytic cycle cannot focus solely on activating Rta and Zta transcription; they must include approaches to stabilize the Rta transcript, likely by NMD inhibition. To investigate this phenomenon, we developed an NMD reporter based on a previously described dual-fluorophore system. By combining this reporter with an EBV fluorescent reporter virus that indicates Zta (red) and Rta (green) promoter activity, we can assess the effects of NMD on Rta expression and lytic activation (measured as the change in blue and far-red fluorescence). This system enables us to determine whether EBV can only reactivate under NMD-low conditions and evaluate how various induction agents influence NMD activity. We can also identify EBV gene products that may act as NMD antagonists, which would establish a positive feedback loop for promoting lytic cycle entry. The insights gained from these studies will provide a deeper understanding of the mechanisms governing viral reactivation and inform the development of next generation lytic induction therapies.

#0221 Single-cell ATAC-sequencing profiling of HPV18 positive head and neck cancer cells reveals heterogeneity of HPV18 genome accessibility and its association with cancer progression.

Chongwen Cao[1], Weiyi Gong[2], Haichang Li[2], Bo Zhao[3], Qingqing Wu[2], Priyanka Bhateja[2], Dukagjin Blakaj[2], Jenny Li[2], Xuefeng Liu[1]

[1]The Ohio State University, Columbus, OH,[2]The Ohio State University College of Medicine, Columbus, OH,[3]Brigham and Women's Hospital, Boston, MA

Background: HPV is a major oncogenic driver of head and neck cancers (HNC). However, the epigenomic heterogeneity of the HPV genome—particularly single-cell chromatin accessibility patterns—and its relevance to cancer progression remain unclear. This study characterizes the chromatin-accessibility landscape of patient-derived HPV positive HNC cells to identify regulatory signatures associated with tumor heterogeneity and potential aggressive subpopulations.
Methods: Primary HPV18$^+$ HNC cells were generated using the conditional reprogramming cell method from patient tumor biopsies. Single-cell ATAC-sequencing was performed to assess chromatin accessibility using a combined human-HPV18 reference genome. Accessibility patterns across the HPV18 genome were encoded by a binary peak matrix. We applied UMAP on genome-wide accessibility profiles and used kernel density estimation to examine the distribution of cells with distinct HPV18 peaks. Differential accessibility, peak-to-gene linkage, and pathway-enrichment were performed across HPV18 accessibility groups.
Results: We identified three major accessible peaks within the HPV18 genome. Cells positive for Peak 1 or Peak 3 showed a dispersed, unbiased distribution on UMAP, whereas Peak 2-positive cells were strongly enriched in discrete clusters, suggesting that accessibility of this peak represents a key marker of intratumoral heterogeneity. We also observed heterogeneous HPV18 integration linking different HPV18 peaks to distinct human genomic loci across cells from the same patient, associated with locus-specific accessibility changes. Sequencing-depth analysis confirmed that differences in HPV18 peak patterns were biological rather than technical artifacts. Peak-to-gene linkage analysis revealed that UGGT1 and COL5A1 transcription start sites were more accessible in the Peak-2-positive subpopulation. Both genes correlate with poor prognosis in cervical cancer and HNC based on TCGA data. Pathway enrichment demonstrated activation of programs associated with neuron migration, epithelial morphogenesis, and tissue morphogenesis, indicating that this subpopulation may possess enhanced invasiveness and stemness features.
Conclusions: This study provides the first single-cell chromatin accessibility map of patient-derived HPV18$^+$ HNC cells and reveals substantial heterogeneity within the HPV18 viral genome. A specific HPV18-accessible peak (Peak 2) marks a distinct, potentially aggressive cellular subpopulation characterized by accessibility of poor-prognosis-associated genes and stemness-related pathways. These findings highlight a novel viral-epigenomic marker that may contribute to HNC progression and could be explored for prognostic or therapeutic applications.

#0222 Aberrant T cell proliferation in HIV associated clonal hematopoiesis.

Haocong Katherine Ma[1], Tsung-Chih Chen[1], Alokkumar Jha[2], Benjamin A. Youngblood[3], Jennifer M. Kwan[1], Irini Sereti[4], Ya-Chi Ho[1]

[1]Yale School of Medicine, New Haven, CT,[2]Weill Cornell Medicine, New York, NY,[3]St. Jude Children's Research Hospital, Memphia, TN,[4]National Institutes of Health, Bethesda, MD

Introduction: Clonal hematopoiesis (CH) is a precursor for acute myeloid leukemia (AML) and predictor of the development of hematologic cancers. Despite suppressive antiretroviral therapy, people living with HIV (PLWH) have higher incidence of clonal hematopoiesis, particularly mutations in *DNMT3A*. While DNMT3A mutations increase inflammation in myeloid cells and increase CD8+ T cell proliferation, the role of DNMT3A mutations in CD4+ T cells remain elusive. Given that CD4+ T cells are the major HIV reservoir, we postulate that HIV-induced systemic inflammation increases DNMT3A mutation, accelerates CD4+ T cell proliferation, and thus promotes HIV persistence in CD4+ T cells.

Methods: To examine the impact of DNMT3A on CD4+ T cell proliferation, we spiked in HIV- and DNMT3A-specific primers in single-cell ECCITE-seq (GoT-seq) and paired HIV- and DNMT3A-targeted long-read sequencing (MAS-ISO-Seq) on peripheral blood CD4+ T cells from four strata (HIV+CH+, HIV+CH-, HIV-CH+, and HIV-CH-). We simultaneously captured HIV RNA, cellular transcriptome, surface proteins, T cell clonality, and *DNMT3A* mutations in the same single cell.

Results: After QC, we captured 420,837 CD4+ T cells from 27 participants (7 HIV+CH+, 7 HIV+CH-, 5 HIV-CH+, and 8 HIV-CH-). Short-read scRNA-seq detected *DNMT3A* RNA in 32,554 cells (10.3%), while Long-read sequencing captured *DNMT3A* in 19,898 cells (8.6%), reflecting low *DNMT3A* expression levels in peripheral blood CD4+ T cells. Importantly, we overcame the 5' sequencing bias of short-read sequencing and captured 767 cells carrying single nucleotide polymorphisms (SNPs) within the DNMT3A. For HIV, short reads identified 170 RNA+ cells (0.055%), whereas long reads detected 3,842 HIV-infected cells, representing a 22-fold increase in sensitivity, and resolved 98 intact proviruses. TCR analysis reconstructed 22,648 unique T cell clones from 76,819 cells having mapped CDR3 region. Larger CD4+ T cell clones were enriched in cytotoxic CD4+ T cells expressing high GZMB/GZMH. Notably, we identified 100 HIV-infected cells (58.8%) in T cell clones. Clone sizes were greater in CD4+ T cells from HIV- CH+ than HIV-CH- donors, consistent with CH-driven T cell proliferation. Importantly, CD4+ T cells from HIV+ CH+ patients exhibited significantly greater clonal expansion and larger clones than those from HIV+CH- patients, suggesting CH mutations also promotes the proliferation of HIV-infected cells. Of note, age distributions did not differ across groups, which excluded age as a confounder for clonal expansion.

Conclusion: Paired single-cell multi-omics with long-read genotyping reveal CH mutations drive the aberrant CD4+ T cell proliferation and promote HIV persistence, highlighting virus-host interaction that elevates cancer risk despite suppressive antiretroviral therapy.

#0223 HPV16 variant lineage in response to treatment in locally advanced cervical cancer.

Monica Morales[1], Jinneth Acosta[2], Gina Malaver[2], Maria Cristina Alarcon[2], Juan G Rodriguez[3], Juan Anzola[3], Nicolas Magne[4], **Pablo Moreno Acosta**[1]

[1]National Cancer Institute, Bogota, Colombia,[2]Universidad Nacional de Colombia, Bogota, Colombia,[3]Corpogen, Bogota, Colombia,[4]Institute Bergonie, Bordeaux, France

Cervical cancer in Colombia ranks third in incidence/mortality, with HPV16 being the most frequent high-risk oncogenic type. The aim of this study was to characterize HPV16 variant lineages in the LCR, E6, and E7 regions and evaluate their association with treatment response in locally advanced cervical cancer. We conducted a retrospective cohort study using 300 formalin-fixed, paraffin-embedded tissue samples from patients with FIGO stages IB1 to IVA cervical cancer treated at National Cancer Institute of Colombia (INC-Colombia) HPV detection was performed using GP5+/GP6+ PCR, with 261 samples successfully sequenced on the Illumina MySeq platform. A custom bioinformatics pipeline was implemented for comprehensive analysis, including viral typing using Mothur Bayesian classifier with PaVE database, and deep sequencing of LCR, E6, and E7 regions using PrimalScheme-designed primers. Variant classification involved reference mapping (BWA), variant calling (FreeBayes), and functional impact analysis (SnpEff) and treatment response were evaluated using RECIST 1.1 criteria, with complete response and non-complete response, encompassing partial response, stable disease, or progression. Statistical analyses were done using Stata 11, R 4.5.0, and jamovi 2.7. Of 300 patients, 227 (75.7%) showed complete treatment response. HPV was detected in 274 cases (91.3%), with HPV16 identified in 242 (80.7%). Among 185 sequenced HPV16 samples, lineage A predominated (76.8%), followed by lineage D (23.2%), mainly D2 (11.4%). No significant differences in SNP frequency (E6, E7, LCR) between response groups were observed, indicating no clear association with treatment outcome. However, However, specific variants E7T678C, LCR 7488T-ins, and LCR 7861del showed suggestive trends ($p < 0.15$), possibly reflecting subtle biological effects warranting further investigation. In summary, while HPV16 lineage A was more frequent than lineage D in this cohort, our findings do not establish an association between HPV16 variant lineages or specific SNPs and treatment response, a result consistent with other studies. Our findings do not allow us to establish an association between HPV16 variant lineages and treatment response, which is consistent with other studies. Our results demonstrated distinct HPV16 lineage distribution patterns in the Colombian cohort. These findings contribute to understanding HPV16 genetic diversity in cervical cancer and its potential implications for treatment response. These results underscore the need for large scale prospective trials to definitively evaluate the role of HPV16 genetic diversity in therapeutic outcomes and encourage further research into viral variants and treatment resistance.

#0224 Analytical validation of viral detection in tumor-derived cell-free DNA.

Hao Wang[1], Lauren Lawrence[2], Jamie Hutchins[1], Tingting Jiang[3]

[1]Bioinformatics, Guardant Health, Palo Alto, CA,[2]Clinical Development, Guardant Health Laboratory, Redwood City, CA,[3]Bioinformatics, Guardant Health, San Diego, CA

Background: Epstein-Barr virus (EBV) and human papillomavirus (HPV) are oncogenic viruses linked to specific malignancies, yet their detection in tumors often goes unassessed in clinical practice. EBV-positive gastric cancer patients may benefit from immunotherapy, but viral status is rarely evaluated routinely. Similarly, HPV-associated malignancies can be missed in cases with unknown primary sites. Cell-free DNA (cfDNA) analysis offers a non-invasive approach to identify these clinically actionable viral signatures. Here, we established the analytical performance of EBV and HPV detection in Guardant360 Liquid (Guardant Health, Palo Alto, CA), a comprehensive blood-based molecular profiling assay for patients with advanced cancer.
Methods: Guardant360 Liquid targets EBV and 14 high-risk HPV genotypes using a targeted hybridization capture cfDNA assay. We evaluated analytical sensitivity, specificity, accuracy, and precision. Accuracy was assessed using 75 clinical samples with orthogonal viral testing results (43 HPV, 33 EBV) and 43 samples with BD Onclarity HPV Assay (Becton Dickinson, Franklin Lakes, NJ) genotyping results. LoB was determined using 120 replicates from 30 self reported cancer-free donor samples. LoD was established through serial titration of WHO HPV reference standards and in-silico down-sampling of clinical samples and reference materials. Precision was evaluated using clinical samples tested in replicate.
Results: For viral detection status, Guardant360 Liquid demonstrated a positive percent agreement (PPA) of 93.48% and a negative percent agreement (NPA) of 96.55% compared to orthogonal methods. For HPV genotyping, PPA was 100% and NPA was 97.39%. The false positive rate was 0% for HPV and 0.83% for EBV in cancer-free donor samples. The class-level LoD was established at 3.36 viral copies per human genome with ≥95% detection rate. Precision testing showed 100% PPA across all replicates at 1-5X LoD.
Conclusions: Guardant360 Liquid demonstrates high analytical sensitivity, specificity, accuracy, and reproducibility for detecting EBV and high-risk HPV genotypes in cfDNA. This validated, non-invasive approach enables viral detection in advanced cancer patients, with potential clinical applications including the identification of EBV-positive gastric cancer patients who may benefit from immunotherapy, and optimization of site-specific treatment pathways for HPV-positive cancers. This capability expands the clinical utility of liquid biopsy beyond genomic profiling to include actionable viral biomarker detection.

#0225 Accelerating precision immunotherapy for HPV-driven cancers.

Tithi Ghosh Halder[1], sam Giannakoulias[2], Juan Montesinos[3], Daniel-Paul Bednarik[3], Corey Casper[4], Ken Carter[3], Raffaella Soldi[1], Sunil Sharma[1]

[1]Honor Health Research Institute, Scottsdale, AZ,[2]Sentauri, Frederick, AZ,[3]Black Canyon Bio, Middletown, MD,[4]University of Arizona, Tucson, AZ

Background: HPV-related cancers affect nearly 48,000 Americans annually, with HPV16-driven cervical and oropharyngeal malignancies progressing rapidly and often outpacing current therapeutic timelines. Despite the success of prophylactic HPV vaccines in preventing infection in uninfected individuals, these agents provide no therapeutic benefit for patients with established invasive disease and fail to address the full spectrum of oncogenic HPV variants. To address this gap, we developed SNAP (Selective Neoantigen Peptide), a personalized therapeutic vaccine platform tailored to each patient's tumor-specific neoantigen expression profile. SNAP has demonstrated potent immunogenicity and tumor control in preclinical models, validating its promise for precision immunotherapy. However, the extended manufacturing timeline-typically exceeding 12 weeks-for generating personalized SNAP vaccine severely limits applicability in rapidly progressing HPV16-positive tumors. To overcome this limitation, we have developed a dual-vaccination strategy that integrates an off-the-shelf (OTS) therapeutic vaccine for immediate immune priming with subsequent administration of the personalized SNAP vaccine. This study covers the development of the OTS HPV vaccine.
Methods: The OTS vaccine is a poly-epitope construct targeting conserved HPV16 oncoproteins E6, E7, and E2, plus recurrent PIK3CA hotspot mutations (detected in >40% of HPV+ cancers), Candidate OTS peptides underwent comprehensive in silico predictive modeling. We used a multi-tiered computational pipeline to identify and prioritize immunogenic peptides for vaccine development, anchored by ProtIQ, a modular antigen selection tool. Top 100 peptides were ranked by immunogenicity, coverage and stability. A subset was synthesized and validated via biolayer interferometry (BLI) for binding kinetics. Human IFN-γ ELISPOT on HLA-matched donor PBMCs assessed T-cell activation to select final candidates.
Results: In silico prediction of OTS peptides yielded high-confidence epitopes with high median immunogenicity scores, across prevalent HLA class I and II alleles. BLI confirmed stable peptide-MHC complexes (KD range 102-103 nanomoles) in a validated subset. ELISPOT on individual peptide pulsed HLA-matched healthy donor PBMCs demonstrated robust IFN-γ responses. Top 30 peptides with highest ELISPOT signals were selected as vaccine candidates. To check the vaccine efficacy in vivo, mouse TC-1 cells engineered to express E2 and PIK3ca mutations will be used as HPV preclinical animal model.
Conclusions: This project will deliver a clinically actionable off-the-shelf vaccine platform that enables early immunologic intervention in HPV16-driven cancers. By priming the immune system ahead of personalized therapy, we aim to reduce time-to-treatment, enhance therapeutic outcomes, and expand access to precision immunotherapy.

#0226 Stochastic mutagenesis at lncBART-KDM5B-bound genomic loci in Epstein-Barr virus-associated nasopharyngeal carcinoma.

Wei Dai[1], Lai Shun Dittman Chung[2], Jiayan Liu[2], Kiu-Wai Cheng[1], Kazi Anisha Islam[2], Zhonghua Liu[3], Honglin Chen[4]

[1]The University of Hong Kong, Pokfulam, Hong Kong,[2]The University of Hong Kong, Hong Kong, Hong Kong,[3]Columbia University, New York, NY,[4]Microbiology, The University of Hong Kong, Hong Kong, Hong Kong

Introduction: The mechanisms linking Epstein-Barr virus (EBV) infection to mutagenesis in nasopharyngeal carcinoma (NPC) remain poorly understood.

Methods: By integrating whole-genome sequencing of 216 NPC tumors with multi-omics profiling, including chromatin isolation by RNA purification (ChIRP)-seq for lncBARTs binding sites, CUT&RUN for the binding sites of KDM5B and CTCF and histone mark H3K27ac, 4C-seq for virus-host chromatin interactions, and ATAC-seq for chromatin accessibility, we uncover a multi-layered model of virus-driven mutagenesis.

Results: We first show that cellular epigenetic regulators CTCF and KDM5B independently define genomic domains of significantly elevated mutation burden (2-fold more than matched controls, $P<0.0001$). Crucially, the viral lncBART does not increase mutation rates but fundamentally reshapes their distribution, randomizing mutations into a stochastic, Poisson-distributed pattern within KDM5B-bound domains ($p=0.3665$), which otherwise exhibit clustered, non-random mutagenesis ($p<0.001$). Furthermore, the lncBART binding sites enriches specific mutation signatures, namely G>T transversions (2.1-fold increase, $p=0.005$) and G>A transitions (1.3-fold increase, $p=0.05$), indicative of oxidative damage and replication stress, without altering the overall mutation density. We developed a computational model that predicts mutation patterns based on CTCF, KDM5B, and lncBART binding together with enhancer status and chromatin accessibility, demonstrating that these factors partially define the landscape of genomic instability. Incorporation of the data from ChIRP-seq and Capture RNA-Protein interactions (CARPID) following mass spectrometry analysis revealed that lncBARTs may act as a central scaffold that directly co-recruits key members of NuRD complex to create chromatin states against large processive mutagens and blockade of the base excision repair (BER) machinery.

Conclusions: Our work establishes a novel paradigm in which a virus co-opts and modulates host epigenetic machinery to create a context-dependent mutagenic environment, providing a new framework for understanding virus-driven cancer evolution.

Acknowledgement: This work was supported by General Research Fund (17101122) and Theme-based Research Scheme (T12-703/22-R; T123-70323-N) from Research Grant Council and Health@InnoHK from Innovation and Technology Commission in the government of Hong Kong (SAR), P. R. China

: Advanced Antibody, Conjugate, and Targeted Therapeutic Platforms
Minisymposium

#1321 Synthbody™- A novel multivalent multispecific antibody drug conjugate platform demonstrates combinatorial logic-gated "synthetic" targeting of cancer antigens with log order enhanced internalization and potency.

R. Baliga, K. Li, K. Mai, H. Horwitz, Z. Dai, S. Ahmed, V. Rao, P. Yakkundi, M. Leabman, **D. S. Chen**;
Synthetic Design Lab, San Carlos, CA

Antibody Drug Conjugates (ADCs), such as trastuzumab deruxtecan, achieve complete responses >20% and duration of response >30 months in patients with metastatic Her2+ breast cancer[1]. However, other mono/bi-specific ADCs have not achieved similar clinical benefit, likely due to the 10-100x higher expression levels of Her2 vs other ADC targets, as well as known heterogeneity of target expression, down-regulation of targets in response to treatment and in some cases, competition from soluble target release.

To address these fundamental limitations, we developed a novel class of engineered multifunctional multivalent multispecific therapeutics (Synthbody™) that enable targeting of combinatorial "synthetic" cancer targets incorporating 6-12 tumor antigen binding domains. This replicates Her2-like high expression and specificity for ADC therapeutics in most tumors without high levels of expression of a single specific tumor antigen.

We engineered an initial human multiple myeloma targeting Synthbody™, referred to as SDF-061390E, that includes affinity-tuned binders for BCMA, GPRC5D and CD38. SDF-061390E (and SDF-061390E-MMAF) demonstrates >30x greater internalization and >80x greater potency when compared, respectively, with the BCMA-targeting antibody Belantamab and Belantamab mafodotin in human myeloma cells. Enhanced internalization and potency are similarly observed when compared against matched mono/bi-specific controls. Additionally, SDF-061390E can bind human myeloma cell lines with both high and low expression of each of the three targets and effectively eliminate low-BCMA expressing cancer cells in ADC killing assays. Further, SDF-061390E can evade impact of soluble BCMA at clinically relevant and higher concentrations, in contrast to belantamab. Similar results are also observed with a NHL targeting Synthbody™, supporting the broad applicability.

Due to biophysical characteristics that can be controlled in the design of Synthbody™ constructs, we generate emergent properties, including conditional activity determined by the geometry and biophysical relationships between the cancer cell antigens, epitopes, and the Synthbody™. This architecture enables the Synthbody™ ADCs to include AND BETTER logic-gated control, layered with AND safety gates and MULTIPLIER functions, yielding synergistic multifunctional activity absent from ADCs. Optimized Synthbody™ constructs show excellent production in CHO cells, developability and IgG-like PK *in vivo*.

The novel Synthbody™ platform demonstrates broad utility as ADC and biologic therapeutics, with capabilities for coordinated targeting, advanced logic-gated control and multifunctional action that may complement or ultimately replace current IgG-based biologics.

[1] *Cortes et al. Nat Med 2024*

#1322 M7437, a novel anti-Ly6E antibody-drug conjugate (ADC) with topoisomerase 1 (TOP1) inhibitor payload: Preclinical antitumor activity and safety.

S. Krah[1], **F. Hart**[1], J. Anderl[1], D. Huels[1], C. Knuehl[1], S. Brandstetter[1], J. N. S. Pereira[1], S. Sweeney-Lasch[1], N. Rasche[1], S. Dickgiesser[1], J. Jabs[1], R. Schneider[1], C. Amendt[1], J. Vahl[1], P. D. Lyne[2];
[1]the healthcare business of Merck KGaA, Darmstadt, Germany, [2]EMD Serono, Billerica, MA

Background: Ly6E, a glycosylphosphatidylinositol (GPI)-anchored protein, is involved in fetal-placenta fusion, immune regulation, and virus-host interaction. It promotes tumor growth, vascularization, and immune evasion. Ly6E is highly expressed across several tumor types including breast cancer, non-small cell lung cancer (NSCLC), ovarian, pancreatic, gastric, and head and neck cancers, and its expression is reported to be correlated with poor survival. M7437 is a novel, highly stable anti-Ly6E ADC with a potent TOP1i payload (exatecan) site-specifically conjugated via an enzyme-cleavable linker.
Methods: The binding of M7437 to cancer cells was assessed using flow cytometry. M7437 potency and bystander effect were tested in viability assays using cancer cell lines. Antitumor activity was evaluated in patient-derived xenograft (PDX) mouse models. In a GLP repeat-dose toxicity study, cynomolgus monkeys were treated 3 times in a Q3W schedule with M7437.
Results: M7437 demonstrated specific binding to and selective killing of Ly6E-positive cancer cells with sub-nanomolar potencies. A potent bystander effect of M7437 was demonstrated in co-culture experiments. Treatment with 7-9 mg/kg M7437 caused strong and long-lasting antitumor activity in PDX models across several indications (triple-negative breast cancer, squamous cell carcinoma of the head and neck, NSCLC, ovarian, pancreatic, and gastric cancer), including models where published TOP1i ADCs showed limited activity. In a pivotal repeat-dose toxicity study in cynomolgus monkeys, the pharmacologically relevant species, M7437 was well-tolerated. M7437 demonstrated favorable pharmacokinetic properties and linker-payload stability in cynomolgus monkey.
Conclusions: M7437 demonstrated strong antitumor activity in PDX models, including a broad range of indications and a potent bystander effect indicating the potential to treat tumors with heterogeneous target expression. Together with an acceptable toxicity profile and favorable pharmacokinetic properties, the observed preclinical data support the clinical development of M7437.

#1323 Preclinical evaluation of target-mediated clearance and alternative payloads in CDH17-directed antibody drug conjugates.

N. A. O'Brien, J. Zhang, M. S. McDermott, K. Gong, M. Lu, B. Hoffstrom, M. Liang, W. Jia, T. Luo, A. M. Madrid, R. Ayala, J. A. Glaspy, L. Presta, D. J. Slamon;
UCLA - University of California Los Angeles, Los Angeles, CA

Cadherin 17 (CDH17), is an emerging target for antibody-based therapeutics in colorectal cancer (CRC), with multiple CDH17-directed chimeric antigen receptor-T/natural killer, bispecific antibodies and antibody drug conjugates (ADCs) in preclinical and early-stage clinical development. Success of these molecules depends on their ability to overcome high expression of P-glycoprotein (P-gp) pumps in CRCs and CDH17 in normal gut epithelium. Here, we investigate the therapeutic potential of CDH17-directed ADCs.High frequency expression of CDH17 in patient tumor microarrays and cell line derived xenografts (CDXs) was confirmed by IHC assay. CDH17-directed ADCs were generated through conjugation of a fully humanized CDH17 mAb to either an anti-mitotic (CDH17-MMAE) or topoisomerase 1 inhibitor (CDH17-exatecan) payload via a cleavable linker. Selective ADC binding and internalization were confirmed by flow cytometry and immunofluorescence.CDH17-MMAE treatment induced significant anti-tumor activity in 5/5 CDH17+ CRC CDXs models, with the strongest and most prolonged responses observed in xenografts that were P-gp low/negative. Head-to-head comparison of CDH17-MMAE and CDH17-exatecan payloads demonstrated improved efficacy for CDH17-exatecan over CDH17-MMAE in high P-gp expressing models. The functional role of P-gp in resistance to MMAE-based ADCs was confirmed using cell lines engineered to either overexpress P-gp through transfection or to lose P-gp expression through CRISPR knockdown. Forced overexpression of P-gp in SNUC1 CDH17+ cells conferred resistance to CDH17-MMAE, while sensitivity to CDH17-exatecan remained. Conversely, CRISPR knockdown of P-gp in CDH17+ LS513 cells reversed resistance to CDH17-MMAE. These findings were confirmed in xenograft studies.Due to lack of binding of the anti-human CDH17-ADCs with mouse or rat CDH17, a mouse model expressing human CDH17 extracellular ECD (B-hCDH17 mice) was used in pharmacokinetic (PK) studies. In wild-type mice, both ADCs exhibited PK profiles consistent with those typically observed for most ADCs. However, in humanized B-hCDH17 mice, both CDH17-MMAE and CDH17-exatecan ADCs were completely cleared from mouse serum less than 96 hours post-dosing, indicating that CDH17 expression in normal colon and ileum may act as a clearance sink for the ADCs.Data presented here support use of topoisomerase 1 inhibitor payloads in cancers where P-gp expression is high. Target-mediated clearance driven by normal gut CDH17 expression presents a pharmacokinetic challenge that may limit clinical utility and require dose optimization or alternative dosing strategies to achieve sufficient tumor exposure while managing potential on-target, off-tumor toxicity.

#1324 Preclinical assessment of HWK-016, a next-generation, MUC16-targeting ADC with novel bioconjugation and linker-payload technology.

Kathy S. Keegan[1], Shihe Hou[1], Ashwini B. Pai[1], Enrico Bellomo[1], Erik Kratzer[1], Victor Peykov[1], Bryan Ball[1], Yifeng Wang[2], Yaohua Hu[2], Xia Wang[2], Zhuozhi Wang[2], Siwei Nie[2], Yunying Chen[2], Jijie Gu[2], David J. Lennon[1], **David Dornan**[1]

[1]Whitehawk Therapeutics, Morristown, NJ,[2]WuXi Biologics, Shanghai, China

Mucin 16 (MUC16) is a cell-surface protein that plays a key role in cancer progression by facilitating tumor cell proliferation, adhesion, invasion, and immune evasion. Proteolytic cleavage of the N-terminal region of MUC16 is known to generate and shed the well-known cancer antigen and biomarker, CA125. MUC16 is highly expressed in multiple tumor types, including ovarian, endometrial, cervical, pancreatic, and lung cancers, and has relatively low expression in normal tissues, making it an attractive target for antibody-drug conjugates (ADCs), chimeric antigen receptor T-cell (CAR-T) therapy, and T-cell engagers. Early clinical trials of MUC16-targeted ADCs, DMUC5754A and DMUC4064A, showed promising efficacy but were limited by targeting an epitope within the shed extracellular domain (ECD) of MUC16, leading to off-target binding to circulating CA125, which created an antigen sink. HWK-016 is a next-generation, MUC16-targeting ADC that was designed to bind to the non-shed ECD of MUC16. HWK-016 comprises an Fc effector-attenuated IgG1 antibody that delivers a novel topoisomerase I inhibitor payload, CPT116. It contains a highly stable, cleavable linker developed using novel bioconjugation technology (carbon bridge cysteine re-pairing) designed to maximize intracellular delivery while minimizing systemic exposure of free payload. HWK-016 has a drug-to-antibody ratio of 6. The mechanism of action of HWK-016 was investigated in preclinical cancer models. Results showed that HWK-016 bound specifically to cell lines expressing the MUC16 non-shed ECD, was internalized through receptor-mediated endocytosis into lysosomes, and induced DNA damage which resulted in loss of cell viability. In contrast to DMUC5754A, addition of exogenous CA125 did not reduce HWK-016 mAb cell-surface binding and internalization, or the effect of HWK-016 on cell viability *in vitro*. Potent antitumor activity was observed in the high CA125-shedding OVCAR-3 xenograft tumor model at lower doses than DMUC5754A, with tumor regression observed with a 1 mg/kg single dose of HWK-016. A bystander killing effect was observed with HWK-016 *in vitro*, suggesting the ability to elicit activity against heterogeneous tumors. HWK-016 demonstrated a favorable pharmacokinetic profile and high stability in cynomolgus monkey and human plasma. Repeat-dose toxicology studies in non-human primates indicated a highest non-severely toxic dose (HNSTD) of 60 mg/kg. Together with preclinical efficacy studies, these data support a therapeutic index suitable for evaluation in humans. In summary, HWK-016 is a highly potent, MUC16-targeted ADC directed to the MUC16 non-shed ECD to avoid circulating CA125 binding. A phase I dose-escalation study is planned to evaluate HWK-016 in patients with advanced malignant solid tumors.

#1325 Preclinical assessment of BT5528 anti-tumor activity in cell-line-derived xenograft (CDX) models of head and neck squamous cell carcinoma (HNSCC).

Lukas Stanczuk[1], Daniel A. Peterson[2], Inma Rioja[1], Michael Method[2], Michael Skynner[1], **Gavin Bennett**[1]

[1]BicycleTx Ltd, Cambridge, United Kingdom,[2]BicycleTx Ltd, Cambridge, MA

Background: Erythropoietin-producing hepatocellular receptor A2 (EphA2) is a receptor tyrosine kinase critical for cell development; it is highly expressed in a range of solid tumors, and its expression correlates with higher grade, later stage disease, and poor prognosis. There is high unmet need for patients with EphA2-expressing tumors, including HNSCC, which has one of the highest EphA2 expression levels across solid tumors. BT5528 is a Bicycle® Drug Conjugate (BDC®), comprising a highly selective EphA2-targeting bicyclic peptide conjugated to the cytotoxin MMAE via a stable valine-citrulline cleavable linker. BT5528 has low molecular weight (4.4 kDa), enabling rapid and efficient delivery of the BDC® to the tumor and subsequent payload release, with minimal systemic exposure to the conjugate. Here we evaluate anti-tumor activity of BT5528 in murine CDX models of HNSCC.
Methods: Three HNSCC CDX models were generated with female NOD SCID (SCC-9 [tongue]) or Balb/c nude (Fadu [hypopharynx] and Cal27 [tongue]) mice by subcutaneous inoculation of cell-line-derived HNSCC tumor cells into the right abdominal flank. Tumor-bearing mice were treated once weekly with either vehicle or BT5528 at 1, 3, or 5 mg/kg IV (n=6 per treatment group per CDX model) once average tumor volume reached ~160 mm^3. EphA2 expression in cell lines was assessed by quantitative FACS. Tumor growth was monitored by caliper measurements and tumor volume calculated as ($width^2$ x length)/2. Average tumor growth inhibition (TGI) was calculated twice weekly for each treatment group per model for up to 28 days.
Results: Average EphA2 expression (receptors/cell) was 29,000 (Fadu, low expression), 46,000 (SCC-9, medium expression), and 135,000 (Cal27, high expression), which are comparable to expression levels observed in previous preclinical work in CDX and patient-derived xenograft models, and which correlated with BT5528 anti-tumor activity. Compared with vehicle treated mice, significant anti-tumor activity was observed for all three models. For Cal27, TGI reached 53% and 92% at 3 and 5 mg/kg IV, respectively, on Day 28 ($p<0.001$ and $p<0.0001$). For SCC-9 and Fadu, the day of measurement was the last day all vehicle-treated mice survived. TGI reached 101% and 107%, respectively, for SCC-9 on Day 21 ($p<0.0001$); and 95% and 107%, respectively, for Fadu on Day 25 ($p<0.0001$). Assessment of tumor volume over time demonstrated a clear dose response for all models tested, with Fadu and SCC-9 being the most sensitive. BT5528 was generally tolerable in line with previous studies.[1]
Conclusions: BT5528 has shown potent preclinical anti-tumor activity in EphA2-expressing CDX models of HNSCC at clinically relevant doses. These data support the potential to further evaluate BT5528 in HNSCC.

1. Bennett et al. *Mol Cancer Ther.* 2020;19(7):1385-1394.

#1326 PRISM AIR: A high-throughput platform for functional validation of ADC targets and antibody candidate prioritization.

J. Eskra, A. Kalathungal, A. Golabi, B. Porter, U. Widocki, A. Bino George, M. Kocak, M. Ronan, M. Rees, J. Roth;
Broad Institute, Cambridge, MA

The development of antibody-drug conjugates (ADCs) remains a resource-intensive process, often hampered by the lack of scalable, early functional assays for validating new tumor targets and prioritizing candidate antibodies with therapeutic potential. To address this technological innovation gap, we developed PRISM AIR (Antibody Internalization Reporter), an assay designed to facilitate discovery of novel cell surface targets and accelerate development of ADCs through integration of large-scale functional cell viability screening with comprehensive molecular data. PRISM AIR utilizes a universal secondary Fab-MMAF conjugate targeting the Fc domain of primary human IgGs. By coupling a secondary drug conjugate with a primary antibody, we hypothesized that we could achieve selective drug delivery mimicking the mechanism of an ADC. This approach would enable early functional screening of candidate antibodies without the need for resource-intensive conjugation of individual antibodies. We screened a panel of antibody and ADC test agents across the entire PRISM cell set of 957 genomically characterized cancer cell lines, validating the platform against several targets including HER2, TROP2, tissue factor and transferrin receptor. Results showed consistent potent, target-selective killing that correlated with antigen expression and analogous conventional ADC efficacy, confirming the assay's ability to functionally prioritize lead candidates. Integration of viability data with comprehensive baseline genomic and perturbational profiles allowed us to disentangle antibody versus linker and payload activity and identify predictive biomarkers. Notably, comparative profiling of AIR against ADCs with distinct payloads revealed differential activity, identifying GPX2 and AKR1C3 as resistance biomarkers specific to deruxtecan versus MMAF. We also identified the lysosomal transporter SLC46A3 as a critical sensitivity biomarker for non-cleavable linkers, a role previously unreported for MMAF conjugates. In conclusion, PRISM AIR represents a significant technological innovation for the antibody field. It is a robust, high-throughput platform that empowers researchers to identify novel ADC targets, prioritize lead candidates based on optimal internalization and functional cytotoxicity, and discover biomarkers predictive of response or resistance. By enabling these critical assessments early in the discovery pipeline, this next-gen tool for ADC development has the potential to significantly streamline the translation of new cancer immunotherapies from bench to clinic.

#4446 STRO-004, an exatecan-based next-generation tissue factor (TF)-targeted ADC, demonstrates superior efficacy across TF-expressing solid tumors in a comprehensive single-mouse PDX trial.

G. Hernandez, K. A. Doshi, M. Armanini, H. Kiefel, S. Zhou, B. Vuillemenot, G. Xu, X. Li, W. Rubas, G. Yin, H. Gerber, A. Yam; Sutro Biopharma, Inc., South San Francisco, CA

Tissue Factor (TF) is aberrantly expressed in multiple solid tumors, including cervical cancer, head and neck squamous cell carcinoma (HNSCC), non–small cell lung cancer (NSCLC), pancreatic ductal adenocarcinoma (PDAC), and colorectal cancer (CRC), and is associated with poor clinical outcomes. Although TF-targeted antibody–drug conjugates (ADCs) such as tisotumab vedotin have demonstrated clinical activity, their utility is limited by on-target/off-tumor and systemic, platform toxicities associated with premature payload release. This study evaluated the preclinical efficacy and safety of STRO-004, a novel site-specific DAR8 β-glucuronidase–exatecan ADC engineered for enhanced stability, reduced off-target toxicity, and an expanded therapeutic index compared with first-generation TF-directed ADCs.Anti-tumor activity was assessed in a single-mouse PDX (patient-derived xenograft) trial comprising diverse solid tumor indications (HNSCC, NSCLC, PDAC, and CRC; up to n=20 models each). Mice were randomized to receive vehicle, STRO-004, or benchmark approved ADCs administered as a single 5 mg/kg dose, which is considered clinically relevant**.** Tumor growth inhibition, best overall response (BOR), and biomarker-response relationships were evaluated. In interim analysis, STRO-004 demonstrated superior anti-tumor activity across all tumor types tested, with complete responses (CR) observed in multiple models. In HNSCC, STRO-004 produced sustained tumor regression in >50% more models vs. benchmark at the same 5 mg/kg dose, confirming enhanced potency at therapeutically translatable exposures. In NSCLC, activity was greater than or comparable to benchmark, with responses in both non-squamous and squamous histologies. STRO-004 also induced robust tumor regression in PDAC and CRC. Biomarker analysis in HNSCC revealed anti-tumor activity across a broad TF-expression range, while limited responses in some TF-high models suggest target-independent resistance mechanisms. In vitro, STRO-004 exhibited reduced cytotoxicity toward corneal and skin epithelial cells relative to approved TF ADC. It was well tolerated in NHPs up to 50 mg/kg, with no ocular or hematologic toxicity and approximately 15-fold higher Cmax and 50-fold greater AUC than first-generation TF ADCs.These data demonstrate that STRO-004 achieves broad, durable responses at clinically relevant dosing, with an improved safety profile and therapeutic index compared with approved TF ADC. Because the single-mouse PDX trial design better reflects patient diversity in human trials, these results provide strong support for STRO-004 as a potential best-in-class TF-targeted ADC. The first-in-human Phase 1 study of STRO-004 is ongoing in solid tumor indications that are expected to have high TF expression or prevalence (NCT07227168).

: Advances in Cancer Epigenetics
Minisymposium

#1356 Chromatin remodeler CHD7 drives lineage plasticity and chemoresistance in neuroendocrine prostate cancer.

M. Shi[1], D. Lin[1], X. Pang[1], H. Xue[2], X. Dong[2], R. Wu[2], A. Classen[1], Y. Ni[3], Z. Maylin[1], W. Dong[4], X. Ci[5], Y. Wang[6], Y. Wang[1], J. Chen[7], N. Kang[2], X. Niu[2], L. Liu[8], V. Wang[9], M. E. Gleave[8], C. Collins[8], C. J. Ong[8], G. Wang[10], Y. Wang[1];
[1]Vancouver Prostate Centre; BC Cancer; University of British Columbia, Vancouver, BC, Canada, [2]Vancouver Prostate Centre; BC Cancer, Vancouver, BC, Canada, [3]Vancouver Prostate Centre; University of British Columbia; Urology Research Institute, The First Affiliated Hospital, Fujian Medical University, Vancouver, BC, Canada, [4]Vancouver Prostate Centre; University of British Columbia ; Union Hospital, Tongji Medical College, Huazhong University of Science and Technology, Vancouver, BC, Canada, [5]Princess Margaret Cancer Centre, University Health Network, Toronto, ON, Canada, [6]Vancouver Prostate Centre; BC Cancer; University of British Columbia; Qilu Hospital, Cheeloo College of Medicine, Shandong University, Vancouver; Jinan, BC, Canada, [7]Vancouver Prostate Centre; BC Cancer; University of British Columbia; Institute of Urology, West China Hospital Sichuan University, Vancouver; Sichuan, BC, Canada, [8]Vancouver Prostate Centre; University of British Columbia, Vancouver, BC, Canada, [9]University of British Columbia, Vancouver, BC, Canada, [10]BC Cancer; University of British Columbia, Vancouver, BC, Canada

Neuroendocrine prostate cancer (NEPC) is a lethal prostate carcinoma subtype that arises through neuroendocrine (NE) transdifferentiation in response to androgen deprivation therapy (ADT) and androgen receptor pathway inhibitors (ARPIs). This process involves profound epigenetic and transcriptional reprogramming, causing loss of luminal features and acquisition of NE traits. Lineage-specific transcription factors (TFs), such as ASCL1, FOXA2, SOX2, and PROX1, have been implicated in orchestrating lineage transition. Critically, both the activation and functional engagement of these TFs depend on upstream chromatin remodeling, which dynamically shapes the chromatin landscape to facilitate lineage reprogramming. The significance of chromatin remodeling in NEPC is underscored by the characteristic “salt and pepper” nuclear morphology, reflecting extensive chromatin reorganization. Together, these molecular and histological features highlight chromatin remodelers as critical regulators of NEPC development and aggressiveness. However, the specific upstream remodelers remain poorly defined.Through integrated analysis of longitudinal RNA-seq data from the clinically relevant LTL331/331R PDX model, which captures the complete temporal progression from adenocarcinoma to castration-induced NEPC, we identified CHD7 as a key chromatin remodeler that is upregulated early during NEPC development, with its expression preceding NE trait acquisition and further increasing in terminal NEPC. Functional studies demonstrated that CHD7 overexpression facilitates NE transdifferentiation of adenocarcinoma cells under AR signaling suppression, while knockdown (KD) in NEPC cells reduces DNA synthesis and cell survival, increases apoptosis, and suppresses NE markers and key NE-TFs. RNA-seq analysis of CHD7-KD cells revealed downregulation of pathways governing NE differentiation, cell cycle progression, and DNA damage response (DDR), further supporting CHD7 in regulating NE-lineage commitment and maintaining genomic stability of NEPC cells. Additionally, CHD7 ChIP-seq and ATAC-seq analysis revealed direct binding and regulating accessibility of regulatory elements of these NE-TFs, supporting its upstream regulatory role in NEPC. Notably, we uncovered that CHD7 modulates replication stress via regulating the ATR-CHEK1 axis. CHD7-KD impairs CHEK1 phosphorylation at key activation sites, leading to DNA damage accumulation and heightened sensitivity to genotoxic stress. Therapeutically, CHD7-KD cells show increased cisplatin susceptibility and pharmacological inhibition of CHEK1 synergistically enhances cisplatin-induced cell death, suggesting that exploiting the CHD7-dependent CHEK1 axis could potentiate cisplatin-based combination therapy in NEPC.

#1357 The essential role of KDM5B/SOX9 signaling Axis in the development and progression of therapy-induced neuroendocrine prostate cancer.

G. Li[1], S. Celada[1], Q. Wang[1], R. Jin[2], T. Kanagasabai[1], Q. Shao[1], B. Liu[1], S. E. Adunyah[1], P. Hurley[3], Z. Chen[1];
[1]Meharry Medical College, Nashville, TN, [2]Vanderbilt University, Nashville, TN, [3]Vanderbilt University Medical Center, Nashville, TN

Therapy-induced neuroendocrine prostate cancer (t-NEPC) represents a subset of lethal prostate cancer (PCa) resistant to androgen deprivation therapy (ADT). Current intervention strategies for t-NEPC are largely undefined, underscoring the urgent need to better understand its molecular mechanisms. Lysine (K)-specific demethylase 5B (KDM5B), a key epigenetic regulator, is frequently elevated in advanced PCa and t-NEPC. Similarly, the transcription factor sex-determining region Y (SRY)-box 9 (SOX9) is a critical regulator of prostate development and has been implicated in PCa. In this study, we investigated the functional role of the KDM5B/SOX9 signaling pathway on the development and progression of t-NEPC. We found that the levels of KDM5B and SOX9 are abnormally elevated in human NEPC cells. Remarkably, KDM5B depletion led to a significant reduction in mRNA and protein levels of SOX9 and neuroendocrine markers (Neuron-specific enolase and Synaptophysin) in PC3 cells. Conversely, KDM5B add-back to KDM5B knockout (KO) cells restored their levels in a dose-dependent manner. Importantly, the recurrent tumors of castrated Pten/Trp53 mice displayed the malignant features of t-NEPC, along with elevated Kdm5b and Sox9 levels. Surprisingly, Kdm5b deficiency abrogated the t-NEPC progression in Pten/Trp53/Kdm5b mutant mice, indicating the essential role of Kdm5b in t-NEPC progression in vivo. Furthermore, we observed an increase in KDM5B and SOX9 levels in LNCaP-MDV cells, a LNCaP-derived NEPC cell line. Mechanistically, KDM5B regulated SOX9 signaling in PCa cells by directly binding to the SOX9 promoter. To further elucidate the contributions of the KDM5B/SOX9 signaling axis to t-NEPC progression, we generated SOX9 KO PCa cells using CRISPR/Cas9 technology. Our results showed that SOX9 KO significantly decreased the proliferation and the levels of neuroendocrine markers in PCa cells, without impacting KDM5B levels. In conclusion, our findings in vitro and in vivo demonstrate the essential role of KDM5B/SOX9 signaling pathway in the development and progression of t-NEPC, suggesting that targeting this pathway could represent a novel and effective therapeutic strategy for controlling t-NEPC.

#1358 Promoter methylation gains in aging and cancer are independent of replication.

S.-J. Thursby[1], Z. Jin[1], N. Patel[1], Y. Tao[1], Y. Bhandari[1], D. Petkovich[1], S. Lu[1], L. Yang[1], T.-H. Wang[1], T. R. Pisanic II[2], S. B. Baylin[3], H. Easwaran[1], J. Blum[1];

[1]Johns Hopkins University, Baltimore, MD, [2]Johns Hopkins Univ., Baltimore, MD, [3]Johns Hopkins University School of Medicine, Baltimore, MD

DNA methylation alterations are observed across multiple cancers, occurring early during tumor initiation. However, the evolution of these changes remains poorly understood and difficult to assess at the clonal level. We addressed the clonal evolution of DNA methylation using our previously established mouse organoid model of *BRAF*^{V600E} oncogene-induced colon cancer (CC) tumorigenesis. We developed a method for profiling genome-wide DNA methylation from low DNA amounts and applied it to that organoid model. Single organoid clones, derived from single stem cells, were profiled every month for 5 months to map nucleotide-level dynamic heterogeneity in methylation changes. Uninduced control organoids exhibit a pattern of epigenetic drift leading towards clonal convergence but not until 5 months. Whereas *BRAF*^{V600E}-induced organoids exhibit a step-wise divergence throughout the different time points, likely explained by progressive clonal takeovers. Although there are differences in the clonal dynamics of epigenetic states in the control and *BRAF*^{V600E}-induced organoids, there is a common basis for the DNA methylation changes in both the lineages explained by the age-in-culture associated methylation changes. This is revealed by the observation that unlike currently proposed models, *BRAF*^{V600E} did not induce or increase the degree of DNA methylation gains. Furthermore, the CpG sites affected in the control and *BRAF*^{V600E} comparison were not shared but mapped to the same genomic elements, indicating common drivers of methylation changes regardless of oncogene. Additionally, investigation of promoter CpG-island methylation gains revealed that they are decoupled from replication. External validation in other pre-cancerous/CC datasets and experimental cell line datasets, show that methylation gains at regulatory elements are a function of “biological aging” and independent of replication or cell division cycles. The sites that acquire DNA methylation changes in *BRAF*^{V600E} -induced organoids, compared to control organoids, are enriched for transcription factor motifs important in colorectal cancers, such as Cdx1, Cdx2, and Pparg. In contrast, control organoids show enrichment for transcription factors involved in stress and viral pathways. Our studies provide new insights into the early epigenetic changes involved in *BRAF*^{V600E}driven carcinogenesis, which is mainly rooted in the age-dependent drivers of epigenetic alterations, and are potentially subject to clonal selection in the context of uncontrolled growth due to oncogenic signaling.

#1359 Cooperativity between DNMT and EZH2 activity drives neuroendocrine phenotype in advanced prostate cancer.

R. Singh[1], V. B. Venkadakrishnan[2], E. Imada[1], N. J. Brady[1], Y. Yamada[2], L. Marchionni[1], B. D. Robinson[1], D. S. Rickman[1], H. Beltran[2];

[1]Weill Cornell Medicine, New York, NY, [2]Dana-Farber Cancer Institute, Boston, MA

Introduction: Upon prolonged anti-androgen treatment, 15-20% of castration resistant prostate cancer (CRPC) progresses to poorly differentiated, androgen-independent neuroendocrine prostate cancer (NEPC) that express neural markers. Studies on clinical samples have elucidated distinct DNA methylome of NEPC tumors compared to other subtypes, suggesting the importance of epigenetic regulation in lineage plasticity of advanced CRPCs.EZH2, catalyzer of repressive H3K27me3, is reported to be overexpressed in NEPC and has been studied as a therapeutic target in advanced prostate cancer. Although evidence from embryonic stem cell studies suggest possible interplay between the two mechanisms, how it contributes to lineage plasticity in advanced CRPCs is unaddressed.

Methods: DNA methylome and H3K27me3 of patient-derived xenografts/organoids and murine model with *MYCN* induction and *Pten/Rb1* co-loss (PRN) were analyzed. DNA methylome upon EZH2 deletion and H3K27me3 profile upon DNMT1 deletion was studied in human and murine NEPC models. To understand their transcriptional impact, expression profiles were analyzed upon EZH2/DNMT1 deletion.

Results: Both DNA methylome and H3K27me3 profile shifts during progression of CRPC to NEPC. H3K27me3 was enriched at hypomethylated regions of NEPC Vs. CRPC tumors across models and was independent of genomic context. EZH2 loss changed DNA methylome in NEPC at regions known to have differential DNA methylation during lineage plasticity. Neuron-related genes were hypomethylated and upregulated while, morphogenesis-related and bivalent genes were hypermethylated and downregulated upon EZH2 deletion. Conversely, DNMT1 deletion altered H3K27me3 landscape in NEPC. Neuron-related genes and bivalent genes were downregulated and enriched with H3K27me3 but upregulated and had depleted H3K27me3 in CRPC upon DNMT1 deletion. H3K4me3 was also decreased upon DNMT1 knockout in NEPC at these regions suggesting loss of bivalency. Short-term DNMT inhibition in NEPC PDX showed similarly altered H3K27me3 as noted in DNMT deleted NEPCs.

Conclusions: DNMT1 and EZH2 activity overlaps and together reprograms the epigenome during lineage plasticity of advanced CRPCs. EZH2 loss was partially compensated by DNMT activity leading to further neuroendocrine differentiation while DNMT1 loss shifted H3K27me3 leading to suppression of neuron-related genes.

#1360 Targeting the ubiquitin reading function of DNMT1 as a next-generation approach for epigenetic cancer therapy.

J. A. Kuleape, Y. Liu, J. A. Hrit, R. Tiedemann, S. B. Rothbart;
Van Andel Institute (VAI), Grand Rapids, MI

DNA methyltransferase 1 (DNMT1) is the key enzyme supporting the epigenetic inheritance of DNA methylation patterns during DNA replication, a process frequently dysregulated across nearly all human cancers. Abnormal DNA methylation patterning is an appreciated mechanism of tumor suppressor gene (TSGs) silencing and immune evasion, motivating the clinical development of DNA methyltransferase inhibitors (DNMTi's). While nucleoside analog DNMTi's are the most clinically advanced epigenetic cancer therapies, their utility has been limited due to pharmacokinetic barriers and adaptive resistance mechanisms. New approaches to inhibit abnormal DNA methylation patterning are therefore needed. Here, we define the DNMT1 ubiquitin interacting motifs (UIMs), which recognize UHRF1-dependent histone H3 mono-ubiquitination, as targetable domains to allosterically inhibit DNMT1 catalytic activity, and we identify a pharmacophore that can be used as a starting point for UIM inhibitor development. To characterize the functional significance of the DNMT1 UIMs, we developed a genetic complementation system in two human colon cancer cell lines to cover the loss of endogenous DNMT1 with wild-type or loss-of-function mutants with disrupted catalytic or UIM activities. Disruption of DNMT1 UIM function mirrored DNMT1 knockdown, catalytic-dead mutant cover, and exposure to nucleoside- and non-nucleoside catalytic DNMT inhibitors. These effects included widespread DNA hypomethylation that correlated with the re-expression of epigenetically silenced TSGs and transposable elements, reduced colony formation, impaired cell proliferation, and impaired growth of xenografted tumors. A pilot screen of a chemical library revealed four compounds with a shared pharmacophore able to disrupt the interaction of DNMT1 with ubiquitinated nucleosomes. Collectively, these studies demonstrate that the oncogenic properties of DNMT1 are supported by its ubiquitin reading function and provide a roadmap for developing next-generation DNMT1 inhibitors targeting this allosteric site.

#1361 KDM2A-driven epigenetic reprogramming promotes barrett's esophagus progression to adenocarcinoma.

Shilpa S. Dhar[1], Johnson Amoah[2], Ferhad Mongal[3], Liyong Zeng[2], Aryana S. Bhati[2], Xueshuai Han[4], Fang Cao[5], Tanaya Alexander Washington[2], MelissaPizzi Pizzi[2], Bansi Vanparia[2], Calena J. Brown[2], Gengyi Zou[1], Min Gyu Lee[6], Linghua Wang[2], Jaffer A. Ajani[2]

[1]GI Medical Oncology, UT MD Anderson Cancer Center, Houston, TX,[2]UT MD Anderson Cancer Center, Houston, TX,[3]University of Houston, Houston, TX,[4]Genome Medicine, UT MD Anderson Cancer Center, Houston, TX,[5]Peking University Health Science Center, Beijing, China,[6]Dept. of Molec. & Cellular Onc., UT MD Anderson Cancer Center, Houston, TX

Purpose: Esophageal adenocarcinoma (EAC), a rapidly increasing and highly lethal cancer arising from Barrett's esophagus (BE), lacks effective preventive strategies. Our study investigates the histone demethylase KDM2A as an early epigenetic driver of BE-to-EAC progression and evaluates whether its inhibition can suppress oncogenic reprogramming and tumorigenesis.
Experimental Procedures: We performed high-plex spatial transcriptomics (COSMx, 1K human panel) on patient tissues spanning BE, low- and high-grade dysplasia, and EAC (n = 20), integrating these results with immunohistochemistry, immunofluorescence, and TCGA (n = 186) datasets. Functional studies employed patient-derived organoids (PDOs), xenografts, and CRISPR-based KDM2A perturbation models. Chromatin profiling (CUT&RUN for KDM2A, ATAC-seq, RNA-seq) was used to map KDM2A-dependent enhancer activation and tumor suppressor repression.
Results: Spatial transcriptomics identified 13 transcriptional clusters delineating epithelial, stromal, and immune compartments. Progression from BE to EAC was characterized by expansion of stem-like epithelial clusters and loss of differentiation markers. PSCA and SPINK1 were consistently upregulated in EAC and correlated with increased EGFR expression, suggesting a convergence of these pathways in promoting therapy resistance and malignancy. KDM2A expression, validated by IHC/IF, was elevated in 4/6 EAC versus 1/3 BE samples and strongly correlated with PSCA and SPINK1. Analysis of TCGA-EAC confirmed KDM2A amplification and overexpression, which correlated with ERBB2, MYC, EGFR, and poor overall survival ($p=8.67\times10^{-3}$). Downstream analysis revealed repression of tumor suppressors DMBT1 and PFN1, implicating KDM2A in chromatin remodeling that silences protective loci while activating oncogenic enhancers. In organoid models, genetic or pharmacologic inhibition of KDM2A reduced PSCA/SPINK1 and EGFR signaling, restored differentiation, and suppressed proliferation.
Conclusions: KDM2A acts as a master chromatin regulator linking histone demethylation, tumor suppressor silencing, and activation of the PSCA-SPINK1-EGFR oncogenic axis during BE-to-EAC progression. Co-targeting KDM2A with EGFR/HER2 or MYC/CDK9 inhibitors represents a rational therapeutic strategy for early intervention and prevention. This study provides mechanistic insight into how epigenetic deregulation establishes a stem-like, therapy-resistant state in EAC and identifies KDM2A as a promising preventive and therapeutic target.

#1362 KMT2D is a master epigenetic regulator of lineage plasticity in lung squamous cell carcinoma.

Y. Jiang[1], **M. Wu**[2], U. Saran[1], L. Campos Clemente[1], S. Jiang[1], A. Ghosh[1], I. Flores[1], D. Morales[1], W. Lu[1], K. Khan[1], L. Zhang[1], L. Maren Solis Soto[1], I. Wistuba[1], M. Gyu Lee[1], K. Rai[1];

[1]UT MD Anderson Cancer Center, Houston, TX, [2]Baylor College of Medicine, Houston, TX

Background The cellular origin of lung squamous cell carcinoma (LUSC) remains poorly understood due to the absence of native squamous epithelium in the lung. While LKB1 loss can promote lung adenocarcinoma (LUAD)-to-LUSC lineage switching, this mechanism does not explain many cases. KMT2D, a histone H3K4 methyltransferase mutated in ~20% of LUSC, is associated with poor outcome in early-stage disease. We investigated whether Kmt2d loss drives initiation of lung adenosquamous (LUAS) lesions and promotes lineage infidelity in AT2 and Club cells.

Methods We evaluated whether Kmt2d loss is necessary and sufficient to induce LUSC in Pik3ca^{H1047R}/p53$^{-/-}$ (PP) and Kras^{Mut}/p53$^{-/-}$ (KP) mouse lung cancer models. A R26-LSL-Tdtomato (TdT) reporter allele was crossed into KP mice, and TdT^{+} tumor cells were isolated at the moribund stage for 10x single-nuclei multiomics profiling (snRNA-seq and snATAC-seq). To define mechanisms underlying Kmt2d-loss-mediated transdifferentiation, cell lines representing different tumor states and histologies were subjected to histone mark ChIP-seq (H3K4me1, H3K4me3, H3K27ac, and H3K27me3) and CUT&RUN for key transcription factors (TFs) and chromatin regulator (FOXA1, FOXA2, SOX2, and MENIN).

Results Kmt2d loss promoted squamous lineage transition and accelerated tumorigenesis in both PP and KP models. Single-nuclei multiomic analyses revealed that Kmt2d deficiency disrupts endodermal differentiation programs, promoting a transition from a highly plastic Itg$\alpha6^{+}/\beta4^{+}$ stem-like adenocarcinoma state toward squamous identity. Regions gaining accessibility in Kmt2d-null tumors were enriched for chromatin remodelers and stress-response TFs, including SMARCC1, EP300, AP-1 members (JUN, FOS), and NFE2L2 (Padj <= 0.01). Mechanistically, KMT2D cooperates with FOXA1/FOXA2 to maintain lineage-specific enhancers and TFs networks required for endodermal differentiation. Upon KMT2D loss, FOXA1 partners with the KMT2A/B-MENIN complex, activating aberrant squamous programs that accelerate tumorigenesis. Consequently, Kmt2d-null cells become dependent on MENIN for their excessive proliferation. NFE2L2 is identified as a key aberrantly activated oncogene contributing to the growth of Kmt2d-null cells.

Conclusions Our findings identify KMT2D as a critical guardian of lung lineage fidelity and reveal how its loss reconfigures core regulatory programs to drive squamous transdifferentiation and aggressive tumor progression.

: Advances in Cancer Research
Minisymposium

#1283 Asymmetric emergence of cardiovascular disease in hematologic malignancy survivors: A national real-world analysis.

Y. Song[1], P. Ma[1], H. Liang[2];
[1]Washington University in St. Louis, Saint Louis, MO, [2]UT MD Anderson Cancer Center, Houston, TX

Background: The link between hematologic malignancies and cardiovascular disease (CVD) is recognized as bidirectional, wherein each condition potentially promoting the onset of the other, thereby creating a complex interplay with significant clinical implications. However, the comparative risk and temporal dynamics of these situations are not clearly established in extensive, heterogeneous populations.
Methods: We utilized Electronic Health Record (EHR) data from the *All of Us* Research Program to construct two real-world cohorts: 5,786 hematologic malignancy survivors (leukemia, lymphoma, multiple myeloma, myelodysplastic syndromes [MDS]) without a history of CVD, and 77,617 CVD patients free of prior blood cancer. We assessed the bidirectional risk of incident disease in both modalities by comparing cumulative incidence, median time-to-event, and risk ratios (RRs), while adjusting for disease subtype, age, sex, race, and socioeconomic status.
Results: Among 5,786 hematologic malignancy survivors, 1,881 (32.5%) experienced new-onset CVD throughout 20-years. The risk was predominantly exhibited in the initial phase, with cumulative incidence reaching 14.7% by year 2, 22.2% by year 5, and 27.7% by year 10. Conversely, merely 1,451 (1.87%) of CVD patients reported a hematologic malignancy by the tenth year. The progression to CVD occurred more rapidly than that of developing cancer after CVD (median: 2.4 vs. 4.0 years; $P<0.0001$), indicating pronounced temporal asymmetry.The extent and duration of CVD risk are affected by the type of malignancy. Survivors of lymphoma and leukemia exhibited a relative risk approximately 20 times greater for developing CVD compared to the risk of cancer development in CVD patients (year 1 RR =19.1 and 20.6, respectively). Multiple myeloma survivors faced even higher risk (year 1 RR = 28.6), remaining elevated at year 10 (RR = 17.1). Among all subtypes, MDS conferred the highest risk during follow-up, with survivors ~40 times more likely to develop CVD in the first year (year 1 RR = 39.9, year 10 RR = 19.9). The incidence of CVD subtypes also varied among hematologic malignancy survivors. Arrhythmias were the most frequent event (10-year incidence: 13.8%), followed by heart failure (8.9%). Patients aged 18-39 had a diminished risk relative to other age groups (OR: 0.78, 95% CI: 0.66-0.91), while female patients similarly demonstrated a reduced risk (OR: 0.86, 95% CI: 0.77-0.96) after controlling for race and ZIP code poverty level.
Conclusion: Survivors of hematologic malignancies face an elevated, immediate risk of CVD that far exceeds the risk of developing cancer following CVD. This asymmetry indicates influences beyond common risk factors and emphasizes the critical necessity for integrated cardio-oncology monitoring, especially within the initial five years post-diagnosis, to alleviate this rapid cardiovascular decline.

#1284 Decoding melanoma immunogenicity: A comprehensive proteogenomic, immunopeptidomic, and metabolomic atlas.

P. Wang, CPTAC Proteomics Characterization Melanoma Study Working Group;
Icahn School of Medicine at Mount Sinai, New York, NY

Melanoma's robust immunotherapy responses are driven by a high mutational load and diverse antigen landscapes, yet the mechanisms linking these features to immune outcomes remain incompletely understood due to the absence of a system-level view. To address this gap, the Clinical Proteomic Tumor Analysis Consortium (CPTAC) performed a large-scale, multi-omics melanoma study spanning 164 primary tumors and metastases. We integrated 13 omic layers — including, for the first time at this scale, immunopeptidomics, metabolomics, and ubiquitination and glycosylation post-translational modifications (PTMs) — to construct a holistic view of tumor immunogenicity. Mass-spectrometry-based HLA-I immunopeptidomics identified 315,225 unique HLA-I-bound peptides, including 1,138 tumor antigen candidates. Of these, 33% are tumor-associated antigens and 22% are lineage-specific antigens, consistent with recent findings that most tumor antigens in cancers derive from unmutated genomic sequences. Tumor antigen load correlates significantly with CD8+ T cell infiltration. Notably, antigens from a few MAGEA-family genes correlates with CD8+ T cell percentages, suggesting MAGEA antigens may drive CD8+ T cell recruitment. We provided the most comprehensive tumor-derived metabolomic profiling in melanoma to date, linking metabolic states to tumor biology and the immune context. In a subset of patients with relatively low tumor antigen loads and limited immune infiltration, ether lipid metabolism emerges as a regulator of primary tumor homeostasis, whereas metastases exhibit upregulated mitochondrial metabolism. Unsupervised clustering of protein ubiquitination data identifies a subgroup with markedly worse survival, characterized by high ubiquitination of the IFN signaling pathway and ubiquitination-dependent activation of AKT1. This ubiquitin-IFN cluster is not detectable in global proteomics, highlighting ubiquitination-mediated regulation of inflammatory signaling and tumor progression. Glycoproteomics-based clustering reveals a lysosome-active subgroup, supported by upregulation of lysosome-associated degradative and lipid-metabolizing pathways. We also observe sex-specific differences: in males, lysosome-active glyco-cluster membership associates with significantly worse survival, a pattern not seen in females. Although sex differences in immunotherapy responses have been reported, mechanisms remain unclear; these data offer insights into sex-specific immunotherapy outcomes. Collectively, this multi-layer resource links tumor genetics, transcriptomics, proteomics, PTMs, and metabolomics to antigen presentation and immune signaling. It unravels the molecular logic underlying immune evasion, offering a comprehensive multi-omic atlas to inform patient stratification and design of combination immunotherapies in melanoma.

#1285 Endocrine therapy adherence and 10-year risk of cardiometabolic outcomes among women with hormone receptor-positive breast cancer.

J. R. Ledesma[1], J. Nugent[1], C. A. Laurent[1], S. R. Thadani[2], R. K. Cheng[3], J. M. Specht[3], J. M. Roh[1], R. Liu[4], H. Greenlee[5], M. L. Kwan[1];

[1]Kaiser Permanente - Northern California, Pleasanton, CA, [2]Kaiser Permanente - Northern California, South San Francisco, CA, [3]University of Washington, Seattle, WA, [4]Kaiser Permanente - Northern California, San Francisco, CA, [5]Fred Hutchinson Cancer Center, Seattle, WA

Background

Adjuvant endocrine therapy (ET) reduces breast cancer (BC) recurrence and mortality but may adversely affect cardiometabolic health. We evaluated, for the first time, the association between ET adherence duration and 10-year cumulative incidence (CI) of hypertension, dyslipidemia, and diabetes among women with hormone receptor-positive BC.

Methods

We conducted a prospective cohort study of 8,365 postmenopausal women with stage I-III hormone receptor-positive BC within Kaiser Permanente Northern California who initiated ET between 2005 and 2013. Adherence was categorized annually over five years and summarized into adherence durations from 0 to 5 years. Cardiometabolic outcomes were identified from diagnoses, labs, and medication dispensings. We estimated 10-year CI under varying adherence durations using sequentially doubly robust (SDR) estimation with Super Learner to flexibly model treatment and outcome mechanisms. Analyses accounted for all-cause death as a competing risk and stratified by ET type (aromatase inhibitor [AI] vs tamoxifen [TAM]).

Results

Overall, 40.8% were adherent for ≥5 years. Compared with never-adherent women, those adherent for ≥5 years were younger (aged 50-70: 73.7% vs 64.0%), lived in higher-income neighborhoods ($80,395 vs $70,417), more often received chemotherapy (34.1% vs 20.9%), and less likely to smoke (5.92% vs 10.5%). Among women never adherent, adjusted 10-year CI of hypertension, dyslipidemia, and diabetes were 22.7% (20.6-24.9), 25.6% (23.3-27.8), and 8.91% (7.65-10.2). Among those adherent for 5 years, CI were 29.1% (27.0-31.2), 32.4% (30.3-34.6), and 12.6% (11.5-13.8), corresponding to CI differences of 6.37% (3.36-9.37), 6.83% (3.79-9.94), and 3.73% (2.06-5.40). CI generally increased with each additional year of adherence. In ET-stratified analyses, 5-year AI adherence was associated with hypertension (CI difference=6.85% [3.74-10.0]), dyslipidemia (8.32% [4.94-11.7]), and diabetes (4.21% [2.28-6.13]) compared with those never adherent. TAM adherence was associated only with hypertension (5.83% [0.53-11.1]). Compared directly with TAM, AI adherence resulted in higher CI of dyslipidemia (difference=10.2% [4.33-16.1]) and diabetes (2.96% [0.07-5.85]).

Conclusion

Longer adherence to AIs was associated with increased 10-year risk of hypertension, dyslipidemia, and diabetes, while TAM use was associated only with elevated hypertension risk. With over 4.3 million breast cancer survivors in the US, findings highlight the need for further research to optimize patient selection for ET, balancing BC benefits with potentially higher cardiovascular disease risk, and strategies for early cardiometabolic management during ET.

#1286 Comprehensive phenotypic mapping of alternative lengthening of telomeres (ALT) regulation expands the landscape of targetable suppressors.

Bill Diplas, Oluchi Ezekwenna, Madison Rex, Mingxuan Wei, Agnel Sfeir

Memorial Sloan Kettering Cancer Center, New York, NY

Background: Alternative lengthening of telomeres (ALT) is used by 10-15% of all cancers as a telomerase-independent mechanism of telomere maintenance. Despite the identification of several ALT regulators, targeting has been challenging due to incomplete penetrance across cell lines and a limited understanding of the broader regulatory landscape. A major barrier to systematic discovery has been the lack of scalable assays compatible with high-throughput screening approaches.
Methods: Native fluorescence in situ hybridization (FISH) detecting ALT-specific single-stranded telomeric DNA was adapted and optimized for hybridization in-suspension with a fluorescent G-rich telomere PNA probe (TelG-647) and fluorescence-activated cell sorting (ALT-FlowFISH). Genome-wide CRISPR knockout screens using the TKOv3 library were performed, followed by selection and ALT-FlowFISH at one week following transduction and selection. Cells with the highest and lowest Native FISH signals were sorted (candidate ALT suppressors and promoters, respectively) and integrated sgRNA sequences were amplified and sequenced. Significantly enriched guides were identified as candidate ALT suppressors and promoters and were validated using targeted depletion (sgRNA/Cas9 RNP) and pharmacological inhibition followed by ALT assay validation (Native FISH and C-circle assay).
Results: ALT-FlowFISH was validated using depletion of established regulators FANCM (suppressor) and BLM (promoter), which resulted in expected increase and decrease of native FISH signal, respectively. Genome-wide phenotypic screens were performed in ALT-positive cell lines U2OS and RPE-ALT, followed by ALT-FlowFISH. These identified established ALT promoters, including components of the BTR complex, and suppressors, including FANCM, validating the screening approach. Overall, ALT suppressors were significantly enriched for known essential genes compared to ALT promoters. Importantly, we discovered and validated multiple novel ALT suppressor pathways, including components of the proteasome, the polyadenylation complex, RNA polymerase II machinery, and previously unrecognized members of the Fanconi anemia pathway. To confirm the functional relevance of these findings, we treated multiple ALT-positive cell lines with the proteasome inhibitor bortezomib, which recapitulated the suppressor phenotype observed in the genetic screens, demonstrating therapeutic potential.
Conclusions: This study establishes the first scalable ALT activity assay and provides the most comprehensive functional map of ALT regulation to date. Our identification of the proteasome and transcriptional machinery as novel ALT suppressors reveals potential precision medicine opportunities for targeting ALT-positive malignancies.

#1287 A spatiotemporal proteome map of chemotherapy response in metastatic breast cancer.

X. Zhao[1], J. Gao[1], G. Qian[1], R. Tiwari[2], J. N. Hansen[3], A. Forget[2], S. Nourreddine[1], Y. Doctor[1], J. Parker[1], P. Mali[1], N. Krogan[2], E. Lundburg[3], T. Ideker[1];

[1]UC San Diego, La Jolla, CA, [2]UC San Francisco, San Francisco, CA, [3]Stanford University, Palo Alto, CA

Cells are not simply aggregates of molecules; they are highly organized entities with dynamic structures and functions that evolve in response to external stimuli, such as drug treatments. Understanding how tumor cells reorganize these structures and functions, both spatially and temporally, is essential for unraveling the mechanisms underlying tumor behaviors including treatment response. Through the NIH Bridge2AI Cell Maps for AI (CM4AI) data generation project, we profiled spatiotemporal proteomics in metastatic breast cancer cells across untreated and chemotherapy-treated conditions using complementary proteomics technologies: immunofluorescence imaging (~11,000 images covering >100,000 single cells to map subcellular localization of >500 proteins), mass spectrometry (protein interactions of >500 proteins and complex organization across >5000 proteins), and single-cell CRISPR sequencing (>120,000 single-cell transcriptomes across 200 gene perturbations). Using self-supervised contrastive learning, we fuse protein embeddings across modalities while preserving treatment-induced protein dynamics. Our analyses reveal that chemotherapy triggers substantial protein reorganization. For example, in untreated cells, HDAC8 forms an assembly in close proximity to TET1, SETDB2, PHF6 and YWHAG. However, after paclitaxel treatment, its expression increases substantially and relocates from cytosol to nucleus. It forms a new seven-protein assembly with PARP1, KAT6B, DNMT3A, HDAC9, HDAC2, and BRD4. Building on this foundation, we will construct an integrated map that (a) delineates how individual proteins assemble into complexes and higher-order structures; (b) annotates these subcellular components with their functional states; and (c) models the dynamics of specific cellular components across drug treatment contexts.

#1288 The protein phosphatase EYA4 is a druggable target for the treatment of breast cancer.

Daniela A. Garcia[1], Chandler Heupel[2], Hannah Palacios[1], Eloise Dray[3]

[1]Greehey Children's Cancer Research Institute, The University of Texas Health Science Center at San Antonio, San Antonio, TX,[2]Neuroscience, Developmental, and Regenerative Sciences, The University of Texas at San Antonio, San Antonio, TX,[3]Department of Biochemistry and Structural Biology, The University of Texas Health Science Center at San Antonio, San Antonio, TX

Eyes Absent Homolog 4 (EYA4) is a dual-specificity phosphatase re-expressed in triple-negative breast cancer (TNBC) through methylation of repressive transcription factor marks. Its overexpression correlates with advanced disease and promotes genomic instability by deregulating Rad51-mediated homologous recombination (HR) and non-homologous end joining (NHEJ), throughout the cell cycle. Here, we characterize a novel property of EYA4: its ability to bind single-stranded DNA (ssDNA), and present a small-molecule inhibitor that abolishes its tyrosine phosphatase activity, possibly through the weakening of the DNA binding. Using a combination of chimeric EYA4 fragments and mutants, mobility shift assays, and biophysical methods including nuclear magnetic resonance (NMR) spectroscopy and microscale thermophoresis (MST), we mapped the DNA-binding interface and identified key residues mediating this interaction. ssDNA binding was found to stimulate the tyrosine phosphatase activity of EYA4, and our small-molecule inhibitor disrupts the phosphatase activity with an IC50 of 1 μM, indirectly suppressing enzymatic function. Functional assays, including homologous recombination reporter systems, immunofluorescence for DNA damage markers, MTT viability assays, and live-cell imaging using the Incucyte system (Essen), showed that EYA4 inhibition impairs HR, leads to DNA double-strand break accumulation, reduces proliferation, and increases apoptosis in MDA-MB-231 TNBC and TKCC PDAC models at concentrations of 1-5 μM. Fluorescent Ubiquitination-based Cell Cycle Indicator (FUCCI) imaging further revealed cell cycle defects, including mitotic failure and chromosomal segregation errors, consistent with disrupted repair during replication. Testing conducted on large panels of patient derived cell lines with the EYA4 inhibitor alone and in combination with standard of care demonstrated broader therapeutic relevance. These findings support targeting EYA4's DNA-binding function as a valid strategy to suppress tumor growth and enhance the efficacy of DNA-damaging therapies in HR-deficient (HRD+) cancers.

#1289 ASP2998, a TROP2-targeted immunostimulatory antibody drug conjugate (iADC) with dual payloads, demonstrates potent efficacy and a favorable safety profile in nonclinical models.

M. Orr[1], T. Chaen[2], M. Shibata[2], N. Ishikawa[2], T. Matsuda[2], Y. Fujita[2], G. Haggerty[3], Y. Ochiai[2], H. Tanaka[2], M. Akaiwa[2], X. Li[4], K. A. Doshi[4], W. Mahauad-Fernandez[4], K. Bajjuri[4], G. Yin[4];

[1]Astellas Pharma Global Development, Inc., Seattle, WA, [2]Astellas Pharma Inc., Tsukuba, Japan, [3]Astellas Research Institute of America LLC, Northbrook, IL, [4]Sutro Biopharma Inc., South San Francisco, CA

Objective: Trophoblast cell surface antigen-2 (TROP2) is a transmembrane glycoprotein implicated in various intracellular signaling pathways that promote cancer cell proliferation, migration, and invasion. TROP2 is frequently overexpressed across multiple tumor types. ASP2998 is a novel TROP2-directed immunostimulatory antibody drug conjugate (iADC) that incorporates two distinct payloads: a cytotoxic topoisomerase 1 inhibitor and an immunomodulator STING agonist. A series of nonclinical studies have been conducted to evaluate the nonclinical efficacy and safety of ASP2998.

Methods: In vitro cytotoxicity, immune cell activation, and cytokine production were assessed using co-culture assays of TROP2-positive cancer cells and human peripheral blood mononuclear cells (PBMCs). Immune cell subsets (dendritic cells, $CD4^+$ and $CD8^+$ T cells, and NK cells) and cytokines (IL-6, IL-1β, TNFα, IFNγ, and IP-10) were analyzed.Tumor immune environment (TME) modulation was evaluated in mice bearing human TROP2-expressing MC38 (MC38-hTROP2) tumors. ASP2998 was administered intravenously and immune cell populations in tumors were analyzed by flow cytometry on Day 5.Primary antitumor efficacy and tumor rechallenge responses were compared between ASP2998 and a TROP2-directed toxin ADC, in a MC38-hTROP2 tumor model.A 4-week GLP-compliant toxicity study (QW x 4) was conducted in cynomolgus monkeys at ASP2988 doses of 3, 10, and 30 mg/kg/week.

Results: ASP2998 exhibited potent cytotoxic activity against TROP2-positive cells and induced dose-dependent activation of human dendritic cells, $CD4^+$ and $CD8^+$ T cells, and NK cells, along with increased secretion of IL-6, IL-1β, TNFα, IFNγ, and IP-10.In vivo, ASP2998 at 1 mg/kg increased the frequency of total monocytes and activated ($CD80^+$) monocytes and dendritic cells in tumors. It also significantly enhanced infiltration and activation ($CD69^+$) of NK cells and increased the frequency of granzyme B^+ NK and $CD8^+$ T cells at both 0.3 and 1 mg/kg.ASP2998 surpassed the efficacy of a TROP2-directed toxin ADC against MC38-hTROP2 in vivo and provided greater protection against tumor rechallenge. ASP2998 demonstrated an acceptable safety profile in monkeys. Target organs included skin, cornea, kidney, urethra, trachea, and red blood cells. The highest non-severely toxic dose (HNSTD) was determined to be 10 mg/kg (QW x 4). Toxicokinetic profiles of the total antibody and ADCs were comparable, with minimal exposure to free payloads.

Conclusion: ASP2998 is a first-in-class dual payload iADC that combines cytotoxic and immuno-stimulatory mechanisms to enhance antitumor efficacy and promote durable antitumor immunity while demonstrating a favorable safety profile in nonhuman primates. A first-in-human (FiH) clinical study is planned.

: Combating T Cell Checkpoints
Minisymposium

#1338 DPP-4: A CD8+ T cell metabolic checkpoint and cancer immunotherapy target.

O. Teran Pumar[1], D. Gannamedi Hinder[1], D. Harwood[2], J. Benedetti[3], C. Ballard[3], E. Ciervo[1], C. Lopez Ruiz[1], C. Rafie[1], J. Mitchell[1], B. E. Leon[1], P. Assenza Tavares Coroa[1], B. Colon[1], M. Ceccarelli[1], Q. T. Ostrom[3], Z. Binder[4], D. Watson[1], E. Stelekati[1], B. W. Kristensen[2], D. Lombard[1], **D. Bayik**[1];
[1]University of Miami, Miami, FL, [2]University of Copenhagen, Copenhagen, Denmark, [3]Duke University, Durham, NC, [4]University of Pennsylvania, Philadelphia, PA

Exhaustion of CD8+ T cells in the tumor microenvironment is intertwined with metabolic dysfunction. Thus, metabolic reinvigoration of T cells is a promising cancer immunotherapy strategy. Here, we identify dipeptidyl peptidase 4 (DPP-4) as an immune checkpoint molecule driving the hypometabolic state of exhausted CD8+ T cells. We found that DPP-4 is highly expressed by CD8+ T cells infiltrating brain tumors, and its expression levels increase with terminal exhaustion. Pharmacological inhibition of DPP-4 with the FDA-approved sitagliptin, which is used for the management of type II diabetes, transcriptionally and metabolically reprogrammed CD8+ T cells to upregulate lymphocyte activation pathways and enhance mitochondrial spare respiratory capacity. Functionally, DPP-4 inhibition increased proliferation, antigen-specific cancer cell killing capability, and cytotoxic mediator production of mouse CD8+ T cells and IL13Ra2 CAR T cells in vitro. Mechanistically, inhibiting DPP-4 upregulated glutamate decarboxylase 1 (GAD1), an enzyme that feeds glutamate into the tricarboxylic acid (TCA) cycle. Pharmacological inhibition of GAD1 abrogated sitagliptin-mediated T cell proliferation and metabolic reprograming of mouse and human CD8+ T cells, underscoring a new role for this enzyme in T cell functional regulation. Systemic inhibition of DPP-4 prolonged survival in preclinical glioblastoma (GBM) models in a CD8+ T cell-dependent manner. Furthermore, retrospective analysis indicated that GBM patients on DPP-4 inhibitors, gliptins, have better outcomes compared to those receive standard of care alone or in combination with metformin. Collectively, our results support repurposing the clinically used and well-tolerated class of DPP-4 inhibitors to enhance cancer immunotherapy responses.

#1339 On-demand GLUT3 expression augments CAR-T cell metabolic fitness and antitumor efficacy while preventing toxicity in glioblastoma models.

K. Watanabe[1], J. Yamaguchi[2], A. Nakamura[2], Y.-T. Lin[1], K. Itahashi[3], S. Koyama[1], D. Sugiyama[2], S. Kato[2], A. Nagata[1], H. Nishinakamura[1], Y. Shiraki[2], A. Enomoto[2], S. Maeda[2], F. Ohka[2], K. Motomura[4], Y. Tsukada[5], M. Ito[5], Y. Maeda[1], R. Ueda[2], A. Natsume[6], R. Saito[2], H. Nishikawa[1];

[1]National Cancer Center Japan, Tokyo, Japan, [2]Nagoya University Graduate School of Medicine, Nagoya, Japan, [3]National Cancer Center Japan, Kashiwa, Japan, [4]Shizuoka Cancer Center, Nagaizumi, Japan, [5]National Cancer Center Hospital East, Kashiwa, Japan, [6]Institute of Innovation for Future Society of Nagoya University, Nagoya, Japan

The clinical success of chimeric antigen receptor T (CAR-T) cell therapy in hematologic malignancies has prompted its application to refractory solid tumors, including glioblastoma (GBM). However, CAR-T cell efficacy against solid tumors remains modest. Here, we demonstrate that the dysfunction of CAR-T cells in GBM is attributed to glucose deficiency in the tumor microenvironment (TME) and that on-demand, but not continuous, metabolic replenishment significantly improves the antitumor efficacy of CAR-T cells. Massive consumption of glucose by cancer cells reduces the glucose level in the TME of GBM, consequently impairing CAR-T cells. Modifying CAR-T cells with stable expression of GLUT3, a high-affinity glucose transporter restored their cytokine production and killing activity. However, while CAR-T cells with stable GLUT3 expression induced tumor reduction in a GBM model, their overactivation led to T-cell apoptosis, exhaustion, and terminal differentiation as well as adverse events and mouse death. On-demand GLUT3 CAR-T cells, in which GLUT3 transcription is driven by the nuclear translocation of nuclear factor of activated T-cells (NFAT) by target antigen stimulation, exhibit enhanced metabolic fitness and increased antitumor efficacy, leading to long-lasting tumor control in intracranial human GBM cell xenograft models while preventing adverse events. Cognitive dysfunction testing and histological analysis using a neuron damage marker, fluoro-Jade C (FJC), in mice treated with on-demand GLUT3 CAR-T cells did not show any signs of toxicity. We propose that on-demand, but not stable, metabolic fitness, such as at the time of exposure to tumor antigens, is a novel concept for maximizing the antitumor efficacy of CAR-T cells against solid tumors.

#1340 The zinc finger 7 motif of TNFAIP3/A20 enforces a critical block in exhausted CD8 T cell degranulation and represents a potent target for enhancing adoptive cellular therapies for cancer.

A. Blaisdell, S. Bachl, L. R. Sandoval, C. Ching, M. Prabandham, R. Advincula, N. Lenci, A. Marson, C. J. Ye, B. A. Malynn, J. Eyquem, J. Carnevale, A. Ma;
University of California San Francisco, San Francisco, CA

Introduction: CD8 T cells eliminate tumors through effector cytokines (IFNgamma, TNF) and cytotoxic granule protein release (perforin, granzymes). The relative contribution of these mechanisms varies across tumor contexts, suggesting distinct modes of regulation. CD8 T cell exhaustion within the tumor microenvironment limits their cytotoxic potential and poses a major obstacle for cancer immunotherapy and adoptive cellular therapies (ACTs). While most studies of exhausted CD8 T cell (Tex) dysfunction have focused on impaired cytokine production, the regulation of perforin- and granzyme-mediated cytotoxicity, as well as the pathways governing CD8 T cell degranulation in general, remain poorly defined.

Methods & Results: We performed a genome-wide CRISPR knockout screen in repetitively stimulated human T cells and identified the multifunctional ubiquitin-modifying enzyme tumor necrosis factor alpha-induced protein 3 (*TNFAIP3*, or A20) as a key suppressor of T cell persistence and cytotoxicity in the face of exhaustive stress. Using a large language model, base editor tiling screen, and tumor models in hypomorphic A20 knock-in mice, we pinpointed the zinc finger (ZF7) motif of A20 as the crucial regulator of CD8 T cell cytotoxicity. We then incorporated base-editing into standard human ACT production workflow to introduce a single inactivating missense mutation in ZF7 that significantly improved ACT efficacy in preclinical leukemia and melanoma models. Although ZF7-edited T cells produced more IFNgamma and TNF, genetic ablation experiments revealed these cytokines were dispensable for improved tumor control. Instead, through in vivo and in vitro functional assays, we revealed an underappreciated block in perforin and granzyme degranulation — rather than expression — that was relieved by ZF7 ablation. Finally, genetic epistasis analyses uncovered a surprising role for receptor-interacting serine/threonine-protein kinase 3 (RIPK3) — a canonical activator of necroptosis without a defined role in CD8 T cell effector function — as the critical orchestrator of degranulation in ZF7-deficient cells.

Conclusions: Our findings highlight an underrecognized yet critical post-translational block in Tex degranulation, regulated independently of cytokine production, and relieved upon targeted disruption of the ZF7 motif in a RIPK3-dependent manner. These results demonstrate that selective targeting of central suppressors such as A20 can not only reverse CD8 T cell exhaustion but also engage alternative signaling programs to unleash cytotoxicity. These insights address critical gaps in our understanding of the biological networks that restrain perforin-dependent cytotoxicity in Tex and provide a foundation for enhancing the potency and durability of ACTs.

#1342 Expression of Galectin-1 in exhausted CD8$^+$T cells restrains their antitumor effector functions.

M. A. Scheidegger[1], J. P. Merlo[2], M. Massaro[1], J. M. Perez Saez[1], S. G. Gatto[1], R. M. Morales[1], A. J. Cagnoni[1], T. Dalotto-Moreno*[1], G. A. Rabinovich*[1];

[1]Instituto de Biologia y Medicina Experimental (IBYME-CONICET), Buenos Aires, Argentina, [2]Instituto de Biologia y Medicina Experimental (IBYME-CONICET); UADE - INTEC, Buenos Aires, Argentina

Antitumor immune responses are constrained by a plethora of inhibitory mechanisms that promote immune evasion. Galectin-1 (GAL1), a glycan-binding protein recognizing N-acetyllactosamine residues in complex N- and O-glycans promotes immunosuppression by expanding regulatory T cells, inducing tolerogenic dendritic cells and activating immunosuppressive circuits in myeloid-derived suppressor cells (MDSCs). Through single-cell RNA sequencing analysis, we identified elevated GAL1 expression in exhausted CD8$^+$ tumor-infiltrating T cells (Tex) compared to effector cells. We validated this observation at the protein level in *in vitro*-generated Tex (iTex) compared to early-activated T cells. *Lgals1*$^{-/-}$ CD8$^+$ Tex cells infiltrating B16 tumors displayed decreased expression of exhaustion-associated transcription factor TOX ($p<0.01$), suggesting a potential role of GAL1 in promoting CD8$^+$ T cell terminal differentiation. To test this hypothesis *in vivo*, we used CRISPR-Cas9 editing on OVA-restricted OT-I CD8$^+$ T cells to generate control and GAL1-deficient antigen-specific T cells (sg*Lgals1*), which we adoptively transferred into B16-OVA tumor-bearing *Rag2*$^{-/-}$ mice. Flow cytometry and RNA-sequencing analysis revealed that sg*Lgals1* tumor-infiltrating Tex conserved effector functions as evidenced by elevated Granzyme B, IFN-γ and TNF-α expression compared to control T cells ($p<0.001$). Mechanistically, we explored whether soluble GAL1 may contribute to T cell exhaustion by interacting with immune checkpoint receptors. Using lectin blot and solid-phase binding assays, we demonstrated that Gal1 differentially binds to a set of immune checkpoint receptors (including VISTA, PD-1, CTLA-4, LAG3, and TIGIT, but not TIM3) in a glycan-dependent manner, as binding was inhibited by lactose. To further pursue this observation, we performed isothermal titration calorimetry and confirmed GAL1-VISTA interaction with a dissociation constant (Kd) of 2.78 µM and GAL1-LAG3 interaction with a Kd of 12.75 µM. Then, we profiled VISTA expression on B16 tumor-infiltrating immune cells and found it to be highly expressed within the myeloid compartment, with minimal or absent expression in the lymphoid compartment and in tumor cells. Collectively, our results suggest a dual function for GAL1 in the tumor microenvironment. Endogenous GAL1 expression by CD8$^+$ Tex cells may promote a terminal dysfunctional state in an autocrine fashion, while simultaneously driving an immunosuppressive phenotype on myeloid cells through paracrine engagement of checkpoint receptors. Thus, targeting Gal1 may have therapeutic implications in cancer immunotherapeutic regimens including immune checkpoint blockade and adoptive cell transfer. Our future perspectives will be to focus both on signaling pathways triggered by GAL1 engagement of checkpoint receptors and on GAL1 intracellular functions during T cell exhaustion.

#1344 PTPN2/N1 inhibition drives a STAT3-mediated response in exhausted T cells and underscores targetable counter-regulatory mechanisms for T cell improvement.

Y. Senent[1], K. Bi[1], H. Keshishian[1], N. Kormshchikov[1], N. Knudsen[1], S. Carr[1], D. Sen[2], K. Yates[1], R. Manguso[1];
[1]Broad Institute of MIT and Harvard, Cambridge, MA, [2]MGH/Harvard Medical School, Cambridge, MA

New strategies to improve T cell function for immunotherapy and cell therapy are urgently needed. PTPN2 and PTPN1 are phosphatases that dephosphorylate members of the JAK–STAT signaling pathway and downstream TCR signaling kinases, positioning them as key negative regulators of cytokine signaling and T cell activation. Genetic deletion of PTPN2 or PTPN1 induces striking T cell–mediated anti–tumor immunity. However, despite the extensive knowledge on the enzymatic targets of PTPN2/N1, the signaling mechanisms leading to enhanced T cell function downstream of PTPN2/N1 loss are unclear. To address this, we performed transcriptional and phospho–proteomic profiling of human T cells treated with a PTPN2/N1 inhibitor (AC484) during chronic antigen stimulation. Using the CytoSig cytokine signaling inference method, we found that PTPN2/N1 loss drives robust activation of STAT3 signaling, accompanied by a counterintuitive inhibition of STAT5 activity. This pattern was consistent across both chronically stimulated human T cells and murine tumor–infiltrating T cells treated with AC484. Phospho–proteomic analyses confirmed a strong upregulation of phosphorylated STAT3, but a marked downregulation of JAK1/2/3 and STAT5 phosphorylation in PTPN2/N1 inhibitor–treated T cells. Conversely, acute PTPN2/N1 inhibition transiently increases STAT5 activity. Transcriptomic analyses further revealed potential mechanisms of feedback inhibition on JAK–STAT5 signaling, as several STAT3–driven counter regulatory factors were highly upregulated in chronically stimulated PTPN2/N1–deficient cells, such as SOCS3. SOCS3 is a well–established inhibitor of JAK1, JAK2, and TYK2, and can dampen STAT5 signaling; our results position SOCS3 as a strong candidate to mediate feedback inhibition. We hypothesize that PTPN2/N1 inhibition causes STAT3–mediated phenotypic changes in T cells, and while this is beneficial for enhancing T cell function, STAT3 also elicits upregulation of counter–regulatory factors that limit JAK–STAT5 signaling during chronic antigen stimulation and may ultimately restrain the persistence of PTPN2/N1–deficient T cells. Our next studies will elucidate the dynamic changes in signaling circuitry in PTPN2/N1–deficient T cells and leverage this knowledge to propose new strategies to counteract T cell exhaustion. These insights could inform the development of next–generation small molecule and cellular immunotherapies with improved efficacy and durability.

: From Real World Data to Medicine-based Evidence
Minisymposium

#1301 Real-world analysis of NSCLC variant-level frequencies from liquid biopsy testing in diverse U.S. populations.
E. K. Longshore, U. G. Sathyanarayana, R. Pestano, B. D'Alessio, T. Petropolis, C. Cochran, M. Sowada, A. Stephen, Z. Velasco, A. Corral, S. Cotten, P. Galvin, G. Johnson, L. Jackson, A. Weaver, G. A. Pestano;
Biodesix, Inc., Louisville, CO

Non-small cell lung cancer (NSCLC) is a highly prevalent and genetically heterogeneous disease, making molecular profiling critical for guiding targeted therapy decisions. However, establishing on-site testing can be complex and costly and thus represents an unmet need in the community. The advent of liquid biopsy has increased accessibility of testing in rural and underrepresented groups in the United States, catalyzing large scale molecular profiling analyses. Data surrounding variant-level mutation frequencies across diverse U.S. populations remain limited, particularly from real-world settings in the community. This study evaluated more than 350,000 tests and 20 ethnically diverse groups for variant level frequencies of actionable molecular markers across the four major mutation classes (Single Nucleotide Variants/INDELs, Fusions, Amplifications, and Exon Skipping) in NSCLC, as identified from send-out liquid biopsy amplicon-based NGS and ddPCR testing over the past 10 years. The overall ddPCR positivity rate over the testing period was 1.5%. Among positive ddPCR results, KRAS G12C was the most frequent mutation (3.9%). NGS testing showed a 46% positivity rate for SNV/INDEL variants, with TP53 as the most frequently mutated gene (34%). NGS fusion positivity was 15%, with EML4-ALK.E6aA20.AB374361 being the most prevalent (12.95%). A disproportionate burden of NSCLC mutations was observed in African American patients, highlighting disparities in lung cancer prevalence. Geographically, the highest positive variant distributions were concentrated in the Southeastern U.S. region. These findings emphasize the utility of centralized molecular testing and the importance of including underrepresented populations in molecular profiling studies. Together, this data may help guide treatment decisions in the community setting.

#1302 Distinct Histology of Lung Cancer inpeople who have never smokedand Prognostic Determinants in Non-Mucinous Adenocarcinoma.

T.-V. Tran[1], M. Saha[1], H. Hoang[1], P. Bhawsar[1], R. Homer[2], M. K. Baine[3], L. M. Sholl[4], P. Joubert[5], C. Leduc[6], W. Travis[3], R. Pfeiffer[1], J. S. Almeida[1], D. R. Jones[3], G. Rocco[3], S. Yang[3], M. Landi[1];

[1]National Cancer Institute, National Institutes of Health, Rockville, MD, [2]Yale School of Medicine, New Haven, CT, [3]Memorial Sloan Kettering Cancer Center, New York, NY, [4]Brigham and Women's Hospital, Boston, MA, [5]Institut universitaire de cardiologie et de pneumologie de Quebec - Universite Laval, Quebec, QC, Canada, [6]Centre Hospitalier de l'Universite de Montreal, Montreal, QC, Canada

Purpose: Lung cancer in people who have never smoked (LCINS) is biologically distinct from smoking-related lung cancer yet remains histologically under-characterized. Prognostic frameworks, including the International Association for the Study of Lung Cancer (IASLC) grading system for non-mucinous adenocarcinoma, were developed in smoker-dominant cohorts and remain untested in LCINS. We characterized the LCINS histologic landscape and, within non-mucinous adenocarcinoma, evaluated the prognostic value of IASLC grade and additional histologic features. To our knowledge, this is the first large-scale study dedicated exclusively to LCINS histopathology.**Methods:** We established the LCINS histologic landscape using the Sherlock-Lung study. Sherlock-Lung H&E-stained whole slide images (n=844) were reviewed independently by ≥2 thoracic pathologists, with consensus resolution. Tumors were classified per WHO 5th edition. Prognostic analyses included non-mucinous adenocarcinoma from Sherlock-Lung (n=634, stage I-IV) and an external MSK cohort of R0-resected stage I-II patients (n=169). We used Kaplan-Meier and Cox models adjusted for age, ancestry, sex, and tumor stage. We evaluated IASLC grade, and pathologist-scored features not included in WHO classification—tumor-infiltrating lymphocytes (TILs; intense/not intense, “intense” indicating high lymphocyte density) for their impact on overall survival (OS) in Sherlock-Lung, and IASLC grade and STAS for OS and disease-free survival (DFS) in MSK.**Results:** LCINS were predominantly adenocarcinomas (84%; 75% non-mucinous), whereas carcinoid tumors accounted for 8%. In Sherlock-Lung (median follow-up 52 months; 202 deaths), Grades 1-2 had significantly better 5- and 10-year OS versus Grade 3 ($HR_{5\ years}$=0.30, 95%CI 0.18-0.50; $HR_{10\ years}$=0.36, 95%CI 0.24-0.53), most strongly in stage I ($HR_{10\ years}$=0.29, 95%CI 0.16-0.53; $p_{interaction}$=0.03). Intense TILs independently improved long-term OS ($HR_{5\ years}$=0.64, 95%CI 0.36-1.11; $HR_{10\ years}$=0.51, 95%CI 0.30-0.86). In MSK (median follow-up 43 months; 21 deaths, 30 DFS events), grades 1-2 showed consistently better OS and DFS, although not statistically significant (OS: $HR_{5\ years}$=0.91, 95%CI 0.28-3.02; DFS: $HR_{5\ years}$=0.61, 95%CI 0.26-1.43) and STAS was not associated with either endpoint.**Conclusion**: In the largest LCINS cohort to date, we defined distinct histologic features and verified the prognostic value of the IASLC grading system, with Grade 3 indicating worse survival. TIL assessment further refined risk stratification, highlighting the need for further smoking-specific histological evaluation and larger prospective studies.

#1303 Real-world overall survival with trastuzumab deruxtecan versus standard chemotherapy in HER2-amplified MSS metastatic colorectal cancer.

Sumbal Aziz[1], **Zunairah Shah**[2], Mariam H. Ahmad[2], Jayasree Krishnan[2], Sohaib Asghar[1], Woojoo Lee[1], Sheheryar Kabraji[2], Kannan Thanikachalam[2]

[1]Adventhealth, Sebring, FL,[2]Roswell Park Comprehensive Cancer Center, Buffalo, NY

Background: HER2-positive (HER2-amplified, IHC3+) microsatellite-stable (MSS), metastatic colorectal cancer (mCRC) represents a small but clinically meaningful subgroup with aggressive biology and limited responsiveness to standard chemotherapy. Trastuzumab deruxtecan (T-DXd), a HER2-targeted antibody-drug conjugate, has shown encouraging activity in DESTINY-CRC01 and DESTINY-CRC02. However, real-world effectiveness of T-DXd remains unclear due to variability in comorbidities, performance status, treatment sequencing, and prior therapy exposure. This study evaluated real-world overall survival (OS) with T-DXd versus standard chemotherapy in patients with MSS, HER2-amplified mCRC to assess effectiveness outside trial settings.
Methods: De-identified TriNetX data (2010-2025) were used to identify adults (>18 years) with HER2-amplified mCRC treated with either second-line chemotherapy (FOLFOX, FOLFIRI, or CAPOX ± bevacizumab) or T-DXd as second-line of treatment. Because anti-EGFR therapy is ineffective in HER2-amplified disease, cetuximab- or panitumumab-treated patients were excluded. Patients were assigned to cohorts based on the line in which T-DXd or standard chemotherapy was initiated. Propensity score matching (1:1) balanced age, sex, comorbidities, metastatic burden, and prior therapies. OS was evaluated using Kaplan-Meier estimates, log-rank tests, and Cox proportional hazards models. Hazard ratios (HRs) with 95% confidence intervals (CIs) were reported; significance was defined as two-sided $P \leq 0.05$.
Results: Two cohorts were identified: standard chemotherapy (n = 9,135) and T-DXd (n = 1,977). Before matching, the T-DXd cohort was slightly older (67.4 ± 13.1 vs 66.5 ± 12.8 years; p = 0.006) and had more females (71% vs 49%; p = 0.0001). Both groups had received one prior line of systemic therapy. After 1:1 propensity score matching (n = 1,870 each), demographics, clinical characteristics, and prior treatments were well balanced. In the matched population, 1-year OS was only slightly different (83.0% vs 84.8%; p = 0.03). However, 5-year OS favored T-DXd (66.6% vs 62.1%; p = 0.0046). Multivariable Cox regression demonstrated a significantly higher mortality risk with standard chemotherapy compared with T-DXd (HR 1.14; 95% CI, 1.05-1.24; p = 0.0024).
Conclusion: Although DESTINY-CRC01 evaluated T-DXd in the third-line or later setting, where patients had received a median of four prior therapies, this real-world analysis demonstrates that T-DXd is associated with improved long-term survival even when used in the second line setting, with fewer treatment-related adverse events. In patients with HER2-amplified mCRC, T-DXd showed a meaningful 5-year overall survival advantage compared with standard chemotherapy.

#1304 Cancer risk with initiation of angiotensin receptor blockers (ARBs) vs. angiotensin converting enzyme inhibitors (ACEIs).

C. Himbert[1], D. K. Addo[1], Y. Xu[1], T. He[1], C. G. Derington[2], T. Greene[1], J. B. Cohen[3], A. Bress[1], S. Hardikar[1];
[1]University of Utah, Salt Lake City, UT, [2]University of Colorado, Aurora, CO, [3]University of Pennsylvania, Philadelphia, PA

Background: The comparative long-term effects of initiation of an angiotensin receptor blocker (ARB) and angiotensin-converting enzyme inhibitor (ACEI) on cancer risk remain uncertain. The objective of this study was to compare risks of cancer and non-cancer mortality between ARB and ACEI initiators among US veterans.
Methods: This prospective cohort included 2,658,758 veterans with hypertension and no history of cancer who initiated either an ARB or an ACEI within the Veterans Health Administration between January 1, 2000, and December 31, 2017. Participants were followed from treatment initiation until the first occurrence of an outcome, death, loss to follow-up, or December 31, 2022 (the end of study). Initiation of ARB or ACEI treatment was determined from pharmacy dispensing records, excluding those with a history of cancer or who filled ARB or ACEI before the study period. The index date (baseline) was defined as the date of initiating either treatment. Inverse probability (IP) of treatment weighting was applied to adjust for 27 baseline covariates and estimate the intent-to-treat effect of ARB versus ACEI initiation. The co-primary outcomes were time to any cancer (ascertained from the VA Cancer Registry) and non-cancer mortality. Secondary outcomes included all-cause mortality, the composite of any cancer or death, incidence of specific cancers, and non-cancer-specific mortality. Cumulative incidence functions and risk ratios (RRs) with 95% confidence intervals (95% CI) were calculated using IP-weighted Aalen-Johansen estimator in the competing risks setting.
Results: Among 2,658,758 veterans (median follow-up, 10 years; mean age, 63 years; 5% women; 76% non-Hispanic White; 15% Black), 90% initiated ACEIs and 10% initiated ARBs. ARB initiation was associated with a lower 10-year risk of any cancer (RR, 0.79; 95% CI, 0.75-0.83) and a similar 10-year risk of non-cancer mortality (RR, 1.03; 95% CI, 0.88-1.07) compared with ACEI initiation. Associations were consistent across most cancer types, except for inconclusive findings for breast and renal cancers. In subgroup analyses, a stronger inverse association between ARB initiation compared to ACEI initiation and cancer risk was observed among older patients (≥70 years).
Conclusions and Relevance: ARB initiators had a lower risk of developing any cancer compared with initiation of ACEIs, with no observed difference in non-cancer or all-cause mortality. We also reported stronger inverse association for ARBs in older adults in subgroup analyses. Further research should clarify underlying biological mechanisms, confirm causality in randomized trials, and evaluate personalized antihypertensive strategies that incorporate cancer risk considerations.

#1305 Assisted reproductive technology and the risk of female sex hormone-related cancers.

E. P. Lin[1], C.-H. Lin[2], C.-Y. Hsu[3], W.-S. Lin[2], J.-C. Chang[2], B.-T. Huang[1], H.-N. Ho[1], Y. Shyr[3];
[1]Taipei Medical University, Taipei, Taiwan, [2]Taichung Veterans General Hospital, Taichung, Taiwan, [3]Vanderbilt University Medical Center, Nashville, TN

Background: Whether assisted reproductive technology (ART) treatment is associated with the risk of female sex hormone-related cancers is inconclusive.
Methods: This study leveraged the national data from Taiwan to assemble the largest ART cohorts. The primary objective was to assess the associations of ART with the risk of breast, ovarian, and endometrial cancers. The secondary objectives included the associations of ART cycle numbers, age at the first ART treatment, and history of childbirth with the risk of these cancers. Cox proportional hazards regression models were used for data analysis.
Results: The cohorts with or without ART exposure for breast, ovarian, or endometrial cancer risk assessment included 104,486, 104,936, or 104,913 subjects, respectively. The results showed that ART was independently associated with an increased risk of breast (HR, 1.11; 95% CI, 1.04 to 1.19) and ovarian (HR, 1.38; 95% CI, 1.13 to 1.69) cancers, but not endometrial cancer. The data also revealed a dose-response relationship between ART cycle numbers ($\geq$2 versus 1) and the risk of breast (HR, 1.13; 95% CI, 1.03 to 1.25) and ovarian (HR, 1.45; 95% CI, 1.10 to 1.90) cancers. No statistically significant associations between age at the first ART and the risk of these cancer types were observed. Subgroup analyses suggested protective effects of childbirth against ovarian and endometrial cancers.
Conclusions: This study demonstrated a statistically significant increase in the risk of breast and ovarian cancers among women with ART treatment. The results suggested that regular checkups for cancer should be considered once ART exposure is established.

#1306 Developing a real-world clinical genomic platform to deliver precision oncology in underrepresented populations.

Shubhankar Sood[1], Daniel Hubschmann[2], Jennifer Wischhusen[3], Andreas Trumpp[3]

[1]Global Precision Medicine (GPM), Heidelberg Institute for Stem Cell Technology and Experimental Medicine, Heidelberg, Germany,[2]Pattern Recognition and Digital Medicine, Heidelberg Institute for Stem Cell Technology and Experimental Medicine, Heidelberg, Germany,[3]Stem Cells and Cancer, Heidelberg Institute for Stem Cell Technology and Experimental Medicine, Heidelberg, Germany

Around 14% of the world's population currently represents more than 75% of oncology clinical trials and genomic datasets, with the majority derived from individuals of Caucasian ancestry. Precision oncology drugs developed over the past decade have been validated largely on this skewed representation. As a result, targeted therapies often perform inconsistently in regions with the highest cancer burden, leading to reduced effectiveness, increased toxicity, and substantial economic losses from failed clinical applicability. To address this unmet need, we developed a global real-world clinical genomic platform through a bilateral collaboration between India and Germany. This platform links major oncology centers in India with the Global Precision Medicine research group in Heidelberg, one of Europe's largest precision-oncology and clinical-trial hubs. At its core, we developed a novel digital interface for structured clinical data capture at source, supported by clinician training and AI-based integration of epidemiological, diagnostic, imaging, and pathology information. We also introduced deep whole genome sequencing with tumor-matched controls using a nationwide snap-frozen workflow, coupled with tumor transcriptome sequencing as part of our multi-omics program. All multimodal data are processed through a validated analytical framework for alignment, variant calling, expression profiling, biomarker annotation, and molecular tumor board integration.

With our platform, we aim to generate real-world multi-omics data for 10,000 genetically diverse patients across India, forming one of the largest clinically annotated oncology datasets from underrepresented populations globally. Initial integration shows that multi-institutional datasets can be harmonized with European pipelines, enabling high-quality sequencing and structured clinical annotation. Early analyses suggest genomic and transcriptional differences compared to European cohorts, including variation in mutational signatures, copy-number profiles, and immune-related states. These insights support the development of context-specific biomarkers and decision-support modules tailored to underrepresented populations.

In conclusion, our platform delivers two parallel value additions. Clinically, it identifies additional actionable mutations, supports combinatorial therapy recommendations, and reveals missed diagnostics. Scientifically, the high-resolution dataset enables biomarker discovery, patient-stratification models, and early identification of therapeutic vulnerabilities. Together, our clinical genomics platform provides a scalable blueprint for integrating underrepresented populations into global cancer genomics and positions these cohorts as essential contributors to the future of precision oncology.

#1307 Pan-cancer landscape of alternative lengthening of telomeres revealed by machine learning analysis of clinical sequencing data.

Harshit Sahay, Bill H. Diplas, Oluchi C. Ezekwenna, Divya Koyyalagunta, Simran Chhabria, Madison Darmofal, Quaid Morris, Agnel Sfeir

Memorial Sloan Kettering Cancer Center, New York, NY

Replicative immortality is a hallmark of cancer, achieved by activating telomere maintenance mechanisms (TMMs), which prevent telomere shortening and senescence. While the majority of tumors achieve this via the reactivation of telomerase, a significant subset (10-15%) relies on alternative lengthening of telomeres (ALT), a recombination-driven mechanism of telomere maintenance. ALT is highly tumor type-specific, most frequently seen in mesenchymal tumors. ALT is strongly associated with inactivating mutations in chromatin remodeling genes ATRX and DAXX, however, many ALT tumors lack alterations in these genes. Additionally, ATRX loss alone in in vitro models is insufficient for triggering ALT. Together, these underscore that the underlying mechanisms of ALT remain incompletely understood. A critical gap has been incomplete characterization of the genetic landscape of ALT, as laborious detection assays restrict studies to specific histologies or to tumors with limited genetic profiling.

To address this, we sought to use the MSK-IMPACT clinical cohort. MSK-IMPACT is an FDA-approved targeted sequencing panel used for routine genetic profiling of tumors, with >100,000 patients profiled across 80+ tumor types. We developed a machine learning framework to infer ALT status by leveraging typically discarded off-target reads. These reads contained telomeric sequences, enabling us to quantify telomere content and repeat composition. We then assessed the presence of ALT experimentally using the C-circle assay (CCA) for 700 patient samples. ATRX/DAXX truncations were strongly associated with ALT but did not show complete correspondence. Using telomeric features from 300 tumors with high-confidence CCA results, we trained an ensemble of Random Forest classifiers with stratified five-fold cross-validation to predict ALT status, achieving robust performance (mean ROC-AUC = 0.84; PRC-AUC = 0.76). Models were then calibrated and ensembled to generate predictions for 78,704 patient tumors in MSK-IMPACT. Model predictions corresponded well with known ALT patterns. Highest prevalence was seen in sarcomas, gliomas, and neuroendocrine tumors, particularly in ATRX/DAXX mutant tumors, with low or no prevalence in TERT-altered tumors. Interestingly, the model predicted low but notable ALT prevalence in ATRX/DAXX wild-type tumors within ALT-relevant pathologies. MSK-IMPACT annotations enabled identification of ALT-associated genetic factors beyond ATRX/DAXX in these tumors.

Our framework enables scalable ALT detection from routine clinical sequencing data and provides an updated picture of ALT prevalence across a wider range of tumor types than previously possible. This resource can be used to identify novel genetic associations, assess differential treatment response and prognosis, and guide therapeutic decisions targeting TMMs.

: Innovative Targeted and Cellular Therapies for Exploiting Cancer Vulnerabilities
Minisymposium

#1329 Preclinical development of EFTX-G12V, a first-in-class EGFR-directed KRAS G12V selective inhibitor.

Lyla J. Stanland[1], Hayden Huggins[1], Snehasudha S. Sahoo[2], Alessandro Porrello[2], Yogitha Chareddy[2], Salma Azam[2], Jillian Perry[2], Pradeep S. Pallan[3], Kristina Whately[2], Lincy Edatt[2], William D. Green[2], Matthew C. Fleming[4], Jonah Im[2], Christina Gutierrez-Ford[2], Imani Simmons[2], Alyaa Dawoud[2], Katherine I. Zhou[2], Vandanaa Jayaprakash[1], Rani Sellers[5], Gabriela de la Cruz[5], Albert Wielgus[5], Justin Milner[2], Martin Egli[3], Albert A. Bowers[2], Chad V. Pecot[2]

[1]EnFuego Therapeutics Inc, Morrisville, NC,[2]Lineberger Comprehensive Cancer Center, University of North Carolina, Chapel Hill, NC,[3]Biochemistry, Vanderbilt University, Nashville, TN,[4]Eshelman School of Pharmacy, University of North Carolina, Chapel Hill, NC,[5]Pathology and Laboratory Medicine, University of North Carolina, Chapel Hill, NC

The KRAS proto-oncogene encodes a small GTPase that is crucial for the activation of intracellular signaling pathways that control cell proliferation, survival and differentiation. *KRAS* is frequently mutated in cancer resulting in its constitutive activation and dysregulation of downstream signaling pathways that drive oncogenic transformation. KRAS G12V is the second most common KRAS mutation in cancer, and occurs frequently in lung, colon and pancreatic cancers. However, while significant advancements have been made in developing KRAS G12C, G12D and pan-KRAS inhibitors, there remain no direct KRAS G12V inhibitors in the clinic. Previously, we developed EFTX-G12V, a fully-modified, mutant-selective, ligand-conjugated siRNA that shows significant anti-tumor activity in multiple cancer models. EFTX-G12V inhibits KRAS G12V expression at both the mRNA and protein level while completely sparing KRAS WT. Further, EFTX-G12V significantly inhibited cancer cell growth *in vitro* and displays no concerning off-target effects. Importantly, our approach takes advantage of high tumor expression of EFGR where our siRNA is conjugated to an EGFR linear ligand that enables high tumor-to-normal tissue payload delivery in models with varying levels of EGFR expression. EFTX-G12V significantly inhibited KRAS G12V mRNA and protein *in vivo* and showed significant anti-tumor activity in lung, colon and pancreatic xenograft models. Critically, EFTX-G12V showed no off-target effects on WT KRAS in somatic tissues. Unexpectedly, we found that EFTX-G12V showed improved efficacy in comparison to a pan-KRAS siRNA which we found is due to increased inhibition of tumor angiogenesis in EFTX-G12V treated groups. Here, we describe further preclinical evaluation of EFTX-G12V including pharmacokinetics in mouse xenograft models and the efficacy and safety profile in an immunocompetent mouse model. We performed a pharmacokinetic evaluation of the antisense strand of EFTX-G12V in plasma, tumors, skin, kidney and liver tissue following a single injection. We observed clearance of the siRNA from the plasma within four hours and uptake of a therapeutic dose level in tumor tissue through 96 hours post injection, with limited exposure to somatic tissues. We evaluated EFTX-G12V in an immunocompetent mouse model and observed significant tumor reduction and a robust anti-tumor immune response that was not a result of a systemic inflammatory response and displayed no concerning toxicities. Lastly, we recently completed non-GLP safety studies in rat and mini-pig models and observed no test article related clinical observations, no injection site reactions and initial gross pathology detected no visible lesions across all tissues. Together these data indicate that EFTX-G12V has therapeutic efficacy in multiple cancer models, is delivered to tumor tissue with minimal somatic tissue exposure, and may be well tolerated.

#1330 Targeting Aurora kinase A for potentiating colorectal cancer to KRAS targeted therapy.

Zhaojin Liu[1], Ning Wei[2], Suisui Hao[1], Xinyan Lu[1], Jian Yu[3], Lin Zhang[3]

[1]USC - University of Southern California, Los Angeles, CA,[2]Montefiore Comprehensive Cancer Center, Bronx, new york, NY,[3]USC Norris Comprehensive Cancer Center, Los Angeles, CA

Colorectal cancer (CRC) is one of the most prevalent and lethal types of cancer worldwide. The development and progression of CRC are driven by the activation of multiple oncogenes, notably KRAS. Mutations in KRAS are among the most common oncogenic alterations, occurring in ~45% of CRC cases. KRAS plays a pivotal role in cell signaling by serving as a binary switch of MAPK/ERK and PI3K/AKT pathways downstream of the epidermal growth factor receptor (EGFR). Two $KRAS^{g12c}$ inhibitors, sotorasib and adagrasib, have been approved for monotherapy against non-small cell lung cancer (NSCLC). However, both drugs have shown limited efficacy in CRC, indicating an intrinsic resistance mechanism. Similarly, the recently developed pan-RAS inhibitor RMC-6236 exhibits only modest activity in KRAS-mutant CRC, highlighting the urgent need for rational combination strategies to overcome therapeutic resistance. Anticancer therapies commonly suppress tumor growth by inducing apoptosis, a major form of programmed cell death. However, $KRAS^{g12c}$ inhibitors alone have been shown to fail in inducing apoptosis in $KRAS^{g12c}$ CRC cells. In this study, we investigated strategies to enhance apoptosis and sensitize KRAS-mutant CRC to KRAS-targeted therapies. We identified Aurora kinase A (AURKA), an oncogenic kinase that regulates the G2/M transition in cell cycle, as a key suppressor of apoptosis in KRAS-mutant CRC cells under KRAS inhibition. Co-inhibition of AURKA and KRAS elicited potent anti-tumor effects both *in vitro* and *in vivo*. Mechanistically, AURKA inhibition enhanced apoptosis by downregulating the anti-apoptotic Bcl-2 family member Mcl-1. Concurrent AURKA blockade suppressed the rebound activation of KRAS downstream signaling, facilitating the degradation of Mcl-1 mediated by GSK3β. Moreover, Mcl-1 inhibition further sensitized KRAS-mutant CRC cells to KRAS inhibitors. Collectively, our findings support AURKA inhibition as a promising combination strategy to overcome intrinsic resistance to KRAS-targeted therapies in CRC.

#1331 The Kinase Library: A global atlas of the human protein kinome and its applications in cancer.

Tomer M. Yaron-Barir[1], Jared L. Johnson[1], Benjamin E. Turk[2], Michael B. Yaffe[3], Lewis C. Cantley[1]

[1]Cell Biology, Dana-Farber Cancer Institute / Harvard Medical School, Boston, MA,[2]Yale University, New Haven, CT,[3]Koch Inst. for Integrative Cancer Research at MIT, West Roxbury, MA

Mass-spectrometry-based phosphoproteomics now profiles phosphorylation at proteome scale, yet converting site-level measurements into coherent, kinase-centered biology remains a persistent barrier to interpretation and action. *The Kinase Library* addresses this gap with the first-in-class, unbiased, experimentally characterized motif atlas of the human kinome, coupled to enrichment frameworks that translate phosphoproteomics data into quantitative maps of kinase activity. Rather than relying on heterogeneous annotations or heuristic rules, KL grounds inference in experimentally derived kinase-substrate relationships, providing a principled basis for comparative signaling analysis. The Kinase Library has broad utility across discovery and translational applications. It enables mechanism-of-action profiling for small molecules and combinations; delineates adaptive signaling and resistance trajectories; supports time-course and dose-response studies to resolve pathway dynamics; and stratifies models and patients in *low-N-high-D* (few samples with high dimensionality of data) settings where conventional statistics underperform. In clinical and preclinical contexts alike — cell lines, organoids, xenografts, and patient specimens — the Kinase Library delivers harmonized, interpretable kinase signatures that are readily integrated with genomic, transcriptomic, and phenotypic readouts to generate and prioritize actionable hypotheses. The novelty of the Kinase Library is twofold. First, scope and provenance: an experimental, unbaised atlas spanning the entire kinome, with comprehensive inclusion of the dark kinome. Second, operationalization: a unified enrichment paradigm that yields robust, rank-ordered kinase programs suitable for decisionmaking — whether the objective is target nomination, combination design, biomarker discovery, or comparative benchmarking across cohorts and studies. Looking forward, the Kinase Library is positioned to empower emerging frontiers in proteomics: single-cell and spatial phosphoproteomics; longitudinal “N-of-1” monitoring to guide therapy; cross-species translation for model selection; and cloudnative workflows that interoperate with community pipelines and public datasets. By elevating kinases from disparate lists of regulated sites to coherent, testable signaling hypotheses, the Kinase Library reframes what phosphoproteomics can deliver — shifting the field from descriptive measurement toward predictive, mechanism-guided intervention.

#1332 Selective targeting of the α3β4 nicotinic acetylcholine receptor by DISCO (dual interacting subunit complex) CAR T cells.

Patrick M. Schurch[1], Vincent P. Zecchino[1], Anna M. Giudice[1], Rebecca S. Kaufman[1], Evan Cresswell-Clay[1], Guillem Pascual-Pasto[1], Sydney L. Roth[1], Brendan C. McIntyre[1], Rawan Shraim[1], Amber K. Hamilton[1], Kush Parikh[1], Karina L. Conkrite[1], Khanh B. Trang[1], Grant P. Grothusen[1], David Groff[1], Pamela Mishra[1], Simona Lombardi[1], Tyler Skinner[1], Andrew D. Wells[1], Struan F. A. Grant[1], Daniel Martinez[1], Wei Li[2], Sharon J. Diskin[1], Kristopher R. Bosse[1]

[1]Division of Oncology, Children's Hospital Of Philadelphia, Philadelphia, PA,[2]Department of Medicine, University of Pittsburgh School of Medicine, Pittsburgh, PA

Developing effective chimeric antigen receptor (CAR) T cell therapies for pediatric solid tumors requires discovery of highly tumor-selective cell surface molecules. Using a multimodal immunotherapeutic target discovery platform, we identified a receptor composed of the nicotinic acetylcholine receptor subunits α3 and β4 as a new previously unrecognized immunotherapeutic target in neuroblastoma. *CHRNA3* (α3) and *CHRNB4* (β4) are robustly differentially overexpressed in neuroblastoma compared with normal tissues, driven by a super-enhancer upstream of the *CHRNA3/B4* locus on chromosome 15q25 that is occupied by neuroblastoma core regulatory transcription factors and physically engages both promoters. Neuroblastoma cells exhibit abundant α3 and β4 protein, which bind and assemble into a stabilized α3β4 complex displayed at high levels on the neuroblastoma cell surface. Functionally, genetic depletion of α3 also reduced β4 levels, induced mesenchymal cell state-associated marker expression, and increased proliferation and invasion in neuroblastoma cell line models. To therapeutically exploit this tumor-restricted α3β4 receptor expression, we engineered Dual Interacting Subunit COmplex (DISCO)-specific single chain variable fragments (scFvs) designed to recognize an epitope requiring simultaneous engagement of both α3 and β4 subunits of the α3β4 cell surface receptor. DISCO CAR T cells generated from these scFvs bound selectively to and were potently activated by the α3β4 receptor, but not either subunit individually. α3β4-targeted DISCO CAR T cells demonstrated potent and selective cytotoxicity across diverse neuroblastoma cell lines and three patient-derived xenograft (PDXs) models, significantly extending the survival of mice harboring PDXs with a range of α3 and β4 expression ($P < 0.05$). Beyond neuroblastoma, *CHRNA3* and *CHRNB4* are also highly expressed in small cell lung cancer (SCLC) and retinoblastoma, among several other tumors. The identical super-enhancer is associated with high levels of *CHRNA3* and *CHRNB4* in SCLC, suggesting similar mechanisms of tumor-driven overexpression. In an intraocular retinoblastoma xenograft model, a single intravitreal dose of α3β4-redirected DISCO CAR T cells achieved marked tumor control and significantly extended ocular survival ($P = 0.0015$), collectively showing disease-relevance and targetability beyond neuroblastoma. Together, these findings broaden the repertoire of actionable CAR T cell targets in pediatric and adult solid tumors by validating the α3β4 receptor, and more broadly the nicotinic acetylcholine receptor family, as bona fide immunotherapeutic candidates. Moreover, these studies demonstrate that CARs can be designed to recognize disease-relevant subunit configurations within multidomain surface receptors.

#1333 REST represses neuroendocrine transcriptional programs and enables anti-tumor immunity in SCLC.

Jackson P. Fatherree, Kelly Heard, Alex Doan, Joseph Hiatt, Daniel S. Hippe, Feinan Wu, Shivani Srivastava, David MacPherson

Fred Hutchinson Cancer Center, Seattle, WA

Small-cell lung cancer (SCLC) is a devastating neuroendocrine carcinoma in critical need of new therapeutic approaches. While a small subset of patients responds well to standard of care chemo-immunotherapy, durable responses are rare. Recent studies have revealed substantial transcriptional and functional heterogeneity, including the identification of multiple low-neuroendocrine SCLC subtypes, which we and others have linked to increased inflammation and response to immunotherapy. A major mediator of neuroendocrine state in SCLC is the transcription factor REST, which is a repressor of neuronal/neuroendocrine genes. While REST is typically silenced in SCLC, it is active in inflamed, low-neuroendocrine SCLC. However, links between REST and immune phenotypes in SCLC have been understudied. To explore the interplay between REST/neuroendocrine status, immune infiltration and response to clinically relevant therapies, we first generated an autochthonous mouse model of SCLC in the *Rb*/*p53*-null (RP) background with conditional REST expression (RP-REST). Transcriptionally, REST expression promoted a low-neuroendocrine SCLC phenotype with decreased expression of ASCL1 target genes compared to RP controls. In contrast, RP-REST tumors displayed a striking enrichment of antigen presentation and inflammatory response gene signatures, which correlated with increased infiltration of CD8+ T cells and F4/80+ macrophages, confirming that REST expression generates inflamed, low-neuroendocrine SCLC. We then overexpressed REST in a panel of murine SCLC cell lines derived from the RP mouse model and confirmed REST-driven repression of a neuroendocrine gene signature. Moreover, REST overexpression potentiated responses to interferon-γ resulting in increased MHC-I antigen presentation and phospho-STAT1. Using murine cell lines to generate syngeneic allografts in immunocompetent mice, we found that REST overexpression sensitized tumors to PD1 checkpoint blockade *in vivo*. Multiparameter flow cytometry reveals that these responses were associated with increased infiltration of activated CD8+ T cells, in addition to an expansion of M1 macrophages. Further, scRNAseq of the tumor compartment identifies a subset of cells in REST-expressing tumors with exceptionally high levels of inflammatory signaling, including secreted cytokines that may serve to recruit the abundant immune cells found in these tumors. Tumor heterogeneity is a critical variable in determining patient outcomes clinically. Here, we show that REST drives a low-neuroendocrine, inflamed SCLC phenotype in an autochthonous mouse model, which is corroborated by isogenic models showing reduced neuroendocrine markers, increased antigen presentation and sensitivity to immunotherapy.

#1334 Age related phenotypic changes in melanoma create a tumor vulnerability to ferroptosis.

Murilo Ramos Rocha[1], Yash Chhabra[2], Alexis Erasta Carey[3], Cheyenne M. Palm[1], Kevin Y. Zhang[3], Joanne Kotelawala[1], Elizabeth Harper[1], Fan Huang[1], Ashani Weeraratna[1]

[1]Johns Hopkins Bloomberg School of Public Health, Baltimore, MD,[2]Fox Chase Cancer Center, Philadelphia, PA,[3]Johns Hopkins University School of Medicine, Baltimore, MD

Aging is an independent poor prognostic factor for melanoma, the most aggressive form of skin cancer. Among the characteristics of aging, the accumulation of iron, polyunsaturated fatty acids, and reactive oxygen species can reshape the skin microenvironment and lead to changes in how melanoma progresses in the aged skin. Here, we investigate the impact of these characteristics of the aged tumor microenvironment and how phenotypic changes in melanoma cells create a tumor vulnerability to ferroptosis, a caspase-independent lipid peroxidation-mediated type of cell death, a possible therapeutic opportunity for older patients. KEGG pathway enrichment analysis on the proteomic data from young and aged mice shows an enrichment in the ferroptosis pathway. Through immunohistochemistry, we confirmed this pro-ferroptosis signature in the skin and using human aged dermal fibroblasts in vitro, observed that their secretome enhanced the cytoxicity of ferroptosis inducers such as RSL-3 (a GPX4 inhibitor) on melanoma cells. To understand how ferroptosis impacts tumor growth in young and aged mice, we used a syngeneic tumor model with intra-dermal administration of Yumm1.7 cells and the treatment with a lipid peroxidation inducer (imidazole ketone erastin - IKE). Although showing a general effect, IKE treatment significantly reduced tumor growth in older mice. Tumors from aged mice showed stronger immunoreactivity to 4-HNE (lipid peroxidation byproduct) when compared to young. This occurred in parallel with increases in AXL and Wnt5a staining. To comprehend the mechanisms driving this age-specific effect, we investigated if the phenotype switch that occurs in melanoma cells present in the aged TME would favor ferroptosis. Correlation between transcriptomic (TCGA-SKCM) and sensitivity data (CTD^2) confirmed that phenotype-switching markers, such as Wnt5a, showed a strong correlation with ferroptosis-related transcripts and an inverse correlation with ferroptosis resistance. Using a panel of melanoma cell lines with distinct Wnt5a levels, we confirmed this association and observed that critical regulators of lipid peroxidation are downregulated with high Wnt5a high: GPX4, AIFM2, and GCH1. The association between Wnt5a levels and ferroptosis regulators were confirmed experiments with the knock down or overexpression of Wnt5a. In a 3D in vitro model, RSL-3 inhibited the invasion of melanoma cells. These results indicate that ferroptosis modulation could be used to prevent metastatic dissemination and is a promising avenue for combined treatment with existing clinical strategies.

#1335 The ubiquitin E3 ligase $SCF^{Skk2/Cks1}$ complex: A critical node coupling cell cycle control, tumorigenesis, and lineage fidelity in small cell lung cancer (SCLC).

Saumen Karan[1], Hongling Zhao[2], Yingjiao Xue[2], Xinrui Zhang[1], Bang Hoang[3], Luc Girard[4], Benjamin Drapkin[4], John D. Minna[4], Edward L. Schwartz[5]

[1]Oncology, Albert Einstein College of Medicine, Bronx, NY,[2]Albert Einstein College of Medicine, Bronx, NY,[3]Orthopedic Surgery, Albert Einstein College of Medicine, Bronx, NY,[4]UT Southwestern Medical Center, Dallas, TX,[5]Oncology & Molecular Pharmacology, Albert Einstein College of Medicine, Bronx, NY

Background: Mutation and inactivation of *RB1* and *TP53* are required and sufficient to drive small cell lung cancer (SCLC) tumorigenesis, both clinically and in mouse genetic models. We previously reported that the knockout of the Skp2 component of the ubiquitin E3 ligase $SCF^{Skp2/Cks1}$ protected *Rb1/Trp53*-deficient mice from SCLC tumorigenesis but also increased the frequency of lung tumors with non-SCLC phenotypes. To explore this observation, we used a SCLC mouse model in which tumorigenesis was induced by CGRP-Cre-mediated deletions of *Rb1, Trp53*, and *Pten* (RPPt) in the neuroendocrine cells of the lungs. We crossed these to mice with either *Skp2* knockout or the knockin (KI) of a mutated, inactivated SCF^{Skp2} accessory protein, Cks1 ($Cks1^{N45R}$), that prevents the binding of p27 to SCF^{Skp2}.

Methods: We generated mouse lung cancer models using neuroendocrine cell-specific *Rb1; Trp53; Pten* triple-knockout mice with Skp2-KO or with $Cks1^{N45R}$ KI. Tumorigenesis, survival, and metastasis were monitored. Lung tumors were analyzed for neuroendocrine, SCLC subtype, squamous and other markers. Primary cell lines were established from lung tumors and characterized for lineage fidelity and sensitivity to cytotoxic and targeted drugs *in vitro* and *in vivo.*

Results: Skp2 mRNA was elevated in human SCLC cell lines and PDXs. In RPPt mice, both *Skp2*-KO and $Cks1^{N45R}$ KI reduced lung tumor and liver metastasis incidence, increased survival, and caused a striking phenotypic shift. RPPt mouse tumors were SCLC with neuroendocrine staining. In contrast, tumors in both Skp2-KO and $Cks1^{N45R}$ KI mice lacked neuroendocrine markers and had squamous cell histology with staining for Sox2, KRT5, and p63. RPPt lung tumors were $ASCL1^{+}$ and $YAP1^{-}$. Conversely, the Skp2-inactivated tumors were $ASCL1^{-}$ and $YAP1^{+}$ and retained SMARCA4 expression. Cell lines derived from the RPPt lung tumors grew more rapidly and were more sensitive to cisplatin and etoposide than were the lung tumor cells from the RPPt-$Cks1^{N45R}$ KI mice. The RPPt lung tumor cells were also more sensitive to growth inhibition by the $SCF^{Skp2/Cks1}$ inhibitors C1 and pevonedistat and the CDK1/2/5/9 inhibitor dinaciclib. Finally, pevonedistat inhibited RPPt tumor growth *in vivo*.

Conclusion: These findings are consistent with the hypothesis that the *Rb1/Trp53*-deficient SCLC neuroendocrine phenotype is not a fixed feature but can vary with the presence of other oncogenic drivers, and document $SCF^{Skp2/Cks1}$ as one such driver. This could reflect an early, deterministic lineage redirection toward a YAP1-high, SMARCA4-intact, non-neuroendocrine phenotype. $SCF^{Skp2/Cks1}$ mediates lung cancer heterogeneity, plasticity and sensitivity to standard cytotoxic and targeted drugs. Furthermore, the *in vivo* efficacy of the neddylation inhibitor pevonedistat highlights SCF^{Skp2} complex assembly as a promising therapeutic target for SCLC.

: Integrative Computational Approaches
Minisymposium

#1292 Multimodal modeling of detailed cancer subtypes and molecular features from >60,000 patients with co-registered H&E images and clinical tumor sequencing.

K. M. Boehm, M. Darmofal, A. Patha, A. Aukmerman, R. Lim, E. Seffar, T. Pollard, N. Rekhtman, J. Chang, J.-F. Chen, A. Kohli, D. Moore, J. Gao, G. Asimomitis, A. Begum, H. Al-Ahmadie, M. F. Berger, N. Schultz, S. P. Shah, F. Sanchez-Vega;
Memorial Sloan Kettering Cancer Center, New York, NY

Background: Optimal oncology treatment depends upon detailed cancer subtyping and molecular characterization. However, due to small datasets, prior digital pathology work often grouped detailed histologic subtypes by anatomy. Furthermore, the role of digital pathology as a complement to DNA sequencing rather than a surrogate remains underexplored. This study develops machine learning for H&E whole-slide images (WSIs) to model detailed cancer subtypes, identify phenotypically-associated biomarkers, and evaluate the added information of digital pathology to clinical tumor sequencing.
Methods: A pan-cancer cohort of 367,535 WSIs matching clinical sequencing data from 62,460 patients across 163 OncoTree subtypes was curated. The first model, Aeon, used a knowledge graph and transformer to classify subtypes from WSIs using self-supervised features. The second model, Paladin, tested the association of molecular features with tumor histopathologic features, conditioned on detailed tumor subtype. This conditioning critically allows the model to identify more detailed phenotypic subtypes than already clinically established. Two independent test sets were used.
Results: Aeon achieved AUROC 0.992 across 163 detailed subtypes, outperforming a genomics-based classifier for 151 subtypes. Reclassified cancers of unknown primary (CUP) exhibited expected prognostic and genomic associations (corrected log-rank $p<0.05$, corrected Fisher's $p<0.05$). For biomarker inference (single nucleotide variants, pathway-level alterations, and higher-order features), Paladin achieved AUROC ≥0.80 for 165 (5%) of 3,541, improving on benchmarks. Importantly, the model also identified phenotype associations for functional states of KEAP1 variants of unknown significance (VUS) in lung adenocarcinoma; VUS cases with H&E-inferred functional significance exhibited shorter overall survival (OS; log-rank $p<0.01$). For STK11, discordant H&E phenotyping and sequencing identified cases with occult phenocopying, supported by immunohistochemistry (H&E score higher for cases with STK11 loss on IHC; Mann-Whitney U (MWU) $p<0.01$) and STK11 RNA abundance (MWU $p<0.01$). This phenocopying had prognostic consequences: wildtype (WT) cases with STK11-mutant phenotype on H&E formed an intermediate prognostic group between STK11-mutant cases and WT cases without STK11-mutant phenotype (log-rank $p=0.01$).
Conclusions: Digital pathology effectively classifies 163 granular tumor subtypes using H&E WSIs, advancing an order of magnitude from the prior state of the art, outperforming a genomics classifier, and clarifying CUP diagnoses. We further established the role of digital pathology in complementing DNA sequencing via VUS annotation and identification of phenocopying, with molecular validation of these phenotypes and prognostic implications.

#1293 A multimodal AI framework integrating spatial omics and radiomics for recurrence prediction in glioblastoma.

J. Louw[1], T. N. Nandi[2], E. Calabrese[1], R. E. Mclendon[3], Y. Sun[1], J. Hickey[1], J. Jepson[1], A. Corcoran[1], K. Zhang[1], R. K. Madduri[2], M. Khasraw[4];

[1]Duke University, Durham, NC, [2]US Department of Energy, Chicago, IL, [3]Duke University Medical Center, Durham, NC, [4]Duke Cancer Institute, Durham, NC

Introduction/Rationale: Glioblastoma (GBM) has a dismal prognosis, yet times to recurrence vary substantially. We integrated multimodal data to identify tumor- and microenvironment-level features associated with timing of recurrence.
Methods: Primary GBMs tumors with documented time to recurrence were analyzed by Xenium spatial transcriptomics (ST). ST data were processed with Seurat, manually annotated, and organized into five reproducible spatial niches. Differential expression was performed within tumor-dense niches comparing that shortest recurrence (SR) and those with the longer time to recurrence (LR). ST embeddings were extracted using the graph attention network based Novae foundation model (FM), while embeddings from the pathology whole-slide Hematoxylin and Eosin (H&E) images were obtained using the vision transformer-based UNI FM and reviewed by a neuropathologist. CODEX spatial proteomics (SP) embeddings will be generated using the vision transformer-based KRONOS FM, and pre-operative MRI features will be incorporated via a PyRadiomics pipeline. Multimodal embeddings from all platforms are being used to train an interpretable tree-based survival model predicting time to recurrence.
Results: ST analyses show that there are marked microenvironmental differences between SR and LR tumors. SR tumors showed malignant-cell infiltration across nearly all spatial niches, indicating disruption of immune and stromal architecture. LR tumors retained distinct vascular, immune, and endothelial-rich regions, reflecting maintained compartmentalization; H&E review confirmed these patterns. Malignant-cell composition also diverged: SR tumors were dominated by AC-like cells (83%) with minimal MES-like (1%), OPC-like (1%), and NPC-like (15%) states. LR tumors were more heterogeneous, with balanced AC-like (38%) and MES-like (36%) fractions and increased OPC-like (16%) and NPC-like (9%) representation. Pseudo-bulk differential expression identified 367 genes (313 up in SR; 54 in LR). SR tumors overexpressed CD38, HLA-DQA1, CX3CR1, TMEM119, and P2RY12, indicating microglial activation and inflammatory signaling. LR tumors upregulated POSTN, LOX, ACKR1, VEGFA, and CAV1, consistent with extracellular matrix organization, angiogenesis, and vascular remodeling. SR GBM exhibits widespread tumor infiltration and immune activation, whereas LR tumors preserve structured vascular-immune niches and more diverse malignant-cell states.
Conclusion: ST, SP, pathology slide H&E imaging, and MRI radiomics provides complementary insights into the cellular and microenvironmental determinants of GBM recurrence. While multimodal model training involving embeddings from all the modalities is ongoing, the preliminary findings highlight the importance of spatial organization of the tumor-immune-vascular interface as a key determinant of recurrence timing.

#1294 Deciphering single-cell heterogeneity and cellular ecosystem dynamics during prostate cancer progression.

F. Zhao[1], H. Zeng[2], J. Zeng[3], C. Chen[1], X. Zhao[1], T. Zhang[1], K. Wang[1], G. Sener[1], J. Liu[4], G. V. Thomas[1], R. C. Sears[1], J. J. Alumkal[5], A. Moran[6], G. B. Mills[7], E. S. Eksi[7], J. Zheng[2], P. S. Nelson[8], Z. Xia[1];
[1]Oregon Health & Science University, Portland, OR, [2]Xinqiao Hospital, Chongqing, China, [3]The University of Texas MD Anderson Cancer Center, Houston, TX, [4]Urologic Surgery Center, Xinqiao Hospital, Chongqing, China, [5]Rogel Cancer Center, Ann Arbor, MI, [6]OHSU, Portland, OR, [7]OHSU Knight Cancer Institute, Portland, OR, [8]Fred Hutchinson Cancer Center, Seattle, WA

Prostate cancer (PC) progresses from benign epithelium through pre-malignant lesions, localized tumors, metastatic dissemination, and castration-resistant stages, with some cases exhibiting phenotype plasticity under therapeutic pressure. However, high-resolution insights into how cellular phenotypes and ecological interactions shift across these successive stages remain incomplete. Here, we present the Prostate Cancer Cell Atlas (PCCAT) by integrating ~710,000 single cells from 197 human samples covering a spectrum of tumor stages. By further incorporating bulk transcriptomic cohorts, spatial transcriptomics, and experimental validations, this comprehensive analysis dissects the multicellular landscape of PC and identifies key epithelial, stromal, and immune programs associated with disease progression. We highlight a dynamic and heterogeneous continuum of malignant and non-malignant epithelial states, and uncover several cell states strongly linked to aggressive progression and poor prognosis, including lineage plasticity-like malignant cells, neuroendocrine tumor cells, matrix cancer-associated fibroblasts (mCAFs), and SPP1-expressing macrophages (SPP1+ Mph). Furthermore, we identify shared immune-suppressive states enriched in advanced disease, including proliferative T cells, activated regulatory T cells, exhausted $CD8^+$ T cells, and SPP1+ Mph, highlighting convergent microenvironmental mechanisms of immune evasion. Among these, SPP1+ Mph emerge as a key immunosuppressive population, progressively accumulate along PC progression, exhibiting an M2-like immunosuppressive phenotype, associating with bone metastasis, and spatially colocalizing with mCAFs at the tumor-stroma interface in NEPC. Functionally, SPP1 blockade restrains bone metastatic progression and alleviates cancer-induced bone pain by reprogramming tumor-associated macrophages and reshaping CAF and $CD8^+$ T-cell phenotypes. Lastly, by integrating PCCAT with spatial transcriptomics, we identify distinct spatial cellular neighborhood (CNs) that transition from epithelial-dominated to stroma-enriched ecosystems along PC evolution. Among tumor-associated CNs, CN1 reflects neuroendocrine and lineage-plasticity features, whereas CN4 captures aggressive luminal malignant programs. Among microenvironmental CNs, mCAF-enriched CN7 expands with tumor progression and predicts adverse prognosis, while iCAF-enriched CN8 diminishes and associates with favorable outcome. Notably, a CN7-CN8-derived ecosystem index robustly predicts biochemical recurrence across multiple patient cohorts. Overall, our study provides a high-resolution reference of PC cellular ecosystems and reveals the dynamic cell states, spatial niches, and immunoregulatory interactions that shape disease progression, offering mechanistic insights and therapeutic opportunities.

#1295 Deep-learning profiling of regulatory somatic variants across clonal cancer evolution.

K. Sokolova, V. N. Kristensen, O. G. Troyanskaya;
Princeton University, Princeton, NJ

Somatic noncoding mutations are abundant in cancer genomes, yet their regulatory functional consequences remain poorly understood. To address this gap, we generated a pan-cancer atlas of variant regulatory effects by profiling >35M SNVs within +/-20 kb of transcription start sites across more than 8,000 TCGA samples. Chromatin impact was predicted with the Sei deep-learning model (>20,000 features across 40 sequence classes), and clonal architecture was inferred with PyClone-VI, enabling genome-wide, evolution aware annotation of proximal regulatory alterations. We then aggregated these variant-level functional predictions into gene-level and patient-level representations of regulatory dysregulation. Despite comparable mutation counts near COSMIC Tier1/2 and non-COSMIC genes, the atlas revealed substantially higher predicted regulatory impact in promoter-proximal mutations, uncovering a noncoding functional dimension not detectable from burden alone. Aggregating these predicted effects into a personalized somatic dysregulation representation across COSMIC Hallmark genes produced a patient-level promoter-proximal regulatory effect score. In a multivariable Cox model of progression-free interval stratified by cancer type and adjusted for log1p(FGA), HRD score, non-silent mutations per Mb, and age at diagnosis, this regulatory score was a strong and independent predictor of adverse progression (HR = 1.10, 95% CI 1.04-1.15, $P < 0.005$), whereas noncoding mutation count contributed no additional information. Partitioning regulatory burden by evolutionary timing revealed distinct processes: clonal promoter-proximal disruption consistently predicted worse pan-cancer outcomes and showed stronger within-cancer associations, whereas subclonal burden was prognostic only in specific cancers. For example, subclonal promoter-proximal disruption within Hallmark genes was significantly associated with progression in Uterine Corpus Endometrial Carcinoma (HR = 1.36, 95% CI 1.10-1.70, $P = 0.01$), possibly indicating late-arising regulatory programs contributing to tumor progression. Finally, deep-learning regulatory sequence classes mapped to tissue-specific vulnerabilities: lower-grade glioma showed disproportionate impact from the E3 brain/melanocyte enhancer class, whereas sarcoma was most strongly associated with PC4 polycomb/bivalent stem-cell-linked disruption. Together, these results show that functional promoter-proximal disruption, not mutational load, captures clinically relevant noncoding dysregulation, shaped by context-specific and evolution-linked regulatory programs. This atlas provides a scalable foundation for integrating noncoding regulatory functions into prognostic modeling and will be made available to the research community.

#1296 Integrated single cell spatial multi-omics landscape of WHO grades 2-4 diffuse gliomas identifies locoregional metabolomic correlates of glioma plasticity and proliferation.

Yanxia Ma[1], Shamini Ayyadhury[2], Sanjay Singh[1], Yashu Vashishath[3], Cagri Ozdemir[3], Keziah Liebenberg[4], Trevor McKee[2], Nhat Nguyen[1], Akshay V. Basi[5], Duncan Mak[5], Javier A. Gomez[5], Jason T. Huse[6], Sana Noor[2], Sharon Wariko[2], Dan Winskowski[7], Regan Baird[8], Jeffrey S. Weinberg[1], Frederick F. Lang[1], Jared K. Burks[5], Livia S. Eberlin[9], Serdar Bozdag[3], Erin Seeley[10], **Chibawanye I. Ene**[1]

[1]Department of Neurosurgery, The University of Texas MD Anderson Cancer Center, Houston, TX,[2]Astraea Bio LLC, Tomball, TX,[3]University of North Texas, Denton, TX,[4]Baylor College of Medicine, Houston, TX,[5]Department of Leukemia, The University of Texas MD Anderson Cancer Center, Houston, TX,[6]Department of Anatomical Pathology, The University of Texas MD Anderson Cancer Center, Houston, TX,[7]Visiopharm A/S, 2970 Horsholm, Denmark,[8]Visiopharm, 2970 Horsholm, Denmark,[9]Division of Surgical Oncology, Baylor College of Medicine, Houston, TX,[10]Department of Chemistry, The University of Texas at Austin, Austin, TX

Introduction: Diffuse infiltrating gliomas are aggressive tumors of the central nervous system driven by intra-tumoral heterogeneity and aberrant normal-tumor cell-cell interactions. Grade-specific and locoregional metabolic dependencies associated with aberrant transcriptional cell-states linked to treatment resistance and proliferation of gliomas remain elusive. We hypothesize that identifying metabolic surrogates of plasticity- and treatment-resistant glioma transcriptional cell states at the recurrence-prone tumor edge will lead to new therapeutic strategies for gliomas.

Methods: We applied spatial transcriptomics (stRNAseq), imaging mass cytometry (IMC) and mass spectrometry imaging (MSI; metabolites, peptides and glycans) to the core and edge tumor tissue from patients with World Health Organization (WHO) grades 2-4 diffuse infiltrating gliomas including isocitrate dehydrogenase (IDH) mutant (mut) oligodendrogliomas (WHO Grades 2 and 3, n= 5) and IDH wildtype (wt) astrocytomas including 'anaplastic' astrocytoma (prior 2016 WHO histological grade 3, n = 3) and IDHwt glioblastoma (GBM, WHO grade 4). To determine if any differentially expressed genes between the core and edge of IDHwt GBM influenced overall survival (OS), we analyzed the association between OS and gene expression levels (low vs. high) in IDHwt GBM samples from the cancer genome atlas (TCGA). To identify grade specific and tumor edge unique metabolites that correlate with plasticity- and therapy-resistance-associated glioma transcriptional cell states and proliferation (Ki-67^{+}), we integrated data from stRNAseq, IMC and MSI within each diffuse glioma grade.

Results: High expression of Neuronatin (NNAT) and Heparin Sulfate-Glucosamine 3-Sulfotransferase 2 (HS3ST2) mRNA, which were significantly over-expressed in the IDHwt GBM edge relative to the core, were associated with significantly worse OS (NNAT^{hi} HR=1.8, *p-value= 0.0043* and HS3ST2^{hi} HR=2, *p-value=0.0096).* Integration of stRNA seq and MSI-derived metabolite expression identified edge unique metabolites overlapping with glioma transcriptional cell states and proliferative states across gliomas profiled.

Conclusion: This comprehensive pan-diffuse infiltrating glioma multi-omics study could serve as a resource for not only uncovering region-specific metabolic signatures of transcriptionally defined cell states across WHO 2-4 diffuse gliomas, but also guide surgical extent of resection in real time, by using metabolic signatures as surrogates for plasticity associated transcriptional cell states and proliferation especially in the infiltrative and non-enhancing portion of the glioma edge.

#1297 ADTnorm enables scalable and interpretable single cell proteomics integration across technologies for incorporating historical cancer data.

T. Le[1], Z. Luo[2], Y. Yan[3], **Y. Zheng**[1];

[1]UT MD Anderson Cancer Center, Houston, TX, [2]Yale University, New Haven, CT, [3]Beijing University of Technology, Beijing, China

CITE-seq enables paired measurement of surface protein and mRNA expression in single cells using antibodies conjugated to oligonucleotide tags. Due to the high copy number of surface protein molecules, sequencing antibody-derived tags (ADTs) allows for robust protein detection, improving cell type identification. However, variability in antibody staining leads to batch effects in the ADT expression, obscuring biological variation, reducing interpretability, and obstructing cross-study analyses. We present ADTnorm (https://github.com/yezhengSTAT/ADTnorm), a normalization and integration method designed explicitly for ADT abundance. Benchmarking against 14 existing scaling and normalization methods, we show that ADTnorm accurately aligns populations with negative- and positive-expression of surface protein markers across 13 public datasets, effectively removing technical variation across batches and improving cell-type separation. ADTnorm enables efficient integration of public CITE-seq datasets, each with unique experimental designs, paving the way for atlas-level analyses. Beyond normalization, ADTnorm includes built-in utilities to aid in automated threshold-gating as well as assessment of antibody staining quality for titration optimization and antibody panel selection. Beyond CITE-seq, single-cell proteomics data are increasingly generated from diverse platforms, including flow cytometry, CyTOF, multimodal assays such as scCUT&Tag-pro, and spatial methods like CODEX. Each technology introduces distinct data characteristics, creating challenges for cross-platform integration. Harmonizing these heterogeneous datasets is essential for leveraging historical cancer data and linking proteomic profiles to clinical outcomes. To address this, we incorporate large language model APIs into ADTnorm for automated parameter tuning tailored to each technology's data characteristics, improving landmark identification and alignment across modalities. We further developed an online platform (https://pvdetector.streamlit.app/) that provides free computational resources for proteomics analysis, with the option to install locally or deploy on servers for enhanced scalability (https://github.com/letian0102/PVdetector). While integration remains grounded in interpretable statistical models, the use of LLMs enables adaptive, data-driven parameter optimization, extending ADTnorm's utility across a broad spectrum of proteomic technologies.

#1298 Structure-sequence integration for peptide:MHC class II binding prediction using AI foundation models (AlphaFold 3 and ESM2).

K. Lahouel[1], M. Mulazimoglu[1], J. Soria-Bustos[1], K. Bates[1], E. Kelley[2], L. Woods[3], K. Upadhyaya[1], G. J. Acevedo[4], S. Penisson[1], M. Munini[1], E. Variani[5], M. E. Feeney[4], J. A. Altin[2], C. Tomasetti[1];

[1]TGen (The Translational Genomics Research Institute), Phoenix, AZ, [2]TGen North (The Translational Genomics Research Institute), Flagstaff, AZ, [3]TGen (The Translational Genomics Research Institute), Phoenix, AZ, [4]University of California San Francisco, San Francisco, CA, [5]Google Research, Mountain View, CA

Background:
Accurate prediction of CD4 T cell epitopes is essential for vaccine design and immunotherapy development but remains challenging due to MHC class II polymorphism and the complexity of antigen presentation. We present a foundation-model-based framework that integrates structural representations from AlphaFold 3 (AF3) and sequence embeddings from ESM2 within a graph neural network (GNN) to predict peptide:MHC II binding.
Model and Experimental Procedures:
For each peptide-MHC II complex, AF3 was used to generate a 3D structural model, from which we constructed a residue-level graph where edges represent geometric proximity. Node features combined AF3-derived spatial descriptors with contextual embeddings from ESM2 corresponding to each amino-acid token in the peptide sequence. The hybrid GNN was trained on experimental data from a multiplexed MHCII-PepSeq assay, a high-throughput platform that directly measures binding of thousands of synthetic peptides across diverse MHC class II molecules (~52,000 non-binders and 633 binders). The model was evaluated on an independent held-out test set encompassing multiple HLA alleles.
Results:
The AF3 + ESM2 GNN achieved an AUC of 0.782 (95% CI: 0.751-0.813), matching exactly the performance of NetMHCIIpan 4.3, a leading model for peptide:MHC II binding prediction on the Immune Epitope Database (IEDB) benchmark—despite being trained on a dataset that is orders of magnitude smaller. A combined ensemble of NetMHCIIpan with the AF3 + ESM2 model further improved performance, reaching an AUC of 0.810. The AF3-only GNN yielded an AUC of 0.775, indicating that ESM2 sequence embeddings may contribute complementary contextual information that enhances prediction accuracy.
Conclusions:
By unifying structure- and sequence-based protein foundation models, our approach achieves state-of-the-art, data-efficient prediction of peptide:MHC II binding. Comparable in accuracy to the gold-standard NetMHCIIpan while trained on orders-of-magnitude smaller datasets, this framework enables scalable and interpretable modeling of antigen presentation. Such structure-informed prediction can accelerate the discovery of CD4 T-cell epitopes relevant to neoantigen identification, vaccine development, and TCR/CAR-T engineering, where precise understanding of peptide:MHC recognition is essential. More broadly, our findings highlight the potential of foundation models to bridge molecular immunology and therapeutic design by providing generalizable, low-data solutions to complex antigen-presentation problems.

: Liquid Biopsy Frontiers: ctDNA, Fragmentomics, and MRD to Guide Precision Oncology Minisymposium

#1310 Serial plasma comprehensive genomic profiling detects therapy resistance and guides management of metastatic non-small cell lung cancer.

W. Bowers[1], M. Conroy[1], J. Wehr[1], V. V. Altiery De Jesus[1], A. Balan[1], S. Scott[1], B. Levy[1], K. A. Marrone[1], V. K. Lam[1], J. Feliciano[1], C. Hann[1], A. Pabani[1], J. Naidoo[2], J. R. Brahmer[1], P. M. Forde[1], J. C. Murray[1], V. Anagnostou[1];
[1]Johns Hopkins University, Baltimore, MD, [2]Beaumont RCSI Cancer Centre, Dublin, Ireland

Introduction: Although plasma comprehensive genomic profiling (pCGP) shows significant potential as a minimally invasive alternative to tissue genotyping in non-small cell lung cancer (NSCLC), its precise clinical utility remains insufficiently studied. To bridge this gap, we conducted a single-center retrospective study of 718 patients with NSCLC who had undergone pCGP in our institution from 2015 through 2022.
Methods: Integrated clinical and genomic data were extracted from the Precision Medicine Analytics Platform as part of a standard workflow of the Johns Hopkins Lung Cancer Precision Medicine Center of Excellence. Fixed gene panel hybrid capture next-generation sequencing (Guardant 360, n = 572 samples and Guardant 360CDx, n = 246 samples) data were retrieved, followed by variant characterization and annotation by an ensemble approach.
Results: Across 718 patients with 818 instances of pCGP, including 79 (11%) patients with serial pCGP, liquid biopsies uniquely informed management in 92 (13%) patients. This primarily occurred when tissue testing was not possible (44%), although pCGP also contributed to clinical decision-making as an adjunct to tissue testing, by improving turnaround time, and by detecting plasma-only mutations. In a subset analysis of first instance of pCGP obtained at the time of diagnosis (n = 427), patients with undetectable ctDNA had significantly prolonged overall survival (OS) (log rank $p < 0.0001$), with similar results when patients were classified as ctDNA undetectable, 1-2 mutations, or 3 or more detected mutations (log rank $p < 0.0001$). Importantly, receipt of genotype-matched therapy informed by pCGP was associated with a significant improvement in OS (log rank $p < 0.0001$). Focusing on 214 patients with *EGFR* mutant (*EGFR*m) NSCLC, pCGP uniquely guided patient management in 28% of cases, benefiting both newly diagnosed patients and those on their second or third iteration of genotyping. Among patients progressing on EGFR tyrosine kinase inhibitors (TKI), 31 (22%) had actionable pCGP findings, of whom 18 (58%) were matched to targeted therapy. pCGP captured differential on-target and off-target resistance genomic alterations based on TKI line of therapy and type of TKI (first or second generation vs. third generation). Mutations in *PIK3CA* most commonly emerged after first-line therapy with third generation TKI, while mutations in the RAS pathway were more frequently detected after third-line therapy, highlighting differential activation of resistance pathways.
Conclusions: Serial pCGP captures actionable genomic alterations and the emergence of drivers of therapy resistance, enabling longitudinal care and timely, effective interventions for patients with NSCLC.

#1311 Feasibility of plasma ctDNA for detecting brain metastasis-specific alterations in lung cancer.

L. P. Stabile[1], K. Shaverdashvili[2], P. H. Rumde[2], X. Wu[3], A. Gaither Davis[2], P. O. Zinn[1], A. Habib[2], N. N. Gecici[2], R. Zhang[4], P. Du[4], S. Jia[4], Y. Huang[4], G. Sica[5], T. F. Burns[6];

[1]UPMC Hillman Cancer Center, University of Pittsburgh, Pittsburgh, PA, [2]University of Pittsburgh, Pittsburgh, PA, [3]University of Pittsburgh and Tsinghua University, Pittsburgh, PA, [4]Predicine, Hayward, CA, [5]Winship Cancer Institute, Emory University, Atlanta, GA, [6]James Cancer Hospital Solove Research Institute, The Ohio State University, Columbus, OH

Brain metastases (BM) are a frequent and devastating complication of non-small cell lung cancer (NSCLC). Molecular divergence between primary NSCLC and BM is common, highlighting the need for non-invasive approaches to detect BM-specific genomic alterations that could guide precision therapy. To address this, we evaluated the feasibility of circulating tumor DNA (ctDNA) to identify BM-specific or enriched alterations by analyzing matched pre- and post-craniotomy plasma samples and corresponding BM tissue. Twenty-eight metastatic NSCLC BM patients undergoing craniotomy were enrolled. Peripheral blood was collected pre-surgery (Day 0, P1) and post-surgery (≥ 8 days, P2) before systemic therapy initiation, and BM tissue was collected during surgery. Following exclusion of 4 patients with insufficient viable tumor, samples from 24 patients were sequenced using the PredicineCARE NGS assay, and data were analyzed using DeepSea, Predicine's proprietary bioinformatics pipeline. After excluding cases with a tumor fraction <0.005 or failed QC, we analyzed 13 complete sets (BM with matched P1/P2 plasma), 3 partial sets (BM with P1 plasma only) and 7 BM tissue-only samples (23 BM samples total). The most frequently detected BM alterations were *TP53* (22/23, 96%), *PIK3CA* (12/23, 52%), *RB1* deletion (del)/mutation (mut), *EGFR* amplification (amp) and *CDKN2A/B* del (each in 11/23, 48%). Additional alterations were found in *BRCA1/2* (10/23, 44%), *MYC* (9/23, 39%), *NF1* (8/23, 35%), and *PTEN* or *BAP1* (7/23, 30%). *MET* amp, *AKT3* amp, or *KRAS* mut were each found in 6/23 patients (26%). Targetable alterations, including *EGFR* (ex19del, L858R, ex20ins), and *KRAS* (G12C) were each detected in 3 patients (13%). While many alterations were shared between BM tissue and the two plasma samples, complete loss of an alteration in post-craniotomy P2 plasma that was detected in both P1 and BM was rare, occurring in only 1/13 patients (*EGFR* amp). However, a decrease of >50% variant allele frequency was seen for multiple variants in an additional 2/13 patients despite similar tumor fractions, suggesting that detecting ctDNA shed from BM is possible. Notably, *NF1*, *KEAP1* and *CD274* del and *ERBB2* amp was only detected in BM and only 1/6 *MET* amps were detected in plasma. Interestingly, one patient who received post-craniotomy brain radiation therapy (RT) one day before P2 collection exhibited new *MET* and *MYC* amps and *TP53* del in P2 plasma. These variants were initially detected in BM but absent in P1, suggesting that RT may enhance tumor DNA shedding. These findings indicate that reliable ctDNA detection of BM-specific alterations may require assays with greater sensitivity, as well as optimized sample collection timing, such as post-RT, to improve yield and clinical utility. To our knowledge, this is the only study that includes pre-/post-craniotomy samples along with matched BM tissue to directly assess the ability of ctDNA to detect BM-specific alterations.

#1312 *AXL* mRNA overexpression in CTCs as a new potential liquid biopsy biomarker in NSCLC.

A. Ntzifa[1], E. Themistokli[1], A. Strati[1], M. Zavridou[1], E. Tsaroucha[2], A. Sfika[3], A. Psyrri[4], A. Kotsakis[5], V. Georgoulias[6], **E. Lianidou**[1]; [1]Analysis of Circulating Tumor Cells, Lab of Analytical Chemistry, Department of Chemistry, National and Kapodistrian University of Athens, Athens, Greece, [2]7th Department of Pulmonary Diseases, "Sotiria" General Hospital of Athens, Athens, Greece, [3]Oncology Unit, 2nd Department of Surgery, Aretaieio Hospital, Medical School, University of Athens, Athens, Greece, [4]Medical Oncology Unit, 2nd Department of Internal Medicine, "Attikon" General Hospital of Athens, Athens, Greece, [5]Department of Medical Oncology, University General Hospital of Larissa, Larissa, Greece, [6]First Department of Medical Oncology, Metropolitan General Hospital, Athens, Greece

Background: AXL is a receptor tyrosine kinase that is over-expressed in NSCLC. It is involved in epithelial-to-mesenchymal transition (EMT), cell survival, invasion, metastasis, and resistance to epidermal growth factor receptor (EGFR) tyrosine kinase inhibitors (TKIs) and immune checkpoint inhibitors (ICIs). Nowadays, clinical trials are investigating the efficacy of AXL-inhibitors such as bemcentinib, that has already received US FDA fast-track designation for the treatment of advanced or metastatic NSCLC combined with a PD-L1 inhibitor. In this study we evaluated *AXL* mRNA expression in circulating tumor cells (CTCs) isolated at different time points from two groups of NSCLC patients: a) under osimertinib treatment and b) under immunotherapy.

Materials and Methods: Group A: Peripheral blood (PB) (15mL) was collected from 39 *EGFR*-mutant NSCLC patients before osimertinib (n=39), after one cycle of treatment (n=31), every 3 months during therapy (n=81) and at progression of disease (PD) (n=30). Group B: PB (10mL) was collected from 116 NSCLC patients before immunotherapy (n=116), after 3 or 4 cycles of treatment with ICIs (n=71) and at PD (n=10). CTCs were enriched using the Parsortix^{TM} system (CellBxHealth plc, UK) and further harvested in Trizol reagent, followed by extraction of total RNA and cDNA synthesis. An RT-qPCR assay was developed and analytically validated for the detection of *AXL* mRNA expression in CTCs using the COBAS z480 system (Roche). PB from healthy donors (n=46) was processed in the same way and used as control group for the estimation of overexpression, based on the $2^{-\Delta\Delta Ct}$ approach.

Results: In Group A (*EGFR*-mutant NSCLC), *AXL* mRNA overexpression in CTCs was detected in 5/39 (12.8%) patients' samples before osimertinib, in 5/31 (16.1%) after one cycle of treatment, in 7/81 (8.6%) samples during treatment and in 4/30 (13.3%) samples at PD. In Group B (treatment with ICIs), *AXL* mRNA overexpression in CTCs was detected in 7/116 (6.0 %) patients prior to treatment, in 8/71 (11.3%) after 3 or 4 cycles of treatment, while no *AXL* transcripts were detected in CTCs at PD.

Conclusions: This is the first time that *AXL* overexpression is detected in CTCs of NSCLC patients undergoing immunotherapy. Our results indicate that NSCLC patients with overexpression of *AXL* in CTCs could benefit from combination therapies with AXL-inhibitors to either overcome resistance to targeted therapies or enhance immune responses. The role of *AXL* as a potential biomarker and therapeutic target in advanced NSCLC needs to be further confirmed through larger clinical studies including liquid biopsy approach.

#1313 Circulating tumor cell (CTC) informed pipeline for rapid personalization of synergistic cytokine-armed CAR-NK cell therapy in PDAC.

Y. Zou[1], M. Tarannum[2], S. Fouladdel[1], Y. Zhang[1], N. Peterson[1], V. Sahai[1], D. Nagrath[1], R. Romee[2], S. Nagrath[1];
[1]University of Michigan, Ann Arbor, MI, [2]DFCI/Harvard Medical School, Boston, MA

Introduction: Pancreatic ductal adenocarcinoma (PDAC) remains highly lethal due to treatment resistance heterogeneity and an immunosuppressive microenvironment, necessitating personalized therapeutics. CAR-NK cell therapy shows promise but faces challenges including target identification in heterogeneous tumors and rapid exhaustion within the TME. Cytokine-armed CAR-NK cells that self-secrete immune-activating cytokines may overcome these barriers. Circulating tumor cells (CTCs) offer dynamic insights into tumor biology, including mutation and protein profiles, enabling personalized CAR target identification. We present a pipeline integrating CTC-informed antigen selection with cytokine-armed CAR-NK therapy, leveraging minimally invasive CTC sampling and allogeneic CAR-NK potential for rapid, adaptive personalized immunotherapy.
Method & Result: Using label-free CTC isolation, we performed multi-omics analysis and identified mucin4 (MUC4) and mesothelin (MSLN), two highly prevalent PDAC antigens, in CTCs across patients (n=13; 6 metastatic, 7 localized). MUC4+CTCs were exclusively detected in 67% of metastatic patients, whereas 92% of all patients exhibited MSLN+CTCs, revealing the potential complementary coverage and enabling patient stratification for dual MUC4&MSLN CAR-NK treatment. We generated anti-MUC4 and anti-MSLN CAR-NK cells showing robust cytotoxicity against target-matched PDAC cell lines.To enhance efficacy, we tested IL-12 (for NK activation) and IL-15 (for NK proliferation) armed CAR-NK cells individually and combined. Anti-tumor efficiency improved in all cytokine-armed CAR-NK cells in short-term assays with no advantage of dual versus single cytokine arming. However, synergistically armed CAR-NK cells displayed drastically higher tumor-specific interferon-γ secretion post 18-hour exposure (4208 pg/mL vs 244 pg/mL for tumor-stimulated vs resting NK) compared to single cytokines (1819 & 252 pg/mL for IL-12 & IL-15), indicating sustained activity. In serial killing assays with repeated 72-hour tumor exposures at 2:1 NK: tumor ratio, unarmed CAR-NK lost efficacy by round 2, IL-15 by round 3, IL-12 by round 4, while synergistically armed CAR-NK sustained cytotoxicity through six rounds (16 days). Suggesting cytokine synergy is not only more physiologically relevant than solo-cytokine, but also more effective in immunotherapy activation.
Summary: Our platform enables adaptive precision immunotherapy, leveraging minimally invasive CTC sampling to identify patient-specific target for rapid CAR-NK administration, while synergistic cytokine arming ensures durable activity against hostile PDAC TME. This real-time molecular monitoring allows dynamic therapeutic adjustments as tumor profiles evolve.

#1314 Circulating tumor DNA (ctDNA) clearance dynamics in microsatellite instability-high metastatic (MSI-H) colorectal cancer (CRC) treated with immune checkpoint inhibitors (ICI).

H. R. Robinson[1], C. H. Lieu[1], V. N. Aushev[2], A. Tin[2], D. Nousome[2], J. Ortiz[2], S. Sharma[2], R. Lentz[2], A. Jurdi[2];
[1]University of Colorado, Aurora, CO, [2]Natera, Inc., Austin, TX

Background: ICI offers durable responses in MSI-H CRC. However, factors for long-term disease control and the optimal ICI duration are unclear, and radiographic assessments can be challenging. ctDNA provides an opportunity to monitor molecular changes during treatment. This retrospective analysis evaluated ctDNA clearance patterns and their relationship to survival in a large real-world cohort of patients with MSI-H metastatic CRC treated with first-line ICI.
Methods: We selected MSI-H metastatic CRC patients treated with first-line ICI (March 2021-June 2025) from Natera's real-world cohort and analyzed Signatera™ ctDNA data linked to an insurance claims database (Forian, CHRONOS™). ctDNA status was assessed pre ICI (within 12 weeks) and longitudinally. ctDNA clearance was defined as early (within 4 months) or sustained (≥6 months of ctDNA negativity). Descriptive analyses assessed ctDNA clearance frequency, timing, and correlation with overall survival (OS).
Results: A total of 465 patients with MSI-H metastatic CRC, treated with first-line IO, predominantly pembrolizumab (67%), ipilimumab + nivolumab (14%), and nivolumab (12%), were identified. Post-IO ctDNA-negativity was observed in 60.5% within 4 months and in 83.5% at any time point. Among 146 patients with pre-ICI ctDNA results, 44% had prior chemotherapy for localized disease, and 77% (106/146) were baseline ctDNA-positive. Of these, 37.7% (40/106) patients had early clearance, 65.1% (69/106 achieved anytime ctDNA clearance (median time to clearance 96 days (range: 12-777), and 19.8% (21/106) remained persistently positive. Of those who cleared, 77.4% achieved sustained ctDNA clearance with a median duration of ctDNA-negativity of 526 days (range: 105-1564). In the entire cohort (N=465), patients ctDNA-positive at their first post-IO ctDNA test had shorter OS (HR 4.75, 95%CI 2.26-9.96, $p<0.0001$) with an estimated 3-year OS of 96% versus 75% for ctDNA-negative versus -positive, respectively. Persistent ctDNA positivity after IO initiation was associated with inferior OS compared to anytime ctDNA negativity (HR 10.04, 95% CI 4.84-20.83, $p<0.0001$).
Conclusions: These findings suggest ctDNA kinetics as a reliable tool for evaluating benefit from ICI in patients with metastatic MSI-H CRC. ctDNA monitoring tracked distinct clearance trajectories. Consistent with ICI efficacy, most patients achieved ctDNA clearance. Importantly, early ctDNA clearance was strongly prognostic for improved OS, while persistent ctDNA-positivity was associated with markedly inferior OS. This supports prospective evaluation of ctDNA to guide ICI use in MSI-H CRC.

#1315 Genomic signatures in red blood cell DNA enable early non-invasive detection of colorectal neoplasia: A multicenter clinical study.

X. Yao[1], H. Sun[1], C. Liu[2], Y. Jiao[2], X. Kong[2], J. Jin[3], K. Ding[2], J. Li[2], X. Gao[4];

[1]Westlake University, Hangzhou, China, [2]Department of Colorectal Surgery and Oncology, Key Laboratory of Cancer Prevention and Intervention, Ministry of Education, The Second Affiliated Hospital, Zhejiang University School of Medicine, Hangzhou, China, [3]Timing Biotech, Hangzhou, China, [4]Research Center for Industries of the Future and School of Life Sciences, Westlake University, Hangzhou, China

Background: Colorectal cancer (CRC) causes substantial mortality, yet most cases arise from precursor lesions that are preventable if detected early. Existing non-invasive tests have limited sensitivity for advanced adenomas (AA), leaving a critical gap in early detection. Cytoplasmic DNA, including micronuclei and chromatin fragments, reflects genomic instability and systemic stress. Solid tumors can remotely induce DNA damage in hematopoietic progenitors, generating persistent DNA remnants in red blood cells (rbcDNA). We recently demonstrated that rbcDNA harbors tumor-associated genomic alterations that can detect early cancers with high accuracy. Here, we report the multicenter validation of an rbcDNA-based assay for early colorectal neoplasia detection.

Methods: We enrolled 1,251 individuals who underwent colonoscopy with histopathologic confirmation and categorized them into three groups: CRC (n = 360), AA (n = 330), and non-advanced neoplasia controls (non-AN, n = 561). rbcDNA was extracted from 1-2 mL peripheral blood using our established workflow (Sun et al., PMID: 40341742), including red blood cell isolation, rbcDNA purification, library preparation, and low-coverage whole-genome sequencing (~2×). Participants were randomly assigned in an 8:2 ratio into a discovery cohort and an internal test cohort, with comparable demographic characteristics. The discovery cohort was used to identify CRC- and AA-associated rbcDNA genomic features and to develop an integrated detection model, which was then evaluated in the internal test cohort to determine the optimal classification cutoff. The locked model was externally validated in two independent cohorts from the Second Hospital of Shandong University (n = 80) and Wenzhou Central Hospital (n = 110).

Results: At a fixed 90% specificity cutoff determined in the internal test cohort, the classifier achieved sensitivities of 85% for AA and 95% for CRC. External validation in two independent cohorts from Shandong and Wenzhou confirmed consistent performance for colorectal neoplasia, with sensitivities of 78% and 80%, respectively. Notably, in the Wenzhou cohort, rbcDNA also detected AA and early-stage CRC cases that were negative by fecal occult blood testing.

Conclusions: Our findings demonstrate that rbcDNA isolated from just 1-2 mL of peripheral blood enables accurate detection of AAs and early-stage CRC, supporting its potential utility for early diagnosis in clinical practice. A larger prospective clinical study (NCT05875584) will further validate the application of rbcDNA in early cancer detection.

#1316 A methylation-based molecular tumor typing classifier for tissue samples from cancers of unknown primary.

E. Forouzmand, L. Lawrence, J. Tung, S. Solomon, W. W. Young Greenwald, **Y. He**;
Guardant Health, Palo Alto, CA

Introduction: Determining tissue of origin is critical for guiding treatment decisions in cancers of unknown primary (CUP), metastatic tumors with ambiguous diagnostic findings, and cases where molecular confirmation may inform therapy selection. We developed a methylation-based molecular tumor type (MTT) prediction algorithm for malignant tissue samples, designed to operate robustly across a wide range of tumor fractions, to aid in determining cell of origin as an adjunct to conventional histopathology and immunohistochemistry.
Methods: The classifier was trained on 24 of the most prevalent solid cancers using the methylation profiles of more than 2,000 differentially methylated regions derived from Guardant360 Tissue (Guardant Health, Palo Alto, CA) from 6,047 FFPE tissue samples. Each MTT prediction was assigned a confidence score between 0 and 1, and the highest-confidence predictions were reported for evaluable samples. Evaluability criteria required a confidence level of the top prediction being greater than 0.5. The MTT classifier reports up to two top predictions based on the confidence scores. Performance was evaluated in 6,056 non-CUP samples and 191 CUP samples (including 35 CUP samples with a suspected diagnosis).
Results: The MTT classifier was first evaluated on 6,056 tumor tissue samples against the clinical diagnoses provided on the test requisition forms. 97.85% (5,926/6,056) were evaluable. The overall accuracy was 91.56% (5,426/5,926) for primary predictions and 93.76% (5,556/5,926) for the top 2 predictions. Among evaluable samples, 91.29% (5,410/5,926) have high-confidence primary predictions, with an accuracy of 94.05% for primary prediction in this subset.A notable subset of discordant primary predictions was among tumor types that could include mixed or closely related subtypes, such as nonsmall cell lung carcinoma (NSCLC) subtypes (22.20% (111/500)), or tumor types with related histogenesis, such as pancreaticobiliary tumors (7.60% (38/500)). The overall accuracy increases to 94.08% (5,575/5,926) and 95.46% (5,657/5,926) for top-1 and top-2 predictions, respectively, when NSCLC subtypes are merged into a single category and the pancreatic and biliary categories are merged to form a pancreaticobiliary category.The MTT classifier was also tested on 191 CUP samples; 88.48% (169/191) were evaluable. In 35 CUP samples with suspected diagnosis, evaluability was 97.14% (34/35) with accuracy of 85.29% (29/34) for primary predictions and 91.18% (31/34) for top-2 predictions.
Conclusions: This methylation-based MTT classifier demonstrates high evaluability and accuracy in determining tissue of origin for both non-CUP and CUP samples, providing valuable information to guide clinical decision-making when used as a supplement to conventional diagnostic methods.

: Modifiers of Inflammation and the Tumor Microenvironment
Minisymposium

#1347 A bone repair external state program drives cancer cell dedifferentiation and immune evasion in melanoma.

J. A. Weir[1], A. Wong[1], P. Liu[1], D. Alakwe[1], J. Wu[1], M. Sade-Feldman[1], N. Hacohen[2], F. Chen[2];
[1]Harvard University, Cambridge, MA, [2]Broad Institute, Cambridge, MA

The spatial organization of immune and stromal cells in the tumor microenvironment is emerging as an important predictor of effective cancer immunity. To systematically probe how multicellular circuits within the melanoma microenvironment drive cancer and immune cell state, we profiled 27 fresh-frozen human melanoma sections with Slide-tags snRNA-seq from 16 patients spanning common metastatic sites. We discovered six recurrent immune hub types representing conserved multicellular structures across melanoma, including an anti-inflammatory niche composed of SPP1+ macrophages, and POSTN+ fibroblasts, and an immune effector hub with NK cells and tumor-specific CD8+ T cells. Using spatial TCR sequencing, we observed a striking enrichment of expanded CD8+ T cell clonotypes in immune effector hubs and an enrichment of singleton CD8+ T cell clonotypes in anti-inflammatory hubs. Further, we found CD8+ T cells in the anti-inflammatory hubs to be more exhausted and less stem-like. Next, we sought to understand how immune niches interact with the malignant compartment. We identified 18 high-quality malignant transcriptional programs spanning the conventional de-differentiation trajectory in melanoma. We revealed that neural crest-like program usage is strongly predicted by the neighborhood presence of SPP1+ macrophages and POSTN+ fibroblasts, but negatively predicted by immune effector hub cells. We find that malignant cells that are more melanocytic-like and less de-differentiated are more immune infiltrated and have less SPP1+ macrophages and POSTN+ fibroblasts in their neighborhoods. Hypothesizing that ligands from the anti-inflammatory niche are shaping tumor state, we perturbed melanoma cell lines with SPP1 and POSTN. We found that when we treat melanocytic-like cells with POSTN, the tumor cells downregulate melanocytic markers and shift towards a more neural crest-like state. Further, when we treat neural crest-like cells with SPP1, the cells become protected from IFNg and TNFa killing. Our integrated spatial and functional analysis delineates six conserved immune hub architectures in metastatic melanoma and maps the spatial trajectory of $CD8^+$ T-cell activation, expansion, and exhaustion. We demonstrate that anti-inflammatory niches composed of $SPP1^+$ macrophages and $POSTN^+$ fibroblasts not only exclude effector T cells but also drive tumor de-differentiation and cytokine resistance. In sum, our results illustrate how specific microenvironmental niches influence CD8 T cell responses, malignant de-differentiation, and tumor cell immune evasion in melanoma.

#1348 Tumor-specific antibodies elicited by engineered bacteria promote bladder cancer immunotherapy.

M. Rouanne[1], N. Chen[2], D. Mariuzza[1], Z. Yang[1], F. Li[1], T. Savage[2], K. de los Santos-Alexis[2], R. Vincent[3], C. L. Mendelsohn[2], T. Danino[1], N. Arpaia[2];

[1]Columbia University, New York, NY, [2]Columbia University Irving Medical Center, New York, NY, [3]Baylor College of Medicine, Houston, TX

The intratumoral microbiome has recently emerged as a new hallmark of cancer, with implications for response or resistance to therapy. While bacteria can either promote or inhibit cancer growth, intratumoral bacteria can also be engineered using synthetic biology to remodel the tumor microenvironment. Here, we engineered the probiotic bacterium *E. coli* Nissle 1917 (EcN) to express the human chemokine CXCL13, a critical component of germinal center (GC) formation. The GC reaction is a fundamental aspect of adaptive immunity by which antibody affinity develops in secondary lymphoid organs for defense against pathogens. Using orthotopic models of bladder cancer, engineered CXCL13-expressing EcN colonized bladder tumors and elicited GC responses in bladder tumor-draining lymph nodes after intravesical delivery. Furthermore, when combined with PD-1 blockade, engineered EcN amplified the antitumor antibody response and promoted long-term survival and protective immunity upon tumor rechallenge. Thus, we demonstrate that synthetically engineered CXCL13-expressing EcN can enhance the efficacy of PD-1 checkpoint blockade immunotherapy by amplifying tumor-specific humoral immunity.

#1349 Deletion of host-derived GPNMB positively regulates anti-tumor response by reprogramming tumor-associated macrophages.

R. Tonea, S. J. Riesenfeld, T. F. Gajewski;
University of Chicago, Chicago, IL

Recent work has suggested that poor T cell infiltration and activation in non-responding tumors to immunotherapy is associated with immunosuppressive tumor-associated macrophages (TAMs). GPNMB is a glycosylated type I transmembrane protein found to be upregulated in multiple human cancers, with several cancer mouse models showing that it is expressed in an anti-inflammatory, highly differentiated subtype of TAMs. Analysis of human breast cancer single-cell RNA-seq data showed GPNMB to be upregulated in the myeloid compartment of non-responders to anti-PD1 therapy, suggesting a possible salvage immune suppressive role. Full knockout (KO), Vav1-Cre, and LysM-Cre GPNMB mouse models were generated to study the effect of this gene on tumor progression in the subcutaneous B16.SIY and orthotopic EO771 tumor systems. KO of GPNMB in the host, but not in tumor cells, led to markedly reduced B16.SIY and EO771 tumor growth. Tumors from KO hosts had more $CD8^+$ T cells, MHC-II^{high} $CD86^+$ macrophages, and enhanced $CD8^+$ T cells activation. $CD8^+$ T cell depletion or in vivo IFN-γ blockade eliminated the difference in the pro-inflammatory macrophages, and depletion of all T cells led to complete loss of tumor control. Single-cell RNA-seq revealed no differences at baseline between WT and KO mice in bone marrow, spleen, and lymph nodes, suggesting GPNMB deficiency did not disrupt normal tissue function. However, it showed significant differences in immune cells isolated from tumors. Relative to WT, KO mice had expanded populations of pro-inflammatory macrophages expressing IFN-induced genes, and smaller populations of macrophages expressing either mitochondrial genes involved in oxidative phosphorylation or lipid metabolism genes. The KO also led to significant changes in the transcriptional profiles of two anti-inflammatory subtypes of macrophages, high in Spp1 and C1q expression respectively. IFN-induced, complement, and inflammasome related genes were upregulated in the KO. Macrophages isolated from tumors of KO mice showed decreased suppression of $CD8^+$ T cells in an in vitro co-culture assay. To better understand the role of host versus bone-marrow-derived GPNMB for tumor control, we generated bone-marrow (BM) chimeras where GPNMB was deleted either from the host only or from the BM only. Slower tumor growth was observed when GPNMB was deleted from the host, and faster tumor growth when GPNMB was deleted from the BM. Conditional deletion of GPNMB in hematopoietic cells using Vav1-Cre mice showed no tumor control, while its conditional deletion in myeloid cells using LysM-Cre mice showed significant reduction in tumor growth. Taken together with previous data showing that the LysM-Cre targets populations of tissue-resident macrophages that the Vav1-Cre does not, those results suggest a potential role of GPNMB-expressing tissue resident-macrophages in shaping anti-tumor immunity.

#1350 Vaccine stimulation of bystander t cells in the lymph node unexpectedly promotes tumor-specific host immunity to regress solid tumors.

L. Ma[1], T. Grzywa[1], R. Tannir[1], G. L. Beatty[2], A. Huang[3];

[1]Children's Hospital of Philadelphia, Philadelphia, PA, [2]University of Pennsylvania, Philadelphia, PA, [3]Alexander Huang (Individual)

Personalized neoantigen cancer vaccines have been at the forefront of therapeutic vaccination. However, although these neoantigen vaccines do induce neoantigen-specific T cell responses, the clinical effects are limited. Logistical challenges, such as the time required for developing personalized neoantigen vaccines, also limit their clinical utility. We were recently intrigued by a case at Penn where one of our patients had a 7.6 cm melanoma tumor and experienced a complete response after receiving the COVID-19 vaccine *alone,* consistent with a recent report that cancer patients who received the SARS-CoV-2 vaccination had improved survival. Further studies identified abundant SARS-CoV-specific T cells present in both the draining lymph node (LN) and in the necrotic tumor bed. At the same time, our preliminary experiment in mice showed a similar phenomenon that the activation of tumor-irrelevant CAR T cells by vaccination reinvigorated the host's tumor-specific immunity and regressed established solid tumors. Specifically, when we used our recently developed lipid polymer vaccine (Ma et al, Science, 2019; Cell, 2023; Grzywa et al, Nat BME, 2025) carrying a chemical ligand Fluorescein (FITC) to specifically stimulate adoptively transferred bystander FITC-targeting chimeric antigen receptor (CAR) T cells in vivo in the lymph node as a negative control, yet unexpectedly we observed distal tumor regression to a level that's comparable to vaccine stimulation of tumor-specific CAR T in syngeneic mouse models of pancreatic cancer and melanoma. In both settings, tumor volume was reduced by>70% within the first 72 hours, and this effect persisted for up to 2 weeks (with some cures of the melanoma). This marked antigen-independent tumor control is completely lost in Rag1-knockout (no endogenous T cells) and BatF3-knockout (deficient in antigen cross-presentation) recipient mice. FITC vaccine boosting of bystander FITC-CAR T induced a rapid and transient cytokine and chemokine release that distally remodels the tumor microenvironment. Notably, IFNg blockade completely abolished this tumor control. In the pancreatic cancer model, IFNg significantly upregulated PD-L1 expression in cancer cells. As a result, co-administration of anti-PD-L1 markedly extended long-term tumor control and animal survival. Collectively, these unexpected findings in both the melanoma patient and syngeneic mouse models of solid tumors suggested a previously unappreciated anti-tumor bystander effect associated with vaccine-mediated T cell activation.

#1351 IL-18 secreting CAR-T cells uncover divergent immune mechanisms of antigen-heterogeneous solid tumor clearance.

A. May, E. Sotillo, P. Xu, A. Malhotra, K. Ho, C. Mackall;
Stanford University School of Medicine, Stanford, CA

CAR-T therapy has improved the outcome for patients with refractory hematological malignancies, however this success has not translated to solid tumors, largely due to an immunosuppressive tumor microenvironment (TME) and heterogenous antigen expression. CAR-Ts capable of reshaping the TME and recruiting endogenous immune cells, could improve outcomes by eradicating cells with low or absent expression of the CAR targeted antigen. However, the biological mechanisms necessary to induce endogenous anti-tumor T cell responses remain unclear. Previous studies have reported that CAR-T cells engineered to secrete IL-18 induced immune priming and an endogenous anti-tumor response. We sought to study tumor clearance rates and endogenous immune responses induced by control and IL-18 secreting CAR-T cells by administering murine CAR-Ts targeting human CD19 (huCD19.28.z-CARs) to mice bearing a mixture of B16F10-Ova+huCD19+/- cells. We profiled endogenous lymphoid and myeloid compartments, as well as engineered CAR-Ts, during tumor clearance within lymphoid and tumor tissues at 14 and 26 days post CAR-T treatment. Additionally, we assessed the induction of CD8 T cells reactive to tumor-derived peptides using ELISPOT. IL-18 secreting CARs demonstrated robust antigen-heterogenous tumor control compared to the control. By day 26 post treatment, tumor measurements in IL-18 secreting CAR-T treated mice were undetectable, while control tumors averaged 680 mm^3. Despite improved tumor control, IL-18 secreting CAR treated mice generated fewer CD8s reactive to Ova, a tumor neoantigen, compared to the CAR only control. Instead, IL-18 secretion induced a strong type II interferon response, skewing effector differentiation of lymphocytes and initiating expansion and activation of myeloid cells, including macrophages and neutrophils. This work reveals that enhanced clearance of heterogenous solid tumors by cytokine secreting CAR-Ts may occur through distinct immunological programs. CAR-Ts secreting IL-18 cleared mixed antigen expressing tumors most effectively, but induced a low/absent anti-tumor CD8 T cell response. In contrast, CAR-Ts alone failed to control tumors, but effectively induced priming of CD8s towards a tumor expressed neoantigen. These findings suggest activated innate myeloid cells as key mediators in eradicating antigen negative cells within a heterogeneous tumor and illustrate distinct biology between tumor clearance via innate immune responses versus induction of persistent adaptive immunity to tumor associated antigens. Taken together, this study can inform next-generation CAR-T design by underscoring the importance of balancing effector potency with durable endogenous anti-tumor immunity to engineer sustained efficacy in solid tumors.

#1353 Emergency myelopoiesis drives immunosuppressive monocyte programming in lymphoma-associated secondary hemophagocytic lymphohistiocytosis.

H. Cho[1], J.-E. Kwak[1], J.-Y. Koh[2], J. Byun[1], Y. Koh[3], J. Hong[1], D.-Y. Shin[1], I. Kim[1], H. Ju[4];
[1]Seoul National University Hospital, Seoul, Korea, Republic of, [2]UCSD, San Diego, CA, [3]Seoul National University School of Medicine, Seoul, Korea, Republic of, [4]Samsung Medical Center, Seoul, Korea, Republic of

Lymphoma-associated secondary hemophagocytic lymphohistiocytosis (sHLH) is a highly fatal manifestation of cancer-induced immune dysregulation, yet how lymphoma reshapes myelopoiesis to generate pathogenic myeloid cells remains unclear. To define the malignant immune ecosystem, we performed single-cell RNA sequencing on paired bone marrow and peripheral blood samples from patients with B-cell lymphoma with sHLH (n=14) or without sHLH (n=7), with primary HLH carrying *PRF1* or *UNC13D* mutations (n=6) included to distinguish cancer-driven remodeling from inherited immune defects (total 110,943 cells). Lymphoma-associated sHLH exhibited tumor-driven emergency myelopoiesis with expansion of myeloid-biased hematopoietic stem cells and granulocyte-monocyte progenitors (GMPs). These progenitors displayed activation of inflammatory pathways (TNF-α, IFN-γ) and were pre-imprinted with the MS1 immunosuppressive transcriptional program (*S100A8/9*, *IL1R2*, *PLAC8*, low *HLA-DR*), indicating that monocytic dysfunction originates at the progenitor stage within the tumor-altered bone marrow niche. MS1-like monocytes diverged into two terminal lineages; one lineage was preferentially expanded in sHLH and expressed pro-inflammatory cytokines (*CXCL2*, *CXCL3*, *IL6*), the regulatory cytokine *IL10*, and multiple immune checkpoint ligands (*VSIG4*, *LILRB4*). Cell-cell interaction and regulon analyses revealed an IL-6/IL-10-STAT3 signaling loop that reinforces MS1 programming and creates a self-sustaining immunosuppressive circuit. Functionally, the abundance of MS1-like monocytes inversely correlated with $CD4^+$ and $CD8^+$ T-cell frequencies, accompanied by loss of conventional dendritic cells, impaired antigen presentation, and metabolic hyperactivation of T cells with increased *PD-1*, *TIM-3*, and *LAG-3* expression, suggestive of dysfunctional activation rather than classical exhaustion. These findings uncover a cancer-driven immunopathogenic mechanism in which lymphoma hijacks myelopoiesis to generate STAT3-dependent immunosuppressive monocytes that simultaneously amplify hyperinflammation and blunt anti-tumor immunity. Targeting emergency myelopoiesis or monocytic STAT3 signaling represents a therapeutic strategy for restoring immune competence in lymphoma-associated sHLH.

: Nonclinical Models of Cancer
Minisymposium

#1383 Defining the role of the Daam2 R414W germline variant in familial glioma.

T. J. Choy[1], Q. Ye[1], M. L. Bondy[2], H. Lee[1];
[1]Baylor College of Medicine, Houston, TX, [2]Stanford Cancer Institute, Stanford, CA

Malignant glioma is the most common primary brain tumor in adults, with high morbidity and mortality due to its aggressive nature and limited treatment options. While advances in molecular genetics have improved glioma classification, these systems rely predominantly on sporadic somatic mutations that cannot predict individual glioma risk. In contrast, the 5-10% of gliomas occurring in families with hereditary predisposition offer a powerful opportunity to identify germline variants that increase glioma susceptibility and may serve as biomarkers for risk assessment. Dysregulation of developmental signaling pathways has been increasingly implicated in gliomagenesis. Through whole-exome sequencing of familial glioma patients, we identified five germline mutations in *Daam2* (Dishevelled associated activator of morphogenesis 2), a key regulator of Wnt signaling. *Daam2* encodes a formin protein crucial for glial differentiation and highly enriched in glial cells. Our prior work demonstrated that Daam2 is sufficient to promote gliomagenesis and essential for glioma growth, prompting us to investigate whether these variants affect tumor progression. We overexpressed each variant in patient-derived glioma stem-like cells and orthotopically xenografted them into immunodeficient mice. Among the variants, Daam2-R414W significantly promoted tumor cell proliferation in vitro and in vivo. To model this patient-observed mutation in an immunocompetent system, we generated a Daam2-R414W knock-in mouse model. Mutant mice exhibited an increased number of proliferating glial progenitor cells in the subventricular zone compared to wildtype (WT) controls, suggesting that Daam2-R414W expands the glial progenitor pool to facilitate glioma initiation. Since the patient harboring the Daam2-R414W mutation was diagnosed with oligodendroglioma, a low-grade glioma (LGG), we induced LGG in Daam2-R414W mutant mice and observed increased tumor cell proliferation and decreased survival compared to WT LGG-bearing mice, suggesting that Daam2-R414W accelerates malignant progression. To identify molecular mechanisms underlying these phenotypes, we performed bulk RNA-sequencing on LGG tumors from Daam2-R414W mutant and WT mice. Sequencing revealed increased expression of Wnt pathway components, actin cytoskeletal genes, and oligodendrocyte progenitor cell (OPC) markers in Daam2-R414W tumors compared to WT. Among these changes, marked upregulation of TCF3, a key transcription factor in canonical Wnt signaling, points to enhanced pathway activation in mutant tumors. These findings suggest that Daam2-R414W accelerates tumor progression by amplifying Wnt-driven proliferative signaling programs that drive glioma growth. Overall, this study identifies a hereditary glioma-predisposing variant and demonstrates how germline mutations in developmental regulators can disrupt normal cellular function to promote malignancy.

#1384 Aging amplifies oncogenic mutant pik3ca 1047R signaling and accelerates mammary tumorigenesis.

T. Mohan, J. Mackay, M. McLaughlin, Y. Li, A. Nazarullah, L.-Z. Sun;
The University of Texas at San Antonio Health Science Center, San Antonio, TX

Breast cancer incidence increases with age, and hormone receptor positive (HR+) and HER2 negative tumors represents the most prevalent subtype among older women. Approximately 70% of early-stage breast cancers are HR+/HER2−, frequently harboring the *PIK3CA* H1047R mutation, a driver of heterogeneous mammary carcinomas. Understanding how PIK3CA H1047R mutant interacts with the aging microenvironment is important for elucidating age-related susceptibility and may enlighten age-specific therapeutic strategies. In this study, we investigated age-dependent susceptibility to PIK3CA H1047R-driven tumorigenesis using intraductal delivery of lentivirus expressing human PIK3CA H1047R in FVB/NJ mice across three age groups (young: 2 mo, n=10; middle-aged: 14 mo, n=8; aged: 22 mo, n=7). Mice were monitored for up to 6 months, and the time to palpable tumor formation was used to generate tumor-free survival curves. qPCR analysis confirmed age-dependent differences in *PIK3CA* H1047R genomic integration and expression. Ductal morphology and histopathology were evaluated using carmine whole-mount and hematoxylin and eosin staining. Morphometric characterization was performed using BD FACS Discover S8 Cell Sorter. High-dimensional flowcytometric analysis (t-SNE, FlowSOM, Cluster Explorer) was used to identify epithelial subsets most susceptible to transformation. Middle-aged and aged mice displayed significantly higher tumor incidence and shorter latency compared with young mice, consistent with increased *PIK3CA* integration and expression. Morphometric analysis revealed that luminal cells ($CD49f^{low}CD24^{high}$) expressed maximal PIK3CA H1047R protein concentration (Max Intensity MFI) than basal cells ($CD49f^{high}CD24^{low}$). Further, Eccentricity and Radial movement imaging features revealed age- and lineage-specific oncogenic responses. Together, these findings indicate that aging is not merely a risk factor but actively modifies PIK3CA-driven oncogenic signaling. These age-associated alterations in mammary epithelial cell populations may inform development of targeted therapies for older patients with HR+/HER2− breast cancer. A limitation of this study is the use of a murine intraductal model, which may not fully capture human breast cancer biology. Further studies incorporating stromal and immune components are needed to comprehensively understand how aging influences oncogenic PIK3CA signaling.

#1385 Evaluation of kinase inhibitor efficacy and cancer-associated fibroblast-organoid crosstalk in a CRISPR-edited mouse model of bladder cancer.

T. Haque, H. Valentine, U. Satyal, L. Bukavina, R. Arya, P. H. Abbosh;
Fox Chase Cancer Center, Philadelphia, PA

Background: The PI3K/AKT/mTOR pathway is altered in more than 40% of bladder cancers (BCa), yet it remains untargeted therapeutically. We developed an immunocompetent, CRISPR-edited BCa mouse model that recapitulates common mutations in this pathway. The tumor microenvironment, particularly cancer-associated fibroblasts (CAFs), plays a critical role in BCa progression, and the molecular mechanisms underlying tumor-CAF crosstalk are incompletely understood in BCa. We focused on identifying genotype-specific kinase inhibitor combinations and elucidating cytokine-mediated crosstalk between CRISPR-edited organoids and CAFs.
Methods: Urothelial organoids from Rosa26-LSL-Cas9/GFP mice were CRISPR-engineered with Trp53 knockout plus either Rb1 knockout or deletion of the region homologous to human chromosome 9p21. A third mutation in the mTOR pathway (PIK3CA H1047R hotspot mutation) was then introduced. Gene edits were confirmed and cell lines were characterized for kinase inhibitor sensitivity. Engraftment studies were assessed in immunocompromised and immunocompetent mice to evaluate therapeutic targeting of genotype-specific kinase inhibitors via bladder engraftment or subcutaneous injection. CAFs were purified from carcinogen-induced murine bladder tumors. Organoid-CAF co-injection experiments were performed to assess CAF dependency for tumorigenesis. Cytokine profiling was performed on organoid monocultures, CAF monocultures, and organoid-CAF co-cultures. GM-CSF knockout organoids were generated and co-cultured with CAFs to evaluate cytokine-mediated crosstalk.
Results: Triple-mutant organoids formed tumors in immunocompromised mice and exhibited sensitivity to PI3K inhibitor treatment (pictilisib or alpelisib) vs double-mutant controls, validating our genotype-specific targeting approach. However, the same organoids were non-tumorigenic in immunocompetent hosts. Co-engraftment with CAFs promoted tumor formation, demonstrating CAF dependency for tumorigenesis in immunocompetent hosts. Cytokine profiling revealed elevated IL-6 and GM-CSF secretion from organoid-CAF co-cultures but not monocultures, with GM-CSF by organoids and IL-6 secreted by CAFs. GM-CSF knockout in organoids reduced IL-6 secretion from CAFs, supporting cytokine-mediated CAF-organoid crosstalk.
Conclusions: Our findings suggest GM-CSF and IL-6 critically mediate CAF-dependent tumor engraftment and targeting this cytokine axis may disrupt CAF-organoid crosstalk to inhibit tumor growth in immunocompetent models. Future studies will evaluate immune contributions and dual cytokine targeting. These findings support precision medicine combining genotype-specific kinase inhibition with microenvironment-directed therapies for BCa patients harboring mTOR pathway alterations.

#1386 NSCLC patient-derived organoids recapitulate tissue signalling and impairment of infiltrated immune cell activation predicting patients' response to therapy.

A. Pasto[1], H. Al-Serori[1], M. Fankhaenel[1], Z. Mokhtari[2], D. Mukherjee[1], R. Drews[1], P. Barber[1], J. Davis[1], L. Wedeken[3], V. Yankova[1], J. Loskutov[3], J. Monypenny[4], N. Patel[4], M. Htun[1], M. Finn[1], S. Ndagire[4], E. Karapanagiotou[5], E. Moon[6], C. Gillett[7], A. Bille[8], T. Ng[1]; [1]GlaxoSmithKline plc, Stevenage, United Kingdom, [2]GlaxoSmithKline plc, Heidelberg, Germany, [3]GlaxoSmithKline plc, Berlin, Germany, [4]King's College of London, London, United Kingdom, [5]Cancer Centre at Guy's St Thomas, London, United Kingdom, [6]GlaxoSmithKline plc, Upper Providence, PA, [7]King's College of London, London, United Kingdom, [8]Guy's and St Thomas' Hospital, London, United Kingdom

Non-small cell lung cancer (NSCLC) with its rapid growth and early metastasis onset, represents the most common cause of cancer-related deaths worldwide. Current treatments offer limited long-term survival, necessitating novel approaches. Immunotherapy, specifically anti-PD1 and anti-PD-L1, has transformed NSCLC treatment, but only a small percentage of patients respond. There is an unmet need to predict immuno-therapy susceptibilities, achieve a cancer patient risk stratification and identify targeted therapies. Patient-derived organoids (PDOs) are in vitro 3D structures that recapitulate the complexity of the tumours from which they derived, showing a great potential as preclinical model for drug screening and tailored treatment. We used 12 PDO models established from chemotherapy-naïve high-risk NSCLC patients tissues collected at the Guy's Hospital, London. Patients' follow-up was performed for more than 24 months post resection/biopsy/surgery. PDOs were treated with cisplatin, then co-cultured with pre-activated immune cells in the presence of IO drugs and subjected to multiple assays including imaging, flow cytometry, genomic and transcriptomic analysis and proteomic from exosome isolation. This multi-omics approach allows for simultaneous analysis of different biological parameters before and after treatment to understand tumour cell interaction with immune cells and drug-induced changes. According to patients' clinical response to standard of care treatment, PDOs were classified as responder (R) and not responder (NR). Cisplatin IC50, elaborated from PDOs cytotoxicity analysis, correlated with R and NR dichotomy, predicting the response status of the patients in vivo. When PDOs were cocultured with PBMC, counterintuitively, we observed a higher immune cells infiltration after cisplatin treatment in the NR-PDOs. Neither baseline CD45 infiltration nor the composition of infiltrating PBMC differed between NR and R-PDOs. However, in the baseline condition, the $CD8^{pos}$ cells infiltrating NR-PDOs presented a predominantly exhaustion profile. Transcriptomic analysis of untreated PDOs revealed higher activation of inflammatory response signalling in the NR-PDOs compared to responders, and the same signalling upregulation was identify from spatial transcriptomic analysis on primary tumour tissues derived from NR patients. Proteomic analysis of extracellular vesicles cargo also identified different protein content in R vs NR-PDO supporting the involvement of EV in the crosstalk between PDO and immune cells. We found that PDOs maintain the transcriptomic profile of the tissue they derived from with different activation of specific signalling that contributes to the creation of an inflammatory microenvironment and correlates with drug response status.

#1387 Live cell visualization of RNA splicing dynamics upon APOBEC3 lentiviral transduction in aged bone marrow using a 3D biosensing nanobioreactor.

E. Klacking[1], I. van der Werf[1], J. Isquith[1], J. Pham[1], T. Whisenant[1], A. A. Khachatrian[2], L. B. Alexandrov[1], C. H. Jamieson[1];
[1]UCSD, La Jolla, CA, [2]Scripps, La Jolla, CA

Background: During aging, hematopoietic stem and progenitor cells (HSPCs) undergo a progressive decline in regenerative capacity, exhibit skewed differentiation toward the myeloid lineage, show increased sensitivity to stressors, and accumulate somatic mutations, a process known as clonal hematopoiesis (CH), which increases susceptibility to hematological malignancies. Additional hallmarks of aging, include genomic instability, chronic inflammation, upregulation of inflammatory cytokines, and deregulated RNA splicing. Prior work demonstrated age-associated splice isoform expression in aged bone marrow (ABM) derived HSPCs (Crews⋯Jamieson, Cell Stem Cell, 2016). Here, we apply a 3D biosensing nanobioreactor (Pham⋯Jamieson, Cell Stem Cell, 2025) to track RNA splicing in aged bone marrow (ABM) derived HSPCs in real-time using confocal microscopy and evaluate age-related splice dysregulation linked to malignant evolution.

Methods: Nanobioreactors were constructed from transparent, gas-permeable, 2-port fluoroethyl polymer (FEP) film bags with a porcine gelatin sponge matrix. Mononuclear ABM cells were isolated by Ficoll density centrifugation, and $CD34^+$ cells were purified by magnetic bead selection. $CD34^+$ cells were lentivirally transduced with a dual fluorescent splicing reporter (van der Werf et al., *Cell Reports Medicine*, 2023), cultured for 48 hours, and co-cultured with autologous $CD34^-$ stromal cells in the nanobioreactor at a 1:4 ratio.

Results: In ABM-derived $CD34^+$ cells, lentiviral transduction of the dual fluorescent splicing reporter resulted predominantly in red fluorescence protein (RFP) expression, indicating exon inclusion, as assessed by confocal microscopy. Based on preliminary whole-transcriptome sequencing analyses showing increased exon-skipping events, we hypothesize that APOBEC3C drives exon skipping in aged HSPCs. To test this, $CD34^+$ selected cells from ABM aspirates were lentivirally transduced with the splicing reporter, followed by either APOBEC3C overexpression or pCDH vector control. Confocal imaging revealed a fluorescence shift consistent with increased exon skipping in APOBEC3C-transduced cells, confirming the reporter's ability to capture dynamic splicing changes in response to APOBEC3C activity.

Conclusion: We developed a 3D biosensing niche nanobioreactor system that enables live-cell visualization of RNA splicing dynamics in primary human HSPCs. Using this platform, we identified predominant exon inclusion in aged bone marrow-derived HSPCs and demonstrated that APOBEC3C overexpression induces exon skipping, a molecular signature associated with leukemic transformation. Future studies will compare aged and young bone marrow to delineate age-related splicing alterations and define RNA splicing-based biomarkers predictive of hematopoietic aging and malignant evolution.

#1388 Ex vivo micro-tumor testing platform to guide patient stratification for clinical development of ADCs.

Esmee Koedoot[1], **Felix M. Behr**[1], Timothy JP Sijsenaar[1], Dieudonne J. van der Meer[1], Lea Le Large[1], Farbod Khoraminia[1], Nelleke Ottevanger[2], Judith R. Kroep[3], Cor D. de Kroon[4], Willemijn Vader[1]

[1]VitroScan, Leiden, Netherlands,[2]Radboud University Medical Center, Nijmegen, Netherlands,[3]Dept. of Medical Oncology, K1-P, Leiden Univ. Medical Ctr., Leiden,[4]Leiden Univ. Medical Ctr., Leiden, Netherlands

Background Antibody-Drug Conjugates (ADCs) are revolutionizing cancer therapy. Yet, more than 90% fail to reach approval and ADC efficacy often poorly correlates with target expression, emphasizing the high need for improved prediction of patient responses to ADCs. Ex vivo micro-tumor testing enables near-clinical evaluation across drug classes, including ADCs, and has been shown to predict clinical responses to platinum therapy (Koedoot et al., npj Precision Oncology, 2025). This study evaluates ex vivo sensitivity to clinically relevant ADCs in ovarian (OC), non-small cell lung (NSCLC), and colorectal (CRC) cancer, aiming to identify predictive biomarkers and guide patient stratification to optimize clinical benefit.

Materials and Methods Ex vivo evaluation of patient specific responses to ADCs was performed by testing mirvetuximab-soravtansine (MIRV) in OC patient samples (N=25), ifinatamab deruxtecan (IFI) in CRC patient samples (N=5) and telisotuzumab vedotin (TEL) in NSCLC patient samples (N=10). Tumor tissue was processed within 48 hours. Enriched patient micro-tumors with preserved tumor microenvironment (TME) were embedded in hydrogel and exposed to standard of care therapy, ADCs and their respective payloads. Screening plates were fixed, stained and imaged, followed by high-dimensional image analysis and phenotypical feature extraction. Drug sensitivity profiles were established based on anti-tumor activity. Target protein expression profiling was performed by immunofluorescence staining of ex vivo micro-tumors.

Results Ex vivo testing of OC, NSCLC and CRC patient samples revealed patient-specific sensitivity to the respective ADCs. For MIRV, 32% (8/25) of the OC patients demonstrated strong sensitivity (Emax < 50%), 48% (12/25) of the patients demonstrated intermediate sensitivity (Emax 50-90%) and 20% of the patients (5/25) demonstrated complete MIRV resistance (Emax > 90%). Reproducible responses were observed for different drainages from the same patient (N=3). A strong correlation was observed between MIRV and paclitaxel sensitivity (R = 0.86), both of which target tubulin. A reduced correlation was observed for MIRV and carboplatin (R = 0.59), that acts by crosslinking DNA. Target protein expression profiling revealed inter- and intra-tumor heterogeneity. Some patients exhibited low target protein expression in all micro-tumors, while others exhibited high expression in a fraction of micro-tumors.

Conclusions This study reports an ex vivo micro-tumor testing platform that enables near clinical assessment of patient responses to ADCs. The platform is future-ready, offering multimodal capabilities including tumor microenvironment (TME) characterization, target protein profiling capturing patient heterogeneity, and assessment of bystander and synergistic responses. The next step is to correlate the ex vivo sensitivity to actual clinical outcome.

#1389 Defining immune phenotypes of checkpoint inhibitor response in human live tumor fragments preserving the native tumor microenvironment.

E. von Euw[1], J. Zweng[1], N. Dana[1], C. Sood[1], H. R. Hernan[1], L. C. F. Hrycyniak[1], P. McDonnell[1], P. Adstamongkonkul[1], C. Johnson[1], N. Marhefke[1], A. Nasreen[1], T. S. Ramasubramanian[1], K. Rexroad[1], S. Schneider[1], C. Scribano[1], A. Sunil[1], E. Wargowski[1], C. Vivelo[1], L. Vedder[1], S. Caenepeel[1], D. A. Braun[2], H. J. Gierman[1], H. Ramos[1];

[1]Elephas Biosciences, Madison, WI, [2]Yale School of Medicine, New Haven, CT

Background: Immune checkpoint inhibitors (ICIs) provide durable benefit for a subset of patients, yet current FDA-approved biomarkers (eg, PD-L1, MMR/MSI, TMB) inaccurately predict clinical response. To address this gap, we have developed an ex vivo platform using live tumor fragments (LTFs) and multiplex cytokine profiling to accurately predict ICI response in patients ($P<0.05$). Ex vivo cytokine profiling of LTFs produced from clinically relevant tumor specimens provides a unique opportunity to elucidate the biology and mechanisms of action of ICI response in the context of the native tumor microenvironment (TME).

Methods: Fresh core needle or forceps biopsy specimens collected as part of three ongoing observational clinical trials (NCT05478538, NCT05520099, NCT0634962) and a biobank biopsy collection study were profiled on the platform. Biopsy specimens were cut into LTFs, encapsulated in hydrogel and treated with ICI (αPD-1, αPD-L1, αPD-1+αCTLA-4 or αPD-L1+αCTLA-4) ex vivo. Longitudinal profiling of 46 cytokines was performed on 193 patient samples representing multiple solid tumor types. Unsupervised hierarchical clustering with Wards method was used to identify cytokine-based response patterns and classify specimens into primary responder and non-responder clusters. Upregulated cytokines within the response cluster were defined using Mann-Whitney-U tests with Bonferroni correction for multiple comparisons, annotated for their function, and subclusters were classified into immune phenotypes.

Results: Comparison of response and non-response clusters identified 21 significantly upregulated cytokines ($P<0.05$) known to be associated with immune response to ICI. Additionally, response subcluster analysis identified 4 distinct tumor-type agnostic immune phenotypes: (1) T-cell inflamed with regulatory counterbalance, (2) mixed regulatory T-reg/myeloid (3) cytotoxic inflamed with T-reg-VEGF counterbalance, and (4) polyfunctional activated with myeloid angiogenic remodeling. Furthermore, subcluster assignment was consistent in 6 of 7 (85%) patient specimens with multiple replicates, demonstrating that profiles of response, when present, are reproducible between replicates from the same tumor. To date, patients with available clinical response data to an ICI therapy were identified across different subclusters.

Conclusions: The ex vivo platform identifies distinct and expected immune phenotypes in response to ICI treatments. These data underscore the platform's potential to accurately predict clinical response to ICI. Future studies will help to understand the relationship between these immune phenotypes and the depth and durability of ICI response in patients.

: Noncoding RNA Regulation of Cancer Hallmarks, Therapeutic Resistance, and Biomarker Discovery Minisymposium

#1365 Regulation of ribosomal RNA synthesis in acute myeloid leukemia.

P. J. Hung, J. A. Henrich, C. Antony, V. R. Paralkar;
University of Pennsylvania, Philadelphia, PA

Acute myeloid leukemia (AML) is an aggressive blood cancer with high rates of relapse and limited second-line treatment options, resulting in a five-year survival of 20-30%. A defining feature of AML cells is their prominent nucleoli, which demarcate sites of active ribosomal RNA (rRNA) synthesis. rRNAs are specialized non-coding RNAs that form the catalytic cores of ribosomes, and their transcription by RNA polymerase 1 (Pol1) is the rate-determining step in ribosome biogenesis. We hypothesized that AML cells require increased rRNA synthesis and protein translational capacities to support their growth and survival. To test this premise, we developed a “FISH-Flow” assay to measure the relative levels of nascent and mature rRNAs in different cell-types across the human hematopoietic tree. Profiling over twenty bone marrow aspirates from healthy donors and AML patients, we found that rRNA synthesis varies widely throughout normal hematopoiesis – peaking in the stem/progenitor cell populations (CMPs, GMPs, MEPs) – and is elevated by 1.5 to 2-fold in AML cells. Our analysis of publicly available single-cell RNA-seq data further showed that the Pol1 gene signature is overexpressed in AML cells.

To assess whether rRNA “hyper-synthesis” is essential for AML cell fitness, we generated a HoxA9 transgene-driven mouse AML cell-line with POLR1A (the catalytic subunit of Pol1) fused to an FKBP degron domain, which enables targeted degradation of Pol1 by a small molecule dTAG. Pol1 depletion led to a rapid decrease in rRNA synthesis, G1 cell cycle arrest, and monocytic differentiation, as evidenced by downregulation of the stem cell marker c-Kit and upregulation of the mature monocyte marker Ly6C. Additionally, dTAG treatment synergized strongly with Bcl-2 inhibitors to induce apoptosis in these cells. This synergy did not extend to other AML chemotherapy agents, such as daunorubicin or cytarabine, indicating a unique, synthetically lethal interaction between the rRNA synthesis and Bcl-2 signaling pathways in AML cells.

In summary, we demonstrate that rRNA synthesis and Pol1 expression are amplified in AML cells to sustain an oncogenic, stem-like state that renders them more resistant to apoptotic stimuli. Notably, our findings identify rRNA synthesis as a therapeutic vulnerability in AML cells and uncover a novel synthetic lethality with Bcl-2 inhibition.

#1366 CYP4A22-AS1-YBX1 axis drives radiation resistance in cervical adenocarcinoma via PGK1 transactivation.

Mingyi Zhou, Chunlai Li, Cristina Ivan, Simone Anfossi, Linda Fabris, Melanie Winkle, Recep Bayraktar, Meng Chen, Lan Pang, Masayoshi Shimizu, Francois Claret, George Calin

The University of Texas MD Anderson Cancer Center, Houston, TX

Background: Cervical adenocarcinoma exhibits poor responsiveness to radiotherapy and inferior survival compared with squamous cell carcinoma. The molecular mechanisms underlying its intrinsic radiation resistance remain largely unknown.
Methods: Integrative analysis of TCGA and our RNA-seq cohort identified CYP4A22-AS1 as one of the most upregulated lncRNAs in cervical adenocarcinoma. qRT-PCR confirmed higher CYP4A22-AS1 expression in tumors with short disease-free survival (DFS). RNA pulldown, mass spectrometry, and RIP assays defined YBX1 as a direct CYP4A22-AS1-binding partner. Immunofluorescence and ChIP-qPCR assays examined YBX1 nuclear localization and promoter occupancy of PGK1, respectively. Functional effects of CYP4A22-AS1, YBX1, and PGK1 silencing were assessed by CCK-8, colony, EdU, and TUNEL assays in HeLa and C33A cells, and validated in xenograft models.
Results: CYP4A22-AS1 was markedly overexpressed in cervical adenocarcinoma relative to normal cervix. Clinically, high CYP4A22-AS1 and PGK1 levels correlated with shorter DFS. Mechanistically, CYP4A22-AS1 binds YBX1 and enhances its nuclear translocation, thereby promoting YBX1 recruitment to the PGK1 promoter and activating glycolytic metabolism. Knockdown of CYP4A22-AS1 or PGK1 suppressed proliferation and markedly increased radiosensitivity both in vitro and in vivo.
Conclusions: This study identifies CYP4A22-AS1 as a novel oncogenic lncRNA that drives radiation resistance through YBX1-mediated PGK1 transactivation. Clinically, CYP4A22-AS1 overexpression predicts poor outcome, while its inhibition restores radiation sensitivity. Targeting the CYP4A22-AS1-YBX1-PGK1 signaling axis offers a promising therapeutic strategy to overcome radioresistance in cervical adenocarcinoma.

#1367 Dual remodeling of RCC-associated fibroblasts via miR-196b antagomir and COUP-TFII inhibitor ultrasmall lactoferrin-lipid nano-assemblies augments immunotherapy.

A. Ziada[1], L. Escalante Gonzalez[2], Z. Sideeka[3], A. Jarrous[4], A. Mayer[5], L. Ren[6], A. Park[5], A. Ajay[4], C. Xin[4], A. Elzoghby[4]; [1]Amherst College, Amherst, MA, [2]Tecnologico de Monterrey, Monterrey, Mexico, [3]The George Washington University, Washington, DC, WA, [4]Brigham and Women's Hospital, Harvard Medical School, Boston, MA, [5]Northeastern University, Boston, MA, [6]Rice University, Houston, TX

Renal cell carcinoma (RCC), a type of kidney cancer, is among the 10 most common cancers in both men and women. Despite the advanced progress of cancer immunotherapy, many RCC patients show resistance to immune checkpoint inhibitors. Cancer-associated fibroblasts (CAFs) play a key role in promoting immunosuppression in RCC, which markedly impairs the antitumor immune response. Several oncogenic miRNAs (OncomiRs) are upregulated in RCC fibroblasts where they drive their differentiation into CAFs by modulating the expression of target genes involved in phenotypic changes associated with CAFs. Moreover, COUP-TFII is an unexplored transcription factor implicated in the differentiation of kidney fibroblasts. In our study, microarray-based miRNA sequencing analysis showed upregulation of some miRNAs (e.g., miR 196b) in RCC patient-derived CAFs compared to normal kidney fibroblasts. Therefore, we engineered novel ultrasmall recombinant lactoferrin (LF)-stabilized lipid nano-assemblies (NAs) co-loaded with antagomir (anti-miR 196b) and COUP-TFII inhibitor (CIA-1) to induce synergistic remodeling of renal CAFs into a quiescent phenotype. LF, a GRAS (Generally Regarded as Safe) glycoprotein, targets tumor fibroblasts through natural tropism to LRP1 and intelectin-1 receptors, over-expressed in fibrotic tissues. In addition, the recombinant form of human lactoferrin (rhLF) has high batch-to-batch consistency, reduced immunogenicity, precise molecular tailoring for drug incorporation and surface modification, and well-tolerated following systemic administration. The rhLF-lipid NAs exhibited ultrasmall and uniform size (5-7 nm) with discoidal morphology. Moreover, the NAs were successfully internalized into RCC patient-derived CAFs without inducing remarkable toxicity. The NAs reprogrammed renal CAFs into quiescence as evidenced by downregulation of fibroblast activation (e.g., αSMA, FAP, and S100A4) and extracellular matrix (e.g., Col1α1, Col3α1, fibronectin, periostin, and tenascin C) markers as well as upregulation of the quiescence marker p27. In addition, the secretion of IL-6, IL-8 and MCP1 by renal CAFs was significantly reduced after treatment with the NAs. Further treatment of renal cancer cells with conditioned media of CAFs pre-treated with the engineered NAs resulted in reduced migration and downregulation of stemness, epithelial to mesenchymal transition and proliferation markers. *In vivo*, the ultrasmall size and LF-targeting properties promoted higher accumulation of the IRDye 800CW-coupled fluorescent NAs in kidney tumors relative to liver and spleen following *i.v.* injection into orthotopic syngeneic kidney tumor-bearing mice. Our strategy represents a paradigm shift in RCC treatment, as it addresses the immunosuppressive role of CAFs by dual mechanistic nano-engineering approach.

#1368 Mitochondrial tRNA fragments as modifiers of breast cancer development and metastasis.

K. L. Swancutt[1], S. Quijano[1], G. Fisette[1], E. Schueddig[1], D. C. Koestler[1], I. Rigoutsos[2], Y. Jing[2], D. R. Welch[1];
[1]University of Kansas Cancer Center, Kansas City, KS, [2]Thomas Jefferson University, Philadelphia, PA

Metastasis accounts for most cancer related morbidity and mortality and is strongly influenced by host genetic background. Using inbred mouse strains, germline single nucleotide polymorphisms (SNP) can shape the tumor microenvironment, immune response, and systemic physiology to permit or restrict metastatic spread. Given the central role of mitochondria in regulating metabolism and cellular signaling, mitochondrial genetics represent an additional, and largely unexplored, dimension of host control over metastasis. To isolate mitochondrial from nuclear contributions, we compared wild-type to mitochondrial nuclear exchange (MNX) mice, in which nuclear genomes from one inbred strain are paired with mitochondrial genomes from another. Across multiple oncogenic drivers, mtDNA significantly alters primary tumor growth and metastatic efficiency. No broad-scope alterations in metabolism distinguish MNX from nuclear genome-matched wild-type mice. So, we focused on a SNP localized to the mitochondrial tRNA for arginine (mt-TR), where distinct SNP correlate with differences in metastasis, nuclear gene regulation, immune profiles, and gut microbial composition. Since nucleus encoded tRNA regulate diverse cellular processes (including transcription, translation, stress responses, and metastasis) via formation of tRNA-derived fragments (tRF), we hypothesized that mitochondrial tRF can function similarly. Using northern blotting, we identified previously unreported mt-TR-derived tRF and found that their expression varies by SNP, sex, and tissues. The fragment patterns indicate that mt-TR undergoes defined site cleavage rather than random degradation. We deduced that tRF derived from mt-TR are highly modified molecules with terminal end modifications and/or base methylations that prevent detection by standard small RNA sequencing. After enzymatic removal of these modifications, the fragments were sequenced, allowing us to map cleavage sites and resolve SNP-dependent fragment populations. These molecules constitute some of the earliest evidence that mitochondrially encoded tRF may contribute to the regulation of complex cancer phenotypes such as metastasis. Ongoing work will determine the molecular interactors which will define molecular networks influenced by mt-tRF. This work has the potential to identify previously unrecognized pathways and metastasis-regulatory mechanisms that can be leveraged to identify new targets for cancer therapy.
Support: Metavivor Inc., Natl. Fndn. Cancer Res., Allison’s Allies, Hall Family Fndn., P30-CA168524

#1369 Urinary extracellular vesicle microRNA profiling enables noninvasive early detection and prognostic stratification of lung cancer.

Y. Ando[1], A. Kiritani[2], S. Mori[2], T. Nojiri[3], J. Watanabe[2], H. Yamaguchi[1], M. Mizunuma[1], Y. Ichikawa[1], Y. Kato[4], J. Araya[2], T. Ohtsuka[2], M. Higashiyama[3], Y. Fujita[2];

[1]Craif Inc., Tokyo, Japan, [2]The Jikei University School of Medicine, Tokyo, Japan, [3]Higashiosaka City Medical Center, Osaka, Japan, [4]Keio University School of Medicine, Tokyo, Japan

Background: Lung cancer remains the leading cause of cancer-related mortality worldwide, and recurrence frequently occurs even after curative-intent therapy. Reliable tools for early detection, prognosis prediction, and recurrence monitoring are critically needed to improve outcomes.

Methods: For early detection of lung cancer, a multicenter case-control study was conducted using urine samples from 278 patients with lung cancer (LC; 50% early-stage) and 213 participants without cancer (NC) collected at four institutions in Japan. Participants were randomly assigned to a training set (208 LC and 159 NC) and a test set (70 LC and 54 NC). Urinary extracellular vesicles-derived microRNAs (EV-miRNAs) were profiled by small RNA sequencing, and machine learning models were developed to evaluate diagnostic performance. For prognosis prediction, urinary miRNA profiles and four-year recurrence-free survival (RFS) were analyzed. Additionally, paired preoperative and postoperative urine samples from 100 surgically treated patients were analyzed, and a subset of patients also provided samples after recurrence to explore temporal miRNA changes during follow-up.

Results: The urinary EV-miRNA classifier demonstrated high diagnostic accuracy, with AUCs of 0.942 (95% CI, 0.918-0.966) in the training and 0.941 (95% CI, 0.899-0.983) in the test sets. Sensitivity and specificity for early-stage LC were 82.0% (95% CI, 73.3%-88.3%) and 92.5% (95% CI, 87.3%-95.6%) in the training set, and 88.2% (95% CI, 73.4%-95.3%) and 87.0% (95% CI, 75.6%-93.6%) in the test set, respectively. Eleven miRNAs were significantly associated with RFS, and a prognostic three-miRNA panel (hsa-miR-181a-5p, hsa-miR-185-5p, and hsa-miR-943) was constructed via fivefold cross-validation, yielding a hazard ratio of 8.3 (95% CI, 1.9-37.0). Furthermore, twelve miRNAs decreased after surgery and re-elevated after recurrence in exploratory analyses, indicating preliminary potential for postoperative monitoring.

Conclusions: This urinary EV-miRNA-based assay enables highly sensitive, noninvasive early detection of LC and demonstrates potential for prognostic assessment and recurrence monitoring. These findings suggest that a urinary EV-miRNA single-assay concept could provide a multifaceted approach for lung cancer management, supporting early detection, risk stratification, and postoperative surveillance.

Keywords: Lung cancer; microRNA; urinary extracellular vesicles; liquid biopsy; early detection; prognosis; recurrence; machine learning

#1370 Developing MTX-5-FU-Gem-miR-15a as a multimodal therapeutic strategy to overcome olaparib resistance in epithelial ovarian cancer.

Amartya Pal, Anushka Ojha, Hersh Bendale, Iwao Ojima, Jingfang Ju

Stony Brook University, Stony Brook, NY

Epithelial ovarian cancer (EOC) is the deadliest gynecological cancer, mainly because of late diagnosis, high relapse (~70%), and drug resistance, including resistance to PARP inhibitors (PARPi). Olaparib, a common PARP inhibitor, is most effective in homologous recombination-deficient (HRD) tumors. However, resistance often develops by activating other DNA repair pathways, such as the ATR/CHK1/WEE1 axis. Several studies show that blocking this pathway can restore olaparib sensitivity in resistant EOC models. miR-15a is often decreased in EOC and targets important regulators of DNA repair, cell-cycle progression, and survival, like WEE1, CHK1, BCL2, and YAP1, indicating that restoring miR-15a could help re-sensitize resistant tumors to PARPi. To enhance therapeutic efficacy, stability and tumor cell specificity, we engineered a multimodal MTX-5-FU-Gem-miR-15a combining the therapeutic power of tumor suppressor miR-15a with methotrexate (MTX), 5-fluorouracil (5-FU), and gemcitabine (Gem). MTX improves tumor specificity by targeting overexpressed folate receptor in EOC cells. Furthermore, the incorporation of 5-FU and Gem allows the construct to both disrupt DNA repair pathways and increase DNA damage burden. Hence, we hypothesized that miR-15a mimic treatment could suppress these pathways and re-sensitize resistant EOC to PARPi.MTX-5-FU-Gem-miR-15a robustly inhibited viability of olaparib-resistant EOC cells (IC50: 5–15 nM) without a delivery vehicle, induced S-phase arrest, and markedly increased apoptosis. The therapeutic efficacy of MTX-5-FU-Gem-miR-15a was improved by over 1000-fold compared to that of Olaparib. Combining MTX-5-FU-Gem-miR-15a with olaparib was significantly more effective than either agent alone. (BLISS Synergy score: 13.2). Transcriptomic profiling revealed downregulation of pathways linked to PARPi resistance, and suppression of pro-survival signaling including PI3K–AKT, mTOR, WNT pathways, consistent with broad disruption of resistance-associated networks. The mimic also retained potency in cancer stem–like (CSCs) spheroids (IC50: ~3 nM) without any delivery vehicle. To evaluate therapeutic efficacy *in vivo*, a metastatic olaparib-resistant EOC model was established by tail-vein injection of olaparib resistant EOC cells into NOD/SCID mice. MTX-5-FU-Gem-miR-15a treatment (3.75 mg/kg) reduced tumor burden by >5.5-fold (~80%) and significantly improved survival without observable toxicity or weight loss. Statistical significance was determined using Student's t-test or two-way ANOVA ($p < 0.05$). Overall, these findings demonstrate that MTX-5FU-Gem-miR-15a is a powerful multimodal miRNA-based therapeutic as it has the potential to exert strong antitumor effects in EOC and overcome drug resistance, supporting its potential as a next-generation strategy to improve patient outcomes.

#1371 POLR1B-derived circular RNA hsa-POLR1B_0014 orchestrates RNA polymerase I transcription and oncogenic hallmarks in lung adenocarcinoma through miR-181b-5p-mediated regulatory networks.

DEEPIKA ANTIL[1], Mansi Sharma[1], karmakar Arpita[1], Srivatsava Naidu[2]

[1]Indian Institute of Technology, Ropar, Rupnagar, India,[2]Biomedical Engineering, Indian Institute of Technology Ropar, Ropar, India

RNA Polymerase I (Pol I) transcription is hyperactive in lung adenocarcinoma (LUAD), underpinning various hallmarks of cancer, including therapeutic resistance. However, the molecular mechanisms, particularly the role(s) of non-coding RNAs, that couple the Pol I transcriptional machinery to oncogenic pathways remain poorly defined. Here, we identify hsa-POLR1B_0014, a circRNA derived from POLR1B gene encoding the core subunit of Pol I, is up-regulated in LUAD in concert with its parent gene. RNA-sequencing analysis of a stable hsa-POLR1B_0014 knockdown LUAD cell line (A549) revealed upregulation of several miRNAs associated with oncogenic pathways. Among these, miR-181b-5p emerged as a key effector predicted to regulate LUAD-relevant malignant networks. Consistently, integrative analyses of public transcriptomic datasets, and LUAD tissues confirmed miR-181b-5p downregulation in LUAD. Furthermore, back-splice junction pull-down and AGO2-RNA immunoprecipitation assays validated a direct interaction between hsa-POLR1B_0014 and miR-181b-5p, with circRNA knockdown enhancing miRNA enrichment, thereby confirming its miRNA-decoy function. Functionally, loss of hsa-POLR1B_0014 elevated miR-181b-5p levels, leading to suppression of TAF1A, an essential Pol I transcription factor, thereby diminishing rRNA synthesis. This reveals a positive feedback circuit in which a Pol I-derived circRNA sustains Pol I output through sequestration of an inhibitory miRNA. Notably, miR-181b-5p also directly targets mTOR, a master regulator of Pol I transcription and malignant proliferation, inducing G1/S cell cycle arrest, apoptosis, and downregulation of Bcl2. Furthermore, miR-181b-5p suppression of ZEB1 attenuates migration, invasion, and enhances chemosensitivity to doxorubicin and cisplatin. In vivo, xenografts derived from hsa-POLR1B_0014-depleted LUAD cells exhibited markedly reduced tumor burden, rRNA synthesis, and Ki-67 expression, and increased apoptosis. Our findings uncover a previously unrecognized Pol I-derived circRNA-miRNA regulatory axis that coordinates ribosome biogenesis, cell growth, and therapeutic resistance in LUAD. By linking Pol I machinery to multiple oncogenic pathways, hsa-POLR1B_0014 emerges as both a driver and a vulnerability within the cancer Pol I network. These results highlight circRNA-mediated regulation of Pol I transcription as a central node controlling cancer hallmarks and a promising therapeutic target in LUAD.

: Population Sciences at the Forefront 1: Risk Factors Influencing Cancer Incidence and Survival Minisymposium

#1374 Adherence to the EAT-Lancet reference diet in adolescence and risk of invasive breast cancer among US women.

P. Le[1], W. Willett[1], B. Rosner[1], W. Y. Chen[2], M. D. Holmes[3], A. Romanos-Nanclares[3], A. Eliassen[1];
[1]Harvard T. H. Chan School of Public Health, Boston, MA, [2]Dana-Farber Cancer Institute, Boston, MA, [3]Brigham & Women's Hospital, and Harvard Medical School, Boston, MA

In 2019, the EAT-Lancet Commission recommended a dietary pattern that is both good for human health and environmentally sustainable. The EAT-Lancet reference diet emphasizes high consumption of vegetables, fruits, whole grains, legumes, nuts, and unsaturated oils, low to moderate intake of seafood and poultry, and no to low intake of red meat, processed meat, added sugar, added saturated fat, refined grains, and starchy vegetables. The Planetary Health Dietary Index (PHDI) was subsequently developed to quantify adherence to this reference diet. Adolescence is marked by rapid breast tissue development and hormonal changes, presenting a susceptible window for breast carcinogenesis. Exposures during this period, including diet, could influence breast cancer risk.This study examines the association between the PHDI during adolescence and subsequent risk of invasive breast cancer in adulthood. We analyzed data from 47,355 women aged 33-52 years old in the Nurses' Health Study II (NHSII) who recalled their adolescent diet using a food frequency questionnaire in 1998. PHDI scores were calculated to reflect adherence to the EAT-Lancet reference diet in adolescence. Participants were followed from 1998 until breast or other cancer diagnosis, death, loss to follow-up, or the end of 2019, whichever occurred first. Multivariable Cox Proportional Hazards models were used to estimate hazard ratios (HR) and 95% confidence intervals (CI).Over 896,674 person-years of follow-up, 1945 invasive breast cancer cases were documented, including 1245 estrogen receptor (ER) - positive and 233 ER-negative cases. Adolescent PHDI was not significantly associated with overall invasive breast cancer risk (HR for highest vs. lowest quartile = 0.89; 95% CI: 0.78, 1.02 ; p trend = 0.29), or with ER-positive breast cancer (HR = 1.00; 95% CI: 0.85, 1.18; p trend = 0.50). However, higher PHDI during adolescence was significantly associated with reduced risk of ER-negative breast cancer (HR = 0.69; 95% CI: 0.47, 1.00; p trend = 0.05), which was slightly attenuated after adjusting for weight change since age 18 (HR = 0.70; 95% CI: 0.48, 1.01; p trend = 0.06). The association between PHDI during adolescence and overall invasive breast cancer risk did not differ by menopausal status or by subgroups of body mass index at age 18.In conclusion, adherence to the EAT-Lancet reference diet during adolescence may reduce the risk of more aggressive breast cancer subtypes, particularly ER-negative cases, but not overall breast cancer. These findings highlight a dietary pattern that could be both health-promoting and environmentally sustainable during a key developmental period.

#1375 Cardiorespiratory multimorbidity and lung cancer risk: A population-based cohort study.

P. Wang[1], Y. Zhang[2], H. Du[1], H. Dai[1], **K. Chen**[1];
[1]Tianjin Medical University Cancer Institute & Hospital, Tianjin, China, [2]Tianjin Medical University, Tianjin, China

Background: Studies have suggested close links between cardiorespiratory diseases and lung cancer. The coexistence of respiratory disease (RD) and cardiovascular disease (CVD) is common. However, the impact of cardiorespiratory multimorbidity (CRM) and its progression trajectory remains poorly understood. This study aimed to explore the relationship of CRM with lung cancer risk and characterize disease trajectories from healthy state through RD, CVD, or subsequent CRM to lung cancer.
Methods: We included 365,735 UK Biobank participants who were free of cancer, RD, or CVD at baseline and had a follow-up time of more than one year. CRM was defined as the co-occurrence of ≥1 RD and ≥1 CVD. RD comprised COPD and asthma. CVD included angina, myocardial infarction (MI), atrial fibrillation (AF), heart failure (HF), peripheral vascular disease (PVD) and stroke. The study outcome was incident lung cancer. Time-varying Cox regression models and accelerated failure time (AFT) regression models were used to assess the associations of CRM with risks of lung cancer incidence and onset time of lung cancer. Multi-state model was further constructed to characterize progression trajectory from healthy state through RD, CVD, or CRM to lung cancer, and to estimate the transition intensity, transition probability and transition time from each state to lung cancer.
Results: During a median follow-up of 13.7 years, 3,464 of the 365,735 participants were diagnosed with lung cancer. Cox models showed that CRM was associated with the highest risk of lung cancer incidence (hazard ratio [HR]=4.11, 95% CI: 3.48-4.85), followed by RD (HR=3.39, 95% CI: 3.01-3.81) and CVD (HR=1.52, 95% CI: 1.36-1.70). AFT models indicated that participants with CRM also showed an earlier onset time of lung cancer (time ratio [TR]=0.20, 95% CI: 0.17-0.23) than those with RD (TR = 0.25, 95% CI: 0.22-0.28) or CVD (TR = 0.53, 95% CI: 0.48-0.59). The multi-state model showed that 22.0% of participants with RD progressed to CRM, compared with 4.9% of those with CVD. The transition proportion to lung cancer was highest for CRM (2.8%), followed by RD (2.1%) and CVD (0.8%). The transition intensity and transition probability curves revealed that the transition intensity and probability from CRM to lung cancer was greater than that from RD or CVD to lung cancer. Additionally, CRM was associated with a significantly shortened progression time to lung cancer (12.39 years) than RD (12.64 years) or CVD (12.87 years).
Conclusion: CRM is associated with a higher lung cancer risk and more rapid progression than individual RD or CVD. These results emphasize CRM may serve as a high-risk clinical phenotype in lung cancer prevention and underscore the potential value of incorporating CRM management into lung cancer prevention strategies.

#1377 Generational immigration status and gastric cancer incidence among Japanese descendants: An analysis of the Multiethnic Cohort study.

Haejin In[1], **Katherine A. De la Torre-Cisneros**[1], Alexandra Adams[1], Chunxia Chen[1], Brijesh Rana[1], Lynne R. Wilkens[2], Meira Epplein[3]

[1]Rutgers Cancer Institute of New Jersey, New Brunswick, NJ,[2]University of Hawaii, Manoa, HI,[3]Duke University Medical Center, Durham, NC

Background: Racial and ethnic minorities in the US experience disproportionately higher rates of gastric cancer (GC) compared to the general population. However, the impact of immigration history on these disparities is not well understood. We aimed to evaluate the association between immigration generation and GC risk among Japanese descendants.
Methods: We conducted analyses using the population-based Multiethnic Cohort Study (MEC), which enrolled residents of Hawaii and California between 1993 to 1996. Individuals who self-identified as being of Japanese ethnic or racial background were included, excluding those who were born or had parents born in locations other than the US or Japan. Cox proportional hazard models were used to examine the association between immigration generation of Japanese descendants and the risk of GC overall and by anatomical subtype, adjusting for demographic, dietary, and lifestyle variables.
Results: Among 94,232 individuals (median age: 61 years; male 47.4%), 716 primary GC cases were identified. The risk of developing GC was higher among all three generations of Japanese descendants compared to non-Hispanic Whites (NHWs). First generation had the highest risk (HR: 4.62, 95%CI 3.24-6.59), followed by the second generation (US-born, with both parents Japan-born; HR: 3.66, 95%CI 2.89-4.64; US-born, with one parent Japan-born, HR: 3.39, 95%CI 2.55-4.50), and the third generation (HR: 2.57, 95%CI 1.93-3.42). The association was strongest among non-cardia GC, with HRs of 5.93, 4.48, and 3.28 for the first, second, and third generations, respectively.
Conclusions: GC risk declined across successive generations of Japanese descendants but remained significantly higher than in NHWs. Recognizing and monitoring these persistently high-risk populations may guide targeted screening and inform research into environmental, biological, and transgenerational factors underlying gastric cancer susceptibility.

Table 1. HRs of gastric cancer incidence by generation status among Japanese descendants

	NHW	1st Generation	2nd Generation, both parents Japanese	2nd Generation, one parent Japanese	3rd Generation	p-trend
All						
Participants	39779	4136	23241	8615	18461	
Cases	103	48	370	99	96	
HR (95%CI)	1.00	4.62(3.24-6.59)	3.66(2.89-4.64)	3.39(2.55-4.50)	2.57(1.93-3.42)	0.001
Men						
Participants	18725	1209	11648	4227	8836	
Cases	65	25	237	67	59	
HR (95%CI)	1.00	5.73(3.75-9.19	3.50(2.60-4.70)	3.42(2.41-4.85)	2.31(1.61-3.32)	0.001
Women						
Participants	21054	2904	11593	4388	9625	
Cases	38	23	133	32	37	
HR (95%CI)	1.00	3.81(2.18-6.66)	3.81(2.54-5.73)	3.24(1.98-5.31)	3.03(1.88-4.88)	0.001

#1378 Development and validation of a parsimonious electronic health record model for pancreatic cancer risk stratification.

L. A. Mavromatis[1], V. Zlatanic[1], E. Agarunov[1], L. Chen[2], S. A. Sanoba[1], L. I. Horwitz[1], N. Razavian[1], A. Maitra[1], T. A. Gonda[1], M. E. Grams[1];

[1]NYU Grossman School of Medicine, New York, NY, [2]New York University, New York, NY

Background Pancreatic ductal adenocarcinoma (PDAC) is projected to become the second leading cause of cancer death in the United States by 2030. Early detection of PDAC improves outcomes. However, screening is impractical in the general population due to low disease incidence. We previously developed a PDAC prediction model using machine learning in an institutional electronic health record (EHR) database. Here, we aimed to improve generalizability, interpretability, and parsimony by developing and validating a Cox model in a national EHR database.

Methods We used Optum Labs DataWarehouse (OLDW), a U.S. EHR and claims database, to develop a Cox model predicting incident PDAC in adults ages ≥40 years in 23 health systems (training cohort; N = 4,836,428). Elastic net with 10-fold cross-validation selected from candidate risk predictors, which included demographics, diagnoses/symptoms measured by International Classification of Diseases (ICD) codes, and routine laboratory values. Performance was assessed by 3-year area under the receiver operating characteristic curve (AUC) and calibration slope and intercept in 31 distinct health systems (validation cohort; N = 5,607,398). Sensitivity analyses excluded adults <50 years, those with abdominal imaging in the prior year, and PDAC diagnosed in the first 6 months, and stratified participants by sex. International validation was performed in the UK Biobank (UKB) (N = 498,754).

Results In the training cohort (mean age 60.4 years), 14,405 patients developed PDAC, with a crude incidence rate (IR) of 56 per 100,000 person-years (PY); in the validation cohort (mean age 60.2 years), 11,693 patients developed PDAC (IR, 55/100,000 PY). The final elastic net model included 19 predictors. Top predictors included chronic pancreatitis and other gastrointestinal conditions, prior cancers, type 2 diabetes, elevated aspartate aminotransferase, current smoking, and male sex. 3-year AUC was 0.75 in both the training and validation cohorts; discrimination was equivalent in males and females. 3-year calibration in the validation cohort was excellent. The hazard ratio of PDAC in the top percentile of predicted risk compared to the 45^{th}-55^{th} percentile was 7.63 (95% CI, 6.85-8.49) and NNS in the top percentile was 128 (95% CI, 117-141). Performance was similar after excluding patients with recent abdominal imaging, PDAC diagnosed in the 6 months following index, and patients under 50. In UKB (IR, 44/100,000 PY), AUC was 0.71 with acceptable calibration.

Conclusions A parsimonious EHR-based PDAC risk model developed in diverse U.S. health systems demonstrated strong 3-year discrimination and good generalizability to cohorts in the United States and United Kingdom. A subsequent prospective validation study will assess the feasibility of EHR-driven PDAC case-finding.

#1379 Age-related differences in predicted basal metabolic rate and survival outcomes after colorectal cancer in the ColoCare Study.

R. Ji[1], P. Erickson[1], T. Lin[1], Y. Zhao[1], J. Van Onselen[1], M. N. Ilozumba[1], I. Strehli[1], M. Mclaws[1], L. Huang[1], J. Cohan[1], E. Siegel[2], M. Extermann[2], A. T. Toriola[3], D. Shibata[4], C. I. Li[5], J. C. Figueiredo[6], D. A. Byrd[2], V. Damerell[7], B. Gigic[7], C. M. Ulrich[1], **S. Hardikar**[1]; [1]University of Utah, Huntsman Cancer Institute, Salt Lake City, UT, [2]Moffitt Cancer Center, Tampa, FL, [3]Washington University School of Medicine, St. Louis, MO, [4]University of Tennessee Health Science Center, Memphis, TN, [5]Fred Hutchinson Cancer Center, Seattle, WA, [6]Samuel Oschin Comprehensive Cancer Institute, Cedars-Sinai Medical Center, Los Angeles, CA, [7]Heidelberg University Hospital, Heidelberg, Germany

BACKGROUND Basal Metabolic Rate (BMR), a key indicator of resting energy expenditure, reflects overall metabolism and varies by age, sex, weight, and height. Younger and overweight/obese individuals exhibit a higher BMR, which has been linked to an increased risk of obesity-related cancers, including colorectal cancer (CRC). The role of BMR in survival after CRC remains unexplored. This study investigates the association between BMR at CRC diagnosis and overall (OS) and CRC-specific survival, evaluating differences by age of onset and obesity status.

METHODS We analysed 3876 patients with stage I-IV CRC from seven ColoCare Study sites. Baseline BMR was estimated using the WHO/FAO/UNU Schofield equation and categorized into sex-specific tertiles. Anthropometric measurements (height, weight) and vital status were obtained through medical records, follow-up mailings and linkage with cancer and death registries. Covariates (demographic, lifestyle, and clinical characteristics) were collected via baseline questionnaires. Cox proportional hazards regression models estimated hazard ratios (HR) and 95% confidence intervals (CI), stratified by age (<50, 50-65, >65 yrs) and BMI (normal weight, overweight, obese) for 5- and 10-year survival. Multivariate models were adjusted for age at diagnosis, study center, sex, BMI, clinical and lifestyle factors.

RESULTS Overall, 25% of participants were <50 yrs old, 43% were 50-65 yrs and 32% were ≥65 yrs; 44% were female. Colon cancer accounted for 51% of the diagnoses and 20% had stage III CRC. Mean BMR was 1673±304 kcal/day with higher values observed among men compared to women (3rd tertile: 2136 ± 202 vs. 1670 ± 156 kcal/day). 74% of participants in the 3rd tertile of BMR were obese compared to only 2% normal weight. BMR declined with age (3rd tertile: 34% in <50 yrs vs.16% in ≥65 yrs). At 5-years post-diagnosis, higher BMR was associated with significantly improved OS [HR (95%CI): 0.84(0.65-1.08)], independent of BMI. This association varied by sex and age, younger men in the 3rd tertile had better survival [HR (95% CI): 0.34 (0.12-0.95)] compared to younger women and older men [HR (95% CI): 0.51 (0.15-1.74)) and 1.46 (0.82-2.61), respectively]. Similar patterns were observed for CRC-specific survival. No significant associations were observed for OS or CRC-specific survival at 10-years post-diagnosis, suggesting that BMR may influence short- rather than long-term survival.

CONCLUSION In the ColoCare Study cohort, BMR varied substantially by sex, age and obesity status. Higher BMR, particularly among younger men, was associated with improved short-term OS, independent of BMI, but not for long-term follow-up. These findings highlight the potential of BMR for early risk stratification in CRC. Incorporating metabolic assessment at diagnosis could inform personalized interventions and targeted survivorship strategies.

#1380 Patient-level and claim-level analysis of telehealth disparities in cancer care: Lower uptake but higher intensity among racial or ethnic minority groups and older adults.

Sakshith Reddy Chintala[1], Margaret Meagher[2], Ceser Delgado[2], Amir Salmasi[2], Micheal Liss[2], Brett Meyer[2], Richard Cripps[3], Elena Martinez[4], Hala Madanat[3], James Murphy[2], Juan Javier-DesLoges[2], Humberto Parada[3]

[1]Radiation Medicine and Applied Sciences, University of California, San Diego, San Diego, CA,[2]University of California, San Diego, San Diego, CA,[3]San Diego State University, San Diego, CA,[4]UCSD Moores Cancer Center, San Diego, CA

Background: Telehealth use expanded rapidly during the COVID-19 pandemic including for cancer care, however, disparities in telehealth access among cancer patients remain poorly understood. While prior studies examined patient-level telehealth adoption, claim-level utilization patterns may reveal different mechanisms.

Methods: We conducted a population-based cohort study using Medicare claims data of patients aged 65+ years diagnosed with bladder, breast, colorectal, gastric, lung, or prostate cancer (2020-2022) with continuous Part A/B enrollment. We examined telehealth utilization within one year of cancer diagnosis using multivariable logistic regression to estimate adjusted odds ratios (aORs) and 95% confidence intervals (CIs) at two levels: (1) patient-level analysis of any telehealth use,and (2) claim-level analysis restricted to cancer-related care identified by cancer-related provider specialties to assess telehealth delivery patterns.

Results: Among 573,328 patients generating 5,276,398 cancer-related claims, 60.6% used telehealth within one year of diagnosis, representing 14.6% of cancer care encounters. At the patient level, compared to non-Hispanic White patients, Asian/Pacific Islander (aOR 0.85, 95%CI 0.82-0.88), Black (aOR 0.78, 95%CI 0.77-0.80), and Hispanic (aOR 0.89, 95%CI 0.86-0.91) patients had lower odds of any telehealth use. Compared to ages 65-69, older adults showed steep age gradients, with 85+ having 52% lower odds (aOR 0.48, 95%CI 0.47-0.484). Rural patients had higher uptake versus urban (aOR 1.17, 95%CI 1.16-1.19). At the claim- level for cancer care delivery, disparities substantially attenuated or reversed: Asian/Pacific Islander (aOR 1.15, 95%CI 1.13-1.17), Hispanic (aOR 1.07, 95%CI 1.06-1.09), Black (aOR 0.96, 95%CI 0.95-0.97), and 85+ years (aOR 0.92, 95%CI 0.92-0.94) . Compared to physicians, advanced practice providers had higher delivery (aOR 1.28); female providers versus male (aOR 1.12) and academic versus non-academic centers (aOR 1.08) showed higher use.

Conclusions: Telehealth disparities in cancer care may be primarily driven by initial access barriers rather than engagement once accessed. Racial/ethnic minorities and older adults who overcome uptake barriers demonstrate high-intensity telehealth use for cancer treatment, suggesting substantial unmet need. Interventions should prioritize addressing initial access barriers such as digital literacy, technology access, and language services-to ensure equitable cancer care delivery.

#1381 The Confluence Project: Largest multi-ancestry genome-wide association study of breast cancer identifies 469 susceptibility loci in over two million participants.

T.-. National Cancer Institute, African-ancestry Breast Cancer Genetic Consortium, Breast Cancer Association Consortium, Consortium of Investigators of Modifiers of BRCA1/2, Latin America Genomics of Breast Cancer Consortium, Male Breast Cancer Genetics Consortium;
National Cancer Inst. Div. of Cancer Epidemiology & Genetics, Bethesda, MD

Background: Genome wide association studies (GWAS) of breast cancer have identified over 230 susceptibility loci, yet much of its heritable risk remains unexplained. Moreover, previous large GWAS included mostly European-ancestry samples, restricting the scope of genetic variation studied and limiting the generalizability of polygenic risk scores trained in these studies. The Confluence Project is a large, international collaboration of breast cancer consortia, biobanks, and other individual studies, studying breast cancer in females, males, and carriers of breast cancer susceptibility genes. With over 300 studies from 62 countries, Confluence includes over 400,000 breast cancer cases and 1,600,000 controls, nearly tripling the effective sample size of previous GWAS and substantially increasing sample diversity (approximate number of cases / controls, by genetic ancestry group: African (AFR)= 24,000 / 67,500, East Asian (EAS) = 49,000 / 429,000, Admixed American (AMR) = 28,500 / 78,000). Confluence is designed as a resource to address a range of breast cancer genetic questions by contributors and the wider scientific community.

Methods: We conducted a multi-ancestry GWAS of overall breast cancer risk (variants analyzed=47,790,460, min allele frequency = 0.03%). Individual-level genotyping data was available on 322,332 cases and 269,357 controls, including 53,058 *BRCA1/2* carriers, 24,883 of which were breast cancer cases. This data was processed through a harmonized quality-control pipeline and imputed by array to the TOPMed reference panel. GWAS were performed separately by array using REGENIE, adjusting for the first ten principal components. Resulting summary statistics were combined with similar statistics from 18 external biobanks (101,579 cases and 1,373,259 controls) through fixed-effect meta-analysis. Novel signals were declared if located more than +/-1Mb from any known locus that were based on previously published GWAS.

Results: We identified 469 independent genome-wide significant loci ($P<5x10^{-8}$) of which 249 (53%) were novel. Among the 240 loci previously reported, 220 (92%) were associated at $p<5x10^{-8}$. Assuming shared effect-sizes across populations, while accounting for ancestry-specific allele frequency differences, the 249 discovered loci increased the logit-scale variance relative to previously known loci from approximately 29% (in AFR) to 36% (in EAS).

Conclusion: This study represents the largest and most ancestrally diverse GWAS of breast cancer. The novel loci identify new candidate genes, substantially improves the proportion of heritability explained, and lay the groundwork for an expanded understanding of breast cancer biology. Ongoing analyses will extend these findings to sex-, ancestry-, and subtype-specific risk, including *BRCA1/2* carriers, and polygenic risk prediction.

Monday, April 20, 2026

: Cancer and Aging: Implications for Outcomes
Poster Session

#2460 Deficit accumulation as a predictor of lung cancer risk in older adults.

Seung Jun Shin[1], Shuyan Qiu[2], Yushu Shi[3], Eunji Choi[3]

[1]Cornell University, Ithaca, NY,[2]Weill Cornell Medicine, New York, NY,[3]Weill Cornell Medicine, Cornell University, New York, NY

Introduction: Lung cancer affects older adults, with a median age at diagnosis of 71. While low dose CT screening is recommended for high-risk smokers, 25% of cases occur in non-smokers, and few risk factors can be repeatedly assessed for early detection, especially in older adults. Age is a major cancer risk factor, and many cancer patients show accelerated biological or epigenetic aging before diagnosis, but chronological age may not reflect their true physiological condition. Deficit accumulation—a geriatric index of multisystem decline and vulnerability—may better reflect overall health than chronological age and has been reported to signal risk for age-related chronic diseases. However, its role in predicting lung cancer is unclear. We examined whether deficit accumulation predicts lung cancer beyond established predictors.
Methods: We analyzed data from the linked SEER-Medicare Health Outcomes Survey (MHOS), including adults aged ≥65 who completed at least one MHOS survey between 1998-2011, followed via 2020. Incident lung cancer was identified using SEER registry data, and all-cause deaths were treated as competing events. Deficit accumulation was measured using a validated 25-item deficit accumulation index for cancer patients (range 0-1), categorized as robust (0-0.2), frail (0.2-0.5), and severely frail (>0.5). For individuals who later developed lung cancer, deficit accumulation was assessed within one year prior to diagnosis. Cause-specific Cox models estimated hazard ratios (HRs) for the association between deficit accumulation and incident lung cancer, adjusting for established predictors including age at survey, sex, smoking, body mass index (BMI), education, and prior cancer history. Variable importance metrics were used to quantify the relative contribution of model features to lung cancer risk.
Results: Among 11,440 older adults, 1,011 developed lung cancer and 115 had a competing event of death before lung cancer diagnosis during follow-up. Frail and severely frail individuals had 1.45 (95% CI: 1.27-1.66) and 1.72 (95% CI: 1.40-2.12) times higher risk of developing lung cancer, respectively, compared with robust older adults. Other established predictors performed as expected, with increased risk associated with smoking and prior cancer history, and decreased risk associated with higher BMI and education. The pre-diagnostic deficit accumulation measure ranked as the third most influential predictor of lung cancer, followed by smoking history and prior cancer history. The predictive effect of deficit accumulation on lung cancer risk was more intensified among non-smokers (vs. active smokers), but interaction terms were not statistically significant.
Conclusions: The 1-year pre-diagnostic deficit accumulation measure was predictive of lung cancer risk in older adults. This finding may help identify high-risk individuals who could benefit from early detection efforts.

#2461 Aging reprograms early oncogenic responses to *Braf*^{V600E} activation in colon organoids through altered growth phenotype, senescence, and secretory signaling.

Shilpa Bisht[1], Kaavya Mahadevan Iyer[1], Akash Sureshkumar[2], Rachael Powers[3], Ying Cui[1], Jinxiao Liang[1], Lijing Yang[4], Daniel Petkovich[5], Damilola Killanin[6], Ray-Whay C. Yen[1], Tina Largent[1], Stephen B. Baylin[1], Rafael de Cabo[7], Hariharan P. Easwaran[1]

[1]Oncology, Johns Hopkins University School of Medicine, Baltimore, MD,[2]Mathematics, Emory University, Atlanta, GA,[3]Department of Neurology, University of Michigan, Ann Arbor, MI,[4]Radiation and Medical Oncology, Zhongnan Hospital of Wuhan University, Hubei, PR, China,[5]Champions Oncology, Rockville, MD,[6]National Institute of Dental and Craniofacial Research, National Institute of Health, Bethesda, MD,[7]Experimental Gerontology, National Institute on Aging, Baltimore, MD

Colorectal cancer (CRC) incidence increases with advanced age, yet how aging affects early epithelial responses to oncogenic mutations remains poorly understood. *Braf*^{V600E} mutation is a major driver of serrated pathway of CRC, but the initial molecular events caused by *Braf*^{V600E} activation in aged intestinal stem cells are largely undefined. In the present study, we used proximal colon organoids (COs) derived from young (2 months) and aged (22 months) male and female mice carrying heterozygous Cre-activable *Braf*^{V600E} (termed Braf$^{+/LSL}$) transgene at the endogenous *Braf* locus and Cre-activable gene encoding red fluorescence marker protein, TdTom (termed TdTom$^{+/LSL}$) to model age-dependent responses to oncogenic *Braf*^{V600E}. We found that *Braf*^{V600E} activation differentially affects epithelial growth depending on age. Following Cre-mediated *Braf*^{V600E} induction, young male and female COs exhibited a pronounced proliferative burst, followed by a sharp growth collapse later passage, indicating an initial oncogene-induced senescence (OIS) response. In contrast, aged COs showed sustained growth across serial passages, indicating a failure to mount an OIS program. qPCR analysis aligned with these phenotypes: in young organoids, senescence-associated genes (*p21*, *p16*, *Cxcl2*, *Il6*) showed strong induction specifically at passage 4, coinciding with growth attenuation. Aged COs showed markedly reduced or absent induction of these transcripts at all passages, supporting an age-related loss of senescence competence. Loss of senescence competence is specific to oncogene response, not to general DNA damaging agents. The secretary profile further distinguished these responses with increases in CXCL2 and IL-6 secretion in young *Braf*^{V600E} activated COs, reflecting SASP activation, whereas aged COs produced minimal amounts of these cytokines. Additionally, IGF2 secretion was significantly diminished in aged COs compared to young counterparts, suggesting altered growth factor signaling that may facilitate continued proliferation under oncogenic stress. Genome wide transcriptome and epigenome analyses indicate emergence of pro-tumorigenic epigenetic states in colon epithelium, which includes disrupted senescence and metabolic pathways. These findings are especially significant given the widely held view that aging is accompanied by increased stem cell senescence. Our studies reveal a paradox: aged epithelial cells exhibit a diminished senescence response when exposed to oncogenes. This novel observation reveals that the ability of aged cells to bypass OIS, together with a reduced inflammatory response, plays a key role in the increased susceptibility to tumor initiation observed with aging.

#2462 Longitudinal change in epigenetic aging and telomere length in breast cancer survivors.

Judith E. Carroll[1], Cynthia Kusters[2], Catherine M. Crespi[3], Michael R. Irwin[1], Patricia A. Ganz[4], Laura Petersen[5], Julienne E. Bower[6]

[1]Psychiatry & Biobehavioral Sciences, UCLA - University of California Los Angeles, Los Angeles, CA,[2]Epidemiology, UCLA - University of California Los Angeles, Los Angeles, CA,[3]University of California, Los Angeles, Los Angeles, CA,[4]Professor, Div. of Cancer Prevention & Control Res., UCLA Jonsson Comprehensive Cancer Center, Los Angeles, CA,[5]UCLA - University of California Los Angeles, Los Angeles, CA,[6]Psychology, UCLA - University of California Los Angeles, Los Angeles, CA

PURPOSE: Cancer treatments may accelerate biological aging, but longitudinal studies of biological markers of aging are needed to better characterize patterns of biological aging over time.
METHODS: We followed 184 women with breast cancer (stage 0-III) from diagnosis to 18 months post treatment. We evaluated biological aging in three treatment groups: chemotherapy (with or without radiotherapy), radiotherapy (without chemotherapy), and neither chemotherapy or radiotherapy. Measures of epigenetic age (PCPhenoAge, GrimAge, DunedinPACE) and telomere length were obtained. Linear mixed models estimated within-group change from pre-treatment to immediate post, 6, 12, and 18 months post-treatment.
RESULTS: Women who received chemotherapy exhibited increased epigenetic age in PCPhenoAge, GrimAge, and DunedinPACE and shortening of telomere length acutely following treatment (Ps<0.001). The change attenuated but remained significantly different than baseline for GrimAge, DunedinPACE, and telomere length out to 18 months. Women treated with radiotherapy exhibited a trend for increases in PCPhenoAge and significant telomere length shortening 6 months following treatment that remained modified at 18 months (Ps<0.05). There were no significant changes in epigenetic age or telomere length among women who did not receive either chemotherapy or radiation.
CONCLUSION: We observed an acceleration of epigenetic age, an increase in the pace of aging, and telomere shortening among women receiving treatment for breast cancer. The effect was predominantly amongst women who received chemotherapy with or without radiation, pointing to this treatment regimen having the most damaging effects. These results support the premise that cancer treatment may accelerate aging and support further research to identify key clinical and biological targets to remediate these effects.

#2463 Microbiota-dependent complex dietary polysaccharide degradation suppresses inflammaging and colorectal cancer susceptibility.

Rekha Jalandra, Mousumi Bhattacharjee, Ruchika Maurya, Radhika R. Gudi, Jayda S. Gilliard, Caroline Westwater, Chenthamarakshan Vasu

The Medical University of South Carolina (MUSC), Charleston, SC

Aging is associated with systemic low-grade inflammation (inflammaging) and increased susceptibility to infections, chronic diseases, and colorectal cancer (CRC). Age-associated gut dysbiosis contributes to a decline in beneficial microbial metabolites, particularly short-chain fatty acids (SCFAs), fostering a pro-inflammatory intestinal microenvironment that promotes tumorigenesis. Dietary strategies that restore microbial balance and enhance SCFA production could mitigate inflammaging and CRC risk. Fermentation of complex dietary polysaccharides (CDPs) by gut microbiota can generate host-beneficial metabolites, including SCFA, and help maintain epithelial barrier integrity and suppress aging-associated inflammation. In this study, using high-pure beta-glucans (BGs) from yeast (yeast beta-1,3/1,6-glucan; YBG) and microalgae (algal beta-1,3-glucan; paramylon, PM), we show that the CDP degradation process alters microbiota composition and metabolite profiles in vitro and in vivo, suppresses aging-associated inflammation and cancer susceptibility in the azoxymethane/dextran sulfate sodium (AOM/DSS) model of CRC. Dietary treatment using BGs significantly altered gut microbial composition, notably increasing the abundance of *Akkermansia muciniphila*, a mucin-degrading bacterium known to produce SCFAs. Fecal microbial cultures of aged mice with BGs showed elevated levels of anti-inflammatory metabolites and reduced levels of pro-inflammatory factors. Aged mice treated with BGs showed significantly lower colorectal tumor burden and disease severity. Bulk RNA sequencing of colon tissue of BG-treated mice revealed suppressed expression of oncogenes, metastasis-related genes, and pro-inflammatory cytokines, along with increased expression of anti-inflammatory cytokines and *Muc2*, a key gene involved in mucin production and gut barrier function. Our findings suggest that the CDP degradation process can rejuvenate the aging gut microbiota, restore host beneficial metabolite production and gut integrity, and suppress inflammaging. Ongoing studies using gnotobiotic animals and colonoid cultures aim to further elucidate the mechanisms by which CDP degradation by gut microbiota modulates gut integrity, inflammation, and CRC susceptibility. Collectively, this work demonstrates the potential of microbiota-targeted dietary strategies for promoting healthy aging, rejuvenating gut microbiota, and reducing CRC risk in elderly populations.

#2464 Novel mechanism driving p53 loss that dictates bladder cancer aggressive phenotypes.

Sabir Salim[1], Sreenidhi Mohanvelu[1], Poorvi Subramanian[1], Afsana Parveen Jahir Hussain[1], Sheeja Aravindan[2], Natarajan Aravindan[1]

[1]Department of Physiological Sciences, Oklahoma State University, Stillwater, OK,[2]OU Health Stephenson Cancer Center, Oklahoma City, OK

Bladder cancer (BLCA) remains a clinically heterogeneous disease, characterized by high mutational burden, recurrence rates, and poor survival in advanced stages. Identifying molecular drivers of progression and therapy resistance is crucial for improving patient outcomes. In muscle-invasive bladder cancer (MIBC), loss of p53 is a major molecular hallmark that drives aggressive basal/squamous-like subtypes, conferring resistance to cell killing and immune evasion. However, the mechanisms underlying p53 inactivation/loss remain thus far unrealized. We previously showed that Retinal Degeneration Protein 3 (RD3) is widely expressed in the body and plays a tumor-protective role. In this study, we investigated the clinical significance of RD3 loss and its interplay with p53 status in a cohort of 107 BLCA patients. Using a custom-archived tissue microarray, RD3 expression was profiled (immunohistochemistry). We observed a complete loss of RD3 in aggressive BLCA tumors when compared with clinically favorable non-muscle invasive bladder cancer (NMIBC). RD3 loss strongly correlated with advanced tumor stage (MIBC), disease dissemination, therapy resistance, metastasis, and recurrence. Survival analysis indicated a strong trend toward decreased overall survival (OS), progression-free survival (PFS), and relapse-free survival (RFS) in RD3-deficient cases. In parallel, p53 expression in the same cohort demonstrated similar associations, confirming that compromised p53 is a defining feature of advanced BLCA. More importantly, our findings indicate a linear association of RD3 loss with p53 loss. Owing to the upstream effector function of RD3 regulating p53 competitor NFκB, the findings throw light on the RD3→p53 signaling flow-through in BLCA evolution. This dual loss could represent a synergistic axis driving disease progression and therapeutic failure in BLCA. These results position RD3 as a potential prognostic biomarker and therapeutic target, especially in p53-deficient tumors. The current focus of our studies are in the line of delineating the RD3-p53 regulatory network and its implications for precision medicine for high-risk BLCA patients.
Funding: DoD CA-210339; OCAST-HR19-045; P20GM103639

#2465 Social support as a predictor of deficit accumulation in older breast cancer survivors and non-cancer controls.

Eunji Choi[1], Iwalola Awoyinka[2], Jaeil Ahn[3], Tim A. Ahles[4], Ashley L. Artese[5], Traci N. Bethea[3], Judith E. Carroll[6], Harvey Jay Cohen[7], Heather S. Jim[8], Brenna C. McDonald[9], Zev Nakamura[10], Sunita Patel[11], James C. Root[4], Andrew J. Saykin[9], Brent Small[10], Ying Wang[3], Wanting Zhai[3], Jeanne S. Mandelblatt[3]

[1]Population Health Sciences, Weill Cornell Medicine, New York, NY,[2]Medical College of Wisconsin, Wauwatosa, WI,[3]Georgetown University, Washington, DC,[4]Memorial Sloan Kettering Cancer Center, New York, NY,[5]Florida Atlantic University, Boca Raton, FL,[6]UCLA - University of California Los Angeles, Los Angeles, CA,[7]Walter Kempner Professor of Med., Duke University Medical Center, Durham, NC,[8]Moffitt Cancer Ctr., Tampa, FL,[9]Indiana University, Indianapolis, IN,[10]University of North Carolina at Chapel Hill, Chapel Hill, NC,[11]City of Hope Comprehensive Cancer Center, Duarte, CA

Introduction: Deficit accumulation is an important construct in oncology, associated with chemotherapy toxicity, cognitive decline, quality of life, and survival. However, longitudinal patterns of deficit accumulation among cancer survivors remain poorly characterized, and the influence of social health on these trajectories is even less understood. We examined long-term deficit accumulation trajectories in older breast cancer survivors compared with non-cancer controls and evaluated the role of social health in predicting these trajectory memberships.

Methods: We included 380 breast cancer survivors and 359 frequency-matched controls enrolled from 2010-2022, each with at least three annual follow-ups through 2024. Social health measures included emotional and tangible support using the Medical Outcomes Study Social Support (MOS-SS) tool, social and family well-being using the Functional Assessment of Cancer Therapy-General (FACT-G) subdomain, and social network size (number of close friends/relatives; categorized as >3 vs. ≤3). Deficit accumulation was assessed at each visit using a 46-item index. Group-based trajectory modeling identified distinct deficit accumulation patterns, and multinomial logistic regression examined predictors of trajectory membership.

Results: Three trajectories were identified: 204 rapid decliners (28%; 5-year increase 0.06 [0.012/year], $p<10^{-5}$), 362 slow decliners (49%; 0.005 increase [0.001/year], p=0.3), and 173 non-decliners (23%; 0.005 decrease [-0.001/year], p=0.4). Breast cancer survivors were more likely to follow a rapid-declining trajectory than non-cancer controls. Among survivors, those who received chemotherapy were most likely to experience rapid deficit accumulation, suggesting persistent treatment-related vulnerability. Higher emotional support predicted lower odds of declining trajectories: each 10-point increase in emotional social support was associated with a 14% lower probability of being a slow decliner (aOR 0.86 [0.74-1.01]) and a 23% lower probability of being a rapid decliner (aOR 0.77 [0.65-0.92]). Higher social and family well-being similarly predicted 15% (aOR 0.85 [0.73-0.99]) and 21% (aOR 0.79 [0.68-0.93]) lower odds of being slow and rapid decliners, respectively. Having more than 3 close friends predicted a 65% lower probability of becoming a rapid decliner (aOR 0.38 [0.17-0.87]).

Conclusions: Deficit accumulation trajectories in older women are heterogeneous, and breast cancer diagnosis and chemotherapy appear to contribute to more rapid deficit accumulation. Social health—including emotional support, social and family well-being, and larger social networks—emerged as a strong protective factor, slowing the pace of deficit accumulation among both breast cancer survivors and non-cancer controls.

#2466 The association between sleep and physical function in the longitudinal TLC cohort study of women.

Cynthia Kusters[1], Wanting Zhai[2], Xingtao Zhou[2], Zev Nakamura[3], Jaeil Ahn[2], Ashley L. Artese[4], Deena Graham[5], Chloe Casagrande[6], Kathleen van Dyk[7], Tim A. Ahles[8], Traci N. Bethea[2], Harvey Cohen[9], Claudine Isaacs[2], Heather S. Jim[10], Brenna McDonald[11], Sunita Patel[7], James C. Root[8], Andrew Saykin[12], Brent Small[3], Jeanne S. Mandelblatt[2], Judith E. Carroll[1], TLC-Age Research Group

[1]UCLA - University of California Los Angeles, Los Angeles, CA,[2]Georgetown University, Washington, DC,[3]University of North Carolina, Chapel Hill, NC,[4]Florida Atlantic University, Boca Raton, FL,[5]Hackensack University Medical Center, Hackensack, NJ,[6]Georgetown, Washington, DC,[7]City of Hope, Duarte, CA,[8]Memorial Sloan Kettering Cancer Center, New York, NY,[9]Duke, Durham, NC,[10]Moffitt Cancer Ctr., Tampa, FL,[11]Indiana University, Indianapolis, IN,[12]Indiana University, Indianapoli, IN

Background: Sleep disturbances, such as insomnia, are common in postmenopausal women and may negatively impact physical functioning. These disturbances are more frequent in breast cancer survivors than in the general female population. Limited data exist on how sleep affects physical function in older breast cancer patients. We analyzed whether sleep quality influences physical function at a one-year follow-up, and vice versa.

Methods: Data were from the Thinking and Living with Cancer study, a multicenter, longitudinal study involving women aged 60 and older, newly diagnosed with breast cancer and frequency-matched non-cancer controls. Participants were followed annually for up to five years. Sleep quality was assessed with the PSQI (range 0-21; higher scores indicate poorer sleep quality); physical functioning was measured by the SF-12 physical component score (PCS) and the Timed Up and Go (TUG). A 3-5 point SF-12 PCS decline was considered clinically meaningful. Random intercept cross-lag panel models (RI-CLPM) analyzed associations using data from 767 women (339 controls and 428 survivors), adjusting for age, race, comorbidities, and recruitment site.

Results: Mean age of participants was 69.5 years (70.0 in survivors vs. 69.3 in controls). Disrupted sleep was more common among survivors at baseline (PSQI above 5: 43.9% vs. 29.0%; p less than 0.001) and remained more prevalent during follow-up. Survivors showed a clinically meaningful decline in PCS (-2.8 points in year 1; -3.0 points over two years), whereas controls had a small, gradual, non-clinically meaningful decline (≈ -0.5 points/year). There was no clear trajectory for TUG, and the RI-CLPM revealed no significant associations between PSQI and TUG.

In survivors, each 1-point higher PSQI predicted 0.4-0.5 points (P less than 0.001) lower SF-12 PCS at the subsequent annual visit during the first three years, decreasing to 0.3 points by year 4 (P = 0.03). Among controls, effects were small initially (-0.25 points, p = 0.10) but from years 2 to 5 a 1-point PSQI increase predicted 0.4-0.65 points lower SF-12 PCS (p = 0.01 to less than 0.001).

For both survivors and controls, a 10-point worsening in a woman's PSQI relative to her usual level would be expected to correspond to about a 4-point lower SF-12 PCS one year later, assuming a 0.4-point decrease in PCS per 1-point increase in PSQI.

Conclusion: Sleep disruption is associated with subsequent declines in physical function among survivors and controls, which can reach clinically meaningful magnitudes as sleep quality worsens. Given the high prevalence of sleep problems among breast cancer survivors, routine monitoring for sleep disturbances and timely intervention may help preserve function in the growing population of older cancer survivors, particularly in the early years following treatment.

This work was conducted with contributions from the entire TLC-Age research team.

#2467 Aging and cancer in the Caribbean: Incidence and mortality trends among older adults during Covid-19: Population-based analysis from Martinique, 2008-2022.

Adrian Puello[1], Murielle Beaubrun-Renard[2], Jonathan Macni[2], Stephen Ulric-Gervaise[2], Manon Boullard[2], Mylene Vestris[2], Aimee Pierre-Louis[2], Sophia Hl George[3], Moustapha Drame[4], Clarisse Joachim[1]

[1]Registre General des Cancers de la Martinique, Pole de Cancerologie-Hematologie-Urologie, CHU Martinique & EpiCliV Research Unit, Faculty of Medicine, University of the French West Indies, Fort de France, France,[2]Registre General des Cancers de la Martinique, Pole de Cancerologie-Hematologie-Urologie, CHU Martinique, Fort de France, France,[3]Department of Obstetrics, Gynaecology and Reproductive Sciences, Miller School of Medicine, University of Miami, Miami, FL,[4]EpiCliV Research Unit, Faculty of Medicine, University of the French West Indies, Fort de France, France

Background: Prostate, breast, stomach, colon-rectum, lung, and hematologic cancers represent a regional public health burden among older adults in the Caribbean. We analyzed 15-year trends in incidence and mortality among older adults in Martinique, including the COVID-19 period, to describe changes in cancer burden, screening and treatment.
Methods: We conducted a population-based cohort study (2008-2022) from the population-based cancer registry of Martinique. Patient selection on all registered residents irrespective of nationality. Segi/WHO age-standardized incidence and mortality rates (ASR) were calculated using the world standard population and Annual Percent Change (APC) in patients ≥65 years, by tumor site and sex with 95% CI.
Results: We recorded 15,400 incident cancers; 9,913 (64.4%) occurred in men. An indicating overall stability with a slight increase from the first to the later periods in age-standardized incidence rates (ASR per 100,000) were 847.80 (95% CI: 801.80-893.90) in 2008-2012 to 862.10 (821.2-903.0) in 2018-2022. Prostate cancer mortality declined; rising female breast cancer incidence with stable mortality; stable colorectal cancer incidence with varying mortality; and declines in stomach cancer incidence and male lung cancer mortality.
Conclusions: Over fifteen years, cancer burden among older adults in Martinique patterns were consistent with Caribbean and global observations, with differences in magnitude and timing by site and sex, reflecting changing screening intensity, new therapeutics, and COVID-19 disruptions. These findings support tailored cancer control strategies for older adults, emphasizing equitable access to diagnostics and treatment, and resilience planning for service interruptions. Future research should integrate socioeconomic and comorbidity factors.

: Community-Engaged Approaches to Equity Across the Cancer Journey: From Prevention to Trial Design
Poster Session

#2471 Accelerating early detection through community-driven cancer wellness hubs and ambassador trainings: Evidence of knowledge gains and real-world impact.

Eduardo B. Ibarra[1], Carolina Aristizabal[1], Elena Nieves[1], Rosa Barahona[1], Freddie Muse[2], Lourdes Baezconde-Garbanati[3]

[1]USC Norris Comprehensive Cancer Center, Los Angeles, CA,[2]The Men's Cancer Network, Los Angeles, CA,[3]Keck School of Medicine of USC, Los Angeles, CA

Background: Communities with limited access to preventive care continue to face higher burdens of late-stage cancer diagnoses and mortality. Persistent barriers including delayed screening, limited navigation support, and low trust in medical institutions slow progress despite national declines in cancer deaths. Sustainable advances in these settings require models that strengthen local capacity, expand screening pathways, and equip residents as credible messengers of cancer information.
Methods: The USC Norris Comprehensive Cancer Center, Office of Community Outreach and Engagement (COE) implements a dual strategy across its catchment area of Los Angeles County and northern Orange County: (1) Cancer Wellness Hubs (CWHs) situated in trusted venues (community centers, YMCA branches, and The Men's Cancer Network Inc.) and (2) Evidence-informed Cancer Ambassador Trainings open to community members. Trained bilingual/bicultural community health workers provide on-site education, navigation to insurance enrollment, cancer screening, and referrals for diagnostic follow-up or clinical-trial enrollment. Ambassador Trainings are two-hour sessions covering epidemiology, risk reduction, early symptoms, treatment basics, survivorship, and effective communication. Standardized pre/post surveys measure knowledge, self-efficacy, and intent to share information.
Results: In 2025, 19 CWHs engaged 714 community members, delivering culturally and linguistically congruent cancer education and resources. Of these, 29 individuals requiring follow-up (screening, diagnostic, or treatment navigation) were successfully connected to USC Norris COE patient navigators.
Twenty-six participants completed Cancer Ambassador Trainings in Los Angeles in 2025. Aggregate knowledge scores increased from 65.0% (pre) to 79.3% (post), with the largest gains observed in pancreatic and prostate cancer awareness. Ninety-six percent of trainees reported intent to disseminate learned information within their social networks. At one prostate-cancer-focused training, nine men aged ≥40 received on-site free PSA screening.
Conclusions: The integrated Cancer Wellness Hub and Cancer Ambassador Training model demonstrates high acceptability, significant knowledge gains, and rapid translation into community action, including direct screening uptake and peer-to-peer education. By training and empowering residents as credible messengers and co-locating services in trusted spaces, this scalable, asset-based approach effectively bridges gaps in prevention, early detection, and clinical-trial access. These findings underscore the value of sustained, bidirectional community-academic partnerships in dismantling structural barriers and accelerating the reduction of cancer differences in underserved populations.

#2472 Using multi-method approaches to develop and refine a tobacco cessation workflow within a Federally Qualified Health Center.

Linda Salgin[1], Jerel P. Calzo[1], Jennifer K. Felner[1], David Strong[2], Marva Seifert[2], Borsika A. Rabin[2]

[1]School of Public Health, San Diego State University, San Diego, CA,[2]The Herbert Wertheim School of Public Health and Human Longevity Science, University of California San Diego, San Diego, CA

Background: The incorporation of implementation science approaches into tobacco control program delivery remains limited. Programs developed using these approaches, including co-creation, are often more feasible and sustainable, as they are designed to consider the operational and cultural context of an organization. This study utilized multiple implementation science approaches to co-create a tobacco cessation workflow within a Federally Qualified Health Center, where tobacco use is disproportionately higher than the national average.

Methods: In this study we conducted six structured meetings across two advisory groups between July-September 2025. Multiple implementation science methods (i.e., forms and functions, brainwriting premortem, and Practical, Robust Implementation and Sustainability Model (PRISM) assessments) were integrated to optimize the tobacco cessation workflow along with co-creation and evaluation methods (i.e., ethnographic observations, engagement survey) to evaluate advisory board engagement. Qualitative and quantitative data were collected and analyzed simultaneously using rapid qualitative analysis and descriptive statistics allowing for a comprehensive understanding and iterative incorporation of the results.

Results: Thirteen individuals participated in this study as co-creation partners who were between the ages 27 to 69 years (M = 31). Participants represent various roles within the FQHC including front-line staff, administrators, providers, and patients. Workflow Optimization: Participants identified 5 core functions and 16 forms in the refinement of the tobacco cessation workflow. Brainwriting Premortem resulted in 29 unique failures and 19 solutions within the workflow across PRISM contextual domains, of which 16 were integrated. The final version of the co-created workflow had high acceptability (M=4.8), appropriateness (M=4.6), and feasibility (M=4.5).

Participant Engagement: A total of 394 interactions were identified across meetings. The most frequent interaction was giving information (53%), followed by seeking information (18%). The quality and frequency of advisory board engagement was rated favorably (average 4.7 of 5). Rapid qualitative analysis of open-ended responses highlighted the value of co-creation with participants stating: “I am glad I participated in this advisory panel... and I am able to bring [this information] back to my team to help our patients.”

Conclusion: This study highlights how co-creation through multiple implementation science methods can be used to conceptualize, adapt, and refine programs responsive to FQHC needs.

#2473 A unified Indigenous Knowledge System (IKS)-integrated biosocial and digital health model to reduce cancer disparity in rural India.

Rupam Das[1], Lekhika Pathak[2], Shirsajit Mitra[2], Tulika Sarma[3], Chayanika Das[3], Upasha Sarmah[2], Riya Kanodia[2], Partha Saikia[2], Sonali Das[4], Manisha Canteenwala[4], Mallika Maral[3], Nayan Bhattacharjee[5], Hem Bhai[5], Uday Shanker Dixit[1], Bikul Das[2]

[1]Center of Indian Knowledge System, Indian Institute of Technology, Guwahati, India,[2]Department of Medical Humanity, KaviKrishna Laboratory, Guwahati, India,[3]KaviKrishna Telemedicine Care, Sualkuchi, India,[4]Department of Medical Humanity, Thoreau Lab for Global Health, Lowell, MA,[5]Center of Indian Knowledge System, KaviKrishna Laboratory, Sualkuchi, India

Background: Through a three decades of community based participatory action research (CBPAR) (Ref.1), we are studying cancer disparity. Since 2010, the "KaviKrishna Satra" program has developed a long-term cancer disparity research platform through an Indigenous Knowledge System (IKS)-based social-network framework (Ref.2) and using ethnography + phenomenology (Ref. 3), plus pancha-padika education (1-2). We are developing a digital IKS-based intervention (KaviKrishna HealArt App + Nigudah Yoga + nutrition + Focussed group discussions/FGDs) and a biosocial resilience scale (Sahasa-Ojash) rooted in Vedic Jiva Upakara Cikitsha Tantra, an Avatar-Kosha-based biosocial healing system (Ref. 1 & 4). We hypothesize that cancer disparity in rural India is a biosocial phenomenon that can be reduced by combining IKS-based communication systems, digital health connectivity, and psychosocial care.
Methods: We mapped the social-support networks of 200 rural cancer patients through home visits, interviews, FGDs, and clinician-interaction analysis to detect the emergence of an IKS-based communication system through CBPAR. We measured Sahasa-Ojash in the first 35 patients, and will longitudinally measure all 200 patients through the Heal-Art app for continuous biosocial analytics. We also evaluated the continuity of care (adherence to scheduled follow-ups, completion of treatment, and persistence in telemedicine contact over 12 months).
Results: The integrated digital-IKS intervention produced measurable biosocial and clinical impact: 1) Sahasa-Ojash increased 2-3-fold after the intervention *(mean increase, p = 0.065; trend toward significance due to sample size).* 2) Fatigue and insomnia reduced by 35-45% *(p = 0.046), whereas appetite increased by 50-60% (p = 0.032)*. 3) Treatment adherence and follow-up continuity increased 3-fold through the KaviKrishna HealArt App. 4) Preliminary IKS-network analysis showed reactivation of indigenous social-communication pathways resembling historical IKIN structures, improving patient navigation and trust. 5) Patients reported greater psychological resilience, enhanced self-care, and improved communication with oncologists. 6) Clinical co-morbidities decreased (anemia, hypertension fluctuations, and GI disturbances). These biosocial gains correlated with a 3-fold improvement in continuity of care, greater chemotherapy completion, and markedly reduced treatment dropout.
Conclusion: We have developed a unified, scalable, and cost-effective IKS-integrated cancer disparity model that Maps biosocial determinants using ethnography and phenomenology.
(1). https://doi.org/10.1158/1538-7445.AM2024-1005 (2). https://doi.org/10.1158/1538-7445.AM2019-3342 (3). https://doi.org/10.1158/1538-7445.AM2024-807 (4). https://zenodo.org/records/8062404

#2474 Non-completion of colorectal cancer screening among Alaska Native people in an intervention trial.

Diana Redwood[1], Christie A. Flanagan[1], Lauren Jeffries[1], Melissa Toffolon[2], Joseph Klejka[3], Lila J. Finney Rutten[4], Judith S. Kaur[5], John B. Kisiel[4]

[1]ANTHC, Alaska Native Epidemiology Center, Anchorage, AK,[2]Actionable Data Consulting, Anchorage, AK, AK,[3]Yukon Kuskokwim Health Corporation, Anchorage, AK, AK,[4]Mayo Clinic, Rochester, MN,[5]Mayo Clinic Florida, Jacksonville, FL

Background: The Alaska Tribal Health System is working to increase colorectal cancer (CRC) screening among Alaska Native peoples. It is unknown why people who initially agree to screening might not follow through to complete their screening.
Methods: As part of a larger intervention investigating multi-target stool DNA (mt-sDNA) test use in rural Alaska communities, we interviewed Alaska Native people who had agreed to scheduling a colonoscopy or having a mt-sDNA kit sent to their home but who did not complete their selected test.
Results: Of 531 Alaska Native people who initially agreed but did not complete screening, 299 (56%) were able to be contacted for a follow-up survey. Of those, 256 (86%) answered the survey; 187/224 (83%) who had chosen mt-sDNA, and 69/75 (93%) who had chosen colonoscopy. Reported reasons for non-completion of stool DNA test kits included being busy or forgetting, being uncomfortable doing a stool test, and not knowing how to do the test or concerns over how to return the kit for processing. Reasons for non-completion of colonoscopy included scheduling issues, physical health issues, travel, and housing barriers, as well as cost, fear, and being too busy. Of note, many respondents in both groups indicated they would still be interested in CRC screening in the future or were currently pursuing screening.
Conclusions: This was the first exploration of reasons for non-adherence to CRC screening after initial test request by Alaska Native people. Many of the identified themes are amenable to health care system changes for future interventions to improve screening outreach and uptake.

#2475 Resource limitations and cancer care access for Native Hawaiian/Pacific Islander veterans in the Pacific region.

Troy Helenihi[1], Akanksha Jain[2], Claire Phibbs[3], Ranak Trivedi[4], Nainwant Singh[5]

[1]Human Biology, Stanford University, Stanford, CA,[2]MD Program, University of Southern California, Keck School of Medicine, Los Angeles, CA,[3]Data Science, University of San Diego, San Diego, CA,[4]Department of Psychiatry and Behavioral Sciences, Stanford University School of Medicine, Stanford, CA,[5]Research & Development, VA Sierra Nevada Health Care System, Reno, NV

Native Hawaiian/Pacific Islander (NHPI) populations may experience poorer cancer-related outcomes, shaped by social determinants such as higher poverty rates and underrepresentation in national data. NHPI Veterans face heightened vulnerability due to military-related exposures and the need to navigate distinct Veterans Health Administration (VHA) pathways for care, adding complexity not experienced by civilians. Limited oncology services across Hawai'i and the U.S.-Affiliated Pacific Islands (USAPI), compounded by geographic isolation and workforce shortages, increase risk for delayed diagnosis and treatment. This qualitative analysis from the PaCiPIC Veterans Study examines key challenges and opportunities to improve access to cancer care among NHPI Veterans residing in the USAPI. Semi-structured interviews were conducted with NHPI Veterans residing within the VA Sierra Pacific Network 21 (n = 8 to date, target = 15-20). Interviews were recorded, transcribed, de-identified, and analyzed thematically in ATLAS.ti. Codes were iteratively developed through team consensus by a multidisciplinary team with clinical, psychological, and qualitative research expertise, guided by Fortney's Access to Care Framework. Veterans described challenges with community care referrals, including delays and uncertainty over follow-up. Many felt resources on the islands remain limited, noting few, if any, noticeable improvements in services or access over time despite advocacy. Long-distance travel for diagnostics and treatment created financial and logistical strain from airfare, lodging, and caregiver support unless Veterans met specified service-related criteria. Teleoncology was viewed as a potential acceptable alternative to reduce travel burden for follow-up care, though Veterans emphasized core aspects—laboratory testing, imaging, and procedures—required in-person encounters. Family and community networks emerged as essential support systems, providing transportation, coordination, and emotional care bridging gaps. Preliminary findings highlight resource limitations as key insular barriers to cancer care for NHPI Veterans in the Pacific, consistent with clinician perspectives from our previously published works. Building on these insights, we will identify feasible strategies to address system-level constraints and inform implementation of services in the region.

#2476 Science and Storytelling: Using a multi-component evidenced based strategy for successful recruitment of Black women with high-risk endometrial cancer to The SISTER Study.

Kemi M. Doll, Julianna Alson, Adrienne Moore, Alvine Ngouonga, Patrice Williams, Liz Sage, Bryan Comstock, Sarah Monsell, The SISTER Study Consortium

University of Washington, School of Medicine, Seattle, WA

Introduction: Black women are underrepresented in national randomized clinical trials. To address known structural and interpersonal barriers to enrollment and for accurate recruitment planning, detailed enrollment statistics from screening to randomization are needed.
Methods: The Social Interventions for Support in Endometrial Cancer Treatment and Recurrence (SISTER) Study is a 13-site national randomized trial that recruited Black/African American women with high-risk EC who were enrolled in the time window between diagnostic confirmation and treatment initiation. In a community-engaged process with Black EC survivors, we created a novel multi-component, evidenced-based recruitment and enrollment process to enhance recruitment and enrollment that was deployed at all SISTER Study sites. In partnership with ECANA, a Black EC cancer advocacy group, we created print and web enrollment materials focused on community-building and self-empowerment during treatment. We also developed an enrollment video that featured the PI and Black EC survivors sharing personal stories about the racial disparities in EC and the importance of the study alongside graphic depictions of randomization and intervention arms. Using an ‘early contact’ and ‘waiting room’ strategy, we identified participants at or prior to their first oncology visit and initiated live conversations occurring several days to weeks prior to their eligibility window. All participants considered for the study were prospectively captured and logged in the study portal allowing for accurate reporting on screening and enrollment rates.
Results: From September 2021 to September 2025, 609 individuals were identified, and 540 officially screened for the trial. Of those screened, 31% (n=166) were ineligible based on clinical and non-clinical exclusion criteria. Of the remaining 374, 16% (n=59) declined being approached. Of the 315 approached for consent, 85% (n=269) consented and 13% (n=46) declined. The trial enrollment goal of 252 was met, representing 41% of all identified, 47% of those official screened, 67% of those eligible, and 80% of those approached for consent.
Conclusions: When approached and invited to participate, Black women with high-risk EC chose to enroll in a randomized controlled interventional trial. Using evidenced-based community-engaged strategies, we successfully enrolled this long-standing underrepresented group requiring active treatment during a narrow eligibility window. Our enrollment rates can be used to accurately plan for appropriate representation of Black women in endometrial cancer trials, and the multi-component strategy can be used nationally to increase equitable clinical trial representation across historically excluded communities.

#2477 Graphic medicine: A patient-centered approach to oncology.

Alexandra Bartholomew[1], Pui Cheng[2], Amelia Jernigan[1], Tara Castellano[1], Counti McCutchen[3], Julia Cazabon[1], Audrey Marsh[1], Ronja Bodola[1], Siyi Cheng[1], Jason Mussell[1]

[1]Louisiana State University Health Sciences Center - New Orleans, New Orleans, LA,[2]Touro Infirmary, New Orleans, LA,[3]University of Chicago, Chicago, IL

Graphic medicine combines graphic narrative with medicine. In this study, we aimed to investigate the potential usefulness of graphics and comics as a therapeutic and teaching tool for gynecologic oncology patients by creating, distributing, and evaluating a narrative about a patient with a newly diagnosed cancer. This project was a multistage mixed methods study. To guide direction and content, focus groups were conducted with members of a gynecologic oncology support group. It was determined that a graphic on coping strategies would be most useful. The first draft underwent several modifications and was translated into Spanish and Vietnamese. The final graphic and survey were implemented into four gynecologic oncology clinics. Patients of any age and at any stage in their treatment were eligible. The survey included demographic questions as well as questions on the usefulness, relatability, and likability of the comic. For statistical analysis, descriptive statistics were used to summarize the study population. The chi-square goodness-of-fit test was used to determine whether participant responses were evenly distributed or skewed in a particular direction. The ANOVA test was used to compare participant responses across categories. 155 patients took the survey. The vast majority found the graphic enjoyable, relatable, useful, and helpful for reducing anxiety ($p<0.001$). Our results suggest that graphic medicine interventions are useful in a gynecologic oncology setting. The project was guided heavily by patient input. This study was successful in determining that graphic medicine interventions are a feasible method of delivering healthcare information to gynecologic oncology patients.

#2478 Advancing equitable preventative cancer screening on the Inova Saville mobile health bus.

Nikita N. Sawant, Elizabeth Stark, Rebecca Kaltman, Victoria Thomas, Bryan Bassig

Saville Cancer Screening and Prevention Center, Inova Health System, Fairfax, VA

Purpose: The INOVA Saville Mobile Health Bus (SMHB), launched in January 2025, aims to expand access to breast and cervical cancer screenings and novel research trials among medically underserved communities in Northern Virginia. Using de-identified, aggregated data, this analysis assessed early program reach, identified race/ethnic and geographic gaps in utilization, and used these insights to improve equitable access to preventive care.

Methods: Screening encounters from February 2025 through August 2025 were summarized by race/ethnicity, ZIP code, and screening type, and encounters were grouped into pre- and post-intervention periods to monitor changes over time. The SMHB catchment area includes five Northern Virginia jurisdictions; the City of Alexandria, Fairfax, Prince William, Loudoun, and Arlington Counties; covering more than 70 ZIP codes. To identify areas with potentially lower breast and cervical cancer screening uptake by race and ethnicity, we used publicly available racial/ethnic demographic data from the U.S. Census Bureau's American Community Survey. Descriptive statistics and geographic information system (GIS) mapping were used to compare bus encounters to community race/ethnic distributions and highlight underserved ZIP codes. Those findings guided adjustments to routes and outreach efforts.

Results: Hispanic/Latino individuals represented 30.5% of early screening encounters, exceeding county estimates (14.4%-24.3%). Several groups were underrepresented: Asian participants accounted for 5.8% of screenings despite representing 10.3%-20.6% of county populations, and Black/African American participation was 4.9% compared to county estimates (7.7%-21.5%). ZIP codes with limited engagement guided new partnerships with community organizations serving Black/African American and Asian residents. After these efforts, participation increased modestly among targeted groups. From January-August to September-mid-November, Black/African American participation increased from 5.9% to 6.6%. Asian participation increased from 8.7% to 13.6%. Hispanic/Latino participation remained stable (29.3% to 28.7%).

Conclusions: This analysis during the early phase of the SMHB program enabled timely identification of outreach inequities and guided practical changes to improve equity in preventive cancer screening. Targeted partnerships with trusted community organizations, including groups serving Black/African American and Asian communities, contributed to early increases in engagement among these populations. These findings underscore the importance of grounding mobile health outreach in continuous quality improvement, community collaboration, and culturally responsive strategies. This approach offers a sustainable framework for building more inclusive and accessible mobile health services as the program continues to expand.

#2479 Embedding community voices in clinical research: The value of community scientists in IIT protocol review.

Reener Balingit[1], Lourdes Barajas[1], Oscar Arroyo[1], Karen L. Reckamp[2], Zul Surani[1]

[1]Cedars Sinai Cancer Center, Los Angeles, CA,[2]Cedars-Sinai Medical Center, Los Angeles, CA

Introduction: Investigator-Initiated Trials (IITs) advance scientific discovery, test interventions, and address unmet clinical needs; however, traditional research processes often overlook the perspectives of communities most affected by cancer disparities, leading to protocols that unintentionally reinforce barriers to participation among underrepresented groups. *Community Scientists*, comprising patients, caregivers, health professionals, and community leaders, offer lived expertise to ensure that study materials, eligibility criteria, and recruitment strategies reflect the realities of the populations affected by cancer.

Methods: Cedars-Sinai Cancer Center Community Outreach & Engagement (COE) identified and trained 11 lay community members as Community Scientists, equipping them with foundational knowledge in clinical trial design, ethical and informed consent considerations, and practical approaches to mitigating participation barriers. COE facilitated engagement between clinical researchers and Community Scientists by integrating them into the IIT protocol review process, resulting in 18 IITs and 243 PRMC reviewed in the past 3 years. To assess the integration and impact of Community Scientist recommendations, COE surveyed 14 clinical researchers (11 initiated, 5 fully completed). Recommendations focused on gender-neutral language, language accessibility, financial toxicity, transportation support, food insecurity, navigation and referral pathways, and health literacy.

Results: Clinical researchers rated COE and Community Scientists as *effective* or *very effective* (80%, n=5) in providing valuable recommendations on IIT protocols, resulting in increased participation and retention of underrepresented communities in clinical trials (1-2 patient referrals yearly from COE). Qualitative feedback from clinical researchers highlighted meaningful practice changes, highlighting that Community Scientists' recommendations were *either already adopted* or *being considered for future studies:* "We adjusted our discussion with patients to improve engagement and retention in trials". Adoption was highest for recommendations related to interpretation and translation services, parking voucher availability, financial and social support navigation, and warm handoffs to internal and external community partners (60%, n=5, respectively).

Conclusion: Clinical researchers recognized the value of collaboration with COE and Community Scientists, and expressed a strong interest in expanding Community Scientists' involvement in early-stage study design, translational and therapeutic science, protocol development, dissemination of findings, and participation in educational activities. The contributions meaningfully enhance the cultural relevance, feasibility, and inclusivity of investigator-initiated trials.

#2480 Exploring social, environmental, and health correlates of lung and bronchus cancer incidence in HMNCC catchment area.

Preeti Sohoni[1], Weishan Bai[2], King David Oware[2], Gang Han[2], Jennifer Cullen[1], Nestor Esnaola[1], **Arica Brandford**[1]

[1]Houston Methodist, Houston, TX,[2]Texas A&M University, College Station, TX

Background: Lung and bronchus cancer drives cancer mortality in the Houston Methodist Neal Cancer Center (HMNCC) catchment area, with profound geographic and racial disparities threatening health equity. The eight-county catchment area exhibits stark variations in demographics, industrial exposures, and health resource access. Characterizing community-level drivers of this excess risk is imperative for targeted prevention strategies that address these inequities.
Methods: County level cancer incidence (2018-2022) was collected through U.S. Cancer Statistics. The sociodemographic, clinical, behavioral, and environmental factors were obtained from the CDC PLACES and ACS 5-year estimates. GIS mapping identified the spatial patterns within the 8 counties: Harris, Montgomery, Fort Bend, Galveston, Brazoria, Chambers, Liberty, and Jefferson. Weighted Spearman correlations (population-weighted) and weighted univariate linear regressions of the log transformed incidence were used to assess the associations. Holm adjustment controlled for multiple testing.
Results: The population-weighted median incidence of lung and bronchial cancer in the eight counties was 77.6 per 100,000 (IQR: 77.6-77.6), with the county-wide rate ranging from 32.5 to 77.6 per 100,000. GIS analyses showed consistently elevated incidence in Liberty, Jefferson, and Chambers counties, with Black residents experiencing the highest race-specific burdens. Several factors exhibited strong positive correlations with incidence, including obesity ($r=0.998$), depression ($r=0.984$), binge drinking ($r=0.976$), asthma ($r=0.893$), and COPD ($r=0.721$) (all raw $p\leq0.05$). After Holm adjustment, obesity, depression, and binge drinking remained significant. Strong negative correlations were observed for the population under 18 ($r= -0.839$), Black ($r= -0.767$), and Asian race ($r= -0.723$), although none survived Holm correction. In weighted univariate regression, depression showed the strongest association with incidence ($\beta=0.102$, $SE=0.013$, $p<0.001$), followed by obesity ($\beta=0.078$, $SE=0.016$, $p=0.003$) and binge drinking ($\beta=0.129$, $SE=0.032$, $p=0.007$). Associations for asthma ($\beta=0.288$, $SE=0.078$, $p=0.010$) and COPD ($\beta=0.130$, $SE=0.047$, $p=0.032$) were also significant. Sensitivity analyses using non-parametric models produced nearly identical rankings.
Conclusion: Across the HMNCC catchment, lung cancer incidence clusters geographically and align closely with modifiable behavioral and clinical risk indicators, especially depression, obesity, and binge drinking. These findings highlight priority communities and population-level factors for targeted prevention, early detection, and community-engaged interventions aimed at reducing inequities in lung cancer burden.

#2481 Psychosocial profiles and pain management patterns among Asian American breast cancer survivors: A cluster analysis.

Dongmi Kim, Jiwon Baek, Seulgi Ryu, **Yeeun Kim**, Wonshik Chee, Eun-Ok Im

The University of Texas at Austin, Austin, TX

Background: Asian American breast cancer survivors represent a diverse population with unique psychosocial needs, yet limited research has identified subgroups based on psychological well-being, pain management beliefs, and social support. Understanding heterogeneity in psychosocial profiles may inform culturally tailored survivorship care. This study aimed to identify distinct psychosocial subgroups among Asian American breast cancer survivors and examine differences in depressive symptoms, pain management attitudes and barriers, social influence, quality of life, coping self-efficacy, loneliness, and perceived social support among the subgroups.
Methods: This is part of an ongoing clinical trial among Asian American breast cancer survivors. Only the baseline data were used for this analysis. A total of 106 women were included in the analysis. K-means cluster analysis was conducted on psychosocial variables, including depressive symptoms, attitudes, and perceived barriers to cancer pain management, social influence, self-efficacy, loneliness, and social support. The optimal number of clusters ($k = 3$) was determined by silhouette analysis. One-way ANOVA with Tukey post-hoc tests compared psychosocial outcomes across clusters.
Results: Three meaningful clusters emerged. Cluster 1 (resilient and supported survivors, $N = 30$) displayed the lowest depressive symptoms, strongest social support, positive pain attitudes, and highest quality of life and coping self-efficacy. Cluster 2 (psychologically vulnerable and socially isolated survivors, $N = 30$) demonstrated the highest depressive symptoms, greatest pain management barriers, and lowest levels of coping self-efficacy, quality of life, and perceived social support, along with the highest loneliness scores. Cluster 3 (moderately coping survivors, $N = 46$) showed intermediate levels across all psychosocial indicators and perceived attitudes towards pain and pain management barriers. All psychosocial and quality-of-life outcomes significantly differed across subgroups ($p < .001$).
Conclusion: Asian American breast cancer survivors demonstrate significant psychosocial heterogeneity. Future culturally responsive, tailored interventions need to target the psychologically vulnerable, socially isolated subgroup, and address emotional distress, social connection, and pain-related attitudes in survivorship care. Findings support cluster-informed personalization strategies in technology-based survivorship programs.

#2482 The CAHR-model: A culturally adaptive hybrid recruitment strategy for Asian American breast cancer survivors.

Dongmi Kim, Seulgi Ryu, **Yeeun Kim**, Wonshik Chee, Eun-Ok Im

The University of Texas at Austin, Austin, TX

Background: Asian American breast cancer survivors remain underrepresented in survivorship and behavioral health research due to cultural stigma, linguistic diversity, and privacy concerns. To address these barriers, culturally aligned outreach strategies leveraging trusted relationships and ethnic-preferred communication channels are needed. This study describes the *Culturally Adaptive Hybrid Recruitment Model (*CAHR-Model), which integrates community consultants with ethnic-specific digital outreach to recruit Asian American breast cancer survivors in the United States.

Methods: The CAHR-Model was developed through an integrative approach combining evidence synthesis, community collaboration, pilot implementation, and iterative refinement. A review of prior research identified barriers such as language discordance, stigma, and privacy concerns as well as facilitators such as collectivist values, community trust, and increasing technology-based communication. Recognizing growing digital connectivity within Asian communities, the research team incorporated technology-enabled outreach as a core strategy. Guided by these insights, consultations with community leaders, survivor advocates, healthcare professionals, and faith-based connectors mapped culturally congruent communication pathways across Korean, Chinese, and Japanese subgroups. Community consultants played a key role in reaching potential participants through trusted networks and providing feedback to refine recruitment messages and delivery. This iterative process led to a dual-channel framework integrating community trust with targeted digital outreach to enhance recruitment.

Results: This hybrid approach enhanced trust, expanded geographic reach, and fostered culturally meaningful engagement. Community consultants, especially healthcare-affiliated connectors such as community health workers and survivor peers, achieved the highest enrollment conversion rates through personal referrals. Korean participants most often engaged digital platforms through *KakaoTalk* and *MissyUSA*, Chinese through *WeChat and RED,* and Japanese survivors through Vivinavi. Digital outreach also effectively reached younger survivors and those less connected to formal networks.

Conclusion: Anchored in community trust and ethnic-specific digital ecosystems, the CAHR-Model demonstrated effectiveness in recruiting Asian American breast cancer survivors. This culturally adaptive and scalable framework offers a practical model to strengthen participation and representation in future breast survivorship and behavioral health research.

#2483 Survivorship and sexual health: What we learned from Black men in community town halls.

Parisa Ghasemi[1], Gaurav Kumar[1], Ernest T. Kaninjing[2], Adanma Ayanambakkam[1], Yaw A. Nyame[3], Amy Siston[4], Jordan M. Neil[1], Adam C. Alexander[1], Andrew G. McIntosh[1], Yan Zhao[1], Zsolt Nagykaldi[1], Kathleen A. Dwyer[1], Mary Ellen Young[5], Sabrina Dickey[6], Daniel Morton[1], Opeyemi Bolajoko[7], Darla E. Kendzor[1], Motolani E. Ogunsanya[1]

[1]University of Oklahoma Health Campus, Oklahoma City, OK,[2]Georgia College & State University, Milledgeville, GA,[3]University of Washington, Seattle, WA,[4]University of Chicago Medicine, Chicago, IL,[5]Mayo Foundation for Medical Education and Research, Jacksonville, FL,[6]Florida State University, Tallahassee, FL,[7]Mayo Clinic Comprehensive Cancer Center, Jacksonville, FL

Background: Prostate cancer (CaP) is among the most common cancers in U.S. men, with Black men experiencing a 1.7-fold higher incidence and nearly twice the mortality rate compared with non-Hispanic White men. While early detection has improved survival, differences remain in recovery and quality of life (QoL). Sexual dysfunction after treatment affects identity, relationships, and well-being, yet stigma, cultural norms, and limited access to patient-centered care prevent open discussion. Few initiatives address the intersection of identity, stigma, and survivorship in this population. Community town halls provide a trusted, culturally responsive space for shared learning, peer connection, and open dialogue on survivorship and sexual health.
Methods: Two community-engaged CaP town halls were convened by the Multidisciplinary Health Outcomes Research and Economics (MORE) Lab at the University of Oklahoma Health Campus (OUHC) to explore survivorship issues among Black CaP survivors. The first, held virtually in June 2024, included watch parties in Georgia and Texas. The second, in November 2024, was hybrid, hosted at OUHC and via Teams with a watch party at the Willa D. Johnson Recreation Center, a community center in Oklahoma City. Panelists included oncologists, psychologists, survivors, partners, and Community Advisory Board members. Both town halls featured survivor storytelling, provider Q&A, and interactive discussion. Post-event surveys captured demographics, satisfaction, and impact. Open-discussion transcripts were analyzed using Braun and Clarke's reflexive thematic analysis, guided by a constructivist framework.
Results: A total of 124 participants attended both town halls. Survey respondents (n=17; 13.7%) provided demographic and satisfaction data; remaining insights came from all participants who engaged in open dialogue. Respondents ranged in age from 19-76 years (mean=48.7 ± 21.8). Of the 17 respondents, 93% rated the events as very good or excellent; 23.5% were CaP survivors, all identifying as Black. Five themes emerged: (1) Masculinity, stigma, and silence limit help-seeking; (2) Sexual dysfunction and identity loss cause major emotional burdens; (3) Navigation challenges highlight systemic barriers; (4) Spousal and psychological support aid coping; and (5) Survivorship empowerment. Participants valued hearing "real stories from real men," validating their experiences.
Conclusions: Community town halls are a feasible and culturally relevant strategy to engage Black CaP survivors in survivorship and sexual health discussions. By centering lived experiences and facilitating two-way communication between survivors, clinicians, and researchers, these events build trust and reduce stigma. Future work will assess changes in knowledge, engagement, and confidence in care navigation and explore scaling this community-academic model to improve survivorship QoL.

#2484 Exercise preferences and barriers in minority cancer patients undergoing chemotherapy.

Huimin Yan[1], Samin Amini[1], James D. Cannon[2], Anton Pecha[1], Rebekah L. Wilson[2], Cami N. Christopher[2], Mary K. Norris[2], Christina M. Dieli-Conwright[2]

[1]University of Massachusetts, Boston, MA,[2]Department of Medical Oncology, Dana-Farber Cancer Institute, Boston, MA

Background: Physical inactivity and comorbid disease burden are disproportionately high among Black and Latinx cancer patients receiving chemotherapy, yet participation in exercise oncology trials remains low in these groups, despite known benefits. The Testing Home-based ExeRcise Strategies to Improve Exercise Participation and CardioVascular Health in UndersErved Minority Patients with Cancer Undergoing Chemotherapy (THRIVE) trial tests the feasibility and acceptability of supervised and unsupervised home-based exercise during chemotherapy in these underrepresented groups. This analysis describes exercise preferences collected through a structured questionnaire administered prior to randomization.

Methods: Participants enrolled in the THRIVE trial completed baseline questionnaires assessing exercise interest, preferred modalities, timing, perceived benefits, and anticipated barriers. Eligible patients were sedentary, self-identified as Black or Hispanic/Latinx, and diagnosed with breast, colorectal, or prostate cancer. Descriptive statistics were used to summarize patient characteristics and survey responses. The Benefit Anticipation Questionnaire was scored using a 7-point Likert scale ranging from −3 (very much harmful) to +3 (very much beneficial). The Exercise Barrier Questionnaire was scored using a 7-point Likert scale, ranging from 1 (not at all) to 7 (very much). Data are reported as mean ± standard deviation.

Results: Nineteen Black or Latinx participants enrolled in the study to date, and 13 participants returned the questionnaire (mean age 55 ± 12 years), including 12 female breast cancer patients and 1 male prostate cancer patient. Most participants expressed interest in participating in an exercise program (84.6%) and felt capable of doing so (76.9%). Walking (69.2%) and strength training (53.8%) were the most preferred modes. Light- or Moderate-intensity exercise (38.5%) performed 30-60 minutes per session (84.6%) three times per week (69.2%) was most common. Surprisingly, the most preferred time to start an exercise program was during cancer treatment (61.5%), followed by before cancer treatment (30.8%). Participants reported high anticipated benefits for the proposed program, with 91.7% rating the impact as “very much beneficial” for both overall quality of life (M = 2.9 ± 0.3) and physical functioning (M = 2.8 ± 0.9). The most frequently cited barriers were feeling sick/not feeling well (M = 4.3 ± 2.1) and feeling tired or fatigued (M = 4.1 ± 2.0), followed by cost (M = 3.8 ± 2.5) and traveling to the fitness center (M = 3.8 ± 2.1).

Conclusion: Black and Latinx cancer patients expressed strong interest and confidence in home-based, supervised exercise programs during cancer treatment. Tailoring exercise schedules and addressing symptoms such as sickness and fatigue may enhance participation. Addressing barriers such as cost and travel may further support adherence.

#2485 Role of social determinants of health on survival in children with acute lymphoblastic leukemia in a Southern California cohort.

Daniel Lee[1], Dennis Kuo[2], Victor Wong[2], Anusha Preethi Ganesan[2], William Roberts[2], Oscar Ramirez[3], Paula Aristizabal[4]

[1]University of California San Diego School of Medicine, San Diego, CA,[2]Department of Pediatrics, University of California San Diego/Rady Children's Health, San Diego, CA,[3]POHEMA Foundation Research Unit, Cali, Colombia,[4]Department of Pediatrics, University of California San Diego/Rady Children's Health & Moores Cancer Center, San Diego, CA

PURPOSE: While survival for Acute lymphoblastic leukemia (ALL) has improved, outcome disparities remain, partly due to limited characterization of Social Determinants of Health (SDoH) and low participation of ethnic minorities. We evaluated clinical outcomes and SDoH in youth with ALL at Rady Children's Health (2015-2023).
METHODS: We assessed demographics, clinical characteristics, outcomes, and parental SDoH (language, interpretation use, acculturation, insurance, neighborhood vulnerability). Analyses included Kaplan-Meier (5-year EFS), multivariable logistic regression (aORs), and Cox regression (aHRs), adjusted by age, clustered by diagnosis year, with 5000 bootstrap replicates.
RESULTS: We included 211 youth, 59% (n=124/211) were male, 64% (n=134/211) were White, 27% (n=56/211) multiracial, 8% (n=16/211) Asian/Pacific Islander/American-Indian, 2% (n=5/211) Black, and 55% (n=117/211) Hispanic. The cohort's median age was 6 years (y), [IQR, 4-13], and 13% of youth was 15-18y (n=28/211). Eighty-seven percent of patients (n=183/211) had B-ALL [SR=57% (n=104/183), HR=35% (n=65/183), VHR=8% (n=14/183)]; and 13% (n=28/211) had T-ALL [SR+IR=68% (n=19/28), HR=32% (n=9/28)]. Eight percent of patients (n=17/211) relapsed once, and 2% (n=4/211) twice. Twenty-two percent of patients (n=46/211) developed bacteremia, and ICU admission occurred in 28% of youth 1-4y vs. 54% of youth 15-18y (P=0.039). Spanish for medical communication was used by 22% of parents (n=46/211). Interpretation use was 85% in parents of youth 1-4y vs. 14% of youth 15-18y (P=0.001). Parental acculturation differed by age: 36% in parents of youth 10-14y vs. 29% of 15-18y (P=0.004). The aOR of public insurance for bacteremia was 3.31 (95%CI 1.47-7.47). Bacteremia was not associated with neighborhood vulnerability (aOR 0.82, 95%CI 0.34-1.96). The cohort's 5-year EFS was 85.7% (SE 2.8%) and differed by age and neighborhood vulnerability (higher vs. lower): In 15-18y, EFS was 57% vs.90% (high vs. low; P=0.036), and in 1-10y, EFS was 78.9% vs.92.9% (high vs. low; P=0.001). The aHR of neighborhood vulnerability for relapse/death was 2.87 (95%CI 1.30- 6.33).
CONCLUSION: In this diverse ALL cohort, we found age-related and SDoH-associated disparities. Adolescents had worse survival, more ICU admissions, and lower interpreter use. Higher neighborhood vulnerability was independently linked to increased mortality, underscoring the need for targeted support for vulnerable groups.

#2486 Racial differences in clinical and cytogenetic features of pediatric acute myeloid leukemia.

Sara Elbanna[1], Hassan Mohammed Abushukair[2]

[1]Jordan University of Science and Technology, Ar-Ramtha, Jordan,[2]University of Oklahoma Stephenson Cancer Center, Oklahoma City, OK

Introduction: Racial disparities in pediatric acute myeloid leukemia (AML) outcomes are well documented, yet the biological basis for these differences remains poorly understood. Despite the availability of molecular technologies, their use in characterizing ancestry-associated disease variation has been limited. In this study, we aimed to profile race-associated clinical and molecular features in pediatric patients with AML.

Methods: We utilized the pediatric TARGET AML 2018 cohort, which included samples from 899 patients with clinical, genomic, and transcriptomic data. All data were retrieved and analyzed through the cBioportal data repository. Analyses were limited to race groups with at least 20 cases (White, Black/African American, and Asian). X2 and Kruskal-Wallis tests were used to compare categorical and continuous features, respectively.

Results: Of 899 patients, 836 patients had data reported on race, of which the majority were White (n = 644, 77.03%), followed by Black/African American (n = 102, 12.20%), Asian (n = 43, 5.14%), and other racial minorities (n=47, 5.62%). Age at diagnosis was comparable across race groups (median 11-12), and there was a trend for increased female percentage in Asian patients (61.22%) compared to Black/African American (50.88%) or White (46.55%) patients (p = 0.255). Compared to White patients, Black/African American patients had worse overall survival (OS) probability (HR: 2.12, 95% CI: 1.46-3.1), while Asian patients did not have a significant difference (HR: 1.65, 95% CI: 0.98-2.8). Median OS was not reached, 59, and 37 months for White, Asian, and Black/African American patients, respectively. Measurable residual disease (MRD) percentage at the end of the first course of treatment varied significantly by race (median: 0, 0, 0.12% in White, Black/African American, Asian, respectively, p = 0.0064). Among cytogenetic abnormalities, t(6;11)(q27;q23) (p = 0.0022) and t(8;21) (p = 0.0059) were most enriched in Black/African American patients (n = 6, 5.26%, n = 23, 20.18%) compared with White (n = 9, 1.29%, n = 82, 11.78%) and Asian patients (n = 1, 2.08%; n = 6, 12.5%) p = 0.0022). In contrast, inv(16) occurred most frequently in White patients (n = 100, 14.34%) compared with Black/African American (n = 10, 8.77%) and Asian patients (n = 1, 2.08%; p = 0.0029). FLT3-ITD positivity was the highest in Asian patients (n = 14, 28.57%), followed by White (n = 134, 18.16%) and Black/African American patients (n = 9, 7.96%, p = 0.0039).

Conclusion: Our findings highlight race-associated clinical variability in outcomes and cytogenetic attributes across pediatric AML patients. Black/African American patients had worse outcomes and more adverse-risk lesions. These patterns show that, beyond socioeconomic factors, potential underlying biological heterogeneity may contribute to racial disparities in AML outcomes and warrant further ancestry-driven investigations.

#2487 Integrating clinical and multiomics data to characterize ethnic disparities in breast cancer on the gulf coast.

Luis del Pozo Yauner[1], **Maha Babker**[1], Rosetta Campbell[1], Veronica Ramirez-Alcantara[2], Huseyin Kilic[1], Elba Turbat-Herrera[2], Hector Chavarria Bernal[1], Bahaaeldin Youssef[1], Ateeqa Mujeeb Ullah[1], Wei Yang[3], Guillermo A. Herrera[1], Ajay Pratap Singh[4]

[1]Pathology, University of South Alabama College of Medicine, Mobile, AL,[2]USA Health Biobank and Histology Service, University of South Alabama College of Medicine, Mobile, AL,[3]Bruker Spatial Biology, Seattle, WA,[4]SOM-Cell and Molecular Biology, School of Medicine at the University of Mississippi Medical Center, Jackson, MS

Ethnic disparities in breast cancer (BC) incidence, subtype distribution, and outcomes remain a significant public health concern in the United States. African American women (AAW) are disproportionately affected by aggressive disease, particularly triple-negative BC (TNBC). Whether these disparities are mirrored in Gulf Coast populations and whether tumor-level molecular features contribute to them remains unclear. This study integrates clinical data with tumor multiomics profiling to characterize ethnic differences among women diagnosed with BC within the USA Health System. Clinical and demographic information from 1,229 women diagnosed with BC from 2016 to 2024 was reviewed; 1,059 women (447 AAW, 612 WAW) with complete datasets were included. Age at diagnosis and BC subtype distribution were compared between ethnic groups. Tumor samples from 20 women (13 TNBC, seven non-TNBC; both AAW and WAW represented) and three normal breast tissues were analyzed using the NanoString BC360 transcriptomic and MO protein panel. Multiomics analyses investigated differences in signaling pathways associated with ethnicity and subtype. AAW exhibited approximately twice the frequency of TNBC observed in WAW and were more often diagnosed before age 55. These patterns parallel national trends and highlight a significant local disparity in disease presentation. The nCounter multiomics assay revealed substantial differences in gene and protein expression profiles between breast cancers from AAW and WAW. At the transcriptomic level, CCNA1, PIK3CA, SOX2, DDX39A, BRCA2, TMPRSS4, and BMP6, among others, showed lower expression in AAW tumors than in WAW tumors.In contrast, CD24 and RAC3 showed higher expression in the former group than in the latter. At the protein level, cyclin A2 and the insulin receptor were underexpressed in AAW tumors. Insulin, Notch1, melanoma GP100, and cIAP2, among others, were overexpressed in AAW tumors compared to those from WAW women. These findings demonstrate that the ethnic disparities in breast cancer observed nationally are also present in the Gulf Coast region and are accompanied by distinct molecular signatures at both the transcriptomic and protein levels. The differential expression of key oncogenic, immune, metabolic, and signaling pathway markers between tumors from AAW and WAW suggests that biological factors may contribute to the more aggressive disease patterns seen in AAW. Further studies with larger cohorts are warranted to validate these results and to explore their implications for personalized risk stratification and targeted therapeutic strategies.

This study was funded by a grant from the Breast Cancer Research Foundation of Alabama (BCRFA) to LPY.

#2488 Transcriptomic landscape for African-specific low-grade prostate cancer.

Eva F. Jensby[1], Korawich Uthayopas[2], Mehedi Hasan[2], Riana Bornman[3], Shingai B. A. Mutambirwa[4], Phillip D. Stricker[5], Karina D. Sorensen[1], Vanessa M. Hayes[2]

[1]Department of Molecular Medicine, Aarhus University, Aarhus, Denmark,[2]Ancestry and Health Genomics Laboratory, Charles Perkins Centre, School of Medical Sciences, University of Sydney, Sydney, Australia,[3]School of Health Systems & Public Health, University of Pretoria, Pretoria, South Africa,[4]Department of Urology, Sefako Makgatho Health Science University, Dr George Mukhari Academic Hospital, Medunsa, South Africa,[5]Department of Urology, St Vincent's Hospital, Darlinghurst, Australia

BACKGROUND

Prostate cancer (PCa) is characterized by large geo-ethnic disparity, with African ancestry being a recognized risk factor of aggressive disease. Globally, ISUP Grade Group 1 (GG1) PCa is considered indolent and is typically treated with active surveillance rather than active treatment. However, this approach is unfeasible in Sub-Saharan Africa due to limited access to PSA testing, imaging, and repeat biopsies. Moreover, ISUP grading developed in European ancestral populations may not reflect African PCa biology.

AIM

This project aimed to explore transcriptional differences between African and European ancestral men presenting with GG1 PCa.

METHODS

Focusing on men from Southern Africa, we performed total RNA sequencing of fresh-frozen (FF) diagnostic prostate biopsy samples from 60 African men with either GG1 PCa (n=28) or without PCa (non-PCa, n=32). FF prostatectomy samples from 47 Australian men of European ancestry with GG1 PCa were sequenced in parallel. This unique data resource enabled ancestry-specific differential gene expression and pathway analysis.

RESULTS

Principal component analysis of the top 1000 most variably expressed genes showed no clear separation between PCa and non-PCa; however, we observed a clear separation between South African and European men. From 24,008 genes, 4,641 were differentially expressed (DE) between African and European-derived GG1 tumors ($P < 0.05$, BH-adjusted). The top 5 candidate genes included downregulation of the tumor suppressor *JUN* in African ancestral tumors. Gene set enrichment analysis (GSEA) of all 24,008 genes and overrepresentation analysis (ORA) of the significant DE genes revealed downregulation of several immune and metabolic pathways ($P < 0.05$, BH-adjusted, NES < -1), indicative of more aggressive PCa driven by unique molecular pathways. Cell type analysis demonstrated lower immune cell, stromal cell, and angiogenesis scores in African compared to European-derived tumors, with stromal cells and angiogenesis reaching statistical significance (P-value < 0.05). The latter indicative of a less diverse tumor microenvironment in African PCa.

Analysis of African ancestry PCa vs. non-PCa identified only 12 DE genes ($P < 0.05$, BH-adjusted). The limited number of significant genes after adjustment may reflect the small sample size or undetected disease in the non-PCa group, which would reduce contrast between the groups. However, GSEA and ORA showed upregulation of proliferative pathways and androgen response ($P < 0.05$, BH-adjusted, NES > 1), which is the expected pattern of PCa vs. non-PCa.

CONCLUSIONS

In this first-of-its-kind study, we reveal distinct transcriptomic profiles between prostate tumors derived from men of African vs. European ancestry. Our results suggest that current active surveillance strategies may not be safe for African ancestral patients with GG1 PCa.

#2489 Distinct HER2- breast cancer traits among subethnic Hispanics of South Florida.

Janice Darkwah[1], Mira G. Spillane[1], Tonya Omlor[1], Sunwoo Han[2], Fei Ye[3], Hoyan Ng-Chen[4], Glenn Fonte[4], **Suzy D. C. Bianco**[4]

[1]University of Miami, Sylvester Comprehensive Cancer Center, Miami, FL,[2]Biostatistics and Bioinformatics Shared Resource, Sylvester Comprehensive Cancer Center, University of Miami, Miami, FL,[3]Division of Biostatistics and Bioinformatics, Department of Public Health Sciences, Sylvester Comprehensive Cancer Center, University of Miami, Miami, FL,[4]Sylvester Comprehensive Cancer Center, University of Miami, Miami, FL

Introduction: Studies with representative numbers of the predominant Caribbean and South American subethnic Hispanics of South Florida (SHFL) are limited. This study explored traits potentially linked to breast cancer susceptibility risk among SHFL, which comprise 45% of Sylvester Cancer Center's breast cancer patients.

Methods: A cohort of 971 SHFL females with breast cancer records between 1/1/2019 and 12/1/2024 was extracted from our medical record database. Data included age, ethnicity, menopausal state, cancer stage, menarche age, BRCA variants, hormone receptors (HR) and HER2 status. Human Epidermal growth factor Receptor-2 negative (HER2-) tumors (n=802) were re-evaluated for reclassification to HER2-Low using criteria: HER2 immunohistochemistry (IHC) = 1+ *or* 2+ with fluorescence *in-situ* hybridization (FISH) negative. Association of risk factors with Triple-Negative Breast Cancer (TNBC) vs non-TNBC (defined as positivity for HR and/or HER2) was assessed using logistic regression. Multiplicity in univariable analysis was reported by Q-values (p-values adjusted for false discovery rate).

Results: At diagnosis, 47% of the cohort was pre-menopausal, with 25% aged ≤45 and 13% aged ≤40. Among those diagnosed with stage 4, 24% were also aged ≤45. 71% of HR+/HER2- tumors were reclassified to HER2-Low, along with 50% of all TNBC. Univariable logistic analysis showed that younger ages (≤45 vs >45: OR=1.69, 95%CI: 1.11-2.56; q=0.042) and greater BRCA burden (1-unit increase OR=2.70, 95%CI: 1.38-5.28; q=0.017) were significantly associated with TNBC. Multivariable analysis including age, HER2-, HER2-Low, BRCA and interaction terms revealed significant positive interaction between BRCA and TNBC ($p_{interaction}$=0.018) which was weakened in HER2-Low tumors. Later cancer stages were associated with less years of estrogen exposure when compared to stages 0/1 (p=0.008 for stages 2/3 and p=0.038 for stage 4). Prevalence of early menarche (age <10) was 7% whereas late menarche (age >14) was 14%.

Conclusions: Our findings reveal distinct patterns and novel associations of BRCA burden, HER2-Low patterns, estrogen exposure and ages at diagnosis and menarche in SHFL with breast cancer. For instance, in contrast to the usual association of breast cancer with older women, nearly half of our cohort was pre-menopausal, with one quarter aged 45 or younger. This is concerning as younger patients may not be old enough to benefit from preventive mammograms and are more likely to have TNBC (the most aggressive tumors with the least treatment options). Reclassification of most HER2- tumors into HER2-Low potentially expands their therapy options to include the first trastuzumab-based therapy for HER2-Low. A weakened interaction of BRCA with TNBC in HER2-Low suggests distinct genetic basis compared to HER2- IHC=0 tumors. Lastly, prevalence of both early and late menarches was elevated compared to the general population.

#2490 Systemic molecular disparities in Black vs. White breast cancer survivors: Beyond socioeconomic determinants.

Ritam Adhikari[1], Chiranjeev Dash[2], Rabindra Roy[3]

[1]The Quarry Lane School, Dublin, CA,[2]Dept. of Oncology, Georgetown Lombardi Comp. Cancer Center, Washington,[3]Georgetown Lombardi Comprehensive Cancer Ctr., Washington

Objective: Mortality from breast cancer (BC) is 27% higher among non-Hispanic Black (NHB) than among non-Hispanic White (NHW) women. The objective of this study is to investigate molecular mechanisms underlying the higher mortality rate in NHB BC survivors, independent of lifestyle and socioeconomic factors.
Experiment: Buffy coats were collected from NHW and NHB BC survivors (n=12 each, 6 months - 3 years post-treatment) and from cancer-free participants (n=6 each). Principal Component Analysis (PCA) and Fisher's exact tests were performed on clinical variables. Gene expression was measured with the nCounter Immunology Panel (594 genes), Metabolic Pathways Panel (768 genes), and Qiagen RT² Profiler PCR Array Human DNA Repair Kit (84 genes). Differential expression analysis was performed for two comparisons: (A) Black vs. White BC survivors, and (B) Black vs. White non-cancer controls. A two-sample Student's t-test with multiple testing correction (Benjamini-Hochberg false discovery rate (FDR)) was performed with $\log_2$FC and filtered for significance ($p < 0.05$, FDR < 0.25, |fold change| > 2). An Ingenuity Pathway Analysis (IPA) was performed, and pathways with -log p value>=1.3 and Z-score >=2 or <=-2 were considered significant.
Result: PCA of clinical factors (age, BMI, and treatments) and stage distribution (Fisher's exact test) showed similar profiles between NHB and NHW BC survivors, suggesting that molecular differences in downstream analyses are unlikely to be driven by clinical or lifestyle factors. Differential expression analysis suggested that only two genes were significantly different between non-cancer NHB and NHW controls, but 92 genes, including IL8 and POLB, were significantly altered between cancer survivors. These findings suggest that the differential expression patterns are driven by cancer survivorship rather than baseline racial differences. Ninety-two genes were then analyzed with IPA, and 17 pathways were deemed significant. The Th1 and TP53 expression and degradation pathways were more active. Abasic site repair pathways were found to be inhibited in NHB survivors, consistent with our previous report.
Conclusion: Our pilot study showed that despite similar clinical profiles, NHB and NHW BC survivors exhibit distinct molecular signatures. In the future, we plan to validate these pathways and use public databases such as TCGA to evaluate how these genes affect cancer survival. Addressing these pathway differences may be key to achieving true equity in breast cancer survivorship.

: Data-Driven Approaches to Precision Oncology
Poster Session

#2494 Prospective organoid drug profiling and clinical response correlation for patients with primary or recurrent ovarian carcinoma (OC) in the PROSPERITY study.

Elizabeth M. Swisher[1], Payel Chatterjee[2], Isabel Rodriguez[1], Kalyan Banda[3], Faith Beers[2], Asal Patterson[4], Enna Manhardt[1], Mayumi Rubin-Saika[2], Emiko Oshima[2], Melanie Dillon[2], Rachele Rosati[5], Vaishnavi Pallem[2], Lauren R. Appleyard[2], Alex C. Rajewski[2], Shalini Pereira[2], Soledad Jorge[2], Renata R. Urban[2], Elise J. Simons[2], John B. Liao[1], Barbara Goff[2], Carla Grandori[6], Christopher J. Kemp[7]

[1]University of Washington, Seattle, WA,[23]University of Washington, School of Medicine, Seattle, WA,[4]Washington State, Pullman, WA,[5]Tempus AI, Inc.,[6]SEngine Precision Medicine, Bothell, WA,[7]Fred Hutchinson Cancer Center, Seattle, WA

We evaluated drug sensitivity profiling of primary and recurrent OC patient-derived organoids (PDOs) from 42 patients prospectively enrolled to the PROfiling Ovarian cancerS to improve PERsonalIzed TherapY (PROSPERITY) study. A total of 50 biopsy samples from 36 participants were received including paired pre- and post- chemo samples for 8 and paired samples from 2-3 different metastatic sites for 6 participants. Short-term PDOs were generated by SEngine Precision Medicine (TEMPUS) and assessed for drug response to a panel of 47 chemotherapeutic or targeted drugs. A filter-based algorithm was applied to each concentration-response curve to generate a sensitivity numerical score (SPM score) ranking drug responses from 15 to 1. Additional metrics were employed to group and assign categories: SPM PDO scores of 15-14 were categorized as exceptional responses, 13-12 as good, 11-9 as moderate to low, and below 9 as no response. Tumor origin and driver mutations were confirmed using whole-exome sequencing. Patient clinical response was assessed post-PARIS test using radiologic response, chemotherapy response score, and KELIM CA-125 kinetics and categorized as concordant or non-concordant relative to the PDO prediction. Drug profiling was successful in 43/50 (86%) samples with a median turnaround time of 20 days for pre-treatment samples and 26 days for post-chemo samples. Tested samples included 16 primary OC collected before chemotherapy, 20 collected after 3-4 cycles of neoadjuvant chemotherapy, and 7 recurrent OCs. 7/21(33%) post-chemo samples failed quality control (QC) metrics compared to 2/17 (11.7%) pre-chemo. Of 9 technically and clinically evaluable primary OC obtained pre-chemo, clinical response to carboplatin-based therapy was concordant with PDO prediction in 7 (77.8%). Of the 9 post-chemo evaluable cases, 6 (66.6%) were clinically concordant with PDO prediction. Of the 6 evaluable participants with recurrent OC, none were treated with a PARIS-guided therapy, preventing assessment of clinical concordance. In both the primary and recurrent OCs, unique PDO drug sensitivity profiles were identified in all profiled samples that would not have been predicted by standard molecular profiling, suggesting actionability. In 5 cases tested at two different metastatic sites, SPM scores were highly concordant (Spearman ranks, 0.48-0.77), one pair in the sixth case failed QC and was non-evaluable. In conclusion, drug profiling of both primary and metastatic OC derived organoids is highly feasible and shows promise for clinically relevant drug response predictions with high concordance in samples from more than one metastatic site. Coverage of off-label drugs with predicted exceptional and good responses has been a major barrier to clinical utilization of PDO profiling in the recurrent setting.

#2495 Rapid clinical diagnostic classification and risk stratification in acute myelogenous leukemia (AML) using whole genome sequencing (WGS).

Wayne M. Jepsen[1], Jonathan J. Keats[1], Sara A. Byron[1], Cherie Wesley[1], Bryce Turner[1], Christophe Legendre[1], Tyler Izatt[1], Tracey White[1], Amy Stouffer[1], Lucy Ghoda[2], Yeneka Campana[1], Courtney Holden[1], Jonathan Beteran[1], Michelle Afkhami[2], Anthony Stein[2], Tibor Kovacsovics[3], Guido Marcucci[2], Jeffrey Trent[1]

[1]TGen (The Translational Genomics Research Institute), Phoenix, AZ,[2]City of Hope, Duarte, CA,[3]City of Hope, Phoenix, AZ

Waiting for test results is a primary cause of delay in the diagnostic classification and risk stratification of patients with AML. With conventional cytogenetic, FISH, and targeted NGS approaches taking a median turnaround time (TAT) of 7-15 days, there is a significant unmet need to deliver these results faster using a more comprehensive testing platform. We have very recently developed, and demonstrated Analytical Validity (AV), Clinical Validity (CV) and Clinical Utility (CU) in accordance with MolDX L38047, for a rapid Whole Genome Sequencing (WGS) approach for AML (DEX Z-Code Z04C0). Importantly, this test (termed ALTseq) was specifically designed to deliver clinically actionable genomic results that encompass those from cytogenetics, FISH, and targeted NGS in under 48 hours (TAT mean = 33 hours). This accelerated turnaround time was enabled by streamlining laboratory workflows, enhancing bioinformatic pipelines, and expediting variant approval for reporting. The assay captures single nucleotide variants, indels (including FLT3-ITDs and KMT2A-PTDs), and 155 distinct structural variants including KMT2A rearrangements, and genome-wide copy number alterations. Additionally, we have recently developed a method to measure monosomal and complex karyotypes from WGS sequencing data. By deploying WGS we are able to gain insight in all genes in the human exome, with the curated clinical reporting covering all current key AML-related aberrations. These include mutations in NPM1, TP53, RUNX1, IDH1/2, FLT3, MEN1, rearrangements involving KMT2A, MECOM, NUP98, and canonical translocations such as PML::RARA, RUNX1::RUNX1T1, and BCR::ABL1. ALTseq has a limit of detection of 9%, 8%, 10%, and 7% for SNVs, indels, CNAs, and SVs, respectively, with sensitivities of 96%, 96.4%, 95.7%, and 100%, respectively. The positive predictive value for all variant types is ≥99.5%. Since implementation, ALTseq has been used in 66 AML cases, achieving a mean TAT of 33 hours from sample receipt to report delivery. Recent evidence of clinical utility includes the incorporation of Mylotarg in induction therapy based on the identification of CBFB::MYH11 fusion gene, and the inclusion of Revumenib for a KMT2A rearrangement that could not be identified with standard breakaway FISH probes. In summary, we will describe the clinical deployment of a high-throughput, fast-turnaround WGS platform for AML, capable of delivering comprehensive genomic profiling in <48 hours from sample receipt to clinical reporting enabling earlier, more informed treatment decisions.

#2496 *In silico* screeening of therapeutics candidates targeting minimal residual disease in glioblastoma.

Harrshavasan Congivaram[1], Shashwat Tripathi[1], Mateo Gomez[1], Katy McCortney[1], Ching Man Wai[2], Ruochen Du[1], Thomas K. Sears[1], Daniel J. Brat[3], Craig M. Horbinski[4], Mark W. Youngblood[1], Jared T. Ahrendsen[5], Adam M. Sonabend[1], Stephen T. Magill[1], Matthew C. Tate[1], Maciej S. Lesniak[1], Sean Sachdev[6], Timothy Sita[6], Priya Kumthekar[7], Karan Dixit[7], Robin Buerki[7], Ditte Primdahl[7], Mustafa Khasraw[8], John de Groot[9], David A. Reardon[10], Rimas V. Lukas[7], Roger Stupp[7], Amy B. Heimberger[1]

[1]Neurological Surgery, Northwestern Univ. Feinberg School of Medicine, Chicago, IL,[2]Biochemistry and Molecular Genetics, Northwestern Univ. Feinberg School of Medicine, Chicago, IL,[3]Professor, Dept. of Path. & Lab Med., Northwestern University - Evanston, IL, Chicago, IL,[4]Department of Laboratory Medicine and Pathology, Mayo Clinic Jacksonville, Chicago, IL,[5]Pathology, Northwestern Univ. Feinberg School of Medicine, Chicago, IL,[6]Radiation Oncology, Northwestern Univ. Feinberg School of Medicine, Chicago, IL,[7]Neurology, Northwestern Univ. Feinberg School of Medicine, Chicago, IL,[8]Duke Cancer Institute, Durham, NC,[9]Neuro-Oncology, University of California San Francisco, San Franscisco, CA,[10]Ctr. for Neuro-Oncology, Dana-Farber Cancer Institute, Boston, MA

Background: Glioblastoma recurrence is inevitable despite aggressive surgical resection of contrast enhancing (CE) tumor. Unlike the deep molecular characterization of CE glioblastoma, unresected infiltrating tumor, representing minimal residual disease (MRD) has not been well profiled. Increasingly, clinical trials are being conducted in the MRD setting for glioblastoma patients, necessitating understanding of unresected infiltrating tumor for targeted therapeutic development.

Methods: Visium HD spatial transcriptomics was used to profile a cohort of newly diagnosed, treatment-naïve glioblastoma patients that underwent supramaximal resection, with both core and infiltrating *in situ* components. Spatial profiles generated expression signatures of infiltrative and CE tumor. For i*n silico* prediction of therapeutics targeting the MRD, expression signatures of infiltrative and CE tumor were compared with drug perturbation signatures from the NIH L1000 database using the sRGES method to predict reversal of disease expression patterns. IC_{50} data from human cell lines were aggregated from the Genomics of Drug Sensitivity in Cancer or individual study data while blood-brain barrier (BBB) penetrance was predicted using the CNS-MPO approach.

Findings: Infiltrative tumor expression profiles were enriched for genes corresponding to neural and oligodendrocyte progenitor like cells. In contrast CE glioblastoma displayed mesenchymal and astrocytic programs, suggesting spatial concentration of glioblastoma states within MRD and CE tumor. For CE glioblastoma, proteasome inhibitors and glucocorticoid receptor agonists were predicted to have the highest antitumor activity. In contrast, histone deacetylase inhibitors (HDACi) were highly ranked for MRD while exhibiting low predicted efficacy in CE tumor. Synergy analysis of drug candidates provided multiple dual treatment options for both the CE and MRD contexts.

Conclusions: Cumulatively, these data indicate that the resected tumor does not reflect the MRD state, providing clarity on why targeted therapeutics for glioblastoma have not been particularly successful. Spatial profiling of the MRD demonstrates vulnerability to unique drug targets, which if utilized in the correct setting could confer greater survival benefit.

#2497 A human pcVMT platform for personalizing chemotherapy route and regimen selection in peritoneal carcinomatosis.

Aaqil M. Khan[1], **Stephanie J. Hachey**[2], Vinodh Kumar Radhakrishnan[2], Fatemeh Tajik[2], Melanie Roman[2], Christopher C. W. Hughes[2], Maheswari Senthil[1]

[1]University of California, Irvine, Irvine, CA,[2]Uc-Irvine, Irvine, CA

Peritoneal carcinomatosis (PC) is a clinically aggressive metastatic disease state marked by diffuse peritoneal involvement and limited responsiveness to systemic chemotherapy due to poor penetration across the mesothelial barrier. Although intraperitoneal (IP) therapy offers a mechanistically rational alternative, clinicians currently lack human-relevant platforms to determine which patients will benefit most from systemic therapy, IP therapy, or a combination of both.To address this unmet need, we developed a dual-chamber peritoneal carcinomatosis vascularized micro-tumor (pcVMT) platform that recreates a human mesothelial-lined peritoneal cavity adjacent to a perfused vascular network, enabling patient-specific, route-specific chemotherapy testing. The pcVMT supports stable vascular perfusion, intact mesothelial barrier function, and tumor adhesion and invasion using both PC cell lines and patient-derived peritoneal metastases. High-resolution confocal imaging confirms robust tumor-stromal-vascular organization across multiple clinical samples.The platform facilitates testing of clinically relevant regimens, including vascular FOLFOX, IP paclitaxel, and bidirectional systemic+IP delivery, and permits real-time visualization of route-dependent tumor responses within each patient's microenvironment. Early patient-derived experiments demonstrate feasibility of individualized assessment, including successful IP paclitaxel administration with observable changes in tumor architecture.By enabling controlled comparison of systemic, IP, and combined delivery strategies within a physiologic human peritoneal model, the pcVMT provides a precision-oncology tool designed to identify the most effective therapy and delivery route for each patient. Ongoing studies will expand patient-derived testing and explore correlations with clinical decision-making to guide personalized treatment selection and future systemic-IP combination strategies in PC.

#2498 OncoKB™, MSK's precision oncology knowledge base: 2025 updates.

Sarah Phillips Suehnholz[1], Ritika Kundra[1], **Moriah Heller Nissan**[2], Calvin Lu[1], Nicole Fernandez[1], Kelly Cavender[1], Kinisha Gala[1], Benjamin Preiser[1], Reshma Ramaiah[1], John Konecny[1], Xiang Li[1], Subhiksha Nandakumar[3], Kseniya Petrova-Drus[1], Mark Ewalt[1], Nikita Mehta[1], Yonina R. Murciano-Goroff[1], James Du[1], Anoop Balakrishnan Rema[1], Aijazuddin Syed[1], A. Rose Brannon[1], Ahmet Dogan[1], Diana Mandelker[1], Zsofia K. Stadler[1], Alexander Drilon[1], David B. Solit[1], Ross L. Levine[4], Maria E. Arcila[1], Marc Ladanyi[1], Michael F. Berger[1], Jianjiong Gao[1], Nikolaus Schultz[1], Debyani Chakravarty[1]

[1]Memorial Sloan Kettering Cancer Center, New York, NY,[2]Memorial Sloan Kettering Cancer Center, San Diego, CA,[3]Memorial Sloan Kettering Cancer Center, Ann Arbor, MI,[4]Assistant Member, Human Onc. Pathogenesis Prog., Memorial Sloan Kettering Cancer Center, New York, NY

OncoKB™, a precision oncology knowledgebase developed at Memorial Sloan Kettering Cancer Center (MSK), provides expert-reviewed interpretations of the biological function and clinical actionability for >8,000 somatic alterations in 950 cancer-associated genes. It remains the only somatic cancer variant knowledgebase partially recognized by the U.S. FDA. At MSK, OncoKB™ has annotated over 100,000 patient sequencing reports so far and it supports thousands of cBioPortal daily users for their variant interpretation needs. In addition, thousands of users globally are utilizing OncoKB™ for annotating and interpreting cancer variants. OncoKB™ is publicly accessible at www.oncokb.org. It can be used for free for academic research and requires a fee-based license for clinical and commercial use.

OncoKB™ classifies alterations based on the level of evidence supporting the alteration as a predictive biomarker of drug response in a specific cancer subtype. To date OncoKB™ includes 58 Level 1 genes as well as MSI-H and TMB-H (included in the FDA drug label), 6 Level 2 genes (included in professional guidelines), 10 Level 3A genes (predictive of response in well-powered clinical studies), 1 Level 4 gene (predictive of response based on compelling biological evidence), and 12 R1/R2 resistance genes.

In 2025, OncoKB™ added 3 novel level 1 biomarkers based on the FDA approval of dordaviprone in *H3F3A, H3C2,* and *H3C3 K28M*-mutant diffuse midline glioma. OncoKB™ also promoted *NPM1* mutations in acute myeloid leukemia and *KRAS* mutations in low-grade serous ovarian cancer to level 1 based on FDA approvals of revumenib and avutometinib + defactinib, respectively. Multiple *EGFR* alterations, including exon 19 in-frame insertions and kinase domain duplications, were also elevated to level 1 following FDA approval of datopotamab deruxtecan for *EGFR* mutant non-small cell lung cancer (NSCLC). NCCN guidelines for pancreatic cancer and NSCLC added erdafitinib for *FGFR1/2* fusion-positive and *FGFR1/3*-mutant tumors, respectively, establishing these as OncoKB™ level 2 biomarkers. Similarly, the NCCN small bowel adenocarcinoma guidelines listed sotorasib and adagrasib for *KRAS* G12C-mutant tumors, and the NCCN breast cancer guidelines listed neratinib + trastuzumab + fulvestrant for tumors with *ERBB2* mutations, also designating level 2 status in these indications. In sum, 3 novel clinically actionable biomarkers and 20 follow-on precision oncology therapies for existing leveled biomarkers were incorporated into OncoKB™ in 2025.

OncoKB™ has started annotating germline variants to enable integrated interpretation of paired tumor-normal sequencing results. Other ongoing efforts include updates to diagnostic and prognostic biomarker annotations, a clinical trial matching module, and piloting AI-based curation workflows to expand OncoKB™ annotation for biomarkers detected by whole genome or transcriptome sequencing and immunohistochemistry.

#2499 Single-cell transcriptomic comparison of tumor before and after chemotherapy reveals therapeutic vulnerabilities in chemo-tolerant osteosarcoma cells.

Parisa Vahidi Ferdowsi[1], Kenny Yeo[1], Tiruneh Adane[1], Qian Wang[1], Nisitha Jayatilleke[1], Sin Wi Ng[1], Janith Seneviratne[1], Daniel R Carter[1], Antoinette Anazodo[2], Richard Boyle[3], Paul Stalley[3], Maurice Guzman[3], Daniel Franks[3], Belamy B. Cheung[1], Glenn Marshall[1]

[1]Children's Cancer Institute, Sydney, Australia,[2]Kids Cancer Centre, Sydney, Australia,[3]Royal Prince Alfred Hospital, Sydney, Australia

Relapse remains the leading cause of treatment failure and mortality in osteosarcoma (OS). There is currently no reliable clinical approach to predict relapse at diagnosis or to inform early, personalised treatment strategies aimed at avoiding relapse. This study aims to address this gap by profiling OS tumors with single-cell RNA sequencing (scRNA-seq) at diagnosis (Dx), after chemotherapy (Rx), and at relapse (Rel). By mapping gene-expression changes across these stages, we identify resistance-associated genes and pathways, define persister cell populations, and prioritise translational combination therapies for high-risk patients. We performed scRNA-seq on 17 primary OS tumor samples (11 Dx, three Rx, and three Rel) from 12 patients including two Dx/Rx and three Dx/Rel pairs. After removing low-quality cells, batch effects were corrected in Seurat using Harmony. Cell types were annotated based on canonical markers, and malignant cells were inferred from copy-number variation (CNV) profiles using CONICSmat. To further increase our sample size and statistical power, we integrated an additional 12 diagnostic and 15 after chemotherapy OS scRNA-seq data from 27 patients using publicly available datasets, applying Harmony to correct for sequencing platform differences and minimise inter-dataset batch effects. Differential expression in malignant cells was assessed between Dx and Rx/Rel using pooled and paired analyses. Genes upregulated at Rx/Rel were prioritised using four filters: patient prognostic association in NCI TARGET, supporting evidence from published studies, gene dependency in DepMap, and small molecule inhibitors suitable for *in vivo* studies. Five candidate genes were selected for functional validation: SNHG6, PFKFB3, MRE11, PLCβ4, and S100A13. PFKFB3 and PLCβ4 were tumor-specific and induced by cisplatin and doxorubicin. Their silencing by siRNA or pharmacologic inhibition with the selective inhibitor sensitised OS cells to chemotherapy. Gene set enrichment identified epithelial-mesenchymal transition (EMT) as the top pathway in Rx/Rel, consistent with therapy-tolerant states. SB-431542, a TGF-β-induced EMT inhibitor, sensitised cisplatin-resistant OS cells to cisplatin and reduced migration of OS cells. Taken together, these findings define chemoresistant tumor states and identify actionable targets and pathways, including PFKFB3 and EMT, for rational combination therapies. They support a scRNA-guided framework for risk stratification and precision treatment selection in high-risk OS.

#2500 *CMTR2* deficiency defines a novel RNA splicing-driven subtype of lung adenocarcinoma with therapeutic vulnerabilities.

Takashi Nakaoku[1], Shigenari Nukaga[1], Kouya Shiraishi[1], Akifumi Mochizuki[1], Hamaguchi Yu[1], Hitomi Nishinakamura[1], Yoshihisa Kobayashi[1], Ayako Ui[2], Yasushi Goto[3], Shun-ichi Watanabe[3], Yasushi Yatabe[3], Hiroyoshi Nishikawa[1], Ryuji Hamamoto[1], Takashi Kohno[1]

[1]National Cancer Center Research Institute, Tokyo, Japan,[2]Institute of Development, Aging and Cancer, Tohoku University, MIyagi, Japan,[3]National Cancer Center Hospital, Tokyo, Japan

Background: RNA splicing is frequently perturbed in cancer, yet upstream genomic drivers and tractable vulnerabilities remain incompletely defined in lung adenocarcinoma (LUAD). CMTR2 catalyzes 2′-O-methylation at the mRNA cap (Cap2), a modification implicated in mRNA maturation. The oncologic significance of *CMTR2* alterations and their impact on splicing have not been systematically characterized. We performed comprehensive splicing analysis to identify novel therapeutic targets in LUAD.

Methods: We analyzed 1,017 primary lung cancer specimens with integrated DNA- and RNA-sequencing to map alternative splicing (AS) events (rMATS) to identify alternative splicing events. t-SNE visualization revealed distinct splicing patterns. *CMTR2* variants were functionally profiled using CRISPR knockout models. Splicing changes were validated by orthogonal assays, including long-read direct RNA sequencing. Physical links between CMTR2 and the spliceosome were assessed by proteomics/Co-IP. Therapeutic dependencies were tested using the RBM39-degrader splicing modulator indisulam in vitro and in vivo, and by evaluating response to anti-PD-1 immune checkpoint blockade (ICB) and combination regimens in immunocompetent models.

Results: Genomic profiling identified 3.8 % of LUAD harboring truncating or functionally impaired *CMTR2* alterations, which associated with a distinct AS signature across multiple event classes. CMTR2 physically interacted with spliceosomal components; these interactions were compromised by truncating variants or loss of *CMTR2*, coinciding with widespread shifts in exon usage and intron retention detected by both short- and long-read sequencing. *CMTR2*-deficient cells exhibited heightened sensitivity to splicing modulation with indisulam, producing robust anti-tumor effects in xenograft models. In immunocompetent settings, *CMTR2* loss increased tumor susceptibility to ICB; combining indisulam with anti-PD-1 further enhanced tumor control. Together, these data establish a mechanistic link between cap modification, spliceosome engagement, and therapeutic vulnerability.

Conclusions: *CMTR2* alterations constitute an upstream genomic driver of splicing dysregulation in LUAD and unveil an exploitable liability to splicing modulation and ICB therapy. Cap-dependent RNA maturation and spliceosome coupling represent a convergent axis of vulnerability with immediate translational potential for patient stratification and combination strategies.

Clinical Relevance: *CMTR2* status may serve as a biomarker to identify patients likely to benefit from splicing modulators and/or ICB, and provides a rationale for clinical exploration of CMTR2-targeted combinations in lung cancer.

#2501 Epigenetic screening in organoids identify KMT5A inhibition as a therapeutic strategy via PGK1in endometrial cancer.

Jingyao Chen, Yinhua Tan, Zhichang Liu, Tong Wang, Kai Xiao, Feifei Na

West China Hospital, Sichuan University, Chengdu, China

Endometrial cancer is the most common malignancy of the female reproductive tract, with a continuously rising incidence in recent years. Genomic analyses, including whole-genome and exome sequencing of large tumor cohorts, have revealed widespread epigenetic abnormalities in endometrial cancer. However, the underlying mechanisms driving tumorigenesis remain unclear, highlighting an unmet clinical need for novel therapeutic targets and drugs. Previously, we established genetically defined endometrial cancer organoids with mutations of Trp53, Pten, and amplification of Myc, which recapitulate the tumor heterogeneity and pathology of the disease. In this study, we employed these organoids to perform a high-throughput screen of an epigenetic-targeted compound library. One of the top candidates was UNC0379, an inhibitor of KMT5A. CRISPR/Cas9-mediated genetic inhibiton of KMT5A, encoding the H4K20me1 methyltransferase, consistently suppressed cell viability in both endometrial cancer organoids and cell lines. To further validate the role of KMT5A in vivo, we applied a gene-delivery approach to knock out KMT5A in tumor cells, which significantly inhibited tumor growth in mouse models. Multi-omics analyses were then utilized to investigate the molecular mechanisms underlying KMT5A function. We found that KMT5A deficiency led to significantly reduced ribosome biogenesis, a corresponding decrease in ribosome number, and dysregulated amino acid metabolism. CUT&Tag revealed that KMT5A directly regulated the expression of PGK1 through histone modification. Moreover, inhibition of PGK1 recapitulated both the anti-tumor effects and the abnormal ribosome biogenesis observed upon KMT5A loss.Clinically, high expression of KMT5A was associated with poor prognosis in endometrial cancer patients. Together, this study identifies the KMT5A/PGK1 axis as a key driver of tumor growth in endometrial cancer, revealing a potential therapeutic target for this malignancy.

#2503 Lung cancer organoid-based diagnostic response prediction (CODRP) for predicting anticancer drug response and progression-free survival.

Seung Joon Kim[1], Sang-Yun Lee[2], Yu-Jeong Seong[1], Yongki Hwang[1], Hyobin Won[1], Eunyoung Lee[1], Dong Woo Lee[3]

[1]The Catholic University of Korea, Seoul, Korea, Republic of,[2]Chungnam National University, Daejeon, Korea, Republic of,[3]Gachon Univ. of Medicine and Science, Suwon-si

Background: Anticancer drug sensitivity analysis using patient-derived lung cancer organoids is being actively investigated as a means to predict individual responses to anticancer therapies. Conventional drug sensitivity analysis methods typically rely on the area under the dose-response curve (AUC) or the half-maximal inhibitory concentration (IC_{50}) to distinguish drug-sensitive and drug-resistant phenotypes, yet these approaches have notable accuracy limitations. To address this issue, we developed Cancer Organoid-based Diagnostic Response Prediction (CODRP), a multiparametric analytical method that integrates AUC values, patient-derived organoid (PDO) growth rates, cancer stage. In progression-free survival (PFS) analyses, CODRP demonstrated superior prognostic accuracy compared with conventional AUC-based methods.

Methods: Lung cancer cells obtained from patient-derived tissue were used to generate PDOs that mimic the characteristics of the original lung cancer tissue. Because patient-derived lung cancer cells could only be obtained in limited amounts, a disposable nozzle-type cell spotter, which enables the precise distribution of minimal cell numbers, was employed for high-throughput screening. The key characteristics of the PDOs were validated through pathological comparison with the corresponding patient tissue slides. Anticancer drug sensitivity testing was performed using the PDOs, and PFS was analyzed according to the therapeutic agents prescribed to the patients.

Results: Anticancer drug sensitivity analysis was performed using lung cancer PDOs derived from 12 patients. The conventional AUC-based approach failed to clearly differentiate drug-sensitive from drug-resistant cases. In contrast, the CODRP index showed strong concordance with actual clinical treatment outcomes. Moreover, whereas AUC analysis revealed only modest differences in PFS between responders and non-responders, CODRP identified a distinct separation, demonstrating its superior predictive capability.

Conclusions: CODRP-based anticancer drug response analysis using lung cancer PDOs provides an effective approach for forecasting and evaluating treatment outcomes in patients with lung cancer. This method has the potential to be incorporated into precision medicine workflows, supporting more individualized treatment planning and enhancing the clinical relevance of therapeutic decision-making.

#2504 Activation of alternative receptor by CCL5 is associated with non-small cell lung cancer disparities.

Briana Alicia Brock, Murugesh Eswaran, Hina Mir, Shailesh Singh

Morehouse School of Medicine, Atlanta, GA

Background and Significance: Lung cancer remains the leading cause of cancer-related mortality in the United States, with persistently lower survival rates among African Americans (AAs) compared to European Americans (EAs). Emerging evidence suggests that race-associated molecular differences in chemokine receptor-ligand networks may underlie these disparities. Chemokine signaling through CC chemokine receptor 5 (CCR5) and its ligand CCL5 has been implicated in tumor growth and immune modulation; however, chemokine ligands often exhibit receptor promiscuity. Hence, in this study, we have demonstrated the activation of other chemokine receptors when CCL5 is unable to activate CCR5, as well as its association with disparities in NSCLC.
Methods: An ELISA assay was used to quantify CCL5, and PCR Immunoprecipitation followed by Western blot was used to evaluate mRNA transcripts and protein expression of CCL5, CCR5, CCR3, and CCR1. An anti-CCR5 antibody and/or a small molecule inhibitor of CCR5 were used during the functional assay, with or without CCL5 stimulation, and blocking other receptors that also share CCL5 as a ligand.
Results: Our findings reveal that CCL5-driven signaling in NSCLC is not restricted to CCR5 and that alternative receptor engagement, such as CCR3 activation, may sustain tumor-promoting pathways. The differential expression of chemokine receptors in AA- versus EA-derived lung cancer cells suggests that ligand-receptor selectivity and compensatory signaling could contribute to racial disparities in lung cancer biology and outcomes. Ongoing work targeting CCR3 will determine whether this receptor mediates escape signaling when CCR5 is unavailable, thereby identifying precision-based therapeutic strategies to disrupt redundant chemokine circuits that reinforce tumor progression and inequities in disease burden.
Conclusions and Implications: These findings highlight the complexity of chemokine signaling in lung cancer, where ligand promiscuity and receptor redundancy can sustain the proliferation and migration of cancer cells. Differences in CCR3, CCR5, and GPR75 expression, cancer-related gene activity, and migratory behavior in AA and EA-derived cells suggest that differences in chemokine receptor utilization may play a crucial role in shaping the molecular landscape and cellular behaviors that contribute to racial disparities in lung cancer outcomes

#2505 Dual siRNAs for precision targeting of synthetic lethal vulnerabilities in Diffuse Pleural Mesothelioma.

Yelixza I. Avila[1], Anand Singh[2], Vivek Singh[3], So-Hyun Yoon[4], Smrity Sahu[3], Nathanael Pruett[3], Chuong D. Hoang[5]

[1]National Cancer Institute, Bethesda, MD,[2]NCI, Bethesda, MD,[3]National Cancer Institute, BETHESDA, MD,[4]NIH-NCI, Bethesda, MD,[5]Assistant Professor, Dept. of Thoracic Surgery, National Cancer Institute, Bethesda, MD

Diffuse pleural mesothelioma (DPM) remains a lethal malignancy with limited benefit from existing therapies, underscoring the urgent need for molecularly precise treatments that act directly at the disease interface. Previously, we identified WEE1 and PKMYT1 as consistently overexpressed in DPM and demonstrated that their combined inhibition induces synthetic lethality. Here, we evaluate a dual-siRNA therapeutic strategy targeting this kinase pair and position it within a platform engineered for localized RNA delivery. Across three DPM subtypes (epithelioid, sarcomatoid, and biphasic), siRNA constructs achieved robust knockdown of WEE1 and PKMYT1, with >70% reduction in mRNA levels at 48-96 h post-transfection. Single-gene silencing induced only modest reductions in cell viability, with >70-80% survival across most lines relative to controls. In contrast, combined WEE1/PKMYT1 knockdown consistently elicited a marked decrease in viability, ranging from 60% to 85% depending on the cell line ($p < 0.001$). Cell-cycle analysis revealed that dual knockdown, unlike individual siRNAs, induced significant G2/M arrest accompanied by a depletion of S-phase cells, indicating disruption of DNA damage checkpoints. Flow cytometry demonstrated a 3- to 5-fold increase in apoptotic cell fractions compared with single knockdowns and controls ($p < 0.0001$), confirming synergistic induction of programmed cell death. These data show that although individual siRNAs exert limited effects, their combination produces robust anti-proliferative, pro-apoptotic, and cell-cycle disruptive phenotypes consistent with synthetic lethality. Collectively, these data validate dual-siRNA synthetic lethality as a promising therapeutic approach for DPM and underscore the potential of a nanoparticle-hydrogel delivery system that we have developed for precise, localized RNA therapy. This work paves the way for RNA nanomedicine in mesothelioma and other anatomically restricted, treatment-refractory cancers.

#2506 Genomic-driven targeted therapy evaluation using patient-derived organoids and xenografts in gastric cancer.

Honyong Zhang, Nicole Halmai, Jasmine Diaz Sezati, Ana Estrada, Luis G. Carvajal-Carmona

University of California, Davis, CA

Background: Gastric cancer (GC) exhibits significant molecular heterogeneity that hampers the effectiveness of standard therapies. Reliable preclinical models that accurately reflect patient-specific biology are urgently needed to inform precision treatments. Patient-derived organoids (PDOs) and xenografts (PDXs) provide complementary platforms for assessing targeted therapies.
Methods: We developed gastric cancer organoids (GCOs) representing diverse molecular subtypes, along with matched PDX and organoid-derived xenograft (ODX) models. Histology, IHC, whole-exome sequencing, and copy-number analysis were used to verify their fidelity to patient tumors. Targeted drug screening was conducted based on actionable genomic alterations (TP53 mutation, PIK3CA mutation/amplification, CDK4/6 amplification). In vivo therapeutic efficacy and resistance mechanisms were evaluated using PDX models, including a Palbociclib-resistant line (3CG-278R) generated through prolonged exposure.
Results: GCOs retained the morphological, immunophenotypic, and genomic features of their parental tumors and PDX counterparts, including recurrent amplifications in PIK3CA, AKT1-3, MTOR, CCND1, CCNE1, and CDK4/6. Genomic-guided drug screening revealed distinct vulnerabilities: CDK4/6-amplified GCOs showed strong sensitivity to Palbociclib (IC_{50} ~0.01 μM); PIK3CA-mutant GCOs exhibited potent responses to PI3K inhibitors (IC_{50} = 0.004-0.013 μM); TP53-mutant GCOs responded robustly to MDM2 inhibitors with clear p53/p21 pathway reactivation. In vivo, Palbociclib and the AKT inhibitor Ipatasertib significantly delayed tumor progression (>40 days to endpoint) and improved survival in CDK4/6-amplified PDXs with minimal toxicity. The Palbociclib-resistant PDX model (3CG-278R) showed CDK6 overexpression and transcriptional reprogramming marked by NF-κB and AP-1 activation, mucin upregulation, and decreased FOX-family tumor suppressor activity. Combination therapy with Palbociclib plus Ipatasertib restored apoptotic signaling and effectively overcame resistance.
Conclusions: This integrated PDO/PDX/ODX platform accurately models gastric cancer biology, supports genomic-guided therapeutic stratification, and uncovers actionable mechanisms behind targeted therapy resistance. These patient-derived systems provide a strong translational framework for discovering effective precision treatments and rational drug combinations in gastric cancer.

#2507 Causal machine learning personalizes endocrine therapy selection for ductal carcinoma *in situ*.

Emma Graham Linck[1], Alex Spicer[2], Marina N. Sharifi[3], Guanhua Chen[1], Mark Craven[1], Nataliya Uboha[3], Mark Burkard[4], Matthew Churpek[2]

[1]Dept of Biostatistics and Medical Informatics, Univ. of Wisconsin Madison School of Medicine & Public Health, Madison, WI, [2]Dept of Medicine, Univ. of Wisconsin Madison School of Medicine & Public Health, Madison, WI,[3]Carbone Cancer Center, Univ. of Wisconsin Madison School of Medicine & Public Health, Madison, WI,[4]Holden Comprehensive Cancer Center, University of Iowa, Iowa City, IA

Background: Standard treatment of ductal carcinoma in situ (DCIS) in post-menopausal women is breast conserving surgery/mastectomy, radiotherapy, and adjuvant endocrine therapy (ET) with either tamoxifen or an aromatase inhibitor. Despite the need to individualize selection of ET based on patient characteristics and side effects, limited tools exist for this purpose. NSABP-B-35, a phase III trial evaluating anastrozole vs tamoxifen in post-menopausal women with DCIS, found that younger patients may benefit more from anastrozole. We hypothesized that causal machine learning methods, which predict treatment effect by accounting for complex interactions between baseline characteristics, would identify treatment benefit more accurately than age alone.
Methods: Individual-level data from the NSABP-B-35 trial (n = 3104) were obtained from the NCI NCTN Data Archive, with administrative approval from NCI. Trial eligibility included: DCIS with no invasive component, hormone receptor positive, and previous lumpectomy (with clear margins and negative nodes), followed by whole-breast irradiation. Baseline variables included age, tumor palpability, presence of comedo necrosis, body mass index (BMI), and black race. The outcome was disease-free survival (DFS). The causal machine learning method, a T-learner with accelerated failure time-Bayesian Additive Regression Trees (AFT-BART), predicted the individualized treatment effect (ITE) of anastrozole vs tamoxifen on the difference in restricted mean survival time at 116 months, conditional on patient characteristics. Three repeats of five-fold cross-validation were used to generate out-of-sample predictions for each patient. Statistical significance ($p < 0.05$) was determined by an aggregate Cauchy association test (ACAT) calculated on the out-of-sample Qini coefficient p-values, a metric that quantifies how well the model orders patients by most to least benefit. Variable importance was quantified using kernelSHAP.
Results: The AFT-BART ITE model was able to significantly prioritize patients in order of most to least benefit from anastrozole vs tamoxifen (p-value = 0.03). Predicted ITE ranged from an increase of DFS by 2.9 months to a decrease in DFS by 4.5 months when on anastrozole vs tamoxifen. Younger age, presence of comedo necrosis, and black race best predicted anastrozole benefit. No statistically significant heterogeneity was found when patient age alone was used to rank patients from most to least benefit (p-value = 0.6).
Conclusions: Our causal machine learning model accurately predicted who would benefit from anastrozole vs tamoxifen, outperforming treatment selection based on age alone. Once validated, this model may help clinicians optimize treatment selection for post-menopausal women with DCIS. This work was supported by NLM 5T15LM007359.

#2508 New precision treatments for glioblastoma.

Lateef Owolabi Anifowose[1], Zhi Sheng[2]

[1]Translational Biology, Medicine, and Health, Virginia Tech, Roanoke, VA,[2]Fralin Biomedical Research Institute, Virginia Tech, Roanoke, VA

The main goal of this study is to develop precision treatments for glioblastoma (GBM). GBM is a deadly brain tumor with few treatment options, mainly due to high intra- and inter-tumoral heterogeneity manifested by diverse genetic alterations and cellular components within an individual tumor or among different patients. Previous efforts targeting molecular features have focused on three molecular subtypes — Classical (CL), Mesenchymal (ME), and Pro-Neural (PN) — but no effective treatments have been developed for each subtype. To overcome this challenge, we recently employed a machine learning algorithm to identify 31 essential survival genes, forming a new GBM progression gene signature (GBM-PGS) that divided patients into high- or low-risk (HR vs LR) of poor prognosis. Because these genes are functionally vital for cancer cell survival/growth, GBM-PGS predicts the progression of GBM patients more accurately than existing biomarkers such as EGFR, MGMT, and IDH1. Given the functional relevance of GBM-PGS to tumor cell survival and disease progression, we hypothesize that combining GBM-PGS with molecular subtyping will stratify GBM patients into distinct treatment groups, enabling the repurposing of FDA-approved drugs for precision medicine in this fatal disease. We stratified TCGA GBM patients and DepMap glioma cell lines into six subgroups: HR-CL, HR-ME, HR-PN, LR-CL, LR-ME, and LR-CL using GBM-PGS and molecular subtyping. The survival of TCGA subgroups was assessed using Kaplan-Meier analysis, and potential drug targets for the HR and LR groups were analyzed using Gene Ontology. Moreover, candidate precision treatments for each subgroup were identified from the DepMap PRISM Repurposing Drug Screen dataset and further verified in a range of GBM cell lines. The LR-PN displayed a significantly better prognosis than the other subgroups. Drugs targeted for HR GBMs were functionally different from those for LR GBMs. The six treatment subgroups exhibited diverse responses to chemical compounds, including FDA-approved drugs. Candidate drugs for each subgroup were validated in GBM cell lines. Our results have verified the crucial roles of GBM-PGS and molecular subtyping in patient stratification and in the development of subgroup-specific precision treatments. Overall, this study has the potential to transform the GBM therapeutic landscape.

#2509 Building a Precision Therapeutics program at a tertiary care Children's Hospital.

Anish Ray[1], Luke Hamilton[1], Riyaz M. Basha[2], Kelly L. Vallance[1], Diana Carrasco[1], Kaitlin Smith[1], Aly Anthony[1], Alejandra Dominguez[3], Megan Gibbs[1], Danielle Miller[1], Heidi Trinkman[1]

[1]Cook Children's Medical Center, Fort Worth, TX,[2]University of North Texas Health Science Ctr., Fort Worth, TX,[3]TCU Burnett School of Medicine, Fort Worth, TX

Background: Pediatric medicine is shifting from population-based approaches to precision medicine, fueled by advances in genomics, pharmacogenomics, and multi-omic data integration. Children, who are disproportionately affected by genetic and rare diseases, stand to benefit significantly from individualized diagnostics and targeted therapies. Cook Children's Health Care System (CCHCS) launched a Precision Therapeutics Program to unify and advance efforts in oncogenomics, pharmacogenomics, genetics, research, and education, establishing a scalable model for pediatric precision care.
Objective: To develop and evaluate a comprehensive, cross-disciplinary precision medicine infrastructure integrating molecular diagnostics, clinical care, research, and education, with measurable outcomes in pediatric oncology and rare disease management.
Methods: CCHCS implemented a unified precision medicine model built on four pillars: oncology-targeted therapeutics, pharmacogenomics, clinical genetics/genetic oncology, and research-education infrastructure. Multidisciplinary teams—led by physician-scientists, pharmacists, geneticists, and informaticians—coordinated efforts across hospital departments. The model included molecular tumor board discussions, precision medicine clinics, pharmacogenomic consultations embedded in the electronic medical record, and genetic oncology surveillance. Utilization, integration, and educational reach were prospectively tracked.
Results: Since 2019, the Molecular Tumor Board has reviewed over 150 pediatric oncology cases, delivering actionable therapies and achieving cost savings through coordinated pharmaceutical oversight. The Precision Medicine Clinic extended targeted and investigational therapies to non-oncologic conditions, improving patient access. Pharmacogenomics services were fully integrated into Epic within 15 months, completing over 100 consultations with high satisfaction and automated decision support. The Genetic Oncology Clinic identified 54 patients with heritable cancer syndromes, enabling early detection and familial cascade testing. Institution-wide education—including monthly accredited conferences, student involvement, and public engagement—further promoted adoption.
Conclusion: The CCHCS Precision Therapeutics Program demonstrates that structured, multidisciplinary integration of genomics, pharmacogenomics, and informatics is feasible and transformative in pediatric care. The model highlights collaboration, education, and patient partnership, offering a replicable framework for other institutions seeking to implement sustainable precision medicine ecosystems. Ongoing innovation, research alignment, and family engagement will be crucial for expanding precision care across pediatric specialties.

#2510 Comprehensive genomic profiling drives precision oncology and expands accessibility to targeted therapies in Uzbek populations.

Zilola Olimova[1], Gowhar Shafi[2], Djuraev Farrukh[1], Yashodhara Bhattacharya[3], Aarthi Ramesh[4], Sandhya Iyer[4], Mohan Uttarwar[4], Hrishita Kothavade[4], Alain D'Souza[4], Bhagwat Jadhav[4], Sangeeta Prajapati[4], Madhura Basavalingegowda[3], Kanchan Hariramani[3]

[1]ILBOZA Med Hospital, Tashkent, Uzbekistan,[2]OneCell Diagnostics India Private Limited, Pune, India,[3]OneCell Diagnostics Pvt Ltd, Mumbai, India,[4]

Background: The current, mortality-to-incidence ratio of 67% indicates most cancers are detected at advanced stages in Uzbekistan. In addition, symptoms appear only when the cancer is large or metastatic and advanced cancer is expensive, difficult to treat, and often fatal. Sophisticated infrastructure requires large funding, trained professional and expensive screening procedures. In several instances, treatment regimen is also administered without information on tumor sensitivity and efficacy. Eventually, patients suffer severe toxicity from multiple tests and treatments. To address these events, personalized molecular tests and treatment monitoring approaches are necessary. This study shows the efficacy of comprehensive genomic profiling (CGP) to append the molecular spectrum of cancer patients from Uzbekistan. This may open several treatment and monitoring possibilities in non-invasive scale.
Methods: A total of 124 genomically profiled patients by our CGP assay were retrospectively investigated for mutational spectrum. All patients belonged to Uzbek ethnicity with ages between 25 to 85 years. CGP was performed on these patients using next-generation sequencing (NGS) with the OncoIndx® panel.

Results: Of the 124 patients profiled genomically, 331 pathogenic/likely pathogenic variants were detected with *TP53* constituting 20.2% (67) of all variants. Several frameshift and truncated *TP53* variants were identified suggesting an impairment of TP53 protein thereby potentially leading to oncogenic stress, DNA damage, and several major pathway malfunctioning. Further, variants in *PIK3CA, APC, KRAS, EGFR, PTEN*, and *BRCA1/2* were also present with high frequencies in the patient cohort at 8.5% (28), 6.3% (21), 6% (20), 4.5% (15), 2.7% (9), and 1.8% (6) respectively. Together, these variants may suggest major impairments in cell proliferation, and DNA repair pathways. Mismatch Repair (MMR) genes including *MSH6, MSH3, MLH1, PMS2, MUTYH*, and *MSH2* were also found to be mutated at frequencies of 1.2% (4), 0.9% (3), 0.9% (3), 0.3% (1), 0.3% (1), and 0.3% (1) respectively showing damages in MMR pathway. Three patients in the cohort with colon and lung cancers exhibited high microsatellite instability (MSI) whilst genomic findings showed impairments in cell proliferation, MMR, and DNA repair pathways.

Conclusion: To conclude, this study highlights the benefit of our CGP assay in identifying diverse oncogenic drivers across multiple pathways and in the study population of the Uzbek ethnicity, it added value in expanding targeted therapeutic opportunities to manage critical pathway impairments.

#2511 Ranking therapeutic recommendations of Molecular Tumor Board with an evidence-based algorithm to deliver optimal care and improve outcomes for cancer patients- continuous study.

Yuliang Sun, Rachel Elsey, Crystal Hattum, Bing Xu, Tobias Meissner

Avera Cancer Institute, Sioux Falls, SD

Background: The Molecular Tumor Board (MTB) has brought about significant advancements in precision oncology, but there is a long-standing challenge in selecting the most effective patient-specific therapeutic strategy due to the molecular rationale, disease relevance, and patient-specific issues. We have developed an algorithm that incorporates both molecular and clinical evidence-based criteria to rank therapeutic strategies to deliver optimal care and improve outcomes in patients with malignancy. This part of our studies was to evaluate the effectiveness and accuracy of our novel algorithm.

Methods: History of present illness and comprehensive genomic profiling results of 571 cancer patients were reviewed by Avera MTB from June 2021 to December 2024. Therapeutic recommendations were provided with the Ranking Score (R, -1 to 12). The progression free survival (PFS) and overall survival (OS) of the patients that received recommended treatments (Cohort 1) or not (Cohort 2) were then assessed.

Results: The median duration of follow-up was 14.1 months by the data cut-off on July 31, 2025. Of the 571 patients, 542 (94.9%) patients with cancer were evaluable in this study, including 286 (52.8%) that received matched therapeutic plans recommended by our MTB, and 256 (47.2%) did not. No significant differences in PFS/OS were observed between patients in Cohort 1 and in Cohort 2. In Cohort1, patients who received early line (≤ line 3, n=236) therapies had longer PFS (median PFS 8.8 vs 4 months, $p<0.0001$) and OS (median OS 24.5 vs 13.7 months, $p=0.0058$) when compared with those that received later lines (> line 3, n=46) of treatment. Among patients in Cohort 1, the median PFS/OS for patients with R≥10 (n=218, 8.6/23.9 months) were longer than patients with R<10 (n=68, 4.9/13.1 months), $p=0.036$/ 0.0009; the OS of patients that received Standard of Care treatments with R≥9 (n=230, 22.2 months) were longer than R<9 (n=27, 13.1 months), $p=0.0053$, whereas no significant difference was found in PFS. The PFS/OS of patients who received Off-Label treatments with R≥7 (n=10, 35.6/not reached months) were longer than R<7 (n=5, 3.5/10 months), $p=0.0095/0.012$; however, no significant differences in PFS/OS were observed among patients treated on Clinical trials.

Conclusion: Our novel molecular and clinical evidence-based algorithm may be used to support oncologists' decision-making to utilize the most clinically appropriate and effective therapeutic options to benefit patients. Further validation studies and development of a user-friendly computational ranking platform based on the algorithm are planned in order.

#2512 A real time imaging based functional precision medicine (FPM) assay for glioblastoma.

Thomas Quinn[1], Anand Panigrahy[1], Dina ElHarouni[1], Mariam A. Oumelloul[2], Smitha Yerrum[1], Kin-Hoe Chow[1], **Sonam Bhatia**[1], Keith L. Ligon[3]

[1]DFCI/Harvard Medical School, Boston, MA,[2]Ecole Polytechnique Federale de Lausanne, Lausanne, Switzerland,[3]Assistant Professor of Path., Dept. of Med. Onc., Dana-Farber Cancer Institute, Boston, MA

Functional precision medicine (FPM) assays, which test drug effects on live patient tumor cells, have the potential of personalizing therapy guidance for cancer patients. A number of FPM assays have been developed, the most common being based on measurements of “cell growth”. However, the majority of these measure “growth” of cells indirectly via bulk viability (e.g. Cell Titer Glo) as a surrogate for increased cell numbers within the assay by a defined time point but interpretation of such low dimensional data from complex tissues is often. We hypothesize that such assays could be improved if one were to ensure that patient cells being tested are healthy and growing before treatment *ex vivo* and could be analyzed for identity and morphology via single cell measurements. Furthermore, overall <50% of patient primary cells are expected to grow in culture and so faster measures could aid in more efficient testing for more patients. To address these areas and provide a simple assay able to be widely implemented in research or clinical labs, we designed and validated a miniaturized real-time growth assay based on Incucyte imaging of patient cells to monitor drug sensitivity response using the brain tumor glioblastoma (GBM) as an example. *Ex vivo* growth response was evaluated for the DNA damaging agent, Temozolomide (TMZ) – currently used as the standard of care for GBM patients, and KRT-232 – an MDM2 inhibitor currently in clinical trials. Patient cells were monitored every 6 hours until they met our treatment enrollment growth criteria of 3 consecutive increases of cell confluence and a minimum confluence of 10%. Patient cells were then eligible to be “enrolled” to the study, cultured as 2D cells in serum-free stem cell media, and treatments were then added. Cells were monitored every 6 hours for an additional 7 days. Initial validation of the method using long-term patient derived cell lines was performed followed by a co-clinical trial conducted in parallel with fresh GBM patient samples following patient consent. To date, 45 GBM patients have been screened in the study with 20/45 (44%) meeting the pre-determined growth enrollment criteria for ex vivo treatment and prospectively followed for which matched the expected rate of long term growth for GBM patient samples under these conditions. The assay was able to be successfully completed, and results generated for 17/20 (85%) of the subjects enrolled. Analysis of the *ex vivo* response profiles from the cohort were correlated with clinical parameters and known biomarkers of response — MGMT and TP53. Initial results suggest positive correlation with known parameters and reveal novel potential patterns of response. These results show feasibility and value of incorporating real-time functional growth monitoring to improve quality-control in functional precision medicine patient diagnostics. With further validation, this assay could become a valuable therapy guidance tool for clinicians.

#2513 Exploring *Ziziphus jujuba* phytochemicals against oral cancer: Network-based profiling and molecular dynamics analyses.

Abdullah A. Assiri[1], Ahmad Alamri[1], Najeeb Khan[2]

[1]King Khalid University, Saudi Arabia, Saudi Arabia,[2]The University of Agriculture Peshawar, Saudi Arabia, Saudi Arabia

Oral cancer remains a major global health challenge due to its complex molecular heterogeneity, limited therapeutic efficacy, and high recurrence rate. This study aimed to identify potential multi-target natural therapeutics derived from *Ziziphus jujuba* using an integrative computational approach. Network pharmacology was employed to map phytochemical-target interactions relevant to oral oncogenic pathways, focusing on EGFR, BCL2, SRC, STAT3, and CTNNB1. Molecular docking was performed to evaluate binding affinities, followed by 200 ns molecular dynamics simulations and MM-GBSA analyses to assess complex stability and energetics. Among the screened compounds, oleanonic acid demonstrated the most favorable interaction profile, with docking scores of approximately -9.0 kcal/mol for BCL2 and -9.3 kcal/mol for EGFR, outperforming reference inhibitors. MD trajectories indicated stable RMSD plateaus, low active-site RMSF, and consistent Rg and SASA profiles, reflecting robust ligand-receptor stability. MM-GBSA results revealed dominant van der Waals and hydrophobic contributions to complex stabilization. Collectively, these findings highlight oleanonic acid as a promising multi-target phytochemical from *Z. jujuba* with potential therapeutic relevance in oral cancer. Further *in vitro* and *in vivo* studies are warranted to validate these computational predictions and advance its development as a candidate for oral cancer management.

#2514 Patient-driven multi-omic longitudinal research study reveals novel insights into uveal melanoma progression.

Amber Smith[1], Ben Kamphaus[1], Katie Campbell[2], Robin Kageyama[1], Benjamin G. Vincent[3], Christopher Heery[1], **Christine N. Spencer**[1], Marshall Thompson[1]

[1]Rare Cancer Research Foundation, Durham, NC,[2]UCLA - University of California Los Angeles, Los Angeles, CA,[3]University of North Carolina at Chapel Hill, Chapel Hill, NC

Introduction: Amid a surging trend in patient engagement in cancer research and the broader cultural shift toward self-advocacy and technology adaptation in healthcare, this study reports findings from a patient-partnered project investigating the mechanistic underpinnings of metastatic uveal melanoma (UM) progression.
Methods: The patient consented voluntarily on IRB-approved protocols under PRISM, a patient-centered research program overseen by The Rare Cancer Research Foundation. Sample collection, processing and distribution for advanced testing was done in collaboration with multiple academic treatment centers and empowered by Pattern.org biologistics and biobanking services. Advanced molecular diagnostic testing was performed on samples collected over a 2 year period from multiple lesion locations, including longitudinal WES/RNA-seq, proteomics, multiplexIF staining, and organoid drug testing. Response to treatment was monitored using longitudinal PET/CT imaging with individual lesion tracking using Mint Medical software, and minimal residual disease monitoring using SignateraTM cell-free DNA testing. All clinical and research data was integrated into the Pattern.org Data Commons (PDC) for downstream analysis.
Results: This patient presented with metastatic UM, initial sequencing revealed germline POT1 (Arg363) and somatic GNAQ (Q20P) and BAP1 (E398, LOF) genetic alterations. Organoid-based drug screening results did not reveal any obvious drug sensitivities to targeted treatment options. The patient experienced disease stabilization with minimal toxicity for 6 months while receiving Pembro/Ipi and an endogenous T Cell therapy. During the course of stable disease, longitudinal sequencing revealed consistent genetic alterations across timepoints and multiple lesion samples. Upon disease progression, defined by increased volumetric measurements in tumor size and increased circulating tumor cfDNA, a new EZH2 (Y641H) variant was identified using WES. Differential variant calling and gene expression analysis collected from samples before and after disease progression highlighted potential resistant mechanisms to immune-based therapies. Further, a comparative study on the tumor microenvironment using multiplex IF staining sheds additional insight into the complexities of UM metastasis and disease progression.
Conclusion: This patient-driven study utilizing multi-omic disease characterization and longitudinal monitoring illuminates immune therapy resistance mechanisms and tumor microenvironment complexities in UM metastasis.

#2515 Preserving predictive power with minimal PDOs: Accelerated drug testing for personalized therapy in metastatic CRC.

Yasmine Abouleila[1], Roel Verkerk[1], Mayke Doorn[1], Timo Voskuilen[1], Gakuro Harada[2], Masahiko Watanabe[2], Lidwien Smabers[3], Hideaki Kyan[2], Takahiko Kumagai[2], Yuichi Hikichi[2], Rene Overmeer[1], Jeanine Roodhart[3], Kiyotaka Matsuno[2], **Carla S. Verissimo**[1], Robert G. J. Vries[1], Sylvia F. Boj[1]

[1]HUB Organoids B.V., Utrecht, Netherlands,[2]Yamaha Motor, Shizuoka, Japan,[3]University Medical Center Utrecjt (UMCU), Utrecht, Netherlands

Patients with relapsed or metastatic colorectal cancer (CRC) face limited treatment options, significant side effects, and prolonged delays in identifying effective therapies. Patient-derived organoids (PDOs; HUB Organoids®) provide a clinically relevant platform that faithfully mirrors individual tumour biology, enabling personalised drug testing. However, conventional drug screening formats typically require several hundred organoids per well, limiting the feasibility of using PDOs to guide real-time treatment decisions at diagnosis or relapse. Translational speed is critical: in metastatic CRC, there is a narrow window to select effective therapy before disease progression or treatment-related toxicity occurs. Traditional preclinical models often take weeks to months, which is too slow to inform immediate patient care. To address this limitation, we developed an automated organoid-handling workflow using the Yamaha CELL HANDLER™ system, enabling precise transfer and image-based quantification while requiring far fewer organoids per well. Miniaturisation reduced input material by 96% (from 250 to 10 PDOs per well) compared to conventional screening. Drug sensitivity of PDOs measured using the miniaturised assay closely mirrored that of conventional screening ($R=0.67$-0.85, $p<0.03$). PDO responses in the miniaturised assay also correlated with patient outcomes, including progression-free survival ($R = -0.85$, $p < 0.01$).By combining automation, miniaturisation, and quantitative readouts, this platform preserves the predictive power of PDOs, drastically reduces the need for organoids, and shortens turnaround time.

#2516 Genomic landscape and patterns of homologous recombination deficiency in Indian ovarian cancer: Clinical implications for precision therapy.

Rahul Katara, Sourabh Kumar, Aditi Agarwal, Kiran Kumar, Deepak K. Sharma, Yuvaraj M, Hardeep Singh, Vipin Kumar, Shivani Sharma

Molecular Pathology, Core Diagnostics, Gurugram, India

Introduction: Ovarian carcinoma remains a leading cause of cancer-related mortality among women globally. However, the genomic characteristics of ovarian cancer in the Indian population are not well defined, limiting insights into ancestry-specific tumor biology and potential therapeutic targets.

Methodology: Whole-exome sequencing data from 619 ovarian tumor samples from Indian patients were analyzed. After stringent quality control and filtering, 5,244 prioritized somatic variants were curated and classified according to AMP guidelines. Homologous recombination deficiency (HRD) scores were integrated with clinical metadata to examine associations between homologous recombination repair (HRR) gene alterations, HRD status, and clinicopathological features.

Results: The median HRD score across the cohort was 47, with 47% of tumors classified as HRD-positive. Among clinically reported variants, 28.2% were classified as pathogenic or likely pathogenic (P/LP), 49.5% as variants of uncertain significance (VUS), and 22.1% remained unclassified. Recurrently altered driver genes included *TP53* (64.9%), *BRCA1* (38.6%), *RAD50* (37.5%), *CHEK1* (21.2%), and *POLE* (17.9%), indicating extensive disruption of DNA damage response (DDR) and HRR pathways. *BRCA1/2* P/LP variants were detected in approximately 40.7% of tumors. HRD positivity was identified in both *BRCA*-mutated (48.0%) and non-*BRCA*-mutated tumors (46.3%), suggesting that HRR deficiency extends beyond *BRCA1/2* alterations to include genes such as *RAD50*, *MRE11*, *CHEK1*,*CHEK2*,*FANCA,andFANCD2.*Age-stratified analysis showed consistent frequencies of *BRCA1/2* alterations and HRD positivity across all age groups (40-50% per stratum), indicating that HRR pathway disruption is widespread across clinical subgroups.

Conclusions: This study represents one of the largest exome-based analyses of ovarian cancer in the Indian population. Nearly half of the tumors demonstrated HRD, and HRR pathway disruption was frequent even in the absence of *BRCA1/2* mutations. These findings highlight the importance of comprehensive HRR gene testing and HRD evaluation to inform precision oncology approaches, including the use of PARP inhibitors and platinum-based therapies, for Indian ovarian cancer patients.

Keywords: Ovarian carcinoma, Indian population, exome sequencing, homologous recombination deficiency, *BRCA1*, *TP53*, DNA repair, PARP inhibitors, precision oncology.

#2517 Real-world clinical performance of a combinatorial functional precision platform, Optim.AI™, in hematological malignancies.

Masturah Rashid[1], Weng Tong Ho[1], Jhin Jieh Lim[1], Sharon Pei Yi Chan[1], William YK Hwang[2], Edward Kai-Hua Chow[1]

[1]KYAN Technologies, Singapore, Singapore,[2]National Cancer Centre, Singapore, Singapore, Singapore

Background:
Ex vivo drug sensitivity testing has been explored for nearly five decades as a strategy to individualize treatment, especially for patients without actionable biomarkers or who have exhausted standard options. Historically, adoption has been limited by challenges such as scarce tumor samples, difficulty recreating indication-specific microenvironments, and inconsistent correlation with clinical outcomes. Advances in functional precision medicine now enable more reliable translation. Optim.AI™, a combinatorial functional precision medicine platform, has shown prospective clinical utility in hematologic malignancies and sarcoma. Here, we report real-world performance data from its use in a clinical-certified laboratory for hematological cancers.
Methods:
Tumor cells from solid tissue, peripheral blood, or bone marrow aspirates were isolated and exposed to 12 FDA-approved chemotherapy and targeted agents in combinatorial formats. Post-treatment cell viability was quantified to generate Optim.AI™ rankings of actionable treatment combinations. Clinical outcomes were retrospectively assessed for patients who subsequently received Optim.AI™-guided therapies.
Results:
Among 154 hematological samples, 91% yielded sufficient cells for testing and 94% of these produced successful reports. Concordance with prior resistance patterns was high: 88% of cases demonstrated predicted normalized cell viability (NCV) > 0.6, consistent with clinically observed resistance. Retrospective analysis of five acute myeloid leukemia (AML) patients treated according to top-ranked Optim.AI™ recommendations showed that the platform was clinically useful in all five cases. Three patients responded to Optim.AI™-guided therapy, including two complete remissions—one successfully bridged to transplant. For the two patients who did not respond, the Optim.AI™ profiles accurately predicted non-response (NCV > 0.6) and supported timely decisions to limit further futile therapy, including transition to palliative care. Across these cases, NCV < 0.3 effectively stratified responders from non-responders.
Conclusion:
Consistent with prior prospective studies, these real-world results validate Optim.AI™'s ability to predict treatment responses in hematological malignancies. Importantly, the platform demonstrated clinical utility in all evaluated patients—by identifying effective therapeutic options when available and by guiding physicians toward appropriate palliative approaches when further intensive therapy was unlikely to help. Larger prospective studies across diverse indications will strengthen its path toward broader clinical adoption.

#2518 Feasibility study of an *ex vivo* functional precision medicine platform, Optim.AI™, in guiding treatment for gynecological cancers.

Masturah Rashid[1], Jhin Jieh Lim[1], Sharon Pei Yi Chan[1], Manavi Sachdeva[2], Hidayah Nabillah Nasit[2], Natalie Ngoi[2], John Chia[3], David Tan[2], Edward Kai-Hua Chow[1]

[1]KYAN Technologies, Singapore, Singapore,[2]National University Hospital, Singapore, Singapore,[3]Curie Oncology, Singapore, Singapore

Background:
Gynecological cancers, like ovarian and endometrial, face therapeutic challenges due to their molecular heterogeneity and high rates of relapse following standard platinum-based chemotherapy. Access to genetic information, such as BRCA mutation and homologous recombination deficiency (HRD) status, can predict potential responders to PARP inhibitors. However, these actionable mutations are amenable for a subset of patients only, underscoring the need for complementary functional precision medicine approaches. This ex vivo screening strategy could potentially support patient treatment management. Optim.AI™, a combinatorial functional precision medicine platform, has previously validated clinical utility for hematological cancers and sarcoma. In this feasibility study, we explored the application of Optim.AI™ on ovarian and endometrial cancers.
Methods:
Tumor cells were isolated from tissue samples from both biopsies and resections. Short-term patient-derived organoids were formed before combinatorial treatment with 12 drugs containing both FDA-approved chemotherapy and targeted drugs. Cell viability was quantified post-drug treatment for Optim.AI™ analysis, ranking all possible top combinatorial therapies for report generation. Retrospective concordance analysis was carried out after clinical responses were collected.
Results:
Based on the samples received, minimum tissue mass of 0.0835g and 0.368g for ovarian and endometrial samples respectively yielded sufficient cells to proceed with Optim.AI™ testing. Reports were successfully generated for 94% of these samples, with a mean turnaround time of seven working days. Z' factor, a statistical, quality measure for high-throughput screening, was demonstrated to be more than 0.5 for all reports generated, indicative of very good assays. Across the eight ovarian cancer reports generated, Gemcitabine-based combinations were among the most frequently top-ranked treatments. Notably, for HRD-negative patients, Optim.AI™ predictions commonly suggested increased sensitivity to gemcitabine paired with doxorubicin and paclitaxel Preliminary retrospective concordance analysis highlights Optim.AI™'s ability to predict response, where general correlation was observed between lower NCV and higher chemotherapy response score.
Conclusion:
This study showcases Optim.AI™ as a viable clinical-decision support platform for aiding treatment management for gynecological cancers, particularly for patients who do not harbor actionable mutations. Prospective clinical concordance analysis of Optim.AI™-guided treatments would further validate its clinical utility in these cancers and provide potential precision medicine insights for HRD-negative patients.

#2519 Characterization of BRAF fusions and their therapeutic and resistance implications in NSCLC.

Kai Wang[1], Chao Yi[2], Xiong Ning[3], Dalin Xiong[3], Song Wang[4], Xiaoying Wu[4], Hua Bao[4], **Haimeng Tang**[4], Xue Wu[4], Yuan Jiang[5], Hongyu Deng[5], Faqing Tang[5]

[1]Pathology Department, Zunyi Medical University Affiliated Hospital, Zunyi, China,[2]Department of Respiratory and Critical Care Medicine, Chongqing University Affiliated Three Gorges Hospital, Chongqing, China,[3]Department of Thoracic Surgery, Yan'an Affliated Hospital of Kunming Medical University, Kunming, China,[4]Nanjing Geneseeq Technology Inc., Nanjing, China,[5]Department of Clinical Laboratory, The Affiliated Cancer Hospital of Xiangya School of Medicine, Changsha, China

Background: *BRAF* fusions are rare but clinically relevant oncogenic events in non-small cell lung cancer (NSCLC). Their molecular characteristics and optimal management remain incompletely understood.

Methods: We retrospectively analyzed 97 NSCLC patients harboring kinase domain-retaining *BRAF* fusions, stratified as *de novo* (N=43) or acquired (N=54). Genomic and clinical features were compared between subgroups and against other oncogenic driver cohorts.

Results: We identified 104 *BRAF* fusions involving 53 unique 5' partners, 29 of which were novel. Frequent partners included *AGK* (12.5%), *IGR* (11.5%), *ZC3HAV1* (7.7%), *TRIM24* (5.8%), and *MKRN1* (5.8%). *IGR*- and *DTNB-BRAF* fusions were enriched in *de novo* cases, while *AGK-BRAF* predominated in the acquired setting. Among *de novo* cases, 65.1% lacked co-occurring drivers. *ZNF703* mutations and NRF2 pathway alterations were recurrent in *BRAF* fusion-only tumors, whereas *CTNNB1* and *NKX2-1* mutations were enriched relative to *ALK*-rearranged cases. *BRAF* fusions co-occurring with other drivers showed enrichment of *KMT2C* and RTK-RAS pathway mutations, and *TP53* mutations were more frequent compared to *RET*-rearranged tumors. One patient harboring *TRIM24-BRAF* and *EGFR* exon 19 deletion achieved clinical benefit from combined MEK and EGFR inhibition. Acquired *BRAF* fusions predominantly emerged after EGFR-TKI therapy (63.0%), consistent with a role in treatment resistance. Median progression-free survival on prior EGFR-TKIs aligned with clinical trial benchmarks.

Conclusions: *BRAF* fusions in NSCLC are molecularly heterogeneous, with distinct genomic landscapes between *de novo* and acquired cases. Their frequent emergence post-EGFR-TKI highlights a key resistance mechanism and supports comprehensive genomic profiling to guide individualized therapy.

#2520 Clinical impact of the personalized medicine for neuroblastoma patients: Six years of experience of the PREME program.

Francesca Parisi[1], Eleonora Ciampi[2], Veronica Bensa[2], Federica Serafino[3], Matilde Tirelli[4], Laura De Rosa[4], Vito A. Lasorsa[4], Mario Capasso[5], Chiara Brignole[2], Loredana Amoroso[6], Massimo Conte[1], Mirco Ponzoni[2], **Fabio Pastorino**[2]

[1]U.O.C. Pediatric Oncology, IRCCS Istituto Giannina Gaslini, Genoa, Italy,[2]Lab Experimental Therapies in Oncology, IRCCS Istituto Giannina Gaslini, Genoa, Italy,[3]University of Genoa, IRCCS Istituto Giannina Gaslini, Genoa, Italy,[4]CEINGE Advanced Biotechnologies Franco Salvatore, Naples, Italy,[5]University of Naples Federico II, Naples, Italy,[6]UO Pediatric Oncology Umberto I Polyclinical University Hospital, Rome, Italy

Background: PREME (PeRsonalizEdMEdicine) program is an Italian, multicentric, prospective study focused on research of possible molecular therapeutic targets for early and relapsed/refractory neuroblastoma (NB).
Methods: From 2019 to 2024, 86 patients were enrolled out of 106 eligible. Molecular alterations (MA) were detected by whole-exome-sequencing (WES) and by Cancer Gene Panel (CGP) sequencing. Somatic Point Mutations (SPM) were classified as either Very-High-Priority (VHP) or High-Priority (HP).
Results: MA, including somatic, germline or copy-number-variations (CNVs): 9 were detected at first diagnosis and 43 at relapse. Specifically, SPM were detected in 94% of patients (n=49), 9 at disease-onset and 40 at relapse. Around 35% (n=17) had VHP alterations, 43% (n=21) HP and 22% (n=11) both. Samples from 11 patients were analyzed at different times during the course of disease: first diagnosis and relapse (n=3), primary and further relapses (n=8); in 9 of those, assessment of molecular tumor changes were detected. An actionable target emerged in 75.5% of patients with SPM (n= 37). A molecular target-therapy was proposed by the study-expert-board, which was implemented in 21 patients. *ALK* was the most frequent mutated gene (43%), but other potentially actionable alterations were detected, both in tumor at first diagnosis and at relapse. Among tumor samples at relapse, from WES analysis emerged alterations in gene encoding for mitogen-activated protein kinase (*MAPK*; 12% of cases), *ATM* mutation (4%), in gene encoding for proteasome subunit member proteins (*PSMC/B*; 6%) and other less common SPMs, such as *CULA4*, *TP53*, *TNKS*, *PIK3R1*, *mTOR*, and *ATR* mutations in 6 corresponding patients. Targeted-therapy was implemented in 11 patients with *ALK* mutations, in 2 patients with *MAPK* alterations, in one patient with *PSMC/B* mutation, in one patient with *ATM* mutation and in those 6 patients harboring the less common SPMs. Generally, among all patients treated, a complete remission was obtained in 3 patients, a partial response in 13, and stable disease as best response in 2 cases. A progression disease and subsequent death occurred in 3 patients. Somatic CNVs were detected in 31 patients (59.61%); among them, 3 patients showed no SPM and a targeted-therapy potentially actionable somatic CNVs was proposed for one of those harboring *TSC2*-deletion. Germline alterations were found in 19.2% of patients (n=10).
Conclusions: PREME program is a useful tool to improve the prognosis of refractory/relapsing NB.

#2521 Illuminating the kinase starmap in NSCLC via tyrosine phosphoproteomics.

Jinfeng Yuan[1], Ying Hu[2], Yilin Wang[1], Tianhui Zhang[3], **Aijuan Yu**[4], Yi Liu[4], Hui Zhou[4], Chao Zhou[4], Junjie Hou[4], Yinyin Xu[4], Xinxin Xu[5], Huan Ding[4], Yuxin Zhang[4], Rujie Zhong[1], Mengjia Yang[1], Chunyan Chang[1], Hongxuan Yan[1], Yuanyuan Shang[1], Weicong Ren[1], Shanshan Li[1], Hongdong Zhong[4], Yun Xiao[4], Zhang Zhang[5], Naizhong Zheng[4], Ming Han[6], Yu Pang[1]

[1]Department of Bacteriology and Immunology, Beijing Chest Hospital, Capital Medical University/Beijing Tuberculosis and Thoracic Tumor Research Institute, Beijing, China,[2]Department of Medical Oncology, Beijing Chest Hospital, Capital Medical University/Beijing Tuberculosis and Thoracic Tumor Research Institute, Beijing, China,[3]Department of Thoracic Surgery, Beijing Chest Hospital, Capital Medical University/Beijing Tuberculosis and Thoracic Tumor Research Institute,, Beijing, China,[4]DeepKinase Biotechnologies Ltd., Beijing, China,[5]State Key Laboratory of Bioactive Molecules and Druggability Assessment, Jinan University, Guangzhou, China,[6]Department of Thoracic Surgery, Beijing Chest Hospital, Capital Medical University/Beijing Tuberculosis and Thoracic Tumor Research Institute, Beijing, China

In lung cancer treatment, understanding kinase activity, particularly tyrosine phosphorylation, is crucial but incomplete. We studied tyrosine phosphoproteomics in 74 patients with non-small-cell lung cancer (NSCLC) using SH2-Superbinder and data-independent acquisition mass spectrometry. We constructed a tyrosine phosphorylation starmap, This starmap is presented as an interactive force-directed network, providing dynamic visualization of intricate signaling pathways that are active in tumor tissues or normal adjacent tissues (NATs). Unlike the dense, unstructured distribution observed in NATs, the tumors showed four well-defined subnetwork constellations: adherens junctions, cytoskeletal dynamics, immune signaling, and blood. Subsequently, patients were stratified by kinase activity for multiple precision medicine perspectives.

#2522 Exploring the impact of RAS mutations in abdominopelvic Rosai Dorfman disease on responsiveness to targeted therapies: A case control study.

Rebecca Denson[1], Fnu Amisha[2], David Pottinger[2], Ling Zhang[3], Lubomir Sokol[2], Samuel Benjamin Reynolds[2]

[1]Medicine, Weill Cornell Medicine, New York, NY,[2]Hematology, Moffitt Cancer Center, Tampa, FL,[3]Hematopathology, Moffitt Cancer Center, Tampa, FL

Introduction: Rosai Dorfman Disease (RDD) is a non-Langerhans cell histiocytic neoplasm characterized histologically by S100, CD68 and CD163 positive sinus histiocytosis with variable emperipolesis. Abdominopelvic RDD represents a rare disease subtype, for which the molecular landscape and associated responses to targeted therapies remain poorly characterized.

Methods: We conducted a single-center matched case-control study comparing 4 patients with *RAS*-mutated multifocal abdominopelvic RDD to 4 with RAS wild-type disease. All patients had confirmed histopathologic diagnoses of RDD with evidence of abdominopelvic disease, confirmed by either direct lesional biopsy or imaging demonstrating extension from a primary extra-abdominal site. Comprehensive genomic profiling was performed for each patient using a next-generation sequencing platform capable of detecting at least 50 mutations and/or fusions. Independent case review was conducted by a panel of investigators to validate diagnoses, molecular findings, and disease localization.

Results: Four similarly aged patients (64-70 years) with *RAS*-mutated abdominopelvic RDD (3 with *KRAS* mutations, 1 with *NRAS* mutation) were evaluated at a single center. Disease localization included peri-colonic soft tissues in 3 patients and with encasement of the abdominal aorta in one patient. Two patients were also diagnosed with clonal hematopoiesis of indeterminate potential, one each respectively harboring DNMT3A and RTEL1 mutations. All 4 patients received frontline cobimetinib with 3 achieving at least a partial response and two demonstrating near-complete resolution of all known disease sites. Dose attenuations were required in three patients due to toxicities. One patient eventually progressed during dose reduction and was transitioned to trametinib; another passed from non-RDD cardiac causes.

We also reviewed an age-matched cohort (63-79) of 4 patients with abdominopelvic RDD lacking baseline RAS/MAPK pathway or other driver mutations. Lesions were collectively identified in the pancreas, lower pelvis, inguinal lymph nodes and soft tissues proximal to the lumbar spine. Management strategies varied as only two patients received frontline systemic therapy, one sequentially with bexarotene followed by rituximab and the other with vinblastine. Three patients underwent radiation during their disease course, one as monotherapy for localized disease and two in consolidation following the systemic therapy. The remaining patient was observed off treatment.

Conclusions: Patients with RAS-mutated abdominopelvic RDD tend to experience a more aggressive disease course compared to wildtype but demonstrate marked sensitivity to MAP Kinase pathway-targeting therapies. The findings of this study are limited by small sample size; ongoing efforts are underway to expand with a multi-center cohort.

: Early Detection Biomarkers 2
Poster Session

#2526 Non-invasive biomarker discovery and validation for the early detection of pancreatic cancer.

Roopali Roy[1], Rama Aldakhlallah[2], Stephen Cobbs[2], Noundy Mazile[3], Kiana Mahdaviani[3], Matthew Kulke[3], Christopher Heaphy[3], Jeanette Dupree[4], David Zurakowski[5], Sarah Danielle Legrand[4], Erkut Borazanci[6], Marsha A. Moses[1]

[1]Vascular Biology Program and Department of Surgery, Boston Children's Hospital and Harvard Medical School, Boston, MA,[2]Vascular Biology Program, Boston Children's Hospital, Boston, MA,[3]Section of Hematology and Medical Oncology, Boston University and Boston Medical Center, Boston, MA,[4]Honor Health Research Institute, Scottsdale, AZ,[5]Department of Anesthesiology, Critical Care and Pain Medicine, Boston Children's Hospital and Harvard Medical School, Boston, MA,[6]Honor Health Research Institute, John Shufeldt School of Medicine and Advanced Medical Engineering ASU, Scottsdale, AZ

Introduction: Pancreatic malignancies are the fourth leading cause of all cancer-related deaths in the United States and this high mortality rate can be attributed to a lack of diagnostic tests for early detection. A majority of patients with pancreatic ductal adenocarcinoma (PDAC) present with advanced disease due to a lack of specific symptoms suggesting that early detection may significantly improve patient outcomes. CA19-9, the only FDA-approved blood biomarker for PDAC, is insufficiently sensitive and specific for detection or surveillance. The goal of our study is to discover and validate non-invasive biomarkers for early PDAC detection.

Methods: We have established a biomarker discovery initiative whose objective is to identify differentially expressed proteins in the urine of cancer patients and validate their diagnostic and prognostic efficacy. For PDAC, our target population(s) include Stage I or II PDAC patients, high risk individuals (HRI, individuals under surveillance for genetic or familial causes) and age- and sex-matched healthy controls (HC). In this study, we have analyzed urinary markers including CTGF, CYR61, TIMP1 and ADAM12, proteins reported to contribute to PDAC development and progression, with the goal of determining their potential to differentiate early (Stage I-II) PDAC from HC, HRI and advanced disease (Stage III-IV).

Results: Urinary TIMP-1 (uTIMP-1) levels were significantly (~19-fold) higher in PDAC patients (all stages; *n*=64) compared to HC (*n*=60) and significantly (~3.5-fold) higher in PDAC patients (all stages) compared to those with benign pancreatic conditions including IPMN (intraductal papillary mucinous neoplasm) or pancreatic cysts (*n*=10). When comparing the HRI cohort (*n*=70, no evidence of disease, NED) to all groups, we found that uTIMP-1 levels were significantly (~13-fold) higher in PDAC patients (all stages) compared to those at high-risk (*n*=37). uADAM12 levels were significantly (~17-fold) higher in PDAC patient samples (all stages) compared to those from HC and significantly (~1.6-fold) higher in PDAC patients compared to those with benign disease, whereas uADAM12 levels were significantly (~5-fold) higher in PDAC patients (all stages) compared to the HRI cohort. While CYR61 levels did not differ between any of the groups tested, CTGF levels were significantly (~700-fold) higher in PDAC patients (all stages) compared to patients with benign disease and significantly (~1500-fold) higher in PDAC patients (all stages) compared to the HRI cohort.

Conclusions: Taken together, our results suggest that the non-invasive detection of uTIMP-1, uADAM12 and uCTGF levels may have diagnostic value in the early detection and/or clinical monitoring of disease status in patients with PDAC.

[The authors gratefully acknowledge the support of *the Robert J. Kleberg, Jr. and Helen C. Kleberg Foundation and the Nile Albright Research Foundation*]

#2528 Effect of COPD diagnosis on TP53-mutated colony size distribution in airway epithelium of subjects with or without lung cancer.

James C. Willey[1], Andrew Boring[2], Erin L. Crawford[3], Daniel J. Craig[3], Chen Heidi[4], Rami Ahmad[3], Kevin Lei[3], Mohamed Omballi[3], Stephen A. Deppen[4], Eric Grogan[4], Thomas M. Blomquist[5]

[1]University of Toledo, Toledo, OH,[2]University of Toledo College of Medicine and Life Sciences, Toledo, OH,[3]University of Toledo Health Science Campus, Toledo, OH,[4]Vanderbilt University Medical Center, Nashville, TN,[5]Medicine, University of Toledo, Toledo, OH

Background: We previously identified a biomarker for the early detection of lung cancer (LC) based on the prevalence of TP53-mutated colonies in airway epithelium, and determined that this biomarker performs well in subjects with or without COPD. To better understand the biological basis for this biomarker, we compared TP53-mutated colony size distributions in subjects with or without COPD and/or LC.

Methods: Airway epithelial cell specimens were collected from subjects undergoing bronchoscopy under an IRB-approved research protocol. DNA was extracted from each specimen and ultra-sensitive NGS was used to measure TP53 mutations, with variant allele fraction (VAF) as low as 0.01%. TP53-mutated colony size was estimated assuming cells were heterozygous for the mutation. Specimens from 59 subjects were assessed in four cohorts: lung cancer with COPD [LC-CO) (N=14), non-lung cancer with COPD (NLC-CO) (N=7), lung cancer without COPD (LC-NCO) (N=16) and non-lung cancer without COPD (NLC-NCO) (N=22). Colony size distributions were assessed by piecemeal slope analysis and Kaplan-Meier analysis.

Results: A total of 192 unique TP53 mutations were identified among the 59 subjects, distributed among the cohorts as follows: LC-CO, 72; NLC-C0, 19; LC-NCO, 87; and NLC-NCO, 14. The mutation VAF values ranged from 0.01% (0.0001) to 6% (0.06), corresponding to a TP53-mutated colony size range of 200 to 30,000 cells. For each cohort, colony prevalence was inversely proportional to colony size, and there was an inflection point (IP1) at 400-600 cells/colony. Prior to IP1 there was little change in colony number relative to size; after IP1 the decline had a steep slope. The IP1 value was smaller for CO subjects (400 cells) than for NCO subjects (600 cells). There was a second inflection point (IP2) at about 1,800 cells, after which there were few surviving colonies for NLC subjects, but many surviving colonies for LC subjects. According to Kaplan-Meier analysis, among LC-CO subjects the higher prevalence of colonies >1,800 cells in LC was key to accuracy of the TP53 biomarker. In contrast for LC-NCO subjects there was a higher prevalence of colonies across the range of sizes.

Conclusions: Interactions between TP53 mutated colonies and the microenvironment are different in CO vs non-CO subjects. This difference may be partly due to the increased adaptive immune inflammation characteristic of CO lung tissue.

#2529 High throughput immunoproteomics for cancer biomarker discovery.

Joshua LaBaer[1], Jin Park[1], Ji Qiu[1], Lusheng Song[1], Karen S. Anderson[2], Jennifer Molloy[1], Gomati Nandedkar[1], Daniel Woodley[1], Deborah Adams[1], Candyce McDaniel[1], Andruw Fierro[1], Renee Turzanski Fortner[3], Toria Trendler[1], Mingyue Wang[4], Leonid Dzantiev[5], Anu Mathew[5], Martin Stengelin[5], Wohlstadter Jacob[5]

[1]Arizona State University, Tempe, AZ,[2]Arizona State Univ. Biodesign Institute, Scottsdale, AZ,[3]German Cancer Research Center (DKFZ), Heidelberg, Germany,[4]Meso Scale Diagnostics, LLC, Rockville, MD,[5]Meso Scale Diagnostics LLC, Rockville, MD

Background: Early detection of lung cancer (LC) remains a critical unmet need. While computed tomography (CT) screening saves lives by detecting cancer at early stages, its utility is limited by high false positive rates and insufficient sensitivity. These limitations lead to unnecessary surgeries and missed malignancies, particularly in individuals presenting with indeterminate pulmonary nodules (IPNs).
Objective: Our overarching goal is to develop circulating biochemical biomarkers that improve the specificity of CT screening for LC by differentiating malignant from benign IPNs.
Methods: We applied a high-throughput systems immunoproteomics strategy to discover serum biomarkers able to discriminate between malignant and benign IPNs. This integrated approach profiles three classes of circulating biomarkers: autoantibodies, anti-microbial antibodies, and serum proteins.
Results: In the discovery phase, we profiled IgG and IgA autoantibodies using Nucleic Acid Programmable Protein Array (NAPPA) against 13,330 full-length human proteins, along with microbial antibodies against 8,820 microbial antigens. These analyses were conducted using serum from 144 lung cancer cases and 143 benign controls from Vanderbilt University Medical Center. Antibodies with significant enrichment in cases (odds ratio $p < 0.05$ in the top decile) were prioritized, yielding 112 autoantibodies and 70 microbial antibodies associated with malignancy, as well as 50 autoantibodies and 230 microbial antibodies associated with benign disease. In the validation phase, we assessed the prioritized antibody candidates in 319 subjects from the Detection of Early Lung Cancer Among Military Personnel (DECAMP-1) cohort using our Multiplexed In-Solution Protein Array (MISPA). In parallel, we quantified 19 well-reported cancer-associated serum proteins across the same samples. A multimodal panel comprising 7 autoantibodies, 4 microbial antibodies, and 4 serum proteins achieved an area under the curve (AUC) of 0.81 in the discovery cohort and 0.74 in independent validation cohorts, showing improved discrimination of malignant versus benign nodules compared to clinical models alone. Additionally, to demonstrate clinical scalability, we confirmed performance of top markers in 46 cases and 230 controls from the German Lung Cancer Screening Intervention Study (LUSI) using the Meso Scale Discovery (MSD) electrochemiluminescence platform.
Conclusions: These results demonstrate a fully integrated immunoproteomics pipeline for the discovery, validation, and potential clinical translation of multiplex antibody and protein biomarkers for lung cancer detection.

#2530 The ELF5 clock: A predictive marker for accelerated breast tissue aging and cancer susceptibility.

Masaru Miyano, Mark A. Labarge

Beckman Research Institute of The City of Hope, Duarte, CA

Aging is the most significant risk factor for breast cancer (BC). It is associated with transformative changes, notably a striking loss of lineage fidelity in luminal epithelial cells. This loss is characterized by a decline in lineage-specific gene expression and the acquisition of EMT- and myoepithelial-like features, along with increased transcriptional and methylome variability. In young women harboring pathogenic mutations in BRCA1, BRCA2, and PALB2, these aging-associated phenotypes, including loss of lineage fidelity in luminal epithelial cells, are accelerated. These changes warrant closer examination as luminal epithelial cells are the likely cells of origin for the BC subtypes most associated with aging. We hypothesize that the loss of lineage fidelity is a critical factor underlying the increased susceptibility to malignant transformation in mammary epithelia. A key age-related alteration in luminal cells is the decreased expression of the transcription factor ELF5. ELF5 is crucial for mammary gland development, maintaining the ER- luminal epithelial cell state, and its dysregulation is observed in BCs. Changes in ELF5 expression and promoter-proximal methylation serve as a biological clock for breast tissue. The expression of ELF5 decreases in luminal cells in an approximately linear fashion with chronological age, driven by changes in regulatory binding factors and promoter-proximal DNA methylation. The age-associated reduction in ELF5 expression, mirrored by alterations in its target genes, suggests that a decline in ELF5 may be a pivotal event leading to the loss of lineage fidelity. We demonstrate that the ELF5 clock predicts breast biological age within ±3 years of chronological age in women at average risk. High-risk carriers of BRCA1, BRCA2, or PALB2 variants, exhibit a biological age acceleration of 10-40 years relative to their chronological age. We hypothesize that ELF5 expression levels in luminal cells reflect the susceptibility of breast tissue to cancer, independent of specific environmental, epigenetic, genetic, or age-related factors contributing to increased risk. We propose that measuring ELF5 could serve as a molecular “canary in the coal mine” for BC risk or as a clinical correlate for monitoring preventive interventions.

#2531 Plasma levels of Serphin-E1 (PAI-1) are significantly increased in patients with colorectal cancer compared to patients with benign colonic disease.

Chandana S. K. Herath Mudiyanselage[1], Yi-Ru Chen[1], Hiromichi Miyagaki[2], Neil Mitra[1], Monica S. Naparst,[1], Vesna Cekic[1], Richard L. Whelan[1]

[1]Department of Surgery, Northwell Health, Lenox Hill Hospital, New York, NY,[2]Department of Surgery, Otemae Hospital, Osaka, Japan

Introduction: Plasminogen activator inhibitor-1 (PAI-1), is an inhibitor for urokinase-type plasminogen activator (uPA) and tissue-type plasminogen activator (tPA). PAI-1 has proangiogenic effects and plays a role in epithelial-mesenchymal transition and metastasis. PAI-1 is a modulator of endothelial cell proliferation and migration in vitro and of angiogenesis and tumor growth in vivo. PAI-1 promotes tumor progression by modulating extracellular matrix proteolysis, cellular adhesion, and detachment; it also facilitates invasion/migration of cancer cells. PAI-1 overexpression has been reported in breast and colorectal cancer(CRC). Plasma levels of PAI-1 in CRC patients (pts) have not been well studied. This study's purpose was to compare preoperative (PreOp) plasmaPAI-1 levels in CRC and benign colonic pathology (BCP) patients.

Methods: Patients (pts) who underwent colorectal resection for BCP or CRC were prospectively enrolled in an IRB-approved tissue and data bank. Preop blood samples, demographic and clinical data, and pathology results were collected prospectively. Plasma PAI-1 levels were measured in duplicate (ng/ml) using ELISA, with results presented as median ± 95% CI. PAI-1 expression levels were also assessed in paired tumor/normal tissues for a subset of pts using QRT-PCR; immunohistochemistry (IHC) was also carried out on CRC and normal tissue samples. The ROC curve and AUC were used to assess plasma PAI-1 as a CRC diagnostic marker. The Mann-Whitney test was used for statistical analysis (significance $p<0.05$.)

Results: A total of 156 CRC (71%colon, 29%rectal) and 101 BCP pts (adenoma 57%, diverticulitis 32%, other11%) were studied. The Stage (S) breakdown for the CRC group was: S 1, 29%; S 2, 29%; S 3, 36%; and S 4, 6%. The median CRC plasma PAI-1 levels were significantly higher (11.75, CI: 9.06, 15.32) vs. BCP pts (2.95, CI: 2.33, 3.49; $P< 0.0001$). A non-significant rise in mean PAI-1 levels was observed in Stage II, III, and IV pts compared to S.I (12% - 33%, p=ns). mRNA PAI-1 expression levels were higher ($p<0.05$) in 50% (9/18) of the CRC tissue samples tested vs. paired normal tissues. IHC confirmed the presence of PAI-1 protein in CRC vs. normal colon tissue. The AUC value for the ROC curve was 0.759 (sensitivity 68%, specificity 77%).

Conclusion: The median Preop plasma PAI-1 was 3.9 X higher in the CRC vs. the BCP group. Although not proven, the added PAI-1 found in the plasma of CRC pts is likely produced by tumor cells and the surrounding inflammatory cells. Elevated PAI-1 levels may be related to neovascularization and inflammation-induced tissue remodeling at tumor sites. The AUC results suggest PAI-1 may have value as a CRC prognostic marker in a panel of proteins. Further studies with a larger population of controls and CRC pts are needed to better determine if there is a correlation between plasma PAI-1 levels and cancer stage or progression.

#2532 Innovative label-free and non-invasive urinary metabolite analysis integrating AI and SERS technology for early cancer detection: A retrospective clinical study involving five cancer types.

Jeehee Kim[1], Hyungseok Choi[1], Eun Hye Koh[1], Thi Nhat Linh Vo[1], Geo Ryu[1], Eun Been Lee[1], Daekeon Kwon[2], Soohyun Lew[2], Si Young Song[3]

[1]SOLUM Healthcare, Yongin, Korea, Republic of,[2]JNPMEDI Inc., Incheon, Korea, Republic of,[3]College of Medicine, Yonsei University, Seoul, Korea, Republic of

Background: Accurate early cancer detection remains a critical clinical challenge due to the high cost and limited sensitivity and specificity of conventional diagnostic methods. Indeed, non-invasive approaches capable of molecular-level characterization of biofluids are urgently needed to improve early diagnostic accuracy and patient outcomes. Artificial intelligence-assisted surface-enhanced Raman scattering (AI-SERS) offers a powerful platform to test complex metabolic signatures in urine with exceptional sensitivity. By integrating high-resolution SERS spectra with deep learning-based classification, AI-SERS platform transcends the limitations of conventional assays, enabling highly precise cancer differentiation and unlocking new avenues for the discovery of metabolite-based biomarkers for early cancer detection.

Methods: This study enrolled a total of 287 clinical urine samples across six groups: prostate cancer (PRC, n = 49), pancreatic cancer (PAC, n = 16), ovarian cancer (OC, n = 64), lung cancer (LC, n = 30), breast cancer (BC, n = 29), and normal controls (NOR, n = 99). A minimal volume (10 μL) of clinical urine samples was applied to a patented SERS sensor to enhance metabolite signals, measured using a Raman spectrometer. The resulting SERS spectra were analyzed using a convolutional neural network (CNN)-based deep learning approach.

Results: The SERS spectra of urine samples from 6 different groups exhibited sharp Raman spectral peaks, providing significant information for analysis. Using the developed CNN model, all cancer types combined could be distinguished from normal controls with an accuracy of 96.6%, sensitivity of 99.3%, and specificity of 94.0%, demonstrating excellent overall classification performance between cancer and non-cancer samples. Further analysis of individual cancer types versus normal controls showed robust predictive performance, with accuracy, sensitivity, and specificity of 98.0%, 98.6%, and 97.3% for PRC; 97.9%, 97.9%, and 97.9% for OC; 97.8%, 97.8%, and 97.8% for LC; and 98.9%, 97.7%, and 100% for BC, respectively. These results demonstrate the strong predictive capability of the AI-SERS platform for noninvasive, cancer-specific detection.

Conclusions: The noninvasive, label-free urine analysis using the AI-SERS platform revealed remarkable test performance in classifying cancers from normal controls, offering a rapid cancer screening approach and highlighting its potential for early cancer diagnosis. Ongoing clinical studies aim to identify cancer-type-specific metabolic biomarkers to further improve diagnostic specificity and contribute to enhanced patient outcomes.

#2533 Blood-based mRNA signature detects pancreatic cancer and distinguishes IPMNs: Discovery and preliminary verification study.

Moritz Robert Eidens[1], Timea Torok[1], **Niamh Nolan**[1], Patrick Lilley[2], Guido Baechler[1], Robert Scott Bresalier[3]

[1]Research, Mainz Biomed Germany GmbH, Mainz, Germany,[2]Liquid Biosciences Inc., Aliso Viejo, CA,[3]Dept. of Gastroenterology, Hepatology & Nutrition, UT MD Anderson Cancer Center, Houston, TX

Purpose: Currently, carbohydrate antigen 19-9 (CA19-9) is recommended for monitoring treatment response and recurrence in PDAC, but its poor sensitivity and lack of expression in ~5-10% of patients limit its use for screening in current guidelines. To address this gap, we sought to discover and verify a dedicated set of blood-based mRNA biomarkers and an algorithmic model that (i) differentiates PDAC from benign/healthy states and (ii) discriminates among healthy, IPMN (high-risk), and PDAC.
Methods: Phase 1 (discovery): Publicly available datasets [NIH Dataset ID GSE68086, GSE28735, GSE18670] including 96 PDACs and 301 controls (including healthy individuals and non-pancreatic cancers) were analyzed. Using machine learning (ML) algorithmic models trained using a quantitative evolutionary-computing platform (Emerge, Liquid Biosciences Inc.), 18 candidate mRNAs with translational feasibility were identified with strict training/selection/test partitioning and cross-dataset validation. Phase 2 (preliminary verification): We performed RNA sequencing on blood PBMCs from 30 individuals (healthy n=15, IPMN n=5, PDAC n=10) sourced from Crown Bioscience Germany GmbH, Hamburg, Germany. Six independent binary classifiers (PDAC vs healthy + IPMN) were trained using distinct subsets of the 18 mRNAs. We assessed diagnostic performance, redundancy, and a simple “voting” scheme (defined as majority vote across our six independent binary models) across the models.
Results: In Phase 1, discovery on blood and tissue/CTC across the three datasets, weighted test performance reached ~95% sensitivity and 98% specificity with multiple ≤6-gene subsets achieving perfect test accuracy on individual datasets. The robust signal was confirmed across diverse modalities and supported reagent availability for all 18 mRNAs, with multiple cross-validated subgroups suitable for clinical translation. In Phase 2 (n=30, PBMCs), the weakest binary model distinguishing between PDAC vs healthy + IPMN made 3/30 errors (all false positives; 100% sensitivity, 85% specificity at 90% accuracy), two models had two errors, two had one, and one model had zero errors. To enhance robustness, we aggregated the six independent binary models via our simple majority voting; the ensemble achieved 100% sensitivity and 100% specificity in the 30-subject cohort. The tri-state classifier achieved 100% three-way accuracy, requiring a minority subset of the 18 biomarkers to resolve healthy, IPMN, and PDAC.
Conclusions: A cross-validated set of blood mRNAs enables accurate PDAC detection and simultaneous discrimination of IPMN. While Phase 2 findings are compelling, they derive from a limited, banked and retrospective cohort and warrant confirmation in a larger study including samples from individuals with other high-risk profiles for PDAC and IPMN types that include malignant and benign characteristics.

#2534 Genomic transposable elements, repetitive sequences, in early-onset melanoma and prostate cancer among West Africans in Nigeria.

Faruk Mohammed[1], Sani Ibrahim[2], Rebecca Garnham[3], Ines Hosni[3], Halimatu Sadiya Musa[3], Sani Kamarudeen Owolabi[4], Adoke Kasimu Umar[4], Jane Carr-Wilkinson[3], Emma Scott[5], Ahmad Bello[2], Kevin Petrie[3]

[1]Ahmadu Bello University, Zaira, Nigeria,[2]Ahmadu Bello University, Zaria, Nigeria,[3]University of Sunderland, Sunderland, United Kingdom,[4]Federal Teaching Hospital, Birnin Kebbi, Nigeria,[5]Newcastle University, Newcastle, United Kingdom

Genomic transposable elements (TEs) constitute a substantial portion of the non-protein-coding genome and play crucial roles in gene expression, regulation, evolution, and genomic variation. The human genome comprises both protein-coding and non-protein-coding regions, the latter often referred to as the “dark genome.” Key components of this non-coding region include non-coding RNAs (ncRNAs), transposable elements (TEs) or “jumping genes,” protein-coding genes of unknown function (e.g., SLX4IP, HSF2BP, and ELFN), and repetitive sequences such as Long Interspersed Nuclear Elements (LINEs), Short Interspersed Nuclear Elements (SINEs), and Human Endogenous Retroviruses (HERVs). While approximately 23,000 genes are known to encode proteins, nearly 98% of the genome is non-coding, previously dismissed as “junk DNA.” This non-coding compartment is composed of LINEs (~21%), SINEs (~15%), HERVs (~8%), and other repetitive elements (~54%). Importantly, transcriptional activation of normally silenced transposable elements, often driven by epigenetic dysregulation such as DNA methylation loss, is a hallmark of cancer. This aberrant activation contributes to malignant transformation and tumor immunogenicity, although the underlying mechanisms remain poorly understood. Notably, HERVs, an important class of repetitive sequences, function as tumor-associated antigens, expressed on the surface of cancer cells, where they influence both innate and adaptive immune responses. The role of HERVs, particularly in early-onset melanoma and prostate cancer (CaP), remains underexplored, especially with respect to prognostication and disease progression. In this study, we investigated the expression and clinical significance of HERV type R (*HERV-R*) in melanoma and CaP. Using malignant melanoma tissues from Nigeria, benign prostatic samples from African men, and comparative tissues from men of European ancestry in Nigeria and the United Kingdom, we applied transcriptomic and molecular biology techniques to characterize *HERV-R* activity. Our findings demonstrate marked expression of HERV-R in malignant melanoma, in glandular regions of metastatic CaP tissues, and in both glandular and partially stromal compartments of benign prostatic lesions. These observations suggest that *HERV-R* holds promise as a prognostic biomarker and potential target for early detection in melanoma and CaP. Furthermore, the consistent glandular expression of HERV-R in both cancerous and benign prostate tissues supports the hypothesis of a mutator phenotype, implicating *HERV-R* in tumor initiation and progression. Collectively, these results underscore the therapeutic and diagnostic potential of *HERV-R* and highlight the urgent need for further investigation into *HERV-R* biology in melanoma and CaP.

#2535 High-resolution mapping of tumor-associated antigens for autoantibody-based lung cancer detection.

Swaralee Kulkarni, Russell D. Williams, Saiful Islam, Ofer Shapira, Jimmy C. Lin, Richard Bourgon, Tanya A. Moreno, Victor Chubukov, Sergey Boyarskiy

Freenome, Inc., South San Francisco, CA

Introduction
Non-invasive, blood-based screening for lung cancer is a promising approach to early cancer detection, but is challenged by low concentrations of tumor-derived biomarkers, especially in early-stage disease. Auto-antibodies (AAbs) are a compelling class of biomarkers to address this gap, leveraging the body's amplified humoral immune response to tumor antigens and providing a unique source of signal not directly linked to tumor shedding. However, natural variation in human immune profiles makes identification of true cancer-specific antigens challenging.
Methods
In this work, we used a Phage Immunoprecipitation and sequencing (PhIP-Seq) method to identify AAbs differentially present in patients with lung cancer. Unlike traditional proteome-wide PhIP-Seq approaches, we used cancer mutation data along with tumor-specific protein expression patterns from GTEx and TCGA databases to narrow the search space to ~4000 proteins with high probability of generating a cancer-specific immune response. By densely tiling these proteins with overlapping 54-mer peptides and requiring overlapping peptides for hit calling, we maximized technical reproducibility while also mapping cancer-specific antigenic regions within proteins to high resolution. Applying this approach to 1,200 samples enabled us to differentiate cancer-specific signals from background antigenicity.
Results
We screened 400 samples from patients with lung cancer and 800 samples from age- and sex-matched healthy controls. Our hit-calling pipeline identified antigens showing significant AAb signal in plasma from multiple cancer patients and little or no signal in healthy controls, taking into account both technical and biological noise. Based on this pipeline, we identified 90 cancer-specific peptide antigens spanning 68 human proteins, including established lung cancer biomarkers such as p53 and NY-ESO-1 as well as proteins not previously associated with lung cancer autoimmunity. Importantly, even in well-established tumor-associated antigen (TAA) proteins, we identified regions with high AAb positivity in healthy individuals, showing that selecting specific antigenic regions of TAA proteins could be crucial for maximizing signal-to-noise. Moreover, we observed distinct AAb profiles across different patient subsets, indicating that a large panel of antigens may help achieve higher sensitivity in a blood-based cancer detection assay.
Conclusions
This work represents a significant step forward in mapping the cancer humoral immunome. By performing PhIP-Seq based AAb profiling in the largest cohort of lung cancer patients and matched healthy controls published to date, and enabling deep peptide-level characterization of the auto-antibody response, we maximize confidence in identification of cancer-specific biomarkers and provide a path to a more accurate AAb-based cancer detection test.

#2537 PD-L1 expression in oral premalignant and malignant lesions and its association with p53 expression.

Oh Run Kim[1], Lewei Zhang[1], Miriam Rosin[2], Cathie Garnis[3], Denise M. Laronde[1]

[1]University of British Columbia, Faculty of Dentistry, Vancouver, BC, Canada,[2]BC Cancer Research Institute, Vancouver, BC, Canada,[3]Dept. of Surgery, University of British Columbia, Faculty of Medicine, Vancouver, BC, Canada

Introduction: Programmed death-ligand 1 (PD-L1) is a key immune checkpoint molecule that allows tumor cells to evade immune surveillance by promoting T-cell exhaustion within the tumor microenvironment (TME). Oral malignant lesions, of which 90% are oral squamous cell carcinoma (OSCC), are known to express abnormally high levels of PD-L1. Extensive research has explored PD-L1 in carcinogenesis and immunotherapy. The tumor suppressor protein p53 is often mutated in cancer, and its immunohistochemistry (IHC) assessment has been found to help predict malignant potential in oral premalignant lesions. Emerging evidence suggests p53 may influence immune activity in the TME by altering PD-L1 levels. However, how developing tumors modify the TME during the premalignant stage, and the role of p53 in this process, remain unclear. This study aims to evaluate the relationship between PD-L1 and p53 in oral premalignant and malignant lesions.

Methods: A comparative cross-sectional study was conducted using patient data and oral tissue samples from the Oral Cancer Prediction Longitudinal Study and the BC Oral Biopsy Service. Inclusion criteria were biopsy confirmed oral epithelial dysplasia (OED) or OSCC. Exclusion criteria included HPV or EBV associated OED or OSCC, actinic cheilitis, and verrucous hyperplasia. IHC was performed on formalin-fixed, paraffin-embedded tissue to assess PD-L1 and p53 expression. We hypothesized that the malignant group (MA), defined as severe OED, carcinoma in situ (CIS), or OSCC, would show increased PD-L1 and mutant p53 expression compared with the premalignant group (PMA), which consists of mild or moderate OED. Samples were considered PD-L1 positive if ≥5% of dysplastic or tumor cells showed moderate to strong membranous staining. p53 was classified as mutant when showing either overexpression or complete loss. Fisher's exact test assessed group differences in categorical variables.

Results: To date, 38 of 138 samples have undergone IHC analysis. PD-L1 positivity was higher in MA than PMA (40% and 17.4%), though not statistically significant with the current sample size. A significantly higher proportion of mutant p53 was observed in MA compared with PMA (86.7% and 34.8%, p=0.002). Thus far, no significant association was observed between PD-L1 and p53 expression, although an inverse trend in expression was noted. Additional samples are being processed to further evaluate expression patterns.

Conclusion: Significant differences in p53 expression were observed between MA and PMA, while PD-L1 expression did not differ significantly between groups. Nonetheless, higher PD-L1 positivity in malignant lesions suggests its potential relevance and warrants further investigation. These findings contribute to a better understanding of immune checkpoint regulation and tumor suppressor dysfunction in the progression of oral premalignant lesions to malignancy.

#2538 Machine learning-derived circulating ncRNA signature for early detection of breast cancer.

Yuanyuan Fu, Mayumi Jijiwa, Zhanwei Wang, Hua Yang, Youping Deng

University of Hawai'i at Manoa, Honolulu, HI

Background: Breast cancer is the most commonly diagnosed cancer and a leading cause of cancer-related mortality among women in the United States. Early detection substantially improves survival, yet current imaging-based screening modalities are limited by reduced sensitivity in certain populations and high false-positive rates. Circulating non-coding RNAs (ncRNAs) represent stable and non-invasive biomarkers with significant potential to complement mammography and enhance diagnostic accuracy. This study aimed to develop and validate a robust circulating ncRNA-based signature for early breast cancer detection using an integrated machine learning framework.

Methods: Circulating ncRNA profiles were generated for 413 individuals (216 breast cancer; 197 non-cancer). A three-stage design—discovery, internal testing, and external validation—was implemented. In the discovery cohort (n=248), we evaluated a broad ensemble of 12 machine learning frameworks and 111 model combinations to establish a consensus-based diagnostic signature (ncRNASig) comprising 16 circulating ncRNAs. Model development emphasized stability, reproducibility, and cross-cohort generalizability. The resulting ncRNASig was evaluated in an independent internal testing cohort (n=175) and further validated using multiple external datasets from The Cancer Genome Atlas (TCGA) and Gene Expression Omnibus (GEO).

Results: The 16-ncRNA diagnostic signature demonstrated high discriminatory power in the discovery cohort, achieving an AUC of 97.4% for distinguishing breast cancer from non-cancer samples. The ncRNASig also differentiated cancer from benign conditions (AUC = 96.1%) and cancer from normal controls (AUC = 100%). Subtype analyses showed consistently strong performance for Luminal A, Luminal B, HER2-enriched, and triple-negative breast cancers (AUCs 96-98%). These results were reproducible in the internal testing cohort and across multiple independent external datasets, supporting the robustness and generalizability of the ncRNASig.

Conclusion: This study identifies and validates a circulating ncRNA-based signature with strong diagnostic performance across breast cancer subtypes and independent cohorts. The findings support the potential of integrating ncRNA-driven liquid biopsy assays with current screening approaches to enhance early breast cancer detection. Further development and clinical translation are warranted.

#2539 miRNA profiling of prostate tissues reveals a molecular continuum from benign to tumor through peritumoral tissue.

Cesar A. Payan-Gomez[1], Dayana Rodriguez-Morales[2], Elizabeth Vargas-Castellanos[2], Jovanny Zabaleta[3], **Rafael Parra-Medina**[2]

[1]Universidad Nacional de Colombia, La Paz, Cesar, Colombia,[2]Pathology, Instituto Nacional de Cancerologia, Bogota, Colombia,[3]Interdisciplinary Oncology, LSU Health New Orleans, New Orleans, LA

Background: Histologically, peritumoral tissue (PTT) or normal adjacent prostate tissue (NAT) surrounding tumors, is considered unaffected by the malignant process. However, emerging evidence suggests that the peritumoral microenvironment may harbor early molecular alterations. We hypothesize that PTT represents an intermediate molecular state between benign (BT) and tumor tissue (TT).

Methods: Micro-RNA sequencing was performed on matched prostate tissues from 40 patients with prostate adenocarcinoma (after quality control 39 Tumor Tissues TT, 38 PTT, and 40 Benign Tissues BT). Differential miRNA expression (DEmiRNAs) was determined using DESeq2 (FDR ≤ 0.05), using BT as the reference group for the contrasts TT vs. BT and PTT vs. BT. Unsupervised principal component analysis (PCA), hierarchical clustering, fold-change comparisons, and pathway over-representation analysis of predicted miRNA targets (miRNet, KEGG/Reactome) were conducted.

Results: PCA of global miRNA profiles revealed a molecular continuum along PC2 (18% of variance), with BT clustering at the negative extreme, TT at the positive extreme, and PTT distributed intermediately between both groups. Comparison of TT vs. BT identified 102 DEmiRNAs, while PTT vs. BT identified 57 DEmiRNAs. Remarkably, 39 miRNAs (68% of PTT vs. BT signature) were shared between both comparisons, and all 39 displayed concordant directional changes, indicating that a substantial fraction of the tumor-associated miRNA dysregulation is already present in PTT. Direct TT vs. PTT comparison revealed only 30 DEmiRNAs, confirming greater molecular similarity between TT and PTT than either with BT. Hierarchical clustering of the top 30 most significant TT vs. BT DEmiRNAs showed that PTT samples formed a distinct cluster with expression levels consistently intermediate between BT and TT, reinforcing the idea of a continuum molecular landscape between BT, PTT and TT. Pathway analysis of miRNA targets showed that nearly all significantly enriched pathways in PTT vs. BT were also altered in TT vs. BT, including key cancer-related pathways (e.g., tight junction, transcriptional dysregulation in cancer, chemical carcinogenesis-receptor activation). Magnitude analysis of the 39 shared DEmiRNAs confirmed stronger dysregulation in TT than PTT, consistent with progression along a continuum rather than an abrupt transition.

Conclusions: miRNA profiling demonstrates that histologically PTT is molecularly altered and occupies an intermediate position between benign and fully malignant states. This molecular continuum supports the existence of a pre-malignant field effect driven by miRNA dysregulation and shared pathway alterations. These findings highlight PTT as a critical component of the tumor ecosystem and a potential source of early detection biomarkers or preventive therapeutic targets.

#2540 A combined bioinformatics, deep learning analysis, and immunohistochemistry approach to define the biomarker potential of advanced glycosylated end products (AGER) complex proteins in colon cancer progression.

Jorge Alberto Guadarrama-Orozco[1], Monica Serrano Arevalo[2], Ariadna Heredia Pulido[3], Jennifer Ramirez-Puente[4], Jose Diaz-Chavez[2]

[1]Tijuana General Hospital, Tijuana, Mexico,[2]Instituto Nacional de Cancerologia, Ciudad de Mexico, Mexico,[3]Oncos Patologia Tijuana, Tijuana, Mexico,[4]Hospital Angeles Tijuana, Tijuana, Mexico

Background: Despite recent advances in colorectal cancer (CRC) diagnosis and population screening programs, the identification of patients with preneoplastic lesions or with early CRC stages remains challenging and is essential for reducing CRC incidence and increasing patients' survival.
Methods: Our study comprehensively investigated the clinical significance and relationship among AGER complex protein/N-Glycosilation genes (DDOST, PRKCSH, and GALECTIN 3) and colon cancer progression in colorectal cancer through a bioinformatics data mining process (STRING, UALCAN, HPA, GEPIA2, TNMplot), their interaction (DMFold-Multimer), and followed by experimental validation. We analyzed 112 colorectal tissue samples originating from CRC stages I to IV, including normal tissue and adenomas. The characterization of three biomarker candidates was performed using immunohistochemistry on normal tissue, precancerous, and cancerous lesions with increasing CRC stages. We selected the ROI in QuPath and analysed it in ImageJ using the DeepLIIF extension to calculate expression percentage.
Results: The distributions of PRKCSH, DDOST, and GALECTIN 3 were validated in tissues, showing different expression levels, especially in early stages of CRC, compared to normal and preneoplastic tissues.
Conclusion: We highlighted three proteins that require further investigation to better characterize their role in early CRC carcinogenesis and their potential as markers of CRC progression.

#2541 Circulating sphingolipids and colorectal cancer risk in African American adults.

Sara Salas[1], Stephanie Richardson[1], Danxia Yu[2], Alan Maschek[1], James E. Cox[1], Joshua Alvarez[1], Emmanuel Onyegba[1], Monowarul Siddique[1], Steve Moore[3], Marc Gunter[4], Anna Ibele[1], Xiao-Ou Shu[5], Scott A. Summers[1], Cornelia M. Ulrich[1], Mary Playdon[1]

[1]University of Utah, Salt Lake City, UT,[2]Vanderbilt University, Nashville, TN,[3]National Cancer Institute, Bethesda, MD,[4]Imperial College London, London, United Kingdom,[5]Vanderbilt, Nashville, TN

Background: Obesity-related metabolic dysfunction may promote colorectal carcinogenesis through sphingolipid pathways. Ceramides and related species regulate insulin resistance, inflammation, and intestinal stem-cell proliferation; however, prospective data linking circulating sphingolipids to colorectal cancer (CRC) are limited, particularly in African Americans.
Methods: We conducted a nested case-control study within the Southern Community Cohort Study (SCCS) including 373 African American CRC cases and 373 matched control participants. Targeted lipidomic analysis quantified 165 sphingolipids including 78 ceramides, 36 sphingomyelins, 30 neutral glycosphingolipids, 14 glycerophosphocholines, 4 sphingoid base-1-phosphates, 4 sphingoid base homologs, and one ceramide-1-phosphate. Conditional logistic regression estimated odds ratios (OR) and 95% CI per standard deviation (SD), adjusting for age, sex, number of aliquot freeze-thaw cycles, education, body mass index, smoking status, physical activity, energy intake, fiber intake, red/processed meat intake, and alcohol intake.
Results: Participants were aged 54±9 years, and 55% were female. In fully adjusted models, several very-long-chain ceramides and one sphingomyelin showed statistically significant inverse associations with CRC risk with adjustment for multiple comparisons at FDR $q<0.05$, including Cer(d16:1/23:0), Cer(d16:1/22:0), Cer(d17:1/22:0), Cer(d17:1/23:0), Cer(d18:2/23:0), and SM(d16:1/23:0) (OR per SD range 0.76 to 0.80, p range 0.001 to 0.009). Some long-chain dihydroceramides and ceramides previously linked to metabolic diseases were positively associated with CRC, though results did not reach statistical significance (e.g., dhCer(d18:0/18:0), OR 1.15, 95% CI 0.98-1.35; Cer(d18:1/18:0), OR 1.08, 95% CI 0.92-1.26).
Conclusions: Pre-diagnostic very-long-chain ceramide species showed protective associations with CRC incidence in African Americans. Findings highlight potential metabolically actionable pathways for CRC prevention.
Acknowledgement: U01CA202979 and U01CA272529

#2542 Assessing the TP53 mutation prevalence biomarker for lung cancer in subjects without COPD.

Andrew Boring[1], Erin Crawford[2], Kevin Lei[1], Daniel Craig[2], Chen Heidi[3], Steven A. Deppen[3], Rami Ahmad[2], Eric L. Grogan[3], Mohamed Omballi[2], James C. Willey[2]

[1]University of Toledo College of Medicine and Life Sciences, Toledo, OH,[2]Department of Medicine, University of Toledo College of Medicine and Life Sciences, Toledo, OH,[3]Vanderbilt University Medical Center, Nashville, TN

Background: COPD increases the risk for lung cancer, but two-thirds of LC cases occur in individuals without COPD. Further, more than half of lung cancers (LC) occur in individuals who do not meet age and/or smoking history eligibility criteria low-dose CT (LDCT) lung cancer screening. Thus, there is a need to develop biomarkers that improve on current demographic criteria to determine eligibility for screening. We previously identified a biomarker for the early detection of lung cancer by quantifying the prevalence of TP53 mutations present in the large airways. In this study we evaluated performance of this LC biomarker in subjects with or without COPD.
Methods: Subjects undergoing standard of care bronchoscopy were recruited into an IRB-approved research study wherein soft brush biopsies of airway epithelial cells (AEC) from the large airways were collected. DNA extracted from bronchial brush specimens was sequenced by PCR-amplicon library NGS. Using synthetic internal standards to control for sequencing error, variant allele fraction (VAF) was observable down to 0.01%. The TP53 biomarker was measured in AEC DNA from 38 non-COPD subjects, including 16 with cancer and 22 without cancer, and 21 COPD subjects, 14 with cancer, and 7 without cancer.
Results: The TP53 biomarker differentiated between cancer and non-cancer subjects in the absence of COPD with a receiver operator characteristics (ROC) area under the curve (AUC) value of 0.84. The TP53 biomarker also differentiated between cancer and non-cancer in patients diagnosed with COPD with an AUC of 0.78 in ROC analysis.
Conclusions: The TP53 biomarker performed well differentiating between cancer and non-cancer status in both COPD and non-COPD subjects. Application of the TP53 mutation prevalence biomarker is expected to have particular value when applied to identify non-COPD subjects at risk for lung cancer. Subjects without COPD who develop lung cancer typically were ineligible for LDCT screening due to correspondingly lower smoking history and age. We plan to validate these associations in larger case-control studies. If validated, this biomarker, alone or in combination with demographic criteria, may enable identification of a large number of subjects at high risk for lung cancer who currently do not qualify for LDCT screening based on demographic criteria alone.

#2543 Serum calreticulin as a promising biomarker for cancer screening.

Jasmine Watts[1], Lucinda Ann Hall[2], Lorenzo Thompson[3], Jacqueline L. Mudd[4], Steven Forsythe[1], Yuvasri Golivi[2], Roheena Panni[4], William E. Gillanders[5], Li Ding[5], Ryan C. Fields[6], Benjamin Larimer[7], Rachael Guenter[1], John B. Rose[2]

[1]Department of Surgery, University of Alabama at Birmingham, Birmingham, AL,[2]University of Alabama at Birmingham, Birmingham, AL,[3]Immunology Institute, University of Alabama at Birmingham, Birmingham, AL,[4]Department of Surgery, Washington University School of Medicine, St. Louis, MO,[5]Washington University School of Medicine, St. Louis, MO,[6]Department of Surgery, University of Rochester Medical Center, Rochester, NY,[7]Department of Radiology, University of Alabama at Birmingham, Birmingham, AL

Background: Calreticulin (CALR) is an endoplasmic reticulum chaperone protein that can translocate to the plasma membrane during cellular stress. Despite its known roles in cancer, CALR levels in the blood have not been extensively studied in cancer patients. We hypothesized that serum CALR is elevated in cancer patients and may serve as a noninvasive biomarker for early detection.
Methods: Serum samples were collected from patients diagnosed with pancreatic ductal adenocarcinoma (PDAC), breast cancer (BC), colorectal cancer (CRC), and healthy donors. CALR concentration was quantified using a RayBiotech Human CALR Sandwich ELISA. Statistical analyses were performed using Mann-Whitney U tests for group comparisons and ROC analysis for evaluating diagnostic performance on GraphPad Prism.
Results: 80 PDAC patients, 25 BC patients, 25 CRC patients, and 60 healthy donors were included in the study. Median (IQR) CALR level increased from 36.22 pg/mL (5.09-264.6) in healthy individuals to 363.1 pg/mL (226.5-729.7) in PDAC patients, 182.5 pg/mL (108.1-344.0) in CRC patients, and 584.9 pg/mL (381.2-823.4) in BC patients. Pairwise testing confirmed significantly higher CLAALR levels in PDAC vs. healthy ($p < 0.0001$), BC vs. healthy ($p < 0.0001$), and CRC vs. healthy ($p = 0.0021$).ROC analysis demonstrated strong diagnostic potential of serum CALR for distinguishing PDAC from healthy individuals (AUC = 0.799). The optimal cutoff, determined using Youden's Index, was 147 pg/mL with a sensitivity of 89% and specificity of 71.7%. Differentiating healthy donors from BC was also significant (AUC = 0.844) with sensitivity of 88% and specificity of 73.33% at the optimal cutoff value of 308.7 pg/mL. CRC was also distinguishable from healthy donors with an optimal cutoff of 52.81 pg/mL, yielding a sensitivity of 96% and specificity of 58.3% (AUC = 0.72).
Conclusion: Serum CALR is significantly elevated in patients with PDAC, BC, and CRC compared to healthy individuals and demonstrates strong diagnostic accuracy. These findings identify CALR as a promising noninvasive biomarker for cancer detection and justifies future validation studies assessing combinatorial biomarker panels.

#2544 Blood- and tissue-derived extracellular vesicle signatures in HPV-positive cervical disease.

Angie Gabriela Rivera-Ramos[1], Mariano Molina Beitia[2], Rafael Parra-Medina[3], Alba Lucia Combita-Rojas[3], Metoboroghene Mowoe[4], Daniel Hagey[4]

[1]Department of Medicine, National University of Colombia, Bogota, Colombia,[2]Laboratory Medicine, Karolinska Institutet, Stockholm, Sweden,[3]Pathology, Instituto Nacional de Cancerologia, Bogota, Colombia,[4]Department of Laboratory Medicine, Karolinska Institutet, Stockholm, Sweden

Background: Extracellular vesicles (EVs) represent promising sources of biomarkers for cervical disease detection. However, optimal EV isolation strategies combining liquid and solid biopsies remain underexplored, particularly in resource-variable clinical settings.
Methods: We implemented a dual-source EV isolation approach in a Colombian clinical cohort of HPV-positive women. Plasma samples and solid biopsies were collected from 17 participants (9 squamous intraepithelial lesion [SIL] cases, 8 controls). Plasma-derived EVs were isolated directly, while tissue-derived EVs were obtained from primary fibroblast cultures established through optimized enzymatic and mechanical dissociation protocols. EVs were characterized using nanoparticle tracking analysis, transmission electron microscopy, and flow cytometry immunophenotyping. mRNA and protein cargo were prepared for RNA sequencing and proteomic analysis.
Results: The dual-source approach successfully yielded EVs from both plasma and tissue samples with appropriate quality and quantity for downstream analysis. Nanoparticle tracking analysis confirmed expected size distributions, while transmission electron microscopy validated EV morphology from cultured cells. Flow cytometry immunophenotyping identified characteristic EV surface markers. The optimized tissue dissociation workflow generated robust primary cultures capable of producing analyzable EVs. Preliminary mRNA sequencing of plasma-derived EVs revealed candidate molecular signatures that distinguished SIL cases from controls and showed association with lesion grade.
Conclusions: This dual-source EV strategy is feasible in Colombian clinical settings and supports the development of liquid biopsy biomarkers for early detection and risk stratification of HPV-related cervical disease. The approach enables comprehensive molecular profiling from complementary biological sources, warranting further validation in larger cohorts.

#2545 Genome-wide analysis of ctDNA-derived DNA palindromes for early detection of breast cancer.

Fumie Igari[1], Hisashi Tanaka[2], Tamami Hyodo[1], Yuko Ishikawa[1], Tomoyuki Fujita[1], Michael Murata[2], Ryan Urbanowicz[2], Armando Giuliano[2]

[1]Juntendo University, Tokyo, Japan,[2]Cedars Sinai Medical Center, Los Angeles, CA

Background and Objective:
Circulating tumor DNA (ctDNA) in the blood provides valuable information about all aspects of patient care, including real-time tumor burden and therapeutic targets. While ctDNA tests currently focus on detecting small mutations and abnormal DNA methylations in targetedgenomic regions, structural variants (SVs) are also common in tumors and could serve as important cancer biomarkers. Despite the growing use of liquid biopsy in cancer detection and management, an effective agnostic SV detection method remains a missing piece. To address this, we target DNA palindromes, a chromosomal structural abnormality also known as fold-back inversions and inverted repeats. We explored the potential of an approach called GAPF-Seq (Genome-wide Analysis of Palindrome Formation: GAPF with NGS) for ctDNA detection. GAPF-seq enriches palindromic DNA from very small amounts of genomic DNAthrough intramolecular annealing (Tanaka et al., Nat Genet 2005). Next-generation sequencing (NGS) analysis of the enriched DNA would enable us to identify SVs across the genome.
Methods:
Breast tumor DNA was processed by the successive denaturation and renaturation. DNA from palindromes would form double-stranded DNA by intramolecular annealing, while normal and nonpalindromic DNA would remain single-stranded, which would be eliminated by S1 nuclease. Tumor-derived DNA palindromes were amplified by PCR, sequenced by NGS, and subjected to bioinformatic analysis, including ROC validation and chromosomal distribution profiling.
Results:
(1) ROC analysis demonstrated high diagnostic accuracy. Using the top 1000 high coverage bins(HCBs) among the 1 million 1-kb bins in the genome, we found that the AUC value for tumor DNA calling was 0.9885, with sensitivity 92.3% and specificity 97.4%, enabling robust distinction between cancer and normal samples, including Stage I tumors. Comparable performance was achieved between 30 ng and 100 ng of DNA.(2) As GAPF-Seq is based on Structural variant detection genome-wide, it allows comprehensive genome-wide screening beyond single-gene mutation or a subset of CpG methylation analyses. Chromosomal mapping revealed uniform distribution of top 1000 HCBs in normal samples, while tumor samples exhibited chromosome-specific enrichment of HCBs. Subtype-specific analysis showed accumulation around the *CCND1* gene on chromosome 11 in Luminal type, and enrichment near the *ERBB2* gene on chromosome 17 in HER2 type.
Conclusion:
GAPF-Seq has the potential to enable accurate detection of early breast cancer even from minimal DNA input. Its agnostic, genome-wide profiling capability provides an additional benefit. Potential clinical applications include cancer screening and monitoring minimal residual disease.

#2546 An alternative screening method for prostate cancer to serum prostate specific antigen.

Yosef Tobi[1], Altin Miraka[2], Noreen F. Rossi[3], Mike Lawson[4], Martin Tobi[5]

[1]Medicine, Medical College of New York, Valhalla, NY,[2]Dept. Surgery, Saginaw VAMC VHA, Saginaw, MI,[3]Detroit VAMC, Detroit, MI,[4]University of California, Sacramento, Davis, Sacramento, CA,[5]Saginaw VAMC, Saginaw, MI

Introduction: After 23 years of follow-up, a recent long-term study by Roobol et al showed a relative reduced mortality rate of 13% and an absolute risk reduction of 0.22% in a group screened for prostate cancer (DOI: 10.1056/NEJMoa2503223). Most prostate cancers (ProC) are not lethal and the death rate is about 15% for lethal tumors versus a majority of more indolent tumors. Prostate Specific Antigen (PSA) blood test is used for screening, but within the grey zone of 4-10ng/mL the positive predictive rate is only 25%, leading to unnecessary invasive biopsies. A more effective non-invasive test would be beneficial.

Methods: Self-collected, unstimulated saliva was obtained. A dot blot p87 assay was performed using Adnab-9 monoclonal antibody (mAb) with binding minus background recorded. The mAb reacts with secretory products in the GI tract usually associated with Paneth cell secretions.

Results: In the figure below, in patients with ProC, the salivary p87 was significantly lower than non-cancer controls ($p<0.005$). We found correlations between salivary products such as blood lysozyme, blood, and stool cancer biomarkers. p87 saliva in breast cancer patients was significantly higher (0.031 ± 0.01) than in prostate cancer patients' saliva ($p<0.031$).

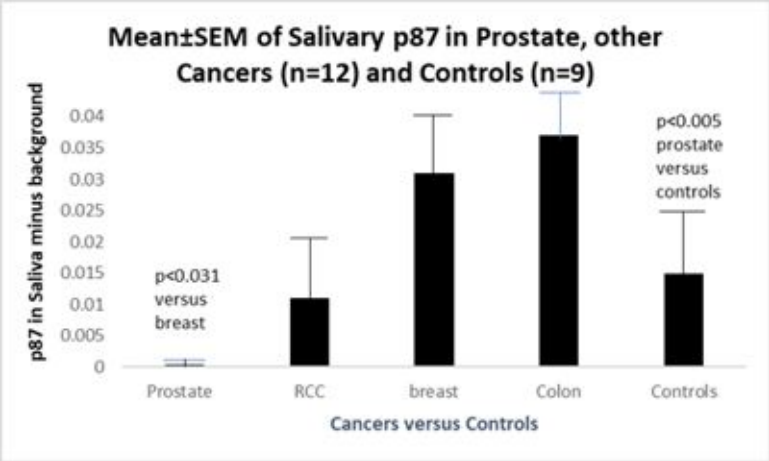

Conclusions: Lower concentrations of salivary lysozyme have been found to be associated with other GI and hemopoietic cancers (Sun et al. https://doi.org/10.1155/2016/8701423). With larger numbers we hope to show that reduced levels of salivary p87, lysozyme, and other biomarkers might be able to detect more aggressive ProC, reducing unnecessary invasive procedures and anxiety.

#2547 Translating to targeted: Bridging discovery lipidomics to multi-omic clinical diagnostic application in ovarian cancer detection.

Rachel Culp-Hill[1], Charles M. Nichols[1], Yu Han[1], Brendan M. Giles[1], Moises Zapata[1], Mattie Goldberg[1], Robert A. Law[1], Enkhtuya Radnaa[1], Shannon Kilkenny[1], Maria Wong[1], Connor Hansen[1], Vuna S. Fa[1], Cory Bystrom[2], Liang Zhao[3], Kim Ekroos[4], Abigail McElhinny[1]

[1]AOA Dx, Denver, CO,[2]Ultragenyx Pharmaceutical Inc., Novato, CA,[3]CompleteOmics, Halethorpe, MD,[4]Lipidomics Consulting Ltd., Espoo, Finland

Ovarian cancer (OC) is often diagnosed at late stages due to a lack of robust diagnostic tools, resulting in one of the highest mortality rates of any gynecologic malignancy. Dramatically altered lipidomic signatures have been observed in OC serum, but barriers exist in translating findings from discovery mass spectrometry (MS) applications to a targeted, clinical diagnostic assay. Discovery lipidomics experiments are challenged by the magnitude of features detected paired with the structural diversity of lipids. This work highlights the importance of feature characterization and identification to discover novel, robust biomarkers for the detection of early-stage OC.Serum samples representing individuals experiencing symptoms of OC as well as OC patients across all stages and a range of subtypes were obtained from University of Colorado, University of Manchester, and commercial vendors . Multi-omic analysis was performed using untargeted and targeted lipidomics and a panel of immunoassay protein biomarkers (CA125, HE4, MUC1, FOLR1). Discovery lipidomics used LCMS/MS with data-dependent acquisition (ddMS2). Data were processed for feature alignment, deconvolution, background rejection, identification, and statistical analysis. Feature exclusion included: (1) no library ID, (2) present in <10% samples, (3) exogenous origin, (4) high technical variability, and (5) not detected. Machine learning (ROC/AUC analysis) and univariate analyses identified features for targeted development. MRM transitions were generated from ddMS2 or targeted MS2 spectra, and targeted MRM methods were built. MRM features were experimentally verified in each polarity. Features were subjected to custom algorithm-informed internal standard normalization prior to inclusion in the model.Our published proof-of-concept multi-omic model reproducibly detects OC with AUCs of 92% (95% CI: 87%-95%) for OC v. controls and 88% (95% CI: 83%-93%) for early-stage OC. We then transferred the discovery lipidomics method to a targeted MRM assay, improving precision and analytical performance, while retaining directionality and/or significance in 82.5% features. Updated multi-omic models using targeted data show reproducible performance with AUCs >90% in an independent cohort of serum samples consistent with the discovery proof-of-concept multi-omic model (lipids + proteins). Here, we describe a workflow for translating discovery lipidomics into a targeted MRM method for a clinical diagnostic assay. Combining feature filtering, statistical analysis, machine learning, and experimental validation across cohorts, we identified a collection of robust lipid biomarkers that reproducibly detect OC. These features, combined with protein biomarkers, are being further developed into a multi-omic assay designed to detect OC earlier in the symptomatic population.

#2548 Circulating proteomic signatures for subtyping NF1 associated peripheral nerve sheath tumors.

Chloe M. Sachs[1], Andrea M. Gross[2], Brigitte C. Widemann[3], Jack F. Shern[4], Russell T. Sundby[1]

[1]Pediatric Oncology Branch, National Cancer Institute, National Institutes of Health, Bethesda, MD,[2]Division of Oncology, Cincinnati Children's Hospital, Cincinnati, OH,[3]Pediatric Oncology Branch, National Cancer Institute, Bethesda, MD,[4]Pediatric Oncology, National Cancer Institute, Bethesda, MD

Purpose: Early detection and interception of malignant transformation in Neurofibromatosis Type 1 (NF1) associated peripheral nerve sheath tumors are challenging due to insensitive clinical symptoms, limited specificity of standard of care imaging, and the limited negative predictive value of invasive tissue biopsy. Novel non-invasive and tumor site-agnostic surveillance assays provide potential for early diagnosis and intervention, especially during the critical transformation from benign plexiform neurofibromas (PN) to pre-malignant atypical neurofibromas (AN), defined by histopathology. We hypothesize that circulating proteins in the plasma accurately distinguish the spectrum of PN, AN, and malignant peripheral nerve sheath tumors (MPNST).

Methods: 118 plasma samples (Healthy $n = 10$, PN $n = 29$, AN $n = 25$, and MPNST $n = 54$) from 79 patients seen at the NIH were analyzed using a proximity extension assay (PEA) panel for 1461 proteins (*Olink*). Unique protein signatures were identified using a one-versus-all comparison: PN-versus-all (PvA) with ANOVA and post-hoc Tukey honestly significant difference (HSD) of normalized protein expression (NPX) outputs from PEA. Significant proteins had an NPX difference ≥ 1.2 and p adj <0.05. Individual proteins' performances were assessed using Youden's index and a receiver operating characteristic (ROC) curve. Given PN's high prevalence in NF1 and the high specificity of the identified proteins, a PN-specific predictive signature was prioritized for downstream analysis due to its clinical utility. Individual PN-associated protein signatures were integrated using a Support Vector Machine Learning Model (SVM) with leave-one-out cross-validation (NPX difference ≥ 1.2 and p adj <0.05).

Results: 114 proteins were significant for PvA comparisons. Individual protein's performance for PvA had a median AUC of 0.64 (IQR: 0.62-0.67), median sensitivity of 0.38 (IQR: 0.33-0.47), and median specificity of 0.97 (IQR: 0.86-1.0). SVM significantly improved the PN-signature's (AUC: 0.954),sensitivity (0.69, 20/29 PN), and specificity (0.99, one AN was misclassified as PN). The integrated PN protein signature predicts with high confidence whether a patient's tumor burden remains PN or has transformed to AN or MPNST (PPV: 0.95, NPV: 0.91).

Conclusions: This pilot demonstrates that circulating proteomics non-invasively distinguish PN from pre-malignant and malignant disease states in NF1. The PN protein profile shows significant dysregulation of protein expression, protein-protein interactions, and biological pathways. Finally, PEA uses just 40 µL of plasma per sample, enabling the integration of non-invasive orthogonal biomarkers, such as cell-free DNA, from a single tube of blood.

#2549 Association of CXCL12 rs1801157 G/A single-nucleotide polymorphism with prevalence and risk of breast cancer in Bangladeshi women.

Md Mustafizur Rahman[1], Shahin Kadir[1], Md Abdur Rahman[1], Amir Hossain[2]

[1]Pharmacy Discipline, Khulna University, Khulna, Bangladesh,[2]Department of Pharmacy, Dhaka International University, Dhaka, Bangladesh

Background: Breast cancer remains the most common cancer among women in Bangladesh. Chemokines play an important role in facilitating intracellular signaling after binding with CXCR4 to promote cell proliferation. CXCL12 plays a pivotal in different stages of tumor development and cancer metastasis. The case-control study assessed the impact of the single-nucleotide polymorphism (SNP) rs1801157 G/A in CXCL12/SDF1 gene in breast cancer patients.
Objective: This study aimed to investigate the association of the single-nucleotide polymorphism (SNP) rs1801157 in CXCL12/SDF1 gene with the prevalence and risk of breast cancer among Bangladeshi women. We also aimed at finding correlation between pathophysiologic variables and polymorphic genotypes in breast cancer patients.
Materials and Methods: The study included 130 breast cancer patients and 142 age matched healthy controls. Genomic DNA was isolated from venous blood collected from breast cancer patients and healthy controls. Genotyping was carried out by PCR-RFLP (polymerase chain reaction followed by restriction fragment length polymorphism) using a restriction enzyme.
Results: The frequencies of the wild type homozygous G/G, heterozygous G/A and variant homozygous A/A were 59%, 31%, and 10% in breast cancer cases whereas in controls were 56%, 38%, and 8%, respectively. The crude genotypic frequencies in breast cancer cases were almost similar to those of the controls. Compared with the homozygous G/G genotype of CXCL12, heterozygous G/A genotypes (OR= 0.7992, 95% CI=0.4784 to 1.3352, p=0.3921) and variant homozygous A/A genotypes (OR= 1.7105, 95% CI = 0.6715 to 4.3572, p=0.2605) were found not to be significantly associated breast cancer prevalence. The G and A content were 74% and 26% respectively for patients whereas it was 75% and 25% for control group, respectively. However, when compared with pathophysiologic characteristics, we found that variant genotypes increased the risk of breast cancer 11 times in non-breast-feeding individuals when compared to breast feeding individuals (X^2 = 11.4953; p =.00319).
Conclusions: rs1801157 SNP may have impact on breast cancer risk among Bangladeshi females. However, Further studies with higher sample size are required to conclude the findings.

#2550 Engineering next-generation EV diagnostics by integrating nanoplasmonic sensing and multiplex enrichment for early PDAC detection.

Tony Hu

School of Biomedical Engineering, Tsinghua University, Beijing, China

Background: Pancreatic ductal adenocarcinoma (PDAC) is typically diagnosed at an advanced stage, when curative options are limited. Circulating extracellular vesicles (EVs) provide a minimally invasive window into tumor biology, yet existing EV assays are slow, sample-intensive, and incompatible with clinical workflows requiring speed, reproducibility, and minimal sample input.
Methods: To confront these challenges, we established a sequential EV liquid-biopsy pipeline that integrates three complementary nanoengineered platforms for PDAC detection. First, a nanoplasmon-enhanced scattering (nPES) assay directly captures EVs from microliter plasma and quantifies tumor-enriched EphA2-positive EVs through dual antibody-nanoparticle coupling, simultaneously enabling the discovery of additional EV surface markers associated with PDAC. Second, we introduce FLARE (Fluctuation-enhanced simultaneous Labeling And Rapid Enrichment), which employs a low-frequency vibrating membrane and a peroxidase-mimicking nanozyme to synchronously enrich, label, and wash EVs in a single 45-minute operation, eliminating the need for multistep centrifugation and improving analytical performance. Third, we refined our plasmonic platform into a multiplex fluorescence assay that assembles plasmonic substrates in situ to enhance EV surface protein emission from unprocessed plasma, allowing simultaneous profiling of multiple PDAC-associated markers within one run.
Results: The EphA2-EV nPES assay enabled highly sensitive quantification of tumor-derived EVs in both small-volume animal samples and patient plasma, distinguished PDAC from pancreatitis and healthy donors, and revealed dynamic EV changes before and after therapy. FLARE achieved more than ten-fold higher EV recovery than conventional methods while maintaining high labeling efficiency, and its amplified colorimetric output enabled smartphone-based quantification of multiple EV biomarkers, discriminating early-stage PDAC with an area under the curve of 0.95. The multiplex plasmon-enhanced fluorescence assay further improved signal-to-noise ratios for rare EV protein detection, enabling multi-marker readout from minimal plasma without prior EV isolation, facilitating personalized prognosis.
Conclusions: By combining plasmonic scattering, vibration-assisted nanozyme enrichment, and plasmon-enhanced fluorescence, this EV-centered pipeline establishes a rapid, low-cost, and sample-sparing framework for PDAC liquid biopsy. Together, these platforms support scalable early detection, longitudinal treatment monitoring, and large-cohort translational studies across both clinical and preclinical settings.

#2551 Dual recognition of β-sheet proteinopathy and glycan moieties enables noninvasive detection of pancreatic ductal adenocarcinoma.

Alfred Akinlalu, Dali Sun

University of Denver, Denver, CO

Early detection of pancreatic ductal adenocarcinoma (PDAC) remains a formidable challenge due to the absence of reliable and accessible screening tools. In contrast to other cancers with established diagnostic methods, PDAC is often detected only after metastasis, resulting in poor survival outcomes. Current biomarkers such as CA19-9 offer limited diagnostic accuracy and frequently yield false positives, emphasizing the urgent need for a more specific and cost-effective approach. Here, we introduce EV-FRET, a biosensing assay that detects PDAC through fluorescence resonance energy transfer (FRET) signaling from tumor-derived extracellular vesicles (EVs). EV-FRET focuses on the molecular cargo of EVs secreted by cancer cells, by simultaneously targeting β-sheet-rich misfolded proteins, indicative of tumor proteinopathy, and N-acetyl-D-galactosamine (GalNAc), a glycan enriched in pancreatic epithelial cells. The assay uses thioflavin T (ThT) and fluorescein-labeled *Dolichos biflorus* agglutinin (FITC-DBA) as the donor-acceptor pair, generating a quantifiable FRET signal only when both tumor and organ markers coexist on EV surfaces. Without requiring EV isolation, the assay provides a single-step, reproducible (coefficient of variation < 4%) and low-cost method. The diagnostic performance revealed an AUC of 0.95 compared with 0.72 for CA 19-9, demonstrating improved specificity. EV-FRET demonstrates the potential for noninvasive PDAC detection and presents a flexible framework for adapting protein structure based diagnostics to other malignancies.

#2552 Cell-free RNA urogentital cancer biomarker detection from urine.

Carrie Ziemniak, Andrea J. O'Hara, Jeff Tio, Yongjun Fan, Haythem Latif

GENEWIZ, LLC, South Plainfield, NJ

Background: Urogenital cancers encompass a variety of tumor types including kidney, bladder and prostate cancer, the most prevalent cancer in men. Current early detection methods rely on blood screening of prostate-specific antigen (PSA), however this method is associated with overdiagnosis and overtreatment, has a high rate of false positives, and the subsequent procedures carry risks. As a result, the search for alternative biomarkers is of much interest. Urine is an ultra-non-invasive analyte ideal for urogenital cancer detection, including prostate cancer. Use of cell free RNA (cfRNA) is ideal for biomarker identification for use in diagnostics, treatment monitoring, and tumor tissue of origin prediction.
Methods: Here we describe urine cfRNA extraction and RNA-Seq analysis on a series of urogenital cancer affected urine samples and normal control urine samples. Several extraction kits were tested, including a novel cfRNA isolation technique that has highly efficient recovery rates of cfRNA with variable input amounts of 1-100 mL of sample. Following extraction, quantitative and qualitative QC were performed directly from the isolate, as well as functional downstream testing via RNA-Seq to assess recovery, transcriptome complexity, and detectability of known cancer biomarkers.
Results: Preliminary testing of the cfRNA isolation methods showed that traditional extraction methods did not achieve the yield required for detection of low-abundance biomarkers. In contrast, the novel extraction method demonstrated high efficiency cfRNA recovery. Along with traditional quantitative and qualitative QC of the extracted cfRNA, functional testing was performed using RNA-Seq. RNA-Seq results demonstrated detection of rare transcripts and cancer-associated biomarkers, confirming this is a reliable method for biomarker detection.
Conclusion: As these results show, cfRNA can be extracted from urine, with the detection of rare biomarkers associated with disease. The high-efficiency extraction method enables sensitive detection of low-frequency transcripts, addressing limitations of conventional techniques. This method is not limited to urine and cfRNA, with the potential for application in other biofluids including plasma and other nucleic acid types such as mitochondrial DNA.

#2553 Multi-omics liquid biopsy approach for sensitive detection of lung cancer via cfDNA and extracellular vesicles-RNA.

Vidyodhaya Sundaram[1], Nisshanthini Sambasivam Durairaju[1], Elim Cheung[1], Vinh Lam[2], Wei Zheng[2], Edwin Haghnazari[3]

[1]BioChain Institute Inc, a CellBio Scientific Company, Newark, CA,[2]System Biosciences Inc, a CellBio Scientific Company, Palo Alto, CA,[3]CellBio Scientific, Newark, CA

Background: Early detection of lung cancer remains challenging due to tumor heterogeneity and the limitations of single-analyte assays. Circulating cell-free DNA (cfDNA) captures genomic alterations, including mutations, copy number variations, and methylation patterns, but does not reflect gene activity. Circulating extracellular vesicles (EVs) carry varieties of small non-coding RNAs reflecting dynamic tumor processes, especially miRNAs that are implicated in regulating the expressions of oncogenes and tumor suppressors in cancer progression.

Methods: Under IRB approval, plasma from 5 normal subjects and 10 pathology-confirmed lung cancer patients, collected with informed consent from BioChain Institute's repository, was analyzed. cfDNA was isolated using BioChain's bead-based automatable cfPure® MAX Cell-Free DNA Extraction Kit and profiled with a targeted lung cancer gene panel. EV-RNA was extracted using SBI's SmartSEC EV isolation kit and EVery EV RNA Isolation Kit, followed by RNA-sequencing. Human normal Cell-Free DNA Control from 5 pooled normal donors from BioChain Institute was used as a control. Integration of cfDNA and EV-RNA readouts was performed to assess complementary genomic and transcriptomic signals.

Results and Conclusions: Combined cfDNA targeted NGS and EV-RNA sequencing from a single plasma sample is feasible and provides complementary insights into tumor biology. This multi-omics liquid biopsy approach reduces false negatives compared with single-analyte tests and enables identification of biomarkers that may be overlooked when assessing DNA or RNA alone. Together, cfDNA and EV-RNA profiling offer a more comprehensive, non-invasive strategy for early detection, monitoring disease progression, and informing treatment decisions in lung cancer.

: Immunomodulatory Effects of Targeted Therapies
Poster Session

#2557 Glucocorticoids inhibit the GARP/TGF-βaxis initiating immune-dependent melanoma control.

Charles H. Earnshaw[1], Poppy Dunn[1], Shih-Chieh Chiang[1], Agrin Moeini[1], Maria A. Koufaki[1], Eduardo Bonavita[1], Massimo Russo[1], Laetita Nebot-Bral[1], Kimberley Hockenhull[1], Erin Richardson[1], Anna Pidoux[1], Charlotte R. Bell[1], Alexander R. Baker[2], Richard Reeves[3], Robert Sellers[3], Sudhakar Sahoo[3], Victoria Fife[4], Matthew G. Roberts[4], Theophile Bigirumurame[5], Caroline Dive[4], Julia A. Newton-Bishop[6], Jeremie Nsengimana[5], Christopher E. M. Griffiths[4], Santiago Zelenay[1]

[1]Cancer Inflammation and Immunity Group, Cancer Research UK Manchester Institute, Manchester, United Kingdom,[2]Visualisation, Irradiation and Analysis, Cancer Research UK Manchester Institute, Manchester, United Kingdom,[3]Computational Biology Support, Cancer Research UK Manchester Institute, Manchester, United Kingdom,[4]Cancer Research UK National Biomarkers Centre, Manchester, United Kingdom,[5]Biostatistics Research Group, Population Health Sciences Institute, Newcastle University, Newcastle, United Kingdom,[6]Institute of Medical Research at St James's, University of Leeds, Leeds, United Kingdom

Melanoma is the form of skin cancer responsible for most patient deaths. Treatment with immune checkpoint blockade (ICB) has led to a significant improvement in outcomes. However, half of melanoma patients do not derive long-term benefit, and improved understanding of this is required to identify novel mechanisms of resistance and treatment. We screened a range of topical treatments, used in non-melanoma skin diseases, for anti-cancer activity in an ICB-refractory murine melanoma model. In particular, and building on previous work by us and others, we focused on topical treatments that had the potential to influence the inflammatory response within tumors, which in turn may improve anti-tumor immune responses.

In a story recently published in *Cancer Discovery*, we found topical glucocorticoids to uniquely trigger acute tumor shrinkage. After just two doses, GC-treated tumors shrank, whereas control-treated tumors doubled in volume. Intriguingly, this effect was lost in *Rag1*$^{-/-}$ mice (deficient in B and T cells) or in mice depleted of CD8^{+}T cells, uncovering a key role for T cells in GC-induced tumor growth control. Of eight cancer models tested for GC-responsiveness, half experienced immune-depended control, and half were unresponsive.

GCs downregulated the expression of Glycoprotein A repetitions predominant (GARP) on the surface of melanoma cells. GARP is a cell-surface protein that plays a critical role in the activation of TGFβ from its inactive latent form. Targeted mutagenesis and genetic knockout confirmed GC-induced GARP downregulation reduced TGFβ signalling, allowing CD8^{+} T cell tumor killing. Of the eight tumor models tested, only the four GC-responsive tumors also responded to TGFβ inhibition, suggesting that GCs triggered immune-dependent tumor control when tumors make use of TGFβ signalling for immune evasion.

Unpublished data expands on this story. We examined the efficacy of using an anti-GARP antibody in mice, with and without immunotherapy, in order to identify further translational opportunities of this finding. Moreover, we have examined in-house melanoma patient biopsies to identify the immune environment of GARPhigh tumors vs GARPlow tumors, and correlated this with response to immunotherapy.

We discovered a paradoxical immune-dependent shrinkage induced by GCs in certain tumor models. Given the widespread use of GCs in patients receiving immunotherapy, these unexpected findings have the potential to result in significant clinical impact. The GARP/TGFβ axis therefore represents a cancer-cell intrinsic immune evasive pathway targetable by steroids, and further studies investigating the approach of inhibiting GARP on tumor cells directly investigate its use as a therapeutic strategy.

#2558 Multi-omic single-cell assessment of castration-resistant prostate cancer patients receiving ^{177}Lu-PSMA-617 and pembrolizumab shows timing of radioligand therapy alters immune response.

Anusha Muralidhar[1], Karen Law[1], Zenghua Fan[2], Shloka Shukla[1], Aram Lyu[1], Serena Kwek[2], David Y. Oh[2], Michael Evans[2], Rahul R. Aggarwal[2], Lawrence Fong[1]

[1]Fred Hutchinson Cancer Center, Seattle, WA,[2]University of California San Francisco, San Francisco, CA

Background: Prostate cancer, a leading cause of cancer-related death in men, is refractory to checkpoint inhibition.[1-3] Lutetium-177-labeled PSMA-617 (^{177}Lu-PSMA, Pluvicto) is an FDA-approved radioligand therapy in CRPC. We have shown that a single dose of ^{177}Lu-PSMA is immunomodulatory, and can be safely combined with the PD-1 blockade, pembrolizumab, in a phase 1 clinical trial (NCT03805594).[4] However, the schedule by which these treatments should be combined is unknown.

Methods: In our phase 1 clinical trial, patients with mCRPC received a single dose of ^{177}Lu-PSMA either before (Schedule 1, n=30), concurrently with (Schedule 2, n=6), or after pembrolizumab (Schedule 3, n=6). Serial peripheral blood mononuclear cells (PBMCs) were collected and analyzed using multi-omic single-cell RNA sequencing (scRNA-seq) to dissect the immune responses with these 3 schedules.

Results: We found that a single dose of ^{177}Lu-PSMA in monotherapy led to an expansion of CD4+ effector T cells as well as in Tregs indicative of direct immunomodulatory activity. This was accompanied by a reduction in NK and B cells. When ^{177}Lu-PSMA was combined with pembrolizumab, we saw dynamic changes in non-Treg T cell subsets ($CD4^+$ and $CD8^+$ T cells), dendritic cells (DCs), NK cells, and B cells across all three dosing schedules. Schedules 1 and 2 demonstrated stable T cell levels accompanied by a gradual increase in DCs, whereas Schedule 3 was characterized by low T cell frequencies and a progressive decline in DCs relative to baseline.

Conclusions: Our study demonstrates the critical importance of treatment sequencing to fully harness the immunomodulatory potential of RLT using a single dose of ^{177}Lu-PSMA and optimize synergy with PD-1 blockade in mCRPC. While initiating with either ^{177}Lu-PSMA or concurrently starting ^{177}Lu-PSMA with pembrolizumab resulted in an increase in DCs, starting with pembrolizumab first resulted in lower frequencies T cells and DCs suggesting that this schedule could be detrimental to immune outcomes.

#2559 Identifying cancer cell intrinsic regulators of radiation-induced interferon signaling.

Olivia Kaneko[1], Bon Ham Yip[1], Arnav Mehta[2], Nir Hacohen[2], Ryan J. Park[1]

[1]Experimental Radiation Oncology, MD Anderson Cancer Center, Houston, TX,[2]Broad Institute, Cambridge, MA and Massachusetts General Hospital, Charlestown, MA, Charlestown, MA

Induction of anti-tumor immunity by radiation therapy (RT) has been observed in multiple preclinical models and in selected patients and can lead to durable systemic tumor regression. Modulation of anti-tumor immunity by RT is thought to act primarily via cGAS-STING activation leading to type I interferon (IFN) response pathways, which coordinate T cell priming and recruitment and adaptive resistance such as PD-L1 induction. Individual studies have demonstrated both immune activating and immune suppressive effects of RT in various contexts, and the determinants of this wide variability are poorly understood. Discovering divergent and convergent mechanisms of type I IFN response to RT across diverse cancer cell states may thus define biomarkers and treatment strategies to enhance RT-driven immune activation. We treated 100 human cancer cell lines with 2 Gy or 8 Gy RT or the STING agonist DiABZI and performed single cell RNA sequencing. We scored cell lines using a composite of IFN response genes as well as individual IFN response genes including ISG15, MX1, CXCL10 and IFNB. We then selected four cell lines with high radiation-induced IFN response for mechanistic studies: two derived from pancreatic ductal adenocarcinoma and two from breast carcinoma. We observed distinct kinetics of ISG15 and MX1 activation between 2 Gy and 8 Gy RT and DiABZI as well as between cell lines. Notably, knockout of STING abrogated DiABZI response but paradoxically increased ISG15 induction by radiation in MDA-MB-231, but not SUIT-2. Our study highlights wide variability among cancer cell states in modulation of IFN response signatures by radiation and emphasizes the need to elucidate mechanisms of radiation-induced immune activation and suppression across diverse cancer types.

#2560 Radiotherapy shapes memory T cell dynamics and region-specific PD-1 expression in the glioblastoma microenvironment.

Hsin-Yu Sherry Liu, Sanghee Lee, Itzel Gutierrez, Jasmine Borroel, Paris Offor, Emily Eastwood, Javier Rodriguez, Kristen Buck, Derrick Gorospe, Elizabeth Valencia, Catherine Elix, Bridget Corcoran, Manuel Reyes, Samantha Lin, Raffaella Pippa

Certis Oncology Solutions, San Diego, CA

Glioblastoma (GBM) is the most common and aggressive malignant brain tumor in adults, where radiation therapy (RT) remains standard care. However, the precise immunomodulatory effects of RT-specifically on T cell checkpoint receptor profiles and memory T cells dynamics -within the tumor microenvironment are not fully elucidated. In this translational study, we utilized an orthotopic patient-derived xenograft (PDX) model, CRT361, engineered with a Luc+ reporter. This system was supported by an HLA-matched peripheral blood mononuclear cell (PBMC) humanization platform, providing a clinically relevant context for immune analysis. CRT361 cells were implanted intracranially into the right hemisphere, and tumors progression was monitored via multimodal imaging, bioluminescence imaging (BLI) and magnetic resonance imaging (MRI). Following successful PBMC engraftment and a single-dose focal irradiation (2 Gy), T cells were harvested from both peripheral blood and distinct brain hemispheres for profiling via spectral flow cytometry. Our results demonstrate that focal irradiation increased the frequency of both $CD8^+$ and $CD4^+$ central memory T cells (T_{CM}) in both blood and brain. Furthermore, irradiation led to elevated programmed cell death protein 1 (PD-1) expression on both $CD8^+$ and $CD4^+$ T_{CM} and naïve T cells in peripheral blood. Crucially, we observed an inverse response in the central nervous system: $CD8^+$ T_{CM} within the brain exhibited lowerPD-1 expression levels exclusively in the irradiated right hemisphere.These novel findings provide critical insight into the capacity of radiotherapy to dynamically influence T cell phenotypes and checkpoint receptor landscapes in a tissue-, region-, and cell type-specific manner within the GBM microenvironment. This study design and results establish a robust foundation for the rationale design and optimization of combinatorial strategies leveraging both radiation and emerging immunotherapies.

#2562 Quantitative and functional immune reprogramming induced by a nanomedicine in breast cancer model.

Mathilde Dacos[1], Lea Plantureux[2], Sarah Giacometti[1], Joseph Ciccolini[1], **Raphaelle Fanciullino**[3]

[1]COMPO SmartC, Aix-Marseille University, Marseille Cedex 07, France,[2]CVN AMUTICYT, Aix-Marseille University, Marseille Cedex 07, France,[3]Aix-Marseille University, Marseille Cedex 07, France

Nanoparticles (NPs) are emerging as a promising strategy in oncology, offering optimised drug delivery and the potential to modulate immune responses. In this study, we developed an innovative nanoparticle encapsulating docetaxel and functionalised with trastuzumab for precise targeting of HER2-positive tumours (called ANC for Antibody Nanoparticle Conjugate). Immunomodulatory effects were performed in C57BL/6 mice administered free docetaxel (1.6 mg-kg-^{1}) and trastuzumab (135 ng-kg-^{1}) by intraperitoneal injection (n = 29) or ANC (nanoparticles at the same docetaxel and trastuzumab doses as the free drugs, n = 40). Immune profiling was performed in blood (J0-J21) and tumor tissue (J21) to evaluate quantitative and functional changes in major lymphoid and myeloid subsets involved in antitumor immunity. Flow cytometric analyses included B cells, T cells ($CD4^+$, $CD8^+$), activated T-cell subsets, NK cells, regulatory T cells (Treg), myeloid-derived suppressor cells (MDSC), and regulatory B cells (Breg). In blood, no significant differences were observed between groups for B cells, NK cells, $CD4^+$ or $CD8^+$ T cells, or their activated subsets. A trend toward reduced Treg frequencies was detected in the ANC group compared with controls ($p = 0.053$), suggesting early systemic modulation of immunosuppressive activity. MDSC levels remained unchanged across all groups. In tumors, global B-cell levels were comparable between groups, but ANC-treated mice showed an increased proportion of Breg, indicating a potential local immunosuppression. NK-cell infiltration and activation tended to be higher in the ANC group ($p \approx 0.08$), suggesting localized immune stimulation. No differences were detected for $CD4^+$ T cells, whereas a reduction in $CD8^+$ T-cell frequency was observed in ANC-treated tumors. Treg levels also showed a decreasing trend ($p = 0.07$), consistent with a partial reduction in immunoregulatory pressure within the tumor microenvironment. MDSC levels did not differ significantly between conditions. ANC formulation exhibited subtle yet biologically relevant immunomodulatory trends, including reduced Treg frequencies and increased activated NK cells within the tumor, potentially favoring antitumor responses. Conversely, the elevated Breg population in ANC-treated tumors may counterbalance these effects by promoting local immunosuppression. These findings suggest that ANC may fine-tune the tumor immune landscape without inducing major systemic alterations. Further investigation with extended cohorts and functional assays will be required to confirm these trends and clarify their implications for therapeutic efficacy.

#2563 mTOR inhibition augments antitumor immune response by reprogramming the *TP53*-mutant, immune-cold HNSCC tumor microenvironment.

Priyatosh Nath, Alok Khandelwal, Tara Moore-Medlin, Chun Li, Cherie-Ann Nathan

Department of Otolaryngology-Head and Neck Surgery, LSUHSC-S, Shreveport, LA

Head and neck squamous cell carcinoma (HNSCC) with *TP53* mutations presents significant therapeutic challenges, characterized by high recurrence rates and treatment resistance. Using a *TP53*-mutant, PD-1 resistant syngeneic mouse flank tumor model, we investigated the immunomodulatory effects of mTOR inhibition (mTORi) followed by comprehensive bulk RNA sequencing analysis. Our transcriptomic analysis revealed profound alterations in multiple biological pathways, indicating significant shifts in the tumor microenvironment (TME). Treatment with the mTOR inhibitor Everolimus increased immune cell infiltration into the tumor through upregulated cytokine, chemokine activity, and enhanced chemokine receptor binding. mTORi also significantly altered the HIF-1α/VEGF angiogenic pathways, which otherwise promote an immune-cold TME and generate immunosuppressive myeloid-derived suppressor cells (MDSCs). Additionally, mTORi treatment interfered with PD-1/PD-L1 interaction between T cells and tumor cells by reducing PD-1 and PD-L1 expression, thereby augmenting T-cell cytotoxic function. These findings provide molecular evidence supporting mTORi as a promising therapeutic strategy for *TP53*-mutant, immune-cold, and immunotherapy-resistant HNSCC.

#2564 Investigating the combination of natural killer immunotherapy with radiation therapy for muscle invasive bladder cancer.

Fatima Inigo[1], Jose Mansure[1], Eva Michaud[1], Brian Meehan[2], Tanner Connell[3], Ciriaco Piccirillo[4], Wassim Kassouf[5]

[1]Cancer Research Program, McGill University Health Centre, Montreal, QC, Canada,[2]Cancer and Angiogenesis, McGill University Health Centre, Montreal, QC, Canada,[3]Medical Physics Unit, McGill University Health Centre, Montreal, QC, Canada,[4]Microbiology and Immunology, McGill University Health Centre, Montreal, QC, Canada,[5]Surgery, Division of Adult Urology, McGill University Health Centre, Montreal, QC, Canada

Background: Muscle-invasive bladder cancer (MIBC) is commonly treated with radical cystectomy (RC) or radiation therapy (RT). However, both approaches have significant limitations: RC is associated with a major impact on quality of life and a high risk of metastasis, while RT, despite preserving the bladder, has a recurrence rate of about 30%, largely due to the presence of radio-resistant tumors. This study explores the potential of combining adoptive Natural Killer (NK) cell immunotherapy with RT to enhance efficacy and offer a more effective bladder-preserving alternative.

Methods: Three human bladder cancer cell lines (UM-UC3, UM-UC1, RT4) were treated with RT (2 × 3 Gy), NK cells (5 × 10^6 cells IV, twice weekly for two weeks), or the combination. Cell viability was assessed using a colorimetric Kit-8 assay at effector-to-target ratios (1:1, 2:1, 5:1). *In vivo* efficacy was tested in a subcutaneous mouse model. Clinical relevance was examined using NanoString GeoMx spatial transcriptomic data from MIBC patients treated with RT (responders n = 107; non-responders n = 35). NK infiltration and NK-associated gene signatures were analyzed via Singscore and xCell deconvolution.

Results: RT significantly reduced viability in UM-UC3 and RT4 cells ($p<0.01$), and the combination of RT+NK further enhanced cytotoxicity ($p<0.001$). In UM-UC1, NK cells alone markedly decreased viability ($p<0.001$), with no additional reduction observed when combined with RT. *In vivo,* combination therapy produced a sustained reduction in tumor growth compared to RT ($p=0.0117$) or NK therapy alone ($p=0.0004$), demonstrating enhanced therapeutic efficacy. Clinically, responders exhibited higher NK infiltration ($p<0.01$), elevated NK anti-tumor scores ($p<0.01$), and increased expression of MICA, NKG2C, and HLA-E, molecules involved in NK-cell activation and target-cell recognition (all $p<0.05$).

Conclusion: Overall, our results suggest that NK cells can play an important role in improving the response to RT in MIBC. We observed that combining NK cell therapy with RT led to better tumor control in preclinical models, and clinical data supported this by showing that patients who responded to RT had higher NK cell infiltration and expression of key immune markers. While further studies are needed to confirm these findings, this work adds to growing evidence that NK cells could play a role in modulating treatment response. Exploring this further may help identify patients who are more likely to benefit from combination strategies and guide future efforts toward more personalized approaches in MIBC.

#2565 mTOR as a mechanistic biomarker of FLASH radiotherapy: Implications for immune-modulated melanoma treatment.

Madison Hawkins[1], Joshua Knight[1], Camden VanTassell[1], Landen Barnett[1], **Gennie Lynne Parkman**[1], Dani Johnson-Erickson[2], Ramesh Rengan[2]

[1]Weber State University, Ogden, UT,[2]Radiation Oncology, University of Washington, Seattle, WA

FLASH radiotherapy (FLASH-RT), which delivers ultra-high dose rate radiation, has emerged as a promising modality that reduces normal tissue toxicity without compromising tumor control. While preclinical data support its tissue-sparing properties, the underlying biological mechanisms remain incompletely defined. Understanding these pathways is critical for integrating FLASH into multimodal cancer therapy.Melanoma, a highly immunogenic and aggressive skin cancer, is increasingly treated with immune checkpoint inhibitors (e.g., anti-PD-1), yet many patients develop resistance. Radiation can enhance immunogenicity, but toxicity often limits dose escalation. The potential for FLASH to synergize with immunotherapy while minimizing side effects presents an exciting opportunity to optimize melanoma treatment.To investigate the immune contributions to the FLASH effect, female BALB/c mice received proton radiation delivered as FLASH (~80 Gy/s) or conventional (~0.5 Gy/s) at 0, 12, or 14 Gy. At 27 days post-treatment, skin tissues were analyzed using Data Independent Acquisition-Mass Spectrometry (DIA-MS). Machine learning-based feature selection identified tryptic peptides that distinguished FLASH from conventional treatment. mTOR (mammalian target of rapamycin)—a master regulator of immune signaling—and its binding partner Raptor were significantly upregulated in FLASH-treated skin, suggesting a distinct mTOR-driven pathway.Given mTOR's known role in modulating PD-L1 expression and immune suppression via interferon and TGF-β signaling, we hypothesized that FLASH may potentiate the efficacy of immune checkpoint blockade. Using in vitro and in vivo melanoma models, we evaluated responses to FLASH or conventional radiation with or without anti-PD-1 therapy. Mice treated with FLASH plus anti-PD-1 demonstrated promising improvements in survival, supporting potential synergy. Immunoblotting and immunofluorescence confirmed increased phospho-mTOR (Ser2448) and downstream effector activation in both normal and tumor tissues following FLASH.These findings identify mTOR as a candidate biomarker and mechanistic driver of FLASH responses and support further development of mTOR-informed, immune-responsive FLASH strategies in melanoma and other cancers.

#2566 KRAS^{G12D} inhibition enhances macrophage-mediated anti-tumor immunity via STING activation.

Xiaoe He, Xiangyan Jiang, Wengui Shi, Long Qin, Tao Wang, **Zuoyi Jiao**

Lanzhou University, Lanzhou, China

The KRAS^{G12D} mutation is a key oncogenic factor in pancreatic cancer, present in over 40% of cases, making it the most prevalent and the most poorly prognostic mutation. However, KRAS^{G12D} has been considered "undruggable," and thus remains a challenging target for therapeutic intervention. The novel KRAS^{G12D} inhibitor, RMC-9805 (Zoldonrasib), has shown promising efficacy and safety in clinical trials, offering hope to address the therapeutic void in KRAS^{G12D}-driven cancers. In this study, we utilized single-cell RNA sequencing to reveal that Zoldonrasib suppresses the SPP1/CD44 intercellular communication between tumor cells and macrophages, while promoting the antigen-presenting function of tumor-associated macrophages. Mechanistically, we observed that Zoldonrasib treatment induces mitochondrial damage and mtDNA release in tumor cells, leading to the activation of the cGAS/STING signaling pathway. Subsequently, STING-mediated phosphorylation of STAT1 inhibits the transcriptional activity of the key SPP1 transcription factor, STAT3, thereby downregulating SPP1 expression in tumor cells. Zoldonrasib enhances macrophage MHC-I antigen presentation by suppressing SPP1/CD44 signaling. In both immune-competent KPC mice and immune-reconstituted PDX models, the use of a clinical-stage STING1 agonist further promoted macrophage antigen presentation and enhanced the therapeutic efficacy of Zoldonrasib, while also sensitizing pancreatic cancer to immune checkpoint inhibitors. This study uncovers the regulatory role of KRAS^{G12D} inhibition via Zoldonrasib in anti-tumor immunity and proposes a promising combinatorial therapeutic approach for clinical trials.

#2567 Axl is a negative regulator of type I IFN in cDC1s hindering anti-tumor immunity.

Isaac Gonzalez[1], Eslam A. Elghonaimy[1], Qiongwen Zhang[1], Isaac Montgomery[1], Peter Q. Leung[1], Arely P. Rodriguez[1], Rolf A. Brekken[2], **Todd A. Aguilera**[1]

[1]Radiation Oncology, UT Southwestern, Dallas, TX,[2]Surgery, UT Southwestern, Dallas, TX

Background: The receptor tyrosine kinase Axl is widely implicated in tumor progression and immune evasion, yet its role in antitumor immunity remains poorly defined.
Methods: Investigate the role of Axl on tumor growth, using animal models, genetic crosses, cellular assays, and single cell RNAseq from human and mouse tumors.
Results: Here, we uncover Axl as a key negative regulator of type I interferon signaling in dendritic cells, with direct consequences for $CD8^+$ T cell priming and tumor control. Axl-deficient mice exhibited delayed tumor growth that was dependent on $CD8^+$ T cells and BATF3, highlighting a requirement for cross-presenting cDC1s. Conditional knockout models confirmed that Axl loss in dendritic cells—but not macrophages—was sufficient to enhance antitumor immunity through type I interferon pathways. Mechanistically, Axl ablation increased cDC1 cross-priming capacity and amplified the therapeutic effects of a STING agonist and radiotherapy.
Conclusion: These findings position Axl as an intrinsic checkpoint in cDC1s that restrains interferon-driven immunity, revealing a mechanism by which innate regulation of dendritic cells shapes adaptive antitumor responses.

#2568 SIRT1 inhibits T cell infiltration and tertiary lymphoid structure formation to promote radioimmunotherapy resistance.

Yunxing Shi[1], Zongfeng Wu[2], Shaoru Liu[2], Renhan Luo[1], Liang Kang[1]

[1]Department of General Surgery (Colorectal Surgery), The Sixth Affiliated Hospital, Sun Yat-sen University, Guangzhou, China,[2]State Key Laboratory of Oncology in South China, Guangdong Provincial Clinical Research for Cancer, Sun Yat-Sen University Cancer Center, Guangzhou, China

Background: Microsatellite stable (MSS) rectal cancer is intrinsically resistant to immunotherapy. Although radiotherapy is often combined with immune checkpoint inhibitor (ICIs) to enhance immunotherapy responses, many immunologically cold tumors remain unresponsive.
Methods: The radiotherapy-induced antitumor immunity effect of SIRT1 inhibition was assessed in murine models. The mechanisms of SIRT1 and DDX5 in tumor immune escape with radiotherapy were determined in vitro and in vivo. The synergistic effects of SIRT1 inhibitor or aspirin plus radiotherapy with PD-1 blockade were also investigated.
Results: We observed a significant increase in electron transport chain activity, acetyl-CoA level, and pan-acetylation level in patients achieving pathologic complete response (pCR) following immunotherapy administered after radiotherapy. Through transcriptomic screening and in vivo experiments, we found that SIRT1, a key executor in regulating protein acetylation, restricted the immunostimulatory effects of radiotherapy. Mechanistically, SIRT1 deacetylates DDX5, promoting its unwinding of irradiation-induced R-loop and inhibiting the accumulation of cytoplasmic RNA: DNA hybrids, thereby suppressing the cGAS/STING pathway and T cell infiltration. Interestingly, we found that radiotherapy forced the tryptophan-SIRT1-SLC36A4 positive feedback, further enhancing SIRT1 activity and competitively uptaking tryptophan in the microenvironment, thereby inhibiting TLS formation and leading to poor efficacy of radioimmunotherapy. Finally, we discovered that both SIRT1 inhibitor and aspirin plus radiotherapy converts ICI-unresponsive rectal cancer into immunogenic tumors that are hyper-sensitive to ICI.
Conclusions: SIRT1 is a potential biomarker and therapeutic target to overcome radioimmunotherapy resistance.

#2569 Particle therapy, ATM and PD-1 inhibition for pMMR rectal cancer.

Cameron M. Callaghan

Radiation Oncology, Mayo Clinic Hospital-Rochester, Rochester, MN

Background and Aims: Colorectal cancer is a leading cause of cancer mortality and most rectal cancers are mismatch repair proficient (pMMR), making them largely resistant to PD-1 inhibitors (PD1i). While PD1i achieves excellent complete response rates in MMR-deficient tumors, these represent <5% of rectal cancers. For the remaining 95% of patients, effective immunotherapy strategies are urgently needed. We evaluated two high-LET radiation approaches to prime pMMR rectal cancers to PD1i and enhance local control: 1) Diffusing alpha emitter Radiation Therapy (DaRT) implants, and 2) LET-optimized (Bragg Peak) protons + ATM inhibitor. An ATM inhibitor was evaluated with protons to evaluate whether it could produce a more alpha/carbon-like effect given the lower comparative LETd achievable in clinical treatment plans.

Methods: In vitro proton irradiation of HCT116, HT29, SW480, and CT26 was performed as previously with dose averaged LET (LETd) values of 2.2 keV/um for ENT and 7.0 keV/um for BP protons. Female Balb/C mice were subcutaneously inoculated with 1×10^6 CT26 cells on one flank and 1×10^5 cells on the contralateral flank to establish primary and secondary (abscopal) tumors, respectively. PD1i monoclonal antibody (RMP1-14 Bio X Cell) was administered i.p. 100ug every 72 hours for 4 total doses. The ATM inhibitor AZD1390 was delivered via oral gavage at 20 mg/kg, PO 1 hour prior to radiation. For in vivo studies, radiation was delivered using a PXI SmART small animal irradiator with opposing lateral beams (225 kVp, 20 mA, 0.3mm Cu filter). Proton irradiation plans were produced as previously described. We used mass cytometry by time of flight (CyTOF) using the TME CD45 lymphocyte subpopulations based on multiple cell markers.

Result: In our preliminary data we demonstrate that both DaRT and BP protons+ATMi synergize with PD1i to dramatically increase complete response rates at both primary and abscopal tumors by increasing DNA damage, activating innate immune pathways, and reducing immunosuppression within the tumor microenvironment. Critically, this effect was observed in a pMMR model which did not respond to PD1i or conventional X-rays+PD1i, highlighting the innovation and potential impact of this work.

Conclusion: DaRT and BP protons ATMi prime pMMR colorectal cancer to PD1i, and all elements are clinically translatable.

#2570 Reprogramming T-cell networks to overcome immune evasion in ovarian cancer relapse.

Denarda Dangaj Laniti

Centre Hospitalier Universitaire Vaudois, Lausanne, Switzerland

Ovarian cancer (OC) remains a major clinical challenge due to its high recurrence rates and resistance to standard therapies. High-grade serous ovarian cancer (HGSOC), the most common and aggressive OC subtype, often presents with tumor-infiltrating lymphocytes (TILs), yet immune checkpoint blockade (ICB) therapies have shown limited efficacy. Our studies aim to dissect the spatiotemporal evolution of the OC tumor microenvironment (TME), reprogram T cell networks, and develop next-generation immunotherapies to restore anti-tumor immunity. We integrated high-resolution spatial proteomics, single-cell transcriptomics, and computational modeling to map TIL dynamics across primary, recurrent, and treatment-resistant OC. Preclinical models, including syngeneic BRCA1-mutant and wild-type mouse models of OC recurrence, are employed to investigate tumor-intrinsic and TME-driven mechanisms of immune suppression during OC relapse. We utilized digital pathology multiplex immunofluorescence (mIF) to classify 697 ovarian cancer (OC) specimens from five independent cohorts, offering the most extensive CD8+ T cell-based immune profiling to date. Our predictive algorithm identified distinct tumor immune phenotypes in OC (i.e. purely inflamed, mixed inflamed, excluded, and desert) based on TIL infiltration and spatial organization, which correlate with HRD status and predict therapeutic outcomes. We observed significant immune and molecular heterogeneity between these tumor immune phenotypes and their dynamics during disease recurrence. Inflamed HRD tumors, maintained T cell-myeloid niches post-chemotherapy. In preclinical models, this was associated with restoration of genomic rearrangements. Recurrent murine HRD tumors upregulated the immunosuppressive PGE2-EP2/4 pathway and targeting of COX-driven PGE2 production during chemotherapy significantly prolonged relapse and survival in preclinical mouse models, identifying a key vulnerability for the recurrence of human HRD OCs. In contrast, homologous recombination repair proficient (HRP) OC tumors evolved into T-cell excluded or desert phenotypes, characterized by malignant cells overexpressing Nduf4l2/Galectins and Trem2/ApoE overactive tumor-associated macrophages (TAMs). Our data suggest that therapeutically targeting of TREM2 overexpressing TAMs may improve anti-tumor immune responses and delay recurrence after first-line chemotherapy in HRP OC. By unraveling the cellular and molecular networks driving immune evasion in recurrent OC, our findings provide a roadmap for precision immunotherapy. Our work highlights novel immune biomarkers and therapeutic targets that can be exploited to retune anti-tumor T cell responses, paving the way for clinically actionable strategies in recurrent OC and other immune-resistant malignancies.

#2572 Pharmacological targeting of CTPS1 elicits macrophage-mediated anti-leukemia immunity.

Meng Liu[1], Lei Zhang[1], Xin He[1], Haojie Dong[1], Yang Li[1], Shuaishuai Ge[1], Guohua Wu[1], Yadav P. Umesh[1], Wei Chen[2], Pinghui Feng[3], Guido Marcucci[1], Ling Li[4]

[1]Beckman Research Institute, City of Hope National Medical Center, Monrovia, CA,[2]Beckman Research Institute, City of Hope National Medical Center, Duarte, CA,[3]Section of Infection and Immunity, University of Southern California, Herman Ostrow School of Dentistry, Los Angeles, CA,[4]City of Hope National Medical Center, Duarte, CA

Immunotherapy has limited efficacy in acute myeloid leukemia (AML), partly because innate immune cells such as macrophages remain inactive. Nucleotide metabolism regulates key cellular processes, and cytidine triphosphate synthase 1 (CTPS1), the enzyme responsible for de novo CTP synthesis, is essential for cell proliferation. We previously showed (Liu, 2024 ASH) that high CTPS1 activity promotes AML growth and suppresses antitumor immunity. Accordingly, the CTPS1 inhibitor STP-B significantly prolonged the survival of immunocompetent leukemic mice in an immune-dependent manner. Across TCGA cancers, CTPS1 expression negatively correlated with M1-macrophage signatures.Here, we show that STP-B exerts anti-AML activity by (1) inducing myeloid differentiation, especially M1-like macrophage polarization through dNTP imbalance, and (2) activating IFN-I signaling by blocking CTPS1-mediated deamidation of IRF3 and histone H1. In a syngeneic MLL-AF9 (MA9) model, daily oral STP-B (100 mg/kg, 3 weeks) reduced leukemia burden and markedly increased $CD11b^+F4/80^+$ macrophages, enriching the M1-like subset. Macrophage depletion completely abolished the survival benefit. Combination with anti-CD47 produced strong synergy. Transcriptomic analysis of MA9 cells and non-malignant myeloid cells showed induction of M1-associated genes (Il6, Il1a, Cxcl9, Cxcl10). Ex vivo, STP-B-treated BMDMs displayed significantly enhanced phagocytosis of MA9 cells. To evaluate human hematopoietic effects, $CD34^+$ cord blood-engrafted NSG mice were treated with STP-B. While total human $CD45^+$ levels were unchanged, myeloid ($CD33^+CD11b^+$), monocyte ($CD14^+CD64^+$), and $HLA\text{-}DR^+CD86^+$ M1-like macrophage populations increased, with higher expression of myeloid transcription factors and human M1 genes. Metabolomic profiling of THP-1 cells confirmed that STP-B markedly reduced intracellular CTP, indicating nucleotide imbalance. Ribonucleotide reductase inhibition partially restored balance, reversed differentiation, and suppressed STP-B-induced M1-gene expression, supporting a nucleotide-driven differentiation mechanism. GSEA demonstrated induction of IFN-I-responsive genes. STP-B increased γH2AX and nuclear S9.6 staining, consistent with DNA damage caused by inhibition of CTPS1-mediated histone H1 deamidation. STP-B also blocked CTPS1-dependent IRF3 deamidation, enhancing ISG expression. Reconstitution of CTPS1-knockout THP-1 cells with a glutaminase-deficient CTPS1 mutant similarly increased ISGs, indicating that CTPS1 deamidation activity suppresses IFN signaling. Together, these findings show that STP-B promotes macrophage specification and innate immune activation, defining STP-B as a leukemia-ablating agent with strong immunostimulatory properties.

#2573 Identification and characterization of platinum agent-induced chemoimmunomodulation in triple-negative breast cancer.

Mariana Makarem, Kathleen Streeks, Claudia Perez Perez, Iasmim Lopes de Lima, Mohammed Gbadamosi

Department of Pharmacotherapy and Translational Research, University of Florida, Gainesville, FL

Triple-negative breast cancer (TNBC) is the most aggressive breast cancer subtype. Although early-stage outcomes have improved, advanced TNBC (aTNBC) continues to have poor outcomes, with a median overall survival < 18 months and heterogeneous benefit from first-line therapy. Although there have been advances in aTNBC therapy, chemotherapy remains central to curative regimens. Among the most critical dimensions of chemotherapeutic efficacy are immunomodulatory effects elicited by chemotherapy (chemoimmunomodulation; (CIM)). Platinum agents are commonly used in aTNBC and induce CIM through ROS generation, immunogenic cell death, DAMP release, and cGAS-STING/interferon signaling. However, platinum-induced CIM induction is heterogeneous and cell type-dependent, thereby limiting its efforts to optimize its use. The goal of this study was to identify and characterize platinum agent-induced CIM to address this challenge. To achieve this, we applied our Chemoimmunomodulation Induction Classifier (CIMIC) pipeline to delta gene expression values (ΔGE; $\Delta\log_2(\text{TPM}+1)$) derived from human TNBC cell lines (N = 8; 3 biological replicates each) profiled via bulk RNA-sequencing pre- and post-48-hour IC_{30} cisplatin exposure. CIMIC is an iterative unsupervised clustering pipeline that classifies samples into distinct groups based on their induction of 3,100 genes spanning 19 CIM pathways. Two distinct CIM states emerged: a functional (Fun-CIM) and a dysfunctional (Dys-CIM) state. The Fun-CIM state exhibited significantly elevated induction of antitumoral inflammatory markers (*TNFAIP8L1* and *TNSF12*) and reactive oxygen species potentiators *(ABL1*) (Fun-CIM vs Dys-CIM all fold change (FC) > 1.50; $p < 0.05$; FDR < 0.10), whereas the Dys-CIM state exhibited elevated induction of DNA-damage repair molecules (*XRCC4* and *XPA*), unfolded protein response genes (*SEC61G*) , and proteostasis mediators (*RPS3A* and *RPS*) (Dys-CIM vs Fun-CIM all fold change (FC) > 1.12 ; $p < 0.05$; FDR < 0.10) Overrepresentation analysis revealed an enrichment for cytokine production, reactive oxygen species response, and phagocytic potentiation for the genes induced within the Fun-CIM group, and proteostasis programs within the Dys-CIM group ($p < 0.05$ FDR < 0.15) corroborating our findings. Together, these data show that CIMIC hold promise in resolving platinating agent-induced immunomodulation into functional and dysfunctional induction states from paired pre-/post- transcriptomes. Our results highlight CIM heterogeneity in response to platinating agent administered at the same potency and highlight tumor-intrinsic stress-adaptation as a potential key determinant of CIM trajectory. To our knowledge, CIMIC is the first unsupervised pipeline built to classify CIM trajectories. Future work will define baseline predictors of CIM trajectories with respect to platinum agents.

#2574 Identification and characterization of chemoimmunomodulatory induction trajectories in breast cancer via unsupervised transcriptomic analyses of pre- and post-treatment specimens.

Iasmim L. de Lima, Kathleen H. Streeks, Elizabeth Molchan, Mariana S. Makarem, Kennedy L. Coleman, Mohammed O. Gbadamosi

Department of Pharmacotherapy and Translational Research, University of Florida, Gainesville, FL

Chemotherapy is key to curative treatment strategies for aggressive breast cancer (BC). Despite this, the molecular features governing the immunomodulatory effects of chemotherapy (chemoimmunomodulation; CIM), which enable efficacy and synergy with other treatment modalities, are understudied, thereby limiting optimization of chemotherapeutic regimens to improve patient outcomes. A key roadblock to these efforts has been the lack of a robust framework for classifying CIM induction trajectories. To address this challenge, we developed the CIM Induction Classifier (CIMIC), an iterative unsupervised clustering pipeline that uses delta gene expression (Δlog2(TPM+1)) of 3,100 genes across 19 CIM pathways from paired pre- and post-treatment tumor transcriptomes to classify CIM induction trajectories. We applied CIMIC to data from two cohorts (GSE191127 (N = 20) and GSE12845 (N = 16)) of BC patients treated with neoadjuvant chemotherapy to identify distinct CIM trajectories and characterize the tumor-intrinsic and tumor-extrinsic programs underlying CIM heterogeneity. In both cohorts, the classifier consistently assigned patients to one of two CIM trajectories, functional CIM (Fun-CIM; N = 17) or dysfunctional CIM (Dys-CIM; N = 19). Overrepresentation analyses of induced genes showed an enrichment for immunostimulatory programs, including immune-effector differentiation, function, and cell killing (FDR ≤ 0.01) and tumor-intrinsic stress adaptation programs, including proteostasis, unfolded protein response, and mitochondrial homeostasis (FDR ≤ 0.01) for the Fun-CIM and Dys-CIM, respectively. Interestingly, Dys-CIM was overrepresented in the basal-like molecular subtype in both cohorts ($p < 0.05$) and, where data were available, was associated with recurrence ($p = 0.041$; N = 20). To further evaluate the clinical relevance of these induction states, we derived trajectory-specific signatures and applied single-sample gene set analysis to baseline tumors from chemotherapy-treated patients in the METABRIC (N = 412) and SCAN-B (N = 2,774) cohorts. In multivariable Cox models adjusted for treatment, clinicopathological features, and molecular subtype, the high Dys-CIM signature was associated with inferior overall survival (METABRIC, HR = 1.83, $p = 0.041$; SCANB, HR = 1.73, $p = 0.014$), poorer disease-specific survival (METABRIC, HR = 1.94, $p = 0.035$), and lower recurrence-free survival (METABRIC, HR = 1.68, $p = 0.019$), suggesting that a predisposition toward Dys-CIM represents a clinically adverse signature detectable at baseline. Taken together, our findings herein provide rationale for dissecting clinically relevant CIM trajectories and responses, supporting future efforts to link induced CIM trajectories to clinical outcomes and personalized immunomodulation strategies.

#2575 Identification and characterization of anthracycline-induced chemoimmunomodulation in triple-negative breast cancer.

Kennedy L. Coleman[1], Kathleen Streeks[2], Mariana Makarem[3], Iasmim Lopes de Lima[4], Mohammed Gbadamosi[2]

[1]Pharmacotherapy and Translational Research, University of Florida, Gainesville, FL,[2]University of Florida, Gainesville, FL,[3]UF Clinical and Translational Science Institute, Gainesville, FL,[4]Department of Pharmacotherapy and Translational Research, University of Florida, Gainesville, FL

Triple-negative breast cancer (TNBC) is the deadliest breast cancer subtype with a median survival < 24 months in advanced cases. While TNBC treatment has advanced, chemotherapy remains a cornerstone of curative treatment. Despite its central role in TNBC treatment, the molecular drivers underpinning the immunomodulatory effects of chemotherapy (chemoimmunomodulation; CIM), which enable long-term efficacy and synergy with other therapeutic modalities, remain understudied, thereby limiting efforts to optimize chemotherapeutic regimens. This study aims to identify and characterize anthracycline-induced CIM states to address this challenge. To achieve this, we applied our Chemoimmunomodulation Induction Classifier (CIMIC) pipeline to delta gene expression values (ΔGE; $\Delta\log_2(\text{TPM}+1)$) derived from TNBC cell lines (N = 6; 3 biological replicates each) profiled by bulk RNA-sequencing pre- and post-48-hour IC_{30} doxorubicin exposure. CIMIC is an iterative unsupervised clustering pipeline that classifies samples into distinct groups based on their induction of 3,100 genes spanning 19 CIM pathways. Using CIMIC, we identified two discrete CIM trajectories in our samples, a functional one (Fun-CIM; N = 3 cell lines) and a dysfunctional one (Dys-CIM; N = 3 cell lines) that were highly distinct (silhouette = 0.95) and stable as determined via standard clustering metrics across multiple bootstraps; proportion of ambiguous clustering = 0.00; cluster consensus score = 1). The CIM states were characterized by significantly differential induction of antitumoral inflammatory markers, including chemoattractants (*CXCL14*) and immune mediators (*IFNB1* and *IL12A/B*) (Fun-CIM vs Dys-CIM all fold change (FC) ≥ 1.3; $p < 0.05$; FDR < 0.15), and protumoral markers, including tumor surveillance inhibitors (*THBS1* and *TGFB2*), immunosuppressive cell population mediators (*NNMT*), and tumor-intrinsic stress adaptation signals (*EIF2A, YARS1,* and *XPOT*) (Dys-CIM vs Fun-CIM all FC ≥ 1.3; $p < 0.05$; FDR < 0.15). Overrepresentation analysis of induced genes identified an enrichment of proteostasis and mitochondrial homeostasis programs within the Dys-CIM Group and metabolic rewiring within the Fun-CIM group (FDR < 0.01). Altogether, CIMIC enabled classification of distinct CIM induction states from paired pre- and post-treatment transcriptomic analysis, allowing interrogation of CIM in a manner not captured via traditional chemoresistance studies alone, the dissection of CIM heterogeneity, and the discovery of underappreciated molecular programs that may underlie dysfunctional CIM in TNBC. To our knowledge, CIMIC is the first unsupervised pipeline specifically designed to classify CIM trajectories. Future work will focus on characterizing baseline molecular features that may influence these CIM induction states, toward the goal of informing personalized TNBC chemotherapeutic regimen.

#2576 Gut-targeted antibiotic modulation enhances radiotherapy response in NSCLC and uncovers epigenetic and microbiome-driven immune programs enabling live biotherapeutic design.

Steven J. Feigenberg[1], Francesca Costabile[1], Ceylan Tanses[1], Kyle Bittinger[1], Divyansh Agarwal[1], Roddy O'Connor[2], Jeffrey Bradley[2], Amit Maity[1], Benjamin A. Garcia[3], **Andrea Facciabene**[2]

[12]University of Pennsylvania, Philadelphia, PA,[3]Washington University School of Medicine in St. Louis, St. Louis, MO

Stereotactic body radiotherapy (SBRT) can induce immunogenic cell death and stimulate systemic antitumor immunity, yet clinical responses remain heterogeneous. Preclinical studies indicate that the gut microbiome modulates host immune tone and influences responsiveness to therapy. We previously demonstrated in lung cancer and melanoma models that oral vancomycin enhances the antitumor effects of radiotherapy by depleting Gram-positive taxa responsible for generating short-chain fatty acids (SCFAs) and other immunosuppressive metabolites. Based on these observations, we conducted the first randomized clinical pilot study evaluating SBRT with or without oral vancomycin in early-stage non-small cell lung cancer (NSCLC). Patients eligible for SBRT (50 Gy in 4-5 fractions) were randomized to SBRT alone or SBRT plus vancomycin administered for one week before and five weeks after SBRT. Serial stool, serum, and PBMC samples were collected at five predefined time points. Primary endpoints were feasibility and safety, while immune activation; progression-free survival; overall survival; and changes in stool SCFAs served as exploratory endpoints. Seventeen patients enrolled; seven completed vancomycin treatment. No grade ≥3 toxicities occurred, and gastrointestinal symptoms were the most frequent adverse events. Cancer recurrence occurred in four patients, three of whom received SBRT alone, with nodal failure as the predominant pattern. Microbiome sequencing revealed marked reductions in specific Gram-positive taxa and compensatory expansion of vancomycin-resistant organisms. Stool metabolomics demonstrated substantial decreases in SCFAs in the vancomycin arm. RNA sequencing of PBMCs showed robust enrichment of antigen-processing and presentation pathways, together with interferon-related immune activation signatures. To extend these findings, we performed epigenetic and functional validation studies. PBMC chromatin profiling confirmed increased accessibility at interferon- and antigen-presentation-associated regulatory regions in vancomycin-treated subjects. Guided by these results, we evaluated whether the vancomycin effect was microbiome-transferable by engrafting stool from SBRT-alone or SBRT+vancomycin patients into antibiotic-conditioned mice. Mice colonized with post-vancomycin human stool reproduced the enhanced radiotherapy response, demonstrating that the immune effects are mediated by the gut ecosystem. These results provide the mechanistic rationale for developing ViRTuE-LTP (RT-enhancing live biotherapeutic) candidates. Consistent with the clinical observations, a defined 3-strain ViRTuE-LTP consortium enhanced APC activation and potentiated RT responsiveness in complementary murine studies.

#2577 Free and encapsulated tunicamycin significantly enhances the suppression of PD-L1 by gemcitabine through blocking K-Ras^{G12D} expression in pancreatic ductal adenocarcinoma cells.

Axel Hugo Breier[1], Sunil P. Upadhyay[2], Ojaswitha Ommi[3], Stefan Bossmann[3], Sushanta K. Banerjee[4], **Snigdha Banerjee**[4]

[1]Kansas City VA Medical Center, Kansas City, MO,[2]Cancer Research Unit, Kansas City VA Medical Center, Kansas City, MO,[3]Cancer Biology, University of Kansas Medical Center, Kansas City, KS,[4]Pathology and Laboratory Medicine, University of Kansas Medical Center, Kansas City, KS

Pancreatic ductal adenocarcinoma (PDAC) remains one of the leading causes of cancer mortality worldwide, including among U.S. Veterans, and it is expected to become the second leading cause by 2040. The standard treatment options include surgical resection (when possible), chemotherapy, targeted therapy, immunotherapy, and radiation therapy. These treatments can be administered individually or in combination. Unfortunately, these treatment options have not significantly improved overall survival rates for patients with PDAC. Thus, currently, the first-line treatments for PDAC are still FOLFIRINOX (a combination of fluorouracil, leucovorin, oxaliplatin, and irinotecan) and Gemcitabine (GEM), either alone or in combination with nab-paclitaxel. While initial responses to chemotherapy, such as Gemcitabine alone or with other agents, can occur, these are often followed by the development of resistance. This resistance leads to increased programmed death-ligand 1 (PD-L1) expression in PDAC cells via the JAK-STAT pathway, posing a significant challenge for immunotherapy. Consequently, there is an urgent need for targeted therapies to overcome these limitations. Our research has identified Tunicamycin (TM), a glycosylation inhibitor antibiotic, as a potent agent that effectively targets PDAC cells and significantly reduces GEM-induced PD-L1 production. We found that treating Panc-1 and KPC cells with free or nanoencapsulated Tunicamycin (^{NP}TM) at a dose of 0.25 μM for 48 hours can overcome the limitations associated with Gemcitabine. Specifically, we observed that Gemcitabine treatment at 0.5 μM did not suppress PD-L1 expression; however, when combined with TM, Gemcitabine significantly reduced PD-L1 levels in these cells *in vitro* and *in vivo*. Although the mechanism by which TM regulates PD-L1 is not fully understood, previous studies have shown that K-RAS mutations can directly influence PD-L1 expression by activating the MAPK/ERK pathway, which Tunicamycin inhibits. Therefore, we hypothesize that TM reduces PD-L1 expression in PDAC cells by suppressing K-RAS^{G12D}. (These studies are supported by the VA Merit grants)

#2578 Clinical feasibility study of Optim.AI 2.0, a co-culture high-content functional precision platform for predicting combinatorial immunotherapy response.

Sharon Pei Yi Chan[1], Masturah Rashid[1], Jhin Jieh Lim[1], Weng Tong Ho[1], **Edward Kai-Hua Chow**[2]

[1]KYAN Technologies, Singapore, Singapore,[2]KYAN Technologies, Los Angeles, CA

Background: Immunotherapies have advanced cancer treatment, but variable outcomes and the lack of robust predictive biomarkers limit their use. Better patient selection and rational combination strategies could expand their effectiveness. Optim.AI™ is a combinatorial functional precision medicine platform previously shown to identify effective combination treatments for hematologic cancers and sarcoma. Earlier versions guided chemo- and targeted therapy choices but lacked immune components, restricting the drugs assessed. Here, we evaluate the clinical feasibility of Optim.AI™ 2.0, which integrates high-content imaging with tumor-immune ex vivo co-cultures to predict responses to immunotherapy combinations across solid and hematologic tumors.
Methods: For Optim.AI™ 2.0, peripheral blood mononuclear cells and tumor cells (non-Hodgkin lymphomas, gynecological cancers or gastrointestinal cancers) were fluorescently labeled to facilitate cell tracking. Combinatorial drug treatment was carried out on co-culture models with indication-specific 12-drug panels, including monoclonal antibodies, antibody-drug conjugates and bispecific antibodies. High-content imaging analysis of tumor-specific cell death was evaluated for Optim.AI™ 2.0 analysis, which searches 531,441 possible permutations derived from 155 ex vivo test combinations to predictively rank all clinically actionable treatments within the drug panel. Clinically relevant immunotherapies were compared with patient-specific factors—disease stage, subtype, and treatment history—to assess concordance with predicted responses.
Results: Optimized effector-to-target ratios were established to effectively quantify immune-mediated tumor killing, including antibody-dependent cellular cytotoxicity. High-content imaging captured tumor-specific killing and key immune-tumor interactions such as immune cell migration and tumor infiltration. Across multiple indications, Optim.AI™ 2.0 demonstrated feasibility by detecting antigen-dependent responses and identifying context-specific immunotherapy combinations in both hematologic and solid tumor models. It accurately predicted sensitivity or resistance to first-line rituximab in naïve and relapsed/refractory diffuse large B-cell lymphoma and revealed additional immunotherapy combinations with potential utility in later treatment lines.
Conclusion: We developed a high-content functional analytics platform that assesses immunotherapy drug sets in a physiologically relevant tumor-immune co-culture system. With further validation, it could help clinicians select effective immunotherapies. When paired with molecular profiling, Optim.AI™ 2.0 may identify novel immunotherapy combinations for specific patient populations defined by known or emerging biomarkers.

#3806 Development of a novel CAR T-cell therapy targeting thymic carcinoma.

Layla Ahmadi[1], Malak Khalifeh[2], Dimitar Donovski[1], DuyKhanh Pham Ceppa[3], Patrick Loehrer[3], Rohan Maniar[3], Huda Salman[2]

[1]Indiana University School of Medicine, Indianapolis, IN,[2]Indiana University Brown Center for Immunotherapy, Indianapolis, IN,[3]Indiana University Melvin and Bren Simon Comprehensive Cancer Center, Indianapolis, IN

Introduction: Thymic carcinoma is a rare, highly aggressive mediastinal malignancy with limited effective therapies and considerable toxicity associated with immune checkpoint inhibitors. Although CAR T-cell therapy has revolutionized the treatment landscape for hematologic malignancies, its application to solid tumors, including thymic epithelial tumors, remains challenging due to disease rarity, a paucity of validated surface targets, and the risk of on-target, off-tumor autoimmune toxicity. In this study, we sought to address these barriers by characterizing antigen expression profiles across thymic carcinoma-relevant cell lines, engineering novel CAR constructs against prioritized candidate antigens, and evaluating antigen-specific cytotoxicity. These efforts aim to inform the development of next-generation cellular therapies tailored to the unique biology of this aggressive and understudied tumor type.
Methods: Surface expression of TROP-2, c-KIT, and CD70 was quantified on candidate cell lines using flow cytometry. CAR T-cells were produced from healthy donor PBMCs via lentiviral transduction and expanded ex vivo. CAR expression was confirmed by detection of Fab fragments on $CD3^+$ T cells. Antigen-specific cytotoxicity was evaluated in vitro using co-culture assays with selected antigen-positive cell lines, and target cell killing was quantified by 7-AAD staining and flow cytometric analysis.
Results: Flow cytometry demonstrated robust surface expression of TROP-2 (83%), c-KIT (88%), and CD70 (99%) across the T1889, Kasumi, and U266 cell lines, respectively. Lentiviral transduction yielded CAR^+ T cell populations of 48.2% (TROP-2), 24.7% (c-KIT), and 47.5% (CD70). All three constructs exhibited potent antigen-specific cytotoxicity substantially exceeding GFP^+ $CD3^+$ control T cells, confirming selective recognition and killing of target cells. These findings provide some of the first in vitro evidence supporting TROP-2, c-KIT, and CD70 as viable immunotherapeutic targets for thymic carcinoma and demonstrate effective CAR expression and selective cytotoxicity. This work establishes a foundation for rational multi-antigen CAR T cell design in a historically understudied solid tumor. Ongoing studies include FACS-based CAR enrichment, characterization of exhaustion markers, development of a dual-antigen synNotch CAR to mitigate off-tumor toxicity, and in vivo validation in murine models to support future clinical translation.

: Liquid Biopsies: Circulating Nucleic Acids 2
Poster Session

#2582 Advancing liquid biopsies via integrated CRISPR-based extracellular vesicle RNA and protein analyses.

Cesar M. Castro[1], Jayeon Song[2], Hakho Lee[3]

[1]Mass General Brigham Cancer Institute, Boston, MA,[2]Sungkyunkwan University, Suwon-si, Korea, Republic of,[3]Center for Systems Biology, Massachusetts General Hospital, Boston, MA

BACKGROUND: We developed REPAIR, an integrated urine-based platform combining extracellular vesicle (EV) mRNA and protein profiling with CRISPR to enable non-invasive, multiparametric disease monitoring. Bladder cancer, our clinical use case, remains the costliest cancer to surveil and treat given the high mortality when advanced. Current surveillance of localized disease relies on invasive cystoscopy, lacking the molecular specificity for risk stratification and frequent treatment monitoring.

METHODS: We significantly advanced our recent mRNA-focused CRISPR-Cas13 assay achieving sub-attomolar sensitivity and single-nucleotide resolution in plasma (*Nature Biotech*, 2025 [cover article]; PMID: 39375445), by: (1) integrating dual EV mRNA *plus* protein detection; (2) automating sample processing with innovative disc-based microfluidics we developed; and (3) translating to urine as the clinical matrix. As proof-of-concept, we designed REPAIR probes targeting EV proteins (CD63, EGFR, EpCAM, PD-L1) and mRNAs (GAPDH, LASS2, GALNT1) also relevant to bladder cancer. For protein detection, aptamers were used as affinity ligands. These aptamers were initially hybridized with complementary RNA sequences (initiator RNAs). When the aptamers bound to targets, the initiator RNAs were released and detected through REPAIR. A non-aptamer based strategy was employed for mRNA detection. Urine samples from 85 bladder cancer patients (mostly non-muscle invasive) undergoing treatment and 98 healthy controls were analyzed using the unified REPAIR protocol.

RESULTS: Multiparametric profiling revealed significantly elevated marker expression in cancer versus control urine ($p<0.05$ for all markers). Integrated logistic regression combining protein and mRNA markers achieved 98% detection accuracy (AUC=0.95; 95% CI: 0.92-0.98). Single-marker analysis showed inferior performance, demonstrating the critical value of a multiparametric CRISPR-based EV approach. Integrated readouts were achieved within 60 minutes.

CONCLUSION: REPAIR greatly facilitates simultaneous EV protein-RNA profiling in urine—a non-invasive, scalable liquid biopsy for bladder cancer surveillance and treatment monitoring. These findings potentially establish a nanotechnology-based platform for same-visit precision monitoring in a disease with an extraordinary economic burden and surveillance challenges. Current experiments in other malignancies where urine serves as a proximal fluid are ongoing.

#2583 Tumor-informed circulating tumor DNA dynamics reflect aggressive histology and radiologic disease status in renal cell carcinoma.

Eric Martin[1], Eun-mi Yu[1], Annika Murthi[1], Hongkun Wang[2], Laura Linville[1], Jeanny B. Aragon-Ching[1]

[1]Inova Schar Cancer Institute, Fairfax, VA,[2]Department of Biostatistics, Bioinformatics, and Biomathematics, Georgetown University, Washington, DC

Introduction: Circulating tumor DNA (ctDNA) enables minimally invasive monitoring of tumor biology and treatment response. Although ctDNA is increasingly used across malignancies, its utility in renal cell carcinoma (RCC) has not been well established. We sought to understand the relationship between ctDNA, tumor histology, and clinical outcomes in locally advanced (laRCC) and metastatic RCC (mRCC).

Methods: Forty-eight patients with laRCC and mRCC underwent serial plasma ctDNA testing with a commercially available, tumor-informed assay (Signatera). Tissue from each patient's tumor was sequenced to identify individualized variants, which were then used to construct a personalized tumor-informed ctDNA assay. Serial plasma testing quantified these patient-specific variants to assess ctDNA dynamics alongside interval imaging. Associations between baseline ctDNA status, peak level of ctDNA in mean tumor molecules per milliliter (MTM/mL), histologic subtype, aggressive morphologic features (sarcomatoid, rhabdoid, necrosis), and radiologic findings were analyzed. Quantitative variables were compared using Kruskal-Wallis and Mann-Whitney U tests. Survival was evaluated using Kaplan-Meier and log-rank testing.

Results: ctDNA was detected at baseline in 39.5% (17/48) of patients overall, including 5.2% (1/19) with laRCC and 55.2% (16/29) with mRCC. Among clear cell (cc) RCC, baseline ctDNA was detected in 66% of cases with aggressive morphologic features (sarcomatoid, rhabdoid, or necrosis) versus 15% of clear cell tumors without these features. Baseline detection in non-clear cell RCC was 42% (3/7). Among ccRCC, the median peak ctDNA level was significantly higher in tumors with aggressive features compared to those without (0.82 vs 0.07 MTM/mL, $p < 0.05$). Peak ctDNA levels were strongly associated with radiologic disease status: patients with progressive disease (PD) had markedly higher median ctDNA levels (8.86 MTM/mL) compared with those demonstrating disease control with complete response (CR, 0.00 MTM/mL), partial response (PR, 0.41 MTM/mL), or stable disease (SD, 0.27 MTM/mL; $H = 9.16$, $p = 0.027$). When stratified by disease control (CR/PR/SD) versus disease progression (PD), patients with disease control exhibited significantly lower peak ctDNA levels (median 0.18 MTM/mL, $n = 12$) than those with progression (median 8.86 MTM/mL, $n = 8$; $p = 0.007$). Conversion from ctDNA-positive to ctDNA-negative during the disease course was associated with improved overall survival ($p < 0.05$). However, baseline ctDNA detection alone did not correlate significantly with survival.

Conclusions: ctDNA may serve as a predictor of aggressive histopathologic features in RCC. Quantitative burden and ctDNA dynamics appear associated with disease status and overall survival. These findings highlight tumor-informed ctDNA as a promising biomarker in RCC.

#2584 Methylation signatures from liquid biopsies predict anti-EGFR therapy response in patients with colorectal cancer.

Xuwen Li[1], Mingyang Cai[1], Shile Zhang[1], Nicole Zhang[1], Reagan Barnett[1], Tingting Jiang[1], Kota Ouchi[2], Yoshiaki Nakamura[3], Kimberly Banks[1], Justin Odegaard[1], Darya Chudova[1]

[1]Guardant Health, Palo Alto, CA,[2]Tohoku University, Sendai, Japan,[3]University of Oxford, Oxford, United Kingdom

Introduction: Anti-EGFR-based regimens are standard treatments for left-sided, *RAS/BRAF* wild-type metastatic colorectal cancer (mCRC), but current biomarkers, including *RAS/BRAF* mutation status and tumor sidedness, do not fully explain the variability in treatment response. Prior tissue-based studies suggest that genome-wide DNA methylation patterns define biologically distinct CRC subtypes. We aimed to develop and validate a circulating tumor DNA (ctDNA)-based methylation classifier to predict anti-EGFR efficacy in mCRC patients.

Methods: Genome-wide methylation profiles from >3,000 CRC liquid biopsy samples were analyzed using Guardant360 Liquid (Guardant Health, Palo Alto, CA). After tumor fraction normalization, unsupervised clustering identified two reproducible subtypes: One cluster exhibited a globally high-methylation pattern consistent with the hypermethylated colorectal cancer (HMCC) state described in prior tissue-based studies, while the other represented a low-methylated colorectal cancer (LMCC) state. A random forest model trained on the top 50 principal components (PCs) of these methylation profiles was applied to a real-world cohort of patients receiving anti-EGFR or anti-VEGF therapies. Real-world survival, measured by time to treatment discontinuation (rwTTD), was assessed by treatment type, methylation status, and genotype (*RAS/BRAF* wild-type vs mutant).

Results: Methylation-based clustering successfully stratified mCRC into HMCC and LMCC groups in samples with evaluable tumor fractions (≥0.5%, N=162). HMCC tumors were enriched for *BRAF* mutations and exhibited significantly shorter PFS on anti-EGFR therapy, particularly among right- or unknown-sided patients. LMCC patients demonstrated improved outcomes on anti-EGFR therapy (HR = 1.76, $p = 0.024$), including in patients with right- or unknown-sided, *RAS/BRAF* wild-type disease, with survival comparable to patients with left-sided disease (HR = 0.94, $p = 0.85$). Combing methylation status with *RAS/BRAF* genotype and tumor sidedness expanded the anti-EGFR-eligible population by 18.8% (from 101 to 120 patients) while maintaining survival comparable to standard eligible patients. Conversely, no significant survival difference was observed between HMCC and LMCC patients treated with anti-VEGF therapy (HR = 1.08, $p = 0.64$), confirming methylation status as a predictive biomarker for treatment selection rather than a purely prognostic factor.

Conclusions: ctDNA methylation profiling enables expanded prediction of anti-EGFR efficacy in mCRC beyond current selection criteria. Methylation-integrated eligibility captures additional patients who might benefit from anti-EGFR therapy that are missed by current sidedness-based guidelines. These findings support ctDNA methylation as a feasible and scalable predictive biomarker for precision therapy in colorectal cancer.

#2585 Plasma cell-free DNA nucleosome footprints in metastatic castration-resistant prostate cancer (mCRPC).

Denisa Bogdan[1], Jan Rekowski[1], George Seed[1], Claudia Bertan[1], Jane Goodall[1], Gemma Fowler[1], Penelope Flohr[1], Christine Geffriaud-Ricouard[2], Mustapha Chadjaa[3], Sandrine Mace[4], Isaac Lazzeri[5], Ellen Heitzer[6], Suzanne Carreira[1], Wei Yuan[1], Johann S. de Bono[1]

[1]The Institute of Cancer Research, London, London, United Kingdom,[2]Medical Oncology Europe Department, Sanofi, Gentilly, France,[3]Clinical Research, Sanofi, Vitry-sur-Seine, France,[4]Sanofi R&D Oncology, Sanofi, Vitry-sur-Seine, France,[5]Division of Oncology, Department of Internal Medicine, Medical University of Graz, Graz, Austria,[6]Institute of Human Genetics, Diagnostic & Research Center for Molecular BioMedicine, Medical University of Graz, Graz, Austria

Background: Transcription factor (TF) activity can be determined by nucleosome footprints in low-pass whole genome sequencing (lpWGS) of plasma cell-free DNA (cfDNA). cfDNA wrapped around nucleosomes is protected from enzymatic digestion, and TFs induce phased nucleosome positioning around their binding sites, which results in oscillatory sequencing coverage and preferential depletion at open chromatin regions. Herein, we quantify nucleosome occupancy at binding sites for hundreds of TFs, evaluating the clinical utility of these functional readouts in plasma taken from subjects treated on the CARD prospective randomized trial of cabazitaxel (CAB) vs second androgen receptor pathway inhibitor (ARPI).
Methods: Plasma cfDNA lpWGS (median coverage ~1.6x) was used to infer nucleosome footprints at TF binding sites (TFBS) of 682 TFs. Overall, 217 CARD trial subjects comprised a Test cohort and 174 patients receiving a taxane on the FIRSTANA and PROSELICA prospective trials comprised a validation set. cfDNA lpWGS of a cohort of 104 healthy participants was used as a control. Hazard ratios (HR) were computed using Cox proportional hazards models. Odds ratios (OR) were computed using logistic regression. Longitudinal changes between baseline and subsequent timepoints were investigated using linear mixed effect models. All analyses were adjusted for tumor fraction.
Results: Out of 682 TFs with available binding site annotations, 357 consistently yielded signal-to-noise ratios of at least 2:1 and were further analyzed. Analytical validation utilizing technical replicates (different samples; same time point) and biological replicates (different samples, taken at baseline and screening, weeks apart) was pursued, determining the dynamic range for these TFs at 1000 TFBS each. Assay limits of detection (LOD) and limits of quantification (LOQ) for sequencing coverage and tumor fraction were determined for each TF. Of 357 TFs, 244 were significantly mCRPC associated (Wilcoxon test, adjusted p-value < 0.05) relative to healthy controls, including AR, NKX3-1, E2F1, MYC, MYCN, and MAZ. Predictive analysis in CARD showed accessibility at UBP1 binding sites at baseline was associated with taxane sensitivity over ARSI (OR 1.44, 95% 1.07-1.95, p-value < 0.05). Furthermore, average FOXP1 accessibility scores increased at progression (average increase 1.76, SE 0.49, p-value 0.02), alongside AR (average increase 1.16, SE 0.49, p-value 0.02) and GRHL2 scores (average increase 1.33, SE 0.53, p-value 0.01). These plasma-derived data suggest patients progress with increased AR signaling.
Conclusions: Evaluating nucleosome footprints at TFBS using lpWGS is a robust approach that identifies valuable functional biomarkers of drug sensitivity. Such studies offer the opportunity to interrogate disease progression through serial clinical samples, where phenotype profiling is otherwise unfeasible.

#2586 Investigating a Wilms tumor DNA methylation signature in liquid biopsies.

Mariusz Shrestha[1], Arteen Torabi-Marashi[1], Marina Dutra[1], Sanaa Choufani[1], Trevor J. Pugh[2], Rosanna Weksberg[1], Jack Brzezinski[3]

[1]The Hospital for Sick Children, Toronto, ON, Canada,[2]UHN Princess Margaret Cancer Centre, Toronto, ON, Canada,[3]Seattle Children's Research Institute, Seattle, WA

For adult cancers, plasma ctDNA interrogation of genomic alterations has the potential to detect cancers before radiographic evidence, supporting prognostication and monitoring of therapeutic response in real-time. Despite its remarkable potential, ctDNA detection is often limited to advanced disease, with very few low-grade tumors shedding sufficient ctDNA with genomic lesions characteristic of the cancer. In contrast to adult tumors, the genomes of early childhood and embryonal tumors are typically stable with low somatic and copy number alterations that are often benign and heterogeneous, making detection even more difficult. Thus, a diagnostic tool that detects DNA methylation (DNAm) changes in ctDNA in addition to genomic alterations could enable earlier cancer detection and improve outcomes. Wilms tumor (WT) is the most prevalent renal cancer in children. Our group has shown that DNAm aberrations exist in all WTs regardless of the presence of genomic aberrations, and that DNAm alterations are often the earliest pathogenic change in early lesions. Here, we present preliminary findings of our methyl-classifiers' ability to detect WT from plasma cfDNA by enzymatic methyl-sequencing (EM-seq). Using EM-seq, we are currently generating DNAm data from plasma drawn at diagnosis in 35 patients with WT and 24 controls. In the initial pilot analysis of 17 patients with Wilms tumors and 4 controls, our WT-methyl-classifier was not only able to reliably identify patients with WT, but also stratified patient cfDNA samples into two subtypes with methylation profiles similar to those reported in primary WT tissues. Additionally, we showed corroborating evidence of WT ctDNA in plasma cfDNA samples: First, copy number alterations associated with WT were present such as chromosome 1p, 11p, and 16q loss, and chromosome 1q gain. Secondly, methylation at commonly differentially methylated regions in WT plasma samples were concordant with tumor tissue - for example increased and decreased methylation at *H19* and *KCNQ1OT1* imprinting control regions respectively. Thirdly, cfDNA from patients with WT had smaller average DNA fragment size compared to controls - a pattern that has been described in other cancer types. Lastly, the majority of matched tumor tissues shared methylation subgroup profiles and CNAs with their cfDNA counterparts, while discordant cases likely resulted from normal tissue contamination. In summary, we demonstrated that WT ctDNA is robustly detected in cfDNA through measurement of DNAm profiles. As prognostic information such as DNAm subgroup can be derived from these data, this assay is well positioned for translation into clinical molecular diagnostics. We are currently optimizing this assay for early detection of WT in patients with predisposition and for monitoring of treatment response.

#2587 Development of a methylated gene panel for detection of cell-free, metastatic prostate cancer DNA in plasma.

Gang Yu[1], Mary Jo Fackler[1], Liqun Zhang[1], Wenfei Xia[1], Roshni Saravanan[1], Ezra Baraban[2], Eunice Van Den Berg[3], Adam Botha[3], Pamela Michelow[3], Reubina Wadee[3], Maureen Joffe[4], Wenlong Carl Chen[4], Thomas Pisanic[5], Michelle Petri[6], Jun Luo[7], Channing Paller[1], Samuel Denmeade[1], Leslie Cope[1], Saraswati Sukumar[1]

[1]Department of Oncology, Johns Hopkins University School of Medicine, Baltimore, MD,[2]Department of Pathology, Johns Hopkins University School of Medicine, Baltimore, MD,[3]Department of Anatomical Pathology, University of the Witwatersrand/National Health Laboratory Service, Johannesburg, South Africa,[4]Strengthening Oncology Services Research Unit, Faculty of Health Sciences, University of the Witwatersrand, Johannesburg, South Africa,[5]Johns Hopkins University School of Medicine, Baltimore, MD,[6]Department of Medicine, Johns Hopkins University School of Medicine, Baltimore, MD,[7]Brady Urological Institute, Johns Hopkins University School of Medicine, Baltimore, MD

Purpose: We sought to develop a highly sensitive, reproducible cell-free methylated DNA assay for accurately detecting metastatic prostate cancer (mPCa) in plasma.
Experimental Design: We identified a new 10-marker panel for accurate detection of PCa in the TCGA prostate adenocarcinoma (PRAD) 450K DNA methylation data. Marker sensitivity and specificity were verified in two independent public prostate cancer datasets (GSE112047, GSE76938). A quantitative multiplex methylation-specific PCR (QM-MSP) assay incorporating these markers was validated in archival benign and prostate cancer tissues from the United States (US, 61 cancer, 26 benign) and South Africa (SA, 80 cancer, 24 benign). We used a newly developed cell-free multiplex methylation-specific PCR (cf-MMSP) assay for the 10-marker panel. Intra-assay and intra-operator reproducibility assays tested its robustness. cf-MMSP performance was assessed in a Training set (40 benign, 40 cancer), and an independent Test set (19 benign, 20 cancer) of plasma. Shapley value regression was used to rank performance of the 10 genes in the cf-MMSP assay. We selected a 5-gene panel based on their high performance. Statistical methods used included the Youden index threshold for ROC analysis and Kruskal-Wallis tests.
Results: In tissues, the 10-gene panel detected all stages of prostate cancer: In tissue from the US (n=87), we achieved ROC AUC = 1.00 (CI. 0.99 - 1.00), sensitivity of 98.36% (CI. 91.28 - 99.91) and specificity of 100.00% (CI. 87.13 - 100.00); in SA samples (n=104), ROC AUC was 0.99 (CI. 0.99 - 1.00), sensitivity of 98.28% (CI. 90.86 - 99.91), and specificity of 100.00% (CI. 86.20 - 100.00). cf-MMSP intra-assay test showed low CVs (1.70-5.70% across copy levels) and strong linearity (R^2 = 0.93). The intra-operator test showed excellent reproducibility, with an ICC of 0.99. In plasma, in the training set, the 10-gene panel showed ROC AUC of 0.89 (CI. 0.81-0.97), sensitivity of 75.00% (CI. 59.81 - 85.81) and specificity of 93.88% (CI: 83.48 - 97.90) in distinguishing mPCa from benign. In the test set, the assay performed with ROC AUC of 0.91 (CI. 0.80 -1.00), sensitivity of 85.00% (CI. 63.96 - 94.76), and specificity of 93.88% (CI. 83.48 - 97.90). Using a standardized Shapley value cutoff of 0.07, we identified the five best-performing genes- HAAO, DLEC1, FBN1, TMEM155 and RTDR1. In the training set of plasma, the refined 5-gene panel subset showed ROC AUC of 0.92 (CI. 0.84 - 0.99), sensitivity of 90.00% (CI. 76.95 - 96.04) and specificity of 90.00% (CI. 76.95 - 96.04). In the test set, this 5-gene panel achieved ROC AUC of 0.92 (CI. 0.84 - 0.99), with a sensitivity of 90.00% (CI. 80.00 - 100.00) and a specificity of 84.20% (CI. 53.00 - 100.00).
Conclusions: The 5-gene cf-MMSP panel showed strong performance indices in detecting mPCa in plasma. The assay shows potential for broadly accessible early detection and disease monitoring for molecular management of mPCa.

#2588 Monitoring ESR1 and other mutations linked to resistance with a tumor-informed MRD test: Analytical validation and real world data.

Jason Harris, John M. Lyle, Gabor Bartha, Sean M. Boyle, Josette Northcott, Devayani Bhave, Claudia Aliguillen, Shuyuan Ma, Rachel M. Pyke, Steven Dea, Dan Norton, Erin Ayash, Richard O. Chen

Personalis, Inc., Fremont, CA

Background
Detecting resistance mutations during cancer surveillance can lead to changes in treatment and improve patient outcomes. For example, a recent study showed HR+/HER2- breast cancer patients with ESR1 resistance mutations detected during surveillance had improved outcomes when switched to a second generation selective estrogen receptor degrader (SERD). To address this emerging need, we analytically validated an option in the tumor-informed NeXT Personal® ctDNA MRD test to report on a set of mutations linked to resistance in the literature ("resistance mutations") across 13 genes, including ESR1. We further performed exploratory analysis on real world data to assess the frequency of these mutations detected during circulating tumor DNA (ctDNA) based molecular residual disease (MRD) testing.
Methods and Results
We performed a number of studies to demonstrate the analytical validity for reporting a set of mutations linked to resistance as part of NeXT Personal. Utilizing a cohort of >7,000 MRD-negative samples, we measured the analytical specificity for detecting these resistance mutations at >99.999%. Orthogonal confirmation of positive mutation detections and negative mutation detections was performed using digital droplet PCR. Finally, using a dilution series of the Seraseq ctDNA Mutation Mix v4, we measure the sensitivity and the analytical range measurements (linearity, precision, and limit of quantification).
We also performed an exploratory retrospective analysis of the detection of mutations linked to resistance across >11,000 cfDNA timepoints from >5,300 patients, across multiple cancer types. We examined resistance mutation detection rates in MRD-positive patients and in a "high-MRD" subset, defined as those whose plasma timepoints reached a MRD level of >1,000 parts per million (PPM). Among ~2,500 MRD-positive patients, we detected a resistance mutation in 15%. Restricting to the ~1,200 high-MRD subset, the detection frequency of resistance mutations increased to 27%. Focusing on high-MRD HR+/HER2- breast cancer patients, we detected ESR1 mutations in 29% of patients.
Conclusions
With recent studies showing the importance of detecting ESR1 mutations as part of breast cancer surveillance, here we validate the ability to additionally report on ESR1 and other resistance associated mutations as a part of longitudinal MRD testing for solid tumors. Using real world data, we also show that these mutations are detected in a significant subset of patients, especially as the ctDNA fraction increases. The added ability to report on these mutations has the potential to inform patient management in the future.

#2589 Prospective verification of OvaPrint and multi-omic profiling for precise adnexal mass classification.

Thomas Simon[1], Lynda D. Roman[2], X. Mona Guo[2], Ben Yi Tew[1], Gerald C. Gooden[1], Monica Neuman[3], Emma Barber[4], Elisa Romeo[5], Todd Holscher[5], Renee Wunderley[6], Danielle Goldberg[7], Krishna Morampudi[7], Dalia Daujotyte[7], Monique Spillman[8], Bodour Salhia[1]

[1]Department of Cancer Biology, Keck School of Medicine, University of Southern California, Los Angeles, CA,[2]Division of Gynecologic Oncology, Keck School of Medicine, University of Southern California, Norris Comprehensive Cancer Center, University of Southern California, Los Angeles, CA,[3]Los Angeles General Medical Center, Los Angeles, CA,[4]Division of Gynecologic Oncology, Feinberg School of Medicine, Northwestern University, Evanston, IL,[5]CpG Diagnostics, Inc., Pasadena, CA,[6]Cpg Diagnostics, Inc., Pasadena, CA,[7]Illumina, Inc., San Diego, CA,[8]Department of Gynecologic Oncology, University of Arkansas Medical Center, Little Rock, AR

Background: Patients with adnexal masses face both overtreatment, when benign disease is misclassified, and undertreatment, when cancers are not managed by gynecologic oncologists. CA125, the most widely used biomarker, lacks specificity. High-grade serous ovarian cancer (HGSOC), the most aggressive subtype of epithelial ovarian cancer (EOC), requires timely specialist management. OvaPrint, a cfDNA methylation liquid biopsy developed to improve adnexal mass evaluation, is currently optimized for HGSOC, with expansion underway. In a prospective multi-site study, we sought to clinically verify OvaPrint, compare it with CA125 and integrate it with 5-base sequencing, next generation proteomics and spatial transcriptomics analysis.
Methods: Plasma was collected from six US sites preoperatively and analyzed with OvaPrint. Eligibility included adnexal mass on imaging without evidence of metastatic disease and planned surgery. Clinical data, including CA125 values, were abstracted from medical records. Diagnosis from surgical pathology reports served as the clinical ground truth. Of 121 cases (7 HGSOC, 16 other EOCs, 5 other cancers, 93 benign), 110 were evaluable (104 had CA125). Endpoints were sensitivity, specificity, positive predictive value (PPV), and negative predictive value (NPV). Samples were also analyzed using the latest Illumina's technology including: Illumina's Protein Preparation (IPP) platform detecting 9500 proteins (80 plasma samples); 5-base sequencing solution for simultaneous whole-genome DNA methylation and variant detection (58 cfDNA samples); spatial transcriptomics for description of the tumor microenvironment (TME) and histologic context (23 fresh frozen tissue samples).
Results: OvaPrint achieved 83.3% sensitivity for HGSOC. Specificity was 96.6% for benign cases and 97.1% for non-HGSOC tumors. The HGSOC-specific PPV and NPV was 62.5% and 99%, respectively. CA125 showed 100% sensitivity for HGSOC but had poor specificity (62.2%, 13% PPV). IPP, 5-base sequencing and spatial transcriptomics data are being evaluated to complement OvaPrint through an integrated multi-omic approach for the discrimination of malignant and benign adnexal masses.
Conclusions: Accurate tools for EOC diagnosis are urgently needed. This prospective, multi-site study demonstrates OvaPrint's exceptional performance for the discernment of HGSOC. The high HGSOC-specific NPV and PPV of OvaPrint means a positive result is a near-certain indicator of HGSOC, supporting timely and appropriate care. OvaPrint is being expanded to other EOCs and is undergoing CLIA validation. Additional integration of other molecular endpoints could further enhance discrimination of adnexal masses. These findings establish it as the first liquid biopsy for HGSOC with potential to transform diagnostic practice and outcomes.

#2590 Urine cfDNA 4-mer end-motif signatures outperform other fragmentomic features for tissue-of-origin classification in genitourinary cancers.

Jessica Linford[1], Pradeep S. Chauhan[1], Irfan Alahi[1], Yohan Kim[1], Arpit Panda[2], Nathan Colon[3], Ryan Mueller[4], Faridi Qaium[1], Eric H. Kim[5], Melissa A. Reimers[4], Zachary L. Smith[6], Woodson W. Smelser[4], Fabrice Lucien-Matteoni[1], Aadel A. Chaudhuri[1]

[1]Mayo Clinic, Rochester, MN,[2]University of Chicago, Chicago, IL,[3]Hoag Foundation, Newport Beach, CA,[4]Washington University School of Medicine, St. Louis, MO,[5]University of Nevada Reno, Reno, NV,[6]AdventHealth Orlando, Orlando, FL

Introduction: Urine cell-free DNA (cfDNA) is a promising ultra-noninvasive analyte for genitourinary cancers (GU) cancers. In this study, we investigated urine cfDNA fragmentomic features and evaluated their ability to predict the tumor tissue of origin.
Methods: A total of 204 GU cancer patients and 34 healthy adults were enrolled in this prospective study. Preoperative urine was collected from 89 bladder cancer (BC) patients (64% muscle-invasive) undergoing cystectomy, 65 renal cell carcinoma (RCC) patients undergoing nephrectomy and 50 metastatic prostate cancer (mPC) patients. Urine cfDNA was isolated and sequenced at 5x genome-wide coverage on a NovaSeq S4 flow cell. To identify malignant tissue of origin, we analyzed somatic copy number alterations (CNAs), genome-wide fragment length ratios, and 4-mer end motifs. CNAs and tumor fraction (TFx) were quantified using ichorCNA in 1-Mb windows, while chromosome arm-level fragment count z-scores and fragment length ratios were calculated in 5-Mb bins across the genome. Relative frequencies of all 256 possible 4-mer end motifs were calculated for each sample. Individual logistic regression models were developed based on each fragmentomic feature using leave-one-out cross validation (LOOCV). Outputs from these models were combined into multi-feature XGBoost models. Cohort-specific end-motif enrichments were identified using Kruskal-Wallis tests with FDR correction. Motifs were then hierarchically clustered based on their cohort-wise median frequencies to define groups of motifs with shared fragmentation patterns.
Results: Across urine cfDNA in the GU cohort, BC showed the highest mean TFx at 10.0%, followed by mPC at 3.6% and RCC at 2.7%. A machine learning model based on 4-mer end motifs achieved a mean ROC AUC of 0.933 with classification accuracies of 63% for healthy, 87% for BC, 72% for mPC, and 83% for RCC. This model outperformed models based on ichorCNA (AUC = 0.767), chromosome arm fragment-count z-scores (AUC = 0.827), and fragment length ratios (AUC = 0.674). Combining end motifs with other fragmentomic features did not improve prediction accuracy. Multi-feature models incorporating end motifs with ichorCNA, chromosome arm-level z-scores, or fragment-length ratios yielded mean AUCs between 0.908-0.924, lower than the end-motif only model. Kruskal-Wallis tests identified 179 of 256 end motifs (79%) as significantly different across healthy, BC, mPC, and RCC. Hierarchical clustering of cohort-level median motifs revealed distinct end motif patterns: Motifs beginning with CT were enriched in RCC; AAAA was strongly enriched in BC; and motifs beginning with CA, AC, and AG were enriched in mPC.
Conclusion: Urine cfDNA 4-mer end motifs capture GU cancer-specific biological patterns that enable accurate tissue-of-origin prediction, underscoring their promise as a diagnostic tool.

#2591 Sequence and structural DNA alterations in the circulation of patients with cancer.

Daniel C. Bruhm[1], Carolyn Hruban[1], Adrianna L. Bartolomucci[1], Akshaya V. Annapragada[1], Sarah Short[1], Shashikant Koul[1], Kaui P. Lebarbenchon[1], Julia S. Johansen[2], Inna M. Chen[2], Andrei Sorop[3], Razvan Iacob[3], Speranta Iacob[3], Liana Gheorghe[3], Simona Dima[3], Katherine A. McGlynn[4], Manuel Ramirez-Zea[5], John Groopman[1], PLCRC-MEDOCC group, Remond J. A. Fijneman[6], Gerrit A. Meijer[6], Zachariah H. Foda[1], Jillian Phallen[1], Robert B. Scharpf[1], Victor E. Velculescu[1]

[1]The Sidney Kimmel Comprehensive Cancer Center, Johns Hopkins University School of Medicine, Baltimore, MD,[2]Department of Oncology, Copenhagen University Hospital-Herlev and Gentofte, Herlev, Denmark,[3]Center of Digestive Diseases and Liver Transplantation, Fundeni Clinical Institute, Bucharest, Romania,[4]Division of Cancer Epidemiology and Genetics, National Cancer Institute, Rockville, MD,[5]Research Center for the Prevention of Chronic Diseases, Institute of Nutrition of Central America and Panama (INCAP), Guatemala City, Guatemala,[6]Department of Pathology, Netherlands Cancer Institute, Amsterdam, Netherlands

The properties of cancer-associated genetic changes in cell-free DNA (cfDNA) are not fully understood. We performed whole-genome sequencing (WGS) of cfDNA as well as tumor tissue and white blood cells (WBCs) from 1,807 samples of 1,064 patients across eight common cancer types. Characterization of single base substitutions, small insertions and deletions, structural variants (SVs), and phased variants in single cfDNA molecules revealed unique properties of tumor-derived alterations as well as differences in error rates that spanned orders of magnitude. Given the low error rate associated with detection of tumor-specific rearrangement junctions in cfDNA, we hypothesized that these types of changes could enable detection of circulating tumor DNA (ctDNA) without prior knowledge of the alterations in the tumor tissue. As an example of this approach, we scanned each sequenced fragment genome-wide in cfDNA samples from the CheckPAC trial of patients with metastatic pancreatic cancer treated with radiation and immunotherapy to identify putative rearrangement junctions. We identified 22,010,911 such fragments but only 1,572 (0.007%) and 58,339 (0.27%) of these were present in the matched tumor or WBC samples, respectively, with the remaining identified only in cfDNA. We characterized each cfDNA fragment by the SV type, SV size, microhomology and insertion at the breakpoint junction, fragment size, and the location of the breakpoint with respect to the nearest fragment end, identifying differences depending on the origin of the SV. Machine learning analyses of SVs from cfDNA resulted in a high cross-validated performance for detection of tumor-specific SVs with an area under the curve (AUC) of 0.97 (95% CI: 0.97-0.98). After enriching for fragments most likely to be tumor-derived, we found that the number of cfDNA fragments containing SVs was highly correlated with the number obtained using a tumor-informed approach (Pearson correlation coefficient = 0.87, $p<0.001$), and could recapitulate longitudinal ctDNA levels and clinical outcomes using only low-coverage (~4x) plasma WGS. The universal nature of tumor-associated sequence and structural alterations in cfDNA may be broadly useful for cancer detection.

#2592 Nocturnal rise in circulating tumor DNA in a subset of metastatic colorectal cancer patients.

Ekaterina S. Kuligina[1], Aleksandr S. Martianov[1], Liliya S. Baboshkina[1], Arina S. Perevalova[1], Yana V. Belysheva[1], Anastasia N. Ershova[1], Tatiana A. Laidus[2], Aram A. Musaelyan[3], Ekaterina M. Anokhina[4], Gulfiia M. Teletaeva[1], Aglaya G. Iyevleva[1], Evgeny N. Imyanitov[1]

[1]N.N. Petrov National Medical Research Center of Oncology, Saint Petersburg, Russian Federation,[2]Department of Medical Genetics, St.-Petersburg Pediatric Medical University, Saint Petersburg, Russian Federation,[3]Department of clinical oncology, Pavlov First Saint Petersburg State Medical University, Saint Petersburg, Russian Federation,[4]Department of Antitumor Drug Therapy, St. Luke Clinical Hospital, Saint Petersburg, Russian Federation

Background: Practical use of ctDNA tests is complicated because many tumors shed into the bloodstream vanishingly low amounts of DNA. Significant efforts have been invested in the identification of factors that influence the performance of ctDNA assays. A recent study demonstrated a nocturnal peak in the amount of circulating tumor cells (CTC) during the deep sleep phase (~4 a.m.). This study questioned whether the same peak is characteristic of circulating tumor DNA (ctDNA).

Methods: Plasma samples were collected from 19 *RAS/RAF*-mutated colorectal cancer (CRC) patients at 12 p.m. (day 1), 4 a.m. (night), and 12 p.m. (day 2). 14 subjects provided a single triplet for the study, and five patients underwent the above procedure twice or thrice. *KRAS, NRAS*, and *BRAF* mutations in plasma were quantified via droplet digital PCR (ddPCR).

Results: *RAS/RAF* mutations (>10 copies/mL) were detected in at least one plasma sample in 20 of 25 (80%) triplets. Among these, 15 showed detectable ctDNA at all time points, with intra-individual variation ranging from 1.7% to 74.8%. In five triplets, ctDNA was undetectable during the daytime but present at night. A nocturnal ctDNA peak occurred in 7 of 9 triplets collected during disease control, while all 10 triplets obtained during tumor progression showed other temporal patterns ($p = 0.005$, Fisher's exact test). Patients sampled multiple times displayed differing ctDNA fluctuation patterns depending on disease status.

Conclusions: ctDNA levels exhibit circadian variation, with a 4 a.m. peak observed in patients with disease control. The results align with prior reports on nocturnal surges in CTC in breast cancer patients and suggest that liquid biopsy results are modulated by circadian or sleep-related physiological changes. This work has been supported by the Russian Science Foundation (grant number 25-45-01051)

#2593 Enspyre MRD: Validation of an ultra-sensitive kitted MRD solution at low sequencing depth.

Magdalena Stolarek-Januszkiewicz[1], Sophie Hackinger[1], Sarah Diels[2], Katarzyna Anton[1], Amy Lovell[1], Ernesto Lowy-Gallego[1], Ana-Luisa Silva[1], Maria Litovchenko[1], Bart Tegenbos[2], Emmanuel Riviere[2], Dirk Goossens[2], Nathalie Bernard[2], Justyna Mordaka[1], Iyelola Turner[1], Lisa Van den Bossche[2], Lien Heyrman[2], Jan Van de Velde[2], Pieter Mestdagh[2], Jurgen Del Favero[2], Barnaby Balmforth[1]

[1]Biofidelity Ltd, Cambridge, United Kingdom,[2]CellCarta, Antwerp, Belgium

Detection of MRD post surgery and monitoring of ctDNA during treatment are gaining increasing traction in patient care and drug development. First-generation assays have considerable clinical datasets, but suffer from limited sensitivity due to low numbers of mutations tracked. Recent 'ultra-sensitive' solutions detect ctDNA at <100 parts per million (ppm), but suffer from high sequencing requirements and costs, limiting their use to large central labs.

Enspyre is a novel sample preparation technique that enriches mutated DNA prior to sequencing, significantly improving signal to noise and reducing sequencing requirements. We present results from two independent sites demonstrating the analytical validation of Enspyre MRD, a kit-based MRD solution utilizing Enspyre.

Specificity was tested with >180 replicates from >50 healthy blood donors at two different DNA input levels. LoD and LoQ were determined through >280 replicates using contrived samples in a 2-phase approach. Assay linearity was assessed using an additional 24 replicates spanning 5 orders of magnitude of ctDNA concentration.

Analytical accuracy and precision were assessed using cell free DNA (cfDNA) derived from patients with NSCLC and serially diluted in cfDNA from healthy donors, as well as DNA extracted from cancer cell lines, fragmented to mimic cfDNA. Different blood collection tubes were also assessed using healthy donors.

The effect of variant panel size on performance was assessed through the design of panels from 500 to 2,000 variants and in-silico downsampling.

Enspyre MRD produced consistent results between sites, with sensitivity, specificity and quantitation all exceeding target specifications and meeting or exceeding that achieved by current ultra-sensitive tests.

Specificity was 100% at all input levels, while LoD was <10ppm for 2,000 variant panels at 20 ng input. Sensitivity was positively correlated with panel size, with potential to trade off cost vs performance for different applications/indications, and was inversely correlated with input mass, with an LoD <40 ppm for 2,000 variant panels at 5 ng input.

Results were replicable and precise across >6 operators, >3 reagent lots, >3 runs, and 2 sites. Consistent results were obtained using low- and mid-throughput sequencing platforms.

Importantly, sequencing requirements were reduced from ~500M read pairs using standard techniques to just 5M, while retaining ultra-sensitive ctDNA detection and negating the need for molecular barcoding.

These results demonstrate the potential of Enspyre as an ultra-sensitive MRD solution, in a format that is much more amenable to adoption in mid- and low-throughput laboratories than existing approaches. Through mutated DNA enrichment, Enspyre enables ctDNA detection at <10ppm with a >98% reduction in NGS requirements, facilitating significant cost reductions and decentralization of MRD testing.

#2594 A deep sampling and single molecule digital counting assay for rare molecule detection.

Danny Overman[1], Cindy Wang[2], Jung won Keum[3], Jesse Soliman[3], Emily Blair[3], Eleen Shum[3], Tricia Zwiefelhofer[2]

[1]Laboratory Corporation of America, Burlington, NC,[2]Laboratory Corporation of America - Sequenom, San Diego, CA,[3]Countable Labs, Palo Alto, CA

Rare molecule detection remains a challenge in liquid biopsy applications. Increasing assay sensitivity requires higher DNA input, yet conventional digital PCR (dPCR) systems are constrained by limited input capacity and partition number, restricting analytical range. We evaluated a next generation PCR platform, Countable PCR, which generates approximately 30 million partitions per 50 µL reaction and supports DNA inputs exceeding 1 µg, enabling “deep sampling” for improved rare variant detection. Using the clinically relevant KIT (*D816V*) mutation associated with systemic mastocytosis (SM) as a model, we analytically validated a multiplexed Countable PCR assay across 15 patient blood and bone-marrow samples at multiple testing sites and compared results with a reference dPCR assay. Standard dPCR achieved a 0.03% mutant allele frequency (MAF) limit of detection only by pooling three wells (78,000 partitions, 100 ng input), as higher inputs caused image saturation and loss of precision. In contrast, Countable PCR demonstrated accurate quantification from 150 to 1,452 ng DNA within a single well, maintaining linearity and low background. Across all samples, MAF values showed near-perfect concordance with the orthogonal method (Pearson coefficient = 0.9997; $p = 1.03 \times 10^{-22}$). Synthetic controls achieved 99.95% variant detection accuracy (5 variant-positive vs. 10,026 wild-type partitions), and contrived samples at 300 ng and 1 µg inputs exhibited 100% concordance across expected variant frequencies. These results demonstrate that Countable PCR enables high-input, single-molecule quantification with exceptional sensitivity and reproducibility, supporting streamlined, cost-efficient workflows for rare variant detection and precision molecular diagnostics in clinical laboratory settings.

#2595 A novel dual-strand whole-genome sequencing (WGS) method for ultra-sensitive molecular residual disease detection (MRD).

Andrew Slatter[1], Jessica Moore[1], Esther Musgrave-Brown[1], Dhamayanthi Pugazhendhi[1], Trevor Ho[1], Alex Calderwood[1], Dale Weekes[1], Seong Won Cha[2], Christopher Edlund[2], Sven Bilke[2], Huihong You[2], Chris Truong[2], **Jeff Tsai**[2], Khai Luong[2], Li Liu[2], Yunjiao Zhu[2], Jeff Fisher[2], Traci Pawlowski[2], James Han[2], Fiona Kaper[2], Cande Rogert[2]

[1]Illumina, Cambridge, United Kingdom,[2]Illumina, San Diego, CA

Whole genome sequencing (WGS) of circulating cell-free DNA (cfDNA) enables ultra-sensitive circulating tumor DNA (ctDNA) detection by leveraging genome-wide mutations. However, the detection sensitivity remains limited by errors. Here we describe the performance of a new, high-Q WGS library prep method, which enables >Q60 cfDNA sequencing, and demonstrate its application in molecular residual disease (MRD) testing. The method enables increased accuracy by sequencing both top and bottom strands of double stranded cfDNA fragments without requiring unique molecular identifiers (UMIs). Briefly, oligonucleotide adaptors are attached to cfDNA samples and are subsequently processed to generate a library structure that contains both top and bottom strands. Samples are appended with barcodes and pooled for sequencing on a standard NovaSeq X™ instrument. Errors originating from DNA damage, library preparation or sequencing are informatically detected and masked, creating duplex consensus reads. A novel q-score prediction algorithm is employed to predict the probability a reported base is an error, as well as substitution-specific error probabilities. Empirical q-score was measured using HG002 cell line DNA. To measure performance in tumor informed MRD application, cfDNA samples extracted from healthy donors were sequenced and analyzed against patient-specific somatic variants derived from tissue WGS using the Illumina Oncology WGS prep. Limit of detection (LoD) was assessed using 5 replicates at each of the 7 target VAF levels from 0-50 parts-per-million (ppm) dilutions of the SeraCare MRD reference material, with analysis by the DRAGEN™ MRD pipeline.Libraries prepared from 10 ng cfDNA delivered ~50x deduplicated duplex consensus coverage with >80% of passed-filter clusters delivering high quality duplex consensus reads. The quality of the resulting base calls was empirically measured at >Q60 accuracy, and certain substitution-specific error rates were measured at >Q70. Healthy plasma was used to establish statistical scores for determining ctDNA presence at different analytical specificity goals. These values were subsequently used to determine the detection in the LoD study. In aggregate, the results showed the method can achieve a LoD95 of 2.5 ppm with analytical specificity of 99.8%. The method presented herein demonstrates the potential of highly sensitive and specific ctDNA detection for MRD testing.

#2596 Ultrasensitive multiplex ddPCR for integrated genomic-epigenomic ctDNA detection in colorectal cancer.

Ya Zhou, Yuwei Ni, Xingyu Yang, Qiancheng You, Jing Su, Yunpeng Zhang, Xiaoling Li, Xinyue Kang, Jiayue Xu, **Zhihong Zhang**, Bingsi Li

Research and Development, Burning Rock Biotech, Shanghai, China

Background: Liquid biopsy is rapidly emerging as a cornerstone of precision oncology, offering sensitive and accurate profiling of tumor-derived information in real-time. Although droplet digital PCR (ddPCR) delivers single-molecule sensitivity, its low-plex design has limited it to interrogating one or a few variants at a time. Here we introduce COMET plus, a 25-plex ddPCR assay that simultaneously detects both genetic and epigenetic changes in a single amplification reaction, enabling highly sensitive detection of circulating tumor DNA (ctDNA) in colorectal cancer (CRC).
Methods: Following analysis of over 500 tumor tissue and more than 1,000 cfDNA specimens, we selected 18 methylation variants that simultaneously display (i) robust tumor-specific hyper-methylation, (ii) negligible signal in healthy donor plasma, and (iii) high recurrence across patients. These loci were co-amplified with somatic mutations and microsatellite instability loci (MSI) markers frequently altered in CRC. The assay runs on a 7- or 6-color ddPCR system (D3200 platform, Pilotgene; QX600^{TM}, Bio-Rad). A classifier was trained and subsequently locked to make sample-level calls of ctDNA positivity or negativity using optimized thresholds for each variant. Limit of detection (LoD) for each analyte was determined by Probit analysis of serially diluted contrived cfDNA and cell-line DNA. Limit of blank (LoB) was established from 10 independent replicates of two healthy donor cfDNA pools.
Results: In 30 ng of contrived cfDNA or cell-line DNA we detected actionable KRAS/BRAF mutations at 0.08% VAF and MSI-H DNA at 0.1% in an MSS background. Individual methylation markers were called to 0.08-0.2%, while the aggregate 18-marker signature reached 0.01% (cell-line) or 0.02% (cfDNA); no false positives were observed across 20 blank replicates.
Conclusions: We developed and validated a high-plex ddPCR assay that sensitively and simultaneously quantifies genetic and epigenetic alterations in colorectal cancer. The multiplexing strategy is compatible with most mainstream ddPCR instruments and readily extendable to other tumor types, offering a simple, streamlined workflow for cancer diagnosis, minimal residual disease (MRD) detection, and therapy selection.

#2597 Baseline cfDNA fragmentomics identifies multiple myeloma patients at risk of early progression.

Dor David Abelman[1], Jenna Eagles[2], Aimee Wong[3], Saumil Shah[4], Jeffrey Bruce[2], Stephanie Pedersen[2], David S. Scott[2], Cecilia Bonolo de Campos[2], Signy Chow[5], Darrell White[6], Irwindeed Sandhu[7], Kevin Song[8], Esteban Braggio[9], Shaji Kunnathu Kumar[10], Alli Murugesan[11], Tony Reiman[12], A. Keith Stewart[2], Suzanne Trudel[1], Trevor J. Pugh[13]

[1]Princess Margaret Cancer Centre and Department of Medical Biophysics, University of Toronto, Toronto, ON, Canada,[2]Princess Margaret Cancer Centre, Toronto, ON, Canada,[3]School of Integrated Health, University of New Brunswick, Saint John, NB, Canada,[4]Department of Biological Sciences, University of New Brunswick, Saint John, NB, Canada,[5]Sunnybrook Health Sciences Centre, Toronto, ON, Canada,[6]Dalhousie University and QEII Health Sciences Centre, Halifax, NS, Canada,[7]Cross Cancer Institute, Edmonton, AB, Canada,[8]Vancouver General Hospital, Vancouver, BC, Canada,[9]Mayo Clinic Arizona, Scottsdale, AZ,[10]Professor of Medicine, Dept. of Hematology, Mayo Clinic, Rochester, MN,[11]Faculty of Medicine, Dalhousie University, and Department of Nursing and Health Sciences, Faculty of Science, Applied Science and Engineering, University of New Brunswick, Saint John, NB, Canada,[12]Saint John Regional Hospital, Saint John, NB, Canada,[13]Princess Margaret Cancer Centre; Department of Medical Biophysics, University of Toronto, and Ontario Institute for Cancer Research, Toronto, ON, Canada

Introduction: Early relapse limits durable remissions in multiple myeloma (MM). Cell-free DNA (cfDNA) fragment patterns capture tumor burden and nucleosome positioning. We tested whether a fragmentomics signature trained at MRD time points stratifies progression-free survival (PFS) when applied to pretreatment plasma.

Methods: We performed 30-40× whole-genome sequencing of plasma cfDNA from 43 newly diagnosed MM patients, with 65 additional MRD timepoint samples from 41 of those patients (post-ASCT n=30; 1-year maintenance n=30; other maintenance n=5) across eight Canadian sites (TFRIM4 and IMMAGINE studies) and one U.S. site (Mayo SPORE). MRD testing used multiparameter flow cytometry for all follow-up samples (n=65) and clonoSEQ in a subset (n=31). Logistic and elastic-net models were trained at MRD timepoints on fragmentomics features (short-fragment burden; a combined model integrating fragment-length distributions with inferred nucleosome positioning at MM-specific chromatin accessibility regions [Ordoñez et al., Genome Res. 2020]). A decision threshold was fixed by the Youden index during training and applied unchanged to diagnosis samples. PFS was analyzed by Kaplan-Meier, log-rank, and Cox models.

Results: After a median follow-up of 49.1 months, 16 of 43 patients (37%) progressed. Using the prespecified locked threshold, patients classified as MRD+ by the proportion-of-short-fragments model had significantly shorter PFS than MRD- patients (HR = 5.12; 95% CI 1.16-22.57; log-rank p = 0.016), with median PFS of 49.2 months for MRD+ cases versus not reached for the MRD- group. Fixed-horizon PFS favored MRD- samples at 24/36/48 months (100/94/87% vs 85/81/53% for MRD+). A combined model integrating weighted fragment lengths with inferred nucleosome positioning also separated outcomes (log-rank p=0.054); the Cox HR was not estimable because no MRD- patients relapsed. At 24, 36, and 48 months, baseline MRD positivity by the short-fragment model identified 100%, 83%, and 86% of patients who relapsed within those intervals (specificity 44%, 43%, and 52%), while the combined model detected all early relapses across the same horizons (specificity 15-21%), indicating consistently high sensitivity but modest specificity for predicting early progression.

Conclusions: A cfDNA fragmentomics signature trained at MRD time points stratified PFS when applied to diagnostic plasma, identifying patients at risk of early relapse. Short-fragment burden was most discriminative, and a combined model with nucleosome positioning recapitulated it with higher sensitivity, albeit lower specificity. These data support cfDNA fragmentomics as a practical liquid-biopsy risk biomarker in MM and suggest higher signals may proxy aggressive disease with greater tumor shedding and chromatin disorganization. Future work will validate findings in larger cohorts and integrate cytogenetic and immune features.

#2598 Analytical validation of an ultra-high sensitivity tumor-informed MRD assay.

Ashley Acevedo, Kelly Colbert, Kyle Trettin, Alexander Ham, Genevieve Gould

Myriad Genetics, Inc., Salt Lake City, UT

Circulating tumor DNA (ctDNA) is a biomarker for molecular residual disease (MRD), i.e., tumor cells that persist during or after cancer treatment. ctDNA can be distinguished from normal cell-free DNA (cfDNA) based on the presence of tumor-specific somatic variants. First-generation tumor-informed MRD assays based on exome sequencing typically interrogate a small number of tumor-specific variants, limiting their sensitivity. We have developed a second-generation, tumor-informed MRD assay using matched formalin fixed paraffin embedded (FFPE) tumor tissue, including core needle biopsies, and normal whole genome sequencing to power expansive variant discovery and selection of panels consisting of up to 1000 targets optimized for assay sensitivity.

Here we validate this assay using more than 100 unique cancer-affected clinical sample sets, more than 30 unique healthy donors and 3 unique sets of matched tumor and normal cell lines. Panels were generated from paired tumor and normal sample sets using as little as 10 ng of DNA, with highly reproducible performance across replicate panel designs. More than 4400 plasma and contrived sample tests were run across a range of assay conditions, including cfDNA input from 7.5 to 40 ng and panel sizes ranging from 500 to 1000 targets. Contrived samples were tested at tumor DNA concentrations ranging from 0.78 to 1,000,000 parts per million (ppm). We found the Limit of Detection with 95% sensitivity (LoD_{95}) to be <5 ppm in units of genome equivalents (comparable to <2.5 ppm in units of variant allele frequency) under typical assay conditions, and that LoD_{95} scales with cfDNA input amount and panel size. We determined the linear range of the assay to be from 1.56 to 1,000,000 ppm, with high quantitative precision down to 18 ppm. Across all tested indications, including breast, renal, colorectal, ovarian, endometrial and lung cancers from stages II-IV, clinical sensitivity is >85% and clinical specificity is >99%, where undetected samples were exclusively in low shedding indications, such as renal and HR+/HER2- breast cancer. Clinical sensitivity is 100% with clinical specificity >99% in colorectal, ovarian, endometrial and lung cancers.

In conclusion, we have developed and validated a quantitative and ultra-high sensitivity tumor-informed MRD assay suitable for challenging, low shedding applications such as breast and renal cancer or post-treatment monitoring.

#2599 Methylation-based circulating tumor DNA predicts recurrence in definitively treated non-small cell lung cancer (NSCLC).

Jisoo Lee, Eun Ji Song, Youngjun Lee, Jongsu Kim, Yuchan Kim, Anthony Wong, Sanghwa Kim, Liam I. Chung, Young Kwang Chae

Northwestern University Feinberg School of Medicine, Chicago, IL

Background: Circulating tumor DNA (ctDNA) is being utilized in detecting molecular residual disease (MRD) and predicting recurrence of non-small cell lung cancer (NSCLC). However, real-world implementation is yet to be reported.
Methods: We retrospectively analyzed 240 longitudinal plasma samples from a real-world cohort of 78 NSCLC patients treated with curative intent, including select stage IV patients who underwent bilateral lung transplantation. MRD was assessed using a tissue-naïve, methylation-based assay (Guardant Reveal), and plasma-based genomic profiling was performed (Guardant360) at the time of MRD positivity. Recurrence-free survival (RFS) and overall survival (OS) were analyzed based on three MRD timepoints post-treatment: within 3 months (Subgroup A, n=42), within 6 months (Subgroup B, n=55), and at any time (Subgroup C, n=78). Recurrence date was determined by biopsy-proven recurrence date when available, otherwise, radiographic recurrence date was used.
Results: 78 patients (median age at diagnosis 65; 33 stage I, 19 stage II, 19 stage III, 7 stage IV) received definitive treatment (surgery alone, n=37; surgery with perioperative therapy, n=33; definitive radiation, n=8). 56 were adenocarcinoma and 21 were squamous cell carcinoma, and 1 was adenosquamous. Targetable alterations (EGFR, ALK, etc.) were found in 31 patients. The median follow-up duration was 22.3 months (range: 2-80.6 months). Among 23 MRD(+) cases, 10 recurrences and 3 deaths occurred, whereas 55 MRD(-) cases showed 5 recurrences and no deaths. MRD(+) was associated with worse OS in all subgroups ($p<0.01$). It was also associated with inferior RFS in Subgroup B (HR = 4.35, 95% CI 1.30-14.50, $p = 0.017$) and Subgroup C (HR = 5.20, 95% CI 1.76-15.30, $p<0.01$), with a similar trend in Subgroup A ($p=0.16$). Among 11 patients who recurred and ever showed ctDNA positivity, ctDNA preceded radiographic relapse in 10 cases with a mean lead time of 5.4 months (range 2 days-20.3 months). In the subset of patients with ≥1 year follow-up from definitive treatment (n=66), MRD(+) showed a sensitivity of 63.6% (7/11) and specificity of 78.1% (43/55) in predicting recurrence. In 13 MRD(+) patients with paired plasma and tissue NGS, 3 (23%) exhibited shared mutations between baseline tissue NGS and post-treatment plasma NGS (matched group). The unmatched group showed a median number of 9 (range 1-14) genomic variations; however, none were biologically relevant.
Conclusion: This is the first real-world analysis evaluating survival outcomes using a methylation-based ctDNA assay in definitively treated NSCLC. MRD(+) can be useful in predicting recurrence and was associated with worse outcomes. Integration of plasma-based NGS may reflect molecular heterogeneity and potential subclonal evolution, supporting its potential utility for personalized post-treatment surveillance.

#2600 Investigating treatment response and resistance in non-small cell lung cancer patients through epigenetic profiling of plasma nucleosomes.

Christoffer T. Maansson[1], Simone Stensgaard[1], Emma Pedersen[1], Anders Lade Nielsen[2], Peter Meldgaard[3], Boe Sandahl Sorensen[1]

[1]Clinical Biochemistry, Aarhus University Hospital, Aarhus N, Denmark,[2]Department of Biomedicine, Aarhus University, Aarhus C, Denmark,[3]Department of Oncology, Aarhus University Hospital, Aarhus N, Denmark

The detection of circulating tumor DNA (ctDNA) through the identification of somatic mutations has shown promising results for monitoring treatment response in cancer patients. However, mutation-based approaches are limited by factors such as clonal hematopoiesis, low sensitivity, and the inability to detect epigenetic tumor signals. Complementary approaches based on epigenetic profiling of cell-free DNA (cfDNA) in liquid biopsies have been developed to infer the gene expression profile in the cells of cfDNA origin. We investigated the application of cell-free chromatin immunoprecipitation (cfChIP) targeting H3K4me3 and H3K36me3 histone modifications of circulating nucleosomes in non-small cell lung cancer (NSCLC) patients treated with immunotherapy or targeted therapies.

ctDNA dynamics were quantified using targeted sequencing of cfDNA to identify molecular responders to treatment based on ctDNA clearance. We performed cfChIP on healthy individuals and cancer patients followed by ddPCR or whole-genome sequencing at baseline, a few weeks after treatment initiation and at progression.

High *FGD2* expression and low *CDH3* expression at baseline were associated with a durable response to immunotherapy. Genes, in which the cfChIP enrichment correlated with ctDNA burden included genes, such as *PLCE1* and *VASH2*, involved in developmental processes. Longitudinal monitoring of *MET* gene activity with H3K36me3 cfChIP ddPCR distinguished patients with crizotinib response from non-responders. cfChIP at progression indicated novel resistance mechanisms to targeted therapy through upregulation of genes such as *FOXG1* and *MT3*, involved in neural development.

In conclusion, cfChIP-seq of cfDNA present in cancer patients' plasma has potential to provide valuable information on tumor specific transcriptional dynamics during treatment in NSCLC. Harnessing this information could enable earlier detection of resistance and guide treatment switching.

#2601 Biomarker tail genes in blood plasma cell-free RNA enable accurate detection of prostate cancer.

Annelien Morlion[1], Philippe Decruyenaere[2], Kathleen Schoofs[1], Jasper Anckaert[1], Nickolas J. Ramirez[1], Justine Nuytens[1], Eveline Vanden Eynde[1], Kimberly Verniers[1], Celine Everaert[1], Guy Brusselle[2], Steven Callens[2], Filomeen Haerynck[2], Dimitri Hemelsoet[2], Eric Hoste[2], Jo Lambert[2], Nicolaas Lumen[2], Fritz Offner[2], Koen Paemeleire[2], Vanessa Smith[2], Lies Van den Eynde[2], Jo Van Dorpe[2], Amber Vanhaecke[3], Hans Van Vlierberghe[2], An Mariman[2], Olivier Thas[4], Jo Vandesompele[1], **Pieter Mestdagh**[1]

[1]Ghent University, Ghent, Belgium,[2]Ghent University; Ghent University Hospital, Ghent, Belgium,[3]Ghent University Hospital, Ghent, Belgium,[4]Hasselt University, Hasselt, Belgium

The purpose of this study was to assess whether transcripts exhibiting strongly deviating abundance in plasma mRNA profiles can reliably differentiate prostate cancer from non-cancer states. To do so, we focused on biomarker tail genes (BTG), defined as protein-coding genes whose cell-free transcript abundance in an individual sample deviates by at least three standard deviations from a healthy control reference distribution. We applied the BTG identification and classification workflow to blood plasma samples from individuals with newly diagnosed prostate cancer (n = 132; 62 early-stage, 70 late-stage) and healthy donors (n = 48). Classification thresholds were established using a train-test cross validation approach (70%), and performance was evaluated in held-out validation samples (30%) and in a separate non-malignant cohort including healthy donors (n=37) and patients with non-malignant conditions (n=88).

Across training and validation analyses, a consensus set of 247 prostate cancer BTG enabled discrimination between prostate cancer samples and healthy controls, with sensitivity and specificity reaching 100% in the validation cohort of male donors. Of note, the number of BTG per plasma sample was not associated with disease stage, and classification remained highly accurate in age-matched subsets, indicating limited influence of age on results. When applied to a cohort of individuals with diverse non-malignant conditions, the established BTG threshold yielded 94.4% specificity, and none of patients with benign prostatic hyperplasia were misclassified (n=5).

To explore redundancy within the BTG set, we evaluated both cluster-derived subsets and algorithmically selected minimal panels. Multiple small subsets, including a ten-gene panel identified by a greedy selection strategy, achieved perfect classification within the validation cohort, demonstrating that strong discriminatory power is retained even when BTG sets are substantially reduced.

In conclusion, blood plasma BTG constitute a highly accurate signature for prostate cancer detection, and the ability of small BTG subsets to reproduce full-set performance highlights opportunities for targeted assays. Further evaluation in broader populations and across cancer stages will refine the potential of BTG-based approaches for early detection and monitoring.

(The last two authors contributed equally to this work)

#2602 Impact of targeted therapies in cancers classified as TMB-high by liquid biopsy: Insights from the Gustave Roussy molecular tumor board.

Adrien Mouren[1], Berenger POIRIER[2], Antoine Italiano[2], Matthieu Roulleaux Dugage[2], Yohann Loriot[3], Antoine Hollebecque[4], Anas Gazzah[2], Barbara Pistilli[2], Christophe Massard[4], Cyril ROUSSEL-SIMONIN[2]

[1]Drug Development Department (DITEP), Gustave Roussy, Villejuif, France,[2]Gustave Roussy, Villejuif, France,[3]INSERM U981 (Gustave Roussy), Villejuif, France,[4]Institute Gustave Roussy, Villejuif, France

Background:
Tumor mutational burden (TMB) has emerged as a biomarker for immunotherapy response, but its predictive value for targeted therapies remains uncertain. In genomically unstable tumors, high TMB may reflect passenger rather than driver events, potentially limiting the efficacy of targeted agents.
Methods:
We retrospectively analyzed adult patients with advanced solid tumors who underwent plasma-based comprehensive genomic profiling (STING master protocol, Foundation Medicine) and had a TMB ≥ 16 mut/Mb. All cases were reviewed by the Gustave Roussy Molecular Tumor Board for orientation toward early-phase trials, phase II-III studies, or MTB-validated off-label targeted therapies. Alterations were classified as driver or non-driver based on integrated molecular and clinical evidence, supported by reference databases such as IntOGen and DriverDB.
Results:
Fifty-six patients were included (mean age 61.6 y; 71% male). The most frequent tumor types were lung (41%), colorectal (11%), and bladder (11%). Brain (20%), bone (38%), and liver (5%) metastases were common; 72% had ≥ 2 metastatic sites. Median plasma TMB was 20 mut/Mb (range, 16-1,450). Patients had received a median 3 prior lines (range 1-6). The most frequent alterations involved *KRAS* (21%), *MET* (11%), and *ERBB2* (11%). Targeted therapies included small-molecule inhibitors (41%), TKIs (27%), ADCs (14%), bispecific antibodies (5%), and PROTACs (5%). Overall, 13 patients (23%) achieved partial response (PR) and 21 (38%) stable disease (SD), resulting in an overall response rate (ORR) of 23% and a disease control rate (DCR) of 61%. Among driver cases (n=43), 12 PR and 17 SD were observed vs 1 PR and 4 SD in non-driver cases (n=13). Median PFS was 3.7 months (95% CI 2.8-4.8). The prior-line PFS was 5.6 months (95% CI 4.0-11.0). A PFS ratio >1/3, indicating clinical benefit compared with the previous treatment line, was achieved in 63.3% of evaluable patients (31/49). Presence of a driver alteration was associated with improved PFS (HR 0.43; 95% CI, 0.22-0.82; p = 0.011). No correlation was found between TMB and PFS (Spearman ρ = 0.10; p = 0.45), and no difference was seen across TMB groups (<20, 20-50, ≥50 mut/Mb).
Conclusions:
Only patients with bona fide driver alterations derived benefit from targeted therapy, irrespective of TMB level. High TMB reflects genomic instability rather than therapeutic sensitivity, underscoring the importance of molecular curation to guide precision oncology decisions. Comparative analyses with TMB-low cases are ongoing to refine the predictive versus confounding role of TMB in targeted therapy response.

#2603 Comparing methylation signatures across 15 cancer types and 7 subtypes.

Harry Mickalide, Joel Rodriguez-Medina, Fernando L. Mendez, Murat Can Cobanoglu, Scott Dashner, Yuqian Jiang, Kevin Chan, Joshua N. Burton, Trupti Kawli, Johannes G. Reiter, Matthew Rabinowitz, Alexey Aleshin

Natera, Inc., Austin, TX

Differentially methylated regions (DMRs), the regions that have a different methylation pattern between tumor and non-tumor genomes, can serve as accurate biomarkers for cancer detection. Here we compare DMRs across 15 cancer types and 7 cancer subtypes. In this retrospective study, tissue samples from 832 patients with 15 different cancer types, including gastrointestinal (GI), genitourinary (GU), gynecological, breast, lung, melanoma, and head & neck cancers, were analyzed to measure methylation levels across genomic regions. Advanced adenoma (AA), an important precursor to colorectal cancer, was also included as a comparator among GI indications. Sets of DMRs were identified in each cancer type based on comparison with methylation levels of healthy samples. DMR signatures were compared across cancer types and subtypes by calculating pairwise overlaps. Across all 15 cancer types, the overlap of shared DMRs ranged from 13% (melanoma vs gastric cancer) to 61% (esophageal cancer vs gastric cancer). Notably, we found strong overlap among GI indications, a group including esophageal, gastric, small intestine, liver, pancreatic, and colorectal cancer, as well as AA. Compared to non-GI cancers, the pairwise overlap of DMRs in GI indications was, on average, 17% higher. Moreover, 65% of DMRs were shared between AA and colorectal cancer, which represented the highest overlap of shared DMRs in any pairwise comparison in this analysis. Among breast and lung cancer samples, we compared subtypes and found strong, but variable, overlap. For instance, among four major subtypes of breast cancer, we found overlaps ranging 53%-68% between subtypes. Among three lung cancer subtypes, overlaps ranged from 34% to 44%. In this study, we demonstrate that each cancer's DMR signature is ultimately unique and can be used as a biomarker for cancer detection even though there is some overlap between DMR signatures of different cancer types. A deeper study of the shared and unique DMR signatures may provide insights into underlying biological mechanisms of cancer development. For example, the high overlap of DMR signatures among GI cancers suggests some shared mechanisms; similarly, while DMR signatures are expected to be similar between subtypes of a cancer, investigation into the patterns unique to each subtype may help resolve observed differences in clinical prognosis and treatment response.

#2604 Postoperative lymphatic exudate as a proximal liquid biopsy source in muscle-invasive bladder cancer.

Zhuosheng Gu[1], Zachary Costliow[1], Seka Lazare[1], Abbey Crittenden[1], Adam Harmon[1], Megan Rivera[1], Ashley Tellis[1], Samuel Espinoza[1], Adam Benson[1], Marra Francis[2], Ankeet Shah[3], Michael R. Abern[4], Gautum Agarwal[5], Wendy Winckler[1]

[1]Droplet Biosciences, Cambridge, MA,[2]Marra S. Francis Consulting, San Antonio, TX,[3]Division of Urology, Duke University Medical Center, Durham, NC,[4]Department of Urology, Duke University School of Medicine, Durham, NC,[5]Mercy Hospital, St. Louis, MO

Introduction: Patients with muscle-invasive bladder cancer (MIBC) experience recurrence rates of up to 50% following radical cystectomy [1,2]. Current monitoring involves imaging scans or peripheral blood ctDNA [3,4], however, there is unmet need for a sensitive molecular test that can identify recurrence early enough to more precisely tailor adjuvant therapy. Our team has pioneered the use of lymphatic exudate collected via surgical drains (“lymph”) as a proximal liquid biopsy fluid. We have previously shown that lymph collected 24 hours after surgery identified molecular residual disease (MRD) in head and neck squamous cell carcinoma (HNSCC) in the immediate post-surgical window [5,6]. Here, we evaluate the feasibility of postoperative lymph to enable sensitive detection of MRD and characterize the dynamics of circulating tumor DNA (ctDNA) in lymph from MIBC patients for 96 hours after surgery.
Methods: Lymph, tumor and whole blood were prospectively collected from 8 MIBC patients undergoing radical cystectomy: 4 patients with disease recurrence (REC) and 4 with no evidence of disease (NED) with >1 year of follow-up. Tumor and peripheral blood were collected at surgery; lymph at 24 ± 6 hours after surgical close. For the serial cohort (n=10), lymph was collected every 8 ± 4 hours for 96 hours after surgery. Next-generation sequencing libraries were prepared from genomic and cfDNA using a 500 gene pan-cancer hybrid capture panel; deduplicated coverage was >250X for tumor and blood and >2500X for lymph. Somatic mutations were identified in tumor with matched blood. Tumor-specific variants were directly genotyped in lymph using a custom bioinformatic pipeline. Mutation calls were filtered by a base-specific error model to eliminate artifacts.
Results: At 24 hours post-surgery, lymph ctDNA was detected in 4 out of 8 patients (50%). Significantly higher variant allele fraction (VAF) was observed in REC lymph than NED ($p = 0.00038$). We classified patients as positive (>1) or negative (<1) for detected mutations and performed a KM survival analysis (sensitivity = 75%, specificity = 75%, Hazard Ratio (HR) = 4.3, $p = 0.17$). To understand the impact of collection timing, serial lymph samples were analyzed. There were no differences across timepoints for either mutation count or mean VAF (repeated measures ANOVA $p = 0.33$ and 0.91, respectively).
Conclusion: We demonstrate the feasibility of analyzing ctDNA in post-surgical lymph in MIBC. ctDNA levels were stable across the first 96 hours after surgery, a pattern consistent with ongoing shed from residual tumor as opposed to decay of DNA from resected tumor debris. While non-significant in this small cohort, the HR and sensitivity in this feasibility pilot are consistent with published larger studies in HNSCC. If these results generalize, postoperative lymph MRD testing has the potential to provide more personalized adjuvant treatment decision-making in MIBC patients.

#2605 Concordance evaluation of plasma whole-exome sequencing (pWES) and tissue whole-exome sequencing (tWES): A pilot study in non-small cell lung cancer (NSCLC).

Bingjie Dong[1], Zhijiao Wang[1], Carol E. Pena[2], Xiaoqiao Liu[1], Gefei Zeng[1]

[1]MSD China, Beijing, China,[2]Merck & Co., Inc., Rahway, NJ

Background: Circulating tumor DNA (ctDNA) analysis by pWES offers the possibility for comprehensive characterization of tumor-derived alterations and longitudinal monitoring of tumor molecular evolution in a minimally invasive manner. Here, we conducted a pilot study to evaluate the analytical performance of a pWES assay with boosted content compared with tWES in NSCLC.
Methods: Cell-free DNA isolated from commercially-acquired plasma samples of patients with stage I-IV NSCLC were analyzed using the PredicineWES+ assay (WES plus a boosted 600-gene panel; Huidu Shanghai Medical Sciences Ltd, China). The copy number burden score (cnbScore; a quantitative measure of genome-wide copy number abnormality as a proxy for tumor fraction [TF]) was derived from low-pass plasma whole-genome sequencing (pWGS). pWES TF was based on the maximum mutation allele fraction of nonsynonymous somatic mutations (single nucleotide variants [SNVs] + indels). Jaccard Index (JI), Spearman correlation (ρ), and Wilcoxon rank-sum test were applied to quantify concordance and differences across measures between pWES and tWES.
Results: 39/40 samples were evaluated by low-pass pWGS (stage II-III, 80%). A high TF (cnbScore ≥5.6) was associated with late-stage tumors and squamous cell carcinoma (SCC) histology. Thirty samples (25 highest and 5 lowest cnbScore samples) were selected for pWES. pWES TF was significantly correlated with pWGS cnbScore ($\rho = 0.64$; $P < 0.001$). Of 30 samples evaluated by pWES, 14 samples were ctDNA-positive (cnbScore ≥5.6) and were included in concordance analyses with tWES. Adenocarcinoma- and SCC-specific driver mutations were highly concordant between pWES and matched tWES (JI = 0.72). NSCLC-dominant smoking-associated mutational signature was identifiable by pWES and was correlated with tWES ($\rho = 0.58$). Considerable concordance of mutation calling was observed between pWES and tWES (median JI = 0.47). Blood tumor mutational burden (TMB) was highly correlated with tissue TMB ($\rho = 0.69$). Compared with nonboosted exome region, boosted region with higher sequencing depth had numerically better TMB correlation ($\rho = 0.81$ vs 0.64) and SNV concordance (median JI = 0.80 vs 0.44) between pWES and tWES. Disconcordant copy number variant results were observed between pWES and tWES, possibly due to low ctDNA TF and copy number gain in tissue.
Conclusions: ctDNA tumor burden metrics by pWES correlated with low-pass pWGS and showed association with tumor stage and histologic subtype of NSCLC. pWES feasibly characterized TMB and SNV in NSCLC especially in ctDNA-positive samples and in the boosted 600-gene WES panel, indicating potential utility for longitudinal tumor profiling and monitoring during treatment.

#2606 A liquid biopsy assay of estrogen receptor activity predicts response to giredestrant in ER+/HER2– advanced breast cancer.

Ann E. Collier[1], Jon Beagan[2], Travis Clark[2], Kristian Cibulskis[2], Corrie Painter[2], Mary McGillicuddy[2], Aparna Gorthi[2], Khoi Nguyen[2], James Sullivan[1], Richard Schwab[1], Jing Zhu[1], Pablo Perez-Moreno[1], Tharu M. Fernando[1], Matthew Eaton[2], Carl J. Barrett[2]

[1]Genentech, Inc., South San Francisco, CA,[2]Precede Biosciences, Boston, MA

Background: Endocrine resistance limits benefit durability in ER+/HER2– advanced breast cancer (aBC), particularly after CDK4/6 inhibition. Prior studies have shown that tumor RNA-based estrogen receptor (ER) activity predicts response to the oral SERD giredestrant and serves as a pharmacodynamic (PD) biomarker of ER pathway suppression. However, tumor RNA profiling requires serial biopsies which are often challenging in aBC. The Precede ER Dependence Index (PERDI) quantifies ER-driven cis-regulatory enhancer activity from circulating chromatin, enabling noninvasive monitoring of ER pathway dependence and treatment response.
Methods: 87 patients (pts) with ER+/HER2– aBC received second or third line giredestrant, alone or in combination. One milliliter of plasma from 87 pre-treatment (tx) and 9 on-tx samples was profiled using Precede's comprehensive epigenomic liquid biopsy assay. PERDI scores were evaluable for 80 pre-tx and 8 on-tx samples. Baseline *ESR1* mutation (m) status was determined using the FoundationOne®Liquid CDx assay. PERDI concordance was assessed against tissue ER activity from matched RNA-seq. Plasma-based gene expression was inferred using Precede's algorithms that integrate enhancer, promoter and DNA methylation features.
Results: Plasma PERDI strongly correlated with tumor tissue ER activity in pts without detectable *ESR1*m and effectively discriminated *ESR1*m status. Plasma-derived predictions of ER signaling-related genes were concordant with tumor RNA-seq results, with identified genes offering biological insights into clinical response. At baseline, PERDI distinguished RECIST 1.1-evaluated responders well compared to tumor ER activity or ctDNA level. Similar to tumor ER activity, a median split of PERDI demonstrated strong predictive power (HR=0.43; CI: 0.20-0.93), with median PFS of 11.4 months in the PERDI-high group and 2.0 months in the PERDI-low group. The effect size was further enhanced when comparing the top versus bottom PERDI tertiles (HR=0.19; CI: 0.07-0.52). PERDI complemented *ESR1*m status and ctDNA levels in predicting response, identifying rapid progressors with *ESR1*m as well as durable responders despite high ctDNA or absent *ESR1*m. PERDI declined on-tx in all partial responders (3/3), suggesting pathway-specific modulation beyond ctDNA effects.
Conclusions: PERDI quantifies plasma-based ER activity and predicts giredestrant benefit, particularly when integrated with *ESR1* genotype or ctDNA tumor fraction. PERDI also showed early evidence of PD change directly from plasma, mitigating the need for serial tumor biopsies. cfDNA-based gene expression modeling enables noninvasive assessment of ER dependence and response-associated transcriptional programs, offering a scalable framework for monitoring endocrine response and adaptation in ER+/HER2– aBC.

: Molecular Imaging, Radiomics, and Theranostics
Poster Session

#2610 Development and clinical evaluation of ^{64}Cu-RAX301: A next-generation PSMA PET tracer for enhanced detection of metastatic prostate cancer.

Fei Chen[1], Min Hong[2], Xupeng Hu[2], Yang Cao[2], Jie Li[1], Zhao Li[1], Shuanglong Liu[2], **Guangzhou Han**[2], Suping Li[1], Gang Chen[2]

[1]Department of Nuclear Medicine, Affiliated Hospital of North Sichuan Medical College, North Sichuan Medical College, Nanchong, China,[2]RadAlliance Therapeutics Inc., San Diego, CA

Prostate-specific membrane antigen (PSMA) PET imaging is widely used for diagnosing and staging prostate cancer, yet the currently approved ^{68}Ga- and ^{18}F-labeled tracers are limited by short half-lives and high urinary excretion, which can obscure small pelvic lesions. To overcome these challenges, ^{64}Cu-RAX301 was developed as a high-affinity PSMA PET tracer designed for improved biochemical stability and extended imaging flexibility. The RAX301 precursor and its ^{nat}Cu-RAX301 analog were synthesized with high purity, and radiolabeling with ^{64}Cu was optimized to achieve high molar activity (≥2000 mCi/μmol) and radiochemical purity (>95%), and remaining stable for over 48 hours post-formulation. Surface plasmon resonance revealed sub-picomolar binding affinity (Kd < 1 pM) for both the precursor and ^{nat}Cu-RAX301, markedly stronger than PSMA-617 (22 pM). Consistent with this, cell-based assays showed two-fold higher affinity, 1.5-fold greater uptake, and four-fold higher internalization compared with ^{64}Cu-PSMA-617 (≈80% vs. ≈20%). In LNCaP xenograft mice, ^{64}Cu-RAX301 demonstrated intense and persistent tumor uptake, with tumor-to-muscle ratios exceeding one hundred at 4 hours post-injection. PET imaging in *Macaca fascicularis* revealed primarily renal clearance with minimal uptake in other organs. In a first-in-human study of ten patients with metastatic castration-resistant prostate cancer (mCRPC), sequential PET/CT scans were performed first with ^{68}Ga-PSMA-11 (5 mCi; imaging at 1 hour post-injection) and then with ^{64}Cu-RAX301 (5 mCi; imaging at 4 and 24 hours post-injection), separated by 1-7 days. ^{64}Cu-RAX301 detected all lesions identified by ^{68}Ga-PSMA-11 while providing higher lesion uptake and superior tumor-to-background contrast. Notably, ^{64}Cu-RAX301 revealed numerous additional small lesions at various sites, including pelvic lymph node metastases that were frequently missed by ^{68}Ga-PSMA-11 due to early bladder activity. The tracer exhibited an excellent safety profile with no significant adverse events. Collectively, these preclinical and early clinical findings demonstrate that ^{64}Cu-RAX301 possesses ultra-high PSMA affinity, favorable pharmacokinetics, and enhanced lesion visualization compared with ^{68}Ga-PSMA-11, supporting its potential as a next-generation PSMA PET imaging agent with improved sensitivity and diagnostic performance in metastatic prostate cancer. Ongoing clinical studies aim to further define its diagnostic impact and broader clinical utility.

#2611 Prospective evaluation of 68Ga-PSMA PET imaging in advanced hepatocellular carcinoma patients undergoing first line immunotherapy.

Nguyen H. Tran[1], Jacob Hirdler[1], Ajith Antony[2], Jacob Teske[1], Sudhakar K. Venkatesh[1], Amit Mahipal[3], Michael S. Torbenson[1], Scott M. Thompson[1], Thor R. Halfdanarson[1], Zhaohui Jin[1], Lionel Aurelien Kankeu Fonkoua[1], Leslie A. Washburn[1], Alexander Revzin[1], Haidong Dong[1], Robert R. Mcwilliams[1], Aminah Jatoi[1], Hani M. Babiker[4], Mitesh J. Borad[5], Tanios Bekaii-Saab[5], Gregory J. Gores[1], Lewis R. Roberts[1], Geoffrey B. Johnson[1], Ajit H. Goenka[1]

[1]Mayo Clinic, Rochester, MN,[2]MD Anderson, Houston, TX,[3]University Hospital, Cleveland, OH,[4]Mayo Clinic Florida, Jacksonville, FL,[5]Mayo Clinic Arizona, Scottsdale, AZ

Prostate-specific membrane antigen (PSMA) is highly expressed in tumor-associated neovasculature in hepatocellular carcinoma (HCC), highlighting its promise as a theranostic target. This prospective study aimed to evaluate the utility of novel biomarkers derived from PSMA positron emission tomography computed tomography (PET/CT) to assess treatment response in advanced HCC patients (pts) receiving first line immune checkpoint inhibitors (ICI).

Methods: This study (NCT05176223) enrolled unresectable, advanced HCC pts eligible for first-line ICI (atezolizumab/bevacizumab [A/B] or durvalumab/tremelimumab [D/T]) with measurable disease according to RECIST criteria. Primary endpoints: progression-free survival (PFS) per RECIST 1.1 and mRECIST; overall survival (OS); and best overall response. The survival distribution was estimated using the Kaplan-Meier method. Observed agreement is defined as the proportion of pts whose responses, as classified by PET/CT or CT, were concordant. Weighted kappa and Cohen's kappa were used to quantify the strength of agreement between PET/CT and CT. Pts completed up to five 68Ga-PSMA PET/CT scans and blood collections.

Results: Twenty-six pts were enrolled (25 evaluable) between Oct 2022 and Nov 2024. Median follow up was 22.1 months (m) (Q1, Q3: 14.5-23.7). Median age 68 yrs, 72% male, 88% White, 68% Child-Pugh [CP] A, 32% CP B, 32% Barcelona Clinic Liver Cancer [BCLC] stage B, 68% BCLC stage C, 36% with microvascular invasion; 56% received A/B and 40% received D/T treatment. PSMA was positive in 96% of pts at baseline with median SUVmax 14.3 (range 5.1-40.5) and median background liver SUVmax 3.9 (range 2.1-6.8). Median (95%CI) PFS was 5.6 m (4.6-12.5) by both RECIST and mRECIST. Median (95%CI) OS was 18.6 m (7.2-not estimable), with 56% deceased. The observed agreement between PET/CT adapted PERCIST criteria compared to RECIST and mRECIST in determining the best response was 46% and 50% and weighted kappa of 0.63 (95% CI: 0.37-0.90) and 0.66 (0.41-0.92), respectively. Observed agreement between PERCIST compared to RECIST and mRECIST for responders' assessment was 67% and 71% with Cohen's kappa of 0.36 (0.03-0.68) and 0.43 (0.11-0.76), respectively.

Conclusion: In this cohort, PSMA PET/CT avidity was observed in all but one pt with advanced HCC, each demonstrating moderate to high SUVmax values. Median OS and PFS were consistent with outcomes reported in clinical trials. Response assessment using 68Ga-PSMA PET/CT according to PERCIST criteria showed good concordance with both RECIST and mRECIST standards. Analysis of immune biomarkers is ongoing.

#2612 Development and preclinical validation of magnetomotive embolization for enhanced targeting of hepatocellular carcinoma.

Ron C. Gaba[1], **Lobna Elkhadragy**[2], Michael E. Sabo[3], David C. Greenspan[4], Francis M. Creighton[5]

[1]Department of Radiology, University of Illinois at Chicago, Chicago, IL,[2]University of Illinois at Chicago, Chicago, IL,[3]UNandUP LLC, Saint Louis, MO,[4]UN&UP, LLC., Saint Louis, MO,[5]UNandUP, LLC, Saint Louis, MO

Background: Hepatocellular carcinoma (HCC) is the most common type of primary liver cancer and remains a leading cause of cancer mortality worldwide. Catheter-directed transarterial embolization (with or without chemotherapy) is the standard treatment for intermediate-stage HCC, but its survival benefit remains modest, reflecting limitations such as incomplete tumor embolization. To address these limitations, we aimed to develop an embolization approach that improves intratumoral bead localization and tumor embolization through biocompatible magnetic embolization beads and magnetic field guidance.
Methods: A dual-cylinder NdFeB magnet system was engineered to generate focused magnetic fields up to 25 mT at 7.5 cm from the magnet surface, creating a stable magnetic trap. Polycaprolactone-based magnetic embolization beads (40-60 μm) incorporating ~30 nm Fe3O4 iron oxide nanoparticles were synthesized using emulsion polymerization and characterized for morphology, uniformity, and magnetization. Magnet-guided bead delivery was assessed in 3D-printed vascular tumor phantoms and validated in vivo using the rabbit VX2 liver tumor model. Tumor-bearing rabbits (n=12) underwent transarterial embolization and were randomized into magnet-guided (5 Hz alternating rotation, 15 minutes) or control groups (n=6 each).
Results: Microscopic analysis confirmed uniform spherical bead morphology with a narrow size distribution, while SQUID magnetometry demonstrated ferrimagnetic behavior of Fe3O4 nanoparticle cores (magnetization 63.6 emu/g, coercivity 20 Oe at 800 kA/m), confirming strong magnetic responsiveness, and supporting MR-safety. Powder X-ray diffractometry confirmed Fe3O4 with no anomalous peaks suggesting the presence of undesirable iron oxide species. In tumor phantoms, the magnet system successfully concentrated magnetic beads within targeted regions at preclinical relevant distances, achieving reproducible spatial control and contrasting with heterogeneous dispersion in controls. In vivo, transarterial delivery was technically feasible and well tolerated in all tumor-bearing rabbits with no acute complications. Histopathologic analysis demonstrated concentration of the magnetic beads in tumor vasculature in magnet-assisted animals. No device-related toxicity was observed.
Conclusion: This study establishes proof-of-concept for magnetomotive embolization as a novel and feasible locoregional therapy for HCC. The findings demonstrate technical feasibility, procedural safety, and effective intratumoral bead localization in both phantom and preclinical animal models. Building on these results, future work will focus on integrating robotic magnetic field control for dynamic targeting and performing quantitative efficacy and safety studies in large-animal models to advance this technology toward clinical translation.

#2613 Multi-omic characterization of imaging invisible prostate tumors reveals microenvironmental drivers of PET visibility.

Jiyoun Seo[1], Raag Agrawal[2], Pranav Movva[1], Camille Motchoffo Simo[1], Paul C. Boutros[3]

[1]Cedars-Sinai Medical Center, Los Angeles, CA,[2]University of California, Los Angeles, Los Angeles, CA,[3]Sanford Burnham Prebys, La Jolla, CA

Background: Up to 20% of aggressive localized prostate tumors are invisible on PSMA PET or MRI, limiting diagnostic accuracy and treatment selection. As both imaging modalities are routinely used in newly diagnosed patients, defining the molecular basis of imaging visibility is critical for imaging-driven precision medicine. Despite prior evidence implicating stromal and metabolic pathways, the biology of imaging visibility has not been resolved using directly linked multi-omic data. To address this, we analyzed prostate tumors with matched imaging and multi-omic profiles to define molecular programs underlying PET and MRI visibility.
Methods: A total 71 grade group 2-3 prostate tumors were obtained from 59 patients who underwent paired PSMA PET and MRI before prostatectomy. Macrodissected tumor regions underwent bulk RNA sequencing, targeted DNA sequencing, and proteomics. Associations with PET SUVmax and MRI visibility (PIRADS≥4) were tested using multivariable models adjusting for clinico-pathologic features (FDR>0.05). Gene set enrichment was performed on ranked test statistics using preranked GSEA with MSigDB Hallmark, KEGG, and Reactome annotations. Concordant molecular features were cross-referenced across DNA and protein datasets to identify pathways consistently associated with imaging visibility.
Results: MRI-invisible tumors showed downregulation of proliferative and metabolic pathways, including DNA repair and glycolysis, consistent with a quiescent phenotype. PET visibility was associated with transcriptionally and metabolically active states. Furthermore, integrative RNA, DNA, and proteomic analyses converged on extracellular matrix remodeling and immune-regulatory processes as major correlates of PSMA PET signal intensity, indicating that stromal and immune architecture shape imaging detectability. Surfaceome profiling further highlighted cell-surface proteins involved in matrix and immune interactions as candidate alternative biomarkers for PET imaging in PSMA low tumors.
Conclusions: These data suggest PSMA PET visibility reflects biologically active tumor states characterized by DNA damage response and extracellular matrix remodeling, while MRI invisibility corresponds to a more quiescent and metabolically repressed phenotype. Integrated molecular and surfaceome analyses indicate that stromal and immune alterations contribute to PSMA uptake and imaging detectability. Together, these findings support imaging visibility as a biologically driven marker with potential to refine risk assessment and guide precision management in prostate cancer.

#2614 Advancing pancreatic cancer theragnostic through claudin-4-selective radiolabeled peptides: Design, optimization, and preclinical validation.

Marian N. Aziz[1], Nisi Zhang[1], Mallesh Pandrala[2], Jongmin An[3], Yutong Guo[2], Marina Raie[2], SPENCER TUMBALE[2], Basit Jan[2], Katherine W. Ferrara[4]

[1]Stanford University School of Medicine, Palo Alto, CA,[23]Stanford University School of Medicine, Stanford, CA,[4]Stanford University, Palo Alto, CA

Accurate cancer imaging is critical for early diagnosis, guiding therapy, and assessing clinical outcomes. Yet pancreatic ductal adenocarcinoma (PDAC) poses major imaging obstacles, mainly due to its complex microenvironment, extensive stromal composition, and rapid disease progression. Claudin-4 (CLDN4), a tight junction protein, is significantly overexpressed in PDAC, making it a promising diagnostic and therapeutic target. Our spatial transcriptomic and proteomic analyses confirmed a 16-fold increase in CLDN4 expression in PDAC compared with normal pancreas. This significant finding supports its accessibility on tumor cell surfaces and suitability for molecular imaging approaches such as positron emission tomography (PET).Methods:We designed selective CLDN4-targeted peptides using solid-phase peptide synthesis, followed by rational optimization through D-amino-acid substitutions to enhance metabolic stability and dimerization strategies to improve affinity and tumor retention. The peptide structures were conjugated to a DOTA chelator through pegylated linkers of varying lengths and evaluated for serum stability. Binding affinity was measured using biolayer interferometry (BLI). Peptides were radiolabeled with ^{68}Ga and ^{64}Cu and tested in subcutaneous and transgenic PDAC-KPTC mouse models using dynamic PET/CT imaging.Results:The synthesized peptides showed good binding affinity for CLDN4 and were successfully radiolabeled with ^{68}Ga and ^{64}Cu. Serum stability studies revealed that tracers with longer PEG linkers exhibited superior stability after 4 hours of incubation. We found a similar observation with D-amino-acid-modified sequences, which showed better stability than the parent peptide. For preclinical testing, we observed that tumor uptake of the tracers gradually increased during the first hour of the dynamic scan, surpassing 10% ID/g at 40 minutes post-injection. This uptake correlated with TdTomato fluorescence, which marks cells expressing CLDN-4 in our genetically engineered model. The in-vitro imaging in a negative control subsequent model confirms the specificity of our tracers to tumors expressing claudin4. Further studies are ongoing to evaluate preclinical imaging of dimeric peptides and D-amino acid-modified sequences. This peptide-based theragnostic strategy has strong potential to improve early detection and guide targeted therapy in PDAC.

#2615 Diffusion kurtosis imaging to predict tumor hypoxia and recurrence in HPV-associated oropharyngeal cancer.

David Gibbes Miller[1], Ramesh Paudyal[2], Bill H. Diplas[1], James E. Han[1], Vaios Hatzoglou[3], Nadeem Riaz[1], Amita Shukla-Dave[2], Nancy Y. Lee[1]

[1]Department of Radiation Oncology, Memorial Sloan Kettering Cancer Center, New York, NY,[2]Department of Medical Physics, Memorial Sloan Kettering Cancer Center, New York, NY,[3]Department of Radiology, Memorial Sloan Kettering Cancer Center, New York, NY

Introduction: A recent phase II trial demonstrated the efficacy of hypoxia-guided chemoradiation (CRT) de-escalation in human papillomavirus-associated oropharyngeal cancer (HPV+ OPC). 18F-fluoromisonidazole (18F-FMISO) positron emission tomography (PET), used to measure hypoxia, is not widely available, limiting use of hypoxia as an imaging biomarker in research and clinical care. Diffusion kurtosis imaging (DKI) quantifies non-Gaussian water diffusion, especially at higher b-values of diffusion weighted (DW) data. DKI captures microstructural complexity, reflects integrity of cell membranes and cellularity, and may serve as a surrogate for hypoxia.
Methods: DW data were obtained from a phase II trial of hypoxia-guided CRT de-escalation in patients with T0-2/N1-N2c HPV+ OPC. Patients received pre-treatment 18F-FMISO imaging and serial MRI scans from pre-treatment through week 4 of CRT. Longitudinal nodal volume was collected. DKI-derived features Dapp and Kapp (mean values, standard deviation, and skewness) from modeling of the multiple b-values DW data were extracted. Associations with pre-treatment hypoxia and nodal recurrence were evaluated using Wilcoxon rank-sum tests. Random forest (RF) models integrating volume and DKI-derived features were developed to predict hypoxia and recurrence, with feature importance assessed using SHAP values.
Results: 90 of 158 trial patients with longitudinal DW-MRI exams were included. Pre-treatment 18F-FMISO PET demonstrated normoxia in 25 patients (27.8%) and hypoxia in 65 (72.2%). Pre-treatment tumor volume was significantly higher in hypoxic tumors than normoxic tumors (mean 25.7 vs. 11.3 cm^3, $p < 0.001$), while pre-treatment DKI-derived features did not differ significantly. Eight patients had nodal recurrence, all in the de-escalated cohort. An RF model incorporating pre-treatment DKI features and tumor volume predicted pre-treatment hypoxia with good discrimination (AUC = 0.77), outperforming a model using volume alone (AUC = 0.65, $p<0.001$). SHAP analysis identified tumor volume, Dapp skewness, Dapp mean, and Kapp mean as the most meaningful predictors. Longitudinal tumor volume in weeks 2-4 was significantly higher in patients who recurred, while longitudinal DKI features did not differ significantly. The model using week 3 volume and DKI features had the best performance (AUC = 0.79). SHAP analysis identified volume, volume change from pretreatment to week 3, Kapp skewness, and mean Dapp as the most meaningful predictors of recurrence.
Conclusion: Changes in cell architecture and metabolism caused by hypoxia may be associated with restricted movement of water molecules in complex tissues. DKI and volumetric measurement demonstrated good predictive ability for both hypoxia and recurrence risk in HPV+ OPC. These findings support further prospective validation of DKI for assessing tumor hypoxia and recurrence risk.

#2616 ECM profiling of patient-matched endometrial PDX-tumors reveals translational drift and TME remodeling.

Dhruva Dave[1], Rebecca Christian Arend[1], Chelsea Crawford[2], Amr Mahmoud[2], Brahma Mubarak K. Budhwani[2], Khidr Kishan K. Budhwani[2], Hunter Segrest[1], Ashwini Katre[1], Rachael E. Guenter[2], Karim Ismail Budhwani[3]

[1]Obstetrics and Gynecology, University of Alabama at Birmingham, Birmingham, AL,[2]CerFlux, Birmingham, AL,[3]University of Alabama at Birmingham, Birmingham, AL

Background: Extracellular matrix (ECM) remodeling, particularly collagen deposition, have been linked with aggressive features of endometrial. It plays a critical role in tissue architecture, deep myometrial invasion, immune infiltration, and therapeutic response. Patient-derived xenograft (PDX) models are widely used in cancer research; however, their ability to preserve patient-specific ECM organization remains uncertain. This study quantified ECM composition and spatial topology to evaluate species-specific translational drift.

Methods: Formalin-fixed, paraffin-embedded tissue from two primary endometrial tumors and matched PDX tumors underwent dual Picrosirius Red (collagen) and Alcian Blue (hyaluronic acid; HA) staining. High-resolution brightfield images were captured under standardized conditions using an Agilent Lionheart system. ECM profiling was performed using the CerFlux PEER AI/ML imaging pipeline, extracting 63 histomorphometric and spatial parameters, including ECM area fractions, HA:collagen ratios, gray-level co-occurrence matrix (GLCM) texture metrics, and Moran's I spatial autocorrelation. Analyses were cross validated in Fiji. Group comparisons used nonparametric statistics, and principal component analysis (PCA) summarized multivariate ECM signatures.

Results: Patient tumors demonstrated substantially higher collagen area fraction than matched PDX tumors (0.20 ±0.01 vs 0.05 ±0.04; $p<0.05$), while HA levels were similar (0.41 ±0.03 vs 0.33 ±0.14). This yielded a marked shift in HA:collagen ratio, from 2.1 ±0.3 in patients to 7.9 ±2.7 in PDX tumors ($p<0.05$). Texture analysis revealed more heterogeneous collagen organization in patient tumors, with higher entropy (8.22 ±0.10 vs 8.07 ±0.02; $p<0.05$) and lower homogeneity (0.15 ±0.02 vs 0.19 ±0.01; $p<0.05$). HA exhibited a similar pattern of increased uniformity in PDX tumors (homogeneity 0.16 ±0.07 vs 0.10 ±0.01; $p<0.05$). Spatial statistics showed a nearly two-fold increase in collagen Moran's I in PDX tumors (0.51 ±0.02 vs 0.26 ±0.07; $p<0.05$), indicating stronger ECM clustering and reduced spatial heterogeneity relative to patient tissue. PCA cleanly separated patient and PDX samples along PC1 (58% variance), driven by HA:collagen balance, textural heterogeneity, and spatial autocorrelation.

Conclusions: Quantitative ECM profiling demonstrates that patient-matched endometrial PDX tumors undergo pronounced translational drift, including collagen depletion, increased HA:collagen ratio, higher ECM homogeneity, and strengthened spatial clustering. These changes reflect species-specific TME remodeling following xenografting and may influence drug penetration, response, and biomarker interpretation. Assessing ECM fidelity is therefore vital when using PDX models to inform translational research and preclinical decision-making in endometrial cancer.

#2617 Rapid assessment of patient derived cancer organoids using label-free imaging and an automated analysis pipeline.

Amani A. Gillette[1], Angela Hsu[1], Shirsa Udgata[2], Alexa Schmitz[2], Dustin A. Deming[3], Melissa Skala[4]

[1]Morgridge Institute for Research, Madison, WI,[2]Univ. of Wisconsin Madison Sch. of Med. & Public Health, Madison, WI,[3]University of Wisconsin Carbone Cancer Center, Madison, WI,[4]Biomedical Engineering, University of Wisconsin - Madison, Madison, WI

Background: Tumor heterogeneity presents a major challenge in effective cancer treatment, particularly in colorectal cancer (CRC), by limiting the efficacy of therapies and driving resistance. Patient-derived cancer organoids (PDCOs) have emerged as powerful preclinical models that faithfully recapitulate the genomic, morphological, and metabolic profiles of primary tumors. However, current methods for rapidly and reproducibly assessing PDCOs are limited. Label-free imaging methods are a promising tool to measure organoid level heterogeneity and rapidly screen drug response in PDCOs. However, manual analysis of wide-field optical redox images is inefficient and laborious for large-scale drug screens. Here, we developed an automated pipeline for PDCO segmentation, single-PDCO tracking, and background correction in autofluorescence images.
Methods: Wide field optical redox imaging (WF ORI) provided organoid-level measurements of treatment response without labels or additional reagents by measuring the autofluorescence intensity of the metabolic co-enzymes NAD(P)H and FAD, and the optical redox ratio, defined as the fluorescence intensity of [NAD(P)H/NAD(P)H+FAD], was used to measure the oxidation-reduction state of multiple CRC PDCO lines. Development of leading-edge analysis tools, isolating the ORI measurement to a 32μm region at the outer edge of the PDCOs, helped to maximize the sensitivity and reproducibility of treatment response measurements using WF ORI in CRC PDCOs. The automated pipeline includes segmentation using a fine-tuned Cellpose model, automated single-PDCO tracking over time via custom python code, and background correction. Glass's delta (GΔ) is used to measure the PDCO treatment effect size.
Results: Leading-edge analysis improves sensitivity to redox changes in treated PDCOs (GΔ = 1.462 vs GΔ = 1.233). Automated segmentation, when compared to manual masks, achieved mean Dice scores ≥0.8, indicating high reproducibility. Additionally, automated PDCO tracking accuracy exceeded 94% by two metrics, recall and Jaccard index, when compared to manual tracking. Importantly, the automated pipeline resolves single-PDCO responses over time with comparable sensitivity to drug treatment with over 127× faster processing time compared to the manual process.
Conclusion: Overall, we demonstrate that combining PDCOs with accessible imaging and analysis techniques enables high-throughput detailed evaluation of tumor heterogeneity and therapeutic response.

#2618 Thoracic ct-derived muscle indices improve prediction of respiratory function beyond standard L3 sarcopenia measures in lung cancer patients.

Kayleigh R. Erickson, Juan Adrover Claudio, Chi-Chen Hong, Ken Batai, Nicolas F. Schlecht, Sai Yendamuri, Andrew Ray

Roswell Park Comprehensive Cancer Center, Buffalo, NY

Background. L3 skeletal muscle index (SMI) is the CT standard for whole-body sarcopenia but does not assess thoracic musculature and may miss muscle morphology tied to respiratory mechanics and upper-body function. This study evaluated whether thoracic muscle measures provide independent or complementary information beyond L3 SMI for functional and pulmonary performance in lung cancer patients.

Methods. Ninety adults with newly diagnosed lung cancer who completed clinically indicated CT imaging and baseline pre-treatment functional assessments were analyzed. SMI was quantified at L3 and thoracic levels (T4, T6, T8, T10). Functional outcomes included handgrip strength (HGS), gait speed, sit-to-stand, and 6-minute walk distance (6MWT). Pulmonary outcomes included maximal inspiratory and expiratory pressures (MIP, MEP), Forced Vital Capacity (FVC), Forced Expiratory Volume in 1 second (FEV1), and Peak Expiratory Flow (PEF). Outcomes were examined continuously and dichotomized at clinically relevant thresholds: weak HGS (< 28 kg for men; <18 kg for women), impaired 6MWT (<300 m), and respiratory muscle weakness (MIP ≤ 62/83 cmH_2O and MEP ≤ 81/≤ 109 cmH_2O in men/women). Correlations, multivariable linear regression (adjusting for age, sex, body mass index (BMI), smoking, and tumor stage), and logistic regression assessed associations; incremental predictive value of thoracic SMI beyond L3 was evaluated using area under the ROC curve (AUC).

Results. Thoracic SMI showed moderate-strong correlations with HGS, MIP, MEP, and PEF (r = 0.24-0.63, all $p < 0.01$). In adjusted models, thoracic SMIs remained associated with HGS (β = 0.20-0.37, $p \leq 0.007$) and several respiratory measures, including MEP at T4/T10 and FVC and PEF at T6/T8. L3 SMI was not independently associated with MEP, MIP, or PEF ($p > 0.10$), but was more strongly related to whole-body mobility (TUG and gait speed, both $p < 0.02$). To connect functional associations with clinical relevance, predictive performance was examined for clinically defined weakness or impairment. For inspiratory muscle weakness, L3 SMI was not predictive (p=0.30; AUC=0.903), and adding thoracic SMI did not improve discrimination (AUCs 0.898 to 0.904). For weak HGS, L3 SMI was not significant (p=0.42, AUC=0.774), whereas adding thoracic SMI increased AUC by 0.06 to 0.12, with T8 showing the largest gain (AUC 0.893). For 6MWT impairment, L3 SMI was predictive (p=0.039, AUC =0.750), while thoracic SMI was not (all p>0.10) and did not meaningfully improve increase AUC (0.75-0.79).

Conclusion. Thoracic CT-derived muscle indices provide domain-specific value beyond L3 SMI, improving prediction of upper-body strength but not inspiratory muscle weakness or whole-body endurance. Incorporating thoracic muscle metrics with standard L3 assessment may enhance functional risk stratification and prehabilitation planning in lung cancer.

#2619 Quantitative modeling of autofluorescence and non-specific staining allows for improved cell phenotyping and marker assessment in highly multiplexed immunofluorescence studies.

Daria I. Mandel, Anton Luis Villamejor, Anthony Colombo, Simeon Mahov, Akil A. Merchant, Joseph Lownik

Cedars-Sinai Medical Center, Los Angeles, CA

While fundamental in cancer diagnostics, immunohistochemistry (IHC) has several significant limitations, including the inability to simultaneously detect multiple markers per slide, which limits true co-expression analysis. In contrast, sequential immunofluorescence (seqIF), a multiplexed protein biomarker detection method, allows for simultaneous detection of multiple markers on a single slide by using antibodies with distinct fluorophores combined with the repeated automated cycles of staining, imaging, and elution. While seqIF has quantitative and scalability advantages over IHC, its use of fluorescence introduces various challenges for downstream computational analysis such as tissue's autofluorescence and non-specific fluorophore accumulation, which are compound by multiple cycles of staining, imaging and elution. The Lunaphore COMET, a seqIF system, allows for an initial background autofluorescence acquisition at the beginning of the protocol. However, we observed that this single baseline measurement did not account changes in the fluorescence of different regions in various tissue types with subsequent imaging and elution cycles, which significantly affected downstream analysis including cell typing.To further investigate these artifacts, we evaluated both autofluorescent quenching on a variety of tissue types during the imaging cycles as well as the non-specific accumulation of fluorophores in all channels (FITC, TRITC, Cy5, and Cy7). We found that the background autofluorescence decreased with sequential cycles in some, but not all cycles, which led to artificially decreased signal intensity for downstream marker analysis. Additionally, we found that non-specific fluorophore accumulation was channel specific, tissue specific, and subcellular localization specific, further confounding interpretability. Overall, these findings suggest that utilizing a single baseline autofluorescence cycle for background subtraction is insufficient and can lead to significant downstream analytical errors.While performing an additional imaging cycle after each elution cycle and subtracting background accordingly may remedy this problem, it is not always feasible or efficient due to increased time, reagent usage, and file size. We found that a total of 5 imaging cycles post-elution accurately predicted the background fluorescence for 20 cycles using a cell-level cubic spline model ($R^2 = 0.94$). These background signal modeling results are then utilized to calculate background-adjusted marker expression values at a cell level for individual cycles, which improved clustering resolution and interoperability. Overall, we demonstrate issues encountered with autofluorescence in seqIF and present a novel method for mitigating them to improve results.

#2620 Comparison of ^{68}Ga-DOTANOC PET/CT with anatomical imaging in opsoclonus-myoclonus-ataxia syndrome in children: A retrospective analysis.

Anish Bhattacharya[1], Rajender Kumar[1], Harmandeep Singh[1], Jitendra Kumar Sahu[2], Naveen Sankhyan[2]

[1]Nuclear Medicine, PGIMER, Chandigarh, India,[2]Pediatric Medicine, PGIMER, Chandigarh, India

Introduction: Opsoclonus-myoclonus-ataxia syndrome (OMAS), also known as “Kinsbourne syndrome” or “dancing eye syndrome,” is a rare immune-mediated paraneoplastic neurological syndrome that may be associated with pediatric neuroblastoma in approximately 2-3% of children aged 1-3 years. OMAS carries a grave prognosis and is characterised by involuntary eye movements, muscle jerks, ataxia and behavioural changes. Paediatric neuroblastoma may be the only cause of OMAS in up to 50% of children. Routine tests to detect occult neuroblastoma include anatomical imaging of the chest and abdomen with USG/ CT/ MRI. ^{131}I-MIBG scintigraphy has also been used; however, its application is limited by its availability, need for strenuous patient preparation, and high radiation exposure. In this retrospective analysis, we evaluated children presenting with OMAS who underwent ^{68}Ga-DOTANOC PET/CT as a single screening study to detect neuroblastoma and stage the disease, in comparison to traditional anatomical imaging.

Methods: Retrospective data from ^{68}Ga-DOTANOC PET/CT scans of 43 pediatric patients presenting with OMAS from January 2019 to June 2024 were evaluated. A somatostatin receptor (SSTR) expressing lesion with corresponding morphological change on the CT image was considered PET-positive, while no abnormal SSTR expression or lesion was considered PET-negative. The results of ^{68}Ga-DOTANOC PET/CT were also compared with prior anatomical imaging studies, which were available for 32 patients (in both PET-positive and PET-negative groups).

Results: Of 43 patients (21 male, 22 female; mean age 1.5 years), 31 (72.1%) were PET-positive and 12 (27.9%) were PET-negative. The mean SUVmax of PET-positive lesions was 12.1 (SD = 6.6). Prior anatomical imaging studies (USG (n=13)/ CT (n=6)/ MRI (n=13)) were available in 32 patients and compared with ^{68}Ga-DOTANOC PET/CT. Discordance was seen in 5 patients with prior USG and 1 patient with prior MRI, in which lesions were missed in 3 patients on USG and 1 patient on MRI. One suspicious lesion was excluded from diagnosis by ^{68}Ga-DOTANOC PET/CT in 1 patient. According to the International Neuroblastoma Staging System (INSS), 24 (80%) were stage 1, 4 (6.4%) were stage 2, 1 (4%) were stage 3, and 2 (6.4%) were stage 4. Repeat ^{68}Ga-DOTANOC PET/CT was done in 7/31 of stage 1 patients after surgical excision, and all were PET-negative.

Conclusion: In this retrospective analysis, we found that approximately 72% of children presenting with OMAS have neuroblastoma as the primary etiology. ^{68}Ga-DOTANOC PET/CT demonstrated high diagnostic performance, accurately identifying neuroblastoma and providing rapid diagnosis, detection of metastasis, and guidance for optimal management.

#2621 A systematic review of radiogenomic applications in prostate cancer.

Thineskrishna Anbarasan[1], Matilda Dichmont[2], Sandy Figiel[1], Bartlomiej Papiez[1], Alastair Lamb[3], Richard Bryant[1], Ian Mills[1]

[1]University of Oxford, Oxford, United Kingdom,[2]Oxford University Hospitals, Oxford, United Kingdom,[3]Barts Cancer Institute, London, United Kingdom

Introduction: A priority in prostate cancer (PCa) research is development of precise risk stratification tools to enable early identification of men with aggressive tumours while minimizing overtreatment of others with indolent disease. With imaging playing a central role in the diagnosis and management of PCa, radiogenomics has been explored as a personalised medicine approach to improve risk stratification. This study aims to review and describe radiogenomic applications reported in the literature.

Methods: Medline, Embase and Cochrane libraries were systematically searched using variations of search terms for articles reporting radiogenomic applications in PCa after 2010. Articles were included if the following were reported (1) genomic platform used; (2) method of determining region of interest (ROI) for radiomic feature extraction; (3) correlation analyses between radiomics and genomics.

Results: A total of 267 articles were screened and 13 met the inclusion criteria following independent review by two authors. Majority (n=10/13) reported MRI-based applications involving 715 patients. Remaining modalities included ultrasound (n=1) and PET scan (n=2). Most (7/10) studies evaluating an MRI imaging modality, correlated bulk RNA-sequencing with radiomic features. Textural radiomics (n=6) features were most commonly reported to correlate with gene expression followed by histogram (n=2) and volumetric features (n=1). MRI radiomics significantly correlated with hypoxia related genes in 4 studies. The textural feature (Gray Level Co-occurrence Matrix) was seen to correlate with *ANGPTL4* expression in 3 studies. Median AUC for a radiogenomic model to predict presence of clinically significant PCa was 0.746. Only 4 studies (MRI-based n=3, ultrasound-based n=1) externally validated the developed model. Most (9/13) studies used a manual qualitative approach to register imaging loci with site of tissue acquisition for genomic analysis.

Conclusion: There is significant heterogeneity in the reporting and design of prostate cancer radiogenomic studies. A signal suggesting and association of MRI textural radiomic features have been consistently observed in several studies but lack validation

: Redefining Targeted Therapy: Bispecific T-Cell Engagers and Antibody-Drug Conjugates 1
Poster Session

#2625 αTIGIT-guided IL-15 mimetics enable potent and safe antitumor immunity.

Xiangming Liu, Nan Li, **Yang-Xin Fu**, Zaopeng Yang

Changping Laboratory, Beijing, China

Cytokines are powerful modulators of antitumor immunity, but their clinical use is constrained by structural instability and systemic toxicity. Although antibody-based cytokine mimetics have recently emerged to activate immune cells *in vitro*, their therapeutic activity *in vivo* remains uncertain. Here, using interleukin-15 (IL-15) as a model, we engineered bispecific antibody-based IL-15 mimetics guided by AlphaFold3-assisted structural modeling. Comparative screening of multiple formats identified tandem IL-15 mimetics with strong *in vitro* bioactivity, but unexpectedly showed minimal antitumor activity *in vivo*. Strikingly, incorporating TIGIT-directed targeting transformed these mimetics into potent and nontoxic cytokine agonists, resulting in strong tumor control associated with enhanced effector activation and expansion of intratumoral $CD8^+$ stem-like T cells. These findings indicate that current cytokine mimetics have limited activity when used alone and require precise T-cell targeting to achieve therapeutic potency. Our study highlights a strategy to use cytokine mimetics to overcome the mismatch between immune checkpoint blockade and low-potency cis-targeted cytokines, offering a path toward safer and more effective cytokine immunotherapy.

#2626 A cleavable IL10-TCE counteracts TCE-induced T cell dysfunction and eradicates solid tumors without toxicity.

Xinxin Wang, **Yang-Xin Fu**, Zaopeng Yang

Changping Laboratory, Beijing, China

The clinical success of T cell engagers (TCEs) in hematologic malignancies has been difficult to replicate in solid tumors due to limited efficacy and on-target toxicities, partly driven by CD3-directed activation-induced cell death (AICD) and exhaustion of tumor-infiltrating lymphocytes (TILs). To overcome T cell dysfunction in the tumor microenvironment, we found that IL-10 receptor expression is enriched on antigen-specific T cells and that exogenous IL-10 markedly reduces T cell death while preserving overall T cell numbers. Guided by this insight, we engineered a series of IL-10-integrated TCE formats and identified an optimized design in which IL-10 is fused to the N-terminus of the anti-CD3 arm in a cleavable configuration, generating a pro-TCE (IL10-TCE) with favorable biochemical properties and potent antitumor activity without detectable toxicity. The IL10-TCE enhanced effector function and substantially expanded both total and antigen-specific T cells within tumors, resulting in complete regression of established solid tumors and metastatic lesions across multiple syngeneic and xenograft models, including colon cancer, melanoma, and pancreatic cancer. These findings establish IL-10 incorporation as a generalizable strategy to overcome TCE-induced T cell dysfunction, enabling robust tumor eradication and durable immune protection.

#2627 ALX006, a PD-1/VEGF bispecific antibody with best-in-class potential demonstrates superior antitumor activity and favorable PK in preclinical models.

Zenglin Pei, Yupeng Zhu, Jinglu Xia, Zhaojun An, **Barry Duplantis**, Yuhao Wang, Yali Wang, Jia Ge, Xiaojin Zhang, Lingjian Yang, Liang Du, Xiangyu He, Yi Li

Shanghai Ailux Biotechnology Co., Ltd., Shanghai, China

Background: PD-1 and VEGF are frequently co-expressed in the tumor microenvironment. PD-1 blockade reverses tumor-induced immunosuppression, while VEGF inhibition normalizes tumor vasculature and modulates immune cell infiltration. Clinical data from bispecific antibodies, such as Ivonescimab, particularly in advanced non-small cell lung cancer, support the synergistic potential of anti-PD-1 and anti-VEGF therapies to enhance efficacy and reduce systemic toxicity. Here we developed a novel PD-1/VEGF bispecific antibody ALX006 with thoroughly preclinical characterization.
Methods: Binding affinities of ALX006 to PD-1 and VEGF were quantified by surface plasmon resonance (SPR). PD-1/PD-L1 pathway blockade was assessed using a luciferase reporter assay. T-cell reactivation was evaluated by mixed lymphocyte reaction assays. Antitumor activity was tested in A375 cell-derived xenograft (CDX) model in PBMC humanized mice and MC38 syngeneic model in human PD-1/PD-L1/VEGF transgenic mice. Biophysical liabilities and developability were profiled. Pharmacokinetics (PK) were evaluated in Sprague-Dawley rats and cynomolgus macaques.
Results: ALX006 is a 2+2 symmetric IgG1 (Fc-null) bispecific antibody that binds to both targets with high affinity. In the presence of VEGF, ALX006 significantly enhanced PD-1 cell binding and PD-1/PD-L1 signal blockade. ALX006 also increased IL-2 and IFN-γ secretion in a dose-dependent manner in mixed lymphocyte reaction. In addition, ALX006 potently suppressed VEGF-induced endothelial cell proliferation. Importantly, superior antitumor efficacy was observed in the A375 CDX model compared with Ivonescimab and two other clinical-stage bispecifics. Consistent activity was also observed in the MC38 syngeneic tumor model in transgenic mice. ALX006 exhibited favorable biophysical properties and overall developability, with an improved PK profile compared with Ivonescimab.
Conclusions: ALX006, a PD-1/VEGF bispecific antibody with best-in-class potential, demonstrates superior antitumor activity and favorable PK in preclinical models, supporting its potential as a therapeutic candidate for immuno-oncology applications.

#2628 AM109, a PSMA×CD137 bispecific antibody with target-dependent T cell activation and potent anti-tumor activity in prostate cancer.

Dong-Wook Kim, Hyun-Jong Lee, Seong Yeol Kim, Min Yoon, Youngha Lee, In-Sik Hwang, Yoon Lee, Jong-Hoon Kim, Jong-Seo Lee

AbClon, Seoul, Korea, Republic of

Metastatic castration-resistant prostate cancer (mCRPC) remains a fatal malignancy with limited responsiveness to current immunotherapies. To achieve tumor-restricted immune activation, we developed AM109, a bispecific antibody that links a PSMA-targeting humanized antibody to a CD137 (4-1BB) affibody, designed to activate T cells exclusively in the presence of PSMA-expressing tumor cells. AM109 elicited robust $CD8^+$ T-cell activation and cytokine secretion (IFN-γ, IL-2, and Granzyme B) in $PSMA^+$ LNCaP cells, but not in $PSMA^-$ MKN45 cells, confirming its target-dependent mode of action. Cytotoxicity assays demonstrated dose-dependent tumor cell killing that correlated with PSMA expression levels. In vivo efficacy was evaluated using human CD137 transgenic mice bearing hPSMA/MC38 tumors, where AM109 achieved complete tumor regression at doses of 0.1-0.3 mpk, exhibiting superior potency compared with the reference CD137 agonist utomilumab. Structural and functional stability were maintained for at least 12 weeks at 4-40 °C. Pharmacokinetic and single-dose toxicity studies in rodents revealed favorable systemic exposure and good tolerability. Collectively, these findings demonstrate that AM109 selectively activates T cells within the tumor microenvironment, eliciting potent and PSMA-dependent anti-tumor responses with an improved therapeutic window. AM109 therefore represents a promising next-generation immunotherapeutic candidate for the treatment of mCRPC.

#2629 A novel ADAM9 ADC with robust anti-tumor efficacy and remarkable preclinical safety profile.

Ruirui Sui, Yin Lu, Furong Gao, Chen Xu, Jiangbo Song, Guoping Jiang, Liuge Gu, Teddy Yang, Ying Lei, Li Tong, **Fei Peng**

Hongcheng Biopharma, Shanghai, China

ADAM9 (A Disintegrin And Metalloproteinase 9) is a transmembrane metalloproteinase overexpressed in a wide range of solid tumors, where it promotes tumor progression, metastasis, and poor prognosis. Internal immunohistochemistry analysis confirmed ADAM9 expressed at very low levels in most normal tissues, significant ADAM9 upregulation in tumor tissues, makes it a highly attractive and viable target for antibody-drug conjugate (ADC) development. An affinity optimized, humanized monoclonal antibody (HC031) was generated against human ADAM9. HC031 cross reacts with cyno ADAM9 with similar affinity. HC031 exhibited specific binding to human ADAM9 with no detectable binding to other ADAM family isoforms. HC031 selectively binds to membrane form of ADAM9 but not to short soluble ADAM9 predicting a regular pharmacokinetic profile unimpeded by soluble ADAM9. Furthermore, HC031 binding is partially dependent of bivalent cation, which may contribute to an improved safety profile. HC031 ADC was generated through conjugation with a novel, proprietary cytotoxic payload (camptothecin derivatives) via a highly stable linker. The resulting ADC demonstrated potent, target-specific cell killing *in vitro* and induced robust and sustained tumor regression in multiple xenograft models. Exploratory toxicology studies in non-human primates revealed an exceptionally maximum tolerated dose (MTD) of 120 mg/kg. No drug-related severe adverse events or significant abnormalities in hematological, biochemical, or coagulation parameters were observed. HC031 ADC exhibited favorable and dose-proportional PK profiles, with extended exposure of the intact ADC. Critically, the linker-payload demonstrated superior plasma stability.HC031 ADC drives potent anti-tumor activity *in vitro* and *in vivo*. Its exceptional stability in circulation and remarkable preclinical safety profile in NHPs predicts a significantly broader therapeutic window compared to existing ADAM9 ADCs.

#2630 MRG008: A novel EGFR and 5T4 bispecific antibody-drug conjugate (ADC) with potent antitumor activity in preclinical studies.

Yuanyuan Yang[1], **Zhijian Cai**[1], Deliang Li[1], Shoujia Liu[2], Wenci Gong[1]

[1]Lepu Biopharma Co., Ltd., Shanghai, China,[2]Shanghai Miracogen Inc., Shanghai, China

Background: Non-small cell lung cancer (NSCLC) is one of the most challenging cancers with unmet medical needs. EGFR (also known as HER1) is an epidermal growth factor receptor with tyrosine kinase activity implicated in both tumorigenesis and tumor progression, and its validity as a therapeutic target for ADC has been clinically confirmed, as exemplified by our approved drug MRG003. Trophoblast glycoprotein, also known as 5T4, is an oncofetal cell surface antigen widely expressed across multiple cancer types. 5T4 expression levels correlate with disease stage and portend poor clinical outcomes. Notably, EGFR and 5T4 are highly co-expressed in most NSCLC patients, while 5T4 exhibits moderate-to-high expression in subsets with low or absent EGFR. Targeting 5T4 thus effectively overcomes the therapeutic limitation of insufficient EGFR expression in this patient population. MRG008 is a bispecific ADC targeting both EGFR and 5T4, comprising an Fc-silenced bispecific antibody, a cleavable linker, and a topoisomerase I inhibitor payload (Topi) with a superior bystander effect. This differentiated design holds promise for broadening the therapeutic scope in NSCLC patients.

Methods: The biological activity and safety profile of MRG008 were investigated in a series of preclinical studies, including (1) binding ability to 5T4 and EGFR by ELISA, Flow cytometry and Biacore; (2) internalization rate in single- and dual- target-expressing cancer cells evaluated by pHAb Reactive Dye labeling; (3) in vitro cytotoxicity against single- and dual-target-expressing cancer cells; (4) anti-tumor activity evaluated in NSCLC cell line-derived xenograft (CDX) and NSCLC patient-derived xenograft (PDX) mouse models; (5) plasma stability evaluated in human and cynomolgus monkey plasma; (6) an exploratory pharmacokinetic (PK) study in cynomolgus monkey.

Results: MRG008 exhibited comparable binding activity to that of the respective parental monoclonal antibody ADC targeting 5T4 or EGFR. Rapid internalization of MRG008 was observed in both EGFR/5T4 single-expressing and EGFR/5T4 dual-expressing cancer cells. MRG008 demonstrated potent in vitro cytotoxic activity, comparable to that of its parental monoclonal antibody ADCs. MRG008 exhibited robust tumor growth inhibition in NSCLC CDX and PDX mouse models with varying levels of 5T4 and EGFR expression. Additionally, MRG008 showed favorable stability in human plasma and a desirable PK profile in cynomolgus monkeys.

Conclusion: MRG008 is a promising dual-targeted ADC with potent anti-tumor efficacy for the treatment of NSCLC. These preclinical findings provide a strong rationale for advancing MRG008 into IND-enabling and clinical studies.

#2631 LPD002, a novel anti-PD-1/IL-2 fusion protein, demonstrates potent antitumor activity in preclinical studies.

Xiaoli Zhang[1], **Zhijian Cai**[1], Shoujia Liu[2], Wenci Gong[1]

[1]Lepu Biopharma Co., Ltd., Shanghai, China,[2]Shanghai Miracogen Inc., Shanghai, China

Background: The advancement of immunotherapy has significantly improved the survival outcomes for patients with malignant tumors. IL-2 therapy has demonstrated potential in activating tumor-infiltrating antigen-specific T cells and inducing durable anti-tumor responses. However, it often triggers severe systemic toxicities. To improve the therapeutic index, a variety of engineered IL-2 analogs have been developed.

Methods: To overcome the challenges of PD-1 blockade and IL-2 therapies, we engineered a novel fusion protein, LPD002, which combines a humanized anti-PD-1 antibody and an engineered IL-2 mutein. The anti-PD-1 antibody portion delivers the IL-2 mutein payload to PD-1$^+$ tumor-infiltrating T cells while blocking the immune-inhibitory signals of the PD-1 pathway. The IL-2 mutein component of LPD002 has been engineered to retain its binding activity to the IL-2 receptor alpha (IL-2Rα) subunit and attenuated affinity for the IL-2 receptor beta and gamma (IL-2Rβγ) complex, which is designed to maintain peripheral tolerance and activate tumor-infiltrating T cells, thereby mitigating the systemic toxicity associated with IL-2 therapy. We systematically assessed the functional properties of LPD002 through PD-1 blockade and IL-2 signaling assays. The anti-tumor efficacy of LPD002 was investigated using PD-1 humanized mouse models. Meanwhile, we also evaluated its PK performance in cynomolgus monkeys.

Results: In IL-2 reporter assays, LPD002 induced enhanced pSTAT5 signaling in PD-1-expressing reporter cells compared with PD-1-null cells. LPD002 also activated pSTAT5 signaling and promoted the proliferation of both activated CD4$^+$ and CD8$^+$ T cells in human PBMCs. Moreover, in both PD-1-sensitive and PD-1-resistant CDX models, LPD002 demonstrated superior anti-tumor efficacy and was well-tolerated. In cynomolgus monkeys, LPD002 displayed a favorable pharmacokinetic profile.

Conclusion: LPD002 represents a novel immunotherapeutic strategy that integrates PD-1 blockade with tumor-focused IL-2 activation, eliciting potent anti-tumor activity while reducing systemic toxicity. These preclinical findings demonstrate that LPD002 is a promising therapeutic candidate for solid tumors and warrants further clinical investigation.

#2632 DXP-106, an anti-IL1RAP monoclonal antibody with enhanced ADCC activity, exhibits both *in vitro* and *in vivo* anti-tumor effects and has successfully completed IND-enabling studies.

Qinghao Liu, Yaqi Ru, Yan Jiang, Huimin Li, Wenbo Li, Lan Yang, **Qian Shi**

Singlomics Biopharmaceuticals, Beijing, China

Background: The Interleukin-1 Receptor Accessory Protein (IL1RAP) is expressed on cancer cells, stromal cells, and infiltrating immune cells within the tumor microenvironment (TME) across various cancer types. By activating the IL-1 superfamily signaling pathways, IL1RAP contributes to tumor progression at multiple stages, making it a promising therapeutic target for cancer treatment.
Methods: The epitope of DXP-106 was identified using cryo-electron microscopy (Cryo-EM). The antibody's inhibitory activity against IL-1, IL-33, and IL-36 signaling was assessed through a range of assays utilizing reporter cell lines, primary HUVEC cells, and the A431 human squamous cell carcinoma model. In vivo efficacy was evaluated using a cell line-derived xenograft (CDX) model. The DXP-106 therapeutic product was manufactured using FUT8 knockout Chinese hamster ovary (CHO) cell lines to enhance the antibody-dependent cellular cytotoxicity (ADCC) activity.
Results: Cryo-EM-based epitope mapping revealed that DXP-106 binds to a unique site within IL1RAP domain 2, an area that overlaps with the key interfaces of IL1β-IL1R1 and IL1RAP. In vitro studies demonstrated that DXP-106 effectively blocked signaling through all six IL-1 family pathways: IL-1α, IL-1β, IL-33, and IL-36α, IL-36β, IL-36γ. Additionally, DXP-106 exhibited strong ADCC activity in tumor cell killing assays and significantly suppressed tumor growth in xenograft models. A robust and high-yield manufacturing process has been successfully established, yielding clinical-ready product. Nonclinical safety evaluations, including GLP-compliant toxicity studies in non-human primates, showed no significant adverse findings.
Conclusions: DXP-106 is a potent monoclonal antibody that specifically binds to a unique epitope on IL1RAP, broadly inhibits all six IL-1 family signaling pathways, and shows robust anti-tumor activity both in vitro and in vivo. IND-enabling studies have been successfully completed, and the first-in-human (FIH) clinical trial is planned for the first quarter of 2026.

#2633 A T-cell engager antibody targeting the non-shed site of mesothelin in solid tumors.

Eber Antonio Guzman-Cruz[1], Masanori Onda[1], Xiufen Liu[1], Tara O'Shea[1], Qi Zhou[1], Wenlong Liu[1], Jing Bian[2], Chin-Hsien Tai[1], Ira Pastan[1], Mitchell Ho[1]

[1]Laboratory of Molecular Biology (LMB), Center for Cancer Research, National Cancer Institute, National Institutes of Health, Bethesda, MD,[2]Collaborative Bioinformatics Resource, Center for Cancer Research, National Cancer Institute, National Institutes of Health, Bethesda, MD

Mesothelin (MSLN) is a cell surface protein that is overexpressed in various cancers, including mesothelioma, pancreatic, and ovarian cancer. Its expression in normal tissue is limited to the mesothelial cells lining the pleura, peritoneum and pericardium; make it an attractive target for antibody-based therapeutics. Many efforts have been dedicated towards the development of these antibody-based approaches but proteases in the tumor microenvironment promote the cleavage of MSLN from cancer cells. High concentrations of shed MSLN in the tumor microenvironment bind to the antibody inhibiting its activity and preventing the death of cancer cells.
To address the presence of shed MSLN, an antibody called 15B6 was designed. It binds the membrane-proximal, protease sensitive region of MSLN that is not shed in the tumor microenvironment. This study investigates the ability of 15B6-targeted bispecific antibodies to eliminate MSLN expressing cancers. We designed humanized and murine versions of a CD3x15B6 bispecific antibody, which binds the CD3 on T cells and the MSLN (15B6) epitope on cancer cells serving as a bridge to promote the activation of T cells to kill MSLN positive cancer cells. These 15B6-based antibodies were compared to SS1-based antibodies that target the distal N-terminal domain of MSLN that is shed by proteases. In-vitro, the SS1 and 15B6 antibodies hold similar cytotoxic activity, but when cocultured with MSLN 296-591, a recombinant protein mimicking shed MSLN, the SS1 antibodies activity is inhibited.
In-vivo, in a human mesothelioma model in immunodeficient mice, tumor shrinkage and growth inhibition were observed when treated with the 15B6-based antibody but not those treated with the SS1-based antibody. In an immunocompetent mouse model, the complete regression of colon and breast tumors was observed when treated with the 15B6-based antibody compared to the SS1 antibody and control samples. Transcriptional analysis revealed that 15B6-treated mice had higher levels of activation of both innate and adaptive immune cells, along with significant upregulation of cytokine and STAT5 signaling pathways. Through in-vitro and in-vivo studies, we have demonstrated that this 15B6-targeted antibody binds to the protease-sensitive region, is highly active against MSLN-expressing cancer cell lines in vitro, is not inhibited by shed MSLN, and promotes upregulation of immune cell populations and signaling pathways that support robust anti-tumor activity.

#2634 HEC-922:A CDH17-4-1BB bispecific antibody targeting CDH17 positive tumors shows potent anti-tumor activity.

Junji Dong, Shushan Lin, Zhou Linjun, Jiang Qiuyue, Chen Cangsha, He Shuiqing, Xiang Li, Ju Peng, Xiaohui Li, Cai Zhao, Ming Li, Xiaoping Li, **Stewart Leung**

HEC Pharma, Dongguan, China

HEC-922 is a novel bispecific agonistic antibody targeting Cadherin-17(CDH17) and the immune agonistic receptor 4-1BB for the treatment of CDH17-positive tumors, particularly gastrointestinal tumors. CDH17 is a tumor associated antigen highly expressed in various tumors, including colorectal cancer, gastric cancer, and neuroendocrine tumors. Activating monoclonal antibodies against 4-1BB have shown clinical efficacy but was limited by systemic toxicity. The design of HEC-922 enables CDH17-dependent agonism of 4-1BB in the presence of CDH17 positive tumor cells, enabling tumor specific T cell activation while minimizing systemic immune toxicity. A high affinity nanobody against CDH17 and a nanobody against 4-1BB were identified for the construction of HEC- 922 containing an ADCC-silenced Fc. HEC-922 shows potent co-binding to both CDH17 and 4-1BB targets and is cross-reactive to the Rhesus macaque. In an assay using 4-1BB high expression 293 cells with NFkB-luciferase reporter, HEC-922 mediated 4-1BB activation in the presence of CDH17 positive cells but not CDH17 negative cells. HEC-922 demonstrated effective tumor growth inhibition in xenograft models of CDH17 positive tumor lines, restored the function of immune cells, reduced the proportion of exhausted T cells, and achieved a sustained and potent anti-tumor effect. Initial drug feasibility and toxicity studies results of HEC-922 were favorable. Overall result demonstrated that HEC- 922 is a promising candidate for CDH17 positive cancer immunotherapy.HEC-921, another bispecific antibody developed on the same 4-1BB platform with Ly6G6D as the targeted tumor antigen, has completed Dose Range Finding (DRF) study in cynomolgus monkeys, with a no-observed-adverse-effect level (NOAEL) of 100 mg/kg, validating the safety of the 4-1BB platform.

#2635 Novel tumor microenvironment (TME) activated interleukin-2 (IL-2) fused to anti-PD-1 or anti-PD-1/VEGF-A antibodies for enhanced anti-tumor immunity.

Rui Zhang, Cheng Liu, **Yuan Liu**

Affinity Biopharmaceutical Co., Ltd., Shanghai, China

IL-2 is a potent immune-activating cytokine that amplifies T-cell responses critical for anti-tumor immunity, yet its clinical use is limited by toxicity. Previous research has focused on receptor-biased IL-2 variants to selectively engage specific IL-2R subunits such as binding only to the dimeric intermediate-affinity IL-2Rβγ rather than the high-affinity trimeric IL-2Rαβγ. IMD-101 is a novel TME-activated WT IL-2 molecule engineered through chemical conjugation with a legumain-cleavable mask entity, which enables full inhibition of IL-2 activity in circulation while restoring WT IL-2 function in the TME. In cynomolgus monkeys, IMD-101 exhibited no-observed-adverse-effect-level (NOAEL) of 2.4 mg/kg with single dose and NOAEL of 0.8 mg/kg with repeated dosing. In phase I dose escalation study, IMD-101 reached markedly reduced systemic toxicity.

Based on this platform, two fusion antibodies, PD1-IL2 TMEAbody (IMD2032) and PD1-VEGF-IL2 TMEAbody (IMD2035), were further developed to match the clinical dose of PD-1 and PD1-VEGF. IMD2032 was conjugated with legumain-cleavable mask entity shielding both the PD-1 antibody and engineered IL-2 (IL-2 receptor abg agonist). IMD2035 was conjugated with legumain-cleavable mask entity blocking the engineered IL-2 (IL-2 receptor a biased agonist). In syngeneic tumor models using PD-1 humanized mice, IMD2032 showed greater tumor growth inhibition compared with the parental anti-PD-1 antibody. And under the same high-dose, once-daily regimen in PD-1 humanized mice, PD1-IL2 antibody induced strong blood lymphocyte elevation and caused 100% mortality by day 4 (after 4 doses), whereas IMD2032 showed no toxicity after 10 days with 10 doses. Similarly, for preclinical tumor models in PD-1/PD-L1/VEGF-A humanized mice, IMD2035 demonstrated superior anti-tumor efficacy relative to parental anti-PD-1/VEGF-A bispecific antibody. Preclinical toxicology studies in cynomolgus monkeys indicated that IMD2035 was well tolerated following repeated doses of 12 mg/kg, exceeding the clinical exposure levels of anti-PD1-VEGF antibodies. Collectively, these findings support the favorable safety profile and therapeutic efficacy of IMD-101, IMD-2032, and IMD-2035, highlighting their potential as next-generation immunotherapeutic candidates for clinical development.

#2636 Tumor microenvironment-activated T-cell engager (TMEA-TCE) targeting claudin 6 demonstrates efficacy without inducing cytokine release syndrome.

Chengli Ding, Cheng Liu, **Yuan Liu**

Affinity Biopharmaceutical Co., Ltd., Shanghai, China

The CD3 protein complex serves as a critical role of T cell activation and signal transduction. While CD3 T-cell engagers (TCEs) are highly potent, they can elicit severe adverse immune effects on various normal tissues due to pervasive T cell activation and excessive inflammatory cytokine release, leading to cytokine release syndrome (CRS) and limiting their therapeutic margin. CLDN6, a member of the claudin family of tight junction proteins, is highly expressed in multiple solid tumors such as ovarian, endometrial, testicular, and gastric cancers, but rarely in healthy adult tissues. The CLDN6-CD3 TCE demonstrates high affinity and specificity for CLDN6, without cross-reactivity to CLDN9 or CLDN4. To enhance tumor selectivity and address CD3-associated toxicity, CLDN6-CD3 TCE is further engineered via chemical conjugation of a legumain-cleavable linker that masks the variable region of the anti-CD3 domain, leading to the formation of a tumor microenvironment-activated (TMEA)-TCEs and the development of CLDN6-CD3 TMEA-TCE (IMD-1743). IMD-1743 can be activated by legumain, an active protease overexpressed extracellularly in the TME, triggering the release of TCE in the TME or in vitro. This activation strategy follows the same proof-of-concept demonstrated by the successful phase 3 studies of legubicin, an albumin-drug conjugate (ALDC). IMD-1743 exhibited dose-dependent anti-tumor activity in human ovarian PA-1 and OVCAR3 as well as human hepatocellular carcinoma HepG2-Luc mouse models at doses of 1, 3, and 10 mg/kg. Complete tumor elimination was observed in the ovarian PA-1 model at 3 and 10 mg/kg, with no associated mouse weight loss. Preclinical toxicology studies in cynomolgus monkeys showed that IMD-1743 was well tolerated after repeated dosing of 15 mg/kg, with no evidence of CRS based on serum cytokine assays. Pharmacokinetic studies in cynomolgus monkeys revealed high concentrations of IMD-1743 and minimal free TCE, indicating that the molecule is highly stable in circulation.
In summary, these findings highlight a favorable therapeutic margin for IMD-1743 as a safe and effective TCE candidate targeting claudin 6. The strong preclinical efficacy combined with its tolerability profile supports further clinical development of IMD-1743 to address the significant unmet medical needs of patients with CLDN6-expressing tumors.

#2637 A DR5-targeting ADC exhibits superior anti-tumor activity and potentially better therapeutic window.

Yang Wang, Lixia Cao, Cui Feng, Yifan Yang, Fangdun Jiang, Lixia Gu, Qi Zhang, Chen Li, Ming Zhou, Cancan Li, Wei Huang, Bonan Yan, Ziping Wei, Yuhong Zhou

Preclinical research & development, Bliss Biopharmaceutical Co., Ltd., Hangzhou, China

Targeting death receptor DR5 with agonist antibody could trigger extrinsic apoptosis via caspase activation in cancer cells while sparing normal tissues. Ozekibart (INBRX109), a tetra-valent anti-DR5 antibody, showed significant efficacy as a monotherapy in patients with advanced or metastatic, unresectable chondrosarcoma, with disease control rate (DCR) of 54%, (compared to 27.5% in the placebo group). Later in a study of advanced Ewing sarcoma, Ozekibart combined with irinotecan and temozolomide demonstrated improved clinical benefit with an ORR of 64% and a DCR of 92%. Encouraged with these results, we designed a DR5-targeting ADC with the aim to synergize the extrinsic apoptosis activity of DR5 engaging and superb cytotoxicity effect of Top-1 inhibitor. In this presentation we show systematic evaluation of this novel ADC including specific tumor cell engaging, anti-tumor efficacy, serum stability, and pharmacokinetics (PK) in target-humanized mice. First, the unique design of the tri-valent DR5-targeting antibody demonstrated superior activity over counterparts. Second,its resulting ADC form showed a robust tumor growth inhibition across diverse xenografts, potentially benefit from its dual mode of action design, surpassing clinically advanced control agents (INBRX109). Our ADC showed dose dependent *in vivo* antitumor activity without hook effect seen with agonist antibodies. Finally, this ADC showed better *in vivo* safety profile: lower on-target off-tumor apoptosis, longer half-life and better tolerability in comparison with that of INBRX109,suggesting a potentially wider therapeutic window. These results may support progression of this novel DR5-tageting ADC into clinical development as a potentially more potent and safer DR5-targeted therapy.

#2638 A rapid patient-derived organoids platform guides the evaluation of ERBB-targeting bispecific T-cell engagers.

Yuhong Liu[1], Chen Wang[2], Jing Zhao[3], Leli Zeng[4]

[1]Centre for Virology, Vaccinology and Therapeutics, The University of Hong Kong, Hong Kong, China,[2]Digestive Diseases Center, The Seventh Affiliated Hospital of Sun Yat-Sen University, Shen Zhen, China,[3]Scientific research centre, The Seventh Affiliated Hospital of Sun Yat-Sen University, Shen Zhen, China,[4]The Biobank, Scientific Research Center, The Seventh Affiliated Hospital of Sun Yat-Sen University, Shenzhen, China

Background: The ERBB receptor family (EGFR/HER1, HER2, HER3, HER4) are well-validated oncogenic drivers. The clinical translation of ERBB-targeted bispecific antibodies (e.g., EGFRxCD3, HER2xCD3,HER2 degrading BsAbs) is bottlenecked by the lack of models that can rapidly and concurrently predict patient-specific efficacy and on-target, off-tumor toxicity. Optimizing these drugs including fine-tuning parameters like affinity, valency, and epitope to maximize the therapeutic window, which requires a predictive platform that provides integrated feedback on both anti-tumor activity and on-target toxicity in a clinically relevant timeframe.
Methods: We established a comprehensive biobank of patient-derived organoids (PDOs) from breast, gastric, and non-small cell lung cancers, alongside matched normal organoids. We developed a high-throughput, standardized co-culture assay with PBMCs or T cells to evaluate a panel of ERBB-targeting bispecific antibodies with varying molecular formats. The entire workflow was designed for speed, generating parallel data on tumor organoid killing and normal organoid toxicity within days.
Results: Our platform delivered robust, quantitative data on the therapeutic index for a series of BsAb candidates within a 3-week window. We demonstrated that affinity-tuning towards tumor-associated antigen levels could preferentially spare normal organoids with low ERBB expression while maintaining potent tumor killing. Furthermore, comparing different BsAbs revealed that certain molecular formats or epitope choices were associated with reduced cytokine release and less severe toxicity in normal organoids, without compromising efficacy in target-positive tumors. This provides a direct, rapid strategy for lead candidate selection and optimization.
Conclusion: We have developed a rapid, reproducible PDO-based platform that not only predicts the therapeutic window of ERBB-targeting BsAbs but also provides critical insights for their molecular optimization. This "fast-feedback" system can significantly de-risk and accelerate the translation of BsAbs by enabling data-driven decisions on affinity, format, and epitope selection early in the drug development process. The ability to rapidly profile multiple candidates against a backdrop of human tumor and normal tissues makes this an invaluable tool for designing safer and more effective bispecific antibodies. This study presents a transformative preclinical optimization tool. By generating predictive safety and efficacy data in weeks, our platform moves beyond mere prediction to active guidance, empowering the rational design of next-generation BsAbs with an inherently improved therapeutic profile for clinical trials.

#2639 Mesothelin-targeted nanobody-drug conjugates to treat pancreatic cancer.

Nisita Dutta[1], Roman Misteli[2], Jessica Hong[1], Julie Becher[2], Francisco Corzana Lopez[3], Christine Alewine[1], Mitchell Ho[1], Goncalo Bernardes[2]

[1]National Cancer Institute, National Institutes of Health, Bethesda, MD,[2]Department of Chemistry, University of Cambridge, Cambridge, United Kingdom,[3]Department of Chemistry, University of La Rioja, La Rioja, Spain

Development of targeted therapies that can penetrate the dense stroma of the pancreatic ductal adenocarcinoma (PDAC) tumor microenvironment (TME) is essential to improve outcomes for pancreatic cancer patients. We have discovered a camel VHH nanobody (A101) using phage display, which effectively binds to mesothelin (MSLN), a cancer antigen that is expressed in PDAC. Using the A101 VHH nanobody with an MMAE payload, we generated nanobody-drug conjugates (NDCs) that can be advantageous compared to existing biologic therapies by enhancing tumor penetration through the PDAC TME and improving pharmacokinetic distribution, while minimizing systemic toxicity.

The structure of the A101 nanobody was computationally predicted and molecular dynamic simulations were run to understand its interaction with MSLN. Site-specific modifications were engineered and small linker-MMAE molecules were synthesized, then bioconjugated to the modified A101 nanobody using maleimide chemistry. The chemical linkers used in these constructs were valine-citrulline, glycine-proline, and AB (a novel small molecule). The NDCs were tested for binding to MSLN via bio-layer interferometry assays. Internalization and cell viability were also assessed using mouse and human PDAC cell lines. Finally, *in vivo* activity was assayed in MSLN+ and MSLN knockout (MLSN-KO) subcutaneous mouse PDAC tumor models to determine efficacy and specificity of each therapeutic.

We found that modified A101 nanobody retains binding to human (K_D = 18 nM) and mouse (K_D = 5.6 nM) MSLN. A101 NDCs displayed a statistically significant difference in internalization into MSLN+ as compared to isogenic MSLN-KO cells. Additionally, the NDCs efficiently killed PDAC cell lines in vitro (IC_{50} = 20-200 nanomolar). In mice, the A101-AB-MMAE NDC (at 20 mg/kg, 3x per week) displayed the most promising inhibition of tumor growth in MSLN+ tumors and had the highest specificity compared to other A101-NDCs tested, showing limited efficacy in analogous MSLN-KO tumors.

We have synthesized A101-based NDCs with high-affinity MSLN binding and promising anti-tumor activity in PDAC cell lines. Our preliminary animal studies suggest that the A101-AB-MMAE conjugate, which has a novel exclusively intracellular cleavable linker, has superior efficacy and specificity compared to other A101-based NDCs tested with known linkers. Future studies will explore A101-AB-MMAE activity in orthotopic humanized MSLN mouse models of PDAC to assess safety, biodistribution, and anti-tumor efficacy.

#2640 XmAb808, a B7H3-targeted CD28 bispecific antibody, costimulates T cells enhancing the anti-tumor activity of clinically active CD3 T cell engagers.

Michael Hedvat, Veronica Zeng, Mayra Montes-Camacho, Charles G. Bakhit, Alex K. Lam, Lizett E. Scott, Jessica Reyes, Heather P. Jimenez, Rosio Padilla, Scott Taylor, Jose Serrato Bucio, Matthew A. Dragovich, Sung-Hyung Lee, Katrina Bykova, Yoon K. Kim, Suzanne Schubbert, Christine Bonzon, Seung Y. Chu, Gregory L. Moore, F. Rena Bahjat, John R. Desjarlais

Xencor, Inc., Pasadena, CA

CD3 bispecific T-cell engagers (CD3-TCEs) represent a promising therapeutic modality for solid tumors, with multiple candidates in clinical development. These agents bridge tumor-associated antigens and CD3 on T cells to form an immune synapse, delivering Signal 1 for T-cell activation. However, solid tumors, unlike professional antigen-presenting cells, typically lack CD28 ligands required for Signal 2 costimulation. T cells receiving Signal 1 without Signal 2 risk developing anergy, potentially limiting CD3-TCE efficacy. A key advancement in costimulatory immunotherapy involves tumor-targeted CD28 bispecific antibodies that strictly depend on concurrent Signal 1 for activation. These bispecifics engage tumor associated antigens to cluster CD28 at the immune synapse, delivering Signal 2 to T cells. We developed XmAb808, a novel B7H3xCD28 bispecific incorporating a nonsuperagonistic, monovalent CD28-binding domain and a high-avidity, bivalent B7H3-binding domain.

In proof-of-concept studies, XmAb808 potently amplified the in vitro and in vivo anti-tumor efficacy of CD3-TCEs targeting prototype tumor antigens. Exploring potential combination opportunities, we found co-expression of B7H3 with CLDN6 in ovarian tumors and co-expression with STEAP1 in prostate tumors. Notably, XmAb808 synergistically enhanced the activity of XmAb541 (CLDN6xCD3) and an analog of xaluritamig (STEAP1xCD3), two programs with clinically observed anti-tumor activity. These XmAb808 combinations induced robust IL-2 secretion from activated T cells, which in turn promoted T cell proliferation and Bcl-xL-dependent survival. Moreover, in a T cell restimulation assay, XmAb808 was able to overcome apparent T cell exhaustion promoted by xaluritamig, strongly recovering xaluritamig’s reduced anti-tumor activity weeks into the assay. The addition of targeted costimulation translated to superior T cell-mediated cytotoxicity in vitro and markedly improved anti-tumor responses in humanized xenograft models, highlighting XmAb808's potential to synergize with TCE-based immunotherapies.

#2642 Pan-cancer GlyTR1 CAR T cells with ‘velcro-like’ density-dependent targeting of β1,6GlcNAc-branched N-glycans.

Paresh Kumar Purohit, Raymond W. Zhou, Michael Demetriou

UC-Irvine, Irvine, CA

Bispecific antibodies and chimeric antigen receptor (CAR) T-cells are some of the most potent cancer immunotherapeutics in clinical use, yet most cancers remain poorly targetable. High-affinity antibodies required to maximize killing detect low antigen expression in normal tissue, risking ‘on-target, off-cancer’ toxicity. This compels identification of cancer-restricted cell surface protein antigens, which are rare and leave most cancers untreatable by CAR T cells. Tumor Associated Carbohydrate Antigens (TACA’s) are the most abundant and widespread cancer antigens known but are poorly targetable by antibodies. With funding from the Cancer Moonshot program at NCI, we recently published in *Cell* a novel pan-cancer immunotherapeutic technology termed Glycan-dependent T cell Recruiter (GlyTR). Unlike antibodies that employ high-affinity ‘key-lock’ binding to target cells regardless of antigen density, GlyTR utilizes high-avidity ‘velcro-like’ lectin binding to kill cells with high but not low TACA expression. The GlyTR1 bi-specific protein binds β1,6GlcNAc-branched N-glycans to overcome immunosuppressive mechanisms in the tumor microenvironment and trigger target-density dependent T cell mediated pan-cancer killing without toxicity in mice having human-like TACA expression. Here we report early development of GlyTR1 CAR T cells, which display similar pan-cancer activity.

#2643 Clinical predictors of cytokine release syndrome in non-single chain CD3 directed therapies among cancer patients.

Harshit Khosla[1], Brian Dinh[1], Rodney Hunter[1], Neha Maithel[1], Natalie Rafaeli[1], Sara Taveras[1], Joan Marie C Bull[2], Syed H. Jafri[1], Adan Rios[3]

[1]The University of Texas Health Science Center at Houston, Houston, TX,[2]Professor of Medicine, Div. of Oncology, UT Health Science Center, Houston, TX,[3]UT Medical School at Houston, Houston, TX

Background: Bispecific T-cell engager (BiTE) antibodies are novel agents in cancer therapeutics which work by simultaneously binding a cancer cell specific antigen and engaging T-Cell. Major safety concern with use of BiTE therapy based on CD3 platforms is cytokine release syndrome (CRS) from massive unchecked T-cell activation. Thus initial dosing of BiTE requires hospitalization for monitoring and treating CRS. This leads to intensive care requirement and mortality if CRS is not identified and intervened early. We assessed the prevalence of CRS in cancer patients receiving non-single chain CD3 based BiTE therapy and contrasted clinical parameters in patient who developed CRS against those who did not.

Methods: A retrospective chart review was performed on patients from our institution who were admitted for the initial and step up dosing of the BiTE therapy for monitoring of CRS between September 2024 - September 2025. The patients were divided in two groups, those who developed CRS and those who did not. Demographic data, previous treatment history, clinical characteristics, laboratory data and duration of hospitalization at the time of admission were noted.

Results: 20 patients were identified with median age of 67 years. 30% were male and 70% were female. 35% received tarlatamab, 30% got glofitamab, 10% got talquetamab and epcoritamab each, 1 patient got mosunetuzumab and linvoseltamab. All 20% patients who had grade two or higher neurotoxicity syndrome had intracranial disease. 35% (n=7) patients had CRS. Three patients had grade I, two patients had grade II and two had Grade IV CRS. Culture data was negative for all CRS patients up to 1 week after the dose. All CRS was seen after first dose of BITE therapy, except 1 patient who developed it after second dose of tarlatamab. Monocyte to lymphocyte (M:L) ratio 24 - 48 hours after the dose of BiTE (1.51 in CRS vs 0.59 in no CRS, p=0.028*), days between diagnosis and BITE therapy (median 864 days in CRS vs 448 days in no CRS patients, p=0.0218*), and previous lines of therapy (LOT)(4 vs 3, p=0.0224*) were noted to be significantly higher in patients with CRS. Logistical regression suggested that only M:L ratio was significantly related to CRS (odds ratio 5.64, p=0.0372*), while previous LOT (OR 6.93, p=0.060) and time of disease before therapy (OR 1.00, p=0.058) were not significantly related.

Discussion: Despite high CRS prevalence in patients receiving BiTE therapy, the literature describing the mechanism of CRS specific to BiTE therapy is very limited. Monocytes get involved in the uncontrolled release of cytokines which may appear early in circulation. The patients who sustain malignancy for longer and had more treatment lines may develop immune build up against the tumor which may increase the chance of CRS in such patients. These factors need to be explored further in the clinical setting to predict CRS and triage clinical resources.

#2644 Enhancing safety to unlock efficacy: A novel class of conditionally-activated T cell engagers for solid tumors.

Aude Segaliny[1], Than Thar Aye[1], Randall Bettman[1], Jui-Yi Chen[2], Yang Zhou[3], Xiaoya Jessie Ma[4], Rodrigo Rivera[5], Ricky Cheng[6], Xianzhi Jiang[3], Yonglei Shang[1], George Wu[1]

[1]Amberstone Biosciences, Inc., Irvine, CA,[2]Valora Therapeutics, San Diego, CA,[3]Aureka Biotechnologies, Laguna Hills, CA,[4]Glaukos Corporation, Aliso Viejo, CA,[5]aTyr Pharma, Inc., San Diego, CA,[6]QLSF Biotherapeutics, Inc., South San Francisco, CA

Background: T cell engagers (TCEs) offer potent anti-tumor activity but remain limited in solid tumors by cytokine release and on-target off-tumor toxicity. Amberstone's Tumor-Microenvironment Activated Therapeutics (T-MATE™) platform enables pH-gated activation of TCEs, exploiting tumor acidity to achieve selective activation within tumors while maintaining potency under heterogenous tumor pHs (up to pH 7.2). We previously demonstrated that T-MATE™ TCEs broaden the therapeutic index and enable selective targeting of tumor antigens such as TROP-2, which were previously intractable due to normal tissue expression.

Methods: The T-MATE technology integrates proprietary pH-dependent anti-CD3 clones identified via *de novo* high-throughput functional screening. These clones undergo pH-dependent conformational changes in their CDRs, conferring tunable affinities and selectivity profiles for plug-and-play integration into next-generation TCEs. ABS-106, a STEAP1×CD3 T-MATE TCE, was evaluated for activity against metastatic castration-resistant prostate cancer (mCRPC) using *in vitro* assays such as cytotoxicity, cytokine release, and repeated-challenge, as well as *in vivo* xenograft models in humanized mice and non-human primates toxicokinetic studies.

Results: ABS-106 demonstrated potent cytotoxicity across tumor-relevant pH ≤7.2 and induced sustained T cell activation and cytokine release comparable to a clinical benchmark TCE. Its pH 7.2 gating minimized activity at physiological pH 7.3-7.5, yielding minimal T cell activation and about 1000-fold lower cytokine release even at high STEAP1 expression. ABS-106 effectively killed STEAP1$^{Med-Low}$ tumor cells and mediated bystander killing of STEAP1^{-} cells, sustaining activity over nine tumor rechallenge cycles. *In vivo*, ABS-106 induced dose-dependent tumor regression with increased intratumoral CD8^{+} T cells infiltration and upregulation of pharmacodynamic markers such as Granzyme B, CD69 and PD-1. ABS-106 is fully cross-reactive to cynomolgus CD3 and STEAP1, and exhibited consistent favorable pharmacokinetics ($t_{1/2}$ 4-5 days) across all animals. Notably, it maintained exposure upon repeat dosing, and was well tolerated at >130× exposure of the benchmark's reported MTD. The molecule demonstrates excellent developability, robust stability under diverse stress conditions, and strong manufacturability characteristics. ABS-106 is currently undergoing IND-enabling studies.

Conclusions: ABS-106 exemplifies the precision-engineered, next-gen T-MATE™ TCE with optimal safety-efficacy balance. This smarter, safer TCE design enables potent anti-tumor efficacy while minimizing systemic toxicity, representing a promising therapeutic strategy for solid tumors and other indications.

#2645 Characterization of osemitamab in pancreatic cancer models and patients.

Fei Teng, Huanhuan Guo, Di Sun, Xinlai Yao, Lei Shi, **Yi Gu**, Chuan Qi, Xueming Qian

Transcenta Therapeutics Co., Limited, Suzhou, China

Background: TST001 (osemitamab) is a high affinity humanized, ADCC enhanced antibody targeting CLDN18.2. It specifically binds to the extracellular domains of CLDN18.2 and eliminates tumor cells by ADCC and CDC. Promising efficacy of TST001 monotherapy in late line G/GEJ cancer patients or plus CAPOX with or without nivolumab as first-line treatment has been observed and reported. TST003 is a novel humanized antibody targeting Gremlin-1, a member of TGF-β superfamily. Gremlin1 promotes epithelial-mesenchymal transition (EMT) and cancer cell proliferation by binding to BMPs and blocking its biological activities. Here we report preclinical anti-tumor activities of TST001 monotherapy or combined with TST003 in pancreatic cancer models and TST001 monotherapy in pancreatic cancer patients.
Methods: The CLDN18.2 expression on the pancreatic cancer cells was evaluated using IHC analysis with 14G11 antibody. The ADCC activity of TST001 on pancreatic cancer cells was assessed by ADCC reporter cell in vitro. Its in vivo anti-tumor activities were investigated in pancreatic cancer models. In a TST001 phase I clinical trial (NCT04495296), pancreatic cancer patients who failed prior available standard therapies were enrolled and received TST001 monotherapy at 10 mg/kg every 3 weeks.
Results: TST001 displayed potent ADCC activities for two pancreatic cancer cell lines (BxPC-3-CLDN18.2 and MIA PaCa-2-CLDN18.2) in vitro. In KRAS wild type BxPC-3-CLDN18.2 model, the tumor growth inhibition (TGI) of TST001 was 61% at 3 mg/kg and 98% at 10 mg/kg. 7 out of 10 mice in the 10 mg/kg group had their tumors completely disappeared from Day 33. In MIA PaCa-2-CLDN18.2 with KRAS mutation, TST001 at 10 mg/kg led to TGI= 49% and combination with gemcitabine (30 mg/kg) improved the TGI to 67%. In the phase 1 trial, a pancreatic cancer patient with liver metastasis and failed prior gemcitabine plus S1 chemotherapy achieved durable clinical benefit. Despite its tumor has low CLDN18.2 expression (5% 1+, 5% 2+, 5% 3+ tested by a validated IHC assay in a central lab) and KRAS G12R mutation (by local test), the primary target lesion shrank 86% at week 6 and complete response was achieved after the patient received TST001 treatment for 270 days. As Gremlin1 is highly expressed in pancreatic cancer, we also tested the anti-tumor activity of the combination of TST001 and TST003 using the BxPC-3-CLDN18.2/Gremlin1 co-expressing tumor model with PBMC co-inoculation. 3 mg/kg of TST001 combined with 30 mg/kg TST003 exhibited significantly better TGI (60%) than monotherapy (34% for TST001 and 28% for TST003).
Conclusions: TST001 displayed significant anti-tumor activity in preclinical pancreatic cancer models and higher efficacy when combined with gemcitabine or TST003. A pretreated pancreatic cancer patient achieved complete response with TST001 monotherapy. These findings support further investigation of TST001 in CLND18.2 positive pancreatic cancer patients.

: Targeted Antigen Therapies and Immunity
Poster Session

#2649 Tumor endothelial cell and cancer cell targeting anti-PRND antibody-drug conjugate to treat hypervascular tumors such as glioblastoma and sarcomas.

Byoungmo Kim[1], Ha Kyeong Lee[1], So-Young Choi[2], Sera Lee[2], Sang Yoon Kim[3], **Youngro Byun**[1], Seong Who Kim[4]

[1]Seoul National University College of Pharmacy, Seoul, Korea, Republic of,[2]New Drug Development Center, Osong Medical Innovation Foundation, Osong, Korea, Republic of,[3]Pharosgen Co. LTD, Seoul, Korea, Republic of,[4]Associate Professor, Dept. of Biochem. & Molec. Bio., University of Ulsan College of Medicine, Seoul, Korea, Republic of

Antibody-drug conjugates (ADCs) have emerged as a major class of targeted therapeutics but remain limited by poor tumor penetration, antigen heterogeneity, and a narrow therapeutic window. To overcome these limitations, we developed an anti-PRND ADC targeting PRND (Doppel), a prion-like glycoprotein selectively expressed in tumor endothelial cells (TECs) and cancer cells but absent in normal tissues except in the testis. This localization enables direct vascular targeting without diffusion barriers and provides a unique opportunity for precise drug delivery to the tumor vasculature. The resulting antibody-drug conjugate, 3H9-KGDEVD-MMAE, is a homogeneous ADC (DAR = 8) free of soluble aggregates. It couples a high-affinity anti-PRND antibody (3H9) with a caspase/cathepsin B-cleavable KGDEVD linker that can be specifically cleaved by both cathepsin B and caspase-3/7. This dual activation allows MMAE release through lysosomal cathepsin B and induces apoptosis of PRND positive cells, and caspase-3/7 from the apoptosis of target cells induces the apoptosis of adjacent tumor tissues. The caspase-mediated cleavage establishes an *in-situ* feedback amplification loop that maintains continuous local drug release, sustained cytotoxicity, and producing a potent bystander effect that overcomes antigen heterogeneity. By combining TEC and cancer cell-specific targeting with a caspase/cathepsin-responsive linker, 3H9-KGDEVD-MMAE (anti-PRND ADC), achieves deep intratumoral penetration, robust vascular disruption, and durable antitumor efficacy. In preclinical models of glioblastoma, sarcoma, and renal cell carcinoma (RCC) - hypervascular malignancies with limited ADC options, anti-PRND ADC induced extensive and durable tumor regressions without systemic toxicity. Collectively, these findings establish anti-PRND ADC as a next-generation vascular-disrupting ADC, integrating endothelial docking with apoptosis-triggered drug amplification for potent and selective control of highly vascularized tumors.
Acknowledgments: This research was supported by the Korea Drug Development Fund (HN21C0264) funded by the Ministry of Science and ICT and the National Research Foundation of Korea (NRF) grant (2020R1A2C2015026) funded by the Korea government (MSIT).

#2650 Breaking immune silence: Tumor-targeted molecular therapy reprograms the tumor-immune interface in progressive neuroblastoma.

Loganayaki Periyasamy[1], Sreenidhi Mohanvelu[1], Sheeja Aravindan[2], Poorvi Subramanian[1], Natarajan Aravindan[1]

[1]Oklahoma State University, Stillwater, OK,[2]OU Health Stephenson Cancer Center, Oklahoma, OK

Progressive neuroblastoma (pNB) that defies intensive multimodal clinical therapy remains a challenging pediatric cancer, characterized by swift clinical deterioration, recalcitrance, and a high degree of immune evasion. Our recent investigations recognized retinal degeneration 3 (RD3) deficiency as a central molecular driver of malignant characteristics, correlating with unfavorable outcomes and dictating immune evasion. Herein, we developed precision-engineered nano-immunotherapeutics targeting RD3-deficient ($RD3^{-/-}$) NB. Five different RD3 peptides were strategically designed and enhanced *via* chemical stabilization through capping modifications and were labeled with a fluorescent marker to assess biodistribution and stability *in vivo*. These peptides were encapsulated into GD2-conjugated immunoliposomes (IL), archiving five RD3[GD2]IL formulations tailored for selective delivery to NB. ILs were assessed for uniform nanoscale distribution (NT Analyzer NS300), encapsulation efficiency, and structural integrity via TEM. Therapeutic efficacy was evaluated using an *in vivo* mouse model established using patient-derived stage 4 progressive pNB cells from a retroperitoneal tumor mass. Systemic administration (IV) of RD3[GD2] ILs (5 µM, thrice weekly × 4 weeks) inflicted immune signatures that were compared to the vehicle control (plain liposomes). High-resolution multiplex immune profiling was performed to characterize the tumor immune landscape, assessing the distribution ($CD4^+$ and $CD8^+$) and activation status ($GITR^+$) of immune subsets. Among the five different formulations, RD3[GD2]IL-1 and RD3[GD2]IL-2 exhibited greater immunogenicity, restoring immune surveillance in $RD3^{-/-}$ tumors. RD3[GD2]IL-2 enhanced the infiltration of $CD4^+$ helper and $CD8^+$ cytotoxic T cells, which was associated with a significant increase in the co-stimulatory receptor GITR, an important factor for T-cell activation and survival. Remarkably, RD3[GD2]IL-2 countered T-cell activation and boosted multifunctional T-cell populations, including $CD4^+GITR^+$, $CD8^+GITR^+$, and a rare, highly functional subset of the $CD4^+CD8^+GITR^+$ triple-positive population. Particularly, RD3[GD2]IL-2 demonstrated impressive homing and tolerability, with no observable systemic toxicity or off-target effects. Collectively, our findings highlight RD3[GD2]IL-2 as a promising therapeutic candidate that synergizes precision tumor targeting with immune reinstatement. This next-generation immunoliposomal delivery reinstates immune responsiveness and treatment sensitivity in refractory pNB, offering a scheme for RD3-based therapies in immunosuppressive “cold” tumors, beyond NB.

Funding: This work was funded by DoD-CA-210339, OCAST-HR19-045, and NIH P20GM103639 to Dr. Aravindan and NCI-P30 CA225520, and NIGMS P30GM154635 awarded to the OU Health SCC.

#2652 MGT-1142, an antibody-drug conjugate targeting a novel glycan for small-cell lung cancer.

Su-Yu Tsai, Maomao He, Ju-Mei Li, Ping Chao, Ting-Chun Hung, Mei-Hsuan Tsai, Charng-Sheng Tsai

Marigold Therapeutics, Inc., Taipei, Taiwan

Background: Aberrant glycosylation is a hallmark of many malignancies, driving tumor growth, immune evasion, and metastasis. Certain tumor-associated glycans are highly expressed in small-cell lung cancer (SCLC) but minimally present in normal tissues, making them attractive yet underexplored targets for antibody-drug conjugates (ADCs). MGT-1142 is an exatecan-based ADC engineered with an optimized Fc domain to recognize a tumor-specific glycosylation pattern and selectively deliver a potent topoisomerase I inhibitor payload.
Methods: Comprehensive in vitro and in vivo evaluations were performed to characterize MGT-1142. Binding affinity, internalization, and cytotoxicity were examined across multiple SCLC cell lines. Anti-tumor efficacy was assessed in both cell line-derived xenograft (CDX) and patient-derived xenograft (PDX) models. Pharmacokinetic (PK) and dose-range-finding (DRF) studies were conducted in cynomolgus monkeys to determine systemic exposure, half-life, and tolerability.
Results: MGT-1142 exhibited high target specificity with no detectable cross-reactivity to structurally related glycans. It demonstrated strong binding and rapid internalization in glycan-positive cells, resulting in potent inhibition of antigen-positive tumor cell proliferation. In vivo, MGT-1142 achieved dose-dependent tumor growth inhibition across multiple CDX and PDX models. Cynomolgus PK studies revealed linear, dose-proportional exposure and a favorable terminal half-life. Dose range finding studies indicated good tolerability and a wide therapeutic window.
Conclusions: MGT-1142 shows potent and selective anti-tumor activity, favorable pharmacokinetics, and an encouraging safety profile in preclinical studies. These findings support MGT-1142 as a potential first-in-class glycan-targeting ADC for the treatment of small-cell lung cancer.

#2653 Sequencing immune checkpoint inhibitors and BRAF/MEK inhibitors in advanced melanoma: A meta-analysis of Kaplan-Meier-reconstructed individual level data.

Anderson Ruiz Simoes[1], Isabella Michelon[2], Wellington Neto[3], Metamia Ciampricotti[4], Ludimila Cavalcante[5]

[1]Federal University of Sao Paulo (UNIFESP), Sao Paulo, Brazil,[2]Universidade Catolica de Pelotas, Pelotas, Brazil,[3]Universidade de Fortaleza, Fortaleza, Brazil,[4]MSKCC, New York, NY,[5]Division of Hematology & Oncology, University of Virginia (UVA), Charlottesville, VA

Objectives: Optimal sequencing of immune checkpoint inhibitors (ICI) and BRAF inhibitors (BRAFi) for BRAFV600-mutant advanced melanoma remains uncertain. We conducted a meta-analysis of Kaplan-Meier (KM)-reconstructed individual-patient data (IPD) comparing two clinically used sequences: First-line ICI followed by BRAFi (ICI-BRAFi) versus first-line BRAFi followed by ICI (BRAFi-ICI).

Methods: We searched MEDLINE, Embase, and Cochrane for phase II/III studies reporting KM curves for stage III/IV melanoma patients treated with either ICI-BRAFi or BRAFi-ICI. Outcomes were progression-free survival (PFS) and overall survival (OS). Secondary endpoints were toxicity and brain-metastasis-free survival (BMFS). Reconstructed IPD were analyzed with Cox proportional hazards (PH) models. We additionally estimated restricted mean survival time (RMST) up to 24 months (m) (Grambsch-Therneau test, $p<0.05$).

Results: Six studies with 832 patients were included, of which 426 patients received ICI-BRAFi, and 406 BRAFi-ICI. Median PFS was approximately 12 m for both groups ($p=0.1$, log-rank). PFS at 24 m was 42.8 and 29 m for ICI-BRAFi and BRAFi-ICI, respectively. The PFS RMST difference at 24 m was 0.32 m (95% CI: -1.1 - 1.8 months; $p=0.66$). Median OS was 58.2 m for ICI-BRAFi and 40.3 m for BRAFi-ICI. OS at 24 m was 65.9% and 60.7% for ICI-BRAFi and BRAFi-ICI groups, respectively ($p=0.4$; log-rank). The RMST revealed a slight and nonsignificant OS difference of -0.49 m (95% CI: -1.64 - 0.67 months; $p=0.41$). In a pooled analysis including the only two randomized studies SECOMBIT and DREAMseq, we found a median PFS of 31.5 m for ICI and 13.1 m for BRAFi ($p=0.003$); and median OS was NA and 32.7 m for ICI and BRAFi ($p=0.005$).

Conclusion: ICI-BRAFi led to significantly longer PFS and OS than BRAFi-ICI when evaluating only randomized clinical trials, supporting ICI-first sequencing.

Survival data in ICI-BRAFi vs BRAFi-ICI cohorts

	ICI-BRAFi	BRAFi-ICI	p value
Overall median PFS	12.5 months (9.6-23.3)	12 (10.7-14)	0.1
PFS at 24 months	42.8 months (36.9-49.7)	29 months (24.2-34.4)	-
Median PFS with RCT only	31.5 months (13.9-44.1)	13.1 months (11.3-16.7)	0.003
Overall median OS	58.2 months (37.5-NA)	40.3 months (32.4-NA)	0.4
Os at 24 months	65.9 % (60.2-72.1 %)	60.7 % (55.6-66.2 %)	-
Median OS with RCT only	NA (55.5-NA)	32.7 (23.1-59.7)	0.005

#2654 DB-1421, an optimized EGFR/MUC1 bispecific ADC, exhibits improved tumor selectivity, promising efficacy and safety in preclinical studies.

Chenggang Li[1], Jun Yao[1], Yongsheng Nie[1], YANG QIU[2], **Haiqing Hua**[2]

[1]Duality Biologics Ltd, Shanghai, China,[2]Dualitybio Inc., Wilmington, DE

Introduction: Epidermal growth factor receptor (EGFR) is a well-known and validated target for anti-tumor therapies. However, anti-EGFR therapy in clinical showed obvious safety concerns because of broad EGFR expression in normal tissue, and such adverse effects limit the efficacy of these products. Mucin 1 (MUC1) is highly co-expressed with EGFR in multiple tumor types including esophageal squamous cell carcinoma (ESCC), non-small cell lung cancer (NSCLC), breast cancer (BC), colorectal cancer (CRC) and others. Dual targeting of both EGFR and MUC1 is a promising therapeutic strategy to enhance tumor-selective targeting and avoid undesired toxicity observed with anti-EGFR therapeutics. DB-1421 is a bispecific ADC comprised of a fully human EGFR/MUC1 bispecific antibody conjugated to a novel DNA topoisomerase I inhibitor via a cleavable linker. The naked antibody of DB-1421 is constructed by an affinity reduced EGFR binding arm and a tumor-associated MUC1 (TA-MUC1) specific binding arm. Based to this optimized format, DB-1421 showed both high tumor cell selectivity and high tolerable in preclinical models.
Methods: The tumor selectivity of DB-1421 between tumor cell and normal cell was evaluated via FACS analysis. The internalization of DB-1421 to tumor cell was tested by Incucyte. CTG assay was used to evaluate the cancer cell killing of DB-1421 on multiple target positive cell lines. Both cell line-derived xenograft (CDX) models and patient-derived xenograft (PDX) models were established to evaluate the in vivo efficacy of DB-1421 monotherapy. The safety and PK of DB-1421 were evaluated by in vivo monkey studies.
Results: The naked antibody of DB-1421 showed significant higher tumor selectivity than EGFR antibody. Internalization assays demonstrated that unconjugated DB-1421 was endocytosed in tumor cells co-expressing EGFR and TA-MUC1. DB-1421 exhibited strong cytotoxicity in vitro against several tumor cell lines across a range of target expression. DB-1421 inhibited tumor growth in vivo in CDX and PDX models by dose dependent manner. Additionally, it was well tolerated with repeat dose administration up to 80 mg/kg in monkeys.
Conclusions: DB-1421 is an EGFR/MUC1 bispecific ADC with a common light chain bispecific antibody and a DNA topoisomerase I inhibitor. Through rational design and engineer of EGFR and MUC1 binding arm, DB-1421 showed improved tumor selectivity, efficacy and very good safety. The promising efficacy and safety profile warrants further clinical development of DB-1421.

#2655 DB-1323, a next-generation mesothelin targeting antibody-drug conjugate, demonstrated anti-tumor activity and favorable safety profile in pre-clinical models.

Haiqing Hua[1], Xi Li[1], Jun Yao[1], Tao Cheng[1], Junjie Yang[1], Xinyue Chen[1], Sang Pil Lee[2], Jiyong Shin[2], Yunseon Choi[2], Gisun Baek[2], Alexandre Joyeux[2], Jung Chae Lee[2]

[1]Duality Biologics Ltd, Shanghai, China,[2]Fatiabgen, Sejong, Korea, Democratic People's Republic of

Background: Mesothelin (MSLN) is highly expressed in many hard-to-treat solid tumors and is associated with metastasis, poor progression-free survival and lower overall survival. Despite 25 years of drug- development efforts across modalities, no MSLN-directed therapy has been approved, hampered by on-/off-target toxicities, intra-tumoral antigen heterogeneity, poor internalization of MSLN-antibody complexes, and soluble MSLN “sink” effects. DB-1323 is a MSLN-ADC composed of a novel fully human anti-MSLN immunoglobulin G1 (IgG1) monoclonal antibody, covalently conjugated to a proprietary DNA topoisomerase I inhibitor via a maleimide-tetrapeptide cleavable linker. In the present study, we evaluated the efficacy and safety of DB-1323 in comprehensive preclinical models.

Methods: Binding affinity of the anti-MSLN antibody to MSLN-expressing cells was quantified by flow cytometry. Cytotoxicity was assessed in MSLN-positive pancreatic cancer cells. Anti-tumor activity was tested in MSLN-positive pancreatic and ovarian cancer xenograft models compared to that of anetumab ravtansine and other MSLN ADCs. The pharmacokinetics and safety profile were also evaluated in cynomolgus monkeys.

Results: DB-1323 showed high affinity to both Human and Cyno MSLN without detectable off-target binding. DB-1323 has unique MSLN binding characteristics (fast on/off kinetics) that allow it to evade soluble MSLN while maintaining high avidity for MSLN on the surface of tumor cells. DB-1323 has faster and more extensive internalization than anetumab ravtansine, especially in the presence of physiologically relevant soluble MSLN concentrations. In vitro, DB-1323 retained cytotoxicity towards MSLN-expressing pancreatic cancer cells in the presence of soluble MSLN. It also showed dose-dependent anti-tumor activity in a pancreatic cancer xenograft model and ovarian cancer patient-derived xenograft model. Moreover, DB-1323 showed stronger tumor growth inhibition than that of anetumab ravtansine at the same dose. The systemic exposure AUC0-last and Cmax of DB-1323 and total antibody increased dose proportionally from 1mg/kg to 10mg/kg with low free payload in serum. DB-1323 also showed good safety profile with highest non-severely toxic dose (HNSTD) of 60mg/kg in cynomolgus monkeys.

Conclusions: DB-1323 overcomes historical MSLN-targeting liabilities through unique rapid-on/off binding, efficient internalization, and potent topoisomerase I inhibition, delivering superior tumor eradication versus at well-tolerated doses. These data support clinical evaluation of DB-1323 for patients with MSLN expressing tumors.

#2656 DB-1329: A novel antibody-drug conjugate targeting CDCP1 demonstrates potent preclinical anti-tumor activity across multiple solid tumors.

Hui Yang, Yujie Liu, YANG QIU, **Haiqing Hua**

Dualitybio Inc., Wilmington, DE

Background: Antibody-drug conjugates (ADCs) are designed to eradicate cancer cells while minimizing damage to healthy tissues. The identification and prioritization of viable tumor-associated antigen (TAA) targets are crucial for ADC development. To address this, we employed an integrative multi-omics approach to systematically discover and prioritize cell surface targets suitable for ADC development.
Methods: We established an integrative framework for the identification and prioritization of tumor-associated antigen (TAA) targets. Following target identification and validation, ADCs were developed and evaluated for anti-tumor efficacy and toxicology.
Results: Our AI-driven multi-omics-based platform identified CUB Domain-Containing Protein 1 (CDCP1), as a cell surface protein that is significantly upregulated in a large proportion of cancer cells across many solid tumors (notably lung, pancreatic, ovarian, and colorectal cancers) with limited expression in normal tissues. Given its role in promoting metastasis and therapy resistance, CDCP1 represents an attractive therapeutic target. We developed a novel antibody-drug conjugate, DB-1329, which consists of a fully human anti-CDCP1 monoclonal antibody with high affinity and specificity, conjugated via a protease-cleavable linker to a potent camptothecin-based TOP1 inhibitor payload. DB-1329 exhibited rapid and efficient internalization upon binding to CDCP1 and demonstrated potent and specific cytotoxicity in CDCP1-positive cancer cell lines. In vivo, DB-1329 induced profound and durable tumor regression across multiple patient-derived (PDX) and cell line-derived xenograft (CDX) models of lung, pancreatic, and colon cancers, demonstrating superior antitumor efficacy compared to benchmark ADC-treated animals. DB-1329 also displayed a favorable pharmacokinetic profile, was well-tolerated in toxicology studies, and exhibited a manageable safety profile.
Conclusion: These compelling preclinical results establish CDCP1-ADC DB-1329 as a promising therapeutic candidate, with potent and targeted anti-tumor efficacy against multiple CDCP1-positive solid malignancies. Our findings strongly support the continued development and clinical translation of CDCP1-ADC.

#2657 DB-1326, a novel dual-payload TA-MUC1-directed antibody-drug conjugate, shows potent antitumor efficacy in pre-clinical tumor model.

Chenggang Li[1], Lei Yi[2], Jun Yao[1], Yang Qiu[3], **Haiqing Hua**[2]

[1]Duality Biologics Ltd, Shanghai, China,[2]Dualitybio Inc., Wilmington, DE,[3]Duality Biologics, Basking Ridge, NJ

Introduction: Tumor-associated mucin-1 (TA-MUC1) is a glycoform of the MUC1 protein that is aberrantly glycosylated and is highly specific expressed by cancer cells. TA-MUC1 is highly expressed in various human epithelial cancers, making it an attractive target for cancer therapies. Several antibody-drug conjugates (ADCs) targeting TA-MUC1 are in development in clinical and preclinical stage, such as DS-3939a, CAT-09-833. However, their application remains limited by inadequate efficacy, highlighting the unmet clinical need for improving the efficacy of single payload ADCs. This study presents the preclinical evaluation of a novel dual-payload TA-MUC1-targeting ADC, DB-1326, composed of a fully human IgG1 antibody specific recognize TA-MUC1 which is conjugated to a topoisomerase I inhibitor and a novel ecteinascidin derivative. The dual mechanism of DB-1326 results in potent anti-tumor effect across different tumor types with a range of MUC1 expression levels.

Methods: Binding activity of DB-1326 to TA-MUC1 was evaluated by ELISA. The tumor selectivity between tumor cell and normal cell was evaluated via FACS analysis. The internalization of DB-1326 to tumor cell was tested by Incucyte. CTG assay was used to evaluate the cancer cell killing of DB-1326 on multiple target positive cell lines. Both cell line-derived xenograft (CDX) models and patient-derived xenograft (PDX) models were established to evaluate the in vivo efficacy of DB-1326 monotherapy.

Results: The naked antibody of DB-1326 showed strong binding ability to TA-MUC1 but not MUC1 peptide without glycosylation and significant higher tumor selectivity than traditional MUC1 antibody. Internalization assays demonstrated that unconjugated DB-1326 was endocytosed in tumor cells expressing TA-MUC1. DB-1326 exhibited strong cytotoxicity in vitro against several tumor cell lines. DB-1326 exhibited dose-dependent tumor growth inhibition and demonstrated superior anti-tumor activity compared to the single payload ADC in both CDX and PDX models across a range of target expression.

Conclusions: DB-1326 is a novel dual-payload ADC with a TA-MUC1 antibody. It displayed high tumor cell selectivity and superior anti-tumor effects in preclinical studies. These findings support the potential of DB-1326 as a promising advanced therapeutic candidate for tumors.

#2658 Distinct biological and immune microenvironment features of MSI-H BRAF^{V600E}colorectal cancer: Potential for combined PD-1, BRAF, and EGFR inhibition.

Lulu He, Feng Guo

the Affiliated Suzhou Hospital of Nanjing Medical University, Nanjing Medical University, Suzhou, China

Purpose: Immune checkpoint inhibitors (ICIs) have shown remarkable efficacy in microsatellite instability-high (MSI-H) colorectal cancer (CRC). However, a substantial subset of patients fails to achieve durable clinical benefit. BRAF mutations—particularly BRAF^{V600E}—are associated with aggressive tumor behavior and poor clinical outcomes, and targeted therapies provide effective treatment options. Epidemiological studies reveal that BRAF mutations frequently coexist with MSI-H status. Nevertheless, the optimal treatment strategy for MSI-H BRAF^{V600E} CRC remains unclear, including whether these patients benefit most from ICIs alone, targeted therapy alone, or combined ICIs and targeted therapy therapy. This study aims to comprehensively characterize the biological properties and tumor immune microenvironment (TME) in MSI-H BRAF^{V600E} CRC, with the goal of improving therapeutic strategies for MSI-H BRAF^{V600E} CRC.

Experimental Design: MSI-H BRAF^{WT} and MSI-H BRAF^{V600E} cell lines were generated from the MC38 background. The biological behaviors of cells were evaluated using colony formation, CCK-8, transwell, and Western bloting. Flow cytometry and multiplex immunofluorescence were performed to evaluate immune cell infiltration. RNA sequencing was conducted to explore underlying molecular mechanisms. Therapeutic efficacy was assessed in vivo across four groups: vehicle, anti-PD-1, BRAFi+EGFRi, and anti-PD-1+BRAFi+EGFRi.

Results: MSI-H BRAF^{V600E} cells exhibited significantly enhanced malignancy. In vivo, MSI-H BRAF^{V600E} tumors displayed profound alterations in the immune microenvironment, including reduced infiltration of CD8$^+$ T cells, along with decreased IFN-γ and GZMB levels. Conversely, M2 macrophages were significantly increased. Multiplex immunofluorescence confirmed reduced CD8$^+$ T cell infiltration, and elevated PD-1$^+$ cell frequencies. Notably, MSI-H BRAF^{V600E} tumors exhibited an increased proportion of PD-1$^+$CD8$^+$ T cells and greater spatial separation between CD8$^+$ T cells and PD-L1$^+$ tumor cells. In vivo, combined PD-1, BRAF, and EGFR inhibition resulted in the strongest tumor suppression in MSI-H BRAF^{V600E} tumors, demonstrating a marked therapeutic advantage, including decreased infiltration of CD8$^+$ T cells, along with decreased IL-2 and GZMB levels.

Conclusions: MSI-H BRAFV600E CRC exhibits distinct molecular and immunological characteristics. Our findings demonstrate that triple-combination therapy targeting PD-1, BRAF, and EGFR substantially enhances antitumor activity in MSI-H BRAFV600E tumors, outperforming ICIs alone or targeted therapy alone. Collectively, these results support a refined molecular subclassification of MSI-H CRC and provide valuable insights for optimizing personalized immunotherapeutic strategies for CRC patients with MSI-H BRAFV600E .

#2659 CD44v9-targeted antibody-drug conjugate as a novel therapy for advanced breast cancer.

Dileep R. Reddy[1], McKenna E. Flynn[2], Yasuaki Anami[3], Zhaoxuan Yang[4], Jayden Aleman[2], Minji Seo[1], Kyoji Tsuchikama[4], Jennifer A. Maynard[2], Naoto T. Ueno[1], **Jangsoon Lee**[1]

[1]Preclinical Core, Cancer Biology Program, University of Hawai'i Cancer Center, Honolulu, HI,[2]Department of Chemical Engineering, University of Texas Austin, Austin, TX,[3]CrossBridge Bio, Houston, TX,[4]The University of Texas Health Science Center at Houston, Houston, TX

Background: Aggressive breast cancers, including triple-negative and inflammatory subtypes, urgently require novel therapeutic strategies. Antibody-drug conjugates (ADCs) have shown improved outcomes in HER2- and TROP2-positive breast tumors; however, the heterogeneous expression of target antigens and the development of acquired resistance often limit their long-term clinical benefit. Identifying tumor-selective antigens that remain expressed in advanced and ADC-refractory breast cancers is critical. CD44 variant isoform 9 (CD44v9), a splice variant of the CD44 family, is highly expressed in aggressive breast cancers but largely absent in normal tissues. Functionally, CD44v9 promotes cancer stemness, oxidative stress adaptation, and therapeutic resistance, making it a promising ADC target.

Methods: CD44v9 expression was evaluated in human breast cancer cell lines, patient-derived xenografts, and tumor specimens by immunohistochemistry, with comparison to normal tissues. A chimeric anti-CD44v9 monoclonal antibody (clone SUM24.1) was conjugated to the microtubule inhibitor monomethyl auristatin F (MMAF). Binding, internalization, and cytotoxicity were assessed in triple-negative, inflammatory, and ADC-resistant breast cancer models. Antitumor efficacy was tested in TNBC xenografts and T-DXd-resistant breast cancer models.

Results: CD44v9 was abundantly expressed across TNBC models and largely absent from a broad panel of normal human tissues, including peripheral blood mononuclear cells. The anti-CD44v9 antibody demonstrated strong binding to its target and efficient internalization, supporting selective MMAF delivery to cancer cells. Anti-CD44v9-MMAF induced potent, target-dependent cytotoxicity in vitro ($p < 0.0001$) and significant tumor growth inhibition (TGI) in TNBC xenografts (SUM149: 50% TGI at 0.5 mg/kg, 90% TGI at 2 mg/kg; HCC1806: 50% TGI at 0.5 mg/kg, 95% TGI at 2 mg/kg; $p < 0.0001$), accompanied by increased apoptosis, reduced proliferation, and minimal systemic toxicity. Notably, CD44v9 expression persisted in breast cancer cells resistant to trastuzumab deruxtecan (T-DXd) and sacituzumab govitecan, and these models remained sensitive to CD44v9-directed MMAF therapy in vitro ($p < 0.0001$) and in SUM190-T-DXd-R xenografts (70% TGI at 2 mg/kg; $p < 0.0001$), demonstrating CD44v9's therapeutic independence from HER2 and TROP2 pathways.

Conclusion: CD44v9 is a tumor-specific, biologically meaningful target for ADC development in advanced breast cancer. The preclinical efficacy and selectivity of anti-CD44v9-MMAF highlight its potential as a next-generation therapy for patients with CD44v9-positive, treatment-refractory breast cancers.

#2660 AV-P138-ADC (ARR-002), a novel MUC16/NaPi2b dual-target tetravalent ADC, for the treatment of ovarian and endometrial cancers.

Sunil Bhakta[1], Levi Blazer[1], Cristina Abrahams[2], Jiang Liu[1], Coen Kuijl[3], Jarrett Adams[1], Marcin Kowanetz[2], Luna Musib[2], Amy Kim[2], Wanda Kwan[2], Viswanatham Katta[1], Vidya S. Jonnalagadda[1], Reva Raghupathi[1], Paul Polakis[1], Stuart Lutzker[2], Sachdev S. Sidhu[1], **Jagath Reddy Junutula**[1]

[1]Aarvik Therapeutics, Inc., Hayward, CA,[2]ArriVent Biopharma, Inc., Burlingame, CA,[3]VU Medical Center, Amsterdam, Netherlands

Antibody-drug conjugates (ADCs) are a class of precision medicines available to oncology clinical practice since 2000. To date, only 15 single-target ADCs (out of >450 entering clinical development) have been approved by the FDA. Dual-target ADCs aim to overcome challenges underlying the high failure rate of single-target ADCs in the clinic including limited internalization, low payload delivery, and heterogeneous target expression in tumors. We designed AV-P138-ADC (also known as ARR-002), a first-in-class, Mucin-16 (MUC16) and sodium-dependent phosphate transport protein 2b (NaPi2b) dual-target, tetravalent (2+2 format) ADC, with site-specific conjugation to vcMMAE at a DAR of 4. Both these cell surface antigens are expressed in ovarian and endometrial cancers with limited expression in normal tissues, making them ideal co-targets. AV-P138-ADC utilizes Aarvik Therapeutics' proprietary MUlti-epitope Targeting Tetravalent Antibody (MUTTA™) platform to engineer multivalent antibodies with precise conjugation sites to improve targeting and broaden the ADC therapeutic window, especially in tumors with heterogeneous target expression. Characterization of AV-P138-ADC showed it effectively bound MUC16 and NaPi2b individually, engaged both targets simultaneously, and enhanced internalization compared to the single-target antibody controls. Robust in vitro activity was maintained in OVCAR-3 cells with moderately high expression of both MUC16 and NaPi2b, as well as OVCAR-3 variant cells enriched for either MUC16 or NaPi2b only. AV-P138-ADC also exhibited better cytotoxicity compared to the combination of the site-specifically-conjugated single-target ADCs, a bivalent (1+1 format) bispecific MUC16/NaPi2b ADC, and a MUC16 DAR2 clinical comparator surrogate. Superior in vivo efficacy compared to single-target ADCs was further confirmed in the OVCAR-3 xenograft model. AV-P138-ADC also exhibited a PK profile resembling a typical IgG antibody and high conjugation stability. It demonstrated a favorable tolerability profile in cynomolgus monkeys, consisting of reversible hematologic findings at a higher maximum tolerated single dose compared with random-conjugated vcMMAE ADCs, suggesting a wider therapeutic window. In conclusion, AV-P138-ADC is a novel, site-specifically-conjugated, dual-target tetravalent ADC that may overcome the limitations of conventional single-target or bivalent (1+1 format) bispecific ADCs to potentially provide a safer and more effective treatment option for a broad spectrum of ovarian and endometrial cancer patients. Aarvik Therapeutics and ArriVent BioPharma collaborated on the pre-clinical development of AV-P138-ADC. ArriVent subsequently exercised an option for an exclusive global license to the molecule, now known as ARR-002.

#2661 AZD5335, a folate receptor alpha-targeted ADC, exerts anti-tumor responses within lung adenocarcinoma.

Jason J. Zoeller[1], Ravinder Tammali[1], Nancy Lee[1], Isabella Tilmont[1], Judith Anderton[2], Shailesh Metkar[3], Michael Ophir[3], Jixin Wang[1], Claire Myers[1], Lara McGrath[3], Alma Andoni[1], Ina Bisha[4], Iris Dino[4], Xhenifer Guza[4], Simon Christ[4], Michael Lehmann[1], Roger Dodd[2], Neki Patel[5], Tim Brier[2], Marc L. Hyer[1], Marco Gymnopoulos[1], Sabina Cosulich[2], Alejandra Negro[1], Elaine Hurt[1], Puja Sapra[1]

[1]AstraZeneca US, Gaithersburg, MD,[2]AstraZeneca UK, Cambridge, United Kingdom,[3]AstraZeneca US, Waltham, MA,[4]AstraZeneca GER, Munich, Germany,[5]AstraZeneca UK, London, United Kingdom

AZD5335 is a folate receptor alpha (FRα)-targeted antibody-drug conjugate (ADC), incorporating a topoisomerase-1 inhibitor (TOP1i) payload. This ADC is currently being developed as a treatment option for FRα-expressing ovarian cancer patients (NCT#05797168-FONTANA). Since FRα has been reported to be expressed in lung adenocarcinoma (LUAD), the purpose of these studies was to pre-clinically evaluate AZD5335 efficacy within LUAD. Employing a panel of FRα-expressing lung cancer cell lines, we demonstrated target-mediated cytotoxicity of AZD5335 and correlated the in vitro sensitivities with FRα expression levels. These studies support ongoing in vivo proof-of-concept studies using cell-derived xenograft models to further define the efficacy and pharmacodynamics of AZD5335. Additional AZD5335 efficacy testing was performed within 9 FRα-expressing patient-derived xenograft (PDX) models of LUAD. Five of these 9 models responded to AZD5335 (2.5mg/kg) and exhibited a ≥ 30% reduction in tumor volumes (ORR ≈ 56%); AZD5335-related tumor stasis occurred in three additional models. These pre-clinical efforts indicated FRα is an actionable target in LUAD and supported expanding clinical assessment of AZD5335 to LUAD in FONTANA.

#2662 MGT-1141, an antibody-drug-conjugate targeting DLL3 positive cancers.

Mei-Hsuan Tsai, Maomao He, Su-Yu Tsai, Ju-Mei Li, Ping Chao, Ting-Chun Hung, Charng-Sheng Tsai

Marigold Therapeutics Inc, Taipei, Taiwan

Background: Delta-like ligand 3 (DLL3) is highly expressed on the cell surface of small cell lung cancer (SCLC) and neuroendocrine cancers (NECs)—among the most lethal malignancies—but is minimally or not expressed in normal tissues, making it an attractive target for DLL3-positive cancers. Here, we describe the preclinical activity of MGT-1141, an anti-DLL3 antibody-drug conjugate (ADC) that delivers a topoisomerase I inhibitor (exatecan) payload *via* Marigold's proprietary linker platform. The IND-enabling study of MGT-1141 is currently ongoing.

Methods: Comprehensive *in vitro* and *in vivo* evaluations were performed to characterize MGT-1141. Binding affinity, internalization, and cytotoxicity were examined across multiple DLL3-expressing cell lines. Anti-tumor efficacy was assessed in both cell line-derived xenograft (CDX) and patient-derived xenograft (PDX) models. Pharmacokinetic (PK) and pilot dose-range-finding (DRF) studies were conducted in cynomolgus monkeys to determine systemic exposure, half-life, and tolerability.

Results: The MGT-1141 antibody exhibited high target specificity with no detectable cross-reactivity toward other Delta-like ligand family proteins. MGT-1141 demonstrated strong binding affinity and rapid internalization in DLL3-expressing cells. *In vivo*, MGT-1141 showed potent and dose-dependent tumor growth inhibition across multiple CDX and PDX models, with a minimal efficacious dose (MED) of 0.5 mg/kg. Pharmacokinetic studies in cynomolgus monkeys revealed linear, dose-proportional exposure and a favorable terminal half-life. Dose-range finding (DRF) studies indicated good tolerability and a wide therapeutic window.

Conclusion: Preclinical evaluations of MGT-1141 have shown potent and selective anti-tumor activity, favorable pharmacokinetic properties, and a well-tolerated safety profile, supporting its further development toward clinical investigation. Collectively, these findings support MGT-1141 as a promising and potential best-in-class DLL3-targeting ADC for the treatment of SCLC and NECs.

#2663 Targeting YAP/TEAD signaling disturbs RNA polymerase II activity and enhances immunotherapy response via activated cytosolic DNA sensing pathway in gastroesophageal cancer.

Yanting Yann Zhang[1], Ayna Mammedova[1], Dipti Athavale[1], Curt Balch[1], Mikel Ghelfi[1], Xiaodan Yao[1], Gennaro Calendo[1], Songjie Liu[1], David Pulipati[1], Yahui Li[2], Xiaoxin Chen[1], Francis Spitz[2], Generosa Grana[2], Vladimir Khazak[3], Shumei Song[1]

[1]Coriell Institute for Medical Research, Camden, NJ,[2]Cooper University Hospital, Camden, NJ,[3]NexusPharma Inc, Hamilton, NJ

Gastroesophageal adenocarcinoma (GEAC) is a significant global cancer burden. Our previous studies demonstrated that YAP/TEAD are highly expressed in GEAC, and play a critical role in tumor progression, therapy resistance and metastasis. Thus, targeting YAP/TEAD signaling presents a promising therapeutic strategy. Here, we tested a novel YAP/TEAD inhibitor VT00278, a chemical analog of CA3, and showed that VT00278 strongly downregulated YAP/TEAD transcriptional activity, and potently suppressed tumor-promoting phenotypes including proliferation, invasion, tumor sphere formation; induced apoptosis and inhibited tumor growth *in vivo* especially in radiation resistant FLO-1 XTR GEAC cells. Mechanistically, in addition to impairing YAP/TEAD signaling, VT00278 or YAP depletion repressed RNA polymerase II (RNAPII) transcriptional regulators, reduced RNAPII S2 phosphorylation and decreased anti-apoptosis MCL-1 expression. More interestingly, VT00278 strongly induced DNA damage, activated cytosolic DNA sensing pathway, upregulated innate immune genes (e.g., INFβ) and PD-L1 expression. In a syngeneic mouse model, combining VT00278 with anti-PD-1 therapy strongly inhibited tumor growth, increased $CD3^+$ and $CD8^+$ T cell infiltration, and induced the production of INFγ from CD3 and CD8 cells. These findings support VT00278 as a promising candidate for GEAC treatment, either alone or in combination with immunotherapy.

#2664 MGT-1143, a novel CDH17-targeting ADC for gastrointestinal cancers.

Maomao He, Ping Chao, Su-Yu Tsai, Ju-Mei Li, Ting-Chun Hung, Mei-Hsuan Tsai, Charng-Sheng Tsai

Marigold Therapeutics, Inc., Taipei, Taiwan

Background: Pan-gastrointestinal cancers represent a heterogeneous group of malignancies arising from the gastrointestinal tract, including esophageal, gastric, pancreatic, and colorectal cancers, which collectively contribute to a major global cancer burden and mortality. Cadherin-17 (CDH17), a Ca^{2+}-dependent adhesion molecule, is overexpressed across multiple GI cancers and has been associated with poor prognosis. Here, we report the development and preclinical evaluation of MGT-1143, a novel Exatecan-based ADC that integrates a fully humanized anti-CDH17 monoclonal antibody (mAb) with Marigold's proprietary linker platform. MGT-1143 is currently undergoing IND-enabling studies.

Methods: The preclinical activity of MGT-1143 was assessed through a series of in vitro and in vivo studies to characterize its pharmacological and safety profiles. Binding affinity, cross-species reactivity, and target specificity of MGT-1143 were evaluated using ELISA and flow cytometry. Antibody internalization was determined by flow cytometry, while cytotoxicity was assessed using the CellTiter-Glo luminescent viability assay. In vivo anti-tumor efficacy was evaluated in CDH17-positive cell line-derived xenograft (CDX) models.

Results: The MGT-1143 antibody exhibited high target specificity with no detectable cross-reactivity toward other cadherin family members. MGT-1143 demonstrated strong binding affinity and rapid internalization in CDH17-expressing cells, resulting in potent cytotoxicity across multiple CDH17-positive cell lines. Furthermore, MGT-1143 induced robust and dose-dependent anti-tumor activity in xenograft mouse models expressing varying levels of CDH17, confirming its target-dependent efficacy.

Conclusions: Collectively, the preclinical data support the continued development of MGT-1143 as a promising therapeutic candidate for the treatment of CDH17-positive gastrointestinal cancers. Ongoing IND-enabling studies will further define its safety and translational potential.

#2665 The MET/HER3 antibody-drug conjugate with dual payload: A dual-target approach to eliminate tumor escape mechanism.

Yuan-Liang Wang, Chi-Huan Lu, Woan-Eng Chan, **Ting-Yu Chang**, Hong-Syuan Lin, Cheng-Yen Wei, Shin-Jin Lin, Lu-Tzu Lu, Meng-Hsin Liu, Wei-Jhen Huang, Ya-Chi Chen

OBI Pharma, Inc, Taipei City, Taiwan

Clinical evidence supports combination approaches such as EGFR plus MET TKIs, which achieve responses in MET-amplified resistance settings and demonstrate the critical role of MET signaling in acquired resistance. Meanwhile, HER3-directed ADCs have shown meaningful activity in refractory tumors, underscoring the therapeutic relevance of HER3 in resistant and heterogeneous cancer populations. Together, these findings highlight the rationale for co-targeting cMET and HER3, as simultaneous inhibition of these complementary pathways provides a strong foundation for the development of a bispecific ADC (BsADC) to overcome resistance and enhance antitumor efficacy. Our MET/HER3 bispecific ADC was constructed using the proprietary glycan-based site specific platform to simultaneously engage c-MET and HER3. The ADC carries two complementary cytotoxins— a microtubule inhibitor, MMAE and a topoisomerase I inhibitor derivative, exatecan, conjugated through the stable linker for controlled intracellular release and maximize antitumor activity. Blue native PAGE (BN-PAGE) and proximity ligation assay (PLA) data confirmed that simultaneous MET and HER3 engagement promote receptor clustering, enhancing internalization and intracellular payload delivery. In preclinical models, the bispecific dual-payload ADC induced stronger tumor regression than monospecific or parental ADCs. Broad activity was observed in c-MET/HER3 dual-positive non-small cell lung cancer and colorectal cancer models. This glycan-based site specific MET/HER3 bispecific dual-payload ADC warrants further clinical investigation as a promising therapeutic option for refractory tumors co-expressing cMET and HER3.

#2666 An open-label, multicenter Phase I clinical study of CVL006, a novel PD-L1/VEGF bispecific antibody, in advanced solid tumors.

Jin Li[1], Ning Li[2], Shuhang Wang[2], Ye Guo[3], Kai Yao[4], Yanjie Zhu[5], Feng Ye[6], Hao Zeng[7], **Steve Shen**[8], Jin Zhang[5]

[1]Shanghai GoBroad Cancer Hospital China Pharmaceutical University, Shanghai, China,[2]Cancer Hospital Chinese Academy of Medical Sciences, Beijing, China,[3]Shanghai East Hospital, Shanghai, China,[4]Sun Yat-sen University Cancer Center, Guangzhou, China,[5]Renji Hospital, Shanghai Jiao Tong University School of Medical, Shanghai, China,[6]The First Affiliated Hospital of Xiamen University, Xiamen, China,[7]West China Hospital, Sichuan University, Chengdu, China,[8]Convalife Pharmaceuticals, Shanghai, China

Background: CVL006 is a novel bispecific antibody designed for synergic antitumor activity by simultaneously blocking two mechanistically distinct pathways VEGF/VEGFR signaling and the PD-L1/PD-1 axis. In this Open-label, Multicenter Phase I Clinical Study of CVL006, Safety, pharmacokinetics (PK) and preliminary efficacy will be assessed in adult subjects with advanced solid tumors, and, thus, the recommended phase II dose (RP2D) will be established (NCT06621615).
Method: All subjects in this study received CVL006 every 2 weeks (Q2W). Primary objectives were to evaluate safety, tolerability, and clinical efficacy by objective response rate (ORR).
Results: As of the data cutoff date of Nov 14, 2025, 29 subjects with various advanced solid tumors received CVL006 at 0.03-20 mg/kg, 12 subjects in phase Ia, 7 subjects in phase Ib and 10 subjects in phase Ic. Phase Ia and phase Ib were completed and Phase Ic is ongoing. Phase Ia results show that CVL006 is well-tolerate, MTD has not reached, and RP2D is 20 mg/kg. All these AEs were recovered after symptomatic treatment. In the 20 mg/kg dose group, CVL006 showed linear pharmacokinetics and a low incidence of ADA positivity.18 subjects had at least one efficacy assessment. In the 10 mg/kg dose group (N=3), 2 stable disease (SD) cases with lesion shrinkage first appeared. At dose of 20 mg/kg, 9 subjects with different tumour types, were evaluated for efficacy and 6 of 9 subjects had a response : 4 SD and 2 partial response (PR).
Conclusion: CVL006 monotherapy appeared to be well tolerated and had encouraging preliminary efficacy in patients with advanced solid tumors, warranting further investigation.

#2667 TM4SF1 as a novel tumor-associated antigen in biliary tract cancers targetable by immune effector cell therapy.

Lorraine Nuniz*, Julia Pham, Juliette Jacques, Josephine Hinneh, Jocelin Chen, Corynn Kasap, Jon Akutagawa, Chih-Hao Chang, Robin K. Kelley, Arun Wiita, Jonathan Chou, Kwun Wah Wen, Vipul Kumar*, Franklin Huang

University of California, San Francisco, San Francisco, CA

Biliary tract cancers (BTC) are a rare set of genetically heterogeneous and aggressive malignancies associated with late presentation, poor prognosis and limited effective therapies. Thus, there is an unmet clinical need for the development of novel therapeutic strategies. Identification of uniquely expressed cell-surface tumor-associated antigens (TAA) holds promise in epithelial tumors more generally, as they can serve as ligands for a variety of therapeutics, including CAR-T cell therapy. However, TAA identification in BTCs has been limited by expression in normal liver tissue. Here, we identify the cell-surface protein transmembrane 4 L six family member 1 (TM4SF1) as a potential BTC TAA targetable by CAR-T therapy. We find TM4SF1 expression is upregulated in BTC relative to normal hepatic/biliary tissue at the mRNA level in the TCGA dataset. Correspondingly, we find that TM4SF1 in primary BTC archival tissue is upregulated at the protein level using immunohistochemistry. To validate TM4SF1 as a targetable TAA in BTC, we show that TM4SF1-directed CAR-T cells demonstrate robust, dose-dependent growth inhibition of human-derived BTC cell lines in vitro and significant anti-tumor activity in a heterotopic BTC cell line-derived xenograft model in vivo. Together, our data provide support for TM4SF1 as a promising TAA in BTCs that can be used for the rational development of therapeutic modalities targeting TM4SF1, including CAR-T cells, in a patient population with significant unmet need.

*Authors contributed equally

#2671 TROP2 expression predicts sensitivity to datopotamab deruxtecan (Dato-DXd) in patient-derived breast cancer organoids.

Won-Ji Ryu[1], Min Hwan Kim[2], Geon-Uk Kim Kim[1], Joohyuk Sohn[3], Yumi Hwang[2], Jeong Dong Lee[1], Shinyoung Park[4], Hyun Myoung Yun[1], Kyoo Hyun Kim[5], Gun Min Kim[6], Hyung Seok Park[5]

[1]Yonsei University Health System, Seoul, Korea, Republic of,[2]Department of Internal Medicine, Division of Medical Oncology, Yonsei University College of Medicine, Severance Hospital, Seoul, Korea, Republic of,[3]Associate Professor, Dept. of Medical Oncology, Yonsei University Cancer Center, Seoul, Korea, Republic of,[4]Yonsei University College of Medicine, Seoul,[5]Yonsei University College of Medicine, Severance Hospital, Seoul, Korea, Republic of,[6]Yonsei Cancer Center, Seoul, Korea, Republic of

Background: Trophoblast cell surface antigen 2 (TROP2) is a transmembrane glycoprotein preferentially expressed in many cancers relative to normal tissues. TROP2 has recently emerged as a promising therapeutic target in breast cancer, leading to the development of TROP2-directed antibody-drug conjugates (ADCs), including datopotamab deruxtecan (Dato-DXd). However, mechanisms underlying heterogeneous responses to Dato-DXd remain poorly defined. In this study, we evaluated the effect of Dato-DXd on the breast cancer patient-derived organoids (PDOs) and analyzed their responses in correlation with the TROP2 H-score of PDOs.
Method: TROP2 expression and Dato-DXd sensitivity were evaluated by western blot analysis in breast cancer cell lines representing different subtypes. The TROP2 band intensity on western blot was quantified across the cell lines to determine TROP2 expression. We obtained surgical or biopsy specimens from patients with breast cancer at Yonsei Cancer Center. PDOs were established and subjected to TROP2 immunohistochemistry (IHC). TROP2 H-scores were quantified using ImageJ IHC Profiler. PDO cell viability following ADC exposure was assessed using the CellTiter-Glo 3D assay.
Results: We evaluated TROP2 expression in a series of breast cancer cell lines. High TROP2 expression was observed in MDA-MB-468 and HCC1937 (triple-negative breast cancer [TNBC]), T-47D (HR+/HER2-), and SK-BR-3 (HER2+). The sensitivity to Dato-DXd in IC50 value was well correlated with the TROP2 protein expression, suggesting TROP2 expression level is an important determinant of Dato-DXd response. In particular, SK-BR3 showed both response to Dato-DXd and T-DXd in line with its high TROP2 and HER2 expression, whereas BT474 showed only response to T-DXd, but not to Dato-DXd. We next evaluated TROP2 expression in PDOs of patients with breast cancer (n=34) and the median TROP2 H-score was 152. The PDOs of high TROP2 expression (H-score ≥ 100, n= 28) exhibited significantly greater sensitivity to Dato-DXd compared to TROP2-low PDOs (H-score < 100, n= 6). Importantly, Dato-DXd showed potent antitumor activity in three treatment-refractory TNBC PDOs, including models derived from tumors progressing after pembrolizumab plus chemotherapy combination (IC_{50}: OSV-001, 0.82 nM; SBO-105, 0.27 nM) and sacituzumab govitecan (IC_{50}: OSV-011, 0.55nM), whereas T-DXd showed lower activity compared to Dato-DXd in these organoids (IC_{50}: OSV-001, 200 nM; SBO-105 = 160 nM; OSV-011, not reached).
Conclusion: These findings demonstrate that TROP2 expression is a key determinant of Dato-DXd sensitivity and provide mechanistic insights into ADC resistance. Our results support the potential of TROP2-guided patient stratification to enhance therapeutic outcomes with Dato-DXd in breast cancer. Dato-DXd showed significant antitumor activity in PDOs from tumors resistant to anti-PD-1 and ADC treatment.

#2672 Characterization of small molecule inhibitors against Lipocalin-2 in inflammatory breast cancer.

Sthephanie Estrada-Mojica[1], Fatma Valiyeva[2], Pablo E. Vivas Mejia[3]

[1]University of Puerto Rico - Rio Piedras, San Juan, PR,[2]Comprehensive Cancer Center, San Juan, PR,[3]University of Puerto Rico Comprehensive Cancer Center, San Juan, PR

Inflammatory breast cancer (IBC) is a rare and very aggressive form of breast cancer (BC) where cancer cells block the lymph vessels in the skin. It only makes up about 1% to 5% of all breast cancers but grows and spreads much faster than other common BC types. No targeted therapies are currently available against IBC. Lipocalin 2 (LCN2) is a secreted glycoprotein involved in transporting small lipophilic ligands, and its abnormal expression plays an important role in the progression and metastasis of IBC. We used a library of 370,000 small molecule inhibitors (SMI) and after bioinformatic and filtering analysis we selected 24 compounds that potentially bind to LCN2. Viability and colony formation assay were performed on the IBC cell line, SUM-149. The majority of the 24 SMIs did not exhibited noticeable reduction on cell viability. However, at 1.0 μM, 12 SMIs achieved >50% reduction in cell proliferation. These results highlight the therapeutic potential and selectivity of SMIs against LCN2. Targeting this protein with our SMIs could provide a novel therapeutic strategy that improves the outcomes of IBC patients. Further studies are needed to validate and optimize the most effective compounds for future clinical development.

: 2026 AACR Undergraduate Scholars and Margaret Foti Undergraduate Prize Recipients
Poster Session

#FOTI01 Margaret Foti Foundation Prizes.

Margaret Foti

American Association for Cancer Research, Philadelphia, PA

The Margaret Foti Foundation was founded by the AACR Chief Executive Officer Margaret Foti. The Margaret Foti Foundation Undergraduate Prizes for Cancer Research were established in 2018 and are presented to meritorious participants at the AACR Undergraduate Student Caucus and Poster Competition during the AACR Annual Meetings. These prizes reward excellence in research conducted and presented by undergraduate students.

: Regulatory Science and Policy
Poster Session

#1392 A mixed-methods evaluation of multilevel barriers and facilitators to inform implementation strategies for advancing equitable clinical trial accrual in a large comprehensive cancer center.

Morgan Gill[1], Syma Iqbal[2], Vibha Kodancha[1], Emmeline Friedman[1], Diana L. Hanna[2], Chanita Hughes-Halbert[3], Anthony El-Khoueiry[2], Jennifer Tsui[1]

[1]Keck School of Medicine of USC, Los Angeles, CA,[2]USC Norris Comprehensive Cancer Center, Los Angeles, CA,[3]USC - University of Southern California, Los Angeles, CA

Introduction: Multilevel interventions and implementation strategies at the system, provider, and patient levels can support clinical trial enrollment. This study examines processes, facilitators, and barriers to clinical trial enrollment across a large comprehensive cancer center to inform interventions and identify opportunities for implementation strategies to sustain equitable trial participation.
Methods: Guided by the Consolidated Framework for Implementation Research (CFIR), we used a mixed-methods design to survey and interview oncology and hematology providers from September 2024 to April 2025. Providers at USC Norris Comprehensive Cancer Center's main medical campus and satellite clinics completed surveys and in-depth interviews that assessed their experiences with trial enrollment, including beliefs, attitudes, and knowledge about clinical trials; workflow and organizational culture; and patient barriers. Survey data were summarized using descriptive statistics, and interview transcripts were coded using CFIR to identify key implementation determinants.
Results: Among survey participants (n=49), 69% practiced at the main campus and 31% at satellite clinics. Although 96% viewed clinical trials as important to patient care, 45% indicated gaps in knowledge of trial accrual. Inner setting barriers differed by site, with 74% of providers at the main campus compared to 20% at satellite clinics citing limited staffing support for clinical trials (p=0.003). Outer setting barriers showed less variation, with 64% of providers at the main campus and 53% at satellite clinics reporting limited language translation resources (p=0.44). Qualitative interviews (n=15) reinforced these CFIR domains; limited access to research coordinators, time constraints, and language translation emerged as key barriers. Provider motivation and interest in trials accrual training were identified as key facilitators to optimize trial enrollment.
Discussion: Barriers to optimal clinical trial recruitment include gaps in provider knowledge, staffing limitations, and insufficient language resources, all of which may constrain equitable enrollment. Despite these challenges, providers remained motivated to offer trials to their patients. Advancing enrollment requires co-designed solutions with providers and clinic teams to address system level and patient barriers. Targeted interventions - such as provider training, enhanced access to trial information, and translation services - may improve inclusive enrollment.

#1393 Design of a prospective implementation study to evaluate the efficacy of an AI-assisted workflow intervention to increase breast cancer clinical trial participation.

Jacob T. Rosenthal[1], Emma Hahesy[2], Sulov Chalise[3], Zhigang Zhang[4], Menglei Zhu[3], Mert R. Sabuncu[5], Anyi Li[6], Lior Zvi Braunstein[7]

[1]Tri-Institutional MD-PhD Program, Weill Cornell Medicine, New York, NY,[2]Department of Radiation Oncology, Memorial Sloan Kettering Cancer Center, New York, NY,[3]Department of Pathology and Laboratory Medicine, Memorial Sloan Kettering Cancer Center, New York, NY,[4]Department of Epidemiology & Biostatistics, Memorial Sloan Kettering Cancer Center, New York, NY,[5]School of Electrical and Computer Engineering, Cornell University and Cornell Tech, New York, NY,[6]Department of Medical Physics, Memorial Sloan Kettering Cancer Center, New York, NY,[7]Memorial Sloan Kettering Cancer Center, New York, NY

We previously developed and retrospectively validated an AI-integrated workflow for conducting rapid, accurate, and cost-effective automated clinical trial eligibility prescreening, but it remains unknown whether this tool can increase trial accrual rates when implemented in real-world clinical workflows. To evaluate its impact on practice, this prospective, controlled implementation study will use a periodic on-off design in which participating clinicians alternate monthly between the AI-assisted workflow and usual care. During intervention periods, the Memorial Sloan Kettering Multi-Agent Trial Coordination Hub (MSK-MATCH) system will conduct automated eligibility prescreening for all upcoming new patient visits. For cases triaged by the AI system for secondary human review, a clinical research coordinator (CRC) will use a secure web interface to verify predictions and resolve ambiguities. The results of this human-in-the-loop eligibility prescreening will be compiled into a single summary report delivered directly to each attending physician in advance of their scheduled clinic each week. The primary endpoint is the rate of accrual to any breast radiation oncology therapeutic clinical trial within 60 days of initial visit. Secondary endpoints include (1) the number of patient-trial pairs evaluated for trial eligibility, and (2) the mean cost of all screening activities per screened pair. Statistical analysis will use a two-sided paired t-test comparing intervention and control periods within each clinician. At the conclusion of the study, semi-structured interviews will be conducted to collect feedback and assess perceptions of this AI workflow intervention among participating clinicians and CRCs. This study is planned to begin in January 2026 in the breast radiation oncology service at Memorial Sloan Kettering Cancer Center. With an enrollment target of 2,500 new patient visits, the design provides 80% power to detect a minimum absolute difference in accrual rate of 1.57% with a type I error rate $\alpha = 0.05$. An interim analysis for efficacy and futility is planned after 1,250 visits, anticipated in June 2026. This quality-improvement study is IRB-exempt, and waivers have been added to all trial protocols to cover screening activities. Findings from this study will provide evidence to guide the responsible and effective adoption of AI-based workflow interventions in clinical oncology.

#1394 Effect of biopsy requirement on patient enrollment to phase I trials in cancer.

Catherine Yang[1], Mona Yuan[1], Sebastian Saenz[1], Marisa Palmeri[1], Mohammad Ghalib[2], Dina Oz[2], Diana Nelson[2], Rita M. Musanti[2], Devika Rao[3], Eugenia Girda[2], Francis Kang[1], Sanjay Goel[2]

[1]Robert Wood Johnson Medical School, New Brunswick, NJ,[2]Rutgers Cancer Institute of New Jersey, New Brunswick, NJ,[3]Memorial Sloan Kettering Cancer Center, New York, NY

Background: A recent trend in clinical trials is the requirement of biopsies (Bx), sometimes mandatory. The main reason is to better understand cancer biology pharmacodynamic effect. We sought to determine whether the requirement for Bx among this vulnerable population had any detrimental effect.

Methods: We included patients (pts) enrolled in phase I trials from June 2022-August 2025 at a single NCI-designated comprehensive cancer center. Data collected included sex, race, age, body mass index (BMI), dates of consent/treatment start/last dose/off treatment/last contact/death, serum lab values, number of prior treatments, metastatic sites, and Bx site/approach/complications. An interventional radiologist reviewed images to assess safety, with targets deemed appropriate biopsied under image guidance. Outcomes were analyzed by Mantel-Cox test in Prism GraphPad v10.

Results: 228 pts [male (n=104, 45.6%)], age 60.5, 23-82 (median, range), NHW-130 (57%), NHB-37 (16.2%), Hispanic-34 (14.9%), and Asian-27 (11.8%) consented to 25 clinical trials. Of these, 8 were mandated paired tumor Bx, 15 mandatory or optional Bx, and 2 did not require Bx. The most common diagnoses were colorectal (54, 23.7%), pancreas (29,12.7%), other GI (26, 11.4%), lung (18, 7.9%), breast (12, 5.3%), prostate (5, 2.2%), and others (84, 36.8%). Image guidance included ultrasound 74 (57.8%), CT scans 49 (38.3%), and others 5 (3.9%). Overall, 91 (39.9%) pts provided 128 Bx samples; 37 paired Bx, 49 only pre-dose Bx, and 5 only on-study Bx. Five pts did not undergo Bx because it was deemed unsafe/high risk. Sites of Bx included liver 63 (49.2%), lung 13 (10.2%), lymph node 15 (11.7%), peritoneum 8 (6.3%), bone 1 (0.8%), and others 28 (21.9%). Two patients developed pneumothorax and recovered without sequelae. The median duration from consent to start of study treatment was 18.5 days among Bx pts vs. 14 among non Bx pts ($p = 0.001$). The median duration of time on study was 62 days among Bx pts vs. 66.5 days among non Bx pts ($p = 0.08$). The overall survival (OS), calculated as time from first dose of treatment to death/last follow up, was 123 days among Bx pts and 163 days among non Bx pts ($p = 0.049$).

In a univariable model, sex (males/women; HR 1.37; p=0.02), albumin (high/low, HR 0.47, p=0.0001), neutrophil-lymphocyte ratio (low/high, HR 0.68, p=0.003), hemoglobin (high/low, HR 0.71, p=0.01), BMI (high/low, HR 0.72, p=0.02), and AST (high/low, HR 0.68, p=0.004), were significant, while age, race/ethnicity, total bilirubin, platelet, ALT, # sites of metastases, and # prior lines of therapy were not.

Conclusions: 40% of pts entering phase I trials underwent study specific Bx, had a median delay of 4.5 days in receiving the first dose of study medication and experienced lower OS by 41 days. Multivariable modeling will be presented to fully understand the intriguing observation of a compromise in OS among patients who underwent biopsies.

#1396 Streamlining combined clinical trial and diagnostic device development: The EMA COMBINE Project Pilot.

Louis-Guillaume Marquier

Biotrial, Rennes, France

The EMA's COMBINE project, is a new pilot initiative designed to streamline the regulatory assessment of trials that combine a medicinal product with an in vitro diagnostic (IVD), such as a companion diagnostic. Currently, these trials must comply with two separate EU regulatory frameworks, the Clinical Trials Regulation (CTR) for medicines and the In Vitro Diagnostic Regulation (IVDR) for diagnostics. This results in duplicative submissions, misaligned timelines, and a substantial administrative burden for sponsors. COMBINE introduces a coordinated, "all-in-one" assessment, enabling sponsors to submit one single submission through the CTIS and to receive unified information requests and approvals from EU authorities. The aim of the pilot is to evaluate whether a harmonized approach can shorten review timelines, enhance cross-country alignment between regulators and ethics committees, and to support a more efficient development of drug-diagnostic combinations. Observations generated through the pilot phase will help shape the future expansion of other possible integrated trial assessments within the EU regulatory framework. This poster provides an overview of the COMBINE project and highlights the core objectives: reducing regulatory submission complexity, supporting integrated precision-medicine development, and improving patient access to innovative therapies and diagnostics.

#1397 Genomic Relational Privacy in AI Era: a scoping review.

Ying Huang[1], Emily Boja[2], Jaime Guidry Auvil[1]

[1]National Cancer Institute, Bethesda, MD,[2]National Cancer Inst. - Bethesda Campus, Rockville, MD

Objective: The concept of privacy is ever evolving and commonly defined as an individual's "right to be let alone". It has been shown that it is foundationally insufficient to address the challenges and opportunities presented by blooming of genomic data, where one individual's decision regarding genomic information to consent to data sharing can directly impact the privacy of their biological and social relations. This scoping review maps the evolution of privacy theory and systematically examines the legal, ethical, and technological conflicts and governance models at the intersection of genomics and artificial intelligence (AI). **Methods:** A scoping review was conducted in 2025 following the Joanna Briggs Institute (JBI) methodology. Systematic searches were performed in three major databases (up to August 2025) - Westlaw, PubMed, and Web of Science databases including foundational privacy scholarship, modern relational and critical data theories, U.S. case law, federal statutes (HIPAA, GINA), international regulations (GDPR), and technical papers on AI and Privacy-Preserving Machine Learning (PPML). **Results:** From 1412 initially retrieved records and after 3 phases of screening, we included 56 studies. The review identified a fundamental and growing conflict between individualistic legal frameworks (based on personal consent) and the interdependent nature of genomic data. Key findings are: (1) The "relational turn" in privacy theory provides a more accurate analytical lens by focusing on context, power imbalances, and interdependence rather than solely on individual control. (2) Escalating real-world conflicts—evident in law enforcement's use of familial DNA searching, DTC data breaches, and clinical "duty to warn" dilemmas—demonstrate the failure of current legal models. (3) AI acts as a powerful risk-amplifier, using its inferential power to deduce familial relationships and perpetuate bias, driven by the economic incentives of surveillance capitalism. (4) A suite of PPML tools (e.g., federated learning, differential privacy) offers technical mitigation, but these are not substitutes for robust ethical governance and risk being co-opted. **Conclusion:** A modernized governance framework for genomic data is a critical and urgent need. This framework shall expand upon, not replace, individual rights, while it should be capable of governing complex, competing interests. We conclude that a durable solution requires a multi-pronged approach based on relational privacy, contextual integrity, and the imposition of legally enforceable fiduciary duties on the powerful entities that steward our collective genomic data.

#1398 Thematic trends in cancer research from sub-Saharan Africa: Insights from a five-year institutional dataset.

Adedayo Joseph[1], Funmilayo Aina-Tolofari[2], Ayodeji O. Ojetunde[2], Philip Ejeikwu[2], Lilian Ekpo[2], Tolulope Adewole[3]

[1]Lagos University Teaching Hospital, Nigeria, Nigeria,[2]Medserve-LUTH Cancer Centre, Lagos University Teaching Hospital, Lagos, Nigeria,[3]Medserve Nigeria Limited, Nigeria Sovereign Investment Authority, Nigeria, Nigeria

Background: The emergence of cancer centres of excellence such as the Medserve - LUTH Cancer Centre (MLCC) in sub-Saharan Africa, provides a unique opportunity to examine evolving research priorities within the region. This study characterizes the thematic distribution, methodological orientation, and funding sources of cancer research output from MLCC over five years (October 2020 - October 2025), offering insights into the maturation of Africa's oncology research landscape.
Methods: A retrospective analysis of the MLCC Research Unit's database was conducted, encompassing all completed manuscripts, abstracts, and ongoing projects. Studies were categorized by disease site (breast, lung, pediatric, gynecologic, prostate, CNS, and cross-cutting), research type (clinical, implementation, translational, educational), and funding origin (institutional, national, international, or industry). Temporal trends were analyzed to assess the evolution of research priorities from descriptive to interventional studies.
Results: A total of 155 publications were identified between 2020 and 2025, comprising articles (70%), abstracts (25%), and posters (5%). Annual output increased more than twofold, from 14 in 2020 to 33 in 2025. Dominant research themes included radiotherapy (n=32), breast (n=23), prostate (n=22), and pediatric cancer (n=17). Early outputs (2020-2021) were primarily descriptive clinical audits and radiation technique utilization studies, while later years (2023-2025) demonstrated a shift toward implementation trials, navigation interventions, molecular characterisation, and technology-driven quality improvement. Collaborative and industry-supported studies rose steadily, accounting for over 30% of research activity by 2025. A keyword heatmap revealed progressive diversification, from "radiotherapy" and "access" in early years to "precision," "financial navigation," and "quality assurance" in recent outputs. Multi-institutional collaborations with partners across North America, Europe, and Africa. International collaborations accounted for 20% of total projects, and funded trials increased from 1 to 8 across the period.
Conclusion: This five-year institutional analysis illustrates a rapid transition in SSA cancer research from descriptive documentation toward hypothesis-driven, interventional, and data-integrated inquiry. The MLCC experience underscores the transformative potential of structured research governance, mentorship, and global partnerships in shifting Africa's oncology research from capacity building to capability and innovation.

#1399 Analysis of regulatory and scientific activities of SFDA oncology and hematology section in sixteen months.

Tariq Hassan AL Qurayshah, SFDA Oncology & Hematology Group

Oncology and Hematology, Saudi Food and Drug Authority, Riyadh, Saudi Arabia

Introduction

Amid the global acceleration of the clinical development of drugs and biologics in oncology and hematology, the Saudi Food and Drug Authority (SFDA) established the Oncology and Hematology (OH) Section to evaluate the efficacy and safety of those drugs. We describe here the OH Section role in advancement of oncology-related regulatory science and policy in Saudi Arabia.

Methodology

We summarize scientific and clinical activities related to the OH efficacy and safety led by OH section's experts from July 2024-October 2025 using the OH excel database.

Results

The SFDA established OH section in July 2024 to evaluate the clinical efficacy and safety of applications of new clinical trials, new OH drugs and biologics and new clinical variations. The section is responsible for the expedited clinical review and designation of orphan drugs in rare OH diseases, breakthrough medicines in high unmet medical need in OH, fast-track and accelerated OH approvals based on validated surrogate endpoints. The OH section presented the oncology efficacy and safety considerations for OH approvals in Saudi Arabia including indications that received expedited review (based on validated surrogate endpoints) or regular review based on evident clinical benefits such as overall survival and patient reported outcomes. Since October 2024, experts in OH section participated with five abstracts in two AACR meetings. The section, experts also are participating in the development of guidelines and recommendations as follows:

- Early-phase clinical development of CAR T cells for patients with hematologic malignancies
- Biomarker and tissue agnostic oncology drug development
- Patient-Reported Outcomes (PROs)
- Regulatory considerations for use of minimal residual disease (MRD) for treatment hematologic malignancies
- Development of products in rare cancers and pediatrics
- Development of products in sickle cell disease
- Gene therapy in hematological diseases

Also, the experts were qualified to join national and international relevant committees and working groups:

- ICH working group: E22 General Considerations for Patient Preference Studies
- The National Scientific Committee in the Saudi Cancer Institute

Moreover, the OH section was responsible for

- The clinical development of the first in-house chimeric antigen receptor T-cells (CAR-T) in Saudi Arabia for acute lymphoblastic leukemia (ALL).
- Positive efficacy and safety opinions granted for at least 10 OH indications as first regulatory drug authority ever.
- First global regulatory approval for mitapivat in thalassemia

Conclusion

Since the formal establishment of the OH section in July 2024, OH experts contributed in hundreds of scientific and regulatory activities related to for OH products including developing clinical guidelines, evaluating the safety and efficacy, and facilitating the timely introduction of OH products and indications.

#1400 Addressing the EU IVDR challenge in targeted oncology trials.

Margaret Curnutte

IVD Regulatory Consulting, Precision for Medicine, Frederick, MD

The European Union (EU) In Vitro Diagnostic Regulation (IVDR 2017/746) went into effect May 2022, dramatically changing the regulatory requirements for oncology clinical trials using an in vitro diagnostic (IVD) for patient enrollment. Sponsors developing experimental targeted oncology drugs are grappling with the new regulatory framework, which lacks alignment between drug and device regulations. This means sponsors may have to manage two parallel submissions and processes: a clinical trial for the drug and a separate performance study for the IVD used for patient selection, adding significant complexity, coordination, and potential delays. This poster outlines key considerations and best practices for drug sponsors managing these requirements. We explore preliminary options to avoid parallel studies—such as running the assay at a qualified Health Institution or utilizing a CE-marked assay—before detailing the necessary steps when a separate device study is unavoidable. The poster provides practical guidance for managing the dual studies that can be required under the new EU IVDR, focusing on two key areas. First, it addresses the critical decision of device sponsorship, clarifying the roles and responsibilities (including regulatory submissions, monitoring, and adverse event reporting) that must be defined between a drug sponsor and a device manufacturer in a partnership. Second, it highlights integrated oversight, outlining crucial areas for coordination where the two studies overlap, such as qualification of clinical trial sites, informed consent forms, shared study objectives, site personnel roles, and joint safety reporting responsibilities. The poster offers actionable insights and lessons learned to help oncology drug sponsors achieve clinical trial readiness in this new regulatory landscape.

#1401 A novel statistical framework for surrogate endpoint prediction of survival in neoadjuvant breast cancer trials.

Keli S. Santos-Parker[1], Jessica R. Santos-Parker[1], W. Fraser Symmans[2], Laura J. Esserman[1], Christina Yau[1], Angie DeMichele[3], Laura van't Veer[1], Doug Yee[4], Fabien Reyal[5], Helena Earl[6], Jean Abraham[6], David Cameron[7], Peter Hall[7], Judy Boughey[8], Matthew Goetz[8], Gabe Sonke[9], Miguel Martin[10], Sara Lopez-Tarruella[10], Priyanka Sharma[11], Rachel Freiberg[1], Jane Perlmutter[12], Aditya Bardia[13], Martin Eklund[14], Rachel Freiberg[1], Lajos Pusztai[15]

[1]Surgery, UCSF - University of California San Francisco, San Francisco, CA,[2]Pathology, MD Anderson Cancer Center, Houston, TX,[3]Medical Oncology, University of Pennsylvania, Philadelphia, PA, USA, Philadelphia, PA,[4]Medical Oncology, University of Minnesota, Minneapolis, MN,[5]Department of Surgery, Institut Curie, Paris, France,[6]Department of Oncology, University of Cambridge, Cambridge, United Kingdom,[7]Department of Oncology, Western General Hospital, Edinburgh, United Kingdom,[8]Surgery, The Mayo Clinic, Rochester, MN,[9]Medical Oncology, Netherlands Cancer Institute, Amsterdam, Netherlands,[10]Instituto de Investigacion Sanitaria Gregorio Maranon, Madrid, Spain,[11]Kansas University Medical Center, Kansas City, KS,[12]The Gemini Group, Ann Arbor, MI,[13]University of California, Los Angeles, Los Angeles, CA,[14]Karolinska Institutet, Stockholm, Sweden,[15]Yale University, New Haven, CT

Introduction

Pathological complete response (pCR) is a strong prognostic marker, but survival outcomes comparing treatment to control do not reliably align with treatment-control differences in pCR rates in breast cancer. A novel Bayesian hierarchical framework models treatments within trials, allowing us to predict treatment effects on distant recurrence-free survival (DRFS) from pCR with greater accuracy.

Methods

We analyzed 12 neoadjuvant breast cancer trials (6,000 patients, all HR/HER2 subtypes; including I-SPY2). The framework of Burzykowski, Molenberghs & Buyse (2005) is extended to a novel arm-based hierarchical structure providing a distribution of pCR and DRFS treatment effects controlling for subtype (HR/HER2), N and T stage, grade, and calendar year. Three held-out trials (877 patients; 26 regimens; med follow-up >4 years) validate predictions of DRFS treatment benefit from pCR. All data was used to estimate treatment-effect correlation and the surrogate threshold effect (STE). Analyses were repeated for Residual Cancer Burden Index (binary RCB01, continuous RCB).

Results

Predicted probability of DRFS benefit closely matched actual DRFS follow-up (mean absolute error 0.06; Pearson r = 0.9). Across all trials, pCR showed moderate surrogacy ($\rho = 0.82$, $R^2 = 0.67$). A 60% increase in pCR odds achieves ≥95% probability of DRFS benefit (STE = OR of 1.60). RCB outperforms pCR across all metrics, with 92% sensitivity and 93% specificity for detecting DRFS benefit in 26 validation regimens (Table 1).

Conclusion

This novel Bayesian meta-analytic framework reveals that pCR, RCB01 and continuous RCB reliably predict survival benefit across heterogeneous trials, with RCB performing the best in an external validation. This provides a statistical foundation for accelerated approval decisions using robust early biomarkers in modern neoadjuvant trial designs by accurately predicting survival at the treatment arm level.

Table 1

	Predicted vs. Actual DRFS Benefit: *26 Held Out Regimens*				**Overall Data Surrogacy Measures**		
	Sensitivity	Specificity	Mean Absolute Error	Pearson r	rho Median Pr[rho>0.5]	R^2 Median PR[R^2>0.5]	STE
pCR	0.83	0.71	0.06	0.90	0.82 (0.87)	0.67 (0.67)	OR 1.60
RCB01	0.91	0.80	0.06	0.94	0.90 (0.95)	0.80 (0.83)	OR 1.37
RCB	0.92	0.93	0.05	0.95	0.89(0.96)	0.80 (0.82)	-9.3%
	Pr[DRFS benefit] > 0.5 Decision threshold used for Sensitivity and Specificity. STE Surrogate Threshold Effect: improvement needed for ≥95% posterior probability of DRFS benefit						

#1402 Real world clinical outcomes with trastuzumab deruxtecan in HER2 expressing ovarian and endometrial cancer.

Oladunni Alomaja[1], Jordyn F. Silverstein[2], Maryam Hajiabbasi[3], Eliya Shachar[2], Shivani Thaker[2], Beth Karlan[4], Aditya Bardia[2], Gottfried E. Konecny[2], First two authors contributed equally and share first authorship

[1]UCLA David Geffen School of Medicine, Los Angeles, CA,[2]Division of Hematology/Oncology, Department of Medicine, University of California, Los Angeles (UCLA), Los Angeles, CA,[3]Department of Medicine, University of California, Los Angeles (UCLA), Los Angeles, CA,[4]Department of Obstetrics and Gynecology, David Geffen School of Medicine at UCLA, Los Angeles, California., Los Angeles, CA

Background: Trastuzumab deruxtecan (T-DXd), a HER2-directed antibody-drug conjugate, is an FDA-approved treatment option for HER2-expressing (IHC 2+/3+) recurrent endometrial (EC) and ovarian cancers (OC) based on DESTINY-PanTumor02. Real-world evidence remains limited.
Methods: We conducted a retrospective study of all patients with recurrent or metastatic OC or EC who received T-DXd between September 2022 and November 2025 at a single academic medical center. Primary endpoints were real-world objective response rate (ORR), disease control rate (DCR; by radiology reports) and median time on treatment (mTOT). Secondary endpoints were median progression-free survival (mPFS), and overall survival (mOS), estimated by Kaplan-Meier.
Results: Thirty-three patients received T-DXd (17 OC, 16 EC, Table 1). The ORR and DCR were 42.4% (14/33) and 66% (22/33), including 4 complete responses and 6 partial responses. The mTOT was 5.5 months (mos) (IQR 1.4-7.6). ORR by HER2 IHC score was 83% for 3+, 42% for 2+, and 0% for 1+. Patients with IHC 1+ had a DCR of 100% and mTOT of 7.3 mos (IQR 2.8-18.6). ORR was 69% in patients with ≤2 prior lines (n=13) and 0% among those with prior topoisomerase-1 inhibitor (topotecan) exposure (n=3) or in BRCA-mutated tumors (n=4). Patients with prior mirvetuximab (n=7) had an ORR of 14% and DCR of 71%.By tumor type: ORR was 47% in OC and 38% in EC; DCR was 76% in OC and 56% in EC; mTOT was 5.5 mos (2.5-9.0) in OC and 4.7 mos (0.8-6.9) in EC. The mPFS was 6.2 mos (95% CI 2.3-15.8) for OC and 6.0 mos (1.4-7.6) for EC. mOS from T-DXd start was 17.3 mos (11.4-27.6) for OC and 10.4 mos (6.3-NR) for EC.
Conclusion: In this real-world cohort, T-DXd demonstrated promising outcomes consistent with DESTINY-PanTumor02. High response rates were observed in IHC 3+ tumors and earlier-line use, while no responses were seen with prior topoisomerase-1 inhibitor exposure or in BRCA-mutated cases. Further studies are needed to validate predictors of response and optimize treatment sequencing.

Baseline Characteristics *HER2 amp by FISH or next generation sequencing. **3 germline, 1 somatic.

	Ovarian cancer N = 17	Endometrial cancer N = 16
Age at diagnosis, mean (std dev)	60.8 (7.6)	66.9 (6.1)
Histology, n (%)		
Serous	13 (76%)	8 (50%)
Clear cell	2 (12%)	1 (6%)
Carcinosarcoma	0	3 (18%)
Endometrioid	1 (6%)	4 (25%)
Other	1 (6%)	0
Lines of treatment prior to T-DXd, median (interquartile range/IQR)	4 (2.5-6.5)	2 (2-3)
Total lines of treatment, median (IQR)	5 (4-9.5)	4 (3-4.8)
HER2 expression		
1+	4 (23%)	1 (6%)
2+	9 (53%)	12 (75%)
3+	3 (18%)	3 (18%)
Amplification*	7 (41%)	6 (37%)
BRCA-mutated**	2 (12%)	2 (12%)
Homologous recombination deficient (HRD)+	5 (29%)	2 (12%)
Prior topoisomerase-1 inhibitor	3 (17%)	0
Prior poly(ADP-ribose) polymerase inhibitor (PARP)	7 (41%)	1 (6%)
Prior ADC	7 (41%)	2 (12%)
Endometrial subgroup		
Deficient mismatch repair (dMMR)	-	1 (6%)
No specific molecular profile (NSMP)	-	1 (6%)
TP53-mutated	-	14 (88%)
POLE-mutated	-	0

: Application of Bioinformatics to Cancer Biology 2
Poster Session

#1407 Single-cell long-read transcriptomics reveals isoform centric molecular features of rare pseudomyxoma peritonei disease.

Kyungtae Lee[1], Anuja Sathe[2], Raegan Wood[2], Dongin Lee[2], Billy Lau[3], Hanlee P. Ji[4]

[1]Oncology, Stanford University School of Medicine, Stanford, CA,[2]Stanford University School of Medicine, Stanford, CA,[3]Biochemistry, Stanford University School of Medicine, Palo Alto, CA,[4]Stanford University, Stanford, CA

Pseudomyxoma peritonei is a rare mucin-producing cancer, most often arising from appendiceal mucinous neoplasm. In the past, investigations into transcriptomic and genomic alterations in this tumor have concentrated on gene-level changes, neglecting the impact of differential isoform usages resulting from alternative splicing and allele specific expression. In this study, we conducted single-cell long-read sequencing on 10 biopsies from 5 tumor patients at various stages of disease. Single cell analysis delineated the individual cell types and long read sequencing revealed the sequence of mRNA transcripts from its 5’ transcript start sites to 3’ polyA-tail - providing insights into disease and cell type specific RNA transcript structures and changes. Across the single cell results, we identified a total of 35,095 expressed genes and 130,272 transcripts, including 50,330 novel transcripts. Based on the identified gene and isoform repertoire, epithelial cells derived from appendiceal mucinous neoplasm showed an upregulation of genes and isoforms linked to goblet cell differentiation, cell proliferation, and mucin production. Furthermore, we identified alternative RNA alternative splicing in genes related to protein degradation and cellular transport within tumor epithelial cells. Our ongoing research focuses on discovering phased somatic mutations at the allele-specific isoform level and uncovering RNA splicing-derived neoantigens expressed in tumor epithelial cells. These efforts may reveal novel oncogenic drivers and potential therapeutic targets for this tumor.

#1408 MicroNucML: A machine learning approach for micronuclei segmentation and the refinement of nuclei-micronuclei relationships.

Nadejda B. Boev, Yukai Wang, Ulises O. Garcia, Kate M. MacDonald, Shane M. Harding, Sushant Kumar

Princess Margaret Cancer Centre, University Health Network, Department of Medical Biophysics at University Toronto, Toronto, ON, Canada

Micronuclei (MN) are structures containing small fragments of DNA, arising from mitotic errors or failed DNA repair attempts. Therefore, MN serve as markers of genomic instability and are typically quantified either manually or through threshold-based methods, which can be tedious and inaccurate, leading to varying degrees of success and throughput. By employing a two-phase labeling approach that utilizes polygon and brush segmentation, along with refinement using SAM2, we developed a high-quality MN segmentation tool. Subsequent data augmentation, which captured heterogeneity in image quality and color diversity, enabled us to train a generalizable Mask-RCNN model optimized for small object detection, achieving state-of-the-art performance in MN detection. Finally, we applied our model to immunofluorescence data obtained from cell lines exposed to DNA damage conditions to gain biological insights into MN dynamics and their role in inducing genome instability. In summary, this work establishes an accessible resource for systematically studying genome instability with significantly greater fidelity and sensitivity, enabling insights into damage biology that were previously unresolved.

#1409 Fusion epigenotyping using cell-free DNA methylation improves detection of actionable ALK fusions in non-small cell lung cancer.

Laura Tung, Anton Valouev, Justin Odegaard, Lauren Lawrence, Nicole Zhang, Martina Lefterova, Matthew Ellis, Tingting Jiang, Sheila Solomon, Darya Chudova

Guardant Health, Palo Alto, CA

Background: Fusion detection with next-generation sequencing is challenging due to short read fragments, which can fail to fully resolve complex genomic rearrangements and map intronic breakpoints that lie outside targeted capture regions. Tumor methylation patterns, which reflect the functional state of cancer cells and do not rely on breakpoint coverage, are less impacted by sequencing fragment length and provide a robust orthogonal signal to augment genomic-based fusion calling. We developed a cell-free DNA (cfDNA) methylation-based fusion epigenotyping method to rescue fusions missed by genomic-based methods, focusing on *ALK* fusion detection in non-small lung cancer (NSCLC) to inform ALK inhibitor therapy selection.
Methods: NSCLC samples were processed using Guardant360 Liquid test (Guardant Health, Palo Alto, CA). Genome-wide cfDNA methylation profiles across thousands of regulatory regions together with genomic molecule support, were used to train a binary classifier that discriminates *EML4-ALK* fusion-positive from fusion-negative NSCLC. A logistic regression model was trained on 175 *EML4-ALK* fusion-positive and 175 fusion-negative samples. Concordance with NSCLC tissue samples was assessed by comparing tissue *EML4-ALK*-associated differentially methylated regions (DMRs, $p<0.05$) from TCGA data to fusion DMRs from Guardant360 Liquid cfDNA samples. To ensure clinical-grade specificity, a decision threshold targeting >99% specificity was calibrated on >11,000 genomic fusion-negative NSCLC samples. Model performance was evaluated on 102 independent positive cases (63 genomically detected, 39 genomically missed) with epigenomic tumor fraction > 0.1% from samples with (a) ALK inhibitor resistance mutations, (b) prior ALK inhibitor treatment, or (c) longitudinal history of genomic fusion detection. Fusion rescue rate was defined as the fraction of genomically missed fusions rescued by the epigenotyping classifier.
Results: Methylation concordance analysis between TCGA NSCLC tissues and Guardant360 Liquid cfDNA samples showed significant overlap, with 64% (1384/2168) of tissue *EML4-ALK*-associated differentially methylated regions (DMRs, $p<0.05$) also significant in cfDNA. In the test cohort, the epigenotyping classifier achieved 74% sensitivity, detecting 100% of fusions identified by the genomic caller. Among genomically missed cases, the classifier rescued 31% (12/39) of fusions.
Conclusion: A cfDNA methylation-based fusion epigenotyping approach provides a high-specificity orthogonal signal that augments genomic fusion detection, recovering a substantial fraction of *EML4-ALK* fusions missed by the genomic method. Clinically, patients with rescued *ALK* fusions could be considered for effective and low toxicity targeted ALK inhibitor therapies.

#1410 Transcriptional silencing of homologous recombination defines a functional HRD in invasive lobular carcinoma.

Yona Kim[1], Yeseul Kim[1], Harim Oh[1], Sung Hak Lee[2], Sangjeong Ahn[1], You-Na Sung[1]

[1]Department of Pathology, Korea University Anam Hospital, Korea University College of Medicine, Seoul, Korea, Republic of,[2]Seoul St. Mary's Hospital, Seoul, Korea, Republic of

Background: Homologous recombination deficiency (HRD) is a key determinant of genomic instability and a major predictor of PARP inhibitor (PARPi) sensitivity in breast cancer. While invasive ductal carcinoma (IDC) commonly exhibits canonical HRD driven by BRCA1/2 loss and characteristic genomic scars, the HR status of invasive lobular carcinoma (ILC) remains poorly characterized. Recent evidence suggests that a subset of ILC displays a *BRCAness-like* phenotype undetected by conventional genomic HRD scores, implying a transcriptionally driven functional HRD mechanism.

Methods: RNA-sequencing data from TCGA-BRCA were analyzed by integrating genomic HRDsum scores with ssGSEA-based pathway scores for a curated HR gene set. Samples were stratified by histological subtype (IDC vs. ILC) and ranked by PARPi7, a seven-gene transcriptomic signature predictive of PARPi response. Correlation analyses and linear interaction models were applied to examine subtype-specific relationships among PARPi7, genomic HRDsum, and HR pathway activity. Differential expression and upstream regulator analyses were performed to identify transcriptomic features and regulators associated with functional HRD in ILC.

Results: In IDC, PARPi7 correlated positively with HRDsum (R = 0.34) and negatively with estrogen receptor expression, consistent with the classical triple-negative breast cancer-like genomic HRD phenotype. HR pathway activity showed minimal association (R = -0.07), supporting a genomically driven HRD. In ILC, this pattern was reversed: PARPi7 correlated negatively with HRDsum (R = -0.20) and strongly with HR pathway suppression (R = -0.48), suggesting that transcriptional silencing of HR genes underlies a functional HRD phenotype in ILC. PARPi7-high ILC tumors exhibited coordinated downregulation of DNA repair and cell-cycle programs with concurrent inflammatory and immune activation. BRCA1 expression was reduced in both subtypes but more markedly in IDC (adj.P = 9.29×10^{-81} vs 1.47×10^{-18}). Upstream regulator analysis identified selective activation of NUPR1 in PARPi7-high ILC - a stress-responsive transcriptional regulator linked to PARP activity and tolerance to DNA damage.

Conclusion: While PARPi7-high IDC reflects canonical, genomically driven HRD with BRCA1-type biology, ILC demonstrates a transcriptionally defined functional HRD lacking genomic scars, implying that PARPi7-high behavior can emerge even in genomically HRD-low tumors. This phenotype involves transcriptional suppression of HR genes and DNA repair machinery, low HRDsum, inflammatory activation, and NUPR1-mediated stress adaptation. These findings define a transcriptomic axis of functional HRD in ILC, suggesting expansion of PARPi strategies beyond genomic HRD to include HR pathway silencing and NUPR1 activation as biomarkers of therapeutic sensitivity.

#1411 Extrachromosomal DNA amplification defines a high-risk subgroup and unique molecular features in gastric cancer.

Jieun Lee[1], Donghyeok Seol[1], Seunghyun Kang[2], Chanmi Bang[1], Mira Yoo[1], Soyeon Kim[2], Hyeongjin Cho[2], So Hyun Kang[1], Young Suk Park[1], Sang-Hoon Ahn[3], Hyung-Ho Kim[4], Eunhee YI[5], Sanghyun Kim[2], Hoon Kim[2], Yun-Suhk Suh[1]

[1]Department of Surgery, Seoul National University Bundang Hospital, Seongnam-si, Korea, Republic of,[2]Department of Biopharmaceutical Convergence, Sungkyunkwan University, Suwon-si, Korea, Republic of,[3]Department of Surgery, Samsung Medical Center, Sungkyunkwan University School of Medicine, Seoul, Korea, Republic of,[4]Department of Surgery, Chung-Ang University Gwangmyeong Hospital, Gwangmyeong-si, Korea, Republic of,[5]Department of Physiology, College of Human Medicine, Michigan State University, Lansing, MI

Gastric cancer (GC) is the fifth most prevalent cancer and the fourth leading cause of cancer mortality. However, clinical strategies targeting these amplifications in GC have been unsuccessful, often leading to treatment resistance and poor prognosis. Extrachromosomal DNA (ecDNA) has emerged as a major mechanism associated with oncogene focal amplification and adverse outcomes. In this study, we performed whole genome sequencing (WGS) and whole transcriptome sequencing (WTS) on paired tumor-normal samples from 76 Korean GC patients collected through Seoul National University Bundang Hospital to understand the prevalence of ecDNAs and their clinical relevance in GC patients. Focal amplification regions amplicons were identified and classified using AmpliconArchitect (AA) and Amplicon Classifier into ecDNA (circular amplification) and non-ecDNA (Chromosomal Amplicons, ChAmps). Focal amplifications were highly frequent and showed a strong association with the chromosomal instability (CIN) subtype (P = 2.37e-09). Of the 76 patients, 17 (22.4%) were classified as "ecDNA positive patients". Notably, 75% of CIN subtype patients carried one or more ecDNA amplicons. Genomic analysis revealed that ecDNA amplicons were significantly larger (P = 0.00056) and more structurally complex than ChAmps, exhibiting a higher frequency of structural variants. ecDNA amplicons also harbored significantly more canonical cancer genes (P = 3.90e-03) and displayed significantly higher copy numbers of these genes compared to ChAmps (P = 6.50e-04). Furthermore, ecDNA regions were significantly enriched with putative transcriptional regulatory elements (P = 1.20e-04) and GC-specific accessible chromatin regions. In WTS data, genes within ecDNA exhibited significantly higher expression compared to in ChAmp (P = 3.59e-05). Gene Set Enrichment Analysis (GSEA) revealed that ecDNA cohorts displayed a significantly more pronounced immunosuppressive phenotype—characterized by downregulation of immune response gene sets—compared to ChAmp patients in both SNUBH and TCGA cohorts. Clinically, the presence of ecDNA conferred a significantly worse Overall Survival (OS) rate compared to ChAmp cohorts (Log-rank test, P = 0.012). Multivariate Cox proportional hazards analysis confirmed that ecDNA status acts as an independent risk factor for OS (HR = 14.4, P = 0.001)Our findings demonstrate that ecDNA amplification is frequent in GC, particularly within the CIN subtype, and is associated with distinct genomic complexity, higher oncogene burden, unique transcriptional consequences (immune suppression), and poor patient prognosis. The presence of ecDNA amplification may serve as a critical prognostic factor in GC, highlighting the need for personalized treatment, including the development of ecDNA-targeted therapies to improve treatment outcomes.

#1412 Informatics-driven spatial-omics for cancer immunotherapy discovery in gynecologic cancers.

Rongting Huang[1], Diane Libert[1], Arslan Kasimov[1], Leandra Kingsley[1], Sahar Nasr[1], Reem Al-Humadi[1], Lindsey A. Finch[1], Elisabeth Diver[1], Ravali A. Reddy[2], Babak Litkouhi[1], Kristin Bixel[1], Sizun Jiang[3], Brooke Howitt[1]

[1]Stanford University, Stanford, CA,[2]The University of Texas MD Anderson Cancer Center, Houston, TX,[3]Harvard Medical School, Boston, MA

Endometrial cancer (EC) remains a highly prevalent and understudied malignancy, with aggressive subtypes disproportionately affecting underrepresented populations and lacking effective targeted therapies. Traditional bulk sequencing approaches have provided limited insight into the spatial and cellular heterogeneity that drive EC progression, particularly with respect to how tumor cells interact with their microenvironment and evade the immune system. Our current research focuses on directly addressing these gaps by leveraging large, well-annotated retrospective EC cohorts to apply advanced spatial multi-omics and computational frameworks.
We propose SPATIAM (Spatial Partitioning of Tumor-Immune Architecture via Multi-omics), a novel computational framework integrating spatial genomics, transcriptomics, and proteomics at single-cell resolution to reconstruct tumor subclonal architecture and map dynamic tumor-immune-stromal interactions in situ. This approach resolves how genetically distinct subclones emerge and interact with their microenvironment and identifies spatially organized immune evasion mechanisms that are invisible in bulk analyses.
Our longitudinal cohort (unpublished) includes patients treated with immune checkpoint inhibitors, with longitudinal sampling of matched primary untreated, post-chemotherapy, interim (on treatment) immune checkpoint inhibition (ICI) and post-ICI samples. This comprehensive collection was processed into tissue microarrays (TMAs) and subjected to multi-modal spatial and molecular profiling. We employed GeoMx Digital Spatial Profiling for high-plex protein and RNA analysis, Multiplexed Ion Beam Imaging (MIBI) for high-resolution spatial proteomics, and single nucleus RNA sequencing for unbiased transcriptional profiling at single cell resolution. This multi-modal approach enabled the systematic characterization of tumor microenvironment evolution throughout the treatment course, capturing both spatial and molecular dynamics of immune responses.
This pioneering study presents the first longitudinal, multi-modal spatial and molecular atlas of ICI treatment evolution, integrating samples across treatment timepoints with cutting-edge spatial proteomics, digital spatial profiling, and single-nucleus sequencing to uncover novel mechanisms of therapeutic resistance.

#1413 Targetable gene dependencies in Ewing sarcoma subtypes.

Dusan Pesic[1], Josh Nash[1], Timmy Wen[1], Pedro Lemos Ballester[1], Livia Garzia[2], Olivier Delattre[3], David Malkin[1], Adam Shlien[1]

[1]Dept. of Genetics & Genome Bio., The Hospital for Sick Children, Toronto, ON, Canada,[2]McGill University, Montreal, QC, Canada,[3]Institute Curie, Paris, France

Ewing sarcoma (EwS) is a bone and soft tissue cancer primarily driven by a FET::ETS fusion protein, most commonly EWS::FLI1. While localized tumors have a five-year survival rate of 70-80% with multimodal treatment, the prognosis for relapsed or metastatic disease remains dismal, with survival rates below 30%. This underscores the urgent need for improved prognostic markers and innovative therapeutic strategies. Using an unsupervised hierarchical clustering approach - RACCOON - we identified three distinct transcriptional subtypes of EwS: EWS::FLI1-high, mesenchymal-like, and muscle-like. The muscle-like group, potentially arising from myofiber infiltration, formed a separate cluster, while the remainder of the cohort was distributed along a continuum of transcriptional states between the EWS::FLI1-high and EWS::FLI1-low/mesenchymal extremes. The same variability in these two transcriptional programs was observed at single-cell resolution and across commonly used preclinical EwS models. Subtype classification in clinical cohorts revealed significant survival differences, with mesenchymal-like tumors showing the poorest prognosis (<35% five-year overall survival) and the highest metastatic potential. An *in vivo* experiment in patient-derived xenografts (PDXs) reinforced these findings, as mesenchymal-like tumors exhibited significantly greater metastatic potential. Additionally, functional genomics data from CRISPR-screened cell lines identified subtype-specific gene dependencies - the Fanconi anemia pathway emerged as a promising therapeutic target for EWS::FLI1-high tumors, while mesenchymal-like tumors showed reliance on distinct transcriptional regulators. By integrating transcriptomic profiling with functional genomics, this study highlights the biological and clinical heterogeneity of EwS, offering novel insights into its molecular underpinnings and paving the way for personalized treatment strategies tailored to specific transcriptional subtypes.

#1414 Shared gut virome profiles highlight potential early colorectal cancer markers in HIV-helminth co-infection.

Botle Precious Damane[1], Thanyani V. Mulaudzi[1], Jonathan Featherston[2], Sayed Shakeel Kader[3], Pragalathan Naidoo[4], **Zodwa Dlamini**[5], Zilungile Lynette Mkhize-Kwitshana[6]

[1]Department of Surgery, Steve Biko Academic Hospital, University of Pretoria, Pretoria, South Africa,[2]Division of National Health Laboratory Service, The National Institute For Communicable Diseases Of South Africa, Sandringham, South Africa,[3]Department of Surgery, University of KwaZulu-Natal, Durban 4001, Congella, South Africa, University of KwaZulu Natal, KwaZulu Natal, South Africa,[4]Department of Medical Microbiology, College of Health Sciences, School of Laboratory Medicine & Medi, University of KwaZulu Natal, KwaZulu Natal, South Africa,[5]Pan African Cancer Research Institute (PACRI), University of Pretoria, Pretoria, South Africa,[6]Biomedical Sciences Department; School of Life and Consumer Sciences, College of Agriculture and Env, University of South Africa, Johannesburg, South Africa

Background: In regions with high HIV and helminth prevalence, co-infection may reshape the gut virome in ways that promote oncogenic processes. Characterizing these alterations may identify early colorectal cancer (CRC) biomarkers in high-risk populations.
Methods: Stool-derived metagenomic data from CRC patients, HIV-infected, helminth-infected, HIV-helminth co-infected individuals, and uninfected controls were analyzed. Viral taxa were quantified at family and genus levels using a metagenomic coassembly pipeline. Hierarchical clustering and heatmap visualisation compared abundance patterns across groups.
Results: CRC samples formed distinct clusters with altered abundance of Siphoviridae (−1.6 ± 0.41; q = 0.0013), Podoviridae (2.3 ± 0.83; q = 0.031), unclassified Caudovirales (−1.6 ± 0.51; q = 0.010), Virus sp. ctWxR2 (−14.7 ± 5.04; q = 0.019), and CrAss-like virus sp. ctt4r3 (22.9 ± 5.00; q = 9.9×10^{-5}). HIV-helminth co-infected samples formed a subcluster overlapping CRC, showing similar enrichments in Siphoviridae (−2.0 ± 0.39; q = 5.3×10^{-6}), unclassified Caudovirales (−2.6 ± 0.48; q = 4.7×10^{-6}), Virus sp. ctWxR2 (−21.1 ± 4.79; q = 0.00011), and CrAss-like virus sp. ctt4r3 (24.8 ± 4.78; q = 2.2×10^{-7}). HIV-only samples resembled controls, while helminth-only samples displayed intermediate profiles.
Conclusion: HIV-helminth co-infected individuals showed closely aligned profiles with CRC, indicating that chronic immune perturbation may create virome states resembling early CRC-associated dysbiosis. These shared viral signatures could serve as potential non-invasive biomarkers for CRC risk stratification in high-burden settings. Longitudinal analyses are needed to clarify temporal dynamics and identify the bacterial hosts and functional pathways through which viral/phage restructuring may promote CRC development.

#1415 A comprehensive computational study of PARP1 isoforms and their interactions with nucleolin: Structural insights and implications for breast cancer.

Nathaniel Zimmerman, Grela Jerliu, Naomi Hutchinson, Anjana Saxena, Shaneen M. Singh

Brooklyn College, Brooklyn, NY

Poly(ADP-ribose) polymerase 1 (PARP1) has emerged as a key player and a promising focal point in dysregulated DNA repair in breast cancer. PARP1 exists in multiple isoforms, each with a unique combination of domains [zinc finger**-**Poly(ADP-ribose) polymerase (zf-PARP), Poly(ADP-ribose) polymerase1domain (PADR1), Tryptophan-Glycine-Arginine domain (WGR), and BRCA1 C Terminus (BRCT)]. High expression of PARP1 is frequently associated with an aggressive type of breast cancer and poor prognosis. We earlier predicted PARP1 as a common interactor of the RNA-binding protein, nucleolin (NCL) and BRCA1 where its BRCT domain is implicated in protein interactions. In a published study we showed NCL-miR interfaces for the six frequently dysregulated miRNA in breast cancer including miR-221. While NCL regulates miR-221 expression, PARP1 is a target of miR-221. These and other studies strongly suggest NCL-PARP1 collaborate at the damaged DNA sites. In this study, we built structural models of the PARP1 isoforms and performed docking analyses using ClusPro and HDOCK using a full-length structural model of NCL to assess their interactions. Our results revealed isoform-specific NCL-PARP1 interaction interfaces. The data is strongly suggestive that differences in domain architecture across PARP1 isoforms can alter protein-protein interactions with potential distinct functional implications. Isoform-specific PARP1-NCL-interactions thus can govern DNA repair processes. Next, we examined how cancer-associated mutations in PARP1 affect these interactions. Using ENSEMBL, COSMIC, and TCGA, we selected key mutations with breast cancer phenotypes and created *in silico* models of PARP1. The generated comparative analyses of mutant and wild-type isoforms revealed mutation-driven alterations in the interaction interfaces. Overall, our study sheds light on the structural and functional diversity of PARP1 isoforms, how they interact with NCL, and how specific mutations could influence breast cancer tumorigenesis. PARP inhibitors are frequently used as targeted cancer therapeutics. Understanding the molecular insights about how PARP-isoforms interact with its protein partners involved in DNA repair process will be valuable and can serve as the initial steps towards the development of potential therapeutic interventions.

#1416 Stress-responsive glucocorticoid receptor signaling shapes the immune tumor microenvironment in lung cancer.

Sabrina Akter[1], Aiman Soliman[2], Robert A. Winn[3], Zeynep Madak-Erdogan[1], Sage J. Kim[4]

[1]Food Science and Human Nutrition, University of Illinois at Urbana-Champaign, Champaign, IL,[2]National Center for Supercomputing Applications, University of Illinois Urbana-Champaign, Champaign, IL,[3]VCU Massey Comprehensive Cancer Center, Richmond, VA,[4]School of Public Health, University of Illinois Chicago, Chicago, IL

Background: Racial disparities continue to exist in lung cancer, while Black individuals tend to smoke less than Whites, indicating potentially additional factors contribute to lung cancer risk. Our previous work showed that social stressors, including neighborhood violent crime, can shape tumor biology via stress-responsive mechanisms. In this study, we investigated how neighborhood violent crime influences tumor microenvironment with a focus on how glucocorticoid receptor activity impacts the spatial pattern of M2 macrophages and $CD8^+$ T cells as indicators of hot and cold immune phenotypes.
Methods: We analyzed 15 lung tumor spatial transcriptomic samples to quantify pathway activity and cell type associations using gene set co-regulation analysis (GESECA). Spatial co-localization was assessed using univariate and bivariate local Moran's I ($p < 0.05$). To enhance spatial resolution beyond the Visium spot size, we extracted latent spatial features using non-negative matrix factorization (NMF), estimated empirical variograms to characterize spatial autocorrelation, and applied ordinary kriging to generate high-resolution spatial maps.
Results: Neighborhood violent crime rates were positively correlated with glucocorticoid receptor activity, as evidenced by high expression of genes involved in the glucocorticoid biosynthesis pathway activity ($p < 0.05$). Regions with elevated glucocorticoid receptor activity also showed higher abundance of epithelial cells, especially in tumors from high-crime neighborhoods. High-resolution spatial maps further revealed that tumors from high-violent crime neighborhoods displayed strong co-localization between M2 macrophages and $CD8^+$ T cells, suggesting that $CD8^+$ T cells are surrounded by immunosuppressive myeloid cells, creating a functionally "cold" tumor microenvironment. In contrast, tumors from low-violent crime neighborhoods showed more mutually exclusive spatial patterns of M2 macrophages and $CD8^+$ T cells, reflecting a "hot" tumor microenvironment.
Conclusions: Our findings suggest that exposure to social stressors, such as neighborhood violent crime, may influence tumor biology by altering stress-responsive pathways and reshaping immune spatial architecture. The distinct hot and cold immune microenvironment may indicate differential treatment effectiveness across neighborhood contexts, potentially contributing to lung cancer disparities. Different immunotherapy strategies depending on immune tumor microenvironment to improve treatment effectiveness.

#1417 Bulk RNA-seq atlas guided annotation of tumor transcriptomes.

Timmy T. Wen, Dusan Pesic, Pedro L. Ballester, Josh Nash, Adam Shlien

The Hospital for Sick Children, Toronto, ON, Canada

Single-cell RNA sequencing (scRNA-seq) enables high-resolution profiling of cellular heterogeneity, revealing novel transcriptomic states. However, many existing generative and foundational single-cell models are trained predominantly on non-neoplastic data, limiting their accuracy in cancer cell annotation. We present SPOTTER (Seed-guided Prediction Of Tumor Transcriptomes with Ensemble Recognition), a framework that integrates bulk RNA sequencing (bulk RNA-seq) cancer atlases with single-cell data. SPOTTER first classifies individual cells using an ensemble neural network classifier OTTER (Oncologic TranscripTome Expression Recognition), trained on the hierarchical RACCOON (Resolution-Adaptive Coarse-to-fine Clusters OptimizatiON) cancer atlas spanning over 15,000 pediatric and adult cancer samples. High-confidence seed labels are selected using a Gaussian mixture model (GMM) and Gini impurity-based filtering of OTTER scores to exclude low-quality cells with uncertain predictions. These labels are then propagated through scANVI (single-cell Annotation using Variational Inference) to achieve per-cell classifications. Across nine diverse pediatric and adult single-cell and single-nucleus cancer datasets, SPOTTER reliably assigned malignant cells to their expected tumor classes. In Ewing sarcoma samples with matched bulk RNA-seq and single-nucleus RNA-seq (snRNA-seq), SPOTTER recapitulated bulk RNA-seq-defined subtypes at single-cell resolution, distinguishing one subtype enriched for neuronal programs, including *SYT1* and *SOX6*, and another with increased *EWS-FLI1* fusion activity and elevated *JAK1* signaling—consistent with subtypes previously identified by OTTER and RACCOON in bulk RNA-seq. By integrating bulk and single-cell analyses, SPOTTER enables characterization of tumor heterogeneity and supports identification of subtype-specific markers to reveal critical insights into the transcriptomic profile of a cancer.

#1418 Uncovering novel splice junctions in prostate cancer using DeepSAP.

Pankaj Vats[1], Fadel Berakdar[1], Thomas D. Wu[2], Tong Zhu[1], Mehrzad Samadi[1]

[1]Nvidia Corporation, Santa Clara, CA,[2]Genentech Inc, South San Francisco, CA

Accurate characterization of alternative splicing and gene fusion events from RNA-seq is crucial for understanding cancer biology, however, this task remains inherently challenging due to factors such as complex splice junction architecture, ambiguous read mapping caused by multi-mapped reads, and the presence of chimeric transcripts that confound standard analysis pipelines. We present DeepSAP, a splice-aware RNA-seq aligner that integrates Transcriptome-Guided Genomic Alignment (TGGA) as implemented in GSNAP with advanced Transformer-based Splice Junction Scoring (TSJS) to overcome these challenges and achieve greater sensitivity and specificity in detecting true splicing events. DeepSAP leverages a fine-tuned DNABERT model, trained on curated splice donor and acceptor site sequences drawn from multiple species, utilizing sequence windows of varying lengths (90, 150, 200, and 400 bp) around the splice junctions. Among the different fine-tuned models evaluated, DNABERT MS150 demonstrated superior performance in distinguishing true splice sites, and is directly integrated into the DeepSAP workflow to re-score and prioritize candidate splice junctions identified by GSNAP TGGA, effectively combining both sequence-driven plausibility in local DNA context and strongly supported by RNA-seq reads. To evaluate DeepSAP in a clinically relevant setting, we applied it to a prostate cancer RNA-seq cohort (PRJNA579899, University Hospital Zurich). In this cohort, DeepSAP consistently identifies numerous high-confidence, novel splice junctions absent from current gene annotations and frequently missed or only weakly detected by current state of the art RNA-seq aligners. Notably, in FOXA1, DeepSAP resolves a novel donor site with a double-adenine substitution that creates a previously unannotated exon-intron boundary. This junction shows coherent read coverage and high transformer derived donor and acceptor probabilities, whereas alternative aligners fail to produce a consistent splice junction at the same locus. A similar pattern is observed in the ERG oncogene, where DeepSAP recovers an additional complex, unannotated splice junction that is not captured by other aligners. The results highlight DeepSAP's ability to recover complex, previously undescribed splice junctions in tumor RNA-seq data and demonstrate that coupling GSNAP TGGA with TSJS substantially improves alignment sensitivity and specificity, enabling improved detection of candidate oncogenic splice events in cancer RNA-seq samples.

#1419 Integrated spatial and genetic lineage tracing uncovers cell state plasticity underlying recurrence in group3 and group4 medulloblastoma.

Bohyeon Yu[1], Emanuele Filiberto Rosatti[2], Jangham Jung[1], Abhinav Jain[1], Joanna Phillips[1], Aaron Antonio Diaz[1]

[1]Department of Neurological Surgery, University of California, San Francisco, San Francisco, CA,[2]Department of Cellular, Computational and Integrative Biology, University of Trento, Trentino, Italy

Recent studies place Group 3/4 medulloblastomas (G3/4 MBs) within the rhombic lip (RL)-derived glutamatergic lineage, indicating that a stalled differentiation program underlies their malignant evolution. However, it remains unclear whether these tumors retain the plasticity to transition within this lineage framework, and how their cellular states are reshaped in response to therapy. To address these questions, we constructed a single-cell multiomics atlas of G3/4 MBs using 84 tumor specimens from 38 patients, including 7 longitudinally matched cases collected through the University of California, San Francisco Brain Tumor Center (UCSF BTC) and the Children's Brain Tumor Network (CBTN). From these samples, we generated single-nucleus transcriptomic and chromatin accessibility profiles from 57 frozen samples, and spatial transcriptomic profiles from 27 FFPE samples using Visium and Xenium. We also incorporated single-cell lineage-tracing data from intracranial xenografts derived from two G3 MB cell lines. Genetic lineage tracing integrating static barcodes with endogenous mutations demonstrated that xenografts recapitulate the developmental cell-type composition of treatment-naive primary human MBs, with barcode-defined individual clones maintaining highly similar and stable cell-type fractions. Comparison of matched primary and recurrent clinical tumors revealed no substantial differences in developmental composition. Despite this stability, phylogenetic analysis uncovered markedly increased plasticity in recurrent tumors, driven by dedifferentiation transitions from unipolar brush cell-like states to RL progenitor-like states. Tumor regions exhibiting high plasticity were spatially clustered and corresponded to structurally disorganized areas. Our work establishes cell-state plasticity as a defining feature of recurrent G3/4 MBs, providing a mechanistic framework for understanding recurrence following therapy.

#1420 Image-based ROI selection for spatial transcriptomic experiments using immune checkpoint inhibitor treatment outcome prediction in gastric cancer.

Sunho Park[1], Minji Kim[1], Jean R. Clemenceau[1], Seock-Jin Chung[1], Eric F. Sha[1], Changjin Hong[1], Soyoung Im[2], Hwanil Choi[3], Soonyoung Lee[3], Jongseong Jang[3], Kohei Shitara[4], Sung Hak Lee[5], Jae-Ho Cheong[6], Tae Hyun Hwang[1]

[1]Vanderbilt University Medical Center, Nashville, TN,[2]St. Vincent's Hospital, College of Medicine, The Catholic University of Korea, Suwon, Korea, Republic of,[3]LG AI Research, Seoul, Korea, Republic of,[4]Department of Gastrointestinal Oncology, National Cancer Center Hospital East, Kashiwa, Japan,[5]Seoul St. Mary's Hospital, College of Medicine, The Catholic University of Korea, Seoul, Korea, Republic of,[6]Yonsei University College of Medicine, Seoul, Korea, Republic of

Introduction

Spatial omics experiments profile only a limited number of regions of interest (ROIs) per section, making ROI selection critical. However, manual selection from tumor annotations may miss critical subregion due to the complexity of tumor structures and the limited capability of human visual processing. We recently reported S2Omics, an AI framework that selects ROIs to maximize cell-type diversity and molecular information in an outcome-agnostic manner. Here, we extend this concept to develop an image-based ROI selection method that directly incorporates immune checkpoint inhibitor (ICI) treatment outcome in gastric cancer (GC), enabling outcome-aware spatial transcriptomic experiments.

Methods

We assembled 157 H&E whole slide images (WSIs) from GC patients treated with ICIs at three centers in Korea and Japan (26 responders, 131 non-responders). WSIs were tiled into 256 µm × 256 µm patches. Tumor tiles were identified using an LG AI Research's EXAONE Path-based cell-type classifier plus a ResNet18 tumor classifier. A weakly supervised model, developed in our previous work, was trained on the tumor tiles to predict responder versus non-responder status, achieving a slide-level area under the curve (AUC) exceeding 0.7 on an independent test set.

Results

Tile-level prediction scores were aggregated into heatmaps representing predicted ICI responsiveness. By applying a sliding window (6.5 mm × 6.5 mm) with rotational adjustments to the prediction heatmap, we identified candidate regions of interest (ROIs) that (i) maximized predicted responsiveness, (ii) maximized predicted non-responsiveness, or (iii) captured heterogeneous ("mixed") patterns. The multiprocessing pipeline efficiently generated ROI suggestions for each slide within seconds. This approach can provide a systematic framework for identifying optimal ROIs for spatial molecular profiling, directly linked to immune responses in gastric cancer.

Conclusion

We developed an image-based approach that selects ROIs according to predicted ICI outcome in GC. By prioritizing regions enriched for predicted response, non-response, or mixed patterns, this strategy samples spatial niches more closely linked to outcome than conventional tumor-enriched or marker-based selection. The framework is adaptable to other spatial platforms by adjusting ROI size and applying user-defined weighting criteria based on predicted outcome, cell composition, or other image-derived features. Ongoing work will validate the method in larger cohorts and profile these ROIs with spatial transcriptomics and multimodal assays to define molecular programs underlying differential ICI response and support biomarker discovery, therapeutic development, and patient selection.

*AI was used for language editing only; authors are responsible for all content and approved the final version.

#1421 Pediatric pan-cancer characterization of transposable elements and their modulation by germline *TP53* variants.

Brianne Laverty[1], Shilpa Yadahalli[1], Safa Majeed[1], Ashby Kissoondoyal[1], Laura Raiti[1], Ann Gong[1], Noa Alon[1], Kashif Daud[1], Alexander Solovyov[2], Scott Davidson[1], Yisu Li[1], Mehdi Layeghifard[1], Adam Shlien[1], David Malkin[1], Vallijah Subasri[3]

[1]Genetics and Genome Biology, The Hospital for Sick Children, Toronto, ON, Canada,[2]Halvorsen Center for Computational Oncology, Memorial Sloan Kettering Cancer Center, New York, NY,[3]Peter Munk Cardiac Centre, University Health Network, Toronto, ON, Canada

Transposable elements (TEs) are dynamic repetitive genomic regions that are silenced through epigenetic repression. Although TE activation is a well-recognized feature of embryonic development and adult cancers, their role in pediatric malignancies is poorly understood. Approximately 15-18% of pediatric cancers arise in the context of hereditary cancer predisposition syndromes, such as Li-Fraumeni Syndrome, caused by germline *TP53* (g*TP53*) variants. *TP53* binds to LINE1 elements to suppress their transcription, and adult tumors with somatic *TP53* mutations exhibit elevated TE activity. These findings suggest that g*TP53* variants may disrupt TE regulation during development, predisposing tissues to malignant transformation. To investigate this, we characterized the germline and tumor TE landscape across a pediatric pan-cancer cohort and evaluated the impact of g*TP53* variants.

We identified TEs in 456 germline and 380 tumor samples. Germline ALU, LINE1, SVA elements were called using MELT, xTEA, and INSurVeyor, while tumor LINE1 elements were called with xTEA and TotalReCall. We excluded 96% of germline and 23% of tumor TEs classified as common (>3% of gnomAD or our additional cancer-free cohort (n=166)).

We observed no difference in germline TE burden between g*TP53* carriers and non-carriers, prompting us to examine insertion-site patterns. Motivated by prior findings of global germline methylation differences in g*TP53* carriers, we tested if g*TP53* variants alter germline insertion location. A support vector machine trained on TE distribution predicted g*TP53* status with an AUPRC of 0.74, suggesting g*TP53* variants influence the position of germline insertions. Germline TEs in cancer-free individuals affected regulatory regions governing cell cycle and mitotic pathways whereas germline TEs in the cancer cohort disrupted immune-related regulatory elements (FDR < 0.05). Preliminary evidence suggests immune pathways are altered in germline blood and fibroblast DNA, indicating a systemic effect.

Half of tumors harboured at least one insertion, with epithelial-origin cancers containing more TEs, reflecting adults-onset cancers. As TEs are active in brain development, we analyzed an additional 102 medulloblastoma samples and found 97% contained no insertions. Unlike adult tumors, somatic or germline *TP53* variants did not increase LINE1 insertion burden. Regulatory regions linked to metabolic pathways were affected in g*TP53* carriers (FDR < 0.05).

Overall, we found g*TP53* variants do not increase germline or tumor TE burden but strongly influence the positional distribution of germline insertions. Tumors in the context of g*TP53* variants contain TEs that affect metabolic regulatory regions**,** highlighting consequences of this altered germline architecture. This work enhances our understanding of tumour susceptibility and *TP53*-associated cancers to guide future therapeutics.

#1422 Characterizing clinical toxicity in cancer combination therapies.

Alexandra M. Wong[1], Cecile Meier-Scherling[1], Lorin Crawford[2]

[1]Center for Computational Molecular Biology, Brown University, Providence, RI,[2]Microsoft Research, Cambridge, MA

Predicting synergistic cancer drug combinations through computational methods offers a scalable approach to creating therapies that are more effective and less toxic. However, most algorithms focus solely on synergy scores without considering toxicity when selecting optimal drug combinations. In the absence of combinatorial toxicity assays, a few models use toxicity penalties to balance high synergy with lower toxicity. Yet, these penalties have not been explicitly validated against known drug-drug interactions (DDIs). In this study, we provide a comprehensive, multifaceted analysis to characterize the relationship between drug synergy, computational toxicity metrics, and clinically reported DDI severity. We focused on five synergy scores: Bliss, Loewe, Zero Interaction Potency (ZIP), Highest Single Agent (HSA), and S. Leveraging the drug synergy data from DrugComb and clinical toxicity annotations (Minor, Moderate, Major) from DrugBank and DDInter, we performed non-parametric tests, including the Kruskal-Wallis and Jonckheere-Terpstra tests, to assess trends between toxicity severity and synergy. We then evaluated three computational toxicity proxies: drug target/pathway overlap (Jaccard Similarity), drug structural similarity (Tanimoto Similarity), and the average distance between drug targets in a protein-protein interaction network (PPIN). Our analysis revealed that prioritizing combinations solely by higher synergy is not associated with lower toxicity. For the DrugBank dataset, all synergy scores exhibited a positive trend with increasing toxicity, indicating that higher synergy is associated with higher DDI severity. Furthermore, we demonstrate that the toxicity proxies used in current models, such as drug target overlap and PPIN distance, are poor predictors of clinical DDI severity. For instance, in DrugBank, the Jaccard Similarity of drug targets showed only a weak, statistically significant difference across toxicity groups ($p \sim 0.000$; effect size ~ 0.098), highlighting its limited practical explanatory power. Our results reveal that while some metrics correlate with general toxicity trends, no single metric robustly captures the complexity of clinically known adverse DDIs across databases. This finding highlights the significant limitations in using simple, readily available proxy metrics as effective toxicity penalties in drug combination prediction models. Ultimately, our study underscores the pressing need for more comprehensive and detailed combination toxicity data to advance the field toward truly safe and efficacious cancer combination therapies.

#1423 Aneuploidy detection from FFPE archived tissues: A computational approach for FFPE-CUTAC data.

Aditya T. Parmar[1], Yiyang Niu[1], Kami Ahmad[2], Steven Henikoff[2], Ye Zheng[1]

[1]Department of Bioinformatics and Computational Biology, The University of Texas MD Anderson Cancer Center, Houston, TX,[2]Basic Science Division, Fred Hutchinson Cancer Center, Seattle, WA

For more than a century, Formalin-Fixed Paraffin-Embedded (FFPE) sample preparation has been the standard for long-term preservation of biological material, but severe molecular degradation has long been a technical barrier to high-quality genomic analysis. We recently introduced FFPE-Cleavage Under Targeted Accessible Chromatin (FFPE-CUTAC) with an antibody to RNA Polymerase II (RNAPII) as a sensitive, cost-effective alternative for profiling transcription in FFPEs. Beyond transcription, these profiles present an opportunity to infer aneuploidy (whole chromosome arm gain or loss), a key cancer hallmark. However, the sparse nature of FFPE-CUTAC data presents a computational challenge with no existing fit-for-purpose tools.

Copy number alterations (CNA) detection methods for whole genome sequencing (WGS) data typically rely on fold change in read depth. However, our analysis shows moderate correlation between FFPE CUTAC and matched WGS read depth across the genome(Pearson correlation coefficient $r = 0.525$, Spearman correlation coefficient $\rho = 0.688$). As a result, directly applying standard read-depth-based CNA methods to FFPE-CUTAC achieves a reasonable but suboptimal recovery rate. These findings indicate the need for a tailored approach that explicitly accounts for the sparsity and noise inherent in FFPE-CUTAC data.

Our new method estimates a read depth baseline for each genomic bin rather than a single baseline for the entire sample to better capture the normal copy number level. We partition the genome into 1 Mb bins and use GC content as a genomic feature to group these bins. Bins with similar GC content share the same read depth baseline, defined as the mean read count across all bins within the corresponding GC content group. We evaluate the performance of our strategy using 30 meningioma samples against a standard WGS reference data from the same patient cohort. Our method demonstrated a 95.4% overall aneuploidy detection accuracy (1116/1170 chromosome arms) and ensured a low false-positive rate by correctly identifying 98.9% of all intact arms. By comparison, aneuploidy detection from matching FFPE RNA-seq profiling was lower, with an accuracy of 86.32% (1010/1170 chromosome arms).

We established a strategy specifically designed for aneuploidy profiling from FFPE-CUTAC data. This method unlocks the ability to sensitively and affordably identify critical chromosome arm variations from the FFPE-CUTAC data, alleviating the need to generate additional costly WGS data.

#1424 Unique tumor ecosystems in metaplastic breast cancer identified through single nucleus RNA sequencing.

Aatish Thennavan, Tuan M Tran, Jianzhuo Li, Clinton Yam, Nicholas E. Navin

UT MD Anderson Cancer Center, Houston, TX

Metaplastic breast cancers (MBC) are rare, aggressive triple negative breast cancers (TNBC) that account for less than 1% of all breast cancers. Patients with MBCs are treated similarly to other TNBCs, however, consistently have a worse prognosis and decreased survival in comparison to other TNBC patients. The main aspect affecting MBCs treatment refractoriness is the heterogeneity of tumor cell differentiation in this tumor towards cells of mesenchymal/sarcoma like phenotype e.g. spindle cells, chondroblasts etc. The objective of this study was to investigate these transdifferentiated MBC tumor cells and tumor microenvironment (TME) changes in comparison to other TNBCs and normal breast tissues using single nucleus RNA sequencing (snRNA). For snRNA we profiled 5000-10,000 nuclei per tumor after running FACS to remove ambient RNA and compared tissue samples from MBCs, TNBC and normal breast tissues. Additionally, we also report that MBCs have different myeloid cell state proportions in comparison to other TNBCs, including a significant increased population of *SIPA1L1* myeloid cells cancer cells in MBCs. We also describe novel fibroblast populations enriched in the MBC that are distinct from normal breast and TNBCs. Overall, the MBC TME also exhibits an increased number of proliferative cells in endothelial, fibroblast and myeloid cell compartments. In the transdifferentiated MBC cancer cells, we also define novel transcriptional metagene programs using non-negative matrix factorization (NMF) analysis. Collectively our data identifies the distinctive cancer cell programs and TME of this rare breast cancer for the first time at a single cell resolution and identifies potential new cell states that define it’s unique tumor biology.

#1425 Identifying tumor-specific membrane targets, therapeutics, and matching cell lines for experimental validation with the Multiomics2Targets2 workflow.

Anna I. Byrd, Lily D. Taub, Avi Ma'ayan

Pharmacological Sciences, Icahn School of Medicine at Mount Sinai, New York, NY

Rapid advancements in the multi-omics profiling of tumors from cancer patients have opened up a range of possibilities for personalized target identification. To this end, we previously developed Multiomics2Targets, a platform that identifies tumor-specific membrane proteins. The tumor-specific membrane targets are highly expressed in the input RNA-seq tumor samples while lowly expressed in hundreds of normal tissues and cell types based on transcriptomics profiling atlases created from GTEx, Tabula Sapiens, and ARCHS4. To further prioritize the identified targets for conducting in-vitro and in-vivo experiments, we upgraded the Multiomics2Targets workflow with data from the Cancer Cell Line Encyclopedia (CCLE) and the Cancer Dependency Map (DepMap). From CCLE we identify correlated cell lines that also express the identified targets, and from DepMap we examine the effects of the identified targets on cell line proliferation when knocked down. We also added to the workflow drug predictions by integrating Connectivity Mapping resources from six databases. Additionally, the updated Multiomics2Targets workflow can be applied to single cell RNA-seq data, or bulk RNA-seq samples can be deconvoluted into single-cell-like profiles. The upgraded workflow also applies the tools ChEA-KG and Enrichr to identify enriched transcription factor regulatory subnetworks, pathways, associated phenotypes, and other enriched terms. The resulting figures and tables are compiled into an automatically generated report which includes introduction, methods, results, and conclusions. We demonstrate the utility of the upgraded workflow by discovering tumor subtype-specific cell-surface targets, enriched pathways, down-regulating chemical perturbations, and most similar cell lines for pancreatic adenocarcinoma tumors from the Clinical Proteomic Tumor Analysis Consortium 3 project. We validate several highly ranked targets and chemical perturbations by literature search, as well as suggest novel targets, therapeutics, and cell lines for future in-vitro and in-vivo validation experiments. The updated drug and target discovery workflow is encoded into a new software application called Multiomics2Targets2 (M2T2).

#1426 A single-cell tumor atlas defines robust pathway and gene signatures enabling cancer cell-line fidelity assessment.

Rosyli F. Reveron-Thornton[1], Chuner Guo[1], James P. Agolia[1], Maria Moozhiyil Korah[1], Peter Yuxin Xie[2], Andrea Delitto[1], Amanda Goncalves[3], Angela Tabora[3], Biren Reddy[4], Wesley Bobst[3], Amanda R. Kirane[4], Monica Dua[1], Brendan Visser[1], Byrne Lee[1], George Poultsides[1], Jeffrey A. Norton[5], Derrick C. Wan[3], Michael T. Longaker[3], Deshka Foster[4], Daniel Delitto[6]

[1]Department of Surgery, Stanford University School of Medicine, Stanford, CA,[2]Department of Bioengineering, Stanford University, Stanford, CA,[3]Hagey Laboratory for Pediatric Regenerative Medicine, Division of Plastic and Reconstructive Surgery, Stanford University School of Medicine, Stanford, CA,[4]Stanford University School of Medicine, Stanford, CA,[5]Professor, Dept. of Surgery, Stanford University Medical Center, Stanford, CA,[6]Stanford Unviersity School of Medicine, Stanford, CA

The aim of this study was to determine whether rigorous quality control applied across multiple single-cell RNA (scRNA-seq) sequencing datasets could generate reproducible transcriptional signatures that accurately reflect tumor biology and support evaluation of cancer model fidelity. We aggregated publicly available scRNA-seq datasets and processed all samples through a high-stringency quality-control pipeline that included thresholds of >5,000 counts, <10% mitochondrial content, removal of samples with < 200 cells, and doublet identification using Scrublet. The resulting atlas included 135,441 high-quality tumor cells across 494 samples representing 36 adult and pediatric tumor types. We identified tumor specific gene signatures through differential expression analysis and computed hallmark pathways analysis. Strict QC markedly improved the clarity and biological coherence of tumor-specific signatures enabling us to group otherwise unrelated primary tumors into reproducible transcriptional archetypes (proliferative, immune-signaling, and metabolic) states. These atlas-derived gene signatures showed strong concordance with independent bulk RNA-seq datasets and spatial transcriptomic signatures validating the approach/model.

To examine the utility of these signatures, we projected gene expression profiles from established cancer cell lines onto the atlas-derived signatures. This analysis scored cell lines based on how representative they remained to their tumor of origin. Culture adaptation, metabolic drift, or the loss or gain of hallmark pathways, are known causes of transcriptional divergence in *in-vitro* models. These findings demonstrate that rigorous QC enables construction of a reproducible, pan-cancer single-cell atlas that yields stable transcriptomic signatures suitable for more reliable tumor characterization than offered by the publicly resources (HTAN, EcoTyper, DepMap, Cancer SCEM etc) which vary significantly in their QC measures. This atlas provides a high-quality reference for tumor biology and a framework for evaluating the fidelity of cancer cell lines, with implications for model selection, assessment of therapeutic vulnerabilities, and translational research.

#1427 Exploring high-resolution subtypes for pancreatic ductal adenocarcinoma via a meta-clustering approach.

Nick Boos Peterson, Jieqiong Wang, **Shibiao Wan**

University of Nebraska Medical Center, Omaha, NE

As the third leading cause of cancer death in the United States, pancreatic cancer (PC) is a malignancy with a very low 5-year survival rate. Early diagnosis and treatment of PC remain challenging due to the lack of reliable clinical indicators such as biomarkers. Pancreatic ductal adenocarcinoma (PDAC) is the most common PC subtype, accounting for over 90% of cases. Identifying PDAC subtypes is essential for downstream risk stratification and tailored treatment design. PDAC is conventionally categorized into four molecular subtypes, i.e., aberrantly differentiated endocrine exocrine (ADEX), immunogenic, squamous, and pancreatic progenitor. However, numerous studies have demonstrated high heterogeneity within these 4 molecular subtypes, indicating that exploring high-resolution subtypes for PDAC is highly needed. Conventional wet-lab techniques like molecular profiling and histopathological studies are time-consuming, costly, and laborious. To fill these gaps, we developed a meta-clustering approach to leverage transcriptomics data to explore high-resolution PDAC subtypes. Specifically, we first leveraged random projection (RP) to reduce the dimensions of the PDAC RNA-seq data, which were then clustered by our base clustering method using the Leiden algorithm. To obtain robust results, we implemented 15 runs of RP-based Leiden clustering. Then, we performed meta-clustering of these 15 clustering results by adopting a weighted meta-clustering (wMetaC) architecture from our previous published single-cell analysis method named SHARP. Results suggested that our proposed approach significantly outperformed state-of-the-art clustering methods for PDAC subtyping. Moreover, our meta-clustering approach performed substantially better than all individual base clustering methods. We further performed cluster-specific differential gene expression analysis, pathway analysis and gene-drug-disease association studies, suggesting that our newly identified PDAC sub-clusters were distinctive among different clusters. We expect our proposed approach will provide a robust framework for high-resolution PC subtype characterization for accurate downstream risk assessment and personalized treatment design.

#1428 Single cell RNA-seq analysis of osteosarcoma reveals conserved and distinct ecosystems across sites and species.

Yogesh Budhathoki[1], Matthew Cannon[1], Troy A. Mceachron[2], Anand G. Patel[3], Matthew Gust[1], Jaime F. Modiano[4], Dylan T. Ammons[5], Kathryn Cronise[5], Daniel Regan[5], Heather Gardner[6], Ryan D. Roberts[1]

[1]Nationwide Children's Hospital, Columbus, OH,[2]National Cancer Institute, Bethesda, MD,[3]St. Jude Children's Research Hospital, Memphis, TN,[4]University of Minnesota, Minneapolis, MN,[5]Colorado State University, Fort Collins, CO,[6]Cummings School of Veterinary Medicine, Tufts University, North Grafton, MA

Osteosarcoma exhibits profound heterogeneity that has long challenged efforts to understand its mechanisms and advance therapeutic progress. To unravel this complexity, we compiled the largest cross-species single-cell transcriptomic dataset, integrating 775,441 cells from human patients, dog patients, patient-derived xenografts, and mouse models. To our knowledge, this dataset represents the first multi-species, multi-technology, and multi-site (primary and metastatic) harmonization of single-cell data for any solid tumor, enabling a unified framework for interrogating inter- and intra-tumor heterogeneity across biological and evolutionary contexts.

Through this work, we define subpopulations of osteosarcoma tumor cells that are conserved across tumors, species, and disease sites. These subpopulations span a continuum of differentiation states, from quiescent progenitor-like cells to more differentiated matrix-producing and inflammatory phenotypes, suggesting a conserved developmental hierarchy. Analysis of the stromal compartment revealed both established and previously unappreciated features of osteosarcoma, including the presence of bone-associated osteoclast-like macrophages in both primary and lung metastatic sites and enrichment of inflammatory and scar-associated macrophages in metastatic lung lesions, which we have previously implicated in metastatic progression.

The resulting atlas provides a rich and unprecedented resource for exploration and discovery. Using this resource, we characterized tumor-host interactions occurring in primary and metastatic sites and compared them across species. This analysis revealed a striking number of matrix-derived signals within metastatic lung lesions, far exceeding those identified in primary bone lesions. For example, we found that tumor-derived fibronectin engages syndecans and integrin receptors on epithelial cells, inducing a pathogenic phenotype remarkably similar to that described in pulmonary fibrosis. Validation of these interactions using spatial transcriptomic data identifies distinct neighborhoods that support specific tumor cell subpopulations, with patterns conserved across samples.

Collectively, this work establishes a transformative resource and conceptual framework for understanding tumor heterogeneity, evolution, and microenvironmental remodeling. It serves as a powerful platform for hypothesis generation, model fidelity assessment, and therapeutic discovery, guiding the next generation of translational advances in osteosarcoma biology.

#1429 Stress-responsive genomic alterations reveal a bi-directional relationship between PTSD biology and breast cancer aggressiveness.

Alakesh Bera[1], Meera Srivastava[2]

[1]USUHS - Uniformed Services University of the Health Sciences, Bethesda, MD,[2]APG Department, Uniformed Services University of the Health Sciences, Bethesda, MD

Background: Breast cancer (BrCa) and post-traumatic stress disorder (PTSD) exhibit a complex, bidirectional relationship. While cancer diagnosis and treatment can induce PTSD, emerging epidemiologic data indicate that pre-existing psychological stress or PTSD may also elevate the risk of developing breast cancer or accelerate tumor progression. The biological mechanisms underlying this interaction remain unclear. We hypothesized that tumor-intrinsic alterations in stress-responsive genes may provide molecular insight into this connection.

Methods: We analyzed 17,605 breast tumors using cBioPortal/TCGA datasets and compared them with a 95,474-sample pan-cancer reference. PTSD- and stress-related over sixty genes were curated from published literature and included: TG, CYP11B1, CYP11B2, CRH, NR3C1, SLC6A4, PRKCA, CHRNA6, RGS2, DRD2, BDNF, FKBP5, SLC6A2, TPH2, and others. Copy number alterations, co-amplification patterns, and clinical outcomes (including metastatic progression) were evaluated.

Results: Stress-related genes exhibited significantly enriched copy number amplifications in breast cancer compared with a pan-cancer reference cohort. Across 17,605 BrCa tumors, more than sixty PTSD-, mood-, and stress-endocrine-associated genes showed recurrent CNAs. Key alterations included TG (19%), CYP11B1/CYP11B2 (16%), RGS2 (12%), CRH (10%), PRKCA (9%), and CHRNA6 (8%), markedly higher BrCa than their frequency across 95,474 tumors from all cancer types (2-5%). TG-amplified tumors demonstrated coordinated co-amplifications involving 8q24 (MYC/PVT1) and 1q32, along with characteristic 8p22 deletions, genomic features strongly associated with aggressive disease biology. Exploratory clinical annotation further showed that TG- or CYP11B-gated BrCa cohorts exhibited rapid metastatic progression, with a median time to metastasis <10 months. Together, these findings identify a robust stress-tumor genomic axis in breast cancer and highlight Thyroglobulin (TG) and Corticotropin-Releasing Hormone (CRH) as high-priority candidates for development as objective, noninvasive serum biomarkers.

Conclusion: Large-scale civilian tumor genomic analyses reveal that stress-responsive and PTSD-linked genes are recurrently amplified in breast cancer and co-cluster with high-risk oncogenic regions. These findings support a biological model in which chronic stress/PTSD and breast cancer aggressiveness intersect through shared neuroendocrine and GPCR-linked molecular pathways. This stress/tumor axis may help explain both PTSD arising after a breast cancer diagnosis and stress-associated increases in breast cancer risk or progression. These insights establish a foundation for developing objective biomarkers and mechanistic studies exploring the PTSD-BrCa interface.

#1430 Conserved tumor imprinted T cell states across cancers revealed by pan cancer single cell atlases.

Yan Zong, Hongru Shen, Yajing Bi, Xiangchun Li

Tianjin Medical Univ. Cancer Inst. & Hospital, Tianjin, China

Tumor immune escape arises not only from intrinsic alterations within tumor cells but also from chronic antigen stimulation, inhibitory checkpoint signaling and an immunosuppressive tumor microenvironment that progressively remodels infiltrating immune cells. In previous single-cell RNA-seq analyses, we repeatedly observed subsets of tumor-infiltrating T cells whose transcriptional profiles closely resemble those of neighboring tumor cells, blurring the boundary between immune and malignant compartments and suggesting that key features of tumor adaptation may be written into T-cell states. However, the shared features of such putative tumor-imprinted T cells across cancer types and tissues, and their systematic differences from healthy T cells, remain poorly defined. To address this gap, we aggregated single-cell RNA-seq data from 371,108 intratumoral T cells spanning 19 cancer types. Matched healthy controls were obtained from Tabula Sapiens across 15 tissue types corresponding to these cancers, from which we identified ~130,000 T cells among 290,334 immune cells. We find that tumor-intrinsic and microenvironmental transcriptional programs are markedly enriched in CD8 terminally exhausted and NK-like CD8 T-cell states in patients with cancer, whereas these signals are only weakly detectable in healthy T cells. In particular, epithelial-mesenchymal transition, TGF-β signaling, hypoxia, angiogenesis, MYC and E2F target programs and cell cycle-related pathways are consistently upregulated in tumor-imprinted CD8 T cells, accompanied by selective depletion of naïve and central memory signatures. Building on these observations, we derive a per-cell tumor-imprint score that integrates these pathways, delineates subset-specific and cancer type-specific imprinting patterns, and robustly separates tumor from healthy T cells across multiple organs and independent cohorts. In single-cell datasets from immune checkpoint blockade cohorts, baseline tumor-imprint patterns align with T-cell states associated with treatment response, indicating that this score may aid patient stratification and response prediction. Collectively, this pan-cancer single-cell study provides evidence that tumor cells “hijack” the immune system by rewiring the transcriptional and pathway programs of infiltrating T cells. The resulting tumor-imprint score offers a biologically grounded and operational framework to quantify the extent of T-cell tumorization, refine immunotherapy strategies and inform the design of next-generation T-cell-targeted and cell-based therapies.

#1431 Functional heterogeneity of neutrophils in hepatocarcinogenesis in animal models and human patients.

Zhihao Huang[1], Wang Xiaopeng[2], Wei Dai[1], Xin-Yuan Guan[1], Feng Gen-Sheng[3]

[1]The University of Hong Kong, Hong Kong, China,[2]Peking University, Beijing, China,[3]Institute of Cancer Research, Shenzhen Bay Laboratory, Shenzhen, China

The role of neutrophils in the tumor microenvironment has been widely reported recently, but the relationship between neutrophil heterogeneity and liver tumorigenesis remains unclear. In this study, we analyzed transcriptomic data from 70707 cells across 184 samples, profiling the progression of liver disease from healthy tissue through non-alcoholic fatty liver disease (NAFLD), non-alcoholic steatohepatitis (NASH), fibrosis, and cirrhosis to hepatocellular carcinoma (HCC). We developed an optimized computational model to evaluate the tumor development index using the single-cell RNA-seq data, which was further validated with independent datasets from various tumor types. Specifically, our analysis revealed a significant positive correlation between the proportion of neutrophils and the tumor development index, suggesting that the neutrophils actively contribute to hepatocarcinogenesis progression. This finding was further confirmed by scRNA-seq data from a c-Myc/Alb-cre mouse model. We also identified neutrophil subtypes with distinct functions, highlighting dynamic functional changes during liver tumorigenesis. These results confirmed that our tumorigenesis model can robustly predict the pre-malignant stage. And they also underscore the role of neutrophils as key mediators in liver tumor progression and provide a framework for targeting the immune microenvironment in HCC.

#1432 Single-cell-derived gene-pair classifiers for prostate cancer prognostication.

Lucio Queiroz, Karnika Singh, Wikum Dinalankara, Luigi Marchionni

Pathology and Laboratory Medicine, Weill Cornell Medicine, New York, NY

Prostate cancer is characterized by marked histologic and molecular heterogeneity, which limits the precision of current prognostic tools based largely on Gleason grading. To better resolve the cellular programs underlying grade progression, we analyzed single-cell RNA-sequencing profiles from multiple prostate cancer specimens and performed high-confidence cell type classification across epithelial, stromal, and immune compartments. Within each annotated cell type, we compared tumors representing distinct Gleason grade groups to identify transcriptional markers that are specifically associated with grade-related biological changes rather than global tumor differences. This cell type-stratified analysis uncovered grade-associated signatures reflecting alterations in differentiation state, signaling pathways, and microenvironmental interactions.

We next leveraged these marker genes to construct k-Top Scoring Pair (k-TSP) classifiers, which rely on relative expression orderings and therefore provide a robust, interpretable, and platform-independent modeling framework. Trained using single-cell-derived grade markers, the resulting classifiers were applied to multiple independent bulk transcriptomic cohorts. Across datasets, the k-TSP models consistently distinguished patients with high- versus low-grade disease and demonstrated strong prognostic performance, including significant associations with biochemical recurrence and progression-free survival.

Overall, our study illustrates how single-cell transcriptomic profiling can reveal cell type-specific determinants of prostate cancer grade and enable the development of clinically relevant, generalizable gene-pair-based classifiers. These results support further evaluation of k-TSP models as practical tools for improving prognostication and guiding risk-adapted management in prostate cancer.

Disclosures: AI tools were used to assist in the preparation of this abstract.

#1433 Evidence of noncontiguous haplotype patterns at chromosome band 13q12 associated with prostate cancer risk in men of African ancestry in the *All of Us* Research Program.

William Peter Letsou, Daniel Galvin Gusmano, Meet Boghani, Ifti M. Gazi, Ashwin Nori

New York Institute of Technology, Old Westbury, NY

Genetic ancestry is known to be an important predictor of prostate cancer (PCa) risk. In particular, PCa incidence and mortality can be up to two times higher in men of African ancestry. While polygenic risk scores based on genome-wide significant polymorphisms can stratify the population into well-defined risk groups, a large portion of the genetic risk remains unaccounted for. Admixture mapping is a technique used to determine the likely genetic origin of a segment of chromosome. We hypothesized that an increase or decrease in local African ancestry in PCa cases vs. controls would implicate regions associated with increased risk, and reveal underlying combinatorial patterns of polymorphisms. To this end, we identified 5,246 PCa cases and controls aged 55 years or older in *All of Us* Research Program (Controlled Tier v. 7), who were of at least 80% global African ancestry, and no two of whom were closer than third-degree relatives. After performing genome-wide admixture mapping using RFMix, we identified a suggestive peak of increased local European ancestry in controls (by 3.2 percentage points) at chromosome band 13q12, near the genes *PCOTH* and *MIPEP* (which we previously found to be more highly expressed in prostate tumors in 51 matched samples from The Cancer Genome Atlas). To study the haplotype structure of this region more closely, we extracted haplotypes from the subset of 926 chromosomes that had a haplotype of unambiguous local European origin—associated with decreased PCa risk (OR = 0.70, $P = 0.026$) compared to haplotypes of non-European origin—and clustered the resulting haplotypes using affinity propagation. Although no haplotype cluster was individually statistically significantly associated with PCa risk in a conditional analysis of carriers of each cluster compared to all other clusters, we found that, after pooling the risk-increasing and risk-decreasing clusters, and comparing the combined clusters to each other, a statistically significant signal could be identified (OR = 3.7, $P = 1.5 \times 10^{-4}$), functional validation of which is being pursued by eQTL analysis in TCGA. The pooled risk-clusters revealed the presence of noncontiguous blocks of variants, suggesting the possibility that combinatorial haplotype patterns could account for increased PCa risk among African-ancestry individuals who locally have a normally protective European-ancestry haplotype. To test this hypothesis, and determine the extent to which higher-order combinatorial interactions can explain additional PCa risk, we are developing a Docker version of our previously published Chromosome Overlap algorithm for use in the *All of Us* Researcher Workbench, to see if the haplotype patterns we reveal mirror those detected by admixture mapping. The authors of this study gratefully acknowledge *All of Us* participants, and the NIH *All of Us* Research Program.

#1434 Scalable, unsupervised deep learning frameworks for rare event detection and single cell phenotyping in enrichment free liquid biopsies.

Dean Tessone[1], Amin Naghdloo[2], Javier Murgoitio-Esandi[3], Jeremy Mason[2], Assad Oberai[4], James B. Hicks[5], Peter Kuhn[6]

[1]Molecular and Computational Biology, University of Southern California, Los Angeles, CA,[2]USC - University of Southern California, Los Angeles, CA,[3]Aerospace and Mechanical Engineering, University of Southern California, Los Angeles, CA,[4]Viterbi School of Engineering, University of Southern California, Los Angeles, CA,[5]USC, Los Angeles, CA,[6]Assoc. Professor, Dept. of Cell Bio., University of Southern California, Los Angeles, CA

Liquid biopsy offers a minimally invasive means to interrogate tumor biology; however, the extreme rarity and phenotypic diversity of circulating tumor cells (CTCs) and related cellular events remain major obstacles to sensitive detection and meaningful analysis. Conventional workflows frequently rely on biophysical enrichment or predefined biomarker panels, both of which can bias cell recovery and constrain discovery. There is therefore a critical need for scalable computational approaches capable of analyzing millions of single-cell observations directly and extracting biological structure without dependence on prior labels. We developed deep learning–based pipelines to analyze nucleated cells isolated from peripheral blood. For each patient, approximately five million cells are obtained via buffy coat preparation, stained with a five-marker fluorescence panel, and imaged by whole-slide microscopy without any enrichment steps. The first pipeline is an unsupervised rare-event detector built on a denoising autoencoder. Applied to samples from 11 breast cancer patients, the method recovered 91 additional events—including CTCs, endothelial cells, cancer-associated fibroblasts (CAFs), and extracellular vesicles—representing a greater than 50% increase with minimal manual tuning. This form of label-free outlier detection is broadly generalizable to high-content imaging studies in which unbiased identification of infrequent or unexpected populations is essential. The second pipeline uses representation learning to derive stable single-cell embeddings. These embeddings support phenotype classification with 92.64% accuracy and also enable unsupervised clustering that reflects intrinsic variation in morphology and marker expression. Notably, the learned features are robust to imaging artifacts, ensuring consistent phenotyping across heterogeneous datasets. Collectively, these deep learning frameworks establish an integrated strategy for enrichment-free rare-event detection, clustering, and cell-type characterization in liquid biopsy, providing a scalable foundation for biomarker discovery

: Digital Pathology 2
Poster Session

#1438 Generative AI improves breast cancer genomic subtype prediction from histology images.

Brennan Geti Simon[1], Clemens L. Weiss[1], Darren Chan[2], Lise Mangiante[1], Nicholas H. Smith[1], Zhicheng Ma[3], Cansu Karakas[4], Christina Curtis[3]

[1]Stanford University School of Medicine, Stanford, CA,[2]Stanford Cancer Institute, Stanford, CA,[3]Stanford University, Stanford, CA,[4]Department of Pathology, Stanford University School of Medicine, Stanford, CA

Breast cancer subtyping is a cornerstone of precision oncology, guiding prognosis, treatment selection, and clinical trial stratification. The Integrative Subtype Classification (IC) scheme is a clinically relevant system that categorizes breast cancer tumors into groups with distinct long-term patient prognoses based on genomic and transcriptomic features. Currently, this approach requires genomic sequencing data to predict tumor subtype, and although genomic profiling continues to drop in cost, it is still not routinely deployed in the clinic at scale, particularly in low-resource settings where adoption is likely to lag. As an alternative, we present PATH-IC, a digital pathology model that predicts ER+ breast cancer IC subtype from routine histology data. Through the novel method BERGERON, which uses generative AI to correct class imbalance and reduce overfitting, we found that synthetic data improved PATH-IC's performance by an amount equivalent to adding 41% more real histology samples for training. PATH-IC reaches a validation AUROC of 0.814 and its predictions correlate with Oncotype DX scores and long-term patient relapse. Using attention-based model interpretation approaches as well as CRAWFORD, a novel embedding-to-image foundation model, we showed that PATH-IC learned expected tumor microenvironment patterns associated with the IC subtypes and identified heterochromatin condensation as a key characteristic of High Risk tumors. Matched single-cell spatial transcriptomics data revealed new IC subtype-specific gene expression patterns discovered by PATH-IC, highlighted by active metabolic, proliferative, and proteostasis pathways. PATH-IC marks a step forward in enabling the routine clinical deployment of IC subtyping while simultaneously advancing the performance of digital pathology models through the implementation of generative AI.

#1439 Foundation model-derived features from immunohistochemistry correlate with recurrence and stage in Merkel cell carcinoma.

Roshan Lodha[1], Kelsey Ouyang[1], Claire Reynolds[2], Allison Vidimos[3], Bryan Carroll[4]

[1]Cleveland Clinic Lerner College of Medicine, Cleveland, OH,[2]Case Western Reserve University School of Medicine, Cleveland, OH,[3]Department of Dermatology, Cleveland Clinic, Cleveland, OH,[4]Department of Dermatology, University Hospitals, Cleveland, OH

Foundation models trained on large histopathology datasets offer broad inference capabilities, yet their performance in Merkel cell carcinoma has not been characterized. We investigated whether a whole slide imaging foundation model could extract clinically informative signals from immunohistochemistry biopsies stained for Merkel cell polyomavirus T antigen. Thirty one digitized slides (12 Stage I, 3 Stage II, 11 Stage III, 3 Stage IV, 2 indeterminate) were processed using a custom tissue masking, tiling, and stain normalization pipeline. High-dimensional features were extracted from the standardized output using a UNI2, a pretrained frozen ViT G/14 encoder developed by the Mahmood Lab. Each tile yielded a 1536 dimensional embedding that was summarized at the slide level by feature means and at the zone level by Moran's I to capture spatial structure. Low dimensional representations were computed with PCA and UMAP. Clinical annotations included recurrence, viral status, immunosuppressed status, and AJCC stage.Across 40 tested correlations, slide level summaries showed the largest associations. Viral status served as a positive control and produced the strongest effects, with slide level PC1 correlating at r equals −0.684 and UMAP1 at r equals 0.594. Binarized American Joint Committee on Cancer (AJCC) stage showed consistent separation in PCA and UMAP spaces, and four individual embedding dimensions correlated with advanced stage at magnitudes up to r equals 0.58. Recurrence also aligned with several embedding axes, including representative correlations of r equals 0.68, 0.63, 0.57, and 0.56. Zone level summaries captured additional biology, with immunosuppressed status reflected in zone level UMAP and PCA components that reached r equals 0.337. The mean absolute correlation across all outcomes was 0.184, and nine correlations exceeded an absolute value of 0.3.These results show that foundation model representations derived from polyomavirus targeted immunohistochemistry contain measurable structure related to viral status, stage, recurrence, and host immunologic state. The ability of slide level and zone level embeddings to recover these signals in a modest cohort suggests that pre trained encoders capture histoarchitectural and spatial cues relevant to Merkel cell carcinoma biology. Larger multi site cohorts with longitudinal follow up will enable validation of these features and support integration with circulating or genomic markers for risk stratification in prospective studies.

#1440 FLEXMIL: A flexible multimodal multiple instance learning framework for clinical and translational research.

Meijian Guan[1], Qifeng Zhou[2], Sneh Lata[3], David Soong[3], Mirna Lechpammer[4], Craig Thalhauser[3], **Han Si**[3]

[1]Genmab, Princeton, NJ,[2]Computer Science and Engineering, The University of Texas at Arlington, Arlington, TX,[3]Translational Data Science, Genmab, Princeton, NJ,[4]Pathology, Genmab, Princeton, NJ

Background: Multiple-instance learning (MIL) provides a powerful framework for training deep neural networks in settings lacking detailed annotations, particularly in digital pathology, where slide-level labels are routinely available, but region- or tile-level annotations are scarce. However, most existing MIL toolkits suffer from limited maintenance, functionality, and restrictive licenses, hindering adoption in clinical-translational research.
Methods: We present FLEXMIL, a flexible, end-to-end MIL framework designed to unify pathology, omics, and clinical data analysis. FLEXMIL was developed in Python (V3.10) to enable survival analysis, classification, and regression with robust cross-validation, automatic data splitting, and standardized reporting to ensure reproducibility. A co-attention fusion module was implemented to integrate multimodal data including clinical information, histopathology images and omics data, while also supporting single-modality experimentations. FLEXMIL generates slide-level predictions, patient-level summaries, and attention-based heatmaps to facilitate biomarker discovery, visual interpretation and hypothesis generation.
Results: We evaluated FLEXMIL across diverse translational use cases, including biomarker discovery, tumor target expression prediction, survival analysis and demonstrated its versatility and robust performance. Importantly, a significant advancement was observed when FOLR1-related transcriptomic signatures were integrated with features extracted from H&E-stained images, leading to enhanced predictive performance for FOLR1 expression levels. Specifically, this multimodal approach boosted not only the AUC from 0.72 to 0.83 in binary classification, but the correlation coefficient for continuous values predicted from 0.5 to 0.78 in TCGA-LUAD (N=460). Same approach further improved the AUC of the predicted FOLR1 protein expression from 0.78 to 0.83 in a commercial cohort (N=69) and enhanced overall survival prediction (C-index increased from 0.59 to 0.62) in TCGA-LUAD (N=334), outperforming models based on image data alone. In the biomarker identification task, we predicted tumor-infiltrating-lymphocytes (TILs) in 85 TCGA-TNBC samples with %TIL annotated by two pathologists. At a 10% TIL threshold, FLEXMIL achieved an AUC of 0.89, highlighting the strong predictive value of histopathology features. In addition, FLEXMIL can generate attention heatmaps for image-only and multimodal (co-attention) models, with support for multi-head views and transcriptomic signature-guided explanations to enable transparent slide-level interpretability.
Conclusions: FLEXMIL provides a flexible, scalable and interpretable platform that bridges computational modeling and clinical insight, advancing the development of integrative biomarkers for precision oncology.

#1441 Whole-slide image and clinical feature integration for superior prostate cancer risk stratification.

Justin Johnson[1], Kingsley Ebare[2]

[1]Creighton University School of Medicine - Phoenix Regional Campus, Phoenix, AZ,[2]Mayo Clinic Arizona, Scottsdale, AZ

Background: Prostate cancer remains one of the most common malignancies in men, with significant heterogeneity in clinical outcomes. Early and accurate diagnosis and risk stratification is crucial for effective treatment and improved outcomes. Although Gleason score is an established risk stratification tool, it does not fully explain outcome variability. We present a multimodal deep-learning framework that integrates attention-based whole-slide image (WSI) features with a clinical variable (Age) to predict survival in patients with prostate adenocarcinoma.

Design: Clinical data and WSI for 500 patients with prostate adenocarcinoma were obtained from TCGA-PRAD. Clinical data were parsed for recurrence or progression (RoP) events and age. RoP was used as the outcome label, and age was used as a patient feature. Diagnostic WSI tumor regions were annotated and tiled at 224×224 pixels using QuPath (Bankhead *Sci Rep* 2017). Tile embeddings were extracted with UNI2-h (Mahmood *Nat Med* 2025). An end-to-end machine learning pipeline was developed to aggregate tile embeddings into slide-level embeddings using Clustering-Constrained Attention Multiple Instance Learning (CLAM) and predict RoP (Lu *Nat Biomed* 2021). A second pipeline used a Gleason score-trained binary cross entropy (BCE) model to predict RoP in the same patients. Three models were evaluated: WSI-only CLAM model, WSI+age CLAM model, and Gleason-only BCE model. All models were trained and evaluated using 5-fold stratified cross-validation. Each fold was repeated 3 times with independent random initialization. AUROC was averaged across all folds and runs per model. Standard deviation was also computed. Model performance was compared using Friedman's test, with post hoc pairwise comparisons by Wilcoxon signed-rank test.

Results: The Gleason BCE model underperformed (AUROC 0.67 ± 0.07). Both WSI-based models outperformed the Gleason BCE model, achieving AUROC 0.76 ± 0.02 (without age), and AUROC 0.76 ± 0.01 (with age). AUROCs were significantly different by Friedman's test ($p = 0.0224$) and showed a trend toward significance in post-hoc comparison between WSI and Gleason-based approaches ($p = 0.06$).

Conclusion: AI models using WSI-derived features, with or without basic clinical context, outperformed traditional Gleason score for recurrence risk prediction in prostate cancer. These findings support the integration of digital pathology and AI into routine prognostic assessment for prostate cancer. Future work will focus on including additional patients, clinical variables, and multi-class prognostic labels to expand prognostic prediction beyond RoP.

#1442 Spatial transcriptomics informed tumor purity estimation from histology slides for triple negative breast cancer.

Minh-Khang Le[1], **Vivek Pujara**[1], I-Chuang Liao[1], Yuan Yuan[1], Joseph Lownik[1], Graeme Murray[2], Jin Sun Bitar[1], Luxi Chen[1], Parisa Najafzadeh[2], Keeyon Dabirian[2], David Lin[1], Fred W Kolling IV[3], Parth S. Shah[4], Jonathan Marotti[4], Xiaoying Liu[4], Louis J. Vaickus[4], Keluo Yao[1], Linda T. Vahdat[4], Zarif L. Azher[5], Joshua Levy[1]

[1]Cedars-Sinai Medical Center, Los Angeles, CA,[2]Huntington Health, Pasadena, CA,[3]Dartmouth Geisel School of Medicine, Hanover, NH,[4]Dartmouth Hitchcock Medical Center, Lebanon, NH,[5]Zarif Azher (Individual), Great Falls, VA

Introduction: Tumor purity, defined as the proportion of malignant cells within a tumor region, is a critical factor in cancer research and clinical practice. Accurate tumor purity estimates (TPEs) are crucial in triple-negative breast cancer (TNBC), where tumor heterogeneity complicates diagnosis, biomarker interpretation, and therapeutic decisions. Traditional pathological assessment of tumor purity is limited by observer variability and scalability. Spatial transcriptomics (ST) integrates whole-transcriptome data with spatial context, enabling high-resolution and scalable estimation of tumor purity directly from H&E-stained slides. This study develops and validates ST-supervised deep learning models for spatially resolved, reliable TPEs that support more precise clinical evaluation and treatment guidance in TNBC.

Methods: Visium ST data and matched 40× H&E whole-slide images from 25 TNBC patients were collected from Dartmouth-Hitchcock Medical Center (DHMC), yielding 120,973 50-µm Visium spots with co-registered 512×512-pixel H&E patches. Tumor regions were segmented using a validated DeepLabv3 model. Cell-type reference profiles were derived by integrating an external breast single-cell atlas with in-house single-cell RNA-seq data from seven TNBC patients using SCANVI. The integrated single-cell data were mapped onto in-house Visium sections with Cell2Location to estimate spot-level tumor cell-type proportions, serving as supervisory labels. A deep learning model (VIDCellTyper), built on the Virchow 2 model, was trained and cross-validated to predict spot-level tumor proportions and produce spatially resolved tumor purity maps. HoVerNet-derived cell counts from each patch were used for slide-level purity computation via cell-count-weighted averaging. The workflow was validated on an independent TNBC cohort (n=29; DHMC and Cedars-Sinai Medical Center), where slide-level purity was derived from aggregated patch-level predictions by the ST-informed model and HoVerNet.

Results: Across tumor regions, the ST-supervised deep learning model achieved a spot-level purity correlation of 0.88 ($p < 0.001$) with spot-level Hovernet-derived TPE. When aggregating across the internal and external cohorts (n=29), slide-level ST-informed TPE showed a Spearman correlation of 0.83 ($p < 0.001$) with Hovernet-derived TPE.

Conclusion: This proof-of-concept study shows that ST can guide computational models to derive TPE directly from H&E slides, yielding accurate and spatially resolved results. The ST-guided model generalized across independent TNBC cohorts, demonstrating robustness across tissue workflows. Future work will refine and validate this approach in clinically relevant contexts, including therapy response, prognosis, and pre- versus post-chemotherapy evaluation, to advance precision in treatment assessment and biomarker development.

#1443 AI-assisted quantitative tissue pathology identifies nuclear morphometric features distinguishing OSCC from normal oral epithelium.

Kelly Y. P. Liu[1], Paul Gallagher[2], Calum Macaulay[3], Catherine FY Poh[4]

[1]Oral Biological and Medical Sciences, University of British Columbia, Vancouver, BC, Canada,[2]Basic and Translational Research, BC Cancer Research Institute, Vancouver, BC, Canada,[3]Clinical Assoc. Professor & Head, Cancer Imaging Dept., BC Cancer Research Institute, Vancouver, BC, Canada,[4]Associate Professor, University of British Columbia Faculty of Dentistry, Vancouver, BC, Canada

Early detection and risk stratification of oral squamous cell carcinoma (OSCC) remain major clinical challenges, and traditional histopathology is limited by subjectivity and interobserver variability. The objective of this study is to investigate the effectiveness using image-analysis pipeline integrating deep-learning nuclei segmentation and multifeature risk scoring of microscopic nuclear morphometric features to distinguish OSCC from normal oral tissue. We hypothesize that nuclear appearance alone contains sufficient biological signal to stratify malignant from non-malignant tissue.

The dataset comprised 34 OSCC and 25 normal mucosa tissue microarray cores from 59 patients that were stained with stoichiometric Feulgen-Thionin stain. Scanned images were converted to 8-bit grayscale, and background brightness was automatically normalized. Nuclear segmentation was performed using a two-stage deep-learning UNet pipeline implemented in PyTorch, with one network detecting nuclear centers and a second network generating full nuclear masks. Following segmentation, 84 nuclear features describing DNA content, morphology, and chromatin texture and spatial organization were extracted. These features were used to train and evaluate three supervised machine-learning classifiers distinguishing OSCC from normal group: Random Forest, XGBoost, and LightGBM. All models were trained on the same feature matrix and identical training/test splits using 5-fold cross-validation. Hyperparameters were tuned using grid search. Model performance was assessed using accuracy, sensitivity, and specificity.

This improved segmentation approach identified 96,000 and 78,000 nuclei in OSCC and normal, respectively. Across all classifiers, LightGBM performed the best (94.2%), followed by XGBoost (93.5%), while Random Forest showed slightly lower, but still strong, performance (91.5%). Malignant nuclei showed consistently larger size, greater irregularity, and more heterogeneous chromatin texture ($p < 0.0001$). Applied to a separate set of 9 oral premalignant samples, the LightGBM model correctly identified 4/5 high-grade lesions, 2 low-grade progressors, and 2 low-grade non-progressors, with 100% specificity.

This approach identifies distinct nuclear morphometric signatures associated with OSCC and provide an objective, quantitative framework for diagnostic classification. Nuclear appearance alone can effectively differentiate malignant from normal epithelium, supporting its potential application in risk assessment and early detection. Ongoing efforts focus on refining the segmentation model and cell-type classification model to retain only squamous epithelial nuclei. Future work will extend this framework to oral epithelial dysplasias to evaluate its utility for progression prediction.

#1444 Lauren subtype classification in gastric cancer using deep learning on real-world H&E images.

Akul Singhania, Qiyuan Hu, Riccardo Miotto, Justin Guinney, Radia M. Johnson

Tempus AI, Inc., Chicago, IL

Introduction:
Gastric cancer (GC) is a heterogeneous disease, with Lauren classification providing a framework to assign diffuse and intestinal subtypes, informing prognosis and therapy. Traditional subtype assignment relies on pathologist review of hematoxylin and eosin (H&E)-stained slides, leading to inter-observer variability and scalability challenges. We developed a deep learning classifier to automate Lauren subtype assignment on real-world H&E images.
Methods:
We analyzed de-identified H&E-stained whole slide images (WSI) from biopsies and resections of 2974 GC patients (3160 samples) from the Tempus real-world database. Samples with pathologist-assigned labels (n=399 diffuse; n=238 intestinal) were used for classifier training. WSI were preprocessed into tissue tiles and tile embeddings were extracted using the H-optimus-0 pathology foundation model. An additive attention-based multiple instance learning model was trained with cross-entropy loss weighted by class prevalence. Data were split 80/20 for development/holdout, with 5-fold cross-validation for model tuning and selection, and ensembled predictions from 5 cross-validation models were used to assign subtypes. An operating point was selected for ~90% positive predictive value (PPV) on the holdout set for each class. Real-world overall survival (rwOS; time from first-line therapy to death) was assessed in patients with available data (31%).
Results:
The model achieved a robust performance (AUC 0.93, 95% CI: 0.88-0.98) on the holdout set. With PPV-optimized thresholds, previously unlabeled samples (n=2523) were assigned by the model as diffuse (n=1321, 52.4%), intestinal (n=749, 29.7%), or indeterminate (n=453,17.95%). For pathologist-assigned samples, diffuse cases had worse median OS (13.3 months, 95% CI: 11.5-15.8) than intestinal (22 months, 95% CI: 15.1-29.8; p=6.2e-4). For classifier-assigned samples, diffuse cases had a shorter median OS (12.6 months, 95% CI: 10.8-15.7) than intestinal (15.3 months, 95% CI: 12.2-17.3; p=0.95). *CDH1* mutations were found in 30.3% of pathologist-labeled and 23.7% of classifier-assigned diffuse tumors, but were rare in intestinal tumors (1.3%, 1.1%). *RHOA* mutations were present in 8.5% of pathologist-labeled and 8.3% of classifier-assigned diffuse tumors, versus 2.5% in intestinal tumors for both groups. Other histologies predominantly aligned with model predictions: signet ring cell carcinoma was predicted diffuse, while tubular, papillary, and mucinous adenocarcinomas were predicted intestinal.
Conclusions:
This deep learning classifier can accurately assign Lauren subtypes in GC from real-world H&E-stained WSI, reducing manual review and variability. Model predictions align with known clinical and molecular differences between subtypes, supporting standardization of Lauren classification and enabling large-scale studies of GC.

#1445 Predicting TCGA molecular subtypes of gastric cancer from H&E whole-slide images using a weakly supervised transMIL-attention framework.

Yesul Jeong[1], Dewan M. Bappy[2], Sangjeong Ahn[3], Sung Hak Lee[4]

[1]Department of Hospital Pathology, St. Vincent's Hospital, College of Medicine, The Catholic University of Korea, Seoul, Korea, Republic of,[2]Department of Computer Science and Engineering, Incheon National University, Incheon, Korea, Republic of,[3]Department of Pathology, Korea University Anam Hospital, Seoul, Korea, Republic of,[4]Department of Hospital Pathology, Seoul St. Mary's Hospital, Seoul, Korea, Republic of

Background:
The Cancer Genome Atlas (TCGA) has defined four molecular subtypes of gastric cancer: Epstein-Barr virus (EBV)- associated, microsatellite instability (MSI)- associated, genomically stable (GS), and chromosomal instability (CIN). These subtypes have distinct clinicopathologic and therapeutic implications. However, the routine determination of these subtypes still relies on multimodal molecular assays that are costly and not universally available. We aimed to develop a weakly supervised deep learning framework that predicts TCGA molecular subtypes directly from hematoxylin and eosin (H&E)-stained whole-slide images (WSIs).
Methods:
As a baseline, we implemented attention-challenging multiple instance learning (ACMIL), which leverages multi-branch attention (MBA) and stochastic instance masking for weakly supervised WSI classification. We then proposed a hybrid multiple instance learning (MIL) model that combines a transformer-based MIL architecture (TransMIL) with an MBA. The features and attention scores from TransMIL-MBA were fused via weighted attention to generate slide-level predictions. The model was trained and evaluated on 484 H&E WSIs at 20× magnification with TCGA molecular subtype labels for gastric cancer from the TCGA ESCA and STAD projects, using an 80%, 10%, and 10% split for training, validation, and testing, respectively. Model performance was assessed using the four-class area under the receiver operating characteristic curve (AUC), accuracy, confusion matrices, and visualization of the latent feature space with UMAP and V-measure.
Results:
Attention heatmaps indicated that the proposed TransMIL-MBA hybrid model consistently highlighted histologically relevant tumor regions compared to ACMIL. On the TCGA test set, the TransMIL-MBA model outperformed ACMIL in four-class subtype classification (AUC: 0.89 vs. 0.87; accuracy: 0.74 vs. 0.67). The hybrid model also showed improved subtype separability in the UMAP embedding (V-measure 0.74 with TransMIL-MBA vs. 0.65 with ACMIL) and clearer confusion matrices.
Conclusions:
A weakly supervised multiple instance learning framework combining TransMIL with MBA shows promising performance for predicting TCGA molecular subtypes of gastric cancer directly from H&E WSIs. By providing a scalable, image-based surrogate method for molecular subtyping, this approach may help move clinical care closer to precision medicine, enabling more tailored treatments and potentially improving outcomes for patients with poor-prognosis gastric cancer.

#1446 Accurate focal plane is crucial for AI assessment of non-monolayer urine cytology specimens for bladder cancer screening and surveillance.

Brody McNutt[1], Sam Harvey[2], Minh-Khang Le[1], I-Chuang Liao[1], Keluo Yao[1], Xiaoying Liu[3], Camille Ng[1], Ahmad Kohsar[2], Daniel Shou[2], Christopher VandenBussche[2], Louis J. Vaickus[3], Joshua Jay Levy[1]

[1]Cedars-Sinai Medical Center, Los Angeles, CA,[2]Johns Hopkins Medical Institutions, Baltimore, MD,[3]Dartmouth-Hitchcock Medical Center, Lebanon, NH

Background: Bladder cancer requires frequent surveillance, and urine cytology is widely used to guide cystoscopic evaluation. Digital image analysis aims to provide quantitative cell-level metrics aligned with The Paris System, but many laboratories use non-monolayer preparations (e.g., SurePath) that place cells in three-dimensional arrangements, complicating automated evaluation. We assessed how focal-plane selection affects nuclear-to-cytoplasmic (NC) ratio estimation and compared several algorithmic strategies for identifying the optimal focal plane.

Methods: We analyzed 300 SurePath whole-slide images scanned on a Roche Ventana DP 200 system (Johns Hopkins), evenly spanning negative, atypical, suspicious, and high-grade carcinoma cases. A published detection model identified clusters, which were reannotated by six pathologists, yielding 343 clusters and 2,435 urothelial cells. Annotators outlined nuclei and cytoplasm areas at each cell's best-focus plane. We evaluated classical focus metrics (Sum of Modified Laplacian [SML], High-Frequency Energy [HFE], Tenengrad, Brenner Gradient, Laplacian, and entropy-based OpenCV methods) and unsupervised vision-transformer approaches (feature-variance [ViT-V], attention-entropy [ViT-A], and supervised Z-stack transformer models [ViT-T, ViT-CLS] that directly predict the focal plane). Algorithms were assessed by within-1-plane accuracy relative to pathologist ground truth. NC ratios were derived from nuclear/cytoplasmic areas. U-Net segmentation generated NC ratios for a held-out test set, and Spearman correlations with ground truth were evaluated using: (1) pathologist-selected planes; (2) off-plane images; and (3) algorithm-selected planes.

Results: Within-1-plane accuracy was 0.416 (ViT-A), 0.594 (Grad), 0.740 (HFE), 0.779 (OpenCV), 0.789 (ViT-V), 0.853 (Laplacian), 0.857 (Tenengrad), 0.862 (SML), and highest for Z-stack transformers ViT-T and ViT-CLS (0.874, 0.872). NC-ratio estimation at the pathologist-selected plane reached a correlation of 0.774. Correlations decreased as images moved off-plane (~0.74 at ±1 plane; ~0.69 at ±2; ~0.65 at ±3; ~0.59 at ±4; ~0.50 at ±5). Using algorithm-selected planes, correlations were 0.639 (ViT-A), 0.687 (Grad), 0.720 (ViT-V), 0.728 (HFE), 0.733 (OpenCV), 0.743 (Tenengrad), 0.744 (Laplacian), 0.746 (SML), and 0.745/0.738 (ViT-T/ViT-CLS).

Conclusion: Accurate focal-plane selection is essential for reliable AI-based cytologic assessment in non-monolayer urine preparations. NC-ratio accuracy and downstream analytic validity degraded quickly off-plane, while algorithm-selected planes recovered much of this loss. Future work will evaluate impacts on cluster- and patient-level tasks and assess extended-focus fusion methods that stitch the sharpest regions across the z-stack into a single optimally focused image.

#1447 DIANNE: Segmentation-free localization of histology differential attributes.

Sergii Domanskyi[1], Jill C. Rubinstein[1], Todd Sheridan[1], Adam Thiesen[1], Javad Noorbakhsh[1], Juliana Alcoforado Diniz[1], Ramalakshmi Ramasamy[1], Dylan S. Baker[1], Riley Sheldon[1], Qian Wu[2], George Kuchel[3], Paul Robson[1], Jeffrey H. Chuang[1]

[1]The Jackson Laboratory for Genomic Medicine, Farmington, CT,[2]Department of Pathology and Laboratory Medicine, UConn Health, Farmington, CT,[3]UConn Center on Aging, UConn Health, Farmington, CT

Pathologist-guided distinctions within histology images provide insights into tissue health, driving advances in understanding of disease mechanisms and clinical decision making. Digital pathology leveraging artificial intelligence is increasingly important to derive insights from histology and spatial omic images. To train computational models, current digital pathology methods rely on upfront manual annotations, which are time-consuming and difficult to scale. This pre-annotation process is also poorly suited for investigating novel spatial behaviors, where annotation is challenging and data requirements are unclear.

To address these issues, we present DIANNE (Differential Image Annotator Environment), a digital pathology approach for rapid computation of spatial differential image attributes based on train-time Positive Class Mixup Augmentation (PCMA) of deep learning imaging features. DIANNE enables localization of differential attributes across whole slide images (H&E or antibody-based multiplex imaging, e.g. CODEX) in seconds on standard workstations, enabling interactive applications for exploratory investigation. Predictive models can be re-trained in real-time after interactive tile annotation changes, clarifying important biological attributes within and across tissue slides.

We first test DIANNE on static histology images for sarcoma tumor detection. We demonstrate that classifiers can be developed with as few as 60 previously unannotated tumor slides to achieve high precision (0.86 ± 0.17) and recall (0.73 ± 0.26), as well as reasonable specificity (0.58 ± 0.3) and low false positives (0.0000 ± 0.0001). These metrics are comparable to more compute intensive pixel-based methods, e.g. [Segmenter. Strudel R et al. arXiv 2105.05633, 2021] (values 0.86 ± 0.15, 0.86 ± 0.22, 0.53 ± 0.28, 0.0062 ± 0.0129) which also required regional annotations, GPU and 6 hours of compute. Moreover, DIANNE has unique capabilities for *interactive* exploration of tissue slides. We show biological structure detection from human pancreatic, placenta and kidney tissue slides, including identification of staining and imaging artifacts. For kidney glomeruli detection we demonstrate tile-level recall, specificity, and false positives of 0.95, 0.95, 0.0002, respectively, based on interactive annotation of only 40 positive and 60 negative patches out of 2884 total patches. Just 9 out of 359 true glomeruli are missed, 7 of which were partially cropped.

DIANNE provides multiple spatial inference workflows (interactive/static, H&E/molecular) implemented in a Jupyter widget-based toolkit. DIANNE enables efficient training of foundation model-based classifiers with only image scale annotation, rather than at the pixel-level. DIANNE's rapid, interactive system allows real-time training from static and exploratory input, providing a practical system for discovery of novel behaviors in spatial datasets.

#1448 Deep learning integration of molecular and histopathological data for prognostic stratification in non small cell lung cancer.

Sanddhya Jayabalan[1], Konstantinos Efthymiadis[2], Alexia Eliades[3], Kyriaki Papadopoulou[2], Abraham Pouliakis[4], Elena Fountzilas[2], Sofia Lampaki[2], Mattheos Bobos[2], Anna Goussia[2], Soultana Meditskou[2], Konstantinos Kyritsis[5], Helena Linardou[2], George Pentheroudakis[2], Dimitrios Bafaloukos[2], Dimitrios Pectasides[2], Epaminondas Samantas[2], Zunamys I. Carrero[1], George Fountzilas[2], Jakob N. Kather[1]

[1]Else Kroner Fresenius Center for Digital Health (EKFZ), Technische Universitat Dresden, Dresden, Germany,[2]Hellenic Cooperative Oncology Group (HeCOG), Athens, Greece,[3]Medicover Genetics, Cyprus, Greece,[4]University General Hospital Attikon, National and Kapodistrian University of Athens Medical School, Athens, Greece,[5]Centre for Research and Technology Hellas, Institute of Applied Biosciences, Thessaloniki, Greece

Background: Co-mutations, PD-L1 and TILs are key NSCLC biomarkers. We applied deep learning to a multimodal patient cohort to identify prognostic patterns integrating morphology, mutations, and clinical features.

Methods: 367 NSCLC patients from 18 Hellenic Cooperative Oncology Group-affiliated centers were retrospectively assessed for PD-L1 status (Dako 22C3 pharmDx), TILs (H&E slides), and somatic pathogenic variants with a 38-gene next-generation sequencing (NGS) panel. Whole slide images (WSI) were digitized by an optical microscope scanner. Ten pathology foundation models were benchmarked for predicting mutation, co-mutation, PD-L1 and TILs status. Mutated genes with >5% prevalence were considered for mutation and co-mutation endpoints (*TP53*, *KRAS*, *STK11*, *PTEN*, *EGFR*). A vision transformer model was trained on WSI features to predict endpoints and evaluate AUROC. Kaplan-Meier analysis assessed prognostic relevance of models and top feature tiles from model attention maps provided morphological explainability. The STAMP digital pathology pipeline supported feature extraction and model training.

Results: Single mutation models yielded AUROC scores of 0.6-0.85, with *STK11* prediction from HOptimus1 features highest. Co-mutation models produced AUROC scores of 0.69-0.77 with *EGFR-TP53* prediction from Uni2 features the best. The *KRAS-TP53* co-mutation model (AUROC 0.69, Uni2) showed significant separation in overall survival curves (p=0.05) between classes. Best-performing PD-L1 and TIL models also demonstrated significant survival separation (p=0.005 and p=0.05).

Conclusion: Findings demonstrate the potential of pathology foundation models to derive complex clinically-relevant prognostic models for NSCLC with multimodal explainability.

AUROC by endpoint and foundation model

	TP53	KRAS	PTEN	STK11	EGFR	EGFR+TP53	KRAS+STK11	KRAS+TP53	PTEN+TP53	TILs	PD-L1
Conch1.5	0.48	0.62	0.24	0.79	0.61	0.58	0.72	0.26	0.41	0.65	0.49
CTranspath	0.52	0.77	0.45	0.17	0.5	0.57	0.33	0.68	0.34	0.6	0.6
Dinobloom	0.43	0.45	0.51	0.58	0.46	0.75	0.75	0.68	0.38	0.65	0.73
Gigapath	0.47	0.5	0.44	0.84	0.31	0.61	0.37	0.12	0.63	0.65	0.6
HOptimus0	0.5	0.72	0.56	0.65	0.55	0.61	0.63	0.08	0.48	0.62	0.65
HOptimus1	0.57	0.66	0.43	0.85	0.64	0.63	0.52	0.39	0.28	0.61	0.55
Musk	0.49	0.49	0.51	0.77	0.54	0.61	0.53	0.58	0.43	0.7	0.54
Plip	0.55	0.52	0.5	0.52	0.43	0.48	0.72	0.44	0.74	0.67	0.6
Uni	0.61	0.58	0.6	0.56	0.48	0.7	0.45	0.26	0.46	0.66	0.61
Uni2	0.52	0.69	0.51	0.81	0.61	0.77	0.41	0.69	0.57	0.59	0.64

#1449 Label free virtual HE from 3D holotomography enables reliable nuclear and microanatomical readouts in thick cancer tissues.

Juyeon Park[1], Su-Jin Shin[2], Geon Kim[1], Dongjoo Kim[3], Hyungjoo Cho[3], Daewoong Ahn[3], Ji Eun Heo[2], Jean R. Clemenceau[4], Dongmin Ryu[3], Isabel Barnfather[4], Minji Kim[4], Inyeop Jang[4], Ji-Youn Sung[4], Jeong Hwan Park[4], Sanggeun Oh[5], Hyun-Seok Min[6], Sumin Lee[6], Kwang Suk Lee[2], Nam Hoon Cho[7], Tae Hyun Hwang[4], YongKeun Park[1]

[1]KAIST, Daejeon-si, Korea, Republic of,[2]Gangnam Severance Hospital, Seoul, Korea, Republic of,[3]Tomocube, Inc., Daejeon Metropolitan, Korea, Republic of,[4]Vanderbilt University Medical Center, Saint Johns, FL,[5]Tomocube, Inc., Daejeon Metropolitan,[6]Tomocube, Daejeon-si, Korea, Republic of,[7]Professor, Dept. of Pathology, Yonsei University College of Medicine, Seoul, Korea, Republic of

Conventional H&E staining is destructive, 2D-limited, and incompatible with longitudinal or scarce-sample studies. Holotomography (HT) enables label-free 3D refractive index (RI) imaging of thick tissue, but pixel-accurate supervision for virtual staining is unattainable due to sectioning-induced deformation. Building on our recent demonstration of 3D virtual H&E for colon and gastric cancer tissues up to 50 µm thick, we developed a framework that learns hematoxylin- and eosin-like contrast directly from HT volumes using weakly aligned chemical H&E supervision. The method produces stable, interpretable nuclear and stromal features, enabling nuclei-centric quantitative readouts in a fully label-free workflow.FFPE breast cancer tissues were imaged with 3D HT to obtain quantitative RI volumes at subcellular resolution. A diffusion-based image-to-image model was trained with weak HT–H&E alignment and a nucleus-aware auxiliary loss applied only during training. Inference requires HT alone, maintaining a consumable-free, non-destructive pipeline. Fidelity was evaluated by (i) nuclear morphology agreement, (ii) patch- and field-level realism, (iii) smooth z-slice consistency, and (iv) standardized nuclei quantification. Cross-tissue generalizability was assessed using previously validated colon and gastric datasets spanning 10–50 µm thickness.The virtual H&E preserved basophilic nuclear contrast and eosinophilic stromal features, accurately reconstructing glandular, stromal, and muscular boundaries even in thick sections. Nuclear contours remained continuous across axial planes without flicker artifacts. Whole-field nuclear counts showed 97.8% concordance with chemical H&E, and nuclear area/shape metrics showed no significant deviation. Appearance error was notably lower than prior virtual-staining approaches, and expert reviewers confirmed faithful chromatin texture, nucleoli visibility, and nuclear crowding patterns essential for cancer grading. The method remained robust across tissue thicknesses (4–50 µm), organ types, and institutional sources.Virtual H&E generated directly from label-free HT enables high-fidelity, nuclei-driven readouts without staining, sectioning artifacts, or tissue loss. This supports rapid, consumable-free tissue assessment and reproducible quantification of nuclei-centric biomarkers. Its compatibility with thick tissue volumes positions the technology for drug-response profiling, mechanism-of-action studies, tumor microenvironment analysis, and high-content phenotypic screening. Ongoing multi-site validation and development of 3D diffusion models for whole-slide inference aim to establish label-free 3D virtual histopathology as a scalable alternative to conventional H&E for research and translational oncology.

#1450 3D holotomography-enabled virtual multiplexed staining of thick medical kidney tissue for comprehensive renal pathology.

Siwon Jeong[1], **Juyeon Park**[1], Hyun-Seok Min[2], Minsun Jung[3], YongKeun Park[4]

[1]KAIST, Daejeon-si, Korea, Republic of,[2]Tomocube, Daejeon-si, Korea, Republic of,[3]Yonsei University College of Medicine, Seoul, Korea, Republic of,[4]Korea Advanced Institute of Science and Technology, Daejeon-si, Korea, Republic of

Renal pathology relies on multiple special stains—including H&E, PAS, AFOG, and PAM—to assess glomerular, tubular, and interstitial changes. These stains require serial sections, are prone to variability, and involve destructive processing, limiting consistency and preventing true 3D interpretation. Holotomography (HT) enables label-free 3D refractive index (RI) imaging of thick tissues, and generative translation models can synthesize stain-equivalent contrast directly from RI inputs. We developed a virtual multiplexed staining framework that generates four major renal stains from a single label-free input, including for thick sections where conventional staining becomes unreliable.Medical kidney samples (thin and thick sections up to 50 μm) were imaged with 3D HT to obtain RI volumes. A conditional generative model was trained on paired RI–stain patches (H&E, PAS, AFOG, PAM) after registration and QC. Similarity metrics—SSIM, PSNR, LPIPS, PCC—were computed on held-out regions. The model was applied to (i) label-free RI and (ii) chemically stained slides to produce cross-stain predictions, enabling direct comparison. Whole-slide virtual staining was performed on 0.5-mm kidney regions.The framework reproduced diagnostic features across stains, with structural similarity typically >0.85. Virtual stains restored key elements—including basement membranes, mesangial matrix, tubular epithelium, and interstitial collagen—closely matching chemical references. Large-region predictions preserved coherent architecture. Virtual PAS and AFOG highlighted basement membranes, glycogen-rich areas, collagen deposition, and casts, supporting interpretation of glomerular injury and interstitial fibrosis. Robust performance was maintained in thick tissues (10–50 μm), where chemical stains often show uneven penetration; virtual stains preserved uniform contrast and delineated overlapping structures. Multiplexing enabled consistent visualization of basement membrane thickening, mesangial expansion, and inflammation within the same section, removing serial-section artifacts.Holotomography with generative translation enables reliable, label-free virtual multiplexed staining, producing H&E, PAS, AFOG, and PAM–equivalent images from a single unstained or singly stained input. The method preserves renal microanatomy and remains robust in thick sections where conventional staining can fail. By eliminating serial sectioning and repeated chemical processing, it provides a unified, non-destructive workflow that improves reproducibility and enables direct cross-stain comparison. This positions virtual multiplexed staining as a scalable, pathology-ready technology for renal disease assessment, translational research, and computational pathology pipelines.

#1451 Visualizing the genotype-phenotype link: Predicting drug-induced tissue dynamics with RNA-based diffusion models.

Vaagn A. Chopuryan[1], Arman Petrosyants[2], Gor A. Chobanyan[1], Dmitrii V. Ivchenkov[1], Eduardo Shugaev-Mendosa[1], **Alexander Bagaev**[1], Viktor Svekolkin[1], Aleksandr Sarachakov[1]

[1]BostonGene Corporation, Waltham, MA,[2]Research Center for Digital Engineering and Innovation, Moscow, Russian Federation

Introduction: Oncology drug development is highly challenging because the chance of obtaining FDA approval is only 4.1%. This underscores the need for predictive models that may de-risk this process and improve the odds of success. We hypothesize that accurate modeling of tissue structures based on gene expression profiles may shed light on genotype-to-phenotype relationships that are crucial for uncovering fundamental biological mechanisms and predicting how drugs affect tissue architecture, with prospects in guiding therapeutic strategies and informing early-phase trial design. Here, we present an RNA-aware diffusion model that produces realistic histological states of tissue samples based on rich RNA vector representations, capturing specific changes in gene signatures.
Methods: RNA embedding based on expression data of 20,062 genes obtained using a variational autoencoder trained on RNA-seq samples from public sources was integrated via cross-attention to condition the diffusion model. The diffusion model was then fine-tuned on paired H&E-RNA-seq samples from TCGA, CPTAC, and GTEx. Board-certified pathologists were consulted to verify the biological relevance of the generated images and the correspondence between the visual histological structures and altered signatures.
Results: Our model generated 512×512-pixel tissue crops (0.5 microns per pixel) with a visually indistinguishable FID of 15. The encoder performance metrics were an MSE of 0.0008 and a median R2 of 0.885. In a simulated H&E analysis, drug-induced gene expression changes were reflected in the anticipated tissue slides over time, showing the dynamics of tertiary lymphoid structures (TLS) and follicles corresponding to changes in TLS and B-cell signature. As such, the model could capture biologically meaningful tissue-level responses, enabling in silico modeling of tissue alterations resulting from specific gene or signature modifications, including those induced by therapeutic interventions.
Conclusion: By translating gene expression profiles into depictable tissue structures, our model enables the prediction of how drugs or drug combinations impact tissue morphology through their effects on gene expression. This approach allows us to gather insights into the underlying mechanisms of action for drugs and drug combinations, thereby promoting the discovery of promising single agents or combinations, such as immune checkpoint inhibitors, T- or NK-cell engagers, or PD-1/VEGF bispecific antibodies, that are tailored to specific diagnoses. Our model is poised to improve drug candidate selection, optimize study design, and reduce drug development costs, aiding both preclinical discovery and early-phase clinical development.

#1452 A high-throughput slide scanning pipeline for digitizing and standardizing legacy genitourinary cancer slides.

Faria Kabir[1], Mitra Shavakhi[2], Akash Parvatikar[1], Adrien Cesaire[1], Egypt Phillips[1], Rachel Trowbridge[2], Liliana Ascione[2], Pablo Barrios[2], Marc Eid[2], Jasmine Lee[2], Sabina Signoretti[3], Eliezer Van Allen[2], Atish Choudhury[2], Linh Hoang[1], Toni K. Choueiri[2], Jeremiah Wala[2]

[1]HistoWiz, Long Island City, NY,[2]Dana-Farber Cancer Institute, Boston, MA,[3]Brigham and Women's Hospital, Boston, MA

Objective:
To build a reproducible digital slide archival pipeline and tissue image repository for genitourinary cancers using archival slides from a large cancer research organization for digital pathology applications and biomarker discovery.
Background:
Digital pathology applies computer vision to digitized H&E to quantify tumor microenvironment and architectural features. Archival tissue with extensive clinical follow-up is essential to this aim, but converting glass slides to high-quality digital images is a significant challenge. We describe a high-throughput, whole slide imaging (WSI) pipeline developed at HistoWiz and its application to over 20,000 legacy cancer slides from the Gelb Center for Translational Research at the Dana-Farber Cancer Institute (DFCI).
Methods:
HistoWiz designed a workflow for (i) standardized intake of archival clinical slides with heterogeneous stain quality, labeling formats, and coverslipping artifacts, (ii) proprietary bulk logistics solutions enabling transport of up to 9,600 slides per shipment with <0.001% damage rate, (iii) high-fidelity scanning using hardware capable of penetrating dirt/film layers commonly found on aging slides, (iv) a real-time, scalable review process via the HistoWiz PathologyMap platform and (v) optical character recognition (OCR) for handwritten slide labels.
Results:
Archived slides from over 20 years (2001 to 2025) of slide collection were scanned at 900 slides per day, using two high-throughput scanning clusters with a >90% initial QC pass rate. A representative subset of images was independently evaluated by a pathologist for issues including tissue folds, cracking, air bubbles, blebs, ink annotations, and out-of-focus regions. We found that most QC failures were caused by four recurring issues: tissue folding from microtomy (30%), cover-slip issues (10%), mounting media residue (2%), and handwritten annotations or processing artifacts (1.5-12.5%). Corrective measures, including rescanning, xylene- or alcohol-based coverslip cleaning, and recoverslipping, resolved >95% of cases with cover-slip or mounting media issues, with limited tissue loss. Final slides were stored as pyramidized OME-TIFF files at 0.248 µm/pixel, averaging 2 GB per slide. In an offline Python pipeline, a Google Vision-derived OCR model yielded superior barcode read rate and accuracy on histology slides, outperforming Microsoft's OCR, Tesseract (v4+), and a Keras-based CRNN baseline.
Conclusion:
Our large-volume and high-throughput WSI archival workflow delivers a scalable imaging pipeline that digitized a 20-year academic tissue biobank and provides on-demand access to AI-ready, high-quality quality full-resolution slide images. This digital image repository will support large-scale digital pathology research to discover biomarkers in genitourinary cancer.

#1453 Association of interpretable histomorphic features with molecular markers: A Computational Histology Artificial Intelligence (CHAI) biomarker development platform analysis.

Asit Tarsode[1], **Haochen Zhang**[1], Viswesh Krishna[1], Vrishab Krishna[1], Snehal S. Sonawane[1], Lesli A. Kiedrowski[1], Trevor J. Royce[1], Anirudh Joshi[1], Richard M. Goldberg[2], Eric A. Collisson[3]

[1]Valar Labs, Palo Alto, CA,[2]Physician-in-Chief/Internal Medicine, West Virginia University Randolph Cancer Center, Morgantown, WV,[3]Hematology/Oncology, UCSF, San Francisco, CA

Background: Biomarkers are needed to guide precision oncology. Ideally, tools have rapid turnaround and integrate into existing workflows. Computational pathology analyzing features on routine hematoxylin and eosin (H&E) stained whole slide images (WSI) provide an accessible system for biomarker discovery. The Computational Histology Artificial Intelligence (CHAI) platform has been validated to predict clinical outcome endpoints across multiple solid tumor types. To explore the unknown overlap of histomorphic features with molecular markers, we assessed associations of CHAI features with markers from multiplex immunofluorescence (MIF).
Methods: The CHAI platform was built on deep learning models trained on >25,000 pan cancer H&E WSI and incorporates >500,000 pathologist annotated nuclei and 100 million μm² tissue, with macro AUC 0.99 for nuclei and tissue segmentation. These models process H&E WSIs, segment comprehensive cancer-relevant cell and tissue types and quantify >30,000 histomorphologic features representing hallmarks of cancer biology (e.g. nuclei size and shape, spatial arrangement, immune infiltration, stromal density). On 41 colorectal cancer WSIs with matched MIF scans from the ORION dataset, CHAI cell/tissue-typing performance was evaluated against MIF by calculating Pearson correlation coefficient between the densities of CHAI's predicted target and matched MIF markers.
Results: Across 289,619 200 x 200 μm² tissue patches, cell segmentation correlation comparing CHAI-segmented nuclei vs MIF DAPI was 0.899 (95% CI 0.898, 0.900). Cell typing correlation was 0.642 (0.640, 0.644) for CHAI-predicted epithelial cells vs MIF cytokeratin (CK) and 0.587 (0.584, 0.590) for CHAI pan-leukocyte vs MIF CD45. Tissue typing correlation was 0.656 (0.653, 0.658) for CHAI tumor-epithelial regions vs MIF CK and 0.543 (0.541, 0.546) for CHAI stromal regions vs MIF smooth muscle actin. All correlations were statistically significant ($p<0.001$).
Conclusion: The CHAI platform measures histomorphic features from H&E WSI at high accuracy; it captures facets of the tumor microenvironment that showed significant overlaps with molecular markers captured by MIF, while also identifying areas to further explore complementarity in these orthogonal modalities. This work underscores the biologic basis of the CHAI system as a novel modality for biomarker development with potential for biomedical research and clinical applications.

#1454 Development of an AI framework for identifying image based digital biomarkers predictive of immunotherapy response in malignant melanoma.

Theresa Koehler[1], Eleftherios Mylonakis[1], Raluca Wroblewski[2], Khalid Daifalla[1], Jasna Kovacevic[2], Gianluca Corradini[2], **Patrick Frey**[1], Markus Tiemann[2], Katharina Tiemann[3], Tobias Lang[1]

[1]Mindpeak GmbH, Hamburg, Germany,[2]MVZ HPH Institut fur Pathologie und Hamatopathologie GmbH, Hamburg, Germany,[3]Faculty of Medicine, Asklepios Campus Hamburg, Semmelweis University, Hamburg, Germany

Background: The MelanomAIX project developed an AI-based framework to identify image-derived digital biomarkers predictive of immunotherapy response in malignant melanoma. Histopathological slides contain rich subvisual information that reflects tumor-immune interactions often missed by conventional assessment. By combining deep learning-based tissue characterization with molecular and clinical data, MelanomAIX leverages routine pathology for biomarker discovery and precision oncology.
Methods: A real-world cohort of 200 melanoma patients was assembled from multiple clinical archives. Each case was curated with digitized H&E and PD-L1 IHC slides, detailed treatment histories, and verified outcome data. Expert pathologists performed specialized, systematic annotations on 138 representative cases, generating detailed region- and cell-level labels to train and validate the AI model. These data complemented an independent larger dataset of 585 cases with over one million manually annotated cells used for model pretraining. The model characterizes the tumor microenvironment by identifying key tissue compartments, immune infiltration patterns, and subvisual morphological features potentially associated with therapeutic response. Building on these explainable image-derived features, the AI framework integrated paired PD-L1 IHC scores to explore AI-driven, multimodal predictive biomarker discovery.
Results: A total of 106,442 manual single-cell and tissue-level annotations across 12 morphological classes were completed. The AI model achieved high segmentation accuracy for tumor-related tissue classes (91.9-95.7%). Extracted image-based features captured spatial and morphological characteristics of the tumor microenvironment, including immune infiltration and tumor-intrinsic heterogeneity. The framework demonstrates promising robust performance in identifying biologically relevant image features that can support response prediction.
Conclusions: MelanomAIX delivers a scalable AI framework connecting histopathologic morphology with clinical outcomes in melanoma. This approach provides a foundation for developing explainable, image-based digital biomarkers predictive of immunotherapy response. Future work will validate the framework on independent and diverse patient cohorts to assess generalizability and clinical utility in predicting immunotherapy response. This abstract text was prepared with assistance from OpenAI’s GPT-5 language model for drafting and refinement purposes.

#1455 Comparison of digital and artificial intelligence (AI)-computational algorithms for quantifying low/ultralow human epidermal growth factor receptor 2 (HER2) protein expression in metastatic breast cancer (mBC) from clinical samples.

Savitri Krishnamurthy[1], Dhanrajan Tiruchinapalli[2], Clara Iam[2], Simon M. Collin[3], Rosemary Taylor[4], Linlin Luo[5], Anupriya Dutta[5], Ehab A. Elgabry[6], Michele S. Woo[7], Grace E. Kwon[8], Robert Egger[9], Jennifer A. Hipp[10], Lauren Brunner[9], Jeppe S. Thagaard[11], Thomas W. Ramsing[12], Henrik Hoeg[13], Wonkyung Jung[14], Heon Song[14], Chang Ho Ahn[15], Vladimir Kravtsov[16], Patrick Frey[17], Ralf Banisch[17], Stella Redpath[2]

[1]Department of Pathology, Division of Pathology and Laboratory Medicine, The University of Texas MD Anderson Cancer Center, Houston, TX,[2]US Medical Affairs, Oncology, AstraZeneca Pharmaceuticals LP, Gaithersburg, MD,[3]Global Medical Affairs, AstraZeneca, Cambridge, United Kingdom,[4]Oncology Biometrics, Oncology R&D, AstraZeneca, Macclesfield, United Kingdom,[5]Global Medical Affairs, AstraZeneca Pharmaceuticals LP, Gaithersburg, MD,[6]Medical Affairs, Daiichi Sankyo Inc., Basking Ridge, NJ,[7]US Medical Affairs, Daiichi Sankyo Inc., Basking Ridge, NJ,[8]Daiichi Sankyo Inc., Basking Ridge, NJ,[9]PathAI, Inc., Boston, MA,[10]Pathology, PathAI, Inc., Boston, MA,[11]Visiopharm, Horsholm, Denmark,[12]Visiopharm, Copenhagen, Denmark,[13]R&D, Visiopharm, Horsholm, Denmark,[14]Lunit, Seoul, Korea, Republic of,[15]Medicine Department, Lunit, Seoul, Korea, Republic of,[16]Machine Learning, Mindpeak GmbH, Hamburg, Germany,[17]Mindpeak GmbH, Hamburg, Germany

Background Based on DESTINY-Breast04 (HER2-low) and -06 (HER2-low/-ultralow) trials, T-DXd is approved for HER2-low (immunohistochemistry [IHC] 1+ or IHC 2+/in situ hybridization negative) or -ultralow (IHC 0 with membrane staining in ≤10% of tumor cells) mBC. Whole slide images (WSIs) from mBC biopsy samples scored HER2 IHC 0/1+ were rescored by pathologists and using digital pathology (DP) to evaluate concordance.

Methods This retrospective real-world evidence study included 384 WSIs collected 2020-2023, stained with PATHWAY HER2 (4B5) assay scored as HER2 IHC 0 (n = 246) or 1+ (n = 138). Three pathologists each performed 2 blinded readings per WSI using 2023 ASCO/CAP guidelines; if readings differed, a reconciled score was used. Consensus was agreement by ≥2 of 3 pathologists. The same WSIs were analysed with 4 AI-computational DP tools in development. Concordance vs manual consensus was measured by overall percentage agreement (OPA) and Cohen κ, with review time recorded.

Results Of 384 WSIs, 375 had aligned HER2 IHC scores by pathologist review; 9 had discordance. Among consensus cases, 2/3 agreement occurred in 154 WSIs (41.1%) and 3/3 in 221 (58.9%); 81 (21.6%) WSIs were reclassified as IHC 0 absent membrane staining, 85 (22.7%) as IHC 0 with membrane staining, 203 (51.4%) as IHC 1+, and 6 (1.6%) as IHC 2+. HER2 IHC rescoring results with the 4 DP tools are shown in Table 1. OPA (95% CI) between consensus and DP-assisted scores across all HER2 IHC score categories was 74% (69-78%), 73% (68-77%), 69% (64-74%), and 55% (50-60%). Cohen κ (95% CI) ranged from 0.33-0.59. Median review times were shorter with DP vs manual review.

Conclusion Preliminary analysis suggests integrating AI-computational DP tools into HER2 IHC clinical workflows may reduce pathologist review time. Further analysis is underway to assess concordance of DP tools with manual scoring.

Table 1. HER2 IHC Re-scores (including HER2-low/ultralow) of WSIs and Median Time to Review

	HER2 IHC 0 absent membrane staining n (%)	**HER2 IHC 0 with membrane staining** n (%)	**HER2 IHC 1+** n (%)	**HER2 IHC 2+** n (%)	**HER2 IHC 3+** n (%)	**Missing results**[a] n (%)	**OPA score between manual consensus and DP Tool,** % (95% CI)	**Cohen κ** (95% CI)	**Review time,** median (range), minutes
Manual consensus N = 375	81 (21.6)	85 (22.7)	203 (54.1)	6 (1.6)	0	0	**Not applicable**	Not applicable	6.7 (3.0-11.5)
DP tool RV73X N = 375	72 (19.2)	100 (26.7)	176 (46.9)	5 (1.3)	0	22 (5.9)	**74 (69-78)**	0.59 (0.52-0.66)	2.1 (0.3-50.2)
DP tool MQ52G N = 375	77 (20.5)	126 (33.6)	168 (44.8)	4 (1.1)	0	0	**73 (68-77)**	0.57 (0.51-0.64)	0.7 (0.1-8.5)
DP tool KL84Q N = 375	82 (21.9)	137 (36.5)	145 (38.7)	10 (2.7)	1 (0.3)	0	**69 (64-74)**	0.53 (0.46-0.60)	2.4 (0.5-25.8)
DP tool ZX19P N = 375	27 (7.2)	201 (53.6)	130 (34.7)	6 (1.6)	3 (0.8)	8 (2.1)	**55 (50-60)**	0.33 (0.27-0.39)	Not available

[a]Full dataset: 375 WSIs; Missing results = WSIs without a DP tool output

#1456 Paletrra^{TM} AI: Automated phenotyping of multiplex immunofluorescence datasets via information maximizing self-training.

Kevin Gallagher[1], Jiong Fei[1], Judy Kuo[1], Maryam Rohafza[1], Mitchell P. Levesque[2], Julia M. Martinez-Gomez[2], Marianne Thio[1], Erinn A. Parnell[1], Qingyan Au[1], Harry Nunns[1]

[1]NeoGenomics Laboratories, Inc., Aliso Viejo, CA,[2]University Hospital of Zurich, Schlieren, Switzerland

Multiplex immunofluorescence (mIF) is a powerful tool for profiling dozens of biomarkers from a single tissue section. Customized mIF panels enable oncology researchers to phenotype cells within the tumor microenvironment, interrogate activation status of immune cells, quantify expression levels of biomarker targets, and explore the spatial organization of cells. Yet, analysis of large mIF datasets remains a bottleneck, largely due to the difficulty of accurately phenotyping single cells across large tissues. The incorporation of deep-learning algorithms into mIF analysis pipelines has helped overcome some limitations of traditional intensity gating by using stain morphology to add robustness to intensity variation, spatial spillover, and tissue artifacts. However, these deep-learning algorithms are costly to develop from a data volume and/or annotation perspective, often requiring fine-tuning on manual labels from target datasets to achieve acceptable performance. Therefore, there is demand for algorithms that efficiently generalize across batches, mIF panels, and tissue types. Here, we present a label-free framework for adapting a pretrained single-channel feature extractor into a mIF whole panel classifier capable of zero-shot cell phenotyping. Our source model is a single-channel feature extractor trained on 20 million annotations spanning over 40 biomarker classes, with text conditioning to encode marker-specific interpretations. We adapt this model into a whole panel classifier by introducing both single-marker binary heads and a multi-marker phenotyping head, jointly trained through self-distillation to enforce per-channel consistency while promoting information maximization across the multiplexed panel. This strategy preserves interpretable single-marker classification while leveraging cross-channel context for accurate and scalable phenotyping of mIF datasets. We applied this framework to 27 FFPE samples stained with a 17-marker mIF TME panel using the Paletrra^{TM} (NeoGenomics Laboratories, Inc) platform. The samples are from a cohort of metastatic melanoma patients treated with pembrolizumab, with our analysis revealing significant differences in immune populations between non-responders and responders. Notably, we showed that our framework achieved higher cell phenotyping accuracy and reduced errors from common mIF issues such as batch effects and spatial spillover, as compared to other mIF image analysis techniques. Overall, our method provides a lightweight, automated method for adapting pretrained mIF algorithms to new panels with strong zero-shot performance to novel biomarkers.

#1457 Prediction of gene expression and molecular pathway activity from H&E whole slide images in non-small cell lung cancer.

Mina Khoshdeli[1], Muhammad Sohaib[2], Mohammed Qutaish[1], Mahesh Bachu[1], Matthew Loya[1], Prianka Chohan[1], Omar Jabado[1], Craig Thalhauser[1], Mirna Lechpammer[1], **David Soong**[1]

[1]Genmab, Princeton, NJ,[2]Electrical and Biomedical Engineering, University of Nevada, Reno, Reno, NV

Predicting transcriptomic profiles from hematoxylin & eosin (H&E) whole slide images (WSIs) remains a challenging but highly desirable task. This is driven by three main factors: (1) H&E WSIs are widely available across patient populations; (2) they are significantly more cost-effective than RNA sequencing; and (3) inferring such information from H&E images can help preserve limited tissue for more critical diagnostic and prognostic tests. Prior studies have explored a variety of models to address this problem and demonstrated potential in predicting genes in key cancer processes. In this study, we developed a two-stage framework that employed state-of-the-art foundation models for patient-level feature extraction, and leveraged robust machine learning methods for efficient model training. Comprehensive evaluation of these models was performed on a carefully curated internal dataset of 67 commercial non-small cell lung cancer (NSCLC) patient samples with matched RNA-seq.

Gigapath, a large-scale pathology foundation model pre-trained on over 170,000 WSIs, was used to extract patch and patient level visual embeddings from H&E-stained NSCLC. Each slide was divided into 256×256 pixel patches, with Gigapath embeddings aggregated via an attention mechanism (LongNet) into slide-level representations. Several regression models were evaluated to predict numerical gene expression and pathway levels from these slide-level embeddings. Ground truth pathway activity was computed using normalized enrichment scores for 50 Hallmark gene sets by single-sample gene set enrichment analysis on the RNA-seq data. Models were trained on 425 slides from The Cancer Genome Atlas Lung -Adenocarcinoma (TCGA-LUAD) cohort and evaluated on the independent dataset of 67 slides. Model performance was assessed using Spearman correlation.

The Gigapath-Random Forest regressor model demonstrated strongest predictive performance across several Hallmark pathways, such as Unfolded Protein Response ($\rho = 0.70$), MTORC1 Signaling ($\rho = 0.69$), and Epithelial-Mesenchymal Transition (EMT) ($\rho = 0.67$). These pathways are not only critical to NSCLC biology but also exhibit distinct histological signatures such as cytoplasmic stress, fibrotic remodeling, and nuclear morphological alterations. The framework was further extended to predict expression levels of individual genes using the same slide-level feature representations. Preliminary results indicate that out of 17,719 expressed genes, 2,223 can be predicted with a Spearman correlation greater than 0.4. These findings demonstrated that pathology foundation models can be efficiently integrated with regression models to capture diverse transcriptomic activities directly from histological imaging features, providing a generalizable framework for biomarker discovery and the development of personalized cancer therapies.

#1458 Deep learning of H&E slides adds prognostic value beyond IASLC grading in non-mucinous lung adenocarcinoma among never-smokers.

Monjoy Saha[1], Thi-Van-Trinh Tran[1], Huu Phuc Hoang[1], Praphulla MS Bhawsar[1], Robert Homer[2], Marina K. Baine[3], Lynette M. Sholl[4], Philippe Joubert[5], Charles Leduc[6], William D. Travis[3], Ruth M. Pfeiffer[1], Jonas S. Almeida[1], Soo-Ryum Yang[3], Maria Teresa Landi[1]

[1]Division of Cancer Epidemiology and Genetics, National Cancer Institute, National Institutes of Health, Bethesda, MD,[2]Yale School of Medicine, New Haven, CT,[3]Memorial Sloan Kettering Cancer Center, New York City, NY,[4]Brigham and Women's Hospital, Boston, MA,[5]Institut universitaire de cardiologie et de pneumologie de Quebec - Universite Laval, Quebec City, QC, Canada,[6]Centre Hospitalier de l'Universite de Montreal, Montreal, QC, Canada

Background: Lung cancer in never smokers (LCINS) most often presents as non-mucinous adenocarcinoma. The International Association for the Study of Lung Cancer (IASLC) system is the current standard for histologic grading, but its use is limited by interobserver variability, time-intensive manual assessment, and limited scalability. We evaluated whether a deep learning model applied to routine hematoxylin and eosin (H&E) slides could predict overall survival and improve prognostic stratification beyond conventional histologic grading.**Methods:** We analyzed 595 stage I-III whole-slide images from the Sherlock-Lung study, each from a unique patient. For the full cohort, median follow-up was 37 months (range 1-120 months); 55 deaths occurred by 5 years and 102 deaths by 10 years from diagnosis, out of 190 events overall. Data were split into training (n=409), internal cross-validation (n=45), and held-out validation (n=141) sets. A convolutional neural network generated continuous patient-level risk scores from H&E images, which were dichotomized into high-risk (n=34) and low-risk (n=107) groups in the validation cohort using the Youden index. Prognostic discrimination for overall survival in the validation set was assessed using time-dependent AUCs and Cox models. We compared AUCs for 5- and 10-year survival probabilities estimated from IASLC grade and deep-learning risks in univariate analyses and based on the following Cox models: (1) baseline (age, sex, ancestry, tumor stage) + IASLC grade; (2) baseline + deep learning; (3) baseline + IASLC grade + deep learning. **Results:** Deep learning yielded higher AUCs than IASLC grade for 5 year (0.84 [0.76-0.92] vs 0.70 [0.62-0.78]; p=0.01) and 10 years overall survival (0.75 [0.61-0.90] vs 0.64 [0.48-0.79]; p=0.59). In multivariable analyses, at 5 years the AUCs were 0.79 for baseline + IASLC, 0.86 for baseline + deep learning ($p<0.01$ vs baseline + IASLC), and 0.87 for the full model (better than simpler models, p=0.04); at 10 years the corresponding AUCs were 0.82, 0.86, and 0.87, with no statistically significant differences overall (p=0.63), possibly reflecting fewer late events. In a Cox model for 5 years of follow-up the deep-learning low-risk group had improved overall survival versus the high-risk group (HR 0.31, 95% CI 0.13-0.76).**Conclusions:** Deep learning on routine H&E slides provides prognostic information independent of IASLC grade in LCINS. Integrating deep learning with grade and clinical factors improves overall survival prediction, supporting AI-augmented pathology for precision risk stratification and personalized treatment/surveillance in non-mucinous lung adenocarcinoma among never-smokers.

: Integrative Computational Approaches 1
Poster Session

#1462 Cell type-specific somatic variants captured from single-cell RNA sequencing underlie transcriptional programs in pre-malignant blood.

Jasmine Ryu Won Kang[1], Mawusse Agbessi[2], June Kim[1], Ido Nofech-Mozes[1], Marie-Julie Fave[3], Philip Awadalla[4]

[1]University of Toronto, Toronto, ON, Canada,[2]Ontario Institute for Cancer Research, Toronto, ON, Canada,[3]Concordia University, Montreal, QC, Canada,[4]University of Oxford, Oxford, United Kingdom

Background: Somatic variants in blood and their prognostic potential in hematological malignancy are well-established in the context of clonal hematopoiesis (CH), but their functional impacts on global gene expression and transcriptional programs remain understudied. We conducted associations between frequently occurring somatic variants, both within and outside of known cancer driver genes, and transcriptional programs to understand phenotypic consequences of genetic mosaicism in blood at the molecular level.
Methods: Single-cell RNA sequencing (scRNAseq), bulk ATAC-sequencing (ATAC-seq), and RipTide whole-genome sequencing (WGS) were conducted on a cohort of 400 samples within the Ontario Health Study. These samples were stratified according to age (<45 or >65 years) and the Intermountain Risk Score (low-risk or high-risk), which is strongly correlated with all-cause mortality. Somatic variants were identified per cell type in each sample with scRNAseq, filtering out germline variants identified with ATAC-seq and RipTide WGS. Cell type-specific gene expression modules were extracted using Hotspot, and pseudobulk profiles were scored for the usage of each module. Linear regressions were conducted to predict module scores for each cell type given somatic variant carrier status and adjusted for covariates.
Results: We identified 6 somatic variants in B cells and 10 in naive T cells which occurred at least 15 times across the cohort. In B cells, somatic variants in AFF3 and IL3RA associated with an upregulation of Module I (AFF3: OR=1.26, adj(p)=0.067; IL3RA: OR=1.26, adj(p)=0.076), which is increased in low-risk samples compared to high-risk (adj(p)=0.020). The variant allele frequency (VAF) of AFF3 somatic variants in B cells was correlated with an upregulation of Module C (ρ=0.510, p=0.0055), which is enriched for heat shock response terms with gene set enrichment analysis. In Naive T cells, MIR4426 VAF correlated with an upregulation of Module H (ρ=0.694, p=4.8e-4), which is increased in young samples compared to aged samples (adj(p)=4.7e-29).
Conclusions: We described how somatic variants shape the landscape of cell type-specific transcriptional programs in blood across 400 individuals. Interestingly, we identified hits in AFF3, of which gene fusion events are well-described in acute lymphoblastic leukemia, and in IL3RA, whose increased expression is an established feature of acute myeloid leukemia. Further work is needed to correlate transcriptional program usage with incident hematological malignancy outcomes.

#1463 DNA methylation driven clonal splicing neoantigens predict immunotherapy response in lung cancer.

Sadegh Saghafinia[1], Carla Castignani[1], Amirhossein Ghorbanpour[2], Carlos Marinez-Ruiz[1], Francisco Gimeno-Valiente[3], Ariana Huebner[1], Cristina Naceur-Lombardelli2[3], Raju Veeriah[3], Mariam Jamal-Hanjani[4], Alan Hackshaw[3], Nnennaya Kanu[3], Charles Swanton[1], Crispin Hiley[1]

[1]The Francis Crick Institute, London, United Kingdom,[2]Agora Cancer Research Center, Lausanne, Switzerland,[3]University College London (UCL), London, United Kingdom,[4]University College London (UCL) Cancer Institute, London, United Kingdom

Immunotherapy has transformed the treatment landscape for previously untreatable cancers, yet its effectiveness is typically associated with high tumour mutational burden. However, additional biological processes can generate immunogenic antigens independently of DNA mutations. Alternative splicing, a major mechanism of transcriptome diversification, can produce cancer-specific isoforms that give rise to neoantigens. Emerging evidence suggests that splicing-derived neoantigens may arise from coordinated dysregulation of splicing factors, including epigenetic alterations such as DNA methylation. Here, we developed an integrated multi-omics framework that combines paired methylome and transcriptome data to identify cancer-specific, splicing-derived epitopes driven by DNA-methylation changes at gene loci. We applied this framework to the DARWIN II cohort of non-small cell lung cancer (NSCLC) patients treated with immune checkpoint inhibitors (CPI), leveraging multi-region paired RRBS and RNA-seq data from 256 tumour regions across 72 patients. Using this approach, we uncovered a compendium of recurrent clonal splicing-derived neoantigens linked to DNA-methylation alterations, several of which were predictive of clinical benefit from CPI therapy. Our findings demonstrate that DNA methylation-mediated splicing regulation represents a source of clonal neoantigens in lung cancer, providing new avenues for patient stratification and informing future vaccine and immunotherapy development.

#1464 CELLama-Perturb: A virtual cell modeling approach for mapping drug sensitivity across spatial tumor heterogeneity.

Haenara Shin, Jeongbin Park, Dongjoo Lee, Hongyoon Choi

Portrai, Inc., Seoul, Korea, Republic of

Background
Predicting how anticancer drugs reshape cellular states in real tissue remains challenging. Perturbation datasets with transcriptomic profiling enable in vitro models of drug response, but how such models transfer to the human tumor microenvironment and capture spatial heterogeneity is unclear. There is a need for frameworks that integrate large-scale perturbation screens with spatial transcriptomics to map intratumoral variation in drug sensitivity.
Method
We developed CELLama-Perturb, a perturbation modeling framework that builds on CELLama-derived foundation embeddings generated by a sentence-transformer cell-embedding strategy. A memory-mapped data pipeline enabled large-scale training on the Tahoe-100M resource. Drug effects were learned from (i) DepMap PRISM drug-sensitivity profiles to model viability responses across cell lines and (ii) paired perturbed transcriptomes used to predict ranked lists of top differentially expressed genes. Drug identity, dose, and cellular state were embedded jointly, and a cross-attention architecture modeled drug-cell interactions. Trained models were then transferred to single-cell and spatial transcriptomics datasets from human tumors to infer spatially resolved drug-sensitivity maps from baseline gene expression.
Results
Across PRISM-derived models, CELLama embeddings captured biologically meaningful expression structure and enabled consistent prediction of drug sensitivity in held-out cell lines, with positive correlations between predicted and observed responses. For gene-expression perturbation tasks, the CELLama-based model accurately reconstructed ranked perturbed-gene profiles (nDCG@16=0.314, MRR=0.660, Recall@16=0.272), corresponding to ~4-5 true perturbed genes among the top 16 predictions out of 17,739 genes. Predicted top-gene sets aligned with experimentally observed differentially expressed genes, indicating that the model encodes transcriptional context relevant to downstream perturbation effects. Applied to lung cancer spatial transcriptomics, CELLama-Perturb produced high-resolution drug-sensitivity maps that revealed marked intratumoral heterogeneity; for example, regions predicted to be sensitive to tubulin inhibitors were spatially distinct from those sensitive to topoisomerase inhibitors, highlighting drug-class-specific vulnerability patterns within the same tumor.
Conclusion
CELLama-Perturb provides a foundation-model-based approach for projecting learned perturbation effects from in vitro systems into complex tissue environments. By generating spatially resolved drug-sensitivity maps, this framework enables virtual cell-to-tissue assessment of therapeutic response and supports refined decisions on drug modality selection, including antibody-drug conjugate payload prioritization.

#1465 Expression-based immune-phenotyping ML model predict ICI response and long-term clinic benefit in lung adenocarcinoma.

Ki Wook Lee[1], Hyun Woo Park[1], Han-En Lo[1], Sehhoon Park[2], Balachandran Manavalan[1], Young-Jun Jeon[1]

[1]Sungkyunkwan University, Suwon, Korea, Republic of,[2]Samsung Medical Center, Seoul, Korea, Republic of

Immune checkpoint inhibitors (ICIs) have transformed the treatment landscape of lung cancer, yet only a subset of patients derive durable clinical benefit, and reliable predictive biomarkers remain limited. To address this challenge, we developed a transcriptome-based artificial intelligence (AI) framework that predicts both ICI response and long-term clinical benefit by leveraging immune phenotype (IP) in lung adenocarcinoma (LUAD). Transcriptomic profiles of 359 TCGA-LUAD samples annotated with IP classes derived from whole-slide images (WSIs) were used to identify immune infiltration-associated AI-informed genes (AIGs) through tree-based classifiers. These features were subsequently trained across 14 machine learning algorithms to classify immune-infiltrated (IF) versus non-infiltrated (non-IF) tumors, followed by ensemble refinement. The resulting AIGs were then applied to ICI-treated LUAD cohorts (N=300) to construct a progression-free survival (PFS) prediction model reflecting long-term therapeutic benefit. The immune phenotyping model achieved strong predictive performance with AUCs of 0.907 in training, 0.810 in the independent test set (N=90), and 0.842 in external validation (N=76). Notably, immune phenotyping based on this model outperformed image-based prediction methods such as Lunit-SCOPE and PD-L1 tumor proportion score (TPS), achieving AUCs of 0.933 for the 1%<TPS<50% subgroup and 0.809 for TPS>50%, compared to 0.733 and 0.559, respectively. The PFS prediction model showed a high correlation between predicted and observed PFS (R = 0.94), and risk scores derived from this model demonstrated excellent predictive accuracy for ICI response (AUCs of 0.964 in training and 0.887 and 0.849 in two external validations). Biological interpretability was further supported by single-cell RNA-seq analysis, which revealed that model-derived genes were enriched in T cell activation and exhaustion compartments, reflecting immune activation linked to therapeutic response. This integrated framework demonstrates dual predictive capacity for short-term ICI response and long-term clinical benefit, offering a biologically interpretable and clinically scalable transcriptome-based platform with strong translational potential in precision immuno-oncology.

#1466 CellNeighbor: A transcriptional atlas of patient tumors and cell line models to inform preclinical model selection.

Caitlin M. A. Simopoulos, Gabrielle Persad, Otto Morris, Carlos A. Origel Marmolejo, Laura M. Richards, Kelly M. Biette

Recursion, Salt Lake City, UT

Preclinical scientists typically select cell line models for compound activity assays based on molecular profiles that support a drug program's hypothesis. However, extensive *in vitro* culturing of these cell lines can influence genetic changes in these models raising concerns about whether these models still represent the patient tumors from which they were derived. To address this translational gap, we developed CellNeighbor, a computational framework that guides model selection by contextualizing cell lines within the landscape of real-world patient transcriptomic data. Building on the established Celligner framework (1), we explicitly identified and removed tumor microenvironment-related gene expression variability before integrating cell line and patient profiles with Harmony (2). Then, we integrated transcriptomic profiles from DepMap (3,4) with patient tumor data from The Cancer Genome Atlas (TCGA) and deidentified patient tumor data from Tempus, creating a unified transcriptomic map of cell lines and tumors. Within this map, we employ a symmetric nearest neighbor approach to identify "patient neighborhoods" centered around each cell line to characterize cell lines most transcriptionally similar to patient tumors. In addition, we have developed novel metrics, such as a neighborhood-tissue homogeneity score, to quantify the confidence of these associations for use in objective and automated decision making. We can now rank cell lines by their transcriptional similarity to neighborhoods of real patient tumors to increase the likelihood that model lines remain representative of the intended patient population. The integrated clinical and molecular data layers produce a cell line-to-patient map that enables cell line selection tailored to specific patient populations. In conclusion, CellNeighbor offers a robust method to identify cell line models that closely resemble patient tumors, ultimately aiming to increase the translatability of preclinical discoveries into clinical applications.

1.Warren, A., Chen, Y., Jones, A. et al. Global computational alignment of tumor and cell line transcriptional profiles. Nat Commun 12, 22 (2021). https://doi.org/10.1038/s41467-020-20294-x
2.Korsunsky, I., Millard, N., Fan, J. et al. Fast, sensitive and accurate integration of single-cell data with Harmony. Nat Methods 16, 1289-1296 (2019). https://doi.org/10.1038/s41592-019-0619-0
3.DepMap, Broad (2025). DepMap Public 25Q3. Dataset. depmap.org
4.Arafeh, R., Shibue, T., Dempster, J.M. et al. The present and future of the Cancer Dependency Map. Nat Rev Cancer 25, 59-73 (2025). https://doi.org/10.1038/s41568-024-00763-x

#1467 Mechanism-aware cancer therapy planning with group-relative policy optimization on a multimodal oncology foundation model.

Eric E. Schadt, Jackson Stokes, Lihua Zhao, Jason Chin, Jonathan Tyler, Lijia Sun, Lauren Beck, Duo Xu, Aviva G. Beckmann, Iker Huerga

Pathos AI, New York, NY

Modern multimodal oncology foundation models (OFMs) can predict patient trajectories and simulate treatment effects from clinical, genomic, transcriptomic, and histologic data, but they remain largely black boxes: they rarely explain which mechanisms drive risk or how to modulate those mechanisms with feasible interventions.

We trained a multimodal OFM on over 1.2 million cancer patients with longitudinal clinical records, tumor DNA and RNA sequencing, and H&E imaging. The model learns a joint latent representation of each patient's evolving disease state and can forecast outcomes and simulate counterfactual treatment trajectories. We then added a mechanism-aware reasoning layer that turns the OFM from a predictor into an engine for mechanism-based therapy design.

Our key innovation is group-relative policy optimization (GRPO), a reinforcement-learning framework that links mechanism states inferred by the OFM (e.g., pathway activation patterns and resistance programs), a drug intervention space built from curated drug-target relationships and perturbation signatures, and an explicit clinical reward. Rather than optimizing an abstract objective for a single patient, we define the reward as improvement in predicted outcomes for cohorts of patients who share similar disease state and driver mechanisms. For each disease context, we identify mechanisms associated with poor outcome, link them to candidate drugs and observed outcomes in real-world data, and then use GRPO to evaluate policies (sets of mechanism-level interventions) by asking whether applying a policy to that cohort improves predicted survival or delays progression relative to matched standard-of-care controls. This group-relative reward stabilizes learning, avoids overfitting to idiosyncratic outliers, and aligns the learned policies with how clinicians naturally reason about "patients like these."

To make outputs biologically and clinically interpretable, we map proposed mechanism shifts to existing drugs and combinations, to mechanism-defined patient clusters whose outcomes are driven by similar latent programs, and to de novo mechanism opportunities where the optimal policy improves outcomes but no current drug fully explains the effect, flagging potential targets for discovery.

Across multiple indications, GRPO recovers known mechanism-therapy relationships, identifies patient subgroups whose outcomes are improved when therapies they receive align with GRPO-suggested mechanism policies compared with matched patients receiving discordant therapies, and proposes novel mechanism-therapy hypotheses involving combined or sequential modulation of programs that are not jointly targeted today. This turns a large-scale OFM into a mechanism-aware decision engine that reasons about resistance and treatment opportunities in the same latent space used for outcome prediction.

#1468 Germline whole exome sequencing implicates homologous recombination repair pathway genes as risk factors in SMARCB1 deficient renal medullary phenotypes without sickle hemoglobinopathies.

Pankaj Kumar Chauhan[1], Panayiotis Kontoyiannis[1], Evan von Eschenbach[1], Jessica P. Cheng[1], Susan S. Thomas[1], Luigi Perelli[2], Christopher J. Logothetis[1], Daria Melikhova[3], Lev Bedniagin[3], Michael Hensley[3], Nizar M. Tannir[1], Pavlos Msaouel[4]

[1]Department of Genitourinary Medical Oncology, UT MD Anderson Cancer Center, Houston, TX,[2]Department of Cancer Biology, UT MD Anderson Cancer Center, Houston, TX,[3]BostonGene Corporation, Waltham, MA,[4]Genitourinary Medical Oncology, UT MD Anderson Cancer Center, Houston, TX

Renal medullary carcinoma (RMC) is a highly aggressive, SMARCB1-deficient kidney cancer classically arising in young individuals of African descent with sickle hemoglobinopathies, most commonly sickle cell trait, due to germline *HBB* variants. Very rare SMARCB1-deficient cases without sickle hemoglobinopathies are classified as renal cell carcinoma, unclassified with medullary phenotype (RCCU-MP). Apart from confirming sickle hemoglobinopathies, there is no established role for germline testing in RMC or RCCU-MP, and germline risk factors for RCCU-MP remain undefined. We performed an integrated germline whole-exome sequencing (WES) and bulk RNA sequencing (RNA-Seq) on 11 patients with RCCU-MP and compared them with 23 patients with canonical RMC associated with sickle hemoglobinopathies (sickle cell trait, n=22; sickle cell-C disease, n=1) and with disease-control cohorts of clear cell RCC (ccRCC; n=11) and chromophobe RCC (chRCC; n=11). RCCU-MP harbored pathogenic germline loss-of-function protein-truncating variants (PTVs) in homologous recombination repair (HRR) pathway genes in 2 of 11 cases (~18%): *ATM* (W2960*, affecting the PIKKc_ATM domain) and *RAD50* (E696*, affecting the Rad50_zn_hook domain). No germline pathogenic HRR pathway PTVs were found in RMC, ccRCC, or chRCC. Furthermore, aside from the expected HBB variants defining sickle hemoglobinopathies in the RMC cohort, no additional germline alterations associated with other hemoglobinopathies - including α-thalassemia and α/β-hemoglobinopathies (*KLF1, ATRX, HBG1, HBS1L, MYB, HBD, HBA1, HBA2, HBG2, HBZ* and *BCL11A*) - were detected in any specific cohort. RNA-Seq cellular deconvolution techniques such as ssGSEA tumor micro-environment (TME) reconstruction and Kassandra cellular deconvolution showed microenvironment with high enrichment for B cells, CD4 and CD8 T cells, and low presence of endothelial cells in both RMC and RCCU-MP cases. These data represent, to our knowledge, the largest germline analysis to date spanning both RMC and RCCU-MP and nominate HRR pathway disruption as a potential germline susceptibility signal specifically for RCCU-MP. Defining HRR-linked germline risk in RCCU-MP refines patient selection for genetic counseling and lays the groundwork for mechanistic and therapeutic studies in SMARCB1-deficient medullary kidney cancers beyond sickle hemoglobinopathies. The ChatGPT-5.1 was used to improve readability and language, and after using this tool, the content was reviewed and edited as needed.

#1469 Multi-omics profiling of neuroblastoma identifies immunological biomarkers associated with higher risk of relapse: Results from the MICCHADO study.

Antonio Colaprico[1], Alexandra Saint-Charles[1], Stelly Ballet[2], Charles Bobin[1], Joffrey Alves-Gasnier[1], Valery Attignon[3], Nathalie Droin[1], Ana Lalanne[4], Doriane Gorret[4], Lydie Cassard[5], Imene Hezam[6], Yasmine Iddir[1], Anthony Ferrari[7], Elnaz Saberi Ansari[1], Gaelle Pierron[2], Julien Masliah-Planchon[2], Angela Bellini[1], Nathalie Chaput[5], Charlotte Butterworth[1], Benoit Dumont[3], Olivier Lantz[4], Olivier Delattre[1], Nadege Corradini[3], Claudia Pasqualini[6], **Gudrun Schleiermacher**[1]

[1]SiRIC RTOP, Translational Research Department, Institut Curie, PSL Research University; Institut Curie-Research Center, INSERM U1330, Childrens' ONCology rEseaRch uniT (CONCERT), Paris, France,[2]Unite de Genetique Somatique, Department of Genetics, Institut Curie Hospital, Paris,France., Paris, France,[3]Department of Pediatric Oncology, Institut d'Hematologie et d'Oncologie Pediatrique/Centre Leon Berard, Lyon, France; Platform of Cancer Genomics, Centre Leon Berard, Lyon, France,[4]Laboratory of Clinical Immunology, Department of Diagnostic and Theranostic Medicine, Institut Curie, Paris, France; Centre d'investigation Clinique en Biotherapie Gustave-Roussy Institut Curie (CIC-BT1428)., Paris, France,[5]Universite Paris-Saclay, Gustave Roussy, AMMICa INSERM US23, Laboratoire d'immunomonitoring en Oncologie , F-94805, Villejuif, France,[6]INSERM US23, CNRS UMS 3655, Gustave Roussy, Villejuif, France; Department of Pediatric and Adolescent Oncology, Gustave Roussy Cancer Campus, Universite Paris-Saclay, Villejuif, France,[7]Synergie Lyon Cancer, Gilles Thomas Bioinformatics Platform, Centre Leon Berard, Lyon, France

BACKGROUND: Neuroblastoma (NB) risk stratification relies on clinical and molecular features, though few molecular markers inform therapeutic interventions. Leveraging multi-omics approaches, we sought to identify biomarkers associated with relapse.
AIMSTo characterize molecular and immunological features associated with relapse inhigh-risk NB (HR-NB), (MYCN-amplified or metastatic >12 months), and correlate findingswith clinical outcomes to identify relapse mechanisms and therapeutic opportunities.
METHODS: For 197 NB patients (145 HR-NB, 52 low/intermediate-risk) in the MICCHADOprogram (NCT03496402, a 600-pediatric patients pancancer cohort), tumor and sequentialblood samples were analyzed using paired tumor/germline whole exome sequencing(WES), bulk RNA sequencing, sequential plasma cell-free DNA (cfDNA) analysis, and bloodflow cytometry by FACS. We assessed DNA alterations, transcriptomic subtypes,stemness, immune infiltration, and blood biomarkers.
RESULTS: In HR-NB higher cfDNA and ctDNA levels were observed at diagnosis compared to non-HR. In addition to previously known genetic features (including MYCN, DDX1 and NBAS amplification, copy number alterations as well as recurrent SNVs), sequential cfDNA analyses identified novel alterations at relapse, including ALK, RAS-MAPK or CDKN2A/B. Transcriptomic profiling revealed a higher stemness index in HR-NB and in patients who experienced relapse, suggesting that a higher stemness index at diagnosis may predict relapse risk. Immune deconvolution of RNAseq from diagnostic samples revealed that patients who experienced relapse had higher levels of CD4+ memory T-cells, but lower natural killer (NK)Cells. Peripheral blood flow cytometry revealed, as expected, more T-cells in younger patients and a significant decrease in CD3+, CD4+, CD8+ T-cells, and NK cells from diagnosis to treatment and relapse.
CONCLUSIONS: Multi-omics profiling of NB identified novel immune biomarkersassociated with relapse. A higher stemness index suggests more undifferentiated, relapse-prone tumors. Immune profiling revealed T-cell and NK cell changes, highlighting the need for integrated molecular and immune profiling in targeted therapies.
Keywords: Neuroblastoma, Relapse, Biomarkers, Multi-Omics, Immune Profiling

#1470 Selecting representative histologic sections for cost-efficient 3D spatial transcriptomics and tumor microenvironment reconstruction.

Minh-Khang Le[1], James Evans[2], Harsimran Kaur[2], Sojung Lee[2], Vivek Pujara[1], Alan Joey Simmons[2], Seungwoo Kang[2], Jai Mehta[3], Louis J. Vaickus[4], Ken Lau[2], Joshua Jay Levy[1]

[1]Cedars-Sinai Medical Center, Los Angeles, CA,[2]Vanderbilt University School of Medicine, Nashville, TN,[3]University of Tennessee Knoxville, Knoxville, TN,[4]Dartmouth-Hitchcock Medical Center, Lebanon, NH

Background: Three-dimensional spatial transcriptomics (ST) is essential for characterizing tumor-microenvironment (TME) heterogeneity but profiling every serial section is cost-prohibitive. Prior work has explored selecting subsets of sections for imputing ST at interleaved positions. However, these approaches do not identify which sections to profile to most efficiently preserve the 3D architecture. An optimal strategy must reinforce high-confidence inference in regions with similar composition while ensuring inclusion of morphologically distinct areas. We developed a computational framework to select histologic sections that optimally preserve 3D TME structure while minimizing the number requiring ST profiling.

Methods: Four 3-mm FFPE colorectal cancer cores (two per patient) were collected to capture tumor-stroma interfaces and tertiary lymphoid structures. ~300 serial 5-µm H&E sections per core (~1500 µm depth) were imaged at 40x resolution; sections with sufficient tissue were retained (reported tissue loss at: TL 1150 µm, TR 350 µm, BL 1005 µm, BR 1100 µm). Retained sections were co-registered with VALIS. Eleven tissue classes—including tumor, desmoplastic stroma (DS), necrosis, smooth muscle, immune aggregates, and mucosa—were segmented using a graph neural network. For each section, we extracted Prov-GigaPath embeddings and tissue class area proportions. Pairwise similarities, incorporating histology features and z-distance, informed a facility location submodular optimization algorithm to select k representative sections (k=3-30). Selected subsets were used to reconstruct 3D TME structure via class-specific α-shape meshes and voxelization. Reconstruction fidelity was assessed using voxelized intersection-over-union (IoU) relative to full-section reconstructions.

Results: Cores differed in composition—TL: normal mucosa 50%, smooth muscle 26%, stroma 11%, DS 10%; TR: tumor 49%, DS 49%; BL: smooth muscle 43%, tumor 32%, stroma 23%, inflammation 2%; BR: smooth muscle 71%, DS 14%, stroma 11%, tumor 3%. Weighted IoU increased with k; mixed-effects models showed each section improved IoU by 0.014 ($p<2\times10^{-16}$), with core-specific slopes TL 0.015, TR 0.019, BL 0.016, BR 0.013. Saturation occurred at TL 18, TR 12, BL 17, BR 16 sections, with maximum weighted IoUs of 0.49, 0.64, 0.68, and 0.50. Class-specific IoUs correlated with tissue class prevalence ($\rho=0.81$, $p=3.6\times10^{-5}$), with abundant classes reconstructing best.

Conclusion: Section-selection algorithms can identify small subsets of H&E sections that preserve 3D TME structure for cost-efficient ST profiling. Although reconstruction fidelity reflects tissue class abundance, 15-20 sections sufficiently capture 3D architecture. Future work will refine selection strategies and integrate selected ST sections with interleaved H&E sections to enhance 3D reconstruction.

#1471 Unsupervised learning with MORPHAEUS enhances conventional tissue spatial phenotyping.

Elias Pavlatos[1], **Benjamin Tate**[1], Gregory Joseph Baker[2], Joanna Pucilowska[1]

[1]Immune Monitoring and Cancer Omics Services, OHSU Knight Cancer Institute, Portland, OR,[2]Division of Oncological Sciences, OHSU Knight Cancer Institute, Portland, OR

Introduction: Identifying unique cell phenotypes in cyclic immunofluorescence (cycIF) images is typically achieved through manual gating or unsupervised clustering of segmented cells based on marker expression profiles. While effective, segmentation-based methods are limited by predefined thresholds and cell type classification schemes. MORPHAEUS is a new Python-based software that infers cell types and multicellular structures directly from pixel-level imaging data using the variational autoencoder (VAE) deep learning architecture. This method enables unsupervised identification of cellular and morphological patterns without relying on image segmentation. Here, we compared segmentation-based phenotyping with MORPHAEUS-derived cell type classifications in a liver metastasis from a patient with PDAC imaged for 32 markers on the Lunaphore COMET platform.
Methods: Cell segmentation was performed on DAPI-counterstained nuclei using the U-net algorithm in Visiopharm. Mean per-cell marker intensities were quantified, and cell types were assigned based on a nested classification scheme using binary thresholding and prior biological knowledge. For MORPHAEUS analysis, 9x9µm image patches centered on nuclear centroids were extracted and stored in Zarr file format for VAE model training. Image patch encoding containing information on marker intensity, morphology, and local neighborhood contexture were clustered using Leiden community detection to identify cell types.
Results: MORPHAEUS identified several clusters consistent with those identified by manual gating, including a cluster with high CD3, CD8, CD69, and CD103 expression corresponding to tissue-resident memory CD8+ T cells. Clusters enriched for PanCK were consistent with tumor cells, with a subset co-expressing Ki67 indicative of proliferating tumor. MORPHAEUS also revealed novel clusters not captured by manual classification, including one with unexpected co-expression of CD4 and CD11C. Inspection of the primary image revealed that this cluster represented cell-cell interactions involving CD4+ T helper cells and CD11C+ dendritic cells, consistent with their known cooperative roles in antigen recognition.
Conclusions: Traditional classification provides a robust framework for quantifying predefined cell populations, but its reliance on manual gating and fixed marker definitions limits the discovery of novel or context-dependent phenotypes. MORPHAEUS offers a complementary, unsupervised approach capable of identifying rare and previously uncharacterized cell states as well as biologically meaningful spatial interactions that may be missed by conventional segmentation-driven analyses. These findings underscore the value of pixel-level deep learning as a powerful adjunct to traditional spatial phenotyping, enabling deeper insights into tissue organization and biomarker discovery.

#1472 AI-derived nuclear morphometrics as a novel prognostic indicator in lung adenocarcinoma.

Bokyung Ahn[1], Hee Sang Hwang[1], Hyun-Jung Sung[1], Se Jin Jang[2], Pil-Jong Kim[3], Heounjeong Go[1]

[1]Asan Medical Center, University of Ulsan College of Medicine, Seoul, Korea, Republic of,[2]Asan Medical Center, University of Ulsan College of Medicine,, Seoul, Korea, Republic of,[3]Seoul National University, Seoul, Korea, Republic of

Background: In lung adenocarcinoma (LUAD), prognostication has largely relied on architectural features, including predominant invasive pattern and tumor invasive size. However, the prognostic relevance of nuclear morphology relatively remains underexplored in LUAD. Using AI-based cell morphology analyzer, this study aimed to systematically quantify various nuclear morphometrics of LUAD and evaluate its prognostic significance.
Method: Whole slide images of surgically resected LUAD cases (n = 160) were retrieved, and CellViT was applied to extract nuclear-level morphometric features. From the generated contours, 114 features—including area, bounding-box area, convex-hull area, Feret diameter, maximum major/minor axis length, aspect ratio, circularity, form factor, eccentricity, compactness, solidity, orientation angle, and fractal dimension—were computed. Case-level features were generated for orientation-related features using orientation variance and entropy of orientation variance, and for all other variables using the median, IQR (interquartile range), IQR-based coefficient of variation, histogram entropy and quantiles (Q10, Q20, Q80, and Q90). Univariate Cox models for disease-specific survival (DSS) and recurrence-free survival (RFS) were fitted using these case-level features.
Results: Multiple nuclear contour features, including maximum Feret diameter, perimeter, major axis length, bounding-box area, and convex-hull area, were significant prognostic factors for both DSS (107/114, 93.9%) and RFS (28/114, 24.6%).
Discussion: These findings demonstrate that nuclear morphometrics can have prognostic implication in LUAD. Incorporating AI-based nuclear features into current grading or risk-stratification frameworks may improve prognostic precision and reduce dependence on subjective visual assessment. AI-driven nuclear shape profiling holds promise as a complementary biomarker in lung cancer pathology.

Univariable analysis of various nuclear morphometrics of LUAD

Disease specific survival feature	Adjusted P-value	Recurrence free survival feature	Adjusted P-value
Maximum Feret diameter_q90	<0.001	Major axis length_q90	<0.001
Perimeter_q90	<0.001	Maximum Feret diameter_q90	<0.001
Major axis length_q90	<0.001	Perimeter_q90	<0.001
Area_bbox_q90	<0.001	Area_bbox_q90	0.001
Area_convex_q90	<0.001	Area_convex_q90	0.003
Area_q90	<0.001	Major axis length_q80	0.004
Maximum Feret diameter_q80	<0.001	Maximum Feret diameter_q80	0.004
Major axis length_q80	<0.001	Area_q90	0.004
Fractal dimension_q20	<0.001	FD_median	0.010
Fractal dimension_q10	<0.001	Perimeter_q80	0.011

#1473 Local indicators of spatial association bioinformatics analysis identifies animmunosuppressive zone at the liver tumor margin.

Yoshiki Nonaka[1], Kanae Echizen[1], Tomonori Kamiya[1], Maho Tsuda[1], Yoshimi Yukawa-Muto[1], Hideki Fujii[1], Ryo Takahashi[2], Takahiro Kodama[2], Naoko Ohtani[1]

[1]Osaka Metropolitan University, Osaka, Japan,[2]Osaka University, Suita, Japan

Immune checkpoint inhibitor therapy has shown effectiveness across several cancer types. However, immune checkpoint inhibitor therapy has limited efficacy for MASLD and MASH associated hepatocellular carcinoma, suggesting that the anti tumor immune response in the tumor microenvironment of MASLD and MASH associated hepatocellular carcinoma may differ from that in other cancers. Therefore, understanding the mechanisms behind MASLD and MASH hepatocellular carcinoma pathogenesis and identifying novel therapeutic targets is essential. Although immune checkpoint inhibitor monotherapy has shown limited efficacy, its combination with agents targeting cancer progression pathways may enhance anti tumor effects. In this study, to elucidate tumor promoting pathways in MASLD and MASH associated hepatocellular carcinoma, we aimed to comprehensively characterize the transcriptomic landscape of cancer cells and stromal cells within the tumor microenvironment. We performed single cell RNA sequencing on 63 samples from 45 hepatocellular carcinoma patients and 8 healthy donors, as well as spatial transcriptomics analysis on 6 samples from 5 patients with non viral hepatocellular carcinoma. Deconvolution analysis of the spatial transcriptomics data revealed that COL1A1 high cancer associated fibroblasts and TIMP1 high cancer associated fibroblasts were enriched at the inner margin of the tumor nodule. In this region, regulatory T cells, monocytes, and SPP1 high macrophages were predominantly co localized with cancer associated fibroblasts, which was determined by local indicators of spatial association analysis. These observations suggest that, in addition to histological wall thickening, the fibrotic tumor margin forms a functionally immunosuppressive niche in MASH associated hepatocellular carcinoma. In this presentation, we will highlight the distinct features of this fibrotic inner margin zone and discuss their therapeutic potential for MASLD and MASH associated hepatocellular carcinoma.

#1475 An evidence-based tool to systematically identify potential adverse drug-drug interactions.

Meetali Sinha, Ansu Kumar, Rajeev K, Vandana Nair, Liptimayee Behura, Deepak Lala, **James Wingrove**

Cellworks Group, Inc., South San Francisco, CA

Background: Combination therapy is routine in oncology, although it may be associated with adverse drug-drug interactions (DDIs). Machine-learning (ML) and Artificial Intelligence (AI) based tools have been applied to this problem, however they often lack predictive rationales. We have leveraged published data, including FDA drug label information, to create a rule-based tool designed to identify and classify potential drug-drug interaction candidates based on shared gene mechanisms, mechanistic impact, and supporting clinical evidence.

Design: A proprietary database was developed and curated from the FDA drug labels of 338 approved drugs (271 small molecules and 67 biologics), capturing detailed information on drug-gene and drug-drug interactions. A rule-based Drug-Drug Interaction (DDI) assessment tool was then developed based on shared gene mechanisms, mechanistic impact, and supported clinical evidence. The performance of the tool was evaluated in 2 independent data sets.

Results: The tool was first tested using a curated set of known DDI-positive and DDI-negative drug pairs, (20 DDI-positive, 10 DDI-negative) yielding 100 percent accuracy. A second set of 544 drug pairs predicted to have efficacy based on a mechanistic model (Cellworks) was then assessed, with 6.8% pairs (37/544) predicted to be DDI-positive. Of these, 34 pairs shared a common gene and showed a clear victim-perpetrator relationship, indicating a strong mechanistic link for possible interactions, while the 3 additional DDI-positive pairs (Fluorouracil, Oxaliplatin; Carboplatin, Nab-Paclitaxel; Trastuzumab, Paclitaxel) showed clinical evidence of interaction in the absence of shared genes. Evaluation of ClinicalTrials.gov showed that 7 of these pairs (18.9%) had failed clinical development due toxicity-related findings. 460 (93%) of the DDI-negative drug pairs lacked shared gene pathways, mechanistic relationships, and clinical corroboration.

Conclusions: Developed specifically for oncology applications, the tool couples FDA label data and clinical information relevant to cancer treatment with mechanistic insights, providing a method to predict and mitigate toxicity risks arising from drug combinations. Future studies will aim to prospectively validate the tool.

#1476 Improve spatial transcriptomic data with integrated hybrid transformer and graph convolutional networks.

Steven Yan[1], Limin Jiang[1], **Yan Guo**[2]

[1]University of Miami Miller School of Medicine, Miami, FL,[2]University of Miami, Miami, FL

Spatial transcriptomics technologies have revolutionized genomics by enabling the measurement of gene expression while preserving the spatial context of cells within tissues. However, their utility is limited by restricted gene coverage and high operational costs. To overcome these challenges, we previously developed generative AI approaches for imputing gene expression [1] and DNA methylation [2]. Building on this foundation, we now present TransGCN, a hybrid neural network model that integrates transformer architectures with graph convolutional networks to enhance spatial transcriptomic datasets through high-fidelity gene expression imputation. For example, TransGCN can expand a 500-gene Xenium panel to more than 1,500 to 2,000 genes. We systematically evaluated TransGCN across three leading spatial transcriptomic platforms: 10x Genomics Visium HD, Xenium, and Bruker CosMx, and six tissue types, including lung, brain, breast, skin, colon, and ovarian. Beyond previously leveraged features (e.g., 3D chromatin interactions from Hi-C, biological pathways, transcription factor networks, and protein-protein interactions), we incorporated spatial and housekeeping features derived from scRNA-seq (19,363 cells) and bulk RNA-seq (418,074 samples). Compared with existing imputation tools, TransGCN consistently achieved higher accuracy while enabling the recovery of a broader gene set, thereby substantially extending the analytical power of spatial transcriptomics.

References

1. Yan, F.Y., et al., *Reinventing gene expression connectivity through regulatory and spatial structural empowerment via principal node aggregation graph neural network.* Nucleic Acids Research, 2024. 52(13).

2. Yan, F., et al., *Genome-wide methylome modeling via generative AI incorporating long- and short-range interactions.* Sci Adv, 2025. 11(15): p. eadt4152.

#1477 Lysosomal routing geometry drives immunosuppressive secretion in triple negative breast cancer.

Sudhanshu Sharma, Manoj K. Mishra

Cancer Research Center, Department of Biological Sciences, Alabama State University, Montgomery, AL

Triple-negative breast cancer (TNBC) shows markedly elevated secretory activity, which contributes to a highly immunosuppressive tumor microenvironment. Lysosomes are central to both degradation and regulated secretion, but how their routing choices influence cytokine release has not been well explored. To investigate this, we developed a Subcellular Causal Geometry Model (SCGM) that maps nanoscale lysosomal routing behavior and identifies patterns in TNBC cells associated with the production of immunosuppressive cytokines. SCGM brings together lysosomal proteomics, LAMP1/LAMP2 vesicle distributions, RAB-GTPase interaction profiles, and intracellular pH gradients derived from patient samples. The mapping of the vesicle-routing paths using a geometry-aware transformer revealed several patterns. Acidic microdomains appeared more fragmented, V-ATPase activity shifted, and the interaction between RAB27A and LAMP1 shifted in a consistent way. To determine the biological impact of these changes, we compared them with cytokine levels, trends in macrophage polarization, exosome characteristics, and interferon-response markers. We also ran perturbation simulations for LAMP1, CTSB, ATP6V1C1, RAB27A, and RAB7A, and evaluated their influence through a geometry-informed Shapley ranking. These findings revealed three distinct routing programs, including a secretory-dominant state, a degradative state, and a recycling-oriented state. The secretory pattern showed fragmented acidic microdomains, stronger interactions between RAB27A and LAMP1, and faster vesicle fusion. Tumors associated with this state released higher levels of TGF-β1, IL-10, galectin-3, and CXCL12 (macro-AUC 0.95) and exhibited nearly fourfold higher M2-like macrophage polarization along with reduced antigen-presenting capacity. Perturbation modeling suggested that reducing RAB27A function could lower immunosuppressive cytokine release by almost two-thirds. Disrupting LAMP1 destabilized the secretory routing framework, and ATP6V1C1 inhibition shifted tumors toward a more immune-activating phenotype. CTSB, RAB7A, ATP6V0A1, and the LAMP1→RAB27A transition repeatedly emerged as major regulators. Taken together, these results outline an unrecognized lysosomal-routing architecture that shapes immunosuppressive cytokine release in TNBC and point to lysosomal geometry as a potential biomarker and intervention point for reshaping the TNBC immune environment.

#1478 Unifying molecular structure and cellular morphology to enhance drug-target interaction modeling in cancer.

Ying-Ju Lai, Yu-Chiao Chiu

UPMC Hillman Cancer Center, Pittsburgh, PA

Accurate drug–target interaction (DTI) prediction is critical for accelerating drug discovery and uncovering therapeutic mechanisms. However, the vast combinatorial space of chemical compounds and protein targets, coupled with the complex nonlinear relationships that govern their interactions, presents significant experimental challenges. Existing computational approaches rely heavily on molecular features, often overlooking perturbation-induced morphological phenotypes and lacking a unified representation that connects molecular properties to responses. To address these limitations, we propose a two-stage contrastive learning framework that integrates structural information of drugs and proteins with cellular morphological profiles derived from the Cell Painting high-content screening into a unified multimodal embedding space. In stage one, two modality-specific contrastive learning models were trained independently: a structure-based model that aligns embeddings of drug structures with protein sequences, and an image-based model that aligns morphological embeddings derived from Cell Painting assays of drug and gene knockout perturbations. In stage two, these modality-specific embeddings were further integrated through cross-modal contrastive learning to construct a shared embedding space that jointly encodes drug structures, protein sequences, and their corresponding cellular morphological profiles. Both embedding spaces from stage 1 (structure- and image-based models) effectively aligned annotated drug–target pairs more closely while pushing non-interacting pairs apart. These models yielded correlation differences of 0.4 and 0.3, respectively, as measured by cosine similarity. In the final unified embedding space, coherent clusters emerged among drugs, targets, and their associated morphological embeddings for known DTI pairs, demonstrating successful cross-modal alignment. Among the top-ranking DTI pairs, gedatolisib and *PIK3CB* showed a similarity of 0.95, consistent with the drug's known activity as a PI3K/mTOR pathway inhibitor. Overall, high-similarity DTI pairs often involved aromatic and heterocyclic compounds whose physicochemical properties closely matched the binding preferences of targets like G protein-coupled receptors (GPCRs) (e.g., *CHRM4*) and kinases (e.g., *PIK3CB*). These patterns align with studies showing that GPCR and kinase ligands share characteristic structural features that facilitate binding. In contrast, low-similarity ones involved molecules whose size, polarity, or geometry posed challenges for targets such as metabolic enzymes and heme-binding proteins. Overall, this study highlights the promise of integrating molecular and morphological representations via contrastive learning, providing a powerful framework for advancing DTI modeling and precision cancer therapeutic discovery.

#1479 CAB: A confidence-aware sequence model enabling high-throughput prediction of mutation-driven binding affinity change in antibody-based cancer therapeutics.

Yuanfei Sun[1], Bing Jiang[1], Huiping Liu[2]

[1]Utah Tech University, St. George, UT,[2]Northwestern University - Chicago, Chicago, IL

Background: Computational prediction of antibody-antigen (Ab-Ag) affinity is increasinglyimportant for designing tumor-targeting therapeutics, enabling rapid in-silico affinity maturation,and optimization of formats such as bispecifics and ADC. However, existing models are trainedalmost exclusively on positive binding cases with measurable affinity, creating a positive-casebias that limits their ability to recognize true loss-of-binding events and often yields unreliableaffinity predictions for Ab-Ag pairs that are experimentally non-binding.

Method: To avoid challenges in predicting accurate structures for mutated proteins, we adopteda sequence-to-function framework and fine-tuned sequence-only protein language models (e.g.,ESM2, DPLM) for mutation-level affinity prediction. We incorporated the AbAgym dataset(~335k measurements) to address the under-representation of weak and non-binding cases. Tobetter separate binding from non-binding regimes, we added a sequence-pair contrastivelearning stage using validated binders as positives and randomly sampled non-binders asnegatives. After contrastive pretraining, we jointly optimized an affinity-change regression headand an AlphaFold-inspired confidence-score head to capture prediction uncertainty and flaglikely non-binders. This combined contrastive and multi-task strategy improves mutation-levelsensitivity and strengthens detection of loss-of-binding events essential for anti-tumor antibodydiscovery.

Result: CAB enabled high-throughput in-silico screening of antibody mutation libraries and wasevaluated on both viral and tumor-associated antigen systems. For SARS-CoV-2 RBD, CABrapidly prioritized thousands of CDR variants and identified high-confidence mutations predictedto yield >10-fold affinity improvements, successfully recovering redesigns known from deepmutational scanning. For tumor targets such as HER2 and Plexin-B2, CAB similarly selected tophigh-confidence mutations with enhanced predicted affinity, consistent with experimentallyengineered antibodies.

Discussion: Unlike conventional models that output a single affinity estimate regardless ofreliability, CAB's confidence head enables explicit identification of low-confidence, likely non-binding variants, addressing a critical limitation of current prediction frameworks. This improvesthe trustworthiness of virtual screening and reduces false-positive redesigns. CAB provides anefficient computational engine for identification of promising variants against tumor-associatedantigens in cancer immunotherapy.

#1480 Transcriptional condensates at super-enhancers mediate pH-dependent transcriptional control in innate immunity.

Shengyuan Wang[1], Zhongyang Wu[2], Zhe Zhong[3], Zhenjia Wang[1], Xu Zhou[2], **Chongzhi Zang**[1]

[1]University of Virginia, Charlottesville, VA,[2]Boston Children's Hospital, Boston, MA,[3]Harvard University, Boston, MA

Tissue acidification is a common feature of hypoxia, inflammation and solid tumor. Acidic pH regulates innate immune response in macrophages by weakening BRD4-containing transcriptional condensates. Yet how disruption of transcriptional condensates leads to gene-specific regulation of immune programs remain unclear. Here, we integrated ATAC-seq, ChIP-seq, and RNA-seq of primary murine macrophages and performed integrative epigenomics analyses to identify transcriptional regulators (TRs) with pH-sensitive regulatory potential and association to BRD4-dependent transcriptional condensates. We determined pH-dependent super-enhancers (SEs) based on dynamic extended profiles of BRD4 binding and H3K27ac marks under pH perturbation. We found RELA, IRF family, and STAT family as candidate TRs enriched at BRD4-associated, pH-sensitive SE regions, particularly in response to LPS stimulation in macrophages. RELA and IRF3 preferentially occupied BRD4-associated and pH-sensitive SEs, and displayed markedly reduced binding under acidic conditions, aligning with BRD4 occupancy change. Correspondingly, immune-response genes within BRD4-associated, pH-sensitive SE regions, including *Ch25h*, *Il20rb*, *Slc2a6*, and *Ifit* family, were significantly higher expressed at pH 7.4 than at pH 6.5. Additionally, analysis of TCGA data for colorectal cancer revealed that chromatin accessibility at potential RELA or IRF binding sites within SEs had significantly elevated association with patient survival, indicating the clinical relevance of TR binding at transcriptional condensates in human cancer. Together, these results reveal a set of TRs involved in BRD4-associated, pH-sensitive transcriptional condensates that coordinate macrophage gene activation under physiological conditions, providing mechanistic insight into how acidic stress modulates transcriptional condensates in immune responses and tumor microenvironment.

#1481 Integrative analysis identifies potential proteomic intermediates associated with renal cell carcinoma and its risk factors.

Ibrahim Hossain Sajal[1], Andrew J. Song[1], Kevin M. Brown[2], Mitchell J. Machiela[2], Peter Kraft[2], Stephen J. Chanock[3], Mark P. Purdue[2], Diptavo Dutta[2]

[1]Integrative Tumor Epidemiology Branch, Division of Cancer Epidemiology & Genetics, National Cancer Institute, Rockville, MD,[2]Division of Cancer Epidemiology & Genetics, National Cancer Institute, Rockville, MD,[3]Sect. Head & Director, CGF/ATC, National Cancer Institute, Rockville, MD

Background: Renal cell carcinoma (RCC), the predominant form of kidney cancer, is influenced by several risk factors (RFs) including obesity, hypertension, and smoking. However, the molecular mechanisms linking these RFs to RCC remain unclear.
Methods: We investigated plasma proteins (PP) as potential intermediates of markers of the effects of RFs on RCC using two-stage Mendelian randomization (TSMR) approach. In stage 1, we identified PPs associated with each of the 19 RFs evaluated (e.g., anthropometric traits, blood pressure, smoking behavior, blood cell counts, and kidney function), leveraging summary-level proteogenetic data on PPs from the UK Biobank Pharma Proteomics Project (N=34,557). In stage 2, we evaluated the effects of these RF-associated PPs on RCC, using the largest-to-date RCC GWAS (N = 864,690; cases=29,020).
Results: Among 2,940 PPs, 2,339 were significantly associated (P<1.7E-05) with at least one of the 19 RFs. Of these, 33 showed a significant effect on RCC (FDR<5%) with 28 mapping outside RCC GWAS loci. Using multivariable MR, we estimated mediation effects of associated PPs, finding that proteins such as CDA and PILRB mediated up to 17.41% of BMI's effect on RCC, and APOL1 mediated 2.76% of white blood cell's effect. Convergent evidence from multiple in silico analyses with cis-MR, colocalization, and TCGA differential expression further prioritized TYMP, UMOD and USP28 as key protein intermediaries of the RF effects on RCC. TYMP and USP28, inversely associated with RCC risk, showed immune-related and tumor-suppressive effects, while UMOD was positively associated, potentially linking renal dysfunction to carcinogenesis. Functional annotation revealed enhancer activity and transcription factor (HIF) binding near these proteins.
Conclusion: Our approach and results identify molecular intermediates that may link epidemiologic risk factors to RCC and highlight actionable candidates for laboratory investigation.

Prioritized PPs associated to RCC and at least one RF, with results from multiple in-silico analyses

Plasma-Protein		Overall-MR		cis-MR		Colocalization	Differential-Gene-Expression(TCGA)		Nearest-GWAS-Signal*	
Name	Region	Beta	P-value	Beta	P-value		FoldChange	P-value(FDR)	RSID	P-value
TYMP	22q13.33	-0.17	2.6E-06	-0.29	4.9E-08	9.95E-01	6.81	1.7E-14	rs131813	5.4E-09
UMOD	16p12.3	0.05	1.4E-06	0.06	1.3E-08	8.93E-01	0.00	5.1E-15	rs7203642	8.2E-06
USP28	11q23.2	-0.31	4.5E-05	-0.46	4.1E-05	9.98E-01	0.85	5.0E-05	rs4288784	1.2E-05
* Strongest GWAS association within +/- 1Mb of the transcription start site of the protein										

#1482 A deep learning-based multimodal integration framework for clinical outcome prediction.

Baoyi Zhang[1], Helen Tian[2], Thanh Bui[1], Yookyung Christy Choi[3], Mona H. Cai[3], Peter Ansell[4], Aditee Shrotre[5], Steven Chirieleison[5], Kevin Kolahi[5], Xi Zhao[1], Josue Samayoa[1], Weilong Zhao[1]

[1]Quantitative Medicine and Genomics, AbbVie, South San Francisco, CA,[2]Computer Science and Mathematics, The University of Chicago, Chicago, IL,[3]Global Epidemiology, AbbVie, North Chicago, IL,[4]Precision Medicine Oncology, AbbVie, North Chicago, IL,[5]Precision Medicine Pathology, AbbVie, South San Francisco, CA

In oncology, a diverse range of advanced approaches, including medical imaging, genomic and transcriptomic profiling, and clinical data analysis, are utilized to comprehensively characterize each patient's tumor. This integrative strategy provides actionable insights that inform personalized care plans and therapeutic decisions, ultimately aiming to optimize patient outcomes. However, practical challenges persist, including how to integrate unstructured imaging data and address missing data modalities.Here, we present a new deep learning based, multimodal integration framework to address these challenges. Our approach incorporates a single modal loss, calculated between each modal representation and the patient's clinical outcome, which encourages the model to learn more clinical outcome relevant features from each modality. Furthermore, a mutual information estimator is implemented to enable the model to explore exclusive features within each data modality. For multimodal fusion, we leveraged a transformer architecture to combine different modalities' embeddings into unified patient-level representations. In our study, we specifically focused on whole slide images, gene expression and mutation. We utilized TCGA non-small cell lung cancer (NSCLC) data (n=989) to develop our model for predicting overall survival (OS), and validated its performance in three independent datasets: CPTAC (n=208), ConcertAI RWD360® linked Caris datasets (ConcertAI/Caris: n=2176), City of hope (COH, n=84). We observed high and robust performance across the four datasets (TCGA: 0.64 ± 0.03; CPTAC: 0.60 ± 0.04; ConcertAI/Caris: 0.59 ± 0.03; COH: 0.61 ± 0.04) using C-index as the evaluation metric. Further evaluating survival association in the three independent datasets indicated significant prognostic values of our model in both univariable (CPTAC: HR = 3.29, p = 0.007; ConcertAI/Caris: HR = 1.50, p = 5e-6; COH: HR = 3.16, p = 0.008) and multivariable (CPTAC: HR = 2.72, p = 0.03; ConcertAI/Caris: HR = 1.40, p = 0.002; COH: HR = 3.81, p = 0.02) Cox proportional hazards model after adjusting for known prognostic clinical factors.To interpret our model, we applied integrated gradients method to understand each feature's contribution to model output. Specifically, we identified 349 core OS-related genes in NSCLC, enriching in cancer-related pathways such as epithelial mesenchymal transition, focal adhesion and TNFA signaling via NFKB. Stratifying patient cohorts by treatment types allowed us to further identify exclusive genes per treatment. As a result, we identified 11 exclusive genes for immunotherapy, with enrichment in immune-related and metabolism pathways.In summary, we developed a multimodal integration framework that predicts clinical outcomes with high and robust performance. Interpretating our framework reveals potential prognostic and predictive markers to advance therapeutic development.

#1483 Cleaved ATP5A1 mediates a poly(ADP-ribose)-dependent regulatory axis for R-Loop homeostasis under oxidative stress.

Aniruddha Mukherjee[1], Kaveri Goel[1], Weiqi Lei[1], Nicholas Hill[1], Rory Greer[2], Yuhua Song[3], Neil Pfister[1]

[1]Radiation Oncology, University of Alabama at Birmingham, Birmingham, AL,[2]Biomedical Engineering, University of Alabama at Birmingham, Birmingham, AL,[3]Associate Professor, Dept. of Biomedical Eng., University of Alabama at Birmingham, Birmingham, AL

Oxidative stress-induced DNA damage potentiates accumulation of R-loops, DNA:RNA hybrid structures with a displaced DNA strand that are resolved in a poly (ADP-ribose) (PAR)-dependent manner via PARP family enzymes. PARylation orchestrates recruitment of DNA repair factors during the oxidative stress response, in addition to multiple mitochondrial proteins also playing a role to protect the nuclear genome. We previously identified cleaved ATP5A1, a mitochondrial stress-responsive proteoform, as an interactor of R-loop resolving proteins including DHX9 and hnRNPU using immunoprecipitation/mass spectrometry (IP/MS) approach. We further investigated its PAR-dependent role in R-loop regulation using *in vitro* assays, cell culture, molecular dynamics (MD) simulation, and RNA-seq approaches in Calu-1, a non-small cell lung cancer cell model. To identify the bioactive R-loop resolving isoform of ATP5A1, mass spectrometry peptide fragments from Peptide Atlas were analyzed to identify potential calpain cleavage sites (cleavage windows that span multiple amino acids). Bioinformatic analyses predicted residue 135 as the primary cleavage site, validated by western blot and MD stability profiles. AlphaFold3 structure prediction and MD simulations demonstrated stable interactions of PAR chains with cleaved ATP5A1 (residues 135-553), with RMSD 0.2-0.3 nm and RMSF of stable residues ranging 0.1-0.2 nm, including ADPR monomers and polymers. IP/MS confirmed PARylation of transiently expressed ATP5A1(135-553) following ionizing radiation-induced oxidative stress. Slot blot was used to quantify R-loops in wild-type, ATP5A1 knockout, and cleaved ATP5A1 rescue conditions. RNA-seq of control and ATP5A1 knock-out (KO) cells identified differentially expressed genes enriching for cellular metabolism, DNA repair, and proliferation/cell cycle pathways in a cleaved ATP5A1-linked R-loop response signature. These findings identify cleaved ATP5A1 as a PAR-interacting protein that modulates R-loop homeostasis under oxidative stress, linking mitochondrial retrograde signaling to nuclear stress responses and revealing a potential R-loop therapeutic target in cancers with dysregulated oxidative stress signaling.

#1484 p-EMT transitional hub and its DC2-macrophage niche define recurrence in oral squamous cell carcinoma.

Yongjoon Jin[1], Jeong-Yeon Ji[2], Hyojung Lee[1], Na-yeon Kim[1], Eun-Jae Chung[3], Jong-Il Kim[4]

[1]Department of Biomedical Science, Seoul National University College of Medicine, Seoul, Korea, Republic of,[2]Department of Otorhinolaryngology-Head and Neck Surgerys, Seoul National University Bundang Hospital, Gyeonggi-do, Korea, Republic of,[3]Department of Otorhinolaryngology-Head and Neck Surgery, Seoul National University Hospital, Seoul, Korea, Republic of,[4]SNU Medicine, Seoul, Korea, Republic of

Background: Partial epithelial-to-mesenchymal transition (p-EMT) is increasingly recognized as a critical driver of invasion and recurrence in OSCC, yet the spatially defined ecosystems and lineage trajectories that sustain p-EMT remain unknown.
Methods: We analyzed 40 tumor-edge TMA cores from 14 patients using Xenium 5k spatial transcriptomics and integrated two-year clinical outcomes (14 non-recurrence, 26 recurrence). Complementary snRNA-seq from 8 matched patients (4 non-recurrence, 4 recurrence) enabled epithelial subclustering, lineage/ontogeny modeling, ligand-receptor inference, and spatial neighborhood reconstruction.
Results: snRNA-seq uncovered a distinctly enriched p-EMT epithelial state (p-EMT_C2) defined by ECM-remodeling genes (MMP11, POSTN, COL11A1), CAF-like markers (PDGFRB, THY1, FAP), and pro-invasive regulators. p-EMT_C2 was significantly expanded in recurrence tumors. Spatial mapping revealed that p-EMT_C2 forms a discrete “transitional zone” positioned between differentiated core epithelium and highly invasive edge cells—a zone that was preferentially amplified in recurrence lesions. Pseudotime reconstruction demonstrated that p-EMT_C2 represents a central branching hub along the core-to-edge invasion trajectory, functionally linking epithelial differentiation to edge aggressiveness.
Strikingly, p-EMT_C2 was embedded within a recurrence-specific multicellular niche composed of DC2 dendritic cells and a pro-metastatic macrophage subset (Macrophage_C1). This tri-cellular niche exhibited strong spatial co-occurrence in recurrence cores. Macrophage_C1 expressed IL1A, IL6, HBEGF, THBS1, VEGFC, DKK1, PTHLH, and FOSL1, while DC2 cells displayed complementary pro-invasive signatures. Ligand-receptor analysis revealed dense reciprocal signaling among the three populations, suggesting that DC2 and Macrophage_C1 collaboratively reinforce and stabilize the p-EMT hub state.
Conclusions: We identify p-EMT_C2 as a transcriptionally and spatially central hub that orchestrates the transition from differentiated epithelium to invasive edge states in OSCC. Its tight association with DC2 and pro-metastatic macrophages defines a recurrence-specific invasive ecosystem. These findings nominate the p-EMT_C2-DC2-macrophage axis as a mechanistically grounded therapeutic target for disrupting the emergence of recurrence in OSCC.

#1485 Multimodal AI for patient subtype discovery in LUSC using real-world data.

Swati Kaushik, Mark Carty, Akul Singhania, Justin Guinney, Radia Johnson

Tempus AI, Inc., Chicago, IL

Introduction: Lung squamous cell carcinoma (LUSC) remains a significant therapeutic challenge due to patient tumor heterogeneity and lack of predictive biomarkers. Prior subtype identification efforts, limited to single-modality data (e.g. gene expression), fail to capture the full spectrum of LUSC's molecular complexity. To define clinically actionable vulnerabilities, we employed a multimodal AI approach integrating gene expression, copy number variation (CNV), and mutation data derived from Tempus real-world data to identify LUSC molecular subtypes, providing a biological landscape essential for improved treatments.

Methods: We analyzed de-identified clinico-genomic records from LUSC patients profiled with Tempus (xT) DNA and RNA (xR) assays. For molecular subtyping, we developed a multimodal autoencoder integrating gene expression, CNV, and mutation profiles from 4,973 tumors of the trachea, bronchus, and lung. Modality-specific encoders were trained and joint embeddings were obtained by averaging and aligning latent spaces with a distance loss to ensure coherent representation across modalities. K-means clustering was applied to joint embeddings to define patient subtypes, which were then functionally characterized via molecular enrichment. Real-world overall survival (rwOS) analysis was performed to assess the clinical and prognostic relevance of the identified subtypes.

Results: The multimodal autoencoder accurately reconstructed all three modalities with low reconstruction errors. Seven distinct subtypes of LUSC were identified with significant differences in rwOS ($p=0.02$). Subtype C1 (12.5% cases) exhibited the lowest median survival (11.7 months; 95% CI 9.4-16.3) and activation of EMT and TGF-β signaling pathways, known to be associated with adverse outcomes, contrasting with subtype C5 (9.5% cases) with the highest median survival (22.4 months; 95% CI 13.28- 31.5). Subtypes derived from joint embeddings showed enrichment for known driver genes, thereby defining distinct molecular characteristics. NFE2L2 mutations were enriched ($p<0.05$) in subtypes C3 (28%) and C7 (29%). RB1 mutations were prevalent in C2 (11%) and C5 (14%), while NF1 mutations were observed in subtypes C1 (15%) and C6 (12%). SOX2 and PIK3CA amplifications are known to be enriched in the classical subtypes (C3, C7). In addition, we identified multiple cluster-specific alterations (e.g. FGF19, CCND1 in C3; ETV5, BCL6 in C7) highlighting extensive intra-subtype heterogeneity. The resulting multimodal subtypes validated established TCGA classifications while providing a significantly deeper molecular resolution by uncovering previously uncaptured intra-subtype variability.

Conclusions: This study validated the potential of multimodal omic integration for high-resolution patient subtyping, establishing a critical foundation for developing integrative AI frameworks to accelerate precision oncology.

#1486 From animals to computational oncology: Digital twins as ethical enablers of next-generation bone metastasis research.

Luca Marsilio[1], Stefan Maksimovic[2], Elisa Serafini[3], Alice Maccarini[1], Sergio Barrios[2], Pietro Cerveri[4], Stefano Casarin[3], **Eleonora Dondossola**[2]

[1]Politecnico di Milano, Milano, Italy,[2]UT MD Anderson Cancer Center, Houston, TX,[3]Houston Methodist, Houston, TX,[4]Politecnico di Milano, milano, Italy

Bone metastasis (BM) is a lethal consequence for advanced prostate and renal cancer patients, contributing significantly to morbidity, elevated mortality risk, and substantial healthcare burden. In vivo biological experiments provide evidence of the cellular mechanisms supporting cancer progression and therapy response, but they are limited in addressing the multi-parameter complexity of BM in a time-cost effective manner and pose ethical concerns about harm and distress. In silico computational models, instead, can explore an unlimited number of experimental combinations avoiding time and resource consumption, providing a valuable alternative to investigate disease biology and microenvironment interactions. Accordingly, this work introduces digital twins to monitor BM progression, response to therapy and impact on bone mechanical properties. By combining three-dimensional multiphoton microscopy and in silico modeling, we generated in vivo inspired, spatially explicit, multicellular A(BM)²s (Agent-Based Models of BM) replicating tumor growth, angiogenesis, and bone resorption. We rigorously retrieved driving coefficients using in vivo data from prostate and kidney tumors and calibrated them through a random forest regressor algorithm to adhere to the in vivo growth rate. We further conducted robust double verification by simulating both the anti-angiogenic effects of cabozantinib and the anti-resorptive effects of zoledronic acid. Our results highlight the predictive character of our A(BM)² in anticipating therapeutic outcomes and increasing our understanding of the complex dynamics of BM. In parallel, we developed a digital twin for mechanical testing of long bones and vertebrae that integrates finite element analysis with micro-CT-derived bone geometry and material properties. Computational compression tests revealed increased fragility in trabecular bone following treatment with the bone-targeting agent Radium-223, whereas three-point bending tests showed no fragility in cortical bone post-treatment. However, they did reveal significantly increased fragility after osteolysis occurred, indicating that these complementary approaches provide a comprehensive understanding of bone mechanical integrity. Overall, our digital twin approach provides a transformative platform to dissect tumor progression, predict therapy response, and evaluate the consequences on bone mechanics. By enabling these insights in silico, we aim to significantly reduce dependence on animal models, directly supporting and strengthening the 3Rs principle.

#1487 Spatial microdomains from histology reveal multi-omic biomarkers for enhanced idiopathic pulmonary fibrosis diagnosis.

Raymond Yan[1], Brian Falkenstein[1], A. Burak Tosun[1], Filippo Pullara[1], **S. Chakra Chennubhotla**[2]

[1]PredxBio, Inc., Pittsburgh, PA,[2]PredxBio, Inc. / University of Pittsburgh, Pittsburgh, PA

Background: Idiopathic pulmonary fibrosis (IPF) is characterized by progressive alveolar injury and extensive tissue remodeling that generate pronounced spatial heterogeneity across affected lung regions. Distinct pathological programs often coexist within adjacent microenvironments, reflecting cellular interactions and molecular circuits that drive disease progression. Although histologic assessment of H&E-stained biopsies remains central to clinical diagnosis, current evaluations lack quantitative measures that connect visual pathology to underlying biology. Integrating spatial transcriptomics with quantitative histologic features enables higher-resolution characterization of heterogeneous disease regions and provides molecular context essential for accurate diagnostic interpretation.
Methods: We applied a multi-omic analytic workflow using the SpaceIQ™ platform to the publicly available Xenium H&E and spatial transcriptomics dataset reported by Vannan et al., Nat. Genet. 2025. Unbiased cell typing was performed on H&E images and spatially aligned to cell-resolved gene expression. Spatial microdomains were derived from differential organization of inferred cell populations in IPF versus healthy tissue. Gene-feature associations were computed to identify molecular markers linked to pathology-associated microdomains. Candidate biomarkers were evaluated in an independent Visium dataset from Mayr et al., Sci. Adv. 2023 to assess reproducibility across platforms and cohorts.
Results: Unbiased H&E-derived cell typing revealed finer structural organization within pathologist-annotated regions and captured subregional distinctions in fibrotic and non-fibrotic compartments. Spatial microdomains identified from cell-type arrangements distinguished IPF-specific architectural patterns and yielded gene signatures associated with epithelial dysregulation, inflammatory macrophages, and extracellular matrix remodeling. These signatures showed consistent enrichment in corresponding molecular niches within the validation cohort. Cross-cohort mapping further demonstrated reproducible cell-type differences and implicated conserved pathways involved in epithelial stress responses, fibroblast activation, and tissue remodeling.
Conclusions: Integrating quantitative histologic features with spatial transcriptomics provides a robust framework for linking visual pathology to molecular mechanisms in IPF. Histology-derived microdomains reveal reproducible biological programs across independent cohorts and support the identification of clinically relevant biomarkers. This multi-omic approach enables more objective, biologically grounded interpretation of heterogeneous fibrotic regions and has the potential to improve diagnostic evaluation and patient stratification in IPF.

#1488 Structure-guided dual targeting of EZH2 and dopamine D1 receptor suppresses TNBC growth and metastasis.

Francesco Drago[1], Libere Ndacayisaba[2], Xilal Y. Rima[3], Gautam Sarathy[1], Deborah Ramsey[4], Gwen Fewell[4], Senthil Saravanamuthu[2], Sanjay Gupta[5], Giovanni Nigita[1], Eduardo Reategu[3], Pierre Giglio[6], Christian Rolfo[1], Eswar Shankar[1]

[1]Division of Medical Oncology, Department of Internal Medicine, Wexner Medical Center, The Ohio State University, Columbus, OH,[2]ONS BIO LLC, Cleveland, OH,[3]Department of Chemical and Biomolecular Engineering, The Ohio State University, Columbus, Ohio, Columbus, OH,[4]SYNVIVO INC., Huntsville, AL,[5]Department of Urology, School of Medicine, Case Western Reserve University, Cleveland, OH,[6]9Department of Neurology, School of Medicine, Wexner Medical Center, The Ohio State University, Columbus, OH

Triple-negative breast cancer (TNBC) is an aggressive subtype with high relapse rates and limited therapies, emphasizing the need for mechanism-based strategies. EZH2, the catalytic subunit of PRC2, drives TNBC proliferation, metastasis, and chemoresistance, while dopamine D1 receptor (D1R) activation induces apoptosis, autophagy, and invasion inhibition. Immunohistochemistry confirmed strong EZH2 expression and elevated H3K27me3, but catalytic inhibition alone is insufficient due to non-enzymatic functions. We hypothesized that dual targeting of EZH2 and D1R would synergistically suppress TNBC by disrupting the EZH2-D1R axis. Computational modeling using a full-length AlphaFold EZH2 structure and three ligands (GSK126, A77636, SKF38393) identified canonical and cryptic binding pockets via PocketMiner and Fpocket, revealing the SET domain as the primary high-affinity site. DiffDock docking showed stable, high-affinity binding of GSK126, while A77636 and SKF38393 displayed dynamic, less-specific interactions. Molecular dynamics simulations over 100 ns confirmed GSK126's stability and persistent contacts at key residues (624, 684, 686), providing mechanistic insight. Immunoprecipitation validated an EZH2-D1R interaction, and D1R knockdown reduced combination efficacy. Experimentally, combination therapy reduced 2D cell viability (CI = 0.24). In droplet-based tumor spheroids (TSIMS), GSK126 + A77636 decreased spheroid diameter by 62% and induced necrosis without apoptosis, with confocal imaging showing EZH2 degradation, H3K27me3 loss, and cytoskeletal disruption. EZH2 knockout cells failed to form spheroids. In a vascularized SynTumor organ-on-chip model, the combination reduced circulating tumor cells by 50% within 96 hours, demonstrating suppression of metastatic spread. Together, these silico-guided and experimental findings establish a translationally actionable dual-target strategy that synergistically inhibits TNBC growth and metastasis. (Supported by DOD: W81XWH2010065, Eswar Shankar.).

#1489 STniche: An approach to identify functional niches in the tumor microenvironment from spatial transcriptomics.

Sasi Arunachalam[1], Oscar Ospina[2], Alex C. Soupir[3], Xiaoqing Yu[3], Brooke L. Fridley[1]

[1]Children's Mercy Research Institute, Kansas City, MO,[2]John Hopkins All Children's Hospital, St. Petersburg, FL,[3]Moffitt Cancer Center, Tampa, FL

Background: Spatial transcriptomics preserves spatial context in the tumor microenvironment (TME), enabling precise mapping of cellular interactions and immune architecture. However, translating these data into functional niche maps remains difficult. We developed STniche, an integrated framework that identifies spatially coherent and biologically interpretable functional niches that link local transcriptomic activity to tissue organization.

Methods: STniche assigns functional phenotypes to spots or cells using pathway signatures, incorporates spatial dependency between neighboring cells with local Moran's I, and detects spatial niches via Gaussian model-based clustering. The optimal number of niches is selected by BIC. We applied STniche to the Meylan et al. (2022) clear cell renal cell carcinoma (ccRCC) dataset containing pathology-annotated tertiary lymphoid structures (TLS). Across ten tumor sections, we used a curated TLS meta-pathway integrating five coordinated programs—chemokine signaling, lymphotoxin axis, antigen presentation, germinal-center B-cell activation, and dendritic-cell maturation—to capture core molecular processes of TLS biology. STniche-identified TLS niches were compared with pathology annotations.

Results: STniche was able to identify spatially coherent functional immune niches corresponding to TLS. TLS meta-pathway-defined clusters showed strong agreement with pathologist annotations, with mean concordance of 0.39 (range 0.28-0.56) and mean relative symmetry of 0.64 (range 0.36-0.96). On average, ~42% of STniche-defined spots overlapped pathology-confirmed TLS, and the clusters captured ~42% of all TLS-positive spots. These findings demonstrate that STniche reliably recovers functional TLS microenvironments directly from spatial transcriptomic data, providing a quantitative and unsupervised framework for immune niche discovery

Conclusion: STniche provides a statistically rigorous and biologically interpretable framework for discovering functional spatial niches in tumor tissues. Its ability to detect TLS-enriched immune architectures highlights potential applications in understanding prognosis, immunobiology, and therapeutic response. Further benchmarking is ongoing.

#1490 A single cell-based protein activity landscape for human small cell lung cancer.

Lucas ZhongMing Hu[1], Anish Thomas[2], Andrea Califano[1]

[1]Columbia University, New York, NY,[2]National Cancer Institute, Bethesda, MD

Small cell lung cancer (SCLC) is a lethal malignancy characterized by rapid metastasis, profound intra-tumor heterogeneity (ITH), and an immunosuppressive tumor immune microenvironment (TIME). The underlying biology of SCLC is poorly understood, and treatment options remain limited. To overcome this, we performed a systematic analysis on a large collection of single-cell RNA-Seq-based SCLC human sample cohort to define the gene regulatory networks and master regulators (MR) driving SCLC ITH and TIME composition. We constructed a single-cell transcriptomic atlas of 182,189 cells from 41 fresh patient-derived SCLC samples (primary and metastatic sites). Tumor and immune cells were cataloged and clustered. To move beyond transcriptional states, we reverse-engineered patient- and cluster-specific regulatory networks using ARACNe and inferred protein activity for >6,500 regulatory and signaling proteins via metaVIPER. This protein activity landscape was used to deconvolute ITH and TIME architecture. The OncoTreat algorithm identified FDA-approved drugs that invert MR activity in matched SCLC cell lines, with subsequent *in vivo* validation. Our protein activity analysis identified distinct, translationally relevant SCLC tumor and TIME subpopulations governed by specific MR programs. In tumor cells, we defined a proliferative "Tumor Checkpoint" module of MRs as a key determinant of this aggressive disease. Within the TIME, we discovered immune subpopulations with unique biological properties. A genome-wide drug perturbation screen identified potent agents that effectively abrogate the activity of tumor-specific MRs. These candidates demonstrated significant efficacy in inducing tumor cell death in preclinical *in vivo* models. We present the largest single-cell protein activity atlas of SCLC, providing a high-resolution view of the regulatory networks underlying its ITH and TIME. We computationally derived and preclinically validated novel therapeutic strategies that target master regulators of distinct tumor and immune subpopulations, offering a promising path to overcome therapeutic resistance in SCLC.

: Sequence Analysis
Poster Session

#1494 Study on acquisition timing of *KRAS* mutations in the pancreatic ductal epithelium.

Tomonori Hirano[1], Yasuhide Takeuch[2], Kazuyuki Nagai[3], Takayuki Anazawa[4], Sachiko Minamiguchi[5], Hiroshi Seno[6], Seishi Ogawa[1], Nobuyuki Kakiuchi[1]

[1]Department of Pathology and Tumor Biology, Graduate School of Medicine, Kyoto University, Kyoto, Japan,[2]Department of Diagnostic Pathology, Graduate School of Medicine, Kyoto University, Kyoto, Japan,[3]Department of Surgery, Graduate School of Medicine, Kyoto University, Kyoto, Japan,[4]Department of surgery, division of gastroenterological surgery, Sapporo Medical University, Hokkaido, Japan,[5]Department of Diagnostic Pathology, Fujita Health University School of Medicine, Aichi, Japan,[6]Department of Gastroenterology and Hepatology, Graduate School of Medicine, Kyoto University, Kyoto, Japan

[Introduction] Pancreatic cancer is a highly aggressive malignancy with a poor prognosis, underscoring the need for early diagnosis *KRAS* mutations are among the earliest genetic events in pancreatic carcinogenesis, but the timing of *KRAS* mutation acquisition in the pancreatic ductal epithelium remains unclear.
[Methods] From surgical specimens, we collected non-neoplastic pancreatic tissues distant from the macroscopic tumor, from which pancreatic duct-derived organoids were established. Paired tumor/normal DNA was extracted and subjected to whole-exome sequencing (WES). Phylogenetic trees were reconstructed based on shared somatic mutations. In patients with pancreatic cancer or intraductal papillary mucinous neoplasm (IPMN), WES was also performed on DNA from formalin-fixed, paraffin-embedded (FFPE) tumor tissue to assess relationships between cancer and non-cancerous *KRAS*-mutant clones. In a subset of bulk organoids, single cell-derived organoids were further established to determine mutation accumulation rates.
[Results] We analyzed 430 organoid samples from patients with (n=25) and without (n=23) pancreatic cancer. A median of 33 mutations per sample was identified. Eighteen *KRAS* mutations were detected in 16 cancer patients compared with four in four non-cancer controls, indicating a higher prevalence and wider distribution of *KRAS*-mutant clones in cancer patients. Phylogenetic analysis showed that 13 of 22 *KRAS* mutations mapped to the major trunk, which typically spread into multiple (n=6 on average) branches, whereas *KRAS*-wild-type clones rarely extended to multiple branches, suggesting more localized expansion. We further analyzed 56 single-cell-derived organoids from 19 cases, of which 7 harbored *KRAS* mutations. In *KRAS*-wild-type cells, the mutational burden positively correlated with age with a rate of 0.29 mutations per exome per year. KRAS-mutant cells carried significantly more mutations than wild-type cells, suggesting an increased mutation rate after KRAS activation. Based on this mutation rate, we estimated that these *KRAS* mutations were acquired between 21 and 44 years of age. Among 16 cases with *KRAS*-mutant PDAC or IPMN, we analyzed 8 FFPE tumors. In one patient with metachronous intraductal papillary mucinous carcinoma, the primary tumor, recurrent tumor, and *KRAS*-mutant organoid clone all arose from a common ancestral clone. Phylogenetic analysis indicated that a clone shared by the primary and recurrent tumors first branched from this ancestor and subsequently gave rise to both lesions. In other cases, *KRAS*-mutant clones in non-neoplastic ducts were phylogenetically independent of the cancer clone, indicating parallel evolution of multiple KRAS-mutant lineages.
[Conclusions] We elucidated the evolutionary history of clones in non-cancerous pancreatic ductal epithelium. These findings improve our understanding of the early events in pancreatic carcinogenesis.

#1495 A novel, deep learning -based filtering tool for enhanced detection of technical artifacts in whole-genome sequencing data.

Julian Gascoyne[1], David Benjamin[2], Juan Gallegos[1], Lee T. Lichtenstein[2], Sachet Shukla[1]

[1]UT MD Anderson Cancer Center, Houston, TX,[2]Broad Institute, Cambridge, MA

Artifactual variants obfuscate the already difficult task of somatic variant calling by mimicking some qualities of low variant allele fraction (VAF) mutations in this low signal-to-noise ratio regime. Statistical callers cannot cover the entire landscape of artifacts, leaving a critical gap. While deep learning tools for variant calling exist, they generally consume enormous amounts of labeled training data, are expensive to run, and can be overfit to a single sequencing technology. Here we present and benchmark Permutect, a lightweight deep learning-based variant caller for identifying artifactual variants across sequencing technologies and genomes. Permutect combines an artifact model for technological context and posterior model for biological context, respectively, allowing it to learn the characteristics not only for the technology but additionally the particularities of a given lab environment. The tool leverages the inherent non-orderedness of a set of reads (and thus their permutation invariance) to ascribe a probability for being a technical artifact. Permutect is therefore a lightweight deep learning model which can use as little as a single (unlabeled) genome for training thereby addressing the shortcomings of existing statistical and deep-learning callers. We tested this novel tool by training on four Genome-in-a-Bottle samples and benchmarking it against Mutect2, Strelka2, and DeepSomatic across well-established callsets: the ICGC Dream Challenge Sets 1-4 and SEquencing Quality Control Phase 2 (SEQC2) HiSeq and NovaSeq replicates. Permutect is an effective and precise tool for filtering, particularly in the paired Tumor-Normal (TN) setting. It achieved the highest mean Precision score (0.928) and the highest mean F1 score (0.899) in the Dream TN cohort, demonstrating superior overall balanced performance relative to its traditional competitors. Performance remained high and consistent across SeqC2 data (e.g., F1 score of 0.941 on HiSeq TN); we exclude scores from DeepSomatic, which was trained on that same data. While the precision of all tools are depressed in the Tumor-Only (TO) setting, it maintains a strong mean Recall (0.810) comparable to that of Mutect2 (0.811) in Dream TO. Though all callers struggled in the TO context, our findings show that Permutect's performance is competitive, and often superior, to established methods, highlighting its potential to address the pervasive issue of artifactual variants. Further work is being done to extend the domain of Permutect to whole-exome and long read sequencing and other improvements such as including the tri-nucleotide context about a variant will further refine the tool to address the shortcomings seen in the TO setting. In doing so, we expect Permutect to enhance downstream genomic analysis with applications ranging from clinical molecular pathology to the design of personalized immunotherapies.

#1496 Long-read sequencing of 15 Ewing sarcoma cell lines uncovers extensive GGAA microsatellite variation shaping the landscape of EWSR1::FLI1 binding.

Andrew Song[1], Xin Li[1], Egor Dolzhenko[2], Helene Neyret Kahn[3], Kristine Jones[1], Difei Wang[1], Komal Jain[1], Aubrey Hubbard[1], Olivia Lee[1], Stephen Chanock[1], Diptavo Dutta[1], Olivier Delattre[3], **Mitchell J. Machiela**[1]

[1]National Cancer Institute, Rockville, MD,[2]PacBio, Menlo Park, CA,[3]INSERM U1330, Children's Oncology Research Unit, PSL Research University, SIREDO Oncology Center, Institut Curie Research Center, Paris, France

Ewing sarcoma (EwS) is a rare, aggressive bone and soft tissue tumor occurring primarily in adolescents and young adults. EwS is defined by acquired chromosomal translocations between a member of the FET gene family and an ETS transcription factor (e.g., EWSR1::FLI1 in >85% of cases) that bind GGAA repetitive sequences and rewire local transcriptional activity. Germline variation in GGAA microsatellite allele length and motif purity can alter binding of EWSR1::FLI1 and disrupt the ability to dysregulate core driver genes. Further investigation into the molecular features underlying these germline-somatic interactions may yield new insights into the genetic etiology of Ewing sarcoma.

We performed whole-genome PacBio Revio HiFi sequencing on high molecular weight DNA extracted from 15 EwS cell lines positive for EWSR1::FLI1 to characterize germline variation in GGAA microsatellites genome-wide. We implemented a custom TRGT pipeline to call microsatellites containing at least 3 GGAA motifs utilizing a genomic repeat library and hidden Markov models. To investigate genomic features that could enhance EWSR1::FLI1 binding, we utilized linear mixed models incorporating PacBio data on microsatellite allele calls and DNA methylation with chromatin accessibility and ChIP-seq of EWSR1::FLI1 binding from the Ewing Sarcoma Cell Line Atlas (ESCLA).

In total, 39,319 GGAA microsatellites were characterized, with notable variation observed in microsatellite length (median=16 bp, interquartile range=13-51) and purity of GGAA motifs (mean=93.4%, standard deviation=9.2%). Allelic variation was present between cell lines with a mean of 4 alleles and a maximum of all 30 haplotypes exhibiting a different allele. Increased microsatellite length was the strongest predictor of EWSR1::FLI1 binding (beta=0.711, 95% CI=0.703,0.719), followed by reduced DNA methylation (beta=-0.023, 95% CI=-0.024,-0.022) and increased H3K27ac measures of open chromatin (beta=0.154, 95% CI=0.138-0.170). Analyses of established core EwS genes dysregulated by EWSR1::FLI1 are underway to identify specific microsatellites and allelic combinations that promote EWSR1::FLI1-altered expression of these genes.

Together, germline data from long-read whole-genome sequencing and multi-omic profiles from the ESCLA enable integrative analyses for disentangling germline-somatic interactions that alter EWSR1::FLI1 binding and downstream transcriptional regulation.

#1497 Long-read RNA-Seq reveals a novel isoform landscape of *SRSF2*-mutant chronic myelomonocytic leukemia.

Nickolas Steinauer, Terra Lasho, Christy Finke, Pankaj Pradeep, Jenna Fernandez, Alejandro Ferrer, Moritz Binder, Abhishek Mangaonkar, Mrinal M. Patnaik

Mayo Clinic Hospital-Rochester, Rochester, MN

While missense somatic mutations in the serine/arginine rich splicing factor 2 (*SRSF2*) occur early in the clonal development of myeloid neoplasms, they are uniquely enriched in chronic myelomonocytic leukemia (CMML), an MDS/MPN overlap neoplasm, where their estimated prevalence is ~50%. Short-read RNA-sequencing experiments have demonstrated that missense alterations of the proline 95 residue hotspot (*SRSF2*^{P95}) globally dysregulate exon inclusion, though the full transcript structures induced by such alternative splicing events remain uncharacterized. Given the striking enrichment of *SRSF2* mutations in CMML, we hypothesized that there exist unique splicing alterations contributing to the biology of this disease, and sought to profile the landscape of alternative transcription induced by *SRSF2* mutations in CMML using long-read RNA-Seq. We conducted bulk long-read RNA-Seq on bone marrow mononuclear cells from 5 CMML patients with *SRSF2*^{P95H} (n=3) and *SRSF2*^{P95L} (n=2) mutations, with VAFs ranging 20-48%, along with 5 CMML splicing factor wildtype patients. Libraries were prepared with the Pacbio Kinnex full-length RNA kit and sequenced on a Revio SPRQ sequencer. Reads were processed and aligned using the IsoSeq pipeline, and isoform collapsing, quality control, reference comparison, and quantification were performed with IsoQuant and SQANTI3. Differential transcript and gene expression was assessed with DESeq2, while differential transcript usage was assessed with the DRIM-Seq and stageR packages. After long-read collapsing and quality control, we identified 255,505 unique transcript isoforms, of which 14,845 (~5.8%) were novel to the reference transcriptome annotation (GENCODE v39). We identified 23 transcripts differentially expressed in *SRSF2*-mutant samples, including 9 novel transcripts, the majority of which (n=7) were upregulated in *SRSF2*-mutant cases. A higher number of transcripts (n=80) and genes (n=65) demonstrated significant changes in proportional transcript usage. Among transcripts with increased expression and usage in *SRSF2*-mutant cases, we identified a novel transcript of the gene *YBX1*, which encodes an RNA- and DNA-binding transcription factor required for cell survival and self-renewal in myeloid neoplasms. This novel transcript, which we termed *YBX1ΔEx4*, has an in-frame loss of exon 4, and is predicted to encode a full-length protein missing a 30 amino acid region of the cold-shock (DNA-binding) domain. Using short read RNA-Seq data from an additional 29 CMML patients, as well as an independent dataset (GSE251806) comprising 43 blast-phase CMML patients, we confirmed increased exclusion of *YBX1* exon 4 in *SRSF2*-mutant cases, with an even greater loss of exon 4 in blast-phase SRSF2-mutant cases. We hypothesize an important role of this isoform in CMML disease progression and are currently performing functional studies to characterize the effect of *YBX1ΔEx4*.

#1498 A generalizable software framework for ultra-rapid sequence analysis and its application in enabling 1 day deep multi-omic data analysis turnaround for brain cancer precision oncology.

Anders Pitman[1], David Bean[2], **Yi Qiao**[2]

[1]Human Genetics, University of Utah School of Medicine, Salt Lake City, UT,[2]Biomedical Informatics, University of Utah School of Medicine, Salt Lake City, UT

BACKGROUND: Pediatric brain cancer patients in relapse lack standard-of-care options and experience poor clinical outcome; and adult glioblastoma is simultaneously the most commonly diagnosed central nervous system malignancy and the most deadly. While they stand to benefit the most from precision-guided, personalized therapy selection supported by multi-omic tumor profiling, they also experience an extremely short post-surgery window-of-opportunity to identify and acquire likely effective drugs. This short clinical timeframe precludes clinical trials utilizing next generation sequencing (NGS) tumor profiling techniques from being designed, as the vast amount of data produced by tumor-normal pair whole genome DNA sequencing and tumor single cell RNA sequencing cannot be analyzed in time using current prevailing methods.
METHODS: We look towards graphics processing unit (GPU) accelerated computation to significantly speed up sequence analysis. We utilize both existing acceleration efforts (most notably the GPU version of BWA-MEM and STAR alignment algorithms as part of the NVIDIA Parabrick package) as well as accelerated versions of software we developed for which no GPU versions currently exist (FreeBayes short variant and FACETS copy number variant calling algorithms). We focus both on result equivalency to the unaccelerated versions, as well as code reusability so that additional software can be ported to GPU platforms by others with ease.
RESULTS: Using the HG008 tumor normal pair from Genome In A Bottle as a test case (2x150bp Illumina NovaSeq 6000, 150X normal and 190X tumor nominal coverage), our pipeline spent < 2 hours in sequence alignment, and < 30 minutes in variant calling and annotation using readily available computer hardware. As a result, the entire sequence analysis workflow can be finished within 1 working day, and produces an annotated variant call set ready for expert review, molecular tumor board discussion, and therapy selection. We further tested our approach on an in-house pediatric brain dataset consisting of 16 patients and both DNA and scRNA sequencing data, and observed similar results.
CONCLUSION: We have developed a generalizable approach to adopting GPU accelerated computation to sequence analysis, and how they can significantly expand the possibilities of applying NGS-based precision oncology approaches to adult / pediatric brain cancer by offering 1 day analysis turnaround. Coupled with logistic optimization at sequencing facilities (e.g. using dedicated flow cells and priority queues), we have achieved <1 week surgery-to-insight turnaround. Our work serves as building blocks for designing next general precision oncology clinical trials that rely on NGS to prioritize treatment options for brain cancer patients.

#1499 Pangenome-based somatic mutation landscape of early- and late-onset colorectal cancer in 99 Korean patients.

Jae-Yoon Kim[1], Soobok Joe[2], Sunwoo Lee[1], Yeo-Gyeong Yoon[1], Jongbum Jeon[2], Jong Hwan Kim[2], Jin Ok Yang[2], Seung-Woo Baek[1], Jong-Lyul Park[3], Seon-Kyu Kim[1], Seon-Young Kim[1]

[1]Genomic Medicine Research Center, Korea Research Institute of Bioscience and Biotechnology, Daejeon, Korea, Republic of,[2]Korea Bioinformation Center (KOBIC), Korea Research Institute of Bioscience and Biotechnology, Daejeon, Korea, Republic of,[3]Genomic Medicine Research Center, Korea Research Institute of Bioscience and Biotechnology, Daejeon, Kosovo, Republic of

Colorectal cancer (CRC) is the third most prevalent cancer type worldwide. Although overall CRC incidence has declined due to improved screening, early-onset CRC (EOCRC) in patients under 50 years old is rapidly increasing globally, including in Korea, unlike the decreasing trend of late-onset CRC (LOCRC). Several studies have attempted to identify EOCRC-specific mutations; however, most were limited to whole-exome sequencing and thus failed to capture CRC-related non-coding variants comprehensively. Moreover, previous mutation-profiling studies relied on the GRCh38 reference genome, a linear and largely European-biased assembly that lacks representation of human genetic diversity, fundamentally limiting the discovery of novel mutations. To address these limitations, we performed whole-genome sequencing (WGS) of paired tumor and matched blood samples from 49 EOCRC and 50 LOCRC Korean patients. Somatic mutations were identified using the graph-based Human Pangenome Reference (Human Pangenome Reference Consortium, released in 2023), which integrates genomic diversity from 49 individuals worldwide. Each sample produced 1.409 billion reads with an average coverage of 37.7×. EOCRC and LOCRC carried an average of 1,673 and 801 somatic mutations in coding regions and 236,610 and 127,616 in non-coding regions—21% and 43% higher than GRCh38-based results. Ten EOCRC-specific coding genes were identified, including LMTK3, GALNT11, and NPHP1, with LMTK3 also reported in a previous Chinese study. In non-coding regions, 32 EOCRC-specific genomic regions were detected, including PRKAG2-GALNTL5, MRGPRF-TPCN2, and ACTRT2-TTC34. Among these, GALNT11, MRGPRF-TPCN2, and ACTRT2-TTC34 contained mutations significantly associated with EOCRC patient survival. Although further expression-level validation is warranted, we propose these three regions as promising genome-level candidates for EOCRC diagnosis and therapy. Additionally, all WGS data have been deposited in the European Genome-phenome Archive (EGA; EGAS50000000544) and are expected to provide a valuable resource for researchers investigating CRC or EOCRC at the genomic level.

#1500 Modeling base-pair level mutation rate in metastatic breast cancer using a sequence-based deep learning model.

Ariaki Dandawate[1], Christina Leslie[2], Ekta Khurana[3]

[1]Physiology, Biophysics and Systems Biology, Weill Cornell Graduate School, New York, NY,[2]Memorial Sloan Kettering Cancer Center, New York, NY,[3]Weill Cornell Medicine, New York, NY

By leveraging a sequence-based deep learning framework, we seek to uncover mechanisms by which mutations arise in noncoding regulatory regions, potentially leading to the discovery of novel targets in metastatic breast cancer.

Research around metastatic breast cancer has largely focused on analyzing coding mutations to characterize progression. Though noncoding mutations are known to affect transcription factor binding and regulation of gene expression, few noncoding mutation drivers have been identified. Previously published work has shown that metastatic mutation rate correlates with open chromatin in the cells-of-origin. However, this work has mostly been done at a coarse, region-level scale, identifying mutational hotspot regions. In this work, we aim to uncover genomic positions in regulatory regions of metastatic breast cancer with elevated mutation rates, and identify their potential mutation mechanism.

We propose a novel deep learning model that uncovers the sequence context-based covariates of per-base mutation rate in regulatory regions of metastatic breast cancer. With access to over 500,000 mutations from the Hartwig Medical Foundation cohort, the neural network is trained on sequences from regulatory regions in normal breast epithelium, and predicts per-base mutation rate profiles for the region. As a result, the model learns how sequence features change mutation likelihood at particular genomic positions.

Analysis of the saliency map of the model allows for identification of specific sites with higher-than-expected mutation rates, which is potentially indicative of increased transcription factor binding that extends beyond selection by pro-metastatic regulatory programs. These findings provide a method to connect noncoding mutation patterns to mutation mechanism and regulatory effects in metastatic genomes.

Future work aims at expanding this model to a pan-cancer level, revealing shared and cancer-specific noncoding mutations that have potential to reveal patterns of metastasis. This scalable sequence model framework provides an advantage over existing methods particularly due to its base-pair level resolution modeling of the metastatic cancer genome. Thus, its implications for modeling and uncovering regulatory mechanisms of cancer is key.

#1501 Cancer gene variant identification and functional interpretation using long-read RNA sequencing with FLAIR3.

Colette Felton[1], Andrea Galvez[2], Tanvi Damle[2], Kevin Levine[3], Mark Diekhans[2], Eunice Lopez Fuentes[4], Taylor Won[2], Christopher Vollmers[2], Alejandro Sweet-Cordero[4], Alice Berger[5], **Angela N. Brooks**[2]

[1]Colette Felton (Individual), UC Santa Cruz, CA,[2]UC Santa Cruz, Santa Cruz, CA,[3]Fred Hutchinson Cancer Center, Seattle, WA,[4]UCSF - University of California San Francisco, San Francisco, CA,[5]Fred Hutchinson Cancer Center, Seattle, CA

Although the impact of single nucleotide variants (SNVs) and changes in transcription and RNA processing are often analyzed separately, a comprehensive analysis facilitates a complete understanding of how cancer gene alterations impact oncogenesis. In traditional short-read RNA sequencing, phasing of alternative exons and cancer variants is lost because the read lengths are much shorter than typical mRNA transcripts (average > 1kb). Here, we show that long-read RNA-seq (lrRNA-seq) can identify full-length transcript isoforms on which variants are expressed, which can be used to more accurately identify the functional impact of oncogenic variants. We developed FLAIR3, which performs an integrated analysis of SNVs, gene fusions, and alternative splicing using lrRNA-seq and predicts functional changes to the amino acid sequence. We performed ONT lrRNA-seq on three osteosarcoma cell lines and PacBio lrRNA-seq on paired normal and tumor tissue from two lung adenocarcinomas. We then used FLAIR3 to identify cancer driver variants and to determine how splicing modulates their expression and function. In the osteosarcoma samples, FLAIR3 revealed alternatively spliced gene fusions in cancer driver genes and TP53 gene fusions with intergenic regions, predicted to cause TP53 truncations. In the lung adenocarcinomas, FLAIR3 revealed isoform-biased expression of oncogenic *BRAF V600E*. Through an isoform-specific analysis of somatic SNVs in *CDKN2A,* we found that *TP53* loss significantly co-occurs with *CDKN2A* missense or nonsense variants of the p16 isoform, but not with *CDKN2A* deep deletion. Damaging variants in the p16 isoform would not have the same damaging effects in p14 isoform, which functions through TP53; therefore, *TP53* loss would be necessary to have complete loss of *CDKN2A* functions. A deep deletion of *CDKN2A* removes both p16 and p14 isoform function and would not need to have additional *TP53* loss. These findings reveal how alternative splicing interacts with and modulates the function of oncogenic variants.

#1503 Single-cell multiomics analysis reveals cell type-specific genetic regulatory programs underlying immunotherapy resistance in hepatocellular carcinoma.

Siyuan Huang, Xiaohang Long, Stephen Lam Chan, Alfred Sze-Lok Cheng

The Chinese University of Hong Kong, Hong Kong, China

Although outcomes for patients with advanced hepatocellular carcinoma (HCC) have improved with the advent of immune-checkpoint inhibitor (ICI)-based therapies, only approximately 30% of patients achieve an objective response. With the rapid development of single-cell technologies, increasing attention has been paid to immunosuppressive cell types in the tumor microenvironment (TME) from a transcriptomic perspective; however, the contribution of genetic variation to immunotherapy resistance remains largely unexplored. Here, we employed single-cell multiomics of 14 treatment-naïve and ICI-resistant HCC patients to investigate cell type-specific genetic regulation underlying chromatin accessibility and gene expression within the HCC TME. High-quality single-cell ATAC-seq data were generated for 155,700 cells and annotated into 11 major cell types, including B cells, CAFs, $CD4^+$ T cells, $CD8^+$ T cells, dendritic cells, endothelial cells, macrophages, monocytes, NK cells, Tregs, and tumor cells. Leveraging genotype information inferred from single-cell ATAC-seq, RASQUAL systematically mapped 23,329 chromatin accessibility-associated quantitative trait loci (caQTLs) across all cell types. We found a wide range of cell number-normalized caQTLs in different cell types (0.01 to 0.22). Notably, tumor cells exhibited the highest frequency of caQTLs, suggesting greater genetic susceptibility within their regulatory landscape. Colocalization with liver cancer-related GWAS signals, combined with peak-to-gene association analyses, identified enhancer-like regulatory elements that may modulate genes involved in tumor progression and immunotherapy resistance. In summary, our study delineates the cell type-specific genetic control and regulatory architecture of HCC TME and provides mechanistic insights into the molecular basis of immunotherapy resistance.

Acknowledgement: This study is supported by Li Ka Shing Foundation and CUHK Strategic Seed Funding for Collaborative Research Scheme.

#1504 Fusobacterium-driven epithelial-stromal remodeling in CRC.

Sabin Park[1], Taeyul Kim[2], Kyung-A Kim[2], Minsun Jung[2], Sang Cheol Kim[3], Han Sang Kim[2], Semin Lee[1]

[1]Ulsan National Institute of Science and Technology, Ulsan, Korea, Republic of,[2]Yonsei University College of Medicine, Seoul, Korea, Republic of,[3]National Institute of Health, Cheongju, Korea, Republic of

Background: Fusobacterium nucleatum is recognized as a key microbial factor accelerating colorectal cancer (CRC) progression. However, the cellular and molecular mechanisms underlying its impact on the tumor microenvironment (TME) are not yet fully understood.

Methods: We performed single-cell RNA sequencing on specimens from 39 CRC patients. Samples were stratified into Fusobacterium-positive (Fuso-pos; n=14) and Fusobacterium-negative (Fuso-neg; n=25) groups using a 1% microbial abundance cutoff. Comparative analyses were conducted across the stromal and epithelial compartments to investigate microbe-associated transcriptional programs, pathway activation, and fibroblast-epithelial interactions.

Results: CRC tumors with high *Fusobacterium* abundance exhibited coordinated remodeling of both stromal and epithelial landscapes. Fibroblasts from Fuso-pos samples showed enhanced interferon-driven inflammatory activity and mesenchymal transition, accompanied by a marked expansion of a specific myofibroblastic cancer-associated fibroblast (myCAF) subtype. In the epithelial compartment, Fuso-pos tumors showed increased genomic instability, elevated stemness, and upregulation of CMS4-related signatures. Gene module analyses demonstrated a strong increase in epithelial-mesenchymal transition-related module in epithelial cells upon *Fusobacterium* infection, which correlated significantly with the myCAF abundance. Analysis of bulk RNA-seq data further confirmed that a higher proportion of the deconvoluted myCAF subtype was associated with unfavorable clinical outcomes. Mechanistically, Fuso-pos tumor cells showed increased *SHH* expression, while the myCAFs exhibited high expression of Hedgehog signaling components, indicating augmented epithelial-stromal Hedgehog signaling.

Conclusions: These findings suggest that *Fusobacterium* infection in CRC promotes epithelial-stromal signaling through the SHH-Hedgehog axis, contributing to CRC progression. It may represent a therapeutically targetable component of the TME in *Fusobacterium*-associated CRC.

Acknowledgments: The authors gratefully acknowledge support from the following funding sources: a grant of the Korea Health Technology R&D Project through the Korea Health Industry Development Institute (KHIDI), funded by the Ministry of Health & Welfare, Republic of Korea (RS-2025-25459033 to H.S.K.). This work is also supported by the National Research Foundation of Korea (NRF) funded by the Ministry of Education (RS-2018-NR031072).

#1505 Long-read sequencing of pancreatic adenocarcinoma transcriptome uncovered aberrant isoforms and tumor progression.

Charny Park[1], Hyeyeong Hwang[1], Daejin Hyung[2], Namhee Yu[3], Sehwa Hong[3], Soo Young Cho[4], Sang Myung Woo[5]

[1]National Cancer Center - Korea, Goyang-si, Gyeonggi-do, Korea, Republic of,[2]Research Institute National Cancer Center, Republi, Research Institute National Cancer Center, Republi, Goyang-si, Korea, Republic of,[3]National Cancer Center, Goyangsi, Korea, Republic of,[4]Department of Molecular and Life Science, Hanyang University, 55 Hanyangdeahak-ro, Sangnok-gu, Ansan, Korea, Republic of,[5]National Cancer Center - Korea, Goyang

Pancreatic cancer remains one of the most lethal malignancies, with a dismal 5-year survival rate of only 13%. Despite multi-omics studies uncovering critical variants and regulatory mechanisms in driver genes and oncogenes, effective therapeutic options remain limited. To address the urgent unmet clinical need for a deeper understanding of the disease, we employed long-read sequencing (LR-seq) to identify complex structural variants and alternative splicing events that are undetectable using short-read sequencing methods.In total, we identified 150,904 isoforms, including 62,111 novel variants. Among these novels, 51.5% showed tumor-specific expression. Novel isoforms were frequently detected in oncogenes such as *CD74*, *B2M*, and *DAXX*, suggesting distinct driver events in pancreatic cancer. Notably, novel alternative transcription start sites were enriched in chromatin-accessible regions marked by H3K4me3 and H3K27ac in tumor cells, and these isoforms appeared to disrupt MHC-associated functions involving *CALR*, *PTK6*, and *TAPBP*.Expression profiling of the novel isoforms clearly distinguished classical and quasi-mesenchymal (QM) subtypes ($P = 0.001$). Furthermore, global analysis of alternative splicing and switch-like isoforms across molecular subtypes revealed that splicing events modulated metastatic characteristics between the classical and QM subtypes through Rho GTPase signaling, GPCR signaling, and extracellular matrix organization.In conclusion, our study underscores the critical role of long-read sequencing in uncovering novel isoforms and alternative splicing events that define the molecular heterogeneity of pancreatic cancer. These findings provide new insights into the regulation of key oncogenes and reveal potential therapeutic targets with implications for improving the diagnosis and treatment of this devastating malignancy.

#1506 Assessing allelic expression variation using somatic mutations vs. polymorphic germline variants.

Kohei Hagiwara, Bensheng Ju, Nadezhda V. Terekhanova, John Easton, Jinghui Zhang

Computational Biology, St. Jude Children's Research Hospital, Memphis, TN

Allele-specific expression (ASE) of somatic mutations can be caused by *cis*-activation of the mutant allele or silencing of the wildtype allele. It has been investigated by examining the enrichment of mutant allele in RNA relative to DNA which can account for increased allelic expression due to somatic copy number alteration. Here we show that this mutation-based approach can be confounded by gene expression differences in tumor and normal cells that co-exist in most bulk tumor samples resulting in enriched mutant allele expression without ASE. By modeling all the relevant co-factors, we show that this confounding effect is exacerbated with low tumor purity and is dependent on mutant allele dosage for mutations that can trigger nonsense-mediated decay (NMD). Our analysis using somatic indels in The Cancer Genomics Atlas (TCGA) dataset found that truncating indel alleles with elevated expression were more prevalent in tumor suppressor genes (TSGs) than in genes not frequently mutated in cancers (non-driver genes) (7.69% vs. 1.76%, Fisher exact $p < 2.2\times10^{-16}$). Consistent with the model, such indels were associated with higher gene expressions in tumor compared to normal and with loss of heterozygosity (LOH) for NMD-sensitive indels in TSGs. By contrast, ASE events of somatic mutations can more accurately be characterized by assessing allelic enrichment of germline heterozygous single nucleotide polymorphisms (SNPs) phased to the somatic mutation. In this SNP-based approach, tumor/normal expression differences and tumor purity exhibit none or minimum confounding effects, discriminating true ASE events caused by *cis*-regulatory change from those caused by confounding factors. To further evaluate the SNP-based ASE analysis, we performed genome-wide haplotype phasing and single-cell full transcriptome sequencing in the B-cell acute lymphoblastic leukemia (B-ALL) cell line Nalm6. We show that that ASE is a heterogenous process with varying degrees of allele expression biases in different cellular subpopulations even in a cell line model and such transcriptional heterogeneity can potentially contribute to clonal evolution under treatments.

#1507 Health behavior associated CCL20 ligand variation contributes to the disparity in non-small cell lung cancer.

Murugesh Eswaran[1], Briana Alicia Brock[1], Hina Mir[1], Sejong Bae[2], Gabriella M. Oprea-Ilies[3], Eric L. Flenaugh[1], Sanjay R. Jain[1], Brian M. Rivers[1], Rick A. Kittles[1], James W. Lillard[1], Rajesh Singh[1], Shailesh Singh[1]

[1]Morehouse School of Medicine, Atlanta, GA,[2]Biostatistics, Data Science and Epidemiology, Augusta Univesrity School of Public Health, Augusta, GA,[3]Pathology, Emory Univesrity School of Medicine, Atlanta, GA

Background: Lung cancer exhibits disparities in incidence, disease prevalence, and treatment outcomes. Chemokines and their corresponding receptors have been shown to be associated with these observed disparities within different ethnic groups. In this study, we have demonstrated that the differential signaling of chemokine receptor CCR6 and its natural ligand is associated with the observed disparity, and this differential CCR6 signaling is primarily due to the diversity in CCL20.
Methods: Bulk RNA-seq data (BioProject ID: PRJNA1039495) from lung cancer cell lines derived from African American (AA) and European American (EA) individuals were analyzed to identify and quantify different isoforms of CCL20. MD simulations were performed to evaluate the binding affinity of CCL20, hydrogen-bond stability, and conformational behavior upon interaction with the CCR6 receptor. Downstream pathway activation potential was inferred by comparing the expression of signaling molecules that support oncogenic pathways and are associated with poor therapeutic outcomes. Furthermore, smoking habits, including higher nicotine intake, distinct metabolite patterns, and alterations in basic cytokine levels, were incorporated into the model as external factors that may influence CCL20 isoforms and CCR6 signaling.
Results: Out of 5 CCL20 isoforms, Isoform-1 (24 TPM) and Isoform-2 (36 TPM) showed stronger interactions with CCR6 compared to EA cells (Isoform-1: 7.5 TPM; Isoform-2: 11.2 TPM). Across smoking groups, AA cells showed higher Isoform-2 levels than EA cells, increasing from non-smokers (Isoform-1: 18 TPM; Isoform-2: 18 TPM) to smokers (Isoform-1: 24 TPM; Isoform-2: 40 TPM), while EA cells showed lower increases from non-smokers (Isoform-1: 18 TPM; Isoform-2: 19 TPM) to smokers (Isoform-1: 24 TPM; Isoform-2: 30 TPM). MD simulations revealed that lung-cancer-cell CCR6 binds both CCL20 Isoform-1 & 2 from AA-derived cell lines with significantly stronger affinity compared to EA-derived cells, reflected by lower binding free energies, more stable hydrogen-bonds, and longer ligand-receptor contact durations. Isoform-2 showed the strongest overall binding affinity, indicating that it may be the dominant activator of CCR6 signaling. Population-level behavioral data, including All of Us cohort metrics, showed that AA smokers tend to use cigarettes with higher nicotine content, inhale more deeply, and exhibit slower nicotine and cotinine clearance, which corresponded with increased Isoform-2 expression.
Conclusion: Lung cancer cells derived from AA exhibit a ligand-rich and affinity-enhanced CCL20-CCR6 signaling axis driven primarily by Isoform-2. Isoform-specific expression, receptor affinity, and smoking-associated inflammation together highlight the significance of Isoform-2 in disparity observation in Lung cancer, as a key player in contributing to disparity.

#1508 A large-scale resource of standardized pediatric somatic cancer variant classifications.

Alex H. Wagner, Kori Kuzma, Kathleen M. Schieffer, Wesley Goar, Don Corsmeier, Michael McCarrick, Kathryn Perry, Jennifer Bowser, James Stevenson, Mohammad Marhabaie, Matthew Cannon, Liana Hernandez, Doug Depoorter, Hongtao Jia, Amy Everest, Jessica Howard, Swetha Ramadesikan, Vijayakumar Jayaraman, Ying-Chen C. Hou, Mariam T. Mathew, Marco L. Leung, Yassmine M. N. Akkari, Daniel Puthawala, Anastasia Bratulin, Ben Kelly, Elaine R. Mardis, Catherine E. Cottrell

Institute for Genomic Medicine, Nationwide Children's Hospital, Columbus, OH

Background: Our ability to interpret pediatric cancer genomes to identify targeted therapeutic strategies is bottlenecked by limited structured knowledge about the clinical significance of detected somatic mutations. Clinical genomics laboratories routinely keep internal records of previously classified variants in *ad hoc* storage systems (e.g., spreadsheets, custom databases), but significant technical barriers exist that prevent the broad dissemination of such knowledge for use across institutions. Recently developed genomic knowledge standards from the Global Alliance for Genomics and Health (GA4GH) provide the foundation to remove these barriers through a shared community framework for disseminating genomic knowledge.

Methods and Results: We implemented these GA4GH standards to produce over 1,500 publicly available somatic variant classification records. These were curated as part of routine pediatric cancer genome assessment in a research hospital setting, 94% (1415/1504) of which were assessed under the Molecular Characterization Initiative of the National Cancer Institute's Childhood Cancer Data Initiative. To broadly disseminate these data, we extended the open-source "ClinVar This!" community software to ingest GA4GH-standardized records for submission to the NIH ClinVar knowledgebase. As a result, we have more than doubled the total number of somatic cancer records submitted to ClinVar (previously 1,325 records across all other community submissions). We anticipate submitting an additional 2,000 records by April 2026. To support this effort, we developed the Variation Categorizer (VarCat) web platform to simplify the structured application of community standards for clinical variant classification in a pediatric setting. The software currently supports community somatic variant classification guidelines for clinical significance (the "AMP/ASCO/CAP guidelines") and oncogenicity (the "ClinGen/CGC/VICC guidelines"). VarCat is an open-source, clinically validated web tool that provides a streamlined mechanism for automating GA4GH-compliant dissemination of pediatric somatic cancer knowledge as part of routine clinical workflows.

Conclusions: This work demonstrates how these novel GA4GH standards enable us to disseminate somatic cancer variant knowledge as part of routine clinical operations. Our presentation will highlight the use of the VarCat platform and the associated standardized variant classification data we have made publicly available. We will also share insights from our applications of these standards to capture nuanced adaptation of community guidelines for clinical variant interpretation. We will conclude with practical guidance about how to best leverage these resources as a scalable approach to addressing the variant interpretation bottleneck in the clinical setting.

#1509 Cost-effective, full-length transcriptome of chronic lymphocytic leukemia patient cd8 t cells reveals the impact of BTKi treatment on mRNA processing and gene expression.

Shanmugapriya Thangavadivel[1], Altan Turkoglu[1], Lianbo Yu[1], Rosario Distefano[1], Alexander Pan[2], Logan Walker[3], Tina Wang[4], Shrilekha Misra[1], Tzung-Huei Lai[1], Britten Gordon[1], Samon Benrashid[1], Alexander He[1], Meixiao Long[1], rosa Lapalombella[1], John C. Byrd[5], Kerry A. Rogers[1], Bradley Blaser[1], Ralf Bundschuh[6], Jennifer A. Woyach[1], **Pearlly S. Yan**[1]

[1]The Ohio State University College of Medicine, Columbus, OH,[2]N-Power Medicine, Inc, Red Wood City, CA,[3]University of Michigan, Ann Arbor, MI,[4]The Ohio State University, Columbus, OH,[5]University of Pittsburgh Medical Center, Pittsburgh, PA,[6]Department of Physics and Department of Chemistry & Biochemistry, The Ohio State University, Columbus, OH

Ibrutinib, a Bruton's tyrosine kinase inhibitor (BTKi), is used to treat chronic lymphocytic leukemia (CLL). It has effects not only on CLL cells but also on the immune microenvironment, particularly T cells. While T cell exhaustion and activation defects are well studied, the role of mRNA processing on the transcriptome and immunome needs investigation. We and others noted such events in CLL cells with shorter isoforms replacing the longer primary transcripts. They enable added regulations via altered mRNA stability, translational efficiency, and protein localization.To conserve precious patient time series samples, we developed a protocol that deposes 300 sorted live cells into cold lysis buffer containing 5' template-switching primers and 3' poly-dT primers to bypass RNA extraction and to capture full-length transcripts. Viewing our data in genome browser, we noted the aligned- and the junction-read tracks reveal exon dropout events as stretches of uncovered exons in a gene-specific manner within- and across patients. For isoform-informed gene expression analysis, we identify a known isoform for each gene that encompasses all the transcribed exons from 10 CLL patients (30 samples: baseline, 3y and 5y ibrutinib treatment) for length-normalized gene expression analysis. For this abstract, we performed global analysis and a subset analysis targeting 187 genes from immune pathways and CD8 T cell activation. For timepoint analysis, differentially expressed gene (DEG) analysis was performed separately for genes without exon dropout and those with exon dropout. The 187-gene timepoint analysis was performed in one list. Key findings are: i) DEGs from subset analysis are also found in the two global analyses; ii) similar DEG trends observed across timepoints in all 3 analyses: highest in BL > 3y and BL > 5y followed by BL > 3y and 5y > 3y with a few 3y > BL and 5y > BL events; iii) 88% of the expressed transcripts contain one or more exon dropout event; iv) STRING analysis using DEGs from subset analysis reveals CD8 activation genes such as *ptprc* and *cd69* interact extensively with Perforin- and PD-1 pathway genes forming a dense network while genes from FAS-, mTOR- and TRAIL pathways form a separate network with few interactions. In summary, with a cost similar to bulk RNA-seq, our full-length data reveals mRNA processing events in both long genes (e.g., *jak1*, 26 exons, full exon coverage in 12/30 samples) and short genes (e.g., *jun*, part of the intronless gene not covered in some samples). An ultralow input of 300 pre- and post-treatment cells allow deep library sampling of both highly expressed genes with no exon dropout and lowly expressed genes with many dropouts. Lastly, DEGs from subset analysis lend support to the ability of the isoform-informed workflow to capture CD8 T cell functional genes in global DEG analysis.

#1510 CASTLE: long-read sequencing panel of cancer cell lines to improve standards of somatic variant calling and benchmarking.

Mikhail Kolmogorov[1], Ayse Gokce Kesus[2], Asher Bryant[2], Tanveer Ahmad[2], Byunggil Yoo[3], Sergey Aganezov[4], Anton Goretsky[2], Ataberk Donmez[2], Lisa Lansdon[5], Joshua Gardner[6], Brandy McNulty[6], Samuel Sacco[6], Jyoti Shetty[2], Yongmei Zhao[2], Bao Tran[2], Giuseppe Narzisi[7], Adrienne Hellend[7], Chengpeng Bi[5], Adam Walter[5], Margaret Gibson[5], Irina Pushel[8], Erin Guest[3], Tomi Pastinen[5], Nicolas Robine[7], Karen H. Miga[9], Midhat S. Farooqi[10], Benedict Paten[6]

[1]NIH-NCI, Bethesda, MD,[2]National Cancer Institute, Bethesda, MD,[3]Children's Mercy Kansas City, Kansas City, MO,[4]Oxford Nanopore Technologies, New York, NY,[5]Children's Mercy Hospital, Kansas City, MO,[6]UC Santa Cruz, Santa Cruz, CA,[7]New York Genome Center, New York, NY,[8]Children's Mercy Kansas City, Kansas City,[9]Biomolecular Engineering Department, University of California, Santa Cruz, Santa Cruz, CA,[10]Children's Mercy Research Institute, Kansas City, MO

Most current large-scale whole-genome sequencing projects rely on short-read sequencing to call germline and somatic SVs, however it provides an incomplete view of the somatic variation landscape because of mappability limitations. In contrast, long-read sequencing can resolve highly repetitive regions of the human genome, and assemble variants into contiguous haplotypes, and therefore is a promising approach to resolve the hidden complexity of a cancer genome. However there is still a limited number of publicly available datasets for benchmarking and development of new methods.

To motivate the development of new short- and long-read tools for cancer genomics, we created the CASTLE panel, based on multi-technology whole-genome sequencing of six commercially available tumor/normal cell line pairs (HCC1954, HCC1937, H1437, H2009, Hs578T and HCC1395). The panel represents two lung and three breast cancer cell lines. Genomic sequencing currently includes PacBio, Oxford Nanopore, Illumina, Hi-C and PoreC, in most cases sequenced from the same DNA extraction or cell line passage. We further generated high-confidence benchmarking somatic variant calls for SNPs, small indels and structural variants using the ensemble method. For structural variants, We used Severus, nanomonsv, SAVANA, Sniffles2, SvABA, GRIDSS, and Manta to generate initial variant calls; confident calls were defined if supported by at least two (out of three) technologies and at least 4 (out of 11) callers. For small variant benchmarking sets, we used a combination of Strelka2, DeepSomatic and ClairS.

Overall, we release a new public resource for cancer genomic developments and benchmarking, which we are aiming to complement with additional genomic and transcriptomic technologies. The data and benchmarking datasets are openly available at: https://github.com/CASTLE-Panel/castle.

#1511 Longitudinal whole genome sequencing to investigate clonal hematopoiesis dynamics.

Rohini Chebbi, Steven Estus, Elif P. Coskun, David W. Fardo, Gregory A. Jicha, Peter T. Nelson, Erin L. Abner, Yasminka A. Jakubek

University of Kentucky, Lexington, KY

Clonal hematopoiesis (CH) is the presence of clonal populations of hematopoietic stem cells, which arise when a cell acquires a somatic mutation and then undergoes clonal expansion. The presence of CH is strongly associated with age. Clonal hematopoiesis of indeterminate potential (CHIP) mutations is defined by having a mutation in a gene commonly altered in blood cancers. CHIP is associated with increased risk of illnesses such as blood cancer and cardiovascular diseases. In addition to CHIP mutations, other somatic mutations can drive CH. To comprehensively characterize CH dynamics, we conducted whole genome sequencing (WGS) of blood samples from a community-based brain aging cohort, sequencing multiple samples that were collected across multiple time points. The University of Kentucky (UK) Alzheimer's Disease Research Center clinical cohort comprises a continuously replenished group of approximately 800 participants followed longitudinally. We selected 12 participants for a pilot study using the following criteria: each individual had 3 blood draws, and a minimum of 2 years between draws. WGS for these samples was performed at the Genomics Core Laboratory at UK. For all participants the age at first blood draw ≤ 89 years (median age: 80.5, range: 66-89), age at last blood draw ≤ 95 (median age: 87, range: 80 - 95). The time in years between first and last blood draw ranged from 6 to 12 years. 75% of participants were female and 25% were male. The mean average coverage was 54.4X. Alignment and variant calling were performed using the Illumina DRAGEN Somatic pipeline. Post pipeline filtering steps include filtering out variants in low complexity and blacklisted regions and removal of putative germline variants. Using stringent quality control metrics, 3/12 (25%) individuals had CHIP in one of the 74 canonical CHIP genes. Of these participants, 2 had DNMT3A CHIP. One participant had DNMT3A CHIP at age 87 (last blood draw), but not at age 80 or 83. For the other participant with DNMT3A CHIP, the mutation was present in all 3 blood draws from age 68, 77, and 80 years and with mutant allele fraction (MAF) ranging between 10-16%. TET2 CHIP was detected in one participant at age 90 (MAF 10%) and 95 (MAF 15%), but not at age 84. Our observations support previous studies showing that CHIP is common in later life. This pilot study provides an opportunity to conduct more in-depth investigations of clonal dynamics in later life and expand these investigations to non-canonical CH driver mutations and mosaic chromosomal alterations. We are pursuing this opportunity and leveraging the longitudinal study design to develop novel approaches for distinguishing germline and somatic variants to improve methods for CHIP mutation calling.

#1512 Enhanced detection of immune and oncogenic signals in HER2-positive breast cancer by a novel data-scaling method.

Chole Gunadi[1], Emily Xue[1], Amy Lei[1], Cindy Hu[2], Qian Wang[1]

[1]iLab Research Institute, Mountain View, CA,[2]

Background: HER2-positive breast cancer, a clinically aggressive subtype accounting for 15-20% of all cases, is characterized by ERBB2 gene amplification and overexpression of the HER2receptor, which drives oncogenic signaling through PI3K/AKT/mTOR and MAPK/ERKpathways. Accurate transcriptomic profiling of tumor tissue versus normal adjacent tissue (NAT)is key to discovering these distinct mechanisms and guiding therapy strategies. However,traditional differential expression (DE) workflows often suffer from data distortions due tooutlier, high-read samples, and normalization limitations, likely obscuring biologically relevantdifferences.
Methods: This study reanalyzed bulk RNA-seq data from HER2-positive breast cancer patients(GSE292823) to compare traditional DE analysis with a novel scaling-based preprocessingmethod.
Results: The scaled data method significantly improved sample clustering in PCA and enhanceddetection of differentially expressed genes, including CCL5, which is associated with resistanceto trastuzumab. Upregulation of IL18, CD86, and NOD2 indicated inflammatory signaling,antigen presentation pathways, and immune cell recruitment, all key factors that can help tumorcells in evading an immune response. Furthermore, several other immune-regulated genes weredownregulated, including CD3G and GZMA, suggesting the suppression and reduced efficiencyof cytotoxic T-cell activity. The downregulation of SATB-AS1, PICSAR and ROR1-AS1,known to be associated with altered chromatin remodeling and long non-coding RNA-mediatedregulation in lung cancers and other types, pointed to similar regulatory mechanisms in HER2-positive breast cancer. These findings demonstrate the value of the novel preprocessing methodin uncovering both activated and suppressed gene networks that shape the tumormicroenvironment and immune response in HER2+ breast cancer. Additionally, Gene ontology(GO) enrichment analysis revealed that the preprocessing method enhanced the detection ofbiologically relevant pathways compared to the original approach. While the traditional methodidentified general immune-related pathways such as leukocyte adhesion and T cell suppression,the new method uncovered several specific immune functions, including regulation of immuneeffector processes, immunological synapse formation, and further downregulation of the T cellreceptor complex activity. Moreover, the new method captured upregulation of vesicle-mediatedsignaling and granule-associated components, suggesting heightened immune cell-tumorengagement.
Conclusion: The scaled preprocessing improves the detection of gene expression differences andsignificant pathways, thereby allowing for a more comprehensive view of tumor-immuneinteractions in HER2-positive breast cancer.

#1513 Gene signatures and infiltration patterns of mast cells in breast cancer revealed by integrated bulk and single-cell RNA sequencing Analyses.

Eva Liu, Benjamin Jin, Cindy Hu, **Qian Wang**

iLab Research Institute, Mountain View, CA

Background: Breast cancer is one of the leading cancers in women, caused by uncontrolledcell growth in breast tissue. Mast cells, a type of immune cell generally responsible forinflammation and allergic reactions, have emerged as key immune players within the tumormicroenvironment. However, the functions of these cells in breast cancer remain incompletelyunderstood and sometimes controversial. This study investigated mast cell infiltration and geneexpression profiles across three breast cancer subtypes by using integrated bulk and single-cellRNA-seq analyses.
Methods: Publicly available transcriptomic datasets GSE45419, GSE254991 were downloadedfrom NCBI and reanalyzed with standard pipelines. Differentially expressed genes (DEGs) wereidentified with |logFC| > 0.2 and FDR < 0.05. UMAPs and Heatmaps were generated tovisualize the data. Gene Ontology (GO) enrichment analysis was subsequently performed toidentify significantly enriched biological pathways.
Results: Bulk RNA-seq data analysis of GSE45419 revealed significant upregulations of mastcell marker genes (KIT, FCER1A, MS4A2, CPA3, HDC and TPSAB1) in ER+, HER2+, TN+(triple negative) breast cancers compared with benign breast lesions (Figure 1). Expressions ofthese genes were the highest in ER+, intermediate in HER2+, lower in TN+, and minimal inbenign breast lesions. Reanalysis of single-cell RNA-seq dataset GSE254991 identified 13clusters of cells in both cancer and adjacent tissues, including a distinct mast cell clusterexpressing canonical markers (KIT, FCER1A, MS4A2, CPA3, HDC and TPSAB1). Theproportion of mast cells is higher in tumor tissue (4.59%) than in paired normal breast tissue(2.89%) from the same patient. Cross-comparison of mast cell gene expression profilesbetween cancerous and adjacent regions identified the core DEGs enriched in mast cellsassociated with breast cancer. GO analysis indicated the significantly up-regulated pathways inbreast cancer including antigen processing and presentation of peptide antigen, antigen binding,MHC Class I and II protein complex assembly, leukocyte mediated immunity and cell-celladhesion, response to type II interferon.
Conclusion: Integrated bulk and single-cell transcriptomic data analysis revealed increasedmast cell infiltration and distinct transcriptional reprogramming in three subtypes of breastcancer. These findings provide new insights into potential immunoregulatory roles of mast cellsin tumor progression and may inform the development of novel therapies targeting mast cells tofight for breast cancer.

#1514 Mapping classifiability in the cancer DNA methylome: A data-learned disease hierarchy.

Hao Xu, Jenny Z. Li, Wanding Zhou

Center for Computational and Genomic Medicine, The Children's Hospital of Philadelphia, Philadelphia, PA

DNA methylation-based tumor classification has been successfully applied in clinical settings. Traditional classifiers assume that diagnostic labels are fixed and mutually exclusive, yet many biological entities are inconsistently defined or intrinsically overlapping. We propose a general framework for quantifying and interpreting classifiability in DNA methylation–based disease classification. Here, we treat classifiability itself as an empirical property of data, measured through cross-validation across more than 13,698 harmonized methylome cohorts drawn from TCGA and GEO, spanning over 324 cancer types. This approach reveals which disease or cancer types are stably separable at the molecular level and which collapse across labels, providing a principled, data-driven view of biological boundaries. By analyzing cross-validation consistency and label confusability, we reconstruct a hierarchical taxonomy derived directly from the methylome, in which relationships between entities emerge without prior human definitions, recapitulating known lineage relationships and uncovering novel cross-entity proximities. We further integrate major public datasets into a pan-disease foundation classifier that reports both predictions and classifiability-aware confidence scores, reflecting separability along the learned hierarchy. Finally, we demonstrate that the same framework can evaluate new or rare cohorts, testing whether a proposed entity forms a distinct, classifiable unit or merges with established types. Together, these advances recast methylation classification from a task of prediction into one of discovering the structure of classifiability itself in the human epigenome, offering a data-driven foundation for refining tumor taxonomies and diagnostic criteria.

#1515 Doublet removal enhances single-cell resolution and uncovers malignant transcriptional programs in NSCLC.

Benjamin Jin, Eva Liu, Amy Lei, **Qian Wang**

iLab Research Institute, Mountain View, CA

Background: Non-small cell lung cancer (NSCLC), accounting for more than 85% of lung cancer cases. includes several subtypes such as adenocarcinoma, squamous cell carcinoma, and large cell carcinoma. Advances in single-cell RNA sequencing (scRNA-seq) have enabled high-resolution profiling of the NSCLC tumor microenvironment, revealed previously unrecognized cellular heterogeneity, and identified potential therapeutic targets, including immune checkpoint inhibitor (ICI) pathways. However, doublets (artificially merged profiles of two cells captured in one droplet) can distort downstream analysis by altering clustering and differential gene expression, ultimately confounding biological interpretation.
Objective: This study evaluated a refined scRNA-seq workflow that incorporates doublet removal to improve cell-type identification and downstream biological insights.
Methods: Public scRNA-seq dataset GSE198099 was downloaded from NCBI and reanalyzed using both routine pipelines and a refined workflow that incorporates the DoubletCatcher algorithm. DoubletCatcher generates artificial doublets, computes doublet scores based on neighbor relationships, and removes cells exceeding the defined threshold. Differentially expressed genes (DEGs) were identified using R-based pipelines (FDR < 0.01; $|\log_2 FC| > 0.2$). Gene Ontology enrichment was performed to identify enriched pathways. UMAPs and heatmaps were generated for visualization.
Results: Routine analysis produced 17 poorly resolved clusters, while the refined workflow yielded 14 well-defined clusters, while eliminating spurious overlaps in immune signatures. Clear cell identities were recovered, including $CD4^+$ T cells, $CD8^+$ T cells, B cells, plasmablasts, macrophages, monocytes, mast cells, endothelial cells, type II epithelial cells, and three distinct cancer cell clusters comprising cancer cells and stem-like cancer cells. DEG analysis revealed significant transcriptional differences of cancer cells and stem-like cancer cells in tumor tissues compared with adjacent Tumor-region cancer cells exhibited de-differentiation, hypoxia-driven metabolic reprogramming, inflammatory and immune-evasive signaling, proliferation and cell-cycle activation, and epithelial-mesenchymal transition (EMT). In contrast, cancer cells from adjacent tissues showed more differentiated states, suggesting potentially greater therapeutic responsiveness before surgical intervention.
Conclusion: Removing doublets markedly improved cluster accuracy and biological interpretability, revealed distinct cancer cell, stem-like cancer cell, and immune cell populations, and uncovered key active malignant programs in tumor-region cancer cells. This refined method enhances the reliability of single-cell analysis and provides further insights into NSCLC tumor biology.

: CAR T Cell Targets and TME Reprogramming
Poster Session

#1519 AI-designed immune sensor-enhanced CAR-T cells for potent solid tumor immunotherapy.

Zoya Alteber, Jitka Sagiv, Reut Nave, Gil Friedman, Dor Shimon, Maayan Shamsian, Megi Cemel David, Dina Listov, Sharon Avkin Nachum, Ofer Levy, Michal Golan Mashiach

Edity Therapeutics, Rehovot, Israel

Immune-based therapies have revolutionized cancer treatment; however, their efficacy in solid tumors remains limited. This is primarily due to the immunosuppressive tumor microenvironment (TME) and insufficient induction of systemic anti-tumor immunity. To overcome these barriers, Edity Therapeutics has developed an AI-guided platform that integrates engineered innate immune sensors into CAR-T cells. These sensors are designed to initiate a localized antiviral-like immune response upon antigen engagement. Immune sensors derived from the STING and MAVS pathways were computationally optimized to generate constitutively active, yet controllable, derivatives that drive Type I interferon and pro-inflammatory cytokine production. These sensor modules were fused to a navigator domain, ensuring their activation is exclusively upon CAR signaling, thereby confining immune stimulation to the tumor site. Hundreds of sensor variants were designed and screened *in vitro* for functional potency. Lead candidates exhibiting strong immuno-stimulatory activity were incorporated into CAR-T constructs and evaluated in SCID-Beige xenograft models. In these models, sensor-enhanced CAR-T cells demonstrated significantly superior tumor control compared to conventional CAR-T counterparts. By locally provoking inflammation, this approach will convert the immune-cold TME into an inflamed tumor milieu, potentially enabling robust anti-tumor responses without inducing peripheral adverse effects. The platform is currently being advanced toward clinical development, with two solid tumor indications selected based on antigen expression, tumor accessibility, and translational readiness. These next-generation CAR-T products represent a new class of cell therapies that couple precise tumor targeting with controlled autonomous immune activation, offering a transformative approach for the treatment of solid malignancies while improving the therapeutic index.

#1520 Improving BCMA-targeted CAR-T cell therapy of myeloma using TGF-β resistance and inducible production of IL-18.

Sandhya Rai[1], Shijing Wang[1], Bin Sun[1], Tyce Kearl[1], Peiman Hematti[1], Joseph Zenga[2], Heather Himburg[3], Musaddiq Awan[3], Deepak Parashar[1], Binod Dhakal[1], Siegfried Janz[1], Fumou Sun[1]

[1]Department of Medicine, Medical College of Wisconsin, Milwaukee, WI,[2]Department of Otolaryngology, Medical College of Wisconsin, Milwaukee, WI,[3]Department of Radiation Oncology, Medical College of Wisconsin, Milwaukee, WI

Background: Although immunotherapy with B cell maturation antigen (BCMA)-targeted chimeric antigen receptor (CAR) T cells, or BCMA CARTs for short, has yielded unprecedented treatment responses in patients with relapsed and/or refractory multiple myeloma (RRMM), efficacy is limited by lack of durability in most cases. This has been attributed, in large part, to the immunosuppressive bone marrow environment (BME) of RRMM, leading to inactivation, exhaustion and attrition of BCMA CARTs. Next-generation CARTs, capable of overcoming BME-dependent inhibitory constraints, may lead to more durable treatment options for RRMM.
Methods: To inform the design of BCMA CARTs that can maintain long-term activity in the myeloma-laden bone marrow, we leveraged a recently published single-cell RNA sequencing dataset, GSE210079, of the BME from 9 patients with RRMM. Based on clinical outcomes, patients were stratified into early relapse (<3 months) and late relapse (>12 months) groups. Biocomputational analyses revealed that activation of TGF-β signaling and T cell exhaustion pathways, along with suppression of IL-18-driven immune responses, were implicated in the mechanisms driving early-relapse post-BCMA CAR-T treatment. Inspired by these findings, we employed standard molecular biology tools to manufacture BCMA CARTs that feature both TGF-β resistance and simultaneously disrupt PD-1 expression and enabling inducible IL-18 secretion.
Result: Compared to T cells from late-relapse myeloma, T cells from early-relapse myeloma demonstrated upregulated oncogenic signaling circuits (p53, FoxO, AMPK), elevated expression of exhaustion-related genes (*PDCD1*, *HAVCR2*, *LAG3*, *CTLA4, TIGIT; p* < 0.01), and increased mRNA levels of key TGF-β pathway genes (*TGFB1*, *SMAD2/3/4*, *TGFBR2*). Early-relapse myeloma exhibits reduced TCR signaling and Th1/Th2 differentiation, which are regulated by IL-18. BCMA CARTs were rendered resistant to TGF-β by enforced expression of a dominant-negative ligand-binding but non-signaling transforming growth factor beta receptor 2 (dnTFGBR2). Monoallelic “knock-in” of an IL-18 encoding gene in the *PDCD1* locus relied on CRISPR/Cas9-mediated editing. The genetically modified BCMA CAR-T cells demonstrated potent cytotoxic activity against myeloma cells in vitro, increased resistance to TGF-β-mediated suppression, and inducible secretion of IL-18 driven by the endogenous *PDCD1* promoter. IL-18 levels increased in correlation with T cell activation, accompanied by a concomitant silencing of PD-1 expression.
Conclusion: TGF-β-resistant BCMA CARTs that produce IL-18 when the cells are challenged by exhaustion in the BME, and thus disrupt PD-1, may be viable way forward to a more potent and durable therapy for patients with RRMM than available today. This hypothesis will be evaluated in greater depth in preclinical in vivo studies ongoing in our laboratory.

#1521 Concurrent targeting of tumors and their microenvironment using CAR-T cells specific for fibroblast activation protein alpha.

Larina Tzu-Wei Shen[1], Afsana Islam[1], Daiki Fujita[1], Kenji Nakamaru[1], Dan Macleod[2]

[1]Optieum Biotechnologies Inc., Toon City, Japan,[2]Optieum Biotechnologies America Inc., Dover, DE

Chimeric antigen receptor T (CAR-T) cell therapy for solid tumors is challenged by the immunosuppressive tumor microenvironment (TME) and physical barriers formed by Fibroblast Activation Protein alpha (FAPα)-expressing cancer-associated fibroblasts (CAFs). Furthermore, high-affinity CAR-T cells often induce trogocytosis and T cell exhaustion, leading to target antigen loss and limiting persistence. We sought to develop FAPα CAR-T cells with optimized binding affinity to overcome these obstacles.

We generated FAPα CAR-T cells (CD28/CD3ζ) by shuffling new light chains fused to the heavy chain of the parental clone of FAPα CAR using a high-throughput scFv library T-cell system (Eumbody System). We identified 3 new clones using this method, FL1, FL8 and FL12, exhibiting slightly lower structural avidity compared to the parental clone. We investigated their function in vitro and in vivo using glioblastoma cell lines.

Unlike the parental clone FAPα-CAR-T, the optimized FL1, FL8 and FL12 clones preserved FAPα expression on target cells, demonstrating successful mitigation of trogocytosis, which was inversely correlated with structural avidity. In in vitro cytotoxicity assays, FL12 CAR-T cells showed superior real-time killing against FAPa-positive U87 cells and better suppression of U87 spheroid growth, while exhibiting a less exhausted T-cell phenotype. In vivo, FL12 CAR-T cells effectively suppressed U87 tumor growth in a subcutaneous xenograft model, with statistically significant improvements compared to both conventional scFv-CAR-T cells and negative control T cells even at low cell doses. To further evaluate their efficacy, FL12 CAR-T cells are currently being tested in in vitro cytotoxicity assays using 3D mixed tumor spheroid (U87 or U251 plus CAFs). This work is designed to confirm their ability to be highly cytotoxic against FAPα-positive CAFs, successfully migrate into mixed tumor spheroids, and achieve a significant reduction in tumor size when compared with conventional scFv-CAR-T cells and tumor-only spheroids.

In conclusion, scFv-optimization successfully generated FAPα CAR-T cells that mitigate trogocytosis and exhibit superior phenotype, persistence, and anti-tumor efficacy. This strategy allows for concurrent targeting of solid tumor cells and the CAF-rich microenvironment, representing a promising and readily translatable approach for refractory solid malignancies.

#1522 FMNL1 overexpression enhances tumor-specific TIL and CAR-T cell accumulation and therapeutic efficacy in solid tumors.

Jeffrey W. Chung, Jessica Olivas-Corral, Ashley M. Wood, Ashton L. Sigler, Edward Ning, Michelle E. Allen, Kayla Fairweather, **Jordan Jacobelli**

Immunology & Microbiology, The University of Colorado School of Medicine, Aurora, CO

Purpose: Adoptive T cell therapies such as tumor-infiltrating lymphocytes (TIL) and chimeric antigen receptor (CAR)-T cells show limited efficacy against solid tumors. This is due in part to physical barriers in solid tumors, including abnormal vasculature and dense extracellular matrix, which limit T cell infiltration and persistence within restrictive tumor microenvironments. We investigated whether overexpression of Formin-like-1 (FMNL1), a cytoskeletal regulator of T cell migration, could overcome these physical barriers and improve T cell accumulation and therapeutic activity in solid tumors.

Methods: We engineered tumor-specific TILs and CAR-T cells to overexpress FMNL1 using a bioengineering platform. We first assessed control and FMNL1-overexpressing T cell activation, cytotoxicity, and restimulation in vitro. Then using murine tumor models, we evaluated tumor infiltration and therapeutic efficacy of adoptively transferred control and FMNL1-overexpressing TILs and CAR-T cells in melanoma and lung carcinoma models.

Results: FMNL1-overexpressing T cells maintained normal activation and tumor cell killing compared to control T cells. In vivo, FMNL1 overexpression significantly increased TIL and CAR-T cell accumulation at melanoma and lung carcinoma solid tumor sites compared to controls. Importantly, adoptive transfer of FMNL1-overexpressing CAR-T cells prolonged survival in melanoma tumor-bearing mice relative to control CAR-T cells, in both immunodeficient and immunocompetent recipient mice.

Conclusions: This is the first demonstration that enhancing cytoskeletal dynamics via FMNL1 overexpression increases T cell accumulation in solid tumors and improves therapeutic efficacy. These findings highlight a novel, tumor antigen and CAR construct independent strategy to overcome physical barriers in the tumor microenvironment and suggest translational potential for improving CAR-T cell therapy in patients with solid tumors.

#1523 Galectin-3 blockade reprograms the tumor microenvironment and improves CAR T-cell therapy in pediatric cancers.

Enrique Conde-Gallastegi[1], Karin Straathof[2], Sergio Quezada[3]

[1]University College London (UCL) Cancer Institute, London, United Kingdom,[2]UCL Great Ormond Street Institute of Child Health, London, United Kingdom,[3]University College London (UCL) Cancer Institute, Berkhamsted, United Kingdom

CAR T-cell therapies have revolutionized the treatment of hematological malignancies, yet their efficacy in solid tumors remains limited. Pediatric solid tumors are particularly challenging due to their low mutational burden, scarce T-cell infiltration, and highly immunosuppressive tumor microenvironment (TME). Although CAR T cells can induce initial responses, sustaining durable activity is difficult.

To identify mechanisms that could be targeted to enhance CAR T-cell function, we performed scRNA-seq analysis of nearly 100 pediatric tumor samples and characterized the T-cell and myeloid compartments. We found that Galectin-3 (Gal3), an immunosuppressive and protumorigenic molecule, was predominantly expressed by myeloid cells and strongly associated with an M2-like macrophage phenotype. Gal3 expression inversely correlated with overall T-cell infiltration and, more specifically, with the proportion of reactive-like T cells. Spatial imaging confirmed Gal3 protein expression in the TME and showed colocalization with immunosuppressive myeloid of T cell markers

Based on these findings, we hypothesized that Gal3 inhibition could synergize with CAR T-cell activity by alleviating myeloid-driven immunosuppression. To deliver Gal3 inhibition directly within the TME, we engineered an “armed” CAR T cell that secretes a protein-based Gal3 inhibitor. Functional characterization is ongoing, and in vivo evaluation in pediatric tumor mouse models is currently in progress.

Our results identify Gal3 as a key barrier to T-cell infiltration and activation in pediatric tumors and provide a strong rationale for combining CAR T-cell therapy with targeted Gal3 inhibition. This engineered CAR T-cell platform represents a promising strategy to enhance therapeutic efficacy in pediatric solid tumors.

#1524 Collagen-binding IL-12-armored STEAP1 CAR-T cells for advanced prostate cancer.

Koichi Sasaki[1], Vipul Bhatia[2], Yuta Asano[3], Jakob Bakhtiari[3], Pooja Kaur[1], Chuyi Wang[1], Takumi Matsuo[1], Olivier Dubois[1], Po-Chuan Chiu[1], Donny Gun[4], Charanjit Singh[1], Ioanna Panagi[1], Laurine Noblecourt[1], Maria Nikolaidi[1], Truman Chong[2], Gerardo Javier[2], Saul J. Priceman[5], Aude G. Chapuis[3], John K. Lee[2], Jun Ishihara[1]

[1]Bioengineering, Imperial College London, London, United Kingdom,[2]Medicine, UCLA, Los Angeles, CA,[3]Translational Science and Therapeutics Division, Fred Hutchinson Cancer Center, Seattle, WA,[4]Microbiology, Immunology and Molecular Genetics, UCLA, Los Angeles, CA,[5]Keck School of Medicine, University of Southern California, Los Angeles, CA

Metastatic castration-resistant prostate cancer (mCRPC) remains an incurable and immunologically cold solid malignancy. Six-transmembrane epithelial antigen of the prostate 1 (STEAP1) is highly expressed in over 85% of mCRPC tumors and represents an attractive therapeutic target. Although chimeric antigen receptor (CAR)-T cell therapy has revolutionized the treatment of hematologic cancers, its efficacy in solid tumors, including prostate cancer, has been limited by the immunosuppressive tumor microenvironment (TME) and heterogeneous antigen expression. Interleukin-12 (IL-12) has the potential to overcome these barriers by activating and recruiting immune cells into tumors and promoting epitope spreading to counter antigen heterogeneity. While armored CAR-T cells engineered to produce IL-12 have been developed, further refinement is needed to optimize both potency and safety. Autologous IL-12-producing T cell therapy has previously shown clinical activity in melanoma, but systemic toxicity constrained its use, indicating that IL-12 secreted by CAR-T cells, though locally produced, can still diffuse into circulation. Here, we present STEAP1-directed CAR-T cells engineered to conditionally secrete a collagen-binding domain-IL-12 fusion protein (CBD-IL-12) upon antigen engagement. We demonstrate that fusing IL-12 to a CBD markedly enhances its retention within prostate tumors while limiting systemic spread in mice. As a result, intra-tumoral levels of IFN-γ, CXCL9, and GM-CSF remained comparably high to those induced by IL-12, yet without associated elevations in serum alanine aminotransferase (ALT) or off-target T cell infiltration in healthy organs. Flow cytometry revealed increased infiltration of T cells, NK cells, and cross-presenting dendritic cells, together with reduced monocytic myeloid-derived suppressor cells, following treatment with CBD-IL-12-expressing STEAP1 CAR-T cells. Immunohistochemistry and spatial transcriptomic analysis confirmed increased immune infiltrates and activation of IL-12 pathway and antigen processing and presentation by major histocompatibility complex-I in the CBD-IL-12 CAR-T treated tumor. Further, tertiary lymphoid structure-related chemokine and chemokine receptors including cxcr4, cxcr5, cxcl12 and cxcl13 as well as co-stimulatory molecules such as cd80, cd86, cd40 and tnfsf4 were upregulated in the tumor. When combined with anti-PD-1 and anti-CTLA-4 antibodies, CBD-IL-12 armored CAR-T cells eradicated established prostate tumors in mice without preconditioning. The CAR-T therapy generated durable anti-tumor immune memory to STEAP1 and other antigens. Our findings suggest that CBD fusion can localize potent but toxic immunomodulators such as IL-12 to the tumor site, offering a promising strategy to improve the safety and effectiveness of CAR-T therapies for solid tumors.

#1525 Optimized CART cell therapy to remodel the tumor microenvironment and eliminate GI malignancies.

Omar L. Gutierrez Ruiz[1], Jennifer Feigin[2], Brooke Kimball[2], R. Leo Sakemura[2], Elizabeth L. Siegler[2], Dominic A. Skeele[2], Ateka Saleh[3], Claudia Manriquez Roman[4], Ismail Can[2], Olivia Sirpilla[2], Kun Yun[2], Carli M. Stewart[2], Mehrdad Hefazi[2], Yoh Yamaguchi[1], Lionel Aurelien Kankeu Fonkoua[5], Long K. Mai[2], Truc Huynh[2], Sophia Y. Goldberg[2], Grace E. DeFranco[2], Sara Foote[6], Ekene Johnkennedy Newton Ogbodo[2], Hong Xia[2], Michael Redig[7], Matthew L. Matthew[8], Tamiel Nichole Turley[2], Skyeler Klinge[8], John Alton Copland[9], Saad J. Kenderian[2]

[1]Hematology, Mayo Clinic, Rochester, MN,[2]Mayo Clinic, Rochester, MN,[3]Molecular Pharmacology and Experimental Therapeutics, Mayo Clinic, Rochester, MN,[4]Mayo Clinic College of Medicine and Science, Rochester, MN,[5]Mayo Clinic Cancer Center Minnesota, Rochester, MN,[6]Immunology, Mayo Clinic, Rochester, MN,[7]Cancer Biology, Mayo Clinic, Rochester, FL,[8]Mayo Clinic, Jacksonville, FL,[9]Assistant Professor, Mayo Clinic Florida, Jacksonville, FL

Gastrointestinal (GI) cancers are rising in people < 50 and remain major causes of cancer mortality despite therapeutic advances. Chimeric antigen receptor T (CART) cell therapy has transformed treatment of hematological cancers. However, its efficacy in GI cancers has been hindered by antigen heterogeneity and immunosuppressive cancer associated fibroblasts (CAFs) in the tumor microenvironment (TME.) Here we aimed to 1) study CART-CAF interactions and 2) engineer CART cells capable of eliminating CAFs to overcome their inhibitory role and enhance their antitumor activity in GI cancers.

We first analyzed primary CAFs from 20 GI cancer patients. CAFs showed high fibroblast activation protein (FAP) expression and significantly suppressed T cells proliferation (26-77%, $p \leq 0.0001$). We next generated CART cells capable of safely eliminating both GI cancer cells and CAFs. To target cancer cells, we developed a novel nanobody (VHH)-based CAR against Claudin18.2, a GI cancer specific target. To avoid off-tumor toxicity in healthy FAP+ tissues, we incorporated an inducible FAP-CAR using the synNotch platform, enabling conditional targeting upon engagement with Claudin18.2$^+$ cells, restricting FAP targeting within the TME.

VHH Claudin18.2 CART cells showed superior specificity and efficacy vs scFv-based CART cells (hu8E85 or zolbetuximab). In Claudin18.2+ SNU-C2B xenografts, tumors were 92mm^3 (VHH) vs 48mm^3 (huE85) vs 211mm^3 (zolbetuximab) on day 23 post-CART, median survival undefined vs 17 days vs 23 days respectively; p=0005. In Claudin18.2+ LS411N xenografts, tumors were 315mm^3 vs 106mm^3 vs 382 mm^3 respectively at 23 days post-CART, median survival undefined vs 19 days vs undefined respectively; p=0004. VHH Claudin18.2 CART cells showed no off-tumor effects, while hu8E85 CART induced significant toxicity.

We next established a co-engraftment model. NSG mice received 1x10^6 SNU-C2B and 6x10^6 CAFs from a GI cancer patient. At 500 mm^3 tumors, mice received 5x10^6 VHH Claudin18.2 or inducible Claudin18.2/FAP CART. Dual-targeting CART cells showed greater antitumor response (728mm^3 vs 320mm^3, p=0.0011 at day 20 post-CART), expansion (61 vs 2,350 CART/µl of blood, p=0.0037), and tumor infiltration (8.71 x 10^5 vs 1.03 x 10^6 CART/g of tumor, p<0.0001). This was also observed in gastric, colon, and pancreatic PDX models, with no observable off-tumor cytotoxic effects with inducible dual-targeting Claudin18.2/FAP CART.

Our findings demonstrate that our novel VHH-based Claudin18.2 CART cells are highly specific and effective against GI malignancies, and that inducible Claudin18.2/FAP dual-targeting CART cells safely remodel the TME into an immune-permissive state. This approach represents a mechanistically innovative and translationally relevant strategy to overcome CAF-mediated immunosuppression, enhance CART cell efficacy, and improve clinical outcomes in refractory solid tumors.

#1526 Nanobody-based, DLL3-directed FAST-CAR T-cell therapy for small cell lung cancer (SCLC).

Qi Dong[1], Wenjie Yin[1], Xiangling Dai[1], Tao Wang[1], Guangyao Zhu[1], Manli Yin[1], Yu Zou[1], Yu Yang[1], Di Wu[1], Mark Cobbold[2], Lianjun Shen[1]

[1]Gracell Biotechnologies Co. Ltd., A Member of the AstraZeneca Group, Shanghai, China,[2]AstraZeneca, Gaithersburg, MD

Introduction: Small-cell lung cancer (SCLC) is aggressive with poor prognosis, and current immunotherapies have limited efficacy. Delta-like ligand 3 (DLL3), expressed in ~80% of SCLC with restricted normal-tissue expression, is a promising CAR T target. We developed nanobody-based, autologous DLL3 CAR T cells armed with a dominant-negative TGFβ receptor II (DNR) to resist TGFβ-driven immunosuppression and enhance antitumor activity.

Methods: Candidate DLL3 binders were derived from a camelid-immunized phage display library and engineered into second-generation CARs. Constructs were tested in vitro for specific lysis with target cell lines. Lead binders were screened for cross-reactivity against Notch ligands. The DLL3 epitope was mapped, and membrane-proximal binders targeting EGF3-6 were prioritized. Off-target interactions were assessed using a membrane proteome array. Multiple CARs—with varying binders/biparatopic combinations, co-stimulation domains, and hinges—were compared in short-term and repeated antigen-stimulation assays across cells with varying DLL3 levels in vitro. Lead CAR T cells with or without DNR were compared in vitro and in vivo. Top constructs advanced to testing in multiple CDX and PDX models to evaluate antitumor efficacy and safety. Manufacturing was compared between a 3-day FasTCAR and an 8-day conventional process.

Results: Three VHH binders demonstrated high DLL3 specificity, with no cross-reactivity to Notch family ligands and no off-target binding, and similar affinity for mouse DLL3. The lead biparatopic CAR construct, B2, demonstrated superior cytotoxicity and durability in short-term and repeated antigen-stimulation assays. When armored with DNR, B2-DNR CAR T cells showed augmented persistence versus the unarmored counterparts. In vivo safety assessments showed no body-weight loss in CAR T-treated mice across multiple dose levels, suggesting a wide therapeutic index. T cells were present in the mouse pituitary pars intermedia, where DLL3-positive cells are enriched, but their DLL3 expression was largely intracellular rather than on the cell surface. B2 did not show on-target, off-tumor toxicity. B2-DNR CAR T cells rapidly cleared established tumor xenografts with high and low DLL3 expression in immunodeficient mice, correlating with robust intratumoral CD3+ T-cell infiltration. In a TGFβ-rich PDX model, B2-DNR CAR T cells outperformed the unarmored counterpart, supporting the functional benefit of DNR. The 3-day FasTCAR manufacturing process demonstrated greater efficacy and durability than the 8-day process.

Conclusions: The camelid nanobody-derived, DLL3-targeted CAR T-cell therapy manufactured by a 3-day FasTCAR process demonstrates the potential to elicit deep and durable antitumor responses with a favorable safety profile. Preclinical data for the lead candidate, B2-DNR, support further clinical development for the treatment of SCLC.

#1527 Conformal external beam radiation increases B7-H3 expression in a murine model of pancreatic cancer liver metastases and promotes CAR T cell function.

Megan C. Purl[1], Alexandria Shick[1], Annaiz Grimm[1], Hind Abdallat[1], Cyrus J. Sholevar[1], Makan Karimzadeh[1], Natalie M. Liu[1], Jinhwan Kim[2], Cameron E. Gaskill[1], Edward J. Kim[3], Arta M. Monjazeb[4], William J. Murphy[5], Robert J. Canter[1], Sean J. Judge[1]

[1]Department of Surgery, UC Davis Medical Center, Sacramento, CA,[2]Department of Surgery and Biomedical Engineering, UC Davis Medical Center, Sacramento, CA,[3]Department of Internal Medicine, UC Davis Medical Center, Sacramento, CA,[4]Department of Radiation Oncology, UC Davis Medical Center, Sacramento, CA,[5]Department of Dermatology, UC Davis Medical Center, Sacramento, CA

Background: Pancreatic ductal adenocarcinoma (PDAC) is a lethal disease characterized by early liver metastases. Chimeric antigen receptor (CAR) modified cells (T and NK) have been largely unsuccessful in PDAC and other solid tumors, despite success in hematologic malignancies. Limitations to CAR therapy success in solid tumors include trafficking, engraftment, and antigen loss. Liver-directed radiation (RT) may improve CAR therapy through altering the tumor and tumor microenvironment. We investigated the impact of liver-directed radiation therapy (RT) to augment B7-H3 CAR T cell homing and function in a xenogeneic model of PDAC liver metastases.

Methods: We evaluated dose-dependent expression of B7-H3 and NKG2D activating ligands by flow cytometry in human PANC-1 and AsPC-1 cells *in vitro* and *in vivo* after RT, including a liver-only metastatic model using a hemi-spleen implantation technique to seed the liver. B7-H3 CAR T cells were generated and assessed by flow cytometry. B7-H3 CAR T cells were then co-cultured with RT-treated target cells, and cytotoxicity was analyzed using Incucyte live cell imaging.

Results: Following RT *in vitro*, PANC-1 and AsPC-1 cells exhibited significant increase in expression of both B7-H3 and NKG2D ligands MICA/B by either median fluorescent intensity or percent expression. Liver-directed RT led to significantly increased expression of B7-H3 and MICA/B on PANC-1 liver metastases compared to untreated mice. Percent killing by B7-H3 CAR T cells against PANC-1 and AsPC-1 cells was significantly increased when target cells were pre-treated with 4 Gy RT prior to killing assay.

Conclusions: RT increases the expression of both B7-H3 and the NKG2D ligands MICA/MICB on pancreas cancer cell lines and this is recapitulated *in vivo* following liver-directed RT to metastasis-bearing mice. Pre-treating target cells with RT results in greater B7-H3 CAR T cell killing *in vitro*. Liver-directed RT may be a strategy to better target PDAC liver metastases with CAR cell therapy.

#1528 AZD5851, a TGF-β-resistant GPC3 CAR-T cell product, prolongs animal survival times in patient derived orthotopic xenograft models of medulloblastoma and atypical teratoid rhabdoid tumor.

Milagros Suarez[1], Aalaa Abdallah[1], Xin Zhai[1], Zilu Huang[1], Yuchen Du[1], Nitin Wadhwani[2], Alicia Lenzen[1], Jee Young Kwon[3], Steven B. Neuhauser[3], Timothy Stearns[4], Jeffrey H. Chuang[3], Emily L. Jocoy[4], Carol J. Bult[4], Beverly Teicher[5], Malcolm A. Smith[6], Xiao Nan Li[7]

[1]Pediatrics, Northwestern University Feinberg School of Medicine, Chicago, IL,[2]Pathology, Northwestern University Feinberg School of Medicine, Chicago, IL,[3]The Jackson Laboratory for Genomic Medicine, Farmington, CT,[4]The Jackson Laboratory, Bar Harbor, ME,[5]Molecular Pharmacology Branch, National Cancer Institute, Bethesda, MD,[6]Clinical Investigations Branch, National Cancer Institute, Bethesda, MD,[7]Departments of Pediatrics, Northwestern University Feinberg School of Medicine, Chicago, IL

BACKGROUND: Glypican-3 (GPC3) is uniquely expressed and has been associated with the development of several pediatric solid embryonal tumors, making it a prime target for GPC3 CAR-T cell killing. TGF-β, a cytokine associated with immunosuppression, has also been shown to be highly expressed in the microenvironment of these tumors, potentially hindering CAR-T cell antitumor activity. In this study, we examined the therapeutic efficacy of AZD5851, an autologous CAR-T product that expresses a CAR specific for GPC3 and a dominant negative (dn)TGFβRII as an armoring strategy.

METHODOLOGY: To assess the drug's *in vivo* efficacy, 5 established patient-derived orthotopic xenograft (PDOX) models of pediatric medulloblastoma (ICb-2123MB, -1299MB, -S1129MB), atypical teratoid rhabdoid tumor (IC-L1115ATRT) and a high grade glioma (IC-2664HGG), with confirmed expression of GPC3 and TGF-β through immunohistochemical staining, were treated with untransduced T cells [dosed at $12x10^6$ cells/mouse, intravenously (IV) once] or GPC3 CAR-T cells (dosed at $5x10^6$ cells/mouse, IV once). 20 eight-week-old SCID mice per model received intra-cerebral (IC) or intra-cerebellar (ICb) tumor cell implantation and were divided into 2 treatment groups (n=10 per group): Untransduced T cells and GPC3 CAR-T cells. Animal survival times were analyzed using Gehan-Breslow-Wilcoxon analysis.

RESULTS: GPC3 CAR-T cell treatment was well tolerated in mice with no loss of body weight or other toxicities. GPC3 CAR-T cell treatment significantly improved the median survival time in 2/5 models, including ICb-2123MB from 90.5 days in the untransduced T cell group to 162.5 days (P=0.02) and IC-L1115ATRT from 136 days to 174 days (P=0.02).

CONCLUSION: Our data identifies single agent antitumor activity for GPC3 CAR-T cells for PDOX models of pediatric medulloblastoma and atypical teratoid rhabdoid tumor. The results support further clinical translational efforts involving the use of AZD5851 alone or in combination with other therapies for the treatment of these tumors.

#1529 ST6GAL1 enhanced CAR-T cells improve persistence and antitumor efficacy in DLBCL.

Lee Seng Mari Lau[1], Maria Suarez[1], Brandon Fernandez[1], Aiza Berdalinova[1], Joseph Souchack[1], Aristotelis Antonopoulos[2], Anne Dell[2], Stuart Haslam[2], Avery D. Posey[3], Charles J. Dimitroff[1]

[1]Cellular and Molecular Medicine, Herbert Wertheim College of Medicine (FIU), Miami, FL,[2]Department of Life Sciences, Imperial College London, London, United Kingdom,[3]University of Pennsylvania, Philadelphia, PA

Diffuse large B cell lymphoma (DLBCL) is the most common and aggressive B cell lymphoma, with poor outcomes for patients who relapse or are refractory to treatment. Chimeric antigen receptor (CAR)-T cell therapy offers a promising therapeutic option, yet limited persistence and functional impairment remain major barriers to durable responses. Galectin (Gal)-3, a carbohydrate-binding protein highly expressed in the DLBCL microenvironment, has been implicated in T cell dysfunction, but its role in CAR-T cell impairment has not been fully defined. We hypothesized that Gal-3 binds to CAR-T cell surface glycans, promoting apoptosis and loss of effector function. ELISA revealed significantly elevated Gal-3 levels in serum from DLBCL patients versus healthy controls ($p<0.001$). Flow cytometry confirmed strong Gal-3 binding to CAR-T cells, which correlated with increased apoptosis ($p<0.01$). To overcome this, we engineered CAR-T cells to overexpress the α2,6 sialyltransferase ST6GAL1 ($ST6^{OE}$)CAR-T cells, which adds α2,6-sialic acids known to mask Gal-3-binding glycans. $ST6^{OE}$CAR T cells displayed markedly reduced Gal-3 binding, lower apoptosis ($p<0.001$), and improved viability and cytotoxicity in Gal-3^{high} DLBCL co-cultures. Cytokine profiling further revealed that control CAR-T cells secreted elevated levels of interleukin-5 (IL-5),a Th2-associated cytokine linked to reduced antitumor activity. In contrast, $ST6^{OE}$ CAR-T cells exhibited significantly lower IL-5 production ($p<0.01$), indicating a shift toward amore cytotoxic, Th1-like functional profile. In a DLBCL xenograft model, $ST6^{OE}$ CAR-T treatment significantly reduced tumor burden and improved survival compared to control CAR-T cells ($p<0.001$). These findings demonstrate that ST6GAL1 overexpression mitigates apoptosis and IL-5-associated dysfunction, enhancing CAR-T cell persistence and antitumor efficacy. Glycoengineering CAR-T cells via ST6GAL1 provides a novel strategy to improve therapeutic outcomes for patients with DLBCL.

#1530 Comprehensive preclinical evaluation of CAR-T cell therapeutics in organoid-fibroblast co-cultures.

Yijie Ren, Tomas Veenendaal, Puxin Wang, Jiawen Gao, Jiawei Meng, Danting Yan, Yingying Li, Meng Zhang, Michelle Kop, Ashgard Weterings, Marten Hornsveld, Gera Goverse, Ludovic Bourre, Peng Wang, Jun Zhou

Crown Bioscience, Inc., San Diego, CA

Introduction: Preclinical assessment of CAR-T cell therapies requires models that recapitulate the complex tumor microenvironment (TME), but conventional 2D cultures fail to model stromal barriers. Patient-derived (xenograft) organoids (PDOs/PDXOs) offer superior clinical relevance, but analyzing 3D immune-tumor-stromal interactions is challenging with bulk assays like LDH release. High-Content Imaging (HCI) overcomes these limitations, enabling high-throughput, multi-parametric quantification of immune infiltration and cytotoxicity. We utilized an HCI-based organoid co-culture platform to evaluate CAR-T therapies in both standard and complex, fibroblast-containing TME models.

Methods: Organoids were co-cultured with PBMCs or engineered CAR-T cells in a 384-well format suitable for automation. HCI analysis allowed quantification of different cell populations and several key readouts, including organoid volume (via actin and DAPI staining), fibroblast network branching (via Cy5 staining) at 96h, and T-cell infiltration at 48h. For a head-to-head lead selection study, seven distinct Claudin18.2-targeting CAR-T candidates were screened against three pancreatic organoid models to comparatively assess their cytotoxic potential. To model a complex TME, ovarian model OV9522B was co-cultured with Normal Human Lung Fibroblasts (NHLF). Triple co-cultures were treated with Mesothelin (MSLN)-targeting CAR-T cells at various Effector-to-Target (E:T) ratios (20:1, 10:1, 5:1).

Results: Baseline Graft-versus-Tumor (GvT) effects were established by co-culturing PBMCs from four healthy donors with four organoid models (LU9906B, CR5082B, CR20155B, PA20077B) revealing variable donor- and model-dependent cytotoxicity (5%-20%). The platform enabled comparison and ranking of seven Claudin18.2-targeting CAR-T candidates against three models. This screen revealed a wide range of killing potency: the most potent CAR-T induced >80% volume reduction in the most sensitive pancreatic model, while the weakest CAR-T showed ~10% reduction in a poor responsive model. Finally, in the triple co-culture model, MSLN-targeting CAR-T cells induced potent, dose-dependent killing of OV9522B organoids (high *MSLN* expression). Despite a stromal network, a significant reduction (>90%) in organoid volume and visualized CAR-T engagement were observed, demonstrating fibroblasts did not affect cytotoxic activity in this case.

Conclusion: Integration of HCI with organoid co-cultures provides a comprehensive, scalable, and clinically relevant platform for evaluating cell therapies. Visualizing and quantifying key parameters like targeted killing in presence of stromal components is a critical advantage and enables confident ranking of therapeutic candidates and provides mechanistic insights, de-risking and accelerating clinical development for next-generation cell therapies.

#1531 Obesity exacerbates cytokine release syndrome (CRS) toxicity associated with chimeric antigen receptor (CAR) T cell therapy in preclinical models.

Wahed A. Firoz[1], Craig P. Collins[1], Logan V. Vick[1], Michael K. Sheng[1], Ryan N. Nielsen[1], Spencer Rosario[2], Robert J. Canter[1], Arta M. Monjazeb[1], Sean J. Judge[1], Anthony E. Zamora[1], Shuchi Gulati[1], William J. Murphy[1]

[1]UC Davis School of Medicine, Sacramento, CA,[2]Roswell Park Cancer Institute, Buffalo, NY

Obesity is characterized by a state of meta-inflammation, excess adiposity, and metabolic perturbations. Although generally considered a negative co-morbidity for cancer progression and immune function, our lab has previously shown obesity to exert a beneficial role in the context of immunotherapy, termed the “obesity paradox”, where obese patients derived greater benefit from immune checkpoint inhibition compared to lean counterparts. Chimeric antigen receptor (CAR) T cells have become a transformative immune cellular therapy for hematological malignancies and are being increasingly applied towards solid tumors and autoimmune conditions. Given the pleiotropy of obesity and the widespread usage of CAR therapy, we aimed to assess the role of obesity in CAR T cell function and toxicity using a novel diet-induced obese (DIO) xenograft model. We utilized immunodeficient NOD-*scid* IL2Rg^{null} (NSG) mice that were fed either a 10% low-fat diet or 60% high-fat diet for four months to generate lean and DIO cohorts, respectively. We observed significant but variable weight gain among the DIO NSG mice compared to lean counterparts. Metabolomic assessment indicated metabolic perturbations in all DIO recipients regardless of adiposity. Interestingly, Raji lymphoma growth was markedly increased in all DIO recipients. We then treated tumor-bearing mice with a tri-specific CD19/CD20/CD22-targeting CAR T cell product on day 9 post-tumor injection, with sub-lethal TBI (135cGy X-ray) conditioning delivered one day prior. Tissues and serum were collected at multiple time-points for flow cytometry immunophenotyping, histopathology, cytokine analysis, and metabolomics as well as imaging for assessment of anti-tumor efficacy. We observed that tumor-bearing DIO mice had comparable anti-tumor effects after CAR therapy and CAR engraftment at various time-points. However, this also coincided with more severe weight loss, increased serum human and mouse pro-inflammatory cytokines (human IL-6, IFNg, TNF; mouse IL-1b, TNF), and mortality in the DIO recipients. This CRS mortality in the DIO recipients precluded ability to assess the CAR recipients long-term for anti-tumor and xenogeneic graft-versus-host disease induction. Overall, we observed negative prognostic effects of obesity on preclinical models of CAR T cells affecting both efficacy and off-target effects. Given the wide application of CAR therapy and high prevalence of obesity, further study of the mechanism driving worse outcomes after treatment and connection to currently available clinical data is warranted.

#1532 *In vivo* genome-wide CRISPR screens in human T cells to enhance T cell therapy for solid tumors.

Qi Liu[1], Peixin(Amy) Chen[1], Esha Urs[1], Shimin Zhang[1], Maya M. Arce[1], Charlotte H. Wang[1], Zhongmei Li[1], Jin Seo[1], Nupura Kale[1], Taylor N. LaFlam[1], Fanglue Peng[1], Eric Shifrut[1], Greg Allen[2], Justin Eyquem[3], Katherine C. Fuh[2], Stacie E. Dodgson[4], Jason Cyster[5], Alexander Marson[2], Julia Carnevale[1]

[1]UCSF School of Medicine, San Francisco, CA,[2]UCSF - University of California San Francisco, San Francisco, CA,[3]University of California, San Francisco, San Francisco, CA,[4]Gladstone Institute, San Francisco, CA,[5]University of California, San Francisco, CA

Large-scale CRISPR screening in human T cells holds significant promise for identifying genetic modifications that can enhance cellular immunotherapy. However, many genetic regulators of T cell performance in solid tumors may not be readily revealed in vitro. In vivo screening in tumor-bearing mice offers greater physiological relevance, but has historically been limited by low intratumoral T cell recovery. Here, we developed a new model system that achieves significantly higher human T cell recovery from tumors, enabling genome-wide in vivo screens with small numbers of mice. Tumor-infiltrating T cells in this model exhibit hallmarks of dysfunction compared to matched splenic T cells, creating an ideal context for screening for genetic modifiers of T cell activity in the tumor microenvironment. Using this platform, we performed two genome-wide CRISPR knockout screens to identify genes regulating T cell intratumoral abundance and effector function (e.g., IFN-γ production). The intratumoral abundance screen uncovered the P2RY8-Gα13 GPCR signaling pathway as a negative regulator of human T cell infiltration into tumors. The effector function screen identified GNAS (Gαs), a central signaling mediator downstream of multiple GPCRs that sense different suppressive ligands, as a key regulator of T cell dysfunction in tumors. Targeted GNAS knockout rendered T cells resistant to multiple suppressive cues and significantly improved therapeutic performance across diverse solid tumor models. Moreover, combinatorial knockout of P2RY8 (trafficking) and GNAS (effector function) further enhanced overall tumor control, demonstrating that genetic modifications targeting distinct T cell phenotypes can be combined to improve therapeutic potency. This flexible and scalable in vivo screening platform can be adapted to diverse tumor models and pooled CRISPR libraries, enabling future discovery of genetic strategies that equip T cell therapies to overcome barriers imposed by solid tumors.

#1533 A universal and switchable CAR T cell therapy platform (zCART) targeting tumor antigens and the immunosuppressive microenvironment.

Ki Hyun Kim[1], Soohwan Kim[1], Eun-Hoe Lee[1], Soo-Youn Lim[1], Tack-Jin Yoo[1], Sung Min Kim[1], E-Young Kim[1], Ji-Hun Park[1], Hyun-Jong Lee[1], Seong Yeol Kim[1], Min Yoon[1], Youngha Lee[1], In-Sik Hwang[1], Yoon Lee[1], Jong-Hoon Kim[1], Jong-Seo Lee[1], Junho Chung[2]

[1]AbClon, Inc., Seoul, Korea, Republic of,[2]Cancer Research Institute, Seoul National University, Seoul, Korea, Republic of

The major hurdles in the treatment of solid tumors with chimeric antigen receptor (CAR) T cell therapies are antigen heterogeneity and the immunosuppressive tumor microenvironment. To address these challenges, we developed a universal and switchable CAR T cell therapy platform (zCART) that utilizes cotinine, a pharmacologically inert hapten, as a molecular bridge between anti-cotinine CAR T cells and tumor cells via cotinine-conjugated affibodies. First, we generated two affibody switches targeting distinct tumor-associated antigens and one affibody switch targeting an immune-oncology molecule. *In vitro* studies demonstrated that all three cotinine-conjugated affibodies, when combined with anti-cotinine CAR T cells, induced potent, dose-dependent cytotoxicity against target-expressing tumor cells. The combination of distinct affibody switches resulted in enhanced anti-tumor activity. These results highlight that the cotinine-based, switchable CAR T cell therapy platform enables flexible, multi-target control of CAR T cell activity and effective elimination of heterogeneous solid tumors. By decoupling antigen recognition from CAR T cell activation, the zCART platform offers a safe, versatile, and next-generation approach to overcoming tumor antigen variability and the immunosuppressive microenvironment, positioning it as a promising strategy for solid-tumor immunotherapy.

#1534 OriC613: A novel therapeutic strategy for gastric and pancreatic cancers utilizing dual-targeting CAR-T cells against MSLN and CLDN18.2 with a favorable safety profile and potent efficacy.

Xiaowen He, Shasha Yang, Hao Guo, Huajing Wang, Xuefeng Kong, Zhongjun Shi

Oricell Therapeutics Co.,Ltd., Shanghai, China

Background: CAR-T cell therapy has demonstrated significant efficacy in hematologic malignancies; however, its application to solid tumors remains limited by on-target, off-tumor toxicity. Mesothelin(MSLN) and claudin 18.2(CLDN18.2) are tumor-associated antigens overexpressed in several solid tumors with minimal co-expression in normal tissues, which presents a therapeutic opportunity for a dual-targeting strategy to enhance tumor selectivity.

Methods: To address gastric toxicity observed with CLDN18.2-directed CAR-T cells in preclinical models, we developed OriC613, a dual-antigen targeting CAR-T based on AND-logic gate. The construct incorporates a high-affinity anti-CLDN18.2 scFv and a moderate-affinity anti-MSLN V_HH, engineered to achieve full T-cell activation only upon engagement of both antigens.

Results: OriC613 demonstrated a favorable safety profile characterized by the absence of cytotoxic activity against CLDN18.2-positive normal gastric models. It exhibited enhanced cytotoxic potency against dual-positive tumor compared to conventional MSLN-targeted CAR-T. In pancreatic cancer re-challenge models, it promoted continued T-cell expansion and maintained cytokine production capacity. OriC613 mediated significant tumor regression in high-burden gastric in-vivo model, demonstrating robust antitumor activity while maintaining the safety profile. It also supported sustained T-cell persistence with detectable engraftment in bone marrow and spleen.

Conclusions: OriC613 demonstrates potent antitumor activity and reduced toxicity profile by leveraging co-expression of MSLN and CLDN18.2. These preclinical findings support further clinical development of this dual-targeting CAR-T approach in patients with gastric or pancreatic adenocarcinoma.

#1535 Preclinical evaluation of allogeneic BCMA/CD70 Dual CAR T cells for high-risk multiple myeloma.

Mark K. O'Dair, David Qu, Duy Nguyen, Kristen Zhang, Zachary Roberts, Elvin Lauron, Cesar Sommer

Allogene Therapeutics, Inc., South San Francisco, CA

Off-the-shelf allogeneic CAR T cells manufactured from healthy donor T cells could potentially address some of the limitations of autologous therapies by providing a more consistent product, immediate availability, and the convenience of scalable manufacturing. However, premature rejection of allogeneic CAR T cells may limit persistence and clinical responses. We previously reported the development of an anti-rejection CD70 CAR that can selectively eliminate $CD70^+$ alloreactive T cells and overcome rejection. Notably, recent studies reported high CD70 expression in high-risk multiple myeloma (MM), supporting the evaluation of CD70-targeted therapies in this patient population.

Here we evaluated the ability of allogeneic CAR T cells targeting BCMA and CD70 to overcome rejection and BCMA antigen loss in preclinical models of multiple myeloma. Human T cells were engineered with CRISPR gene-editing technology to knock out the TRAC locus and to allow site-specific integration (SSI) of a BCMA/CD70 Dual CAR construct. Following expansion, TRAC KO Dual CAR T cells were characterized by flow cytometry and through various in vitro assays including cytotoxicity, cytokine release, target-mediated expansion and mixed lymphocyte reactions (MLR). In vivo efficacy and expansion of Dual CAR T cells were evaluated in mice engrafted with MOLP-8 MM cells.

Allogeneic BCMA/CD70 Dual CAR T cells produced from multiple donors exhibited high efficiency of TRAC KO (98-99%), sustained expression of the BCMA and CD70 CARs, and a balanced effector and memory phenotype. In MLR assays with previously-primed T cells, BCMA/CD70 Dual CAR T cells showed resistance to allorejection and expanded > 5-fold, whereas control cells not expressing the CD70 CAR were rapidly eliminated. In response to target cells, BCMA/CD70 Dual CAR T cells produced high levels of IFN gamma, TNF alpha, and IL-2, and exhibited sustained killing and expansion following repeated stimulation. In addition, BCMA/CD70 Dual CAR T cells displayed high efficacy and expansion in a xenograft model of multiple myeloma. Compared with single targeting BCMA CAR T cells, BCMA/CD70 Dual CAR T cells showed improved cytotoxic activity and expansion in an in vitro model of antigen-escape.

Taken together, these results demonstrate that BCMA/CD70 Dual CAR T cells produced using site-specific integration show specific cytotoxic activity, rejection avoidance, and the ability to eliminate tumor cells that have downregulated BCMA. Our findings underscore the promise of allogeneic BCMA/CD70 Dual CAR T cells as an accessible, off-the-shelf treatment option for high-risk multiple myeloma patients and those who have progressed after BCMA-directed therapies, with the potential to extend beyond multiple myeloma toward broader applications in autoimmune disorders.

#1536 CADM1-CAR T cells targeting neuroendocrine subtypes of small cell lung cancer.

Shiva Krishna Katkam[1], Sergei Chuikov[1], Zhefan Wang[1], Venkateshwar Keshamouni[2]

[1]Internal Medicine, University of Michigan, Ann Arbor, MI,[2]University of Michigan, Ann Arbor, MI

Small cell lung cancer (SCLC), accounting for approximately 15% of all lung cancer cases, represents an aggressive carcinoma characterized by rapid proliferation, early dissemination, and the development of therapeutic resistance. Recent transcriptomic profiling has delineated SCLC into distinct molecular subtypes defined by the expression of lineage-specifying transcription factors ASCL1, NEUROD1, YAP1, and POU2F3. Among these, the neuroendocrine subtypes SCLC-A (ASCL1-driven) and SCLC-N (NEUROD1-driven) predominate in 80% of patient populations. Due to the intrinsically low expression of major histocompatibility complex (MHC) molecules and the consequent poor responsiveness to immune checkpoint blockade, the development of MHC-independent immunotherapeutic strategies is imperative for SCLC. Cell Adhesion Molecule 1 (CADM1), a membrane glycoprotein with context-dependent tumor suppressor and pro-tumorigenic functions, is aberrantly expressed in SCLC and implicated in regulating cellular adhesion, immune evasion, and metastatic dissemination. Our analyses revealed that CADM1 expression inversely correlates with MHC expression scores and is enriched in treatment-naïve tumors with high neuroendocrine differentiation (ASCL1- and NEUROD1-dominant subtypes). The overexpression of CADM1 in tumor cells, makes it an attractive target for antigen-specific immunotherapy. To exploit this vulnerability, we engineered a CADM1-specific chimeric antigen receptor (CADM1-CAR) T cell. CADM1-CAR T cells exhibited robust antigen-dependent cytotoxicity, enhanced secretion of effector cytokines (IFN-γ, TNF-α), and upregulation of cytolytic mediators (granzyme A/B, perforin), resulting in potent SCLC cell lysis in vitro. In NSG mice bearing disseminated H82 xenografts, CADM1-CAR T cell treatment significantly inhibited tumor progression and extended overall survival. These findings establish CADM1 as a promising tumor-associated antigen and support the therapeutic potential of CADM1-targeted CAR T cell therapy for high-grade neuroendocrine SCLC.

#1537 Anti GPC3 CAR T lymphocytes effectively target NSCLC, including chemoresistant stem like cells.

Lucilla Minori[1], Alessia Proment[1], Francesca Napoli[1], Luisella Righi[1], Gabriella Doronzo[1], Elisa Vigna[1], Katherine Chaney[2], Woo Jin Shim[2], John Stone[3], Paolo Bironzo[1], Ashley Hamilton[3], Silvia Novello[1], Dario Sangiolo[1]

[1]University of Torino, Orbassano, Italy,[2]AstraZeneca, Gaithersburg, MD,[3]AstraZeneca, Trumpington, Cambridge, United Kingdom

Purpose: The aim of our study was to explore a preclinical strategy of cell-based immunotherapy using anti-GPC3 CAR-lymphocytes in the context of lung cancer, with a particular focus on eradicating a chemoresistant tumor subset displaying stem-like features.

Procedures: GPC3 expression was confirmed on a large series of surgical specimens from squamous non-small cell lung cancer (NSCLC) and on a panel of tumor cell lines. Functional assays were performed using CAR-T lymphocytes engineered from healthy donors with an anti-GPC3 2nd generation CAR construct. To visualize the cancer stem cell (CSC) subset, tumor cell lines were transduced with a lentiviral CSC-detector vector in which GFP expression is driven by the stem-gene promoter OCT4, rendering green the cells with stem-like features.

Results: GPC3 expression was confirmed on 21/50 squamous NSCLC samples and 5 tumor cell lines (EBC1; H226; NCI-H23; NCI-H596; A-427), by immunohistochemistry and flow cytometry respectively. Anti-GPC3 CAR-T lymphocytes (mean surface CAR expression 40%) effectively killed all tested tumor cell lines (n = 5), with mean specific cytotoxic activity ranging from 71% ±13 to 42%±21 at effector-to-target (E:T) ratios of 10:1 and 2:1, respectively ($p<0.0001$ vs unmodified T cell controls), while showing no activity against the GPC3-negative A-549 cell line. The cytotoxic activity fully included the putative cancer stem cell (CSC) compartment (GFP^+), previously shown with increased resistance to cisplatin in vitro, but also displayed preferential killing toward this subset compared with GFP^- differentiated counterparts resulting in approximately twofold greater reduction ($p<0.05$, E/T 5:1).

Conclusions: GPC3 emerges as an effective and promising target for cell-based immunotherapy in lung cancer. Although preliminary, our data support the concept that anti-GPC3 CAR-T cells can effectively eliminate the CSC-enriched tumor compartment, which is believed to drive chemoresistance and recurrence, thus providing a rationale for future clinical development of cell-based immunotherapies in advanced or relapsed non-responsive lung cancer.

#1538 Oncostatin-M ligand-based CAR T-cell therapy targets and eliminates lung adenocarcinoma.

Kayla Klatt, Daniel Feinberg, Reshmi Parameswaran

Case Western Reserve University School of Medicine, Cleveland, OH

Background: A major barrier to effective CAR T-cell therapy in solid tumors is the dense extracellular matrix and the presence of cancer-associated fibroblasts (CAFs), which together impede CAR T-cell infiltration. To overcome this limitation, our lab has developed an oncostatin-M (OSM) CAR T-cell that targets heterodimers formed between GP130 and either OSMR or LIFR. These heterodimers are expressed on both tumor cells and CAFs, making them attractive therapeutic targets. Here, we evaluate the therapeutic potential of OSM CAR T-cells in lung adenocarcinoma (LAC), a subtype of non-small cell lung cancer that accounts for approximately 40% of all lung cancers.

Methods: To measure OSM CAR T-cell killing of CAFs, we co-cultured patient-derived CAFs with untransduced T cells (UT) or OSM CAR T-cells at 1:1 effector-to-target ratios for 48 hours. Interval confocal imaging of co-cultures were performed and cytotoxicity was assessed by quantifying CAF confluence. Next, we used flow cytometry to evaluate the surface expression of GP130, OSMR, and LIFR on four LAC cell lines (PC9, H1975, H2009, H2087) to determine if LAC could be putatively targeted by OSM CAR T-cells. To directly assess OSM CAR T-cell killing of LAC, we performed co-culture assays as described above, with the addition of Incucyte Cytotox dye to assess cytotoxicity by quantifying mean red fluorescence. To further assess the efficacy of OSM CAR T-cell therapy against LAC, we generated luciferase-expressing H1975 cells for subcutaneous implantation into NSG immunodeficient mice. Tumors were monitored until palpable, after which mice were randomized and treated intratumorally with PBS, UTs, or OSM CAR T-cells, with regular monitoring of tumor growth and body weight.

Results: Flow cytometry revealed heterogeneous expression of GP130, OSMR, and LIFR across LAC cell lines, with notably higher OSMR expression on H1975 and H2009. OSM CAR T-cells induced robust in vitro cytotoxicity against both LAC cells and patient-derived CAFs, with cytotoxicity correlating positively with OSMR expression levels. In the subcutaneous H1975-luc model, intratumoral administration of OSM CAR T-cells reduced tumor burden without evidence of significant toxicity.

Conclusions: These findings support the therapeutic promise of OSM CAR T-cells for targeting LAC. Importantly, depletion of CAFs may enhance CAR T-cell penetration into the tumor microenvironment, addressing a key barrier to efficacy in solid tumors. Future work will be aimed at testing OSM CAR T-cell therapy using an H1975-luc orthotopic model.

#1539 Harnessing NOPE: A key oncofetal protein driving β-catenin signaling through peptidic antigen receptor macrophages in hepatocellular carcinoma.

Carmen Oi Ning Leung[1], Rainbow Wing Hei Leung[1], **Terence Kin-Wah Lee**[2]

[1]The Hong Kong Polytechnic University, Hong Kong, Hong Kong,[2]Applied Biology and Chemical Technology, The Hong Kong Polytechnic University, Hong Kong, Hong Kong

Background: Tumor cells utilize the embryonic stem cell (ESC) pathway, which enhances cell plasticity, to evade targeted therapies. Oncofetal proteins, reactivated in tumors and regulating ESC properties, act as markers for liver tumor-initiating cells (T-ICs). Glypican-3 (GPC-3) is a promising therapeutic target for hepatocellular carcinoma (HCC), but the limited identification of functionally significant cell surface oncofetal proteins restricts clinical application. Identifying novel oncofetal proteins with specific T-IC functions is crucial for developing strategies to combat tumor recurrence and drug resistance in HCC.
Methods: Integrated OMICs analysis identified liver T-IC populations with increased expression in TCGA datasets. We used AP-MS and stable isotope labeling coupled with SILAC to identify NOPE's binding partners. The functional role of NOPE in liver T-IC regulation was assessed through various cancer stem cell assays. GSEA and β-catenin pathway analysis elucidated the molecular pathways involved. We targeted NOPE-expressing HCC cells with a peptidic chimeric antigen receptor macrophage approach (pCAR-Ms).
Results: Through a comprehensive analysis of our in-house T-IC OMICS profiling datasets in clinical HCC samples, alongside a model of human hepatocyte differentiation, we identified IGDCC4, also known as NOPE, as being highly expressed in liver T-ICs and shows particular expression pattern of oncofetal protein. Consistently, Gene Ontology Biological Process (GOBP) and Chemical and Genetic Perturbation (CGP) analyses revealed that pathways related to stem cell differentiation were enriched in NOPE-high HCC patients. We observed a stepwise increase in NOPE expression from normal liver to cirrhosis and to progressive HCC stages, with NOPE overexpression correlating with poor overall patient survival. In MHCC-97L cells, NOPE overexpression enhanced T-IC features, including self-renewal, tumorigenicity, cell invasiveness, expression of liver T-IC markers, and resistance to lenvatinib treatment. Using AP-MS combined SILAC analysis, we identified PABPC1 as a direct binding partner of NOPE, a finding confirmed through co-immunoprecipitation (co-IP) analysis. The NOPE/PABPC1 complex regulates cell state and drug resistance by directly affecting the β-catenin signaling pathway, potentially through its impact on YB-1 mRNA stability. We have developed a novel pCAR-Ms with designed peptides specifically targeting NOPE-expressing HCC cells. Our pCAR-Ms demonstrated specificity and potency in inducing phagocytosis of NOPE-expressing HCC cells.
Conclusions: We identified NOPE as a functional oncofetal protein that promotes liver cancer stemness by activating the β-catenin signaling pathway, which can be targeted by a novel pCAR-Ms approach.

#1540 Development of EPHA2 car t cell therapy for solid tumors.

Ali Cihan[1], Daoqi You[1], Armaan Siddiquee[1], Kristina Guillan[1], Tamar Feinberg[1], Erin Burns[2], Jasmine Um[2], Samantha Brosius[1], Joan Rou-En Choo[2], Andrew L. Kung[1], Anthony F. Daniyan[2], Filemon S. Dela Cruz[1]

[1]Department of Pediatrics, Memorial Sloan Kettering Cancer Center, New York, NY,[2]Department of Medicine, Memorial Sloan Kettering Cancer Center, New York, NY

Background: Efforts to apply CAR (Chimeric Antigen Receptor) T cell therapy to solid tumors are challenged by antigen heterogeneity, immunosuppressive microenvironments, and insufficient T-cell persistence. EPHA2, a receptor tyrosine kinase, is broadly overexpressed across solid tumors, including osteosarcoma (OS), non-small cell lung cancer (NSCLC), and glioblastoma, and is linked to metastatic progression and poor outcomes. The need is especially urgent in OS, where no new systemic therapy has been approved in over four decades. This study evaluates EPHA2 expression in OS and preclinically validates EPHA2-directed CAR T cells with enhanced tumor clearance and immune activation.

Methods: EPHA2 expression was evaluated by immunohistochemistry on an OS patient-derived xenograft (PDX) tissue microarray (n = 55) and assigned H-scores. Fully human EPHA2 antibodies were engineered into 2nd generation CAR constructs containing antibody that recognizes and binds to EPHA2 antibody and costimulatory signaling domain. Cytotoxicity assays were employed to screen EPHA2-directed CAR T cells against EPHA2-high A549 (NSCLC) and 143B (OS) cell lines, enabling identification of the most active construct, EP10. EP10 was then evaluated in immunodeficient MHC-DKO (MHC class I and II double knockout) mice bearing metastatic A549 or 143B xenografts. Tumor burden was quantified by bioluminescence imaging. Event-free survival (EFS) was was assessed by log-rank test with events defined a moribund status.

Results: EPHA2 showed broad expression across OS PDX models (range 1.8-265.1; median 99.7), with 88% of models scoring ≥20. EP10 CAR T cells demonstrated potent in vitro cytotoxicity, achieving 75% growth inhibition in A549 and 90% in 143B at a 1:8 effector-to-target ratio, outperforming reference CAR 4H5. EPHA2 surface expression was confirmed by flow cytometry. In A549 xenografts, EP10 significantly reduced tumor burden ($p < 0.0001$) and markedly improved EFS compared to both the non-targeting mCherry ($p=4e-04$) and 4H5 ($p=4e-04$). In 143B xenografts, EP10 significantly prolonged EFS compared to the non-targeting mCherry control ($p=0.01$; EP10 median survival = 53.5 days vs 44 days) and 4H5 ($p=0.01$; EP10 median survival = 53.5 days vs 49.5 days).

Conclusions: EPHA2 is widely expressed in OS and represents a compelling therapeutic target in OS and other solid tumors. We developed a novel EPHA2-targeting CAR T cell demonstrating potent cytotoxicity, tumor control, and survival benefit in OS and NSCLC models. Ongoing armoring efforts aim to enhance T-cell fitness, infiltration, and resistance to antigen-negative escape. Together, these data support ongoing clinical translation efforts of EPHA2-directed CAR T cells.

#1541 Development of MUC4-directed CAR-T cells against chemoresistant colorectal carcinoma.

Avik Chattopadhyay[1], Erin O'Connor[1], Anna Tingler[2], Kristi L. Helke[3], Melinda A. Engevik[2], Leonardo M. R. Ferreira[1]

[1]Department of Pharmacology and Immunology, Medical University of South Carolina, Charleston, SC,[2]Department of Regenerative Medicine and Cell Biology, Medical University of South Carolina, Charleston, SC,[3]Department of Comparative Medicine, Medical University of South Carolina, Charleston, SC

Colorectal adenocarcinoma remains a leading cause of cancer mortality, with chemoresistance and metastatic progression severely limiting treatment options. MUC4, a membrane-bound mucin normally confined to the apical epithelial surface, becomes aberrantly overexpressed across the tumor cell membrane in colorectal and other epithelial cancers. This dysregulated expression promotes immune evasion, cancer survival and metastasis. Therefore, MUC4 serves as a promising candidate for the development of targeted CAR-T therapies. We engineered MUC4-specific CAR-T cells and evaluated their activity against human colorectal cancer cell lines representing distinct clinical features: HT29 (parental), HT29-MTX (methotrexate-resistant), and T84 (metastatic). MUC4 expression was quantified by flow cytometry. Tumor cell responsiveness to IFN-γ and CAR-T-mediated cytotoxicity were assessed *in vitro*. For *in vivo* studies, HT29-MTX cells were injected intraperitoneally into NSG mice, creating a highly aggressive and lethal tumor model in which tumor-bearing mice succumb within 30-35 days, to determine the therapeutic impact of MUC4 CAR-T cells. All lines expressed high MUC4 levels. Interestingly, MUC4 CAR-T cells efficiently eliminated HT29-MTX and T84 cells but not HT29 cells. IFN-γ treatment upregulated MHC-I and PD-L1 expression across all lines. However, only HT29-MTX and T84 cells underwent robust IFN-γ-induced apoptosis, paralleling CAR-T cell killing, suggesting that IFN-γ secreted by MUC4 CAR-T cells might contribute to tumor clearance. Strikingly, in an intraperitoneal HT29-MTX tumor growth model, MUC4 CAR-T treatment significantly reduced tumor burden, demonstrating therapeutic efficacy in a setting where chemotherapy typically fails. Mouse necropsy analysis revealed no off-target *in vivo* toxicities associated with MUC4 CAR-T cell therapy. Our findings establish MUC4 as a potent and clinically relevant CAR-T cell target and demonstrate that MUC4 CAR-T cells control tumor progression in an aggressive human colorectal cancer *in vivo* model. These results highlight the potential of MUC4-targeted CAR-T cell therapy to fill a critical treatment gap for patients with chemoresistant colorectal cancer and may extend to other MUC4-expressing solid tumors.

Funding: This work was supported by Swim Across America Grant 23-1579 to LMRF and an MUSC Specialized Center of Research Excellence (SCORE) 5U54DA016511-18 Pilot Project Award to AC. This study was supported in part by the Flow Cytometry and Cell Sorting Shared Resource, Hollings Cancer Center, Medical University of South Carolina (P30 CA138313).

#1542 ALK expression identifies a therapeutically targetable subset of Merkel cell carcinomas responsive to ALK.CAR-T cell therapy alone or in combination with ALK inhibitors.

Alessandro Gasparetto[1], Jasna Metovic[2], Elisa Landoni[3], Carmen Mecca[2], Gabriele Saccu[2], Simone Piane[2], Nirmala Tilija Pun[4], Umberto Mortara[5], Chiara Anselmo[5], Marco Campisi[6], Haley Ohlson[2], Maria Vittoria Di Marco[7], Giulia Mura[7], Mauro Papotti[7], Rebecca Senetta[7], Claudia Voena[7], Gianpietro Dotti[3], Elisa Bergaggio[2], Roberto Chiarle[2]

[1]Pathology, University of Turin / Boston Children's, Boston, MA,[2]Boston Children's Hospital, Boston, MA,[3]University of North Carolina at Chapel Hill, Chapel Hill, NC,[4]Pathology, Boston Children's Hospital, Boston, MA,[5]Pathology, University of Turin, Turin, Italy,[6]Dana Farber Cancer Institute, Boston, MA,[7]University of Turin, Turin, Italy

Background: Merkel cell carcinoma (MCC) is a rare and highly aggressive neuroendocrine skin cancer with limited treatment options. While chemo-immunotherapy remains the standard of care, nearly 50% of patients experience disease progression, with a median overall survival of 10 months. Anaplastic lymphoma kinase (ALK) has emerged as a promising therapeutic target in various malignancies, including MCC, where it is detected in 40-80% of cases. Our group recently developed novel chimeric antigen receptor T-cell against ALK (ALK.CAR-T), demonstrating potent anti-tumor activity against ALK$^+$ neuroblastoma. This ALK.CAR-T product is currently under clinical investigation in a Phase I/II clinical trial (NCT06803875). In the present study, we evaluated the relevance of ALK.CAR-T immunotherapy in ALK$^+$ MCC tumors.

Methods: We tested ALK and Merkel cell polyomavirus antigen (MCPyV) expression in a cohort of 181 patients with MCC using immunohistochemistry. In addition, we characterized a panel of MCC human cell lines and two patient-derived xenografts (PDX) to identify potential immunotherapeutic targets (ALK, GD2, and HLA-I). ALK.CAR-T cells were co-cultured either in 2D with MCC cell lines or in 3D-microfluidic devices with xenograft-derived organotypic tumor spheroids (xDOTS) to assess their killing efficacy *in vitro*, either alone or in combination with ALK inhibitors. For *in vivo* testing, NSG mice were injected intravenously with human MCC cell lines and, after engraftment, treated with ALK.CAR-T cells, either alone or in combination with the ALK inhibitor lorlatinib. Tumor monitoring was performed weekly using IVIS imaging.

Results: We found ALK expression in approximately 90% of MCC tumors and observed a significant association between ALK expression and poor clinical outcomes. *In vitro*, ALK.CAR-T treatment effectively killed ALK$^+$ MCC cell lines and xDOTS, associated with an increased production of IFNγ and granzyme B. Moreover, the combination with an ALK inhibitor (lorlatinib or nadelalkib) enhanced ALK.CAR-T antitumor activity, even when the ALK inhibitor showed no effect alone. *In vivo*, ALK.CAR-T outperformed GD2.CAR-T, extending the overall survival of mice in two MCC metastatic models. Nonetheless, ALK.CAR-T efficacy was enhanced by lorlatinib, improving tumor control without altering the safety profile.

Conclusions: We identified ALK as a clinically relevant target in MCC and demonstrated that ALK.CAR-T cells, especially when combined with ALK inhibitors, have a potent anti-tumor activity against ALK$^+$ MCC. Our study provides a preclinical rationale for expanding the ongoing Phase I/II clinical trial in relapsed/refractory neuroblastoma patients to include patients with MCC, thus broadening the therapeutic indication of ALK.CAR-T.

#1543 B-cell activating factor plays a critical role in CAR-T cell-associated cytokine release syndrome.

Claire Fritz[1], Leland Metheny[2], David N. Wald[3], Paolo Caimi[4], Reshmi Parameswaran[5]

[1]Case Western Reserve University, Cleveland, OH,[2]University Hospitals, Cleveland, OH,[3]Assistant Professor, Dept. of Path., Case Western Reserve University, Cleveland, OH,[4]Cleveland Clinic Foundation, Cleveland, OH,[5]Department of Medicine, Case Western Reserve University School of Med., Cleveland, OH

Introduction: Despite the growing success of chimeric antigen receptor (CAR) T cell therapy in treating previously incurable cancers, toxicities remain a major concern. Cytokine release syndrome (CRS) and immune effector cell-associated neurotoxicity syndrome (ICANS) are the most common and potentially life-threatening adverse events (AEs) associated with CAR-T cell therapy and are related to a heightened immune effector state. We explored a previously unidentified role of B-cell activating factor (BAFF), a cytokine that plays a prominent role in B-cell tumor microenvironments, in the pathophysiology of these AEs.

Methods: A Luminex multi-analyte assay was used to measure serum levels of BAFF and known CRS cytokines in patients who experienced CAR-T CRS. To identify the cell types contributing to the release of BAFF in vitro, monocytes, CD19 CAR-T cells, and Jeko-1 cancer cells were incubated alone or at a 1:1:1 ratio, and a multiplex assay was performed on the supernatant. After IFN-γ stimulation of monocytes, BAFF secretion and expression of the BAFF receptors (BAFF-R, TACI, BCMA) were measured by ELISA and flow cytometry, respectively. To determine the impact of BAFF on cytokine release, this tri-culture was co-incubated in the presence of a BAFF or BCMA neutralizing antibody, and cytokine release was measured by multiplex assay (IL-6, IL-1β, GM-CSF, IL-10, CXCL8, CCL2). To determine if BAFF neutralization interferes with CAR-T cell function, cancer cells were cocultured with CD19 CAR-T cells in the presence of monocytes and a BAFF-neutralizing antibody. Cytotoxicity was measured by propidium iodide uptake in cancer cells, and activation and degranulation of CD3+ cells was measured by percent positivity of CD69 and CD107a by flow cytometry.

Results: First, we observed that patients who experienced CAR-T cell-related CRS have elevated serum BAFF levels that coincide with increased IL-6 and other known CRS and ICANS-associated cytokines. In the tri-culture system of monocytes, cancer cells, and CAR-T cells, monocytes were the primary cellular producer of BAFF. Mechanistically, we show that IFN-γ, produced by activated CAR-T cells, stimulates monocytes to release BAFF. Additionally, monocytes derived from CRS patients express BCMA, which is further induced by IFN-γ stimulation. In the tri-culture system of cancer cells, monocytes, and CD19 CAR-T cells, neutralization of BAFF or BCMA significantly reduces production of various CRS and ICANS-related cytokines without impairing CAR-T cell function.

Conclusion: We demonstrate that BAFF plays a role in CAR-T-cell-related AEs, and that its neutralization may be a novel strategy for treating both CRS and ICANS. In our model, we suggest that activated CAR-T cells secrete IFN-γ, which can increase the expression of BCMA on monocytes as well as the secretion of BAFF. BAFF binds to BCMA and induces increased release of cytokines that contribute to CRS and ICANS.

: Combination Immunotherapies
Poster Session

#1547 IDH1-R132H enhances oncolytic HSV-1 therapy by facilitating viral entry and immune activation in glioma.

Eleni Panagioti[1], Hunter J. Kelley[2], Alexander L. Ling[2], William Goins[3], Daniel Roberts[1], Sotiris Sotiriou[4], Bryan J. Iorgulescu[5], Karen Dixon[6], Michael B. Yaffe[7], Maria G. Castro[8], Sean E. Lawler[9], Gordon J. Freeman[10], Vijay K. Kuchroo[11], E Antonio Chiocca[12], Charles H. Cook[1]

[1]Department of Surgery, Beth Israel Deaconess Medical Center, Boston, MA,[2]Department of Neurosurgery, Brigham and Women's Hospital, Boston, MA,[3]Department of Microbiology and Molecular Genetics, University of Pittsburgh School of Medicine, Pittsburgh, PA,[4]Department of Pathology, Aristotle University of Thessaloniki, Thessaloniki, Greece,[5]Department of Pathology and Laboratory Medicine, The University of Texas MD Anderson Cancer Center, Houston, TX,[6]Department of Biomedicine, University of Basel, Basel, Switzerland,[7]Department of Biological Engineering, Massachusetts Institute of Technology, Boston, MA,[8]Department of Neurosurgery, University of Michigan Medical School, Ann Arbor, MI,[9]Department of Pathology and Laboratory Medicine, Brown University, Providence, RI,[10]Department of Medical Oncology, Dana-Farber Cancer Institute, Boston, MA,[11]Department of Neurology, Brigham and Women's Hospital, Boston, MA,[12]Department of Neurosurgery, Brigham and Women's Hospital, Boston, MA

Oncolytic virotherapy represents a promising yet under-explored therapeutic avenue for precision cancer treatment, particularly when tailored to tumor-specific molecular alterations. Patients with high-grade IDH-mutant astrocytomas continue to face limited treatment options and poor outcomes, emphasizing the need for novel strategies. In this study, we evaluated the therapeutic potential of rQNestin34.5v.2, an engineered oncolytic HSV-1, in the context of IDH1-R132H-mutant high-grade diffuse gliomas. We show that the IDH1-R132H mutation increases glioma susceptibility to viral infection by upregulating Nectin-1, the main HSV-1 entry receptor in gliomas. Concurrently, IDH1-R132H-driven DNA hypermethylation suppresses interferon (IFN) signaling, an essential antiviral defense pathway, creating a permissive environment that supports enhanced viral replication and increases tumor cell sensitivity to virus-induced apoptosis. In immunocompetent IDH1-R132H murine glioma models, intratumoral delivery of rQNestin34.5v.2 induced robust immune activation, marked by increased immune-cell infiltration into the tumor and systemic release of IFN-γ. However, elevated expression of poliovirus receptor (PVR-CD155) and the inhibitory immune checkpoint T-cell immunoreceptor with immunoglobulin and ITIM domain (TIGIT) on tumor-infiltrating lymphocytes, suggested the emergence of an adaptive resistance mechanism following virotherapy. Combining rQNestin34.5v.2 with TIGIT blockade enhanced therapeutic efficacy and improved survival outcomes compared to monotherapy. Collectively, these data demonstrate that IDH1-R132H reshapes both viral entry pathways and antiviral immune defenses, identifying it as a predictive biomarker for oncolytic virotherapy response.

#1548 T-cell acute lymphoblastic leukemia (T-ALL) drives robust T cell responses that can be harnessed with aCD40 and aPD1 combination therapy.

Faizah Alabi[1], Alex Somma[2], Todd Triplett[3]

[1]Immunotherapeutics and Biotechnology, Texas Tech University Health Sciences Center, Abilene, TX,[2]Livestrong Cancer Institutes, Department of Oncology, Dell Medical School, The University of Texas at Austin, Austin, TX,[3]Immunotherapeutic and Biotechnology, Texas Tech University Health Sciences Center, Abilene, TX

T-cell acute lymphoblastic leukemia (T-ALL) is a malignancy of immature T cells characterized by a low mutational burden and limited neoantigens. Despite improved survival rates, the standard of care has not progressed from an intensive chemotherapy regimen, which is highly toxic with a high relapse rate. Therefore, there is a need for more targeted therapies. Immunotherapy, like checkpoint blockade, that aims to harness the patient's pre-existing anti-tumor T cells, is a viable alternative. However, whether or not T-ALL is responsive to this approach is unknown due to low tumor mutational burden. Using murine models transplanted with CD45.2$^+$ T-ALL cells from spontaneously leukemic mice into immune-competent CD45.1$^+$ hosts, we investigated host (CD45.1$^+$) T-cell responses over time. Employing NUR77, RAG knock-out, OT-I, OT-II mouse models and in vitro models, we confirmed leukemia-specific, TCR-driven activation, while single-cell RNA sequencing identified expanded antitumor effector subsets.We found that T-ALL elicits leukemia-specific T cells despite its low mutational burden. Immune profiling revealed elevated effector-memory T cells expressing PD-1, TOX, and FoxP3$^+$ Tregs, consistent with chronic exhaustion and an ongoing immune response. Ex vivo cytokine assays demonstrated reduced IL-2 but increased IFN-γ production, further indicating partial exhaustion. To confirm antigen specificity, we transplanted T-ALL into OT-I and OT-II mice, whose fixed TCRs recognize OVA (absent in our leukemia model). These mice lacked PD-1$^+$TOX$^+$ T cells, confirming that exhaustion observed in wild-type mice was leukemia-specific. NUR77 transgenic analyses verified that TCR signaling drove this activation. Myeloid cells exhibited upregulated PD-L1 and enrichment of suppressive subsets, suggesting inhibitory crosstalk restraining leukemia-specific T cells. Based on this, we evaluated combined immunotherapy using αCD40 to activate myeloid antigen-presenting cells and αPD-1 to reverse T-cell exhaustion. While either monotherapy modestly prolonged survival, dual treatment induced robust, durable responses with ~50% of mice achieving complete remission. Re-challenge experiments confirmed long-term immune memory. Collectively, our findings demonstrate that despite low antigenicity, T-ALL can generate leukemia-specific T-cell responses that can be therapeutically harnessed. Co-targeting myeloid activation and PD-1 inhibition represents a promising immunotherapeutic avenue for T-ALL.

#1549 Non-clinical characteristics of BH3120, a clinical stage bispecific antibody targeting PD-L1 and 4-1BB, in combination with CD3 T cell engagers.

Jing Wang, Jun Wang, Yang Liu, Aibo Sun, Aihong Zhang, Haixia Zhao, Renai Guo, Jie Feng, **Jiangcheng Xu**, Jiawang Liu, Kyoungwoo Lee

Beijing Hanmi Pharm. Co. Ltd., Beijing, China

In the tumor microenvironment (TME), T cell activation often leads to upregulation of immune checkpoints such as PD-1 and PD-L1. This adaptive resistance mechanism, combined with insufficient co-stimulatory signals, creates an immunosuppressive milieu that compromises T cell cytotoxicity and contributes to resistance against T cell-targeted immunotherapies.
Activation of T cells with CD3 stimulation alone is often associated with cytokine-related safety concerns and limited efficacy in solid tumors. To overcome the limitation with CD3 T cell engagers, different combination strategies have been discussed and co-stimulatory signals have been suggested as potential combination partner of T cell stimulators.
BH3120 is a clinical-stage bispecific antibody designed to induce 4-1BB co-stimulation in a PD-L1-positive tumor tissue-localized manner, promoting immune activation within the TME while minimizing immune-related adverse events (irAEs), including liver toxicity. The therapeutic potential of BH3120 in combination with CD3 T cell engagers was evaluated, demonstrating enhanced T cell activation and specific lysis of tumor cells in vitro. Furthermore, this combination regimen exhibited synergistic tumor growth inhibition across different animal models without significant safety concerns.
These findings support BH3120 as a rational combination partner for T cell-engaging therapies, offering a promising strategy to overcome adaptive immune resistance while minimizing systemic toxicities.

#1551 Intratumoral biodegradable nanofluidic platform for localized multimodal immunotherapy enhances tumor eradication and immune memory.

Jingyi Wang, Francesco Manfredi, Eleonora Molinari, Madison A. Deeson, Danilo Settis, Casey Lewis, Junjun Zheng, Junhua Mai, Shu-Hsia Chen, Corrine Ying Xuan Chua, Alessandro Grattoni

Houston Methodist Research Institute, Houston, TX

Introduction: Tumor-infiltrating lymphocytes (TILs) are key mediators within the tumor immune microenvironment (TIME) and are often associated with favorable prognosis across multiple cancers. Despite the transformative success of immunotherapy, its clinical efficacy remains limited by immune evasion and systemic toxicity. Multi-agent immunotherapy targeting complementary pathways holds great potential, yet its application is constrained by dose-limiting toxicities.
Hypothesis: We hypothesize that localized, sustained delivery of multiple immunomodulators through a biodegradable nanofluidic drug-eluting seed (b-NDES) can enhance antitumor efficacy, generate durable immune memory, and minimize systemic adverse effects.
Methods: A fully implantable, biodegradable nanofluidic platform (b-NDES) was engineered for intratumoral release of α-CTLA4, STING agonist, resiquimod (TLR7/8 agonist), IL-12, and α-CD40. Efficacy was evaluated in murine models of triple-negative breast cancer (4T1), pancreatic cancer (KPC), and lung cancer (KLN205). Three- to five-drug combinations were compared for tumor regression, systemic immune activation, and toxicity. For the KPC abscopal model, bilateral tumors were established, and only one lesion received b-NDES implantation to assess systemic immune activation. Immune memory was assessed via tumor rechallenge and IFN-γ ELISpot assays. Tumor immune remodeling was profiled using Olink proteomics, CyTOF, and imaging mass cytometry (IMC).
Results: The five-drug b-NDES achieved complete tumor eradication in 5 of 6 mice in the 4T1 model and induced robust antitumor responses across KPC and KLN205 models. In the KPC abscopal model, b-NDES induced regression of untreated contralateral tumors, indicating systemic immune activation. Rechallenged mice demonstrated full tumor rejection and elevated IFN-γ-secreting splenocytes, indicating durable memory responses. IMC and CyTOF revealed enriched $CD8^+$ T-cell infiltration, dendritic-cell activation, and M1 macrophage polarization in responders. Cytokine profiling showed a robust pro-inflammatory signature in the five-drug group. Importantly, localized b-NDES delivery avoided the weight loss, hypothermia, and liver toxicity observed with systemic administration.
Conclusion: The b-NDES platform enables safe, sustained, and synergistic delivery of multiple immunotherapies directly into tumors, achieving complete regression, systemic immune activation, and long-term memory without systemic toxicity. This approach represents a promising strategy for localized, multimodal immunotherapy against aggressive, treatment-resistant cancers.

#1552 Epigenetic induced increased chromatin accessibility of immune activation loci is associated with response to anti-PD-1 therapy.

Otega Oviri[1], Tyler Gross[2], Md Imran Khan[2], Sean Henry Colligan[3], Jonathan E. Bard[4], Roberto Pili[5]

[1]Pathology and Anatomical Sciences, University at Buffalo, State University of New York, Buffalo, NY,[2]Genetics, Genomics and Bioinformatics, University at Buffalo, State University of New York, Buffalo, NY,[3]University at Buffalo, Buffalo, NY,[4]Department of Biochemistry, University at Buffalo, State University of New York, Buffalo, NY,[5]Division of Hematology/Oncology, University at Buffalo, State University of New York, Buffalo, NY

Immune checkpoint inhibitors (ICIs), including anti-PD-1 antibodies, have transformed the management of genitourinary malignancies, yet a substantial proportion of patients exhibit primary or acquired resistance. Resistance to PD-1 blockade has been associated with an immunosuppressive tumor microenvironment characterized by elevated regulatory T cells (Tregs) and myeloid-derived suppressor cells (MDSCs). Histone deacetylase inhibitors (HDACi) such as vorinostat may overcome these barriers by reprogramming immune and chromatin landscapes to favor antitumor activity. In this study, we integrated transcriptomic, epigenomic, and immunogenetic analyses from a Phase I/IB clinical trial of vorinostat plus the PD-1 inhibitor pembrolizumab and a preclinical mouse model to investigate the mechanisms driving response. ATAC-seq of peripheral blood mononuclear cells (PBMCs) revealed that patients with clinical response maintained global chromatin accessibility from baseline to on-treatment, including at promoter regions of immune activation genes such as *IRF1*, *IRF4*, and *IRF8*. Gene Ontology and motif enrichment analyses demonstrated enrichment of IRF-family transcription factor motifs within regions of increased accessibility. Corresponding RNA-seq analyses showed upregulation of *IRF4* and reduced expression of immunosuppressive genes including *FOXP3* and *TIGIT*, consistent with a less suppressive immune phenotype and enhanced effector activation. Interestingly, HLA genotyping identified an overrepresentation of HLA-B44 supertype alleles among responders, suggesting a potential immunogenetic predictive marker. Building on the immune profiling results, we next examined how the combination therapy of vorinostat and anti-PD-1 shaped immune programs in a murine model of kidney cancer (RENCA). We observed significantly reduced tumor burden, decreased metastases, and improved overall survival relative to monotherapies. Single-cell RNA-seq of splenocytes revealed downregulation of myeloid-associated immunosuppressive genes (*Saa1*, *Saa3*, *S100a8*, *S100a9*) in the combination group, implicating HDAC inhibition in the attenuation of MDSC and neutrophil-mediated resistance pathways. Flow cytometry studies are ongoing to further characterize the immune cell composition and validate these transcriptomic findings at the protein level. In summary, these findings suggest that HDAC inhibition may enhance PD-1 blockade efficacy by maintaining chromatin accessibility at immune activation loci, reducing immunosuppressive signaling, and potentially interacting with host HLA genotype to shape therapeutic outcome. These results support further exploration of HDAC inhibitors as a rational combination strategy to overcome immune resistance in cancer.

#1553 Combining PD-1 blockade with DLL3-targeted T cell engager potentiates antitumor efficacy in small cell lung cancer.

Tongxin Huo[1], Ting Ni[1], Jingjing Wang[1], Panpan Wang[2], Yuhe Han[3], Yawen Zhang[1], **Jian Xiang**[1], Zhixiang Zhang[2]

[1]WuXi AppTec, Suzhou, China,[2]WuXi AppTec, Shanghai, China,[3]WuXi AppTec, Nantong, China

Small cell lung cancer (SCLC) is an aggressive neuroendocrine malignancy characterized by rapid proliferation, early metastasis, and poor prognosis. Despite initial sensitivity to chemotherapy and immune checkpoint blockade, most patients experience disease relapse, highlighting the urgent need for novel therapeutic strategies. Delta-like ligand 3 (DLL3) is highly expressed on the surface of SCLC cells but minimally on normal tissues, making it an ideal target for T-cell-engaging therapies. However, limited immune infiltration and the immunosuppressive tumor microenvironment often restrict the efficacy of TCEs in SCLC. Given the complementary mechanism of TCE (T cell engager) mediated cytotoxicity and PD-1 blockade-induced T-cell activation, our research found that combining a DLL3-targeted TCE with PD-1 inhibition could enhance antitumor immune responses significantly and improve therapeutic outcomes in SCLC. In PBMC-humanized mouse models bearing SHP77 (DLL3-high expression) or NCI-H69 (DLL3-low expression) xenografts, DLL3 TCE combined with pembrolizumab achieved significant antitumor efficacy than DLL3 TCE monotherapy. To elucidate the underlying mechanisms, we found a marked increase infiltration of human $CD45^+$ immune cells in tumors after combination treatment. In tumors treated with DLL3 TCE alone, PD-1 expression on tumor-infiltrated T cells was upregulated, suggesting T-cell activation accompanied by the inhibitory immune regulation. Notably, PD-1 expression decreased upon co-administration with pembrolizumab, indicating that PD-1 blockade effectively reversed immunosuppressive microenvironment and enhanced immune-mediated tumor clearance. Furthermore, the combination treatment not only promoted T-cell priming and activation but also enhanced recognition between cancer cells and T cells within the tumor microenvironment, indicating a more inflamed immunologically active phenotype. This strategy provides a strong preclinical rationale for clinical evaluation of DLL3-targeted TCEs in combination with immune checkpoint inhibitors for the treatment of SCLC.

#1554 Combining an optimized irinotecan formulation with self-amplyfing RNA to treat an immunosuppressive lung metastasis melanoma model.

XuXin Sun[1], Nasim Sarrami[1], Irafasha C. Casmil[2], Sijie Zhang[1], Marcel B. Bally[3], Anna K. Blakney[2]

[1]BC Cancer Research Institute, Vancouver, BC, Canada,[2]Michael Smith Laboratory, University of British Columbia, Vancouver, BC, Canada,[3]Sr. Research Scientist & Unit Head, Adv. Therapeutics, BC Cancer Research Centre, Vancouver, BC, Canada

Background: Melanoma is an aggressive skin cancer that frequently metastasizes to the lungs in its advanced stages. The tumor microenvironment of melanoma is typically immunosuppressive; lacking immune cells with strong antitumor activity. While interleukin-12 (IL-12) based immunotherapy has shown potential for treating melanoma, its clinical application is limited by significant toxicity. To address this, we are developing a self-amplifying RNA (saRNA)-lipid nanoparticle (LNP) system to produce IL-12 in vivo. The formulation selected is similar to that used for Onpattro, a clinically approved formulation of siRNA designed to deliver RNA to liver hepatocytes. IL-12 saRNA delivery to hepatocytes will increase plasma levels of IL-12 and sustain expression which should stimulate an immune response. This saRNA LNP formulation is being combined with a novel liposomal formulation of irinotecan (Irinosome High C). This formulation can improve the tumor immune microenvironment (TIME)from an immunosuppressive one to an immunosupportive one. We believe that this formulation is ideally suited for combination with IL-12 saRNA-LNPs.
Method: The safe and effective (as judged by IL-12 levels on the plasma) dose of saRNA-LNPs was determined in C57BL/6 mice following intravenous (iv) administration. A safe and effective (as judged by assessments of anti-tumor activity) was determined for Irinosome High C following iv administration. These treatments were used alone and in combination to treat a model lung metastasis model where mice were injected iv with B16F10 melanoma cells. Tumor burden in the lungs was determined 18 days after cell injection (6 days after last treatment) and overall survival data was collected along with health status data. As a function of time after treatments splenocytes from mice were isolated and co-cultured with B16F10 cells in vitro and immune mediated cell kill was determined.
Results: The combination of IL-12 saRNA-LNP and Irinosome High C significantly improved survival and reduced lung tumor burden in B16 tumor bearing mice compared to those receiving either treatment alone. Splenocyte assays confirmed that IL-12 treatment enhanced levels of key immune cytokines, including IL-12, IL-2, and IFN-γ, indicating a robust antitumor immune response.
Conclusion: The combination of Irinosome High C and IL-12 saRNA-LNPs represents a promising new approach for treating lung metastatic disease a life-threatening complication seen in patients with late-stage melanoma. This strategy may offer a safer, more effective treatment option through use of a TIME modulatory agent with IL-12 mediated immune activation. Studies are on going to better understand the underlying mechanisms driving enhanced antitumor responses and the development of strategies to see this approach transition in various tumor models and from the lab to patients.

#1555 Differential tumor and immune responses to anti PD-1 and DGK inhibition in patient-derived tumor spheroids reveal additive killing effect.

Bihui Melidosian[1], Julia Vail[2], Xiaodi Ren[1], Danielle Hagee[2], **Michael A. Perricone**[2], Cynthia Timmers[1]

[1]Incyte Corporation, Wilmington, DE,[2]Xsphera Biosciences, Inc, Cambridge, MA

PD-1 checkpoint blockade has transformed cancer therapy, yet durable responses remain confined to a subset of patients. Diacylglycerol kinase (DGK) inhibition has been proposed as a complementary strategy to enhance T-cell activation and reprogram the tumor microenvironment. We tested a novel dual DGKA and DGKZ inhibitor using a patient-derived organotypic tumor spheroid (PDOTS) platform that preserves tumor, stromal, and immune architecture, enabling functional assessment of therapeutic response in a physiologic ex vivo context. PDOTS from 22 patient tumors were treated with retifanlimab-dlwr (PD-1 inhibitor), DGK inhibitor (INC-DGKi) at two doses, or the combination. Tumor response was defined as a $\log_2$ fold-change < -0.5 in epithelial tumor load ($EpCAM^+$) or a composite epithelial marker set to account for squamous cell carcinomas. Immune activation was profiled by multiplexed gene expression emphasizing $CD8^+$ effector activity, interferon-stimulated genes, cytokine induction, and antigen presentation. Baseline PD-L1 and MHC-I were measured by flow cytometry. Responsive (R) and non-responsive (NR) tumors were defined by tumor killing and/or immune activation and compared by differential expression and pathway analyses. Retifanlimab induced tumor regression in 6 of 22 (~27%) tumors and triggered immunologic activity in 10 of 22 (~46%), including increased $CD8^+$ and NK activity and interferon gene induction. DGKi elicited tumor regression in 5 of 22 (~23%) and stimulated immune-related transcriptional programs in 11 of 22 (~50%), representing largely distinct responders, with pro-inflammatory and leukocyte recruitment pathways enriched. Combination treatment induced tumor regression in 9 of 22 (~41%) and elicited immune activation in 6 of 22 (~27%), exceeding monotherapy cytotoxicity. Baseline PD-L1 and MHC-I variably correlated with response, indicating contextual, not universal, biomarkers. Retifanlimab and DGKi each elicited antitumor and immune responses in distinct tumor subsets, with comparable single-agent activity. Combination therapy improved tumor killing but not immune engagement, suggesting complementarity of the two agents and merits additional studies to clarify the observed discordance between tumor regression and immune signals in the combination setting. These data support biomarker-guided approaches and highlight PDOTS as a translational platform for defining rational immunotherapy combinations.

#1556 NK cells activated by monoclonal antibody-coated target cells enhance bispecific antibody-induced T cell proliferation, activation and cytotoxicity.

Reza Amani, Jyoti Arora, George J. Weiner

University of Iowa, Iowa City, IA

Background: We previously demonstrated that T cell help can enhance the viability and cytotoxic potential of Natural Killer (NK) cells activated by monoclonal antibody (mAb)-coated target cells. Here we evaluated whether the reverse is also true, and that NK cells coated by mAb can enhance proliferation, activation, and the cytotoxic potential of bispecific antibody (bsAb) retargeted T cells.
Methods: Raji lymphoma cells and normal donor peripheral blood mononuclear cells depleted of NK cells were mixed at an effector to target ratio of 5:1. Autologous NK cells were added back in controlled concentrations (0%, 5% or 20% of total effector cells). Co-cultures were treated with anti-CD3×CD19 bispecific antibody (blinatumomab), anti-CD20 monoclonal antibody (rituximab) or both. Media and antibodies were refreshed on days 2 and 4. After 5 days, T cell proliferation (Ki67) and production of cytotoxic molecules (including granzyme B) was assessed as was the number of remaining Raji cells as a measure of cytotoxicity.
Results: Treatment with the combination of blinatumomab and rituximab enhanced T cell proliferation and activation when larger numbers of NK cells were present. The presence of NK cells also enhanced elimination of Raji cells. The impact of NK cells on T cell proliferation and activation in response to single agent blinatumomab or rituximab was less pronounced. Similar results were seen with other mAb and bsAb combinations.
Conclusion: NK cells, activated by mAb-coated tumor cells, promote the proliferation, activation and cytotoxic capacity of bsAb-retargeted T cells. These data provide evidence that NK cells activated by mAb and T cells activated by bsAb are synergistic and provide cross help to each other. This provides additional rationale for evaluating therapeutic strategies involving concurrent administration of mAb and bsAb that allows for simultaneous co-engagement of NK cells (via mAbs) and T cells (via bsAbs).

Number T cells ($\times 10^3$)	**No Ab**	**Rituximab**	**Blinatumomab**	**Rituximab & Blinatumomab**
0% NK	54±13	57±16	56±62	77±74
5% NK	56±20	68±34	60±64	153±137
20% NK	67±39	92±34	81±86	212±147
T cell Granzyme B				
0% NK	96±204	128±351	2328±1534	3660±1277
5% NK	265±500	1412±834	4508±2754	11409±5077
20% NK	1043±1491	6882±2830	10876±3252	27083±9834
Remaining Raji cells ($\times 10^3$)				
0% NK	314±72	230±82	184±26	145±27
5% NK	259±84	93±80	174±20	50±79
20% NK	241±68	21±35	124±11	9±15

#1557 PHST001 combination with standard-of-care chemotherapy enhances macrophage-mediated elimination of tumor cells.

Giovanni C. Forcina, Kelsey E. Hart, Joseane Sampaio, Joshua D. Rudolph, Suzana A. Kahn, Raphael F. Rousseau, Amira A. Barkal, Ravindra Majeti, Irving L. Weissman, Roy L. Maute, Jennifer Yinuo Cao

Pheast Therapeutics Inc., Redwood City, CA

Chemotherapy exposure induces cellular stress and can upregulate ‘Eat me’ signals on the surface of cancer cells thereby targeting these cells for clearance by macrophage phagocytosis. However, this phagocytosis can be inhibited by ‘Don’t eat me’ (DEM) signals like CD24 on the surface of tumor cells. The clinical-stage anti-CD24 monoclonal antibody PHST001 blocks the CD24 DEM signal and promotes macrophage phagocytosis of target cells, raising the possibility that cotreatment with PHST001 and chemotherapy could provide combinatorial benefit to patients. To identify potential PHST001 and chemotherapy combinations, we screened 17 standard-of-care chemotherapy agents with PHST001 in coculture of peripheral monocyte-derived human macrophages and each of 13 cell lines representing 6 different cancer indications. We identified several common classes of chemotherapy drugs, including taxanes, platins, topoisomerase inhibitors, and anti-metabolites that enhance PHST001-induced macrophage clearance of cancer cells. We found that while cancer cells are generally sensitive to chemotherapy, macrophages display remarkable resistance to many chemotherapy agents. We further validated PHST001 combination with several chemotherapies in two-way dose-response experiments and identified chemotherapies that synergize with PHST001 to clear cancer cells in macrophage coculture. We subsequently validated select chemotherapy and PHST001 combinations (e.g. cisplatin) in vivo with mouse xenograft studies. Mechanistically, we discovered that certain chemotherapy agents increased the surface expression of the ‘Eat me’ signal phosphatidylserine (PS) on cancer cells, while others directly enhanced the phagocytosis capacity of macrophages. Taken together, these data support therapeutic combination of PHST001 with multiple standard-of-care chemotherapies to deepen tumor-killing response in patients.

#1558 Preclinical activity of ziftomenib and CAR T cell immunotherapy in *KMT2A*-rearranged (R) acute leukemias.

Sarah E. Haines[1], Shubhmita Bhatnagar[1], Michael C. Yarnell[2], Samantha M. McClellan[1], Catherine D. Falkenstein[1], Linda Kessler[3], Francis J. Burrows[3], Lisa M. Niswander[4], Terry J. Fry[2], Sarah K. Tasian[5]

[1]Children's Hospital of Philadelphia, Philadelphia, PA,[2]University of Colorado Anschutz Medical Center and Children's Hospital Colorado, Aurora, CO,[3]Kura Oncology, San Diego, CA,[4]Roswell Park Cancer Institute, Buffalo, NY,[5]Children's Hospital of Philadelphia and University of Pennsylvania School of Medicine, Philadelphia, PA

Introduction: Many patients with *KMT2A*-R acute leukemias experience chemoresistance and/or subsequent relapse despite intensive frontline therapies. While CD19 chimeric antigen receptor T cells (CD19CART) induce initial remission in most children with relapsed/refractory B-acute lymphoblastic leukemia (ALL), post-CD19CART relapse occurs in ~50% of patients, many of whom experience CD19 antigen loss and/or lineage switch (LS) to fatal acute myeloid leukemia (AML). To address this unmet need, we previously developed CAR T cells targeting the FLT3 receptor (FLT3CART) and reported potent anti-leukemia activity in preclinical models of wild-type FLT3-overexpressing *KMT2A*-R ALL and LS AML. In the current study, we tested the hypothesis that co-targeting of a highly-expressed cell surface antigen with CARTs and critical intracellular biology with the selective menin inhibitor (MENi) ziftomenib in *KMT2A*-R ALL would have therapeutic synergy and ameliorate resistance mechanisms of single agent therapies.
Experimental procedures: Human *KMT2A*-R and non-R ALL cell lines were co-incubated *in vitro* with FLT3CART or CD19CART +/- ziftomenib in viability assays. CART-induced IFN-γ production was measured via ELISA. Patient-derived xenograft (PDX) models of infant, pediatric, and young adult non-*KMT2A*-R (n=1), *KMT2A*-R ALL (n=6), and *KMT2A*-R LS AML (n=1) were treated intravenously with saline, mock T cells, FLT3CART, or CD19CART +/- ziftomenib daily *per os* as previously described (Loftus *Haematologica* 2021, Falkenstein *Blood* 2022, Niswander *Haematologica* 2023). Human CART and leukemia cells were quantified weekly via flow cytometry (FC) analysis of murine peripheral blood and in end-study bone marrow and/or spleens. *In vivo* IFN-γ production was measured weekly in murine plasma.
Results: Ziftomenib monotherapy induced robust inhibition of leukemia proliferation *in vitro* and *in vivo* in all tested *KMT2A*-R ALL or LS AML models. Importantly, ziftomenib did not impair CART functionality, as assessed by cytokine production and FC immunophenotyping of T cell subsets and activation/exhaustion markers. Ziftomenib co-therapy significantly augmented *in vivo* FLT3CART or CD19CART activity in most *KMT2A*-R ALL and the LS AML PDX models. Paradoxically, *in vivo* IFN-γ production in murine blood and CART cells in end-study spleens were decreased in all ziftomenib + CART co-treated *KMT2A*-R ALL or LS AML PDX models versus FLT3CART or CD19CART alone, which we posit was due to rapid cytotoxic efficacy of ziftomenib against target antigen-expressing leukemia cells necessary for CART activation and expansion.
Conclusions: Our preclinical data strongly support combinatorial efficacy of the MENi ziftomenib and FLT3CART or CD19CART immunotherapy in *KMT2A*-R ALL that may overcome or even prevent subsequent LS relapse. Studies in additional *KMT2A*-R ALL and LS AML PDX models are ongoing to validate and extend these results.

#1559 First-in-class Zα-domain-targeted ADAR1 p150 inhibitor demonstrates potent antitumor efficacy in high IFN syngeneic melanoma.

Aditya Kulkarni[1], Avijit Goswami[2], Sandeep Goyal[2], Princy Khurana[2], Kawaljit Singh[2], Barnali Deb[2]

[1]Avammune Therapeutics, Coatesville, PA,[2]Avammune Lifesciences, Bangalore, India

Background: ADAR1 (Adenosine deaminase acting on RNA) exists in two isoforms: the nuclear p110 and the p150, which shuttles between the nucleus and cytoplasm. ADAR1 p150 promotes immunotherapy resistance by suppressing immunogenic dsRNAs, and by preventing the accumulation of Z-RNA structures. Loss of ADAR1 leads to Z-RNA buildup, activating ZBP1 and triggering necroptosis. Tumors exhibiting high IFN signatures enhance synthetic lethality when ADAR1 is inhibited, while also upregulating PD-L1. This dual effect presents an opportunity for synergistic efficacy for ADAR1 inhibition and checkpoint inhibitors. In this context, we report the discovery of a novel, first-in-class inhibitor that specifically targets the Zα domain of ADAR1 p150 for cancer immunotherapy. Additionally, we evaluated the potential of this ADAR1 p150 inhibitor as a novel payload delivered via PD-L1-targeted ADCs.
Methods: A series of ADAR1 p150 inhibitors (AVA-ADR) were identified using a high-throughput binding assay, Zα domain binding confirmed by FRET assay. The anti-tumor efficacy of AVA-ADR compounds was assessed in a B16F10 syngeneic melanoma mouse model, both as a monotherapy and in combination with anti-PD-1 therapy in a high interferon condition. AVA-ADR compounds were also evaluated as a novel payload for PDL1 targeted ADCs.
Results: We identified a novel series of small-molecule inhibitors of ADAR1 p150 that elicits a robust interferon response. Binding studies showed AVA-ADR compounds exhibit submicromolar Zα-domain affinity, surpassing prior inhibitors. AVA-ADR inhibitors displayed nanomolar EC50 values and significant anti-tumor activity in the B16F10 melanoma model. AVA-ADR compounds demonstrate additive efficacy in combination with anti-PD1 treatment (~1.5 X vs anti-PD1). AVA-ADR compounds demonstrate strong anti-tumor potency in high interferon environment, >1.5x superior mIFN- β alone. Tumor samples from the combination group showed significantly elevated expression of interferon-stimulated genes and T-cell activation markers.
Conclusion: To our knowledge no selective small molecule inhibitors of ADAR1 p150 targeting the Za domain have been reported so far. Our SAR approach yielded several next generation Zα binders with nM potency demonstrating effective and competitive displacement of the tightly bound Z-DNA. Next generation compounds demonstrate low nM interferon dependent toxicity in OE21 cell lines. In vivo efficacy study in B16F10 melanoma model demonstrates synergistic efficacy of AVA-ADR compounds with mIFN-β. This is the first disclosure of a selective ADAR1 p150 inhibitor that was systemically administered demonstrating strong anti-tumor potency in high IFN tumors. Furthermore, these inhibitors show promise as payloads for antibody-drug conjugates (ADCs), enabling targeted delivery and enhanced therapeutic index in IFN-responsive cancers.

#1560 Targeting the non-canonical immune checkpoint MUC1-C enhances anti-PD-1 therapy in solid tumors.

Dae Young Kim, **Hee Young Kang**, Young Ha Yoon, Sung Min Kim, Hoil Choi

Peptron, Inc., Daejeon, Korea, Republic of

Immune checkpoint inhibitors (ICIs), particularly monoclonal antibodies targeting PD-1 and PD-L1, have revolutionized cancer therapy by enhancing antitumor immune responses. Despite their clinical success across multiple tumor types, several challenges remain, such as suboptimal response rates, which underscores the need for novel combinatorial strategies. MUC1-C, a transmembrane glycoprotein aberrantly expressed in many cancers, has recently emerged as a non-canonical immune checkpoint associated with T cell depletion and dysfunction within tumor microenvironment, thereby promoting immune evasion. Here, we present a novel immunotherapeutic strategy that concurrently targets canonical and non-canonical immune checkpoints by combining anti-PD-1 with PAb001, a humanized IgG1 antibody developed by Peptron that binds MUC1-C with high affinity (K_D < 1 nM). In a syngeneic tumor model utilizing MC38-hMUC1, a murine colon adenocarcinoma cell line engineered to express human MUC1, combinatorial treatment with 1H7 (a surrogate murine antibody targeting human MUC1-C) and an anti-mouse PD-1 antibody exhibited robust antitumor activity, resulting in marked tumor growth inhibition (TGI = 91.3%). Ongoing studies are evaluating the combinatory efficacy of additional anti-MUC1 antibodies and ICIs to further define the selective advantages of PAb001 in treating malignant tumors, and are also aimed at elucidating the molecular mechanisms underlying its therapeutic activity. In conclusion, these findings support the therapeutic potential of a dual-checkpoint blockade strategy that concurrently targets canonical and non-canonical pathways, which offers a promising approach to address limitations inherent to current ICI-based therapies.

#1561 Overcoming immunosuppression in pancreatic cancer: Efficacy of polyamine blockade and anti-PD-1 combinational therapy.

Joseph A. Goode[1], Diana Estefania Gaete-Alvarez[2], Savannah Harris[1], Otto Phanstiel[2], Deborah A. Altomare[2]

[1]College of Medicine, University of Central Florida, Orlando, FL,[2]University of Central Florida, Orlando, FL

Pancreatic ductal adenocarcinoma (PDAC) is an extremely aggressive cancer with an 88% mortality rate. This high mortality rate is due to its dense microenvironment, late-stage diagnosis, and limited treatment options. Polyamines, small molecules essential for cell growth, play a critical role here because their dysregulation is linked to PDAC tumor growth, invasion, and metastasis. Polyamine accumulation also reinforces an immunologically “cold” tumor microenvironment by supporting the recruitment of immunosuppressive cell populations and promoting immune-evasion pathways such as PD-1 signaling. This study aims to explore the interaction between polyamines and the PDAC immune microenvironment, and to evaluate the effectiveness of combining Polyamine Blockade Therapy (PBT) with anti-PD-1 inhibitors as a novel immunotherapy strategy. Using an orthotopic mouse model of PDAC with syngeneic GFP-Luc2 cells, we assessed the impact of PBT, consisting of Difluoromethylornithine (DFMO) and the polyamine transport inhibitor (PTI) Trimer44NMe (Trimer PTI), in conjunction with anti-PD-1 therapy. Tumor progression was monitored via in vivo bioluminescence imaging, and immune cell populations were analyzed using both tumor multiplexing and flow cytometry of peripheral tissues. The combined PBT and anti-PD-1 treatment led to a significant reduction in tumor mass, increased infiltration of anti-tumor immune cells, and enhanced systemic anti-tumor immune responses. The combination of Polyamine Blockade Therapy with anti-PD-1 inhibition shows promise as an effective immunotherapy for PDAC, potentially improving patient outcomes by disrupting the polyamine-mediated immunosuppressive network while enhancing anti-tumor immunity.

#1562 Rewiring the immune-excluded tumor microenvironment: Vactosertib/anti-PD-1/VEGF inhibitor triplet therapy reinstates antitumor immunity in CRC.

Seong-Jin Kim, Dong Woo Kang, Hye Jin Kim, Seonho Yoo, Jin Beom Bae, June Myoung Kim, Min Kyu Kim, Jinhwan Kim, Jin Su Kim, Ye Seon Kim, Jeong Su Lee, Kwiyeom Yoon

MedPacto, Inc., Seoul, Korea, Republic of

Introduction: Despite the clinical success of immune checkpoint inhibitors (ICIs), microsatellite-stable (MSS) tumors, which account for the majority of colorectal cancer (CRC), remain resistant to anti-PD-1 therapy. While VEGF/VEGFR-targeted combination therapies can provide partial remission, they fail to sufficiently reconstitute the immunosuppressive tumor microenvironment (TME). TGF-β signaling induces immune exclusion and stromal fibrosis in CRC, contributing to resistance to VEGF and PD-1 blockade. In this study, we investigated whether vactosertib (Vac), a TGF-β receptor type I inhibitor, could overcome this resistance when administered in combination with anti-PD-1 and VEGF inhibitors in the CT26 CRC model with PD-1 resistance.
Methods and Results: To establish a clinically meaningful PD-1 resistance model, CT26 tumors that initially responded to anti-PD-1 therapy but later progressed according to RECIST criteria were serially passaged to establish the CT26-αPD-1/R2 cell line. Maintained PD-1 antibody binding during progression indicated that resistance was not due to reduced target engagement. BALB/c mice bearing tumors were treated with the FDA-approved pan-VEGFR inhibitor fruquintinib (Fru), an anti-PD-1 antibody, and/or Vac. Vac enhanced the efficacy of Fru (TGI 10% → 47%) and anti-PD-1 (TGI 17% → 42%) monotherapy. Triple combination therapy showed a complete response rate of 20-33%, demonstrating a significantly greater antitumor effect (TGI 86%) than dual blockade of anti-PD-1 and anti-VEGF (TGI 50%). Subsequent RNA-seq analysis revealed that the triple combination therapy was the only treatment that induced a robust intratumoral immune response. Specifically, the triplet activated T cells and upregulated genes involved in myeloid activation, phagocytosis, and antigen presentation, while also increasing B cell activation. TIL analysis showed that the triplet increased $IFN\gamma^{+}CD8^{+}$ T cells by 6.0-, 12.6-, and 3.9-fold compared to Vac + Fru, anti-PD-1 + Fru, and Vac + anti-PD-1 combination therapy, respectively. The ratios of activated $CD4^{+}$ T cells and M1/M2 macrophages showed a similar pattern. Furthermore, the triplet preferentially enhanced effector memory T cells, suggesting persistent and memory-rich adaptive immunity. In a second trial using a VEGFR2-selective inhibitor, Vac similarly improved the efficacy of VEGFR2 inhibitor plus anti-PD-1 therapy (TGI 39% → 63.3%).
Conclusions: Triple blockade using Vac, an anti-PD-1 inhibitor, and a VEGFR inhibitor achieved superior antitumor efficacy and broad immune activation compared to all other dual combination therapies in PD-1-resistant CRC. These results suggest that TGF-β inhibition is essential for overcoming treatment resistance in an immunosuppressive TME, supporting the clinical evaluation of this triple combination in refractory CRC.

#1563 Intratumoral IL-12 in combination with HDAC inhibition overcomes checkpoint-refractory tumors.

Asma S. Khelifa[1], **Ainara Meler**[1], Christine M. Minnar[1], Katherine E. Lothstein[1], Masaya Miyamoto[1], Nicholas Roller[1], Lisa K. Poppe[1], David Peeney[1], Sailaja Battula[2], Howard L. Kaufman[2], Jeffrey Schlom[1], Sofia R. Gameiro[1]

[1]Center for Immuno-Oncology, National Cancer Institute, Bethesda, MD,[2]Ankyra Therapeutics, Inc., Cambridge, MA

Background: Clinical resistance to immune checkpoint blockade (ICB) is prevalent across solid malignancies, thus prompting the need for novel therapies. Interleukin-12 (IL-12) is an important cytokine for cancer immunotherapy due to its ability to bridge innate and adaptive immunity. However, the narrow therapeutic index and toxicity associated with systemic IL-12 administration has hampered its clinical development. ANK-101 is an alum-anchored human IL-12 providing tumor retention upon intra-tumoral delivery. In this study, we investigated the anti-tumor activity and mechanism of action of murine ANK-101 (mANK-101) delivered intra-tumorally in combination with the class I histone deacetylase (HDAC) inhibitor entinostat, in different ICB-refractory murine tumor models, including CT26 (colorectal) and MOC-1 (HPV16^{neg} head and neck).

Methods: Mice receiving Entinostat diet and/or mANK-101 were monitored for anti-tumor activity, survival and protective memory. The contribution of CD8$^+$, CD4$^+$, and NK lymphocytes to antitumor effects were investigated via immune depletion. Analysis of tumor-specific T cell responses and comprehensive proteomic, transcriptomic, and tumor architecture analysis of the immunome was performed in MOC-1 tumors, tumor-draining lymph node (tdLN), and spleen. In addition, functional analysis of CD8$^+$T cells in the periphery were performed.

Results: We demonstrate that mANK-101 synergizes with Entinostat to suppress CT26 (colon, Kras G12D^{mut}) and MOC-1 (oral, HPV16^{neg}) tumors, resulting in significant anti-tumor effects, survival benefit, and protective memory. Immune depletion studies demonstrated a role for CD8$^+$ T cells, CD4$^+$ T cells, and NK cells in the anti-tumor activity elicited by combination therapy. Mechanistically, combination therapy elicited significant activation of peripheral CD8$^+$ T cells and NK lymphocytes, increased CD8$^+$ T effector memory, tumor-specific T cell responses, and multifunctional IFNγ$^+$TNFα$^+$CD8$^+$ T cells, with concomitant decrease in CD4$^+$ Tregs and increased CD8/Treg ratio. Notably, spatial analysis of tumor architecture indicates the development of B-cell rich stemness hubs exclusive to combination therapy. Ongoing in-depth studies including single cell transcriptomics in the tumor and tDLN, and investigation of the role of immune stemness hubs in the observed anti-tumor activity will allow for an in-depth understanding of the synergistic effect of mANK-101 with HDAC inhibition.

Conclusion: Collectively, these findings provide a rationale for the combination of intratumoral delivery of anchored IL-12 with epigenetic modulation for patients with ICB-refractory solid tumors, such as colorectal and HPV16^{neg} head and neck cancers.

#1564 Bortezomib enhances anti-tumor efficacy of PD-1 blockade in lung squamous cell carcinoma via innate immune activation.

Xin Jin, Jianguo Zhong, SIbo Peng, **Song Xu**

Tianjin Medical University General Hospital, Tianjin Medical University, Tianjin, China

Background: Immune checkpoint inhibitors have improved survival outcomes for patients with lung squamous cell carcinoma compared to conventional chemotherapy. However, challenges such as low response rates and acquired resistance remain. Although proteasome inhibitors have shown antitumor potential owing to their unique mechanism of action, their ability to synergistically enhance immunotherapy is not well established. This study aimed to investigate a novel combinatory strategy of bortezomib and PD-1 blockade in lung squamous cell carcinoma.
Methods: We established co-culture systems to assess lymphocyte cytotoxicity and cytokine production by flow cytometry. Syngeneic and humanized mouse models of lung squamous cell carcinoma were used to evaluate tumor growth and immune infiltration in response to bortezomib, alone or in combination with anti-PD-1. Immune infiltration in tumor tissues was analyzed by immunohistochemistry. Signaling pathway activation and chemokine expression were examined by Western blot and polymerase chain reaction. Key molecules of innate immune pathways were perturbed using genetic knockdown or pharmacological inhibition to delineate the underlying mechanism.
Results: Pre-treatment of lung squamous cell carcinoma cells with bortezomib enhanced lymphocyte-mediated killing and increased secretion of IFN-γ and granzyme B in co-culture. In syngeneic models, bortezomib promoted intratumoral lymphocyte infiltration and synergized with PD-1 blockade, leading to increased $CD8^+$ T cell and granzyme B^+ cell accumulation. These findings were corroborated in humanized mouse models. Mechanistically, bortezomib triggered chemokine expression (e.g., CCL5) and activated components of the innate immune pathway, including TBK, IRF3, IKK, and NF-κB. This effect was not abrogated by STING or RIG-I knockdown. In contrast, pharmacologic inhibition of MYD88 suppressed TBK and IKK phosphorylation and reversed CCL5 upregulation induced by bortezomib.
Conclusion: Bortezomib augments the efficacy of PD-1 blockade in lung squamous cell carcinoma by activating a TLR/MYD88-dependent innate immune pathway, enhancing chemokine-mediated immune infiltration. These results support the further development of this combination as a promising therapeutic strategy.

#1565 Analyzing Tumor Treating Fields (TTFields) therapy concomitantly with checkpoint inhibitors in a GBM mouse model.

Si Yeon Lee, Kwang Bog Cho, Caren Wu, Justin Liu, Joe Ha, Adam Sjoholm, Michael Lim, Gordon Li, Ryan Nitta

Neurosurgery, Stanford University School of Medicine, Stanford, CA

Glioblastoma (GBM) is the most common malignant form of adult brain tumor, with a median survival of around 1.5-2 years. Despite multimodal treatments (tumor resection, radiotherapy, and chemotherapy) achieving an effective cure remains a significant challenge due to its highly aggressive nature. Immune checkpoint inhibitors have emerged as a promising strategy to combat GBM; however, limitations have hindered clinical success, largely due to the “cold” and immunosuppressive tumor microenvironment (TME). Tumor Treating Fields (TTFields) therapy is a non-invasive, FDA approved treatment for GBM that employs specific frequency ranges (100-500 kHz) delivered through transducer arrays placed on the head. Our initial in vitro studies, using the inovitro system, confirmed that TTFields (72 hours, 200kHz) enhanced the immune response in GBM by inducing immunogenic cell death, which led to the recruitment of immune cells through the release of damage-associated molecular patterns (DAMPs). Additionally, we demonstrated that TTFields increased T-cell activity (IFNγ and perforin) and enhanced the motility and phagocytic activity in antigen presenting cells (Raw 264.7) and dendritic cells (JawsII). We then studied the therapeutic potential of directly applying the TTFields (10-14 days, 200kHz), using the inovivo system, to an orthotopic syngeneic GBM mouse model (CT2A-luciferase) with the checkpoint inhibitor anti-PD-1**.** Consistent with previous findings, the single arm treatments of TTFields and anti-PD-1 reduced tumor volume and slightly modulated the immune environment. Concomitant treatment of TTFields with systemic anti-PD-1 therapy reduced tumor volume and significantly increased immunomodulation, as observed via an increase in T cells and myeloid cells. Our findings suggest that concomitant treatment of TTFields with checkpoint inhibitors has the potential to help transform GBM into a “hot” tumor, making it an attractive target for immunotherapy.

#1566 Genetic and pharmacologic targeting of host ATF4 sensitizes pancreatic ductal adenocarcinoma to CAR T and immune checkpoint blockade.

Nektarios Kostopoulos[1], Rohan Ganesh[1], Tej Patel[1], Frank Chinga[2], Dan Boehmler[1], Arjun Sengupta[2], Aalim Weljie[2], Costa Koumeis[2]

[1]Radiation Oncology, University of Pennsylvania, Philadelphia, PA,[2]University of Pennsylvania, Philadelphia, PA

Activating Transcription Factor 4 (ATF4) is a central mediator of the Integrated Stress Response (ISR), a conserved adaptive pathway activated under conditions of nutrient deprivation, hypoxia, and oxidative stress. In pancreatic ductal adenocarcinoma (PDAC), this pathway supports tumor survival and contributes to the establishment of an immunosuppressive tumor microenvironment (TME). Here, we demonstrate that global ATF4 deletion in the host - affecting the non-tumor, non-CAR T compartments - in combination with mesothelin-CAR T cell therapy, significantly delays tumor progression in syngeneic PDAC models. ATF4 loss in the host was associated with reduced numbers of myeloid-derived suppressor cells (MDSCs) and regulatory T cells (Tregs), alongside enhanced cytotoxicity and reduced exhaustion in both meso-CAR T and endogenous $CD8^+$ T cells. Spatial metabolomic profiling revealed that ATF4-deficient tumors exhibit focal oxidative stress and depletion of key amino acids, including leucine, suggesting impaired metabolic adaptability that may hinder Treg and MDSC maintenance. Preliminary *in vitro* differentiation assays further showed that ATF4 loss or pharmacologic ISR inhibition with ISRIB impaired Treg polarization under amino acid-limiting conditions, indicating a metabolic link between ATF4 activity and Treg stability. Importantly, *in vivo* ISRIB treatment recapitulated the host ATF4-knock out effects, leading to slower tumor growth and improved CAR T cell responses. Finally, combinatorial experiments with anti-PD-1 and anti-CTLA-4 therapy revealed enhanced tumor control in ATF4-KO mice, suggesting that targeting the ISR can sensitize PDAC to immune checkpoint blockade. Collectively, these findings identify ATF4 as a key regulator of PDAC immune evasion and establish ISR inhibition as a promising strategy to enhance both CAR T-cell and checkpoint immunotherapy efficacy in pancreatic cancer.

#1567 Reprogramming of exhausted T cells in pancreatic cancer with SBRT/IL-12 therapy.

Sarah Eckl[1], Gary Hannon[2], Angela Hughson[2], Scott A. Gerber[2]

[1]Microbiology & Immunology, Univ. of Rochester School of Medicine & Dentistry, Rochester, NY,[2]Surgery, Univ. of Rochester School of Medicine & Dentistry, Rochester, NY

Pancreatic ductal adenocarcinoma (PDAC) has a poor 13% 5-year survival rate and is the 3rd leading cause of cancer related deaths in the US. Current treatment options include surgical resection, chemotherapy, and radiation. Surgical resection is the only treatment with curative potential, however, few PDAC patients are eligible, and recurrence rates are high. The limited efficacy of targeted interventions is largely attributed to the highly immunosuppressive tumor microenvironment (TME) in PDAC. The PDAC TME has a dense stromal peripheral layer that restricts effector cell infiltration and a myeloid cell compartment that suppresses the anti-tumor function of intratumoral T cells. Chronic antigen presentation to T cells also induces T cell exhaustion in the PDAC TME, further limiting anti-tumor responses. T cell exhaustion is typically described by increased expression of inhibitory receptors and limited cytotoxic potential and is a major barrier to effective PDAC therapeutics. Our lab has developed a pre-clinical orthotopic KP2 PDAC mouse model that recapitulates the immunosuppressive PDAC TME. However, the functionality and subsets of exhausted T cells (Tex cells) present in this model have not been fully understood. To examine Tex cell dynamics in the PDAC TME, we have used flow cytometry to identify progenitor, intermediate, and terminally exhausted T cells based on their differential expression of PD-1, Ly108, and Tim3. Using additional markers of exhaustion and activation, we show that the intermediate Tex population (PD-1+, Ly108+, Tim3+) has the most effector-like phenotype in the PDAC TME, suggesting a potential role of intermediate Tex cells in tumor control. To target the PDAC TME, we developed a novel therapeutic that combines stereotactic body radiation therapy (SBRT) and IL-12 immunotherapy. SBRT/IL-12 therapy repolarizes the PDAC TME and results in abrogation of PDAC tumor burden and long-term survival. Single-cell RNA sequencing reveals a decrease in the exhausted T cell phenotype after SBRT/IL-12 therapy, and cytotoxicity assays demonstrate restoration of anti-tumor functions of T cells post-therapy. Flow cytometry analysis of Tex subsets in the PDAC TME demonstrates repolarization towards cytotoxicity and activation of each subset, including the most severely exhausted terminally exhausted T cells. These findings suggest that the reprogramming of Tex cells in the PDAC TME is important for the efficacy of SBRT/IL-12 therapy. This work also informs the broader application of SBRT/IL-12 therapy to other solid tumors.

#1568 Synergistic antitumor effects of immune checkpoint inhibitors and targeted therapy in an orthotopic RCC mouse model.

Balaji Ramachandran[1], Satheeshkumar Rajendiran[2], Abhilash Reddy[2], Girish Joshi[2], Krishnappa Haladasappa[2]

[1]In vivo Pharmacology, Adgyl Lifesciences Private Limited, Bangalore, India,[2]In Vivo Pharmacology, Adgyl Lifesciences Private Limited, Bangalore, India

With the development of checkpoint inhibitors and immunotherapy treatment for Renal cell carcinoma (RCC), syngeneic orthotopic mouse models are advantageous as suitable preclinical models due to the presence of immune system. Orthotopic renal subcapsular inoculation tumor models are challenging and offer strong clinical relevance by closely mimicking the native tumor microenvironment. The In Vivo Imaging System (IVIS) further enhances these studies by enabling non-invasive, real-time tracking of tumor growth/regression during the study period without interim animal sacrifice. In the present study, we have evaluated the preclinical efficacy of anti-PD1, anti-CTLA-4 antibody and Cabozantinib and Bevacizumab as standalone and combination regimen in orthotopic renal cell carcinoma (RCC) model of immunocompetent BALB/c mice. Subcutaneous tumor was generated in donor mice by inoculation of RenCa luciferase reporter cell line. Tumor fragments ($1mm^3$) harvested from the donor mice were orthotopically implanted into the sub-renal capsule (SRC) space of the fresh batch of mice. Tumor growth was monitored twice weekly by IVIS optical imaging system. Mice were randomized based on total flux signal intensity ($1\text{-}2 \times 10^6$ photons/second). Standalone and combination treatment was initiated with Cabozantinib at 10mg/kg; p.o; QD for 2 weeks and Bevacizumab at 5mg/kg; i.p; Q4Dx4 dose, anti-PD-1 at 10mg/kg; i.p; Q4Dx4 dose and Anti-CTLA4 at 10mg/kg; i.p; Q4Dx4 dose. Total flux (photons/second), changes in body weight, clinicals signs, mortality were monitored twice weekly up to 3 weeks. At the study's endpoint, tumors were excised and both ex-vivo bioluminescence signal intensity and tumor mass were quantified to assess treatment efficacy. In the current, orthotopic renal cell carcinoma model, treatment with standalone anti-PD1, anti-CTLA-4, and Cabozantinib and Bevacizumab resulted in moderate tumor regression. Whereas combination of anti-PD1 and anti-CTLA-4 with Cabozantinib and Bevacizumab demonstrated in improved efficacy when compared with individual treatments which was evident from the reduction in signal intensity, organ metastasis and resulted in prolonged survival. The findings of this study indicate that combining targeted therapy with immune checkpoint inhibitors can effectively suppress tumor progression and potentially overcome therapeutic resistance. This combinatorial strategy represents a promising multimodal translational approach to enhance the efficacy of chemotherapy in renal cancer. Assessing treatment outcomes in preclinical orthotopic tumor models using IVIS imaging offers a valuable, non-invasive method for accurate and longitudinal monitoring of tumor growth over time.

#1569 Treatment of PAX3-FOXO1 alveolar rhabdomyosarcoma with ICP34.5-armed G47Δ oncolytic herpes simplex virus confers survival benefit when co-administered with anti-Pd1 antibody.

Cole W. D. Peters[1], Miriam Valenzuela-Cardenas[2], Moe Kawakami[1], Andrew Dinh[1], Jaden Nguyen[1], Allison Flores[2], Theodore S. Nowicki[2]

[1]UCLA - University of California Los Angeles, Los Angeles, CA,[2]UCLA, Los Angeles, CA

Background. Patients diagnosed with PAX3-FOXO1 (P3F) positive alveolar rhabdomyosarcomas (aRMS) have much worse prognosis than those with fusion-negative aRMS or embryonal rhabdomyosarcomas. The low immunogenicity of P3F+ aRMS tumors has impaired efforts to treat patients with immune checkpoint blockade, and the lack of an accessible PAX3-FOXO1 expressing murine tumor model has limited efforts to address this unmet therapeutic need. Here we generate a novel oncolytic herpes virus (oHSV) and show it improves mouse survival in a PAX3-FOXO1 expressing M3-9-M murine tumor model, when combined with anti-PD1 treatment.
Methods. We designed a P3F-responsive promoter by combining a PRS1 element with a minimal Myogenin promoter. This synthetic promoter was inserted into the oHSV G47Δ, to drive the cytotoxic ICP34.5 gene. We tested rG47-PRS1 cytotoxicity and growth in human and murine RMS cell lines, as well as safety in normal human muscle. To determine efficacy of oncolytic herpes viruses in RMS tumor bearing C57/BL6 mice, we implanted M3-9-M:PAX3-FOXO1 tumors into the gastrocnemius muscle, followed by intratumoral injection of 1E8 PFU of virus with or without IP injection of anti-PD1 antibody. Tumor infiltrating lymphocytes were observed via flow cytometry and IHC upon harvest. Additionally, we explored the gene expression response of human and murine RMS cell lines to infection via RNA sequencing, RTqPCR, and western blot.
Results. In vitro assays showed the PRS1 promoter resulted in expression of GFP or luciferase transgene in the presence of PAX3-FOXO1, but not its absence. Infection of RMS cells with rG47-PRS1 resulted in ICP34.5 protein expression. Recombinant rG47-PRS1 kills RMS lines faster than its parental virus while displaying the same safety profile as parental G47Δ in normal human muscle cells in vitro and is safe for intra-muscular injections in mice up to 1E9 PFU. Mice harboring M-3-9M RMS tumors expressing PAX3-FOXO1 had no response to anti-PD1 treatment alone but responded to combination therapy with either G47Δ or rG47-PRS1 virus (mean tumor volume $p<0.001$; survival G47Δ+PD1 vs PD1 alone $p<0.0012$). Tumors from combination treated mice had higher CD45+ lymphocyte infiltration of their tumors and significantly reduced PD1 positive CD4 and CD8 T cells as compared to mock or single treatment. RNA sequencing data revealed increased NF-kB pathway activation in aRMS tumor lines after infection, which we observed via p65, p100, cFOS, JNK1, and PI3K western blot and RTqPCR for AP-1 transcription factor elements.
Conclusions. We observe oHSV sensitizes PAX3-FOXO1 aRMS to anti-PD1 therapy in mice. Infection of aRMS leads to upregulation of the NF-kB pathway, which may have a role in T cell engagement or tumor biology for this pediatric malignancy.

#1570 Preclinical assessment of EGFR and checkpoint inhibitor combination therapy in spontaneous colon cancer model.

Balaji Ramachandran, Satheeshkumar Rajendiran, Girish Joshi, Krishnappa Haladasappa

In Vivo Pharmacology, Adgyl Lifesciences Private Limited, Bangalore, India

Spontaneous colon cancer models closely mimic human disease, enabling translational research and therapeutic evaluation. The ApcMin/+ mouse, with a mutation in the APC gene, is a well-established model for intestinal neoplasia. In recent years, immunotherapy has shown promise in colorectal cancer, the combination of EGFR inhibitors and immune checkpoint blockers remains underexplored in polyp models. This research looks at how well these two treatments work together in stopping early tumors, using real time colonoscopy to watch how tumors grow in APC mice. In this study we have evaluated the preclinical efficacy of immune checkpoint inhibitors (anti-PD-1/ CTLA-4) and EGFR inhibitors like Erlotinib and as standalone and in combination regimen in spontaneous colon cancer model of C57BL/6J-*Apc*^{Min}/J mice. Four-week-old mice were randomized, and treatment was initiated with anti-PD1 10mg/kg, i.e., BIW for 8 weeks, anti-CTLA-4 dosed at 10mg/kg, i.p; BIW for 8 weeks and Erlotinib 50mg/kg, po; QD for 8 weeks, as standalone and combination with Erlotinib. Weekly colonoscopies with image capture tracked tumor progression. Body weight, clinical signs, and mortality were monitored biweekly. At the study end, mice were euthanized, and their small intestines and colons were collected, imaged, and assessed for polyp load using ImageJ software. Colon samples were rolled and processed for histological analysis. In the current spontaneous colon cancer model, endoscopy assessment revealed that the anti-PD-1, CTLA-4, and Erlotinib monotherapies significantly reduced lesions, tumor burden, inflammation, and polyp area compared to controls. Significantly reduced the total area of intestinal polyps relative to the control group. The percentage (%) reduction in polyp area in the small intestine (proximal, middle, and distal) and colon was found to be 38%, 27%, and 68% respectively. However, the combination of Erlotinib with anti-PD-1 and anti-CTLA-4 antibodies showed a substantial reduction in colonic tumor burden. The % reduction in polyp area in the small intestine (proximal, middle, distal) and colon was found to be 88% and 74%, respectively. Histology showed less inflammation and dysplasia in the combination group versus monotherapy. In summary, combination therapy led to a marked decrease in both the number and size of small intestinal polyps in ApcMin/+ mice, with potential survival benefits. These findings indicate that dual targeting of EGFR signalling and immune checkpoints may enhance antitumor efficacy, presenting a promising approach for colorectal cancer treatment

#1571 CAF-mediated cancer immunotherapy resistance can be overcome via selective inhibition of NOX1, 2 and 4.

Jihyun Um, Heesu Kim, Hye Ji Jang, Eun Sil Lee, Yeonhee Ahn, Sung Hwan Moon, Soo Jin Lee

Aptabio Therapeutics Inc., Yongin, Korea, Republic of

Cancer-associated fibroblasts (CAFs) represent a functionally heterogeneous population forming a major component of the tumor stroma. CAFs interact with cancer cells and immune cells via cytokine secretion, contributing to extracellular matrix (ECM) remodeling and immune suppression in the tumor microenvironment (TME). Through these mechanisms, CAFs promote tumor progression and induce resistance to chemotherapy and immunotherapy, driving tumor aggressiveness and correlating with poor prognosis in various types of cancers. The primary function of NADPH oxidases (NOXs) is to generate reactive oxygen species (ROS). NOXs are key drivers of CAF activation, thereby facilitating tumor progression and resistance to anticancer therapies. In particular, NOX1, NOX2, and NOX4 are highly expressed in CAFs and contribute to regulation of CAF functions. Herein, we demonstrate for the first time that NOX1 and NOX2, in addition to NOX4, play critical roles in promoting fibrotic and immunosuppressive responses in CAFs. These findings indicate that selective inhibition of NOX1, NOX2, and NOX4 may prevent CAF activation, suppress tumor growth, enhance antitumor immunity, and represent a promising approach to overcome resistance. As a result, we found that NOX1, 2, and 4 are markedly elevated in human pancreatic CAFs (pCAFs) compared with human pancreatic fibroblasts (PFs). Moreover, knockdown of NOX1, 2, or 4 effectively decreased fibrosis-related markers and immune cytokines/chemokines in pCAFs, respectively. Furthermore, treatment of Compound-19 (Com-19), a selective NOX inhibitor, significantly reduced the expression of fibrosis-related factors and immune cytokines/chemokines in pCAFs and also inhibited tumor fibrosis and immune cytokines via NOX inhibition in CAF-rich colorectal cancer mouse model. Importantly, Com-19 increased the intratumoral infiltration of CD8+ T cells, resulting in synergistic anti-cancer efficacy when co-administered with immune check inhibitors (ICIs) in the model which poorly responses to ICIs. Collectively, the results indicate that NOX1, 2, and 4 play a crucial role in CAF-mediated resistance to ICIs in cancers and NOX inhibition can be an effective strategy to overcome the resistance. Notably, Com-19 effectively modulated the fibrotic and immune-suppressive properties of CAF-rich tumors via NOX inhibition, thereby resensitizing tumors to ICI therapy. Therefore, Com-19 has the potential to enhance the efficacy of cancer immunotherapy by overcoming CAF-mediated ICI resistance. Phase 1 clinical trials are underway, with administration beginning in 4Q 2025. This open-label, dose-escalation study is designed to evaluate the safety, tolerability, PK, and preliminary efficacy of Com-19 as monotherapy (Part A) and in combination with pembrolizumab (Part B) in patients with advanced solid tumors. The study aims to identify the MTD and/or RP2D of Com-19.

#1572 Cocktail immunotherapy: Plant virus immunomodulator, HER2 antibody, and co-delivered IL-12 cytokine for the treatment of HER2+ cancer.

Ayumi E. Pottenger[1], Miguel A. Moreno Gonzalez[1], Manuel L. Penichet[2], Nicole F. Steinmetz[1]

[1]Chemical and Nano Engineering, UC San Diego, La Jolla, CA,[2]Professor, Dept. of Surgery, University of California (UCLA), Los Angeles, CA

Cowpea Mosaic Virus (CPMV) is a plant virus which infects legumes such as cowpea plants. It has been used as a powerful intratumoral immunotherapy in murine cancer models and canine veterinary clinical trials. CPMV is a multi- Toll-Like Receptor (TLR) agonist which induces a strong anti-tumor immune response both locally and systemically. While highly potent as a monotherapy, the most robust immunotherapy approaches are those which target cancer through multiple axes. In the present work, we tested the combination of intratumoral immunotherapy using CPMV with human epidermal growth factor receptor 2 (HER2) monoclonal antibody (mAb) therapy targeting HER2+ tumors. More specifically, we combined CPMV with an anti-HER2 mAb or anti-HER2 antibody-(IL-12) fusion protein (anti-HER2 antibody-(IL-12))—an anti-HER2 antibody genetically fused to the cytokine IL-12. Amplification of HER2 is known to occur in several cancers and is associated with poor prognosis as well as cancer recurrence. Mice with HER2+ tumors from colorectal cancer cell lines (MC38-HER2+ and CT26-HER2+) were treated with CPMV and HER2 mAb or anti-HER2 antibody-(IL-12). Tumor volume and overall survival were measured over the course of 8 weeks. While animals were refractory to HER2 mAb therapy alone, reduced tumor growth and increased survival was achieved using CPMV and the combination therapies- with the combination therapies outperforming CPMV therapy alone. These results indicate that CPMV can synergize with targeted antibody therapies for greater anti-tumor efficacy.

This work was funded in part through NIH grants R01-CA274640 and R01-CA253615-02S1, NIH training grant T32-CA121938, the American Cancer Society Extramural Discovery Science (EDS) Accelerator Award EDS-24-1330440-01-EDS, and the American Cancer Society - F.M. Kirby Foundation Inc. - Mission Boost Grant MBGI-23-1030244-01-MBG.

The authors declare the following competing financial interests: Dr. Steinmetz is a co-founder and CEO of and has equity in PlantiosX Inc. Dr. Steinmetz is a co-founder of and has equity in Mosaic Immunoengineering, Inc. Dr. Steinmetz is a cofounder and manager of Pokometz Scientific LLC, under which she is a paid consultant to Ring Therapeutics, Inc. The other authors declare no potential conflicts of interest.

#1573 Thermal trapping of MMC7 induces G2/M arrest, autophagy, and cGAS-STING signaling to augment anti-PD-1 efficacy.

Shan Li, Xiaofeng Ding, Zhilian Zhou, Huanlin Zhang, **Tingting Lin**, Lifeng Zhu, Yingming Sun

Affiliated Sanming First Hospital of Fujian Medical University, Sanming, China

Background: Overcoming resistance to immune checkpoint blockade, such as anti-PD-1 therapy, remains a critical challenge in oncology. This study investigates the potential of mild hyperthermia to modulate tumor cell biology and enhance immunotherapy efficacy.
Methods: Human tumor cell lines were subjected to mild hyperthermia (42°C) for 4 hours. Chromatin binding of MMC7 was assessed by chromatin fractionation and immunofluorescence. Cell cycle distribution was analyzed by flow cytometry. Autophagy induction was evaluated using LC3B-II conversion and autophagosome formation assays. Activation of the cGAS-STING pathway was measured via phosphorylation of STING and TBK1, and interferon-stimulated gene (ISG) expression. In vivo efficacy was validated using syngeneic mouse tumor models treated with hyperthermia (localized 42°C for 4 hours) combined with anti-PD-1 antibody.
Results: Sustained mild hyperthermia (42°C for 4 hours) specifically inhibited the dissociation of MMC7 from chromosomes, resulting in prolonged G2/M phase arrest in tumor cells. This arrest triggered significant induction of autophagy and robust activation of the cGAS-STING innate immune signaling pathway, characterized by increased cGAS activity, STING/TBK1 phosphorylation, and downstream ISG expression. Critically, this hyperthermia-induced immunogenic state synergistically enhanced the anti-tumor efficacy of PD-1 blockade therapy. Mouse tumor models recapitulated these findings, demonstrating significantly improved tumor control and survival in cohorts receiving the combination of localized hyperthermia and anti-PD-1 compared to either treatment alone.
Conclusion: Our findings demonstrate that controlled mild hyperthermia (42°C, 4h) induces persistent MMC7-chromatin binding, leading to G2/M arrest, autophagic activation, and potent stimulation of the cGAS-STING pathway within tumor cells. This creates a favorable tumor microenvironment that overcomes resistance and synergistically enhances the effectiveness of PD-1 checkpoint blockade immunotherapy. This combination strategy presents a promising novel approach for improving cancer treatment outcomes.

#1574 Chronotherapy of hyperthermia: Circadian rhythm governs HSP expression and modulates anti-tumor immunity.

Tingting Lin, Chunyan Lin, Zhilian Zhou, Shan Li, Lifeng Zhu, Yingming Sun

Affiliated Sanming First Hospital of Fujian Medical University, Sanming, China

Background: Heat shock protein (HSP) expression is a key mechanism underlying hyperthermia-induced anti-tumor immunity. However, whether HSP expression exhibits circadian rhythmicity and how this impacts therapeutic efficacy remains unclear.
Methods: Murine tumor models received localized hyperthermia at different times of day (specifically comparing afternoon and nighttime). Core circadian clock proteins (e.g., Bmal1 or Clock) were genetically ablated. Tumor tissues were analyzed for: (1) HSP expression levels post-hyperthermia; (2) release of damage-associated molecular patterns (DAMPs), including HMGB1 and ATP; (3) infiltration of CD8+ T cells. The effect of hyperthermia timing on treatment efficacy, both alone and in combination with anti-CTLA-4 antibody, was evaluated.
Results: HSP expression induced by hyperthermia showed significant circadian variation: it was highest when hyperthermia was administered in the afternoon and lowest when administered at nighttime. Genetic ablation of core circadian clock proteins abolished this time-dependent difference in HSP expression, confirming the critical regulatory role of the biological clock. Compared to afternoon hyperthermia, nighttime hyperthermia triggered significantly greater release of immunogenic DAMPs (HMGB1, ATP) from tumor tissue and induced markedly enhanced infiltration of CD8+ T cells.Crucially, nighttime hyperthermia demonstrated a significantly stronger synergistic anti-tumor effect when combined with anti-CTLA-4 immune checkpoint blockade therapy.
Conclusion: The circadian rhythm profoundly influences the immunogenic effects of hyperthermia by regulating HSP expression. Although inducing lower HSP levels, nighttime hyperthermia is more effective at releasing immunogenic DAMPs (HMGB1, ATP), promoting CD8+ T cell infiltration, and potently enhancing the efficacy of anti-CTLA-4 therapy. This study identifies timing of hyperthermia administration (specifically nighttime) as a critical factor for optimizing immunogenic cell death and augmenting the effectiveness of combined immunotherapy.

#1575 Immune implications of dual PIKfyve and KRAS inhibition in pancreatic ductal adenocarcinoma.

Jasmine P. Wisniewski[1], Caleb Cheng[1], Ruya Pakkan[1], Sydney Peters[1], Gabriel Cruz[2], Yuanyuan Qiao[2], Costas A. Lyssiotis[3], Arul M. Chinnaiyan[2]

[1]University of Michigan, Ann Arbor, MI,[2]Pathology, University of Michigan, Ann Arbor, MI,[3]Molecular and Integrative Physiology, University of Michigan, Ann Arbor, MI

BackgroundPancreatic Ductal Adenocarcinoma remains one of the deadliest cancers, with an overall 5 year survival rate of 13 percent. The majority of PDAC cases are driven by mutations in KRAS, making it a critical therapeutic target. Although many KRAS inhibitors have been developed and show promise in preclinical and clinical settings as single agents, the emergence of resistance and adaptive mechanisms has highlighted the need for combinatorial therapies. We recently demonstrated that the concurrent targeting of KRAS-MAPK and the lipid kinase PIKfyve disrupts lipid homeostasis in PDAC and has potent antitumor effects, curing the majority of mice in a syngeneic orthotopic mouse model. Interestingly, PIKfyve and KRAS-MAPK inhibition independently increase MHC Class 1 surface expression and enhance effectiveness of anti-PD-1 therapy. Thus, building on these findings, we hypothesized that dual inhibition of PIKfyve and KRAS-MAPK signaling modulates the immune landscape of PDAC.

Methods & Results Using a syngeneic orthotopic PDAC model, mice underwent 19 days of treatment with PIKfyve inhibitor ESK981 in combination with RAS inhibitor RMC-6236. Those that achieved a complete cure at the end-point were left untreated for 2 months, and it was observed that tumors grew back for all mice, highlighting the need for additional therapy. Notably, PIKfve or KRAS-MAPK inhibition alone increased expression of immune signaling markers MHC Class I and PD-L1, suggesting that the addition of anti-PD-1 therapy could further enhance efficacy.

To investigate the effect of PIKfyve and RAS inhibition on the PDAC tumor microenvironment, we performed single-cell RNA sequencing on tumors harvested after 5 days of treatment with ESK981 and RMC-6236. The combination therapy resulted in an increased proportion of immune cells, particularly T and B cells, along with a decreased proportion of epithelial cells and fibroblasts, which are associated with immune evasion. These suggest that PIKfyve and RAS inhibition alter immune function and prime the microenvironment for immune therapy.

Together, our preliminary findings suggest that the combined inhibition of PIKfyve and KRAS-MAPK exerts both direct antitumor effects and enhances the immune response in PDAC. Our goal is to build upon this strategy by leveraging its immune-enhancing effects, particularly with the addition of immune checkpoint blockade.

#1576 Combination treatment of mertki and immunomodulatory chemotherapy results in cxcl9 positive macrophage reprogramming and anti tumor adaptive memory in triple negative breast cancer.

Alex J. Smith[1], Zachary Schrank[2], Nan Guan[1], Diego Pedroza[1], Sebastian Calderon[1], Xueying Yuan[1], Na Zhao[3], Zoe Gabriel[1], Yang Gao[3], Charlotte Rivas[1], Fengshuo Liu[1], Chuck Perou[4], Shelton Earp[5], Jeffrey M. Rosen[3]

[1]Molecular and Cellular Biology, Baylor College of Medicine, Houston, TX,[2]UNC Chapel Hill, Chapel Hill, NC,[3]Baylor College of Medicine, Houston, TX,[4]UNC School of Medicine, Chapel Hill, NC,[5]UNC Lineberger Comprehensive Cancer Center, Chapel Hill, NC

Breast cancer is the most prevalent cancer and accounts for the second-highest cancer mortality rate in women. Recently, immune checkpoint blockade (ICB) in combination with chemotherapy has become the standard-of-care for Triple-Negative Breast Cancer (TNBC) patients. CD8 T cell infiltration is a predictive marker for ICB and is associated with a better prognosis, whereas suppressive myeloid cell infiltration is associated with a poor prognosis. Tumor-associated macrophages (TAMs) are suppressive myeloid cells that are common targets for solid tumor microenvironment (TME) re-education. While it is known that TAMs orchestrate lymphoid cell activation/inhibition, little is known about TAM programming, derivation, and functionality in tumors. MerTK and Axl (TAMr) are receptor tyrosine kinases expressed by monocytes and TAMs that act as negative regulators of STAT1 signaling in these cells. TAMr inhibition with a MerTKi, MRX-2843, synergizes with Interferon (IFN) to reprogram TAMs in vitro. These reprogrammed cells produce anti-tumor markers such as Cxcl9 and iNOS. Reprogramming of the bone marrow, with immunomodulatory cyclophosphamide drives myeloid cells into the monocytic lineage resulting in increased activated monocyte production. Moreover, IFN signaling is increased within the tumor. When CTX is combined with MRX-2843 long-term durable responses (LTR) are observed in the basal 2153L model, but not in the claudin low T12 model which recurs. Through scRNAseq we identified that IFN signaling maintains lymph activating Mo.Macs that release high levels of Cxcl9 in 2153L. Furthermore, 2153L ‘heats up’ early during treatment by Cxcl9 monocytes recruiting both antigen experienced effector CD8 and stem-like memory CD4 T cells to the TME. Importantly, germinal center formation with the tumor draining lymph of combination treated 2153L tumor bearing mice was observed, suggesting that CD4 and B Cell interactions may drive anti-tumor adaptive immunity. In addition, CD8 T Cells express PD-1 and IFN signaling drives PD-L1 expression on monocytes in combination treated mice. The addition of ICB to the CTX + MRX-2843 regimen prevented recurrence in 60% of mice. This study revealed that MRX-2843 synergizes with CTX to drive Cxcl9 and antigen presentation in monocytic cells, resulting in adaptive memory activation via germinal centers. Furthermore, TAM RTK receptors regulate IFN signaling in monocytic derived cells and when inhibited can synergize with chemotherapy to drive long term durable responses in TNBC pre-clinical models. TAM reprogramming with MRX-2843 + CTX + ICB, therefore, may represent a novel therapeutic approach for patients with basal TNBC.

: Innate Immunity in Cancer
Poster Session

#1580 Virus like particles enable targeted gene engineering and pooled CRISPR screening in primary human myeloid cells.
Hyuncheol Jung[1], Pascal Devant[1], Carter Ching[1], Minetoa Ota[1], Jennifer Hamilton[2], Zachary Steinhart[1], Wayne Ngo[1], Luis Sandoval[1], Jae Hyung Jung[1], Da Xu[3], Merui An[4], Esha Urs[1], Peixin Amy Chen[1], Vincent Allain[1], Takuya Tada[5], James K. Nunez[3], Nathaniel R. Landau[5], David R. Liu[4], Justin Eyquem[1], Jennifer A. Doudna[1], Alexander Marson[1], Julia Carnevale[1]

[1]Genomic Immunology, Gladstone-UCSF Institute, San Francisco, CA,[2]Azalea Therapeutics, San Francisco, CA,[3]Department of Molecular and Cell Biology, University of California, Berkeley, Berkeley, CA,[4]Merkin Institute of Transformative Technologies in Healthcare, Broad Institute of MIT and Harvard, Cambridge, MA,[5]Department of Microbiology, NYU Grossman School of Medicine, New York, NY

Primary human myeloid cells are promising candidates for immunotherapy, yet efficient and scalable technologies for genetic engineering and screening in these cells are limited. Here we present a virus-like particle (VLP)-based toolkit that delivers diverse CRISPR genome editing modalities to human monocytes, macrophages, and dendritic cells with high efficiency while preserving viability and innate immune responsiveness. VLP-mediated delivery of ribonucleoprotein payloads supports gene knockout, base editing and epigenetic silencing, and enables site-specific integration of large DNA sequences when combined with AAV donors for homology-directed repair. Leveraging sgRNA delivery via VPX-lentivirus combined with Cas9 protein delivery via engineered virus-like particle (eVLP) treatment (SLICeVLP), we performed the first pooled loss-of-function screens in human macrophages. We uncovered regulators of TNF production and CD80 expression in human macrophages, converging on TNFAIP3 as a central regulator of inflammatory polarization. TNFAIP3 ablation promoted a pro-inflammatory cell state that is resistant to suppressive polarization, and augmented cytotoxicity of engineered HER2 CAR-macrophages. Taken together, this technology platform enables unbiased discovery and characterization of functional gene targets in primary human myeloid cells.

#1581 Driver and mechanism of t-cell dysfunction and immune cold microenvironment in deadly developmental tumor in infants.

Poorvi Subramanian[1], Sreenidhi Mohanvelu[1], Sheeja Aravindan[2], Sabir Salim[1], Sivasubramani Narayanan[1], Natarajan Aravindan[1]

[1]Oklahoma State University, Stillwater, OK,[2]OU Health Stephenson Cancer Center, Oklahoma City, OK

Neuroblastoma (NB), a prevalent extracranial pediatric malignancy, is characterized by an immunologically “cold” tumor microenvironment (TME), yet the mechanisms underlying its immune evasion remain poorly understood. Here, we identify a novel immunoregulatory role for **Retinal Degeneration 3 (RD3)** in shaping host immunity and T-cell fate during NB progression. Using immune-competent mouse models, neural crest cell (NCC)-specific RD3 knockout **(RD3$^{-/-}$)**, ALK phosphor-mimetic mutated (**ALKF1174L** knock-in), or **RD3$^{-/-}$ALKF1174L** (aggressive NB phenotype), we demonstrate that RD3-loss does not impair thymic T-cell development, but profoundly alters peripheral T-cell maturation and activation. RD3-deficient mice exhibit enhanced thymic commitment of CD3^{+} T-cells, increased TCR rearrangement, and elevated CD8^{+} cytotoxic T lymphocyte (CTL) maturation, while CD4^{+} helper T-cell development is markedly suppressed. In NB-bearing RD3$^{-/-}$ mice, we observed tumor-driven reprogramming of effector T-cell populations, with increased CD8^{+} CTLs and diminished CD4^{+} activation, indicating a skewed immune response. Splenic microenvironment revealed robust homing of TCR-programmed cells but a blockade in CD4^{+} T-cell activation. Wild-type controls maintain balanced T-cell activation and effector composition, underscoring the immune detour induced by RD3 deficiency. Multiplex immunofluorescence highlights a depletion of CD4^{+} and CD8^{+} effector T-cells, reduced activation markers (CD44, GITR), and elevated exhaustion marker CD244.2. Innate immune compartments are similarly compromised, with diminished CD206^{+}, CD86^{+}, and STING^{+} populations, reflecting impaired antigen presentation. Notably, RD3$^{-/-}$ tumors exhibit heightened adenosinergic suppression via the CD73/CD39/A2AR axis, establishing a metabolic barrier to immune activation. New to science, these findings reveal RD3-loss as a central orchestrator of immune collapse in NB, promoting T-cell exhaustion, suppressing antigen presentation, and fostering a metabolically suppressed TME. This study provides mechanistic insight into tumor-intrinsic immune evasion and lays the groundwork for therapeutic strategies to restore immune competence in NB.

Funding: Department of Defense CA-210339; OCAST-HR19-04; NIH-P20GM103639; and supported by P30CA225520 and P30GM154635.

#1582 Integrative functional and multi-omics profiling reveals divergent natural killer cell responses and tumor cell plasticity in breast and ovarian cancer.

Jennifer C. Wischhusen[1], Rebecca Weber[1], Syed A. Ali[2], Brenda Besemer[1], David Palmero-Canton[1], Viktoria Sokolova[1], Christina Kohler[1], Elisa Donato[1], Andreas Trumpp[1]

[1]Division Stem Cells and Cancer, German Cancer Research Center (DKFZ), Heidelberg Institute for Stem Cell Technology and Experimental Medicine (HI-STEM gGmbH), Heidelberg, Germany,[2]Division Proteomics of Stem Cells and Cancer, German Cancer Research Center (DKFZ), Heidelberg, Germany

Natural killer (NK) cells are key mediators of innate antitumor immunity and promising candidates for cell-based therapies, yet tumor cells frequently evade NK surveillance, particularly in advanced disease. To dissect these evasion mechanisms and identify points of intervention to enhance anti-tumor immunity, we evaluated the cytotoxic response of human primary NK cells toward primary breast cancer (BrCa) and ovarian cancer (OvCa) cells.

NK cytotoxicity was assessed by cell surface expression of the CD107a degranulation marker, tumor cell (TC) survival by DAPI exclusion, and TC susceptibility using a fluorogenic protease assay. Responsive and non-responsive NK cells, as well as susceptible and resistant TCs from serial TC:NK co-cultures, were profiled by mini-bulk transcriptomics, low-input proteomics, and secretomics. NK degranulation and killing were consistently higher toward OvCa cells, whereas repeated BrCa exposure induced progressive loss of NK activity. NK receptor-ligand profiling showed stable receptor expression after OvCa co-culture but extensive remodeling upon BrCa contact. Secretome analysis revealed convergence of OvCa and NK secretory programs into a mixed phenotype, whereas BrCa suppressed NK-derived secretion and dominated the BrCa:NK secretome. These data highlighted a heterogenous NK response to different cancer entities and the control of NK activity by TCs. Multi-omics analysis of NK subsets showed glycolytic and proliferative enrichment in degranulating NK cells, whereas non-degranulating NK cells upregulated exhaustion and immunosuppressive markers absent in mono-cultured NK cells. These signatures were consistent across donors, across exposure to six BrCa/OvCa samples, and detected in NK cells from patients with advanced disease, underscoring clinical relevance. Across all six cancer cultures, NK-resistant TC subsets emerged with enhanced survival and a quiescent, metabolically low phenotype. In an orthotopic BrCa model, *in vitro*-generated resistant cells showed delayed tumor growth. Upon cell cycle re-entry during extended culture, resistant TCs regained NK susceptibility. Control and resistant TCs isolated from tumors two months post-engraftment were equally sensitive to NK killing, and *in vivo* NK therapy did not preferentially eliminate resistant TCs, indicating a plastic, reversible resistance state.

These findings revealed reciprocal reprogramming between NK cells and TCs. NK cells acquired exhaustion, while TCs adopted temporary quiescence to evade killing. Targeting both NK dysfunction and TC plasticity will be essential for effective NK cell-based therapies for solid tumors.

#1583 Galectin9 targeted therapy for aiming cure in oncogenic driver alterations-positive non-small cell lung cancer.

Takanori Kondo, Toshiyuki Minami, Hidemi Kitai, Yoko Higashiguchi, Takashi Kandori, Naoki Kawamura, Misa Murakami, Jotaro Kiyota, Mayuko Tokuda, Tomoki Higashiyama, Akio Tada, Yoshiki Negi, Kazue Yoneda, Daichi Fujimoto, Taiichiro Otsuki, Koji Mikami, Ryo Takahashi, Kozo Kuribayashi, Takashi Kijima

Department of Respiratory Medicine, Hyogo Medical University, Hyogo prefecture, Japan

Small-molecule tyrosine kinase inhibitors (TKIs) exert dramatic antitumor effect in patients with oncogenic driver alterations-positive non-small cell lung cancer (driver-positive NSCLC). However, it is inevitable for those patients to experience recurrence because of the existence of intrinsic drug-resistant subpopulation called drug-tolerant persisters (DTPs). Therefore, elimination of DTPs is crucial toward complete cure. We examined whether innate immunity could eliminate DTPs for complete cure in driver-positive NSCLC. To identify the key immune checkpoint molecule (ICM) to eradicate DTPs, *EGFR* mutation-positive NSLC cells (HCC827 and PC-9) and *ALK* fusion-positive NSLC cells (H3122 and H2228) were exposed to specific TKI osimertinib and alectinib, respectively. Among ICMs, galectin-9 (Gal-9) transcripts were most dramatically upregulated in both driver-positive NSCLC cells via activation of interferon regulatory factor 1 in nucleus. Gal-9 was also overexpressed in both HCC827 osimertinib-resistant cells (HCC827OR) and H3122 alectinib-resistant cells established by continuous exposure to respective TKI. Moreover, TCGA database analysis showed the possibility for Gal-9 to be a negative prognostic factor in lung adenocarcinoma. We next examined whether Gal-9 expression in cancer cells affected the cytotoxicity of natural killer (NK) cells. Cytotoxicity was evaluated by co-incubating cancer cells and NK leukemia cells (NKL) under continuous monitoring using xCELLigence. While exogenous Gal-9 expression weakened NKL-mediated cytotoxicity for HCC827 cells, anti-Gal-9 antibody enhanced the cytotoxicity against HCC827OR cells. We then generated CRISPR/Cas9-mediated Gal-9-knockout (KO) HCC827 cells (HCC827-sgLGALS9) and performed long-term NKL killing assay in the presence of osimertinib for evaluating the cytotoxicity against DTPs. While HCC827-sgLGALS9 cells were completely depleted by osimertinib exposure plus NKL mediated-cytotoxicity, scramble guide RNA-transfected HCC827 cells (HCC827-scr) reproliferated, which suggested that NKL-mediated cytotoxicity failed to eliminate DTPs in HCC827-scr cells. We further engrafted HCC827-scr and HCC827-sgLGALS9 cells into the flank of athymic nude mice and administered osimertinib orally for 30 days. Xenografts in both groups rapidly shrank and disappeared by osimertinib, however, the regrowth rate was higher in HCC827-scr group. Since human Gal-9 has low affinity for mouse immune cells, we transfected mutant human *EGFR* into NIH 3T3 cells (3T3-EGFRmt) and established allograft model. As expected, osimertinib significantly suppressed the growth of mouse sgLGALS9 transfected 3T3-EGFRmt allografts compared with that of scramble control allografts. Collectively, targeting Gal-9 is promising for aiming cure in driver-positive NSCLC by activating innate immunity against DTPs.

#1584 Metastasis associated macrophages drive immunosuppression and fibrosis in gastric peritoneal carcinomatosis.

Lilia Turcios[1], Neelima Hosamani[1], Ellen Beswick[2], Maria Carey[1], Joseph Kim[1], **Mautin Barry-Hundeyin**[1]

[1]University of Kentucky, Lexington, KY,[2]University of New Mexico, Albuquerque, NM

Gastric cancer peritoneal metastasis (GC-PM) remains a lethal disease with 5-6% overall survival. Macrophages are the predominant antigen presenting cells in the peritoneum initiating innate and adaptive responses. Thus, macrophage-based therapies may be an important avenue for immune based therapeutic strategies. However, the role and regulators of metastasis associated macrophages (MAMs) in GC-PM remain uncertain. Comparative transcriptomic analysis of malignant ascites and solid peritoneal tumor implants demonstrated that MAMs are a predominant cell type in the tumor microenvironment. Using syngeneic murine models of gastric carcinomatosis, we observed that targeted macrophage depletion restricted tumor growth as evidenced by 80% reduction in tumor weights, total body tumor volume, number of nodules, and malignant bowel obstruction. Bulk RNA sequencing of the malignant ascites demonstrated upregulation of pathways associated with T cell activation, differentiation and proliferation with macrophage depletion. In addition, bulk RNA sequencing of the macrophage-depleted tumor tissue showed downregulation of pro-fibrotic genes Col1a1, Fgf2 and Itgb1 compared with controls. Multiplex cytokine array revealed inhibition of immunosuppressive chemokines IL-10, IL-6 and CXCL1 with macrophage depletion. Functionally, co-cultured isolated MAMs isolated from malignant ascites and tumor nodules inhibited naïve polyclonal CD4+ T cell activation ex-vivo. Taken together, we elucidate dual mechanisms by which metastasis associated macrophages promote oncogenesis through altering adaptive anti-tumor immunity and promoting fibrosis in gastric peritoneal metastasis. Future studies will identify macrophage subsets that can be targeted for potential therapies.

#1585 Kinetic profiling of ILC and ILTC responses during early hepatocellular carcinoma development reveals IL-15-ILC1 axis.

Patrick Huang[1], Rajiv Trehan[1], Benjamin Ruf[2], Chi Ma[1], Dana Soika[1], Lorenz Kocheise[1], Gabriel B. Prata[1], Tim F. Greten[1], Firouzeh Korangy[1]

[1]Thoracic & GI Malignancies Branch, NIH/DHHS, Bethesda, MD,[2]Malignome, Metabolome and Microbiome, University of Tubingen, University of Tubingen, Germany

Cancer immunotherapy has largely focused on conventional T cells due to their recognition of precise peptide-antigens. However, despite recent breakthroughs, including the adoption of immune checkpoint inhibitor therapy as first-line therapy for unresectable hepatocellular carcinoma (HCC), the overall mortality associated with HCC continues to rise. Innate lymphoid cells (ILC) and innate-like T cells (ILTC) are lymphoid populations that play critical roles in inflammation, tissue repair, and immune tolerance. Using single cell RNA sequencing and flow cytometry on tumor samples from patients with established HCC, we have previously shown that the tumor cytokine milieu controls ILC composition and HCC outcome (Heinrich et al. Gut 2022). However, their dynamic roles during tumor development and progression particularly in the early phases of tumor initiation are poorly understood. We decided to study ILCs and ILTCs in murine HCC models, which allows us to perform temporal analysis and functional studies during very early tumor development. Using a combination of high-dimensional flow cytometry, single-cell RNA sequencing, and histologic imaging, we characterized the temporal shifts in these populations in a plasmid-induced (MYC-Luc;sg-p53) HCC mouse model. Most ILC and ILTC populations including mucosal-associated invariant T (MAIT) cells, group 1 ILCs, ILC2s, and ILC3s expanded by day 4, but lost cytotoxic granule production as the tumors progressed. We identified liver resident Hobit-expressing ILC1s as pivotal effectors of anti-tumor immunity, as their loss led to a significant increase in early tumor burden. Single-cell RNA sequencing demonstrated substantial phenotypic diversification in group 1 ILCs which ultimately shift towards an exhausted state as tumors progressed. Additionally, cytokine and transcriptional data suggested early tumor-derived IL-15 to be an early mediator and activator of hepatic ILC1s. Together, our findings position ILCs and ILTCs as rapid responders to oncogenic transformation, with ILC1s functioning as critical mediators of early anti-tumor defense.

#1586 Surgery-induced long term innate immune changes facilitate tumor progression.

Zhengyi He, Hamza O. Yazdani, Tony Haykal, Ruiqi Yang, Celine Tohme, Rihito Kanamaru, Krish Wasson, Anthony Gebran, Silvia Liu, David A. Geller, Jian-Hua Luo, Samer Tohme

University of Pittsburgh, Pittsburgh, PA

Introduction: Surgical intervention is crucial in managing cancer patients, yet it can increase tumor recurrence risk due to pro-tumorigenic innate immunity. We hypothesized that surgical stress can induce prolonged rewiring of bone marrow cells that can differentiate into a pro-tumorigenic phenotype upon stimulation.
Methods: Wild type C57BL/6J mice were subject to surgical stress including laparotomy, liver ischemia reperfusion and hepatectomy. Sham surgery includes anesthesia without further manipulation. MC38 (murine colorectal cancer cells) were subcutaneously inoculated 1- or 3-weeks post-surgery. Neutrophil depletion is done by anti-Ly6G monoclonal antibodies administration.
Results: Wild type mice subjected to different surgical stress showed significantly increased tumor volumes when tumor was inoculated subcutaneously 1- or 3-weeks post-surgery. However, neutrophil-depleted mice subjected to surgical stress showed no significant increase of cancer growth compared to wild type mice. These findings are correlated with transcriptomic analysis on tumor-associated neutrophils which exhibited enhanced production of pro-inflammatory factors that promote tumor growth. Circulating neutrophils after surgical stress also showed similar pro-inflammatory markers persistently upregulated after surgery in the absence of cancer. Furthermore, mice showed increased tumor volume when received bone marrow cells from surgery-preconditioned mice compared to sham mice. Analysis on bone marrow progenitor cells specifically showed enhanced proliferation of granulocyte-monocyte progenitors (GMPs) after surgery compared to sham mice. Additionally, proliferation of GMPs is enhanced in surgery-preconditioned mice compared to sham mice in response to cancer inoculation. Single-cell analysis of bone marrow progenitor cells revealed persistent transcriptomic changes post-surgery, while transcriptional factor enrichment revealed CCAAT/enhancer binding proteins (C/EBP) to be potential drivers of these persistent changes. Analysis of post-surgical plasma revealed acute increase of IL-1β and HMGB1 post-surgery. *In vitro* short-term (3 days) treatment of bone marrow progenitor cells with IL-1β or HMGB1 resulted in enhanced proliferation of GMPs and persistent upregulation of pro-tumorigenic gene markers in induced neutrophils.
Conclusions: Surgery-induced IL-1β and HMGB1 can induce persistent changes in bone marrow progenitor cells that can produce pro-tumorigenic neutrophils in response to cancer cells. IL-1β and HMGB1 can serve as targets to improve cancer patient prognosis after surgical resection.

#1587 *In Vivo* CRISPR screen of dendritic cells identifies Traf2 as a critical regulator of anti-tumor immunity via modulation of non-canonical NF-kB pathway.

Chang Yoon Moon[1], Meriem Belabed[2], Steven Chen[1], Jessica Le Berichel[1], Alexander Tepper[1], Camillia Azimi[1], Natalie Vaninov[1], Prerna Suri[1], Adam Marks[2], Alessandra Gurtner[1], Matthew D. Park[2], Alessia Baccarini[2], Brian Brown[2], Miriam Merad[2]

[1]Immunology, Icahn School of Medicine at Mount Sinai, New York, NY,[2]Icahn School of Medicine at Mount Sinai, New York, NY

For their ability to sample and present tumor antigens and prime cognate adaptive immune responses, the critical role of dendritic cells (DCs) in potentiating anti-tumor immune has been increasingly recognized. Yet despite their instrumental function in empowering tumoricidal adaptive immune responses, they have also been found in several cancers to foster tolerogenic immunity towards cancer antigens—underscoring the need to better understand the regulatory mechanisms that enable DCs to orchestrate a more tumoricidal response rather than a tolerogenic one. To investigate such mechanisms, we performed pathway analysis on transcriptional signatures of mature DCs found in several tumor types in both mice and humans, which identified non-canonical NF-kB (ncNF-kB) signaling as a potential regulatory pathway. Through an *in vivo* ProCode-based CRISPR knockout (KO) screen targeting ncNF-kB signaling molecules in DCs in $Kras^{G12D}Tp53^{-/-}$ (KP) tumors in mice, we discovered Traf2, a negative regulator of ncNF-KB pathway, as a key modulator capable of enhancing the expression of immunostimulatory molecules, particularly IL-12. Both CRISPR-mediated Traf2 knockout and DC-specific deletion using Zbtb46-Cre demonstrated that KO of Traf2 in DCs lead to elevated IL-12 production and increased frequencies of $CCR7^{+}CD40^{+}$ mature DCs upon dead-cell uptake. In congruence with their immunogenic phenotype, Traf2-KO DCs demonstrated a heightened capacity to activate OT-1 T cells. Reflective of enhanced DC immunogenicity in vitro, mice with DC-specific Traf2 knockout, when challenged with orthotopic lung tumors, showed increased IL-12 production in DCs and enhanced T cell activation—all of which led to a significantly reduced tumor burden compared to their wildtype controls. Collectively, these findings position DC-specific Traf2 inhibition as a promising strategy to reprogram dendritic cells toward potent tumoricidal immunity and enhance the efficacy of cancer immunotherapy.

#1588 TOX functions as a cytotoxicity checkpoint in human NK cells and is reversibly regulated by SLAMF7 receptor.

Yasser Ali Aldhamen, Rana K. Alrabiah, Maram Alshuwaymi, Rita Alonaizan

King Faisal Specialist Hospital & Research Centre, Riyadh, Saudi Arabia

The thymocyte selection-associated high mobility group box protein (TOX) is the master regulator of T cell exhaustion, but its function in human NK cell is not well defined. Here, we identified TOX as a cytotoxicity checkpoint in human NK cells and uncovered a previously unknown role for SLAMF7 as a selective and negative regulator of TOX-mediated NK cells dysfunction. Human PBMCs-derived NK cells were stimulated with IL-2, IL-10, IL-15, and IL-18, or cross-linked with agonistic antibodies targeting NKp46, NKp30, NKp44, CD16, 2B4, NKG2D, DNAM-1, 4-1BB, IL-2Rβ, SLAMF7, or NKG2A, alone or in combination with SLAMF7. Expression of TOX, IFNγ, CD107a, Granzyme B, PD-1, and SLAMF7 was quantified by flow cytometry. IL-2 and IL-15 induce rapid, dose-dependent TOX upregulation, with IL-15 showing greater potency. IL-10 and IL-18 failed to upregulate TOX. NKp30, NKp46, CD16, and 2B4 stimulation also upregulated TOX alongside IFN-γ, CD107a, and Granzyme B induction. SLAMF7 alone did not induce TOX but selectively modulated TOX during co-engagement with other activating receptors. Specifically, SLAMF7 + NKp46 and SLAMF7 + NKp30 co-stimulation suppressed TOX to baseline while preserving strong IFNγ, CD107a, and Granzyme B responses. SLAMF7 did not alter DAP12-, DAP10-, or FcRγ- dependent signaling, demonstrating that SLAMF7 specifically counteracts CD3ζ-dependent signaling. In contrast, SLAMF4 (2B4) synergistically amplified TOX and PD-1 across NK cytotoxicity receptor (NCR) and NKG2D pathways, implicating it as a strong exhaustion-promoting receptor. Additionally, SLAMF7 + CD16 increased TOX above CD16 alone. Moreover, SLAMF7 co-stimulation with NKp44, NKG2D, DNAM-1, 4-1BB, IL-2Rβ, or NKG2A did not alter TOX levels. Functionally, TOX^{low} NK cells represented the dominant $IFN\gamma^{+}$, $CD107a^{+}$, and Granzyme B^{+} subset**,** confirming TOX as a negative regulator of NK cell cytotoxicity. Consistent with these findings, SLAMF7 + NKp46 co-stimulation produced synergistic killing of MDA-MB-231 cells, whereas SLAMF7 + CD16 co-stimulation, which augments TOX, reduced cytotoxicity compared to CD16 alone. Importantly, tumor-induced TOX modulation strongly correlated with NK susceptibility. We observed that NK-sensitive MDA-MB-231 cells induced strong TOX downregulation, resulting in robust effector responses, whereas NK-resistant PANC-1 cells failed to downregulate TOX and elicited weak activation. Together, these results identify TOX as a checkpoint regulating NK cytotoxicity and define a previously undescribed SLAMF7-CD3ζ axis that modulates NK cell exhaustion. Targeting TOX or modulating SLAMF7 signaling may enhance NK-based immunotherapies for resistant solid tumors.

#1589 Spatial and molecular profiling of multinucleated giant macrophages in pancreatic ductal adenocarcinoma.

Marika Viatore[1], Rebecca Polidori[1], Anna Rita Putignano[2], Arturo Bonometti[2], Silvia Uccella[2], Silvia Bozzarelli[2], Gianluca Basso[2], Marco Erreni[3], Capretti Giovanni[2], Vincenzo Corbo[4], Alberto Mantovani[5], Massimo Locati[1], Federica Marchesi[1]

[1]University of Milan, Milan, Italy,[2]IRCCS Humanitas Research Hospital, Rozzano, Italy,[3]Dept of Immunology and Inflammation, Humanitas Clinical and Research Center, Milano, Italy,[4]University of Verona, Verona, Italy,[5]IRCCS Istituto Clinico Humanitas, Pieve Emanuele, Italy

Macrophages constitute a dominant and heterogeneous immune population within the microenvironment of pancreatic ductal adenocarcinoma (PDAC), but how specific macrophage states contribute to tumor behavior remains poorly understood. In an institutional series of 145 PDAC specimens, we identified a distinct subset of multinucleated giant cells (MGCs) of macrophage origin, an entity well described in chronic inflammation but rarely characterized in cancer. $CD68^+$MGCs were found in about 28% of cases, enriched in squamous, non-glandular regions, and more frequent after neoadjuvant chemotherapy. Spatial and high-dimensional profiling, including NanoString GeoMx® Digital Spatial Profiling, Hyperion Imaging System, and AI-guided histopathology, defined the morphological, phenotypic, and transcriptional features of these cells. PDAC-associated MGCs lacked canonical polarization markers (HLA-DR, CD163) and instead displayed a unique transcriptional program involving POLR2K, TUBA8, COX5B, and VDAC1, genes linked to oxidative stress, DNA repair, and MYC signaling. Gene set enrichment and spatial analyses indicated that MGC-rich regions coincide with hypoxic and extracellular matrix-remodeling niches. Experimental hypoxia promoted MGC formation *in vitro*. Morphometric assessment revealed abnormal nuclear architecture and increased $53BP1^+/Ki67^+$ nuclei in MGCs, suggesting proliferative activity despite DNA damage. A macrophage MGC gene signature was enriched in the squamous subtype of PDAC and correlated with shorter overall survival in TCGA datasets ($p = 0.018$). Collectively, these data identify multinucleated macrophages as a previously unrecognized immune cell state driven by microenvironmental stress and hypoxia. Their distinctive transcriptional and spatial profiles associate with aggressive tumor phenotypes, highlighting potential diagnostic and prognostic relevance in pancreatic cancer.

#1590 The oncometabolite D2HG reprograms macrophages to drive immunosuppression in IDH1-mutant cholangiocarcinoma.

Sara E. Young[1], Emma Kartalia[1], Johnathan DeBetta[2], James Leatherman[1], Kayla J. Bendinelli[1], Tamara Lopez-Vidal[1], Edwin Y. He[3], Mark Yarchoan[4], Daniel J. Zabransky[3]

[1]Johns Hopkins University School of Medicine, Baltimore, MD,[2]Johns Hopkins University Bloomberg School of Public Health, Baltimore, MD,[3]Johns Hopkins University, Baltimore, MD,[4]Sidney Kimmel Comprehensive Cancer Center, Baltimore, MD

Background: Intrahepatic cholangiocarcinoma (CCA) is an aggressive primary liver cancer, with ~20% of cases driven by mutations in isocitrate dehydrogenase 1 (mIDH1). Compared with IDH1 wild-type tumors, mIDH1 CCA exhibits an immunosuppressive microenvironment enriched for M2-like macrophages and may derive reduced benefit from immune checkpoint therapy than the general CCA population, suggesting tumor-immune interactions contribute to therapeutic resistance. mIDH1 tumors secrete the oncometabolite D2HG, but its effects on macrophages within the tumor microenvironment (TME) remain incompletely understood.
Methods: We exposed THP-1 monocytes, a human myeloid leukemia cell line commonly used to model macrophage differentiation, and PBMC-derived macrophages to D2HG. Flow cytometry, RT-qPCR, and Luminex were used to assess expression of immunosuppressive markers (CD206, CD163, IL-10) and cytokine secretion (IL-10, IL-4, IL-13). Lipid uptake and accumulation was quantified by BODIPY staining, and CD36 expression was measured by flow cytometry and RT-qPCR. Seahorse metabolic assays and fatty acid oxidation analyses evaluated metabolic activity, while phagocytosis assays with live-cell imaging assessed macrophage function.
Results: Exposure to pathologically relevant levels of D2HG that mirror those in the mIDH1 TME led THP-1 and PBMC-derived macrophages to upregulate immunosuppressive markers including CD206, CD163, and IL-10, while also increasing secretion of IL-10, IL-4, and IL-13. Functionally, D2HG-treated macrophages showed a 51% reduction in phagocytic capacity compared to untreated cells. Mechanistic studies revealed that D2HG enhanced lipid uptake and strongly upregulated the lipid transporter CD36. Despite increased lipid accumulation, Seahorse analyses and fatty acid oxidation assays showed no rise in energy production, indicating lipids were not metabolically utilized. BODIPY staining confirmed neutral lipid accumulation, supporting the development of a lipid-laden macrophage phenotype. Metabolic lipidomic analyses of mIDH1 tumors revealed higher lipid content than IDH1 wild-type tumors, suggesting that the mIDH1 CCA TME is enriched in lipids. This tumor-derived lipid abundance, together with D2HG-induced upregulation of lipid uptake in macrophages via CD36, likely promotes a cooperative process in which macrophages take up excess lipids, reinforcing their lipid-laden, immunosuppressive phenotype.
Conclusion: The oncometabolite D2HG reprograms macrophages into a lipid-rich, metabolically altered, immunosuppressive state. This mechanism reveals how mutant IDH1 tumors shape the immune microenvironment and highlights CD36 and lipid metabolism as potential therapeutic targets to restore antitumor macrophage function in mIDH1 CCA.

#1591 microRNA-25 drives initial resistance to immune checkpoint therapy by repressing innate and humoral immunity via Syndecan3.

Zhouting Zhu[1], Wenyan Han[2], Yufei Deng[3], Zhaoyang Jia[2], Lujing Wu[2], Shweta Jakhmola[2], Gulshanbir Baidwan[2], Tongyun Wang[2], Dhenugen Logeswaran[2], Amanda Y. Sun[2], Bill Bray[2], Na Li[2], Lingling Wang[2], Hui Hui[2], Jiaqian Wu[1], Sandip Pravin Patel[4], Tariq M. Rana[2]

[1]Graduate School of Biomedical Sciences, Sanford Burnham Prebys Institute, La Jolla, CA,[2]Department of Cellular and Molecular Medicine, University of California San Diego, La Jolla, CA,[3]Cancer and Cell Biology program, Graduate School of Biomedical Science, Baylor College of Medicine, Houston, TX,[4]San Diego Center for Precision Immunotherapy, Moores Cancer Center, La Jolla, CA

Immune Checkpoint Therapy (ICT) has demonstrated durable responses and long-lasting immunologic memory in cancer treatment. However, overcoming primary and acquired resistance remains a major challenge. Here, we show that CRISPR-Cas9-mediated deletion of miRNA-25 (miR-25) sensitizes tumors to cancer immunotherapy across three syngeneic mouse tumor models. Single-cell RNA sequencing (scRNA-seq) of the tumor microenvironment (TME) revealed that miR-25 deficiency induces innate immunity by upregulating major histocompatibility complex class II (MHC II) in antigen-presenting M1-like macrophages and enhances the classical complement cascade in cancer-associated fibroblasts (CAFs) to drive a humoral immune response. The complement activation polarizes CAFs from myofibroblastic CAFs (myCAFs) toward inflammatory CAFs (iCAFs) while simultaneously reduces immune-suppressive interactions between CAFs and tumor associated macrophages (TAMs). This shift results in a reduced macrophage population and fosters a pro-inflammatory, anti-tumor TME. Syndecan-3 (Sdc3), a membrane proteoglycan expressed in tumors, is repressed by miR-25 through miRISC (microRNA induced silencing complex) upon IFN-γ exposure. Using an adenine base editor (ABE8e) to mutate the miR-25 binding site in the 3' untranslated region (3' UTR) of Sdc3 effectively overcomes the resistance. The repression of SDC3 by miR-25 is further validated in five human cancer cell lines upon IFN-γ exposure but remains unaffected in non-cancerous cells. These findings identify miR-25 as a key driver of initial resistance through the repression of SDC3 and demonstrate that miR-25 deletion or stabilization of SDC3 could transform immune resistant "cold" tumors into immune responsive "hot" tumors, offering therapeutic avenues to enhance cancer immunotherapy.

#1592 Age-driven changes in tumor-associated macrophages contribute to slower tumor growth in murine melanoma and breast cancer models..

Manasa Suresh[1], Marie Durr[1], Bryan Weselman[1], Xintang Li[1], Francisco Tapia Belmonte[2], Sonia Sebaoui[1], Adhithi Rajesh[3], Katherine Fisher[3], Megan Winakur[3], Matias Hepp[4], Alexis Salas-Burgos[2], Satish Noonepalle[1], Alejandro Villagra[1]

[1]Georgetown Lombardi Comprehensive Cancer Ctr., Washington, DC,[2]Concepcion University, Concepcion, Chile,[3]Georgetown University, Washington, DC,[4]Universidad Catolica de la Santisima Concepcion, Concepcion, Chile

Introduction: The global cancer incidences are significantly higher between 50 to 70 years of age and decline thereafter. The age-driven factors contributing to this decline beyond 70-75 years of age is unknown, but it can help identify novel anticancer targets. It is now well established that tumor-associated macrophages (TAMs) secrete angiogenic growth factors that promote an immunosuppressive tumor microenvironment (TME). While novel strategies try to modulate TAMs for anticancer benefits, the impact of aging is often neglected. We have previously characterized the changes in macrophage phenotype and functions with aging. Considering their significant role in the TME, this study further determines the changing landscape of TAMs with aging and their impact on melanoma and breast tumors.

Objective: To elucidate the impact of age-driven changes in tumor-associated macrophages in murine melanoma and breast cancer models.

Methods: Wildtype mice of four ages (2-3, 6-8, 12-14, and 22-24 months) were implanted with SM1 melanoma and 4T1 breast tumor cells. In addition to tumor growth kinetics, changes in macrophage, T cell, and NK cell populations within the aging tumors were determined. At the end of the study, single-cell transcriptomic and proteomic analyses were performed on CD45-positive and F4/80-positive cells, respectively, to characterize TAMs and their interactions with other immune cells with aging. To study the impact of cancer on macrophage aging, we compared RNA sequencing data from bone marrow-derived macrophages from tumor-bearing and healthy mice of the above four age groups. Using a multiplex ELISA, we also determined age-associated changes in the secretion profile of macrophage cytokines, chemokines, and growth factors.

Results: The melanoma and breast tumor growth kinetics were significantly slower in aged mice compared to younger mice. The macrophage population within melanoma tumors increased, whereas that within breast tumors decreased with aging. The aged TAMs, however, exhibited dysfunctional properties, including reduced secretion of cytokines, chemokines, and growth factors. The transcriptomic analyses of tumor-associated and bone marrow-derived macrophages highlighted a unique age-driven signature that complements previously observed changes in macrophage function with aging and emphasized the potential cancer-driven acceleration of macrophage aging. In addition to the secretome profile, changes in the epigenetic and metabolic landscapes of aged macrophages further identified potential targets contributing to slower tumor growth.

Conclusions: Aging of TAMs significantly affects tumor growth and the TME in murine melanoma and breast cancer models. The changes observed in transcriptomic and proteomic landscape further reveal the age- and cancer-driven impact on macrophages and their significance to cancer development.

#1593 Mitochondrial enzyme A promotes macrophage-dependent antitumor responses in colorectal cancer.

Lin Chung, Shi-Chuen Miaw

National Taiwan University College of Medicine, Taipei, Taiwan

Colorectal cancer (CRC) remains one of the leading causes of cancer-related mortality worldwide, with the immunosuppressive tumor microenvironment (TME) posing a major barrier to effective therapy. Previous studies have shown that the mitochondrial enzyme A promotes CRC progression and may represent a potential therapeutic target. However, enzyme A is also highly expressed in M1 macrophages, where it drives inflammatory gene expression, underscoring the need to clarify its role specifically within tumor-associated macrophages (TAMs). Our findings demonstrate that mice with a global deletion of enzyme A develop significantly larger tumors compared to littermate controls. Similarly, $LysM^{cre}$ mediated macrophage-specific knockout mice displayed a marked increase in tumor burden. Moreover, adoptive transfer of bone marrow-derived macrophages (BMDMs) suppressed tumor growth and prolonged survival, whereas enzyme A-deficient BMDMs failed to exert these antitumor effects. These results indicate that macrophage-intrinsic enzyme A is essential for effective antitumor immunity. Mechanistically, enzyme A deficiency in macrophages resulted in reduced frequencies and total numbers of IFN-γ^+, TNF-α^+, and granzyme B^+ tumor-infiltrating NK cells, indicating impaired NK-cell activation and cytotoxic function. Further analysis revealed that enzyme A regulates the expression of key macrophage-derived cytokines and chemokines, including Ccl2, Cxcl9/10, and Il12, that are critical for NK-cell recruitment and functional activation.

#1594 Cyproheptadine and its derivatives inhibit tumor growth by eliciting NK cell-mediated anti-tumor responses in bladder cancer.

Himani Kumari[1], Chin Pui Chan[1], Ciao-Ni Chen[1], Hsin-An Shih[2], Tsung-Yu Tseng[3], Chao-Ling Yao[3], Steven Lin[2], Cheng-Huang Shen[4], **Michael W.Y. Chan**[1]

[1]National Chung Cheng University, Chiayi County, Taiwan,[2]Academia Sinica, Taipei, Taiwan,[3]National Cheng Kung University, Tainan, Taiwan,[4]Ditmanson Medical Foundation Chia-yi Christian Hospital, ChiaYi, Taiwan

Bladder cancer, the second most common malignancy of the urothelial system, exhibits a strong capacity to evade innate immune surveillance through multiple pathways, underscoring the need for innovative therapeutic strategies. We previously observed that cyproheptadine (CPH) induces anti-tumor effects in bladder cancer, although the underlying mechanism remained unclear. In this study, RNA-seq analysis of CPH-treated BFTC905 bladder cancer cells revealed significant enrichment of natural killer (NK) cell-mediated anti-tumor immune responses following CPH exposure. Using *in vitro* co-culture systems, we demonstrated that pre-treatment with CPH or CPH-SAHA conjugates markedly enhanced NK cell-mediated killing of bladder cancer cell lines by NK-92 cells and by human primary NK cells. This enhancement results from the epigenetic activation of NKG2D ligands, driven by increased H3K27ac and reduced H3K27me3 enrichment at the ULBP2 promoter in bladder cancer cells. *In vivo*, treatment with CPH in a syngeneic MB49 bladder cancer mouse model significantly suppressed tumor growth and increased NK cell infiltration. This elevated infiltration is likely mediated by upregulated expression of the NK-recruiting chemokine CCL3 in CPH-treated urothelial cancer cells. In conclusion, our findings demonstrate that CPH suppresses tumor growth and enhances immune surveillance by modulating epigenetic pathways that activate NK cell responses. These results highlight CPH and its derivatives as promising candidates for developing new immunomodulatory therapies for bladder cancer.

#1595 Combining DNA methylation inhibition and STING agonist in the treatment of metastatic triple-negative breast cancer.

Sofiane Berrazouane[1], Rhea Dumitrescu[1], Xiaoting You[2], Jack Su[1], Margarita Bartish[3], Marios Langke[1], Benjamin Lebeau[4], Young Im[1], Valerie Sabourin[1], Sonia del Rincon[1], Josie Ursini-Siegel[1], Michael R. Witcher[1]

[1]McGill University, Montreal, QC, Canada,[2]University of Toronto, Toronto, ON, Canada,[3]Karolinska Institutet, Stockholm, Sweden,[4]Nanyang Technological University, Singapore, Singapore

Triple negative breast cancer (TNBC) is an aggressive cancer associated with early metastatic events leading to a poor prognosis. According to the American Cancer Society, the 5-year relative survival rate is 91% in patients with localized TNBC but only 12% for those with distant metastatic TNBC. Thus, there is an urgent need to understand the mechanisms that drive TNBC metastasis to uncover more effective therapeutic approaches. In this regard, we profiled RNA Seq and DNA methylation in 8 metastatic TNBC cell lines with lung, liver, and bone organotropism compared to 3 parental TNBC lines. RNA-Seq revealed downregulation of IFN-I pathways associated with metastatic organotropism in the lung, liver and bone. Surprisingly, DNA methylation is enriched within the promoters of STING/IFN-related genes in these metastatic TNBC cells. In line with these findings, the analysis of TCGA human TNBC tumors showed a decreased expression of STING, an IFN-I pathway activator, in metastases versus primary tumors. In addition, a low STING expression associates with poorer TNBC patient survival. Consistent with transcriptomic data, the treatment with decitabine, a DNA methylation inhibitor, restored IFNβ and STING expression in metastatic TNBC cells, supporting epigenetic silencing with decitabine. Furthermore, combining decitabine with a STING agonist synergistically reduced viability in metastatic TNBC lines, indicating that targeting DNA methylation and activating the IFN-I pathway may represent therapeutic vulnerabilities in metastatic TNBC. More importantly, the decitabine/STINGa therapy showed a potent effect in targeting TNBC metastatic lesions in vivo with lung and liver organotropisms and increased the median survival of mice by almost 50% compared to the control single drug-treatment groups. Mechanistically, the inhibition of IFNβ with specific blocking anti-IFNβ mAb and the knockdown of TBK1, a mediator of IFN-I pathway, both abrogate the synergy between decitabine and STINGa in targeting metastatic tumor xenografts suggesting that the decitabine/STINGa targets metastatic TNBC via TBK1/IFNβ pathway. Furthermore, the spectral flow cytometry profiling of metastatic TNBC xenografts revealed that decitabine/STINGa therapy significantly enhanced NK cell infiltration and activation within metastatic tumors. Finally, the in vivo NK cell depletion showed that decitabine STINGa therapy is dependent on NK cells in treating metastatic TNBC. Altogether, this work suggests that the DNA methylation inhibition with decitabine and the stimulation of the IFNβ pathway with STINGa represent a new approach to efficiently target the metastatic TNBC that currently lacks effective targeted therapies and immunotherapies. This study also brought new evidences that decitabine/STINGa combination therapy is dependent on the TBK1/IFNβ pathway and NK cells in targeting metastatic TNBC in vivo.

#1597 A spontaneous arthritis mouse model driven by TNF-α overexpression.

Qingqing Qi, Shuang Li, Xiaolei Qiu, Yi Li, Ruilin Sun

GenoBioTX LLC, Sugar Land, TX

Rheumatoid arthritis (RA) is the most prevalent autoimmune arthropathy characterized by persistent inflammation, pain, swelling and progressive destruction of the synovial joints. Tumor necrosis factor α (TNFα) plays a central role in the autoimmune response leading to RA, as evidenced by the significant therapeutic benefits observed upon its inhibition. However, certain inhibitors targeting human TNFα (hTNFα), such as Infliximab, failed to cross-neutralize mouse TNFα (mTNFα). This limitation has impeded mechanistic and therapeutic investigations of hTNFα inhibitors *in vivo*, necessitating the development of humanized mouse models expressing hTNFα.Here, we developed an hTNFα transgenic mouse model (hTNFα-Tg) in C57BL/6 background, which carries the native promoter and coding sequences of the human *TNFα* gene, thereby driving robust overexpression of the human TNFα, as a relevant model for RA. By measuring serum hTNFα levels through ELISA following LPS stimulation, we confirmed significant overexpression of both hTNFα and endogenous mTNFα. Regarding the RA phenotype, macroscopic evaluation of arthritis revealed visible joint swelling in hTNFα-Tg mice compared to wild-type mice. Micro-CT imaging further confirmed prominent joint bone loss in hTNFα-Tg mice, validating their utility as an RA mouse model. To assess the in vivo therapeutic efficacy of hTNFα-targeted inhibitors, we administrated Infliximab to hTNFα-Tg mice and observed that Infliximab significantly reduced pathological scores of joint swelling and paw thickness, along with a significant increase in body weight gain. Concurrently, the treated mice exhibited amelioration of the joint space widening caused by bone destruction or inflammation, as well as phalangeal deformity.Overall, our hTNFα-Tg mouse model provides a powerful preclinical platform for the development of drugs targeting the hTNFα protein and for evaluating their efficacy and toxicity in vivo.

#1598 Preclinical efficacy of a bispecific NK cell engager studied using a humanized multiple myeloma mouse model.

Mari I. Suominen[1], Katja M. Fagerlund[1], Mervi Ristola[1], Justyna Zdrojewska[1], Yumei Diao[2], Carina Norstrom[2], Kristina Witt-Mulder[2], Ellen Santangelo[2], Thorstein Boxaspen[3], Hannah Cuthbertson Husbyn[3], Kim A. Giang[4], Caterina Heinz[5], Silje Z. Krokeide[3], Fredrik Schjesvold[6], Per-Ake Nygren[4], Ebba Sohlberg[5], Karl-Johan Malmberg[3], Stefan Svensson Gelius[2], Jukka P. Rissanen[1], Jenni H. E. Maki-Jouppila[1]

[1]Pharmatest Services Ltd., Turku, Finland,[2]Oncopeptides, Stockholm, Sweden,[3]Institute for Cancer Research, Oslo University Hospital, University of Oslo, Oslo, Norway,[4]KTH Royal Institute of Technology, Stockholm, Sweden,[5]Karolinska Institutet, Stockholm, Sweden,[6]Oslo University Hospital, Oslo, Norway

Natural killer (NK) cells are an essential part of the innate immune system as they can recognize and eliminate various cells in distress, such as virus-infected and tumor cells. Several promising therapeutics based on NK cell function are currently being developed and under preclinical and clinical investigation. This study aimed to evaluate the efficacy of an affibody-derived bispecific NK cell engager engineered to target CD16a on NK cells and BCMA on multiple myeloma (MM) cells, both *in vitro* and *in vivo*.

In vitro, efficient lysis of MM cells was observed across a panel of cell lines with varying BCMA expression using NK cells from healthy donors. The bispecific engager also achieved MM cell clearance in a 48-hour real-time cytotoxicity assay at a 2:1 effector-to-target ratio when combined with ADAPT-NK cells—*ex vivo* expanded adaptive NK cells from healthy donors (Haroun-Izquierdo A et al., J Immunother Cancer 2022). The engager did not induce IL-6 release measured in the presence of PBMCs and target cells.

In vivo, a humanized mouse model of MM was used to assess preclinical efficacy of the engager. In this model, human MM.1S cells - tagged with GFP and luciferase (BPS Bioscience) and xenograft-derived from mouse bone marrow - were combined with ADAPT-NK cells. The NSG-Tg(huIL-15) mice (The Jackson Laboratory) were given an intravenous injection of 0.5 million bone marrow-derived MM.1S cells, and tumor growth was followed by bioluminescence imaging (BLI). At study day 4, the dosing of the engager was started and continued daily until study day 18. Belantamab was used as a positive control and administered every fourth day, for a total of four doses, beginning on study day 4. ADAPT-NK cells were administered on study days 4, 8 and 13. Blood samples were obtained for flow cytometry throughout the study, and the mice were sacrificed on study day 33 when bone marrow was harvested for flow cytometry analysis.

Body weight developed similarly in all groups. Inhibition of tumor growth was observed by BLI from day 18 onward in the engager-treated group in comparison to vehicle controls. In the *ex vivo* BLI, lower tumor burden was observed in bones, liver, lungs and spleen in the engager treated group compared to the control. Flow cytometry of bone marrow showed fewer BCMA+CD138+ cells, indicating MM cells, in the engager- and belantamab-treated groups compared to vehicle controls.

These findings support the potential of the bispecific NK cell engager combined with ADAPT-NK cells as a treatment for MM. The study also demonstrates the utility of the humanized MM mouse model for evaluating NK cell engagers using BLI and flow cytometry.

#1599 mTOR enables alveolar macrophage survival and GM-CSF-STAT5-PPARγ signaling: Genetic and temsirolimus evidence.

Samson Hennessy-Strahs[1], Xiaojun Su[2], Si Sun[2], Ge Deng[2], Wen Muo[2], Tasha Miller[2], Xiang Xiao[2], Xian C. Li[2]

[1]Texas A&M College of Medicine, Bryan, TX,[2]Immunobiology and Transplant Science Center, Houston Methodist Research Institute, Houston, TX

Mechanistic target of rapamycin (mTOR) inhibitors, widely used in transplant and oncology settings, can induce a noninfectious pneumonitis linked to disrupted alveolar macrophage (AM) function. AMs uniquely require granulocyte-macrophage colony-stimulating factor (GM-CSF) signaling through CSF2RA, STAT5, and PPARγ to maintain identity and survival, yet the extent to which mTOR participates in this pathway in AMs remains undefined. Given that alveolar and interstitial macrophages (IMs) occupy distinct microenvironments with potentially divergent dependencies, the purpose of this study was to determine whether AMs exhibit a unique, non-redundant requirement for mTOR downstream of GM-CSF and how this requirement preserves AM survival and alveolar niche homeostasis.

To investigate mTOR dependence in AMs, we generated conditional myeloid mTOR knockout mice ($LysM^{Cre}mTOR^{f/f}$) and performed lung histopathology, flow cytometry, and signaling analyses across AMs and IMs. GM-CSF stimulation assays evaluated STAT5 phosphorylation in wild-type versus knockout AMs. Bone-marrow cultures were used to generate AM-like cells with GM-CSF to test mTOR-dependent differentiation and survival. WT AM-like cells were treated with rapamycin and GM-CSF. Intraperitoneal temsirolimus was administered to WT mice three times per week at 30 mg/kg/wk for four weeks. Human Protein Atlas datasets were interrogated for expression patterns of key signaling pathways in human AMs.

$LysM^{Cre}mTOR^{f/f}$ mice were generated and developed pulmonary alveolar proteinosis with AM loss, lipid-laden foamy AMs, and surfactant accumulation, while IMs and other tissue macrophages remained intact, indicating niche-specific mTOR dependence. Temsirolimus produced a similar AM depletion in vivo. AMs displayed higher baseline mTOR activity, CSF2RA, phosphorylated STAT5, and PPARγ than IMs. GM-CSF induced robust STAT5 phosphorylation in wild-type but not knockout AMs, whereas IMs showed neither basal nor inducible STAT5 activation. Human datasets demonstrated concordant AM-selective enrichment of CSF2RA, JAK2, STAT5, mTOR, phosphorylated S6, PPARγ, C/EBPβ, and downstream effectors (CD36, MerTK, Bcl-2 family proteins).

In vivo, mTOR-deficient AMs underwent progressive apoptosis with loss of PPARγ despite preserved CSF2RA. *In vitro*, GM-CSF drove AM-like differentiation marked by Siglec F, CD206, and CD11c regardless of genotype. In contrast, mTOR-deficient AM-like cells failed to upregulate p70 S6 kinase, C/EBPβ, PPARγ, CD36, MerTK, Bcl-2, and Bcl-xL. Rapamycin impaired survival of wild-type AM-like cells in a dose-dependent manner, partially rescued by increasing GM-CSF.

Together, these findings identify mTOR as a non-redundant regulator of GM-CSF survival signaling in AMs—a dependency absent in IMs—supporting an AM mechanism for mTOR inhibitor-associated alveolar injury.

#1600 Improved humanization of peripheral blood mononuclear cells in NSG-SGM3xIl15xDKO (SDKO) over that of NSG-MHC I/II DKO mice for immuno-oncology modeling.

Leandro Salati D'Abronzo, Xiaoqing (Nancy) Zheng, Beau Parry, Guoxiang Yang, Destanie Rose, Li-Chin Yao, James Keck, Jiwon Yang

The Jackson Laboratory-West, Sacramento, CA

Introduction Immunotherapies are the largest growing therapeutics applied to cancer and autoimmune disorders, rapidly transforming the drug development landscape. Despite significant improvements in immunotherapy research and available treatments, ample variation in clinical outcomes exposes gaps in our understanding of their mechanisms of action and specific response biomarkers. The development of the NSG-MHC I/II double-knockout (DKO) mice improved significantly the availability of models that can delay graft-versus-host disease (GvHD) while still achieving strong T cells engraftment. Nonetheless, DKO mice perform better with irradiation and engraftment with high doses of PBMCs to achieve these results and there is a challenge on producing multilineage human immune subsets such as natural killer (NK) cells and myeloid populations. Here, we characterize a next-generation DKO strain, SDKO (NSG-SGM3xIL15xDKO) designed for enhanced humanization with lower PBMC doses and improved immune diversity without the need for irradiation.

Methods Nonirradiated SDKO (Jax #037320, n=20) and DKO (Jax #025216, n=20) mice between 7-10 weeks of age were intravenously (IV) injected with 10 million PBMC using a total of five different donors. Mice were bled weekly via retro-orbital bleeds to assess engraftment status up for 12 weeks. Half the mice per strain were euthanized at SD21 for spleen engraftment checks. Survival was assessed up to 84 days.

Conclusions Survival between the two strains was comparable throughout the entire length of the studies. The newly developed mouse strain, NSG-SGM3xIL15xDKO (SDKO) offers improved overall humanized engraftment over the industry standard NSG-MHC I/II double-knockout (DKO), with higher hCD45+ numbers than DKO strain without the need for irradiation. Also, the SDKO strain present a higher T cell subpopulation (CD4+ and CD8+), higher number of Natural Killer (CD56+) cells and B (CD19+) cells. Noteworthy, SDKO presents high number of differentiated Plasma Cells (CD138+) in the spleen, a population that is not usually observed in engrafted DKO strain. Based on these results, we conclude that the novel SDKO mice better recapitulates the development of human innate and adaptive immunity than its counterpart DKO model.

#1601 A novel preclinical tool to unlock the potential of IL-18 in cancer immunotherapy: genO-hIL-18-hIL-18R mice.

Angela Pappalardo, Gaelle H. Martin, Patricia Isnard-Petit, **Fabiane Sonego**, Kader Thiam

genOway, Lyon, France

Interleukin-18 (IL-18) has emerged as a promising immunomodulatory cytokine in immuno-oncology due to its ability to enhance both innate and adaptive immune responses. It promotes IFN-γ production by T and NK cells, thereby amplifying anti-tumor immunity, especially when combined with checkpoint inhibitors or engineered pro-drugs to resist natural inhibition by IL-18BP. Recent studies suggest that IL-18-based therapies may overcome resistance mechanisms in "cold" tumors, making them more responsive to immunotherapies. Humanized mouse models expressing human IL-18R are essential to accurately assess efficacy and guide development of human-directed IL-18-based therapies. Therefore, we describe here a new IL-18-IL-18R double humanized mouse model to assess the efficacy of therapeutics targeting the IL-18/IL-18R axis. The generated genO-hIL-18-hIL18-R mice show expression of human IL-18Ra on NK, monocytes and T cells under steady state conditions. Functional validation of genO-hIL-18/hIL18-R mice demonstrates robust *in vitro* IFN-γ production by splenocytes upon stimulation with exogenous human IL-18, suggesting that hIL-18R is functional. Similarly to mouse IL-18 in wild-type mice, human IL-18 is not detected in naïve mice. However, its secretion can be induced *in vivo* by treatment with lipopolysaccharide (LPS), which also triggers IFN-γ secretion. Importantly, humanization of the IL-18/IL-18Ra axis does not alter the physiological distribution of immune cells, as immune-profiling reveals comparable frequencies of main immune cells between genO-hIL-8-hIL-18R mice and wild-type control mice. Finally, the effectiveness of the genO-hIL-18-hIL-18R model in supporting drug efficacy was demonstrated by evaluating an engineered IL-18. Splenocytes from genO-hIL-18-hIL-18R mice treated with this engineered IL-18 exhibited enhanced cell proliferation and increased IFN-γ production compared to those treated with an inactive IL-18. Altogether, these data support the suitability of the genO-hIL-18-hIL-18R mice for assessment of new therapies targeting this axis.

#1602 Quaking regulates macrophage MHC II-mediated antigen presentation and immune function in glioblastoma.

Spring Yewon Hwang

Cancer Biology, MD Anderson, Houston, TX

Glioblastoma (GBM) remains one of the most lethal brain tumors, in part due to profound immunosuppression driven by tumor-associated macrophages (TAMs). A central deficit within the GBM microenvironment is the failure of macrophages to execute effective MHC class II (MHC II)-mediated antigen presentation, a process essential for priming anti-tumor $CD4^+$ T cell responses. We identified the RNA-binding protein Quaking (Qki), frequently lost or mutated in GBM, as a critical regulator of macrophage antigen processing and presentation.

Across human GBM datasets and the QPP (Qki-/-; Trp53-/-; Pten-/-) glioma model, Qki expression positively correlates with MHC II and its master regulator CIITA. Using bone marrow-derived macrophages, we found that Qki deficiency does not impair IFNγ-driven induction of MHC II transcripts. However, Qki knockout (KO) macrophages were unable to effectively activate $CD4^+$ T cells in OT-II co-culture assays, indicating a defect downstream of transcription. Functionally, phagocytosis and DQ-OVA assays revealed that Qki KO macrophages display reduced phagocytosis and proteolytic activity, suggesting that Qki mediates multiple steps of antigen processing and presentation.

To define Qki-dependent programs, we performed RNA sequencing in wild-type and Qki-KO macrophages. Qki loss led to coordinated downregulation of pathways involved in extracellular matrix interactions, focal adhesion signaling, and protein uptake. Using qPCR, we confirmed decreased expression of key regulators, including Cav1 and Thbs1, demonstrating that Qki orchestrates post-transcriptional programs that enable cytoskeletal dynamics, vesicle trafficking, and antigen processing required for MHC II function.

To explore therapeutic potential, we tested the Qki co-activator agonist KD3010, which enhanced MHC II expression and $CD4^+$ T cell activation in vitro, and improved survival in QPP mice. Proteomic analysis identified osteopontin (OPN), a protein elevated in GBM, as a tumor-derived factor suppressing Qki. In vitro, OPN treatment reduced Qki expression in macrophages, suggesting that it acts as a mechanism of immune suppression.

In conclusion, our findings identify Qki as a central regulator of macrophage antigen processing and MHC II functionality and uncover a GBM-driven pathway that disrupts this axis. Restoring Qki represents a promising strategy to reawaken macrophage immunity in glioblastoma.

#1603 Opposing control of MHC-II antigen presentation by FAK and PYK2: Implications for therapeutic intervention.

Terrance James Haanen[1], Xiao Lei Chen[1], David D. Schlaepfer[2]

[1]Obstetrics, Gynecology, and Reproductive Sciences, University of California, San Diego, San Diego, CA, [2]University of California, San Diego, San Diego, CA

High-grade serous ovarian cancer (HGSOC) is the most lethal gynecologic malignancy in the U.S. and is marked by resistance to chemo- and immunotherapy. Although focal adhesion kinases (FAK and PYK2) are known to induce tumor microenvironment immunosuppression, their role in altering tumor-cell major histocompatibility complex class-II (MHC-II) presentation requires further investigation. HGSOC tumors have few mutations but frequently show FAK amplification (~75%). Notably, elevated MHC-II expression correlates with longer progression-free survival in recurrent HGSOC, likely through enhanced $CD4^+$ T-cell activation and improved anti-tumor immunity. Flow cytometry analysis revealed that ATP competitive small molecule inhibition of FAK kinase activity (FAKi) increases MHC-II antigen presentation *in vitro and in vivo*. Targeted FAK protein degradation following treatment with a FAK proteolysis targeting chimera (FAK-PROTAC) produced a similar effect. In a syngeneic orthotopic mouse model, FAK depletion induced MHC-II to levels comparable to kinase-dead FAK, consistent with the loss of FAK activity in promoting tumor MHC-II expression. As ovarian tumor cells also express the FAK-related homolog PYK2, CRISPR was employed to selectively inactivate FAK and or PYK2 expression in human OVCAR3, murine KMF, and murine HGS2 ovarian tumor models. Notably, loss of FAK, but not PYK2, resulted in enhanced MHC-II presentation in these cells. As tumor cell treatment with a dual FAK-PYK2 inhibitor or PROTAC that targets FAK and PYK2 does not induce MHC-II expression as does selective loss of FAK, our results support a distinct immunogenic role for PYK2 in ovarian tumor cells. Ongoing studies are evaluating PYK2 mechanism of action upon FAK inhibition and the regulation of CIITA (class II, major histocompatibility complex, transactivator) transcription. Collectively, our findings suggest roles for FAK-specific inhibitors that may potentiate MHC-II-related adaptive immune responses as a therapeutic strategy for advanced ovarian cancer.

#1604 PTEN-L/CD68 axis regulates diet-induced obesity, monocyte-to-macrophage polarization, and signaling via IL-4 and AKT pathways.

Tiphaine C. Martin[1], Sait Ozturk[1], Benjamin Kepecs[1], Nicolas de Azevedo[1], Ivan Reyes-Torres[1], Royce Zhou[1], Kaitlyn Bosch[1], Emily Gallagher[1], Miriam Merad[2], Ang Cui[3], Alexander Tsankov[1], Ramon Parsons[1]

[1]The Tisch Cancer Institute, Icahn School of Medicine at Mount Sinai, New York, NY,[2]Precision Immunology Institute, The Tisch Cancer Institute, Icahn School of Medicine at Mount Sinai, New York, NY,[3]Harvard Medical School, Boston, MA

Obesity has emerged as a major health issue in the developed world, including in the development and treatment of cancer. Immune regulation is crucial for maintaining adipose tissue balance; however, the early events that convert a noninflammatory state to inflammation, contributing to obesity and cancer, remain poorly understood. PTEN is well known as a tumor suppressor that inhibits the PI3K/AKT pathway and has been linked to cancer, obesity, and macrophage (MΦ) function. However, the role of its secreted isoform, PTEN-L, remains unclear. We previously observed that PTEN-L affects the function of MΦs in mice during *Pseudomonas aeruginosa* infection and tumor development. Here, based upon a yeast two-hybrid screen, we identified that PTEN-L interacts with CD68, a MΦ marker encoding a scavenger receptor with an unknown function. We studied PTEN-L and CD68 in the context of induced obesity with a high-fat diet (HFD) by knocking them out in mice. We observed that CD68 facilitates entry of PTEN-L into MΦs and human tumor cells, and that Pten-l and Cd68 knockout mice fed a HFD are protected from obesity. Adipose tissue from Pten-l and Cd68 knockout mice exposed to a HFD showed similar immune phenotypes, including expansions of $CBR2^{+}$ and immature monocyte-derived MΦs and depletion of $Apoe^{+}$ and lipid-associated MΦs, which displayed characteristics of IL-4-stimulated polarization and elevation of AKT activation. Our findings suggest that Pten-l and Cd68 play a role in regulating MΦ polarization by attenuating IL-4-AKT signaling and are important factors in the high-fat diet-induced remodeling of white adipose tissue, contributing to obesity and insulin resistance. Interestingly, treating patients with Atopic Dermatitis using an antibody targeting the IL-4 receptor has been demonstrated to be associated with a noteworthy increase in body weight. Meanwhile, IL-4 influences the phenotype of tumor-infiltrating monocyte-derived MΦs and plays a role in mediating resistance to immunotherapy through macrophage regulation. Thus, we define a mechanism of adipose tissue homeostasis controlled by the expression of PTEN-L and CD68 in myeloid populations, which may have clinical relevance for immune and metabolic responses due to PI3K/AKT inhibitor and IL4R targeted therapy.

#1605 Motif neoepitopes demonstrate immunogenic signal in CCL21-gene modified dendritic cell vaccination trial (NCT03546361).

Amy Lauren Cummings[1], Andy Han[1], Michael Oh[2], Camelia Dumitras[2], Seung J. Park[1], Sai S. Kollapaneni[1], Daniel Li[1], Arjan Gower[2], Maria Antonia Velez Velez[3], Aaron Lisberg[2], Monica Cappelletti[1], Steven M. Dubinett[2], Bin Liu[2], Edward B. Garon[4]

[1]UCLA Health, Los Angeles, CA,[2]UCLA David Geffen School of Medicine, Los Angeles, CA,[3]UCLA - University of California Los Angeles, Los Angeles, CA,[4]Asst. Prof., Dept. of Hem./ Onc., University of California (UCLA), Santa Monica, CA

Background: Inefficient prediction of functional tumor neoantigens and subsequent host anti-tumor immune responses limit optimization of immunotherapeutic approaches. We recently demonstrated that programmed cell death 1 inhibitors have greater efficacy in those with charged human leukocyte antigen (HLA)-B binding pockets whose tumors harbor mutation(s) leading to “motif” neoepitopes (those that generate new charged HLA anchors). Whether peptides derived from motifs are capable of inducing host tumor-specific immune responses was previously unknown.

Methods: Matched tumor and peripheral blood mononuclear cell (PBMC) biospecimens from participants (pts) in NCT03546361 underwent whole exome sequencing (WES) and HLA/supertype/neoepitope prediction using established pipelines. Pts were grouped as (1) 1+ B44/B27 allele with 1+ motif, (2) B44/B27 without motifs, and (3) no B44/B27 alleles. For (3), neoepitope prediction was run with classic B44/B27 supertype alleles (B*40:01, B*27:05) as a negative control. Nonamer peptides were created from pt motif and non-motifs and their wildtype sequence. For those with more than 2 non-motifs, the highest variant allele fraction (VAF), lowest IC50 (binding), and/or highest fold change (fold) were selected. T-cell activation and expansion assays were run using pt PBMC collections on days 0, 21, 42, and 63 by co-incubating peptide-pulsed dendritic cells ($2x10^5$) with autologous CD8+ T cells ($2x10^6$) in RPMI containing 10% pooled human serum, 10 mM HEPES, 2mM L-Glutamine, and 50 µM β-mercaptoethanol supplemented with IL-15 (10 ng/mL) and IL-2 (50 IU/mL) for both 18 hours and 10 days. Negative controls included vehicle only (0.1% DMSO); positive controls included PMA (25 ng/mL), ionomycin (1 µg/mL) and BFA. Activated T cells were assessed by flow cytometry based on intracellular staining of INF-ɣ and TNF-α.

Results: 18 pts underwent analysis: 14 had sufficient WES, 11 exhibited a B44/B27 allele. Of these, 8 pts had predicted neoepitopes with VAF ≥10%: 3 pts were (1), 2 were (2), 3 were (3). From this cohort, 23 peptides represented 6 motif, 6 VAF, 4 binding, 4 fold, and 3 multiple categories. Positive controls yielded activated T cell peaks at day 42 (4.78%). One participant in the B44/B27 motif category (1) had one peptide that elicited T cell activation at day 42 (2.51%), which was motif/VAF, and confirmed in a subsequent assay (0.63%). All other peptide experiments did not demonstrate T cell activation, and there were no pts who demonstrated meaningful clinical benefit from the trial.

Conclusion: Current neoepitope prediction continues to provide limited insight into functionality. In a limited sample size of those without clinical benefit to NCT03546361, possible functionality of one motif neoepitope was demonstrated. Additional studies are ongoing to validate these findings and further define the functional relevance of motif neoepitopes.

#1606 Transcriptional regulation of human NK cells: TAL1 as a modulator.

Baomou Feng, Dandan Wang, Subramaniam Malarkannan

Molecular Immunology, Versiti Blood Research Institute, Milwaukee, WI

Background - Natural killer (NK) cells are major cytotoxic lymphocytes subset with potent activity against hematopoietic malignancies and are strong candidates for immunotherapy. However, their clinical application is limited by our incomplete understanding of the transcriptional programs that control NK cell development and function. Human NK cells development from hematopoietic stem cells to mature NK cells is orchestrated by a network of lineage-committing transcription factors (TF). TAL1—a class II basic helix-loop-helix TF—is essential for early hematopoiesis and is maintained in several mature myeloid lineages, but it is absent from mature B- and T-cells. However, we recently discovered that mature human NK cells express TAL1, making them a rare lymphoid population retaining TAL1 expression. We also identified three TAL1 isoforms, suggesting isoform-specific roles in NK cell maturation and function. This suggests that TAL1 may shape NK cell identity and function. We hypothesize that TAL1 is a previously unrecognized regulator of human NK-cell development and cytotoxic activity. To test this, we used (a) an inducible TAL1 knockout mouse model to identify TAL1-dependent checkpoints in NK cell development and (b) TAL1 overexpression in NK-92 cells to characterize TAL1 binding partners.

Method - For development and differentiation of NK cells, we generated an inducible *TAL1*$^{fl/fl}$*Mx1*^{Cre} knockout (KO) mouse model, in which poly(I:C) was used to activate Cre. Bone marrow and spleen tissues were then analyzed by flow cytometry. We used CRISPR/Cas9 to generate HEB, ID2, and E2A KO NK-92 cells and created a TAL1-overexpressing NK-92 line. Protein expression and interactions were assessed by Western blot and co-immunoprecipitation.

Results - TAL1 KO in mouse showed a significantly increased percentage of NK progenitor cells (CD3ε$^-$CD122$^+$NK1.1$^-$NCR1$^-$; 91.3% in KO vs 33.0% in WT) and a reduction of immature and mature NK cells (CD3ε$^-$CD122$^+$NK1.1$^+$ and CD3ε$^-$CD122$^+$NCR1$^+$) in the bone marrow compared to control. Co-immunoprecipitation of TAL1 in NK92 cells revealed protein interactions with methylase SETD1A, and E-proteins HEB, and ID2.

Conclusion - TAL1 KO mice show NK cell maturation arrested at the CD122$^+$NK1.1$^+$ progenitor stage, suggesting a central role for TAL1 in NK cell development. Co-immunoprecipitation in NK-92 cells revealed TAL1 interactions with SETD1A, HEB, and ID2. We propose that TAL1 forms a heterodimer with HEB that recruits the demethylase LSD1 to repress genes required for NK cell maturation. When ID2 joins the complex, it blocks LSD1 recruitment and instead brings in the methylase SETD1A to activate maturation-associated genes. Together, these findings raise the possibility that TAL1 recruits specific partners that influence NK cell maturation. Understanding the role of TAL1 in human NK cell development may enable the therapeutic modulation of NK cell function for clinical applications.

: T Cell Engagers 1
Poster Session

#1609 Unlocking pMHC target space for next generation T cell engagers in oncology and autoimmunity.

Roberto Magliozzi, Haydn Prosser, Hanif Ali, Amy Li, Luca Pellegrinet, Ni Huang, Petra Mlcochova, Wei Wang, Ruben Cabanillas, E-Chiang Lee, Allan Bradley

T-Therapeutics Ltd, Cambridge, United Kingdom

Peptide-MHC (pMHC) complexes represent a compelling and emerging class of targets for oncology and autoimmune diseases. Their presentation on the cell surface enables the targeting of peptides from non-membrane bound proteins which could be highly specific to pathogenic cells. The lack of disease cell-surface specific targets is currently limiting the potential of bispecific T cell engagers (TCEs) for solid tumours and autoimmune diseases. Despite their promise, pMHC targeting TCEs face two significant challenges. Firstly, a pMHC targeting entity needs to bind to the pMHC of interest with high affinity and specificity to ensure drug efficacy and safety. Secondly, since cell surface density of pMHC is generally low (typically ~10 -1,000 copies per cell), the bispecific format and anti-CD3 moiety need to work concordantly to mediate efficient killing with minimal cytokine release. We have developed unique technology platforms to overcome these major challenges for delivering first-in-class pMHC directed TCEs for solid tumours and autoimmunity. To harness the natural ability of TCRs to bind pMHC with high specificity and overcome the constraints for TCR discovery against self antigens in humans due to negative selection in T cell development, we generated a humanised transgenic mouse, OptiMus® mouse, by introducing human TCRα, TCRβ, CD8α, CD8β, HLA- A02, and β2M genes in situ by precision genome engineering. Over a decade, 1.6 million bases of human DNA were introduced into the mouse to fully humanise the entire TCRαβ repertoire, CD8 co-receptor and MHC class I. The immune compartment of this mouse strain is phenotypically normal, and importantly, it allows TCR discovery against human antigens without the self-antigen constraint. The diverse TCR repertoire produced by OptiMus® mouse enables the discovery of hundreds of antigen-reactive TCRs as a starting point for drug discovery. Drug efficacy at low pMHC target density requires a TCE format that is optimised for immune synapse engagement. The anti-CD3 moiety must be fine-tuned in terms of epitope selection and affinity modulation to maximize the therapeutic window. We have explored over 500 formats to identify a novel design in which a TCR, anti-CD3 and Fc are accommodated to allow efficient immune synapse formation and target cell killing, and which has an antibody-like developability and pharmacokinetics profile. Furthermore, we discovered de novo anti-CD3 moieties that are optimised with our format for desired properties: durable serial killing, high *in vivo* potency, low cytokine release and no T cell mediated drug disposition. By maximising the power of our technology platforms, from human TCR discovery to TCE engineering, we are advancing a pipeline of first-in-class TCEs for oncology and autoimmune indications. Our approach unlocks previously inaccessible targets and redefines the potential of TCEs in precision immunotherapy.

#1610 A novel and versatile Prodrug T cell engager platform with a novel candidate demonstrating potent and tumor-restricted activity.

Zhou Lv, Yinhui Ding, Jingjing Mao, Huifeng Lv, Yang Yang, Yi Ren, Yu Zhang, Lijun Wang, Danqing Wu, Xuan Wu, **Shiyong Gong**

Shanghai EpimAb Biotherapeutics Co., Ltd., Shanghai, China

T-cell engagers (TCEs) have emerged as a powerful modality of immunotherapies. However, their clinical application, particularly in solid tumors, is limited by on-target, off-tumor toxicities and potentially life-threatening systemic immune activation, such as severe cytokine release syndrome (CRS). To address these challenges, conditionally activated prodrug TCEs (ProTCEs) represent a promising next-generation strategy. Recent efforts have focused on masking either the CD3 binding domain or both CD3 and TAA (tumor associated antigen) binding domain of TCEs. The masking peptide is fused to ProTCE molecules usually through a cleavable linker that can be cleaved by tumor-specific proteases. Despite recent progress, there is still a challenge for balancing efficient masking and tumor-specific activation to achieve a wider therapeutic window. Here, we present a modular ProTCE design that includes a masking peptide screening platform, allowing rapid identification of masking peptides that effectively suppress the antibody binding ability. Moreover**,** we engineered a proprietary peptide linker that can be recognized and cleaved by multiple tumor specific proteases. This novel linker exhibits exceptional stability in serum to prevent systemic activation, while demonstrating enhanced cleavage efficiency by tumor-associated proteases, ensuring tumor-specific drug activation and exposure. In addition, our platform is flexible to generate single masking (mask CD3 binding domain) or dual masking (mask both TAA and CD3 binding domains) ProTCEs. With this platform, we have generated a pipeline of ProTCE molecules targeting various TAAs. Most notably, we have developed a ProTCE, EM33, targeting a TAA that is highly expressed on multiple solid tumors but also expressed on normal tissues at a low level. This molecule was designed to have both TAA and CD3 binding domains masked. EM33 exhibits minimal activity in its prodrug form; however, upon exposure to proteases, its activity is fully restored, demonstrating a 1000-fold therapeutic window. In a high density PBMC assay, our ProTCE does not induce T-cell activation and cytokine release, in contrast to its unmasked variant. In vivo, this molecule demonstrated significant tumor growth inhibition in multiple PBMC engrafted tumor cell xenograft models. EM33 also exhibited comparable anti-tumor activity to the unmasked TCE while inducing significantly less cytokine release, indicative of its potential enhanced benefit/risk ratio in human.Our ProTCE platform enables the rapid development of conditionally activated TCEs with an improved therapeutic window. The preclinical data for our first candidate highlights the potential of our platform to generate new TCE therapies for cancer patients targeting TAAs, that currently have posed significant safety and/or efficacy challenges to the classical T-cell engaging approach.

#1611 Development of a T cell engager against IGFBPL1: A novel target for small cell lung cancer and other neuroendocrine cancers.

Lauren A. Pitt, Eleanor Leung, Ruban Kannan, Shereen Jabar, Nicole Church, Zariah Rosenes, Ben Kiefel, Matthew Beasley

Myrio Therapeutics Pty Ltd, Melbourne, Australia

Small cell lung cancer (SCLC) is an aggressive neuroendocrine malignancy with dismal clinical outcomes defined by treatment resistance. FDA approval of tarlatamab, a T cell engager targeting DLL3, has delivered a new treatment option for patients with relapsed disease and spurred enthusiasm for T cell engagers and other DLL3-targeted therapies for SCLC. Notably, SCLC is transcriptionally complex with multiple molecular subtypes. Additional treatment options are required for DLL3-negative patients and to combat acquired resistance associated with intratumoral heterogeneity. Insulin growth factor binding protein-like 1 (IGFBPL1) is a member of the insulin-like growth factor binding protein (IGFBP) family, secreted proteins regulating the biological activity of insulin-like growth factors (IGFs). *IGFBPL1* is normally silenced in healthy adult tissues, but is highly expressed in SCLC, as well as other neuroendocrine-phenotype cancers, as shown in human cell lines and patient samples. Using Retained Display (ReD^{TM}) technology, we isolated several fully human single chain variable fragments (scFvs) specifically recognising a peptide derived from IGFBPL1 presented by HLA-A*02:01, one of the most common HLA alleles worldwide. We generated a half-life extended T cell engager based on a lead candidate scFv displaying picomolar range binding to the target IGFBPL1/HLA-A*02:01 complex. Potent killing of HLA-A*02:01-positive SCLC cell lines naturally expressing IGFBPL1 was observed in vitro, including models with low HLA surface expression - a common feature of SCLC. We are currently characterising IGFBPL1 expression at the total protein and surface peptide level, in addition to evaluation of in vivo efficacy and other IND enabling studies in progress. Our data support development of a novel T cell engager for SCLC based on IGFBPL1 targeting. This potential therapy provides another option to DLL3-targeting therapies in the clinic and under investigation, to overcome this challenging and devastating disease.

#1612 Novel CD3 binders enable T cell engagers with potent tumor control, limited cytokine release, and safe pairing with co-stimulation.

Sinduja Marx, Ian Blumenthal, Kristina Pilat, Shelli M. Morris, Emily J. Girard, Kenneth Brasel, Ray Ruff, Alison M. Williams, Hailey Hentschel, Steven Chen, Chunfeng Yin, James M. Olson, Jason Price

Seattle Children's Research Institute, Seattle, WA

Introduction: T cell engagers (TCEs) have demonstrated clinical promise in hematologic malignancies, but their application in solid tumors has been held back by significant side effects and limited efficacy. TCEs that bind CD3 with SP34-derived clones exhibit marked polyreactivity, leading to off-target activation and narrow therapeutic windows. Leveraging a unique nanoparticle-based immunization platform, we discovered non-polyreactive, non-human primate (NHP) cross-reactive CD3 binders, many against novel CD3 epitopes. As exemplified by a CD3δε selective clone, SCRI-6, these binders drive potent anti-tumor activity with reduced cytokine production. Our data suggests that these novel binders are uniquely positioned to pair with TCE designs that incorporate costimulation strategies to improve T cell antitumor activity and persistence.

Methods: Our antibody campaign used a novel immunization strategy in the OmniRat transgenic platform incorporating whole-cell and protein-nanoparticle immunogens. Identified hits from the campaign were produced as recombinant monoclonal antibodies and biochemically and biophysically characterized. Clinical benchmark TCEs incorporating our novel CD3 binders were evaluated for non-specific activation, antigen-dependent tumor-cell killing and cytokine release in vitro and in vivo.

Results: We identified 12 distinct sequence families, 7 of which bound and activated human T cells. Among these, 5 showed no detectable polyreactivity. Four clones recognized both CD3δε and CD3γε subunits, whereas one clone (SCRI-6) bound exclusively to CD3δε. Notably, 3 of these sequence families, including SCRI-6, also activated NHP T cells. TCEs (targeting PD-L1, DLL3, and CD19) that incorporate our novel CD3 binders demonstrated antigen-dependent cytotoxicity comparable to SP34-based TCEs but with reduced cytokine release (e.g., IFNγ, IL-2, TNFα, and IL-6). In an assay to assess tumor-independent activation of T cells, TCEs including SCRI-6 exhibit dramatically less non-specific T cell activation than matched-TCEs containing SP34. Adding CD28 or 4-1BB costimulation to this assay dramatically exacerbated the non-specific activation caused by SP34-containing TCEs; however, swapping the CD3 binder for SCRI-6 eliminated this activity. TCEs incorporating SCRI-6 demonstrate equivalent potency to clinical benchmark comparators in both solid and liquid in vivo tumor models, but with substantially lower cytokine release.

Conclusion: Non-polyreactive CD3 engagers may be incorporated into TCEs to improve therapeutic index without sacrificing potency and allowing for therapeutic strategies that safely engage T cell costimulatory targets.

#1613 Expanded therapeutic window of potent bispecific PD-L1:CD3 T cell engager using a novel best-in-class CD3 binder.

Andrew J. Mhyre, Emily J. Girard, Sinduja Marx, Shelli M. Morris, Kristina Pilat, Alison M. Williams, Parvathi Muthuraman, Ray Ruff, Hailey Hentschel, Steven Chen, Chunfeng Yin, Zachary Crook, Jason Price, James M. Olson

Seattle Children's Research Institute, Seattle, WA

Introduction: Bispecific T cell engagers (TCE) are potent, off-the-shelf immune modulators that have been hugely successful against hematologic malignancies and are beginning to demonstrate utility in solid tumors. PD-L1 targeting bispecific TCE with an SP34 variant CD3 binder showed exceptionally potent activity against intracranial tumor models in mice. To further expand the potential therapeutic index, we engineered SCRI-6, a novel, high-affinity, non-polyreactive CD3 binder, into a next generation PD-L1 TCE and compared the SP34 and SCRI-6 versions for efficacy and tolerability.

Methods: The efficacious dose range of systemically administered PD-L1:CD3 TCE was interrogated using SP34 or SCRI-6 CD3 binders against intracranially implanted NCI-H1975-GFP/ffLuc, modeling metastatic lung cancer. Activity of SP34 or SCRI-6 TCE with a murine PD-L1 binder was evaluated in mice transgenic for human CD3ε.

Results: Bioluminescent tumor burden of mice treated with the SP34 TCE was eliminated in 85-100% of mice across the entire dose range of 0.3 to 8.5 mg/kg. However, despite the loss of luminescent signal at 2.1, 4.2, and 8.4 mg/kg, 28-85% of these mice met humane end point criteria and were removed from study early, suggesting that these doses exceeded the maximum tolerated dose. SCRI-6 TCE eliminated bioluminescent tumor signal and 100% of mice remained healthy at doses from 0.03 to 2.12 mg/kg (the highest dose tested). Doses of 0.0005-0.008 mg/kg did not alter tumor growth, and the median survival was similar to the negative control group, establishing the lower limit of efficacy for this TCE. A dose titration from 0.01 to 5 mg/kg of both the SP34 and SCRI-6 TCE in human CD3ε transgenic mice showed pharmacodynamic responses with similar, modest, and transient loss of body weight and transient depletion of circulating lymphocytes at doses of 0.4-5mg/kg. Cytokines associated with cytokine release syndrome (IL-6, IFNγ and TNFα) were found to be elevated at higher levels in SP34 TCE treated mice compared to those in SCRI-6 TCE mice. INFγ was significantly higher in the SP34 TCE at 5, 2.5, and 0.1mg/kg ($p=0.03$, 0.05, and 0.01 respectively), TNFα at 5mg/kg ($p=0.003$), and IL-6 at 1.3mg/kg ($p=0.03$), suggesting a higher tolerated threshold for the SCRI-6-based TCE. In the NCI-H1975 brain metastases model, the SCRI-6 TCE induced complete and durable remissions for the entirety of the study, whereas remissions tended to be variable and transient with the SP34 version.

Conclusion: Incorporation of the novel SCRI-6 CD3 binder into a potent PD-L1 targeted TCE showed superior efficacy with lower cytokine secretion, demonstrating potential to expand the therapeutic index.

#1614 Novel anti-CD3 single domain antibodies for the development of T cell engager.

Jieying Liu, Yongqing Cheng, Mengmeng Sun, Xiaoqian Zhang, Hui Cong, Rumeng Bao, Changchang Zhang, Yu Dan, Shuang Wang, Jie Yang, Donghui Wu, Lei Wu, Jijie Gu

WuXi Biologics, Shanghai, China

In cancer immunotherapy, CD3 T-cell engager (TCE) bispecific antibodies (BsAbs) represent a pivotal direction in drug development due to their ability to directly recruit T cells for precise elimination of tumor cells. Currently, all approved TCE BsAbs are based on conventional anti-CD3 antibodies consisting of both heavy and light chains. However, these TCEs face challenges in bispecific format design and complicate manufacturing, due to their structural complexity. In contrast, TCEs based on anti-CD3 single-domain antibodies (sdAbs, or VHHs) enable modular assembly into compact bispecific molecules. This approach avoids the light chain mispairing issue and allows for more flexible molecular design. Their simpler architecture streamlines production, especially for multi-specific constructs. Moreover, smaller VHHs may facilitate formation of more effective immune synapses. WuXi Biologics has developed a panel of anti-CD3 VHHs with novel sequences derived from immunized llama phage display libraries. These VHHs exhibit a range of binding affinities to CD3 and varying potencies in T-cell activation. TCE molecules constructed using these CD3 VHHs demonstrate potent T cell-dependent tumor cell killing efficacy both in vitro and in vivo. Compared with some marketed TCEs, our VHH-based CD3 TCE molecules show superior in vivo efficacy with comparable cytokine profiles. Additionally, these humanized VHHs display excellent developability characteristics.

#1615 Discovery of CD28 targeting single domain antibodies to facilitate the development of costimulatory T cell engager.

Siwei Nie[1], Yali Wan[2], Hang Zhou[2], Xinyan Ji[2], Jianqing Xu[2], Lei Wu[2], Jijie Gu[1]

[1]WuXi Biologics, Wuxi, China,[2]WuXi Biologics, Shanghai, China

Optimal T-cell activation is a multistep process requiring T-cell receptor engagement by peptide-MHC complexes (Signal 1) coupled with costimulatory signals (Signal 2). The lack of Signal 2 increases the TCR activation-induced cell apoptosis and decreases T cell proliferation, which may lead to compromised therapeutic activity of anti-PD1 therapy or CD3 T cell engagers (TCEs) in the clinic. The purpose of this study is to identify CD28 single domain antibodies to develop co-stimulatory T cell engager to improve T cell proliferation, survival and response durability, and therefore further expand the utility of checkpoint blockade and/or CD3 TCE therapies for treatment of a broad range of solid tumors. The agonistic propriety of CD28-targeting VHH or CD28-based bi-specific TCE (BiTCE) or tri-specific TCE (TriTCE) was evaluated by analysis of IL-2 secretion in PBMC/T cell activation assay. T cell survival was measured by the expression of anti-apoptosis marker Bcl-xl after treatment of CD28-based antibody. Tumor cells were incubated with T cells together with CD28-based bi- or tri-TCE in the presence of CD3 TCE or anti-PD-1 mAb. Viability of target cells were then measured to reflect T cell killing activity. Xenograft mice models were further used to confirm the benefit of integrating CD28-targeting agonist into CD3 TCE. A series of CD28-targeting agonistic VHHs binding to CD28 with different binding affinities in a non-superagonistic manner were obtained. The co-stimulatory effect of CD28-targeting T cell engagers were demonstrated: (1) CD28xB7-H3 BiTCE significantly improved T cell killing potency and durability on OVCAR-3 cells when combined with CD3 TCE and strongly activated T cells and enhanced T cell killing potency of A375 cells when combined with anti-PD-1 mAb; (2) CD3/CD28/TAA TriTCE were generated by screening of the most suitable CD28 agonist and delicate format design. Both CD3xROR1xCD28 and CD3xMUC16xCD28 significantly improve T cell survival which in turn allows more persisted T cell killing of target tumor cells in vitro and in vivo, compared to CD3xROR1 and CD3xMUC16, respectively. Therefore, including CD28 signaling during CD3 TCE and immune checkpoint blockade treatment may improve the therapeutic benefit in patients with solid tumors.

#1616 CLSP-5282, a first-in-class T cell engager targeting KRas^{G12V} mutant peptide presented on HLA-A*03:01.

Amanda Ford[1], Lenore Cullen[1], Alec R. Andrews[1], Justina X. Caushi[2], Catherine Souza[1], Veselin S. Dobrev[2], Raffaello Verardi[2], Hayden Jones[2], Brena Williams[2], Kai Li Tan[2], Michael Alloway[2], Anthony S. Gizzi[2], James Bingham[2], Gillian A. Kingsbury[1], **Jessica Kohler**[1]

[1]Clasp Therapeutics, Cambridge, MA,[2]Clasp Therapeutics, Rockville, MD

Background: Mutant KRas is one of the most common driver oncogenes in solid tumors. Approximately 25% of pancreatic cancer, 9% of colorectal cancer (CRC), and 5% of non-small cell lung cancer (NSCLC) tumors harbor KRas^{G12V} mutations. We describe the nonclinical characterization of CLSP-5282, a first-in-class T cell engager that selectively targets the KRas^{G12V}[7-16] mutant peptide presented on HLA-A*03:01.

Methods: Functional activity was assessed *in vitro* in co-culture assays of T cells and target cells expressing KRas^{G12V} and HLA-A*03:01, including models with acquired resistance to Ras-targeted small molecule inhibitors. Since CLSP-5282 does not cross react with any preclinical toxicology species, an extensive panel of secondary pharmacology and in vitro toxicology studies was performed. A Jurkat reporter assay with a positional scanning peptide library was used to identify potential cross-reactivity to other peptides presented on HLA-A*03:01. Specificity was further assessed by T cell reactivity with a panel of normal human tissues and a panel of the most common Class I HLA alleles, and cytokine release in high density PBMC cultures was determined to evaluate CRS risk. In vivo anti-tumor activity of CLSP-5282 was investigated in PBMC engrafted mouse models.

Results: CLSP-5282 induces T cell activation and target cell killing specifically against cells expressing KRas^{G12V} and HLA-A*03:01, but not wild-type KRas. Cell lines with acquired resistance to KRas inhibitors maintain sensitivity to CLSP-5282, suggesting continued presentation of the KRas^{G12V} neoantigen. In vitro studies did not identify potential cross-reactivity to any peptides presented on HLA-A:03:01 and showed minimal T cell reactivity or cytokine release with a panel of normal human tissues, a panel of the 50 most common Class I HLA alleles, or in high-density PBMC cultures. In vivo, CLSP-5282 induces regression of established tumors in a humanized mouse model.

Conclusions: These preclinical data support clinical evaluation of CLSP-5282 in HLA-A*03:01 positive patients with solid tumors harboring the KRas^{G12V} mutation. CLSP-5282 is expected to be the first TCE in the clinic directed against mutant KRas, providing tumor targeting without the risk of on-target, off-tumor toxicity. Our data demonstrate the potential for CLSP-5282 to be efficacious even in the context of resistance to small molecule KRas inhibitors.

#1617 AI-assisted development of a TCR-like T cell engager targeting MAGE-A4 against melanoma.

Yang Liu, Qi Zhao

Faculty of Health Science, University of Macau, Taipa, Macao

MAGE-A4 is a promising immunotherapeutic target due to its frequent overexpression in cancers and limited expression in normal tissues. Intracellularly processed MAGE-A4 peptides, frequently presented by HLA-A*02:01 on the cell surface, can be recognised by T-cell receptor-mimetic agents. Utilising artificial intelligence-driven in silico screening and experimental validation, we generated a T-cell receptor-like antibody that specifically binds to the HLA-A*02:01-restricted GVY230-239 peptide complex. We subsequently engineered a T cell engager (TCE) in an IgG(L)-scFv format by fusing it with an anti-CD3 scFv. This MAGE-A4-targeting TCE demonstrated potent and specific cytotoxicity against multiple HLA-A*02:01^{+}/MAGE-A4^{+} tumour cell lines. To eliminate potential interference from Fc-mediated ADCC on T-cell-mediated killing, an N297A mutation was introduced into the Fc region, and the loss of ADCC activity was confirmed using a CD16 reporter cell line. Furthermore, in an HLA-A*02:01^{+}/MAGE-A4^{+} cell-derived xenograft (CDX) mouse model, the TCE exhibited significant antitumor efficacy in vivo. Compared to most currently available TCR-like antibodies, which primarily target haematological malignancies, this TCE showed superior tumour-killing activity against melanoma in vitro and in vivo. This work is supported by FDCT/009/2023/RIC and FDCT/0150/2025/AFJ.

#1618 A novel pan-gamma-delta T cell engager platform for next-generation cancer therapeutics.

Baotian Yang[1], Yuan Wu[1], Tengfei Yu[1], Sha Cheng[1], Qun Sun[1], Siwei Nie[2], Lei Wu[1], Jijie Gu[2]

[1]WuXi Biologics, Shanghai, China,[2]WuXi Biologics, Wuxi, China

Bispecific T cell engagers (TCEs) are potent immunotherapeutic molecules that redirect the body's T cells to kill tumor or pathogenic cells by bridging CD3 and tumor-associated antigen (TAA). Over the past decade, TCE-based therapies have achieved great success for the treatment of liquid tumors. However, although there is a multitude of TCEs with solid tumor targets in preclinical and clinical development, only one DLL3-targeting TCE was approved by FDA. For most TCEs targeting solid tumors, the main concern is on-target/off-tumor cytotoxicity, that is target organ toxicity due to redirection of T cells to normal tissues expressing the TAA. In addition, excessive release of cytokines may also translate to potentially life-threating cytokine release syndrome (CRS). To expand the therapeutic index and bring more treatment options to patients, there are intense efforts to overcome these challenges. Gamma-Delta T (γδT) cells can leverage both innate and adaptive immunity to combat target cells. Gamma-delta T cell engager (γδTCE) is a novel antitumor therapeutic to redirect γδ T cells to eliminate tumor or other pathogenic cells without pan T cell activation, therefore resulting in improved therapeutic index compare to pan T cell engager. To test this hypothesis, WuXi Biologics has developed a novel and unique pan-γδ TCE platform for the undruggable or hard-to-drug TAAs, that CD3 TCE can't target. Epidermal growth factor receptor (EGFR) is highly expressed in many solid tumors (e.g. non-small cell lung cancer and colorectal cancer) and low in normal tissues. EGFR has been clinically validated by multiple drug modalities, such as monoclonal antibodies and antibody-drug conjugates. However, EGFR x CD3 TCE, which may be the most powerful therapeutic modality, remains undruggable due to severe adverse effects of cytokine release and on-target/off-tumor toxicities. WuXi Biologics' EGFR-γδTCE is able to motivate diverse γδ T cell populations with equivalent activity, inducing significant expansion of γδ T cells without causing exhaustion. Compared with the clinical Vδ1 and Vδ2 benchmarks, WuXi Biologics' EGFR-γδTCE showed more efficient cytotoxicity against tumor cells, while sparing healthy cells and maintaining low cytokines. In in vivo antitumor studies of human colorectal cancer HCT116 xenograft models, the EGFR-γδTCE also exhibited superior antitumor efficacy than the clinical benchmarks. The studies support WuXi Biologics' EGFR-γδTCE as a promising novel therapeutic to target multiple solid tumors with EGFR expression and also demonstrate that WuXi Biologics' γδTCE platform has the potential to become best-in-class and can be applied to the undruggable or hard-to-drug TAAs.

#1619 Discovery and optimization of XTX601, a masked claudin 18.2-targeting T cell engager.

Jason Hedges, Pyae Hein, David Crowe, Aaron Bogle, Jing Ying Eng, Manoussa Fanny, Wilson Guzman, Sami Kahloun, Bernard Lanter, Janice Lee, Natalia Malkova, Haley Saxton, Kyle Smith, Sallyann Vu, Yihong Zhang, Kurt Jenkins, Elsie DiBella, Benjamin Nicholson, Scott Coleman, Carl Uli Bialucha

Xilio Therapeutics, Waltham, MA

T cell engagers (TCEs) are bispecific molecules engineered to bind to tumor-associated antigens on cancer cells and simultaneously engage T cells via CD3 interaction. Multiple TCEs have been approved for treating hematological malignancies, but approvals against solid tumor antigens have been limited to-date due to on-target, off-tumor toxicities. Aberrant protease dysregulation in solid tumors presents an opportunity for tumor-selective activation of biotherapeutic molecules including TCEs. To optimize the therapeutic index of TCEs by maximizing tumor exposure and minimizing peripheral activity, we have developed a masked TCE format we call ATACR (Advanced Tumor-Activated Cell Engager). In the ATACR format, peripheral engagement of CD3 is limited by a masking domain that is designed to prevent the TCE's anti-CD3 domain from binding CD3. By incorporating a protease cleavable linker between the half-life extension domain and the anti-CD3 domain, cleavage of the ATACR molecule by tumor associated proteases results in the release of a short half-life, fully active TCE locally within the tumor microenvironment. Here we report preclinical data for XTX601, a masked TCE in the ATACR format designed to target the clinically validated tumor associated antigen Claudin 18.2 (CLDN18.2), which is aberrantly expressed in gastrointestinal cancers, such as gastric, esophageal, and pancreatic cancer. A comprehensive CLDN18.2 TCE discovery and optimization effort yielded XTX601, which was found to be 1) highly selective for CLDN18.2; and 2) demonstrated efficient masking with a significant reduction in the levels of CD3 binding compared to the proteolytically activated molecule. Consistent with the CD3 binding data, intact XTX601 was effectively masked relative to proteolytically activated XTX601 when tested in T cell-dependent cellular cytotoxicity (TDCC) assays across multiple cancer cell lines that endogenously express CLDN18.2. XTX601 demonstrated robust anti-tumor activity in humanized, murine xenograft models adoptively transferred with human T cells. In both mice and non-human primates, XTX601 exhibited favorable pharmacokinetics and tolerability, highlighting the potential for an improved therapeutic index compared to systemically active TCEs targeting CLDN18.2. Collectively, these preclinical data demonstrate the effectiveness of our ATACR masked T cell engager format in reducing systemic activation of T cells while retaining potent anti-tumor activity. XTX601 is the first masked CLDN18.2-targeting TCE and has the potential to address a significant unmet need for patients with CLDN18.2 expressing malignancies including gastric, esophageal, and pancreatic cancers.

#1620 ATG-112, a novel ALPP/G x CD3 bispecific T cell engager, for the treatment of ALPP/G^{+} solid tumors.

Jishun Chen[1], Yu Bai[1], Suya Bai[1], Huiling Liu[1], Zaoshun Hu[1], Jay Mei[2], Peng Chen[3], **Bing Hou**[2]

[1]Antengene (Hangzhou) Biologics Co., Ltd, Hangzhou, China,[2]Antengene Corporation, Shaoxing, China,[3]Shanghai Antengene Corporation Limited, Shanghai, China

Background Placental alkaline phosphatase (ALPP) and related placental-like/germ-cell isoforms (ALPPL2 / ALPG) are cell-surface alkaline phosphatases that are aberrantly expressed in various solid tumors (e.g., ovarian, endometrial, germ cell, gastric, and pancreatic cancers), while being virtually absent from normal adult tissues except the placenta, making them highly promising tumor-selective targets for immunotherapy. T-cell engagers (TCEs) demonstrate robust clinical activity by co-engaging T cells with tumor cells, thereby inducing T cell activation and T cell-dependent cellular cytotoxicity (TDCC) against tumors. Here we developed ATG-112, an ALPP/G × CD3 bispecific TCE using the AnTenGager™ platform, featuring bivalent antigen binding for improved low-antigen tumor recognition and a sterically-masked CD3 binding arm to restrict T-cell activation to the tumor microenvironment.
Methods ATG-112 was engineered in a 2+1 IgG-based format, enabling bivalent binding to ALPP/G and monovalent engagement of CD3. We characterized its binding kinetics, TDCC, immunogenicity, and cytokine release profile using ALPP/G-positive cell lines, recombinant proteins, and human PBMCs. Antitumor efficacy was assessed in humanized mice with HPAC and NCI-H1650 xenografts.
Results Tissue microarray (TMA) IHC analysis revealed that ALPP/G expression was restricted to placental tissue in healthy organs and not detected in other normal tissues. In human tumors, ALPP/G was frequently expressed in endometrial (58.50%) and ovarian cancers (51.01%), with lower prevalence in bladder (26.14%), gastric (25.00%), and pancreatic cancers (16.67%). ATG-112 showed high binding affinity to both ALPP/G-positive tumor cells and recombinant protein, with EC_{50} and KD values in the sub-nanomolar range. ATG-112 induced robust TDCC activity against target positive cells with pico-molar range EC50, confirming potent antigen-dependent T-cell redirection. *In vitro* cytokine-release assays demonstrated minimal cytokine secretion from human PBMCs, suggesting low risk of excessive immune activation. Immunogenicity assessment showed that humanized ATG-112 molecules exhibited low immunogenic potential. *In vivo*, ATG-112 achieved potent tumor suppression across multiple dose levels, demonstrating strong antitumor activity and dose responsiveness. Safety studies revealed a favorable *in vivo* safety profile, including low cytokine release and controllable CRS risk at efficacious doses. ATG-112 also exhibited excellent developability.
Conclusion ATG-112 is a 2+1 T-cell engager that potently and selectively targets ALPP/G and CD3. It demonstrates potent in vitro and in vivo efficacy with minimal cytokine release. These findings support ATG-112 as a differentiated and promising therapeutic candidate for ALPP/G-positive solid tumors and justify its advancement toward clinical development.

#1621 ATG-106, a novel “2+1”format CDH6-targeted T-cell Engager (TCE), shows potent T cell dependent cytotoxicity and in vivo anti-tumor efficacy.

Tengteng Li[1], Peng Chen[1], Huiling Liu[2], Zaoshun Hu[2], jiaqi yan[2], jie huang[2], Jay Mei[3], **Bing Hou**[3]

[1]Shanghai Antengene Corporation Limited, Shanghai, China,[2]Antengene (Hangzhou) Biologics, Hangzhou, China,[3]Antengene Corporation Co., Ltd, Shaoxing, China

Background

CDH6 is crucial in embryonic kidney development but shows negligible expression in the adult kidney. Its overexpression in cancers like ovarian and renal cancer, contrasted with limited normal tissue expression, makes CDH6 an attractive target for cancer therapy, as supported by promising ADC clinical efficacy. However, T-cell engagers (TCEs) show limited efficacy and carry cytokine release syndrome (CRS) risks in solid tumors. In this study, we developed a novel "2+1", stericly-masked CDH6xCD3 bispecific TCE, ATG-106, demonstrating potent anti-tumor activity with a potentially reduced CRS risk.

Method

ATG-106 was developed by introducing a novel conformational epitope-targeted anti-CD3 single chain fragment variable (scFv) antibody to the hinge region of a novel humanized CDH6 monoclonal antibody. The CD3 binding site is concealed by the anti-CDH6 Fab arm before binding to CDH6, due to the steric hindrance. It was evaluated through a series of preclinical in *vitro* and *in vivo* assays for efficacy and safety, including binding affinity, cell based CD3 signal pathway activation, T cell dependent cytotoxicity (TDCC) and cytokine release. The *in vivo* efficacy of ATG-106 was evaluated in human PBMC reestablished 786-O kidney cancer and OVCAR-3 ovarian cancer xenograft mouse model. The safety profile of ATG-106 was characterized in intermittent intravenous dosing studies in rhesus monkeys using surrogate antibody (ATG-106-RM).

Results

ATG-106 exhibited reduced binding affinity to CD3+ cells before CDH6 crosslinking, while inducing 100-400 folds more potent cytotoxicity against CDH6-positive tumor cells compared to a 1+1 control TCE. It induced minimal ex-vivo cytokine release in the whole blood assay. In PBMC humanized 786-O xenograft model, ATG-106 demonstrated promising *in vivo* efficacy, resulted in tumor shrinkage in all mice dosed, with complete remission observed in 0.1 mg/kg (4 out of 6 mice) and 0.3 mg/kg (6 out of 6 mice) treatment groups . Notably, the serum concentration of pro-inflammatory cytokines was very low in ATG-106 treated group, suggesting low risk of CRS . ATG-106 also induced tumor shrinkage and complete remission in OVCAR-3 model. ATG-106-RM was well tolerated in rhesus monkey at doses up to 10mg/kg.

Conclusions

ATG-106 demonstrated powerful T cell dependent cytotoxicity and *in vivo* anti-tumor efficacy against ovarian and renal cancer preclinically, which warrants further clinical evaluation.

#1622 The affinity-optimized bispecific T cell engager W308051 selectively kills PSMA-expressing tumor cells with limited cytokine secretion.

Johannes Breuning[1], Yi Qin[2], Yunying Chen[2], Xia Wang[2], Jijie Gu[2]

[1]GlaxoSmithKline plc, Stevenage, United Kingdom,[2]WuXi, Shanghai, China

Metastatic castration-resistant prostate cancer (mCRPC) remains a therapeutic challenge with limited treatment options. Here, we report the preclinical characterization of W308051, a bispecific T cell engager developed by GSK under license from WuXi, designed to target prostate-specific membrane antigen (PSMA) on malignant cells and CD3 on T lymphocytes. W308051 demonstrates a higher binding affinity to PSMA compared to the competitor molecules AMG160 and AMG340 with a K_D of 16 pM as shown by surface plasmon resonance and also stronger binding in ELISA and cell-based binding assays. However, its affinity for CD3 with a K_D of 60 nM is lower than AMG160 but higher than AMG340, a rationale design choice to increase the therapeutic index. *In vitro* studies reveal that W308051 induces potent cytotoxicity against PSMA-positive cancer cells, achieving efficacies comparable to AMG160 and surpassing those of AMG340 across multiple cell lines with variable PSMA expression levels. Furthermore, *in vivo* experiments utilizing a cell line-derived xenograft model with the LNCaP cell line in immunodeficient mice engrafted with human peripheral blood mononuclear cells demonstrated complete tumor growth inhibition at higher dosing regimens, reflective of AMG160's profile. Importantly, *in vitro* cytokine release associated with W308051 treatment was reduced relative to AMG160 and marginally elevated compared to AMG340, suggesting a potentially improved safety profile and an expanded therapeutic window. Pharmacokinetic analyses indicate that the use of T cell receptor domains for bispecific antibody assembly confers properties akin to those observed with conventional monoclonal antibodies. Collectively, these findings support the further clinical investigation of W308051 as a promising therapeutic modality for mCRPC.

#1623 A novel pH dependent T cell engager platform for next generation cancer therapeutics.

Jie Li[1], Wenqian Fang[1], Nan Feng[1], Tengfei Yu[1], Siwei Nie[2], Lei Wu[1], Jijie Gu[2]

[1]WuXi Biologics, Shanghai, China,[2]WuXi Biologics, Wuxi, China

On-target off-tumor toxicity is a big challenge for the treatment of solid tumors using T cell engager (TCE) therapy because solid tumor associated antigens (TAAs) often expressed in not only tumor tissue but also normal healthy tissues. The acidic tumor microenvironment (TME) is a key characteristic of cancer and is leveraged to develop conditional tumor-selective therapy, which has been demonstrated with effective tumor control alongside manageable adverse events by encouraging preliminary clinical evidence emerged recently. WuXi Biologics has developed an innovative platform to identify pH dependent TAA binders that selectively bind to tumor and spare normal healthy tissues. As a clinically validated target, FolR1 overexpressed on multiple cancers, especially in ovarian and lung cancers, and associated with high-grade tumor progression & poor prognosis. Low expression of FolR1 in normal tissues is restricted to the luminal surface of lung, kidney, intestine, etc. ELAHERE, the approved FolR1 ADC demonstrated great clinical efficacy to FolR1^{high} patients but is ineffective to FolR1^{low} patients. FolR1 targeting TCE might be a promising therapy, though currently several TCEs stopped in pre-clinical stage due to on-target-off-tumor effect or lack of efficacy. To address these challenges, WuXi Biologics identified a novel pH-dependent FolR1 binder that binds to tumor at acidic pH over normal tissue at neutral pH, and then discovered a conditional FolR1 TCE which could kill tumor cell specifically by TME triggered activation and turning off at normal tissue, mitigate on-target-off-tumor toxicity and potentially widen therapeutic window and dose to achieve better clinical benefits. As a potential first-in-class conditional FolR1 TCE candidate, WuXi Biologics' FolR1 TCE showed potent binding to FolR1^{+} tumor cells at acidic pH and very weak binding to FolR1^{low} cells at neutral pH (representing normal tissue). Designed with fine-tuned CD3 and FolR1 affinity balance, it exhibited efficient *in vitro* on-tumor cytotoxicity at acidic pH and minimal cytotoxicity on normal tissue at neutral pH, and correlating cytokine levels released by T cells. WuXi Biologics' FolR1 TCE showed dose-dependent and efficient tumor growth inhibition in human ovarian cancer and NSCLC CDX models. In exploratory cynomolgus monkey tox study, WuXi Biologics' FolR1 TCE was well-tolerated up to 1 mg/kg with better safety profile than 16D5, one conventional benchmark FolR1 TCE which showed severe toxicity as low as 15 μg/kg. These findings suggest that WuXi Biologics' FolR1 TCE offers significant therapeutic potential as a next-generation TCE with minimal on-target-off-tumor cytotoxicity and enhanced therapeutic window. The pH dependent design provided an innovative strategy to offer safer and more effective therapeutic overcome for solid cancer patients.

#1624 Logic-gated switch-DARPin T cell engager with CD2 co-stimulation for improved safety and efficacy in MSLN and EpCAM co-expressing ovarian cancer.

Matteo Bianchi, Sarah Jetzer, Simon Haberle, Aline Eggenschwiler, Albulena Toska, Anja Schlegel, Justin D. Walter, Stephan Wullschleger, Tamara Lekishvili, Yvonne Kaufmann, Rocio Evangelista Vaz, Marcela Guzman Ayala, Alexander Link

Molecular Partners AG, Zurich-Schlieren, Switzerland

Introduction

The development of T cell engagers (TCEs) for solid tumors is challenged by the scarcity of specific tumor-associated antigens (TAAs), which limits selectivity and increases the risk of on-target/off-tumor toxicity due to antigen expression in normal tissues. In ovarian cancer (OC), immunotherapy has shown limited success, largely due to the lack of “clean” TAAs, dysfunctional T cells, and an immunosuppressive tumor microenvironment. To overcome these challenges, we engineered a multi-specific, logic-gated CD3 TCE targeting the TAAs mesothelin (MSLN) and EpCAM, with CD2-mediated co-stimulation. This conditional Switch-DARPin design employs an AND-gate mechanism, enabling CD3 engagement only upon simultaneous recognition of both TAAs. This strategy aims to deliver potent, sustained antitumor activity while minimizing systemic toxicity and off-tumor effects on single TAA-expressing healthy cells.

Methods

The MSLNxEpCAM-targeting Switch-DARPin was developed using our DARPin platform. It features a masked CD3 binder that is unmasked upon dual binding to MSLN and EpCAM on tumor cells, a CD2 binder for co-stimulation, and includes a silent Fc domain for extended half-life. Preclinical safety and antitumor efficacy were evaluated *in vitro* and *ex vivo* using tumor and reporter cell lines, primary T and mesothelial cells from healthy donors, whole blood cytokine release assays, and *in vivo* using an OVCAR-3 xenograft model in PBMC-humanized NXG mice.

Results

Using our computational workflow DARPin Compass, we identified MSLN and EpCAM as a promising TAA pair in OC, with low co-expression in healthy tissues. *In vitro*, the Switch-DARPin induced selective T cell cytotoxicity against tumor cells co-expressing MSLN and EpCAM, with markedly reduced activity on cells expressing only one antigen. Notably, substantially lower activity against primary human mesothelial cells was observed, compared to other clinically tested MSLN-targeting TCEs. CD2 co-engagement promoted sustained activation and proliferation of T cells, preventing exhaustion. *In vivo*, the Switch-DARPin exhibited suitable pharmacokinetics and achieved significant tumor regression in MSLN+EpCAM+ xenografts without systemic cytokine release. The absence of cytokine induction in human whole blood assays confirmed the favorable safety profile despite CD2 co-stimulation.

Conclusions

Co-targeting of MSLN and EpCAM may lower the risk of on-target/off-tumor toxicity compared to single-targeting approaches. Preclinically, our logic-gated CD3xCD2 Switch-DARPin demonstrates selective antitumor activity against MSLNxEpCAM dual-positive tumors such as OC. CD2 co-stimulation further enhances T cell function without systemic activation. Together, our approach has the potential to overcome key limitations that TCE therapy faces in solid tumor indications.

#1625 VHH nanobody-masked conditionally active CDH17 T cell engager for colorectal cancer.

Lei Wu, Guoxin Ni, Xiaoyue Liu, Sha Cheng, Senfeng Xiang, Yi Liu, Xia Wang, Donghui Wu, Tengfei Yu, Jijie Gu

WuXi Biologics, Wuxi Shi, China

T cell engagers (TCEs) bind antigens on tumor cells on one arm and CD3-TCR complex on the other arm to induce cytotoxic immune synapses and redirect nonspecific T cells to kill in a specific manner. TCEs have demonstrated convincing efficacy in multiple blood cancers and have recently with Tarlatamab made breakthrough in solid tumors. However, major hurdles remain for the realization of the full potential of this exciting modality in solid tumors - most importantly the lack of clean and specific antigens. CDH17 is a type-1 transmembrane glycoprotein of the cadherin superfamily and its expression is normally restricted to the lateral area of epithelial tight junctions of the intestines and the pancreatic duct. CDH17 is highly expressed in over 95% of colorectal cancers, and its upregulation and tumor tissue disorganization results in disoriented CDH17 expression susceptible to T cell surveillance In order to accommodate CDH17 that is highly expressed on tumor cells but is indeed present on some normal tissues, we developed a next-generation conditionally active masked CD3 TCE platform. Instead of using traditional linear peptide masks that oscillate and are prone to digestion, we generated anti-idiotypic VHH nanobody specifically for our clinical stage CD3 binder (NCT05579132). The structured VHH masking moiety prevents premature unmasking and activation. In addition, we designed enzyme cleavable linker specifically to be resistant to enzymes that are highly expressed in normal tissues. These designs ensured good tolerability. Anti-idiotypic VHH mask binds CD3 binder with high affinity and fine-tuned kinetics. VHH-masked CD3 binder is no longer able to induce effective T cell killing. The newly designed cleavable linker can be effectively cut by certain MMPs and other enzymes enriched in the tumors. The resulting masked CDH17xCD3 TCE showed good serum stability and remained inactive after extensive incubation. Once activated with corresponding enzymes, the VHH mask is effectively released and the TCE is activated to induce potent tumor cell killing. In multiple CDX models of human tumors, masked CD3 TCE demonstrated convincing in vivo efficacy on par with the corresponding non-masked TCE. Moreover, exploratory toxicity study in NHP showed significantly higher MTD and improved safety profile. WuXi Biologics has developed a conditionally active CDH17 TCE with the proprietary VHH-masked CD3 TCE platform. The molecule has demonstrated great efficacy and better tolerability preclinically, and is to be further evaluated in the clinic.

#1626 A novel machine-learning derived nectin-4 x CD3 bispecific T-cell engager, LGTX-101, demonstrates high degrees of tumor selectivity and potently induces tumor regression *in vivo*.

Lucrecia Alberdi, Sabrina Bouhafs, Dan Foxler, Justin Grace, Winston Haynes, Catherine Howsham, Leo Kassimatis, **Sylwia Marshall**, Lida Mavrogonatou, James McClory, Portia McGhan, Rebecca Mighell, Michael Mullin, Sandra Pasternakiewicz, Sujata Ravi, Nush Sarvaria, Gino Van Heeke, Angus Sinclair

LabGenius Therapeutics, London, United Kingdom

Nectin-4 is a tumor-associated antigen (TAA) that is commonly overexpressed on numerous solid tumor types, including urothelial, head and neck, and triple-negative breast cancer. Nectin-4 is also expressed at low levels on normal, healthy tissues, which limits current ADC therapies due to high rates of dose-limiting, on-target, off-tumor toxicities. Furthermore, patients previously benefiting from ADC therapy become resistant to treatment. This highlights a need for alternative approaches for anti-cancer therapeutics that can selectively target Nectin-4 expressing solid tumors with an improved mechanism of action. A highly selective and potent trivalent VHH based Nectin-4 x CD3 T-cell engager (TCE) was generated using LabGenius Therapeutics' proprietary discovery engine (EVA™). By harnessing avidity-driven selectivity, LabGenius' Nectin-4 x CD3 TCE (LGTX-101) is able to differentiate between healthy and diseased cells based on differential TAA expression. LALA mutations were introduced to abrogate FcyR activity. The potency and selectivity of the lead molecule LGTX-101 was tested in a range of tumor cell line cytotoxicity models with varying expression of Nectin-4, including primary bladder cancer cells. Furthermore, the *in vivo* efficacy was established using a humanised BT-474 CDX model. LGTX-101 has a 3:1 Nectin-4:CD3 stoichiometry capable of high affinity binding to Nectin-4 expressing cells and low-moderate affinity to human CD3. In *in vitro* tumor cell cytotoxicity assays, LGTX-101 potently induced cytotoxicity in cancer cell lines with Nectin-4 receptor expression levels within 2-fold of healthy control model cell lines, with mean EC_{50} potency of 0.712 +/- 0.132 pM. No evidence of cytotoxicity of the healthy cell model was observed, demonstrating a >1,000-fold therapeutic window between Nectin-4 positive normal and tumor cell cytotoxicity. These observations were further extended to primary bladder cancer co-cultures, where LGTX-101 induced activation of T cells at concentrations of <5 pM. Furthermore, no evidence of T cell activation was observed when PBMCs were cultured with human primary keratinocytes, known to express low levels of Nectin-4. Finally, LGTX-101 demonstrated robust reduction of the growth of established tumors *in vivo* in a humanized BT-474 xenograft model (>90% tumor growth inhibition) and a preliminary PK profile that supports a Q2W - Q4W dosing regimen in the clinic. LGTX-101 is a highly selective and highly efficacious Nectin-4 x CD3 TCE currently in preclinical development for treatment of advanced solid tumors. With an increased selectivity and potency profile, LGTX-101 has the potential to provide a safer, more effective treatment option for patients.

#1627 DS-2243a, an HLA-A*02/NY-ESO-directed bispecific T-cell engager, shows potent anti-tumor activity in preclinical models of solid tumors.

Junya Ichikawa, Ayaka Yatsu, Ryuichi Nakamura, Akemi Kita, Shingo Noguchi, Yoko Ishimoto, Chikako Maru, Kento Tanaka, Kensuke Nakamura, Shinji Furuzono, Makiko Nakayama, Toshiaki Ohtsuka, Reimi Kawaida

Daiichi Sankyo Co., Ltd., Tokyo, Japan

Background: NY-ESO-1 and LAGE-1 are homologous proteins commonly expressed in various tumor tissues but not in normal tissues other than the testis and placenta, making them potential tumor-specific therapeutic targets. Tumor types with prevalent NY-ESO-1 and/or LAGE-1 expression include SS, MRCLS, NSCLC, and UC. Following the intracellular processing of NY-ESO-1 and LAGE-1 proteins (hereafter referred to as NY-ESO) by the proteasome, the same highly immunogenic NY-ESO peptides are presented extracellularly by HLA-A*02. DS-2243a is a first-in-class bispecific T-cell engager (BiTCE) with an effectorless Fc region. It is designed with a novel TCR-like antibody that engages both HLA-A*02/NY-ESO-expressing tumor cells and T-cells, redirecting T-cell-mediated cytotoxicity toward the tumor.

Methods: The binding affinity of DS-2243a to HLA-A*02/NY-ESO peptide complex was evaluated by surface plasmon resonance (SPR) analysis, and specificity of DS-2243a for the human HLA-A*02/NY-ESO complex was evaluated by a flow cytometry-based binding assay using T2 cell line supplemented with HLA-A*02/NY-ESO peptide and various HLA-A*02/NY-ESO homologous peptides. Anti-tumor cytotoxicity, T-cell activation, and cytokine release were evaluated by co-culturing tumor cells with human peripheral blood mononuclear cells (hPBMCs) in the presence of DS-2243a. The anti-tumor efficacy of DS-2243a was evaluated against various HLA-A*02 positive tumors with different NY-ESO expression levels in human T-cell-transferred mouse models.

Results: DS-2243a specifically bound to human HLA-A*02/NY-ESO peptide complex with a high affinity of 1.31×10^{-9} mol/L, but not to other HLA-A*02/homologous peptide complexes. DS-2243a induced T-cell activation, cytokine release, and target cell cytotoxicity in a dose-dependent manner. It demonstrated robust anti-tumor efficacy across multiple tumor types, including those with low NY-ESO expression, and also demonstrated efficacy in a tumor-mixture model of NY-ESO-positive and NY-ESO-negative tumors, supporting potential effectiveness in tumors with heterogeneous NY-ESO expression. Furthermore, DS-2243a exhibited efficacy in combination with immune checkpoint inhibitors, providing a rationale for combination therapies.

Conclusions: Preclinical data indicate that DS-2243a has strong potential to deliver clinically meaningful anti-tumor activity in patients with HLA-A*02 and NY-ESO-expressing cancers. The first-in-human study DS2243-054 (NCT06644755) is being conducted to evaluate DS-2243a monotherapy in patients with advanced or metastatic solid tumors.

#1628 A bispecific PDL1:CD3 T-cell engager potently kills intractable primary and metastatic intracranial tumors.

Emily J. Girard, Shelli M. Morris, Kristina Pilat, Alison M. Williams, Kenneth Brasel, Heather Conti, Parvathi Muthuraman, Ray Ruff, Hailey Hentschel, Steven Chen, Chunfeng Yin, Zachary Crook, Jason Price, Andrew J. Mhyre, James M. Olson

Seattle Children's Research Institute, Seattle, WA

Introduction: Central nervous system tumors represent a huge unmet medical need. Many pediatric and adult brain cancers and cancers (e.g., lung, colon, breast) with CNS involvement remain largely intractable despite standard of care and advanced treatment strategies. We engineered a bispecific PD-L1 targeted T-cell engager (TCE) and discovered promising efficacy in a wide range of pre-clinical intracranial tumor models, including some models with intact blood brain barriers.
Methods: Anti-tumor activity of a systemically administered PD-L1:CD3 TCE was interrogated in 14 intracranially implanted tumor xenografts representing poor-prognosis pediatric brain tumors, adult glioblastoma, and metastatic lung, breast, and colorectal cancers. On-target/off-cancer toxicity was evaluated in mice transgenic for human PD1/PD-L1 or CD3ε with surrogate chimeric TCEs for species appropriate binding over 2- and 4-week treatment periods with repeated dosing. Dose range finding study in non-human primates was conducted to establish the safety profile of the lead TCE.
Results: Median and overall survival were significantly extended by TCE treatment in 4 of 5 models of pediatric brain tumors (2 diffuse midline glioma, 1 medulloblastoma, 2 high-grade glioma), 2 of 3 models of adult glioblastoma, and all 6 models of intracranial metastases (3 lung adenocarcinoma, 2 triple-negative breast cancer, 1 colorectal carcinoma). One of the adult GBM and the 6 metastatic models were transduced for bioluminescent monitoring of tumor burden: 53% of tumors across model types were eliminated by TCE treatment, 39% showed tumor presence without progressive growth, and 8% of tumors continued to grow with or without an initial delay. Dose range tolerability in transgenic mice showed dose dependent pharmacodynamic effects on body weight, lymphopenia, cytokine stimulation, CD3+ cell biodistribution, and tissue PD-L1 expression with no overt toxicity. A dose range finding study in non-human primates revealed the TCE was well tolerated with pharmacodynamic responses observed at 0.03 mg/kg and limited to grade 1 toxicities. At 0.3 mg/kg grade 2-4 toxicities were observed.
Conclusion: Bispecific PD-L1:CD3 TCE is safe at doses that show efficacy in intracranial xenograft tumor models. This PD-L1 TCE presents a novel therapeutic strategy for patients with primary and metastatic intracranial tumors that are typically fatal.

#1629 An innovative approach to improve bispecific T-cell engagers for solid tumor therapy.

Hing C. Wong, Xiaoyun Zhu, Varghese George, Hamidreza Farzaneh, Crystal Gilkes, Natalia Valderrama, Alyssa Thompson, Lijing You, Lucas Gomez, Christian Echeverri, Niraj Shrestha, Peter R. Rhode, Jack Egan

HCW Biologics Inc., Miramar, FL

T cell engagers (TCEs), mainly in the format of Bispecific T-cell Engagers (BiTE), are promising anti-cancer immunotherapies for hematological malignancies. However, solid tumors create immunosuppressive microenvironments and physical structures that hinder the effectiveness of T- cell engagers and preclude tumor infiltration by $CD8^+$ T cells. Our hypothesis for overcoming these barriers is to add components to the BiTE format that alleviate immunosuppression and promote activation and tumor infiltration of $CD8^+$ T cells. To test this hypothesis, we used our novel TRBC platform to construct HCW11-018b, a tetravalent heterodimeric TCE. The BiTE portion of HCW11-018b contains an antibody that targets human tissue factor (TF), which is overexpressed in a wide spectrum of solid tumors; an anti-CD3 single-chain antibody; and an IL-15Rα domain. The other chain of HCW11-018b comprises a dimeric soluble TGFβRII domain (i.e., TGFβ trap), TRβC1 and a soluble IL-15. The plasmids carrying the coding regions of the two fusion proteins were co-transfected into CHO cells and the fully functional TCE was purified from culture supernatant. *In vitro*, we found HCW11-018b induced robust, antigen-specific tumor cell killing, which was sustained up to five rounds. Increased phosphorylation of STAT5, expression of activation markers (CD69, CD25), chemokine receptor (CCR5), and anti-apoptosis marker (BCL2) were observed on T cells by HCW11-018b treatments. RNAseq analysis revealed that increased expression of *BCL2* and other genes associated with T-cell effector function were specifically attributable to the IL-15 component of HCW11-018b. In SCID mice subcutaneously (s.c.) implanted human AsPC-1 pancreatic cancer cells with human PBMCs, we demonstrated that s.c. administered HCW11-018b could infiltrate into implants and activate bystander $CD8^+$ T cells for potent anti-tumor activities. In AsPC-1 tumors (NSG mice models) and adoptively transferred human T cells, HCW11-018b stimulated expression of CCR5 and promoted tumor infiltration of human T cells, upregulated T cell expression of CD25, NKG2D, DNAM1, Granzyme B, and IFNγ, and enhanced their cytotoxicity against cancer cells. Treatment also reduced tumor cell metastasis from the primary site. We further demonstrated that the upregulation of NKG2D and DNAM1 on HCW11-018b-activated $CD8^+$ T cells played a role in the cytotoxicity against AsPC-1 tumor cells. In a PDX model, we further demonstrated the potency of HCW11-018b which directed hPBMCs against TF^+ patient-derived pancreatic cancer tissues. HCW11-018b was well tolerated in mice and non-human primates with s.c. administration. HCW11-018b is currently in IND-enabling studies for clinical development against solid tumors. In summary, we demonstrate that the addition of TGFβ-trap and IL-15 components onto BiTE using our novel TRBC platform can overcome the deficiencies of BiTE for solid tumor therapy.

#1630 Preclinical investigation of a novel tumor associated antigen, cb02, as a bispecific t-cell engager in cancer.

Mary Mathieu

Cartography Biosciences, Inc., South San Francisco, CA

Therapeutic success in next-generation cancer immunotherapy is dependent on identifying highly effective targets that allow selective eradication of tumor cells while sparing healthy tissues to maximize the therapeutic window. The novel target CB02 (target undisclosed), a highly tumor-specific antigen, was nominated from our comprehensive ATLAS platform that analyzes healthy and tumor tissues at single cell level. Based on target expression profile and target cleanliness, we built a bispecific T cell engager, CB02 TCE. Analysis of relevant patient tissues using quantitative flow cytometry (qFlow) and IHC indicated high prevalence across hematological and solid tumor indications.

Through strategic antibody discovery and engineering, we designed a TCE optimized for the tumor specific CB02 expression profile with balanced CD3 binding affinity. Selection criteria focused on maximizing functional potency while maintaining molecular stability and manufacturability. *In vitro* characterization across multiple CB02 expressing preclinical tumor models allowed binder screening, kinetic analysis, cytotoxic function and profiling of T-cell activation and cytokine release. Functional assays showed robust, dose-dependent T-cell activation and cytotoxicity in 2D co-cultures as well as 3D spheroid models. Furthermore, we demonstrate robust in vivo efficacy of the CB02 TCE in systemic and subcutaneous cell-line derived xenograft models as well as good PK properties.

The preclinical investigation successfully identified and validated CB02 as a promising, highly selective T-cell engager target, significantly enriched on malignant cells over critical healthy cell types. The associated TCE exhibits high affinity and compelling in vitro and in vivo efficacy across both hematological and solid tumor models. These data strongly support the continued development of this CB02-targeted bispecific TCE antibody for clinical evaluation.

#1631 Leveraging off-the-shelf T cells to enhance bispecific T cell engager therapy efficacy in patients with suboptimal T cell responses.

Saghar Pahlavanneshan, Stephen J. Forman, Xiuli Wang

Cellular Immunotherapy Center, Department of Hematology and Hematopoietic Cell Transplantation, Beckman Research Institute of City of Hope, Duarte, CA

Bispecific T cell engagers (BiTEs) have showed potent antitumor activity in hematologic malignancies but are often limited by T-cell dysfunction in patients. To overcome this challenge, we developed an off-the-shelf immunotherapy platform using healthy donor-derived multi-virus-specific T cells (mVSTs) as effectors for BiTE-mediated redirection. These memory-derived mVSTs recognize cytomegalovirus (CMV) and Epstein-Barr virus (EBV) antigens, exhibit central and effector memory phenotypes, and carry minimal graft-versus-host disease (GVHD) risk, providing a bankable, and functional T-cell source.mVSTs were expanded from CMV/EBV-seropositive donors and evaluated in multiple myeloma and lymphoma models. Two BiTE-loading strategies were tested: pre-incubation with T cells (armored) or direct addition to co-culture. mVSTs alone exhibited minimal cytotoxicity, whereas BCMAxCD3 BiTE-redirected mVSTs mediated robust tumor lysis in both approaches (89.8 ± 1.7% and 88.7 ± 0.4%, respectively at 72h and E:T 1:4) and expanded ≥3-fold versus no-BiTE controls. Both loading methods triggered robust activation, with marked upregulation of CD137 and CD25 and substantial increases in effector cytokines. In Raji lymphoma models, CD19×CD3 and CD20×CD3 BiTEs produced 48-52% cytotoxicity with armored mVSTs, and direct BiTE addition further enhanced killing to 73-74% with a comparable activation profile. Collectively, BiTE-redirected mVSTs exhibit potent cytotoxicity, robust activation, and strong effector cytokine release across myeloma and lymphoma targets, validating their function as an effective, off-the-shelf T-cell platform. A single donor-derived mVST source can be paired with multiple BiTEs to address tumor heterogeneity or antigen-loss relapse without engineering. These data support the feasibility and translational promise of combining BiTEs with healthy donor-derived mVSTs to generate scalable, non-engineered allogeneic T-cell immunotherapies for diverse malignancies.

#1632 Preclinical characterization of DBXO-1, a multi-pMHC targeted bispecific T cell engager for major solid tumors.

Johanna K. Kaufmann, Jason Lajoie, John L. Silberstein

Deck Bio, Inc., Cambridge, MA

Bispecific T cell engagers (TCEs) are a well-established therapeutic modality in heme malignancies, and recent regulatory approvals in select solid tumors highlight their promise more broadly. However, adoption in major solid tumor indications and across large patient populations remains limited, in part by the scarcity of surface targets with cancer-exclusive expression patterns. Cancer-specific intracellular targets can be accessed by TCEs via peptide-MHC complexes (pMHCs), but individual pMHCs are expressed at low copy numbers which impacts TCE potency and breadth of response. DBXO-1 is designed to address this limitation by targeting a defined set of cancer-restricted intracellular proteins that generate multiple target pMHCs that can be recognized by a single binder, addressing copy number and heterogeneity concerns. Here, we describe the specificity profile and functional activity of DBXO-1 preclinically.A T cell receptor recognizing HLA-A*02:01-restricted target peptides was affinity- and specificity-engineered using yeast and phage display, aided by structural modelling. Optimized binders were formatted into Fc-containing TCEs using clinically validated anti-CD3 sequences. Affinity was measured by biolayer interferometry. Specificity was characterized using yeast display workflows and a T2/Jurkat reporter assay, cytotoxicity was assessed by LDH release. The DBXO-1 discovery campaign identified multiple pMHC binders with single digit nanomolar affinities to the relevant target pMHCs. When formatted into TCEs, this led to potent T cell activation with EC_{50}s <10 pM. Mutational analyses confirmed a shared structural recognition mode across target pMHCs, underlining the basis for the intended multi-targeting mechanism. Importantly, the specificity of final leads was assessed sequence-agnostically by testing binding against 13,849 HLA-A*02:01-presented peptides that were found in healthy tissues by immunopeptidomics. This comprehensive assessment revealed only a very small number of low-affinity interactions, a profile superior to a clinical stage benchmark pMHC-TCE. When T2 cells were pulsed with these peptides at supraphysiological concentrations for additional stringency, >100x EC_{50} windows for T cell activation were observed. Further derisking on healthy cells is ongoing. Finally, DBXO-1 mediated potent, dose-dependent cytotoxicity on multiple HLA-A*02:01^{+} cell lines expressing the target signature, while no activity was observed in absence of either target expression or HLA restriction.Taken together, these data support continued preclinical development of DBXO-1, with the goal of entering a first-in-human clinical trial in 2027. Initial clinical development is anticipated in biomarker-selected patient populations across major solid tumors, including non-small cell lung, head and neck, and gastroesophageal cancers.

#1633 MAIT engagers: Avoiding Treg suppression to deliver stronger activity in solid tumors..

Simon E. Plyte[1], Marie Fraudeau[1], Dorothee Winterberg[2], Claire Germain[1], Camille Rousseau[1], Maxime Audin[1], Alexandre Ivagnes[1], Sothea Touch Dumoitier[1], Sarah Ducellier[1], Lise Fenou[3], Hans Heinrich Oberg[2], Pierre Emmanuel Gerard[1], Isabelle Teulon[3], Daniela Wesch[2], Matthias Peipp[2], Julie Prigent[1]

[1]Biomunex Pharmaceuticals, Paris, France,[2]Universitats Klinikum Schleswig-Holstein,, Kiel, Germany,[3]IRCM, Univ Montpellier, ICM, INSERM, Montpellie, France

MAIT engagers are part of the immune cell engager drug modality and specifically target Mucosal Associated Invariant T cells (MAITs) via their unique T cell receptor (TCR) and tether them to cancer cells, via a tumor antigen, to elicit MAIT-mediated cell death. MAIT cells are an abundant cytotoxic subset of non-conventional T cells that are present in blood and all major organs and are particularly enriched in barrier tissues. Classical CD3 engagers activate all T cell subsets, including the regulatory T-cell (T-regs) population whose activation in the tumor microenvironment (TME) will dampen the intended cytotoxicity of the CD8 cytotoxic T cells and will limit CD3 engager efficacy. Unlike CD3 engagers, MAIT engagers only activate MAIT cells and do not cause increased immune suppression via T-reg activation or cytokine release syndrome (CRS) via general CD4 T cell activation. MAIT engagers were generated using Biomunex's proprietary bispecific, tetravalent antibody platform, BiXAb. MAIT-cell activation, proliferation, degranulation and cytotoxicity assays were established in co-culture between tumor cells, immune cell subsets (CD8 or PBMCs) and BiXAb MAIT engagers. Analysis of activation, degranulation and proliferation was followed by FACs whilst cytotoxicity was assessed by chromium release. Regulatory T cells were enriched from PBMCs and used in co-culture assays to assess CD8 T cell repression as judged by IL-2 release. General cytokine release was measured by Legend Plex or ELISA. Cytotoxicity of tumor-resident MAITs, from fresh patient samples, was determined by impedance measurements. *In vivo* efficacy studies were performed in humanized mouse models by co-injection of CD8s, cancer cells and the MAIT engager. MAIT engagers are as potent as classical CD3 engagers in terms of activation, degranulation, proliferation and cytotoxicity towards cancer cells. However, in co-culture assays of cancer cells and PBMCs, CD3 engagers induce large quantities of cytokines, especially IL-6 which is known to initiate CRS whilst MAIT engagers induced similar levels to control antibodies suggesting greater safety. CD3 engagers induced Treg activation proliferation and release of IL-10 in a dose dependent manner and induced Treg suppression of CD8 activation. MAIT engagers had no impact on Treg biology and increased immune suppression. *Ex vivo* cytotoxicity of tumor-resident MAIT cells using dissociated Ovarian cancer samples at "real E:T ratios" showed that MAITs in human tumors can respond to MAIT engagers, proliferate and eliminate tumor cells. *In vivo* efficacy studies showed that MAIT engagers can control human tumors in mice models of cancer. MAIT engagers are as potent as CD3 engagers but have a significantly improved safety profile. More importantly, they do not cause Treg activation which can dampen T-cell cytotoxicity in the TME and are expected to show greater efficacy in the clinic for the treatment of solid tumors.

#1634 A conditionally-active, dual-targeting TCE with superior tumor selectivity for the treatment of solid tumors.

Steffen Dickopf, Jorge A. Lerma Romero, Jessica Seib, Laura Perucho-Aznar, Steffen Runz, Abdul-Habib Maag, Anna Pryszlak, Anja Schreiber, Martha Gschwandtner, Christoph Erkel, Richard J. Austin

VERAXA Biotech GmbH, Heidelberg, Germany

Background

T cell engagers (TCEs) represent a rapidly advancing class of immunotherapies that have demonstrated remarkable clinical efficacy in hematologic malignancies. However, their application in solid tumors remains limited by on-target, off-tumor toxicities resulting from antigen expression in healthy tissues. Moreover, off-target, off-tumor effects can arise from systemic T cell engagement and nonspecific activation, leading to cytokine release syndrome (CRS). To overcome these challenges, we have developed an innovative TCE platform incorporating an AND-gated safety mechanism that enables selective killing of tumor cells while sparing healthy cells.

Method

The Bi-targeted Tumor-Associated Cytotoxicity (BiTAC) T cell engager builds up on the previously described hemibody concept[1] and employs an on-cell assembly mechanism of two complementary compounds to achieve conditional activation. Each compound comprises a tumor-binding domain recognizing a distinct tumor-associated antigen (TAA) and a split T cell-binding moiety. Individually, the compounds do not engage T cells. Productive T cell activation occurs only when both compounds co-bind and accumulate on tumor cells co-expressing the respective antigens, leading to reconstitution of an active CD3 binder. The BiTAC-TCE was optimized for developability, stability, and potent functional activity in both in vitro and in vivo settings.

Results

Our bioinformatics pipeline identified a TAA pair highly co-expressed in colorectal and lung cancers. Constitutively active drugs targeting each TAA individually have been tested in humans and revealed target-associated toxicities. An antibody format with favorable manufacturability and developability was subsequently selected. Using in vitro T cell-dependent cellular cytotoxicity (TDCC) assays across multiple cell lines in 2D and 3D cultures, we demonstrate that the combinatorial design of BiTAC-TCE enables T cells to selectively eliminate dual-target-positive tumor cells while sparing single-positive healthy cells. Individual compounds/BiTAC precursors don’t bind T cells and don’t induce TDCC in vitro and in vivo. Furthermore, BiTAC-TCE exhibits strong antitumor efficacy in PBMC-engrafted mice bearing colorectal tumors and displays a favorable pharmacokinetic (PK) profile in preclinical mouse studies.

Conclusion

Our BiTAC-TCE platform enables precise targeting of solid tumors through TAAs not druggable by current immunotherapies. Both TAAs addressed are broadly expressed but not co-expressed on healthy cells of different tissues, leading to failure of monotargeting T cell engagers in clinical settings. Our lead BiTAC-TCE for the treatment of colorectal and lung cancers has recently entered formal preclinical development and IND-enabling studies.

[1]Banaszek, A. et al. Nat Commun 10, 5387 (2019)

#1635 CBX-663, a first-in-class TCR-mimetic T-Cell Engager targeting the TERT peptide-HLA complex, mediates potent cytotoxicity *in vitro* and tumor inhibition *in vivo* in preclinical models of solid malignancies.

Yu Huang[1], Ricard Masia[1], Bhupal Ban[1], Qunyan Yu[1], Jennifer Helble[1], Jessica Jimenez[1], Delainey O'Connor[1], Preethi Sankaran[1], Christine A. Devlin[1], Melissa Bikowitz[1], Emily McNally[1], Sarah Jaffe[1], Tanzila Rahman[1], Alona Kulesha[1], Andrew Wolpert[1], Shawn O'Malley[1], Yue Li[1], Michael Jennings[1], Galina Gabriely[1], Mathilde A. Poussin[2], Daniel J. Powell[2], Nga Sze Amanda Mak[1], Tao Wang[1], Geraldine L. C. Paulus[1], Michi Schebesta[1], Benjamin Lee[1], Dmitri Wiederschain[1]

[1]Crossbow Therapeutics, Inc., Cambridge, MA,[2]Department of Pathology and Laboratory Medicine, University of Pennsylvania, Philadelphia, PA

While T-cell engager (TCE) therapies have demonstrated clear clinical benefit, their broader application remains limited by the restricted repertoire of tumor-specific surface antigens. Targeting HLA-restricted peptides (pHLA) derived from intracellular tumor antigens offers an opportunity to expand the reach of TCEs to solid tumors. Telomerase reverse transcriptase (TERT) represents such an intracellular target, as it is highly expressed in approximately 85-95% of human tumors. We have previously described CBX-663, a potent and specific TCR-mimetic (TCRm) TCE targeting the $TERT_{540}$/HLA-A*02:01 complex, and its activity in hematologic cancer models. Here, we characterize its therapeutic potential in preclinical solid tumor models. CBX-663 consists of a single humanized CD3-binding domain and two fully human TCRm domains that recognize $TERT_{540}$/HLA-A*02:01 in a bivalent format. CBX-663 binds $TERT_{540}$ pHLA with sub-nM affinity and low-pM avidity, leading to potent T-cell-mediated cytotoxicity across multiple TERT- and HLA-A*02:01-positive solid tumor cell lines. Subsequent analysis revealed that responsive cell lines exhibit higher HLA-A*02:01 expression than non-responders. Notably, some of the highest responding cell lines carry TERT promoter mutations, which are well known to elevate TERT transcription and may increase pHLA presentation. CBX-663 achieved robust tumor control in a disseminated NSCLC COR-L23-A2 model using PBMC-humanized NSG mice and induced tumor growth delay in a subcutaneous NSCLC NCI-H1703 model established in humanized CD34+ (huCD34) mice. Additional efficacy studies are ongoing. To further characterize specificity, X-scan analysis of $TERT_{540}$ peptide was conducted and revealed multiple residues critical for CBX-663 recognition of $TERT_{540}$ pHLA. A screen of >6,000 human membrane proteins identified no detectable off-target interactions of CBX-663. In addition, no activity was observed against TERT- or HLA-A*02:01-negative cells, unrelated HLA alleles, or normal HLA-A*02:01-positive primary cells from diverse tissues. CBX-663 induced moderate cytokine release upon treatment of HLA-A*02:01-positive PBMCs in the absence of tumor cells, consistent with previously reported targeting of monocytes and B cells by TERT-directed T cell therapies in preclinical models. Cytokine induction with CBX-663 was markedly lower than that elicited by a CD123-targeting TCE tested under identical conditions. Importantly, repeat dosing of CBX-663 was well tolerated in non-tumor-bearing huCD34 mice reconstituted with human hematopoietic cells, with minimal cytokine release and transient changes in leukocyte populations. Collectively, these data support the therapeutic potential of CBX-663 in solid tumors. IND-enabling studies are currently underway.

#1636 TNF-driven paracrine killing determines the cytotoxic efficacy of Teclistamab in Myeloma.

Allison Carr[1], Elise Sintim-Aboagye[2], Adrian Ting[1]

[1]Immunology, Mayo Clinic, Rochester, MN,[2]Medical Oncology, Mayo Clinic, Rochester, MN

Multiple Myeloma is the second most common hematologic malignancy among US adults and remains incurable. Immunotherapies, including bispecific T cell engagers (BiTEs) targeting BCMA, have greatly improved outcomes. However, a significant fraction of patients still fail to respond, or develop resistant disease. Conventional models of T cell cytotoxicity focus on delivery of perforin- and granzyme-containing granules following antigen recognition and T cell activation, an inefficient mode of killing that requires effector-to-target cell contact. Activated T cells, however, also secrete cytokines capable of diffusing and acting on distant targets. This raises the possibility of paracrine killing, in which these cytokines induce tumor cell death independently of cell-cell contact.Tumor necrosis factor (TNF) is a key cytokine released during T cell activation and is unique in that it can drive either cell survival or cell death. Although most cells default to cell survival and NFkB-mediated inflammation, several modulators can shift this survival signaling toward cell death. We therefore hypothesized that sensitizing Myeloma cells to TNF could enable T cell paracrine killing and enhance the efficacy of anti-Myeloma T cell immunotherapies.To test this, we first established an in vitro model of clinical response to Teclistamab, a BCMA-directed BiTE, using Multiple Myeloma cell lines that displayed sensitive, intermediate, or resistant responses to T cell killing. Combining these data with assays of cytokine sensitivity and receptor expression, we found that susceptibility to TNF-mediated cell death was a major determinant of Teclistamab sensitivity. This correlation was further supported by reduction or complete abrogation of Teclistamab T cell killing of sensitive Myeloma cell lines when soluble TNF was neutralized from these co-cultures using monoclonal antibodies. Pharmacologic inhibition and CRISPR-mediated deletion of known regulators of TNF survival-signaling further sensitized Myeloma cells to both TNF and T cell killing. In the absence of these regulators, BCMA-negative myeloma targets retained sensitivity to Teclistamab, supporting the idea that the main mechanism of cell death was indeed paracrine killing.Together, these findings establish a direct link between TNF sensitivity and T cell-mediated killing of Myeloma cells, and support TNF-driven paracrine killing as a dominant mechanism of response to Teclistamab. Enhancing this TNF-mediated death signaling may therefore represent a strategy to overcome resistance and improve clinical efficacy of T cell-based immunotherapies in Multiple Myeloma.

#1637 Human-cynomolgus cross-reactive CD3 nanobody-centric TCE platform enhances clinical translation.

Yuanyuan Wang, Ce Gu, Liang Xiao, Huijuan Lu, Ruhan Lin, Tingchu Wu, Peipei Hu, Chang Zhou, Fan Wu, Jian Guo, Yongting Huo, Di Lu

Guangdong Fapon Biopharma Inc., Guangdong, China

T-cell engagers (TCEs) have emerged as a research hotspot in recent years, owing to their ability to precisely mediate T cell killing of target cells. However, their clinical translation is frequently hindered by core challenges: insufficient target specificity, inadequate preclinical safety risk assessment, and poor developability. Thus, an advanced technological platform is urgently needed to break through these barriers and facilitate the efficient translation of TCEs from basic research to clinical applications.
Here, we established a TCE platform with distinctive technological advantages. Its core highlight lies in the integration of nanobodies targeting the first and second signals of T-cell activation, which possess cross-reactive binding activity between human and cynomolgus monkey, a feature provides crucial support for the preclinical safety assessment. Verification data demonstrates that the TCEs armed with our CD3 nanobody not only exhibit excellent cytotoxicity but also demonstrate favorable safety profiles and robust developability. Nanobodies not only meet the requirements of diverse structural design but also, due to their relatively small molecular weight, are best suited for in vivo TCE development. Currently, relying on the core components of this platform, we have initiated the development of three types of differentiated TCE projects:secondary signal enhanced TCEs, biased activation TCEs and dual-target TCEs. These core components and TCE projects will provide crucial support for achieving excellent therapeutic efficacy in oncology and autoimmune diseases.

#1638 A high-throughput luciferase cancer cell panel driving DLL3-targeted TCE discovery.

Chen Cai, Yue Zhai, Kejun Mao, Yixiao Zhao, Mingying Li, Qian Wang, Yan Zhang, Lili Chai, **Tj (Tiejun) Bing**

ICE Bioscience, Beijing, China

Background: T-cell engagers (TCEs) have rapidly moved into the spotlight as a next-generation immunotherapy, lauded for their (1) “off-the-shelf” convenience, (2) dual-arm precision that re-directs, rather than re-engineers, a patient’s own T cells, and (3) capacity to deliver deep, durable responses even after conventional checkpoint blockade has failed. Solid-tumor TCE development is now a major frontier, yet conventional assays—confined to few cell lines—offer limited throughput and cannot probe the full antigen expression spectrum, leaving a blind spot for candidate triage. To close this gap, we selected delta-like ligand 3 (DLL3)—an embryonic Notch inhibitor that is transcriptionally resurrected in high-grade neuroendocrine tumors yet absent from normal adult tissues—and constructed a fully integrated discovery platform anchored by a 20-member luciferase-reporter tumor panel that systematically recapitulates clinically relevant expression gradients.

Methods: The platform merges four modules: (1) biophysical profiling via SPS binding kinetics and cell-based affinity screens; (2) parallel 2-D/3-D tumor co-culture assays as well as ICI combination to evaluate T-cell mediated cytotoxicity; (3) multiparametric T-cell activation readouts (CD69/CD25, proliferation); and (4) 10-plex cytokine release assays to map safety-relevant inflammatory signatures.

Results Here we showcase several DLL-3 targeting TCEs using a diverse luciferase-neuroendocrine cell panel. Preclinical studies demonstrate their binding, activation, antitumor activity, and T cell expansion in DLL3+ cell lines across cancer types, juxtaposed with a diminished impact on DLL3- cell lines.

Conclusions: This platform enables high-throughput evaluation of TCEs across the full antigen expression spectrum, systematically linking target density to therapeutic activity and safety outcomes. By linking target density to TCE performance, this system guides candidate selection and accelerates solid-tumour TCE development, while being readily adaptable to other antigens.

: Antibody Technologies and Platforms 1
Poster Session

#1642 A pan-RASi antibody-drug conjugate platform with high activity in RAS-mutant cancers.

Graham A. E. Garnett, Victoria K. Harman-McKenna, Taixiang Wang, Jodi Wong, Truman Hirkala-Schaefer, Michael G. Brant, Mark E. Petersen, Catalina Suarez, Khushi Lodaya, Rehan Higgins, Jesse H. Leblanc, Linglan Fu, Cathy Fu, Sara Weeres, Manuel Lasalle, Kaylee J. Wu, Vidhi Khanna, Sam Lawn, Kurt Stahl, Vincent Fung, Raffaele Colombo, Stuart D. Barnscher, Jamie R. Rich

Zymeworks Inc., Vancouver, BC, Canada

Aberrant activation of RAS protein by oncogenic mutation is a critical driver of tumorigenesis, yet effective and tolerable inhibition of RAS signaling remains a major unmet need. Tricomplex RAS inhibitors (RASi) are an emerging class of drugs that disrupt RAS signaling by forming a ternary complex with cyclophilin A (CypA) and the active, GTP-bound conformation of RAS [RAS(ON)], thereby blocking downstream signaling through the MAPK and PI3K pathways. RMC-6236 is an orally administered, potent pan-RAS inhibitor and is a prototypical drug in this class. Despite promising initial results in the clinic, treatment-related adverse events such as skin and gastrointestinal toxicities have emerged, likely as a result of on-target, off-tumor inhibition of RAS in normal tissues. We hypothesized that targeted delivery of a potent pan-RASi as an antibody-drug conjugate (ADC) payload could enhance anti-tumor efficacy and improve tolerability, thereby overcoming the limitations of orally administered RASi small molecules. Here we report the generation of a novel antibody-drug conjugate platform designed for the treatment of RAS-mutant cancers.

To identify suitable ADC payloads, novel pan-RAS inhibitors were synthesized with a focus on high potency, favorable polarity, and suitable functionality for linker attachment. A library of over 100 novel linkable pan-RAS inhibitors was synthesized and screened, with multiple candidates demonstrating significantly higher potency than RMC-6236 across a panel of KRAS-mutant cell lines. Mechanistic characterization of RAS binding was achieved via surface plasmon resonance, demonstrating formation of the binary (CypA:inhibitor) and ternary (RAS:CypA:inhibitor) complexes. Disruption of RAS–RAF interaction was profiled using homogeneous time resolved fluorescence.

Drug-linkers were generated from selected payloads and used to produce ADCs with a drug-to-antibody ratio of 8. Linker format and payload attachment site were tuned to improve drug-linker hydrophilicity and ADC pharmacokinetic characteristics. Pan-RASi ADCs were profiled for targeted antitumor activity in tumor cell lines. More than 20 ADCs with distinct drug-linkers were evaluated and >10 were selected for evaluation in cell line derived xenograft models. Strong regressions were observed with single doses as low as 1 mg/kg in multiple models. Evaluation in mice demonstrated no significant toxicity at doses up to 200 mg/kg. Safety was further assessed in non-human primate studies. Collectively, the promising antitumor activity and manageable tolerability profile support the application of this novel pan-RASi ADC platform to clinically meaningful targets across NSCLC, PDAC, and CRC.

#1643 Targeting LANCL1 with a humanized monoclonal antibody suppresses tumorigenesis in hepatocellular carcinoma.

Chui-Yee Diana O, Yu-Man Tsui, Irene Oi-Lin Ng

Pathology, The University of Hong Kong, Hong Kong, China

Background: The limited efficacy of current hepatocellular carcinoma (HCC) treatments drives the need for novel molecular targets. Building on our previous discovery that LANCL1 promotes HCC tumor initiation by reducing cellular reactive oxygen species (ROS), this study aims to validate it as a druggable target and develop a first-in-class humanized antibody therapeutic.
Methods: We generated a parental murine monoclonal antibody (mAb) against LANCL1. Its efficacy was evaluated *in vitro* using sphere-formation, cytotoxicity, migration, and invasion assays on HCC cell lines, and *in vivo* in an orthotopic HCC model. For clinical translation, we created humanized variants, with binding affinity assessed by Surface Plasmon Resonance (SPR).
Results: *In vitro*, the parental murine mAb potently inhibited cancer stemness (>90% reduction in sphere formation), induced significant cytotoxicity (<55% viability), and suppressed migration and invasion (67.6% and 85.3%, respectively). *In vivo*, it impaired tumor growth by 50.3%. This efficacy was demonstrated in an orthotopic NOD SCID model established with implanted human hepatic tumor cells. We next evaluated nine humanized variants, finding that all exhibited binding affinity comparable to the parental antibody. Specifically, Variant 1 showed strong inhibition at 62.8%, an efficacy close to the chimeric antibody (83.5%). Although Variant 2 was less potent, it still achieved significant inhibition at 44.5%. This confirms the humanization process successfully retained anti-tumor efficacy.
Conclusion: This work is novel as it presents the first therapeutic antibody targeting LANCL1. Our findings not only confirm the therapeutic potential of LANCL1 inhibition but also demonstrate the potent anti-tumor activity of a novel humanized antibody, providing a strong foundation for future clinical development.

#1646 Maximizing therapeutic index using fully Fc-silent antibody platform.

Kihwan Chang

CrossPoint Therapeutics, Hwaseong-si, Gyeonggi-do, Korea, Republic of

Antibody drug conjugates (ADCs) have transformed the clinical landscape for the treatment of cancers over the last two decades spear-headed by intensive research of linker and payload chemistries. However, toxicities remain a concern where impairing dosage and administration frequency of the ADCs could impact overall clinical benefit. We developed Stealth-Body (SB) by introducing specific mutations in the Fc region of the antibody to limit Fc-Fcγ receptor interactions without compromising efficacy and maintaining manufacturing scalability, when compared to LALA mutations, the SB Fc showed improved pharmacokinetic (PK) parameters such as half-life in serum studies in double transgenic mice (huFcRn and hualbumin) and complete loss of binding to all Fcγ receptors as well as C1q. Based on these characteristics, we are developing a ADCs containing SB Fc for selective anti-tumor efficacy and limiting interaction with Fcγ receptors to reduce off-target toxicities. Antibodies containing WT Fc and SB Fcs were conjugated with MMAE and efficacy was determined in in vitro and in vivo studies. Currently, PK studies in mice and preliminary toxicology studies in non-human primates are ongoing. To determine whether SB Fc conjugates were able to avoid off-target toxicities, cancer cell lines expressing FcγRs were treated with SB Fc containing conjugates or WT Fc conjugates. As expected, the SB Fc conjugates displayed no off-target cell killing toxicities in these cell lines compared to WT Fc conjugates. Conjugates containing the SB Fcs maintained potent efficacy in vitro in cancer cell lines similar WT Fc containing conjugates, indicating that efficacy was not compromised by the mutations in the SB Fc. In in vivo cell line derived xenograft (CDX) models, the SB Fc conjugates showed strong tumor growth inhibition (TGI) as single injection doses and similar potent minimum efficacious dose (MED) was observed in CDX models and determined to be 0.6 mg/kg. These preclinical data demonstrate the potential of SB Fc containing ADCs as promising for the treatment of various cancer indications and supports their use for clinical development.

#1647 RenNano platform enables efficient discovery of fully human VHH antibodies.

Frank An, Xun Xu, Jun Du, Yiqing Hu, Baihong Liu, Guan Wang, Hao Cai, Lijun Zhang, Huizhen Zhao, Jiawei Yao, Chengzhang Shang, Qiuhong Yu, Xueyuan Jiang, Fengping Yao, Jing Huang, Gao An, Yi Yang

Biocytogen, Waltham, MA, MA

VHH antibodies stand at the forefront of biomedical research, driven by their distinctive structural properties and versatile applications. The clinical potential of this technology was formally validated in 2018 with the approval of caplacizumab, the world's first VHH antibody-based drug. Currently, a growing pipeline of VHH antibody-based therapies is under investigation in clinical trials, targeting a broad spectrum of diseases, including various cancers (with a focus on PD-L1 and EGFR pathways), cardiovascular disorders, inflammatory conditions, and neurodegenerative diseases like Alzheimer's and Parkinson's. With a molecular weight of merely 12-15 kDa—approximately one-tenth that of conventional IgG antibodies—and a compact structure, VHH antibodies possess unparalleled tissue penetration capabilities. The complementary determining region (CDR) of VHH antibodies, particularly the CDR3 loop, is significantly longer, forming a protruding "finger-like" structure. This unique conformation allows VHH antibodies to penetrate deep into hidden antigen epitopes, such as enzyme active sites or viral conformational epitopes, that are inaccessible to traditional antibodies. However, the production of VHH antibodies requires the use of camelid animals (such as llamas and alpacas) or the construction of phage display libraries via genetic engineering techniques. Compared with the production of traditional mouse monoclonal antibodies, its production process may be more complex, and the cost may also be higher. Our RenNano mice produce fully human heavy chain-only antibodies that eliminate the need for *in vitro* humanization, thereby accelerating the development process and reducing costs. Owing to their small size and structural flexibility, these VHH antibodies have demonstrated significant utility in key applications such as conditional activation (e.g., 4-1BB), half-life extension (e.g., ALB), and enhanced blood-brain barrier (BBB) penetration through improved receptor-mediated transcytosis (e.g., TFR1). Leveraging the RenNano platform, we have developed a fully human VHH antibody library for the treatment of cancer, autoimmune diseases, and metabolic disorders. Preliminary evaluations indicate that these VHH antibodies possess developability profiles comparable to those of marketed VHH antibody drugs.

#1648 Real-time imaging for quantitative assessment of antibody-drug conjugate internalization.

Tian Wang[1], Yunfei Pu[1], Ryan Raver[2], **Xiaoyu Zhang**[2], Peifang Ye[1], Nancy Li[2]

[1]Agilent Technologies, Hangzhou, China,[2]Agilent Technologies, La Jolla, CA

Antibody-drug conjugates (ADCs) represent a major advancement in cancer therapy, relying on efficient target-mediated internalization for optimal efficacy. This underscores the need for precise, convenient, and cost-effective methods to monitor antibody internalization for candidate selection, mechanism-of-action studies, and safety evaluation. We present a robust, real-time quantitative assay using the Agilent xCELLigence RTCA eSight system combined with CypHer5E-NHS-Ester labeling. CypHer5E is a pH-sensitive cyanine dye that fluoresces in acidic environments, enabling dynamic tracking of antibody trafficking into intracellular compartments. Using this approach, we demonstrated selective internalization of CypHer5E-labeled trastuzumab in HER2-positive cell lines via receptor-mediated uptake. Both primary CypHer5E labeling and secondary Fab-CypHer5E conjugation enabled clear visualization of internalization events. Furthermore, secondary Fab-CypHer5E labeling facilitated comparative analysis of multiple HER2-targeting therapeutic antibodies. This integrated platform provides a powerful tool for mechanistic studies and drug-screening assays, offering critical insights to optimize antibody efficacy, safety, and pharmacokinetics in biopharmaceutical development.

#1649 FcRn humanized mice with an immunodeficient background can be used to evaluate the pharmacokinetics of antibody drugs while avoiding anti-drug antibodies.

Hannah Horton, Ruili Lv, Suman Zhao, Qingqing Xu, Xiaofei Zhou

Biocytogen, Waltham, MA

Introduction: FcRn is a pH-dependent receptor that binds and recycles IgG, preventing its lysosomal degradation to extend plasma half-life. Separately, Rag2 is essential for V(D)J recombination in lymphocyte maturation, and its absence results in a lack of functional T and B cells, preventing the formation of Anti-Drug Antibodies (ADA).Biocytogen's B-hFcRn, Rag2 KO mouse model is a tool for PK/PD/safety evaluation of human IgG therapeutics that circumvents ADA via T and B cell deficiency.

Methods: l B-hFcRn mice (110001) were generated by replacing exons 2-4 of the mouse *Fcgrt* gene with a coding sequence (CDS) that encodes full-length human *FCGRT*, while the mouse *Fcgrt* gene transcription and translation will be disrupted.B-Rag2 KO mice (110809) were produced through targeted knockout of exon 3 and the 3' UTR region of the *Rag2* gene. This knockout leads to the inactivation of Rag2.To generate B-hFcRn, Rag2 KO mice, B-hFcRn mice (110001) were mated with B-Rag2 KO mice (110809).l For protein expression analysis, spleen, lung tissue lysates were collected from wild-type C57BL/6N mice (+/+), homozygous B-hFcRn mice (H/H), and homozygous B-hFcRn, Rag2 KO mice (H/H, -/-), and then analyzed by western blot with species-specific anti-FcRn antibody. l The frequency of leukocyte subpopulations was analyzed in B-hFcRn, Rag2 KO mice. Using flow cytometry, immune cells (including T and B cells) in the spleen, blood, and thymus were quantified and compared to wild-type C57BL/6 mice.l The *in vivo* PK of YTE-mutated and control antibodies was assessed in C57BL/6, B-hFcRn, B-Rag2 KO, and B-hFcRn, Rag2 KO mice following tail vein injection and serial blood collection.

Results: l Western blot analysis results indicated that human FcRn was detected in the spleen and lung of B-hFcRn, Rag2 KO mice.l Flow cytometry analysis revealed that T cells and B cells were undetectable in the spleen, blood, and thymus of homozygous B-hFcRn, Rag2 KO mice.l PK data suggest ADA formation against our YTE antibody in immunocompetent mice, its absence in Rag2 KO mice, and a half-life-extending effect that was confined to hFcRn humanized mice.

Conclusions: The B-hFcRn, Rag2 KO mouse model, deficient in T and B cells yet expressing human FcRn, provides a valuable tool for assessing the PK/PD of antibody candidates that are susceptible to ADA interference in immunocompetent mice.

#1650 MPSA-AB5000: A high-throughput cell-based membrane protein screening array for accurate early-stage off-target assessment to accelerate safer antibody therapeutic development.

Liping Wang, Guoqian Wang, Yao Peng, Jinying Ning, **Feng Hao**

Kyinno Biotechnology Co., LTD, Beijing, China

Antibody drug development is a lengthy and complex process, often hindered by off-target binding that affects approximately 25-30% of preclinical candidates. With the growing importance of advanced modalities such as CD3 bispecific antibodies, antibody-drug conjugates (ADCs), and CAR-T therapies, early and accurate off-target assessment has become essential. However, conventional assays—including immunohistochemistry (IHC), ELISA, and flow cytometry (FACS)—remain limited in sensitivity, specificity, and throughput.To address these limitations, we developed the Membrane Protein Screening Array (MPSA-AB5000), a high-throughput, cell-based platform for comprehensive identification of antibody targets and off-targets. The MPSA-AB5000 expresses a broad spectrum of human membrane proteins in live cells, maintaining native conformation and post-translational modifications to ensure physiologically relevant binding analysis. MPSA-AB5000 is a high-throughput, cell-based platform for identifying antibody targets and off-targets, enhancing antibody specificity screening and reducing development risks. To provide the highest level of sensitivity, MPSA-AB5000 uses luciferase reporter cell line detection. The wash-free strategy reduces false negatives, and signal amplification makes remarkable discrimination. Furthermore, the platform integrates a Protein A-based reporter system, leveraging Protein A's strong Fc-binding affinity—particularly for human IgG1, IgG2, and IgG4—to immobilize antibodies on reporter cells. This allows detection of off-target-induced signaling even in Fc-modified formats such as IgG1-LALA or IgG4. Collectively, the MPSA-AB5000 provides a robust, versatile, and physiologically relevant solution for antibody target deconvolution and specificity evaluation, accelerating the discovery and optimization of safer antibody therapeutics.

#1651 Automated imaging-based verification of monoclonality in single-cell cloning confirms higher efficiency of the Pala single cell sorter and dispenser compared to limiting-dilution assays.

Ahmed Shaaban[1], Benjamin Werdelmann[2], Anna Willms[2], Matthias Pirsch[2], Sebastian Kollenda[2], Aleks Guledani[2], Ankit Vaghasiya[2], Susanne Sebens[3], **Ryan McComb**[1], Reinhild Geisen[2]

[1]Bio-Techne, San Jose, CA,[2]Synentec GmbH, Elmshorn, Germany,[3]Institute for Experimental Cancer Research and University Hospital Schleswig-Holstein Campus Kiel, Kiel, Germany

Establishing monoclonal cell lines is a common process in cancer research and drug discovery, ensuring genetic uniformity and reproducibility in functional assays, therapeutic antibody production, and clinical manufacturing. However, isolating single cells and confirming their monoclonal origin remain major bottlenecks due to the low efficiency and high hands-on time of conventional limiting-dilution assays (LDA). We therefore assessed a workflow combining the Pala Single Cell Sorter and Dispenser (Bio-Techne) with SYNENTEC's automated imaging system for reliable, traceable proof of monoclonality and compared it to LDA.

One cell per well was dispensed into 10 × 96-well plates using Pala, and parallel LDA controls were prepared at 0.5 cells/well. We used CHO-K1 cells as the main production cell line as a robust cell model for process validation, before testing the system with cancer cell lines. Wells were automatically imaged on days –1, 0, 1, 4, and 8 using SYNENTEC's high-throughput imaging system. Automated segmentation, clone tracking, and confluence analysis were performed with YT-SOFTWARE®. Wells were classified as clonal, non-clonal, empty, or 'ghost' based on initial and subsequent images. Single-cell dispensing efficiency, colony formation rate, and growth kinetics were compared between methods.

Pala dispensing yielded 828 monoclonal colonies versus 329 from LDA, representing a >2.5-fold increase. The average number of monoclonal wells per 96-well plate was higher (71.2 vs. 32.8), while the number of non-clonal (7.2 vs. 13.4) and empty wells (16.6 vs. 49.5) was reduced. Average clonal outgrowth per single cell (89.8 % vs. 78.4 %) and growth rate (0.86 vs. 0.83) were higher for Pala, indicating gentle handling and improved viability. The automated workflow reduced hands-on time and provided clear documentation for regulatory compliance.

Combining Pala single-cell dispensing with SYNENTEC's automated imaging enhances clonal yield, efficiency, and traceability while reducing resource consumption. This approach accelerates the establishment of standardized, reproducible cell models and supports high-throughput biotherapeutic and translational oncology research.

#1652 Binding to bridging: Complete suite of FcγR assay tools accelerates antibody therapeutic development.

Julia K. Gilden, Denise Garvin, Kristin Riching, Brock F. Binkowski, Richard Moravec, Pete Stecha, Rod Flemming, Becky Godat, **Kai Hillman**, Marjeta Urh, Mei Cong, Jamison Grailer

Promega, Madison, WI

Antibodies are effective therapeutics because of their specificity in binding to an antigen and ability to activate an immune response through Fc effector functions like antibody-dependent cellular cytotoxicity (ADCC), antibody-dependent cell phagocytosis (ADCP), and complement-dependent cytotoxicity (CDC) by engaging with immune cells like NK cells and macrophage. However, traditional methods for characterizing these interactions are highly variable and labor-intensive. We developed a suite of luminescent assays for characterizing antibody effector functions for robust, streamlined measurement across antibody development: Lumit® Binding Immunoassays, Fc Effector Reporter Bioassays for ADCC/ADCP, and HiBiT Target Cell Killing Bioassays using MoA-qualified primary cells. We demonstrate application to anti-CD20 biosimilar antibodies, showing concordant rank order from binding to functional killing studies. These rapid, high-throughput assays support comparability, stability, and lot-release decisions.

#1653 FcRn humanized rats for pharmacokinetics assessment of antibody drugs.

Kelvin Yin, Suman Zhao, Zhi Zhang, Yanling Wang

Biocytogen, Waltham, MA, MA

Introduction: Biocytogen's B-hFcRn rat model serves as a practical tool for assessing the pharmacokinetics/pharmacokinetics and safety of human IgG therapeutics. The model capitalizes on the rat's larger size, which allows for serial blood sampling and thus more efficient and continuous data collection compared to mice, where animal welfare considerations necessitate staggered sampling across subgroups. This is combined with the presence of human FcRn, a pH-dependent receptor that binds and recycles IgG, protecting it from lysosomal degradation to extend its plasma half-life.

Methods: l B-hFcRn rats were generated by inserting a chimeric cDNA encoding full-length human *FCGRT,* followed by its 3'UTR and stop codon right after the rat *Fcgrt* start codon, thereby replacing exons 2-4 and placing human FcRn expression under the control of the endogenous rat promoter while disrupting the native rat gene.l For protein expression analysis, liver, kidney, and spleen tissue lysates were collected from wild-type SD rats (+/+), homozygous B-hFcRn rats (H/H), and then analyzed by western blot with species-specific anti-FcRn antibody. l SD rats and B-hFcRn rats were intravenously injected with Bevacizumab (commercial), and serum was collected for pharmacokinetic (PK) analysis.

Results: l Western blot analysis results indicated that Rat FcRn was only detectable in wild-type SD rats. Human FcRn was exclusively detectable in the liver, kidney, and spleen of homozygous B-hFcRn rats.l Linear pharmacokinetics were observed in B-hFcRn rats after a single intravenous bolus administration of the monoclonal antibody and serial blood collection. PK data suggest that the B-hFcRn rat model enables reliable prediction of the FcRn-mediated pharmacokinetics and efficacy of IgG antibodies in humans.

Conclusions: The B-hFcRn rat model is used for pharmacokinetics, pharmacodynamics, and safety evaluation of human immunoglobulin G (IgG) and is based on the Fc domain therapeutics.

#1654 Bioluminescent and cell-based assays for comprehensive characterization of antibody-drug conjugate mechanisms of action.

Mei Cong[1], Yitong Li[1], virginia Kincaid[2], Morten Seirup[1], Christopher Eggers[3], Rod Flemming[4], Jim Hartnett[4], Kristin Riching[4], Jamison Grailer[1], Julia K. Gilden[1]

[1]Promega, Madison, WI,[2]R&D, Promega, Madison, WI,[3]Promega Corp., Madison, WI,[4]

The growing field of targeted therapeutics has led to the emergence of Drug Conjugates, including antibody-drug conjugates (ADCs), protein-drug conjugates (PDCs), and other payload-conjugated biologics that integrate selective delivery with potent cytotoxic payloads. These modalities exert therapeutic effects via multiple mechanisms of action (MoA), including direct cytotoxicity following receptor binding and internalization, bystander killing via cleaved payload diffusion, antigen function blockade, and immune-mediated cytotoxicity such as ADCC and ADCP, driven by Fc effector function. Effective characterization and potency assessment of ADCs require robust in vitro tools that capture these complex MoA. Here we present a panel of bioluminescent and cell-based assays to support the pharmacological profiling of ADCs. The Lumit® Ligand Binding Assay provides a homogeneous solution-phase format to quantify antigen engagement by mAbs and ADCs, enabling efficacy and QC assessments. The Lumit® FcRn Binding Immunoassay evaluates FcRn-ADC interactions to inform half-life predictions and Fc engineering. Fcγ receptor binding, uptake, and C1q engagement are assessed through Lumit®-based and cell-based formats, offering insights into immune effector functions and FcγR-mediated toxicity. Additionally, a bioluminescent ADC Internalization Assay tracks intracellular trafficking, enabling payload delivery characterization and identification of dose-limiting toxicity risks. Together, these assays offer scalable, reproducible platforms for PK, PD, and toxicity evaluation in ADC development.

#1655 Building a recombinant Factor C assay to enable sustainable endotoxin testing in antibody development.

Yingjie Liu[1], **Peter Hsueh**[2], An Ouyang[2], Spencer Chiang[1], YuehChun Hsieh[1]

[1]ACROBiosystems Co., Ltd., Beijing, China,[2]ACROBiosystems Inc., Newark, DE

Endotoxins, lipopolysaccharide components of the outer membrane of Gram-negative bacteria, are among the most potent pyrogens known. Even at trace levels, endotoxins can trigger severe inflammatory responses in humans, including fever, hypotension, septic shock, and multi-organ failure, particularly when introduced intravenously. Consequently, accurate detection and quantification of endotoxins are essential at every stage of biopharmaceutical development, from early-stage antibody discovery to large-scale manufacturing and final product release. In the context of antibody discovery, residual endotoxins in cell culture supernatants or during purification can confound in vitro bioassays, misrepresent functional activity, and affect downstream characterization. During manufacturing, endotoxin contamination poses a serious safety risk and regulatory non-compliance, necessitating rigorous quality control measures. Regulatory agencies globally, including the FDA and EMA, mandate strict endotoxin limits for injectable therapeutics, emphasizing the importance of robust and reliable endotoxin assays in maintaining both patient safety and product efficacy. Traditionally, the Limulus Amebocyte Lysate (LAL) assay has been the industry standard due to its high sensitivity, rapid turnaround, and broad adoption across biopharmaceutical laboratories. However, LAL relies on lysates derived from horseshoe crab blood, raising sustainability, ethical, and supply chain concerns. In response, recombinant Factor C (rFC) assays have emerged as a viable animal-free alternative. rFC assays leverage recombinant expression of Factor C, the key enzyme initiating the LAL coagulation cascade, with fluorescence-based detection of endotoxin binding. This study describes the development and validation of an rFC-based endotoxin detection method specifically optimized for antibody discovery and production workflows. The method was benchmarked against conventional LAL assays in accordance with established bioanalytical validation guidelines, demonstrating comparable sensitivity with a lower limit of quantitation (LLOQ) of 0.005 EU/mL. Notably, the absence of Factor G in rFC assays eliminates interference from β-glucans, as verified by spiking experiments with 10 μg/mL β-glucan, which produced no detectable non-specific signal. Extensive matrix testing across 25 common buffers and culture supernatants revealed recovery rates ranging from 75% to 109%, underscoring the assay's robustness and versatility. Overall, the rFC assay provides a reliable, sensitive, and ethically responsible approach to endotoxin monitoring, aligning with the 3Rs principles while maintaining rigorous analytical performance.

#1656 Luminescent assay platforms accelerate therapeutic antibody development in veterinary immuno-oncology.

Jun Wang, Denise Garvin, Ildiko Kasza, Jim Hartnett, Mei Cong, Jamison Grailer

Promega, Madison, WI

Advances in immuno-oncology increasingly depend on translational animal models to inform mechanism of action (MoA), pharmacokinetics, and therapeutic potential. Beyond their preclinical utility for human therapies, these models are critical for developing novel biologics in veterinary oncology, particularly in canine cancers, which share key demographic, immunologic and molecular features with human disease. A major limitation in this research is the lack of robust analytical tools to characterize species-specific antibody function and receptor engagement. We developed a suite of luminescent, cell-based bioassays to quantify Fc-mediated effector mechanisms, including antibody-dependent cellular cytotoxicity (ADCC). Each assay incorporates canine Fcγ receptors and features luciferase reporters, providing sensitive, quantitative, and reproducible readouts suitable for potency and MoA evaluation. In addition, cell-based reporter bioassays were developed to measure the potencies of antibodies that modulate canine immune checkpoints (PD-1/PD-L1) or co-stimulatory receptors (CD40). Complementing these cell-based tools, an improved canine antibody binding assay offers a rapid, homogeneous alternative to ELISA and SPR methods for characterizing antibody-target interactions. The assay supports antibody development from screening to potency release testing of veterinary antibody therapeutics. Together, these luminescent assay platforms streamline veterinary immuno-oncology research, accelerating translation of therapeutic antibodies across species.

#1657 BCG015:A first-in-class antibody-drug conjugate targeting TM4SF5 for the treatment of hepatocellular carcinoma.

Guan Wang, Zhi Qi, Yu Qi, Gao An, Cong Shen, Yanan Guo

Biocytogen, Waltham, MA, MA

Background: Hepatocellular carcinoma (HCC) is one of the leading causes of cancer-related mortality worldwide, and patients with HCC respond poorly to current therapies. Currently, no antibody-drug conjugate (ADC) has been approved or is in late-stage clinical development for the treatment of HCC. To address this unmet medical need, Biocytogen developed a novel ADC targeting TM4SF5 for HCC treatment.
Results: TM4SF5 expression was detected in 70% of HCC patient samples, with limited expression in normal tissues. Target abundance studies in HCC cell lines revealed TM4SF5 protein levels comparable to or higher than those of other HCC-associated tumor antigens. TM4SF5 demonstrated internalization activities in HCC cell lines.The lead anti-TM4SF5 mAb generated from Biocytogen's RenLite® transgenic mice exhibited high affinity, good specificity, strong cancer cell binding, and efficient internalization *in vitro*. It also demonstrated excellent physicochemical properties and stability under accelerated and stress conditions.BCG015, the BLD1102-conjugated ADC, showed potent and TM4SF5-dependent tumor growth inhibition activity in HCC cell lines. *In vivo*, BCG015 exhibited significant antitumor efficacy across multiple HCC CDX and PDX models with TM4SF5 expression. In four CDX models, BCG015 demonstrated comparable or superior efficacy compared to ADCs targeting other HCC-associated antigens. Preliminary safety studies in canine and cynomolgus monkey models are ongoing.
Conclusion: BCG015 represents a novel, first-in-class ADC targeting TM4SF5 with strong preclinical efficacy. These findings highlight its potential as a promising therapeutic option for HCC patients with TM4SF5 expression, addressing a significant unmet need in liver cancer treatment.

#1658 Preclinical study of NW008, a novel dual-functional anti-MICA/B antibody-drug conjugate.

Afang Zhou[1], Juanjuan Li[1], Changcheng Li[1], Xueying Zhong[1], Yiran Wu[1], Li Liu[1], Gang Liu[1], Jiaoyi Zhong[1], Lijia Yang[1], Junkui Yang[1], Dan Mi[1], Jiabao Liu[1], Yaolan Dai[1], Yan Gao[1], **Zhijian Li**[2], Bin Liu[1], Zhigang Guo[1], Wenting Luo[1]

[1]Chengdu Chipscreen Newway Biosciences Co., Ltd., Chengdu, China,[2]Chipscreen Biosciences (United States) Ltd, Somerset, NJ

Background: The MHC class I polypeptide-related sequences A and B (MICA and MICB; collectively MICA/B) are stress-induced antigens. They are minimally expressed in healthy tissues but overexpressed in a wide range of solid tumors. Membrane-bound MICA/B activates antitumor immunity by engaging the NKG2D receptor on immune effector cells, such as CD8-positive T cells, natural killer (NK) cells and γδ T cells. However, proteases in the tumor microenvironment (TME) cleave MICA/B from the tumor cell surface, which impairs NKG2D-mediated tumor recognition and facilitates immune evasion. Furthermore, soluble MICA/B induces sustained NKG2D activation, resulting in receptor downregulation and lymphocyte dysfunction. Elevated serum levels of soluble MICA are associated with poor patient survival, highlighting the therapeutic potential of targeting MICA/B.
Methods: Mice were immunized with recombinant proteins containing the α3 domain derived from multiple MICA/B alleles. A humanized anti-MICA/B antibody that binds with high affinity to various MICA/B alleles was obtained through high-throughput screening. Each antibody molecule was site-specifically conjugated to four molecules of a highly potent topoisomerase I inhibitor via a specially designed, hydrophilic, enzyme-cleavable linker that suppresses the retro-Michael reaction, resulting in the ADC candidate NW008. The in vitro antitumor activity of NW008 was evaluated using multiple MICA/B-expressing tumor cell lines. Its in vivo efficacy was assessed in several cell-derived xenograft (CDX) models.
Results: The humanized anti-MICA/B antibody exhibited high internalization efficiency and sub-nanomolar affinity for multiple MICA/B alleles. It also inhibited MICA/B shedding from tumor cells and enhanced MICA/B-NKG2D interactions. The ADC molecule NW008 demonstrated high homogeneity and favorable stability, and it showed potent cytotoxicity against a variety of MICA/B-expressing tumor cell lines, with half-maximal effective concentration (EC_{50}) values in the nanomolar range. In multiple mouse xenograft models bearing human MICA/B-expressing tumors, NW008 exhibited significant antitumor efficacy in vivo, with maximum tumor growth inhibition (TGI) exceeding 85% in all models, and was well tolerated.
Conclusion: MICA/B represents a highly attractive target for ADC development. NW008 is a first-in-class dual-functional ADC that acts by restoring antitumor immunity through inhibition of MICA/B shedding and directly eliminating tumor cells via targeted delivery of a topoisomerase I inhibitor. NW008 demonstrates robust antitumor efficacy in preclinical models, supporting its clinical development as a promising therapeutic candidate for MICA/B-positive solid tumors.

#1659 Development of a novel PSCA-targeting antibody-drug conjugate with high potency and stability for prostate cancer therapy.

Yanyang Cao, Evelyn A. Kono, Robert E. Reiter

Department of Urology, UCLA David Geffen School of Medicine, Los Angeles, CA

Antibody-drug conjugates (ADCs) enable the selective delivery of highly cytotoxic payloads to tumors and are emerging as new, promising therapeutic options for prostate cancer. Prostate stem cell antigen (PSCA) is a cell-surface antigen that is highly overexpressed in prostate cancer and upregulated in advanced disease states, while minimally expressed in normal tissues, making it an ideal target for ADC therapy. In this study, we identified and generated full-length human anti-PSCA antibodies, exhibiting high binding affinity and rapid internalization into PSCA-expressing cancer cells. Various cytotoxic drugs (e.g., monomethyl auristatin E (MMAE), DM1, etc.) were conjugated to the lead anti-human PSCA antibody (A2) using a chemically validated linker. Among the resulting ADC candidates, A2-MMAE demonstrated the most potent, concentration-dependent cytotoxicity against PSCA-positive human prostate cancer cell lines, with an IC_{50} range of 0.18-2.17 nM, while exhibiting no cytotoxicity in PSCA-negative cells. Hydrophobic interaction chromatography (HIC-HPLC) analysis revealed a heterogeneous distribution of drug-to-antibody ratios (DARs), with an average DAR of 4.84. Furthermore, A2-MMAE retained a high level of total ADC integrity following 10 days of incubation in mouse plasma, indicating a robust plasma stability. These findings suggest that the novel anti-PSCA ADC (anti-PSCA-VC-PAB-MMAE), characterized by its strong target specificity, high potency, and excellent stability, holds promise as a safer and more effective therapeutic for prostate cancer. Ongoing studies will evaluate its in vivo antitumor efficacy, tolerability, safety, and pharmacokinetic/pharmacodynamic (PK/PD) profiling in mouse models.

#1660 Design of a synthetic non-natural antibody (NoNabody) against GRP as a new therapy for small cell lung cancer.

Pablo Garrido Rodriquez[1], Jahaziel Gasperin Bulbarela[2], Alexei Fedorovish Licea Navarro[2], Alfredo Martinez[3]

[1]Centro de Investigacion Biomedica de La Rioja (CIBIR), Logrono, Spain,[2]Biomedical Innovation Department, Centro de Investigacion Cientifica y Educacion Superior (CICESE), Ensenada, Mexico,[3]Angiogenesis Group, Oncology Area, Center for Biomedical Research of La Rioja (CIBIR), Logrono, Spain

(a) An introductory sentence indicating the purposes of the study; Gastrin-releasing peptide (GRP) has been described as an autocrine growth factor for small cell lung carcinoma (SCLC) and the use of a monoclonal antibody (MoAb) against GRP was shown to reduce tumor growth in animal models and had a positive profile in a phase 2 clinical trial. Here we aim to develop a synthetic non-natural antibody (NoNabody) as a potential new therapeutic tool for SCLC.
(b) A brief description of pertinent experimental procedures; The first step to obtain a NoNabody against GRP was to study the interaction between a well-characterized anti-GRP MoAb and the peptide itself. After obtaining the sequence of the variable binding region, ColabFold was used to predict the antibody structure and VMD, together with NAMD, were used to analyze the antibody-peptide interaction.
(c) A summary of the new, unpublished data; An *in silico* evaluation of the interaction between the anti-GRP antibody and the peptide identified the last seven residues of GRP, including the terminal amide group, as the main target of the antibody.Throughout all the molecular dynamics simulations, the MoAb remained structurally stable, whereas the full-length GRP peptide exhibited limited stability. In contrast, simulations performed with only the last 10 or 7 amino acids of the peptide showed increased stability.A comparison of the interactions between the amidated versus the free-acid peptide with the MoAb showed that amidation greatly enhances the antibody's affinity for GRP.Analysis of the antibody-peptide interface revealed that the interaction is distributed between the heavy and light chains, with GRP positioned right in between them. CDR3 (light chain) interacts with the last three residues of GRP, whereas CDR1 and CDR2 (heavy chain) interact with residues 16-22.
(d) A statement of the conclusions; NoNanobodies represent a new tool for employing antibodies in *in vitro* and *in vivo* studies. This work focuses on generating a NoNanobody against GRP. An initial *in silico* analysis showed that antibody-peptide binding occurs at the C-terminal amino acids and that this interaction is strengthened when GRP is amidated. This information is critical for developing new synthetic binding moieties against GRP that may improve drug performance through their small size, improved tissue penetrability and low immune responses to the small synthetic forms.
This work was supported by the Science and Innovation System of the Government of La Rioja (25658-2025/0000000016).

#1661 Preclinical characterization of XB773, a novel anti-DLL3 antibody-drug conjugate.

Marlene Hennessy, Ganapathy Sarma, Yutaka Matsuda, Jenny Chang, Suprit Deol, Zhenzhen Mo, Yan Hu, Maoyin Li, Rajesh Kumar, Hui Zhao, Brian A. Mendelsohn, Minjong Park, Summer Park, Janice Kim, Ragadeepthi Tunduguru, Kathleen R. Gogas, Seema Kantak

Exelixis Inc, Alameda, CA

Background: Delta-like ligand 3 (DLL3) is a single transmembrane protein that is a member of the Notch ligand family and an inhibitor of the Notch signaling pathway involved in cell signaling. DLL3 has low cytoplasmic expression in normal tissue but is selectively overexpressed and trafficked to the membrane in small cell lung cancer (SCLC) as well as some other neuroendocrine cancers, where its expression is correlated with aggressive disease. XB773 is an antibody-drug conjugate comprising a humanized VHH Fc antibody with high affinity for DLL3 that is conjugated to a topoisomerase 1 inhibitor using site-specific AJICAP® technology. Here, we describe the preclinical characterization of XB773, including its in vitro cytotoxicity and internalization and in vivo efficacy in cell line-derived xenograft (CDX) and patient-derived xenograft (PDX) models.
Methods: In vitro cytotoxicity, internalization, and bystander activity of XB773 were evaluated in DLL3-overexpressing cell lines using luminescence and fluorescence assays. In vivo tumor growth inhibition was evaluated in the SHP77 CDX model of SCLC and the NCI-H660 model of neuroendocrine prostate cancer (NEPC) using 1, 3, and 6 mg/kg dose levels in a single or repeat dose schedule. Tumor growth inhibition was additionally assessed in a PDX model of SCLC at 5 and 10 mg/kg (single dose).
Results: XB773 displayed in vitro cytotoxic activity at nanomolar concentrations and demonstrated internalization properties. Bystander effect was illustrated through the cytotoxic activity of XB773 against non-DLL3-expressing Jurkat cells when cocultured with DLL3-overexpressing cells compared with monoculture where no cytotoxicity was observed. In vivo, XB773 demonstrated significant dose-dependent antitumor activity in PDX and CDX models of SCLC as well as in a model of NEPC expressing DLL3. Tumor regression was observed in the SHP77 model.
Conclusions: XB773 demonstrated target-mediated tumor cell cytotoxicity and in vivo efficacy across several xenograft cell lines and PDX models of SCLC and neuroendocrine cancers. Taken together, these preclinical results support further development of XB773. Investigational New Drug-enabling studies are ongoing.

#1662 GSPT1 degrader antibody conjugate, BLB-201, for the treatment of high-risk acute myeloid leukemia.

Rakesh Bam[1], Wenjian Qian[1], John Liu[1], Peipei Zheng[2], Haoyang Wang[1], Jinna Yu[2], Wenfeng Hou[2], Xiaoying Wei[1], Dengqi Xue[1], Wen Zhang[1], David Yi[1], Alice Chen[1]

[1]Baylink Biosciences, Palo Alto, CA,[2]Asieris Pharmaceuticals, Shanghai, China

Targeted degradation of GSPT1, a translation termination protein, is a novel approach for Acute Myeloid Leukemia (AML) treatment. We developed a degrader antibody conjugate (DAC) BLB-201 to (i) improve the systemic tolerability of GSPT1 degrader, and (ii) selectively kill AML blasts and leukemia stem cells expressing the tumor antigen, CD123/IL3RA. The BLB-201 DAC was optimized for activity, safety, physiochemical properties, and stability. BLB-201 rapidly degraded GSPT1 and caused cellular stress-driven apoptosis in AML cells, and showed high degree of homogeneity, solubility, and linker-payload stability in serum. A panel of CD123-positive cell lines and patient AML blast samples, with high-risk abnormalities, such as FLT3-ITD mutation, TP53 mutation and MLL1 gene re-arrangements, were evaluated for cell killing by BLB-201. BLB-201 was potent against CD123-positive AML cell lines but did not affect the viability of CD123-negative cells in the cell killing assays. BLB-201 had strong cytotoxic effects on patient AML blasts (n=17 samples) and leukemic stem cells *ex vivo*. *In vivo*, BLB-201 exhibited excellent synergy at low doses (0.1-0.3mg/kg) with clinical anti-AML agents (venetoclax, azacitidine and quizartinib) in systemic MV-4-11 and MOLM-13 models. In the systemic PDX models representing relapsed AML with high-risk mutations, BLB-201 monotherapy significantly suppressed circulating CD45+ AML cells, prolonged survival as well as produced complete response in combination with venetoclax and azacitidine regimen. As a single agent both in the *in vitro* and in CDX AML models, BLB-201 showed better efficacy compared to a CD33-targeted GSPT1 DAC benchmark. We did not observe any effects of BLB-201 on normal erythroid, megakaryocytic and myeloid cell differentiation from CD34+ hematopoietic stem cells *in vitro*, while the CD33-targeted antibody drug conjugate, gemtuzumab ozogamacin, was highly toxic in these assays. BLB-201 DAC allows selective targeting of CD123-positive AML blasts and leukemia stem cells, minimizing direct exposure of GSPT1 degrader to healthy tissues. This unique mechanism of action may improve response rates when combined with existing targeted therapies for AML patients with high-risk or relapsed/refractory disease.

#1663 Monoclonal antibodies targeting the B-cell receptor complex directly induce widespread kinase inhibition and B-cell killing for the treatment of leukemia and lymphoma.

Rachel Welt[1], Virginia Raymond[2], David Kostyal[3], Sydney Welt[1]

[1]Welt Bio-Molecular Pharmaceutical, Briarcliff Manor, NY,[2]Biogent Consultants, Armonk, NY,[3]ARDL, Akron, OH

Welt Bio-Molecular Pharmaceutical (WBMP) aims to develop cytotoxic monoclonal antibody (mAb) therapies binding driver membrane receptors on malignant cells. Such membrane targets control growth, survival, and proliferation signals in healthy cells and their increased activity is often implicated in the oncogenesis of tumor cells. In B-cells, the B-cell Receptor Complex (BCRC), a signalosome comprising several membrane proteins, is involved in transmitting signals that determine cellular fate. Dysregulation of BCRC proteins, or those in downstream signaling pathways, result in a diversity of B-cell cancer subtypes, making the BCRC a rational drug target. WBMP has previously described WBMP-4, a pro-apoptotic anti-membrane IgM antibody. Using a proprietary mAb-target-discovery platform, we have developed mAbs against two additional sites across the BCRC. All pipeline mAbs mediate apoptosis individually upon target binding. Here we investigate the therapeutic potential of this suite of mAbs via *in vitro* kinase and cytotoxicity analyses.
Antibodies against designated regions of the BCRC, identified via WBMP's drug-discovery platform, were developed using hybridoma technology. Candidate mAbs were selected for their target-reactivity, and biologic effect was measured via preliminary growth assays of various lymphoma cell lines treated with hybridoma supernatant. These mAb supernatants have been tested for their ability to modulate B-cell kinase activity using the Pamgene phosphotyrosine kinome assay. Biacore assays will select unique, high affinity mAbs binding at distinct BCRC epitopes. Cell growth, MTT, and additional kinome assays will define the cytotoxicity characteristics of mAbs at varying doses and compared to existing B-cell therapeutics (i.e. ibrutinib, acalabrutinib, venetoclax, rituximab).
WBMP has successfully applied a drug discovery system to develop a pipeline of B-cell cancer therapeutics. Each candidate mAb in this pipeline binds to a specific BCRC epitope and modulates the function of this signalosome. Here we show the potent effect of each of these mAbs as monotherapies, *in vitro*, in inducing widespread kinase inhibition, and, at sufficient doses, apoptosis. Activity of these mAbs will be studied in mouse xenograft systems and safety will be assessed with comprehensive normal tissue and non-target protein cross-reactivity assays. Those mAbs which are determined to be safe and effective will be considered for further clinical development. Together, this pipeline of novel mAbs covers the spectrum of B-cell malignancies, and the availability of multiple, distinct, directly effective mAbs against B-cells offers the potential for combination treatment strategies that can be optimized for specific tumor-types.

#1664 Novel GPC3-targeting antibody-drug conjugate using novel payload or dual payloads to treat hepatocellular carcinoma and non-small-cell lung cancer.

Suk Lee, John Liu, Alice Juang, Aastha Jain, Xiaoying Wei, Wen Zhang, David Yi, Alice Chen

Baylink Biosciences, Palo Alto, CA

Glypican-3 (GPC3) is a highly promising therapeutic target due to its selective, abundant overexpression in hepatocellular carcinoma (HCC) and certain subsets of non-small cell lung cancer (NSCLC), while being largely absent in normal adult tissues. A Phase 1 trial with a GPC3-targeted CAR-T therapy showed an objective response rate of 57 percent in heavily pre-treated patients with advanced HCC, highlighting the potential of GPC3 as a viable tumor-specific antigen for targeted therapy. ADC modality offers distinct advantages over CAR-T therapies, including off-the-shelf availability, lack of risk of cytokine release syndrome, and significant accessibility and cost advantages. However, HCC is known to be resistant to traditional chemotherapy thus traditional ADC payloads likely won't work. We have developed a series of next-generation anti-GPC3 antibody-drug conjugates that combine our proprietary GPC3-targeting antibody and distinct payload classes including topoisomerase inhibitor and a novel protein degrader. Compared to benchmark GPC3-targeting antibodies, our antibody binds a unique epitope on GPC3, resulting in enhanced internalization and significantly improved ADC-mediated cytotoxicity in GPC3-positive cells. Our novel protein degrader payload showed broad anti-proliferative activity in vitro, including potent cytotoxicity in DXd-resistant cell lines and HCC cell lines. In vivo, our GPC3 single-payload or dual-payload ADC molecules showed robust anti-tumor efficacy in multiple HCC and NSCLC CDX and PDX models. We believe that our anti-GPC3 ADC can be an effective off-the-shelf biologic therapy for HCC and NSCLC patients.

#1665 Preclinical characterization of IPN60300, a first-in-class ITGA2 antibody-drug conjugate for cancer therapy.

Aurelie Courtin[1], Benjamin Beaufils[1], Karl Brendel[1], Sophie Colombo[1], Isabel Esteves[1], Marie-Odile Galcera[1], Thierry Guyon[1], Pei Han[2], Feng He[3], Wei Li[2], Weihong Nian[3], Vincent Martin[1], Lou-Amelia Revellin[1], Sylvain Roqueviere[1], Pierre Roubert[1], Yu Song[2], Amath Thiongane[1], Catherine CL Wong[2], Chuanying Xu[3], Qing Zhou[3], Mary Jane Hinrichs[4], Elisabetta Leo[5]

[1]Ipsen, Paris, France,[2]Foreseen Biotechnology, Shangai, China,[3]Escugen Biotechnology, Shangai, China,[4]Ipsen, Boston, MA,[5]Ipsen, London, United Kingdom

Background: Integrin alpha-2 (ITGA2), a component of the heterodimeric transmembrane receptor integrin α2/β1, plays a key role in cell adhesion and transduction. Although ITGA2 is expressed at low levels across normal tissues, it is notably overexpressed in various solid tumors, including pancreatic, gastric and colorectal, where it contributes to tumor progression via extracellular matrix signaling and epithelial-mesenchymal transition. We report the development of IPN60300, a novel antibody-drug conjugate (ADC) targeting ITGA2, designed to specifically deliver exatecan, a potent topoisomerase I inhibitor, to ITGA2 expressing cancer cells. IPN60300 consists of a humanized Fc mutated monoclonal antibody site-specifically conjugated to exatecan via a cathepsin-cleavable linker, with a drug-to-antibody ratio of 8.
Methods: The pharmacological characteristics of IPN60300 were assessed through comprehensive in vitro and in vivo studies including analysis in ITGA2-expressing cell lines, cell-derived xenograft models, and cynomolgus monkey, chosen for its homology with human ITGA2.
Results: IPN60300 demonstrated a specific and high-affinity binding to ITGA2, efficient internalization into tumor cells, and intracellular release of exatecan, resulting in potent cytotoxicity in ITGA2-positive cell lines. The engineered Fc region of the antibody decreased FcγRI binding, reducing off-target toxicity while maintaining FcRn interaction. In tumor-bearing mice, IPN60300 exhibited plasma stability and led to significant exatecan accumulation in xenograft tumors, resulting in high, dose-dependent anti-tumor activity in models of cholangiocarcinoma, pancreatic ductal adenocarcinoma, gastric, and colorectal cancers. Toxicology studies in cynomolgus monkeys revealed favorable tolerability and pharmacokinetic characteristics supporting an acceptable therapeutic index.
Conclusion: These preclinical findings support IPN60300 as a promising first-in-class ITGA2-targeting ADC, combining potent anti-tumor efficacy with a favorable safety profile. IPN60300 holds potential to improve clinical outcomes for patients with ITGA2-expressing malignancies and is advancing to First-in-Human clinical trial (NCT07213817).

#1666 Targeting the extra-cellular matrix in the tumor microenvironment with a novel antibody-drug conjugate.

Matthew J. Edwards, Kovilen Sawmynaden, Aurelie Michelet, Edward Long, Rachel Evans, Dhruv Chauhan, Cecilia Pennica, Nafia Guljar, Cherie Akpotor, Luca Frenguelli, Gareth Muirhead, Sam Cooper, Athiva Shankar, TuVinh Luong, Emma Huang, Giuseppe Mazza, Chris Stevenson

Discovery Sciences, Engitix Therapeutics, London, United Kingdom

Background: Tumors with high stromal content are associated with poor prognosis, in part due to these tumors' resistance to standard of care therapies and increased aggressiveness. A common, highly deregulated program of extensive ECM remodeling exists in most solid tumors. Therefore, targeting the tumor ECM with an antibody drug conjugate (ADC) offers a promising strategy to improve tumor selectivity and treatment efficacy.
Methods: Proteomic analysis of decellularized tumor tissues processed to preserve ECM-bound proteins, and pan-cancer transcriptomic profiling of CAF-associated ECM genes was used to identify and validate target selection. Antibodies were developed against a novel, tumor microenvironment (TME)-specific antigen expressed in multiple solid tumors, including PDAC and CRC. High-affinity antibodies were conjugated to exatecan *via* a cleavable linker and efficacy was evaluated in an in vitro transwell-based tumor cell cytotoxicity assay.
Results: Integrative analysis transcriptomic and proteomic analysis revealed numerous ECM proteins that are selectively expressed by CAFs and biochemically stable within the tumor matrix. Among these, we identified a target, EGTX004, that was consistently upregulated across multiple solid tumor types, and not expressed in adjacent non-tumor tissue or healthy control tissue samples. The increased and tumor-specific expression of EGTX004 was confirmed by IHC using proprietary antibodies against the target. EGTX004 expression is elevated early in tumorigenesis and increases as tumors progress to become more invasive.The antibodies against EGTX004 demonstrated positive target engagement in biochemical, cell-based stromal deposition with sub- to low nanomolar affinities (0.5 - 2 nM). EGTX004 ADCs were also demonstrated to have tumor killing activity in vitro. EGTX004 expression has also been found to be increased in a number of CDX and PDX models. The induction EGTX004 in these models appears to be driven by the mouse fibroblast response to the human tumor cell insult, and EGTX004 expression progresses as the tumors grow larger.
Conclusions: Integrating transcriptomic and proteomic analyses of CAF-derived ECM proteins enables discovery of novel, broadly applicable ADC targets. Our findings provide compelling evidence that targeting the TME with a rationally designed ADC can yield robust anti-tumor responses.

#1667 Antibody encapsulated drug: Tr-ACT2 for targeted treatments of various cancers.

C. J. Yu[1], Linrong Li[2], leslie Wang[1], Kinsley Wang[1], Mengmeng Liu[1], Faqing Huang[3], Warren A. Chow[4], Xiaojiang Cui[5]

[1]Sunstate Biosciences, LLC, Pasadena, CA,[2]Cedars Sinai Medical Center, Los Angeles, CA,[3]The University of Southern Mississippi, Hattiesburg, MS,[4]University of California at Irvine, Irvine,, CA,[5]Cedars-Sinai Medical Center, Los Angeles, CA

Purpose: HER2 is overexpressed in 15-20% of breast cancers and some other cancers, and the development of HER2-targeted therapies has revolutionized cancer treatment in past 20 years. Trastuzumab (Tr) has demonstrated efficacy in treatment of HER2+ breast cancer and advanced gastric cancer. Recently, Tr-based antibody drug conjugates (ADCs), Kadecyla and Enhertu, have emerged as a new class of anti-HER2 therapies by combining targeted antibodies with cytotoxic agents via linkers. However, ADC approach faces great challenges, such as *in vivo* instability, manufacturing processes, limited availability of antitumor payloads and suboptimal payload release. Therefore, smarter and more efficient designs are urgently needed.

Methods: Our patented single protein encapsulation (SPE) platform, allowing encapsulation of small-molecule drugs by a single protein (albumins or globulins) without artificial nanoparticles and chemical modifications to drugs and proteins, has achieved great success in development of 2 drug products, SPEDOX-6 under human clinical trial (NCT0764018) and SPESN38-8 (IND #: 164346) under IND-enabling study based on albumin, which have prompted us to utilize antibody, such as Tr to encapsulate cytotoxic payload, actinomycin D (ACT, RNA polymerase inhibitor), forming antibody encapsulated drugs (AEDs). We developed Tr-ACT2 as a first-in-class AED drug, featuring each Tr molecule to encapsulate two ACT molecules without linkers. Tr-ACT2 was well characterized by UV, fluorescence, membrane dialysis, particle size distribution and molecular docking. *In vitro* and *in vivo* anticancer efficacy of Tr-ACT2 against various HER2+ & HER2- cancers were evaluated.

Results: Tr-ACT2 has been investigated in following. *In vitro* cytotoxicity of Tr-ACT2 against breast cancers, HER2+ (SKBR3, JIMT1) and HER2- (BT549, MDA-MB-231) and A549 (NSCLC, HER2-) was evaluated, leading to a time-dependent and significant reduction in cell viability, induction of apoptosis and reduction of Akt activation. Tr-ACT2's cytotoxic activity appeared to be independent of HER2 expression levels. The internalization study on Tr-ACT2 demonstrated that early-stage internalization of Tr-ACT2 is HER2 dependent, but the rate of late-stage internalization of Tr-ACT2 is not limited by HER2 expression level, confirming that Tr-ACT2 could be effectively internalized into both HER2+ and HER2- cancer cells. *In vivo* anticancer efficacy of Tr-ACT2 at 1 mg/kg vs irinotecan at 50 mg/kg using A549 mouse model has been evaluated, showing that Tr-ACT2 was significantly more effective in suppressing growth of A549 than irinotecan.

Conclusions: We have developed the first-in-class AED nanocomplex, Tr-ACT2, as a potent anticancer agent, demonstrating that the SPE technology can be applied to antibody for encapsulating small-molecule drugs without covalent conjugation and marking a significant advancement in antibody-based therapeutics.

#1668 MAC-8001: A KRAS-targeting molecular glue-antibody conjugate with robust antitumor activity in KRAS-mutant cancers.

Feilong Sun, Shuaishuai Chi, **Carlos Chai**, Yi Chen, Xuan Zhang

DaCure Therapeutics, Shanghai, China

Background
KRAS mutations are among the most frequent oncogenic drivers, occurring in approximately 10-15% of all human cancers and in over 90% of pancreatic ductal adenocarcinomas (PDAC). Although KRAS G12C inhibitors have achieved clinical success, the majority of KRAS mutations (>85%), predominantly G12D and G12V, remain without approved targeted therapies. Recently, several G12D/V-selective inhibitors and pan-RAS molecular glues (MGs) have emerged as promising strategies to address this unmet need. Converting KRAS-targeting MGs into molecular glue-antibody conjugates (MACs) offers an attractive avenue to further optimize their therapeutic window by limiting systemic exposure, improving pharmacokinetics, and enhancing clinical translatability.
Methods
A series of KRAS-modulating MG payloads were developed through structure-based optimization and subsequently site-specifically conjugated to an anti-B7H3 antibody via a cleavable linker, yielding the conjugate MAC-8001. The conjugate was characterized by reversed-phase liquid chromatography (RPLC) and size-exclusion chromatography (SEC) to determine its drug-to-antibody ratio (DAR) and aggregation profile, respectively. The capacity of the payloads to interfere with RAS-BRAF RBD interactions was evaluated using a TR-FRET assay. *In vitro* antiproliferative activities were evaluated across cancer cell lines harboring KRAS G12C/D/V mutations, while in vivo efficacy and pharmacodynamic responses were examined in corresponding xengraft models.
Results
The conjugate exhibited a DAR of approximately 8.0 with no detectable aggregation. MAC-8001 demonstrated potent and selective inhibition of KRAS-mutant cancer cells (IC_{50} <10 nM) compared with KRAS wild-type counterparts, accompanied by pronounced, dose-dependent suppression of downstream p-ERK and p-AKT signaling. Consistent with its scaffold-derived mechanism, TR-FRET assays confirmed that the payloads disrupted RAS-BRAF interactions, thereby attenuating MAPK signaling. In xenograft mouse models, a single intravenous dose of MAC-8001 produced durable antitumor responses, achieving over 90% tumor growth inhibition. Moreover, MAC-8001 was well-tolerated, without body-weight loss or detectable systemic toxicity.
Conclusions
MAC-8001 represents a potent KRAS-targeting MAC that selectively inhibits KRAS-driven signaling and exhibits robust antitumor efficacy both *in vitro* and *in vivo*. The modular design of this MAC platform allows straightforward adaptation to other tumor-associated antigens,
such as TROP2, thereby broadening its translational potential across RAS-driven malignancies. Collectively, these findings establish a novel therapeutic paradigm that may overcome the inherent limitations of systemic KRAS modulation.

#1669 S DUAL™: An Advanced Bispecific Antibody Platform Delivering Practical Manufacturability and Enhanced Therapeutic Efficacy.

Jina Kim, **Wooseok Yang**, Kihong Kim, Hyunbum Kim, Siwon Park, Haewon Ahn, Hyebeen Hong, Hyunseung Sun, Soyeon Lee, Gwangsu Shin, Jihoon Kim, Seonkyeong Jeong, Hyunsik Lee, Sungjin Han, Joseph H. Jeong, Yeumin Kim, Brian Hosung Min

Samsung Biologics, Incheon, Korea, Republic of

Background - Receptor tyrosine kinases (RTKs) drive tumor progression through ligand-dependent or ligand-independent dimerization, which brings the intracellular kinase domains into proximity, triggers autophosphorylation, and recruits adaptor proteins such as GRB2 and Shc. The resulting RAS-MAPK and PI3K-AKT cascades sustain cancer cell proliferation, survival and differentiation. Among RTKs, HER2 (ErbB2) is an orphan receptor that preferentially forms homodimers and heterodimers with other ErbB family members. HER2 over-expression or the generation of truncated forms (e.g., p95HER2) is strongly associated with aggressive disease and resistance to HER2-directed therapies.

Clinically - approved HER2 antibodies—trastuzumab (domain IV) and pertuzumab (domain II)—bind distinct extracellular epitopes yet only partially inhibit HER2-driven signaling, especially in tumors with high HER2 density or in which the receptor is mutated/truncated. Consequently, patients often develop intrinsic or acquired resistance.

Approach - To overcome these limitations, we employed Samsung Biologics' S-DUAL^{TM} platform to generate a heterodimeric bispecific antibody (BsAb) that simultaneously engages HER2 epitopes II and IV. The two Fab arms are engineered to heterodimerize via a "knob-into-hole" Fc architecture, preserving native IgG1 Fc effector function while enforcing defined Fab geometry.

Results - In HER2-positive cell lines, S-DUAL^{TM} reduced HER2 autophosphorylation by ~27.9 % ($p < 0.05$) and downstream p-ERK1/2 and p-AKT levels by 18.6 % and 25.3 %, respectively, resulting in a maximal inhibition (Emax) of 64.4 % in cell proliferation ($IC_{50} \approx 1.64$ nM). Cell surface binding affinity and Fc-mediated ADCC activity remained comparable to reference platform. In HER2-positive xenograft models, weekly intravenous administration of S-DUAL^{TM} substantially reduced tumor growth relative to the isotype control, achieving a marked suppression of tumor volume without evident toxicity.

Conclusion - Simultaneous blockade of two non-overlapping HER2 extracellular domains by a biparatopic BsAb can fully suppress ligand-independent HER2 signaling while preserving immune effector mechanisms. This "dual-epitope, Fab-geometry-tuned" strategy defines a new design principle for next-generation HER2 therapeutics and offers a potential solution to overcome resistance arising from HER2 over-expression, truncation, or mutation.

: Antibody-Drug Conjugates and Linker Engineering 1
Poster Session

#1672 Enhanced delivery and activity of a novel antibody-drug conjugate, PF-08052667, for treatment of non-muscle invasive bladder cancer.

Christopher M. Carosino, Devra Olson, David Ortiz, Steven Duniho, Maddy Burcher, Eliana Moskovitz, Rebecca Mazahreh, Iliyana Mikell, Matthew R. Levengood, Sharsti Sandall, Joeseph D. Dekker

Pfizer, Inc., Bothell, WA

PF-08052667 is a novel antibody-drug conjugate (ADC) under investigation for intravesical treatment of non-muscle invasive bladder cancer (NMIBC). Intravesical administration remains the standard approach patients with high-risk NMIBC. While this route allows direct access to the bladder lumen and tumor cells, drugs such as Bacillus Calmette-Guérin (BCG) and other chemotherapies are typically retained for less than two hours and evacuated after instillation. Current BCG supply issues, along with a documented lack of sustained response in about two-thirds of cases, highlight the demand for alternative treatment options such as ADCs which have proven activity in bladder cancer. PF-08052667 is an integrin beta-6 (IB6)-directed MMAE ADC specifically designed for intravesical treatment of NMIBC with eight MMAE molecules per ADC via a pegylated glucuronide linker. Prior to ADC administration, a bladder prewash is performed to increase urothelial permeability, enhance drug uptake into bladder tissue, and improve antitumor activity while maintaining low systemic exposure and a favorable safety profile. Here, we present the optimization of PF-08052667 for local delivery through ADC design and incorporation of a n-dodecyl-β-D-maltoside (DDM)-containing bladder prewash. In vitro and in vivo studies assessed tissue retention, tissue penetration, and antitumor efficacy with PF-08052667 or a rodent-specific surrogate ADC administered alone or following a bladder prewash. Additionally, tolerability and systemic exposures were evaluated in pharmacologically relevant animal models. High IB6 expression was confirmed across a panel of NMIBC tumors. In vitro, PF-08052667 demonstrated robust cytotoxic activity in a variety of IB6-expressing bladder cancer cell lines and NMIBC patient-derived organoids. The combination of PF-08052667 with bladder prewash resulted in up to 42-fold higher bladder tissue MMAE concentrations, improved tissue penetration and residence time, and achieved significant tumor control in orthotopic NMIBC mouse models. Following repeated local administration of PF-08052667 with bladder prewash, systemic exposure remained minimal, and no systemic toxicity was detected. Overall, these findings support the clinical development of PF-08052667 with bladder prewash, which is being evaluated for safety and antitumor efficacy in a Phase I trial (NCT07206225) involving patients with NMIBC.

#1673 PF-08046033 (GPS): A novel first in class auristatin S antibody-drug conjugate for treatment of GPNMB-expressing solid tumors.

Parul Katoch, Gabriele Blahnik-Fagan, Xiao Di Yang, Marlena Gray, KC Crowder, Vineet Kumar, Midori Clarke, Kaveh Alizadeh, Samantha Sarrett, Serena Wo, Gardenia Zaki, Andrea Lim, Elizabeth Gray, Philip Moquist, Michael Flister, Sharsti Sandall

Pfizer, Bothell, WA

Glycoprotein non-metastatic melanoma protein B (GPNMB) is a type 1a transmembrane protein that is markedly upregulated in several cancers, including NSCLC, ESCC, HNSCC, and BRCA. GPNMB is associated with poor patient prognosis and plays diverse roles in cancer biology, contributing to processes such as cell differentiation, proliferation, invasion, and migration. Low GPNMB expression in normal tissues, contrasted with high expression in primary and metastatic tumors, makes GPNMB a compelling target for antibody-drug conjugate (ADC) therapies. A previous GPNMB-targeting ADC, Glembatumumab vedotin (GV), comprised of a monoclonal antibody (mAb) conjugated to the microtubule disrupting agent monomethyl auristatin E (MMAE), showed early signs of efficacy. However, its development was constrained by dose-limiting toxicities, the majority of which were likely driven by the released MMAE payload. We hypothesized that pairing the GPNMB-targeted mAb with the novel Auristatin S (AurS), a payload engineered to be less permeable compared to MMAE, may widen the therapeutic window. Thus, we developed PF-08046033 (GPS), a novel investigational ADC composed of the human IgG1 anti-GPNMB mAb (hCR011) conjugated to the novel microtubule disrupting agent AurS using the clinical validated, protease-cleavable MC-Val-Cit linker with an average drug-to-antibody ratio (DAR) of 4. In this study, we evaluated the expression of GPNMB across multiple solid tumors, assessed the antitumor activity of GPS in vitro and in vivo in a variety of xenograft tumor models, and examined its safety profile in non-human primate (NHP) toxicology studies. GPS bound and internalized the GPNMB/ADC complex from the surface of cancer cells, leading to release of the AurS payload that induced apoptosis following G2/M cell-cycle arrest. GPS demonstrated comparable efficacy to GV in multiple GPNMB-expressing xenograft models. Notably, in NHP toxicology studies, GPS was tolerated at 15 mg/kg, which is five-fold higher than GV. Altogether, these data support the evaluation of PF-08046033 (GPS) in a first-in-human phase 1 clinical trial for the treatment of multiple solid tumors.

#1674 Diversity-oriented dpADC discovery with high throughput dual-conjugation platform and predictive resistant disease models.

Meijun Xiong, Yanchun Li, Qingsong Wu, Chong Liu, Shanshan Xie, Zhongsheng Hu, Yajun Sun, Zengyan Mu, Haibo He, Yanwen Feng, Xinju Gao, Paul H. Song, Gang Qin

GeneQuantum Healthcare (Suzhou) Co., Ltd., Suzhou, China

Acquired resistance to antibody-drug conjugate (ADC) therapy remains a major clinical challenge, often leading to diminished efficacy of subsequent ADCs that share the same payload class even based on different targets. For instance, reduced response has been observed in patients receiving sequential treatment with the Top1 inhibitor-based ADCs sacituzumab govitecan and trastuzumab deruxtecan, irrespective of treatment sequence. This underscores payload cross-resistance as an emerging limitation in ADC-based regimens. Dual-payload ADCs (dpADCs) represent a novel therapeutic modality with the potential to overcome such resistance. However, conventional dpADC discovery is often constrained by limited molecular designs, as the vast structural complexity—arising from variations in payload pairing, stoichiometric ratios, linker release mechanisms and kinetics, and antibody properties—poses significant challenges for systematic synthesis and evaluation. To address this challenge, we developed a comprehensive linker-payload (LP) library featuring diverse linker designs and multiple payload classes—including LPs based on Topoisomerase I inhibitors, Topoisomerase II inhibitors, PARP1 inhibitors, ATR inhibitors, and CHK1/2 inhibitors. Using our automated, high-throughput dual-conjugation platform (iScreener), we efficiently constructed a diversity-oriented dpADC library targeting HER2 and TROP2 respectively. These dpADCs were systematically evaluated in resistant in vitro and in vivo models, including patient-derived organoid/xenograft (PDXO/PDX) systems. Notably, several candidates with novel designs demonstrated significantly enhanced therapeutic efficacy while maintaining favorable safety profiles compared to benchmark and conventional mono-payload ADCs, revealing clear enhanced effects between payload classes. In summary, our shift from a purely rational design paradigm to a high-throughput screening approach—enabled by efficient dpADC library construction and predictive resistant disease models—offers a robust discovery framework. This strategy identifies potent dpADC candidates through empirical screening rather than traditional design perception, and we are currently expanding our evaluation of additional payload combinations in dpADC format using resistant preclinical models that recapitulate unmet clinical needs.

#1675 Payload-recycling ADCs (PR-ADCs): A novel ADC platform for reducing free-payload toxicity and enhancing therapeutic index.

Jianmin Fang[1], Dong Li[2], Jing Jiang[1], Yuanhao Li[1], Wei Zhang[3], Xiaoshan Min[3], Zhulun Wang[3]

[1]RemeGen Co., Ltd, Yantai, China,[2]RemeGen Co., Ltd., Shanghai, China,[3]RemeGen Biosciences (U.S.), South San Francisco, CA

Background: Antibody-drug conjugates (ADCs) have emerged as an important class of cancer therapeutics in clinical application. Many ADC drugs, however, failed during clinical studies due to excessive toxicity. Even approved ADC drugs also often face challenges in balancing clinical efficacy and safety. A major cause of ADC toxicity is due to free-payload (small molecule toxin) released from ADC drug into circulation. Free-payload often appears rapidly in plasma after ADC administration which causes systemic toxicity. To overcome ADC toxicity caused by free-payload, we have developed a novel technology, payload-recycling ADC (PR-ADC), that allows ADC drugs to re-capture, or recycle, small molecule toxin in circulation, thus reducing free-drug concentration in plasma.
Methods: To develop PR-ADC technology, we first generated a high affinity anti-MMAE monoclonal antibody through hybridoma screening. This anti-MMAE antibody exhibits exceptional specificity to free-MMAE with no detectable cross-reactivity to linker-MMAE or conjugated MMAE. Then an anti-mesothelin (MSLN) single domain antibody was attached to the anti-MMAE antibody to create a bispecific antibody that can simultaneously bind to both tumor antigen MSLN and free-MMAE. This bispecific antibody was then conjugated with MMAE to become the PR-ADC molecule which is basically a mesothelin-directing ADC with an additional ability to capture free-MMAE.
Results: This PR-ADC can effectively kill MSLN-expressing tumor cells *in vitro* in a potency similar to or even higher than a conventional MSLN-targeting ADC. On the other hand, this PR-ADC can prevent MMAE-induced cytotoxicity in cell-protection assays, highlighting its ability to effectively shield normal cells or tissues from free-MMAE-induced damage, thus increasing safety of ADC drugs. *In vivo*, this PR-ADC molecule, compared to conventional ADC, significantly reduced free-MMAE concentration in serum after administrated in mice or rats. In toxicity studies in rats, the PR-ADC significantly improved safety profile, showing larger therapeutic window than the conventional ADC. The increased safety profile of PR-ADC *in vivo* was further supported by favorable tissue distribution, drug metabolism and pharmacokinetics (DMPK) profiles. In xenograft tumor model studies, the MSLN-targeting PR-ADC achieved robust tumor growth inhibition, outperforming the conventional ADC.
Conclusions: The PR-ADC platform improves ADC safety by minimizing free payload-mediated toxicity while maintaining or enhancing anti-tumor efficacy. By enabling active payload recapture, PR-ADCs may support higher clinical dosing, increased effective DAR through captured payload, and an overall superior therapeutic index. This technology represents a promising next-generation strategy for advancing ADC development.

#1676 HA-00495: A development candidate ADC featuring a novel protein translation inhibitor payload with broad efficacy and a favorable non human primate safety profile.

Tara L. Arvedson, Victor Cee, Corey Reeves, Madhura Deshpande, Natacha Le Moan, Kyle Dunbar, Amandeep Gakhal, Chris Kimberlin, Cynthia Bailey, Edres Babacarkhial, Nolan Carney, Xufeng Cao, Yi-Ming Chiang, Amber Cornelius, Natalie Duong, Colin Harvey, Yingxia Hu, Dimitri Kharakovsky, Jose Leighton, Dennis Liu, Luca Lizzardo, Octovia Monteiro, Samuel Oteng-Pabi, Bruno Perlatti, Rajani Marthappa Shenoy, Joseph Spraker, Melanie Uguen, Jakub Vaith, Sandeep Venkataram, Kendra Wheeler, Shiyan Xu, Danielle Yee, Clarence Yeung, Eva Yuan

Hexagon Bio, Menlo Park, CA

Antibody drug conjugates (ADCs) have demonstrated clinical benefit across multiple cancers, yet resistance to existing payload classes, particularly topoisomerase and microtubule inhibitors, remains a major barrier to durable efficacy. To address this limitation, Hexagon Bio is leveraging its natural product discovery platform to identify new ADC payloads with mechanisms of action (MOAs) that are non-overlapping with currently approved payload classes. Enabled by our proprietary natural product library, we identified a protein translation inhibitor as a highly potent ADC payload. We conjugated the payload to a diverse panel of antibodies recognizing tumor-associated antigens and observed consistent ADC-mediated cytotoxicity across cell lines, supporting broad applicability across tumor types. In vivo, ADCs generated using anti-TROP2 (sacituzumab) and anti-HER2 (trastuzumab) antibodies demonstrated deep and durable antitumor activity in bladder, gastric, breast and lung cancer models, including models with known resistance to topoisomerase inhibitor-based ADCs. Here, we provide updated efficacy data across multiple tumor models and, for the first time, report the non-human primate (NHP) safety profile of an ADC incorporating this payload. Our new data include a comprehensive assessment of the HER2 ADC HA-00495 in NHPs, evaluating multiple dose levels as well as repeat-dose regimens. These studies reveal an acceptable safety and tolerability profile. We will present the clinical observations, clinical pathology, histopathology and key findings from these studies.In summary, we have identified a novel protein translation inhibitor payload class for ADCs that demonstrates strong efficacy, activity in resistance settings and a favorable NHP safety profile. These results support the potential of HA-00495 to address critical gaps in current ADC therapies and development activities for this candidate are now underway.

#1677 NL019: A next-generation TROP2/NECTIN4 dual-target nanobody-based ADC developed from the NanoOne™ Platform.

Meiguang Xiong, Binbin Wang, Jie Ni, Chenchen Lu, Fang Yu, **Yu Zhang**

Naliean Therapeutics Co. Ltd, Suzhou, China

Background:
While antibody-drug conjugates (ADCs) have transformed oncology treatment, conventional IgG-based ADCs are constrained by suboptimal tumor penetration, heterogeneous antigen expression, and Fc receptor-mediated immune toxicity. NanoOne™, developed by Naliean Therapeutics, is an innovative nanobody-based modular ADC platform that redefines ADC engineering through molecular miniaturization, structural precision, and payload flexibility.
Methods:
NanoOne™ integrates multiple VHH nanobody modules (<54 kDa) to achieve deep tumor penetration and broad recognition of tumors with diverse tumor-associated antigen (TAA) profiles. Its proprietary Site-Specific Dual-Payload Conjugation enables precise stoichiometric control (1:2, 2:1, 2:2, etc.) for single or dual payloads with outstanding homogeneity. The design incorporates a highly hydrophilic and stable linker that confers excellent developability. Fc domains are removed to avoid Fc receptor-mediated toxicity to immune cells while maintaining optimal half-life and enhancing tumor microenvironment accumulation.
Results:
NL019, a TROP2/NECTIN4 dual-target ADC armed with a microtubule inhibitor, demonstrated potent and synergistic activity in vitro—including dual-target binding, internalization, and cytotoxicity—while minimizing on-target toxicities seen in single-target ADCs. In multiple xenograft and CDX models, NL019 achieved superior, dose-dependent antitumor efficacy versus benchmark ADCs targeting TROP2 or NECTIN4.
Conclusions:
NL019 exemplifies the disruptive potential of NanoOne™, combining advanced molecular architecture, precision one/dual-payload conjugation, and superior tumor selectivity. Supported by strong preclinical efficacy and developability, NL019 is advancing toward first-in-human trials. Given the broad expression of TROP2 and NECTIN4 across epithelial malignancies, NL019 has the potential to establish a new generation of broad-spectrum ADC therapeutics.

#1678 Integrated ADC platform: From discovery to functional evaluation.

Meimei Yin, Xiaoming Miao, Yang Zheng, Jingbo Ding, **Jun Liu**, Fang Zhang, Zhongyao Ma, Letian Kuai, Wenji Su

WuXi AppTec, Shanghai, China

Antibody-Drug Conjugates (ADCs) represent a rapidly advancing modality with elegantly simple and compelling mechanisms. They have proven successful not only in combating cancer but have also recently expanded into other therapeutic areas such as autoimmune diseases. Despite these advancements, challenges such as new payload exploration, antibody penetration, increasing ADC uptake and processing, and overcoming ADC resistance continue to persist. Our comprehensive antibody discovery platform excels in generating high-affinity antibodies against challenging antigens, particularly multi-pass transmembrane proteins. By combining this with advanced high-throughput screening capabilities, we efficiently identify potent antibody candidates, thereby accelerating the antibody discovery process. To further expedite ADC discovery with high efficiency, we have developed a state-of-the-art high-throughput conjugation platform integrated with various downstream biological assays. Utilizing parallel synthesis and analytics, we can generate and evaluate ADCs with diverse linkers and payloads at microgram to milligram scales within 2-3 weeks. IgG1 antibodies are used, and products are isolated through resin purification. These ADCs exhibit uniform Drug-to-Antibody Ratios (DAR), consistent analytical size-exclusion chromatography (aSEC) profiles, and precise concentration ranges, with less than 0.1% free drug residue. This facilitates the simultaneous construction of hundreds of conjugate variants per run, allowing for rapid cytotoxicity and stability assays to triage and prioritize candidates for further development. In addition to high-throughput antibody screening and conjugation, our well-established full-spectrum ADC platform provides comprehensive services from payload assessment and ADC in vitro efficacy evaluation to supporting in-depth mechanistic exploration. This includes studying antibody internalization, killing effects, bystander evaluation and the development of potential resistance. Through continuous expansion of this platform, we are not only enabling early-stage ADC drug discovery but also addressing emerging challenges in the field.

#1679 Plate-based conjugation for antibody and payload optimization in ADC development.

Zeinab Fereshteh, Madhavi Latha S. Chalasani, Rupa Sarkar, **Julien Dugal-Tessier**, Nareshkumar Jain

NJ Bio, Inc., Princeton, NJ

ADCs are typically synthesized one by one and not amenable to early screening using a platform method. We developed a plate-based conjugation platform that integrates early screening with in vitro characterization using maleimide-based linker-payloads. With a standardized, assay-compatible protocol, this high-throughput system rapidly assesses DAR, purity, yield, cytotoxicity, and binding. It supports antibody screening with fixed linker-payloads, payload screening with fixed antibodies, and ADC characterization under varied conditions, providing a powerful tool for rational ADC design.

#1681 RenLite® transgenic mice provide a high-quality platform for accelerating the development of fully human bispecific antibodies or ADCs worldwide.

Jade Hsu, Wenjiao Zhang, Jun Du, Zhuolin Li, Yifu Zhang, Yanfei Han, Chengzhang Shang, Yi Yang

Biocytogen, Waltham, MA, MA

Global development of bispecific antibodies (BsAbs) and bispecific antibody-drug conjugates (BsADCs) is undergoing explosive growth. However, key pain points persist—heavy-light chain mismatch, inadequate target synergy, poor toxicity control, and complex manufacturing. While novel technologies have been developed to address these issues, drug development still faces hurdles in target combination selection, lengthy antibody discovery cycles, and low clinical translation success rates.Biocytogen RenLite® mice generate fully human antibody candidates with a common light chain, enabling subsequent assembly of BsAbs with minimized chain mismatch and excellent developability—conferring advantages for downstream CMC development. Additionally, the common light chain facilitates screening of different BsAb formats, payload conjugation, and function evaluation—supporting the discovery of diverse BsAb or BsAb-ADC modalities.To date, leveraging RenLite® and its novel BsADC platform, Biocytogen has generated multiple preclinical BsAb-ADC candidates. For example, DM001 (anti-TROP2×EGFR), with good developability, demonstrates potent tumor-suppressive activity in seven various patient-derived xenograft (PDX) models; DM005 (anti-EGFR×MET), with high purity and good conjugation property, exhibits outstanding specificity and anti-tumor efficacy in lung cancer PDX models. These BsADC candidates hold great clinical development potential.Leveraging its RenLite® platform and preliminary screening, Biocytogen has built an antibody library covering over 200 tumor-associated antigens (TAAs). This lets researchers easily conduct rapid screening, flexible pairing, and target synergy validation using *in vitro*/*in vivo* efficacy platforms, speeding up BsAb/ BsADC development and boosting clinical translation success of anticancer therapies.

#1682 Potency-Attenuated analogues of PNU-159,682 in conjugation with GlycoConnect® and HydraSpace® technologies provide ADCs with improved tolerability and efficacy.

Marcel Scheepstra, Remon van Geel, Jorin Hoogenboom, Lianne Lelieveldt, Sorraya Popal, Mick Verhagen, Oleksandr Zagorodko, Finn McSorley, Cağla Koc, Margarida Espadinha, Floris van Delft, Anette Sommer, Sander van Berkel

Synaffix/Lonza, Oss, Netherlands

PNU-159,682, an oxidized secondary metabolite of nemorubicin, exhibits extraordinary cytotoxic potency, being 2,100-6,400 fold more active than the clinically established doxorubicin. Despite promising antitumor activity, antibody-drug conjugates (ADCs) utilizing PNU-159,682 have not advanced beyond phase I clinical trials. The high potency and associated poor tolerability of PNU-based ADCs likely result in suboptimal clinical dosing, limiting the potential efficacy in patients. Based on these concerns, we designed and synthesized PNU analogues with attenuated cytotoxic potency, aiming to increase the tolerability while retaining robust antitumor activity, thus improving the therapeutic index (TI). Our approach involved multiple modifications to improve the properties. Conjugation of these new PNU analogues using GlycoConnect® site-specific conjugation technology, combined with HydrasSpace® polar spacer, yielded highly homogeneous ADCs with improved PK properties. Comprehensive in vitro and in vivo studies demonstrated that ADCs incorporating these attenuated PNU analogues maintained potent antitumor efficacy, inducing complete tumor regression in relevant xenograft models. Importantly, the maximum tolerated dose (MTD) of these ADCs was increased by up to 8-fold compared to ADCs based on the original PNU-159,682 payload, translating into a significantly expanded TI. Our findings demonstrate that potency-attenuated PNU analogues, when combined with GlycoConnect® and HydraSpace® technologies, represent a promising alternative to overcome the limitations of highly potent DNA-damaging payloads. This approach may enable higher clinical dosing paving the way for next-generation anthracycline-based ADCs with broad applicability in oncology.

#1683 Enhancing therapeutic efficacy and overcoming resistance with a novel dual-payload antibody-drug conjugate technology.

Antoine Attinger[1], Leo Marx[2], Diana Bianca Rocha Gomes[1], Vincent Gerusz[2], Min Ma[1], Viktoriia Postupalenko[2], Alain Monjardet[1], Nicolas Quesnot[1], Christophe Chardonnens[2], Rene Wuttke[1], Noemie Luong[1]

[1]Debiopharm International SA, Lausanne, Switzerland,[2]Debiopharm Research & Manufacturing SA, Martigny, Switzerland

Antibody-Drug Conjugates (ADCs) are promising oncology therapeutics that deliver cytotoxic payloads selectively to tumors. However, their efficacy is often limited by tumor heterogeneity, acquired resistance to single-agent payloads and off-target toxicity caused by premature linker cleavage. There is a critical need for next-generation ADCs to address these issues and broaden the therapeutic use of such modality. To address these challenges, we developed MLINK Duo, a dual-payload ADC technology combining plasma stability and controlled tumor-specific dual payload release. This technology enables the conjugation of a diverse range of dual payloads to antibodies, including combinations of well-established cytotoxic agents such as DM1, DM4, MMAE, and exatecan, as well as innovative new payload combinations. Here we show a proof of concept using a trastuzumab MLINK Duo ADC simultaneously delivering MMAE and exatecan (TmAb-MLINK Duo-MMAE/exatecan) at different drug-to-antibody ratios. The payload release mechanism was characterized biochemically, and the ADC stability was evaluated in mouse and human plasma. The TmAb-MLINK Duo-MMAE/exatecan was characterized for efficacy, pharmacokinetics and safety in non-clinical models. We also provide proof of synergy with other new dual-payload ADCs. The MLINK Duo ADCs exhibited low aggregation, high stability in circulation with minimal premature payload release, suggesting an improved therapeutic window. The specific enzymatic cleavage mechanism of the MLINK Duo linker technology was confirmed, demonstrating effective payload release. Crucially, the TmAb-MLINK Duo-MMAE/exatecan showed enhanced anti-tumor activity in several Cell-Derived Xenograft (CDX) models, maintaining efficacy and achieving tumor regression in CDX models that were resistant to the corresponding mono-payload ADCs (MMAE-ADC or exatecan-ADC). In addition, other MLINK Duo ADCs demonstrated clear synergistic anti-tumor effects compared to the treatment with single-payload ADCs. The pharmacokinetic profile of the TmAb-MLINK Duo-MMAE/exatecan supported favorable dosing schedules, and preliminary safety data showed a tolerable profile, validating the platform's clinical viability. In conclusion, we have developed a novel, stable, and versatile linker technology enabling the generation of innovative ADCs, including a highly promising dual-payload (MMAE/exatecan) configuration. The tested MLINK Duo ADCs could overcome resistance mechanisms prevalent against mono-payload ADCs and demonstrate potent synergy *in vivo*. This technology marks an important advancement in antibody-drug conjugate (ADC) technology, providing a promising approach to overcoming tumor resistance and potentially improving clinical outcomes in cancer therapy. Further translational development is ongoing. AI was used to assist abstract writing

#1684 ALM-502: A highly effective ADC for solid tumor therapy - enhancing payload delivery through molecular design.

Graham Cotton[1], Estelle McLean[2], Paul Trumper[1], Mark Wappett[3], Stephanie Gatdula[2], Stacey Dodd[1], Greg Papadakos[1], Stephanie Burton[2], Georgiana Parau[2], Aidan McCann[2], Chiara Saladino[2], Jennifer Thom[1], Aaron N. Cranston[2], Tim Harrison[2]

[1]Almac Discovery, Edinburgh, United Kingdom,[2]Almac Discovery, Belfast, United Kingdom,[3]Almac Discovery, Manchester, United Kingdom

Antibody-drug conjugates (ADCs) have transformed cancer therapy, yet their efficacy in solid tumors remains constrained by heterogeneous antigen expression, limited tumor penetration, low therapeutic index and the emergence of resistance mechanisms. ALM-502 is a highly differentiated, biparatopic ADC designed to address these challenges through innovative antibody architecture, enabling enhanced payload delivery.

ALM-502 targets ALPP/ALPPL2, developmental proteins which are over-expressed in multiple solid tumor indications but have undetectable protein expression on normal adult tissues. Additionally, ALPP/ALPPL2 are upregulated in response to standard of care treatments, providing additional therapeutic opportunities in the drug-resistant setting. The upregulation in multiple solid tumors, undetectable normal tissue expression and role in drug resistance make ALPP/ALPPL2 highly attractive targets for ADC approaches.

ALM-502 exploits multiple design features to deliver optimized performance:

• A biparatopic binding mode increases the effective number of binding sites on the tumor cells and increases payload delivery.
• A clinically proven, small antibody architecture is employed for enhanced tumor penetration.
• A low payload drug-to-antibody ratio (DAR) of 2 is used to enable higher ADC dosing and plasma levels.
• Payload attachment is via site specific conjugation to engineered sites providing a homogeneous product with excellent stability.
• A clinically proven payload matched to indications of interest is used which delivers a strong bystander effect and is a potent inducer of immunogenic cell death.
• The single chain antibody architecture coupled with site specific payload attachment and optimized physicochemistry facilitate high yield manufacture.
• Improved payload delivery (for a given amount of circulating ADC) drives the therapeutic index.

ALM-502 targets two distinct epitopes and is highly selective for ALPP/ALPPL2. In *in vitro* assays, this biparatopic mode of binding delivers enhanced internalization into cancer cells compared to a canonical ADC. The design features of ALM-502 translate into excellent anti-tumor efficacy in ALPP/ALPPL2 positive cell-line derived xenograft (CDX) and patient-derived xenograft (PDX) models of gastric, pancreatic, ovarian and bladder cancers, which display a range of target expression. In benchmarking studies, ALM-502 consistently delivers improved efficacy over a full length DAR4 ADC on a payload equivalents basis, in both single dose and multi-dose studies.

ALM-502 has an excellent PK profile in preclinical species together with strong developability and manufacturability characteristics. These features, coupled with an ultra-low immunogenicity profile mean that ALM-502 has the potential to deliver significantly improved patient outcomes across a range of solid tumor indications with high unmet need.

#1685 The HER2-targeting dual-payload antibody-drug conjugate combining a topoisomerase I inhibitor and a microtubule inhibitor demonstrates superior efficacy and overcomes resistance to single-payload ADCs in xenograft models.

Angela Matcham, Robert Yuan, Brian Vuillemenot, Rhoneil Pena, Young Park, Abigail Yu, Jeffrey Hanson, Cuong Tran, Xiaofan Li, Miao Wen, Daniel Calarese, Werner Rubas, Krishna Bajjuri, Guifen Xu, Alice Yam, Hanspeter Gerber

Sutro Biopharma, San Francisco, CA

The genetic and phenotypic heterogeneity of human cancers is a primary driver of drug resistance, posing a major challenge to achieving durable therapeutic responses. To overcome this, Sutro has developed a dual-payload antibody-drug conjugate (dpADC) platform that enables precise co-delivery of two cytotoxic payloads via a single, homogeneous molecule. Sutro's HER2-targeting dpADC demonstrates that simultaneous delivery of two cytotoxic payloads provides greater anti-tumor activity than single-payload ADCs and overcomes preclinical, in-vivo-derived treatment resistance. Combining Sutro Biopharma's XpressCF+® cell-free expression system with site-specific conjugation technology, we engineered a HER2-targeting dpADC combining exatecan (topoisomerase I inhibitor; TOPO1i) and monomethyl auristatin E (MMAE) (microtubule inhibitor; MTi) payloads at an 8:4 ratio. The resulting dpADC exhibited favorable pharmacokinetics in vivo and minimal linker-payload loss over a 21-day study. In *in vitro* cell killing assays, the dpADC performed better than Enhertu and DAR8 exatecan ADC across multiple tumor cell lines. In *in vivo* efficacy studies, the dpADC exhibited greater anti-tumor activity than both single-payload ADC comparators across multiple xenograft models. To further evaluate the dpADC concept's potential, we examined its utility in addressing resistance induced by ADC treatment. To mimic resistances to single payload ADCs observed in the clinic, we continuously dosed xenograft tumors with Enhertu on a weekly dosing schedule until the tumors progressed. These Enhertu-resistant tumors were then continuously dosed with a MTi ADC until *de novo* resistance developed. Dual-resistant tumors were then treated with a dpADC resulting in deep and durable anti-tumor responses. Even in tumors that were rendered resistant to both payloads, the dpADC treatment was able to achieve substantial tumor regression, demonstrating the potential for benefit in mono payload ADC refractory settings. Overall, these results indicate that Sutro's HER2 dpADC can enhance anti-tumor activity beyond that of single-payload ADCs and can overcome prior treatment-induced resistance in a preclinical setting.

#1686 Development of ZW418, a biparatopic PTK7-targeting antibody-drug conjugate incorporating a novel pan-RAS inhibitor payload for the treatment of non-small cell lung cancer.

Luying Yang, Alex Wu, **Vincent Fung**, Kaylee J. Wu, Sara Weeres, Katina Mak, Taixiang Wang, Victoria Harman-McKenna, Allysha Bissessur, Jesse Leblanc, Vidhi Khanna, Matthew Bonderud, Jodi Wong, Rehan Higgins, Linglan Fu, Dunja Urosev, Raffaele Colombo, Graham A. E. Garnett, Jamie R. Rich, Stuart D. Barnscher

Zymeworks Inc., Vancouver, BC, Canada

Mutations in the RAS oncogene family occur in approximately 25-30% of lung adenocarcinomas and represent one of the most common oncogenic drivers in non-small cell lung cancer (NSCLC). These alterations lead to constitutive activation of downstream MAPK signaling, promoting tumor growth and therapeutic resistance. Protein tyrosine kinase 7 (PTK7) is prevalently overexpressed in NSCLC but has limited expression in normal tissue, making it an attractive therapeutic target for NSCLC.
Existing mutant-specific and pan-RAS inhibitors (RASi) have demonstrated clinical benefit in NSCLC but patients often experience on-target off-tumor toxicities and acquire resistance. These challenges may be improved upon by enhancing delivery of a RASi via an antibody drug conjugate (ADC) mechanism. We have developed ZW418, a biparatopic PTK7-targeting ADC that leverages a cleavable linker designed to deliver a novel pan-RASi payload with optimized stability and bystander effect for the treatment of NSCLC.
A biparatopic antibody recognizing two non-overlapping epitopes on PTK7 was engineered and conjugated to a cleavable pan-RASi drug-linker. Binding affinity, internalization, spheroid penetration, and in vitro cytotoxicity were characterized across a panel of PTK7-expressing RAS-mutated cancer cell lines. Additional mechanistic evaluation of RAS inhibition was also performed in vitro. Pharmacokinetic properties were evaluated in non-tumor bearing mice, and antitumor activity was investigated in RAS-mutated cancer xenograft models.
Across RAS-mutated cancer cell lines with varying PTK7 expression level, the biparatopic antibody demonstrated greater cell surface decoration, internalization, and spheroid penetration compared to cofetuzumab and other PTK7-targeted clinical benchmark antibodies. ZW418 exhibited potent target-dependent cytotoxicity in vitro and demonstrated strong anti-tumor activity in multiple RAS-mutated cancer cell line derived xenograft models. The pan-RASi ADC platform showed encouraging tolerability in mice with no significant toxicity observed up to a dose of 200 mg/kg. Overall, the data supports the potential of ZW418 as a novel, highly differentiated therapeutic agent against PTK7-expressing RAS mutant cancers.

#1687 Engineering multi-specific and multi-payload ADCs to address tumor heterogeneity and drug resistance.

Greg Liang, Songyan Huang, Fan Feng, Mingqi Shao, Qikuan Chen, Kaijian Bi, Haixia Chen, Yanjie Chen, Yan Zhu, **Hu Liu**

Shanghai ChemPartner Co., Ltd., Shanghai, China

Antibody-drug conjugates (ADCs) are advancing beyond single-target, single-payload formats to address the challenges of heterogeneity and resistance to treatment. We previously generated ADC's based on monospecific, bispecific, biparatopic, and tri-specific antibodies, as well as dual-payload conjugates. *In vitro* and *in vivo* evaluation of these constructs demonstrated enhanced internalization and cytotoxicity. In this study, we combine these design strategies to generate next generation ADCs that incorporate multi-specific antigen recognition and multi-payload delivery, aiming to further improve therapeutic efficacy. A biparatopic anti-PD-L1 antibody was produced by combining two humanized parental antibodies via scFv integration. The antibody was expanded into tri-specific formats by incorporating additional binding domains targeting VEGF, HER2 and TROP2 tumor associated targets, enabling differential tumor engagement. Three cytotoxic payloads with distinct mechanisms of action (DNA damaging, microtubule inhibition, and topoisomerase I inhibition) were individually conjugated to generate monospecific single-payload ADCs. Based on the relative potency of these conjugates, dual and tri-payload ADCs were developed using the tri-specific antibodies with each payload conjugated at a Drug -to-Antibody Ratio (DAR) calibrated to achieve comparable cytotoxic effects. *In vitro* cytotoxicity was assessed across a panel of tumor cell lines with heterogenous target expression to evaluate the therapeutic potential of combining multi-specific antigen recognition with multi-payload delivery. The biparatopic anti-PD-L1 construct showed enhanced binding and internalization compared to its parental antibodies. Tri-specific formats retained cooperative engagement of multiple-antigens, supporting their potential for broader tumor targeting.

Among these, the HER2/TROP2 targeting tri-payload ADC maintained molecular integrity and exhibited enhanced potency in mixed-resistance models, outperforming corresponding monospecific or single-payload ADCs. All three PD-L1-based tri-specific tri-payload ADC's exhibited stronger and more widespread cytotoxic activity across diverse cell lines. *In vivo* studies confirmed that ADC's combining multi-specificity with multi-payload delivery achieved better tumor growth inhibition relative to monospecific or single-payload controls. Multi-specific antibody mechanisms and multi-payload delivery are complementary strategies to improve ADC performance by promoting efficient internalization, expanding the range of cytotoxic mechanisms, and addressing tumor resistance. These modular approaches offer a flexible framework for next-generation ADCs targeting heterogeneous solid tumors.

#1688 Empowering development of next generation ADCs & XDCs through advanced WuXiDARx conjugation technologies.

Qirui Fan, Hu Chen, Jingjie Huang, Lin Zhang, Zekun Wang, Ding Wei, Guoguang Wei, Yanjie Zhao, Laisen Wang, Cindy Cheng, Marie Zhu

Discovery and Development, WuXi XDC, Shanghai, China

Background: Antibody drug conjugates (ADCs) and various types of bioconjugates (XDCs) have garnered increasing attention over the past decade. These novel payloads and payload combinations require advanced conjugation technologies to fully achieve their therapeutic potential. Conventionally, interchain cysteine coupling serves as the most clinically validated conjugation technologies. However, such methods have two major flaws: (1) heterogeneity from stochastic coupling (except for DAR8); and (2) instability during circulation due to maleimide retro-Michael addition.
Solutions: To address these needs, WuXi XDC has built a platform through internal development and external collaboration. This platform includes two parts: (1) WuXiDARx™ conjugation technology WuXiDARx™ conjugates at interchain cystines which are the most clinical validated site, as 13 out of 18 commercial ADCs are developed through cysteine conjugation. This technology features: • Flexible DAR choices (WuXiDAR1^{TM}, WuXiDAR2^{TM}, WuXiDAR4^{TM}, WuXiDAR6^{TM}) • Improved homogeneity: ≥ 85% for DAR1 and DAR2; or ≥ 65% for DAR4 and DAR6 • Enhanced efficacy and safety profiles • Compatibility with IgG1 mAb • Compatibility with novel ADCs (e.g., dual-payload ADCs, bispecific ADCs) and XDCs (e.g., AOCs, APCs) • Simple and robust conjugation process • Validated technology: 7 ADCs in clinical trials, 10 CMC projects, up to > 2 kg batch size (2) Thiol reactive connector technologies Conventional interchain cysteine conjugation uses maleimide connector to react with the thiol groups from the antibody. However, the reverse reaction (retro-Michael addition) may result in premature release of the payload-linkers in circulation. To solve this problem, X-LinC connector is developed to replace the maleimide connector, which has shown good plasma stability and is fully compatible with WuXiDARx^{TM}. A different way to create homogeneous DAR4 ADCs is by using thiol-rebridging connectors. CysLink technology incorporates a stable thiol-rebridging connector into the platform. Unlike traditional connectors, the CysLink version produces ADCs with fewer thiol mismatches and half-antibody ratios, and it works with WuXiDARx^{TM} to offer additional DAR options (e.g., DAR1).
Conclusion: The combination of WuXiDARx^{TM}, X-LinC, and CysLink offers an integrated solution to utilize the most clinically validated conjugation sites, which is helping accelerate ADCs/XDCs pipeline development from clients.

#1689 Next generation ConjuAll BCMA antibody-drug conjugates (ADCs) LCB14-2524 and LCB14-2516 show increased efficacy in preclinical models of multiple myeloma.

Matthew Sender[1], Joe Ponte[1], Stephen Slocum[1], Yun-Hee Park[2], Yunjoo Jung[2], Chul Woong Chung[2], Rodrigo Ruiz-Soto[1], Jeiwook Chae[2]

[1]AntibodyChem Biosciences, Newton, MA,[2]LigaChem Biosciences, Daejeon, Korea, Republic of

LCB14-2524 and LCB14-2516 are Antibody-Drug Conjugates (ADCs) targeting B cell maturation antigen (BCMA). This target has emerged as one of the most important for targeted therapies in relapsed/refractory multiple myeloma (RRMM) as demonstrated by the recent approval of the ADC belantamab mafodotin in combination with bortezomib and dexamethasone. While belantamab mafodotin has delivered meaningful benefit to patients, the high rate of keratopathy leaves room for improvement. We present data for next generation anti-BCMA ADCs designed for robust efficacy with the potential for reduced ocular toxicity. LCB14-2524 is an ADCC enhanced IgG1 anti-BCMA ADC utilizing the second generation β-glucuronide (LBG) ConjuAll platform linker delivering a homogenous drug-antibody-ratio (DAR) of 2 monomethyl auristatin F (MMAF) microtubule inhibitor payloads. LCB14-2516 is an Fc silenced IgG1 anti-BCMA ADC that also utilizes the ConjuAll platform to deliver the highly potent pyrrolobenzodiazepine (PBD) DNA cross linking payload. These molecules were selected for progression through comparison of payload, conjugation method (ConjuAll vs maleimide), and antibody Fc properties (ADCC enhanced or silenced) to a belantamab mafodotin biosimilar in vitro and in vivo. In a panel of in vitro cytotoxicity assays the LBG-proPBD based ADCs were more potent than the belantamab mafodotin biosimilar or LBG-MMAF ADCs which demonstrated similar potency across cell lines. ADCC reporter assay showed potent activation by the Fc enhanced ADCs and antibodies, with no signal from the silenced ADCs or antibodies. The parental antibodies and the ADCs displayed similar activity in the ADCC reporter assay, suggesting no impact on function following conjugation. In vivo, both LCB14-2516 (LBG-proPBD) and LCB14-2524 (LBG-MMAF) were more active than the belantamab mafodotin biosimilar across OPM2, MM.1S and NCI-H929 CDX models. Both LCB14-2516 (LBG-proPBD) and LCB14-2524 (LBG-MMAF) ADCs utilize clinically validated LCB technology with promise to increase the therapeutic index of BCMA targeted ADCs and are progressing through IND enabling studies for clinical development.

#1690 Preclinical development of XNW27011, an antibody drug conjugate targeting claudin18.2 for treatment of CLDN 18.2-positive solid tumors.

Yonghan Hu[1], Yuanbao Li[2], Zhenwei Wu[2], Yuzhen Hou[2], Liang Kong[2], Shihua Wang[2], Zhe Zhang[2], Ka Ruan[2], Wengui Wang[2], Hui Zhao[2], Qifeng Shi[2], Haiyang Wei[2], Xiaojun Liu[2], Meijie Le[1], Jing Qiang[1]

[1]Evopoint, Shanghai, China,[2]Evopoint, Suzhou, China

Claudin (CLDN) 18.2, a member of a large family of transmembrane proteins with distinct functions, is highly expressed in cancers including gastric and pancreatic adenocarcinomas. Unlike in normal tissue, CLDN18.2 is exposed on epithelial surfaces in malignancy. It is suggested that CLDN18.2 is an ideal target for cancer therapy. So far, drug targeting CLDN18.2 has been approved for treating gastric cancer. XNW27011, an antibody-drug conjugate (ADC) composed of a monoclonal antibody (mAb) targeting CLDN18.2 with a toxin (payload, YL0010014) site-specifically conjugated via a cleavable linker with a drug-antibody ratio (DAR) of 8. XNW27011 is under development by Evopoint Biosciences for the treatment of patients with various CLDN 18.2-positive solid tumors including gastric cancers and pancreatic cancers in China. Here we present the preclinical development of a novel therapeutic CLDN18.2 ADC. In preclinical pharmacology studies, XNW27011 specifically binds to cells expressing human CLDN18.2 with high affinity but not to the closely related Claudin 18.1. XNW27011 demonstrated potent antiproliferative activity with CLDN 18.2 highly-expressed cell lines including arresting the cell cycle at the G2/M stage and inducing apoptosis in a variety of *in vitro* pharmacology studies. XNW27011 also exhibited similar activities to the naked antibody (XNW27011-mAb), including antibody-dependent cell-mediated cytotoxicity (ADCC), complement dependent cytotoxicity (CDC), internalization activities, and bystander effect. XNW27011 as a single agent displayed potent antitumor activities in multiple *in vivo* xenograft models of human gastric and pancreatic cancer, including PDX models (PDX001 [gastric cancer] and PDX002 [pancreatic cancer]) and CDX models (NUGC-4 and NUGC-4 CLDN 18.2) with low or high CLDN18.2 expression., XNW27011 achieved partial tumor regression (PR) and complete tumor regression (CR) in most mouse xenograft models at well tolerated iv doses (3 or 10 mg/kg). In nonclinical pharmacokinetics of XNW27011 in SD rats and Cynomolgus monkeys by intravenous infusion, XNW27011 showed good ADME characteristics in that it was stable in the bloodstream and exposure to the payload is very low. In toxicity studies, XNW27011 displays good tolerability with wide therapeutic windows in both SD rats and Cynomolgus monkeys. It is particularly important to note that XNW27011 has no toxic effects on the lungs in both rats and monkeys. In summary, XNW27011 has demonstrated potent *in vitro* and *in vivo* antitumor effects, favorable pharmacokinetic and an acceptable safety margin. XNW27011 is expected to be a potent therapeutic ADC candidate in cancer treatment of CLDN 18.2-positive solid tumors including gastric and pancreatic adenocarcinomas. Clinical activity of XNW27011 is currently under evaluation in a Phase III clinical trial (CTR20252730).

#1691 Site-specific dual-payload antibody conjugation enhances antitumor efficacy.

Wei-Ting Sun[1], Shih-Hsien Chuang[1], Shih-Chong Tsai[2], Cheng-Chou Yu[2]

[1]Honeybear Biosciences Inc., Taipei City, Taiwan,[2]Development Center for Biotechnology, Taipei City, Taiwan

We have developed a site-specific conjugation platform enabling controlled dual-payload delivery on antibodies. The antibody is enzymatically trimmed and modified to allow sequential bioorthogonal attachment of two payloads. This approach permits precise control of payload type and DAR number, enabling combinations that improve in vivo tumor suppression at lower payload doses. Here we present dual-payload HER2 ADCs as a proof-of-concept. A trastuzumab-based ADC carrying DM1 (DAR 2) and seco-DUBA (DAR 2) demonstrated potent inhibition of JIMT-1 xenograft tumors, a model known to be resistant to T-DM1. Additionally, a dual-payload MMAE/exatecan ADC (DAR 2+2) achieved antitumor activity comparable to T-DXd (DAR 8), despite using substantially lower total payload. These results show the versatility and therapeutic potential of our dual-payload site-specific conjugation strategy. The platform provides a method to overcoming drug resistance and expanding therapeutic windows for next-generation ADCs.

#1692 STX-1, a first-in-class ADC targeting DPP4 protein, acts as an anticancer and senolytic treatment.

Benjamin Le Calve[1], Delphine Dayde[1], Gregoire Jouffroy[1], Omayma Asbai[1], Virginie Lelarge[1], Justine Choeur[1], Thierry Mathieu[1], Florence Lhospice[1], Eric Angevin[2]

[1]StarkAge Therapeutics, Lille, France,[2]INSERM U981 (Gustave Roussy), Villejuif, France

Antibody-drug conjugates (ADCs) are innovative cancer therapies which, unlike conventional chemotherapies, enhance the anti-tumor effect while limiting adverse effects. However, it is necessary to discover new therapeutic targets that will enable the development of future generations of ADCs. Here we present an original ADC, called STX-1, targeting DPP4 protein and exhibiting both anticancer and senolytic activities. DPP4 is a type II glycoprotein that has intrinsic dipeptidyl peptidase IV (DPPIV) activity and is implicated in broad and various physiological processes, including metabolism of glucose, activation of T lymphocytes, and cell adhesion. This protein has also been known as a cell surface marker associated with varied malignancies and as a part of cancer stem cells in mesothelioma and colon carcinoma. More recently, studies have shown that its expression is a major hallmark of senescence. DPP4 therefore appears to be a promising therapeutic target in the treatment of certain types of cancer, targeting not only tumor but also senescent tumor cells.STX-1 is composed of a humanized IgG1 antibody directed against DPP4 (anti-DPP4 mAb) conjugated to four topoisomerase I inhibitor Exatecan with cathepsin B sensitive linker. The preclinical datasets display *in vitro* complete characterization of STX-1 associated to high internalization of the ADC, strong affinity to DPP4 protein and cytotoxic activity on several cancer models specifically related to target expression. Moreover, senescence induction in cancer cell lines through chemo- or radiotherapy exposure, boosts DPP4 expression and increases significantly antigen density at the plasma membrane. Despite the cell cycle arrest induced by senescence, cancer cells remain sensitive to STX-1 treatment. *In vivo*, administration of intravenous (IV) doses of STX-1 is associated with potent anti-tumor activity in pancreas and liver cancer xenograft models whose effectiveness depends on the level of DPP4 expression. However, pretreatment of mice by a combination of Trametinib/Palbociclib induces senescence in tumor, boost expression of DPP4 and allows a better anti-tumor activity of STX-1. Finally, in toxicology studies in mice expressing human form of DPP4, STX-1 was well tolerated, at dose levels up to 100 mg/kg, 21 days after administration. To conclude, STX-1 is associated with strong anti-tumor activity in different cancer models, whereas synergistic combination activity to senescence phenotype induction in tumors. The data presented support future clinical development of STX-1 for the treatment of gastric, pancreatic and liver cancer indications.

#1693 Targeting MET-LGR5 crosstalk using an antibody-drug conjugate combination with diverse payloads to overcome adaptive resistance in colorectal cancer.

Shraddha Subramanian[1], Peyton Christian High[2], Zhengdong Liang[3], Cara Guernsey-Biddle[3], Adela Aldana[3], Kendra S. Carmon[2]

[1]The University of Texas MD Anderson Cancer Center UTHealth Houston Graduate School of Biomedical Sciences, Houston, TX,[2]UT Health Houston, Houston, TX,[3]UTHealth Houston, Houston, TX

Off-target side effects and drug resistance often hamper the therapeutic benefits of existing anti-cancer therapies against colorectal cancer (CRC), the second deadliest malignancy worldwide. CRCs contain tumor-initiating cancer stem-like cells (CSCs) that survive toxic drugs and give rise to metastatic disease. Antibody-drug conjugates (ADCs) are a revolutionary class of therapeutics that leverage monoclonal antibody (mAb) specificity to deliver cytotoxic payloads to tumor cells. We generated ADCs targeting leucine-rich repeat-containing G protein-coupled receptor 5 (LGR5), a bona fide CSC biomarker frequently overexpressed in CRCs. Our LGR5 ADC exhibited high potency in CRC xenograft models with minimal toxicity. However, it failed to prevent tumor relapse after treatment cessation. Interestingly, we found that recurrent tumors evade LGR5 ADC-mediated elimination by transiently converting into an LGR5-negative ($LGR5^-$) state, accompanied by concomitant MET upregulation and activation of the downstream pathway. MET is a receptor tyrosine kinase frequently upregulated in CRCs and promotes metastatic progression. We identified that the activation of STAT3, a downstream effector protein in the MET pathway, undermines LGR5 ADC efficacy in CRC cells. To eliminate drug-resistant $LGR5^-$ cells, we generated MET-targeted ADCs by attaching a highly selective MET mAb (ABT700) backbone to the DNA-crosslinking payload pyrrolobenzodiazepine (PBD) via site-specific conjugation. This MET ADC (ABT700-PBD) demonstrated dose-dependent cytotoxicity in CRC cells. Furthermore, ABT700-PBD did not affect CRC cells with genetically induced MET ablation, demonstrating its specificity. Safety studies in immunocompetent mice showed that ABT700-PBD exhibited a favorable safety profile. Moreover, in CRC xenograft models, ABT700-PBD induced marked tumor regression. However, in the residual tumors following dose-dependent ABT700-PBD monotherapy, LGR5 protein expression was upregulated. These observations suggest that the MET-LGR5 crosstalk may be a potential driver of adaptive resistance in CRC. Cytotoxicity assays testing ABT700-PBD and our previously reported camptothecin-derived (CPT2) LGR5-targeted ADC (8E11-CPT2) demonstrated synergistic cell-killing activity in vitro. Combination treatment with ABT700-PBD and 8E11-CPT2 in CRC patient-derived xenograft models extended survival compared to single-agent ADCs. Collectively, our findings support MET and LGR5 ADC combination therapy as a novel treatment strategy to overcome adaptive resistance-driven relapse in CRC.

#1694 Application of tangential flow-filtration (TFF) to enable solvent exchange and precipitation process for the production of payload-linkers of antibody-drug conjugates.

Sudhir Patil, Feng Xu, Minglin Wang, **Jianwei Bian**, Xudong Wei

Payload-linker Department, WuXi XDC, Cranbury, NJ

Tangential Flow Filtration (TFF), also known as Crossflow Filtration, is a technique in which the fluid mixture flows tangentially (parallel) across the surface of the filter rather than being forced directly through it. This method is widely utilized in bioprocessing. We have demonstrated that TFF can be effectively applied in the enrichment process for the payload-linker prep HPLC purification, enabling significant volume reduction. The process works by allowing solvents to pass into the exchange buffer while retaining and concentrating the payload-linker product in the retentate. This approach facilitates solvent exchange, which in turn enables direct precipitation, eliminating the need for the time-consuming lyophilization step. The process has been successfully validated under GMP conditions at a production scale of 1 kg.

#1695 Preclinical characterization of STRO-227: A PTK7-targeting dual-payload ADC with topoisomerase 1 and tubulin inhibitors.

Daniel Calarese, Kshama Doshi, Garrett Gross, Brian Vuillemenot, Xiaofan Li, Mark Armanini, Guifen Xu, Miao Wen, Krishna Bajjuri, Gang Yin, Werner Rubas, Alice Yam, Hanspeter Gerber

Sutro Biopharma, Inc., South San Francisco, CA

PTK7 is a catalytically inactive, cell surface protein tyrosine kinase and a marker of tumor-initiating cancer stem cells. It plays a key role in tumor biology by regulating pathways involved in cell migration, invasion, and metastasis, and is upregulated in multiple solid tumors, including ovarian, triple-negative breast, non-small cell lung, esophageal, and head and neck cancers. Its combination of tumor-restricted expression and functional relevance in cancer stem cells makes PTK7 an attractive target for antibody-drug conjugates. We present the preclinical characterization of STRO-227, an investigational PTK7-targeting antibody-drug conjugate (ADC) generated using Sutro's XpressCF+® cell-free protein synthesis platform, which enables the site-selective incorporation of non-natural amino acids. This platform allows precise conjugation of two distinct payloads: exatecan, a topoisomerase I inhibitor, and monomethyl auristatin E (MMAE), a tubulin inhibitor. Each of these potent payloads is attached via a hydrophilic β-glucuronidase-cleavable linker. The final ADC possesses a defined drug-to-antibody ratio (DAR) of 8 exatecan to 2 MMAE payloads. In preclinical studies, STRO-227 demonstrated favorable pharmacokinetics and *in vivo* stability. In multiple xenograft and patient-derived xenograft (PDX) models, STRO-227 exhibited superior anti-tumor activity compared to the corresponding single-payload ADCs. In addition, STRO-227 demonstrated a favorable safety and pharmacokinetic profile in non-human primates, with a highest non-severely toxic dose (HNSTD) comparable to established MMAE- and topoisomerase I-based single-payload ADC benchmarks.

#1696 IN30758, an integrin-targeted antibody drug conjugate (ADC) demonstrating strong therapeutic effects in multiple solid tumors.

Baoyuan Zhang, Shiqiang Lu, Yue Ma, Jiaming Gao, Fengmin Xi, Ran Pang, Leo Liu, Zaiqi Wang

InxMed (Shanghai) Co., Ltd., Shanghai, China

Integrins represent a promising target for the development of antibody-drug conjugates (ADCs). The integrin alphaVbeta6 has already been leveraged in the creation of a clinical-stage ADC, which has demonstrated favorable efficacy and safety profiles in early assessments. The integrin family consists of 24 heterodimers formed by 18 alpha and 8 beta subunits. In this study, we present ADC IN30758, which comprises the integrin antibody A28 and a clinically validated linker payload, LD38. The binding affinities of both the unconjugated antibody and the ADC to the human integrin antigen are comparable. A28 exhibits strong antibody-antigen binding characteristics, facilitating effective association and dissociation. Both the unconjugated antibody and the ADC demonstrate significant internalization capabilities in cancer cells. Immunohistochemistry (IHC) staining assays indicate that A28 can bind to various solid tumors, including non-small cell lung cancer (NSCLC), pancreatic ductal adenocarcinoma (PDAC), and ovarian cancer (OC). Various animal models, including cell line-derived xenograft (CDX) and patient-derived xenograft (PDX) trials, were conducted to assess the tumor growth inhibition effects of IN30758, revealing that the ADC shows promising sensitivity across multiple solid tumors. Currently, the Investigational New Drug (IND) package, which includes preclinical efficacy, pharmacokinetics, and toxicity data, has been compiled, with the IND application expected to be submitted in December 2025.

#1697 NW024-1, a novel ALPP/ALPPL2-targeting antibody drug conjugate with a topoisomerase 1 inhibitor payload, demonstrates potent antitumor efficacy.

Juanjuan Li[1], Wenting Luo[1], Li Liu[1], Yiran Wu[1], Gang Liu[1], Changcheng Li[1], Yaolan Dai[1], Jiabao Liu[1], **Zhijian Li**[2], Lixia Wang[1], Dan Wang[1], Dan Mi[1], Jiaoyi Zhong[1], Bin Liu[1], Desi Pan[1], Zhigang Guo[1]

[1]Chengdu Chipscreen NewWay Biosciences Co., Ltd., Chengdu, Sichuan, China,[2]Chipscreen Biosciences (United States) Ltd., Somerset, NJ

Background: Placental alkaline phosphatases, ALPP and ALPPL2, are highly homologous (97%) membrane-bound proteins involved in fetal development. They are highly expressed in a variety of tumor cells including ovarian (70%), endometrial (41%), lung (NSCLC, 25%) and gastric (25%), but have limited expression levels in normal tissues, making them ideal targets for the development of antibody-drug conjugates (ADCs). Here, an ALPP/ALPPL2-targeting ADC NW024-1 was developed, consisting of a humanized IgG1 anti-ALPP/ALPPL2 antibody conjugated via a hydrophilic linker to a topoisomerase 1 inhibitor payload (TOP1i), designed to selectively deliver the cytotoxic agent to ALPP/ALPPL2-expressing cells. NW024-1 was tested in vitro and in vivo to evaluate its therapeutic potential.
Methods: A library of ALPP/ALPPL2-binding clones was screened for cell binding, internalization and affinity. The humanized antibody was conjugated to the TOP1i payload with DAR8 using a cleavable linker. The in vivo efficacy of NW024-1 was evaluated in a mouse xenograft model of gastric cancer (NCI-N87), administered with a single dose of 3 mg/kg and 10 mg/kg to evaluate anti-tumor activity.
Results: The antibody showed strong binding to human ALPP/ALPPL2 (EC50 = 1.32 nM) low expressing cells, but no binding to human ALPI /ALPL high expressing cells. In vitro, it displayed robust internalization into ALPP/ALPPL2 positive cells and low nanomolar affinity to ALPP (KD = 1.32 nM) and ALPPL2 (KD = 0.85 nM). NW024-1 showed ALPP/ALPPL2-dependent cell killing. In vivo, NW024-1 achieved near-complete tumor regression (TGI > 95%) at 3 and 10 mg/kg for single dose, and was well tolerated in mice as indicated by body weight.
Conclusions: NW024-1 is a novel ADC exhibiting a favorable profile and potent antitumor efficacy. These findings highlight its promising therapeutic potential for ALPP-expressing tumors and support its further advancement into clinical investigation.

#1698 A novel synergistic dual-payload FRα ADC (CTPH-08) that can potentially offer benefits for low IHC+ ovarian cancer patients by improving MTD and MED.

Soyeon Lim, Myeong Joo Kim, Junho Ha, Heegoo Jun, Jongchan Lee, So Hee Im, Seo Ha Kim, Young Sang Kim, Seung Chan Kim, Hyo Jin Kang, **Chang-Sun Lee**

Celltrion Pharm, Inc., Incheon, Korea, Republic of

Dual-payload antibody drug conjugates (ADCs) have achieved increasing traction as a next-generation ADC technology to improve the therapeutic window of single-payload ADCs. By integrating two different payloads having distinct modes of actions, dual-payload ADC platforms can offer opportunities to counter tumor heterogeneity, or to reduce the likelihood of resistance that often emerges with the single-payload ADCs. We have pursued novel dual-payload ADC formats that can provide synergistic activity as well as minimal overlapping toxicity due to complementary acting mechanisms from two different payloads. A few combinations of payloads have been found to demonstrate synergistic cytotoxicity, which have been successfully incorporated into ADCs to confirm the novel dual-payload ADC(AD^2C) concept. Although folate receptor-alpha (FRα) represents a clinically validated antigen as highlighted by the approval of Elahere, clinical benefit is yet to remain limited due to dose-limiting toxicities and suboptimal response durability. To address these shortcomings, we have generated dual-payload FRα ADC (AD^2C) designed to enhance anti-tumor activity without exacerbating systemic toxicity. This presentation covers a comprehensive characterization of FRα AD^2C including *in vitro* cytotoxicity for cancer cells with different levels of FRα expression, *in vivo* anti-tumor activities in FRα-positive CDX models, *in vivo* stability of FRα AD^2C via pharmacokinetic assessment in rats, and preliminary safety evaluation in mice. We are currently advancing dual-payload FRα ADC(AD^2C) toward PDX efficacy studies and GLP toxicology studies in order to proceed to Ph1 IND filing in due course.

#1699 GlycoConnect® ADC toolbox expansion with dual payload ADC (dpADC) technology.

Remon van Geel, Lieke Kraaijvanger, Mick Verhagen, Nick Burgers, Marie Nassiet, Margarida Espadinha, Elias Post, Sander van Berkel, Floris van Delft, Marcel Scheepstra, Anette Sommer

Synaffix - A Lonza Company, Oss, Netherlands

Intratumoral heterogeneity and interpatient tumor heterogeneity have been recognized as hurdles for efficacious cancer treatments and may result in short duration of response and resistance to classical chemotherapies. It has been shown that combinations of chemotherapy drugs with an independent mode-of-action (MoA) controls tumor growth and enhances survival in both, hematological and solid tumors.

In the past years, antibody-drug conjugates (ADCs) have successfully been included in cancer treatment paradigms. Recently, there has been a growing interest in dual-payload ADCs (dpADCs), i.e. ADCs consisting of two payloads conjugated to a tumor targeting antibody, for developing more efficacious ADCs. Similar to combining chemotherapy drugs, combining two payloads with independent MoA in one ADC might be an attractive strategy to address interpatient and intratumoral heterogeneity and increase response rate, duration of response, overall survival and overcome resistance. These payloads may act on (1) different cellular pathways (complementary MoA), (2) the same cellular pathway, or (3) the payloads may have a different pharmacokinetic profile, and by this dpADCs may enhance anti-tumor activity.

Previously, we have shown that the native glycan of monoclonal antibodies is a privileged site for attachment of cytotoxic payloads[1] (GlycoConnect© technology), while the therapeutic index is further elevated by a highly polar spacer technology (HydraSpace©)[2]. Here we show that GlycoConnect© technology can readily be extended to generation of dpADCs. We have developed a modular method enabling generation of dpADCs with tailored payload ratios. In vitro and in vivo studies will be presented showcasing these GlycoConnect© dpADCs combining payloads with different MoAs.

[1]Wijdeven et al., Enzymatic glycan remodeling-metal free click (GlycoConnect™) provides homogenous antibody-drug conjugates with improved stability and therapeutic index without sequence engineering. *mAbs* 2022, 14, doi: 10.1080/19420862.2022.2078466.

[2]Verkade et al. A Polar Sulfamide Spacer Significantly Enhances the Manufacturability, Stability, and Therapeutic Index of Antibody-Drug Conjugates. *Antibodies* 2018, 7, 12, doi:10.3390/antib7010012.

: Antibody-Drug Conjugates and Linker Engineering 2
Poster Session

#1704 Method development of purity and assay HPLC method for unstable antibody-drug conjugate linker regulated starting material BCN-OH.

Yilin Hao, Yujie Guo, Jing Zhuang, Shijuan Xu, **Lynn Wang**, Xudong Wei, Gengcheng Jack Yang

Payload-linker Department, WuXi XDC, Cranbury, NJ

BCN-OH is a critical raw material in an innovative payload-linker platform utilizing azido-sugar site-specific conjugation technology, which offers superior conjugation efficiency and therapeutic index. However, BCN-OH exhibits extreme instability, with solution stability of less than one hour and high susceptibility to oxidation upon air exposure. These characteristics pose significant challenges for impurity profiling and specification setting during manufacturing. To address this, we aimed to develop a robust and reproducible HPLC method capable of accurately identifying and characterizing related substances in BCN-OH, ensuring reliable quality control and regulatory compliance. Through systematic optimization of chromatographic conditions—including column selection, temperature, mobile phase composition, sample diluents, and gradient profiles, the method achieved baseline separation of five specified impurities and resolved the main peak from its isomer. Incorporation of BHT as an antioxidant extended BCN-OH solution stability from under one hour to 24 hours, greatly improving operational feasibility. Additional measures, such as nitrogen storage and glove box handling, further minimized oxidation risk. The validated method demonstrated robustness, intermediate precision, and suitability for PPQ and routine QC, providing essential data for impurity specification setting and ensuring consistent quality of this highly unstable payload-linker intermediate.

#1705 Compatibility study of routine chromatographic analytical testing of antibody-drug conjugate payload-linkers.

Tingting Xu, Yupei Deng, Xinsheng Yang, **Lynn Wang**, Jianqiang Li, Xudong Wei

Payload-Linker Department, WuXi XDC, Cranbury, NJ

Payload-linkers are essential components of antibody-drug conjugates (ADCs), connecting the antibody to the cytotoxic drug through complex chemical structures that include PEG chains, peptide sequences (e.g., GGFG, VC, etc.) linked by disulfide, carbonate, amide, or pyrophosphate bonds. These features make payload-linkers highly sensitive to hydrolysis, oxidation, photodegradation, moisture absorption, and metal ion complexation, posing significant challenges during analytical testing. Their instability requires strict control of sample preparation, storage, and analysis conditions to ensure accurate and reliable data. This study aimed to identify suitable analytical conditions for different structural types to support robust characterization and quality control. We systematically evaluated preparation processes, diluents, mobile phases, consumables, and instrumentation to minimize degradation and variability. The optimized method incorporates inert consumables, chromatography columns with appropriate packing material and pore size, and stability-preserving diluents to reduce analytical instability. These measures enable reproducible and accurate analysis of payload-linkers, supporting specification setting and quality assurance in ADC development. Our findings underscore the importance of tailored analytical strategies for structurally complex and highly reactive intermediates in bioconjugation platforms.

#1706 An integrate comprehensive *in vitro* and *in vivo* strategies for antibody drug conjugate development.

Ismahene Benzaid, Peggy Provent, Aurelie Durgeau, Didier Grillot, **Marc Hillairet de Boisferon**

Oncodesign Services, Dijon, France

Antibody-drug conjugates (ADCs) have transformed the landscape of modern drug development, offering a powerful way to deliver chemotherapy with precision. But translating an ADC concept into a successful candidate requires an integrated approach to identify targets, optimize payload delivery directly to the tumor, and validate efficacy across ex vivo and in vivo preclinical models. The challenge remains to develop improved preclinical tools and select the right pipeline supporting ADC development that will be more predictive of clinical outcome.

Oncodesign Services has generated a comprehensive preclinical platform to support ADC functional characterization by integrating in vitro binding and internalization assays to pharmacokinetics, pharmacodynamics along with efficacy studies in translational models. We offer a wide range of specialized assays and validation tools that examine both antibody and target characterization including a wide range of biological activity (MoA) functional cell-based assays. Available assays include target binding, ADC internalization, payload function and tumor cell kill potency, while available organoid platforms for enhanced translational relevance.

Oncodesign Services includes over 500 tumor models across 35 cancer indications, offering a wide selection of translational models to support your efficacy studies, including patient-derived xenografts (PDX) as well as syngeneic and humanized models.

In this poster we show different pre-clinical experiments steps including cellular assays, relevant in vivo models tested with FDA approved ADC payloads in validated target expression tumor combined with imaging technologies and radiopharmaceutical ADCs. The application of preclinical molecular imaging techniques by conjugating an ADC to a fluorescent tag or radioactively labeled improve the identification of effective candidate ADC molecules for therapeutic success.

From concept to proof-of-efficacy, Oncodesign Services present a platform combining biological and pharmacological expertise to accelerate the identification of effective candidate ADC molecules with the best chance of clinical translation and cancer patient benefit.

#1707 ZW191 - a differentiated FRα-targeted topoisomerase I antibody drug conjugate active in combination with standard of care drugs.

Sam Lawn, Andrea Hernandez Rojas, Jodi Wong, Araba Sagoe-Wagner, Vincent Fung, Kurt Stahl, Ambroise Wu, Lemlem T. Degefie, Steve Seredick, Pranshul Chauhan, Raffaele Colombo, Jamie R. Rich, Stuart D. Barnscher, Paul A. Moore

Zymeworks Inc., Vancouver, BC, Canada

ZW191 is a clinical stage differentiated FRα-targeted ADC under ongoing investigation for tolerability and efficacy in patients with advanced cancers, including ovarian, endometrial, and NSCLC (NCT06555744). ZW191 markedly improves on the FDA-approved FRα-targeted ADC mirvetuximab soravtansine in its efficacy in patient-derived xenograft tumors with both high and low level of FRα by virtue of its novel and highly effective FRα-targeted antibody and its novel ZD06519 TOPO1i payload. The by-design moderate potency of ZW191's payload confers a best-in-class nonclinical tolerability profile, with an HNSTD of 60 mg/kg in NHP, potentially enabling its clinical application in combination with multiple other clinically relevant drug modalities and in various lines of treatment. Here, we demonstrate ZW191's strong antitumor activity in a xenograft model of ovarian cancer when dosed in combination with each of the platinum-based drug carboplatin, the microtubule inhibitor paclitaxel, and the anti-angiogenic antibody bevacizumab. In multiple 3D spheroid tumor cell models in vitro, ZW191 demonstrates combination effects with poly (ADP-ribose) polymerase (PARP) inhibitor and platinum-based drugs as determined by the Bliss independence model of drug interactions. Mechanistically, ZW191's TOPO1i payload and platins both drive DNA strand breaks in tumor cells, and we show the enhanced target-dependent cytotoxic activity of these drugs in combination is associated with greater levels of the DNA damage marker gamma H2AX (γH2AX). A clinical landscape analysis demonstrates that moderate potency ADC payloads facilitate higher dosing levels in the clinic. Together with encouraging early clinical data that highlight ZW191's single agent activity and differentiated safety profile, these data reinforce its potential to achieve meaningful efficacy gains through combination with other agents.

#1708 Novel DLL3 x B7H3 bispecific ADC demonstrated superior efficacy in preclinical studies.

Sipeng Li, Chong Liu, Meijun Xiong, Yajun Sun, Zhongsheng Hu, Xinju Gao, Haibo He, Yanwen Feng, Zengyan Mu, Paul H. Song, Gang Qin

GeneQuantum Healthcare (Suzhou) Co., Ltd., Suzhou, China

Background: Small Cell Lung Cancer (SCLC) is a highly aggressive neuroendocrine carcinoma accounting for approximately 15% of all lung cancer diagnoses. It is characterized by rapid proliferation, early metastasis, and a dismal prognosis, with a 5-year survival rate of only 3% for patients with metastatic disease. Research over the past decade has revealed significant molecular heterogeneity in SCLC, leading to a classification into four major subtypes based on distinct transcriptional signatures: there are defined by the expression of specific transcription factors—ASCL1 high (SCLC-A), NEUROD1 high (SCLC-N), and POU2F3 high (SCLC-P)—and the fourth, SCLC-I, is characterized by low expression of these three factors. Notably, the SCLC-P subtype has been associated with inferior outcomes following chemo-immunotherapy, suggesting it may represent a more treatment-resistant variant. This high heterogeneity is likely a key driver of therapeutic resistance. DLL3, an inhibitory ligand of the Notch pathway, is overexpressed in up to 85% of SCLC tumors and varies significantly across SCLC subtypes, while its expression is negligible in normal tissues. B7H3, a type I transmembrane protein belonging to the B7 immune checkpoint family, is another promising target. It is expressed at low levels in normal tissues but is highly and homogeneously overexpressed across all SCLC subtypes, as well as in other solid tumors.
Methods: To address tumor heterogeneity in SCLC and improve responses for treatment-resistant patients—particularly those with the SCLC-P subtype—we pursued a rational design of a bispecific antibody-drug conjugate (ADC) targeting both DLL3 and B7H3. We engineered a diverse library of bispecific antibodies with varying sequence combinations and structural formats, which were then conjugated to diverse linker-topoisomerase 1 inhibitor (Top1i) payloads. Through a systematic screening campaign involving comprehensive in vitro and in vivo evaluations, we successfully identified a superior lead bispecific ADC candidate.
Results: The lead bispecific antibody exhibited potent cellular internalization in vitro, while the bispecific ADC demonstrated concentration-dependent and target-specific cytotoxicity in antigen-positive cells. In vivo, across multiple patient-derived xenograft (PDX) models, the lead bispecific ADC exhibited robust and sustained antitumor activity, outperforming both clinical-stage monospecific ADC benchmarks and its parental monospecific ADC. Notably, in refractory SCLC-P PDX models, it maintained superior efficacy compared to clinical monospecific ADC benchmarks. These results support a synergistic mechanism of action conferred by the bispecific ADC.
Conclusions: In conclusion, the next-generation bispecific ADC holds great potential to overcome SCLC heterogeneity and improve outcomes for treatment-resistant patients.

#1709 BCG042: A promising anti-LILRB4 antibody with ADCC enhancement demonstrates superior efficacy in preclinical models of monocytic AML.

Jade Hsu, Peiran Li, Yanan Guo

Biocytogen, Waltham, MA, MA

Monocytic acute myeloid leukemia (AML; FAB M4/M5) is an aggressive disease characterized by limited response to standard therapies, including chemotherapy and hypomethylating agent (HMA) plus venetoclax combinations. LILRB4, a validated immunosuppressive receptor highly expressed on monocytic AML blasts, drives immune evasion and tissue infiltration via APOE engagement and SHP-1/2 signaling. To overcome the limitations of current therapy, we engineered BCG042, a fully human anti-LILRB4 IgG1 antibody with an Fc mutant designed to enhance effector function and targeted clearance of AML cells. BCG042 binds to human LILRB4 with nanomolar affinity, demonstrates cross-reactivity to the cynomolgus ortholog, and exhibits high specificity within the LILRB family. Epitope binning analysis confirmed that BCG042 shares the same epitope as IO-202. BCG042 demonstrated strong binding to LILRB4-positive AML cell lines (THP-1, MV-4-11), and critically, exhibited superior inhibition of APOE-LILRB4 signaling compared to an IO-202 analog at 1 μg/mL *in vitro*. BCG042 mediated robust antibody-dependent cellular cytotoxicity (ADCC) against LILRB4+ AML cells, without antibody-dependent cellular phagocytosis (ADCP) or complement-dependent cytotoxicity (CDC) activity. This cytotoxicity was further amplified in an Fc-enhanced SI variant. This antibody exhibits favorable biophysical properties and developability profiles. *In vivo*, BCG042 induced significant dose-dependent tumor regression in a THP-1 xenograft model in B-NDG mice (dosed at 0.1, 0.5, and 1 mg/kg, Q3D×2), markedly outperforming an IO-202 analog. This potent antitumor effect was achieved with a favorable safety profile, evidenced by no body weight loss or signs of systemic toxicity. BCG042 uniquely combines targeted blockade of the LILRB4 immunosuppressive axis with potent Fc-engineered ADCC effect. This dual mechanism of action translates into superior antitumor efficacy and a favorable therapeutic window in preclinical models. These compelling data provide a strong rationale for the clinical development of BCG042 as a novel therapeutic for patients with relapsed/refractory monocytic AML.

#1710 ORM-1153: A novel CD123-targeting degrader antibody conjugate with proprietary GSPT1 degrading payload for the treatment of acute myeloid leukemia.

Dongki Choi[1], Adam Boutin[2], Jessica Alves[2], Sang Hyun Lee[1], Maysoun Shomali[2], Anna Skaletskaya[2], Hangyeol Jeong[1], MinSoo Kim[1], Da-Yeong Kim[1], Khuloud Takrouri[2], Qinsi Zheng[2], Nadia Cherkassky[2], Teresa Mako[2], Vineetkumar B. Patil[1], Olaf Christensen[2], YeonHee Yang[1], James Palacino[3]

[1]Orum Therapeutics, Daejeon, Korea, Republic of,[2]Orum Therapeutics, Lexington, MA,[3]Littlecastle, Lexington, MA

Acute myeloid leukemia (AML) is a devastating hematological malignancy, with limited treatment options and an overall poor prognosis. Due in part to the complex cytogenetics and clonal heterogeneity, targeted therapies have demonstrated some success in disease control, albeit with frequent relapse due to clonal selection. The only approved ADC for AML therapy is gemtuzumab ozogamicin (GO). However, its clinical utility is restricted by safety concerns. Therefore, there exists an unmet need for effective therapies for AML with superior safety and tolerability profiles as compared to standard of care treatment options. Because of its high expression on leukemic blast and stem cells compared with normal hematopoietic stem cells and progenitors, CD123 has emerged as a rational candidate for molecularly targeted therapeutic approaches in this disease. In addition, recent studies have reported that small-molecule GSPT1 degraders, such as CC-90009, exhibit potent antileukemic cytotoxicity in AML and demonstrate activity against TP53-mutant disease, one of the highest unmet needs. However, their therapeutic window may be potentially narrow. Therefore, we have developed ORM-1153, a CD123 targeting Degrader Antibody Conjugate (DAC) generated by conjugating our proprietary GSPT1 degrading payload SMol006 to the OR000559 antibody, which is characterized by significantly enhanced cellular internalization, via clinically validated β-glucuronide release linker. ORM-1153 showed robust in vitro activity in CD123+ AML cell line and AML blast. This in vitro activity is comparable to GO and ~3-log greater than venetoclax. Though the TP53 isogenic model study, TP53 null status did not affect MoA and potency of ORM-1153. Moreover, ORM-1153 showed lower cytotoxicity than Mylotarg in healthy hematopoietic progenitor lineages via colony formation assays. We evaluated ORM-1153 in vivo MV4-11 xenograft model, and treatment with ORM-1153 demonstrated superior activity than standard of care treatment option. Our results indicate that ORM-1153 may represent a viable therapeutic agent for the treatment of AML, including in patients with TP53-mutant status who face limited options and an overall poor prognosis, and warrants further investigation in clinical trials.

#1711 GS002, a novel anti-PD-L1 ADC with targeted cytotoxic delivery and immune checkpoint inhibition.

Lin Jun, An Deqiang, Song Liwei, Zhu Hongju, Yuan Qiwei, Li Jianshi, Miao Zhongyi, Gao Zhen, Zhou Fang, Wang Xiaolei, Chen Tao, Zhuang Lu, Zhou Kaiyue, Yang Bo, Si Xinjuan, Hu Wenwen, Chang Genqiong, Xu Maosen, Liu Bin, Luo Shun

Shanghai Ginspire Biologics Co., Ltd, Shanghai, China

GS002 (also designated 002mAb-GSLP003) is an investigational anti-PD-L1 antibody-drug conjugate (ADC) with a drug-to-antibody ratio (DAR) of 8. It comprises a high-affinity, Fc-silent IgG1κ antibody engineered to promote endocytosis, site-specifically conjugated via a solubility-enhanced linker to a novel topoisomerase I inhibitor payload. A key distinguishing feature of GS002 is its optimized linker-payload system, which enhances solubility and stability, and incorporates a payload that is superior to DXd, exhibiting potent bystander killing while resisting drug efflux. Preclinically, GS002 demonstrates a dual mechanism of action, combining potent PD-L1-targeted cytotoxicity with immune checkpoint blockade. In vitro, GS002 mediated enhanced endocytosis relative to two competitor ADCs and induced potent cytotoxicity in PD-L1-positive tumor cells, with minimal impact on antigen-presenting cells such as M0 macrophages and myeloid dendritic cells. In vivo, GS002 elicited sustained antitumor activity across multiple cell-derived xenograft models, including EMC-1, KARPAS-299, and H1975, matching or exceeding the efficacy of 002mAb-GGFG-DXd and two competitor ADCs. The solubility-enhanced linker-payload design of GS002 conferred favorable pharmacokinetics in rats following a single 6 mg/kg IV dose, exhibiting closely overlapping plasma concentration-time curves for total and conjugated antibody. GS002 also demonstrated high plasma stability across species, with minimal premature payload release after 21 days at 37°C. Furthermore, its developability profile was comparable to the unconjugated antibody (002mAb), showing similar hydrophobicity and thermostability as evidenced by identical HIC retention times and closely matched Tm and Tagg values. In summary, GS002 represents a highly differentiated PD-L1-targeting ADC candidate with synergistic dual mechanisms, compelling efficacy in vitro and in vivo, a favorable pharmacokinetic profile, and excellent developability properties, supporting its advancement into further IND-enabling development.

#1712 PA289: A first-in-class prodrug payload with a novel mechanism of action and favorable efficacy/safety profile.

Alicja Turska, Marc Lee, Bryony Moss, Yong Yi, Iris Britwum, Samuel Barton, Zoe Jukes, Toni Pringle, Adam Lodge, Justyna H. Mysliwy, Jutta Deckert, Robert J. Lutz

Iksuda Therapeutics Limited, Newcastle upon Tyne, United Kingdom

Background: PA289 is a novel seco-CBI based linker-payload with a differentiated protein alkylation (ProAlk) mechanism of action, killing cells via alkylation of cytosolic proteins (Wirth *et al*, 2012). It uses IKSUDA's stable, cysteine-specific PermaLink conjugation technology and glucuronide triggers to enhance tolerability. Tumor overexpressed lysosomal glucuronidase leads to selective activation after ADC uptake and limits systemic release of the active payload. PA289's unique MOA and prodrug format lead to controlled activation support improved therapeutic performance and help address the clinical challenge of ADC sequencing.
Methods: The prodrug linker-payload PA289 was conjugated using PermaLink technology to generate ADCs with a drug to antibody ratio of approximately 4. *In vitro* cell-killing and bystander activity was evaluated by CellTiter-Glo assay and impact on cell cycle was determined by propidium iodide staining. An HMGB1 ELISA was used to monitor immunogenic cell death. Induction of apoptosis was measured by Caspase-Glo® 3/7 assay. Efficacy studies were conducted in immunodeficient mice engrafted with human cancer xenografts. Toxicology studies were conducted in cynomolgus monkeys.
Results: The free payload shows potent *in vitro* activity against 248 cancer cell lines from 15 solid cancer indications (IC50 from 1-100 pM). Both the free payload and a PA289 ADC induce S-phase cell cycle arrest and apoptosis *in vitro*. The payload triggers immunogenic cell death and, unlike MMAE or deruxtecan, is a poor substrate for ABCB1 and ABCG2 drug efflux pumps. A PA289 ADC demonstrates stronger bystander cell-killing than an MMAE-ADC in co-cultures *in vitro*. Both the payload and a PA289 ADC retain activity against a trastuzumab deruxtecan-resistant cell line *in vitro*. This latter finding was confirmed in vivo, where a PA289 ADC shows durable tumor regressions in a trastuzumab deruxtecan-resistant xenograft. PA289 ADCs against multiple targets are active *in vivo* across several lung, esophageal and breast cancer xenograft models with a single dose of 0.3 mg/kg and show 10 to 20-fold greater potency than clinical benchmark ADCs with topoisomerase I inhibitor payloads. Despite this high *in vivo* potency, a PA289 ADC was well-tolerated in cynomolgus monkeys at 8 mg/kg (single dose) and 5 mg/kg repeat dose (Q3Wx2), with minimal test-article related findings.
Conclusions: PA289 is an ADC linker-payload with a unique protein alkylation mechanism and a novel glucuronide prodrug design, showing strong in vitro potency and low susceptibility to drug efflux pumps. PA289-based ADCs demonstrate superior in vivo activity compared with deruxtecan ADCs across multiple tumor models, with excellent tolerability in monkeys at doses well above those required for durable tumor regressions.

#1713 STRO-006: An Integrin beta-6-targeting ADC demonstrates favorable safety profile and potent antitumor activity in preclinical solid tumors.

Kshama A. Doshi, Stephanie Armstrong, Eunice Kim, Dan Shen, Sihong Zhou, Rhoneil Pena, Robert Yuan, Mark Armanini, Brian Vuillemenot, Xiaofan Li, Guifen Xu, Krishna Bajjuri, Miao Wen, Jeff Hanson, Cuong Tran, Amandeep Gakhal, GARRETT GROSS, Gang Yin, Werner Rubas, Genevive Hernandez, Daniel Calarese, Hans-Peter Gerber, Alice Yam

Sutro Biopharma, Inc., South San Francisco, CA

Integrin beta-6 (ITGb6) is a heterodimeric, cell-surface glycoprotein highly expressed in multiple solid tumor indications, including non-small cell lung cancer, esophageal cancer, head and neck cancers, breast and gastric cancers. Its expression has been associated with pro-tumorigenic activities including proliferation, migration, and invasion. ITGb6 has restricted expression in adult tissues, making it a highly promising target for cancer therapy using antibody drug conjugates (ADCs). STRO-006 is an investigational ADC composed of an ITGb6 targeted human IgG1 antibody conjugated to exatecan, a topoisomerase 1 inhibitor, via a b-glucuronidase-cleavable linker. The anti-ITGb6 antibody was discovered from a Fab ribosome display library using Sutro's XpressCF+® system. The drug-linker is functionalized with dibenzylcyclooctyne (DBCO) and allows rapid and selective site-specific conjugation to the azide-containing non-natural amino acid *p*-azidomethylphenylalanine (pAMF) incorporated into the antibody (Ab) sequence using XpressCF+®. This site-specific conjugation is highly efficient, resulting in a well-defined, homogeneous ADC with a drug-antibody ratio (DAR) of 8. The STRO-006 antibody binds specifically to the alpha-v beta-6 heterodimer and has high affinity to human and cynomolgus ITGb6. It demonstrates rapid and efficient internalization, ideal for an ADC mechanism of action. Importantly, the STRO-006 antibody does not compete for LAP binding and therefore does not interfere with TGFb signaling. STRO-006 is optimized for a stable pharmacokinetic profile and exhibits extended half-life of ~7 days, low clearance of ~5 mL/d/kg and maintains a stable DAR over the course of 21-days in non-human primates. In preclinical studies, STRO-006 demonstrates potent anti-tumor activity at clinically relevant dose in both PDX and xenograft models of non-small cell lung, head and neck squamous cell and pancreatic carcinomas. STRO-006 demonstrates a favorable safety and pharmacokinetic profile in non-human primates. These results suggest that STRO-006 is a promising candidate for the treatment of multiple carcinomas and supports further clinical investigation. A Phase 1, first-in-human study is planned to assess the safety and activity of STRO-006.

#1714 First-in-class CHK1 inhibitor antibody-drug conjugate overcomes limitations of current ADC payloads and provides a new option for HER2-positive and TOP1 inhibitor-resistant tumors.

Thanos D. Halazonetis[1], Giacomo G. Rossetti[2], Daniela Carraturo[3], Michalis Petropoulos[2], Camilla Trugenberger[4], Theodoros Rampias[5], Dennis Gillingham[3]

[1]Cancentus Pharma and University of Bern, Bern, Switzerland,[2]University of Bern, Bern, Switzerland,[3]University of Basel, Basel, Switzerland,[4]University of Geneva, Geneva, Switzerland,[5]Biomedical Research Foundation Academy of Athens, Athens, Greece

Background:
Current ADCs rely almost exclusively on two payload classes -TOP1 poisons and microtubule inhibitors- leading to significant toxicity, frequent dose interruptions and reductions, and limited options once resistance develops. To address these limitations, we developed a first-in-class ADC incorporating a novel payload class: a CHK1 inhibitor (CHK1i). The novel payload exploits the presence of DNA replication stress in cancer, leading to greater selectivity.
Methods:
Trastuzumab variants containing engineered cysteines were generated to enable site-specific conjugation. A proprietary cleavable linker was synthesized and conjugated to the CHK1i payload. The resulting ADC was evaluated for HER2-dependent activity in vitro and tested in vivo in a HER2-positive breast cancer xenograft model (HCC1569).
Results:
As a small molecule, the CHK1i was about 50-fold less toxic to normal cells than a TOP1 poison (deruxtecan) while maintaining comparable potency in cancer cell lines. When bound to the ADC linker, the CHK1i was not toxic to cells, in contrast to the deruxtecan-linker, which retains toxicity.
Trastuzumab with five engineered cysteines, combined with a novel cleavable linker and a CHK1i as payload, enabled enhanced ADC potency and selective killing of HER2-positive cancer cells. In vivo testing of the ADC, administered intravenously once per week for five consecutive weeks, demonstrated antitumor efficacy at 10 mg/kg in the HCC1569 xenograft model. Mice were monitored for three weeks after treatment completion, and tumor growth inhibition was still observed. No body weight loss or obvious signs of toxicity were detected.
Conclusions:
This first-in-class CHK1i ADC expands payload diversity, aims to address resistance to existing ADCs and reduce nonspecific toxicity, offering the potential for a wider therapeutic window.

#1715 JS212, a novel bispecific ADC targeting EGFR and HER3, demonstrates superior and broad antitumor activity in preclinical evaluation.

Wenli Shi[1], Ning Song[1], Qiang Fu[1], Li Ye[1], Aikun Xia[1], Mingxing Yang[1], Jiaming Wang[1], Xuan Wu[1], Yue Deng[1], Yanghua Xu[1], Xin Wang[1], Honglin He[1], Yuyuan Yan[1], **Ziyang Zhong**[2]

[1]Shanghai Ruotuo Biosciences Co., Ltd., Shanghai, China,[2]Anwita Bioscience, Inc., San Carlos, CA

Background: EGFR and HER3 are frequently co-expressed across multiple epithelial tumors. HER3 overexpression is a recognized resistance mechanism to EGFR tyrosine kinase inhibitors (TKIs) in NSCLC. The HER3-targeting antibody-drug conjugates (ADC), such as patritumab deruxtecan, has shown encouraging clinical benefit in NSCLC patients with EGFR mutations. Additionally, an EGFR and HER3 dual targeting ADC, BL-B01D1, demonstrated promising antitumor activities in patients with EGFR-mutated advanced NSCLC, confirming simultaneous targeting of EGFR and HER3 with a bispecific ADC as a promising strategy to achieve good therapeutic efficacy. We have developed JS212, a bispecific ADC targeting EGFR and HER3 with molecular design to enhance antitumor activity while maintaining a favorable safety and pharmacokinetic profile.

Methods: JS212 is composed of a Fab arm targeting EGFR, a scFv arm targeting HER3, and DNA topoisomerase I inhibitor, exatecan, linked through a cleavable linker with a homogeneous drug-to-antibody ratio (DAR) of 6. In vitro potencies were measured through cytotoxicity assays. Antitumor activities were evaluated in cell line-derived xenograft (CDX) models. Preclinical safety pharmacokinetics were assessed in cynomolgus monkeys.

Results: JS212 exhibited high-affinity binding to tumor cells expressing either or both of EGFR and HER3, resulting in efficient killing of tumor cells with a broad spectrum of EGFR and HER3 expression levels. It also demonstrated superior antitumor activities to BL-B01D1 in CDX models. In the EGFR-dominant NCI-H1975 model, JS212 demonstrated a significant tumor growth inhibition, with a TGI of 113% after the administration of a single dose of 1.9 mg/kg. In comparison, BL-B01D1 at the same molar dose, could only achieve a 75% TGI. In the HER3-dominant SW620 model, JS212 at a single dose of 1.3 mg/kg resulted in complete tumor regression in all 5 mice, whereas BL-B01D1 only suppressed tumor growth at 2.5 mg/kg, D1D8 Q3W. JS212 also had better antitumor activity than BL-B01D1 in an osimertinib-resistant HCC827 model. Additionally, JS212 induced near complete regression in either BL-B01D1 or patritumab-deruxtecan resistant SW620 model. In cynomolgus monkeys, JS212 was well tolerated with repeated doses at 30 mg/kg. It also showed favorable pharmacokinetics profiles with half-life > 3 Days.

Conclusion: JS212 is a promising EGFR and HER3 dual targeting ADC that shows superior and broad-spectrum antitumor activities and a favorable safety and pharmacokinetic profiles in preclinical evaluation, supporting its first-in-human studies. Its phase I clinical trial is ongoing, and results will be reported elsewhere.

#1716 AT06 is a bispecific antibody drug conjugate targeting DLL3 and SEZ6 with potent activity in small cell lung cancer (SCLC) models.

Bin Zou, **Bryan K. S. Yeung**, Nannan Lang

Axcynsis Therapeutics, Singapore, Singapore

Small cell lung cancer (SCLC) and other high-grade neuroendocrine neoplasms (NENs) are therapeutically challenging malignancies with limited treatment options. For patients with extensive-stage SCLC the median survival is 6 to 12 months with current treatment options making it the most aggressive type of pulmonary tumor. Delta-like ligand 3 (DLL3) and seizure-related homolog 6 (SEZ6) are selectively expressed in SCLC, neuroendocrine carcinomas, and glioblastomas with minimal expression on normal adult tissues, making them attractive targets for antibody-drug conjugates (ADC) therapy. While DLL3 and SEZ6 single-target ADCs have shown clinical benefit, tumor heterogeneity and antigen downregulation may limit their long term efficacy. Moreover, as much as 88% of all SCLC patients display DLL3 and SEZ6 co-expression making bispecific ADCs a promising approach for improving efficacy and broadening patient coverage. Our approach utilizes a 2+2 VHH format fused to a human Fc region and engineered to bind both SEZ6 and DLL3 antigens. VHH domains were optimized for improved affinity, internalization, and developability over the parental VHH and conjugated to a proprietary topoisomerase I inhibitor payload with strong bystander effect, high DAR homogeneity, and a hydrophilic enzyme-cleavable linker. In vitro cytotoxicity, internalization efficiency, and target-dependent activity were evaluated across a panel of SCLC cell lines. In vivo efficacy was assessed in xenograft tumor models with varying SEZ6 and DLL3 expression profiles. In a low DLL3/SEZ6-expression model of SCLC (NCI-H82), AT06 displayed strong and durable tumor growth inhibition (>99%) at a 1 mg/kg dose. These data reflect a promising dual-targeting bispecific ADC therapeutic with the potential to address tumor heterogeneity and resistance mechanisms across a broader range of patients.

#1717 SCR-A014, a novel bispecific ADC targeting B7H3 and DLL3 for SCLC therapy, exhibits potent anti-tumor efficacy.

Guangcun Cheng, Yayuan Fu, Jiajing Wang, Shuai Wang, Guimei Yang, Chunlei Xia, Xiaoxing Huang, Renhong Tang

Simcere Zaiming, State Key Laboratory of Neurology and Oncology Drug Development. Simcere Pharmaceutical Group, Shanghai, China

Background: Small cell lung cancer (SCLC) is a most aggressive lung neuroendocrine tumor, accounting for approximately 15% of all lung cancers. Delta-like ligand 3 (DLL3) is an inhibitory Notch ligand that is highly expressed in SCLC and other neuroendocrine tumors but minimally expressed in normal tissues. B7H3, also known as CD276, is a type I transmembrane protein belonging to the B7 family that includes immune checkpoint molecules such as PD-L1, B7-1, and B7-2. DLL3 and B7H3 are highly overexpressed in small cell lung cancer (SCLC) tumor tissues, with limited presence in normal tissues, making them attractive therapeutic targets. Both B7H3 and DLL3 target shows a high positivity rate (>80%) in SCLC patient samples. However, the expression levels of DLL3 and B7H3 are not high, most samples are at a 1+ level. Moreover, B7H3 exhibits relatively slow internalization, whereas DLL3 demonstrates rapid internalization. Based on these complementary characteristics, we propose a dual-antibody drug conjugate strategy targeting both B7H3 and DLL3. This innovative approach aims to enhance antitumor efficacy.
Methods & Results: We developed a novel B7H3 x DLL3 targeted bispecific antibody-drug conjugate (ADC) called SCR-A014, which is comprised of B7H3/DLL3 bispecific antibody conjugated with topoisomerase 1 inhibitor (CPT116). SCR-A014 specifically bind B7H3 and DLL3 with high affinity, and showed enhanced internalization and binding capacity compared to parental monoclonal antibody ADC separately in the B7H3/DLL3 co-expressing cell line. SCR-A014 induced tumor cell lysis in various tumor cell lines, and showed remarkable anti-tumor efficacy in several CDX models in a dose dependent manner. SCR-A014 exhibits significantly stronger anti-tumor activity than their parental monoclonal-ADC or clinical ADC in B7H3+DLL3+ double positive tumor cells. SCR-A014 also have very good stability and favorable developability.
Conclusion: These findings suggest that SCR-A014 is a potential first-in-class bispecific ADC and may offer a novel therapeutic strategy for SCLC cancers positive for B7H3 and DLL3.

#1718 RT023, a first-in-class CEACAM5/EGFR targeted bispecific antibody drug conjugate (ADC) in colorectal cancer (CRC).

Shuting Huang, Lulu Zhou, Jingjing Cao, Lingli Bi, Qiang Fu, Xuan Wu, Aikun Xia, Jiaming Wang, Yue Deng, Yanghua Xu, Xin Wang, Wenli Shi, Honglin He, Yuyuan Yan, Ziyang Zhong

Shanghai Ruotuo Biosciences Co., Ltd., Shanghai, China

Background: CEACAM5 and EGFR are highly expressed in several cancers, including colorectal, gastric, and lung, with greater specificity than in normal tissues. EGFR antibodies like cetuximab are standard first-line therapy for colorectal cancer (CRC) patients with wild-type KRAS, but are less effective in those with KRAS mutations, creating an unmet clinical need. ADCs targeting CEACAM5 or EGFR, such as M9140 and MRG003, are under clinical development for CRC; however, single-target ADCs have shown limited efficacy, likely due to variable antigen expression among patients. To address this, we developed RT023, a CEACAM5/EGFR bispecific ADC designed to treat patients positive for either marker, including those with KRAS mutations and those who relapse after EGFR antibody treatment.
Methods: RT023 is an ADC composed of an anti-CEACAM5/anti-EGFR bispecific antibody and a DNA topoisomerase I inhibitor, exatecan, linked through a cleavable linker, with a homogeneous drug-to-antibody ratio (DAR) of 6. In vitro potency was measured through cytotoxicity assay. Its anti-tumor activities were evaluated in cell line-derived xenograft (CDX) models. Toxicity and pharmacokinetics of RT023 were assessed in cynomolgus monkey.
Results: RT023 exhibited high affinity binding to CEACAM5 and EGFR. It had higher internalization rate than its respective parent monospecific antibodies, resulting in efficiently killing to tumor cells with a wide spectrum of CEACAM5 and EGFR expression levels. RT023 demonstrated superior tumor growth inhibition than M9140 and Cetuximab ADC in several CRC CDX models. In the EGFR-dominant HCT116 model, RT023 exhibited impressive tumor growth inhibition with a TGI of 88.5% after single dose of 0.77 mg/kg, whereas the Cetuximab ADC at the same molar dose achieved only a 58% TGI, and M9140 did not inhibit tumor growth. In the CEACAM5-dominant GP2D model, a single dose treatment of RT023 at 2.3 mg/kg resulted in 80% (4/5) complete tumor regression (CR), whereas M9140 treatment group only achieved 20% (1/5) CR. In the CEACAM5 /EGFR double-driven SW1116 model, RT023 induced tumor repression with a higher TGI than Cetuximab ADC (117% vs 105%) after two doses of 2.3 mg/kg, Q3W, and showed more durable anti-tumor effect than M9140 (64 days vs 47 days). RT023 was well tolerated in cynomolgus monkeys up to 30 mg/kg, with only minimal skin and hematological adverse effect. It also had a favorable PK profile with a half-life of approximately 120 hours. RT023 remained stable in circulation with less than 0.02% free drug release.
Conclusion: RT023, with its unique bispecific design and differentiated features in affinity, linker-payload, has shown promising potential as a first-in-class ADC candidate for CRC treatment. Preclinical discovery studies have revealed favorable efficacy and toxicity profiles, supporting advancing RT023 into first-in-human studies.

#1720 Preclinical study of BCG039, a Nectin-4×TROP2 bispecific ADC, in urothelial carcinoma and other solid tumor models.

Frank An, Liu Yang, Chengzhang Shang, Junlan Han, Yi Yang, Frank An

Biocytogen, Waltham, MA, MA

Background: Urothelial carcinoma (UC) affects over 600,000 patients worldwide annually, with the incidence rate increasing over the past decade. Metastatic urothelial carcinoma (mUC) has a poor prognosis, with the 5-year survival rate estimated to be as low as 10-15%.Nectin-4 is highly expressed in mUC. It is a clinically validated target for mUC with enfortumab vendotin (EV) and pembrolizumab combination as the newly established SOC for first-line metastatic and locally advanced UC. TROP2 is also highly expressed in UC, and sacituzumab govetecan (SG) has shown therapeutic activity in later-line mUC. Nectin-4xTROP2 bsADC aims to target these two clinically validated targets in mUC to further improve efficacy and reduce toxicity.

Method: Fully human antibodies against Nectin-4 and TROP2 were generated with Biocytogen's RenLite® transgenic mice. We selected the arms of the bispecific antibody based on their internalization activities in constructing and evaluating the bispecific antibody in a 1+1 format. The bispecific antibody was conjugated to both vcMMAE at DAR of 4 and Biocytogen's proprietary linker-payload BLD1102 at DAR of 4, respectively. BLD1102 is composed of a novel TOP1 inhibitor payload and a highly hydrophilic and enzyme-cleavable linker. The resulting ADCs were tested in CDX and PDX tumor models in mice, along with relevant benchmark ADCs for anti-tumor activity.

Results: We selected the arms based on their internalization activities, with the nectin-4 arm and the TROP2 arm showing enhanced internalization capability in the format of 1+1 bispecific antibody vs the respective monovalent parental arms, suggesting cooperative interactions of the two arms. Consistent with this *in vitro* observation, the vcMMAE conjugated bispecific ADC (bsADC) exhibited markedly increased anti-tumor activity compared with the monovalent parental ADCs in mouse CDX/PDX models. BCG039, the BLD1102-conjugated bsADC, also demonstrated tumor growth inhibition superior to benchmark anti-nectin-4 and certain benchmark anti-TROP2 ADCs. The bispecific antibody has excellent developability and is now in CMC development.

Conclusion: BCG039, a bsADC targeting Nectin-4 and TROP2, showed superior anti-tumor efficacy in mice compared to single-targeting parental ADCs and relevant benchmark ADCs. The cooperative interaction of the two arms may also help reduce the toxicity observed with single-targeting ADCs against these targets in mUC.

#1721 BCG041: A first-in-class bispecific ADC targeting B7-H3 and the proximal membrane region of MUC1 with superior antitumor activity.

Icy Niu, Peiran Li, Ying Zhu, Yanan Guo

Biocytogen, Waltham, MA, MA

BCG041 is a first-in-class fully human IgG1κ bispecific antibody-drug conjugate (ADC) targeting both B7-H3 (CD276) and the proximal membrane region of MUC1. These two tumor-associated antigens are broadly overexpressed in a wide range of epithelial malignancies and correlate with poor prognosis individually. The frequent co-expression provides a convincing rationale for dual targeting of B7-H3 and MUC1. The effectiveness of B7-H3 ADCs, such as ifinatamab deruxtecan (DS-7300), in treating small-cell lung cancer, even in patients who have received extensive prior treatment, emphasizes the significant potential of this target. On the other hand, therapies targeting MUC1 have historically encountered several obstacles: variations in glycoforms, the production of soluble MUC1 decoys due to SEA-domain cleavage, and the poor internalization of certain epitopes. These challenges can restrict the delivery of therapeutic agents and affect the therapeutic index. Targeting the proximal region of MUC1, which can decrease the shedding and enhance internalization, offers a feasible strategy to overcome these challenges. Based on this strategy, BCG041 was developed with a hydrophilic, protease-cleavable linker and a Topoisomerase-I inhibitor payload (BCPT02, DAR≈8) to enhance binding, internalization, and antitumor potency through the avidity-driven co-engagement of its two targets. The naked antibody exhibits high affinity and full cross-reactivity with both human and cynomolgus B7-H3 and MUC1. *In vitro*, BCG041 demonstrated stronger binding and faster internalization than naked DS-7300 or Gatipotuzumab analogs across multiple tumor cell lines. *In vivo*, BCG041 achieved superior antitumor efficacy compared to ADCs of naked DS-7300 or Gatipotuzumab conjugated to either BCPT02 or DXd in several patient-derived xenograft (PDX) models of lung and breast cancer. Treatment was well-tolerated, with no observed body-weight loss or overt systemic toxicity. Pharmacokinetic evaluation revealed a favorable ADC profile, and this drug demonstrates excellent developability, with CMC cell-line development currently ongoing. Together, these data position BCG041 as a highly promising next-generation bispecific ADC for B7-H3/MUC1-positive malignancies, addressing significant unmet clinical needs in breast, lung, gastro-esophageal, head-and-neck, colorectal, prostate, and ovarian cancers.

#1722 Optimal targeting of heterogeneous tumors using highly developable bispecific antibody drug conjugates based on an improved heterodimerization platform and precisely controlled conjugation of a novel payload.

Dongsop Lee[1], Younggyu Kong[1], Seong-Hyun Park[2], Hyeonseok Jin[1], Aera Lee[1], Haerynn Chung[1], Jungwoo Kim[1], Jinhoon Jung[1], Haedueok Jung[1], Yunjung Um[1], Youngjee Jeong[1], Su jin Jung[1], Haneol Kim[1], Kyoung-Ho Pyo[2], Hyungseok Choi[1], Mi-Kyung Kim[1]

[1]Dong-A ST Research Headquarter, Yongin, Korea, Republic of,[2]AbTis Co., Ltd, Yongin, Korea, Republic of

We describe the construction of bispecific antibody drug conjugates (ADCs) against multiple target combinations that are clinically correlated, and show that bispecific ADCs have the potential for improved efficacy in heterogeneous tumors compared to single targeted ADCs. Although single-target antibody drug conjugates (ADCs) are highly efficacious in numerous tumor indications, many patients still relapse following ADC therapy due to multiple factors, including inefficient tumor delivery, drug resistance, and antigen escape due to tumor heterogeneity. Thus, there is a high need for developing next generation ADCs that can overcome these limitations. Dual targeting using bispecific antibody-drug conjugates (bsADCs) is an approach that can address important issues such as insufficient targeting due to intra-tumoral expression heterogeneity. Bispecific ADCs are currently being investigated in discovery and early clinical pipelines, but challenges still remain such as selecting optimal target combinations, generating high-quality homogeneous ADC compounds, and optimizing the various ADC components to establish an effective therapeutic window. To develop bispecific antibody drug conjugates, we selected target combinations based on bioinformatics and clinical co-expression. Several in-house platforms were leveraged to create a workflow for rapidly generating bispecific ADCs: (1) an efficient heterodimerization platform for rapidly obtaining native IgG bispecific antibodies from parental monoclonal antibodies, (2) a novel hydrophilic TOPO1 inhibitor payload with an enzyme-cleavable linker, and (3) site-specific conjugation to create ADCs with precisely controlled drug-to-antibody ratio (DAR). A series of bispecific antibodies were constructed against rational combinations of co-expressed targets, and highly homogeneous DAR2 ADCs were obtained by conjugating the payload using Abclick® platform. The bsADCs thus created are less prone to CMC and developability liabilities due to their low hydrophobicity and minimal structural deviation from native IgG. Furthermore, the bispecific ADC showed improved anti-tumor activity in vitro and in vivo compared to the parental mono-targeted ADCs. Together, these results highlight a practical path toward the development of ADCs with improved efficacy in heterogeneous tumors.

#1723 Application of clinical stage GlycoConnect® technology to bispecific antibodies yields improved bispecific ADCs in comparison to randomly conjugated bsADCs.

Lianne Lelieveldt[1], Nazli Hilal Turkmen[1], Kinneret Rozales[2], Maya Wadmany[2], Anna Kaliakatsou[3], Floris van Delft[1], **Anette Sommer**[1]

[1]R&D, Synaffix - a Lonza Company, Oss, Netherlands,[2]R&D, Lonza, Haifa, Israel,[3]R&D, Lonza, Slough, United Kingdom

Several bispecific antibodies (bsAbs), with the ability to bind selectively and in a concerted fashion to two tumor associated antigens (TAAs) or in the form of a biparatopic antibody, have meanwhile been approved for cancer therapy. Another increasingly successful modality for anti-cancer therapy are antibody-drug conjugates (ADCs). Although typically based on random conjugation to cysteine or lysine residues, we have shown that the native glycan of monoclonal antibodies is a privileged site for attachment of cytotoxic payloads[1], while the therapeutic index is further enhanced by a highly polar spacer technology (HydraSpace®)[2]. Complemented by a broad choice of payloads with various modes-of-action (toxSYN® platform), these technologies have jointly been applied in multiple clinical ADC programs with the most advanced now in phase 3.

As multiple different bsAb formats have been introduced and are currently in clinical trials[3] we wanted to understand how GlycoConnect® conjugation technology would work in context of different bsAb formats to create site-specific ADCs with defined DAR. To this end, GlycoConnect® bispecific ADCs (bsADCs) were generated with high yield and purity and the successful application of the GlycoConnect® technology was demonstrated for several different bsAb formats. In addition, we will show the advantages of GlycoConnect® conjugation in generating bsADCs compared to random cysteine conjugation. GlycoConnect® bsADCs are more homogeneous than randomly conjugated bsADCs, have improved stability and provide for compelling antitumor activity in in vivo cancer xenograft models.

[1] (a) van Geel *et al*. *Bioconj. Chem.* 2015, *26*, 2233-2242. (b) Wijdeven *et al. MAbs* 2022, DOI: 10.1080/19420862.2022.2078466. [2] Verkade *et al*. *Antibodies* 2018, *7*, 12, doi:10.3390/antib7010012. [3] Herrera *et al. Trends in Cancer* 2024, 10, 10, doi.org/10.1016/j.trecan.2024.07.002.

#1724 NEOK001 (ABL206): A first in class B7-H3xROR1 bispecific ADC demonstrated enhanced efficacy and promising tolerability.

Min Ji Ko, Junga Kwon, Suyoun Lee, Juhee Kim, Ilhwan Ryu, Junyoung Kim, JaeHyun Eom, Byeong Min Yoo, Hyeon Ji Park, Yong-Gyu Son, Donghoon Yeom, Arim Seo, Byungje Sung, Jinwon Jung, Jinhyung Ahn, Weon-Kyoo You, Sang Hoon Lee

ABL Bio, Inc., Seoul, Korea, Republic of

NEOK001 (ABL206) is a bispecific antibody-drug conjugate (ADC) designed to overcome limitations of monospecific targeting of B7-H3 and ROR1. NEOK001 is a heterodimeric 2+2 bispecific ADC with a drug-antibody ratio (DAR) of 4, conjugated with SYNtecan E™, a linker-payload containing the topoisomerase I inhibitor exatecan. B7-H3 is a tumor-associated immune regulator which has been associated with poor prognosis and is overexpressed in multiple cancers as well as several normal tissues. ROR1 is an embryonic protein which is associated with poor prognosis in multiple cancers. ROR1 is upregulated in various solid and hematological cancer types and plays a role in cancer stem cells, epithelial-mesenchymal transition, and chemoresistance, but is restricted in its expression in normal adult tissues. By selectively targeting two distinct, co-expressed tumor associated antigens with minimal co-expression in normal tissue, NEOK001 leverages this co-expression to achieve enhanced efficacy while reducing normal tissue binding/toxicity. In vivo efficacy studies were performed in B7-H3 and ROR1 expressing cancer cell line-derived xenograft (CDX) or patient-derived xenograft (PDX) models. NEOK001 at 6-10mg/kg or monospecific ADCs at the equivalent molar doses were administered. Non-human primate toxicity was evaluated with NEOK001 administered in two doses (Days 1 and 22) at 30, 60 and 90 mg/kg. NEOK001 demonstrates enhanced *in vitro* cytotoxicity compared to ROR1 and B7-H3 monospecific ADCs. *In vivo*, NEOK001 demonstrates tumor growth inhibition in 81% (n=37) and regression in 54% of PDX models across multiple tumor types including SCLC (3/4), HNSCC (3/4), ovarian (4/5), NSCLC (3/5), prostate (2/5), TNBC (2/5) and sarcoma (2/5). NEOK001 demonstrates greater efficacy compared to monospecific ADCs such as zilovertamab vedotin (ROR1 ADC) and I-Dxd (B7-H3 ADC) in SCLC, ovarian and NSCLC xenograft models ($P<0.01$-0.001). In the repeat-dose GLP tox study in non-human primates, dose dependent payload class effects were observed, including minimal to mild reversible cytopenias and minimal to moderate reversible gastrointestinal toxicity observed at 30 and 60 mg/kg with an HNSTD of 60 mg/kg. NEOK001 is a first in class B7-H3xROR1 bispecific ADC, combining the broad expression of B7-H3 with the selective expression of ROR1 to enhance tumor-specific binding while reducing toxicity to normal tissue. Therefore, NEOK001 will be a promising therapeutic drug and will enter the clinic in early 2026.

#1725 Dual modality of EpiTAC bispecific degrader ADCs combines c-MET degradation with cytotoxic payload delivery to overcome limitations of current c-MET-targeted therapies.

Lisa Marshall, Jonathan Sitrin, Kenneth Ng, Shruti Yadav, May Dayao, Hai Tran, Josef Gramespacher, Jacob Cohen, Kimberly Hoi, Zhong Huang, Noah Solomon, John Coan, Andy Goodrich, Adison McLaggan, Sarah Yan, Brian Hillier, Danica Manalo-Hebert, Lichao Zhang, Maia Vinogradova, Isaac J. Rondon, Shyra J. Gardai

EpiBiologics, San Mateo, CA

Extracellular targeted protein degradation (eTPD) is a new therapeutic modality designed to eliminate pathogenic extracellular and transmembrane proteins by leveraging proteosome and endosomal-lysosomal protein degradation pathways. EpiTACs are bispecific antibody-based eTPD therapeutics in which one arm binds to a pathogenic target protein and the other arm binds to a tissue-enriched degrading receptor to drive selective and potent protein removal. For the oncogenic receptor tyrosine kinase cMET, existing therapies such as tyrosine kinase inhibitors (TKIs) and antibody-drug conjugates (ADCs) face limitations due to acquired resistance or off-target toxicities and dependence on high target expression in the case of ADCs. We developed EpiTACs and EpiTAC-ADCs to cMET to overcome these challenges using a novel mutation-independent mechanism of action to degrade oncogenic cMET and deliver a cytotoxic payload to drive deep, durable and broad responses across cMET tumors. We screened a panel of cancer-focused degrading receptors in cMET exon 14 skipping mutant and wild type amplified tumor cell-based assays and identified potent cMET-degrading EpiTACs that drove internalization and degradation independent of form in multiple tumor cell-based assays. Degradation of mutant cMET in vitro translated to strong tumor growth suppression in vivo, but not all tumor cell models responded to degradation alone. We developed EpiTAC-ADCs to solve for tumors that express cMET but do not rely exclusively on its oncogenic signaling. EpiTAC-ADCs demonstrated robust anti-tumor activity in vitro and in vivo xenograft tumor models, including cMET responsive and non-responsive models. Combining protein degradation with cytotoxic payload delivery induced strong anti-tumor activity against models with low cMET, where standard ADCs are ineffective. The dual mechanism of EpiTAC-ADCs also demonstrates robust activity at lower drug-antibody ratio (DAR), independent of cMET expression levels or oncogenic signaling dependence. EpiTAC-ADCs represent a novel class of eTPD therapeutics that can effectively degrade oncogenic receptors including cMET independent of mutation and form, while delivering a potent cytotoxic payload. This approach has the potential to address oncogenic driver and resistance mechanisms broadly across cMET-driven tumors. In addition to targeting cMET-high tumors, EpiTAC-ADCs have the potential to target low and medium cMET tumors in patients whose needs are not addressed by standard of care therapeutics including ADCs.

#1726 NEOK002 (ABL209): Redesigning an EGFRxMUC1 bispecific TOP1i ADC with promising anti-tumor activity and enhanced therapeutic window.

Bora Lee, Hyeon Ji Park, Byeong Min Yoo, Hangil Kim, Junyoung Kim, Arim Seo, Youngeun Hong, Donghoon Yeom, Yong-Gyu Son, Jaehyun Eom, Byungje Sung, Jinhyung Ahn, Jinwon Jung, Weon-Kyoo You, Sang Hoon Lee

ABL Bio Inc., Seoul, Korea, Republic of

NEOK002 (ABL209) is a bispecific antibody-drug conjugate (ADC) designed to enhance the impact of dual targeting of Epidermal Growth Factor Receptor (EGFR) and Mucin-1 (MUC1). NEOK002 is a heterodimeric 1+1 bispecific ADC with a drug-antibody ratio (DAR) of 4, conjugated with SYNtecan E^{TM}, a linker-payload containing the topoisomerase I inhibitor exatecan. EGFR is a key oncogenic driver in multiple tumor types, however, clinical targeting of EGFR is limited by dose-dependent skin toxicity. MUC1 is a well-established tumor-associated antigen characterized by aberrant glycosylation and overexpression, but expression can be heterogeneous and the MUC1 extracellular domain is shed from the tumor, limiting monospecific targeting of MUC1. NEOK002, a dual targeting ADC, was designed to reduce EGFR affinity to minimize interference with EGFR signaling and potential toxicity while targeting the SEA domain of membrane-bound MUC1, avoiding binding to the shed, circulating form. Internalization was assessed with the Incucyte system, and *in vitro* cytotoxicity by WST-8 assay. We have selected 36 patient-derived xenograft (PDX) models across six indications, based on their expression of EGFR and MUC1 and tested efficacy of NEOK002. The *in vivo* potency of NEOK002 was also assessed on CFPAC-1, NCI-H1373, and an osimertinib-resistant PDX model. Non-human primate multi-dose GLP toxicity studies were carried out at 20, 40, and 60 mg/kg with dosing on Day 1 and Day 22 with four weeks recovery. NEOK002 demonstrated enhanced cell binding and internalization compared to monospecific EGFR or MUC1 ADC. NEOK002 did not inhibit proliferation of human epidermal keratinocytes *in vitro*, unlike cetuximab-based ADC molecules. *In vivo*, NEOK002 resulted in complete regressions with single doses as low as 1.5 mg/kg in a CFPAC-1 pancreatic CDX model. In a PDX screening study, NEOK002 caused tumor growth inhibition in all 36-tested models and induced tumor regressions in 75% of PDXs across lung, head and neck, esophageal, pancreatic, colorectal, and bladder tumors, and showed strong efficacy in 6 of 9 KRAS-mutant models. Co-treatment of the KRAS-mutant NCI-H1373 model with the KRAS G12C inhibitor sotorasib demonstrated rapid and prolonged tumor regression, which was sustained up to Day 57. In non-human primates, anticipated, reversible gastrointestinal toxicity, cytopenias, and skin erythema/hyperpigmentation were observed in a dose-dependent manner. The HNSTD of NEOK002 in cynomolgus monkeys was established at 40 mg/kg, which is associated with a free exatecan C_{max} of <3 ng/mL. NEOK002 is a potential best-in-class bispecific EGFRxMUC1 ADC effectively leveraging the benefits of co-targeting these antigens yielding enhanced antitumor activity across a wide range of tumors, and reducing the liabilities through attenuated EGFR-related toxicity and reduced impact of binding to shed MUC1.

#1727 Dual targeting of HER2 and AXL by an eKiH-engineered bispecific ADC to overcome resistance in solid tumors.

Kyoung-Ho Pyo[1], Seong-Hyun Park[1], Dongsop Lee[2], Haneol Kim[2], Younggyu Kong[2], Younggeun Lee[1], Hojin Yeom[1], Sowon Aum[1], Sun Hee Park[1], Huijo Oh[1], Cheyeon Kim[1], Hyeonseok Jin[2], Aera Lee[2], Hojeong Hong[2], Ju Hwan Kim[1], Hyungseok Choi[2], Mi-Kyung Kim[2], Taedong Han[1]

[1]AbTis Co., Ltd, Yongin, Korea, Republic of,[2]Dong-A ST Research Headquarter, Yongin, Korea, Republic of

Background: AXL signaling is a key mediator of drug resistance, metastasis, and immune modulation in solid tumors. Its activation drives epithelial-mesenchymal transition (EMT) and promotes tumor aggressiveness, underscoring its role in therapeutic resistance. HER2, a clinically validated ADC target, is similarly associated with oncogenic signaling and metastatic progression. Dual targeting of HER2 and AXL offers a rational approach to suppress complementary resistance pathways and overcome tumor heterogeneity, particularly in patients refractory to standard therapies. We therefore developed a HER2×AXL bispecific ADC using Dong-A ST BsAb platform with an enhanced knob-into-hole (eKiH) interface to improve heavy-chain pairing fidelity and bispecific assembly.
Methods: Lead HER2 and AXL antibodies were selected for high affinity and improved internalization; the AXL lead outperformed benchmark anti-AXL antibodies in binding and internalization assays. Bispecifics were assembled using Dong-A ST BsAb platform and site-selectively conjugated to monomethyl auristatin E (MMAE), exatecan (a topoisomerase-I inhibitor), or dual-payload configurations. Single-cell RNA-seq (scRNA-seq) datasets from lung, breast, and gastric cancers were analyzed to profile HER2 heterogeneity and AXL-associated epithelial-mesenchymal transition (EMT) signatures. Multiplex immunohistochemistry (mIHC) on tissue microarrays quantified spatial co-expression and heterogeneity. Combination potential with immune checkpoint inhibitors (ICIs) was explored via immune-correlative analyses and ongoing co-treatment studies.
Results: scRNA-seq revealed pronounced intra- and inter-tumoral HER2 heterogeneity across indications, while AXL-high tumors exhibited elevated EMT-related markers. mIHC confirmed mosaic/cluster-type co-expression and heterogeneous distribution of HER2 and AXL across multiple tumor types. HER2xAXL BsAb retained high-affinity binding to both targets and efficient internalization, with preliminary in-vitro cytotoxicity observed in HER2-high, AXL-high, and co-expressing models using MMAE, exatecan, and dual-payload ADCs. Immune-correlative data support the mechanistic rationale for ICI combinations, and formal co-treatment evaluations are in progress.
Conclusions: HER2xAXL is a rationally engineered HER2×AXL bispecific ADC designed to mitigate target heterogeneity and therapy resistance. These preclinical data support investigation in HER2-expressing solid tumors—including lung, breast, and gastric cancers—particularly in patients who have failed standard first-/second-line regimens.

#1728 Overcoming target heterogeneity in gastric cancer with an eKiH-engineered CLDN18.2×HER2 bispecific ADC.

Kyoung-Ho Pyo[1], Seong-Hyun Park[1], Dongsop Lee[2], Haneol Kim[2], Younggyu Kong[2], Younggeun Lee[1], Hojin Yeom[1], Sowon Aum[1], Sun Hee Park[1], Huijo Oh[1], Cheyeon Kim[1], Hyeonseok Jin[2], Aera Lee[2], Hojeong Hong[2], Ju Hwan Kim[1], Hyungseok Choi[2], Mi-Kyung Kim[2], Taedong Han[1]

[1]AbTis Co., Ltd, Yongin, Korea, Republic of,[2]Dong-A ST Research Headquarter, Yongin, Korea, Republic of

Background: Target heterogeneity, mosaic and cluster expression of CLDN18.2 and HER2 is common in gastric cancer (GC) and undermines the efficacy of single-antigen therapies. We previously developed DA3501 (AT-211), a CLDN18.2-targeting ADC currently advancing toward Phase 1 evaluation. The DA3501 antibody clone demonstrates enhanced affinity and internalization compared with zolbetuximab. To more comprehensively address heterogeneous tumors, we engineered a CLDN18.2×HER2 bispecific ADC built on Dong-A ST BsAb platform incorporating an enhanced knob-into-hole (eKiH) interface to improve heavy-chain pairing fidelity and bispecific assembly.
Methods: Antibody discovery and optimization yielded lead clones for CLDN18.2 and HER2 with improved binding and internalization. Bispecifics were assembled using Dong-A ST BsAb platform. Conjugation to monomethyl auristatin E (MMAE), exatecan (a topoisomerase-I inhibitor), or dual-payload configurations was performed using site-selective chemistry. Target prevalence and co-expression were evaluated in human GC using single-cell RNA sequencing (scRNA-seq) of tumor specimens and multiplex immunohistochemistry (mIHC) on tissue microarrays (TMAs). Immune correlates were analyzed to assess combinatorial potential with immune checkpoint inhibitors (ICIs).
Results: scRNA-seq revealed CLDN18.2 and HER2 expression in mutually exclusive as well as co-expressing tumor cell subsets, corroborated by mIHC showing intra-tumoral mosaic and clustered patterns. The DA3501 anti-CLDN18.2 clone exhibited superior binding kinetics and internalization versus zolbetuximab. ATS1002 retained high-affinity binding to both targets and demonstrated efficient internalization in dual-positive and single-positive (CLDN18.2 or HER2) models, supporting a “catch-all” approach for heterogeneous lesions. ADCs conjugated with MMAE, exatecan, or dual payloads showed potent in vitro cytotoxicity across CLDN18.2-high, HER2-high, and co-expressing GC lines. Immune-correlative analyses indicated potential synergy with ICIs in tumors exhibiting activated T-cell and myeloid signatures.
Conclusions: This BsAb is a rationally engineered CLDN18.2×HER2 bispecific ADC designed to overcome target heterogeneity in GC. Together with the DA3501 program, it broadens therapeutic coverage of CLDN18.2/HER2-expressing tumors and combination-strategy studies, including ICI co-therapy.

#1729 OBI-904, a next-generation nectin-4-targeting exatecan ADC, demonstrates enhanced cytotoxicity and overcomes enfortumab vedotin resistance.

Yuan-Liang Wang, Chi-Huan Lu, Woan-Eng Chan, Shin-Jin Lin, Ting-Yu Chang, Hong-Syuan Lin, Wei-Jhen Huang, **Ya-Chi Chen**

OBI Pharma, Inc., Taipei, Taiwan

Nectin-4 is a validated therapeutic target for several epithelial cancers. Enfortumab vedotin (EV), the first FDA-approved Nectin-4-directed ADC, has demonstrated significant clinical benefit. However, its efficacy remains limited by multiple mechanisms, P-glycoprotein (P-gp)-mediated efflux, the emergence of EV-resistant tumor cells contribute to reduce cytotoxic activity where its short plasma half-life necessitates more frequent dosing. In addition, off-target hematological toxicities have been observed, potentially resulting from suboptimal linker stability and premature payload release in circulation. To address these limitations, we developed OBI-904, a next-generation Nectin-4-targeting ADC. OBI-904 is a homogeneous ADC and consists of a novel anti-Nectin-4 antibody (10K06) conjugated to an exatecan payload through a stable glycan-based site-specific linker platform.

The 10K06 and Enfortumab antibody epitopes were compared by sequence and structural analysis. Cell binding, internalization, and keratinocyte binding were evaluated by flow cytometry and confocal microscopy. Cross-species reactivity was tested by ELISA. Cytotoxicity was tested in Nectin-4 low 3D spheroid models, bystander activity in co-cultures of Nectin-4-positive and -negative cells, and resistance mechanisms in P-gp-overexpressing and EV-resistant cell lines.

The 10K06 antibody binds to the Nectin-4 IgV domain (amino acids 86-92) and shows good binding affinity and internalization in cell-based assays, ensuring efficient target engagement. In addition, OBI-904 shows reduced binding to keratinocytes compared with EV, suggesting a lower risk of skin toxicity. We also confirmed that 10K06 recognizes human and cynomolgus Nectin-4 but not murine Nectin-4, supporting its suitability for preclinical evaluation in non-human primates. OBI-904 exhibited superior cytotoxic potency in Nectin-4 low-expressing cell lines under 3D spheroid culture conditions, consistent with the high potency and membrane permeability of its exatecan payload. Moreover, OBI-904 mediated a robust bystander effect in co-culture systems with Nectin-4-positive and -negative cells, indicating efficient payload diffusion into neighboring tumor cells. Importantly, OBI-904 retained strong cytotoxic activity in P-gp-overexpressing and EV-resistant tumor cells.

Collectively, these findings establish OBI-904 as a potent, next-generation Nectin-4 ADC with reduced skin binding, enhanced cytotoxicity, a pronounced bystander effect, and the ability to overcome P-gp-mediated and EV-acquired resistance. These attributes position OBI-904 as a promising clinical candidate with the potential to achieve improved therapeutic outcomes in Nectin-4-expressing cancers.

#1730 Guide-effector bsADCs: Driving co-endocytosis for enhanced payload delivery.

Wei-Jhen Huang, Woan Eng Chan, Meng-Hsin Liu, Yueh Chin Wu, **Ya-Chi Chen**

OBI Pharma, Inc., Taipei, Taiwan

Bispecific antibodies (BsAbs) are engineered to simultaneously engage two distinct receptors, offering a powerful approach to enhance receptor internalization and intracellular payload delivery. By exploiting differences in endocytic capacities between receptors, dual targets can convert poorly internalizing target into efficiently internalized complexes—a mechanism particularly advantageous for bispecific antibody-drug conjugates (BsADCs).

BsAbs targeting HER2×TROP2 and cMET×HER3 were engineered, expressed in ExpiCHO cells, and purified via Protein A affinity chromatography. BsADCs were conjugated by the glycan-based site-specific platform via a cleavable linker-payload system. The drug-antibody ratio (DAR) was determined per candidate. Internalization kinetics of BsAbs and their monospecific counterparts were assessed in receptor-coexpressing tumor cell lines (HER2/TROP2^{+} and cMET/HER3^{+}) using a pH sensor dye. Upon antibody binding and internalization, the dye transitions from the neutral extracellular pH (7.4) to the acidic lysosomal environment (pH 4.5-5.5), resulting in increased fluorescence. Fluorescence signals were monitored in real time at 37 °C using a Cytation 5 imaging system.

In this study, the internalization of two BsAb pairs—HER2 × TROP2 and c-MET × HER3, was compared with their respective monospecific antibodies. Using a guide-effector mechanism, BsAbs pair a rapidly internalizing receptor (e.g., HER2 or c-MET) with a poorly internalizing one (e.g., TROP2 or HER3), leveraging the guide receptor's endocytic capacity to drive co-endocytosis and lysosomal trafficking.

HER2 × TROP2 BsADC (OBI-201) illustrates this concept: HER2 facilitates co-internalization of TROP2 (1.7-fold increase compared to the mono-ADC), enhancing lysosomal trafficking and intracellular payload delivery in tumors co-expressing both receptors, overcoming resistance seen with monospecific antibodies and improving cytotoxic efficacy. Similarly, c-MET × HER3 BsAbs exploit c-MET's rapid internalization to drive HER3 uptake (5.5-fold increase compared to the HER3 mono-Ab), inducing receptor clustering, coordinated lysosomal trafficking, and increased intracellular payload delivery, thereby enhancing antitumor activity.

These findings show that BsAbs enhance receptor internalization via co-endocytosis, using a guide-effector mechanism to improve intracellular payload delivery and therapeutic potency. This strategy offers a generalizable approach for BsADC development, enabling targeting of low-expression or non-internalizing antigens and addressing resistant or heterogeneous tumors.

#1731 Hydrophilicity-enhanced linker technology enables site-specific degrader-antibody conjugates with improved stability and enhanced activity.

Yu-Hung Chen, Wei-Chien Tang, Chi-Dian Lu, Hung-Yi Lin, Wei-Jhen Huang, Nan-Hsuan Wang, Ya-Chi Chen, Teng-Yi Huang

OBI Pharma, Inc, Taipei City, Taiwan

Proteolysis-targeting chimeras (PROTACs) have emerged as a novel modality for targeted protein degradation, enabling catalytic removal of disease-related proteins rather than transient inhibition. Despite their mechanistic advantages, most PROTACs suffer from poor drug-like properties—high molecular weight, highly hydrophobic, and with limited permeability—leading to suboptimal pharmacokinetics and formulation challenges. To overcome these limitations, the concept of degrader-antibody conjugates (DACs) has recently gained attention, leveraging antibody-mediated delivery to transport degraders selectively into target cells. DACs can reduce systemic exposure and overcome permeability barriers, thereby expanding the therapeutic utility of degraders. However, bioconjugation of PROTAC payloads remains hindered by issues such as antibody aggregation, inefficient conjugation, and constraints in achieving optimal drug-to-antibody ratios (DAR). Here, we selected a representative BET degrader as the proof-of-concept payload to evaluate the feasibility of DAC construction. Leveraging glycan site-specific technology, we achieved DAC construction with tunable DARs and robust conjugate stability. To address the intrinsic physicochemical challenges of PROTACs, proprietary linker technology was incorporated to enhance hydrophilicity and mitigate aggregation. Proprietary linker also provides high serum stability and enables precise release in the tumor site, potentially broadening the therapeutic index. This BET DAC is anticipated to be applicable to both solid and hematologic malignancies. *In vitro* studies showed that glycan site-specific DACs preserved antibody binding, maintained high stability, and facilitated efficient intracellular delivery of active degraders. Functional analyses confirmed target protein degradation with time- and dose-dependent kinetics, accompanied by strong cytotoxicity in antigen-positive models. These results establish clear proof of concept for our linker-enabled DAC platform. Through the integration of site-specific glycan conjugation and proprietary linker chemistry, this DAC platform offers a versatile and scalable solution to overcome hydrophobic degrader limitations, paving the way for next generation of targeted degradation therapeutics.

: DNA Damage and Repair 2
Poster Session

#1735 Expanding the therapeutic potential of TXNRD inhibitors for triple-negative breast cancer.

Brenna Flowers[1], Abigail Rullo[2], An Zhang[3], Iria Lloshi[1], Keacha Chang[4], Valentina Petukhova[5], Pavel A. Petukhov[5], Irida Kastrati[6]

[1]Cancer Biology, Loyola University Chicago, Chicago, IL,[2]Loyola University Chicago, Oak Park, IL,[3]Loyola University Chicago, Maywood, IL,[4]Loyola University Chicago, Chicago, IL,[5]Medicinal Chemistry and Pharmacognosy, University of Illinois at Chicago, Chicago, IL,[6]Loyola University Chicago - Health Sciences Campus, Maywood, IL

Triple negative breast cancer (TNBC) has the lowest 5-year survival of all breast cancersubtypes, and for many patients the standard of care is limited to a multiagent chemotherapyregimen. Therefore, there is a need to explore improved therapeutic targets and strategies. We havepreviously demonstrated that elevated levels of both thioredoxin reductase 1 (TXNRD1) andthioredoxin reductase 2 (TXNRD2) correlates with lower recurrence-free and overall survival inTNBC and are both relevant targets for TNBC.We have developed new non-covalent TXNRD inhibitors (TXNRD(i)s) that successfullyinhibit TXNRD1 and TXNRD2 in TNBC models as demonstrated through fluorescent biochemicalassays and qPCR of TXNRD related genes. Additionally, these TXNRD(i)s show pleiotropic anti-cancer activity against aggressive phenotypes in both *in vitro* and *in vivo* TNBC models. Treatmentwith TXNRD(i)s reduces 2D viability, mammosphere formation, collagen invasion, and primaryxenograft growth in TNBC models.Mechanistically, we have identified ribonucleotide reductase (RNR) dysfunction causedby our TXNRD(i)s. Given that RNR provides dNTPs, the building block for both DNA synthesisand repair, this led to the hypothesis that TXNRD(i)s induce DNA damage and replicative stress.Furthermore, this is aggravated by poly (ADP-ribose) polymerase (PARP) inhibition, leading toa synergistic effect in BRCA wild-type TNBC cell lines. Using COMET and fork stall assays,microscopy, and western blotting, we concluded there is evidence of replicative stress and DNAdamage induced by our TXNRD(i)s and validated the inhibitors are acting on target by using agenetic approach with inducible TXNRD1 and TXNRD2 knockdowns of our model cell line.Using our TXNRD(i)s in combination with Olaparib, we observed synergistic effects with the twoinhibitors in BRCA wild-type TNBC models. The synergy shown between our TXNRD(i)s andPARP inhibitors in BRCA wild-type TNBC cell lines expands the therapeutic potential of ourTXNRD(i)s as well as opening the possibility to an expansion of PARP inhibitors.

#1736 Synergistic anticancer activity of ciclopirox and prexasertib in non-small cell lung cancer cells.

Zhu Huang, Bing Cheng, **Shile Huang**

Biochemistry and Molecular Biology, LSU Health Sciences Center, SHREVEPORT, LA

Lung cancer is a leading cause of cancer-related deaths worldwide. Non-small cell lung cancer (NSCLC) is the most prevalent lung cancer subtype. Ciclopirox olamine (CPX), an off-patent fungicide, has been identified as a new anticancer agent. Prexasertib (PRE), a Chk1 inhibitor, is in Phase 1/2 clinical trials in various tumors. The anticancer effect of the combination of CPX with PRE on NSCLC cells is unknown. Here, we show that CPX is synergistic with PRE in inhibiting cell proliferation and inducing apoptosis of NSCLC (A549 and A427) cells. Combined treatment with CPX and PRE significantly increased the cell population in the G1/G0 and sub-G1 phases, compared to the single treatment with CPX or PRE. Concurrently, the combined treatment downregulated the protein levels of cyclins (A, B1), cyclin-dependent kinases 4, 6, 2 (CDK4, CDK6, CDK2), cell division cycle 25 B, C (Cdc25B, Cdc25C), and upregulated the protein levels of the CDK inhibitors p21 and p27, leading to decreased phosphorylation of Rb. In addition, the combined treatment increased DNA damage, evidenced by increased expression of γH2AX. In line with this, the combined treatment induced more apoptosis than either single treatment. This was associated with increased expression of DR4, DR5, Fas, and FADD and decreased expression of survivin, resulting in activation of caspase-8 and caspase-3 as well as cleavage of poly (ADP ribose) polymerase (PARP). Taken together, the results indicate that inhibition of Chk1 with PRE can enhance the anticancer activity of CPX at least partly by decreasing cell proliferation and increasing apoptosis in NSCLC cells. Our finding suggests that combination of CPX and PRE may represent a novel therapeutic approach for NSCLC.

#1737 Direct measurement of NER activity using sSTRIDE-NER.

Olga Wojcikowska, Julita Imioło, Magdalena Bartyńska, Zsombor Prucsi, Magdalena Kordon-Kiszala, **Kamil Solarczyk**

intoDNA S.A., Krakow, Poland

Nucleotide Excision Repair (NER) removes bulky DNA adducts and intrastrand crosslinks generated by ultraviolet light and chemotherapeutic agents such as cisplatin. NER capacity profoundly influences tumor response and resistance to DNA-damaging therapies. Despite its biological and clinical importance, direct and quantitative methods for measuring NER activity *in situ* are lacking. Current approaches provide indirect or bulk measurements that fail to capture the spatial and temporal dynamics of repair at the single-cell level. We developed sSTRIDE-NER, a new assay based on the STRIDE (SensiTive Recongition of Individual DNA Ends) platform, designed to visualize and measure single-strand breaks (SSBs) generated during active NER. The assay targets XPD, a core helicase of the TFIIH complex that localizes near incision sites where transient SSBs occur during the repair process. Incorporation of XPD detection into the STRIDE workflow enabled selective visualization of NER-associated DNA ends in individual nuclei. Validation experiments demonstrated high specificity: multiple negative technical controls yielded minimal background signal. Cisplatin was used as a positive control, as it induces bulky intrastrand crosslinks that robustly activate NER. Following cisplatin exposure, sSTRIDE-NER revealed a time-dependent increase in nuclear signal intensity, consistent with accumulation of NER-associated SSBs. sSTRIDE-NER provides the first single-cell, image-based method for direct measurement of NER activity through detection of SSBs proximal to XPD. This assay offers new opportunities to functionally profile NER capacity in cancer cell models and patient-derived samples. It can be applied to investigate mechanisms of resistance to platinum drugs, to evaluate DNA repair-targeting agents, and to support the development of functional biomarkers predictive of therapy response.

#1738 Alnodesertib (ART0380) in combination with irinotecan is highly efficacious in preclinical models of ATM null pancreatic cancer.

Helen M. R. Robinson, Elias Elinati, Eeson Rajendra, Paula Costales, Aurora Cerutti, Lerin Geo, Emily Graham, Kirsty Lawrence, Joana F. B. P. Neves, Marina Roy-Luzarraga, Ozgun Ozer, Vera Grinkevich, Jayesh B. Majithiya, Ian Smith, Graeme C. Smith

Artios Pharma, Cambridge, United Kingdom

Ataxia telangiectasia mutated (ATM) and Ataxia telangiectasia and Rad3-related (ATR) proteins function in concert to regulate the cellular response to both intrinsic and extrinsic factors that induce replication stress such as oncogene activation and DNA damaging agents. Data from the ongoing STELLA Phase II clinical trial (NCT04657068), exploring the safety and efficacy of the ATR inhibitor, alnodesertib (ART0380), in combination with low-dose irinotecan in an ATM negative setting has shown promising response rates of up to 50% across eight different tumor types*. This data has highlighted the effectiveness of a three pronged approach of targeting ATR via alnodesertib in a replication stress high background e.g. ATM loss, with an agent that induces further replication stress e.g. topoisomerase I inhibition. Here, mechanistic preclinical evidence is provided for this novel therapeutic approach across a range of *in vitro* and *in vivo* ATM negative pancreatic cancer models. In all of the CDX and PDX models studied, the combination of alnodesertib and irinotecan induced tumor stasis or regression. Our data highlights that PDAC may represent a highly sensitive tumor type for further development of this new treatment modality exploiting cancer cell specific replication stress

* Ulahannan et al. Cancer Res (2025) 85 (8_Supplement_2): CT267

#1739 Deciphering the molecular links between DNA damage response and autophagy in cancer: Implications for chemotherapy resistance.

Kavya Ajit Pandya, Neeru Singh

School of Biotechnology and Bioengineering, Institute of Advanced Research, Gandhinagar, India

DNA damage response (DDR) guards the cells against DNA damage through coordinated detection and repair of DNA lesions. However, cancer cells rewire this mechanism to mitigate genotoxic insults induced by chemotherapy, thereby attenuating treatment efficacy. This adaptive DDR represents a critical barrier to effective cancer treatment, necessitating elucidation of molecular determinants conferring chemoresistance. Concomitantly, autophagy is activated as a cytoprotective mechanism under genotoxic stress, and emerging evidence suggests functional crosstalk between DDR and autophagy pathways in orchestrating cellular survival. Mediator of DNA damage checkpoint 1 (MDC1) is an indispensable anchor protein of double strand break repair, while Beclin-1 is canonically characterized as a cytoplasmic autophagy regulator. However, their functional convergence during genotoxic stress remains unexplored. We utilized a comprehensive approach combining computational modeling (molecular docking) with cellular assays, including co-immunoprecipitation (Co-IP), immunofluorescence microscopy, and immunoblotting in HeLa cell models with differential MDC1 expression. Here, we report an interaction between MDC1 and Beclin-1 that is dynamically enhanced following genotoxic insult. Remarkably, we demonstrate that genotoxic agents induce nuclear translocation of Beclin-1, a process that is MDC1-dependent. Further, we also show that nuclear Beclin-1 supports the accumulation and retention of various DDR effectors and hence promotes DNA repair. Additionally, we have analyzed the effect of CHK2 kinase activity on this interaction and presence of phospho-CHK2 probably supports the nuclear activity of Beclin-1 through its phosphorylation, but is dispensable for the nuclear translocation of Beclin-1. We believe that the cancer cells rely on this crosstalk to evade chemotherapy induced cytotoxicity. Given that the cytotoxic efficacy of most chemotherapeutic agents relies on inducing irreparable DNA damage, the MDC1-Beclin-1 axis may constitute a pivotal cytoprotective mechanism exploited by malignant cells to enhance DNA repair capacity and thereby circumvent therapeutic intervention. These findings establish a compelling rationale for pharmacological disruption of the MDC1-Beclin-1 interaction as a strategy to resensitize refractory tumors to DNA-damaging chemotherapy. This work offers mechanistic insights for developing next-generation combination therapies targeting the DDR-autophagy interface to surmount treatment resistance.

#1740 Quantitative helicase and polymerase assays to accelerate DNA damage repair targeted drug development.

Oganinma Okakpu, Kasia Zientara-Rytter, Veronique Baron, Michelle Kinbara, Guillermo Cardenas, Jonathan Mikolosko, Henry Zhu, Pavel Shashkin

BPS Bioscience, INC, San Diego, CA

Repairing DNA damage is essential for maintaining cellular health and genomic stability. Mammalian cells therefore rely on multiple repair mechanisms, each activating specific response pathways that recruit defined sets of proteins to initiate and execute repair. Beyond their roles in DNA maintenance, many repair proteins also regulate cell-cycle progression, stress responses, and apoptosis. Proteins involved in DNA damage repair (DDR) pathways have become important therapeutic targets in oncology. Some DDR inhibitors enhance the effectiveness of DNA-damaging cancer treatments such as chemotherapy and radiotherapy, while others induce synthetic lethality when combined with genetic alterations or inhibition of complementary DDR pathways. Among emerging targets, DNA polymerases and helicases offer considerable promise. Helicases unwind complex DNA and RNA structures during replication, recombination, and transcription, and their ATPase activity provides the energy required for this unwinding function. Inhibiting ATPase activity disrupts helicase function, leading to increased DNA damage, cell-cycle arrest, and apoptosis in cancer cells. As a result, small molecules that interfere with ATPase or helicase activities represent compelling therapeutic strategies. To support drug discovery and development efforts, we have established quantitative enzymatic assays that measure the activity of multiple DNA polymerases and helicases. These include assays that selectively assess helicase activity or ATP hydrolysis for targets such as WRN, DHX9, and BLM. Each protocol was optimized to account for dual enzymatic functions and substrate preferences. Together, these assays enable robust evaluation of candidate inhibitors, providing insights into potency, mechanism of action, and target selectivity.

#1741 Nanoparticle co-delivery of microtubule inhibitors and cisplatin overcomes DNA repair-mediated resistance in head and neck cancer.

Xin Li[1], Liubov Palchak[2], Ling Wang[1], Marina Sokolsky[2], Alexander Kabanov[2], Aimin Peng[1]

[1]UNC Adams School of Dentistry, Chapel Hill, NC,[2]UNC Eshelman School of Pharmacy, Chapel Hill, NC

Cisplatin remains a foundational chemotherapeutic for head and neck squamous cell carcinoma (HNSCC), but its effectiveness is often limited by intrinsic or acquired resistance driven largely by enhanced DNA interstrand crosslink (ICL) repair. Through a combined screen of ICL repair and cisplatin resistance modulators, our current study identifies a strong synergy between cisplatin and microtubule-targeting agents (MTAs), including taxanes and colchicine. MTAs suppress ICL repair and overcome cisplatin resistance in HNSCC cells. Mechanistically, MTAs impair the resolution of cisplatin-induced lesions, consistent with reduced recruitment of the ERCC1-XPF endonuclease required for ICL unhooking. MTAs also diminish homologous recombination, accompanied by reduced DNA damage recruitment of RPA32 and RAD51. Moreover, MTAs disrupt DNA damage checkpoint activation in response to cisplatin, permitting cell cycle transit through S-phase despite persistent DNA damage. Together, these effects drive enhanced DNA damage accumulation and apoptosis in HNSCC cells treated with the cisplatin-MTA combination. To further harness this synergy for therapeutic benefit, we employ poly(2-oxazoline)-based micelles to co-encapsulate paclitaxel and a hydrophobic cisplatin prodrug with two aliphatic hexane chains. This nanoformulation is developed to improve drug solubility and release profiles, resulting in optimized pharmacokinetics and enhanced tumor delivery and retention. Indeed, in a syngeneic HNSCC model, nanoparticle co-delivery of paclitaxel and cisplatin prodrug produced markedly superior antitumor efficacy compared to the free drug combination. Collectively, our findings define a mechanism-guided, nanoparticle-enabled therapeutic approach for sensitizing HNSCC to platinum-based chemotherapy through selective disruption of DNA damage responses.

#1743 A novel brain-penetrant dual ATR-mTOR inhibitor for PTEN-deficient cancers.

Sarah Truong[1], Beibei Zhai[1], Louise Ramos[1], Mona Marzban[1], Fariba Ghaidi[1], Marshall Drew-Brook[2], Peter Guzzo[2], Ahmad Issa[2], Mehran Khodabandeh[2], Sara Omar[2], Jason Rolfe[2], Seyed A. Saberali[2], Kally Singh[3], John Langlands[3], Dennis Brown[3], Jeffrey Bacha[3], Mads Daugaard[4]

[1]Vancouver Prostate Centre, Vancouver, BC, Canada,[2]Variational AI, Vancouver, BC, Canada,[3]Rakovina Therapeutics Inc., Vancouver, BC, Canada,[4]University of British Columbia, Vancouver, BC, Canada

Ataxia telangiectasia and Rad3-related protein serine/threonine kinase (ATR), a master regulator of DNA damage repair, maintains genomic stability in cancer cells and allows cancer cells to survive with high replication stress. Inhibition of ATR thus causes genomic instability, leading to mitotic catastrophe and apoptosis. ATR inhibitors (ATRi) have been found to be particularly effective against cells harboring PTEN deficiencies due to synthetic lethality. PTEN regulates the cell cycle and interacts with key proteins like p53 and Chk1, and PTEN deficient cells show increased genomic instability due to compromised DNA repair. Inhibition of ATR in PTEN-deficient cells therefore leads to accumulation of DNA damage and cell death. PTEN loss/mutation also leads to activation of mTOR through activation of PDK1 and AKT, contributing to cell survival and growth. Therefore, simultaneous inhibition of ATR and mTOR seems rational in the context of PTEN-deficient tumor cells. PTEN deficiency can be found in up to 40% of gliomas and 63% of breast cancers, which often metastasize to the brain. Since combination treatments can be clinically difficult due to overlapping toxicities and differing pharmacokinetics, we sought to develop a CNS-penetrating dual inhibitor of ATR and mTOR for the treatment of PTEN-deficient cancers. A generative artificial intelligence platform called Enki™ was used to identify *de novo* molecules with optimized properties for CNS penetrance and specificity for ATR and mTOR. Enki uses a latent diffusion model to optimize many properties simultaneously within the search space, including maximal potency against the primary target, selectivity, ADMET, and physicochemical properties. The most promising molecules were synthesized and tested, and data on potency, selectivity, ADME and *in vivo* efficacy will be presented. Enki™ has enabled deep exploration of chemical space and rapid generation of *de novo* molecules, accelerating the drug discovery process and allowing discovery and development of CNS-penetrating dual ATR and mTOR inhibitors.

#1744 CRISPR screening identifies SMARCAL1 and MRN as modulators of WRN dependency in MSI-H colorectal cancer.

Tiantian Ma, Jibo Wu, Siting Li, **Junjie Chen**

UT MD Anderson Cancer Center, Houston, TX

Microsatellite instability-high (MSI-H) colorectal cancers (CRCs) rely on the Werner syndrome helicase (WRN) to resolve cruciform DNA structures that arise from expanded TA-dinucleotide repeats. Pharmacologic inhibition of WRN with the selective small molecule HRO761 recapitulates WRN loss, causing replication stress and double-strand breaks (DSBs). However, mechanisms modulating WRN dependency remain incompletely understood.

To systematically identify genetic determinants of WRN inhibitor sensitivity, we performed genome-wide CRISPR/Cas9 knockout screens in MSI-H colorectal cancer cell lines treated with or without HRO761. Top candidates were validated using individual gene knockouts, RAD50 degron (dTAG) knock-in systems, and biochemical and imaging assays for DNA damage and replication stress. SMARCAL1 emerged as the strongest resistance hit, and its depletion conferred a 3-5-fold reduction in HRO761 sensitivity and attenuated γH2AX induction. SMARCAL1 likely antagonizes WRN helicase activity and promotes cruciform DNA stabilization via its annealing helicase function. In contrast, loss of structure-specific nucleases MUS81 or ERCC1-XPF did not affect HRO761 response. Instead, acute degradation of RAD50 disrupted the MRE11/RAD50/NBS1 (MRN) complex and conferred ~10-fold resistance to WRN inhibition, accompanied by reduced DSB signaling. ATM, recruited by the MRN complex, also mediated WRN inhibitor sensitivity, as ATM knockout similarly induced resistance.

Our results identify SMARCAL1 and the MRN-ATM axis as critical regulators of WRN dependency in MSI-H CRC. These findings redefine the mechanism of WRN synthetic lethality and provide a framework for predicting and overcoming resistance to emerging WRN-targeted therapies.

#1746 Dual inhibition of TREX1 and polymerase theta uncovers a synergistic DNA repair vulnerability in BRCA-deficient tumors.

Roger Shen, Daniel S Higginson

Radiation Oncology, Memorial Sloan Kettering Cancer Center, New York, NY

Alternative End Joining (Alt-EJ) becomes a key DNA double-strand break (DSB) repair mechanism in tumors with homologous recombination (HR) deficiencies, including BRCA1/2-mutant cancers. Because these tumors depend heavily on POLQ-mediated repair, we sought to identify additional druggable regulators of Alt-EJ that could be leveraged for combination therapy. We used CRISPR-based perturbations, three Alt-EJ reporter systems, and DSB repair pathway analyses in HR-proficient and HR-deficient models. TREX1 subcellular localization after DNA damage was assessed using confocal microscopy and fractionation. To evaluate therapeutic potential, we tested a TREX1 inhibitor alone and in combination with the POLQ inhibitor ART558. Our results reveal TREX1 as a potent suppressor of Alt-EJ and a complementary regulator to POLQ. TREX1 loss markedly increased Alt-EJ frequency, enhanced POLQ-dependent repair, and shifted pathway choice toward more mutagenic mechanisms. Following DNA damage in mitosis, TREX1 translocated from the cytosol into the nucleus, indicating a direct role in DSB repair engagement. Pharmacologic TREX1 inhibition reduced Alt-EJ activity, and co-inhibition of TREX1 and POLQ produced strong synergy, leading to substantial suppression of Alt-EJ and significant loss of viability in BRCA2-deficient cells. Genetic co-depletion of TREX1 and POLQ similarly enhanced sensitivity to ionizing radiation, demonstrating that dual targeting amplifies therapeutic impact across modalities. These findings identify TREX1 as a druggable modulator of DSB repair and establish a mechanistically informed combination strategy in which TREX1 and POLQ inhibitors cooperatively exploit the repair dependence of HR-deficient tumors. Dual inhibition may represent a rational therapeutic approach for BRCA-deficient cancers that rely on Alt-EJ for survival.

#1747 A combination of PG3 and PARP inhibitors exhibits antitumor effects in both BRCA1-mutated and BRCA1-wild-type TNBC.

Xiaobing Tian, Wafik S. El-Deiry

Brown University Warren Alpert Medical School, Providence, RI

DNA double-strand break (DSB) repair can be mediated by non-homologous end joining (NHEJ) and homologous recombination (HR). Homologous recombination repair (HRR) is important because it accurately repairs DNA DSBs using a sister chromatid as a template, which is crucial for maintaining genome stability and preventing mutations. Deficiency in HRR makes cancer cells sensitive to DNA damage drugs. BRCA1/2 and RAD51 proteins play very important roles in HRR. PARP is a key enzyme in the repair of DNA single-strand breaks (SSB). Unrepaired SSBs will convert to DSBs in cells. Therefore, BRCA1/2 -mutated cancer cells are sensitive to PARP inhibitors.

However, PARP inhibitor resistance develops quickly, mainly through mechanisms that restore homologous recombination repair. This can happen through secondary mutations that restore function in genes of BRCA1 or BRCA2, and overexpression of RAD51. RAD51 overexpression is reported in many cancers, such as breast, prostate, and glioblastoma, and has been involved in chemotherapy resistance. Inhibition of RAD51 creates an HR-deficient status, which can sensitize cancer cells to PARP inhibitor treatments. It has been reported that ISR (integrated stress response) leads to downregulation of RAD51. We reported before that PG3 treatment induced potent ISR. Hence, we hypothesized that PG3 can sensitize PRAP-resistant tumor cells (both BRCA1-mutant and wild-type) to PARP inhibitors by downregulating RAD51.

The combination treatments of PG3 and Olaparib/Talazoparib showed synergistic inhibitory effects on triple-negative breast cancer cells, BRCA1-mutated SUM149 and MD-MB-436, and BRCA1-wildtype MD-MB-231 and MD-MB-468. Western blots showed that two BRCA1-mutated cell lines, SUM149 and MD-MB436, express very low levels of BRCA1 protein compared to wild-type cell lines MD-MB231and MD-MB468. On the other hand, SUM149 and MD-MB436 show much higher RAD51 expression than MD-MB231 and MD-MB468. PG3 downregulates RAD51 in both SUM149 and MD-MB231 cells, but not in MD-MB436 and MD-MB468 cells. Transcriptional factors c-Myc, E2F1, and FoxM1 regulate RAD51 gene expression. We found that PG3 induced downregulation of c-Myc, E2F1, and FoxM1 in both SUM149 and MB231 cells, but not in MB436 and MB468 cells. That is consistent with previous publications. PG3 also downregulates wild-type BRCA1 in MD-MB231 cells but not in MD-MB468 cells. We found that olaparib treatment induced upregulation of RAD51 in SUM149 cells and upregulation of both BRCA1 and RAD51 in MD-MB231 cells. PG3 blocked the olaparib-induced upregulation of RAD51 in SUM149cells, and the upregulation of BRCA1 and RAD51 in MD-MB231 cells. The combined treatment induced more DNA damage than olaparib or PG3 alone in SUM149 and MB231 cells, as indicated by increased γH2AX level.

#1748 FORX-428: Exploiting PARG inhibition to target replication stress in cancer cells.

Frank Tadashi Zenke[1], Ulrich Lucking[1], Olivier Querolle[1], Luca Iacovino[1], Marta Malattia[1], Alessandro Potenza[1], Nicolas Bocquet[1], Serena Bologna[1], Hanna Kok[1], Anika Kuster[1], Roxanne Lourman[1], Jason Clochard[1], Irena Konstantinova[1], Thanos D. Halazonetis[2], Jens Wuerthner[1], Tarig Bashir[1]

[1]FoRx Therapeutics AG, Basel, Switzerland,[2]Department of Molecular and Cellular Biology, University of Geneva, Geneva, Switzerland

PARylation/dePARylation is essential for sensing and repairing replication-associated DNA damage. Inhibitors of the PARP enzymes catalyzing the build-up of poly(ADP-ribose) chains have become a mainstay of breast and ovarian cancer therapy over the past decade. Inhibiting PARG, the enzyme responsible for degrading poly(ADP-ribose) chains, has rapidly gained momentum as a therapeutic approach to benefit cancer patients which develop resistance to PARP inhibitor therapy. FORX-428 is a highly potent, reversible, selective, and orally bioavailable PARG inhibitor with the expected mechanism of action and exquisite efficacy in PARP inhibitor-resistant cancers. Of note, PARG inhibition demonstrated un-precedented antitumor activity in cancers with oncogene-induced replication stress suggesting therapeutic potential even outside of the label of PARP inhibitors. FORX-428 entered a Phase 1 clinical trial in July 2025. We will present the structure of FORX-428, in-depth pharmacology data as well as up-to-date results from the ongoing Phase 1 study. Collectively, these findings provide evidence supporting PARG inhibition as a novel and promising therapeutic strategy to treat PARP inhibitor-resistant and other hard-to-treat cancers.

#1749 Modeling response to alkylating chemotherapy in a syngeneic model of MGMT overexpression and MMR-deficient glioma.

Ranjini K. Sundaram[1], Deepti Bhatt[2], Ranjit S. Bindra[3], Juan Vasquez[1]

[1]Yale School of Medicine, New Haven, CT,[2]Yale University School of Medicine,[3]Yale University, New Haven, CT

Glioblastoma (GBM) is associated with dismal prognosis, having a median survival of less than 15 months. The frontline chemotherapeutic agent used in the treatment of GBM patients, temozolomide (TMZ), is limited by predictable resistance mechanisms. TMZ-induced O^6-methylguanine (O^6-MeG) lesion is repaired directly by O^6-Methylguanine Methyltransferase (MGMT). In tumor cells with loss of MGMT, the unrepaired methyl adducts result in a mismatched nucleotide base pairing. The mismatch repair (MMR) pathway recognizes the damage and promotes cell death through futile cycles of MMR. Loss of function mutations in MMR proteins are now recognized as a key mechanism of acquired TMZ resistance in gliomas, specifically in tumors with MGMT promoter methylation. MGMT serves as a prognostic marker in GBM and is found to be related to improved response to TMZ. Although alkylator therapy has shown relative efficacy in treating MGMT-methylated tumors, standard treatments are largely ineffective for GBM patients with MGMT-unmethylated tumors. For this, it is crucial to overcome intrinsic resistance to TMZ, which can be possible with the use of MGMT inhibitors such as O^6-benzylguanine (O^6-BG) and Lomeguatrib. Fluoroethylating agents, KL-50, is a recently developed agent which acts through a unique DNA-modifying mechanism involving evolution of a primary alkyl lesion to a DNA interstrand crosslink particularly in the absence of MGMT.Using CRISPR/Cas9, isogenic SB28 murine glioma cell lines with knockout of MSH6 and MLH1 were generated and MGMT overexpression models created by overexpressing FLAG-tagged MGMT. We performed in vitro short-term viability and clonogenic survival assays demonstrating that cells with loss of MMR displayed resistance to TMZ while retaining sensitivity to KL-50. MGMT overexpression showed resistance to TMZ and KL-50 and this resistance was reversed when cells were treated with O^6-BG or Lomeguatrib as MGMT inhibitors. We assessed the TMZ and KL-50 efficacy in flank and intracranially implanted tumor models and observed that KL-50 extended the median survival in comparison to TMZ or vehicle control in the MLH1 KO setting. Therefore, this suggested that KL-50 forms DNA interstrand crosslinks selectively in MGMT-silenced tumor models and maintains its efficacy even in the loss of functional MMR, emphasizing its potential to fill a critical therapeutic gap in recurrent, treatment-refractory tumors.Furthermore, in MGMT+ models, Lomeguatrib given concurrently with KL-50 demonstrated a significantly increased survival benefit, indicating that KL-50 in combination with the MGMT inhibitor can be used as a potential clinical approach for GBM patients with MGMT-unmethylated tumors. Our findings suggest that KL-50 may provide a new treatment approach for TMZ-resistant gliomas and in the MGMT+ setting, combination with Lomeguatrib could be beneficial.

#1750 Building an integrated platform for drug discovery in DNA damage response.

Bruno Vaz[1], Julien Brustel[1], Marie Cargnello[1], Marie Lafitte[1], Frederique Dol-Gleizes[1], Rahul Valiya Veettil[2], Andrei Zinovyev[1], **Anne-Sophie Casagrande**[1], Francisco H. Cruzalegui[1], Stephen Durant[3]

[1]Evotec, Toulouse, France,[2]Evotec, Verona, Italy,[3]Evotec, Abingdon, United Kingdom

The DNA Damage Response (DDR) consists of a network of cellular pathways that recognize, signal, and repair different DNA lesions in coordination with other cellular activities. While DDR deregulation contributes to tumor initiation, it also confers therapeutic vulnerabilities specific to cancer cells. Currently, more than 50 chemotherapeutic drugs approved by FDA act primarily through general DNA damage mechanisms. Furthermore, the identification of synthetic lethal interactions in the last years has further paved the way for a new wave of precision drugs that target DDR. PARP inhibitors have revolutionized the treatment of patients with BRCA mutations. Similarly, WRN inhibition shows promising activity in microsatellite-unstable cancers, and ATR inhibition confers therapeutic benefit in ATM-deficient cancers. We have established an integrated platform designed to characterize and decipher the DDR defects and mechanisms associated with a specific target or pre-clinical drug candidates. Leveraging a comprehensive suite of biochemical assays, high content imaging multiplex panels that detect DNA damage and replication stress markers, GFP-based reporter assays for double strand break (DSB) repair, hematotoxicity and replication-related toxicity, and *in vivo* pharmacology DDR models for PK/PD and efficacy, we can support every stage of cancer drug discovery. Additionally, we have developed a knowledge-based DDR modelling tool to predict the impact of target depletion on the choice of DSB repair pathway and potentially identify novel synthetic lethal interactions. Using this in silico tool, we were able to recapitulate one of the mechanisms of resistance to PARP inhibition in BRCA deficient tumors. In conclusion, Evotec's comprehensive DDR toolkit enables mechanistic understanding of targets and drug candidates in the DDR network.

#1751 Deletion of the DACH1 gene tumor suppressor increases replication fork stress, epithelial mesenchymal transition and sensitivity to WEE1 kinase inhibitors in prostate cancer.

Danni Li[1], Arijit Ghosh[2], Zhiping Li[1], Kenneth Iczkowski[3], Hidetoshi Mori[4], Samiha Nasser[5], Csaba Kerepesi[5], Andras Benczur[5], Hallgeir Rui[6], Ritika Harish[1], Li Lan[7], **Xuanmao Jiao**[1], Fred Saad[8], Janne Purhonen[7], Anthony W. Ashton[9], Richard G. Pestell[1]

[1]Baruch S. Blumberg Institute, Wynnewood, PA,[2]Duke University School of Medicine, Durham, NC,[3]UC Davis Health, Sacramento, CA,[4]UC Davis, Davis, CA,[5]Hungarian Research Network, Budapest, Hungary,[6]Thomas Jefferson University, Philadelphia, PA,[7]Karolinska Institutet, Stockholm, Sweden,[8]Centre de Recherche du Centre Hospitalier de l'Universite de Montreal, Montreal, QC, Canada,[9]Lankenau Institute for Medical Research, Wynnewood, PA

• Introduction: Patients with metastatic prostate cancer have poor survival with DNA damage repair pathway abnormalities. The cell fate determination factor DACH1 is deleted (shallow or deep deletion) in ~5-12% of PCa patients, but up to 65% of metastatic PCa. WEE1 kinase is one of the most upregulated kinases in the human prostate cancer kinome associated with metastatic progression in prostate cancer (mCRPC). We determined the potential for differential sensitivity of PCa to Wee1 Kinase inhibitors (WEE1Ki) based on DACH1 expression profiles.

• Methods: Analysis of patient gene expression, tumor histology, organoids derived from prostate epithelial cell-specific DACH1 deletion prostate onco-mice, DNA replication fork assays, tissue culture.

• Findings: DACH1 deficient (*Dach1*$^{-/-}$) cells showed enhanced cell killing by WEE1Ki, that was reversed by reintroduction of DACH1a. Increased sensitivity to WEE1Ki was shown in fibroblasts, prostate cancer cell lines and in organoids derived from human prostate cancer cell lines or the prostate epithelium of Dach1 deletion onco-mice. DACH1 deletion dramatically enhanced non replicating S phase in the presence of WEE1Ki. *Dach1*$^{-/-}$ cells showed increased replication fork stress, that was reversed by reintroduction of the DACH1a isoform. DACH1 epithelial cell deletion onco-mice, and the prostate organoids derived therefrom, was associated with the induction of epithelial mesenchymal transition (EMT) with a corresponding increase in AKT^{Ser473P}, ATR^{Thr1989p} and CHK1 ^{Ser345P}. Increased sensitivity to WEE1Ki is associated with reduced SETD2 or NSD1/KMT3B expression, and reduced RRM2, a ribonucleotide reductase subunit, thereby inducing dNTP starvation. DACH1 expression was highly correlated with SETD2, NSD1 and RRM2. Gene ontology terms associated with DACH1 DNA binding templates included nucleoside metabolic processes. Like several other tumor suppressor genes (RB, FOXO3), DACH1 restrained dNTP production. dNTP production also requires NDPK (Nucleoside Diphosphate Kinase) encoded by NME genes. Consistent with the inhibition of dNTP production, DACH1a expression in prostate cancer PC3 cells reduced NME1 and NME7 (NDPKA expression), and DACH1 was strongly inversely correlated with NME1 in human prostate cancer (N=491. P 9.9e-24).

• Conclusions: As *DACH1* deletion PCa subclass conveys specific therapeutic sensitivities, that is dependent upon the DACH1a isoform, testing for DACH1a in patient samples may be warranted.

#1752 APOBEC3B enhances PARP inhibitor response by suppressing ovarian cancer stem cells.

Maria Rivera[1], Lucy Liu[1], Chae-Eun Lim[1], Sabina Enlund[2], Haoran Zhang[1], Kaifu Yang[1], Roman Sasik[3], Kathleen Fisch[3], Frida Holm[2], Leslie A. Crews[1], Qingfei Jiang[1]

[1]UCSD Moores Cancer Center, La Jolla, CA,[2]Karolinska Institutet SE, Stockholm, Sweden,[3]University of California, San Diego, La Jolla, CA

Poly(ADP-ribose) polymerase inhibitors (PARPi) provide substantial benefit to high-grade serous ovarian cancer (HGSOC) patients with BRCA mutations or homologous recombination deficiency (HRD), yet resistance remains a major clinical challenge. Cancer stem cells (CSCs) are thought to drive recurrence and therapeutic failure, highlighting the need to define molecular determinants governing CSC biology and PARPi response. APOBEC3 (A3) cytidine deaminases, particularly A3B, represent key enzymatic mutators in cancer and are highly expressed in HGSOC. However, their roles in CSCs and therapeutic sensitivity remain poorly understood.

Using previously published scRNA-seq datasets from six HGSOC patients, including one BRCA2-mutant case, we found that A3B is the predominantly expressed A3 family member, followed by A3C and A3A. In patient-derived xenografts (PDXs) and cell lines, CSC-enriched tumorspheres consistently exhibited reduced A3B levels relative to adherent non-CSC cells, whereas other A3s showed no CSC-specific changes. This pattern mirrors observations in myeloproliferative neoplasms, where stem cell populations display reduced A3 mutational burden relative to bulk tumor cells. Functionally, A3B knockdown increased tumorsphere formation and SOX2 expression, indicating that low A3B supports a self-renewing CSC state. Notably, among three HGSOC PDX models, only OV033 readily formed tumorspheres and exhibited the highest A3B expression, suggesting that BRCA status, HRD, and other genomic features may influence both tumorsphere capacity and A3B levels.

We further demonstrate that A3B loss promotes olaparib tolerance by reducing A3B-induced replication stress in S/G2 cell line tumorspheres. Because PARPi induces ssDNA accumulation and replication stalling, A3B-high cells may experience increased DNA damage under PARPi, contributing to heightened sensitivity. This aligns with clinical data linking A3B overexpression to improved platinum responses. Together, these findings support A3B expression and activity as potential biomarkers for predicting PARPi response in HGSOC.

In conclusion, our findings position A3B as a critical molecular switch linking CSC biology to PARPi response, revealing an immediately actionable biomarker and therapeutic vulnerability in HGSOC.

: Engineering the Next Wave of Antibody-Based Cancer Therapeutics
Poster Session

#1756 Novel HER2 antibody drug conjugates with stable hydrophilic linkers.

Zhiying Zou[1], Sichang Zhou[1], Jin Chu[1], Xueping Jiang[1], Zhongliang Jiang[1], Jing Ming Dong[2], Feng Bai[2], Jing Pan[1], Yuzhong Chen[1], Can Mao[1], Qun Sun[1], Lucas Pan[3], Greg Witham[1], Xiaoyu Wang[1], Gann Xu[1], Bingsen Zhou[2], Kai Qi[1], Lin Wang[1], Ray Yin[1]

[1]Fulgent Pharma, Newark, DE,[2]Fulgent Pharma, El Monte, CA,[3]Newark Charter School, Newark, DE

Background: The success of Trastuzumab deruxtecan (T-DXd) was previously attributed to its unique cleavable linker and membrane permeable payload. However, the robust efficacy in cancers with ultralow HER2 expression demands further understanding of its anti-tumor mechanisms. In addition, the occurrence of severe adverse events and the development of drug resistance in clinical settings highlights the importance of designing new ADCs with improved pharmacokinetics (PK) and alternative payloads. Here we present the mechanistic study of a novel HER2-directed ADC with an attempt to improve drug biodistribution, therapeutic window, and sustained efficacy.
Methods: HER2-targeting ADC (FID-031) with a proprietary linker and a topoisomerase I inhibitor payload has been developed with an estimated drug to antibody ratio of 7 and evaluated by HPLC, SEC, HIC, ELISA, flow cytometry and cell viability assays in vitro. PK and tissue distribution of the ADC were evaluated in CD-1 mice and tumor bearing SCID mice. In vivo efficacy and anti-tumor mechanism were explored in CDX mouse models.
Results: FID-031 showed both HER2-dependent cytotoxicity and a bystander killing effect comparable to the control ADC (T-DXd). In various CDX models, FID-031 demonstrated significantly improved and more sustained tumor growth inhibition than T-DXd at 1-3 mg/kg dose levels. In CD-1 mice, the levels of FID-031 and total antibody exhibited a prolonged half-life in circulation. In HER2-positive tumor-bearing mice, the free payload level from FID-031 was relatively low in plasma but significantly higher in tumor tissue compared to T-DXd, correlating with its superior efficacy in animal models. Immunohistochemistry of FID-031 revealed higher antibody distribution in the tumor microenvironment and deeper penetration in tumor parenchyma compared to T-DXd control. In both HER2 high- and low-expression CDX models, cancer-associated fibroblast and tumor-associated macrophage colocalized with ADC in the tumor microenvironment, suggesting critical roles of these cells in the ADC biological metabolism. Comparable levels of free payload accumulation were observed in normal tissues (i.e., lung, liver, kidney and spleen) for both FID-031 and T-DXd. Significantly lower level of free payload was observed in intestine tissue within the FID-031 treatment group compared to the T-DXd control group. In vivo toxicology studies in NHP are in progress.
Conclusions: FID-031 is a novel HER2-targeting ADC with improved PK profile, tissue distribution, and efficacy. This study provides fresh insights on the design considerations for ADC development aimed towards improving safety and overcoming drug resistance.

#1757 Synergy of BCL-2 and MEK/HDAC inhibition in IBC and non-IBC models: Potential for a first IBC specific therapy.

Hassan Zbib[1], Habib Serhan[1], Maryam Nakhjiri[1], Rhea Raghavan[1], Tusharika Rastogi[1], Peter J. Ulintz[1], Aki Morikawa[2], Nathan Merrill[1], Sofia Merajver[1]

[1]Department of Internal Medicine, University of Michigan, Ann Arbor, MI,[2]Medical Student, University of Michigan, Ann Arbor, MI

Background: Inflammatory breast cancer (IBC) is an aggressive subtype of breast cancer characterized by rapid progression. Despite its unique clinical presentation, there are no IBC specific therapies. IBC growth is not faster than non-IBC, so evasion of apoptosis, mediated by the B-cell lymphoma 2 (BCL-2) family, is hypothesized to be a major mechanism for IBC persistence. Aberrant BCL-2 expression favors tumor survival. Although BCL-2 inhibition can restore apoptotic activity, single-agent activity remains limited by compensatory signaling. Our initial high-throughput screen indicated that certain drug classes including: HSP90, BCL-2, MEK, and HDAC inhibitors showed a trend toward greater activity in IBC compared to non-IBC models. This led us to explore rational combination strategies across our panel of IBC and non-IBC breast cancer models.
Methods: We screened eight breast cancer cell lines (3 IBC: SUM-149, SUM-190, IBC-1; and 5 non-IBC: MDA-MB-231, JIMT-1-GFP, BT-474, MUM51, HCC1143) with a library of more than 1,200 compounds to identify drug classes with increased sensitivity in IBC relative to non-IBC. This initial screen identified HSP90, BCL-2, MEK, and HDAC inhibitors as classes of interest. We then performed follow-up combination screens using Pimitespib (HSP90 inhibitor) and Navitoclax (BCL-2 inhibitor), the top hits within their respective classes, testing them against the same 1,200+ compound library to identify synergistic partners. In parallel, we rationally combined inhibitors of multiple active pathways (e.g., BCL-2 + MEK or BCL-2 + HDAC), which have shown synergy in other cancers, to evaluate additional synergistic interactions. Combination effects were assessed using the Chou-Talalay method (CI < 1 indicating synergy).
Results: Our high-throughput screen identified HSP90, BCL-2, MEK, and HDAC inhibitors as more sensitive in IBC relative to non-IBC. Secondary screens pairing Pimitespib (HSP90 inhibitor) or Navitoclax (BCL-2 inhibitor) with the same compound library identified synergistic partners. Pimitespib synergized with taxanes and PI3K/MAPK inhibitors in select lines such as MDA-231 and BT474, whereas Navitoclax consistently showed strong synergy with MEK and HDAC inhibitors in IBC models. Distinct subtype-dependent trends emerged: synergy between BCL-2 and MEK inhibition was strongest in IBC, while BCL-2 and HDAC synergy predominated in non-IBC lines.
Conclusions: This study shows for the first time a trend towards IBC-specific synergistic drug interactions. These findings suggest potential mechanistic differences in apoptotic regulation and may guide rational development of targeted combination therapies for IBC. Future studies will assess whether these *in vitro* synergy trends translate into subtype-specific therapeutic responses in vivo.
AI disclosure: AI was used only for language editing; content was verified by the authors.

#1758 Targeted DNA damage through SSTR2: Preclinical development of a novel peptide-drug conjugate for neuroendocrine tumors.

Gianluca Fossati[1], Daniela Modena[1], Luca Menin[1], Michela Bottani[1], Andrea Stevenazzi[1], Barbara Vergani[1], Elisabetta Galbiati[1], Andrea Resovi[1], Matteo Tironi[1], Serena Cecchetti[2], Francesca Spadaro[2], Maria Carollo[2], Rosita Lupi[3], Barbara Valsasina[3], Paolo Orsini[3], Silvia Castelli[3], Italo Beria[3], Christian Steinkuhler[4]

[1]Italfarmaco S.p.A., Milan, Italy,[2]Istituto Superiore di Sanita, Rome, Italy,[3]Nerviano Medical Sciences, Nerviano, Italy,[4]Italfarmaco SpA, Milan, Italy

Targeted induction of DNA damage in tumor cells offers a promising strategy to efficiently kill cancer cells while sparing healthy tissues. Precise tumor targeting can be achieved by the exploitation of the differential expression of specific molecular targets on the surface of tumor cells. Somatostatin receptor 2 (SSTR2) has emerged as a valuable tumor-associated target, due to its high expression in gastroenteropancreatic neuroendocrine tumors (GEP-NETs). SSRT2 is not only expressed in these differentiated, slow-proliferating NET, but also in highly proliferative and metastatic neuroendocrine carcinomas, such as small cell lung cancer (SCLC). SSTR2 overexpression occurs in up to 50% of primary tumors from SCLC patients and is correlated with poor prognosis, highlighting SSTR2 as an optimal candidate for targeted therapeutic intervention in a subset of SCLC patients. To exploit this opportunity, we designed a peptide drug conjugate (PDC), named ITF3912 which combines a modified octreotide analog with a novel and potent duocarmicin via a cathepsin-cleavable linker. In preclinical studies in vitro ITF3912 demonstrated high affinity and selectivity for SSTR2, acting as an agonist with an IC_{50} of 8 nM and a selectivity index of at least 10 over SSTR3/5, with no significant binding observed for SSTR1 or SSTR4. ITF3912 induced cytotoxicity in SSTR2-expressing cells, with efficacy correlated to SSTR2 expression levels. In high level SSTR2 expressing NCI-H524 cells, ITF3912 was rapidly internalized and localized in lysosomes where enzymatic cleavage of the linker released the active toxin. Once in the nucleus, the toxin induced an S-phase replication block and a potent and lethal DNA damage as evidenced by the activation of key biomarkers such as the phosphorylation of ATM, ATR, CHK1, CHK2, RPA32 and γ-H2AX, leading to cell death with an IC50 of 4 nM. The NCI-H69 cell line that expresses lower level of SSTR2 can still be targeted by ITF3912 but with lower efficiency (60 nM). The activity on NCI-H727 cell line that expresses very low level of SSTR2 diminished as expected (400 nM). Consistent with the in vitro findings, ITF3912 showed strong antitumor efficacy in vivo. It effectively reduced the tumor growth of NCI-H524 with a survival rate of 50% after 80 days of treatment and several mice showed complete tumor remission. In contrast, ITF3912 was less effective on NCI-H727 cell line by inducing a tumor growth reduction of 30%. Collectively, these data establish ITF3912 as a potent and selective SSTR2-targeted PDC, whose efficacy in vitro and in vivo correlates with receptor expression levels. These results support the use of ITF3912 as a therapeutic option for patients with SSTR2-positive neuroendocrine tumors, addressing a significant unmet medical need. Encouraging preliminary toxicology results, further support the progression of ITF3912 toward clinical development.

#1759 Targeting LRRC15 with an aptamer-drug conjugate achieves complete tumor growth inhibition.

Kristin Thompson[1], Aaron Ball[1], Jin Yuan[1], Yuxun Wang[1], Doo Young Jung[2], Shuhao Zhu[1]

[1]Guardian Therapeutics, Lowell, MA,[2]Pinotbio, Inc, Suwon, Korea, Republic of

Antibody-drug conjugates (ADCs) have demonstrated the clinical potential of targeted payload delivery for cancer therapy. However, their large molecular size can limit tumor penetration, leaving regions of the tumor insufficiently exposed to the cytotoxic payload. To address this limitation, GRX2672 has been developed as a novel aptamer-drug conjugate (ApDC) designed to target LRRC15-expressing tumors while maintaining a small molecular size to enable deep tumor penetration. LRRC15 (leucine-rich repeat-containing protein 15) is a transmembrane member of the LRR superfamily involved in cell-cell and cell-matrix interactions. It is highly expressed in mesenchymal-derived tumors such as sarcoma, glioblastoma, and melanoma, making it an attractive target for therapeutic intervention. Aptamers are short, structured oligonucleotides that bind their targets with high affinity and specificity. Compared with monoclonal antibodies, their compact size enables superior tissue and tumor penetration. Moreover, aptamers can be engineered to neutralize oncogenic targets, deliver cytotoxic payloads, or achieve both simultaneously. Incorporating a proprietary half-life-extension moiety preserves the aptamer's small size and tumor-penetrating capability while markedly improving its pharmacokinetic properties. Here, we describe an LRRC15-targeting aptamer with high affinity and selectivity that has been conjugated to 2DAR of a novel topoisomerase I inhibitor (PBX-7016) at the 5′ end and a half-life-extending fatty acid at the 3′ end. The resulting ApDC, GRX2672, selectively kills LRRC15-positive cells in vitro and achieves complete tumor growth inhibition in vivo without observed toxicity. These findings support the potential of LRRC15-targeted ApDCs as an emerging therapeutic strategy to improve outcomes for patients with LRRC15-positive tumors.

#1760 Preclinical characterization of XB404, a masked anti-ROR1/2 antibody-drug conjugate.

Kathleen R. Gogas[1], Christine M. Janson[1], Hui Zhao[1], Fang Wang[1], Bee-Cheng Sim[1], Brian A. Mendelsohn[1], Penelope M. Drake[2], Robyn M. Barfield[2], Thomas Linz[2], Maxine Bauzon[2], Dharmaraj Samuel[2], Minjong Park[1], Inna Vainshtein[1], Jackie Cheng[1], Seema Kantak[1]

[1]Exelixis, Inc., Alameda, CA,[2]Catalent, Inc., Emeryville, CA

Background: Receptor tyrosine kinase-like orphan receptors (ROR) 1 and 2 are single-pass transmembrane proteins that are part of the ROR family that mediates Wnt signaling. ROR1 and ROR2 are aberrantly expressed in various cancers, including lung, breast, ovarian, and endometrial cancers, and their expression can be associated with poor disease outcomes. XB404, a masked anti-ROR1/2 antibody-drug conjugate (ADC) developed using the Adagene masking platform and the SMARTag® ADC platform, is designed to deliver a cytotoxic payload to ROR1/2-expressing tumors while minimizing on-target, off-tumor side effects. XB404 is composed of a tandem-cleavage topoisomerase 1 inhibitor-based linker-payload conjugated to a masked monoclonal antibody that binds to both ROR1 and ROR2 with high affinity. Here, we describe the preclinical characterization of XB404, including its in vitro cytotoxicity and internalization and in vivo efficacy in cell line-derived xenograft (CDX) and patient-derived xenograft (PDX) models.
Methods: In vitro cytotoxicity of XB404 was evaluated in ROR1- and ROR2-overexpressing cell lines using the CellTiter-Glo® luminescent cell viability assay. In vitro internalization for the unmasked XB404 antibody was assessed in ROR antigen-expressing MDA-MB-231 tumor cells using flow cytometry. A rat pharmacokinetics (PK) study at 5 mg/kg was used to assess and compare PK properties for a non-masked ROR1/2 ADC and XB404. In vivo tumor growth inhibition was evaluated in Jeko-1 and MDA-MB-231 CDX models using XB404 at 7.5 mg/kg in a QWx2 dose schedule. Tumor growth inhibition was assessed in non-small cell lung cancer (NSCLC) and triple-negative breast cancer (TNBC) PDX models using 1, 3, 6, and 10 mg/kg dose levels.
Results: Unmasked XB404 displayed potent in vitro cytotoxic activity, and unmasked XB404 antibody demonstrated internalization properties. XB404 demonstrated improved clearance and half-life compared with the non-masked ROR1/2 ADC in rats. In addition, overlapping total antibody and total ADC curves for XB404 indicated good in vivo stability. In vivo antitumor activity was observed in the Jeko-1 and MDA-MB-231 xenograft models. XB404 demonstrated dose-related tumor growth inhibition and improved survival in both NSCLC and TNBC PDX models. Tumor regression was observed in both PDX models and complete responses were observed in the TNBC PDX model.
Conclusions: XB404 demonstrated in vitro cytotoxicity and internalization, in vivo stability, and in vivo efficacy across multiple CDX and PDX models. Taken together, these preclinical results support further development of XB404. Investigational New Drug-enabling studies are ongoing.

#1761 Tissue Factor expression is associated with B7-H4-mediated immune evasion in ovarian clear cell carcinoma and with response to tisotumab vedotin in preclinical models.

Yutaro Mori, Ryo Tamura, Kotaro Takahashi, Kosuke Yoshihara

Niigata University, Niigata, Japan

Objective: Ovarian clear cell carcinoma (OCCC) characteristically overexpresses Tissue Factor (TF; *F3*), yet its biological significance and therapeutic implications remain unclear. We aimed to elucidate the impact of TF expression in OCCC and evaluate the antitumor efficacy of the anti-TF antibody-drug conjugate, tisotumab vedotin (TV), *in vitro and in vivo* models.

Methods: We performed bulk RNA sequencing (RNA-seq) of 112 clinical OCCC cases to identify transcriptomic features of *F3*-high tumors. We then applied single-nucleus RNA-seq (snRNA-seq) to three *F3*-high and three *F3*-low cases to characterize tumor biology at the single-cell level. Based on these transcriptomic results, we focused on immune-related pathways and immune-checkpoint molecules, with emphasis on *VTCN1* (B7-H4). Immunohistochemistry for TF and B7-H4 was performed on 57 OCCC specimens. Finally, we assessed TV activity in patient-derived OCCC spheroids and xenografts.

Results: *F3*-high tumors exhibited lower immune scores with upregulation of MYC and cell cycle pathways, and suppression of inflammatory and immune pathways in bulk RNA-seq. Consistently, snRNA-seq showed similar trends in cancer cells, and immune fractions were significantly reduced in *F3*-high tumors, indicating an immunologically “cold” state. Notably, the immune-checkpoint molecule *VTCN1* was highly expressed in *F3*-high tumors and positively correlated with *F3* expression. Immunohistochemistry confirmed that B7-H4 was significantly overexpressed in TF-positive tumors, showing a positive correlation between TF and B7-H4 expression.TV activity correlated with TF abundance *in vitro* and induced marked growth inhibition in *F3*-high xenografts; residual tumors showed decreased TF and B7-H4 expression.

Conclusions: TF-high OCCC shows a distinct gene expression pattern, particularly an immunologically cold subtype with B7-H4-mediated immune evasion. TV demonstrates TF-dependent activity, supporting TF as a therapeutic target, and providing rationale for TV-based monotherapy or combinations with immunotherapy in OCCC.

#1762 An avidity-driven, dual-targeting ADC with superior tumor selectivity for the treatment of solid tumors.

Steffen Runz, Paul Sauter, Sebastian Latwiel, Jennifer Volkind, Jawad Iqbal, Wilma Neumann, Helga Groetsch, Dina Osmanovic, Abdul-Habib Maag, Anja Schreiber, Christine Kohler, Tatjana Schneidt, Anna Pryszlak, Christoph Erkel, Richard J. Austin

VERAXA Biotech GmbH, Heidelberg, Germany

Background
Antibody drug conjugates (ADCs) represent one of the most promising therapeutic modalities in recent years. However, the full therapeutic potential of ADCs is hampered because many tumor antigens are also expressed in healthy tissues, causing *on-target, off-tumor* toxicities. Other toxicities are caused by *off-target* uptake of ADCs in healthy cells or by systemic payload exposure as consequence of unstable conjugation. These issues have restricted a successful implementation of highly potent payloads such as pyrrolobenzodiazepine dimers (PBD).
Method
We developed a bispecific ADC (bsADC) which requires the simultaneous binding to two tumor-associated antigens (TAAs) to mediate cytotoxic activity (AND-gate approach). Co-expression of the TAAs is only found in tumor cells. Cell killing is therefore restricted to tumor cells. Healthy cells, which express only one of the TAAs, are spared. Our lead candidate comprises a bispecific antibody linked to a PBD prodrug at a DAR of 2 via a tumor-selective glucuronide linker using our proprietary site-specific, click-based glycan conjugation platform, which minimizes *off-target* toxicity by two mechanisms: first, using a highly stable linker, the payload is not released in circulation but only inside cells expressing both targets; second, hydrophilic chemistry prevents target-independent uptake.
Results
We identified a TAA pair that is highly co-expressed in various solid tumors including TNBC and NSCLC, while co-expression in healthy tissues is limited. It therefore represents a promising target combination for the development of an AND-gated bsADC with enhanced tumor-selectivity. Our lead candidate makes use of a pronounced avidity binding due to low monovalent affinities for both targets. This translates into superior internalization as well as potent killing of tumor cell lines expressing both targets in comparison to healthy cells expressing one target, resulting in an increased therapeutic window. In co-culture assays, the bsADC induced bystander killing of target-negative cells, indicating the bsADC should be efficacious in tumors where co-expression of both targets is not 100% penetrant. In vivo, our candidate dose-dependently reduced the tumor burden in mice bearing cell line-derived xenograft (CDX) models of breast cancer. In addition, the bsADC was well-tolerated up to high dose levels in mice and showed high stability in vitro and in vivo.
Conclusion
By combining an AND-gated, dual-targeting approach with our hydrophilic, highly tumor-selective, and stable ADC conjugation platform, we have generated a bsADC with superior tumor specificity. This enables the application of a potent PBD prodrug for highly efficient anti-tumor activity. Our lead bsADC for the treatment of lung and breast cancers has entered formal preclinical development and IND-enabling studies.

#1763 BSI-737, a best-in-class B7H3xPD-L1 bi-specific ADC with dual function to eliminate tumor via selective killing and exacerbated anti-tumor immune response.

Hui-Han Hu[1], Xiaoyao Hao[1], Yue Gao[1], Hongyan Li[1], Jinyu Liu[1], Jinge Zhao[1], Yi Lu[1], Liezhou Ji[1], Zhigang Ma[1], Mingjiu Chen[1], Kedan Lin[2]

[1]Biosion Inc., Nanjing, China,[2]Biosion USA Inc., Delaware, DE

Background: B7H3 and PD-L1 are both inhibitory immune checkpoints. The dual targeting of B7H3 and PD-L1, which are prevalently co-expressed in various malignancies, may synergistically enhance anti-tumor immune response. PD-L1-directed ADCs have shown modest efficacy with no target-related safety issues. B7-H3, by comparison, is a clinically validated ADC target that tolerates high-dose exposure without target-mediated toxicity and supports added immune-checkpoint blockade. B7H3xPD-L1 bi-specific ADC may hold promise via bi-specific binding mode, cytotoxic agent-mediated immunogenic cell death, and exacerbated anti-tumor immune response.

Methods: The B7H3xPD-L1 bi-specific antibody was composed of humanized anti-PD-L1 and anti-B7H3 antibodies identified from A/J mice immunized with PD-L1-ECD-Fc and HG5042 mice immunized with B7H3-EDC-Fc, respectively. The final bi-specific construct was selected based on simultaneous binding to B7H3 and PD-L1, efficient cell internalization, and strong PD-1/PD-L1 signal blocking. The bi-specific antibody was conjugated to exatecan via a glycol-site-specific conjugation technology in a DAR of 4. The anti-tumor activity of BSI-737 was investigated in cell-derived xenograft models with various expression levels of B7H3 and PD-L1. The CMC developability as well as the stability of BSI-737 in mouse and human plasma were also assessed.

Results: BSI-737 simultaneously bound to B7H3 and PD-L1 with high affinity and showed strong PD-1/PD-L1 signal blocking activity. The binding of BSI-737 resulted in efficient antibody-induced internalization across cell lines expressing various levels of B7H3 and PD-L1. When conjugated to exatecan via a cleavable linker in DAR of 4, BSI-737 demonstrated an outstanding anti-tumor activity compared to clinical benchmarks. A single administration of BSI-737 resulted in a complete tumor regression in a CDX model expressing high level of B7H3 with a survival rate of 100% by the end of the study. A significant anti-tumor activity of BSI-737 after a single administration was also observed in a B7H3-medium expressing model. BSI-737 possessed a favorable CMC developability profile.

Conclusion: BSI-737 is a B7-H3 × PD-L1 bispecific ADC with best-in-class potential, leveraging dual targeting to enable selective tumor cell killing while amplifying anti-tumor immune responses. The current pre-clinical data highlight the potential of BSI-737 across expression levels of B7H3 and further pharmacokinetics, toxicity, and IND-enabling studies are underway.

#1764 MC003: A novel bi-epitope, dual-payload, fixed-combination chemoimmunotherapy antibody drug conjugate for the treatment of folate receptor alpha-expressing ovarian cancer.

Seah H. Lim[1], Hailiang Zheng[2], Peipei Zhong[2]

[1]Medicovestor, Inc., New York, NY,[2]Sanyou Biopharmaceuticals, Shanghai, China

Background: Folate receptor alpha (FRα) is overexpressed in approximately 80% of epithelial ovarian cancers (EOC), but with limited expression in most normal tissues. FRα is, therefore, an ideal therapeutic target for antibody drug conjugates (ADCs). In patients with platinum-resistant ovarian cancer, where treatment options are scarce and outcomes remain dismal, FRα-targeted ADCs have emerged as a promising approach. To enhance therapeutic efficacy and overcome drug resistance, we developed a novel bi-epitope, dual-payload FRα-targeted ADC, designated MC003 (ADoTope FRα ADC), and evaluated its preclinical pharmacology, efficacy, and safety profile.

Methods: A panel of fully human monoclonal antibodies specific for FRα was isolated from a human v-gene phage display library. Through biolayer interferometry (BLI), two high-affinity antibodies, Clone 65 and Clone 91, were identified to bind distinct, non-overlapping epitopes on FRα with comparable KD values. Clone 65 was conjugated to gemcitabine, a nucleoside analog, and Clone 91 to exatecan, a potent topoisomerase I inhibitor, both via enzyme-cleavable linkers. Each ADC achieved an average drug-to-antibody ratio (DAR) of approximately 8. The fixed 1:1 combination of the two ADCs constituted MC003, representing the ADoTope dual-payload format.

Results: Both Clone 65 and Clone 91, in their unconjugated forms, demonstrated robust antibody-dependent cellular cytotoxicity (ADCC) against FRα-positive SKOV3 ovarian cancer cells but lacked complement-dependent cytotoxicity (CDC). When conjugated, MC003 exhibited markedly enhanced cytotoxic potency in vitro compared to either single-payload ADC, indicating synergistic antitumor activity. In SCID mice bearing established SKOV3 xenografts, MC003 achieved superior tumor growth suppression relative to mirvetuximab soravtansine, a clinically approved FRα ADC. Histological analysis revealed increased intratumoral $CD8^+$ T-cell infiltration, dendritic cell maturation, and upregulation of MMP9, suggesting immune activation within the tumor microenvironment. Single-dose toxicology studies in Sprague Dawley rats and cynomolgus monkeys demonstrated that MC003 was well tolerated up to 20 mg/kg—approximately 6.5-fold above the pharmacologically active dose—with no evidence of bone marrow suppression, hepatotoxicity, or nephrotoxicity.

Conclusions: ADoTope enhances FRα targeting by simultaneously engaging two distinct epitopes, effectively functionally increasing the antigen density and enabling the co-delivery of mechanistically distinct cytotoxic payloads. MC003 also mediates efficient ADCC and induces immune activation. These preclinical findings support the advancement of MC003 into IND-enabling studies as the next-generation therapeutic for platinum-resistant ovarian cancer.

#1765 YL413: A novel dual-payload anti-HER2 antibody-drug conjugate demonstrating potent preclinical activity.

Hanwen Deng, Tao Wang, **Wei Lian**, Tingting Mao, Qing Zong, Chun Deng, Bingsong Xie, Tongtong Xue, Jiaqiang Cai

MediLink Therapeutics (Suzhou) Co., Ltd., Suzhou, China

Antibody Drug Conjugates (ADC) have achieved great success as anti-cancer therapies, with 21 ADC drugs approved in the global market. Despite the initial response to ADC treatment, drug resistance and tumor relapse inevitably happen, driven by high heterogeneity in advanced tumors. Overcoming these resistance mechanisms is a critical challenge to next-generation ADC development for cancer therapy. To address these challenges, we developed YL413, a novel anti-HER2 ADC with two payloads of different MOAs: a topoisomerase 1 inhibitor and a microtubulin inhibitor. This dual-payload strategy is designed to mitigate resistance associated with single-agent therapies. YL413 was engineered with an appropriate drug-to-antibody ratio (topoisomerase I inhibitor to microtubule inhibitor) to optimize the therapeutic window. Trastuzumab, topoisomerase I inhibitors, and microtubule inhibitors were expected to demonstrate anti-tumor activity in clinical trials. In vitro, YL413 demonstrated comparable binding and internalization in the HER2+ cell line to Trastuzumab. YL413 demonstrated better cytotoxicity than Mon-payload ADCs against tumor cells in vitro. In Vivo, the dual-payload ADC exhibited superior efficacy in CDX models and the Ehertu-resistance models. In summary, we developed HER2 dual-payload ADCs to address Topo1 inhibitor-induced tumor resistance. The dual-payload HER2 ADC exhibited strong anti-tumor activity in vitro and in vivo, indicating potential to overcome Enhertu® resistance. YL413 retains Topo1 inhibitor efficacy, supplemented by a microtubule inhibitor, with possible use in earlier treatment lines.

#1766 Dual EGFR and Bcl-2 inhibition overcomes resistance in sinonasal squamous cell carcinoma.

Rhea Raghavan[1], Athena Apfel[1], Habib Serhan[1], Angel Qin[1], Chia-Jen Liu[2], Maryam Nakhjiri[1], Sofia D. Merajver[1], Aaron Udager[2], Nathan Merrill[1]

[1]Department of Internal Medicine, University of Michigan, Ann Arbor, MI,[2]Department of Pathology, University of Michigan, Ann Arbor, MI

Background: Sinonasal cancers are rare head and neck malignancies. Although outcomes for other head and neck cancers have improved, those for sinonasal cancers remain stable, with 5-year overall survival at 55%. This study focuses on sinonasal squamous cell carcinoma (SNSCC), which develops in the mucosal epithelium and accounts for nearly 61% of sinonasal malignancies. A strong association exists between inverted sinonasal papilloma (ISP) and the development of SNSCC, with approximately 50% of cases progressing to malignancy that harbors epidermal growth factor receptor (EGFR) exon 20 mutations. These EGFR-mutated SNSCCs have a significantly poorer prognosis than other sinonasal tumors, underscoring the need for more effective therapies.
Methods: We sought to identify therapeutic partners for EGFR inhibitors that could enhance the effectiveness of EGFR blockade. We focused on pairing pathways orthogonal to EGFR activation, such as apoptosis inhibition. To identify synergistic drug pairings with optimal activity, we screened a library of >1,000 signaling inhibitors. Drug sensitivity scores (DSS3) were calculated, identifying Bcl-2 inhibitors as potential synergistic partners with EGFR inhibition. Dose-response curves for EGFR and Bcl-2 inhibitors were generated, and synergy was assessed using the Chou-Talalay method across four cell lines (UM-SCC-112, UM-SCC-33, SCCNC4, MOP-IPST-1) in 3D culture. Western blotting examined expression of EGFR, pro-apoptotic markers (Bax), and pro-survival proteins (Bcl-2).
Results: Drug screening revealed that ISP-associated sinonasal carcinoma (SNC) cell lines were highly resistant to both standard and targeted single-agent therapies. In 3D *ex vivo* cultures, sinonasal papilloma and carcinoma PDOs showed partial responses to EGFR inhibitors, and EGFR inhibition alone failed to suppress growth or induce apoptosis. In contrast, dual or triple combinations of EGFR inhibitors with Bcl-2 and/or PI3K/AKT/mTOR pathway inhibitors produced synergistic cytotoxic effects, suggesting that co-targeting EGFR and anti-apoptotic pathways may overcome intrinsic resistance. Western blot analysis showed that resistant lines had reduced Bcl-2 expression, while lines with higher Bcl-2 levels demonstrated greater synergy with EGFR/Bcl-2 co-inhibition, including those with EGFR mutations, indicating reliance on alternative survival mechanisms.
Conclusions: Dual EGFR and Bcl-2 inhibition demonstrate synergistic anticancer potential in ISP-associated SNC, overcoming de novo resistance to EGFR-targeted therapy. These findings underscore the importance of targeting anti-apoptotic pathways in EGFR-mutant sinonasal cancers. Ongoing studies aim to define EGFR-Bcl-2 crosstalk and identify optimal drug combinations for *in vivo* testing.
AI disclosure: AI was used for language editing only; content was verified by the authors.

#1767 Preclinical efficacy of a first-in-class anti-SLC3A2 ADC in hard-to-treat solid and hematologic malignancies.

Qinhong Ma, Daizong Li, Kewei Zhao, Mary Q. Xu, **Mason Lu**

MedAbome, Inc., Fremont, CA

SLC3A2 (CD98 heavy chain, CD98hc, or 4F2hc) is a type II transmembrane glycoprotein that functions primarily as the heavy chain component of heterodimeric amino acid transporters (HATs). The aberrant overexpression of SLC3A2 has been linked to many types of cancer, such as lung cancer, breast cancer, colorectal cancer (CRC), pancreatic cancer (PDAC), and various types of hematologic malignancies. Using our proprietary live-cell immunization (LC-I) and high-throughput screening (LC-HTS) platforms, we developed MAb52-4.2, an anti-SLC3A2 monoclonal antibody that selectively recognizes a tumor-associated conformational epitope of SLC3A2, which significantly elevated expression levels in cancer cell lines, and exhibits minimal or no cross-reactivity with normal cells or tissues. Both the chimeric and humanized versions of MAb52-4.2 bound to recombinant SLC3A2-ECD with high affinities in the low single-digit nanomolar range. MAb52-4.2 cAb, containing two Fc point-mutations, was conjugated to MMAE through an MC-Vc-PAB linker to produce MAb52-4.2-ADC (DAR4). MAb52-4.2-ADC demonstrated potent antiproliferative effects *in vitro*, with cytotoxicity correlating with the target abundance and antibody internalization efficiency across a variety of cancer cell lines. A single intraperitoneal (*i.p.*) dose of MAb52-4.2-ADC at 4, 7, or 10 mg/kg effectively inhibited tumor growth in cell line-derived xenograft (CDX) mouse models of triple-negative breast cancer (TNBC), non-small cell lung cancer (NSCLC), gastric cancer (GC), and other tumor types, with subcutaneously inoculated tumors completely regressing within 24~30 days post-treatment. Preliminary toxicology studies indicated that MAb52-4.2-ADC did not raise any safety concerns. These findings support MAb52-4.2-ADC as a promising therapeutic candidate for treating solid and hematologic malignancies, and potentially mitigating toxicity concerns. Ongoing studies aiming to support further clinical investigation include MAb52-4.2-ADC in patient-derived xenograft (PDX) gastrointestinal (GI) cancer models, along with retrospective analyses of its target expression in clinical tumor samples.

#1768 High-sensitivity targeted mass spectrometry enables quantification of HLA-presented antigens for TCR-T therapeutic target discovery.

Simonas Savickas[1], Anamarija Pfeiffer[1], Arthur Viode[1], Liliana Malinovska[1], Oliver Bernhardt[1], Veronique Laforte[1], Lucy Yang[1], Roland Bruderer[1], Daniel Redfern[1], **Yuehan Feng**[1], Wayne Paes[2]

[1]Biognosys AG, Schlieren, Switzerland,[2]Greywolf Therapeutics, Oxford, United Kingdom

Background

Human leukocyte antigens (HLA) are key mediators of adaptive immunity, presenting antigenic peptides derived from self and non-self proteins for immune surveillance. Tumor-specific neoantigens generated by somatic mutations represent key determinants of immune recognition and are central to the development of targeted immunotherapies. Recent advances in immunopeptidomics have enabled systematic identification of these peptides; however, accurate quantification of immunogenic epitopes remains essential to assess their therapeutic relevance. Precise measurement of (neo)antigen abundance can inform the design of T-cell receptor (TCR)-based therapeutics, as well as personalized vaccines and cell therapies. Highly sensitive, quantitative methods for profiling peptide presentation across cell or tissue materials are therefore critical to advancing precision immuno-oncology and immune-modulatory therapies.

Method

Current methodologies to measure presented antigens are hampered by low sensitivity, and laborious optimization procedures. To overcome these issues, we applied a targeted mass spectrometry approach (FAIMS-PRM) combined with a one-step collision energy (CE) optimization, as described in a recent publication (Salek et al. 2024) workflow to systematically optimize collision energy and improve assay sensitivity. This streamlined method enables robust, cost- and time-efficient development and optimization of targeted assays for immunopeptides using minimal input material: 25 million cells or 15 mg of fresh-frozen tissue. Incorporating stable isotope-labeled internal standards (SIS peptides) allowed absolute quantification and estimation of copy number per cell.

Results

To demonstrate the performance of the optimized workflow, we quantified HLA I-presented (neo)antigens in multiple cell lines, including SK-MEL-5, Raji and HCT116. The analysis panel comprised peptides derived from well-established TCR-T and tumor-specific antigen (TSA) targets such as PRAME, MAGE-A1, and NY-ESO-1, alongside candidate antigens identified in prior discovery studies. Application of the collision energy-based optimization improved signal intensity for approximately 50% of targeted peptides compared with default settings. The method achieved lower limits of quantification (LLOQ) in the low single-digit range (1-3 copies per cell), enabling precise quantification of low-abundance immunopeptides. These results illustrate the sensitivity and robustness of the workflow for accurate measurement of clinically relevant HLA-presented targets.

In conclusion, these advances provide a sensitive and efficient workflow for quantitative assessment of HLA-presented peptides across disease and healthy samples, supporting identification of promising targets for immunotherapy development.

#1769 LY4170156, an antibody-drug conjugate targeting folate receptor alpha, exhibits enhanced antitumor activity in combination with standard-of-care therapies in preclinical ovarian cancer models.

Zhaohai Lu[1], Chun Ping Yu[2], Jack A. Dempsey[1], Wei Guo Xu[2], Lisa Kays[1], Bonita D. Jones[1], Andrew Capen[1], Xueqian Gong[1]

[1]Eli Lilly and Company, Indianapolis, IN,[2]Lilly (China) R&D Center, Shangai, China

LY4170156 is an antibody-drug conjugate targeting folate receptor alpha (FRα). It is composed of a humanized IgG1 monoclonal antibody with silenced Fc function, a proprietary polysarcosine hydrophobicity-masking agent with a dipeptide-cleavable linker, and a topoisomerase I inhibitor exatecan payload with a drug-to-antibody ratio of 8:1. In preclinical studies, LY4170156 was active against various FRα-expressing tumors[1], including those with low/moderate (0 - <75%)[2] FRα expression.[1] The Phase 1 trial (NCT06400472) indicated that LY4170156 was well-tolerated and resulted in durable clinical efficacy in heavily pretreated patients with platinum-resistant ovarian cancer (PROC), regardless of FRα levels or prior mirvetuximab soravtansine-gynx treatment, and without grade ≥3 drug-related ocular, neuropathy, or alopecia events.[3] The Phase 3 study (NCT07213804) evaluates LY4170156 as monotherapy in patients with PROC and in combination with bevacizumab in patients with platinum-sensitive ovarian cancer (PSOC). This study reports the preclinical activity of LY4170156, as a single agent and in combination with standard of care therapies (SoC) in ovarian cancer (OC) cell lines using in vitro 3D cell culture, and cell line-derived or patient-derived xenograft models. Sequencing of treatments was also assessed. CellTiter-Glo assay was used for evaluating cell viability in vitro after treatment of 7 days. Tumor volume and mice body weight were measured twice a week throughout the in vivo study. Assays using 5 OC cell lines demonstrated that when LY4170156 was combined with various SoC, it exerted enhanced growth inhibitory effects, independent of FRα expression levels. In vivo efficacy studies showed that LY4170156 combined with cisplatin with or without bevacizumab, bevacizumab, doxorubicin, or carboplatin plus paclitaxel resulted in superior and more durable antitumor responses compared to SoC alone. In addition, LY4170156 plus bevacizumab was highly effective as both first- and second-line treatment in tumor models with moderate responses to SoC. Furthermore, LY4170156 plus olaparib demonstrated enhanced antitumor activity in DNA repair-deficient models. Collectively, these findings offer further support for the clinical assessment of LY4170156 in patients requiring improved treatment options, including those with PROC and PSOC. [1]Viricel et al. AACR; Cancer Res. 2023; 83(7). [2] Moore K, et al. *N Engl J Med.* 2023;389(23):2162-2174 [3]Ray-Coquard et al. Presented at ESMO 2025.

#1770 Differential *in vitro* activity of amivantamab, cetuximab, and panitumumab against EGFR ECD resistance mutations.

Stacey L. Lehman[1], Himanshu Gupta[1], Rosa MF Cardoso[2], Laura A. Struzyna[3], Stephen W. Jarantow[3], Xuesong Lyu[4], Elsie Samakai[3], Emrullah Yilmaz[5], Sanjib Chowdhury[6], Joshua C. Curtin[1], Bharvin Patel[1]

[1]Johnson & Johnson, Oncology Translational Research, Spring House, PA,[2]Johnson & Johnson, In Silico Discovery, Spring House, PA,[3]Johnson & Johnson, Biologics Discovery, Spring House, PA,[4]Johnson & Johnson, Oncology Translational Research, Shanghai, China,[5]Johnson & Johnson, Clinical Oncology, Raritan, NJ,[6]Johnson & Johnson, Oncology Translational Research, Cambridge, MA

Epidermal growth factor receptor (EGFR) ectodomain (ECD) mutations are a known acquired resistance mechanism to EGFR monoclonal antibodies cetuximab and panitumumab in metastatic colorectal cancer (mCRC). Amivantamab, an EGFR-MET bispecific antibody with immune cell-directing activity, has demonstrated meaningful antitumor activity in several solid tumor types. Amivantamab, cetuximab, and panitumumab bind to EGFR domain III; however, the precise epitopes vary, which could lead to differential binding and activity against EGFR ECD resistance mutations. Here, we compare the activity of these EGFR-targeting agents against a panel of 29 EGFR ECD mutations historically associated with resistance to cetuximab and panitumumab. HEK293Ta cells expressing EGFR ECD-mutated variants were used for binding and functional assays of amivantamab, cetuximab, and panitumumab. Amivantamab demonstrated increased binding and functional activity against a wider range of EGFR ECD mutations, including the most prevalent V441, G465, and S492 mutations, relative to cetuximab and panitumumab. Furthermore, structural modeling of amivantamab bound to EGFR indicated that the amivantamab epitope is shifted away from EGFR residues 441-444 and 464-465, which are the regions that form more extensive interactions with cetuximab and panitumumab. Of note, amivantamab was inactive against ECD mutations occurring at K489 and I491, which were previously identified as a part of the amivantamab EGFR epitope. The preclinical activity of amivantamab against EGFR ECD mutations was corroborated in a clinical case study. In OrigAMI-1 (ClinicalTrials.gov Identifier: NCT05379595), a phase 1b/2 study evaluating amivantamab monotherapy among heavily pretreated *RAS/BRAF* wild-type mCRC, one participant was retrospectively found to carry an EGFR ECD S492R mutation by baseline tissue next-generation sequencing. This participant achieved a partial response, providing preliminary clinical evidence that amivantamab is active against a mutation demonstrated to confer resistance to cetuximab. In conclusion, amivantamab may be more active against a wider range of EGFR ECD resistance mutations compared with cetuximab and panitumumab.

#1771 Synergistic lethality of combination treatment with Trop2-directed antibody-drug conjugate (IMMU-132) and Apo2L/TRAIL in triple negative breast cancer (TNBC).

Yonit Addissie, Yoshimi Endo Greer, Stan Lipkowitz

National Cancer Institute, Bethesda, MD

Background: Sacituzumab govitecan (IMMU-132) is an antibody drug conjugate targeting trophoblastic cell surface antigen 2 (Trop2) that's approved for treatment of patients with metastatic TNBC who have received two or more prior systemic therapies. The cytotoxic payload of IMMU-132 is a topoisomerase I inhibitor (SN-38) that kills cancer cells by causing DNA damage. Efforts to enhance the efficacy of IMMU-132 treatment include combination therapy with other agents. Apo2L/TRAIL interacts with death receptors on the cell surface to induce apoptosis in cancer cells, sparing normal cells. We previously have shown that TNBC is most sensitive to Apo2L/TRAIL. We investigated whether combination treatment with IMMU-132 and Apo2L/TRAIL synergistically inhibit TNBC cell growth.

Methods: Human TNBC cell lines treated *in vitro* with IMMU-132 and Apo2L were assessed for cell viability via a propidium iodide-based cell death assay and ATP cell viability assay. The mode of cell death elicited by combination treatment was also investigated by using inhibitors of apoptosis, necroptosis and ferroptosis. Effects of treatment on cell cycle arrest were explored using flow cytometry. *In vivo,* NCr athymic nude (nu/nu) female mice with HCC1806 TNBC xenografts were treated with IMMU-132 and Apo2L after which tumor growth and survival were monitored.

Results: Combination treatment with IMMU-132 and Apo2L synergistically induced cell death in triple negative breast cancer cell lines with high Trop2 expression (e.g. HCC1806, MDA-MB-468) but did not in the Trop2 low expressing MDA-MB-231 cell line. In some Trop2 low TNBC cell lines (e.g. BT-549, SUM-159), combination treatment also showed synergistic induction of cell death, suggesting extracellular deconjugation of the SN-38 cytotoxic payload and diffusion into cells. The synergy seen in Trop2 low TNBC cell lines was abrogated by limiting drug incubation periods - which minimizes the extracellular deconjugation. In contrast, the synergy seen in Trop2 high cells was maintained in these short incubation assays. Caspase activation assays and viability assays with caspase inhibitors showed that the primary mechanism of cell death for Apo2L and combination treatment with IMMU-132 is through apoptosis. Furthermore, flow cytometry-based cell cycle assays showed that IMMU-132 and combination treatment with Apo2L induce cell cycle arrest at the G2/M stage. Our xenograft model also showed significant antitumor effects with SG and TRAIL agonist combination treatment including decrease in tumor growth and improved survival in HCC1806 bearing mice.

Conclusions: The data suggest a synergistic effect of combination treatment with Trop2 antibody drug conjugate IMMU-132 and TRAIL agonists in killing TNBC cells.

#1772 HER3-targeted nano-bioparticles deliver 5′-triphosphate-modified FOXC1 siRNA to induce tumor regression and immune activation in HER3$^+$ cancers.

Amirhesam Babajani[1], Felix Alonso-Valenteen[1], James Teh[1], Nelyda Gonzalez[1], Simoun Mikhael[1], Michelle Wong[1], Xiaojiang Cui[1], Ravinder Abrol[2], Lali K. Medina-Kauwe[1]

[1]Cedars-Sinai Medical Center, Los Angeles, CA,[2]California State University, Northridge, Los Angeles, CA

Purpose: HER3 is frequently overexpressed in a range of solid tumors and contributes to resistance against both targeted and chemotherapies. To address this, we developed a triple-function therapeutic approach using HER3-targeted HPK nanocapsid (NC) to deliver FOXC1-specific siRNA, thereby silencing this master transcriptional regulator of tumor aggressiveness and metastasis. The siRNA was synthesized with T7 polymerase to incorporate a 5′-triphosphate (5′-ppp) moiety, which serves as an activator of cellular immune responses. This strategy enables targeted and protected delivery of siRNA cargo, while simultaneously achieving FOXC1 silencing and tumor-intrinsic activation of cellular Interferon response.
Methods: HPK proteins were engineered to self-assemble into virus-like NCs capable of encapsulating siRNA. We evaluated the properties, stability, and morphology of the nanoparticles. HPK design incorporates the adenovirus penton base protein for membrane penetration and neuregulin for HER3-targeted binding. T7-transcribed FOXC1 siRNAs (HSiFox-T7) were packaged into HPK NCs and evaluated in HER3$^+$ tumor cell lines and mouse models. We assessed cytokine production, cell viability, interferon role in cell cytotoxicity, FOXC1 knockdown, migration, immune cell infiltration, and in vivo therapeutic efficacy in both HER3$^+$ immunodeficient melanoma and immunocompetent triple-negative breast tumor (TNBC) models.
Results: The HPK and T7-transcribed siRNA formed stable and smaller nanoparticles compared to synthetic siRNAs. In vitro, T7-derived 5′-ppp siRNAs induced greater cytotoxicity than synthetic controls mainly via activated type I interferon response. HSiFox-T7 achieved robust FOXC1 knockdown, significantly reducing cell migration and viability. In vivo, systemic administration of HSiFox-T7 suppressed tumor growth and increased type I interferon response in immunocompromised HER3$^+$ melanoma models. It also suppressed FOXC1, reduced metastatic lung burden, and increased tumor apoptosis with minimal off-target toxicity while protecting siRNA content in the circulation of immunocompetent TNBC mice model. Treatment enhanced infiltration of NK cells and CD8$^+$ T cells into both primary tumors and metastases, indicating strong immunostimulatory effects.
Conclusions: HPK NCs represent a multifunctional platform that combines HER3-targeted delivery, master gene silencing, and immune activation. The HSiFox-T7 system effectively suppressed HER3$^+$ tumor growth and metastasis while reprogramming the tumor microenvironment toward immune responsiveness. This triple-action strategy overcomes major barriers in siRNA therapeutics including protecting nucleic acid content in circulation and avoiding off-target effects while offering translational potential for treating aggressive cancers such as TNBC and melanoma.

#1773 Development and characterisation of a novel monoclonal antibody against overexpressed integrin α6β4 on human pancreatic cells.

Gustavo Arias[1], Angus G. Dalgleish[2], Izhar Bagwan[3], Said Khelwatty[1], Satvinder Mudan[2], Tony Walker[1], **Helmout Modjtahedi**[1]

[1]Kingston University London, Kingston upon Thames, United Kingdom,[2]St George's Hospital, University of London, London, United Kingdom,[3]Royal Surrey Hospital, Guildford, United Kingdom

Despite major advances in the diagnosis and treatment of patients with cancer, pancreatic cancer remains one of the most aggressive and fatal cancer types. There is an urgent need for the discovery of additional therapeutic targets and the development of more effective therapeutics. Monoclonal antibody (mAb) technology is an excellent tool for the discovery of overexpressed cell surface tumour antigens, and antibodies generated may have significant diagnostic and therapeutic value. Here, we report the generation and characterisation of a novel antibody KU44.71 against the human ductal pancreatic adenocarcinoma metastasised to the liver cell line CFPAC-1, using hybridoma technology. Following screening, mAb KU44.71 which was directed against overexpressed cell surface antigens on pancreatic cancer cells was selected and purified by affinity chromatography. Further characterisation of the mAb was performed by ELISA, flow cytometry, cell proliferation assay, internalisation studies, immunoprecipitation and mass spectrometry, western blotting, and immunohistochemistry. We discovered that KU44.71 recognises the external domain of integrin α6β4 that is overexpressed by varying amounts in pancreatic cancer cell lines, derived from different sources including primary pancreatic cancer, liver metastasis, ascites and lymph node metastasis. Treatment with the naked antibody did not affect growth of α6β4 expressing pancreatic cancer cells. In contrast, exposure to anti-α6β4 KU44.71 induced internalisation of integrin α6β4 in pancreatic cancer cells. Furthermore, KU44.71 was found to be effective in detecting α6β4 expression by western blot and immunohistochemistry. Our results suggest that mAb KU44.71 is an useful tool for studying the role of α6β43 in the complex biology of human cancer, and for investigating the relative expression, prognostic significance, and predictive value of integrin α6β43 in patients with pancreatic cancer. Further studies are warranted to elucidate the therapeutic potential of this novel mAb including its humanised or drug conjugated versions in patients with α6β43 overexpressing pancreatic and other type of cancer.

#1774 ACR317, a novel CDH17-ADC, shows potent efficacy in preclinical gastrointestinal cancer models.

Zhenwei Miao, Feng Wang, Yaowu Li, Shanhui Weng, Li Yang

Hangzhou Adcoris Biopharma Co., Ltd., Hangzhou, China

Background:Cadherin-17 (CDH17) is a well-validated target with high expression in gastrointestinal (GI) cancers, including colorectal (CRC) and gastric cancer, while its expression in normal tissues is restricted to the basolateral membrane of intestinal epithelial cells. This unique expression pattern makes CDH17 an attractive therapeutic target for antibody-drug conjugates (ADCs). The development of effective ADCs for GI malignancies, particularly for CRC, remains a significant challenge. The landscape is largely dominated by DS-8201, with many other candidates failing due to efficacy or safety concerns. Here, we present the preclinical profile of ACR317, a novel CDH17-targeting ADC developed using Adcoris' proprietary platform, designed to address this unmet need.
Methods: IBR217 antibody, was isolated from a naïve fully human phage display library based on its high specificity and affinity for human CDH17. The binding affinity of IBR217 was determined by bio-layer interferometry (BLI), tumor cell binding activity was evaluated by flow cytometry, and internalization efficiency was assessed using a Fab-ZAP cytotoxicity assay. ACR317 was generated by site-specifically conjugating IBR217 to a novel topoisomerase I inhibitor payload using Adcoris' proprietary MuSC™ conjugation platform, achieving a drug-to-antibody ratio (DAR) of 8. *In vivo* antitumor activity was evaluated in multiple CDH17-positive and negative gastric and colorectal cancer cell-derived xenograft (CDX) models, with an IBR217- Dxd ADC included as a benchmark.
Results: IBR217 exhibited high affinity for human CDH17, with a binding affinity (KD) of 2.47 nM, and demonstrated excellent specificity by showing no binding to other cadherins. It also displayed potent binding to CDH17-positive tumor cells, with a half-maximal effective concentration (EC50) of 0.30 nM, and was subsequently efficiently internalized by these cells. ACR317 was successfully generated with a drug-to-antibody ratio (DAR) of 8. The resulting ADC ACR317 demonstrated significant tumor growth inhibition in preclinical CDX models, showcasing superior efficacy compared to the IBR217-Dxd benchmark in two CDH17-positive gastric cancer and four CRC CDX models. As expected, it showed minimal activity in a CDH17-negative gastric model, confirming its target-dependent mechanism. In these studies, ACR317 was well tolerated, with no significant body weight loss or other observable toxicities noted. Pharmacokinetics and safety studies in cynomolgus monkeys are ongoing.
Conclusions: ACR317 is a novel, highly specific CDH17-targeting ADC. The compelling preclinical efficacy observed suggest its therapeutic potential and form a solid foundation for subsequent clinical investigation in CDH17-positive gastrointestinal cancers.

#1775 ACR335, a novel cMET/EGFR bispecific dual-payload antibody-drug conjugate, demonstrates potent and broad antitumor activity in preclinical models of solid tumors.

Zhenwei Miao, Feng Wang, Shanwei Weng, Li Yang, Wu Yao

Hangzhou Adcoris Biopharma Co., Ltd, Hanghzou, China

Background: cMET and EGFR are frequently co-expressed oncogenic drivers in solid tumors, with pathway crosstalk driving therapeutic resistance. This combination is clinically validated by amivantamab, a bispecific antibody (BsAb) targeting cMET and EGFR approved for EGFR-mutant NSCLC. To enhance efficacy and overcome resistance, we developed ACR335, a bispecific ADC (BsADC) that simultaneously targets both receptors. Furthermore, ACR335 is engineered as a dual-payload ADC, combining a Topoisomerase I (Top1) inhibitor and a non-Top/non-Tubulin inhibitor, a strategy designed to synergistically maximize tumor cell killing.
Methods: The BsAb IBR335 combines a fully human anti-cMET antibody (isolated from a naïve phage library) with an engineered version of panitumumab (anti-EGFR). Binding affinity for cMET and EGFR was determined by BLI, tumor cell binding by flow cytometry, and internalization efficiency by a Fab-ZAP cytotoxicity assay. ACR335 was generated by site-specifically conjugating IBR335 to a Top1 inhibitor and a non-Top/non-Tubulin inhibitor using the MuSC™ platform, achieving a DAR of 4+4. Antitumor efficacy was evaluated in multiple cMET/EGFR-positive CDX models, including KATO-III (gastric), H1650 (NSCLC, EGFR Ex19del), Calu-6 (NSCLC, EGFR-wt), HT1376, and SW780 (bladder), with single-payload ADCs or a Dxd-ADC as benchmarks.
Results: IBR335 exhibited a 27.5-fold higher binding affinity for human cMET (KD = 0.149 nM) than for EGFR (KD = 4.1 nM), with sub-nanomolar EC_{50} binding to cMET/EGFR-positive tumor cells comparable to amivantamab and efficient internalization. This preferential targeting strategy mitigates potential on-target off-tumor toxicity associated with broad EGFR inhibition. The resulting ADC, ACR335, was homogeneous with a DAR of 4+4. It demonstrated potent *in vitro* cytotoxicity and induced significant tumor growth inhibition and regression across multiple CDX models, showing superior efficacy to single-payload ADCs and the Dxd-ADC benchmark. ACR335 was well-tolerated with no significant toxicity observed. Pharmacokinetic and safety studies in cynomolgus monkeys are ongoing.
Conclusions: ACR335 is a first-in-class cMET/EGFR bispecific dual-payload ADC with a unique pharmacological profile. The compelling preclinical data underscore its potential as a targeted therapy with an optimized safety profile. Phase I clinical trials are expected to commence in Q2 2026.

#1776 ALK101sc, a novel afucosylated bispecific antibody targeting EGFR and c-MET with common light chain demonstrates potent, broad-spectrum antitumor activity.

Li Li, Hongwang He, Mengfan Peng, Meiyu Yang, Jiajia Pan, Hui Feng

Allink Biotherapeutics, Shanghai, China

Acquired resistance to EGFR tyrosine kinase inhibitors (TKIs) represents a major clinical challenge in treating EGFR-mutant non-small cell lung cancer (NSCLC). This resistance arises either from secondary EGFR mutations (e.g., C797S) or via bypass signaling through the c-MET pathway—including c-MET mutation, gene amplification, or hepatocyte growth factor (HGF) upregulation. To overcome these mechanisms, we developed ALK101sc, an afucosylated IgG1 bispecific antibody (bsAb) co-formulated with hyaluronidase, designed to simultaneously target EGFR and c-MET. ALK101sc (120 mg/mL) was produced using a single-cell common-light-chain (CLC) platform, which ensured correct heterodimerization and scalable manufacturing without chain mispairing or exchange. In vitro functional assays demonstrated that ALK101sc effectively bound to EGFR/c-MET double-positive tumor cells, inducing receptor internalization and lysosomal degradation, and potently suppressed ligand-induced downstream signaling of both EGFR and c-MET, including phosphorylation of ERK and AKT. The afucosylated Fc region enhanced antibody-dependent cellular cytotoxicity (ADCC), thereby boosting FcγR-mediated antitumor immunity. In vivo, ALK101sc monotherapy induced significant tumor regression in both cell line-derived xenograft (CDX) and patient-derived xenograft (PDX) models, including those with EGFR mutations and/or c-MET-driven resistance. Furthermore, combining ALK101sc with osimertinib produced synergistic antitumor efficacy, even in the presence of TKI-insensitive mutations. Pharmacokinetic (PK) and GLP toxicology studies in cynomolgus monkeys following subcutaneous administration revealed typical antibody-like PK profiles, with systemic exposures comparable to amivantamab at equivalent doses and a bioavailability of approximately 89%. No significant abnormalities in safety pharmacology or toxicity were observed, with a no-observed-adverse-effect level (NOAEL) of 120 mg/kg. Together, these results demonstrate that ALK101sc exhibits antitumor potency comparable to amivantamab across preclinical models. Moreover, its CLC-based design provides a streamlined CMC development pathway, positioning it as a promising therapeutic candidate for overcoming EGFR TKI resistance. Compared with intravenous formulations, subcutaneous ALK101sc can substantially reduce administration time, improve patient convenience, and is expected to have a more favorable safety profile—characterized by meaningful reductions in infusion-related reactions (IRR) and venous thromboembolism (VTE) rates.

#1777 FL116, a PD-1/IL-18 bispecific antibody, enables cis-activation of PD-1$^+$ T cells and reshapes the suppressive tumor microenvironment (TME).

Haiming Huang[1], Quanxiao Li[1], Xiaotuan Zhang[1], Liwen Ji[1], Yanling Wu[2], Dong Wei[1], Tianlei Ying[2]

[1]Suzhou Forlong Biotechnology Co., Ltd, Shanghai, China,[2]Key Laboratory of Medical Molecular Virology (MOE/NHC/CAMS), Shanghai Institute of Infectious Disease and Biosecurity, School of Basic Medical Sciences, Fudan University, Shanghai, China

Background: IL-18 is a potent immune cytokine that promotes CD8$^+$ T-cell and NK-cell-mediated antitumor responses but is neutralized by IL-18BP. We previously engineered a panel of IL-18 variants which are completely resistant to IL-18BP inhibition. FL116 is a dual-function immunocytokine, in which an anti-PD-1 IgG was fused with one such IL-18 variant to achieve cis-delivery of IL-18R agonism to PD-1$^+$ T cells while bypassing IL-18BP in TME. The molecule aims to re-ignite pre-existing tumor immunity within the TME with minimal systemic toxicity.

Methods: FL116 was constructed by fusing the DNA coding sequence of an IL-18 variant that fully escapes IL-18BP neutralization with that of one heavy chain of an anti-PD-1 IgG to produce recombinant protein. Both binding domains of FL116 were confirmed by ELISA. The cis-acting of FL116 was evaluated by an engineered mammalian cell line which expresses both IL-18 receptors and PD-1. In vitro, the IFN-γ-inducing activity of FL116 was further validated using PBMC assays. In vivo, FL116 was assessed in MC38, CT26 and B16-F10 tumor models to evaluate its antitumor efficacy and safety.

Results: Both parts of FL116 preserved their binding and biological functions as validated by ELISA and PBMC assays. In vivo, FL116 produced strong and durable antitumor activity across tumor models. In MC38, FL116 achieved 98% tumor growth inhibition (TGI) and 2/5 complete response(CR). In CT26, FL116 showed 93% TGI and 3/5 CR. CT26 rechallenge revealed cured mice fully rejected tumor re-implantation without further treatment, indicating durable immune memory. In B16-F10 tumors, FL116 induced dose-dependent tumor regression and elevated intratumoral IFN-γ(8-fold) compared to the vehicle treatment, consistent with type-1 immune activation. TIL profiling showed substantial expansion of CD8$^+$ Tem(6-fold) and NK cells, increased cytotoxic markers(granzyme B), and enhanced DC activation. Suppressive myeloid cells were significantly reduced, with PMN-MDSC decreasing ~5-fold, leading to improved effector/suppressor ratios (CD8/MDSC 20-fold, CD8/Treg 6-fold). Peripheral blood composition remained stable, with slightly increases in CD8$^+$ Tem and NK maturation, indicating localized pharmacodynamic amplification rather than systemic inflammation. No body-weight loss was observed, and only mild, pharmacologically driven hepatosplenic enlargement occurred.

Conclusions: FL116 achieves potent antitumor activities, high CR rates, and rechallenge-confirmed immune memory while maintaining systemic immune homeostasis. By delivering decoy resistant IL-18 variant directly to PD-1$^+$ T cells, FL116 re-ignites intratumoral cytotoxic immunity and reshapes the TME toward a highly inflamed, effector-dominant state. These results support FL116 as a promising candidate for next-generation cytokine-fusion immunotherapy.

: Mechanisms of Drug Resistance 2
Poster Session

#1781 Improving response of pancreatic cancer to losartan: Mechanistic insights and implications for personalized therapy.

Heena Kumra[1], Ryo Morisue[1], Benjamin E. Wolf[1], Vasiliki Salameti[1], Sonu Subudhi[1], Nilesh P. Talele[1], Eric F. Zaniewski[2], Robert Morris[2], Tsion H. Tale[1], Karim El-Marouk[1], Cora Schueller[1], Mariagiovanna Barresi[1], Jennifer Schulz[1], Halil I. Corbali[1], Rieke Schleinhege[1], Peigen Huang[1], Pascal Bernatchez[3], Wilhelm Haas[2], Yves Boucher[1], Dai Fukumura[1], Rakesh K. Jain[1]

[1]Edwin L. Steele Laboratories, Department of Radiation Oncology, Massachusetts General Hospital and Harvard Medical School, Boston, MA,[2]Massachusetts General Hospital Cancer Center and Department of Medicine, Massachusetts General Hospital and Harvard Medical School, Boston, MA,[3]Centre for Heart Lung Innovation and Department of Anesthesiology, Pharmacology & Therapeutics, University of British Columbia, Vancouver, BC, Canada

Introduction: Pancreatic ductal adenocarcinoma (PDAC) is the third leading cause of cancer-related death in the United States, with a 5-year overall survival of ~13%. Delayed diagnosis, limited response to current treatments, and the predominance of locally advanced or metastatic disease contribute to poor outcomes. Leveraging our preclinical findings in PDAC murine models, we showed that adding losartan—an angiotensin II type-1 receptor (AT1) blocker—to FOLFIRINOX followed by chemoradiation doubled R0 resection rates to ~70% in locally advanced PDAC in a phase II trial (NCT01821729) (PMID: 31145418). However, the patient-response was variable. Here we recapitulated this variability in orthotopic PDAC mouse models and revealed the underlying mechanism.
Methods and Results: To investigate potential causes of the variable response, we mapped AT1 expression using light-sheet microscopy in AT1 reporter mice bearing orthotopic PDAC. We observed abundant AT1 throughout the tumor microenvironment. To define its functional relevance, we generated *Agtr1a* knockout (KO) PDAC cell lines and inducible KO mouse models. AT1 deletion in either cancer cells or stromal cells (but not α-SMA$^+$ myCAFs or pericytes) significantly reduced tumor growth. Because losartan is a pro-drug that needs activation by liver enzymes CYP3A4 and CYP2C9, we next examined its metabolism. We subcutaneously administered two major losartan metabolites, EXP3179 and EXP3174, to orthotopic PDAC-bearing mice and found that EXP3174 mediated the anti-tumor effects of losartan. Mass spectrometry of plasma samples revealed that while some tumor-bearing mice efficiently converted losartan to its active metabolite, others showed limited or no conversion. To determine the cause, we assessed CYP2C9 and CYP3A4 activity in liver microsomes from non-metastatic PDAC-bearing mice. CYP2C9 activity was markedly reduced and inversely correlated with tumor burden, providing a mechanistic basis for differential losartan activation. Ongoing work aims to determine whether PDAC patients likewise display variable plasma levels of losartan and EXP3174.
Conclusion: These findings identify impaired hepatic metabolism as a key driver of variable losartan responses in locally advanced PDAC. Mass-spectrometry-based assessment of losartan and EXP3174 levels may help determine which patients can effectively activate the drug. Given losartan's safety and low cost, its oral administration remains appropriate for most patients; however, in individuals with compromised CYP2C9 activity, administration of the active metabolite — EXP3174 may represent a more effective therapeutic option.

#1782 Exome-scale CRISPR screening reveals master controllers of cell state maintenance in high-risk neuroblastoma.

Grace McKay-Corkum, Stephanie Nance, Noha AM Shendy, Shilpa Narina, Shondra Miller, Alex Carisey, Qiqi Jin, Jiyang Yu, Adam D. Durbin

St. Jude Children's Research Hospital, Memphis, TN

A major limitation in cancer treatment is chemoresistance, particularly at relapse. Previously, relapse was thought to be driven by chemoresistance arising from new acquired genetic mutations; however, emerging evidence indicates that cancer cells exploit non-genetically-driven processes such as epigenetically regulated transcriptional plasticity to drive chemoresistance, invasion and proliferation. High-risk neuroblastoma (NB) demonstrates transcriptional plasticity with defined cell states and low mutational burden. NB cells exist primarily in two distinct states: a chemosensitive adrenergic state (ADRN) and a less common drug-tolerant persister cell state, the mesenchymal (MES) state. MES cells are enriched at relapse, suggesting that cells switch to this state under therapeutic pressure. Despite a myriad of approaches to treating high risk NB, relapsed patients have exceptionally poor survival. Unfortunately, mechanisms maintaining cell state and permitting state switching in NB are poorly understood. We hypothesize that dissection of the pathways promoting NB cell state plasticity will reveal new approaches to drive cell state interconversions that facilitate chemosensitivity. Thus, here, we took advantage of a recently developed novel fluorescent reporter system of the NB MES cell state developed by the Durbin Lab, to perform whole exome-CRISPR-cas12 knockout screening and identify master controllers of cell state maintenance in ADRN and MES-dominant cell lines. Integrated pathway analysis demonstrated conserved pathway modules involved in maintenance of cells in distinct cell states. To validate these findings, we performed targeted CRISPR knockouts in reporter carrying cells and identified changes in chemoresistance by chemosensitivity assays. To profile the effects of chemotherapy directly on cell state maintenance, we performed fluorescence reporter assays, followed by RNAseq to confirm changes in target loss nominated from CRISPR screens. Cell state switching is an intriguing paradigm by which NB cells may evade conventional therapies. We have identified pathways playing a role in maintaining either the ADRN or MES cell state in NB. Continued interrogation of these fundamental mechanisms represents a new approach that may potentially be leveraged for therapeutic gain.

#1783 ELF3-driven epigenetic reprogramming creates ERK pathway dependency in SERD-resistant ER+ breast cancer.

Na Zhang[1], Myles A. Brown[1], Rongbin Zheng[2], Kaifu Chen[3]

[1]Dana-Farber Cancer Institute, Boston, MA,[2]Boston Children's Hospital, Boston, MA,[3]Boston Children's Hospital, Bosotn, MA

Selective estrogen receptor degraders (SERDs) such as fulvestrant represent a promising therapeutic strategy for endocrine-resistant ER+ breast cancers. However, acquired resistance to SERDs remains a significant clinical challenge, and mechanisms underlying SERD resistance without ESR1 mutations are poorly understood. With the new generation of oral SERDs entering clinic, there is urgent need to understand the mechanisms of SERD resistance. Using genome-wide CRISPR knockout screens in parental and fulvestrant-resistant MCF7 cells, we identified ELF3 as a critical driver of SERD resistance. We then performed multi-omics profiling including RNA-seq, ATAC-seq, H3K27ac ChIP-seq, ER ChIP-seq and ELF3 ChIP-seq to characterize the parental and fulvestrant-resistant cell models. We found that SERD-resistant cells exhibited a stable $ER^{low}/ELF3^{hi}$ phenotype driven by a dysregulated ERα-ELF3 reciprocal negative feedback circuit. Multi-omics profiling revealed that ELF3 motifs ranked as the top enriched transcription factor binding motif in both gained ATAC-seq and H3K27ac peaks in the resistant cells. ELF3 ChIP-seq identified ~ 5,000 gained binding sites in resistant cells that co-localized with dramatic increases in chromatin accessibility and H3K27ac signals, confirming robust ELF3-driven enhancer activation of ER-independent survival programs. To assess ELF3-driven transcriptional changes associated with SERD resistance, we integrated ELF3 ChIP-seq data with RNA-seq data from both parental and SERD-resistant cells. We derived an ELF3 signature consisting of the top 500 genes that showed both increased ELF3 binding and elevated expression in the resistant cells. Pathway enrichment analysis revealed that ELF3 target genes are highly enriched in ERK signaling components. Experimental validation showed that resistant cells exhibited marked ERK pathway activation and developed strong dependency on ERK signaling, with increased sensitivity to MEK inhibitor trametinib. Re-analysis of single-cell RNA-seq from a metastatic breast cancer cohort confirmed that $ER^{low}/ELF3^{hi}$ tumor cells show enrichment of the ELF3 signature and increased ERK signaling compared to $ER^{hi}/ELF3^{low}$ cells. We define a novel mechanism of SERD resistance where the $ER^{low}/ELF3^{hi}$ state drives resistance by activating an ELF3-ERK signaling axis. Targeting this pathway may overcome resistance in $ER^{low}/ELF3^{hi}$ tumors.

#1784 Mechanistic characterization of (Z)-endoxifen in ESR1-mutant and endocrine-resistant breast cancer.

Sandra Suarez Hammer[1], Alina Ustiugova[2], Anastasia Shneyderman[3], Alexander Veviorskiy[2], Khadija M. Alawi[2], Mikhail Korzinkin[3], Lucia Beaulieu[1], Hayley Erickson[1], Scott M. Blackburn[1], H. Lawrence Remmel[4], Steven Quay[1]

[1]Atossa Therapeutics Inc., Seattle, WA,[2]Insilico Medicine AI Limited, Abu Dhabi, United Arab Emirates,[3]Insilico Medicine Hong Kong Ltd., Hong Kong, China,[4]University Medical Center Utrecht, Utrecht, Netherlands

Background: ESR1 mutations (e.g.Y537S and D538G) drive ligand-independent ER activation and resistance in ER-positive breast cancer. (Z)-Endoxifen, the active tamoxifen metabolite, inhibits ER signaling, but its impact on ESR1-mutant signaling and therapy-resistant disease is not yet fully defined.

Methods: HEK293T cells were transfected with ESR1-WT or mutant plasmids together with an ERE-luciferase reporter and Renilla control. After 24 h, cells were treated with endoxifen, elacestrant (10 μM-0.01 nM), or 0.1% DMSO for an additional 24 h. Firefly luciferase activity was normalized to Renilla, and mean ± SD values from three independent experiments were used to generate dose-response curves. Transcriptomic analyses of 166 ESR1 Y537S and 45 ESR1-WT MCF-7 samples from PandaOmics were performed, and differential expression after endoxifen treatment was assessed using 27 treated and 25 untreated samples processed with limma and gseapy. Plasma and tumor samples were extracted by methanol precipitation with deuterated endoxifen-d_5 and quantified by UPLC-MRM on a Poroshell 120 EC-C18 column using a six-point calibration curve.

Results: (Z)-Endoxifen (ENDO) and elacestrant (ELAC) both produced dose-dependent inhibition of ER signaling in wild-type and mutant ESR1 constructs. At 100 nM, ENDO and ELAC showed comparable suppression of WT and three common ESR1 mutants, consistent with the ~80 nM steady-state ENDO plasma level in women taking 20 mg tamoxifen. At higher doses, ENDO more effectively inhibited Y537S and D538G than ELAC.

Test Agent	Wildtype	ESR1-Y537N	ESR1-Y537S	ESR1-D538G	ESR1-K303R
Endoxifen, 100 nM	94 ± 2 %	94 ± 0.1%	62 ± 15%	91 ± 2.4%	90 ± 3.5%
Endoxifen, 400 nM	95 ± 1.5%	94 ± 0.3%	69 ± 13.8%	91 ± 2.1%	91 ± 2.9%
Elasctrant, 100 nM	97 ± 1.8%	98 ± 0.2%	61 ± 19.7%	79 ± 3.2%	91 ± 2.7%

Transcriptomic analyses revealed that ENDO reversed key mutant-associated transcriptional programs in MCF-7 cells. ENDO significantly downregulated estrogen response, apoptosis, E2F-target, and Myc-target pathways while restoring oxidative phosphorylation, xenobiotic and fatty acid metabolism, p53 signaling, and DNA repair (FDR < 0.05). Transcription factor enrichment showed suppression of resistance-associated POU5F1 and SOX11, and reactivation of FOXA1, ELF3, and SPDEF. ENDO also reduced expression of three genes (MTMR7, IL20, CA12) from a six-gene poor-prognosis ESR1-mutant signature. In the ongoing EVANGELINE phase 2 trial (NCT05607004), mean (Z)-endoxifen plasma levels at 40 mg/day reached 278.5 ng/mL (≈746 nM).

Conclusion: In summary, (Z)-endoxifen and elacestrant both suppress ER-dependent transcription in ESR1-WT and mutant models, and clinically relevant (Z)-endoxifen concentrations are sufficient to inhibit mutant ESR1 activity. Endoxifen additionally reprograms key transcriptional and metabolic pathways associated with ESR1-mutant resistance and metastasis. These results support further evaluation of (Z)-endoxifen's pathway-level effects in ESR1-mutant breast cancer, and ongoing studies are testing its ability to block mutant ESR1-driven proliferation in preclinical models.

#1785 Aspects of the YBX1-dependent mechanism of drug resistance in hepatocellular carcinoma.

Yamile Abuchard Anaya[1], Ana Ayala Pazzi[2], Veerababu Nagati[1], Kaylee Renteria[1], Denise Soto[1], Manish Tripathi[1]

[1]Oncology and Medicine ISU, South Texas Center of Excellence in Cancer Research, The University of Texas Rio Grande Valley, Mcallen, TX,[2]UT Southwestern, Dallas, TX

Background: Hepatocellular carcinoma (HCC) is the most common type of primary liver cancer. In the Rio Grande Valley (RGV), high rates of obesity, diabetes, and MAFLD elevate HCC incidence, further worsened by socioeconomic disparities and limited healthcare access. Consequently, late-stage diagnoses and therapeutic resistance lead to poor patient outcomes, emphasizing the importance of understanding the molecular mechanisms behind HCC progression. Y-box binding protein 1 (YBX1) is a multifunctional regulator of transcription and translation involved in EMT, metastasis, and drug resistance in various cancers, including HCC. To investigate the downstream signaling pathways activated by YBX1 overexpression (OE), we developed puromycin-stable GFP-tagged YBX1 OE SK-HEP1 cell lines. These cell lines have been evaluated for their invasion, migration, proliferation, colony formation, and cell impedance properties. YBX1 OE influenced multiple downstream kinases. We identified a specific kinase responsible for oncogenicity and drug resistance. We will continue to characterize and validate the kinase activity using specific activators and inhibitors.
Methods: The TCGA was analyzed for the YBX1 profile in the human HCC cohort. SK-HEP1 cells were used to develop a puromycin-stable YBX1 OE cell line using lentiviral plasmids. The cell lines were also enriched for GFP expression. Functional assays included cell proliferation, colony formation, migration, invasion, and real-time impedance analysis using the xCELLigence system. MTT assays determined IC50 values. The Human Proteome Profiler Array was used for kinase array analysis. Kinase activator and inhibitor assays were also performed.
Results: Analysis of the TCGA revealed elevated YBX1 expression in HCC tumors compared to normal tissues, which correlates with poor survival and increased metastasis. In vitro, YBX1 overexpression boosted proliferation, migration, invasion, and colony formation, while knockdown diminished these effects. xCELLigence analysis confirmed faster growth kinetics in cells overexpressing YBX1. Phosphoproteomic profiling identified several YBX1-regulated kinases, including members of the Src family.
Conclusion: Stable SK-HEP1 models with differential YBX1 expression have been successfully established and characterized. These findings confirm YBX1's oncogenic role in HCC. Ongoing research involving kinase pathway inhibitors and activators may uncover new therapeutic targets to overcome resistance and enhance outcomes for HCC patients in the RGV and beyond.

#1786 Convergent FGFR-JAK signaling reprograms luminal identity and drives endocrine resistance in HR$^+$ breast cancer.

Yucheng Zeng[1], Ruixin Liu[2], Xiaoyan Qiang[1], Jean Fan[1], Caixia Sun[1], Hanlin Zeng[2], **Peng Peng**[1]

[1]TransThera Sciences (Nanjing), Inc., Nanjing, China,[2]Shanghai Institute of Precision Medicine, Shanghai, China

Endocrine therapy has substantially improved outcomes in hormone receptor-positive (HR$^+$) breast cancer, yet resistance remains a major clinical challenge. Such resistance arises via two axes: spatially from tumor-intrinsic alterations or microenvironmental cues; temporally as de novo or acquired phenotypes. How these diverse drivers converge to reprogram cancer cell states remains poorly understood. Through single-cell transcriptomics of resistant HR$^+$ breast cancers, we uncovered a recurrent luminal-to-basal transition with ER/PR downregulation - plasticity that emerged in primary tumors and amplified in metastases, particularly malignant pleural effusions (MPE).

Using serial drug selection and MPE coculture, we recapitulated both therapy-induced and microenvironment-driven resistance, both of which converged on FGFR and JAK pathways activation—a phenotype reversible by genetic knockdown or pharmacological inhibition of these pathways.

Mechanistically, FGFR and JAK activation regulated transcription factors to repress luminal genes (*ESR1, PGR*) and conferred resistance. Tinengotinib (TT-00420), a first-in-class dual FGFR and JAK small molecular inhibitor, restored luminal identity and resensitized resistant models to endocrine therapy *in vitro* and *in vivo*. Thus, lineage plasticity unified intrinsic/extrinsic inputs in endocrine resistance, supporting dual FGFR-JAK blockade as a translational strategy.

Planned trials of tinengotinib combined with endocrine therapy in advanced HR$^+$ breast cancer will assess its clinical potential, with results reported in due course.

#1787 Inhibition of MAOA suppresses intracrine androgen biosynthesis and enhances abiraterone treatment in castration-resistant prostate cancer.

Kaisheng Yuan, Hongling Li, Wen Guan, Jing Wei, Boyang Wu

Department of Pharmaceutical Sciences, College of Pharmacy and Pharmaceutical Sciences, Washington State University, Spokane, WA

Background: Androgen receptor signaling inhibitors (ARSIs), such as enzalutamide (Enz) and abiraterone (Abi), have become cornerstone treatments for castration-resistant prostate cancer (CRPC). Despite initial favorable responses, tumors often develop resistance to these agents, partly due to activation of intracrine androgen biosynthesis, underscoring the need for effective strategies to overcome resistance and prolong the utility of ARSIs. This study investigates the role of monoamine oxidase A (MAOA), a mitochondrial enzyme that degrades monoamines and has recently been implicated in prostate cancer, in intracrine androgen biosynthesis, and assesses the potential of MAOA inhibitors to improve Abi efficacy, an ARSI that blocks androgen biosynthesis.
Methods: Multiple ARSI-resistant CRPC models were used, including C4-2B EnzR, VCaP EnzR, and C4-2B AbiR cell lines, as well as LuCaP147CR EnzR and AbiR patient-derived xenograft (PDX) models. Western blot and qPCR were used to analyze the expression of key steroidogenic enzymes involved in androgen biosynthesis in control and MAOA-knockdown cell lines. ELISA and mass spectrometry were used to measure testosterone and dihydrotestosterone (DHT) levels in cell conditioned media. Cell viability, colony formation, and in vivo tumorigenesis assays were used to evaluate the effects of MAOA inactivation by gene silencing or pharmacological approaches, combined with Abi, in both Abi-sensitive and -resistant CRPC models, including cell lines, PDX-derived organoids, and tumor xenografts.
Results: The ARSI-resistant CRPC cells and PDXs showed increased expression levels of MAOA and select steroidogenic enzymes, including CYP17A1 and AKR1C3, compared to their sensitive counterparts. Silencing MAOA reduced the protein expression of CYP17A1 and AKR1C3, in EnzR and AbiR cells, likely through TWSIT1, a known MAOA downstream effector that mediates MAOA's multifaceted functions in prostate cancer. MAOA knockdown also decreased testosterone and DHT levels, both with and without the androgen precursor androstenedione, in EnzR and AbiR cells. Further, antagonizing MAOA with gene silencing or pharmacological inhibitors, including clorgyline and phenelzine, enhanced Abi effectiveness in Abi-sensitive cells and restored Abi sensitivity in resistant cells both in vitro and in vivo.
Conclusion: Our findings reveal that MAOA is essential for maintaining intracrine androgen biosynthesis associated with ARSI resistance and suggest that MAOA inhibitors could enhance Abi treatment in CRPC.
Funding Acknowledgements: This work was supported by NIH/NCI grants R37CA233658, R01CA258634, and R01CA279528 to BJW.

#1788 Cysteine accumulation as a driver of resistance to bortezomib.

Jennifer A. Brain[1], Sarah M. Chang[2], Maximilian Kobiesa[1], Leah G. Rector[1], Kelli J. Che[1], Zhaoqi Li[2], Sky H. Kim[2], Matthew G. Vander Heiden[2], Lucas B. Sullivan[1]

[1]Fred Hutchinson Cancer Center, Seattle, WA,[2]Koch Institute for Integrative Cancer Research at MIT, Cambridge, MA

Covalent drugs targeting key oncogenic drivers are promising cancer therapies, but resistance limits their clinical benefit. Many covalent inhibitors rely on reacting with nucleophilic residues on proteins, and thus we hypothesized that these inhibitors could interact directly with intracellular pools of nucleophiles, like cysteine, diminishing the drug's efficacy. To investigate the possibility that intracellular cysteine drives resistance to chemotherapies, we performed a high throughput screen of clinically available chemotherapeutics in high and low cysteine conditions. We identified cells to be more resistant to boronic-acid proteasome inhibitors in high cysteine conditions (Bortezomib (Btz) and Ixazomib (Ixa)), but not to the epoxyketone-containing proteasome inhibitor Carfilzomib (Cfz). We confirmed the potential of proteasome inhibitors to react with free cysteine and found that Btz and Ixa both formed a covalent conjugate with cysteine as detected via LC-MS. Upon treating cells with the cysteine-drug conjugate, we find nearly all of the toxicity of the drug has been abolished, supporting the hypothesis that cysteine could be a detoxification mechanism in cells.

Using cancer cell lines derived from diverse cancer types, we modulated the cysteine availability and treated cells with two classes of proteasome inhibitors: those with either a boronic-acid or an epoxyketone moiety. In conditions known to increase intracellular cysteine such as high media cystine or co-treatment with the cysteine pro-drug NAC, we found that cells are more resistant to boronic acid-containing inhibitors. Conversely, when we decrease intracellular cysteine levels by co-treating with erastin, an inhibitor of SLC7A11, we measured that cells become more sensitive to Btz and Ixa. In either low or high cysteine, sensitivity to Cfz was unchanged. Collectively, these results indicate that a direct interaction between cysteine with the boronic acid group of Btz and Ixa is responsible for cysteine mediated resistance to these compounds, upstream of proteasome inhibition.

We next explored cysteine's role in rescuing proteasome function by measuring proteasome activity and ubiquitylation in cells. In both assays, we observed that high cysteine prevented the effects of proteosome in cells treated with boronic acid-containing inhibitors. We did not measure a difference in proteasome function in carfilzomib-treated cells in high cysteine, once again implying a unique direct interaction between boronic acid-containing inhibitors and cysteine.

In summary, we uncovered a novel mechanism of resistance to boronic acid-containing proteasome inhibitors with straightforward possibilities to reverse resistance. This work has clinical implications for cancer treatment, especially those with ATF4 or NRF2 stabilization which both drive cysteine accumulation in a SLC7A11-dependent manner.

#1789 RNA isoform discovery and quantification with SMART-Seq® mRNA Long Read (v1 and v2) kits.

Jackson Peterson[1], Yue Yun[1], Lisa Welter[1], Kazuo Tori[1], Alan Du[1], Yana Ryan[1], Ning Ma[1], Rachana Kumar[1], Shiyi Yin[1], Mike Covington[1], Shuwen Chen[1], Elena Shagisultanova[2], Mohammad Fallahi[1], Bryan Bell[1], Andrew Farmer[1]

[1]Takara Bio USA, Inc., San Jose, CA,[2]Department of Medicine/Medical Oncology, University of Colorado, Aurora, CO

RNA serves a central role in biology by converting genomic information into effector molecules, either as functional non-coding RNAs or as protein-coding mRNAs. While it has long been appreciated that complex RNA transcript profiles can be produced through alternative splicing, numerous discoveries have highlighted the essential role of alternative splicing in cell and developmental biology. Furthermore, aberrant splicing has recently been linked to diseases like cancer, neurodegeneration, and autoimmunity. Of particular interest, cancer-specific splice isoforms have emerged as a potential source of neo-antigens targetable by novel immune therapeutics. Thus, understanding the expression and function of RNA isoforms has become increasingly important in cancer biology research. A current limitation of long-read RNA sequencing (LR-RNA-seq) is the requirement of large amounts of input RNA, which can be unachievable for samples such as resected tumors or sorted single cells. Here, we describe SMART-Seq® mRNA Long Read kit, a new LR-RNA-seq library preparation technology that enables full-length RNA sequencing from single cells (~10 pg RNA/cell) up to 100ng total RNA. In high-quality bulk RNA inputs, we demonstrate the ability to reliably sequence at an average read length (N50) of 2 kb and to detect full-length transcripts as long as 8 kb, enabling the discovery and quantification of novel mRNA isoforms in samples from both healthy tissues and cancer cells. Analysis of cancer cell lines with evolved resistance to targeted therapies identifies differential isoform usage associated with the evolution of cancer therapeutic resistance. We further describe an update to this technology, SMART-Seq® mRNA Long Read version 2, which expands the input range to 2µg, improves read-length performance, and enables UMI-based analysis. Comparison studies demonstrate that SMART-Seq mRNA Long Read technology substantially outperforms existing bulk and single-cell LR-RNA-seq methods. With PCR barcoding of up to 96 samples at a time, this technology will accelerate discovery as scientists catalog and study splice isoforms in both routine long read cDNA sequencing workflows and in settings where sample input is limited.

#1791 Targeting succinate dehydrogenase impairs the proliferation of ER+ breast cancer cells.

Anil Kumar Yadav, Lu Jin, Robert Clarke

The Hormel Institute, University of Minnesota, Austin, MN

Endocrine therapies (ET) for estrogen receptor positive (ER+) breast cancer directly block either estrogen biosynthesis (aromatase inhibitors) or estrogen receptor function (Fulvestrant or tamoxifen). However, due to intrinsic and acquired resistance, disease progression often resumes despite continued ET. Succinate dehydrogenase (SDH) enzyme catalyzes the reversible conversion of succinate to fumarate. It contains four different subunits and SDH assembly factor 2 (SDHAF2). In our study, we found elevated SDH enzymatic activity and protein expression of SDHB (catalytic subunit) in LCC9 (ET-resistant cells) comparison with LCC1 or MCF-7 (ET-sensitive cells). T47D-4HT (ET-resistant) also showed significantly higher protein levels of SDHB in comparison with their parental T47D-A18 cells (ET). Pharmacological inhibition of SDH activity using dimethylmalonate (DMM) reduced cell growth, colony and spheroid formation in both LCC9 and T47D-4HT. DMM treatment induced caspase-dependent apoptosis and reduced mitochondrial membrane potential in both LCC9 and T47D-4HT cells. Importantly, succinate accumulation was accompanied by HIF 1-α stabilization and SDH inhibition led to lower levels of HIF1-α, which indicates that SDH may function in the conversion of fumarate to succinate in LCC9 cells. Genetic ablation of SDHB confirmed the importance of SDH activity in growth, colony and spheroid formation of LCC9 and T47D-4HT cells. Taken together, SDH enzymatic activity is crucial for the proliferation and mitochondrial function of ET-resistant ER+ breast cancer cells. We propose that SDH is a potentially novel therapeutic target for ER+, endocrine therapy resistant breast cancer.

#1792 Comprehensive identification of factors involved in the resistance mechanism of a novel cereblon modulator in multiple myeloma cells.

Sho Osawa[1], Tomofumi Yamamoto[2], Rina Tamaru[1], Natsumi Seki[1], Maiko Matsushita[1]

[1]Keio University, Tokyo, Japan,[2]National Institute of Health Sciences, Tokyo, Japan

Background: Multiple myeloma (MM) is a hematologic malignancy characterized by clonal proliferation of plasma cells. Although novel agents such as antibody-based drugs and T cell engagers have improved outcomes, MM remains incurable and relapse is inevitable. Immunomodulatory drugs (IMiDs), including lenalidomide and pomalidomide, are central to MM therapy, but resistance frequently develops with long-term use. Cereblon modulators (CELMoDs), a new generation of IMiDs, are expected to overcome such resistance mechanisms. Mezigdomide, a novel CELMoD, demonstrated an overall response rate of approximately 40% in patients with relapsed/refractory MM (Richardson et al., *N Engl J Med*, 2023). However, early relapse after an initial response remains a clinical concern.

Methods: To elucidate the mechanisms of mezigdomide resistance, we utilized MM cell lines with differential sensitivity to the drug. Expression levels of cereblon (CRBN), IKZF1, and IKZF3—key mediators of IMiD and CELMoD activity—were analyzed by Western blotting. RNA sequencing was then performed to identify gene expression changes associated with resistance. Candidate resistance genes were further validated by RT-PCR, and comparative analyses were conducted with lenalidomide- and pomalidomide-treated cells.

Results: CRBN, IKZF1, and IKZF3 expression levels did not differ between mezigdomide-sensitive and -resistant cells. RNA sequencing revealed several differentially expressed genes potentially associated with resistance. Validation studies confirmed distinct gene expression patterns between resistant and sensitive cell lines.

Conclusions: This study provides the first insights into molecular mechanisms underlying mezigdomide resistance in MM. Identification of these candidate resistance factors may contribute to the development of predictive biomarkers and strategies to overcome CELMoD resistance.

#1793 RAC2 as a mediator of drug resistance in triple-negative breast cancer.

Antonisha R. McIntosh[1], Ngoc Voung[1], Destiny Ball[2], Perrin Black[2], Alayjha Edwards[1], Qingguo Wang[2], Amos M. Sakwe[3]

[1]Biomedical Science, Meharry Medical College, Nashville, TN,[2]Meharry Medical College, Nashville, TN,[3]Assistant Professor, Cancer Biology, Meharry Medical College, Nashville, TN

Triple-negative breast cancer (TNBC) is a highly aggressive and heterogeneous subtype of breast cancer, defined by the absence of estrogen receptor (ER), progesterone receptor (PR), and low or absent human epidermal growth factor receptor 2 (HER2) expression. The lack of these therapeutic targets limits treatment options and contributes to poor clinical outcomes. Tyrosine kinase inhibitors (TKIs) offer a targeted approach by disrupting receptor tyrosine kinase (RTK) signaling pathways that drive tumor growth and survival. However, the emergence of resistance, mediated by compensatory signaling, genetic alterations, and epithelial-to-mesenchymal transition (EMT), remains a major barrier to sustained therapeutic efficacy. In this study, we hypothesized that chronic exposure to TKIs induces transcriptional reprogramming in epithelial TNBC cells, promoting drug resistance. Using RNA sequencing, we profiled differentially expressed genes (DEGs) in control and lapatinib-resistant MDA-MB-468 cells, an EGFR/HER2-driven TNBC model. We identified 129 DEGs and validated five of the most significantly modulated genes by qPCR and Western blotting. These genes were also associated with relapse-free survival in basal-like breast cancer patients. Notably, RAC2, a small Rho GTPase, emerged as a top candidate, showing robust upregulation in resistant cells. Compared to similar small GTPases, we found that this upregulation is specific to RAC2. RAC2 expression was found to be heterogeneous across TNBC cell lines and patient-derived xenograft (PDX) models, suggesting cell type-specific regulation. Ectopic overexpression of RAC2 in MDA-MB-468 cells conferred increased viability following treatment with lapatinib and neratinib and supported the resistance of TNBC cells to neratinib significantly. Furthermore, RAC2 upregulation significantly enhanced migratory and invasive behavior, as demonstrated by Transwell migration and Matrigel invasion assays. Our findings implicate RAC2 as a novel mediator of TKI resistance in TNBC and support its potential as a therapeutic target to restore drug sensitivity in resistant TNBC cells.

#1794 m^{6}A-mediated control of kinase reprogramming in endocrine therapy-resistant breast cancer.

Attila Szenasi[1], Enakshi Sivasudhan[2], Santiago Haase[1], Austin Whitman[1], Kate D. Meyer[2], Philip M. Spanheimer[1]

[1]Lineberger Comprehensive Cancer Center, University of North Carolina, Chapel Hill, NC,[2]Department of Biochemistry, Duke University School of Medicine, Durham, NC

Endocrine therapy resistance (ETR) in estrogen receptor-positive breast cancer arises through multiple adaptive mechanisms, with kinase reprogramming representing a central driver of therapeutic escape. *N*^{6}-methyladenosine (m^{6}A), the most abundant internal RNA modification, has emerged as a key regulator of RNA fate, yet its role in restructuring kinase networks during ETR is unclear. Using GLORI sequencing, a single-nucleotide-resolution method for stoichiometric m^{6}A quantification, we profiled parental, tamoxifen and exemestane resistant MCF7 derivatives. Tamoxifen-resistant cells exhibited ~2,600 m^{6}A sites with canonical DRACH motifs with widespread hyper- and hypomethylation across transcripts encoding MAPK regulators, receptor tyrosine kinases, and cell-cycle-associated kinases. Multi-omic integration including RNA-seq and quantitative proteomics indicate differentially methylated kinase mRNAs gained stability, enhanced translational efficiency and increased protein output, establishing an m^{6}A-dependent mechanism of kinase reprogramming. Resistant cells also displayed selective upregulation of m^{6}A-associated RNA-binding proteins, including YTHDF1 and IGF2BP2, consistent with a remodeled post-transcriptional landscape. Together, our findings uncover a previously underappreciated epitranscriptomic layer integrating quantitative m^{6}A dynamics and RNA-binding protein shifts that drives kinase reprogramming and promotes ETR in breast cancer.

#1795 Cooperative role of ESR1 mutations and midasin in endocrine resistance and the therapeutic potential of dual targeting.

Mounika Pamukuntla[1], Bipika Banjara[2], Manasa Kotina[3], Afia Ohemeng[4], Alicia Hudson[4], Michael Davidson[4], Jillian L. Pope[5], Selina F. Darling-Reed[6], Elizabeth Henderson[7], Simak Ali[8], Syreeta Tilghman[2]

[1]Department of Pharmacology/Toxicology, Florida A&M University, Tallahassee, FL,[2]Florida A&M University College of Pharmacy & Pharmaceutical Sciences, Tallahassee, FL,[3]Florida A&M University, Tallahassee, FL,[4]Basic Pharmaceutical Sciences, Florida Agriculture and Mechanical University, Tallahassee, FL,[5]Department of Bilological sciences, Florida A&M University, Tallahassee, FL,[6]Assistant Professor, Florida A&M Univ. College of Pharmacy, Tallahassee, FL,[7]Hampton University, School of Pharmacy, Hampton, VA,[8]Professor of Molec. Endocrine Onc., Imperial College London, London

While most cases of estrogen receptor-positive (ER+) breast cancer initially respond to endocrine therapy, inevitably many women acquire resistance. A major hurdle hampering the response of metastatic breast cancer patients to endocrine therapy is constitutively active point mutations in the ER ligand binding domain (LBD). We previously identified midasin (MDN1), a novel ribosomal protein, which was significantly overexpressed in MCF-7 endocrine-resistant breast cancer stem cells. Additional studies also indicated that midasin was required for growth, and stemness, but there was a mutation-dependent impact of midasin inhibition on mammosphere morphology and protein expression. However, the consequences of increased MDN1 expression and *ESR1* mutations remain unclear. We hypothesize that *ESR1* mutations along with dysregulated MDN1 cooperate to alter the microenvironment and position breast cancer cells for a survival advantage. The objective of this study was to elucidate the mechanism by which midasin inhibition alters the biology of breast cancer cells with *ESR1* mutations. To address this, breast cancer patient tumor samples were queried using CPTAC, and MDN1 protein expression was significantly elevated in luminal, HER2+, and triple-negative tumors compared with normal breast tissue. In a metastatic breast cancer cohort (n = 379), 10% of patients exhibited alterations in MDN1, whereas 25% exhibited ESR1 alterations, primarily amplifications and missense mutations. A significant co-occurrence ($\log_2$ OR = 1.60; q = 0.027) between these alterations suggested functional interplay between midasin and ER signaling. Molecular docking identified Rbin-2 as a compound interacting with midasin (docking score: –5.70). Proliferation assays using MCF-7 wild-type, MCF-7^{D538G}, and MCF-7^{Y537S} cells showed that 12 µM Rbin-2 produced ~50% growth inhibition. In 3D spheroid assays, Rbin-2 significantly decreased invasion, disrupted spheroid integrity, and promoted cell death, particularly in ER-mutant cells. Given these results and the clinical data, we examined co-targeting ER point mutations and midasin. Cells treated with 12 µM Rbin-2 plus 2.5–10 µM elacestrant exhibited ~79% growth inhibition. Combination Index analysis showed the strongest synergy in MCF-7^{Y537S} and MCF-7^{D538G} cells compared with the wildtype cells. Immunoblots demonstrated that elacestrant reduced ER and midasin expression, while the combination produced a synergistic decrease in MDN1, supporting a cooperative mechanism between ER signaling and midasin. Overall, our results indicate that aberrant ESR1 activity and elevated MDN1 cooperate to drive aggressive tumor phenotypes, and that simultaneous inhibition of ER and midasin may offer a novel therapeutic avenue for patients with ESR1-mutant, endocrine-resistant breast cancer.

#1796 Lineage-specific survival vs proliferative enzalutamide resistance states as potential drivers of prostate cancer disparities.

Richard Van[1], Mira V. Han[1], Desh P. Sharma[2], Ajay Singh[3], **Ranjana Mitra**[4]

[1]University of Nevada Las Vegas, Las Vegas, NV,[2]U.S. Department of Veterans Affairs, Las Vegas, NV,[3]Cancer Center and Research Institute, Department of Cell and Molecular Biology, University of Mississippi Medical Center, Jackson, MS,[4]Roseman Univ. of Health Sciences, Las Vegas, NV

African American (AA) men bear a disproportionate burden of prostate cancer, exhibiting higher incidence and mortality rates than their non-Hispanic White American (NHWA) counterparts. Therapeutic resistance is a major driver of prostate cancer-related mortality, and AA patients often show poorer responses to available treatments. Enzalutamide is a second-generation androgen receptor signaling inhibitor widely used to treat advanced metastatic prostate cancer. To investigate lineage-specific mechanisms of enzalutamide resistance, we generated resistant derivatives of the AA-origin MDAPCa2b and the NHWA-origin LNCaP cell lines by gradually increasing enzalutamide exposure. We then performed RNA sequencing-based transcriptomic profiling and integrated gene set enrichment analysis (GSEA), overrepresentation analysis (ORA), and KEGG pathway analysis. Comparison of Enz-R cells with their respective parental lines identified several resistance-associated differentially expressed genes (DEGs), revealing lineage-specific transcriptional programs. Notably, MDAPCa2b Enz-R cells exhibited a robust survival program characteristic of aggressive, therapy-refractory prostate cancer. Although these cells retained a measurable proliferative capacity, they adopted a persister-like, metabolically minimized state, marked by the coordinated downregulation of oxidative phosphorylation, glycolysis, pentose phosphate pathway, amino acid and tRNA biosynthesis, ribosome biogenesis, and proteasomal activity. KEGG analysis revealed apoptosis suppression, including loss of TRAIL/TNFRSF10 signaling and reduced CASP10, BID, and TP53. This combination of metabolic quiescence and anti-apoptotic protection reflects a survival-optimized phenotype associated with lineage plasticity, therapeutic tolerance, and the aggressive disease trajectories commonly observed in AA prostate cancer. In contrast, Enz-R LNCaP cells exhibited a distinct proliferative resistance state, marked by coordinated upregulation of cell-cycle progression, DNA replication, homologous recombination, mismatch and base-excision repair, p53 signaling, and pyrimidine metabolism. Immune response and adhesion pathways were broadly downregulated, consistent with an immune-evasive, AR-independent phenotype. This proliferative remodeling represents a canonical escape route driven by AR bypass and strengthened genome maintenance pathways. Together, these findings highlight two distinct resistance strategies: a survival-optimized, metabolically repressed, apoptosis resistant program in MDAPCa2b cells and a proliferative, DNA-repair enhanced program in LNCaP cells. These biologically divergent trajectories may contribute to observed clinical disparities and underscore the need for tailored, lineage-informed therapeutic strategies.

#1798 Nicotinamide phosphoribosyltransferase (NAMPT) inhibitor-resistant rhabdomyosarcoma (RMS) models exhibit alterations in metabolic and genomic profiles.

Ariana Elizabeth Nelson[1], **Abantika Chakraborty**[2], David Bell[3], Victor J. Collins[2], Ali Mokhtar Mahmoud[2], Ying Wu[4], SOPHIA VARRIANO[2], Arnulfo Mendoza[5], Sameer Issaq[6], Parthav Jailwala[4], Jack F. Shern[7], Ernesto Suarez[3], Joseph Ivanic[3], Christine M. Heske[8]

[1]National Cancer Institute Center for Cancer Research,[2]Pediatric Oncology Branch, National Cancer Institute, National Institutes of Health, Bethesda, MD,[3]Advanced Biomedical Computational Science, Frederick National Laboratory for Cancer Research, Frederick, MD,[4]Advanced Biomedical Computational Science, Frederick National Laboratory for Cancer Research,, Frederick, MD,[5], National Cancer Institute, National Institutes of Health, Bethesda, MD,[6]National Cancer Institute, Bethesda, MD,[7]Pediatric Oncology,NIH, NCI-CCR, Bethesda, MD,[8]Pediatric Oncology Branch, National Cancer Institute, National Institutes of Health,, Bethesda, MD

RMS is a common pediatric soft tissue sarcoma for which new therapies are critically needed. We previously demonstrated that RMS is highly sensitive to inhibitors of NAMPT, which catalyzes the rate-limiting step of the NAD^+ salvage pathway and is the only pharmacologically targetable NAD^+ production enzyme. Treatment with the NAMPT inhibitor OT-82 results in complete tumor regressions *in vivo,* however, upon intermittent treatment, acquired resistance develops in some models. As acquired drug resistance is a known impediment to the clinical efficacy of targeted agents, we sought to elucidate potential mechanisms of OT-82 resistance in RMS. Mice with orthotopic fusion-positive (FP) and fusion-negative (FN) RMS xenograft tumors were treated with OT-82 for 8 weeks on the clinical dosing schedule. After stopping treatment, mice were observed for recurrence and retreated when tumors regrew to >900 mm^3. Tumors that progressed on treatment were harvested and converted to cell lines. Two resistant cell lines (1 FP - Rh30-mRes and 1 FN - RD-mRes) were selected for further study. Incucyte live cell analysis confirmed retention of OT-82 resistance *in vitro* with resistant cells maintaining proliferation at doses of OT-82 up to 30X above the IC_{50} of parental cells. Resistant cells exposed to OT-82 maintained ATP levels consistent with that of untreated controls. After 24h of OT-82 treatment, NAD^+ loss was observed in both parental and resistant cells, however resistant cells recovered NAD^+ levels within 48-96h. Effects on glucose metabolism, measured using extracellular flux and metabolomic analyses demonstrated that in the presence of OT-82, only resistant cells maintained glycolytic function. Specifically, metabolites downstream of the NAD^+-dependent enzyme glyceraldehyde-3-phosphase dehydrogenase were reduced in parental cells but maintained in resistant cells. Analysis of protein expression of NAD^+ synthesis enzymes NAMPT, NAPRT, and QPRT revealed that Rh30-mRes expresses more QPRT, however, genetic silencing of *QPRT* did not reverse resistance, suggesting upregulation of compensatory NAD production enzymes is not a primary mechanism of resistance. Whole exome sequencing revealed that each resistant cell line has a distinct, previously unreported mutation in *NAMPT*. Protein modeling suggests each mutation affects the drug binding pocket of NAMPT, with the S17F variant in Rh30-mRes resulting in a collapse of the pocket and the S241C variant in RD-mRes reducing binding affinity of OT-82. These findings are consistent with functional studies demonstrating that Rh30-mRes is resistant to multiple other NAMPT inhibitors whereas RD-mRes is resistant only to OT-82. Together, these data suggest that acquired resistance to NAMPT inhibitors in RMS models involves the development of mutations in the target protein affecting drug binding and affinity.

#1799 Ferroportin mediates bevacizumab resistance and ferroptosis evasion in ovarian cancer.

Zonghao Tang[1], Amir A. Jazaeri[1], Weiche Wu[1], Mark Kim[2], Shannon N. Westin[3], Timothy A. Yap[1], Sanghoon Lee[1], Anil K. Sood[1]

[1]UT MD Anderson Cancer Center, Houston, TX,[2]The University of Texas MD Anderson Cancer Center, Houston, TX,[3]Gynecologic Oncology and Reproductive Medicine, UT MD Anderson Cancer Center, Houston, TX

Adaptive drug resistance remains a major barrier in cancer therapy, driving poor patient outcomes. Bevacizumab (Bev) is a mainstay of ovarian cancer (OC) treatment, yet prolonged exposure frequently leads to resistance and diminished clinical benefit. Understanding the mechanisms underlying Bev response and tumor adaptation is therefore critical for improving therapeutic strategies. To investigate these mechanisms, we established a SKOV3 Bev-resistant tumor model. RNA-seq analysis revealed that two ferroptosis-inhibitory genes, *SLC40A1* (fold change 4.01) and *AKR1C2* (fold change 3.81) among the top five differentially expressed genes, implicating ferroptosis regulation as a potential determinant of Bev sensitivity. Consistently, public datasets indicate that OC cells with high *SLC40A1* expression are resistant to ferroptosis, whereas low SLC40A1 correlates with ferroptosis susceptibility. In vitro experiments further demonstrated that OC cell lines with elevated *SLC40A1* levels exhibit reduced labile iron pools and enhanced ferroptosis resistance. Likewise, Bev-resistant OVCAR5 and OVCAR8 cell lines derived from in vivo models showed significant upregulation of ferroportin (FPN), the protein encoded by SLC40A1, compared to parental controls. Pharmacologic inhibition of FPN increased labile iron across multiple OC cell lines, and the FPN inhibitor VIT-2763 markedly sensitized Bev-resistant cells to ferroptosis ($P<0.01$). Proteiomic profiling revealed that Bev-sensitive tumors accumulate higher levels of polyunsaturated fatty acids and lower glutathione ($P<0.05$) compared with both untreated controls and resistant tumors. Collectively, these findings indicate that Bev induces ferroptosis in OC models, while tumor-associated upregulation of FPN enables escape from this lethal stress. These data highlight FPN as a promising therapeutic target to overcome Bev resistance.

#1800 Mitochondrial dysfunction induces asparaginase resistance in R-spondin fusion colorectal cancer.

Su Hyun Lee, Yun-Cheol Chae, Alejandro Gutierrez

Department of Oncology, St. Jude Children's Research Hospital, Memphis, TN

Improved therapies are required for the thousands of patients who die of colorectal cancer (CRC) every year. We previously found that asparaginase, a cancer therapeutic that degrades asparagine, has efficacy in R-spondin fusion CRCs because these fusions block upregulation of proteasomal protein degradation, a source of intracellular amino acids, when asparagine is lacking from the environment (Hinze et al., Cancer Discovery, 2020). To anticipate mechanisms of treatment resistance that may emerge, we applied a CRISPR-based genetic screen to identify modifiers of asparaginase response in R-spondin fusion CRC. We found that guide RNAs targeting multiple mitochondria-localized proteins were enriched in asparaginase-treated cells, as these genes comprised 59% of the top 100 “hits” on the screen. This finding suggested that impairing mitochondrial function induces asparaginase resistance, which was surprising because mitochondrial function is required to produce intracellular aspartate, a key substrate for asparagine biosynthesis. Indeed, in R-spondin fusion CRC driven cells, we confirmed that shRNA knockdown of multiple mitochondrial factors, or a pharmacologic inhibitor of mitochondrial translation, each induced asparaginase resistance. Mitochondria contain >1100 proteins, 99% of which are nuclear-encoded, cytoplasmically-synthesized, and then imported into mitochondria. We found that induction of mitochondrial dysfunction led to a marked increase in total K48-linked polyubiquitinated proteins, along with cytoplasmic accumulation of multiple nuclear-encoded mitochondria proteins. Our findings support the model that triggering mitochondrial dysfunction impairs mitochondrial import of nuclear-encoded mitochondrial proteins, which are then degraded via the ubiquitin proteasome system. This provides an alternative mechanism through which these cells can increase protein degradation despite expression of the R-spondin fusion. Protein degradation releases free amino acids, providing these cells with a catabolic source of intracellular asparagine that allows them to survive during asparaginase-induced depletion of asparagine. Our findings provide a molecular understanding of how the failure of import of mitochondrial proteins may be an anticipated mechanism of resistance to asparaginase in patients.

#1801 *H. pylori* infection induces WEE1 to promote drug resistance in gastric adenocarcinoma.

Md Obaidul Islam[1], Krishnapriya Thangaretnam[2], Jialun Lyu[1], Zhenzhen Zhang[3], Heng Lu[2], Dunfa Peng[3], Nadeem Sidiq Bhat[3], Mohammed Soutto[3], Wael El Rifai[3], Zheng Chen[3]

[1]University of Miami Miller School of Medicine, Miami, FL,[2]University of Miami, Miami, FL,[3]University of Miami, Miller School of Medicine, Miami, FL

Background: Gastric cancer (GC) is the 5th leading cause of cancer-related mortality worldwide, with a poor prognosis and frequent resistance to therapy. Identifying key molecular drivers of this resistance and novel therapeutic vulnerabilities is urgently needed. This study investigates the non-canonical role of the nuclear kinase WEE1 in GC progression and drug resistance, particularly in the context of *Helicobacter pylori (H. pylori)* infection.

Methods: Integrative analyses of over 2,000 gastric cancer patient samples from various datasets, cell line models, and patient-derived xenografts (PDXs) were employed to elucidate WEE1-associated signaling pathways. Gene set enrichment analysis (GSEA) was conducted to identify transcriptional programs associated with high WEE1 expression. Functional validation was performed using siRNA knockdown, overexpression, Western blot, RT-qPCR, immunofluorescence, and *in vivo* xenograft models. A high-throughput screen of 892 FDA-approved drugs was conducted to identify effective drug combinations with the WEE1 inhibitor MK1775.

Results: WEE1 was found to be aberrantly overexpressed and mis-localized to the cytoplasm in gastric cancer cells. GSEA across 14 datasets consistently showed enrichment of MYC and E2F target genes in WEE1-high tumors. Mechanistically, WEE1 activated E2F1 through the phosphorylation of RB, leading to the transcriptional upregulation of MYC. MYC, in turn, enhanced expression of WEE1 and E2F1, forming a feedforward oncogenic loop. Notably, *H. pylori* infection robustly induced WEE1 and MYC expression, as well as their downstream effectors, linking microbial etiology to transcriptional reprogramming and tumor progression. Targeting WEE1 with MK1775 suppressed MYC-driven transcriptional activity, reduced anti-apoptotic gene expression (BCL2, BCL2L1), and sensitized GC cells to DNA-damaging agents. A high-throughput screen identified Afatinib, an EGFR/HER2 inhibitor, as a potent synergistic partner with MK1775. Combination therapy demonstrated enhanced anti-tumor efficacy *in vitro*, in PDX models, and in 3D organoid systems derived from GC patients.

Conclusions: This study identifies a novel *H. pylori*-WEE1-E2F1-MYC signaling axis that contributes to GC pathogenesis and resistance. Given the lack of clinically available MYC inhibitors, targeting WEE1 provides a promising alternative approach. The discovery of synergistic efficacy with Afatinib supports a new therapeutic strategy for overcoming resistance in MYC-driven gastric cancer.

#1802 Fibroblast-driven tamoxifen resistance in ER+ breast cancer: Experimental validation and development of a high-throughput co-culture screening assay.

Elisabet Rodriguez-Tomas[1], Francesco Massai[2], Arne Ostman[1]

[1]Karolinska Institutet, Stockholm, Sweden,[2]SciLifeLab, Stockholm, Sweden

New strategies are needed to overcome tamoxifen resistance in ER+ breast cancer. While the contribution of the tumor microenvironment to drug resistance remains incompletely understood, fibroblasts have emerged as potential therapeutic targets, due to their ability to modulate tumor behavior and drug sensitivity via paracrine signaling, extracellular matrix remodeling, and immune regulation. This study aimed to validate the protective role of fibroblasts against tamoxifen and to establish a co-culture assay suitable for high-throughput drug screening.

We first performed functional assays to assess fibroblast-mediated protection using human ER+ breast cancer (MCF-7) and human fibroblast (BJhTERT) cell lines. Flow cytometry experiments with the CD140 marker distinguished BJhTERT (CD140+) from MCF-7 (CD140-) in co-culture and revealed that tamoxifen induced close to 90% cell death in MCF-7 monocultures measured by a viability dye 7-AAD (7-aminoactinomycin D), whereas only 25% of MCF-7 cells died under co-culture conditions with BJhTERT. In parallel, qPCR analysis confirmed that tamoxifen downregulated proliferative (CCND1) and estrogen response (ESR1, PGR, TFF1, GREB1) genes.

Building on these findings, we developed a high-throughput co-culture assay. MCF-7 and BJhTERT cells were transduced with mCherry and GFP lentiviral reporters, respectively, and seeded into 384-well plates at optimized densities (500 and 1,000 cells/well). Cells were treated with tamoxifen or DMSO, fixed at defined time points, and mCherry, GFP, and Hoechst nuclear stain signals were analyzed using high-content imaging. Sixteen hours post-seeding was chosen as the optimal time for treatment initiation. Over that time, MCF-7 monocultures showed a fold change of 1.3 (30% increase) in cell numbers relative to the initial count, whereas MCF-7 in co-culture showed a fold change of 1.9 (90% increase), indicating a significantly greater growth-promoting effect of fibroblasts. Tamoxifen at a concentration of 20 µM reduced MCF-7 cell numbers by 63% in monoculture versus 38% in co-culture, confirming the protective stromal effect.

In conclusion, our experiments validate fibroblast-ER+ breast cancer crosstalk as a mechanism of tamoxifen resistance. Furthermore, the development of a co-culture-based high-throughput assay, that models fibroblast-mediated tamoxifen resistance, provides a platform for novel screening strategies aimed at targeting the tumor-stroma interactions in ER+ breast cancer.

#1803 Dynamic copy number changes and *de novo* generation of extrachromosomal DNA modulate therapy resistance.

Tim Vorberg[1], Manuel Reitberger[2], Bernardo Rodriguez Martin[3], Maja Starostecka[4], Dominique Schulz[2], Arlou K. Angeles[5], Kate I. Glennon[6], Tasneem Cheytan[2], Roberto Wurth[7], Vera Thiel[8], Paul Schwerd-Kleine[2], Verena Thewes[9], Laura Michel[10], Ewgenija Gutjahr[11], Simon J. Ogrodnik[6], Heike Conrad[12], Steffi O. Mehlhorn[2], Vanessa Vogel[2], Corinna Klein[2], Albrecht Stenzinger[13], Peter Lichter[14], Andreas Schneeweiss[15], Martin Granzow[16], Marc Zapatka[17], Anna Jauch[16], Holger Sultmann[18], Jan Korbel[4], Andreas Trumpp[19], **Martin R. Sprick**[2]

[1]DKFZ German Cancer Research Center, Heidelberg, Germany,[2]German Cancer Research Center/HI-STEM, Heidelberg, Germany,[3]3Genome Biology Unit, European Molecular Biology Laboratory (EMBL), Heidelberg, Germany,[4]Genome Biology Unit, European Molecular Biology Laboratory (EMBL), Heidelberg, Germany,[5]4Division of Cancer Genome Research, German Cancer Research Center, Heidelberg, Germany,[6]Division of Cancer Genome Research, German Cancer Research Center, Heidelberg, Germany,[7]HI-STEM gGmbH, Heidelberg, Germany,[8]DKFZ German Cancer Research Center/HI-STEM, Heidelberg, Germany,[9]Gynecologic Oncology, National Center for Tumor Diseases (NCT), Heidelberg, Germany,[10]National Center for Tumor Diseases (NCT), University of Heidelberg, Heideberg, Germany,[11]Heidelberg Institute for Stem Cell Technology and Experimental Medicine (HI-STEM gGmbH), Heidelberg, Germany,[12]Institute of Pathology, Heidelberg University Hospital (UKHD), Heidelberg, Germany,[13]Heidelberg University Hospital (UKHD), Heidelberg, Germany,[14]6Division of Molecular Genetics, German Cancer Research Center (DKFZ), Heidelberg, Germany,[15]Gynecologic Oncology,, National Center for Tumor Diseases (NCT), Heidelberg, Germany,[16]Institute of Human Genetics, University Heidelberg,, Heidelberg, Germany,[17]Computational Cancer Genomics, German Cancer Research Center (DKFZ), Heidelberg, Germany,[18]Division of Cancer Genome Research, German Cancer Research Center (DKFZ), Heidelberg, Germany,[19]German Cancer Research Center, Heidelberg, Germany

Extrachromosomal DNA (ecDNA) is increasingly recognized as a driver of cellular plasticity, yet its role in therapy adaptation in pancreatic ductal adenocarcinoma (PDAC) remains poorly defined. In patient-derived PDAC models, we identify extrachromosomal ABCB1 amplification as a mechanism of resistance to paclitaxel and KRAS inhibitors and show that ABCB1 copy number dynamically adjusts to selective pressure. Notably, paclitaxel-resistant cells remain primed for rapid de novo ecDNA generation: after eliminating pre-existing ABCB1 ecDNA through single-cell cloning, new and structurally distinct ABCB1 ecDNA rapidly emerges, indicating treatment-induced molecular changes that prime these cells for ecDNA formation. In metastatic breast cancer, taxane-associated ABCB1 amplification is likewise observed and can be tracked in cell-free DNA (cfDNA), underscoring clinical relevance beyond PDAC. Finally, gemcitabine co-treatment suppresses ABCB1 ecDNA generation, suggesting potential strategies to counteract ecDNA-mediated resistance. Together, these findings demonstrate that dynamic ecDNA modulation and inducible ecDNA biogenesis enable rapid, reversible drug resistance, providing a rationale for ecDNA-targeted combination therapies and longitudinal monitoring.

#1804 Midasin inhibition disrupts the sumoylation axis to impair mammosphere stability through alteration of transcriptional network.

Bipika Banjara[1], Mounika Pamukuntla[2], Manasa Kotina[2], Afia Ohemeng[2], Alicia Hudson[3], A. Michael Davidson[3], Jillian L. Pope[4], Selina F. Darling-Reed[5], Syreeta Tilghman[6]

[1]Basic Pharmaceutical Sciences, Florida A&M University College of Pharmacy & Pharmaceutical Sciences, Tallahassee, FL,[2]Florida A&M University, Tallahassee, FL,[3]Basic Pharmaceutical Sciences, Florida A&M University, Tallahassee, FL,[4]Biological Sciences, Florida A&M University, Tallahassee, FL,[5]Assistant Professor, Florida A&M Univ. College of Pharmacy, Tallahassee, FL,[6]Florida A&M University College of Pharmacy & Pharmaceutical Sciences, Tallahassee, FL

Endocrine resistance remains a major barrier to effective treatment of estrogen receptor–positive (ER+) breast cancer, necessitating identification of molecular drivers that sustain tumor growth, plasticity, and cancer stem cell (CSC) associated phenotypes. Midasin (MDN1), a key regulator of ribosome biogenesis, is elevated in endocrine-resistant tumors, yet its contribution to aromatase inhibitor (AI) resistance is not well defined. Here, we examined differential responses to MDN1 inhibition in AI-sensitive AC-1 and AI-resistant LTLT-Ca cells cultured in 2D and 3D. Basal characterization showed higher aromatase (1.2-fold) and ERα (1.6-fold) expression in AC-1 cells, while LTLT-Ca cells exhibited 7-fold and 3.85-fold increase in EGFR and HER2, respectively, with further EGFR and HER2 amplification (up to 4-fold) in 3D mammosphere. Although MDN1 levels were higher in AC-1 cells under 2D conditions, MDN1 was enriched in LTLT-Ca mammosphere, linking elevated ribosome biogenesis to the resistant, stem-like phenotype. Treatment with the MDN1 inhibitor, Rbin-2 (18 μM) significantly reduced MDN1 expression and disrupted spheroid architecture in both models. AC-1 spheroids displayed moderate size reduction (1010.5 μm² to 731.7 μm² by day 12), whereas larger LTLT-Ca spheroids (1204.5 μm²) became fragmented and irregular (1539.3 μm²), indicating structural collapse rather than shrinkage. Acridine Orange/Ethidium Bromide staining revealed a 65% decrease in the live-to-dead fluorescence ratio in AC-1 versus 14% in LTLT-Ca, consistent with extensive degeneration in sensitive cells and instability in resistant spheroids. Spheroid invasion assays showed modest reduction in matrix outgrowth in both AC-1 and LTLT-Ca after Rbin-2 exposure. LTLT-Ca mammospheres expressed elevated OCT4 and SOX2, which decreased by 49% and 45% respectively, following MDN1 inhibition, implicating MDN1 in sustaining CSC transcriptional networks. Analysis of SUMOylation dynamics revealed intrinsically higher SUMO2/3 in resistant cells, with a further increase upon Rbin-2 treatment, consistent with decreased midasin associated cell death. Conversely, the deSUMOylase SENP3, also elevated in resistant cells, was reduced by Rbin-2 in both lines. This increase in SUMO2/3 coupled with decreased SENP3 reflects MDN1-dependent disruption of homeostasis and aligns with reduced ALDH1A1 and loss of CSC properties. Collectively, these findings identify a SUMO2/3–SENP3–MDN1 regulatory axis that supports, stemness and invasiveness in AI-resistant breast cancer, and demonstrate that MDN1 inhibition disrupts this axis to impair mammosphere integrity, attenuate CSC programs, and suppress invasion. This work establishes MDN1 as a promising therapeutic vulnerability for overcoming AI resistance.

#1805 Ancestry-dependent differences of PASK (Per-Arnt-Sim Kinase) inhibitor efficacy in triple-negative breast cancer under variable glucose conditions.

Ayomide Olayiwola, Sree Aramgam, K. Sean Kimbro

Morehouse School of Medicine, Atlanta, GA

Breast cancer mortality rates are nearly 40% higher in African American women than in women of European ancestry. A major contributor to this outcome is triple-negative breast cancer (TNBC), which disproportionately affects African American women and is associated with more aggressive disease. Per-Arnt-Sim Kinase (PASK) is a nutrient-sensitive protein kinase that regulates glucose and lipid metabolism. Previous studies have shown that PASK plays a significant role in breast cancer progression by promoting tumor growth through several metabolic and signaling pathways. Preliminary evidence suggests that the PASK inhibitor, BioE-1115, exhibits differential efficacy across TNBC cell lines of distinct ancestral backgrounds across varying glucose levels. TNBC cell lines representing African ancestry (HCC-1806 and MDA-MB-468) and European ancestry (MDA-MB-231) were cultured in media containing physiologically relevant glucose concentrations representing hypoglycemia (2.5 mM; 45 mg/dL), normoglycemia (5.5 mM; 100 mg/dL), hyperglycemia (11 mM; 198 mg/dL), and severe hyperglycemia (17.5 mM; 315.1 mg/dL). Cell viability assays were performed following BioE-1115 treatment to quantify ancestry- and glucose-dependent differences in the response to the inhibitor. Half-maximal inhibitory concentration (IC_{50}) values were calculated for each condition. BioE-1115 demonstrated distinct efficacy profiles across TNBC cell lines. The African-ancestry HCC-1806 and MDA-MB-468 cells displayed markedly reduced sensitivity to BioE-1115, with IC_{50} values 1.3x-1.5x higher compared with the European-ancestry MDA-MB-231 cells under equivalent glucose conditions. Variability in inhibitor response was observed across glucose concentrations, indicating that metabolic state modifies PASK inhibitor efficacy. PASK inhibition preliminarily suggests ancestry-dependent differences in therapeutic response that are further modulated by glucose availability. These findings highlight the importance of integrating ancestry-informed genetic and metabolic context when evaluating targeted metabolic therapies for TNBC. This work provides foundational data supporting the need for precision-oncology approaches that consider both ancestry-linked biology and metabolic stressors.

#1806 WRN under the scalpel: Helicase-domain hotspot & splice-site knock-ins in HCT116 and RKO.

Yue Huang, Xiaomeng Gou, Jinying Ning, **Feng Hao**

Kyinno Biotechnology Co., LTD, Beijing, China

The WRN helicase is a synthetic-lethal vulnerability in microsatellite-instability-high (MSI-H) tumors, yet allele-specific resistance is a foreseeable risk as small-molecule WRN inhibitors advance. Endogenous point-mutation models, built in the native regulatory context, more faithfully capture drug-target engagement and pathway compensation than overexpression systems. Such models enable rigorous mechanism-of-action confirmation, resistance-liability mapping, chemotype backup selection, patient-stratification/biomarker hypotheses, and faster SAR and combination design.Across isogenic HCT116 and RKO models, two WRN-targeting chemotypes diverged at specific liability nodes. WT HCT116 was highly sensitive (VVD-214 48.47 nM; HRO761 86.89 nM), and baseline RKO remained responsive (366/720 nM). C727 dictated VVD-214 resistance: C727A drove VVD-214 to >10 μM while preserving near-WT HRO761 (153-179 nM); C727S pushed HRO761 to 2.1-3.5 μM and VVD-214 to >10 μM; in RKO-C727S, both exceeded 10 μM. I852F showed the reciprocal pattern—VVD-214 stayed potent (62-77 nM) but HRO761 was inactive (>10 μM). G729D and F730L caused bilateral right-shifts, larger for HRO761 (VVD-214 0.71-1.34 μM; HRO761 2.9-8.0 μM); combining G729D+I852F abolished HRO761 (>10 μM) while VVD-214 remained sub-μM (0.78-0.82 μM). The splice variant c.1577-1G>C was hypersensitive to VVD-214 (36-37 nM) yet right-shifted for HRO761 (~1.11 μM). Collectively, C727 → VVD-214 resistance and I852 →HRO761 resistance, while G729/F730/splice confer a broader HRO761 bias—guiding chemotype switching and backup selection.Alleles were introduced by CRISPR-Cas9 HDR using ~200-nt ssODN donors; single-cell clones were sequence-verified (Sanger/NGS), STR-authenticated, and mycoplasma-free banked. Dose-response viability assays (72-96 h, 10-point curves) were fit with four-parameter logistic models to derive IC_{50}; each clone included n≥2-3 biological replicates. This WRN allele panel is immediately deployable to (1) build allele-resolved resistance maps, (2) prioritize chemotype backups based on the C727/I852 complementarity, (3) generate patient-selection/biomarker hypotheses for MSI-H settings, and (4) accelerate SAR and combination strategies—thereby front-loading chemical and clinical derisking for VVD-214- and HRO761-class WRN inhibitors.

#1807 RLIP depletion suppresses ovarian cancer growth and metastasis.

Sharad S. Singhal[1], Madhu Krishna[1], Prakash Kulkarni[2], David Horne[2], Ravi Salgia[2]

[1]Beckman Research Institute of The City of Hope, Duarte, CA,[2]Beckman Research Institute of City of Hope, Duarte, CA

Ovarian tumor metastasis is a leading cause of cancer-related deaths worldwide. Ovarian cancer (OC) cells frequently metastasize to the peritoneum. OC cells, after detaching from the primary tumor, can float in the ascitic fluid (fluid that accumulates in the abdominal cavity due to cancer) and attach to the peritoneum, the lining of the abdominal cavity. Peritoneal metastasis is strongly linked to poor prognosis in OC patients. In the current study, we evaluated the anti-proliferative and anti-metastatic effects of RLIP inhibition in an array of OC cell lines and an orthotopic mouse model of ovarian metastasis. Compared to control treatment, RLIP inhibition and/or depletion reduced *in-vitro* cell viability and suppressed the migratory and invasive potential of OC cells. Further, mice intraperitoneally implanted with luciferase-expressing HeyA8 OC cells were treated with RLIP antisense (RAS; 4 mg/kg, b.w.), RLIP antibody (Rab; 4 mg/kg, b.w.) or a combination of RAS+Rab. RAS-, and Rab-treated mice exhibited significantly lower primary tumor weight and reduced metastasis compared to control mice. Mice treated with a combination of RAS+Rab exhibited no metastasis and significantly lower tumor weight than the single agent-treated mice. *In-vivo* studies showed that the RLIP targeting agent's treatment prolonged the survival of NSG mice inoculated with HeyA8-luc OC cells. Collectively, our results suggest that RLIP antisense has potential to be combined with RLIP antibodies to more effectively suppress primary ovarian tumor growth and metastasis to the peritoneum that warrants further investigation. (This work was supported in part by the Department of Defense grant W81XWH-22-1-0331. Funding from the Beckman Research Institute of City of Hope is also acknowledged).

#1808 METTL7A and METTL7B confer resistance to the oral thiol-based histone deacetylase inhibitor ST7612AA1.

Omotola D. Gbadegesin, Robert W. Robey, Michael M. Gottesman

Laboratory of Cell Biology, Center for Cancer Research, National Cancer Institute, Bethesda, MD

As modulators of chromatin structure and gene expression, histone deacetylase (HDAC) inhibitors are emerging as an important class of epigenetic therapeutics in cancer treatment. These agents exert their activity by targeting HDAC enzymes, primarily through zinc-binding groups (ZBGs) that chelate the catalytic zinc ion essential for HDAC function. The FDA-approved HDAC inhibitor, romidepsin, and some pre-clinical HDAC inhibitors, including ST7612AA1, KD-5170, and NCH-51, are prodrugs that are converted to their active forms containing thiol as ZBGs. We have previously shown that the sulfhydryl methyltransferases, METTL7A and METTL7B, cause the methylation and subsequent detoxification of thiol-containing compounds, including romidepsin. The goal of this study is to evaluate METTL7A and METTL7B as drivers of resistance to ST7612AA1 in the HepG2 liver cancer cell line. Parental HepG2 cells were selected with ST7612AA1 and valspodar continuously for 3 months to generate ST7612AA1-resistant HepG2 cell lines. The resulting resistant cell lines were characterized using cell proliferation, colony formation, and ATP-based viability assays. The expression of METTL7A and METTL7B by the resistant cells was validated by Western blotting. Our result shows that HepG2-STV50, the ST7612AA1-resistant liver cancer cell line that was selected with 50 micromolar ST7612AA1 and 1 micromolar valspodar, had approximately 80% confluency 6 days post-incubation with 10 micromolar ST7612AA1 and showed 8.7-fold resistance to ST7612AA1, compared to the parent HepG2 cell line. HepG2-STV50 also showed cross-resistance (6.7-fold compared to HepG2) to romidepsin. To compare the effect of METTL7A and METTL7B expression on ST7612AA1 in other cell lines, HT1080 cells transfected with METTL7A and METTL7B were treated with ST7612AA1 and KD5170. Compared to the empty vector-transfected HT1080 cells, the METTL7A-overexpressing cells were more resistant (100-fold) than the METTL7B-overexpressing cells (10-fold). Similarly, MCF-7DpVp300, an MCF-7-derived resistant breast cancer cell line that highly expresses METTL7A, which was selected with romidepsin in the presence of the P-gp inhibitor verapamil, showed approximately 100-fold resistance to ST7612AA1 and KD5170, compared to the parent MCF-7 cell line. The ST7612AA1-resistant HepG2 cell lines overexpressed METTL7B more than METTL7A. Since METTL7B does not confer as much resistance as METTL7A, it may be responsible for the relatively low-fold resistance seen for the ST7612AA1-resistant HepG2-STV50 cells compared to the parental HepG2 cells. While HDAC inhibitors have been effective against T-cell lymphomas, they have not shown success in treating solid tumors. This work establishes METTL7A and METTL7B overexpression as a novel mechanism of resistance to thiol-containing HDAC inhibitors and a potential target for the treatment of solid cancer types.

: Quantitative Pharmacology and Translational Modeling
Poster Session

#1813 A sensitive MSD-ECL platform for in vivo pharmacokinetic profiling of ADCs.

Carla N. Castro, Jonas Hummel, Philipp Metzger, Cynthia Obodozie, **Holger Weber**

Reaction Biology Europe GmbH, Freiburg, Germany

Antibody-drug conjugates (ADCs) are a rapidly evolving class of targeted cancer therapeutics that combine the specificity of monoclonal antibodies with the potency of small-molecule cytotoxic drugs. It is critical for ADCs to be stable in the systemic circulation in order to prevent premature release of the payload, which can lead to off-target toxicity and reduced therapeutic efficacy. The pharmacokinetic (PK) behavior of ADCs is influenced by several factors, such as antibody structural heterogeneity, linker type, and payload physicochemical properties. Stability is a key quality attribute that directly affects dosing strategies, the therapeutic window, and clinical outcomes. Therefore, robust and sensitive analytical platforms are essential for monitoring ADC integrity and payload release over time. While traditional ELISA-based methods are widely used, they often lack the sensitivity and dynamic range required to detect subtle changes in ADC composition during circulation. In this study, we use the Meso Scale Discovery® (MSD) platform, which uses plate-based electrochemiluminescence (ECL) technology, to evaluate the in vivo PK and stability of ADCs. By applying this technology to preclinical in vivo models, we aim to generate high-resolution PK profiles and stability data that support the rational design and optimization of ADCs for clinical development.
Standard 1-Spot SECTOR plates were used to detect the antibody backbone by coating them with a specific capture antibody. Small Spot Streptavidin SECTOR plates were used to detect the intact ADC, capturing the molecule via anti-payload antibodies. In both assays, detection was performed using a sulfo-tagged anti-human IgG antibody. After optimizing the setup, it demonstrated a broad dynamic range of 4-5 orders of magnitude and a lower limit of detection of less than 100 pg/mL for both the antibody and the intact ADC. Subsequent in vivo PK studies involved administering ADCs via a single intravenous injection to SCID beige mice. Serum samples were diluted 1:1000 in PBS containing 1% BSA, and 25 µL per well was applied to the MSD plates. This high dilution factor permits minimal blood volume collection per time point, thereby reducing the number of animals required. The assay demonstrated excellent reproducibility with minimal variability between replicates. To further increase the relevance of the results, future studies may use mFcRn$^{-/-}$ hFcRn transgenic mice or HSA/hFcRn/hFcγR triple transgenic models. These models more accurately reflect the serum half-life of human IgG and correlate well with data from cynomolgus monkeys and humans.
In summary, this MSD-based assay platform offers a highly sensitive and reproducible approach for in vivo PK analysis of ADCs that spares animals. There is potential to further refine this approach using humanized mouse models to improve clinical predictability.

#1814 An integrated DMPK and bioanalytical platform for comprehensive characterization of antibody-drug conjugates (ADCs).

Kefeng Gong[1], Xinhe Feng[1], Zhengyi Hua[1], Yanting Ma[1], Rui Wang[1], Xiaolong Tu[1], Luke Yu[2]

[1]Crown Bioscience, Taicang, China,[2]Crown Bioscience, Inc., San Diego, CA

Introduction: Antibody-drug conjugates (ADCs) represent a transformative class of targeted oncology therapeutics; their complex structure introduces significant challenges in characterization, necessitating a holistic DMPK strategy to understand their *in vitro* stability, *in vivo* PK and biodistribution, and biotransformation. The success of this strategy hinges on the precise quantification of key analytes—including total antibody (Tab), conjugated antibody (ADC), free payload, and the drug-to-antibody ratio (DAR)—in diverse biological matrices. Here, we present an integrated DMPK platform evaluating Trastuzumab Deruxtecan (T-DXd), Enfortumab Vedotin (EV), and Trastuzumab Emtansine (T-DM1), with distinct linkers/payloads, to delineate PK behavior and biotransformation pathways.
Methods: For three marketed ADCs, including T-DXd, EV, and T-DM1, *in vitro* plasma stability was assessed in human, monkey, rat, and mouse plasma (37 °C, 7-21 days) and followed a single 10 mg/kg i.v. dose for *in vivo* PK in naïve C57BL/6 mice. Quantitation used ligand binding assay (total and conjugated antibody), LC-MS/MS for free payload (LLOQ 10-50 pg/mL), and hybrid immunocapture LC-HRMS for DAR and biotransformation assessment.
Results: T-DXd, with a cleavable peptide linker and high baseline DAR (~7.6), demonstrated high stability *in vitro*, showing less than 40% DAR decrease (to ~4.8) over 7 days and minimal free DXd release (<2% across species). It's *in vivo* DAR gradually declined to ~4.0 by Day 14, with highly overlapped PK curves for Tab and conjugated ADC. EV, incorporating a protease-cleavable linker and a baseline DAR of ~3.5, exhibited faster degradation *in vitro*, with DAR dropping to ~1.6 and significant MMAE release (~74 ng/mL at 24 h in mouse plasma). *In vivo*, ADC levels displayed a more rapid decline than Tab, accompanied by a marked DAR decrease to ~0.5 by Day 21. T-DM1, featuring a non-cleavable thioether linker and DAR ~3.5, displayed very high plasma stability and negligible free DM1 release (<0.1 ng/mL). It's *in vivo* PK profiles for Tab and ADC were nearly identical, confirming minimal payload release in circulation. For ADCs lacking anti-payload reagents, we also developed a hybrid approach combining DAR-insensitive Tab assay with LC-HRMS-based DAR profiling. This flexible bioanalytical strategy enabled comprehensive characterization across diverse ADC formats.
Conclusion: Our integrated DMPK platform provides comprehensive and robust ADC characterization capability, promoting critical insights into ADC stability, biotransformation, and exposure profiles. This supports direct correlation between ADC design, *in vitro* properties, and *in vivo* PK behavior, thereby de-risking candidate selection and accelerating the development of novel ADC therapeutics.

#1815 Nonclinical characterization of SBE303: A nectin-4 targeted antibody drug conjugate (ADC) with novel topoisomerase 1 inhibitor shows a favorable safety margin.

Ji Yeon Kim, Sungwoo Hyung, Hyun-Ji Choi, Songhyun Lim, Jae Hee Lee, Seokuee Kim, Donghyun Kim, So-Shin Ahn, Donghoon Shin

Samsung Bioepis Co., Ltd., Incheon, Korea, Republic of

Antibody-drug conjugates (ADCs) targeting Nectin-4 have emerged as a promising therapeutic approach particularly in urothelial carcinoma (UCs). However, currently available Nectin-4 directed ADCs are often limited by narrow therapeutic index and dose-limiting toxicities. SBE303 is a novel Nectin-4 targeting ADC engineered to improve the therapeutic window by combining a highly specific anti-Nectin-4 antibody conjugated with a potent novel topoisomerase I inhibitor via a proprietary beta-glucuronide-based cleavable linker, OHPAS^{TM}.

For nonclinical characterization of SBE303, a comprehensive set of pharmacology, pharmacokinetics, and toxicology studies was performed. In vitro studies have shown that the antibody of SBE303 exhibits specific binding to the human Nectin-4. Upon binding, SBE303 internalizes into cancer cells, which then traffics to the lysosomal compartment where payload is released via beta-glucuronidase cleavage of the linker. Released payload induces DNA topoisomerase I inhibition, triggering cytotoxicity in various cancer cells.

The antitumor efficacy of SBE303 was evaluated across multiple Nectin-4 positive cell-derived xenograft models including UC. SBE303 treatment resulted in marked and statistically significant tumor growth inhibition compared to vehicle controls on week 3, supporting the broad therapeutic potential in solid cancers.

Pharmacokinetic properties were evaluated in mice, rats, and monkeys. Comparable profiles between SBE303 and total antibody showed the linker stability in systemic circulation, supported by minimal free payload exposure. Novel free payload showed low risk of drug-drug interaction potential for metabolic enzymes and drug transporters.

In repeat-dose toxicity study in cynomolgus monkeys, IV administration of SBE303 was well tolerated at 40 mg/kg/dose. No severe systemic toxicity or unexpected target-related findings were observed, including skin toxicity. SBE303-related findings were limited to minimal-to-moderate changes and were reversible at the end of the recovery period. The absence of significant histopathologic changes indicated a favorable systemic safety profile.

These nonclinical findings support the advancement of SBE303into clinical development with a favorable therapeutic index based on higher tolerated doses and wider exposure margins compared to known approved anti-Nectin4 ADC. A first-in-human study is expected to initiate in 2026.

#1816 ACSL4 mediated ferroptosis and its potential role in enhancing the efficacy of antibody-drug conjugates.

Shigehiro Koganemaru[1], Hirobumi Fuchigami[2], Hiroshi Tsugawa[3], Hiroko Shinohara[1], Yasutoshi Kuboki[1], Toshimitsu Uenaka[4], Toshihiko Doi[5], Masahiro Yasunaga[6]

[1]National Cancer Center Hospital East, Kashiwa, Japan,[2]National Cancer Ctr. Hosp. East, Kashiwa, Japan,[3]Tokyo University of Agriculture and Technology, Tokyo, Japan,[4]Eisai Co., Ltd., Tsukuba, Japan,[5]National Cancer Centre Hospital East, Kashiwa, Japan,[6]Investigative Treatment Div., National Cancer Center Hospital East, Kashiwa, Japan

Purpose: While antibody-drug conjugates (ADCs) are generally assumed to preserve the pharmacokinetic/pharmacodynamic (PK/PD) properties of their payloads, the extent to which conjugation alters their mechanism of action remains underexplored. This study investigated whether ADC conjugation can fundamentally reprogram payload pharmacology and clarified the downstream consequences for antitumor efficacy and immune activation beyond conventional delivery advantages.
Experimental Design: Using MORAb-202, an ADC consisting of the clinically approved eribulin linked to a folate receptor alpha (FRα)-targeting antibody, we performed intratumoral pharmacokinetic/pharmacodynamic (PK/PD) and pharmacometabolomic analyses in xenograft models with varying FRα expression. Intratumoral concentrations of released eribulin and phospholipid profiles were quantified by liquid chromatography-mass spectrometry. We compared effects of MORAb-202 and free eribulin on ferroptosis, immunogenic cell death (ICD), and tumor immune infiltration. Therapeutic efficacy was tested as monotherapy and in combination with pembrolizumab in a human peripheral blood mononuclear cells co-implantation model.
Results: ADC-conjugated eribulin achieved >20-fold higher intratumoral retention of eribulin compared to the free eribulin in AUC value. Metabolomics analysis revealed that MORAb-202 robustly induced ferroptosis, characterized by ACSL4 upregulation, GPX4 depletion, lipid peroxidation, and arachidonic acid remodeling. Unlike free eribulin, MORAb-202 triggered ICD, evidenced by HMGB1 expression and enhanced recruitment of total/activated/PD-1$^+$ T cells and dendritic cells. Furthermore, ferroptosis responses induced by free eribulin were reversible, whereas ADC-conjugated eribulin induced irreversible and sustained responses. The combination of MORAb-202 with pembrolizumab enhanced tumor control beyond either monotherapy.
Conclusions: ADC conjugation reprograms payload's pharmacodynamics, inducing ferroptosis and ICD unattainable with free payload, even at clinically equivalent doses. This highlights a pharmacodynamic threshold unique to the ADC formulation. These findings stress the need for intratumoral PK/PD evaluation and identify ferroptosis-linked lipid remodeling as a novel ADC mechanism, supporting rational combination with immunotherapy in precision oncology.

#1818 Overcoming resistance with OBI-902: Preclinical evaluation of a next-generation TROP2 ADC.

Ren-Yu Hsu, **Chi-Huan Lu**, Chi-Sheng Shia, Jing-Rong Huang, Hsin-Shan Wu, Lu-Tzu Chen, Jhih-Jie Yang, Tzu-Min Yen, Jyy-Shiuan Tu, Yu-Hsuan Tsao, Ya-Chi Chen

OBI Pharma, Inc, Taipei, Taiwan

Trophoblast cell surface antigen 2 (TROP2) is a clinically validated target. However, existing TROP2 ADCs show distinct toxicities, such as myelosuppression (sacituzumab govitecan) and stomatitis/interstitial lung disease (datopotumab deruxtecan). These toxicities underscore the need for safer ADCs. OBI-902 is a novel, site-specific ADC designed to address this gap. It consists of a humanized anti-TROP2 antibody conjugated to a topoisomerase I inhibitor via glycan-based site-specific platform, which generates a highly stable and homogeneous ADC optimized for enhanced antitumor activities and reduced systemic toxicity. This study investigates the exposure-response relationships to further characterize its pharmacologic and therapeutic profile.

A comprehensive preclinical data package was generated for OBI-902. The pharmacokinetic-pharmacodynamic (PK-PD) relationship was characterized to define exposure-response parameters in non-small cell lung cancer (NSCLC) xenograft models. Antitumor efficacy was evaluated across multiple dosing regimens in NSCLC models, patient-derived xenografts (PDX) from various cancer types, and cell line-derived xenografts (CDX) engineered for TROP2 resistance. The safety profile was formally established in a GLP-compliant toxicology study in non-human primates, supporting further development.

In an NSCLC xenograft model, OBI-902 exhibited a predictable and dose-proportional PK profile at doses ≥3 mg/kg, establishing a clear exposure-response relationship. This translated to durable anti-tumor activity at extended dosing intervals (3 mg/kg): the Q3W regimen induced complete regressions (CRs) in 2/5 animals by day 35, while both Q4W and Q6W regimens achieved sustained tumor stasis through day 62. OBI-902 demonstrated robust tumor growth inhibition, including regressions, across a diverse panel of ten PDX models encompassing NSCLC, triple-negative breast cancer (TNBC), and gastric cancer. To address acquired resistance, In TOP1 ADC-resistant NSCLC and TNBC CDX models, OBI-902 demonstrated superior efficacy, yielding >3-fold and >2-fold smaller mean tumor volumes, respectively, compared to the TOP1 inhibitor-based ADCs, highlighting its potential to overcome resistance. In a GLP-compliant toxicology study in cynomolgus monkeys, OBI-902 was well-tolerated with a NOAEL of 30 mg/kg, supporting a wide therapeutic index for clinical development.

OBI-902 exhibits broad and potent antitumor activity across multiple cancer models, including those resistant to prior TOP1 ADCs, along with a favorable safety profile. Taken together, these preclinical results support the clinical development of OBI-902, which is currently being evaluated in a Phase 1/2 clinical trial as a potential best-in-class TROP2-targeted ADC.

#1819 OBI-904, a glycan-based site-specific Nectin-4-targeted ADC, demonstrates potent and durable antitumor activity with an improved PK profile and overcoming EV-resistance in non-clinical studies.

Chi-Huan Lu, Ren-Yu Hsu, Jing-Jie Ciou, Tzu-Min Yen, Jyy-Shiuan Tu, Yu-Hsuan Tsao, Jing-Rong Huang, Ya-Chi Chen

OBI Pharma, Inc, Taipei, Taiwan

Nectin-4 is a type I transmembrane adhesion molecule with low expression in normal tissues but is highly overexpressed in multiple cancers. Its expression is associated with tumor proliferation, metastasis, and poor prognosis, making it a clinically validated target for ADC development. Although *Padcev* (enfortumab vedotin, EV) has demonstrated meaningful clinical benefit, safety concerns, suboptimal dosing schedules, and emerging resistance underscore the need for next-generation Nectin-4-targeted ADCs. OBI-904 is a Nectin-4-targeted ADC conjugated with the topoisomerase I inhibitor Exatecan (DAR 8) via glycan conjugation platform and dual-action enzymatic technology, designed to provide homogenous DAR, improve ADC stability, and optimal payload delivery. In vitro linker-payload stability was evaluated in human serum albumin by LC-MS. Pharmacokinetics (PK) were assessed in serum and tumor using HNSCC xenograft models. Antitumor activity was tested in CDX models of HNSCC, CRC, TNBC, prostate cancer, cholangiocarcinoma, and in PDX models of cervical and sarcoma, as well as in an EV-resistant bladder CDX model, with Padcev and ETx-22 as benchmarks. GLP toxicology studies were conducted in cynomolgus monkeys at 5, 15, and 30 mg/kg Q2W for three doses (Days 1, 15, 29), followed by a six-week recovery period. OBI-904, the glycan conjugated ADC, maintained a 100% DAR in serum albumin, longer half-life, overcoming the instability associated with conventional cysteine-based linkers. OBI-904 exhibited improved pharmacokinetics and slow release of payload in tumor cells for prolonged anti-tumor responses. In vivo, OBI-904 demonstrated potent antitumor activity across multiple models, including CDX models of HNSCC, CRC, TNBC as well as PDX models of cervical and sarcoma, showing antitumor effect independent of Nectin-4 expression levels. Durable responses were observed in prostate (high Nectin-4) and cholangiocarcinoma (low Nectin-4) CDX models. Notably, OBI-904 effectively overcame EV-resistant bladder cancer, highlighting its potential to address acquired resistance. In the GLP toxicology studies, a highest non-severely toxic dose (HNSTD) of 30 mg/kg was determined in non-human primates with favorable toxicology findings. OBI-904, a next-generation Nectin-4-targeted ADC with optimized stability and payload delivery, demonstrated potent antitumor activity across multiple models, including EV-resistant tumors, independent of Nectin-4 expression. Favorable pharmacokinetics and toxicology support its further clinical development as a promising therapy for Nectin-4-expressing cancers.

#1820 Pharmacokinetic-tumor growth inhibition modeling of raludotatug deruxtecan (R-DXd) to support phase 3 dose selection in platinum-resistant ovarian cancer (PROC).

YoungJun Yoo[1], Kevin Koloskoff[2], Sandra Re[1], Izna Ali[1], Felipe K. Hurtado[1], Raouf El Cheikh[2]

[1]Daiichi Sankyo, Inc., Basking Ridge, NJ,[2]Daiichi Sankyo France, SAS, Rueil-Malmaison, France

Background: R-DXd is a novel cadherin 6 (CDH6)-directed antibody-drug conjugate (ADC) under clinical investigation. In ongoing Phase 1 DS6000-A-U101 (NCT04707248) and Phase 2/3 REJOICE-Ovarian01 (NCT06161025) studies, preliminary data showed promising results in patients with platinum-resistant ovarian cancer (PROC). To support dose selection in PROC, a pharmacokinetic-tumor growth inhibition (PK-TGI) model was developed to investigate the effect of R-DXd exposure on tumor size and predict percent change from baseline in tumor size across R-DXd doses of interest (4.8, 5.6, and 6.4 mg/kg), as well as explore the effect of CDH6 expression levels on tumor response.

Methods: The analysis dataset comprised 229 patients enrolled from either study who completed at least 18 weeks of follow-up (ie, 3 postbaseline tumor scans). Time-course data of PK (ADC and released payload [DXd] plasma concentration) and tumor size (sum of longest diameters [SLD], assessed by blinded independent central review [BICR]) were collected from PROC patients treated with R-DXd monotherapy at 1.6-9.6 mg/kg IV Q3W in DS6000-A-U101 and the dose optimization part of REJOICE-Ovarian01. The PK-TGI model was developed using nonlinear mixed-effects modeling and adapted from previously published TGI modeling frameworks by Claret et al. Simulations accounting for parameter uncertainties were conducted to predict tumor response of R-DXd treatment across dose levels for a typical reference patient.

Results: Model parameters were estimated with good precision, and goodness-of-fit plots showed that model predictions describe data appropriately. The final model was comprised of three components: 1) a drug-induced tumor killing rate (k_{kill}) driven by R-DXd concentration, which is 2) attenuated over time by a resistance term ($e^{-\lambda \cdot t}$), and 3) tumor growth described as a saturated logistic function, $k_{ge} \times TS \times (1 - TS/TS_{max})$, in which k_{ge} represents the intrinsic growth rate, TS tumor size, and TS_{max} the maximum tumor size. The simulations demonstrated a clear exposure-response relationship, with higher doses of R-DXd associated with stronger tumor shrinkage: predicted median tumor shrinkage at 24 weeks was –52%, –58%, and –64% for 4.8, 5.6, and 6.4 mg/kg, respectively. Additionally, baseline CDH6 protein expression was identified as a significant covariate on k_{kill} parameter, positively associated with tumor shrinkage, with its effect tending to plateau with increasing expression levels.

Conclusions: The PK-TGI model could adequately characterize changes in tumor size as a function of R-DXd concentration as well as quantify the effect of target expression on tumor shrinkage. Combined with the totality of clinical data and an overall assessment of benefit-risk, the analyses supported the selection of 5.6 mg/kg Q3W as the optimal monotherapy dose of R-DXd for the Phase 3 part of the REJOICE-Ovarian01 study.

#1821 Preclinical efficacy and safety of CS5006, a novel integrin β4-targeting antibody-drug conjugate with a topoisomerase 1 inhibitor payload.

Chuan Wang, Xinling Zhang, Ning Zhang, Yamin Wang, Yongwang Li, Mengyao Zhu, Xuelian Liu, Yaxin Chen, Yuxin Qian, Yongli Yang, Jingyu Sun, Fei Ma, Jianxin Yang

CStone Pharmaceuticals, Suzhou, China

Background: Integrin β4 (ITGB4) is highly expressed in colorectal carcinoma (CRC), non-small cell lung cancer (NSCLC), squamous cell carcinoma of the head and neck (SCCHN), esophageal squamous cell carcinoma (ESCC), and other solid tumors. CS5006 is a novel ITGB4-targeting antibody-drug conjugate (ADC) composed of an ITGB4-specific humanized IgG1 antibody (H86.2) conjugated to the clinically validated exatecan (Exa) payload via a highly stable, hydrophilic tandem-cleavage CSL linker, with a drug-to-antibody (DAR) value of 4.

Methods: The potency of CS5006 was evaluated in viability assays across a panel of cancer cell lines with varied ITGB4 expression levels. Its antitumor efficacy was evaluated in cell-derived xenograft (CDX) mouse models. ITGB4 expression level on tumor cell lines applied *in vitro* and *in vivo* studies was determined by quantitative flow cytometry and immunohistochemistry (IHC) assays. Its NHP safety and pharmacokinetics (PK) were assessed at three dose levels including 10, 30, 50 mg/kg. The physical stability under accelerated conditions (40°C for 2 weeks and freeze-thaw for 5 cycles) was assessed by SEC-HPLC for purity and by RP-HPLC for DAR value.

Results: CS5006 demonstrated potent, target-dependent killing of ITGB4-positive cancer cell lines with potency positively correlating with antigen expression levels (nanomolar range IC50 against high-expressing cells). A single 10 mg/kg dose of CS5006 induced tumor regression across all 9 CDX models, representing NSCLC (n=4), CRC, SCCHN, urothelial carcinoma (UC), gastric cancer (GC) and breast cancer (BC). In a repeat-dose toxicity study, CS5006 was well tolerated in cynomolgus monkeys during the study. Systemic exposure of the ADC was comparable to the total antibody, and increased dose-proportionally, suggesting CS5006's remarkable circulating stability. CS5006 exhibited excellent developability, maintaining stable after five freeze-thaw cycles and after 2 weeks at 40°C.

Conclusions: CS5006 demonstrates high potency, robust antitumor activity, a manageable safety profile, and excellent developability in preclinical studies, supporting its clinical translation. An IND application for CS5006 is planned for H2 2026 to support clinical development in patients with advanced solid tumors.

#1822 Preclinical efficacy and safety of CS5008, a novel SSTR2×DLL3 bispecific antibody-drug conjugate (ADC) with topoisomerase 1 inhibitor payload for small cell lung cancer and neuroendocrine tumors.

Chuan Wang, Yongwang Li, Ning Zhang, Yamin Wang, Xinling Zhang, Xuelian Liu, Yuxin Qian, Hui Dai, Xueqin Dai, Yaxin Chen, Zicong Zheng, Wenjing Xiang, Fei Ma, Jianxin Yang

CStone Pharmaceuticals, Suzhou, China

Background: CS5008 is a first-in-class bispecific ADC targeting SSTR2 and DLL3, constructed on CStone's proprietary modular ADC platform. It comprises a bispecific antibody with high affinity for both targets, a proprietary tandem-cleavable β-glucuronide linker (CSL20), and the topoisomerase 1 inhibitor exatecan as payload (drug-to-antibody ratio = 4). CS5008 is designed to overcome tumor heterogeneity in small cell lung cancer (SCLC) and neuroendocrine tumors (NETs) by simultaneously targeting two clinically validated antigens with complementary expression profiles. SSTR2 is a well-established target in neuroendocrine tumors (NETs/NECs). DLL3 is a clinically validated target in SCLC, serving as the target of tarlatamab, a T-cell engager. However, tumor heterogeneity and subtype plasticity often limit the effectiveness of single-target approaches in SCLC. CS5008 is a first-in-class bispecific ADC designed to address this challenge by simultaneously targeting SSTR2 and DLL3. It is constructed on CStone's proprietary modular ADC platform and comprises a bispecific antibody with high affinity for both targets, a proprietary tandem-cleavable β-glucuronide-cathepsin linker (CSL20), and the topoisomerase 1 inhibitor exatecan as payload (drug-to-antibody ratio = 4).

Methods: CS5008 was evaluated *in vitro* for binding affinity, internalization, and cytotoxicity using tumor cell lines with varied SSTR2/DLL3 expression levels. *In vivo* efficacy was assessed in multiple SCLC xenograft (CDX) models (e.g., H524, H69, H82, H446, COR-L279, SHP77). Pharmacokinetics (PK) and tolerability were studied in rodents and non-human primates, including preliminary toxicology assessments at doses of 30, 45, and 60 mg/kg administered every three weeks (Q3W).

Results: CS5008 exhibited nanomolar binding affinity for both DLL3 and SSTR2, both of which were determined by flow cytometry (FACS) on SCLC tumor cells. It induced rapid internalization and potent, antigen-dependent cell killing in SSTR2+/DLL3+ models (e.g., IC50 of 1.54 nM in H524 cells). A single treatment with 10 mg/kg CS5008 achieved significant tumor growth inhibition in all 5 tested SCLC CDX models with different expression level of DLL3 and SSTR2 assessed by FACS, indicating the designated character of CS5005 to overcome the heterogeneity of SCLC. PK profiles in rodents and non-human primates demonstrated CS5008's high circulating stability. In cynomolgus monkeys, CS5008 was well-tolerated at doses up to 60 mg/kg.

Conclusions: CS5008 demonstrated potent antitumor activity against SCLC by dual targeting of SSTR2 and DLL3, effectively addressing heterogeneity. Its favorable preclinical safety and robust PK support further clinical development. An IND application is expected by the end of 2026.

#1823 Preclinical efficacy and safety of CS5007, an EGFR×HER3 dual-targeting antibody-drug conjugate with a topoisomerase 1 inhibitor payload.

Chuan Wang, Yamin Wang, Ning Zhang, Xinling Zhang, Yongwang Li, Yuxin Qian, Yaxin Chen, Yongli Yang, Xuelian Liu, Mengyao Zhu, Hui Dai, Wenjing Xiang, Xueqin Dai, Fei Ma, Jianxin Yang

CStone Pharmaceuticals, Suzhou, China

Background: EGFR and HER3, members of the ErbB receptor family, are key oncogenic drivers that are frequently co-overexpressed across a variety of human epithelial malignancies, Both EGFR and HER3 are clinically validated therapeutic targets for cancer therapies. Therefore, simultaneously targeting both EGFR and HER3 offers a promising strategy to overcome tumor heterogeneity and adaptive resistance commonly observed with single-target approaches. CS5007 is constructed with 1) functional EGFR&HER3 arm to tackle tumor heterogeneity; 2) hydrophilic beta-glucuronide linker (our proprietary CSL20 linker) to ensure that the ADC has a mAb-like PK profile, stability and tumor selective cleavage; 3) potent, well-tolerated and clinically validated topoisomerase 1 inhibitor exatecan (Exa) conjugated to the antibody with a drug-to-antibody ratio (DAR) of 4.

Methods & Results: CS5007 demonstrated high-affinity binding (single digit nM) to EGFR/HER3 single- and double-positive tumor cells, comparable to its naked bispecific antibody and its parental antibodies. Western blot analysis of tumor cell lines revealed that naked bispecific antibody treatment led to strong inhibition of ligand-induced EGFR/HER3 downstream signaling, indicating effective blockade of proliferative pathways and induction of apoptosis. CS5007 induced rapid internalization and potent cell killing in tumor cell lines, demonstrating its potential to overcome tumor heterogeneity. It also showed superior *in vitr*o cytotoxicity over a bispecific control ADC (BL-B01D1 analog) and monospecific EGFR- or HER3-targeting ADCs in various tumor cell lines, including an osimertinib-resistant NSCLC model. A single treatment with 5 mg/kg CS5007 demonstrated robust, antigen-dependent antitumor activity across multiple xenograft (CDX) models, including EGFR+, HER3+, and dual-positive tumors. CS5007 showed strong tumor growth inhibitory ability comparable to or exceeding that of the anti-EGFR and anti-HER3 monospecific ADCs, as well as the bispecific control BL-B01D1. CS5007 exhibited a mAb-like PK profile in the rodent model. *In vitro* human, mouse, and cyno serum studies showed minimal payload release after 7 days, suggesting robust stability in circulation. CS5007 was well tolerated in cynomolgus monkeys at 30 mg/kg, with dose-dependent hematolymphoid and intestinal effects being its major toxicity findings, consistent with other EGFR targeting treatment. Cyno TK data further confirmed its excellent circulating stability.

Conclusions: With demonstrated enhanced signaling inhibition, superior efficacy across multiple solid tumor models, and a favorable safety margin in preclinical studies, CS5007 is planned for an IND submission in early 2026 to support clinical development in advanced solid tumors.

#1824 ORM-1153: A Next-Generation CD123-Targeting Degrader Antibody Conjugate (DAC).

Adam T. Boutin[1], Dong-Ki Choi[2], YeonHee Yang[2], Jessica Alves[1], MinSoo Kim[2], Da-Yeong Kim[2], Khuloud Takrouri[1], Qinsi Zheng[1], Nadia Cherkassky[1], Anna Skaletskaya[1], Teresa Mako[1], VineetKumar Patil[2], Hangyeol Jeong[2], Olaf Christensen[1], Maysoun Shomali[1], Sang Hyun Lee[2], James Palacino[3]

[1]Orum Therapeutics, Boston, MA,[2]Orum Therapeutics, Daejeon, Korea, Republic of,[3]Little Castle Consulting, Boston, MA

ORM-1153 is a next-generation CD123-targeting Degrader Antibody Conjugate (DAC) designed to improve safety and therapeutic index through advanced antibody and linker engineering. DACs combine the tissue selectivity of antibody-mediated delivery with the well-validated catalytic mechanism of targeted protein degradation, offering opportunities to expand beyond conventional cytotoxic ADC payloads. ORM-1153 is comprised of a proprietary GSPT1-degrading payload (SMol006) conjugated to a high-affinity anti-CD123 antibody via a novel β-glucuronide cleavable linker. The antibody was engineered to minimize Fc gamma receptor interactions, reducing off-target and immune cell engagement, while the linker was optimized for enhanced plasma stability. Together, these modifications combined to produce a molecule with a robust preclinical therapeutic index (TI), suggesting the potential for ORM-1153 in the clinic. ORM-1153 was determined to have a minimal efficacious dose (MED) of 0.1 mg/kg in a disseminated AML model. Efficacy was superior to standard of care (SoC) and to a competitor ADC: anti-CD123/TOP1i. Improved efficacy correlated with a better PK profile consisting of a longer plasma half-life and minimal or undetectable free payload at most timepoints with a LLOQ of 1 ng/ml. Because SMol006 is a CRBN-based molecular glue degrader; rodent species have amino acid differences in CRBN that renders their cells insensitive to the MoA. Therefore, the relevant species for assessing tolerability is non-human primates (NHP). ORM-1153 had a favorable safety profile in repeat-dose monkey studies with clinical pathology findings limited to transient, reversible reductions in platelets and transient, reversible increases in clotting times, fibrinogen and C-reactive protein. Of note, hepatic biomarkers remained within the normal range. Consistent with a common ADC toxicity of thrombocytopenia and prior findings with our DACs, we observed transient and reversible decreases in platelet levels. These results highlight how molecular engineering of both the antibody and linker can dramatically shift the balance between efficacy and tolerability for complex bioconjugates. Collectively, ORM-1153 exemplifies a rationally engineered DAC with superior pharmacologic properties, including robust potency and a broad therapeutic window, supporting advancement toward clinical introduction

#1825 QSP modeling to inform dose and regimen selection for TAK-280: A bi-specific antibody.

Agnish Dey[1], Tao Long[1], Sabrina Collins[1], Dean Bottino[2], Jaydeep Srimani[1], John Gibbs[1]

[1]Takeda Pharmaceuticals, Cambridge, MA,[2]DMPK&M, Oncology Therapeutic Area, Takeda Development Center Americas, Cambridge, MA

Background: CD3-targeting T cell engagers (TCE) have been approved as therapy for various hematological and solid tumor oncology indications; however, they can often induce unwanted safety issues, including cytokine release syndrome (CRS) and liver enzyme elevations. TAK-280 is an investigational B7-H3 x CD3ε conditional bispecific redirected activation (COBRA) TCE. In its masked prodrug form, TAK-280 binds to B7-H3, but not to CD3ε. Once in the protease-rich tumor microenvironment, proteases mediate cleavage of the linker resulting in unmasking the prodrug, which allows for the formation of active CD3ε-binding dimers and ultimately CD3 T-cell activation and cytotoxic anti-tumor response against co-engaged B7-H3 expressing cells. We developed a mechanistic PK/PD modeling framework to describe the PK and safety of TAK-280, based on clinical data from a Phase 1 dose escalation study (NCT05220098) investigating TAK-280 for the treatment of patients with advanced, unresectable or metastatic cancer, with a focus on tumor types with enhanced B7-H3 expression.

Methods: In the tumor compartment of the model, TAK-280 binds to B7-H3 expressed on tumor cells. Once the dimer is formed, it binds to CD3 to form the desired trimer complex composed of TAK-280, B7-H3 and CD3. It is assumed that this trimer complex is the only species that triggers cytokine release in the tumor compartment. Once cytokines are secreted in the tumor, they are assumed to move to systemic circulation. In the central compartment, cytokines undergo basal production and degradation.

Results: A two-compartment model with linear elimination was sufficient to describe the PK. Cytokine dynamics were described using a three-population immune cell pool[1] (non-secreting, secreting and refractory) framework. Immune cell dynamics reveal that the cytokine Cmax attenuation over time is a consequence of immune cell de-sensitization by transitioning to the refractory state. This concept of de-sensitization or decreased cytokine release following TCE dosing is clinically well established and mechanistically it is attributed to fewer non-secreting immune cells that are available by the time the top dose is administered (in a lead-in dosing regimen).

Conclusion: Using the model, we were able to show that lead-in dosing led to lower cytokine peak concentrations and therefore predicted lower probability for an adverse event. Model simulations demonstrated comparable safety outcomes for both QW and BIW dosing of the bispecific antibody.

References: 1.Weddell et. al. *CPT Pharmacometrics Syst Pharmacol.* 2023; 12:1726-1737

#1826 Exposure-response analysis and quantitative systems pharmacology modeling for an optimal dose selection of surovatamig in patients with DLBCL.

Xu (Sue) Zhu[1], Damilola Olabode[1], Massimo Lai[2], Cesar Pichardo-Almarza[2], Meenu Pillai[3], Denise Brennan[1], David Sermer[4], Robin Lesley[5]

[1]AstraZeneca, Waltham, MA,[2]AstraZeneca, Cambridge, United Kingdom,[3]AstraZeneca, Gaithersburg, MA,[4]AstraZeneca, New York, NY,[5]AstraZeneca, South San Francisco, CA

Introduction: Surovatamig (formerly AZD0486) is a novel, IgG4 fully human CD19xCD3 bispecific T-cell engager that is being evaluated in an ongoing phase 1 study (NCT04594642) in patients (pts) with relapsed or refractory (R/R) B-cell non-Hodgkin lymphoma (B-NHL). Here, we present our quantitative approaches for determining an optimal dose for surovatamig in pts with R/R diffuse large B-cell lymphoma (DLBCL) with population pharmacokinetics (popPK), exposure-response (ER) analysis, and quantitative systems pharmacology (QSP) modeling.

Methods: Pts with R/R B-NHL received escalating doses of surovatamig IV with fixed dosing, single step-up dosing (SUD), or double SUD schedules in cycle 1, followed by target dose (TD) every 2 weeks in 28-day cycles for up to 24 months. PK data from serial sampling was used to develop a popPK model in NONMEM®. ER relationships between surovatamig PK and overall response rate (ORR) or complete response rate (CRR) were characterized in pts with DLBCL. Further, QSP modeling was developed to link the surovatamig PK to the trimeric complex formation. A total of 185 pts with all histology (DLBCL, follicular lymphoma [FL], and mantle cell lymphoma/marginal zone lymphoma) were analyzed for PK and safety, and 100 pts with DLBCL were analyzed for efficacy (based on data cutoff of August 2025).

Results: Following IV infusion, the observed mean half-life of surovatamig is ~11 days across the dose cohorts after the cycle 1 day 15 dose. A dose-proportional increase in exposure is observed across the dose ranges (≥0.27 mg). Surovatamig PK was best described by a 2-compartment PK model with linear clearance and was comparable in pts with FL and DLBCL. No covariates (eg, disease type, race, age) other than body weight were identified to have a significant impact on PK parameters (clearance and volume of distribution). Exposure-efficacy analysis in pts with R/R DLBCL showed higher probability of ORR and CRR with increasing exposures (eg, $C_{avgcycle1\&2}$ or C_{trough}) across the dose range, supporting a TD of 25 mg in pts with DLBCL. Based on the QSP model calibrated with preclinical and emerging clinical data (eg, sum of the long diameter of target lesions), the maximal median trimer concentration at the tumor site increases across the TD of 2.4-37.5 mg. Predictions suggested no significant increments in ORR by increasing the TD from 25 mg to 37.5 mg. Overall, QSP modeling and simulation results support the TD of 25 mg as an optimal recommended phase 2 dose (RP2D) for efficacy. Exposure-safety analysis showed no clear association of exposure after TD with Gr2+ CRS or ICANS, or Gr4+ neutropenia.

Conclusion: ER analysis and QSP modelling confirmed the clinical benefit with increased TD from 2.4 to 25 mg in pts with R/R DLBCL, with no clear TD-dependent clinically relevant toxicity, supporting 25 mg as the RP2D.

#1827 Combining PRC2 inhibitors with metronomic chemotherapy: A promising therapeutic strategy for diffuse large B-cell lymphoma.

Marta Banchi[1], Maryam Latarani[2], Paola Orlandi[3], Kayleigh Orchard[2], George Bryant[2], Francesco Crea[2], Guido Bocci[1]

[1]Department of Translational Research and of New Surgical and Medical Technologies, University of Pisa, Pisa, Italy,[2]Cancer research Group, School of Life, Health and Chemical Sciences, The Open University, Milton Keynes, United Kingdom,[3]Department of Clinical and Experimental Medicine, University of Pisa, Pisa, Italy

Diffuse large B-cell lymphoma (DLBCL) is the most common aggressive non-Hodgkin lymphoma (NHL). Most attempts to combine standard chemo-immunotherapy with targeted drugs have failed due to limited synergy or excessive toxicity. Enhancer of zeste homolog 2 (EZH2) is the catalytic subunit of the polycomb repressive complex 2 (PRC2) acting as a transcriptional repressor by methylating histone H3 at lysine 27 (H3K27me3). Activating mutations in EZH2 in NHL correlate with poor survival. We aimed at using metronomic chemotherapy (mCHEMO)—the frequent, regular administration of low-dose cytotoxic drugs that maintain prolonged and active drug-plasma levels—in combination with new epigenetic therapies as a promising, more effective and less toxic approach for DLBCL treatment. In vitro proliferation assays were performed on both $EZH2^{Y641F}$ mutant (SU-DHL10) and EZH2 wild-type (OCI-LY3, Toledo) DLBCL cell lines exposed to thrice-weekly vinorelbine (mVNR) and daily PRC2 inhibitors (PRC2i: tazemetostat, valemetostat, ORIC-944), alone and in concomitant combination, for 144h. Synergism was measured by the Combination Index method and the Loewe additivity model. PRC2i target engagement was assessed by H3K27me3 western blot. The modulation of gene expression in DLBCL cells treated with 144h-daily valemetostat was evaluated by RNA sequencing. The 144h exposure of daily PRC2i and mVNR inhibited the DLBCL cell viability in a concentration-dependent manner. Among the PRC2i, valemetostat exhibited the greatest cytotoxic effect on SU-DHL10, OCI-LY3 and Toledo cells (IC_{50}s: 3.09nM, 371nM, and 303nM, respectively). ORIC-944 also effectively reduced DLBCL cell growth (IC_{50}s: 8.7nM, 721nM, and 1,388nM, respectively). Tazemetostat significantly inhibited DLBCL cell viability, with higher IC_{50} values (1,389nM, 3,481nM, and 8,597nM, respectively). mVNR substantially arrested the proliferation of all cell lines (IC_{50}s: 508.9pM, 62.9pM, and 675.6pM, respectively). The strongest synergistic effect was observed for the mVNR+valemetostat combination, while mVNR+ORIC-944 showed synergism only for high percentage of affected DLBCL cell fractions. PRC2i markedly reduced H3K27me3 levels in DLBCL cells. Among the differentially expressed genes, we observed more up-regulated than down-regulated transcripts upon PRC2 inhibition, and an increased expression of key p53-dependent pro-apoptotic genes. These findings offer a solid rationale for combining PRC2i and mCHEMO as an encouraging therapeutic approach for DLBCL, particularly in elderly or fragile patients, due to their low toxicity profiles. Overall, these results warrant additional in vitro investigations to elucidate the mechanisms underlying the reported effects and in vivo experiments in DLBCL models to validate our new therapeutic strategy, which holds potential for rapid translation into future clinical trials.

#1828 Preclinical evaluation of selective and potent EP300 degraders demonstrates robust antitumor activity and favorable tolerability in hematologic malignancies.

Meiyun Lin, Wesley Austin, Qianhe Zhuo, Rieko Arimoto, Karolina Mizeracka, Abira Ramakrishnan, Kevin Wilson, Elizabeth Wittenborn, Laura La Bonte, Steven Bellon

Foghorn Therapeutics, Watertown, MA

E1A binding protein P300 (EP300) is a histone acetyltransferase and transcriptional coactivator that regulates gene expression programs essential for proliferation and survival in hematologic malignancies. Developing selective EP300 agents has been challenging due to the high degree of homology between EP300 and its paralog CREB binding protein (CBP). Current pharmacological inhibitors targeting EP300 are not very selective and result in adverse effects, such as thrombocytopenia. Therefore, the development of agents that selectively target EP300 is of high interest as it has the potential to broaden the therapeutic window. To address this, we developed heterobifunctional compounds with exquisite selectivity, achieving rapid and sustained EP300 degradation *in vivo* while sparing CBP. Our previous work demonstrated that selective degradation of EP300 has strong anti-proliferative activity in a broad range of hematologic malignancies *in vitro*, including diffuse large B-cell lymphoma (DLBCL), multiple myeloma (MM), and follicular lymphoma. In MM.1S xenograft studies, both immediate-release and long-acting injectable formulations of EP300 degraders achieved robust, dose-dependent tumor growth inhibition at well-tolerated exposure levels. Pharmacokinetic and pharmacodynamic analyses revealed a positive correlation between systemic exposure, EP300 degradation, and anti-tumor response. Importantly, selective EP300 degradation *in vivo* showed minimal impact on body weight and no adverse hematologic effects, such as anemia or thrombocytopenia, in contrast to dual CBP/EP300 inhibitors, indicating a favorable therapeutic window. Collectively, our results establish selective EP300 degradation as a novel and promising therapeutic strategy to treat multiple hematologic malignancies.

#1829 Treating breast cancer brain metastases in the leptomeninges through p-selectin targeted delivery of EZH2 PROTACs.

Raashed Raziuddin, Logan Hillger, Annie Ikemoto, Daniel Heller

Memorial Sloan Kettering Cancer Center, New York, NY

Breast cancer brain metastases (BCBMs) occur in 10-15% of all breast cancer patients with dismal median survival rates as low as 1 month for patients with leptomeningeal metastases (LMs). In BCBMs, EZH2, a histone methyltransferase, has been found to have non-enzymatic oncogenic function promoting metastatic proliferation and decreased overall survival. Thus, degradation versus inhibition of EZH2 in brain metastases could be a powerful strategy to treat BCBMs and LMs if a therapeutic could accumulate to therapeutic doses in the cerebrospinal fluid.

In this study, we use an EZH2 proteolysis-targeting chimera (PROTAC) enabling degradation of EZH2 in BCBMs and LMs. We find that an EZH2 PROTAC administers cytotoxic efficacy in brain metastatic (Br) and leptomeningeal (LM) derivatives of breast cancer cell lines while inhibitors have no effect. Proteomics data and mitochondrial assays suggest this discrepancy can be attributed to mitochondrial complex I and electron transport chain dysfunction.

PROTACs often have poor brain penetrance due to their hydrophobic nature and large molecular weight, but they can be encapsulated in P-selectin targeted nanoparticles (nanoPROTACs). We have previously shown that P-selectin can be presented selectively on primary brain tumor cells to deliver nanoparticles across the blood brain barrier *in vivo*. Here, we discover using humanized models of BCBMs that P-selectin is selectively presented on tumor and leptomeningeal vasculature. Only intraperitoneal delivery of P-selectin targeted EZH2 nanoPROTACs demonstrate remarkable degradation of EZH2 in LMs 48 hours after administration. This work demonstrates the ability to deliver PROTACs selectively to brain metastases and offers a therapeutic platform to extend BCBM patient survival.

#1830 SP09253, an orally bioavailable, highly potent RAS(ON) molecular glue inhibitor demonstrates robust anti-tumor activity in KRAS-mutant tumors.

Zherong Zhang, Xiaoyu Di, Qiming Sun

Hefei Shengpu Pharmaceutical Co., Ltd., Hefei, Anhui, China

KRAS is the most frequently mutated cancer driver gene. Approximately 30% of human tumors harbor KRAS mutations, with particularly high prevalence in pancreatic, colorectal, and non-small cell lung cancers (NSCLC), among others. Patients carrying KRAS mutations often exhibit poor efficacy and low response to current clinical therapeutics. Although $KRAS^{G12C}$ mutant-selective inhibitors have shown success in treating patients with G12C mutations, more than 85% of other “undruggable” KRAS mutations still lack effective treatment options. Next-generation KRAS inhibitors that target multiple oncogenic RAS variants while sparing wild-type RAS hold the potential to address broader indications and patient population. SP09253 is an orally bioavailable, highly potent pan-RAS molecular glue inhibitor that demonstrates robust activity against key RAS mutations including KRAS G12C, G12D, G12V, G13D, while exhibiting high selectivity over wild-type KRAS. Importantly, SP09253 exhibits more favorable ADME and PK profiles compared to positive control, and the *in vivo* anti-tumor efficacy of SP09253 is superior to that of a positive control, a first-in-class pan-RAS molecular glue currently undergoing Phase III clinical trial.SP09253 is a potent pan-RAS molecular glue that has been proven to selectively inhibits KRAS mutants but spares wild type KRAS. SP09253 potently inhibits ERK phosphorylation and cellular viability in KRAS mutantt cell lines *in vitro*. SP09253 demonstrates robust *in vivo* efficacy in KRAS mutant xenografts harboring different mutant types, including G12C, G12D, G12V, etc., while showcasing a favorable PK profile and oral bioavailability.<!--EndFragment-->

#1831 First-in-human clinical pharmacokinetic prediction of D3S-003, an orally bioavailable dual-state KRAS G12D inhibitor.

Shaonan Wang, Zhiqiang Zheng, Jing Zhang, Tienan Wang, Xin Xiong, Hui Wang, Zhijian Chen

D3 Bio Inc., Shanghai, China

Background: D3S-003 is a potent and selective KRAS G12D inhibitor that engages both GDP-bound (OFF) and GTP-bound (ON) KRAS G12D and demonstrates broad preclinical antitumor activity. To support rational first-in-human (FIH) dose selection, translational pharmacokinetic (PK) modeling and allometric scaling were applied to predict human PK characteristics from multi-species data.
Methods: PK data from mouse, rat, and dog were analyzed using two-compartment models with first-order absorption and linear elimination. Allometric scaling of clearance (CL), central and peripheral distribution volumes (Vc, Vp), and intercompartmental clearance (Q) was performed to derive human PK parameters. Absorption rate constant (Ka) and bioavailability (F) were explored over a broad range to capture interspecies variability, and human simulations were conducted for oral doses of 60-1200 mg once daily. Exposure metrics (Cmax, AUC_{0-24}, Cmin, Cavg) were predicted for both single- and multiple-dose regimens to assess dose proportionality and steady-state PK.
Results: Allometric extrapolation yielded predicted human parameters of CL = 0.869 L/h/kg, Vc = 2.151 L/kg, Q = 0.693 L/h/kg, and Vp = 16.664 L/kg. Results shown here reflect simulations using mid-range absorption and bioavailability assumptions. Simulated profiles indicated rapid absorption (Tmax ≈ 1-2 h) and biexponential decline consistent with moderate distribution and linear clearance. Across 60-1200 mg QD, predicted Cmax rose from ~26 to ~520 ng/mL and AUC_{0-24} from ~91 to ~1824 ng·h/mL after a single dose. At steady state (τ = 24 h), Cmin and Cavg ranged ~2-46 ng/mL and ~6-127 ng/mL with minimal accumulation (~1.7-fold). Simulated exposures at clinically feasible doses exceeded unbound exposure level (Cave of ~2.3nM) associated with complete tumor regression in preclinical models, suggesting a high likelihood of achieving pharmacologically active concentrations and early clinical responses during dose escalation.
Conclusions: A translational PK and allometric-scaling strategy successfully predicted human PK for D3S-003. Simulations under mid-range absorption conditions demonstrated linear exposure and favorable oral PK, supporting model-informed dose selection for the planned FIH study. Ongoing integration of clinical data will refine dose-exposure-response relationships and guide dose optimization in later-phase clinical development.

#1832 *In silico* calmodulin-PCAIs binding affinities versus *in vitro* anticancer cell viability: Strategies for the development of anti-pan-mutant KRAS agents.

Jahnissi Frimpomah Odoom[1], Kweku Ofosu-Asante[1], Joshua Kofi Ablordeppey[1], Desmond Kwakye[1], Amarender Burra[2], Nazarius Lamango[3]

[1]Florida A&M University, Tallahassee, FL,[2]R&D Department, Lee Pharma Ltd., Hyderabad, Telangana, India,[3]Professor, Florida A&M Univ. College of Pharmacy, Tallahassee, FL

About 90% of pancreatic cancers are pancreatic ductal adenocarcinoma (PDAC), and roughly 90% of PDAC cases are driven by *KRAS* mutations, which render them very aggressive and resistant to treatments. Therefore, there is a critical need for cancer therapy designed specifically to disrupt and suppress hyperactive G-protein signaling, such as those caused by various mutant RAS isoforms. We previously developed polyisoprenylated cysteinyl amide inhibitors (PCAIs) as potential anticancer agents and showed their efficacies against cell viability, migration, and angiogenesis. We recently identified the pharmacological target of the PCAIs as calmodulin (CALM). To further understand the mechanistic interactions of PCAIs with calmodulin, *in silico* studies were performed. CALM plays a significant role in cancers driven by KRAS proteins. The X-ray crystal structure of CALM with ID 6OS4 and a resolution of 2.05 Å was obtained from the RCSB Protein Data Bank. The crystal structure contained CALM co-crystallized with s-farnesyl-l-cysteine methyl ester (native ligand) and 4 calcium ions. For docking, all water molecules and bound ligands were removed, polar hydrogens were added, and Gasteiger charges were assigned using AutoDockTools. PCAIs were docked onto CALM, and the binding energies were plotted against cell viability EC_{50} values obtained using MIAPaCa-2 cells which harbor the $KRAS^{G12C}$ mutation. PCAIs with low EC_{50} values also displayed lower binding energies. CALM binds to the farnesylated hypervariable region of KRAS4B. Upon docking analysis, the same key residues were observed in docking interactions between CALM and the PCAIs. Redocking the native ligand produced a binding affinity of -5.9 kcal/mol, while the PCAIs showed stronger affinities that ranged from -8.9 to -6.5 kcal/mol, with similar CALM amino acid to PCAIs interaction patterns. The CALM hydrophobic residues, Leu39, Phe92, Leu105, Leu112, Met124, and Met144, which mediate its association with KRAS4B farnesylated cysteine, also contribute to PCAIs binding. The CALM-KRAS4B interaction is further stabilized through Asp20, Asp22, Asp56, Asp58, and Glu67 residues, which form ionic interactions with the polybasic hypervariable region KRAS4B domain. Although Ser-181 of KRAS4B does not directly contact a specific CALM residue, its phosphorylation state negatively impacts the CALM-KRAS4B interaction, providing an additional regulatory layer to KRAS4B growth stimulation through repulsion of CALM negatively charged residues that attract the polybasic region. Basic N atoms on the PCAIs form defined electrostatic contacts with specific Glu residues of CALM, including N3-Glu14, N4-Glu114, and N4-Glu14, further demonstrating the strong and specific PCAIs disruption of CALM-oncogenic KRAS4B complexation that can be harnessed for effective anticancer drug development.

#1833 Polyisoprenylated cysteinyl amide inhibitors suppress growth, induce cytoskeletal and transcriptomic remodeling in multiple *KRAS*-mutated lung cancer cells.

Desmond Kwakye[1], Chase Lilly[1], Kweku Ofosu-Asante[1], Jahnissi Frimpomah Odoom[1], Joshua Kofi Ablordeppey[1], Bianca Dal Bo[2], KARLA GONZALEZ[3], Chunli Yan[3], Matthew A. Gladstone[3], Kyle R. Phillips[4], Benjamin J. Ryder[4], Yong Huang[4], Ite A. Offringa[5], Nazarius Lamango[1]

[1]College of Pharmacy and Pharmaceutical Sciences. Institute of Public Health, Florida A&M University, Tallahassee, FL,[2]Keck School of Medicine of USC, Los Angeles, CA,[3]University of Southern California, Los Angeles, CA,[4]University of Florida, Gainesville, FL,[5]USC Norris Comprehensive Cancer Center, Los Angeles, CA

Lung cancer remains the leading cause of cancer-related deaths globally, with *KRAS* mutations driving approximately 30% of cases. Although $KRAS^{G12C}$ protein inhibitors such as Sotorasib and Adagrasib have improved therapeutic outcomes, intrinsic resistance and mutation heterogeneity such as $KRAS^{G12A}$ limit their long-term efficacy. Therefore, novel agents capable of targeting multiple mutant KRAS variants are urgently needed. Polyisoprenylated cysteinyl amide inhibitors (PCAIs) are molecular mimics of the essential post-translational modifications of G-proteins such as KRAS, RHOA, CDC42, and RAC1 that are important for their interactions as part of functional protein complexes. PCAIs were designed to interfere with and disrupt the polyisoprenylation-dependent protein-protein interactions required for KRAS signaling. Here we evaluated the long-term effects of PCAIs (NSL-YHJ-2-27), versus Adagrasib and Sotorasib on NCI-H23, which normally carries mutant $KRAS^{G12C}$, and a derivative in which $KRAS^{G12C}$ was replaced by $KRAS^{G12A}$. Treatment of NCI-H23 carrying $KRAS^{G12C}$ with 3 µM Adagrasib or NSL-YHJ-2-27 showed consistent inhibition of cell proliferation, down by 82 and 87% respectively. However, Adagrasib at 3 µM inhibited proliferation of NCI-H23 carrying $KRAS^{G12A}$ by just 19%, while Sotorasib had little to no effect. At the same time NSL-YHJ-2-27 inhibited NCI-H23 carrying $KRAS^{G12A}$ by 88%. Proliferation of Sotorasib-treated mutant $KRAS^{G12C}$ NCI-H23 rebounded to 54% by day 18 of continuous treatment, showing $KRAS^{G12C}$ mutants can quickly adapt to resist Sotorasib. NSL-YHJ-2-27 inhibited the viability of NCI-H23 carrying either $KRAS^{G12C}$ or $KRAS^{G12A}$, with respective EC_{50} values of 2.0 and 2.5 µM. NSL-YHJ-2-27 and Adagrasib at 2 µM disrupted F-actin filaments, increased cell rounding, and reduced mean cell area by 89 and 92%, respectively. Sotorasib showed a slight decrease in mean cell area of 15%. Transcriptomic profiling of NSL-YHJ-2-27-treated NCI-H23 cells carrying $KRAS^{G12C}$ revealed three genes that were significantly upregulated and two that were downregulated. Proapoptotic genes such as *CXCL2, WNT9A, PTX3* were elevated by 9, 12 and 10-fold, whereas motility and angiogenesis-associated genes such as *TMSB15A* and *POSTN* were downregulated by30 and 9-fold, respectively. Pathway enrichment highlighted alterations in cytoskeletal organization, adhesion, and KRAS-associated signaling networks. These findings support PCAIs as promising pan-mutant-KRAS-targeting therapeutic candidates against lung cancer.

#1834 A mathematical model for fitting adjusting azacytidine in AML or SMD patients.

Quentin Gerbault[1], Loic Osanno[1], Joseph Ciccolini[1], Laure Farnault[2], Geoffroy Venton[2], **Raphaelle Fanciullino**[1]

[1]COMPO SmartC, Aix-Marseille University, Marseille Cedex 07, France,[2]Hematology Unit, Aix-Marseille University, Marseille Cedex 07, France

Background: Azacitidine (Aza) is a hypomethylating agent (HMA) used to treat patients with acute myeloid leukaemia (AML) or myelodysplastic syndrome (MDS) who are not eligible for intensive chemotherapy. The standard Aza dose and schedule is 75 mg/m² daily for seven days, administered in 28-day cycles until disease progression occurs or severe toxicities arise. Recent protocols have associated it with venetoclax. However, only half of patients respond, and almost all will eventually relapse. Azacitidine undergoes metabolic detoxification driven by cytidine deaminase (CDA) in the liver. However, CDA is encoded by a highly polymorphic gene, resulting in significant variability: some patients do not respond to treatment, while others experience toxic death. Fifty per cent of patients with acute myeloid leukaemia (AML) or myelodysplastic syndrome (MDS) have deficient CDA enzyme activity (1). This variability suggests the need to consider individualising doses and understanding the kinetics of Azacytidine. In this real-world study, we monitored azacitidine plasma concentrations in order to develop a mathematical model to predict its pharmacokinetics (PK).
Method: Twenty-one adult patients (13 male/8 female), with a mean age of 78.7 years (range 59-89), were treated with azacitidine, either alone or in combination with venetoclax. Aza plasma concentrations were measured at the first cycle (C1) at multiple time points. Aza was analysed using a validated mass spectrometry method. PK parameters were derived using a population model with the SAEM algorithm within the Monolix® software. The influence of various factors, including CDA activity, on the pharmacokinetics (PK) of Azacytidine was investigated using a stepwise multivariate procedure.
Results: A one-compartment population pharmacokinetic (popPK) model with zero-order absorption and linear elimination was developed. This model incorporated CDA status as an absorption covariate, as well as basal serum albumin and body surface area as distribution volume covariates, and sex and renal impairment as clearance covariates.
Conclusions: This initial characterisation of a population model marks the beginning of the process of dose individualisation, which aims to optimise efficacy while minimising undesirable toxicities. Validating this model and determining toxicity parameters (concentration-dependent, exposure-dependent and time-dependent toxicity) and survival parameters will improve the management of these complex diseases with poor prognoses.
(1): High incidence of CDA deficiency in patients with hematological malignancies: perspectives and therapeutic implications. Donnette M, Ciccolini J, Pissier C, Costello R, Duffaud F, Salas S, Farnault L, Tichadou A, Arcani R, Jarrot PA, Ouafik LH, Venton G, Fanciullino R. Ann Oncol. 2021 May;32(5):684-686.

#1835 Evaluation of busulfan stability in infusion bags and biological matrix: Application to routine therapeutic drug monitoring with adaptive dosing in children.

Marielle Jehanno, Jasmine Bettayeb, Guillaume Sicard, Arthur Sterin, **Joseph Ciccolini**

La Timone University Hospital of Marseille, Marseille, France

Purpose: High Dose Busulfan is administered using pharmacokinetically guided dosing for conditioning protocols before hematopoietic stem cell transplantation. To be reliable, this strategy requires that administered doses and drug levels measured from samples are not affected by degradation before being assayed.
Methods: Busulfan stability at clinically meaningful concentrations was monitored by liquid chromatography/mass spectrometry in infusion bags as well as in human blood and plasma, using various storage conditions. Next, TDM (Therapeutic Drug Monitoring) with adaptive dosing was implemented in routine setting to customize the dosing in a child scheduled for High dose Busulfan.
Results: Busulfan was stable up to 72h in 0.25 mg/mL infusion bags, up to 24 hours in plasma regardless of the storage condition, and up to 16 hours in whole blood at 4°C. Conversely, blood samples of Busulfan left at room temperature showed a rapid degradation, suggesting that they should be rapidly proceeded in a temperature-controlled fashion. When applied next to children treated with High Dose Busulfan following 8 to 16 administrations over 4 consecutive days, TDM with PK-guided dosing was successfully performed to tailor the dosing and reached the desired target exposure. Upon initial standard dosing, deviation from the target AUC ranged from -52.3% to +11.5%. Busulfan dosing was subsequently adapted from Dose-9 for the 7 remaining administrations) and final cumulative AUCs showed deviation from the target from -22% to +13.6%.
Conclusion: Busulfan blood samples must be rapidly proceeded in refrigerated condition upon sampling to allow reliable TDM and adaptive dosing in paediatric oncology.

#1836 Nivolumab exposure and efficacy in metastatic melanoma patients: A real-world study.

Quentin Gerbault, Clara Boeri, Nausicaa Malissen, Caroline Gaudy, **Joseph Ciccolini**

Cancer Research center of Marseille, Marseille, France

Background: The PK/PD relationships of immune checkpoint inhibitors are not fully understood. In this real-world study, we monitored plasma concentrations of nivolumab and investigated to what extent they could predict clinical outcome in a cohort of unresectable stage III or IV melanoma patients.
Methods: 52 adult patients (26M/26F), mean age 64.3 years (range 31-89), performance status 0 (79.2%) or 1 (20.8%) were treated with 1 mg/kg nivolumab + 3 mg/kg ipilimumab (35 patients) or single agent nivolumab 240 mg Q2W or 480 mg Q4W flat dose (17 patients). Radiological response was assessed every 3 months per clinical practice. Nivolumab plasma concentrations (Cmax: end of infusion and Cmin: trough levels) were measured at the first cycle (C1). Nivolumab was analysed using a validated mass spectrometry method. PK parameters were derived using a standard population PK approach on Monolix using a two-compartment model. Statistical analyses were performed using R.
Results: confirmed response rates were 5.7% complete response, 32% partial response, 17% stable disease and 45.3% progressive disease. Patients with objective response or stable disease were next categorised as having clinical benefit (CB). There was no difference in efficacy between single-agent and combination therapy (odd ratio = 0.28, [0.06-1.087], Fisher test). After the first cycle (C1), nivolumab Cmax concentrations were 67.1 µg/mL ±64.1 (CV = 95%) and trough levels were 26.9 µg/mL ±23, (CV = 87%). In patients treated with the nivolumab + ipilimumab combination, there was no statistical difference in Cmax levels (37.9 µg/mL vs. 33.9 ug/mL $p > 0.05$) and trough levels (24.0 µg/mL vs. 15.4 µg/mL $p > 0.05$), between those achieving a CB and PD patients despite a +56% numerical difference in trough levels. Similarly, no statistical difference was seen in Cmax levels between CB and PD patients treated with nivolumab monotherapy (203.1 µg/mL vs. 159.6 µg/mL, $p > 0.05$) despite a numerical difference of +35%. There was a statistical difference in Cmin between CB and PD patients (54.2 µg/mL VS. 34 ug/mL $p = 0.03$). ROC analysis showed that a threshold of <42.6 µg/mL was significantly associated with treatment failure ($p = 0.016$).
Conclusions: This proof-of-concept study suggests that when nivolumab is given as a single agent, trough levels after the first cycle may help predict clinical outcome, as patients with plasma concentrations <42.6 µg/mL are at significantly higher risk of experiencing PD. The marker inter-patient variability observed in nivolumab pharmacokinetics warrants the use of therapeutic drug monitoring to check that exposure levels are within the expected range since patients with trough levels < 42.6 µg/mL after the first cycle are at risk of treatment failure.

#1837 Targeting Hippo/YAP-TEAD increases the antitumor activity of darovasertib in uveal melanoma.

Rodolfo Daniel Cervantes-Villagrana[1], Elena Sofia Cardenas Alcoser[1], Kuniaki Sato[1], Simone Lubrano[1], Tomohiko Ishikawa[1], Andrew E. Aplin[2], J. Silvio Gutkind[3]

[1]Pharmacology, University of California San Diego, San Diego, CA,[2]Jefferson Health Sidney Kimmel Cancer Center, Philadelphia, PA,[3]UCSD Moores Cancer Center, La Jolla, CA

Activating mutations in *GNAQ* and *GNA11* (*GNAQ* oncogenes) are found in ~93% of uveal melanoma (UVM) and 4% of skin cutaneous melanoma (SKCM), where they act as driver oncogenes. UVM is the most common primary cancer of the eye in adults, affecting more than 2,500 patients each year in the US alone, nearly 50% of whom will die from liver metastasis. To date, there are limited effective therapeutic options to prevent or treat UVM metastatic disease (mUVM), which typically also fails to respond to immunotherapies. By combining synthetic biology approaches, CRISPR/Cas9 genome-wide screens, and high-throughput chemogenetic drug screening, our team has revealed that classical and novel non-canonical GNAQ signaling circuits converge to promote UVM growth, survival, metastasis, and treatment resistance. Ultimately, elucidating GNAQ oncogenic signaling networks may reveal system vulnerabilities that can be exploited to develop new precision therapies for mUVM. In this regard, we have recently shown that darovasertib acts as a dual PKC-PKN inhibitor and exhibits the highest activity among thousands of drugs tested. Darovasertib has demonstrated encouraging activity in UVM patients, and clinical trials using darovasertib as a single agent in primary UVM lesions and in combination with crizotinib in mUVM are currently ongoing. However, few patients achieve complete responses, and tumors often progress due to the acquisition of resistance mechanisms. We aim to identify new targets that can overcome resistance to darovasertib. RNA-seq analysis revealed that long-term treatment with darovasertib increased the expression of YAP-target genes, and we hypothesized that YAP/TEAD activation may contribute to darovasertib resistance. Indeed, expression of an active YAP mutant (YAP2-5SA) or LATS1/2 inhibition was sufficient to induce darovasertib resistance in UVM cells. In turn, knockdown of YAP or TEAD, or the expression of a doxycycline-induced TEAD inhibitor (TEADi) peptide, increases darovasertib-induced apoptosis. Remarkably, co-targeting with small molecule TEADi decreases the expression of darovasertib-induced YAP targets and acts synergistically to reduce cell viability and increase UVM cell death. Ongoing studies are now exploring the preclinical benefit of combining darovasertib with small-molecule TEADi for the treatment of human UVM tumor xenografts in mice. Emerging evidence will be presented supporting that the Hippo YAP/TEAD pathway represents an adaptive mechanism of resistance to darovasertib treatment, and that the combination of TEADi with darovasertib may prevent the development of treatment resistance, thereby increasing the depth and duration of the anti-tumor response in UVM.

#1838 Optimal epigenetic therapies in triple-negative breast cancer.

Simone Bruno[1], Alexandra Indeglia[2], Sophia Lichterfeld[3], Karen M. Cichowski[2], Franziska Michor[4]

[1]Dana-Farber Cancer Institute, Boston, MA,[2]Brigham and Women's Hospital, Boston, MA,[3]Harvard College, Cambridge, MA,[4]Assoc. Professor, Dept. of Biostatistics & Computational Bio., Dana-Farber Cancer Institute, Boston, MA

Triple-negative breast cancer (TNBC) is the most aggressive form of breast cancer and is characterized by a very high recurrence rate. The primary treatment for this cancer type is systemic chemotherapy, often combined with immunotherapy. However, these treatments typically result in only short-term responses. Recent experimental studies have highlighted the critical role of chromatin modifications, such as DNA methylation and histone modifications, in TNBC development and progression. Consistent with these findings, epigenetic therapies targeting these modifications have shown promise in preclinical and early clinical studies. Building on these insights, we developed a predictive computational modeling platform to gain a deeper understanding of how different chromatin modifications influence TNBC and to identify optimal therapeutic strategies targeting these modifications. The platform integrates experimental data, pharmacokinetics, and mechanistic insights into the role of chromatin regulation in TNBC. We focused on therapies combining an EZH2 inhibitor, which reduces the establishment of repressive H3K27me3 marks and promotes chromatin opening, and an AKT inhibitor, which enhances the expression of GATA3 and BMF. Using this framework, we confirmed the experimentally observed synergy between the two inhibitors and uncovered its mechanistic basis: EZH2 inhibition quickly reaches a plateau once chromatin becomes fully accessible, whereas the effect of AKT inhibition increases more gradually across a broader concentration range. In-silico clinical trials involving 1,500 virtual patients further showed that optimized combination schedules markedly outperform monotherapies. Based on these predictions, we conducted in-vitro experiments using live-cell imaging, which validated the model's predictions on how different inhibitor doses and combinations shape treatment response, and confirmed the combination regimen identified by the platform as optimal. Beyond TNBC, the generalizable framework developed here can potentially be adapted to other types of cancer in which chromatin modifications play a similar role. This research can then also help establish the basis for the discovery of common therapeutic targets, contributing to a broader range of cancer treatment strategies. Overall, this research could lead to the development of novel, more effective, and more durable treatment strategies for TNBC, thereby improving patient outcomes and providing new possibilities for cancer therapy research.

: Targeting Drug Resistance 1: Apoptosis and Autophagy
Poster Session

#1841 Venetoclax rewires Notch signaling to drive resistance in North American adult T-cell leukemia/lymphoma.

Ankit Tanwar[1], Salman Sadullah Usmani[1], Sovira Chaudhry[1], Aditi Shastri[1], Marina Konopleva[1], Murali Janakiram[2], Ali Bazarbachi[3], B. Hilda Ye[1], Xingxing Zang[1], Amit Verma[1], R. Alejandro Sica[1]

[1]Albert Einstein College of Medicine, Bronx, NY,[2]City of Hope National Medical Center, City of Hope Duarte, NY,[3]American University of Beirut-Medical Center., Beirut, Lebanon

Purpose: North American Adult T-cell leukemia/lymphoma (NA-ATLL) is an aggressive HTLV-1-associated T-cell malignancy with median survival of less than 2 years. NA-ATLL cases are distinct from those in endemic regions like Japan and exhibit a correlation with poor prognosis and therapeutic resistance. Interferon-alpha/Zidovudine, when combined with other chemotherapy regimens, has shown efficacy in acute and chronic malignancies. We previously showed that Venetoclax induces mitochondrial apoptosis in NA-ATLL; however, resistance inevitably emerges despite initial sensitivity. As limited epidemiologic data delay ATLL research, our center accomplishes one of the nation's first cohorts, with ~150 cases annually, predominantly among Caribbean-descent patients. In this study, the use of Venetoclax-treated patient-derived NA-ATLL cells led to prominent Notch pathway activation, highlighting a key adaptive resistance mechanism.
Methods: Preclinically, patient-derived NA-ATLL cell lines (Pt-4a, 5a, 6a, 15a) along with Japanese patient-derived ATLL cell lines [ATL43Tb(−)] (J-ATLL) were treated with Venetoclax. RNA-seq identified adaptive survival pathways. Clinically, several patients with aggressive subtypes of NA-ATLL (Shimoyama types: lymphomatous and acute) were treated with Venetoclax-based treatment at our Institution.
Results:
Preclinical: Both NA-ATLL and J-ATLL cells responded heterogeneously to Venetoclax. In responsive lines, Venetoclax-treated cells enhanced apoptotic priming with caspase-3/PARP-1 activation, and reduced HTLV-1 HBZ and Tax expression whereas non-responders showed minimal effect, while ferroptosis was excluded. BH3 profiling confirmed NA-ATLL has unique apoptotic priming compared to J-ATLL. RNA-seq revealed robust induction of NOTCH1/2, DLL1/4, JAG1/2, and canonical targets HES1. Noteworthy, Venetoclax also upregulated the Fring*e* glycosylation genes (LFNG, MFNG, RFNG), which augment Notch receptor responsiveness, indicating a glycan-optimized Notch activation program that supports survival under BCL-2 inhibition.
Clinical: NA-ATLL patients received Venetoclax-based combinations across multiple therapy lines. Mutation profiling (TP53, NOTCH1) by NGS was correlated with outcomes. Notably, the Venetoclax-based regimes (PEG-IFN + Biktarvy + VEN) produced durable complete responses, with patients remaining alive beyond 95 and 234 days at data cutoff.
Conclusion: Venetoclax shows a significant effect in NA-ATLL both at preclinical and clinical settings, but emerging adaptive Notch signaling activation represents a crucial resistance mechanism. Our study supports evaluating Notch-directed agents (γ-secretase inhibitors/Nirogacestat) in combination with Venetoclax to overcome therapeutic resistance and improve outcomes in NA-ATLL.

#1843 Venetoclax-resistant AML cell models as a platform for exploring new generation drug for BCL2 inhibitor resistance.

Jinjin Wang, John Liu, Lin Teng

BioDuro, Irvine, CA

BCL2 is a key regulatory protein in the apoptotic pathway. Venetoclax (ABT-199), an orally bioavailable and highly selective BCL-2 inhibitor, has demonstrated promising efficacy in acute myeloid leukemia (AML) when used in combination with hypomethylating agents (HMA), leading to high remission rates and significantly prolonged overall survival. However, a considerable number of patients developed resistance or experienced relapse, highlighting the need for new strategies to overcome acquired venetoclax resistance. To investigate this issue, we established venetoclax-resistant models in three AML cell lines (RS4;11, MOLM-13, and MV 4-11) through prolonged exposure to progressively increasing concentrations of venetoclax (ranging from 1 nM to 500 nM). The resulting resistant cells exhibited a marked reduction in venetoclax sensitivity, with resistance levels exceeding 160-fold compared to their parental counterparts. These models serve as a valuable platform for evaluating novel BCL-2 inhibitors, combination treatment regimens, and other targeted agents. Moreover, they provide a crucial resource for elucidating the underlying mechanisms of venetoclax resistance.

#1844 Epigenetic rewiring of BCL6 drives responses and unveils synthetic dependencies in large B cell lymphoma.

Haopeng Yang[1], Kevin Bowman[1], Wenzhi Ji[2], Sai Gourisankar[2], Ashley L. Wilson[1], Zihan Yang[1], Ethan Marszalek[1], Stephen M. Hinshaw[2], Tinghu Zhang[2], Xiaofan Liu[2], Andrey Krokhotin[2], Sabin Nettles[2], Suprateek Kundu[1], Gerald R. Crabtree[2], Nathanael S. Gray[2], Michael R. Green[1]

[1]UT MD Anderson Cancer Center, Houston, TX,[2]Stanford University, Stanford, CA

Diffuse large B cell lymphoma (DLBCL) is a clinically and molecularly heterogeneous malignancy that can be classified into germinal center (GCB) and activated B cell (ABC) subtypes. Clinically, these subsets are often classified by immunohistochemistry (IHC) with CD10 and BCL6 expression being characteristic of GCB and IRF4 (MUM1) expression being characteristic of ABC. Efforts to inhibit signaling pathways active in ABC DLBCL by addition of targeted therapies to frontline chemoimmunotherapy have failed to meet their primary endpoints, and mechanisms of resistance to targeted therapies in DLBCL have not been extensively explored in clinically relevant models. Targeting BCL6 has recently emerged as an exciting therapeutic direction, with multiple BCL6 degraders now being tested in early phase clinical trials. BCL6-targeting transcriptional/epigenetic chemical inducers of proximity (TCIP) are an innovative approach to recruit transcriptional coactivators that flip BCL6 from a transcriptional repressor to an activator and induce the expression of its target genes. We thoroughly tested the efficacy of a TCIP that recruits BRD4 to BCL6-bound site (TCIP1) using our extensive PDX repository, evaluating models with uniformly high (n=5), heterogeneous (n=6) or negative (n=2) expression of BCL6 by IHC. PDX models with high BCL6 expression all responded rapidly to TCIP1, with eradication of tumors in 4/5 models including those from CAR T refractory tumors with p53 mutation. As expected, BCL6 negative models showed no response. Interestingly, BCL6 heterogeneous models also showed no response compared to vehicle control. Mechanistic studies by RNA-sequencing following short term *in vivo* exposure to TCIP1, its constituent components (BCL6 BTB binder; BRD4 binder) or vehicle control in BCL6 high (n=3) or heterogeneous (n=3) models revealed a selective up-regulation of IRF4 activity in BCL6 heterogeneous models. Evaluation by IHC showed that, at baseline, BCL6 heterogenous models consisted of mixed populations of BCL6+IRF4- and BCL6-IRF4+ cells that were polarized to a uniformly BCL6-IRF4+ state under TCIP1 pressure, then returned to heterogeneous states following secondary implantation. IRF4 can be indirectly targeted using lenalidomide (len), thus we evaluated the activity of TCIP1+len combination in two BCL6 heterogeneous models. Single agent TCIP1 or len treatment resulted in no significant reduction in tumor volume compared to vehicle control. However, TCIP+len drove significant *in vivo* responses. In conclusion, we present the first data implicating epigenetic mosaicism and plasticity as a resistance mechanism to targeted therapy in DLBCL. Using a large array of PDX models we show impressive efficacy for TCIP1 in BCL6 high DLBCL and identify a rational strategy to overcome escape via epigenetic plasticity using a combination of TCIP1 and lenalidomide to target polar epigenetic states.

#1845 Targeting mitochondrial and glutathione metabolism sensitizes leukemia cells to DNA-hypomethylating agents and venetoclax combination therapy.

Pony Yu-Ling Lee[1], Joy Khag[2], Marvin A. Aberin[2], Ta-Yu Liu[2], Ya-Ting Lu[2], Kun-Yuan Lin[1], Chao-Di Chang[1], Shan-Yun Cheng[1], Ya-Wen Hung[1], Chih-Chieh Yang[1], Yu-Hsien Chang[1], Chien-Chang Shen[1], Yao-Ming Chang[2], Hsing-Chen Tsai[3], Shih-Yu Chen[2], Shu-Ping Wang[2]

[1]Pharmacology Discovery Services Taiwan, Ltd., New Taipei City, Taiwan,[2]Institute of Biomedical Sciences, Academia Sinica, Taipei, Taiwan,[3]National Taiwan University College of Medicine, Taipei, Taiwan

Acute myeloid leukemia (AML) is the most common acute leukemia diagnosed in adults. DNA-hypomethylating agents (HMAs), such as decitabine and azacitidine, are widely used to treat AML and myelodysplastic syndromes (MDS). Although HMAs demonstrate only modest efficacy as monotherapies, clinical responses improve substantially when HMAs are combined with other therapeutic agents, notably venetoclax (VEN) in older patients, FLT3 inhibitors (FLT3i) for FLT3-mutated AML, and IDH inhibitors (IDHi) for IDH1/2-mutated disease. Nevertheless, drug resistance frequently emerges, emphasizing the need to elucidate resistance mechanisms and develop new therapeutic strategies. The typical schedule of HMA treatment, several consecutive days of sequential dosing followed by a rest interval, suggests that epigenetic memory may contribute to resistance. To investigate potential mechanisms of resistance, we examined the effects of transient low-dose decitabine in AML cell lines, observing that three consecutive treatment days markedly suppressed cell proliferation and viability. However, after three weeks of drug-free recovery, surviving cells regained robust growth, indicating that a subset of cells adapts and potentially acquires relapse-associated drug-resistance. We found that decitabine induces persistent mitochondrial dysfunction, characterized by altered mitochondrial networks, ultrastructure, and activity, that remains evident even after drug withdrawal and likely contributes to initial growth inhibition. Notably, surviving cells exhibit strong enrichment of the glutamate-glutathione metabolic pathway, suggesting a compensatory mechanism that mitigates mitochondrial stress. Integrated RNA sequencing and metabolomic profiling identified a key enzyme in the glutamate-glutathione metabolic pathway for this metabolic adaptation. In human AML xenograft models, inhibition of this enzyme significantly restored sensitivity to HMA (decitabine or azacytidine)-VEN combination therapy in resistant or poorly responsive AML cells. Together, our findings identify glutathione-based metabolic adaption as a potential mechanism of HMA resistance and highlight targeting mitochondrial and glutathione metabolism as a promising therapeutic strategy to enhance the efficacy of HMA-containing combination regimens.

#1847 Improve proteasome inhibitor response by targeting NHE6-mediated endosomal-autophagic machaniery in multiple myeloma.

Yutong Wang[1], Liuting Chen[1], Winston Huang[1], Jin He[1], Li Bao[2], Yihui Fan[3], Pei Lin[4], Qing Yi[1], Jing Yang[1]

[1]Houston Methodist Neal Cancer Center, Houston Methodist Research Institute, Houston, TX,[2]Department of Hematology, Beijing Jishuitan Hospital, Capital Medical University, Beijing, China,[3]Department of Pathogenic Biology, School of Medicine, Nantong University, Nantong, China,[4]Department of Hematopathology, Division of Pathology and Laboratory Medicine, The University of Texas MD Anderson Cancer Center, Houston, TX

Multiple myeloma (MM) remains incurable, and resistance to frontline proteasome inhibitors (PIs) is a major barrier to improving patient survival. Identifying new therapeutic targets that overcome PI resistance is therefore essential. Through transcriptomic analysis of PI resistance gene signatures across public datasets, we identified NHE6 (*SLC9A6*) as a regulator of MM cell survival under treatment-induced stress. NHE6, an endosomal Na^+/H^+ exchanger that controls vesicular pH and membrane trafficking, has not previously been implicated in MM. We found that NHE6 is highly expressed in patient-derived primary MM cells and human MM cell lines, with further upregulation in PI-resistant cell lines. Elevated NHE6 expression levels correlated with inferior survival across independent patient cohorts. To examine the role of NHE6 in MM therapeutic response, we knocked out NHE6 expression (*sgSLC9A6*) in a panel of MM cell lines (ARP-1, MM1S, RPMI8266 and H929). We found that sg*SLC9A6* cells exhibited markedly enhanced PI-induced apoptosis *in vitro*, and significantly reduced tumor burden with prolonged survival *in vivo*. Since autophagy is a key survival mechanism under PI stress, we inhibited autophagy pharmacologically and found that PI-induced apoptosis was increased in sg*Ctrl* cells, making them similarly sensitive to sg*SLC9A6* cells. These results demonstrate that the enhanced drug response caused by NHE6 loss is autophagy dependent. Consistent with this, sg*SLC9A6* cells exhibited higher LC3B and p62 levels than sg*Ctrl* cells, and autophagy inhibition raised their accumulation in both groups to comparable levels, indicating that NHE6 loss blocks autophagic flux. Cellular fractionation localized NHE6 predominantly to early endosomes. Immunoprecipitation studies revealed that NHE6 promotes Rab7 recruitment and GTP loading, thereby accelerating early-to-late endosomal maturation and facilitating endosome–autophagosome fusion and amphisome formation. Pharmacologic inhibition of Rab7 enhanced bortezomib efficacy, like the effect of NHE6 loss. Analysis of the CoMMpass^{SM} cohort supported the clinical relevance of this pathway: non-responders displayed significantly higher Rab7 and NHE6 levels, which correlated with poorer survival. In summary, our study identifies NHE6 as a regulator of endosomal maturation, contributing to PI resistance in MM. Suppressing NHE6 restores drug sensitivity and prolongs survival in preclinical MM models. Targeting NHE6-mediated endosomal dynamics presents a promising therapeutic strategy for MM patients.

#1848 IL-1-driven signaling promotes resistance to PI3K and BCL2 inhibitors in B-cell lymphoma preclinical models.

Alberto J. Arribas[1], Federica Fuzio[1], Eleonora Cannas[1], Michela Chiappa[2], Luciano Cascione[1], Giulio Sartori[1], FIlippo Spriano[1], Andrea Rinaldi[1], Georg Stussi[3], Emanuele Zucca[1], Davide Rossi[1], Anastasios Stathis[3], Andrea Alimonti[1], Giovanna Damia[2], Massimo Broggini[2], Francesco Bertoni[1]

[1]Institute of Oncology Research, Universita della Svizzera italiana, Bellinzona, Switzerland,[2]Istituto di Ricerche Farmacologiche Mario Negri IRCCS, Milan, Italy,[3]Oncology Institute of Southern Switzerland, Bellinzona, Switzerland

Background: IL-1 is a central inflammatory cytokine with context-dependent effects in B-cell lymphomas, capable of supporting anti-tumor immunity but also promoting a pro-tumorigenic microenvironment. Here, we investigated the role of IL-1 in driving resistance to PI3K and BCL2 inhibitors in B-cell lymphoma preclinical.
Methods: Cell lines, including derivatives with acquired resistance to PI3K/BCL2 inhibitors obtained by long exposure to the PI3K inhibitor copanlisib in the marginal zone lymphoma (MZL) cell line VL51 (Arribas, ENA 2020), were analyzed using transcriptomics, proteomics, and immunoblotting. Functional assays assessed drug sensitivity, pathway activation, cytokine responses, and the impact of IL-1 stimulation and blockade. A 1,400-compound FDA-approved library was used in combination with copanlisib/venetoclax.
Results: VL51 cells with acquired resistance to PI3K/BCL2 inhibitors were characterized by an upregulation of IL1α and IL1β, elevated ERK and STAT3 phosphorylation, and increased expression of pro-survival and cytokine-responsive proteins. Recombinant IL-1α and IL-1β activated NF-κB and Ox-Phos in parental cells. IL-1α induced MYC and SRC targets, while IL-1β activated PI3K and STAT signaling. Either IL-1α or IL-1β reduced sensitivity to PI3K and BCL2 inhibitors in models of MZL (VL51, ESKOL), mantle cell lymphoma (REC1), and diffuse large B-cell lymphoma (OCI-Ly10). IL-1R1 blockade restored drug response. Notably, the combination of both IL-1α and IL-1β further enhanced resistance to copanlisib and to the BCL2 inhibitor venetoclax in VL51 cells. IL-1R1 blockade restored drug response. Notably, the combination of both IL-1α and IL-1β further enhanced the resistance to copanlisib and venetoclax in VL51. The drug-screen identified compounds targeting WNT, CDK, HDAC, HSP, PLK, ALDH1, AURKA, proton pump function, and microtubule dynamics that improved treatment efficacy, particularly in resistant cells. Validation studies demonstrated that several inhibitors effectively counteracted IL-1-associated resistance. The ALDH1 inhibitor disulfiram strongly restored copanlisib/venetoclax sensitivity in resistant models. Additional combinations, including ganetespib, rigosertib, panobinostat, alisertib, and AZ6102, also enhanced responses, indicating that IL-1-responsive stress, epigenetic, and mitotic pathways represent actionable vulnerabilities.
Conclusions: IL-1-driven reprogramming promotes resistance to PI3K and BCL2 inhibition in B-cell lymphoma via activation of NF-κB, STAT3, and metabolic survival pathways. Targeting IL-1 signaling or downstream effectors may overcome resistance and offer a promising therapeutic strategy for relapsed or refractory B-cell lymphomas.

#1849 Dual inhibition of AURKA and ERBB overcomes resistance to PI3K/BTK/BCL2 inhibitors in marginal zone lymphoma models.

Emma Pesenti[1], **Alberto J. Arribas**[1], Maidel Carpio[1], Eleonora Cannas[1], Georg Bischof[2], Francesco Bertoni[1]

[1]Institute of Oncology Research, Universita della Svizzera italiana, Bellinzona, Switzerland,[2]Puma Biotechnology, Inc., Los Angeles, CA

Background: Despite recent therapeutic advances, resistance to targeted agents remains a major barrier to durable responses in B-cell lymphomas, including marginal zone lymphoma (MZL). Aurora kinase A (AURKA) inhibition has shown promise in overcoming chemotherapy resistance and improving outcomes in MYC-driven B-cell lymphomas (Park et al., 2019). In parallel, ERBB4 signaling mediates resistance to PI3K and BTK inhibitors through activation of the PI3K-AKT pathway (Arribas et al., 2024). The AURKA inhibitor alisertib is currently in clinical development, while the pan-ERBB inhibitor neratinib is FDA/EMA-approved for use across several malignancies, providing an opportunity for rapid translation. Here, we evaluated the antitumor activity and mechanisms of alisertib and neratinib, alone or combined with the BTK inhibitor ibrutinib, in MZL models with acquired resistance to PI3K/BTK/BCL2 inhibitors.**Methods**: MZL cell lines Karpas1718 and VL51, along with their derivatives resistant to PI3K/BTK/BCL2 inhibitors (Arribas et al., 2022; 2024; 2025), were treated with alisertib, neratinib, and ibrutinib individually or in combination. Cell viability, apoptosis, and immunoblotting assays were used to assess drug activity, synergy, and modulation of signaling pathways.**Results**: Alisertib and neratinib displayed strong, dose-dependent anti-lymphoma activity and maintained efficacy in models resistant to PI3K, BTK, and BCL2 inhibitors. Their combination with ibrutinib produced additive/synergistic effects, significantly enhancing apoptosis compared with ibrutinib alone, including in BTK-resistant cells. The alisertib/ibrutinib/neratinib triple combination induced the most profound suppression of cell growth, outperforming the dual-agent regimens. Mechanistically, triple therapy suppressed phosphorylation of AURKA and its downstream target, PLK1, reduced ERK activation, and downregulated the prosurvival protein MCL1. Notably, alisertib plus neratinib overcame ibrutinib resistance in both Karpas1718 and VL51, despite not directly enhancing BTK inhibition.**Conclusions**: Dual inhibition of AURKA and ERBB pathways with alisertib and neratinib synergizes with BTK blockade to overcome resistance to multiple targeted therapies in MZL. Given the clinical availability of neratinib and emerging safety data for alisertib, these findings highlight a therapeutically actionable strategy that could be rapidly advanced into early-phase trials for relapsed/refractory MZL. This combination approach may expand treatment options for patients with limited responses to current PI3K, BTK, or BCL2 inhibitors.

#1850 Co-targeting EZH2 and TEAD elicits apoptosis through tumor-intrinsic innate immune signaling in Hippo pathway-mutated cancers.

Antja-Voy Hartley[1], Mustafa Al-Dulaimi[1], Navin R. Mahadevan[2], Pinar Eser[3], William W. Feng[1], Tran Thai[1], Jeanelle A. Tsai[1], Caitlyn Weston[1], Nicholas Tourtillot[1], Matthew Booker[1], Joseph Kulesza[1], Zhaorong Li[1], Elizabeth Cohen[1], Sean Lenahan[1], Choudhury Fabliha Yusuf[1], Abeba Teshager[1], Prafulla C. Gokhale[1], Shweta Kukreja[1], Sonsoles Liria Veiga[1], Rong Li[1], Xintao Qiu[1], Henry W. Long[1], Michael Y. Tolstorukov[1], Matthew G. Oser[1], Nathanael S. Gray[4], David A. Barbie[1], Pasi A. Janne[1]

[1]Dana-Farber Cancer Institute, Boston, MA,[2]University of Michigan, Ann Arbor, MI,[3]Broad Institute, Boston, MA,[4]Stanford University, Stanford, CA

TEA/TEF-domain [TEAD] inhibitors are being evaluated in clinical trials for cancers with alterations in the Hippo pathway including mesothelioma. We recently developed and showcased the potency of TEAD palmitoylation inhibitors MYF-03-69 and MYF-03-176 in mesothelioma cell lines. However, TEAD inhibition results in cell cycle arrest in cell line models with Hippo pathway alterations without inducing cell death, potentially limiting their long-term clinical efficacy. Using a genome-wide CRISPR/Cas9 screen, we identified EZH2 as a critical modulator of the cellular response to TEAD inhibition. Compared to single agent treatments, EZH2i/TEADi robustly triggered apoptosis and suppressed the growth of Hippo-mutated cells *in vitro* and *in vivo.* Mechanistically, EZH2i/TEADi-treated cells exhibited heightened activation of tumor-intrinsic innate immune signaling which resulted in DNA damage and subsequent apoptosis. Taken together, we propose this novel combinatorial strategy as a potential approach to enhancing the anti-tumor efficacy of single agent TEAD targeting therapies in Hippo pathway altered tumors.

#1851 Overcoming drug resistance in ccRCC through inhibition of protein phosphatase 5 (PP5).

Sarah J. Backe[1], Rebecca Sager[1], Jennifer Heritz[1], John Chisholm[2], Mark Woodford[1], Dimitra Bourboulia[1], Gennady Bratslavsky[1], Mehdi Mollapour[3]

[1]SUNY Upstate Medical University, Syracuse, NY,[2]Syracuse University, Syracuse, NY,[3]Postdoctoral Research Fellow, Urologic Onc. Branch, SUNY Upstate Medical University, Syracuse, NY

BACKGROUND: Belzutifan is an FDA approved small molecule inhibitor used for the treatment of patients with advanced clear cell renal cell carcinoma (ccRCC). Belzutifan inhibits HIF2α, a transcription factor that promotes tumor angiogenesis and metastasis. Although ccRCC patients can potentially develop resistance to belzutifan there are currently no strategies to counteract this drug resistance in patients. We have identified that serine/threonine protein phosphatase-5 (PP5) expression and activity is elevated in ccRCC, contributing to its pro-survival role. We have designed and developed small molecule inhibitors of PP5. The objective of this study was to examine whether PP5 inhibition can cause apoptosis in belzutifan-resistant ccRCC cells.
METHODS: Belzutifan-resistant ccRCC cells were developed by treating 786-O cells with 10μM belzutifan. Once 70% confluent, the cells were split and treated with 10μM belzutifan again. This process was repeated until the cells appeared healthy and grew at a similar rate to 786-O without belzutifan treatment. Belzutifan was removed from the cells for at least 24 hours before additional drug treatments and/or protein extraction. Compound P053 is a second-generation small molecule inhibitor of PP5. Belzutifan-resistant ccRCC cells were treated with either 1μM or 10μM of P053 for 24 hours and apoptotic markers were evaluated by immunoblotting to examine cleaved caspase-3 and cleaved-PARP.
RESULTS: The second generation PP5 inhibitor P053 has the ability to bind to the catalytic domain and inhibit the phosphatase activity of PP5. Belzutifan-resistant ccRCC cells are able to maintain growth in the presence of 10μM belzutifan and do not display any hallmarks of activation of apoptosis. Treatment of belzutifan-resistant cells with either 1μM or 10μM of P053, however, induced apoptosis, as evidenced by elevated levels of cleaved caspase-3 and cleaved-PARP.
CONCLUSIONS: PP5 inhibition with our novel small molecule inhibitor retains the ability to cause apoptosis in belzutifan-resistant cells. This suggests PP5 is a viable therapeutic target in advanced ccRCC even after belzutifan resistance.

#1852 CRISPR screening identifies BMF loss as a drug-tolerant persister cell survival factor in ALK-rearranged lung cancer.

Ryohei Katayama[1], Takahiro Utsumi[1], Ken Uchibori[2], Makoto Nishio[3]

[1]Japanese Foundation for Cancer Research, Tokyo, Japan,[2]Cancer Institute Hospital, Japanese Foundation for Cancer Research, Tokyo, Japan,[3]Department director, Department of Thoracic Medical Oncology, Japanese Fndn. for Cancer Res. Cancer Institute, Tokyo, Japan

Anaplastic lymphoma kinase (ALK) tyrosine kinase inhibitors (ALK-TKIs) have significantly improved the clinical outcomes of patients with ALK-rearranged non-small cell lung cancer (NSCLC). However, the development of resistance remains a major obstacle to long-term therapeutic success. Drug resistance is believed to develop from drug-tolerant persister (DTP) cells that survive drug treatment. Therefore, understanding the molecular mechanisms underlying DTP formation and survival is critical for developing strategies to overcome resistance and extend patient survival.To identify the factors related to the survival of DTP cells, we conducted a genome-wide CRISPR-Cas9 knockout screening using patient-derived ALK-positive NSCLC cells. From the Crispr screening, we identified the pro-apoptotic factor BMF (Bcl-2 modifying factor) as a critical determinant of DTP formation. BMF expression was rapidly induced following ALK-TKI exposure or dual inhibition of ERK and PI3K signaling, suggesting its role as a mediator of apoptotic induction by ALK-TKIs. Strikingly, BMF knockout cells exhibited impaired apoptosis and an increased fraction of DTPs under ALK-TKI treatment, highlighting its essential function in limiting drug tolerance.Mechanistic studies revealed that pharmacologic or siRNA-mediated inhibition of MCL-1 restored apoptosis and eliminated BMF-deficient DTP cells, underscoring the therapeutic potential of targeting anti-apoptotic pathways. Furthermore, knockdown of FOXO1 resulted in the upregulation of BMF, indicating that FOXO1 acts as a transcriptional repressor of BMF. These findings suggest the existence of a regulatory axis in which FOXO1 suppresses BMF, thereby promoting the survival of DTP cells.In addition, patient tumor samples collected before and after ALK-TKI therapy, together with publicly available datasets, were analyzed to evaluate the clinical relevance of these findings. The clinical analyses revealed that low BMF expression was associated with poor treatment response and shorter overall survival in patients with ALK-positive non-small cell lung cancer (NSCLC). Moreover, BMF genomic loss was found relatively frequently across diverse cancer types, suggesting that BMF deficiency may be a common mechanism contributing to drug tolerance and resistance beyond ALK-driven lung cancer.In summary, our study demonstrates that BMF deficiency promotes the formation of DTP cells and contributes to therapeutic resistance in ALK-positive NSCLC. Importantly, targeting MCL-1 or FOXO1 may be a promising strategy for eradicating DTPs and enhancing the durability of ALK-TKI responses. These findings provide mechanistic insight into the regulation of persister cell apoptosis and highlight actionable vulnerabilities that could be exploited to improve patient outcomes.

#1853 NAT10-mediated ac^{4}C RNA modification promotes colorectal cancer stemness and 5-FU resistance via ATG5-dependent autophagy.

Xin Kong[1], Junyong Weng[1], Zhe Wang[2], Ajay Goel[1]

[1]Department of Molecular Diagnostics and Experimental Therapeutics, Beckman Research Institute of City of Hope, Monrovia, CA,[2]Department of Pathology, The First Affiliated Hospital of USTC, University of Science and Technology of China, Hefei, China

Background: Colorectal cancer (CRC) is the third most common malignancy and the second leading cause of cancer-related death globally. Although 5-fluorouracil (5-FU)-based chemotherapy remains a mainstay, acquired resistance severely limits its clinical benefit. The objective response rate to first-line combination therapy remains only 40-50%, and the 5-year survival for metastatic CRC hovers around 12%. Autophagy enables tumor cells to survive chemotherapy-induced stress, and targeting protective autophagy has emerged as a promising approach to reverse chemoresistance. RNA modifications can influence this process. N-acetyltransferase 10 (NAT10), the sole RNA N^4-acetylcytidine (ac^{4}C) acetyltransferase, has been implicated in cancer progression, but its role in autophagy-driven 5-FU resistance remains undefined. This study explores how NAT10 regulates autophagic activity and contributes to 5-FU resistance in CRC.

Methods: Integrative clinical and bioinformatics analyses were conducted to examine the association between NAT10 expression and 5-FU resistance in CRC. Complementary in vitro assays assessed the functional role of NAT10 in CRC progression and chemoresistance. Mechanistic studies, including pathway enrichment analyses, autophagic flux assays, and genetic epistasis experiments, were conducted to elucidate the signaling pathways downstream of NAT10. RNA immunoprecipitation (RIP) and ac^{4}C-specific RIP were used to identify direct molecular targets, and pharmacologic inhibition was applied to evaluate NAT10 as a therapeutic target.

Results: NAT10 was found to play a key oncogenic role in CRC by promoting cell proliferation, migration, and stemness. NAT10 expression was significantly higher in 5-FU-resistant CRC cells (p<0.001). NAT10 depletion markedly suppressed proliferation (p<0.001) and restored sensitivity to 5-FU. Mechanistically, NAT10 stabilized ATG5 mRNA through ac^{4}C modification ($t_{1/2}$ = 12.2 h vs. 20.1 h), thereby enhancing autophagic flux, which sustains cancer stemness and supports resistance to 5-FU. Loss of NAT10 resulted in reduced LC3-II accumulation and increased p62 expression, indicating impaired autophagy, and significantly decreased sphere-forming ability (p<0.001), along with downregulation of stemness markers, ultimately sensitizing resistant cells to 5-FU. Similarly, pharmacological inhibition of NAT10 repressed autophagy and significantly lowered the 5-FU IC50 values (~2.2-fold), thereby restoring 5-FU sensitivity in CRC models.

Conclusion: The NAT10-ATG5-autophagy axis represents a critical mechanism underlying chemoresistance in CRC. Targeting NAT10-mediated RNA acetylation disrupts autophagy-driven survival and restores 5-FU responsiveness, offering a promising therapeutic strategy for overcoming treatment resistance in colorectal cancer.

#1854 Selective Mcl-1 inhibition with KS18 overcomes apoptotic resistance and enhances FLT3-targeted therapy in acute myeloid leukemia.

Sahil Jethi[1], Krishne Gowda[2], Tulin Budak-Alpdogan[3], Subash C. Jonnalagadda[4], Manoj K. Pandey[1]

[1]Department of Biomedical Sciences, Cooper Medical School of Rowan University (CMSRU), Camden, NJ,[2]Department of Pharmacology, Penn State College of Medicine, Hershey, PA,[3]Cooper University Health Care, MD Anderson Cancer Center at Cooper, Camden, NJ,[4]Department of Chemistry and Biochemistry, Rowan University, Camden, NJ

Acute myeloid leukemia (AML) remains the most common adult leukemia and continues to have a dismal 5-year survival rate below 30 percent, largely due to relapse driven by therapy-resistant leukemic clones. Overexpression of the anti-apoptotic protein Mcl-1 is a major mechanism of such resistance, particularly against FLT3 and BCL-2 inhibitors, making selective Mcl-1 blockade a compelling therapeutic strategy. Here, we evaluate KS18, a highly selective small-molecule Mcl-1 inhibitor developed in our laboratory, as a single agent and in rational drug combinations in AML models (MOLM-13, MV4-11, THP-1) including a venetoclax-resistant line (MV4-11 VR). KS18 potently restored intrinsic apoptotic signaling by targeting the BH3-binding groove of Mcl-1 and releasing bound pro-apoptotic effectors (BIM, BAK, BAX), resulting in mitochondrial outer membrane permeabilization, cytochrome-c release, and robust caspase-dependent apoptosis. Mechanistically, KS18 induced mitochondrial dysfunction as evidenced by altered oxygen consumption (OCR) and extracellular acidification (ECAR) profiles. Combination treatment with either the FLT3 inhibitor quizartinib or the multi-kinase inhibitor sitravatinib yielded strong synergistic cytotoxicity through concurrent Mcl-1 suppression and inhibition of upstream survival pathways including FLT3/STAT5, AKT, and ERK. These combinations markedly enhanced cleaved caspase-3 and PARP levels, confirming extensive mitochondrial apoptosis. Together, these findings identify KS18 as a promising next-generation therapeutic candidate with both single-agent efficacy and strong combination potential for overcoming drug resistance and relapse in AML. Ongoing studies are generating FLT3 inhibitor-resistant models and evaluating KS18 in vivo across diverse FLT3 mutation backgrounds to accelerate its translational development for relapsed and refractory AML.

#1855 PI3K/mTOR dual inhibitor overcomes ceritinib resistance in ALK-rearranged NSCLC via both apoptosis and autophagy.

Hyun-Min Ryu[1], Joo Young Ha[2], Shinkyo Yoon[1], Yunkyung Sung[1], Deokhoon Kim[3], Chang Hoon Lee[4], Wanlim Kim[5], Seyoung Seo[1], Sang-We Kim[1], Kang-Seo Park[1], Dae Ho Lee[1]

[1]Oncology, Asan Medical Center (AMC), Seoul, Korea, Republic of,[2]Internal Medicine, Veterans Health Service Medical Center, Seoul, Korea, Republic of,[3]Pathology, Asan Medical Center (AMC), Seoul, Korea, Republic of,[4]SCBIO Inc, Daejeon, Korea, Republic of,[5]Orthopaedic Surgery, Asan Medical Center (AMC), Seoul, Korea, Republic of

Anaplastic lymphoma kinase-Tyrosine kinase inhibitors (ALK-TKIs) have substantially improved the treatment landscape for ALK-rearranged NSCLC; however, resistance to these agents remains a persistent clinical challenge. Whereas on-target resistance caused by secondary ALK mutations can be addressed with next-generation inhibitors, off-target resistance driven by activation of alternative RTKs is highly variable and often difficult to predict, making the development of a unifying therapeutic strategy complex. We investigated whether targeting the common downstream PI3K/AKT signaling pathway shared across multiple RTKs could provide an effective strategy to counter ALK-TKI resistance. In NSCLC cells resistant to ceritinib, a second-generation ALK-TKI, we observed that the PI3K/AKT signaling was robustly reactivated despite sustained suppression of ALK activity. Surprisingly, pharmacologic inhibition of AKT alone produced minimal anti-tumor effects, suggesting the presence of additional survival pathways beyond AKT itself. Based on previous reports showing that ALK contains an LC3-interacting region (LIR) motif whose dephosphorylation enhances autophagy, we investigated mTOR signaling as a potential compensatory pathway. Notably, PI3K/mTOR dual inhibition, rather than AKT inhibition alone, induced a markedly stronger anti-cancer response. Dual inhibition resulted in coordinated activation of apoptosis and autophagy-associated cell death, supported by significant changes in both apoptotic and autophagic markers, indicating a synergistic elimination of resistant cells. Because off-target resistance involves diverse and often unpredictable RTK-bypass activations, our findings suggest that PI3K/mTOR dual inhibition can target a broader range of downstream resistance mechanisms whenever ALK function is already pharmacologically suppressed. These results position PI3K/mTOR dual inhibitors as a promising therapeutic option for overcoming non-ALK-mutation-driven resistance in ALK-positive NSCLC, with potential translational relevance for patients who experience repeated TKI failure due to complex RTK-bypass signaling.

#1856 Downregulation of ETV4 mediates trametinib resistance via AMPK-ULK1-dependent protective autophagy in breast cancer.

Xiaodong Liu, Ji Won Kim

Jeju Research Institute of Pharmaceutical Sciences, College of Pharmacy, Jeju National University, Jeju, Korea, Republic of

Trametinib is a selective MEK1/2 inhibitor initially approved for melanoma and later extended to BRAF-mutant non-small cell lung cancer and thyroid cancer, either as monotherapy or in combination with a BRAF inhibitor. The favorable pharmacologic profile of trametinib has prompted broader evaluation across cancers driven by MAPK/ERK signaling. However, its efficacy as monotherapy in breast cancer (BCa) remains limited, partly due to adaptive resistance mechanisms. Therefore, we aimed to elucidate the molecular mechanisms underlying trametinib resistance in BCa and to validate therapeutic strategies that restore sensitivity. Here, we first found that trametinib responsiveness was associated with suppression of ETV4 expression. In T47D, SKBR3, and MDA-MB-453 cells, trametinib treatment suppressed ETV4 and promoted autophagic flux. Mechanistically, both trametinib treatment and ETV4 silencing activated AMPK-Thr172 phosphorylation, which in turn phosphorylated ULK1 at Ser555 while simultaneously inhibiting mTOR, thereby triggering protective autophagic flux. Combination treatment with trametinib and the autophagy inhibitors chloroquine (CQ) or 3-methyladenine (3-MA) induced apoptotic pathways in vitro and suppressed T47D xenograft tumor growth in vivo. Our results reveal that trametinib-induced downregulation of ETV4 enables cancer cells to acquire a survival advantage by activating AMPK-ULK1-mediated protective autophagy. We further identified that inhibiting autophagy reverses trametinib resistance and induces apoptotic cell death, providing a readily translatable combination therapeutic strategy to enhance MEK1/2-targeted therapy in BCa.

#1857 Mechanisms of acquired resistance to BTK and BCL2 inhibitors reveal clinically actionable vulnerabilities in B-cell lymphoma.

Alberto J. Arribas[1], Camilla Scalise[1], Eleonora Cannas[1], Maria Elena Carazzolo[2], Luciano Cascione[1], Andrea Rinaldi[1], Carlo Visco[2], Davide Rossi[1], **Francesco Bertoni**[1]

[1]Institute of Oncology Research, Universita della Svizzera italiana, Bellinzona, Switzerland,[2]Department of Engineering for Innovation Medicine, Section of Biomedicine, University of Verona, Verona, Italy

Background: BCL2 inhibitors (i) and BTK-directed agents, including BTK degraders (d), are essential components of modern therapy for B-cell lymphomas. However, acquired resistance often limits long-term benefits. Identifying the molecular mechanisms that underlie resistance and understanding reciprocal drug sensitivities may help guide the rational sequencing of treatments. Here, we investigated the mechanisms of secondary resistance to the BCL2-i venetoclax and the BTK-d bexobrutideg (NX-5948) in models of marginal zone lymphoma (MZL) and mantle cell lymphoma (MCL).
Methods: Derivatives of Karpas1718 (MZL) and REC1 (MCL) with acquired resistance were developed through chronic exposure to increasing doses of venetoclax or bexobrutideg. Parental and resistant lines were characterized using drug sensitivity assays, apoptosis and cell cycle analyses, molecular profiling, and immunoblotting of apoptotic regulators and BCR signaling components.
Results: Venetoclax-resistant models from both lymphoma subtypes exhibited broad cross-resistance to other BCL2-i and upregulation of BCL-xL, with MZL cells also resistant to MCL1-i. Regulation of anti-apoptotic proteins varied among models: BCL-xL increased in both venetoclax-resistant models, whereas MCL1 increased only in Karpas1718. All venetoclax-resistant cell lines retained sensitivity to BTK-d, revealing a potential therapeutic vulnerability. Resistance to BTK-d was highly model-specific. In Karpas1718-resistant cells, no BTK degradation occurred after bexobrutideg exposure, and these cells were also resistant to BGB-16673, another BTK-d. Nonetheless, they remained sensitive to BTK-i and all BCL2-i, suggesting that switching to a different drug class could restore their response. Conversely, REC1 derivatives became resistant to both BTK-d and BTK-i. Since resistance was linked to continued drug-induced BTK degradation, these findings indicate a BTK-independent resistance mechanism. Interestingly, the bexobrutideg-resistant REC1 cells were also resistant to BCL2-i. No mutations were observed in *BTK, PLCG2, or BCL2*.
Conclusions: In two distinct B-cell lymphoma models, resistance to venetoclax and BTK-d developed through target-specific and model-specific adaptations involving anti-apoptotic reprogramming, altered BCR signaling dependence, and incomplete BTK degradation. Notably, cross-drug sensitivities persisted in several contexts: venetoclax-resistant MZL and MCL cells remained susceptible to BTK degradation, while BTK-d-resistant MZL cells continued to respond to BCL2 inhibition. These insights emphasize clinically actionable strategies for treatment sequencing and support precision approaches to overcome therapeutic resistance in B-cell lymphoma.

#1858 FAK inhibition by APG-2449 enhances the antitumor activity of MAPK pathway blockade in *BRAF* V600E-mutant tumor models.

Zhou Yu[1], Zhiyan Liang[2], Xinyi Yao[1], Shujie He[1], Dajun Yang[1], Yifan Zhai[2]

[1]Ascentage Pharma (Suzhou) Co., Ltd., Suzhou, China,[2]Ascentage Pharma Group Inc., Rockville, MD

Background: *BRAF* mutations are present in approximately 4% to 8% of all cancers, predominantly in colorectal cancer (CRC), melanoma, and non-small-cell lung cancer. Among them, the V600E mutation is the most common and functionally activating form, leading to constitutive activation of the mitogen-activated protein kinase (MAPK) signaling cascade. Combined BRAF and MEK inhibition has shown substantial clinical benefit in *BRAF* V600E-mutant melanoma and CRC. However, resistance frequently develops through feedback reactivation of ERK or compensatory activation of the PI3K-AKT signaling pathway. Recent evidence indicates that focal adhesion kinase (FAK) signaling is also adaptively reactivated upon MAPK inhibition, contributing to therapeutic resistance. This study evaluated the effects of APG-2449, a potent and selective multikinase (FAK) inhibitor, on the antitumor activity of BRAF inhibitor dabrafenib and MEK inhibitor trametinib in *BRAF* V600E-mutant CRC and melanoma preclinical models.

Methods: Cell proliferation was measured by CellTiter-Glo® assay or clonal formation assay. Apoptosis was assessed using flow cytometry. Protein expression levels were examined by western blot. Antitumor effects of APG-2449, alone or combined with dabrafenib and trametinib, were evaluated in C32 and RKO xenograft models *in vivo*.

Results: Cell proliferation assays across a panel of human cancer cell lines revealed that cell lines harboring *BRAF* V600E were more sensitive to APG-2449 than those without MAPK pathway alterations. APG-2449 synergistically enhanced the antiproliferative efficacy of dabrafenib and trametinib in both BRAF inhibitor-sensitive (C32 and Colo205) and -insensitive (RKO and LS411N) cells. The triple combination (APG-2449 + dabrafenib + trametinib) caused synergistic growth inhibition in C32 and RKO cells compared with BRAF/MEK dual blockade. Mechanistically, APG-2449 attenuated feedback reactivation of ERK signaling and bypass activation of the PI3K-AKT pathway induced by BRAF/MEK inhibition, resulting in sustained suppression of p-ERK and p-AKT expression, prolonged cell growth inhibition, and enhanced cell apoptosis. In *in vivo* studies, the triple combination (T/C: 4.55% for C32; 17.18% for RKO) outperformed APG-2449 alone (T/C: 106.09% for C32; 96.93% for RKO) or dabrafenib + trametinib (T/C: 35.39% for C32; 78.45% for RKO) in tumor growth inhibition. APG-2449 synergistically enhanced the antitumor activity of trametinib + dabrafenib in C32 and RKO xenograft models, with synergy ratios of 8.25 and 4.43, respectively.

Conclusions: APG-2449 suppresses compensatory signaling activation induced by MAPK pathway blockade and synergistically enhances the antitumor activity of dabrafenib + trametinib. These results warrant clinical development of APG-2449 for patients with melanoma or CRC harboring *BRAF* V600E.

#1859 Overexpression of fructose transporter increases pro-survival signaling and confers venetoclax resistance in Ph-like B-cell acute lymphoblastic leukemia.

Serene Xavier[1], Sonia Rodriguez[1], Zhaohui Gu[1], Lucy Ghoda[1], Stuart Blakemore[2], Lukas Frenzel[2], Alexey Danilov[1], Vinod Pullarkat[1]

[1]City of Hope National Medical Center, Duarte, CA,[2]University Hospital Cologne, Colonge, Germany

Philadelphia chromosome-like (Ph-like) B-cell acute lymphoblastic leukemia (B-ALL) represents a high-risk subtype characterized by therapy resistance and an adverse clinical profile similar to Ph+ ALL. Recent evidence highlights the growing significance of metabolic reprogramming in drug resistance in B-ALL. We have identified increased fructose transporter GLUT5 expression in Ph-like and Ph+ primary samples and cell lines compared to other B-ALL subsets. In this study, we aim to investigate the novel mechanistic roles of GLUT5 in pro-survival signaling and drug resistance in Ph-like B-ALL. Firstly, to study the role of GLUT5 and fructose availability in cell proliferation, Ph-like B-ALL cell lines (MHH-cALL4 and MUT5Z) stably expressing GLUT5 or empty vector control, were cultured in glucose- or fructose-rich standard media. GLUT5-overexpressing B-ALL cell lines in glucose- or fructose-rich media showed increased proliferation (quantified by CFSE) when compared to control in glucose-rich media. GLUT5-overexpressing cells showed increased colony formation in glucose- or fructose-rich media, while control cells showed the same effect only in fructose-rich media when compared to those in glucose-rich media, indicating that GLUT5-mediated fructose uptake provided a proliferation advantage. To gain better insights on the significance of GLUT5 expression in high-risk B-ALL, bulk RNA-Seq was performed on control or GLUT5-overexpressing Ph-like B-ALL cell lines in glucose- or fructose-rich media. Pro-survival signaling pathways (such as PI3K/AKT, MAPK, NFKB, HIF-α and others) were significantly upregulated in GLUT5-overexpressing cell lines in glucose- or fructose-rich and control cells in fructose-rich conditions (vs. control in glucose-rich condition). We confirmed increased expression of p-AKT/AKT, MYC and NFKB in GLUT5-overexpressing Ph-like B-ALL cell lines in glucose- or fructose-rich conditions by immunofluorescence and immunoblotting. Further, increased BCL-2 expression was observed in GLUT5-overexpressing Ph-like cell lines in fructose-rich conditions only, indicative of the potential role of GLUT5 and fructose availability in conferring venetoclax resistance. Consistent with this, GLUT5-overexpressing B-ALL cell lines treated with venetoclax in fructose-rich media showed significantly increased resistance vs. control. A combination of venetoclax with serine synthesis pathway (SSP) inhibitor partially reversed venetoclax resistance. This suggests that GLUT5 expression and fructose availability may divert glycolytic pathway intermediates to SSP as an alternative cell survival mechanism. In summary, GLUT5 may have clinically relevant role in high-risk B-ALL where it modulates pro-survival signaling and confers therapy resistance.
AD and VP – equally contributing senior authors

#1860 Determining mechanisms of ONC212-resistance in uveal melanoma to develop combination therapy strategies.

Md Alauddin, Chandrani Chattopadhyay

Department of Melanoma Medical Oncology, UT MD Anderson Cancer Center, Houston, TX

Uveal melanoma (UM) is the most common primary eye cancer in adults, affecting ~2,500 people annually in USA. Metastasis in ~50% of UM patients is predominantly to the liver (>95%), resulting in poor prognosis. Only two FDA-approved therapies exist for metastatic UM (mUM), with poor response rates. There is an urgent need for developing new therapeutic strategies to achieve effective response. Our preliminary studies indicated that mUM has high Oxidative Phosphorylation (OXPHOS). Indirect targeting of OXPHOS with the imipridone compound ONC212, significantly inhibited UM cell survival, reduced tumor burden and improved survival in orthotopic liver mUM mouse models. However, extended treatment resulted in tumor recurrence, suggesting acquired resistance. Thus, successful translation of the growth inhibitory effect of ONC212 in mUM depends on identification of ONC212 resistance mechanisms and new targets. In this study, we generated and characterized multiple ONC212-resistant UM cell clones. More than thirty ONC212-resistant clones were generated from MM28 and MP46 parental UM cells via prolonged treatment with high-dose ONC212 (0.3 μM). Cell viability assays were done to calculate IC_{50} and resistance index (RI) for ONC212, and mitochondrial function was assessed using the Seahorse Mito Stress Test. Whole-genome sequencing (WGS) was used to identify acquired mutations in resistant clones, while proteomic profiling via Reverse Phase Protein Array (RPPA) was used to determine alterations in cell signaling pathways. A high throughput drug screen was completed to identify sensitivities of ONC212-resistant cells to approved anticancer drugs. Orthotopic liver-mUM mouse models were generated with resistant cells and growth of tumors monitored by bioluminescence imaging. ONC212-resistant clones exhibited higher $IC_{50,}$ and RI compared to parental cells and showed cross-resistance to other imipridones (ONC201, ONC206), suggesting shared mechanisms of resistance. Resistant clones displayed reduced sensitivity to ONC212-mediated OXPHOS inhibition. WGS of each resistant clone confirmed mutations in CLPP, the target of ONC212 action in UM cells. RPPA data revealed alterations in multiple cell signaling pathways. Bioluminescence imaging of liver mUM *in vivo* models revealed rapid proliferative capacity of ONC212-resistant clones. Using these preclinical models and the compounds identified in drug screen, combination therapy strategies will be tested and validated for clinical studies in future. Importantly, ONC201, the first imipridone was recently approved for therapy of midline gliomas. Therefore, lessons learned from this study may benefit patients acquiring resistance to ONC201 in future as well.

#1861 Acquired drug resistance with autophagy is suppressed by fatty acid oxidation inhibition in pancreatic ductal adenocarcinoma.

Soo-Youl Kim, Sang M. Woo, Wonyoung Choi, Joon Hee Kang, Sung Hoon Sim, Jung Won Chun

National Cancer Center, Goyang, Korea, Republic of

Purpose: We found that irinotecan treatment of pancreatic ductal adenocarcinoma (PDAC) induces autophagy. Autophagy enhances fatty acid oxidation (FAO), resulting in increased ATP production. Elevated ATP levels subsequently are linked to mTOR activation. As a result, prolonged chemotherapy paradoxically co-activates mTOR and autophagy, which are two pathways traditionally known to suppress each other, resulting in the promotion of acquired drug resistance.
Experimental Design: To test whether blocking FAO reverses the acquired drug resistance, inhibition of FAO achieved by dual knockdown of carnitine-acylcarnitine carrier and acetyl-CoA acyltransferase 1 or inhibited the targets by KN510 and KN713. Anti-cancer effect was examined by xenograft model using human pancreatic cancer cells. Synergy of KN510 and KN713 with chemotherapeutic drugs also tested using a xenograft model.
Results: We found that a combination treatment of KN510 and KN713 accompanied with irinotecan abolished autophagy activation and suppressed mTOR, resulting absence of drug resistance. In a PDAC xenograft model, combination treatment with irinotecan and the FAO inhibitor KN510713 significantly decreased acquired resistance, whereas irinotecan alone led to tumor regrowth.
Conclusion: These findings highlight that the FAO pathway is a key mechanism of cancer-specific autophagy, supporting its role in the development of acquired drug resistance during chemotherapy.
Funding source: Basic Science Research Program through the National Research Foundation of Korea (NRF) funded by the Ministry of Science and ICT to SK (NRF-2019M3A9G1104345) and was supported by a grant from the National Cancer Center of Korea to WC (NCC 2410891-2).

#1862 Targeting nucleolin overcomes MCL-1-mediated venetoclax resistance in acute myeloid leukemia.

Kyung Jin Kim, Jihyun Um, Eun Jung Shin, Yu Mi Ji, Sung Hwan Moon, Soo Jin Lee

Aptabio Therapeutics Inc., Yongin, Korea, Republic of

BCL-2 inhibitors, such as venetoclax, have become a standard treatment for acute myeloid leukemia (AML), particularly for patients ineligible for intensive chemotherapy. However, a significant number of patients are refractory or acquire resistance, which remains a major clinical challenge. MCL-1, an anti-apoptotic Bcl-2 family protein, is well recognized to play critical roles in resistance to venetoclax treatment and there is a significant unmet need for the development of effective therapies that inhibit MCL-1 to overcome venetoclax resistance. Nucleolin (NCL) is a multifunctional protein frequently overexpressed on the surface of AML cells and is implicated in promoting cancer cell survival and drug resistance by regulating various oncogenic transcripts. This study provides the first evidence that NCL acts as an upstream regulator of MCL-1 and that inhibition of NCL can effectively overcome venetoclax resistance in AML by downregulating MCL-1. As a result, we found that the expression levels of NCL and MCL-1 were significantly elevated in venetoclax-resistant AML cell lines, and that siRNA-mediated genetic knockdown of NCL led to a significant reduction of MCL-1 expression levels along with a corresponding induction of cleaved caspase-3, confirming the activation of apoptosis. APTA-16 is a first-in-class therapeutic for AML that specifically targets NCL developed using aptamer-drug conjugation (APTA-DC) technology. To confirm the role of NCL in MCL-1-mediated venetoclax resistance, we treated venetoclax-resistant AML cell lines with Apta-16, and Apta-16 significantly reduced in both NCL and MCL-1 expression levels and activated caspase-3. Furthermore, in a C1498 syngeneic mouse model of venetoclax-resistance in vivo, Apta-16 monotherapy significantly improved the survival rate, whereas venetoclax showed no therapeutic benefit. In addition, we also confirmed that in vivo Apta-16 treatment markedly decreased intratumoral levels of NCL and MCL-1 expression.In conclusion, our findings demonstrate that the NCL-MCL-1 axis plays a critical role in mediating venetoclax resistance in AML and inhibition of NCL can be a promising strategy to disrupt this axis and overcome venetoclax resistance. Therefore, the results suggest that Apta-16 has strong potential as an effective therapy approach to overcome venetoclax resistance in in patients with relapsed or refractory AML. GLP safety/toxicity studies of APTA-16 have been completed, and orphan drug designation (ODD) was granted by FDA.

#1863 Development and characterization of the venetoclax-resistant AML model to enable preclinical drug discovery.

Jifan Yuan[1], Miaomiao Yu[1], Gaoxiang Liu[1], Jian Xiang[1], **Xiangnan Qiang**[2], Zhixiang Zhang[2]

[1]In Vivo Pharmacology Unit, WuXi Biology, WuXi AppTec, Suzhou, China,[2]In Vivo Pharmacology Unit, WuXi Biology, WuXi AppTec, Shanghai, China

Acute myeloid leukemia (AML) is an aggressive type of hematological cancer, causing over 100,000 death per year globally. Venetoclax, a BCL-2 antagonist, was approved in 2018 for the treatment of AML in combination with Azacytidine. Through neutralizing BCL-2 function, Venetoclax restores the apoptotic cascade in tumor cells. However, long-term efficacy of Venetoclax is often limited by the development of drug resistance, underscoring the need for preclinical Venetoclax-resistant (Ven-R) tumor models. In this study, we successfully established two Venetoclax-resistant cell lines, Ven-R-MV4-11 and Ven-R-MOLM-13, through chronic exposure to Venetoclax. Compared to the parental cell lines, both resistant cell lines exhibited increased expression of MCL-1, an anti-apoptotic protein that plays a crucial role in Venetoclax resistance. Cell viability assays in these resistant cell lines demonstrated strong synergy between Venetoclax and two MCL-1 inhibitors, AMG-176 and MIK665. *In vivo*, both Ven-R-MV4-11 and Ven-R-MOLM-13 models showed increased growth rate and substantial resistance to Venetoclax alone and in combination with Azacytidine (standard therapy). Interestingly, the MCL-1 inhibitor, MIK665 effectively overcame the resistance in the Ven-R-MV4-11 tumor model when used in combination with Venetoclax and Azacytidine. In conclusion, we have developed two Venetoclax-resistant AML models, which serve as a promising tool for mechanistic research and drug discovery aimed at overcoming the BCL2 inhibitor resistance.

#1864 G3BP1 knockdown sensitizes the acute myeloid leukemia cell line HL60 to venetoclax by inducing apoptosis.

Naoko Hosono[1], Rie Nishi[1], Naoko Ida[2], Chantana Polprasert[3], Rosesanun Pavaputanont[3], Takahiro Yamauchi[4]

[1]University of Fukui, Fukui, Japan,[2]University of Fukui Hospital, Japan,[3]Center of Excellence in Translational Hematology, Chulalongkorn University, Bangkok, Thailand,[4]Asst. Professor, First Dept. of Internal Med., University of Fukui, Fukui, Japan

Background: G3BP1 is an RNA-binding protein that acts as the primary nucleation factor for the assembly of stress granules (SG). Its functions are central to the cellular stress response, survival, and fate decisions. G3BP1 is located on the long arm of chromosome 5 and deletion of this region is a recognized poor prognostic factor in acute myeloid leukemia. Given that G3BP1 is highly expressed in hematopoietic stem cells and functions to stabilize p53, its deficiency is hypothesized to be implicated in the tumorigenesis and therapeutic resistance of leukemic cells.
Methods: To investigate the role of G3BP1, a G3BP1 knockdown cell line was generated by introducing shRNA into the HL60 AML cell line. We performed analyses of expression changes and drug sensitivity, using cell lines in which the expression level was reduced to 15% by knockdown .
Results: Expression profiling via RNA sequencing demonstrated an upregulation of WT1, SAMD9L, and BCL2 expression in HL60/shG3BP1 cells (G3BP1-knockdown cells). Confirmation by Western blot analysis revealed increased protein levels of WT1 and SAMD9L. We also observed upregulation of both mTOR and its phosphorylated mTOR. HL60/shG3BP1 cells exhibited reduced sensitivity to Ara-C compared to control cells (IC50 value: 7 μM, 0.5 μM, respectively), while conversely demonstrating increased sensitivity to venetoclax (IC50 value: 4nM, 900nM, respectively). Sensitivity to other tested agents, including daunorubicin, etoposide, and Decitabine, remained unchanged. In HL60/shG3BP1 cells, venetoclax treatment led to an increased induction of apoptosis, which was accompanied by an increase in cleaved caspase-3 levels.
Conclusion: Knockdown of G3BP1 in HL60 cells resulted in enhanced sensitivity to venetoclax. This enhanced sensitivity might be explained by the impairment of G3BP1-mediated SG formation.

: Targeting Drug Resistance 2: RAS Signaling
Poster Session

#1868 Resistant cell panel-based discovery of multi-target combinations and mechanisms to overcome KRAS inhibitor resistance.

Lili Chai, Yue Zhai, Xue Yang, Zhengtai Li, Ying Bi, Yan Zhang, **Tj (Tiejun) Bing**

ICE Bioscience, Beijing, China

Background: KRAS mutations are common oncogenic drivers in solid tumors, and KRAS-targeted inhibitors have revolutionized treatment. However, inherent and acquired resistance limits long-term clinical benefit, highlighting the need for effective combination strategies and their mechanisms.
Methods: 1) Generation of KRAS inhibitor-resistant cell lines: Over 10 resistant cell lines were established by long-term exposure of KRAS-mutant cancer cells to clinically approved KRAS inhibitors and novel agents (e.g., KRAS molecular glues, PI3K/RAS breakers). 2) Resistance mechanism exploration: Multi-omics bioinformatics analyses (transcriptomics, proteomics) were performed to dissect molecular drivers of resistance and predict potential synergistic combination partners. 3) High-throughput combination screening: More than 100 drug combinations (including KRAS inhibitors, targeted agents against bypass pathways, and novel scaffolds) were tested using a customized resistant cell panel to identify regimens that overcome resistance. 4) Mechanistic validation: Key signaling pathways (e.g., MAPK, PI3K-AKT, STAT3) were interrogated via Western blot, and phospho-protein arrays to confirm the functional relevance of predicted resistance mechanisms and combination efficacy.
Results: Bioinformatics analyses of resistant cell lines revealed diverse resistance mechanisms, including upregulation of bypass signaling cascades, KRAS isoform switching, and adaptive metabolic rewiring. High-throughput screening identified several promising drug combinations that restored sensitivity to KRAS inhibitors in resistant cells, with combinations of KRAS inhibitors plus PI3K/RAS breakers or pathway-specific inhibitors showing the most potent synergistic effects. Mechanistic validation confirmed that these combinations effectively abrogated aberrantly activated resistance-related signaling pathways, reversing the resistant phenotype. Additionally, the customized cell panel enabled rapid ranking of KRAS inhibitor monotherapy and combination efficacy across distinct KRAS mutation subtypes.
Conclusions: Our study establishes a robust platform of KRAS inhibitor-resistant cell lines and a high-throughput screening system for identifying resistance-overcoming combinations. The identified synergistic regimens and their validated mechanisms provide critical preclinical evidence to guide the development of next-generation KRAS-targeted combination therapies, addressing the unmet clinical need of overcoming resistance in KRAS-mutant cancers.

#1869 Combining FGTI-2734 and MRTX1133 to suppress ERK-driven resistance in KRAS G12D pancreatic cancer.

Deblina Ghosh[1], Aslamuzzaman Kazi[1], Hitesh Kumar Kantilal Vasiyani[1], Vignesh Vudatha[1], Nicolas Lecomte[2], Christine A. Iacobuzio-Donahue[2], Jose G. Trevino[3], Said M. Sebti[1]

[1]VCU Massey Comprehensive Cancer Center, Richmond, VA,[2]David M. Rubenstein Center for Pancreatic Cancer Research, Memorial Sloan Kettering Cancer Center, New York, NY,[3]Div. of Surgical Oncology, VCU Massey Cancer Center, Richmond, VA

The KRAS G12D-selective inhibitor MRTX1133 marks a significant step forward in targeting mutant KRAS; however, its therapeutic impact is dampened by adaptive resistance driven by ERK pathway reactivation, a process requiring membrane localization of wild-type (WT) RAS. In this study, we introduce a rational approach to circumvent this resistance by using FGTI-2734, a dual inhibitor of farnesyltransferase (FT) and geranylgeranyltransferase-1 (GGT-1) that impairs WT RAS and mutant RAS membrane Localization. FGTI-2734 suppresses the ERK rebound elicited by MRTX1133 and acts synergistically with MRTX1133 to inhibit cell growth and trigger apoptosis in KRAS G12D pancreatic cancer cell lines. In patient-derived organoids from 12 individuals with KRAS G12D pancreatic cancer, including organoids originating from both primary and metastatic sites and spanning diverse co-mutation patterns (KRAS, TP53, CDKN2A, SMAD4, RTKs, PI3K/AKT, JAK/STAT, DNA repair/cell-cycle genes, and chromatin modifiers), the FGTI-2734/MRTX1133 combination produced consistent strong synergy. This effect was observed regardless of prior treatment, disease stage, or intrinsic sensitivity or resistance to MRTX1133. In vivo, FGTI-2734 potentiated MRTX1133's anti-tumor effects, leading to tumor regression in orthotopic patient-derived xenografts established from a KRAS G12D pancreatic cancer patient who progressed after radiation and chemotherapy, as well as in xenografts derived from KRAS G12D human pancreatic cancer cell lines. Importantly, FGTI-2734 treatment prevented MRTX1133-driven ERK reactivation in these KRAS G12D xenograft models. Collectively, these results define a mechanistically grounded combination strategy that neutralizes a key resistance pathway limiting MRTX1133 efficacy, and they highlight a promising therapeutic option for KRAS G12D pancreatic cancers.

#1870 Characterizing drug-induced transcriptional reprogramming in KRAS mutant lung cancer.

Wafa Malik[1], Anurag Singh[1], Laurent Sansregret[2], Aaron N. Hata[1]

[1]Massachusetts General Hospital, Krantz Family Center for Cancer Research, Boston, MA,[2]Novartis Institutes for BioMedical Research, Basel, Switzerland

KRAS mutations define the largest genomic subset of non-small cell lung cancer (NSCLC). Recently, inhibitors that selectively target the $KRAS^{G12C}$ mutation (G12Ci) have been developed, however, clinical responses are incomplete and short-lived due to intrinsic and adaptive drug resistance. Combination drug strategies designed to inhibit adaptive resistance by targeting reactivation of the MAPK pathway have demonstrated limited efficacy and significant dose-limiting toxicity. Therefore, new strategies to overcome drug resistance are needed. In some contexts, resistance to oncogene-directed therapies in NSCLC can be linked to dysregulation of the Hippo pathway, a key cell growth control pathway that is conserved across species. Recent preclinical studies have suggested that dysregulation of the Hippo pathway and activation of YAP and its corresponding transcription factor TEAD promote adaptive resistance in *KRAS*-mutant lung cancer models, which can be overcome by combining YAP-TEAD inhibitors with G12Ci. However, our mechanistic understanding of how YAP drives adaptive resistance is incomplete. Using patient-derived $KRAS^{G12C}$-mutant models, we show that G12Ci induces progressive YAP-dependent and YAP-independent transcriptional reprogramming. We identify lineage programs regulated by YAP during adaptation to G12Ci that are derepressed upon co-treatment with a YAP-TEAD inhibitor. These results reveal insights into non-genomic adaptive drug resistance in lung cancer and will enable future development of rational drug combination strategies to overcome therapeutic resistance.

#1871 Combined RAS and ICB inhibition targets NF-KB-driven immune evasion in chemoresistant pancreatic cancer.

Kevin Christian Gulay, Alexei Martsinkovskiy, Isabella Ng, Deepa Sheik Pran Babu, Jay Patel, Rithika Medari, Ponmathi Panneerpandian, Tatiana Hurtado de Mendoza, Andrew Lowy, Herve Tiriac

Department of Surgery, University of California San Diego, San Diego, CA

Pancreatic ductal adenocarcinoma (PDAC) is one of the most lethal malignancies, with surgery as the only potentially curative option. However, 85% of patients present with inoperable disease. For these patients, chemotherapy remains the standard treatment, though nearly all develop resistance and disease progression. We hypothesize that resistance to chemotherapy and RAS inhibitors reshapes the tumor microenvironment (TME), and understanding these changes is key to developing effective combination therapies. To investigate resistance mechanisms, we generated chemoresistant (CR) PDAC models. Parental (PT) and CR cells were orthotopically implanted into syngeneic mice and treated with vehicle or MRTX1133. The TME was analyzed using flow cytometry, single-cell RNA sequencing (scRNA-seq), multiplex immunohistochemistry, and immunofluorescence. RNA sequencing and cytokine arrays characterized cancer-TME crosstalk. NF-κB signaling was interrogated for its effects on cytokine and immune checkpoint expression. In addition, human PDAC organotypic slice cultures were treated with RMC6236 and immune checkpoint blockade (ICB). In vivo experiments tested MRTX1133 in combination with anti-CTLA-4 or dual anti-CTLA-4 + anti-PD1 therapy. RNA-seq revealed significant KRAS pathway upregulation in CR tumors and NF-κB pathways in RASi-treated tumors. MRTX1133 treatment of CR tumors significantly reduced tumor volumes and weights compared to vehicle controls and PT tumors ($P=<0.01$). Histological and scRNA-seq analyses demonstrated that CR tumors had expanded epithelial and fibroblast compartments and decreased T cell and macrophage populations, which were rescued by MRTX1133 treatment ($P=<0.001$). Cytokine profiling showed that CR tumors treated with MRTX1133 exhibited increased CXCL10 and CCL2, and decreased GM-CSF and LIF. NF-κB signaling regulated expression of CCL2, GM-CSF, and LIF, and also influenced immune checkpoint expression in T cells, linking tumor-intrinsic signaling with T cell exhaustion pathways. Human PDAC organotypic slice cultures treated with anti-CTLA-4 antibody showed reduced epithelial cell populations compared to controls, suggesting improved therapeutic response. In vivo, MRTX1133 combined with anti-CTLA-4 and anti-PD1 antibodies significantly reduced tumor volumes and prolonged survival compared to MRTX1133 and anti-CTLA-4 or monotherapy with MRTX1133. KRAS inhibition controls tumor growth in chemorefractory PDAC and improves immune infiltration. Mechanistically, RASi in tumor cells activate NF-κB signaling, driving cytokine changes that enhance PD-1 and CTLA-4 expression in T cells. Targeting these NF-κB-driven cytokines and immune checkpoints alongside RAS inhibition represents a promising combinatorial strategy to overcome chemoresistance and improve PDAC outcomes.

#1872 A high-throughput combination screen identifies NT-1 as a superior compound to overcome KRAS^{G12D} inhibitor resistance.

Natalie Thielen[1], Chaoyuan Kuang[2], Ning Wei[3], Seiya Kitamura[1], Emiko Nagai[1]

[1]Albert Einstein College of Medicine, Bronx, NY,[2]Albert Einstein Cancer Ctr., Bronx, NY,[3]Montefiore Comprehensive Cancer Center, Bronx, New York, NY

Background: Colorectal cancer (CRC) is the second leading cause of cancer-related mortality. KRAS mutations, present in approximately 40% of CRC cases. FDA-approved inhibitors exist for KRAS^{G12C}, but this mutation represents only a small subset of CRC, and resistance frequently develops through canonical or alternative survival pathways. KRAS^{G12D} is the most prevalent allele in CRC; however, there are currently no FDA-approved inhibitors and few agents in advanced development. To address KRAS resistance, we developed a high-throughput combinatorial screening platform using both cell lines and patient-derived organoids (PDOs) with fully annotated molecular profiles to identify synergistic drug combinations capable of overcoming resistance.
Method: To demonstrate the utility of this platform for identifying G12D inhibitor (G12Di) resistance mechanisms and synergistic partners, we performed a large-scale combinatorial drug screen in both parental and resistant KRAS^{G12D} mutant CRC cell lines. The screening library consisted of approximately 2,600 kinase inhibitors and 3,500 FDA-approved or clinical-stage compounds, tested both as single agents and in combination with a preclinical KRAS^{G12D} inhibitor. Viability was assessed using the ATP-based luminescence assay CellTiter-Glo. Compounds demonstrating robust synergy were prioritized for secondary validation using 8×8 dose-response matrices. The most promising compounds were validated in KRAS^{G12D} PDOs to confirm translational potential.
Result: Multiple compounds displayed synergistic activity with KRASi. Notably, "NT-1," a novel analog of the FDA-approved EGFR inhibitor osimertinib, demonstrated significant synergy (synergy score >10) at nanomolar concentrations across both sensitive and resistant CRC models. Compared with other EGFR inhibitors (osimertinib, erlotinib, afatinib), NT-1 achieved greater inhibitory effects at lower doses. These findings were extended to combinations with emerging pan-KRAS inhibitors, where NT-1 consistently outperformed approved EGFR inhibitors and cetuximab, producing deeper suppression of p-EGFR and p-ERK, and stronger induction of apoptosis. Ex vivo validation using KRAS^{G12D} PDOs confirmed the translational potential of these combinations, demonstrating that NT-1 can mitigate both intrinsic and acquired resistance to G12Di. Ongoing in vivo studies are assessing NT-1 in combination with G12D selective and pan-KRAS inhibitors to delineate mutation-specific versus pathway-level vulnerabilities.
Conclusion: Our combinatorial screening platform provides novel biological insights into KRAS^{G12D} resistance mechanisms in CRC and effectively identifies drug combinations with immediate clinical utility. The combination of NT-1 with G12D selective or pan-KRAS inhibitors represents a promising therapeutic strategy to overcome KRAS^{G12D} resistance.

#1873 Atebimetinib's deep cyclic inhibition of MEK constrains MAPK-axis adaptive and acquired alterations in patients with RAS-mutant tumors.

Jason S. Kim[1], Jason Funt[2], Jenny Zhang[1], Sarah Kolitz[3], Praveen Nair[2], Vinny Hayreh[2], Benjamin J. Zeskind[3], Igor Matushansky[1], Brett M. Hall[2]

[1]Immuneering, New York, NY,[2]Immuneering, San Diego, CA,[3]Immuneering, Cambridge, MA

Purpose: This study characterized acquired molecular alteration patterns arising in patients with RAS mutant tumors during treatment with the pulsatile MEK inhibitor atebimetinib (IMM-1-104), a once daily oral drug in clinical development that drives Deep Cyclic Inhibition (DCI) to modulate the MAPK pathway without continuous suppression.
Methods: 64 patients with RAS-mutant, advanced solid tumors received monotherapy atebimetinib, and serial circulating tumor DNA (ctDNA) analyses were performed to assess emergent genomic alterations detected with treatment over time. The evaluable patient population included a broad range of tumor types, disease stages and prior therapeutic exposures.
Results: Atebimetinib treatment did not lead to meaningful reactivation of the RAS/MAPK pathway, as canonical resistance events such as secondary RAS mutations, RAS-mutant allele amplification, or activating RAF variants were rarely observed. These events occurred less frequently than reported under continuous MEK, ERK, KRAS-selective, or pan-RAS inhibition, suggesting that intermittent DCI-based MAPK suppression reduces selective pressure for classical pathway signaling restoration. Rather than reestablishing MAPK dependence, emergent acquired mutation patterns were heterogeneous. Tumors frequently carried alterations spanning multiple pathway classes, for example combinations of cell-cycle deregulation, growth-factor and PI3K signaling, and transcriptional or epigenetic remodeling, including MYC-linked programs, without convergence on a single bypass mechanism. This pattern is consistent with distributed multipathway adaptive changes rather than reliance on a discrete secondary driver.
Conclusions: Atebimetinib-treated patient data demonstrate that deep, pulsatile MEK inhibition prevents the sustained loss of adaptive feedback commonly observed with chronic MAPK-pathway blockade, thereby reducing selective pressure for MAPK-reactivating resistance mechanisms. The resulting shift toward non-MAPK pathways suggests that atebimetinib's DCI mechanism, unlike chronic target engagement, limits MAPK-axis evolution. The low incidence of RAS/MAPK reactivation events supports evaluation of atebimetinib as a preferential combination backbone with either mutant-selective RAS inhibitors or mechanistically complementary therapies to enhance response durability and constrain RAS/MAPK pathway-mediated escape.

#1874 Prolonged KRAS-MAPK inhibition activates interferon signaling to promote cellular plasticity and uncover novel targets for combination therapy.

Ashenafi Shiferaw Bulle[1], Yali Chen[1], Huaping Li[1], Hung-Po Chen[1], Iftikhar Ali Khawar[1], Lin Li[1], Yu Wang[1], Peng Liu[1], Vikas Kumar Somani[1], Richard Kurupi[1], Sapana Prakashrao Bansod[1], Son Bang Le[2], Marianna Ruzinova[1], David D Tran[2], Kian-Huat Lim[1]

[1]Washington University School of Medicine, Saint Louis, MO,[2]Keck School of Medicine of USC, Los Angeles, CA

KRAS-MAPK cascade inhibition shows promise for treating PDAC. However, resistance arises through secondary mutations that restore MAPK signaling and trigger epithelial-to-mesenchymal transition (EMT), key mechanisms of acquired resistance. Here, we show that human PDAC specimens and cells treated long-term with an ERK inhibitor exhibit upregulation of EMT and interferon signaling, with similar pattern also seen following prolonged KRAS inhibition in PDAC cells. Using the GeneRep-nSCORE framework, we identified TRIM22, an interferon-inducible E3 ubiquitin ligase, as a key mediator of EMT and resistance by promoting proteasomal degradation of IκBα and activating NF-κB signaling. Searching for druggable targets, we found TACSTD2 (TROP2), an NF-κB target gene upregulated after EMT. Combining ulixertinib or the KRAS inhibitor MRTX1133 with the TROP2-directed antibody-drug conjugate sacituzumab govitecan effectively suppressed growth of PDAC patient-derived xenografts. This study highlights TRIM22's role in linking interferon signaling with EMT and identifies TROP2 as a therapeutic vulnerability to overcome acquired resistance.

#1875 Synergistic co-targeting of KRAS G12V and pan-TEAD by an EGFR-directed, inverted chimeric RNAi molecule.

Lyla Stanland[1], Alessandro Porrello[2], Sarah R. McLarnon[3], Lori L. O'Brien[3], Chad V. Pecot[2]

[1]EnFuego Therapeutics Inc, Morrisville, NC,[2]Lineberger Comprehensive Cancer Center, University of North Carolina, Chapel Hill, NC,[3]Cell Biology and Physiology, University of North Carolina, Chapel Hill, NC

While KRAS has long been considered an “undruggable” oncoprotein, advancements in structural and chemical biology have resulted in KRAS G12C, G12D, pan-KRAS and pan-RAS small molecule inhibitors. Although several have shown clinical promise, therapeutic resistance remains a significant problem. Recently, YAP/TAZ activation has emerged as a common resistance mechanism to KRAS inhibition. YAP and TAZ act as transcription coactivators with the TEAD1-4 transcription factors as part of the Hippo signaling pathway. Several groups have already shown that pan-TEAD (pTEAD) inhibition synergizes with KRAS inhibition, and YAP and KRAS exhibit pathway crosstalk in cancer. Previously, we developed EFTX-G12V, a first-in-class EGFR-directed KRAS G12V selective siRNA that displays excellent single agent efficacy in lung, colon and pancreatic cancers. Further, we developed a novel inverted chimeric siRNA design that incorporates two oncogene-targeting siRNAs linked by an endo-nucleolytic DNA bridge. The chimeric siRNA design ensures equivalent molar targeting of both gene transcripts in the same cell with enhanced metabolic stability and tumor accumulation. Here, we describe the development of chemically modified pTEAD targeting siRNAs and subsequent development of a KRAS G12V, pTEAD targeting chimeric siRNA. We used a structure-activity relationship screening approach to identify a highly potent fully chemically modified siRNA that inhibits TEAD1-4 at both the mRNA and the protein level. This pTEAD siRNA inhibited cancer cell growth *in vitro* and showed no concerning off-target effects. Using this siRNA and EFTX-G12V we developed EFTX-G12V-pTEAD, that inhibits KRAS G12V, TEAD1-4 and downstream signaling at both the mRNA and the protein level. Importantly, EFTX-G12V-pTEAD showed improved inhibition of downstream targets when compared to each single agent siRNA highlighting the value of the chimeric siRNA. Similar to our previously described siRNAs, EFTX-G12V-pTEAD is conjugated to an EGFR linear ligand that enables high tumor-to-normal tissue payload delivery and limits systemic exposure. *In vivo* evaluation of EFTX-G12V-pTEAD in comparison to single agent EFTX-G12V in both xenograft and immunocompetent cancer models are planned to evaluate durability, efficacy and safety. Importantly, small molecule pTEAD inhibitors cause kidney toxicity including podocyte effacement, proteinuria and albuminuria, which has limited their clinical utility. Using spatial profiling in the kidney, we found that our siRNA molecules do not enter podocytes and largely clear through the proximal tubules, therefore we anticipate the potential for less kidney toxicity and a wider therapeutic window using this therapeutic modality. Together our findings represent a technological advance in multi-oncogene targeting using RNAi and a therapeutic modality capable of addressing resistance to KRAS inhibitors.

#1876 Pre-treatment with azacytidine sensitizes *RAS* mutated secondary AML to the pan-RAS inhibitor RMC-7977.

Xinghan Zeng[1], Yuju An[1], Brandy Perkins[1], Tessa Seale[2], Erotokritos Georgantzinos[1], Theodora Chatzilygeroudi[1], Bogdan Paun[1], Maximillian Stahl[1], Mark J. Levis[3], Styliani Karanika[1], Alexander Ambinder[1], Sandra Misale[2], Theodoros Karantanos[1]

[1]Johns Hopkins University, Baltimore, MD,[2]Johns Hopkins University School of Medicine, Baltimore, MD,[3]Johns Hopkins Sidney Kimmel Cancer Center, Baltimore, MD

Patients with acute myeloid leukemia (AML) arising from antecedent myeloid neoplasms (secondary AML, sAML) continue to have poorer outcomes than those with de novo AML, characterized by a high incidence of refractory disease and relapse after initial response. Most patients with sAML are treated with combinations of hypomethylating agents, such as azacytidine, together with venetoclax, a BCL-2 inhibitor. However, *RAS* mutations, present in approximately 20-30% of these patients, confer resistance to venetoclax and are associated with shorter overall survival. Although *RAS* oncogenes were long considered “undruggable,” KRAS mutant-specific inhibitors have recently shown promise in clinical trials for solid tumors. Notably, treatment with the RAS-Multi^{ON} inhibitor RMC-7977 has been reported to sensitize AML cells to FLT3 and BCL-2 inhibition. In this study, we found that pretreatment with azacitidine enhances the sensitivity of *RAS*-mutated sAML cells to RMC-7977.Analysis of the BEAT AML 2.0 dataset revealed that mutations affecting RAS signaling—particularly in *KRAS*, *NRAS*, and *PTPN11*—rank among the top alterations associated with resistance to azacytidine treatment in AML samples. These findings suggest that combining azacytidine with RAS inhibition may represent a promising therapeutic strategy for *RAS*-mutated AML. To evaluate this, we compared three treatment approaches in SKM1 cells: concurrent administration of azacytidine and RMC-7977, sequential treatment with azacytidine followed by RMC-7977, and the reverse sequence. Only pretreatment with azacytidine followed by RMC-7977 produced synergistic effects. This sequential regimen also produced synergistic effects on inducing apoptosis in the MDS/sAML cell lines MDS92, MDS-L, and SKM1. Consistently, treatment of primary *RAS*-mutated sAML samples with azacytidine followed by RMC-7977 significantly reduced clonogenic growth compared with either agent alone, without impairing the clonogenicity of healthy hematopoietic cells. Finally, pretreatment of SKM1 xenografts with azacytidine (5 mg/kg for 5 days) markedly improved RMC-7977-mediated control of leukemic burden.We found that azacytidine treatment sensitizes *RAS*-mutated sAML cells to RAS inhibition by RMC-7977 in both *in vitro* and *in vivo* models. Ongoing studies aim to elucidate the underlying molecular mechanisms, including the potential role of methylation changes in modulating oncogenic signaling dependencies. Together, these findings provide a strong rationale for continued evaluation of RAS inhibitors as part of combination treatment strategies for *RAS*-mutated AML.

#1877 Acquired resistance to Tri-complex inhibitors in colorectal cancer.

Sabine Jurado, Simone Lieb, Marco H. Hofmann, Mark Pearson, Phillipp Schmalhorst, Krzysztof Zak

Boehringer Ingelheim RCV, Vienna, Austria

KRAS is the most frequently mutated oncogene, with high prevalence in indications with significant unmet clinical needs, such as lung, pancreatic and colorectal cancer. The most frequent alterations result in an amino acid exchange at position 12 from Glycine to Aspartic Acid (G12D), Valine (G12V) or Cysteine (G12C). The approval of mutant specific KRAS G12C inhibitors by the FDA opened a new field of treatment options for patients with KRAS G12C mutation and additional KRAS targeted therapy approaches are currently being clinically tested in the hope to provide benefit to cancer patients with cancers harboring other KRAS mutant alleles. These therapies include pan-RAS, pan-KRAS and allele selective inhibitors as well as degraders. For patients with advanced solid tumors harboring a KRAS G12D mutation, several selective inhibitors have entered clinical trials (MRTX1133, RMC-9805, QTX3034/46, LY3962673...) and RMC-6236, a pan-RAS inhibitor from Revolution Medicines, has recently shown promising early clinical data. However, alongside the great hopes placed in (K)RAS targeting therapy, resistance is likely to occur, as it was already observed in patients relapsing in response to KRAS G12C inhibitors. We aimed to use this pre-clinical study to predict and understand potential resistance mechanisms that may arise during targeted treatment against (K)RAS in the CRC setting. To this aim, the colorectal cancer cell line GP2d, expressing KRAS G12D, was continuously treated with a pan-RAS inhibitor to generate resistance. Once the resistance was confirmed, individual outgrowing clones were subsequently profiled in a series of assays to identify potential mechanism(s) and cross-tested with other inhibitors. Interestingly, cells were cross resistant to both pan-RAS (RMC-6236) and KRAS G12D (RMC-9805) inhibitors from Revolution Medicine, highlighting a common mechanism of action, while remaining sensitive to other KRAS G12D inhibitors. These findings were then confirmed in an orthogonal assay. Collectively our *in vitro* preclinical study identified a resistance mechanism to Tri-complex inhibitors in colorectal cancer cells. This resistance can still be addressed by other KRAS G12D inhibitors, opening options for patients harboring this characteristic post RMC-therapy. Future investigations may focus on characterizing tumors from patients who relapse on RMC-6236 and RMC-9805 to validate these findings clinically.

#1878 Cotargeting B-Raf and ACLY in Ras mutant cells leads to synergistic loss of cell viability and apoptosis.

Nancy A. Krucher, Bryce D. Aierstok, Sabrina Bergesio, Gabriella J. Galgano, Morgan E. Strecker

Biology, Pace University, Pleasantville, NY

Ras mutation is found in several tumor types including pancreatic and colon cancer. Downstream from Ras is the B-Raf kinase, also often found mutated in tumor cell types such as melanoma. B-Raf inhibitors Vemurafenib, Dabrafenib and Encorafenib are used clinically in combination with MEK inhibitors Trametinib, Cobimetinib and Binimetinib. Together, these agents serve to inhibit the MAPK pathway, but the PI3K/AKT pathway is often upregulated leading to treatment resistance. AKT functions in numerous cellular processes including metabolism. In fact, AKT activates lipogenesis by direct phosphorylation and activation of the enzyme ATP-Citrate Lyase (ACLY). ACLY expression and activity are elevated in various cancer cell types. A new inhibitor of ACLY, NDI-091143, was recently identified based on the structure of ACLY and was used in this study. A panel of Ras mutant cell lines was used to investigate the effect of combining the ACLY inhibitor NDI-091143 with the BRAF inhibitor Vemurafenib on cell proliferation and apoptosis. Using concentrations of each drug that reduced cell viability individually by 25%, we found that the combination exhibited synergistic reduction of cell viability in Ras mutant A375 melanoma cells, MDA-MB-231 breast cancer cells, MIA Paca-2 pancreatic cancer cells and HCT116 colon cancer cells. Cancer cells with WT Ras such as MeWo melanoma and T47D breast cancer showed no synergistic loss of viability in response to the combination. Non-transformed cells such as colon epithelial (CCD-18Co) and normal pancreatic cells (H6c7) are unaffected by the same concentrations used in the Vemurafenib and NDI-091143 combination treatment. The mechanism of reduction in viability appears to be due to activation of apoptosis. All four Ras mutant cell lines showed increased expression of cleaved PARP and the activation of the ER stress pathway regulator ATF4. Finally, the apoptosis stimulated by the combination was shown to be dependent on Caspase-3 activity using Annexin V analysis of HCT116 cells treated with Vemurafenib plus NDI-091143.

#1879 Characterization of intrinsic and acquired resistance to KRAS^{G12C} inhibitors across a broad collection of cancer cell line models.

Jeffrey J. Kooijman, Kirsten J. W. Kevenaar, Imke P. M. Smits, Daphne J. F. Kluitmans, Laura D. R. van Zelst, Bente Timmers, Tsang W. Lam, Jeroen A. D. M. de Roos, Yvonne Grobben, Janneke J. T. M. Melis, Guido J. R. Zaman, Jorg C. J. Benningshof

Oncolines B.V., Oss, Netherlands

Mutations in *KRAS* are among the most common oncogenic driver events in human cancer. A glycine-to-cysteine mutation at position 12 (KRAS^{G12C}) impairs GTP hydrolysis, keeping KRAS in the GTP-bound active state. For decades, the KRAS^{G12C} mutation was considered undruggable, until the discovery of a new pocket beneath the effector switch II region of KRAS. Covalent binding of inhibitors into this pocket locks KRAS in its inactive, GDP-bound state. This breakthrough led to the accelerated approval of the first-generation inhibitors sotorasib (AMG 510) and adagrasib (MRTX849). However, their clinical benefit remains limited by modest response rates and the rapid emergence of drug resistance. To address these limitations, next-generation KRAS^{G12C} inhibitors such as divarasib (GDC-6036) have been developed, showing improved selectivity, potency and clinical response rates. Nevertheless, resistance is expected to arise, underscoring the importance of early insights into both intrinsic and acquired resistance to guide the most effective use of these emerging agents in the clinic.

To investigate intrinsic resistance, adagrasib, sotorasib and divarasib were profiled across 140 cancer cell lines using nine-point dose ranges in cell viability assays. KRAS^{G12C}-mutant cell lines exhibiting limited potency or efficacy were classified as intrinsically resistant. To study acquired resistance, inhibitor-sensitive KRAS^{G12C}-mutant cell lines were cultured with escalating doses of inhibitor. For both intrinsic and acquired resistant cell lines, resistance mechanisms were characterized using genomic and transcriptomic analyses, determination of MAPK and PI3K pathway phosphorylation after drug exposure, and broad therapeutic and combination profiling to identify pathway dependencies and strategies to overcome resistance.

Our analyses revealed heterogeneous responses of KRAS^{G12C}-mutant cell lines to the inhibitors, mirroring clinical responses. The KRAS^{G12C}-mutant cell lines SW1573 and OV56 were intrinsically resistant to all three KRAS^{G12C} inhibitors. Co-mutation analysis revealed a *PTEN* loss-of-function mutation in OV56, suggesting enhanced PI3K pathway activity. Although *PTEN* loss was restricted to OV56, both OV56 and SW1573 were resistant to inhibitors of various MAPK pathway components, including RAF (tovorafenib, belvarafenib), MEK (trametinib), and ERK (ulixertinib), suggesting MAPK pathway independence. Cross-resistance to adagrasib, sotorasib and divarasib was also observed in the acquired resistant models.

Intrinsically KRAS^{G12C} inhibitor-resistant cell lines, along with acquired resistant models, represent valuable systems for evaluating next-generation KRAS inhibitors and identifying new drug combinations to optimize therapeutic benefit of KRAS^{G12C} inhibitors in patients.

#1880 Deconstructing the paradigm of oncogene cooperation: Targeting MYC to enhance response and overcome resistance to KRAS inhibitors.

Daniel Capitan-Leo[1], Inigo Gonzalez-Larreategui[1], Magda Arnal[2], Judit Grueso[1], Lorena Sansegundo-Barbosa[2], Hugo Thabussot[2], Irene Ferrer[3], Silvestre Vicent[4], Marie-Eve Beaulieu[2], Silvia Casacuberta-Serra[2], Laura Soucek[1]

[1]VHIO Vall D'Hebron Institute of Oncology, Barcelona, Spain,[2]Peptomyc S.L., Barcelona, Spain,[3]H12O-CNIO Lung Cancer Clinical Research Unit, Health Research Institute Hospital 12 de Octubre, Spanish National Cancer Research Center (CNIO), Madrid, Spain,[4]Program in Solid Tumors and Biomarkers, Center for Applied Medical Research (CIMA), Pamplona, Spain

Background: Activating mutations in *KRAS*, particularly at codon G12, are common in non-small cell lung cancer (NSCLC, ~30%), pancreatic ductal adenocarcinoma (PDAC, ~90%), and colorectal cancer (CRC, ~35%). Although KRAS-G12C inhibitors (KRASi) such as sotorasib and adagrasib are approved for NSCLC, their clinical benefit is frequently limited by intrinsic and acquired resistance. MYC, a key transcription factor downstream of KRAS, is often deregulated in cancer and contributes to tumorigenesis and therapeutic resistance. Omomyc (OMO-103), the only direct MYC inhibitor currently in Phase II clinical trials, offers a unique opportunity to evaluate the impact of MYC blockade in KRAS-driven tumors.
Methods: We used NSCLC, CRC, and PDAC tumor cell lines and patient-derived xenograft (PDX) models to characterize KRAS-dependent signaling and to assess the effects of KRASi, Omomyc, and their combination on proliferation, cell-cycle progression, and apoptosis. Mechanistic studies included Western blotting and RNA-seq analyses.
Results: Dual KRAS and MYC inhibition synergistically impaired proliferation and induced robust apoptosis across models. Omomyc sensitized KRAS-mutant cells with intrinsic resistance to KRASi and restored drug responsiveness in models with acquired resistance. Transcriptomic and proteomic analyses revealed extensive reprogramming of oncogenic pathways upon combination therapy. In vivo, co-treatment with OMO-103 and KRASi resulted in significantly greater tumor regression than either monotherapy.
Conclusions: These findings demonstrate critical cooperation between MYC and KRAS in driving tumor survival and resistance to KRAS inhibition. Direct MYC blockade enhances the therapeutic activity of KRAS inhibitors and represents a promising strategy to overcome both intrinsic and acquired resistance in multiple KRAS-mutant cancer types.

#1881 Understanding evolutionary and ecological mechanisms of sotorasib resistance in KRAS G12C-mutant non-small cell lung cancer.

Jinling Wu[1], Mina Nguyen Dinh[2], Arda Durmaz[2], Maximilian Strobl[3], Jacob G. Scott[4]

[1]School of Medicine, Case Western Reserve University, Cleveland, OH,[2]Genomic Medicine and Systems Biology, Cleveland Clinic Research, Cleveland, OH,[3]Imperial College London, London, United Kingdom,[4]Case Comprehensive Cancer Center, Cleveland, OH

KRAS G12C mutation is a major oncogenic driver in non-small cell lung cancer, with targeted therapy using sotorasib offering clinical promise. However, resistance inevitably emerges. Evolutionary therapies based on collateral sensitivity exploit molecular and pharmacologic vulnerabilities that arise in evolved resistant populations and provide a promising strategy to guide evolution-informed sequential or combination therapies to delay resistance. We developed a novel *in vitro* experimental evolution framework using a KRAS G12C-mutant H358 cell line. Multiple independent replicates were continuously exposed to 25nM sotorasib for around 3 months across 8 sequential treatment cycles, while independent control replicates were treated without drug. Most treated replicates (4/6) developed robust resistance at cycle 8. To map evolutionary shifts in drug response, we performed collateral sensitivity screening using a panel of 10 FDA-approved agents targeting pathways relevant to KRAS signaling. Drug sensitivity shifted over time and resistant replicates evolved cross-resistance to EGFR/HER2-targeted inhibitors (e.g. Gefitinib and Lapatinib). In contrast, a statistically significant increase in paclitaxel sensitivity was detected, suggesting a collateral vulnerability associated with altered cell-cycle regulation as a compensatory response to KRAS inhibition. Bulk RNA-Seq revealed clear transcriptional changes accompanying resistance acquisition. Gene set enrichment analysis identified upregulation of several hallmark pathways in resistant group, including epithelial-mesenchymal transition, mTORC1 signaling, and inflammatory signaling by the end of experiment. Moreover, further analysis revealed that while replicates initially respond similarly at cycle 4, their molecular profiles diverge over time and give rise to considerable heterogeneity by cycle 8, despite a shared evolutionary origin. Drug resistance is also shaped by dynamic ecological interactions, so we evaluated ecological vulnerabilities using a co-culture framework that quantifies ecological coefficients based on relative growth rates of resistant and sensitive cells. Preliminary assays show that several resistant populations outcompete sensitive cells even without drug, contradicting the expected fitness cost of resistance and suggesting that certain resistance mechanisms may enhance baseline fitness. Competition outcomes shifted across sotorasib concentrations, indicating that ecological interactions are dose-dependent, highlighting the potential for ecology-informed dosing strategies to reduce competitive release and delay resistance. Together, we provide novel insights into the eco-evolutionary processes underlying sotorasib resistance and identify vulnerabilities that may be leveraged to design therapies that delay or redirect resistance.

#1882 Generation of daraxonrasib-resistant patient-derived xenograft models of pancreatic cancer.

Nina Dashti-Gibson[1], Amy L. Olex[1], Rachel K. Myrick[2], Alexa M. Barber[3], David C. Boyd[2], Emily K. Zboril[2], Katarzyna M. Tyc[4], Mikhail G. Dozmorov[4], Guang-Yu Yang[2], Nicholas T. Woods[3], Jose G. Trevino[5], J. Chuck Harrell[2]

[1]Wright Center for Clinical and Translational Research, Virginia Commonwealth University, Richmond, VA,[2]Department of Pathology, Virginia Commonwealth University, Richmond, VA,[3]University of Nebraska Medical Center, Omaha, NE,[4]Department of Biostatistics, Virginia Commonwealth University, Richmond, VA,[5]Department of Surgery, Virginia Commonwealth University, Richmond, VA

Background: Patients diagnosed with pancreatic ductal adenocarcinoma (PDAC) face limited treatment options and a dismal survival rate. KRAS is mutated in over 90% of PDAC and is a critical driver of tumor initiation and progression. Daraxonrasib (RMC-6236), a newly developed pan-RAS inhibitor, has shown promise in extending the survival of patients with PDAC in ongoing clinical trials. However, acquired resistance to daraxonrasib is anticipated and may limit the efficacy of this new therapeutic. To address this challenge, we developed a biobank of over 60 patient-derived xenograft (PDX) models, including 24 new models of PDAC, and aimed to generate daraxonrasib-resistant lines to investigate mechanisms of resistance and explore strategies to prolong daraxonrasib efficacy.

Methods: PDX cells from six patients with PDAC were injected subcutaneously in NSG mice, and tumor volume was measured weekly by caliper. Daraxonrasib (25 mg/kg) was administered daily by oral gavage when tumor volume reached 10-30 mm^3. Following 4-6 weeks of treatment, tumors that were initially responsive were digested and injected into additional mice which were again treated with daraxonrasib. Tumors that grew through treatment were collected for histological analysis and single cell RNA-sequencing.

Results: PDAC was found to be the most KRAS-dependent cancer type in our PDX biobank. Initial daraxonrasib treatment resulted in 63-97% reduction in tumor volume area-under-the-curve (AUC) compared to untreated controls across six models of PDAC. Response was significantly correlated with KRAS dependency score, while no association was found with patient demographics, KRAS mutation, or PDAC subtype. The PDXs with the greatest response were selected to generate resistant lines. Within two passages, the reduction in AUC was no longer significant based on Welch's t-test, indicating that resistance had developed. Transcriptomic analysis of treated tumors revealed upregulation of mucin production and YAP1 signaling, which likely represent early resistance mechanisms.

Future directions: Daraxonrasib was effective in reducing tumor volume in PDX models of PDAC, but prolonged treatment resulted in acquired resistance. Comparing the transcriptomic profiles of newly generated resistant lines and their sensitive counterparts will elucidate the mechanisms by which PDAC develops resistance to daraxonrasib. Furthermore, these models will provide a platform to test strategies to overcome resistance and maximize the efficacy of this promising new therapeutic.

#1883 Predicting resistance mechanisms in pancreatic cancer organoids under KRAS^{G12D} inhibition via pooled CRISPR-Cas9 druggable library screen.

Lauryn E. Flannagan[1], Michela Cadarso[1], Md Shahadat Hossan[1], Molly A. Nellen[2], Sean J. McIlwain[3], C. Dustin Rubinstein[4], Sean Ronnekleiv-Kelly[5], Jeremy D. Kratz[1]

[1]Medicine, University of Wisconsin-Madison, Madison, WI,[2]UWBC Advanced Genome Editing, University of Wisconsin-Madsion, Madison, WI,[3]School of Medicine and Public Health Dept. Biostatistics and Medical Informatics, University of Wisconsin-Madison, Madison, WI,[4]UWBC Advanced Genome Editing, University of Wisconsin-Madison, Madion, WI,[5]University of Wisconsin-Madison, Madison, WI

Background: Pancreatic ductal adenocarcinoma (PDAC) is the third leading cause of cancer mortality, with a median 5-year survival of 13%. Acquired resistance to single agent targeted inhibitors plays a critical role in progression, however there is a lack of predictive tools on resistance that incorporate functional genomics. Here, we evaluate the resistance mechanisms with early treatment of MRTX1133, a small non-covalent inhibitor of KRAS^{G12D}, using a pooled CRISPR-Cas9 lentivirus screen in patient derived cancer organoids (PCO).

Methods: PCOs were collected and transduced at a 1:5 cell to lentivirus ratio using a lentiviral-based CRISPR-Cas9 library with 2,292 genes targets from the 'druggable genome' (Milipore-Sigma). Transduced PCO's were expanded in Cultrex matrix and underwent puromycin selection for 6 days. A baseline group was collected post selection to control for basal expression over the course of media treated control. In parallel, PCOs were treated with MRTX1133 (30nM) or control with collection at 6 days post-treatment. Digital PCR was used to normalize lentiviral transduction efficiency to background. PCR libraries were prepared against targets and DNA sequencing was done to assess resistance mechanisms via the Model-based Analysis of the Genome-wide CRISPR/Cas9 Knockout (MAGeCK) analysis. Results from MAGeCK were also used for HALLMARK gene set analysis to evaluate pathway disruption specific to MRTX1133 treatment.

Results: Digital PCR showed optimal lentiviral copy number for baseline (0.863 ± 0.025) post puromycin selection. Pearson correlation plot showed increased variance between control groups when treatment was extended from a 6-day collection (PC1 16%, PC2 15%, PC total 31%) to a 9-day collection (PC1 18%, PC2 18%, PC total 36%). MAGeCK analysis revealed a list of 130 significant gene targets from the druggable screen ($p<0.05$). Top targets from basal PDAC expression included epithelial-mesenchymal transition pathways with knockout of interleukin-6 ($p<0.001$) and the E2F transcription family pathway with knockout of CDKN1B ($p<0.05$). HALLMARK analysis revealed 168 expressed pathways expressed in the control against PCO's treated with MRTX1133 following a 0.05 false discovery rate threshold. These pathways include KRAS signaling ($p<0.05$), adipogenesis ($p<0.05$), and E2F targets ($p<0.05$). Individual gene knockouts observed consistent targets included KCNQT ($p<0.05$) in KRAS signaling, UQCRC1 ($p<0.01$) in adipogenesis, and CDKN1B ($p< 0.01$) in E2F targeting.

Conclusions: By scaling a druggable lentiviral based CRISPR-Cas9 screen, we show potential signaling pathways that aid in resistance to tool compound MRTX in PDAC organoids. Thus, addressing the unmet need of predictive resistance modeling in PDAC organoids. Further work includes selective knockout of key targets to confirm synthetic lethality with MRTX1133.

#1884 Molecular determinants of sensitivity and resistance to the pan-RAS(ON) inhibitor daraxonrasib(RMC-6236) across KRAS-mutant patient-derived models.

Kayla Tyskiewicz[1], Markus Hippich[1], Tristan Cates[1], Gervaise Henry[1], Gilad Silberberg[1], Nicole Spanburg[1], Madeline Westcott[1], Daniel Ciznadija[2], Michael Boice[1], Paul Heverly[1], Frank Smith[1], Marianna Zipeto[1], Stefano Cairo[3], Sebastian Brabetz[1]

[1]Champions Oncology (Rockville, MD), Rockville, MD,[2]Champions Oncology, Hackensack, NJ,[3]Champions Oncology, Inc. (Hackensack, NJ), Rockville, MD

CHAMPIONS Abstract Body: KRAS mutations define a major therapeutic opportunity across solid tumors but often align with limited response durability and resistance to targeted therapies. Daraxonrasib (RMC-6236), a selective pan-RAS(ON) inhibitor, demonstrates activity across KRAS G12X-mutant tumors; however, the molecular and clinical features governing sensitivity or promoting resistance remain incompletely understood. We screened a >50-model KRAS-mutant PDX cohort spanning NSCLC (n=16), colorectal cancer (n=19), and pancreatic ductal adenocarcinoma (n=19). Models reflect clinically relevant KRAS variants and diverse co-mutational landscapes, accompanied by pre-treatment patient histories, enabling classification of responders and non-responders through integration of molecular and clinical contexts. Tumors were evaluated for intrinsic response, and longitudinal sampling captured acquired-resistance outgrowths for subsequent genomic analysis. We performed integrated NGS (omics?) analyses on (i) baseline data from responding vs non-responding models, (ii) resistant tumors emerging after initial regression, and (iii) associations with prior patient treatments. Daraxonrasib produced a broad range of activity across the array of models screened. Heterogeneity in the depth and durability of responses correlated with KRAS allele type, co-driver mutations, and specific pre-treatment exposures. These studies establish an annotated, translational system for defining determinants of RAS(ON) inhibitor response that shape resistance and inform rational therapeutic combination strategies.

#1885 USP7 inhibitor synergistically enhanced the anticancer effect of the KRAS G12C inhibitor by effectively countering feedback signaling pathways.

Yuanyuan Gao[1], Keqiang Zhang[1], Wendong Li[1], Chunxia Su[2], John Liu[1], Lilian Gu[1], Mahima Raul[1], Dan Raz[1]

[1]Division of Thoracic Surgery, City of Hope National Medical Center, Duarte, CA,[2]School of Basic Medical Science, Ningxia Medical University, Yinchuan, China

Background: KRAS mutations are the most frequent oncogenic drivers in non-small cell lung cancer (NSCLC), with the KRAS G12C variant accounting for nearly half of KRAS-mutant cases. While KRAS inhibitors show strong antitumor activity, their efficacy is often limited by adaptive and acquired resistance, highlighting the urgent need for effective combination strategies. The deubiquitinase USP7, frequently overexpressed in cancers and linked to malignancy, therapeutic resistance, and poor prognosis. However, its role in KRAS-mutant lung cancer remains unclear.

Methods: USP7 mRNA and protein expression levels in human and mouse KRAS-mutant lung cancers were analyzed using TCGA data mining and immunohistochemistry (IHC) analysis. KRAS G12C-mutant NSCLC cells and in vivo xenograft models were treated with KRAS G12C specific inhibitor (GDC-6036) and USP7 inhibitor (P5091), either alone or in combination, to evaluate the combinatorial antitumor effects. Cell viability and apoptosis assays were performed to evaluate treatment outcomes. Western blotting and RNA sequencing (RNA-seq) analyses were conducted to investigate alterations in this related cancer signaling pathways and elucidate the underlying molecular mechanisms.

Results: USP7 mRNA expression was found to be significantly elevated in human cancer tissues and cell lines compared with normal controls. Combination index (CI) analysis using the Chou-Talalay method showed CI < 1, confirming that the USP7 inhibitor synergistically enhanced the efficacy of the KRAS G12C inhibitor. Mechanistically, USP7 synergistically inhibits the KRAS feedback signaling pathways, possibly due to suppression of cell proliferation through the MAPK and AKT pathways in cancer cells. RNA-seq revealed that the combination treatment elicited broader and more pronounced pathway modulation, with simultaneous inhibition of proliferative mechanisms (MYC, MTORC1, G2M) and suppression of DNA repair pathways. In line with RNA-seq findings, low-dose KRAS or USP7 inhibitors did not trigger significant apoptosis, while the combination markedly enhanced apoptosis and delayed KRAS signaling reactivation. Importantly, in vivo xenograft studies further demonstrated that the combination therapy produced a markedly stronger antitumor effect, significantly suppressing tumor growth (reduced p-ERK and Ki-67) and inducing substantially higher levels of apoptosis (increased Caspase-3) compared with KRAS or USP7 inhibition alone.

Conclusion: The combination of KRAS G12C and USP7 inhibitors significantly enhances the anticancer effect by suppressing KRAS feedback signaling, modulating multiple oncogenic and metabolic pathways, and promoting apoptosis in cancer cells, representing a promising novel approach to achieve durable therapeutic benefits of KRAS blockade in NSCLC, warranting further investigation.

#1886 Ligand links EGFR reactivation to resistance against KRAS G12C inhibitors in NSCLC.

Shigeki Nanjo, Yifeng Liu, Hayato Koba, Seiji Yano

Kanazawa Univ. Hospital, Kanazawa, Japan

KRAS G12C inhibitors have shown meaningful clinical efficacy against Kirsten rat sarcoma viral oncogene (KRAS) G12C-mutant non-small cell lung cancer (NSCLC), providing a long-awaited therapeutic option for this historically difficult-to-target oncogene. However, both intrinsic and acquired resistance frequently limit the durability of response. To overcome these limitations, rational combination strategies based on molecular mechanisms are urgently needed. Although multiple combination approaches—such as co-targeting EGFR or PD-L1—are being evaluated in ongoing trials, biomarker-driven therapeutic selection remains underdeveloped. To elucidate the mechanisms underlying resistance, we established intrinsic and acquired KRAS G12C inhibitor-resistant tumor models using mouse and patient-derived xenografts (PDX). Mechanistic analyses, including western blotting and enzyme-linked immunosorbent assay (ELISA), were conducted to characterize resistance-associated signaling. Combination treatment efficacy was validated in vitro and in vivo. In addition, immunohistochemistry (IHC) and RNAscope in situ hybridization (ISH) were performed on xenograft tissues and tumor samples from patients with KRAS G12C-mutant NSCLC treated with sotorasib. Our findings reveal that tumor cell-autocrine ligand-mediated epidermal growth factor receptor (EGFR) phosphorylation plays a central role in both intrinsic and acquired resistance to KRAS inhibitors. Strikingly, this same EGFR signaling axis was also detected in central nervous system (CNS) metastatic recurrence in a leptomeningeal carcinomatosis model, indicating its relevance to disease progression in sanctuary sites. Moreover, RNAscope ISH enabled spatial visualization of ligand expression, suggesting its potential as a diagnostic marker for identifying patients with EGFR-dependent resistance. Importantly, combined inhibition of KRAS and EGFR effectively suppressed tumor growth and overcame resistance in vitro and in vivo. Consistent with these preclinical results, elevated EGFR ligand mRNA expression was observed in two of seven clinical tumor samples from patients with KRAS G12C-mutant NSCLC who exhibited poor response to sotorasib. In conclusion, ligand-mediated EGFR activation serves as a key driver of both intrinsic and acquired resistance to KRAS G12C inhibitors in NSCLC. These results establish a mechanistic rationale for biomarker-guided combination therapy using concurrent KRAS and EGFR inhibition to enhance therapeutic efficacy and prevent resistance in KRAS G12C-mutant lung cancer.

#1887 Real-time dissection of SCLC emergence in a *KRAS^{G12C}* LUAD tumour: A case study of targeted therapy resistance.

Priyanka Gopal

Robert H. Lurie Comprehensive Cancer Ctr. of Northwestern Univ., Chicago, IL

Background: Lineage plasticity is an emerging mechanism of resistance in non-small cell lung cancer (NSCLC). We present a case study of a KRASG12C-mutant lung adenocarcinoma (LUAD) PDX that underwent neuroendocrine transdifferentiation into small-cell lung cancer (SCLC) after treatment with the KRASG12C inhibitor sotorasib.
Methods: KRASG12C PDX CBX336 was treated with sotorasib and monitored using high-content imaging, fluorescence lineage tracking, DNA barcoding, and whole-exome clonal tracing. Pre- and post-treatment tumours underwent genomic, transcriptomic, and morphometric profiling. PDX-derived ex vivo cultures supported functional studies, including CRISPR knockout and cDNA overexpression.
Results: CBX336 showed an initial response to sotorasib followed by rapid regrowth. Post-treatment samples demonstrated a histologic shift from LUAD to SCLC, marked by elevated NEUROD1 and neuroendocrine markers. Lineage tracking revealed a coordinated, not stochastic, transition toward the neuroendocrine state. Multi-omic analysis identified ZEB1 as an upstream regulator linked to RB1 loss, increased p16, and N-cadherin. ZEB1 knockout suppressed neuroendocrine marker induction and partially restored LUAD-like differentiation, confirming ZEB1 as a driver of lineage reprogramming.
Conclusions: This case study shows that KRASG12C-targeted therapy can induce neuroendocrine transdifferentiation via ZEB1 upregulation. Real-time monitoring of CBX336 evolution reveals actionable plasticity mechanisms and supports development of strategies to prevent or reverse therapy-induced SCLC emergence.

#1888 Unveiling mechanisms of MRTX1133 resistance in PDAC models.

Qin Li

WuXi AppTec, Suzhou, China

Recent years have witnessed significant advances in the development of therapeutics targeting KRAS G12D in cancer patients. However, the emergence of drug resistance remains a formidable clinical challenge, and the underlying mechanisms remain largely unknown. To investigate these mechanisms, we established resistant cell lines through stepwise escalation of MRTX1133, the first covalent inhibitor of KRAS G12D to enter clinical evaluation, in KRAS G12D-mutant modelsThese resistant cells maintain stable phenotypes to MRTX-1133 both in vitro and in vivo, and exhibited broad cross-resistance to other KRAS G12D inhibitors, such as RMC9805 and HRS-4642, with partial resistance observed toward the pan-RAS inhibitor RMC6236.Bioinformatic analysis of both resistant models revealed a spectrum of convergent adaptive mechanisms, including: (1) altered oncogenic signaling networks, (2) upregulation of cell cycle and drug efflux regulators, and (3) epithelial-mesenchymal transition (EMT). Interestingly, the MRTX1133-R-GP2D model acquired secondary KRAS mutations (specifically H95Q, Y96H, Y96N, and D92N), indicating on-target resistance. In a contrast, the MRTX1133-R-KPC model exhibited chromosome 5 amplifications encompassing key metabolic and detoxification genes (notably CYP51 and CYP3A), accompanied by tumor microenvironment (TME) reprogramming and immune evasion.Together, these findings reveal comprehensive mechanisms of resistance to KRAS G12D inhibition. The established resistant models serve as physiologically relevant platforms for biomarker discovery and the development of rational combination therapies. Using these models, functional studies demonstrated that targeting core vulnerabilities—including the cell cycle, DNA damage repair, compensatory signaling pathways, metabolic modulators may overcome resistance phenotype.

#1889 Elucidation and therapeutic strategies to overcome intrinsic resistance mechanisms in KRAS G12D-mutant tumors.

Ryo Sawada, Tadaaki Yamada, Yuki Katayama, Koichi Takayama

Department of Pulmonary Medicine, Kyoto Prefectural University of Medicine, Kyoto, Japan

[Background and Aim] KRAS, a small GTPase transmitting signals from receptor tyrosine kinases to MAPK and PI3K pathways, plays a pivotal role in cell proliferation and survival. Oncogenic KRAS mutations cause constitutive activation of downstream signaling and are common in pancreatic, colorectal, and lung cancers. The G12D variant is particularly prevalent in pancreatic and colorectal cancers and also occurs in non-small cell lung cancer, especially among never-smokers. While the success of covalent KRAS G12C inhibitors has validated KRAS as a druggable target, KRAS G12D remained challenging. Recently, selective non-covalent inhibitors such as MRTX1133 have shown potent preclinical efficacy. However, the efficacy of KRAS G12D inhibitor monotherapy remains limited, underscoring the need to clarify and overcome resistance mechanisms.
[Method] KRAS G12D-mutant lung and pancreatic cancer cell lines (A427, SK-LU1, AsPC1, Panc1, T3M10, and HPAF-II) were used to evaluate the antitumor effects of MRTX1133 monotherapy and combination therapies. In vitro, three combinations were assessed: MRTX1133 plus an AXL inhibitor, MRTX1133 plus both AXL and FGFR1 inhibitors, and MRTX1133 plus a SHP2 inhibitor. Cell viability was determined by MTT assay, signaling alterations were analyzed by Western blotting, and apoptosis was evaluated by flow cytometry. In vivo, the efficacy of MRTX1133 combined with a SHP2 inhibitor was validated using cell-derived xenograft (CDX) mouse models.
[Results] MRTX1133 monotherapy exhibited variable efficacy across cell lines. Knockdown or pharmacological inhibition of AXL (dual therapy) significantly enhanced the antiproliferative effects of MRTX1133. However, some cell lines showed ERK reactivation, indicating incomplete pathway suppression. Further addition of the FGFR1 inhibition (triple therapy) effectively suppressed ERK reactivation and markedly improved antitumor activity. Moreover, targeting adaptor proteins such as SHP2 amplified the therapeutic efficacy, suggesting that convergence nodes downstream of RTKs play a crucial role in resistance mechanisms. While SHP2 inhibition alone showed limited activity, its combination with MRTX1133 prevented ERK reactivation and achieved substantial growth suppression.
[Discussion and Conclusion] Resistance to MRTX1133 in KRAS G12D-mutant tumors is driven by AXL and FGFR1 activation, which can be suppressed through dual or triple combination therapies. Inhibition of adaptor proteins such as SHP2 further provides a strategy to overcome heterogeneous RTK-mediated resistance, supporting combination approaches targeting adaptor signaling.

#1890 Targeting ribonucleotide reductase to overcome FLT3 inhibitor resistance in acute myeloid leukemia.

Zhen Tian[1], Peng Wang[1], Stacia Octaviani[1], Yahui Li[2], Yun Liao[1], Xiaolei Liu[3], Zhaorui Lian[1], Hong Zheng[4], Elliot Stieglitz[5], Catherine C. Smith[6], Jian Huang[1]

[1]Coriell Institute for Medical Research, Camden, NJ,[2]Surgical Research Lab, Department of Surgery,, Cooper University Health Care, Camden, NJ,[3]Department of Medicine, Perelman School of Medicine at the University of Pennsylvania, Philadelphia, PA,[4]Penn State Cancer Institute, Penn State University College of Medicine, Hershey, PA,[5]Pediatrics, UCSF, San Francisco, CA,[6]Adjunct Instructor, Dept. of Med./Hem.-Onc., UCSF, San Francisco, CA

Acute myeloid leukemia (AML) is a malignant hematopoietic disorder characterized by the clonal proliferation and impaired differentiation of myeloid progenitor cells. It is the most common type of acute leukemia in adults and is associated with high rates of chemotherapy resistance and relapse. Mutations in the FMS-like tyrosine kinase 3 (*FLT3*) gene occur in approximately 30% of AML cases and are linked to poor prognosis. The discovery of FLT3 inhibitors (FLT3i) has represented a breakthrough in targeted AML therapy; However, resistance to FLT3i remains a significant clinical challenge that limits long-term efficacy. Previously, we identified Sprouty RTK Signaling Antagonist 3 (*SPRY3*)—a negative regulator of RAS/MAPK signaling—as a key determinant of FLT3i sensitivity. Loss of *SPRY3* activated RAS signaling and conferred robust FLT3i resistance in AML. Consistent with these findings, activating *NRAS* mutations (such as $NRAS^{G12C}$ and $NRAS^{Q61K}$) —present in approximately 15% of AML cases—also drive resistance to FLT3i. In our recent studies, we identified ribonucleotide reductase (RNR) as a critical downstream effector upregulated by *NRAS*-activating mutations ($NRAS^{mut}$) in AML, driving FLT3i resistance. RNR catalyzes the conversion of ribonucleoside diphosphates (NDPs) into deoxyribonucleoside diphosphates (dNDPs), which are subsequently phosphorylated to deoxyribonucleoside triphosphates (dNTPs)—the essential building blocks for DNA replication and repair. We found that $NRAS^{mut}$ AML cells exhibit significantly elevated expression of *RRM1*, *RRM2*, and *RRM2B*, the three subunits of RNR, following FLT3i treatment. Mechanistically, RAS activation enhances RNR expression through the RAS-MAPK-E2F1/MYC signaling axis. Inhibition of E2F1 or MYC markedly reduced *RRM1* and *RRM2* expression, confirming their transcriptional regulation of RNR. Furthermore, knockdown of Dual Specificity Phosphatase 6 (DUSP6)—a negative feedback regulator of RAS/MAPK signaling—further increased RNR activity and sensitized $NRAS^{mut}$ AML cells to RNR inhibition. Functionally, both pharmacologic inhibition of RNR using clofarabine and siRNA-mediated knockdown of RNR subunits effectively restored FLT3i sensitivity in $NRAS^{mut}$ AML. Combination therapy with gilteritinib and clofarabine in both cell line-derived xenograft (CDX) and patient-derived xenograft (PDX) models significantly reduced leukemic burden and prolonged survival compared with either agent alone. In summary, our findings identify RNR as a critical downstream effector of RAS/MAPK signaling and a promising therapeutic target to overcome FLT3i resistance in $NRAS^{mut}$ AML. These results provide a strong mechanistic and preclinical rationale for the combined inhibition of *FLT3* and RNR as a novel therapeutic strategy to improve outcomes in resistant AML.

#1891 Minnelide enhances the antitumor activity of pan-KRAS inhibitor RMC-6236 in preclinical models for pancreatic cancer.

Edgar Banuelos[1], Jaeger Moore[1], Mohana Velagapudi[2], Ashok Saluja[2], Daniel D. Von Hoff[1], **Haiyong Han**[1]

[1]Translational Genomics Research Institute, Phoenix, AZ,[2]Minneamrita Therapeutics LLC, Tampa, FL

Triptolide, a natural compound from *Thunder God Vine*, and its water-soluble prodrug Minnelide have shown potent antitumor activity, including promising single-agent efficacy in patients with pancreatic cancer. We previously demonstrated that triptolide suppresses super-enhancer activity in pancreatic cancer and stromal cells by inhibiting the XPB subunit of TFIIH, leading to downregulation of c-Myc and transcriptional effectors of mutant KRAS signaling. In this study, we assessed whether triptolide/Minnelide can enhance the antitumor activity of RMC-6236, a pan-KRAS inhibitor in clinical development for KRAS mutant cancers. We first evaluated the synergistic effects of triptolide and RMC-6236 on pancreatic cancer cell growth across multiple KRAS-mutant lines, including HPAC ($KRAS^{G12D}$), Capan-1 ($KRAS^{G12V}$), Hs766T ($KRAS^{Q61H}$), and BxPC3 ($KRAS^{wt}$). The combination demonstrated strong synergy across a range of concentrations in HPAC and Capan-1 cells and additive effects in BxPC3 and Hs766T. To validate these findings *in vivo*, we assessed Minnelide in combination with RMC-6236 using an HPAC xenograft model (3×10^6 cells, subcutaneous implantation). Mice received oral Minnelide (0.10 or 0.15 mg/kg, QDx21) with or without a low dose of oral RMC-6236 (15 mg/kg, QDx21; n = 10/group). While Minnelide alone showed modest tumor inhibition, both doses of Minnelide significantly enhanced the antitumor efficacy of low dose RMC-6236 after 21 days ($p < 0.01$, two-way ANOVA). No weight loss or other toxicities were observed in the single agent or combination groups. Taken together, these results demonstrate that triptolide/Minnelide augments the activity of RMC-6236 *in vitro* and *in vivo*, supporting further preclinical and potentially clinical evaluation. (This work was supported by Minneamrita Therapeutics, Purple Pansies, and the Pancreas National Advisory Council)

: Cell Cycle
Poster Session

#1893 Inhibiting CDK9/13 decreases progression of multiple myeloma and myeloma-induced bone disease in preclinical studies.

Tiina E. Kahkonen[1], Gergana Gababova[1], Ru Yang[2], Jie Wen[2], Michael Thormann[1], Jussi M. Halleen[1]

[1]OncoBone Therapeutics Ltd, London, United Kingdom,[2]PharmaLegacy LLC, Shanghai, China

Cyclin-dependent kinases (CDKs) are promising targets in many cancers. OBP-004 is an oral highly potent and selective small-molecule dual inhibitor of CDK9/13 with a half-life of 17-20 hours, high tissue biodistribution in brain, lung, spleen and kidneys, and with no observed safety issues. Multiple myeloma (MM) is a plasma cell malignancy that is primarily growing in bone marrow and has a strong association with bone. At advanced stages, MM patients develop bone disease leading to increased bone loss and bone pain. In this study, we used OBP-004 to study if CDK9/13 is a suitable drug target in MM and MM associated bone disease.
For studying efficacy on hematological cancers, female NMRI nude mice were inoculated intravenously with luciferase-labelled MV4-11 human acute myeloid leukemia cells and randomized to treatment groups at day 15 based on body weight and bioluminescence imaging (BLI) signal. OBP-004 was given orally at a dose of 1.0 mg/kg three times a week (3-day on, 4-day off). Tumor burden was monitored by BLI and the study was terminated at day 32. In the MM model, NPG mice were inoculated intratibially with luciferase-labelled RPMI-8226 human MM cells and randomized to treatment groups at day 3 based on body weight and BLI signal, and treatments were started at day 3. OBP-004 was given orally at a dose of 0.6 mg/kg daily. The standard-of-care therapies bortezomib (0.8 mg/kg, ip, BIW) and zoledronic acid (0.1 mg/kg, sc, QW) were used as reference compounds. Tumor burden was monitored by BLI and cancer-induced bone loss by scoring X-ray images. The study was terminated at day 56.
The initial 1.0 mg/kg dosing (3-day on, 4-day off) of OBP-004 in the MV4-11 study resulted in slight decrease of body weight without any clinical signs. After optimizing the dose and the dosing schedules, the daily dose of 0.6 mg/kg showed no body weight loss or clinical signs during the 54 days treatment period. In the MV4-11 model, OBP-004 showed strong decrease (>97%) of brain, lung and lymph node metastases, and almost complete (>99.99%) abolishment of bone metastases. In the RPMI-8226 model, bortezomib inhibited tumor growth but zoledronic acid showed no effects, and zoledronic acid inhibited cancer-induced bone loss but bortezomib showed no effects. OBP-004 showed significantly stronger tumor growth inhibition than bortezomib and decreased cancer-induced bone loss similarly to zoledronic acid.
We conclude that CDK9/CDK13 is a potential target in hematological malignancies including MM. By targeting CDK9/13, it is possible to affect both tumor growth and cancer-induced bone loss.

#1894 Proteome-wide target engagement and selectivity profiling of CDK2 inhibitors using CETSA®.

Tomas Friman, Merve Kacal, Tuomas Tolvanen

Pelago Bioscience AB, Solna, Sweden

Mitosis and the cell cycle is a pivotal part of cancers and other neoplastic diseases. The cell cycle is tightly regulated, yet frequently deregulated in tumors, making its core regulators attractive targets for anti-tumor therapy. Cyclin-dependent kinases (CDKs) form complexes with cyclins to phosphorylate key proteins that drive cell-cycle progression. Dual CDK4/6 inhibition is an established treatment strategy in subsets of breast cancer, but resistance is common. Targeting CDK2 has therefore emerged as a strategy to overcome resistance to CDK4/6 inhibition. While CDK4/6 primarily controls early cell-cycle progression by regulating phosphorylation of the retinoblastoma-associated protein (RB1), CDK2 participates in this phase and regulates later cell-cycle transitions. CDK2 inhibitors may thus offer additional therapeutic benefits compared with CDK4/6 inhibitors. Several CDK2-selective inhibitors have recently been developed, including Tagtociclib (PF-07104091), Cirtociclib (BLU-222), and INX-315. Here, we investigated the proteome-wide target engagement and selectivity profiles of these CDK2-selective kinase inhibitors and compared them with those of approved CDK4/6 inhibitors (palbociclib, ribociclib, and abemaciclib) and pan-CDK probes. We utilized the cellular thermal shift assay (CETSA®) coupled with mass spectrometry (MS). CETSA monitors drug-induced changes in protein thermal stability and can be applied in intact cells or cell lysates without modifying proteins, ligands, or cells. An MS-based readout enables unbiased, proteome-wide detection of small-molecule-protein interactions, including non-kinase targets and downstream pathway components. All tested CDK2-selective inhibitors engaged CDK2 and additional kinases at high concentrations of 30 µM. Compared with CDK4/6 inhibitors, they showed weaker engagement of CDK4/6 but, like CDK4/6 inhibitors, induced thermal destabilization of RB1, indicating a shared impact on RB1-dependent pathways. Target engagement of CDK1 was restricted to CDK2-selective and pan-CDK inhibitors and was only observed at higher compound concentrations. Together, these data illustrate the utility of CETSA MS for mapping target engagement and selectivity across the proteome, as well as for characterizing the evolution of CDK inhibitors from early pan-CDK compounds to modern CDK2-selective agents.

#1895 Distinct metabolic adaptations to resistance to CDK4/6 inhibitors in ER+ breast cancer identified using microfluidic mass spectrometry platform.

Gianna A. Slusher[1], Yuan Gu[2], Sunil S. Badve[3], Andrei G. Fedorov[1], **Yesim Gokmen-Polar**[3]

[1]George W. Woodruff School of Mechanical Engineering, Parker H. Petit Institute for Bioengineering, Georgia Institute of Technology, Atlanta, GA,[2]Pathology and Laboratory Medicine, Emory University School of Medicine, Atlanta, GA,[3]Department of Pathology and Laboratory Medicine and Emory Winship Cancer Institute, Emory University School of Medicine, Atlanta, GA

Background: Cyclin-dependent kinase inhibitors, CDK4/6i, have been one of the most significant practice-changing advances in the treatment of estrogen receptor positive (ER+) breast cancer in the recent decade. Despite their clinical success, CDK4/6i resistance remains a major clinical challenge. Importantly, therapeutic response does not correlate with expression levels of CDK4, CDK6, or other canonical cell cycle proteins, suggesting that resistance arises from complex adaptive mechanisms.
Methods: To address this challenge, we generated drug-tolerant persister cell populations (DTPs) from LCC2, LCC9 and T47D breast cancer cell lines to both palbociclib and abemaciclib. Transcriptomic profiling of these DTPs revealed significant alterations in the expression of metabolic enzymes, suggesting that metabolic reprogramming plays a central role in the survival and maintenance of CDK4/6i-tolerant cells. To further identify and quantify changes in metabolites and metabolic pathways, we analyzed these DTP populations using a dynamic sampling platform (DSP) integrating a sample introduction mechanism, a microfabricated processing device, and electrospray ionization mass spectrometry (ESI-MS) analysis. The device, manufactured via advanced microfabrication techniques, enables integration of real-time multiple processing and metabolic profiling. Full untargeted metabolomics data were evaluated using pathway level gene set enrichment analysis (GSEA).
Results: Across resistant cell states, multiple metabolic pathways exhibited coordinated shifts associated with DTP-like adaptation. Palbociclib resistant LCC2-DTPs exhibit a distinct metabolic remodeling trajectory characterized by consistently elevated ubiquinone biosynthesis, an adaptation absent in abemaciclib-resistant LCC2-DTPs and other DTP sublines. This drug-specific metabolic signature suggests that palbociclib engages mitochondrial pathways in a unique manner, potentially influencing therapeutic resistance. On the other hand, pathways involving electron transport chain and fatty acid oxidation were upregulated in abemaciclib DTPs, suggesting differential metabolic regulation in response to each CDK4/6i.
Conclusions: These findings highlight divergent metabolic consequences for palbociclib and abemaciclib in endocrine-resistant ER+ breast cancer and underscore the utility of microfluidic ESI-MS workflows for resolving drug-specific adaptive states relevant to therapeutic resistance and tumor progression.

#1896 'Translating' CDK9 inhibitor effects to target prostate cancer.

Shivani Yalala[1], Pedro Durao[2], Agata Carreira[2], Joyeeta Chatterjee[3], Muskan Kumari[1], Antti Sakari Rannikko[4], Eileen E. Parkes[2], Fadi Issa[2], Ian G. Mills[2], **Harri M. Itkonen**[1]

[1]University of Helsinki, Helsinki, Finland,[2]University of Oxford, Oxford, United Kingdom,[3]University of Oslo, Oslo, Norway,[4]HUS Helsinki University Hospital, Helsinki, Finland

Introduction Prostate cancer (PC) is the most common male cancer, and more effective treatments are needed to control the late-stage disease. In the lethal disease, termed castration-resistant PC (CRPC), cancer cells sustain a pro-proliferative gene expression program despite the presence of anti-androgens. This gene expression program is ultimately dependent on CDK9, and compounds targeting it are currently in clinical trials for solid tumors. All cells depend on CDK9 to sustain gene expression, although it is not clear why cancer cells are particularly sensitive to CDK9 targeting drugs.

Experimental procedures Multi-omics profiling of prostate cancer cell lines was used to understand how cells respond to CDK9 inhibition. Patient samples were used to correlate some of the findings, with data validation ongoing in syngeneic mouse models.

Summary of the data We show that CDK9 inhibition activates the innate immune response through viral mimicry in PC cells. As expected, targeting CDK9 suppresses overall transcription; however, some genes are expressed in significantly higher levels in this situation. Mechanistically, CDK9 inhibition uncouples the mRNA-processing machinery from RNA polymerase II, and we show that in this situation intron retention is significantly increased. The generated mis-spliced RNAs are prone to form double-stranded RNAs (dsRNA), and full activity of (dsRNA)-activated kinase is required for the CDK9 inhibitor-induced anti-proliferative effects. Accumulation of dsRNAs is known to activate the innate immune response and indeed we show that CDK9 inhibition leads to excessive secretion of immunogenic cytokines.

Conclusions Our data reveal that targeting the transcription elongation kinase CDK9 activates immuno-modulatory signalling *in vitro* by selectively augmenting translation of certain mRNAs. We are now validating these effects in syngeneic animal models, patient derived organoids, and probing the extent to which the transcriptional and translational programs are rewired. In the long run, our aim is to develop an effective treatment strategy against CRPC.

#1897 Targeting RB-deficient small cell lung cancer with selective CDK2 inhibition by AZD8421.

Rajita Vatapalli, Michael Grondine, Jun Fan, Grace Guo, Zhan Liu, Tam Nguyen, Deepa Bhavsar, Christopher Denz

AstraZeneca Pharmaceuticals LP, Waltham, MA

Retinoblastoma (RB) loss is a hallmark of small cell lung cancer (SCLC), yet its therapeutic vulnerabilities remain underexplored. DepMap analysis identifies Cyclin-dependent Kinase 2 (CDK2) as a top vulnerability in SCLC with RB mutations and RB1 protein loss in cell lines corresponds with increased sensitivity to CDK2 KO. CDK2 is a Ser/Thr kinase activated via interaction with its cyclin partners cyclin E (CCNE) and cyclin A (CCNA), driving G1 and S phase progression of the cell cycle. Here, we demonstrate that RB-deficient SCLC exhibits sensitivity to AZD8421, a highly selective inhibitor of CDK2.

Within a panel of SCLC cell lines, AZD8421 demonstrates selective growth inhibition in RB-mutant lines, with the average IC50 value being more than 45-fold lower than that observed in RB-wildtype counterparts. Mechanistically, CDK2 inhibition results in G2 cell cycle arrest and robust activation of cleaved PARP and cleaved caspase 3/7 specifically in RB-deficient models, distinguishing this cytotoxic phenotype from cytostatic effects previously observed in disease indication outside of SCLC, including CCNE1 over-expressing cancer models.

In vivo, 4 RB-expressing SCLC PDX models exhibited substantial tumor growth inhibition following treatment with AZD8421, with an average TGI of 58%. In contrast, 6 RB-deficient PDX models demonstrated more profound and sustained responses with monotherapy, achieving an average TGI of 90%. Pharmacodynamic studies confirm dose-dependent target engagement via p-NPM1 suppression and evidence of apoptosis in vivo.

These findings support further evaluation of CDK2 inhibition as a possible targeted strategy for RB-mutant SCLC that could offer a precision-medicine approach for a historically refractory disease subtype.

#1898 CDK2 partners with cyclin E or cyclin A to support distinct roles in cell cycle regulation: Implications for anti-tumor efficacy and potential toxicity of CDK2 inhibitors.

Haoran Jing, Neil Umbreit, Rens Janssens, Kimberly Rizzolo, Thao Duong, Huyen Nguyen

Novartis, Cambridge, MA

Cyclin-dependent kinase 2 (CDK2) is the primary regulator of the S phase of the cell cycle, phosphorylating numerous substrates involved in controlling DNA replication origin firing and fork progression. CDK2 initially becomes activated in late G1 via binding to cyclin E (CCNE1/CCNE2), and contributes to phosphorylating RB1 to drive G1/S transition. As S phase progresses, CDK2 activity becomes increasingly dependent on cyclin A (CCNA2) to support the completion of DNA replication and promote activation of CDK1 in the G2 phase. In certain physiological and pathological circumstances, cyclin E overexpression has been shown to hyperactivate CDK2 and promote endoreduplication, inhibit cellular senescence, and/or override cell cycle checkpoints. Many of these features are hallmarks of cancer cells; indeed, copy number amplification of CCNE1 or CCNE2 are observed in subsets of solid tumors (e.g. gastroesophageal, ovarian, and breast cancers), highlighting CDK2 as a promising therapeutic target in these contexts. However, the development of CDK2 inhibitors has been hindered by dose-limiting gastrointestinal (GI) toxicities, and it is unclear whether this is caused by off-target (e.g. CDK1) or on-target inhibition of one or more CDK2-cyclin complexes. Using a combination of genetic and pharmacologic perturbations, we investigated how the different CDK2-cyclin complexes contribute to cell cycle regulation in both cancer and normal GI cell models. Our findings shed light on the underlying mechanisms by which CDK2 inhibition contributes to both anti-cancer efficacy and normal tissue toxicity.

#1899 Thymidine kinase activity as a translational biomarker to support dose optimization in oncology drug development and a tool for monitoring patients.

Hanna Ritzen, Mattias Bergqvist

Biovica International AB, Uppsala, Sweden

IntroductionThymidine Kinase (TK) is a cell-cycle regulated enzyme essential to DNA synthesis and a marker of cell proliferation and tumor aggressiveness. TK is released into the bloodstream and measurement of its activity (TKa) serves as a predictive and dynamic biomarker providing valuable insights in drug development. These studies aim to demonstrate the role of TKa—from evaluating drug effects in cells and preclinical studies to guiding dosing, patient stratification and monitoring in clinical trials. The FDA Project Optimus underscores the need for biomarkers that can support drug dosing optimization based on biological responses rather than maximum tolerated dose.MethodsTKa was investigated as a translational biomarker of pharmacodynamic (PD) response across preclinical and clinical settings, studying cell cycle inhibitor drugs effect on TKa levels. In HR+ breast cancer cell lines, the effects on both sensitive cells (CDKS) and cells with acquired resistance (CDKR) to CDK4/6 inhibition were studied. Clinically, the effects of CDK2 inhibition were evaluated in a phase 1/2 dose escalation study and CDK4/6 inhibition in the real-world setting, including dose adjustments, from TKa monitored breast cancer patients treated at US institutes. TKa was measured with the FDA cleared DiviTum® TKa assay (Biovica, Sweden). ResultsTKa was significantly reduced in CDKS cells treated with increasing doses of palbociclib for 3 days compared to drug vehicle (DMSO) with the highest dose of palbociclib suppressing TKa >95% vs DMSO ($p < 0.05$). No significant impact on TKa were observed in CDKR cells at any palbociclib dose.CDK-2 inhibition impact on TKa and pRb was demonstrated, with significant correlation between increasing drug exposure and decreasing TKa levels ($p < 0.05$). Combination of CDK2- and 4/6 inhibitors plus fulvestrant achieved the greatest TKa suppression ($p < 0,05$). Real-world evidence from breast cancer patients demonstrates how TKa monitoring can support individualized dose adjustments of CDK4/6 inhibitors. A lack of drug-induced TKa suppression may indicate suboptimal efficacy, justifying either dose escalation or a different therapy combination, while a strong and sustained drug-induced TKa suppression signals therapy efficacy and disease control. Dose adjustments of CDK4/6 inhibitors show how different dosing impact TKa levels and PD suppression of tumor proliferation reflects cell-cycle control. Examples of dose adjustments and drug concentration on TKa levels will be presented. ConclusionsTKa acts as a translational biomarker and a surrogate for anti-tumor activity, offering an evidence-based approach to balance efficacy and tolerability. TKa patterns can provide early signals of drug efficacy, identify patients with sustained cell-cycle inhibition, refine dose-response understanding and improve patient monitoring.

#1900 PTEN loss of function encodes sensitivity to multitargeted small molecule CDK4/6-CDK9-AURKA/B inhibitor, LCI133, and other CDK9 inhibitors.

Halle Goodwin[1], Qi Zhang[1], Vaidehi Mujumdar[1], Krishaniah Maddeboina[2], Cody McHale[2], Bharath Yada[2], Hailey Dryden[2], Robert Wendel Naumann[1], Yovanni Casablanca[1], Erin K. Crane[1], Jubilee Brown[1], Allison Puechl[1], Brittany Lees[1], Donald Durden[2], Dhananjaya Pal[2]

[1]Gynecologic Oncology, Atrium Health, Wake Forest University, Levine Cancer Institute, Charlotte, NC,[2]Molecular Targeted Therapeutics Laboratory, Atrium Health, Wake Forest University, Charlotte, NC

ObjectiveTargeted therapies for endometrial cancer (EC) have shown promise, making multitargeted therapeutics of particular interest. LCI133 is a novel, in *silico*-designed triple inhibitor of CDK4/6-CDK9-AURKA/B that demonstrated nanomolar potency by 48-hour IC_{50} and selective dose-dependent apoptosis induction in *PTEN* mutant EC cell lines. *In vivo*, LCI133 showed antitumor activity against *PTEN* mutant EC xenografts and presented an acceptable safety profile. Given these data, our objective is to define the mechanism by which *PTEN* status serves as a biomarker for LCI133 and other transcriptional inhibitor sensitivity in EC.

Methods1. *PTEN* WT HEC-1-B cells were transfected with *PTEN* shRNA and control shRNA to generate *PTEN* knockdown and control HEC-1-B cell lines. *PTEN* null AN3 CA cells were transduced with lentivirus to generate a doxycycline (Dox) inducible *PTEN* WT AN3 CA cell line.2. Isogenic *in vitro* studies were performed to determine potency of LCI133 and AZD4375 (single agent CDK9 inhibitor) by luminescent viability assay, 7-AAD/Annexin V and DNA dye flow cytometry assays. Nascent RNA (nRNA) was detected by Click-it Nascent RNA Capture Kit and assessed by qRT-PCR or confocal microscopy. Co-immunoprecipitation (Co-IP), reciprocal Co-IP, and Western blotting were used to examine protein-protein interactions.3. HEC-1-B *PTEN* shRNA or control shRNA xenografts were established in NSG mice, which were randomized and treated with LCI133 (50mg/kg) or vehicle (VEH) by daily intraperitoneal injection for 21 days. Tumor volume and animal mass were monitored, and biosamples were collected at end point.

Results1. *PTEN* knockdown in HEC-1-B cells increased sensitivity to LCI133 and AZD4375 compared to control by viability assay ($p \leq 0.0001$) and apoptosis assays ($p \leq 0.001$). Conversely, Dox induced *PTEN* expression reduced sensitivity to LCI133 by apoptosis assay ($p \leq 0.001$).2. In isogenic HEC-1-B cells, *PTEN* knockdown resulted in augmented relative nRNA transcription, followed by a significant decrease in nRNA after LCI133 treatment. A *PTEN*-dependent protein-protein interaction between RNA Polymerase (Pol) II and PTEN was shown in isogenic HEC-1-B-shRNA and *PTEN*-reconstituted AN3 CA cells.3. Tumors reached 50-75 mm^3 more quickly in the HEC-1-B *PTEN*-shRNA group compared to control ($p \leq 0.0001$). In the *PTEN* knockdown group, treatment with LCI133 resulted in slower tumor growth compared to VEH ($p \leq 0.0001$), while in the control-shRNA group, there was no difference in tumor growth between LCI133 and VEH.

ConclusionsThese data prove that the absence of *PTEN* is causally linked to sensitivity to LCI133 and AZD4375 via facilitating RNA Pol II dependent transcriptional elongation followed by a marked decrease in nRNA in *PTEN* knockdown EC cells. *PTEN* expression may be useful as a biomarker in selecting targeted therapeutics for EC driven through transcriptional activation.

#1901 Mechanisms of sensitivity and resistance to CDK2 inhibitors.

Sabrina L. Spencer

Univ. of Colorado Denver School of Medicine, Aurora, CO

CDK2 is a core cell-cycle kinase that phosphorylates many substrates to drive progression through the cell cycle. We used several CDK2 inhibitors in clinical development to interrogate CDK2 substrate phosphorylation, cell-cycle progression, and drug adaptation in preclinical models. Whereas CDK1 is known to compensate for loss of CDK2 in *Cdk2-/-* mice, this is not true for acute inhibition of CDK2. In normal mammary cells and estrogen receptor-positive breast cancer cells, CDK2 inhibition causes a rapid loss of substrate phosphorylation that is rapidly restored by a hard-wired cell-cycle buffering mechanism in which CDK4/6 maintains Rb hyper-phosphorylation, E2F transcriptional activity, and Cyclin A2 expression, enabling re-activation of CDK2. Thus, we hypothesized that sensitivity to CDK2 inhibition is linked to the absence of this CDK4/6-mediated compensatory mechanism. Indeed, we found that Cyclin E1-driven ovarian cancers often co-express the tumor suppressor p16, which inhibits CDK4/6. We show that ovarian cancer cells expressing p16 exhibit heightened sensitivity to CDK2 inhibitors and that depletion of p16 renders them resistant. Multiplexed immunofluorescence of 225 ovarian patient tumors reveals that at least 18% of tumors express high Cyclin E1 and high p16, a group that we expect to be particularly sensitive to CDK2 inhibition. These data further reveal two cell-cycle entry paths that are readily detectable in patient tumors - the canonical CDK4/6-Cyclin D path, and the CDK2-Cyclin E path ‘bypass’ path. Thus, p16 may be a useful biomarker for identifying the patients that are most dependent on the CDK2-Cyclin E path and are thus most likely to benefit from CDK2 inhibitors.

#1902 Comparative biochemical evaluation of small-molecule inhibitor efficacy on CDK/Cyclin complexes across diverse mammalian species.

Andreas Gericke[1], Frank Totzke[1], Constance Rademann[2], Carolin Heidemann-Dinger[1], Daniel Mueller[1]

[1]Reaction Biology Europe GmbH, Freiburg im Breisgau, Germany,[2]Reaction Biology Europe GmbH, Freiburg, Germany

Cyclin-dependent kinases (CDKs) and their associated cyclins are central regulators of cell cycle progression and transcriptional control. Dysregulation of CDK/Cyclin complexes is a hallmark of many cancers, driving uncontrolled proliferation and tumor development. Consequently, these complexes have become critical targets in oncology, with CDK4/6 inhibitors already established as a cornerstone in the treatment of e.g. hormone receptor-positive breast cancer and under investigation for other malignancies. Early preclinical development of CDK inhibitors relies on biochemical screening assays to identify small molecules capable of inhibiting CDK/Cyclin activity. These assays, frequently based on kinase activity measurements, enable high-throughput evaluation of compound libraries and provide essential insights into inhibitor potency and selectivity. These approaches are mandatory for rational drug design, guiding the optimization of lead compounds toward improved efficacy and reduced off-target effects. Despite their obvious limitations in predicting cellular and in vivo responses, these early screening strategies are instrumental in shaping the current generation of CDK- and other kinase-targeted therapeutics. In subsequent development stages, cellular and in vivo model systems are employed to validate inhibitor activity and assess pharmacodynamics and toxicity. Many of these models are based on non-human mammalian species, such as murine or primate systems. These studies are essential for bridging the gap between biochemical screening and clinical application, ensuring that candidate molecules demonstrate efficacy and safety before entering human trials. However, despite the importance of such data, it is rarely assessed in early biochemical screening whether results from human and non-human assays are consistent. Such early biochemical evaluation of potential differences in the effects of drug candidates on the kinase target from different species could generate valuable insights to select the most relevant cellular or in-vivo model systems for advanced drug-development. Here, we present comparative biochemical data for late-stage development or already approved CDK inhibitors tested against CDK/Cyclin complexes from human, rat, mouse, dog and primate origin, focusing on CDK4/CycD1. Notably, differential inhibitory potency was observed for several compounds, including palbociclib, which showed an approximately ten-fold difference in CDK4/CycD1 inhibition between human and murine enzymes.

#1903 Targeting autophagy and the cell cycle in mesothelioma.

George Scaria, Marian Kratzke, Stephen Porter, Betsy Kren, **Mark A. Klein**

Minneapolis VA Health Care System, Minneapolis, MN

Introduction. Mesothelioma is considered incurable for the majority of patients, and current systemic therapies are inadequate for most patients. Targeting 1) autophagy and 2) autophagy in combination with the inhibition of select cyclin-dependent kinases (CDKs) have potential for mesothelioma, as the cell cycle is altered in the majority of mesotheliomas.

Methods. We conducted cell proliferation assays in mesothelioma cell lines to determine the IC_{50} for the autophagy inhibitors ULK-101 and hydroxychloroquine (HCQ). ULK-101, HCQ, or control were incubated with mesothelioma cells for 72 hours, and cell viability was determined using a Cell Counting Kit-8 spectrophotometric assay. We then determined mRNA expression via RNA-sequencing (RNA-Seq) after CDK4/6 inhibition with abemaciclib. Subsequently, we conducted cell proliferation assays to determine if the combination of ULK-101 plus abemaciclib or HCQ plus abemaciclib could be additive or synergistic. Lastly, we obtained micrographs of H2452 cells treated with abemaciclib and subsequent organelle labeling stain (LysoTracker Red and mitoview green).

Results. ULK-101 exhibited potency against mesothelioma cell lines (H2373 and H2452) with IC_{50} values ranging from 11.9 μM to 13.3 μM, while the IC_{50} values for HCQ against these cell lines were 32.5 μM and 45 μM. When H2373 and H2452 cells were exposed to varying combinations of abemaciclib plus ULK-101, or H2452 cells were exposed to varying combinations of HCQ plus abemaciclib, synergy was exhibited at several combinations of concentrations, with several Combination Indices < 1 as calculated via the Chou-Talalay method. This suggests a synergistic effect of these combination of drugs on decreasing cell proliferation. After exposure to abemaciclib, ULK1 (ATG1) and ATG5 (role in autophagy activation) transcript expression increased as identified via RNA-Seq. Micrographs of organelle tracking after exposure to abemaciclib demonstrated increased lysosome size and number, suggesting autophagy activation.

Conclusions. ULK-101 is active against mesothelioma cells, while ULK-101 plus abemaciclib act synergistically against mesothelioma. Also, abemaciclib was associated with increased lysosome size and number, suggesting autophagy activation. Collectively, the results suggest that autophagy and the cell cycle pathways may be targeted in mesothelioma and could be co-targeted in a synergistic fashion.

#1904 Dual-targeting CDK4 and CDK2 overcomes resistance to CDK4/6 inhibitors in HR+ breast cancer.

Wenqing Cai, Siwen Liu, Lu Su, Quang Fu, Chen Liao

Hengrui pharmaceuticals Co. Ltd., Shanghai, China

Cyclin-dependent kinase 4/6 inhibitors (CDK4/6i)have proven clinical efficacy in hormone receptor-positive (HR+) breast cancer (BC) patients. However,current clinical challenges are frequent hematologic toxicities mediated by CDK6 inhibition and acquired drug resistance driven in part by cyclin E/CDK2 activation. The next generation of CDK inhibitors such as atirmociclib targeting CDK4 and tagtociclib targeting CDK2 have demonstrated encouraging early efficacy, and the combination of a selective CDK4 inhibitor and a selective CDK2 inhibitor has entered clinical trials. We propose that simultaneous targeting CDK4 and CDK2 with a small-molecule may provide a new therapeutic option.

To address the efficacy of dual-targeting CDK4 and CDK2, compound-1308 (Cpd-1308) were synthesized. In NanoBRET assay measuring cellular target engagement, Cpd-1308 had an IC50 against CDK4 of 24nM, an IC50 against CDK2 of 123nM, and an IC50 against CDK6 of 521nM, suggesting a CDK4/2 inhibitor over CDK6. Antiproliferative potency and inhibition of retinoblastoma (RB) phosphorylation were tested in multiple cancer cell lines. Human primary hematopoietic stem and precursor CD34+ cells (CD34+ HSPC) were used to estimate impact on the inhibition of hematopoietic cells proliferation. Cpd-1308 and palbociclib are nearly equipotent in MCF7 cells, whereas Cpd-1308 showed a 7-fold reduced impact on CD34+HSPC cells when compared to palbociclib. These results suggested that CDK4:CDK6 selectivity of Cpd-1308 was greater than that of palbociclib.

Further kinetic characterization using surface plasmon resonance (SPR) spectroscopy revealed that Cpd-1308 has long residence time on CDK2 in comparison with tagtociclib. Long residence time on CDK2 may potentially lead to improved efficacy against drug resistance driven in part by cyclin E/CDK2 activation. Cpd-1308 indeed showed superior potency on antiproliferation of derived palbociclib resistant MCF7 cells (MCF7-palbo-r) and derived abemaciclib resistant MCF7 cells (MCF7-abema-r). We tested the in vivo efficacy of Cpd-1308 in CDK4/6i-resistant HR+ breast cancer patient-derived xenografts tumors (PDX). Tumor growth was inhibited in a dose-dependent manner and significant growth inhibition was observed. Cpd-1308 demonstrated significant resistance-overcoming activity.

Taken together, we demonstrate activity of Cpd-1308 in HR+ breast cancers and CDK4/6i-resistant breast cancers. Our research results indicate that co-targeting CDK4 and CDK2 with a small-molecule may grant new therapeutic opportunities for patients.

#1905 Discovery of ABK-CDK4, a selective and brain-penetrant CDK4 inhibitor.

Weiling Pan, Hui Wang, Fangfei Qi, Zheng Li, Xinming Du, Jie Zhang, Jie Wang, Manqi Zhang, Haibing Deng, Hongping Yu, Yao-chang Xu, **Haiyan Ying**

Abbisko Therapeutics, Shanghai, China

Introduction: Cyclin-dependent kinase (CDK)4/6 play important roles in the G1-S phase transition in the cell cycle. Although the first generation dual CDK4/6 inhibitors— such as palbociclib, ribociclib, and abemaciclib—have demonstrated clinical efficacy in advanced breast cancer, inhibition of CDK6 would cause dose-limiting hematological toxicity. Sparing CDK6 inhibition could improve therapeutic window and enhance CDK4 target coverage. Meanwhile, brain metastases occur in 20%-40% of patients with breast cancer during their course of disease. A selective CDK4 inhibitor with reduced CDK6 inhibition and good brain penetration could provide a differentiated therapeutic option, especially for patients with brain metastasis. Through advanced computational structural analysis and medicinal chemistry effort, we have discovered ABK-CDK4, a highly selective and brain-penetrant CDK4 inhibitor. Preclinical studies demonstrate its good selectivity over CDK6, robust anti-tumor efficacy, and favorable pharmacokinetics.

Methods: Biochemical assays were performed to assess the potency of ABK-CDK4 against CDK4 and to evaluate selectivity across a kinase panel, including CDK6. Anti-proliferative effect and inhibition of retinoblastoma (Rb) phosphorylation were tested in multiple cancer cell lines. *In vivo* anti-tumor activity was evaluated in cell-derived xenograft (CDX) mouse models. Pharmacokinetic and safety profiles were also examined.

Results: ABK-CDK4 exhibited potent inhibition of CDK4 with >70-fold selectivity over CDK6. In HR^+HER2^- cancer cell lines, it effectively suppressed Rb phosphorylation and cell proliferation. ADME profiling demonstrated superior brain-penetration (Kpuu>0.5) and favorable drug-like properties. Orally administration of ABK-CDK4 led to robust tumor growth inhibition in HR^+HER2^- breast cancer xenograft models.

Conclusion: ABK-CDK4, developed by Abbisko Therapeutics, is a highly selective and brain-penetrant CDK4 inhibitor with the potential to address limitations of current CDK4/6 inhibitors. Its promising efficacy, selectivity, and other properties support further preclinical advancement toward clinical development.

#1906 Novel treatment: CDK11 inhibition in rhabdoid tumor of the kidney.

Kamhung Lam, Yuki Murakami, Shinsuke Fukui, Elizabeth Helmke, Noriko Satake

UC Davis, Sacramento, CA

Rhabdoid tumor of the kidney (RTK) is an aggressive pediatric malignancy with extremely poor outcomes despite extensive treatment. Its high treatment resistance and disease relapses necessitates a search for new therapeutic strategies. RTK is marked by the loss of SMARCB1 gene, leading to downstream dysfunctions in cell cycle, cell proliferation, and RNA splicing. Cyclin dependent kinases (CDKs) are known to regulate these processes, with several CDK inhibitors already being used in cancer treatment. CDK11's known function in regulating cell cycle and RNA splicing via splicing factor SF3B1 and its overexpression in various cancers makes it a potential therapeutic target. In this study, we evaluated the therapeutic potential of CDK11 inhibition in RTK. Based on the Therapeutically Applicable Research To Generate Effective Treatments (TARGET)-RT database, RTK tissues (n = 63) have significantly higher CDK11 expression compared to normal kidney tissues (n = 6). We also confirmed higher CDK11 protein expression in two RTK cell lines (G401 and JMU-RTK-2) than in human embryonic kidney cells (HEK293) ($p = 0.05$, 0.13, respectively). A CDK11 inhibitor, OTS964, showed significant dose-dependent cytotoxicity with IC50 of 33.1 nM in G401 and 19.3 nM in JMU-RTK-2. Next, we treated nude mice engrafted with JMU-RTK-2 tumors with 25 mg/kg of OTS964 or vehicle control. OTS964 monotherapy significantly prolonged survival (median survival: 46.5 days vs 37.0 days) and suppressed tumor progression ($p = 0.002$) without clinical signs of toxicity. Finally, we investigated OTS964's mechanisms of action. OTS964 treatment at IC80 of 80 nM (G401) and 30 nM (JMU-RTK-2) significantly increased expression of cleaved PARP, cleaved caspase-3, and p53. G2/M cycle arrest was demonstrated at 8 hours (G401) and 12 hours (JMU-RTK-2). OTS964 is known to inhibit phosphorylation of the splicing factor SF3B1, a core component of the spliceosome, thereby regulating RNA splicing. We confirmed SF3B1 inhibition by increased accumulation of the unspliced transcript DNAJB1, a known SF3B1-dependent transcript. In conclusion, our data demonstrated the therapeutic efficacy of CDK11 inhibition in RTK. CDK11 inhibition using OTS964 suppressed RTK cell growth and prolonged survival in mouse xenograft model. OTS964 induced apoptosis via caspase-3 activation with G2/M cell cycle arrest, p53 upregulation, and RNA splicing disruption via SF3B1 inhibition. In future studies, we plan to investigate synergistic combination of CDK11 inhibition with existing therapies.

#1907 CDK2 controls RIPK2 ubiquitination and stability in prostate cancer cells.

Lili M. Guerra, Ahmed M. Elgehama, Jaceline G. P. Sanches, Leslie Chiu, Wei Yang*

Department of Pathology, Stony Brook University - Cancer Center, Stony Brook, NY

Background: Prostate cancer (PC) metastasis drives PC-related mortality and morbidity, yet the molecular mechanisms underlying this lethal process remains incompletely understood. Previously, we demonstrated that RIPK2 is critical for PC progression and metastasis (*Nat. Commun.*, 2022). However, the regulatory mechanisms controlling RIPK2 protein levels in PC cells remain unclear. This study aims to address this knowledge gap by investigating the regulation of RIPK2 ubiquitination and degradation in PC cells, with a particular focus on CDK2, which we identified as a key mediator of RIPK2 regulation of the c-Myc oncoprotein.
Methods: PC cells—22Rv1 (androgen receptor-positive) and PC3 (androgen receptor-negative)—were treated with two clinically evaluated, CDK2-selective inhibitors, INX-315 and PF-07104091. Changes in RIPK2 protein levels were measured by western blotting. RIPK2 stability was assessed using cycloheximide (CHX) chase assays, and proteasomal degradation was evaluated with MG132 treatment. K48-linked ubiquitination of RIPK2 was examined by immunoprecipitation followed by western blotting with K48-linked ubiquitin antibodies. Cell cycle synchronization was achieved by serum starvation or treatment with Ro-3306, hydroxyurea, thymidine, or monastrol. Proximity ligation assays (PLA) were used to assess protein-protein interactions between RIPK2 and CDK2, its E3 ligase ZNRF4, or deubiquitinases YOD1, OTUB2, and OTUB5. Statistical analyses were performed using unpaired, two-tailed Student's *t*-tests.
Results: CDK2 inhibition significantly reduced RIPK2 protein half-life in a proteasome-dependent manner and increased RIPK2 K48-linked ubiquitination. RIPK2 protein abundance peaks in the G2 phase, lagging behind the S-phase peak of active CDK2, its stabilizing kinase. Proximity ligation assays showed that RIPK2 associates with CDK2, ZNRF4, YOD1, and OTUB5 primarily in the cytoplasm. Notably, CDK2 inhibition disrupted RIPK2 association with YOD1 but not ZNRF4 in a dose-dependent manner, implicating YOD1 in CDK2-mediated control of RIPK2 stability. Together, these findings identify CDK2 as a key regulator of RIPK2 ubiquitination and stability in PC cells.
Conclusion: Kinase-active CDK2 inhibits the K48-linked ubiquitination of RIPK2 and protects it from proteasomal degradation. This protection is potentially mediated by regulating the association between RIPK2 and its deubiquitinase YOD1 in PC cells. The findings support further investigation into the molecular mechanisms by which CDK2 stabilizes RIPK2 in PC and other cancer types.
*Corresponding Author: Wei.Yang@stonybrook.edu

#1908 Activity of dual BET and CDK9 inhibition in murine models of pancreatic ductal adenocarcinoma.

Michela Cadarso[1], Austin Stram[1], Lucas Koeppel[1], Robert J. Millikin[2], Md Shahadat Hossan[1], Eleanor Riedl[1], Ron Stewart[2], Jeremy D. Kratz[1]

[1]University of Wisconsin-Madison, Madison, WI,[2]Morgridge Institute for Research, Madison, WI

Background: Pancreatic ductal adenocarcinoma (PDAC) remains a leading cause of cancer related mortality in the U.S. with a 13% 5-year survival rate. Acquired resistance plays a critical role in progression, however targeted therapeutics have been developed for rare molecular subsets. Prior phenotypic screening efforts showed activity of bromodomain and extraterminal (BET) and cyclin dependent kinase 9 (CDK9) in PDAC organoid models. Here, we examine two independent heterotopic patient derived xenograft (PDX) murine models for the activity of BET inhibitor (ZEN3694) and CDK9 inhibitor (VIP152).

Methods: Immunodeficient $Rag2^{KO}/Il2rg^{KO}$ (R2G2) mice received subcutaneous injections of two PDAC models, PDX1 and PDX2. The models shared pathologic variants including $KRAS^{G12D}$, MTAP loss, and CDKN2A/B loss. PDX2 had concurrent loss of SMAD4. Mice colonies were treated with ZEN3694 (50 mg/kg), VIP152 (6 mg/kg), or the combination. VIP152 was administered once per week at the start of each treatment cycle and ZEN3694 was administered for five consecutive days followed by a two-day rest period. Four seven-day cycles were administered with primary endpoint of tumor volume comparison at day 28. Body weight and tumor volumes were measured biweekly by a blinded co-investigator. Toxicity was assessed by animal condition, complete blood count (CBC), and comprehensive metabolic panel (CMP) testing.

Results: All treatments were well tolerated, with no treatment group achieving weight loss >20% over the study duration. For PDX1, median weights increased by +1.21%, with non-significant change in weight for the combination of VIP152 with ZEN3694 (-14.1%). For PDX2, median weights decreased by -4.17%, with non-significant change in weight for the combination group (-8.85%). CBC and CMP results reveal no significant differences at terminal draws across treatment groups. For PDX1, median tumor growth was found to increase by +308%, with non-significant change in growth for VIP152 (+223%) or ZEN3694 (+210%), while the combination of VIP152 with ZEN3694 yielded growth arrest (-1.56%, $p<0.036$). For PDX2, median tumor growth was found to increase by +1,127%, with non-significant change in growth for VIP152 (+1,083%) or ZEN3694 (+643%), while the combination group yielded significant reduction in growth (+375%, $p<0.024$).

Conclusions: Across two independent PDAC PDX models, ZEN3694 and VIP152 yield tumor growth inhibition. All treatments were well tolerated in two independent PDAC models, PDX1and PDX2. Ongoing studies are analyzing early timepoints for a putative mechanism involving transient disruption in the activation of RNA polymerase II. Parallel analysis is examining the selectivity of this disruption in cancer tissues as opposed to background liver to index the selectivity of this drug combination in cancer types, including those where Myc can be dynamically overexpressed in response to therapeutic challenge.

#1909 CDK7 inhibition by SY5609 suppresses tumor growth in gastric cancer through inhibiting RNA pol II mediated transcription and Hippo/YAP1 signaling .

Dipti Athavale, **Yan-ting Yann Zhang**, Mikel Ghelfi, Anthony Pompetti, Junsong Zhao, Xiaodan Yao, Shumei Song

Coriell Institute for Medical Research, Camden, NJ

Background: Cyclin-dependent kinases (CDKs) are a family of serine/threonine kinases that catalyze protein phosphorylation to regulate key cellular processes. CDK7 is transcription-associated CDK which participates in both transcriptional regulation and cell cycle control. CDK7 forms a complex with cyclin H to phosphorylate the C-terminal domain (CTD) of RNA polymerase II, thereby promoting transcription initiation and elongation. In addition, CDK7 has been shown to phosphorylate the Hippo pathway coactivator YAP1 at serine 128 in mammalian cells, leading to YAP stabilization and enhanced its transcriptional activity. These findings suggest that CDK7 may represent an attractive therapeutic target. SY5609 treatment demonstrated acceptable tolerability and preliminary antitumor activity in patients with advanced pancreatic cancer. However, the expression profile of CDK7, its association with Hippo/YAP1 signaling, and its therapeutic value in advanced gastric cancer (GC) remain poorly understood. This study aimed to explore the anticancer effects of CDK7 inhibition and its potential interaction with Hippo/YAP1 signaling in GC model.
Methods: CDK7 expression was evaluated by immunohistochemistry and Western blotting in human GC tissues, patient-derived xenografts (PDXs), and GC cell lines, and further analyzed using public datasets. Functional assays, including cell proliferation, invasion, colony formation, tumor sphere formation and *In vivo* antitumor efficacy were performed to assess the effects of CDK7 inhibition by SY5609.
Results: CDK7 expression was significantly elevated in GC tumor tissues compared with adjacent normal tissues in two public datasets (cistrome.shinyapps.io/timer; GSE33335). SY5609 treatment markedly reduced cell viability and colony formation in a dose-dependent manner in GC cell lines. It also inhibited migration and tumor spheroid formation at low concentrations. Mechanistically, SY5609 decreased RNA Pol II mediated transcription and induced apoptosis. SY5609 also significantly inhibited TEAD-YAP1 transcriptional activity. Unexpectedly, SY5609 increased PD-L1 mRNA and protein expression in GC cell lines, suggesting a potential rationale for combination therapy with PD-1/PD-L1 immune checkpoint blockade. Oral administration of SY5609 significantly suppressed tumor growth and reduced tumor weight in PDX models without affecting mouse body weight.
Conclusion: Mechanistically, SY5609 treatment suppressed transcription and induced apoptosis by decreasing RNA Pol II Ser2/Ser5 phosphorylation, and reduced YAP1-TEAD transcriptional activity. Thus, targeting CDK7 with SY5606 represents a promising therapeutic strategy for advanced gastric cancer and may provide synergistic benefit when combined with immune checkpoint inhibitors.

#1910 GDC-4198, a next-generation CDK4/2 inhibitor, induces durable cell cycle arrest and shows combination benefit with giredestrant.

Marc Hafner[1], Steffan Vartanian[1], Luca Gerosa[1], Nont Kosaisawe[1], Michael S. Hwang[1], Eva Lin[1], Yi-Chang Wang[1], Jason Oeh[1], Tianyi Chen[1], Kazi N. Islam[2], Alice Zheng[2], Karen Samy[1], Udi Segal[1], John G. Moffat[1], DANIEL ZINGG[1], Annie Collier[1], Ioannis Sanidas[2], Zhi Xie[3], Seth A. Wander[2]

[1]Genentech, Inc., South San Francisco, CA,[2]Massachusetts General Hospital, Boston, MA,[3]Regor Pharmaceuticals Inc, Cambridge, MA

While CDK4/6 inhibitors (CDK4/6i) have improved the treatment of hormone receptor-positive (HR+) breast cancer (BC), resistance remains a major clinical challenge. Resistance to CDK4 inhibition can be driven by higher CDK2 activity, due to overexpression of cyclin E1/E2 or p53 loss of function, and other mechanisms. As such, targeting both CDK4 and CDK2 is hypothesized to achieve more durable cell cycle arrest. This study evaluated the preclinical activity of GDC-4198, a novel CDK4/2 inhibitor currently in early clinical trials, and its potential to overcome CDK2-driven resistance to CDK4 inhibition as a single-agent and in combination with giredestrant, a novel selective estrogen receptor (ER) degrader and full ER antagonist.

GDC-4198 has sub-nanomolar potency against CDK4/CycD1 and is a more potent inhibitor of CDK2/CycE or CDK2/CycA than CDK6/CycD3, unlike approved CDK4/6i. Western blots and immunofluorescence data demonstrated that GDC-4198 can directly decrease levels of pNCL, a direct marker of CDK2 activity. Cells engineered with a CDK2-activity reporter further confirmed the difference in inhibition profile of GDC-4198 compared to first generation CDK4/6i. In cell viability assays, we observed that GDC-4198 can maintain more durable growth arrest than CDK4/6 or CDK4-targeted inhibitors. Moreover, the introduction of TP53 knock-out had limited effects on GDC-4198 activity, and its potency was not changed by the overexpression of CCNE1/2, in contrast to other CDK inhibitors. Notably, across these different assays, the single-agent activity of GDC-4198 was comparable to the combination of CDK4- and CDK2-targeting agents. Additional studies in patient-derived cell lines obtained in the setting of metastatic HR+ breast cancer following progression on letrozole/ribociclib, as well as in cell lines with acquired in vitro resistance to palbociclib, confirmed the enhanced anti-proliferation activity of GDC-4198 compared to CDK4/6i.

When combined with giredestrant, GDC-4198 showed strong combination benefits across a range of HR+ BC cell lines. In xenograft HR+ BC models, GDC-4198 demonstrated dose-dependent tumor growth inhibition as a single agent and further improved antitumor activity in combination with giredestrant. Pharmacokinetic and pharmacodynamic analyses indicated pRb modulation in tumor samples correlated with drug exposure.

Taken together, these preclinical findings demonstrate that GDC-4198 induces more durable cell cycle arrest than first generation CDK4/6i and CDK4-targeting agents by overcoming CDK2-driven adaptive and intrinsic resistance to CDK4 inhibition. These results suggest that GDC-4198 is a promising next generation CDK4/2 inhibitor with the potential to prolong clinical benefit by delaying adaptation in earlier disease settings, as well as to provide benefit to patients who have progressed on approved CDK4/6i.

#1911 Targeting PLK1 or WEE1 uncovers a therapeutic vulnerability in BRCA1/2 wild-type, homologous recombination-proficient high-grade serous ovarian cancer.

Akiko Kunita[1], Qian Xi[2], Masanori Kawakami[3], Miho Ogawa[1], Mirei Ka[2], Kousuke Watanabe[1], Tetsuo Ushiku[4], Hidenori Kage[3], Kazuhiro Katayama[5], Katsutoshi Oda[2]

[1]Next-Generation Precision Medicine Development Laboratory, University of Tokyo, Tokyo, Japan,[2]Division of Integrative Genomics, University of Tokyo, Tokyo, Japan,[3]Respiratory Medicine, University of Tokyo, Tokyo, Japan,[4]Pathology, University of Tokyo, Tokyo, Japan,[5]Laboratory of Molecular Targeted Therapeutics, School of Pharmacy, Nihon UniversityKeio University, Chiba, Japan

Background: High-grade serous ovarian cancer (HGSOC) with BRCA1/2 wild-type (BRCA-WT) and homologous recombination proficiency (HRP) responds poorly to platinum agents and PARP inhibitors and lacks effective targeted therapies. We aimed to determine whether inhibition of PLK1 or WEE1, two G2/M checkpoint kinases, could uncover a therapeutic vulnerability in BRCA-WT/HRP HGSOC.

Methods: We evaluated the effects of the PLK1 inhibitor volasertib and the WEE1 inhibitor adavosertib in BRCA-WT/HRP (and BRCA-mutant/HR-deficient (HRD) ovarian cancer models. Cell viability, cell-cycle distribution, apoptosis markers, and DNA damage responses were quantified, including γH2AX, RAD51, and 53BP1 foci. DNA-PKcs inhibition or siRNA was used to assess NHEJ dependence. Antitumor activity was further validated in BRCA-WT cell line-derived xenografts and two PDX models with confirmed BRCA status.

Results: BRCA-WT cells demonstrated substantially higher sensitivity to PLK1 or WEE1 inhibition than BRCA-mutant cells. In BRCA-WT models, volasertib induced abnormal spindle assembly, polyploidy, and delayed mitotic progression, whereas adavosertib abrogated the G2/M checkpoint and triggered premature mitotic entry. Both agents increased DNA damage and markedly reduced RAD51 foci, demonstrating HR suppression. Although NHEJ activation was observed, it was insufficient to compensate for impaired HR. In contrast, BRCA-mutant cells showed minimal response and displayed constitutively high DNA-PKcs expression with persistent 53BP1 foci. Pharmacologic or genetic DNA-PKcs inhibition restored sensitivity to PLK1 or WEE1 inhibition in BRCA-mutant cells. *In vivo*, PLK1 or WEE1 inhibition significantly reduced tumor growth and increased apoptosis in BRCA-WT xenografts and BRCA-WT PDX, whereas BRCA-mutant PDX exhibited limited response.

Conclusion: BRCA-WT/HRP HGSOC exhibits distinct susceptibility to PLK1 or WEE1 inhibition through disruption of HR repair and mitotic regulation, revealing a DNA repair-based vulnerability not observed in BRCA-mutant/HRD tumors. These findings provide a strong rationale for biomarker-guided development of PLK1 or WEE1 inhibitors as therapeutic strategies for HRP ovarian cancers, a patient population with significant unmet clinical needs.

#1912 Extrachromosomal DNA (ecDNA)-mediated replication stress as a potential targetable vulnerability in high-risk medulloblastoma.

Jessica Wang[1], Hui Hui[1], Jon D. Larson[2], Rishaan Kenkre[3], Owen Chapman[4], Yan Yuen Lo[1], Emerald Adeyan[1], Lukas Chavez[1]

[1]Sanford Burnham Prebys Med. Discovery Inst., La Jolla, CA,[2]Sanford Burnham Prebys, La Jolla, CA,[3]Sanford Childrens Health Research Center, San Diego, CA,[4]Nagoya City University, Nagoya, Japan

Extrachromosomal DNA (ecDNA) amplification is a key driver of cancer evolution and progression. In medulloblastoma, ecDNA is present in approximately 18% of cases and is associated with poor patient survival. However, its role in tumor progression and treatment resistance for patients with medulloblastoma remains poorly understood. This study investigates ecDNA-mediated replication stress (RS) as a potentially targetable vulnerability in high-risk medulloblastoma with a focus on tumors harboring MYC amplifications. Using RNA sequencing data from a cohort of 186 patients from the Pediatric Brain Tumor Atlas, we performed gene set enrichment analysis (GSEA) and found RS to be significantly enriched in medulloblastomas with amplifications compared to those without amplifications. We then investigate the effects of pharmacological checkpoint kinase 1 (CHK1) inhibition using BBI-2779—a novel, selective, and potent inhibitor developed by Boundless Bio—on MYC ecDNA-positive (D425 and D458) and MYC-HSR (D283) medulloblastoma cell lines. Our results show that ecDNA-positive lines exhibit greater sensitivity and a stronger dose-dependent response to CHK1 inhibition than MYC-HSR cells. Moving forward, we will use patient-derived xenografts (PDXs) generated from tumor biopsies collected at Rady Children's Hospital-San Diego, along with cell line models, to monitor tumor response and ecDNA copy number dynamics following CHK1 inhibition. We will then perform multiome single-cell sequencing to identify therapy-induced emergence of novel ecDNA variants.

Keywords: Medulloblastoma, Extrachromosomal DNA, ecDNA, genomic instability, therapy resistance, tumor heterogeneity

#1913 KMT2D deficiency alters CDK-cyclin regulation of Rb in endometrial cancer.

Madelyn Maurer[1], Swornalata Pukhrambam[1], Jessica Long[1], Sanjeev Ganesh[1], Sophia Agrusa[1], Maya Paytas[1], Katherine Gurdziel[2], Paul Stemmer[3], Mike R. Wilson[1]

[1]Wayne State University School of Medicine, Detroit, MI,[2]Wayne State University Genomic Sciences Core, Detroit, MI,[3]Wayne State University Proteomics Core, Detroit, MI

Endometrial cancer (EC) is the most common gynecological cancer and ranks fourth overall among all cancers affecting women in the United States. Its incidence, especially among premenopausal women, continues to increase in contrast to many other malignancies. Recent genomic investigations, including our lab's preliminary findings, have identified KMT2D, a histone methyltransferase that modulates enhancer activity, as being highly mutated in early onset EC. Our initial observations suggest that KMT2D deficiency triggers aberrant histone methylation at the Rb/E2F pathway genes, leading to upregulation of the pathway. These findings motivated the development of a KMT2D CRISPR knockout (KO) cell line to explore the mechanistic consequences of KMT2D deficiency. We are employing 12Z endometrial epithelial cell lines, derived from endometriosis, with and without CRISPR-mediated KMT2D KO to examine the mechanistic basis of Rb/E2F pathway dysregulation at both the gene expression and post-translational levels. Preliminary data indicate that KMT2D deficiency enriches retinoblastoma (Rb) phosphorylation levels, consistent with upregulation of the Rb/E2F pathway. Additionally, cyclin E, cyclin D, p21, and CDK1 were more highly expressed in KMT2D KO cells compared to the control. To further investigate upstream regulators, we examined CDK1/2 pathway dynamics. In control and KMT2D KO cells, we found pharmacologic inhibition of CDK1/2 activity led to increased expression of cyclin A2 and cyclin E1. There was also a divergent effect on Rb phosphorylation following CDK1/2 inhibition, with phospho-Rb increasing expression in control cells but reducing in KMT2D KO cells. This indicates KMT2D deficiency alters CDK-Rb signaling pathways. To explore additional mechanisms contributing to altered Rb regulation, we performed Rb immunoprecipitation followed by mass spectroscopy to identify changes in Rb protein interactions in the absence of KMT2D. Ongoing analysis of these datasets aims to determine whether KMT2D deficiency exposes novel regulatory interactions affecting Rb phosphorylation. This study builds on preliminary findings implicating KMT2D in Rb pathway dysfunction in early-onset EC. By investigating the contribution of CDK-mediated phosphorylation, we have sought to clarify the mechanistic basis of elevated Rb activity in KMT2D-deficient cancer. These findings may reveal novel therapeutic vulnerabilities that can be exploited for targeted treatment strategies in patients with early-onset EC.

#1914 Sequential inhibition of CDK4/6 and the mitotic kinase TTK as a potential treatment in triple-negative breast cancer cell lines.

Gretchen M. Albarran-Acosta, Janangelis Lopez-Ramos, Magda N. Alvarez-Rodriguez, Alexandra N. Aquino-Acevedo, Harold I. Saavedra-Lugo

Basic Sciences Department Pharmacology Division, Ponce Health Sciences University, Ponce, PR

Triple-negative breast cancer (TNBC) is a poor-prognostic subtype. TNBC cells have uncontrolled cell proliferation, genetic instability, and elevated rates of metastasis. Lacking targeted therapies, chemotherapy is the primary treatment option. Mitotic kinases that maintain genomic stability, such as Threonine Tyrosine Kinase (TTK), exhibit increased expression in TNBC patients. TTK regulates the spindle assembly checkpoint, and its overexpression contributes to centrosome amplification, chromosome instability, and early metastasis. Palbociclib, a CDK4/6 inhibitor known to induce cellular senescence in tumors, is approved against luminal BC but not TNBC. Due to the reduced sensitivity of non-cycling cells to chemotherapeutic drugs, simultaneous association between Palbociclib and different chemotherapeutic agents has shown antagonistic effects. Preliminary data shows no significant decrease in the viability of TNBC cell-lines after simultaneous inhibition of TTK and CDK4/6. Based on studies stating that a sequential treatment with Palbociclib followed by a chemotherapeutic agent (paclitaxel) decreases TNBC cell-line viability, and our preliminary data showing that TTK inhibition restores the expression of G1/S regulators such as Rb, our study aims to evaluate if resistant TNBC cells may be sensitive to sequential treatment of CDK4/6 inhibition followed by mitotic kinase TTK inhibition. Twenty-four hours after seeding MDA-MB-231 and MDA-MB-157 TNBC cell lines, Palbociclib (PD0332991) was added at increasing concentrations. Twenty-four hours later, TTK inhibitor (BAY1217389) was added at a constant IC_{50} concentration. The MTT Assay was performed after 96 hours of incubation. Pre-treatment with Palbociclib followed by a constant IC_{50} concentration of TTK inhibitor showed significant decrease in MDA-MB-157 cell line viability. Results state that a sequential treatment strategy with Palbociclib followed by TTK inhibitor treatment can be a potential therapeutic approach for certain populations with TNBC. Differences associated with drug responses can be attributed to the difference in levels of cell cycle regulators in TNBC cell lines, which will be investigated further on. Results allowed the reduction of drug levels and toxicity, while potentially improving safety and efficacy for clinical use.

#1915 Serpine2 promotes melanoma progression through the modulation of the DDX3X/MITF/p21 signaling pathway.

Qirui Liu[1], Xin Huang[1], Xiao Zhang[2], Xinyu Ye[1], Yi Lu[1], **Jian Zhang**[1]

[1]School of Medicine, Southern University of Science and Technology, Shenzhen, China,[2]The Affiliated Foshan Hospital of Southern University of Science and Technology, Southern University of Science and Technology, Shenzhen, China

Melanoma is the most lethal form of skin cancer, characterized by an increasing incidence and high mortality rates globally. However, the mechanisms underlying melanoma tumorigenesis and progression remain poorly understood. Analyses of public repositories have identified SERPINE2 as a key differentially expressed gene involved in the biological processes associated with melanoma. As a member of the serpin superfamily, SERPINE2 plays diverse roles in regulating proteolytic activity, inflammation, and tissue remodeling; however, its specific functions in melanoma warrant further investigation. This study aims to explore the potential mechanisms by which SERPINE2 influences tumorigenesis and progression in melanoma. In this study, we evaluated the expression and clinical relevance of SERPINE2 in melanoma by analyzing data from TCGA, GTEx, and TIMER2.0, and identified SERPINE2-associated biological processes through GO and KEGG enrichment analyses. Our findings revealed that SERPINE2 is significantly upregulated in melanoma tissues compared to normal skin tissues, and its expression correlates with cell growth, epithelial-mesenchymal transition, and immune response. Knockdown of SERPINE2 markedly inhibited cell viability, proliferation, and invasion of melanoma cells both *in vitro* and *in vivo*. RNA sequencing analysis of SERPINE2-knockdown cell lines demonstrated that silencing SERPINE2 induced cell cycle arrest in the G0/G1 phase and promoted apoptosis. To investigate the underlying mechanisms, we identified DDX3X as a binding partner of SERPINE2 through co-immunoprecipitation (CO-IP) and immunoprecipitation-mass spectrometry (IP-MS) analyses. We found that SERPINE2 attenuates the protein stability of DDX3X, promoting its degradation via the ubiquitin-proteasome system. Furthermore, silencing DDX3X resulted in the downregulation of nuclear protein expression of MITF and p21, suggesting that DDX3X downregulation may influence the transcription of downstream genes associated with cell cycle progression, thereby impacting melanoma growth. Additionally, downregulation of SERPINE2 enhanced CD8+ T cell infiltration, stimulated T-cell activation-related cytokines and chemokines, and improved the cytotoxic function of CD8+ T cells *in vitro*. Furthermore, in both the Lauss cohort and the IMvigor210 cohort, we observed that SERPINE2 expression correlated with the prognosis of melanoma patients undergoing immunotherapy; specifically, patients with low SERPINE2 expression exhibited better prognoses compared to those with high SERPINE2 expression. In summary, the expression level of SERPINE2 is a predictor of therapy response and prognosis in melanoma patients, suggesting its potential as a biomarker for melanoma immunotherapy. This work was supported by the National Natural Science Foundation of China (No. 82173336), and the MRI Project (G030410001).

#1916 Identifying changes in cell cycle regulatory proteins during clobetasol-induced quiescence in UMSCV-4 vulvar cancer cells.

Claudia M. Marsello, Trinity A. Trojanowski, **Jani E. Lewis**

Biology, State University of New York at Geneseo, Geneseo, NY

Quiescence is a reversible state in which cells temporarily exit the cell cycle in response to stress, with the capacity to re-enter the cycle once the given stress is relieved. Growing evidence suggests that quiescent cancer cells may underlie long-term tumor dormancy and late relapse. We found that a subpopulation of the vulvar squamous cell carcinoma line UMSCV-4 enters quiescence following exposure to the corticosteroid clobetasol (clob). Upon removal of clob, these cells re-enter the cell cycle. To characterize this process, we quantified changes in proliferation using BrdU incorporation and assessed the timing of cell cycle re-entry after clob withdrawal. We hypothesized that clob treatment would downregulate key cell-cycle-promoting proteins while upregulating cell-cycle inhibitors, and that these changes would reverse within three days of clob removal, coinciding with increased DNA synthesis and the reappearance of mitotic figures. Using Western blot analysis, we examined the expression of cell-cycle promoters (cyclin D1, cyclin D3, CDK2, CDK4, CDK6) and inhibitors (p21Waf1/Cip1 and p18INK4C). RNA seq analysis is being used to evaluate corresponding changes in mRNA abundance and to identify additional regulators associated with clob-induced arrest. Together, these studies aim to define the molecular mechanisms by which clobetasol promotes quiescence in vulvar cancer cells.

#1918 CRISPR screening in human iPSC-derived glioblastoma models reveals RNA-binding protein dependencies associated with TERT promoter mutation.

Christopher C. Chie[1], Daisuke Kawauchi[1], Shunichiro Miki[1], Nicholas O. Stevers[2], Joseph F. Costello[2], Chun-Yuan Chen[3], Gene W. Yeo[4], Frank B. Furnari[1]

[1]Division of Regenerative Medicine, Department of Medicine, University of California San Diego, San Diego, CA,[2]Department of Neurological Surgery, University of California San Francisco, San Francisco, CA,[3]Sanford Stem Cell Institute, Innovation Center, San Diego, CA,[4]Department of Cellular and Molecular Medicine, University of California San Diego; Sanford Laboratories for Innovative Medicines; Sanford Stem Cell Institute, Innovation Center; Center for RNA Technologies and Therapeutics; Institute for Genomic Medicine, San Diego, CA

IDH-wildtype glioblastoma (GBM) is a highly aggressive adult brain tumor with an extremely poor prognosis, characterized by multilayered intratumor heterogeneity. Telomerase reverse transcriptase (TERT) promoter mutation, the most frequent driver mutation in GBM, is homogeneously present within tumors, offering the potential for comprehensive and selective eradication of heterogeneous GBM populations. However, targeting cells expressing TERT in a mutation-dependent manner has not been feasible, largely due to the adverse effects of existing telomerase inhibitors and the inability to block GABPA, a transcription factor that selectively activates the mutant promoter. These obstacles highlight the need to identify novel actionable vulnerabilities. Previous GBM models, such as patient-derived xenografts and genetically engineered mouse models, have failed to provide such insights due to lack of experimental standardization and human-to-mouse variations in telomere biology and TERT promoter. To bypass these challenges, we leveraged human iPSCs to engineer GBM models harboring either wildtype or mutant TERT promoter, enabling discovery of synthetic lethal therapeutic targets. Performing a pooled CRISPR knockout screen targeting 1078 RNA-binding proteins (RBPs), we identified 40 RBPs whose depletion selectively impaired survival of TERT promoter-mutant (TPM) cells without affecting wildtype (TPW) cells. Intriguingly, these included 3 RBPs that form a methyltransferase complex governing N^6-methyladenosine (m^6A) modification; METTL14, METTL3, and RBM15. Functional analyses showed that METTL14 depletion downregulates GABPA mRNA level independent of TERT promoter status but reduces TERT expression specifically in TPM cells. m^6A-targeted eCLIP-seq revealed m^6A-independent regulation of GABPA and TERT, indicative of regulatory factor(s) mediating this gene expression cascade. Integrated analysis of m^6A-eCLIP-seq and RNA-seq uncovered enrichment of transcription factors (TFs) among METTL14 target genes for m^6A methylation, identifying potential mediators linking METTL14 with GABPA and TERT. These TFs are downregulated upon METTL14 depletion and m^6A-methylated, with public databases showing ChIP-seq peaks at the GABPA promoter and highly correlated expression with METTL14 and GABPA. We hypothesize that m^6A methyltransferase machinery stabilizes transcripts of these TFs via m^6A methylation, driving GABPA transcription and sustaining TERT expression in TPM cells. This study uncovers a novel epitranscriptomic axis regulating TERT and lays the groundwork for developing new therapeutic strategies by leveraging stem cell-derived disease models.

#1919 Longer leukocyte telomeres and specific alleles of telomere maintenance genes are independently associated with improved survival of colon cancer patients.

Estela M. Cruz Garcia[1], Gobinda Sarkar[2], Jun Chen[2], Shubham Sood[3], Kim Kossick[2], Daniel Schupack[2], Rondell Graham[2], Brooke Druliner[2], Zahra Heydari[2], Lauren Helgeson[2], Richard G. Cawthon[4], Lisa A. Boardman[2]

[1]University of Puerto Rico, San Juan, PR,[2]Mayo Clinic, Rochester, MN,[3]University of Central Florida/ HCA Florida West Hospital, Pensacola, FL,[4]Human Genetics, University of Utah, Salt Lake City, UT

Background: Aberrations in telomere length have important implications in cancer development and progression. This study aimed to determine whether leukocyte telomere length (LTL) in patients with colorectal cancer (CRC) is associated with survival outcomes. We also investigated whether genetic variants in telomere maintenance genes are associated with survival in these patients.
Methods: Blood specimens were collected from 1,007 patients prior to receiving chemotherapy or radiation. Genomic DNA was extracted using the Promega Maxwell RSC instrument. LTL was measured in triplicate using monochrome multiplex PCR, where the average amplification value of telomeric repeats was termed T. Similarly, PCR amplification of a single-copy reference gene was performed, and its average amplification value was termed S. The telomere length for each sample was expressed as the T/S ratio. Genotyping of single-nucleotide polymorphisms (SNPs) in TERC, TERT, and OBFC1 genes was conducted at the institutional Genome Analysis Core facility. Kaplan-Meier survival curves were generated to evaluate patient survival outcomes.
Results: Younger individuals (~25 years) exhibited nearly a twofold longer LTL compared with older individuals (~75 years). No significant difference in LTL was observed between stage II and stage III CRC patients. A strong inverse correlation was observed between patient age and LTL (Spearman's $r = -0.48$; $p = 1.13 \times 10^{-58}$). Females had significantly longer LTL than males ($p = 3.97 \times 10^{-5}$). The TERC SNP rs1317082 was significantly associated with both overall survival (OS) and disease-free survival (DFS) in the combined stage II and stage III patient cohort ($p = 0.017$ and $p = 0.023$, respectively). Similarly, the OBFC1 SNP rs9419958 was significantly associated with OS ($p = 0.016$). Importantly, LTL itself was significantly associated with both OS and DFS ($p = 0.008$ and $p = 0.044$, respectively) among the combined stage II and stage III patients. Kaplan-Meier survival analyses demonstrated that age- and sex-adjusted LTL was predictive of long-term survival outcomes.
Conclusions: Survival among patients with stage II and III colorectal cancer is significantly influenced by LTL. Additionally, specific allelic variants of telomere maintenance genes, including TERC and OBFC1, are independently associated with improved survival, irrespective of LTL. These findings suggest that peripheral blood LTL measurement, along with telomere-related genotyping, may serve as a valuable prognostic marker for colorectal cancer outcomes. Funding: Individualizing colorectal cancer patient care using the host and tumor telomere phenotype (RO1 CA204013), Curtiss Fund (92541775), C-SiG Core(s): Epigenomics & Spatial Biology Core, and Clinical Core of the Mayo Clinic Center for Cell Signaling in Gastroenterology (P30DK084567)

#1920 Resolving telomere length dynamics in breast cancer evolution through single-cell DNA sequencing.

Nicolaas Baudoin, Lei Yang, Chenling Tang, Hanghui Ye, Kaile Wang, Jianzhuo Li, Yun Yan, Nicholas E. Navin

UT MD Anderson Cancer Center, Houston, TX

Telomeres serve as a critical tumor-suppressive barrier by limiting the accumulation of genomic mutations through two checkpoints: replicative senescence and telomere crisis. Cells that bypass senescence and enter telomere crisis experience rampant chromosomal instability driven by end-to-end fusions and mitotic defects, which typically results in cell death. Rare cells that activate a telomere maintenance mechanism (e.g., telomerase) can re-lengthen telomeres, escape crisis, and stabilize their genome while potentially leveraging transient instability to fuel punctuated copy number evolution and tumorigenesis. Despite their importance in replicative mortality and maintaining genomic stability, the dynamics of telomere length during tumor evolution remain poorly understood due to limited longitudinal patient samples and technical challenges in telomere measurement, which often require large input material and lack compatibility with multiomic profiling. To overcome these barriers, we developed a method to infer telomere length from single-cell DNA sequencing and multiomic data. We validated this approach in cell lines and applied it to study the telomere length dynamics in ER-positive (N = 7) and ER-negative (N = 14) breast tumors with unprecedented resolution. Our analysis revealed substantial telomere length changes during subclonal diversification, highlighting telomere dynamics as a key feature of breast tumor evolution. Phylogenetic reconstruction uncovered tumor-specific patterns of telomere length evolution, which may have clinical implications. Furthermore, we found that telomere length variation among subclones was associated with differences in fitness and telomere maintenance pathway activity. This work introduces a powerful tool to interrogate telomere biology directly in patient tumors at single-cell resolution, providing new insights into the role of telomere dynamics in cancer evolution and laying the foundation for future studies to clarify the biological and clinical significance of telomere regulation in cancer

#1921 Proximity labeling and thermal profiling proteomic analysis unveil mechanistic role of YWHAZ and YWHAB in CDK4/6 inhibitor resistance.

Min-Jyun Dong[1], Wei-Ting Chung[2], Yi-Ru Tseng[2], Chun-Yu Liu[2], Chi-Cheng Huang[2], Ling-Ming Tseng[2], Ta-Chung Chao[2], **Jiun-I Lai**[1]

[1]National Yang Ming Chiao Tung University, Taipei, Taiwan,[2]

CDK4/6 inhibitors are currently standard of care in both early and metastatic hormone positive breast cancer. With the expanded use of CDK4/6 inhibitors in early breast cancer, identifying and addressing resistance mechanisms become increasingly important for improving patient outcome. In our prior work, using proximity labeling approaches, we identified the YWHAB/YWHAZ complex (both members of the 14-3-3 family) as important mediators for CDK4/6 inhibitors resistance. Genetic silencing of YWHAB sensitized resistant hormone positive breast cancer cells towards CDK4/6 inhibitors. We further demonstrated that YWHAB-YWHAZ existed as a dimer and suppressed proteosomal function for CDK6 degradation, leading to CDK4/6 inhibitor resistance. To elucidate the interactome of YWHAZ, and to probe for proteosomal roles in CDK4/6 inhibitor resistance, we performed Thermal Proximity Co-aggregation (TPCA) proteomics on cells with/without YWHAZ silencing. TPCA analysis identified proteins involved in proteosomal processing and confirmed a role of YWHAZ in mediating proteosomal degradation. Further functional studies validate novel mechanisms for CDK4/6 inhibitors. Our findings were correlated with TCGA and other public cohorts to demonstrate a prognostic and predictive role of YWHAZ in CDK4/6 inhibitors. In summary, our findings indicate a role for proteosomal selectivity that mediates CDK4/6 inhibitor resistance and could serve as future therapeutic targets for hormone positive breast cancer.

: Chromatin Structure and Function
Poster Session

#1924 Retrotransposon reactivation to elicit innate immunity in squamous cancers while sparing normal tissues.

Mande Xue, Ying Lyu, **Yejing Ge**

UT MD Anderson Cancer Center, Houston, TX

Transposons make up over 40% of the human genome, and while most are inactive, a few retrotransposons remain capable of jumping, contributing to mutations and genetic variation. Squamous cell carcinomas (SCCs) including those from the head and neck, esophagus, lung, cervix, anogenital sites and skin show particularly high retrotransposon activity among all cancers analyzed, yet their pathogenic mechanisms and therapeutic potential remain poorly understood.
We tackle these challenges by using a genetic model lacking a crucial epigenetic repressor of endogenous retroviruses (ERVs, a type of retrotransposons resembling retroviruses) in the adult murine skin. We saw in our model robust ERV induction, accompanied by retroviral peptides production and viral like particles assembly, leading to stem cell exhaustion and hair loss phenotypes, which can be reversed in vivo by antiviral drugs that inhibit reverse transcriptase (Lyu Y et al, Ge Y. Cell. 2024).
In the current study, we dissect host mechanisms restraining and responding to ERV reactivations, and leverage these pathways to inhibit SCCs while sparing normal tissues. Retrotransposon reactivation elicits host antiviral responses in the tumors, known as viral mimicry, which we recapitulated in the skin. Interestingly, we observed two genetically and biochemically diverging pathways elicited by ERVs versus SINEs (short interspersed elements, another type of retrotransposons), that are responsible for skin pathogenesis and tumor progression. Moreover, while retrotransposon reactivations are widely associated with antiviral responses in cancer patients, such correlations remain context dependent, and their decoupling often occurs unexplained. We saw intriguing decoupling of retrotransposon induction and antiviral response in our model. We further noted that distinct heterochromatin repressors cooperate to not only dictate retrotransposon-independent antiviral responses, but also blunt antiviral responses despite the presence of retrotransposon reactivations. Finally, we propose retrotransposon related SCC specific vulnerabilities that can be tackled while sparing normal tissues.

#1925 De novo enhancer formation at human-viral junctions drives hybrid extrachromosomal DNA amplification in HPV-associated cancer.

Takuya Nakagawa[1], Jens Luebeck[2], Kaiyuan Zhu[2], Sasik Roman[2], Brin Rosenthal[2], Kathleen Fisch[2], Toyoyuki Hanazawa[1], Atsushi Kaneda[1], Paul S. Mischel[3], Vineet Bafna[2], Joseph A. Califano[4]

[1]Chiba University, Chiba, Japan,[2]UC San Diego, La Jolla, CA,[3]Stanford University School of Medicine, Stanford, CA,[4]UC San Diego School of Medicine, La Jolla, CA

Introduction: Extrachromosomal DNA (ecDNA) contributes to oncogene amplification in human cancers, yet the mechanisms underlying the formation and function of human-viral hybrid ecDNA (hybrid ecDNA), circular elements harboring both HPV and human sequences, remain unclear. We recently identified hybrid ecDNA in human papillomavirus-associated oropharyngeal cancer (HPVOPC), a rapidly increasing malignancy. Here, we show that *de novo* enhancer formation at viral-human junctions activates viral oncogenes and promotes hybrid ecDNA self-amplification, revealing a tractable therapeutic vulnerability.

Methods: Hybrid ecDNA was identified in HPVOPC cell lines and patient-derived xenografts (PDX) using whole-genome sequencing and AmpliconArchitect. Validation was performed by multicolor FISH. Chromatin accessibility and enhancer activity were profiled by ATAC-seq and H3K27ac ChIP-seq. Hi-C sequencing was used to assess 3D chromatin interactions and potential contacts among distinct ecDNA species. Functional significance was evaluated by CRISPR interference (CRISPRi) targeting ecDNA-derived enhancers. Therapeutic relevance was assessed by BET inhibition in vitro and in vivo.

Results: Hybrid ecDNA was detected in both cell lines and PDX tumors and validated by overlapping human and HPV FISH signals. Epigenomic profiling revealed *de novo* active enhancers flanking HPV sequences exclusively in hybrid ecDNA(+) tumors. Hi-C demonstrated enhancer-promoter loops linking host enhancers to HPV oncogenes. CRISPRi targeting these enhancers significantly inhibited proliferation in hybrid ecDNA(+) models only ($P = 0.006$). BET inhibition selectively suppressed hybrid ecDNA(+) tumor growth in vivo ($P = 2\times10^{-5}$). Importantly, Hi-C contacts also indicated enriched interaction patterns among distinct ecDNA species, suggesting potential extrachromosomal cooperation that enhances viral oncogene expression.

Conclusions: Hybrid ecDNA is a functionally critical structure in HPVOPC by generating *de novo* enhancers and reorganizing chromatin interactions to activate viral oncogenes, creating a therapeutic vulnerability. Contact enrichment among distinct ecDNA species further suggests participation in a broader extrachromosomal regulatory network in HPV-driven malignancies.

#1926 The VPS72-H2A.Z-axis is an underappreciated oncogenic vulnerability in lung adenocarcinoma.

Xzaviar Kaymar Solone, Selim Reza, Kalpana Subedi, Nirmal Parajuli, Li Zhou, Qing-Sheng Mi

Dermatology Research, Henry Ford Health System, Detroit, MI

Lung adenocarcinoma (LUAD), the most common subtype of non-small cell lung cancer (NSCLC), frequently relies on epigenetic plasticity to support growth, stress adaptation, and therapeutic escape. Among the chromatin mechanisms enabling this plasticity, histone variant exchange is central. Incorporation of specific variants reshapes DNA accessibility and transcriptional programs, underpinning cancer cell adaptability. VPS72, a histone chaperone shared by the SRCAP and TIP60 complexes, mediates ATP-dependent deposition of the H2A.Z-H2B dimer into regulatory chromatin, thereby promoting proliferation, lineage state, immune evasion, and treatment tolerance transcriptional programs. H2A.Z deposition is linked to aggressive malignancy; however, the contribution of VPS72 itself to LUAD progression remains undefined. Given its central role in H2A.Z loading, the VPS72-H2A.Z axis may represent a key epigenetic driver and potentially targetable vulnerability. TCGA LUAD datasets were analyzed to profile VPS72 expression, genomic correlates, and functional relevance. VPS72 was significantly upregulated relative to normal tissue and associated with greater genomic instability, higher tumor mutational burden, stronger hypoxia signatures, earlier clinical detectability, and reduced overall survival. High VPS72 expression was also observed in female patients and ever-smokers, indicating exposure-linked modulation. Functional evaluation in LUAD models showed that genome-wide CRISPR and RNAi screens identified VPS72 as a major fitness gene. shRNA-mediated VPS72 depletion reduced proliferation and Ki-67 expression, reduced colony formation, impaired migration and invasion, and abrogated anchorage-independent growth. Transcriptional profiling revealed that VPS72 loss strongly repressed MYC- and E2F-driven cell-cycle programs and disrupted metabolic pathways, including heme biosynthesis, mitochondrial respiration, calcium signaling, and hypoxia adaptation. Although H2A.Z itself is not directly targetable, VPS72 role in its deposition creates a druggable interface. To exploit this, we developed cell-permeable peptides that block the VPS72-H2A.Z interaction, which phenocopied VPS72 knockdown by inducing apoptosis and suppressing LUAD cell growth in a dose-dependent manner. Collectively, these findings identify VPS72 as a central epigenetic regulator and therapeutically actionable vulnerability in LUAD. Disrupting the VPS72-H2A.Z axis attenuates oncogenic transcriptional programs and malignant behaviors, offering a promising strategy to overcome epigenetic plasticity and treatment resistance in aggressive NSCLC.

#1927 Epigenetic CRISPR screen identifies chromatin regulators essential for ovarian cancer spheroid formation.

Deren Demirel Yavuz[1], **Irem Durmaz Sahin**[2]

[1]Graduate School of Health Sciences, Koc University, Istanbul, Turkey,[2]School of Medicine, Koc University, Istanbul, Turkey

Background: Cancer stem-like cells (CSCs) contribute to recurrence and chemoresistance in high-grade serous ovarian cancer (HGSOC). Spheroid formation in ultra-low attachment (ULA) cultures models CSC self-renewal, yet the epigenetic regulators and molecular dependencies sustaining this 3D phenotype remain largely undefined.
Methods:A focused CRISPR knockout screen targeting 800 epigenetic and chromatin regulators was performed in OVCAR-3 spheroids. sgRNA enrichment after 3D selection identified genes essential for spheroid growth. Top candidates were functionally validated in BRCA1-wildtype, BRCA1-LOH, and BRCA1-mutant cell lines by assessing spheroid morphology, compaction, viability, and proliferative behavior.
Results: The screen identified a high-confidence set of regulators required for spheroid formation, including DNA damage response genes (BRCA1, PARG), Polycomb complex members (SUZ12, BMI1), RNA-binding proteins (NCL, SYNCRIP), and cell cycle regulators (CDK2, PBRM1). These hits converge on chromatin remodeling, histone methylation, and transcriptional control pathways, linking epigenetic regulation with DDR signaling.Functional assays revealed a striking BRCA1 dependency: while BRCA1-WT and LOH cell lines formed compact, viable spheroids, BRCA1-mutant cells produced disorganized, loosely aggregated, hyperproliferative structures with poor architectural integrity. This indicates that BRCA1 is essential not for proliferation per se, but for establishing and maintaining 3D stem-like organization. Integration of the CRISPR hits with phenotypic outcomes suggests a cooperative network between DDR factors, RNA-binding regulators, and chromatin modifiers in sustaining CSC-like behavior.
Conclusions: Our findings demonstrate that BRCA1 function underpins the epigenetic and chromatin-based control of spheroid architecture, revealing a mechanistic link between DNA repair fidelity, chromatin integrity, and cancer stemness. The identified vulnerabilities highlight potential therapeutic targets for BRCA1-deficient ovarian and breast cancers.

#1928 SMARCB1-Mediated chromatin remodeling underlies sex differences in gliomagenesis.

Adham Halaoui, Najla Kfoury-Beaumont, Thomas Beaumont

UCSD Medical Ctr., San Diego, CA

Glioblastoma (GBM), the most prevalent primary malignant brain tumor has significant sex disparities with a higher incidence and poorer prognosis in males. SMARCB1 is a key component of SWI/SNF chromatin remodeling complexes, including canonical BAF (BAF) and polybromo-associated BAF (PBAF), and has been shown to have tumor-suppressive functions in a wide range of cancers. Using a panel of 20 human glioma samples, we have shown that SMARCB1 expression is significantly downregulated in GBM compared to IDH wild-type gliomas. However, its role in GBM development remains unclear. Using a murine model of GBM, we performed SMARCA4 immunoprecipitation coupled with mass spectrometry in syngeneic male and female tumor cells and demonstrated BAF complex assembly. We then performed knockdown (KD) of SMARCB1 using CRISPR CRISPRi in male and female tumor cells. Growth assays revealed strong sex-dependent differences, as depletion of SMARCB1 markedly increased proliferation and clonogenic potential in male cells, while having the opposite effect in female cells. RNA-seq analysis uncovered sex-specific transcriptional reprogramming following SMARCB1 knockdown. Gene set enrichment analyses revealed strong enrichment (NES = 2.08-2.19, FWER < 0.001) in proliferation- and oncogenesis-associated pathways in male tumor cells, and an inflammatory pathway (NES = 1.73-2.72, FWER = 0) in female cells. Additionally, we observed pronounced sex-dependent expression in O-6-methylguanine-DNA methyltransferase (MGMT) gene expression wherein male cells displayed three-fold higher MGMT expression compared to females. Importantly, SMARCB1 KD further amplified this sex-biased MGMT expression. Based on this observation, we treated male and female tumor cells with Temozolomide (TMZ), the standard-of-care chemotherapy for patient with GBM and performed a metabolic viability assay. Consistent with the expression profiling data, female cells exhibited a 25 % greater reduction in metabolic activity following TMZ treatment than their male counterparts, indicating heightened intrinsic sensitivity. MGMT expression levels correlate with the relative TMZ resistance of male cells, implicating a potential sex-specific response to treatment. To further assess sex-specific SMARCB1 function at the epigenetic level, we performed ATAC-seq and ChIP-seq experiments on male and female control and SMARCB1 KD GBM cells. These experiments demonstrated increased chromatin access at the MGMT locus in male cells and facultative heterochromatin in female cells. Additionally, 3D-genome studies using HiC are underway to identify sex-specific topographical associated domains (TADs). Collectively, our data underscore an important sex-specific role for SMARCB1 in GBM tumorigenesis and identifies a potential new biomarker for TMZ responsiveness during treatment.

#1929 Stag2-cohesin mediates 3d genome dynamics to regulate MYCN driven oncogenic transcriptome in neuroblastoma..

Jee-Youn Kang[1], Kaitlyn Tremble[2], Zhihui Liu[3], Carol J. Thiele[2]

[1]Pediatric Oncology Branch, National Cancer Institute, Center for Cancer Research, Bethesda, MD,[23]Staff Scientist, Pediatric Oncology Branch, NCI-CCR, Bethesda, MD

Neuroblastoma(NB) is characterized by an abnormal transcriptome driven by a network of core regulatory circuitry (CRC) transcription factors (TFs) and cell type-specific enhancer landscapes. Neuroblastoma arises due to defects in cellular differentiation, either through a failure to terminally differentiate or a reversion to a pluripotent-like state. While CRC TFs are known to bind cell type-specific enhancers and promoters to define transcriptomes necessary for proper differentiation, their functional interplay with 3D nuclear architectural proteins, such as cohesin (comprising SMC1A, SMC3, RAD21, and STAG1 or STAG2), remains largely unexplored. 3D genome organization plays a critical role in defining the cell type-specific transcriptional landscape by facilitating enhancer-promoter looping, which undergoes dynamic rewiring during differentiation. Beyond their canonical roles in DNA replication and repair, cohesin mediates chromatin looping between enhancers and promoters, enabling precise regulation of target gene expression. Understanding how CRC TFs collaborate with cohesin to establish and maintain NB-specific transcriptional programs could provide valuable insights into the mechanisms underlying neuroblastoma pathogenesis and differentiation defects. **To define roles of STAG1- and STAG2-cohesin in MYCN target regulation**, genome-wide RNA-seq and ChIP-seq analyses were performed to uncover the distinct yet overlapping roles of these complexes in regulating the oncogenic transcriptome of NB cells. STAG1 Knockdown (KD) has minimal impact on NB cell proliferation or transcriptional activity. In contrast, STAG2 KD reduces cell proliferation, accompanied by downregulation of MYCN target genes and upregulation of neuronal differentiation genes. Genome-wide ChIP-seq analysis revealed that MYCN/STAG1 peaks are associated with promoters of canonical MYCN target genes. In contrast, MYCN/STAG2 peaks are primarily associated with promoters and enhancers of neural differentiation genes. STAG2 KD decreases chromatin-bound MYCN, particularly at enhancers and promoters, with no change in total MYCN protein levels. This reduction correlates with the observed downregulation of MYCN target genes. In contrast, STAG1 KD does not affect MYCN chromatin binding. Ectopic induction of MYCN in MYCN-nonamplified SHEP cells significantly increased STAG2 chromatin binding, whereas STAG1 binding remains unchanged. In contrast, chromatin-bound STAG1 and STAG2 levels remained unaffected by MYCN KD despite the reduction in their total protein levels. These findings underscore the critical role of STAG2-cohesin in sustaining the NB oncogenic transcriptome by selectively modulating MYCN chromatin binding. This study highlights STAG2-cohesin's functional specialization, establishing it as a pivotal regulator of cohesin dynamics and NB transcriptional programs.

#1930 Unveiling ecDNA spatial organization and epigenetic landscapes through long-read multi-omic sequencing and high-content microscopy.

Yanbo Wang[1], Xiaowei Yan[2], Natasha E. Weiser[2], Shu Zhang[2], Ivy Tsz-Lo Wong[2], Yung-Hsin Huang[1], Rui Li[3], Nicolas Altemose[4], Paul S. Mischel[1], Howard Y. Chang[5]

[1]Stanford University School of Medicine, Stanford, CA,[2]Department of Pathology, Stanford University School of Medicine, Stanford, CA,[3]Center for Personal Dynamic Regulomes, Stanford University, Stanford, CA,[4]Department of Genetics, Stanford University School of Medicine, Stanford, CA,[5]Amgen, Stanford, CA

Oncogene amplification is one of the most common genetic alterations in cancer, playing a central role in tumorigenesis. A major mechanism of oncogene amplification is extrachromosomal DNA (ecDNA), which is present in nearly 20% of cancer patients and found across half of all cancer types. Patients with ecDNA-positive tumors have significantly shorter survival compared to those without ecDNA. Despite its prevalence and strong association with poor treatment outcomes, there is no approved treatment targeting ecDNA-positive cancers. Developing such treatments requires identifying unique and actionable features of ecDNA.

Two unique features of ecDNA warrant special attention because they are seemingly paradoxical. On one hand, proliferation of cancer cells depends on high-level oncogene expression from ecDNA. On the other hand, ecDNA molecules preferentially cluster at the nuclear periphery, a region typically associated with transcriptional repression. Why would cancer cells position most of their ecDNA at the nuclear periphery? What molecular mechanisms control this localization, and what are its functional consequences? These are longstanding questions in the field that have remained unanswered largely due to the lack of experimental approaches capable of deciphering the molecular heterogeneity of ecDNA and linking its spatial organization to oncogene expression.

To fill the technical gap and answer these fundamental ecDNA biology questions, we developed DINO-seq, a long-read single-molecule sequencing technology that enables simultaneous profiling protein binding, DNA accessibility and CpG methylation on individual ecDNA molecules. Using DINO-seq, we discovered that ecDNA carries a bivalent epigenetic landscape—coexisting active and repressive epigenetic marks—that is distinct from chromosomal DNA and enables ecDNA to remain transcriptionally active even at the nuclear periphery. Combining a CRISPR screen with high-content microscopy, we further identified molecular anchors that tether ecDNA to the nuclear periphery. Functionally, we show that peripheral ecDNA localization alters replication timing, promotes ecDNA hub formation, and enhances RNA transcription and export. Together, these findings reveal that ecDNA possesses unique spatial and epigenetic properties that distinguish it from chromosomal DNA and represent potential vulnerabilities that could be exploited to target ecDNA-positive cancers.

#1932 TIP-ChIP: Tagmented, indexed and pooled ChIP-seq to generate high-throughput, multi-sample results for low input samples.

Sarah Traynor[1], Shuxiong Wang[1], Shakiba Mahmoudi[1], Sumati Gonuguntla[1], Justin Cayford[2], Theresa K. Kelly[3], Brian Egan[1]

[1]Active Motif, Carlsbad, CA,[2]Volition, Carlsbad, CA,[3]Pictor, Carlsbad, CA

Epigenetic profiling approaches have greatly expanded our understanding of the mechanisms underlying gene regulation and disease. Histone modifications and transcription factors play a crucial role in chromatin organization and transcriptional control, with dysregulation often linked to various pathological conditions. Chromatin immunoprecipitation followed by sequencing (ChIP-seq) remains the gold standard for genome-wide mapping of histone modifications; however, its high input requirements, susceptibility to batch effects, and labor-intensive workflow limit its scalability and efficiency. Here we present Tagmented, Indexed and Pooled ChIP (TIP-ChIP), a high-throughput alternative that enables the simultaneous profiling of histone modifications and transcription factors across up to 96 samples in a single reaction. This method substantially reduces batch effects, enhances reproducibility, and requires significantly lower input material compared to conventional ChIP-seq. Furthermore, the streamlined workflow can be completed in as little as 3 days, minimizing hands-on time and reducing overall costs while maintaining high sensitivity and resolution. By leveraging an optimized plate-based workflow and a tagmentation barcoding strategy that enables pooling, our method allows for efficient sample multiplexing without compromising data quality. To validate its performance, we apply this approach across multiple cell types, including human primary cells, and demonstrate strong concordance with conventional ChIP-seq for both histone modifications and transcription-factor targets. Further, TIP-ChIP captured dynamic chromatin and transcriptional responses in LPS-stimulated THP-1 cells, revealing time-resolved changes in H3K27ac, H3K4me3, RNA polymerase II Ser2P, and NF-κB (p50). This advancement makes large-scale epigenomic and TF-profiling studies more accessible and cost-effective, enabling the investigation of regulatory dynamics across diverse biological contexts with unprecedented efficiency

#1933 Pan-cancer 3D genomic analysis revealed extremely long Polycomb loops as the biomarker for sensitivity to Polycomb inhibition.

Zhong Fan[1], Sean Moran[2], Miriam Zanovello[1], Jie Liu[2], Chao Lu[3], **Xiaotian Zhang**[1]

[1]Biochemistry and Molecular Biology, University of Texas Health Science Center At Houston, Houston, TX,[2]University of Michigan, Ann Arbor, MI,[3]Columbia University Irving Medical Center, New York, NY

Polycomb targeted loci form long-range chromatin interactions independent of CTCF-cohesion and are demarcated by low DNA methylation. Polycomb targets form extremely long-range loops (long Polycomb loops) that can span up to 60 Mb. These loops predominantly occur in cells of self-renewal status, such as human hematopoietic stem cells (HSC) and mouse embryonic stem cells (ESC). But it was rarely studied in any cancers, in which extensive epigenetic alterations of DNA hypermethylation and loss of Polycomb binding occurs at Polycomb target loci.To identify long Polycomb loops in cancer, we initiated a pan-cancer survey of long Polycomb loops in a collection of 247 tumor samples (33 acute myeloid leukemias, 29 Breast cancer samples, 63 pediatric brain tumors, 70 prostate cancers, and 42 colon cancers). We found most cancers, displayed reduced levels of long Polycomb interactions in comparison with the normal HSC. Solid tumors including all prostate cancers and colon cancers, lack detectable level long Polycomb loops. Additionally, the long Polycomb loop signals are the weakest in cancer cell lines. Pediatric brain tumors and certain AMLs however displayed high long Polycomb loops similar or even stronger than HSC. In pediatric brain tumors, we found the over 20% ependymoma PFA subtypes (in which EZHIP over expression drives Polycomb protein segregation at the canonical Polycomb target loci) notably displayed strong long Polycomb loop interactions with low differentiation. AML displayed more diverse levels of long Polycomb loop interactions. Most AMLs lost both long Polycomb loops with Polycomb binding loss at the loop anchors. Whereas 10% of AMLs retain long Polycomb loops as strong as in HSCs. These AMLs recurrently carry mutations in *CEBPA* and *STAG2*, which are not associated with the Polycomb complex or DNA methylation machinery. Further, while the normal HSC and developing brains contain strong long Polycomb loop, such signal is undetectable in normal colon, suggesting the strong long Polycomb loop is inherited from the tissue of origin. The deletion or inhibition of Polycomb repressive complex (PRC) 1/2 have been shown to eradicate the long Polycomb loops. We found that long Polycomb loop strong AML is sensitive to PRC2 key enzyme EZH2 inhibition, which inhibits cell cycle and induces cell differentiation. Conversely, CRISPR DepMap PRC1 component dependency can be used to predict long Polycomb loop formation in cell lines, identifying cell lines with rare occurrence of long Polycomb loops. Our analysis suggests that the oncogenesis process antagonizes the long Polycomb loop maintenance in most cancers, yet certain cancers may still preserve strong long Polycomb loops from cell-of-origin. The maintenance of long Polycomb loops sensitizes cells to Polycomb inhibition, indicating that such loops could be an epigenomic biomarker for pharmacological or genetic Polycomb inhibition.

#1934 The relationships between the stability of the +1 nucleosome and DNA superhelicity.

Peter Nanasi Jr.[1], Laszlo Imre[1], Istvan Szatmari[2], Viktor Dombradi[3], **Gabor Szabo**[1]

[1]Biophysics and Cell Biology, University of Debrecen, Debrecen, Hungary,[2]Biochemistry and Molecular Biology, University of Debrecen, Debrecen, Hungary,[3]Medical Chemistry, University of Debrecen, Debrecen, Hungary

When the effect of various posttranslational histone tail modifications (PTMs) on nucleosome stability was compared in an *in situ* assay involving agarose-embedded nuclei, a subpopulation of the promoter proximal H3K4me3, H3K27ac positive nucleosomes exhibited relative sensitivity to intercalators as compared to bulk H3-GFP or nucleosomes carrying any of the following marks: H3K27me1, H3K27me2, H3K27me3, H3K9me1, H3K9me2, H3K9me3, H3K36me3, H3K4me0, H3K4me1, H3K4me2, H3K9ac, and H3K14ac. Nickase or DNase I treatment of the nuclei, or bleomycin treatment of live cells, did not affect the stability of nucleosomes carrying H3K4me3 or H3K27ac, while those of the second group were all destabilized upon treatment with intercalators. These observations support the possibility that the promoter proximal marks specifying dynamic nucleosomes are juxtaposed with relaxed DNA sequences due to DNA breaks generated *in vivo*. In line with this interpretation, endogeneous, 3'OH nicks were mapped within the nucleosome free region of promoters in human mononuclear cells as well as in mES. We also present evidence that the chromatin regions harboring the breaks are topologicaly separated from the domains containing superhelical chromatin. Regarding the mechanism eliciting the breaks, two alternative models were tested experimentally using kncok out cells, inhibitors and degrader systems, based on TOP2 activity or on histone demethylation induced oxydative DNA lesions and their repair. These observations lend support for a model where the role of DNA strand discontinuities in transcriptional regulation and in higher-order chromatin organization are integrated. Grants: OTKA/NKFIH 138524, ERA-Net NEURON 2024-1.2.2-ERA_NET-2024-00009 *PN and LI contributed equally

#1936 Druggable dependency on histone demethylase LSD1 in MITF-low therapy resistant melanoma.

Shinichiro Kato[1], Anlun Xu[1], Hongyan Xie[2], Simone Sidoli[3], Genevieve Boland[2], Russel W. Jenkins[4], Dave S. B. Hoon[5], Hiroyoshi Nishikawa[6], David E. Fisher[2]

[1]Kyoto University, Kyoto, Japan,[2]Massachusetts General Hospital, Boston, MA,[3]Albert Einstein College of Medicine, Bronx, NY,[4]Medical University of South Carolina, Charleston, SC,[5]Saint John's Cancer Institute, Santa Monica, CA,[6]National Cancer Center Japan, Tokyo, Japan

Acquired and intrinsic resistance to targeted and immune therapies in melanoma is associated with an undifferentiated, mesenchymal-like tumor cell state characterized by low expression of the melanocytic lineage regulator MITF and high expression of the receptor tyrosine kinase AXL. Because MITF governs lineage-specific survival and differentiation programs, therapy-resistant MITF-low/AXL-high melanomas appear to evade these programs and instead depend on alternative survival mechanisms. To uncover such dependencies, we systematically interrogated genome-scale CRISPR-Cas9 knockout screens from the Cancer Dependency Map and identified a selective vulnerability to the epigenetic regulator lysine-specific demethylase 1 (LSD1/*KDM1A*). Intriguingly, domain-focused CRISPR screening spanning whole LSD1 coding locus further revealed that this dependency is mediated through non-catalytic, scaffold-like functions of LSD1 rather than its demethylase activity. Mechanistically, integrated LSD1 ChIP-seq, histone ChIP-seq (H3K4me1/2/3 and H3K27ac) and RNA-seq analyses demonstrated that LSD1 sustains a survival program characterized by chromosome segregation and neuronal dedifferentiation in MITF-low melanoma, orchestrated through distinct super-enhancer activation at key regulators, such as CDC6, related to these pathways. Disruption of LSD1's non-catalytic activity by a LSD1 allosteric inhibitor induced G2/M arrest, transcriptional reprogramming, and growth inhibition selectively in MITF-low melanomas via downregulation of CDC6. Strikingly, genetic and pharmacological ablation of LSD1's non catalytic function significantly prevented or delayed the emergence of resistance to BRAF inhibition and anti-PD-1 therapy in vitro, in vivo, and in patient-derived melanoma organoids. Furthermore, pan-cancer analyses revealed a similar LSD1 dependency in other poorly differentiated malignancies, including pancreatic cancer, that share an undifferentiated transcriptional state. Collectively, these findings define an epigenetically determined, therapeutically targetable state that underlies treatment resistance across multiple cancer types. By targeting the non-catalytic scaffolding function of LSD1, either alone or in combination with targeted and immune therapies, it may be possible to eradicate undifferentiated, drug-tolerant tumor cell populations and overcome therapeutic resistance in melanoma and other aggressive cancers.

#1937 FOXK2^{+} malignant epithelial cells promote platinum resistance via KANSL1-MOF-mediated redox sustaining mechanism in ovarian cancer.

junzui li, Hao Huang, Yinu Wang, Didi Zha, Shannon Glynn, Ujin Kim, Jennifer Heo

Northwestern Univ. Feinberg School of Medicine, Chicago, IL

Platinum resistance remains a major obstacle in ovarian cancer therapy, yet the molecular programs that enable malignant cells to maintain redox balance and survive oxidative stress remain incompletely defined. Through integrated analyses of bulk RNA-seq, spatial transcriptomics, and single-cell datasets, we identify a distinct FOXK2-positive epithelial cancer population that is reproducibly detected across multiple patient cohorts. This FOXK2-high malignant cell state expands after chemotherapy, preferentially accumulates in recurrent and platinum-resistant tumors, and is consistently associated with inferior patient survival, indicating a potential role in therapy failure. Functional studies demonstrate that FOXK2 is required to maintain redox resilience in ovarian cancer cells. FOXK2 depletion increases intracellular ROS, disrupts mitochondrial respiration, and markedly sensitizes both in vitro cultures and in vivo xenografts to platinum treatment. These vulnerabilities are reversed by antioxidant supplementation, supporting a causal link between FOXK2 loss, ROS accumulation, and enhanced chemosensitivity. To uncover the molecular mechanism underlying FOXK2-mediated redox control, we performed immunoprecipitation-mass spectrometry and identified a previously unrecognized physical interaction between FOXK2 and the KANSL1-MOF chromatin-remodelling complex-an association not previously linked to redox biology, stress adaptation, or chemoresistance in ovarian cancer. FOXK2 leverages this newly defined interaction to recruit KANSL1-MOF to antioxidant gene promoters and enhancers, including SLC7A11, GCLC, and GPX2. This recruitment maintains H4K16 acetylation, preserves chromatin accessibility, and sustains transcriptional activation of key antioxidant programs. Loss of KANSL1 phenocopies FOXK2 depletion, leading to ROS accumulation and heightened platinum sensitivity, establishing KANSL1 as a critical FOXK2-dependent cofactor. Strikingly, this regulatory system is responsive to oxidative stress. Exposure to ROS increases FOXK2 and KANSL1 protein levels and enhances FOXK2-KANSL1 binding, creating a self-reinforcing, redox-sensitive positive feedback loop that sustains antioxidant capacity under therapeutic stress. Together, our findings reveal a therapy-selected FOXK2-positive malignant cell state and uncover a novel epigenetic FOXK2-KANSL1-MOF axis that couples chromatin remodeling to redox homeostasis and platinum resistance in ovarian cancer. Targeting FOXK2-high cellular states or disrupting their chromatin-associated cofactor network may offer a therapeutic strategy to overcome chemoresistance.

#1938 Epigenetic regulation of histone lysine demethylase 4B on cancer therapy in tamoxifen-sensitive and -resistant breast cancer cells.

Tian Zheng, Ju Ri Kim, Hyun Ji Noh, Hyung Sik Kim

Sungkyunkwan University College of Pharmacy, Suwon, Korea, Republic of

Background: Histone lysine demethylase 4B (KDM4B), a key histone lysine demethylase, is aberrantly overexpressed in breast cancer and functions as an essential epigenetic co-activator of ERα signaling. Although its oncogenic role in breast tumorigenesis has been established, the functional distinctions and underlying molecular mechanisms of KDM4B in tamoxifen-sensitive versus tamoxifen-resistant states remain poorly defined. Elucidating KDM4B's contribution to the evolution of endocrine resistance will be critical for identifying novel therapeutic targets and advancing precision strategies to overcome resistance to endocrine therapy.
Methods: KDM4B expression across human cancers and normal tissues was evaluated using TCGA and GTEx datasets. To investigate its functional role, we compared the effects of KDM4B modulation in ERα-positive MCF-7 cells and their tamoxifen-resistant derivative, MCF-7 TamR. KDM4B was suppressed either by siRNA-mediated knockdown or by pharmacological inhibition using the selective KDM4B inhibitor B3. Cell proliferation was measured through MTT and colony formation assays. Protein expression levels of ERα, Bcl-2, H3K9me3, Cyclin D1, c-Myc, and related signaling molecules were examined via Western blotting. Cell-cycle progression and apoptosis were analyzed using flow cytometry. Metabolic reprogramming was evaluated using the Seahorse glycolytic stress test.
Results: TCGA and GTEx analyses revealed that KDM4B is significantly overexpressed in breast cancer compared with normal breast tissue. Consistently, KDM4B levels were markedly elevated in tamoxifen-resistant MCF-7 (TamR) cells relative to parental MCF-7 cells. Suppression of KDM4B through siRNA-mediated knockdown or pharmacological inhibition substantially reduced the proliferative capacity and colony-forming ability of both MCF-7 and TamR cells. KDM4B depletion restored H3K9me3 enrichment, decreased ERα expression, and induced G1/S cell-cycle arrest. In addition, metabolic profiling demonstrated that KDM4B inhibition attenuated glycolytic activity, indicating a role in metabolic reprogramming.
Conclusion: KDM4B serves as a critical epigenetic regulator in both tamoxifen-sensitive and tamoxifen-resistant ERα-positive breast cancer. Inhibition of KDM4B restores repressive histone marks, suppresses ERα-dependent transcription, and attenuates cellular proliferation and metabolic activity. The heightened dependence of tamoxifen-resistant cells on KDM4B further underscores its potential as a promising therapeutic target for overcoming endocrine therapy resistance.

#1939 Oncogenic NSD2 drives Eph-ephrin signaling between myeloma and bone marrow stromal cells.

Austin Boese[1], Lindsey Rosas Togo[2], Qing Wu[1], Bethany Kaplan[1], Sungmi Park-Chouinard[2], Jonathan D. Licht[3], Ho Man Chan[2], Lisa Drew[1], Omid Tavana[1], Neeraj Aryal[1], Jessie Hao-Ru Hsu[1]

[1]Hematology Discovery R&D, AstraZeneca, Waltham, MA,[2]Oncology Targeted Discovery, AstraZeneca, Waltham, MA,[3]University of Florida Health Cancer Center, Gainesville, FL

The t(4;14) translocation occurs in 15-20% of multiple myeloma cases and upregulates the histone methyltransferase NSD2 to drive oncogenic transcriptional dysregulation. Patients with t(4;14)+ myeloma are high risk with shorter survival and higher incidence of bone lesions when compared to patients with other cytogenetic subtypes, suggesting an oncogenic role of NSD2. Counterintuitively, under standard culture conditions, NSD2 knockout in t(4;14)+ models only demonstrated a modest growth inhibition phenotype. Therefore, we hypothesized that oncogenic NSD2 epigenetically modulates signaling between myeloma cells and the bone marrow microenvironment (BMME) to drive myeloma progression. To test this, we utilized both pharmacological inhibition and CRISPR/Cas9 knockout of NSD2 in human myeloma cells lines with varying genetic backgrounds. We assessed proliferation and viability under standard conditions, in co-culture with bone marrow stromal cells (BMSCs), or in BMSC-conditioned media. BMSC co-culture or exposure to BMSC-conditioned media strikingly increased the sensitivity of myeloma lines to NSD2 inhibition, thereby supporting our hypothesis. RNA-sequencing and pathway analysis revealed that oncogenic NSD2 regulates Eph-ephrin signaling, and epigenetic profiling showed NSD2-dependent remodeling of H3K36me2 and H3K27me3 at corresponding Eph-ephrin genomic loci in myeloma cells, suggesting a direct regulation by NSD2. To assess the importance of ephrin receptor signaling between myeloma cells and the BMME, we conducted CRISPR/Cas9 knockout of Eph-ephrin genes and assessed myeloma growth and viability. CRISPR/Cas9 knockout of Eph-ephrin signaling genes caused significantly stronger growth inhibition of myeloma cells with oncogenic NSD2 status in BMSC-conditioned media, while overexpression of ephrin receptor partially rescued the growth defect of NSD2 knockout myeloma cells in BMSC-conditioned media. To assess the clinical relevance of our findings, we analyzed publicly available data from the MMRF CoMMpass patient cohort, which confirmed higher tumor expression of Eph-ephrin genes in t(4;14)+ myeloma patients, correlating with inferior overall and progression-free survival. These findings implicate Eph-ephrin signaling as a key mediator of t(4;14)+ myeloma biology and an attractive therapeutic target. In summary, oncogenic NSD2 reshapes the chromatin of myeloma cells to promote Eph-ephrin signaling, thereby conferring bone marrow microenvironment-dependent fitness in t(4;14)+ multiple myeloma. These data highlight Eph-ephrin signaling as an actionable therapeutic pathway for t(4:14)+ and NSD2 mutant myeloma.

#1940 Dissecting the function of NSD1 in intestinal epithelium and inflammation.

Arum Kim, G Greg Wang

Duke University School of Medicine, Durham, NC

NSD1 (nuclear receptor-binding SET domain protein1, KMT3B) is a histone H3 lysine 36 methyltransferase, which is critical to normal growth and development, and its loss-of-function mutation causes Sotos syndrome, a genetic disorder characterized by overgrowth in childhood, a distinctive facial appearance and developmental delay. Given the prior reports showing that NSD1 decreases H3K27ac at active enhancers and that the H3K27 is associated with intestinal inflammation, we here show that NSD1 maintains intestinal epithelial integrity and inhibits intestinal inflammation in a mouse model that mimics the symptoms and pathology of ulcerative colitis (UC) in humans. Specifically, intestinal epithelial cell (IEC)-specific Nsd1 KO mouse exhibits a significant decrease in antimicrobial peptides (AMPs) genes, which are essential to maintain intestinal homeostasis and mediate epithelial host defense against infection. Collectively, this work uncovered the function of NSD1 in intestinal epithelium sustaining intestinal integrity and protecting that from damage-induced inflammation, which may contribute to prevent the development of GI (gastrointestinal) malignancy caused by chronic intestinal inflammation.

#1941 KMT2D loss drives gastric cancer tumorigenesis through an RCOR3-dependent mechanism.

Liyong Zeng, Fang Cao, Calena J. Brown-Abel, Aryana S. Bhati, Bansi R. Vanparia, Melissa P. Pizzi, Yibo Fan, Gengyi Zou, Tanaya S. A. Washington, Johnson Amoah, Shay Patel, Arman Dhar, Elisha Deewan, Feng Yin, Yuan-Hung Lo, Min Gyu Lee, Jaffer A. Ajani, Shilpa S. Dhar

GI Medical Oncology, The University of Texas MD Anderson Cancer Center, Houston, TX

Gastric adenocarcinoma remains a major cause of cancer mortality worldwide. KMT2D, a histone H3K4 methyltransferase, is recurrently altered across solid tumors, yet its role in gastric cancer is not fully defined. We show that KMT2D expression is frequently reduced in gastric tumors, and its loss correlates with significantly poorer overall survival, independent of sex or age. KMT2D-negative tumors exhibit markedly higher EGFR expression compared with KMT2D-positive tumors. Functionally, KMT2D knockdown promotes gastric cancer cell proliferation, migration, invasion, and tumor growth, whereas KMT2D reconstitution suppresses tumor progression in a KMT2D-null model. Conditional Kmt2d deletion in mouse stomach induces gastric enlargement and dysplasia, and Kmt2d-deficient gastric organoids develop low-grade dysplasia with increased proliferation. Mechanistically, KMT2D loss downregulates key transcriptional corepressors, including NCOR2 and RCOR3, leading to activation of multiple oncogenic pathways. KMT2D directly binds and catalyzes H3K4 methylation at the RCOR3 enhancer, supporting its regulatory role. Collectively, these findings define a mechanistic basis for KMT2D loss in gastric tumorigenesis and highlight its potential as a diagnostic biomarker.

#1942 MIRAGE: A ctDNA methylation-driven computational algorithm designed for sensitive detection of minimal residual disease.

Gowhar Shafi, Aarthi Ramesh, Sandhya Iyer, Aparna Sornapudi, Alain D'Souza, Sumit Halder, Bhagwat Jadhav, Sangeeta Prajapati, Mohan Uttarwar

OneCell Diagnostics India Private Limited, Pune, India

Background: Detection of minimal residual disease (MRD) following surgical resection or a treatment regimen remains a significant clinical challenge, primarily due to the typically low concentrations of circulating tumor DNA (ctDNA) in the bloodstream post-treatment. In situations where circulating tumor cells (CTCs) are undetectable or ctDNA levels fall below the thresholds of conventional detection methods, DNA methylation analysis has emerged as a promising alternative. Utilizing computational algorithms further improve the detection of tumor signal in cancers with as low as 0.001% circulating tumor fraction.
Methods: MIRAGE (Minimal Residual Assessment using Genome-wide Epigenomics) algorithm was validated using 156 samples, among which 16.7% (n=26) were control reference samples. The algorithm assessed DNA methylation patterns across genome-wide differentially methylated regions (DMRs). The algorithm quantifies methylation by evaluating the number of methylated and unmethylated cytosines at each CpG site and integrating these values into a composite methylation score, reflecting overall hyper- or hypomethylation. The resulting methylation score is further normalized against a predefined cut-off established from a reference cohort of non-cancerous healthy individuals to enable standardized interpretation.
Results: MIRAGE achieved a specificity of 96.8% from 127 clinical samples (64 tumor, 63 non-cancerous healthy controls) tested. Among the clinical tumor samples, 64% (n=41/64) were detected as ctDNA-positive which showed an overall sensitivity of 64.1%.
Conclusion: The study demonstrates the specificity of MIRAGE algorithm for ctDNA classification-based minimal residual detection with high specificity. Further validation on larger cohort is still warranted to show more clinical insights.

#1943 Epigenomic evolution during tumorigenesis in colorectal cancer.

Chang Hyun Nam[1], Yunah Lee[1], Yeonjin Kim[1], Hyein Won[1], Jinhee Ryu[1], Ji Won Park[2], Seung-Yong Jeong[2], Min Jung Kim[2], Young Seok Ju[1]

[1]Korea Advanced Institute of Science and Technology, Daejeon, Korea, Republic of,[2]Department of Surgery, Seoul National University College of Medicine, Seoul, Korea, Republic of

Cancer cells exhibit distinct features compared with normal cells, such as genomic instability and phenotypic plasticity. Growing evidence suggests that epigenomic reprogramming during tumorigenesis, in addition to genomic mutations, plays a critical role in establishing cancer hallmarks. However, the genome-wide landscape of epigenomic alterations and the interplay among the genome, epigenome, and transcriptome during tumorigenesis remain poorly understood, particularly at single-cell resolution. Here, we investigated the genome, DNA methylome, and transcriptome of 129 single-cell-derived cancer clones and 142 single-crypt-derived matched normal clones from 13 patients with colorectal cancer. Compared with normal clones, in which ~75% of CpG sites were fully methylated, cancer clones exhibited pervasive global demethylation, with only ~50% of CpGs remaining fully methylated. We estimated the somatic epimutations using the consensus methylation states of normal clones and found that, on average, 7.5 million CpG sites (~25% of all CpGs) were demethylated in cancer clones. The burden of somatic demethylation increased linearly with the endogenous somatic SNV burden in cancer, suggesting that widespread demethylation primarily results from imperfect DNMT1-mediated maintenance of DNA methylation. The estimated timing of chromosomal gains inferred from genomic mutations and CpG demethylation was largely consistent, supporting the clock-like accumulation of demethylation across broad genomic regions during tumorigenesis. Interestingly, promoter CpG methylation was slightly increased in cancer compared with normal clones, despite pervasive demethylation. We identified genes with differentially methylated promoters, including hypermethylated tumor-suppressor genes and hypomethylated oncogenes, and correlated these methylation changes with gene-expression profiles, supporting their role as driver epimutations. In addition, despite the activation of L1 elements during tumorigenesis, demethylation rates in L1HS promoters were lower than in the rest of the genome in both normal and cancer clones, suggesting that L1 activation in cancer is a passive consequence of global demethylation rather than an active regulatory process. Overall, our single-cell multi-omics analysis provides a comprehensive view of epigenomic reprogramming during tumorigenesis and offers valuable insights into how epigenomic alterations contribute to cancer hallmarks.

#1944 Hypermethylation of Sox21 masks its oncogenic role in glioblastoma.

Shu-Huei Hsiao, Jui-Ming Sun, Tun-Wu Wang, Yu-Wei Leu, and Shu-Huei Hsiao

Biomedical Sciences, National Chung Cheng Univ., Chiayi County, Taiwan

The transcription factor Sox21, a member of the SRY-related HMG-box (SOX) family, is known to promote neuronal differentiation and regulate stem cell function; however, its role in brain tumors remains largely unexplored. Because epigenetic dysregulation contributes to aberrant gene expression and malignant progression, we aimed to elucidate the expression and function of Sox21 in U87 human glioblastoma cells. A marked reduction in Sox21 mRNA and protein expression was observed by RT-PCR and Western blot analysis. Methylation-specific PCR (MSP) and bisulfite sequencing further revealed that the Sox21 promoter is hypermethylated, indicating that Sox21 expression is epigenetically regulated in U87 cells.To determine the functional consequences of restoring Sox21, U87 cells were transfected with a Sox21-expressing vector, resulting in a robust increase in Sox21 expression. Forced Sox21 expression significantly enhanced cell proliferation, as shown by MTT assays and flow cytometry, and was accompanied by a decreased proportion of cells in the sub-G1 phase, suggesting a growth-promoting role for Sox21 in glioblastoma cells. In addition, Sox21 overexpression accelerated cell migration, as demonstrated by wound-healing and transwell assays.These findings indicate that Sox21 downregulation in glioblastoma is mediated, at least in part, by promoter hypermethylation. However, restoring its expression facilitates tumor cell growth and migration. Collectively, our results demonstrate that Sox21 functions as an oncogene that is epigenetically silenced through promoter hypermethylation in glioblastoma.

#1945 Epigenetic silencing of ESR1 in primary breast tumors from young women compared to those from older women: An integrative methylation and expression analysis.

Praveen Kumar Raj Kumar[1], Anupama Praveen Kumar[1], Mariano Russo[1], Jianfang Liu[1], Craig D. Shriver[2], Hai Hu[1], Xiaoying Lin[1]

[1]Bioinformatics, Chan Soon-Shiong Institute of Molecular Medicine at Windber, Windber, PA,[2]Uniformed Services University, Bethesda, MD

Young women with primary breast cancer (<40 years) often present with more aggressive disease and show lower estrogen receptor alpha (ESR1) expression than older women (≥60 years), but the underlying mechanisms remain unclear. We hypothesized that DNA methylation contributes to ESR1 repression in tumors from young women. We analyzed TCGA-BRCA HumanMethylation450 data from 108 primary tumors (54 young, 54 older) matched by PCAPAM50 subtype and race. After preprocessing, the dataset contained 363,870 CpG sites. Differential methylation was performed using limma, adjusting for subtype and race. Gene set enrichment analysis (GSEA) used preranked t-values for 21,582 genes mapped from CpGs. Matched TCGA RNA-seq data were used to evaluate correlations between ESR1 methylation and expression. Validation was conducted using the Lund cohort (GSE75067; n = 61); genome-wide modeling was not feasible due to smaller sample size, so Wilcoxon tests assessed ESR1-associated CpGs. We identified 3,012 differentially methylated CpGs (FDR < 0.05, fold change > 2), with 36 hypermethylated and 2,976 hypomethylated in tumors from young women, indicating a global trend toward higher methylation in older tumors. Among 53 ESR1-associated CpGs in TCGA, seven were significantly hypermethylated exclusively in young luminal tumors and all 7 are significantly hypermethylated in both luminal A/B. Notably, none of the ESR1 CpGs were hypermethylated in older women. ESR1 methylation of these 7 sites was inversely correlated with expression ($\rho = -0.35$ to -0.51), consistent with transcriptional silencing. In the Lund dataset, of 61 ESR1 CpGs, 2 were hypermethylated in young Luminal A and 16 in Luminal B tumors, whereas 1 showed hypomethylation in Luminal B. Of the 7 CpGs hypermethylated in TCGA, one each was significant in young LumA and LumB; others showed similar trends, though not statistically significant, likely due to small sample size. Methylation-based GSEA showed enrichment of hypermethylation within the early estrogen response pathway in the older group, consistent with previous studies reporting heightened estrogen pathway activity in younger women. We report consistent ESR1 promoter hypermethylation in young breast cancer, especially in Luminal A/B subtypes, supported by inverse correlation with transcript levels. These findings suggest that ESR1 silencing is a recurrent feature of young breast tumors and reinforce the potential utility of methylation-based biomarkers for age-stratified cancer profiling. Disclaimer: The contents of this publication are the sole responsibility of the author(s) and do not necessarily reflect the views, opinions or policies of USUHS, HJF, the DoW or the Departments of the Army, Navy or Air Force. Mention of trade names, commercial products, or organizations does not imply endorsement by the U.S. Government.

: DNA Methylation
Poster Session

#1949 Clonal expansion of leukocytes harboring mosaic chromosomal alterations accelerates epigenetic aging and reshapes local DNA methylation.

Corey D. Young[1], Charles Breeze[1], Derek W. Brown[1], Rebecca Lynn Kelly[1], Kara Marie Barnao[1], Aubrey K. Hubbard[2], Amy Hutchinson Hutchinson[1], BELYNDA HICKS[3], Aurelie L. Vogt[3], Wen-Yi Huang[4], Steven C. Moore[1], Stephen J. Chanock[5], Mitchell J. Machiela[6]

[1]Division of Cancer Epidemiology and Genetics, National Cancer Institute, NIH, Rockville, MD,[2]National Cancer Institute, Montgomery Village, MD,[3]Cancer Genomics Research Laboratory, Frederick National Lab for Cancer Research, Fredrick, MD,[4]National Cancer Institute, Bethesda, MD,[5]Sect. Head & Director, CGF/ATC, National Cancer Institute, Rockville, MD,[6]Division of Cancer Epidemiology and Genetics, Division of Cancer Epidemiology and Genetics, National Cancer Institute, NIH, Rockville, MD

Mosaic chromosomal alterations (mCAs), a type of age-related clonal hematopoiesis, arise from postzygotic chromosomal gains, losses, or copy-neutral loss of heterozygosity (CN-LOH) in hematopoietic cells. DNA methylation serves as a molecular measure of biological aging and can be quantified through methylation-based epigenetic clocks. The extent to which mCAs accelerate epigenetic aging or induce local methylation remodeling is poorly understood.
We analyzed 482 cancer-free participants from the Prostate, Lung, Colorectal, and Ovarian (PLCO) Cancer Screening Trial aged 54-77 at sample collection. Selection was based on mCA status (mCA carriers=261), prior genotyping, adequate DNA age and sex. Illumina MethylationEPIC array data raw IDATs were processed using the ChAMP pipeline with BMIQ normalization and ComBat batch correction. Six established methylation clocks (Horvath2013 and 2018, Hannum, PhenoAge, GrimAge, and DunedinPACE) were implemented using the dnaMethyAge R package to compute residual-based age acceleration. Multivariable linear models adjusted for age, sex, ancestry, smoking, and BMI compared mCA carriers to mCA-free individuals, as well as autosomal, mLOY, mLOX, and multi-mCA subtypes. Immune cell composition was estimated with EpiDISH using the IDOL-optimized FlowSorted.BloodExtended.EPIC reference. To identify local methylation effects, ordinary least squares regression tested per-CpG β-values for differential methylation within mCA-affected regions and functional enrichment was performed using Ingenuity Pathway Analysis (IPA).
Across six epigenetic clocks, mCA carriers showed higher epigenetic age acceleration vs mCA-free (e.g., PhenoAge β=3.46, 95% CI 1.670-5.22, $p=1.32x10^{-4}$), with the largest effect sizes observed for autosomal mCAs. Methylation-based deconvolution of whole blood revealed shifts in leukocyte composition, including higher memory B-cell and lower CD4memory-cell proportions in participants with multiple mCAs (B-cell: β=0.024, $p=2.0x10^{-8}$; CD4: β=-0.017, p=0.017). Analyses of methylation levels at each CpG site within mCA regions identified 2,553 significant probes (1,973 hypo- and 580 hyper-methylated) with significant clusters visible across several CN-LOH and Gain regions. IPA revealed subtype-specific pathway perturbations, including growth-factor/GPCR signaling in Loss events , NAD biosynthesis and circadian regulation in CN-LOH, and suppressed interferon and TLR signaling in Gain events, with TGFB1 and TNF emerging as key upstream regulators.
These findings suggest mCAs are associated with accelerated epigenetic aging, altered immune-cell composition, and localized epigenetic remodeling, with subtype-specific pathway disruptions that may reflect distinct compensatory mechanisms permitting clonal expansion in hematopoietic cells.

#1950 Integrated transcriptomic and epigenomic analysis to study the mechanism by which smoke-induced hypomethylation of cg05575921 increases lung cancer risk.

Matthew Gladstone[1], Khoi Huynh[2], Chunli Yan[1], Kimberly D. Siegmund[3], Aram Modrek[2], Ite Offringa[1]

[1]Surgery, Cancer Biology, USC Norris Comprehensive Cancer Center, Los Angeles, CA,[2]USC Norris Comprehensive Cancer Center, Los Angeles, CA,[3]USC, Los Angeles, CA

Lung cancer is the leading cause of cancer death in the US. The most common subtype is lung adenocarcinoma (LUAD), arising out of the alveolar epithelium. Tobacco smoke and pollution play a key role in LUAD risk and have been associated with changes in DNA methylation in numerous epigenome-wide association studies. Hypomethylation of cg05575921 is one of the most significant changes, predicting over 30% of the increased risk of lung cancer seen in smokers. However, the mechanism by which this methylation loss is linked to lung cancer risk remains unknown. We previously showed that cg05575921, located in intron 3 of the gene aryl hydrocarbon receptor repressor (*AHRR*), borders a tobacco smoke-inducible enhancer. Upon smoke exposure *AHRR* is the only gene within a two megabase window whose expression increases. AHRR is a negative feedback regulator of aryl hydrocarbon receptor (AHR) induced detoxification responses. Like AHR, AHRR binds to the partner protein ARNT. However, unlike the AHR/ARNT heterodimer, which turns on detoxification genes, the AHRR/ARNT heterodimer downregulates the detoxification response. We hypothesize that prolonged tobacco smoke exposure triggers maladaptive expression of *AHRR*, that hypomethylation of cg05575921 is a byproduct of the adjacent enhancer activation, and that constitutive expression of *AHRR* prevents protective xenobiotic detoxification responses, thereby increasing lung cancer risk. Using our unique immortalized human alveolar epithelial cells, we are determining what role the enhancer and cg05575921 play in *AHRR* expression by i) using Oxford Nanopore long-read sequencing to study DNA methylation changes in the region over time during tobacco smoke exposure, ii) using CRISPR/Cas 9 to heterozygously delete the known enhancer and/or the CpG to determine the effects on the expression of *AHRR* from the enhancer/CpG-deleted and control alleles, iii) using an inducible *AHRR* gene to test the effects of constitutive expression of *AHRR* on the xenobiotic response genes induced by cigarette smoke. Understanding why cg05575921 hypomethylation is strongly associated with lung cancer risk may help devise strategies to mitigate the effects of smoke exposure.

Supported T31IP1913 from the Tobacco-Related Disease Research Program, an Epigenomic Regulation in Cancer Pilot ward from the USC/Norris Comprehensive Cancer Center, the Norris Comprehensive Cancer Center core grant NIH/NCI P30CA014089, and a Keck School of Medicine Dean's Fellowship. MAG and IAO are members of CaRE^2, the Cancer Research Education and Engagement Health Center, supported by NIH/NCI grants U54CA233396, U54CA233444, and U54233465.

#1951 Non-destructive methylation sequencing enables concurrent detection of genetic and epigenetic variation in FFPE and cfDNA samples.

Max Boeck[1], Jennifer Pavlica[1], Craig MARSHALL[1], Travis Sanders[2], Kristina Giorda[1], Martin Ranik[1], Eduard Casas[1], Thomas D. Harrison[1], Kailee Reed[1], Aaron Garnett[1], Doug Wendel[1], Brian Kudlow[1]

[1]Watchmaker Genomics, Boulder, CO,[2]Travis Sanders (Individual)

Comprehensive tumor characterization increasingly requires both genomic and epigenomic information, yet current methylation profiling methods, such as bisulfite-based workflows, limit sensitivity and accuracy due to DNA degradation and reduced sequence complexity. To address these constraints, we developed an improved positive-conversion chemistry that directly converts methylated cytosines while preserving unmethylated ones to enable simultaneous detection of cytosine modifications and genetic variants from a single NGS library. This approach is designed to support oncology research applications where high accuracy from limited or damaged material, such as FFPE tissue and cell-free circulating tumor DNA (ctDNA), is essential.

To assess performance, FFPE, fresh-frozen, and cfDNA samples were processed using an optimized oxidation–reduction workflow. Libraries were sequenced on standard short-read platforms, and methylation accuracy, F1 scores, CNV concordance, and tumor–normal methylation contrast were evaluated. Performance was compared to whole-genome sequencing (WGS) controls and conventional bisulfite and enzymatic methylation sequencing methods.The chemistry demonstrated efficient reduction of modified cytosines, enabling high-confidence methylation calling with low false positive rates. Sequence complexity was maintained, allowing robust SNV and CNV detection from the same library. FFPE samples exhibited improved CpG coverage, fewer sequence artifacts, and improved library complexity compared to enzymatic methylation sequencing. cfDNA libraries generated from as little as 1 ng yielded reliable global methylation profiles suitable for tissue-of-origin analyses. The nondestructive nature of the chemistry preserved cfDNA fragments, opening the door to fragmentomics analyses. In tumor–normal comparisons, there was clear resolution of differentially methylated regions (DMRs), supporting more precise identification of tumor-specific epigenetic alterations.

This enhanced positive-conversion chemistry enables unified genomic and epigenomic analysis from a single assay, making it highly suited for oncology research applications such as tumor classification, biomarker discovery, minimal residual disease (MRD) assessment, and liquid biopsy. Its gentle conditions, compatibility with degraded FFPE DNA and low-input cfDNA, and ability to capture both methylation and variants position it as a powerful tool for advancing translational research and precision oncology.

#1952 Novel mouse models enabling locus-specific manipulation of DNA methylation.

Julia M. Salamat, Li Yang, Xiaomin Chen, Eduardo Lopez, Lanlan Shen

Baylor College of Medicine, Houston, TX

Introduction: DNA methylation is a key epigenetic mechanism that regulates development and disease, including cancer. However, current tools for precise, locus-specific epigenetic gene editing remain limited. Because phenotypic outcomes often result from interactions among multiple genes, there is a critical need for systems that can modulate methylation across several genomic loci simultaneously. Equally important, tight spatial and temporal control of such epigenetic modulation is essential to accurately dissect causal relationships between DNA methylation and gene function. To address these challenges, we developed mouse models that enable controlled, cell type-specific, and time-dependent epigenetic modulation in vivo.

Methods: We applied the CRISPR-dCas9-SunTag system for targeted DNA methylation editing, using TET1 for demethylation and DNMT3A/3L for methylation. To generate mouse models, we employed homologous recombination to introduce knock-in constructs at genomic safe harbors. Specifically, the dCas9-SunTag-TET1-GFP system was inserted into the Rosa26 locus and the dCas9-SunTag-DNMT3A/3L-mCherry system was integrated into the Hipp11 (H11) locus. Expression of the dCas9-based epigenetic editors was regulated through recombinase systems: Cre or Flp recombination activated expression, while Dre recombination removed the entire construct, thereby terminating expression. Specific guide RNA (gRNAs) directed targeted demethylation or methylation at single or multiple genomic sites.

Results: For both mouse lines, correct knock-in was confirmed by Southern blot and DNA sequencing. Germline transmission was successful, and offspring developed normally with the expected Mendelian ratios. Mouse embryonic fibroblasts (MEFs) derived from these lines were used to validate inducible expression mediated by Cre or Flp recombination. Inducibility was confirmed by Cas9 Western blot, RT-PCR analysis of TET1 or DNMT3A/3L transcripts, and fluorescent reporter expressions. Using gRNA targeting multiple promoters, including tumor suppressor genes p16 and Hic1 and oncogenes Tfap2a and VEGF, we observed robust and site-specific DNA methylation editing. Furthermore, targeted methylation of the p16 promoter in MEFs resulted in transcriptional silencing and bypass of the senescence checkpoint.

Conclusion: We successfully established mouse models that enable precise, locus-specific manipulation of DNA methylation through inducible CRISPR-dCas9-SunTag-based epigenetic editing. These models provide a versatile platform for dissecting the causal relationships between DNA methylation and gene function in vivo. Given their flexibility and inducible control, these systems will be broadly applicable to researchers investigating functional epigenomics, developmental regulation, and the epigenetic mechanisms underlying human diseases.

#1953 A novel synthetic lethal combination of FERMTs obtained by screening using DNA methylation-silenced genes.

Takahiro Ebata, Ryoma Mashiko, Yumi Furuichi, Qichun Wang, Yui Ohashi, Toshikazu Ushijima

Hoshi University, School of Pharmacy and Pharmaceutical Sciences, SHINAGAWA-KU, Japan

Synthetic lethality with a methylation-silenced gene is a promising strategy for cancer treatment. Here, we aimed to identify such a synthetic lethal combination using genome-wide DNA methylation data and the gene dependency database (DepMap) in 92 gastrointestinal cancer cell lines. First, we isolated 108 genes frequently methylation-silenced in the cell lines, using criteria of a gene with a promoter CpG island and frequent methylation among the cancer cell lines. Next, we searched for their synthetic lethal partners by calculating a correlation coefficient between the methylation level of each candidate gene and dependency of the gene upon 16,836 genes in the DepMap database. As a result, we identified 21 candidate combinations. Among them, to avoid false positive combinations, we focused on one paralog combination; *kindlin1* dependency on a high methylation level of its paralog *kindlin2*. The 92 cell lines could be classified into *kindlin1* knock-down-sensitive and resistant groups by *kindlin2* methylation. In addition, incorporation of methylation of *kindlin3*, another paralog in the kindlin family, made the classification clearer. The synthetic lethality of the three genes was confirmed by rescue experiments in which overexpression of *kindlin2* or *kindlin3* decreased *kindlin1* dependency. Mechanistically, suppression of all the three *kindlin* genes caused severe adhesion deficiency, which induced YAP inactivation through its re-localization from nucleus to cytosol, independent of its phosphorylation status. In mouse xenograft models, suppression of *kindlin1* by inducible knockdown resulted in tumor regression and it was rescued by overexpression of one of other two paralogs. Methylation analysis of 927 clinical samples from TCGA database showed that 5-10% of gastrointestinal cancer had *kindlin2* and *kindlin3* methylation. Our research showed that *kindlin1* is a new therapeutic target for *kindlin2* and *kindlin3*-methylated cancers and that a search for synthetic lethal combinations with methylation-silenced genes is a promising strategy.

#1954 Spatial and single-cell DNA methylation analysis of primary breast cancer reveals lineage independent epigenetic plasticity.

Ruslan Strogantsev[1], Aysegul Ors[2], Jamie Endicott[3], Aaron R. Doe[4], Hugo Cros[5], Joseph Hwang[5], **Hisham Mohammed**[5]

[1]Knight Cancer Institute, Oregon Health & Science University, Portland, OR,[2]Aysegul Ors (Individual),[3]OHSU Knight Cancer Institute, Portland, OR,[4]Oregon Health and Science University, Portland, OR,[5]CEDAR, Knight Cancer Institute, Oregon Health & Science University, Portland, OR

Introduction: Intra-tumoral heterogeneity is governed by the interplay between rigid genetic evolution and plastic epigenetic states. However, dissecting the distinct contributions of these forces remains a challenge. While single-cell methods have traced genetic phylogeny, the spatial logic of epigenetic evolution and the extent to which it acts as an independent driver of phenotype remains unresolved. We present a comprehensive spatial and single-cell multi-omic atlas to decouple these mechanisms.
Methods: We generated a large-scale dataset comprising single-cell DNA methylation profiles from >22 patients, matched single-cell NMT-seq (nucleosome, methylation, transcription) from 8 patients, and spatial DNA methylation maps from 11 patients. We utilized our spatial sequencing approach achieving high-quality DNA methylation recovery at 50-micron resolution across tumor sections.
Results: We observed widespread, dramatic demethylation in Partially Methylated Domains (PMDs) characteristic of the cancer genome as expected. By leveraging variable/fluctuating DNA methylation sites as native barcodes, we reconstructed the phylogenetic lineage of each tumor. We demonstrate that epigenetically defined clones are not randomly dispersed but form spatially coherent, adjacent domains, confirming that tumor expansion follows a spatial logic. Integrating matched genetic data, we found that methylation lineages align with Copy Number Variation (CNV) sub-clone status. However, our multi-omic analysis revealed a critical divergence. While sub-clone specific DNA methylation patterns tracked with genetics, we observed dominant epigenetic states characterized by coordinated shifts in chromatin accessibility, transcription factor enrichment, and RNA expression that emerged independently of the underlying genetic phylogeny.
Conclusion: This study provides the first high-resolution spatial map of epigenetic architecture in cancer. We demonstrate a dual-layer model of evolution: while single CpG epimutations can record the genetic history of the clone, DNA methylation can also simultaneously drive broad, phylogenetically independent state changes that dictates cell phenotype. These findings establish epigenetic plasticity as a distinct, key driver of tumor heterogeneity beyond the constraints of the genome.

#1955 Early-life gut microbiota programs intestinal stem cell epigenetics to protect against colon cancer later in life.

Li Yang[1], Shirui Zhou[2], Xiaomin Chen[1], Fabiola Gutierrez[3], Stephanie Fowler[3], Lanjing Zhang[4], Julia M. Salamat[1], Karen Riggins[1], Jiejun Shi[2], Lanlan Shen[1]

[1]USDA Children's Nutrition Research Center, Department of Pediatrics, Baylor College of Medicine, Houston, TX,[2]Department of General Surgery, Shanghai Tongji Hospital, School of Life Sciences and Technology, Tongji University, Shanghai, China,[3]Gnotobiotic Facility, Molecular Virology & Microbiology, Baylor College of Medicine, Houston, TX,[4]Department of Pathology, Princeton Medical Center, Plainsboro, NJ

Background: Colorectal cancer (CRC) arises from both genetic and epigenetic alterations. Epidemiological and animal studies suggest early-life exposures, including gut microbiota changes during weaning, can influence long-term CRC risk. However, the mechanisms linking early microbial interactions to durable disease protection remain unclear. We hypothesize that early microbial exposure epigenetically programs long-lived intestinal stem cells (ISCs), shaping immune regulation and disease susceptibility.

Methods: *Lgr5-GFP* reporter mice were used to isolate colonic ISCs and intestinal epithelial cells (IECs) under specific-pathogen-free (SPF) and germ-free (GF) conditions. Whole-genome bisulfite sequencing (WGBS) and RNA sequencing were performed to assess microbiota-associated transcriptional changes mediated by DNA methylation from weaning into adulthood. Gut microbe transplant (GMT) experiments defined the critical developmental window during which ISC epigenetics are most sensitive to microbial influences. A maternal low-dose penicillin (LDP) model combined with shotgun metagenomics identified specific bacterial taxa contributing to epigenetic effects. Dextran sulfate sodium (DSS)-induced colitis and azoxymethane (AOM)/DSS-induced CRC models were used to evaluate long-term consequences.

Results: We identified 683 differentially methylated regions (DMRs) that were persistently associated with the microbiome in both adult ISCs and IECs. Among these, 51% were located in enhancers, and the majority DMRs (79%) exhibited loss of methylation under SPF conditions. The hypomethylated genes were enriched for immune and host defense functions, including MHC class II genes (*Cd74*, *H2-Aa*, *H2-Eb1*, and C*iita*). Loss of methylation occurred post-weaning and correlated with increased gene expression. GMT experiments demonstrated the post-weaning as the optimal window to restore methylation patterns, compared to adolescence or adulthood. Mechanistically, a transient IFN-γ burst during weaning drove epigenetic reprogramming via the IFN-γ-STAT3-TET3 axis. In addition, microbiota-derived metabolites, including short-chain fatty acids (SCFAs), α-ketoglutarate (α-KG), and methionine-γ-lyase-dependent products, reinforced the establishment of proper methylation patterns. Early-life LDP exposure reduced Gram-positive bacterial abundance, altered IFN-γ expression, disrupted MHC-II epigenetics, and increased susceptibility to colitis and CRC.

Conclusion: Early-life microbial and immune signals establish durable epigenetic programs that protect against CRC. Timed microbial interventions may provide long-lasting protection against adult-onset diseases.

#1956 Efficacy of DNA methyltransferase inhibition in combination with immune-checkpoint/PARP-inhibitor in colorectal cancer preclinical model.

Pooja Mittal, Jae Ho Lo, Ben Yi Tew, Goar Smbatyan, Sandra Algaze, Lesly Torres Gonzalez, Unnati Hemant Shah, Michela Bartolini, Yan Yang, Steve Soto Trujillo, Wu Zhang, Josh Millstein, Gangning Liang, Bodour Salhia, Shivani Soni, Heinz Josef Lenz

Keck School of Medicine of USC, Los Angeles, CA

Background. Epigenetic alterations in the form of DNA methylation changes in genes have been associated with colorectal cancer (CRC) progression. DNA methyltransferase (DNMT) enzyme plays central role in epigenetic regulation. In this study, we evaluated the therapeutic potential of epigenetic modulation using DNMT inhibitor 5-AZA-2´-deoxycytidine (5AZA) in combination with immune-checkpoint inhibitor (ICI) anti-PD1 or PARP inhibitor BMN673 in syngeneic CRC mouse model.

Methods. 8 weeks old C57BL/6 J female mice were subcutaneously injected with 10^6 MC38 cells in the right flank. Mice (n=10 per group) were randomized into following treatment groups: control, 5AZA 0.5 mg/kg, anti-PD1 100µg/mouse, BMN673 0.3 mg/kg, combinations 5AZA+anti-PD1, and 5AZA+BMN673. Upon endpoint, mice were euthanized, tumors and plasma were collected. Plasma cytokine levels were subsequently measured using V-PLEX Proinflammatory Panel 1 kit (MSD). Isolated DNA was subjected to reduced representation bisulfite sequencing, followed by analysis of statistically significant (adjusted $p<0.05$) differentially methylated regions (DMRs) and their associated genes using metilene and Ingenuity Pathway Analysis (IPA). RNA sequencing was performed using Novaseq (Illumina) and significant differentially expressed genes (DEGs) (adjusted $p<0.05$) were analyzed using DESeq2.

Results. We showed that combining 5AZA with anti-PD1 significantly reduced ($P<0.0001$) tumor volume compared to control and with either 5AZA or anti-PD1 alone. Similarly, combination of 5AZA and BMN673 significantly reduced ($P<0.0001$) the tumor volume compared to control and BMN673 alone. Methylation profiling revealed 940 and 299 DMRs in the combination 5AZA+anti-PD1 and 5AZA+BMN673, respectively when compared to single agent treated groups. IPA analysis revealed upregulation of RHO GTPase cycle and downregulation of adipogenesis in all 5AZA-treated groups. Furthermore, proinflammatory cytokines were differentially expressed among treatment groups, with cytokines IL-1β and TNF-α detected at higher concentration in BMN673 treated groups and higher levels of IL-10 and IL-2 in 5AZA treated groups. Transcriptomics profiling showed 203 and 135 upregulated, and 126 and 237 downregulated DEGs in 5AZA+anti-PD1 and 5AZA+BMN673, respectively. Notably, both combination groups showed significant downregulation of *Hba* and *Hbb* genes which encode the hemoglobin subunits, suggesting increased reactive oxygen species and associated apoptosis in tumors as a countereffect to the observed upregulation of *Tuba3a*, *Tuba3b* and *Trap1a* genes all associated with hypoxia in both combination groups.

Conclusion. Our findings suggest that administration of DNMT inhibitors in combination with ICI or PARP inhibitors could be a promising strategy to substantially improve the treatment and survival outcomes in CRC.

#1957 DNA methylation differentiates early-stage lung adenocarcinoma cells-of-origin with distinct smoking history and grade.

Xuan Cindy Li[1], Diego Almanza[2], Phuc Huu Hoang[1], Thi-Van-Trinh Tranh[1], Nicholas H. Juul[2], Maximilian Diehn[2], Tushar J. Desai[2], Maria Teresa Landi[1]

[1]Division of Cancer Epidemiology & Genetics, National Cancer Institute, Rockville, MD,[2]Stanford University, Stanford, CA

Lung cancer is a major cause of cancer-related mortality worldwide. Approximately 10%-20% of lung cancers occur in patients with no smoking history and are mostly lung adenocarcinoma (LUAD). Studies in mouse models showed that LUAD cases arising from alveolar epithelial type I (AT1) cells transitioning to alveolar type II (AT2) are less aggressive than those that originate directly from type 2 (AT2), but the origin of human LUAD remains unclear. Leveraging the bulk methylation array data from the EAGLE and Sherlock-*Lung* studies, two large multi-omics studies of lung cancer in people with and without smoking history, respectively, we infer the cells-of-origin for early-stage tumor samples and examine their associations with smoking history and grade.

We impute cells-of-origin from bulk methylation array data of tumor and normal samples collected from 388 stage I LUAD cases without smoking history and 238 with smoking history. For the methylation reference profiles of normal lung cell types, we combined a published normal human cell methylation data set (Loyfer et al. 2023) from whole-genome bisulfite sequencing (WGBS) as well as purified AT1 and AT2 enzymatically converted methylation profiles sequenced in-house. We then perform principled feature engineering to select methylation sites that best distinguish cell types and represent each cell type in a balanced manner. To estimate the proportion of each lung cell type in the samples, we employ a combinatorial optimization strategy by formulating and solving the deconvolution as a quadratic program. The inferred compositions of tumor origins are then evaluated in relation to smoking history and tumor grade based on the International Association for the Study of Lung Cancer (IASLC) grading system.

The tumor samples of LUAD cases without smoking history (n=238) have 11% higher AT1 presence compared to those with smoking history (n=388, $p<0.05$). Among cases without smoking history and with coherent grades, the tumor samples with well or moderate grade (n=96) have on average 13% higher AT1 presence than those with poor grade (n=102, $p<0.05$). Notably, tumor samples of stage I LUAD cases with no smoking history have the highest overall AT1 presence among all groups (on average 26%). All normal samples, regardless of smoking history and grade, have no significant difference in AT1 presence (on average 10%).

Our study establishes a principled deconvolution framework to infer tumor origins in LUAD using DNA methylation data. Mirroring findings in mouse models, our results indicate that AT1 cells may generate LUAD in humans, and that this appears to occur more frequently in patients without smoking history and with better tumor grades. Our work adds a new dimension to the understanding of early-stage LUAD and sheds light on patient stratification, prognostic evaluation, and therapeutic targeting of tumor origin-specific vulnerabilities.

#1958 Targeting UHRF1-SUV39H1/H2 crosstalk enhances DNMT1 inhibitor efficacy in colon cancer.

Yanqing Liu[1], Joel A. Hrit[1], Alison A. Chomiak[1], Stephanie Stransky[2], Jordan Hoffman[3], Rochelle L. Tiedemann[1], Ashley K. Wiseman[1], Leena S. Kariapper[1], Bradley M. Dickson[1], Evan J. Worden[1], Christopher J. Fry[3], Simone Sidoli[2], Scott B. Rothbart[1]

[1]Van Andel Institute (VAI), Grand Rapids, MI,[2]Albert Einstein College of Medicine, Bronx, NY,[3]Cell Signaling Technology, Inc., Danvers, MA

DNA hypomethylating agent (DNMTi) efficacy is associated with the re-expression of epigenetically silenced tumor suppressor genes (TSGs) and transposable elements (TEs) in preclinical cancer models, yet their clinical efficacy in solid tumors is limited. An emerging mechanism of resistance to DNMTi involves compensation through repressive histone post-translational modifications (PTMs). Here, we define a targetable chromatin-based mechanism through UHRF1-SUV39H1/H2 crosstalk that reinforces transcriptional silencing in colon cancer cells exposed to DNMTi's. Leveraging integrative epigenomic profiling and biochemical analyses, we discovered that transient DNA hypomethylation triggers UHRF1-dependent mono-ubiquitination of lysine 18 on histone H3 (H3K18ub), which in turn stimulates SUV39H1/H2 methyltransferases to deposit H3K9me3 at CpG island promoters of DNA methylation-silenced TSGs. This UHRF1-SUV39H1/H2 crosstalk establishes new heterochromatin domains that stabilize repression despite global DNA demethylation. Disrupting UHRF1 enzymatic function or an identified H3K18ub-recognition motif in SUV39H1 prevents H3K9me3 accumulation, increases TSG re-expression, and enhances DNMTi-induced antiproliferative effects in colon cancer cells. These findings reveal a compensatory heterochromatin signaling mechanism that limits DNMTi responses and identify the UHRF1-SUV39H1 pathway as a novel therapeutic target to improve epigenetic therapy efficacy in solid tumors.

#1959 The potential of methylated DNA markers for accurate detection of high-risk, HPV-positive cervical lesions.

Roshni Saravanan[1], Mary Jo Fackler[1], Madison Pleas[1], Wenfei Xia[1], Tomisin Adebari[1], Gang Yu[1], Liqun Zhang[1], Suzette Jordaan[2], Eunice Van Den Berg[2], Pamela Michelow[2], Reubina Wadee[2], Maureen Joffe[3], Wenlong Carl Chen[3], Youxiang Wang[4], Leslie Cope[1], Saraswati Sukumar[1]

[1]Department of Oncology, Johns Hopkins University School of Medicine, Baltimore, MD,[2]Department of Anatomical Pathology, University of the Witwatersrand/National Health Laboratory Service, Johannesburg, South Africa,[3]Strengthening Oncology Services Research Unit, Faculty of Health Sciences, University of the Witwatersrand, Johannesburg, South Africa,[4]Atila Biosciences, Sunnyvale, CA

Purpose: Cervical smear cytology exhibits high variability and limited sensitivity in detecting cervical lesions. While the HPV test, recommended by WHO, offers high sensitivity, it has limited specificity. Our goal was to determine whether DNA methylation markers could improve both sensitivity and specificity, thereby enabling more effective triage to colposcopy and biopsy than cytology and HPV testing.

Experimental Design: We previously published a 5-gene (*TBXT, MOS, FMN, EDNRB,* and *ZNF671*) DNA methylation assay with high sensitivity and specificity for detecting cervical cancer in cytology and histology samples [1]. In the current study, we tested cervical brush samples (n = 222) with known cytology but no available histology that were preserved in CytoLyt, selected and deidentified at the National Health Service screening clinic in Johannesburg, South Africa. Samples were tested for both high-risk HPV variants (Atila Biosystems) and for cumulative 5-gene methylation utilizing Quantitative Multiplex Methylation-Specific PCR (QM-MSP). Statistical tests included the Youden Index for gene-specific thresholds, odds ratio scores for individual genes, Mann-Whitney test, and Receiver Operating Characteristic Area Under the Curve (ROC AUC); a P value ≤ 0.05 was considered significant.

Results: Among the 222 cervical brush samples, HPV was prevalent in similar numbers of HSIL (87/95, 92%) and LSIL (47/57, 82%), and in about half of the NIEL (39/70, 56%). Thus, HPV was highly sensitive for the detection of HSIL, but very poorly specific for low-risk LSIL or NIEL. In contrast, among HPV+ samples, to distinguish between high risk HSIL and low risk LSIL/NEIL, the QM-MSP assay showed a high level of sensitivity: 78.16% [CI 68.39 - 85.55] and, in addition, a high level of specificity: 95.35% [CI 88.64 - 98.18], and ROC AUC = 0.890 [CI 83.71 - 94.37]. A highly significant (P<0.0001) difference in methylation levels was observed between HSIL and LSIL/NIELs. In the small set of HPV-negative samples, hypermethylation of the 5-gene panel was observed in 5/8 (63%) HSIL, 0/10 (0%) LSIL, and 1/31 (3%) NIEL, suggesting that QM-MSP may be independent of the HPV status.

Conclusions: These findings suggest that the 5-gene panel detected a large proportion of HSIL, while the majority of LSIL and NIEL remained negative. Thus, this assay could serve as an effective triage tool for HPV+ cases, expediting care for women with HSIL while potentially reducing referrals for colposcopy in LSIL and NIEL by up to 95%. This could reduce costs and risks associated with repeated biopsy procedures for low-risk lesions.

Reference: [1] DOI: 10.1186/s13148-024-01669-z

#1960 The stability of epigenetic cell identity in cancer.

Cameron Cloud[1], Benjamin Steinberg[2], Yitzhak Reizel[2], Wanding Zhou[3]

[1]Department of Bioengineering, University of Pennsylvania, Philadelphia, PA,[2]Biotechnology and Food Engineering, Technion - Israel Institute of Technology, Haifa, Israel,[3]Center for Computational and Genomic Medicine, The Children's Hospital of Philadelphia, Philadelphia, PA

Cell-type-specific DNA methylation patterns encode cell identity and are largely preserved over mitotic divisions across the organism’s lifespan. These patterns have shown strong potential as diagnostic markers in cancer. However, DNA methylation is also plastic, dynamically remodeled in development and diseases, including cancer, due to interaction with genetic, cellular, and environmental factors. Despite wide utilities, a unified and quantitative framework for assessing the stability of cell-identity-defining methylation signatures during tumorigenesis is lacking. We systematically quantified the extent to which the DNA methylation-based definitions of cell identity, as established in healthy tissue, are maintained or disrupted in 324 human cancer types. We found that cell-type-specific methylation signatures are remarkably stable across diverse cancer types, including metastatic lesions and tumors harboring mutations in epigenetic regulators. While signature erosions were common, particularly in in vitro cell lines, complete loss in primary tumors was rare and often pointed to mischaracterized or ambiguous cells of origin. Based on these insights, we developed computational strategies to infer tumor cell-of-origin from cancer methylomes, enabling a better understanding of cancers with poorly defined origins. Our findings deepen the understanding of epigenetic maintenance in cancer and guide the development of more robust methylation-based cancer diagnosis.

#1961 DNA methylation signatures associated with tumor location in early-onset colorectal cancer identified across two independent cohorts.

Aniruddha B. Rathod[1], Sandi L. Pruitt[2], Amit G. Singal[2], Caitlin C. Murphy[3]

[1]Epidemiology, University of Arkansas for Medical Sciences, Little Rock, AR,[2]UT Southwestern Medical Center, Dallas, TX,[3]Pediatrics, University of Chicago, Chicago, IL

Background: Incidence of early-onset colorectal cancer (EOCRC; ages 18-49) continues to rise globally, with rectal cancers increasing more rapidly than proximal or distal colon cancers. Germline variation does not fully explain these trends or the disproportionate rise in rectal tumors, suggesting a role for epigenetic mechanisms. However, the association of DNA methylation (DNAm) to EOCRC tumor location remains poorly understood.

Methods: We used The Cancer Genome Atlas (TCGA) as the discovery cohort to identify tumor location-specific DNAm markers in EOCRC. First, we conducted an epigenome-wide association study, screening Cytosine-Phosphate-Guanine site, (CpGs) at FDR< 0.2, followed by multivariable logistic regression adjusting for age, sex, stage, and treatment. CpG sites were modeled as independent variables and tumor location (rectum [defined as rectum and rectosigmoid] vs. colon) as the outcome; significant CpGs were defined at <fdr 0.05.="" to="" validate="" these="" findings,="" we="" tested="" the="" tcga-identified="" cpgs="" in="" an="" independent="" eocrc="" cohort="" of="" patient="" tumor="" tissue="" from="" ut="" southwestern="" medical="" center="" (utsw)="" using="" same="" analytic="" framework.="" for="" replicated="" cpgs,="" evaluated="" dnam="" patterns,="" mapped="" annotated="" genes,="" and="" conducted="" pathway="" enrichment="" analysis.="" tcga="" served="" as="" discovery="" dataset,="" utsw="" dataset="" replication="" cohort.

Results: Among the TCGA cohort of 67 patients, (31.3% rectum, mean age 44 years, 55.2% women, 73% White, 41.8% stage III), 766 CpG sites differed significantly between rectal and colonic tumors (FDR < 0.05); 27.7% were hypermethylated and 72.3% were hypomethylated in rectum tumors. The UTSW replication cohort included 72 patients (31.9% rectum, 45.8% women, 56.9% White, 37.5% stage III). Of the 504 CpGs available for replication testing, 266 showed the same direction of association, with 14.3% hypermethylated and 85.7% hypomethylated in rectal/rectosigmoid versus colonic tumors. Principal component analysis on replicated CpGs demonstrated separate clusters of rectum and colonic tumors. Replicated CpGs mapped to 202 genes, including SRC, IGF1R, EPHB3, and MAP4K4. Pathway enrichment analysis highlighted processes related to epithelial cell migration, cell-cell adhesion, and immune activation.

Conclusion: Tumor location-specific DNAm signatures differentiate rectal from colonic tumors in EOCRC, and nearly half of TCGA-identified CpGs showed directional replication in independent patient tumor tissue samples. These findings support a biological role for DNAm in anatomic heterogeneity of EOCRC and identify a focused set of CpGs and pathways for future mechanistic investigation to uncover epigenetic drivers.

#1962 Epigenetic remodeling of BCOR-PRC1.1 complex dictates response and resistance to IDH inhibitors in AML.

Sarah Hanache[1], Xiaoyan Zhang[2], Satoko Ogata[1], Hidetaka Uryu[1], Ken Furudate[1], Zongrui Li[1], Abhinav Jain[3], Erika Thompson[4], Courtney D. Dinardo[1], Margaret A. Goodell[2], Koichi Takahashi[1]

[1]Leukemia, MD Anderson Cancer Center, Houston, TX,[2]Molecular and Cellular Biology, Baylor College of Medicine, Houston, TX,[3]Epigenet & Mol Carcinogenesis, MD Anderson Cancer Center, Houston, TX,[4]Genetics, MD Anderson Cancer Center, Houston, TX

Background: IDH1/2 mutations occur in about 20% of AML and generate 2-hydroxyglutarate, which blocks TET-mediated hydroxymethylation, induces CpG island hypermethylation, and enforces a differentiation arrest. Although mutant-specific IDH inhibitors induce remissions, relapse is common. Our prior study identified recurrent acquisition of BCOR Loss of Function mutations at resistance. Because BCOR/PRC1.1 recruitment is regulated by CpG methylation, we hypothesized that IDH-driven hypermethylation disrupts BCOR binding, that IDH inhibitor mediated demethylation restores PRC1.1 occupancy, and that relapse associated BCOR loss prevents this restoration.

Methods: Using isogenic TF-1 IDH2-R140Q models, we performed EvoC 6-base sequencing, BCOR ChIP-seq, and RNA-seq across WT, IDH2 mutant, and enasidenib treated cells. Published CRISPR-Cas9 screening data from IDH1 mutant AML (Liu et al. Cancer Research 2022) were reanalyzed to define major key genes in IDH-inhibitor-induced differentiation.

Results: IDH2 mutation induced coordinated promoter hypermethylation and 5hmC loss. EvoC sequencing showed that about 60% of DMRs were hypermethylated and enriched upstream of transcription start sites. 5hmC was markedly reduced and fully restored by enasidenib, consistent with impaired TET2 activity. Notably, 87% of hypermethylated DMRs with 5hmC loss underwent demethylation after 28 days of treatment, coinciding with normalized 2HG. BCOR occupancy decreased at promoter-proximal regions in IDH2 mutant cells and was restored by enasidenib.Integration of methylation, BCOR ChIP-seq, and RNA-seq showed that most BCOR-loss promoters were hypermethylated, transcriptionally activated, and normalized with treatment. Restored BCOR targets were enriched for Wnt, PI3K/Akt/mTOR, RTK, and MAPK pathways. Promoters of *JUNB* and *WNT11* showed concordant hypermethylation, reduced BCOR binding, and increased expression in IDH2 mutant cells, all reversed by enasidenib.CRISPR-Cas9 data identified *Bcor* as a top gene required for differentiation upon IDH inhibition, exceeding canonical regulators such as *Cebpa* and *Cebpb.* Bcor targets (*Junb* and *Wnt11*) also ranked as essential effectors in the differentiation arm, matching our multi-omics findings.

Conclusions: IDH2 mutation establishes an epigenetic blockade marked by promoter hypermethylation, 5hmC loss, and loss of BCOR-PRC1.1 occupancy, enabling aberrant activation of stemness programs. Enasidenib reverses these defects by restoring 5hmC, promoter methylation balance, BCOR binding, and PRC1.1-mediated repression. These data support a model in which IDH-inhibitor-induced differentiation requires intact BCOR function and repression of BCOR targets such as JUNB and WNT11, defining how IDH-mutant epigenetic dysregulation and BCOR loss converge to limit therapeutic efficacy.

#1963 The landscape of epigenetic alterations in the prostate cancer patient cohort from India.

Promit Ganguly[1], Tanay Biswas[1], Atin Singhai[2], Alok Srivastava[3], Abhishek Chauhan[4], Manzoor Ahmad[5], Piyush Tripathi[6], Sanjeev Mehrotra[6], Anjali Tewari[6], Nuzhat Husain[7], Apul Goel[8], Bushra Ateeq[1]

[1]Department of Biological Sciences and Bioengineering, Indian Institute of Technology Kanpur, Kanpur, India,[2]Department of Pathology, King George's Medical University, Lucknow, India,[3]Department of Urology & Renal Transplant, Dr. Ram Manohar Lohia Institute of Medical Sciences, Lucknow, India,[4]Department of Radiodiagnosis, Dr. Ram Manohar Lohia Institute of Medical Sciences, Lucknow, India,[5]Department of Surgery, Jawaharlal Nehru Medical College, Aligarh Muslim University, Aligarh, India,[6]Regency Hospital, Kanpur, India,[7]Department of Pathology, Dr. Ram Manohar Lohia Institute of Medical Sciences, Lucknow, India,[8]Department of Urology, King George's Medical University, Lucknow, India

Prostate cancer (PCa) ranks as the third most prevalent malignancy among men in India, where it is frequently diagnosed at its advanced stage due to a lack of routine screening and awareness. PCa is a highly heterogeneous disease, comprising multiple molecular subtypes and exhibiting significant ethnic disparities. Its progression is driven by a cascade of genetic and epigenetic alterations that dysregulate key gene networks and signaling pathways. The global molecular landscape of PCa patients of Indian ethnicity has remained unaddressed. Hence, as a prospective study, we characterized the aberrant DNA methylation pattern in PCa specimens of Indian origin and performed Illumina EPICv2 array-based profiling of fresh, treatment-naïve PCa (N=32), Benign Prostatic Hyperplasia (BPH; N=7) and one high-grade prostatic intraepithelial neoplasia tumor specimens. Using Sesame pipeline, we have identified genome-wide differentially methylated loci in PCa specimens to understand the epigenetic aberrations prevalent in this cohort. We observed significant hypermethylation in the regulatory regions of *GSTP1*, *APC*, *RARB,* and *RASSF1,* while *TDRD1*, *CTBP1,* and *KLK3* showed hypomethylation. Moreover, key cancer and development-linked processes such as stem cells pluripotency signaling, and synaptic signaling were observed to be dysregulated in PCa specimens compared to BPH. Additionally, hypermethylated regulatory regions exhibited reduced chromatin occupancy of PCa-driving transcription factors such as AR and ERG, while hypomethylated regions showed increased occupancy. Unsupervised hierarchical clustering identified a distinct subset of PCa patients with elevated DNA methylation levels independent of their Gleason grade. Moreover, mapping genetic alterations in matched Indian PCa patients would offer a framework for patient stratification, enabling tailored therapeutic interventions driven by distinct epigenomic and genomic aberrations. In conclusion, our study for the first time, explored the global epigenetic profile of Indian PCa patients while identifying key DNA methylation aberrations and dysregulated pathways driving disease progression that would help improve PCa diagnostics and forward our understanding of PCa pathogenesis.

#1964 Age-related *p16* epimutation is a targetable driver of *Kras*-mutant lung cancer.

Xiaomin Chen[1], Li Yang[1], Eduardo Lopez[1], Lili Ma[2], Chao Cheng[2], Lanjing Zhang[3], Lanlan Shen[1]

[1]USDA Children's Nutrition Research Center, Department of Pediatrics, Baylor College of Medicine, Houston, TX,[2]Department of Medicine, Epidemiology and Population Science, Baylor College of Medicine, Houston, TX,[3]Department of Chemical Biology, Earnest Mario School of Pharmacy, Rutgers University, Piscataway, NJ

Background: Lung cancer is a leading cause of cancer death worldwide; however, current targeted therapies have limited efficacy for most patients. *p16* epimutation, characterized by epigenetic silencing of *p16* by promoter DNA hypermethylation, is common in lung cancer. Elucidating how *p16* epimutation drives lung tumorigenesis may uncover new therapeutic opportunities.

Methods: We developed a mouse model combining the conditional Cre-inducible *Kras*^{G12D}-mutation with epigenetically engineered *p16* epimutation and conducted time-course study to analyze the tumor phenotype and survival. Organoids derived from normal and tumorous lung tissue were used to assess the role of *p16* epimutation in tumor initiation and maintenance. Moreover, spatial transcriptomic analysis was used to characterize tumor heterogeneity and define distinct cell populations. To test the therapeutic potential of reversing *p16* epimutation, we evaluated the efficacy of hypomethylating agents 5-Aza-2'-Deoxycytidine (DAC) and GSK3685032 on *p16* reactivation in organoid and *in vivo*. Furthermore, we developed mice enabling conditional, inducible and site-specific DNA demethylation using a CRISPR-dCas9-Tet1 based epigenetic editing system. We assessed the effect of targeted *p16* promoter demethylation on tumor progression *in vivo*.

Results: Mice with combined *Kras*-mutation and *p16* epimutation developed malignant tumors more rapidly and had significantly shorter survival than mice with *Kras*-mutation only (Median survival: 161 days vs. 223 days, n=50, p=0.0003). Histopathological analyses confirmed the tumor progression to adenocarcinoma with distinct papillary and intraluminal growth patterns in combined mice, but not in *Kras*-mutation only mice. Spatial transcriptomic analysis confirmed that tumors with this growth patterns were enriched in transitional airway progenitors co-expressing Sox2, Nkx2-1, and ciliated markers. Moreover, normal and tumor organoids derived from the combined mice proliferated robustly whereas organoids from *Kras*-mutation only mice stopped growing shortly after establishment. While global hypomethylation agents significantly reactivated *p16* and inhibited proliferation in tumor organoids, these agents failed to block tumor development *in vivo* (Fold change of tumor burden to control: DAC 1.41 ± 0.11, GSK3685032 1.33 ± 0.18, n=5, p=0.07). In contrast, CRISPR-mediated targeted *p16* promoter demethylation significantly reduced both tumor number and size *in vivo* compared with control mice (Tumor number: 16.17 vs. 6.33 per mouse, n=6, p=0.04).

Conclusion: Our work identifies *p16* as a bona fide epigenetic driver and therapeutic target for Lung cancer. Importantly, this study provides proof-of-concept that precise, locus-specific DNA demethylation can restore tumor suppressor function, highlighting a promising strategy for targeted epigenetic therapy in lung cancer patients.

#1965 Conserved endothelial cell-specific DNA methylation alterations in colorectal and breast tumor microenvironments.

Barbara Karakyriakou[1], Ze Zhang[2], Lucas A. Salas Diaz[3], Brock C. Christensen[3]

[1]Epidemiology, Molecular and Systems Biology, Dartmouth Geisel School of Medicine, Lebanon, NH,[2]Division of Population Sciences, Dana-Farber Cancer Institute, Boston, MA,[3]Dartmouth Geisel School of Medicine, Lebanon, NH

DNA methylation alterations are well-established contributors to carcinogenesis, yet, within the tumor microenvironment (TME), lineage- and cell-specific patterns remain poorly characterized. We applied a bulk DNA methylation deconvolution approach (HiTIMED) combined with a cell-type-specific differential methylation framework (CellDMC) to identify and validate tumor endothelial cell (TEC) specific DNA methylation alterations in colorectal cancer and nontumor normal tissue. We previously identified TEC-specific DNA methylation alterations in breast cancer. Here, we evaluate the shared endothelial-specific epigenetic programs between breast and colorectal tumors. Endothelial cells, key regulators of angiogenesis and vascular homeostasis, often acquire molecular and structural abnormalities that promote tumor progression. Using genome-scale DNA methylation data from a discovery and validation framework (tumor n = 725; nontumor n = 989) of colorectal tissues, we identified 38,647 CpGs (FDR ≤ 0.05) with altered DNA methylation specific to TECs in both discovery and validation sets, corresponding to 13,249 genes. The majority of CpGs were hypermethylated in TEC compared to endothelial cells in normal tissue. Clusters of CpGs mapped to genes known to regulate angiogenesis, endothelial cell biology, genes in the VEGF signaling pathway, and members of the hallmark angiogenesis gene set. Comparative analysis of TEC-specific methylation alterations in the colorectal and breast TME showed a 24% overlap at the CpG level, and an 81% overlap at the gene level, suggesting conserved endothelial-specific methylation dysregulation programs between tumor types. Nearly all genes whose expression correlated with endothelial cell proportion in our previous breast cancer analysis were also identified in the colorectal datasets. These findings indicate a shared epigenetic architecture underlying endothelial cell reprogramming in distinct tumor contexts. Ongoing expression analyses will extend these comparisons in colorectal tumors to further link DNA methylation with transcriptional regulation. Together, our results demonstrate that high-resolution, lineage-specific DNA methylation landscapes can be reconstructed from bulk tumor DNA methylation profiles and establish conserved TEC-specific epigenetic signatures with implications for tumor vascular biology and precision therapeutic targeting.

#1966 Vitamin C delays mouse embryonic cells immortalization by maintaining enhancer hypomethylation of senescence-related genes.

Guillermo A. Urrutia[1], Minmin Liu[2], Rachel Shereda[1], Stacey L. Thomas[1], Gangning Liang[3], Peter A. Jones[4]

[1]Van Andel Institute, Grand Rapids, MI,[2]Van Andel Research Institute, Grand Rapids, MI,[3]Department of Urology, Keck School of Medicine, University of Southern California, Los Angeles, CA,[4]Van Andel Institute (VAI), Grand Rapids, MI

Immortalization is the first step necessary for cancer cells to overcome replicative senescence and proliferate indefinitely, and it is known to be influenced by DNA cytosine methylation. Vitamin C (vitC) is a known cofactor for the Ten-eleven-translocation (Tet) enzymes, which are involved in active DNA demethylation. However, its role during this key process remains unclear. In this study, we evaluated vitC´s potential to prevent cell immortalization and its associated DNA methylation changes in a mouse embryonic cell culture model. Our findings demonstrate that vitC at physiological concentrations delays embryonic cell immortalization, inducing β-Galactosidase positive senescence, and increasing the global levels of 5-hydroxymethylcytosine in DNA. DNA methylation arrays revealed that immortalization induces a substantial reprogramming of the DNA methylation landscape, characterized by hypomethylation of Partially Methylated Domains (PMDs) and hypermethylation of enhancers, while vitC treatment prevented the immortalization-acquired DNA methylation. Gene expression analysis confirmed the upregulation of senescence and adipogenesis-related genes in vitC-treated cultures. Additionally, DNA hypomethylation was detected in key regulatory regions associated with these upregulated genes, particularly in enhancers. Interestingly, treated cultures sometimes acquired deletions of the *Cdkn2a* gene, suggesting that additional genetic insults are necessary for cells to overcome vitC-induced senescence. Collectively, our findings provide insight into how vitC modifies the epigenetic landscape of embryonic cells, inducing hypomethylation of DNA regulatory elements, thus preventing cells from overcoming replicative senescence and becoming immortal.

#1967 Methylation-based classification of circulating tumor DNA using enzymatic methyl-seq in a pan-cancer clinical cohort.

Kimberly A. Holden[1], Ashraf Shabaneh[1], Dennis D. Krutkin[1], Adib Shafi[1], Tong Liu[1], Kerry D. Fitzgerald[1], Eyad Almasri[1], Yuanyu Cao[1], Xiaojun Guan[1], Graham McLennan[1], Nathan Faulkner[1], Shakti Ramkissoon[2], Marcia Eisenberg[2], Brian Caveney[2], Eric Severson[2], Taylor J. Jensen[2], Jonathan Williams[1]

[1]Labcorp, San Diego, CA,[2]Labcorp, Durham, NC

Circulating tumor DNA (ctDNA) offers a minimally invasive approach for cancer detection and monitoring. The addition of DNA methylation-based biomarkers into liquid biopsy workflows has the potential to enhance analytical performance. We evaluated the performance of the NEBNext® Enzymatic Methyl-seq (EM-seq) kit for ctDNA-based cancer classification in a pan-cancer clinical cohort. A cohort consisting of 99 plasma-derived cfDNA samples (29 healthy donors; 70 cancer patients across five organ sites) were processed using a semi-automated EM-seq workflow and sequenced to a target depth of 10X. Multiple machine modeling methods were evaluated using DNA methylation ratio values segmented into bin sizes ranging from 10 bp to 350 bp, increasing in 10 bp increments. For each window size, a leave-one-out cross-validation strategy was applied to differentiate cancer from healthy samples. This resolution study resulted in the testing of over 31,000 models, and the predictive capacity of models was evaluated using sensitivity, specificity, and area under the curve (AUC). For each model, performance was evaluated by assessing the ability of the model to differentiate cfDNA from healthy donors and cancer patients. Logistic regression with a bin size of 290bp achieved the highest performance with an AUC of 0.98, sensitivity of 0.96, and specificity of 0.9. Model agnostic feature selection identified 15 features that highly overlap amongst cross-validation sets. Some bins mapped to known oncogenes such as *NOTCH2* and *CASC15*, or regions known to contribute to cell growth and tumor progression, including *TGFA* (a proto-oncogene), regulatory RNA LINC00665, and genes implicated in cancer biology such as *HS3ST5*, *SPOCK3*, *ATG13*, and *ERGIC1*. Other bins fell in intergenic regions or within genes with no known roles in oncogenesis (*EPS15L1*, *ARMC9*). The misclassified samples (n = 6; 3 healthy and 3 cancer) had a lower average mapping efficiency (mean = 87.5%) than correctly classified samples (mean = 94.5%; p = 0.003), suggesting that sequencing quality may influence classification outcomes. Different combinations of modeling methods and resolution levels (bin size) were also highly predictive of disease status. Methylation-based classification of ctDNA using EM-seq enables high-sensitivity cancer detection across multiple tumor types. Ongoing improvements in conversion efficiency, consistency across workflows, and expansion of sample cohorts may further enhance model robustness. These findings support the potential of methylation-informed liquid biopsy as a diagnostic tool in oncology.

#1968 Epigenetic reprogramming via DNMT1 inhibition reduces invasion and migration in docetaxel-resistant prostate cancer.

Carmen M. Ortiz-Sanchez[1], Gabriela Castro[2], Shakira Abad[2], Solimar Esteves[1], Valerie Rodriguez[1], Stephanie Montalvo[3], Rodniel Aviles[1], Ralphdy Vergne[1], Gustavo Alayon[1], Caleb Santiago[1], Lenin Godoy[1], Kosj Yamoah[4], Gilberto Ruiz-Deya[1], Jong Y. Park[4]

[1]Ponce Health Sciences University, Ponce, Puerto Rico,[2]Pontificia Universidad Catolica de Puerto Rico, Ponce, Puerto Rico,[3]University of Puerto Rico at Mayaguez, Mayaguez, Puerto Rico,[4]H. Lee Moffitt Cancer Center and Research Institute, Tampa, FL

Background: Metastatic castration-resistant prostate cancer (mCRPC) is associated with poor prognosis and high mortality, largely due to the emergence of androgen and chemotherapy resistance. Resistance to docetaxel occurs in nearly 50% of patients and remains a major clinical challenge. DNA methylation is known to contribute to therapy resistance through gene silencing and reprogramming of cellular pathways. This study investigated whether global DNA hypomethylation achieved through DNMT1 inhibition could reduce cell invasion and motility in docetaxel-resistant (DR) prostate cancer (PCa) cells.
Methods: Parental and docetaxel-resistant cells (22Rv1, PC3, and DU145) were treated with 5-AZA (0.5-16 μM, 72 h). Viability was measured by MTT. Protein markers (AR, ARv7, MDR1, GSTP1, DNMT1) were assessed by Western blot; invasion and migration by Matrigel and wound-healing assays; and EMT markers (*CDH1*, *SNAI2*, *VIM*) by RT-PCR.
Results: Treatment with 5-AZA reduced cell viability in a dose-dependent manner in all cell models except DU-145DR cells. DNMT1 inhibition was confirmed in all cell lines, while re-expression of GSTP1, indicating successful DNA hypomethylation, was observed in DU145-DR and PC3/PC3-DR cells. No changes were observed in AR, AR-V7, or MDR1 protein expression. Invasion capacity was significantly reduced in DU145-DR (1 μM: $p<0.05$; 2 μM: $p<0.0001$) and PC3-DR (1 μM: $p<0.0001$; 2 μM: $p<0.01$) cells. Migration capacity was also reduced in DU145-DR and PC3-DR cells following 5-AZA treatment. 5-AZA induced upregulation of *CDH1* (DU145-DR: $p<0.05$; PC3-DR: $p<0.01$) and downregulation of *TJP1* (DU145-DR: $p<0.01$; PC3-DR: $p<0.01$) compared to parental cells. Additionally, SNAI2 ($p<0.05$) and VIM ($p<0.01$) were significantly downregulated only in DU145-DR cells, suggesting a cell line-specific modulation of epithelial-mesenchymal transition (EMT) markers.
Conclusions: These findings demonstrate that DNMT1 inhibition modulates EMT-related pathways, leading to reduced invasion and migrations in docetaxel-resistant PCa cells. The effect of 5-AZA appears to be mediated by upregulation of *CDH1* and suppression of *SNAI2* and *VIM*, highlighting the role of DNA methylation as a regulator of metastatic potential. This study provides mechanistic insight into the epigenetic regulation of therapy resistance and supports the potential of DNMT1 inhibition as a strategy to mitigate aggressive behavior in docetaxel-resistant mCRPC.
Funding: Sponsored by U54 PHSU-MCC Grants: U54CA163071 & U54CA163068; NIH-NIMHD Grant MD007579, and NIH-NIGMS Grant U54GM133807.

#1969 Hypomethylating activity of zebularine suppresses migration in docetaxel-resistant prostate cancer cells.

Gabriela Castro Morales[1], Daniela Gonzalez[1], Gustavo Alayon[1], Ralphdy Vergne[1], Lenin Godoy[1], Jong Y. Park[2], Gilberto Ruiz-Deya[1], Carmen M. Ortiz-Sanchez[1]

[1]Ponce Health Sciences University, Ponce, PR,[2]Moffitt Cancer Center, Tampa, FL

Background: Prostate cancer (PCa) is one of the most common types of cancer diagnosed in men. According to the Centers for Disease Control and Prevention (CDC), for every 100 men, 13 will develop PCa during their lifetime. DNA methylation has been investigated as a biomarker for disease aggressiveness and therapy resistance in PCa. Although PCa is considered a slow-growing disease, it can progress into metastatic castration resistant prostate cancer (mCRPC). Docetaxel is the standard first-line chemotherapy for mCRPC; however, drug resistance occurs in almost 50% of patients. Therefore, this study aimed to determine whether altering DNA methylation patterns in docetaxel-resistant (DR) PCa cell lines modifies key cellular functions, including proliferation, migration, and expression of resistance-related proteins. We hypothesized that Zebularine, a DNA methyltransferase (DNMT) inhibitor, would induce changes proliferation and migration in both parental and DR PCa cell models.
Methods: To evaluate the effects of Zebularine (12.5 - 400 µM) on the proliferative capacity of PCa cell lines (PC-3, DU-145, and 22Rv1) and their DR counterparts, the MTT assay was performed. Protein expression changes in DNMT1, DNMT3A, and MDR1 were evaluated through Western Blot. Effects over cell migration capacity were evaluated using the Wound Healing assay.
Results: Zebularine treatment reduced cell viability in a concentration-dependent manner in all cell lines. Based on these results, non-toxic concentrations of Zebularine (25 µM and 100 µM) were selected for further experiments. Zebularine reduced DNMT1 expression across all cell lines except DU145-DR; no changes were observed for DNMT3a or MDR1. In migration assays, Zebularine reduced the migration capacity of DR cell lines compared with their parental counterparts, particularly in PC3-DR and DU145-DR cells at 48 and 72 hours.
Conclusions: Zebularine led to successful inhibition of DNMT1, providing evidence of its hypomethylating action in the cell models used. Moreover, it led to a reduction in cell migration specifically in DR cell lines. This study sheds light on the importance of DNA methylation in the regulation of biological processes in DR cell lines.
Funding: Sponsored by U54 PHSU-MCC Grants: U54CA163071 & U54CA163068; NIH-NIMHD Grant MD007579, and NIH-NIGMS Grant U54GM133807.

#1970 Epigenetic modulation with 5-Azacytidine reduces aggressive phenotypes in 3D spheroid models of docetaxel-resistant prostate cancer.

Alanis Paola Torres Rosado[1], Gabriela Castro Morales[2], Lenin J. Godoy[1], Jong Y. Park[3], Gilberto Ruiz Deya[1], Carmen M. Ortiz-Sanchez[1]

[1]Ponce Health Sciences University, Ponce, PR,[2]Pontifical Catholic University, Ponce, PR,[3]Moffitt Cancer Center, Tampa, FL

Background: Prostate cancer (PCa) remains a significant health burden in the US, making it the second most frequently diagnosed malignancy in men. While the 5-year survival rate for localized tumors is 98%, metastatic prostate cancer presents a marked difference, with a 5-year survival rate of only 32%. The disparity in treatment effectiveness is largely due to low response rates and rapid resistance to docetaxel. Increasing evidence suggests that epigenetic mechanisms, particularly DNMT1-mediated hypermethylation, play a critical role in developing and maintaining this resistance by suppressing tumor-suppressor gene expression, leading to increased invasion, migration, and chemoresistance.Previous studies have shown that 5-azacytidine (5-AZA) can decrease epithelial-mesenchymal transition (EMT)-related markers and aggressive phenotypes in prostate cancer models. However, its effects in 3D spheroid systems, which better mimic the in vivo tumor microenvironment, remain unclear.
Methods: To evaluate the impact of 5-AZA on epigenetic regulation, EMT markers, and aggressive phenotypes in 3D spheroids generated from PC3 and PC3-DR cells, spheroids were formed in ultra-low attachment plates and treated with 1-2 μM of 5-AZA. Protein expression of DNMT1 and resistance related markers was evaluated through Western blot.
Results: PC3-DR spheroids in Matrigel showed strong invasion at 24 hours with outward cellular extensions and interaction with the matrix. Treatment with 5-AZA reduced this invasion in a dose-dependent manner. Protein analysis revealed significant suppression of DNMT1 in nuclear extracts, confirming effective targeting of epigenetic factors, whereas MDR1 remained abundant in cytosolic fractions, consistent with its role in chemoresistance. 5-AZA induced the re-expression of GSTP1 and shifted EMT programs toward an epithelial phenotype, corroborating previously reported findings in 2D models. Notably, PC3-DR spheroids demonstrated a stronger response to treatment than the parental PC3 cells, suggesting a greater reliance on methylation-driven pathways.
Conclusions: Overall, 5-AZA appears to reverse aggressive phenotypes in 3D spheroid models of docetaxel-resistant prostate cancer by reducing DNMT1 activity, restoring epithelial identity, and suppressing invasion. These findings support the use of epigenetic modulation as a potential therapeutic strategy to overcome chemoresistance and emphasize the importance of 3D systems for modeling treatment-resistant diseases. Future studies integrating genome-wide methylation profiling and in vivo validation are needed to establish 5-AZA as a viable strategy to counteract docetaxel resistance in metastatic prostate cancer. Sponsored by U54 PHSU-MCC Grants: U54CA163071 & U54CA163068; NIH-NIMHD Grant MD007579, and NIH-NIGMS Grant U54GM133807.

#1971 Distinct genome wide DNA methylation signatures due to pathogenic germline variants in *DKC1*, *TERC*, and *TINF2*.

Kelvin Cesar De Andrade[1], Gina Ney[1], Tianna Zhao[2], Shilpa Gaddam[2], Jia Liu[2], Kristine Jones[2], Lisa J. McReynolds[1], Neelam Giri[1], Sharon A. Savage[1]

[1]National Cancer Inst. Div. of Cancer Epidemiology & Genetics, Bethesda, MD,[2]Division of Cancer Epidemiology and Genetics, National Cancer Institute, National Institutes of Heal, Cancer Genomics Research Laboratory, Leidos Biomedical Research, Frederick National Laboratory for Cancer Research, Bethesda, MD

Germline pathogenic variants (GPVs) in *DKC1*, *TERC*, or *TINF2* lead to defective telomere maintenance and cause the cancer-prone telomere biology disorders (TBDs). DNA methylation (DNAm) can contribute to disease expressivity and penetrance in TBDs; however, epigenetic signatures across patients with TBDs remain undefined. As telomere shortening is a hallmark of aging, TBDs also offer a framework to study its link to epigenetic aging. We sought to identify DNAm alterations and evaluate epigenetic aging in patients with TBDs. Genome-wide DNAm profiling was performed using the Illumina Infinium Methylation EPICv2 array on blood samples from individuals with heterozygous *TERC* (n=15) or *TINF2* (n=13) GPVs, hemizygous *DKC1* males (n=7), and 41 controls participating in our IRB-approved study (NCT00027274). Differentially methylated probe (DMP) analysis was conducted using *limma*, adjusting for age, sex, DNAm-derived cell type composition, and family structure (FDR < 0.05 and $|\Delta\beta| \geq 0.20$); group differences were evaluated with mixed-effects regression models. Differentially methylated regions (DMRs) were identified with *DMRcate* (HMFDR < 0.05; $|\text{mean } \Delta\beta| \geq 0.10$). Functional enrichment of DMP-associated genes was assessed via KEGG pathway analysis using *missMethyl*. Epigenetic aging was estimated using the DunedinPACE algorithm. We identified 499, 167, and 164 DMPs in *TINF2*, *DKC1*, and *TERC*, respectively. Hypermethylation was mainly found in OpenSea regions (59-79%), except for *TERC*, which showed enrichment in CpG islands (45%). Hypomethylated probes were largely OpenSea (≥90%) across all cohorts. Genomic mapping showed enrichment of hypermethylation on chromosome X in *TERC* carriers, whereas *TINF2* and *DKC1* showed widespread autosomal changes. We detected 403 DMRs in *TINF2*, 158 in *DKC1*, and 119 in *TERC*, predominantly within promoter-proximal (21-30%) and intronic (27-38%) segments. Promoter hypermethylation was most common in *TERC* and *DKC1*, whereas *TINF2* exhibited intronic hypermethylation (36%). Nine genes with promoter hypermethylation and five with hypomethylation were recurrently detected across all patients. Pathway analysis showed enrichment in hematopoietic lineage and calcium signaling, with gene-specific trends in immune (*DKC1*), stem cell (*TERC*), and growth factor (*TINF2*) pathways. Epigenetic aging was accelerated in all patients, most prominently in *DKC1* (β=0.225, $p<0.001$) and *TINF2* (β=0.190, $p<0.001$). We detected distinct yet convergent DNAm signatures across individuals with TBDs. Individuals with GPVs in *TINF2* exhibited the most extensive methylation remodeling. All patients demonstrated accelerated epigenetic aging. These findings suggest that DNAm alterations accompany telomere dysfunction in TBDs and underscore the need for integrated multi-omic and longitudinal studies to clarify its mechanistic basis, tissue specificity, and clinical implications.

: Genomic Drivers of Cancer Pathogenesis
Poster Session

#1975 Genomic drivers of plasticity in transformed small cell lung cancer.

Swanand Rakhade, Mamie Wang, Lena Morrill Gavarro, Emmanuel Spanos, Alvaro Quintanal-Villalonga, Amin Sabet, Parvathy Manoj, Rishika Giri, Ronan Chaligne, Xinjun Wang, Helena A. Yu, Esther Redin, Dana Pe'er, Charles M. Rudin, Joseph Chan

Memorial Sloan Kettering Cancer Center, New York, NY

Background:
An emerging mechanism of resistance to targeted therapies in lung cancer is the lineage switch from lung adenocarcinoma (LUAD) to a neuroendocrine (NE) histology, the most aggressive subtype being small cell lung cancer (SCLC). In *EGFR*-mutant tumors, concurrent *TP53/RB1*mutations are enriched in transformed tumors, but the mechanisms underlying transformation remain poorly defined. We present a single-cell atlas of transformed (T)-SCLC and identify genomic and transcriptional drivers of NE transformation.
Methods:
We curated a cohort of 97 T-SCLC, 777 *de novo* SCLC, and 10,140 LUAD patients from a single institution, with mutational profiling performed using MSK-IMPACT. A subset of 47 tumors from 24 patients with transformed or admixed LUAD-SCLC histology underwent 10x single-cell RNA sequencing compared to 10 *EGFR/TP53/RB1*-mutant LUAD (triple-mut), 17 *de novo* SCLC, and 4 normal lung samples, yielding ~140,000 cells. Analysis was performed using scanpy, scVI, CellRank, Palantir, SPECTRA, and GSEApy.
Results:
Among stage IV patients, we observed worse median overall survival (OS) in *EGFR*-wt T-SCLC (9.70 mos) and *de novo* SCLC (10.22 mos) compared to *EGFR*-wt LUAD (19.33 mos) and *EGFR*-mut T-SCLC (27.58 mos). T-SCLC showed a higher mean mutational burden (12.4 mut/Mb) compared to LUAD (6.7 mut/Mb) and *de novo* SCLC (9.0 mut/Mb). *TP53* and *RB1* were the most common mutations in both T-SCLC and *de novo* SCLC. Only 38% of T-SCLC had *EGFR* mutations. Mutation enrichment differed by genotype. *EGFR*-mut tumors displayed higher rates of *NFKB1, NKX2-1, FOXA1, CARD11, ELF3, RRAS2*, and *MDM4* mutations. *EGFR*-wt T-SCLC tumors were enriched in *MYC, KRAS, KEAP1, CDKN2A, SF3B1, CCND1,* and *FGF3* mutations. *PI3K/AKT* pathway alterations were enriched across both *EGFR*-wt and *EGFR*-mut T-SCLC compared to *de novo* SCLC. Single-cell analysis revealed enrichment of *MYC*, *PI3K/AKT*, chromatin remodeling, and stemlike gene programs in T-SCLC, especially early in transformation. We identified a basal-like signature highly active in LUAD immediately prior to transformation that was previously unrecognized in patients. The basal-like signature persisted in T-SCLC samples that had the highest intratumoral heterogeneity. A subset of triple-mut LUAD also expressed the basal-like signature, indicating a potential ‘pre-transformation’ stage. We observed trajectories leading to alternative squamous and mesenchymal fates as well.
Discussion:
Our data show that NE transformation is shaped by interplay between genotype and underlying transcriptional rewiring. While *EGFR*-mut and *EGFR*-wt tumors display differential mutational patterns, they converge on *PI3K/AKT* activating mutations and a shared basal-like precursor state, which primes tumors for transformation to NE, squamous, and mesenchymal fates. Our study underscores the clinical need to better understand NE transformation and highlights potential therapeutic vulnerabilities.

#1976 Pathogenic germline KEAP1 variants drive constitutive NRF2 hyperactivation and enhanced oncogenic fitness in non small cell lung cancer.

Laura Eibler, Miika M. Mehine, Rebecca Caeser, Esther Redin, Michael F. Berger, Chaitanya Bandlamudi, Charles M. Rudin

Memorial Sloan Kettering Cancer Center, New York, NY

KEAP1 is a key tumor suppressor, which is mutated in 15-20% of non-small cell lung cancers (**NSCLC**), ranking as the third most frequently altered gene. Somatic loss-of-function mutations disrupt the Cullin 3-based E3 ubiquitin ligase complex, preventing *NRF2* degradation and enabling its nuclear translocation. This drives metabolic reprogramming, ferroptosis resistance, and adaptation to oxidative stress, which are hallmarks of aggressive disease and poor survival. While somatic *KEAP1* alterations are established drivers of adverse prognosis, **the role of germline *KEAP1*** variants in cancer predisposition remains largely unknown. Using MSK-IMPACT paired tumor-normal sequencing, we analyzed 49.000 patients across 65 cancer types for rare germline variants predicted to be deleterious by VEP, REVEL, and AlphaMissense. We identified 35 carriers of pathogenic *KEAP1* candidates (12 truncating, 23 missense). In tumors from these carriers, we observed recurrent loss of the wild-type allele in NSCLC, and enrichment of somatic co-mutations in *STK11*.In this study we selected five novel *KEAP1* germline missense mutations (1438G>C, 1244G>A, 779G>T, 1524C>G, 1649T>A) to investigate their pathogenic impact on *NRF2* signaling and tumor cell fitness in NSCLC. *KEAP1* variant and wild-type (WT) plasmids were generated by site-directed mutagenesis and introduced via lentiviral transduction into NSCLC cell lines (A549, H460) using CMV-driven expression constructs. A549 and H460 harbor *STK11* and *KEAP1* co-mutations and were transduced with the *NRF2*-mediated ARE luciferase reporter plasmid. All five selected germline *KEAP1* variants exhibited significant **loss-of-function**, failing to suppress *NRF2* activity and resulting in **5-10-fold elevated ARE-luciferase reporter signal** compared to WT *KEAP1* ($P<0.001$) across all time points. Western blotting confirmed **disruption of KEAP1-NRF2 binding**, with **marked nuclear *NRF2* accumulation and cytoplasmic depletion** - phenocopying known somatic pathogenic mutants (959G>T). Functionally, variant-expressing NSCLC cells demonstrated **2-3-fold increases in colony number and size** ($P<0.01$), enhanced proliferation rates and increased expression of ferroptosis protective proteins (*AKR1C2, AKR1B10*), directly linking germline *KEAP1* dysfunction to oncogenic gain-of-function via *NRF2* hyperactivation. This study provides the first functional validation of germline *KEAP1* variants as **pathogenic drivers of inherited *NRF2* hyperactivation** in NSCLC, with loss-of-function severity equivalent to somatic mutations. These findings establish germline *KEAP1* testing as a critical tool for hereditary cancer risk assessment, enabling personalized therapeutic targeting strategies in high-risk families. This work has transformative implications for precision oncology and improved long-term outcomes in NSCLC.

#1977 Whole-genome sequencing of >8,000 TCGA samples reveals diverse and atypical spectra of homologous recombination deficiency in primary human cancers.

Joonoh Lim[1], Chunyang Bao[1], Hansol Park[1], Gang-Hee Lee[1], Ryul Kim[1], Won-Chul Lee[1], Jonghoon Lee[1], Yoonsuh Lee[1], Beomki Lee[2], David Lehotzky[3], Ron Solan[3], Antonia Kowalewski[3], Xavi Loinaz[3], Vasuki Narasimha Swamy[3], David I. Heiman[3], Samantha Van Seters[3], Saveliy Belkin[3], Sam Wiseman[3], Andrew D. Cherniack[3], Luis Antonio Corchete Sanchez[3], Brian P. Danysh[3], Zachary Everton[3], Chip Stewart[3], Haruna Tomono[3], Gengchao Wang[3], Esther Rheinbay[4], Gad Getz[4], Young Seok Ju[1]

[1]Inocras Inc., San Diego, CA,[2]Graduate School of Medical Science and Engineering, Korea Advanced Institute of Science and Technology, Daejeon, Korea, Republic of,[3]Broad Institute of MIT and Harvard, Cambridge, MA,[4]Massachusetts General Hospital, Boston, MA

Mutations not only drive carcinogenesis but also record the evolutionary history of cancer. Homologous recombination deficiency (HRD), a defect in high-fidelity DNA double-strand break repair, produces characteristic mutational footprints that define an HRD phenotype. HRD has major clinical relevance as a predictor of response to DNA-damaging agents and targeted therapies, yet current HRD assays were developed primarily in breast and ovarian cancers, and their applicability to other tumor types remains unclear. We conducted a pan-cancer whole-genome analysis of >8,000 primary tumors from The Cancer Genome Atlas (TCGA), spanning ~30 cancer types, including ~900 breast and 300 ovarian cancers. We developed HRDecide, an HRDetect-derived framework that uses comprehensively annotated germline and somatic mutations in homologous recombination (HR) pathway genes, including structural variants and non-canonical splice alterations informed by recent advances in variant-effect prediction, to refine HRD identification across cancer types. Applying HRDecide to TCGA whole-genome sequencing data, we identified HRD-positive tumors and delineated their mutational signatures. HRD-associated features were broadly shared across cancers, extending beyond breast and ovarian tumors to include tumor types such as prostate, pancreatic, gastric, and hepatocellular carcinomas. These signatures encompassed canonical short deletions with microhomology as well as cancer type-specific patterns across substitution, indel, and structural variation profiles. Notably, we also characterized atypical HRD-like phenotypes that showed only a subset of components of the classical HRD signatures. The spectrum of inactivated HR pathway genes, and the predominant modes of disruption, point mutation, structural variation, and allelic loss, varied substantially by cancer type. The scale of this cohort enabled robust associations between HRD phenotypes and pathogenic mutations in HR pathway genes, such as *ATM*, *CHEK2*, and *RAD51B*, often truncated by structural variations and LINE-1 retrotranspositions, extending beyond the classical BRCA1/2, PALB2, and RAD51C events reported in PCAWG and Hartwig datasets. In summary, this pan-cancer study provides a comprehensive whole-genome landscape of HRD in primary tumors, revealing tissue-specific modes of repair failure and expanding the HRD spectrum beyond the BRCA-centered paradigm. These findings establish a reference framework for tissue-agnostic HRD biomarker development and therapeutic stratification across cancer types.

#1978 Copy number analysis of regulatory regions reveal recurrent promoter/enhancer somatic copy number alterations across >8,000 TCGA samples.

Haruna Tomono[1], Chunyang Bao[2], Antonia Kowalewski[1], David Lehotzky[1], Ron Solan[1], Matthew Leventhal[1], Luis Antonio Corchete Sanchez[1], David I. Heiman[1], Samantha Van Seters[1], Saveliy Belkin[1], Sam Wiseman[1], Brian P. Danysh[1], Chip Stewart[1], Vasuki Narasimha Swamy[1], Gengchao Wang[1], Xavi Loinaz[1], Zachary Everton[1], Gang-Hee Lee[2], Won-Chul Lee[2], Hansol Park[2], Ryul Kim[2], Young Seok Ju[2], Esther Rheinbay[1], Gad Getz[1], Andrew D. Cherniack[1], Matthew L. Meyerson[3], Rameen Beroukhim[3]

[1]Cancer Program, Broad Institute of MIT and Harvard, Cambridge, MA,[2]Inocras Inc., San Diego, CA,[3]Department of Medical Oncology, Dana-Farber Cancer Institute, Boston, MA

Somatic copy number alterations (SCNAs) are frequent oncogenic events. Previous studies have identified recurrent gene-level SCNAs using DNA microarray and whole exome sequencing data. These studies have also identified focal amplifications of regulatory regions. High-throughput whole genome sequencing enables deeper, comprehensive analysis of these focal SCNAs in non-coding regions, potentially revealing novel drivers of oncogenesis. To this end, we systematically analyzed SCNAs and structural variants in WGS data from >8,000 tumor-normal pairs across 31 cancer types from The Cancer Genome Atlas (TCGA) using GISTIC2.0 to identify focal, recurrent promoter and enhancer SCNAs near known oncogenes and tumor suppressor genes. We leveraged structural variant calls to orthogonally validate our primary focal SCNA findings. We identified a recurrent amplification event specific to the *EGFR* promoter/enhancer region in a subset of IDH-wildtype glioblastoma samples. This suggests an additional SCNA-driven mechanism for *EGFR* upregulation, distinct from canonical gene body amplification or point mutations, in a fraction of these aggressive tumors. Our ongoing work aims to broaden the landscape of regulatory SCNAs across cancers and validate their transcriptional impact to provide new biological insights and candidate therapeutic targets.

#1979 Genomic profiling of 1,104 consecutive, prospective meningiomas defines the population prevalence of molecular alterations and elucidates potential biomarkers of treatment response.

Minh P. Nguyen, Kanish Mirchia, **Brooke C. Braman**, Ramin A. Morshed, Nancy Ann Oberheim Bush, Javier E. Villanueva-Meyer, William C. Chen, Walter Patrick Devine, Arie Perry, David R. Raleigh

University of California San Francisco, San Francisco, CA

Background: Molecular profiling of meningioma has revealed biologic drivers and therapeutic vulnerabilities that have refined risk stratification and guided clinical trials. Most molecular studies of meningioma are limited to retrospective cohorts, and the population prevalence of meningioma genomic alterations is incompletely understood.
Methods: DNA mutations and copy number alterations (CNAs) were defined across a consecutive cohort of 1,104 meningiomas that were prospectively analyzed using the next-generation UCSF500 DNA sequencing assay at a single institution from 2019 to 2025.
Results: Meningiomas were CNS WHO grade 1 (49.4%), grade 2 (30.9%), grade 3 (7.0%), or undefined (12.7%). Median patient age was 60 years (range 2-91) and 64.1% were female. Patient race included white (39.2%), Asian (10.4%), Black or African American (3.6%), Native American or Alaska Native (0.6%), Native Hawaiian (0.3%), other Pacific Islander (0.3%), other (9.5%), or unknown. Ethnicity was reported as Hispanic or Latino in 125 cases (11.3%). Loss of chromosomes 22q (64.1%), 1p (40.7%), and 14q (22.3%) were the most common CNAs. Multivariate regression identified male sex, increasing age, and Asian vs. white race as significant predictors of multiple CNAs that are associated with poor clinical outcomes, including co-occurrent 1p loss/1q gain (odds ratio [OR] for male sex: 2.79, $p<0.001$; increasing age OR 1.02, $p=0.028$; Asian vs. white race OR 2.77, $p=0.001$). CNA burden was enriched in high grade meningiomas ($p<0.001$), and male sex (OR 10.1, $p<0.001$), increasing age (OR 1.04, $p=0.026$), and Asian vs. white race (OR 4.31, $p=0.047$) were significant predictors of higher CNA burden. The most common short somatic variants (SSVs) were in NF2 (53.6%) and TRAF7 (16.3%), which were mutually exclusive in all but 2 meningiomas. CDKN2A/B homozygous deletions and TERT promoter mutations were identified in 3.1% and 3.6% of meningiomas, respectively. Increasing age was a significant predictor of NF2 (OR 1.02, $p<0.001$) and TERT promoter mutation (OR 1.06, $p=0.001$), and Asian vs. white race was a significant predictor of CDKN2A/B mutation (OR 4.26, $p=0.003$). Median tumor mutation burden (TMB) was 3.4/megabase. Mutations in ARID1A ($p<0.001$), ARID2 ($p=0.028$), CDKN2A/B ($p=0.017$), KMT2D ($p=0.011$), SMARCB1 ($p=0.0061$), TERT ($p<0.001$), TET2 ($p=0.019$), and TP53 ($p=0.0033$) were associated with elevated TMB. Increasing age (OR 1.01, $p=0.02$) and Asian (OR 5.02, $p<0.001$) and Black (OR 2.54, $p=0.004$) vs. white race were significant predictors of higher TMB.
Conclusion: Prospective next-generation DNA sequencing of consecutive meningiomas defines the population prevalence of molecular alterations. These data fill a critical gap in the understanding of biological drivers of meningioma behavior and therapeutic response across demographic groups.

#1980 Pan-cancer LINE-1 retrotransposition landscapes in TCGA whole-genome sequences.

Beomki Lee[1], Ryul Kim[2], Chunyang Bao[2], Hansol Park[2], Gang-Hee Lee[2], Jonghoon Lee[2], Yoonsuh Lee[2], Won-Chul Lee[2], David Lehotzky[3], Ron Solan[3], Antonia Kowalewski[3], Xavi Loinaz[3], Vasuki Narasimha Swamy[3], David I. Heiman[3], Samantha Van Seters[3], Saveliy Belkin[3], Sam Wiseman[3], Andrew D. Cherniack[3], Luis Antonio Corchete Sanchez[3], Brian P. Danysh[3], Zachary Everton[3], Chip Stewart[3], Haruna Tomono[3], Gengchao Wang[3], Esther Rheinbay[3], Gad Getz[3], Cheng-Zhong Zhang[3], Young Seok Ju[2]

[1]Graduate School of Medical Science and Engineering, Korea Advanced Institute of Science and Technology, Daejeon, Korea, Republic of,[2]Inocras Inc., San Diego, CA,[3]Broad Institute, Cambridge, MA

Overexpression of LINE-1 (L1) elements is recognized as a hallmark of many cancers, yet their activity and the number of somatic LINE-1 retrotranspositions (soL1Rs) vary markedly across tumor types. Despite their ubiquity in certain cancers, such as esophageal and colorectal carcinomas, the biological significance of transposable elements in cancer development remains underappreciated. To elucidate the contribution of L1 activity to oncogenesis, we analyzed whole-genome sequencing (WGS) data from >8,000 tumor-normal pairs in The Cancer Genome Atlas (TCGA). In total, we identified over 132,000 soL1R events, with their distribution differing widely across cancer types. The highest soL1R burdens were observed in esophageal carcinoma (ESCA, 134.2 events per case), bladder carcinoma (BLCA, 74.0), head and neck squamous cell carcinoma (HNSC, 56.3), lung squamous cell carcinoma (LUSC, 53.3), colon adenocarcinoma (COAD, 29.7), and rectal adenocarcinoma (READ, 16.8). The number of transductions correlated strongly with the overall soL1R burden in each cohort. Activity of germline LINE-1 source elements, inferred from transduction counts, identified 22q12.1-2 as the most active locus, followed by Xp22.2-2, 5q14.3-2, and 14q23.1. Using L1 transduction events, we further discovered 12 previously unreported germline LINE-1 source loci. Functional analysis revealed that soL1R events contribute to oncogenesis through both direct disruption of tumor suppressor genes and complex genomic rearrangements mediated by retrotransposition. In summary, this population-scale WGS analysis delineates the pan-cancer landscape of somatic LINE-1 retrotranspositions, uncovers novel germline source elements, and highlights the multifaceted role of soL1R activity in cancer genome evolution.

#1981 Absence of somatic copy number alterations in non-neoplastic prostate epithelium.

Ajay Vaghasia[1], Levent Trabzonlu[2], Anuj Gupta[3], Ibrahim Kulac[4], Busra Ozbek[5], Jiayu Chen[1], Qizhi Zheng[3], Jessica L. Hicks[3], Tracy Jones[3], Roy Elias[6], Alyza Skaist[3], Jennifer Meyers[3], Kornel Schuebel[3], Christopher M. Heaphy[7], Alan K. Meeker[6], William G. Nelson[8], Angelo Michael De Marzo[3], Srinivasan Yegnasubramanian[1]

[1]Oncology, Johns Hopkins University School of Medicine, Baltimore, MD,[2]Pathology, University of Illinois Chicago, College of Medicine, Chicago, IL,[3]Johns Hopkins University School of Medicine, Baltimore, MD,[4]Johns Hopkins Univ., Baltimore, MD,[5]Kocaeli University, İzmit, Turkey,[6]Johns Hopkins University, Baltimore, MD,[7]Boston University, Boston, MA,[8]Sidney Kimmel Comprehensive Cancer Center, Cockeysville, MD

Somatic copy number alterations (CNA) in cancer driver genes are a hallmark of human cancers, but have recently been reported in benign tissues in a handful of organ systems, including the prostate. However, these recent findings may be confounded by technical limitations and challenges in accurately ruling out cancer precursors such as intra-epithelial neoplastic lesions, particularly in frozen tissue. To address this, we used a panel of molecular markers to definitively distinguish benign glands from prostatic intra-epithelial neoplasia (PIN) and invasive cancer in frozen tissue sections, and used this as a guide for laser capture microdissection followed by whole genome sequencing to assess copy number alterations. Our analysis of 171 benign samples from 138 subjects revealed a complete absence of large copy number alterations (LCNA) in benign epithelium, including at key driver genes such as MYC, PTEN, RB1, and APC. In contrast, a significant fraction of PIN exhibited intermediate LCNA levels between benign and cancer. A post-hoc review of these copy number altered PIN lesions indicated that they would have been highly difficult to distinguish morphologically from benign prostate without the use of the panel of molecular markers. These results highlight the importance of rigorous molecular approaches for tissue diagnosis in frozen tissue and suggest that previous reports of CNA in benign prostate may reflect misidentified PIN.

#1982 Genomic analyses of patient-derived xenografts reveal novel molecular subsets of PDAC and their association with clinical features.

Chani Stossel[1], Rotem Tal[2], Rouven Hoefflin[2], Maria Raitses-Gurevich[1], Dikla Atias[1], Yulia Glick Gorman[1], Gali Altman[1], Tamar Beller[1], Talia Golan[1], Itay Tirosh[2]

[1]Sheba Medical Center, Tel Hashomer, Israel,[2]Weizmann Institute of Science, Rechovot, Israel

Pancreatic ductal adenocarcinoma (PDAC) is a dismal disease with limited therapeutic options. We have established a large-scale RNA-seq dataset comprised of >120 PDAC patient-derived xenograft (PDX) models and >300 bulk RNA-seq specimens (when counting biological replicates). This cohort includes diverse PDAC clinical manifestations, such as patients with particularly low survival (<8 weeks) that are under-represented in other large-scale efforts (e.g. TCGA). Our analysis identified two transcriptional programs with a highly heterogeneous expression among the basal-like models: a unique partial-Epithelial-to-Mesenchymal program (Basal-Mesenchymal) and an epithelial senescence-associated program (Basal-EpiSen), reminiscent of the pan-cancer epithelial senescence-associated program that we recently described in other epithelial malignancies. Notably, high expression of the Basal- Mesenchymal program is strongly associated with low-survival and with models established from patient's tumors at terminal stage. Next, we compared representative Basal- Mesenchymal and Basal-EpiSen PDAC cell lines across the comprehensive Cancer Cell Line Encyclopedia (CCLE) drug response dataset. Our initial results show differential drug sensitivity and gene dependencies between the Basal- Mesenchymal and Basal-EpiSen subsets, highlighting their potential clinical significance. We show that the Basal-like subtype diverges into two distinct clinically-relevant subsets. Taken together, our work provides an unprecedented resource towards improving PDAC molecular classification, an essential step for PDAC precision medicine.

#1985 Optimizing precision oncology: A large scale clinico-genomic analysis of WES versus targeted panels in 37,898 patients.

Jing Hu[1], Minghui Wang[2], Junqiang Yin[3], Aibo Xia[1], Zanmei Xu[4], Shaohua Yuan[4], Yannan Zhu[4], Kunxu Xu[4], Yimin Guan[4], Haiyin Huang[4], Kai Wang[4]

[1]The First People's Hospital of Yunnan Province, KunMing, China,[2]Sun Yat-sen Memorial Hospital, Guangzhou, China,[3]First Affiliated Hospital of Sun Yat-sen University, Guangzhou, China,[4]OrigiMed, Shanghai, China

Background: Next-generation sequencing (NGS) is now routine in oncology practice, but clinicians still face uncertainty about how whole-exome sequencing (WES) compares with large targeted panels for identifying actionable alterations and guiding immunotherapy decisions. We addressed this by benchmarking these platforms within a massive clinico-genomic cohort to define their specific clinical utility.

Methods: We retrospectively analyzed 37,898 tumor-normal pairs tested in a CAP/CLIA-certified laboratory: 3,360 WES tests (covering ~20,000 genes) and 34,538 hybrid capture targeted panels (covering ~500 cancer genes). We compared detection rates for single nucleotide variants (SNVs), copy number variants (CNVs), and rearrangements. Clinical variables, including stage and treatment history, were integrated to evaluate molecular patterns.

Results: WES cases were enriched for lung adenocarcinoma, gastric, and colorectal cancers, whereas panel testing was dominated by lung adenocarcinoma, colorectal cancer, and hepatocellular carcinoma. Across all tumors, 701,119 somatic alterations were identified. WES yielded a mean of 76.7 alterations per patient and panels 12.8 per patient. Although WES covered the entire exome and detected clinically expected events such as >20% *ERBB2* amplification in breast cancer and >4% *ALK* fusions in lung adenocarcinoma, its overall CNV and fusion detection remained clearly lower than panel, which showed much higher sensitivity due to deeper, specially targeted coverage. Mean TMBs were 6.5 muts/Mb (WES) and 8.8 muts/Mb (panel), with good agreement between platforms; overall, 17.0% of patients were TMB-High (≥10 muts/Mb). On both platforms, TMB-H was most frequent in endometrial carcinoma, lung squamous cell carcinoma, and urothelial carcinoma, while pancreatic and clear cell renal carcinomas showed very low TMB. Importantly for clinical decision making, early stage patients also harbored TMB-H tumors, indicating that potential candidates for immune checkpoint inhibitors are not restricted to advanced disease. Treatment-naïve patients had higher TMB-H rates than previously treated patients (22.5% vs 16.2%), consistent with therapy-driven clonal selection and supporting baseline TMB testing at initial diagnosis. The most frequently mutated genes were similar across platforms (*TP53*, *EGFR, KRAS*). Actionable alterations were common: 68.1% of panel cases carried at least one actionable gene.

Conclusions: In this largest real world clinico-genomic cohort of Chinese cancer patients, we define the complementary utility of each platform. Whereas targeted panels excel at detecting clinically actionable alterations, WES delivers a comprehensive genomic blueprint that is well suited as a baseline for future minimal residual disease monitoring and the identification of novel biomarkers.

#1986 The pan-cancer landscape of chromosome Y alterations.

Luis Antonio Corchete Sanchez[1], Chunyang Bao[2], Saveliy Belkin[3], Andrew D. Cherniack[3], Brian P. Danysh[3], Zachary Everton[3], David I. Heiman[3], Ryul Kim[2], Antonia Kowalewski[3], Gang-Hee Lee[2], Won-Chul Lee[2], David Lehotzky[3], Xavi Loinaz[3], Vasuki Narasimha Swamy[3], Hansol Park[2], Ron Solan[3], Chip Stewart[3], Haruna Tomono[3], Samantha Van Seters[3], Gengchao Wang[1], Sam Wiseman[3], Young Seok Ju[2], Gad Getz[3], Esther Rheinbay[1]

[1]Krantz Family Center for Cancer Research, Massachusetts General Hospital Cancer Center, Charlestown, MA,[2]Inocras Inc., San Diego, CA,[3]Broad Institute of MIT and Harvard, Cambridge, MA

Background: Despite the well-documented male bias in the incidence and mortality of most non-sex-specific cancers, the Y chromosome (chrY) remains as a genomic blind spot. Major pan-cancer genomic consortia, including The Cancer Genome Atlas (TCGA) and PCAWG, have historically excluded the chrY from somatic analyses due to computational challenges related to its haploid state, repetitive structure, and homology with the X chromosome. Consequently, the somatic landscape of chrY alterations, including complete loss of Y (LOY), structural variants (SVs), single-nucleotide variants (SNVs), and INDELs, remains largely uncharacterized.
Methods: We implemented a pan-cancer computational framework utilizing deep whole-genome sequencing (WGS) data from a comprehensive re-analysis of 26 cancer types from the TCGA cohort. We developed and applied a novel bioinformatic pipeline to accurately call somatic LOY, complex SVs, SNVs, and INDELs. The pipeline was specifically designed to overcome analytical challenges of the chrY, including its repetitive structure and the correct handling of pseudoautosomal regions (PARs). Potential artifacts were flagged using variant-support metrics and by identifying breakpoints in problematic regions.
Results: The analysis revealed a highly heterogeneous landscape of chrY alterations across tumor types. We found a high prevalence of somatic SVs in some tumor types, such as bladder (BLCA), head and neck (HSNC), stomach (STAD), and prostate (PRAD) cancers, while others, like thyroid (THCA) and renal clear cell carcinoma (KIRC), were rarely affected. In affected tumors, the SV landscape included numerous inter-chromosomal translocations, which often showed low variant allele frequency (VAF), suggesting a subclonal origin. In contrast, the clonality of chrY deletions varied across cancer types. The SNV/INDEL burden was substantial in certain cancers, for example, in glioblastoma (GBM) and PRAD, but was concentrated in non-coding regions, with protein-coding mutations being infrequent. Interestingly, we observed a chrY SNV spectrum enriched in C>T and T>C substitutions across several tumor types.
Conclusion: We developed a computational framework to systematically analyze the Y chromosome across multiple cancer types, overcoming historical analytical challenges. Our results reveal a diverse spectrum of somatic alterations, including structural variants and point mutations. These findings provide the first comprehensive, pan-cancer map of the somatic chrY landscape.

#1988 Human and viral whole genome sequencing identify HPV and APOBEC as oncogenic drivers in sinonasal squamous cell carcinoma.

Harrison B. Chong[1], Michael E. Bryan[2], Maoxuan Lin[1], Magdy Gohar[1], William C. Faquin[3], Lisa J. Mirabello[4], James S. Lewis[5], Michael S. Lawrence[6], **Daniel Faden**[7]

[1]Krantz Family Center for Cancer Research, Massachusetts General Hospital, Boston, MA,[2]Otolaryngology-Head and Neck Surgery, Mass General Brigham, Boston, MA,[3]Pathology, Massachusetts General Hospital, Boston, MA,[4]NCI Div. of Cancer Epidemiology & Genetics, Bethesda,[5]Otolaryngology-Head and Neck Surgery, Vanderbilt University Medical Center, Nashville, TN,[6]Broad Institute of Harvard and MIT, Cambridge, MA,[7]Mass General Brigham, Boston, MA

Background:
Sinonasal squamous cell carcinoma (SNSCC) is a rare, aggressive malignancy with limited molecular characterization. Emerging evidence implicates human papillomavirus (HPV) in a subset of cases, but the genomic interplay between viral and host factors remains poorly defined.

Methods:
We performed paired host and viral whole-genome sequencing (WGS) on 21 SNSCC tumors with matched normal samples, including ultra-deep viral WGS (10,000×) and comprehensive HPV PCR genotyping. Somatic mutations, viral integration, structural variants, and mutational signatures were analyzed using established computational pipelines.

Results:
Eighteen of 21 (86%) tumors were HPV-positive by WGS or PCR, with 94% concordance across assays. Unlike oropharyngeal squamous cell carcinoma (OPSCC), where HPV16 predominates, SNSCC exhibited nine HPV genotypes, including HPV11, 18, 35, 39, 45, 51, 56, and 59. Viral integration events were detected in most HPV-positive tumors, including an HPV45-TP63 fusion amplified as extrachromosomal DNA (ecDNA), representing, to our knowledge, the first HPV-associated ecDNA-like amplicon in SNSCC. Multi-genotype infections showed a single dominant integrating type, indicating that one “driver” genotype typically initiates tumorigenesis. Host mutational analysis revealed recurrent clonal mutations in PIK3CA, CHEK2, and KDM6A, with depletion of TP53 and CDKN2A alterations in high-risk HPV+ cases. Mutational signature analysis identified predominant APOBEC3 activity, independent of smoking, which extended to viral genomes, providing direct evidence of concurrent host-virus APOBEC mutagenesis. Structural variants were common, including focal PTEN loss and complex rearrangements such as chromothripsis and chromoplexy, underscoring pervasive genomic instability.

Conclusions:
Paired human and viral WGS reveals that HPV drives tumorigenesis in SNSCC through diverse genotypes, APOBEC-mediated mutagenesis, and integration-linked ecDNA formation. These mechanisms expand the known spectrum of viral oncogenesis beyond the oropharynx, highlighting novel routes of genomic instability and supporting the inclusion of broad HPV genotyping and viral-genomic assays in diagnostic and translational frameworks for SNSCC.

#1989 Systematic discovery and classification of structural variant drivers across >8,000 TCGA whole genomes.

Antonia Kowalewski[1], Xavi Loinaz[1], Hansol Park[2], Vasuki Narasimha Swamy[1], David Heiman[1], Samantha Van Seters[1], Saveliy Belkin[1], Sam Wiseman[1], Chunyang Bao[2], Andrew D. Cherniack[1], Luis A. Corchete Sanchez[1], Brian P. Danysh[1], Zachary Everton[1], Ryul Kim[2], Gang-Hee Lee[2], Won-Chul Lee[2], David Lehotzky[1], Ron Solan[1], Chip Stewart[1], Haruna Tomono[1], Gengchao Wang[1], Rameen Beroukhim[1], Young Seok Ju[2], Esther Rheinbay[1], Gad Getz[1]

[1]Broad Institute, Cambridge, MA,[2]Inocras Inc., San Diego, CA

Structural variants (SVs)—large-scale genomic deletions, duplications, inversions, and translocations—can promote tumorigenesis by activating proto-oncogenes, disrupting tumor suppressors, generating oncogenic fusions, rewiring gene regulation, and mediating catastrophic events such as chromoplexy and chromothripsis. Yet, the role of SVs as cancer-driving mutations remains less comprehensively characterized than that of single-nucleotide variants or indels, largely due to the historic scarcity of tumor whole-genome sequencing data required for accurate SV detection. In this study, we analyzed whole-genome sequencing data from >8,000 tumor-normal pairs spanning 31 cancer types from The Cancer Genome Atlas (TCGA) to systematically characterize SVs at unprecedented scale. Compared with the flagship Pan-Cancer Analysis of Whole Genomes (PCAWG) project, our analysis includes roughly four times as many samples and six additional cancer types. Somatic SVs were identified using a custom pipeline combining Manta and dRanger with optimized downstream filters. Across all tumors, we detected >1 million somatic SVs. We developed two complementary frameworks to interpret these variants. First, to classify SVs by their genomic architecture, we inferred genomic segments and their associated copy number alterations driven by SVs ranging from a single to hundreds of breakpoints, enabling the generalization of distinct patterns through unsupervised clustering. Second, to identify candidate driver genes, we developed SVelfie, a statistical framework that detects genes significantly enriched in functional SVs predicted to confer gain- or loss-of-function effects. Applying SVelfie to 385 prostate and 333 ovarian cancer genomes revealed multiple novel candidate driver genes, with additional discoveries expected as analysis extends to the full >8,000-sample dataset. This work represents the most comprehensive analysis to date of SV drivers in cancer. By uniting large-scale WGS data with new computational frameworks for SV classification and driver detection, we expand the catalog of SV-driven cancer genes, illuminate mechanisms of SV-mediated oncogenesis, and advance the clinical utility of whole-genome sequencing in precision oncology.

#1990 Pan-cancer PCR-free whole-genome sequencing refines the somatic driver landscape beyond exome sequencing alone.

Gengchao Wang[1], David I Heiman[2], Vasuki Narasimha Swamy[2], Chip Stewart[2], Xavi Loinaz[2], Ron Solan[2], Chunyang Bao[3], David Lehotzky[2], Brian P Danysh[2], Luis Antonio Corchete Sanchez[1], Zachary Everton[2], Sam Wiseman[2], Antonia Kowalewski[2], Samantha Van Seters[2], Saveliy Belkin[2], Haruna Tomono[2], Andrew D Cherniack[2], Ryul Kim[3], Gang-Hee Lee[3], Won-Chul Lee[3], Hansol Park[3], Rebecca Jang[3], Young Seok Ju[3], Gad Getz[2], Esther Rheinbay[1]

[1]Krantz Family Center for Cancer Research, Massachusetts General Hospital Cancer Center, Charlestown, MA,[2]Cancer Program, Broad Institute of MIT and Harvard, Cambridge, MA,[3]Inocras Inc., San Diego, CA

Background: The initial TCGA exome sequencing project established a foundational catalog of somatic mutations. However, capture biases and limited coverage in GC-rich and repetitive regions may have obscured bona fide driver events and introduced systematic “blind spots” in the landscape of protein-coding genes. Leveraging high-depth, PCR-free whole-genome sequencing (WGS), we revisited the somatic mutation landscape in multiple tumor types to enhance driver discovery by improving sensitivity in GC-rich regions and reducing artifact-driven false positives.

Methods: We analyzed matched tumor–normal PCR-free WGS data from >8,000 TCGA cases across several cancer types with existing previously published somatic mutation calls from whole exome sequencing (WES) data, applying a unified best-practice pipeline for SNV/indel detection and stringent post-calling filters. We focused on (i) concordance between WGS and exome across coding regions, (ii) coverage, allele fraction, and local sequence context (GC content, segmental duplications) of discordant sites, and (iii) recurrence and positional clustering of variants in established cancer genes.

Results: PCR-free WGS identified substantially more high-confidence coding mutations than WES, with the greatest gains in GC-rich exons and difficult-to-capture loci. This increased sensitivity uncovered additional pathogenic or likely pathogenic variants in canonical drivers, including *TP53* and *FOXA1* in breast cancer, *EGFR* in glioblastoma, and *BAP1* in uveal melanoma (UVM), thereby strengthening known genotype–phenotype associations. In UVM, we observed an indel in the *BAP1* 5′UTR/promoter region that was systematically missed by WES but supported by robust read evidence in WGS data, nominating an expanded spectrum of BAP1-disrupting events with potential regulatory and clinical relevance. Conversely, we found a subset of WES-only calls localized to segmental duplications or low-support sites, consistent with technical artifacts. Integrated re-annotation of discordant calls thus both eliminates spurious events and reveals underappreciated driver mutations and mechanisms.

Conclusions: Our systematic comparison demonstrates that PCR-free WGS can refine the somatic mutation and driver landscape beyond exome-based catalogs, particularly in GC-rich and regulatory regions. These results advocate for re-interrogation of previously profiled tumor types with contemporary WGS to achieve a more complete and accurate map of cancer-driving alterations.

#1991 Germline predisposition in The Cancer Genome Atlas (TCGA) whole-genome sequencing datasets.

Ryul Kim[1], Owen Hirschi[2], Matthew Leventhal[3], Chunyang Bao[1], Hansol Park[1], Gang-Hee Lee[1], Won-Chul Lee[1], Jonghoon Lee[1], Yoonsuh Lee[1], Beomki Lee[4], David Lehotzky[5], Ron Solan[5], Antonia Kowalewski[5], Xavi Loinaz[5], Vasuki Narasimha Swamy[5], David I. Heiman[5], Samantha Van Seters[5], Saveliy Belkin[5], Sam Wiseman[5], Andrew D. Cherniack[5], Luis Antonio Corchete Sanchez[5], Brian P Danysh[5], Zachary Everton[5], Chip Stewart[5], Haruna Tomono[5], Gengchao Wang[5], Esther Rheinbay[5], Gad Getz[5], Cheng-Zhong Zhang[3], Matthew L. Meyerson[2], Young Seok Ju[1]

[1]Inocras, San Diego, CA,[2]Department of Medical Oncology, Dana-Farber Cancer Institute, Boston, MA,[3]Department of Data Science, Dana-Farber Cancer Institute, Boston, MA,[4]Korea Advanced Institute of Science and Technology, Daejeon, Korea, Republic of,[5]Cancer Program, Broad Institute of MIT and Harvard, Cambridge, MA

The goal of The Cancer Genome Atlas (TCGA) has been to continually characterize the genomic and transcriptomic landscapes across diverse malignancies. In this analysis, we assess matched tumor-normal Whole-Genome Sequencing (WGS) data from a previously sequenced set of adult cancer patients to identify germline pathogenic variations. These latest TCGA data consist of cancer patients from varied ancestral backgrounds with solid tumors and lymphoid cancers and patient-matched normal samples, consisting of blood or tissue. We have now obtained high-quality tumor and normal WGS data from over 8,000 samples, including normal samples derived mainly from the patient-matched blood samples. To discover novel links between genetics and cancer predisposition, we are analyzing germline variants—including single-nucleotide variants (SNVs) and structural variants (SVs)—in known cancer genes, as well as in genes with recurrent mutations that may have been missed or previously could not be assessed using exome or low-coverage genome studies.We have conducted a preliminary analysis focused on identifying Pathogenic or Likely Pathogenic (P/LP) variants, classified according to American College of Medical Genetics and Genomics guidelines, in cancer predisposition genes. This initial pass on a majority of samples confirmed the presence of P/LP variants across the cohort in canonical cancer predisposition genes, including *BRCA1*, *BRCA2*, *ATM*, and other genes integral to the mismatch and DNA repair pathways. Across cohorts, we identified known P/LP germline variants in established cancer predisposition genes in less than 10% of all cases, with the largest number of variants identified in *BRCA1/2*, aligning with previous published work. The prevalence of P/LP variants was not uniform across cancer types, with some showing an enrichment, including breast cancer, while other cancer types, like low-grade gliomas, demonstrated a lower prevalence than the average. These findings underscore the highly variable, tumor-specific landscape of germline predisposition.We continue to leverage this comprehensive WGS dataset as a key resource for ongoing analyses of germline-somatic interactions. We are actively investigating how these germline P/LP variants shape the tumor's somatic mutational landscape and contribute to oncogenesis. We are also investigating whether haplotype-specific copy number alterations contribute to the pathogenicity of identified germline cancer risk alleles. Further work includes characterizing both structural and complex non-coding pathogenic variants that were previously inaccessible in exome or low-coverage WGS studies.

#1992 Delineating genomic instability dynamics in breast cancer by bulk and single-cell whole genome sequencing.
Konstantinos L. Georgiadis, Sen Li, Thomas Hatschek, Theodoros Foukakis, Nicola Crosetto

Karolinska Institutet, Stockholm, Sweden

The aim of this study is to chart the evolution of genomic instability in response to treatment in hormone receptor-positive/HER2-negative ($HR^+/HER2^-$) breast cancer, the most prevalent breast cancer subtype, comprising approximately 70% of cases. Copy number alterations (CNAs) are a hallmark of aggressive $HR^+/HER2^-$ tumors and have been proposed as prognostic biomarkers; however, their temporal dynamics during therapy remain insufficiently characterized. Here, we utilized tissue biopsies collected in the context of the PREDIX Luminal B clinical trial (NCT02603679), which aims to evaluate the role of paclitaxel chemotherapy versus the combination of endocrine treatment with the CDK4/6 inhibitor palbociclib in the neoadjuvant setting. We conducted bulk whole genome sequencing (WGS), whole exome sequencing (WES) and RNA sequencing of tissue biopsies (n = 169 patients) collected before and after treatment. In a subset of the study cohort, we also performed single-cell WGS (n = 15 patients, 8,387 cells) on samples before and after each treatment modality. Bulk sequencing data analysis and correlation with clinical outcomes indicated candidate genomic regions linked to therapeutic response, including arm-level gains and losses selectively enriched in post-treatment samples of patients who responded to treatment. Integration with RNA-sequencing data revealed gene-dosage relationships on amplified or deleted chromosomal regions and highlighted genes with potential functional impact. Moreover, single-cell WGS further resolved the subclonal architecture of these tumors, indicating that most patients exhibit limited subclonal complexity. Neoadjuvant treatment reshaped the tumor genomic landscape through expansion or contraction of pre-existing subclones rather than emergence of new subclones. Correlation of response to treatment with subclonal shift patterns demonstrated that non-responding tumors display pronounced alterations in their subclonal composition whereas responding tumors present heterogeneous patterns of subclonal dynamics. Our findings suggest that interpatient variability in treatment response is driven by clonal remodeling of pre-existing subclones rather than de novo subclone generation, and that recurrent CNAs may serve as predictive biomarkers of neoadjuvant treatment efficacy.

#1993 Real-world landscape of KMT2A and NPM1 variants and fusions in hematologic malignancies (2020-2025).

Roisin Puentes, Madhuri Paul, Ryan Bender, Amber Chevalier, Nathan Montgomery

NeoGenomics, Fort Myers, FL

Background: KMT2A rearrangements and NPM1 mutations are key genomic drivers in myeloid neoplasms, informing diagnosis, prognostication, MRD assessment, and emerging targeted therapies. Large-scale real-world data are needed to clarify testing trends, positivity rates, and co-mutational patterns across hematologic indications.
Methods: We analyzed all KMT2A and NPM1 tests performed in a national reference laboratory cohort from 10/1/2020-9/30/2025. Test modality, indication, and positivity were evaluated, as well as variant classification, fusion partners, and aggregated co-mutations for positive cases.
Results: Across the study period, 201,381 KMT2A and 202,902 NPM1 tests were performed, with positivity rates of 2.6% and 3.1%, respectively. Annual testing volume increased substantially for both markers, driven by hospital-based ordering and expanding NGS utilization. Testing spanned both sexes and all ages, with most samples originating from patients ≥65 years. Top testing indications were MDS, AML, and MPN/CMML. KMT2A positivity was most frequent in AML (1,964), MPN (1,369), and MDS (353). NPM1 positivity was enriched in MDS (6,170), AML (1,191), and CMML (541). Over time, use of NGS expanded significantly from 2021 onward, becoming the dominant modality for NPM1 testing and complementing ongoing FISH testing for KMT2A, with positivity detected across both platforms. Among KMT2A-positive cases, SNVs (86%) and fusions (9%) were observed, with most pathogenic findings occurring in fusion-positive samples. Common fusion partners included MLLT3, AFF1, ELL, MLLT4, and MLLT10. Recurrent co-mutations involved TP53, KRAS/NRAS, TET2, FLT3, DNMT3A, and ASXL1. Within AML, 273 of 1,964 KMT2A-positive patients harbored a fusion. NPM1-positive variants were predominantly pathogenic (65%), with co-alterations spanning SNVs, insertions/deletions, and rare fusions. The most frequent co-mutations involved TET2, DNMT3A, FLT3, IDH2, NRAS, and SRSF2.
Conclusions: Testing for KMT2A and NPM1 nearly doubled over five years, driven by widespread adoption of NGS, continued FISH utilization, and increasing clinical relevance of genomically guided therapies for KMT2A- and NPM1-mutated disease, particularly in AML. These findings define a comprehensive real-world genomic profile of KMT2A-rearranged and NPM1-mutated hematologic malignancies and support ongoing efforts in diagnosis, prognostication, and therapeutic development.

#1994 Integrative multi-omic analysis reveals subtype-specific impact of extrachromosomal DNA in melanoma.

Sharadha Sakthikumar, Bryce Turner, Jeffrey Trent, ALEKSANDAR SEKULIC

TGen (The Translational Genomics Research Institute), Phoenix, AZ

Extrachromosomal DNA (ecDNA) drives oncogene amplification, transcriptional deregulation, and therapeutic resistance in cancer, but its prevalence and impact in melanoma remain unclear. We analyzed 470 TCGA-SKCM samples with whole-genome (n = 223), whole-exome (n = 247), and RNA sequencing (n = 469). Tumors were classified as BRAF/NRAS/NF1-mutant (BNN, n = 396) or triple wild-type (TWT, n = 74). ecDNA detection was performed using *AmpliconArchitect* (AA) and *Gene-level Circular Amplicon Prediction* (GCAP). Multi-omic analyses assessed transcriptional, immunologic, and clinical correlates. ecDNA was detected in 133 tumors (28%; 47 by AA, 133 by GCAP, 39 overlapping), with higher prevalence in TWT tumors (51%) than BNN tumors (26%; $\chi^2 = 17.88$, $p = 2.4 \times 10^{-5}$). Frequently amplified ecDNA genes included *MDM2, CDK4, CCND1, BIRC2/3, PAK1, GAB2,* and *RSF1*, implicating proliferation, apoptosis evasion, and chromatin regulation. In an effort to assess putative functional impact, we performed various transcriptomic analyses which identified upregulation of amplified oncogenes (*GAB2, MDM2, RSF1, CCND1, PAK1*). In addition, gene set enrichment analyses with MutSigDB (against Hallmark genes) shows strong enrichment of pathways associated with enhanced cell proliferation, such as MYC and E2F targets in ecDNA+ tumors. In addition, cell deconvolution methods reveal immune cell composition varies across subtypes, highlighting potential unique immunomodulatory effects. Survival analysis indicated worse overall survival in ecDNA+ tumors ($p = 0.016$), driven by TWT cases ($p = 0.0048$). ecDNA is prevalent in melanoma, particularly in TWT tumors, where it promotes oncogene amplification, immunomodulatory reprogramming, and poor prognosis. These results highlight ecDNA as a potential biomarker for stratification and targetable vulnerability in TWT melanoma.

#1995 Clinicogenomic landscape of IPMN-derived pancreatic cancer.

Peter Y. Yu, Joseph R. Habib, Jonah Levine, Brock Hewitt, Michael D. Kluger, Katherine A. Morgan, Anirban Maitra, Christopher Wolfgang, Ammar A. Javed, Greg Sacks

NYU Langone Health, New York, NY

Further understanding of the genomic alterations in intraductal papillary mucinous neoplasm (IPMN)- derived pancreatic cancer and associations with survival outcomes is necessary to identify tailored therapy and improve outcomes. We reviewed resected IPMN-associated pancreatic cancer cases from 2012 to 2025 and identified cases of pancreatic ductal adenocarcinoma (PDAC) where pathology demonstrated that the invasive component arose from an IPMN (not concomitant PDAC). 38 patients with corresponding comprehensive genomic profiling results were identified and clinical characteristics and outcomes data were collected. 30 patients (79%) had KRAS mutated (mt) and 8 patients (21%) had KRAS wild type (WT) tumors. 12 tumors (32%) were mtGNAS and 26 tumors (68%) were GNAS WT. Further examining mtKRAS in the context of mtGNAS, 23 patients' tumors (61%) had mtKRAS alone, 7 (18%) with KRAS and GNAS co-mutation, 5 (13%) with mtGNAS alone, and 3 patients (8%) had neither mutation. KRAS wild type (WT) tumors associated with better overall survival (OS) and disease-free survival (DFS) compared with mtKRAS tumors. mtGNAS tumors associated with better DFS compared with GNAS WT tumors. In the 5 mtGNAS-only tumors, there was an enrichment of CCND2 and MYC gene family co-amplifications (3 out of 5). The other two mtGNAS-only cases had BRAF and MAP2K1 (MEK) mutations. 7 cases (18%) harbored ATM mutations and 2 cases (5%) of RNF43 mutations were identified. In univariate cox regression analysis, only lymphovascular invasion (LVI) was significantly associated with OS. LVI and node positivity were significantly associated with DFS. Despite limited numbers of patients, we have identified KRAS WT and mtGNAS as potential prognostic biomarkers for IPMN-derived PDAC.

#1996 Base editing for systematic reclassification of variants of unknown significance in NF1.

Sara Galavotti[1], Elena Endrizzi[1], Emanuele Bonetti[1], Gabriele Picco[2], Gianmaria Frige[1], Pier Giuseppe Pelicci[1], Luca Mazzarella[1]

[1]Department of Experimental Oncology, Fondazione Istituto Europeo di Oncologia e Centro Cardiologico Fondazione Monzino, Milano, Italy,[2]Wellcome Sanger Institute, Hinxton, United Kingdom

NF1 is an established tumor suppressor, frequently mutated in cancer genomes and responsible for the cancer-predisposing syndrome neurofibromatosis. NF1 is very large (~350 kb) and has one of the highest mutation frequency in the human genome. Due to incompletely understood biology of the coded protein, high sequence homology, allelic heterogeneity and lack of functional assays, the interpretation of NF1 variants is highly challenging in clinical practice. According to the *ClinVar* database, 13460 NF1 variants are listed (data extracted up to July 2024) with missense variants being the most represented type, of which 84.8% are variant of unknown significance - VUS.We recently identified a novel function in microtubular damage repair for NF1 (Duso et al Biorxiv 2025). NF1-deficient cells become highly sensitive to microtubule-depolymerising maytansinoids like DM1. We designed a high-throughput base editing screen that exploits this differential sensitivity to identify NF1 variants that lead to its loss of function.SpliceR was employed to design control guides (non targeting, intragenic and splice essential and non essential targeting regions) while for gRNAs directing to NF1, the BEstimate tool was utilised. As a model, we generated HER2+ breast cancer cell line, HCC-1954 and to 293T cells to stably express lentiviral cytidine-(CBE) and adenosine-base editors (ABE). Editing efficiency is evaluated through the BEAR-GFP reporter plasmid.

We obtained a library covering 8191 variants with 5569 total guides. Of these, the majority are nonsynonymous. We analysed the coverage of known NF1 variants. Based on ClinVar classification, we cover 882 VUS, 68 conflicting interpretation of pathogenicity (CIP), 202 pathogenic/likely pathogenic (P/LP) variants, and 25 benign/likely benign (B/LB) variants. Based on our RENOVO tool for VUS reinterpretation, 4968 covered variants are considered Low-precision Pathogenic or Benign.Key functional domains in NF1 are covered with high density, in particular with 573 variants covering the functional GTPase-activating domain (GAP), 2745 covering the HEAT domain, likely to mediate interactions with microtubules, and 267covering the SecPH domain, essential for membrane localization. 4257 variants in splicing sites and 3 prime untranslated regions (UTR) variants are covered.The results of the functional screen are integrated with public data to develop a novel NF1 predictor based on our RENOVO architecture (Favalli V et al., Am J Hum Genet. 2021 and Bonetti E, et al., Hum Genomics 2025).These tools will be essential to overcome key diagnostic challenges in neurofibromatosis and precision oncology.

#1997 Integrative single-nuclei spatial transcriptomic profiling of primary and recurrent human glioblastoma reveals cell-specific EGFRvIII expression and ANXA1 signaling axis.

Simon G. Gregory[1], Lauren Whaley-Powers[1], Vaibhav Jain[1], Michael Aksu[1], Emily Hocke[2], Alan Smith[2], Stephanie Arvai[2], Ellora Haukefrers[2], Kevin Stevenson[3], Khooshbu Patel[3], Diane Satterfield[3], Elizabeth Thomas[3], Karen Abramson[2], Giselle Y. Lopez[4], Roger E. McLendon[4], David M. Ashley[1]

[1]Neurosurgery, Duke University School of Medicine, Durham, NC,[2]Duke Molecular Physiology Institute, Duke University School of Medicine, Durham, NC,[3]Preston Robert Tisch Brain Tumor Center, Duke University School of Medicine, Durham, NC,[4]Pathology, Duke University School of Medicine, Durham, NC

The World Health Organization provides clear criteria for diagnosing IDH1-wildtype glioblastoma (GBM), relying on traditional approaches to define pathoetiological features, genomic mutations, copy number variation, and aberrant expression of prognostic genes. While these methods guide diagnosis, they may lack the resolution to fully capture tumor heterogeneity, therapeutic response, or outcomes. To address this, we applied leading-edge technologies to 14 primary and recurrent tumors to add granularity to current diagnostic metrics and clinical classification. Aiming to better inform tumor subtyping and improve patient care, this integrative approach enabled us to identify malignant gene programs and localize prognostically relevant features at both single-cell and spatial levels. We analyzed 14 GBM tumors from 6 patients using spatial *in situ* sequencing (ISS) and single-nuclei RNA-sequencing. A custom ISS gene panel enabled spatial mapping of tumor-associated cell types and state markers, while matched snRNA-seq from adjacent tumor tissue provided transcriptome-wide profiles. The dataset enabled subcellular and spatial localization of the prognostic GBM biomarker, EGFRvIII, being enriched in oligodendrocyte progenitor (OPC)-like tumor cells, which provides and exciting insight into the putative cell of origin for GBM. Finally, one patient contributed 5 serially collected during tumor recurrence which enabled longitudinal analysis of tumor evolution. Characterizing these tumors using ligand-receptor interaction analysis of snRNA-seq and spatial data identified an evocative ANXA1 signaling axis that progresses across recurrent tumors, which suggests novel therapeutic opportunities. By extending beyond conventional diagnostic benchmarks, our molecular profiling reveals new insight into GBM biology that may support more refined tumor subtyping and prognostic assessment.

#1998 Minerva: High-Resolution Allele-Specific Copy Number and Complex SV Harmonization with Long Reads.

Ayse G. Keskus, Tanveer Ahmad, Isabel Rodriguez, Anton Goretsky, Ataberk Donmez, Sonam Tulsyan, Nicholas Syracuse, Michael Dean, Mikhail Kolmogorov

NIH-NCI, Bethesda, MD

Copy-number alterations (CNAs) and structural variations (SVs) are major drivers of cancer evolution, yet accurately resolving allele-specific copy number (ASCN) in highly rearranged tumor genomes remains challenging. Conventional approaches often struggle with limited phasing information and inaccurate segmentation. Long-read sequencing offers unique advantages for genome reconstruction, but current CN tools do not fully exploit its long-range phasing or breakpoint-level resolution.We present Minerva, a long-read framework for ASCN calling and complex SV clustering. Minerva integrates high-fidelity structural variation calls from Severus into a breakpoint graph that defines segmentation directly on rearrangement breakpoints. This approach enables chromosome-arm–scale phasing, allowing haplotypes to be followed through long and structurally complex regions. It further provides haplotype-specific coverage estimates and accurate CN assignment even across SV clusters. Minerva supports both tumor–normal and tumor-only workflows, delivering stable ploidy estimation and haplotype-aware CN inference even in the absence of matched normals.
Using the CASTLE long-read somatic cancer cell line panel, we benchmarked Minerva against established short-read and long-read CN methods. Across nearly all cell lines, Minerva achieved higher chromosome-scale CN accuracy, more consistent purity/ploidy estimates, and markedly improved detection of focal CN changes, including deletions, duplications, or more complex events like translocations with deletions. Leveraging the precision of long-read SV breakpoints, Minerva resolves sub-100 bp CN segments, representing orders-of-magnitude finer resolution than short-read approaches. Performance gains were strongest in genomes with dense rearrangements, including fold-back inversions, sysmic amplifications, templated insertions, and ecDNA.
We further applied Minerva to (i) a breast cancer long-read cell-line panel and (ii) a long-read breast tumor cohort. Across both datasets, Minerva identified distinct and recurrent amplification patterns in key oncogenic regions, including MYC, ERBB2, and CCND1, and revealed allele-specific focal events and complex rearrangement architectures missed by existing CN/SV methods.
Minerva provides a unified, phasing-aware solution for high-resolution CN and SV interpretation in tumor-only long-read cancer genomics, enabling more accurate reconstruction of cancer genome structure, selective pressures, and oncogenic amplification landscapes.

#1999 Founder Wnt alterations guide the evolutionary trajectories of colorectal tumorigenesis.

Yoshikage Inoue[1], Nobuyuki Kakiuchi[1], Satoshi Nagayama[2], Yutaro Kuwashima[3], Sekine Shigeki[4], Kenichi Yoshida[5], Koichi Watanabe[1], Satoshi N. Omura[6], Kazutaka Obama[7], Toshiro Sato[3], Seishi Ogawa[1]

[1]The Department of Pathology and Tumor Biology, Kyoto University, Kyoto, Japan,[2]The Department of Gastrointestinal Surgery, Uji-Tokusyukai Medical Center, Uji, Japan,[3]The Department of Integrated Medicine and Biochemistry, Keio University, Tokyo, Japan,[4]The Department of Pathology, Keio University, Tokyo, Japan,[5]National Cancer Center, Division of Cancer Evolution, Japan,[6]The Department of Biological Sciences, The University of Tokyo, Tokyo, Japan,[7]The Department of Gastrointestinal Surgery, Kyoto University, Kyoto, Japan

Colorectal cancer (CRC) is classically divided into hypermutated (HM) and non-hypermutated (NHM) subtypes based on mutation burden. Although NHM tumors account for ~80% of CRC, no widely accepted genetic framework is available to understand CRC heterogeneity. In this study, we analyzed a total of 4,437 CRCs using targeted-capture sequencing across 169 driver genes, along with RNA sequencing of 2,833 tumors. Based on the bimodal distribution of mutation burden, 3,986 were classified as NHM, while HM cases were further resolved into MSI- and *POLE*-mutated CRC. Notably, within NHM CRCs, *APC* mutations, *CTNNB1* alterations affecting exon 3, biallelic *RNF43* mutations, and *RSPO2/3* fusions were almost completely mutually exclusive, a pattern that also held in hypermutated tumors. Leveraging this mutual exclusivity, we classified NHM CRCs into five non-overlapping subgroups: *APC*-mutant (*APC*^{mut}; 90%), *CTNNB1* exon 3-altered (*CTNNB1*^{Exon3}; 2.4%), biallelic *RNF43*-mutant (*RNF43*^{biallelic}; 1.7%), *RSPO2/3* fusion-positive (*RSPO2/3*^{fusion}; 1.7%), and Wnt-negative (Wnt^{WT}; ~1.5%). Accounting for ~10% of NHM CRCs, the *APC*-wild-type subtypes —*CTNNB1*^{Exon3}, *RNF43*^{biallelic}, *RSPO2/3*^{fusion}, and Wnt^{WT}—showed distinct genomic and transcriptomic features and consistently poorer outcomes than *APC*^{mut} CRCs. Among them, the Wnt^{WT} subtype exhibited attenuated Wnt signaling with prominent inflammatory and immune-response signatures, representing a highly inflamed subset distinct from Wnt-pathway-altered CRCs. To further dissect the heterogeneity of *APC*^{mut} CRCs, we quantified the selection pressure acting on different *APC* mutations by calculating amino-acid-level dN/dS values. This analysis revealed five segments within the *APC* coding region with distinct profiles. Mutations within three segments were mutually exclusive even after accounting for biallelic *APC* inactivation. Leveraging this mutually exclusive architecture, we classified *APC*^{mut} tumors into four subgroups (APC1-4). As expected, these CRC subgroups were characterized by different Wnt activation levels as assessed by *AXIN2* expression or GSVA analysis of Wnt-pathway gene sets. Subgroups with lower-Wnt activation (APC3-4) were enriched for *AMER1* or *CTNNB1* minor-hotspot mutations, whereas those with higher-Wnt activation (APC1-2) frequently harbored *TCF7L2/TCF7* mutations. These mutational patterns indicate that colorectal tumors avoid excessively high or low Wnt activity, instead maintaining signaling within a relatively restricted range. The *APC*^{mut} subgroups also differed in their co-mutation profiles, chromosomal instability, tumor location, and clinical outcomes, suggesting that founder *APC* mutations dictate evolutionary trajectories and clinical behavior.In conclusion, we provide an integrated view of how founder Wnt alterations and the positional effects of *APC* truncations shape the molecular and evolutionary landscape of CRC.

#2000 A spontaneous *CTNNB1* driver mutation reversion in a primary ovarian clear cell carcinoma.

Rania Bassiouni[1], Yuxin Jin[1], Lee D. Gibbs[2], Jing Qian[2], Solomon O. Rotimi[2], Heather Miller[2], Michelle G. Webb[2], David W. Craig[1], Javier Arias-Stella[1], Lynda Roman[2], John D. Carpten[1]

[1]City of Hope, Duarte, CA,[2]University of Southern California, Los Angeles, CA

Ovarian clear cell carcinoma (OCCC) is a histologically and clinically distinct subtype of epithelial ovarian cancer that typically demonstrates genomic instability and recurrent copy number (CN) alterations.

Here, we describe an OCCC case from a 46-year-old patient. The primary tumor, staged IIIC, was surgically removed prior to administration of adjuvant treatment. We subjected a fresh-frozen specimen of the primary tumor to nuclear isolation and single cell whole genome sequencing. For single cell CN analysis, sequencing data was processed with the Cell Ranger DNA pipelines (10x Genomics). Following stringent quality filtering, cells were clustered by CN to resolve clonal mixtures.

In addition to diploid cells (cluster 1), the sample contained two clones with distinct CN profiles (clusters 2 and 3), each comprised of additional subclones. The two clones shared some identical CN alterations, suggesting a common ancestor. To determine the order of clone emergence, we performed CN-based phylogenetic analysis, which identified cluster 3 as the earlier clone. This was supported by single cell loss of heterozygosity (LOH) determination, which revealed that LOH in cluster 2 equaled and exceeded that of cluster 3.

Using the diploid component of the sample as a matched germline, we performed somatic variant calling to identify consequential mutations. The two clones shared several hundred somatic passenger mutations, supporting a shared lineage. However, only one candidate driver mutation was identified, a heterozygous *CTNNB1* S37C activating mutation. Interestingly, only cluster 3 - the early clone - harbored the mutation. Examination of B-allele frequencies revealed LOH on chromosome 3, encompassing *CTNNB1*, in cluster 2. Haplotype determination confirmed the loss of the B-allele and a duplication of the wild-type A-allele in cluster 2. Thus, the evidence suggests that the *CTNNB1* driver mutation was lost via a copy-neutral LOH event that retained the wild-type allele.

To determine whether this reversion was reflected in gene expression programs, we performed spatial transcriptomics (10x Genomics) on a formalin-fixed, paraffin embedded specimen of the primary tumor. We identified regions of the tumor corresponding to both clones by positional gene set enrichment. The clones occupied spatially discrete locations and were histologically and transcriptionally distinct. Gene set enrichment analysis confirmed that regions corresponding to cluster 3 were enriched in programs reflecting WNT/β-catenin signaling and epithelial-mesenchymal transition, consistent with an activating *CTNNB1* mutation. Conversely, cluster 2 was enriched in programs for TNFA signaling, hypoxia, and KRAS signaling.

This is the first evidence of an oncogenic driver mutation reversion in an untreated primary tumor and reflects a surprising consequence of chromosomal instability on intra-tumoral heterogeneity.

#2001 Discovery of coding and non-coding driver mutations across >8,000 TCGA whole genomes.

David Lehotzky[1], **Ron Solan**[1], Antonia Kowalewski[1], Nick Haradhvala[1], Xavier Loinaz[1], Hansol Park[2], Vasuki N. Swamy[1], David Heiman[1], Samantha Van Seters[1], Saveliy Belkin[1], Sam Wiseman[1], Chunyang Bao[2], Andrew Cherniack[1], Luis A. Corchete Sanchez[1], Brian P. Danysh[1], Zachary Everton[1], Ryul Kim[2], Gang-Hee Lee[2], Won-Chul Lee[2], Chip Stewart[1], Haruna Tomono[1], Gengchao Wang[1], Young Seok Ju[2], Esther Rheinbay[1], Gad Getz[1]

[1]Cancer Program, Broad Institute, Cambridge, MA,[2]Inocras, San Diego, CA

Cancer driver genes are oncogenes and tumor suppressor genes whose changes in function or expression promotes tumorigenesis. They are used to study cancer behavior, to classify cancer types, and to guide precision medicine. Cancer driver genes are usually identified by statistical analysis of coding mutations in tumor genomes. However, studies searching for new drivers are limited by statistical power, since mutations in each specific driver are often rare, and drivers are often specific to tumor subtypes. In addition, studies relying on whole-exome sequencing miss functionally important noncoding regions, such as promoters, and sequencing using PCR amplification often misses GC-rich and GC-poor regions. As a result, PCR-free whole-genome sequencing (WGS) of larger cohorts is required to continue the discovery of cancer drivers. To comprehensively identify single nucleotide variant (SNV) and indel drivers in cancer, we analyzed >8,000 tumor-normal pairs spanning 31 cancer types from The Cancer Genome Atlas (TCGA) sequenced using PCR-free WGS. We identified somatic SNVs and indels using a custom pipeline, then used MutSig2CV and dNdScv to identify genes under positive selection in coding regions and used Dig to detect increased mutation rates in coding and non-coding regions, including 5'-UTR, 3'-UTR, and promoter sequences. Our analysis identified well-known noncoding drivers, including TERT promoter mutations, TP53 5’-UTR mutations, and NFKBIZ 3’-UTR mutations, as well as some novel candidate cancer drivers, including in non-coding regions. We believe that the new drivers we discovered will provide new insights into the genetic mechanisms of tumorigenesis, aid in the development of cancer therapeutics, and offer a foundation for the use of noncoding driver events in precision oncology.

#2002 The landscape of X chromosome copy number alterations in cancer.

Matthew Joseph Leventhal[1], Chunyang Bao[2], Ron Solan[3], Haruna Tomono[3], Andrew D. Cherniack[3], Luis A. Corchete Sanchez[3], Rebecca Jang[2], Jeehee Suh[2], Antonia Kowalewski[3], Sam Wiseman[3], Samantha Van Seters[3], Saveliy Belkin[3], David I. Heiman[3], Chip Stewart[3], David Lehotzky[3], Vasuki N. Swamy[3], Brian P. Danysh[3], Gengchao Wang[3], Xavi Loinaz[3], Zachary Everton[3], Gang-Hee Lee[2], Won-Chul Lee[2], Hansol Park[2], Ryul Kim[2], Young Seok Ju[2], Esther Rheinbay[3], Gad Getz[3], Cheng-Zhong Zhang[3]

[1]Data Sciences, Dana-Farber Cancer Institute, Boston, MA,[2]Inocras Inc., San Diego, CA,[3]Broad Institute of Harvard and MIT, Cambridge, MA

Copy number alterations are frequent, early events in cancer evolution. Previous pan-cancer analyses have not characterized recurrent copy number alterations on the actively and inactively transcribed X chromosome. The monoallelic expression of the active X chromosome predicts a higher sensitivity of cell fitness to copy number alterations on the active X chromosome than expected from autosomal copy number alterations. Large deletions on the active X chromosome are likely intolerable due to loss of expression of essential genes; a duplication of the active X chromosome will increase chromosome X expression by 100% instead of 50%,which is the expected increase of gene expression from duplication of a single autosome homolog. Recurrent copy number alterations on the X chromosomes could lead to the discovery of new, therapeutically actionable drivers of tumor evolution. We have developed a new method to accurately determine the copy number alterations on the active and inactive X from combined whole genome sequencing and RNA-seq of >8,000 TCGA tumors. We found recurrent copy number gains on the active X chromosome q-arm spanning the telomere. The active X chromosome copy number gains overlapped previously identified cancer genes in the Cancer Gene Census from other tumors such as ATP2B3, FLNA, MTCP1, RPL10, PHF6 and GPC3. These segmental and arm-level gains were not significantly more frequent in patients with whole genome doubling or TP53 mutations. These results suggested that recurrent gains of the q-arm of the active X chromosome were not a result of genomic instability, suggesting that these gains were putative driver events that could be truncal in tumor evolution. Telomere-spanning segmental copy number gains on the q-arm were less common in female glioblastoma or uveal melanoma tumors, which are cancer types that affect both male and female patients. This work shows that copy number gains on the active X chromosome are a new source of cancer driver mutations. The sensitivity of the active X chromosome to selection suggests that genes in recurrent X chromosome amplifications could be new genetic dependencies or therapeutic targets in treating female cancers. The results of this study may identify previously unknown drivers of cancer on the active X chromosome that could be new, effective therapeutic targets in cancer.

#2003 Comprehensive genomic profiling of angiosarcoma cells reveals widespread activation of the RAS pathway.

Donghee Lee, Sun Hee Choi, Md Abdullah, Eslenur Nipa, Jong Hyuk Kim

University of Florida, Gainesville, FL

Angiosarcomas are a heterogeneous group of an aggressive vascular malignancies, with a 40% five-year survival rate and a median overall survival of 16 months for half of patients. These tumors exhibit a high degree of genomic complexity, encompassing a broad spectrum of cancer-related mutations, including *TP53*, *KDR, PTPRB, PIK3CA, NRAS,* and *CDKN2A*. Despite recent advances in genomic and molecular profiling in angiosarcomas, the development of effective therapies targeting these genetic alterations and their downstream functional pathways has been hampered. This limitation is possibly due to incomplete molecular characterization and the scarcity of preclinical research models. Specifically, only a small number of angiosarcoma cell lines are available, and their molecular features and functional properties remain incompletely defined. This hinders the development of robust preclinical models and the discovery of reliable, effective drug targets. The aim of this study is to systematically characterize the genetic landscape of previously uncharacterized angiosarcoma cell lines to identify novel molecular targets and propose clinically relevant therapeutic strategies. First, we established comprehensive genomic profiles, including single nucleotide variants (SNVs), copy number variation (CNV), DNA methylation, and gene expression patterns, across a panel of angiosarcoma cell lines (AS5, ISO-HAS-B, HAMON, KU-CAS3, and KU-CAS5) using Whole Exome Sequencing and Oxford Nanopore sequencing. Our integrated analysis identified alterations in *CDNK2A*, *PTPRB*, and *RAS*, suggesting CDK4/6, TIE2/VEGFR2, and RAS/MAPK as potential molecular targets involved in the proliferation and survival of angiosarcoma cells. Through anti-cancer drug screening, we found that a RAS inhibitor RMC-7977 effectively suppressed angiosarcoma cell growth. Remarkably, RMC-7977 was effective in both RAS-mutated and wild-type angiosarcoma cells, concurrently leading to a reduction in phosphor-ERK and phosphor-S6K levels. In addition, the RAS signaling pathway was broadly activated across primary angiosarcoma patient tissues (n=13), irrespective of the RAS mutation status. These data suggest that RMC-7977 effectively targets the widespread, pathway-level activation of RAS arising from various upstream alterations in genomically complex angiosarcomas. Our ongoing work involves evaluating the *in vivo* efficacy of RMC-7977 in angiosarcoma xenograft models harboring both mutant and wild-type RAS. Furthermore, we will dissect the molecular mechanism underlying this broad RAS dependency by assessing the impact of RMC-7977 on activated RAS and downstream signaling, further supporting the rationale for its clinical use in angiosarcoma.

#2004 Interrogating the genomic co-evolution of the immune system and cancer along the time and treatment continuum.

John Roy Lozada[1], Christine Luo[1], Devin Schmeck[1], Jeffrey S. Miller[1], Akash Patnaik[2], Emmanuel S. Antonarakis[1], Frank Cichocki[3], Justin Hwang[1]

[1]University of Minnesota, Minneapolis, MN,[2]University of Chicago, Chicago, IL,[3]Medicine, University of Minnesota, Minneapolis, MN

Clonal hematopoiesis (CH) is exemplified by the expansion of mutant hematopoietic stem and progenitor cells that may give rise to altered immune repertoires. Driven largely by age and chronic inflammation, CH is historically linked to myeloid malignancies. Although emerging evidence points to a modest prevalence of CH within solid tumors, the impact of these naturally occurring alterations on anti-tumor immunity and therapeutic responses remain less defined.

Here, we employed somatic mutation calling algorithms to detect single nucleotide variants (SNVs) in both epithelial and immune compartments of tumors. Our preliminary analyses of single-cell RNA-sequencing (scRNA-seq) of 32 primary, therapy-naïve prostate tumors encompassing 11 patients identified mutations representative of both CH and prostate cancer. Within the tumor-epithelial compartment, we identified recurrent *FOXA1* class 1C mutations in 27% (3/11), alongside *NCOR1* mutations in 18% (2/11), *IDH1* in 9% (1/11), and *SPOP* in 9% (1/11) of patients. Of note, these SNVs were detected across multiple samples for the same patient. Interestingly, we also detected germline *HOXB13* G84E variants, associated with increased risk for prostate cancer, in 2 cases at a high clonality within epithelial cells (>75%). CH alterations were identified in 27% (3/11) of patients based on the detection of exonic, nonsynonymous SNVs in myeloid cells. Specifically, these variants affected *SF3B2* (variant allele frequency; VAF = 0.30), *UBE2A* (VAF = 0.30), and *KMT2C* (VAF = 0.43) that are predicted deleterious across multiple classifier algorithms. Patients with detectable CH alterations displayed immunologically hotter tumor microenvironments, with CH+ patients having significantly higher proportions of tumor-infiltrating monocytes (16.22% vs 7.13%, Fisher's exact test $p<0.0001$), macrophages (6.49% vs 2.88%, $p<0.0001$), $CD8^+$ T cells (10.35% vs 3.33%, $p<0.0001$), $CD4^+$ T cells (2.81% vs 0.74%, $p<0.0001$), and B cells (1.81% vs 0.59%, $p<0.0001$), and lower epithelial fractions (50.94% vs 69.81%, $p<0.0001$).

In summary, we leveraged de novo mutational algorithms to detect CH alterations in prostate cancer at the single-cell resolution. Further work will integrate our mutational signatures with transcriptomics to elucidate the impact of both cancer- and immune-intrinsic alterations on anti-tumor immunity. Additionally, we will incorporate mitochondrial DNA-based lineage tracing algorithms on matched peripheral blood, primary, and metastatic tumor samples across diverse solid tumor types to deconvolute the spatiotemporal regulation of naturally occurring CH alterations across cancer progression. We envision our findings will illuminate novel drivers of immune function and regulation within solid tumors that may be exploited for future immunomodulatory therapies.

: Metabolic Regulation in Breast and Gynecologic Cancers
Poster Session

#2008 Fasting induces ferroptosis by modulating lipid metabolism in breast cancer.

Claudio Vernieri[1], Giovanni Fuca[2], Francesca Ligorio[2], Laura Tronci[1], Paola A. Corsetto[3], Giulia Salvadori[1], Arta Ajazi[1], Antonino Belfiore[2], Andrea Vingiani[2], Beatrice Cantarelli[1], Mattia Pavani[1], Keagile Bati[1], Lorenzo Drufuca[1], Saverio Minucci[4], Pagani Massimiliano[1], Filippo de Braud[2], Pruneri Giancarlo[2], Angela Bachi[1], Marzia Santamaria[5]

[1]IFOM ETS, the AIRC Institute of Molecular Oncology, Milan, Italy,[2]Fondazione IRCCS Istituto Nazionale dei Tumori, Milan, Italy,[3]University of Milan, Milan, Italy,[4]IEO - European institute of Oncology, Milan, Italy,[5]IFOM-FIRC Institute of Molecular Oncology, Milan, Italy

Introduction: Cyclic fasting and fasting-mimicking diets (FMDs) showed broad antitumor activity in mice with breast cancer (BC), with promising results in patients (pts) enrolled in conpleted or ongoing clinical trials (NCT03340935; NCT03454282; NCT04248998; *NCT05763992*). However, with the exception of glucose and growth factor modulation, the mechanistic determinants of fasting/FMD antitumor activity are poorly understood.

Methods: We combined *in vitro* and *in vivo* experiments in BC models with *ex vivo* analyses of blood and tumor samples collected from BC pts undergoing FMD in the context of clinical trials (NCT03454282; NCT04248998) to investigate the role of lipid metabolism modulation in mediating fasting/FMD antitumor effects. In *in vitro* experiments, we used six murine and human BC cell lines to study the role of polyunsaturated fatty acids (PUFAs) in affecting cell proliferation (IncucyteS3), survival (propidium iodide), apoptosis (cleaved PARP/caspase 3), lipid peroxidation (malondialdehyde, MDA) and ferroptosis during nutrient starvation. In *in vivo* experiments, orthotopic mouse BC models (4T1-bearing BALB/c mice, E0771-bearing C57BL/6J mice and MDA-MB-231-bearing NOD-scid IL2rgnull (NSG) mice) were randomized to control conditions (ad libitum diet), intermittent fasting (IF), oral administration of the PUFAs arachidonic acid (AA) or docosaexahenoic acid (DHA), or a combination of IF and PUFAs, with or without carboplatin. We assessed primary tumor growth, lung metastasis formation (through IVIS) and animal survival. Mass Spectrometry analysis was used to quantify plasma and intratumor free fatty acids (FAs), as well as FAs in lipid fractions, in mice and in patients.

Results: In both mice and pts (n=112) with BC, fasting/FMD-induced reduction of blood glucose and insulin activated lipolysis in fat tissue, followed by an increase of blood and intratumor AA and DHA. Inhibiting lipolysis through BAY 59-9435 reversed the *in vivo* antitumor effects of fasting in mice, thus revealing a crucial role of blood FA increase in nutrient starvation antitumor activity. Among several FAs modulated by fasting, AA and DHA accumulate in mitochondrial phospholipids, where they promote radical oxygen species (ROS) formation, lipid peroxidation and ferroptosis. Combining cyclic fasting with AA/DHA administration resulted in cooperative delay of *in vivo* tumor progression, reduced metastasis formation and prolonged animal survival via ferroptosis activation. These effects were enhanced when chemotherapy was combined with IF plus AA/DHA. Conversely, vitamin E reversed the antitumor effects of nutrient starvation plus AA/DHA.

Conclusions: Ferroptosis emerges as a novel determinant of fasting/FMD anticancer activity via PUFA accumulation. Cyclic fasting/FMD plus AA/DHA supplementation is a new, safe and effective antitumor metabolic combination that deserves investigation in phase I/II clinical trials.

#2009 Targeting metabolic vulnerabilities in basal-like breast cancer.

Amanda Linke[1], Kevin Mott[2], Felix Olivares[1], Michael East[1], Chengheng Liao[3], Qing Zhang[3], Gary L. Johnson[1], Charles M. Perou[2]

[1]Pharmacology, UNC School of Medicine, Chapel Hill, NC,[2]Department of Genetics, UNC School of Medicine, Chapel Hill, NC,[3]UT Southwestern Medical Center, Dallas, TX

Triple Negative Breast Cancers (TNBC) are a biologically heterogeneous clinical subtype of breast cancer with limited treatment options and generally poor prognosis. Basal-like breast cancer (BLBC), which accounts for ~75% of TNBCs by gene expression profiling, is particularly aggressive, highlighting an urgent need to develop targeted therapies for this subtype. Our lab previously identified an enrichment of pyrimidine synthesis metabolites in tumors from BLBC patients. Further, an analysis of the Chinese Breast Cancer Genome Atlas (PMID: 38347143), a multi-omics dataset including 443 breast cancer metabolomics samples, also revealed a similar feature of pyrimidine-enriched metabolites in both BLBC and TNBC tumors. Therefore, we hypothesize that pyrimidine biosynthesis is essential for BLBC survival and may represent a therapeutic vulnerability. To investigate this unique metabolic phenotype, we utilized a panel of syngeneic, serially transplanted, genetically engineered mouse (GEM) model mammary tumors representing multiple breast cancer subtypes (luminal, basal-like, mesenchymal). Metabolomic mass spectrometry of 20 GEM models, including 6 BLBC models and normal mammary glands, identified 2 distinct metabolic subtypes, namely a Nucleotide-enriched and Fatty Acid-enriched groups, mirroring the patterns observed in human breast tumors. To evaluate the dependency of these murine tumors on pyrimidine biosynthesis, we used leflunomide, an FDA-approved dihydroorotate dehydrogenase (DHODH) inhibitor. *In vivo* testing across 4 tumor models, including the basal-like p53-null 2225L model, showed that leflunomide slowed tumor growth and extended survival in 3 models. However, 1 model exhibited resistance, suggesting that combination therapies may still be needed. To identify potential combination therapies based upon DHODH inhibitors, we conducted a drug combination screen using both the murine 2225L and human SUM102 basal-like cell lines. Notably, we found that kinase inhibitors with off-target activity against ENT1 sensitized cells to DHODH inhibition. These findings are currently being validated *in vivo*, which may support a strategy of co-targeting pyrimidine biosynthesis and the nucleotide salvage pathways to overcome resistance.

#2010 Ovarian cancer drives mitochondrial dysfunction via WT1 in tumor associated stroma.

Roja Baruwal[1], Huda Issa Atiya[1], Paige Matusiak[2], Angelina Li[3], Swathi Suresh[1], Geyon Garcia[1], Benjamin K. Johnson[2], Hui Shen[4], Leonard Frisbie[5], Lan G. Coffman[6]

[1]University of Pittsburgh School of Medicine, Pittsburgh, PA,[2]Van Andel Institute Graduate School, Grand Rapids, MI,[3]North Allegheny Senior High School, Pittsburgh, PA,[4]Graduate Student, Van Andel Research Institute, Grand Rapids, MI,[5]University of Pittsburgh, Pittsburgh, PA,[6]University of Pittsburgh Medical Center, Wexford, PA

Ovarian cancer (OvCa) is the deadliest gynecologic cancer with most of its lethality attributed to late diagnosis and early metastasis. Prior work demonstrates that carcinoma associated mesenchymal stem cells (CA-MSC) enhance OvCa metastasis by donating their mitochondria to metabolically vulnerable OvCa cells thus increasing OvCa cell oxidative phosphorylation (OXPHOS). Although we have shown a crucial role for these donated mitochondria in OvCa progression and metastasis, the functionality of CA-MSC mitochondria and how they differ from normal MSC (nMSC) mitochondria is not known. The purpose of this study is to characterize differences in mitochondrial form and function in CA-MSC compared to nMSC with the goal of targeting CA-MSC mitochondria to decrease OvCa progression and metastasis. We discovered that CA-MSC derived mitochondria persist in OvCa cells over multiple passages but fail to incorporate into the host mitochondrial matrix and instead take a donut and punctate shaped morphology which is indicative of mitochondrial stress. Interestingly, mitochondrial ATACseq revealed that CA-MSC, compared to their nMSC counterparts, are enriched in pathogenic mitochondrial mutations. GSEA analysis on RNAseq dataset comparing CA-MSC to nMSC show OXPHOS as one of the top altered pathways. Here we demonstrate that CA-MSC have altered mitochondrial functionality and morphology compared to nMSC. Using 11 patient derived CA-MSC lines and 7 patient derived nMSC lines in a cell mito stress test assay, we found that CA-MSC have increased mitochondrial respiration compared to nMSC. Although CA-MSC mitochondria consume more oxygen, we demonstrate that they are not as efficient as their normal counterparts in coupling this to ATP production. Using confocal and TEM microscopy, we demonstrate that CA-MSC have more networked mitochondria consistent with increased mitochondrial respiration, but we also observe increase in donut and punctate mitochondria, morphologies linked to oxidative stress. Importantly, CA-MSC have increased mitochondrial ROS and decreased mitochondrial membrane potential compared to nMSC, suggesting mitochondrial dysfunction. Using a fluorescent reporter protein, MitoTimer, we demonstrate that CA-MSC accumulate more oxidatively stressed mitochondria and preferentially donate these dysfunctional mitochondria to OvCa cells. Finally, using knockdown and overexpression models, we demonstrate that expression of the Wilm's Tumor 1 (WT1) gene mediates oxidative stress in CA-MSC. Our current study elucidates the functional consequences of the unique mitochondrial phenotype of CA-MSC in OvCa to enable novel targeted strategies to improve outcomes in OvCA.

#2011 Integrin α6β4 stimulates glucose metabolism and NAD(H) production needed to drive invasive growth of triple negative breast cancer cells.

Yiming Sheng, Parvarnee A. Karimpour, Andrew Elliott, Jayla L. Fenderson, Teresa A. Cassel, Penghui Lin, Richard M. Higashi, Andrew N. Lane, Teresa W. M. Fan, Min Chen, Kathleen L. O'Connor

University of Kentucky, Lexington, KY

Integrin α6β4, a laminin receptor preferentially expressed on cells of epithelial origin, is highly expressed in over 80% of TNBC cases and contributes to the aggressive nature of this deadly breast cancer subtype. We recently demonstrated that integrin α6β4 enhances Hif-1α nuclear accumulation, suggesting its role in a pseudohypoxia signature. Hif-1α reprograms cellular metabolic processes, such as glycolysis, as a hallmark of cancer. However, whether glucose metabolism is part of this signature and how integrin α6β4 impacts TNBC glucose metabolism remain unclear. To examine how integrin α6β4 signaling impacts glycolysis, we first applied a Seahorse XF glycolysis stress test to measure the extracellular acidification rate in BT549 cells that stably express integrin β4 (BT549-β4) or an empty vector (BT549-EV). The BT549-β4 cells had significantly increased glycolysis and glycolytic capacity. Next, we used $^{13}C_6$ glucose stable isotope resolved metabolomics to define how integrin α6β4 impacts glucose metabolic pathways. Integrin α6β4 overexpression increased glucose uptake and shunted it into the pentose phosphate pathway compared to control, resulting in increased production of ribose phosphate. Interestingly, the increased ribose phosphate production in BT549-β4 cells was used for ATP synthesis, which is a precursor of NAD, both of which are essential coenzymes and co-substrates for TNBC metabolism. We then measured the expression levels of key proteins in the glycolysis pathway and found that glucose transporters (Glut1 and Glut3) and several enzymes, such as hexokinases and LDHA, are upregulated by integrin α6β4. We further validated that integrin α6β4 promotes invasive growth and upregulates hexokinase I and II protein levels using the EMT6 syngeneic model (EV vs β4). To assess the impact of integrin α6β4-promoted glucose metabolism on cell proliferation and invasive growth, we treated EMT6 cells (EV vs. β4) with various doses of the glucose analog, 2-DG, and monitored cell viability by MTT assays. The results demonstrated that EMT6-β4 cells are more sensitive to 2-DG compared to EMT6-EV cells. Similar results were obtained from BT549 cells grown in 3D. Culturing BT549 (EV vs. β4) and MDA-MB-231 (control vs. β4 KO) cells in low vs. high glucose media, we found that integrin α6β4-driven cell proliferation depends on the levels of glucose. Using shRNAs and specific inhibitors, we found glucose transporters are regulated through integrin α6β4 signaling-driven Hif-1α and KLF5 activation. We further found that integrin α6β4 increased AMPK activation under energy stress and the NAD^+/NADH ratio in cells is significantly decreased by integrin α6β4 signaling. In summary, our data highlights a novel function of integrin α6β4 in altering glucose metabolism and the significant impact on the dynamics of NAD^+/NADH to promote an invasive phenotype of TNBC cells.

#2012 Spatial proteomic profiling of metabolic and cell signaling heterogeneity in breast cancer tumor microenvironment using imaging mass cytometry.

Qanber Raza, **Nick Zabinyakov**, Liang Lim, Christina Loh

Standard BioTools, Markham, ON, Canada

The tumor microenvironment (TME) is a complex ecosystem of tumor and immune cells with dysregulated metabolic and signaling pathways that drive tumor heterogeneity, progression and differential treatment response. Targeting these pathways has emerged as a promising strategy to enhance immunotherapy efficacy. Imaging Mass Cytometry™ (IMC™) systems, leveraging CyTOF™ technology, enable simultaneous detection of >40 markers, providing scalable, high-throughput spatial characterization of the TME with true dynamic range, free from spectral overlap and autofluorescence limitations inherent to fluorescence-based approaches.

We applied IMC technology to interrogate metabolic and signaling programs in human breast cancer using integrated antibody panels: the Human Immuno-Oncology IMC Panel (PN 201509) combined with either the Human Cell Metabolism (PN 201521) or Human Cell Signaling (PN 201522) IMC Panels. This approach enabled simultaneous assessment of energy production, cellular homeostasis and mitogenic signaling. Whole tissue sections were initially imaged in Preview Mode, followed by high-resolution analysis of regions of interest using Cell Mode or Tissue Mode to phenotype tumor and immune cells and evaluate immune activation.

IMC technology revealed spatial heterogeneity in metabolic and signaling states within breast tumors. Tumor regions demonstrated differential energy utilization: Immune cells predominantly infiltrated areas enriched for fatty acid oxidation, whereas tumor regions with anaerobic or aerobic glycolysis corresponded to immune-excluded zones. Signaling pathway activity also varied by cell type. Elevated glycolysis and mTOR activation indicated adaptation to hypoxic and anabolic demands. Wnt signaling and PTEN expression were enriched in tumor cells, whereas MAP kinase signaling was localized primarily to stromal compartments. Unsupervised pixel-clustering and hierarchical analysis using MCD™ SmartViewer further resolved region-specific metabolic and signaling heterogeneity.

IMC systems enable comprehensive spatial profiling of metabolism and signaling in breast cancer, revealing tumor-immune interactions and intratumoral heterogeneity. This high-dimensional spatially resolved approach provides a powerful framework for identifying clinically relevant targets, informing prognostic assessments and guiding development of personalized therapeutic strategies.

For Research Use Only. Not for use in diagnostic procedures.

#2013 Mitochondrial protein translation supports metabolic rewiring of chemo-refractory triple negative breast cancer.

Mariah Joy Berner, Steven W. Wall, Mokryun L. Baek, Audra Lane, Allison S. Greer, Karen Wang, Lacey E. Dobrolecki, Bing Zhang, Jonathan T. Lei, Michael T. Lewis, Gloria Vittone Echeverria

Baylor College of Medicine, Houston, TX

Nearly 45% of patients with triple negative breast cancer (TNBC) treated with chemo-immunotherapy have residual cancer burden, which is associated with relapse and mortality. Previously, our group reported that TNBCs rely heavily on mitochondrial structural and functional adaptations to survive treatment (PMIDs 30996079, 36813854). Additionally, mitochondrial translation-related proteomic profiles of TNBC patients (n=55, PMID 36001024) and orthotopic PDX tumors (n=42, PMID 39713418) reveal a significant association with resistance to carboplatin (CRB), docetaxel (DTX), or their combination. Furthermore, on-treatment biopsies were collected from a subset of patients, and mitochondrial translation proteomic signatures were significantly elevated relative to their matched pre-treatment counterparts. Leading-edge proteins in those pathways included 30 mitoribosome proteins and the accessory protein Oxidase (Cytochrome C) Assembly 1-Like (OXA1L). OXA1L plays two crucial roles in the mitochondria: 1) it promotes translation termination for the 13 mtDNA-encoded mitochondrial respiratory chain (MRC) proteins, and 2) it aids in inner mitochondrial membrane insertion of mtDNA- and nDNA-encoded MRC proteins. Therefore, we hypothesized that mitochondrial translation, supported by OXA1L, is critical for maintaining mitochondrial function and chemoresistance in TNBC.

Knock-down (KD) of OXA1L in TNBC cells significantly reduced MRC protein levels, mitochondrial ‘respirasome’ supercomplex formation, and oxidative phosphorylation (oxphos). Notably, the characteristic elevation of oxphos in ‘residual’ cells surviving CRB treatment was abolished by the KD. Concomitantly, OXA1L KD cells exhibited significantly improved CRB sensitivity relative to control cells. These results underscore the significance of OXA1L in MRC assembly and function in TNBC, as well as its role in supporting chemoresistance.

Though there are no existing inhibitors of OXA1L, we tested the translational potential of our findings by leveraging the mitochondria’s bacterial ancestry through repurposing FDA-approved antibiotics to inhibit mitochondrial translation (PMID 25625193). We demonstrated inhibition of mitochondrial translation, MRC protein production, respirasome formation, and oxphos with low-dose tigecycline (TIG) treatment in TNBC cells. While we observed minimal toxicity to TNBC cells from TIG as a single agent, we found a significant enhancement of sensitivity to conventional chemotherapies, both in vitro and in vivo, in a PDX. In summary, our data reveal the vital role of mitochondrial translation for the metabolic adaptation and survival of chemo-refractory TNBC. Moreover, these data provide evidence that disrupting MRC assembly by inhibiting mitochondrial translation may be a promising approach to overcome mitochondrial vulnerabilities in chemo-refractory TNBC.

#2014 Metabolic adaptations of obesity-accelerated breast cancer..

Amandine Chaix[1], Keren I. Hilgendorf[2], Gregory S. Ducker[2], Edgar J. Hernandez[3]

[1]Nutrition & Integrative Physiology, University of Utah, Salt Lake City, UT,[2]Biochemistry, University of Utah, Salt Lake City, UT,[3]Biomedical Informatics, University of Utah, Salt Lake City, UT

Obesity, defined by a body mass index (BMI) ≥ 30 kg/m^2, increases the incidence, morbidity, and mortality of breast cancer (BC). However, the specific mechanisms linking obesity to BC risk remain poorly understood. Obesity is a complex condition that alters both systemic metabolism and the local tumor microenvironment, creating conditions that can promote tumor growth. Among these changes, the specific contribution of elevated lipid levels to BC growth has not been experimentally tested, despite hyperlipidemia being a common feature of obesity and dysregulated lipid metabolism a hallmark of cancer biology.Using dietary and genetic approaches in immune-competent mice, we demonstrate that elevated circulating lipids are sufficient to accelerate the growth of orthotopic models of triple-negative BC, even in the absence of obesity or changes in blood glucose and insulin levels. Conversely, pharmacological reduction of systemic lipids attenuates BC growth in obese mice, implicating circulating lipids as direct drivers of tumor expansionWeight loss (WL), achieved through lifestyle interventions or bariatric surgery, remains the only recommended strategy for women with obesity who are at risk for, BC patients and BC survivors. However, evidence-based dietary guidelines tailored to this population are lacking. In our model, a ketogenic diet which evoked WL but failed to lower systemic lipids, failed to protect against BC growth, underscoring the importance of directly targeting lipid metabolism in obesity-associated BC.Incretin mimetics (IM) or GLP-1 receptor agonists are revolutionizing the treatment of obesity and its metabolic complications, by inducing substantial WL and improving multiple health outcomes. As their use expands, IMs will increasingly be part of the therapeutic landscape for BC patients and survivors with obesity. Yet emerging epidemiological data suggest that IM-induced WL may not reduce postmenopausal BC incidence or improve disease-free survival. Consistent with these observations, our mouse data show that IM-mediated WL alone does not prevent BC progression unless accompanied by healthy dietary changes. Our data further suggest that both systemic improvements and local changes to the tumor mammary fat pad microenvironment play a key role in controlling BC growth. Together, our findings identify lipids as critical drivers of BC growth and highlight the importance of lowering circulating and local lipid levels, beyond achieving weight loss, to mitigate BC risk in individuals with obesity.

#2015 Beta-hydroxybutyrate alters one-carbon and branched-chain amino acid metabolism in glucose-restricted ER+ breast cancer cells.

Cynthia Cheung[1], Natalija Glibetic[2], Rylee Maldonado[3], Tia Skaggs[3], Scott Bowman[4], Louise Torres[3], Katelynn A. Perrault Uptmor[5], **Michael Weichhaus**[6]

[1]Laboratory of Forensic and Bioanalytical Chemistry, School of Natural Sciences and Mathematics, Chaminade University of Honolulu, Honolulu, HI,[2]Department of Cell and Molecular Biology, John A Burns School of Medicine, University of Hawaii at Manoa, Honolulu, HI,[3]Undergraduate Biology Program, School of Natural Sciences and Mathematics, Chaminade University of Honolulu, Honolulu, HI,[4]Undergraduate Biochemistry Program, School of Natural Sciences and Mathematics, Chaminade University of Honolulu, Honolulu, HI,[5]Nontargeted Separations Laboratory, Chemistry Department, William and Mary, Williamsburg, VA,[6]Laboratory of Molecular Cancer Research, School of Natural Sciences and Mathematics, Chaminade University of Honolulu, Honolulu, HI

Ketogenic diet interventions show promise in breast cancer treatment, yet precise metabolic adaptations remain incompletely characterized. We investigated amino acid metabolic reprogramming in estrogen receptor-positive (ER+) breast cancer cells subjected to glucose restriction with beta-hydroxybutyrate (BHB) supplementation to model ketogenic conditions. MCF-7 and T47D cells were cultured in glucose-restricted medium (5% standard concentration) with graded BHB supplementation (2.5-15 mM) for four days. Metabolomic profiling was performed using comprehensive two-dimensional gas chromatography-mass spectrometry (GC×GC-MS) with Fisher ratio analysis. Targeted quantification of glycine and branched-chain amino acids (BCAAs) was conducted using colorimetric and fluorometric assays. SHMT1 protein expression was measured by ELISA. Bioinformatic analysis of TCGA Breast Invasive Carcinoma data (n=1,084) assessed co-expression patterns between one-carbon metabolism genes (SHMT1/2), BCAA metabolism (BCAT1), and ketone body catabolic enzymes (OXCT1, ACAT1, BDH1). Differential expression analysis was performed on paired ER+ tumor and adjacent normal tissue samples (n=20) from GSE58135. R-code for DEG analysis was partially created using Anthropic Claude (version Sonnet 4.5). Metabolomics analysis revealed significant perturbations in one-carbon and BCAA metabolism pathways. Direct quantification confirmed dose-dependent glycine accumulation, with peak elevation at 5 mM BHB in both MCF-7 (51.1±29.5 µM vs. 27.7±3.9 µM low glucose, $p<0.05$) and T47D cells (40.7±9.8 µM vs. 29.6±9.5 µM, $p<0.05$). Despite altered glycine levels, SHMT1 protein expression remained stable across treatments in both cell lines. TCGA analysis showed weak positive correlations between SHMT1 and ketone catabolic genes BDH1 ($r=0.18$, $p=2.88\times10^{-9}$) and ACAT1 ($r=0.05$, $p=0.133$), while BCAT1 showed moderate negative correlation with BDH1 ($r=-0.36$, $p=3.69\times10^{-35}$). Differential expression analysis revealed significant downregulation of OXCT1 (log2FC=-1.41, $p=5.75\times10^{-7}$), SHMT1 (log2FC=-1.31, $p=1.62\times10^{-5}$), and ACAT1 (log2FC=-1.07, $p=1.07\times10^{-4}$) in ER+ tumors versus normal tissue, indicating selective suppression of ketone catabolism and cytoplasmic one-carbon metabolism. BHB supplementation under glucose restriction induces specific alterations in glycine homeostasis without corresponding SHMT1 changes, suggesting post-translational regulation or altered metabolic flux. Downregulation of ketone catabolic enzymes in ER+ tumors may represent a metabolic vulnerability exploitable through ketogenic interventions, warranting investigation of one-carbon metabolism as a therapeutic target in ER+ breast cancer.

#2016 Metabolic and inflammatory crosstalk underlying cancer-related fatigue (CRF) in a mouse model of breast cancer (BC).

Abigail A. Koomson[1], Susana C. B. Nakandakari[1], Andin Fosam[1], Rosalie M. Grijalva[1], Rachel J. Perry[2]

[1]Cellular and Molecular Physiology, Yale School of Medicine, New Haven, CT,[2]Yale University School of Medicine, New Haven, CT

Cancer-related fatigue (CRF) is among the most prevalent and debilitating side effects of breast cancer and its treatment in women, severely reducing adherence to treatment and quality of life. However, standardized, preclinical metrics for CRF remain poorly defined, impeding the development of therapeutic interventions. We hypothesized that breast cancer-induced physical fatigue is due to metabolic dysregulation in skeletal muscle mitochondria. Using the syngeneic E0771 mouse model of breast cancer, we characterized physical fatigue, assessed cytokine profiles, and performed targeted metabolomic analyses of muscle. Tumor-bearing mice showed significantly reduced survival and fat mass although overall body weight and lean mass were stable. Physical performance declined after three weeks of tumor growth as shown by reduced grip strength, maximum speed and peak oxygen consumption. Metabolic cage activity of mice revealed reduced oxygen consumption, carbon dioxide production, respiratory exchange ratio, energy expenditure, and water intake, consistent with suppressed metabolic function. Metabolomic profiling of skeletal muscle revealed upregulation of pipecolate and pyridoxamine, metabolites linked to amino acid metabolism and oxidative stress signaling, while key mitochondrial and antioxidant metabolites including glutathione, riboflavin and isocitrate were suppressed. These alterations suggest mitochondrial dysfunction, redox imbalance, and impaired energy production as contributors to the physical fatigue phenotype. These changes were accompanied by reduced IL1β, IL-2, MIP-1α and increased IP-10 in the plasma implicating inflammation-driven metabolic reprogramming. Breast cancer induced coordinated inflammatory and metabolic changes in the skeletal muscle, disrupting mitochondrial pathways that contribute to physical fatigue. This study identifies distinct metabolic signatures associated with CRF and highlights mitochondrial pathways as promising targets for therapeutic intervention to improve the quality of life in breast cancer patients.

#2017 Time restricted eating potentiates chemotherapy in obesity-driven breast cancer mouse models.

Manasi Das, Yunpeng Yang, Isabella Maranan, Yanting Wang, Liping Zeng, Samantha Lu, Nicholas Webster

Medicine, University Of California, San Diego, CA

Time-restricted eating (TRE) has emerged as a metabolic intervention with potential to improve cancer treatment responses. In this study, we investigated whether TRE enhances the therapeutic efficacy of chemotherapy in murine breast cancer models. Different chemotherapies, such as Letrozole, Tamoxifen, Doxorubicin, and Paclitaxel, were used in combination with TRE. Female obese mice were assigned to high-fat diet ad libitum feeding or an 8-hour TRE schedule. Mice bearing orthotopic breast tumors from ad libitum and TRE groups were treated with or without standard chemotherapeutic treatment to evaluate the TRE-Chemotherapy combination effect. The combination of TRE and chemotherapy (Doxorubicin and Paclitaxel) resulted in significantly reduced tumor growth compared with chemotherapy or TRE alone. TRE in combination with Letrozole demonstrated improved survival benefits over chemotherapy or TRE alone. These findings suggest that aligning feeding patterns with circadian rhythms can potentiate chemotherapeutic efficacy. TRE represents a lifestyle-based non-pharmacologic approach that may improve treatment outcomes in breast cancer and warrants further investigation of metabolic timing strategies in cancer treatment.

#2018 Investigating the role of Wnt/planar cell polarity signaling in the reprogramming of energy metabolism in breast cancer.
Liliana Loza Sanchez, Kacey VanderVorst, Kermit L. Carraway

UC Davis Medical Center, Sacramento, CA

This study aims to investigate how non-canonical Wnt/planar cell polarity (Wnt/PCP) signaling contributes to metabolic reprogramming and supports breast cancer progression. Breast cancer is the most prevalent cancer affecting women, and the 5-year survival rate for women diagnosed with metastatic breast cancer remains below 30%. For breast tumors to progress and ultimately result in metastatic disease, large increases in energy demands must be met. Tumors gain bioenergetic versatility by undergoing metabolic reprogramming through the upregulation of glycolytic and oxidative phosphorylation (OXPHOS) activity, and through alterations in mitochondrial biogenesis and degradation (mitophagy). However, the signal transduction pathways critical to sustaining the high levels of ATP production remain largely undefined. The non-canonical Wnt/PCP signaling pathway has been implicated in promoting tumor cell migration and metastasis in diverse tumor types. Our laboratory has reported that the Wnt/PCP-specific transmembrane protein Vangl mediates breast cancer collective migration and metastasis. Further, our recent proteomics and metabolomics studies indicate that Vangl1 regulates the expression of critical components in the OXPHOS pathway in vivo and in vitro, and that the Wnt/PCP ligand Wnt5a alters the phosphorylation of proteins involved in mitochondrial biogenesis and mitophagy. Thus, I propose that Wnt/PCP signaling regulates the reprogramming of energy metabolism to drive cell proliferation and motility in breast cancer. This will be tested by investigating the contribution of Wnt/PCP signaling to OXPHOS activity and the regulation of mitochondrial biogenesis and mitophagy in breast cancer. This study will promote our understanding of Wnt/PCP involvement in breast cancer progression and provide new insights into the mechanisms contributing to cancer metabolic reprogramming.

#2019 Comparison of non-metastatic and metastatic breast cancer cell and lipid droplet proteomes.

Chaylen Andolino, Kimberly K. Buhman, Dorothy Teegarden

Nutrition Science, Purdue University, West Lafayette, IN

Metastatic breast cancer cells often have increased cellular storage of neutral lipids, such as triacylglycerol (TAG), in cytoplasmic lipid droplets (LDs). Although LD accumulation is associated with increased cancer aggressiveness, the role of these organelles in contributing to metastatic disease remains unclear. Aside from TAG storage within the core of the LD, the phospholipid monolayer is also decorated with a variety of proteins. Given that LD-associated proteins reflect the organelle's function within a given physiological context, we characterized the proteome of LDs from a human metastatic compared to non-metastatic breast cancer cell line to assess potential candidate protein pathways that may associate with LDs to promote metastasis.

Untargeted shotgun proteomics of LDs isolated via sucrose density gradient ultracentrifugation from non-metastatic MCF10CA1h (less LDs) and metastatic MCF10CA1a (more LDs) cell lines was performed. The LD proteomes, as well as the proteome of each cell line's whole cell lysate (WCL), were compared utilizing MaxQuant, MassDynamics, Metascape, and STRING.

We identified that LDs from metastatic cells are highly enriched in proteins related to LD organization and protein localization compared to LDs from non-metastatic cells. Interestingly, proteins involved in the sequestering of NFκB were the most highly enriched lipid-related protein category in LDs of metastatic compared to non-metastatic cells. Further, NFκB was similarly enriched in the WCLs of both cell lines; however, was only identified in the isolated LD fraction from metastatic cells. Additionally, the negative regulator of LD catabolism, hypoxia inducible lipid droplet associated protein (HILPDA), was only identified in the metastatic cell LD fractions. Given the role of NFκB and HILPDA in tumor progression and therapy resistance, results from this study provide testable hypotheses that can elucidate how LDs contribute to breast cancer metastasis. For example, LDs may act as scaffolds for signaling to coordinate lipid metabolism and metastatic processes or as a stress-adaptive platform to enable rapid lipid-mediated signaling under hypoxia inducible factor (HIF) activation. Additionally, given that HILPDA stabilizes LDs which store precursors for eicosanoid synthesis, which in turn modulate NFκB activity and subsequent inflammatory response, the interactions of these mediators may integrate into a metabolic-inflammatory axis to promote tumor progression and immune evasion.

Together, our results indicate that though the global proteome of non-metastatic and metastatic breast cells derived from the same parental line are similar, the proteins associated with LDs vary greatly. This study provides a list of candidate proteins for additional experimentation to determine their role in sustaining LD accumulation and metastatic progression.

#2020 Fatty acid metabolism supports survival in normoxia and migration upon reoxygenation in lung-metastasizing breast cancer cells.

Marjorie Anne Layosa[1], Morgan Conrad[1], Chaylen Jade Andolino[1], Michael K. Wendt[1], Stephen D. Hursting[2], Dorothy Teegarden[1]

[1]Purdue University, West Lafayette, IN,[2]University of North Carolina at Chapel Hill, Chapel Hill, NC

Breast cancer is the most common cancer among women, and metastasis remains the leading cause of mortality. While fatty acid metabolism plays a critical role in cancer progression, its specific contribution to supporting breast cancer metastasis to distinct organs, particularly the lungs and liver, remains poorly understood. This study aims to characterize the lipid metabolic profiles of breast cancer cells with preferential metastasis to the lung versus the liver, and to determine how lipid metabolism supports cell survival under normoxia and drives migration upon reoxygenation after exposure to hypoxia. We utilized a unique murine breast cancer cell model with preferential metastasis to either lung (metM-Wnt^{Lung}; MLg) or liver (metM-Wnt^{Liver}; MLr). The metastatic cells were exposed to normoxia or hypoxia (1% O_2, 48 hrs) and reoxygenation to mimic dynamic tumor microenvironmental stress. Fatty acid metabolism was assessed using ^{13}C isotopic tracing, and cell viability and migration were evaluated following inhibition of key metabolic enzymes. Results showed that $^{13}C_6$-glucose and $^{13}C_5$-glutamine were significantly incorporated into the synthesis of both saturated (16:0 and 18:0) and unsaturated (16:1 and 18:0) fatty acids, indicating higher *de novo* fatty acid synthesis in MLg cells compared to MLr cells. Despite this, both cell lines exhibited similar triacylglycerol levels without evident lipid accumulation. A pulse-chase experiment showed that $^{13}C_6$-glucose-labeled fatty acids declined more rapidly in MLg than in MLr cells at 24 and 48 hrs (48.8% vs 30.3%, and 58.5% vs 48.3%, respectively), indicating more rapid fatty acid turnover in MLg than MLr cells. Inhibition of key enzymes in fatty acid metabolism, including *de novo* fatty acid synthesis (FASN via TVB-3166), esterification (DGAT2 via PF-06424439), lipolysis (ATGL via ATGListatin), and β-oxidation (CPT1A via etomoxir), induced a significantly greater reduction in cell viability of MLg than MLr cells, indicating that dynamic fatty acid synthesis, storage, lipolysis and oxidation are necessary to support survival in MLg cells. Under hypoxic conditions, MLg cells sustained higher *de novo* fatty acid synthesis accompanied by lipid accumulation. Upon reoxygenation following hypoxia, inhibition of either lipolysis or β-oxidation reduced MLg cell migration by 57% and 42%, respectively, an effect not observed in MLr cells. Overall, these results support that dynamic and rapid fatty acid turnover in lung-metastatic breast cancer cells is necessary to support survival, with lipids accumulated during hypoxia subsequently mobilized and oxidized to fuel migration upon reoxygenation. These findings identify lipid metabolism as a critical driver of lung-specific metastasis and a promising therapeutic target to reduce metastatic spread and improve outcomes for patients with breast cancer.

#2022 Tryptophan metabolites drive ferroptosis resistance in triple-negative breast cancer cells.

Jamshid Motalebzadeh, Hossein Anani, Chloe Thompson-Peach, Theresa Hickey, Lisa Butler, Nirmal Robinson, Daniel Thomas

Adelaide Medical School, University of Adelaide, Adelaide, Australia

Introduction

Tryptophan (Trp) metabolites are increased in various cancer types due to elevated expression of Trp dioxygenases, TDO2, IDO1, and IDO2. While recent studies have highlighted the immunosuppressive functions of these metabolites, their intrinsic significance to cancer cell survival remains poorly understood. This study explores the role of formylkynurenine and kynurenine, the first two metabolites in Trp catabolism on triple-negative breast cancer (TNBC) resistance to ferroptosis.

Methods

We performed comprehensive gene expression analysis using 46 ER+, 103 TNBC tumours, and 21 adjacent normal tissue samples from the SRA database. BRCA-TCGA RNA-seq and DNA-seq data were analysed to identify alterations in three Trp dioxygenases in TNBC patients. RNA-seq was conducted on BT549 cell line cultured with 50 μM formylkynurenine and kynurenine. Gene expression changes were validated using western blotting and real-time qPCR. Intracellular glutathione (GSH) and oxidized glutathione (GSSG) levels were quantified by LC-MS and MS/MS approach. Cell sensitivity to ferroptosis was evaluated by treating cells with 300 nM RSL3.

Results

Our analysis revealed increased expression of all three Trp dioxygenases, TDO2, IDO1, and IDO2, in TNBC tumours compared to luminal and adjacent normal tissues. DNA amplification was detected in IDO1 and IDO2, and reduced IDO1 promoter methylation in TNBC samples compared to luminal subtypes. Formylkynurenine and kynurenine both at concentrations of 50-100 μM significantly enhanced BT549 cell line proliferation. Transcriptomic analysis indicated that these metabolites regulate genes involved in ROS metabolism and iron transport. Metabolomics analysis further demonstrated alterations in the intracellular GSH/GSSG ratio. Notably, we report for the first time that kynurenine upregulates GPX4 protein expression, while formylkynurenine does not. However, both metabolites increased cellular resistance to RSL3-induced ferroptosis.

Conclusion

Formylkynurenine and kynurenine both increase GSH/GSSG ratio. While kynurenine upregulates GPX4 expression, formylkynurenine does not alter its levels. These findings establish a novel metabolic axis linking Trp catabolism to ferroptosis resistance in TNBC, suggesting that targeting this pathway could represent a promising therapeutic strategy for this aggressive subtype of breast cancer.

#2023 Tryptophan and serine metabolic axis reveals novel therapeutic vulnerabilities in triple-negative breast cancer.

Jamshid Motalebzadeh, Hossein Anani, Chloe Thompson-Peach, Theresa Hickey, Lisa Butler, Nirmal Robinson, Daniel Thomas

Adelaide Medical School, University of Adelaide, Adelaide, Australia

Tryptophan (Trp) metabolism is recognised to have immunomodulatory effects in cancer, with downstream metabolites such as kynurenine suppressing T cell responses. However, the role of Trp catabolism in cancer cell biosynthesis and tumor growth is poorly understood. Herein, we investigated for the first time the role of Trp as a source of one-carbon metabolism through formate production in triple-negative breast cancer (TNBC) and its effect on serine synthesis via phosphoglycerate dehydrogenase (PHGDH), a rate-limiting enzyme for de novo serine synthesis.

CRISPR-Cas9 system was used to generate tryptophan 2,3-dioxygenase (TDO2) and/or indoleamine 2,3-dioxygenase (IDO1) knockout TNBC cell lines. Multi-omics approach using LCMS Q-TOF system and RNA-seq was employed to integrate targeted and untargeted metabolomics, ^{13}C fluxomics, and transcriptomics in TNBC cell lines. For fluxomics studies, cells were cultured with ^{13}C-labeled tryptophan to trace the metabolic flux of carbon atoms through Trp metabolism into kynurenine pathway.

While serine is recognised as a major source of one-carbon metabolism, our fluxomics data revealed that one-carbon units are released during the conversion of N-formylkynurenine to kynurenine. Labelled metabolites derived from tryptophan that give rise to tetrahydrofolate and methionine cycles were identified and these were subsequently incorporated to generate de novo purines. Integrated transcriptome and metabolomic analysis of tryptophan dioxygenase KO versus WT, as well as formylkynurenine and kynurenine treated cells, revealed a link between Trp catabolism and serine anabolism via alteration in PHGDH expression. Moreover, KO cells deprived of one-carbon units derived from Trp metabolism showed upregulation of PHGDH gene expression. Interestingly, KO cells showed a significantly lower growth rate in serine-glycine free media and also when PHGDH was inhibited with 2.5 μM NCT-503.

This study provides evidence that Trp metabolism contributes to one-carbon metabolism in TNBC beyond its immunosuppressive functions. We also show that disruption of Trp metabolism upregulates PHGDH as a compensatory mechanism. This study identifies simultaneous inhibition of both pathways as a promising dual-targeting therapeutic strategy for TNBC treatment.

#2025 Zinc promotes aerobic glycolysis in breast cancer by promoting PKM2 dimerization and nuclear localization.

Wenyou He, Jiali Xu, Yihuizhi Zhang, Weijian Ding, Xinyu Chen, Yirui Ye, Linyue Li, Baotong Zhang, **Siyuan Xia**

Southern University of Science and Technology (SUSTech Shenzhen), Shenzhen, China

Zinc regulates breast cancer progression by modulating cellular proliferation and hormone-dependent signaling pathways, yet its role in glucose metabolic reprogramming remains incompletely understood. In our study, we found that elevated Zn^{2+} enhances aerobic glycolysis while markedly suppressing mitochondrial oxidative phosphorylation and inhibiting the pentose phosphate pathway. Transcriptomic profiling further reveals that Zn^{2+} treatment selectively upregulates glycolysis-associated genes, including the glucose transporter GLUT1 (SLC2A1) and pyruvate kinase, highlighting a coordinated shift toward glycolytic metabolism under zinc-replete conditions. Mechanistically, Zn^{2+} directly binds to pyruvate kinase M2 isoform (PKM2), stabilizing its dimeric state and promoting its nuclear translocation. Nuclear PKM2 subsequently enhances the transcription of glycolytic genes (i.e., *LDHA*). Consistent with this mechanism, Zn^{2+} treatment sensitizes tumor cells to the LDHA-specific small-molecule inhibitor NHI-2, resulting in a synergistic anti-tumor effect. Furthermore, the zinc efflux transporter ZnT1 (SLC30A1) is transcriptionally induced following Zn^{2+} exposure, functioning as a feedback mechanism to maintain zinc homeostasis. Conversely, ZnT1 knockdown leads to intracellular zinc accumulation, which further enhances aerobic glycolysis through similar mechanisms of PKM2 dimer stabilization and nuclear translocation. Collectively, this study elucidates a molecular mechanism by which zinc promotes aerobic glycolysis through direct binding to PKM2, stabilizing its dimeric conformation and facilitating its nuclear localization. These findings propose a therapeutic strategy that combines Zn^{2+} supplement with LDHA inhibition, revealing a previously unrecognized metabolic vulnerability that may be leveraged for precision oncology.

#2026 Scd1 overexpression in cancer-associated adipocytes drives breast cancer development and metastasis.

Zander Esh[1], Pascal Naef[1], Justice Williams[1], Johnny Le[1], Gautham Prabhakar[1], Jacob Insua Rodriguez[1], Hannah Savage[2], Ayisha Bushra[1], Cholsoon Jang[1], Kai Kessenbrock[1]

[1]Biological Chemistry, UCI School of Medicine, Irvine, CA,[2]Department of Physiology and Biophysics, UCI School of Medicine, Irvine, CA

Throughout the course of tumor development in breast cancer (BC), adipocytes within the tumor microenvironment undergo modifiable changes that promote tumor growth and invasive capacity, notably including the upregulation of Scd1, an enzyme integral to lipid metabolism. The timing of this metabolic reprogramming of healthy adipocytes to cancer-associated adipocytes (CAAs), as well as interventions that can reverse this process are poorly understood. To elucidate this progression, we used a polyoma middle T antigen (PyMT) transgenic mouse model that spontaneously develops luminal B-like tumors specific to the mammary fat pad (MFP). Using this model, we performed single-nucleus RNA sequencing (snRNA-seq) and metabolic profiling of MFP from healthy and tumor-bearing PyMT littermates. Among the many differences found when comparing healthy to tumor-bearing tissue at several time points throughout the progression of hyperplasia to invasive carcinoma, we discovered a consistent upregulation of Scd1, a stearoyl-CoA desaturase that performs the rate-limiting step in the conversion of saturated fatty acids (SFAs) to monounsaturated fatty acids (MUFAs), in adipocytes. However, despite the persistent upregulation of Scd1, we noticed an overall depletion of MUFAs in PyMT tumor-bearing tissue, indicating that tumor cells consume MUFAs during their malignant progression to invasive carcinoma and eventual metastasis. First, we recapitulated our snRNA-seq findings from mice in both snRNA-seq and spatial transcriptomics data from human breast tissue through gene signature scoring. We found that our progressive gene signatures accurately map to ductal carcinoma in situ, as well as invasive ductal carcinoma, providing confidence that interventions we establish in our mouse and in vitro models will translate to human BC. Next, to target the malignant transformation observed in our PyMT model, we cultured BC cell lines in adipocyte-conditioned medium, either when adipocyte Scd1 is selectively inhibited (iACM) or when adipocytes are allowed to function normally (ACM). Exposure to ACM alone increased cell viability, spheroid formation, and invasiveness, while iACM led to a marked decrease in all three parameters. Finally, to extend these results back into our mouse model, we injected C57BL/6 mice intracardially with BC cells conditioned in either ACM, iACM, or control media. While ACM led to aggressive metastasis with tropism selective for bone, iACM abolished the tropism and greatly decreased the metastatic capability of the injected cells. Taken together, our data show that the consistent upregulation of Scd1 throughout tumor progression in BC can be inhibited to reduce tumor growth and metastasis, thus identifying Scd1 expression in CAAs as a therapeutic target in BC, both in the early stages of progression and during metastatic spread.

#2027 ATP citrate lyase fuels lipid storage to support triple negative breast cancer chemoresistance.

Katherine E. Pendelton[1], Mokryun L. Baek[1], Mariah J. Berner-Wu[1], Steven W. Wall[1], Audra Lane[1], Jonathan T. Lei[1], Iqbal Mahmud[2], Lin Tan[2], Lacey E. Dobrolecki[1], Philip L. Lorenzi[3], Michael T. Lewis[1], Blake R. Rushing[4], Gloria V. Echeverria[1]

[1]Baylor College of Medicine, Houston, TX,[2]MD Anderson Cancer Center, Houston, TX,[3]City of Hope, Duarte, CA,[4]UNC Chapel Hill, Chapel Hill, NC

Triple negative breast cancer (TNBC) is an aggressive breast cancer subtype in which neoadjuvant chemotherapy (NACT) is the backbone of standard of care. Unfortunately, ~45% of patients have residual tumor burden following NACT, which is strongly associated with poor prognoses. Our group previously demonstrated that mitochondrial oxidative phosphorylation is upregulated and is a therapeutic vulnerability of chemo-refractory TNBC. We used metabolomic flux tracing to show a heightened contribution of glucose oxidation to the tricarboxylic acid (TCA) cycle in residual human TNBC cells surviving several conventional chemotherapies. We found significantly elevated abundance of citrate and acetyl-coA (AcCoA) in residual cells. Further, glucose, but not palmitate, glutamine, or acetate, derived heavy carbon was more strongly incorporated into citrate and AcCoA in residual relative to naïve cells. Concomitantly, we observed drastic lipidomic remodeling, largely characterized by elevation of triglycerides, long chain fatty acids, and poly unsaturated fatty acids (PUFAs) in cultured TNBC cells and orthotopic patient-derived xenograft (PDX) tumors following chemotherapy relative to their treatment naïve counterparts. This was accompanied by a significant increase in the number of lipid droplets (LDs) in residual cells. Together, these data suggest glucose oxidation supports fatty acid synthesis (FAS) and storage in chemoresistant TNBC. Our analyses of human TNBC proteomic and transcriptomic data affirmed the significant association of fatty acid metabolism with TNBC chemoresistance, as well as its upregulation in chemotherapy-treated tumors relative to their pre-treated counterparts. Mining those data led us to ATP citrate lyase (ACLY), the rate limiting enzyme for cytosolic AcCoA production from citrate. We hypothesized that ACLY converts excess citrate, generated by heightened TCA cycling, to AcCoA to promote FAS and storage in chemoresistant TNBC. We found elevated protein levels of ACLY and an activating phosphorylation mark in TNBC cells surviving treatment with conventional chemotherapies doxorubicin and carboplatin. ACLY knockdown or inhibition potently reduced chemotherapy-induced accumulation of AcCoA and LDs and elicited lipidomic rewiring largely characterized by increased PUFAs. Notably, combining ACLY inhibition or KD with conventional chemotherapy treatments provided significant improvement of tumor cell growth inhibition. These data indicate that NACT can cause accumulation of citrate, AcCoA, LDs, and overall lipidomic rewiring through ACLY. ACLY is a novel functional dependency of chemo-refractory TNBC and should be further explored as a potential therapeutic target. We posit that TNBC cells adapt to the stress of NACT by upregulating lipid synthesis and storage in conjunction with glucose catabolism, enhancing metabolic flexibility and cell survival.

#2028 Hyperlipidemia drives tumor growth in a mouse model of obesity-accelerated breast cancer growth.

Renan Fudoli Lins Vieira, Sawyer Sanchez, Menusha Arumugan, Peyton Mower, Meghan Curtin, Abigail Jackson, Jillian Wright, Alexis Bowles, Gregory S. Ducker, Keren Hilgendorf, Amandine Chaix

University of Utah, Salt Lake City, UT

Obesity is an established risk factor for breast cancer (BC), yet the specific mechanisms driving this association remain unclear. Dysregulated lipid metabolism has emerged as a key factor in cancer cell biology, and, while obesity is often accompanied by hyperlipidemia, the isolated impact of elevated lipid levels on BC growth has not been experimentally tested. Using the E0771 and Py230 orthotopic models of obesity-accelerated BC growth in immune-competent mice, we investigated the role of systemic lipids on tumor growth. Combining dietary and genetic mouse models, we show that elevated circulating lipids are sufficient to accelerate BC tumor growth even in the absence of obesity or alterations in blood glucose and/or insulin levels. Pharmacological lowering of systemic lipid levels attenuates BC growth in obese mice, suggesting a direct role for lipids in fueling tumor expansion. Notably, we also show that weight loss alone, without a corresponding reduction in lipid levels such as that induced by a ketogenic diet, fails to protect against BC, highlighting the necessity of targeting lipid metabolism in obesity-associated BC. Our findings establish hyperlipidemia as a critical driver of BC progression and suggest that lipid-lowering interventions may be a promising strategy to mitigate BC risk in individuals with obesity.

#2029 Regulation of metabolic and stress adaptation in triple-negative breast cancer.

Emilia F. Carlo[1], Columba de la Parra[1], Erna Mitaishvili[2], Blessing Ukandu[1]

[1]Chemistry, Herbert H. Lehman College, City University of New York, Bronx, NY,[2]Ph.D. Program in Biology, The Graduate Center, City University of New York, New York, NY

Triple-negative breast cancer (TNBC) is a highly aggressive breast cancer subtype characterized by rapid progression, metabolic reprogramming, and limited therapeutic options. Under stress conditions such as nutrient deprivation or oxidative stress, TNBC cells suppress canonical translation initiation and rely on alternative mechanisms to maintain the production of stress-adaptive proteins. Death-Associated Protein 5 (DAP5), a member of the eIF4G family, facilitates an alternate cap-dependent translation under conditions in which canonical translation is inhibited. Our data suggest that DAP5 plays a critical role in orchestrating metabolic adaptation for TNBC progression and metastasis. To investigate the role of DAP5 in metabolic and oxidative stress adaptation, we used the well-characterized TNBC cell line MDA-MB-231 with either control or DAP5 silencing. We found that DAP5 activity persists under oxidative stress when canonical translation is suppressed, enabling sustained expression of glycolytic enzymes and supporting glycolytic flux. DAP5 silencing resulted in reduced translation of glycolytic proteins, including GLUT1 and hexokinase II. It also decreased proteins related to redox response singling pathways, including CDK12. Metabolomic profiling following DAP5 depletion indicated significant alterations in nucleotide cofactors and disruptions in metabolic pathways commonly enriched in metastatic cancers, including amino acid and glucose metabolism. Consistently, ATP assay measurement showed a significant reduction upon DAP5 silencing, suggesting impaired energy metabolism in TNBC cells. Our findings support a model in which DAP5-mediated translation preserves a subset of metabolic mRNAs critical for metastasis when translation is attenuated. DAP5 acts as a key regulator of TNBC metabolism by selectively translating metabolic mRNAs, particularly those involved in glucose metabolism, thereby sustaining stress adaptation and promoting metastatic behavior.

#2030 Differential impact of metformin based prevention and therapeutic strategies on aberrant metabolic signals/ molecular signatures associated with triple negative breast cancer (TNBC) during high fat/ high fructose diet feeding.

Md. Imtiazul Kabir[1], Robin Kumar[1], Lakshmi Sai Pratyusha Bugata[1], M. Nurul Islam[2], Sanjida Afroz Mitu[2], Komal Raina[1]

[1]Dept. of Pharmaceutical Sciences, South Dakota State University, Brookings, SD,[2]Dept. of Chemistry and Biochemistry, South Dakota State University, Brookings, SD

Metformin is routinely used in the management of type-2 diabetes (T2D) and is known for its potential to alter mitochondrial respiration-driven energetic stress. Interestingly, metformin has also been the focus of cancer research because various study outcomes have associated its intake with anti-cancer benefits. In the present study, we determined the comparative anti-cancer effects of preventive *versus* therapeutic regimen of oral metformin against TNBC tumorigenesis. Given that the anti-cancer benefits of metformin are observed mostly in cases associated with metabolic aberrations such as obesity/T2D, accordingly, the *in vivo* preclinical study was performed in diet-induced obese mice model (DIO mice) wherein four week old C57Bl/6 female mice were fed either a high fat diet (HFD, 60 kcal% fats) or high fructose diet (HFR, 60 kcal% fructose) throughout the course of the study so as to induce obesity-associated changes in both systemic and local mammary gland microenvironment that could impact breast tumorigenesis. After 10 weeks of respective DIO feeding (at 14 weeks of mice age), orthotopic mammary tumors were induced by subcutaneous injection of $2x10^6$ PY230 breast cancer cells in the 4^{th} mammary fat pad (either left or right). In the preventive regimen metformin (pre) treatment (daily oral gavage: 300mg/kg body wt.) was started 4 weeks before the cell inoculation and continued till 2 weeks after the cell inoculations followed by a wash out period of 6 weeks till study end (8 weeks following cell inoculations). On the other hand, in the therapeutic regimen, metformin (post) treatment (daily oral gavage: 300mg/kg body wt.) was started 2 weeks after the cell inoculation and continued till 6 weeks after the cell inoculations (till study end). Overall, the results indicated that while both preventive and therapeutic regimens of metformin had an anti-tumorigenic effect on TNBC growth and progression, the preventive regimen even after the washout period (no drug administration) had long lasting anti-cancer effect which was comparatively better than therapeutic treatment of TNBC tumors. In untargeted metabolomic profiling, the observed metabolic alterations in both the HFD and HFR groups suggest that metformin has the potential to restore metabolic homeostasis in the tumor microenvironment. In untargeted lipidomics profiling, metformin's preventive and therapeutic effects were evident in the modulation of multiple lipid classes. Specifically, the preventive regimen appeared to yield more pronounced lipid alterations, indicating the potential benefits of early intervention in modulating cancer progression.

#2031 Reproducible serum metabolomics drives biomarker discovery in ovarian cancer.

Rachel Culp-Hill[1], Brendan Giles[1], Mattie Goldberg[1], Robert A. Law[1], Enkhtuya Radnaa[1], Shannon Kilkenny[1], Maria Wong[1], Connor Hansen[1], Benjamin G. Bitler[2], Kian Behbakht[2], Vuna Fa[1], Abigail McElhinny[1]

[1]AOA Dx, Denver, CO,[2]University of Colorado Anschutz Medical Campus, Aurora, CO

Ovarian cancer (OC) remains one of the deadliest gynecologic malignancies, with a clear unmet need for novel biomarker strategies. Altered metabolism has emerged as a cancer hallmark, with serum reflecting rewired cellular pathways supporting tumor growth and survival. Advancements in mass spectrometry (MS) have improved precision and confidence in feature identification, allowing for impressive analytical depth in extremely low volumes (<10µL) of biofluid. Our previous work has focused on lipidomics, but the biological mechanisms revealed through metabolomics can offer novel and complementary insight into tumor metabolism. Metabolomics, therefore, has the potential to become a powerful tool for biomarker discovery through the characterization of systemic metabolic alterations in individuals diagnosed with OC.Two independent, clinically annotated cohorts of serum representing the population of women experiencing symptoms of OC were analyzed using untargeted metabolomics (UHPLC-HRMS). Cohort #1 (N=519), obtained from University of Colorado and commercial vendors comprised patients diagnosed with OC across stages and subtypes (N=219: 80 stage I/II, 139 stage III/IV), benign gynecological disorders (N=168), gastrointestinal disorders (N=50), and healthy donors (N=82). Cohort #2 (N=400) comprised patients diagnosed with OC (N=116: 50 stage I/II, 66 stage III/IV), benign adnexal masses (N=116), borderline tumors (N=19), other symptomatic individuals (N=114), and healthy donors (N=35). We observed alterations in several key metabolic pathways, many of which have been individually implicated in OC biology, including decreased amino acids and bile acids, with increased acyl-carnitines and fatty acids. To evaluate cohort reproducibility, we compared statistical trends (cancer v. non-cancer) from each cohort. Of the significantly altered features in both cohorts, 68% maintained directionality. 90% of those maintaining directionality are a part of the key pathways above. The consistency in metabolic alterations across two independent cohorts suggests these pathway intermediates transcend batch-to-batch variability and could be leveraged as diagnostic biomarkers . In fact, initial machine learning-based modeling shows that models combining metabolites, lipids, and proteins result in AUCs >90%. MS-based metabolomics represents a snapshot of an individual’s disease state, offering insight into metabolic alterations indicative of early-stage cancer through a non-invasive sample. Here, we identified consistent metabolic alterations in OC serum across two independent, clinically annotated cohorts that align with previously reported pathway alterations. This demonstrates the analytical robustness of our approach and highlights the potential of MS-based metabolomics to move beyond discovery, toward development of clinically viable biomarkers for early-stage OC detection.

#2032 MEX3A sustains mitochondrial integrity and metabolic resilience to drive ovarian clear cell carcinoma progression and liver colonization.

Priyanka Vinothkumar[1], Pei-Yi Lin[2], Li-Tzu Cheng[3], Chen-Hsin Albert Yu[4], Pang-Hung Hsu[5], Yu-Chi Chou[6], Wendy W. Hwang-Verslues[7]

[1]Molecular and Cell Biology, Taiwan International Graduate Program, Academia Sinica; Graduate Institute of Life Sciences, National Defense Medical University, Genomics Research Center, Academia Sinica, Taipei, Taiwan,[2]Genomics Research Center, Genomics Research Center, Academia Sinica, Taipei, Taiwan,[3]Graduate Institute of Life Sciences, National Defense Medical University, Taipei, Taiwan,[4]Institute of Molecular Biology, Taipei, Taiwan,[5]Department of Bioscience and Biotechnology, Department of Bioscience and Biotechnology, National Taiwan Ocean University Keelung City, Keelung, Taiwan,[6]Biomedical Translation Research Center, Academia Sinica, Taipei, Taiwan,[7]Genomics Research Center, Academia Sinica, Taipei, Taiwan

Background and Aim: Ovarian clear cell carcinomaOCCC is a metabolically distinct and chemo-resistant subtype of ovarian cancer characterized by poor prognosis and high recurrence rates. OCCC exhibits unique metabolic adaptations that enables survival under nutrient deprivation and oxidative stresses. Mitochondrial integrity is central to this adaptive capacity, yet the molecular mechanisms that preserve mitochondrial homeostasis in OCCC remain poorly defined. Recent evidence has identified the RNA-binding protein MEX3A as an oncogenic regulator in several cancers, including OCCC, where it promotes tumor progression. However, its role in regulating mitochondrial metabolism and stress adaptation is largely unexplored. This study aims to elucidate whether and how MEX3A sustains mitochondrial homeostasis to drive OCCC progression, focusing on its impact on tumor growth, mitochondrial structure and transcriptional responses to metabolic and mitochondrial stress.
Methods: Endogenous MEX3A protein levels were evaluated across an OCCC cell panel by western blotting. Stable MEX3A knockdown and control cells were generated using a lentivirus shRNA system. Functional studies were performed using OCCC cell lines TOV21G,JHOC5 and *in vivo* orthotopic intrabursa and intrasplenic xenograft models to assess tumor growth and liver colonization. Mitochondrial function was analyzed by Seahorse metabolic flux assays, ATP quantification and NAD^+/NADH measurements. Morphological and ultrastructural alterations were examined by confocal and transmission electron microscopy. Mitochondrial biogenesis genes and mitophagy markers were assessed by qPCR and immunoblotting.
Results:MEX3A expression was significantly elevated in OCCC tissues and correlated with poor overall survival. Knockdown of MEX3A in OCCC cells markedly reduced primary tumor growth and significantly reduced the number of liver metastatic nodules in mouse models, demonstrating its functional importance for metastatic colonization. At the cellular level, MEX3A depletion led to loss of mitochondrial cristae integrity, fragmented morphology, reduced oxygen consumption and decreased ATP generation, indicating a dysfunctional in oxidative phosphorylation. Under mitochondrial stress induced by FCCP or liver-extract, control cells activated transcriptional programs for mitochondrial biogenesis, upregulating PGC1A, NRF2 and TFAM. In contrast, MEX3A-deficient cells failed to induce this adaptive response, leading to TOM20 degradation and defective mitochondrial recovery.
Conclusion: Our study reveals MEX3A as a crucial RNA-binding protein that preserves mitochondrial integrity and enables metabolic adaptation in OCCC. By sustaining mitochondrial biogenesis and recovery following stress, MEX3A enhances OCCC fitness, tumor growth and liver colorization

#2033 LSR suppresses ferroptosis through alpha-tocopherol uptake and promotes tumor growth in gynecological cancers.

Masashi Akada, Kosuke Hiramatsu, Yoshikazu Nagase, Tatsuo Masuda, Mamoru Kakuda, Satoshi Nakagawa, Tadashi Iwamiya, Shinya Matsuzaki, Michiko Kodama

The University of Osaka, Suita, Japan

Background
Lipolysis-stimulated lipoprotein receptor (LSR) plays an important role in lipid uptake and is overexpressed in gynecologic cancers, where its high levels are correlated with unfavorable outcomes. However, the lipid metabolic mechanisms via LSR are not well understood. In this study, we investigated how LSR-dependent lipid uptake promotes tumor growth in gynecologic malignancies.
Methods
To explore the lipid metabolic mechanism mediated by LSR, we first demonstrated the effect of high-fat diet (HFD) on tumor growth of LSR-positive ovarian cancer in vivo, and compared the antitumor efficacy of anti-LSR antibody (Ab) between HFD-fed and normal diet (ND)-fed mice. Next, we assessed whether serum from HFD-fed mouse promotes proliferation of ovarian cancer cells in vitro. To identify lipid metabolites responsible for HFD-induced tumor promotion, we performed metabolomic analysis of HFD and ND mouse serum. Based on the identified metabolite, we further investigated its mechanistic contribution to tumor growth.
Results
HFD significantly promoted ovarian cancer growth ($p < 0.05$), and the antitumor effect of anti-LSR Ab was strongly effective in HFD-fed mouse in vivo ($p < 0.05$). HFD mouse serum also significantly enhanced cell proliferation of ovarian cancer cells in vitro ($p < 0.05$). Metabolomic analysis of HFD and ND mouse serum identified alpha-tocopherol (vitamin E) as the most discriminative metabolite. Alpha-tocopherol is a lipid-soluble antioxidant known to suppress ferroptosis; thus, we hypothesized that LSR-mediated alpha-tocopherol uptake inhibits ferroptosis in gynecological cancer cells. At first, we demonstrated that LSR knockdown (KD), using siRNA, significantly suppressed cell proliferation in endometrial and ovarian cancer cells ($p < 0.05$). LSR-KD also reduced GPX4 expression and increased reactive oxygen species (ROS) and lipid peroxidation, indicating enhanced ferroptosis sensitivity. Importantly, these effects were completely reversed by ferroptosis inhibitors but not by apoptosis or necroptosis inhibitors, suggesting that LSR inhibits ferroptosis specifically. In control endometrial and ovarian cancer cells, alpha-tocopherol supplementation restored cell proliferation ($p < 0.05$), GPX4 expression, and reduced ROS and lipid peroxidation under oxidative stress (H_2O_2 exposure). However, in LSR-KD cells, alpha-tocopherol did not show a rescue effect, consistent with impaired uptake via LSR.
Conclusion
LSR promotes tumor progression of gynecological cancers through alpha-tocopherol uptake, leading to ferroptosis suppression. Inhibition of alpha-tocopherol uptake via LSR may sensitize endometrial and ovarian cancers to ferroptosis-inducing treatments.

#2034 H6PD as a metabolic target of DAP5 regulating NADPH homeostasis in TNBC.

Blessing Ukandu[1], Erna Mitaishvili2[2], Emilia CARLO[3], Columba de la Parra[3]

[1]Chemistry, Lehman College - CUNY, Bronx, NY,[2]CUNY Graduate Center, New York, NY,[3]Lehman College - CUNY, Bronx, NY

Triple-negative breast cancer (TNBC) is an aggressive malignancy defined by the absence of estrogen receptor (ER), progesterone receptor, and HER2 expression. This lack of receptor expression makes TNBC particularly challenging to treat using standard targeted therapies. TNBC cell proliferation is driven in part by cellular stress responses, such as oxidative stress and nutrient deprivation, that activate adaptive mechanisms supporting survival and growth under hostile conditions. H6PD (Hexose-6-phosphate dehydrogenase) is a key enzyme of the endoplasmic reticulum (ER)-associated pentose phosphate pathway (PPP) that generates NADPH, a reducing agent crucial for managing oxidative stress, facilitating protein folding, and supporting anabolic metabolism. Although the cytosolic PPP enzyme G6PD is extensively characterized, the role of H6PD in cancer metabolism and stress adaptation remains underexplored. Its ER localization provides a unique capability to buffer redox imbalance and maintain protein quality in cells with high anabolic demands. We investigated the regulation of H6PD by DAP5/eIF3d-dependent non-canonical translation in TNBC. Our analysis indicates that H6PD is a target of this translational mechanism. Targeted metabolomic profiling and DAP5 silencing revealed significant reductions in the levels of nucleotide cofactors (ADP, ATP, CTP, GTP, and UTP) and impaired nucleotide biosynthesis, indicating disruption of ER-associated PPP activity. These results suggest that DAP5-dependent translation maintains H6PD expression to support NADPH production, which is essential for anabolic metabolism in TNBC.

#2035 Cell density drives glutamine synthesis in fibroblast—like cells in the tumor microenvironment.

Lisa Shakachite, Natalya N. Pavlova

University of Utah, Salt Lake City, UT

Dense fibrous tissue, a hallmark of increased breast cancer risk, is composed of abundant extracellular matrix (ECM) and fibroblast-like cells that shape the tumor microenvironment (TME). These fibroblast-like cells can create regions of variable cell density, which in turn influences local nutrient availability. In solid tumors, poor vascularization generates a nutrient-deprived environment where amino acids, particularly glutamine, become limiting. Glutamine is essential for many cell processes, including replenishment of the TCA cycle, antioxidant defense, protein synthesis, and nucleotide production. Aggressive triple-negative breast cancer cells are often unable to synthesize their own glutamine *de novo* using glutamine synthetase (GS) and rely on exogenous sources for growth and survival. Fibroblast-like cells within the TME may compensate by producing and supplying glutamine through GS activity. Although this metabolic dependency has been demonstrated in ovarian cancer, how GS is regulated in fibroblast-like cells within the breast TME, and whether it is influenced by cell density, remains unknown. We hypothesize that high cell density acts as a non-cell-autonomous metabolic cue, upregulating GS in fibroblast-like cells under glutamine-deprived conditions. To test this, fibroblasts from mammary, skin, and lung tissue, as well as progenitor fibroblast-like cell lines (10T1/2 and MC3T3), were cultured at varying densities in the presence or absence of exogenous glutamine. Preliminary data show that near-confluent fibroblast-like cells upregulate GS and maintain active protein translation despite glutamine deprivation, suggesting that dense cultures adopt a metabolic state that gives them an added advantage compared to less-confluent cells. These findings point to a potential mechanism by which fibroblast-like cells in the breast TME promote glutamine availability and, consequently, tumor progression. Because direct GS inhibition is neurotoxic, identifying upstream, density-dependent regulators of GS represents a promising therapeutic avenue for selectively disrupting glutamine supply to aggressive breast cancers.

#2036 Post-transcriptional regulation of cancer by a metabolic pathway: modulation of HuR by the mevalonate pathway.

Mana Heidari[1], Raymond J. Hohl[2]

[1]Biomedical Engineering/Molecular and precision Medicine in Cancer Institute, Penn State University, Hershey/State College, PA,[2]Professor, Hem./Onc., Penn State Hershey Cancer Institute, Hershey, PA

Background: Mevalonate (MVA) pathway, the metabolic pathway essential for producing cholesterol, is inhibited by statins to manage hypercholesterolemia and reduce the risk of cardiovascular diseases. Increasing evidence has shown that dysregulation of this pathway also contributes to cancer development and progression. Its role in cancer has been well established through its production of isoprenoid intermediates enabling the prenylation and activation of small GTPases that drive tumor cell proliferation, migration, and metastasis. While the direct prenylation-dependent effect of the MVA pathway have been well characterized, there is growing evidence that it can also indirectly affect other oncogenic regulators. In this study, we aim to determine whether the MVA pathway is involved in regulating HuR, an RNA-binding protein that plays a central role in stabilizing numerous oncogenic transcripts. Demonstrating an MVA-dependent influence on HuR would establish a promising regulatory mechanism can modulate multiple oncogenic pathways simultaneously. Also, as HuR is consistently upregulated across diverse cancer types, defining how the MVA pathway affects HuR in a few cancer types will lay the foundation for generalizing these findings to other malignancies.
Methods & Results: Cell viability was assessed by MTT assay to determine the IC_{50} of simvastatin in MDA-MB-231 breast cancer cells. Cells were subsequently treated with simvastatin at concentrations below, at, and above the IC_{50} for 24 and 48 hours. HuR protein expression was then measured by Western blot. We observed a clear dose-dependent reduction in cell viability, along with a pronounced suppression of HuR expression at extremely low simvastatin concentrations (nanomolar doses) compared with vehicle control at the 24-hour timepoint. To determine whether the effect of simvastatin on HuR is specifically mediated through inhibition of the mevalonate pathway, rescue experiments are being performed in which mevalonate and isoprenoid intermediates are added following simvastatin treatment. To evaluate downstream consequences of HuR suppression, Western blot analysis is being performed for Cyclin B1 and BCL2, two HuR-regulated targets involved in cell-cycle progression and apoptosis. Transcript levels of HuR, Cyclin B1, and BCL2 are being quantified by qPCR to validate the observed protein-level changes. Also, as HuR overexpression is frequently accompanied by its cytoplasmic accumulation, immunofluorescence staining is being performed to assess HuR distribution and quantify the nuclear/cytoplasmic ratio in treated cells.
Conclusions: Our findings demonstrate that mevalonate-pathway inhibition reduces HuR expression in breast cancer cells, supporting a mechanistic connection between metabolic signaling and post-transcriptional control of oncogenic pathways. This abstract was revised with AI assistance.

#2037 Engineering multiplexed NRF2 reporters to decipher single cell oscillations in real time.

Naurisha Kapoor[1], Yasemin Ceyhan Ozdemir[2], James V. Alvarez[2]

[1]University of Washington, Seattle, WA,[2]Fred Hutchinson Cancer Center, Seattle, WA

Tumor cell survival after therapy and the emergence of recurrent disease are major contributors to breast cancer mortality. NRF2, a master regulator of antioxidant and metabolic stress responses, is frequently activated in therapy-resistant and recurrent tumor cells, yet its regulation in the absence of canonical Nfe2l2/Keap1 mutations remains poorly understood. To enable real-time visualization of NRF2 dynamics, we developed a dual fluorescent reporter system to independently monitor NRF2 protein stability and transcriptional activity at single-cell resolution. The first reporter (Neh2-YFP) fuses YFP to the NRF2 Neh2 degron domain, providing a readout of KEAP1-dependent NRF2 protein turnover. The second reporter (ARE-CFP) places CFP under control of antioxidant response elements (AREs), enabling measurement of NRF2-dependent transcriptional output.

Using confocal live-cell imaging in NMuMG mammary epithelial cells, we validated both reporters by demonstrating increased fluorescence after exposure to NRF2 activators (H_2O_2, TBHQ) and decreased signal with NRF2 inhibitors (ML385, luteolin). Building on this foundation, we will use the reporters to define how NRF2 activity fluctuates over short timescales and how these dynamics change during transitions from therapy-naïve to drug-tolerant, recurrent, or metastatic cell states. Because the two reporters disentangle protein stabilization from transcriptional competence, this system will also allow us to identify noncanonical mechanisms of NRF2 activation - such as altered kinase signaling or autophagy - specifically in breast cancer models lacking Nfe2l2/Keap1 mutations.

Together, this dual-reporter platform enables dynamic, single-cell characterization of NRF2 regulation and will provide new insight into how NRF2-driven stress tolerance and metabolic adaptation contribute to tumor persistence, recurrence, and metastatic progression.

: MicroRNAs as Cancer Biomarkers, Therapeutic Targets, and Modulators of Treatment Response
Poster Session

#2041 Short-term pre-operative caloric restriction downregulates miR-21 and modulates gut microbiome in breast cancer and prostate cancer patients.

Meera Gupta[1], Anuradha A. Shastri[1], Pramila Anne[1], Tiziana DeAngelis[1], Leonard G. Gomella[2], Adeseye Adekeye[1], Melissa Lazar[1], Nicole L. Simone[1]

[1]Thomas Jefferson University Sidney Kimmel Medical College, Philadelphia, PA,[2]Thomas Jefferson University, Philadelphia, PA

Purpose: Calorie restriction (CR) has been shown to improve oncological markers in numerous studies, the mechanism and extent to which it can modulate clinical outcomes remain of interest. In this study, we sought to determine the effect of a 2-5-week preoperative CR intervention on the oncogenic microRNA miR-21, as well as other clinical, microbiome and metabolic markers in patients with breast cancer and prostate cancer. We hypothesized that caloric restriction would lower miR-21-mediated inflammation, inducing a favorable shift in patient characteristics and enhancing anti-tumor responses.

Methods: Breast cancer and prostate cancer patients from a large academic medical center were recruited to participate in a 25% reduced calorie diet intervention up to 12 weeks before definitive surgery. Adherence was maintained via a diet journal, regular check-ins, as well as nutritional and behavioral counseling. Clinical labs, weight, body composition, biomarkers and microbiome samples were collected pre and post-intervention. Paired t-tests were used to identify significant clinical parameters. Microbiome data was analyzed with QIIME2 and microbiome pathway analysis was conducted with PiCrust2.

Results: From August 2016 to October 2018, 35 patients enrolled in the study and completed the pre-operative CR intervention, lasting an average of 21 days. The intervention resulted in significant weight loss, with an average of 7.8 pounds lost ($p<0.0001$). Patient fatigue was decreased, as measured by the Promis Fatigue scale ($p < 0.01$). Leptin ($n=23$) and IGFBP-3 ($n=25$) were both significantly decreased ($p<0.05$). MiR-21 expression was found to be significantly downregulated post-intervention ($p<0.05$). Microbiome analysis did not find any significant differences in alpha or beta diversity. Picrust2 analysis revealed 10 differentially expressed functional microbiome pathways, with the three greatest changes being decreased benzoyl-CoA degradation, decreased L-arabinose degradation IV, and decreased glycogen degradation. Serum biomarker microarray analysis revealed significantly post-intervention downregulation of Eotaxin 2 and IP 10 chemokines in breast cancer patients (FDR < 0.05), and significant upregulation of IGFBP-1 in prostate cancer patients (FDR < 0.05).

Conclusions: This study demonstrates that short term preoperative caloric restriction is feasible and elicits rapid biologic changes in breast and prostate cancer patients, including significant downregulation of the oncogenic miR-21 and modulation of inflammatory chemokines. Microbiome pathway and taxa shifts suggest coordinated host/microbiome adaptation during the intervention. These findings support CR as a low-risk short-term intervention that warrants further investigation to determine the potential impact on long-term cancer outcomes.

#2042 A mechanosensitive RNAi machinery regulates pro-tumorigenic transformation in the colon.

Carlos Gomez, Joyce Nair-Menon, Amanda Daulagala, Antonis Kourtidis

Medical University of South Carolina, Charleston, SC

Background: Up to 90% of all cancers are of epithelial origin, such as the cancers of the gastrointestinal tract. A hallmark of the epithelial tissue is that cells that comprise it form a barrier that depends on the integrity of the adherens junctions (AJs), an essential cell-cell adhesion complex. However, a common observation in cancer is that this barrier and the AJs are compromised, promoting cancer progression. We have particularly discovered mislocalization of the AJ and barrier component PLEKHA7 in colon cancer, resulting in pro-tumorigenic cell behavior, caused by dysregulation of a PLEKHA7-associated RNA interference (RNAi) machinery and oncogene upregulation. However, the reasons for this PLEKHA7-RNAi disruption in colon tumors are unclear. To investigate what causes this disruption, we will perturb the extracellular matrix (ECM), which is commonly found to increase in stiffness as cancer progresses, potentially promoting tumor behavior. Our hypothesis is that mechanical changes that occur during cancer progression cause disruption of the PLEKHA7-RNAi machinery.
Methods: To test this hypothesis, we have generated several substrates of polyacrylamide gels and functionalized them with collagen to simulate the ranges of elastic moduli seen in normal and diseased colonic tissues. We will be plating non-malignant colon Caco2 cells on these substrates to investigate how ECM stiffness impacts localization of PLEKHA7 and RNAi components at AJs, as examined by immunofluorescence and confocal microscopy.
Results and Conclusions: Currently, our results show that increasing ECM stiffness disrupts formation of this AJ complex, suggesting that the elastic modulus of the ECM indeed impacts PLEKHA7-RNAi function and epithelial integrity. We will be conducting further analyses to delineate the exact properties of the elastic moduli of the ECM that result in PLEKHA7-RNAi disruption and the extent that this ECM-PLEKHA7-RNAi crosstalk contributes to disease progression.

#2044 Single-cell spatial profiling microRNA in human colon cancer tissue using high-plex multiomic Spatial Molecular Imaging (SMI).

Rachel Liu, Joe Phan, Rustem Khafizov, Kimberly Young, Ashley Heck, Dwayne Dunaway, Sayani Bhattacharjee, Courtney Anderson, Mirko Corselli, Prajan Divakar, Margaret L. Hoang, Joseph M. Beechem

Research and Development, Bruker Spatial Biology, Seattle, WA

MicroRNAs (miRNAs) are small, conserved noncoding RNAs that play an important role in cancer mechanisms and translational research, acting as oncogenes (e.g., miR-21), tumor suppressors (e.g., miR-200 family), and immune modulators (e.g., miR-155). However, miRNAs and their spatial and temporal implications, until now, have not been spatially profiled on an “omics-scale,” as short sequence length complicates traditional in situ hybridization probe design. The CosMx® Spatial Molecular Imager (SMI) fills this gap by providing a multiomics platform that profiles over 800 miRNAs spatially in tandem with 64+ proteins and over 1,000 RNAs, allowing the collection of a rich dataset that enables precise cell typing, miRNA imaging, and observation of the tumor microenvironment. Detection is achieved through the attachment of barcode oligos to miRNA targets and rounds of readout reporter binding and fluorescence imaging of these barcodes. Although over 38,000 miRNA sequences are cataloged, only a subset is considered biologically or clinically relevant per the latest miRBase database release. The CosMx miRNA Expression Panel targets these most impactful 827 human miRNAs, including key molecules such as miR-21, miR-200 isoforms, and miR-155, among others.Using the CosMx SMI multiomics workflow, we spatially profiled sections of formalin-fixed paraffin-embedded (FFPE) colon adenocarcinoma miRNA at the highest plex ever achieved at subcellular resolution in combination with same-section protein or RNA data. Results showed distinct miRNA enrichment in tumor cells, revealed miRNA-mRNA interactions, and highlighted regulatory networks across tissue compartments. These results underscore the power of high-plex spatial miRNA imaging for translational and clinical research.

#2046 Streamlined workflow generates small RNA and RNA-seq libraries from the same sample for deeper insights into tumor and normal matched tissues.

Heather M. Raimer Young, Gautam Naishadham, Bradley W. Langhorst, Louise Williams

Applications and Product Development, New England Biolabs, Inc., Ipswich, MA

Small noncoding RNAs (sncRNAs) play fundamental roles in many biological processes including cancer development and drug resistance. Increasing evidence shows that sncRNA expression signatures can be used to discriminate between normal and cancer tissues, highlighting their potential as diagnostic and prognostic biomarkers of the disease. Differentially expressed sncRNAs can be investigated using small RNA next generation sequencing methods and can be used to infer downstream effects on the transcriptome. However, performing RNA-seq from the same samples is necessary to confidently determine expression of any given affected transcript and understand the overall transcription profile. Making both small RNA and standard RNA-seq libraries can be challenging when sample material is limiting. Workflows that enable multiple data types to be generated from a single sample are needed for comprehensive understanding of disease.

Here we demonstrate the use of the NEB Monarch RNA size fractionation workflow to allow a single sample to be used for both small RNA and ribosomal depleted RNA-seq library preps. The Monarch RNA cleanup columns were used to enrich small RNA (< 200 nucleotides) and recover large transcripts (> 200 nucleotides) from 6 different human tissues (brain, testis, placenta, bladder, ovary, and esophagus) as well as 5 sets of matched normal and tumor samples (breast, stomach, rectum, colon, and liver).

Small RNA libraries were prepared using either total RNA or enriched small RNA samples (from the Monarch RNA column) with the NEBNext® Low-bias Small RNA Library Prep Kit. Ribosomal depleted RNA-seq libraries were prepared from the large transcript fractions using the NEBNext UltraExpress® RNA Library Prep Kit downstream of NEBNext rRNA Depletion Kit v2. We correlated expression of individual sncRNAs between total RNA and enriched small RNA libraries across all six normal tissues. In matched tumor and normal samples, we evaluated the relationships between miRNAs and their targets within the differentially expressed transcripts from both small RNA and transcriptome datasets. Overall, generation of small RNA and RNA-seq libraries from the same starting material permits a better understanding of the biological regulation of transcriptomes in individual samples.

#2047 Overcoming drug resistance by novel gemcitabine-modified miR-15a in colorectal cancer.

Anushka Ojha, Amartya Pal, Max Chao, Ramana Davuluri, Jingfang Ju

Stony Brook University, Stony Brook, NY

Colorectal cancer (CRC) is the third most prevalent cancer globally. Despite therapeutic advances, chemoresistance remains a major challenge, with ~20-30% of advanced-stage CRC patients experiencing recurrence within the first five years of treatment. Growing evidence suggests that targeting DNA damage response proteins, such as ATR/ATM, WEE1, and CHK1, is critical for overcoming resistance. In this regard, microRNAs (miRNAs) offer great therapeutic potential, as they can simultaneously target multiple signaling pathways and their dysregulation is widely implicated in cancer. Notably, tumor-suppressor miRNA-15a (miR-15a) is frequently downregulated in CRC and has been associated with poor patient prognosis. While miR-15a restoration has shown great promise, effective miRNA delivery remains a significant challenge due to its instability. Various chemical modifications have been shown to greatly enhance the stability of miRNAs. One such modification, 5-FU modified miR-15a (5-FU-miR-15a) was demonstrated as a promising therapeutic in CRC by our lab. Building on this, we engineered a new gemcitabine-modified miR-15a (Gem-miR-15a), which integrates the tumor-suppressive properties of miR-15a with the chemotherapeutic ability of gemcitabine. Though not a standard therapy in CRC, gemcitabine is emerging as an alternative for advanced refractory and resistant cases. Thus, we hypothesized that Gem-miR-15a would have an enhanced therapeutic advantage in overcoming chemoresistance to standard drugs, such as 5-FU. In this study, we assessed the effects of Gem-miR-15a on cell viability, apoptosis, and cell cycle progression of various parental (HCT116, SW480, SW620, HT-29) and 5-FU resistant CRC cell lines. Gem-miR-15a drastically reduced cell viability in both parental (IC_{50}=1-10nM) and resistant cells (IC_{50}=4.08 nM) without any delivery vehicle, significantly induced apoptosis, and caused an S-phase cell cycle arrest. Gem-miR-15a demonstrated dramatically increased cytotoxicity, with an almost 1000-fold reduction in IC_{50} as compared to the standard drug, 5-FU. The effects were consistent in 3D spheroids (IC_{50}=9.76 nM) and patient-derived organoids (IC_{50}=6-14 nM), too. The modification retained the target specificity of the native miR-15a, and downregulated key oncogenes like WEE1, CHK1 and BMI1 which was confirmed by western blotting. Additionally, Gem-miR-15a demonstrated strong synergy with oxaliplatin (Synergy score: 11.03). Experiments were done in triplicate (n=3) and analyzed using Student's t-test ($p < 0.05$). Gem-miR-15a (4mg/kg) was also significantly able to reduce the tumor growth in *in vivo* metastatic mouse models, as compared to the mice treated with vehicle alone, with no visible toxicities. Hence, our findings establish Gem-miR-15a as a potent and multi-targeted therapeutic candidate capable of overcoming chemoresistance in CRC.

#2048 Exosomal micrornas as epigenetic biomarkers of disease progression in Hispanic men with metastatic castration-resistant prostate cancer.

Carmen M. Ortiz-Sanchez[1], Jarline Encarnacion[1], Stephanie Montalvo[2], Shakira Abad[3], Gabriela Castro[3], Lenin Godoy[1], Ralphdy Vergne[1], Jong Y. Park[4], Gilberto Ruiz-Deya[1]

[1]Ponce Health Sciences University, Ponce, Puerto Rico,[2]University of Puerto Rico at Mayaguez, Mayaguez, Puerto Rico,[3]Pontificia Universidad Catolica de Puerto Rico, Ponce, Puerto Rico,[4]Moffitt Cancer Center, Tampa, FL

Background: Metastatic castration-resistant prostate cancer (mCRPC) arises when localized prostate tumors become unresponsive to androgen deprivation therapy (ADT) and develop metastatic potential. Despite therapeutic advances, mCRPC remains incurable, with a median survival of only 9-13 months. Identifying epigenetic biomarkers, such as exosomal microRNAs (exo-miRNAs), that can aid in early detection and monitoring disease progression is therefore critical, particularly among underrepresented populations such as Hispanic men.

Methods: Matched plasma samples from Puerto Rican men with prostate cancer at localized and metastatic stages (n=11) were analyzed to identify exo-miRNAs associated with progression to mCRPC. Exosomes were isolated from plasma, total exo-miRNAs were extracted, and expression profiling was performed using the nCounter Human v3 miRNA Expression Assay (NanoString Technologies) at Moffitt Cancer Center. Data were normalized, and statistical significance was evaluated using two-sample t-test and the Welch's t-test. All analyses were performed in R (v4.5.1) using the tidyverse, readr, and ggplot2 packages.

Results: The initial expression matrix (M) contained 798 miRNAs after excluding controls and spike-ins. Homogeneity assessment yielded a refined matrix of 66 targets. Applying an SD=1 threshold identified 18 candidate miRNAs differentially expressed during disease progression. Among these, miR-302d-3p ($p=0.01$) and miR-23a-3p ($p=0.045$) were significantly altered between localized and metastatic disease. Six additional candidates (miR-1246, miR-16-5p, miR-199a-3p/miR-199b-3p, miR-2053) showed borderline significance ($p<0.05$), suggesting potential biological relevance. This study provides novel insight into the epigenetic landscape of prostate cancer progression among Hispanic men, highlighting circulating exo-miRNAs as minimally invasive biomarkers for disease monitoring. Given the limited availability of clinical specimens from this population, these findings are particularly significant. The identification of circulating exo-miRNA signatures offers a minimally invasive approach to monitor disease progression and could ultimately support the development of blood-based biomarkers for early detection and risk stratification in advanced prostate cancer.

Funding: Supported by the American Cancer Society Institutional Research Grant (ACS-IRG Subaward No. 60-21510-99-20), the Catalyzer Research Grant from the Puerto Rico Science, Technology & Research Trust (PRST), and the NIH/NCI U54 Partnership Grants (U54CA163071 & U54CA163068) between Ponce Health Sciences University and Moffitt Cancer Center.

#2049 miR-1260a promotes proliferation and migration in breast cancer.

Marina Bataller[1], Andrea Feliciano[1], Yilin Sun[2], Daniela Gala[1], Marc Biasini[1], Almudena Sanchez-Garcia[1], Cristina Mir[1], Josep Castellvi[3], Sergi Benavente[4], Yoelsis Garcia-Mayea[1], **Matilde Esther LLeonart Pajarin**[1]

[1]Otorhinolaryngology, Vall d'Hebron Research Institute (VHIR), Barcelona, Spain,[2]CNIC, Madrid, Spain,[3]Pathology, Vall d'Hebron Research Institute (VHIR), Barcelona, Spain,[4]Radiotherapy, Vall d'Hebron Research Institute (VHIR), Barcelona, Spain

Background: MicroRNAs (miRNAs) regulate cellular and pathological processes, including cancer. As previously described by our group, miR-1260a was upregulated in breast cancer tissue. The aim of this research was to characterize miR-1260a in the breast cancer model.

Methods: MiR-1260a levels were studied by RNA array and qRT-PCR in breast cancer patients. The role and mechanisms underlying miR-1260a-mediated breast cancer cell growth, invasion and target proteins were studied using proliferation assays, colony formation assays, western blot, RT-qPCR and immunohistochemistry.

Results: Here, we found that miR-1260a expression is higher in luminal B tumors, followed by triple-negative tumors, and luminal A tumors in a clinical database of 50 breast cancer patients. Moreover, miR-1260a expression correlates positively with cyclin D1 protein. On the other hand, miR-1260a overexpression promotes the proliferation of MCF7, MDA-MD-231, MDA-MB-468, and T47D cells. In addition, miR-1260a induces the invasion of MCF7 and MDA-MB-231 cells. Moreover, our results suggest that the oncogenic properties of miR-1260a are linked to GCDH and ERP29 inhibition, two tumor suppressor proteins downregulated in breast cancer.

Conclusion: These findings indicate that miR-1260a promotes the oncogenic properties of cancer cells and may be useful as a new potential therapeutic target in hormone-dependent (luminal A and B) and triple-negative breast cancer.

#2050 Adipocyte-conditioned medium enhances the proliferation, motility and invasion of prostate cancer cell lines: Involvement of the microRNAs.

Masatoshi Watanabe[1], Hitoshi Nakano[2], Yoshifumi Hirokawa[1], Kazutoshi Iijima[3], Yuhei NIshimura[2]

[1]Department of Oncologic Pathology, Mie University Graduate School of Medicine, Tsu, Japan,[2]Department of Integrative Pharmacology, Mie University Graduate School of Medicine, Tsu, Japan,[3]Faculty of Engineering, Yokohama National University, Yokohama, Japan

Adipocytes (e.g., periprostatic adipose tissues, bone marrow) are one of the critical components in the prostate cancer tumor microenvironment. It has been reported that adipocytes influence the behavior of prostate cancer cells through adipocytokines and exosomes. We have previously shown effects of conditioned medium (CM) from adipocytes in behaviors of DU145 prostate cancer cells, and analyzed the microRNA profile of DU145 cells cultured in CM by a microarray. In this study, two additional cell lines (LNCaP and PC-3)were added to analyze cell behaviors. CM enhanced the proliferation, motility and invasion of PC-3 cells as same as DU-145 while not enhanced these behaviors of LNCaP, suggesting that CM promote androgen-independent cancer cell behaviors. However, in the invasion assay under CM, DU145 and PC-3 cells showed different amoeboid-mesenchymal transition plasticity, suggesting that effects of CM involve different mechanisms depending on the cell line. In addition, we re-analyzed the microRNA profiles of DU145 and PC-3 cells, verified target scores using miRDB and Target Scan, assessed overall survival and disease-free survival using GEPIA and Human Protein Atlas to identify candidate target genes. We also confirmed the expression levels of these candidate target genes in DU145 and PC3 cells using the DepMap. These results suggest that CM may affect behaviors of prostate cancer cells through microRNA-5787 and its multiple target genes such as WWOX and FLNA.

#2051 Simultaneous quantification of microRNA155 and let-7a using digital PCR.

Yu Zhao, Lindsey Cambria

Roche Diagnostics, Wilmington, MA

MicroRNAs (miRNAs) are small, non-coding RNAs that regulate gene expression post transcriptionally. Detection of miRNAs remains technically challenging due to the short length and high sequence similarity among family members. Accurate and sensitive quantification methods are therefore desired for clinical research. Digital PCR (dPCR) provides absolute quantification without the need for standards, offering high sensitivity and tolerance to inhibitors. These features make dPCR a powerful tool for miRNA analysis. In this study, a single well multiplex assay for the simultaneous detection of miR155, let-7a, and U6 snRNA as an internal control was developed with an advanced TaqMan-like probe design. Target specific reverse primers were used for cDNA synthesis, with or without 10-12 nt artificial sequence at the 5' end, followed by using Roche Digital LightCycler® dPCR system with universal nanowell plates equipped with 28,000 partitions. Each target was amplified with four primers in optimized ratios. The TaqMan-like probe incorporated a target specific reverse primer extended with an additional 20-22 nt sequence labeled with a 5' fluorophore, paired with a complementary primer containing a 3' quencher to block extension. Synthetic mature miR155 and let-7a miRNAs, along with commercial cell line RNAs were used to test assay performance. Ten-fold serial dilutions of mature miRNAs demonstrated robust detection down to 4-6 copies per reaction in singleplex and multiplex for both targets. No cross reactivity or competitive inhibition was observed when one target was present at 1000-fold excess relative to the other through spiked samples. In control RNA from Raji cell line, the assay quantified let-7a at 165 ± 21 copies and miR155 at 1,185 ± 141 copies, while in universal human reference RNA with pooled cell lines, it measured let-7a at 120 ± 14 copies and miR155 at 33 ± 8 copies in 25 pg total RNA. Furthermore, the assay successfully discriminated let-7a from closely related family members let-7b (two nucleotides difference) and let-7c (single nucleotide difference). Intermediate fluorescence (rain) is one of the major challenges for accurate quantification by using dPCR. To achieve reliable quantification results in this study, assay required supplement with 20-37.5 mM dNTPs per reaction, as well as optimized thermocycling parameters. In addition, to address unexpected clusters, multiplexing required distinct TaqMan-like probe sequences for each target. Together, these findings demonstrate that advanced TaqMan-like multiplex dPCR assay provides sensitive, specific, and reliable quantification of clinically relevant miRNAs, with potential applications in biomarker discovery and cancer research.*Data on file at Roche Diagnostics, Wilmington, MA, USA

#2052 miR-342-5p: A promising tumor suppressor in diffuse pleural mesothelioma.

So-Hyun Yoon, Anand Singh, Nathanael Pruett, Vivek Singh, Smrity Sahu, Yelixza Avila, Chuong Hoang

NIH-NCI, Bethesda, MD

Diffuse pleural mesothelioma (DPM) is an incurable, aggressive neoplasm with limited therapies. Moving beyond conventional approaches, we posit that microRNAs (miRNA), short, non-coding RNA that coherently regulate gene expression, can uniquely disrupt the molecular networks involved in DPM. In this study, we identified miR-342-5p as a novel DPM-associated miRNA. We used a human miRNA mimic library to screen for miRNAs with antiproliferative effects on a panel of DPM cell lines. Among the most potent candidates was miR-342-5p. We profiled the downregulation of miR-342-5p in DPM patient specimens compared to normal pleura (Normal=22, Tumor=50). TCGA-MESO analysis revealed that miR-342-5p downregulation is significantly associated with poor survival outcomes. Our results demonstrated that the re-expression of miR-342-5p significantly impaired DPM cell viability, reduced 2D colony foci formation, and inhibited anchorage-independent cell growth in soft-agar and sphere assays. Additionally, Annexin-V assays showed a significant increase in early and late apoptotic cells in miR-342-5p transfected DPM cells compared to controls. Furthermore, we confirmed the induction of apoptosis in miR-342-5p-treated DPM cells through PARP cleavage and the activation of caspase-3/7. Importantly, no significant biological effects were observed when normal human mesothelial cells (NP1 line) were treated with miR-342-5p. Next, we performed a Biotin-miRNA (Bi-miR) pull-down assay, a direct binding assay in which a biotin-tagged miR-342-5p probe captures its associated mRNA transcripts in a pooled lysate. Then, RNA-seq analysis is conducted to identify direct target genes associated with apoptosis and cell death pathways in DPM. We identified the top transcripts targeted by miR-342-5p that are also involved in its tumor-suppressive activity in DPM. Overall, our findings highlight the tumor suppressive effects and therapeutic potential of miR-342-5p for DPM treatment.

#2053 Developing the miR-888 cluster members as an antimiRNA therapy for aggressive prostate cancer.

Alex Cain[1], Katherine Routon Stanton[1], Vishal Kasina[2], Raman Bahal[2], Aurora Esquela Kerscher[1]

[1]Biomedical and Translational Sciences, Macon and Joan Brock Virginia Health Sciences at Old Dominion University, Norfolk, VA,[2]Department of Pharmaceutical Sciences, University of Connecticut, Storrs, CT

Metastatic prostate cancer (PCa) represents an unmet treatment need, with a 5-year survival rate of only 30%. MicroRNAs (miRNAs) are small noncoding RNAs that hold therapeutic promise for PCa and act as important tumor suppressors and pro-oncogenic factors in the prostate. The Kerscher lab identified the miR-888 cluster as preferentially enriched in human metastatic PCa cell lines and prostatic fluids from patients with high-grade PCa compared to low-grade or non-cancer patients. We showed that cluster members promoted prostate growth and aggressiveness in vitro, particularly miR-888 and miR-891a, and these miRNAs accelerated tumor load in mice. Reciprocally, inactivation of miR-888 and miR-891a using antisense oligos reversed these effects, highlighting their potential as antimiR targets for PCa. AntimiRs are valuable tools for inhibiting miRNA function, but current antimiR therapies require high dosage and suffer from poor tissue specificity. To address these shortcomings, the Kerscher lab collaborated with Dr. Raman Bahal's group to test the efficacy of their acid-sensing peptide pHLIP (pH low insertion peptide) as a novel prostate tumor delivery reagent conjugated to peptide nucleic acids (PNAs) designed to inhibit miR-888 or miR-891a. We hypothesized that pHLIP-PNA-antimiRs against miR-888/-891a would allow efficient delivery to prostate tumors (with inherently acidic microenvironments) and inhibit progression to lethal disease. We also predicted more pronounced effects in castration-resistant PCa. Indeed, when endogenous miR-888/891a levels were analyzed by qRT-PCR across a panel of human PCa cell lines representing the spectrum of this disease, we noted that miR-888 & miR-891a expression was especially elevated in castration-resistant, neuroendocrine PCa lines. pHLIP-PNA-antimiR-888 and antimiR-891a reagents were further validated in vitro to reduce miRNA levels and suppress cancer phenotypes in PCa cell lines. For these experiments, PCa cells were treated with 4 uM pHLIP-PNA-antimiR or control reagents in pH 6.0 media for 3 hours, recovered for 24-48 hours, and harvested for qRT-PCR, WST-1 (proliferation), and soft agar (anchorage-independent growth) assays. As predicted, pHLIP-PNA-antimiR treatment reduced growth more effectively in metastatic PC3-ML than in indolent LNCaP cells. Ultimately, we sought to determine pHLIP-PNA-antimiR efficacy in a xenograft mouse model. We first validated that cy5-pHLIP alone efficiently targeted PC3-ML xenografts in mice, with low signal in kidney and liver. In a pilot efficacy study, we then injected PC3-ML cells into the flanks of mice. When tumor volume reached ~300 mm^3, animals were injected with pHLIP-PNA-antimiR-891a or -NC67 controls by tail vein on days 1, 4, 8, and 11. This preliminary study showed that antimiR-891a reduced tumor load. These novel pHLIP-PNA-antimiR reagents demonstrate clinical promise for late-stage PCa.

#2054 Melatonin and estradiol action on let-7 family members in triple-negative breast cancer cells.

Bruna Cristine De Almeida, Kelly Pedrozo Ferreira, Jose Maria Soares-Junior, **Katia Candido Carvalho**, Edmund Chada Baracat

Obstetrics and Gynecology, Faculdade de Medicina da Universidade de Sao Paulo, Sao Paulo, Brazil

The widely studied tumor suppressor miRNAs of the let-7 family are involved in many cellular processes through the regulation of several signaling pathways. They shared identical seed sequences and have variable stem-loop regions. The let-7 family regulates crucial physiological functions in cells. However, low expression is frequently found, and it was associated with cell proliferation, migration, and metastasis in triple-negative breast cancer (BC). Although the MDA-MB231 BC cell line is triple-negative, it has been shown to express estrogen receptor beta. Let-7 has a regulatory relationship with estrogen, acting as a negative regulator of estrogen receptors. The recovery or restoration of let-7 expression seems to be a key point to prevent breast cancer growth and development. In this context, melatonin (Mel) has gained notoriety due to its versatile and essential mechanisms for antagonizing tumor features, which involve modulation of differential miRNA expression. Studies have demonstrated that Mel can alter the expression of some members of the let-7 family in some contexts. Objective: We aimed to demonstrate the effects of Mel and 17beta-estradiol (E2) treatments on the proliferation of triple-negative BC and assess the expression profile of six let-7 family members (let-7a/b/c/g/i/f). Methods: MDA-MB231 cells were treated with 3 mM Mel and 100 nM E2, and the two drugs were combined (ME2) and were replaced daily for up to 96h. Cell proliferation was evaluated in treated cells. RNAs were extracted, and reverse transcription was performed. RT-PCR was carried out for the detection of selected let-7 family members. Results: Our preliminary results showed a significant decrease in the proliferation assay in the cell line after Mel and ME2 treatments. Cells presented a lower rate of proliferation at 72h of Mel and ME2 treatments. Mel treatment leads to slightly and significantly increased expression of let-7c/g/f (Fold:1.939; 1.132; 1.624, respectively), and the let-7c/g also showed higher expression related to ME2. Cells treated with ME2 showed a significant increase of let-7b/i/f (Fold:1.112; 1.123; 1.506, respectively) compared to CC and E2. Let-7c (Fold: 0.879) presented a significant decrease compared to CC. Additionally, lower expression of let-7a/b/g/i (Fold: 0.707; 0.823; 0.662; 0.759, respectively) was observed in cells treated with E2. Conclusion: Our results indicate that Mel can minimize E2 effects and inhibit the proliferation of triple-negative BC cells through the regulation of specific miRNAs. It seems to recover the expression of tumor suppressor miRNAs of the let-7 family in triple-negative BC. Supported by: FAPESP 2025/08621-1, 2022/04174-2, and 2018/24224-9, and CNPq 444345/2024-8.

#2055 Isoform-aware miRNA network mapping in NSCLC via computational consensus targeting and functional clustering.

Shaopeng Gu[1], Junhao Liu[2], Shaohong Feng[3], Rosario Distefano[4], Sebastiano Di Bella[5], Francesco Orilio[5], Rosario Brancaccio[5], Giulia Romano[6], Eswar Shankar[7], Mario Acunzo[6], Federica Calore[8], Christian Rolfo[7], Qin Ma[1], Giovanni Nigita[7]

[1]Department of Biomedical Informatics, The Ohio State University Comprehensive Cancer Center, Columbus, OH,[2]College of Engineering, The Ohio State University, Columbus, OH,[3]Department of Biomedical Informatics, The Ohio State University, Columbus, OH,[4]The Ohio State University Comprehensive Cancer Center, Columbus, OH,[5]University of Palermo, Palermo, Italy,[6]LUM University, Casamassima, Italy,[7]Department of Internal Medicine, Division of Medical Oncology, The Ohio State University Comprehensive Cancer Center, Columbus, OH,[8]Department of Cancer Biology and Genetics, The Ohio State University, Columbus, OH

MicroRNA (miRNA) isoforms (isomiRs), generated by alternative processing, RNA editing, and tailing/trimming, broaden regulation and can differ from canonical miRNAs in targets and function. Yet most cancer genomics workflows still collapse reads to canonical miRNAs or ignore non-canonical variants, obscuring isoform-specific regulatory networks. This gap is especially relevant in NSCLC, where heterogeneity and unmet needs in biomarkers and targets are high. Building on our pan-cancer data showing that isomiR-aware profiling improves clinicopathologic classification, we assumed that systematic isoform-level analysis would uncover NSCLC-specific biological signatures and vulnerabilities missed by traditional miRNA analyses.

Data from TCGA LUAD and LUSC were processed with an isoform-aware pipeline. Differentially expressed isomiRs between tumors and matched normals were defined using |fold-change|>1.5 and FDR<0.05. Consensus targets were predicted across six algorithms, retaining interactions supported by ≥4 tools and downregulated in isomiR-high versus isomiR-low tumors. Isoform functions were compared across subtypes using Jaccard distances on pathway-level target matrices, hierarchical clustering, and pathway-frequency summaries across lung cancer-related pathways.

We identified ~1,300 deregulated isomiRs in LUAD and ~1,100 in LUSC. Pathway-based clustering grouped isomiRs into functional clusters that separated LUAD and LUSC. Clusters enriched for hallmark oncogenic signaling networks (e.g., PI3K-AKT, MAPK, p53, VEGF) contained ~14% shared isomiRs that converged on these pathways. miR-183-5p, which contributed the largest isoform repertoire, aligned with high cluster activity and PTEN/p53-AKT signaling. Oncogenic clusters were further shaped by miR-17-5p/miR-93-5p and context-dependent miR-130b-3p, whereas tumor-suppressive isomiRs (e.g., miR-128-3p) marked restraint of cell-cycle progression and invasion.

Isoform-aware miRNA analysis uncovers NSCLC regulatory networks beyond traditional views. Integrating consensus targeting with cohort-level expression and pathway-based clustering enables functional identification of isomiRs and prioritization of isoform-target pairs, including subtype-specific and shared oncogenic networks, as potential biomarkers and therapeutic targets. These results are still limited by current challenges in isomiR quantification, context-specific target prediction, cohort variability, and the need for functional validation.

#2056 Cross-species microRNA expression patterns identify potential therapeutic targets in osteosarcoma.

Sophia C. Fernandes[1], Emma N. Vanderboon[1], Alicia Viloria-Petit[2], R. Darren Wood[1], Geoffrey A. Wood[1]

[1]Pathobiology, University of Guelph, Guelph, ON, Canada,[2]Biomedical Sciences, University of Guelph, Guelph, ON, Canada

Osteosarcoma is the most common primary bone tumour in both humans and dogs. In both species, osteosarcoma displays a marked propensity for pulmonary metastasis, making canines a robust and clinically relevant translational model of the disease. With current standard-of-care treatment, the 5-year survival rate for humans with localized osteosarcoma is approximately 60-70%, but falls to around 20-30% for patients presenting with metastatic disease. In dogs, amputation followed by chemotherapy yields a median survival time of roughly 10-12 months, with fewer than 20% surviving beyond two years. Despite incremental improvements in supportive care, therapeutic strategies for osteosarcoma have remained largely unchanged for more than three decades in both species, highlighting the need for novel prognostic indicators and therapeutic targets. MicroRNAs (miRNAs) are small, non-coding RNAs that can function as tumour suppressors or oncogenes. They are expressed across diverse tissues and are known to exhibit dysregulation in cancer. In this study, 20 osteosarcoma cell lines (6 human and 14 canine), derived from both primary and metastatic tumours, were evaluated for key malignant behaviours using a series of in vitro functional assays. These included measurements of proliferation (doubling time), migration (scratch and transwell assays), anchorage-independent survival (anoikis assay), invasion (drop invasion assay), and colony formation (clonogenic assay). RNA was subsequently isolated from each cell line, and expression of 48 candidate miRNAs was quantified using real-time quantitative polymerase chain reaction (RT-qPCR). Each miRNA was correlated with measured behaviours using Pearson's r and false discovery rate (FDR) analysis. Ten miRNAs were significantly associated with at least one behaviour at $p < 0.05$ following FDR correction. Notably, miR-708-5p demonstrated significant correlations with multiple malignant phenotypes, including doubling time, migration, and colony formation. MiRNA expression profiles, therefore, revealed several candidates associated with malignant behaviour, suggesting that select miRNAs may contribute to disease progression and represent promising targets for future therapeutic development.

#2057 Subtype-dependent modulation of mir-655-3p by melatonin in breast cancer cell lines.

Kelly Pedrozo Ferreira[1], Bruna Cristine De Almeida[2], Edmund C. Baracat[1], **Katia C. Carvalho**[3]

[1]Faculdade de Medicina da Universidade de Sao Paulo, Sao Paulo, Brazil,[2]Fundacao Faculdade de Medicina, Sao Paulo, Brazil,[3]Obstetrics and Gynecology, HCFMUSP, Sao Paulo, Brazil

Background: Breast cancer (BC) is a highly heterogeneous disease composed of distinct molecular subtypes that influence tumor behavior and therapeutic response. Melatonin (MEL) has been widely investigated for its oncostatic properties, partly mediated through the modulation of microRNA (miRNA) expression—key post-transcriptional regulators of genes involved in proliferation, invasion, and metastasis. Among these, miR-655-3p has been described as a potential tumor-suppressive miRNA associated with reduced aggressiveness in several cancer types. However, the effects of MEL on miR-655-3p expression across different BC subtypes remain poorly defined. Therefore, we aimed to evaluate the impact of MEL treatment on miR-655-3p expression in BC cell lines with distinct molecular profiles, including luminal A and triple-negative (TN) subtypes.
Methods: Human BC cell lines MCF-7 and T47D (luminal A; ER+/PR+) and MDA-MB-231 (TN) were cultured under standard conditions and treated with 3000 µM MEL or left untreated (control group — CC). Total RNA was extracted using the mirVana™ miRNA Isolation Kit. cDNA synthesis was performed with the High-Capacity cDNA Reverse Transcription Kit, and miR-655-3p expression was quantified by qRT-PCR using specific TaqMan® assays. Relative expression levels and normalization to endogenous controls were obtained using ExpressionSuite™ Software v1.3.
Results: MEL treatment resulted in a significant upregulation of miR-655-3p in MDA-MB-231 (TN) cells compared with untreated controls. In contrast, luminal A cell lines (MCF-7 and T47D) exhibited a significant decrease in miR-655-3p expression under the same MEL exposure conditions.
Conclusion: Melatonin differentially modulates miR-655-3p expression across BC molecular subtypes, increasing its expression in TN cells while reducing it in luminal A cells. These opposite expression patterns suggest that MEL's regulatory effects on miR-655-3p are subtype-dependent, potentially reflecting differences in signaling pathways associated with hormone receptor status. Together, these findings indicate that miR-655-3p may serve as a biomarker of subtype-specific responses to melatonin and a potential therapeutic target involved in the modulation of tumor aggressiveness. Further studies are warranted to identify its direct gene targets and elucidate the biological relevance of this regulation.

#2058 Melatonin modulates mir-340-5p expression in breast cancer molecular subtypes: Implications for subtype-specific regulation and therapeutic targeting.

Kelly Pedrozo Ferreira[1], Bruna Cristine De Almeida[2], **Katia C. Carvalho**[3]

[1]Faculdade de Medicina da Universidade de Sao Paulo, Sao Paulo, Brazil,[2]Fundacao Faculdade de Medicina, Sao Paulo, Brazil,[3]Obstetrics and Gynecology, HCFMUSP, Sao Paolo, Brazil

Background: Breast cancer (BC) comprises highly heterogeneous subtypes with distinct molecular and clinical features. Triple-negative breast cancer (TNBC) is characterized by poor prognosis and limited therapeutic options, whereas luminal A tumors exhibit hormone receptor positivity and more favorable outcomes. Emerging evidence suggests that melatonin (MEL) exerts oncostatic effects through the modulation of gene expression, including microRNAs (miRNAs), which regulate key oncogenic pathways. Among these, miR-340-5p has been implicated in tumor suppression and in the regulation of epithelial-mesenchymal transition (EMT). However, its modulation by MEL across BC molecular subtypes remains poorly understood. Therefore, we investigated the differential expression of miR-340-5p in BC cell lines representing distinct molecular profiles (luminal A and TN) following melatonin treatment.
Methods: Human BC cell lines MCF-7 and T47D (luminal A) and MDA-MB-231 (TN) were cultured and either left untreated (control) or treated with 3000 μM MEL. Total RNA was extracted using the mirVana™ miRNA Isolation Kit. cDNA synthesis was performed with the High-Capacity cDNA Reverse Transcription Kit, and miR-340-5p expression was quantified by qRT-PCR using specific TaqMan® assays. Relative expression levels, endogenous control normalization, and data processing were performed using ExpressionSuite™ Software v1.3.
Results: MEL treatment resulted in an upregulation of miR-340-5p in MDA-MB-231 (TN) cells compared with untreated controls. Conversely, luminal A cell lines (MCF-7 and T47D) exhibited a reduction in miR-340-5p expression following MEL treatment relative to control cells.
Conclusion: Melatonin modulates miR-340-5p expression in a molecular subtype-dependent manner, increasing its expression in TN cells while reducing it in luminal A cells. This differential regulation highlights the potential of miR-340-5p as a biomarker for subtype-specific responses to melatonin and may contribute to distinguishing aggressive from hormone-responsive BC phenotypes. Additional studies are needed to identify downstream targets and elucidate the biological significance of this regulatory pathway.

#2059 Auro-Liposome miR-195 delivery system impedes ovarian cancer progression and enhances cisplatin-sensitivity.

Arpan Dey Bhowmik, Pallab Shaw, Prasanta Panja, Geeta Rao, Resham Bhattacharya, Priyabrata Mukherjee, Shailendra Kumar Dhar Dwivedi

Peggy and Charles Stephenson Cancer Center, University of Oklahoma Health Sciences Campus, Oklahoma City, OK

Background: Ovarian cancer (OvCa) accounts for the highest mortality rate among all gynecological malignancy. This is mainly due to late-stage detection, early metastasis and drug-resistance. While most patients initially respond to chemotherapy, Cancer Stem-like Cells (CSCs) facilitate chemoresistance and tumor relapse. WNT7A, a key activator of β-catenin signaling, is overexpressed in OvCa and promotes CSC characteristics, epithelial-mesenchymal transition (EMT), chemoresistance, whereas the tumor-suppressive miR-195 is downregulated. In this study, we investigated whether restoring miR-195 expression could inhibit cancer progression and improve drug-sensitivity by targeting WNT7A mediated β-catenin signaling.
Methods: CSCs were enriched using anchorage-independent spheroid culture conditions. miR-195 expression levels were assessed by qRT-PCR. Functional assays were performed to determine the effect of miR-195 on CSC markers, EMT, drug-sensitivity. A luciferase reporter assay was utilized to validate the direct miR-195 binding within the WNT7A 3'UTR. β-catenin activation and nuclear localization were analyzed by immunoblot, immunofluorescence. To mimic tumor microenvironment, multicellular aggregate model was generated using OvCa cell line (A2780-CP20), cancer-associated fibroblast (CAF19) and human microvascular endothelial cells (HMEC1) and for assessing AuLPs's potential as a miR-195 delivery system.
Results: Spheroid-derived CSCs displayed enhanced expression of stem cell markers NANOG, OCT4, cMYC, KLF4, accompanied by a significant reduction in miR-195 levels. Restoration of miR-195 expression inhibited spheroid growth, caused downregulation of stemness markers and enhanced cisplatin-sensitivity. miR-195 directly targeted WNT7A, leading to decreased nuclear localization of active β-catenin and inhibition of WNT/β-catenin signaling, EMT pathway. Furthermore, *in vivo* homing assay revealed that stable miR-195 re-expression significantly reduced A2780-CP20 adhesion to the mice omentum, highlighting its anti-metastatic role. Noticeably, our novel AuLPs system conferred superior intracellular delivery of miR-195 compared to commercial agents and more striking inhibition of oncogenic WNT7A/β-catenin pathway and profound anti-tumor effect against multicellular aggregate.
Conclusions: miR-195 suppress OvCa progression by targeting cancer stemness, EMT and enhance cisplatin-sensitivity via directly modulating WNT7A/β-catenin pathway and formulations of novel AuLPs delivery system offers a promising miRNA-based therapeutic strategy.
Acknowledgments: PHF and DOD'S Ovarian Cancer Academy grant (HT94252310772) to SKD.

#2060 Targeting microRNA-mediated copper homeostasis dysregulation to enhance intratumoral susceptibility to oncolytic herpes simplex virus-1 in glioblastoma.

Tae Jin Lee[1], Min Hye Noh[1], Citu Citu[2], Alexandra A. Miller[1], Jiyeon Kim[1], Grace Nguyen[1], Minxin Huang[1], Amanda S. Kouaho[1], Stephanie M. Bean[1], Dohyoung Lee[1], Lily Nguyen[1], E. Antonio Chiocca[3], Zhongming Zhao[2], Ji Young Yoo[1]

[1]Department of Neurosurgery, UT Health Houston, Houston, TX,[2]Center for Precision Health, UT Health Houston, Houston, TX,[3]Department of Neurosurgery, Brigham and Women's Hospital and Harvard Medical School, Boston, MA

Glioblastoma (GBM) is a WHO grade IV astrocytoma characterized by diffuse infiltration, rapid proliferation, and resistance to conventional therapies, resulting in dismal patient outcomes. Oncolytic virotherapy, particularly utilizing genetically engineered oncolytic herpes simplex virus-1 (oHSV), has demonstrated tumor-selective cytolysis and immunogenic cell death. Despite promising preclinical data, clinical efficacy remains limited due to poorly defined intrinsic resistance mechanisms within the tumor microenvironment (TME) of GBM. Our study identified microRNA-155 (miR-155) as a critical modulator of oHSV therapeutic resistance. We found elevated miR-155 expression in GBM compared to low-grade gliomas, which correlates with a poor prognosis and reduced response to OV therapy. These findings were further supported by The Cancer Genome Atlas (TCGA) data. Ectopic overexpression of miR-155 significantly attenuated oHSV replication and cytopathic effects. Transcriptomic profiling and pathway enrichment analyses revealed that miR-155 upregulates metallothioneins *MT1E* and *MT1F*, key regulators of intracellular copper sequestration and antiviral defense. Mechanistically, miR-155 disrupts copper homeostasis via the MT1 axis, impairing viral replication and therapeutic efficacy. Functional ablation of miR-155 via CRISPR/Cas9-mediated knockout or Locked Nucleic Acid (LNA)-based inhibition restored copper homeostasis, oHSV replication kinetics, and enhanced oncolysis in vitro and in orthotopic GBM xenograft models, resulting in prolonged survival. These data suggest that the miR-155/MT1E-MT1F/copper signaling axis represents a novel barrier to oHSV therapy. This work elucidates a previously uncharacterized antiviral resistance pathway in GBM and validates miR-155 inhibition as a rational therapeutic strategy to potentiate oHSV efficacy. Our findings provide a mechanistic framework for overcoming innate resistance and advancing the clinical translation of virotherapy in neuro-oncology. This abstract was originally written by the authors and then edited and revised with generative artificial intelligence (AI).

#2061 MicroRNAs targeting tumor suppressor GRK2: Novel potential therapeutic strategies for restraining MALT1-dependent DLBCL.

Jing Cheng[1], Mei Smyers[2], Matt Trotta[2], Neil M. Carleton[3], Lisa M. Maurer[2], Uma R. Chandran[4], Min Xia[5], Ari M. Melnick[5], Peter C. Lucas[1], Linda M. McAllister-Lucas[6]

[1]Laboratory Medicine and Pathology, Mayo Clinic, Rochester, MN,[2]Pediatrics, University of Pittsburgh, Pittsburgh, PA,[3]Pathology, University of Pittsburgh, Pittsburgh, PA,[4]Biomedical Informatics, University of Pittsburgh, Pittsburgh, PA,[5]Medicine, Weill Cornell Medical College, New York, NY,[6]Comprehensive Cancer Center, Mayo Clinic, Rochester, MN

Introduction/Objectives: The CARMA1-BCL10-MALT1 (CBM) signalosome plays crucial role in mediating antigen receptor-induced activation of NF-κB transcription factor and subsequent lymphocyte activation. The effector protein of the signalosome, MALT1, functions both as a scaffold to recruit downstream NF-κB signaling machinery, and as a protease to cleave and inactivate multiple substrates including negative regulators of NF-κB. Constitutive MALT1 activation, which can occur as a result of gain-of-function mutations of the B cell receptor, CARMA1, BCL10 or chromosomal translocation involving the *MALT1* gene, underlies the pathogenesis of multiple lymphoid malignancies including activated B-cell type-diffuse large B-cell lymphoma (ABC-DLBCL) and MALT lymphoma. We previously identified G-protein-coupled receptor kinase 2 (GRK2) as a tumor suppressor in MALT1-dependent lymphomas which binds MALT1 and inhibits MALT1 scaffolding and proteolytic activities. Accordingly, *GRK2* mRNA levels are markedly lower in a subset of DLBCL tumors compared to normal B cells and lower *GRK2* level in ABC-DLBCL is associated with reduced patient survival. In current study, we sought to investigate the mechanism of how GRK2 levels are regulated in ABC-DLBCL. **Methods/Results**: Using DICER1 depleted cells, we showed that globally impaired miRNA processing leads to increased GRK2 protein levels. We then conducted bioinformatic analyses of patient tumor samples and performed screening via microRNA Data Integration Portal to identify microRNAs that target GRK2 in ABC-DLBCL. Further GRK2 3'UTR reporter assay confirmed direct targeting of GRK2 by candidate miRNAs. ABC-DLBCL cell lines, OCI-LY3 and TMD8, which demonstrate reduced *GRK2* mRNA expression compared to primary B cells, show elevated expression of candidate GRK2-targeting microRNAs. Stable overexpression of miR-125a, 125b, or 148b in OCI-LY3 or TMD8 cells led to reduced GRK2 expression, enhanced MALT1 activity and increased cell proliferation. Conversely, in vitro inhibition of candidate miRNAs using anti-miRNA Locked Nucleic Acids (LNA) inhibitors led to enhanced GRK2 expression, reduced MALT1 activity and decreased cell proliferation. Importantly, treatment of mice with inhibitors of miR-125b and miR-148b abrogates the growth of ABC-DLBCL xenograft tumors in vivo. **Conclusion**: We have identified miRNAs that negatively regulate *GRK2* expression in ABC-DLBCL. These GRK2-targeting miRNAs serve a pro-tumorigenic role by promoting MALT1 oncoprotein's scaffold and protease activity. Furthermore, inhibitors of these miRNAs can enhance *GRK2* expression and thereby suppress MALT1 activity and MALT1-dependent tumor cell proliferation, both in vitro and in vivo. These studies suggest that microRNA inhibitors which enhance GRK2 expression could represent a novel approach for restraining MALT1-dependent lymphomagenesis.

#2063 The impact of 4-thiouridine posttranscriptional modification on the oncosuppressive activity of bioengineered let-7e-5p in NSCLC cells.

Katherine K. Wang[1], Mei-Juan Tu[1], Yufan Zhou[1], Ziyuan Wang[2], Patrick A. Limbach[3], Hongxu Ding[2], Ai-Ming Yu[1]

[1]Department of Biochemistry and Molecular Medicine, UC Davis School of Medicine, Sacramento, CA,[2]Department of Pharmacy Practice and Science, Statistics and Data Science GIDP, University of Arizona, Tucson, AZ,[3]Department of Chemistry, Rieveschl Laboratories for Mass Spectrometry, University of Cincinnati, Cincinnati, OH

Current microRNA (miRNA) research and therapeutic development primarily rely on miRNA mimics chemically synthesized *in vitro*. While effective, miRNA mimics may not fully recapitulate the properties of natural miRNA agents synthesized *in vivo*. Our lab has developed a novel tRNA-fused pre-miRNA carrier-based RNA bioengineering platform technology, enabling consistent, high-yield, and large-scale production of biologic miRNAs (BioRNAs) through *in vivo* bacterial fermentation, which have shown strong potential in experimental therapeutics for non-small cell lung cancer (NSCLC). Among the tumor suppressive let-7-5p isoforms, BioRNA/let-7e-5p was identified as the most effective to suppress human NSCLC cell viability. Further, while we observed species-conserved posttranscriptional modifications, such as dihydrouridine (D) and 2′-*O*-methylguanosine (Gm) in the D-loop as well as 5-methyluridine (m^5U) and pseudouridine (Y) in the T-loop, liquid chromatography tandem mass spectrometry (LC-MS/MS) and nanopore-based direct RNA sequencing studies revealed the presence of a bacteria-specific 4-thiouridine (s^4U) modification at position 8 (s^4U8) of the human tRNA segment. To re-innovate our BioRNA technology and generate BioRNA/let-7e-5p molecules free of s^4U modification, we employed two strategies: (1) change of U8 through deletion or substitutions, and (2) expression of U8 BioRNAs in an *E. coli* strain deficient in s^4U synthesis. Both approaches proved successful, allowing us to produce milligrams of pure, ready-to-use BioRNA/let-7e-5p molecules per 200 mL bacterial culture, and LC-MS/MS and nanopore sequencing analyses confirmed the escape from s^4U modification. Surprisingly, comprehensive comparative studies showed minimal effects of the distal s^4U modification on the release of let-7e-5p from BioRNAs and consequently, downregulation of multiple targeted oncogenes in NSCLC cells. These findings will guide the development of BioRNA/let-7e-5p as potential therapeutics for NSCLC treatment.

#2064 miR-1293 suppresses diffuse pleural mesothelioma growth by targeting a novel S100A16-Hippo-EMT axis.

Vivek Singh[1], Anand Singh[1], Nathanael Pruett[2], So-Hyun Yoon[3], Smrity Sahu[2], Yelixza Avila[2], Chuong D. Hoang[4]

[1]Laboratory of Integrative Cancer Immunology (LICI), Center for Cancer Research, Bethesda, MD,[23]NIH-NCI, Bethesda, MD,[4]Assistant Professor, Dept. of Thoracic Surgery, National Cancer Institute, Bethesda, MD

Background: Diffuse pleural mesothelioma (DPM) features frequent NF2 loss, Hippo pathway disruption, and limited therapies. We identify miR-1293 as a tumor-suppressive miRNA that targets an S100A16-centered Hippo/EMT axis involving Hippo/YAP and epithelial-mesenchymal transition (EMT) in DPM. **Methods:** We performed a high-throughput human miRNA mimic screen across multiple DPM cell lines with proliferation assays to identify anti-tumor miRNAs. miR-1293 expression was measured by qRT-PCR in DPM tumors and normal pleura. Targets were mapped by biotin-miR-1293 pulldown plus RNA-seq and in silico prediction, then integrated with pathway and DepMap data to define an S100A16-Hippo/EMT module. Functional effects of miR-1293 re-expression were tested in NF2-wild-type and NF2/Hippo-deficient DPM lines and in MB52 xenografts using local hydrogel-based (SFH-miR-1293) delivery in subcutaneous and orthotopic pleural models. **Results:** The screen identified miR-1293 as a top antiproliferative miRNA, and miR-1293 was significantly underexpressed in DPM versus normal pleura. Re-expression in miR-1293-low DPM lines reduced proliferation, colony and soft-agar growth, with minimal impact on non-malignant mesothelial cells, and induced apoptosis and cell-cycle arrest. Target mapping yielded 345 genes enriched for Hippo signaling and EMT, with additional mTORC1, IL-2/STAT5, and hypoxia signatures, and a 19-gene core S100A16-Hippo-EMT module. Within this module, S100A16 was the most essential and strongest adverse prognostic gene, highly expressed in NF2/Hippo-deficient lines (H2052, MB52, MB24) with activated YAP/TAZ/TEAD and EMT-like features. miR-1293 re-expression preferentially impaired viability and clonogenicity in these NF2/Hippo-deficient cells, with coordinated suppression of S100A16, YAP/TAZ/TEAD, and EMT markers. In vivo, SFH-miR-1293 significantly reduced tumor burden, Ki-67, and bioluminescence, increased cleaved caspase-3, and prolonged survival in xenograft and orthotopic pleural models. **Conclusions:** miR-1293 is a tumor-suppressive miRNA in DPM that targets an S100A16-Hippo-EMT axis and shows preferential activity in NF2/Hippo-deficient mesothelioma. Local hydrogel-based delivery elicits strong antitumor effects in vivo, supporting miR-1293 as a therapeutic candidate for DPM and a rational partner for Hippo/YAP-directed and immunotherapy strategies.

#2065 Prognostic potential of microRNA-encoding gene signatures in gynecologic cancers.

Elizabeth Miller[1], Amber Hoskins[1], Natalie Gierat[2], Aneth Ochoa Negrete[2], **Riyaz Basha**[2]

[1]Texas College of Osteopathic Medicine, University of North Texas Health Science Center, Fort Worth, TX,[2]University of North Texas Health Science Center, Fort Worth, TX

Background/Significance: Effective early-stage biomarkers are needed for improving outcomes in gynecologic cancers. Micro RNAs (miRNAs) are small non-coding RNAs that function in post-transcriptional gene regulation and their dysfunction can play key role in cancer development and progression. Recently, the role of miRNAs is gaining attention as circulating biomarkers for various malignancies. However, there is a gap in studies involving gynecologic cancers with high-mortality rates such as ovarian serous cystadenocarcinoma (OV), uterine corpus endometrial carcinoma (UCEC), and uterine carcinosarcoma (UCS). The objectives of this study are to analyze the expression profiles of selected miRNA-coding genes such as hsa-mir-6511b-1, hsa-mir-6820, and hsa-mir-3198-2 in tumor specimens from patients with OV, UCEC, and UCS cancers using The Cancer Genome Atlas (TCGA) datasets. Additionally, we evaluated the prognostic significance of these miRNAs by correlating their expression levels with overall survival and clinical outcomes.

Methods: Data were obtained from TCGA, an online portal for analyzing tumor genes and survival curves. A comparison was made between the common miRNA-coding genes in OV vs UCS, OV vs UCEC, and UCS vs UCEC. Survival curves were obtained for OV (n=474) vs UCS (n=56). Clinical trials information was accessed through clinicaltrials.gov. Data was analyzed and the statistical significance was assessed by Student's t-test (comparisons between two-groups), or one-way ANOVA (for multiple-groups), and survival curves were analyzed using Kaplan-Meier method with log-rank test. A p-value of 0.05 or less was considered significant.

Results: Analyses revealed differences in patient survival based on the expression of the miRNA-coding genes of interest, hsa-mir-6511b-1, hsa-mir-6820, and hsa-mir-3198-2, in OV and UCS. High expression of hsa-mir-6511b-1 was associated with a shorter survival period in both OV (p=0.021) and UCS (p=0.035) patients. In contrast, high expression of hsa-mir-6820 showed opposite effects: it was linked to shorter survival in OV patients (p=0.024) but longer survival in UCS patients (p=0.028). High expression of hsa-mir-3198-2 was associated with longer survival in both OV (p=0.027) and UCS (p=0.046) patients. Data suggest that the role of miRNAs in these gynecologic cancers appears to be complex, showing both oncogenic and protective effects.

Conclusions: These preliminary findings emphasize that miRNAs behave in a context-dependent manner in gynecologic cancers. Importance of miRNAs should be further studied to validate their potential as biomarkers for early detection, prognosis, and treatment strategies. Our laboratory is conducting translational studies to precisely understand the role of miRNA-coding genes on drug resistance to address platinum-resistance in gynecologic cancer models.

#2066 Non-invasive screening of gynecologic tumors using miRNAs in urinary extracellular vesicles.

Hiroko Matsumiya[1], **Atsushi Satomura**[2], Hiroshi Asano[1], Hiroyuki Yamazaki[1], Ryutaro Yamamoto[1], Keiichiroh Akabane[1], Ryo Tamaki[1], Hiroyuki Kurosu[1], Kei Ihira[1], Daisuke Endo[1], Takashi Mitamura[1], Yosuke Konno[1], Takeshi Umazume[1], Motoki Mikami[3], Yuki Ichikawa[3], Hidemichi Watari[1]

[1]Hokkaido University Graduate School of Medicine, Hokkaido, Japan,[2]Craif USA, San Diego, CA,[3]Craif, Tokyo, Japan

Background:
Gynecologic malignancies constitute the second leading cause of cancer-related morbidity and mortality among women worldwide, following breast cancer. Despite the availability of effective screening programs, participation remains limited in several regions because of psychological reluctance toward pelvic examinations (e.g., approximately 40% in Japan) and constrained clinical resources. To address this issue, we explored a non-invasive screening strategy based on comprehensive microRNA (miRNA) profiling of urinary extracellular vesicles (uEVs).

Methods:
This study enrolled both pregnant and non-pregnant women with gynecologic diseases, along with healthy counterparts. In total, 456 urine samples were collected, from which uEVs were isolated and subjected to comprehensive miRNA profiling. A subset comprising 121 disease cases (84 malignant and 37 benign tumors) and 121 age-matched healthy non-pregnant controls was used to establish a diagnostic model. The dataset was randomly divided into training (N = 90) and holdout (N = 31) sets for performance evaluation. The resulting model was subsequently applied to pregnant women with gynecologic diseases and healthy pregnant women to assess its generalizability and diagnostic performance.

Results:
Differential expression analysis in the training set between disease cases and healthy controls identified 25 miRNAs with significant expression changes. A diagnostic model constructed using these differentially expressed miRNAs achieved an AUC of 0.907, with sensitivity and specificity of 0.867 and 0.856, respectively. When applied to the holdout set, the model maintained high performance (AUC = 0.937; sensitivity = 0.889; specificity = 0.944). Both malignant and benign tumors were detected with high scores in non-pregnant women, irrespective of cancer type or disease stage. Although healthy pregnant women, who were not included in model training, showed low predicted cancer probabilities, pregnant women with gynecologic diseases exhibited slightly reduced scores compared with their non-pregnant counterparts.

Conclusions:
Our results suggest that urinary uEV-miRNA profiling combined with machine learning enables accurate screening of gynecologic diseases. This non-invasive approach may complement general health checkups and enhance gynecologic screening rates, thereby contributing to earlier diagnosis and improved outcomes.

#2067 PiR-60643 is a novel inhibitor of fatty acid binding protein 5 (FABP5) in lung cancer cells.

Yousef G. Amaar, Mark E. Reeves

Loma Linda VA Medical Center, Loma Linda, CA

Introduction: It is important to discover and characterize new pathways and their associated gene networks in cancer cells to develop effective diagnostic and therapeutic tools. Our laboratory is focused on the impact of the RASSF1C-PIWIL1-piRNA pathway on non-small cell lung cancer (NSCLC) cell growth; and our studies have resulted in identifying specific PIWI-interacting RNAs (piRNAs) that appear to function both as oncogenes and tumor suppressors. Among the recent piRNAs identified, we found that piR-60643 targets fatty acid bind protein 5 (FABP5) in lung cancer and appears to function as a tumor suppressor.

Methods: In previously published work we reported on a global microarray screen which identified potential piRNA genes in non-small lung cancer cells over-expressing RASSF1C. We were able to detect several piRNAs that are modulated by RASSF1C. The expression of specific piRNAs that appear to be down or up-regulated by RASSF1C were confirmed by RT-PCR. We evaluated the impact of selected RASSF1C-target piRNAs on lung cancer cell proliferation and migration *in vitro*. We also have identified both host and target genes for specific piRNAs and have used piRNA mimics to down regulate target gene expression.

Results: We show that piR-60643 is down regulated by RASSF1C and seems to function as a tumor suppressor in non-small cell lung cancer cells. Consistent with this, treatment of lung cancer cells with piR-60643 mimics reduced cell proliferation and migration, supporting the idea that piR-60643 could be a new inhibitor of lung cancer cell growth and progression. To learn more about how piR-60643 may hinder lung cancer cell growth, we searched for genes that could be targeted by piR-60643. Interestingly, we identified FABP5 as a piR-60643-target gene. FABP5 is up regulated in lung tumor tissue and in tissues of other cancers and is associated with poor patient survival. FABP5 plays a key role in regulating lipid metabolism and fatty acid oxidation (FAO). FAO is critical to supply the high energy (ATP) demand of rapidly growing cancer cells and contributes to cell cycle progression, EMT, migration, and metastasis. We found that treatment of lung cancer cells with piR-60643 mimics resulted in down regulation of FABP5 expression both at the mRNA and protein levels, implying that piR-60643 could disrupt FAO-associated metabolic pathway(s) in lung cancer cells. Interestingly, we found that PIWIL1 overexpression up-regulates FABP5 expression in lung cancer cells, suggesting that the PIWIL-FABP5 gene axis may play a role in lipid metabolism/FAO. This novel finding has not been previously reported.

Conclusion: Targeting FABP5 by piR-60643 could prove a novel mechanism of inhibiting lipid metabolism/FAO and impeding tumor growth and progression. As such, piR-60643 could prove to be a useful diagnostic/therapeutic tool for lung cancer.

: Aging and Host Determinants of Tumor Progression: The Macroenvironmental Axis
Poster Session

#2071 Aging impairs NK-cell surveillance to promote metastatic outgrowth in breast cancer.

Pulkit Datt, Jhon Pasamonte, Kelly Coutant, Anastasiia Burtseva, Mitchell Fane

Cancer Signaling and Microenvironment Research Program, Fox Chase Cancer Center, Philadelphia, PA

Metastasis is the main driver of breast cancer mortality and is more common in older patients (55-85 years), yet most experimental work still relies on young (~8-week-old, equivalent to 20 human years) mice, which fail to capture the age-related dynamics of metastasis. Moreover, most studies focus exclusively on lung metastasis, even though breast cancer often spreads to the liver, which responds poorly to immune checkpoint inhibitors and other systemic therapies. Prior work shows that an aged lung microenvironment can promote breast cancer progression via stromal factors, but how aging reshapes immune surveillance, particularly natural killer (NK) cells, in lung and liver niches remains unclear. To address this, we developed syngeneic breast cancer metastasis models in young (8 weeks), middle-aged (12-16 months), and geriatric (22-26 months) C57BL/6 mice, generating primary tumors and lung or liver metastases. Strikingly, primary tumors progressed rapidly in geriatric mice and were associated with larger lung metastases, whereas young and middle-aged mice showed limited outgrowth. Tail-vein models recapitulated this whereby older mice had increased lung metastasis. Immune profiling of pre-metastatic lung revealed that NK cells were decreased in aged and geriatric mice relative to young mice. We then depleted NK cells in young mice to test their role in restraining outgrowth. NK-cell depletion significantly increased primary tumor size and lung metastatic burden, and surprisingly, in the tail-vein model, produced large liver metastases, a phenotype not seen in any age group with tail-vein injection. Pre-metastatic liver analysis confirmed reduced NK cells in middle-aged and geriatric mice. To assess their role, we used hydrodynamic tail-vein injection, which promotes colonization of the liver specifically. Interestingly, liver metastases peaked in middle-aged mice but were reduced in both young and geriatric mice, recapitulating human data where breast cancer incidence is low in young adults (<45 years), peaks between 65-75 years and then declines in women ≥80 years. Immune profiling showed overall NK cells in lung and liver were largely unchanged across ages in tumor-bearing mice; however, NK cells in middle-aged mice livers alone exhibited a dysfunctional phenotype, with increased expression of inhibitory receptors. Importantly, immunosuppressive PMN-MDSCs and regulatory T cells were elevated in middle-aged livers but remained low in young and geriatric mice. Together, these findings define an age- and organ-specific regulation of immune cells that drives metastatic outgrowth in middle-aged and geriatric lungs and enhances liver metastasis in middle-aged mice but, surprisingly, limits liver metastasis in geriatric mice. This work underscores the need for age-appropriate models and highlights NK cells as a key target to prevent metastatic outgrowth in older breast cancer patients.

#2072 Role of the aging on the γδ T-cells in metastatic cutaneous melanoma progression.

Kelly Coutant[1], Christopher Price[1], Jhon Pasamonte[2], Pulkit Datt[2], Mitchell Fane[1]

[1]Fox Chase Cancer Center, Philadelphia, PA,[2]Temple University, Philadelphia, PA

Melanoma incidence, metastasis, and mortality are significantly associated with age. Interestingly within the clinic, melanoma incidence is low in young adults, peaks between ages 65-79, and decreases thereafter (79+). This phenomenon has never been studied as pre-clinical studies predominantly focus on young (8-week-old) mouse models.

Syngeneic melanoma cells have been injected by IV (lung colonization) and hydrodynamic tail vein injection (liver colonization) into C57/Bl/6 young (8 weeks), aged (12 months) and geriatric (18-24 months) male mice. Spleen, lungs and liver have been collected to analyze metastasis and immune infiltration by flow cytometry. H&E and IHC staining have been performed to quantify the number of metastases and to determine different immune markers (e.g. CD45, CD8, CD4). Our data highlighted that middle aged mice had significantly increased γδ T cell infiltration in the metastatic lung and liver relative to young and geriatric mice, which had less metastasis. Based on this, we used a γδ T cell mouse model of depletion coupled with depletion antibodies against gamma delta in young and geriatric mice respectively. Finally, our preliminary data indicated that upon reactivation in middle-aged mice, melanoma cells secreted PROS1, which drives cancer proliferation. Its effects on the immune system within our model have not been studied. We overexpressed PROS1 in melanoma cells and injected them via IV and HDTV and analyzed metastasis and γδ T cell infiltration.

Our data shows that middle-aged mice have significantly increased lung and liver metastasis relative to young mice. Interestingly, geriatric mice have lower levels of metastasis, replicating what is seen in the clinic. Assessment of immune cell infiltration confirmed that γδ T-cells were significantly reduced in middle-aged mice relative to young and geriatric mice. We hypothesized that they may play an anti-tumor role in metastasis. To study this, we injected tumor cells as a primary tumor, IV, and HDTV into a transgenic γδ TCR diphtheria toxin depletion model and found that while the primary tumor grew slower, γδ depleted mice had increased lung and liver metastasis. Use of a γδ depletion antibody in geriatric mice replicated this phenotype. Finally, IV and HDTV injection of PROS1 overexpressing melanoma cells significantly increased lung and liver metastasis while subsequently decreasing δ T cells infiltration in young mice.

Age induced decrease of γδ T cell infiltration in middle-aged mice, induced largely by PROS1 secretion from melanoma cells, promotes aggressive metastases. Adoptive treatment with γδ T cells or use of a PROS1 inhibitor may be a viable therapeutic option for metastasis in elderly individuals.

#2073 In vivo single-cell CRISPR screens identify targets to restore T cell function in aged tumors.

Alex C. Y. Chen, Keely Ji, Cansu Yerinde, Daniela Martinez, Thomas J. LaSalle, Kazuhiro Taguchi, Marc A. Schwartz, Maria Zschummel, Thorsten R. Mempel, Nir Hacohen, Debattama R. Sen

MGH/Harvard Medical School, Boston, MA

Aging brings significant changes to the immune system, which slow down the immune response and make it less effective at detecting and fighting cancer. However, the mechanisms behind this are not fully understood. To address this open question, we focus on studying $CD8^+$ T cells, a type of immune cell that specifically recognizes and kills tumor cells, to understand how aging alters their antitumor function. Here, we demonstrated that the aged tumor microenvironment in older individuals has a stronger effect in weakening these T cells than the intrinsic aging impacts on these T cells. Even when young, healthy, naive T cells were transferred into older hosts, they quickly lost their ability to fight tumors, indicating that therapies relying on replenishing new T cells, such as adoptive T cell transfer therapy or CAR-T cell therapy, may not be effective if the aged environment drives them toward dysfunction. One strategy to further identify candidate genes associated with T cell dysfunction is to perform in vivo single-cell CRISPR screening. To achieve this, we designed a CRISPR library pool targeting genes encoding transcriptional regulators in $Cas9^+$ OT-1 $CD8^+$ T cells, with 6 sgRNAs targeting each gene to maximize statistical confidence. After transducing T cells with vectors containing the library pool and mAmetrine marker, these successfully transduced $mAmetrine^+$ naive T cells were sorted and transferred into aged mice one day before B16-OVA tumor inoculation. After 15 days, T cells were sorted from aged B16-OVA tumors and tumor-draining lymph nodes for Perturb-seq analysis. We found T cells lacking *Bcl6*, *Dusp4*, *Dusp5*, *Ets1*, *Ikzf2*, *Irf2bp2*, *Prdm1*, or *Zfp219* showed better T cell expansion and persistence in aged tumors and lymph nodes. Notably, Dusp5 acts as a negative feedback regulator of the ERK1/2 pathway. Dusp5 deletion promotes T cell proliferation and effector-like T cell differentiation, resulting in enhanced tumor control and survival benefit. Overall, our work fills a critical knowledge gap in the field of immune aging and cancer therapy, establishing Dusp5 as a novel and promising therapeutic target to restore T cell antitumor responses, particularly in older cancer patients.

#2074 Adenosine-driven inflammatory reprogramming of aged cancer-associated fibroblasts promotes immune suppression in pancreatic ductal adenocarcinoma.

Shuncang Zhu[1], Jinpeng Lu[1], Ziyi Tu[1], Hongyi Lin[2], Yinhao Chen[1], Yiting Chen[3], Haoxiang Zhang[4], Zuwei Wang[2], Shi Chen[2]

[1]Shengli Clinical Medical College of Fujian Medical University, Fuzhou, China,[2]Department of Hepatobiliary Pancreatic Surgery, Fuzhou University Affiliated Provincial Hospital, Fuzhou, China,[3]College of Biological Science and Engineering, Fuzhou University, Fuzhou, China,[4]University of Kentucky, Lexington, KY

Background: Aging exerts a profound influence on the tumor immune microenvironment of pancreatic ductal adenocarcinoma (PDAC). In elderly patients, PDAC is frequently characterized by pronounced stromal desmoplasia, enhanced immune evasion, and increased resistance to chemotherapy. The molecular underpinnings of these age-associated alterations remain largely undefined. Emerging evidence indicates that aging-related metabolic reprogramming can profoundly reshape the cellular and immunologic composition of the tumor microenvironment (TME). Yet, the mechanistic interplay between metabolic perturbations, stromal cell dynamics, and immune regulation in aged PDAC has not been fully elucidated.

Methods: Two PDAC clinical cohorts stratified by age and survival were analyzed using bulk and single-cell transcriptomics, and metabolomics. Nucleotide metabolism was assessed by targeted metabolomics. Functional studies included adenosine stimulation of aged and young cancer-associated fibroblasts (CAFs), B cell migration and co-culture assays, cytokine profiling, and orthotopic PDAC mouse models with adenosine receptor blockade. Multiplex immunohistochemistry (mIHC) was applied to spatially validate the proximity of $A2B^+CXCL13^+$ CAFs and $IL\text{-}10^+$ Bregs in aged human PDAC tissues.

Results: Aged PDAC exhibited increased regulatory B (Breg) cell abundance, which correlated with shorter overall survival. Multi-omic analyses identified age-related adenosine accumulation as the most dysregulated metabolite linked to both poor prognosis and Breg infiltration. Direct adenosine exposure failed to expand Bregs but reprogrammed aged CAFs toward a proinflammatory state. Aged CAFs expressed elevated adenosine receptor A2B and secreted the B cell chemoattractant CXCL13 upon adenosine stimulation. The adenosine-A2B-CXCL13 axis promoted $IL\text{-}10^+$ Breg recruitment, which suppressed $CD8^+$ T cell cytotoxicity and accelerated tumor growth. mIHC confirmed close spatial association between $CXCL13^+$ CAFs and Bregs within aged PDAC tissues. Pharmacologic inhibition of A2B signaling or CXCL13 neutralization reduced Breg infiltration, restored T cell activity, and prolonged survival in orthotopic aged PDAC models.

Conclusion: Age-associated adenosine accumulation reshapes the fibroblastic niche through A2B receptor-dependent inflammatory reprogramming, inducing CXCL13-mediated Breg recruitment and immune suppression. Targeting the adenosine-A2B-CXCL13 axis represents a promising strategy to restore anti-tumor immunity in elderly patients with PDAC.

#2075 Lactate-driven cholesterol reprogramming induces fibroblast senescence and immune suppression in aged pancreatic cancer.

Ziyi Tu[1], Jinpeng Lu[2], Shuncang Zhu[1], Hong-yi Lin[1], Yi-ting Chen[1], Yinhao Chen[1], Haoxiang Zhang[2], Zu-Wei Wang[1], Shi Chen[1]

[1]Shengli Clinical Medical College of Fujian Medical University, Fuzhou, China,[2]University of Kentucky, Lexington, KY

Background: Aging profoundly remodels the pancreatic tumor microenvironment (TME), where senescent cancer-associated fibroblasts (senCAFs) accumulate and promote tumor progression. However, the metabolic cues derived from aged tumor cells that induce fibroblast senescence and mediate immune suppression remain poorly understood.
Methods: Integrated analyses of murine and human single-cell RNA-sequencing datasets combined with multiplex immunofluorescence (mIF) revealed a marked enrichment of $p16^+$ senCAFs in aged pancreatic ductal adenocarcinoma (PDAC). Targeted metabolomics and isotope tracing identified lactate as a key metabolite driving fibroblast senescence. Lactyl-proteomics, ATAC-seq, CUT&Tag, and site-directed mutagenesis were used to define functional lactylation sites. Multiplex cytokine profiling identifies the secretome of senCAFs that modulates the immunosuppressive microenvironment.
Results: Aged PDAC exhibited a marked expansion of senCAFs, validated by scRNA-seq and mIF. Metabolomic and isotope-tracing analyses revealed that lactate secreted by aged tumor cells was preferentially imported by fibroblasts through upregulated MCT1 transporters, triggering metabolic and phenotypic senescence. Proteomic profiling identified enhanced histone A-protein lactylation (H3K18la) as a key senescence-associated modification strongly correlated with poor prognosis. Mutation of the lactylation site (K18R) restored fibroblast proliferative capacity and reduced SASP secretion. Mechanistically, histone lactylation reprogrammed cholesterol metabolism by transcriptionally activating SQLE (squalene epoxidase), a rate-limiting enzyme in cholesterol biosynthesis. Cholesterol accumulation further reinforced fibroblast senescence and sustained inflammatory SASP signaling, including IL-8, CXCL12, and TGF-β, establishing an immunosuppressive tumor microenvironment. Pharmacologic inhibition of SQLE or blockade of lactate import markedly decreased senCAF accumulation, restored $CD8^+$ T cell infiltration, and improved survival in aged PDAC models.
Conclusion: Aged PDAC cells metabolically reprogram fibroblasts via lactate-driven histone lactylation, reactivating cholesterol biosynthesis and maintaining senescence. This metabolic-epigenetic axis fuels immune suppression and tumor progression. Targeting the lactate-H3K18la-SQLE pathway offers a promising therapeutic strategy to reprogram the aged tumor stroma and enhance anti-tumor immunity in PDAC.

#2076 FGFR1 drives progression of ER+ breast cancer brain metastases in young and aged hosts.

Morgan S. Fox[1], Jenny A. Jaramillo-Gomez[1], R. Alejandro Marquez-Ortiz[1], Karen L. F. Alvarez-Eraso[1], Maria J. Contreras-Zarate[1], Trinh C. Pham[1], Elaina N. Barela[1], Stella Koliavas[1], Peter Kabos[2], Carol A. Sartorius[1], Elizabeth A. Wellberg[3], Diana M. Cittelly[1]

[1]Pathology, University of Colorado, Aurora, CO,[2]Medical Oncology, University of Colorado, Aurora, CO,[3]University of Oklahoma Health Sciences Center, Oklahoma City, OK

The purpose of these studies is to define mechanisms that drive estrogen receptor positive (ER+) breast cancer brain metastasis (BCBM) colonization and outgrowth. Most ER+ BCBMs arise in postmenopausal women due to prior endocrine therapies or age, yet most *in vivo* ER+ breast cancer (BC) models require estrogen (E2) supplementation and use young hosts. Thus, the mechanisms underlying metastatic progression in the aged/E2-depleted brain tumor microenvironment (TME) remain unknown. FGFR1-amplification (amp), an established driver of ER+ BC endocrine therapy resistance, was the only genomic alteration associated with increased late recurrence in post-menopausal women with ER+ BC on aromatase inhibitors, and FGFR aberrations are enriched in BCBM patients compared to non-BM metastatic BC. While FGFR1amp often causes auto-activation, TME-dependent FGFR1 activation has emerged as an important mechanism modulating its activity. Here, we tested the hypothesis that canonical and non-canonical activation of FGFR1 by astrocytes and neurons promotes FGFR1-dependent ER+ BCBM in E2-high young and E2-low aged hosts. Intracardiac injection of ER+ cells showed that FGFR1amp lines had higher BM incidence, and were E2-dependent in young but not aged hosts. FGFR1 knockdown (KD) did not alter proliferation but decreased BCBM in both E2-high/young and E2-low/aged mice. Spatial transcriptomics of the ER+ BCBMs TME showed that aging and E2-depletion reduced FGF2 expression and FGF/FGFR signaling in surrounding glial cells, suggesting that TME-driven FGFR1 activation may be distinct in young and aged hosts. In the normal brain, NCAM1, an adhesion molecule expressed on neurons and astrocytes, can activate FGFR1. We found that NCAM1 activated FGFR1 kinase activity and downstream signaling in ER+ BC cells, and induced differential expression of neuronal gene signatures including neural cell adhesion. FGFR1 KD reduced ER+ BC cell migration along neurites in co-culture with primary neurons and decreased synaptic puncta. NCAM1 KD in neuron-like SH-SY5Y cells also decreased ER+ cell migration, suggesting that FGFR1/NCAM1 facilitates ER+ BC interactions with neurons, contributing to early brain colonization. Activated FGFR1 was higher in young versus aged mice at early stages of colonization but absent in late-stage ER+ BCBMs, suggesting that paracrine FGFR1 activation and interactions with neurons and astrocytes are critical for early colonization. Consistently, an FDA-approved FGFR inhibitor blocked ER+ BCBM when administered at early stages of colonization in young mice but had no effect at late stages or in aged mice. Together, these studies suggest a novel mechanism whereby canonical and non-canonical activation of FGFR1 promote ER+ BCBM colonization in young and aged/E2-depleted hosts, and caution that FGFR1 inhibition may only be effective to prevent but not to treat BMs.

#2077 Remodeling the aged bone marrow niche: LRG1-mediated immunosuppression promotes prostate cancer metastasis.

Lele Xu[1], Yuanhao Song[2], Wenlin Zhao[2], Peter Ka Fung Chiu[1], Anthony Chi-Fai Ng[1], **Dinglan Wu**[1]

[1]SH Ho Urology Centre, Department of Surgery, The Chinese University of Hong Kong, Hong Kong, Hong Kong,[2]Shenzhen Hospital of Southern Medical University, Shenzhen, China

Prostate cancer (PCa) bone metastasis arises from intricate interactions between tumor cells and the bone marrow microenvironment. Chronic inflammation in the aging bone marrow is thought to foster an immunosuppressive niche that facilitates metastatic progression. Here, we identify Leucine-Rich Alpha-2-Glycoprotein 1 (LRG1) as a central mediator of this process. LRG1 protein is significantly elevated in the circulation of patients with metastatic castration-resistant prostate cancer (mCRPC), where its levels correlate with worse overall survival. In both human PCa tissues and our established RM1-BM3 mouse model of PCa bone metastasis, LRG1 expression is markedly upregulated. Functionally, LRG1 overexpression enhances tumor growth in bone and correlates with immunosuppressive bone microenvironment by accumulation of polymorphonuclear myeloid-derived suppressor cells (PMN-MDSCs). Mechanistically, MS and CO-IP assays reveal that LRG1 interacts directly with ITGA6 (CD49f) on prostate cancer cells to activate pro-metastatic pathways and with the inflammatory protein S100A9 to recruit and expand PMN-MDSCs. Furthermore, we show that interleukin-1 (IL-1) stimulates LRG1 expression in an androgen receptor (AR)-independent manner via NF-κB pathway activation. Collectively, we propose a model wherein IL-1 signaling in the aging bone marrow upregulates LRG1, which then acts dually: it promotes cancer cell aggressiveness via ITGA6 and fosters an immunosuppressive niche via S100A9-PMN-MDSC axis, thereby driving bone metastasis in CRPC. Our findings nominate LRG1 and its associated pathways as promising therapeutic targets for metastatic prostate cancer.

#2078 Aging promotes liver and lung melanoma metastasis via tissue-infiltrating Tregs.

Anastasiia Burtseva, Kelly Coutant, Jhon Pasamonte, Christopher Price, Mitchell Fane

Fox Chase Cancer Center, Philadelphia, PA

Metastasis is the leading cause of melanoma-related deaths, yet its age-related mechanisms remain poorly understood. This gap stems partly from reliance on young mouse models (~8 weeks old, equivalent to 20 human years) in most studies. Additionally, research has largely focused on lung metastasis, even though melanoma often spreads to other sites like the liver, which is notably more resistant to immune checkpoint inhibitors (ICIs).Using syngeneic melanoma cells, we optimized intravenous (IV) injections to model lung colonization and developed a novel liver colonization model using hydrodynamic tail vein injections. Tumor cells were injected into young (8 weeks) and aged (12-16 months) male C57BL/6 mice. Spleen, lungs, and liver were harvested to assess immune infiltration of lymphocyte and myeloid populations via flow cytometry. Hematoxylin and eosin (H&E) and immunohistochemistry (IHC) staining were used to quantify metastases and examine spatial immune cell locations. Upon observation that regulatory T cells (Tregs) increased consistently in aged mice in both lung and liver metastatic sites, we treated additional aged cohorts with either anti-mouse CD25 antibody, which we show decreased Tregs while not changing CD3+, CD4+ or CD8+ T cell infiltration, or an IgG control (200 µg/mouse, intraperitoneally) to evaluate the role of Tregs and in metastasis.Aging significantly increased melanoma colonization in both the lungs and liver compared to young mice. Analysis of common changes in the immune microenvironment of both the lung and the liver revealed elevated Treg infiltration in both metastatic sites of aged mice. Notably, Tregs were not elevated in the pre-metastatic niche, suggesting an age- and tumor-specific mechanism of immune suppression. Depletion of Tregs in aged mice using anti-CD25 antibody significantly reduced lung metastases compared to IgG controls. Moreover, depletion of Tregs decreased secretion of TGF-β and the number of myeloid cells in metastatic sites and increased the number of $NK1.1^+$ NK cells, $CD4^+$ and $CD8^+$ T cells.Our findings indicate that age-associated Treg infiltration promotes metastasis to the lung and liver, suggesting that targeting Tregs could offer a promising approach to mitigate age-related metastatic progression in melanoma.

#2079 Aging attenuates brain metastasis in lung cancer through the MT1G/NF-κB/SPARC signaling.

Abhishek Tyagi[1], Shih-Ying Wu[1], Jee Won Kim[1], Kerui Wu[2], Ravindra Deshpande[1], Kounosuke Watabe[3]

[1]Wake Forest University School of Medicine, Winston Salem, NC,[2]The Joint School of Nanoscience and Nanoengineering University of North Carolina, Greensboro, NC,[3]Associate Director for Basic Science, Wake Forest University Health Sciences, Winston-Salem, NC

Aging is a major risk factor for cancer, with incidence and mortality increasing significantly with age across most cancer types. With the global population aged over 60 projected to rise from 12-22 percent by 2050, understanding the relationship between aging and cancer is critically important. Aging and cancer share several hallmarks—including cumulative genetic damage, immune senescence, altered nutrient sensing, and chronic low-grade inflammation. This overlap implies that age-related biological changes may not only correlate with increased cancer incidence but also influence tumor progression and metastasis. Despite this preconceived notion, population-based epidemiological studies have revealed an inverse association between aging and brain metastasis incidence in lung cancer, with unclear molecular mechanism(s). Here, we show a significantly lower incidence of brain metastasis in aged lung cancer patients compared to younger patients or those with brain metastasis from other cancers, based on analysis of the SEER population-based cancer registry. Mechanistically, aging activates MT1G/NFκB signaling in reactive astrocytes within the brain, leading to increased secretion of SPARC from A1 type reactive astrocytes, which suppresses tumor growth by inhibiting ITGB1 signaling in tumor cells, thereby limiting brain colonization. Notably, therapeutic targeting of ITGB1 using liposome-encapsulated SPARC peptide effectively suppresses brain tumor growth and metastasis, supporting its tumor-suppressive role. These findings uncover an age-associated protective mechanism and provide a compelling rationale for developing targeted therapies to prevent or treat brain metastasis in younger lung cancer patients.

#2080 Aged-induced increases in IL-11 leads to immune escape and PD-1 resistance in melanoma through myeloid cell polarization.

Michael F. Emmons[1], Chao Zhang[1], ethan vallebuona[1], Richard L. Bennett[2], Manali Phadke[1], Jonathan D. Licht[2], Keiran Smalley[1]

[1]Moffitt Cancer Center, Tampa, FL,[2]University of Florida, Gainesville, FL

Background: Stress-like states, associated with hypoxia, drug treatment and aging, can contribute to immune escape in cancer through mechanisms that remain poorly understood. IL-11 is a poorly studied cytokine whose expression increases with age. In previous work, we have identified histone deacetylase (HDAC)-8, as an epigenetic regulator whose expression increases in response to multiple stresses. Here, we identify HDAC8 as a regulator of IL-11 expression, leading to immune escape and immunotherapy resistance in melanoma. <
strong>Objectives: We investigated the role of IL-11 in modulating the immune microenvironment and its impact on melanoma progression and resistance to immunotherapy in young vs aged mice.
Methods: Intrinsically sensitive and resistant melanoma cells were assayed for cytokine secretion by cytokine arrays and ELISAs. Chromatin accessibility, histone modifications, and transcriptional changes of IL-11 were assessed in human melanoma cells overexpressing HDAC8 using ATAC-seq, ChIP-seq, and scRNA-seq. ELISA, immunohistochemistry (IHC), and flow assays were employed to evaluate IL-11 expression and its effects on myeloid-derived suppressor cells (MDSCs) and T cell interactions in young vs aged mice. Young (<3M) and old (>18M) mice were treated with an IL-11 blocking antibody and/or anti-PD-1 antibody to determine drug efficacy. TMAs and IHCS from patients were stained for IL-11.
Results: IL-11 expression was upregulated in melanoma cells in response to hypoxia as well as intrinsic and acquired targeted therapy treatment. Expression of IL-11 accelerated melanoma growth in vivo and led to increased accumulation of PMN-MDSCs and reduced CD8+ T cell infiltration. IL-11 expression reduced the efficacy of anti-PD-1 therapy in melanoma models, whereas IL-11 blockade enhanced anti-PD-1 responses. Old mice (>18M) had increased circulating levels of IL-11 levels compared to young mice (<3M), as well as increased IL-11 expression in the liver. Therapeutic blockade of IL-11 led to complete anti-tumor responses to anti-PD-1 in aged mice with melanomas. In melanoma patient samples, IL-11 expression was correlated with increased age, and was spatially expressed in areas of the tumor that had reduced CD8+ T cell infiltrate.
Conclusions: IL-11 promotes a "cold" immune microenvironment in aged mice by increasing accumulation of PMN-MDSCs and suppressing T cell recognition and infiltration. Blocking IL-11 in aged mice contributed to increased immunotherapy efficacy. Targeting IL-11 represents a promising therapeutic strategy to limit immune escape and boost responses to anti-PD-1 in melanoma, particularly in aged patients.

#2081 Age of host impact on epigenetics in tumors derived from early or late onset Hispanic colorectal cancer patients.

Lesly Torres-Gonzalez[1], Shivani Soni[1], Zeyi Yang[1], Ben Y. Tew[1], Jae H. Lo[1], Pooja Mittal[1], Unnati H. Shah[1], Michela Bartolini[1], Steve Soto Trujillo[1], Yitzher Goretsky[1], Sandra Algaze[1], Wu Zhang[1], David W. Craig[2], John D. Carpten[3], Salhia Bodour[1], Heinz-Josef Lenz[1]

[1]USC Norris Comprehensive Cancer Center, Keck School of Medicine, University of Southern California, Los Angeles, CA,[2]City of Hope Comprehensive Cancer Center, Duarte, CA,[3]City of Hope, Duarte, CA

Introduction Over the past decade, the incidence of early-onset (EO) colorectal cancer (CRC) in adults under 50 has shown a significant increase compared to late-onset (LO) CRC rates, especially in the Hispanic/Latino (H&L) population. EO CRC exhibits unique molecular features compared to LO CRC, associating this distinct disease with a more aggressive presentation. Investigations on the effect of age within both the tumor and host environments could provide insight into key differences between EO and LO CRCs. This study, as part of Cancer Moonshot Program, explores how age of the host influences epigenetic changes in CRC tumors.
Methods CRC patient derived tumor samples from an EO 36 year old (young patient, YP) and a LO 66 year old (old patient, OP) H&L male were implanted into both young (2 months, YM) and old male NSG mice (13-14 months, OM) to establish four PDX models: YP in YM, OP in YM, YP in OM, and OP in OM. Tumor samples were collected at endpoint (15mm length or width). Tumors were processed for epigenomic analysis using the Illumina EPIC Array Epigenetics Kit. Methylation data was used to identify differentially methylated regions ($\Delta\beta>0.1$) in YP in OM compared to YP in YM and OP in YM compared to OP in OM. Identified regions were mapped to the nearest gene using the human genome (GRCh38 Genome Reference Consortium Human Reference 38) from UCSC. The differentially methylated genes ($\Delta\beta>0.2$) were input into Ingenuity Pathway Analysis to identify relevant biological pathways.
Results There were 8916 differentially methylated regions identified in YP in OM when compared to YP in YM. Of these regions, 5529 showed hypermethylation and 3387 showed hypomethylation. Regions were mapped to 5886 unique gene symbols, of which 1061 were hypermethylated and 999 were hypomethylated. YP in OM showed predicted activation of key genes, including TNF, WNT1, MYB, ERBB3, GLI3, EGR2, and EGR3, involved in the development and progression of gastrointestinal cancers. There were 28032 differentially methylated regions ($\Delta\beta>0.1$) identified in OP in YM when compared to OP in OM. If these regions, 17590 showed hypermethylation and 10442 showed hypomethylation. Regions were mapped to 11888 unique gene symbols, of which 4273 were hypermethylated and 2936 were hypomethylated. OP in YM showed predicted inhibition of key genes, including RELA, TNF, EGFR, YAP1, WNT3A, FGF2, IFNG, SP1, IGF1, ERBB2 and TEAD1, involved in cell transformation and tumor cell metastasis.
Conclusions Our current findings show differences in epigenetic DNA methylation patterns in EO and LO CRC PDX models. Differentially methylated region analysis in both EO and LO CRC suggests that an older host age may correlate with activation of cancer related genes while younger host age may inhibit similar pathways, regardless of tumor age. Further studies are warranted to understand the epigenetics modifications that influence the observed differences.

#2082 Multiplex immunofluorescence reveals compartment-specific immune cell correlations associated with age and immunotherapy response in ovarian carcinoma.

Kathy Kwock[1], Okan Gultekin[2], Hanim I. Ozkizilkaya[3], Lynda D. Roman[3], William Dean Wallace[3], Tirzah Petta[3], Joseph W. Carlson[4]

[1]University of Southern California, Los Angeles, CA,[2]Karolinska Institute, Stockholm, Sweden,[3]Keck School of Medicine of USC, Los Angeles, CA,[4]CIty of Hope, Duarte, CA

BackgroundOvarian carcinoma, an aggressive malignancy typically diagnosed at advanced stages, has shown limited response to immune checkpoint inhibitors. Increasing evidence suggests that age-related immune alterations and spatial heterogeneity within the tumor microenvironment influence immunotherapy outcomes. This study investigates whether immune cell organization across tissue compartments correlates with clinical response to immunotherapy.

MethodTwenty patients treated with immunotherapy were identified. FFPE tumor blocks were retrieved, and slides were stained using a multiplex immunofluorescence panel (DAPI, PD-L1, CD4, CD8, CD20, FoxP3, PanCK). Regions of interest were annotated by a pathologist and analyzed using supervised learning in inForm and PhenoChart. Immune cell phenotypes were quantified across tissue compartments, and correlation analyses were performed using RStudio, Excel, and GraphPad Prism.

ResultOlder patients demonstrated significantly improved immunotherapy outcomes, including longer progression-free survival and duration of effective immunotherapy, confirming an age-associated advantage in therapeutic response. Multiplex immunofluorescence revealed distinct immune correlation networks between responders and non-responders, driven by tissue compartmentalization. Among immunotherapy responders, stromal regions showed a positive correlation between $FoxP3^+$ and $PanCK^+$ tumor cells, whereas tumoral regions exhibited a negative correlation between $CD8^+$ cells and $PanCK^+$ cells. Whole-tissue analysis revealed a strong correlation between $FoxP3^+$ and $CD8^+$ cells in responders. In contrast, non-responders displayed a different pattern of immune cell organization, characterized by strong correlations between $CD4^+$ and $CD8^+$ T cells in the stroma and between $CD20^+$ B cells and $PanCK^+$ cells in the tumor compartment. Spatial proximity heatmaps demonstrated that responders had higher local clustering of $CD8^+$, $CD4^+$, and $CD20^+$ cells across multiple radii within both tumor and stromal regions, while non-responders exhibited limited spatial clustering consistent with “immunologically cold” tumors.

ConclusionThis study identifies distinct, compartment-specific immune cell relationships associated with immunotherapy response in ovarian carcinoma highlights age as a significant modifier of immune architecture. Responders, predominantly older patients, exhibited coordinated stromal $FoxP3^+$ interactions and tumoral $CD8^+$ engagement, whereas non-responders, predominantly younger patients, showed stromal $CD4^+$/$CD8^+$ clustering and tumoral $CD20^+$ associations characteristic of cold immune phenotypes. These findings suggest that immune cell correlations, rather than absolute densities, may serve as informative spatial biomarkers for predicting immunotherapy response.

#2083 Spatial profiling reveals distinct immune microenvironments in early vs late onset colorectal cancer.

Niti Jani[1], Michael Martinez[1], Christopher Flynn[1], Hatano Yuichiro[1], Zhongqiu Zhang[2], Daniel W. Rosenberg[3]

[1]University of Connecticut Health Center, Farmington, CT,[2]Waterbury Hospital, Waterbury, CT,[3]Professor of Med. & Co-Director, Colon Cancer Prev. Prog., University of Connecticut Health Center, Farmington, CT

Colorectal cancer (CRC) is the fourth most common cancer and the second leading cause of cancer related deaths in the United States. While CRC incidence increases with age, rates are rising among individuals younger than 50 years old (early-onset CRC; EOCRC). Most sporadic EOCRC tumors are microsatellite stable (MSS), and MSS tumors generally do not respond favorably to immunotherapy. The age-associated differences within the tumor microenvironment (TME) remain poorly understood. We hypothesize that EOCRC tumors have a more immunosuppressive microenvironment, which may influence treatment response. Methods: Tumor tissues were collected under an approved IRB protocol from Waterbury Hospital and UConn John Dempsey Hospital. Patients ≤50 years were classified as EOCRC (n = 8) and ≥60 years as late-onset (LOCRC; (n = 10). A total of eighteen regions of interest (ROIs) from tumor sections were selected by a pathologist. Imaging mass cytometry (IMC; 27-marker panel) was performed to spatially characterize the epithelial and immune cell populations. Images were processed to identify single cells, the data were adjusted to remove technical differences, and cells were grouped based on markers and visualized using MCD Viewer software. We also examined how different cell types were spatially arranged and interacted within the tissue. Statistical comparisons were performed using Welch's t-test and permutation-based tests. Results: Using IMC, a total of 142,992 single cells across 18 ROIs were analyzed. Unsupervised clustering identified 19 cell populations, including epithelial (40%), stromal (18%), $CD45^+$ lymphocytes (11%), myeloid subsets (11%), and rare intra-epithelial lymphocytes (<1%). Cluster identities were validated by marker expression and spatial localization. EOCRC tumors showed a significantly higher abundance of $FoxP3^+$ $CD4^+$ Tregs (P = 0.047), indicating an immunosuppressive TME. LOCRC samples trended toward higher intra-epithelial lymphocytes. Spatial analysis suggested a direct Treg-M2 macrophage interaction due to their colocalization, suggesting the possibility of suppressive niches forming within EOCRC. Immune-enriched stromal regions were slightly more abundant in EOCRC (20.3% of cells) than in LOCRC (16.5%). These regions were enriched with Tregs, CTLs, and M2 macrophages, with Treg infiltration being significantly higher in EOCRC (P = 0.032). These findings support a localized immunosuppressive phenotype. Conclusion: EOCRC tumors display a more immunosuppressive microenvironment, characterized by increased Treg infiltration and a higher M2 macrophage presence in immune cell-enriched regions. These findings suggest that age-related immune differences may exist within tumors of CRC patients. Ongoing validation by multiplexed immunohistology will strengthen these results and inform the development of age-tailored therapeutic strategies.

#2084 Angiotensin-II-induced chronic hypertension reprograms the antitumor-immune-response in pancreatic ductal adenocarcinoma.

Benjamin Wolf[1], Heena Kumra[1], Ryo Morisue[1], Karim El-marouk[1], Igor L. Gomes-Santos[1], Rieke Schleinhege[1], Tsion H. Tale[1], Marc Charabati[1], Sonu Subudhi[1], Dai Fukumura[1], Rakesh K. Jain[2]

[1]Massachusetts General Hospital, Boston, MA,[2]Harvard Medical School/Massachusetts General Hospital, Boston, MA

Introduction: Chronic arterial hypertension (CAH) is one of the most prevalent medical conditions worldwide and plays a causal role in cardiovascular diseases. Cancer patients with CAH have inferior outcomes compared to non-hypertensive cancer patients, especially in pancreatic ductal adenocarcinoma (PDAC). Furthermore, retrospective analyses have shown that antihypertensive therapy targeting angiotensin signaling is associated with improved oncological outcomes compared to other anti-hypertensive treatments in cancer patients. Methods and Results: To investigate this relationship, we employed a syngeneic, orthotopic PDAC model in mice with chronic hypertension induced by subcutaneously implanted osmotic minipumps delivering angiotensin II. Using highly multiplexed spectral flow cytometry, we found that chronic angiotensin II administration re-wires the anti-tumor immune response, leading to an increased presence of myeloid cells, particularly Ly6C+ monocytes, and CD206+ macrophages. Blockage of the angiotensin II receptor type I (AT1) with losartan leads to a marked decrease in tumor growth and a reduction in MDSCs. This effect was observed only with the synchronous administration of angiotensin II and losartan, not with losartan alone, and was consistent across different PDAC treatment regimens. In addition, we observed a trend toward improved tumor vessel perfusion in hypertensive mice treated with losartan, indicating vascular repair. Additional findings suggest that inhibition of the angiotensin II receptor type 2 (AT2) and the Mas receptor (which physiologically counterbalance AT1 signaling) abrogated the beneficial effect of AT1 blockade with losartan, suggesting a role for AT2 and the Mas receptor in shaping the immune microenvironment. Conclusion: Overall, our findings show that CAH reprograms the tumor microenvironment in PDAC and that inhibition of angiotensin signaling reverses these changes. This may indicate that inhibition of angiotensin signaling in cancer patients with CAH may exert its beneficial effect by reprogramming the anti-tumor immune response.

#2085 Novel obesity-associated adipokine modulates the malignant phenotype of endometrial cancer cells.

Chi Lam Au Yeung, Gaayathri Binoj, Qian Zhang, Yadira Pacheco, Samuel Mok

UT MD Anderson Cancer Center, Houston, TX

Endometrioid Endometrial Cancer (EEC) is the most common gynecologic malignancy in the United States. Around 60% of women with EEC are believed to be associated with being overweight or obese. This fraction of patients is likely to increase as the obesity epidemic continues in the United States. Omentin (ITLN1) is a novel adipokine that is expressed in mesothelial cells covering the omental adipose tissue. The serum omentin level is inversely correlated with Body Mass Index and it increases with weight loss. We demonstrated that serum omentin level is significantly lower in patients with EEC compared to healthy women. Besides, immunocompetent mice fed with high-fat diet demonstrated a significantly higher tumor burden and lower circulating omentin level than those fed with low-fat diet, suggesting that obesity suppresses circulating omentin level and promotes EEC progression. To determine the roles of omentin in EEC pathogenesis, both human and mouse EEC cell lines were treated with recombinant omentin to evaluate cell growth and cell motility. We found that EEC cells treated with recombinant omentin have a significantly lower cell proliferation rate compared to control cells treated with PBS. Omentin-treated EEC cells also resulted in a significantly reduced migration rate compared to control cells. Since omentin was previously reported to bind to alpha-v-beta-3 (αvβ3) integrin to exert biological functions, we treated the EEC cells with αvβ3 blocking antibody to see if the effects of omentin on cell growth and motility would be abrogated. We found that αvβ3 blocking antibody abrogated the suppressive effect of omentin on cell growth compared to normal mouse IgG control. Similarly, αvβ3 blocking antibody counteracted the effect of omentin on cell migration. These suggest that omentin binding to the αvβ3 integrin inhibited cell proliferation and motility. In addition, Western blot analysis showed that omentin downregulated key αvβ3 downstream signaling molecules, such as p-ERK and p-CREB. Addition of αvβ3 blocking antibody in omentin-treated cells reversed the suppressive effect of omentin on p-ERK, further suggesting that omentin/αvβ3 integrin axis may play an important role in mediating the tumor suppressive effect of omentin.In conclusion, the above findings suggest that omentin suppresses EEC cell growth and migration potentially through binding to αvβ3 integrin. Further study is needed to characterize the specific pathways involved in omentin-mediated suppression on EEC cells and to develop omentin as a low toxicity chemopreventive and therapeutic agent for EEC patients

#2087 Intermittent fasting remodels gut ecosystem to influence initiation and therapy responses in pancreatic cancer.

Le Li[1], Vidhi Chandra[2], Fuduan Peng[2], Luca S. Santovito[3], Olivereen Le Roux[2], Rian M. Howell[2], Thais Bartelli[2], Virginia Tahan[2], Erika Y. Faraoni[2], Seyda Baydogan[2], Haiyan D. Miller[4], Kejing Song[4], Vasanta Putluri[5], Badrajee Piyarathna[5], Abu Hena Kamal[5], Nagireddy Putluri[6], Joseph Petrosino[5], Arun Sreekumar[5], Jay Kolls[4], James R. White[7], Zheng Sun[5], Lora V. Hooper[8], Linghua Wang[2], Faraz Bishehsari[3], Florencia McAllister[2]

[1]Department of Genetics, UT MD Anderson Cancer Center, Houston, TX,[2]UT MD Anderson Cancer Center, Houston, TX,[3]UT Health Center Houston, Houston, TX,[4]Tulane University, New Orleans, LA,[5]Baylor College of Medicine, Houston, TX,[6]Baylor College of Medicine, Sugar Land, TX,[7]Resphera Biosciences, Baltimore, MD,[8]UT Southwestern, Dallas, TX

Pancreatic ductal adenocarcinoma (PDAC) has one of the lowest cancers related-survival rates with high resistance to therapies and no available preventive strategies. Even immunotherapy, which has transformed cancer treatment by providing survival benefits in many solid tumors, has shown limited efficacy in PDAC. Eating patterns can modulate the composition and metabolic activity of the gut microbiota, thereby affecting anti-tumor immune responses. Fasting, a common treatment for pancreatic inflammatory conditions, can affect the composition of gut microbiota, regulates immunity and host metabolic responses. Although fasting is known to offer therapeutic benefits in pancreatic disorders such as pancreatitis and diabetes, its potential role in the prevention or treatment of pancreatic cancer remains unclear. Intermittent fasting (IF) refers to dietary regimens that limit food intake to specific time windows while allowing ad libitum calorie consumption during those periods. Using multiple spontaneous genetically engineered premalignant and orthotopic murine cancer models, we show that IF delays pancreatic tumorigenesis and induces sensitivity to immunotherapy in PDAC. IF-mediated reversal of PD-1 blockade resistance is dependent on gut microbiota mediated $CD8^+$ T cells activation and migration. IF modulates the relative abundance of gut microbiota as well as the serum metabolite levels, which activates intratumoral dendritic cells (DCs). Timeseries single cell transcriptomic analysis revealed that IF remodels the circadian clock of $CD8^+$ T cells and promotes anti-tumor immune responses through shifting the oscillation of genes, including *Kat2b*, *E2f4*, *Carns1* and *Ccnc*. Integration of these gene-expression profiles enables stratification of survival among PDAC patients. Spatial analysis confirmed that long-term fasting was associated with increased the proportion of $CD8^+$ T cells which were in proximity to DCs compared to short-term fasting, suggesting clinical evidence supporting a role for fasting in the redistribution of immune cells within the tumor microenvironment of PDAC. Our findings demonstrate the efficacy of IF in PDAC prevention and reversal of therapy resistance by modulating the activation and egress of rhythmic $CD8^+$ T cells, ultimately affecting the pancreas tumor ecosystem.

#2088 Prostaglandin E_2 signaling promotes adverse survival outcome in B-cell acute lymphoblastic leukemia.

Michael Cohen[1], Nayaonika Vasishtha[1], Byourak Shabane[1], Jia Tan[1], Tyler Kuk[1], Neha Chandra[1], In Sook Ahn[1], Xia Yang[1], Etan Orgel[2], Steven D. Mittelman[1]

[1]UCLA - University of California Los Angeles, Los Angeles, CA,[2]Children's Hospital Los Angeles, Los Angeles, CA

Obesity increases risk and worsens treatment outcome of acute lymphoblastic leukemia (ALL). To explore how adipose tissue may contribute to these effects, we previously performed single cell RNA sequencing in obese mice to compare gene expression in ALL from adipose tissue to ALL from marrow. We identified 577 differentially expressed genes (DEGs) with a $\log_2$-fold threshold of ±0.25 and Bonferroni corrected p-values <0.05. Using *ex-vivo* coculture of ALL and human adipose explants, we confirmed that adipose tissue upregulates a top DEG, *TNFSF11*, in ALL cells via secretion of prostaglandin E2 (PGE_2). Additionally, we observed that PGE_2 conferred modest resistance *in vitro* to vincristine and daunorubicin chemotherapies. In the present study, we explored whether adipose tissue PGE_2 might contribute to poor ALL treatment outcome. We identified six additional genes in the top 50 DEGs that may be induced by PGE_2-cAMP signaling and confirmed that these genes were upregulated *in vitro* by 200 ng/mL PGE_2 in BV173 and RS4;11 ALL cell lines (Table)(N=6). To investigate the relevance of these genes to ALL survival, we analyzed data from the TARGET-ALL P2 clinical trial using the NCI GDC Data Portal. TARGET-ALL P2 included pediatric and young adult B-precursor ALL patients treated on Children's Oncology Group protocols, enriched for patients who experienced relapse within 4 years of diagnosis. Survival and RNAseq expression on diagnostic specimens were available for 466 subjects. Expression of these six genes, as well as *TNFSF11*, was associated with significantly worse survival, with hazard ratios ranging from 1.7 to 3.7 (Table). Overall, our data shows that adipose tissue PGE_2 can upregulate genes that are associated with a worse prognosis in ALL patients. Further work is needed to test whether adipose tissue PGE_2 is a contributing factor for worse ALL outcomes in obese patients.

Gene name	Symbol	Log_2 FC adipose vs. marrow (scRNAseq)	Fold change with PGE_2 (qPCR) BV173, RS4;11	p-value BV173, RS4;11	Hazard ratio	Log-rank p-value
TNF superfamily member 11	*TNFSF11*	2.195	5.50, 7.34	0.0020, 0.0365	1.731	0.0043
Fos proto-oncogene, AP-1 transcription factor subunit	*FOS*	1.809	2.18, 4.31	0.029, 0.0004	2.025	0.0004
Fos like 2, AP-1 transcription factor subunit	*FOSL2*	1.561	4.8, 7.67	0.0015, 0.0008	2.289	<0.0001
JunB proto-oncogene, AP-1 transcription factor subunit	*JUNB*	2.730	1.70, 1.24	0.034, 0.023	3.523	<0.0001
JunD proto-oncogene, AP-1 transcription factor subunit	*JUND*	1.616	1.51, 1.87	0.076 (n.s.), 0.0017	3.748	<0.0001
Nuclear receptor subfamily 4 group A member 1	*NR4A1*	2.184	3.07, 6.63	0.016, 0.0008	2.483	<0.0001
Nuclear receptor subfamily 4 group A member 2	*NR4A2*	1.871	2.41, 8.10	0.0005, 0.0022	3.431	<0.0001

#2089 Sex-specific IgA secretion in muscle-invasive bladder cancer: A preliminary study.

Yasmine Ilkhani[1], Sirine Bouabda-Barc[1], Rachel Chevalier[1], Orlando Yuan[1], Jose Joao Mansure[1], Madhuri Koti[2], Wassim Kassouf[3], **Eva Michaud**[3]

[1]Urologic Oncology Research Division, Cancer Research Program, Research Institute of the McGill University Health Center, Montreal, QC, Canada,[2]Department of Biomedical and Molecular Sciences, Queen's University, Kingston, ON, Canada,[3]Department of Surgery, Division of Surgery, Cancer Research Program, McGill University, Montreal, QC, Canada

Background: Males are 3 times more at risk to develop muscle-invasive bladder cancer (MIBC), yet females present with higher-grade disease, worse prognosis, and reduced response to available treatments. The biological basis of these sex differences remains elusive. Secretory IgA (SIgA), including SIgA1 and SIgA2, maintains mucosal homeostasis by binding commensal microbes. SIgA is secreted *via* pIgR-mediated transcytosis and microbe-bound SIgA2 can traffic back to the *lamina propria* by binding to Dectin-1 and Siglec-5 (reverse transcytosis). This is known in other mucosae but not the bladder. Urinary IgA is elevated in MIBC patients, yet existing studies suggest conflicting roles: IgA is linked to reduced immunosuppression and improved immunotherapy response, yet also to poor survival in cohorts largely dominated by male cases. This leaves sex-specific IgA biology uncharacterized in urinary immunity. *Hence, we hypothesize that bladder IgA secretion is distinct in males and females and may influence MIBC outcomes.*

Methods: Digital Spatial Profiling (GeoMx) was performed on pre-treatment MIBC tumors (n=171; 35F/136M). RNAscope pan-bacterial 16S and multiplex IHC (IgA1, IgA2, ER, AR) were applied to the same tissues. Urinary IgA1/IgA2 were quantified by ELISA (n=20F/20M). Wild-type (n=20F/20M), gonadectomized (n=15F/15M), and sex-reversed FCG mice (FCG, n=5-8 XX-F, XY-F, XY-M and XX-M) received 0.05% N-butyl-N-(4-hydroxybutyl)-nitrosamine (BBN) for 20 weeks. HBLAK cells were cultured on inserts for stratification± β-estradiol then exposed to commercial IgA (2h). Q-omics was used to query TCGA MIBC datasets.

Results: Female tumors were enriched for *IGHA1*, with increased urinary IgA2. In TCGA, high tumoral *IGHA2* correlated with improved survival in women only, particularly in tumors with low ESR1 expression. We also found increased *CLEC7A* (dectin-1) and *SIGLEC5* expression in tumors compared to matched normal area. Female mice displayed higher urinary and urothelial IgA, with ovariectomy modulating IgA only after tumor establishment. We found a staining gradient in the urothelium and IgA-positive vesicles, indicating active transport of complexed IgA. No differences in urinary IgA were observed between sex-reversed FCG and WT mice, supporting hormonal rather than autosomal control of IgA. HBLAK pIgR expression was downregulated by β-estradiol. In stratified cultures, IgA added to either side of culture inserts was detected on the opposite side, demonstrating both transcytosis and reverse transcytosis. Long-term exposure to β-estradiol led to significantly less transcytosis, but not reverse-transcytosis.

Impact: This is the first investigation of bladder IgA biology in MIBC; we show human and mice tumors are broadly poised for IgA secretion and retro-transport, modulated by female hormones. IgA may represent a novel sex-specific biomarker, its integration in a predictive response model is pending.

#2090 Modifiable lifestyle factors and immune gene expression in breast tumor and normal-adjacent tissue.

Kristen D. Brantley[1], Cheng Peng[2], Clara Bodelon[3], Deborah A. Tadesse[4], Peter Kraft[5], Rulla M. Tamimi[6]

[1]Dana-Farber Cancer Institute, Boston, MA,[2]Brigham and Women's Hospital, Boston, MA,[3]American Cancer Society, Atlanta, GA,[4]Trans-Divisional Research Program, Division of Cancer Epidemiology and Genetics, National Cancer Institute, Rockville, MD,[5]National Cancer Institute, Rockville, MD,[6]Weill Cornell Medicine, New York, NY

Background: The tumor immune microenvironment may provide key information on breast cancer prognosis. Several modifiable risk factors influence the immune response, including weight, physical activity, and diet; however, whether these factors alter the breast tumor immune microenvironment remains unknown.

Methods: Participants enrolled in the Nurses' Health Studies diagnosed with invasive breast cancer and available tumor and/or normal adjacent tissue were included (N=945). Immune cell abundance was deconvoluted using CIBERSORTx. Gene expression signatures were derived for components of the immune profile such as immune checkpoint markers, co-regulatory signal and antigen presentation, and cytokine signaling. Participant weight, BMI, alcohol use, and smoking status were collected via bi-annual questionnaires. Overall diet was summarized by the alternative healthy eating index (AHEI) and the empirical dietary inflammatory pattern (EDIP), derived from food frequency questionnaires completed every 4 years. Linear regression was used to test the association between pre-diagnostic exposures (from questionnaires closest to diagnosis) and immune cell abundance and gene expression. Tumor and normal-adjacent tissue were analyzed separately. Models were adjusted for year and age of diagnosis, menopausal status, and estrogen-receptor (ER) status. Multiple testing of immune components was controlled via the false discovery rate. Models were also stratified by ER and menopausal status.

Results: Among 875 women with available tumor tissue, mean age at diagnosis was 59 years (SD=11.4). The majority (73%) were post-menopausal, had ER-positive tumors (77%), and were diagnosed at stage 1-2 (91%). In ER-positive tumor tissue of postmenopausal women, weight gain since age 18 was positively associated with interferon signaling, MHCII, and PD1 expression (all $p_{adj}<0.05$). Higher physical activity was associated with enriched CD8:CD68 ratio in this group. In ER-negative tumor tissue of pre- and postmenopausal women, consuming more drinks per week was associated with higher PDL1 and lower CSR expression. In normal-adjacent tissue, current smoking was associated with enriched cytokine signaling in premenopausal women and total pack-years was associated with higher B cell plasma in postmenopausal women. Higher EDIP was associated with heightened MHCII and IL12 expression in ER-negative tumor tissue while higher AHEI was associated with lower lymphocyte infiltration expression in normal adjacent tissue, regardless of menopausal status.

Conclusions: Weight gain, smoking, alcohol use, and diet (AHEI and EDIP) are associated with differences in the breast cancer immune microenvironment, with distinct associations by ER and menopausal status. Changes in lifestyle behaviors may influence the tumor immune response and impact patient prognosis, though further studies are needed.

#2091 Progesterone promotes immunosuppression in murine mammary tumors by modulating CD4 T cell viability and helper functions, promoting T cell apoptosis and a shift from inflammatory to anti-inflammatory cytokine profiles.

Amanda Glen Heard

Cancer Biology, Univerisity of Kansas Medical Center, Kansas City, KS

Breast Cancer is the most common cancer diagnosed in women in the US. Breast cancer results in the second greatest number of cancer deaths for women. Hormone receptor positive (HR+) breast cancers - cancers expressing the nuclear receptors for steroid hormones estrogen and progesterone, termed the estrogen receptor (ER) and progesterone receptor (PR) - make up the 70% of diagnosed breast cancers, making the HR+ subtype the largest contributor to breast cancer mortality despite a favorable prognosis compared to other breast cancer subtypes. Treatment consists of anti-endocrine therapies, targeting ER/estrogen signaling pathways. Most women respond well to these therapies, but for women who do not, there are few alternative options. It is accepted that lifetime exposure to estrogens increases the risk of developing of HR+ breast cancer, but both estrogen and progesterone are part of the normal menstrual cycle. Prior work from our lab has uncovered a novel immune-modulatory role for progesterone, pivotal to promoting the growth of PR-positive mammary tumors. Single cell RNA sequencing data from these PR+, progesterone treated tumors show a significant decrease in tumor-infiltrating T cells, specifically of the CD4+ helper T cell subset. Interestingly, *in vitro* progesterone treatment increases the percentage of CD4+ T cell undergoing apoptosis post T cell activation. Progesterone treatment also significantly decreases IFNγ production in CD4+ T cells, while increasing Th2 cytokine production. Our lab show that the culmination of these effects provides protection against T cell killing in a co-culture with mouse mammary tumor cells. Our lab has also found that mouse mammary tumor cells do not express select progesterone metabolism genes to efficiently metabolize progesterone, and that the human orthologs for these genes are also downregulated in human breast cancer. These results suggest that progesterone in the tumor microenvironment could modulate T cell functions, providing tumor cells with protection from immunosurveillance and contributing to HR+ breast cancer development. These data also argue for the use of anti-progestins to boost anti-tumor immune activity and synergize with current cancer immunotherapy regimens, providing an alternative option for women who have failed anti-estrogen therapies.

#2092 Single-cell RNA sequencing reveals ancestry-associated molecular and cellular immunosuppressive features in non-small cell lung cancer.

Liang Liu[1], **Pengbo Zhang**[2], Enzo Palma[1], Ashley Ballard[1], Lance Miller[1], Gregory Hawkins[3], Cristina M. Furdui[3], Edward Levine[4], Alberto de Hoyos[5], Wencheng Li[6], Fang-Chi Hsu[7], Ralph D'Agostino[7], David Foureau[8], Wei Zhang[1]

[1]Cancer Biology, Wake Forest University School of Medicine, Winston Salem, NC,[2]Atrium Wake Forest Baptist Comprehensive Cancer Center, Winston Salem, NC,[3]Biochemistry, Wake Forest University School of Medicine, Winston Salem, NC,[4]General Surgery, Wake Forest University School of Medicine, Winston Salem, NC,[5]Cardiothoracic Surgery, Wake Forest University School of Medicine, Winston Salem, NC,[6]Pathology, Wake Forest University School of Medicine, Winston Salem, NC,[7]Biostatistics and Data Science, Wake Forest University School of Medicine, Winston Salem, NC,[8]Cancer Medicine, Wake Forest University School of Medicine, Winston Salem, NC

Background: Racial disparities in non-small cell lung cancer (NSCLC) outcomes persist, with Black American (BA) patients having inferior survival compared to White American (WA) patients, even after adjusting for stage, treatment, and socioeconomic factors. We hypothesize that distinct molecular and cellular features in the tumor microenvironment (TME) contribute to ancestry-specific heterogeneity and these disparities.

Methods: We performed 10x scRNA-seq on treatment-naïve, early-stage NSCLC from 42 patients: 29 adenocarcinomas (15 WA, 14 BA) and 13 squamous (10 WA, 3 BA). Unsupervised clustering and annotation of 220,591 cells identified six major cell types: epithelial, endothelial, fibroblasts, myeloid, mast, and lymphocytes-each further subdivided into lineage-specific phenotypes. Analyses stratified by ancestry include: differential gene expression and cell abundance, gene set enrichment analysis, trajectory inference, and ligand-receptor analysis.

Results: Malignant epithelial cells showed significant pathway enrichment of OXPHOS, fatty acid metabolism, and G2/M checkpoint in BA tumors ($q \leq 0.01$) and TNF-α signaling via NF-κB, IFN-γ response, and heme metabolism in WA tumors ($q=0.004$, 0.008, and 0.02, respectively). Endothelial cells showed enrichment in IL-2/STAT5 signaling and fatty acid metabolism in BA tumors ($q=0.01$ and 0.03, respectively) and in proliferation pathways in WA tumors (Myc Targets V1, $q=0.005$).BA and WA tumors exhibited distinctive immunosuppressive features. BA tumors showed higher numbers of FAP- cancer associated fibroblasts (CAF; $q=0.07$) and M2 macrophages ($q=0.004$) but low effector CD8+ ($p=0.02$) and γδ T cells ($p=0.018$). BA tumor associated macrophages (TAM) showed preserved activation (CD40, CD80) but impaired antigen presentation (HLA-DM/DQ/DR, all $q<0.05$) and were enriched for hypoxia and TGF-β signaling gene signatures ($q<0.01$). In contrast, WA tumors contained more FAP+ CAFs and macrophages displayed M0/M1-like features with prominent antigen presentation and IFN-I/II responses ($q<0.01$). Also, BA tumors showed active innate immune networks, particularly SPP1-CD44 signaling ($p<0.001$), whereas WA tumors exhibited stronger adaptive stimulatory (MHCII-TCR) and inhibitory (CD86-CTLA4) signaling ($p<0.001$). Furthermore, $CD8^+$ T cells in BA tumors adopted an early exhaustion phenotype associated with TGF-β signaling ($q<0.01$), while in WA tumors they showed progressive exhaustion (high PDCD1, HAVCR2, LAG3) in an IFN-α/γ-driven environment ($q<1E-5$).

Conclusions: This first large-scale, ancestry-stratified scRNA-seq atlas of NSCLC reveals molecular mechanisms underlying distinctive immunosuppressive programs in BA and WA patients and highlights molecular and cellular TME features that may contribute to racial disparities in NSCLC.

#2093 Elucidating the mechanistic connection between the elevated occurrence of EGFR mutation in Hispanic/Latinx lung adenocarcinoma patients.

Jonathan Castillo[1], William D. Wallace[2], Leonidas Arvanitis[3], Dan Raz[4], Crystal N. Marconett[1]

[1]Department of Integrative Translational Sciences, City of Hope, Duarte, CA,[2]Department of Pathology, USC Keck School of Medicine, Los Angles, CA,[3]Department of Pathology, City of Hope, Duarte, CA,[4]Division of Thoracic Surgery, Department of Surgery, City of Hope, Duarte, CA

Hispanic/Latinx (H/L) patients with lung adenocarcinoma have higher rates of epidermal growth factor receptor (EGFR) mutation than those who identify as non-H/L White. Although the overall survival outcome of H/L patients is better than non-H/L White patients, the subset of H/L patients with EGFR mutations have poorer survival outcomes. Immunotherapy has improved survival outcomes for lung adenocarcinoma, but their role in EGFR-mutant lung adenocarcinoma has been underwhelming, as EGFR-mutant tumors are often associated with an immunosuppressive tumor microenvironment and non-response to immunotherapy. Understanding how EGFR mutations and race/ethnicity shape the tumor immune microenvironment is critical to close gaps in health disparities. To address this, we utilized spatial transcriptomics (Visium HD) on lung adenocarcinoma patients from H/L and non-H/L patients stratified by EGFR status and sex (n=4 per group, n=24 total) to characterize spatial patterns of immune infiltration, immune cell composition, and changes to signaling pathways within the tumor-immune microenvironment. To validate and extend these findings to a larger population, bulk RNA-seq data (n=237) from a diverse cohort will be used to quantify immune-cell composition via cell deconvolution (CIBERSORT). In addition, associations between EGFR mutational status, race/ethnicity, and clinical variables including survival, smoking history, and therapy response are also considered. We hypothesize that EGFR-mutant tumors in H/L patients display distinct spatially organized immune-suppressive, resulting in the observed poorer survival outcomes. Taken together, this work integrates spatial and bulk transcriptomic approaches with EMR chart records to uncover mechanistic, race/ethnicity-specific immune features associated with EGFR mutation prevalence in H/L lung adenocarcinoma patients, with the goal of bridging the gaps in health outcomes.

#2094 Investigating the influence of genetic background on TNBC-T cell interactions in TNBC organoids and co-cultures.

Batoul Farran[1], Moses Kamita[2], Shuk Mei Wong[1], Sylvester Antwi[1], Valerie Ofori Aboah[1], Harriet Larrious-Lartey[1], Jessica Jessica Bensenhaver[1], Ali Haythem[1], Walker Eleonor[1], Foster Amponsah[3], Josephine Nsafu.[3], Rose Dampson[3], Patrick Kafui Akapko[3], Evelyn Jiage[1]

[1]Henry Ford Health System, Detroit, MI,[2]Fox Chase Cancer Institute, Philadelphia, PA,[3]PMABC, Accra, Ghana

Triple negative breast cancer (TNBC) is an aggressive form of breast cancer (BC) characterized by early relapse and poor prognosis. The TNBC mortality burden is unequally distributed among populations of different genetic ancestry, with populations of African descent displaying higher incidence of TNBC with high mortality rates. The tumor microenvironment (TME) plays a key role in TNBC development. Interactions between different TME components, such as T cells, can modulate TNBC progression and resistance to therapies. Additionally, the TME can contribute to the disparities in outcomes observed between TNBC patients of EA versus African ancestry. However, the immunomodulatory mechanisms that mediate immune evasion in TNBC in women of African descent remain understudied. To investigate these mechanisms, we developed organoids from TNBC patients of African American and Ghanian ancestry. TNBC tumors from EA, AA and GH patients were implanted into immunosuppressed mice and PDX-derived organoids (PDXos) were established from these tissues. The expression of epithelial, mesenchymal, stromal and immune markers in PDXos and matching PDXs and primary tissues was assessed using multiplex IF and qRT-PCR. T cells were isolated from healthy control PBMCs and activated as per previously published protocols. 5 different TNBC organoids, including 1 EA, 2 AA and 2 GH PDxOs, were co-cultured with T cells, following which the responsiveness of organoids to T cells was assessed using flow cytometric analysis. Finally, immune-resistant organoids were co-cultured with T cells then sorted for downstream analysis. We have successfully established 8 TNBC organoids (PDxOs) from patients of different genetic ancestries, including 1 EA TNBCs, 3 GH TNBCs and 5 AA TNBCs. Multiplex IF and qRT-PCR analysis revealed that the obtained PDXos retained the epithelial (EpCAM) and mesenchymal (vimentin) signatures of their tissues of origin. Co-culture with T cells revealed that the organoids displayed differing patterns of immune responsiveness and exerted distinct effects on T cell exhaustion and activation. Flow cytometric analysis showed that epithelial TNBC organoids were more responsive to T cells whereas mesenchymal-like organoids were more immune resistant. qRT-PCR analysis of organoids grown in co-culture with T cells revealed that they had increased vimentin expression, suggesting a role for EMT in immune evasion in these organoids. These findings reveal that PDXos recapitulate the epithelial and mesenchymal patterns of their tissues of origin and represent a valuable platform for investigating ancestry-specific pathways of immune responsiveness and resistance in TNBC patients of African ancestry.

#2095 Smoking is associated with reduced tumor-infiltrating lymphocyte density in breast cancer.

Annelie Marika Augustinsson[1], Karolin Isaksson[2], Aniko Kovacs[3], **Helena Jernstrom**[4]

[1]Department of Clinical Sciences, Lund, Lund University, Lund, Sweden,[2]Clinical Sciences Lund and Surgery, Lund University and Skane University Hospital Kristianstad, Lund and Kristianstad, Sweden,[3]Clinical Pathology and Institute of Biomedicine, Sahlgrenska University Hospital and Sahlgrenska Academy Gothenburg University, Gothenburg, Sweden,[4]Clinical Sciences Lund, Lund University, Lund, Sweden

Purpose: Previous studies examining the relationship between smoking and stromal tumor-infiltrating lymphocytes (TILs) in breast cancer (BC) have reported conflicting findings, ranging from no significant association to evidence suggesting that smoking may modify the immune tumor microenvironment (TME) and potentially increase TIL density. This study aimed to clarify whether smoking is associated with TIL density in BC.

Methods: Within the prospective Melanoma in Southern Sweden (MISS) study, tissue micro arrays (TMAs) were available for 1,276 women diagnosed with a primary invasive BC between March 1, 1992, and October 31, 2013. The presence of TIL was successfully annotated in 1,173 (91.9%) tumors by a breast pathologist and classified into three categories based on the percentage of stained TILS as low (<10%), intermediate (10-49%), or high (≥50%). Associations between TIL categories and ever smoking at study inclusion between 1990-1993, age at BC diagnosis, tumor size, nodal status, histological grade, and triple-negative subtype were assessed using Pearson's Chi² test and multivariable linear regression. Two-tailed *p*-values <0.05 were considered statistically significant.

Results: Median age at BC diagnosis was 61 years (interquartile range 53-69 years). Of the TMAs with TILs scored, 839 (71.5%) were classified as low, 259 (22.1%) as intermediate, and 75 (6.4%) as high. Smoking was significantly associated with lower TIL density (p = 0.033, adjusted P_{trend} = 0.013). Age at BC diagnosis showed a borderline association with lower TIL density (adjusted P_{trend} = 0.060). Higher TIL density was associated with larger tumor size (p < 0.001, adjusted P_{trend} = 0.023), higher histological grade (p < 0.001, adjusted P_{trend} < 0.001), and triple-negative subtype (p < 0.001, adjusted P_{trend} < 0.001). Nodal positivity was highest in the intermediate group, with no linear association (p = 0.006, adjusted P_{trend} = 0.57).

Conclusions: In this large prospective cohort, smoking was independently associated with significantly lower TIL density in breast cancer, while associations between TILs and other clinicopathological factors were as expected. These findings suggest that smoking may negatively influence immune TME and shed new light on a mechanism through which smoking could modify response to breast cancer treatments. Further studies are warranted to explore the clinical impact of smoking on TILs in breast cancer.

#2096 Investigating the effect of SGLT2 inhibitor dapagliflozin on acute lymphoblastic leukemia in obese mice.

Jia Tan[1], Thomas Tran[1], Tyler Kuk[1], Houfu Leng[1], Michael Cohen[1], Etan Orgel[2], Steven D. Mittelman[1]

[1]UCLA - University of California Los Angeles, Los Angeles, CA,[2]Children's Hospital Los Angeles, Los Angeles, CA

Patients who are obese at diagnosis of acute lymphoblastic leukemia (ALL) have a 50% higher relapse rate. We showed that diet and exercise can improve ALL treatment outcome in mice and patients, but these interventions can be difficult due to financial and logistical barriers. Alternative interventions that induce weight-loss or metabolic changes could prove more accessible in real-world treatment. The SGLT2 inhibitor dapagliflozin (DAPA) is a diabetes medication that inhibits renal glucose reabsorption, lowers blood glucose, and induces modest weight loss. It has been shown to improve outcomes of heart failure and chronic kidney disease. In mice, SGLT2 inhibitors have been shown to slow tumor growth and synergize with chemotherapy in liver, colon, and breast cancer. However, no studies have tested SGLT2 inhibitors on ALL. We investigated whether SGLT2 inhibition might be an alternative to diet and exercise to improve ALL outcome. Human (BV173, RS4;11) and mouse (8093) ALL cell lines expressed *Sglt2* by qPCR (n=4). DAPA showed synergistic effects with chemotherapy vincristine (VCR) *in vitro* (Table). DAPA treatment (3 mg/kg/day in water, 28 days) in obese male C57Bl/6 mice induced glucose loss in urine (2 g/dL vs. undetectable, n=12) and decreased blood glucose (179±17 vs. 203±14 mg/dL, p=0.008, n=6). As monotherapy, DAPA slowed but did not halt ALL progression in a syngeneic ALL model (median survival: 18 vs. 21 days, p=0.027 log rank, n=6). Surprisingly, combining DAPA with VCR resulted in higher mortality than VCR alone (83 vs. 33% mortality, p=0.047 log rank, n=6). Developing medication-based alternatives to diet/exercise interventions is important to ensure all patients with ALL can benefit from metabolic-interventions. Our study shows that SGLT2 inhibition is effective in vitro, but in vivo data imply it may not be a viable option for improving ALL treatment outcome.

Table

Cell Line	Control (x10^6)	VCR (2-2.5 nM)	DAPA (10 μM)	VCR+DAPA	P value (VCR vs VCR + DAPA)
BV173	1.95±0.45	1.70±0.25	1.73±0.38	1.21±0.51	0.037
RS4;11	1.27±0.42	1.15±0.28	1.19±0.33	0.71±0.19	0.035
8093	3.61±0.58	3.30±0.46	2.74±0.48	1.95±0.63	0.048

#2097 Fibroblast galectin-3 remodels the obese breast tumor microenvironment to promote cancer progression.

Ellen E. Bamberg[1], Kiran Vinod-Paul[1], Amy L. Pyo[1], Kirk C. Hansen[2], Carol A. Sartorius[3], Paul S. MacLean[4], Peter Kabos[1], Heather Brechbuhl[1]

[1]Medicine - Division of Medical Oncology, University of Colorado Anschutz Medical Campus, Aurora, CO,[2]Biochemistry and Molecular Genetics, University of Colorado Anschutz Medical Campus, Aurora, CO,[3]Pathology, University of Colorado Anschutz Medical Campus, Aurora, CO,[4]Medicine - Division of Endocrinology, Metabolism, and Diabetes, University of Colorado Anschutz Medical Campus, Aurora, CO

Background: Obesity, affecting 42.4% of U.S. adults, correlates with higher tumor grade, increased metastasis, and reduced survival in breast cancer (BC). Our prior work revealed obesity-induced secretion of collagen-crosslinking enzymes, basement membrane proteins, and the matricellular protein galectin-3 (LGALS3) in the breast. These extracellular matrix (ECM) changes were positively associated with the fibroblast population in obese breast tissue. Elevated LGALS3 expression predicts poorer overall survival in estrogen receptor-positive (ER+) BC. We *hypothesize* that obesity amplifies LGALS3 fibroblast signaling to disrupt ECM composition and organization, supporting BC progression.

Methods: Rag1-/- mice were fed a high-fat high-sugar (HFHS) or low-fat low-sugar (LFLS) diet for 16 weeks to establish obese and lean phenotypes. ER+ UCD65 BC cells were implanted bilaterally into the mammary fat pad alone or with $CD146^{neg}$ (HS5) fibroblasts, generating four groups: LFLS, HFHS, LFLS + $CD146^{neg}$, and HFHS + $CD146^{neg}$. All mice received 1 mg of estrogen at implantation and remained on their assigned diets for eight weeks. Tumors, plasma, lungs, and mammary fat pads were collected at endpoint for analyses. LGALS3 was knocked down in $CD146^{neg}$ fibroblasts and overexpressed in $CD146^{pos}$ (HS27) fibroblasts for in vitro studies. Conditioned media was generated under starvation conditions and concentrated 20x for western blotting.

Results: Obese mice implanted with $CD146^{neg}$ fibroblasts exhibited a 2.7-fold increase in tumor growth and 8.8-fold increase in metastasis compared with lean controls. $CD146^{neg}$ fibroblasts significantly enhanced angiogenesis in both lean and obese settings but did not affect lymphangiogenesis. Obesity significantly disrupted the collagen organization of the mammary fat pads. In obese mice, with $CD146^{neg}$ fibroblasts, increased collagen deposition, macrophage infiltration, and circulating levels of LGALS3. Genetic manipulation of LGALS3 showed that it specifically regulates collagen I secretion without altering intracellular levels. This loss of secretion triggered unfolded protein response activation and reduced TGF-β signaling, further supporting a secretion-focused mechanism. LGALS3 was diet-responsive, with time-restricted feeding and intermittent fasting lowering circulating levels by 2.1 and 2.7-fold, respectively.

Conclusions: Obesity synergizes with $CD146^{neg}$ fibroblasts to accelerate BC aggression through LGALS3-mediated ECM remodeling, supported by a novel post-transcriptional control of collagen secretion. LGALS3 can serve as a therapeutic target and is modifiable by dietary strategies to mitigate obesity-associated BC risks, potentially improving outcomes for millions of at-risk patients.

#2098 CNTF governs exercise-induced myofibroblast reversion in prostate cancer.

Pengju Gong[1], Yuan Liu[2], Leng Han[2], Liuqing Yang[1], Chunru Lin[1]

[1]Department of Molecular and Cellular Oncology, The University of Texas MD Anderson Cancer Center, Houston, TX,[2]Department of Biostatistics and Health Data Science, Indiana University School of Medicine, Indianapolis, IN

Prostate cancer (PCa) remains a major cause of cancer-related morbidity and mortality in the United States, with more than 2.5 million new cases reported annually. Epidemiological studies suggest that physical exercise reduces PCa risk and progression, yet the underlying molecular and stromal mechanisms remain poorly defined. Here, we demonstrate that long-term and moderate exercise significantly suppresses primary tumor growth and metastatic spread in the Transgenic Adenocarcinoma of the Mouse Prostate (TRAMP) model. Single-cell RNA-seq and spatial analyses of the tumor microenvironment (TME) revealed an abundance of myofibroblast populations in PCa, a hallmark associated with tumor progression and immunosuppression. Exercise robustly reversed this myofibroblast transition, shifting fibroblasts toward a resting phenotype in the TRAMP model. Mechanistically, we identified ciliary neurotrophic factor (CNTF) as an exercise-induced cytokine that restrains myofibroblast transition and enhances $CD8^+$ T-cell infiltration within the TME. This CNTF-dependent remodeling of the TME emerged as a key determinant of the anti-tumor effects of exercise. Therapeutically, recombinant CNTF suppressed PCa tumor growth in vivo and demonstrated synergy with immune checkpoint blockade, suggesting that CNTF restoration provides a promising strategy to sensitize PCa to immunotherapy. Collectively, our findings reveal a previously unrecognized CNTF-mediated axis that links physical exercise to fibroblast plasticity and anti-tumor immunity in PCa. This work also provides critical insights into mitigating potential risk factors for PCa patient survival outcomes, offering an avenue for further studies that may serve as a foundation for future clinical considerations for patients with this cancer type.

#2099 Iron supplementation rescues anemia of chronic disease in pancreatic ductal adenocarcinoma.

Yichi (Tony) Zhang[1], Cindy Pyo[1], Anna Barbeau[1], Davey Feng[1], Amit Roopan[1], Matthew Vander Heiden[1], Kendra Libby[2], Alison Epstein Ringel[3]

[1]Koch Inst. for Integrative Cancer Research at MIT, Cambridge, MA,[2]Ragon Institute, Cambridge, MA,[3]Massachusetts Institute of Technology (MIT), Cambridge, MA

Pancreatic cancer is a devastating malignancy that is rising in incidence and has nearly universal poor outcomes. We find rates of iron deficiency are high in pancreatic cancer patients and track with the high prevalence of anemia in these patients. From an evolutionary perspective, anemia of chronic disease is a condition seen where our bodies respond to an inflammatory insult, such as an infection, by sequestering iron from circulation to store the iron in peripheral tissues, such as muscle, to make this iron unavailable for pathogens. Our recent preliminary data suggest pancreatic cancer may act as the inflammatory stimulus to cause iron dysregulation and anemia. Analysis of a large cohort of pancreatic cancer patients shows both iron and hemoglobin decrease early in pancreatic cancer patients, suggesting of dysregulated iron metabolism. When pancreatic cancer is modeled in mice, decreases in hemoglobin and iron are also observed, as are increases in circulating hepcidin. Interestingly, supplementing mice with pancreatic cancer with iron improves anemia. Mechanistically, we want to understand why mice with PDAC develop anemia and analyzed Ter119-expressing erythrocyte differentiation and maturation in the bone marrow. We found that there is no defect in erythroid maturation in PDAC mice therefore its unlikely that defective erythropoiesis is the cause for anemia in PDAC. We also profiled Ter119-expression on the surface of F4/80-positive macrophages as a measure of hemophagocytosis and found that there is decreased Ter119-positive macrophages in PDAC so hemophagocytosis in the bone marrow is not the caused of anemia in PDAC. We find that iron-sequestering proteins such as hepcidin are increased throughout PDAC progression and iron sequestration in tumors and we find iron sequestration by many different cell types and tissues during PDAC. Hepcidin is known to cause iron sequestration in macrophages, which are the largest source of iron recycling and supply for heme and hemoglobin synthesis in the body. Furthermore, we observed decreased macrophage numbers in the bone marrows of PDAC mice. Hence, we proposed that PDAC leads to reduced iron-recycling by macrophages and this causes anemia of chronic disease. Therefore, iron supplementation is sufficient to rescue anemia in PDAC.

: Characterization of Metastases by Imaging and Profiling
Poster Session

#2103 Genome-wide DNA methylation profiling uncovers epigenetic alterations in key oncogenic pathways and prognostic biomarkers of metastatic thyroid cancer.

Sara Alnassar, Jana Almusallam, Nada Almutairi, Najla Albader, Amal Qattan, **Yufei Shi**

King Faisal Specialist Hospital & Research Centre, Riyadh, Saudi Arabia

Background: Thyroid cancer is the most prevalent endocrine malignancy with its incidence rising worldwide. Distant metastases are the leading cause of patient morbidity and mortality. While aberrant DNA methylation is known to drive thyroid cancer progression, the methylation landscape of metastatic thyroid cancer cells remains poorly characterized. This study aims to investigate DNA methylation dynamics in metastatic cells and to identify aberrantly methylated genes with potential clinical significance.
Methods: Whole-genome bisulfite sequencing (WGBS) was performed on four paired primary and metastatic thyroid cancer cell lines, each derived from genetically engineered mouse models of PTC, FTC, PDTC, and ATC. GO and KEGG analyses were conducted to annotate the functions and pathways associated with differentially methylated regions (DMRs). The cBioPortal for Cancer Genomics was utilized to access the TCGA-ThCa database for biomarker screening and to construct a prognostic multi-gene signature.
Results: DNA hypomethylation was markedly increased in metastatic cells. Comparative methylome analysis identified more than 3,500 DMRs in each cancer pair. Among these, 133 hypomethylated and 20 hypermethylated regions were consistently detected across all metastatic cancer types, representing a set of common metastatic DMRs. Pathway enrichment analysis revealed that the hypomethylated genes were significantly overrepresented in several key signaling pathways implicated in cancer progression, including focal adhesion, ECM-receptor interaction, PI3K-Akt, Wnt, and MAPK pathways. Notably, these epigenetic alterations were positively correlated with the transcriptional upregulation of the corresponding genes as determined by RNA-Seq analysis. Several metastasis-driven genes were found to be hypomethylated, such as Col4a1, lamc1, Il6ra, Rptor, Tcf7l2, and Nfatc1, suggesting their potential as therapeutic targets. Furthermore, a five-gene hypomethylation signature comprising DEDD, TJAP1, CAVIN4, YWHAG, and FABP4 was identified, the overexpression of which was significantly associated with poor overall survival ($p < 10^{-10}$), poor disease-specific survival ($p < 10^{-10}$), and poor progression-free survival. Clinically, overexpression of these genes exhibited a statistically significant correlation with older age at diagnosis, higher aneuploidy and hypoxia scores, and advanced disease stage.
Conclusions: Metastatic thyroid cancer cells demonstrated significant global DNA hypomethylation, resulting in the transcriptional activation of numerous metastasis-driving genes. The hypomethylated gene signature may serve as a potential prognostic biomarker to stratify patients at elevated risk for distant metastasis and to guide individualized therapeutic strategies.

#2104 RNA editing based risk model to predict extrahepatic metastasis in colorectal cancer liver metastasis.

Eiki Miyake, Kunitoshi Shigeyasu, Toshiaki Takahashi, Kazuya Moriwake, Masashi Kayano, Yuhei Kondo, Yuya Sakurai, Shunsuke Nakamura, Masafumi Takahashi, Kaori Nitta, Kazuya Yasui, Tomokazu Fuji, Kosei Takagi, Hiroshi Tazawa, Toshiyoshi Fujiwara

Gastroenterological Surgery, Okayama Univ. Graduate School of Med., Dentistry & Pharm. Sci., Okayama, Japan

Background: The management of colorectal cancer liver metastases (CRLM) remains an urgent challenge in metastatic colorectal cancer. The efficacy of liver transplantation for unresectable CRLM has recently introduced a new treatment option. However, extrahepatic metastasis (EHM), which is one of the key exclusion criteria for liver transplantation, is a poor prognostic factor in CRLM. Therefore, establishing a method to accurately detect EHM prior to treatment is needed. Existing imaging diagnostics have limitations in detecting small lesions, necessitating complementary biomarkers. Adenosine-to-inosine RNA editing, which is a post-transcriptional modification driven by adenosine deaminase acting on RNA (ADAR), promotes tumor malignancy and the acquisition of metastatic potential. We have previously reported that ADAR1 expression in liver metastases is a predictor of residual liver recurrence, but the significance of RNA editing in extrahepatic metastasis remains unclear. This study aimed to analyze RNA editing profiles in primary tumors and liver metastases to clarify the clinical significance of RNA editing in EHM.
Methods: We analyzed gene profiling datasets from normal tissue, primary tumor and liver metastasis in silico discovery from GEO (Gene Expression Omnibus) for both gene expression analysis and RNA editing analysis. For clinical validation, we analyzed 70 CRLM cases (39 EHM and 32 non-EHM).
Results: Public data analysis revealed significantly higher ADAR1 expression in primary tumors and liver metastases compared to normal colon tissue ($P = 0.03$, $P < 0.001$, respectively). RNA editing analysis identified numerous RNA editing events specific to both primary tumors and liver metastases, in addition to common editing events shared between the two sites. These findings suggest that the RNA editing program regulated by ADAR1 changes according to the metastatic site, implying involvement in organ specificity and multiorgan metastasis. In clinical validation, primary tumor ADAR1 expression was an independent predictor of EHM alongside sex (female) and poorly differentiated histology. Furthermore, a risk model that incorporated CEA and the presence of multiple CRLM in addition to the three independent predictors effectively predicted EHM (AUC = 0.78), suggesting clinical utility. Further characterization of site-specific RNA editing events may improve predictive performance.
Conclusion: ADAR1 expression is a promising biomarker for predicting EHM in patients with CRLM. Identification of EHM-specific RNA editing events may enable the development of non-invasive and highly accurate metastasis prediction models with clinical applicability.

#2105 Transcriptomic insights into MAO B inhibition and bevacizumab synergy in colorectal cancer model.

Unnati Hemant Shah[1], Shivani Soni[1], Pooja Mittal[1], Lesly Torres-Gonzalez[1], Michela Bartolini[1], Steve Soto Trujillo[1], Yitzhar Goretsky[1], Francesca Battaglin[1], Goar Smbatyan[1], Yan Yang[2], Joshua Millstein[2], Karam Ashouri[1], Sandra Algaze[1], Wu Zhang[1], Jean Chen Shih[3], Heinz-Josef Lenz[1]

[1]USC Norris Comprehensive Cancer Center, Los Angeles, CA,[2]Department of Population and Public Health Sciences, Keck School of Medicine, University of Southern California, Los Angeles, CA,[3]Department of Pharmacology and Pharmaceutical Sciences,, Afred E. Mann School of Pharmacy and Pharmaceutical Sciences, Los Angeles, CA

Background: Monoamine oxidase B (MAO B) plays a critical role in colorectal cancer (CRC) by influencing oxidative stress, angiogenesis, and therapy resistance. Building on preclinical evidence of MAO B inhibition in CRC, this study aimed to characterize transcriptomic alterations following treatment with MAO B inhibitors—Deprenyl, Rasagiline, and Safinamide alone and in combination with the anti-angiogenic agent Bevacizumab (Bev), to elucidate potential mechanisms underlying their antitumor synergy.
Methods: RNA sequencing was performed on HT29 CRC xenograft model tumor samples treated with MAO B inhibitors as single agents and in combination with Bev. Differential gene expression (DEG) analysis ($|\log2FC| > 2$; adjusted $p < 0.05$) identified distinct gene signatures across treatment groups. DEGs were clustered using Gene Ontology (GO), and enrichment was assessed using Fisher's exact test. Canonical pathway analysis was performed to characterize major signaling changes. To assess clinical relevance, DEGs were evaluated for correlation with MAO B expression in TCGA CRC datasets.
Results: Distinct and overlapping transcriptional signatures were observed across treatment groups. Tumor-suppressive genes: *VSIG1, GLIPR1, GUCY2C, SMPD3, CDX1, CDX2*, and *GJA1* were strongly upregulated with MAO B inhibitor treatment, indicating enhanced apoptotic and anti-angiogenic signaling. Oncogenic drivers: *MAGEA12, SOX5, OXCT1, VCAM1*, and *TNC* were significantly downregulated, in combination therapy groups, suggesting suppression of epithelial mesenchymal transition and metastatic potential. Long non-coding RNA (lnc) *TPTEP1* and anti-inflammatory mediator *LYPD8* were upregulated in Rasagiline-treated tumors, while oncogenic lncRNA *XIST* was downregulated in Safinamide-treated samples. When compared with TCGA CRC datasets, these treatment-responsive genes showed significant correlation with MAO B expression. Upregulated genes: *GUCY2C, CDX1, BTNL3,* and *SMPD3* showed negative correlation with MAO B, whereas downregulated genes including *SOX5, OCT1, VCAM1*, and *TNC* exhibited a positive correlation, further supporting the clinical relevance of MAO B associated gene expression patterns. GO analysis showed enrichment of oxidation reduction and neural signaling pathways in the Deprenyl group, whereas Bev combinations were associated with inhibited Wnt signaling and activation of the CDX pathway which is associated with the upregulation of CDX1/2 gene that plays a crucial role in the development and maintenance of the intestinal epithelium.
Conclusion: MAO B inhibition modulates key oncogenic, apoptotic, and angiogenic pathways in CRC tumors. Combination treatment with Bev amplifies tumor-suppressive gene expression and attenuates pro-angiogenic signaling, highlighting the therapeutic potential of MAO B inhibitors as complementary agents in CRC treatment strategies.

#2106 High-throughput and accurate intrasplenic injection in mice for metastatic cancer modeling using a robotic injection device.

Alexis Stanley, James Tseng, Ryan Gessner, **Tomasz J. Czernuszewicz**, Jeffrey D. Peterson

Revvity, Waltham, MA

Intrasplenic injections represent a critical technique for establishing metastatic cancer models, particularly for hepatic metastases from colorectal, pancreatic, and gastric cancers. However, traditional intrasplenic injection methods have distinct challenges: blind percutaneous approaches suffer from targeting inaccuracy and variable outcomes, while surgical methods, though more precise, significantly increase procedural complexity and limit experimental throughput. Ultrasound-guided percutaneous injection combines the reproducibility of surgical visualization with the efficiency of minimally invasive delivery. To this end, we have developed a standardized protocol using the Revvity VivoJect (VJ) instrument to enable precise, high-throughput intrasplenic cell delivery in mice. The VJ platform combines real-time ultrasound imaging with motor-controlled needle positioning for accurate target identification and injection. To demonstrate feasibility of spleen injection with VJ, a pilot study was conducted comparing percutaneous (N=7) and surgical (N=5) spleen injections in nude mice. For the percutaneous group, mice were sedated with isoflurane, positioned in right lateral recumbency, coupled to the VJ transducer with ultrasound gel, and injected using ultrasound guidance to identify the spleen. Mice received 50 µL injections of HT-29-RedF-Luc human colorectal adenocarcinoma cells (1×10^6 cells) mixed with IVISense 750 fluorescent tracer. The FLI tracer was used for ex vivo confirmation of injection delivery, while Luc-tagged cells were used for in-vivo tracking of metastasis. For traditional surgical group, anesthetized mice underwent mini-laparotomy to expose the spleen for direct injection of the same cancer cell suspension, followed by surgical staple closure and standard post-operative monitoring. Injection accuracy was confirmed through immediate ex vivo fluorescent imaging (FLI) in a small subset of mice (N=2) and subsequent bioluminescence (BLI) monitoring. VJ achieved 100% successful percutaneous intrasplenic delivery across all test animals, as confirmed by FLI tracer localization and absence of peritoneal spillage. Day 4 in vivo BLI demonstrated successful establishment of hepatic metastases in all injected mice, with consistent tumor burden distribution to the surgical group. VJ reduced procedure time to under 5 minutes per animal with immediate animal recovery and no adverse effects. These results suggest VJ can transform intrasplenic injection from a technically challenging, low-throughput invasive surgical procedure into a reproducible, high-efficiency method suitable for large-scale metastasis studies. This advancement enables more robust preclinical evaluation of anti-metastatic therapies and biomarker validation in clinically relevant models of hepatic metastasis from gastrointestinal cancers.

#2107 Genomic landscape of melanoma brain metastases: Real-world analysis and comparison with public melanoma cohorts.

Dina Elantably[1], **Joseph B. Parker**[1], Jakob Hamilton[1], Ahmed Abdelhakeem[1], Oluwatayo Adeoye[1], Saivaishnavi Kamatham[1], Winston Tan[1], Arkadiusz Z. Dudek[2], Anastasios Dimou[2], Matthew S. Block[2], Robert McWilliams[2], Svetomir Markovic[2], Mahesh Seetharam[3], Roxana Dronca[1], Ruqin Chen[1]

[1]Mayo Clinic Comprehensive Cancer Center, Jacksonville, FL,[2]Mayo Clinic Comprehensive Cancer Center, Rochester, MN,[3]Mayo Clinic Comprehensive Cancer Center, Phoenix, AZ

Background: Melanoma brain metastases (MBM) represent a biologically distinct and clinically aggressive subset of melanoma. Comprehensive molecular characterization focused on intracranial disease remains limited. We aimed to define the genomic landscape of MBM and compare these findings with public melanoma datasets.
Methods: We retrospectively identified 166 patients with histologically confirmed MBM across Mayo Clinic tri-sites (2011-2025). Molecular testing was performed in 123 patients (74.1%). Comprehensive next-generation sequencing (NGS; ≥300-gene platforms including Tempus, FoundationOne, Caris, NeoGenomics, and MayoComplete Solid Tumor Panel) was available in 41 patients (24.7%). Intermediate-depth profiling using the MayoComplete Melanoma Panel (17 genes) was performed in 21 patients (12.7%), and a targeted 5-gene melanoma driver panel (BRAF, NRAS, KIT, GNAQ, GNA11) in 52 patients (31.3%). cfDNA-based NGS was available in 12 patients (7.2%). Genomic alterations were summarized and benchmarked against TCGA-SKCM and MSK-IMPACT datasets via cBioPortal. We considered assay heterogeneity, as Mayo panels varied in sequencing depth and CNV coverage, and hybrid-capture platforms often under-detect TERT promoter hotspots.
Results: Patients had a median age of 67 years, and 63% were male. BRAF mutations occurred in 48.8% (BRAF V600E/K 41.6%; non-V600 7.2%). Additional MAPK alterations included NRAS (17.5%), KIT (5.4%), GNAQ (1.2%), and GNA11 (0.6%). In the comprehensive NGS subset, tumor-suppressor alterations included CDKN2A (17.5%), PTEN (7.8%), NF1 (9.0%), TP53 (8.4%), and TERT promoter mutations (22.9%). Median TMB was 11.55 mut/Mb (IQR 5.0-25.5). Co-alterations included BRAF+CDKN2A (7.2%), BRAF+PTEN (4.2%), NRAS+CDKN2A (4.2%), NRAS+PTEN (1.2%), and CDKN2A+PTEN (3.6%); overall, 18.1% harbored MAPK driver + tumor-suppressor co-alterations. Compared with TCGA and MSK cohorts, MBM showed similar MAPK driver frequencies but fewer MAPK + tumor-suppressor co-alterations and lower CDKN2A, PTEN, and TP53 disruption, alongside a more prevalent of TERT promoter mutations (22.9% vs 7% and 2.1%), which may partly reflect coverage differences.
Conclusion:MBM exhibit a distinct genomic profile characterized by reduced tumor-suppressor loss, fewer MAPK-tumor-suppressor co-alterations, and higher prevalence of TERT promoter mutations. While assay heterogeneity limits direct cross-cohort comparisons, these patterns suggest potentially distinct biological features of intracranial melanoma and underscore the need for harmonized, MBM-specific molecular studies to guide therapeutic development.

#2108 Proteomic insights into metastatic small cell lung cancer using patient derived xenograft models.

Sara Surguta[1], Laura Svajda[2], Zsolt Megyesfalvi[3], Bence Ferencz[3], Ildiko Kovacs[3], Vivien Teglas[3], Lilla Horvath[3], Szilvia Torok[3], Balazs Dome[3], Melinda Rezeli[4], Jozsef Tovari[1]

[1]National Institute of Oncology, Budapest, Hungary,[2]KINETO Lab Ltd., Budapest, Hungary,[3]National Koranyi Institute of Pulmonology, Budapest, Hungary,[4]BioMS Swedish National Infrastructure for Biological Mass Spectrometry, Lund, Sweden

Small cell lung cancer (SCLC) is one of the most aggressive solid malignancies with limited treatment options. Access to clinically relevant SCLC tissue is restricted because surgical resection is rare in metastatic disease, making this cancer type difficult to study. Through our multicenter rapid research autopsy (RRA) program, however, we are able to collect not only primary tumors but also multiple metastatic lesions, providing a unique and rare collection of SCLC specimens. In this program, rapid autopsies are performed within four hours after death to ensure optimal tissue quality for downstream analyses. In the current project, we analyzed samples from seven patients with histologically confirmed SCLC, including clinical and metastatic lesions, as well as their corresponding patient-derived tumor xenografts (PDTXs) serially passaged through three generations. To assess whether the original tissue architecture and intratumoral heterogeneity are preserved across PDTX generations, we performed immunohistochemical and proteomic analyses, comparing molecular profiles between the original tumors and their corresponding PDTX models. A subset of SCLC clinical specimens, including matched PDTX-clinical pairs, confirmed that the histologic landscape of the tumors of origin is preserved in the derivative PDTX models. Samples were grouped by patient and anatomical site, and pairwise Pearson correlations of global protein abundance profiles were computed within each group. The mean within-lineage correlation was high (typically >0.8), and correlation heatmaps showed tight clustering across PDTX generations from the same lineage. Across all patients, the only pathways consistently and significantly downregulated in PDTX models compared with the original tumors were the ECM-receptor interaction and Complement and Coagulation Cascade pathways. When analyzing metastatic PDTX samples, we compared liver and lymph node metastases with their corresponding primary patient tumors across PDTX generations. In lymph node metastases, proteins involved in ECM-receptor interaction and EMT pathways were upregulated. In contrast, liver metastases showed upregulation of fatty acid metabolism and peroxisome proliferator-activated receptor signaling pathways, with downregulation of EMT, ECM-receptor interaction, E2F targets, and G2M checkpoint. These findings demonstrate that the proteomic identity of SCLC tumors is largely preserved during serial passaging in PDTX models, while site-specific adaptations emerge in distinct metastatic microenvironments.

#2109 Analysis of collagen architecture in brain metastasis and paired primary tumors in Non-small cell lung cancer supports the recruitment of fibroblasts originating outside the brain.

Jordi Alcaraz[1], Alejandro Bernardo Suarez[1], Gabriela Caballero[2], Patricia Fernandez-Nogueira[1], Marc Rico-Pasto[1], Victoria Batto[1], Iban Aldecoa Ansorregui[2]

[1]Universitat de Barcelona, Barcelona, Spain,[2]Clinic Barcelona, Barcelona, Spain

Lung adenocarcinoma (LUAD) is the most common subtype of non-small cell lung cancer (NSCLC) and frequently metastasizes to the brain. Lung brain metastases arise in a microenvironment that is structurally and mechanically distinct from the collagen-rich, highly desmoplastic stroma of primary LUAD tumors, which is driven by the chronic activation of cancer-associated fibroblasts (CAFs). In contrast, the normal brain lacks fibroblasts and is virtually devoid of fibrillar collagens. Although recent work suggests that disseminated tumor cells may co-travel with fibroblasts to recreate a primary tumor-like stroma at metastatic sites, the extent to which LUAD brain metastases recapitulate the fibrotic landscape of the primary tumor remains poorly defined. We retrospectively analyzed collagen architecture and common markers of immunosuppressive CAF phenotypes in LUAD patient samples, including primary tumors, paired brain metastases (n=17), and normal brain tissue from epilepsy patients (n=5). Collagen organization was assessed by picrosirius red staining, polarized light microscopy, and quantitative extraction of collagen fiber descriptors using CT-FIRE (Almici et al., Mod Pathol 2023). As expected, collagen fibers were virtually absent in normal brain. In contrast, LUAD brain metastases displayed prominent fibrillar collagen deposition. However, collagen architecture differed substantially from that of primary tumors, with brain metastases exhibiting fewer, shorter, and less aligned fibers. To explore whether EMT contributes to collagen production, LUAD cells and normal pulmonary fibroblasts were stimulated with TGF-β1. Although TGF-β1 increased vimentin and fibrillar collagens in cancer cells, their levels remained substantially lower than in activated fibroblasts. Consistently, brain metastases contained numerous elongated, fibroblast-like stromal cells expressing α-SMA but not markers of activated astrocytes and pericytes, supporting a fibroblast origin. Our findings demonstrate for the first time that LUAD brain metastases develop a fibrotic stroma characterized by de novo collagen deposition driven by fibroblast-lineage cells originating outside the brain, rather than by cancer cells undergoing EMT. These results indicate that collagen-rich fibrosis is a defining feature of the LUAD metastatic niche in the brain and may influence immune cell localization, tumor progression, and therapeutic response. Ongoing studies are examining CAF heterogeneity and functional differences between primary tumors and brain metastases.

#2110 Characterizing drivers of invasiveness in basal-like triple negative breast cancer.

Perrin Black[1], Destiny Ball[1], Antonisha McIntosh[1], Alayjha Edwards[1], Sewedo Ajisegiri[1], Nobelle I. Sakwe[1], Ngoc Vuong[1], Olga Korolkova[2], Qingguo Wang[2], Amos M. Sakwe[3]

[1]Biomedical Sciences, Meharry Medical College, Nashville, TN,[2]Meharry Medical College, Nashville, TN,[3]Assistant Professor, Cancer Biology, Meharry Medical College, Nashville, TN

PURPOSE: Triple-negative breast cancer (TNBC) is characterized by aggressive tumor growth, resistance to treatment, higher likelihood of relapse, and overall worse prognosis when compared to other breast cancer subtypes. The TNBC tumor microenvironment is molecularly heterogeneous, containing various numbers of rapidly growing basal-like (BSL), and invasive mesenchymal-like (MSL) stromal and TNBC cells. Annexin A6 (AnxA6) is a multifunctional calcium-dependent scaffolding protein that is highly expressed in MSL TNBC cells but expressed at low levels in BSL TNBC, and is implicated in cell proliferation, motility, and drug resistance. It is currently unclear how altered AnxA6 levels influence the invasiveness of MSL and BSL TNBC cells. We hypothesize that altered expression of AnxA6 differentially contributes to the invasiveness of BSL and MSL TNBC subgroups.
METHODS: Short hairpin RNAs were used to downregulate AnxA6 in parental (PAR) subpopulations of model MSL (BT-549) and BSL (MDA-468) TNBC cell lines. The invasive subpopulations (INV) of these cell lines with or without AnxA6 downregulation were isolated from control and AnxA6 downregulated cells by sequential invasion assays in Boyden chambers. The parental and invasive subpopulations were then assessed for markers of invasiveness, cancer stem cell (CSC) expression, drug sensitivity, oncoprotein expression, and differential gene expression.
RESULTS: Invasiveness increased AnxA6-dependently in BSL TNBC INV subpopulations compared to the PAR population. Sensitivity to doxorubicin was decreased in the INV subpopulations of both MSL and BSL TNBC. Flow cytometry revealed an increase in CD49f+/EpCAM+ CSC expression among BSL TNBC INV subpopulations. Carbonic anhydrase IX (CA9) was found upregulated only in the INV subpopulations of BSL TNBC, and that downregulation of CA9 results in decreased invasiveness and viability within BSL TNBC INV subpopulations. RNA sequencing and RT-qPCR validation has revealed an upregulation of *EDN2* and *PDXN* among INV BSL TNBC subpopulations, while *BIRC3* and *PARP9* were found to be upregulated in MSL TNBC INV subpopulations.
CONCLUSION: Our data suggest that the invasive subpopulations of both TNBC subgroups differentially modify key oncogenes with respect to their parental controls. Altered AnxA6 expression is associated with differential invasive potential and sensitivity to chemotherapy for MSL versus BSL TNBC cells. Sequential invasion assays have successfully isolated invasive subpopulations that upregulate TNBC subgroup-dependent biomarkers. Targeting the upregulated genes and proteins identified in this study may yield promising results in the future for treating TNBC metastatic disease.

#2111 Mapping immuno-vascular signatures to characterize blood brain barrier disruption and tumor colonization in triple negative breast cancer brain metastasis..

Shruti Rodrigues[1], Maria Jose Godoy Calderon[2], Manali Patwardhan[2], VK Gadi[3]

[1]College of Medicine, University of Illinois at Chicago, Chicago, IL,[2]Medicine, University of Illinois at Chicago, Chicago, IL,[3]Hematology/Oncology, University of Illinois at Chicago, Chicago, IL

Introduction: The incidence of brain metastases in breast cancer patients is rising, with brain metastases affecting 25-40% of women with triple-negative breast cancer (TNBC), with a median survival of under six months. Disruption of the blood-brain barrier (BBB) leads to the formation of a blood-tumor barrier (BTB), which is a critical event in brain colonization. We hypothesize that metastatic tumor cells disrupt neurovascular integrity via specific molecular mechanisms, thereby enabling BTB formation. Elucidating the molecular mechanisms and key players underlying TNBC brain tropism—focusing on BBB disruption and immune evasion— will help identify and manipulate key players in this metastatic process, offering potential for preventing or reversing colonization.

Methods: We performed bulk RNA sequencing to compare brain-tropic 4T1-Br5 cells with parental 4T1 cells and characterized the transcriptional programs supporting brain adaptation. We also established a dual-phased *in vivo* injection model (orthotopic mammary fat pad injection (MFP) followed by intracardiac injection (IC) 7 days later) to obtain BrM tissue for spatial analysis.

Results: For the *in vivo* study, 10 mice got hybrid injections of 4T1-Br5 cells; however, only 5 mice survived to the endpoint. Robust, histologically confirmed brain metastases were detected in 1 of 5 mice (20%). This rate aligns with literature reports and also highlights modeling challenges in immunocompetent settings. RNA-seq showed upregulation of cell cycle drivers (MYC,E2F) and DNA repair pathways, indicating rapid proliferation and genomic resilience. altered BRCA1/TP53 balanced instability with survival often observed with aggressive metastasis. Adaptive pathways for brain colonization, including neuronal signaling (via NGFR-BDNF), cytoskeletal remodeling, and ESR1 activation, exhibited distinct upregulation. Immune-evasive signatures were characterized by the reduced expression of IL-1β, IFN-γ, as well as impaired antigen presentation (MHC I/II), and the activation of CCL5 and the complement cascade. As expected with brain vasculature remodeling, angiogenesis/vascular markers, such as VEGF, HCN, and BGN, were upregulated, while THBS2 and NOTCH signaling were downregulated.

Conclusion: Overall, the brain-tropic 4T1-Br5 cells exhibit a coordinated reprogramming of proliferation, immune evasion, angiogenesis, epigenetic plasticity, and neuronal mimicry pathways, collectively empowering them cells to overcome the unique barriers of the brain, thus supporting their metastatic growth. This establishes a strong scientific foundation for identifying actionable targets for therapeutics. I*n vivo* model dose optimization will yield more consistent brain metastases, enabling a comparative spatial analysis of mouse tissue with patient-derived tissue samples.

#2112 Image activated cell sorting reveals distinct morpholomic manifolds in breast cancer cell lines.

Andres Jose Nevarez[1], Lan Zheng[2], Songyun Li[2], Nicholas E. Navin[1]

[1]Systems Biology, UT MD Anderson Cancer Center, Houston, TX,[2]Graduate School of Biomedical Sciences , UT MD Anderson Cancer Center, Houston, TX

Background: Breast cancer progression is driven by genomic alterations that fundamentally reshape cellular architecture. However, the specific mapping between genomic drivers and the resulting quantitative morphological phenotype—the "morpholome"—remains poorly understood. We hypothesize that distinct breast cancer subtypes occupy unique, stable morphological "attractor states" defined by high-dimensional features invisible to standard microscopy, and that this morpholome is a direct, quantifiable readout of underlying genomic identity.

Methods: To decode these morpholomic states, we established a multimodal, high-throughput imaging pipeline applied to a controlled model system of three genetically distinct breast cancer cell lines: MCF10A (normal-like), SKBR3 (HER2+), and MDA-MB-231 (TNBC). We generated a massive dataset of single-cell images using two complementary platforms: (1) DeepCell for high-resolution, label-free brightfield structural analysis, and (2) BD FACSDiscover S8 for multi-channel, image-based flow cytometry to capture molecularly-defined morphological features. We then extracted deep, self-supervised (DINOv3) features from >150,000 single cells to construct a high-dimensional morpholomic atlas.

Results: Our analysis revealed that genomic identity dictates a robust and quantifiable morphological manifold. (1) **Distinct Attractor States:** In latent space analysis (PHATE), each cell line occupied a distinct, non-overlapping morphological manifold, confirming that the "morpholome" faithfully captures subtype-specific genomic differences without the need for molecular labels. (2) **Robust Biological Signal:** This morphological separation was highly robust, with independent biological replicates of the metastatic MDA-MB-231 line showing near-perfect overlap in feature space (e.g., Area, Intensity SD, Elongation), demonstrating that these are stable biological properties rather than technical artifacts. (3) **Intra-line Heterogeneity:** Crucially, we resolved distinct morphological sub-clusters within the clonally derived MDA-MB-231 population, suggesting that even isogenic cancer populations fluctuate between distinct morphological states that may correspond to functional plasticity.

Conclusions (Future Directions): These findings establish the single-cell morpholome as a powerful, high-dimensional biomarker of breast cancer cell state. Having validated that genomic subtypes drive distinct morphological manifolds in cell lines, we are now applying this framework to patient samples. Our next steps will utilize this approach to identify the specific "morpho-genomic metaprograms" that drive metastasis, using generative AI to causally link these subtle morphological shifts to their genomic drivers in primary tumors.

#2113 Optical imaging and digital pathology evaluation increases the translational value and robustness of patient-derived metastatic breast cancer models.

Philipp Meyer[1], Laura Neagu-Lund[2], Eva Oswald[1], Aleksandra Zuraw[3], Loreen Weichert[1], Michael Staup[4], **Julia B. Schueler**[1]

[1]Charles River Laboratories, Freiburg, Germany,[2]Charles River Laboratories, Laval, QC, Canada,[3]Charles River Laboratories, Reno, NV,[4]Charles River Laboratories, Wilmington, MA

Breast cancer remains the most prevalent malignancy among women and a leading cause of cancer-related death, primarily due to metastatic progression. Reliable preclinical models that recapitulate the metastatic cascade are essential for understanding disease mechanisms and evaluating novel therapies. Traditional methods, while informative, often lack the sensitivity and dynamic resolution needed to track metastatic spread *in vivo*. This study demonstrates the utility of integrating *in vivo optical* digital image analysis with *histopathological* digital image analysis to enhance the detection, characterization, and translational relevance of patient-derived xenograft (PDX) models of metastatic breast cancer. The metastatic potential of three breast cancer models first was classified *in-vitro* using two assays: 2D scratch wound and 3D spheroid invasion. Next, five PDX models, composed of two Her2+(1162, 1322) and three triple negative models (401, 857, 1387), were developed and evaluated for spontaneous *in-vivo* metastasis in mice. The breast cancer cell line MDAMB231 served as positive control. To enable in vivo tracking, tumor cells were infected with a fluorescent reporter or a bioluminescent reporter (luciferase) and visualized using optical imaging systems (IVIS Lumina S5 and Licor Pearl). In the in-vitro assays, MDAMB231, MCF-7, and 401 (triple negative PDX) were classified as high, low, and non-metastatic respectively. In the in-vivo lung metastasis assay, two triple negative models (401, 1387) and one HER2+ model (1387) were classified as low-metastatic. The other triple negative model (1162) and HER2+ model (1162) displayed no metastases at all. Unfortunately, it was not possible to create a PDX with a reporter that was stably expressed because the reporters reduced with passages over time. However, these results demonstrate that transient transfection is a promising tool to follow tumor growth in vivo. Finally, the organs were harvested, and metastases were evaluated via histology (H&E) and human-specific immunohistochemistry (IHC, hLaminB1). The hLaminB1+ metastasis were quantified by digital image analysis (DIA) using the Visiopharm software. MDAMB231 metastasized mainly to the lung and to a lower extend to the liver and the brain. Its metastatic level was much higher than all the PDXs, reflecting the aggressive growth of the cell line. The DIA provided a robust interpretation of the PDX models, illustrating that this integrated workflow supports the selection and quantification of metastatic models, with applications in therapeutic testing and mechanistic studies.

#2114 Murinemodels of bone and brain metastasis for preclinical cancer research.

Hongyan Sun, Fang Zhu, Yan Wang, Yuan Fang, Yuqing Han, Jianming Xu, Huixin Yang, Xiang Gao

GemPharmatech Co., Ltd., Nanjing, China

Tumor metastasis remains a daunting challenge in cancer treatment and is a major driver of poor prognosis and therapy resistance. Despite remarkable advances in oncology, effective therapies for metastatic disease remain scarce—highlighting an urgent need for clinically relevant preclinical models to dissect metastasis mechanisms and validate anti-metastatic strategies. To bridge this gap, we developed robust mouse models of bone and brain metastasis that faithfully recapitulate clinical metastatic progression. For the bone metastasis model, MDA-MB-231-Luc human breast cancer cells were injected into the left ventricle of immunodeficient mice via ultrasound-guided intracardiac injection. Through in vivo selection, we derived a subclone with enhanced metastatic potential that preferentially colonizes the spine and lower limb bones. This model recapitulates key clinical hallmarks of bone metastasis—including tumor-mediated bone destruction and osteolytic lesions—with tumor colonization confirmed via bioluminescence imaging (BLI). For the brain metastasis model, LLC1-Luc lung cancer cells were injected into the common carotid artery to enable direct dissemination to the brain. Bioluminescence imaging demonstrated progressive tumor colonization over time, and this model provides a valuable platform to dissect brain metastasis mechanisms and test novel therapeutic strategies targeting central nervous system (CNS) metastases. Collectively, these models offer clinically relevant platforms to investigate metastasis mechanisms, identify therapeutic targets, and discover novel biomarkers. Furthermore, we generated a panel of luciferase-labeled cancer cell lines to facilitate advanced metastasis research. Our preclinical models accurately recapitulate the metastatic cascade, serving as a translational bridge for drug discovery, therapeutic validation, and biomarker development—ultimately accelerating the translation of next-generation cancer therapeutics into the clinic.

#2115 Development of the cf-MMSP assay for enhanced detection of methylated cfDNA in breast cancer by liquid biopsy.

Liqun Zhang, Wenfei Xia, Mary Jo Fackler, Gang Yu, Madison Pleas, Leslie Cope, Saraswati V. Sukumar

Johns Hopkins University School of Medicine, Baltimore, MD

Background: While mammography remains a standard screening tool for breast cancer, its high false positive rate and invasiveness of subsequent biopsies highlight the need for improved technologies. Liquid biopsy, leveraging circulating cell-free DNA (cfDNA), offers a noninvasive alternative, yet the low levels of cfDNA in blood demand highly sensitive detection techniques. In this study, we sought to improve our two-step lab assay, cMethDNA (1), by testing three commercial DNA isolation kits, and through innovative use of primer combinations to specifically enrich for methylated cfDNA in blood.
Methods: Circulating cfDNA was isolated using three kits: QIAamp MinElute Virus Spin Kit (Virus kit), QIAamp MinElute ccfDNA Mini Kit (ccfDNA kit), and MAGicBead cfDNA Isolation Kit. A 9-gene panel consisting of AKR1B1, COL6A2, HIST1H3C, HOXB4, RASGRF2, RASSF1A, TM6SF1, TMEFF2, and ZNF671 (2) was amplified using bisulfite-converted DNA and optimized primer combinations in a cell free, multiplexed, methylation-specific PCR (cf-MMSP) assay. Technical validation of the assay was performed with normal plasma spiked with 12.5-50 copies of fully methylated human genomic DNA and 10 copies of STDHOXB4 plasmid. We quantified relative methylation levels for each gene, and cumulative methylation (CM) of all 9 markers in each sample. The cf-MMSP assay was validated in a pilot study of plasma samples from 21 stage IV breast cancer patients and 20 healthy controls or women with benign disease.
Results: The Virus Spin kit outperformed the MAGicBead and ccfDNA kits in cfDNA recovery, showing a significant improvement in the detection of STDHOXB4 reference DNA ($p < 0.0001$ vs. MAGicBead). Using a combination of a methylation-agnostic (ExtF) and a methylation sequence-specific primer (IntMR) set in the first multiplex PCR step significantly reduced Ct values of target genes (median 17.9 vs. 19.8, $p = 0.0001$) and STDHOXB4 (median 16.8 vs. 18.8, $p < 0.0001$), enhancing detection sensitivity by at least 4-fold compared to cMethDNA. In clinical samples, the cf-MMSP assay distinguished stage IV breast cancer patients from controls with 86% sensitivity (95% CI = 65.4-95.0) and 90% specificity (95% CI = 69.9-98.2), achieving an area under the curve (AUC) of 0.8929 ($p < 0.0001$).
Conclusions: The cf-MMSP assay, which included the use of the Virus kit for cfDNA isolation, choice of primers that selectively amplified methylated products, and a single STDHOXB4 standard, significantly reduced assay cost and time and enhanced its sensitivity for detecting methylated cfDNA in plasma from breast cancer patients.
Reference: 1) Fackler et al, PMID: 24737128. 2) Fackler et al, PMID: 36046124.

#2116 Genomic landscape of 1007 pan-cancer brain metastases.

Ramzi Homsi[1], Henry Walch[1], Roshal Patel[1], Anna Skakodub[1], Emily Miao[1], James Lee[1], Chengcheng Gui[1], Mitchell Parker[1], Zachariya Yazdani[1], Michel A. Padilla Mazzeo[1], Claire Cooper[1], Kyle Sporn[1], Brandon Imber[1], Yao Yu[1], Jessica Wilcox[1], Nelson Moss[1], Ahmet Turan Ilica[2], Rabih Bou-Nassif[1], Joseph Stember[1], Christopher Jackson[1], Connor Kinslow[1], Gustav Cederquist[1], Caleb Lareau[1], Helena A. Yu[1], Soo Ryum Yang[1], Pedram Razavi[1], Joseph Chan[1], Kenny Kwok Hei Yu[1], Walid Khaled Chatila[1], Nikolaus Schultz[1], Luke R. G. Pike[1]

[1]Memorial Sloan Kettering Cancer Center, New York, NY,[2]University of Miami, Miami, FL

Background: The pan-cancer genomic landscape of brain metastases (BM) has not been well-characterized. Herein, we evaluate genomically profiled BM tumor samples and additional sequenced tumor samples from other sites to further understand disease evolution.

Methods: We analyzed BM specimens from 1007 patients who underwent craniotomy between 2014 and 2024. Targeted sequencing was performed with MSK-IMPACT, a next-generation sequencing assay which detects genomic alterations in up to 505 genes. The FACETS algorithm was used to estimate tumor purity, fraction of genome altered (FGA) and whole-genome duplication (WGD) status. We analyzed matched sample pairs from patients who had additional sequenced tumor samples resulting in 227 primary-BM (P-BM) pairs, 189 extracranial metastasis-BM (ECM-BM) pairs and 60 BM-BM pairs. One pair per patient was selected for each category based on maximum purity. For paired comparisons, the Wilcoxon signed-rank test was used to compare continuous features and McNemar's test was used to compare WGD, with Benjamini-Hochberg p-value adjustment. The Jaccard index was computed to assess mutational concordance between pairs. Private mutation analysis was limited to genes with driver mutations in >5 pairs in each P-BM/ECM-BM group.

Results: Median intracranial progression-free survival (iPFS) and overall survival (OS) from craniotomy were 11.3 and 25 months, respectively. The most frequent histologies in the cohort were non-small cell lung cancer (NSCLC; n = 360), breast (n = 181), and melanoma (n = 128). The genes with the highest proportion of oncogenic alterations were *TP53* (62.0%), *CDKN2A* (25.0%), *TERT* (23.4%), *KRAS* (19.7%), and *ERBB2* (12.3%). At least one structural variant or mutation was shared by 88.1% of P-BM pairs, 90.0% of ECM-BM pairs and 98.3% of BM-BM pairs. The mean number of shared driver mutations was 2.48 for P-BM pairs, 2.43 for ECM-BM pairs and 4.02 for BM-BM pairs. In a pan-cancer paired analysis, FGA, WGD and tumor purity were higher in BM in P-BM pairs ($q < 0.01$ for all) and in ECM-BM pairs ($q < 0.01$ for all). FGA and purity were higher in BM for P-BM pairs in upper gastrointestinal (GI) and NSCLC ($q < 0.01$), and in ECM-BM pairs for NSCLC ($q < 0.01$). By histology, in P-BM pairs, lower GI (n = 22) had the highest mean Jaccard index (J = 0.71) and prostate cancer (n = 10) had the lowest (J = 0.33), while in ECM-BM pairs melanoma (n = 23) had the highest (J = 0.77) and sarcoma (n = 9) had the lowest (J = 0.36). *TP53* was the most commonly mutated gene in both P-BM (n pairs = 147, shared proportion = 0.816) and ECM-BM pairs (n pairs = 111, shared proportion = 0.869). Mutations in *NFE2L2* and *KMT2B* were most commonly private to the BM in P-BM pairs (4/6 and 5/8 pairs with driver mutations private to BM, respectively), while *NF1* mutations were most often BM-private in ECM-BM pairs (4/7).

Conclusion: There is a high degree of concordance in alterations between P-BM and ECM-BM pairs. Alterations more commonly private to BM warrant further investigation.

#2117 Single cell chromatin accessibility profiling of human metastatic tumor cells.

Valentina Opazo-Mellado[1], Maria Jose Oviedo[1], Diego Figueroa[1], Carlos Perez[1], Laura Hernandez[1], Joanna Phillips[2], Jeroen Roose[3], **Hugo Gonzalez**[4]

[1]Tumor Microenvironment and Metastasis Laboratory, Centro Basal Ciencia & Vida, Fundacion Ciencia y Vida., Santiago, Chile,[2]Department of Neurological Surgery, University of California San Francisco, San Francisco, CA,[3]Department of Anatomy, University of California San Francisco, USA., San Francisco, CA,[4]Tumor Microenvironment and Metastasis Laboratory, Centro Basal Ciencia & Vida, Fundacion Ciencia y Vida; Universidad San Sebastian., Santiago, Chile

Metastasis is responsible for the vast majority of cancer deaths, yet the regulatory programs that enable metastatic tumor cells (MTCs) to survive, adapt, and expand in distant organs remain incompletely understood. Brain metastasis (BrM) is particularly lethal, marked by limited therapeutic options and profound resistance to existing treatments. Although chromatin accessibility orchestrates transcriptional states and cellular plasticity, its contribution to metastatic colonization has been largely unexplored.Here, we present the most comprehensive single-cell chromatin accessibility atlas of human BrM MTCs to date, spanning 15 metastases originating from diverse primary carcinomas. Following immune-cell depletion, nuclei were profiled using 10x Genomics single-cell ATAC-seq and analyzed with Cell Ranger ATAC, Signac, and Seurat, integrating inferred gene expression from published BrM datasets. We reconstructed gene regulatory networks (GRNs) with Pando to connect transcription factor activity, DNA accessibility, and downstream gene regulation.Across 49,907 high-quality single cells and 147,139 shared accessible peaks, we uncovered three dominant regulomes: two aligned with known inflammatory and proliferative programs, and a third non-proliferative, developmentally biased state not previously characterized in BrM or any other distant metastasis. We performed mechanistic validation of key markers from these modules, complemented by protein-level validation in human specimens. We also identified 22,242 conserved cis-regulatory elements (CREs), with 91% mapping to known human enhancers—yet with previously unknown implications for metastatic fitness. Notably, we discovered abundant CREs located in non-coding regions linked to developmental and mesodermal transcription factors, highlighting a core regulatory architecture underlying metastatic adaptation. This work provides an expansive reference map of the cis-regulatory landscape of human BrM and reveals previously unappreciated developmental regulatory circuits in MTCs, offering new avenues for therapeutic targeting in metastatic cancer.

#2118 Cell surface anchored ratiometric probes for heparan sulfate enable live cell bioimaging and suppression of cancer cell migraion.

Minwoo Jeong[1], Hyun Jung Hwang[2], Donghee Kang[2], Min-Ji kim[2], Lee Keun-Hyung[2], Jae-Seon Lee[1]

[1]Program in Biomedical Science and Engineering, Inha University, Incheon, Korea, Republic of,[2]Research Center for Controlling Intercellular Communication, Inha University, Incheon, Korea, Republic of

Heparan sulfate (HS) proteoglycans are essential molecular components of the cell surface glycocalyx that play critical roles in tumor growth, cell migration, and cancer invasion. Despite their biological significance, the development of fluorescent probes capable of selectively and quantitatively visualizing HS in live cells has been highly challenging due to poor water solubility, limited cell-surface retention, and insufficient molecular selectivity. Here, we synthesized a rationally designed peptide-based fluorescent probe (probe 2) that selectively binds to HS on live cell membranes. This probe exhibits prolonged membrane localization and produces a distinct ratiometric fluorescence response. Under physiological conditions, probe 2 achieves stable anchoring on the cell surface and enables quantitative detection of HS through red-shifted emissions upon aggregation. Importantly, this probe allows real-time visualization of HS downregulation in live cells following siRNA-mediated gene silencing or chemical inhibition of HS biosynthesis. Moreover, probe 2 significantly inhibited cell migration and wound healing in vitro, suggesting that HS modulation by the probe may influence tumor-associated cellular behaviors. Collectively, this study introduces a new class of membrane-anchored fluorescent probes that enable dynamic and quantitative imaging of HS in live cells. These findings suggest that probe 2 is both a diagnostic imaging tool for heparan sulfate and a molecular modulator of HS-related cancer biology, with potential implications for cancer research and therapeutic development.

#2119 Spatial gene expression profile of primary tumor is associated with the release of aggressive CTCs from the invasive front, leading to early recurrence in OSCC.

Geeta S. Boora[1], Anshika Chauhan[1], Suvradeep Mitra[2], Arindam Maitra[3], Sushmita Ghoshal[4], Arnab Pal[1]

[1]Biochemistry, Postgraduate Institute of Medical Education & Research (PGIMER), Chandigarh, India, Chandigarh, India,[2]Histopathology, Postgraduate Institute of Medical Education & Research, Chandigarh, India,[3]BRIC-NIBMG, Kalyani, India,[4]Radiotherapy, Postgraduate Institute of Medical Education & Research (PGIMER), Chandigarh, India

Background Oral squamous cell carcinoma (OSCC) exhibits high incidences of relapse and treatment failure. To understand the molecular mechanisms driving these poor outcomes, we explored the spatial and temporal heterogeneity of primary tumors and their circulating tumor cells (CTCs) using whole transcriptome analysis.

Methods Bulk RNAseq was performed on three tumor regions (T1-invasive front, T2, T3) and the tumor-free margin (TFM) from early (EarlyR) and no recurrence till 2 years (NoR) patients (N=5 per group). Ultra-low cell RNAseq of CTCs was performed at diagnosis and at post-therapy/recurrence. Differential gene expression analysis and pathway enrichment using fgsea and clusterProfiler, with the Hallmark and Reactome databases, were performed to identify biologically relevant genes/pathways.

Results Spatially distant tumor regions of EarlyR patients were highly diversified from their adjacent free margin in comparison to the NoR group, as indicated by a significantly high number of DEGs - T1 vs TFM (EarlyR-2969, NoR-23), T2 vs TFM (EarlyR-4220 vs NoR-50), and T3 vs TFM (EarlyR-3883 vs NoR-1239). We ruled out that these increases in DEGs were not due to differences in TFMs of the EarlyR and NoR groups (DEGs-17). The pathway analysis revealed enrichment of metastasis-related pathways, including EMT, TNFA signalling via NFκB, and ECM remodelling, in the T1-invasive front of the EarlyR tumor, while the other regions(T2/T3) showed enrichment of proliferation-related pathways, indicating that the invasive front -T1 might be the source of release of aggressive CTCs. We identified SERPINE1, BMP2, CXCL10, CXCL11, ICAM1, IFIH1, IFIT2, IL15, IL15RA, IRF1, JUNB, TGFB1, and TNC as hub genes across multiple pathways enriched in T1, which may contribute to the aggressiveness of this tumor region. Among these genes, IFIT2, IRF1, and JUNB were also upregulated in baseline CTCs of the EarlyR group, indicating the importance of tracking these genes as markers of aggressive CTCs. The PCA analysis of CTC data revealed that, although baseline CTCs are transcriptomically similar between the EarlyR and NoR groups, the post-therapy CTCs are more evolved in the EarlyR group than in the NoR group. We also identified a key molecular marker, FNBP1L, overexpressed in the tumor invasive front (T1) of EarlyR and in their CTCs at pretherapy and posttherapy. However, FNBP1L was downregulated in other regions of the primary tumor (T2/T3), suggesting that aggressive CTCs originate primarily from the invasive front, and FNBP1L (implicated in cytoskeletal reorganisation) might be a key player driving early recurrence and metastasis.

Conclusion OSCC tumors from EarlyR patients undergo extensive spatial and temporal transcriptomic evolution, and the invasive front is plausibly involved in the release of aggressive CTCs marked by expression of IFIT2, IRF1, JUNB, and FNBP1L.

#2120 Spatially resolved transcriptomic analysis revealed the molecular characteristics of the worst pattern of invasion in oral squamous cell carcinomas.

Seungeun Lee[1], Yeonbi Han[2], Dohoon Kim[3], Sumin Lee[3], Amos Chungwon Lee[3], Wonjae Cha[4], Jin-Ku Lee[5]

[1]Biomedical Sciences, Seoul National University, Seoul, Korea, Republic of,[2]Seoul National University Bundang Hospital, Gyeonggi-do, Korea, Republic of,[3]Meteor Biotech, Seoul, Korea, Republic of,[4]Otorhinolaryngology-Head & Neck Surgery, Seoul National University Bundang Hospital, Seoul, Korea, Republic of,[5]Department of Anatomy and Cell Biology, Department of Biomedical Sciences, Seoul National University, Seoul, Korea, Republic of

Worst pattern of invasion (WPOI), defined by the presence of dispersed satellite nodules ≥1 mm from the primary tumor, is strongly associated with LNM; however, the molecular features that functionally link invasive histopathology to metastasis are not fully characterized. We aimed to elucidate the relationship between histopathology invasion pattern and metastatic progression at the molecular level, and to determine whether invasion patterns share early metastatic features. Accordingly, we performed full-length single-cell mRNA sequencing using Spatially resolved Laser Activated Cell Sorting (SLACS), which isolates regions of histologically interest from Hematoxylin and Eosin (H&E) stained tissue slides and obtains transcriptomic and genomic while preserving pathological context. A total of 849 spatially annotated regions of interest (5-10 cells/ROI) were captured from matched tumor, WPOI, tumor-stromal interface, and lymph node metastasis sites from five OSCC patients. Integration of single-cell transcriptomic and genomic features revealed heterogeneous tumor characteristics associated with distinct pathological patterns. We identified a WPOI-associated malignant subpopulation (Cluster 2) characterized by upregulation of IQCE and SMPD2 and an elevated partial epithelial-to-mesenchymal transition (p-EMT) phenotype, indicative of invasive plasticity. In contrast, LNM-enriched populations exhibited re-acquisition of epithelial differentiation programs, including increased expression of CRNN and SPRR3, suggesting epithelial resurging following metastatic colonization. These findings support a dynamic invasion-metastasis continuum in OSCC, especially WPOI represents an intermediate state enabling metastasis in molecular level. We are ongoing reconstruct the evolutionary trajectories. A molecular understanding of pathological invasion patterns such as WPOI may inform precision stratification and guide personalized surgical and adjuvant strategies for OSCC patients.

#2122 Integrative transcriptomic analysis identifies malaria-associated signaling pathways and repurposable drug candidates for ovarian cancer metastasis.

Dr. Muhibullah Ghafoorzai[1], Arsalan Riaz[2], Dr. Faisal F. Khan[1]

[1]Precision Medicine Lab, Peshawar, Pakistan,[2]Centre for Genomics Sciences, Rehman Medical Institute, Peshawar, Pakistan

Ovarian cancer metastasis remains a leading cause of cancer-related mortality and presents major challenges for effective therapy. This study aimed to identify pivotal genes, proteins, and pathways involved in ovarian cancer metastasis and to explore already approved drugs with potential to inhibit these metastatic mechanisms through a drug repurposing framework. A comparative in silico analysis was conducted using transcriptomic data from matched primary and metastatic ovarian tumors. In Phase 1, gene expression profiles from three microarray and four RNA-sequencing datasets were analyzed using R (v4.3.1) to identify differentially expressed genes (DEGs). In Phase 2, pathway enrichment and protein–protein interaction analyses were performed to pinpoint key signaling networks, followed by systematic drug repurposing using dgiDB and PanDrug databases. Top significant 100 DEGs were identified among 27,985 transcripts from the microarray datasets, while RNA-sequencing analysis revealed DEGs from 25,551 transcripts. KEGG pathway analysis highlighted ten major pathways, of which three, malaria, TGF-β, and PPAR signaling, were common to both datasets and significantly associated with metastatic transformation. Gene literature mining identified eight genes (THBS1, VCAM1, ADIPOQ, LPL, ACKR1, CD36, FABP4, HBA1) overlapping malaria-associated and metastasis gene sets. Network analysis using the STRING database showed strong interactions among 14 of 17 key genes, with VCAM1 emerging as a central hub protein linked to adhesion and immune-related pathways. Subsequent drug–gene interaction screening identified 37 potential repurposed drug candidates, with highest-priority agents including chloroquine (ACKR1, interaction score 0.711), fenofibrate and pioglitazone (ADIPOQ/LPL, 0.622), pirfenidone (THBS1, 0.702), and bevacizumab (THBS1/VCAM1, 0.908), all approved drugs with established clinical safety profiles.These findings emphasize the convergence of TGF-β, PPAR, and malaria-associated signaling in ovarian cancer metastasis, suggesting that repurposed drugs targeting these pathways, particularly chloroquine and PPAR agonists, may have therapeutic potential in this context. The computational identification of bevacizumab, an agent already approved for ovarian cancer, corroborates the approach. Future work will focus on in vitro validation of prioritized drug candidates, including chloroquine, PPAR agonists, and pirfenidone, against ovarian cancer cell lines to substantiate the in silico predictions and support the development of new treatment strategies derived from existing pharmacologic agents with reduced development timelines.

#2123 A high resolution spatial transcriptomic atlas of the bone marrow microenvironment pre and post prostate cancer seeding.

Haley du Bois[1], Alberto Chaves[2], Mostafa Nasr[2], Tao Li[3], Karl Nyman[2], Ryan Bishop[3], Conor C. Lynch[3]

[1]Tumor Microenvironment & Metastasis, Moffitt Cancer Center, Tampa, FL,[2]University of South Florida, Tampa, FL,[3]Moffitt Cancer Center, Tampa, FL

Prostate cancer is the second leading cause of cancer-related death in men, and nearly 80% of patients develop skeletal metastases. However, how primary prostate tumors sculpt the bone microenvironment prior to or during the earliest stages of metastatic spread remains poorly understood. To fill this gap, we generated a spatiotemporal map of tumor-induced changes in the bone marrow using an immunocompetent syngeneic mouse model of prostate cancer (RM1; C57BL/6).Using whole-genome Visium HD spatial transcriptomics, we profiled bone microenvironments from (1) tumor-naïve mice, (2) mice bearing primary prostate tumors but lacking bone metastases (pre-metastatic), and (3) early metastatic mice following intra-arterial delivery of RM1 cells. We interrogated these datasets using a comprehensive bioinformatic workflow (Seurat, GPTcelltype, Banksy, STenrich, Monocle, and CellChat) to resolve coordinated stromal and immune remodeling as disease progresses. We discovered that primary prostate tumors initiate *mixed bone-remodeling programs* characterized by sustained osteoclast activation and a progressive collapse of osteoblast differentiation. Consistent with this, microCT imaging revealed measurable bone loss in pre-metastatic mice, which intensified upon metastatic colonization. Within the immune compartment, we found a concomitant disruption of plasma cells, possibly driven by the loss of osteoblasts which are key niche cells required for normal plasma cell recruitment and survival. Unexpectedly, despite inoculation with a genetically homogeneous RM1 line, we observed that early metastatic lesions diverged into two transcriptionally distinct tumor populations occupying separate spatial neighborhoods. The proximal, trabecular-associated lesion is embedded in a stromal-rich niche and shows upregulation of hypoxia- and oxidative stress-related programs. In contrast, the distal lesion in a more immune-dense region exhibits heightened interferon signaling. These findings demonstrate that *local bone microenvironments impose divergent selective pressures on metastatic tumors*, shaping their phenotypic evolution. Together, our work provides a high-resolution spatiotemporal atlas of prostate cancer progression to bone, illuminating early stromal and immune perturbations that may prime the bone for metastatic takeover. This dataset serves as a platform for hypothesis generation and identifies potentially targetable microenvironmental mechanisms for preventing or treating bone metastatic prostate cancer.

#2124 Patient-derived CSF and ascites organoids reveal divergent metastatic mechanisms in advanced gastric cancer.

Byeong Gyu Yoon, Chan Hee Park, Woo Sun Kwon, Tae Soo Kim, Sun Young Rha

Yonsei University College of Medicine, Seoul, Korea, Republic of

Gastric cancer most frequently metastasizes to the peritoneum (PM), whereas leptomeningeal metastasis (LM) is extremely rare but highly lethal. Although LM shows markedly worse outcomes than PM, the mechanisms driving LM remain poorly understood due to the absence of appropriate experimental models. To address this limitation, we established organoid models derived from PM and LM from the same patient and compared their morphological and genomic characteristics. Organoids were generated from ascites and Cerebrospinal fluid obtained from a 50-years old female patient with stage IV diffuse-type gastric cancer, with passage 5 defined as the establishment point. Organoid cultures were initiated under optimized 3D conditions and maintained through multiple passages to ensure stability and expansion. Morphological and phenotypic features were characterized using 3D bright-field imaging, scanning electron microscopy (SEM), and hematoxylin and eosin (H&E) staining. For molecular characterization, targeted panel sequencing and whole-genome sequencing were performed. Copy number variations of selected genes were validated by qPCR. The ascites-derived organoids (AS2 and AS4) required approximately 34-39 days to reach establishment, while the Cerebrospinal fluid-derived organoid (CSFO) required about 39 days. At morphological characterization, AS2 formed a lumen structure and displayed pronounced pseudopodia with elongated cellular shape, indicative of stronger cell-cell interactions. In contrast, CSFO and AS4 exhibited rounder cellular shapes with grape-like clustered architectures and weaker intercellular adhesion. Despite the different metastatic microenvironments, 136 mutations common among all organoids, 20 mutations were CSFO-specific, 19 mutations were AS2-specific, and 28 mutations were AS4-specific. Subsequently, we conducted Gene Ontology analysis. CSFOs were enriched for mutations associated with vascular morphogenesis. In contrast, ASOs harbored mutations related to epithelial proliferation and organ development. Patient-derived peritoneal tissues exhibited mutations predominantly in immune-regulatory pathways, including MHC class I/II-mediated antigen presentation. Notably, MET amplification and CDKN2A deletion were consistently detected in all organoid models but not in the original patient tissues, highlighting culture-associated genomic selection. MAP2K4 deletion was observed in CSFOs and GO15-5, while MYCN and ADGRA2 amplification were detected only in GO15-5, suggesting additional clonal evolution during extended in vitro passage, and genomic variants were validated using qPCR. Overall, this study demonstrates the feasibility of using patient-derived organoids to model atypical metastatic routes of gastric cancer and provides novel insights into the biology of LM through integrative morphological and genomic analyses.

#2125 Patient-derived orthotopic xenograft models recapitulate the peritoneal dissemination of pancreatic cancer and delineate its transcriptomic, regulatory, and spatial programs.

Takaaki Furukawa[1], Kohei Kumegawa[1], manabu takamatsu[2], Kenichi Miyata[1], Sumito Saeki[1], Chikako Shibata[1], Takafumi Mie[3], Takeshi Okamoto[3], Tsuyoshi Takeda[3], Takashi Sasaki[3], Masato Ozaka[3], Miwa Tanaka[1], Shunji Takahashi[4], Tetsuo Noda[5], Yao Ryoji[6], Naoki Sasahira[3], Reo Maruyama[1]

[1]Division of Cancer Epigenomics, Cancer Institute, Japanese Foundation for Cancer Research, Tokyo, Japan,[2]Division of Pathology, Cancer Institute, Japanese Foundation for Cancer Research, Tokyo, Japan,[3]Division of Hepato-Biliary-Pancreatic Medicine, Cancer Institute Hospital of Japanese Foundation for Cancer Research, Tokyo, Japan,[4]The Cancer Institute Hospital of JFCR, Tokyo, Japan,[5]Director, Japanese Fndn. for Cancer Res. Cancer Institute, Tokyo, Japan,[6]The JFCR Cancer Institute, Tokyo, Japan

BACKGROUND: The mechanisms of peritoneal dissemination in pancreatic ductal adenocarcinoma (PDAC) remain unclear partly owing to the lack of patient-derived models that recapitulate this process. This study aimed to establish an orthotopic model of PDAC peritoneal dissemination and to uncover the transcriptional and regulatory programs underlying this process.
METHODS: Organoids were established from primary pancreatic tumors and malignant effusions of patients with PDAC and orthotopically transplanted into the pancreas of immunodeficient mice to generate patient–derived orthotopic xenograft (PDOX) models. Subsequently, the organoids were rederived from pancreatic and peritoneal lesions of a representative model (PDOX12) and orthotopically reimplanted to assess the dissemination capacity. Single-nucleus RNA sequencing (snRNA-seq), single-cell ATAC sequencing (scATAC-seq) and spatial transcriptomic analysis were performed to analyze the tumors from these models.
RESULTS: The organoids that were derived from malignant effusions reproducibly generated peritoneal metastases after orthotopic implantation. To dissect this process more precisely, we focused on one representative model (PDOX12) and rederived organoids from its pancreatic and peritoneal lesions (PDXO12P and PDXO12A, respectively). These organoids generated matched PDOX models that differed only in dissemination potential when reimplanted orthotopically. The results of snRNA-seq revealed a distinct subpopulation enriched in the high-dissemination model, suggesting a dissemination-primed state. Integration with scATAC-seq identified potential upstream regulators of the gene programs in the subpopulation. Furthermore, the cellular plasticity was revealed by the PDOX system. In vitro, PDXO12P and PDXO12A organoids exhibited nearly indistinguishable transcriptional and proliferative profiles. However, their latent differences were unmasked when placed in vivo: PDXO12A demonstrated stronger peritoneal dissemination, accompanied by the clear transcriptional divergence. We hypothesized that these differences were unveiled by the influence of the tumor microenvironment (TME) and performed spatial transcriptomic analysis to profile the TME in the high-dissemination model and comprehensively characterize the transcriptional features of fibroblasts.
CONCLUSIONS: We established PDOX models that isolate the peritoneal dissemination phenotype and reveal the transcriptional and regulatory programs driving this process.

: In Vivo Imaging
Poster Session

#2129 Pharmacodynamics of Akt drugs revealed by a kinase-modulatedbioluminescent indicator withBBB-permeable substrate.

Yan Wu[1], Chenzhou Hao[1], **Chao Gao**[2], Matt Hageman[2], Sungmoo Lee[1], Thomas A. Kirkland[3], Nathanael S. Gray[1], Yichi Su[4], Michael Z. Lin[1]

[1]Stanford University, Stanford, CA,[2]Promega Corporation, San Luis Obispo, CA,[3]Head of ATG Chemistry Research, Promega Corp., Madison, WI,[4]Department of Nuclear Medicine, Fudan University, Shanghai, China

Noninvasive imaging tools that enable real-time visualization of biological events in living subjects are highly valuable in biomedical research. Bioluminescence imaging (BLI), with its high sensitivity and low background, provides an ideal platform for developing molecular sensors to monitor intracellular signaling *in vivo*. Here, we report the development of a kinase-modulated bioluminescent indicator (KiMBI) for rapid, noninvasive pharmacodynamic (PD) assessment of Akt-targeted therapeutics, substantially reducing compound use and animal requirements. This ATP-independent reporter, based on NanoLuc luciferase, produces light upon administration of the brain-penetrant substrate cephalofurimazine (CFz9). Using KiMBI, we performed a structure-PD relationship analysis of the brain-active Akt inhibitor ipatasertib by designing and characterizing two novel analogs. One analog, ML-B01, exhibited robust Akt inhibition in both brain and peripheral tissues. Remarkably, capivasertib, ipatasertib, and ML-B01 all demonstrated prolonged PD effects that outlasted their pharmacokinetic (PK) profiles. Furthermore, KiMBI imaging revealed that the PD effect of an Akt-targeted proteolysis-targeting chimera (PROTAC) degrader persisted for more than three days following a single dose. Together, these results establish bioluminescence imaging with the Akt KiMBI as a sensitive and efficient method for real-time, longitudinal visualization of Akt inhibitor and degrader activity in vivo. This platform offers a powerful approach for early-stage drug optimization and for elucidating the pharmacodynamics of kinase-targeted therapies in live animals.

#2130 High-throughput imaging approaches to characterize CAR T therapies for solid tumor microenvironments.

Ernest Heimsath, Paul Held, Peter Brescia, Joe Clayton

Agilent Technologies, Inc., Winooski, VT

CAR T therapies have revolutionized hematologic cancer treatment but face significant barriers in solid tumors, primarily due to the tumor microenvironment. Dense extracellular matrix (ECM) regions impede lymphocyte migration and infiltration, reducing therapeutic efficacy. To model these clinical challenges, we developed a high-throughput imaging assay to evaluate CAR T cytotoxicity in three-dimensional (3D) ECM-embedded tumor spheroids.

The epithelial cell adhesion molecule (EpCAM), typically overexpressed in epithelial cancers, provides a clinically relevant target for CAR T therapy. EpCAM-targeted CAR T cells were tested against T-47D spheroids embedded in ECM to mimic solid tumor architecture. Our imaging-based approach revealed dose-dependent cytotoxicity and deep infiltration of spheroids by CAR T cells, despite delayed cytopathic responses compared to suspension cultures. Furthermore, this cytotoxicity is distinct to EpCAM-engineered CAR T cells when compared to nonengineered T lymphocytes. Importantly, elevated IC_{50} values under embedded conditions underscore the impact of ECM on therapeutic kinetics. These results offer actionable insights for optimizing CAR T design and dosing strategies to overcome microenvironmental barriers. By quantifying migration, infiltration, and killing in physiologically relevant models, this work supports translational efforts to improve CAR T efficacy in solid tumors and informs clinical development pathways for next-generation immunotherapies.

#2131 Hyperpolarized carbon-13 MRI for early treatment response assessment in pancreatic ductal adenocarcinoma patients.

Minjie Zhu[1], Hsin-yu Chen[1], Tanner Nickles[1], Robert Bok[1], Andrew H. Ko[2], Zhen Wang[1], Jeremy W. Gordon[1]

[1]Radiology and Biomedical Imaging, UCSF School of Medicine, San Francisco, CA,[2]UCSF School of Medicine, San Francisco, CA

Current methods for monitoring treatment response in pancreatic ductal adenocarcinoma (PDA), primarily relying tumor size measurement using response evaluation criteria in solid tumors (RECIST), are often delayed and limited by the infiltrative nature of the disease. Timely, non-invasive assessment is crucial for adapting therapies for non-responders. PDA tumor cells are characterized by significant metabolic reprogramming, driven by KRAS oncogene mutations, which enhance glycolysis and lactate production while downregulating alanine aminotransferase, which mediates pyruvate to alanine conversion. Hyperpolarized (HP) carbon-13 (^{13}C) magnetic resonance imaging (MRI) offers a non-invasive solution to interrogate these metabolic changes. Utilizing dynamic nuclear polarization, this technique provides unprecedented sensitivity(> 10,000-fold signal increase) and chemical specificity for rapid and pathway-specific investigation of dynamic metabolic processes that were previously inaccessible by ^{1}H MRI or CT. Pre-clinical studies have shown HP ^{13}C MRI using [1-^{13}C]pyruvate as substrate can detect and monitor PDA precursor lesion progression, with an increase in the lactate-to-pyruvate ratio and decrease in the alanine-to-pyruvate ratio observed in the affected mice pancreas. Initial clinical studies have further demonstrated the feasibility and safety of HP ^{13}C MRI for quantifying metabolism in PDA patients. In this ongoing study, five PDA patients underwent multiparametric ^{1}H MRI and HP ^{13}C MRI both pre- and at 4&8 weeks post-treatment. ^{13}C pyruvate, lactate, alanine signal intensities and their respective ratios in the primary tumor and normal pancreas were assessed. All five patients exhibited elevated pre-treatment primary tumor lactate-to-pyruvate ratios. A significant decrease (approximately 25%) in the primary tumor lactate-to-pyruvate ratio post-treatment correlated with partial response by RECIST in four patients, while one patient with stable disease showed minimal change (<5%). Reduced alanine-to-pyruvate ratios were observed in pre-treatment tumors for two patients, though their relationship to treatment response could not be fully quantified. No significant changes in tumor ADC from diffusion-weighted ^{1}H MRI were observed pre- and post-treatment, suggesting that metabolic alterations detectable by HP ^{13}C MRI precede significant changes in cellularity at this early time point. These initial findings indicate that HP ^{13}C MRI can detect early metabolic changes in PDA tumors in response to therapy, holding significant potential for providing timely treatment response information, facilitating adaptive treatment strategies, and improving patient outcomes in PDA.

#2132 Near-Infrared Claudin-1 antibody enables accurate detection of primary and metastatic colorectal tumors in mice.

Javier Bravo[1], Shanglei Liu[1], Siamak Amirfakhri[1], Blackberrie Eddins[1], Keita Kobayashi[1], Jasmin Zaker[1], Robert Hoffman[1], Sumbal Talib[2], Aaron M. Mohs[3], Punita Dhawan[4], Michael Bouvet[1]

[1]UC San Diego Health, San Diego, CA,[2]University of Nebraska Medical Center, Omaha, NE,[3]Pharmaceutical Sciences, University of Nebraska Medical Center, Omaha, NE,[4]University of Kansas Medical Center, Kansas City, KS

Background: Claudin-1, a tight-junction protein frequently overexpressed in colorectal cancer (CRC), is an attractive target for antibody-mediated near-infrared (NIR) fluorescence imaging. This study evaluates an anti-Claudin-1 antibody conjugated to IRDye800CW for detecting and validating colorectal tumors using bioluminescence correlation in orthotopic and metastatic mouse models.

Methods: Luciferase-expressing LS174T human colon cancer cells were implanted into athymic nude mice to establish orthotopic (n = 10) and hepatic (n = 9) tumor models. Mice received 50 µg of Claudin-1-IRDye800CW intravenously 48 hours before imaging. In vivo imaging was performed using both the Pearl Trilogy Small Animal Imaging System and the Arthrex Synergy Vision System equipped for 800 nm fluorescence. Mean fluorescence intensity (mFI) was used to calculate tumor-to-background (TBR) and tumor-to-liver (TLR) ratios. Co-registration with luciferase bioluminescence was used to confirm probe specificity, and ex vivo imaging validated biodistribution.

Results: In the orthotopic model, Claudin-1-IRDye800CW achieved a mean TBR of 3.92, clearly delineating tumor margins, while sub-millimeter peritoneal metastases (< 1 mm) produced a mean TBR of 2.9. In the hepatic model, the mean TLR was 3.42, confirming selective tumor contrast over surrounding tissue. Ex vivo analysis further increased contrast (TBR = 16.4; TLR = 4.78). Fluorescent signals consistently co-localized with luciferase activity, confirming targeting specificity. Both imaging systems demonstrated high-resolution detection, and the Arthrex clinical laparoscope enabled real-time intraoperative visualization under clinically relevant conditions.

Conclusion: The anti-Claudin-1-IRDye800CW conjugate selectively and accurately identifies both primary and metastatic colorectal tumors in vivo. Strong tumor contrast and spatial concordance with bioluminescence validate its specificity, while compatibility with a clinical laparoscopic platform underscores the translational promise of Claudin-1-targeted NIR fluorescence imaging for colorectal cancer detection and fluorescence-guided surgery.

#2133 Fibronectin extra-domain B-recognizing gold nanoparticles as an innovative tool for neuroblastoma targeting.

Chiara Barisione[1], Silvia Ortona[2], Veronica Bensa[3], Caterina Ivaldo[1], Eleonora Ciampi[3], Simonetta Astigiano[4], Michele Cilli[4], Luciano Zardi[1], Mirco Ponzoni[3], Domenico Palombo[5], Giovanni Pratesi[6], Pier Francesco Ferrari[7], **Fabio Pastorino**[3]

[1]Department of Surgical and Integrated Diagnostic Sciences, University of Genoa, IRCCS Ospedale Policlinico San Martino, Genoa, Italy,[2]Department of Experimental Medicine, University of Genoa, Genoa, Italy,[3]Lab of Experimental Therapies in Oncology, IRCCS Istituto G. Gaslini, Genoa, Italy,[4]Animal Facility, IRCCS Ospedale Policlinico San Martino, Genoa, Italy,[5]Department of Surgical and Integrated Diagnostic Sciences, University of Genoa, Research Center for Biologically Inspired Engineering in Vascular Medicine and Longevity, University of Genoa, Genoa, Italy,[6]Department of Surgical and Integrated Diagnostic Sciences, University of Genoa, Research Center for Biologically Inspired Engineering in Vascular Medicine and Longevity, University of Genoa, Clinic of Vascular and Endovascular Surgery, IRCCS Ospedale Policlinico San Martino, Genoa, Italy,[7]Research Center Biologic Inspired Engineering in Vasc Med and Long, Civil, Chem and Envir Eng UNIGE, IRCCS Ospedale Policlinico San Martino, Genoa, Genoa, Italy

Background/Objectives: Neuroblastoma (NB) is the most common extracranial solid tumor in children and accounts for 12-15% of pediatric cancer-related deaths. Current multimodal therapies still lack of specific cellular targets, causing systemic toxicity and drug resistance. The development of innovative tumor-targeted nanoformulations might represent a promising approach to enhance NB diagnosis and antitumor efficacy, while decreasing off targets side effects. Fibronectin extra-domain B (FN-EDB) is upregulated in the tumor microenvironment.
Methods: Here, FN-EDB expression was evaluated by immunohistochemical (IHC) staining in several animal models of NB. A gold nanoparticle, decorated with an antibody (Ab) recognizing FN-EDB (L19-AuNP) was developed by the company Nano Flow and its tumor binding was tested by ELISA *in vitro* and in Patient-Derived Xenografts (PDX) models of NB by photoacoustic imaging *in vivo*.
Results: All models of NB used expressed FN-EDB, at the tumor cell, stroma and tumor vasculature levels. Compared to the non-targeted (no L19 Ab) Au-NP (size: 35.59 ± 2.54 nm; PDI: 0.47 ± 0.08; zeta potential: -51.18 ± 0.84), L19-AuNP was found to be stable (size: 108.70 ± 1.37 nm; PDI: 0.29 ± 0.07; zeta potential: -28.34 ± 0.48) and able to specifically bind to FN-EDB *in vitro*. *In vivo*, L19-AuNP specifically homed into PDX of NB, accumulating more in the tumor expressing higher levels of FN-EDB.
Conclusions: In this preliminary study, L19-AuNP was shown to be a novel diagnostic tool specific for binding NB expressing FN-EDB, paving the way for the development of theranostic nanoformulations co-encapsulating gold moiety and standard-of-care for NB.

#2134 Targeting primary gastric tumors and peritoneal metastases in cell-derived xenograft mouse models using an anti-mucin-4-antibody conjugated near infrared fluorophore.

Blackberrie Eddins[1], Sunidhi Jaiswal[1], Abhijit Aithal[2], Siamak Amirfakhri[1], Javier Bravo[1], Jasmin Zaker[3], Sumbal Talib[4], Kavita Bantwal Mallya[2], Aaron M. Mohs[4], Maneesh Jain[2], Robert M. Hoffman[5], Surinder K. Batra[2], Michael Bouvet[1]

[1]Department of Surgery, University of California San Diego, La Jolla, CA,[2]Department of Biochemistry and Molecular Biology, University of Nebraska Medical Center, Omaha, NE,[3]VA San Diego Healthcare System, La Jolla, CA,[4]Department of Pharmaceutical Sciences, University of Nebraska Medical Center, Omaha, NE,[5]President, AntiCancer, Inc., San Diego, CA

Introduction: The purpose of the present study is to validate the use of an anti-MUC4 antibody conjugated near infrared dye to target primary and metastatic gastric cancers in nude mouse models.

Methods: Subcutaneous models were created in nude mice by injecting 10^6 cells of human gastric cancer cell lines SNU-16 or NCI-N87 into their flanks. These tumors were excised after 2 months and 1 mm^3 fragments were implanted into the stomachs of nude mice to establish orthotopic gastric cancer models of SNU-16 and NCI-N87. Experimental metastasis models were established by injecting 10^6 SNU-16 or 10^6 NCI-N87 cells intraperitoneally in nude mice. 2-3 months after tumor implantation mice were injected via tail vein with a mucin4 antibody conjugated to a near infrared fluorescent dye IRDye800CW (MUC4-IRDye800CW). Mice were sacrificed 72 hours after tail vein injection of 50 µg MUC4-IRDye800CW and imaged with the LI-COR Pearl Imaging System and a Stryker laparoscope. The tumor-to-background ratios (TBR) were calculated by dividing the mean fluorescence intensity of the tumors by that of the surrounding stomach. Histopathological analysis was performed on tumors with immunohistochemical (IHC) staining with anti-mucin-4 and anti-immunoglobulin G (IgG) as a negative control.

Results: 20 total mice were imaged, including 14 primary gastric cancer models and 4 intraperitoneal metastatic gastric cancer models. Primary gastric SNU-16 tumors (n = 6) had a mean TBR of 1.99 (SE ± 0.58), and primary gastric NCI-N87 tumors (n = 8) had a mean TBR of 2.81 (SE ± 1.04). Metastatic SNU-16 tumors (n = 3) had a mean TBR of 3.7 (SE ± 0.75), and metastatic NCI-N87 tumors (n = 3) had a mean TBR of 3.91 (SE ± 0.98). Tumor borders were clearly visualized with both Pearl and the Stryker laparoscope fluorescence imaging systems. Representative tumors stained with anti-mucin-4 stained brown while those stained with anti-IgG did not.

Conclusions: Anti-MUC4-IRDye800CW can be used to accurately localize both primary and metastatic gastric cancer models in nude mice with fluorescence imaging and is promising for identifying both primary tumor margins and intraperitoneal metastasis intra-operatively.

#2135 Optimized iron-carbon nanoparticles demonstrate superior; in vivo antitumor efficacy in magnetic hyperthermia treatment.

Mariam Elabbasi[1], Sofia Cooper[1], Ahmed El Gendy[2]

[1]Environmental Sciences and Engineering, The University of Texas at El Paso, El Paso, TX,[2]The University of Texas at El Paso, El Paso, TX

This study aims to develop and evaluate iron-carbon (Fe/C) nanoparticles synthesized for magnetic hyperthermia-based cancer therapy, as a continuation of our previously published in vitro work on the same cell lines. The Fe/C nanoparticles were prepared using a co-precipitation method with optimized precursor ratios to enhance magnetic performance. Structural and magnetic characterization revealed improved properties, with a saturation magnetization of 148.6 emu/g. In vitro cytotoxicity assays in MCF-7 breast cancer cells showed significant cell death at lower nanoparticle doses, confirming effective hyperthermic activity. In vivo experiments were performed using DU145 prostate and MCF-7 breast cancer xenograft models, where intratumoral injections of SPINs at 50 µg/mL and 100 µg/mL were followed by alternating magnetic field exposure. The 50 µg/mL dose led to gradual tumor reduction, while the 100 µg/mL dose induced rapid and uniform shrinkage, with near-complete regression in several cases. Thermal imaging verified temperature increase within the tumors. These findings indicate that Fe/C SPINs are promising agents for targeted and minimally invasive magnetic hyperthermia monotherapy in cancer treatment.

#2136 Optimizing an S100A9 probe to enhance CD147 targeting for image guided surgery of pancreatic ductal adenocarcinoma.

Barish H. Edil, Rohit Singh, Ryan C. Bynum, Karl N. Thomas, Lacey R. McNally

Surgery, University of Oklahoma Health Science, Oklahoma City, OK

Background: Pancreatic ductal adenocarcinoma, PDAC, remains of the deadliest cancers with the 5-year survival rate being 10-15%. Surgery is one of the only curable treatments for PDAC with up to 70% of patients that are candidates for surgery having positive margins; it is critical to have accurate imaging of PDAC which can contribute to patient stratification. S100A9 is a calcium binding ligand that binds to CD147, also designated as extracellular matrix metalloproteinase inducer (EMMPRIN), a membrane-bound glycoprotein. To better visualize PDAC cells, an S100A9 derivative Near-infrared fluorescent probe was created to have increased binding to CD147 while minimizing off-target accumulation.
Methods: The pancreatic adenocarcinoma cancer cell lines, MiaPaca2, Panc1, Suit2, S2VP10 and S2013 were assessed for CD147 levels using western blot. The 114 amino acid S100A9 was synthesized using microwave chemistry and lyophilized. Hilyte 750 succinimidyl ester and Hilyte 750 amine reactive dyes were independently conjugated to the S100A9 peptide to determine the ideal orientation. Spectroscopy confirmed the conjugation of the probes. NIR imaging determined 750-S100A9 probes binding to S2VP10 cells. S100A9 peptide length was reduced to 89 or 80 amino acids and conjugated to HiLyte Fluor 750 acid SE dye on the C-Terminal end. Conjugation was tested with spectroscopy and the full length and cut down probes binding to S2VP10L were tested with NIR imaging.
Results: The western blot demonstrated that MiaPaca2, Panc1 and S2013 were highly positive for CD147 while Suit2 and S2VP10 were less positive. Successful conjugation of peptides to the reactive dyes resulted in an OD of 0.1 each. 750 dye conjugated to the C-terminal of the S100A9 probe determined stronger binding to S2VP10 at 279,600 a.u. at 500 nM compared to 4,055 a.u. of N-terminal 750-S100A9 ($p< 0.05$). The 89 amino acid probe resulted in the highest expression at 291,760 a.u. compared to the full-length at 46,580 a.u. and the S100A9-750 80 amino acid probe at 115,200 a.u. when assessed with binding to S2013Q ($p< 0.05$).
Conclusion: CD147 is a suitable target for PDAC using an S100A9 ligand conjugated near infrared fluorescent dye. In addition, S100A9 cut down to 89 amino acids on the C-Terminal with the HiLyte Fluor 750 acid SE dye determines to be a strong target for PDAC. The findings suggest that off-target accumulation of S100A9 could be minimized with the use of the smaller probe. The results also suggest that the S100A9 probes can improve detection and treatment of PDAC specificity with contrast agents or nanoparticles.

#2137 *In vivo* short-wave infrared imaging for liquid tumor and immuno-oncology models.

Tiffany W. Leong[1], Pavel Abdulkin[2], Ameena A. Moghe[1], Vidya Ganapathy[3], Mark C. Pierce[4], Mark Ravera[1]

[1]Nanoink Imaging Inc., Bernardsville, NJ,[2]SMALL Bio GmbH, Zug, Switzerland,[3]Rider University, Lawrenceville, NJ,[4]Biomedical Engineering, Rutgers University, Piscataway, NJ

In vivo imaging challenges in cancer drug discovery include imaging liquid tumors and tracking immune cell activity after checkpoint immunotherapy for solid tumors. Current methods for real-time *in vivo* imaging of tumor models include bioluminescence imaging (BLI), which involves using genetically modified cell lines that can confound study data due to potential changes in the cell lines' biology. This risk of potentially aberrant data is especially a concern with patient-derived xenograft (PDX) models. Our earlier work utilized targeted albumin-coated nanoparticles encapsulating rare earth-containing cores to image tumors in *in vivo* models of solid tumors and to image T cells in the tumor microenvironment. These biocompatible nanoparticles enable imaging without the need for genetic modification by emitting short-wave infrared (SWIR) light after excitation by a 980 nm light source. SWIR light travels through blood and tissue more efficiently than does visible bioluminescent light, providing deeper tissue illumination and sharper images. By functionalizing this technology with targeting antibodies, we were able to not only specifically image a range of solid tumors but also visualize CD8+ T cell activity around tumor sites. More recently, we have shown that our nanoparticles can be used to image and track an increase in liquid tumor burden within bone marrow and spleen over a three-week period in a lymphoma model. Briefly, U937 cells (50,000 per mouse) were injected i.v. into NSG mice on Day 0. Nanoparticles targeted to CD45 were injected on Days 10, 16, and 21, and the animals were imaged four hours post-injection using a SWIR-based imaging system. Tumor burdens were confirmed using flow cytometry. Since this initial lymphoma imaging study, we have improved our nanoparticle formulation by encapsulating the rare earth cores with a combination of biocompatible lipids and polymers, and by switching from a batch synthesis process to a microfluidics-based fabrication process. This microfluidics-based approach enables scalability and a high degree of batch-to-batch reproducibility. We tested these next-generation nanoparticles *in vivo* and showed that they are ≥5-fold brighter than our original albumin formulation, providing researchers with a highly sensitive imaging modality to interrogate the tumor microenvironment and to visualize liquid tumors in real time, all without the risks inherent in genetic modification of the tumors and immune cells being studied.

#2138 Development of a bioluminescence imaging-guided CTC liquid biopsy procedure to identify the optimal time window for achieving superior photothermal therapy efficacy.

Abhijit De, Chetna Patnaik

Molecular Functional Imaging Laboratory, ACTREC, Tata Memorial Centre, Navi Mumbai, India

Global cancer burden represents one of the most significant challenges in public health. Notable concern for the mainframe therapeutic procedures is the high incidence of relapsed disease among majority patients availing those. This problem is frequently attributed to the evolving state of cancer cell dissemination, where circulating tumor cells (CTCs) begin to appear in the blood circulation. However, due to CTC enrichment requirement, high-volume blood withdrawal repeatedly during initial or follow up diagnosis, raises an ethical concern, and therefore CTC determination not integral in practice. Given the sparse nature of CTC applications in preclinical experiments using mouse model, where the total blood volume is limited to only 1.5 ml/mouse, in this study we challenged this dogma, and established a luminescence-based CTC detection method using preclinical mouse tumor models. The optimized liquid biopsy process using bioluminescence imaging-guidance allowed detection of up to two cells from as low as 100µl blood volumes, allowing us to follow the CTC surge dynamics from a very low blood volume. We examined both CTC dynamics and metastatic potential in mice bearing highly aggressive 4T1-FLuc2 and a relatively indolent ZR-75-1-Nanoluc orthotopic breast cancer models. To test the case, we further used our well-standardized photothermal therapy (PTT) procedure using gold-coated solid lipid nanomaterial (Au-SLN) and demonstrate that when PTT is performed in a temporally optimized window, the therapy application does not induce a detectable CTC flux ($p < 0.05$), nor distant spread of malignant tumors in the vital organs, both in highly aggressive and less aggressive breast cancer models. Imaging signal from CTC was confirmed further by molecular biomarker and transcriptomic characterization, revealing a close association of EpCAM positive CTCs with tumor aggressiveness and their metastatic propensity. These effects essentially improve mice longevity and relapse-free survival of the mice. Our findings highlight that Au-SLN mediated PTT could provide a relapse-free efficacious treatment, when performed before viable CTCs are released and underscore the importance of integrating a sensitive liquid biopsy method for monitoring metastatic risk and chance of disease relapse.

#2139 [^{18}F]-FMISO-PET imaging to characterize the impact of obesity on the hypoxic tumor microenvironment during immunotherapy.

Corinne Crawford[1], Shannon Elizabeth Lynch[2], Jonathan Moye[2], Chloe T. DeMellier[2], Patrick N. Song[2], Kelsey M. O'Brien[2], Benjamin P. Lee[2], Benjamin Larimer[2], Anna G. Sorace[2]

[1]Department of Biomedical Engineering, University of Alabama at Birmingham, Birmingham, AL,[2]Department of Radiology, University of Alabama at Birmingham, Birmingham, AL

Introduction: 40% of patients with triple-negative breast cancer (TNBC) also have obesity (BMI>30 kg/m^2). Clinical studies have demonstrated that obesity worsens cancer outcomes, urging investigation of novel therapeutic targets within the obese tumor microenvironment (TME). Preclinical studies have shown that obesity increases tumor hypoxia, diminishing immunotherapy (IMT) response via reduced IMT distribution and pro-tumoral immune shifts. [^{18}F]-fluoromisonidazole (FMISO) positron emission tomography (PET) can non-invasively quantify hypoxia, allowing for patient stratification by hypoxia levels to predict IMT response and inform the use of secondary hypoxia-activated prodrugs, like evofosfamide (EVO).

Methods: C57/Bl6J mice were fed a high-fat diet (HFD, n=68) or low-fat diet (LFD, n=19) for 13 weeks prior to E0771 implantation in the 3rd mammary fat pad on day -12. To explore the impact of obesity on baseline tumor hypoxia, a cohort of LFD and HFD were imaged with [^{18}F]-FMISO PET. A second HFD cohort was split into controls (saline, n=19) or IMT (anti-CTLA-4 and anti-PD-1 every 3 days, n=49). Mice were imaged with [^{18}F]-FMISO PET on days 0, 5, and 12, and signal was quantified via standard uptake value (SUV) metrics. On day 6, IMT mice were randomized to continue with IMT (n=30) or also receive EVO (n=19). Based on ROC analysis, a threshold of day 5 tumor to background ratio (TBR) of the muscle of 1.3 was used to categorize tumors as hypoxic/normoxic. A correlation evaluated the predictive ability of day 5 TBR on long-term response (defined by RECIST criteria). A subset of treatment groups was euthanized at imaging timepoints for flow cytometry of immune populations. A two-way ANOVA was used for statistical analysis.

Results: HFD mice demonstrated significantly increased tumor hypoxia (SUV_{mean}) compared to LFD mice on day 0 ($p<0.0001$) without tumor volume differences. In HFD, IMT resulted in a 25% response rate by day 21. Day 5 TBR was inversely correlated with long term survival for IMT-treated mice ($p=0.003$, $r^2=0.5$). When stratifying tumors as normoxic or hypoxic, adding EVO to IMT demonstrated a 21% reduction of tumor hypoxia (SUV_{max}) within hypoxic tumors compared to IMT alone ($p=0.008$). Interestingly, combination therapy led to a 330% and 173% increase in M2-like macrophages ($p=0.06$) and regulatory T cells ($p=0.06$) compared to IMT alone and did not reveal improvements in long-term tumor volume.

Conclusions: Our study supports ongoing literature demonstrating increased hypoxia in tumors in a HFD environment and that [^{18}F]-FMISO stratification predicted response to immunotherapy in a TNBC model. Previous studies showed that lean tumor models have additive response when adding EVO to IMT in hypoxic tumors; however, our study demonstrated that EVO reduces hypoxia in hypoxic, obese tumors, but this did not salvage IMT response, likely due to increased tumorigenic immune changes.

#2140 Diet composition - A critical variable in fluorescence imaging for preclinical cancer research.

STEVEN YEUNG[1], Phuong Dang[2], Jeffrey D. Peterson[3], Sridhar Radhakrishnan[1]

[1]Research Diets, Inc., New Brunswick, NJ,[2]The Jackson Laboratory, Bar Harbor, ME,[3]Revvity, Durham, NC

Background: Fluorescence based imaging is a cornerstone of preclinical cancer research, enabling noninvasive, real time assessment of tumor growth, metastasis, and therapeutic response. However, dietary ingredients can impact image quality and data integrity. Grain-based chow diets contain nonnutritive components such as phytochemicals and potential toxins including endotoxins, mycotoxins, and heavy metals, that vary by batch and influence animal phenotype, metabolism, and imaging outcomes. Dyes (FD&C Blue #1, Yellow #5, Red #40) commonly added to diets for visual differentiation may introduce background fluorescence, while alfalfa and other chlorophyll-rich dietary ingredients fluoresce strongly in the red and near infrared (NIR) range, overlapping with wavelengths used by many NIR fluorescent cancer imaging probes. The effect of different dietary ingredients on fluorescence imaging quality was evaluated in this study.

Methods: Direct fluorescence imaging measurements of diet pellets were acquired on the IVIS™ Spectrum 2 using excitation wavelengths from 640 to 750 nm. For *in vivo* studies, 8 wk old male C57BL/6J and NU/J mice were initially fed alfalfa containing chow for a week, then transitioned to either purified diets (with or without dyes) or chows (with or without alfalfa) for two weeks. Multiple excitation wavelengths were used with appropriate excitation/emission filter sets to capture the range of diet- and dye-related signal from 500-750 nm with most analysis focused on the 640-750 nm range. Datasets were analyzed using Living Image™ 4.8.3 system software to quantify gastrointestinal fluorescence, using spectral unmixing algorithms to separate the signal from chlorophyll/dye and a relevant NIR fluorescent probe.

Results: *In vitro*, both alfalfa (640 nm and 675 nm) and incorporated dyes (640 nm) contributed to strong fluorescence signal. However, only the alfalfa containing diets produced strong background signal at 640 and 675 nm *in vivo*, sufficient to obscure tumor and inflammation probe signals. Alfalfa free and purified diets, with or without added dyes, cleared the background chlorophyll signal within 1-2 weeks, improving signal to noise ratios and image clarity. Data were similar in both NU/J and C57BL/6J strains.

Conclusions: Diet composition strongly influences fluorescence imaging. Alfalfa derived chlorophyll in chows introduces substantial NIR autofluorescence, which is minimized in alfalfa-free diets. Although dyes in purified diets fluoresce strongly *in vitro*, they likely degrade upon consumption contributing to minimal in vivo signal. Standardizing diet offers a simple, cost effective approach to improve image quality, reproducibility, and translational relevance in preclinical cancer imaging.

#2141 Progression of blood brain barrier leakage in orthotopic glioma SRG rat model using contrast enhanced MRI.

Tuulia Huhtala, Jussi Rytkonen, Riikka Immonen, Ayhan Korkmaz, Torsten Giesemann, Julia B. Schueler

Charles River Laboratories, Inc., Kuopio, Finland

Gliomas are the most common type of primary brain tumors. Innovative therapies are vital to improve treatment outcomes but to be efficient, trafficking across the blood brain barrier (BBB) is required. For this advent, animal models provide important information prior to clinical studies. Among the different in vivo models, orthotopic models mimic the biological environment. In addition to traditional mouse models, novel immunocompromised rat models offer new approach to preclinical efficacy testing facilitating PK/PD studies for IND enabling studies. SRG rats enable high engraftment rates and rapid growth of a variety of human tissues and tumors. Severe immunodeficiency ensures high engraftment rates and larger organism size allows larger sample collection e.g. for blood biomarker analysis. Especially in the brain tumor research, imaging has a central role in clinical diagnosis and as a prognostic factor to monitor therapy response. It enables longitudinal monitoring in a fully translational manner. Magnetic resonance imaging (MRI) offers unprecedented soft tissue contrast, high spatial resolution and non-invasive nature renders MRI in rodents a perfect tool for preclinical work in oncological applications. In addition to monitor tumor growth, cerebral blood flow (CBF) and leakage of BBB can be measured with a contrast agent. Perfusion indicates angiogenesis in tumor, one hallmark of most malignant gliomas as well the leakage status of glioma is critical to understand for possible therapeutic intervention. The purpose of this work was to establish orthotopic glioma model in SRG rats using U87MG cells. Development of brain pathologies were longitudinally monitored in vivo using MRI. Key readouts were anatomical visualization of abnormalities, tumor volumetry, vascularization in tumor, CBF and development of BBB leakage. Differences in CBF represents mass effect from brain tumors impairing blood flow in the surrounding brain parenchyma. As a conclusion, translational in vivo imaging techniques were applied to study orthotopic tumor progression. These readouts provide a powerful and translational research tool together with oncological disease animal models with detailed understanding about disease progression and improved treatment intervention design.

#2142 MRI radiomic features to differentiate aggressive and indolent renal tumors.

Huan Lu, Salim Rukhsar, Xueqing Yin, Garima Suman, Ashish Khandelwal, Ananth J. Madhuranthakam, Durga Udayakumar

Mayo Clinic, Rochester, MN

Renal tumors are highly heterogeneous, ranging from benign lesions and indolent renal cell carcinoma (RCC) to highly aggressive phenotypes. Accurately determining tumor aggressiveness before treatment remains a major clinical challenge. Conventional MR imaging lacks sensitivity to microarchitectural differences underlying tumor biology, and biopsy is limited by sampling error and tumor heterogeneity. Radiomics offers a noninvasive approach to extract high dimensional features that may capture biologically relevant patterns. In this IRB-approved retrospective study, we evaluated MR-based radiomics combined with machine learning (ML) to differentiate indolent from aggressive tumors. Pre-operative clinically acquired MR images obtained from eighty-two RCC patients (aggressive, n = 56; indolent, n = 26) who underwent nephrectomy were included for the analysis. Regions of interest (ROIs) of the entire tumor were manually drawn using 3D Slicer on the morphological T2-weighted images and four phases (pre-contrast [PRE], corticomedullary [CM], nephrographic [NG], and delayed [DEL]) from the contrast-enhanced MR images, normalized, and used for radiomic feature extraction (PyRadiomics, v3.1.0). Independently, tumors were grouped into aggressive and indolent phenotypes based on the established histological classification of Mayo Clinic. Statistical analysis used two-sided t-test. Features selected based on mutual information were used for ML classification (Random Under-Sampling Boosting (RUSBoost)) and performance assessed using accuracy, sensitivity, precision, specificity, F1-score, and area under the curve (AUC). Of 107 radiomics features extracted, the following numbers showed statistically significant differences between aggressive and indolent tumors ($p < 0.05$): CM phase (n = 19), NG phase (n = 24), DEL phase (n = 22), and T2-weighted images (n = 29). Several features consistently differed among contrast-enhanced images and included first-order (length, surface area, volume), GLCM (correlation, IDM, IMC1, IMC2), GLDM (dependence entropy, dependence non-uniformity, dependence variance), GLRLM (gray-level non-uniformity, run entropy, run-length non-uniformity), GLSZM (high gray-level emphasis, zone entropy), and NGTDM (coarseness). Using the 15 features with highest mutual information across 50 patients (aggressive, n = 31; indolent, n = 19), a five-fold cross-validation RUSBoost classifier achieved accuracy 0.81, sensitivity 0.84, precision 0.87, specificity 0.77, F1-score 0.85, and AUC 0.80 for identifying the aggressive phenotype. MRI radiomics features show potential to differentiate aggressive from indolent renal tumors. ML-based classification using these features demonstrates promising accuracy. Further optimization and validation in larger cohorts, may help guide individualized care, including consideration of active surveillance for indolent renal tumors.

#2143 From local growth to distant metastasis: A versatile in vivo imaging platform for modeling cancer progression.

Na Li, Hao Huang, Xinyu Zhong, Xuyang Duan, Xing Lan, Jinying Ning, **Feng Hao**

Kyinno Biotechnology Co., LTD, Beijing, China

Background: A comprehensive understanding of cancer progression requires experimental models capable of dynamically capturing both localized tumor growth and the multi-step process of systemic dissemination. Conventional models often recapitulate isolated aspects of this cascade, thereby limiting their translational relevance.
Objective: To establish and validate an integrated in vivo platform that utilizes luciferase-based imaging to quantitatively model distinct stages of cancer progression—from primary engraftment to organotropic dissemination.
Methods: We engineered a series of site-specific cancer models in immunodeficient mice, with disease progression continuously monitored by bioluminescent imaging (BLI). These included: 1. Intracardiac injection of MDA-MB-231-Luc2 cells to model disseminated metastatic seeding. 2. Intratibial and intracranial inoculation to evaluate site-specific growth of breast cancer cells in bone and brain microenvironments. 3. Intravenous injection of Ba/F3 and lymphoma cells to simulate hematogenous dissemination. 4. A systematic analysis of intracranial engraftment topography, where A375-GFP-Luc cells were inoculated at stereotactic coordinates 0.5 mm anterior, 1.5 mm anterior, and 0.5 mm posterior to the bregma.
Results: The platform robustly recapitulated diverse disease phenotypes. Intracardiac injection resulted in widespread bioluminescent signals indicative of metastatic colonization. Orthotopic tibial and intracranial inoculations led to progressive, quantifiable local tumor growth. Intravenous injection of hematopoietic cells produced a systemic pattern of leukemic proliferation. Importantly, the intracranial implantation site emerged as a key determinant of disease progression: injections posterior to the bregma were associated with a significantly greater propensity for metastatic dissemination compared to anterior sites.
Conclusion: We present a validated and versatile in vivo platform that enables the spatiotemporal quantification of tumor dynamics across multiple disease contexts. This integrated system provides a powerful tool for investigating organ-specific tumor biology and evaluating therapeutic efficacy against both primary and metastatic disease.

#2144 Sodium nitrite alters perfusion and hypoxia in preclinical models of breast cancer.

Kelsey M. O'Brien[1], Patrick N. Song[2], Katrina Ricart[3], Seth N. Lee[2], Chloe T. DeMellier[2], Zora Paschel[4], Urvi Rawal[4], Hailey Houson[2], Suzanne E. Lapi[2], Rakesh P. Patel[3], Anna G. Sorace[2]

[1]Graduate Biomedical Sciences, University of Alabama at Birmingham, Birmingham, AL,[2]Radiology, University of Alabama at Birmingham, Birmingham, AL,[3]Molecular and Cellular Pathology, University of Alabama at Birmingham, Birmingham, AL,[4]Biomedical Engineering, University of Alabama at Birmingham, Birmingham, AL

Breast cancer is known to have high levels of hypoxia, leading to poor prognosis and reduced treatment response. Sodium nitrite is an exogenous agent that has been shown to decrease hypoxia in ischemic limb injury and is being explored to improve hypoxia in the tumor microenvironment. The goal of this study is to use non-invasive imaging to characterize changes in perfusion, hypoxia, and drug delivery in vivo following exposure to sodium nitrite.

Mouse models of breast cancer (BT474 human and 4T1 syngeneic cell lines) were treated with saline or sodium nitrite (165μg/kg IP) twice daily. Dynamic contrast-enhanced (DCE) MRI was used to monitor changes 20 minutes after the administration of a single dose of sodium nitrite. [^{18}F]-fluoromisonidazole ([^{18}F]FMISO) positron emission tomography (PET) enabled visualization and quantification of hypoxia within both models, with the BT474 model receiving one week of treatment and the 4T1 model receiving three doses of treatment before imaging. Sodium nitrite-induced changes to drug delivery were measured via dynamic [^{89}Zr]Zr-atezolizumab PET in the 4T1 model, which informed on delivery alterations and the 24-hour retention of an antibody drug delivery. Mice were given sodium nitrite 24 hours, 12 hours, and 20 minutes prior to scan. Modeling of dynamic PET was performed with a two-tissue compartment model to extract biological metrics of perfusion (*K1*) and retention (*k3*). For all molecular studies, tracer uptake was quantified using the mean and distribution of the standardized uptake value (SUV) in the tumor. The Wilcoxon rank sum test was used to assess differences in K^{trans} extracted from Kety-Tofts analysis of DCE-MRI data. One-way and two-way ANOVAs were used to determine the effects of treatment. Independent t-tests were used to examine differences between treatment groups.

Mice treated with sodium nitrite showed increased perfusion (K^{trans} from DCE-MRI) compared to those treated with saline (p=0.03). In both models, hypoxia was shown to be significantly reduced with the introduction of sodium nitrate compared to controls, with a decrease observed after 10 doses in BT-474 (p=0.01) and after two doses in 4T1 (p=0.02). Compartmental modeling showed that adding sodium nitrite increased the rate of delivery of the tracer (*K1*) compared to control (p=0.02) and improved retention (*k3*) at 24 hours (p=0.015).

Non-invasive imaging revealed tumor microenvironment alterations in perfusion and oxygenation following sodium nitrite in two breast cancer models. Further, sodium nitrite was able to increase delivery of an antibody PET tracer, serving as a measure of antibody therapy delivery. As perfusion and hypoxia are key drivers in response to therapy, the addition of sodium nitrite can modulate hypoxia, perfusion, and drug delivery in solid tumors and could potentially offer new therapeutic insights for optimizing treatment in breast cancer.

#2145 Biophysical enhancement of radiation-activated photodynamic therapy (radioPDT) and translational brain tumor models.

Manjusha Muralidharan[1], Deepak Dinakaran[2]

[1]Biological Sciences, Sunnybrook Health Sciences Centre, Toronto, ON, Canada,[2]University of Toronto, Toronto, ON, Canada

Background: Radiation-activated photodynamic therapy (radioPDT) uses X-ray-excited nanoscintillators to activate photosensitizers deep within tissues, generating cytotoxic reactive oxygen species without requiring receptor expression. This biophysical strategy is well suited for heterogeneous tumors such as glioblastoma (GBM), where receptor-targeted approaches often fail. A major translational barrier is the blood-brain barrier (BBB), which restricts nanoparticle entry. Physical modulation via focused ultrasound (FUS) and microbubble cavitation can enhance nanoparticle delivery and potentially improve radioPDT efficacy. To evaluate this approach, we established a multi-model pipeline incorporating flank xenografts, intracranial GBM models, and the chick CAM system, allowing visualization of nanoparticle transport, vascular effects, and treatment response.

Methods: SCID mice bearing PC3 flank tumors received control, radiation, FUS, NP+RAD, NP+FUS+RAD, or NP+microbubbles+FUS+RAD. Tumors were analyzed using multiplex immunofluorescence for proliferation/apoptosis (Ki67, cleaved Caspase-3), DNA damage (γ-H2AX, 53BP1), oxidative injury (4-HNE, TUNEL), vascular structure (CD31, NG2), hypoxia (CA9, HIF-1α), and inflammation (CD45, Iba1). For translational studies, U87 and U251 GBM cells expressing LUC-GFP were validated and used to generate intracranial xenografts for bioluminescence imaging and a CAM model enabling rapid assessment of nanoparticle behavior and radioPDT effects.

Results: radioPDT alone disrupted endothelial cells, while radioPDT combined with microbubble-enhanced FUS produced both endothelial and pericyte disruption, suggesting potential for BBB modulation. Multiplex tumor analysis is ongoing. LUC-GFP GBM models have been established, and intracranial and CAM tumors provide complementary systems to study FUS-mediated BBB opening and nanoparticle delivery during radioPDT.

Conclusions: radioPDT may amplify ultrasound-mediated vascular modulation without requiring receptor-specific targeting. The integrated PC3, intracranial GBM, and CAM platforms establish a translational pathway to evaluate BBB-penetrant, physics-based radioPDT. These studies are designed to define how physical forces—rather than receptor-mediated uptake—shape nanoparticle distribution, vascular response, DNA damage, oxidative injury, and overall radioPDT potency.

#2146 Innovative preclinical platform to highlight the impact of macro and microenvironment on pancreatic cancer development and therapy response.

Isabella Manni[1], Francesca Romana Auciello[1], Giulia Cristinziano[1], Clizia Maccaroni[1], Elena di Gennaro[2], Maria Serena Roca[2], **Giulia Piaggio**[1]

[1]IRCCS Regina Elena National Cancer Institute, Rome, Italy,[2]Inst. Nazionale Tumori IRCCS - Found. Pascale, Napoli, Italy

The poor outcome of pancreatic adenocarcinoma (PDAC) is due to the lack of early biomarkers and therapeutic options. The impact of the systemic temporal and spatial activation response, defined as macroenvironment, on PDAC is not fully understood. Key questions remain about the timing and occurrence of early systemic responses. This knowledge gap is primarily due to the absence of human and animal models that can intercept early tumor-related systemic perturbation before tumor uptake. We have developed the MITO-Luc reporter mouse model to measure physiological and/or aberrant proliferation in any body district by non-invasive bioluminescence imaging. To design new therapeutic protocols< with precise timing, targeting systemic aberrant proliferation before tumor appearance, we crossed MITO-Luc mouse with PDAC models carrying oncogenic Kras alone (KC) or with mutant p53 (KPC) in pancreatic cells. This mice model allows for the non-invasive tracking of early and late stages of PDAC development in live animals. Taking advantage of this model, we have been able to intercept early systemic events in the hematopoietic organs occurring significantly before the appearance of pre-cancerous lesions and/or a palpable tumor. We also have results regarding the molecular and cellular critical players involved in the early steps of PDAC development. To generate a preclinical platforms to explore the efficacy of new combination therapies, targeting both PDAC cells and microenvironment, we inoculated cell lines with different ability to recruit microenvironment derived from KC and KPC mouse models into MITO-Luc mice. We found a different immune cells and CAFs recruitment in tumors that recruit lower or higher number of proliferating endogenous cells. Furthermore, taking advantage of tumor slice cultures reflecting the state of tumor behavior and heterogeneity, we highlighted a simple approach to study cancers with intact microenvironment. We observed that, upon 72 hours of culture, PDAC, stromal and immunological cells are present and still alive.

: In Vivo Models 1: Mouse, Zebrafish, and Alternative Species
Poster Session

#2150 *Drosophila*-based screening identifies ferroptosis induction via NAD-GPx4 axis inhibition as a therapeutic strategy for PDAC.

Masahiro Sonoshita

Institute for Genetic Medicine, Hokkaido University, Sapporo, Japan

Pancreatic ductal adenocarcinoma (PDAC) remains one of the most lethal malignancies, and substantial progress has been made using mammalian models to elucidate its pathogenic mechanisms. To enable systematic discovery of actionable vulnerabilities, we generated a Drosophila PDAC model library that recapitulates key genetic alterations observed in human disease. Among these models, the *"4-hit"* flies—harboring alterations in *KRAS*, *TP53*, *CDKN2A*, and *SMAD4*, a genotype associated with the poorest clinical prognosis—exhibited robust tumorigenic manifestations, including epithelial transformation and impaired organismal viability. A genetic screen using this high-fidelity model uncovered a critical role for the nicotinamide adenine dinucleotide (NAD) biosynthesis pathway in promoting PDAC progression. Within this pathway, we identified glutathione peroxidase 4 (GPx4) as a key effector that mitigates reactive oxygen species (ROS)-mediated cytotoxicity. Combined inhibition of GPx4 and MEK using ML210 and trametinib, respectively, markedly ameliorated lethality and tumor-like phenotypes in the *4-hit* flies. Importantly, this combinatorial treatment synergistically suppressed proliferation of human PDAC cells and their corresponding xenografts, primarily by inducing ROS accumulation and triggering ferroptotic cell death.Collectively, these findings reveal a conserved dependency of PDAC on the NAD-GPx4 redox axis and demonstrate that therapeutic induction of ferroptosis represents a promising strategy to target genetically refractory PDAC.

#2151 Understanding the mechanisms by which environmental arsenic elevates the risk of urothelial bladder cancer.

Yuyang Huang[1], Britton C. Goodale[1], Jordan E. Magurk[1], Xiaoying Liu[2], Yang Zheng[1], Stephen A. Watts[3], Steven D. Leach[1]

[1]Department of Molecular and Systems Biology, Geisel School of Medicine at Dartmouth, Hanover, NH,[2]Department of Pathology and Laboratory Medicine, Dartmouth Hitchcock Medical Center, Lebanon, NH,[3]Department of Biology, The University of Alabama at Birmingham, Birmingham, AL

Arsenic (As) in drinking water is associated with increased risk of multiple malignancies, particularly urothelial bladder cancer (UBC), yet the underlying mechanisms remain poorly understood. We previously demonstrated that zebrafish possess a contractile urinary bladder with a specialized urothelium closely resembling the human bladder structurally and functionally. We and others have further shown that zebrafish As metabolism parallels that of humans and that zebrafish express the key As metabolism genes AS3MT and MTHFR. AS3MT is essential for methylating inorganic As into less toxic metabolites, while MTHFR is required for generating the universal methyl donor SAM; hypoactive SNPs in both genes are associated with increased UBC risk. Using both adult zebrafish and human cell lines, we aim to investigate how As impacts the bladder urothelium and elevates UBC risk. In a 28-day study, adult zebrafish exposed to 500 ppb As (III) exhibited histological evidence of As-induced hyperplasia and urothelial thickening. Bulk RNA-seq of As-exposed zebrafish bladders revealed upregulation of cancer-related pathways including MYC, mTOR, and unfolded protein response. Single cell RNA-seq further identified female-specific urothelial and non-urothelial clusters and revealed distinct clusters altered by As that differed between sexes, suggesting a potential link to the known sex bias in UBC. In both female and male urothelial clusters, As induced a shift of cells from a UPK+ phenotype to a less-differentiated UPK- phenotype. Loss of both luminal and basal markers including UPK3B, KRT5, and KRT15 was observed, while lineage-regulating factors like FOXA1 are retained. Induction of the AP-1 transcriptional complex, implicated in promoting tumor growth and invasion, was also observed. To validate, we employed the spontaneously immortalized human urothelial cell line HBLAK. While HBLAK cells are homogeneously basal, they can be induced with EGFR inhibition and PPARγ activation to express luminal markers, providing a platform to study urothelial differentiation. Upon induction, As-exposed HBLAK cells exhibited a dose-dependent decrease in both basal (KRT14) and luminal (UPK2) markers while retaining FOXA1 expression, accompanied by upregulated AP-1 components, consistent with zebrafish *in vivo* findings. As also induced global loss of histone and DNA methylation, with reduced SAM levels. We will employ newly generated AS3MT and MTHFR knockout zebrafish lines and human urothelial cell lines to understand As-induced epigenetic dysregulation and its link to disrupted differentiation. Our findings establish zebrafish as a powerful model for studying As-induced changes in urothelial differentiation and suggest that As induces urothelial cell dedifferentiation in both zebrafish and human models, which may lead to the early emergence of tumor-initiating cells during tumorigenesis.

#2153 The Miniature Oncopig® cancer model as an innovative large animal platform for preclinical pharmaceutical evaluation.

Taeyoung Shin[1], Jennifer J. Meudt[1], C. Dustin Rubinstein[1], Brent Lehman[1], **Lobna Elkhadragy**[2], Matthew M. Niemeyer[1], Jamie Reichert[1], Kathryn M. Nelson[1], Jennifer Frank[1], Ashley Nelson[1], Paige Munns[1], Devon Klipsic[1], Eric Schmuck[1], Mahmoud Khalafalla[3], Navin Viswakarma[3], Jessicca Rege[3], Ali Pirasteh[1], Lawrence B. Schook[3], Tanja Dominko[1], Dhanansayan Shanmuganayagam[1], Kyle M. Schachtschneider[3]

[1]University of Wisconsin-Madison, Madison, WI,[2]University of Illinois at Chicago, Chicago, IL,[3]Sus Clinicals, Inc., Chicago, IL

Background: Advances in cancer care rely on human-like preclinical animal models to evaluate safety, metabolism, pharmacokinetics, and efficacy of novel therapeutics in a translational manner. We previously developed the transgenic Oncopig®, a genotypically, anatomically, metabolically, and physiologically relevant large animal model that develops inducible tumors on demand. While the Oncopig® platform is ideal for short-term device-based therapeutic and diagnostic studies, its rapid growth and large size limits use for pharmaceutical and long-term efficacy studies. To overcome this limitation, we used the Wisconsin Miniature Swine™ (WMS™) to develop a miniature version of the Oncopig® (WMS™-Oncopig®). The WMS™-Oncopig® is a valuable model for preclinical drug studies due to its reduced size in addition to predisposition to obesity, metabolic disorders, and other clinically relevant cancer comorbidities.

Methods: The WMS™-Oncopig® transgene cassette was designed to harbor Cre recombinase-inducible *KRAS*^{G12D} and *TP53*^{R167H} driver mutations. The cassette also includes a mScarlet fluorescence gene flanked by LoxP sites, serving as a negative marker of Cre-induced recombination and driver mutation expression. Using CRISPR/Cas9 technology, the transgene cassette was inserted into the Rosa26 locus of WMS™ fibroblasts. After validation, the modified fibroblasts were used for reproductive cloning of WMS™-Oncopigs® by somatic cell nuclear transfer. Tumor induction studies were conducted on WMS™ -Oncopig® clones (n=2) with established Oncopig® liver tumor induction protocols, while the remaining clones were used for breeding.

Results: WMS™-Oncopig® fibroblasts were selected based on fluorescent imaging (mScarlet) and sequencing. Transgene cassette functionality was confirmed based on *KRAS*^{G12D} and *TP53*^{R167H} expression, increased proliferation, and loss of red fluorescence following nucleofection with a Cre recombinase-expressing plasmid. WMS™-Oncopigs® formed liver tumors within 2 weeks of induction using established Oncopig® tumor induction protocols. Finally, cells isolated from 3 of 5 fetuses generated by breeding WMS™-Oncopig® clones to wild-type WMS™ displayed red fluorescence, with genomic PCR confirming germline transmission of the transgene cassette.

Conclusions: The WMS™-Oncopig® model enables on-demand tumor induction in a clinically relevant pig breed with reduced size and growth compared to the current Oncopig® model. This, combined with predisposition to obesity and other clinically relevant cancer comorbidities supports the translational relevance of the WMS™-Oncopig® for preclinical oncologic drug metabolism, pharmacokinetic, safety, and efficacy studies. The WMS™-Oncopig® thus fulfills the current unmet need for translationally relevant models for preclinical investigation of novel cancer therapeutics.

#2154 Modeling olaparib resistance in prostate cancer PDXs to elucidate PARP inhibitor escape mechanisms.

Nadege BIDAN[1], Claire BERAUD[1], Emilie INDERSIE[2], Marie TAVERNIER[2], Clementine KRUCKER[3], Eric POTIRON[4], Philippe LLUEL[1], Olivier DEAS[2]

[1]Urosphere, Toulouse, France,[2]XenTech, Evry-Courcouronnes, France,[3]Department of Pathology, Institut Curie, Paris, France,[4]Department of Urology, Clinique Urologique, Nantes, France

Patient-derived xenografts (PDXs) are essential preclinical tools for modeling prostate cancer (PCa) biology and assessing therapeutic responses. Over the past years, we have established and comprehensively characterized a panel of 15 prostate cancer PDX models that recapitulate the histological and molecular heterogeneity of human disease. While PARP inhibitors such as olaparib provide clinical benefit to patients harboring BRCA1/2 mutations or homologous recombination deficiency (HRD), resistance inevitably emerges and remains a major clinical challenge. Here, we present insights that pave the way for characterizing mechanisms of PARP inhibitor resistance and identifying strategies to circumvent PARPi escape using our panel of PCa PDX models. Therapeutic responses to olaparib were evaluated across the biobank, alongside assessment of homologous recombination repair (HRR) status. Most PDX models displayed intrinsic resistance, whereas three showed marked sensitivity. Notably, a neuroendocrine prostate cancer (NEPC) PDX harboring DNA damage-repair alterations exhibited pronounced olaparib sensitivity, providing the first preclinical evidence supporting PARP inhibitor activity in a neuroendocrine context. These three sensitive models were then exposed to chronic treatment until tumor recurrence, generating acquired olaparib-resistant derivatives. Resistant PDXs were compared with their isogenic sensitive counterparts through histopathological analysis and transcriptomic and genomic profiling, with a focus on DNA repair and compensatory pathways. Multi-omic analyses indicate involvement of mechanisms such as partial restoration of homologous recombination and activation of alternative DNA repair pathways. Overall, this unique PCa PDX panel, together with the newly generated olaparib-resistant derivatives, constitutes a valuable preclinical resource for deciphering PARP inhibitor resistance mechanisms and informing the development of next-generation therapeutic combinations for prostate cancer.

#2156 Syngeneic mouse models of prostate cancer driver mutations.

Jean C. Tien[1], Yunhui Cheng[1], Fan Yang[1], Christina E. Wheeler[1], Abigail J. Todd[1], Somnath Mahapartra[1], Shuqin Li[1], Jie Luo[1], Rahul Mannan[1], Arul M. Chinnaiyan[2]

[1]Pathology, University of Michigan, Ann Arbor, MI,[2]University of Michigan, Ann Arbor, MI

Immunotherapy, such as immune checkpoint blockade, has emerged as a highly successful treatment for cancers including melanoma. While prostate cancer has been termed a “cold malignancy”, generation of models that effectively recapitulate the tumor immune environment offers an avenue by which immunotherapeutic approaches with potential clinical viability can be developed. Syngeneic mouse systems—in which implanted tumor tissue is genetically similar to that of a host animal—represent one such model. At present, syngeneic mouse models of prostate cancer—Myc-CaP, TRAMP-C2, RM1 and PPSM (*Pten*-/-; *P53*-/-; *Smad4*-/-)—do not encompass most driver mutations implicated in tumorigenesis. We therefore sought to broaden the suite of available syngeneic systems, by generating mice harboring tumors with the following mutations: *Cdk12* inactivation, *ERG* overexpression, *Myc* overexpression, *SPOP* mutation, *FOXA1* mutation, *BRAF* fusion, *Brca2* mutation, and MMR deficiency. In producing these lines, we applied a variety of molecular approaches, subjecting prostate tumor cells from pre-existing genetically modified mouse models (GEMMs e.g. *p53* knockout) to *in vitro* overexpression of fusion oncogenes (e.g. *ACPP-FGFR2*) or CRISPR-based knockout of tumor suppressor genes (e.g. *Msh2*). Growth of the resultant tumor lines in immunocompetent mice provided a platform for novel therapeutic testing. For instance, we generated organoids from *Rosa26*^{ERG}*;Pten* mice, then subcutaneously implanted them in C57Bl/6 hosts. Upon histological examination, resultant tumors exhibited classical adenocarcinoma histology strongly immunopositive for ERG. While tumors were essentially non-responsive to classical immune checkpoint blockade (anti-PD1), they exhibited reduced growth upon treatment with CBPD-409, a degrader of the key prostate cancer transcriptional coactivator CBP/p300. Strikingly, combination therapy with the aforementioned agents yielded overt tumor regression and marked tumor lymphocytic response encompassing CD4, CD8 and NK cells. This proof of concept experiment highlights the utility of our syngeneic models for *in vivo* combinatorial pharmacologic testing aimed at generating novel immunotherapy vulnerabilities.

#2157 Feasibility and challenges of developing PDX models of neuroendocrine cancers.

Caleb A. Morgan[1], Alexandria A. Peterson[1], Carlos H.F. Chan[2], Andrew M. Bellizzi[1], James R. Howe[3], **Po H. Ear**[1]

[1]University of Iowa, Iowa City, IA,[2]Carver College of Medicine, University of Iowa, Iowa City, IA,[3]Univ. of Iowa Hospitals and Clinics, Iowa City, IA

Neuroendocrine neoplasms (NENs) are a family of heterogenous cancers with neuronal and hormone-secreting features. NENs are subdivided into slow growing well-differentiated neuroendocrine tumors (NETs) and rapidly growing poorly differentiated neuroendocrine carcinomas (NECs). The incidence and prevalence of NENs have been steadily rising over the last twenty years. Yet, few effective therapeutic options are available for curing these complex diseases. The main bottleneck has been linked to the lack of preclinical NEN models for therapy testing. Recent advances in NET patient-derived organoid or spheroid models have significantly improved and contributed to accelerating the drug discovery pipeline. In addition, efforts in developing patient-derived xenograft (PDX) models of NECs have also been successfully reported by several research groups. However, efforts to develop PDX models of NETs remained largely unsuccessful. Our group aimed to prioritize the development of novel NET PDX models. We performed subcutaneous implantation of tumor cells isolated from 50 patient tumor samples from small bowel and pancreatic NETs (sbNETs and pNETs) in NOD scid IL2R gamma null (NSG) mice. Nine engraftments produced detectable tumors within 3-6 months. Of these, 2 sets of mice harbored spontaneously developed mouse tumors with no neuroendocrine feature, and 7 sets of mice harbored human tumor samples confirmed by short tandem repeat analyses to match with the original patient NET samples. Six of the 7 PDX tumors measured less than 5 mm in diameter at 4-6 months post-tumor cell implantation. Although these tumors were small, they recapitulated NET features and expressed NET markers such as synaptophysin (SYP), chromogranin A (CgA), or somatostatin receptor 2 (SSTR2), and have Ki67 staining in less than 25% of the tumor cells. One pNET PDX model yielded large tumors measuring over 10 mm in diameter at 3 months post-tumor cell implantation. Interestingly, these large tumors stained negative for SYP, CgA, or SSTR2, and displayed elevated Ki67 levels (over 35%). Analyses of the mutational landscape of these PDX models are underway and will reveal insights into key genetic regulators that hinder the development of NET PDX models. Overall, these findings highlight both the feasibility and challenges of developing NET PDX.

#2159 Establishment of new preclinical tumor models for pancreatic neuroendocrine carcinoma.

Takuto Yasuda[1], Ryota Tanaka[1], Daisuke Inoue[1], Koichi Nakanishi[1], Kosuke Hatta[1], Shigeaki Kurihara[1], Jun Tauchi[1], Sadaaki Nishimura[1], Masahiko Kinoshita[1], Kohei Nishio[1], Hiroji Shinkawa[1], Ken Kageyama[2], Akira Yamamoto[2], Takeaki Ishizawa[1]

[1]Hepatobiliary-Pancreatic Surgery, Osaka Metropolitan University, Osaka, Japan,[2]Diagnostic and Interventional Radiology, Osaka Metropolitan University, Osaka, Japan

Introduction: Pancreatic neuroendocrine carcinoma (PanNEC) is an extremely aggressive and rare malignancy with a poor prognosis. Owing to its rarity, therapeutic development has been significantly delayed, highlighting the urgent need for novel treatment strategies. Although preclinical models such as cell lines and patient-derived xenograft (PDX) models are essential tools for drug discovery, only one PanNEC cell line has been reported to date. In this study, we successfully established novel PanNEC cell lines and multiple PDX models and aimed to clarify their biological features and drug responses.

Experimental procedures: Tumor tissue obtained from a PanNEC patient was sutured onto the pancreatic tail of severe combined immunodeficient (SCID) rats to generate orthotopic pancreatic PDX models. In addition to orthotopic models, subcutaneous models and peritoneal dissemination models were created. Tumor tissue and malignant ascites obtained from orthotopic PDX models were subjected to primary culture, leading to the establishment of two novel PanNEC cell lines. Drug sensitivities to etoposide, irinotecan, cisplatin, and carboplatin were assessed using the CCK-8 assay. Furthermore, cell line-derived xenograft (CDX) subcutaneous models were generated to validate in vivo tumorigenicity.

Summary of the data: The engraftment rate of the orthotopic pancreatic PDX was 100% (2/2), with engraftment requiring approximately two months. Both tumor-derived and ascites-derived cell lines exhibited semi-adherent morphology. Tumor-derived cells showed planar adherent proliferation, whereas ascites-derived cells demonstrated three-dimensional spheroid-forming growth. The doubling times were 2.7 and 2.5 days, indicating strong proliferative capacity. Immunohistochemistry showed consistent expression of markers such as synaptophysin and chromogranin A across the primary tumor, PDX models, CDX models and the established cell lines. CCK-8 assays revealed growth-inhibitory effects for all four drugs without notable resistance, and the combination of etoposide and cisplatin demonstrated a synergistic effect.

Conclusion: We successfully established novel PanNEC cell lines and multiple PDX models, including orthotopic, subcutaneous, and peritoneal dissemination models, as well as CDX models. These rare models provide a valuable platform for future preclinical studies and may facilitate the development of new therapeutic strategies for PanNEC.

#2161 Paired PDX-PDXO models serve an integrated preclinical platform for high-throughput payload screening and ADC drug development.

Jinxi Wang, Leilei Chen, Qingzhi Liu, Jiawen Gao, Jun Zhou, Wubin Qian, Likun Zhang, Ludovic Bourre, Jessie Jingjing Wang

Crown Bioscience, Inc., San Diego, CA

Introduction Antibody-drug conjugates (ADCs) offer an effective and targeted strategy to kill tumor cells by delivering potent cytotoxic payloads directly to tumor cells. However, payload activity can lead to the emergence of resistance through ADC mechanisms such as altered metabolism, efflux pumps, or impaired intracellular activation. Here, we describe an integrated strategy using patient-derived xenograft (PDX) models and paired PDX-derived organoids (PDXOs) for high-throughput payload screening to guide the selection of optimal ADCs and the preclinical validation.

Methods PDX models were successfully established from a metastatic triple-negative breast cancer patient who showed resistance to Sacituzumab Govitecan (Trodelvy®), an ADC incorporating a topoisomerase I (TOP1) inhibitor payload (SN-38). The phenotypic and biomolecular characteristics of these models were thoroughly validated via RNA sequencing and whole-exome sequencing (WES). PDX-derived organoid (PDXO) model was developed from fresh PDX tumor tissue. *In vivo* efficacy was evaluated by tumor growth inhibition (TGI) ratio of each treatment group was calculated by formula: 1-Delta (Treatment group)/ Delta (Vehicle group). *In vitro* response to different payload of organoids were tested using CellTiter-Glo (CTG) assay and assessed by IC50 values.

Results Biomarker analysis showed the PDXO models faithfully recapitulated key features of the corresponding PDX tumors, including high TROP2 expression and reduced sensitivity to Trodelvy. High-throughput *in vitro* cytotoxicity screening of various ADC payloads revealed a distinct sensitivity profile in these PDXOs: they were insensitive to TOP1 inhibitor payloads (SN-38: IC50>0.008 and DXD: IC50>0.007) but exhibited sensitivity to the tubulin-targeting agent monomethyl auristatin E (MMAE: IC50≤0.0004). Subsequent *in vivo* efficacy studies of the PDX models with ADCs with different payloads shown consistent sensitivity with the PDXO screening results. The PDX models showed less sensitivity to Trodelv Dato-Dxd and SKB264 which carry TOP1 inhibitor payloads (TGIs rang 24%-57%) but were more sensitive to Dato-MMAE, which showed obvious tumor regression with a TGI of more than 90%, thereby showing correlation with the *in vitro* predictions.

Conclusion This study validates an efficient and integrated preclinical platform for early-stage ADC development. The combined PDX/PDXO approach significantly streamlines the ADC discovery process by enabling high-throughput payload screening, helping prioritize the most promising ADC candidates before advancing to more resource-intensive *in vivo* studies. This streamlined strategy accelerates data-driven decision-making for developing more effective, patient-tailored ADC therapies and for overcoming clinical resistance mechanisms.

#2162 GliomaPDOX - A direct brain-to-brain glioma xenograft library for drug discovery and development.

Elizabeth G. Fernandez[1], Christopher Tse[1], Jennifer Salinas[1], Nicholas Bayley[1], Lisa H. Ta[1], Laura Gosa[1], Henan Zhu[1], Michael Vigman[1], Francesco Sanvito[1], Benjamin M. Ellingson[2], Linda M. Liau[3], Timothy Cloughsey[1], Thomas G. Graeber[1], Nathanson David[1]

[1]University of California, Los Angeles, Los Angeles, CA,[2]Assistant Professor of Radiology; Dept. of Radiological Sciences, University of California, Los Angeles, Los Angeles, CA,[3]UCLA David Geffen School of Medicine, Los Angeles, CA

Cancer drug discovery and development rely on preclinical models that accurately reflect the molecular and functional characteristics of human tumors, while accounting for *in vivo* factors that influence drug efficacy, such as pharmacokinetics, metabolism and toxicity. Malignant gliomas are highly aggressive brain tumors that develop within the brain parenchyma, where their heterogeneous cellular composition engage in complex interactions with highly specialized brain cells, and a blood brain barrier that restricts drug penetration. When removed from this native environment, such as in culture or heterotopic *in vivo* environments (e.g., flank), gliomas either lose their molecular diversity or fail to grow altogether. Therefore, there is a critical need for physiologically relevant models that capture both the intra and inter-tumor diversity of glioma, as well as the organismal context required for drug development. Here, we present GliomaPDOX - a direct brain to brain glioma orthotopic xenograft biobank, consisting of more than 200 unique models that faithfully recapitulate the key molecular, histopathological, and proliferative features of their parental tumors. By incorporating a non-invasive, secreted reporter system to monitor tumor burden in real time—including drug-induced changes in intracranial tumor growth—we demonstrate the utility of GliomaPDOX for therapeutic evaluation. Together, this robust platform provides a physiologically relevant system to accelerate drug discovery and development for glioma.

#2163 Triple-negative breast cancer PDX models with acquired resistance to Enhertu®: A preclinical platform to uncover mechanisms of escape.

Emilie INDERSIE, Benjamin GUERRIN, Eugenie DELHORBE, Eva CYPRIEN, Elena DARBINEAN, Delphine NICOLLE, Marie TAVERNIER, **Olivier DEAS**

R&D, XenTech, Evry-Courcouronnes, France

Triple-negative breast cancer (TNBC) remains an aggressive and heterogeneous subtype with a poor prognosis. Although the antibody-drug conjugate Enhertu® (trastuzumab deruxtecan, T-DXd) has shown clinical activity in a subset of TNBCs with low HER2 expression, the rapid emergence of resistance limits its long-term efficacy. Robust preclinical models are therefore essential to investigate resistance mechanisms and evaluate novel therapeutic combinations. Within our panel of 40 TNBC patient-derived xenografts (PDXs), 14 were exposed *in vivo* to Enhertu®, of which 11 were sensitive. Among these, some PDX models were treated until the development of acquired resistance. To date, we have established five resistant derivatives from three initially sensitive models through continuous T-DXd exposure. Transcriptomic profiling was performed by RNA sequencing (HTSeq), followed by DESeq-based normalization and differential expression analysis. Functional enrichment analyses focused on predefined pathways related to endocytosis, receptor recycling, lysosomal trafficking, drug efflux, and DNA repair. Differential expression analysis revealed hundreds of significantly modulated genes. HER2 expression was assessed by immunohistochemistry, and RNA-Seq expression levels and mutational status of lysosomal cathepsins (CTSD, CTSB, CTSL) were examined in detail, given their potential involvement in the observed resistance mechanisms. In addition, resistant models were tested with HER2-targeting agents and a topoisomerase I inhibitor to evaluate the respective contributions of the two pharmacological targets of Enhertu® in the resistance mechanisms. Overall, resistance to Enhertu® in TNBC PDX models involves multifactorial adaptations, including signaling pathway reprogramming, altered drug efflux, and modulation of DNA repair. This collection of resistant models represents a valuable preclinical resource to investigate resistance mechanisms and to support the development of novel therapeutic strategies.

#2164 Breast cancer PDX models with acquired resistance to olaparib: A preclinical platform to uncover mechanisms of PARP inhibitor escape.

Emilie INDERSIE, Benjamin GUERRIN, Eugenie DELHORBE, Eva CYPRIEN, Elena DARBINEAN, Delphine NICOLLE, Marie TAVERNIER, **Olivier DEAS**

XenTech, Evry-Courcouronnes, France

PARP inhibitors (PARPi), such as olaparib, have significantly improved the prognosis of breast cancer patients harboring BRCA1/2 mutations or with homologous recombination deficiency (HRD). However, the emergence of acquired resistance remains a major clinical obstacle. Robust preclinical models are therefore essential to elucidate the mechanisms of resistance and evaluate new therapeutic strategies. Within our cohort of 55 patient-derived breast cancer (PDX) xenografts, 51 were exposed *in vivo* to olaparib, of which 19 showed sensitivity. Several HRD models were then chronically treated with olaparib until tumor recurrence, indicating acquired resistance. Resistant tumors and their parental sensitive counterparts were comprehensively compared using histopathological, transcriptomic (RNA-seq), and genomic (whole-exome sequencing) analyses. To date, we have established a panel of nine olaparib-resistant derivatives from six initially sensitive PDX models through continuous *in vivo* exposure. These resistant models exhibit heterogeneous resistance mechanisms, including BRCA1 mutation reversion, partial restoration of homologous recombination, and overexpression of DNA repair pathways. Overall, this panel of olaparib-resistant PDX breast cancer models represents a valuable preclinical resource to investigate PARPi resistance mechanisms and to guide the development of second-line combination therapies for HRD breast cancer.

#2165 An integrated preclinical platform for comprehensive evaluation of T-Cell engagers.

Hongyan Sun, Xinjie Lian, Shiying Guo, Yujing Zhang, Huixin Yang, Xiang Gao

GemPharmatech Co., Ltd., Nanjing, China

T-cell engagers (TCEs) are bispecific antibodies designed to bind both CD3 on T cells and a tumor-associated antigen (TAA) on cancer cells, representing a promising class of immunotherapies. Given their complex mechanisms of action, physiologically relevant preclinical models are essential for accurately evaluating the efficacy and safety profiles of TCE candidates. We developed a panel of medium- to high-throughput in vitro assays to screen TCEs based on target binding, T-cell activation, and tumor cell killing capabilities. Lead candidates were further assessed using in vivo efficacy studies in both xenograft and syngeneic models. In xenograft studies, we utilized NCG mice and NCG-MHC-dKO mice—the latter generated by deleting murine MHC class I and II genes in the NCG background—to reduce graft-versus-host disease (GvHD) after human PBMC engraftment and extend the experimental observation period. AMG509 (targeting STEAP1), AMG757 (targeting DLL3), and IBI-389 (targeting CLDN18.2) were evaluated in models of prostate cancer, small-cell lung cancer, and patient-derived xenografts (PDX), respectively. For syngeneic studies, we used BALB/c-hCD3EDG mice, in which endogenous Cd3e, Cd3d, and Cd3g genes were replaced with human versions. These mice were engrafted with A20-hCD20 lymphoma cells to test a CD3/CD20 bispecific antibody.

Both AMG509 and AMG757 significantly suppressed tumor growth in PBMC-humanized NCG and NCG-MHC-dKO models, with no major adverse effects on animal health. The efficacy of AMG509 varied across prostate cancer cell lines with different levels of STEAP1 expression. In NCI-H69 tumor-bearing mice treated with AMG757, the degree of tumor response correlated with the extent of human immune cell reconstitution observed three weeks post-treatment. IBI-389 exhibited marked tumor growth inhibition in two gastric cancer PDX models and one pancreatic cancer PDX model. In the BALB/c-hCD3EDG syngeneic model, administration of the CD3/CD20 bispecific antibody led to 81.5% tumor growth inhibition after 18 days.

GemPharmatech's integrated strategy—combining in vitro screening with a range of in vivo models such as NCG, NCG-MHC-dKO, and CD3-humanized mice—enables rapid, scalable, and translationally relevant assessment of T-cell engager candidates. This comprehensive platform supports robust and efficient immuno-oncology drug discovery and development.

#2166 Robust *in vivo* CAR-T efficacy evaluation in a PBMC-reconstituted NCG-MHC-dKO model with delayed GVHD.

Hongyan Sun, Xiaoliu Yang, Shiying Guo, Yujing Zhang, Huixin Yang, Xiang Gao

GemPharmatech Co., Ltd., Nanjing, China

Background: Humanized mouse models are critical for evaluating in vivo CAR-T therapies, but their utility is limited by rapid onset Graft-versus-Host Disease (GVHD). We employed a novel NCG-MHC-dKO model to mitigate GVHD, enabling prolonged assessment of anti-tumor efficacy for different in vivo CAR-T modalities. **Methods:** The NCG-MHC-dKO model was reconstituted with human PBMCs, confirming delayed GVHD. Mice bearing Nalm-6 tumors were treated with a single dose of either a lentiviral vector or an LNP formulation delivering a CD19-targeting CAR. Tumor growth was monitored via bioluminescence imaging. **Results:** The PBMC-NCG-MHC-dKO model demonstrated a significantly extended observation window due to postponed GVHD. In this model, both lentiviral and LNP-based in vivo CAR-T therapies potently suppressed Nalm-6 tumor growth. Functional CAR-T cells generated in vivo were detected and expanded in treated mice. **Conclusion:** The PBMC-reconstituted NCG-MHC-dKO model provides a robust and durable platform for in vivo CAR-T evaluation by overcoming early GVHD. We successfully validated its utility for both lentiviral and LNP delivery platforms, demonstrating significant and comparable anti-tumor efficacy.

#2167 A novel humanized mouse model for preclinical assessment of anti-CD47 and anti-SIRPAtherapeutics.

Hongyan Sun, Shaotong Ma, Yujing Zhang, Huixin Yang, Xiang Gao

GemPharmatech Co., Ltd., Nanjing, China

Background: CD47, a ubiquitously expressed "don't eat me" molecular signal, mediates the evasion of tumor cells from phagocytic clearance through specific interaction with signal regulatory protein alpha (SIRPA) expressed on the surface of macrophages and dendritic cells. Therapeutic agents targeting the CD47-SIRPA pathway promote tumor cell eradication through two well-characterized mechanisms: 1. Blocking antibodies, including monoclonal and bispecific antibodies, interfere with the CD47-SIRPA interaction to enhance macrophage-driven phagocytosis of tumor cells; 2. The Fc domain mediates antibody-dependent cellular cytotoxicity (ADCC) and complement-dependent cytotoxicity (CDC). These biological processes further strengthen dendritic cell-mediated antigen presentation and initiate anti-tumor adaptive immune responses, which collectively establishes the CD47-SIRPA axis as a high-priority target in immuno-oncology.
Methods: To support the translational assessment of CD47-targeted therapies, GemPharmatech developed a BALB/c-derived double humanized hCD47/hSIRPα knock-in mouse model, in which the extracellular domains of human CD47 and SIRPA were expressed. Successful model construction was verified by detecting the protein expression levels of hCD47 and hSIRPA in BALB/c-hCD47/hSIRPA mice. This model was used to evaluate the anti-tumor efficacy of the anti-hCD47 antibody Magrolimab (5F9) using a CT26-hCD47 colorectal tumor model—established by engrafting CT26 overexpressing human CD47 into BALB/c-hCD47/hSIRPA mice. Given the well-documented toxicity of CD47 blockade, anti-SIRPA antibodies were also tested to explore an alternative targeting strategy. Additionally, the anti-tumor efficacy of the hSIRPA × hClaudin18.2 bispecific antibody (BsAb) was evaluated in BALB/c-hCD47/hSIRPA mice bearing the EMT6-hCD47-hClaudin18.2 triple-negative breast tumor model, where EMT6 cells overexpress both human CD47 and human Claudin18.2.
Results: Expression of hCD47 and hSIRPA in BALB/c-hCD47/hSIRPA mice was successfully verified. Administration of the anti-hCD47 antibody induced dose-dependent tumor regression in the established colorectal tumor model. Notably, the hSIRPA×hClaudin18.2 bispecific antibody (BsAb) exerted a significant anti-tumor effect in BALB/c-hCD47/hSIRPA knock-in mice implanted with EMT6-hCD47-hClaudin18.2 tumor cells.
Conclusions: The BALB/c-hCD47/hSIRPA mouse model serves as a clinically relevant tool for evaluating therapeutics targeting the CD47-SIRPA pathway within an immuocompetent model. Notably, it addresses key limitations of traditional immunocompromised murine models while providing critical insights into the mechanisms underlying CD47 pathway-mediated tumor clearance, toxicity management, and immune activation.

#2168 Human IgG1-expressing mouse models for tolerance induction and reliable assessment of IgG1-based therapeutic antibodies.

Angela Pappalardo, Gaelle H. Martin, Patricia Isnard-Petit, **Fabiane Sonego**, Kader Thiam

genOway, Lyon, France

Mouse models expressing human targets offer strong translational relevance for evaluating human antibody-based therapies in IO. However, when treated with human antibodies, these models frequently develop anti-drug antibodies (ADA), which can compromise the interpretation of preclinical data. ADA formation may alter pharmacokinetics, reduce therapeutic efficacy, and introduce immune-related artifacts that do not reflect human responses. This immune recognition limits the duration and reliability of treatment studies, especially for repeated dosing or long-term efficacy assessments. Therefore, careful selection and engineering of preclinical models that minimize ADA formation are essential to accurately predict clinical performance and support the development of safe and effective biologics. We generated a model expressing humanized IgG1, the most used isotype in clinical development, which was designed to induce tolerance to human IgG1-based therapies. Herein, we describe the investigation of the tolerance induced by the expression of hIgG1 in a mouse model humanized for serum albumin, FcRn, which was developed to investigate PK profile of antibodies in a context of tolerance to hIgG1. Both hSA and FcRn have already been shown to be expressed and enable half-life extension of compounds with enhanced binding to hFcRn and hSA in genO-hSA/hFcRn mice (Viuff *et al.*, 2016). Humanization has been confirmed by the detection of circulating human IgG1 levels in mice. Other immunoglobulins are also present in their serum, with only minor differences relative to WT mice, and suggesting no impairment on class switch. To test the tolerance to hIgG1, mice received a weekly injection of Teropavimab (anti-gp120- hIgG1κ) for 7 weeks. Blood was collected 2 hours after each injection for quantification of circulating Teropavimab. Expression of hIgG1 in mice leads to better tolerance to multiple cycles of Teropavimab compared to WT and genO-hSA/hFcRn mice. Indeed, one week after the last injection (day 49), Teropavimab is not detected in genO-hSA/hFcRn mice, whereas is detected in 2/5 WT mice, and in 5/5 mice expressing hIgG1 mice. Taken together, these results indicate that constitutive expression of hIgG1 promotes immunological tolerance to repeated administrations of therapeutic hIgG1 in murine models. Moreover, hIgG1 expression has been integrated into advanced mouse models such as genO-PanhCD3 and genO-FcγR to enable tolerance induction in experimental systems designed for the evaluation of T-cell engagers and Fc-mediated effector functions, respectively. In addition, an hIgG1-expressing variant of genO-TFRC model is available to support the characterization of hIgG1-based antibodies engineered for TFRC-mediated transcytosis, facilitating targeted delivery of therapeutic antibodies across the blood-brain barrier.

#2170 Patient-derived orthotopic xenograft models predict chemotherapeutic response in pancreatic ductal adenocarcinoma: an emerging platform for translational research.

Xin Zhang[1], Nathan Bolton[2], Alicia Ray[1], Grace Maresh[1], Rachel Graham[3], Li Li[1]

[1]Institute of Translational Research, Ochsner Health System, New Orleans, LA,[2]Department of Surgical Oncology, Ochsner Health System, New Orleans, LA,[3]Multi-specialty Clinical Research, Ochsner Health System, New Orleans, LA

Background: Pancreatic Ductal Adenocarcinoma (PDAC) is the third leading cause of cancer death. Current chemotherapy options are centered on a gemcitabine as backbone. However, the chemotherapy responsive rate and prognosis are still very poor with a five-year survival rate of 13%. Animal models mimicking tumor microenvironment have been used for pre-clinical and therapeutic studies, but the subcutaneous xenograft model does not replicate the clinical location and human PDAC chemotherapy responses. In this study, we used patient-derived orthotopic xenograft (PDOX) mouse models, with tumors localized to the pancreases, that mimic the natural tumor microenvironment, to test the efficacy of chemotherapeutic gemcitabine on PDAC progression and compare to their clinical response.
Methods: Totally 71 PDAC patients were consented and their tumor/blood specimens were collected after reviewed by pathologists. Tumor cells from one representative partial/moderate chemo-responding PDAC patients (PaCa23) and one representative poor chemo-responding PDAC patient (PaCa54), were expanded, isolated and intra-pancreas injected to NOD/SCID mice. Gemcitabine (100 mg/kg) was administered weekly by intravenous infusion for 4 weeks. Tumor volumes and mouse body weights were monitored weekly. After mice were euthanized, tumors were collected for tumor weight measurement. Hematoxylin & Eosin staining and OpalTM 4-color immunofluorescence staining were performed for tumor cell profile and tumor microenvironment study.
Results: Our PDOX model in both PaCa23 and PaCa54 retains the principal histologic characteristics of their donor tumor with similar infiltration patterns of stromal cells and remains stable across passages. No significant body weight loss was observed in the gemcitabine group. PaCa23 tumor responded to gemcitabine with significantly decreased tumor volume and tumor weight compared to control group ($p=0.007$ and $p=0.01$, respectively). PaCa54 tumor poorly responded to gemcitabine without significant tumor weight decrease compared to controls ($p>0.05$).
Conclusion: Our PDOX mouse model successfully recapitulates key histopathological and microenvironmental features of human PDAC and reflects patient-specific responses to gemcitabine treatment. The differential tumor response observed in PaCa23 and PaCa54 models mirrors their respective clinical outcomes, underscoring the predictive value of this platform. This orthotopic model holds significant promise as a preclinical tool for evaluating chemotherapeutic efficacy, guiding personalized therapy strategies, and studying tumor biology within a clinically relevant microenvironment.

#2171 Maintaining blood-brain barrier integrity in translational brain tumor models.

T. Liz Bailey, Melissa Tran, Cheryl Davis, Ben Hoerner, Victoria Caruso, Kathleen Hutchinson, Helen Ketteringham, Corrine Silvio, Shannan Paul, Chris Holding, Aliccia Koznecki, Dawn Lusk, Shorena Nadaraia-Hoke

Reaction Biology Corp, Malvern, PA

Brain metastases remain exceptionally challenging to treat, in part because many candidate therapies fail to demonstrate the clinical benefit observed in preclinical studies. A major contributor to this gap is the limited ability of traditional animal models to accurately replicate the functional blood–brain barrier (BBB). Conventional intracranial orthotopic tumor models are commonly used but inherently compromise BBB integrity, reducing their utility for evaluating drug penetration and therapeutic performance. Other implantation routes, such as intravenous or intracardiac delivery, better preserve the BBB but often produce extensive extra-cranial metastases, shortening study duration and diminishing relevance for brain-specific disease.

To overcome these limitations, we established an intra-carotid tumor cell delivery method that selectively seeds the brain while minimizing systemic spread. This technique enables localized tumor growth in disease relevant brain regions without disrupting BBB architecture. Tumor progression and spatial distribution were followed longitudinally using magnetic resonance imaging (MRI) together with bioluminescence imaging (BLI). These modalities consistently demonstrated reliable brain colonization and supported high-resolution tracking of tumor growth dynamics.

Our intra-carotid model provides a more physiologically faithful system for studying metastatic brain disease. By retaining BBB functionality and supporting reproducible, long-term monitoring, this platform offers a powerful tool for assessing BBB-permeant therapeutics and may enhance the translational value of preclinical studies in for brain targeted therapies, particularly in the context of metastatic disease.

#2172 Differential expression of the Kv3.4 channel in *in vitro* and *in vivo* models of cervical cancer: Potential clinical implications.

Ana Alejandra Ramirez[1], Andrea Jazmin Chiliquinga[2], Ingrid Ogonaga-Borja[2], Brenda Acosta[2], Patricio Gariglio[3], Rodolfo Ocadiz-Delgado[3], Jaime de la Garza[4], Elisabeth Hernandez-Gallegos[5], Maria de Guadalupe Chavez-Lopez[5], J. Martha Noyola[5], Javier Camacho[5]

[1]Faculty of Chemical Sciences and Engineering, Autonomous University of Baja California, Tijuana, B.C., Mexico,[2]Technical University of the North, Ibarra, Ecuador,[3]Department of Genetics and Molecular Biology, Center for Research and Advanced Studies of the National Polytechnic Institute, Mexico City, Mexico,[4]National Institute of Cancerology, Mexico City, Mexico,[5]Department of Pharmacology, Center for Research and Advanced Studies of the National Polytechnic Institute, Mexico City, Mexico

Introduction: Cervical cancer remains a major global health concern, and current diagnostic methods have significant limitations, highlighting the need for improved molecular biomarkers. Its progression is primarily linked to HPV infection, estrogen exposure, and ion channel deregulation. Ion channels such as Kv3.4 have gained relevance due to their involvement in carcinogenesis. This study examines the gene and protein expression of the Kv3.4 (KCNC4) channel in cervical cancer models and evaluates the effects of its pharmacological blockade as a potential diagnostic and therapeutic strategy.
Experimental procedure: KCNC4 gene expression was study in HeLa and SiHa cells by qRT-PCR, while Kv3.4 protein was evaluated by immunocytochemistry in HeLa, SiHa, normal keratinocytes (KN) and keratinocytes with HPV16 E6/E7 oncogenes (KT E6E7). The effect of Kv3.4 functional inhibition was assessed by metabolic activity assays following treatment with the Kv channel blocker BDS-I. In vivo model from four mouse groups: transgenic K14E7 mice treated with 17β-estradiol (K14E7+E2), untreated K14E7 mice, non-transgenic FvB mice treated with 17β-estradiol (FvB+E2), and untreated FvB controls, were examined by immunohistochemistry to determine the impact of HPV oncogenes and estrogen exposure on Kv3.4 regulation in cervical epithelium.
Results: Gene expression analysis showed a significantly higher KCNC4 expression in HeLa cells compared with SiHa cells, consistent with their differing HPV copy numbers. Immunocytochemistry confirmed Kv3.4 protein expression in HeLa, SiHa, and KT E6E7 cells, but not in KN cells. BDS-I treatment significantly reduced metabolic activity only in KT E6E7 cells, with no effect in KN cells. In mouse cervical tissues, Kv3.4 expression was strongest in FvB+E2 mice, followed by K14E7 and untreated FvB at 4 months. At 7 months, expression remained highest in FvB+E2, then K14E7+E2, K14E7, and FvB, indicating that estrogen exposure and HPV oncogenes enhance Kv3.4 expression in vivo.
Conclusion. Our findings show that the Kv3.4 channel is linked to HPV-related cervical carcinogenesis. Kv3.4 protein was detected in HeLa, SiHa, KT E6E7, and in cervical tissues from FvB+E2, K14E7+E2, and K14E7 mice, indicating that estrogen and HPV oncogenes upregulate the channel in vivo. Notably, Kv3.4 blockade selectively reduced proliferation in KT E6E7 cells, suggesting a greater dependence of HPV-transfected keratinocytes on this channel. Overall, these results support Kv3.4 as a potential biomarker and therapeutic target in early HPV-mediated cervical cancer. Partially supported by Conacyt grant A1-S-9783 to JdlG.

#2173 Development of novel syngeneic mouse models of mHSPC and mCRPC for evaluation of radiopharmaceuticals on the immune tumor microenvironment (TME).

Brian Ragaishis[1], Andrei Molotkov[2], Shruti Bansal[1], Krishan Saini[1], Meirdan Palihati[1], Chelsea Rahiman[2], Courtney Buress[1], Jasleen Kaur Virk[1], Mikhail Doubrovin[2], Catherine Spina[2]

[1]Radiation Oncology, Columbia University Irving Medical Center, New York, NY,[2]Columbia University Irving Medical Center, New York, NY

Introduction Radiopharmaceutical therapy (RPT) offers a safe and effective treatment for metastatic castrate resistant prostate cancer (mCRPC), however little is known about the differential impact of α- and β-emitters at the single cell level and on the immune tumor microenvironment (TME). This investigation aims to design novel mHSPC and mCRPC syngeneic mouse models to compare the therapeutic efficacy of α- and β-emitting RPTs and understand how different RPTs influence immune cell dynamics within the TME.

Methods We developed two novel murine PC cell lines that over express FOLH1/PSMA, MyC-CaP^{PSMA+} and MyC-CaP$^{HER2+PSMA+}$ (HER2 serving as a tumor antigen to quantify anti-tumor immune responses). Cell lines were developed by lentiviral transduction using EGFP+ as a positive selection marker. Transduction stability was confirmed by EGFP positivity by flow cytometry. We characterized expression of FOLH1 (the gene encoding PSMA) and PSMA by qPCR and western blot (WB), respectively, and quantified uptake of 68Ga-PSMA-11 in vitro. In immunocompetent FVB/NJ mice, MyC-CaP and MyC-CaP^{PSMA+} growth kinetics were evaluated and tumor PSMA expression was quantified by qPCR and WB. In vivo, we conducted biodistribution studies with 177Lu-PSMA-617 in mice bearing bilateral subcutaneous MyC-CaP and MyC-CaP^{PSMA+} tumors. After delivery of 3-5MBq, tumor and normal tissues were collected at 4 timepoints post-treatment (1h, 24h, 72h, 168h) and activity in the tumor and normal tissues was estimated using a HIDEX gamma-counter. Tumor and tissue percent injected dose per gram (%ID/g) was calculated. Mice bearing single flank 200mm^3 MyC-CaP^{PSMA+} tumors were chemically castrated with degarelix (25mg/kg body weight) to generate a mCRPC model.

Results MyC-CaP^{PSMA+} and MyC-CaP$^{HER2+PSMA+}$ showed a 10x increase in FOLH1 gene and protein expression compared to parent MyC-CaP and MyC-CaP^{HER2+}. In our in vitro uptake assay, we demonstrated a 30-50x increase in 68Ga-PSMA-11 uptake by transduced cell lines. In vivo, MyC-CaP^{PSMA+} tumors showed 1000x increase in expression of FOLH1 compared to parent MyC-CaP tumors. However, compared to in vitro, FOLH1 expression decreased by 10-fold in 33-day old tumors, likely due to immunoediting. Biodistribution studies demonstrated tumor MyC-CaP^{PSMA+} %ID/g was 33x higher compared to MyC-CaP tumors, with a Tumor/Kidney absorption ratio of 0.39, on par with other well-characterized models of mHSPC. 100% of MyC-CaP^{PSMA+} tumors treated with degarelix regressed for 20 days before rebounding.

Conclusion Here we reveal translationally relevant models of mHSPC and mCRPC for mechanistic investigations of α- and β-emitting RPTs. Leveraging these tools, we aim to study DNA damage and immune responses to generate foundational data to guide the development of combination therapies to improve outcomes of RPT for patients with mHSPC and mCRPC.

#2174 A comprehensive CRISPR/Cas9-based RAS knock-in cell line platform (50+ models) for assessing efficacy of KRAS-targeted inhibitors in RAS-mutant malignancies..

Lin Zhou, Guoqian Wang, Tingduo Lv, Zidan Su, Yue Huang, Jinying Ning, **Feng Hao**

Kyinno Biotechnology Co., LTD, Beijing, China

The rat sarcoma gene (RAS) was the first discovered human proto-oncogene. Its product, the RAS protein, is a small guanine nucleotide-binding protein with intrinsic guanosine triphosphatase (GTPase) activity. Currently, three subtypes are known in the RAS family: KRAS, NRAS, and HRAS.RAS is a key mediator of the MAPK pathway. Activated RAS proteins bind GTP, while inactivated RAS proteins bind GDP; thus, the function of RAS proteins primarily depends on their GTP/GDP ratio. Missense mutations in the RAS protein alter the GDP/GTP homeostasis and lead to sustained activation of signaling pathways by reducing GTP hydrolysis (G12, Q61), increasing GTP loading rates (G13, K117), or affecting nucleotide exchange (A146). This uncontrolled signaling promotes unregulated cell proliferation and ultimately leads to carcinogenesis. RAS mutations occur most frequently in the KRAS subtype (>80%), followed by NRAS and HRAS. Notably, KRAS mutations are found in 97.7% of pancreatic ductal adenocarcinomas. In colorectal adenocarcinoma, multiple myeloma, lung adenocarcinoma, and cutaneous melanoma, the overall prevalence of RAS mutations is 52.2%, 42.6%, 32.2%, and 29.4%, respectively.For decades, RAS was notoriously considered an "undruggable" target, posing significant challenges for drug development. The approval of AMG510 (sotorasib) broke this barrier, proving that direct targeting of RAS is achievable. Since then, the field of RAS-targeted therapy has advanced remarkably, moving the "undruggable" label into the past. With deepening understanding, targeting RAS is poised to drive the next wave of breakthroughs in cancer treatment.Using CRISPR/Cas9 technology, we have developed over 50 knock-in cell line models with KRAS and NRAS mutations for evaluating KRAS-targeted inhibitors. These include common mutations such as G12C, G12D, and G12V, as well as various double and triple mutation combinations. This Ras knock-in mutant cell line platform stands as a powerful tool for developing and evaluating the next generation of RAS inhibitors.

#2175 Towards ethical and robust drug development: comprehensive validation of an animal-free matrix for in vivo tumor models.

Julia B. Schueler[1], Kanstantsin Lashuk[1], Philipp Meyer[1], Alejandra Ferrer Diaz[2], Eva Oswald[1], Kalhara Menikdiwela[2], JOHN HUANG[2]

[1]Charles River Laboratories, Freiburg, Germany,[2]theWell Bioscience, Monmouth Junction,, NJ

The 3R principles are embedded in regulatory frameworks and industry standards. However, drug development pipelines are highly standardized and validated over decades. Introducing new and adapting existing models requires extensive validation. The need to compare data before and after these adaptions can lead to inconsistencies and complicating interpretation. The aim of the current project is to introduce an animal-free matrix, VitroGel® (TheWell Bioscience), in our experimental pipeline, focusing on subcutaneously implanted human and murine cancer cell lines into mice. Of the 250 human and 38 murine cell line-derived models in our panel, 92 require the use of a matrix for optimal growth. To introduce the new matrix in a comprehensive way, we implemented a two-step process. At first, we validated the technical feasibility and the influence of the new matrix in two models, which are known to have low take rates and show experiment-limiting characteristics such as the onset of ulceration. The ovarian cancer cell line SKOV-3 and the breast cancer cell line MDA-MB-468 were implanted with two different cell numbers and three different matrices into NSG mice. Tumor volume was followed twice weekly, and in the case of SKOV-3, the time and degree of ulceration were plotted as well. In this experiment, we could show that SKOV-3 tumor growth and ulceration rate are independent of the matrix. For MDA-MB-468, the synthetic hydrogel induced faster tumor growth in the group receiving the higher cell numbers and vice versa. The histological examination of the tumors did not show any differences. Based on those results, we decided to fully implement the VitroGel hydrogel across all models. For each cell line, we injected 5 animals using hydrogel and 5 animals using Matrigel. Again, tumor volume was monitored by twice-weekly caliper measurements. To better understand the influence of the matrices in relation to other biological and technical parameters that influence tumor growth, we compared the actual wet lab data with our database of control groups, which is annotated for cell line passage, mouse strain, and control vehicle (Clark et al, Cancer research. 2023;83(7_Supplement):4676-4676). By feeding these data into the database, we were able to quantify the biological variability and determine whether the matrix had an influence on tumor growth beyond or within the range of the biological variability of the specific model. So far, we have tested 32 of 92 lines and have not observed significant differences driven by the choice of matrix. With this combination of wet lab experiments and in silico analysis, we can refine our in vivo experiments while minimizing the use of additional animals. Furthermore, this workflow ensures the consistency of data output from those experiments and enables the comparison of data before and after the implementation of the animal-free hydrogel.

#2176 Mutating E-cadherin in rats to model invasive lobular breast cancer.

Yuxiang Lin, Luyu Jia, Derrick Manosh Thomas, Wen Bu, Carolina Gutierrez, Yi Li

Baylor College of Medicine, Houston, TX

Background: Invasive lobular carcinoma (ILC) is the most common special histologic subtype of breast cancer, accounting for 8-14% of cases. Nearly 95% of ILCs are estrogen receptor positive (ER+) and managed with endocrine therapy. However, optimal rodent models are limited for studying ILC evolution and therapeutic vulnerabilities. Although mouse ILC models have been generated by mutating CDH1 (which encodes E-cadherin), a hallmark of ILC, but these tumors rarely show estrogen dependence. Rats, which have mammary biology more similar to humans, can easily generate ER+ and estrogen-dependent tumors. Our lab has successfully established ER+, estrogen-dependent ductal tumors in rats using intraductal CRISPR/Cas9 editing. Here, we aim to develop a rat model of ILC by targeting CDH1 and PIK3CA, the most frequently mutated driver in human breast cancer.
Methods: AAV-sgRNA constructs targeting CDH1 and activating PIK3CA^{H1047R} were delivered intraductally to induce somatic CDH1 loss and PIK3CA activation in rat mammary epithelial cells and drive tumor formation.
Results: AAV targeting CDH1 (AAV-C) efficiently induced knockout in Cas9-expressing rat primary cells in vitro, and deep sequencing confirmed high editing rates. Intraductal delivery of AAV inducing CDH1 loss and PIK3CA^{H1047R} activation (AAV-rPC) generated tumors with a latency of 2-3 months, significantly shorter than tumors induced by AAV-PIK3CA^{H1047R} alone (AAV-rP, ~4 months). Importantly, AAV-C alone did not induce tumors in the rat mammary gland, and AAV-rP did not generate lobular lesions. Somatic CDH1 knockout combined with PIK3CA^{H1047R} activation efficiently induced widespread LCIS and ILC. Mammary tumors induced by AAV-rPC were characterized by high ER and progesterone receptor (PR) expression with moderate Ki67 and were hormone-dependent. Ongoing studies are profiling tumor transcriptomes and immune features and comparing them with human ILCs.
Conclusion: CRISPR/Cas9-mediated targeting of CDH1 and PIK3CA in rats produces a clinically relevant ER+ ILC model.

#2177 Characterization of a panel of PDX models derived from PARP inhibitors pretreated breast and ovarian cancer patients for therapeutic evaluation.

Qingzhi Liu, Jinxi Wang, Leilei Chen, Wubin Qian, Likun Zhang, Ludovic Bourre, Jessie Jingjing Wang

Crown Bioscience, Inc., San Diego, CA

Introduction: Poly (ADP-ribose) polymerase (PARP) inhibitors benefit patients with homologous recombination-deficient cancers, especially BRCA-mutated, but resistance frequently emerges through multiple adaptive mechanisms, limiting long-term efficacy. To better recapitulate clinical resistance and advance precision therapy development, we established a panel of patient-derived xenograft (PDX) models from PARP inhibitors pretreated breast and ovarian cancers, providing a translational platform to investigate resistance mechanisms and assess novel treatment strategies.

Methods: Ten PDX models from patients pretreated with PARP inhibitors (Olaparib, Niraparib ± Bevacizumab), and Talazoparib + Avelumab) were established subcutaneously in immunodeficient mice (NOD.SCID, BALB/c nude, NSG-like) and characterized by histology and RNA sequencing. Homologous recombination-related alterations (BRCA1/BRCA2 mutations, PALB2 deletions) were present in some patients, and all had disease progression after PARP inhibitor therapy. For *in vivo* efficacy studies, three breast cancer PDX models were treated with Olaparib (100 mg/kg, p.o., QD) for 3-5 weeks following clinical schedule. Tumor growth inhibition (TGI) was calculated as [1 - (mean treated tumor volume / mean control tumor volume)] * 100%. Homologous recombination deficiency (HRD) scores from whole exome sequencing via scarHRD and PureCN used a cutoff of 38; high HRD scores (≥38) correlated with PARP inhibitors sensitivity.

Results: A panel of PAPR inhibitor clinical pretreated PDX models, including three breast cancer (BR9671, BR9679, BR9815) and seven ovarian cancer (OV9576, OV9670, OV9692, OV9563, OV9568, OV9803, OV9805), were established with comparable genomic profiles to the clinic. To evaluate the PARP inhibitor efficacy *in vivo*, BR9671, BR9679 and BR9815 derived from the same Olaparib-treated BRCA1 mutated patient were re-challenged with Olaparib. Tumor progression was observed in all three PDX models (TGI: BR9671=29.68%, BR9679=-9.30 %, BR9815=13.77%) despite high HRD scores (58, 59, and 64, respectively), indicating pronounced genomic instability. Besides, each model carried the MDM4-S367L mutation and had high MDM4 (BR9671: 3.654, BR9679: 3.755, BR9815: 4.539) and MDM2 (BR9671: 6.028, BR9679: 6.118, BR9815: 6.524) expression. As MDM2/MDM4 are known p53 suppressors, these findings suggest impaired p53 function may contribute to PARP inhibitor resistance; but further investigation is required.

Conclusion: By developing this panel of clinically PARP inhibitor pretreated PDX models, we established a translational platform that reflects clinical disease progression. These models enable investigation of resistance mechanisms and evaluation of next-generation therapies and combinations, supporting preclinical decision-making.

#2178 Integrating patient-derived tumor models into translational oncology and drug discovery.

Umar Khalid, Thomas Quinn, **Cong Fu**, Lucia Arabit Loosbrock, Anand Panigrahy, Aniket Shetty, Keith Ligon, Sonam Bhatia

Dana-Farber Cancer Institute, Boston, MA

Patient-derived tumor models provide powerful tools to investigate cancer biology and therapeutic responses in clinically relevant contexts. The Center for Patient-Derived Models (CPDM) at the Dana-Farber Cancer Institute is a collaborative research hub specializing in the generation, characterization, and application of patient-derived xenografts (PDX), patient-derived cell lines (PDCLs), and organoid/spheroid cultures to accelerate translational oncology. CPDM partners with both academic and industry researchers to enable data-driven drug discovery, preclinical validation, and functional precision medicine. The center maintains an extensive repository of patient-derived models spanning brain tumors, hematologic malignancies, and a broad range of solid tumors, each annotated with corresponding clinical and genomic data. These models are available to collaborators worldwide to advance translational and precision oncology research. To support precision oncology and preclinical research, CPDM has established automated imaging pipelines and standardized quantitative assays for real-time monitoring of growth and drug response in both 2D and 3D culture systems. In addition, the center's Functional Precision Medicine (FPM) platform integrates live-cell imaging and patient-specific drug screening to inform therapeutic selection and improve translational predictive accuracy. Together, these efforts position CPDM as a translational bridge between preclinical modeling and clinical application, facilitating data-driven collaborations that advance personalized cancer treatment.

#2876 Influence of transgenic MUC13 expression on gut microbiota and chemokine profile.

Swati Dhasmana, Anupam Dhasmana, Shweta Singh, Iris A. Perez, Shabnam Malik, Bilal B. Hafeez, Sheema Khan, Murali M. Yallapu, Subhash C. Chauhan

University of Texas Rio Grande Valley, McAllen, TX

Background: MUC13 is an important oncoprotein that is often overexpressed in cancers, including colorectal cancer, and is linked to worse outcomes, although its exact role is not fully understood. Using a MUC13 transgenic mouse model, we examined how MUC13 overexpression affects gut microbiome and cytokines that can influence cancer risk and treatment responses.
Methods: Fecal specimens were collected from MUC13-overexpressing transgenic mice (MUC13Tg) and wild-type mice. To assess the fecal bacterial communities, we performed DNA extraction followed by 16S rRNA metagenomic sequencing on the Illumina MiSeq platform. Additionally, colon tissues from MUC13Tg and wild-type mice were assessed by IHC to confirm the overexpression of MUC13. Furthermore, chemokine profiling analyses were performed using chemokines arrays in serum samples of MUC13-overexpressing mice and wild-type mice, respectively.
Results: IHC confirmed elevated MUC13 expression in the colon of transgenic mice, leading us to investigate associated changes in the gut and immune environment. 16S rRNA sequencing showed clear shifts in the gut microbiota, with increases in Alistipes, Clostridium_XIVa, Oscillibacter, and TM7 (25→35%, 1.6→11.6%, 8.3→16.6%, 2.5→6.6%) and decreases in Parabacteroides and Akkermansia (31.6→11.6%, 15→3.3%) compared with wild-type mice. These microbial alterations were accompanied by cytokine changes, including elevated EGF, FGF21, CD93, and Leptin, as well as reduced levels of cytokines such as Angiopoietin-1, CD14, HGF, and CCL17. Together, these results demonstrate that MUC13 overexpression not only shifts gut microbial composition but also modifies systemic inflammatory signaling.
Conclusion: This study suggests that MUC13 overexpression markedly alters the gut microbiome and cytokine expression profile in mice. The increased Firmicutes/Bacteroidetes ratio, enrichment of pro-inflammatory species, and repression of beneficial bacteria collectively indicate a shift toward gut dysbiosis and a pro-tumorigenic environment. These findings suggest that MUC13 plays a key role in shaping the gut microbial landscape and influencing immune modulation, both of which are important drivers of cancer development.

: Metabolic and Transcriptional Control of Cancer Stem Cell Plasticity
Poster Session

#2182 Upregulation of mitochondrial sirtuins in prostate cancer stem-like cells.

Shiv Verma[1], Leah Tharian[2], Jason A. Mears[3], **Sanjay Gupta**[4]

[1]Urology, Case Western Reserve University, Cleveland, OH,[2]Case Western Reserve University, Cleveland, OH,[3]Pharmacology, Case Western Reserve University, Cleveland, OH,[4]Case Western Reserve University School of Medicine, Cleveland, OH

Bone metastasis represents one of the most aggressive and painful late-stage manifestations of prostate cancer. Current treatments, primarily docetaxel-based chemotherapy with or without radiation, provide only temporary benefit, as relapses driven by therapy-resistant cancer stem-like cells (CSCs) are common. These CSCs are maintained by active gene networks that promote self-renewal through symmetrical division while retaining the ability for asymmetrical division and differentiation. However, the molecular mechanisms that govern CSC differentiation and therapy resistance remain poorly understood. To elucidate transcriptomic signatures associated with CSC differentiation, we profiled gene expression in androgen-repressive human prostate cancer C4-2B cells. CSC-enriched and non-CSC fractions were isolated using magnetic bead separation with CD133 antibody, followed by fluorescence-activated cell sorting and ALDH1 assay to identify the $CD133^{+}/ALDH1^{high}$ and $CD133^{-}/ALDH1^{low}$ populations. RNA sequencing revealed 33,676 expressed genes, of which 615 were significantly differentially expressed ($p < 0.05$). After false discovery rate correction, 56 genes remained significant ($q < 0.05$). Pathway analysis using QIAGEN Ingenuity Pathway identified activation of the sirtuin signaling pathway as a key feature in the CSC fraction, alongside enrichment of oxidative phosphorylation (OXPHOS), mitochondrial dysfunction, B cell receptor, CXCR4, Th2, IL17A, and TNFR2 signaling pathways. Transcript profiling of the sirtuin gene family (SIRT1-SIRT7) revealed marked upregulation of mitochondrial sirtuins: SIRT3, SIRT4, and SIRT5 in the $CD133^{+}/ALDH1^{high}$ population, consistent with enhanced OXPHOS activity relative to the $CD133^{-}/ALDH1^{low}$ cells. Network analysis further demonstrated that the SIRT3-SIRT4-SIRT5 interactome integrates into the NAD^{+} metabolic framework, connecting key enzymes involved in NAD^{+} synthesis and utilization, including NADSYN1, NMNAT1/2, NADK2, BST1, NNMT, and ENPP3. Notably, SIRT3 emerged as the central regulatory hub, coordinating interactions with SIRT4 and SIRT5 to sustain oxidative metabolism and suppress reactive oxygen species accumulation. This coordination promotes metabolic flexibility, redox balance, and resistance to differentiation cues which are hallmarks of CSC persistence and therapeutic resistance. Collectively, these findings identify mitochondrial sirtuins, particularly SIRT3, as key regulators of metabolic reprogramming and redox homeostasis in castration-resistant CSCs. Targeting mitochondrial sirtuin signaling, alone or with chemotherapy, represents a promising strategy to eliminate CSCs and prevent prostate cancer progression and bone metastasis.

#2183 FABP4 functions as a novel cancer stem cell marker in triple-negative breast cancer.

Huiyi Feng[1], Jinquan Xia[2], Fuhua Zhong[2], Yinghuan Cen[1], Lu Jiang[2], Pan Zhao[2], Lin Gao[2], Chang Zou[2]

[1]Shenzhen Hospital, Shenzhen Hospital of Southern Medical University, Shenzhen, China,[2]Shenzhen People's Hospital, Shenzhen, China

Anthracycline-paclitaxel (A/P)-based chemotherapy remains a cornerstone of triple-negative breast cancer (TNBC). However, chemo-resistance continues to compromise durable clinical benefit. Cancer stem cells (CSCs) are major contributors to tumor heterogeneity and therapeutic resistance. Identifying novel CSC-associated genes may provide new strategies for overcoming drug resistance in TNBC. Single-cell RNA sequencing on five paired TNBC tumors and adjacent normal tissues. FABP4 exhibited the strongest enrichment within the CSC-like population compared with luminal and basal epithelial cells. Spatial transcriptomics further confirmed the expression of FABP4 within CSC-enriched cell clusters. Integrated transcriptome profiling demonstrated significant upregulation of FABP4 in paclitaxel-resistant 4T1 cells, which was further validated in resistant and sphere-forming TNBC models across both 4T1 and MDA-MB-231 cells. Knockdown of FABP4 by siRNA markedly reduced spheroids-forming capacity of these breast cancer cells, supporting its functional role in maintaining the stemness in TNBC. Moreover, FABP4 was identified highly expressed and accompanied by CSC markers in TNBC clinical tissue by immunofluorescence, indicating its spatial and biological association with the CSC niche. Further studies are warranted to elucidate the mechanistic pathways through which FABP4 contributes to chemo-resistance and CSC stemness maintenance.

#2184 Defining cancer initiating cells and their vulnerabilities in renal cell carcinoma.

Zohreh Mehrjoo[1], Hellen Kuasne[2], Ariel M. Aguirre[1], Ozge Saatci[3], Ali Shahini[1], Matthew G. Annis[2], Anne-Marie N. Fortier[2], Tianyuan Lu[1], Larisa M. Soto[1], Hong Zhao[2], Dongmei Zuo[2], Virginie Pilon[2], Matthew Dankner[2], Tamiko Nishimura[1], Kevin Petrecca[4], Jonathan D. Spicer[5], Peter Siegel[2], Simon Tanguay[6], Hamed S. Najafabadi[1], Sahin Ozgur[3], Morag Park[2], Yasser Riazalhosseini[1]

[1]Department of Human Genetics, McGill University, Victor Dahdaleh Institute of Genomic Medicine at McGill University, Montreal, QC, Canada,[2]Rosalind and Morris Goodman Cancer Research Institute, McGill University, Montreal, QC, Canada,[3]Department of Biochemistry and Molecular Biology, Hollings Cancer Center, Medical University of South Carolina, Charleston, SC,[4]Montreal Neurological Institute and Hospital, Department of Neurology and Neurosurgery, McGill University, Montreal, QC, Canada,[5]Cancer Research Program, Research Institute of the McGill University Health Centre, Montreal, QC, Canada,[6]Department of Surgery, Division of Urology, McGill University Health Center, McGill University, Montreal, QC, Canada

Tumor initiating cells (TICs) drive tumor initiation, growth, therapy resistance, and metastasis, yet their molecular characteristics remain poorly defined in clear cell renal cell carcinoma (ccRCC). ccRCC is the most common form of kidney cancer, leading to 179,000 cancer-related deaths annually. We aim to identify ccRCC-TICs and their essential genes using a cell marker-agnostic strategy.We performed scRNA-seq on five ccRCC patient-derived xenograft (PDX) models and applied RNA velocity and CytoTRACE analyses to identify malignant cells that are origin for other cancer cells in each tumor. We identified a minor cell population (less than 15% of cells) as the origin of other tumor cells, representing putative CICs. Pathway and network analyses on the genes that were specifically up-regulated in the origin cells, suggested that a core network of proteins, regulated by PLK1-FOXM1 axis, conventionally known to regulate mitosis, are highly active in TICs and may be essential for their function.We validated the role if these proteins in tumor initiation in PDX and 3D patient-derived models of ccRCC, through functional experiments. These proteins were expressed in spheroids established following a TIC enrichment protocol. Spheroid cells exhibited higher tumorigenicity and colony formation ability compared to parental tumor cells, as confirmed by in-vivo injection in nude mice and in-vitro colony formation assays. Successive in vivo passaging confirmed the self-renewal capacity of spheroid-derived tumors. Pharmacological blockade of PLK1 with Volasertib elicited dose-dependent inhibitory effect on spheroid and colony formation, with in-vivo validation showing that blocking PLK1 significantly delayed tumor growth and more efficiently prevented tumor formation in nude mice. Cultivation of tumor cells isolated from treated PDX demonstrated loss of self-renewal and tumor-propagating capacity in these cells. Notably, RCC-TICs remained vulnerable to PLK1 inhibition despite bypassing mitotic arrest using TCMps1-12, revealing that PLK1 elicit its TIC-related functions independently from its canonical G2/M regulatory roles. RNA-seq analysis of treated models identified pathways in adhesion, cytokine signaling, immune evasion, and developmental self-renewal circuits, as potential processes mediating PLK1 roles in RCC stemness.Overall, we identified and validated essential proteins in RCC-TICs using single-cell transcriptome data, RCC spheroids, and PDX models. Targeting PLK1 disrupts the fundamental self-renewal and tumor-initiating capacities of ccRCC, offering a promising avenue for therapeutic intervention through PLK1 inhibition. Furthermore, our data uncover novel and non-canonical functions for PLK1, which upon further characterization may open new ways for combinational therapeutic strategies involving PLK1 and its effectors with standard of care in advanced ccRCC.

#2185 Trem1 sustains liver cancer stemness in hepatocellular carcinoma.

Ashwin Ajith[1], Arsha Sreekumar[1], Kanza Mamouni[2], Anatolij Horuzsko[2]

[1]Augusta University, Augusta, GA,[2]Augusta University, August, GA

Hepatocellular carcinoma (HCC) is the most common primary liver malignancy and a leading cause of cancer-related mortality worldwide. Although the Triggering Receptor Expressed on Myeloid Cells 1 (TREM1) is well known for shaping tumor-infiltrating myeloid populations and promoting an immunosuppressive tumor microenvironment, its tumor-intrinsic function remains poorly defined. Here, we identify a previously unknown function of TREM1 in sustaining the stem-like properties of liver cancer stem-like cells (LCSLCs). Flow cytometric analyses revealed high TREM1 expression within the $CD133^{+}EpCAM^{+}$ LCSLC population. CRISPR-Cas9-mediated knockout of TREM1 in HCC cell lines markedly impaired proliferation and migration while enhancing apoptosis. Specifically, in LCSLCs TREM1 deficiency reduced clonogenic growth and spheroid formation, indicating loss of self-renewal and stemness. Consistently, cell line-derived xenografts generated from TREM1-deficient LCSLCs exhibited substantially diminished tumorigenicity in vivo. Transcriptomic profiling of FACS purified LCSLCs demonstrated that TREM1 loss disrupted various nuclear and extracellular signaling programs associated with oncogenic and stemness pathways. Moreover, pharmacologic inhibition of TREM1 using the small-molecule antagonist VJDT phenocopied the tumor-suppressive effects observed in genetic knockout models. Collectively, these findings establish TREM1 as a critical intrinsic regulator of LCSLC survival and tumorigenic potential, independent of its immunomodulatory activity in the tumor microenvironment. Therapeutically, targeting TREM1 may offer a dual-action approach to simultaneously suppress cancer stem-like cell function and attenuate cancer progression in HCC.

#2186 Galangin effectively inhibits the proliferation and stemness characteristics of liver cancer stem cells by knocking down the expression of TINCR..

Amira S. Fyala[1], Mohamed M. H Elkewedi[2], Ahmed S. Sultan[3]

[1]Biochemistry Department, Faculty of Science, Alexandria University, Alexandria, Egypt,[2]Biochemistry Department, Faculty of Pharmacy, Alexandria University, Alexandria, Egypt,[3]Oncology Department, Lombardi Comprehensive Cancer Center, Georgetown University Medical Center, Washington, DC

Hepatocellular carcinoma (HCC) is a leading cause of cancer-related deaths worldwide. Liver cancer stem cells (LCSCs) are thought to play a crucial role in its pathology, but their mechanisms in HCC remain poorly understood. TINCR (terminal differentiation-induced long non-coding RNA) influences cancer cell behavior in various malignancies, including HCC. Recent research has highlighted the potential of natural anticancer agents, particularly Galangin (GLN). This compound is recognized for its antibacterial, antifungal, and antiviral properties, and it may also contribute to managing conditions like hypertension, diabetes, and cancer prevention. However, the specific effects of GLN on HCC are still not fully understood. The present study aims to explore the molecular mechanism and anticancer properties of GLN on TINCR expression, which may influence the stemness characteristics of liver cancer stem cells (LCSCs). Our findings demonstrate that TINCR is highly expressed in LCSCs, suggesting that it is essential for maintaining the stemness properties and tumorigenesis of these cells. In the Wst-1 assay, GLN treatment exhibited a dose-dependent inhibitory effect on proliferation and induced significant morphological changes in LCSCs, indicative of apoptosis induction after 24 h of treatment. Furthermore, the expression of TINCR was significantly inhibited after 24 h of GLN treatment compared to the control. Western blot analysis and qRT-PCR were conducted to assess oncogenic signaling pathways, including β-catenin, mTOR, and STAT3, along with downstream targets. Our results indicated a significant reduction in cell viability and oncogenic signals, as well as in LCSC stemness markers, following GLN treatment combined with TINCR knockdown, suggesting that inhibiting TINCR expression alongside GLN treatment effectively disrupts oncogenic signals and inhibits LCSC stemness characteristics. In addition, TINCR knockdown significantly enhanced the antiproliferative effects and sensitivity to Doxorubicin. Our data introduce GLN as a promising, natural, and non-toxic anticancer compound, demonstrating its therapeutic potential for treating HCC by regulating the expression pattern of TINCR.

#2187 Direct regulation of the cancer stemness by eIF4A1 in triple-negative breast cancer.

Azeezat Oluwatobiloba Osikoya, Shobhit Srivastava, David Terrero, Dayanidhi Raman

Cell and Cancer Biology, College of Medicine & Life Sciences, University of Toledo-Health Science Campus, Toledo, OH

Triple-negative breast cancer (TNBC) is very aggressive with relapses after chemotherapy and high mortality due to metastases. Though there is an initial response to neoadjuvant chemotherapy (NACT) it frequently recurs leading to chemoresistance. Prior evidence points to a small population of chemoresistant tumor-initiating cells termed breast cancer stem-like cells (BCSCs). These cells exhibit intrinsic drug resistance and self-renewal capacity driven by pluripotency transcription factors (PTFs) such as SOX2, OCT4, NANOG, and KLF4. BCSCs survive following NACT, resulting in minimal residual disease (MRD), a clinically significant state of tumor persistence that seeds relapse, aggressive regrowth and metastasis. Our prior studies identified eukaryotic translation initiation factor 4A1 (eIF4A1) as an important regulator of cancer stemness in TNBC. Here, we investigate the mechanistic basis by which eIF4A1 helicase activity regulates cancer stemness that promotes MRD. To establish clinical relevance, we analyzed human TNBC biospecimens and matched adjacent normal tissues for PTFs expression. To demonstrate a causative role for eIF4A1 in sustaining cancer stemness *in vitro*, eIF4A1-knockout (KO) TNBC cells generated by CRISPR/Cas9 were rescued by ectopic expression of wild type (WT)-eIF4A1 and its helicase-defective mutants. Expression of PTFs was assessed by immunoblotting and qPCR, while measures of cancer stemness were evaluated by ALDH activity, tumorsphere formation, anchorage-independent growth, and 3D growth assays. To directly determine translational regulation of PTFs by eIF4A1, we employed a luciferase reporter system to measure eIF4A1-dependent translation through mutational analysis of 5′ untranslated regions (UTRs) of SOX2, OCT4, NANOG and KLF4 mRNAs. A significantly higher eIF4A1 and PTF protein levels were observed in TNBC but lower in adjacent normal area. Consistent with this, ectopic WT-eIF4A1 in the eIF4A1-KO background robustly significantly rescued PTF expression, tumorsphere formation efficiency, 3D-colony growth on Matrigel, and anchorage-independent growth. The helicase-defective mutants failed to restore PTF levels and stemness traits. Furthermore, total ALDH activity and expression of some ALDH isoforms followed a similar trend. Cloning of WT or mutant 5′-UTRs of PTFs and analysis of reporter luciferase activity confirmed that eIF4A1 can directly regulate the translation of PTF mRNAs and hence the PTF-driven cancer stemness program. Our findings demonstrate for the first time that eIF4A1 helicase activity directly governs a cancer stemness program in TNBC by promoting translation of PTF mRNAs harboring structured 5′ UTRs. Ongoing studies are assessing tumor initiation frequency *in vivo*. Thus, targeting the helicase activity of eIF4A1 may suppress cancer stemness, restore sensitivity to therapy, reduce relapses and improve longevity in TNBC.

#2188 Integrative transcriptomic profiling and flow cytometry analysis of AML PDX models identify purine-pyrimidine metabolic dependency shared in LSCs and blasts.

Kangsan Kim[1], Haiming Xu[1], Geoff Nelson[2], Tim Nieuwenhuis[2], Huiyun Liu[1], Justine Roderick-Richardson[1], Jessie Hao-ru Hsu[1], Brandon Willis[1], Lisa Drew[1], Omid Tavana[1]

[1]Hematology R&D, AstraZeneca, Waltham, MA,[2]Oncology Data Science & AI, AstraZeneca, Waltham, MA

Acute myeloid leukemia (AML) comprises a heterogeneous population in which leukemic stem cells (LSCs) can drive initiation, persistence, and relapse. While current standard of care effectively reduces disease burden, 30-80% relapse rates emphasize the need of investigating LSC as a potential driver of relapse. To better understand biology of LSC, we performed RNA-seq and flow cytometry analysis in AML patient-derived xenograft (PDX) models with defined LSC, progenitor, and blast compartments. Ex vivo culture conditions were optimized for AML PDXs to preserve subpopulation heterogeneity in vitro by supplementing cytokines. For RNA-seq, CD34/CD38 markers-based sorting isolated LSCs, progenitors, and blasts; differential expression analyses identified LSC-specific genes and shared vulnerabilities that could enable dual targeting of LSCs and blasts. For immunophenotyping, we developed a 20-color flow cytometry panel incorporating LSC, differentiation, and classic AML surface markers to quantify expression patterns across compartments. RNA-seq of sorted LSCs and blasts demonstrated differential expression between LSCs and blasts with a clear upregulation in the LSC17 score, consistent with previous results and confirming our data purity/quality. Flow cytometry panel also displayed differential surface marker expression across LSCs and blasts. Focusing on LSC-enriched biology first, we identified around 160 genes consistently upregulated in LSCs across 2 independent AML PDX models. These LSC-elevated targets showed limited dependency in DepMap (which have AML cell lines that represent blast), suggesting these genes may exert functional effects only in LSC, and not in blasts. To identify targets showing a dependency in all subsets, we implemented a blast-centric filter. We first selected AML dependency genes from DepMap and then intersected this set with genes highly expressed in both LSCs and blasts. This approach yielded 16 candidate genes with dual relevance. Functional annotation indicated that half of these genes map to purine/pyrimidine biosynthetic pathways, pointing to a metabolic vulnerability and supporting a potential dual-targeting strategy to impact both the LSC and blast population. Integrated transcriptomic profiling and flow cytometry analysis exhibit LSC-restricted programs while uncovering shared metabolic dependencies across LSCs and blasts. By combining expression with AML dependency data, we prioritized 16 dual-compartment candidates, where about half align to purine/pyrimidine biosynthesis nominating nucleotide metabolism as a potential axis for dual targeting. Together elevated LSC17 scores that confirm dataset quality, these findings provide a roadmap for target selection, patient stratification, and rational combinations aimed at durable remission and reduced relapse in AML.

#2189 Metabolic control of pancreatic cancer stemness through PDK3 dependent SOX2 lactylation.

Neelanjana Gayen, Nivedeta Krishna Kumar, Ayoola O. Ogunleye, Palanisamy Nallasamy, Venkatesh Varadharaj, Saravanakumar Marimuthu, Surinder K. Batra, Moorthy P. Ponnusamy

University of Nebraska Medical Center, Omaha, NE

Cancer stem cells (CSCs) pose a critical challenge in Pancreatic cancer (PC) management because of their unique ability to survive treatment and drive tumor relapses. CSCs exhibit metabolic flexibility to adapt to stress by switching between glycolysis and oxidative phosphorylation. Pyruvate dehydrogenase kinase 3 (PDK3) governs this transition by phosphorylating and inactivating the pyruvate dehydrogenase complex (PDHA), thereby promoting a glycolytic phenotype. Understanding the metabolic reprogramming that sustains cancer stem cells may reveal strategies to disrupt their survival and propagation. In this study, RNA sequencing of spheroid-based PCSC model followed by unbiased *in-silico* analysis identified 14 upregulated metabolic regulatory genes, with *PDK3* emerging as the top candidate. PDK3 expression was elevated in CSC subtype population, pancreatic tumor tissues from patients and Kras; PdxCre (KC) mouse models, but minimal in normal pancreatic tissues. Dual-IHC staining demonstrated co-expression of PDK3 with the stemness marker *CD44* in human pancreatic tumor tissues, highlighting its association with CSC phenotypes. Stable lentiviral-mediated shRNA knockdown (KD) or pharmacologic inhibition with artesunate (a PDK3 targeting compound identified in this study) significantly reduced stemness markers (CD44, SOX2, and CD133), glycolytic genes (GLUT1 and LDHA), and phosphorylated PDHA levels. Functionally, PDK3 depletion decreased the side-population fraction, impaired sphere-formation, and colony-forming capacities, suggesting suppressed sustenance and self-renewal properties. Metabolomic profiling by LC-MS revealed lactic acid as one of the most enriched metabolites in scramble PC cells compared to PDK3 KD cells. Consistently, metabolomic analysis revealed a significant reduction in lactic acid release and glucose uptake upon PDK3 KD. Seahorse analysis further demonstrated that PDK3 depletion lowered ECAR and elevated OCR, indicating a metabolic shift from glycolysis toward oxidative phosphorylation. Interestingly, elevated lysine lactylation and SOX2 expression were observed in control and lactate-treated PC cells, whereas both were markedly reduced upon glycolysis inhibition and PDK3 KD, indicating a strong dependence on PDK3-mediated metabolic activity. Mechanistically, immunoprecipitation and immunofluorescence revealed that PDK3 promotes lactate-dependent lysine lactylation of SOX2, enhancing its stability and stemness activity. Orthotopic implantation of PDK3 KD human PC cells resulted in significantly reduced tumor growth *in vivo*, underscoring PDK3's pivotal role in driving CSC-mediated tumor progression. In conclusion, our findings establish PDK3 as a central metabolic regulator of PCSC maintenance and tumor progression, offering new opportunities to develop therapies that disrupt lactate-fueled stemness in pancreatic cancer.

#2190 Trib3 identified as a key therapeutic target for pancreatic cancer stem cells.

Nirjhar M. Aloy[1], Kyle McAndrews[2], Adam Zulli[1], Kathryn Baldwin[1], Kristine Von Maltzan[1], Sarah Thayer[1]

[1]Surgery, LSU Health Shreveport (LSUHS), Shreveport, LA,[2]University of Nebraska Medical Center, Omaha, NE

Background: Pancreatic ductal adenocarcinoma (PDAC) is among the most lethal cancers, exhibiting early dissemination and chemoresistance. These features are attributed to a specialized subpopulation of cancer stem cells (CSCs). Our lab has defined the cell of origin for PDAC within the pancreatic duct gland (PDG) stem cell compartment, a region crucial for epithelial renewal. Creation and maintenance of the CSC pool is hypothesized to underlie aggressive tumor biology, but transcriptional networks in this compartment remain poorly characterized.
Objective: To define molecular pathways unique to pancreatic cancer stem cells (CSCs) that can be exploited as targeted therapies to eradicate CSCs while sparing normal pancreatic stem cells.
Methods: Genetically engineered mouse models and single-cell RNA sequencing were used to trace and compare CSC-enriched (TTKS) and normal (TT) PDG organoids. Key findings were validated in other mouse and human PDAC models.
Results: Single-cell analysis revealed broad upregulation of stem cell and CSC markers (Mthfd2, Slc7a5, Gadd45a), supporting conserved stem-like signatures in CSCs. Twelve genes were uniquely upregulated in PDAC CSCs, revealing new CSC-selective pathways. Trib3 was most strongly and widely upregulated among these, with multiple downstream regulators (β-catenin, FOXO1, ATF4) also enriched, indicating robust Trib3-driven network activation.
Conclusion: Identification of a discrete PDG stem cell origin for PDAC enables detailed interrogation of CSC biology. Our model demonstrates that PDAC CSCs activate unique survival and adaptation pathways, with Trib3 emerging as a central regulator. Collectively, this provides new mechanistic insight and positions Trib3 as a compelling CSC-targeted therapeutic candidate. Work is going on to understand the biological role of Trib3 in progression of CSCs in PDAC.

#2191 NQO1 inhibits FBXL14-dependent SNAIL degradation to promote EMT-mediated stemness in colorectal cancer cells.

Ha Gyeong Kim, Yunmi Cho, Eun-Taex Oh

Department of Biomedical Sciences, Inha University College of Medicine, Incheon, Korea, Republic of

Overexpression of NAD(P)H:quinone oxidoreductase 1 (NQO1) is associated with poor prognosis in various human cancers. In colorectal cancer (CRC), NQO1 overexpression is frequently associated with tumor progression and the formation of cancer stem cells (CSCs), which can drive therapy resistance, recurrence, and metastasis via their self-renewal and differentiation capacities. However, the precise mechanisms by which NQO1 regulates CSC traits remain poorly understood. Here, we investigated the functions of NQO1 in modulating CSC properties in human CRC cells. Knockdown of NQO1 in CRC cell lines markedly reduced colonosphere formation and downregulated the key stemness-related marker genes, *Nanog*, *Oct4*, and *Sox2*. Conversely, restoration of NQO1 expression in NQO1-knockdown cell lines rescued colonosphere-formation and restored the levels of these CSC marker genes. Further investigation revealed the modulation of NQO1 changed the expression and stability of Snail, a key transcription factor involved in CSC maintenance. Suppression of NQO1 downregulated Snail and its targeted CSC marker genes. NQO1 was found to directly bind the nuclear export signal (NES) domain of Snail to prevent its interaction with the E3 ubiquitin ligase FBXL14, which targets Snail for proteasomal degradation. This protective interaction stabilized Snail and enhanced its downstream stemness-related transcriptional activity. In line with these results, NQO1 knockdown enhanced the sensitivity of CRC cells to 5-FU and ionizing radiation. Importantly, Snail overexpression partially restored the resistance to these treatments in NQO1-suppressed cells, suggesting that NQO1 promotes therapy resistance by stabilizing Snail. Analysis of clinical CRC datasets demonstrated that there is a strong positive correlation between NQO1 and Snail-targeted CSC marker gene expression, and this was further correlated with poor prognosis in CRC patients. Our findings collectively suggest that NQO1 promotes CRC stemness and poor patient prognosis by stabilizing Snail. Targeting NQO1 may therefore represent a promising therapeutic strategy to eliminate CSCs and improve treatment outcomes in CRC.

#2192 SLFN5 mediates liquid-to-solid phase transition of NOTCH1 to suppress stemness and radioresistance of non-small cell lung cancer.

Mi Tang, Lu Zhang, Jiaxin Zhao, Hongji Dai, Zhiyong Yuan, Zeyun Mi, **Zhiqiang Wu**

Tianjin Medical Univ. Cancer Inst. & Hospital, Tianjin, China

Background: Radiotherapy remains one of the principal therapeutic modalities for non-small cell lung cancer (NSCLC), yet its therapeutic efficacy is frequently compromised by tumor recurrence, metastasis, and the development of radioresistance. Accumulating evidence identifies cancer stem cells (CSCs) as a critical driver of radioresistance. Therefore, elucidating the underlying molecular mechanisms and developing therapeutic targets to enhance radiosensitivity are of critical importance.
Methods: To identify key mediators of adaptive radioresistance in NSCLC, we established radioresistant NSCLC cell lines through repeated cycles of irradiation and subsequently performed RNA-seq analysis comparing them with their parental counterparts. The effects of SLFN5 on radiosensitivity were evaluated by flow cytometry and colony formation assays, and further validated in vivo using a nude mouse xenograft tumor model. Cancer stem-like properties were assessed by RT-PCR, Western blot, flow cytometry, sphere formation assay, and in vivo limiting dilution tumorigenesis assays. Subsequently, we employed mass spectrometry, co-immunoprecipitation, and proximity ligation assay to identify the interaction between SLFN5 and NOTCH1. Furthermore, phase separation assay, fluorescence recovery after photobleaching, CUT&Tag-seq, and ATAC-seq were used to investigate the role of NOTCH1 phase separation in promoting stemness and radioresistance, and the regulatory effect of SLFN5 on this process. Finally, the methylation status of the SLFN5 promoter was analyzed using bisulfite sequencing PCR.
Results: Our results demonstrate that SLFN5 was significantly downregulated in radioresistant NSCLC cell lines. Overexpressing SLFN5 effectively suppressed cancer stemness and epithelial-mesenchymal transition, thereby enhancing radiosensitivity both in vitro and in vivo. Conversely, knockdown of SLFN5 had significantly opposite effects. Mechanistically, liquid-liquid phase separation property is critical for NOTCH1 mediated stemness and radioresistance. Notably, SLFN5 interacts with NOTCH1 and induces the liquid-to-solid phase transition of NOTCH1, thereby impairing NOTCH1 signaling and the subsequent stemness and radioresistance. Finally, we identified DNMT3A and DNMT3B as the epigenetic regulators responsible for promoter hypermethylation and consequent silencing of SLFN5.
Conclusion: Our study reveals that DNA methylation downregulated SLFN5 resulting in radioresistance of NSCLC via liberating NOTCH1 from gel-like phase to liquid droplet to potentiating stemness of cancer cells. This research provides a potential therapeutic strategy to overcome radioresistance in NSCLC.

#2193 UPP1 promotes cisplatin-induced cancer stem cell enrichment in ovarian cancer via metabolic reprogramming.

Jessica J. Miao[1], Linzhou Wang[1], Ananya Banerjee[1], Na Li[1], Yajing Yang[1], Aidan Li[1], Kevin Wang[2], Patrick Stevens[2], Xiaoli Zhang[3], Qi-En Wang[1]

[1]Department of Radiation Oncology, Comprehensive Cancer Center, The Ohio State University, Columbus, OH,[2]Department of Bioinformatics, College of Medicine, The Ohio State University, Columbus, OH,[3]Biostatistics Core, College of Nursing, University of South Florida, Tampa, FL

Epithelial ovarian cancer (EOC) remains one of the leading causes of cancer-related mortality in women, largely due to late-stage diagnosis, recurrence, and resistance to chemotherapy. Growing evidence suggests that cancer stem cells (CSCs), a subpopulation of cancer cells that exhibit enhanced tumorigenicity and chemoresistance, are major drivers of these challenges. However, it remains unclear how CSCs maintain their stemness properties and survive chemotherapy. To gain deeper insights into the heterogeneity of ovarian cancer cells in response to cisplatin treatment, single-cell RNA sequencing (scRNA-seq) was conducted on spheroid-cultured ovarian cancer cells exposed to cisplatin. Following a two-week treatment period and a subsequent two-week recovery phase, several distinct clusters of cisplatin-surviving ovarian cancer cells were identified, exhibiting enhanced growth advantages. Analysis of the gene expression profiles of the cell clusters revealed that Uridine Phosphorylase 1 (UPP1) is highly expressed in clusters that survived cisplatin treatment compared to those eliminated by cisplatin. Given that cisplatin enriches CSCs and upregulates UPP1 expression, we sought to determine if UPP1 is linked to CSC properties. Our studies demonstrated that downregulation of UPP1 in CSCs impairs their self-renewal capability and their tumorigenic potential, establishing a causal relationship between UPP1 and the maintenance of CSC fitness and stemness in ovarian cancer. Further untargeted metabolomics analysis by LC-MS/MS indicated that UPP1 knockdown impacts several potential metabolic pathways, such as the “Superpathway of glycolysis, pyruvate dehydrogenase, TCA, and glyoxylate bypass” and “Superpathway of pentose and pentitol degradation”. This implies that UPP1 may bolster the stemness of ovarian cancer cells by reprogramming their metabolism, especially under cisplatin-induced stress. In summary, our findings reveal a novel mechanism through which cisplatin treatment enhances the stemness of ovarian cancer cells and promotes the expansion of the CSC population. Targeting UPP1 or UPP1-mediated metabolic reprogramming may represent a promising therapeutic strategy to improve ovarian cancer outcomes and reduce tumor recurrence after conventional platinum-based chemotherapy.

#2194 A PLK1-OCT4 regulatory axis controls lineage plasticity and neuroendocrine differentiation in prostate cancer.

Mohammad Esfini Farahani, Yanquan Zhang, Meng Wu, Ruixin Wang, Fatemeh Seilani, Xinyi Wang, Xiaoqi Liu

University of Kentucky, Collage of Medicine, Lexington, KY

Prostate cancer remains the most frequently diagnosed malignancy and a major cause of cancer-related death among men in the United States. A particularly aggressive subtype, neuroendocrine prostate cancer (NEPC), often emerges as a treatment-induced state in patients receiving prolonged second-generation anti-androgen therapies. NEPC tumors progress rapidly, respond poorly to conventional treatments, and are associated with markedly worse outcomes. This therapy-driven lineage switch highlights the need to define the molecular mechanisms governing neuroendocrine transformation and identify actionable vulnerabilities. PLK1 (Polo-like kinase 1) is a key regulator of mitosis and has been increasingly linked to prostate cancer progression. Our work identifies OCT4, a core pluripotency transcription factor, as a novel PLK1 substrate. We demonstrate that PLK1 phosphorylates OCT4 and promotes its degradation. In CRPC cells, short-term enzalutamide treatment elevates both stemness and neuroendocrine markers; however, with prolonged exposure, stemness features decline while neuroendocrine markers remain elevated, suggesting a transition from a transient stem-like state to a stable NEPC phenotype. We observed a similar plasticity pattern in 16D cells treated with enzalutamide, and in a DOX-inducible LNCaP Rb/p53 knockdown model, where DOX induction likewise promoted a shift toward neuroendocrine features. In N2P1 as a NEPC cells, knockdown or degradation of OCT4 further increased MYC and neuroendocrine markers, emphasizing OCT4's role in lineage balance and tumor plasticity. RNA-sequencing of N2P1 cells revealed significant elevation of MYC and BRD2, a BET-family chromatin regulator associated with MYC transcriptional control. Increased BRD2 expression, combined with enhanced MYC signaling, prompted us to investigate whether dual inhibition of PLK1 and BET proteins could more effectively suppress NEPC growth. To test this, we performed in vivo xenograft studies using pre-castrated NSG mice bearing N2P1 tumors and treated animals with vehicle, the PLK1 inhibitor Onvansertib, the BET inhibitor AZD5153, or the combination. Both single agents reduced tumor growth, but the combination therapy produced the most robust and sustained suppression, suggesting a synergistic effect and supporting co-targeting of PLK1 signaling and BET-driven chromatin regulation. Collectively, our findings reveal a critical role for the PLK1-OCT4 axis in prostate cancer plasticity and neuroendocrine differentiation. These results support a therapeutic strategy that simultaneously inhibits PLK1 and BET proteins as a promising approach to slow NEPC progression and improve patient outcomes.

#2195 The morphological discovery of the natural killer cells and enhancement of their activity using micellized nutraceuticals.

Jerry T. Thornthwaite[1], Olufemi Emmanuel Akanni[2], Daniel Strasser[3], Kyle A. Thornthwaite[1]

[1]Immunogenicity- Oncology, Cancer Research Institute of West TN, Henderson, TN,[2]Osun State University, Osogbo, Nigeria,[3]Immunogenicity- Oncology, miVital AG, St. Gallen, Switzerland

We observed that sheep erythrocytes and, later, Cancer Stem Cells (CSCs) are spontaneously destroyed by circulating lymphocytes without prior immunization. These lymphocytes, subsequently referred to as Natural Killer Cells (NKC), are the first line of defense in the blood against viruses and cancer stem cells. Much of our research has used nutraceuticals to enhance NKC activity against cancer cells. Our initial discovery of the NKC occurred while carefully observing non-immunized mouse lymphocytes centrifuged onto a lawn of sheep Red Blood Cells (SRBC) on a microscope slide. These “killer” lymphocytes would completely destroy the surrounding foreign erythrocytes on contact within a 15-minute incubation at 37 °C, forming clear plaques in a lawn of SRBC. We were able to purify these killer cells at least fivefold using continuous isotonic bovine serum albumin gradients (density = 1.0498) of normal mouse spleen cells. After glutaraldehyde fixation and Giemsa staining, Nomarski microscopy showed that the killer cells were small to medium lymphocytes. Scanning electron microscopy revealed a rough surface for these cells. Subsequently, a lawn of K562 leukemic stem cells was used as a target for the lymphocytes. We observed binding to the cancer cells, followed by the destruction of their cell membranes, as shown by Nomarski microscopy. The “blebbing” destruction of the K562 membranes is visualized in the transmission and scanning electron microscopy images. Interestingly, the NKCs exhibit pseudopodia membranes that resemble fangs, allowing them to deposit their venom into the cancer cell. Additionally, one can observe the rough endoplasmic reticulum aligning itself on the side where destruction occurs, indicating the production of cytolytic proteins. We have devoted significant research to identifying nutraceuticals that enhance NKCs and overall immunity, with an emphasis on increasing bioavailability through micellized formulations, which will be presented.https://youtu.be/HNP1EAYLhOs?si=QmsD3xDo5C9FrRZw

#2196 Matrix softness and fluid shear forceact through TRPV4 to promote ovarian cancer stemness, tumorigenicity and metastasis.

Zhenchuan LEI

The Chinese University of Hong Kong, Hong Kong, Hong Kong

Matrix stiffness and fluid shear force are key mechanical cues in ovarian cancer microenvironment that can impact cancer stemness, tumorigenicity and metastasis. However, the molecular identity of mechanosensors and/or mechanosensitive mediators that can be respond to matrix stiffness and fluid shear force in ovarian tumor microenvironment is unclear. TRPV4 is a mechanosensitive Ca^{2+}-permeable channel expressed in ovarian cancer cells. In the present study, we used 3D fibrin gel to enrich ovarian cancer stem cell (OCSC)-like cells. We found that matrix softness can increase the expression level of TRPV4 in OCSC-like cells. The activity of TRPV4 subsequently stimulates the growth of OCSC-like cells in tumor spheroids and increases the expression of OCSC markers in vitro, and promotes the growth of tumor xenografts in NOD/SCID mice in vivo. Atomic force microscope measurement of patients' samples and spatial transcriptome analysis of ovarian tumor database demonstrated that softer tumor regions have lower TRPV4 expression. Light-induced photolysis of 3D CarHc hydrogel, which rapidly dissipates the gel stiffness, elicited a TRPV4-mediated Ca^{2+} transient in the gel-encapsulated OCSC-like cells. Furthermore, we found that TRPV4 activity has positive feedback regulation on its own expression and that matrix softness may act through integrin β3 to stimulate TRPV4 activity. In another series of experiments, fluid shear force was found to directly stimulates the activity of TRPV4 channels, consequently elevating the expression level of OCSC markers, and promoting transwell migration of OCSC-like cells in vitro and peritoneal tumor metastasis in vivo. Taken together, the present study provides strong evidence that soft matrix and fluid shear act though mechanosensitive TRPV4 channels to promote ovarian cancer stemness, consequently aggravating ovarian cancer malignancy.

#2197 Mechanistic basis of panobinostat, venetoclax, and anti-CD40 combination therapy in the immune elimination of cancer stem cells.

Yishu Xu[1], Juraj Jakubik[2], Leoni Moldaner[1], Gautami Atul Gaidhani[1], Zuzana Tatarova[1]

[1]DKFZ German Cancer Research Center, Heidelberg, Germany,[2]Georg-Speyer-Haus, Frankfurt, Germany

Resistance in breast cancer treatment drives the search for new therapies. Cancer stem cells (CSCs) contribute to metastasis, recurrence, and therapy resistance. Our data suggest that combining panobinostat, venetoclax, and anti-CD40 (aCD40) immunotherapy effectively eliminates CSCs through immune modulation. This triple combination showed superior outcomes in three breast cancer mouse models, though its precise mechanism remains unclear. To dissect these mechansims, we use a multiplex implantable microdevice assay (MIMA) for precise drug delivery, cyclic immunofluorescence for tumor microenvironment characterization, and computational analyses to investigate treatment response and resistance. Single-cell RNA sequencing and multiplex tissue imaging map drug-induced cellular changes. Our results demonstrate that the panobinostat and venetoclax combination (PV) increase intratumoral immune infiltration, recruiting neutrophils, macrophages, and dendritic cells (DCs). Spatial analysis reveals APOE+ myeloid cells accumulating in PV-treated regions. Systemic PVaCD40 treatment enhances tumor killing, reduces CSCs, and improves antigen presentation by activating DCs and macrophages. Mechanistically, macrophages upregulate interferon-induced genes, boosting antigen presentation, while DCs regulate T cell migration and also increase antigen presentation. Interactions between CSCs and DCs/macrophages are elevated, and ligand-receptor analyses indicate that Mif-Cd74 and App-Cd74 signaling mediate CSC-immune cell communication. Collectively, these results provide a mechanistic framework for how Panobinostat-Venetoclax-Anti-CD40 triple combination therapy remodels the tumor microenvironment to eliminate breast CSCs and potentiate antitumor immunity.

#2198 Targeting Bmi-1 suppresses cancer stemness and tumor growth in mucoepidermoid carcinoma.

Satoshi Yamada, Kristy Warner, Jaqueline Vaz Vanini, Zhaocheng Zhang, Ririko Tsuboi, Jacques Eduardo Nor

Department of Cariology, Restorative Sciences, Endodontics, University of Michigan School of Dentistry, Ann Arbor, MI

Salivary gland carcinomas display considerable histopathological diversity and mucoepidermoid carcinoma (MEC) is recognized as the most frequent malignant subtype. However, chemotherapy provides limited benefit in MEC, highlighting the need for novel therapeutic approaches. Recent studies have highlighted the impact of cancer stemness in treatment resistance and tumor progression. Bmi-1 is a polycomb group protein and master regulator of stemness in head and neck cancers and therefore is a potential therapeutic target. This study aimed to evaluate the impact of therapeutic Bmi-1 in salivary gland MEC. Three MEC cell lines (UM-HMC-1, UM-HMC-3A, UM-HMC-3B) were treated with the Bmi-1 inhibitor PTC596 (Unesbulin), currently under clinical evaluation for solid tumors. Western blotting, flow cytometry, and sphere formation assays were performed. For Western blotting and flow cytometry, PTC596 was administered at 0-500 nM for 24-72 hours. Sphere assays in ultra-low attachment plates were performed with 0-100 nM for 10 days. Xenograft models were generated by implanting cell-seeded scaffolds of UM-HMC-3A and UM-HMC-3B into immunodeficient mice. When tumors reached 200 mm^3, mice were randomized to receive vehicle, 5 mg/kg or 10 mg/kg PTC596 every three days for 30 days. Tumor volume and body weight were recorded throughout treatment. We observed dose- and time-dependent inhibition of Bmi-1 protein expression in all MEC cell lines following PTC596 exposure. Flow cytometry revealed marked reductions in the fraction of $ALDH^{high}CD44^{high}$ cells, indicating effective targeting of cancer stem cells. Sphere formation assays further confirmed a significant dose-dependent decrease in sphere-forming capacity. *In vivo*, PTC596 induced rapid tumor regression, with tumors shrinking and remaining stably suppressed thereafter. Both 5 mg/kg and 10 mg/kg PTC596 regimens produced comparable antitumor effects. Importantly, mice maintained or gained body weight, and no overt treatment-associated toxicity was observed. Notably, PTC596 ablated cancer stem cells ($ALDH^{high}CD44^{high}$) and produced antitumor responses in preclinical salivary gland MEC models. Collectively, these findings provide compelling preclinical evidence that Bmi-1 represents a promising and clinically relevant therapeutic target for salivary gland mucoepidermoid carcinoma, supporting further translational and clinical investigation.

#2199 Dissecting ROBO4 function in regulating breast cancer cell plasticity.

Isobel J. Fetter[1], Veronica Haro Acosta[1], Paloma Medina[2], Shaheen S. Sikandar[1]

[1]Molecular, Cell, and Developmental Biology, UC Santa Cruz, Santa Cruz, CA,[2]Biomolecular Engineering, UC Santa Cruz, Santa Cruz, CA

Breast cancer is the most common cancer in women and the second-leading cause of cancer-related deaths in women. Breast cancer tumors are highly heterogeneous, with small populations of stem-like tumor-initiating cells that exhibit high cellular plasticity and often display both epithelial and mesenchymal characteristics (hybrid). These plastic stem-like cells contribute to tumorigenesis, so identifying and targeting these populations can lead to improved patient survival. ROBO1-4 proteins are transmembrane receptors that, with their SLIT1-3 ligands, regulate axon guidance, cell adhesion, mammary gland development, and angiogenesis. This signaling pathway is tightly regulated and has a wide variety of roles in normal development, but cancer is defined as abnormal development and frequently has alterations in signaling pathways. SLIT-ROBO signaling has been implicated in cell adhesion regulation in breast, lung, and colorectal cancer, but there is conflicting evidence on whether it is tumor-promoting or tumor-suppressive. Previous studies have shown that ROBO4 expression in endothelial cells suppresses breast cancer growth; however, ROBO4 has not been investigated in tumor epithelial cells. We have found that ROBO4 is expressed in epithelial breast cancer cells, and a high ROBO4+ epithelial fraction in basal-like tumor cells predicts worse survival in patients. ROBO4 knockdown in breast cancer cells reduces colony formation and proliferation, and increases apoptosis. Using patient-derived xenografts (PDXs) *in vivo,* constitutive ROBO4 knockdown reduced tumorigenesis, and inducible knockdown halted further tumor growth in pre-established tumors. Transcriptomic and proteomic analyses reveal enrichment of cancer stem cell and plasticity markers in control cells compared to ROBO4 knockdown, including *ALDH3A1, MSI2*, *CD44,* and *S100A4.* Flow cytometry analysis of tumor cells shows that knocking down ROBO4 reduces hybrid cells as measured by co-expression of CD44 (mesenchymal cells) and CD104 (epithelial cells). Preliminary results from ROBO4 overexpression tumors show an increase in hybrid $CD44^{+}/CD104^{+}$ cells, suggesting that ROBO4 maintains stem and hybrid populations in breast cancer. Gene Set Enrichment Analysis (GSEA) suggests Rho GTPase, Wnt/β-catenin, and Notch signaling are downregulated in *ROBO4* knockdown cells. These findings reveal a novel role for ROBO4 in maintaining stem-like and hybrid cell populations in breast cancer, with ROBO4's location on the cell surface providing an attractive target for potential therapeutic applications.

#2200 The mesenchymal state drives stemness and limits differentiation in glioblastoma.

Emanuele Filiberto Rosatti, Denise Sighel, Anna Veronese, Toma Tebaldi, Alessandro Quattrone

Department of Cellular, Computational and Integrative Biology, University of Trento, Trento, Italy

Glioblastoma is a highly heterogeneous and lethal brain cancer with limited therapeutic options. Recent single-cell omics studies have emphasized the importance of the proneural-mesenchymal axis and strengthened the link between glioblastoma and neurodevelopment, yet the identity and regulatory drivers of glioblastoma stem cells remain poorly defined. In this work, we combined published single-cell datasets with in vitro models to investigate glioblastoma stemness and the tumor's response to differentiation cues. Through integrative analysis of single-cell RNA sequencing and single-nucleus ATAC sequencing, we refined the landscape of glioblastoma cellular states. Comparison with human subventricular zone profiles reveals a striking similarity between a mesenchymal-like subpopulation and adult radial glia. We further established a comprehensive differentiation assay incorporating phenotypic, transcriptomic, and proteomic readouts. Using this system, we show that glioblastoma cells exhibit heterogeneous responses to differentiation signals and that mesenchymal-like cells, in particular, display pronounced resistance to lineage commitment. Together, these findings highlight the mesenchymal state as a key barrier to differentiation in glioblastoma and lay the groundwork for targeting its underlying drivers to restore differentiation capacity and potentially improve therapeutic outcomes.

#2201 Multidimensional transcriptomic alas of recurrent uterine leiomyosarcomas uncovers stem-like hormonal cells with high drug sensitivity and improved patient outcomes.

Maria Moozhiyil Korah[1], James P. Agolia[1], Biren Reddy[1], Renceh A. B. Flojo[1], Amanda Goncalves[1], Lilin Wang[2], Rosyli F. Reveron-Thornton[1], Chuner Guo[1], Beatrice Sun[1], Amanda R. Kirane[1], George Poultsides[1], Deshka Foster[1], R. Stephanie Huang[3], Gregory W. Charville[1], Michael T. Longaker[1], Daniel Delitto[1]

[1]Stanford University, Stanford, CA,[2]University of Minnesota, Minneapolis, MN,[3]Asst. Professor, Dept. of Medicine, University of Minnesota, Minneapolis, MN

INTRODUCTION: Uterine leiomyosarcomas (ULMS) are rare, aggressive tumors with profound genomic heterogeneity, which has precluded the identification of effective targeted therapies. The overall purpose of this study was to investigate the transcriptomic and spatial landscape of ULMS to identify new therapeutic avenues.

METHODS: We performed single-cell RNA sequencing (scRNA-seq) on fresh ULMS tumors using the 10X Genomics platform and spatial transcriptomics on FFPE sections using the Singular G4X platform. Resulting cells were integrated with scVI or resolVI and annotated using canonical markers. Tumor signatures were correlated with patient outcomes using bulk RNA sequencing data and novel drugs predictions for each tumor cell subtype were computed using the scIDUC algorithm.

RESULTS: ScRNA-seq was performed on 15 recurrent, metastatic ULMS tumors from 13 patients at the time of debulking surgery, which yielded 204,250 high quality cells. Spatial transcriptomics was performed on 29 sections from 10 patients, which yielded 2.3 million spatially resolved cells. Both assays revealed heterogenous tumor microenvironments comprised of several types of cells, including myeloid cells, lymphoid cells, endothelial cells, and tumor cells. Among the tumor cells, three prevalent subtypes emerged: 1) interferon-signaling cells that were distributed throughout sections, 2) mesenchyme-like cells arranged in nest-like configurations and around blood vessels, 3) ischemic cells with a high ribosomal signature organized around necrotic penumbras. Additionally, dedifferentiated stem-like cells with high expression of *ESR1*, *PGR*, and *AR*, along with Wnt signaling pathway markers, were scattered throughout tumor sections. These hormonal cells clustered into two subtypes on scRNA-seq: 1) those with high ESR1 and low AR/PGR and 2) those with low ESR1 and higher AR/PGR expression. These cells were the most sensitive to all interrogated drugs, including current first-line therapies gemcitabine, docetaxel, and doxorubicin. All other tumor subtypes were highly resistant to most drugs, though several alternative drug candidates uniquely targeting each tumor subtype were identified. Furthermore, by correlating with bulk RNA sequencing, each tumor subtype was shown to be associated with unique patient outcomes. AR and PGR hormone receptor-expressing cells correlated with improved patient survival, whereas ischemic cells correlated with the worst survival outcomes.

CONCLUSIONS: We present a comprehensive atlas of ULMS, identifying several transcriptomic subtypes of tumor cells, including dedifferentiated stem-like hormonal cells that correlate with better drug sensitivity and improved patient outcomes. Findings from this study may further facilitate patient prognostication and guide targeted therapeutic management.

#2202 APOBEC3C rewires RNA splicing and self-renewal in hematopoietic stem and progenitor cells.

Inge van der Werf[1], Jane Isquith[1], Emma Klacking[1], Jessica Pham[1], Wenxue Ma[1], Shuvro P. Nandi[2], Rongjie Wu[2], Claire Engstrom[1], Neha Katragadda[1], Anna A. Khachatrian[3], Thomas Whisenant[2], Ludmil Alexandrov[2], Catriona Jamieson[1]

[1]Sanford Stem Cell Institute, UC San Diego, La Jolla, CA,[2]UC San Diego, La Jolla, CA,[3]Scripps Health, La Jolla, CA

Introduction Inflammatory cytokine-responsive APOBEC3 cytosine deaminases promote antiviral defense through DNA and RNA editing and, when deregulated, drive somatic mutations and cancer progression. While APOBEC3A and APOBEC3B are well studied, the role of APOBEC3C remains less defined. However, our recent whole genome and whole transcriptome analyses of myeloproliferative neoplasm (MPN) derived hematopoietic stem and progenitor cells (HSPCs) revealed that APOBEC3C is highly expressed in this context, suggesting a context-specific function in hematopoiesis. This observation prompted us to investigate the effects of APOBEC3C, alongside other APOBEC family members, on HSPC biology, with an emphasis on their roles as drivers of clonal hematopoiesis (CH) and myeloid disorders in the context of aging and inflammation.

Methods We collected healthy cord blood (CB) and aged bone marrow (ABM), and lentivirally transduced immunomagnetic bead-selected $CD34^+$ cells with APOBEC3B, C, D, F, or G, or pCDH lentiviral backbone controls. Subsequently, we performed whole genome and transcriptome analyses and assessed C-to-T DNA mutations, C-to-U RNA edits and differential gene expression. As widespread changes in RNA splicing where observed as well as widespread changes in expression of genes implicated in CH upon lentiviral transduction of APOBEC3C, we also performed dual fluorescent splicing reporter assays, survival and self-renewal assays, and in vivo engraftment studies, respectively.

Results We discovered that APOBEC3C and 3F, induce more DNA mutations, whereas APOBEC3B, 3C and 3G disrupt RNA splicing. We observed differential expression of genes crucial for hematopoiesis, such as ZRSR2, U2AF1, and SRSF2, as well as differential exon usage and enrichment of the spliceosome pathway. Additionally, we demonstrated that APOBEC3C induced substantially greater transcriptomic effects in ABM HSPCs compared to CB HSPCs. We observed a 10-fold increase in differential gene expression, including alterations in ribosomal genes (RPS19 and RPL5), alongside splicing factors (U2AF1, ZRSR2, and SF3B2) implicated in CH, MPN, and myelodysplastic syndrome (MDS) pathogenesis. Moreover, in ABM HSPCs, APOBEC3C was found to affect CH-associated transcripts, including DNMT3A, enhance ADAR1-mediated RNA editing, and increase self-renewal capacity. Consistent with these findings, APOBEC3C is elevated in $JAK2^+$ MPN HSPCs, while its knockdown reduced $JAK2^+$ MPN $CD34^+$ self-renewal and ADAR1 reporter activity.

Conclusion In conclusion, these findings demonstrate that APOBEC3C modulates RNA splicing and C-to-U RNA editing in CB derived HSPCs, with more pronounced effects in ABM derived HSPCs. In ABM, this also includes increased ADAR1p150 expression and elevated A-to-I editing, which combined with increased HSPC expansion, may contribute to the pathogenesis and progression of myeloid disorders.

#2203 PSMD2 Suppression Disrupts Autophagy Turnover and Creates an Autophagy-Dependent Vulnerability in ER+ Breast Cancer.

Yejoo Lee[1], Ju Hee Kim[2], So-Youn Jung[3], Wonshik Han[4]

[1]Integrated Major in Innovative Medical Science, Seoul National University Graduate School, Seoul, Korea, Republic of,[2]Center for Medical Innovation, Seoul National University Hospital, Seoul, Korea, Republic of,[3]National Cancer Center - Korea, Goyang-si, Korea, Republic of,[4]Seoul National Univ. College of Medicine, Seoul, Korea, Republic of

Background: The ubiquitin-proteasome system (UPS) and autophagy cooperate to maintain protein homeostasis, yet how these pathways interact to regulate breast cancer stem cells (BCSCs) remains unclear. PSMD2, a 19S regulatory subunit of the proteasome, has been linked to poor outcomes in several cancers, but its role within the autophagy-proteostasis network in ER$^+$ breast cancer has not been defined. Here, we examined how PSMD2 influences CSC maintenance and drug response through UPS-autophagy crosstalk and explored how its suppression alters autophagy regulation and CSC vulnerability in ER$^+$ breast cancer.
Methods: Stable PSMD2 knockdown (ShPSMD2) lines were generated in ER$^+$ breast cancer cells (MCF-7, ZR-75-1). Autophagy was modulated using hydroxychloroquine (HCQ). Western blotting assessed CSC-related markers (SOX2, OCT4, NANOG), EMT markers (E-cadherin, N-cadherin, Vimentin), and autophagy proteins (LC3B-II, p62, p-mTOR). Functional assays, including MTT viability, colony formation, migration, and invasion, were performed to evaluate PSMD2-dependent phenotypes. Mammosphere and viability assays assessed CSC formation and HCQ sensitivity. Tumor growth and metastasis were tested using mammary fat-pad and tail-vein xenografts in NSG mice.
Results: PSMD2 depletion reduced CSC frequency, mammosphere formation, and colony formation, with decreased stemness markers (SOX2, OCT4, NANOG) and reversal of EMT features, shown by lower N-cadherin, Vimentin, and Snail. Loss of PSMD2 resulted in LC3B-II and p62 accumulation with mTOR suppression, indicating impaired autophagy turnover and disrupted proteostasis. PSMD2-deficient cells displayed reduced migration and invasion and were more sensitive to HCQ-induced cytotoxicity. HCQ treatment further lowered PSMD2 protein levels in a dose-dependent manner, implying feedback destabilization of the proteasome under lysosomal stress. This correlated with loss of $CD44^+/CD24^-$ CSC-like populations and reduced sphere-forming ability. In xenografts, PSMD2 knockdown suppressed tumor growth and lung, liver metastasis, suggesting that PSMD2 is a critical node linking proteostasis to metastatic progression.
Conclusions: PSMD2 depletion disturbs UPS-autophagy coordination, leading to loss of proteostasis and CSC depletion in ER$^+$ breast cancer. This insight reveals PSMD2 as a key regulator of proteolytic balance and a potential target for autophagy-based therapeutic strategies.

#2204 ID proteins regulate IL-6 expression and cancer stem-like cell features following chemotherapy in ovarian cancer.

Megan A. Keene[1], Mikella Robinson[2], Darren Lighter[3], Carrie D. House[2]

[1]Cell and Molecular Biology, San Diego State University / University of California San Diego, San Diego, CA,[2]San Diego State University, San Diego, CA,[3]Cell and Molecular Biology, San Diego State University, San Diego, CA

Ovarian cancer (OC) remains the most lethal gynecological cancer. Discreet OC symptoms lead to late stage diagnosis, limiting treatment options. Most patients are initially responsive to chemotherapy, but over 80% of advanced cases relapse with treatment-resistant disease within 2 years. Cancer recurrence has been attributed to a small subpopulation of cancer stem-like cells (CSCs) that possess the ability to resist chemotherapy, self-renew, and asymmetrically divide. ID1-4 proteins, also known as inhibitors of differentiation, regulate cell fate and differentiation in normal stem and progenitor cells. In gliomas, ID1-4 proteins have been identified as master transcriptional regulators of CSC identity, signaling to downstream pathways important for self-renewal, tumor initiation, and survival; however, their role in OC CSCs and recurrence is unclear. Recently, we found that ID1-3 gene expression significantly increased following chemotherapy treatment in OC clinical samples and cell lines, and higher gene expression of ID1 and ID3 was associated with worse clinical outcomes. We hypothesize that ID proteins are required for OC CSC survival, self-renewal, and tumor recurrence following chemotherapy. In a subcutaneous xenograft mouse model, we found that cancer cell ID2 and ID4 protein expression significantly increased within 3 days following carboplatin treatment compared to vehicle groups, but this trend waned at later time points. Furthermore, we saw ID1-4 gene expression significantly increased stepwise following one and two cycles of chemotherapy in OVCAR8, OVCAR4, OVCAR5, and OV90 OC cell lines. Using a pan-ID inhibitor, AGX51, we have significantly knocked down ID expression in the four OC cell lines, and quantified CSC presence and function. Our data shows ID inhibition in OC cell lines reduces chemotherapy-dependent increases in CSC marker expression by flow cytometry (ALDH), spheroid formation, and gene expression of SOX2 and IL-6. Future studies will utilize siRNA silencing to elucidate the ID-dependent mechanisms of chemotherapy-induced SOX2 and IL-6 expression and how this contributes to OC survival. These studies highlight a novel target important in CSC maintenance that contributes to tumor progression and relapse. Understanding these mechanisms will enable development of therapies to overcome chemotherapy resistance and relapse, ultimately improving clinical outcomes.

#2205 Isoform-level transcriptome analysis for enriched cancer stem cells from patient-derived ovarian cancer cell lines.

Rachel S. Perkins[1], Jisun Kang[1], Matthew S. Jung[1], Sue Chin Lee[2], Wenjing Zhang[1], Won-Young Choi[1]

[1]Department of Pathology, University of Tennessee Health Science Center, Memphis, TN,[2]Department of Physiology, University of Tennessee Health Science Center, Memphis, TN

Background: In high-grade serous ovarian cancer (HGSOC), the abilities of tumor cells to resist cytotoxic treatment and relapse are largely driven by ovarian cancer stem cells (CSCs). CSCs are a population of cells within a tumor that maintain stem-like qualities, such as self-renewal and asymmetric division, but also have the capacity to produce metastasis and drive drug resistance. Despite extensive research over the past two decades, no specific CSC target has been identified in ovarian cancer, and no drug has proven effective in neutralizing the CSC population. Therefore, identifying the molecular mechanisms underlying CSC development in HGSOC is urgently needed, as eradicating CSCs represents one of the most formidable challenges in oncology, yet also offers one of the most transformative opportunities to alter the course of cancer therapies. Based on the emerging evidence of linking differential isoform usage to the regulatory mechanisms of developmental process, we hypothesize that CSCs exploit isoform diversity to sustain stemness, drive therapy resistance, and shape prognosis while gene-level programs shape general differentiation status.
Methods: We employed CSC-enriched sphere culture system to emphasize the features of CSC population from 3 patient derived high grade serous ovarian carcinomas (PD-HGSOC) with different metastatic abilities and tumor aggressiveness. For these cell lines, we generated RNA-seq data for genome-wide transcriptome profiling to investigate stemness and differentiation status comparing standard culture condition and CSC-enriched spheres. In this study, we analyzed RNA-seq data in gene-level as well as in isoform-level with the most up-to-date transcript annotation to identify patient-specific CSC features and define the mechanism of cancer related stemness and plasticity.
Results: We analyzed gene-level transcriptome profiles focusing on stemness signatures in PD-HGSOC and CSC-enriched spheres. We observed that CSCs exhibited markedly higher stemness characteristics and identified differentially expressed gene sets across PD-HGSOCs. We noted that each cell line had a distinct subset of genes regulating stemness which suggested multiple mechanisms of CSC development and maintenance. In result of isoform-level analysis, we found that a large proportion of gene-level expression changes were driven by the differential expression of a single predominant isoform. Importantly, our isoform-level analysis enabled the identification of differential isoform usage that would not be detected at the gene level expression analysis, as changes in isoform composition can occur while total gene expression remain unchanged. These results are instrumental for foundational understanding of CSC plasticity and for next generation drug design, increasing target specificity and reducing adverse effects.

#2206 Uncovering a pancreatic ductal adenocarcinoma sub-population with stemness and unique therapeutic response.

SHIFA KHAN, Wen-Cheng Chung, Charles D. Moore, Keli Xu

University of Mississippi Medical Center, Jackson, MS

Pancreatic ductal adenocarcinoma (PDAC) remains one of the most lethal malignancies, primarily due to its detection at advanced stages, with therapy resistance being the second major cause, leading to limited treatment options. It is well established that pancreatic differentiation is controlled by Notch during organogenesis, and its reactivation is seen in pancreatic tumorigenesis. The regulation of Notch signaling and its relationship with pancreatic exocrine and endocrine cells in pancreatic cancer is still unclear. Therefore, this study was designed to investigate the role of Notch in PDAC initiation and progression with respect to different cells of origin, along with a significant focus on understanding the potential of these cells to behave like cancer stem cells. The two different types of PDAC cells, derived from primary mouse tumors with Kras mutation and p53 deletion, were tested for their sensitivity to various pharmacological inhibitors. These cells originated from Lunatic Fringe (Lfng)-expressing centroacinar cells (CAC) and Mist1-expressing acinar cells. The subsets of $Lfng^+$ tumor cells in these two types of PDAC were sorted for the tests in comparison with their $Lfng^-$ counterparts. The protein expression of Notch receptors was analyzed along with their downstream targets. The cells isolated from mice harboring PanIN lesions (not yet developed into PDAC) were examined for their organoid-forming capability to trace which lineage of PDAC cells carries the stem-like properties. Finally, the organoids were analyzed for various markers of pancreatic progenitors and stem-like characteristics to gain insight into the subset of pancreatic cells involved in the initiation of PDAC. It was found that the PDAC cells derived CAC population has an inherent property of behaving as cancer stem-like cells. These cells were highly resistant to the inhibitory effects of the chemotherapy drug gemcitabine compared to acinar-derived PDAC cells. However, they were uniquely sensitive to a gamma-secretase inhibitor, which blocks Notch activation. High expression of Notch3 and Hes1 was predominantly found in the CAC-derived PDAC cells, along with the high efficiency in forming 3D organoids, even at the early stage of tumor initiation. The organoids were found to co-express ductal (CK19) and acinar (Amylase) cell markers, containing cells expressing the pancreatic progenitor marker (Pdx1), stem cell marker (Aldh1a1), and Vimentin-expressing cells, which represent a more aggressive and metastatic subpopulation. These findings hold significant potential in unraveling treatment options and screening patients based on the subtype of the PDAC population. The full potential of GSI needs to be explored for its use as a treatment option alongside other available chemotherapy drugs. Targeting Lfng-dependent Notch signaling may offer an option for treating patients with CAC-derived PDAC.

#2207 The impact of tumor treating fields (TTFields) on the transcriptome and the secretome of cancer stem-like cells isolated from the sub-ventricular zone of glioblastoma patients.

Rachel B. Sidebottom[1], Antonia E. Sajche Sapon[1], Yamhilette Licon-Munoz[1], Christian A. Bowers[2], **Sara G.m. Piccirillo**[1]

[1]Cell Biology and Physiology, University of New Mexico Health Sciences Center, Albuquerque, NM,[2]Neurosurgery, University of New Mexico Health Sciences Center, Albuquerque, NM

Glioblastoma (GBM) is the most aggressive brain tumor in adults that almost inevitably recurs despite radical treatments. Recurrence is driven by residual disease, which is extremely difficult to identify and target. We were the first to identify and characterize specific anatomic/functional areas of residual disease in GBM patients, including the sub-ventricular zone (SVZ), the most well-characterized neurogenic area in the mammalian brain. Specifically, we showed that the SVZ is a reservoir of cancer stem-like cells (CSCs) seeding recurrence. Thus, the SVZ holds the key to identifying novel therapeutic targets for GBM patients. We previously evaluated the impact of Tumor Treating Fields (TTFields) - electric fields exerting physical forces on tumor cells - on the morphology and proliferation of CSCs isolated from the SVZ of GBM patients. We observed that the proliferation of CSCs resistant to Temozolomide and ionizing radiation is significantly inhibited by TTFields when cells are exposed for 48 hours to the optimized frequency for GBM (200 kHz). Moreover, we observed that this antiproliferative effect of TTFields is maintained among patients. In our recent work, we examined the impact of TTFields on the transcriptome and secretome of CSCs isolated from the SVZ of GBM patients using single-cell transcriptomics and functional phenotyping. First, we isolated and characterized 10 CSCs. These cells were maintained in conditions that preserve the molecular profile of the original patient tumor, thus representing *bona fide* models to study the impact of TTFields on GBM residual disease. Second, we used the 10x Genomics platform and the Bruker single-cell proteomic barcoding solution to perform single-cell transcriptomics and functional phenotyping. Our results indicate changes in the transcriptomic profile of CSCs after TTFields compared with matched untreated cells. Specifically, TTFields altered the expression of genes related to cell cycle and GBM cell states. Moreover, functional phenotyping analysis of the innate immune cytokine secretome revealed that CSCs treated with TTFields secrete less VEGF and more soluble CD137 (sCD137) than untreated cells. CD137 is a member of the TNF family contributing to the activation of cytotoxic responses in T cells, while sCD137 exhibits immunoinhibitory functions. Clinical trials involving agonistic anti-CD137 antibodies(Abs) that also counteract sCD137-mediated immunoinhibition are currently underway in patients with advanced tumors. Combined with TTFields, these Abs offer a novel therapeutic opportunity for the treatment of GBM. Collectively, our results point to the effectiveness of TTFields in GBM and identify a novel therapeutic target in GBM residual disease.

#2208 MAP2-mediated integrin dysregulation reprograms cancer cell plasticity to drive liver cancer cell transition to a mesenchymal and stemness state in hepatocellular carcinoma.

Ut Kei Lou[1], Tin-Lok Wong[1], Huajian Yu[1], Ki-Fong Man[1], Ka-Hei Lam[1], Jia Jian Loh[1], Lei Zhou[2], Yuan Gao[3], Cheng-Han Yu[1], **Stephanie Ma**[1]

[1]School of Biomedical Sciences, Li Ka Shing Faculty of Medicine, The University of Hong Kong, Hong Kong, Hong Kong,[2]Precision Medicine Institute, The First Affiliated Hospital, Sun Yat-Sen University, Guangzhou, China,[3]State Key Laboratory of Cancer Biology, Biotechnology Centre, School of Pharmacy, Fourth Military Medical University, Xi'an, China

Targeting tumor cell plasticity is central to overcome drug resistance and metastasis, two major obstacles in eradicating cancer. Through lineage-tracing and lineage-ablation studies, our team has previously shown hepatocellular carcinoma (HCC) cells marked by prominin-1 (CD133) to represent a functional subset displaying dedifferentiated status with stemness traits, yet there are limited therapies effective for eradicating such resilient cell populations. To address this unmet clinical need, we explore the therapeutic potential of repurposing an existing drug estramustine phosphate (EMP) for targeting HCC plasticity through inhibiting microtubule associated protein 2 (MAP2), a gene uniquely enriched in CD133+ 'HCC' stemness subset but not in CD133+ 'normal' regenerative cells. MAP2 is transcriptionally activated by p300-driven histone 3 lysine 27 acetylation, and its upregulation is associated with aggressive clinical features. Functional characterization demonstrates that MAP2 confers tumor-initiating and migratory abilities to HCC cells both in vitro and in vivo, and enables cells to resist cell apoptosis upon sorafenib treatment. Comparative transcriptome profiling and pathway analysis by Gene Set Enrichment Analysis and Gene Ontology identifies a pan-deficiency of integrin α expressions and depletion of integrin-directed adhesion pathways upon MAP2 overexpression. Mechanistically, MAP2 sustains tumor plasticity and transition to a mesenchymal phenotype through inducing filamentous actin polymerization and activation of yes-associated protein (YAP), which subsequently disrupts integrin-mediated cell adhesion behaviors on type I collagen. Of note, pharmacological inhibition of MAP2 effectively sensitizes HCC to targeted therapy sorafenib in HCC cells lines, patients-derived organoids and immunocompetent HCC mice model. Collectively, our research offers a promising opportunity for drug repurposing using EMP in combination with sorafenib to target HCC at its stemness roots.

#2209 RelB drives integrin-mediated stress tolerance and relapse in high-grade serous ovarian cancer.

Omar Lujano Olazaba[1], Mikella Robinson[1], Greg J. Jordan[1], Sofia Howe[1], Cassidy Lucht[1], Anna Platen[1], Dishant Vandra[1], Mena Shammas[1], Katelyn Shelby[2], Ingrid Niesman[1], Christina M. Annunziata[3], **Carrie Danielle House**[1]

[1]San Diego State University, San Diego, CA,[2]BioLegend, San Diego, CA,[3]American Cancer Society, McLean, VA

High-grade serous ovarian cancer (HGSOC) initially responds to chemotherapy but frequently relapses with chemoresistant disease, potentially driven by cancer stem-like cells (CSCs), a minority tumor cell population with enhanced chemoresistance and tumor-initiation capacity that persists following treatment. We previously demonstrated that NF-κB signaling is upregulated in HGSOC and promotes stemness features in ovarian cancer cells including drug resistance, asymmetric division, tumor-initiation capacity, and epithelial to mesenchymal transition (EMT). Here, we investigated potential mechanisms by which this signaling cascade supports stress tolerance and tumor regrowth following chemotherapy to identify new therapeutic targets to prevent relapse. We found that NF-κB transcription factors RelA and RelB commonly regulate extracellular matrix organization genes but differentially regulate specific integrin subunits, including *ITGAV* (αV) by RelA and *ITGB3* (β3) by RelB. Given the clinical feasibility of targeting integrins we investigated αVβ3 in ovarian CSCs. We show that $\alpha V\beta 3^{+}$ cells have significantly enhanced tumor-initiation capacity relative to $\alpha V\beta 3^{-}$ cells and αVβ3 and αVβ5 are enriched on ovarian CSCs following standard of care chemotherapy. We developed a relapse model that demonstrates αVβ3 expression on ~90% of cells derived from re-established tumors and $\alpha V\beta 3^{+}$ cells exhibit preferential growth on mesentery, which is mediated by RelB. Importantly, knockdown of RelB combined with inhibition of αVβ3 and αVβ5 eradicated stress-tolerant cells, reduced overall tumor burden, and significantly prolonged survival following chemotherapy. Studies are underway to elucidate stromal responses to cytotoxic chemotherapy in peritoneal tissues that generate a modulated matrisome characterized by increased vitronectin and fibronectin. These tissues, which include the mesentery, may be susceptible to colonization of stress tolerant cells expressing αVβ3 and αVβ5 following chemotherapy and thus may play a significant role in relapse. Crucially, this work proposes integrins as promising therapeutic targets for HGSOC and indicates distinct roles for NF-kB transcription factors in regulating integrin expression and metastatic growth in this disease.

#2210 Ouabain exerts both anti-tumor and senolytic effects in brain cancer stem and tumor cells.

Alaa Daoud Sarsour[1], Gila Kazimirsky[1], Moran Dvela-Levitt[1], Chaya Brodie[1], Heidrun Weidemann[2], Iris Frid[3]

[1]The Mina and Everard Goodman Faculty of Life Sciences, Bar-Ilan University, Ramat Gan, Israel,[2]Internal Medicine,, Saint Georg Clinics, Eisenach, Germany,[3]Pediatric Hematology Oncology Unit, Shaare Zedek Hospital, Jerusalem, Israel

Glioblastoma (GBM) and diffuse intrinsic pontine glioma (DIPG) are highly aggressive brain tumors with dismal prognoses. These tumors contain therapy-resistant cancer stem cells (CSCs) that drive tumor progression and relapse. Standard treatments such as radiation and temozolomide (TMZ) induce senescence in a subset of tumor cells, generating a persistent, treatment-refractory population. Senolytic agents that selectively eliminate senescent cells may overcome this resistance. Here, we investigated the anti-tumor and senolytic effects of the cardiac glycoside ouabain in glioblastoma stem cells (GSCs), DIPG stem cells, and glioma cell lines. Neurosphere formation and transwell assays were used to assess self-renewal and migration, and senolytic activity was examined in TMZ-treated cells using β-galactosidase staining. RT-PCR quantified stemness-associated gene expression.Ouabain inhibited the self-renewal of GSCs and DIPG stem cells in a dose-dependent manner and reduced their migratory capacity. TMZ pre-treatment sensitized GSCs to ouabain, resulting in a more pronounced suppression of neurosphere formation and an enhanced inhibition of migration. Ouabain decreased the expression of stemness and EMT-related genes, including SOX2, YKL-40, OCT4, and NANOG.In addition, ouabain selectively eliminated TMZ-induced senescent cells in both glioma cell lines and differentiating GSCs. Together, these findings demonstrate that ouabain exerts dual anti-tumor and senolytic effects in GBM and DIPG cells by suppressing CSC stemness, migration, and eliminating senescent, stem-like populations. These combined effects highlight ouabain as a potential therapeutic strategy for targeting treatment-resistant cells in malignant gliomas.

#2211 STAT1 and STAT3 cooperatively control cancer stem cell (CSC) fate and IFNγ-dependent CSC maintenance.

Sophia Hidalgo[1], Anushka Poola[1], Yipeng Zhang[1], Rachel Zhou[1], Kourosh Kouhmareh[2], Jack D. Bui[1], **Magalie Dosset**[1]

[1]Department of Pathology, UC San Diego, La Jolla, CA,[2]UC San Diego School of Medicine, La Jolla, CA

Background: Cancer stem cells (CSCs) are a rare tumor cell subset with self-renewal and differentiation capacity that drives tumor initiation, heterogeneity, metastasis, and therapy resistance. Interferon-γ (IFNγ) has been implicated in regulating CSC fate, but its effects are highly context dependent. How the intrinsic balance between opposing IFNγ pathway effectors such as STAT1 and STAT3 shapes CSC properties remains poorly understood.
Methods: Breast (4T1, PY230) and sarcoma (F244, F236, H74) cell lines were exposed to high acute or persistent IFNγ stimulation. STAT1/STAT3 were deleted via CRISPR-Cas9. Retroviral transfection was used to restore STAT1 in STAT1-deficient H74 sarcoma cells. CSC induction was monitored using molecular and sphere formation assays for in vitro and in vivo experiments. Bioinformatic analyses include single-cell and bulk-RNA sequencing from public databases of human breast cancer.
Results: In this study, we found that cancer cell lines with higher expression of stem-cell-associated markers at baseline tend to have a lower STAT1/ STAT3 ratio and/or constitutive STAT3 activation. Exposure to acute high dose of IFNγ or persistent exposure to IFNγ led a progressive increase of CSC-associated genes (e.g. *Zeb1, Bst2, Tert*). STAT1 depletion favored CSC induction, while STAT3 loss led to increased cell death both with or without IFNγ stimulation. Interestingly, combined STAT1/STAT3 depletion markedly increased sphere size independently of IFNγ treatment, indicating that those two transcription factors may cooperate to restrain CSC proliferation. In vivo, STAT1-deficient H74 sarcoma cell line exhibited accelerated tumor progression and CSC induction in an IFNγ-dependent manner. By contrast, restoration of STAT1 completely abrogated H74 tumor growth in immunocompetent but not immunodeficient mice, confirming that STAT1 limits CSC induction by sensitizing tumor cells to immune-mediated cytotoxicity. Finally, single-cell RNAseq of human breast cancer cells revealed an inverse correlation between STAT1 and STAT3 expressions. STAT1-negative tumor cells with high IFNγ score were enriched in EMT- and apoptosis-related programs. Consistently, $IFN\gamma^{hi}/STAT3^{hi}$ breast tumors exhibited a stronger EMT signature and were associated with poorer clinical outcomes compared with $IFN\gamma^{hi}/STAT3^{lo}$ tumors.
Conclusions: Modulating the STAT1/STAT3 balance can suppress CSC expansion and preserve tumor cell vulnerability to immune-mediated killing. STAT1-sufficient tumors respond to IFNγ typically by increasing immunogenicity and limiting CSC potential, whereas STAT1-deficient tumors respond to IFNγ by increasing CSC properties. These results suggest that STAT1 serves as a toggle for anti- and pro-tumor effects of IFNγ.

: Tertiary Lymphoid Structures in Cancer
Poster Session

#2215 Tertiary lymphoid structure score associates with unique immune profile and therapeutic response in triple negative breast cancer.

Kei Kawashima[1], Akimitsu Yamada[2], Itaru Endo[2], Kazuaki Takabe[1]

[1]Roswell Park Comprehensive Cancer Center, Buffalo, NY,[2]Yokohama City University, Yokohama, Japan

Background: Tertiary lymphoid structures (TLSs) are aggregates of immune cells that resemble secondary lymphoid organs in both morphology and function, and are frequently observed within the tumor microenvironment (TME) of solid cancers including breast cancer. TLS have emerged as a predicter of anti-tumor immune activation and improved responses to immune checkpoint inhibitors (ICIs). However, TLS evaluation typically relies on histology that limits its generalizability. We hypothesize that TLS score is associated with distinct immune profiles and therapeutic response in triple negative breast cancer.
Methods: Clinical and transcriptomic data from 12 independent TNBC cohorts (TCGA(n=170), METABRIC(n=335), SCAN-B(n=174), GSE194040(n=363), GSE25066(n=133), GSE163882(n=90), GSE123845(n=86), GSE20271(n=63), GSE50948(n=17), GSE230881(n=49), GSE41998(n=151), GSE176078(n=10)) were analyzed using established 12-gene TLS signature score. The patients in each cohort were divided into TLS-high and low groups by median cutoff. For validation of the TLS score, we utilized pathological and spatial transcriptomic data from GSE17703(n=30) and EGAC50000000323(n=96). Associations between the TLS score and clinicopathologic features, genomic features and therapeutic outcomes were assessed.
Results: The TLS score was significantly higher in tumors with histologically confirmed TLSs. Spatial transcriptomic analysis revealed that high TLS scores colocalized with histologically confirmed TLSs, suggesting that the TLS score reliably reflects the presence of TLS. High-TLS score tumor had higher histological grade and lymph node involvement, and associates with significant enrichment of Hallmark cell proliferation-related pathways. Immune-related pathways were also significantly enriched in the TLS-high group, which exhibited significantly greater infiltration of CD8+ T cells, B cells, regulatory T cells, macrophage M1, and dendric cells. Among immune cells, macrophages displayed particularly elevated TLS scores, and TLS-high immune cells showed stronger intercellular communication. TLS scores were not associated with HRD or mutation burden, however, TLS-high tumors showed higher intratumoral genomic heterogeneity, suggesting that they are genomically stable yet immunologically inflamed and likely to be aggressive. Across 8 independent neoadjuvant chemotherapy cohorts, TLS scores were significantly higher in patients who achieved pathological complete response, with the largest effect observed in the ICI-treated cohort. Despite their association with features of aggressive biology, TLS-high tumors demonstrated more favorable clinical outcomes.
Conclusions: TLS-high TNBC were highly proliferative but immunologically active, and the TLS score was strongly associated with better treatment response and improved prognosis.

#2216 Spatial multi-omics reveals functional diversity of tertiary lymphoid structures in brain metastases.

Sadaf Shabbir Mughal[1], Jennifer H. Lun[2], Karina Martinez[1], Jadranka Macas[2], Jonathan Schupp[2], Tatjana Starzetz[2], Stefanos Voglis[3], Benedikt Brors[1], Karl H. Plate[2], Yvonne Reiss[2]

[1]Division of Applied Bioinformatics, German Cancer Research Center, Heidelberg, Germany,[2]Institute of Neurology (Edinger Institute), University Hospital Goethe University, Frankfurt, Germany,[3]Department of Neurosurgery, University Hospital Zurich, Zurich, Switzerland

Tertiary lymphoid structures (TLS) are increasingly recognized as important drivers of anti-tumor immunity and predictors of survival and immunotherapy response in multiple non-central nervous system cancers. However, their role in brain metastases (BrM) remains poorly understood. To better advance understanding of their role in the immunosuppressive brain tumor microenvironment, we applied a multimodal approach to examine TLS prevalence, spatial organization, and clinical relevance in a retrospective cohort of 461 BrM samples from diverse primary tissues, collected between 2015 - 2022 at the University Cancer Center Frankfurt. CD20 immunohistochemistry was used to screen for lymphoid aggregates, and a subset of TLS-positive and negative tumors were subjected to comprehensive molecular and spatial profiling. For an in-depth characterization of TLS, we employed multiple spatial technologies, including 7-plex immunofluorescence imaging for spatially resolved cellular phenotyping and TLS identification, whole-transcriptome spatial profiling of regions of interest, subcellular-resolution spatial transcriptomics (468-gene panel) for whole-tissue mapping, and spatial proteomic profiling using 40 markers to assess immune and stromal interactions. TLS were detected in 50% of BrM, most frequently in lung-to-brain metastases. Notably, the majority of TLS lacked features characteristic of mature germinal centers, indicating a potentially attenuated or dysregulated immune response within the BrM microenvironment. Survival analyses revealed a favorable prognosis associated with TLS-positive tumors and an improved response to immune checkpoint inhibitors. Spatial characterization of the BrM tumor immune microenvironment revealed cellular niches that promote distinct patterns of immune cell aggregate formation and cell-cell interactions, underlying phenotypic heterogeneity within patients and across primary sites. Analysis of whole transcriptomic data further revealed remodeling of extracellular matrix and evidence of metabolic reprogramming in tumor rich areas and enrichment of processes such as antigen presentation, regulation and activation of immune response in B cell-rich niches. Integrative single-cell spatial transcriptomics and proteomics, enabled phenotyping of TLS subtypes across patients, capturing different stages of maturation and levels of organization. This spatially resolved, multimodal approach provides a comprehensive resource for understanding TLS biology in BrM and may guide microenvironment-informed strategies to improve immunotherapeutic outcomes in metastatic brain disease.

#2217 Immune-active and mesenchymal endothelial programs define TLS presence in the tumor microenvironment.

Shoko Kure[1], Giorgia Brambilla Pisoni[1], Saba Tabasum[1], Xiaoyu Li[1], Jingjing Li[1], Yao Yu Yeo[2], Sizun Jiang[2], Harrison Olszewski[3], Nicholas C. Weaver[3], Kathleen L. Pfaff[3], Jason L. Weirather[4], Ian D. Dryg[4], Scott J. Rodig[5], Frank S. Hodi[1]

[1]Medical Oncology, Dana-Farber Cancer Institute, Boston, MA,[2]Center for Virology and Vaccine Research, Beth Israel Deaconess Medical Center, Boston, MA,[3]Tissue Biomarker Lab, Dana-Farber Cancer Institute, Boston, MA,[4]Department of Data Sciences, Dana-Farber Cancer Institute, Boston, MA,[5]Department of Pathology, Brigham & Women's Hospital, Boston, MA

Introduction: Tertiary lymphoid structures (TLSs) are ectopic lymphoid formations. In cancer, they promote antitumor immunity by supporting B-cell maturation, antibody production, and sustained T-cell activation. TLSs can convert immunologically non-inflamed tumors into inflamed ones. However, the vascular and molecular cues that govern TLS induction in human tumors remain poorly defined.

Methods: Formalin-fixed paraffin-embedded tissue sections from twelve primary lung adenocarcinomas were analyzed. Tumor-associated vasculature was histologically annotated and stratified into three categories based on TLS status: (1) noTLS (absence of TLS), (2) iTLS (presence of immature TLS), and (3) mTLS (presence of mature TLS). GeoMx spatial transcriptomics was performed on endothelial regions. Protein-level validation was conducted using sequential immunofluorescence on the COMET platform.

Results: Endothelial cells in noTLS regions showed high expression of COL5A1, COL3A1, FN1, ERRFI1, COL1A1, IFI6, SPP1, MDK, and BGN, whereas CXCL13 and CCL19 were enriched in mTLS. Gene-set analyses revealed that noTLS endothelium exhibited a myofibroblast-like, extracellular matrix-producing, EndoMT-associated program consistent with a fibrotic, immunosuppressive microenvironment. In contrast, mTLS endothelium displayed immune-activated signatures aligned with lymphoid organogenesis and fibroblastic reticular cell-like function. Receptor-ligand analysis showed preferential Wnt signaling in noTLS, while chemokine signaling dominated in mTLS. COMET immunofluorescence confirmed that FN1 was highly expressed in noTLS regions, whereas CXCL13 was highly expressed in mTLS.

Conclusion: Tumor endothelial cells display striking context-dependent plasticity. noTLS vasculature undergoes EndoMT and adopts a matrix-producing, immunosuppressive phenotype that may actively suppress TLS formation. Conversely, mTLS endothelium acquires immune-organizing properties that favor TLS maturation and lymphoid compartmentalization. These findings identify endothelial reprogramming as a potential therapeutic strategy to induce TLSs and enhance response to immune checkpoint blockade.

#2218 Tertiary lymphoid structures in colorectal cancer: Clinical significance and their interaction with CAFs and the immune microenvironment.

Zizhou Wang[1], Hiroaki Kasashima[1], Yukina Kusunoki[2], Yasuhiro Fukui[1], Iguru Omori[1], Nobuhiro Naito[1], Hideki Tanda[1], Yuki Seki[1], Kenji Kuroda[1], Yuichiro Miki[1], Mami Yoshii[1], Tatsuro Tamura[1], Masatsune Shibutani[1], Takahiro Toyokawa[1], Yu Muta[3], Yuki Nakanishi[3], Masakazu Yashiro[4], Kiyoshi Maeda[1]

[1]Department of Gastroenterological Surgery, Osaka Metropolitan University, Osaka, Japan,[2]Department of Pathophysiology, Osaka Metropolitan University, Osaka, Japan,[3]Department of Gastroenterology and Hepatology, Kyoto University, Japan, Kyoto, Japan,[4]Department of Molecular Oncology and Therapeutics, Osaka Metropolitan University, Osaka, Japan

Colorectal cancer (CRC) is a major malignancy with high global mortality. The tumor immune microenvironment, particularly tertiary lymphoid structures (TLSs), has gained increasing attention for its role in antitumor immunity. However, their specific functions in CRC and the prognostic relevance of TLS-associated cells remain unclear. We analyzed 166 CRC patients who underwent curative resection, evaluating TLSs by hematoxylin and eosin (H&E) staining and immunohistochemistry for CD20, α-SMA, CD8, CD4 and CD103. We additionally performed Opal-based multiplex immunofluorescence (mIF) with a two-plex panel (CD20 and α-SMA) to validate the presence of cancer-associated fibroblasts (CAFs) within TLSs. Patients were categorized by TLS density and immune-cell infiltration levels. TLSs were predominantly located at invasive margins, and higher TLS density correlated with better prognosis ($P < 0.05$). In contrast, high CAF density within TLSs was associated with poorer outcomes ($P < 0.01$), whereas a high abundance of $CD8^+$ T cells predicted improved survival. Furthermore, using Xenium Explorer spatial transcriptomics, we confirmed the spatial coexistence of CAFs and immune cells within TLSs in colorectal cancer. In particular, CAF accumulation within TLSs may reshape the immune microenvironment and potentially impair antitumor T-cell activity.

#2219 CXCL13 secretion and immobilization show distinct geographies within secondary and tertiary lymphoid structures (TLS).

Jonathan Rex Skidmore, Aleksandra Ogurtsova, Grant Salvucci, Victoria Jacobs, Logan Engle, Robert A. Anders, Drew M. Pardoll, Janis Marie Taube

Johns Hopkins Bloomberg-Kimmel Inst. for Cancer Immunotherapy, Baltimore, MD

The purpose of this study is to investigate the formation and maintenance of germinal centers in TLS by defining mechanisms and spatial patterns of CXCL13 chemokine gradients in tumor tissue. In secondary lymphoid tissue, it is recognized that CXCL13 is immobilized by follicular dendritic cells (FDCs), but the mechanisms of immobilization remain unclear. Furthermore, spatial patterns and mechanisms of CXCL13 immobilization in TLS are unknown. We developed a CXCL13 Immunohistochemistry /in situ hybridization (ICH/ISH) dual stain to determine which cells are responsible for CXCL13 production and display. We stained 3 formalin-fixed paraffin-embedded tonsil specimens and found that CXCL13 protein and mRNA staining have distinct localizations. Specifically, spatial analyses were performed on 10 individual follicular structures from each tonsil to compare the percent surface area of either germinal centers or mantle zones (n=30) demonstrating staining by IHC or ISH. This analysis revealed that CXCL13 protein was highly expressed in germinal centers and expressed relatively lower in mantle zones (31% vs 12% surface area, $p<0.0001$). However, CXCL13 ISH staining was the inverse: mRNA expression was lower in germinal centers, and higher in mantle zones (20% vs 37%, $p<0.0001$). Flow cytometry analysis of fresh tonsil tissue revealed stromal cells displaying CXCL13, ($PDPN^{+}CD31^{-}CXCL13^{+}$), supporting the CXCL13 IHC findings. Similarly, spatial transcriptomics showed similar findings to the CXCL13 ISH, providing additional validation of the spatial expression pattern. Together, these results support a model where CXCL13 is primarily secreted from mantle zones, then immobilized in germinal centers.

To investigate if these findings extend to TLS in tumor tissues, we applied our CXCL13 IHC/ISH dual stain to lung cancer tissue from the definitive resection specimen from patients treated with neoadjuvant anti-PD-1 immunotherapy. Spatial analyses revealed that similar to what was observed in tonsil, the density of CXCL13 mRNA is highly correlated with CXCL13 protein staining (n=3, Spearman's r: 0.9, $p<9.311e-19$), though these do not immediately overlap spatially, with an average distance of 30 µm between mRNA and protein expression, suggesting capture of the diffusing CXCL13. We also observed that stromal cells in mature TLS immobilize CXCL13, but stromal cells in immature TLS do not. In addition, we found CXCL13 immobilized on elastin fibers near mRNA staining.

These findings show that CXCL13 immobilization may contribute to the formation and maintenance of TLS. New therapies enhancing the formation and maturation of TLS by modulating CXCL13 may warrant exploration. Ongoing single cell RNA sequencing and in vitro studies are focused on determining the mechanisms responsible for the immobilization of CXCL13 in lymphoid and tumor tissue.

#2220 A spatially resolved multi-omics atlas of tertiary lymphoid structures in ovarian cancer.

Zhihan Liang[1], Ada Junquera[1], Hanna Elomaa[1], Joona Sarkkinen[2], Iga Niemiec[1], Ziqi Kang[1], Oskari Lehtonen[1], Lina Maltrovsky[1], Saundarya Shah[1], Aleksandra Shabanova[1], Matilda Salko[1], Ulla-Maija Haltia[3], Eliisa Kekalainen[2], Anni Virtanen[4], Anniina Farkkila[1]

[1]Research Program in Systems Oncology, University of Helsinki, Helsinki, Finland,[2]Translational Immunology Research Program, University of Helsinki and Helsinki University Hospital, Helsinki, Finland,[3]Department of Obstetrics and Gynecology, and Clinical Trials Unit, Comprehensive Cancer Centre, Helsinki University Hospital, Helsinki, Finland,[4]Department of Pathology, University of Helsinki and HUS Diagnostic Center, Helsinki University Hospital, Helsinki, Finland

Tertiary lymphoid structures (TLSs) coordinate localized immune responses in the ovarian tumor microenvironment. However, the maturation transitions of TLS remain poorly understood at both cellular and molecular levels. We constructed a spatially resolved multi-omics atlas that integrates histopathology, spatial transcriptomics, proteomics, and immunogenomics to characterize TLS organization, maturation, and clinical relevance in ovarian cancer. H&E-stained tumor sections from a prospective cohort of 334 ovarian cancer patients across histologies were analyzed using deep learning-assisted segmentation to identify lymphoid aggregates (LAggs), immature TLSs (iTLSs), and mature TLSs (mTLSs) with germinal centers (GCs). From these, 45 post-neoadjuvant chemotherapy omental samples were used for tissue cyclic immunofluorescence (t-CyCIF) imaging with a 30-marker immune panel, followed by Mesmer segmentation and spatial phenotyping. 30 adjacent sections underwent spatial transcriptomic profiling by GeoMx DSP. Data were batch-corrected and analyzed for differential expression, pathway enrichment, and cell-type deconvolution. B-cell receptor (BCR) repertoires were reconstructed from bulk RNA-seq data with MiXCR. Preliminary analyses indicate substantial heterogeneity in TLS and LAgg abundance and spatial localization across ovarian cancer histologies. LAggs were present in 46% of samples, whereas iTLSs or mTLSs appeared in 16% and were confined to omental metastases. Spatial metrics quantified TLS distribution and proximity to tumor nests. Early t-CyCIF results revealed distinct TLS microstructures at different maturity stages: mTLSs contain well-defined GCs while iTLSs exhibited only early B/T compartments. Processed t-CyCIF data are being analyzed using the SPACEStat spatial analysis algorithm to uncover functional spatial immune composition in TLSs. 268 selected regions of interest (ROIs) were profiled in GeoMx. GC, T-B zone, and stromal signature scores enabled molecular labeling of TLS regions. SCORPIUS pseudotime analysis delineated a maturation trajectory from LAggs to iTLSs and mTLSs. By integrating spatial data, gene expression dynamics are mapped across maturation stages to investigate key chemokine axes and pathway enrichment. Cell-type deconvolution is expected to reveal maturation-associated spatial remodeling and functional specialization of immune subsets. Ongoing BCR profiling aims to explore clonotype patterns that may reflect class switching and somatic hypermutation. Our spatially resolved multi-omics atlas captures coordinated cellular and molecular remodeling that underlies TLS maturation and functional specialization, providing mechanistic insights into anti-tumor immune activation linked to clinical outcomes.

#2221 Tumor-associated CD207$^+$ cDC2 drives TLS formation via TNF family cytokines in non-small cell lung cancer.

Youngtaek Kim[1], Gang-Taik Lee[2], Dong Kwon Kim[2], JuHyeon Lee[2], So Young Park[2], Jae Hwan Kim[3], Hyun Jung Yoo[2], Byoung Chul Cho[3]

[1]Yonsei University College of Medicine, Seoul, Korea, Republic of,[2]Department of Research Support, Yonsei Biomedical Research Institute, Seoul, Korea, Republic of,[3]Yonsei New Il Han Institute for Integrative Lung Cancer Research, Seoul, Korea, Republic of

Background: Dendritic cells (DCs) are specialized antigen-presenting cells that orchestrate innate and adaptive immunity, and within the tumor microenvironment (TME) they extend their function to modulate anti-tumor immune responses. The heterogeneity of DCs underlies their diverse immune functions, with conventional type 2 DCs (cDC2s) showing particularly high phenotypic and functional complexity, which enables context-dependent immune modulation. However, the characteristics and functions of tumor-associated DCs remain incompletely defined. Elucidating how these subsets arise and function could broaden our understanding of tumor immunity and contribute to the development of effective cancer immunotherapies.

Methods: Tumor tissues (n=35) and adjacent normal tissues (n=24) from treatment-naïve, EGFR-wildtype NSCLC patients were enzymatically dissociated and subjected to single-cell RNA sequencing using the 5′ Chromium platform (10x Genomics). Trajectory and SCENIC analyses were performed to delineate cDC2 lineage programs. Functional validation included differentiation of CD207$^+$ DCs from human monocytes, co-culture with HUVECs, and multiplex IHC (mIHC) on FFPE tumor slides from NSCLC patients. Deconvolution analyses of TCGA-LUAD and an in-house immunotherapy bulk RNA-seq cohort were conducted to assess clinical relevance.

Results: We identified 10 transcriptionally distinct DC subtypes and found that CD207$^+$ cDC2s were markedly enriched in tumors. Trajectory analysis defined CD207$^+$ cDC2s as a distinct TME-enriched lineage characterized by reduced NF-κB signaling, chemotaxis, and T cell-regulatory programs, while enhanced TNF superfamily cytokine production and retinoic acid metabolism. SCENIC analysis implicated RARA/RXRA as key regulators of CD207$^+$ cDC2 differentiation. CD207$^+$ cDC2 frequency correlated with higher immune cell infiltration, especially CXCL13$^+$ T cells. Consistently, LTB expression in CD207$^+$ cDC2 correlated with high endothelial venule (HEV) and tertiary lymphoid structure (TLS) gene signatures, suggesting a role in lymphoid organization. Functionally, monocyte-derived CD207$^+$ DCs induced adhesion molecules in endothelial cells *in vitro*, and mIHC confirmed that their co-localization with HEVs and increased TLS density. Higher CD207$^+$ cDC2 abundance was associated with improved survival and immunotherapy response, highlighting their specialized role within TME in supporting lymphoid structuring and favorable outcomes in EGFR-wildtype NSCLC.

Conclusion: CD207$^+$ cDC2s constitute a distinct TME-enriched DC subtype that mediates endothelial activation and drives HEV and TLS formation via LTB. Their enrichment in tumors correlates with improved survival and enhanced immunotherapy response, indicating that CD207$^+$ cDC2s promote lymphoid organization and favorable immune outcomes in EGFR-wildtype NSCLC.

#2222 Mapping lymphoid responses to tumor growth and lymph node metastasis: multiomic spatial analysis of pancreatic ductal adenocarcinoma reveals tertiary lymph node structures.

James P. Agolia[1], Chuner Guo[1], Rosyli F. Reveron-Thornton[1], Xiaomo Li[2], Maria Moozhiyil Korah[1], Angela Tabora[1], Byrne Lee[1], Amanda R. Kirane[1], George Poultsides[1], Brendan Visser[1], Gregory W. Charville[2], Michael T. Longaker[1], Deshka S. Foster[1], Daniel Delitto[1]

[1]Surgery, Stanford University, Stanford, CA,[2]Pathology, Stanford University, Stanford, CA

Introduction**:** Within the next five years, pancreatic ductal adenocarcinoma (PDAC) will become the second-highest cause of cancer death in the United States; even with surgical resection and chemotherapy, median overall survival remains less than three years. Spatial transcriptomic and proteomic analysis is one pathway toward therapeutic target discovery for PDAC. While previous spatial transcriptomic studies have uncovered remarkable intratumoral heterogeneity in primary and metastatic samples, most lack subcellular resolution and multiomic scale.

Methods**:** Using the Singular G4X platform, we performed spatial multiomic analysis of 31 regions of interest in formalin-fixed, paraffin-embedded matched primary tumor and metastatic lymph nodes from eight patients. All patients had a pathological diagnosis of PDAC and received neoadjuvant chemotherapy at a single cancer center, and 7/8 patients showed pathological treatment effect with partial response to therapy. Data were analyzed in python.

Results**:** After quality control, 2.4 million cells were integrated. Major cell types were manually annotated: acinar cells (*CPB1*+ *GATM*+), adipocytes (*ADIPOQ*+ *PLIN1*+), B cells (*MS4A1*+ *HLA-DRA*+), cancer-associated fibroblasts (*COL1A1*+ *LUM*+), plasma cells (*JCHAIN*+ *IGHA1*/*IGHM*+), macrophages (*CD163*+ *CD68*+), mast cells (*KIT*+), neuroendocrine cells (*NRXN1*+ *NCAM1*+), pericytes/endothelial cells (*PECAM1*+ *RGS5*+), smooth muscle cells (*TAGLN*+ *MYH11*+), and T cells (*CD3D*+ *IL7R*+). Tumor cells formed three distinct clusters: *KRT19*+ *MUC1*+ ductal cells, *PIGR*+ *GATM*+ ductal cells, and *STAT1*+ *CD44*+ cells (from one patient with sarcomatoid dedifferentiation). The predominant cell type in the tumor microenvironment, cancer-associated fibroblasts (CAFs) could be subclustered into inflammatory CAF (*CXCL12*-high *IL6*-high), mechanoresponsive CAF (*PDGFRB*-high *ACTA2*-high), and steady-state CAF phenotypes. Although we did not select regions of interest explicitly with tertiary lymphoid structures (TLSs) in mind, we found that 7/8 patients and 9/19 tumor sections contained putative TLSs, with 4 sections containing more than one TLS area. TLS morphology appeared similar to that of lymphoid aggregates in tumor-positive lymph nodes. A predominance of CAFs was also noted in the involved lymph nodes. B cells within TLSs stained positive for CD20 protein and expressed *CXCR5* transcripts; they were surrounded by T cells that stained positive for CD3 and CD4/CD8 proteins. *CXCR5* colocalized closely with its binding partner *CXCL13,* a known trigger of TLS formation.

Conclusion**:** In a cohort of PDAC patients with lymph node metastasis, multiomic spatial analysis revealed TLSs in nearly all patients, suggestive of immune potential within the PDAC stroma. The CXCR5-CXCL13 axis should remain a target of active investigation in TLS formation.

: Therapies Targeting Metastasis
Poster Session

#2226 Novel targeted therapies for malignant ascites in pancreatic cancer.

Kuntal Halder[1], Ruben Munoz[1], Wei Lin[1], Annie Yang[2], Yanghee Woo[2], Erkut Borazanci[3], Haiyong Han[1], Daniel D Von Hoff[1]

[1]TGen (The Translational Genomics Research Institute), Phoenix, AZ,[2]City of Hope National Medical Center, Duarte, CA,[3]Honor Health Research Institute, Scottsdale, AZ

Malignant ascites (MA) remains a severe, untreatable complication in patients with late-stage cancers including pancreatic cancer, contributing to their poor prognosis. Using single-cell RNA sequencing (scRNA-seq), we characterized 12,084 cells isolated in MA samples from patients with pancreatic cancer. We found that immune cells were the dominant (90%) cell population with M2-like macrophages (62.4%) and T cells (23.1%) prevailing, while tumor cells constituted only 7.5% of the total cell population. The M2-like macrophages, marked by high CD163 and low CD80 expression, expressed elevated vascular endothelial growth factor (VEGF) and colony-stimulating factor-1 receptor (CSF1R), potentially promoting tumor proliferation, survival, and ascites formation via increased endothelial permeability. The T cells were mostly CD8-negative, indicating suppressed cytotoxic function, consistent with findings in ovarian cancer ascites. We hypothesize that targeting VEGF, CSF1R, and immune checkpoint proteins (e.g., PD-1 and CTLA-4) can reprogram the MA immune microenvironment, reducing ascites and peritoneal tumor growth. To test this hypothesis, we established an MA model for pancreatic cancer by intraperitoneally implanting murine pancreatic cancer cells derived from the KPC model into C57BL/6 mice. These mice develop ascites 7-10 days after cell injection and succumb to the disease within 4-5 weeks. We then evaluated the activity of anti-PD-1 and anti-CTLA-4 antibodies as a single agent or in combination in the KPC MA model. Both antibodies significantly reduced the formation of MA and extended the survival of the mice. The anti-PD-1 antibody (300 µg/dose for 3 weekly doses) extended the median survival from 25 days in the isotype control antibody group to 55 days, while the median survivals for both the anti-CTLA-4 group (100 µg/dose for 3 weekly doses) and the combination group were not reached 96 days after the initiation of treatment. We are in the process of assessing the efficacy of an anti-VEGFA antibody (2G11-2A05) and a CSF1R inhibitor (PLX3397) in the same model. Results from the studies could establish preclinical evidence supporting the utility of these novel therapeutic regimens for treating MA in pancreatic cancer patients and lead to clinical trials to address this critical unmet need.

#2227 Selectively eliminating senescent cancer-associated fibroblasts via chidamide and chemo-immunotherapy in metastatic pancreatic cancer: phase 2 clinical trial results (PANDA-1706).

Tianxing Zhou[1], Jingrui Yan[2], Jihui Hao[2]

[1]Pancreas Center, Tianjin Medical Univ. Cancer Inst. & Hospital, Tianjin, China,[2]Tianjin Medical Univ. Cancer Inst. & Hospital, Tianjin, China

Lymph node metastasis (LNM) in early-stage pancreatic ductal adenocarcinoma (PDAC) predicts systemic dissemination and poor survival, yet its underlying mechanisms remain elusive. Here, we demonstrate that senescent cancer-associated fibroblasts (senCAFs) drive lymphatic remodeling and LNM in early-stage PDAC and predict distant metastasis. Genetic or pharmacologic elimination of senCAFs suppresses LNM and distant metastasis. Mechanistically, senCAFs promote lymphangiogenesis and LNM by augmenting glucose metabolism and lactate production, which activates lactylation-mediated serine metabolism to protect lymphatic endothelial cells from oxidative stress. Moreover, using advanced multiplex imaging techniques, we have discovered that $CCR4^+$ Tregs from the draining lymph nodes accumulated around lymphatic vessels. This localized accumulation is facilitated by lymphatic endothelia enriched in senCAFs, which established an immunosuppressive peri-lymphatic niche. Furthermore, high throughput drug screening platform determines selective clearance of senCAFs via chidamide, one HDAC inhibitor, attenuates tumor progression and improves chemo-immunotherapeutic efficacy at low concentrations. We subsequently initiated a phase 2 clinical trial in metastatic PDAC patients. Here we report the results of the chidamide arm (chidamide and nab-paclitaxel/gemcitabine plus anti-PD-1/CTLA-4). The pre-specified primary endpoint of this arm was met, with a confirmed objective response rate. Collectively, these findings reveal a closed link between cellular senescence, metabolic reprograming, spatial immusuppressive niche and PDAC metastasis, offering the potential senolytic means to improve chemo-immunotherapy efficacy in PDAC patients. Clinical Trials.gov. identifier: NCT06951997.

#2228 Biofield therapy inhibits pancreatic cancer invasion and metastasis by modulating multiple steps of metastatic cascade.

Peiying Yang[1], Sharmistha Chakraborty[1], Phuong Nguyen[1], Defeng Deng[1], Amanda Eckstrom[1], Andrew Cusimano[1], Daoyan Wei[2], Lorenzo Cohen[1]

[1]Palliative, Rehabilitation and Integrative Medicine, The University of Texas MD Anderson Cancer Center, Houston, TX,[2]Gastroenterology and Hepatology, The University of Texas MD Anderson Cancer Center, Houston, TX

Biofield therapies (BTs) are gaining attention as potential complementary treatments for cancer. Some devices have been developed to mimic the energetic or electromagnetic fields emitted by BT practitioners. We previously reported that BT significantly inhibited growth and invasiveness of pancreatic cancer cells in vitro and in relevant animal models. To identify which steps of the metastatic cascade are affected by BT and to elucidate potential antimetastatic mechanisms in pancreatic ductal adenocarcinoma (PDAC), we conducted in vivo studies using metastatic mouse models. In a KPCY orthotopic model, BT treatment significantly reduced the percentage of visible liver nodules by 61.3% and 54.6% compared with the colony control (CC) and sham control (SC) groups, respectively ($p < 0.05$). Imaging of YFP+ cells in the liver tissues revealed a significant reduction in disseminated tumor cells in the BT group relative to CC and SC groups ($p < 0.05$). In a tail-vein injection model, lung tissues from BT treated mice exhibited a significant 59.6% reduction in YFP+ signal intensity compared with SC mice, supporting the conclusion that BT suppresses metastatic dissemination of PDAC cells. BT treated mice bearing PANC-1 orthotopic tumors had significantly lower levels of tumor cell-free DNA (11.5 ± 4.6 ng/µl) compared with sham control (24.7 ± 7.9 ng/µl; $p < 0.01$), suggesting that BT treatment impairs tumor cell intravasation. This is consistent with our previous findings that BT inhibits EMT in human PDAC PANC-1 cells. Additionally, BT induced anoikis in PANC-1 cells, indicating that BT may also reduce PDAC cell survival in circulation. To investigate whether BT affects metastatic colonization, both PANC-1 and KPCY cells were exposed to BT and subjected to adhesion assay using phalloidin staining and fibronectin quantification, as fibronectin is a key regulator of cell adhesion. PANC-1 cells exposed to BT for 15 mins showed an average of 14 ± 4 adhered cells per field, compared with 96 ± 35 in the SC group ($p < 0.0001$). Similarly, fibronectin-based cell adhesion measurements showed a 58.3% decrease in BT-treated PANC-1 cells relative to SC ($p < 0.001$). BT also significantly reduced F-actin intensity in PANC-1 cells ($p < 0.01$), with similar results observed in KPCY cells after 30 min of treatment. Epigenetic profiling further revealed that BT modulated the expression of genes involved in actin cytoskeleton regulation. Collectively, these results demonstrated that biofield therapy suppressed multiple metastatic steps including cell invasion/migration, intravasation, survival in circulation, and colonization ultimately contributing to its antimetastatic effects in PDAC models. These processes may be mediated in part through alterations in cytoskeleton organization, particularly actin dynamics.

#2229 RIPK2 and CDK2 form a targetable positive feedback loop in prostate cancer cells.

Ahmed Elgehama[1], Jaceline Pires Sanches Sanches[2], Lili Guerra[3], Wei Yang[2]

[1]Stony Brook University, Renaissance School of Medicine, Stony Brook, NY,[2]Stony Brook University, Stony Brook, NY,[3]Stony Brook UNIVERSITY, Stony Brook, NY

Background: Prostate cancer (PC) metastasis is the leading cause of PC-related mortality, yet effective therapies targeting this lethal process remain lacking. We previously identified RIPK2 as a promising drug target in PC metastasis, functioning in part through a noncanonical RIPK2/MKK7/c-Myc phosphorylation pathway (*Nat. Commun.*, 2022). However, additional downstream effectors and upstream regulators of RIPK2 remain poorly characterized. This study aims to address this knowledge gap, which represents a major barrier to developing highly effective and low-toxicity combination therapies.

Methods: Genetic manipulation was performed using CRISPR/Cas9 knockout, siRNA knockdown, and overexpression of wild-type or mutant genes. The metastatic potential of PC cells was assessed by cell proliferation, Matrigel invasion, clonogenicity, and soft-agar assays. RIPK2 activation of CDK2 was evaluated by western blotting and *in vitro* kinase assays. RIPK2-CDK2 interaction was examined using co-immunoprecipitation, GST pulldown, proximity-ligation assay, fluorescence colocalization, and fluorescence resonance energy transfer. Gene transcription and expression were measured by RT-qPCR. Protein stability was determined using cycloheximide chase and ubiquitination assays. Synergistic effects of RIPK2 and CDK2 inhibitors are assessed with a 6x6 matrix. At least two independent cell lines were used for each cell assay.

Results: RIPK2 enhanced the metastatic potential of PC 22Rv1 and PC3 cells primarily through its kinase activity, cytoplasmic localization, and induction of c-Myc expression. RIPK2 bound directly to CDK2 and activated it, leading to phosphorylation of c-Myc at S62. Notably, active CDK2 increased both transcription and protein stability of RIPK2, establishing a positive feedback loop. Co-inhibition of RIPK2 and CDK2 synergistically reduced c-Myc protein levels and suppressed PC cell invasion and colony formation.

Conclusion: RIPK2 and CDK2 form a multi-layered positive feedback loop that sustains c-Myc expression and drives PC metastatic progression. Low-dose co-inhibition of these two kinases using clinically evaluated inhibitors represents a promising therapeutic strategy to overcome c-Myc-dependent PC metastasis with high efficacy and minimal toxicity.

#2230 Combined treatment with agonists for CXCR4 and CB2 receptors reduces prostate cancer growth and metastasis.

Nakea Michelle Pennant[1], Alifiani Bonita Hartono[2], Shiqin Liu[2], Sidharth Paparaju[2], Chung Lee[2], Christopher Massey[2], Tanya Ivanova Stoyanova[2], Cimona V. Hinton[3]

[1]Biological Sciences, Clark Atlanta University, Atlanta, GA,[2]UCLA - University of California Los Angeles, Los Angeles, CA,[3]Microbiology, Biochemistry & Immunology, Morehouse School of Medicine, Atlanta, GA

CXCR4 is a G-protein-coupled receptor (GPCR) widely expressed in tumors, regulates cell migration, survival, and immune responses through activation by stromal cell-derived factor-1α (SDF-1α), contributing critically to metastasis and tumor aggressiveness. Our previous *in vitro* studies demonstrated that CXCR4 forms heterodimers with the cannabinoid receptor 2 (CB2) in human breast and prostate cancer cell lines. Simultaneous stimulation of CXCR4 and CB2 with SDF-1α and the CB2 agonist AM1241 induced the formation of a physical dimer, which markedly suppressed CXCR4-mediated pro-tumorigenic signaling, reduced cell migration, disrupted cytoskeletal organization, and downregulated motility-associated proteins. Given the reported anti-metastatic effects of cannabinoids and the results of our heterodimer, we hypothesized that simultaneous activation of CXCR4 and CB2 could attenuate tumor progression *in vivo*. To test this, we established a spontaneous metastasis model using luciferase-expressing human prostate cancer cells (DU145 RFP/Luc or PC3 GFP/Luc) implanted subcutaneously into male NSG mice. Once tumors reached ~40 mm^3, mice were randomized into four treatment groups: vehicle, SDF-1α, AM1241, or simultaneous SDF-1α+ AM1241. Primary tumors were surgically resected at ~400 mm^3, and treatments continued post-resection to assess metastasis and recurrence. Mice that received the combined agonist treatment exhibited no local tumor recurrence, a significant reduction in tumor volume, and a markedly lower incidence of distant metastases compared to all other groups. These findings demonstrate that concurrent CXCR4 and CB2 activation inhibits tumor growth and dissemination, as we observed *in vitro,* suggesting that targeting the CXCR4-CB2 receptor complex represents a promising alternative to traditional CXCR4 antagonists for managing metastatic prostate cancer.

#2231 Resensitizing therapy-resistant anoxic metastatic melanoma cells.

Gustavo Untiveros[1], Daryl Forney[1], Mariella Andrews[2], Tekaswini Kannan[1], Luigi Strizzi[3]

[1]Midwestern Univ. - Downers Grove Campus, Downers Grove, IL,[2]Loyola University - Chicago, Chicago, IL,[3]Pathology, Midwestern Univ. - Downers Grove Campus, Downers Grove, IL

Introduction: Metastatic melanoma significantly reduces patient survival. Metastatic growth can outpace vascularization creating areas of extreme hypoxia or anoxia. HIF-1α is a master transcriptional regulator of cellular survival response to hypoxia that can facilitate the selection of more stem cell-like, drug-resistant cancer cells. BRAF inhibitors (BRAFi), commonly used to treat melanoma, targets cell signaling involving pERK-dependent melanoma growth. Resistance to BRAFi can lead to melanoma recurrence and poor survival. Dual specificity phosphatases (DUSP), such as DUSP6 can reduce ERK activity; moreover, DUSP6 has been shown to be upregulated by HIF-1α during cellular responses to hypoxia. We hypothesize that HIF-1α levels increase in metastatic melanoma cells as these adapt to the anoxic metastatic niche, which then increases DUSP6 expression, which in turn reduces ERK activity that causes resistance to BRAFi.

Methods: Western blot (WB) was used to compare the expression of HIF-1α, pERK, and DUSP6 in lysates from A375 melanoma cells grown in anoxia or normoxia. An MTT cell proliferation, and a cell apoptosis assay were used to compare the effect of the BRAFi, Dabrafenib between treated normoxic and anoxic A375 cells. Lysates were collected for WB to assess effects on pERK between anoxic A375 treated with the DUSP6 inhibitor, BCI, and untreated control. Finally, to see if BCI can increase drug sensitivity, MTT and cell apoptosis assays were performed on anoxic A375 treated with both BCI and Dabrafenib.

Results: WB results show that anoxic A375 cells express higher levels of HIF-1α, and lower levels of pERK compared to normoxic control cells. Dabrafenib treatment reduced cell proliferation of normoxic but not anoxic A375 cells, presumably due to reduced expression of the pERK target in these cells. Inhibition of DUSP6 with BCI significantly increased pERK expression and when combined with Dabrafenib significantly reduced proliferation and increased cell death of the anoxic A375 cells.

Conclusion: We show that melanoma cells cultured in anoxia express higher levels of HIF-1α. This in turn led to an increase in DUSP6 expression. In these anoxic cells, DUSP6, in turn, reduces pERK level, which is an important component of the signaling cascade targeted by Dabrafenib. Finally, our results from the combination treatment with both BCI and Dabrafenib suggest that by inhibiting DUSP6 it may be possible to re-express pERK in drug-resistant anoxic metastatic melanoma cells and reestablish drug sensitivity.

#2232 Investigating the combined inhibition of RAF, MEK, and FAK in melanoma molecular subtypes.

Jared Almazan

University of Utah Huntsman Cancer Institute, Salt Lake City, UT

Despite promising results from FDA-approved therapies, many patients with advanced melanoma develop resistance to standard-of-care therapy, which includes immunotherapy in all molecular subtypes and targeted therapy for $BRAF^{V600E/K}$ melanoma. Most melanomas harbor alterations in the mitogen-activated protein kinase (MAPK) pathway, including mutations in BRAF, NRAS, and NF1 genes. While $BRAF^{V600E/K}$ melanomas initially respond to mutant BRAF and MEK inhibitors, resistance develops in the majority of cases. Furthermore, there are currently no FDA-approved targeted therapies for patients with tumors harboring NRAS or NF1 alterations following immunotherapy failure. Therefore, novel and effective therapeutic approaches are urgently needed to treat these molecular subtypes of melanoma, both in primary and resistant settings. The PI3K/AKT pathway is often activated in melanoma, contributing to poor clinical outcomes and promoting brain metastases, yet clinical attempts to target this pathway have been hindered by limited efficacy or intolerable toxicity. Proteomic analysis comparing non-metastatic and metastatic primary tumors in mice revealed focal adhesion kinase (FAK) as an AKT1-specific effector and a potential alternative therapeutic target. In mutant BRAF-driven models, the combination of the FAK inhibitor VS-4718 and the RAF/MEK clamp avutometinib, with or without the mutant BRAF inhibitor encorafenib, significantly delayed tumor onset, induced regression of established tumors and brain metastases, and prolonged overall survival. These findings support an ongoing clinical trial evaluating the efficacy of avutometinib and the FAK inhibitor defactinib, with or without encorafenib, in patients with brain metastases from cutaneous melanoma (DETERMINE; NCT06194929). Early observations indicate that the triplet combination is safe and well-tolerated. Additionally, in melanoma models harboring RAS mutations or NF1 loss, the combination of VS-4718 and avutometinib significantly reduced melanoma cell growth and viability in vitro, delayed tumor progression in autochthonous mouse models, and inhibited tumor growth in patient-derived xenografts driven by these alterations. Lastly, we are investigating the non-canonical roles of FAK in modulating the tumor microenvironment to determine whether this treatment strategy alters immune cell composition, chemokine and cytokine production, and enhances the efficacy of immune checkpoint inhibition.

#2233 Novel anticancer mechanisms of melanin: Effects on cancer cell adhesion, survival, and migration.

Dorie Liu, Wei Zhu

SCI research institute, Jericho, NY

Melanoma is the deadliest form of skin cancer, with 330,000 new cases diagnosed and 60,000 deaths globally each year. While early-stage melanoma is often treatable, metastatic melanoma usually has poor prognosis with a high mortality rate.
Melanin, a pigment synthesized through the melanogenesis pathway, has been reported to exert anti-cancer effects. However, the molecular mechanisms underlying its protective role remain poorly understood. We hypothesize that melanin may exert anticancer activity by reducing cancer cell survival and suppressing metastatic potential.
This study uses 3 different cancer cell lines, including U937 (monocytic), HTB-11 (neuronal), and Colo320 (colorectal), and utilizes a combination of methods, including in silico molecular docking, cell attachment assays, and MTT assays, to evaluate the effects of melanin on cancer cell adhesion, proliferation, and survival.
The results revealed that melanin decreased U937 (monocytic) cancer cell adhesion in a dose dependent manner: at a lower concentration, melanin increased cell adhesion by 29.5%, while in a higher concentration, it decreased cell adhesion. In HTB-11 cells, high concentration of melanin decreased cell proliferation by 48.61%, while in Colo320 cells, low concentration of melanin significantly suppressed cell growth by 63%.
Data also showed that melanin has a strong binding affinity to cancer-related target proteins, including MMP2, MMP9, CDH1, and ITGB1, the possible molecular and genetic mechanisms of melanin in working with known cancer target proteins to regulate cancer growth.
In conclusion, these findings suggest novel molecular pathways by which melanin may regulate cancer cell survival, adhesion, and migration. Collectively, this study provides new evidence for melanin as a potential anticancer agent with differential, dose-dependent effects, underscoring its relevance as a therapeutic lead for targeting diverse cancer types.
D.L. is with Manhasset Secondary School, Manhasset, NY, USA. W.Z. is with SCI research institute, Jericho, NY, USA

#2234 Antibodies that bind to primitive human growth factor NME7-AB block interaction with MUC1* growth factor receptor to inhibit cancer growth and metastasis.

Cynthia Carol Bamdad, Benoit J. Smagghe, Mark G. Carter, Kevin R. Yi, Michael J. Nash, Trevor J. Grant, Daniel S. Miller, Natalie K. Miller, Andrew K. Stewart

Minerva Biotechnologies, Woburn, MA

Purpose: Develop therapeutic antibodies that block the tumorigenic action of MUC1* ligands and bacterial mimics thereof.
Methods: Ligand fishing using the MUC1*ecd-45 peptide as bait identified NME1 and NME7-AB as ligands of MUC1*. Dimeric NME1 and monomeric NME7-AB, which has two MUC1* binding domains, dimerize MUC1* extracellular domain (ecd) and activate MAP kinase growth pathway. IF microscopy showed NME7-AB is secreted by all Day 3 cells of a human blastocyst, then only by cells of the Inner Cell Mass by Day 5. NME7-AB is then replaced by adult form, NME1, which only binds MUC1* when a dimer. At higher concentration, NME1 switches from dimer to hexamer, which doesn't bind MUC1* but instead triggers differentiation. NME7 is cytoplasmic until cleavage removes an N-terminal DM10 fragment, which allows secretion, then 'NME7-AB'. Alternative splice variant NME7-X1 is transcribed without the DM10 domain, so is always secreted and active. Cancer cells that have acquired resistance to cancer drugs, increase expression of MUC1*, NME7-AB and NME7-X1. We mapped the MUC1* interaction site on NME7-AB and generated antibodies that block the interaction. We discovered a subset of antibiotic-resistant bacteria that make NME7-AB mimics that function like human NME7-AB. We developed monoclonal antibodies that specifically bind to these bacterial mimics.
Results: Growing cancer cells with recombinant NME7-AB as the only growth factor, enabled anchorage independent cell growth, induced upregulation of metastasis markers and formed tumors as well as metastasis from injection of as few as 10,000 cells within 10-20 days. 50-times as many parent cells did not. A novel antibody, prevented NME7-AB from inducing upregulation of metastatic markers, and prevented anchorage independent growth. In animals, NME7-AB monoclonal antibodies reversed total metastasis in a few days. They also inhibited metastasis of established sub-cu tumors. Similarly, bacterial mimics of NME7-AB induced upregulation of metastatic markers and, in animals, accelerated tumor growth and their metastasis. We developed monoclonals antibodies that bind to the interaction region on bacterial mimics.
Conclusions: MUC1 has long been an elusive target for cancer therapeutics. However, there has been little focus on its onco-embryonic ligand NME7-AB. NME7-AB is turned off early in embryogenesis but is turned on again in all MUC1-positive cancers. Levels of NME7 determine growth rate and metastatic potential of human cancers. Demonstration of NME7-AB antibodies inhibiting cancer and metastasis in animals xenografted with human cancers supports the further clinical development of NME7-AB targeted therapeutics. Discovery of a molecular link between specific bacteria and acceleration of human cancers may be an important area for future research.

#2235 Intercepting metastasis: 8-step CRISPR design via multi-modal foundation models.

Fahad Kiani

CrisPRO.ai, New York, NY

Background: Metastasis accounts for >90% of cancer deaths, yet CRISPR design tools prioritize on-target efficiency alone (CRISPOR, Benchling), ignoring stage-specific biology (EMT, extravasation, colonization). No existing tool integrates essentiality (DepMap), chromatin accessibility (ENCODE), and metastatic cascade relevance into guide selection. We present Interception, a stage-aware CRISPR framework targeting vulnerabilities across the metastatic cascade.
Methods: We compute three orthogonal signals: (i) Functionality (Evo2): predict variant impact on protein function; (ii) Essentiality (DepMap): prioritize genes critical for metastatic survival; (iii) Regulatory (GTEx eQTLs): predict expression changes. Target-Lock score quantifies gene relevance to specific metastatic stages (e.g., EMT vs. extravasation) using literature-derived weights. Guide candidates are generated with PAM constraints, scored for efficacy (Evo2-predicted expression change via sigmoid transformation) and safety (minimap2 genome-wide alignment with exponential mismatch decay), then ranked by Assassin score (0.40×efficacy + 0.30×safety + 0.30×mission fit). Weights were optimized via ablation study on 304 gene-stage pairs. All outputs include full provenance and are reproducible via frozen scripts/environment.
Results: Target-Lock significantly outperformed single-metric baselines: AUROC 0.976 (ours) vs. 0.61 (DepMap alone), 0.58 (Evo2 alone), 0.52 (random); AUPRC 0.948 vs. 0.42 (DepMap), 0.39 (Evo2); Precision@3 = 1.000 (perfect top-3 enrichment) vs. 0.33 (random). All 8 metastatic steps showed significant enrichment (Fisher's exact $p < 0.001$ for 6/8 steps) with large effect sizes (Cohen's $d > 2.0$). Guide validation on 20 designs showed mean efficacy 0.548 ± 0.119, safety 0.771 ± 0.210. Structural validation of 15 guide:DNA complexes via AlphaFold 3 Server achieved 100% pass rate (pLDDT 65.6 ± 1.8, iPTM 0.36 ± 0.01)—the first metastasis-targeted CRISPR framework with structural validation.
Conclusions: Interception delivers reproducible, mission-aware CRISPR design for metastasis, integrating multi-modal signals, genome-wide safety, and structural validation. Future work will (i) integrate Enformer for chromatin predictions, (ii) expand structural validation to 40 guides (complete 8-step coverage), and (iii) validate in metastatic mouse models (PDX/CDX) to assess in vivo efficacy.

#2236 Evaluation of novel medicinal compounds for therapeutic efficacy against liver cancer.

Aarya M. Tripathi[1], Veerababu Nagati[2], Yamile AbuchardAnaya[2], Kaylee Renteria[2], Denise Soto[2], Miguel Salazar[1], Subhash C. Chauhan[2], Debasish Bandyopadhyay[1]

[1]School of Integrative Biological and Chemical Sciences, The University of Texas Rio Grande Valley, Edinburg, TX,[2]Oncology and Medicine ISU, South Texas Center of Excellence in Cancer Research, The University of Texas Rio Grande Valley, McAllen, TX

Hepatocellular carcinoma (HCC), the most common type of liver cancer, makes up over 90% of cases and remains a significant global health issue. Early-stage HCC can be treated with hepatectomy or liver transplant, but advanced disease has a poor outlook due to treatment resistance and widespread drug resistance. Sorafenib, the first-line tyrosine kinase inhibitor for advanced HCC, provides only modest gains in overall survival, highlighting the urgent need for new treatments. This need is especially urgent in the Rio Grande Valley (RGV), where liver cancer rates and mortality are higher than the national average due to high rates of obesity, diabetes, metabolic dysfunction-associated steatotic liver disease (MASLD), hepatitis infections, and limited healthcare access. To address these regional and global disparities, this study evaluates four medicinally privileged molecules: 1. DB5 OTFE, 2. DBMG-5, 3. DBNJ-1, and 4. DB-3-OCAS, for their potential anti-cancer effects. Out of these four compounds, 1 and #4 are natural product mimics with beta-lactam moiety at the core, synthesized by a multi-step procedure. Compound#2 is a macrocycle-fused gamma-lactone and #3 is a pentacyclic triterpene, isolated from plants. Human HCC cell lines SK-HEP1, Hep G2, C3A, and Huh7 will be treated with logarithmic dilutions of each compound (10 mM DMSO stocks) and assessed using the MTT viability assay to determine IC_{50} values. Phase-contrast microscopy will be used to observe morphological changes and confirm cell viability. We hypothesize that these natural compounds will exhibit dose-dependent cytotoxicity against liver cancer cells and that at least one will have significantly lower IC_{50} values compared to Sorafenib. Expected outcomes include decreased confluency, alterations in cell morphology, and the identification of a lead compound with strong cell-killing activity. The most effective compound will then undergo structural optimization of its functional groups, followed by re-evaluation against HCC cell lines and comparison with Sorafenib to assess its therapeutic potential. Long-term goals include conducting mechanistic studies and potentially progressing to *in vivo* models. This research supports developing locally relevant therapies aimed at reducing liver cancer disparities in the RGV and contributes to the broader search for accessible, natural-product-based treatments for HCC.

#2237 Novel MACC1 transcriptional inhibitor act via reduced NFκB signaling pathway to reduce metastasis formation.

Ulrike S. Stein

Translational Oncology of Solid Tumors, Max Delbruck Center for Molecular Medicine, Berlin, Germany

Metastasis Associated in Colon Cancer 1 (MACC1) is a key metastatic molecule, used as a prognostic and predictive biomarker for metastasis formation and therapy outcomes. A high expression predicts poor survival and therapy resistance to common chemotherapeutics. Recently we have identified a novel transcriptional inhibitor of the MACC1 gene. This tetrazolo-pyridazine-based compound (compound 22) was discovered through a high-throughput screen (HTS) using the human MACC1 promoter coupled to a luciferase reporter gene. 1,2,3,4-tetrazolo[1,5-b]pyridazine-based compounds can act as effective MACC1 inhibitors in vitro by reducing MACC1-induced cancer cell motility. This translates in reduced metastasis formation in mice, and thus pose them promising candidates for anti-metastatic therapies particularly for patients with MACC1-overexpressing cancers, that are at high risk to develop metastases. To identify the mode of action, we used RNA-sequencing to reveal the gene expression changes under compound 22 treatment which displayed the TNF-α signaling via NFκB was attenuated. Subsequent gene ontology analysis of the differentially expressed genes showed changes in biological functions such as cell cycle progression and intermediate filament-based processes. These render the cells less proliferative and with more epithelial characteristics. Molecular analysis of the NFκB pathway revealed a reduced p65 and p50 activity with reduced nuclear translocation and activity on the MACC1 promoter. In silico predictions revealed p105 as a possible protein target. Further, the novel compound blocks the TNF-α induced phosphorylation of p105. Although further experimental data is needed to address the potential binding of the identified tetrazolo-pyridazine-based compound to p105, this study revealed that the NFκB signaling pathway is strongly reduced under the treatment with this novel compound. This in turn reduces the MACC1 gene expression and thereby the metastatic potential of cancer cells.

#2238 Anti-metastatic properties of the triterpene diosgenin on lung carcinoma cells.

Laurie Mar Santos[1], Edwin Figueroa[2], Juan Figueroa[2], Yamixa Delgado[3], Daraishka Perez[3], Yancy Ferrer[4]

[1]Universidad Central del Caribe, Bayamon, PR,[2]University of Puerto Rico, Cayey, PR,[3]San Juan Bautista School of Medicine, Caguas, PR,[4]University of Puerto Rico, Medical Science Campus, San Juan, PR

Lung cancer remains the leading cause of cancer-related mortality worldwide, with non-small cell lung carcinoma (NSCLC) accounting for ~85% of all cases. Although chemotherapy is a standard treatment option, its success is limited by dose-dependent toxicity and the development of chemoresistance. These challenges have increased interest in phytochemicals such as triterpenes, natural metabolites with broad pharmacological activities and potential anticancer properties. Diosgenin (Dios), a steroidal triterpene present in numerous medicinal plants, has been reported to modulate pathways central to cancer cell survival and metastasis. This study evaluated the effects of Diosgenin on NSCLC cells to elucidate its mechanism of action. Diosgenin demonstrated strong cytotoxic activity in the micromolar range in a dose-dependent manner within 24 hours. Functional assays showed that Diosgenin significantly inhibited A549 cell migration and induced cell cycle arrest at the S and G2/M phases. Protein analysis revealed reduced expression of proliferative and survival markers, including Ki67, MAPK, and PI3K, accompanied by a notable increase in Caspase 3/7 activation. Metastasis-related gene expression profiling showed that Diosgenin downregulated key pro-metastatic genes such as MMP2, MMP9, and PREX1, all of which contribute to extracellular matrix degradation, cytoskeletal remodeling, and invasive potential. In contrast, Diosgenin upregulated NDRG1, a well-established metastasis suppressor involved in inhibiting epithelial-to-mesenchymal transition and limiting cell motility. Collectively, these findings indicate that Diosgenin exerts multi-targeted anticancer activity by suppressing proliferation, inducing apoptosis, and significantly impairing metastasis-associated pathways. Diosgenin represents a promising natural therapeutic candidate for slowing NSCLC progression and reducing metastatic potential.

Acknowledgement: This research was supported by an Institutional Development Award (IDeA) from the National Institute of General Medical Sciences of the National Institutes of Health under grant number P20GM103475.

#2239 The transcobalamin receptor, CD320, is a therapeutic target for metastatic triple negative breast cancer.

Joanne Tejero, Felicia Lazure, Stanislav Drapela, Eduardo Miranda, Nadir Sarigul, Devesh Raizada, Didem Ilter, Ana Gomes

Moffitt Cancer Center, Tampa, FL

Vitamin B12 is an essential micronutrient that functions as a cofactor for enzymes in the folate and propionate metabolism pathways, placing it at the center of nucleotide metabolism, redox balance, and cell fate decisions. Following dietary intake of vitamin B12, vitamin B12 binds to transcobalamin (TC), which protects it from degradation. Cellular uptake of vitamin B12 is mediated by the TC receptor, CD320, positioning CD320 in a prime position to regulate vitamin B12 availability and govern cell fate decisions. Triple negative breast cancer (TNBC) is a highly aggressive subtype of breast cancer with limited treatment options and poor survival rates once metastasis to distant sites occurs, highlighting the need for novel therapeutic strategies for metastatic TNBC. Using publicly available datasets, we found that CD320 was highly expressed in TNBC cell lines and patient samples compared to hormone receptor-positive and HER2-positive subtypes. High expression of CD320 was associated with poor prognosis specifically in TNBC, unlike in other subtypes. Metastasis accounts for the majority of breast cancer-related deaths, and progression into metastatic disease requires cancer cells to adapt to the different pressures throughout the metastatic cascade. Thus, we hypothesized that upregulation of CD320 represents a metabolic adaptation of TNBC metastasis to meet the steep vitamin B12 demand that drives this aggressive phenotype. Consistent with this hypothesis, we observed that CD320 expression was significantly higher in TNBC metastases compared to the expression in primary tumors. Strikingly, suppression of CD320 induced TNBC cell death while having no cytotoxic effect on mammary epithelial cells and markedly impaired metastatic progression *in vivo*, as demonstrated in orthotopic and experimental models of metastasis. Conversely, overexpression of CD320 in transformed mammary epithelial cells conferred aggressive properties, such as increased proliferation, suggesting that CD320 is not only required for TNBC metastasis but also sufficient to enable TNBC aggressiveness. Together, these findings establish CD320 as a critical regulator of TNBC growth and metastasis and reveal CD320 as a promising therapeutic target to selectively eliminate TNBC cells without eliminating the normal tissue counterpart.

#2240 Inhibition of STAT3 and PARP1 reduces TNBC invasion through cytoskeletal remodeling.

Arielle McGlone[1], Ali Andalibi[2], Pranabananda Dutta[3]

[1]Charles R. Drew University of Medicine & Science, Los Angeles, CA,[2]Office of the Provost, Charles R. Drew University of Medicine & Science, Los Angeles, CA,[3]Division of Cancer Research and Training, Charles R. Drew University of Medicine & Science, Los Angeles, CA

Triple Negative Breast Cancer (TNBC) is an aggressive, treatment-resistant subtype that disproportionately affects African American women, leading to high mortality. TNBCs have significantly higher metastasis rates compared to the receptor-positive Luminal subtype. Although research is ongoing, the biological mechanisms underlying metastasis in TNBC, particularly those related to cytoskeletal organization, remain unclear. Understanding how TNBC cells migrate, particularly through actin cytoskeleton remodeling, is crucial. Here, we demonstrate that combined inhibition of PAPR1 and STAT3 reduces cytoskeletal remodeling, particularly actin filament remodeling, a key factor in TNBC invasiveness. We used TNBC cell lines BT-549 (mesenchymal phenotype) and MDA-MB-468 (Basal-like 1/Immunomodulatory) to test Olaparib (a PARP1 inhibitor), Stattic (a STAT3 inhibitor), or both. Co-immunoprecipitation was used to study the interaction between PAPR1 and STAT3. We assessed cytoskeletal remodeling by western blotting, phalloidin staining, and cell motility using wound-healing and Boyden chamber invasion assays. The results show that PARP1 interacts with STAT3 in TNBC and poly-ADP-ribosylates STAT3. We observed reduced migration with inhibitors, especially with combined treatment, and disruption of actin cytoskeletal organization with the inhibition of STAT3 and PARP1. Combined PARP1 and STAT3 inhibition led to decreased peripheral actin and stress fiber formation, driven by Cofilin phosphorylation. Additionally, we noted downregulation of LIMK2 (Cofilin kinase) and PDXP (Cofilin phosphatase) with Stattic and dual-inhibitor treatment. The inhibitor treatment also downregulated CCL2 and other cytokines in both cell lines, potentially impacting cytoskeletal organization, possibly via the MAP kinase pathway. These findings suggest potential implications for combination therapies and the development of targeted treatments to improve outcomes, particularly by reducing metastasis. Our research enhances understanding of TNBC metastasis by identifying PARP1 and STAT3 as key regulators of actin cytoskeletal remodeling.

#2241 Galectin 1 as a regulator of hormone driven mammary remodeling and early dissemination with therapeutic potential in breast cancer.

Magali Berton[1], Ramiro Perrotta[2], Luis Valencia Salazar[3], Tomas Dalotto Moreno[1], Yamil D. Mahmoud[4], Juan Manuel Perez Saez[1], Sabrina Gatto[1], Rosa Morales[1], Julio Aguirre-Ghiso[3], Gabriel A. Rabinovich[5], Mariana Salatino[6]

[1]IBYME, CONICET, Buenos Aires, Argentina,[2]Department of Genetics, Harvard Medical School, Boston, MA,[3]Montefiore Einstein Comprehensive Cancer Center, New York, NY,[4]Department of Medicine, Weill Cornell Medicine, New York, NY,[5]Institute de Biologia y Medicina Experimental, Ciudad de Buenos Aires, Argentina,[6]Instituto de Biologia y Medicina Experimental, Buenos Aires, Argentina

Galectin-1 (GAL1) is a glycan-binding protein broadly known to shape tumor progression by promoting immune evasion and metastatic dissemination. While GAL1 is well recognized as an immunomodulator in multiple cancer types, its role in hormone-driven mammary gland biology and early tumor evolution remains poorly defined. Using our established MMTV-PyMT model WT or KO for GAL1 (Lgals1-/-), we previously demonstrated that GAL1 deficiency delays tumor onset, reduces metastatic burden, and diminishes mammary branching morphogenesis. Unexpectedly, we also observed a decreased Progesterone Receptor (PR) expression in luminal cells from Lgals1-/- mice in both normal and transformed mammary glands. These findings suggested that GAL1 may act as a critical regulator of hormone-driven mammary gland development. To test this hypothesis, we stimulated C57BL/6 Lgals1+/+ and Lgals1-/- mice with a pellet containing Medroxyprogesterone acetate (MPA), a synthetic progestin, and observed that GAL1-deficient mice exhibited a significantly reduced branching index in response to MPA stimuli. RNA-seq analysis of MPA-treated or control mammary glands further revealed that canonical progesterone-responsive genes such as Tnfsf11 (Rankl) and Wnt4 were attenuated in Lgals1-/- glands. To determine if GAL1 absence perturbs epithelial cell hierarchies, we profiled mammary epithelial cell populations by spectral flow cytometry using EpCAM, CD49f, CD49b and Sca1 markers among CD45neg cells. GAL1-deficient glands exhibited reduced MaSC and ER+ luminal progenitor cell compartments, suggesting that GAL1 helps maintain lineage balance during the development of the mammary gland. This finding is particularly relevant given that this population has been recognized as an early cell of origin in neoplastic transformation. To further interrogate the therapeutic relevance of GAL1 blockade, we used an MMTV-HER2+ model of breast cancer. We developed a GAL1 (clone 3) neutralizing monoclonal antibody and treated MMTV-HER2+ mice (15mg/kg, twice a week) from week 14 of age (preneoplastic stage), through week 19. Therapeutic blockade of GAL1 reduced branching morphogenesis, curtailed the release of early circulating tumor cells (CTCs), decreased the number of transformed ducts, and reduced lung metastasis. Importantly, anti-GAL1 treatment led to reduced PR expression in mammary luminal cells and depleted GAL1 in serum, further confirming the blockade's effectiveness. Together, these findings introduce Galectin-1 as a regulator of progesterone-driven epithelial remodeling and early metastatic spreading. By linking GAL1 to hormone signaling, epithelial hierarchy, and early dissemination, our study positions GAL1 as a promising therapeutic target for treating metastatic breast cancer progression.

#2242 Dual TTK/PLK1 inhibition combined with G-CSF treatment synergistically suppresses metastatic progression in triple-negative breast cancer.

Sunwoong Kim[1], Hanyoung Kim[1], Sung-Dae Cho[2], Jaehan Lee[2], Mi Kyung Park[3], Minkyung Kang[4], Seunghyun Ma[5], Hee-Joo Choi[1], Jeong-Yeon Lee[1]

[1]Department of Pathology, Collegy of Medicine, Hanyang University, Seoul, Korea, Republic of,[2]Department of Oral Pathology, School of Dentistry and Dental Research Institute, Seoul National University, Seoul, Korea, Republic of,[3]Biomedical Science, Hwasung Medi-Science University, Seoul, Korea, Republic of,[4]SillaJen, Inc., Seoul, Korea, Republic of,[5]SillaJen Biotherapeutics, Inc., San Francisco, CA

Threonine tyrosine kinase (TTK) and polo-like kinase 1 (PLK1), critical regulators of the spindle assembly checkpoint (SAC) required for faithful mitotic progression, are frequently overexpressed and dysregulated in human cancers. In recent years, strategies targeting the SAC, including TTK and/or PLK1, have emerged as promising therapeutic approaches in cancer treatment. However, these SAC inhibitors are known to induce adverse effects, including neutropenia. Granulocyte-colony stimulating factor (G-CSF) is widely used to prevent anti-cancer therapy-induced neutropenia, but growing evidence suggests that G-CSF may also promote tumor progression. Here, we demonstrate the broad anti-cancer activity of a novel dual TTK/PLK1 inhibitor, BAL0891, and its functional link to the G-CSF/G-CSF receptor (G-CSFR) axis in metastatic breast cancer. In patients with breast cancer, both TTK and PLK1 were markedly upregulated in triple-negative breast cancer (TNBC), which exhibits aggressive behavior, compared with other subtypes, and their expression levels were positively correlated among TNBC patients. The expression of G-CSFR was upregulated in breast tumors compared with normal tissues and was further elevated in metastatic tumors. In multiple human and murine TNBC cell lines, BAL0891 exerted potent anti-proliferative activity, accompanied by G2/M cell-cycle arrest and apoptosis. BAL0891 showed markedly higher potency in TNBC cells (GI50 ≈ 50—90 nM) than in immortalized MCF10A and ER+ MCF7 cells GI50 > 700 nM). In addition, BAL0891 treatment suppressed the migratory and invasive capacities of metastatic TNBC cells, with a concomitant reduction in vimentin expression, an epithelial-mesenchymal transition (EMT) marker. When comparing the effects of BAL0891 alone and in combination with G-CSF on TNBC progression, G-CSF treatment did not alter the anti-proliferative or apoptotic responses to BAL0891 in TNBC cells harboring moderate to high G-CSFR levels. However, combined BAL0891 and G-CSF treatment further potentiated BAL0891-mediated suppression of migration and invasion in these cells. Taken together, these findings suggest that dual TTK/PLK1 inhibition in combination with G-CSF may represent a valuable therapeutic strategy to suppress metastatic TNBC while potentially reducing the risk of neutropenia.

#2243 Lasofoxifene is a bone protective treatment option for estrogen receptor positive breast cancers.

Emily Kate Zboril[1], David C. Boyd[2], Rachel K. Myrick[2], Nina Dashti-Gibson[3], Faith E. Parker[2], Carson Walker[2], Amy Olex[2], Chuck Harrell[2]

[1]VCU Massey Comprehensive Cancer Center, Richmond, VA,[2]Virginia Commonwealth University, Richmond, VA,[3]Virginia Commonwealth University - VCU, Richmond, VA

Estrogen receptor positive (ER+) breast cancer primarily metastasizes to the bone microenvironment, and patients with ER+ disease are almost twice as likely to develop bone metastasis as those with other subtypes. Treatment with current endocrine therapies frequently results in osteoporosis and subsequent bone turnover which can potentially accelerate metastatic progression. This underscores the need for new treatments which will simultaneously inhibit tumor growth and preserve the bone microenvironment. Standard treatments like aromatase inhibitors and ER-antagonists, like fulvestrant, indiscriminately suppress ER signaling, in both breast and bone. Lasofoxifene, a selective ER modulator, exhibits tissue-selective ER-agonist activity in bone and is currently being evaluated in the ELAINE-III clinical trial [NCT05696626] in combination with abemaciclib for the treatment of ESR1-mutant advanced or metastatic ER+ breast cancer. Here, we investigated the physiological relevance of lasofoxifene's bone-selective ER-agonist activity and its impact on metastatic progression. Animal models of ovariectomy-induced osteoporosis were treated with lasofoxifene or standard endocrine therapies, and femurs were analyzed by histology and micro-CT histomorphometry. In parallel, anti-tumor effects of lasofoxifene were evaluated in vitro and in vivo in clinically relevant endocrine therapy-sensitive and -resistant primary and metastatic Patient-Derived Xenograft models. Additionally, drug synergism studies with lasofoxifene and the NCI NExT Oncology Interrogation Tools Set of 555 drugs were performed which identified pathways that were vulnerable to pharmacological inhibition in lasofoxifene-treated cells. We found that lasofoxifene protected against hormone withdrawal-induced bone loss and maintained a robust anti-tumor response in primary and metastatic models of ER+ breast cancer. Drug synergy screens have defined choices for rational combination with lasofoxifene to further potentiate its anti-tumor activity. Overall, this study supports the use of lasofoxifene-based treatment combinations which will concurrently protect bone architecture while suppressing ER+ metastasis progression in the bone niche.

#2244 Pro-metastatic kinase network inhibition to treat drug-resistant triple-negative breast cancer.

Margarite Matossian[1], Madeline Henn Bungert[1], Kent Schechter[1], Long Chi Nguyen[1], Michael East[2], Denis O. Okumu[2], Rita Nanda[1], Gary L. Johnson[2], Marsha R. Rosner[1]

[1]University of Chicago, Chicago, IL,[2]University of North Carolina, Chapel Hill, NC

Metastatic triple-negative breast cancer (mTNBC) has high mortality rates and limited therapeutic options. Chemotherapy, the basis of standard approved therapy for mTNBC, targets rapidly dividing cells but fails to eliminate the stem-like cells that drive metastasis. While kinases are promising drug targets, single-kinase inhibitors have been largely ineffective in mTNBC due to tumor heterogeneity, drug resistance, and the absence of predictive biomarkers. Our strategy is to identify and target kinase networks in pro-metastatic tumor cells that are upregulated in drug-resistant cells or specifically targeted by physiological regulators of metastasis. We initially utilized this approach to overcome AKT resistance in mTNBC. Employing a kinase activity assay (MIB-MS profiling), we demonstrated upregulation of Src family and ATM/ATR kinase networks following treatment of patient-derived, drug-resistant mTNBC organoids with the AKT inhibitor capivasertib. Sequential administration of capivasertib and dasatinib to target the Src family did not reduce organoid viability but did disrupt organoid formation and self-renewal, suggesting effective inhibition of metastatic potential. Building on our previous work, we then optimized a multi-kinase inhibitor regimen that mimics a physiological metastasis suppressor by targeting key stress-responsive kinase networks (ERK1/2, p38, JNK, and MLK). This low-dose drug combination (4MAPKi) prevented both TNBC metastasis and activation of compensatory pathways. We further refined this to a three-drug regimen (Ralimetinib, JNK-in-8, and Trametinib) that inhibits stress kinase networks, pro-motility gene expression and TNBC cell invasion in organoid assays. Importantly, combining this antimetastatic regimen with standard chemotherapy sensitized both TNBC cells and organoids to treatment. Ongoing studies focus on optimizing treatment efficacy with antibody-drug conjugates, characterizing kinase network targets specific for other metastasis regulators such as transcription factors, and exploring kinase networks as biomarkers for treatment resistance. Our long-term goal is to develop a low-toxicity, multi-kinase inhibitor strategy that reprograms metastatic TNBC cells, enhancing the efficacy and durability of their response to chemotherapy and improving clinical outcomes.

#2245 DNMTi in combination with PARPi inhibits aberrant Wnt/β-catenin signaling and tenasin-C pathways, cancer stemness and metastasis in triple negative breast cancer.

Lora Stojanovic[1], Kaushlendra Tripathi[2], Zahra Gohari[1], Julia L. Rutherford[1], Saranya Rajendran[3], Tara X. Metcalfe[3], Shu Zhang[3], Stephen B. Baylin[4], Michael Topper[5], Kenneth P. Nephew[6], Feyruz V. Rassool[7]

[1]University of Maryland, Baltimore, Baltimore, MD,[2]The National Institutes of Health, Bethesda, MD,[3]Indiana University Bloomington, Bloomington, IN,[4]Johns Hopkins University School of Medicine, Baltimore, MD,[5]Johns Hopkins University, Baltimore, MD,[6]Indiana University School of Medicine, Bloomington, IN,[7]Univ. of Maryland School of Medicine, Baltimore, MD

Triple-negative breast cancer (TNBC) has a higher rate of metastasis; a poor prognosis and survival compared with other breast cancer types. Poly-ADP ribose polymerase inhibitors (PARPis) are used to treat TNBC patients that harbor germline BRCA1/2 mutations, inducing synthetic lethality, but responses are not durable. We previously reported that PARPis in combination with DNA methyltransferase inhibitors (DNMTis) exert synergistic cytotoxicity in TNBC, independent of BRCA mutations, but the effects of these drugs on metastasis and stemness, which are associated with poor survival outcomes, are not known. Aberrant Wnt/β-catenin signaling in TNBC is known to drive cancer stemness, metastasis, and resistance to apoptosis and chemotherapy. Genome-wide transcriptomic analysis in TNBC cell line MDA MB 231 demonstrated that combining DNMTis azacytidine (AZA) and PARPis talazoparib (TAL) down-regulated cancer stemness and metastases pathways, and key leading-edge genes including those involved in Wnt/β-catenin signaling and tenasin-C (TNC), a multimodular glycoprotein that promotes the migration of cancer cells, were decreased. The effects of this drug combination on cell migration were functionally validated using scratch and transwell migration and invasion assays in multiple TNBC cell lines, including MDA MB231 and SUM159, and patient-derived organoids (N=3). Xenograft studies of MDA MB 231 by tail vein and SC injection showed decreased metastasis to the lung with this drug combination. Notably, stem cell assays, including spheroid assays and stem cell markers, SOX2, ALDH1a1 and CD44, were also decreased with AZA and TAL treatment. Notably, we show for the first time in TNBC that Beta-catenin/TCF12 transcriptionally regulates TNC by binding to its promoter region and that inhibition or KD of WNT/Beta catenin or TNC expression decreases the cell migration, metastasis and stemness, mimicking the effects of the drug combination in TNBC cells. Taken together, our results show for the first time that PARPi and DNMTi combination therapy targets WNT/Beta-catenin signaling and TNC regulation in driving aggressive disease, metastasis, stemness and poor survival in TNBC.

#2246 GLUT3 inhibition reduces metastatic potential of triple-negative breast cancer cells by modulating cell mechanics via the TEAD-VASP-Actin axis.

Seeun Oh[1], Wonkyung Lee[2], Song Kim[2], Donghoon Yoon[3], Jun-Yong Choe[4], **Tae-Hyung Kim**[2]

[1]Department of Molecular Genetics & Microbiology, University of New Mexico, Albuquerque, NM,[2]Department of Pathology, University of New Mexico, Albuquerque, NM,[3]University of Arkansas for Medical Sciences, Little Rock, AR,[4]Department of Chemistry, University of New Mexico, Albuquerque, NM

Triple-negative breast cancer (TNBC) is an aggressive breast cancer subtype lacking hormone (estrogen and progesterone) receptors and human epidermal growth factor receptor 2 (HER2), limiting the development of targeted therapies and contributing to poor patient outcomes. Metastasis, a major contributor to TNBC mortality, is closely linked to cancer cell mechanics—such as deformability and contractility—yet the molecular signaling cues from the tumor microenvironment (TME) that regulate these mechanical properties remain poorly understood.

This study investigates the role of glucose metabolism, particularly the role of glucose transporter 3 (GLUT3), in modulating TNBC cell mechanics and metastatic behavior. GLUT3, which has the highest glucose affinity among GLUT isoforms, is upregulated in various cancers including TNBC and is associated with poor prognosis and metastasis in TNBC patients. We demonstrate that GLUT3 inhibition by a selective inhibitor G3iA reduces glucose uptake, glycolysis and ATP production by 30% in TNBC cells, leading to AMP-activated protein kinase (AMPK) activation and suppression of myosin activity. The decreased myosin activity reduces cell contractility and ultimately cell invasion. AMPK activation also increased YAP phosphorylation resulting decreased YAP target gene expressions. We also identified VASP, an actin filament nucleator and polymerase, is a novel YAP-TEAD target gene that regulated by the glucose-AMPK signaling axis. Additionally, GLUT3 inhibition triggers the cAMP-Protein Kinase A (PKA) pathway, which impairs actin polymerization through vasodilator-stimulated phosphoprotein (VASP). The decreased F-actin levels correlates with reduced cell stiffness, which was measured by Atomic Force Microscope. Using pharmacological inhibitors that activate the AMPK signaling or the cAMP-PKA signaling pathways, we show that these altered cell mechanics—cell stiffness and contractility—diminishes cell motility *in vitro.* Furthermore, we confirmed our findings that GLUT3 null TNBC cells show reduced lung metastasis *in vivo*.

In summary, we delineate molecular pathways that translate extracellular glucose signaling into regulation of cell mechanics and motility via actin rearrangement. For the actin rearrangement, we discovered that regulation of VASP in transcriptional level and post-translational modification is critical. Our findings reveal a novel mechanistic link between glucose metabolism and cancer cell mechanics with detailed molecular mechanisms, offering a promising therapeutic avenue for mitigating TNBC metastasis.

#2247 Intracellular complement signaling plays a critical role in s1p/s1pr1 mediated inflammasome activation and tumor metastasis.

Salih Gencer[1], Alhaji H. Janneh[2], Natalia Oleinik[1], Charles Chalfant[3], Besim Ogretmen[1]

[1]The Medical University of South Carolina (MUSC), Charleston, SC,[2]Memorial Sloan Kettering Cancer Center, New York City, NY,[3]University of Virginia, Charlottesville, VA

Sphingolipid metabolism, specifically sphingosine 1-phosphate (S1P), has been demonstrated to regulate cancer progression and metastasis. Our previous research showed that oncogenic S1P and S1P receptor 1 (S1PR1) signaling activated intracellular C3 complement processing to enhance migration/metastasis through inflammasome activation by the C3-PPIL1 complex. This study addressed how the S1PR1/C3 axis mediates inflammasome/NLRP3 activation in various solid tumors, including melanoma and triple-negative breast cancer (TNBC). To better understand the roles of S1PR1 and C3 in mouse mammary tumorigenesis and metastasis, we crossed the MMTV-Cre S1pr1$^{fl/fl}$; MMTV-Cre or C3^{Tdt}; MMTV-Cre mice with MMTV-PyMt expressing mice to generate S1pr1$^{fl/fl}$; MMTV-Cre; MMTV-PyMt or C3^{Tdt}; and MMTV-Cre; MMTV-PyMt (controls) animals. Our preliminary data show that silencing C3 and S1PR1 selectively in mammary tumors significantly reduces tumor burden in MMTV-PyMt mice, consistent with decreased inflammasome signaling. Mechanistically, our data also showed that PPIL1-C3 complex requires SNU13 to induce cell migration in response to S1P signaling by mediating the alternative splicing of various factors involved in activating NLRP3/inflammasome in metastatic tumors. These findings suggest that attenuation of the S1PR1/C3 and PPIL1-SNU13-inflammasome signaling inhibits cancer cell migration and metastasis.

#2248 Inhibition of the mitochondrial antioxidant response blocks ex vivo lung colonization in pediatric osteosarcoma.

Elli Maria Tiliakou, Michael Lizardo, Yue-Zhou Huang, Taras Shyp, Poul Sorensen

Department of Molecular Oncology, BC Cancer Research Institute, Vancouver, BC, Canada

Osteosarcoma (OS) is the most common type of bone cancer affecting children and adolescents. Pulmonary metastasis is the primary cause of OS mortality, yet treatments have not improved patient outcomes in four decades. This gap emphasizes the urgent need to identify and vet novel anti-metastatic therapies. When OS tumor cells spread to the lung, they are subjected to oxidative stress caused by high levels of reactive oxygen species (ROS) secreted from microvascular endothelial cells and alveolar macrophages. This stress is further amplified by limited antioxidant capacity and other redox-imbalancing features of the lung microenvironment. We previously demonstrated that metastatic OS cells upregulate NFE2-like BZIP Transcription Factor 2 (NRF2), promoting cell survival in this stressful environment. In addition to being a master regulator of redox balance, NRF2 also influences mitochondrial function by controlling the expression of thioredoxin system members, including the antioxidant enzyme peroxiredoxin 3 (PRDX3) located in the mitochondrial matrix. Therefore, we hypothesize that PRDX3 upregulation promotes metastatic cell survival during the early stages of lung colonization, and disrupting this response will impair adaptation to the lung microenvironment. We evaluated thiostrepton (TS), a *Streptomyces*-derived thiopeptide antibiotic with demonstrated PRDX3-inhibitory activity in preclinical and clinical cancer studies, to determine its effect on metastatic OS tumor cells. To mimic the oxidative stress of the lung microenvironment in vitro, we treated cells with *tert*-butyl hydroperoxide (tBHP), which chemically induces oxidative stress. Through cell viability assays we showed that subtoxic levels of TS sensitize metastatic OS cells to tBHP-induced oxidative stress. In addition, we determined that PRDX3 is upregulated when metastatic OS cells are subjected to oxidative stress via confocal microscopy. Through protein immunoblots, we demonstrated that TS acts by dimerizing PRDX3, inactivating the catalytic site of the enzyme. Furthermore, we found that combining TS with the chemotherapeutic agents doxorubicin or etoposide, which are commonly used to treat pediatric pulmonary OS metastasis, produced a synergistic increase in cell death compared to either drug alone. Lastly, we studied TS as a single agent therapy using the pulmonary metastasis assay, an ex vivo lung explant system, and found that treatment significantly decreased OS lung tumor burden. Our findings provide promising preclinical data supporting the use of TS as a possible anti-metastatic therapeutic for pediatric OS.

: Tumorigenesis and Early Microenvironmental Trajectories
Poster Session

#2252 Resolving the initiating changes in the immunomodulatory glycome during early tumorigenesis of head and neck squamous cell carcinoma in living animals.

Sarah M. Hammoudeh, Thomas D. Madsen, Roberto Weigert

CCR-LCMB, NIH-NCI, Bethesda, MD

Cancer cells exploit the intricate network of stimulatory and inhibitory pathways to prevent immune-mediated clearance and thrive in an immunocompetent biological system. While targeting immune checkpoints (ICs) to reactivate the immune response has proven to enhance tumor-immune infiltration and patient prognosis, efficacy is limited only to a subset of patients. Hence, identifying alternative approaches to enable anti-tumor immune response is crucial. Aberrant protein glycosylation is a hallmark of cancer; in particular, increased cell-surface sialylation has been shown to inhibit immune-mediated clearance of tumor cells. This is mediated by the sialic-acid-binding immunoglobulin-like lectins (Siglecs), a family of surface receptors that mediate inhibitory signals by binding to sialic acid. Several factors complicate targeting the Sialic acid-Siglec axis in cancer therapy, including (1) the systemic adverse effects of broad abrogation of sialylation or Siglecs binding, (2) the diverse binding affinities of Siglecs based on sialic acid linkage, scaffold glycan and carrying protein. To enable the full use of this regulatory pathway, we set out to determine how the sialoglycome is dysregulated during early tumorigenesis. To this end, we used longitudinal intravital microscopy to record premalignant growth within the same animal at cellular resolution over 24 weeks in a carcinogen-induced model of head and neck squamous cell carcinoma (HNSCC). This allowed us to stratify lesions into progressing, regressing and stable growth signatures. We employ spatially resolved glycomics, transcriptomics and multiplex staining to generate a longitudinal signature of premalignant lesions. We observe an increased abundance of glycans decorated with α2,3-linked sialic acid (α2,3Sia). The elevated levels of α2,3Sia reflected a significant upregulation of α2,3-Sialyltransferases expression, indicating control mechanisms at the transcriptional levels. In the epithelial compartment, α2,3Sia was particularly enriched in CD44+ de-differentiated tumor cells. Using Siglec-Fc Chimeric constructs, we observed a binding preference of the CD44+ tumor-cells to Siglec-E. α2,3Sia was also elevated in the lesion stroma, strikingly in ly6G+ CD11b+ neutrophils recruited to progressing lesions. Our findings suggest a potential engagement of the Siglec-E - α2,3Sia axis in premalignant HNSCC lesions. Ongoing analysis is dissecting the tumor-immune interactions implicated in this axis as a potential regulator of the immune spatio-temporal landscape during early tumorigenesis. This study offers a groundwork to delineate glycomic and transcriptomic signatures in premalignant lesions with the opportunity to identify potential preventative measures in harnessing the immune response in patients.

#2253 Multimodal and multikingdom spatial transcriptomics identify bacterial niches implicated in oral cancer development.

Fushun Chen[1], Lorena Isabel Gomez[1], Tieling Zhou[1], Yuejiang Liu[1], Inti C. Tarifa Reischle[1], Sujuan Yang[1], Manvi Sharma[1], ,Jiping Feng[1], Jaafar Hadi[1], Fuduan Peng[1], Yibo Dai[1], Mhenaz Hossain[1], Ratna Veeramachaneni[1], Ansam Sinjab[1], Sean Anderson[2], Dhrishit Mangrolia[2], Deborah Rodriguez[1], Nadim Ajami[1], Jennifer Wargo[1], Adel El-Naggar[1], Roberto Rangel[1], Nadarajah Vigneswaran[2], Linghua Wang[1], Jeffrey N. Myers[1], Humam Kadara[1]

[1]UT MD Anderson Cancer Center, Houston, TX,[2]UT Health School of Dentistry, Houston, TX

Background: Oral squamous cell carcinoma (OSCC) of the tongue is the most common head and neck malignancy. OSCC develops from oral precancerous lesions (OPL) such as dysplasias which provide a window for preventive intervention. OSCC pathogenesis is influenced by genetic alterations, host immune responses, and the oral microbiome. Still, how microbial niches and their interactions in the tumor microenvironment (TME) promote oral carcinogenesis remains poorly defined.

Materials and Methods: Multimodal and multikingdom (host and bacterial) spatial transcriptomics (ST) analysis using the Visium and Xenium 5K platforms was performed on matched OSCC, dysplastic and normal regions from 16 cross-sectional tumor-normal specimens and from 21 longitudinally transforming dysplasia and OSCC biopsies, and on tissues from carcinogen-driven mouse models of OSCC. Custom add-on panels targeting key oral cancer genes and bacterial probes (16S rRNA, 20 oral taxa including *F. nucleatum*) were included which enabled cross-platform mapping of host-microbe interactions. Copy number alterations (CNAs) were spatially inferred and analyzed phylogenetically. Neighborhood analysis was performed to probe proximity of epithelial-microbial-TME interactions.

Results: Following quality control, over 120,000 spots from Visium ST and over 3.5 million Xenium-resolved cells were retained which comprised diverse epithelial, immune, and stromal lineages. Trajectory analysis revealed major differentiation states mapping to distinct layers in the oral epithelium. Along the normal to dysplasia to OSCC continuum, basal cells progressively expanded while more differentiated cells (e.g., granular) were reduced, accompanied by increased EMT and inflammatory signatures. Spatial analysis of CNAs showed elevated aneuploidy across the normal-dysplasia-OSCC spectrum, with basal cells among all epithelial layers harboring the highest CNA burdens. Spatial phylogenetic analysis identified shared clones between dysplasias and OSCC, marking early events in OSCC evolution. Multikingdom ST identified bacteria-enriched niches that harbored tumor cells and *IL1B* high granulocytic myeloid cells. Epithelial cells in these niches displayed genes with roles in host defense (*DEFB4A*, *LCN2*) as well as chemokines that promote myeloid cell recruitment (e.g., *CXCL1*, *CXCL8*), suggesting epithelial-microbe-immune interactions with both tumor restricting and promoting properties that together tune OSCC progression. These niches and their properties were recapitulated in tumors from 4NQO-exposed mice.

Conclusions: Our study suggests that epithelial remodeling, inflammatory signaling, and bacteria-rich niches result in epithelial-microbial-immune interactions that shape the pathogenesis of OPL and OSCC and, thus, harbor high-potential targets that can guide early treatment strategies for OSCC.

#2254 3D multimodal spatial profiling of pre-gastric cancer progression using same-slide RNA-protein and fluorescent H&E.

Eric Sha[1], Seock-Jin Chung[2], Jean R. Clemenceau[2], Sunho Park[2], Minji Kim[2], Inyeop Jang[2], Youngwon Cho[2], Seunghyi Kook[2], Soonyoung Lee[3], Jongseong Jang[3], Eunyoung Choi[2], Tae Hyun Hwang[2]

[1]Vanderbilt University, Nashville, TN,[2]Vanderbilt University Medical Center, Nashville, TN,[3]LG AI Research, Seoul, Korea, Republic of

Background: Gastric cancer arises through a cascade from intestinal metaplasia to dysplasia and invasive adenocarcinoma, but only a subset of precancerous glands progress. The spatial features that distinguish progressing from non-progressing niches are unknown. We applied a multimodal platform that combines same-slide, subcellular RNA and protein profiling on the G4X Spatial Sequencer with fluorescent H&E (fH&E) and 3D holotomography (HT) to characterize pre-gastric cancer (pre-GC) niches and their transition toward carcinoma.

Methods: FFPE gastric tissues from 12 patients (38 regions of interest) were profiled on G4X flow cells using a custom 358-gene gastric cancer/pre-cancer panel, a 16-plex protein panel, and fH&E on the same slide. We used multimodal clustering and classification of spatial transcriptomic, morphology, and protein features to define cell states and associated niches. For matched regions, 3D HT from the same tissues was used to embed 2D molecularly defined states into their gland and mucosal context and to assess whether pre-GC states share or segregate across glandular units, extend through the mucosal depth, and how immune populations are positioned around them in 3D. By aligning subcellular G4X coordinates with HT volumes, this method enables us to visualize the x-y-z localization of transcripts within individual cells, providing a molecular level 3D model of the tumor-stroma-immune microenvironment.

Results: Multimodal analysis of integrated RNA, protein, and morphology data resolved distinct epithelial, stromal, and immune compartments in precancerous tissue, whereas cancerous regions showed expansion of epithelial and immune states and altered compartment boundaries. Within the epithelial layer, regions of metaplasia and dysplasia localized to discrete gland-associated zones enriched for intestinal or gastric gene signatures. Same-slide RNA-protein measurements enabled mapping of $CD4^+$ helper and $CD8^+$ cytotoxic T-cell distributions relative to the gastric epithelium. Incorporating 3D HT enabled us to investigate whether 2D-defined pre-GC foci represented continuous lesions or separate glands and refined estimates of lesion extent and immune proximity along the gland axis in 3D.

Conclusions: This 3D-enabled, same-slide G4X platform with fH&E, RNA transcript profiling, and a 16-plex protein panel generates multi-scale maps of pre-GC and gastric cancer niches. In particular, 3D spatial multimodal modeling improves interpretation of pre-cancer epithelial programs and immune positioning and supports discovery of 3D niche features linked to progression risk beyond conventional 2D histology.

Generative AI assistance was limited to language editing of this abstract. The scientific content, interpretation, and conclusions are the sole responsibility of the authors, who have reviewed and approved the final version.

#2255 Spatial transcriptomics reveals evolving tumor microenvironmental archetype along the lung premalignancy-adenocarcinoma continuum.

Yibo Dai[1], Fuduan Peng[1], Ansam Sinjab[1], Yunhe Liu[1], Sujuan Yang[1], Lorena I Gomez Bolanos[1], Tieling Zhou[1], Minyue Chen[1], Alejandra G Serrano[1], Jianlong Liao[1], Guangsheng Pei[1], Yang Liu[1], Jiahui Jiang[1], Kyung Serk Cho[1], Kai Yu[1], Jiping Feng[1], Zahraa Rahal[1], Naoe Jimbo[2], Takuo Hayashi[3], Satsuki Kishikawa[3], Kazuya Takamochi[3], Avrum Spira[4], Steven M. Dubinett[5], Tomoo Itoh[2], Takashi Yao[3], Kenji Suzuki[3], Stephen G. Swisher[1], Mingyao Li[6], Junya Fujimoto[7], Ignacio Wistuba[8], Jared K. Burks[1], Kadir Caner Akdemir[1], Hind Rafei[1], Katayoun Rezvani[1], Jeffrey N. Myers[1], Humam Kadara[1], Linghua Wang[1]

[1]UT MD Anderson Cancer Center, Houston, TX,[2]Kobe University Hospital, Kobe, Japan,[3]Juntendo University Graduate School of Medicine, Tokyo, Japan,[4]Lung Cancer Initiative at Johnson and Johnson, Boston, MA,[5]UCLA David Geffen School of Medicine, Los Angeles, CA,[6]University of Pennsylvania, Philadelphia, PA,[7]Hiroshima University Hospital, Hiroshima, Japan,[8]Moffitt Cancer Center & Research Institute, Tampa, FL

Background: Lung adenocarcinoma (LUAD) is one of the most lethal cancer types worldwide, yet how the tumor microenvironmental (TME) archetypes are remodelled during the transition from premalignant lesions (PMLs) to LUAD remains poorly understood. This study aims to systemically characterize the dynamic evolution of tumor immune archetypes across the PML-LUAD continuum using spatially resolved transcriptomics.

Methods: Spatial profiling was conducted on 56 samples from 25 patients with paired PMLs and LUADs using the Visium (spot-level) platform. Among them, 12 paired samples from 6 patients were also profiled with the Xenium 5K (single-cell-resolution) platform. TME cellular organizations and interactions were investigated, and distinct spatial TME archetypes were defined. Subsequently, signature scores representing these microenvironmental architectures were derived from spatial data and validated in bulk RNA-sequencing cohorts. Finally, single-cell RNA sequencing (scRNA-seq) was performed on serial lung samples from a carcinogenesis mouse model with *Gprc5a* knockout (*Gprc5a*$^{-/-}$) and exposure to nicotine-derived nitrosamine ketone (NNK), and the dynamic transition of TME archetypes during LUAD development was characterized.

Results: Compared with PMLs, LUADs displayed an expansion of cancer-associated fibroblasts, alongside intratumoral enrichment of mature tertiary lymphoid structures and depletion of natural killer cells. Additionally, multiple immune-suppressive signals were observed in LUADs and showed progressive upregulation from distal normal to tumor regions. Altogether, these findings indicate dynamic TME remodelling during malignant progression. Spatial mapping of TME cells revealed four distinct immune archetypes, termed IMmune Phenotype spAtial Contextual Typing in LUAD and PML (IMPACT). PMLs were dominated by IMPACT-1, with enrichment of macrophages in the tumor regions, alongside concurrent intratumoral enrichment of T (subtype 1a) or B (subtype 1b) cells. In contrast, LUADs exhibited mixed lymphocyte infiltration (IMPACT-2) or lymphocyte exclusion (IMPACT-3). These subtypes displayed distinct molecular profiles, showing evidence of tumor-promoting inflammation, immune activation, and different mechanisms of immune evasion. IMPACT signatures applied to bulk RNA sequencing cohorts recapitulated key immune features of different IMPACT subtypes and their associations with disease stages. Finally, scRNA-seq analysis on lung samples from the *Gprc5a*$^{-/-}$ carcinogenesis mouse model further validated the dynamic transition of IMPACT subtypes overtime.

Conclusions: PML-LUAD progression is accompanied by profound TME reprogramming. Patient stratifications by spatial immune archetypes may enable predicting disease developmental trajectories and inform strategies for early cancer interception.

#2256 Age-related transcriptional and alternative splicing changes in lung progenitor cells predisposing to immune dysfunction.

Mohammed Toufiq[1], Florentina Marches[2], Hyeon Gu Kang[2], Te-Chia Wu[2], Ryan Englander[2], Sanaz Keshavarz Shahbaz[2], Marina Yurieva[2], Phylip Chen[3], Mark E Peeples[4], Adolfo Garcia-Sastre[5], Michael Schotsaert[6], Damien Chaussabel[2], Karolina Palucka[1], Olga A. Anczukow-Camarda[1]

[1]The Jackson Laboratory for Genomic Medicine, Institute for Systems Genomics, University of Connecticut, Farmington, CT,[2]The Jackson Laboratory for Genomic Medicine, Farmington, CT,[3]Center for Microbe and Immunity Research, Abigail Wexner Research Institute at Nationwide Children's Hospital, Columbus, OH,[4]Center for Microbe and Immunity Research, Abigail Wexner Research Institute at Nationwide Children's, Department of Pediatrics, College of Medicine, and Infectious Disease Institute The Ohio State University, Columbus, OH,[5]Department of Microbiology, Global Health and Emerging Pathogens Institute, Department of Medicine, Division of Infectious Diseases, The Tisch Cancer Institute, Department of Pathology, Molecular and Cell-Based Medicine, Icahn School of Medicine at Mount Sinai, New York, NY,[6]Department of Microbiology, Global Health and Emerging Pathogens Institute, Icahn Genomics Institute, Marc and Jennifer Lipschultz Institute for Precision Medicine, Icahn School of Medicine at Mount Sinai, New York, NY

Purpose: Aging is the greatest risk factor for lung cancer, the leading cause of cancer-related deaths worldwide. With advancing age, impaired immune surveillance and cellular senescence create a pro-tumorigenic microenvironment that disrupts epithelial homeostasis and promotes oncogenic remodeling. However, the molecular mechanisms by which age-related transcriptional and splicing changes in lung contribute to immune dysregulation and cancer susceptibility remain poorly understood. We performed integrated transcriptomic profiling of lung progenitor cells to identify age-associated molecular alterations predisposing to immune dysfunction and early tumorigenic changes.

Methods: Primary human broncho-epithelial cells from young (age: 18y to 27y, n=5) and old (age: 42y to 67y, n=5) donors were enriched for progenitor cells in 2D culture for seven days following Fulcher et al. We performed Illumina short-read and PacBio long-read RNA-sequencing. Isoform-level analysis on long-reads was performed through IsoSeq3 and SQANTI3. Differential expression was analyzed using DESeq2 (FDR < 0.05) and alternative splicing using rMATS (>10% Delta PSI, FDR < 0.05) with a long-read derived transcriptome. Functional consequences of splicing events were predicted using SpliceDecoder.

Results: We identified 47 differentially expressed genes (36 upregulated, 11 downregulated with age). Notably, IL18, MMP25, PGLYRP4, THY1, CDH2, MFAP5, and PLXNC1 were upregulated in older donors, reflecting activation of inflammatory and immune response programs alongside altered epithelial and extracellular matrix remodeling. We also detected 991 age-related differentially spliced events in 632 genes. Among these, intron retention occurred in immune genes including HLA-A, HLA-B, HLA-C, TRIM65, and FOSB, while splicing of cassette exons was observed in IFNAR2-IL10RB, DMKN, HLA-F-AS1, and NOD1. SpliceDecoder predicted that these age-related splicing alterations introduce premature stop codons, alter coding sequences, and modify protein domains, potentially leading to gain- or loss-of-function effects. Finally, long-read RNA-sequencing identified 42,206 full-length spliced isoforms, the majority of which were novel and absent from reference transcriptomes, revealing extensive isoform diversity in lung progenitor cells.

Conclusions: Our integrated approach demonstrates that aging reshapes the transcriptomic landscape through changes in gene expression and splicing, that may contribute to immune dysfunction and epithelial remodeling. These changes may create a pro-inflammatory environment that enhances susceptibility to oncogenic transformation and disrupts tissue homeostasis. Together, these findings uncover molecular mechanisms linking aging to lung cancer risk and identify potential biomarkers and therapeutic targets for prevention and intervention.

#2257 Eric Medina.

Eric F. Medina[1], Jacob I. Rodriguez[1], Alyssa Bujnak[2], Devon Lawson[1], Kai Kessenbrock[1]

[1]Biological chemistry, University of California, Irvine, Irvine, CA,[2]University of Chicago, Chicago, IL

Most high-grade serous carcinomas are thought to originate from the fallopian tube epithelium and progress through pre-malignant states that are more susceptible to transformation in BRCA1/2 mutation carriers. However, the early epithelial and stromal programs that arise during transformation remain poorly defined. To address this gap, we analyzed 49 FFPE scRNA-seq samples from 28 patients, including normal ovary and fallopian tube tissues, BRCA1/2 pre-malignant tissues, and matched primary ovarian tumors and metastatic lesions. FASTQ files were aligned to GRCh38 with the Cell Ranger pipeline, followed by doublet removal. Integration was performed using reciprocal principal component analysis separately for normal and pre-malignant ovary or fallopian tube samples, and primary tumor and metastatic samples. Cell type annotation was guided by a custom reference derived from publicly available human fallopian tube scRNA-seq datasets and validated using canonical marker genes. Across samples, we identified major epithelial, immune, and stromal compartments, including distinct secretory and ciliated epithelial populations. Early analyses revealed that malignant epithelial cells from both primary tumor and metastatic lesions overwhelmingly mapped to secretory epithelial lineages, with minimal contribution from ciliated cells. Normal and BRCA1/2 pre-malignant ovary tissues similarly showed a strong enrichment for secretory cells, whereas fallopian tube tissue displayed a more balanced secretory-ciliated distribution. In addition, primary and metastatic samples displayed markedly increased immune infiltration compared with normal and pre-malignant tissues. This comprehensive single-cell dataset provides new insight into early epithelial and microenvironmental changes associated with BRCA1/2 mutation status. Ongoing analyses aim to determine whether specific stromal cell states, such as fibroblast subpopulations, emerge in pre-malignant tissues and persist into malignant and metastatic lesions, suggesting the presence of early tumor-promoting stromal phenotypes. Overall, this study establishes a framework for discovering early microenvironmental drivers of ovarian carcinomas initiation.

#2258 SLC12A2 drives a tumor-promoting microenvironment and poor prognosis in hepatocellular carcinoma by suppressing lipolysis.

Yotaro Kudo, Ryosuke Tateishi, Mitsuhiro Fujishiro

Gastroenterology, Graduate School of Medicine and Faculty of Medicine, The University of Tokyo, Bunkyo City, Japan

Hepatocellular carcinoma (HCC) frequently arises from steatotic and fibrotic livers, yet molecular factors linking metabolic dysregulation to tumor-promoting hepatic microenvironments remain incompletely defined. We aimed to identify transporter genes associated with HCC risk and elucidate their mechanistic role in steatohepatitis-related hepatocarcinogenesis. Using the GSE10143 cohort, we screened 617 transporter genes curated from the Transporter Classification Database for prognostic relevance based on Cox proportional hazards modeling of overall survival. Candidate genes were validated by RNA sequencing of liver biopsy specimens from 94 patients with metabolic dysfunction-associated steatotic liver disease (MASLD) (12 with HCC) obtained between 2016 and 2020, following institutional ethical approval. Functional studies were conducted in C57BL/6 mice with hepatic overexpression of solute carrier family 12 member 2 (SLC12A2)—a Na^+-K^+-Cl^- cotransporter—via AAV8, followed by feeding with a choline-deficient, L-amino acid-defined, high-fat diet (CDAHFD) for six weeks to induce diet-associated steatohepatitis. In vitro assays were performed using a normal hepatocyte cell line and Hep3B cells with stable SLC12A2 overexpression or shRNA-mediated knockdown. From the transporter gene screening, SLC12A2 showed the highest hazard ratio for poor survival and was also associated with increased late (>2 years) post-hepatectomy recurrence, implying enhanced carcinogenic potential of background liver tissue. In the MASLD cohort, hepatic SLC12A2 expression was significantly higher in HCC cases and positively correlated with fibrosis stage and liver stiffness. In mice, hepatic SLC12A2 overexpression exacerbated CDAHFD-induced steatohepatitis—evidenced by increased liver weight, serum ALT levels, hepatic triglyceride content, Sirius red-positive area, and fibrogenic gene expression. Cleaved caspase-3 and Ki-67 staining indicated increased hepatocellular apoptosis and compensatory proliferation, features typical of chronic liver injury. Orthotopic implantation of Hepa1-6 cells resulted in significantly larger tumors, demonstrating a tumor-promoting microenvironment. In vitro, SLC12A2 overexpression enhanced palmitate-induced lipid droplet formation, whereas shRNA-mediated knockdown suppressed it. Expression of genes involved in fatty acid synthesis and oxidation remained unchanged, but glycerol release was decreased, indicating suppression of lipolysis as the primary mechanism. Our findings suggest that SLC12A2 promotes hepatic steatosis and fosters a tumor-promoting microenvironment by repressing lipolysis. Its overexpression identifies high-risk MASLD livers predisposed to HCC and represents a potential therapeutic target for metabolic liver disease-associated hepatocarcinogenesis.

#2259 Reprogramming of the stromal and immune microenvironment in preinvasive breast cancer.

Siyuan He[1], Aatish Thennavan[1], Runmin Wei[1], Shanshan Bai[1], Jianzhuo Li[1], Chante Bethell[1], Emi Sei[1], Mitchell Rao[1], Tapsi Kumar[1], Chenling Tang[1], Ivan Marin[2], Jessica Montalvan[2], Chandandeep Nagi[2], Bora Lim[1], Savitri Krishnamurthy[1], Alastair Thompson[3], Nicholas E. Navin[1]

[1]UT MD Anderson Cancer Center, Houston, TX,[2]Baylor College of Medicine, Houston, TX,[3]Baylor College of Medicine, Dan L. Duncan Cancer Center, Houston, TX

Ductal carcinoma in situ (DCIS) is the most common form of preinvasive breast cancer. However, our knowledge of the DCIS tumor microenvironment (TME) remains limited. Here, we investigated the TME of estrogen receptor positive DCIS using fresh tissues samples from DCIS, invasive breast cancers and normal breast tissues. In total, 795,585 cells were analyzed from 153 patients by single cell RNA sequencing and 39 samples were profiled with spatial transcriptomics methods (Visium, Xenium). Our data identified reprogrammed vascular cells, fibroblasts and basal cells that encircled the DCIS regions, forming cancer stromal loops (CSL) that support the preinvasive cancer cells. The DCIS regions were highly immunosuppressive, and only lipomacrophages (APOC1+) and interferon T-cells infiltrated. The preinvasive cancer cells showed activation of cell cycling and interferon signaling, while reducing cell growth regulation, RNA processing, secretion and cell adhesion. Collectively, these data show extensive remodeling of the TME in DCIS that persists during invasive progression.

#2260 Macrophage immunometabolism as a targetable driver of early lung cancer progression.

Tyler Faith[1], Amrita Roy[2], Dikshaya Prabhakara[2], Yaron Zaret[1], Samuel Weinberg[3], Alicia Hulbert[4], Frank D. Weinberg[5]

[1]College of Medicine, University of Illinois at Chicago, Chicago, IL,[2]Division of Hematology and Oncology, University of Illinois at Chicago, Chicago, IL,[3]Department of Pathology, Northwestern University, Chicago, IL,[4]University of Illinois at Chicago, Chicago, IL,[5]University of Illinois Cancer Center, Chicago, IL

Background Lung cancer is a leading cause of cancer-related mortality and early progression is driven by interactions between epithelial cells and the tumor-immune microenvironment. Macrophages shape cancer progression through both inflammatory and immunosuppressive programs. Prior work has shown dysbiosis, cytokine enrichment, and increased stearic acid (SA) levels in tumor affected lobes of early-stage lung cancer patients. To better understand the role of SA within the tumor microenvironment, we consider its effect on macrophage polarization, altered immune signaling, and epithelial response. We modeled the effect of macrophage-derived signals on the early transformation of lung epithelial cells to identify conserved transcriptional programs that may be leveraged to improve prevention and treatment strategies.

Methods To characterize the effect of SA on macrophages, U937 pro-monocytic cells were differentiated into macrophage-like cells (M0, M1, M2) with PMA and further stimulated with some combination of LPS, IFN-γ, IL-4, SA, or BSA (vehicle). Conditioned media from macrophage cell cultures was collected before RNA was extracted using TRIzol and sequenced on an Illumina platform. To characterize the effect of SA on macrophage immune signaling, BEAS2B epithelial cells were treated with macrophage-like conditioned media and malignant potential was assessed with a methylcellulose-based soft agar assay. Total RNA was extracted using NEB Monarch Total RNA Miniprep kit and sequenced on an Illumina platform. Differential gene expression for U937 and BEAS2B treatment groups were analyzed, and pathway enrichment was assessed using GO terms and KEGG analysis.

Results SA exposure modified transcription across M0-, M1-, and M2-like macrophage phenotypes and lead to altered expression of 83 common genes. Gene ontology (GO) functional analysis showed evidence of modified cholesterol and alcohol metabolism and steroid biosynthesis in M0- and M2-like macrophages. SA exposure was associated with increased expression of *MVK*, *STARD4*, and *INSIG1* related to sterol and lipid metabolism. SA exposure was also associated with decreased expression of *KIF4A*, *TOP2A*, and *BRCA2* related to cell cycle regulation and genomic stability. Modified expression of these and other genes identified during our analysis may be involved in early tumor processes.

Conclusions Stearic acid modulates macrophage transcription across phenotypes, supporting our hypothesis that immunometabolic signaling plays an important role in lung cancer initiation. These findings provide a molecular foundation for future studies characterizing the transcriptional changes identified and their effect on lung cancer initiation. Furthermore, they highlight macrophages as potential targets for preventive or early therapeutic interventions in lung cancer.

#2261 Deciphering the role of macrophages in the development of pancreatic ductal adenocarcinoma.

Maria F. Wissler[1], Jessie Kanacharoen[1], Daniel J. Salas-Escabillas[1], Shalini Datta[1], Naziheh Assarzadegan[2], Eugene Shenderov[1], Ashley Kiemen[3], Won Jin Ho[3], Laura DeLong Wood[1]

[1]Johns Hopkins University School of Medicine, Baltimore, MD,[2]Department of Pathology, Immunology, and Laboratory Medicine, University of Florida, Gainsville, FL,[3]Johns Hopkins University, Baltimore, MD

Pancreatic ductal adenocarcinoma (PDAC) is one of the most aggressive forms of cancer. Intraductal papillary mucinous neoplasms (IPMNs) are a well-documented precursor of invasive PDAC; however, the molecular and cellular alterations that drive malignant progression of IPMNs are poorly understood. Genetic alterations drive progression in only a minority of cases, highlighting the likelihood that the surrounding tumor microenvironment (TME) may play an important role. PDAC is characterized by an immunosuppressive TME with abundant macrophages, but the temporal accumulation of immunosuppressive macrophages in PDAC precursors and their role in the progression to invasive cancer has not been explored. A deeper understanding of the TME in IPMN and PDAC may reveal actionable mechanisms of progression, potentially identifying novel therapeutic targets or biomarkers of progression risk. To investigate the temporal recruitment, polarization state, and spatial localization of macrophages, we leveraged immunohistochemistry (IHC) and imaging mass cytometry (IMC) datasets of human IPMNs and adjacent PDAC. IHC from 24 patients showed significant upregulation of CD68+ macrophages in PDAC. IMC allows quantification of the densities and spatial distribution of distinct subtypes. IMC analysis of IPMN, transition zone, and PDAC regions from 12 patients identified heterogeneous changes in total macrophage count and proportions of macrophages subsets over the transition from IPMN to invasive PDAC. In addition, spatial transcriptomics was performed on a subset of samples from 4 patients to interrogate mechanisms of macrophage-epithelial crosstalk across the transition from IPMN to PDAC. *In vitro* culture of primary human macrophages and PDAC organoids further enables characterization of the functional impact of macrophage-epithelial crosstalk. Organoid-conditioned media treatment of macrophages demonstrates that the PDAC secretome is capable of polarizing macrophages toward an immunosuppressive phenotype with increased expression of IL-10 and CD163. This study provides a comprehensive molecular analysis of macrophages present in the TME of IPMN and PDAC, revealing heterogeneous patterns across patients. The results suggest a role for macrophages in malignant progression and pathways by which PDAC cells reprogram the macrophage population, offering new insights into the interaction between macrophages and neoplastic epithelial cells, which can be used to identify signaling dependencies that could serve as novel biomarkers of therapeutic targets.

#2262 Cell division regulates macrophage invasion in mammary epithelia.

Emily A. Pratt, Mariia Akhmanova

Cell Biology, Memorial Sloan Kettering Cancer Center, New York, NY

Macrophages survey the mammary epithelium and are found between the myoepithelial and luminal layers of the ducts where they aid in tissue remodeling during branching morphogenesis. These ductal macrophages expand as more bone marrow derived macrophages arrive during puberty and pregnancy, when there is extensive remodeling of the gland, increased cell proliferation, and luminal apoptosis to maintain the ductal lumen. Interestingly, early macrophage infiltration is also observed in triple negative breast cancer (TNBC) and is associated with poor prognosis. TNBC-associated macrophages resemble the polarized state and tissue remodeling function of ductal macrophages during normal mammary development and are not as commonly found in luminal or human epidermal growth factor receptor 2-positive (HER2+) breast cancers. While it is well documented that mammary macrophages are present within the gland, the mechanisms by which macrophages infiltrate epithelial barriers in both developmental and disease contexts remains unknown. Thus, to address this gap in our understanding of macrophage biology, we employ 3D mammary epithelial and macrophage co-cultures compatible with live imaging. We hypothesize that macrophages respond to transient disruption in epithelial integrity-such as those occurring during mitosis or programmed cell death-and use these short-lived losses of epithelial-epithelial adhesions as opportunities to access epithelial compartments. To examine this hypothesis, we have live imaged 3D mammary epithelial spheroids generated from healthy (MCF10A) and TNBC (MDA-MB-231) cells in co-culture with macrophages. Mammary acini form polarized lumen where apoptotic cells are extruded into the luminal space, like *in vivo.* Mammary spheroids present an *in vitro* model where apoptosis can be driven pharmacologically, resulting in increased epithelial turnover, allowing us to model dynamic conditions of the mammary duct. Our data support the hypothesis that macrophages traverse epithelial layers at sites of cell division, consistent with a model in which transient junctional instability guides macrophage positioning. During involution, luminal epithelial cells undergo apoptosis and release “find-me” signals into the tissue microenvironment. We hypothesize macrophages respond to these local attractants, exploiting the transient losses in epithelial-epithelial cell adhesion, to traverse the myoepithelial layer. Together, this work aims to define the epithelial cues that regulate macrophage infiltration into mammary tissues and to understand how these processes shape both normal developmental programs and early disease transition in TNBC. Elucidating the mechanisms of macrophage entry into epithelial environments may reveal new opportunities for targeting immune-epithelial interactions in aggressive breast cancers while enriching our understanding of underappreciated immune-epithelial crosstalk.

#2263 Microenvironmental rewiring in giant cell tumor of bone: Stromal lineage hierarchy, immune diversion, and novel osteoclastogenic and angiogenic circuits.

Chao Zhang[1], Jilong Yang[1], Xiangchun Li[2], Kexin Chen[2], Hongru Shen[2], Zhichao Liao[1]

[1]Department of Bone and Soft Tissue Tumor, Tianjin Medical Univ. Cancer Inst. & Hosp., Tianjin, China,[2]Department of Epidemiology and Biostatistics, Tianjin Medical University Cancer Institute & Hospital, Tianjin, China

Giant cell tumor of bone (GCTB) is a locally aggressive osteolytic neoplasm characterized by neoplastic stromal cells and abundant osteoclast-like giant cells, yet the microenvironmental architecture and regulatory networks that sustain tumor progression remain incompletely understood. Here, we performed integrated single-cell RNA sequencing and spatial transcriptomics on six treatment-naïve primary GCTB specimens to generate a high-resolution atlas of stromal, immune, myeloid, osteoclastic and vascular compartments. We identify a structured mesenchymal hierarchy linking pericytes, osteoblast precursors and tumor stromal cells through a continuous transcriptional trajectory, providing evidence that the neoplastic stromal population arises from, or co-evolves with, osteogenic and perivascular lineages. Tumor cells display marked inter- and intra-patient heterogeneity, characterized by discrete EMT-, coagulation-, myogenesis- and androgen-responsive subclusters, indicating diverse functional specializations within the stromal tumor compartment.Despite substantial cytotoxic T-cell infiltration across all patients, ligand-receptor inference revealed that effector immune signals—including CCL and PARs pathways—are preferentially directed toward osteoclast-like giant cells rather than tumor cells, suggesting an “immune diversion” or “immune sink” mechanism that may blunt anti-tumor immunity despite preserved T-cell functional states. Beyond confirming the canonical tumor-derived RANKL engagement of giant cells, we uncover two additional regulatory circuits: (i) a tumor-specific CHAD-ITGA2 signaling axis, with ITGA2 expression uniquely restricted to giant cells, implicating a selective osteoclastogenic mechanism with therapeutic potential; and (ii) a multisource CSF1/IL34-CSF1R network arising from tumor cells, osteoblast precursors and pericytes, cooperatively shaping myeloid recruitment and giant-cell formation, further supporting a shared stromal origin among these lineages.Finally, we identify a tumor-exclusive APELA-APLNR (APJ) angiogenic axis linking ligand production strictly in tumor cells to receptor expression exclusively in endothelial cells. Spatial transcriptomics confirmed that APELA is enriched within RANKL-high tumor niches, revealing a spatially confined angiogenic microdomain functionally distinct from the broadly distributed VEGF pathway.Together, this atlas defines the cellular logic and intercellular circuitry underlying GCTB progression and identifies multiple stromal, immune, osteoclastogenic and vascular vulnerabilities—including the CHAD-ITGA2 and APELA-APLNR axes—that may guide therapeutic strategies beyond RANKL inhibition.

#2264 Spatial trajectories and niche rewiring from ground-glass to solid transition in lung adenocarcinoma.

Kwon Joong Na, Hongyoon Choi, Jaemoon Koh, Taeyoung Yun, Jihyeon Park, Bubse Na, Samina Park, In Kyu Park, Chang Hyun Kang, Young Tae Kim

Seoul National University Hospital, Seoul, Korea, Republic of

BackgroundGround-glass nodules (GGNs) are frequently detected by screening, yet how they acquire invasion in situ is unclear. We asked how epithelial states, stromal architecture, and immune circuits reorganize during the GGN-to-solid transition.
MethodsWe generated paired spatial transcriptomes (10x Visium, fresh-frozen) from GGN-predominant and solid-predominant regions of three resected stage I LUADs. Cell composition and epithelial states (tS1-tS3) were inferred using a single-cell reference. We quantified ligand-receptor (L-R) communication, inferred pathway activities (PROGENy; Hallmark), and constructed diffusion-based spatial trajectories within sections to model the preinvasive-to-invasive continuum.
ResultsTwo tumors converged on an epithelial-high, fibroblast-low, myeloid-inflamed solid region, while one showed a stroma-dominant solid phenotype; myeloid influx was shared across all cases. The malignant-potential epithelial state (tS2) expanded in 2/3 tumors (the third was approximately flat), whereas benign-like states receded focally. Fibroblast programs consistently showed myofibroblast enrichment, supporting early ECM stiffening. T-cell lineages shifted toward exhaustion ($CD8^+$; modest Tfh) with variable Treg increases, yielding an inflamed-but-immunosuppressed niche. Spatial L-R maps highlighted strengthening of complement-B-cell axes (C3-CR2/CD19) and ECM-anchored signals (SDC4-TGM2, FN1-TNFRSF11B), with contraction of NK/T-cell-supportive interactions (HLA-E-KLRD1; IL-7-IL7R). Pathway scores corroborated a state of EGFR and hypoxia upshift with glycolytic/fatty-acid programs increased, apical junction and E2F programs reduced—compatible with proliferation under metabolic stress rather than indiscriminate cell-cycle acceleration. In a case spanning adjacent normal-GGN-solid, spatial trajectories captured early endothelial/fibroblast loss between normal and GGN, followed by consolidation of invasion marked by tS2 gain, myofibroblast accumulation, and monocyte/DC recruitment toward the solid core.
ConclusionsPaired spatial transcriptomes indicate that the GGN-to-solid shift is assembled by coordinated epithelial state change, stromal myofibroblast enrichment, and immune rewiring toward exhaustion with myeloid influx. L-R and pathway profiles converge on complement-biased, ECM-anchored signaling with attenuated NK/T-cell support, nominating candidate axes for risk stratification of GGNs and prospective validation in larger cohorts.

#2265 Stromal cyclin D1 promotes prostate cancer stemness via the transcriptional regulatory E domain.

Xuanmao Jiao[1], Danni Li[1], Rita Pancsa[2], Ritika Harish[1], Zhiping Li[1], Gideon Tolufashe[3], Hallgeir Rui[4], Beatrice S. Knudsen[5], Yanming Du[1], Hsin-Yao Tang[6], Peter Tompa[7], Richard G. Pestell[1]

[1]Pennsylvania Cancer and Regenerative Medicine Research Center, Baruch S. Blumberg Institute, Wynnewood, PA,[2]Institute of Molecular Life Sciences, HUN-REN Research Centre for Natural Sciences, Budapest, Hungary,[3]Baruch S. Blumberg Institute, Doylestown, PA,[4]Sidney Kimmel Cancer Center, Thomas Jefferson University, Philadelphia, PA,[5]University of Utah, Salt Lake City, UT,[6]The Wistar Institute, Philadelphia, PA,[7]HUN-REN Office for Supported Research Groups, Cell Cycle Laboratory, National Institute of Oncology, 1122 Budapest, Hungary, Budapest, Hungary

• **Introduction.** Prostate cancer “stemness” increases with tumor progression, predicts poor prognosis and contributes to therapy resistance. The *cyclin D1* gene (CCND1), which encodes the regulatory subunit of a holoenzyme that phosphorylates RB and conveys transcriptional properties, is expressed in prostate cancer and augments growth of some castrate resistant prostate cancers. Clinical trials are targeting the kinase activity of cyclin D1 in prostate cancer. The functional significance of the cyclin D1 E domain remained to be further defined. We investigated a potential kinase-independent function of cyclin D1 in prostate cancer. • **Methods**. Analysis of patient gene expression, tumor histology, gene knockout transgenic mice, tissue culture stem cell assays, proteomic analysis. • **Findings**. We show cyclin D1 expression is increased in PCa tumor stroma compared with adjacent tissue. Using single cell sequencing cyclin D1 we identified cyclin D1 in cancer associated fibroblasts. In vivo, cell markers of PCa stemness including Trop2^{ICD} activity. Deletion of both epithelial cell and stromal cyclin D1 further reduced markers of PCa stem cells suggesting a role for extra epithelial stromal cell cyclin D1 in the induction of PCa stemness. In vitro, cyclin D1 rescue of cyclin D1 deficient fibroblasts demonstrated cyclin D1 governed a secretome that augmented prostate cancer stemness, assessed by prostate cancer sphere size and number, and expression of pro-stemness chemokine receptors (CXCR2, CX3CR1). Mutational analysis showed the cyclin D1 heterotypic induction of stemness and chemokine receptor expression required an intrinsically disordered acidic rich “E domain” (AA 272-280) within the cyclin D1 carboxyl terminus. Integrated proteomics and ChIP Seq identified transcriptional targets governing cancer stemness and pro-tumorigenic inflammation. • **Conclusions.** Cyclin D1 augments prostate cancer stemness through heterotypic functions via an intrinsically disordered carboxyl terminal domain.

#2266 Unexpected role of nuclear receptor CAR in cholangiocarcinoma development.

Inyoung Cheon[1], Ji Ho Suh[2], Mi Jeong Heo[3], Sung Ho Lee[4], Hyun-Jung Jung[2], Young-Ho Ahn[1], David D. Moore[5], Kang Ho Kim[2]

[1]Molecular Medicine, Ewha Womans University School of Medicine, Seoul, Korea, Republic of,[2]Anesthesiology, Critical Care and Pain Medicine, University of Texas Health Science Center at Houston, Houston, TX,[3]University of Texas Health Science Center at Houston, Houston, TX,[4]Biomedical Laboratory Science, Gwangju Health University, Gwangju, Korea, Republic of,[5]University of California, Berkeley, Berkeley, CA

Cholangiocarcinoma (CCA), the second most common primary liver cancer, arises from the biliary epithelium, either within the liver parenchyma or in the hepatoduodenal ligament. Several cholestatic liver diseases, such as primary sclerosing cholangitis, developmental bile duct malformation, and progressive familial intrahepatic cholestasis (PFIC), have been implicated as CCA risk factors. Cholestatic conditions exhibit a cocarcinogenic effect when combined with chronic liver injuries, as supported by a recently reported CCA animal model in which partial bile duct ligation is combined with repeated treatments of the carcinogen diethylnitrosamine. The nuclear receptor Constitutive Androstane Receptor (CAR, NR1I3), a central regulator of xenobiotic metabolism, is known to drive hepatocellular carcinoma (HCC) when chronically activated, while CAR ablation prevents it in multiple liver cancer models. We have recently characterized the impact of endogenous CAR activation in a mouse model of human PFIC5 disease (*i.e.*, *Fxr;Shp* double knockout, FS-DKO) that exhibits cholestatic liver injury and develops spontaneous HCC at 1 year of age. In this study, we demonstrated the role of endogenous CAR activation in cholestasis-driven liver cancer development. Based on the strong correlation between CAR activation and liver cancer development in FS-DKO liver, we initially hypothesized that chronic CAR activation mediates hepatic carcinogenesis in FS-DKO liver. However, in contrast to our expectations, further deletion of CAR in *Fxr;Shp;Car* triple knockouts (FSC-TKO) did not reduce tumor incidence compared to FS-DKO. Instead, highly hypertrophic as well as hyperplastic cholangiocytes became much more abundant in FSC-TKO livers than in FS-DKO livers. Accordingly, about half of the visible FSC-TKO tumor nodules were CCA or combined HCC-CCA types, while most tumors in FS-DKO livers were hepatocellular types. Using RNA-seq and TRRUST transcription factor analysis, we found that CAR/PXR targets were significantly depleted in FSC-TKO, while ETS1 targets were significantly enriched, consistent with emerging evidence that ETS1 biases liver tumor fate toward CCA lineage. These findings suggest that, under cholestatic stress, loss of CAR unexpectedly promotes CCA development by unleashing a microenvironment that favors CCA. Targeting the CAR-ETS1 axis may offer new opportunities to modulate HCC-CCA lineage specification and improve therapeutic strategies.

#2267 Microenvironmental CTHRC1 has a pro-tumorigenic role in colorectal cancer.

Haylee Duval[1], Barbara Toomey[2], Michelle Karam[2], Brian Nestor[2], Sergey Ryzhov[2], Volkhard Lindner[2], Michaela Reagan[2]

[1]University of Maine, Orono, ME,[2]MaineHealth Institute for Research, Scarborough, ME

In the United States, colorectal cancer (CRC) is the third leading cause of cancer-related deaths in both men and women, with a projected 154,270 new cases in 2025 alone. These statistics highlight the need for a better understanding of the underlying mechanisms of CRC and the development of improved therapies, which are both critical steps in improving patient outcomes. CRC is characterized by extensive stromal cell involvement, which is believed to be tumor-supportive, and thus components of the tumor microenvironment (TME) are promising targets. Collagen triple helix repeat containing 1 (CTHRC1) is a secreted protein with known roles in metabolism, bone and joint homeostasis, tissue remodeling, extracellular matrix synthesis and organization, and, by unknown mechanisms, oncogenesis. Despite its known expression in tumor-associated stroma and correlations with poor prognosis in many cancers, causative evidence that host-derived CTHRC1 influences CRC progression is lacking, and its function within the TME remains poorly understood. Here, we assess the role of host-derived CTHRC1 in three independent *in vivo* studies using male and female wild-type (WT) and global *Cthrc1* null (KO) mice subcutaneously inoculated with MC38 colon cancer cells. Across all studies, our results clearly demonstrate that host-derived CTHRC1 drives CRC progression. Survival analysis showed significant improvement in *Cthrc1* KO mice ($p = 0.0012$, Kaplan-Meier), with median survival more than doubling from 28 days post-inoculation in WT ($n = 10$) to 69 days in *Cthrc1* KO ($n = 10$). Notably, initial tumor growth followed by tumor regression occurred in all three *Cthrc1* KO cohorts between Days 9-14 post-inoculation, while most WT tumors continued growing, suggesting CTHRC1 supports tumor cell immune evasion and contributes to a tumor-permissive TME. *Cthrc1* KO mice also developed significantly smaller tumors across all studies compared to WT, as measured by bioluminescent imaging, calipers, and postmortem tumor weights.Histological staining further revealed that the absence of CTHRC1 in the TME alters tumor microarchitecture and cellularity, with tumor density markedly reduced in *Cthrc1* KO mice by H&E staining and Likert scoring ($p = 0.0017$). Immune profiling identified clear differences in the composition of tumors and spleens between groups, with *Cthrc1* KO mice exhibiting an increased percentage of $CD3^+$ T cells in tumors ($p = 0.0014$) and spleens ($p = 0.0010$) and decreased splenic $Gr\text{-}1^+$ cells ($p = 0.0369$) by Mann-Whitney tests, consistent with reduced myeloid-driven T cell suppression, and suggests both stromal and circulating CTHRC1 may contribute to immunosuppression in WT mice. Together, these results identify CTHRC1 as a key driver of CRC by aiding in immune evasion and supporting tumor growth. In humans, CTHRC1 may hold great potential as a novel target in future CRC therapies.

#2268 Elucidating the role of *p21*$^{+}$ senescent cells in early-stage lung tumorigenesis.

Yuanning Du, Luis I. Prieto, Karthikbabu Jeganathan, Cheng Zhang, Hu Li, Darren Baker

Mayo Clinic, Rochester, MN

Cellular senescence is a dynamic, multistage biological program that exerts context-dependent effects on tumor initiation, progression, and overall carcinogenesis. Our laboratory has previously demonstrated that the early accumulation of $p16^{Ink4a}$-expressing (representing strong cyclin-dependent kinase inhibition) senescent alveolar macrophages during tumorigenesis actively facilitates tumor formation and progression by inhibiting the infiltration of cytotoxic T lymphocytes. However, considering the dynamic nature of cellular senescence, distinct senescent cell populations could express high amounts of the alternative cell cycle inhibitor $p21^{Waf1/Cip1}$ independently of $p16^{Ink4a}$ to potentially catalyze distinct functions. To test this, we have employed transgenic p21-*ATTAC* (p21-driven apoptosis through targeted activation of caspase 8) mice to investigate the role of p21-expressing cells during *Kras*-driven adenoma formation. In agreement with our previous observations following clearance of p16-expressing senescent cells, we found that removal of p21+ cells attenuates early tumor development. Western blot and immunofluorescence analyses corroborates a reduction in p21, p16, and multiple members of a putative senescence-associated secretory phenotype (SASP). Although senescent alveolar macrophages remain a critical therapeutic target, here we found that senescent endothelial cells also exhibited elevated expression of p21, p16, and SASP with a high senolytic response. Future studies will include identifying the predominant p21-expressing senescent endothelial subpopulations and elucidating the mechanisms by which endothelial senescence contributes to lung tumorigenesis. Collectively, our findings have unveiled additional senescent cell populations with the potential to drive lung tumorigenesis.

#2269 Two-step mechanism of plexiform neurofibroma formation: Role of the NF-κB pathway in neurofibroma formation.

Ramya Ravindran[1], Noemi Kedei[2], Eui-Kyung Youn[1], Kwangmin Choi[1], Avery Volz[1], Jay Pundavela[1], David A. Largaespada[3], Jack F. Shern[4], Nancy Ratner[1]

[1]Division of Experimental Hematology and Cancer Biology, Cincinnati Children's Hospital Medical Center, Cincinnati, OH,[2]Collaborative Protein Technology Resource, OSTP, Center for Cancer Research, National Institutes of Health, Bethesda, MD,[3]Departments of Pediatrics and Genetics, Cell Biology, and Development, University of Minnesota, Minneapolis, MN,[4]Pediatric Oncology Branch, Center for Cancer Research, National Institutes of Health, Bethesda, MD

Rationale: *NF1-/-* Schwann cells are the cells of origin in plexiform neurofibroma (PNF). This benign tumor formation occurs long after *Nf1* loss in mouse models of the disease, suggesting that Schwann cells undergo secondary changes during tumor formation. However, additional genetic hits are not observed in this tumor type. Single cell RNA-sequencing implicated NF-κB signaling as upregulated in established tumor formation. Consistent with the idea that NF-κB signaling is a tumor driving signal, in human and mouse neurofibromas p-65 was nuclear (active) in neurofibroma cells, some of which were Schwann cells (Kershner et al., 2022).
Methods: To test if activation of NF-κB signaling is a second step in neurofibroma formation we used a combination of multiplexed antibody staining, flow cytometry and RNA sequencing in tumors over their development. *In vitro* assays were utilized to determine the effect of NF-κB pathway modulation in *Nf1-/-* Schwann cells. Finally, we tested if blocking IKK2 activity *in vivo* reduces tumor formation or growth.
Results: We identified markers of Schwann cells, fibroblasts and immune cells in PNF by multiplex imaging and flow cytometry. Tumor Schwann cells, but not pre-tumor Schwann cells in the same mice, expressed the cell surface markers CD44 and CD49f; cultured *Nf1-/-* Schwann cells upregulate these markers and nuclear (active) p65 when exposed to stressors known to activate NF-κB signaling, including prolonged serum depletion, Poly I:C, IL1β, and TNFα, or when infected with activated IKK2, which activates the NF-κB pathway; these Schwann cells increased secretion of cytokines that are immune cell chemoattracts. Concurrent increases in EMT genes were observed *in vivo* and *in vitro*. Treatment of *DhhCre;Nf1fl/fl* mice with the NF-κB pathway inhibitor BAY 11-7082 combined with MEK inhibitor Mirdametinib reduced the CD44+ CD49f+ Schwann cell population, tumor cell proliferation, the tumor immune cell population, and tumor cytokines.
Conclusion: A two-step process to PNF formation is proposed, with *Nf1* loss in Schwann cells an initiating step and the formation of an inflammatory microenvironment via activation of the NF-κB pathway and Schwann cell reprogramming as a second step. (Supported by DOD-HT9425-1-0435 (to NR and JS), NIH NS115438R01 (to DAL and NR) and a Children’s Tumor Foundation Young Investigator Award to RR)

#2270 A MUC1-overexpressing epithelial population is associated with CDH1 loss-of-function gastric adenocarcinoma.

Chuner Guo[1], Rosyli F. Reveron-Thornton[1], Xiaomo Li[2], James P. Agolia[1], Maria Moozhiyil Korah[1], Peter Yuxin Xie[3], Amanda Goncalves[1], Angela Tabora[1], Lily Xia[4], Natali Barakat[4], George Poultsides[1], Byrne Lee[1], Amanda R. Kirane[1], Deshka Foster[1], Michael T. Longaker[1], Gregory W. Charville[2], Daniel Delitto[1]

[1]Department of Surgery, Stanford University School of Medicine, Stanford, CA,[2]Department of Pathology, Stanford University School of Medicine, Stanford, CA,[3]Department of Mechanical Engineering, Stanford University School of Medicine, Stanford, CA,[4]Stanford University School of Medicine, Stanford, CA

Germline mutations in CDH1 are associated with early-onset diffuse gastric adenocarcinoma. There is no gold standard for screening and management, and endoscopic surveillance is often insufficient for detecting early disease. Prophylactic gastrectomy is maximally preventive but is a major operation associated with significant morbidity and extensive lifestyle modifications. Therefore, there is a need to better understand the pathophysiological features underlying carcinogenesis in the setting of CDH1 mutation. To address this gap, we performed spatial transcriptomic profiling on 29 formalin-fixed paraffin-embedded sections from 8 patients with various stages of gastric adenocarcinoma, including one patient with a germline CDH1 mutation (c.1936+5G>A) found to have multifocal intramucosal poorly cohesive signet-ring cell carcinoma. Image-based cell segmentation and subcellular transcript detection enabled identification of diverse epithelial cell types, as well as their stromal and immune neighborhoods. Epithelial cells from the specimen harboring the germline CDH1 mutation expressed lower levels of CDH1 compared with other samples. Although morphologically normal-appearing, mucosal layers in these sections exhibited altered transcriptomic profiles characterized by an expanded epithelial population with high MUC1 expression. MUC1 is a transmembrane glycoprotein frequently upregulated in various cancers, with a cytoplasmic domain capable of interacting with several intracellular signaling partners, particularly β-catenin. Gene regulatory network analysis revealed a gradient of CTNNB1/β-catenin activation program, suggesting a potential interplay between CDH1 loss-of-function, MUC1 overexpression, and β-catenin pathway dysregulation. These findings reveal a novel MUC1-overexpressing epithelial population associated with CDH1 mutation and early-onset gastric adenocarcinoma, providing new rationales for developing surveillance biomarkers and targeted therapies.

#2271 p53-null cells act as supercompetitors in gastroesophageal tumor initiation.

Kyle LaBella, Efren Reyes, Mathijs Verhagen, Priyanka Kulkarni, Shadi Tarazi, Shawn Gillespie, Oana Ursu, Louis Vermeulen

Genentech, Inc., South San Francisco, CA

TP53 is the most frequently mutated gene in cancer and is often detected in histologically normal tissues decades before malignant transformation. p53-null cells possess a competitive advantage over neighboring wildtype cells, yet the mechanisms that restrain their outgrowth within healthy tissue or drive their expansion in disease remain poorly understood. Here, we investigated the role of p53 inactivation in a new model of Barrett's esophagus using long-term live-cell clonal tracing coupled with single-cell RNA sequencing. Using an epithelioid co-culture system of gastric stem cells and esophageal squamous epithelium, we found that gastric epithelial p53-loss confers a strong competitive advantage over neighboring wildtype esophageal squamous cells, leading to the expansion of mutant clones via the active suppression of adjacent wildtype cell proliferation. Mechanistically, these p53-null cells exhibit high levels of chromosomal instability, which drives an altered secretome that represses the growth of wildtype basal cells. Strikingly, p53-null cells remain resistant to these inhibitory factors. Additionally, neutral competition was restored either by deleting cell cycle checkpoint pathways in p53-wildtype neighbors or by blocking the pathways in p53-null cells that confer resistance to secreted inhibitory factors. Collectively, these findings reveal how p53 inactivation alters competitive stem cell dynamics at the gastroesophageal junction and suggest potential strategies for cancer interception in individuals with Barrett's Esophagus.

#2272 Dichotomous immunogenetic landscape of lung adenocarcinoma associated with usual interstitial pneumonia.

Akifumi Mochizuki[1], Ayako Suzuki[2], Kouya Shiraishi[3], Masahiro Torasawa[4], Takayuki Honda[1], Susumu Kirimura[5], Yasunari Miyazaki[1], Kenichi Okubo[6], Syuzo Kaneko[7], Yukihiro Yoshida[8], Shun-ichi Watanabe[8], Masahiro Tsuboi[9], Genichiro Ishii[10], Issei Imoto[11], Ryuji Hamamoto[12], Yasushi Yatabe[13], Yutaka Suzuki[2], Takashi Kohno[3]

[1]Department of Respiratory Medicine, Institute of Science Tokyo, Tokyo, Japan,[2]Department of Computational Biology and Medical Sciences, Graduate School of Frontier Sciences, The University of Tokyo, Kashiwa, Japan,[3]National Cancer Center Research Institute, Tokyo, Japan,[4]Division of Genome Biology, National Cancer Center Research Institute, Tokyo, Japan,[5]Division of Pathology, Institute of Science Tokyo, Tokyo, Japan,[6]Department of Thoracic Surgery, Institute of Science Tokyo, Tokyo, Japan,[7]Division of Medical AI Research and Development, National Cancer Center Research Institute, Tokyo, Japan,[8]Department of Thoracic Surgery, National Cancer Center Hospital, Tokyo, Japan,[9]Department of Thoracic Surgery, National Cancer Center Hospital East, Kashiwa, Japan,[10]Department of Pathology and Clinical laboratories, National Cancer Center Hospital East, Kashiwa, Japan,[11]Dept. of Human Genetics, Inst. of Health Biosciences, Aichi Cancer Center Research Institute, Nagoya, Japan,[12]Associate Professor, National Cancer Center Japan, Tokyo, Japan,[13]Chief, Dept. of Pathology & Molec. Diagnostics, National Cancer Center, Nagoya, Japan

Background: Interstitial pneumonia increases the risk of lung cancer; however, the underlying carcinogenic pathways remain poorly understood. Usual interstitial pneumonia (UIP) frequently co-localizes with lung adenocarcinoma (LADC), providing a model to understand chronic inflammation-driven carcinogenesis.

Method: We conducted whole-genome and RNA sequence of 44 UIP (+) LADCs and compared them with 216 UIP (-) LADCs. To address intra-tumoral heterogeneity and characterize the tumor microenvironment, we performed spatial transcriptomics using a whole-transcriptome platform (Visium, 55 µm resolution) and single-cell-resolution platforms (Xenium lung panel, 302 genes; Xenium 5K, 5,018 genes).

Results: UIP (+) LADCs exhibited unique molecular features: low tumor mutation burden, absence of EGFR mutations, and a pervasive presence of myofibroblastic cancer-associated fibroblasts (myCAFs), likely derived from fibrotic myofibroblasts in UIP. The most common genetic alteration was in NKX2-1 (41%), encoding the lung-lineage transcription factor TTF-1. A dichotomous immunogenetic landscape was observed: NKX2-1-deficient tumors showed gastrointestinal differentiation, frequent ERBB2 amplification with super-enhancer formation, and immune "cold" characteristics; NKX2-1-proficient tumors exhibited immune "hot" characteristics with abundant intra-tumoral CD8+ T cells and elevated PD-L1 expression. Spatial transcriptomics analysis revealed intratumor heterogeneity associated with NKX2-1 expression status, suggesting illegitimate gastrointestinal differentiation. In addition, the presence of WNT5A- and CTHRC1-expressing myCAFs were identified, which may originate from UIP-associated myofibroblasts. Paired tumor and UIP regions demonstrated that CTHRC1+WNT5A+ myCAF population was markedly enriched in tumor tissues relative to matched UIP regions, suggesting their expansion during carcinogenesis.

Conclusion: We propose a dual model of UIP-associated lung carcinogenesis determined by NKX2-1 status, wherein myCAFs derived from UIP-associated myofibroblasts drive both carcinogenic pathways. These findings offer targeted therapeutic strategies based on the dichotomous immunogenetic landscape and highlight targeting the myofibroblast-to-myCAF transition as a potential approach for cancer prevention in chronic pulmonary fibrosis.

#2273 Obesogen co-exposure promotes triple-negative breast cancer growth via adipocyte-mediated mechanisms.

Sarah M. Bernhardt, Mikella Robinson, Carrie House

San Diego State University, San Diego, CA

Introduction: Bisphenol A (BPA) and dichlorodiphenyldichloroethylene (DDE; the primary metabolite of DDT) are environmental 'obesogens' that independently associate with altered adipocyte function and increased breast cancer risk. While the effects of obesogens alone are well studied, particularly in hormone receptor (HR)-positive breast cancer, the biological consequences of combined exposure and their impact on HR-negative disease through adipocyte-tumor interactions remains poorly understood. Here, we investigate how obesogen co-exposure alters mammary adipocyte function and promotes tumorigenesis in a mouse model of triple-negative breast cancer (TNBC).

Study design: Post-pubertal BALB/c mice (n=10/group) were exposed to obesogens via drinking water for the duration of the study, at environmentally relevant doses (Vehicle (ethanol); BPA (4µg/kg/day); DDE (0.8µg/kg/day); combination (BPA+DDE)). After 2 weeks exposure, murine mammary cancer cells (4T1; 20,000 cells) were injected bilaterally into the fourth inguinal mammary fat-pads, and investigator-blinded tumor growth tracked for 21 days. To assess how obesogens affect adipocyte function *in vitro,* 3T3-L1 preadipocytes were differentiated in the presence of vehicle (0.03% ethanol), BPA (1nM), DDE (1µM), or combination (BPA+DDE), and adipokine secretion profiles assessed using an adipokine array.

Results: Mouse body weight did not differ between treatment groups. In tumor-free mammary glands, obesogen exposure associated with increased adipocyte size (BPA 1029±231µm^2, DDE 957±350µm^2, Combo 1011±344µm^2) compared to vehicle-treated mice (766±187µm^2; $p<0.05$). Interestingly, while individual exposures induced adipocyte hypertrophy, only combined exposure increased epithelial cell proliferation (Ki67), compared to vehicle-treated mice (2.8-fold, $p=0.02$). In tumors, combination treatment associated with increased tumor burden (1.4-fold, $p=0.02$) and proliferation (1.3-fold, $p=0.04$), compared to vehicle-treated mice. *In vitro,* obesogen exposure altered adipocyte secretion of 11/38 adipokines (>2-fold change), 6 of which were unique to combination-treated adipocytes (up: LIF; down: IGF-II, VEGF, M-CSF, CCL2, adiponectin). Exposure of 4T1 cells to this conditioned media increased proliferation (EdU), compared to vehicle controls (1.5-fold, $p=0.04$). Future directions will investigate whether inhibition of LIF/LIFR signaling abrogates obesogen-induced proliferation.

Conclusions: Co-exposure to BPA and DDE synergistically promotes TNBC proliferation at environmentally relevant doses, underscoring the need to study obesogens in the context of real-world co-exposures. The effects on HR-negative disease occurred independent of obesity and were mediated, at least in part, through adipocyte-derived mechanisms, highlighting the need to expand research beyond HR-positive breast cancer.

#2274 Cigarette smoke-induced sphingosine-1-phosphate drives cancer-associated fibroblasts activation and esophageal cancer carcinogenesis.

Xinying Yue[1], Jialing Ma[1], Zifei Yang[1], Yutong Wu[1], Qianqian Su[1], Lina Song[1], Miaoxin Pan[1], Dongxu Li[2], Qingyi Liu[2], Shasha Liu[1], Yueping Li[1], Shaokai Zhang[3], Siyuan Wang[4], Li Zhang[5], Ni Zhang[5], Wei Ping[5], Catherine C. L. Wong[4], Dongxin Lin[2], Chen Wu[2], **Jiang Chang**[1]

[1]Huazhong University of Science and Technology, Wuhan, China,[2]Cancer Hospital, Chinese Academy of Medical Sciences, Beijing, China,[3]The Affiliated Cancer Hospital of Zhengzhou University, ZhengZhou, China,[4]Chinese Academy of Medical Science & Peking Union Medical College, Beijing, China,[5]Tongji Hospital, Tongji Medical College, Huazhong University of Science and Technology, Wuhan, China

The metabolic impact of cigarette smoke on tumor microenvironment remodeling remains poorly defined. Here, we identify a missense variant in *ACER1* that confers elevated risk of esophageal squamous cell carcinoma (ESCC) specifically among smokers, based on a gene-smoking interaction analysis involving 10,716 cases and 12,637 controls. Functional assays demonstrate that the risk allele synergizes with nicotine and benzo[a]pyrene to enhance sphingosine-1-phosphate (S1P) biosynthesis and secretion in ESCC epithelial cells. Integrated single-cell RNA sequencing, spatial proteomics, and multiplex immunofluorescence analyses across multi-stage ESCC samples reveal that this ACER1-driven sphingolipid reprogramming promotes the activation of myofibroblastic cancer-associated fibroblasts (myCAFs). Mechanistically, epithelial-secreted S1P engages the S1PR3-ERK-AKT signaling cascade in fibroblasts, promoting a pro-tumorigenic stromal state. Pharmacological inhibition of S1PR3 markedly suppresses ESCC growth *in vivo*. These findings uncover a critical gene-environment interaction driving pro-tumorigenic microenvironmental remodeling in esophageal tumorigenesis and highlight a metabolic vulnerability for early detection and therapeutic intervention.

#2275 Biological impact of nanoplastics on the tumor microenvironment.

Tetsuya Fukui[1], Ryota Sumitomo[1], Kosuke Tanaka[2], Toshi Menju[1]

[1]Thoracic Surgery, Kyoto University Graduate School of Medicine, Kyoto, Japan,[2]Material Cycles Division, National Institute for Environmental Studies, Tsukuba, Japan

Objectives: Nanoplastics (NPLs), generated through the degradation of environmental plastics, are emerging contaminants with potential biological risks. Although recent studies have detected NPLs in human lungs and blood, their effects on human cells remain poorly understood due to the lack of standardized particles. Previous research has predominantly relied on commercially available polystyrene particles, which may contain impurities and display heterogeneity in size and shape, leading to concerns regarding reproducibility. To overcome these limitations, standardized NPLs with uniform size and shape, free from contaminants, have recently been developed by the National Institute for Environmental Studies. In this study, we aimed to investigate the effects of these standardized NPLs on immune responses and tumor progression.

Methods: Standardized polypropylene (PP)-based NPLs were subjected to UV irradiation to simulate environmental weathering. The particles were then dispersed in distilled deionized water by sonication. Particle size distribution was confirmed by dynamic light scattering. THP-1 cells (a human monocytic cell line) were treated for 24 h with phorbol 12myristate 13-acetate to differentiate them into macrophages. A549 cells (a human lung adenocarcinoma cell line) and THP-1-derived macrophages were exposed to these NPLs. Additionally, A549 cells and NPL-exposed macrophages were co-cultured using a six-well Transwell system for 48 hours. Cytotoxicity was evaluated using MTT assays, and protein expression was assessed by Western blotting. Phenotypic changes associated with EMT were evaluated by transwell migration and invasion assays.

Results: NPLs were stably dispersed with an average diameter of approximately 400 nm as measured by dynamic light scattering. No significant cytotoxicity was observed in A549 cells at PP concentrations up to 250 μg/mL. Direct exposure of A549 cells to NPLs did not induce epithelial-mesenchymal transition (EMT). In contrast, THP-1-derived macrophages exposed to NPLs exhibited increased expression of CD163, suggesting polarization toward a tumor-promoting phenotype. When NPL-exposed macrophages were co-cultured with A549 cells in a Transwell system, co-cultured A549 cells displayed EMT-like features, including reduced E-cadherin and elevated vimentin expression compared to parental cells. Functionally, co-cultured A549 cells exhibited significantly enhanced migratory and invasive abilities compared to parental cells.

Conclusions: This study demonstrates that PP-based NPLs can alter immune cell behavior and indirectly promote tumor progression by shaping the tumor microenvironment. We established an exposure model using standardized NPLs that reflect the intrinsic physicochemical properties of the particles.

: Hormone Receptor Signaling and Therapeutic Targeting
Poster Session

#2279 DNA methylation-based classifier predicts SERD benefit in *ESR1* wild-type HR+/HER2- breast cancer.
Shile Zhang, Nicole Zhang, Vishnu Ramani, Tingting Jiang, Marisa Juntilla, Amar Das, Martina Lefterova, Justin Odegaard, Darya Chudova, Matthew Ellis

Guardant Health, Palo Alto, CA

Background: Resistance to aromatase inhibitors (AIs) in hormone receptor-positive (HR+) metastatic breast cancer (mBC) is inevitable and frequently driven by *ESR1* mutations. Selective estrogen receptor degraders (SERDs) target estrogen receptors for degradation and provide clinical benefit in this setting. *ESR1* mutations are established biomarkers guiding transition from AI to SERD-based endocrine therapy. However, many patients lack detectable *ESR1* mutations, and no validated biomarker exists to guide SERD use in *ESR1* wild-type (*ESR1-wt*) patients. We investigated whether a blood-based, DNA methylation-derived hormone receptor (mHR) activity score could predict SERD benefit in *ESR1-wt* patients.
Methods: An mHR activity score was developed using a logistic regression model integrating over 400 most informative regions from genome-wide methylation capture of Guardant360 Liquid test. mHR-high/-low thresholds were defined using >2,000 clonal *ESR1-mutant* mBC samples. Validation was performed in a real-world *ESR1-wt* cohort (N=765) with post-AI progression plasma samples from the GuardantINFORM database. Clinical outcomes defined by time to treatment discontinuation (TTD) of SERD or chemotherapy were evaluated across mHR-high/-low groups using Kaplan-Meier methods and multivariable Cox models, adjusting for tumor fraction, age, and treatment type.
Results: Across >12,000 breast cancer samples tested with Guardant360 Liquid, the mHR activity score was positively correlated with *ESR1* mutation status and higher in tumors with clonal versus subclonal *ESR1* mutations. In the *ESR1-wt* validation cohort, mHR-high patients showed significantly longer median TTD with SERD treatment (Fulvestrant mono or combination) compared to mHR-low patients (adjusted hazard ratio: 0.44, 95%CI: 0.21-0.89; $p = 0.02$; median TTD 107 vs. 89 days). Moreover, mHR status predicted relative benefit from SERD versus chemotherapy: among mHR-high patients, SERD treatment yielded significantly longer TTD than chemotherapy (adjusted hazard ratio: 0.41; 95%CI: 0.21-0.81; $p = 0.01$; median TTD 107 vs. 87 days), while mHR-low patients exhibited a trend towards shorter TTD on SERD versus chemotherapy (adjusted hazard ratio: 1.83; 95% CI: 0.87-3.87; $p = 0.11$; median TTD 89 vs. 108 days).
Conclusions: A blood-based DNA methylation-derived mHR score captures hormone receptor-driven epigenetic activity and predicts benefit from SERD therapy in *ESR1*-wt HR+ mBC. This classifier enables real-time, noninvasive stratification of *ESR1*-wt patients, identifying a molecularly defined subset more likely to derive benefit from SERD-based therapy. These findings support the potential clinical utility of methylation-based biomarkers to extend precision endocrine therapy beyond *ESR1* mutation profiling.

#2280 Ligand-activated AR promotes the survival of endocrine therapy-responsive ER+ breast cancer.

Patrick Aouad[1], Eliah Shamir[2], Jackson Liang[3], Liang-Fu Chen[1], Vasumathi Kameswaran[4], Lisa Crocker[5], Marc Hafner[6], Bence Daniel[4], Antonina Hafner[1], Ciara Metcalfe[1]

[1]Discovery Oncology, Genentech, Inc., South San Francisco, CA,[2]Pathology, Genentech, Inc., South San Francisco, CA,[3]Translational Medicine - Oncology, Genentech, Inc., South San Francisco, CA,[4]Proteomic and Genomic Technologies, Genentech, Inc., South San Francisco, CA,[5]Translational Oncology, Genentech, Inc., South San Francisco, CA,[6]Oncology Bioinformatics, Genentech, Inc., South San Francisco, CA

Giredestrant, a next-generation oral selective ERα degrader (SERD), is a potent and full antagonist that recently demonstrated statistically significant and clinically meaningful improvement in progression free survival (PFS) in the phase III evERA Breast Cancer trial (NCT05306340). Given its potent ER antagonism, giredestrant is currently under evaluation in multiple clinical studies, including those involving premenopausal participants with an intact hypothalamus-pituitary-ovary (HPO) axis, both with and without gonadotropin-releasing hormone (GnRH) agonists. To anticipate potential mechanisms of tumor cell survival and resistance, we sought to investigate the biology of giredestrant response in tumor-bearing mice with an intact HPO axis, using the intraductal xenograft model- a physiologically relevant system for ER+ breast cancer that supports tumor growth without exogenous estrogen. We established and characterized multiple ER+ breast cancer cell lines and patient-derived intraductal xenografts with distinct growth and metastatic profiles. Giredestrant treatment significantly suppressed tumor proliferation and reduced invasive and metastatic burden. Transcriptomic and chromatin profiling of giredestrant-treated tumors revealed a marked decrease in gene sets and chromatin sites associated with ER signaling and proliferation, as anticipated. Unexpectedly, giredestrant treatment also consistently led to the activation of androgen receptor (AR) signaling, which was accompanied by increased AR motif accessibility and chromatin occupancy. We find that systemic ER inhibition engages the HPO axis, resulting in increased ovarian production of testosterone, and thus driving ligand-dependent AR activation in tumor cells. Dual inhibition of ER and AR demonstrated enhanced anti-proliferative effects compared to ER antagonism alone. Transcriptomic data suggest that this is mediated by the suppression of proliferation-associated programs, potentially through PI3K/mTOR pathway inhibition. By leveraging the novel mouse intraductal model, we identified dual ER and AR blockade, as well as ER-PI3K/mTOR pathway co-targeting, as promising therapeutic strategies to improve outcomes for premenopausal women with ER+ breast cancer, particularly those not receiving GnRH agonists.

#2281 AZD4241, an orally bioavailable ERα PROTAC, degrades wild-type and mutant ERα and delivers anti-tumour activity in preclinical breast cancer models.

Mandy Lawson[1], Natalie Cureton[1], Lynet Nyoni[1], Sophie D'Arcy[1], Lydia Parkinson[1], Ana Quiroga[1], Pablo Morentin Gutierrez[1], Ji Li[2], Hana Baakza[1], Thomas Hayhow[1], Claire Crafter[1], Lucy Ireland[1], Gemma Hardman Fowler[1], Georgia M. Simmons[3], Lakjaya Buluwela[3], Simak Ali[3], Neil Gibson[1]

[1]Oncology Targeted Discovery, AstraZeneca R&D, Cambridge, United Kingdom,[2]Translational Medicine, AstraZeneca R&D, Waltham, MA,[3]Department of Surgery and Cancer, Imperial College London, London, United Kingdom

Estrogen receptor alpha (ERα) is a member of the nuclear hormone receptor superfamily and a key driver of hormone receptor-positive (HR+) breast cancer. Current ER-pathway inhibitors include aromatase inhibitors (letrozole, anastrozole, exemestane), selective estrogen receptor modulators (SERMs; tamoxifen), and selective estrogen receptor degraders (SERDs; fulvestrant, elacestrant, imlunestrant). In metastatic ER-positive disease, resistance is common and often involves the emergence of ESR1 mutations (e.g., Y537S, D538G). These mutations occur in the ligand-binding domain of ERα and enable ligand-independent ER activation, reducing the effectiveness of aromatase inhibitors and some antagonists. This underscores the need for novel treatments that target ER in both wild-type (ESR1wt) and mutant (ESR1m) settings, including more effective ERα degraders, as demonstrated clinically by SERDs. Here we characterise AZD4241, a novel ER-targeting proteolysis targeting chimera (PROTAC), that degrades both wt and mutant ERα and delivers anti-tumour efficacy in preclinical breast cancer models. AZD4241 degraded ERα in ESR1wt cell lines (IC_{50} 0.4 nM in MCF7 cells) and showed good oral bioavailability across species. ERα half-life was reduced through PROTAC-mediated degradation requiring cereblon engagement and proteasomal activity. In MCF7 cells engineered to express clinically relevant ESR1 mutations, AZD4241 reduced ERα with degradation potency (IC_{50} 0.2-1.0 nM) comparable to ESR1wt controls. AZD4241 completely inhibited estradiol-induced gene expression (e.g., GREB1, PGR, and TFF1) and suppressed proliferation of ER-dependent breast cancer cell lines with low-nanomolar IC_{50} values. In vivo, AZD4241 induced dose-dependent anti-tumour activity and, in some cases, tumour regressions across ESR1wt and ESR1m patient-derived xenograft (PDX) models, including a palbociclib-resistant model. Efficacy was associated with marked reductions in ERα protein levels and decreased ER pathway activity, supporting a pharmacodynamic link between target degradation, suppression of ER signalling and efficacy. Collectively, these data confirm that AZD4241 is a potent, orally bioavailable degrader of wt and mutant ERα, driving anti-tumour efficacy in ESR1wt, ESR1m, and CDK4/6 inhibitor-resistant PDX models. These findings support the use of AZD4241 as a novel ER-PROTAC with potential to overcome key resistance mechanisms to current standards of care and deliver clinical benefit for patients with ER-positive breast cancer.

#2282 Targeting estrogen receptor mutations and aberrant myelopoiesis in hormone resistant breast cancer.

Maria Belen Villegas[1], Mario Morales Martinez[1], Javier Mansilla[2], Eduardo Mauricio Gonzalez[1], Begona Comin-Anduix[1], Marisol Chavez[1], Brian Aguirre[3], Gang Deng[2], Nalo M. Hamilton[4], Madhuri Wadehra[3], Michael E. Jung[2], Richard J. Pietras[1], Diana C. Marquez Garban[1]

[1]Medicine, UCLA David Geffen School of Medicine and Jonsson Comprehensive Cancer Center, Los Angeles, CA,[2]Chemistry and Biochemistry, UCLA and Jonsson Comprehensive Cancer Center, Los Angeles, CA,[3]Pathology and Laboratory Medicine, UCLA David Geffen School of Medicine and Jonsson Comprehensive Cancer Center, Los Angeles, CA,[4]UCLA School of Nursing, Los Angeles, CA

Breast cancer (BC) is the most commonly diagnosed cancer among women worldwide. In the U.S., it is the second leading cause of cancer-related mortality among women and the leading cause of cancer death among Hispanic and African American women. Approximately 70% of BCs express estrogen receptor alpha (ERα), which plays a central role in driving tumor development and progression. Endocrine therapy provides durable clinical benefit, as evidenced by significant reductions in local, contralateral and distant recurrence and by improvement in overall survival, with effects persisting long after treatment cessation. Despite its efficacy, development of acquired or intrinsic resistance remains a major obstacle in BC management. A key mechanism of resistance involves somatic mutations in the ESR1 gene, most commonly Y537S and D538G, which stabilize the ligand-binding domain in a constitutively-active conformation, thereby enabling ligand-independent ER signaling and diminishing effectiveness of aromatase inhibitors and tamoxifen. Until recently, fulvestrant was the only selective estrogen receptor degrader (SERD) available to counteract endocrine resistance; however, two next-generation SERDs, elacestrant and imlunestrant, have now received FDA approval. This underscores the continued need for advanced SERDs capable of effectively targeting both wild-type (WT) and mutant ERα while minimizing adverse effects. We have developed novel oral SERDs designed to degrade both WT and mutant ERα. To assess their anti-tumor activity, we evaluated these compounds in BC cell lines with and without Y537S and D538G ERα mutations. Treatment with our SERDs significantly reduced cell proliferation in a dose-dependent manner ($P<0.01$) and consistently decreased ERα protein levels in both WT and mutant cell lines. These effects were comparable to, or exceeded, those observed with current FDA-approved SERDs such as fulvestrant and elacestrant. Additionally, SERD treatment resulted in reduced ESR1 mRNA levels. ERα knockdown in BC cells abrogated SERD activity, confirming that their mechanism of action is ERα-dependent. Moreover, SERD JD128 demonstrated potent *in vivo* efficacy against MCF7-Y537S xenografts in humanized BLT-NSG-SGM3 mice ($P<0.01$). Analysis of the tumor immune microenvironment (TME) revealed that JD128 treatment increased T-cell infiltration compared with controls. These findings indicate that our SERDs represent promising therapeutic candidates for ERα-positive BC that has developed resistance to existing endocrine therapies. Furthermore, combining endocrine agents with immunotherapy may help mitigate immune suppressive myeloid populations within the TME and enhance T-cell-mediated anti-tumor responses. Funding: CIRM DISC2-14166, UCLA JCCC BC Award, Tower Cancer Res Found, Hickey Foundation, NIH/NCI U54 CA143930 CDU-UCLA JCCC Partnership, CBCRPB27IB3869, DOD BCRPBC181420.

#2283 Obesity predicts greater changes in Ki67 after neoadjuvant aromatase inhibitor therapy in early-stage ER+ breast cancer.

Mary Dickinson Chamberlin[1], **Lillian A. Lawrence**[2], Roberta M. DiFlorio-Alexander[1], Victoria Jones[1], Eugene Demidenko[1], Jonathan Marotti[1]

[1]Dartmouth Cancer Center, Lebanon, NH,[2]Geisel School of Medicine at Dartmouth, Hanover, NH

Background: Nearly 70% of breast cancers are ER positive (ER+), and anti-estrogen therapy, such as tamoxifen and aromatase inhibitors (AI), are a mainstay of treatment. Neoadjuvant endocrine therapy (NET) with aromatase inhibitors is effective at reducing tumor burden and may be predictive of better long-term outcomes. A significant decrease in Ki-67 is prognostic but additional predictive clinical factors for improved response to NET are not well understood. Preliminary data from our post-menopausal cohort of women with ER+ early-stage breast cancers treated with NET presented at the San Antonio Breast Cancer Symposium 2025, showed correlation between larger tumor sizes and greater radiographic response to NET with 68% of tumors exhibiting a radiographic response. Women with higher BMI have a higher risk of breast cancer recurrence and mortality, hypothesized to be due to incomplete suppression of aromatase but specific data on response to NET is lacking.
Objective: Determine the association between BMI and change in Ki67 expression after NET in patients with early-stage breast cancer.
Methods: 150 post-menopausal women with Stage I-III ER+, HER2- breast cancer were treated with an aromatase inhibitor for 7-168 days (mean 42.83 days) prior to surgery and had BMI, pre- and post-NET Ki67 immunohistochemistry available. Digital Ki-67 analysis on the diagnostic biopsy before NET was compared to Ki-67 on the surgical specimen. Statistical analysis determined p-values from the pairwise t-test. Control group analysis is in progress.
Results: The mean Ki-67 prior to NET was 18.62% (range 0.69%- 61.56%). The mean Ki-67 after NET was 4.17% (range 0.04%-46.07%). The mean radiographic baseline tumor size 20.9 mm. We found that both BMI and the baseline tumor size significantly correlated with Ki-67 expression difference ($p=0.038$ and $p= 0.026$, respectively). For example, based on our analysis, it is expected that women with a BMI = 30, there will be a two-fold decrease in post-NET Ki-67 expression. There was no significant correlation between change in Ki-67 and number of days on NET.
Discussion: In our cohort, higher BMI was associated with a greater decrease in Ki-67 expression compared to women with BMI <30, suggesting greater suppression of cell proliferation by NET in obese women. Suppression of Ki-67 is considered a good prognostic indicator, therefore this preliminary data contradicts the hypothesis that poorer outcomes for women with breast cancer and a BMI >30 are due to insufficient response to aromatase inhibitors. Additional research is needed to further elucidate these findings and validate this data against long-term AI adherence and other predictors of outcomes.

#2284 Progesterone receptor modulates the antigen processing and presentation machinery: Decreasing MHC class I expression on tumor.

Julio Tinoco[1], Eilidh Chowanec[2], Amanda Glen Heard[3], Christy R. Hagan[2]

[1]University of Kansas Cancer Center, Kansas City, KS,[2]University of Kansas Medical Center, Kansas City, KS,[3]University of Kansas Medical Center, Kansas City, MO

Hormone receptor (HR)-positive breast cancers, which account for approximately 75% of all breast cancers and express both estrogen receptor (ER) and progesterone receptor (PR), have been the focus of extensive research. Anti-estrogen and ER-targeted therapies have been highly successful in treating HR+ breast cancer; however, more than one-third of patients eventually develop resistance, underscoring the need for new targeted strategies. Unlike ER, the role of PR in breast cancer progression and immune modulation remains less explored. In previous work, we found that a mouse mammary tumor cell line (E0771) engineered to express mouse progesterone receptor (mPR) and the ovalbumin (OVA) peptide exhibited reduced T-cell-mediated cytotoxicity following progesterone treatment compared with control cells. This progesterone-mediated protection occurred only in mPR+ cells. Flow cytometric analysis further demonstrated decreased MHC class I surface expression in progesterone-treated E0771-Ova-mPR cells relative to vehicle controls. To investigate the underlying mechanisms, we analyzed the expression of genes involved in antigen processing and presentation (APP) of MHC class I molecules. Progesterone treatment reduced RNA levels of Tap1, Tap2, Tapbp, Nlrc5, B2m, and Psmb8, which are essential components of the APP pathway. These findings suggest that progesterone receptor activation suppresses the antigen presentation machinery, leading to reduced MHC class I expression and impaired recognition by cytotoxic T cells. Collectively, our data indicate that progesterone signaling may contribute to immune evasion in HR+ breast cancer through transcriptional regulation of MHC class I APP genes.

#2285 TGFβ Induction: An essential tumor suppressive arm of next generation SERDs in ER+ breast cancer models *in vitro*.

Kareem Heslop[1], Jackson Liang[1], Steffan Vartanian[2], Jinchu Vijay[1], Liang-Fu Chen[1], Marc Hafner[3], Michael Costa[1], Ciara Metcalfe[4]

[1]Discovery Oncology, Genentech, Inc., South San Francisco, CA,[2]Genentech, SOUTH SAN FRANCISCO, CA,[3]Scientist, Genentech, South San Francisco, CA,[4]Genentech, Inc., South San Francisco, CA

Breast cancer is the most diagnosed cancer globally, with a significant need for improved treatments for the most prevalent Estrogen Receptor α (ER)-positive subtype, where ER signaling drives cell proliferation.The next-generation oral Selective ER antagonist and degrader (SERD), giredestrant, is a potent investigational agent that robustly suppresses tumor cell proliferation. However, primary and acquired resistance pose a major challenge to all endocrine therapies including oral SERDs, necessitating a deeper understanding of resistance mechanisms.

In a comprehensive whole-genome CRISPR screen, we sought to identify genetic perturbations that confer a growth advantage in the presence of giredestrant. Notably, knockout of multiple TGFβ signaling components (TGFβ3, SMAD4, IPO8, TGFβR2) consistently freed ER+ cells from giredestrant-induced cell cycle arrest. We establish an unexpected autocrine mechanism: by suppressing the ER pathway, giredestrant induces the expression and signaling of the tumor suppressor TGFβ3. This induced TGFβ signaling then elevates CDKN1A (p21) levels, which precedes the inhibition of its natural target, CDK2.

We demonstrate that this TGFβ→p21-|CDK2 axis is necessary for giredestrant to achieve its maximal inhibitory effect in vitro. Molecular profiling confirmed CDKN1A was among the most significantly suppressed genes when TGFβ signaling was inhibited in combination with giredestrant. Crucially, combining giredestrant and a TGFβ inhibitor led to resistance, but this was partially overcome by a combination of CDK4/6 and CDK2 inhibition. This finding shows that CDK4/6/2 blockade can bypass, in-part, the requirement for the p21 cell cycle brake.

Collectively, our results reveal that giredestrant's in vitro efficacy relies on an autocrine TGFβ loop to mediate the necessary G1 arrest. The inhibition of TGFβ creates a resistance mechanism by neutralizing this essential tumor-suppressive signaling component.

#2286 Monitoring response to camizestrant next-generation oral SERD in ER+ advanced breast cancer patient-derived xenografts via circulating tumor DNA profiling.

Susana Ros*[1], Paul Labrousse*[2], Hugh Russell[2], Fryer Henderson[3], Sara Talbot[1], Benjamin Phillips[4], Teresa Klinowska[5], Christopher Morrow[5], Claire Crafter[1], Daniel Stetson[2], Darren Hodgson[6], James Hadfield[6]

[1]Research and Early Development, Oncology R&D, AstraZeneca, Cambridge, United Kingdom,[2]Cancer Biomarker Development, Oncology R&D, AstraZeneca, Waltham, MA,[3]Cancer Biomarker Development, Oncology R&D, AstraZeneca, Gaithersburg, MD,[4]Discovery Sciences, BioPharmaceuticals R&D, AstraZeneca, Cambridge, United Kingdom,[5]Late Development, Oncology R&D, AstraZeneca, Cambridge, United Kingdom,[6]Cancer Biomarker Development, Oncology R&D, AstraZeneca, Cambridge, United Kingdom

Background: While circulating tumor DNA (ctDNA) is widely used clinically for disease monitoring, its preclinical application has been limited by perceived constraints of small blood volumes in animal models. Patient-derived xenograft (PDX) models offer unique advantages for ctDNA analysis, as human tumor DNA can be distinguished from murine background DNA, enabling clearer assessment of treatment-induced changes compared to clinical samples where tumor and normal DNA separation is more complex.
Methods: We developed a preclinical ctDNA monitoring platform using ER-positive advanced breast cancer PDX models, including both wild-type and ESR1-mutant tumors. Digital Droplet PCR (ddPCR) informs whether sufficient human ctDNA levels are present (human repeat elements) to perform next generation sequencing (NGS). This feature allows the ability to monitor ctDNA levels over time, in response to various therapies. Mice received camizestrant, a next-generation oral selective estrogen receptor degrader (SERD), as monotherapy and in combination with CDK4/6 inhibition. Human-specific LINE-1 DNA levels and variant allele frequency (VAF) of tumor-specific somatic mutations were quantified in mouse plasma samples and correlated with tumor volume measurements.
Results: Treatment with camizestrant, either as monotherapy or in combination with CDK4/6 inhibition, resulted in significant reductions in tumor volume and growth rate in both wild-type and ESR1-mutant PDX models which correlated with marked decreases in human-specific LINE-1 in mouse plasma, as measured by ddPCR. Variant allele frequency in ctDNA decreased significantly, correlating with anti-tumor efficacy following treatment with camizestrant monotherapy or in combination with CDK4/6 inhibition.
Conclusions: This study establishes a robust, minimally invasive preclinical platform for evaluating ctDNA-based biomarkers and treatment efficacy in oncology research. The approach enables investigation of ctDNA release biology and treatment response in preclinical models that are difficult to address using human samples alone. These findings demonstrate the translational potential of preclinical ctDNA monitoring to inform clinical biomarker strategies and optimize therapeutic development in ER+ breast cancer.

#2287 Minimal-length CAG repeats in AR define a hyperactive AR-LSD1 axis driving metabolic reprogramming in prostate cancer.

Songqi Zhang[1], Muqing Li[1], Mingyu Liu[1], Nolan D. Patten[1], Maryam Labaf[1], Jaeweon Jeong[1], HyeonYeong Sun[1], Jared G. Lourie[2], Kai Zou[2], Susan Patalano[1], Jill A. Macoska[1], Shuai Gao[3], Dong Han[1], Maria Pennuto[4], Steven P. Balk[5], Changmeng Cai[1]

[1]Center for Personalized Cancer Therapy, University of Massachusetts Boston, Boston, MA,[2]Department of Exercise and Health Science, University of Massachusetts Boston, Boston, MA,[3]Department of Cell Biology and Anatomy, New York Medical College, Valhalla, NY,[4]Department of Biomedical Sciences, University of Padova, Padova, Italy,[5]Hematology-Oncology Division, Department of Medicine, Beth Israel Deaconess Medical Center, Boston, MA

Background: Racial disparities in prostate cancer (PCa) incidence and mortality are well recognized, with men of African ancestry (AA) exhibiting more aggressive disease. One germline genetic factor contributing to this disparity is the polymorphic CAG trinucleotide repeat in the first exon of the androgen receptor (AR) gene, which encodes a variable-length polyglutamine (polyQ) tract within the AR N-terminal domain. Shorter polyQ tracts, commonly found in the AA population, are reported to associate with enhanced AR transcriptional activity and increased PCa risk. Notably, minimal-length CAG repeats, defined as ≤17, are present in ~10% AA men but are rare among men of European ancestry (EA). These encode ultrashort polyQ tracks, however, how such variations alter AR chromatin function, its transcriptional output, metabolic reprogramming, and therapeutic response remains unclear.
Methods: We performed CRISPR/Cas9 editing to generate isogenic LNCaP-derived prostate cancer cell lines harboring minimal-length CAG repeats (10Q) AR alleles. Integrated analyses combining RNA-seq, ChIP-seq, and functional studies in vitro and in vivo were conducted to define the transcriptional, epigenetic, and metabolic consequences of ultrashort polyQ AR.
Results: The 10Q AR variant exhibited markedly reduced proteasomal degradation, leading to enhanced AR protein stability and resistance to AR antagonist-induced protein degradation. Genome-wide analyses revealed markedly expanded AR chromatin binding and redistribution of the pioneer transcription factor FOXA1, accompanied by transcriptional activation of lipid biosynthesis and glycolysis genes. Mechanistically, the ultrashort polyQ tracks strengthened AR interaction with the epigenetic coactivator LSD1, enhancing its coactivator activity. Pharmaceutical inhibition of LSD1 with iadademstat (ORY-1001) suppressed AR-mediated metabolic reprogramming and significantly reduced tumor growth in 10Q xenograft models.
Conclusion: Minimal-length CAG repeats in AR establish a hyperactive AR-LSD1 chromatin axis that drives transcriptional and metabolic reprogramming, leading to prostate cancer progression. These findings link inherited germline AR polymorphism to epigenetic-metabolic remodeling and identify LSD1 inhibition as a promising therapeutic strategy for aggressive and racially disparate PCa subtypes harboring minimal-length CAG repeats.

#2288 Neoadjuvant treatment of ER-positive/HER2-negative breast cancer with aromatase inhibitors in sequence: Ki67 dynamics and biology shifts.

Kamilla Fjermeros[1], Julius Johannes Grindahl Hettich[1], Stephanie Beate Geisler[1], Unn-Cathrin Buvarp[1], Hilde Presterud Odegard[1], Elin Edda Seland Agustsdottir[2], Laurens Cornelus Reitsma[3], Nazli Bahrami[3], Vessela N. Kristensen[4], Xavier Tekpli[5], Torben Luders[6], Andliena Tahiri[7], Manouchehr Seyedzadeh[8], Torill Sauer[9], Silje Mathiassen[10], Sofie Flovik Ranestad[10], Clara Hammarstrom[10], Jurgen Geisler[11]

[1]Department of Oncology, Akershus Univ. Hospital, Lorenskog, Norway,[2]Department of Breast & Endocrine Surgery, Akershus University Hospital, Lorenskog, Norway,[3]Department of Breast & Endocrine Surgery, Akershus Univ. Hospital, Lorenskog, Norway,[4]Oslo University Hospital, Institute for Cancer Research, Oslo, Norway,[5]Department of Medical Genetics & Department of Pathology, Oslo University Hospital, Oslo, Norway,[6]Institute of Clinical Medicine, Faculty of Medicine, Oslo University Hospital, Oslo, Norway,[7]Department of Clinical Molecular Biology (EPIGEN), Akershus Univ. Hospital, Lorenskog, Norway,[8]Department of Radiology, Akershus Univ. Hospital, Lorenskog, Norway,[9]Institute of Clinical Medicine, Faculty of Medicine, University of Oslo, Oslo, Norway,[10]Department of Pathology, Akershus Univ. Hospital, Lorenskog, Norway,[11]Department of Oncology & Institute of Clinical Medicine, Faculty of Medicine, Akershus Univ. Hospital/Oslo University Hospital, Lorenskog/Oslo, Norway

Background. Neoadjuvant endocrine treatment (NET) is used for locally advanced hormone receptor (HR)-positive, HER-2-negative breast cancer in highly selected patients. Aromatase inhibitors (AI) are the preferred option in this setting. Although NET has been proposed to be similarly effective as neoadjuvant chemotherapy (NCT) for certain patients, there are no reliable markers currently available to guide post-surgery decisions. Changes in Ki67 levels and results provided by multi-gene arrays (MGA) before and after neoadjuvant treatment have been suggested to be promising and clinically relevant markers for further decision making.
Methods. The NEOLETEXE trial was an open-label, intrapatient cross-over trial including patients with locally advanced HR-positive, HER2-negative breast cancer. Patients were randomized 1:1 to NET with either letrozole or exemestane for 3 months, followed by an intrapatient cross-over to the alternative treatment for another 3 months. Extensive biobanking was performed at multiple time points before and during neoadjuvant therapy. In a subset of patients, gene expression profiling was performed using the Prosigna® (PAM50) assay on both the diagnostic biopsy and the final surgical specimen. Immunohistochemical Ki67 expression was assessed in core biopsies obtained at baseline and in excision specimens collected at the time of surgery.
Results. A total of 84 patients were included in the intention-to-treat analysis. The median age was 76 years. Pathological complete responses (pCR) occurred in 6% (n=5). The median follow-up time was 6,3 years. Only nine patients (10,7%) relapsed during the follow-up period. An analysis of Ki67 at baseline (Ki67b) and at the time of surgery (Ki67s) was performed, with levels of Ki67 10% or higher classified as Ki67high. Kaplan-Meier analysis showed that patients with low Ki67 levels at surgery (<10%) experienced significantly better recurrence-free survival (RFS) compared to the Ki67 high group (HR 0,07, CI 0.02-0.31, $p < 0.001$).Prosigna testing was performed at baseline and at the time of surgery in a cohort of 20 patients. At baseline, 35% (n = 7) of the Prosigna cohort were classified as Luminal A, 57,9% (n = 11) as Luminal B, and one patient was identified as HER2-enriched. At the time of surgery, most tumors were classified as Luminal A (80%, n = 16), two patients were categorized as HER2-enriched, and only one patient remained in the Luminal B category.
Conclusions. Our trial strongly underlines that NET involving AI as monotherapy for locally advanced HR-positive breast cancer is a pragmatic and effective alternative to NCT in highly selected patients. Ki67 expression data and MGA data at surgery turned out to be promising markers to potentially guide post-neoadjuvant decision-making and should be tested in future clinical trials.

#2289 Newly-designed selective estrogen receptor downregulators and their role in the tumor microenvironment and hematopoiesis in breast malignancies.

Mario Morales Martinez[1], Javier Mansilla[2], Eduardo Mauricio Gonzalez[1], Begona Comin-Anduix[1], Marisol Chavez[1], Brian Aguirre[3], Julia Aguade Gorgorio[4], Gang Deng[2], Nalo M. Hamilton[5], Hannah Mikkola[4], Madhuri Wadehra[3], Michael E. Jung[2], Richard J. Pietras[1], **Diana C. Marquez Garban**[1]

[1]Medicine, UCLA David Geffen School of Medicine, Los Angeles, CA,[2]Department of Chemistry and Biochemistry, UCLA, Los Angeles, CA,[3]Pathology and Laboratory Medicine, UCLA David Geffen School of Medicine, Los Angeles, CA,[4]Molecular, Cell and Developmental Biology, UCLA, Los Angeles, CA,[5]UCLA School of Nursing, Los Angeles, CA

Breast cancers (BC) with estrogen receptor-alpha (ERα) expression represent 70% of newly-diagnosed patients in the US. Endocrine therapies with antiestrogens or aromatase inhibitors, either alone or combined with CDK 4/6 inhibitors, are an important intervention for BCs that express ERα, and these remain among the most effective targeted treatment strategies. However, a number of patients with localized BC, and essentially all patients with advanced BC, eventually become resistant to current endocrine therapy regimens. In contrast, immunotherapy is transforming the landscape of treatment for many cancers. However, most breast cancers, apart from a minority of triple-negative breast cancers (TNBC), are resistant to this promising immunotherapeutic approach. Several mechanisms of immune resistance have been described. Of note, BCs are reported to drive expansion and differentiation of hematopoietic stem and progenitor cells in the bone marrow to skew hematopoiesis toward an immunosuppressive myeloid lineage. This dysregulation of myelopoiesis in breast malignancy leads to aberrant expansion of immunosuppressive and tumor-promoting myeloid subpopulations such as myeloid-derived suppressor cells (MDSCs). Our newly-designed selective estrogen receptor down-regulator JD128 (SERDs) markedly reduces *in vitro* proliferation of several ERα+ BC cell lines, alone and combined with CDK 4/6 inhibitors, when compared with FDA-approved SERDs Fulvestrant and Elacestrant ($P < 0.01$). This was accompanied by a significant decrease of ERα protein as well as mRNA levels, confirming ERα protein degradation. Further, estrogen stimulated proliferation of CD34+ bone marrow stem cells, multipotent progenitors and MDSCs derived from normal female donors, an effect that was inhibited by SERD JD128 and Fulvestrant indicating that hematopoietic stem and progenitor cells express estrogen receptors and respond to estrogen. In addition, SERD JD128 inhibited proliferation of BC cell mammospheres and reduced expression of cancer stem cell markers. Importantly, accumulation and activity of MDSCs that occupy the tumor microenvironment (TME) appear to occur in both ER-positive and ER-negative tumors. Moreover, estrogen-responsive MDSCs in the TME can be targeted by SERD therapy to block estrogen signaling. These estrogen-mediated effects on hematopoietic cell expansion/activation have implications for potential clinical use of SERDs in ER-positive or ER-negative BCs. [Funded by: CIRM DISC2-14166, UCLA JCCC Breast Cancer Award, Tower Cancer Research Foundation, Hickey Foundation, NIH/NCI U54 CA143930 CDU-UCLA JCCC Partnership, CBCRP B27IB3869, DOD BCRP Level 2-BC181420]

#2290 Therapeutic targeting of ATAD2 in endocrine-resistant breast cancer.

Anil Kumar Devakrishnan[1], **Murugesan Palaniappan**[2]

[1]Baylor College of Medicine, Houston, TX,[2]Pathology and Immunology, Baylor College of Medicine, Houston, TX

Introduction: ATPase family AAA domain-containing protein 2 (ATAD2) is a highly conserved protein that functions as a coactivator of oncogenic transcription factors, and its bromodomain is critical for its association with acetylated chromatin. ATAD2 is frequently amplified in multiple types of cancer, including breast cancer. The upregulation of ATAD2 is often associated with poor patient outcomes and can be used as a prognostic marker. In breast cancer, ATAD2 is proposed to act as a coactivator of estrogen receptor (ER) α, which is selectively recruited upon estradiol stimulation, leading to the induction of a subset of ER target genes, including c-Myc, cyclin D1, and E2F1, which are required for breast cancer cell proliferation. Here, we examined the role of ATAD2 in hormone-resistant metastatic ER-positive breast cancers with activating mutations in ESR1, which currently have limited therapeutic options.
Methods: We examined the expression of ATAD2 in human breast tumors and subtype-specific breast cancer cells, including endocrine therapy-resistant breast cancer cells. To investigate the therapeutic potential of ATAD2 in Y537S and D538G mutant breast cancer cells, we conducted genetic and pharmacological modulation of ATAD2 in endocrine-resistant breast cancer cells. Additionally, we established stable suppression of ATAD2 using shRNA in the Y537S mutant MCF-7 and T47D cells. We also performed a co-immunoprecipitation assay, which demonstrated an interaction between ATAD2 and ERα in Y537S MCF-7 cells.
Results: Analysis of The Cancer Genome Atlas (TCGA) and Clinical Proteomic Tumor Analysis Consortium (CPTAC) data sets revealed elevated mRNA and protein levels of ATAD2 across all major subtypes compared with normal breast tissues. Additionally, ATAD2 was overexpressed in endocrine-resistant breast cancer cells, including Y537S palbociclib resistance and long-term estrogen-deprived (LTED) cell line models. Pharmacological and siRNA-mediated inhibition of ATAD2 significantly reduced the expression of ERα and its target genes in Y537S and D538G mutant breast cancer cells. More importantly, the inhibition of ATAD2 by a genetic or pharmacological agent potentially blocks ligand-dependent and ligand-independent ER signaling in endocrine-resistant breast cancer cells. Finally, our co-immunoprecipitation experiments showed that ERα directly interacts with ATAD2.
Conclusion: Collectively, our study highlights that ATAD2 is necessary for ESR1 mutant signaling in endocrine-resistant breast cancer. Therefore, blocking ATAD2 is a promising therapeutic strategy for endocrine-resistant breast cancer, including *ESR1* mutant breast cancer.

#2291 Exposure to plastic additives suggests potential androgen receptor agonism in prostate cancer.

Wylie K. Watlington[1], Sophia Colmenares[1], James Carter[1], Sophie Vincoff[2], Andrew A. Armstrong[1], Daniel Reker[1], Jason A. Somarelli[1]

[1]Duke University, Durham, NC,[2]University of Pennsylvania, Philadelphia, PA

Introduction: Plastic is the most abundant human-made substance in the world, and routine ingestion represents a global public health threat. Plastics are comprised of solid hydrocarbon polymers with over 10,000 chemical “additives” that augment the material properties of plastic. These additives include known carcinogens, endocrine disrupting compounds, and DNA damaging agents. Endocrine disruptors are of particular concern, as they may promote growth of hormone-dependent cancers or inhibit hormone therapies used in treatment. Perhaps more alarming is how little we know about the thousands of additives not yet characterized. Here we developed a computational platform to identify additives with potential binding activity to androgen receptor (AR), the key hormone receptor used for prostate cancer growth signaling. The goal for this work is to better understand how these routine exposures may impact endocrine signaling and potentially fuel prostate cancer growth.

Methods: We developed a pairwise deep learning model to enhance AR agonist prediction accuracy by leveraging relative potency relationships among compounds. After training this model on 469 compound structures and half-maximal effective concentration (EC_{50}) values, we screened 2,712 plastic additives and identified eight commonly used additives as potential AR agonists. We treated AR-dependent LNCaP cells engineered with a fluorescent prostate-specific antigen (PSA) reporter with each additive, ranging from 100 µM to 0.0001 µM. Cell growth rate and AR activity via PSA reporter were quantified using the analysis features on the Incucyte S3® (Sartorius).

Results: Upon ranking predicted candidates from our deep learning model, we selected eight compounds for experimental validation based on favorable prediction values, cost, and availability. Out of seven additives initially screened, four showed significant increases in PSA reporter expression upon additive exposure at 10 µM (edetic acid, sebacic acid, 2,4,6-tribromophenol, and TTBP-TAZ). Two additives (TTBP-TAZ and 2,4,6-tribromophenol) showed significant growth proliferation at doses ranging from 1-100 µM. Cross-checking these additives with human biomonitoring data shows that decabromodiphenyl ether and 2,4,6-triboromophenol have been detected in human samples and are being monitored for potential detection.

Conclusions: We have developed and deployed a pairwise deep learning approach to screen a database of plastic additives for predicted AR activity and validated experimentally the AR activation for three of these additives. This work could help identify areas of environmental exposure to AR agonists that increase risk of prostate cancer development or progression. Future work is focused on expanding this platform to identify compounds acting as regulators of other hormones relevant in cancer and developing assays to detect these additives in patient samples.

#2292 Interleukin-6 increases glucocorticoid inactivation in a castration resistant prostate cancer cell line model.

Olivia M. Tonini[1], Lina Schiffer[2], Nima Sharifi[2]

[1]Cancer Biology Graduate Program and Sylvester Comprehensive Cancer Center, University of Miami Miller School of Medicine, Miami, FL,[2]Urology, Desai Sethi Urology Institute and Sylvester Comprehensive Cancer Center, Miami, FL

Prostate cancer is the second leading cause of cancer deaths in men in the United States. It is dependent on androgen receptor (AR) signaling and initially is responsive to therapies blocking AR signaling. Unfortunately, it is common for the cancer to reoccur and become resistant to these therapies and become a form known as castration resistant prostate cancer. This resistance to AR blockers is in part mediated by the glucocorticoid receptor (GR) taking over the regulation of AR-target genes driving proliferation. As shown by our group and others, this GR take over in AR blocker resistant tumors is in part due to increases in GR levels and due to loss of the glucocorticoid-inactivating enzyme 11βHSD2. Studying the regulation of the tumor-specific levels of the active glucocorticoid, cortisol, is essential as they determine local GR activity and are hence tied to therapeutic resistance. In this work, we set out to determine how cytokines regulate 11βHSD2 activity and affect glucocorticoid levels in prostate cancer.

Using a cell line model of castration resistant prostate cancer (VCaP) and tracing of radiolabeled steroids by High Performance Liquid Chromatography, we show that interleukin-6 (IL-6) increases 11βHSD2 activity, promoting metabolic inactivation of glucocorticoids. We show that interleukin-6 increases transcript levels of *HSD11B2* (encoding 11βHSD2) and 11βHSD2 protein abundance indicating that IL-6 drives increased glucocorticoid inactivation by upregulating *HSD11B2* at the transcriptional level. Using transient siRNA knockdowns and selective, pharmacological inhibitors, we show that blocking JAK1/2, gp130, and STAT3 results in reversal of this glucocorticoid inactivation and are therefore required signaling elements that mediate the interleukin-6 induced upregulation of *HSD11B2* expression, protein level and activity in VCaP cells. Taken together, we have discovered interleukin-6 and JAK/STAT signaling as a potential new regulator of glucocorticoid metabolism in prostate cancer. Further work will elicit the physiological and therapeutic implications in the context of disease progression and therapy resistance. Ultimately, this research aims to deepen the understanding of glucocorticoid metabolism regulation in prostate cancer and its role in disease escalation and treatment responsiveness.

#2293 The LncRNA XIST mediates resistance to estrogen receptor beta targeted therapies in triple negative breast cancer.

Michael Emch[1], Kirsten Aspros[1], Matthew P. Goetz[2], John Hawse[1]

[1]Mayo Clinic, Rochester, MN,[2]Mayo Clinic College of Medicine and Science, Rochester, MN

Breast cancer accounts for nearly a quarter of all cancers in women with an estimated 2.3 million new diagnoses and over 670,000 deaths annually. Triple-negative breast cancer (TNBC) is an aggressive subtype characterized by lack of estrogen receptor alpha (ERα) and progesterone receptor (PR) expression in the absence of HER2 amplification. TNBC accounts for ~15% of all incident breast cancers and is associated with poor patient outcomes. Problematically, TN tumors exhibit vast inter-patient molecular heterogeneity making the identification of novel therapeutic vulnerabilities difficult and the development of alternative treatment strategies problematic. We and others have demonstrated that estrogen receptor beta (ERβ) is expressed in about 20% of TN tumors and potently suppresses proliferation, invasion, and migration in TNBC cells *in vitro* and *in vivo*. We thus hypothesized that endocrine therapies that selectively activate ERβ would be an effective treatment approach for this subset of patients. We also anticipated that some tumors would display de novo or acquired resistance to ERβ targeted therapies despite ERβ protein expression. We therefore sought to define mechanisms of resistance to ERβ targeted therapy and to identify synthetic lethal vulnerabilities. We generated the first models of ERβ resistant TNBC through chronic exposure to estradiol or an ERβ specific agonist (LY500307) and through a CRISPR genome wide knockout screen. We identified the LncRNA XIST as one of the most upregulated transcripts in multiple models of ERβ resistant disease, and knockdown of XIST expression was shown to resensitize resistant cell to estradiol and LY500307 treatment. XIST was not found to be directly regulated by ERβ in TNBC further suggesting that its overexpression is a bona fide mechanism of resistance to ERβ mediated suppression of proliferation. The phenomena of chronic ligand exposure leading to activation of XIST expression in ERβ+ cells is not shared with ERα suggesting that the mechanism by which XIST expression is elevated during the development of resistance is distinct between the two sister receptors. We further characterized *XIST* expression in patient samples of TNBC and found that XIST expression varies, but largely exhibits a bimodal distribution with most tumors displaying either low or high transcript levels. In conclusion, we have identified the X-inactivating transcript as a driver of resistance to ERβ targeted therapies in TNBC. Future studies aimed at uncovering the consequences of XIST over-expression on global gene expression, functionality of ERβ, and aggressiveness of TNBC are ongoing.

#2294 Examining the effect of second-generation antiandrogens in androgen receptor-overexpressing prostate cancer cells.

Kia Vaalavirta, Hanna Rauhala, Tapio Visakorpi

Faculty of Medicine and Health Technology, Tampere University, Tampere, Finland

Antiandrogens inhibit androgen receptor (AR) signaling, a critical driver of prostate cancer (PCa) growth and survival. While these agents are initially effective, prolonged therapy frequently results in resistance, often associated with AR overexpression or the emergence of constitutively active splice variants. To better understand how AR overexpression influences antiandrogen efficacy, we examined cell proliferation and AR target gene expression under second-generation antiandrogen treatment in AR-high PCa cells.
In this study, we used darolutamide, enzalutamide, and apalutamide and systematically compared their effects on cell proliferation and AR-mediated gene expression using identical experimental setups. LNCaP-ARhi cells, expressing 4-6-fold higher AR than their parental cell line LNCaP-pcDNA3.1, were hormone-deprived and treated with increasing concentrations (0.001 nM-10 nM) of the synthetic androgen, R1881. Cell proliferation and morphology were monitored with Incucyte phase-contrast imaging for 7 days. Direct AR target gene expression (KLK3 and FKBP5) was quantified by qPCR. For co-treatment, we used two R1881 concentrations (0.01 nM and 0.1 nM): the lower promoted proliferation, the higher suppressed it, and both significantly increased KLK3 expression in AR-overexpressing cells. The cells were hormone-deprived, then treated with DMSO, 0.01 nM or 0.1 nM R1881, and antiandrogens (1 μM, 10 μM, and 25 μM). Cell proliferation and morphology were monitored for 5 days, and AR target gene expression was measured as previously described.
Our results support previous findings that AR overexpression enhances androgen responsiveness and sustains cell growth even under low androgen concentrations (0.01 nM R1881). We also found that LNCaP-ARhi cells shifted from elongated, spindle-shaped cells to a flattened, polygonal morphology at R1881 0.03 nM-10 nM. Co-treatment with R1881 and antiandrogens restored the original morphology.
All tested second-generation antiandrogens reduced R1881-stimulated growth and KLK3/FKBP5 gene expression in both cell lines, suggesting effective AR signaling inhibition in a dose-dependent manner. However, in LNCaP-ARhi cells, KLK3 expression remained elevated compared to DMSO control even at high antiandrogen concentrations. Overall, second-generation antiandrogens suppress AR signaling and growth in PCa cells, but AR overexpression may limit inhibitory efficacy, highlighting the need for strategies targeting AR-high conditions.

#2295 KMT2D loss rewires estrogen-PI3K crosstalk in endometrioid adenocarcinoma.

Jessica L. Long[1], Swornalata Pukhrambam[1], Areebah Qazi[1], Michele L. Cote[2], Greg Dyson[1], Anna Gottschlich[1], Mike R. Wilson[1]

[1]Wayne State University School of Medicine, Detroit, MI,[2]Richard M. Fairbanks School of Public Health, Indianapolis, IN

BACKGROUND: Endometrioid adenocarcinoma is defined by pervasive PI3K-pathway dysregulation and estrogen-driven growth. More than 80% of tumors harbor PI3K-pathway alterations, and approximately 20% exhibit loss-of-function mutations in the histone methyltransferase KMT2D, often at high variant allele frequencies, suggesting biological relevance rather than mutational noise. While estrogen enhances PI3K signaling through genomic and non-genomic mechanisms, the epigenetic factors governing this interaction remain poorly understood in endometrial cancer. In ER+ breast cancer, KMT2D governs regulatory crosstalk between these two pathways, raising the possibility that loss-of-function mutations in endometrial cancer alter estrogen-responsive transcription and shift oncogenic dependencies.

METHODS: KMT2D was depleted via siRNA in 12Z-ESR1 endometrial epithelial cells, followed by estradiol or vehicle treatment (n=3/group). Bulk RNA-sequencing assessed transcriptional changes. To evaluate in vivo function, a conditional Kmt2d-SET-fl/fl mouse model, yielding a catalytically impaired protein, was analyzed by uterine RNA-seq. Clinical relevance was assessed using an integrated dataset of whole-exome sequencing and transcriptomics from endometrioid adenocarcinomas. Tumors were stratified by KMT2D loss-of-function status for differential expression and pathway enrichment analyses.

RESULTS: KMT2D knockdown markedly altered estradiol-driven transcription, shifting ER-related signaling pathways that remained intact in control cells. In Kmt2d-SET-deficient mouse uteri, PI3K-Akt pathway genes were significantly upregulated even without estrogen stimulation or neoplastic change, demonstrating that KMT2D enzymatic activity constrains baseline PI3K signaling in vivo. In patient tumors, KMT2D-mutant cancers showed enrichment of oncogenic pathways consistent with convergence of estrogen and PI3K programs. Across models, KMT2D loss amplified PI3K pathway activity and altered estrogen receptor-directed transcription, suggesting increased reliance on PI3K signaling.

CONCLUSION: This supports a model in which KMT2D loss disrupts ER-regulated transcriptional programs, enhances PI3K pathway activation, and creates a potentially targetable dependency in endometrioid adenocarcinoma. Given the mixed clinical efficacy and toxicity of PI3K inhibitors, identifying molecular contexts that heighten PI3K dependence is critical. This work highlights KMT2D loss as a potential biomarker for PI3K-targeted therapy and provides new insight into epigenetic regulation of hormone-oncogenic crosstalk.

#2296 Anti-tumor actions of novel tamoxifen-melatonin drug conjugates on estrogen-resistant tumors and actions on tumor- and uterine-expressed ESR1 in SCID_BEIGE mice.

Asef Faruk[1], Sophie Dietrich[2], Yong Myoung[1], Afsana Jahan[1], Mohamed Marzouk[3], Jane E. Cavanaugh[1], Simak Ali[4], Matthew Burow[2], Darius Zlotos[5], Paula Witt-Enderby[1]

[1]Pharmaceutical Sciences, Duquesne University School of Pharmacy, Pittsburgh, PA,[2]Section of Hematology & Medical Oncology, Tulane School of Medicine, New Orleans, LA,[3]Institute of Pharmacy and Food Chemistry, University of Wu̇rzburg, Wu̇rzburg, Germany,[4]Department of Surgery & Cancer, Imperial College London, Hammersmith Hospital Campus, London, United Kingdom,[5]Dept. of Pharmaceutical Chemistry, The German University in Cairo, Cairo, Egypt

Background: Often, prolonged use of tamoxifen, an FDA approved SERM to treat ER+ breast cancer (BC), has untoward effects on the uterus and can lead to tamoxifen resistance. Novel tamoxifen-melatonin drug conjugates, C1-C5, with varying CH2- spacer lengths were developed (US Patent No. 8,785,501 B2) to offset tamoxifen-mediated tumor resistance and uterotropic actions. Two candidate compounds, C4 and C5, demonstrated anti-BC actions in MCF7, TNBC, and tamoxifen-resistant MCF7 cells (doi:10.1124/mol.119.116202).

Methods: The goal of this study was to evaluate C4- and C5-mediated actions on estrogen resistant BC in vivo and ESR1 levels in the uterus in vivo using SCID/BEIGE mouse xenografts and western blot analyses.

Results: Using CCK-8 assays, C4- and C5-mediated potency and efficacy to inhibit proliferation of ESR1 mutant (MCF7-luc Y537S, MCF7-luc D538G, MCF7-E380Q) and parental (MCF7-luc parental, MCF7-PE parental) lines revealed MCF7-lucD538G to be most sensitive to C4 (IC_{50}= 3.8μM; 43% inhibition) and C5 (IC_{50}=1.2μM; 26% inhibition). Preliminary testing using MCF7-lucD538G or parental cells bilaterally implanted into fat pads of SCID/BEIGE mice given additional estrogen or not demonstrated 60% to 90% greater tumor volumes compared to parental controls by 3 weeks, suggesting estrogen-independence. MCF7-luc D538G cells ($5x10^6$), were bilaterally implanted in the mammary pads of SCID/BEIGE mice and grown for 28 days in the absence of estrogen to allow for tumor formation. Next, treatments with C4 or C5 (1mg/kg/mouse/day, sc,), DMSO (10% in HP-β-CD), tamoxifen (5mg 60-day release pellet implanted), fulvestrant (200mg/kg/week, sc) began and continued for 28 days. Significant tumor inhibition occurred with C4 and C5 vs DMSO- and tamoxifen-treated mice; and similar tumor-inhibiting effects were observed when compared to fulvestrant (% change from baseline: DMSO=211%; tamoxifen=169%; C4=134%; C5=95%; fulvestrant=96%, n=5/group). Analysis of ESR1 levels in tumor and uterine tissue demonstrated increases in levels in tamoxifen-treated mice and no changes in C4-, C5- and fulvestrant-treated mice vs control. ESR1 stability assays were conducted in wildtype MCF7 cells exposed to vehicle (DMSO), and 10μM each of tamoxifen, C4 or C5 for 24h, followed by a withdrawal period (0, 6, 12, 24h) using media containing cycloheximide (100μg/mL). Increases in the half-life ($T_{1/2}$) of ESR1 were observed in cells exposed to tamoxifen ($T_{1/2}$=13.2h) or C4 ($T_{1/2}$=12.6h) while decreases were observed in MCF7 cells exposed to C5 ($T_{1/2}$=5.1h) compared to DMSO-treated ($T_{1/2}$=9.6h) and no treatment cells (($T_{1/2}$=7.4h).

Conclusion: Our findings indicate that tamoxifen-melatonin drug conjugates may be a viable BC treatment option for estrogen-resistant and potentially other resistant cancers while offering uterine protection.

#2297 Effects of AVA-291 (d3-testosterone) versus testosterone on MCF-7 estrogen receptor positive breast cancer cells - lack of aromatization to estradiol leads to a highly differentiated cellular proliferation profile.

Paul M. Tarantino[1], **Judith A. Boice**[2], Pamela A. Trail[3], Bradford C. Sippy[2]

[1]PMT Pharma Consulting LLC, Holden, MA,[2]Aviva Biopharm Inc, Concord, MA,[3]AGL Biotechnology Consultants LLC, Kiawah Island, SC

Introduction: Conversion of androgens to estrogens within breast tumors by aromatization plays a pivotal role in the proliferation of tumor cells expressing the estrogen receptor (ER). Testosterone (T) has demonstrated breast cancer (BC) cell proliferation effects *in vitro* and clinically has been linked to a breast cancer signal in postmenopausal women. Given this link, the increasing number of women using T therapy and its potential association with an increased risk of breast cancer is of concern. However, the androgen receptor (AR) in general, which T binds to, has been postulated to have BC suppressive effects and in certain clinical situations T has been reported to be an effective BC treatment. The ability to decouple these countervailing proliferative and antiproliferative effects of T in BC cell growth is of interest. AVA-291 (d3-testosterone) is a structurally identical, deuterium-substituted isotopologue of T that retains T's androgen effects and hepatic metabolic profile but is highly resistant to aromatization. In the studies described here, the ER+ BC cell line MCF-7 was used to assess the relative proliferative effects of T or AVA-291 (ranging from 0.1 nM to 3 μM) *in vitro*. Single 10 nM concentrations of estradiol (E2) and dihydrotestosterone (DHT) were included as positive and negative controls, respectively.
Results: Consistent with literature reports, T stimulated MCF-7 cell proliferation in a concentration-dependent manner. The proliferative effects of T were observed starting at 1 nM reaching a maximum effect at 10 nM. In contrast, AVA-291 did not stimulate proliferation over a broad concentration range with a proliferative effect only observed at concentrations ≥1 μM. As expected, the positive control (10 nM E2) demonstrated maximal stimulation and the negative control (10 nM DHT) resulted in no proliferative effect.
Conclusions: We demonstrate that T has a proliferative effect on the ER+ BC cell line MCF-7 and that AVA-291, a non-aromatizing form of T, did not stimulate cell proliferation at similar concentrations. These findings confirm prior literature reports on this effect by T and the purported underlying mechanism of androgen aromatization by MCF-7 ER+ BC cells. These results suggest that AVA-291 may be a useful alternative to T in clinical situations where the aromatization of T limits its therapeutic potential, such as hormone replacement therapy in postmenopausal women.

#2298 Spatial immune profiling reveals varying tumor microenvironments in papillary thyroid microcarcinoma.

Rhitajit Sarkar[1], Shilpa Thakur[2], Gus Fridell[3], Elijah Edmondson[2], Sonam Kumari[2], Joanna KLUBO-GWIEZDZINSKA[4]

[1]Metabolic Diseases Branch, NIH National Institute of Diabetes and Digestive and Kidney Diseases (NIDDK), Bethesda, MD,[2]National Institutes of Health, Bethesda, MD,[3]Johns Hopkins University, Baltimore, MD,[4]National Institutes of Health, Reston, VA

Introduction: Papillary thyroid microcarcinomas (PTMC) are usually indolent, but up to 10% present with clinically significant lymph node metastases or very rarely with distant metastases (M1). This study analyzes transcriptomic signatures and spatially resolved tumor microenvironment profiles in metastatic versus non-metastatic PTMC to refine risk stratification.

Methods: Patients diagnosed with indolent non-metastatic (N0/Nx) PTMCs and with primary tumors (PT) metastatic to the lateral neck lymph nodes or distant sites (N1b/M1) were selected, and RNA sequencing was done on PT and adjacent normal tissues. Multiplex immunofluorescence was performed, staining using CD8a and CD20 antibodies. Images were analyzed in a single-blinded manner using HALO (Indica Labs), and differential spatial expression was tested using a t-test or a Mann-Whitney test, depending on data distribution. Spatial proteomic profiling was performed using the NanoString (Bruker) GeoMX® platform, including Human Immune Cell Profiling, Typing and Activation Status, and MAPK Signaling Protein Modules for the nCounter analysis. Protein expression data were log2-transformed, and between-groups differential expression was assessed using Welch's two-sample t-tests with Benjamini-Hochberg adjustment. Proteins with adjusted $p<0.05$ and absolute log2 fold-change >0.5 were considered significant.

Results: The N0/Nx and N1b/M1 study cohorts consisted of 17 and 19 patients, respectively. No difference in the clinical characteristics, viz., age ($p=0.64$), sex ($p=0.24$), and median PT size ($p=0.27$), was found between the groups. Transcriptome analysis indicated significant downregulation of pathways involved in the B cell activation without a significant difference in B cell ($CD20^+/CD8a^-$) infiltration in the PT ($p=0.43$) nor in the PT rims ($p=0.92$) from the N1b/M1 compared to N0/Nx group. However, cytotoxic T cells ($CD8a^+/CD20^-$) significantly populated the rims of the PT from N1b/M1 group compared to N0/Nx ($p=0.007$). Spatial immune profiling revealed that N1b/M1 PT had significantly higher T-cell infiltration (CD3; padj=0.02) than N0/Nx tumors and showed pronounced expression of the immune evasion molecule PD-L2 (padj=0.02). N1b PT also showed high stemness (CD44, padj=0.001). Compared to N1b PT, M1 showed higher immune evasion (PD-L1, padj=0.01; PD-L2, padj=0.049).

Conclusion: Metastasis-prone PTMC is characterized by enhanced stemness, and increased T cell infiltration, accompanied by upregulation of immune evasion molecules, suggesting that immune evasion may play a critical role in pathogenesis of metastases.

: Biomarkers of Endogenous or Exogenous Exposures, Early Detection, Biological Effects, and Prognosis
Poster Session

#2302 Prognostic biomarkers associated with the progression of cervical premalignant lesions to cancer: A scoping review.

Luis Giraldo-Barrios, Salome Andrade-Romero, Jonathan Villalobos-Escorcia, Gerardo Barboza-Guevara, **Ines Benedetti**

School of Medicine, Histopathology Research Group, Universidad de Cartagena, Cartagena, Colombia

Introduction: Cervical cancer is the fourth most common cancer and the fourth leading cause of cancer-related death in women, worldwide. Advances in understanding the molecular biology of premalignant cervical lesions have shown that not all low-grade squamous intraepithelial lesions progress to high-grade squamous intraepithelial lesions and, nor will all of these progress to invasive carcinoma. Prognostic biomarkers make it possible to predict the evolution of high-grade squamous intraepithelial lesions and to identify patients at risk of progression to cancer. Biomarkers related to cell proliferation, DNA methylation, and immune regulation have been proposed, although the evidence is extensive and heterogeneous.We conducted a scoping review to search possible promising biomarkers for risk stratification of high-grade squamous intraepithelial lesions progression.
Methods: We followed the methodological framework proposed by Arksey and O'Malley and the guidelines established by PRISMA-ScR. A systematic literature search was conducted in Web of Science, PubMed, and Embase using terms such as "high-grade squamous intraepithelial lesions," "uterine cervical neoplasms," "biomarkers," and "disease progression," from the inception of each database through May 30, 2025.
Results: A total of 11,795 articles were identified; after removing 4,447 duplicates with Rayyan®, 7,348 records remained for title and abstract screening. Of these, 619 were assessed in full text and 34 were included in the qualitative synthesis. In high-grade squamous intraepithelial lesions, p16, Ki-67, and detection of E6/E7 were associated with a higher risk of progression, whereas FAM19A4/miR124-2 methylation was associated with regression. Overexpression of markers such as RFC4, RIPK4, ATAD2, EZH2, IMP3, ADAR1, AEG-1, TK1, PAK1, aPKCι/λ, tenascin-C, HABP1, CFTR, CPE, and the Np63/TAp63 ratio was linked to greater aggressiveness, lymph node metastasis, and poorer survival.
Conclusions: The most promising biomarkers for risk stratification of high-grade squamous intraepithelial lesions progression are p16, Ki-67, FAM19A4/miR124-2 methylation, and E6/E7 mRNA. Their combined use could optimize the identification of patients who require active management and reduce overtreatment in cases with a high probability of regression. Standardization of methods and cut-off values is required for their clinical validation.

#2303 Androgen receptor expression in breast cancer and its prognostic significance: A systematic review and meta-analysis.

Elias Ferreira[1], Luis Giraldo-Barrios[1], Laura Suarez[1], Maria P. Valera[1], Jose Aldana[1], Pedro Araujo[2], **Ines Benedetti**[1]

[1]School of Medicine, Histopathology Research group, Universidad de Cartagena, Cartagena, Colombia,[2]School of Medicine, Universidad de Cartagena, Cartagena, Colombia

Background: Molecular classification of breast cancer subtypes is based on the expression of estrogen, progesterone and HER2 receptors. The androgen receptor has emerged as a biomarker however, its prognostic role remains incompletely elucidated. Objective: to determine androgen receptor expression value as a biomarker and its potential impact on the clinical course of breast cancer.
Methods: We conducted a systematic review and meta-analysis in accordance with the PRISMA statement, protocol was registered in PROSPERO (CRD420251166750). PubMed, Embase, and Web of Science were searched from inception to May 2025. We included analytical observational studies that enrolled histologically confirmed breast cancer, of any molecular subtype, and evaluated tumor androgen receptor expression by immunohistochemistry using a predefined positivity cut-off. Definitions of androgen receptor positivity were accepted as reported in each study, given the limited number of studies per outcome, which precluded formal subgroup analyses by cut-off. Studies were eligible if they reported hazard ratios (HRs) with 95% CIs for survival outcomes. Two reviewers independently assessed study eligibility, extracted data, and evaluated risk of bias using the Newcastle-Ottawa Scale; disagreements were resolved by consensus. Given the between-study heterogeneity, hazard ratios were pooled using an inverse-variance random-effects model, and heterogeneity was quantified with the I^2 statistic.
Results: From a total of 966 records identified, 118 full texts were assessed after removing 228 duplicates, including 15 studies for qualitative synthesis. Seven of these reported hazard ratios for the predefined outcomes and were included in the meta-analysis. For overall survival in patients with triple-negative breast cancer and androgen receptor expression, the pooled HR was 0.60 (95% CI 0.29-1.21; $I^2 = 85.8\%$, $p = 0.0009$), showing a non-significant trend toward better survival in AR-positive tumors. For breast cancer-specific survival in AR-positive breast cancer, the pooled HR was 0.55 (95% CI 0.20-1.49; $I^2 = 88.2\%$, p for heterogeneity < 0.0001), also indicating a non-significant trend toward reduced breast cancer mortality.
Conclusions: Although our meta-analysis did not demonstrate a statistically significant association between androgen receptor expression and overall or breast cancer-specific survival, these findings are relevant because they highlight substantial heterogeneity across studies. Differences in how androgen receptor status was assessed, along with variability in the definition and reporting of prognostic outcomes, likely contribute to the inconsistent estimates. Developing standardized criteria for positivity and harmonized outcome reporting will be crucial to clarify the true prognostic role of androgen receptor in breast cancer.

#2306 Gene polymorphisms in LEPR and PTGS2 contribute for prognostic evaluation in breast cancer.

Alessandra Brandao de Souza[1], Daniely Regina Freitas-Alves[1], Taiana Sousa Lopes da Silva[2], Mario da Silva Ramos[3], Matheus de Oliveira Afonso[3], Jessica Vilarinho Cardoso[4], Jamila Alessandra Perini[4], Rosane Vianna-Jorge[3]

[1]Fundacao Oswaldo Cruz (Fiocruz), Rio de Janeiro, Brazil,[2]Instituto Nacional do Cancer, Rio de Janeiro, Brazil,[3]Universidade Federal do Rio de Janeiro, Rio de Janeiro, Brazil,[4]Universidade Estadual da Zona Oeste, Rio de Janeiro, Brazil

Breast cancer is the second most frequent neoplasm worldwide and is considered a heterogeneous disease, with distinct genetic backgrounds and diverse histological and molecular presentations that influence prognosis. Besides tumor-specific characteristics, individual genetic variations may also potentially impact disease outcomes, and need to be assessed in prognostic models. Here, we employed a candidate gene approach, focusing on biologically relevant pathways, such as inflammation, to investigate the effects of single nucleotide polymorphisms (SNPs) on breast cancer outcomes. The investigation involved a 10 year follow-up of a prospective cohort of Brazilian women (N = 1038) with unilateral, nonmetastatic breast cancer treated at the National Cancer Institute (CAAE 55929416.8.0000.5240). Blood samples were genotyped for 14 SNPs from five genes (*LEP*, *LEPR*, *PTGS2*, *VEGFA* and *EGFR*) using Real-Time PCR. Linkage disequilibrium and haplotypes were evaluated using Haploview. Survival curves were estimated using the Kaplan–Meier method. The effects of SNPs on disease-free survival (DFS) and breast cancer specific survival (BCSS) were estimated using hazard ratios (HR) and 95% confidence intervals (95% CI). Adjusted hazard ratios (HRadj) were obtained through Cox regression multivariate models. Improved DFS was detected for *LEPR* rs1137101 when considering the whole population (HR = 0.45; 95%CI 0.26 - 0.77), post-menopausal women (HR = 0.57; 95%CI 0.37 - 0.88), or among patients with luminal tumors (HR = 0.44; 95%CI 0.25 - 0.80). In contrast, *PTGS2* rs689466 was associated with worse outcomes of DFS (HR = 1.70; 95%CI 1.21 - 2.37) and BCSS (HR = 1.67; 95%CI 1.13 - 2.47) among post-menopausal women, as well as among obese patients (HR = 1.68; 95%CI 1.08 - 2.64 for DFS and HR = 1.82; 95%CI 1.08 - 3.04 for BCSS). Because *LEPR* rs1137100 and *LEPR* rs1137101 showed significant linkage disequilibrium (R^2 = 0,89), they were also evaluated together, in combination with *PTGS2* rs689466, considering the three SNPs (A>G, A>G, A>G). The occurrence of at least two variant alleles in either *LEPR* rs1137100 or *LEPR* rs1137101, in combination with the reference genotype of *PTGS2* rs689466 showed improved DFS (HR = 0.60; 95%CI 0.37 - 0.96) within the whole population of the study. In contrast, the occurrence of *PTGS2* rs689466 variant alleles in combination with both *LEPR* rs1137100 and *LEPR* rs1137101 reference genotypes showed the worst outcomes even in multivariate models, significantly affecting both DFS (HRadj = 1.75; 95%CI 1.18 - 2.60) and BCSS (HRadj = 1.72; 95%CI 1.07 - 2.75) for the whole population, as well as for post-menopausal women, with DFS (HRadj = 2.09; 95%CI 1.16 – 3.77) and BCSS (HRadj = 2.60; 95%CI 1.35 - 5.0). The present results indicate the importance of tailoring prognostic models for breast cancer considering both tumor and individual biomarkers.

#2307 Body mass index-associated transcriptomic signatures reveal immune, stromal, and metabolic rewiring in non-small cell lung cancer: Insights into the obesity paradox.

Roberto Borea, Eswar Shankar, Francesco Drago, Carlos Ayala de Miguel, Estela Puchulu-Campanella, Christian Rolfo, Giovanni Nigita

Division of Medical Oncology, Department of Internal Medicine, The Ohio State University Comprehensive Cancer Center, College of Medicine, Columbus, OH

Although obesity increases cancer risk, obese patients with non-small cell lung cancer (NSCLC) paradoxically exhibit better survival. The biological basis of this "*obesity paradox*" remains unclear. High-throughput profiling can reveal body mass index (BMI)-linked transcriptional networks that shape immune, metabolic, and stromal responses, clarifying whether this "obesity paradox" reflects true tumor-microenvironment interactions rather than clinical confounders.We analyzed whole-transcriptome samples from 263 NSCLC patients in the ORIEN Avatar data at The Ohio State University. Patients were stratified into Lean (BMI<25; n=93), Overweight (25≤BMI<30; n=78), and Obese (BMI≥30; n=92) groups. Differential expression (DE) analyses (Lean vs Overweight, Lean vs Obese, Overweight vs Obese) were performed across all groups. Significantly deregulated transcripts ($p<0.01$ and $|\text{fold-change}|>1.5$) were retained for downstream analyses. Canonical pathway enrichment was conducted using Ingenuity Pathway Analysis ($p<0.05$).Distinct BMI-dependent transcriptomic signatures emerged. In Obese vs Lean, 40 transcripts were deregulated and enriched for metabolic processes (NAD^+ biosynthesis, non-oxidative PPP), suggesting metabolic reprogramming. Overweight vs Lean revealed 358 deregulated transcripts with upregulated immune activation (Th1/Th2, ICOS-ICOSL, IL-2 family, PI3K signaling in B cells), indicating enhanced adaptive, particularly T-cell, immunity. Obese vs Overweight revealed 304 deregulated transcripts enriched for extracellular matrix, platelet-collagen, and osteoclast signaling, implying stromal remodeling suppression in obesity. Overlap of deregulated transcripts was modest (OvsL∩OvsOw=1; OvsL∩OwvsL=7; OvsOw∩OwvsL=52; triple overlap≈0), implying group-specific biology.Our findings delineate three BMI-linked programs in NSCLC: immune activation in overweight tumors, ECM suppression and platelet signaling in obesity, and metabolic rewiring in obese versus lean tumors. Moderate adiposity appears to foster an immune-active microenvironment, whereas higher adiposity induces stromal quiescence and redox adaptation, consistent with reports of improved immunotherapy outcomes at higher BMI. The obese subgroup's ECM/platelet and NAD^+ salvage/PPP signatures nominate combinatorial strategies (e.g., stromal or antiplatelet agents with PD-1/PD-L1 blockade, NAMPT inhibition) and suggest that BMI-associated molecular heterogeneity may contribute to the "obesity paradox."

#2308 A pan-system approach for mutational signature identification and etiology assignment in cancer genomics.

Maria Zhivagui[1], Shams Al-azzam[2], Jessica Au[2], Peter Nguyen[1], Zichen Jiang[2], Mark D. Barnes[2], Ludmil B. Alexandrov[2]

[1]University of Nevada, Las Vegas (UNLV), Las Vegas, NV,[2]University of California San Diego, San Diego, CA

Purpose: Somatic mutations accumulate in the genomes of both normal and cancer cells. Mutagens imprint characteristic genomic patterns of somatic mutations, termed, mutational signatures. Accurate identification of mutational signatures is essential for linking genotoxic exposures and endogenous processes to cancer etiology. However, technical artefacts, sequencing noise, and platform heterogeneity often compromise the fidelity of signature detection, limiting mechanistic insights and biomarker discovery.

Methods: We developed *SigRescueR*, a pan-system computational tool that performs noise correction and robust mutational signature identification across diverse sequencing platforms. The framework integrates adaptive artefact filtering, robust signature reconstruction, and cosine similarity-based signal rescue across diverse mutational classes, including single base substitutions (SBS), insertions and deletions (indels), doublet base substitutions (DBS), and strand-bias mutation categories.

Results: We applied *SigRescueR* to the largest collection of experimentally derived mutational profiles assembled to date, encompassing over 4,200 genome-wide sequencing profiles across 42 model systems exposed to 120+ mutagenic agents under standardized experimental conditions. Comparative analysis across human, mouse, rat, chicken, and C. elegans models revealed 49 robust experimental mutational signatures. Several experimentally derived signatures reflected conserved DNA damage patterns across species and models exposed to the same agent or related chemicals, while others were species- or model-specific, suggesting system-dependent variability in mutational response. Moreover, several experimental mutational signatures corresponded to established COSMIC patterns, while others represented previously uncharacterized DNA damage processes in human cancers. Importantly, this compendium enabled causal assignment of previously unexplained COSMIC signatures, namely SBS94 and SBS95, to defined environmental exposures.

Conclusion: Together, *SigRescueR* and this compendium provide a unified, high-resolution view of mutagenesis, connecting molecular toxicology, cancer genomics, and biomarker discovery. This integrative framework refines how we trace, interpret, and incite measures to prevent the genomic imprints of carcinogenesis.

#2309 Exposure to solid fuel burning and transcriptomic changes in the nasal epithelium in never smoking women in Guatemala.

Batel Blechter[1], Lingge Yu[2], Wei Hu[3], Kaytlyn Salmons[4], Maggie Clarke[5], Dana Barr[4], Shuguang Leng[6], Gang Liu[2], Jennifer E. Beane-Ebel[2], Kyle Steenland[7], Nathaniel Rothman[1], Qing Lan[8]

[1]National Cancer Institute, Rockville, MD,[2]Boston University, Boston, MA,[3]National Cancer Inst. Div. of Cancer Epidemiology & Genetics, Bethesda, MD,[4]Colorado State University, For Collins, CO,[5]Colorado State University, Fort Collins, CO,[6]University of New Mexico, Albuquerque, NM,[7]Emory University, Atlanta, GA,[8]NCI Div. of Cancer Epidemiology & Genetics, Bethesda, MD

Introduction Understanding environmental-exposure associated gene expression alterations provides insights into how they contribute to cancer risk. We previously showed that individuals exposed to diesel engine exhaust (DEE) or smoky coal exhibit gene expression changes overlapping with those of smokers, suggesting shared mechanisms of toxicity. Wood smoke, produced by incomplete combustion of biomass fuels, is classified as probably carcinogenic (Group 2A), yet studies of its gene expression effects are limited. Here, we conducted a pilot study to examine whether genes associated with smoking, DEE, and smoky coal exposure are also differentially expressed in individuals exposed to wood smoke. **Methods** We studied 16 never-smoking women from Guatemala in the Household Air Pollution Intervention Network trial who use wood as their primary fuel. $PM_{2.5}$ exposure was measured with monitors, and urinary 1-Hydroxypyrene (1-OHP) was assessed as a biomarker of polycyclic aromatic hydrocarbons exposure. Nasal turbinate brush samples underwent bulk RNA-seq and were processed via a GTEx-based pipeline. Differential expression (DE) analysis to compare high vs. low $PM_{2.5}$ and 1-OHP was conducted using limma. Gene Set Enrichment Analysis was used to evaluate whether previously reported gene signatures associated with smoking, DEE exposure, and smoky coal use, were enriched among genes up- and down-regulated for each exposure, ranked by t-statistics. **Results** We found that both up-regulated and down-regulated smoking-associated signatures were concordantly enriched in wood smoke exposed women with high levels of $PM_{2.5}$ ($p = 0.001$ and $p=0.04$, respectively) and among women with elevated 1-OHP levels ($p < 0.001$ and $p = 0.015$, respectively). Genes down-regulated with exposure to smoky coal and DEE were also suppressed in participants with high levels of $PM_{2.5}$ ($p=0.005$ for smoky coal signature) and 1-OHP ($p<0.001$ & $p=0.008$ for smoky coal and DEE signatures, respectively). Notably, the signatures included genes such as *CYP1A1, CYP1B1,* and *CDH1,* which are involved in activation and detoxification of carcinogens. **Conclusions** Wood smoke exposure in never smokers was associated with airway gene expression changes with similarities to those associated with smoking, DEE, and smoky coal, suggesting shared molecular response to combustion pollutants and pathways linked to lung cancer development. Larger studies are needed to replicate these findings and further examine biomass smoke in lung carcinogenesis.

#2310 Development and validation of a plasma proteomics signature for earlier diagnosis of ovarian cancer using prospectively collected blood samples.

Nan Lin[1], Ngo Long[2], Allison F. Vitonis[1], Tara Eicher[3], SHELLEY TWOROGER[4], Simon T. Dillon[2], Towia A. Libermann[2], Daniel W. Cramer[1], John Quackenbush[3], Kathryn L. Terry[1], Naoko Sasamoto[5]

[1]Department of Obstetrics and Gynecology, Brigham and Women's Hospital and Harvard Medical School, Boston, MA,[2]Department of Medicine, Beth Israel Deaconess Medical Center and Harvard Medical School, Boston, MA,[3]Department of Biostatistics, Harvard T.H. Chan School of Public Health, Boston, MA,[4]Division of Oncological Sciences, Knight Cancer Institute, Oregon Health & Science University, Portland, OR,[5]Department of Obstetrics and Gynecology, University of Washington, Seattle, WA

Background: There is currently no ovarian cancer biomarker appropriate for screening which is partially due to using retrospective clinical samples obtained at the time of diagnosis for biomarker discovery. Thus, we sought to discover novel plasma proteomic biomarkers for ovarian cancer early detection using prospectively collected blood samples.
Method: We evaluated 10,778 plasma proteins measured using the SomaScan v5.0 assay in blood drawn at least three years prior to ovarian cancer diagnosis and matched controls in the Prostate, Lung, Colorectal and Ovarian Cancer Screening Trial (PLCO; n=98, training dataset) and the Nurses' Health Studies (NHS; n=99, replication dataset). We used a conditional logistic regression to identify individual proteins associated with ovarian cancer in the two datasets separately. We also compared plasma proteins for early-stage and late-stage ovarian cancer in blood collected at diagnosis in the PreOperative Pelvic Mass Study to age-matched population-based controls (PreOp; n=134). Then we used Elastic Net to develop a proteomic-based score to discriminate ovarian cancer cases from controls in PLCO, compared to a model with CA125 alone, and validated the proteomic-based score performance in NHS by calculating the area under the receiver operating characteristic curve (AUC) and 95% confidence interval (CI).
Results: Plasma proteins associated with ovarian cancer in blood samples collected prospectively differed from those associated with blood samples collected at diagnosis of early-stage disease compared to controls. There were 99 proteins associated with ovarian cancer diagnosed at least 3 years from blood collection ($p<0.05$) in PLCO, where 2 proteins, RCN3 and OBP2B, replicated in NHS ($p<0.05$). Of these 99 proteins, majority were not associated with ovarian cancer in PreOp and only three proteins overlapped (i.e., SERPINF2, ASAH2, BAGE3). In PLCO, adding a proteomic-based score comprised of 56 proteins to a model with CA125 alone significantly ($p=0.02$) improved discriminating ovarian cancer cases from controls with an AUC (95%CI) from 0.65(0.50-0.80) to 0.86(0.67,1.00). In NHS, proteomic-based score resulted in an AUC of 0.60(0.49-0.72) with marginal significance.
Conclusion: Our results revealed plasma proteomic profiles differ between prospectively collected blood samples at least 3 years prior to diagnosis and blood samples collected at time of diagnosis regardless of stage. We developed a proteomics-based score that improved upon CA-125 alone, although application to an independent cohort did not demonstrate a strong improvement. However, differences between studies (e.g., menopausal status and hormone therapy use) may explain this variation.

#2311 Natural history and biomarker discovery in gastric preneoplasia: Insights from the TUMMIE longitudinal study.

Tyler Anthony Simi[1], Fabian Leonardo Castro Valencia[2], Nanci Chavarria Villa[1], Ana Patricia Estrada-Florez[1], Angelica Michelle Rolon[1], Krish Jagasia[3], Alexa Morales-Arana[1], Alex Zhornitskiy[1], Asha Gupta Cogdill[1], Jeffrey Zheng-Hsien Ko[1], Joseph Marsano[1], Luis G. Carvajal-Carmona[1]

[1]UC Davis, Davis, CA,[2]Sciences and Health Sciences, University of Tolima, Ibague, CA,[3]UC San Diego, La Jolla, CA

Background: Gastric cancer remains a leading cause of cancer mortality worldwide, with marked racial and ethnic disparities in incidence and outcomes. Gastric intestinal metaplasia (GIM) is a key preneoplastic lesion, yet its natural history and progression biomarkers are poorly understood, particularly in diverse U.S. populations.
Methods: The TUMMIE study is a longitudinal cohort of patients with gastric preneoplasia at UC Davis Health. In a pilot phase, we enrolled 69 individuals (mean age 66 years) with histologically confirmed GIM. The cohort demographic composition was 67% female and 33% male, with race/ethnicity distributed as 67% non-Hispanic White, 15% Asian, 7% Black, 7% Hispanic White, and 4% multiracial, Native Hawaiian/Other Pacific Islander, or missing. Twenty-two patients (32%) reported a personal history of cancer and nearly half (48%) reported a family history of gastric conditions.. Among these, 39 participants provided stool and saliva samples, which were analyzed for Helicobacter pylori (H. pylori) strain detection using digital droplet PCR (ddPCR). We assessed concordance between clinical testing and ddPCR-based detection in both sample types. Additionally, we conducted a scoping review of published biomarkers associated with gastric preneoplasia progression.
Results: Of the 39 biospecimen donors, 8 tested high positive for H. pylori by ddPCR. Strain typing revealed clear variation in H. pylori virulence profiles, with ddPCR detecting both CagA-positive and CagA-negative strains across participants, including several samples with strong high-droplet signals (>100 to >1000) thereby indicating strain diversity in the cohort. Clarithromycin resistance mutations were detected by ddPCR, this indicates the presence of both antibiotic-resistant and antibiotic-sensitive H. pylori strains. Several samples carried VacA toxin-associated alleles and EPIYA motifs. Preliminary analyses show correlations between ddPCR detection and clinical test results. Demographic characteristics and infection rates varied across racial/ethnic groups, highlighting potential disparities in risk profiles. The scoping review identified candidate biomarkers in pathways related to inflammation, immune response, and epithelial transformation.
Conclusions: This pilot phase demonstrates feasibility of biospecimen collection and molecular characterization in a multiethnic cohort with GIM. Integration of ddPCR-based H. pylori detection and biomarker discovery may inform risk stratification and surveillance strategies for gastric cancer prevention. Expanded longitudinal follow-up will enable validation of progression biomarkers and clarify racial/ethnic differences in disease trajectory.

#2312 ASH-MARCC: Assessment of smoking history via methylation and reference-based cell composition in human tissue samples.

Minghui Zhang, Brock C. Christensen, Lucas A. Salas Diaz

Dartmouth Geisel School of Medicine, Lebanon, NH

Introduction: Cigarette smoking (CS) is associated with adverse health effects, including an increased risk of cancer development. Epigenome-wide association studies (EWAS) show that CS significantly alters DNA methylation (DNAm). While several DNAm-based predictors of smoking history have been trained using blood samples, their accuracy in tissue types remains limited. We aimed to develop a predictive model for smoking history that integrates DNAm data with reference based cell composition estimates in human tissue samples.

Methods: We utilized Infinium MethylationEPIC array data from the Genotype-Tissue Expression (GTEx) project as training and testing, and the Clinical Proteomic Tumor Analysis Consortium Lung Adenocarcinoma (LUAD) cohort as external validation. Quality control and beta value extraction were performed with ENmix. Cell type proportions (CPs) were estimated by HiTIMED. Surrogate variables (SVs) were derived from GTEx to account for batch effects. EWAS was conducted to identify differentially methylated CpGs (DMC), adjusting for tissue type, sex, age, CPs, and SVs. GTEx was split into training and testing (70:30) sets. DMC, CPs, sex, age, and tissue type were used to train an Elastic Net model predicting smoking history (smoker vs. non-smoker). Model accuracy was assessed by the area under the receiver operating characteristic curve (AUC) comparing the reported smoking status to the predicted probabilities. LUAD normal samples were classified into 3 groups based on predictions for survival analysis using Coxph.

Results: After QC, 654 GTEx normal, 183 normal adjacent and 199 primary tumor LUAD samples were retained. 198 DMC sites were enriched for cellular response to xenobiotic stimulus pathways. The model selected 83 features at min lambda, including 79 CpG sites, age, NK and CD8 CPs, and breast tissue type. cg21566642 (*Lnc-ECEL1-1*) overlapped with 3 published blood predictors; cg07339236 and cg11554391 with one. The ASH-MARCC model demonstrated near-perfect internal performance (training AUC 0.98, 95% CI 0.97-0.99; testing AUC 0.91, 95% CI 0.88-0.95). In external validation, the model maintained high accuracy on normal samples (AUC 0.81, 95% CI 0.75-0.87), while performance decreased but remained informative on tumor samples (AUC 0.66, 95% CI 0.58-0.74). The highest risk group showed a non-significant risk (adj-HR 2.1, 95% CI 0.98-4.56) versus the lowest.

Conclusions: We developed ASH-MARCC, a DNA methylation based model to assess smoking history in human tissue. An objective and accurate smoking classification enhances clinical decision-making across cancer types by treatment personalization and prognostic precision. By enabling direct evaluation of smoking exposure in cancer tissues, especially when self-reported information is unavailable, ASH-MARCC offers a powerful tool with crucial applications in both research and clinical settings.

#2313 Association of NMR-based metabolomics and lung cancer risk in the UK biobank.

Beiwen Wu[1], Jennifer D. Brooks[1], Joanne Kotsopoulos[2], Rayjean J. Hung[3]

[1]Dalla Lana School of Public Health, University of Toronto, Toronto, ON, Canada,[2]Women's College Research Institute, Toronto, ON, Canada,[3]Lunenfeld-Tanenbaum Research Institute, Sinai Health System, Toronto, ON, Canada

BackgroundLung cancer remains the most common type of cancer and the leading cause of cancer-related death globally. Nuclear magnetic resonance (NMR) techniques enable detailed profiling of lipoprotein subclasses by concentrations and compositions, offering potential opportunity for lung cancer risk screening.

MethodsWe included 273,375 participants (2164 developed lung cancer) from the UK Biobank, with 251 metabolites (170 absolute and 81 ratio metabolites) measured at baseline. Cox proportional hazards models were used to estimate the individual hazard ratio (HR) between each metabolite and lung cancer risk, adjusting for core and extended covariates. P-values were corrected for multiple testing. Subgroup analyses were conducted by sex, age group, and smoking status. Principal component analyses (PCA) were performed separately on absolute and ratio metabolites. PCs explaining 90% of the variance in each set were incorporated into Cox models to assess patterns in metabolomic profiles on lung cancer risk. A LASSO penalty was applied to identify key metabolites for lung cancer risk and their associations were obtained using multivariable Cox regression.

ResultsA total of 163 metabolites (98 absolute and 65 ratios metabolites) were found to be significant. Among absolute metabolites, glycoprotein acetyls showed the strongest association with increased risk [HR per SD = 1.19, 95% CI = 1.14-1.25], whereas the degree of unsaturation in fatty acids showed the strongest protective association [HR per SD = 0.84, 95% CI = 0.80-0.88]. Across all lipoprotein compositions, only triglycerides consistently showed increased risk in the main and subclasses of lipoproteins [HR range: 1.00-1.07], with 5 associations reaching statistical significance. Similar patterns were observed for ratio metabolites, except for phospholipid percentages, which showed increased risk. These patterns remained largely unchanged after adjustment for extended covariates, except for triglycerides, whose associations were attenuated and even reversed in some cases. In subgroup analyses, the largest differences were observed for triglycerides, where stronger positive associations were seen among females, former smokers, and people aged <60 years. In absolute metabolites, PC1 (VLDL-driven), PC2 and PC3 (HDL-driven) showed increased risk; PC8 and PC9 (glycolysis- and fatty acids-driven) showed decreased risk. In ratio metabolites, PC1, PC4, and PC6 (LDL and VLDL-driven) showed increased risk, PC5, PC7 and PC9 (fatty acids-driven) showed decreased risk. The LASSO-Cox models selected 15 metabolites and the direction and magnitude of these metabolites were largely consistent with those observed in the individual CoxPH models.

ConclusionFindings from this study highlighted the complexity of metabolic patterns and their role in lung cancer risk, warranting further investigation through pathway analyses.

#2314 Plasma metabolomics profiles in the progression of adverse liver conditions to liver cancer.

Xinyuan Zhang[1], Longgang Zhao[2], Yun Chen[2], Lu Cai[3], Michelle Lai[4], Wenjie Ma[5], Andrew T. Chan[5], Xuehong Zhang[2]

[1]Brigham and Women's Hospital, Boston, MA,[2]Yale School of Nursing, Orange, CT,[3]University of Louisville, Louisville, KY,[4]Beth Israel Deaconess Medical Center, Boston, MA,[5]Massachusetts General Hospital, Boston, MA

Background: Circulating metabolites may mark the progression from metabolic dysfunction-associated steatotic liver disease (MASLD) and liver cirrhosis to liver cancer. We characterized metabolomic patterns and evaluated prospective associations with stage-specific transitions.

Methods: We used data from 47,972 participants in Mass General Brigham Biobank with Nightingale metabolomics and longitudinal medical records before and after assessment. Stage at metabolomics was defined based on if MASLD, liver cirrhosis, or liver cancer had occurred by International Classification of Diseases codes. For participants with no adverse liver condition, we excluded those with Charlson comorbidity index >5 or death in 1 year of assessment to limit the impact of other diseases. Adjusted means and linear trends were estimated with covariates including demographics, comorbidities, and lifestyles. Adjusted Cox models examined the associations of pre-cancer metabolite and incident liver cancer. Interactions between metabolite and the hepatic fat-associated polygenic risk score (PRS) were tested.

Results: At metabolomics assessment, 17,869 participants had no adverse liver condition, 2041 had MASLD, 1774 had liver cirrhosis, and 206 had liver cancer. In the 249 metabolomic variables, 181 displayed significant linear trends by stage (FDR <0.05), e.g., small HDL cholesterol and very large HDL cholesterol / total lipids ratio decreased while large HDL free cholesterol / total lipids ratio and tyrosine increased with progression. These metabolites also show significant associations (FDR <0.05) with liver cancer incidence in participants with no liver disease or cirrhosis. We did not observe metabolite × PRS interactions (FDR >0.05).

Conclusions: Metabolomic profiles capture signals along the MASLD - cirrhosis - liver cancer continuum. These markers may improve risk stratification, timing of surveillance, and inform the biological mechanisms along the liver conditions spectrum.

Top metabolites in the progression of adverse liver conditions to liver cancer.

	Adjusted mean level					Association with incident liver cancer					
						No liver disease		MASLD		Liver cirrhosis	
Metabolite	No liver disease	MASLD	Liver cirrhosis	Liver cancer	FDR-linear	HR (95% CI)	FDR	HR (95% CI)	FDR	HR (95% CI)	FDR
Small HDL cholesterol	-0.21	-0.11	-0.60	-0.83	<0.001	0.72 (0.62, 0.82)	<0.001	0.65 (0.32, 1.29)	0.67	0.66 (0.54, 0.81)	0.004
Small HDL cholesteryl esters	-0.20	-0.11	-0.62	-0.88	<0.001	0.72 (0.63, 0.82)	<0.001	0.62 (0.31, 1.23)	0.65	0.66 (0.55, 0.80)	0.003
Small HDL particle concentration	-0.20	-0.10	-0.59	-0.79	<0.001	0.72 (0.62, 0.83)	<0.001	0.67 (0.32, 1.40)	0.69	0.65 (0.52, 0.80)	0.005
Very large HDL cholesterol / total lipids ratio	0.01	0.08	-0.24	-0.45	<0.001	0.74 (0.63, 0.87)	0.006	0.63 (0.35, 1.14)	0.62	0.53 (0.38, 0.75)	0.04
Large HDL free cholesterol / total lipids ratio	0.03	-0.09	0.19	0.47	<0.001	1.39 (1.16, 1.66)	0.008	1.71 (1.21, 2.42)	0.85	1.71 (1.21, 2.42)	0.03
Tyrosine	0.03	0.05	0.06	0.20	0.03	1.19 (1.03, 1.37)	0.11	1.30 (0.68, 2.50)	0.76	1.57 (1.28, 1.93)	0.003

#2315 Metabolomics and liver cancer risk: A systematic review of prospective studies.

Longgang Zhao[1], Mengjie Hu[2], Yun Chen[1], Xinyuan (Cindy) Zhang[3], Xuehong Zhang[1]

[1]Yale University, School of Nursing, Orange, CT,[2]Yale University, School of Public Health, New Haven, CT,[3]Brigham and Women's Hospital, Boston, CT

Introduction Emerging metabolomic studies have identified circulating metabolites associated with liver cancer, yet evidence remains inconsistent across populations. To address these gaps, we conducted the most comprehensive systematic review of prospective metabolomic studies to date, integrating results across different populations to identify metabolic signatures of liver cancer.
Methods We followed Preferred Reporting Items for Systematic Reviews and Meta-Analyses guidelines to report our findings. We systematically searched PubMed through January 2025, for prospective cohort or nested case-control studies examining pre-diagnostic circulating metabolomic profiles with liver cancer. Two reviewers independently screened, extracted, and evaluated studies. Due to heterogeneity in study design and outcome reporting, findings were synthesized descriptively. Direction and effect size of metabolite associations was summarized. Enrichment analysis was conducted for those metabolites significantly associated with liver cancer.
Results Twenty-four prospective studies were included, of which eight nested case-control or cohort studies with 1,626 cases of liver cancer, providing risk estimates for per standard deviation (SD) increase. Seven studies used liquid chromatography-mass spectrometry and one used nuclear magnetic resonance. Across these studies, 98 unique metabolites were evaluated, and consistent metabolic alterations preceding liver cancer were observed. Elevated aromatic amino acids (tyrosine, phenylalanine), glutamate, arginine, and conjugated bile acids were positively associated with liver cancer risk with risk ratios (RRs for per SD increase) ranging from 1.49 to 5.82, whereas branched-chain amino acids (leucine and isoleucine), lysine, glutamine, and lysophosphatidylcholines showed inverse associations with RRs ranging from 0.15 to 0.75. Saturated phosphatidylcholine, sphingosine, and select amino acid derivatives (cystathionine, kynurenine) were positively associated (RRs, 1.62-3.32), while androgen sulfates and creatine were inversely related (RRs, 0.20-0.56). The direction was generally consistent across the majority of the 24 prospective studies. Three most enriched pathways were taurine and hypotaurine metabolism, valine/leucine and isoleucine biosynthesis, and arginine biosynthesis.
Conclusions Our systematic review indicates that liver cancer risk was associated with increased aromatic amino acids, bile acid conjugation, and lipid remodeling, and decreased branched-chain amino acids and androgenic steroids. The identified metabolic signatures may inform future efforts in risk prediction, early detection, and targeted prevention for liver cancer.

#2316 Circulating lipid and bile acid metabolites as predictors of colorectal cancer risk: A multi-cohort metabolomics meta-analysis.

Mary Playdon[1], Emma Braun[2], Kelly Santucci[2], A. Heather Eliassen[3], Edward L. Giovannucci[4], Marc Gunter[5], Steven Moore[6], Lorelei A. Mucci[7], Xiao-Ou Shu[8], Mingyang Song[9], Ying Wang[10], Danxia Yu[8], Wei Zheng[8], Cornelia M. Ulrich[11], Jennifer Ose[12]

[1]Nutrition and Integrative Physiology, University of Utah Huntsman Cancer Institute, Salt Lake City, UT,[2]University of Utah, Salt Lake City, UT,[3]Assistant Professor, Harvard University, Boston, MA,[4]Professor of Nutrition & Epidem., Harvard TH Chan School of Public Health, Boston, MA,[5]Imperial College London, London, United Kingdom,[6]National Cancer Inst. Div. of Cancer Epidemiology & Genetics, Bethesda, MD,[7]Harvard T.H. Chan School of Public Health, Boston, MA,[8]Vanderbilt University Medical Center, Nashville, TN,[9]Harvard TH Chan School of Public Health, Boston, MA,[10]American Cancer Society, Atlanta, GA,[11]University of Utah Huntsman Cancer Institute, Salt Lake City, UT,[12]Hochschule Hannover - University of Applied Sciences and Arts, Hanover, Germany

Background: Metabolic dysregulation has been implicated in colorectal cancer (CRC) development but not fully characterized. We conducted a large-scale metabolomics meta-analysis to identify circulating metabolites associated with future CRC risk across heterogeneous populations.

Methods: We harmonized pre-diagnostic metabolomic and covariate data from seven prospective cohorts: the Cancer Prevention Study II Nutrition Cohort (CPS-II), the Prostate, Lung, Colorectal, and Ovarian Cancer Screening Trial (PLCO), the Women's Health Initiative Metabolomics in Nutrition Study (WoMIN), the Nurses' Health Study (NHS), the Health Professionals Follow-up Study (HPFS), the Shanghai Women's Health Study (SWHS), and the Shanghai Men's Health Study (SMHS). Using multivariable logistic regression, we applied fixed-effects meta-analysis to evaluate associations between 1,039 harmonized metabolites and CRC risk, adjusting for body mass index and other covariates.

Results: Across seven cohorts (N = 3,779, 50% cases), participants were predominantly female (59.5%), with a median age of 68 years (IQR 62-73) and median BMI of 25.0 kg/m² (IQR 23.0-28.0). Fourteen metabolites were significantly associated with CRC risk (FDR < 0.05). Inverse associations were observed for phospholipids and ether lipids enriched in polyunsaturated fatty acids (e.g., PE(20:0/18:2), PE(22:6/P-18:1), PC(22:6/18:0); OR range 0.47-0.63, p-value range 6.2E-04 to 6.8E-13). Positive associations included monoacylglycerols (MG(18:3)), bile acids (e.g., glycochenodeoxycholate), and xenobiotic compounds (e.g., N-undecylbenzenesulfonic acid). Heterogeneity was low (mean I^2 across the significant metabolites was ~ 15%), and directionality was consistent across studies.

Conclusions: This multi-cohort analysis identified lipid metabolism and bile acid signaling as key pathways in CRC etiology, among others, independent of adiposity. The inverse associations with polyunsaturated lipid species and the positive association with bile acids and xenobiotics suggest that membrane lipid remodeling, gut-liver axis perturbations, and environmental exposures may play mechanistic roles in CRC development. Ongoing external validation in the European Prospective Investigation into Cancer and Nutrition (EPIC) cohort using untargeted metabolomic data will inform the utility of these metabolites as biomarkers for CRC risk stratification and prevention.

#2317 Plasma metabolomic profiles of oral contraception use associated with breast and ovarian cancers among premenopausal women in Nurse's Health Study II.

Jennifer M. Mongiovi[1], Nan Lin[1], Oana Alina Zeleznik[2], Naoko Sasamoto[3], Britton Trabert[4], Julian Avila-Pacheco[5], Clary B. Clish[5], A. Heather Eliassen[6], Shelley TWOROGER[7], Kathryn L. Terry[8]

[1]Brigham and Women's Hospital, Boston, MA,[2]Harvard Medical School/Brigham and Women's Hospital, Boston, MA,[3]Fred Hutchinson Cancer Center, Seattle, WA,[4]University of Utah Huntsman Cancer Institute, Salt Lake City, UT,[5]The Broad Institute, Cambridge, MA,[6]Assistant Professor, Harvard University, Boston, MA,[7]Oregon Health and Science University, Portland, OR,[8]Asst. Professor, Dept. of OB/GYN, Brigham and Women's Hospital, Boston, MA

BACKGROUND: While over 80% of sexually active premenopausal women use oral contraception (OC), the biological mechanisms linking OC to hormone-sensitive cancers are not well understood. OC use lowers ovarian cancer risk while current use modestly increases breast cancer risk, suggesting complex underlying pathways. We sought to identify plasma metabolites associated with OC use in premenopausal women and relationships with ovarian and breast cancer. METHODS: Analysis included 2,072 premenopausal women in Nurses' Health Study II with self-reported OC history. OC use was defined as ≥1 years of previous use, excluding current users. All metabolite values were transformed to probit scores to achieve normality. Associations of prior use ≥1 years versus never and per 5 years use with individual metabolites were evaluated through multivariable linear regression, accounting for the number of effective tests (NEF) based on the number of principal components explaining 90% of the variance. Metabolite groups were identified through metabolite set enrichment analysis (MSEA) using false discovery rate (FDR) for multiple testing. OC use models were adjusted for blood draw variables (age, time, season, fasting status), BMI smoking, diet (Alternative Healthy Eating Index score), alcohol consumption, and physical activity at the time of blood draw. Associations of metabolite groups (FDR<0.20) and metabolites (NEF<0.20) were considered nominally associated with OC use. Associations with incident breast (n=663) and ovarian cancers (n=34) diagnosed at least ≥3 years after blood draw were assessed using conditional logistic regression, using controls matched 1:1 on blood draw variables, adjusting for age, OC duration, parity, and family history of breast or ovarian cancer and using MSEA. RESULTS: Of 2,703 women, 1,681 (81.1%) reported having previously used OC for ≥1 year, with a mean duration of 4.0±3.9 years. Each additional 5 years of OC use was associated with higher C40:6 phosphatidylethanolamines (PE) levels (β=0.09; 95% CI: 0.04, 0.14), and both phosphatidylcholines and PEs were negatively associated with OC use and duration but positively for breast and ovarian cancer risk. Increasing OC duration was associated with lower tryptophan (β=-0.11; 95% CI: -0.16, -0.05) and higher 1,7-methyluric acid (β=-0.11; 95% CI: -0.16, -0.05), which were both lower among breast cancer cases and higher among ovarian cancer cases, but the overall organoheterocyclic compound group was not significantly associated with OC use. CONCLUSION: Our results suggest long-lasting alterations of systemic metabolism may in part explain associations of OC use with breast and ovarian cancers, particularly among metabolites that contribute to lipid metabolism. Analyses are ongoing and will include a deeper investigation into timing and formulation of OC use as well as cancer subtypes.

#2318 Environmental exposures, metabolomic profiles and mutational signatures in never and ever smokers with lung cancer.

Kathryn Demanelis[1], Sonali Dayal[1], Autumn Gaither Davis[1], Arjun Pennathur[1], Riyue Bao[1], Jennifer Walker[1], Patricia Lynn Opresko[1], James G. Herman[2], Brenda B. Diergaarde[3], Laura P. Stabile[1]

[1]University of Pittsburgh, Pittsburgh, PA,[2]UPMC Hillman Cancer Center, Pittsburgh, PA,[3]University of Pittsburgh School of Public Health, Pittsburgh, PA

Non-small cell lung cancer in never smokers (LCINS) accounts for ~25% of all cases and is the fifth highest cause of cancer death. LCINS disproportionately affects women and has been reported to be associated with environmental exposures, such as air pollution and radon. Prior LCINS studies investigating environmental risk factors often relied on geospatial estimates of exposures rather than individual-level exposures. In addition, information on the relationship between these exposures and tumor characteristics, such as mutational signatures (MutSigs), is limited. Liquid chromatography-high resolution mass spectrometry (LC-HRMS) profiling of plasma enables identification of chemical and metabolic exposures, i.e. the chemical exposome (CE), encountered by an individual. We conducted an exposome-wide analysis of compounds in the CE among 86 matched early-stage non-small cell lung cancer in smokers (LCIS) and LCINS cases. Whole-genome sequencing (WGS) on tumor and blood was performed on a subset of LCINS cases (N=16) to assess associations of chemical compounds and metabolites with tumor mutational burden (TMB) and MutSigs. Residential addresses were geocoded and geospatially integrated with environmental and radon data. Untargeted CE profiles were generated, and 539 annotated compounds were reproducibly detected in >75% of samples. Associations between LCIS/LCINS and CE compounds were evaluated using logistic regression; the correlation with TMB and MutSigs was assessed using Spearman's rho. The study population consisted of 28% women; mean age was 70 years. Among the LCINS cases sequenced, most exhibited common driver mutations. After exposome-wide analysis, 37 and 9 compounds were respectively higher and lower in plasma from LCINS vs. LCIS ($P < 0.05$). Compounds higher in LCINS included trifluoroacetic acid (TFA, a degradation product of polyfluorinated hydrocarbons), methocrifos (a pesticide), and aspartame (artificial sweetener). Among the sequenced LCINS cases, 18 single base-substitution (SBS) signatures were identified, including SBS18 (reactive oxygen species damage) in 4/16, SBS26 (defective DNA mismatch repair) in 6/16, and SBS40a in 16/16 (unknown etiology). We identified 44 compounds that were positively correlated with SBS18 ($P < 0.05$), including the histamine precursor and inflammatory agent, histidine, and microbial metabolites. Our pilot study identified differential CE profiles between LCINS and LCIS cases, where LCINS cases showed higher exposure to environmentally relevant exposures (e.g., TFA, pesticides, food additives). Chemical and metabolic compounds were positively correlated with several MutSigs, suggesting a role in carcinogenesis potentially via relevant mechanisms such as oxidative stress and DNA repair. These findings support a role for environmental carcinogens in LCINS etiology and warrant further investigation.

#2319 Variation in urinary estrogen levels according to breast parenchymal texture in postmenopausal women.

Onyedikachi Adike[1], Kajita Yukie[1], Xianming Tan[1], Gretchen Gierach[2], Cherie Kuzmiak[1], Despina Kontos[3], Eric A. Cohen[3], Walter C. Mankowski[3], Sarah J. Nyante[1]

[1]Department of Radiology, University of North Carolina at Chapel Hill, Chapel Hill, NC,[2]Division of Cancer Epidemiology and Genetics, National Institute of Health(NIH), Bethesda, MD,[3]Center for Innovation in Imaging Biomarkers and Integrated Diagnostics (CIMBID), Columbia University Irving Medical Center, New York City, NY

Background: Estrogen levels and breast parenchymal texture are both risk factors for breast cancer, but the relationship between the two is incompletely understood. This study evaluated associations between urinary estrogens, their metabolites, and parenchymal texture features in postmenopausal women to clarify how hormonal pathways contribute to radiomic breast tissue characteristics.
Methods: Urinary concentrations of estradiol, estrone, and 13 estrogen metabolites were quantified using liquid chromatography/tandem mass spectrometry (LC-MS/MS) and standardized to urinary creatinine levels (pmol/mg creatinine) among 294 postmenopausal women undergoing screening mammography at the University of North Carolina between 2020 and 2022. Women who were using menopausal hormones, oral contraceptives, or chemoprevention, or who had breast implants were excluded. An automated radiomic pipeline was used to quantify 344 parenchymal texture features from bilateral mammograms. Features were harmonized using ComBat to reduce batch effects. Principal components analysis and unsupervised clustering of features were used to define texture groups. Multinomial regression was used to assess associations between texture groups and estrogen levels, with and without adjustment for age and body mass index (BMI).
Results: Participants had a median age of 64 years (IQR: 59-71), a median BMI of 28 kg/m2 (IQR: 24-33), and a median total estrogen level of 20.9 pmol/mg creatinine. Participants clustered into three groups (Group 1: n=120, Group 2: n=154, Group 3: n=21). In the unadjusted analysis, Group 1 had lower levels of all parent estrogens and metabolites compared with Group 2, including lower levels of estrone (β =-0.046, p=0.04), 2-hydroxyestrone (β=-0.064, p=0.03), 16-epiestriol (β=-0.177, p = 0.03), and 17-epiestriol (β=-0.449, p=0.02). Differences in some, but not all, metabolites were attenuated after adjustment. In contrast, there was no consistent difference in estrogens between Group 3 and Group 2 in unadjusted or adjusted analyses.
Conclusion: For some postmenopausal women, estrogen metabolism, particularly through the 2- and 16-hydroxylation pathways, was associated with distinct mammographic parenchymal texture profiles. Identification of texture patterns linked to specific hormonal profiles may help explain the biological factors that shape breast composition and inform strategies for prevention of hormonally driven breast cancers.

#2320 Assessing endometrial cancer etiology by histologic subgroups.

Deirdre A. Hill[1], Carolyn Y. Muller[1], Kimberly K. Leslie[1], David G. Mutch[2]

[1]Internal Medicine, University of New Mexico, Albuquerque, NM,[2]Obstetrics and Gynecology, Gynecologic Oncology, Washington University, St. Louis, MO

Introduction: Endometrial cancer incidence has increased substantially in the past two decades, with the increases occurring primarily in tumors of non-endometrioid histology, which have a poor prognosis. Evidence regarding the origin(s) of the increase is sparse. We sought to determine whether women who had particular molecular signatures of endogenous and exogenous exposures had an increased risk of non-endometrioid histology, particularly serous tumors.

Methods: We investigated single-base substitution (SBS) signatures in exome sequencing data from The Cancer Genome Atlas (TCGA). Standard algorithms for mutational signature assessment were applied. Signatures were evaluated on a continuous scale, and also using a high/low cut point determined by maximally selected rank statistics. Relative risks (RR) and 95% confidence intervals (CI) were computed for 49 signatures, comparing risk for serous in relation to endometrioid histology. Disease-specific survival (DSS) was also evaluated in Cox proportional hazard models, with calculation of hazard ratios (HR) and 95% CI. The proportional hazards assumption was verified by Schoenfeld residuals. All analyses were adjusted for age at cancer diagnosis, and DSS analyses were also adjusted for stage.

Results: Included were n=414 women with endometrioid and n= 134 with serous non-endometrioid tumors. High Mismatch Repair defective (dMMR) (SBS6 and SBS15) and Polymerase Epsilon mutation (POLE) (SBS10a; SBS10b) signatures were less common in serous than endometrioid tumors, as expected from the literature (dMMR: SBS6 RR 0.21;95% CI 0.12-0.39; SBS15 0.22;95% CI 0.12-0.40;SBS26 0.21;95% CI 0.12-0.40); SBS15 RR 0.22;95% CI 0.12-0.40 and POLE SBS10a RR 0.23;95% CI 0.10-0.54 and SBS10b 0.33; 95% CI 0.19-0.58). A signature related to tobacco use (SBS4) was also less common in serous tumors (RR 0.32;95% CI 0.15-0.71). Women with high dMMR (SBS6: HR 0.06;95%CI 0.01-0.47; SBS15 HR 0.23;95%CI 0.08-0.64; SBS26: HR 0.42;95% CI 0.21-0.84)) or high POLE (SBS10a HR 0.06;95% CI 0.01-0.46; SBS10b HR 0.13; 0.03-0.54) signatures had a reduced risk of endometrial cancer-specific mortality.

Discussion: Endometrioid and serous tumors differ in mutational signatures. The reduced dMMR and POLE signature risk in relation to both serous tumors and DSS are in agreement with other findings. Our results open up new prospects for exploration of serous tumor etiology

#2321 Expression of 27-hydroxycholesterol metabolizing enzymes and breast cancer clinicopathological characteristics: The Multiethnic Cohort Study.

Lenora W. M. Loo[1], Yuqing Li[2], Kami K. White[3], Jose A. Aparicio[4], Veronica Wendy Setiawan[5], Brenda Y. Hernandez[3], Anna H. Wu[4], Christopher Haiman[5], Loic Le Marchand[3], Lynne R. Wilkens[3], Iona Cheng[2]

[1]Cancer Biology Program, University of Hawai'i Cancer Center, Honolulu, HI,[2]Department of Epidemiology and Biostatistics, School of Medicine, University of California San Francisco, San Francisco, CA,[3]Population Sciences of the Pacific, University of Hawai'i Cancer Center, Honolulu, HI,[4]Department of Population and Public Health Sciences, University of Southern California, Keck School of Medicine, Los Angeles, CA,[5]USC Norris Comprehensive Cancer Center, Los Angeles, CA

Background: Obesity is a major modifiable risk factor for postmenopausal breast cancer prognosis. Mechanisms underlying the association between obesity and post-menopausal breast cancer include higher levels of estradiol, cholesterol, and inflammation. Circulating cholesterol is metabolized into 27-hydroxychlolesterol (27HC) by the sterol 27-hydroxylase enzyme (CYP27A1). 27HC is catabolized by the oxysterol 7α-hydroxylase enzyme (CYP7B1). 27HC can regulate breast cancer pathobiology by functioning as an endogenous selective estrogen receptor modulator in breast tumors. In this study, we examined the associations of expression levels of *CYP27A1* and *CYP7B1* in tumor tissue with clinicopathological characteristics of breast cancer in a multiethnic population.
Methods: Invasive breast tumor tissue from 510 postmenopausal females (62 African American, 114 Japanese American, 93 Latino, 135 Native Hawaiian, and 106 White) in the Multiethnic Cohort Study were used for targeted profiling of gene expression using the NanoString nCounter Breast Cancer 360™ (BC360) Panel, including 51 additional custom genes. Generalized odds logistic regression analysis was conducted to examine associations of gene expression levels for *CYP27A1* and *CYP7B1* with clinicopathological characteristics -- stage, PAM50 molecular subtype (Luminal A, B, HER2-enriched, Basal-like) and NanoString Risk of Recurrence (ROR) score.
Results: *CYP27A1* expression was associated with a lower likelihood of advanced versus localized stage at diagnosis (OR=0.87; 95% CI 0.74, 1.02). No association was observed for *CYP7B1* with stage. *CYP27A1* expression was associated with a lower likelihood of HER2-enciched (OR=0.71; 95% CI 0.55, 0.92) and Luminal B (OR=0.71; 95% CI 0.58, 0.89) subtypes in comparison to Luminal A subtypes. *CYP7B1* expression was associated with Basal-like (OR=1.23; 95% CI 1.02, 1.49), HER2-enriched (OR=0.59; 95% CI 0.43, 0.80), and Luminal B (OR=0.43; 95% CI 0.32, 0.58) subtypes in comparison to Luminal A. No significant association was observed for *CYP27A1* and ROR categories (low, intermediate, and high). In contrast, *CYP7B1* expression was associated with lower risk of recurrence score (ROR intermediate vs. low: OR=0.77; 95% CI 0.62, 0.96; ROR high vs. low: OR=0.56; 95% CI 0.40, 0.79).
Conclusion: This study identified that gene expression levels of 27HC metabolizing enzymes, *CYP27A1* and *CYP7B1,* in breast tumors were associated stage, breast cancer subtype, and risk of recurrence among a multiethnic population of women.

#2322 Protective role of abundant healthy stroma against breast cancer: A prospective cohort study of healthy women in the Susan G. Komen Tissue Bank.

Garrett S. Hendley[1], Shaoqi Fan[1], Scott Lawrence[2], Karun Mutreja[2], Ruth M. Pfeiffer[1], Maire A. Duggan[3], Gretchen L. Gierach[1], Jill E. Henry[4], Mustapha Abubakar[1]

[1]Division of Cancer Epidemiology and Genetics, National Cancer Institute, National Institutes of Health, Bethesda, MD,[2]Molecular and Digital Pathology Laboratory, Leidos Biomedical Research, Inc., 21702, Frederick, MD,[3]Department of Pathology and Laboratory Medicine, University of Calgary, Calgary, T2N2Y9, AB, Canada,[4]Biospecimen Collection and Banking Core, Susan G. Komen Tissue Bank at the IU Simon Comprehensive Cancer Center, Indianapolis, IN

Background

Breast cancer (BC) remains a leading cause of morbidity and mortality in women worldwide. To mitigate this trend, future BC risk reduction strategies need to be grounded in BC etiologic histogenesis, i.e., the tissue pathways in the normal breast by which etiologic factors impact BC risk. Results from previous studies have indicated that the tissue composition of the breast may offer clues into the etiologic histogenesis of BC. However, many prior studies were conducted among women with benign breast disease (BBD), a tissue state characterized by underlying pathological changes that may obscure studies of etiologic histogenesis. Here, we investigated the associations of histologic tissue composition metrics of the normal breast with subsequent BC risk.

Methods

This prospective cohort study includes 3,435 healthy females (aged 18-75 years) who donated normal breast tissue to the Susan G. Komen Tissue Bank (KTB) between 2009-2019 and met study-specific inclusion criteria. Of these, 109 women developed BC after a median follow-up of 6 years (range: 1-16 years). Supervised machine-learning algorithms were used to analyze digitized histologic sections of normal breast tissues to generate quantitative data on percent epithelium, stroma, and adipose tissue for each woman. Associations between histologic metrics and breast cancer incidence were assessed in multivariable Cox proportional hazard regression models with age as the time-scale. Analyses were performed overall and following stratification by age at study entry and menopausal status. Models were adjusted for race, education, parity, body mass index, smoking status, alcohol use, and whole slide tissue area.

Results

Overall, abundant stroma was associated with decreased BC risk (hazard ratio (HR) per 1 standard deviation (SD) increase = 0.55, 95% confidence interval [CI] = 0.38 to 0.80, $P < 0.01$). The stromal protective effect was most profound among women younger than 55 years at tissue donation (HR/1-SD = 0.45, 95% CI = 0.26 to 0.79, $P < 0.01$) and in premenopausal women (HR/1-SD = 0.48, 95% CI = 0.26 to 0.87, $P = 0.015$), irrespective of age. Elevated epithelium and adipose tissue were associated with significantly increased BC risk in these same groups. However, when including stroma and adipose tissue in the same regression model, the mutual adjustment for stromal tissue mitigated adipose-related risk in women overall (HR/1-SD = 0.26, 95% CI = 0.06 to 1.16, $P = 0.077$), women younger than 55 years (HR/1-SD = 0.17, 95% CI = 0.04 to 0.71, $P = 0.015$), and in premenopausal women (HR/1-SD = 0.16, 95% CI = 0.04 to 0.65, $P = 0.01$).

Conclusion

Findings from this cohort of healthy women provide insights into the role of stroma in BC histogenesis during normal homeostasis, with potential implications for BC risk prediction and risk-reduction strategies.

#2323 Associations of stromal markers with breast terminal duct lobular involution.

Yaileen D. Guzman-Arocho[1], Lusine Yaghjyan[2], Laura C. Collins[3], Brian R. Sardella[1], Maisey Ratcliffe[2], **Rulla M. Tamimi**[3], Yujing J. Heng[1]

[1]Beth Israel Deaconess Medical Center, Boston, MA,[2]University of Florida, Gainesville, FL,[3]Weill Cornell Medicine, New York, NY

Background: Elevated expression of stromal markers in breast cancer (BrCa) has been linked to more aggressive disease and poorer prognosis. In contrast, data on stromal marker expression in premalignant breast tissues are limited, and it remains unclear whether these markers may inform future BrCa risk. Terminal duct lobular involution (TDLU), a physiologic process characterized by a decreased number of TDLUs and acini within breast lobules, has been associated with lower BrCa risk and is considered a potential surrogate risk marker for BrCa. In this study, we examined the associations between five stromal markers and TDLU involution in premalignant breast tissues.

Design: Tissue microarrays from 260 cancer-free women with biopsy-confirmed benign breast disease within the Nurses' Health Study (NHS) and NHSII were stained and evaluated for alpha-smooth muscle actin (αSMA), fibroblast activation protein (FAP), matrix metallo-peptidase (MMP14), tenascin-C (TNC), and calcyclin (s100A6). For each core, the % positivity was quantified by the inForm software. Our previously published computational algorithm computed six measures of TDLU involution assessing the number of TDLUs (TDLU counts/non-adipose tissue area), TDLU size (median TDLU span, median TDLU area, and TDLU area/% of non-adipose tissue area), and TDLU development (median acini counts/TDLU and median acini density). The associations of each marker's expression (binary with 1% cut-off) with each feature (log-transformed) was examined using generalized linear regression, adjusting for established BCa risk factors.

Results: The expression of αSMA and MMP14 was positively associated with four out of five features related to TDLU size and development (all $p<0.05$). FAP expression was positively associated with three features of TDLU size and development: median TDLU span, median TDLU area, and median acini counts/TDLU (all $p<0.05$). TNC expression was positively associated with median TDLU span but inversely associated with median acini density and TDLU counts/non-adipose tissue area (all $p<0.05$). No associations were found for s1006a.

Conclusions: The expression of several stromal markers in benign breast tissue was associated with larger TDLUs and more acini, i.e., lower degrees of lobular involution. Studies are underway to evaluate if these findings translate into associations with increased BCa risk.

#2324 Associations of circulating insulin-like growth factor-1 and insulin-like growth factor binding protein-3 with the expression of stromal markers in women with benign breast tissue.

Lusine Yaghjyan[1], Yu Jing J. Heng[2], Brian R. Sardella[2], Maisey Ratcliffe[1], **Rulla M. Tamimi**[3]

[1]University of Florida, Gainesville, FL,[2]Beth Israel Deaconess Medical Center, Boston, MA,[3]Weill Cornell Medicine, New York, NY

Purpose: The breast tissue microenvironment, and specifically stroma, is important for maintaining the normal tissue structure, and alterations within this environment may influence breast cancer (BCa) risk. The resident (normal) fibroblasts are the most abundant stromal cells. In breast tumors, cancer-associated fibroblasts have been associated with more aggressive phenotypes, and resistance to treatment. The insulin-like growth factor (IGF) pathway is involved in breast epithelial cell growth and extracellular matrix remodeling and may potentially influence normal fibroblasts. To date this association has not been explored in epidemiological studies. We examined, for the first time, the associations of circulating IGF-1 and IGF binding protein-3 (IGFBP-3) with the expression of breast stromal markers related to fibroblast activation: alpha-smooth muscle actin (αSMA), tenascin-C (TNC), fibroblast activation protein (FAP), calcyclin (s100a6), and matrix metallo-peptidase (MMP14).

Methods: This study included 145 cancer-free women with incident biopsy-confirmed benign breast disease (BBD) from the Nurses' Health Study II (NHSII) cohort. The data on BCa risk factors were obtained from biennial questionnaires. Immunofluorescence (IF) of stromal markers was performed on tissue microarrays with commercial antibodies (αSMA: 1:400 dilution; FAP: 1:50; MMP14: 1:150; TNC: 1:200; s100a6: 1:300). For each core, the % positivity was quantified by inForm v2.6.0. Generalized linear regression was used to examine the associations of plasma IGF-1 and IGFBP-3 (continuous log-transformed and quartiles) with log-transformed positivity for each stromal marker, adjusted for BCa risk factors and BBD subtype.

Results: In multivariate analysis, circulating IGF-1 was positively associated with s100a6 expression both when modeled continuously (β=0.89, 95% 95% Confidence Interval [CI] 0.07, 1.71) and as quartiles (β for 4^{th} vs. 1^{st} quartile=0.82, CI 0.16, 1.48; p-trend=0.03). Women whose circulating IGFBP-3 levels were in the top quartile appeared to have lower expression of TNC (β=-2.51, 95% CI -4.75, -0.27; p-trend=0.08). No associations were seen for αSMA, FAP, and MMP14.

Conclusion: Our findings suggest positive associations of circulating IGF-1 with s100a6 and inverse associations of IGFBP-3 with TNC, consistent with previously reported positive associations of IGF-1 and inverse associations of IGFBP-3 with BCa risk. Future studies are warranted to confirm our findings.

#2325 Association between widowhood and ovarian tumor gene expression.

Jaileene Perez Morales[1], Kathryn Berns[1], Cassandra Copp[1], Joseph Grieco[1], Mark K. Townsend[2], Steven A. Eschrich[3], Guillermo Armaiz-Pena[4], Lauren Cole Peres[3], Shelley TWOROGER[2]

[1]Knight Cancer Institute, Portland, OR,[2]Oregon Health & Science University, Portland, OR,[3]H. Lee Moffitt Cancer Center, Tampa, FL,[4]Ponce Health Sciences University, Ponce, PR

Background: Distress increases the risk of developing epithelial ovarian cancer (EOC). This can lead to the activation of the sympathetic nervous system (SNS) and the release of norepinephrine (NE). NE promotes inflammation, angiogenesis, and cell motility, which influence early and late stages of tumor progression. Widowhood is one form of chronic psychosocial stress that is associated with an increase in EOC risk. We hypothesize that women who experienced widowhood prior to EOC diagnosis will have higher tumor gene expression of inflammation-related and immune suppression pathways when compared to women who are married.
Methods: RNA sequencing was performed on 167 high-grade serous or poorly differentiated ovarian cancer tumors from the Nurses' Health Study (NHS), NHSII, and the New England Case-Control study who had information on pre-diagnosis marital status. The primary exposure was ever reported widowhood up to 1 year before diagnosis. Linear regression was used to identify differentially expressed genes associated with widowhood, adjusted for age. Gene set enrichment analysis (GSEA) using the Cancer Hallmarks, KEGG, and Reactome databases was employed to identify biological pathways associated with widowhood.
Results: Five genes (KCNE3, ACHE, C3orf52, RPL19P9, and AC116366) were significantly upregulated in the ovarian tumors of widowed versus married individuals. The top upregulated genes are associated with wound healing and cancer progression. Two genes (GABBR2 and RPS3AP29) were significantly downregulated and have been demonstrated to be involved in inhibitory neurotransmission and elevated tumor immune cell infiltration. GSEA identified six pathways that exhibited significant associations with widowhood, specifically related to inflammation (TNF-α), proliferation (G2M checkpoint), and tumor immunity (interferon-α and γ response).
Conclusions: Our results provide insight into biological pathways that link widowhood to ovarian cancer development, particularly through inflammatory and tumor immunity pathways.

#2326 Differentiating epigenetic marks and DNA adducts at the KRAS codon 12 mutation hotspot using ONT/ELIGOS sequencing.

Gunnar Boysen[1], Alongkorn Kurilung[2], Visanu Wanchai[2], Intawat Nookaew[2], Sarah Shuck[3]

[1]University of Arkansas for Medical Sciences, Little Rock, AR,[2]Biomedical Informatics, University of Arkansas for Medical Sciences, Little Rock, AR,[3]Diabetes and Cancer Metabolism, Beckman Research Institute at the City of Hope, Duarte, CA

Mutations—whether inherited or acquired—are central to cancer development, and reducing mutagenesis is an effective strategy for lowering cancer rates. At its simplest, DNA mutations arise from error-prone DNA replication or from the replication of DNA following incorrect repair of DNA lesions. Mechanistically, mutations occur when polymerases erroneously replicate DNA, with error rates increasing significantly in the presence of DNA modifications or DNA adducts. Among DNA modifications, epigenetic marks such as 5-methyl-deoxycytidine (5mdC) are the most abundant, occurring at a frequency of approximately one methylated cytosine per 100 cytosines. This is substantially higher than the frequency of endogenous DNA adducts (about one in 10,000 nucleotides) and exogenous DNA adducts (often less than one in 100 million normal nucleotides). Therefore, it remains unclear whether a specific mutation arises from errors in epigenetic processes, or from endogenous- and exposure-induced DNA adducts. Chemically specific methods for DNA adduct detection, unfortunately, often do not provide information about their position within the genome, prohibiting identification of the DNA adduct causing specific mutations. To address these knowledge gap, our group developed a nanopore-based DNA sequencing approach, called “ELIGOS” (Oxford Nanopore Technology-Epitranscriptional/ Epigenomical Landscape Inferring from Glitches of ONT Signals) that can (i) detect and (ii) differentiate between various types of epigenic marks and exposure-induced DNA adducts at base pair resolution while sequencing the DNA. ONT/ELIGOS provides an innovative tool to study the DNA lesions and mutations in pre-selected DNA regions. In this work, we present our latest ONT/ELIGOS findings demonstrating the detection and identification of DNA adducts at codon 12 within the KRAS cancer driver gene. In addition to common epigenetic marks and exposure-derived DNA adducts, our current panel of DNA adducts includes common endogenous lesions. Together these novel approaches can reveal the dynamics changes in single DNA molecules.

#2327 Thymic radiation and oncologic outcomes.

Vasco Prudente[1], Simon Bernatz[1], Suraj Pai[1], Katelyn M. Atkins[2], Keno Bressem[3], Christian V. Guthier[1], Leonard Nurnberg[1], Christopher E. Kehayias[4], Christopher Abbosh[5], Charles Swanton[6], Mariam Jamal-Hanjani[7], Nicolai Juul Birkbak[8], Raymond H. Mak[9], Hugo Aerts[1]

[1]Artificial Intelligence in Medicine, Harvard Medical School, Boston, MA,[2]Department of Radiation Oncology, Cedars-Sinai Medical Center, Los Angels, CA,[3]Technical University of Munich, Munich, Germany,[4]Department of Radiation Oncology, Dana-Farber Cancer Institute, Boston, MA,[5]Christopher Abbosh (Individual), London,[6]The Francis Crick Institute, London, United Kingdom,[7]University College London (UCL) Cancer Institute, London, United Kingdom,[8]Aarhus University, Aarhus, Denmark,[9]Instructor, Dept. of Radiation Oncology, Dana Farber/Brigham & Women's Cancer Center and Harvard Medical School, Boston, MA

BackgroundThe thymus plays a crucial role in early life, serving as the primary source of T-cell development, a vital component of adaptive immunity. Despite its central role in immune biology, the thymus is not currently considered an organ-at-risk in Radiotherapy (RT). RT, a cornerstone of treatment for locally advanced non-small cell lung cancer (NSCLC), has effects extending beyond local tumor control. In particular, it can trigger immunogenic cell death, releasing tumor antigens that prime systemic antitumor immunity. These immune-mediated effects are particularly important when RT is combined with immunotherapy, where consolidation immunotherapy has been shown to improve survival after chemoradiation.
MethodsIn this multicohort study, we assessed whether thymic irradiation was associated with distant metastases and all-cause mortality across 882 locally-advanced NSCLC patients treated with RT (RTOG-0617 n=460 | HARVARD-CRT n=422). For each patient, we measured the mean thymic radiation dose (MTD). Thymic health was determined based on thymic radiographic representation on CT scans, automatically inferred using a self-supervised deep learning model. Associations with clinical outcomes were assessed using multivariable Cox models, adjusting for key clinical factors. Sensitivity analyses evaluated the incremental contribution of MTD. To demonstrate the clinical feasibility of thymic sparing with modern RT techniques and AI-based volume delineation, we replanned the RT treatment plan in a representative case with high cumulative thymic dose exposure.
ResultsIn RTOG patients with preserved thymic health, higher thymic radiation dose was progressively associated with worse clinical outcomes. An MTD of 35Gy was identified as the lowest dose linked to a significant deterioration in outcomes. This threshold was validated in both cohorts, where exceeding the 35Gy MTD in patients with preserved thymic function was associated with increased risk of distant metastases (RTOG-0617: adjusted hazard-ratio [aHR]=1.32; p=0.002 | HARVARD-CRT: aHR=2.15; p=0.018) and worse overall survival (RTOG-0617: aHR=1.20; p=0.002 | HARVARD-CRT: aHR=2.02; p=0.014). No significant associations emerged in patients with low thymic health prior to radiation therapy. One-year follow-up imaging demonstrated dose-dependent declines in AI-quantified thymic health, supporting a mechanistic link between thymic irradiation and loss of immune competence. In a feasibility test case, thymic dose was successfully reduced below 35 Gy without compromising tumor coverage or cardiopulmonary constraints.
ConclusionsThymic radiation exposure was independently associated with higher risks of metastasis and death in NSCLC patients with preserved thymic function. These findings suggest that the thymus should be recognized as an organ-at-risk in radiotherapy and that thymus-sparing strategies may be crucial to preserve immune health and improve patient outcomes.

#2328 Gut microbiome and breast cancer-related endogenous hormone risk factors in US women: findings from the Nurses' Health Study II.

Tengteng Wang[1], Tong Cheng[1], Walter C. Willett[2], Curtis Huttenhower[2], Yang-Yu Liu[3], A. Heather Eliassen[4]

[1]Rutgers Cancer Institute, New Brunswick, NJ,[2]Harvard T.H. Chan School of Public Health, Boston, MA,[3]Brigham and Women's Hospital, Boston, MA,[4]Harvard T.H. Chan School of Public Health; Brigham and Women's Hospital, Boston, MA

Background: Endogenous estrogens are well-established risk factors for breast cancer. A subset of gut microbes, collectively termed the estrobolome, plays a fundamental role in estrogen metabolism and reabsorption. However, existing studies examining associations between the gut microbiome and circulating estrogen levels in humans have been few and small in scale, and no prior work has established an estrobolome linked to circulating estrogen levels using shotgun metagenomic sequencing.
Methods: This study included 141 non-hormone users from a microbiome sub-study nested within the Nurses' Health Study II. Stool samples were collected using a home-based self-collection protocol, followed by blood collection approximately 3-4 months later. Circulating estrone (E1), estradiol (E2), and testosterone levels were assayed at the Mayo Clinic Laboratory by liquid chromatography-tandem mass spectrometry. Shotgun metagenomic sequencing was conducted using the 100 nt Illumina HiSeq platform. Taxonomic and functional profiling were performed using the bioBakery 4.0 workflow. Microbial α-diversity (Inverse Simpson index) and β-diversity (Bray-Curtis dissimilarity) were calculated. LASSO regression was applied to identify microbial features predictive of hormone levels, and age and BMI-adjusted generalized linear models were used for association analyses with multiple comparisons correction.
Results: Taxonomic and functional profiling identified 1,860 species and 512 MetaCyc pathways. Microbial α-diversity was inversely correlated with E1 ($R = -0.16$, $p = 0.07$) and E2 ($R = -0.16$, $p = 0.06$), and positively correlated with testosterone ($R = 0.12$, $p = 0.16$). In age-adjusted models, α-diversity was significantly inversely associated with E2 (β = -0.39; 95% CI: -0.70, -0.07), though the association attenuated after further adjustment for BMI at stool collection (β = -0.16; 95% CI: -0.47, 0.15). PERMANOVA analyses revealed significant associations between taxonomic variation and E1 ($R^2 = 0.28\%$), E2 ($R^2 = 0.34\%$), and testosterone ($R^2 = 0.16\%$) (all $p < 0.005$). LASSO feature selection identified 23 species predictive of E1 and 16 predictive of E2, with the majority belonging to the genera *Bacteroides*, *Clostridium*, *Eubacterium*, and *Alistipes*. E2 was further associated with microbial pathways related to glycogen degradation and queuosine biosynthesis.
Conclusion: This study represents the first and largest shotgun metagenomic investigation of gut microbiome composition in relation to circulating sex hormones in an epidemiological cohort. Reduced microbial diversity and higher abundance of estrobolome species with β-glucuronidase activity (e.g., *Bacteroides fragilis*) may be associated with elevated circulating estrogen levels, suggesting that structural variation in gut microbial communities contributes to inter-individual differences in estrogen metabolism.

#2329 Role of inflammatory markers in the development of cardiovascular conditions in breast cancer survivors and matched comparison groups.

Talar S. Habeshian[1], Michael R. Irwin[2], Lie H. Chen[1], Jiaxiao Shi[1], Richard Olmstead[2], **Reina Haque**[1]

[1]Research and Evaluation, Kaiser Permanente Southern California, Pasadena, CA,[2]Jane and Terry Semel Institute for Neuroscience and Human Behavior, University of California, Los Angeles, Los Angeles, CA

Background: Inflammation in breast cancer survivors (BCS) may play a role in developing cardiovascular disease (CVD). Prior studies have not included cancer-free comparison cohorts (CC) that can help elucidate if BCS have an increased risk of CVD. We evaluated whether incident CVD is greater in BCS compared with CC, and if the excess risk can be attributed to different levels of inflammatory markers, adjusting for pre-existing cardiovascular risk factors, demographic, and clinical characteristics. This preliminary analysis focuses on C-reactive protein (CRP), which has been strongly correlated with CVD.

Methods: We conducted a prospective cohort study of 315 BC survivors aged 55-85 years and 321 CC from the KPSC health plan. Of these, 70% in each group (N=218 BCS, N=222 CC) agreed to blood draws for assessment of inflammatory markers at baseline and every 8 months until month 32. Participants were followed a maximum of 5 years or until a CVD event, death, or health plan disenrollment, whichever came first. Person-year (PY) rates for CV events were calculated by cumulative CRP levels over the 32 months. Bivariate and multivariable Cox models were used to estimate hazard ratios (HRs) and 95% confidence intervals (CIs) for the associations between cumulative CRP (using CVD risk-related cut points: <1.0 (low), 1.0-3.0 (moderate), and >3.0 mg/dL (high) and 5-year composite CV event. The association was also evaluated by cumulative CRP levels, with CC as the reference group. Multivariable models were adjusted for age, demographic characteristics, and cardiometabolic risk factors.

Results: BCS had a higher crude CV event PY rate (33.3 per 1,000 PY) vs. CC (24.7 per 1,000 PY). In BCS, the 5-year CV event rate rose from 32.3 per 1,000 PY in the lowest CRP level (<1.0 mg/dL) to 34.4 per 1,000 PY (1.0-3.0 mg/dL), and then 40.8 per 1,000 PY (>3.0 mg/dL) (p-trend=0.68). Further, the CV event rates were greater in BCS than in CC in each of these CRP levels. In the crude model stratified by cohort, BCS with higher cumulative CRP levels had a greater CVD risk compared to those with normal CRP levels ($HR_{>3.0\ mg/dL}$=1.24, 95% CI: 0.45-3.43; $HR_{1.0\text{-}3.0\ mg/dL}$=1.05, 95% CI: 0.44-2.45), although results were not statistically significant. We observed similar trends in the CC. In the crude model stratified by CRP, BCS had a higher CVD risk than CC across all CRP categories, although the results were not significant ($HR_{BCS\ CRP\ <1.0\ mg/dL}$=1.36, 95% CI:0.53-3.46; $HR_{BCS\ CRP\ 1.0\text{-}3.0\ mg/dL}$=1.39, 95% CI: 0.49-3.91; $HR_{BCS\ CRP\ >3.0\ mg/dL}$=1.01, 95% CI:0.26-3.98). These risks attenuated in both multivariable models.

Conclusions: Preliminary results signal higher cumulative CRP levels may differentially affect CVD risk in BCS than in CC, but larger studies are needed for confirmation. Further analyses will examine if other inflammatory markers (IL-6, Il-8, IL-10, and TNF) predict long-term CVD risk in BCS.

#2330 Mosaic loss of the Y chromosome in leukocytes is associated with increased incidence of non-aggressive prostate cancer in 278,998 cancer-free males.

Rebecca L. Kelly[1], Anqi Wang[2], Yifan Zhang[3], Weyin Zhou[4], Kara M. Barnao[4], Corey D. Young[4], Aubrey K. Hubbard[4], Wen-Yi Huang[4], Steven C. Moore[4], Christopher A. Haiman[3], Stephen J. Chanock[4], Ying Wang[5], Konrad H. Stopsack[6], Lorelei A. Mucci[7], Fei Chen[3], Mitchell J. Machiela[4]

[1]Division of Cancer Epidemiology and Genetics, Division of Cancer Prevention, National Cancer Institute, Rockville, MD,[2]USC School of Pharmacy, Los Angeles, CA,[3]Department of Population and Public Health Sciences, University of Southern California Keck School of Medicine, Los Angeles, CA,[4]Division of Cancer Epidemiology and Genetics, National Cancer Institute, Rockville, MD,[5]American Cancer Society, Atlanta, GA,[6]Leibniz Institute for Prevention Research and Epidemiology, Bremen, Germany,[7]Harvard T.H. Chan School of Public Health, Boston, MA

Background: Mosaic loss of the Y chromosome (mLOY), a type of clonal hematopoiesis, is the most frequently detected chromosomal alteration in the leukocytes of aging males. Prostate cancer (PCa) increases exponentially in aging males and previous studies have shown a positive association between genetic risk of mLOY and PCa diagnosis. Confirmation of this association in population-based studies is needed to determine if mLOY could be an informative biomarker for PCa risk.
Methods: To evaluate the potential association between mLOY and prostate cancer risk, we detected mLOY using the MoChA algorithm on existing high-density genotyping array data from blood-derived DNA of 278,998 cancer-free males across six prospective cohorts: UK Biobank (UKBB, N=210,103); Prostate, Lung, Colorectal, and Ovarian Cancer Screening Trial (PLCO, N=26,275); Health Professionals' Follow-Up Study (HPFS, N=4,933); Physicians' Health Study (PHS, N=1,148); Multiethnic Cohort (MEC, N=24,370); and Cancer Prevention Study II (CPSII, N=12,169). Cox proportional hazards models with age as a timescale estimated hazard ratios (HR) and 95% confidence intervals (CI) for the association of mLOY on prostate cancer incidence adjusted for body mass index, smoking status, genotyping array, and the top 10 genetic principal components. Association tests were performed in each cohort and then meta-analyzed.
Results: The average mLOY detection and PCa diagnosis across cohorts were 23.4% and 17.9%, respectively. Fixed effects meta-analysis of the adjusted HRs identified a positive association of mLOY with overall PCa risk (HR=1.09, CI 1.05, 1.13; P-Value (*P*)=2.25 x 10^{-6}). mLOY was associated with a Gleason score ≤6 at diagnosis (HR=1.13, 95% CI 1.04, 1.23; *P*=0.0029), a greater hazard of non-aggressive PCa diagnosis (HR=1.15, 95% CI 1.05, 1.26; *P*=0.0022), and PSA <10ng/mL at diagnosis (HR=1.11, 95% CI 1.02, 1.22; *P*=0.015). We did not observe evidence for mLOY associations with Gleason score ≥8, aggressive PCa or metastasis at diagnosis. We confirmed germline genetic risk of mLOY was positively associated with PCa incidence in participants with genetic similarity to European reference populations (HR=1.02 per 1 SD mLOY PRS, 95% CI 1.00, 1.03; *P*=0.0083), there was less evidence in participants similar to African reference populations (HR=1.01 per 1 SD mLOY PRS, 95% CI 0.94, 1.08; *P*=0.769).
Conclusion: Our investigation of the relationship between mLOY and PCa diagnosis provides evidence for an association between mLOY detected in the blood and increased risk of non-aggressive PCa, suggesting mLOY could have utility in PCa risk stratification.

#2331 Clinical performance of Signatera Genome assay to predict treatment response and prognosticate outcomes in patients with locally advanced (LAR) resectable gastric or gastroesophageal junction (G/GEJ) adenocarcinoma: Results from the PLAGAST Study.

Aziz Zaanan[1], Michael Khayat[2], Erik Spickard[2], **George Laliotis**[3], Punashi Dutta[2], Meenakshi Malhotra[2], Shruti Sharma[2], Gabrielle Heilek[2], Adham Jurdi[2], Minetta C. Liu[2], Pierre Laurent-Puig[4]

[1]Department of Digestive Oncology, Georges Pompidou European Hospital, Assistance Publique - Hopitaux de Paris, University of Paris Cite, Paris, France,[2]Oncology, Natera, Inc., Austin, TX,[3]Natera, Inc., Austin, TX,[4]INSERM, Sorbonne Universite, Universite de Paris F-75006, Centre de Recherche des Cordeliers, Paris, France

Background: Circulating tumor DNA (ctDNA) is a clinically validated biomarker across multiple gastrointestinal cancers, used to predict recurrence risk, monitor response to neoadjuvant therapy (NAT), and detect molecular residual disease (MRD) post-definitive treatment. Signatera™ is a personalized, tumor-informed, multiplex PCR-NGS ctDNA assay that can be developed using either whole-exome sequencing (WES) or whole-genome sequencing (WGS). Initial clinical validation of Signatera Genome in select clinical contexts of a pancancer cohort showed robust performance. Here, we evaluated the performance of Signatera Genome in pts with LAR G/GEJ cancer enrolled in the PLAGAST prospective study (NCT02674373).

Methods: A retrospective analysis was conducted using residual samples from pts with LAR G/GEJ cancer in the PLAGAST study (N=54). Signatera Genome assays were designed from matched tumor and normal WGS data and used to detect ctDNA in the corresponding pts' plasma samples collected at pre-NAT (or pre-surgery for NAT-naive), during-NAT, post-NAT, and post-surgery in the MRD window (within 2–12 weeks, before adjuvant treatment). ctDNA levels were quantified as mean tumor molecules per mL of plasma (MTM/mL). Longitudinal blood samples represented time points pre-/post-definitive treatment until recurrence or the end of follow-up. The correlation between ctDNA status and disease-free survival (DFS)/overall survival (OS) was assessed using Cox regression analysis.

Results: The median pt age was 66 (34-86) years. The majority of pts were males (65%), had gastric cancer (57%), and received NAT (87%). Pts with post-NAT, pre-surgery ctDNA positivity had significantly worse outcomes (RFS: HR: 5.4, 95% CI: 1.68-17.37; p=0.005; OS: HR: 5.42, 95% CI: 1.5-28.73; p=0.0085). Postoperative survival analysis demonstrated that ctDNA positivity during the MRD window was also associated with worse RFS (HR: 9.78, 95% CI: 3.41-28.07, p<0.0001) and OS (HR: 12.98, 95% CI: 3.69-45.67; p<0.0001). Multivariate analyses showed ctDNA status post-NAT and within the MRD window to be the most significant independent risk factor for both RFS and OS compared to other clinicopathological features (post-NAT: RFS: HR: 5.53, p=0.005; OS: HR: 6.51, p=0.029; MRD window: RFS: HR: 4.97, p=0.014; OS: HR: 4.28, p=0.031).

Conclusions: Persistent ctDNA positivity at post-NAT/pre-surgery timepoint and in the MRD window were strongly prognostic of inferior outcomes. These data indicate the robust clinical performance of Signatera Genome in pts with LAR G/GEJ adenocarcinoma and support its potential clinical utility in this disease setting. Prospective clinical trials are warranted to establish the clinical utility of the assay for guiding treatment decisions.

: Epidemiology: Cancer Incidence, Mortality, Patterns, and Methodology
Poster Session

#2335 A population-based study on thyroidectomies in Mexico from 2010 to 2023.

Adrian Cortes-Valencia, Giovanni Garfias-Becerril, Lina Sofia Palacio-Mejia, Evelyn Mitzy Flores-Salas, Juan Eugenio Hernandez-Avila, **Martin Lajous**

Instituto Nacional de Salud Publica, Cuernavaca, Mexico

Background. Thyroid cancer is the fourth most common cancer in Mexico. Overdiagnosis and subsequent overtreatment have increased as diagnostic tests have become more readily available. Also, an increasing share of total thyroidectomies relative to partial thyroidectomies was observed in many high-income countries in the early 2000s. There is limited understanding of the frequency of thyroidectomies and surgical approach in low- and middle-income countries. We aimed to estimate time trends and geographic patterns of thyroidectomies in Mexico by sex, age groups, type of procedure (total and partial thyroidectomies), and discharge diagnosis.
Methods. We used a national hospital discharge database collected by the Ministry of Health for individuals without health insurance coverage from 2010 to 2023. We identified hospital discharges where a total (ICD-9: 064X, 0650, 0652) or partial (ICD-9: 0639, 0651) thyroidectomy were performed. We classified discharge diagnoses into four groups: malignant neoplasms, benign tumors, goiter and thyroid-related morbidities, and other diagnoses unrelated to the thyroid. We calculated crude and age-standardized incidence rates for men and women by region in Mexico (North, Central, Southeast, West, and Mexico City) and for three time periods: 2010-2012, 2013-2018, and 2018-2023.
Results. The national standardized rate of thyroidectomies was 4.8 per 100,000 in women and 0.74 in men. The rate showed a downward trend throughout the period, particularly among women with goiter. Overall, the rate of thyroidectomies for malignant disease remained stable, however, the percentage of thyroidectomies for malignant tumors increased in both women (34.3%, 36.0%, and 45.2%) and men (36.6%, 43.6%, and 51.7%) when comparing the three periods. We observed important regional differences, with the highest rate in Mexico City (17.9 per 100,000 in women) and the lowest in the central region. The proportion of total thyroidectomies in the examined period increased from 49% to 63% in women and from 47% to 66% in men.
Conclusions. The downward trend in thyroidectomies in Mexico may be the result in changing guidelines. Our results do not reveal thyroid cancer overdiagnosis but show potential for more conservative surgical treatment.

#2336 Rectal and sigmoid colon cancers drive rising early-onset colorectal cancer incidence in the United States.

Michelle O. Nagata[1], Scott K. Kuwada[2], Linda Wong[1], Loic Le Marchand[1], Brenda Y. Hernandez[1]

[1]University of Hawai'i Cancer Center, Honolulu, HI,[2]John A. Burns School of Medicine, Honolulu, HI

Background: Early-onset colorectal cancers (EOCRCs) diagnosed in people younger than 50 are increasing in incidence in the U.S., though the causes are unclear. We studied recent trends in EOCRC incidence and survival in the U.S.
Methods: De-identified data from the National Cancer Institute Surveillance, Epidemiology, and End Results Program (SEER 21) was used to evaluate colorectal cancer (CRC) cases diagnosed in the U.S. in 2013-2022 (excluding 2020) by demographic and clinic-pathologic characteristics including age, sex, race, tumor site, stage, histology, and county-level measures of rurality, annual household income, poverty, and education using SEER*Stat. Average annual percent change was calculated using Joinpoint. Age-standardized 5-year relative and disease-specific survival rates were calculated using time from cancer diagnosis to death or last contact.
Results: Overall CRC incidence declined from 2013-2022 in a manner that was more pronounced for colon and rectosigmoid junction cancers than rectal cancers. Among individuals aged 50+, incidence significantly declined for all subsites except for the rectum. Among individuals younger than 50, colon and rectal cancers significantly increased 2.50% and 4.15% annually, respectively. Rectal cancers showed the highest annual increase among EOCRCs, followed by sigmoid colon (3.86%, $p = 0.002$), splenic flexure (2.97%, $p = 0.048$), overlapping lesion/not otherwise specified (NOS) colon (1.79%, $p = 0.01$), transverse colon (1.38%, $p < 0.001$), and ascending colon (1.08%, $p < 0.001$). Increases in EOCRCs were observed for all sex, race/ethnicity, stage, and county-level rurality, income, poverty, and education groups, with significantly higher annual increases for metropolitan compared with nonmetropolitan counties (3.05% vs. 1.78%, $p < 0.001$). Adenocarcinomas (NOS) and neuroendocrine tumors (NET) accounted for increases in both early-onset colon (3.05% and 1.50%) and rectal cancers (4.15% and 7.42%). Survival was lower for individuals aged 50+; males compared with females; Blacks compared with Whites; regional and distant stages compared with localized; single individuals compared with married; and nonmetropolitan, lower income and education, and higher poverty counties. Survival was significantly lower for mucinous adenocarcinomas and higher for NET and hematologic cancers compared with adenocarcinomas (NOS).
Conclusions: The recent increase in EOCRC incidence has been driven by increases in rectal and sigmoid colon cancer incidence, which showed the steepest growths and equally across all demographic and socioeconomic groups, and were diagnosed at younger ages and at more advanced stages compared with other anatomical subsites. These findings highlight the need to elucidate biological and environmental mechanisms underlying the rise in EOCRC to inform prevention and intervention efforts.

#2337 Mapping the associations of 144 incidence risk factors with 39 cancers: An AI-driven systematic review and meta-analysis.

Changfa Xia[1], **Shiyuan Tong**[2], Yongjie Xu[1], Hui Yu[2], Fang Liu[2], Shiqing Chen[2], Fei Zhao[2], Junyi Ye[2], Jing Liu[2], Baoliang Zhu[2], Xiaohui Wu[2], Sibo Zhu[2], Wanqing Chen[3]

[1]Office of Cancer Screening, National Cancer Center/National Clinical Research Center for Cancer/Cancer Hospital, Chinese Academy of Medical Sciences and Peking Union Medical College, Beijing, China,[2]Shanghai Xiaohe Medical Laboratory Co. Ltd., Shanghai, China,[3]Office of Cancer Registry, National Cancer Center/National Clinical Research Center for Cancer/Cancer Hospital, Chinese Academy of Medical Sciences and Peking Union Medical College, Beijing, China

Background: A comprehensive understanding of the associations between multiple risk factors and cancer incidence is crucial for evidence-based cancer control. While many studies have examined specific risk-cancer pairs, none have yet estimated the entire network of risks across cancer types. This study aims to quantity the associations between 144 cancer-related risk factors and the incidence of 39 cancer types.
Methods: Using risk records from CanRisk-DB, a well-established repository that employs graph-based retrieval-augmented generation large language model agents within the PICOS-PRISMA framework, we synthesized relative risks (RRs) or hazard ratios (HRs) of cancer incidence from cohort studied between 1980 and 2024. We meta-analyzed the effect sizes using harmonized definitions and both graph-based and inverse variance approaches. The reliability of this artificial intelligence (AI)-driven meta-analysis was validated by comparing our estimated effects with those from published meta-analyses.
Results: A total of 2,388 combinations between 144 risk factors and 39 cancer types were identified from CanRisk-DB. Among these, 131 and 120 risk factors were linked to 36 and 33 cancer types in females and males, respectively. Of 144 risk factors, 92.4% were modifiable. 67 factors were identified as causal risk factors only, such as family history of cancer, immunosuppressive agents, non-alcoholic fatty liver disease, and nitrogen dioxide pollution. However, 77 risk factors showed either causal and protective roles across cancer types, such as tobacco use, alcohol consumption, and type 2 diabetes. For instance, alcohol consumption was positively associated with several cancers (e.g., liver [RR = 1.46; 95% CI, 1.27-1.69], breast [RR = 1.09; 95% CI, 1.06-1.12], and colorectal [RR = 1.08; 95% CI, 1.02-1.13]) but inversely with kidney cancer (RR = 0.81; 95% CI, 0.76-0.87). The cancers with the greatest number of associated risk factors were lung (73 factors), colorectal (57), and liver (53). Overall, the majority of cancer types were associated with multiple modifiable risk factors: 34 cancers (87.2%) with at least 5 risks, 28 cancers (71.8%) with at least 10 risks, and 20 cancers (51.3%) with at least 15 risks. The effect sizes in our analysis are highly consistent with those reported in published meta-analyses (Spearman's $\rho = 0.93$).
Conclusion: AI-driven systematic reviews and meta-analyses accurately captured the complex network of associations between cancers and risk factors. Mapping these relationships facilitated a better understanding of the attributable risk of cancer, thereby informing strategies for cancer prevention and control.

#2338 Oral bacteriome and its association with cancer-specific mortality.

Shelly Han[1], Morgan Byrd[2], Ayush Khanna[1], Tammara L. Watts[3], Katharine Ciarrocca[4], Nosa Osazuwa-Peters[2]

[1]Duke University, Durham, NC,[2]Duke University School of Medicine, Durham, NC,[3]Duke Cancer Institute, Durham, NC,[4]Head and Neck Surgery & Communication Sciences, Duke University, Durham, NC

Objectives: Cancer is the leading cause of death in the United States, with more than 600,000 deaths annually. Emerging evidence suggests that alterations in the oral microbiota, one of the body's most diverse microbial communities, may influence cancer outcomes. However, associations between microbial diversity and composition with cancer mortality remain poorly understood. We aimed to identify associations between oral microbiome diversity and bacterial abundance with cancer-specific mortality.
Methods: We analyzed 441 participants from the 2009-2012 National Health and Nutrition Examination Study (NHANES) linked to National Death Index (NDI). Oral rinse samples were 16S rRNA V4 amplicon-sequenced and resolved to the genus level using SILVA v123. Alpha diversity was calculated after rarefaction to 2,000 reads. Cancer deaths were defined using ICD-10 malignant neoplasm codes. As an exploratory analysis, supervised random forest models (1,000 trees; 100 random seeds; "randomForest" R package) were applied to centered log-ratio (CLR) transformed abundance values to identify genera associated with cancer-mortality, with importance measured by Mean Decrease Accuracy. Survey-weighted multivariable Cox proportional models estimated adjusted hazard ratios for cancer-specific mortality by alpha diversity and genus abundance, adjusting for age, sex, race/ethnicity, poverty income ratio, lifetime smoking history, and self-rated oral health. Bonferroni correction accounted for multiple hypothesis testing.
Results: Higher alpha diversity was associated with lower cancer-specific mortality, with significant inverse associations for Shannon (aHR 0.72, 95% CI 0.53-0.98) and Inverse Simpson's Index (aHR 0.13, 95% CI 0.02-0.73), while Faith's Phylogenetic Diversity and observed ASV richness were not significant. In the exploratory random analysis using random forest, Prevotella_7, Gemella, Bergeyella, Fusobacterium, Ruminococcaceae_UCG-014, Alloprevotella, and Oribacterium emerged as potential discriminatory genera for cancer deaths versus non-cancer deaths (MDA > 5.75). In adjusted Cox models, participants with Bergeyella abundance above the median (aHR 0.59; 95% CI 0.35-0.99) and participants with Oribacterium (aHR 0.52; 95% CI 0.32-0.81) had lower cancer-specific mortality. After adjustment, the other genera identified in the exploratory analysis were not significant for cancer-mortality.
Conclusion: The oral microbiome harbors bacteria that may be potentially predictive of cancer-specific mortality. Although prior literature provides limited support for Bergeyella's and Oribacterium's roles in cancer mortality, our results underscore the need for further studies to validate our results and for examining biomarkers and targets for microbiome-informed prevention strategies.

#2339 Cardio-kidney metabolic health among adult cancer survivors in the Hispanic Community Health Study/Study of Latinos.

Myunhee Lee[1], Matthew Allison[2], Linda C. Gallo[1], Carlos Rosas[3], Daniela Sotres-Alvarez[4], Frank J. Penedo[5], Martha Daviglus[6], James Lash[6], Humberto Parada[1]

[1]San Diego State University, San Diego, CA,[2]University of California San Diego, San Diego, CA,[3]California State University San Marcos, San Marcos, CA,[4]University of North Carolina at Chapel Hill, Chapel Hill, NC,[5]University of Miami, Miami, FL,[6]University of Illinois Chicago, Chicago, IL

Background: Compared to the general population, cancer survivors are at higher risk for cardiovascular, kidney, and metabolic (CKM) diseases. However, the prevalence and progression of CKM diseases among Hispanic/Latino adults with a history of cancer remain underexplored. Using data from the community-based Hispanic Community Health Study/Study of Latinos (HCHS/SOL), we examined the changes in CKM diseases and predictors of CKM disease progression over an average of six years, stratified by baseline cancer history.

Methods: We included 16,415 participants from the HCHS/SOL with a history of cancer (n=644) and without a history of cancer (n=15,771) at Visit 1 in 2008-2011. CKM stage at Visit 1 and Visit 2 in 2014-2017 was defined according to the 2023 American Heart Association(AHA)'s CKM stage framework. The 2023 AHA advisory defines five CKM stages (0-4), progressing from no CKM risk factor (stage 0) to excess or dysfunctional adiposity (stage 1), metabolic syndrome or chronic kidney disease (stage 2), subclinical cardiovascular disease or risk equivalent (stage 3), and established cardiovascular disease (stage 4). Descriptive statistics were used to assess the prevalence and transition of CKM stage between visits. Survey-weighted multivariable logistic models and Fine-Gray competing risk models were used to evaluate the associations (odds ratios, ORs, and 95% confidence intervals, CIs) between cancer history and sociodemographic factors and CKM stage progression.

Results: Compared to those without a history of cancer, those with a history of cancer were older (mean age±standard error = 55.8±1.0 versus 47.4±0.2 years), more likely to be female (65.4% versus 52.7%), retired (29.0% versus 10.6%), have an annual household income <$20,000 (54.9% versus 47.5%), and be physically inactive (45.0% versus 36.4%). Cancer survivors had a higher prevalence of advanced CKM stages (≥ stage 3) at both Visit 1 (24.2% versus 10.0%) and Visit 2 (35.3% versus 16.9%). While the proportions of CKM worsening were similar between groups, cancer survivors had a significantly higher mortality rate (12.2% vs 4.8%) during follow-up. Cancer history itself was not a predictor of CKM worsening after adjusting for sociodemographic factors (OR = 1.03; 95% CI = 0.75-1.43). After accounting for competing mortality, cancer survivors were 37% less likely to experience CKM stage progression than those without a cancer history (HR = 0.63; 95%CI = 0.47-0.83; $P<0.01$).

Conclusion: CKM diseases are prevalent among Hispanic adults, with cancer survivors experiencing more advanced CKM stages and higher mortality rates over time than those without a history of cancer.

#2340 African ancestry, Duffy-null genotype, and epithelial ovarian cancer in a cohort of Black women.

Joellen M. Schildkraut[1], Jeffrey R. Marks[2], Xintian Song[3], Yao Xin[4], Anthony J. Alberg[5], Lauren C. Peres[6], Katherine Anne Lawson-Michod[7], Lindsay Jane Collin[8], Jennifer A. Doherty[9], Andrew B. Lawson[10], on behalf of the African American Cancer Epidemiology Study

[1]Emory University, Rollins School of Public Health, Atlanta, GA,[2]Surgery, Duke University, Durham, NC,[3]Epidemiology, Emory University, Rollins School of Public Health, Atlanta, GA,[4]Medical College of South Carolina, Charleston, SC,[5]Epidemiology, University of South Carolina, Columbia, SC,[6]Moffitt Cancer Institute, Tampa, FL,[7]Fred Hutchinson Cancer Center, Seattle, WA,[8]Emory University, Rollins School of Public Health, Salt Lake City, UT,[9]University of Utah Huntsman Cancer Institute, Salt Lake City, UT,[10]Biostatistics, Medical College of South Carolina, Charleston, SC

Background: Black women experience poor survival from epithelial ovarian cancer (EOC), for all stages at diagnosis and EOC histotypes. We present findings of the contribution of African ancestry and an ancestry-related genotype in the Atypical Chemokine Receptor 1 (*ACKR1*) gene to EOC survival among a cohort of Black/African American women. We also report associations with tumor molecular features that may explain the potential underlying biology related to the Duffy-null *ACKR1* genotypes.

Methods: The relationship between global African ancestry and the rs2814778 SNP in the promotor region of the *ACKR1* gene and survival was determined in a cohort of 408 Black women with EOC (275 with high grade serous ovarian cancer (HGSC)) who participated in the population-based African American Cancer Epidemiology Study (AACES) using a Bayesian modeling approach adjusting for stage, age at diagnosis, the Yost index for socioeconomic status, education, and ovarian cancer family history. Proportion of global African ancestry and the *ACKR1* genotype (Duffy-null (CC) vs. TC/ TT) were determined from germline DNA. Tumor molecular features including gene expression using RNAseq, tumor immunity (i.e., T-cell abundance) measured using multiplex immunofluorescence (mIF), and homologous recombination deficiency (HRD) derived from whole exome sequencing data were generated from HGSC tumors.

Results: The Duffy-null genotype was present in 70.6% EOC cases overall, and 72.0% of HGSC. The prevalence was higher among individuals with high African ancestry (African ancestry >83.6%) than those with lower African ancestry (83.2% and 58.3%, respectively). The Duffy-null genotype was associated with improved survival among EOC cases (adjusted Hazard Ratio (HR)=0.59, 95% credible intervals (CI): 0.35-0.96). The corresponding HR for HGSC was 0.61 (95% CI: 0.34-1.12). However, global African ancestry—as indicated by a 1% increase in percent African ancestry on the logit scale—was suggestively associated with worse survival, especially for HGSC, with an HR of 1.31 (95% CI: 0.89-1.90). Additionally, we examined the relationship between the CC vs. TC/ TT genotypes and tumor molecular features in HGSC. The Duffy-null genotype was associated with lower *ACKR1* expression, lower cytotoxic T cell abundance, and higher HRD in HGSC. Among EOC subjects, mIF-derived myeloid cells (CD11b+) showed lower abundance in those with high African ancestry, which is consistent with worse survival.

Conclusion: The Duffy-null genotype is associated with ~40% decreased EOC mortality in Black women. Lower T-cell infiltrates may reflect lower immune surveillance and may coincide with higher HRD in HGSC among Duffy-null individuals. The HRD finding, in particular, may explain the improved prognosis observed with the Duffy-null genotype, as our group has previously shown that HRD status was associated with better survival in Black women with HGSC.

#2341 Using geospatial methods to analyze associations of neighborhood change on breast cancer mortality in Maryland, 2000-2019.

Katherine L. Ho[1], Kassandra I. Alcaraz[2], Avonne E. Connor[1], Michael R. Desjardins[1]

[1]Johns Hopkins Bloomberg Sch. of Public Health, Baltimore, MD,[2]Johns Hopkins School of Medicine, Baltimore, MD

Purpose: To examine whether neighborhood change status (declining, stable, or upgrading) is associated with the risk of breast cancer (BC)-specific mortality.

Background: Neighborhood-level social determinants of health are associated with BC mortality, but few studies have investigated how dynamic neighborhood conditions over time and geography (i.e., neighborhood trajectories) can modulate the risk of BC-specific mortality.

Methods: We identified primary BC cases diagnosed among women age ≥18 in the Maryland Cancer Registry (NPCR) between 2005-2019 with valid census tract information at diagnosis (proxy for neighborhood). Observed and expected BC deaths were calculated by tract using 2000 standard female population and referent BC mortality rates for Maryland from 2018-2022 (age <50: 4.4 deaths/100k; age ≥50: 60.8 deaths/100k). Tracts were linked to a continuity-adjusted version of the Social Vulnerability Index (CA-SVI), which harmonized SVI component variables across years. Neighborhood change was defined as the difference in CA-SVI percentiles between consecutive 5-year periods (2000-2004, 2005-2009, 2010-2014, 2015-2019). Tracts were classified as stable (Low, Low-Medium, Medium-High, High CA-SVI)), upgrading (–25 to –49 or ≤–50 %ile; becoming moderately/substantially less disadvantaged), or declining (+25 to +49 or ≥+50 %ile; becoming moderately/substantially more disadvantaged). We evaluated the relationship between neighborhood change and BC mortality using Bayesian negative binomial space-time models that captured effects for geographic clustering and temporal trends. Models were adjusted for individual-level covariates (age, stage, grade, receipt of treatment [surgery, chemotherapy, radiation, hormone], and tumor characteristics [ER, PR, HER2 status]), starting/ending CA-SVI categories, and county-level rurality (2013 USDA Beale Rural-Urban Continuum Codes).

Results: Among 60,388 BC cases, 8,946 died as a result of their diagnosis. Women residing in neighborhoods that modestly improved (+1 cat.) had a slightly elevated risk of BC mortality compared to those living in areas of stably low CA-SVI (Relative risk $[RR]_{Inc}$ =1.11, 95% Credible Interval [CrI] 1.01-1.22). Women living in neighborhoods that became more disadvantaged had between 11 to 24% higher risk of BC mortality ($RR_{Decl1\ cat.}$=1.11 [1.01-1.02], $RR_{Decl2\ cat.}$=1.24 [1.04-1.48]).

Conclusion: Both sustained vulnerability and shifts in neighborhood conditions were associated with BC-specific mortality. Marked declines showed the highest risk for BC mortality, but sustained vulnerability and modest upgrades also indicated elevated risk. These results highlight the importance of neighborhood contexts on cancer outcomes, emphasizing the need for longitudinal research evaluating how neighborhood trajectories might affect place-based inequities.

#2342 Neighborhood concentrated disadvantage and risk of recurrence or breast cancer death in a nationwide study of US Black women.

Sabrina Mellinghoff[1], Etienne Holder[1], Nora Xu[1], Mollie Barnard[2], Julie R. Palmer[3]

[1]BU School of Medicine, Boston, MA,[2]Boston University, Boston, MA,[3]Professor of Epidemiology, Boston University, Boston, MA

Purpose: US Black women with breast cancer experience higher rates of recurrence and disease-specific mortality.[1] We previously found that Black breast cancer patients living in areas of high neighborhood concentrated disadvantage (nDIS) have poorer breast cancer-specific survival when compared to those living in areas with low nDIS.[2] The present analysis incorporates recurrence events to assess the association of nDIS with disease-free survival. We hypothesize that the association will be weaker than with mortality, an outcome more clearly influenced by neighborhood-level factors such as access to care.
Methods: We included 2,290 Black Women's Health Study (BWHS) participants diagnosed with incident breast cancer (stages I-III). Recurrence was defined as an invasive cancer in the ipsilateral breast or in a common metastatic site (lung, liver, brain, or bone) occurring more than four months after the initial breast cancer diagnosis. Medical records were reviewed to distinguish true metastases from new primary tumors. Data on death and cause of death were determined from the National Death Index. We used geocoded participant addresses from the time of breast cancer diagnosis in conjunction with US Census Bureau and American Community Survey data to calculate nDIS. Hazard ratios (HRs) and 95% confidence intervals (CI) were estimated from multivariable Cox proportional hazards models with control for tumor characteristics, treatments, education, insurance, and lifestyle factors.
Results: There were 399 poor breast cancer outcomes (recurrence or death) among 2,290 breast cancer cases followed for a median of 10.5 years. Compared to women in the lowest quartile of nDIS, HRs for a subsequent breast cancer outcome were 1.00 (95% CI 0.93-1.89), 1.19 (95% CI 0.89-1.59) and 1.29 (95% CI 0.94-1.75), for quartiles 2, 3, and 4, respectively. A statistically significant trend was observed across quartiles (*p*-trend=0.03), indicating increasing risk of poor outcomes with greater neighborhood disadvantage.
Conclusions: Breast cancer survivors living in the most disadvantaged neighborhoods were estimated to have 1.29 times the rate of breast cancer death or recurrence compared to those living in the most advantaged neighborhoods. While our findings were statistically significant, the magnitude was lower than the 1.47-fold increase in mortality rate that we previously observed in the same study population, suggesting that factors captured by nDIS may be more important to survival than to recurrence.
[1] Black Women Have Higher Risk of Recurrence Than Other Ethnicities. Oncology Times 41(1):p 24, January 5, 2019. | DOI: 10.1097/01.COT.0000552839.22529.72[2] Holder EX, Barnard ME, Xu NN, Barber LE, Palmer JR. Neighborhood Disadvantage, Individual Experiences of Racism, and Breast Cancer Survival. *JAMA Netw Open.* 2025;8(4):e253807. doi:10.1001/jamanetworkopen.2025.3807

#2343 Reproductive factors associated with breast cancer risk by subtypes: Findings from the Southern Community Cohort Study.

Rajat Das Gupta, Wanqing Wen, Wei Zheng

Medicine, Vanderbilt University Medical Center, Nashville, TN

Background:
Breast cancer is the most common cancer among U.S. women. Reproductive factors may influence breast cancer etiology through hormonal pathways that differ by molecular subtypes. We investigated the associations between reproductive factors and breast cancer risk by subtypes in the Southern Community Cohort Study.

Methods:
After excluding the first year of follow-up to minimize potential reverse causation, 42,922 women aged 40-79 years (69.2% Black) remained for the study. Cohort members were followed for up to 213 months. Breast cancer cases were classified by estrogen receptor (ER), progesterone receptor (PR), and human epidermal growth factor receptor 2 (HER2) status as luminal A-like (ER/PR+, HER2-), luminal B-like (ER/PR+, HER2+), HER2-enriched (ER/PR-, HER2+), and triple-negative breast cancer (TNBC; ER/PR/HER2-). To account for competing risk, cause-specific Cox proportional hazards models were used to estimate hazard ratios (HRs) and 95% confidence intervals (CIs) for associations between reproductive factors and each breast cancer subtypes. Models were adjusted for age, enrollment source, education, race, income, family history of breast cancer, personal history of breast cysts or fibroids, smoking, alcohol intake, body mass index, leisure-time physical activity, healthy eating index, and ever use of oral contraceptive pills and hormone replacement therapy. Subgroup analyses were conducted among Black women. We repeated the above analyses using Fine-Gray subdistribution hazard models.

Results:
Over follow-up, 1,257 breast cancers occurred (luminal A-like = 612; luminal B-like = 105; HER2-enriched = 62; TNBC = 180; unclassified = 298). In the overall cohort, multiparity, particularly ≥3 births, was inversely associated with luminal A-like (HR = 0.74; 95% CI: 0.57-0.96) and luminal B-like (HR = 0.53; 95% CI: 0.30-0.94) subtypes, but positively with ER-/PR- disease (HR = 1.71; 95% CI: 1.06-2.77). Among Black women, it was also positively associated with TNBC (HR = 2.30; 95% CI: 1.12-4.72). Among parous women, first live birth at ≥ 30 years was associated with a higher risk of ER+/PR+ (HR = 1.59; 95% CI: 1.05-2.40) but a lower risk of ER-/PR- (HR = 0.25; 95% CI: 0.08-0.76) breast cancer. Fine-Gray models showed consistent results with cause-specific models.

Conclusions:
Parity and age at first birth demonstrate subtype-specific associations with breast cancer risk. Multiparity is associated with a reduced risk of luminal breast cancer subtypes but an increased risk of ER–/PR– tumors. A later age at first childbirth is associated with an increased risk of ER+/PR+ disease and a decreased risk of ER–/PR– subtypes. These findings highlight etiologic heterogeneity by hormonal receptor status and underscore the importance of incorporating reproductive history in subtype-specific risk prediction and prevention strategies.

#2344 Cardiometabolic health and risk of breast cancer subtypes among US Black women.

Yifei Shan, Sarah M. Rothbard, Lynn Rosenberg, Julie R. Palmer, **Mollie E. Barnard**

Boston University Chobanian & Avedisian School of Medicine, Boston, MA

Background: In the United States (US), Black women are more likely to be diagnosed with estrogen receptor (ER)-negative breast cancers as compared with White women. Cardiometabolic conditions are also more common among Black women. Understanding their associations with risk of breast cancer subtypes may help to explain racial differences in breast cancer risk. Prior studies have identified obesity as a risk factor for postmenopausal ER+ breast cancer and type 2 diabetes as a probable risk factor for ER- breast cancer. The goal of the present study was to comprehensively evaluate the associations of cardiometabolic factors with breast cancer subtypes in a large population of US Black women.

Methods: The Black Women's Health Study is a prospective study of 59,000 self-identified US Black women. Cardiometabolic factors that have been queried every two years since the start of the study in 1995 include high body mass index (BMI ≥30 kg/m^2), type 2 diabetes, hypertension, and hypercholesterolemia. Breast cancer cases were identified through self-report on biennial questionnaires, review of death certificates, and linkage to cancer registries. Hospital or registry-recorded pathology data were used to classify cases by ER status and to assign breast cancer subtypes (luminal A-like, luminal B-like, HER2-overexpressed, and triple negative). We used competing risk Cox proportional hazards models to estimate the associations between cardiometabolic factors and breast cancer subtypes, adjusting for age, reproductive factors, and lifestyle factors.

Results: In comparisons of women with each cardiometabolic exposure to those without that exposure, elevated BMI was associated with an increased risk of luminal A-like breast cancer among postmenopausal women (hazard ratio [HR] 1.32 (1.03-1.68) for BMI ≥30 kg/m^2 versus <25 kg/m^2). All other results were not statistically significant. When we repeated the analyses using a common referent group (those with no cardiometabolic conditions), no patterns of association were observed among premenopausal women. Among postmenopausal women, HRs for all cardiometabolic factors were above 1.00 for ER+ breast cancers, although none of the HRs were statistically significant. In analyses of combined groups of cardiometabolic factors, the HR for three or more cardiometabolic conditions versus none was 1.32 (0.98-1.77) for ER+ breast cancer in postmenopausal women.

Conclusions: In this large study of US Black women, poorer cardiometabolic health was associated with a higher risk of postmenopausal ER+ breast cancer. The observed association seems to be driven by the positive association of obesity with postmenopausal luminal A-like breast cancer, as has been seen in other racial and ethnic groups.

#2345 Pre-diagnostic circulating 25-hydroxyvitamin D and prostate cancer survival: A collaborative analysis of 13 prospective studies.

Jiaqi Huang[1], Aurora Perez-Cornago[2], Ruth Travis[2], Timothy J. Key[2], Naomi Allen[2], **Demetrius Albanes**[3], on behalf of the Endogenous Hormones Nutritional Biomarkers and Prostate Cancer Collaborative Group

[1]National Clinical Research Center for Metabolic Diseases, Key Laboratory of Diabetes Immunology, Ministry of Education, and Department of Metabolism and Endocrinology, The Second Xiangya Hospital of Central South University, Changsha, Hunan, China,[2]Cancer Epidemiology Unit, Nuffield Department of Population Health, University of Oxford, Oxford, United Kingdom,[3]National Cancer Inst. Div. of Cancer Epidemiology & Genetics, Bethesda, MD

Previous research suggests increased risk of prostate cancer in men with higher vitamin D serology, but there are limited data related to prostate cancer survival. In this study, we examined the association between pre-diagnostic blood concentrations of 25-hydroxyvitamin D [25(OH)D] and the risk of prostate cancer-specific mortality, as well as mortality from other causes, in men diagnosed with prostate cancer. This prospective international collaborative analysis of circulating 25(OH)D, the major biochemical indicator of vitamin D status, was based on data for 12,635 incident prostate cancer cases from 13 cohorts. Multivariable-adjusted Cox proportional hazards regression models estimated hazard ratios (HRs) and 95% confidence intervals (CIs) for the associations between study-specific/season-standardized categories as well as clinically defined 25(OH)D categories (<30, 30-50, 50-75, and ≥75 nmol/L) and death from prostate cancer (n=1,316) and other causes (n=2,129). In fully adjusted models that included demographic and lifestyle factors, as well as information on stage and grade of prostate cancer at diagnosis (available for 5,363 and 5,928 cases, respectively), men who had higher pre-diagnostic 25(OH)D concentrations experienced lower prostate cancer-specific mortality (HR for 80-percentile increase=0.75, 95% CI: 0.64-0.88; P_{trend}<0.001) and somewhat lower risk of mortality from other causes (HR=0.85, 95% CI: 0.75-0.96; P_{trend}=0.009). When analyses were restricted to cases with complete stage and grade information (5,078 cases (40.2% of all cases) and 761 deaths from prostate cancer [57.8% of all deaths]), the association between 25(OH)D and prostate cancer mortality was only slightly attenuated in the model that was further adjusted for these clinical factors (HR for 80-percentile increase=0.76, 95% CI: 0.62-0.93; P_{trend}=0.009). Vitamin D was not associated with risk of death from other causes in this same subset of cases (HR=0.97, 95% CI: 0.83-1.12; P_{trend}=0.7). In this pooled prospective cohort analysis, higher pre-diagnostic circulating vitamin D (25(OH)D) was associated with lower prostate cancer-specific mortality in men with prostate cancer. Further research is required to establish whether the association may be contributed to by biases such as the earlier detection of disease and thus better survival in men with higher vitamin D in these populations, as well as to investigate possible biological impacts of vitamin D on prostate cancer progression.

#2346 Uptake of conservative management, and uptake of curative-intent treatment following conservative management, in low and favorable-intermediate risk prostate cancer patients.

Isaac Allen[1], Jane Bailey Vaselkiv[2], Hannah E. Guard[2], Sinead Flanagan[2], Hari Iyer[3], Kevin Kensler[4], Jaime E. Hart[5], Mark A. Preston[6], Andreas Pettersson[7], Keyan Salari[8], Edward L. Giovannucci[9], Adam S. Kibel[6], Lorelei A. Mucci[2], Timothy Rebbeck[1]

[1]Dana-Farber Cancer Institute, Boston, MA,[2]Harvard T.H. Chan School of Public Health, Boston, MA,[3]Rutgers Cancer Institute of New Jersey, New Brunswick, NJ,[4]Weill Cornell Medicine, New York, NY,[5]Department of Medicine, Brigham and Women's Hospital and Harvard Medical Schoo, Boston, MA,[6]Department of Urology, Brigham and Women's Hospital, Boston, MA,[7]Department of Medicine Solna, Karolinska Institutet, Stockholm, Sweden,[8]Department of Urology, Massachusetts General Hospital, Boston, MA,[9]Professor of Nutrition & Epidem., Harvard TH Chan School of Public Health, Boston, MA

Background

Low-risk and favourable-intermediate risk prostate cancer patients are eligible for conservative management. We estimated the probability of conservative management uptake and 10-year rates of curative treatment initiation following conservative management in a prospective cohort of 2,872 health professionals diagnosed with low or favorable-intermediate risk prostate cancer.

Methods

The study included males with low-risk (grade group 1, stage≤cT2a, prostate-specific antigen (PSA)<10ng/ml) and favourable-intermediate risk (grade group 1, stage cT2b-cT2c or PSA 10-20ng/ml, or grade group 2, stage≤cT2a and PSA<10ng/ml) prostate cancer whom were diagnosed 1986-2019 and were participants in the Health Professionals Follow-up Study. We estimated the variation in conservative management uptake by age and calendar year at diagnosis, prostate cancer risk group, and pre-diagnostic lifestyle using Poisson regression. We estimated 10-year rates of curative treatment initiation in patients that initially received conservative management using Fine and Gray models adjusted for competing risks of lethal progression (prostate cancer death, metastasis, or initiation of hormone therapy) and other-cause death, censoring at December 2022. We assessed the variation in continuation to curative treatment with Cox models.

Results

The uptake of conservative management was 16% (444/2872). Conservative management was higher in older patients (1 year of additional age - Relative Risk (RR): 1.08, 95% CI: 1.06 - 1.11), in later calendar years (1 additional year - RR: 1.07, 95% CI 1.05 - 1.10)), and in neighborhoods of higher socioeconomic status (1 standard deviation rise - RR: 1.16. 95% CI 1.03 - 1.30). Uptake was lower in favorable-intermediate risk, rather than low-risk, prostate cancer (RR: 0.47. 95% CI 0.35 - 0.61). Among the 444 patients who initially received conservative management, when adjusted for competing risks of lethal progression and other-cause death, the 10-year curative treatment incidence was 22%. Patients were more likely to continue to curative treatment if they were younger at diagnosis (1 year of additional age - Hazard Ratio (HR): 0.96, 95% CI: 0.93 - 0.99) or had healthier post-diagnostic lifestyles (increase of 1 in joint measure of physical activity, BMI, and smoking, scored 0-3 - HR: 1.47, 95% CI 1.01 - 2.15).

Conclusion

We found age at diagnosis, calendar year at diagnosis, prostate cancer risk group, and neighborhood-level socioeconomic status to affect conservative management uptake, and age at diagnosis and post-diagnostic lifestyle to affect rates of curative treatment initiation following conservative management, in low/favorable-intermediate risk prostate cancer patients. These results could inform the clinical management of low/favorable-intermediate risk prostate cancer.

#2347 Lethal progression risks of low risk and favorable-intermediate risk prostate cancer in a prospective cohort of US health professionals.

Isaac Allen[1], Jane Bailey Vaselkiv[2], Hannah E. Guard[2], Sinead Flanagan[2], Hari Iyer[3], Kevin Kensler[4], Jaime E. Hart[5], Mark A. Preston[6], Andreas Pettersson[7], Keyan Salari[8], Edward L. Giovannucci[9], Meir Stampfer[10], Adam S. Kibel[6], Lorelei A. Mucci[2], Timothy Rebbeck[1]

[1]Dana-Farber Cancer Institute, Boston, MA,[2]Harvard T.H. Chan School of Public Health, Boston, MA,[3]Rutgers Cancer Institute of New Jersey, New Brunswick, NJ,[4]Weill Cornell Medicine, New York, NY,[5]Department of Medicine, Brigham and Women's Hospital and Harvard Medical School, Boston, MA,[6]Department of Urology, Brigham and Women's Hospital, Boston, MA,[7]Department of Medicine Solna, Karolinska Institutet, Stockholm, Sweden,[8]Department of Urology, Massachusetts General Hospital, Boston, MA,[9]Professor of Nutrition & Epidem., Harvard TH Chan School of Public Health, Boston, MA,[10]Department of Epidemiology, Harvard T.H. Chan School Public Health, Boston, MA

Background

Low-risk (grade group 1, stage≤cT2a, PSA<10) or favorable-intermediate risk (grade group 1, stage cT2b-cT2c or PSA 10-20, or grade group 2, stage≤cT2a and PSA<10) prostate cancer patients are at risk of progressing to lethal disease (prostate cancer death or metastasis, or receipt of hormones). We estimated 35-year lethal progression risks in a prospective cohort of health professionals with low/favorable-risk prostate cancer.

Methods

We followed 2872 men from diagnosis (1986-2019) to lethal progression, censoring at other-cause death or December 2022. We estimated 35-year cumulative incidences using Kaplan-Meier techniques and assessed lethal progression risk by treatment, sociodemographics, PSA, stage, grade group, and lifestyle with Cox models.

Results

We saw 260 lethal progressions over a median follow-up of 15.7 years (IQR: 8.6 years). The 35-year cumulative lethal progression incidence was 16.7% (95% confidence interval (CI): 13.3 - 20.4%). Lethal progression risks were higher in patients older at diagnosis (Hazard Ratio (HR): 1.08, 95% CI: 1.06 - 1.10) and with higher PSA at diagnosis (HR: 1.08, 95% CI: 1.05 - 1.12), and were lower in patients that received curative-intent treatment (radical prostatectomy, radiotherapy, brachytherapy, or cryosurgery) (HR: 0.34, 95% CI: 0.24 - 0.48) or or had healthier post-diagnostic lifestyles (increase of 1 in joint measure of physical activity, BMI, and smoking, scored 0-3 - HR: 0.74, 95% CI: 0.60 - 0.91).

Conclusion

Over 35 years of follow-up, we saw higher lethal progression risks in patients older at diagnosis or with higher PSA at diagnosis, and lower risks in patients that had curative-intent treatment or with healthier post-diagnosis lifestyles. These results may inform clinical management of low/favorable-intermediate risk prostate cancer.

#2348 Impact of transportation infrastructure on differentially expressed miRNAs in triple negative breast cancer stages at diagnosis.

Nathan Xiang[1], Amjila Bam[2], Nubaira Rizvi[2], Micheal Celestin[2], Ty-Runet Bryant[2], Tung Sung Tseng[2], Bingbing Mao[2], Xiao-Cheng Wu[2], Qingzhao Yu[2]

[1]Tulane University, New Orleans, LA,[2]School of Public Health, Louisiana State University Health Science Center, New Orleans, LA

Purpose: Triple negative breast cancer (TNBC) is a subtype of breast cancer (BC) characterized by the absence of estrogen, progesterone, and HER2 receptors, accounts for 10-15% of all BC cases, and is associated with poor clinical outcomes. Environmental factors such as residential proximity to major transportation infrastructure may influnce disease severity, yet evidence and molecular mechanism remain fragmented. MicroRNAs (miRNAs) regulate tumor growth and treatment response, acting as either tumor suppressors or oncogenes. Here, we investigated miRNA expression across varying environmental exposure groups in TNBC, aiming to evaluate the impact of proximity to high volumes of transportation infrastructure on clinical outcomes in TNBC patients.
Methods: Total 434 TNBC patients diagnosed between 2009 and 2019 in Louisiana were included. Clinical and environmental data were integrated from Louisiana Tumor Registry (LTR) and Environmental Justice Index (EJI). RPL_EBM_DOM4 is the environmental variable representing the percentile rank of domain consisting of proximity to high volume roads, railways, and airports, and is categorized into 4 groups. TNBC stages were categorized as early or advanced. All of their Formalin-Fixed, Paraffin-Embedded (FFPE) TNBC tumor specimens were collected. MiRNA expression was profiled using high-throughput sequencing and normalized via the TMM method. Differentially expressed (DE) miRNAs were identified using edgeR, adjusting for plate effects. Shared DE miRNAs across TNBC stage and RPL_EBM_DOM4 were visualized using a Venn Diagram. All the analysis were performed using R.4.5.0. Statistical significance was considered as $p<0.05$.
Results: Advanced TNBC patients resided closer to major transportation infrastructure. There was a statistically significant association between RPL_EBM_DOM4 and TNBC stages ($p=0.005657$), indicating that environmental exposure to transportation infrastructure may increase the risk of advanced TNBC. A total of 196 miRNAs were identified as differentially expressed in relation to proximity to high-volume transportation infrastructure, and 69 miRNAs were associated with TNBC stage. Of these, 32 miRNAs were commonly differentially expressed across both RPL_EBM_DOM4 and TNBC stage.
Conclusion: Our study identified miRNAs potentially mediating the influence of environmental exposures on TNBC progression. The discovery of shared DE miRNAs offers insights into the molecular mechanisms underlying TNBC and suggests potential targets for intervention and prevention strategies tailored to environmentally influenced cancer outcomes. Futher studies by incorporating additional TNBC-related outcomes (such as patient survival) and other environmental risk factors may gain more comprehensive understanding of TNBC and provide strategies for equitable healthcare.

#2349 An investigation of etiologic heterogeneity across transcriptomic subtypes of clear cell renal cell carcinoma in two case-control studies.

Eun Mi Jung[1], Kristine Jones[2], Diptavo Dutta[1], Jonathan N. Hofmann[1], Helena Furberg Barnes[3], Stephen J. Chanock[1], Nat Rothman[1], Paul Brennan[4], Kai Yu[1], Mark P. Purdue[1]

[1]Division of Cancer Epidemiology and Genetics, National Cancer Institute, Rockville, MD,[2]Cancer Genomics Research Laboratory, Frederick National Laboratory for Cancer Research, Frederick, MD,[3]Memorial Sloan Kettering Cancer Center, New York, NY,[4]Section of Genetics, International Agency for Research on Cancer, Lyon, France

The well validated Clearcode34 transcriptomic subtypes of clear cell renal cell carcinoma (ccRCC) are clinically distinct, with ccB tumors having poorer patient survival than ccA tumors, yet few studies have evaluated whether the subtypes possess distinct risk factor profiles. To address this question, we investigated potential etiologic heterogeneity between the ccA and ccB subtypes in two case-control studies conducted in Europe (144 ccA, 106 ccB, 1,476 controls) and the U.S. (75 ccA, 27 ccB, 1,235 controls). We measured expression levels of the 34-gene Clearcode panel to classify ccRCC tumors by subtype. For each study we conducted (1) case-only analyses (ccB vs. ccA) using logistic regression to assess subtype differences in tumor characteristics and control matching factors (e.g., age, sex, race/ethnicity) and (2) case-control analyses using polytomous regression to compute subtype-specific associations with established and suspected RCC risk factors [e.g., body mass index (BMI), smoking, hypertension, polygenic risk score (PRS) derived from genome-wide association studies (European-ancestry subjects)]. Study-specific findings were combined through meta-analysis using random effects models. We also computed associations with additional suspected risk factors that were assessed in the US study only. In the meta-analysis of case-control findings, we found ccA tumors to be more strongly associated with obesity [odds ratio (OR)=3.75, 95% confidence interval (CI)=1.14-12.35] than ccB tumors (OR=1.56, 95% CI=0.96-2.52). Conversely, ccB tumors were more strongly associated with a PRS based on 13 risk variants (90^{th} vs. 10^{th} percentile: OR_{ccA}=1.96, 95% CI=1.23-3.11; OR_{ccB}=3.34, 95% CI=1.83-6.11). From the U.S study, we identified that ccB tumors were more common among US Black vs. White patients (case-only OR=6.71, 95% CI=1.22-36.98), more strongly associated with chronic renal failure (OR_{ccB}=22.12, 95% CI=6.22-78.72; no exposed ccA cases), and more highly associated with a recent PRS based on 108 risk variants (90th vs. 10th percentiles: OR_{ccA}=3.26, 95% CI=1.39-7.60; OR_{ccB}=13.12, 95% CI=1.61-107.02). We did not observe any notable differences by subtype for the associations with smoking, hypertension, hysterectomy, oophorectomy, physical activity, and alcohol consumption. Our findings suggest the existence of etiologic heterogeneity between the Clearcode34 subtypes, with ccA tumors more strongly associated with excess weight and ccB tumors more common among Black patients and more strongly associated with chronic renal failure and genetic risk scores. This evidence suggesting risk factor heterogeneity across subtypes highlights the importance of accounting for tumor molecular characteristics in investigations of ccRCC etiology and risk prediction models.

#2350 Subtype-specific patterns of peripheral T-cell lymphoma in diverse Asian populations.

Xuanxi Kuang[1], Esther Lam[2], Mallory P. Bernstein[3], Nicole Foley[3], Lauren Pinter-Brown[4], Megan S. Lim[5], Wendy Cozen[3]

[1]University of California, Irvine, Irvine, CA,[2]UCI Health, Orange, CA,[3]Medicine, Division of Hematology-Oncology, UCI School of Medicine, Irvine, CA,[4]Medicine, UCI School of Medicine, Irvine, CA,[5]Pathology, Memorial Sloan Kettering Cancer Center, New York, NY

Peripheral T-cell lymphomas (PTCLs) are rare, aggressive non-Hodgkin T-cell lymphomas with a poor prognosis. Black individuals have a higher incidence compared to White individuals, but little is known about incidence rates for specific Asian populations. We obtained average annual age-adjusted incidence rates (AAIR)/100,000 based on the age distribution for the US 2000 Census for PTCL-not otherwise specified (ICD-O-3: 9702), angioimmunoblastic T-cell lymphoma (AITL, 9705), and anaplastic large cell lymphoma (ALCL, 9714) within Asian subpopulations, in addition to rate ratios(RR) comparing racial/ethnic groups with non-Hispanic whites (NHW) as a reference group. Data was obtained from the Surveillance, Epidemiology, and End Results (SEER) 9 registry (1990-2014). The combined-subtype analysis showed no significant difference between Asian-Pacific Islanders overall and NHW (RR 0.94; p=0.0976), but stratified analysis in SEER showed striking differences. Southeast Asians had the highest incidence rates, followed by Filipinos, while Chinese had the lowest incidence rates (Table 1). By subtype, Southeast Asians had the highest incidence rates of PTCL-NOS (0.72/100,000, RR= 2.40, p=0.002, based on 21 cases), followed by Filipinos (0.45/100,000, RR=1.49, p<0.001). Both Filipinos (p=0.0004) and Vietnamese (p=0.05) had higher incidence rates of AITL (0.18/100,000) compared to NHW (0.1/100,000) with RR=1.73. NHW had the highest incidence rates of ALCL (0.23/100,000). Compared to NHW, Chinese, Japanese, and Koreans showed significantly lower ALCL rates (RRs = 0.45-0.57, p < 0.01). These findings highlight distinct subtype-specific PTCL risk patterns across Asian subgroups. Given the low case counts, results should be interpreted cautiously. Disaggregation of Asian subgroups in PTCL subgroups remains essential to identify high-risk groups and improve prognostic accuracy.

Table 1. AAIR and RR for PTCL by racial/ethnic group.

	AAIR/100,000	95% CI	N	Rate Ratio	95% CI	P-value
Non-Hispanic Whites	0.63	0.62. 0.65	6,778	1.0		
Chinese	0.50	0.43, 0.59	171	0.80	0.68,0.93	0.0031
Japanese	0.60	0.51, 0.71	141	0.96	0.80, 1.13	0.6544
Filipino	0.80	0.71,0.91	260	1.27	1.12,1.44	0.0004
Korean	0.51	0.39, 0.65	64	0.80	0.61,1.03	0.0932
Vietnamese	0.73	0.58,0.92	87	1.16	0.91,1.45	0.2260
Pacific Islander	0.73	0.54,0.96	54	1.16	0.86, 1.52	0.3385
SE Asian	0.94	0.59,1.41	28	1.49	0.94,2.23	0.0882

#2351 Population awareness of HBV, HCV, and their association with cancer in the US.

Eric Adjei Boakye[1], Chaitali Dagli[2], Minerva So[1], Pranali G. Patel[2], Mrudula Nair[1], Joel Fokom Domgue[3]

[1]Henry Ford Health, Detroit, MI,[2]University of Alabama at Birmingham, Birmingham, AL,[3]MD Anderson Cancer Center, Houston, TX

Introduction: It is estimated that there will be 42,240 new cases and 30,090 deaths of liver cancer in the US in 2025. Chronic hepatitis B and C infections are the leading risk factors of liver cancer, yet public awareness of their oncogenic potential remains limited. Understanding population-level awareness of this link is essential for improving prevention, screening, and vaccination efforts. We examined the prevalence and association between sociodemographic characteristics and awareness of the link between hepatitis B or C and cancer among U.S. adults.

Methods: We analyzed data from the Health Information National Trends Survey (HINTS 7), a nationally representative survey of U.S. adults conducted in 2024. The outcome was awareness about the link between hepatitis B or C and cancer (yes/no). The outcome was accessed with the question “Do you think the Hepatitis B virus (also known as Hep B or HBV), or Hepatitis C virus (also known as Hep C or HCV) can cause cancer?” Weighted prevalence of awareness of hepatitis B or C as a cause of cancer was estimated among respondents. A weighted multivariable logistic regression model was used to estimate the association between sociodemographic characteristics (age, gender, race/ethnicity, marital status, education level, household income, rural-urban status, # of healthcare visits, and health status) and awareness of the link between hepatitis B or C and cancer.

Results: A total of 7,278 participants were included in the analysis, including 51% of individuals aged 18-48 years, 52% of female, 61% of non-Hispanic White, 56% of married, 33% of college graduates, and 27% with household annual income of <$35,000. Of these, 26.9% were aware that hepatitis B or C can cause cancer. Compared with respondents aged 18-49 years, those aged ≥65 years were less likely to know that hepatitis B or C can cause cancer (aOR=0.57; 95% CI: 0.44-0.76). Similarly, compared to respondents who were married, those who were divorced/separated/widowed were less likely to know that hepatitis B or C can cause cancer (aOR=0.73; 95% CI: 0.53-0.98). However, respondents who were college graduates were more likely to know hepatitis B or C can cause cancer (aOR=2.03; 95% CI: 1.39-2.95) compared with those with high school diploma or less.

Conclusion: Despite the growing burden of liver cancer in the US, population awareness that hepatitis B or C viruses can cause cancer remains low and varies substantially across sociodemographic groups. These findings suggest critical information/knowledge gaps persist across the U.S. population and call for targeted, health-literacy-appropriate educational interventions to enhance public awareness of preventable cancer risks.

#2352 Disability patterns and subjective cognitive decline among adults with and without cancer history.

Elham Samami[1], Sayantani Sarkar[2], Hermine Poghosyan[3]

[1]School of Nursing, Yale University, Orange, CT,[2]University of California, Berkeley, Greater Sacramento, CT,[3]Yale University, Orange, CT

Background: Subjective cognitive decline (SCD) is a self-reported experience of worsening confusion or memory loss, which increases the risk of dementia and may be influenced by disabilities. This study compared disability types and counts and SCD of people with or without a cancer history and examined the potential association between disability counts and SCD.
Methods: We used cross-sectional survey data from the 2024 Behavioral Risk Factor Surveillance System Cognitive Decline module. The sample included adults aged ≥45 years, with (n=12,601) and without (n=61,575) cancer history. The outcome was self-reported SCD confusion or memory loss worsening in the past 12 months. Disability types included limitations in hearing, vision, mobility, self-care, and independent living, and were categorized by count as 0, 1, 2, 3-5 disabilities. We conducted descriptive statistics and multivariable logistic regression, incorporating an interaction term between cancer history and disability count.
Results: About 73.0% of participants were aged ≥75 years, 53.2% were female, and 66.1% self-identified as White. Overall, 15.4% self-reported SCD, with higher prevalence among cancer survivors than those without cancer history (19.7% vs. 14.7%, p≤.001). The most prevalent disability type was mobility among adults with (31.0%) and without (20.4%) a cancer history. Among cancer survivors, SCD prevalence increased with disability count: 11.8% with no disabilities, 21.5% with one, 32.8% with two, and 47.2% with 3-5 disabilities. Similar patterns were observed in the non-cancer group: 8.9%, 19.8%, 30.2%, and 47.2%, respectively. In subgroup regression models, cancer survivors with 3-5 disabilities have 341% increased odds of reporting SCD compared to those without disabilities (AOR=4.41, 95% CI 3.07-6.33). Individuals without a cancer history who have 3-5 disabilities have 403% higher odds of reporting SCD compared to their no-disability counterparts (AOR=5.03, 95% CI 4.05-6.25). In the full model, both disability count and cancer status were independently associated with SCD; however, the interaction term was not statistically significant, suggesting that cancer status does not influence the relationship between disability count and SCD.
Conclusions: We estimated that SCD affects many individuals with (1.1million) and without (4.8million) cancer history aged ≥45 years. Routine screening for cognitive health, particularly for individuals with disabilities, is crucial for the early identification, proactive management, and tailored care of health needs in the adult population that may potentially lower the risk for dementia. Building personalized and need-based cognitive support resources, such as decision aids, checklists, digital and manual reminders, will help to promote care to this vulnerable group.

#2353 Geospatial analysis of incidence and mortality rates of gastrointestinal cancer and socioeconomic status across Puerto Rico during 2013-2022.

Brenda C. Torres-Velasquez[1], Liliana M. Castro-Jimenez[1], Yoel Velazquez Oliver[1], **Hilmaris Centeno-Girona**[1], Carlos R. Torres-Cintron[2], Elba V. Caraballo[1]

[1]Division of Shared Resources and Scientific Operations, University of Puerto Rico Comprehensive Cancer Center, San Juan, PR,[2]Puerto Rico Central Cancer Registry, University of Puerto Rico Comprehensive Cancer Center, San Juan, Puerto Rico

Colorectal (CRC), gastric, and pancreatic cancers are classified as gastrointestinal (GI) malignancies. Collectively, they rank among the top ten leading causes of cancer-related death in Puerto Rico (PR) for both men and women with CRC being the second most diagnosed and second leading cause of cancer death in PR. This study examines spatial and temporal variations of GI cancer incidence and mortality across municipalities in PR, while evaluating the role of sociodemographic factors and major disruptions -such as Hurricanes Irma and Maria (2017), subsequent earthquakes, and the COVID-19 pandemic- on these patterns across two periods. Age-adjusted incidence rates (AAIRs) and age-adjusted mortality rates (AAMRs) at municipality level were obtained from the PR Central Cancer Registry for 2013-2017 and 2018-2022. Sociodemographic data came from the American Community Survey. Global spatial autocorrelation was assessed using Global Moran's Index (I) and visualized through choropleth maps (Jenks Natural Breaks). Getis-Ord Gi* analysis identified clusters of municipalities with high-incidence or mortality (hot spots) and low-incidence or mortality (cold spots), using Bonferroni correction at a 90% confidence level. Wilcoxon rank-sum tests compared AAIRs, AAMRs, and socioeconomic indicators between periods and spot classifications. Statistical significance was set at $p<0.05$. Analyses were conducted by period using R (version 4.4.1) and R-Studio. Spatial clustering of AAIRs was significant across PR for the full period (Moran's I 0.17, $p<0.05$). Clustering in 2013-2017 was marginal (Moran's I 0.08, $p=0.1$) but became pronounced in 2018-2022 (Moran's I 0.19, $p<0.05$). Furthermore, AAMRs showed positive spatial autocorrelation for 2013-2017 period (Moran's I 0.22, $p<0.001$). In 2013-2017, 11 municipalities were hot spots and 12 were cold spots. In 2018-2022, 10 hot spots emerged—Juana Díaz and Guánica persisted across both periods while nine new cold spots appeared with no overlap. In 2013-2017 period, hot spots had 13% higher AAMRs than cold spots ($p<0.001$), while hot spots had significantly higher AAIRs in the latter period. Socioeconomic status did not correlate with hot or cold spots from 2013-2017; however, cold spots showed significantly higher socioeconomic status than hot spots in the 2018-2022 period: lower household income, and higher rates of poverty and SNAP participation ($p<0.05$). GI cancer in Puerto Rico exhibits persistent spatial clustering: AAIRs intensified in 2018-2022 and AAMRs shifted from higher AAMRs in hot spots during 2013-2017 to an income-related gradient in 2018-2022, where higher socioeconomic levels were linked to lower mortality. These findings suggest that systemic disruptions such as natural disasters and the COVID-19 pandemic may have deepened existing inequalities in vulnerable regions of Puerto Rico.

#2354 Predictors of mortality in patients with hepatobiliary and pancreatic cancers.

Jieun Lee, Sunhee Hwang, Suhyeon Hwang, Junglyun Kim

Chungnam National University, Daejeon, Korea, Republic of

Background Hepatobiliary and pancreatic cancers are the most lethal malignancies, with consistently poor survival outcomes due to delayed diagnosis and limited therapeutic options. Identifying factors associated with mortality is essential for improving prognosis and tailoring supportive care. However, evidence remains limited regarding comprehensive predictors of mortality in this population. This study aimed to identify determinants of mortality using a biopsychosocial approach that incorporates demographic, clinical, laboratory, and psychological factors, including quality of life (QoL).

Methods Patients diagnosed with hepatobiliary or pancreatic cancers were recruited from a university hospital between September 2022 and November 2023, and their mortality was followed up at 1 year from enrollment. Pain, anxiety, depression, and QoL were assessed using the Numeric Rating Scale, Hospital Anxiety and Depression Scale, and Functional Assessment of Cancer Therapy-General, respectively. Clinical information and death records were obtained from electronic health records. Cox proportional hazards regression was performed to identify factors influencing mortality using SPSS 30.0.

Results Among the 204 participants, Among the 204 participants, 81 (39.7%) of deaths were recorded. Higher physical well-being (HR = 0.95, 95% CI: 0.90, 0.99) and undergoing surgical treatment for cancer (HR = 0.38, 95% CI: 0.21, 0.70) were associated with lower mortality. In contrast, higher social well-being predicted increased mortality (HR = 1.12, 95% CI: 1.06, 1.19), which may indicate that patients with advanced disease receive more social support and caregiving. Elevated blood urea nitrogen also predicted higher mortality (HR = 1.03, 95% CI: 1.01, 1.07), suggesting that metabolic burden or renal dysfunction worsens outcomes.

Conclusions Physical well-being, received surgical treatment, and blood urea nitrogen levels were significant predictors of mortality in patients with hepatobiliary and pancreatic cancers. Enhancing physical functioning, surgical treatment history, and monitoring metabolic indicators may improve prognostic assessment. While psychological factors, except QoL, did not directly predict mortality. The findings highlight the value of an integrated biopsychosocial approach for managing high-risk cancer populations.

#2355 The association between metabolic syndrome and cancer: A systematic review.

Rebecca Mattson[1], Mary Barger[2], Arjan De Van Der Star[1], Uduak George[1]

[1]San Diego State University, San Diego, CA,[2]University of San Diego, San Diego, CA

Background: Metabolic syndrome (MetS), a cluster of central adiposity, hypertension, dysglycemia, hypertriglyceridemia, and low HDL cholesterol, has been identified as a possible determinant of lung cancer incidence and mortality.
Objective: To evaluate the association between MetS and lung cancer incidence and mortality, and examine sources of heterogeneity across studies.
Methods: A systematic review was conducted in accordance with PRISMA 2020 guidelines. CINAHL, Web of Science, and PubMed were searched from January 2000 through March 2025 for studies in adults that reported adjusted effect estimates for the relationship between MetS, defined by NCEP ATP III, IDF, or similar criteria, and cancer outcomes. Two reviewers independently screened studies, extracted data, and assessed risk of bias using the Newcastle-Ottawa Scale. Narrative synthesis and random effects meta-analysis were performed, with subgroup analyses by sex, smoking status, geographic region, and MetS definition. Heterogeneity was evaluated with the I^2 statistic and Cochran's Q, and publication bias was examined using Egger's test.
Results: Of 2,607 records screened, 11 studies met the inclusion criteria. In the meta-analysis of lung cancer incidence, the pooled hazard ratio was 1.18 (95% CI 1.04-1.33, p =.010), indicating a higher hazard of lung cancer among individuals with MetS. Heterogeneity was substantial (I^2 = 97.6 percent, $p < .001$).
Conclusions: The reviewed studies indicate that MetS has an association with increased lung cancer incidence. Clinical evaluation for MetS may identify individuals at elevated cancer risk, supporting early lung cancer screening and preventive strategies. Further research should determine whether integrating cancer prevention into MetS management influences long-term cancer outcomes.

#2356 Reliability of stromal markers multiplex immunofluorescent staining: Pathologist assessment compared to quantitative image analysis.

Lusine Yaghjyan[1], Yaileen D. Guzman-Arocho[2], Yu Jing J. Heng[2], Brian R. Sardella[2], Gurzhikhan Murtazaalieva[2], Graham A. Colditz[3], Dongtao Fu[1], Krishna Patel[4], Bernard Rosner[4], **Maisey Ratcliffe**[1], Rulla M. Tamimi[5]

[1]University of Florida, Gainesville, FL,[2]Beth Israel Deaconess Medical Center, Boston, MA,[3]Washington University School of Medicine in St. Louis, St. Louis, MO,[4]Brigham and Women's Hospital and Harvard Medical School, Boston, MA,[5]Weill Cornell Medicine, New York, NY

Purpose: Prior studies show the importance of stroma in breast tumorigenesis. However, there is no data on the expression of stromal markers alpha-smooth muscle actin (αSMA), fibroblast activation protein (FAP), matrix metallo-peptidase (MMP14), tenascin-C (TNC), and calcyclin (s100A6) in the breast tissue of cancer-free women. We compared the immunofluorescence (IF) expression assessment of these markers in histologically normal terminal duct-lobular unit tissue cores between an expert pathologist and an automated image analysis. We also assessed the homogeneity of these markers across multiple cores pertaining to each woman.
Methods: We included 73 cancer-free women with biopsy-confirmed benign breast disease in the Nurses' Health Study (NHS) and NHSII cohorts. IF was conducted with commercial antibodies (αSMA: 1:400 dilution; FAP: 1:50; MMP14: 1:150; TNC: 1:200; s100A6: 1:300). For each core, the % positivity was quantified by the pathologist and inForm v2.6.0. Using the pathologist scores as the gold standard, correlations between the two methods were evaluated with Spearman correlation (for categorical positivity: 0, >0 -<1, 1- 10, >10-50, and >50%) and sensitivity/specificity (for binary positivity with 1%, 10% and 25% cut-offs).
Results: Pathologist and inForm readings were available for 149 and 134 cores, respectively; 105 cores had both manual and automated readings. The correlation in the expression across available cores for a woman (median=3, range 1-6) was strong for FAP, MMP14, and S100A6 (Intra-class correlation [ICC]=0.69, 0.72, 0.63, respectively), moderate for αSMA (ICC=0.35), and poor for TNC (ICC=0.21). Correlation between pathologist and inForm was strong for s100A6, FAP, and MMP14 (0.77, 0.70, and 0.78, respectively) and moderate for αSMA (0.37) and TNC (0.42). With a 1% cut-off, sensitivity was the lowest for TNC (0.30) and ranged between 0.84-0.93 for other markers. Specificity ranged between 0.43-0.98 with the lowest estimates for αSMA. Sensitivity declined for all markers while using 10% and 25% cut-offs, while specificity increased.
Conclusion: Our findings show that computational assessments for αSMA, FAP, MMP14, TNC, and s100A6 exhibit variable correlations with manual assessment. These findings support the use of computational platforms for IF evaluation of stromal markers in large-scale epidemiologic studies and the importance of pilot studies for identification of appropriate cut-offs for defining staining positivity.

#2357 Feasibility of survey-based data collection in a diverse colorectal cancer cohort: Early-onset vs. average-onset.

Citlalli F. Lopez[1], L. Joseph Su[1], Luis Gonzalez[1], Yu-Lun Liu[1], Rasmi Nair[1], Lindsay Cowell[1], Emina Huang[2], Syed Mohammad Ali Kazmi[3]

[1]Peter O'Donnell Jr. School of Public Health, University of Texas Southwestern Medical Center, Dallas, TX,[2]Department of Surgery, University of Texas Southwestern Medical Center, Dallas, TX,[3]Division of Hematology Oncology, University of Texas Southwestern Medical Center, Dallas, TX

BACKGROUND: The incidence of early-onset colorectal cancer (EOCRC) is rising, yet a robust model of underlying factors across diverse populations is unknown. Most studies have examined a single factor or were performed in non-diverse population. The collection of comprehensive, patient-reported data across different populations in CRC will enable a deeper understanding of these associations to inform early intervention strategies.
METHODS: A pilot survey study was conducted at UT Southwestern Simmons Comprehensive Cancer Center (SCCC) and its affiliated safety-net hospital, Parkland Health and Hospital System (PHHS). The objective was to evaluate the feasibility of a multidomain survey in colorectal cancer patients. Eligible patients (≥18 years, stage I-IV adenocarcinoma, diagnosed within 12 months) completed baseline surveys in English or Spanish on demographics, lifestyle, symptom burden, nutrition (Dietary History Questionnaire), quality of life (EORTC QLQ-30, CR29), and financial toxicity (COST-FACIT). Surveys were administered in REDCap at baseline and three months follow-up. The primary endpoint was survey completion; feasibility was assessed by recruitment, participation, and completion rates. Descriptive comparisons were made between EOCRC (<50 years) and average-age onset colorectal cancer (AOCRC; ≥50 years).
RESULTS: From March 2024 to April 2025, 66 patients were approached, and 60 (91%) consented; all completed the baseline survey (100%), confirming feasibility across academic and safety-net settings. However, for the three-month follow-up survey participation decreased by 50%. The cohort was evenly distributed by sex (48% female, 52% male) and site (50% Parkland, 50% UTSW). Participants were diverse (42% Hispanic, 18% Black, 42% Non-Hispanic White) with variable socioeconomic status: 38% reported income <$35,000, 23% >$100,000, 28% were unable to work, and 23% were employed. Hospital utilization differed: 96% of Non-Hispanic Whites were treated at SCCC, while most Hispanic and Black patients were seen at PHHS. Parkland Financial Assistance was reported by 77%, highest among Hispanic patients. Nineteen patients (32%) had EOCRC (median age 42, range 30-48) and 41 (68%) had AOCRC (median age 64, range 51-82). EOCRC patients were more often Hispanic (58% vs. 32%), treated at Parkland (58% vs. 46%), and received assistance more frequently (47% vs. 34%).
CONCLUSION: This pilot study confirms that comprehensive, survey-based data collection is feasible in a racially, ethnically, and financially diverse CRC cohort. These preliminary findings highlight the clinical and sociodemographic differences of EOCRC and AOCRC across distinct groups. Future work will expand longitudinal follow-up, incorporate electronic health record data, and leverage tumor registry phenotypes to enable low-touch, systematic patient recruitment for a more robust sample.

#2358 Mining social determinants of health documentation patterns for genitourinary cancer patients using natural language processing.

Nikita Thakur[1], Natalie Reizine[1], Karine Tawagi[1], Charbel Hobeika[1], Ashwani Tanwar[2], Guanyu Tao[2], Marzana Chowdhury[2], Evan Garrad[3], Ahsan Wahab[1], Jingqing Zhang[2], Vibhor Gupta[4], VK Gadi[1], Sandeep Kataria[1]

[1]University of Illinois Cancer Center, Chicago, IL,[2]Pangaea Data, London, United Kingdom,[3]University of Illinois Chicago, Chicago, IL,[4]Pangaea Data, South San Francisco, CA

Mounting evidence demonstrates that social determinants of health (SDOH) significantly impact cancer care, contributing to persistent disparities in prevention, diagnosis, treatment access and survival rates that disproportionately affect vulnerable populations. However, SDOH are frequently underreported in clinical notes, obscuring barriers for patients to receive appropriate care. The systematic extraction from clinical notes remains challenging. We developed an advanced Natural Language Processing (NLP) based Artificial Intelligence (AI) platform to automatically extract SDOH from genitourinary cancer clinical notes.

We analyzed 757,757 clinical notes from 5,585 patients (prostate:n=3,772; bladder:n=619; renal:n=1,194, based on ICD) using the AI platform. The platform used NLP to extract 19 types of SDOH features (e.g. race, ethnicity, health literacy, substance abuse, financial strain, social isolation, etc) across four note types: Progress Notes, Consults, Care Plans, Patient Instructions.

The AI platform extracted 767,000 SDOH mentions from 4,464 patients (80% of patients). 140 clinical notes across 21 patients were randomly selected to evaluate AI accuracy. Of 140 notes, AI found SDOH features in 131 notes and clinicians from University of Illinois Cancer Center manually determined that 124 notes contained fully accurate SDOH extractions, while 7 notes had partially inaccurate SDOH extractions, yielding 95% accuracy (124/131). The study showed high prevalence of mentions of health literacy (96.71%), substance use (93.15%), and mood/affect issues (81.41%). 65% patients had minimal SDOH documentation (1.4 features per patient) and 35% patients had multiple SDOH documentation (6.9 features per patient).

Among 2,900 patients who were diagnosed with genitourinary cancer in 2018-2023 (317,143 SDOH mentions after removing boilerplate SDOH mentions), by analyzing COVID-19 impact (pre vs post March 2020), we found that documentation of demographic SDOH decreased, e.g. home address (-37%), race (-34%), ethnicity (-36%), but the social SDOH increased, e.g. social isolation (+65%), financial strain (+76%), stress (+63%).

This study shows the feasibility and effectiveness of using NLP to systematically extract SDOH from genitourinary cancer clinical notes. The high prevalence of documented SDOH underscores their potential impact on cancer care delivery and emphasizes the importance of routine SDOH documentation for every patient. COVID-19 caused a significant shift in SDOH documentation patterns with more pandemic-exacerbated social barriers. Future work should focus on validating the clinical impact of SDOH-informed decision making. Additional directions include leveraging large language models (LLMs) to infer the presence or impact of SDOH features and analyzing extracted SDOH information for clinical and societal insights.

#2359 Validation of prostate cancer diagnosis and cause of death in a national cohort of male veterans with type 2 diabetes mellitus.

Mulugeta Gebregziabher[1], Kinfe G. Bishu[2], Andrew Schreiner[3]

[1]Public Health Sciences, The Medical University of South Carolina and Charleston VAMC, Charleston, SC,[2]Research, The Medical University of South Carolina and Charleston VAMC, Charleston, SC,[3]Medicine, The Medical University of South Carolina and Charleston VAMC, Charleston, SC

Background: Accurate diagnosis and determination of cause of death are essential for effective disease surveillance, health planning, and research. This study seeks to validate the diagnostic accuracy and cause of death data related to prostate cancer (PCa) among Veterans with type 2 diabetes mellitus (T2DM).

Methods: We conducted a retrospective cohort study of Veterans with type 2 diabetes (T2DM) diagnosed between 2010 and 2019, using data from the Veterans Health Administration (VHA) Corporate Data Warehouse (CDW). Diagnostic codes and cause of death information were obtained from the Prostate Cancer Data Core (PCDC) and the National Death Index (NDI), which served as the gold standard for validating CDW data. Concordance between data sources was evaluated using Cohen's Kappa statistic, along with measures of diagnostic performance such as sensitivity and specificity.

Result: Among 763,424 Veterans with T2DM, 37,048 were diagnosed with PCa in the CDW and 36,861 in the PCDC, with concordance rate of 98.7%. Mortality data from the NDI revealed 2,723 deaths with PCa as the underlying cause, of whom 75.4% had a recorded diagnosis of PCa in CDW. For all-cause mortality, 328,156 Veterans were identified as deceased in the CDW Vital Status File (VSF) and 326,707 were reported as deceased in the NDI, with a concordance rate of 99.3% deaths between the two sources. Comparing incident PCa diagnoses for all patients, we found that the CDW had a high sensitivity 98.6% and specificity 99.9%. Similarly, for cause specific death, the sensitivity rate was 75.5% and specificity was 100.0%.

Conclusions: The findings demonstrate a high level of concordance in key outcomes of interest, specifically, prostate cancer (PCa) diagnosis between the CDW and PCDC, and all-cause mortality between CDW VSF and NDI data sources. Given the time-consuming nature of data retrieval and management from the CDW, we recommend using the PCDC for PCa diagnosis and CDW VSF for all-cause mortality ascertainment.

#2360 Differences in oral HPV prevalence estimation via Bayesian and frequentist methodologies from people living with HIV in Puerto Rico.

Erick M. Ivanovich-Mendez[1], Luis R. Pericchi[2], Brenda Torres-Velasquez[2], Vivian Colon Lopez[2], Josue Perez Santiago[2]

[1]Cancer Control Division and Population Sciences, University of Puerto Rico Comprehensive Cancer Center, San Juan, PR,[2]University of Puerto Rico Comprehensive Cancer Center, San Juan, PR

Introduction: Puerto Rico faces significant public health challenges due to a high rate of HPV-related cancers and a high prevalence of HIV, consistently ranking among the U.S. states and territories with the most AIDS cases. While population-based data on oral HPV infection for Puerto Rico remains scarce, studies focusing on high-risk groups have found a 12.5% prevalence rate among drug users in the San Juan metropolitan area. Logistic regression, a common method for frequentist estimation, often fails to account for the accuracy of a screening method. Studies confirm that Bayesian statistical models overcome these limitations by incorporating test performance. Despite these advantages, the use of Bayesian prevalence estimation is rare. Specifically, they have proven useful in scenarios where screening methods are suboptimal; limited sample size, or the core assumptions of frequentist models are unable to be met. These challenges are commonly encountered in studies addressing site-specific HPV prevalence, making Bayesian prevalence estimation a particularly well-suited and recommended alternative. **Objective**: To compare point estimates of oral HPV prevalence derived from frequentist and Bayesian models.

Methods: HPV genotyping data from an on-going study titled Multi-omics Predictors of Oral HPV Outcomes among People Living with HIV in Puerto Rico (P20GM148324) was used to estimate population prevalence. HPV status of this data was determined using the SPF10-LiPA25 method. R-statistical software and was used for prevalence estimation. The *rjags* library in R will provide the connection to run Markov Chain Monte Carlo (MCMC) simulations in JAGS software, Rogan-Gladen (RG) model will be utilized as the frequentist model since it compensates for diagnostic misclassifications. The comparison metrics to determine the best estimate will include error distribution for the point estimate and length of the confidence interval, or credible interval for the Bayesian case.

Results: The Bayesian estimation was 0.121 ± 0.0261 (CrI95%: 0.073 - 0.176) whilst the Rogan-Gladen model was 0.117 ± 0.0465 (CI95%: 0.032 - 0.212). While estimates are similar for both models, there is a slight improvement for both standard errors (SE) and corresponding intervals for the Bayesian estimation compared to the RG estimation.

Conclusion: The Bayesian method outperformed in both SE and Interval estimations as expected. A disadvantage of applying RG estimation is lack of interval estimation in the default function; intervals were manually calculated. Likewise, the number of iterations in MCMC impacts the SE for the Bayesian approach, further research must be done to determine if a cut-off point should be considered.

#2361 MELD 3.0 policy and evolving socioeconomic disparities in liver transplantation.

Tehyun Phillip Eom[1], Junho Song[2], Hyungjune Ku[3], **Sungsu Park**[4], Minkwan Kim[5], Sunghan Kim[1], Sangsoo Lee[3], Heekyoo Kim[3], Seoyeong Ku[6], Hyewon Kim[7], Amy Choi[2], Changmin Jo[8]

[1]CHA University School of Medicine, Seongnam-si, Korea, Republic of,[2]Penn State College of Medicine, Hershey, PA,[3]Kosin University College of Medicine, Busan, Korea, Republic of,[4]Daegu Catholic University School of Medicine, Daegu, Korea, Republic of,[5]Independent researcher, Gwangmyeong-si, Korea, Republic of,[6]Seoul Women's University, Seoul, Korea, Republic of,[7]Hanyang University College of Natural Sciences, Seoul, Korea, Republic of,[8]Chung-Ang University College of Medicine, Seoul, Korea, Republic of

Background: The MELD 3.0 policy, implemented by UNOS on July 13, 2023, updated the liver allocation scoring system to better reflect 90-day mortality risk. While intended to improve transplant equity, questions remain about its impact on socioeconomic disparities. We examined how MELD 3.0 affected DDLT access across socioeconomic groups and whether it narrowed or widened existing disparities.

Methods: We analyzed 12,479 adult HCC patients in the 21-month periods before (n=6,154) and after (n=6,325) MELD 3.0 implementation using UNOS data. Competing risks analysis with Aalen-Johansen estimators assessed DDLT rates accounting for death/deterioration. Gray's test evaluated socioeconomic disparities in DDLT access by race/ethnicity, insurance, education, employment, citizenship, gender, and region. Era-specific censoring used listing date as time origin.

Results: MELD 3.0 implementation significantly improved DDLT rates at 12 months: 53.3% pre-policy vs. 62.2% post-policy (+8.9 percentage points, p<0.001). Socioeconomic disparities showed mixed patterns. Race/ethnicity disparities persisted and slightly widened: Asian patients improved from 49.0% to 54.7%, while White patients increased from 55.1% to 64.3%. Black patients rose from 55.1% to 59.5%, and Hispanic patients from 46.1% to 64.8%, with differences remaining significant (pre p<0.001, post p<0.001).

Education disparities remained minimal: less than college vs. college graduates had similar rates pre-policy (53.0% vs. 53.2%) and post-policy (62.5% vs. 62.1%), with significance reflecting sample size rather than meaningful differences (p<0.001 both eras).

Insurance disparities showed mixed results: private insurance maintained advantage over public insurance, though significance weakened (p=0.015 pre, p=0.043 post).

Citizenship disparities showed a slight reduction in absolute difference (US vs. non-US: 53.4% vs. 51.0% pre; 62.3% vs. 60.7% post), while statistical significance strengthened (p=0.047 pre, p=0.010 post).

Employment and regional disparities persisted: post-policy, employed patients had slightly higher access, and substantial regional variation continued (p<0.001 both eras). Gender differences remained non-significant.

Conclusions: MELD 3.0 improved overall DDLT access for HCC patients but had varied effects on socioeconomic disparities. Education disparities remained minimal, while race/ethnicity, insurance, employment, citizenship, and regional differences continued. Although MELD 3.0 enhanced transplant access, persistent disparities highlight the need for additional interventions targeting socioeconomic determinants beyond allocation score refinements.

: Cancer Disparities
Poster Session

#2365 Demographic and socioeconomic disparities in access to curative-intent surgery for thymic carcinoma: A population based study..

Chinemerem M. Emeasoba[1], Chiugo Okoye[2], Gilbert-Roy Kamoga[1], Olanipekun Ntukidem[3], Hannah Jensen[1]

[1]Internal Medicine, UAMS Northwest, Fayettville, AR,[2]Internal Medicine, Northeast Georgia Medical Center, Gainesville, GA,[3]Internal Medicine, Trinity Health Ann Arbor Hospital, Ann Arbor, MI

Thymic carcinoma is a rare, aggressive thoracic malignancy in which surgery is the only potentially curative therapy. National inequities in surgical evaluation and treatment access remain poorly defined. We performed the largest population-based analysis to evaluate demographic and socioeconomic disparities in stage presentation and curative-intent surgery.

SEER (2010-2022) was queried for adults with histologically confirmed thymic carcinoma (ICD-O-3: 8586/3). Variables included age, sex, race/ethnicity, median household income, rural-urban classification, stage (Derived EOD 2018), surgery, chemotherapy, radiation, and "Reason for No Cancer-Directed Surgery." "Surgery not recommended" was used as a proxy for clinical inoperability or limited access to surgical evaluation. Associations were assessed using χ^2 and multivariable logistic regression, adjusting for age, sex, income, rurality, and stage group. Survival was evaluated using observed survival months.

Among 1,009 patients, the cohort was 62% male and racially diverse (White 51%, Black 17%, Asian/Pacific Islander 16%, Hispanic 15%). Stage was undocumented in 66%. Among staged cases, metastatic disease predominated (18%); early-stage (I-II) disease comprised 10%. Surgery was performed in 54%, while 41% had surgery "not recommended." Early-stage patients underwent surgery in 87% of cases versus 33% of metastatic cases ($p < 0.001$). Marked racial disparities were noted: surgery "not recommended" among Black (53.5%), Hispanic (45.7%), Asian/Pacific Islander (41.1%), and White (42.9%) patients. After adjustment, Black patients had significantly higher odds of surgery "not recommended" versus White patients (OR 1.61; 95% CI 1.11 - 2.35; $p = 0.01$). Advanced and unknown stage strongly predicted surgery not being recommended ($p < 0.001$). Treatment delays >90 days occurred more frequently in non-metropolitan counties (8.8% vs 4.6%). Median survival was markedly longer for patients who received surgery compared with those for whom surgery was not recommended (45 vs 15 months).

Substantial racial and socioeconomic inequities limit access to curative-intent surgery for thymic carcinoma in the United States. Black patients experienced significantly higher adjusted odds of surgery being deemed "not recommended," independent of stage, income, and rurality. High rates of missing stage documentation and prolonged treatment delays in non-metropolitan regions further hinder equitable care delivery. These findings highlight urgent needs for standardized staging, equitable referral pathways to thoracic surgical oncology, and system-level interventions to improve access to curative treatment for this rare malignancy.

#2366 HRSNs and CRC screening recommendation in NHIS.

Isaiah Casarez[1], Humberto Parada[1], Matthew P. Banegas[2], Uriel Nataren Geronimo[1], Benjamin Aceves[3]

[1]San Diego State University, San Diego, CA,[2]Cancer Prevention Fellow, UC San Diego, San Diego, CA,[3]Health Promotion and Behavioral Science, San Diego State University, San Diego, CA

Background: Health-related social needs (HRSNs), including food insecurity, housing instability, and financial hardship, are increasingly recognized as barriers to preventive care. Clinician recommendation is a primary driver of colorectal cancer (CRC) screening uptake. However, little is known about how specific HRSNs and co-occurring social risk patterns relate to clinician recommendations in nationally representative populations.

Methods We analyzed pooled 2021 and 2023 National Health Interview Survey (NHIS) cross-sections among adults 45-75 years without cancer history (unweighted n = 6,500; weighted = 27.6 million). Survey-weighted logistic regression estimated adjusted odds ratios (aORs) for clinician recommendations in the past 12 months. We examined granular food insecurity categories, HRSN burden counts, and latent social-risk subgroups using latent class analysis (LCA). Analyses were stratified by race/ethnicity and nativity; interaction terms tested effect modification.

Results: Overall, roughly 16% of adults reported a clinician's screening recommendation in the past 12 months. Among non-Hispanic White adults, financial hardship was associated with increased odds (aOR = 1.32, 95% CI: 1.11-1.56). Among Hispanic adults, food insecurity was associated with higher odds (aOR = 2.94, 95% CI: 1.59-5.42) while housing instability was associated with lower odds (aOR = 0.38, 95% CI: 0.16-0.88). LCA identified three distinct HRSN configurations: Low/No HRSN (85%), Moderate/Mixed (5%), and High HRSN Burden (10%). High-burden adults had marginally higher odds of recommendation (aOR = 1.33, 95% CI: 0.99-1.78). Race-by-HRSN interactions were statistically significant for housing instability.

Conclusions Specific and clustered social needs are associated with clinician recommendations for CRC screening, with differential patterns by race/ethnicity and nativity. Social risk assessment may support more equitable preventive care engagement. Disclosure: During the preparation of this work, the author used OpenAI ChatGPT to assist with wording and clarity. After using this tool, the author reviewed and edited the content and takes full responsibility for the accuracy and integrity of the abstract.

#2367 *KRAS* mutations worsen overall survival (OS) in Black but not White colon cancer patients.

Susan Ahmedyar, Minoru Koi, John M. Carethers

Medicine, UC San Diego, La Jolla, CA

Background. Disparities between Black (BA) and White Americans (WA) exist for incidence and OS among colon cancer (CC) patients. Identifying race-associated markers for OS may elicit CC treatment approaches to improve OS. We previously demonstrated that low-levels of microsatellite instability (MSI-L) and elevated microsatellite alterations at selected tetranucleotide repeats (EMAST) are associated with shorter CC recurrence-free survival. We also showed that MSI-L/EMAST with loss of heterozygosity (LOH) at chromosome 9p21-24 (9p-LOH) improves OS of CC patients. Additionally, we and others have observed high prevalence of *KRAS* and *BRAF* mutations in BA and WA CCs, respectively. Here, we examined race-associated differences in *KRAS* and *BRAF* mutations, 9p-LOH, and MSI-L/EMAST, and examined their prognostic values.

Methods. Three hundred-fifty CC cases (175 WA and 175 BA) from the North Carolina Colon Cancer Study were analyzed for associations between race and genetic alterations. Chromosome 9p-LOH was determined at 4 single nucleotide polymorphism (SNP) loci present on 9p21-24 by digital PCR. MSI-L/ EMAST was determined from 14 microsatellite markers, including 2 mono-, 5 di-, and 7 tetra-nucleotide markers by fragment analysis. *KRAS* G12/13 and *BRAF*^{V600E} mutations were determined by Sanger sequencing of PCR products generated from targeted regions.

Results. Among the 175 BA CC cases, 82 (46.8%) had *KRAS* mutations compared to 31.1% (53/169) of WA cases (O.R.: 1.97, 95%CI: 1.27-3.06, *P*=0.002). More WA CC cases (10.9%: 19/156) exhibited *BRAF* mutations than BA CC (6.1%: 10/165) but this difference did not reach significance (*P*=0.075). There was no association between MSI-L/EMAST and race (*P*=0.5). Chromosome 9p-LOH was detected in 15.2% of BA CC cases (19/125) and 9p-LOH with MSI-L/EMAST was detected in 8.6% of BA cases (12/140). Chromosome 9p-LOH prevalence was higher among WA CC vs BA CC in our initial subset analysis of 42 patients. Among BA CC cases, *KRAS* mutations were associated with shorter 5yr OS (H.R.: 1.91, 95%CI: 1.11-3.29, *P*=0.018) and 10yr OS (H.R.: 1.55, 95%CI: 1.02-2.37, *P*=0.04), and when adjusted for MSI-L/EMAST, tumor stage/location, and smoking status, *KRAS* mutations were associated with shorter 5yr OS (H.R.: 2.20, 95%CI: 1.27-3.8), *P*=0.0045) and 10yr OS (H.R.: 1.8, 95%CI: 1.17-2.78: *P*=0.0075). Among WA CC cases, there was no association between *KRAS* mutations and either 5yr OS (*P*=0.85) or 10yr OS (*P*=0.82).

Conclusions. *KRAS* G12/13 mutations are more frequent in BA CC than WA CC and are a poor prognostic factor for BA CC OS. The significance of 9p-LOH and 9p-LOH plus MSI-L/EMAST in WA CC is being currently assessed.

#2368 Social determinants and lifestyle factors driving colorectal cancer mortality disparities in younger Black and White patients.

Chinenye M. Okafor[1], Lauren Rose Fanning[2], Tami L. Crawford[3], John Pearce[3], Kathy Williams[3], Alexander V. Alekseyenko[3], Kristin Wallace[4]

[1]The Medical University of South Carolina (MUSC), Florence, SC,[2]The Medical University of South Carolina (MUSC), Summerville, SC,[3]The Medical University of South Carolina (MUSC), Charleston, SC,[4]MUSC Hollings Cancer Center, Charleston, SC

Background: Disparities in colorectal cancer (CRC) mortality in Black compared to White patients are more evident at younger ages. Emerging data suggests that earlier age of diagnosis in Blacks is associated with socioeconomic and lifestyle factors such as smoking and alcohol use; however, whether these factors contribute to differences in race- and age-specific CRC mortality remains unclear.
Methods: Data from the Medical University of South Carolina (MUSC) Hollings Cancer Center cancer registry was used to identify analytic CRC cases from 2000 - 2021 with ≥12 months of follow-up. This study was approved by the MUSC Institutional Review Board. Cox proportional hazards regression estimated risk of death (HR, [95% CI]) for Black versus White patients adjusting for age, sex, stage, year of diagnosis, and treatment. Interactions assessed were race x age (continuous), race x social deprivation index (SVI, high vs low), race x alcohol use (current vs not), race x smoking (current vs not).
Results: Of 1,324 patients, 43.5% were female, and 31.7% Black. Median age 62 years; 60 years for Black, 63 years for White. Median survival of 68 months for Blacks and 95 months for Whites. Blacks had higher adjusted risk of death (1.19 [1.01-1.40] vs Whites). There was significant interaction for race by age (p=0.01): Blacks <65 years had greater mortality than Whites (HR 1.38 [1.10-1.69]), with no racial difference observed for those ≥65 years (HR 0.99 [0.76-1.28]). We observed a significant race by SVI interaction (p=0.04): among those with higher SVI, Black patients had modest decrease in risk of death (HR 0.88 [0.66-1.16]) whereas Whites had an increased risk (HR 1.24 [1.02-1.49]); this difference was confined to those <65 years. A significant race by alcohol interaction was also present (p=0.0001): current drinkers who were Black had an increased risk of death (HR 1.63 [1.20-2.22]), while those who were White had a lower risk (HR 0.82 [0.67-1.00]), again limited to patients <65 years. Current smoking increased risk of death in both Blacks (HR 1.70 [1.23-2.35]) and Whites (HR 1.33 [1.05-1.67]), with no significant race x smoking interaction (p=0.22) or age-specific effect. Ever smoking or ever drinking yielded similar but attenuated results. Mortality risk did not differ by sex.
Conclusion: Black CRC patients <65 years had higher mortality risk than Whites, and specifically those with current alcohol use and concurrent smoking/alcohol use. No racial difference observed for those ≥65 years. Younger Black people with higher SVI (more vulnerability) had lower mortality than Whites with similar SVI, suggesting that access to health services in poorer Black communities improves outcomes. These findings identify a particularly vulnerable subpopulation that may benefit from targeted interventions focused on improving care access, addressing social barriers, and enhancing smoking and alcohol screening

#2369 Determinants of clinical outcomes: A pooled analysis of 71 phase I clinical trials evaluating metastatic colorectal cancer.

Ahan Bhatt[1], Hasan Zaidi[2], Shobi Venkatachalam[3], Lawanya Singh[2], Abhiraj Saxena[2], Radha Patel[3], Christina Boatwright[3], Demmie Aguilar[3], Jay Shah[3], Mohammad Ghalib[3], Imran Chaudhary[4], Simran Goel[4], Radhashree Maitra[4], Eugenia Girda[5], Sanjay Goel[5]

[1]Department of Internal Medicine, Jacobi Medical Center, Albert Einstein College of Medicine, Bronx, NY,[2]Department of Internal Medicine, Rutgers Robert Wood Johnson Medical School, New Brunswick, NJ,[3]Rutgers Robert Wood Johnson Medical School, New Brunswick, NJ,[4]Montefiore Medical Center, Bronx, NY,[5]Rutgers Cancer Institute of New Jersey, New Brunswick, NJ

Background: Minority patients are historically underrepresented in clinical trials. Their clinical outcomes are often reviewed retrospectively after drug approval, leaving uncertainty about efficacy in the broader population, including patients with metastatic colorectal cancer (mCRC). In phase I trials for mCRC, patient selection criteria remain challenging, and objective clinical and laboratory markers may improve uniform screening and outcome prediction.

Methods: We retrospectively reviewed medical records of patients with mCRC enrolled in phase I trials at two institutions between 1999-2018 and 2021-2025. Data collected included demographics, clinical and laboratory findings, treatment responses, and overall survival (OS). Variables were dichotomized using institutional or clinically relevant cutoffs. OS was defined from the date of first dose to death or last follow-up (censored if alive). Univariate analyses were performed using the Mantel-Cox test (Prism GraphPad v10), with hazard ratios (HRs) and 95% confidence intervals (CIs) reported.

Results: We analyzed 295 patients across 71 trials. Median age was 59 years (range, 29-83 years). 50.5% of patients were female. 24.4% were Non-Hispanic Black (NHB), 24.4% Hispanic, 6.1% Asian, 43.0% Non-Hispanic White (NHW). OS was 9 months and did not differ significantly among the different races/ethnicities ($p = 0.71$). The median duration on the trial was 59 days (range, 54-65 days). Median number of prior lines of therapy was 3 (range, 0-11), and the median number of sites of metastasis was 3 (range, 0-10). In a univariate model, poor performance status (PS ≥2; HR 2.665, $p=0.0026$), ≥3 metastatic sites (HR 1.497, $p=0.0049$), and > 3 prior lines of therapy (HR 1.358, $p=0.0167$) were associated with decreased OS. Laboratory markers including low albumin (<3.9 g/dL; HR 1.596, $p=0.0002$), high LDH (>281.5 U/L; HR 1.751, $p<0.0001$), high CEA (>119.5 ng/mL; HR 1.513, $p=0.0031$), elevated liver enzymes (AST>40 U/L, HR 1.696, $p=0.0004$; ALP>150 U/L, HR 2.102, $p<0.0001$), elevated bilirubin (≥1 mg/dL; HR 1.852, $p=0.0204$), and cytopenias (WBC<6 K/µL, HR 0.66, $p=0.0011$; ANC<4 K/µL, HR 0.63, $p=0.0004$; hemoglobin <11.5 g/dL, HR 1.435, $p=0.0043$) also predicted worse OS.

Conclusion: Patients with mCRC, regardless of age, sex, or race/ethnicity, had similar outcomes in phase I studies. The OS was at par with published data with similar exposure to prior therapies. Heavily pre-treated patients, low performance status, and spread to >3 sites were all associated with decreased survival. High LDH and high CEA, along with liver function tests, are key parameters and may refine eligibility and stratification in early-phase mCRC studies. A multivariate analysis will be presented, looking into the interplay of these key clinical findings.

#2370 American Indian and Alaska Native community perspectives on HPV vaccination: Insights from providers and parents in a shared tribal clinic setting.

Dakota K. Jones[1], Morgan Gill[1], Claradina Soto[1], Philip Farabaugh[2], Jennifer Tsui[1]

[1]Keck School of Medicine of USC, Los Angeles, CA,[2]Riverside San Bernardino Indian Health Clinic, Riverside, CA

INTRODUCTION

Human papillomavirus (HPV) vaccination prevents infection of HPV types that cause most cervical cancers, yet American Indian and Alaska Native (AI/AN) youth remain disproportionately under-vaccinated due to structural and community-level barriers. This mixed-methods pilot study assessed multilevel factors among providers and parents within the Riverside-San Bernardino County Indian Health (RSBCIHI) clinic system.

METHODS

This study aimed to identify multilevel barriers to HPV vaccination by integrating provider and parent perspectives from the same Tribal clinic setting, an area with limited empirical data. Survey items assessed provider-level barriers to HPV vaccine delivery, including communication challenges influencing uptake. Concurrently, pilot qualitative focus groups with AI/AN parents and caregivers explored individual and community influences on vaccine decision-making. Thematic analysis identified emergent sociocultural factors relevant to implementation refinement.

RESULTS

In October 2025, a baseline survey was administered among 15 clinical staff, including medical assistants (60%), physicians (13%), nurse practitioners (13%), and registered nurses (13%). While 92% of providers viewed HPV vaccination as “very important,” system-level barriers included limited training on addressing parental hesitancy (61%) and inconsistent reminder systems (47%). Reported challenges among parents included limited time with providers during visits (55%), cultural or trust-related concerns (48%), and vaccine safety concerns (67% rated as somewhat of a barrier). Over half of providers (53%) had worked in the clinic for less than one year, indicating high staff turnover. Parent focus group findings (n=3) revealed hesitancy rooted in healthcare provider mistrust, vaccine misinformation, and a desire for increased provider communication on sensitive topics.

DISCUSSION

This study identified several structural and interpersonal barriers to HPV vaccination within the RSBCIHI Tribal clinic system. Emergent themes from provider surveys included limited time during visits, inconsistent reminder systems, vaccine safety concerns, and frequent staff turnover. Parent perspectives further highlighted hesitancy rooted in vaccine misinformation, limited trust with healthcare providers, and discomfort discussing sensitive topics including sexual health and vaccinations. Together, these provider- and parent-level barriers illustrate the multilevel challenges influencing AI/AN HPV vaccination uptake, which will inform future sustainment strategies to strengthen vaccine confidence and culturally adapted cancer prevention efforts in Native communities.

#2371 Outcomes after introduction of cervical cancer screening in an opioid treatment program (OTP) by offering HPV self-collect testing to an under-screened population.

Elizabeth M. Swisher[1], Mallory Davis[2], Mayumi Rubin-Saika[1], Enna Manhardt[1], Emiko Oshima[1], Renata Urban[1], Stephem L. Cherne[1], Eric Huang[1], Tom Hutch[2]

[1]University of Washington, Seattle, WA,[2]We Care Daily Clinic, Auburn, WA

Individuals with opioid use disorder (OUD) have lower cancer screening rates. Cervical cancers are preventable through screening and treatment of human papillomavirus (HPV)-related pre-cancers. HPV self-collect tests provide opportunities to expand screening access to previously unreached populations, offering advantages of privacy, autonomy, and negating a clinic requirement for gynecological services. We evaluated a novel, low-barrier model for integrating HPV self-collect screening into a brick-and-mortar OTP and its four associated mobile medication units in a major metropolitan area in Washington state. Screening was offered with self-collection kits during annual medical update visits to eligible patients (those age 25 or above with a cervix who were overdue for screening or unsure) and collected privately in the clinic restroom. HPV swabs were analyzed at the University of Washington HPV Molecular Pathology Laboratory or Labcorp and included all 14 known high-risk HPV (hrHPV) types. Screened subjects with positive results received education and recommendations for guideline concordant care. Clinic staff facilitated referrals to local providers with gynecologic services and follow-up was tracked. The study's primary outcomes were the rates of screening uptake, HPV positivity, and successful linkage to follow-up care. From June 24, 2024 through October 31st, 2025, 186 patients were evaluated including 29 (15.6%) American Indian/Alaskan Native, 2 (1.1%) Asian, 20 (10.8%) Black, 2 (1.1%) Native Hawaiian/Pacific Islander, 125 White (67.2%) and 9 (4.8%) Hispanic. The majority were current (72.9%) or former (17.6%) tobacco users. Of 168 (90.1%) eligible for screening (median age 40 years, range 22-65 years), 150 (89.3% of those eligible) completed screening. There were no failed or inconclusive test results. Of 150 resulted tests, 120 (80%) were HPV-negative, 7 (4.7%) were HPV16/18+, and 23 (15.3%) were “other” (non-16/18) hrHPV+. Patients encountered a variety of structural and social barriers in following up hrHPV+ tests. Of the 30 hrHPV+ tests, no one has been lost to follow-up and 12 (40%) patients have completed follow-up, which often required multiple coordination attempts by providers. The remainder are in various stages of referral and scheduling. Providing cervical cancer screening was feasible in an OTP using HPV self-collection and resulted in high patient uptake. This population was both under-screened and high-risk with approximately double the hrHPV positivity rate found in most U.S. screening studies. Our patient-centered model promotes health equity and provides a scalable solution to reduce the burden of cervical cancer in under-screened communities.

#2372 Uncovering cervical cancer screening disparities among Asian American subgroups in California.

Alice W. Lee[1], Elinita Pollard[2], Minh Tung Phung[3], Meng-Han (Mina) Tsai[4]

[1]Public Health, California State University, Fullerton, Fullerton, CA,[2]Health Behavior, University of North Carolina, Chapel Hill, NC,[3]University of Wisconsin-Madison, Madison, WI,[4]Augusta University, Augusta, GA

Background: Cervical cancer is a highly preventable and treatable malignancy when detected early. Despite the availability of Pap test, clear racial/ethnic disparities in screening uptake exist, with Asian American women having significantly lower rates than Non-Hispanic White (NHW) women. To improve cervical cancer screening rates among Asian American women, it is important to understand which Asian subgroups are more inclined to be underscreened. However, research on this topic remains limited. Our study aims to examine recent Pap test rates and factors associated with screening uptake across disaggregated Asian subgroups.
Methods: Using cross-sectional data from the 2016, 2018, and 2020 California Behavioral Risk Factor Surveillance System, we calculated the weighted prevalence of women ages 21-65 who reported being up-to-date with Pap test based on the most recent U.S. Preventive Services Tasks Force's recommendations (i.e., having been tested in the past three years) for the six largest Asian American subgroups (Asian Indian, Chinese, Filipino, Japanese, Korean, Vietnamese) and NHW women as a comparison group. Multivariable logistic regression was fitted with reporting being up-to-date with Pap test as the outcome, regressing on race/ethnicity and adjusting for sociodemographic (age, education, income, marital status, poverty status, metropolitan statistical area) and access to care factors (having a primary care provider, health insurance type). In addition, the weighted prevalence of Pap test uptake for each Asian subgroup was calculated for factors found to be statistically significant in the adjusted model.
Results: Our analysis included 517 Asian American and 3,061 NHW women. While the percentage of NHW women who reported being up-to-date with Pap test was 83%, this percentage was lower for all Asian American subgroups (32% for Vietnamese, 54% for Asian Indian, 59% for Japanese, 66% for Korean, 67% for Chinese, 75% for Filipino). After adjusting for covariates, the Asian subgroups had 46-91% lower odds of reporting being up-to-date with Pap test, with the most notable disparities being among Vietnamese (OR=0.09, 95% CI 0.02-0.33) and Asian Indian women (OR=0.20, 95% CI 0.08-0.45). Interestingly, while all Asian subgroups with a primary care provider showed a prevalence of Pap test uptake of over 70%, this percentage was only 30% for Vietnamese women.
Conclusions: Although all Asian American subgroups reported lower Pap test adherence to screening guidelines than NHW women, the disparities were particularly striking for Vietnamese and Asian Indian women. Our results also suggest further exploring the role of primary care providers in the context of cervical cancer screening, particularly among Vietnamese women. Furthermore, the ethnic-specific disparities noted in our analysis highlight the importance of disaggregated data so interventions can be appropriately tailored.

#2373 Barriers to mammography screening among US women aged 40 and older: Disparities by race, region, and age.

Anas Al-Zubaidi

UTMB Health at Galveston, Galveston, TX

Background: Screening mammography is recommended for women aged 40 years and older. Understanding barriers to screening mammogram and identifying disparate populations is critical for implementing these recommendations equitably.
Methods: This cross-sectional study used National Health Interview Survey data from 2021 and 2023. Women aged 40+ who reported not having a mammogram in the past 2 years or ever were included (N=47.9 million weighted). Self-reported reasons were categorized as knowledge/awareness barriers (no reason, didn't know needed, doctor didn't order, no problem), behavioral barriers (put it off, too painful), cost/access barriers (too expensive, no doctor), age-related perceptions (too young/old), and other reasons. Complex survey design examined barrier patterns by race/ethnicity, region, urban-rural status, and age group (P<.05).
Results: Overall, knowledge/awareness barriers dominated (58.2%), followed by behavioral (14.0%), other (12.7%), age-related (9.0%), and cost/access barriers (6.2%). Significant disparities existed across race/ethnicity (P<.001), region (P<.001), and age (P<.001), but not urban-rural status (P=.40) (Table). Non-Hispanic Asian women had highest knowledge barriers but lowest cost barriers. Hispanic women had highest cost barriers. Women aged 50-64 had highest behavioral and cost barriers, while women 65+ had minimal cost barriers but high age-related misperceptions. Southern women faced both high knowledge and cost barriers versus other regions.
Conclusions: While knowledge and awareness gaps are the primary barriers to mammography screening among US women aged 40 and older, the specific types of barriers vary substantially by race/ethnicity, geographic region, and age. These disparities underscore the need for targeted, population-specific strategies to improve equitable access to mammography screening.

#2374 Neighborhood and language influences on mammography receipt among latinas in community health centers.

John D. Heintzman[1], Jennifer A. Lucas[1], Jorge Kaufmann[1], Cirila Estela Vasquez Guzman[2], Wyatt Bensken[3], Amelie G. Ramirez[4], Miguel Marino[1]

[1]Oregon Health & Science University, Portland, OR,[2]OHSU Knight Cancer Institute, Portland, OR,[3]OCHIN, Inc, Portland, OR,[4]UT Health Science Center at San Antonio, San Antonio, TX

Background: Breast cancer is a significant source of mortality and morbidity for Latinas in the United States. Literature has shown that breast cancer survival and diagnosis stage may be associated with neighborhood factors, but less is known about how these factors affect mammogram receipt specifically. Therefore, we performed an analysis of mammography receipt in Latina patients, by language preference, compared to non-Hispanic White women, by multiple community level factors (transportation access, economic level, education level).
Methods: We used electronic health record data from 59,646 Latina and non-Hispanic White patients between the ages of 50 and 74 receiving care at 594 community health centers across 21 states, along with geocoded census-tract-level neighborhood data to evaluate the prevalence of mammogram completion by neighborhood characteristics, including high school graduation rates, community poverty as percent of the federal poverty level, percent of households with a vehicle and with a 60+minute public transit commute. We stratified Latina patients by language preference and adjusted for common individual demographic and clinical characteristics.
Results: In the sample, 3,987 patients were non-Hispanic White, 11,338 were English-preferring Latinas, and 44,381 were Spanish-preferring Latinas. A higher proportion of Latinas lived in high poverty census tracts. A higher prevalence of non-Hispanic White women were smokers. Spanish-preferring Latinas (67.2%) had a higher unadjusted prevalence of mammogram receipt than English-preferring Latinas (57.7%) and non-Hispanic white women (54.6%). In covariate-adjusted analyses, Spanish preferring Latinas had the highest prevalence of being up-to-date with their mammograms, and of having completed mammograms if ordered, regardless of community characteristics. Across community characteristics, there was no difference in outcome prevalence within ethnicity language groupings.
Conclusion: In an analysis of mammogram completion in Latina and non-Hispanic white women by neighborhood-level factors in a national network of community health centers, mammogram
prevalence was low. Spanish-preferring Latinas had the highest prevalence of mammogram receipt.There was no outcome difference in any group across neighborhood-level factors. Community health centers are vital in the early detection of breast cancer for Latinas, but clinics should understand the limitations of community level factors in targeting improved mammogram completion and be aware of individual barriers that may reduce mammography in Latinas.

#2375 Stress-responsive immune microenvironment in triple-negative breast cancer among African American women.

Aminah M. Lawal[1], Fulya Koksalar Alkan[1], Hilmi Kaan Alkan[1], Ahmet Burak Caglayan[2], Neva Celiker[1], Brianna Temby[1], MAX WICHA[2], Morhaf Al Achkar[1], Kristen Purrington[1], Hasan Korkaya[1]

[1]Wayne State University, Detroit, MI,[2]University of Michigan, Ann Arbor, MI

African American (AA) women experience higher incidence and mortality from triple-negative breast cancer (TNBC) compared to White women, particularly at younger ages. While socioeconomic determinants contribute to this disparity, emerging evidence indicates that chronic social stress becomes biologically embedded, reshaping systemic inflammation and the tumor immune microenvironment (TIME). We hypothesize that stress-responsive inflammatory signaling drives the accumulation of immune suppressive myeloid cell populations contributing mechanistically to enhanced cancer stemness and aggressive tumor behavior in AA TNBC.Using spatial transcriptomics on TNBC tumors from (n=4) AA and (n=4) White patients enrolled in the Karmanos Cancer Institute Biobank, we identified distinct immune and stress-response programs enriched in AA tumors. AA samples displayed a marked increase in immunosuppressive myeloid populations, including TAM-like and MDSC-like clusters, accompanied by heightened expression of IL1B, TNFA-associated cytokine modules, S100A8/S100A9, and other innate inflammatory cytokines. These inflammatory programs correlated with activation of stress-response pathways, most notably HSP70, a central regulator of cellular stress, danger signaling, and antigen presentation. Mechanistically, these pathways were tightly linked to a transcriptional activation of cancer stemness signatures, including NQO2, IRF3-associated stress modules, and other stem-associated genes, consistent with a more plastic, therapy-resistant phenotype in AA TNBC tumors.Previous studies have shown that chronic social stressors such as perceived discrimination, inadequate support, and neighborhood disadvantage have been associated with systemic inflammation and altered immune response. Our tumor-level analyses suggest that this stress activated signaling may converge on innate immune pathways within the TIME, amplifying myeloid suppression, cytokine activation, and stress-induced stemness that collectively worsened outcomes.Hypothesizing that AA patients experience higher social stress than White patients, these results support a mechanistic model in which psychosocial stress primes the innate immune microenvironment toward immune dysfunction and myeloid dominance, promoting tumor plasticity and metastatic potential in AA TNBC. Understanding how stress-responsive immunologic programs shape tumor evolution may reveal actionable targets to mitigate biologically mediated cancer disparities and guide interventions integrating immunology, social determinants, and precision oncology.

#2377 Heavy-metal exposure and cancer incidence in Puerto Rico.

Ingrid M. Montes-Rodriguez, Yoel A. Velazquez-Oliver, **Hilmaris Centeno-Girona**, Camille Zenon, Elba V. Caraballo

University of Puerto Rico Comprehensive Cancer Center, San Juan, PR

Background: Puerto Rico (PR) exhibits geographic variation in overall cancer incidence, with rising early-onset cases suggesting region-specific factors that shape cancer risk. Persistent toxic exposure to heavy metals associated with industrial activity and legacy pollutants may underlie these regional differences. Heavy metals are pervasive environmental contaminants; accumulating exposures have been linked to disruptions in DNA methylation and other epigenetic mechanisms that regulate the cell cycle, DNA repair, and immune function, providing a plausible biological basis for increased cancer susceptibility. Evidence from diverse populations links metal exposure to cancer risk, suggesting regional metal profiles may affect local cancer burden. To date, there have been only a limited number of studies testing the association between regional metal exposures and cancer incidence across PR.
Objective: This study tests the hypothesis that population-wide exposure to heavy metal toxic releases aligns with cancer incidence patterns across PR when analyzed at the municipal level. Leveraging existing data, we integrated industrial-emission data from federal databases and cancer incidence records from the Puerto Rico Central Cancer Registry (PRCCR) spanning 2018-2022.
Methods: Age-adjusted incidence rates for overall and early-onset cases of the most prevalent cancer types in PR were obtained from the PRCCR for the period 2018-2022. Metal emission data were sourced from the U.S. EPA Toxics Release Inventory for 2008-2018 and aggregated at the municipality level. Out of 78 municipalities, 23 were identified with positive emissions values and were included in the analysis. Spearman correlations with p-values were used to quantify relationships between heavy metal emissions and cancer rates. Bivariate choropleth maps using Jenks Natural Breaks and proportional symbols were used to visualize geographic patterns. Statistical analyses were conducted in R 4.3.2 using RStudio, and spatial mapping was done in QGIS 3.40.
Results: Mercury and lead exposure showed the strongest associations with overall cancer incidence, with $r = 0.70$ ($p < 0.001$) and $r = 0.68$ ($p < 0.001$), respectively. Lead and mercury also correlated with prostate cancer ($r = 0.53$, $p < 0.01$; $r = 0.65$, $p < 0.001$). Mercury and nickel were associated with leukemia ($r = 0.40$, $p < 0.05$; $r = 0.41$, $p < 0.05$). Cobalt and zinc were associated with thyroid cancer ($r = 0.467$, $p < 0.05$; $r = 0.69$, $p < 0.001$). Additionally, these metals correlated with early-onset thyroid cancer ($r = 0.42$, $p < 0.05$; $r = 0.45$, $p < 0.05$). Manganese showed associations with both overall and early-onset uterus cancer ($r = 0.40$, $p < 0.05$; $r = 0.38$, $p < 0.05$).
Conclusion: Collectively, these patterns suggest that specific metal exposure may contribute to cancer risk. Future work should incorporate other exposure routes and pursue hypothesis-driven studies to identify targeted prevention strategies for high-exposure regions.

#2378 Cancer of unknown primary (CUP) mortality as a surrogate for imaging inequity in the United States (1999-2023).

Sophia Ahmed[1], **Fareed Baksh**[2], Bilal Ahmad[3], Salman Mustafa[4], Elangovan Krishnan[5], Oshaz Fatima[6]

[1]Medicine, Allama Iqbal Medical College, Lahore, Pakistan,[2]Internal Medicine, Community Health Systems - Flowers Hospital: Dothan, Alabama, US, Dothan, AL,[3]Dow Medical College, Karachi, Pakistan,[4]Medicine, Dow Medical College, Karachi, Pakistan,[5]AIM DOCTOR, Thiruverkadu, India,[6]King Edward Medical University, Lahore, Pakistan

Background: Cancer of Unknown Primary (CUP) remains a major diagnostic and clinical challenge in oncology. Despite advances in imaging, CUP continues to account for a significant number of cancer deaths in the United States. Limited access to high-quality diagnostic imaging may delay identification of the primary tumor and contribute to persistent disparities. This study examines national, regional, and demographic trends in CUP mortality from 1999 to 2023 and evaluates mortality patterns as a potential marker of imaging inequity. We analyzed national mortality data from the CDC WONDER database using ICD-10 code C80. Variables included sex, age group (15+), race, census region, metropolitan status, and state. Age-adjusted mortality rates (AAMR) were calculated for all subgroups. Temporal trends were assessed for 1999-2023. ARIMA forecasting was used to project trends to 2035. A total of 679,020 CUP deaths occurred between 1999 and 2023. The national AAMR declined from 13.24 in 1999 to 7.19 in 2023. Males had higher mortality (AAMR: 11.83) than females (8.82), though both decreased over time. Mortality was concentrated in adults aged 45 years and older. Racial disparities were marked: Black (12.09), White (10.38), and American Indian or Alaska Native populations (9.70) had nearly double the mortality of Hispanic or Latino (6.47) and Asian American or Pacific Islander groups (5.50). Nonmetropolitan areas had higher mortality (9.08) than metropolitan areas (7.84). Among regions, the Northeast (11.18), Midwest (10.55), and South (10.08) showed higher mortality than the West (8.74). ARIMA projections to 2035 suggest rising mortality for males (10.64), females (8.48), the Northeast (10.97), and the West (10.09). CUP mortality has declined nationally but remains uneven across demographic and geographic groups. Higher mortality in rural areas, high-burden regions, and populations with historically limited diagnostic access suggests that imaging inequity may contribute to persistent disparities. The rising projected mortality in select groups and regions underscores the need for targeted investments in diagnostic infrastructure, earlier access to advanced imaging, and equitable oncology services. Future research should integrate imaging and mortality data to refine strategies for early detection and intervention.

#2379 Increased stromal ERV methylation in African American compared to European American prostate cancer patients: Enrichment on chromosome 19.

Tara S. K. Jennings[1], Lucas Ueta[1], Vinay Kumar[1], Ali Afsari[2], Elham Arbzadeh[3], Patricia Castro[4], Michael M. Ittmann[4], Yan Zhao[1], Michael Daneshvar[5], Farah Rahmatpanah[1]

[1]Department of Pathology and Laboratory Medicine, University of California Irvine, Irvine, CA,[2]Department of Pathology, University of California Irvine Medical Center, Orange, CA,[3]Department of Pathology, George Washington University, Washington, DC,[4]Department of Pathology and Immunology, Baylor College of Medicine, Houston, TX,[5]Department of Urologic Oncology, University of California Irvine Medical Center, Orange, CA

Background: African American (AA) men experience worse prostate cancer (PCa) outcomes than European American (EA) men, including higher PSA levels, larger tumors, earlier onset, and more aggressive disease progression. These disparities persist even after accounting for healthcare access and socioeconomic factors, suggesting underlying biological contributors. Endogenous retroviruses (ERVs), normally silenced through DNA methylation, have emerged as regulators of anti-tumor immune activity and as effective prognostic markers in PCa. Despite constituting 8% of the human, ERVs' role in the tumor microenvironment remains incompletely understood. In our previous study, pathways associated with anti-tumor immune activity were significantly more methylated and silenced in AA PCa patients in the tumor-adjacent stroma (TAS) compared to EA patients, indicating potential epigenetic differences that may contribute to observed disparities.

Methods: We performed methyl-binding domain sequencing (MBD-seq) and RNA sequencing (RNA-seq) on TAS tissue from 17 AA and 15 EA PCa patients. Two custom bioinformatic pipelines were developed: one for ERV methylation analysis and another for ERV expression analysis. For methylation, sequencing reads were mapped to ERVs curated from the Human Endogenous Retrovirus Database (HERVd) to quantify locus-specific methylation. For expression, RNA-seq data were aligned to the same database to assess ERV expression profiles. ERV methylation patterns and their chromosomal distribution were visualized using chromoMap.

Results: In tumor-adjacent stroma, African American patients demonstrated significantly higher global ERV methylation with lower expression, while European American patients exhibited reduced methylation with elevated transcriptional activity ($p<0.05$). ChromoMap and statistical analysis revealed non-random chromosomal distribution of methylated ERVs, with the most significant ancestry-related differences on chromosome 19 (AA: 2.09 vs. EA: 1.76, $p<10^{-159}$), which harbored the highest methylation levels, consistent with its enrichment for repetitive elements and ERV sequences. Chromosome Y showed no significant difference ($p=0.148$), potentially due to constitutive heterochromatin status across ancestries.

Conclusion: In TAS, enhanced ERV silencing through hypermethylation in AA patients may represent a potential epigenetic mechanism contributing to disease aggressiveness through altered immune response genes. Conversely, hypomethylated and transcriptionally active ERVs in EA patients may enhance antitumor immune signaling, potentially explaining distinct clinical outcomes between populations.

#2380 Apolipoprotein E gene & PSA levels in Black men.

Lauryn Janelle Denise Jones[1], Jabril Johnson[2], Deyana Lewis[1], LaKendria K. Brown[1], Rick Kittles[1]

[1]Community Health & Preventative Medicine, Morehouse School of Medicine, Atlanta, GA,[2]Microbiology, Biochemistry and Immunology, Morehouse School of Medicine, Atlanta, GA

Background/Significance: Prostate cancer (Pca) is more prevalent among African American (AA) men compared to men of other racial and ethnic groups. Apolipoprotein E (APOE) plays a critical role in lipid metabolism and facilitates cholesterol and lipid transport, with its isoforms potentially impacting cancer progression. Prostate-specific antigen (PSA) is a biomarker of Pca and elevated PSA levels may predict the presence of Pca in patients. Our study investigates the genetic factors underlying this disparity, with a specific focus on the APOE gene and its role in prostate cancer cell proliferation. In this study, we aim to conduct an in-depth analysis of the APOE gene locus, examining isoform differentiation and its relationship to PSA elevation in African American men.
Methods: APOE SNP-level (rs429358, rs7412, rs440446) and haplotype-level analyses were performed using linear and logistic regression and haplotype-based modeling (R package haplostats). Models adjusted for age, West African genetic ancestry (WAA), vitamin D, case-control status, and PSA when applicable. Analyses were conducted separately after quality control in 1,370 men of west African ancestry from Washington DC (N=648), Columbia, SC (N=632) and Cameroon west Africa (Bamileke, N=90).
Results: Among AA men, PSA levels were strongly predicted by age ($\beta = 0.050$, $p = 1.39 \times 10^{-5}$) and case status ($\beta = 0.52$, $p < 1 \times 10^{-12}$). APOE haplotypes demonstrated no association with PSA (E4: $p = 0.80$; E2: $p = 0.36$) or prostate cancer status (logistic regression: E4 $p = 0.71$, E2 $p = 0.58$). Vitamin D ($p = 0.12$) and WAA ($p = 0.25$) were also non-significant predictors. Among men from Cameroon west Africa, we observed a nominal association suggesting higher PSA in E2 haplotype carriers ($\beta = 1.03$, $p = 0.045$), but this was not observed among AAs. No significant associations were detected for E4 ($p = 0.69$) or E3. In the combined analysis, APOE SNPs and haplotypes were not significantly associated with PSA (E4: $p = 0.93$; E2: $p = 0.67$) or case-control status (allelic tests: $p > 0.50$ for all SNPs). Across all models, age ($p < 2 \times 10^{-9}$) and PSA ($p < 6 \times 10^{-15}$) remained the strongest predictors of prostate cancer status.
Conclusion and Implications: Across three groups totaling more than 1,300 Black men, APOE genetic variation including the E2, E3, and E4 haplotypes did not significantly predict PSA levels or prostate cancer risk. Associations observed in the stratified analyses were not replicated and did
not withstand combined analysis. More studies are needed to confirm if APOE plays a biologically meaningful role in prostate cancer etiology or PSA regulation in these populations.
Acknowledgment of Funding: This research is supported by the Health Equity Research Career Advancement Program funded by the American Cancer Society's Diversity in Cancer Research Institutional Development Grant 885016.

#2381 Race-specific trajectories of prostate cancer evolution: Distinct temporal and spatial progression patterns in African American and Caucasian men.

Josiah Harsh[1], Shannon Carskadon[2], Nilesh S. Gupta[3], Sangeetha Jyothilingam[2], Jessica Ryba[3], Craig G. Rogers[2], James O. Peabody[2], Sunita Ghosh[4], Nallasivam Palanisamy[2]

[1]College of Human Medicine, Michigan State University, Detroit, MI,[2]Urology, Henry Ford Health, Detroit, MI,[3]Pathology, Henry Ford Health, Detroit, MI,[4]Public Health Sciences, Henry Ford Health, Detroit, MI

African American (AA) men experience a higher incidence and mortality from prostate cancer, traditionally attributed to more aggressive tumor biology. However, emerging evidence suggests that when access to care is equal, AA men often have outcomes comparable to—or better than—Caucasian men, showing that biological behavior may be distinct rather than inherently worse. To clarify early evolutionary trajectories, we performed a detailed race-stratified analysis of temporal and spatial progression patterns using serial 12-core and saturation biopsies.Longitudinal biopsy datasets were evaluated to measure time-to-progression across key histologic transitions from benign to HGPIN, benign to high-grade Gleason patterns, and within-grade upgrading. Site-specific progression proportions were compared across 12 anatomical regions. Statistical significance for temporal and spatial differences was assessed using proper parametric tests.In 12-core biopsies, AA men showed significantly slower progression from benign tissue to Gleason 5+5 carcinoma (140.77 vs. 8.49 months; $p<0.0001$) and a trend toward delayed progression from benign to HGPIN ($p=0.051$). In contrast, AA men showed faster progression from Gleason 3+4 to 4+3 (15.84 vs. 42.37 months; $p = 0.0005$), exhibiting a distinct—not uniformly aggressive—pattern of disease evolution. Spatial mapping showed higher progression rates in Caucasian men at the right lateral base and apical regions. In contrast, AA men showed greater progression in the left-sided areas (left base, lateral base, mid, and lateral mid).In saturation biopsies, AA men again displayed slower transitions from benign to Gleason 3+3 (22.36 vs. 18.35 months; $p=0.073$), benign to Gleason 4+4 (24.1 vs. 15.14 months; $p=0.021$), and from Gleason 3+3 to 3+4 (21.29 vs. 14.05 months; $p=0.021$). Anatomically, Caucasian men showed higher progression at the left lateral base, while AA men showed higher progression at the right lateral base.Our serial biopsy analyses reveal that AA men experience slower early biological progression from benign and low-grade disease compared to Caucasian men, challenging the long-standing assumption that AA prostate cancer is intrinsically more aggressive. Instead, these findings support a model of biologically distinct evolutionary pathways, with AA men exhibiting delayed early transitions but accelerated intermediate-grade shifts, and displaying unique spatial patterns of progression. These results align with recent clinical and genomic studies showing equal or better outcomes for AA men when access to care is equivalent. Collectively, our findings offer mechanistic insight into race-specific prostate cancer evolution and underscore the need for tailored surveillance and sampling strategies.

#2382 Achieving prostate cancer equity globally: Multinational advances from the iCCaRE consortium.

Folakemi T. Odedina[1], Arnold Merriweather[2], Roxana S. Dronca[3], Ernest T. Kaninjing[4], Solomon Rotimi[5], Gerardo Colon-Otero[6], Kimlin Ashing[7], Ademola A. Popoola[8], Gladys Asiedu[9], Opeyemi Bolajoko[1], Ewan COBRAN[10], Emelina Asto-Flores[1], Floyd Willis[1], Christopher Williams[11], Monica L. Albertie[12], Michelle Fudge[1], Oluwaseyi Toye[13], Collisa Mahin[1], Jada Melton[1], Inclusive Cancer Care Research Equity (iCCaRE) Consortium, Prostate Cancer Transatlantic Consortium (CaPTC)

[1]Mayo Clinic Florida, Jacksonville, FL,[2]Prostate Health Education Network, Quincy, MA,[3]Mayo Clinic College of Medicine and Science, Jacksonville, FL,[4]Georgia College & State University, Milledgeville, GA,[5]Covenant University, Ota, Ogun State, Nigeria,[6]Mayo Clinic Cancer Center Florida, Jacksonville, FL,[7]City of Hope National Medical Center, Duarte, CA,[8]Department of Surgery, University of Ilorin Teaching Hospital, Ilorin, Nigeria,[9]Mayo Clinic, Rochester, MN,[10]Mayo Clinic, Phoenix, AZ,[11]Urology Consultants, Jacksonville, FL,[12]Cancer Services, Mayo Clinic Florida, Jacksonville, FL,[13]Prostate Cancer Transatlantic Consortium (CaPTC), Jacksonville, FL

Background: Black men across the African Diaspora experience a disproportionate burden of prostate cancer (CaP). The Inclusive Cancer Care Research Equity (iCCaRE) Consortium aims to eliminate CaP burden through global scientific collaboration, innovative research, community-engaged interventions, and next-generation workforce development. The primary objective for this Consortium was to optimize CaP diagnosis, treatment, and survivorship through research, research training and education, community engagement and community outreach. The Consortium integrates digital health technologies, community navigation, precision communication and precision science.

Methods: Five full projects and one pilot project were launched across partner institutions in North America and Africa. Supported by multiple cores and services, the research activities included (1) implementation of a Point of Prostate Cancer Diagnosis Virtual Robot Assistant (PPCD-ViRA); (3) initiation of a cancer care at home trial; (4) migrant health studies of Caribbean and Sub-Saharan African immigrants; (5) expansion of genomic and metabolomic research; and (6) digital, psychosocial, and survivorship intervention development. Training and dissemination activities were deployed through iCCaRE TV, webinars, and community engagement programs including the Global Prostate Health Dialogue (Glo-PHD).

Results: In one year, accomplishments included 45 presentations, 17 publications, 16 grant submissions, and 3 awards. The consortium delivered 408 live webinar engagements and reached more than 400 men globally through Glo-PHD. PPCD-ViRA was fully developed and prepared for clinical deployment (see https://www.youtube.com/watch?v=1mI-HS5R6sk). The African cohort expansion for genomic and metabolomic profiling was activated across several countries, with biospecimen collection underway. Media dissemination generated more than 15,000 views across platforms, including high-impact educational videos (see: www.youtube.com/@iCCaREConsortium). Training achievements included 13 early-career investigators and 7 trained prostate cancer advocates.

Conclusions: In just one year, the iCCaRE Consortium Phase 2 made substantial progress toward transforming CaP equity globally. Through multidisciplinary science, digital innovation, and community partnerships, the consortium is building scalable infrastructure to address diagnosis experiences, treatment quality, and survivorship among Black men. Ongoing efforts will continue to advance precision medicine, culturally grounded interventions, and global capacity building.

#2383 The stress survival gene CCNB1 drives colorectal cancer progression and represents a novel target to address ethnic disparities.

Md Zahirul Islam Khan, Urbashi Basnet, Soumya Nair, Sourav Roy

Biological Sciences, University of Texas at El Paso, El Paso, TX

Background: Colorectal cancer (CRC) is the second leading cause of cancer-related mortality in the U.S., marked by significant racial and ethnic disparities in incidence, stage at diagnosis, and survival. While highly curable with early detection, Hispanics, who comprise over 17% of the U.S. population, face disproportionate barriers to timely diagnosis, leading to presentation with more advanced disease and poorer outcomes. This study investigates the functional role of the stress-survival pathway (SSP) gene, Cyclin B1 (CCNB1), as a potential early detection biomarker and therapeutic target to mitigate disparities between Hispanic and Non-Hispanic White (NHW) populations.

Methods: Our investigation utilized a multi-platform approach, integrating computational and experimental cancer biology. Initial screening involved in-house in-silico RNA-sequencing, differential expression analysis of tumor and adjacent non-tumor CRC tissue samples, from Hispanic and NHW cohorts. CCNB1 was identified as one of the most differentially expressed gene among the two races. To validate this finding, we performed qRT-PCR in CRC cell lines and tissue samples. The stage-specific expression was further evaluated using cDNA microarray whereas protein-level expression was determined using immunohistochemical assay of tissue microarrays. The oncogenic role of CCNB1 was further evaluated *in vitro* using CRC cell lines, and highly translational patient derived organoid model after CCNB1 knockdown. The RNA sequencing and Mass spectrometry will subsequently be employed to identify underlying molecular mechanisms of CCNB1-mediated CRC progression.

Results: Our results showed significant upregulation of CCNB1 in CRC cell lines and tissues at both transcript and protein levels. Notably, Hispanic CRC samples exhibited significantly higher expression of CCNB1 compared to NHWs, with marked upregulation of CCNB1 in early-onset and late-stage Hispanics. These results are in line with traditional delayed in diagnosis for Hispanic populations. The functional study demonstrated that CCNB1 knockdown in CRC cell lines significantly reduced proliferation, growth, invasion and migration of cells by inducing cell cycle arrest and apoptosis. In organoid model, the knockdown of CCNB1 reduced organoid growth by inducing apoptosis. In addition, multi-omics based molecular mechanisms associated with CCNB1-mediated cancer progression will be further evaluated using western blotting and qRT-PCR respectively.

Conclusions: This study identifies CCNB1 as a key oncogenic driver in CRC, highlighting its potential as a diagnostic biomarker and therapeutic target to enhance disease management and reduce ethnic disparities in outcomes among Hispanics and NHWs.

#2384 Demographic representation in randomized controlled trials of colorectal polyp prevention: A systematic review and meta-analysis.

Frankie Fan[1], Namrata Trivedi[2], Ryan Ford[2], Ajay Verma[1], Karen Brown[1]

[1]University of Leicester, Leicester, United Kingdom,[2]University Hospitals of Leicester NHS Trust, Leicester, United Kingdom

Background: Colorectal cancer (CRC) is an increasing global health burden. With incidence rising, there is a need to develop effective preventive strategies. Polyp-prevention randomized controlled trials (RCTs) are central to testing CRC-preventive therapies, using colorectal polyp development as an established endpoint. Marked ethnic disparities in CRC incidence, particularly in early-onset disease, are well documented. However, no systematic evaluation of demographic representation in polyp-prevention RCTs exists.
Methods: We conducted a systematic review and meta-analysis of RCTs assessing chemopreventive or immunopreventive interventions for polyp recurrence. The protocol was registered in PROSPERO (CRD420251102449). Eligible trials enrolled adults with prior polyps while excluding those with prior CRC, inflammatory bowel disease, or hereditary cancer syndromes. Of 9,127 screened records, 27 RCTs met inclusion. Demographic data including age, sex, geography, race, ethnicity, and socioeconomic status (SES) were extracted. Multi-arm data were pooled. Geography was grouped as Western, Non-Western, or multinational (Western and Non-Western). Race and ethnicity were harmonized to OMB-1997 categories. Age was meta-analysed using inverse-variance random-effects models. Sex, race, and ethnicity proportions were analysed using logit-transformed random-effects models. Temporal trends were visualised with sample-size-weighted bubble plots. All analyses were performed using R Statistical Software (v4.1.2; R Core Team 2024).
Results: All trials reported age, geography, and sex. Other demographics were often incomplete or collapsed. Race was reported in 41% of trials, and only 11% reported SES. The pooled mean age was 60.7 years (95% CI 59.2-62.2). Participants were 67.9% male. Studies were predominantly Western (74.07%), with Non-Western (18.52%) and multinational studies (7.41%) comprising the remainder. Of the 12 trials reporting race, pooled representation was White 87.9% (95% CI 82.5-91.8), Black 6.8% (95% CI 3.5-12.8), and Asian 2.2% (95% CI 1.1-4.1). Only 8 trials reported ethnicity, with Hispanic representation of 5.0% (95% CI 3.1-8.1). Bubble plots demonstrated persistently low non-White representation across three decades.
Conclusion: This review highlights inconsistent demographic reporting in CRC polyp-prevention RCTs. The persistent demographic underrepresentation, particularly of Black and Asian participants, fails to reflect the disproportionate disease burden. This limits the generalisability of prevention strategies and may worsen existing disparities in CRC outcomes. There is an urgent need for standardised demographic reporting and intentional equity-focused recruitment strategies to ensure that therapeutic prevention approaches are effective and applicable across all populations.

#2385 Examining structural and social drivers of hepatitis B vaccination across diverse clinical settings.

Alisa Vidwans[1], Anita Narkhede[1], Lisa Sanders[2]

[1]USF Health Morsani College of Medicine, Tampa, FL,[2]Pediatrics, USF Health Morsani College of Medicine, Tampa, FL

Hepatitis B is a major cause of liver cancer in the United States and is also associated with increased risks of non-Hodgkin lymphoma, pancreatic, and head and neck cancers. Although the Hepatitis B vaccine is highly effective at preventing chronic infection and subsequent cancer development, vaccination rates remain low: In 2021, Hepatitis B vaccination coverage was 34.2% among adults 19 and older. This study evaluates Hepatitis B vaccination series completion among adolescents and young adults across clinic settings, demographics, and social determinants of health (SDOH) to identify gaps in vaccine coverage and reduce the incidence of Hepatitis B infection. We performed a retrospective, cross-sectional analysis using electronic health record data from adolescent medicine, pediatric infectious diseases, internal medicine-pediatrics, and family medicine clinics within the University of South Florida health system, and Ybor Youth Clinic, a community sexual health clinic within the USF pediatrics department. The sample included 456 patients aged 16-24 who were seen between January and March 2025 and had documented immunization histories. Completion of the Hepatitis B vaccination series was analyzed by clinic type and demographic and SDOH variables, including age, gender, race, ethnicity, insurance status, primary language, primary care provider, HPV and tetanus vaccination status, and comorbid conditions. Across 20 clinics, 422 patients (92.5%) completed the Hepatitis B vaccination series. Completion rates varied significantly across clinic types ($p=0.012$). Demographic factors such as gender, race, and ethnicity were not significantly associated with vaccination status ($p=0.092$, $p=0.787$, $p=0.956$). However, younger patients were more likely to have completed the vaccine series ($p<0.001$). Uninsured patients demonstrated lower completion rates compared to those with public or private insurance ($p=0.045$). Completion of other routine vaccines (HPV series/tetanus) was strongly correlated with Hepatitis B vaccination completion (all $p<0.001$). Having a primary care provider was not significantly linked to completion ($p=0.271$), and comorbidities such as HIV infection showed no significant association ($p=0.092$, $p=0.124$). Hepatitis B vaccination rates in this cohort were substantially higher than national averages. However, disparities persisted based on various SDOH factors. Structural and access-related factors, particularly clinic type and insurance coverage, were more predictive of vaccine completion than demographic characteristics, suggesting structural factors have a greater influence than patient attributes in determining vaccination status. These findings highlight the need for system-level interventions to support series completion, particularly among underserved populations, to support Hepatitis B prevention and mitigate cancer-related disparities.

#2386 Evaluating ABCC1 as a potential prognostic biomarker in laryngeal cancer health outcomes.

Christina Gobin[1], Matthew Chang[1], Jai Walker[2], Kristianna Fredenburg[1]

[1]University of Florida, Gainesville, FL,[2]Labcorp, Jacksonville, FL

Background: Overexpression of ABCC1 is associated with poor overall survival across many cancers and has been associated with decrease response to chemotherapy. Our *in vivo* and *in vitro* studies have shown that ABCC1 expression is higher in laryngeal squamous cell carcinoma (LSCC) from individuals with African heritage. Here, we further investigate ABCC1 as a potential prognostic and predictive marker in laryngeal cancer health outcomes.

Methods: ABCC1 gene expression was assessed in tumor tissue from 32 advanced-stage LSCC patients from differing populations via RT-PCR. Immunohistochemistry (IHC) for ABCC1 protein expression was performed on tissue microarrays (TMAs) generated from 61 paraffin-embedded tissues of advanced stage LSCC from patients of differing heritages. Machine learning based digital pathology software (QuPath) was used to semi-quantitate ABCC1 IHC protein expression as H scores. Age, treatment, self-reported heritage, N stage, tumor histologic grade, and ABCC1 H-scores were evaluated as predictors of patient mortality risk via multivariable Cox proportional hazards (CPH) model. The median Cox risk score (cutoff > 0.971) was used to stratify patients into low and high mortality risk groups. The relationship among the clinical features and ABCC1 in low and high mortality risk groups was explored by Chi Square analysis. Overall survival was assessed using the Kaplan-Meier method.

Results: LSCCs from patients with African heritage demonstrated a 2.2-fold elevation in ABCC1 gene expression and higher ABCC1 protein expression (H-score) compared with the reference population ($p < 0.05$). Controlling for treatment, African heritage patients with low ABCC1 H-scores had a high mortality risk ($p < 0.05$), and patients from the reference population with metastatic disease and high ABCC1 H-scores had a low mortality risk ($p < 0.05$). Overall, high-risk patients had significantly worse overall survival (HR = 2.46, 95% CI [1.27-4.74], log rank $p < 0.01$) and high mortality risk was associated with low ABCC1 H-scores and regional metastatic disease ($p < 0.05$).

Conclusion: Although LSCC patients with African heritage have higher ABCC1 expression compared with the reference population, low ABCC1 H-scores carry a higher mortality risk in this group. LSCC patients from the reference population with high ABCC1 H-scores have reduced mortality risk despite having regional metastatic disease. Future studies will involve exploring mechanistic implications of ABCC1 expression on treatment outcomes across differing heritages.

#2387 Colorectal cancer equity and impact (CLEAR-CRC): The colorectal cancer alliance's community-based model for advancing biomarker testing.

Kimberly Lynn Newcomer, Erin Siegel, David Fenstermacher, Marianne Pearson, Lindsey Gladspell, Marc Mason

Colorectal Cancer Alliance, Washington, DC

Background: Despite the growing importance of comprehensive biomarker testing in precision oncology, only approximately 65% of colorectal cancer (CRC) tumors undergo some level of molecular testing. Rural CRC patients are 20% less likely to receive recommended molecular testing (e.g. MSI) compared to urban patients. Barriers include limited provider awareness, logistical hurdles, financial constraints, and fragmented provider-patient communications. The Colorectal Cancer Alliance convened a collaborative partnership including non-profit, academia, community clinics and industry to launch a prospective study to increase the uptake of comprehensive biomarker tests among patients with CRC in these underserved populations.
Methods: The initiative is designed as both a regional health communication campaign and a multi-modal quality improvement effort. Core components include hybrid patient navigation, education for patients and physicians, improved access to biomarker testing, and prospective longitudinal data collection. The study aims to recruit 100-120 patients with advanced CRC from two rural and one urban clinical sites. The study leverages the Alliance's BlueHQ digital support platform to support consent, navigation, patient and provider education, and longitudinal data collection. The health communications campaign will be developed based on focus group input and evaluated by pre- and post-surveys. Longitudinal study endpoints will include knowledge of biomarker testing, updates on biomarker testing, and biomarker-driven care delivery.
Results: Preliminary results are expected to be released after the study launch in early 2026. Outcomes will be measured through patient-reported data, navigation logs, and longitudinal tracking of testing uptake and treatment decisions. Key milestones before study launch include completion of messaging materials, site selection, navigator recruitment and training, and IRB protocol submission.
Conclusions:This project models a scalable, equity-driven approach to improving access to biomarker testing in CRC care through collaborative, multi-stakeholder partnerships led by a mission-driven patient advocacy organization. This study adopts a patient-centric approach through community-informed messaging, flexible navigation strategies, and centralized patient engagement via BlueHQ to address persistent gaps in CRC precision oncology. The effectiveness of our comprehensive quality improvement intervention will inform future efforts to reduce disparities and support advancing comprehensive biomarker testing as a standard of care in oncology.

#2388 Racial and ethnic differences in interest in cancer screening.

Ya Yang

Public Health Davis, University of California, Davis, Davis, CA

Background: Although research has shown lower cancer screening uptake among racial and ethnic minority groups, few studies have examined whether these groups are interested in screening. Understanding interest helps clarify whether disparities stem from differences in personal preference or from structural barriers. This study examines racial and ethnic differences in interest in obtaining a cancer screening test.

Methods: This cross-sectional study used national data from the 2022 Health Information National Trends Survey. The sample included adults aged 18 and older (n = 3,774). The outcome was a four-level measure of interest in having a cancer screening test within the next year. Ordinal logistic regression was used to examine associations between race/ethnicity and screening interest, adjusting for sociodemographic and health-related factors, including family history of cancer.

Results: Compared with non-Hispanic Whites, non-Hispanic Black (AOR=1.72, 95% CI: 1.20-2.46) and Hispanic adults (AOR=2.02, 95% CI: 1.49-2.73) reported significantly higher interest in getting screened for cancer within the next year. Females reported higher interest than males (AOR=1.75, 95% CI: 1.44-2.14). Adults aged 40-44 (AOR=1.69, 95% CI: 1.11-2.57) and 45 and older (AOR=1.68, 95% CI: 1.27-2.22) had higher odds of interest compared with those aged 18-34. Individuals without a family history of cancer had lower odds of reporting greater interest in screening (AOR=0.68, 95% CI: 0.53-0.87).

Conclusions: Despite lower cancer screening uptake among racial and ethnic minority groups, Black and Hispanic adults reported higher interest in cancer screening. This suggests that individual interest is not the limiting factor; instead, structural and access barriers likely drive lower screening completion. Future research should identify the specific points in the screening process where racial and ethnic disparities occur, since higher interest among minority groups does not translate into completed screening.

#2389 Geospatial mapping of health-linked risk factors and cancer outcomes in Puerto Rico: Data from the Puerto Rico BioBank.

Jose A. Oliveras Torres[1], Edna Gordian[2], W. Douglas Cress[3]

[1]Ponce Health Sciences University, Ponce, PR,[2]Moffitt Cancer Ctr. Research Inst., Tampa, FL,[3]Moffitt Cancer Center, Tampa, FL

The Puerto Rico BioBank (PRBB), established through a partnership between the Ponce Health Sciences University and the Moffitt Cancer Center with support from the National Cancer Institute, was the first centralized cancer-focused biorepository in Puerto Rico. It was designed to collect, store, and distribute well-annotated biological specimens and associated clinical data from individuals diagnosed with cancer across the island. The PRBB supports translational research by providing high-quality biospecimens linked to demographic, diagnostic, and geographic data. As of 2025, the biobank has accrued over 5,000 participants. The aim of this study is to describe the current structure and contents of the PRBB and highlight how its integrated dataset enables the mapping of health-linked factors such as comorbidities, geographic distance to care, sociodemographic factors, and diagnosis.Since 2019, the PRBB has enrolled 2,550 individuals diagnosed with cancer through academic-affiliated hospitals and clinics in southern Puerto Rico. All participants provided consent for the collection of tissue samples, clinical information, and zip code at the time of diagnosis. The dataset includes clinico-pathological variables, comorbidities, treatment pathways, and demographic variables. Biospecimens and data are collected, processed, and stored under standardized protocols consistent with national biobanking best practices and managed under institutional IRB-approved procedures. Statistical analysis was conducted using descriptive statistics. Analysis was performed using R statistical software version 2025.09.1+401.Preliminary analysis shows that over 50% of PRBB participants live more than 30 km from Ponce, the primary site for diagnostic and specialty care for patients from the central municipalities often traveling 45-90 minutes each way for services. Sociodemographic data further reveal that 35% of participants have only completed grades 8-12. Most participants report household annual incomes under $40,000 (83%), and 37% are publicly insured. Additionally, 73% have a family history of cancer and 29% report current or past tobacco use.The PRBB serves as a robust and expanding research platform for investigating region-specific factors that influence cancer outcomes across the island. By integrating biospecimens with clinical, geographic, and sociodemographic data, the PRBB enables the identification of spatial patterns related to stage at diagnosis, access to care, and treatment variability. This infrastructure supports future studies aimed at improving early detection, guiding mobile screening initiatives, and informing resource planning to address cancer burden in Puerto Rico.

#7560 Understanding the reasons for declining to participate in cancer genetics and genomic studies in the United States: A scoping review.

Joel Sanchez Mendez[1], Diego Alvarez-Lopez[1], Jessica Sanchez[2], Fibi Berhane[1], Vernon S. Pankratz[2], Andrew L. Sussman[2], Ursa Brown-Glaberman[2], Nicole N. Hamblet[2], Saira Khan[3], Christine Marx[3], Jennifer W. Mack[4], Shiraz I. Mishra[2], Mariana C. Stern[1]

[1]USC - University of Southern California, Los Angeles, CA,[2]University of New Mexico, New Mexico, NM,[3]Washington University School of Medicine, St. Louis, MO,[4]Dana-Farber Cancer Institute, Boston, MA

INTRODUCTION: Cancer is the second leading cause of death in the United States (US). Genetics and genomic cancer studies have improved understanding of risk, onset, progression, and have informed treatment options. However, many populations are underrepresented in existing studies, and reasons why some individuals decline to participate remain unclear. To address this gap, we conducted a scoping review to summarize the reasons associated with declining participation in cancer genetics and genomic studies among cancer patients in the US.

METHODS: A standardized search strategy was developed and deployed in Medline (PubMed), Embase (Ovid), and Scopus from database inception until March 13th, 2025. The search covered three concepts: cancer, genetics and genomic research, and declination to participate. A two-step screening process ensued against predefined inclusion criteria. Study characteristics were summarized descriptively. Reported reasons were harmonized into common data elements (CDEs). A network analysis was conducted to evaluate co-occurrence of CDEs and identify barriers. Recommendations to address barriers were mapped to specific themes and discussed with community members during the PE-CGS annual meeting.

RESULTS: A total of 18,114 studies were imported, after the selection process, 19 studies were included in the review. Most studies were cross-sectional (42%), published after 2019 (58%), and reported on clinical genetic testing (58%). The most evaluated cancer sites were breast (n=13), ovary (n=9), and colon-rectum (n=7). The mean declination rate was 22.7% (SD=5.3). Non-Hispanic White, non-Hispanic Black, and Asian individuals reported lower declination rates than the mean, while Hispanic/Latino/a/x, American Indian/Alaska Native, and Native Hawaiian or other Pacific Islander individuals had higher rates of decline (27-28%). Network analysis showed that financial concerns with emotional distress or low perceived utility often co-occurred. Physical or medical limitations and sample collection issues were common reasons for declining genetic testing, and financial or insurance concerns and low perceived relevance were more frequent in testing done to guide clinical decision-making only. Three overarching barriers were identified: behavioral, logistical, and structural. Educational interventions, flexible participation strategies, and system-level improvements are key recommendations, endorsed by community members with whom we discussed results.

CONCLUSION: Declining participation arises from behavioral, logistical, and structural barriers. Emotional, financial, and perceived utility concerns were most common and interrelated. Tailored education, provider engagement, and improved system accessibility may enhance equitable participation in cancer genetics and genomic studies.

: Antibodies, Antibody-Drug Conjugates, and Nucleic Acids
Poster Session

#2393 DXC016, a novel cMET-targeting dual payload antibody-drug conjugate, demonstrates potent antitumor activity and favorable PK for potential subcutaneous use.

Yong Du[1], Jiaojiao Yu[1], Huihui Guo[1], Lingli Zhang[1], Xiaoqiang Xie[1], Jialei Hu[1], Xiafen Wu[1], Yunxia Zheng[1], Yuanyuan Huang[1], Junxiang Jia[1], Wei Liu[1], Zhouyang Zhou[1], Qingliang Yang[1], **Robert Y. Zhao**[2]

[1]Hangzhou DAC Biotechnology Co., Ltd, Hangzhou, China,[2]Hangzhou DAC Biotechnology Co., Ltd., Hangzhou, China

DXC016 is a next-generation cMET-targeting antibody-drug conjugate (ADC), composed of a novel anti-cMET monoclonal antibody (DXA016) and a functional dual payload designed to overcome limitations of conventional cMET-ADCs. Across multiple cMET-expressing tumor models, including SNU-5 (gastric), EBC-1 (NSCLC), HCT116 (colorectal), SW1990 (pancreatic), and an osimertinib-resistant NSCLC model, DXC016 demonstrated potent in vitro and in vivo antitumor activity, archived tumor regression at doses below 1.5 mg/kg and outperformed DXd and MMAE-based benchmark ADCs, highlighting the superior efficacy enabled by the dual-payload design. In mouse subcutaneous pharmacokinetic studies, co-administration with the recombinant hyaluronidase DXE001 markedly accelerated absorption, as indicated by a substantially earlier Tmax, while overall exposure remained similar between groups due to the thin and low-resistance subcutaneous tissue in mice. Given the higher hyaluronan content and greater diffusional resistance in human skin, DXE001 is expected to produce a more pronounced enhancement of subcutaneous absorption and bioavailability in clinical settings. In preliminary safety studies in rats and cynomolgus monkeys with once-weekly dosing for three administrations, DXC016 was well tolerated up to 80 mg/kg in rats and 50 mg/kg in monkeys, with no treatment-related mortality observed, indicating a favorable early safety profile. Collectively, the strong antitumor efficacy, improved subcutaneous absorption profile with DXE001, and encouraging preliminary safety characteristics support DXC016 as a promising clinical development candidate of next-generation cMET-targeting ADC.

#2394 A novel 2+2 IgG-like bispecific antibody-drug conjugate targeting EBV GP220/350 and EGFR for selective treatment of nasopharyngeal carcinoma.

Saihong Yu[1], Yunxia Zheng[1], Junxiang Jia[1], Xiangfei Kong[1], Juan Wang[1], Yi Luo[1], Hangbo Ye[1], Xueqing Ma[1], Qingliang Yang[1], **Robert Y. Zhao**[2]

[1]Hangzhou DAC Biotechnology Co., Ltd, Hangzhou, China,[2]Hangzhou DAC Biotechnology Co., Ltd., Hangzhou, China

Nasopharyngeal carcinoma (NPC) is endemic in East and Southeast Asia, with Epstein-Barr virus (EBV) infection as a primary etiological factor. The EBV envelope glycoprotein GP220/350 is highly expressed on EBV-positive NPC cells, serving as a tumor-specific antigen. Epidermal growth factor receptor (EGFR) is also overexpressed in >80% of NPC cases and is a validated therapeutic target (e.g., cetuximab). Bispecific antibodies (bsAbs) offer unique advantages by co-targeting two antigens, enhancing tumor selectivity and internalization efficiency. Here, we report the development of a 2+2 IgG-like bispecific antibody-drug conjugate (ADC) co-targeting GP220/350 and EGFR for precise NPC therapy. The bsAb was engineered as a 2+2 IgG-like molecule. The GP220/350-binding arm was derived from a fully humanized synthetic VHH (single-domain antibody) library and a high affinity binder C2 was selected via phage display. The EGFR-binding arm was based on nimotuzumab, a low-affinity EGFR antibody chosen to minimize on-target/off-tumor toxicity. The bsAb designated as DXA038 was conjugated to a topoisomerase I inhibitor payload CPT113 via a cleavable linker, with an average drug-to-antibody ratio (DAR) of 4. Binding affinity, in vitro cytotoxicity and in vivo efficacy were assessed. DXA038-CPT113 showed superior activity both in vitro and in vivo compared to nimotuzumab-CPT113.This bispecific ADC represents a promising therapeutic strategy for EBV-positive NPC, addressing unmet needs in precision oncology.

#2395 DXC011, a novel dual-payload antibody-drug conjugate targeting folate receptor alpha.

Zhicang Ye[1], Huihui Guo[1], Wei Zheng[1], Junpeng Wang[1], Yifang Xu[1], Hui Xia[1], Yuanyuan Huang[1], Junxiang Jia[1], Wei Liu[1], Xiang Chen[1], You Zhou[1], Qingliang Yang[1], **Robert Y. Zhao**[2]

[1]Hangzhou DAC Biotechnology Co., Ltd, Hangzhou, China,[2]Hangzhou DAC Biotechnology Co., Ltd., Hangzhou, China

Folate Receptor alpha (FRα) is highly expressed in epithelial ovarian cancer and selected solid tumors, making it an attractive target for antibody-drug conjugates (ADCs). Although an FRα-directed ADC Elahere has already achieved clinical approval, this microtubule inhibitor-based agent faces challenges, such as ocular toxicity, narrow therapeutic windows, and limited activity beyond ovarian cancer. To address these limitations, we developed DXC011, a next-generation FRα-targeting ADC engineered to enhance antitumor efficacy while improving tolerability. DXC011 comprises DXA011, a humanized IgG1 antibody specific for FRα, an optimized cleavable linker and a dual functional payload. This dual-payload strategy introduces complementary cytotoxic mechanisms and may help overcome resistance associated with single-mechanism ADCs. DXC011 demonstrated potent activity across multiple FRα-expressing in vitro and in vivo tumor models, encompassing ovarian cancer as well as additional solid tumor types. Beyond established ovarian cancer settings, DXC011 showed notable efficacy in gastrointestinal tumor models, supporting its potential for broader clinical application. Moreover, DXC011 displayed favorable tolerability in mouse, with an improved safety profile relative to microtubule inhibitor-based ADC while maintaining robust antitumor potency. Collectively, these findings indicate that DXC011 offers an improved therapeutic index and may enable expanded indication coverage. DXC011 represents a novel FRα-targeted dual-payload ADC that achieves potent and broad antitumor activity with enhanced tolerability, supporting its advancement toward clinical development.

#2396 A novel 2+2 IgG-like bispecific antibody-drug conjugate with dual payloads for targeted therapy of heterogeneous gastrointestinal cancers.

Wei Zheng[1], Junxiang Jia[1], Xiaolei Liu[1], Gengxiang Zhao[1], Yongxiang Chen[1], Xia Zhou[1], Simin Zhao[1], Qingliang Yang[1], **Robert Y. Zhao**[2]

[1]Hangzhou DAC Biotechnology Co., Ltd, Hangzhou, China,[2]Hangzhou DAC Biotechnology Co., Ltd., Hangzhou, China

Gastrointestinal (GI) cancers, including colorectal, gastric, and pancreatic cancers, remain a leading cause of cancer-related mortality globally due to their high incidence, aggressive progression, and profound intratumoral heterogeneity. This heterogeneity often leads to treatment resistance and limits the efficacy of monotherapies. Cadherin-17 (CDH17) and Guanylate Cyclase C (GUCY2C) are two promising tumor-associated antigens (TAAs) that are broadly and specifically overexpressed in various GI cancers, making them ideal targets for dual-specific therapy. Bispecific antibodies (bsAbs) offer a strategic advantage by co-targeting two distinct antigens, potentially enhancing tumor selectivity, overcoming heterogeneity, and improving therapeutic outcomes. Here, we report the development of a novel 2+2 IgG-like bispecific antibody-drug conjugate (ADC) targeting both CDH17 and GUCY2C, engineered to address the unmet needs in GI cancer treatment. The bispecific antibody was constructed as a 2+2 IgG-like molecule. The CDH17-binding arm was derived from a humanized single-domain antibody (VHH) isolated from an immunized alpaca library, selected for high affinity and specificity. The GUCY2C-binding arm was a fully human IgG1 kappa antibody identified through biopanning of a human phage display library. The resulting bsAb was site-specifically conjugated to a proprietary dual-payload linker-drug system from Hangzhou DAC, consisting of a potent antimetabolite drug and a topoisomerase I inhibitor. The bsAb exhibited high-affinity binding to both CDH17 and GUCY2C (KD values in the low nanomolar range) and demonstrated dual-specific binding to cells expressing either or both antigens. This ADC agent also demonstrated potent cytotoxicity against both single and dual antigen-expressing tumor cells. The promising preclinical efficacy profile of this ADC support its potential as a targeted therapy for patients with advanced GI cancers, offering a new strategy to overcome treatment resistance and improve clinical outcomes.

#2397 Cell based payload release highlights design, site, and cell dependent ratio shifts in dual payload ADCs.

Nan Hsuan Wang, Wei-Han Lee, Evelyn He, Li Chuan Huang, Yu-Chao Huang, David Teng-Yi Huang, Ya-Chi Chen

OBI Pharma, Inc, Taipei City, Taiwan

Dual-payload antibody-drug conjugates (ADCs) are designed to deliver two cytotoxic payloads in a defined ratio, yet whether this designed composition is maintained upon cellular processing is poorly understood. Conventional enzymatic payload release assays confirm linker cleavability but fail to reflect the biological complexity governing intracellular release. To address this, we established a quantitative cell-based liquid chromatography payload-release assay to monitor intracellular drug liberation after ADC treatment across multiple tumor cell lines. Using this platform, we examined how linker design, conjugation site, drug-to-antibody ratio (DAR), and steric environment affect payload release of mono- and dual-payload ADCs. While all constructs exhibited analytically confirmed enzymatic cleavability, the intracellular release profiles frequently diverged from the designed A:B payload ratios. Notably, the extent and direction of these ratio shifts were cell-type dependent, even for the same ADC construct, indicating that differences in protease abundance, endolysosomal trafficking, and microenvironmental pH strongly modulate payload liberation. Furthermore, conjugation site and DAR configuration introduced steric shielding effects that altered linker accessibility and release kinetics, resulting in distinct and less than optimal intracellular payload ratios despite identical chemical designs. Importantly, cell-based release results correlated closely with cytotoxicity outcomes in animal models, underscoring their functional relevance. Together, these findings reveal that the custom-designed dual-payload ratio does not necessarily reflect the effective intracellular ratio, and that cellular context, linker architecture, and conjugation geometry collectively determine the eventual payload balance. This framework provides a mechanistically informative tool for rational optimization of dual-payload ADC design, enabling more predictive control of intracellular pharmacology.

#2398 Dissecting ADC pulmonary toxicity: A murine ADC-associated ILD model to guide and inform ADC discovery.

Suresh Anaganti, Arti Bhujade, Steven Murkli, Zachary Sparta, Nabin Panth, Alexander Weig, Richa Vartak, Julien Dugal-Tessier, Nareshkumar Jain

NJ Bio, Inc., Princeton, NJ

Antibody drug conjugates (ADCs) built upon topoisomerase I inhibitors such as deruxtecan have reshaped the therapeutic landscape of solid tumors, yet their promise continues to be constrained by interstitial lung disease (ILD), a clinically significant toxicity whose mechanistic origin remains incompletely understood. Herein, using a translational murine ILD platform, we dissect the architectural determinants of ADC-induced lung injury and reveal a striking divergence in pulmonary responses driven by drug-linker chemistry. Trastuzumab-GGFG-DXd reproduced the delayed-onset alveolar inflammation, macrophage-rich infiltrates, and fibrotic remodeling characteristic of clinical and non-human primate ILD, whereas structurally distinct comparators including an SN38-based ADC, novel camptothecin ADCs, and ADCs featuring payload-free linkers result in unexpected findings that suggest ILD is much more than a payload-derived toxicity. This data highlights the importance of evaluating ILD-related toxicity in the discovery process whereas previously toxicity screening is reserved for lead optimization stages. Employing our murine ILD platform, we were able to study and evaluate numerous combinations of novel camptothecin payloads and novel linkers arriving at significantly reduced or no ILD without compromising the efficacy in low HER-2 expressing JIMT1 efficacy model. These findings establish a predictive and scalable murine platform for ADC-associated ILD and propose a conceptual reframing of ADC safety engineering, one in which ILD related toxicity evaluation can guide rational ADC design.

#2399 Discovery of ZL-6201, a novel LRRC15-targeting antibody drug conjugate (ADC) for the treatment of sarcomas and epithelial solid tumors.

He Xu[1], Zengxia Li[2], Jiaqing Yi[1], Wilson Peng[1], Qiuping Ye[1], Xinchao Xia[2], Lei Wang[2], Xinchuan Dai[2], Yue Ge[2], Donghui Li[1], Ziruo Wen[2], Changwei Lv[2], Joshua Zeng[1], Qidong Hu[1], Lina Wang[2], Jelveh Lameh[1], Nathan Ihle[1], Bing Wan[2], Linda N. Liu[1]

[1]Zai Lab (US) LLC, Cambridge, MA,[2]Zai Lab (Shanghai), Co. Ltd, Shanghai, China

Leucine-rich repeat-containing protein 15 (LRRC15) is a transmembrane protein involved in cell-cell and cell-extracellular matrix interactions. It is overexpressed in tumors of mesenchymal origin which include sarcomas, glioblastoma and melanoma, where its expression has been implicated in promoting metastasis. Additionally, LRRC15 is upregulated in cancer-associated fibroblasts (CAFs) that are found in the tumor microenvironment (TME) of multiple epithelial tumors. Its predominant expression in tumors and CAFs, coupled with minimal or absent expression in normal cells, makes LRRC15 a selective and potentially effective therapeutic target for antibody-drug conjugate (ADC) development.

ZL-6201 is an innovative ADC targeting LRRC15, built on the tumor microenvironment-activable linker-payload (TMALIN®) platform. It comprises a humanized anti-LRRC15 antibody, a hydrophilic protease-cleavable linker, and a novel camptothecin-derived topoisomerase I inhibitor payload C24. Site-specific conjugation yields an average drug-to-antibody ratio (DAR) of 8. ZL-6201 binds human and cynomolgus monkey LRRC15 with high affinity and specificity.

In vitro, cell-surface binding and target-dependent internalization selectively occurred in tumor cells expressing LRRC15. This resulted in C24 payload release, the induction of DNA damage response, cell cycle arrest, and ultimately cytotoxicity to tumor cells. The internalization of ZL-6201 in LRRC15-expressing human tumor cells and CAFs, followed by payload release and diffusion, mediated cytotoxicity against LRRC15-negative tumor cells in co-culture via the bystander effect.

In vivo studies demonstrated efficacy of ZL-6201 in human patient-derived xenograft (PDX) sarcoma models expressing endogenous LRRC15. Additionally, CAF-mediated payload release and the resultant efficacy were evaluated in two model systems: (1) cell-derived xenograft (CDX) models with low or no endogenous LRRC15 expression in tumor cells but high LRRC15 expression in mouse-derived CAFs using a mouse-reactive ZL-6201 surrogate, and (2) syngeneic tumor models with human LRRC15 knock-in CAFs using ZL-6201. Both ZL-6201 and the surrogate were well tolerated and demonstrated dose-dependent anti-tumor activity. Finally, ZL-6201 showed acceptable toxicokinetic and safety profiles in non-human primates (NHP).

Collectively, these data support advancing ZL-6201 into clinical development as a therapeutic candidate for sarcomas and epithelial solid tumors characterized by LRRC15 expression within the tumor microenvironment.

#2400 Design and evaluation of mRNA translation inhibitors for use as antibody drug conjugate payloads.

Mark Petersen[1], Jodi Wong[1], Samir Das[2], Vidhi Khanna[1], Kurt Stahl[1], Micheal G. Brant[1], Truman Hirkala-Schaefer[1], Jesse Leblanc[1], Victoria K. Harman-McKenna[1], Manuel Lasalle[1], Graham A. E. Garnett[1], Rehan Higgins[1], Catalina Suarez[1], Kaylee J. Wu[1], Linglan Fu[1], Germanna Righetto[1], Devika Sim[1], Adele Chan[1], Allysha Bissessur[1], Ambroise Wu[1], Araba Sagoe-Wagner[1], Luying Yang[1], Andrea Hernandez Rojas[1], Dunja Urosev[1], Sam Lawn[1], Vincent Fung[1], Stuart D. Barnscher[1], Raffaele Colombo[1], Jamie R. Rich[1]

[1]Zymeworks Inc., Vancouver, BC, Canada,[2]Abcellera, Vancouver, BC, Canada

Introduction: Eukaryotic initiation factor 4A (eIF4A) mediates recruitment of ribosomes to mRNA and catalyzes the unwinding of mRNA secondary structure, thereby facilitating ribosome scanning and translation initiation. Inhibitors of eIF4A (e.g., silvestrol, zotatifin, and other rocaglates) block translation of select mRNAs that contain a high degree of secondary structure (e.g. mRNAs encoding MYC, KRAS, and CDK4/6, among others), resulting in inhibition of cell proliferation and induction of apoptosis. Despite limited efficacy observed for zotatifin in a phase I clinical trial, antibody conjugation of a novel eIF4A payload offers the possibility of enhanced exposure and improved tolerability, which could lead to more robust responses. Furthermore, eIF4A antibody-drug conjugates (ADCs) would constitute a novel mechanism with the potential to address payload-specific resistance mechanisms that have been reported following progression on ADCs with camptothecin payloads.
Methods: A panel of novel rocaglamide-derived eIF4A inhibitors containing linkable functional groups were synthesized and evaluated for potency, hydrophilicity, and DMPK properties. Select analogs were elaborated into drug-linkers containing a hydrophilic polyethylene glycol (PEG) side chain to minimize hydrophobicity. Conjugation to endogenous cysteines using maleimide chemistry provided ADCs targeting diverse tumor associated antigens that were evaluated for in vitro potency, in vivo efficacy, and tolerability.
Results: ADCs carrying eIF4A inhibitors with a drug-to-antibody ratio of 8 required use of hydrophilic PEG groups to minimize aggregation. In vitro, trastuzumab ADCs showed potent antigen-dependent activity in HER2-expressing cell lines and bystander activity in mixed co-cultures of HER2+ and HER2- cells. Selection of lead drug-linkers was based on robust in vivo anti-tumor activity of HER2 targeted ADCs in NCI-N87 and SKOV-3 CDX models as well as tolerability in non-tumor bearing mice and Sprague Dawley rats. The breadth of efficacy of the lead drug-linkers was evaluated in vivo using Ly6E, PTK7, TROP2, cMET, and EGFR targeted ADCs.
Conclusions: Novel eIF4A ADCs constructed using hydrophilic drug linkers demonstrated potent and target-specific in vitro cytotoxicity. Promising in vivo efficacy was observed across multiple tumor associated targets, however the observed toxicity level in both mice and rats suggests a potentially lower than anticipated preclinical therapeutic window.

#2401 Developing a single B cell platform to accelerate antibody discovery and screening.

Spencer Chiang[1], **Wenlin Ren**[1], An Ouyang[2], Yu Sun[1], Xiaoli Li[1]

[1]ACROBiosystems Co., Ltd., Beijing, China,[2]ACROBiosystems Inc., Newark, DE

Rapid and efficient isolation of antigen-specific B cells is a critical bottleneck during antibody discovery, especially for antigens that are complex, maintain small and specific epitopes, or have a low immunogenicity. To solve this challenge, we developed a next-generation single B cell discovery platform focusing around utilizing both fluorescence-activated cell sorting(FACS) and CellCelector(CC) to maximize the recovery of low-population, high-value B cells. By performing an initial screen concurrently, this platform is able to maximize its complementary strengths: FACS with the deep sampling of large lymphocyte populations with precise multi-parametric gating, while CC can ensure a flexible, image-guided recovery of more fragile B cell subsets. This dual-mode workflow increases single-cell retrieval efficiency, reduces sampling bias, and improves downstream recombinant antibody expression success rates. To demonstrate platform performance, we employed a case study targeting DM1, a maytansinoid payload widely used in ADC development. Antigen-specific memory B cells were enriched and screened using fluorescent DM1 conjugates. FACS revealed a success rate of 73%, and after setting the gating parameters, 96 Abs with rIgGwith rIgG+/hIgG-DM1+/rIgM- binding was selected. Out of the 49 unique CDR3 Abs, 45 were specific to DM1 and first screened by ELISA. Antibodies with an affinity above nanomolar levels were further confirmed by biolayer interferometry (BLI) and ELISA, highlighting 19 potential candidates against DM1. Binding characterization revealed that 19 antibodies exhibited affinities above the nanomolar range, confirming robust recognition of the DM1 moiety. These results highlight the power of combining parallel FACS and CellCelector workflows to capture diverse, high-affinity antibody repertoires, even against complex small-molecule payloads. Overall, the platform provides a scalable, high-confidence route for antibody discovery supporting ADC payload targeting, mechanistic studies, and the development of next-generation biotherapeutics.

#2402 Rapid lead generation with the Pioneer Antibody Discovery Platform.

Birthe Jessen-Park[1], Sarah-Jane Kellmann[2], Mateusz Putyrski[2], Manuel Cavada[2], Hanh Hanuschka[2], Christian Frisch[2], Achim Knappik[2], Francisco Ylera[2]

[1]Bio-Rad Laboratories, Hercules, CA,[2]Bio-Rad Laboratories, Munich, Germany

The Pioneer™ Antibody Discovery Platform is Bio-Rad's biotherapeutic antibody generation service, centered around the Pioneer Antibody Library—one of the largest functional Fab libraries (225 billion unique sequences). Informed by over 18 years of phage display expertise, the library is optimized for therapeutic antibody selection. It integrates SpyDisplay, a proprietary SpyTag-based selection system, and TrailBlazer, a modular platform for rapid format assembly. We showcase data on antibody selection against IL-6R, C5aR, and CXCR4, demonstrating that the Pioneer Platform yields diverse, high-affinity, and functional leads for difficult targets. These candidates show comparable or superior performance to clinically developed or marketed antibodies across key parameters.

#2403 Advancing precision oncology through innovative bioconjugation and linker architecture strategies.

Shuhui Chen, **Dan Hart**, Matt Giese, Erika Leonard, Bowu Luan, Shamali Roy, Michael Fiebig, Catherine Bladen

Vector Laboratories, Inc., Newark, CA

The purpose of this study is to showcase how Vector Laboratories' proprietary bioconjugation technologies enable the development of highly specific and stable biomolecule conjugates, driving improvements in cancer detection and targeted therapy. We utilized Vector's advanced conjugation chemistries—including site-specific labeling and click chemistry—combined with optimized linker systems to create antibody-drug conjugates (ADCs) and diagnostic probes. Conjugates can be characterized using LC-MS, SEC, fluorescence imaging, and functional assays in tumor-derived cell lines to assess binding specificity, payload release, and signal amplification. Summary of New Data: The successful development of new antibody drug conjugates (ADCs) requires expert knowledge of antibody engineering, chemical biology, and linker architecture. BioDesign by Absolute Antibody and Vector Laboratories, provides drug developers ease of access to trusted antibody engineering, crucial bioconjugation products, and unique linker IP. These critical elements in the BioDesign toolbox help to maximize life science development versatility, overcome resource constraints, manufacturing at scale, and decrease time-to-market. Vector will showcase data highlighting how dPEG-based linkers have enhanced the therapeutic profile of ADCs, supported by recent bioassay results. In summary, Vector Laboratories' bioconjugation capabilities deliver precise, reproducible, and scalable solutions for oncology research and clinical applications. These findings underscore the potential of our platform to enhance therapeutic efficacy and diagnostic accuracy in cancer care.

#2404 Selective tumor immune activation by novel nucleic acid drug.

Akimitsu Okamoto[1], Kunihiko Morihiro[1], Makoto Yamamoto[2]

[1]University of Tokyo, Tokyo, Japan,[2]TKG Therapeutics, Inc., Tokyo, Japan

Introduction: Cancer-selective immune activation by artificial nucleic acids holds promise as a potent therapeutic modality for cancer treatment. We developed a hairpin DNA self-assembly technology and found it effectively suppresses tumor growth. Specifically, our developed compound TKG-002 activated cellular innate immunity and demonstrated potent tumor growth inhibition. Here, we discuss the results of tumor growth suppression by TKG-002.

Experimental Design: Two hairpin DNA sequences (oHP) were designed. Among these, the oHP showing the strongest cancer growth suppression effect in B16 tumor-bearing mice was selected and named TKG-002. In vitro tests confirmed TKG-002's self-assembly triggered by binding to miR-21. We also investigated the induction of innate immune activation that causes cancer growth suppression.

Results: TKG-002 was confirmed to aggregate under conditions of abundant miR-21 expression, forming long double-stranded DNA to which cGAS binds. Administration of TKG-002 to cancer cells induced apoptosis via the cGAS-STING pathway, including the production of phosphorylated IRF3. When TKG-002 was administered intra-tumorally to B16-bearing mice using an appropriate DDS, tumor growth was strongly suppressed. Aggregates of $CD8^+$ T cells and $CD4^+$ T cells were observed at the periphery of the shrinking tumor tissue. While TKG-002 alone demonstrated sufficient tumor growth suppression, combination with anti-PD-1 antibody resulted in even greater tumor growth inhibition.

Conclusions: The suppression of miR-21-overexpressing cancer growth by TKG-002 represents a potent therapeutic modality enabling selective tumor lysis through intracellular DNA self-assembly. The engineered TKG-002 induced autoimmunity toward targeted tumor lysis by forming long double-stranded DNA via miR-21. Further safety evaluation and condition optimization of TKG-002 are expected to establish it as an efficient cancer treatment modality.

#2405 A first-in-class IKZF1/3 degrader antibody conjugate (DAC) as a potential myeloma treatment.

Shuai Wu[1], Jinyu Yang[2], Mo Dan[2], Xiwu Hui[3], Bing Yao[3], Miaomiao Wei[2], Bin Bao[1], Qiwen Zhu[1], Linlin Xiao[2], Penghui Wen[2], Xiaodan Zhang[1], Wei Fang[1], Xiao Li[2]

[1]CSPC Megalith Biopharmaceutical Technology, Shanghai, China,[2]CSPC Pharmaceutical Group Ltd., Shijiazhuang, China,[3]CSPC Megalith Biopharmaceutical Technology, Shijiazhuang, China

Antibody-drug conjugates (ADCs) deliver potent cytotoxins to tumors but are limited by off-target toxicity and resistance. This drives the development of Degrader Antibody Conjugates (DACs) platform, which combine the catalytic activity of targeted protein degradation (TPD) with the tissue specificity of antibodies. We applied this innovative approach to multiple myeloma, where most patients relapse after frontline regimens (e.g., RVd, PVd), creating a critical need for novel therapies that overcome IMiD resistance. Emerging novel IKZF1/3 degraders, which allosterically reprogram CRBN, offer a potent solution by overcoming IMiD resistance in the clinic. We hypothesized that conjugating these catalytic degraders to CD38 antibody would create a synergistic therapeutic, migrating this potent mechanism from late-line to frontline treatment. Here we describe the rational design and pre-clinical profile of ADC-2419, the first-in-class CD38-directed DAC that delivers the potent IKZF1/3 degrader P5 to tumors. From a panel of candidate payloads, we identified P5 that binds CRBN with an 80-fold higher affinity (Kd <10 nM) than lenalidomide. This ultra-high affinity enables robust ternary-complex formation even at low intracellular CRBN levels, thereby bypassing the resistance mechanisms that cripple IMiD efficacy. P5 exhibits low-picomolar degradation potency (IKZF1 EC_{50} < 0.1 nM; IKZF3 EC_{50} < 0.1 nM) and drives deep target degradation (≥ 90% D_{max}) in tumor cells. Quantitative proteomics of >8,000 proteins confirmed exquisite selectivity; no endogenous CRBN neosubstrates were significantly reduced. Consequently, P5 shows potent cytotoxicity against MM cells (IC_{50} < 1 nM) while exhibiting limited cytotoxicity toward PBMCs up to 1 μM. P5 exhibited favorable PK *in vitro* and *in vivo* and was well tolerated in cynomolgus monkey toxicity study, supporting its development as a next-generation payload. Therefore, conjugation of P5 to the human CD38 antibody via a cathepsin-cleavable linker generated ADC-2419. ADC-2419 demonstrates potent cytotoxicity against CD38-expressing cells in vitro. In NCI-H929 xenograft model, a single 1 mpk dose achieved complete tumor regression, outperforming parental CD38 antibody at the same dose. In the PBMC-humanized mouse model, ADC-2419 demonstrated enhanced efficacy and maintained significant superiority over the CD38 antibody. Furthermore, pronounced tumor accumulation was observed in tumor-bearing mice, aligning with the in vivo efficacy and validating the targeted-delivery capability of our DAC platform. Collectively, the robust preclinical evidence for ADC-2419, which synergizes antibody targeting with catalytic protein degradation, supports its translational promise in overcoming key limitations in myeloma treatment.

#2406 A novel BRD4 degrader-HER2-targeting antibody-drug conjugate (DAC) overcomes trastuzumab deruxtecan resistance in HER2-positive cancers.

Xin Yu[1], Bin Yang[1], Wendi Ni[2], Haibo Liu[2], **Jan Willem Theunissen**[2], Jesse Chen[2], Jin Wang[1]

[1]Baylor College of Medicine, Houston, TX,[2]Fortitude Biomedicines, Boston, MA

Trastuzumab deruxtecan (T-DXd), an antibody drug conjugate (ADC), has transformed the treatment landscape for HER2-positive cancers. However, its long-term efficacy is limited by the inevitable development of resistance, which is often driven by altered internalization dynamics, impaired payload activation, or drug efflux. Therefore, next-generation ADCs capable of overcoming these resistance mechanisms are urgently needed to extend durable benefit. We have developed a next-generation degrader antibody conjugate (DAC) that combines a HER2 targeting antibody, trastuzumab, and a selective BRD4 molecular glue degrader, bromoseradeg (BsD), as the payload. BsD is a highly potent, BRD4 degrader and exhibits single digit nanomolar (nM) or sub-nM potency across diverse HER2+ cancer models. Trastuzumab bromoseradeg (T-BsD) was synthesized by cysteine conjugation chemistry via the cleavable Valine-Citrulline-para-aminobenzyl carbamate (Val-Cit-PABC; VCP) linker with an average drug-to-antibody ratio (DAR) of ~4. T-BsD preserved strong Her2-dependent cytotoxicity and consistently outperforming T-DXd in multiple HER2+ cell models and is also highly active in the T-DXd-insensitive xenograft model. To directly interrogate different resistance mechanisms, we first engineered HER2^{+} cancer lines to carry the clinically relevant TOP1 R364H mutation, which abolishes TOP1 inhibitor binding and confers robust T-DXd resistance. T-BsD retained cytotoxic potency in these mutant cells ex vivo and showed no loss of antitumor activity in corresponding xenograft models. Separately, we also evaluated resistance driven by overexpression of the efflux transporter ABCC1, a common mechanism that exports the DXd payload. In HER2^{+} cells with high ABCC1 expression, T-Dxd activity was abrogated, whereas T-BsD completely bypassed ABCC1-mediated efflux and maintained potent activity in both 2D culture and 3D xenograft tumors. Collectively, these compelling preclinical findings establish T-BsD as a mechanistically distinct therapeutic agent designed to overcome potentially key drivers of acquired resistance. By integrating potent BRD4 degradation with HER2-targeted delivery, T-BsD achieves superior activity and effectively bypasses the two most clinically relevant T-DXd resistance pathways. Together, these data strongly support the selective BRD4 degrader as a promising payload for developing next-generation ADCs that can benefit patients who are refractory or resistant to current ADC therapies.

#2407 DAC-1522: A novel Trop2-targeting degrader-antibody conjugate for precision oncology.

Chuanjie Chen[1], Qianqian Shen[1], Xinhui Cai[1], Yaqi Ding[1], Xiaoyu Yang[1], Yanfen Fang[1], **Carlos Chai**[2], Jian Ding[1], Yi Chen[3], Xuan Zhang[3]

[1]Shanghai Institute of Materia Medica, Chinese Academy of Sciences, Shanghai, China,[2]DaCure Therapeutics, Shanghai, China,[3]Shanghai Institute of Materia Medica, Chinese Academy of Sciences/DaCure Therapeutics, Shanghai, China

Background

Antibody-drug conjugates (ADCs) have revolutionized cancer therapies by enabling the targeted delivery of cytotoxic payloads to tumor cells. However, their efficacy and safety are constrained by the limited diversity of cytotoxic payloads. Notably, all FDA-approved Trop2-targeting ADCs employ topoisomerase I inhibitors as payloads, which may lead to both intrinsic and acquired drug resistance. Degrader-antibody conjugates (DACs) have emerged as a next-generation modality that integrates the selective targeting of ADCs with the mechanistic versatility of protein degraders, thereby offering a means to overcome these limitations. In this study, we sought to develop a TROP2-directed DAC capable of addressing the constraints of conventional ADCs and enhancing therapeutic outcomes.

Methods

A library of BET degraders was screened in MDA-MB-231 and BT-474 cells using CCK8 assays, and their degradation efficacy was subsequently confirmed by Western blot analysis. The selected payload candidates were converted into linker-drug precursors and conjugated to antibodies to generate the corresponding DACs. The drug-to-antibody ratio (DAR) and aggregation profiles were characterized using reversed-phase liquid chromatography (RPLC) and size-exclusion chromatography (SEC), respectively. *In vitro* cytotoxicity and selectivity were evaluated across multiple cancer cell lines, including MDA-MB-231, JIMT-1, BXPC-3, and KP-4. Furthermore, the DACs were evaluated in an Enhertu-resistant NCI-N87 model. *In vivo* anticancer efficacy was investigated in JIMT-1, MIA PaCA-2, and BXPC-3 cell-derived xenograft (CDX) models.

Results

Several BET degraders demonstrated potent cytotoxic and degradation activities. The corresponding DACs achieved the designated DAR without detectable aggregation. *In vitro*, DAC-1522 exhibited potent and Trop-2 dependent antiproliferative effects across multiple human cancer cell lines. Notably, DAC-1522 maintained robust activity in an Enhertu-acquired drug resistance model, whereas Enhertu and SKB264 showed markedly compromised efficacy, highlighting its potential to overcome resistance associated with conventional ADC therapies. *In vivo*, a single intravenous dose of DAC-1522 induced complete tumor regression in the BXPC-3 xenograft model without body weight loss.

Conclusion

DAC-1522 represents a novel Trop2-targeting DAC that demonstrates superior in vivo antitumor efficacy and the ability to overcome drug resistance, underscoring its promise as a therapeutic candidate for TROP2-positive malignancies.

#2408 ADCs in cancer treatment: SPR-driven insights into discovery and characterization .

Soraya Diez-Posada[1], **Cynthia Shuman**[2], Narashima Murthy Bandaru[2], Anna Moberg[2], Bryan Edwards[1], Sam Ness[1], Lowri Davies[1], Anja Pomowski[1], Laura Bouche[1], Isabel Perez-Castro[1], Howard Desmond[1], Gokhan Yahioglu[1], Mahendra P. Deonarain[1]

[1]Antikor Biopharma Ltd, Stevenage, United Kingdom,[2]Cytiva, Marlborough, MA

Antibody-drug conjugates (ADCs) have significantly advanced cancer therapeutics. Yet their efficacy in solid tumors remain limited due to poor tumor penetration, large molecular size and systemic toxicity. To address these challenges, we present a novel class of antibody fragment-drug conjugate (FDC) engineered for improved pharmacokinetic/pharmacodynamic (PK/PD) profiles and enhanced tumor accessibility. Surface plasmon resonance (SPR) was used to perform high-resolution kinetics and affinity analyses across multiple FDC targets. This approach provided rational candidate selection and optimization of binding kinetics, which supported the development of FDCs with superior tumor penetration and therapeutic potential. Integration of SPR data into the early discovery workflow has proven instrumental in identifying FDCs with optimal kinetic and affinity profiles. In preclinical development, SPR data supported assessment of safety and toxicology of FDCs through precise binding kinetics profiling. SPR data also deepened our understanding of target biology and mitigated development risk by eliminating the need for surrogate antibodies. This integrated approach streamlined the transition from discovery to preclinical evaluation, accelerating therapeutic development. These findings highlight FDCs as promising candidates for solid tumor treatment and provide a strategic path to overcome the limitations of conventional ADCs.

: Structural and Chemical Biology
Poster Session

#2412 Malic enzyme inhibition as a strategy to exploit metabolic reprogramming in cancer: A structure-based approach.

Ben Andrew Krinkel[1], Yuliana Yosaatmadja[1], Mark Daniel Slayton[2], Jin Heon Jeon[2], Jack Copping[1], Jack Flanagan[1], Sofia Merajver[2], Chris Squire[1], Kerry Loomes[1]

[1]University of Auckland, Auckland, New Zealand,[2]University of Michigan, Ann Arbor, MI

Background: Cancer remains a global health challenge and urgently requires therapies that improve clinical outcomes and patient quality of life. Tumor cells commonly reprogram metabolism to sustain proliferation and survival, notably by increasing glutamine dependence and upregulating mitochondrial malic enzyme 2 (ME2), which produces pyruvate and NAD(P)H. ME2 is overexpressed in pancreatic, melanoma, and lung cancers, making it a compelling therapeutic target that remains underexplored.
Methods: Recombinant human ME1, ME2, and ME3 were expressed and kinetically characterized in the presence and absence of inhibitors. We solved a complete set of X-ray crystal structures for the three isoforms with a potent malic enzyme inhibitor bound, revealing ligand and metal coordination. These structures guided virtual screening of a curated library of up to 14 million drug-like and fragment molecules to identify novel malic enzyme inhibitors. Biochemical hits were advanced to cellular assays to evaluate efficacy; lead compounds NPD-389 and FLA were tested for antiproliferative activity in melanoma and triple-negative breast cancer cell lines.
Results: Kinetic analyses show distinct activity and inhibition patterns across ME isoforms. X-ray crystallography visualized the potent, isoform-nonselective inhibitor NPD-389 bound in a metal-coordinating mode and captured an unexpected malic enzyme conformation. Structure-based virtual screening against this conformation identified multiple novel scaffolds with biochemical inhibitory activity. One scaffold, FLA, exhibited a unique selectivity profile and was found bound to ME2 in a previously cryptic pocket that rearranges upon ligand engagement and sits adjacent to the NAD^+ cofactor and malate-binding site. In a panel of melanoma and triple-negative breast cancer cell lines, NPD-389 and FLA reduced proliferation in most models, supporting their potential as chemical leads for further development.
Conclusions: These results establish mitochondrial malic enzymes, particularly ME2/ME3, as tractable targets for cancer therapy. Structural elucidation of NPD-389's metal-binding mode and of FLA's cryptic/allosteric binding pocket provides a robust foundation for rational optimization of potency and isoform selectivity. Selective ME inhibitors—either isoform-specific or mitochondrially targeted—have potential as adjuncts to checkpoint inhibitors or chemotherapy, enabling more effective, metabolism-directed cancer treatment.
References:1.Heon, J., Slayton, M., Krinkel, B., et al., Interplay Between Malic Enzyme 2, de novo Serine Synthesis, and the Malate-Aspartate Shuttle Drives Metabolic Adaptation in Triple-Negative Breast Cancer. *Cancer & Metabolism*, 2025.

#2413 Insights in CYP2E1-mediated ferroptosis in hepatocellular carcinoma.

Kristy L. Thomas, Kylie R. Driggers, Hyland C. Gonzalex, Jessica H. Hartman

The Medical University of South Carolina, Charleston, SC

Introduction: CYP2E1, a cytochrome P450 enzyme mainly found in hepatocytes, is crucial for metabolizing xenobiotics including fatty acids and drugs. In hepatocellular carcinoma (HCC), CYP2E1 acts as a tumor suppressor. However, CYP2E1 has significantly reduced RNA and protein expression in HCC and its expression correlates positively with patient survival. We hypothesized that CYP2E1 promotes ferroptosis—a regulated, iron-dependent cell death involving iron accumulation, ROS generation, glutathione depletion, and lipid peroxidation—which may underlie its beneficial effects in HCC.

Methods: HCC cell lines were cultured per ATCC guidelines and transduced with adenoviral vectors expressing GFP or CYP2E1, confirmed by Western Blot. To assess palmitic acid (PA) toxicity, cells were treated with 0-5mM PA for 24 and 48h, followed by cell death analysis. For ferroptosis sensitivity, cells were exposed to graded concentrations of inducers (FINO2, FIN56, Erastin, RSL3) for 24h, then analyzed for cell death.

Results: Cell lines exhibited a variation in sensitivity to palmitic acid (PA) treatment, with HepG2 exhibiting a stronger response than SNU398 and SNU449 cells. However, there was no statistically significant effect of CYP2E1 expression in the response to PA feeding. Sensitivity to ferroptosis inducers also varied widely across cell lines and appeared to be cell type-specific rather than dependent on CYP2E1 expression.

Conclusion: Our results provide new insight into the sensitivity of different HCC cell lines to ferroptosis induced by PA feeding and by pharmacological inducers of ferroptosis. Further studies are needed to determine the mechanism of CYP2E1 tumor suppression, which our data suggests may not be through ferroptosis.

#2414 Targeting the interferon-inducible isoform, p150 of ADAR1 for the treatment of oral squamous cell carcinoma (OSCC).

Annie Wai Yeeng Chai[1], Pei San Yee[1], Xavier Wezen Chee[2], Stephanie Hao Ling Cheah[2], Jie Ying Teo[3], Keng Yoon Yeong[4], Siew Kit Ng[3], Siaw San Hwang[2], Sok Ching Cheong[1]

[1]Translational Cancer Biology, Cancer Research Malaysia, Subang Jaya, Malaysia,[2]Faculty of Engineering, Computing and Science, Swinburne University of Technology Sarawak, Kuching, Malaysia,[3]Advanced Dental and Medical Institute, Universiti Sains Malaysia, Penang, Malaysia,[4]School of Sciences, Monash University Malaysia, Subang Jaya, Malaysia

Oral squamous cell carcinoma (OSCC) is the fourth most common cancer in low- and middle-income countries (LMIC) and is one of the leading causes of cancer deaths in Asia, accounting for nearly three-quarters of global oral cancer mortality. Five-year survival rates remain poor, reflecting both the scarcity of actionable genetic drivers and the absence of Asian patient-derived models in global cancer datasets. This underrepresentation has slowed therapeutic innovation for populations that bear the greatest burden, leaving a significant unmet clinical need. To address this gap, we conducted genome-wide CRISPR/Cas9 dependency screens on a panel of unique Asian-derived OSCC cell lines that reflect the genetic and etiological diversity of these patients to identify vulnerabilities for therapeutic development. We have identified Adenosine deaminase acting on RNA (ADAR1) as an essential gene for OSCC survival. ADAR1 is an RNA-editing enzyme, whereby its dysregulation has been associated with tumor progression in various cancers. There are two isoforms of ADAR1 (p110 and p150), which are identical except that p150 has a unique Zα domain, which binds Z-DNA and offers a unique targeting opportunity to treat this deadly OSCC. To take this forward, we applied a proprietary computer-aided drug discovery pipeline, termed the Multi-layer Ultra-large Screening and Exploration (M.U.S.E), to identify potential Zα-targeting ADAR1 inhibitors. Approximately six billion compounds were evaluated through integrated filters for solubility, drug-likeness, binding affinity, and stability. A total of 51 compounds were shortlisted from the in-silico screening, and their binding affinities and specificities were evaluated. The intrinsic tryptophan fluorescence (ITF) spectroscopy was used to determine the binding affinity, while the electrophoretic mobility shift assay (EMSA) was used to determine the on-target effect of the compounds in disrupting the Zα-Z-DNA binding. From ITF analysis, 21 compounds demonstrated strong binding affinity with Stern-Volmer constants (K_{SV}) exceeding 10,000 M^{-1}. Using EMSA, we identified eight compounds with robust evidence of disruption of Zα-Z-DNA binding complexes. Our selected top hits demonstrated better binding affinity and on-target efficacy in disrupting ADAR1-Zα function, compared to other reported experimental candidates of ADAR1 inhibitors. While further effort in the hit-to-lead optimization and validation of its anti-tumor efficacy in OSCC cells are still ongoing, the discovery of these top hits with validated binding affinity and functional efficacy assures a promising outlook of our drug discovery strategy.

#2415 First-in-class stabilizing inhibitor of CHD4 that traps and disassembles the NuRD complex.

Anthony Sanchez[1], Minkyu Kim[2], Ivan Babic[3], Kyle Miller[1], **Elmar Nurmemmedov**[3]

[1]Emory University, Atlanta, GA,[2]University of Texas, San Antonio, TX,[3]CellarisBio, San Diego, CA

CHD4, the catalytic core of the NuRD complex, regulates chromatin remodeling, transcriptional repression, and DNA repair. Its overexpression in glioblastoma correlates with poor prognosis, yet CHD4 has remained undruggable. Employing a novel cell target engagement strategy, we identified CH41, a first-in-class small molecule that covalently engages cystine residues in the CHD4 chromodomain. The compound stabilizes CHD4 on chromatin, blocks its remodeling activity, and induces NuRD complex dissociation and proteasomal degradation. MICRO-TAG® cellular target engagement assay system applied in both discovery and validation stages, confirms direct CHD4 binding and real-time intracellular stabilization consistent with mechanistic trapping. CH41 disrupts CHD4 interaction with ZMYND8 and RBBP4/7, represses RAD51 expression, and impairs homologous-recombination repair, leading to reduced RAD51 foci and increased γH2AX and 53BP1 accumulation. Functionally, CH41 disables CHD4-dependent DNA repair and transcriptional control, re-sensitizing temozolomide-resistant glioblastoma cells. The data establishes CH41 as the first selective CHD4 inhibitor and illustrates how advances in cellular biophysics and cellular target engagement profiling are transforming the discovery of small molecule modulators of challenging transcription factor targets, such as chromatin remodelers.

#2416 Analyzing non-cancerous and cancerous protein structure using a novel Elliptical Dichroism Spectrometer.

Tommy Gao[1], Dali Sun[2]

[1]KIHA, University of Denver, Denver, CO,[2]KIHA, Univerisity of Denver, Denver, CO

Protein structure analysis is important as structure often dictates a proteins function. Currently, there are many instruments for analyzing protein structural features, such as Circular Dichroism (CD) Spectrometry. However, the large size and high cost of this method limit its applicability to well-organized and funded research environments only. Previously, we constructed an Elliptical Dichroism Spectrometer (EDS) instrument for the analysis of micromolecules (amino acids) chirality, as well macromolecule (protein) secondary structure analysis using both theoretical simulation methods and experimental validation. Furthermore, we demonstrated the EDS potential in distinguishing between protein derived from non-cancerous and cancerous pancreatic cell lines. We demonstrated the potential of the EDS for use as a protein secondary structure analysis instrument with potential application for noninvasive cancer detection using structural features exhibited by cancerous proteins as the source of detection. The simplified design of the EDS additionally tackles issues faced by current CD spectrometry by being smaller in size and lower in cost, allowing for greater applicability.

#2417 Proteome-wide target engagement and ternary complex mapping of molecular glues using LiP-MS.

Martin Soste[1], Polina Shichkova[1], Matevz Stefancic[1], Daniel Redfern[1], Francesca Cavallo[2], Lorna Charge[2], Ka Ying Lee[2], Ricardo Canavate del Pino[2], Denise Swift[2], Roland Hjerpe[2], Stuart Thomson[2], Allan Jordan[2], **Yuehan Feng**[1]

[1]Biognosys AG, Schlieren, Switzerland,[2]Sygnature Discovery, Nottingham, United Kingdom

Deciphering molecular targets and interaction networks of small molecules within native cellular contexts remains essential for both target-based and phenotypic drug discovery. This is particularly critical for molecular glues (MGs), which promote selective protein degradation through induced protein-protein interactions. Two mechanistic axes define MG action: (1) direct binding of the compound to an E3 ligase that subsequently recruits a neosubstrate, and (2) compound engagement with a primary protein target that promotes E3 ligase recruitment and ternary complex formation.

Limited proteolysis coupled with mass spectrometry (LiP-MS) has emerged as a powerful, label-free approach for elucidating small-molecule target engagement and mapping binding sites in complex proteomes without chemical tagging or genetic manipulation. Here, we expand the application of LiP-MS to two complementary experimental formats that interrogate distinct stages of molecular glue activity.

In the first scenario, an in-lysate LiP-MS workflow was implemented to identify primary drug-protein interactions across the proteome. Using quantitative data-independent acquisition mass spectrometry (DIA-MS) and a seven-point concentration series, we monitored conformational and accessibility changes across >250,000 peptides from >8,000 proteins. Machine learning-based LiP scoring enabled peptide-level resolution of binding sites and quantitative ranking of target engagement.

In the second scenario, a live-cell LiP-MS assay was developed to capture compound-induced protein-protein interaction changes under physiological conditions. This live-cell format enables detection of secondary, compound-dependent protein recruitment events, including ternary complex formation with E3 ligases and other associated proteins.

To evaluate LiP-MS performance in characterizing molecular glue mechanisms, we conducted global target identification experiments using two representative compounds: SR-4835, a cyclin K degrader that binds CDK12 and recruits DDB1, and MRT-2359, a GSPT1 degrader that engages CRBN. Live-cell LiP-MS experiments were performed at two time points (1 hour and 6 hours) to monitor compound-dependent conformational changes and protein recruitment dynamics associated with primary target engagement and potential ternary complex formation.

Together, LiP-MS provides a comprehensive, high-resolution platform for mapping small-molecule target engagement and for characterizing dynamic protein recruitment events associated with molecular glue activity directly in the cellular environment.

#2418 Non-covalent small molecule probe discovery of large intrinsically disordered protein.

Yichen Xiang[1], Marc Ramos Sala[1], Jose I. Vergara Panzone[1], Nancy Jiang[1], Diya Rana[2], Eliot Ebert[3], Angela N. Koehler[1]

[1]Massachusetts Institute of Technology (MIT), Cambridge, MA,[2]Massachusetts Institute of Technology (MIT), Cambrudge, MA,[3]Koch Institute For Integrative Cancer Research, Cambridge, MA

Fusion-positive alveolar rhabdomyosarcoma (ARMS), is a rare pediatric cancer often characterized by the pathognomonic fusion protein PAX3::FOXO1. Similar to other highly disordered transcription factors, PAX3::FOXO1 lacks typical small-molecule binding pockets thus making drug development difficult by conventional structural oriented design or traditional screening. Currently, there is no direct therapeutic approach to treat children with fusion-positive ARMS and patients are treated with ineffective traditional chemotherapeutic agents. Previously, we screened a library of small molecules against PAX3::FOXO1 via Small-Molecule Microarrays (SMMs) and identified a compound that shows selective target engagement in thermal shift assay but no apparent cellular activity. Furthermore, we are exploring targeted degradation with PROTACs due to the slow turn-over rate of this target. We have identified a scalable protein purification strategy to achieve stable, functional recombinant PAX3::FOXO1 and we are in the process of expanding the SMMs libraries up to 300,000 compounds. To validate hits from those high throughput screenings, we developed lentiviral transduced ARMS cell lines expressing HiBiT-tagged PAX3::FOXO1, enabling plate-based reporter assays as well as thermal shift assays. Small molecules are highly advantageous in their administration, delivery, and patient accessibility. We hope to address some of the unmet needs in the space of small molecule drug discovery against intrinsically disordered oncoprotein and transcription factors.

#2419 Synthesis and evaluation of novel functionalized β-lactams as potent anti-melanoma agents targeting PI3K/MAPK and JAK/STAT pathways.

Joy Temiloluwa Folahan[1], Ojasvi Dutta[1], Tolulope Omole[1], B. Donji[2], Konstantin Kousoulas[1], Timothy Beng[2], Jean Christopher Chamcheu[1]

[1]Louisiana State University, Baton Rouge, LA,[2]Central Washington University, Ellensburg, WA

Background: Skin cancers represent the most prevalent malignancies in the United States, affecting approximately 9,500 individuals daily and contributing to an annual economic burden exceeding $8.1 billion. Cutaneous melanoma skin cancer (CMSC), accounted for more than one million affected individuals and over 7,600 deaths in the US in 2022. Despite advances in targeted interventions, durable responses remain limited by systemic toxicity, low-bioavailability and rapid development of drug resistance. These challenges highlight the critical need for novel molecular scaffolds with improved pharmacological profiles and multi-target mechanisms.
Methods: To address this need, we leverage diversity-oriented synthesis, a powerful approach for creating structurally diverse, drug-like scaffolds with enhanced pharmacological potential. This strategy is becoming increasingly relevant in oncology drug discovery pipelines. A focused library of 40 novel, functionalized β-lactams were synthesized and screened against human (A375, SK-MEL-28) and murine (B16F10) CMSC cell lines. Cytotoxicity was assessed via IC_{50} determination, followed by phenotypic and mechanistic assays evaluating clonogenicity, migration, redox modulation, and apoptosis.
Results: Several derivatives demonstrated potent anti-melanoma activity, from which two lead molecules, W035 and W038, were selected for detailed characterization. W035 showed IC_{50} values of 14 μM (B16F10) and 24 μM in A375 cells, while W038 exhibited IC_{50} values of 24 μM in both A375 and B16F10 cells. Both compounds significantly inhibited colony formation (60% reduction at $0.75\times IC_{50}$) and suppressed wound closure and migration by 80%, indicating strong anti-metastatic potential. Mechanistically, W035 and W038 disrupted redox homeostasis, evidenced by 50% reduction in intracellular reactive oxygen species, and robustly activated caspase-3/7, confirming induction of apoptotic cell death. ADME profiling using SwissADME web-tool, predicted favorable drug-likeness, including high skin permeation (log Kp), good gastrointestinal absorption, Lipinski rule compliance, optimal lipophilicity (Log P_o/w<5), and favorable biodegradability. SwissTargetPrediction analysis indicated that the lead compounds possess a multi-target melanoma-inhibitory profile involving targeting MAPK, PI3Ks and JAK/STAT signaling pathways. Immunoblotting further therapy dose-dependent downregulation of these targets, indicating convergence on key melanoma signaling nodes.
Conclusions: This study identifies rationally designed β-lactam-based scaffolds with multi-target anti-melanoma activity. The lead compounds modulate apoptotic signaling, redox homeostasis, and MAPK/PI3K and JAK/STAT pathways, supporting rationale their further optimization and preclinical development for melanoma therapy.

#2421 Combining deep mutational scanning and next-generation protein sequencing to harness dominant protein variants to develop DNA repair inhibitors.

Nigel O'Neil[1], Lina Ma[2], Anthony Oppedisano[1], Esteban Lenoir[1], Philip Hieter[2], Peter C. Stirling[1]

[1]Arrowsmith Genetics, Vancouver, BC, Canada,[2]Michael Smith Laboratories, University of British Columbia, Vancouver, BC, Canada

The most clinically effective DNA repair enzyme inhibitors not only inhibit but also convert the target itself into a therapeutic agent. For example, topoisomerase poisons block the completion of the topoisomerase reaction resulting in a genotoxic DNA-protein adduct. Similar mechanisms underlie clinically relevant PARP inhibitors and other emerging DNA repair inhibitors. The challenge is identifying which repair proteins can be converted into gain-of-function therapeutic agents and how to elicit a gain-of-function phenotype. We developed an approach, Mutational Target Mapping, that uses deep mutational scanning to identify dominant missense variants that define structure-function relationships in drug targets that can direct therapeutic development. Dominant missense protein variants can be used to model the behavior of a potential drug to validate mechanisms of action and define genetic dependencies. Combining this platform with benchtop Next-Generation Protein Sequencing on the Quantum-Si Platinum® instrument, we can identify, track, and characterize the phenotypic effects of dominant missense variants in cells and biochemical assays. We applied this approach to several therapeutic targets discovering key residues in orthosteric and allosteric sites that can be mutated to elicit a dominant phenotype. Here, we describe our complementary genetic (high throughput screens) and proteomic (benchtop protein sequencing) approaches to find and model the behavior of therapeutics targeting DNA repair enzymes.

#2422 Next-generation chemical biology: Mapping the Purinome druggable space reveals genotype-specific vulnerabilities via phenotypic screening.

Ali Khateb, Ritika Gangaraju, Eric Gonzalez, Maizie Lee, Akshat K. Nigam, Jessica San Juan, Agnes Tan, Imran S. Haque, Thilo J. Heckrodt, Jack D. Sadowsky, Stig K. Hansen, Raymond V. Fucini

Kimia Therapeutics, Berkeley, CA

Background: Phenotypic screening enables discovery of biologically active compounds without prior knowledge of specific molecular targets. When combined with systematic chemical-space analysis, it represents a next-generation framework for mapping the druggable space across diverse genetic backgrounds. The human Purinome - a family of purine-interacting proteins composed of kinases and other nucleotide-binding enzymes - contains many attractive drug targets. Here, we applied our ATLAS (Active Learning with Automated Synthesis and Screening) platform which integrates high-throughput precision chemistry, direct to biology (D2B) screening, and machine learning, to survey the Purinome druggable space using diverse purine-directed libraries, aiming to identify genotype-specific dependencies within this critical protein network.

Methods: Using ATLAS, we generated proprietary, structurally diverse small molecule libraries of over 100,000 purine-directed samples, synthesized at nanoliter scale and directly screened in a high-throughput 1536-well cell viability assay. Screening was conducted in two colorectal cancer cell lines with distinct genotypes: HCT-116 and NCI-H747. Active D2B hits were validated by full dose-response curves, followed by pure resynthesis to confirm activity, selectivity, and potency. High-resolution chemical-space analysis was applied to visualize the diversity of active compounds, map activity across the surveyed chemical space, and define structure-activity relationships (SAR) enabling the identification of uniquely active scaffolds.

Results: ATLAS enabled exploration of a diverse chemical space which yielded thousands of cell-active compounds, many with strong cell line selectivity. Iterative application of ATLAS rapidly improved potency. As SAR was refined through the triage, hits clustered into distinct, non-overlapping chemical scaffolds, suggesting engagement with different biological targets. Importantly, activity maps differed between the two cell lines, revealing genotype-specific dependencies. One prominent chemotype contained structurally related molecules to known Aurora kinase inhibitors with clear cell line selectivity, while others represent novel, uncharacterized dependencies. These results demonstrate the platform’s efficiency in simultaneously discovering genotype-selective, cell-active compounds and accelerating their refinement toward optimal biological activity.

Conclusion: Using ATLAS, we performed phenotypic screening combined with high-resolution mapping of Purinome-directed chemical space. This approach identified small molecule compounds linked to genotype-specific vulnerabilities, establishing ATLAS as a powerful strategy for dissecting the druggable proteome and uncovering genotype-tailored therapeutic targets.

#2423 Evaluation of novel small molecule inhibitors targeting Polycomb repressive complex 1 as chemical probes.

Geoffrey Hewett[1], Haiqing He[2], Yiwu Yao[2], Se Ra Park[2], Sydney Musser[3], Trupta Purohit[2], Jolanta Grembecka[1], Tomasz Cierpicki[1]

[1]Pathology, University of Michigan, Ann Arbor, MI,[23]University of Michigan Medical School, Ann Arbor, MI

Background: Polycomb Repressive Complex 1 (PRC1) is an epigenetic regulatory complex responsible for monoubiquitylation of lysine 119 on histone H2A (H2AK119Ub). This ubiquitylation activity is mediated by a canonical heterodimeric E3 ligase involving Ring1B (or its paralog Ring1A) bound to BMI1. Deposition of H2AK119Ub is associated with gene repression at loci involved in determining cell fate and identity. Notably, genetic depletion of Ring1A and Ring1B results in reduction of H2AK119Ub, derepression of PRC1 target genes, and cell growth arrest in a leukemia model. Therefore, small molecules targeting the ubiquitylation activity of Ring1A/B are useful chemical probes towards studying PRC1 biology.
Results: We have previously developed RB-3: a first in class small molecule inhibitor of PRC1. Here we report the next generation of novel small molecule PRC1 inhibitors. Employing structure-based design, we have developed a potent cell permeable next generation inhibitor RB-322. RB-322 is a mixture of two atropisomers which were separated yielding RB-322-1 and RB-322-2. To validate direct binding of our inhibitors to Ring1A/B we used 2D HSQC. Notably, RB-322-1 demonstrates slow exchange while RB-322-2 demonstrates fast exchange indicating strong and weak binding respectively. We then used an AlphaScreen competition assay to evaluate RB-322-1 mediated disruption of the PRC1-nucleosome interaction *in vitro* in which it shows low nanomolar activity. A novel radiometric ubiquitylation activity assay (RadUb) was then developed to quantitatively assess inhibition of PRC1 E3 ligase activity. Using this assay we found RB-322-1 demonstrates sub-micromolar activity. RB-322-2 is 2 orders of magnitude weaker in these assays. We then investigated the on-target activity of RB-322 in leukemia cell lines. First, we developed a biotinylated RB-322 probe and performed streptavidin-based pull downs followed by proteomics analysis revealing enrichment of multiple PRC1 proteins. We then evaluated the effects of RB-322-1 on cellular H2AK119Ub and gene expression. We found RB-322-1 demonstrates rapid and dose-dependent reduction of the H2AK119Ub mark after 6-hours and derepresses PRC1 target genes in AML cell lines. Crucially, these effects have not been observed for the weak atropisomer RB-322-2.
Conclusions: Extensive medicinal chemistry optimization has yielded a potent cell permeable next generation small molecule inhibitor of PRC1: RB-322. RB-322 demonstrates low nanomolar activity in biochemical assays *in vitro* and demonstrates on-target derepression of PRC1 genes providing novel mechanistic insights. RB-322 represents a useful chemical probe for studying PRC1 biology and serves as the foundation for a potential novel anti-cancer agent.

#2424 Evaluating the biochemical activity and endogenous engagement of covalent small molecule inhibitors of NSD1 and NSD3 in cancer cell lines.

Joshua Ray, Bradley Clegg, Sergei Zari, Kibum Kim, Se Ra Park, Jolanta Grembecka, Tomasz Cierpicki

University of Michigan, Ann Arbor, MI

Background: The nuclear receptor-binding SET domain (NSD) family of proteins consists of NSD1, NSD2, and NSD3, each with histone methyltransferase (HMT) activity responsible for mono and di-methylation of histone 3 lysine 36 (H3K36me2). NSD1 expression and genetic alterations are implicated in 17% of head and neck squamous cellular carcinoma (HNSCC) patients, and knockdown of NSD1 inhibits the growth of HNSCC cell lines. Additionally, amplification of chromosome 8p11-12 (amplicon encoding *NSD3* among other genes), overexpression, or activating mutations of NSD3 drive the progression of non-small cell lung cancer (NSCLC) subtypes. In NSCLC cell lines with NSD3 amplification, knockdown of NSD3 results in growth inhibition. In multiple cancer cell lines, methyltransferase activity of NSD1 and NSD3 has been implicated in promoting cell growth, rationalizing the development of small molecule inhibitors.

Results: Optimization of our previously reported covalent inhibitors of the NSD1 SET domain led to the development of separate series of NSD1 and NSD3 inhibitors, which demonstrate potent growth inhibition in various cancer cell lines. To evaluate the potency of these inhibitors, we developed an *in vitro* engagement assay utilizing intact protein mass spectrometry. These experiments validated nearly complete covalent engagement of NSD1 and NSD3 after 2 h of incubation with small molecule inhibitors. We have also determined second order rate constant K_{inact}/K_I confirming effective covalent inhibition of NSD1 and NSD3. To assess inhibition of NSD1 and NSD3 SET domains, we employed an enzymatic histone methyltransferase activity assay and found mid-nanomolar IC_{50} values. To determine the covalent engagement of endogenous methyltransferases in cancer cells, we have developed and optimized an immunoprecipitation followed by bottom-up proteomics workflow. Our current experiments evaluate the inhibition of H3K36 methylation in these cell lines.

Conclusions: We have developed small molecule covalent inhibitors of NSD1 and NSD3 SET domains with strong engagement in *in vitro* mass spectrometry analyses and potent inhibition in histone methyltransferase assays. Furthermore, IP bottom-up proteomics methodology has enabled confirmation of covalent engagement to NSD3 in cancer cell lines, supporting on-target growth inhibitory effects of NSD3 inhibitors. These covalent inhibitors can be used as chemical probes to further study the effects of NSD1 and NSD3 inhibition in cancer and represent potential therapeutic modalities.

#2426 The cryo-EM structure of ADGRL4 provides functional insights into its mechanism of activation.

David M. Favara[1], Qingchao Chen[1], Anastasiia Gusach[1], Aurora Diamante[2], Jayesh C. Patel[2], Patrcia C. Edwards[1], Christopher G. Tate[1]

[1]Structural Studies Division, MRC Laboratory of Molecular Biology, Cambridge, United Kingdom,[2]Nxera Pharma UK Limited, Cambridge, United Kingdom

Background

ADGRL4 (also known as ELTD1) is an orphan adhesion G protein-coupled receptor (aGPCR) upregulated in multiple aggressive malignancies where it promotes angiogenesis, proliferation and epithelial-mesenchymal transition. Its molecular activation mechanism however was previously unknown. We demonstrated that ADGRL4 couples weakly to the heterotrimeric G protein G_q and determined the first active-state cryo-EM structure of ADGRL4. We then combined the structural data with systematic mutagenesis and G protein recruitment assays to define the molecular determinants of tethered agonist (TA) mediated activation.

Methods

A split NanoLuc-proximity assay using engineered ADGRL4 and mini-G protein constructs was used to quantitate Gq coupling. We purified the active-state ADGRL4-mini-G_q-βγ complex and determined its structure by cryo-EM. Guided by the structure, we performed alanine-scanning mutagenesis on TA residues contacting the orthosteric binding pocket and selected residues within the receptor core, assessing effects on G_q recruitment in HEK293T cells.

Results

Cryo-EM analysis yielded the first high-resolution structure of active-state ADGRL4 to 3.1 Å resolution. The TA region forms a short α-helix that occupies the orthosteric site and promotes outward displacement of transmembrane helix 6 (TM6). Alanine substitution of seven out of eight TA residues that interact with the orthosteric pocket significant impaired G_q recruitment. Mutation of six residues (H408A, F409A, I411A, L412A, M413A, S414A) reduced coupling by >50%; M413A abolished coupling completely (p<0.0001) and F409A reduced coupling by 88% (p<0.0001). Previous aGPCR structures have proposed three conserved core activation motifs: the upper quaternary core motif (UQC), the hydrophobic P/F/W/LφφG motif, and the H(N)L(M)Y motif. Structure-guided mutagenesis of corresponding positions in ADGRL4 showed that mutation of any UQC residue to alanine (F505A, M508A, W631A) abolished G_q recruitment. In the P/F/W/LφφG motif, L627A and G628 eliminated activity, whilst F625A and L626A caused partial impairment. In the H(N)L(M)Y motif, L515A and Y516A abolished coupling, whilst H514A produced partial impairment. Together, these findings clarify ADGRL4's activation mechanism: exposure of the TA permits engagement with the orthosteric pocket, which in turns facilitates TM6 displacement and formation of a cytoplasmic cleft for G_q engagement, with all activation motifs functioning as essential structural elements of this process.

Conclusions

These findings define how ADGRL4's TA and conserved 7TM activation motifs cooperatively stabilise its active conformation and engage G_q. These findings establish a structural framework for developing ADGRL4-selective antagonists (nanobodies, synthetic binders or small molecules) with potential therapeutic utility in ADGRL4-associated malignancies.

#2427 Optimizing the detection of pH-dependent conformational changes in pH-low insertion peptides using microfluidic modulation spectroscopy (MMS).

Emma Sanderson, Ryan Bynum, Happy Agarwal, Lacey McNally

Surgery, University of Oklahoma, Oklahoma City, OK

Introduction: The acidic microenvironment of pancreatic ductal adenocarcinoma (PDAC) can be targeted by pH-responsive peptides that undergo conformational changes upon protonation of their negatively charged residues. While microfluidic modulation spectroscopy (MMS) has been successfully used to detect higher-order structure in large proteins, there is room for optimization in the reliable detection of secondary structure for small peptides (< 30 amino acids). We utilized two pH-responsive peptides, V7 and V3, and an inactive peptide, K7, to investigate the effects of buffer conditions and the presence of liposomes on the ability of MMS to detect pH-based conformational changes in these small peptides.
Methods: Peptides were synthesized using the CEM LibertyBlue microwave technology. 10 mM and 20 mM phosphate buffer solutions (PBS) were prepared at pH 7.4 and 6.6. Liposomes were prepared using the thin film hydration technique, and then characterized with dynamic light scattering (DLS) to find size, polydispersity index, and surface potential. The RedShiftBio Aurora MMS system was used to analyze the secondary structure of V7, V3, and K7 at either pH 7.4 or 6.6 PBS with liposomes or without liposomes. Each buffer solution was prepared with 1 mg/mL of peptide and sonicated for 30 minutes before MMS reading. RedShiftBio higher-order structure and Gaussian analysis software were used to compare conformational changes between pH 7.4 to 6.6 for each peptide in the various buffer conditions.
Results: DLS revealed the liposomes to be 122 nm with a polydispersity index of 0.207 and a surface potential of +32.9 mV. The expected conformational changes for V7 and V3 based on pH could not be adequately detected without the presence of liposomes in the solution. 10 mM PBS with a concentration of 10^6 liposomes per mL was the optimal solution for characterizing the peptides, with V7 and V3 experiencing an increase in alpha-fold at pH 6.6 compared to 7.4, and K7 experiencing either no change or less alpha-fold at pH 6.6 compared to 7.4.
Conclusion: A low salt concentration solution containing liposomes was the ideal environment for the peptides V7 and V3 to undergo a pH-dependent conformational change that could be detected by MMS. MMS is a relatively quick method for determining peptide secondary structure with a low limit of quantification.
Funding: R01CA2810190

#2428 Structural proteomics and AI powers PROTAC rational design.

Nitzan Simchi, Michal Ran Shchory, Joseph Rinberg, Alon Shtrikman, Yaron Ben Shoshan-Galeczki, Gali Arad, Katharina Lange, Sagie Brodsky, Anjana Shenoy, Dimitri Kovalerchik, Yonatan Kedem, Iris Alchanati, Galina Otonin, Noam Cohen, **Kirill Pevzner**, Eran Seger

Protai, Ramat Gan, Israel

Proximity-inducing drugs are an emerging class of protein interaction modulators, as many cellular processes rely on the coordinated activity of proteins to support cell growth, homeostasis, regulation and communication. This is most famously exemplified by proteolysis-targeting chimera (PROTAC). PROTACs are heterobifunctional compounds consisting of two ligands joined by a linker to bring together an E3 ligase and a protein of interest and induce ubiquitination and subsequent degradation. Dozens of PROTAC drugs are being investigated in clinical trials, most notably targeting androgen receptor (AR) and BTK. The efficacy of a PROTAC molecule is driven by ternary complex formation and stability, rather than relying solely on the binary affinity of a single molecule to a single protein. Therefore, the major challenge in rational development of PROTACs is deep understanding of the dynamics and functions of complex assembly. However, protein complexes and interactions have traditionally been hard to model and are not well represented in existing protein structure resources, both experimental and computational.In this work, we present the AIMS™ platform, which integrates structural mass spectrometry (MS) data and AI modeling tools. We apply our AIMS™ platform to multiple PROTAC systems, allowing us to improve the confidence of predicted structures compared to AI alone and support rational PROTAC design.

#2429 Nanoformulation enabling repurposing of niclosamide for the treatment of pancreatic cancer: Rapidly soluble oral formulation for enhanced bioavailability.

Bhoomi Mukeshbhai Dholariya, Ketankumar Patel

St. John's University, Queens, NY

Pancreatic ductal adenocarcinoma (PDAC) is relatively uncommon yet remains one of the most lethal cancers worldwide. Its asymptomatic nature leads to delayed diagnosis, and by the time PDAC is detected, it has often progressed to an advanced, metastatic stage. Consequently, there is a critical need to identify new therapeutic strategies that can improve patient survival. Drug repurposing has emerged as a promising approach for rapidly expanding treatment options in PDAC. Our *in-vitro* screening suggested niclosamide (NIC) as a promising repurposed drug candidate for the treatment of PDAC. Various PDAC cell lines including gemcitabine resistant mia paca2 cells were susceptible to NIC induced apoptosis. Prior studies from various researchers also revealed role of NIC in killing cancer cells while compromising the tumor stromal barriers. However, its extremely poor water solubility often resulted in <10% oral bioavailability, which is not sufficient for anticancer activity. Poor lipid and organic solvent solubility limit the choices of nanoformulation approaches for NIC. We have explored a hydrophobic ion pairing approach with ionizable lipid for the development of self-nanoemulsifying drug delivery system (SNEDDS). Complexation between negatively charged NIC and lipophilic cation resulted in improved drug loading in SNEDDS while preventing the precipitation of drug in aqueous media. Different batches of NIC-SNEDDS were prepared using oleyl amine and ionizable lipid DLin-DMA. The particle size and zeta potential of the DLin-DMA based blank formulation were 18.35±0.99 nm and +18±0.69 mV, respectively, whereas the oleyl amine based blank formulation exhibited a particle size of 23.97±0.89 nm and a zeta potential of +32±0.77 mV. Due to very high positive charge blank formulation containing oleyl amine showed higher cytotoxicity. In contrast, the DLin-DMA blank formulation showed negligible cytotoxicity due to their ionizable nature - neutral at physiological pH and cationic at lower pH. Based on these results, DLin-DMA based nanoformulation was optimized for NIC. The optimized formulation NIC-SNEDDS exhibited a particle size of 23.67±1.2 nm and a zeta potential of +15.5±0.56 mV. NIC alone showed the IC_{50} of 2.33±1.5 µM in MIA PaCa2. The final formulation demonstrated an IC_{50} of 2.20±1.4 µM in MIA PaCa2 cells, confirming its promising anticancer activity. In PANC-1 cells, NIC-SNEDDS exhibited an IC_{50} of 3.09±1.1 µM IC_{50} compared to NIC alone (14.8 µM). Predictive pharmacokinetic modelling using Gastroplus indicated >75% oral bioavailability of the NIC oral formulation compared to suspension. Thus, a hydrophobic ion pairing approach with ionizable lipid enabled the development of a self-nanoemulsifying drug delivery system of niclosamide. Currently, we are investigating the effect of NIC on *in vivo*pancreatic tumor bearing mice.

: Biomarkers Predictive of Therapeutic Benefit 3
Poster Session

#2431 Clinical outcome of patients with early stage and metastatic non-small cell lung cancer (NSCLCa) harboring high genomic scarring score (GSS).

Panteleimon Konstantoulakis[1], Georgia Christopoulou[1], Apostolos Klinakis[2], Katerina Tsilingiri[2], Ioannis Vatselas[2], Natalia Asimakopoulou[3], Vassilis Georgoulias[3], Ioannis Pateras[4], Konstantinos Ntostoglou[5], Georgios Christodoulopoulos[6], Athanasios Kotsakis[6], Vasiliki Anastasopoulou[2], Dora Hatzidaki[5], Abdriani Harpidou[7], Emilia Tsaroucha[8], Gary Karponi[9]

[1]GENOTYPOS Science Labs, Athens, Greece,[2]Biomedical Research Foundation Academy of Athens, Athens, Greece,[3]Medical Oncology, Metropolitan Hospital, Athens, Greece,[4]Pathology, Attikon University Hospital, Athens, Greece,[5]Hellenic Oncology Research Group, Athens, Greece,[6]Medical Oncology, University Hospital of University of Thessaly, Larissa, Greece,[7]Medical Oncology, Sotiria Hospital, Athens, Greece,[8]Pulmonary Diseases, Sotiria Hospital, Athens, Greece,[9]Pathology, Microdiagnostics Lab, Thessaloniki, Greece

Background: DNA damage and genomic instability represent hallmarks of cancer. Tumors with defects in repairing double strand breaks have been shown to respond to platinum compounds, immune checkpoint inhibitors (ICI) and PARP inhibitors. We have previously reported that 28% of early-stage Non-Small Cell Lung Cancer (NSCLC) patients present high Genomic Scarring Score (h-GSS), an indicator of genomic instability, while patient-derived xenografts from those patients respond favorably to olaparib. The aim of this study was to investigate the immune landscape of h-GSS early-stage and metastatic NSCLC patients, and to assess their clinical outcome.
Material and Methods: Sixty-seven (early stage I-III) and 52 (stage IV) patients with no actionable genomic alteration were enrolled in the study. Their GSS was assessed using a commercial panel (AmoyDx® HRD Complete), which also identifies mutations in 20 homologous recombination repair (HRR) genes. PD-L1 expression (tumor proportion score-TPS) and early and late exhausted ($TCF1^+PD1^+$ and $TCF1^-PD1+$, respectively) $CD8^+$ cells were assessed using immunohistochemistry. All patients with early-stage disease received platinum-based adjuvant chemotherapy while stage IV patients received immunotherapy-based regimens.
Results: h-GSS was detected in tumors from 28/67 (41.8%) patients with stage I-III NSCLC and in 16/52 (30.8%) with stage IV. *TP53* mutations (*TP53mut)* were observed in 27/28 (96.4%) and 22/39 (56.4%) of stage I-III h-GSS and l-GSS tumors, respectively ($p<0.001$), and in 12/16 (75.0%) and 15/34 (44.1%) of h-GSS and l-GSS tumors stage IV tumors, respectively ($p=0.067$). Early-stage but not stage IV *TP53*mut patients presented a better DFI and OS, compared to wild-type *TP53* tumors ($p=0.002$ and 0.026, respectively). Early-stage h-GSS/TP53mut and l-GSS/TP53mut patients had better DFI ($p=0.012$ and $p=0.002$, respectively) compared to l-GSS/*TP53*wt counterparts, whereas only the h-GSS/*TP53*mut status was associated with a better OS ($p=0.031$). PD-L1 expression in l-GSS but not in h-GSS stage IV tumors was associated with a significantly better OS (HR=0.2, 95%CI: 0.1-0.6, $p=0.009$). Finally, there was a statistical trend towards an increased density of both PD1+TCF1+ (0.067) and PD1+TCF1- (0.054) exhausted tumor-infiltrating lymphocytes in h-GSS compared to l-GSS tumors in patients with stage IV disease.
Conclusions: The findings of this study clearly suggest that genomic instability in NSCLC, as assessed by GSS, could become an important tool for better stratification of patients regarding prognosis and treatment choice.

#2432 Precision genomics in leukemiareveals mutational and fusion landscapes in South Asian patients driving clinical decisions.

Puja Sinha, Amit Kumar, Shobit Gupta, Rama Chandran, **Giulliana Tessarin**

Genes2Me Pvt Ltd, Gurugram, India

Background: The integration of next-generation sequencing (NGS) into routine diagnostic workflows is revolutionizing molecular characterization in cancer care, enabling precise detection of pathogenic variants and other fusion transcripts. Particularly in malignant haematological diseases, NGS has significantly enhanced diagnostic accuracy and prognostic assessment, providing critical insights that directly inform and optimize clinical decision making. To support precision oncology in routine clinical practice, various in-house developed and commercial NGS based leukemia panels have been adopted. In this study, leukemic patient samples from an Indian cohort were analysed to identify the most statistically significant gene mutations and chromosomal fusions implicated in leukemic disorders.

Methods: Genomic profiling, including fusion detection, was performed on 98 leukemic samples using the G2M Hemat NGS assay, which targets 208 clinically relevant genes including DNA fusion and 94 RNA fusion genes and approximately 650 kb of genomic regions and was sequenced on the Illumina platform. Bioinformatics analysis was conducted using the GATK v4.1.2 somatic variant calling pipeline, and downstream visualization of mutational landscapes and hotspot regions was achieved using MAF tools.

Results: Comprehensive genomic profiling revealed recurrent mutations in ASXL1, FLT3, PTPN11, NRAS, KRAS, BCOR, ABL1, NF1, KIT, and EZH2, with variant allele frequencies ranging from 2% to 16%, emphasizing their potential role in leukemogenesis. Additionally, seven clinically significant RNA fusion genes were identified across 19 patient samples, with RUNX1-RUNX1T1 and ETV6-RUNX1 emerging as the most prevalent, followed by the hallmark BCR-ABL1 fusion. Key substitutions including Gly→Val (ASXL1), Asp→Tyr (FLT3) at specified position, and multiple changes in signalling genes define a clinically relevant spectrum of amino acid changes in leukemia. These findings highlight a complex mutational and fusion landscape with critical implications for risk profiling and targeted therapy development.

Conclusion: The ability to detect clinically relevant mutations and fusion genes that inform diagnosis, prognostic stratification, and precision treatment decisions in hematologic malignancies, establishes the assay's value as a comprehensive genomic tool for precision oncology.

#2433 BAP1 loss confers ferroptosis resistance to cholangiocarcinoma via TLCD1-mediated membrane phospholipid remodeling.

Yu Zhao[1], Peyton Classon[2], Danielle Marie Carlson[3], Jayla Millender[1], Irene K. Yan[2], Sumera Ilyas[1], Rory L. Smoot[4], Gregory J. Gores[5], TUSHAR PATEL[2], Davide Povero[1]

[1]Mayo Clinic, Rochester, MN,[2]Mayo Clinic, Rochester, MN, MN,[3]Mayo Clinic Hospital-Rochester, Rochester, MN,[4]Surgery, Mayo Clinic, Rochester, MN,[5]Professor of Medicine, Mayo Clinic, Rochester, MN

INTRODUCTION: Cholangiocarcinoma (CCA) is a deadly cancer of the hepatic bile duct epithelial cells. Loss-of-function mutations of epigenetic regulator ubiquitin C-terminal hydrolase deubiquitinase BRCA1-associated protein 1 (BAP1) occur in 26-32% of human CCA and are associated with worse prognosis and resistance to cytotoxic therapy. The goal of this study is to identify how BAP1 loss promotes cell death evasion through metabolic rewiring.
MATERIALS & METHODS: Isogenic wild-type and BAP1-deficient human and murine CCA cell lines were generated with shRNA/siRNA or CRISPR/Cas9 and were used to assess ferroptosis sensitivity by treatment with ferroptosis inducers. In vitro, ferroptosis was assessed by phospholipid peroxidation (C-11BODIPY), mitochondrial phospholipid peroxidation (MitoPeDPP, MitoCLox), iron oeverload (MitoFerro green) and cell death (CellTiter-Glo). Phospholipidomics and proteomics were performed in isogenic cells by LC-MS/MS. Isogenic liver orthotopic CCA murine models were used for in vivo pre-clinical studies.
RESULTS: Our findings indicate that BAP1 loss confers CCA ferroptosis resistance. BAP1 loss protects CCA against mitochondrial iron overload, ROS accumulation, and phospholipid peroxidation. Strikingly, BAP1 loss protects from mitochondrial phospholipid peroxidation and cardiolipin oxidation. Unbiased phospholipidomic profiling revealed that BAP1 loss remodels membrane phospholipid composition, enriching for ferroptosis-blocking monounsaturated phospholipids (MUFA-PLs) at the expense of ferroptosis-inducing polyunsaturated (PUFA-PLs). We found that BAP1 loss upregulates TLCD1, a phosphatidylethanolamine acyltransferase that incorporates MUFAs into membrane phospholipids, thereby stabilizing membranes against peroxidation. TLCD1 knockdown in BAP1-deficient CCA cells, restored ferroptosis sensitivity Notably, TLCD1 is significantly upregulated in human BAP1-mutant CCA as compared to WT tumors. We identified TLCD1 in the endoplasmic reticulum, Golgi and by mitochondrial outer membrane. In syngeneic liver orthotopic CCA murine models, engineered EpCAM-aptamer-coated lactosomes carrying GPX4 siRNA selectively targeted CCA cells, inducing ferroptosis and robustly suppressing tumor growth without systemic toxicity. Lastly, BAP1-mutant patient-derived xenografts (PDXs) and organoids were resistant to ferroptosis inducers, as compared to WT controls.
CONCLUSIONS: Our findings reveal that BAP1 loss rewires mitochondrial phospholipid metabolism thus conferring CCA resistance to ferroptosis, identifying TLCD1 as a targetable metabolic vulnerability in BAP1-mutant CCA.

#2434 Prognostic and predictive effects of *TP53* co-mutations and *RET* fusion partners in *RET*-rearranged advanced NSCLC.

Daniela Miliziano[1], Julia K. Rotow[2], Meghanne Lomibao[3], Tolulope Adeyelu[4], Arianna Marinello[1], Helena Bote-de Cabo[5], Jamie Feng[6], Andrea De Giglio[7], Mariana Brandao[8], Florian Guisier[9], Michael Duruisseaux[10], Christina Falcon[3], Massimiliano Cani[11], Francesca Colamartini[12], Barliz Waissengrin[13], Isabelle Monnet[14], Anna Eisert[15], Emilio Bria[16], Amin H. Nassar[17], Ayesha Aijaz[18], Patricia Iranzo[19], Colin R. Lindsay[20], Elizabeth Fabre[21], Vladmir Cordeiro de Lima[22], Judith Raimbourg[23], Laura Mezquita[24], Nicolas Minatta[25], Sophie Cousin[26], Katarzyna Szymczak[27], Vincent Fallet[28], Clarisse Audigier-Valette[29], Helene Doubre[30], Philippe Rochigneux[31], Annarita Avanzo[32], Antonio Calles[33], Marco Tagliamento[34], Diego Cortinovis[35], Balazs Halmos[36], Nicholas Girard[37], Andrew Elliott[4], Jair Bar[38], Alessio Cortellini[39], Diana N. Ionescu[40], Frances A. Shepherd[41], Fabrice Barlesi[42], Karen L. Reckamp[13], David Planchard[1], Benjamin Besse[1], Alexander Drilon[3], Mihaela Aldea[1]

[1]Department of Medical Oncology, Gustave Roussy, International Center for Thoracic Cancers, Villejuif, France,[2]Lowe Center for Thoracic Oncology, Dana-Farber Cancer Institute, Boston, Massachusetts, MA,[3]Memorial Sloan Kettering Cancer Center and Weill Cornell Medical College, New York, NY,[4]Caris Life Sciences, Phoenix, AZ,[5]Department of Medical Oncology, Hospital Universitario 12 de Octubre, Madrid, Spain,[6]Department of Medical Oncology, British Columbia Cancer Agency, Vancouver, BC, Canada,[7]Medical Oncology, IRCCS Azienda Ospedaliero-Universitaria di Bologna, Bologna, Italy,[8]Clinic of Thoracic Oncology & Phase 1 Clinical Trials Unit, Institut Jules Bordet-Hopital Universitaire de Bruxelles, Universite Libre de Bruxelles, Brussels, Belgium,[9]Normandie Univ, UNIROUEN, AIMS Lab QuantIF team, CHU Rouen, Department of Pneumology and Inserm CIC-CRB 1404, Rouen, France,[10]Respiratory Department and Early Phase (EPSILYON), Louis Pradel Hospital, Hospices Civils de Lyon Cancer Institute, Lyon, France; Cancer Research Center of Lyon (INSERM U1052, CNRS 5286), Lyon, France; Universite Claude Bernard Lyon 1, Universite de Lyon, Lyon, France,[11]Department of Oncology, University of Turin, S. Luigi Gonzaga University Hospital, Orbassano, Turin, Italy,[12]Medical Oncology, Santa Maria Della Misericordia Hospital, University of Perugia, Perugia, Italy,[13]Department of Medicine, Cedars-Sinai Medical Center, Los Angeles, CA,[14]Pneumology and Thoracic Oncology Department, Intercommunal Hospital of Creteil (CHI), Creteil, France,[15]Department of Medical Oncology, University Hospital of Cologne, Cologne, Germany,[16]Universita Cattolica del Sacro Cuore, Rome, Italy; Fondazione Policlinico Universitario Agostino Gemelli IRCCS, Rome, Italy; Ospedale Isola Tiberina - Gemelli Isola, Rome, Italy,[17]Division of Oncology, Yale University School of Medicine, New Haven, CT,[18]Stephenson Cancer Center, University of Oklahoma Health Sciences Center, Oklahoma City, OK,[19]Medical Oncology Department, Vall d'Hebron Hospital Universitari / Vall d'Hebron Institute of Oncology (VHIO), Barcelona, Spain,[20]Division of Cancer Sciences, University of Manchester, Manchester, United Kingdom,[21]Department of Thoracic Oncology, European Hospital Georges Pompidou, Paris, France,[22]Department of Medical Oncology, A. C. Camargo Cancer Center, Sao Paulo, Brazil,[23]Institut de Cancerologie de l'Ouest, St Herblain, France,[24]Medical Oncology Department, Hospital Clinic of Barcelona, Barcelona, Spain,[25]Department of Medical Oncology, Hospital Italiano, Buenos Aires, Argentina,[26]Department of Medical Oncology, Institut Bergonie, Bordeaux, France,[27]Department of Oncology and Radiotherapy and Early Phase Clinical Trials Center, University of Gdańsk, Gdańsk, Poland,[28]Department of Pneumology and Thoracic Oncology, Tenon Hospital, AP-HP - Sorbonne Universite, Paris, France,[29]Department of Thoracic Oncology, Hospital Sainte Musse, Toulon, France,[30]Department of Pulmonary Medicine, Hopital Foch, Suresnes, France,[31]Department of Medical Oncology, Paoli-Calmettes Institute, Aix Marseille University, Marseille, France,[32]Department of Clinical Medicine and Surgery, University of Naples "Federico II", Naples, Italy,[33]Department of Medical Oncology, Hospital General Universitario Gregorio Maranon, Madrid, Spain,[34]Department of Internal Medicine and Medical Specialties, University of Genova, Genova, Italy,[35]Medical Oncology, Fondazione IRCCS S. Gerardo dei Tintori, Monza; Department of Medicine, Universita Milano-Bicocca, Milan, Italy,[36]Montefiore Medical Center - Albert Einstein College of Medicine, New York, NY,[37]Department of Medical Oncology, Institut Curie, Paris, France,[38]Gray Faculty of Medical and Health Sciences, Tel Aviv University, Tel Aviv, Israel,[39]Department of Medical Oncology, Fondazione Policlinico Universitario Campus Bio-Medico, Rome, Italy,[40]Department of Pathology, British Columbia Cancer Agency, Vancouver, BC, Canada; Department of Pathology and Laboratory Medicine, University of British Columbia, Vancouver, BC, Canada,[41]Division of Medical Oncology, Princess Margaret Cancer Centre, University Health Network (UHN), Toronto, ON, Canada,[42]Universite Paris-Saclay, Gustave Roussy, Inserm, Predicteurs moleculaires et nouvelles cibles en oncologie (U981), F-94805, Villejuif, France

Background: *RET* fusions occur in ~1-2% of advanced NSCLC (aNSCLC). Selective RET inhibitors (SRIs) significantly improve outcomes, yet ~10% of patients progress by 6 months and ~30% by 12 months. Predictors of response or early progression remain poorly defined.
Methods: A multicenter retrospective analysis (RET-MAP) of RET+ aNSCLC from 47 international centers evaluated clinical/genomic correlates of SRI outcomes. Multivariable Cox models estimated progression-free (PFS) and overall survival (OS) and tested interactions with first-line (1L) SRI versus chemotherapy ± immune checkpoint inhibitor (CH±ICI). In parallel, genomic/transcriptomic features were characterized in an external Caris Life Sciences (CLS) RET+ aNSCLC cohort.
Results: Among 510 RET-MAP patients (median age 63; 59% female; 36% ever-smokers; 92% adenocarcinoma), 401 received an SRI (1L n=151; later lines n=250). Median PFS on SRI (any line) was 17.1 months (95% CI, 14.5-21.1), median OS 30.4 months (95% CI, 27.0-41.1). *TP53* co-mutation was present in 27% (78/292 tested) and was associated with shorter PFS (8.9 vs 19.2 months; p<0.001) and OS (22.7 vs 30.9 months; p=0.002), without a significant treatment-by-*TP53* interaction for 1L SRI versus CH±ICI (p=0.22). Fusion partner contributed with additional signal: *KIF5B* (73%, 274/373) had inferior PFS (13.4 vs 60.2 months; p<0.001) and OS (26.6 vs 73.0 months; p=0.002) compared with *CCDC6* (17%, 65/373), and a significant treatment-by-fusion interaction favored SRI over CH±ICI in *CCDC6* versus *KIF5B* (p=0.007). On multivariate analysis, shorter PFS and OS were independently associated with *TP53* mutation (HR 1.74, p<0.001; HR 1.77, p=0.001), *KIF5B* fusion (HR 1.98, p=0.002; HR 1.64, p=0.040), ECOG ≥2 (HR 2.20, p<0.001; HR 3.06, p<0.001), and brain metastases (HR 1.59, p=0.003; HR 1.88, p<0.001); worse OS was associated with non-adenocarcinoma histology (HR 1.74, p=0.049) and smoking (HR 1.42, p=0.034). Notably, *KIF5B* fusions were enriched for *TP53* mutations versus *CCDC6* (40% vs 19.6%, p=0.011), suggesting partially overlapping biology. In the CLS cohort (N=211), *TP53*-mutant tumors (74/211) were enriched for *RB1* mutations, had higher PD-L1 expression and tumor mutational burden, and demonstrated increased M1 macrophage/B-cell infiltration with reduced neutrophils; by fusion partner, *CCDC6* showed higher PD-L1, while global transcriptomes were otherwise

similar to *KIF5B*.
Conclusions: In RET+ aNSCLC, *TP53* mutation is prognostic for inferior outcomes on SRIs but not predictive of differential benefit versus CH±ICI. Fusion partner carries both prognostic and predictive relevance; *CCDC6* is associated with a more indolent course and greater relative benefit from SRI. External profiling supports an inflammatory microenvironment in *TP53*-mutant disease, reinforcing biologically distinct—and clinically meaningful—subsets within *RET*-driven lung cancer.

#2435 Tertiary lymphoid structures induction predicts and enhances response to famitinib plus PD-L1 blockade in advanced thyroid cancer.

Wei Kou, Yue Che, Qiwu Zhao, Haoran Feng, Zhuoran Liu, Jie Kuang, Weihua Qiu

Ruijin Hospital, Shanghai, China

Background: Therapeutic options for advanced thyroid cancer (TC) remain limited once standard treatments fail. In our phase II trial (NCT 06146985), the multi-target kinase inhibitor famitinib combined with the PD-L1 antibody adebrelimab showed early antitumor activity. However, the immunologic basis of this synergy, particularly the contribution of tertiary lymphoid structures (TLSs), remains unclear. To determine whether TLS induction underlies treatment sensitivity, we integrated histopathology, single-cell transcriptomics, and patient-derived organoid (PDO) assays.

Methods: TLS density and maturity were evaluated by H&E staining and multiplex immunofluorescence (mIHC). Pre- and on-treatment tumor biopsies underwent single-cell RNA-sequencing to define TLS-associated transcriptional features, including chemokine modules, lymphoid-organogenesis signatures, and T follicular helper (Tfh)-B-cell interaction pathways. PDOs were generated from fresh papillary thyroid cancer (PTC) tissues, and autologous $CD3^+$ T cells and $CD20^+$ B cells, the principal TLS-associated lymphocyte subsets, were isolated. PDO-TIL 3D co-culture assays assessed baseline immune killing, the response to famitinib plus PD-L1 blockade, TLS-pathway activation using CpG ODN with Mn^{2+}, and the combination of TLS activation with drug treatment. Apoptosis, proliferation, and TLS-signaling molecules were quantified after 48-72 hours.

Results: TLS density and the presence of mature TLSs strongly correlated with tumor shrinkage and successful surgical conversion. Single-cell analysis showed that TLS-positive tumors exhibited an immune-activated microenvironment enriched in Tfh cells, B cells/plasma cells, dendritic cells, and activated $CD8^+$ cytotoxic T cells. TLS-associated transcriptional features, including CXCR5- and CXCR3-driven chemokine recruitment pathways, were robustly enhanced, whereas TLS-negative tumors were dominated by Tregs and suppressive myeloid cells. Functionally, CpG plus Mn^{2+} induced TLS-related signaling and markedly enhanced TIL-mediated killing. Activating TLS-pathway synergized with famitinib plus adebrelimab, producing the strongest apoptotic and antiproliferative effects, surpassing drug treatment alone. These findings demonstrate that TLS activation potentiates the efficacy of TKI-immunotherapy combination.

Conclusions: Mechanistic evidence from this phase II study identifies TLS induction and maturation as key determinants of therapeutic response to famitinib plus adebrelimab. TLS enhances Tfh-B-cell interactions and cytotoxic T-cell activation, thereby increasing treatment sensitivity. TLS represents a mechanistic driver of response, a predictive biomarker, and an actionable immunologic target to sensitize advanced TC to TKI-immunotherapy combination.

#2436 Gastric cancer-derived tertiary lymphoid structure score from single-cell spatial transcriptomics with pan-cancer validation for immunotherapy response.

Wenbo Zhu, Hongru Shen, Huijun Wang, Ben Liu, Xiangchun Li, **Kexin Chen**

Tianjin Medical University Cancer Institute and Hospital, Tianjin, China

Background: Gastric cancer (GC) is a leading cause of cancer-related death, with poor 5-year survival rates for advanced stages, emphasizing the need for biomarkers to guide immunotherapy. Tertiary lymphoid structures (TLSs) in the tumor microenvironment have been linked to favorable prognosis and immune checkpoint blockade response, but the specificity of GC-derived TLS transcriptional signatures and their utility across tumor types remain unclear. We used single-cell-resolution spatial transcriptomics to construct a GC-derived TLS score and evaluated its prognostic and immunotherapy-predictive value in GC and pan-cancer cohorts.
Methods: In a cohort of 100 GC patients, TLS presence and maturation were assessed on surgical specimens by H&E, immunohistochemistry, and multiplex immunohistochemistry. A subset of 20 fresh GC tumors underwent high-resolution CosMx single-cell spatial transcriptomics to map immune and stromal cell distribution in TLS-positive versus TLS-negative regions. These spatial data were used to identify TLS regions, define major cell populations, and derive a 78-gene TLS signature, from which we constructed the GC-derived TLS score. The score was applied to pan-cancer bulk transcriptomic datasets and anti-PD-1 melanoma cohorts to assess its prognostic and immunotherapy-predictive performance. Patient-derived xenograft (PDOX) GC tumors were established in huCD34^{+} HSC-NCG mice and treated with anti-PD-1/CTLA-4 antibodies to test functional associations with TLS score.
Results: Patients were stratified into TLS-negative, immature TLS, and mature TLS groups. CosMx spatial transcriptomics resolved 10 major cell populations and mapped their distribution in TLS versus non-TLS regions. From mature TLS regions, we derived a 78-gene signature and constructed a GC-derived TLS score. Higher scores were associated with improved survival and better response to immune checkpoint blockade across multiple tumor types, including low-grade glioma, melanoma, NSCLC, metastatic melanoma, and metastatic GC (AUCs up to 0.857); in melanoma immunotherapy cohorts, high-score patients consistently had superior overall survival. In the humanized GC PDOX model, high TLS score tumors showed enhanced response to anti-PD-1/CTLA-4, with increased tumor cell apoptosis and higher T- and B-cell infiltration, potentially enhancing anti-tumor immunity.
Conclusions: We developed the first GC-derived TLS score using single-cell-resolution spatial transcriptomic data and validated its performance across multiple tumor types and in a humanized GC model. This high-resolution score was consistently associated with improved response and survival after immune checkpoint blockade, supporting its use as a precise biomarker for patient stratification and immunotherapy guidance across cancers.

#2437 A comparative scoring framework for BCMA-, GPRC5D- and CD38-targeted therapies in multiple myeloma.

Konstantin Chernyshov, Stanislav Kurpe, Maria Kuzmicheva, Kseniia Fede, Sargis Margaryan, Daria Goncharova, Anastasiya Evdokimova, Dmitry Grachev, Oleg Baranov, Polina Turova, Alexander Nesmelov, Andrey Kravets, Eduardo Shugaev-Mendosa, Nikita Kotlov

BostonGene Corporation, Waltham, MA

Selecting patients for T-cell engager (TCE) and CAR-T therapy in multiple myeloma (MM) relies on prior therapy lines, lacking predictive biomarkers. No tools guide target (e.g., BCMA vs GPRC5D) or modality (e.g., CAR-T vs TCE) selection. We developed an NGS-based framework computing a “Target Readiness” score (ReadyScore, RS) to predict response using malignant and tumor microenvironment (TME) features.

Public MM cohorts, including bulk (n=715, n=290) and scRNA-seq (n=6, n=5), were used to develop the framework. RS was developed for anti-BCMA CAR-T and TCE, anti-GPRC5D TCE, and anti-CD38 monoclonal antibodies (mAb). RS is a normalized, weighted score integrating expression activity of related genes (e.g., targets *TNFRSF17, GPRC5D, CD38*; resistance *STAT3*, γ-secretase; immune factors *CD274* (PD-L1), *CD55, CD59, ICAM1*) and relevant TME signatures (e.g., T-cell exhaustion, T-reg fraction).

We observed heterogeneous profiles in MM (CoMMpass): 36% of patients (pts) had high $RS^{BCMA\text{-}CAR\text{-}T/TCE}$, 33% high $RS^{CD38\text{-}mAb}$, and 31% high $RS^{GPRC5D\text{-}TCE}$, reflecting potential treatment benefit. Notably, 21% of pts had a low RS (< 0.5) for all tested immunotherapies. Within this 'low-RS' group, the tool identified other actionable pathways potentially linked to resistance (e.g., 2% high γ-secretase, 3% high *STAT3*), highlighting intervention opportunities. To illustrate the tool's predictive utility, we applied it to anti-BCMA CAR-T treated pts (Table 1). All 3/3 pts with a high $RS^{BCMA\text{-}CAR\text{-}T}$ had long PFS. For pts with short PFS on CAR-T, the tool highlighted potential alternative therapies: pt 8 had a high value for $RS^{BCMA\text{-}TCE}$, pt 32 for $RS^{GPRC5D\text{-}TCE}$, and pt 16 for $RS^{CD38\text{-}mAb}$.

This work introduces a molecular stratification framework with potential to support biomarker-driven selection of MM pts for TCE and CAR-T therapies. While validation in expanded cohorts is needed, this approach could help prioritize predictive profiles that can enhance trial design and translational decision-making.

Table 1. Target ReadyScore applied to the GSE210079 dataset

Patient	PFS	$RS^{BCMA\text{-}CAR\text{-}T}$	$RS^{BCMA\text{-}TCE}$	$RS^{GPRC5D\text{-}TCE}$	$RS^{CD38\text{-}mAb}$
Pt 1	long	0.69	0.23	0.01	1
Pt 19	long	1	0.66	0.48	0
Pt 33	long	0.71	0	0	0.3
Pt 8	short	0	1	0.51	0.16
Pt 16	short	0.6	0.38	0.56	0.61
Pt 32	short	0.09	0.29	1	0.24

#2438 Discovery of predictive circulating proteomic biomarkers for therapy response in HRR-driven solid tumors.

Anamarija Pfeiffer[1], Wouter van Bergen[1], Martin Mehnert[1], Polina Shichkova[1], Vanessa Buhlmann[1], Amaury Lachaud[1], **Yuehan Feng**[1], Takayuki Yoshino[2], Norio Nonomura[3], Taigo Kato[3]

[1]Biognosys AG, Schlieren, Switzerland,[2]Department of Gastroenterology and Gastrointestinal Oncology, National Cancer Center East, Kashiwa, Chiba, Japan,[3]Department of Urology, The University of Osaka, Graduate School of Medicine, Suita, Osaka, Japan

Background

The IMAGENE trial (jRCT2051210120) is a multicenter, tumor-agnostic, phase II basket study evaluating the combination of the PARP inhibitor niraparib and PD-1 inhibitors in patients with homologous recombination repair (HRR) gene mutations who have progressed following prior immune checkpoint inhibitor (ICI) therapy. In this tumor-agnostic setting, patients were enrolled with unresectable, locally advanced urothelial carcinoma (UC), renal cell carcinoma (RCC), gastric cancer (GC), esophageal cancer (EC), head and neck cancer (HNC), and melanoma (MC), all harboring HRR gene alterations. A total of 45 patients were enrolled in the primary cohort between April 2022 and April 2024.

Existing biomarkers such as PD-L1 expression and tumor mutation burden (TMB) have shown limited predictive power in ICI-treated and HRR-driven tumors. To address this gap, we performed unbiased deep plasma proteomic profiling, complemented by a targeted inflammatory marker panel, on baseline and on-treatment samples from HNC participants enrolled in the IMAGENE trial.

Methods

Citrate plasma samples were collected from patients at baseline and two post-dose time points after treatment with niraparib plus anti-PD-1 therapy. To study proteomic differences between responders and non-responders, and their temporal dynamics, we employed two complementary approaches: (i) unbiased plasma proteome profiling using the P2 enrichment system combined with mass spectrometry (DIA-MS), and (ii) targeted quantification of inflammatory proteins using a proximity ligation assay (NULISA) panel of ~250 markers.

Results

A total of 4,875 proteins and 67,311 peptides were quantified by P2-enriched LC-MS/MS across all samples. Comparative analysis of post-treatment samples identified 160 proteins differentially abundant between responders and non-responders, with enrichment in complement activation and immune-related pathways. Longitudinal analysis revealed 46 proteins significantly altered between pre- and post-treatment samples in responders, again highlighting immune and complement system activation as key features. Targeted NULISA profiling confirmed 20 markers differing between responders and non-responders and 11 markers dynamically regulated during response. Collectively, these findings suggest that complement activation, humoral immune response, and B-cell-mediated immunity are critical determinants of therapeutic response to niraparib plus anti-PD-1 combination therapy.

#2439 Predictive modeling of venetoclax/azacitidine response in acute myeloid leukemia using inflammatory cytokine profiling and clinical data from the NCT04267081 trial cohort.

Ankita Srivastava[1], Bahar Tercan[2], David L. Gibbs[2], Heikki Kuusanmaki[1], Mika Kontro[1], Caroline A. Heckman[1], Guangrong Qin[2]

[1]Institute for Molecular Medicine Finland (FIMM), HiLIFE, University of Helsinki, Helsinki, Finland,[2]Institute for Systems Biology, Seattle, WA

Cytokines in acute myeloid leukemia (AML) remodel the bone marrow microenvironment, drive disease progression, and contribute to chemoresistance. Cytokines such as IL-8 and CXCL12 promote AML cell survival and drug resistance, while some others influence therapeutic response, making cytokine signaling a key factor for predicting outcomes. Venetoclax (VEN) plus azacitidine (AZA) is standard therapy for older patients or those unable to receive intensive chemotherapy, yet responses vary widely. To address this, we developed predictive models for VEN/AZA response and survival using cytokine and clinical data.

Cytokine profiling was performed on samples from 85 AML patients in the VenEx trial (NCT04267081). Using the Olink Target 48 platform, the protein expression of 44 inflammatory cytokines was measured and normalized for downstream analysis. Clinical measurements and VEN/AZA treatment responses were collected, including 68 responders and 17 non-responders. T-test was used to compare the difference in cytokine expression between responders and non-responders. Elastic net regression models incorporating cytokine profiles and clinical variables were used to predict patient response and identified key cytokines associated with treatment response. To assess survival risk, we performed univariate Cox regression for each cytokine and generated Kaplan-Meier curves by stratifying patients into high-expression (above the third quartile) and low-expression groups.

Comparing the responders vs non-responders, we found potential biomarkers, including IL13 had higher expression in responders, while IL18, IL10, VEGFA, OSM, and CSF1 were expressed higher in non-responders. Using cytokine profiling to predict patient response, the model achieved an accuracy of 0.74 using 5-fold cross validation. Adding cell population measurements in the model, the accuracy increased to 0.83. All potential biomarkers are the top predictors for ven/aza response. Beyond that, we also identified TSLP, IL15, IL1B and TNFSF12 are among the top 10 predictors. Cox's proportional hazard model identified cytokines linked to poor survival, including CSF1, CCL3, CCL19, IL18, HGF, IL1B and OSM (ranked by hazard ratio). Stratification by FAB type revealed distinct cytokine associations with survival and drug response, TNFSF10 was siginificantly higher in non-responders in FAB M0-M2 (n=51; 41 responders, 10 non-responders).

Integrating cytokine and clinical data enables robust prediction of VEN/AZA response and survival in AML. Key cytokines such as CSF1, IL18 and IL13 may guide risk stratification and personalized therapy. Future work will map pathways linked to these cytokines and explore their roles in survival and treatment response.

#2440 Single-cell MRD profiling identifies CXCR4-high AML as a responder population to CXCR4 inhibition with Motixafortide.

Enise Ceran[1], Sonia Jaramillo-Segura[1], Anne Kahtrin Merbach[1], Christian Rohde[1], Robert Durruthy-Durruthy[2], Adam Sciambi[2], Marc Arribas-Layton[2], Michelle Lotze[1], Maxi Wass[3], Kathrin Rieger[4], Mathias Hanel[5], Regina Herbst[5], Christoph Rollig[6], Edgar Jost[7], Richard Schlenk[1], Katharina Gotze[8], Marina Scheller[1], Marion Subklewe[9], Simone Kowoll[10], Jorg Steighardt[10], Bayram Edemir[3], Lutz P. Muller[3], Irit Glicko-Kabir[11], Abi Vainstein-Haras[11], Cora Gromann[10], Ella Sorani[11], Shaul Kadosh[11], Andreas Wienke[12], Claudia Baldus[13], Uwe Platzbecker[14], Hubert Serve[15], Martin Bornhauser[16], Carsten Muller-Tidow[1]

[1]Department of Internal Medicine V, Heidelberg University Hospital, Heidelberg, Germany,[2]Mission Bio, San Francisco, CA,[3]Department of Internal Medicine IV, Hematology and Oncology, Martin Luther University Halle-Wittenberg, Halle, Germany,[4]Department of Hematology, Oncology and Tumor Immunology, Universitatsmedizin Berlin, corporate member of Freie Universitat Berlin and Humboldt-Universitat zu Berlin, Berlin, Germany,[5]Klinik fur Innere Medizin III, Klinikum Chemnitz, Chemnitz, Germany,[6]Department of Internal Medicine I, University Hospital Carl Gustav Carus, Dresden, Germany,[7]Department of Hematology, Oncology, Hemostaseology, and Stem Cell Transplantation, Faculty of Medicine University Hospital RWTH Aachen, Aachen, Germany,[8]Department of Medicine III, Technical University Munich School of Medicine and Health, Munich, Germany,[9]Department of Medicine III, University Hospital LMU Munich, Munich, Germany,[10]Coordination Centre for Clinical Trials Halle, Martin-Luther University Halle-Wittenberg, Halle, Germany,[11]BiolineRx, Modi'in, Israel,[12]Institute of Medical Epidemiology Biometrics and Informatics, Martin Luther University Halle-Wittenberg, Heidelberg, Germany,[13]Department of Hematology and Oncology, University Hospital Schleswig-Holstein, Campus Kiel, Kiel, Germany,[14]Department of Hematology, Cellular Therapy, Hemostaseology and Infectious Diseases, University Leipzig Medical Center, Leipzig, Germany,[15]Department of Medicine, Hematology/Oncology, Goethe-University Frankfurt, University Hospital, Frankfurt am Main, Germany,[16]Med. Klinik und Poliklinik I, Carl Gustav Carus Univ. Hospital, Dresden, Germany

Background: The CXCL12-CXCR4 axis mediates bone marrow niche mediated protection of leukemic stem cells and contributes to chemoresistance. Motixafortide is a potent CXCR4 antagonist that disrupts leukemic cell retention in the microenvironment. We leveraged single-cell minimal residual disease (scMRD) profiling to quantify CXCR4 expression and clonal persistence after consolidation therapy within the BLAST trial (NCT02502968), aiming to define predictive biomarkers of Motixafortide response.
Methods: Among 128 randomized AML patients in first complete remission (CR), 56 underwent bone marrow scMRD analysis using the Tapestri platform (Mission Bio) targeting 40 recurrent mutation hotspots and 19 surface markers including CXCR4. CXCR4 expression was quantified at single-cell resolution and dichotomized by cohort median. Clinical outcomes were correlated with treatment and scMRD metrics.
Results: Although relapse-free survival (RFS) was not different between treatment arms in the ITT population (median RFS: 10.3 vs. 11.5 months, p=0.98), scMRD profiling uncovered a CXCR4 dependent treatment effect. In the placebo arm, high CXCR4 expression correlated with increased relapse risk (p=0.02). In contrast, in the Motixafortide arm, high CXCR4 expression was associated with reduced relapse (p=0.047). A multivariable Cox model confirmed a significant treatment by CXCR4 interaction (HRinteraction 0.032, 95% CI 0.004 to 0.269, p=0.0015), supporting CXCR4 as a predictive biomarker for Motixafortide benefit. scMRD revealed persistent clonal diversity, but conventional MRD positivity did not associate with outcome.
Conclusion: While the BLAST trial showed no overall difference in RFS, single-cell MRD analysis revealed differential treatment effects according to CXCR4 expression. These findings suggest that CXCR4 may serve as a biomarker for response to Motixafortide and highlight the potential of single-cell profiling to inform patient stratification.

#2441 The myCAF and ECM landscape in KRAS-mutated cancer: Utilizing liquid biomarkers to track KRAS-induced fibrosis and KRAS inhibitor efficacy.

Martin Birkmose Rasmussen[1], Rasmus Sund Pedersen[2], Nicholas Willumsen[2], Morten Karsdal[2]

[1]Oncology, Nordic Bioscience, Copenhagen, Denmark,[2]Nordic Bioscience, Copenhagen, Denmark

Background: KRAS-driven cancer represents ~25% of cancers, with high rates in pancreatic cancer (PDAC), colorectal cancer (CRC), and non-small cell lung cancer (NSCLC). Mutated KRAS and TGF-β signaling activate cancer-associated fibroblasts (CAFs), creating a fibrotic extracellular matrix (ECM). The fibrotic ECM promotes immunosuppression and tumor growth but is potentially reversible with KRAS inhibitors (KRASi). We have recently demonstrated that myofibroblast CAFs (myCAFs) in KRAS-mutated PDAC express high levels of collagens III, V, VIII, XI, and XII. In this study, we investigated the landscape of KRAS-induced myCAF activation and ECM change across KRAS-mutated cancers. We utilized these changes to identify biomarkers for KRASi efficacy.
Methods: Patients with KRAS-mutated PDAC (n=141), CRC (n=223), or NSCLC (n=74) were evaluated for collagen expression and gene-set variation analysis (GSVA) was used for hallmark KRAS and TGF-β signaling. Correlations of KRAS and TGF-β signaling, and collagen expressions across cancers, were evaluated using Spearman correlation. Single-cell RNA-seq data from KRASi treated KPPC mice was analyzed using Seurat. CAFs were subclustered and subtypes identified from marker genes (myCAF, inflammatory CAF, and antigen-presenting CAF). CAF subtype and collagen expression were compared between KRASi and vehicle with Fisher's exact test and Wilcoxon rank-sum test, respectively. Biomarkers for formation of collagens I (PRO-C1), III (PRO-C3), V (PRO-C5), VIII (PRO-C8), XI (PRO-C11), and XII (PRO-C12) were measured in serum from healthy controls and patients with PDAC, CRC, or NSCLC. Differences between cancer and control were evaluated by Wilcoxon rank-sum test.
Results: KRAS signaling was significantly correlated with TGF-β signaling and expression of COL3A1, COL5A2, and COL8A1 across patients with KRAS-mutated PDAC, CRC, and NSCLC ($R>0.4$, $p<0.05$). Significantly increased expression of Col3a1, Col5a2, Col8a1, Col11a1, and Col12a1 was observed from fibroblasts in KRASi treated PDAC compared to vehicle ($p<0.001$). Significantly fewer myCAFs in KRASi treated PDAC ($p<0.001$) suggested reduced myCAF-derived ECM with KRAS inhibition. Serum biomarkers for formation of myCAF collagens (PRO-C3, PRO-C5, PRO-C8, PRO-C11, and PRO-C12) were significantly upregulated in patients with PDAC, CRC, and NSCLC compared to healthy controls ($p<0.001$). Type I collagen formation was unaffected (PRO-C1, $p=0.37$), suggesting KRAS-specific collagen formation.
Conclusion: KRAS-mutated tumors have a myCAF-enriched microenvironment with a unique collagen expression profile that is altered by KRAS inhibition. Non-invasive myCAF-derived collagen biomarkers that are elevated in serum from patients with KRAS-driven cancers, can potentially quantify KRAS signaling and track KRASi efficacy to guide clinical decision-making.

#2442 Baseline single-cell mass distributions correlate with clinical response to acalabrutinib, venetoclax, and obinutuzumab in mantle cell lymphoma.

Mingzeng Zhang[1], Ye Zhang[2], Lydie Debaize[1], Grace Chen[1], Sona Baghiyan[1], Shogo Miura[1], Nezha Senhaji[1], Juniper Mai[1], Clare Phinney[1], Alexa Batingana[1], Jenalyn Weekes[1], Salah Abdulkarim[1], Haocheng Wang[1], Svitlana Tyekucheva[3], Jerome Ritz[1], Christine E. Ryan[1], Austin I. Kim[1], Scott R. Manalis[2], Mark A. Murakami[1]

[1]Department of Medical Oncology, Dana-Farber Cancer Institute, Boston, MA,[2]Koch Institute for Integrative Cancer Research, Massachusetts Institute of Technology, Boston, MA,[3]Department of Data Science, Dana-Farber Cancer Institute, Boston, MA

Background: Mantle cell lymphoma (MCL) exhibits heterogeneous responses to targeted therapy, which are incompletely explained by genomic and immunophenotypic markers. Building on our prior work linking single-cell mass to BCR signaling activity and Bruton's tyrosine kinase inhibitors (BTKi) sensitivity, we hypothesized that baseline biophysical mass distributions may integrate proliferative, metabolic, and signaling states and predict clinical responses to BTKi-based therapy.

Methods: Baseline tumor cells from treatment-naïve MCL patients in a phase 1/2 trial of Acalabrutinib, Venetoclax, and Obinutuzumab (NCT04855695) were enriched by fluorescence-activated cell sorting and analyzed via suspended microchannel resonators (SMR) without drug exposure to measure distributions of single-cell buoyant mass. Durable response (DR) was defined as achieving complete metabolic remission ≥12 months; non-durable response (NDR) as refractory disease or relapse within 12 months. Of the nine cases analyzed by SMR, seven also underwent parallel CyTOF profiling.

Results: Baseline median mass of MCL cells was higher in NDR (n = 3; mean of patient medians 13.1 pg) than in DR (n = 6; mean of patient medians 13.1 pg; $p = 0.02$). The fraction of cells >15 pg—a threshold previously linked to BTK inhibitor response—was elevated in NDR (p=0.02) and correlated with clinical Ki-67 index (available in 6/9, r^2=0.87). Eight of nine cases exhibited classic MCL morphology; the single blastoid case (NDR) had a median mass of 14.6 pg. In CyTOF-profiled samples, the >15 pg tumor cell fraction correlated with B-cell expression of Ki-67 ($r^2 = 0.99$), the glucose transporter GLUT1 ($r^2 = 0.55$), and the immune checkpoint ligand PD-L1 ($r^2 = 0.99$), but not with the amino acid transporter CD98 or fatty acid transporter CD36. These associations are consistent with sequelae of heightened BCR. Across the cohort, an increased proportion of tumor cells >15 pg correlated with increased PD-1 expression on $CD4^+$ T cells ($r^2 = 0.66$) and expansion of T follicular helper (Tfh) cells ($r^2 = 0.74$). Increased tumor cell mass distributions also positively correlated with Tfh activation markers, including ICOS, Ki-67, and checkpoint molecules TIGIT ($r^2 = 0.56$-0.69). Taken together, these features raise the possibility of chronic B-cell antigen stimulation driving both Tfh activation and immune-regulatory feedback.

Conclusions: Baseline MCL cell biophysical mass distributions correlate with tumor-intrinsic proliferation and metabolic activity as well as systemic Tfh activation and immune checkpoint expression. These results suggest that tumor biophysical properties ex vivo may capture in vivo BTKi sensitivity through tumor-intrinsic and immunologic mechanisms. Evaluation in larger cohorts and deeper mechanistic analyses are required to clarify its potential as a predictive biomarker.

#2443 Urinary pesticide biomarkers and liver disease risk in Thailand: A machine-learning-based risk-prediction model.

Daxeshkumar P. Patel[1], Christopher Loffredo[2], Majda Haznadar[3], Mohammed Khan[4], Amelia Parker[4], Benjarath Pupacdi[5], Siritida Rabibhadana[6], Panida Navasumrit[7], Nirush Lertprasertsuke[8], Anon Chotirosniramit[9], Chawalit Pairojkul,[10], Vor Luvira,[11], Ake Pugkhem[12], Wattana Sukeepaisarnjaroen[12], Teerapat Ungtrakul[13], Thaniya Sricharunrat[14], Kannika Phornphutkul[15], Frank J. Gonzalez[16], Anuradha Budhu[17], Chulabhorn Mahidol[6], Xin Wei Wang[18], Mathuros Ruchirawat[7], Curtis C. Harris[18], TIGER-LC Consortium

[1]LHC, CCR, NIH-NCI, Bethesda, MD,[2]Georgetown University, Washington, DC,[3]FDA, Silver Spring, MD,[4]Laboratory of Human Carcinogenesis, Center for Cancer Research, National Cancer Institute, Bethesda, Maryland, USA, Bethesda, MD,[5]Translational Research Unit, Chulabhorn Research Institute, Bangkok, Thailand,[6]Laboratory of Chemical Carcinogenesis, Chulabhorn Research Institute, Bangkok, Thailand,[7]Laboratory of Environmental Toxicology, Chulabhorn Research Institute, Bangkok, Thailand,[8]Department of Pathology, Faculty of Medicine, Chiang Mai University, Chiang Mai, Thailand,[9]Department of Surgery, Faculty of Medicine, Chiang Mai University,, Chiang Mai, Thailand,[10]Faculty of Medicine,, Khon Kaen University, Khon Kaen, Khon Kaen,, Thailand,[11]Khon Kaen University, Khon Kaen, Thailand;, Khon Kaen, Thailand,[12]Faculty of Medicine,, Khon Kaen University, Khon Kaen, Thailand;, Khon Kaen, Thailand,[13]Princess Srisavangavadhana Faculty of Medicine,, Chulabhorn Royal Academy, Bangkok, Thailand;, Bangkok, Thailand,[14]Princess Srisavangavadhana Faculty of Medicine, Chulabhorn Royal Academy, Bangkok, Thailand,[15]Rajavej Hospital, Chiang Mai, Thailand,[16]Cancer Innovation Laboratory, Center for Cancer Research, National Cancer Institute, National Institutes of Health, Bethesda, MD,[17]Laboratory of Human Carcinogenesis, Center for Cancer Research, National Cancer Institute, Bethesda, MD,[18]National Cancer Institute, Bethesda, MD

Background Building on evidence linking urinary glyphosate to chronic liver disease (CLD) and hepatocellular carcinoma (HCC), we developed urinary pesticide profiling integrated with machine learning risk prediction (MLRP) to stratify risk in high-exposure populations.Methods We conducted a case-control study within the Thailand Initiative in Genomics and Expression Research for Liver Cancer (TIGER-LC; 2011-2016; n=593): 228 CLD, 116 HCC, and 249 controls. Eight urinary pesticides were quantified by LC-MS/MS (pendimethalin, oxadiazon, metsulfuron-methyl, butachlor, 2,4-dichlorophenoxyacetic acid [2,4-D], cypermethrin, flocoumafen, bromadiolone). A composite Pesticide Load Score (PLS), with and without glyphosate, estimated burden. Two predictive models were developed: a logistic-regression Pesticide-Informed Liver Cancer Risk Score (PILCRS) and an Extreme Gradient Boosting (XGBoost) classifier that incorporated age, sex, alcohol use, occupation, and PLS. Internal validity used 1,000 bootstrap resamples with optimism-corrected calibration.Findings Predicted CLD probability increased from 30% in the lowest PLS quartile to over 70% in the highest, and HCC from 10% to 40% ($p<0•0001$). Relative estimates were consistent; the highest versus lowest quartile yielded odds ratios of 2•84 (95% CI 1•66-4•91) for CLD and 4•76 (2•30- 10•29) for HCC. Cypermethrin remained independently associated. After optimism correction, both models demonstrated strong discrimination and calibration.Interpretation This framework establishes a scalable, exposure-informed tool for liver disease prediction. Findings underscore pesticide burden as a modifiable risk factor and align with Sustainable Development Goal 3•9 and WHO-FAO priorities in low- and middle-income countries (LMICs). External validation is essential.

#2444 Multi-agent-augmented analysis of PD-1 checkpoint inhibitor response.

Ada Shaw[1], Christina Vivelo[2], Nicholas Dana[2], Chetan Sood[2], Michelle Garred[1], Aqib Hasnain[1], Shara Balakrishnan[1], Vivek Adarsh[1], Hinco Gierman[2], Erika von Euw[2]

[1]Mithrl, San Francisco, CA,[2]Elephas, Madison, WI

Purpose: While checkpoint inhibitors have revolutionized treatment for cancer patients, only 20% of patients respond to PD-1 blockade, underscoring a need to better understand the mechanisms of response. Here, we deploy a multi-agent system for biological discovery that autonomously integrated functional cytokine readouts with multi-omics data to: (i) map patient clustering patterns and biological drivers; (ii) identify cytokine biomarkers differentiating response; and (iii) generate pathway-level mechanism narratives.
Methods: The analytical workflow involved: (1) unsupervised stratification of patient cohorts by clinical response using integrated transcriptomic and cytokine features (data from patients enrolled in NCT05478538, NCT05520099, NCT0634962, and a biobank biopsy collection study), (2) pathway enrichment analysis coupled with autonomous generation of mechanistic hypotheses, and (3) systematic comparative analyses against the public pan-cancer PD-1 resistance dataset. To contextualize the findings, a comparative study was performed against public pan-cancer datasets of checkpoint inhibitor response [Ref: Nature Scientific Data, 2025; data in CELLXGENE collection].
Results: The analysis revealed distinct patient clusters with separable cytokine profiles and immune-pathways that associated with response categories. The comparative overlay highlighted shared resistance hallmarks with the public resource while surfacing cohort-specific cytokine features and pathway combinations not captured in prior meta-analyses.
Conclusions: This work demonstrates that an agentic AI system enables the integration of cytokine profiling and transcriptomic datasets, yielding insights into mechanisms of checkpoint inhibitor response. In combination with clinical data, the mechanistic insights garnered from this approach will enable the improved prediction of immunotherapy response, providing the potential to improve patient outcomes.

#2445 LAPNET-01: Translational results of a Phase 1b evaluating NP137, an inhibitor of the epithelial-to-mesenchymal transition in combination with mFOLFIRINOX for the first-line treatment of locally advanced pancreatic ductal adenocarcinoma.

Gael Roth[1], Pascal Artru[2], Olivier Bouche[3], Marc Manceau[4], Nicolas Williet[5], Julien Ghelfi[6], Anthony Turpin[7], Astrid Lievre[8], Jean Frederic Blanc[9], Camille Evrard[10], Jean Baptiste Bachet[11], Pauline Parent[12], Matthieu Roustit[4], Hector Hernandez-Vargas[13], Elise Georges[14], Sebastien Hazard[14], Benjamin Ducarouge[14], Agnes Bernet[15], Patrick Mehlen[15]

[1]Department of Hepato-Gastroenterology and Digestive Oncology, CHU Grenoble Alpes, Grenoble, Grenoble, France,[2]Department of Hepato-Gastroenterology, Hopital Jean-Mermoz, Lyon, France,[3]CHU Reims, Reims, France,[4]Inserm, HP2 - U1300, CHU Grenoble Alpes, Grenoble, France,[5]Department of Hepatogastroenterology and Gastrointestinal Oncology, CHU St Etienne, Grenoble, France,[6]Department of Radiology, CHU Grenoble Alpes, Grenoble, France,[7]Medical Oncology Department, Lille University Hospital, Lille, France,[8]Department of Gastroenterology, CHU Rennes, Rennes, France,[9]Department of Hepato-Gastroenterology and Digestive Oncology, CHU Bordeaux, Bordeaux, France,[10]Department of Medical Oncology, CHU Poitiers, Poitiers, France,[11]Department of Gastroenterology, APHP - Pitie Salpetriere, Paris, France,[12]Medical Oncology Department, CHU Lille, Lille, France,[13]Genomics Consulting, Lyon, France,[14]NETRIS Pharma, Lyon, France,[15]Apoptosis, Cancer and Development Laboratory, Centre de Recherche en Cancerologie de Lyon (CRCL), INSERM U1052-CNRS UMR5286, Lyon, France

Background: Pancreatic ductal adenocarcinoma (PDAC) is a highly lethal malignancy characterized by aggressive tumor dissemination and resistance to therapy; processes significantly driven by the epithelial-to-mesenchymal transition (EMT). Netrin-1 is a key regulator for EMT. NP137, an anti-netrin-1 antibody, has shown to inhibit EMT in preclinical models and in a phase 1 monotherapy trial.
Methods: LAPNET-01 is a single arm phase Ib clinical study to assess the combination of NP137 with mFOLFIRINOX in locally advanced, unresectable PDAC. Laser capture microdissection was performed on pre-therapeutic biopsies and surgical specimens to allow microbulk RNA sequencing.
Results: 43 patients were included in this trial and received mFOLFIRINOX plus NP137 once every two weeks for up to 12 cycles (6 months). NP137 was well tolerated. Median PFS was 10.9 months (95% CI, 10.0 - 15.6) and median OS was 16.4 months (95% CI, 12.8 - NR) with 21 patients still alive at time of the data cut-off. Surgery was made possible by the combination therapy in 23% of patients. Microbulk RNA sequencing was successfully performed on 22 pre-therapeutic and 6 surgery samples and revealed that the main pathway downregulated with the combination mFOLFIRINOX+NP137 is EMT, bringing a clinical validation of the main mechanism of action of NP137. Moreover, bioinformatic analyses supported an extended OS and PFS in tumors expressing high levels of the netrin-1 receptor neogenin (NEO1) at baseline. In the high-NEO1 subgroup, NP137 treatment demonstrated an improved outcomes compared to the low-NEO1 subgroup including longer median PFS (15.7 vs 10.2 months, $p<0.001$) and longer median OS (not reached vs 16.5, $p<0.024$). These observations are consistent with experimental data that demonstrated the implication of neogenin in pancreatic cancer EMT and its progression.
Conclusion: NP137 in combination with mFOLFIRINOX demonstrates a favorable safety profile, promising clinical activity, and a mechanistically distinct mode of action supported by translational analyses. These results warrant further investigation of netrin-1 blockade in randomized trials and provide a rationale for biomarker-driven development of NP137 in pancreatic cancer.

#2446 High PRMT5 expression is associated with decreased immune infiltrate and worse outcomes to immune checkpoint inhibitors in non-small cell lung cancer.

Natalie Vokes[1], Stamatina Fragkogianni[2], Pooja A. Shah[3], Santiago G. Trevino[1], Konstantinos Leventakos[4], Lei Deng[5], Matthew Lee[6], Tali Azenkot[7], KAYLA LAYNG[2], JACOB MERCER[2], Jyoti Patel[2], Jordi Rodon Ahnert[8]

[1]MD Anderson Cancer Center, Houston, TX,[2]Tempus, Chicago, IL,[3]UT MD Anderson Cancer Center, Houston, TX,[4]Mayo Clinic Cancer Center Minnesota, Rochester, MN,[5]Fred Hutchinson Cancer Center, Seattle, WA,[6]City of Hope, Duarte, CA,[7]University of California San Diego - UCSD, San Diego, CA,[8]UT MD Anderson Cancer Center, Conroe, TX

Background: Deletions in *MTAP* occur in 10-15% of cancers and are associated with poor prognosis. MTAP deletion (MTAPdel) leads to accumulation of MTA which causes partial inhibition of PRMT5, creating a synthetic lethality approach with PRMT5 inhibitors. Multiple investigational MTA-cooperative PRMT5 inhibitors have demonstrated early clinical efficacy in MTAPdel NSCLC and other cancers. MTAPdel, PRMT5 expression, and clinical outcomes to standard of care immune checkpoint inhibitors (ICI) and chemotherapy (chemo) have not been well characterized.

Methods: The Tempus Lens Platform (Tempus AI, Inc., Chicago, IL) was used to query the Tempus multimodal de-identified database and establish and subsequently analyze a cohort of patients (pts)with NSCLC and DNA (Tempus xT) and RNA (Tempus xR) testing, treated with front-line (1L) ICI with or without chemo (N=3,676). PRMT5 expression was normalized as transcripts per million (TPM) and reported as log2(TPM + 1). Pts were classified into high vs low groups based on median PRMT5 expression and into MTAPdel vs intact (MTAPwt) based on MTAP biallelic loss. Immune infiltration was estimated using Quantiseq. Real-world overall survival (rwOS) was defined as the time from 1L start to death or last known follow-up. Real-world progression-free survival (rwPFS) was defined as the time from 1L start to death, progression or last known follow-up. Hazard ratios (HR) were calculated using Cox proportional hazards models and adjusted for age, sex, histology, smoking status and PDL1 status.

Results: PRMT5 expression was moderately increased in pts with MTAPdel (6.65 v 6.70, p=0.012). Alterations in *MYC*, *SMARCA4* and *KEAP1* were enriched in PRMT5-high tumors in both MTAPdel and MTAPwt pts (p<0.03). Pts with PRMT5-high tumors had decreased infiltrate of multiple immune cells, including B cells, macrophages (M1 and M2), NK cells, CD4 and CD8 T cells (p<0.001). Pts with MTAPdel/PRMT5-high expression had shorter rwOS compared to MTAPwt/PRMT5-low when treated with ICI alone (HR 1.58, 95% CI 1.11-2.24, p=0.011) or with ICI + chemo (HR 1.65, 95% CI 1.34-2.03, p<0.001). These associations persisted on multivariate analysis. Pts with MTAPdel/PRMT5-high expression were also associated with worse rwPFS when treated with ICI + chemo (HR 1.5, 95% CI 1.22-1.86, p<0.001) on univariate and multivariate analysis, but did not associate with rwPFS in pts treated with ICI alone (HR=0.97, 95% CI 0.66-1.42, p=0.9).

Conclusion: PRMT5 expression defines an immune suppressed subpopulation of pts with NSCLC. Pts with elevated PRMT5 expression and MTAPdel have poor outcomes with ICI+/- chemo, indicating PRMT5 RNA expression levels can be used to inform clinical trial designs, particularly those that are testing novel combinatorial strategies.

#2447 Epigenomic liquid biopsy-based biomarkers of platinum and PARP inhibitor response in patients with germ line BRCA-associated PDAC: A pilot study.

Maria Raitses-Gurevich[1], Gulfem Guler[2], Yuhong Ning[2], Ceyda Coruh[3], Micah Collins[3], Shimul Chowdhury[3], Samuel Levy[3], Talia Golan[4]

[1]Cancer Center, Sheba Medical Center, Tel Hashomer, Israel,[2]ClearNote Health, San Mateo, CA,[3]ClearNote Health, San Diego, CA,[4]Cancer Center, Sheba Medical Center, Ramat Gan, Israel

Background: Despite favorable overall response, pancreatic ductal adenocarcinoma (PDAC) patients with germline *BRCA* mutations show varied response to platinum-based chemotherapy and PARP inhibitor treatment. While some patients demonstrate long term response, others develop acquired resistance after an initial durable response and a third group are refractory to first-line platinum-based therapy. 5-hydroxymethylation (5hmC) analysis of plasma-derived cell-free DNA (cfDNA) of PDAC patients present a non-invasive approach to investigate treatment response biomarkers. Here, we investigated 5hmC profiles of plasma-derived cfDNA obtained from PDAC patients prior to treatment and while on treatment. Additionally, samples were evaluated for response by CA19-9 measurements and the Avantect Pancreatic Cancer Test (Avantect, a non-invasive, blood-based assay designed to detect PDAC using epigenomics and genomics biomarkers.

Methods: A total of 80 blood samples were collected in EDTA tubes from 32 PDAC patients pre-treatment or while on-treatment, with 2-5 timepoints for each patient. Blood samples were processed to obtain plasma. Cell-free DNA extracted from plasma were analyzed using Avantect. Germline *BRCA1/2* mutations were confirmed for all study subjects.

Results: Of the 32 patients included in the study, 6 were refractory, 14 developed acquired resistance and 12 were long term responders to platinum/PARP-inhibitor treatment. Differential 5hmC analysis at the earliest available timepoint for each patient revealed refractory patients to have distinct cfDNA profiles relative to both acquired resistance and long-term responders. Analysis with Avantect showed that the refractory group exhibited the highest cancer scores when compared to the acquired resistance and long-term responder groups (p value 0.001). Stratification of stage IV patients according to Avantect test results revealed that cancer signal-detected patients have poor overall survival relative to cancer signal not-detected patients (9.3 months vs 25.9 months, Hazard ratio 4.17, p = 0.017). Furthermore, evaluation of on-treatment timepoints demonstrated that Avantect detected disease progression in 78.6% (11/14) of PDAC patients who developed acquired resistance.

Conclusions: cfDNA 5hmC analysis revealed clear differences between long-term responders and patients with resistance, highlighting potential blood-based biomarkers of treatment durability and mechanisms of resistance. Cancers with worse response to therapy were detected at a higher rate by the Avantect test. These findings suggest that larger studies using Avantect can be performed to identify patient subpopulations with limited treatment response and to monitor treatment response.

#2448 Somatic DDR mutations as potential predictive biomarkers of platinum benefit in metastatic pancreatic cancer.

Ethan L. Low, Aakash Shah, Eunji Jo, Aliya Lackan, Susan Hilsenbeck, Benjamin L. Musher

Dan L Duncan Comprehensive Cancer Center, Baylor College of Medicine, Houston, TX

Background: Next-generation sequencing (NGS) has faciliated widespread identification of genetic alterations in pancreatic ductal adenocarcinoma (PDAC). Germline DNA damage repair (DDR) mutations, including BRCA1/2, PALB2, and ATM, predict sensitivity to first-line platinum-based chemotherapy (CTX). However, the predictive role of somatic DDR mutations remains undefined.
Methods: We retrospectively identified patients with metastatic PDAC (mPDAC) harboring a somatic DDR mutation (sDDR) who were treated at the Dan L Duncan Comprehensive Cancer Center (Houston, TX) between January 2018 and June 2025. Patients with germline DDR mutations or MSI-high tumors and those who < 2 cycles of CTX were excluded. Best response (RECIST 1.1), progression-free survival (PFS), and overall survival (OS) were assessed. OS was defined as the interval between CTX initiation and death, hospice enrollment, or last follow-up. Outcomes for sDDR patients receiving first-line platinum vs non-platinum CTX within our cohort were compared using Fisher's exact test. Outcomes for sDDR patients receiving first-line platinum CTX were compared with unselected PRODIGE controls using a one-sample binomial test (ORR) and a one-sample χ^2 test under exponential survival assumptions (PFS, OS).
Results: Eighteen patients met inclusion criteria; 14 (77.8%) had *de novo* mPDAC and 4 (22.2%) had recurrences post-resection. sDDR mutations included ATM (11, 61.1%), BRCA2 (5, 27.8%), BRCA1 (1, 5.6%), and PALB2 (1, 5.6%). Twelve patients received first-line FOLFIRINOX (5-fluorouracil, irinotecan, and oxaliplatin): 4 (33.3%) had partial response, 4 (33.3%) had stable disease, and 4 (33.3%) had progressive disease, yielding an overall response rate (ORR) of 33.3% and disease control rate (DCR) of 66.6%. The remaining 6 patients received non-platinum CTX (n=6): 5 (83.3%) had stable disease and 1 (16.7%) had progressive disease, yielding an ORR of 0% and DCR of 83.3%. Median PFS was 13 months in the platinum group versus 16 months in the non-platinum group (p=0.5), and median OS was 27 vs 31 months (p=0.6). Compared to the unselected population who received FOLFIRINOX in PRODIGE, sDDR patients who received platinum CTX in our cohort demonstrated a comparable ORR (33.3% vs 31.6%, p=1.0), but longer PFS (13 vs 6.4 months, χ^2 =70.6, p < 0.001) and OS (27 vs 11.1 months, χ^2 =87.5, p < 0.001).
Conclusion: In this exploratory single-institution cohort, PFS and OS were longer in sDDR-mutated mPDAC patients treated with FOLFIRINOX compared to unselected patients treated with FOLFIRINOX in PRODIGE. Within our small sDDR cohort, outcomes were not statistically superior with platinum versus non-platinum CTX. These hypothesis-generating findings are limited by small sample size, retrospective design, and selection bias toward patients completing ≥2 CTX cycles. Larger studies are needed to clarify whether sDDR mutations predict mPDAC outcomes.

#2449 Comparison of liquid versus solid tissue genomic profiling for the prediction of chemo-immunotherapy benefit in advanced NSCLC.

Charu Aggarwal[1], Prashant Nair[2], Anagha Jenu[2], Poornachandra G[2], Ansu Kumar[2], Swati Khandelwal[2], Jyoti Chauhan[2], Susheel George[2], Neelsh Lunkad[2], Vijayashree PS[2], Nagendra Prasad[2], Shweta Kapoor[2], Drew Watson[2], **James Wingrove**[2], Tejas Patil[3]

[1]University of Pennsylvania, Philadelphia, CA,[2]Cellworks Group, Inc., South San Francisco, CA,[3]University of Colorado Anschutz Medical Campus, Aurora, CO

Background: Front-line genomic profiling in advanced NSCLC typically utilizes solid tissue, although assessment via liquid biopsy is becoming more frequent. In addition to detecting the presence of actionable mutations, genomic profiling can also be used to inform on the use of immune checkpoint inhibition (ICI), alone and in combination with chemotherapy (ICI+C). Using genomic profiling obtained from solid tissue (Foundation One CDx), we previously validated an algorithm capable of distinguishing advanced NSCLC patients with favorable ICI+C benefit from those with no benefit [1]. We have evaluated this algorithm in a cohort of advanced NSCLC patients receiving both liquid and solid tissue genomic profiling.

Design: The ΔTRI algorithm uses Cellworks' computational model of a patient's tumor genomics to predict biomarker changes related to disease progression and potential benefit from ICI+C therapy. The previously validated ΔTRI and clinical threshold (ΔTRI score of 16, which equates to a 15% increase in 24 month OS when receiving ICI+C) were evaluated in 20 non-squamous, advanced NSCLC patients with complete clinical and genomic information (Foundation One Solid and Liquid), derived from the nationwide (US-based) de-identified ConcertAI Genomics360 database. Differences in solid and liquid-derived ΔTRI scores were assessed for association with clinical factors as well as genomic markers.

Results: Mutational profiles were highly similar between both platforms (median Jaccard index = 0.84), with 20% (4/20) of the patients having a Jaccard index < 0.5. In the 16 patients with differences between solid and liquid aberrations, discordance was driven 81% of the time by novel mutations identified in the liquid samples. Despite these differences, the ΔTRI scores generated from liquid biopsy samples were significantly correlated with those generated from solid tissue (R^2 = 0.61, *p* value < 0.001), with a median difference in ΔTRI score of 2.39, equating to roughly 2% difference in ICI+C benefit. Using the pre-defined clinical threshold of 16, 15% (n=3) of the samples switched from high ICI+C benefit category obtained from solid tissue (≥ 16 increase in 24 median OS with ICI+C) to a low/no benefit category ΔTRI score obtained with liquid samples, with an median difference in ΔTRI score of 7.4. Clinical factors such as the number of days between tissue and blood collection and number of metastatic sites were not associated with panel differences.

Conclusions: Good similarity was observed in ΔTRI scores generated from liquid biopsy samples compared to scores generated from solid tissue, suggesting that with additional exploration liquid samples could be used for ΔTRI score generation. Discordant cases appeared to be driven by novel mutations identified via liquid biopsy.

1 Aggarawal et al, WCLC 2025

#2450 Peritumoral adipose tissue as a prognostic imaging biomarker for immunotherapy response in HNSCC.

Kyle Harris[1], Nazila Godfrey[2], Dalia El-Gamal[2], Shesh Rai[3], Jianmin Pan[3], Brady Williamson[1], Trisha Wise-Draper[2]

[1]University of Cincinnati College of Medicine, Cincinnati, OH,[2]Division of Hematology/Oncology, University of Cincinnati Cancer Center, Cincinnati, OH,[3]Department of Biostatistics, Health Informatics and Data Sciences, University of Cincinnati, Cincinnati, OH

Introduction: Obesity is a well-known risk factor for many cancers, including head and neck squamous cell carcinoma (HNSCC), yet greater systemic adiposity has been linked to improved responses to immune checkpoint inhibitors (ICIs). Increased adipose tissue modulates the tumor microenvironment via immune cell infiltration and PD-1 signaling. While prior work has focused on systemic obesity, the role of peritumoral adipose tissue remains unexplored. How peritumoral adiposity impacts ICI response may reveal mechanisms driving immunotherapy efficacy.

Methods: We retrospectively analyzed 36 HNSCC patients treated with neoadjuvant and adjuvant pembrolizumab concurrent with adjuvant radiation +/- chemotherapy. Tumors were segmented on pre-treatment CT scans using 3D Slicer, and a 1 cm peritumoral shell was generated in 24 patients with available imaging. Adipose volumes were quantified using patient specific Hounsfield unit thresholds: peritumoral adipose fraction (peritumoral adipose volume / peritumoral volume) and adipose:tumor ratio. Pathologic response was determined histologically. Group differences were tested using Wilcoxon rank-sum and Fisher's exact tests. Survival was censored at 2 years with Kaplan-Meier and log-rank testing. Adipose—volume correlations used Spearman's rho. In a subset of patients with paired tissue samples pre- and post-pembrolizumab, RNA-seq assessed differential pathway enrichment. Gene set enrichment analysis (GSEA) was performed using curated Reactome and KEGG pathways.

Results: Among 24 patients, median peritumoral adipose fraction was 0.017 (IQR 0.026), median adipose:tumor ratio was 0.096 (IQR 0.194), and the median tumor volume was 8.5 cm^3 (IQR 23.3). Pathologic responders had higher peritumoral adiposity compared to non-responders (median 0.0314 vs 0.0076; Wilcoxon rank-sum, $p = 0.026$). When dichotomized by the median, higher peritumoral adiposity was associated with pathologic response (Fisher's exact test, OR = 8.9, 95% CI 1.1-132.4, $p = 0.036$). Kaplan-Meier analysis showed a significantly improved survival in the high-adipose group (2-year OS 100% vs 58%; log-rank $p = 0.0098$). Transcriptomic analysis identified ~60 genes changed significantly pre- to post-pembrolizumab in responders (adjusted $p<0.1$). GSEA demonstrated that responders had significant activation of pathways involving TGF-β receptor signaling, regulation of gene expression by HIF1A, TRAF6-mediated cytokine induction, and innate and adaptive immune signaling.

Conclusion: Greater peritumoral adiposity was associated with improved pathologic response and 2-year survival in HNSCC patients treated with pembrolizumab. Transcriptomic analysis reveals activation of TGF-β, HIF1A, and immune signaling pathways in responders, suggesting peritumoral adipose tissue may shape a treatment-permissive microenvironment that enhances response to PD-1 blockade.

#2451 Dual-function platform for chemotherapy prediction and mutation detection in pancreatic cancer by *tCAM-seq*.

Arturo Orlacchio[1], Erik Ladewig[2], Adrienne K. Chandra[1], Anwesha Dhara[1], Sharon M. James[1], Steven D. Leach[3], Kenneth H. Yu[4], **Surajit Dhara**[1]

[1]Episteme Prognostics, Inc, Brooklyn, NY,[2]Memorial Sloan Kettering Cancer Center, New York, NY,[3]Dartmouth Cancer Center, Hanover, NH,[4]Gastrointestinal Oncology Service, Memorial Sloan Kettering Cancer Center, New York, NY

Predicting chemotherapy response by chromatin accessibility and detecting actionable mutations are two independent paradigms, but here we demonstrate their integration in an all-in-one platform. We addressed two fundamental questions, 1) whether clinically actionable mutations can be detected from a Tn5-accesible genome instead of a traditional whole genome or exome, and 2) whether the higher depth of sequencing would compromise the quantitative ability of chromatin accessibility. We designed the panel using Illumina's standard deep-sequencing platform, encompassing the canonical driver mutations of pancreatic ductal adenocarcinoma (PDAC), e.g., KRAS, TP53, BRCA1/2 etc. On the same panel, we included our previously discovered 1092-chromatin signature regions that distinguishes gemcitabine resistant and sensitive tumors. We named this method targeted chromatin accessibility and mutation sequencing (*tCAM-seq*). First, we applied this *tCAM-seq* approach on four PDAC cell lines (AsPC1, BxPC3, MiaPaCa2, and PANC1), which accurately identified canonical driver mutations. The 1092-chromatin signature exhibited distinct accessibility patterns between gemcitabine resistant (AsPC1, BxPC3) and gemcitabine sensitive (MiaPaCa2, PANC1) cell lines. Next, we performed a head-to-head comparison of *tCAM-seq* with *ATAC-seq* on an archival cohort of Tn5-accessible DNA libraries prepared from surgically resected PDAC patients (n=24) between 2015 - 2017 at MSKCC. We observed high concordance (median R^2=0.77, range 0.61-0.85) among the two methods in terms of chromatin accessibility estimation. Our *tCAM-seq* maintained the predictive accuracy, even with >100× sequencing read depth. Kaplan-Meier analysis (n=24) of overall survival demonstrated a significant segregation between chemotherapy responder and non-responder patients (p=0.0184, HR=0.2958, 95% CI=0.066-1.323; median follow-up 8.98 years) using the *tCAM-seq*-derived 1092-chromatin accessibility profiles. Owing to the higher sequencing depth, tCAM-seq identified canonical driver mutations with high confidence which were otherwise not possible with traditional bulk *ATAC-seq*. Our results suggest clinically actionable mutations in PDAC reside within "accessible" chromatin regions and therefore can be detected from the Tn5-accessible genome, while accurately quantifying the chromatin accessibility profiles on the same sample. This clinically translatable "dual-purpose" *tCAM-seq* panel surpasses *mutation-only* panels by enabling both mutation-matched targeted therapies and prediction of chemotherapy response from the same assay. This will enable oncologists to provide a more comprehensive and better-informed treatment decision.

#2452 Proteomic aging biomarkers predict survival in immunotherapy-treated tumors.

Michal Harel[1], Coren Lahav[1], Yehonatan Elon[1], M. Austin Argentieri[2], Surbhi Singhal[3], Adam P. Dicker[4]

[1]OncoHost, Binyamina, Israel,[2]Massachusetts General Hospital, Boston, MA,[3]UC Davis Comprehensive Cancer Center, Binyamina, CA,[4]Professor & Chair, Dept. of Radiation Oncology, Thomas Jefferson University Kimmel Cancer Center, Philadelphia, PA

Introduction:
Plasma proteomics provides a comprehensive view of the biological processes active in an individual. Studies in healthy populations have shown that the plasma proteome undergoes changes with aging, and that proteomics-based models can predict biological age. The difference between biological and chronological age, known as the “age gap,” reflects an individual’s risk of disease. Extending this approach, organ-specific aging models have demonstrated that accelerated aging of individual organs is associated with organ-related disorders. Here, we examined age-associated effects on the plasma proteome of cancer patients across multiple tumor types and applied organismal and eleven organ-specific proteomic aging models to identify links between aging, tumor characteristics, and clinical features.
Methods:
Baseline plasma samples were collected from patients with metastatic solid tumors (non-small cell lung cancer [NSCLC], n=818; small cell lung cancer [SCLC], n=99; renal cell carcinoma [RCC], n=297; melanoma, n=163) and healthy subjects (n=278). Deep plasma proteomic profiling was performed using an aptamer-based assay. Bioinformatic analyses identified age-associated proteomic signatures, and organismal and organ-specific predictors were applied to estimate biological ages for each patient and organ.
Results:
Proteins involved in multiple signaling pathways, including Wnt, PI3K-Akt, IGF, and Ephrin receptor signaling, were upregulated in older patients (≥65 years) compared with younger patients, along with immune-regulatory proteins, reflecting immune remodeling associated with aging. These trends were consistent across tumor types. The organismal biological age gap was significantly higher in all cancer cohorts versus healthy controls, largest in SCLC and smallest in melanoma, with the most substantial effect in younger patients. Organ-level analyses revealed distinct patterns: lung age gap was highest in NSCLC and SCLC, and kidney age gap was most significant in RCC. Elevated organ-specific gaps correlated with corresponding comorbidities (e.g., cardiac age gap with arrhythmia, ischemic heart disease, and vascular disease) but much less with organ-specific metastases. Focusing on the immune age gap, patients treated with immune checkpoint inhibitor-based therapy who exhibited a high immune age gap had significantly shorter overall survival compared with patients with a low immune age gap (median OS, 16.4 vs. 31.8 months; HR = 0.67, $p < 0.0001$). The effect varied by indication, being strongest in melanoma (HR = 0.27, $p = 0.0007$) and absent in SCLC (HR = 0.87, $p = 0.65$).
Conclusions:
Proteomic aging predictors capture systemic and organ-specific aging processes in cancer. Distinct age-gap patterns across tumor types, along with their association with survival and comorbidities, highlight the biological and clinical relevance of proteomic aging in oncology.

#2453 Valproic acid enhances immune reprogramming in locally advanced rectal cancer: Insights from the VshoRTR3 trial.

Maria Serena Roca[1], Elena Di Gennaro[1], Federica Iannelli[1], Alfonso De Stefano[2], Carmen Romano[2], Francesca Collina[3], Cristina Testa[1], Rossella De Cecio[3], Palmina Bagnara[1], Susan Costantini[1], Roberto De Gregorio[4], Sean Houghton[4], Shauna Lee Houlihan[4], Dario Righelli[5], Andrea Sboner[4], Alicia Alonso[6], Antonio Avallone[2], Alfredo Budillon[7]

[1]Experimental Pharmacology Unit Laboratory of Naples and Mercogliano (AV), National Cancer Institute of Naples IRCCS G. Pascale Foundation, Napoli, Italy,[2]Experimental Clinical Abdominal Oncology, National Cancer Institute of Naples IRCCS G. Pascale Foundation, Napoli, Italy,[3]Pathology Unit, National Cancer Institute of Naples IRCCS G. Pascale Foundation, Napoli, Italy,[4]Systems and Computational Biomedicine, Weill Cornell Medicine, New York, NY,[5]Department of Electrical Engineering and Information Technology, University of Naples Federico II, Naples, Italy,[6]Medicine, Weill Cornell Medicine, New York, NY,[7]Scientific Directorate, National Cancer Institute of Naples IRCCS G. Pascale Foundation, Napoli, Italy

Rectal cancer, a common subtype of colorectal cancer, is rising worldwide due to lifestyle factors and aging population. Patients with locally advanced rectal cancer (LARC) are commonly treated with neoadjuvant chemoradiotherapy and surgery; however, recurrence rates remain high, ranging from 25% to 40%, depending on disease stage. Among the hallmarks of cancer, metabolic dysregulation and immune suppression play a critical role in tumor recurrence. Valproic acid (VPA), a histone deacetylase inhibitor, has shown potential in modulating these processes. The V-shoRT-R3 clinical trial (NCT01898104) have investigated the combination of VPA with short-course radiotherapy (SCRT) and capecitabine in LARC patients, aiming to enhance therapeutic efficacy by targeting some cancer hallmarks._To assess the biological effects of VPA within the V-shoRT-R3 trial, a multi-omic approach was employed. Peripheral blood samples were collected at baseline and after 10 days of VPA treatment, and analyzed by cytokine profiling (48-plex Bio-Plex assay) and metabolomics (1H-NMR and LC-MS). Gene expression was profiled (770-plex Nanostring panel) on matched biopsy and surgical specimens. Validation studies are ongoing using spatial transcriptomics and immunohistochemistry in an expanded patient's cohort. Preliminary data from 48 patients suggest that adding VPA to SCRT and capecitabine improves clinical outcomes. Specifically, the VPA-based regimen was associated with a significant increase in relapse-free survival compared to standard treatment. At a median follow up of 70,14 months (IQR 63-77) 3 pts in SCRT arm relapsed, with a RFS rate of 83% (cv scrt), 71% SCRT 66% CSCRT 40% V SCRT respectively. Cytokine analysis revealed a significant downregulation of IL1β, LIF, CSF1, and CSF2, following VPA treatment, suggesting suppression of the myeloid compartment. Metabolomic analysis revealed altered amino acid and energy metabolism, with enrichment in immune-related pathways. Notably, VPA induces increased tryptophan and decreased kynurenine levels suggesting a reduction of indoleamine 2,3-dioxygenase (IDO) activity confirmed also by its reduced expression indicating a shift away from immunosuppressive metabolism. Moreover, gene expression analysis revealed activation of NK cell, IL10, and cytotoxicity signatures in VPA-treated patients, indicating marked immune modulation. VPA promotes immune activation and metabolic reprogramming, improving outcomes in LARC. Multi-omics analyses and ongoing validations will define VPA-driven mechanisms to inform for more personalized therapeutic strategies.

#2454 A Drug Response Predictor (DRP®) is associated with enhanced overall survival in the phase 2 trial in advanced, recurrent ovarian cancer patients treated twice daily with 2X-121/ Stenoparib (NCT03878849).

Steen Knudsen[1], Annette Nielsen[1], Thomas Jensen[1], Peter Gimsing[1], Anker Hansen[1], Mogens Winkel Madsen[1], Michele Gargano[1], Jose Iglesias[1], Fernanda Musa[2], Kathleen N. Moore[3], **Jeremy Graff**[1]

[1]Allarity Therapeutics Inc, Tarpon Springs, FL,[2]Swedish Cancer Institute, Seattle, WA,[3]OU Health Stephenson Cancer Center, Oklahoma City, OK

2X-121 (stenoparib) inhibits PARP1/2 (1nM ~IC50) and Tankyrase 1/2 (IC50 ~50nM) limiting DNA repair while inhibiting WNT/ß-catenin oncogenic signaling. A 2X-121- specific Drug Response Predictor (DRP®) comprised of 414 genes was developed and highlights the gene expression profiles correlated with 2X-121 sensitivity, many of which are involved in the WNT/ ß-catenin pathway. In a ph1 clinical study, 2X-121 treatment showed clinical response by RECISTv1.1, notably in ovarian cancer patients. Blinded, retrospective analysis revealed that the 2X-121 DRP® identified the patients most likely to benefit from 2X-121. A follow-on, open label phase 2 trial in 3L+ ovarian cancer patients (DRP score > 50) began in May 2023 with 2X-121 dosed BID for the first time. 15 heavily pre-treated patients were enrolled independent of *BRCA* or Homologous DNA Repair status. Prior treatment included PARP inhibitors, mirvetuxumab, bevacizumab and immunotherapy. 14 of these patients were platinum resistant, 1 was primary platinum refractory. Collectively, the data show durable clinical benefit in patients with varied genetic and treatment backgrounds. Two patients (one $BRCA^{mut}$, one $BRCA^{WT}$) remain on therapy > 26 mos. An additional patient (prior PARP inhibitor treatment) showed a complete, confirmed response and stayed on treatment > 10 mos. The patient with primary platinum refractory disease was on therapy > 10 mos and remains alive beyond 2 years. Kaplan-Meier analyses show that the median Overall Survival (OS) is now > 25 mos, having not been reached with >23 mos median time to follow-up. We assessed whether the DRP score from pre-treatment biopsies might be related to enhanced OS. Indeed, patients with higher DRP scores reliably showed the greatest OS. In a continuous cox proportional hazard analysis, a 50-point difference in DRP score was associated with a hazard ratio of 0.03 (95% CI, 0.0-1.4). Applying a fixed DRP cutoff of 80 yielded a hazard ratio of 0.13 (95% CI, 0.02-0.9). To address whether the DRP was prognostic vs predictive, we assessed RNA expression data from biopsies in the public TCGA dataset of 481 high grade serous ovarian cancer samples from patients treated with platinum/ taxane. The DRP scores ranged from 0 to 100 in this cohort. The 2X-121 DRP® did not correlate with better OS (continuous cox HR=0.76 (95% CI, 0.54-1.1)). Among the 90 samples from patients with platinum resistant disease, the hazard ratio was 0.96 (95% CI, 0.39-2.3). These results indicate that the 2X-121 DRP may be a predictive- rather than prognostic- biomarker, highlighting extended OS in patients treated twice daily with 2X-121. A new ph2 clinical trial protocol is currently enrolling platinum-resistant Ovarian Cancer patients to further explore and delineate the relationship between 2X-121 DRP® score and clinical benefit.

#2456 Profiling the expression of antibody-drug conjugates in fibrolamellar hepatocellular carcinoma.

Waqar Arif[1], Elsa Hallab[2], Franshisca Hayek[2], Howard Liu Li[2], Mari Nakazawa[2], Mark E. Furth[3], Andrew S. Liss[4], Patricia Cogswell[3], Ezra G. Baraban[1], Jacqueline Birkness-Gartman[1], Marina Baretti[2], Robert A. Anders[1], Mark Yarchoan[2]

[1]The Johns Hopkins University School of Medicine, Baltimore, MD,[2]Sidney Kimmel Comprehensive Cancer Center, Baltimore, MD,[3]Fibrolamellar Cancer Foundation, Greenwich, CT,[4]Massachusetts General Hospital, Boston, MA

Background: Fibrolamellar carcinoma (FLC) is a rare and aggressive primary liver cancer that primarily affects adolescents and young adults. It is biologically distinct from other forms of primary liver cancer, such as hepatocellular carcinoma (HCC) and cholangiocarcinoma (CCA). There are no standard or approved systemic therapies for advanced FLC, and most patients present with unresectable disease or experience recurrence after surgery. These factors underscore the need for new therapeutic approaches. Antibody-drug conjugates (ADCs) have shown efficacy in several solid tumors by delivering cytotoxic payloads to tumor-associated surface antigens with improved specificity, but their utility in FLC is not known. To evaluate the relevance of ADC-based therapies in FLC, we assessed the expression of five clinically actionable ADC targets (NECTIN4, TROP2, CLDN18.2, HER2, and B7-H3) in an expanded cohort of FLC specimens.

Methods: Archival FFPE samples were obtained from consented patients through the Johns Hopkins Liver Cancer Tissue Bank and the Fibrolamellar Cancer Foundation, including FLC tumors (n=58; 38 primary and 20 metastatic lesions). Immunohistochemistry (IHC) was performed for all five markers. Expression patterns of interest in FLC were compared with control cohorts of HCC (n=10) and CCA (n=10). Three pathologists, blinded to clinical data, independently scored staining using both a 0 to 3 plus ordinal IHC scale and a semi-quantitative H-score.

Results: Among the five ADC targets evaluated, only B7-H3 and HER2 showed detectable staining in FLC. NECTIN4, TROP2, and CLDN18.2 were uniformly negative, scored as 0+ in all tumors, and had H-scores of 0. B7-H3 demonstrated the strongest expression. 3+ staining was observed in 20 of 58 tumors (34.5%). Tumor-cell H-scores ranged from 10 to 240, with a mean of 132. B7-H3 was also expressed in the tumor microenvironment, with prominent staining in cancer-associated stroma and fibroblasts. Stromal H-scores ranged from 40 to 300, with a mean of 199, often exceeding tumor-cell expression. HER2 showed detectable 3+ staining in 12 of 58 tumors (21.7%), with H-scores ranging from 2 to 270 and a mean of 70. One patient in this cohort with 3+ HER2 expression received fam-trastuzumab deruxtecan-nxki, and experienced a durable partial response lasting approximately one year.

Conclusions: B7-H3 and HER2 are promising ADC targets in FLC. While a subset of patients may already be eligible for fam-trastuzumab deruxtecan-nxki under its tumor-agnostic indication, B7-H3 shows particularly strong and widespread expression across both tumor and stromal compartments. These findings support further preclinical and clinical evaluation of B7-H3- and HER2-directed ADCs as targeted treatment strategies for advanced FLC.

: Application of Bioinformatics to Cancer Biology 3
Poster Session

#2676 Subtyping cancer cachexia through automated body composition.

Sonia Boscenco[1], Venise Jan Castillon[1], Perry J. Pickhardt[2], John W. Garrett[2], Nathaniel C. Swinburne[3], Ed Reznik[1]

[1]Computational Oncology, Memorial Sloan Kettering Cancer Center, New York, NY,[2]Professor of Radiology, University of Wisconsin School of Medicine, Madison, WI,[3]Department of Radiology, Memorial Sloan Kettering Cancer Center, New York, NY

Understanding how patients lose body mass during cachexia is critical for improving diagnosis and developing meaningful clinical endpoints. Yet, which body compartments drive the wasting phenotype remains unknown. We hypothesized that distinct patterns of changes to body composition might stratify patients into clinically relevant subtypes of cachexia. To test this hypothesis, we computed changes in body composition across periods of weight loss in a cohort of over 6000 pan-cancer patients from MSKCC and identified that loss of subcutaneous fat, loss of skeletal muscle, and unexpectedly, gain of liver volume, were the principal alterations during cachexia. Although all patients underwent periods of weight loss, unsupervised clustering of all body composition changes identified two broad subtypes of wasted and non-wasted patients. Wasted patients had significantly inferior overall survival, increased C-reactive protein, decreased albumin, and lower rates of weight recovery. Bulk RNA-sequencing analysis from a subset of BLCA, RCC, and PDAC patients identified a unique transcriptional phenotype of wasted patients, with marked upregulation in inflammatory response, interferon gamma response, and IL6-JAK-STAT3 signalling pathways. A subset of wasted patients exhibited pronounced hepatomegaly accompanied by markers of steatosis such as decreased radiographic liver density and increased alkaline phosphatase. This wasted-hepatomegaly subgroup, characterized by pronounced systemic inflammation, showed the poorest overall survival, suggesting a potential liver-driven axis of cachexia severity. Together, our data leverages opportunistic screening of computed-tomography scans to classify weight loss episodes using a radiographic biomarker that identifies bona fide wasting cachexia in a human patient cohort.

#2677 Identifying and analyzing clinicopathological features of uterine endometrial endometrioid tumors discordant by p53 and copy number status.

Sreekar B. Challa[1], Jessica D. St. Laurent[2], Zehra Ordulu[3], Alexander J. Neil[3], Melissa S. Gildenberg[3], Matthew L. Meyerson[1], Yvonne Y. Li[1], Andrew D. Cherniack[4], Elizabeth H. Stover[1]

[1]Department of Medical Oncology, Dana-Farber Cancer Institute, Boston, MA,[2]Division of Gynecologic Oncology, Brigham and Women's Hospital, Boston, MA,[3]Department of Pathology, Brigham and Women's Hospital, Boston, MA,[4]Cancer Program, Broad Institute, Cambridge, MA

The Cancer Genome Atlas (TCGA) identified four molecular subtypes of endometrial carcinoma: POLE, high microsatellite instability (MSI-H), copy number-low and copy number-high. These classifications were eventually adopted into clinical practice in the form of ProMisE, a molecular classifier for endometrial cancers based on TCGA. While TCGA used hierarchical clustering to define copy-number high and low clusters, ProMisE utilizes *TP53* mutation as a marker of the copy-number (CN) high and low subgroups. We have observed discordances between TP53 mutation call and copy-number status. We developed a method to redefine CN-high based on the presence of a single chromosomal arm-level deletion in a tumor. Arm-level copy number calls were generated by running the algorithm ASCETS (Arm-level Somatic Copy-number Events in Targeted Sequencing) on copy number segmentation data to give arm-level copy number calls. We validated this approach using molecular subtypes from both TCGA and CPTAC (Clinical Proteomic Tumor Analysis Consortium) data after taking out MMR-D/MSI-H and POLE patients, yielding accuracies of 0.823 and 0.865, respectively. Next, we applied this approach to a cohort of 446 endometrioid endometrial tumors profiled using a next-generation targeted sequencing panel (OncoPanel). After removing MSI-H/POLE tumors, we found 167 tumors concordant with regards to CN and *TP53* mutation status (31 CN-high/*TP53* mutant; 136 CN-low/*TP53* wild-type), and 92 discordant tumors (84 CN-high/*TP53* wild-type; 8 CN-low/*TP53* mutant). Survival analysis stratified by *TP53* mutation and copy number status called by arm-level deletion yields significantly worse overall survival for patients with both *TP53* mutation and high copy number in both the CPTAC ($p = 0.027$) and OncoPanel ($p < 0.0001$) cohorts, but no significant difference in survival between *TP53* WT/CN-high and *TP53* WT/CN-low patients. Overall, we find that *TP53* WT tumors have similar prognosis regardless of copy number status and have also found that CN-high/ *TP53* mutant tumors may have significantly worse prognosis than CN-low/ *TP53* mutant tumors ($p = 0.036$). Additional data will be used to confirm this.

#2678 A multimodal model to forecast prostate cancer metastasis from primary tumor transcriptomics and histopathology morphology.

Itzel Valencia[1], Priyanka Vasanthakumari[1], Pier V. Nuzzo[2], Edoardo Francini[3], Francesco Ravera[4], Giuseppe N. Fanelli[2], Sara Bleve[5], Cristian Scatena[6], Luigi Marchionni[2], Mohamed Omar[7]

[1]Cedars-Sinai Medical Center, Los Angeles, CA,[2]Weill Cornell Medicine, New York, NY,[3]Department of Experimental and Clinical Medicine, University of Florence, Florence, Italy,[4]University of Genoa, Genova, Italy,[5]IRCCS Istituto Romagnolo per lo Studio dei Tumori (IRST), Meldona, Italy,[6]Department of Translational Medicine and New Technologies in Medicine and Surgery, University of Pisa, Pisa, Italy,[7]Cedars-Sinai Medical Center, West Hollywood, CA

Prostate cancer (PCa) is the most commonly diagnosed non-cutaneous malignancies in men in the United States, and metastatic dissemination remains the principal driver mortality. While advanced disease is typically managed with androgen deprivation therapy, most patients eventually progress to castration-resistant PCa, underscoring the need for early identification of tumors predisposed to metastasis. Clinicopathological metrics, including PSA, tumor stage, and Gleason grade, provide only coarse estimates of risk and fail to capture the molecular and spatial heterogeneity underlying disease progression. To address this limitation, we developed *Met-Score*, a transcriptomic signature derived from meta-analysis of primary tumor expression profiles from 1,239 PCa patients. Using a rigorous training (n=1000) and independent validation (n=239) design, we computed gene-level Hedges' effect sizes across cohorts, pooled them using a random-effects model, integrated evidence across datasets using Fisher's and log-sum methods, and applied false discover rate correction to identify genes most strongly associated with metastatic progression. In the validation cohort, *Met-Score* achieved an AUC of 0.72 for predicting metastasis, and maintained independent prognostic value for overall, metastasis-free, and progression-free survival across two independent datasets, even after adjustment for Gleason score, demonstrating its clinical relevance beyond standard pathology. To investigate whether *Met-Score* reflects morphological phenotypes encoded in routine histopathology, we quantified morphometric features from digitized H&E slides of prostate biopsies and prostatectomies. *Met-Score* showed significant associations with multiple architectural and cytological descriptors, suggesting that the signature captures transcriptional programs tightly coupled to microanatomical patterns observable on standard tissue sections. Building upon this link between molecular and morphological readouts, we trained a multimodal risk model that integrates *Met-Score* with an image-derived *Morph-Score*, and benchmarked its performance against unimodal predictors. Our preliminary analysis indicates that the multimodal framework substantially enhances risk discrimination and more accurately identifies patients likely to develop metastasis compared to transcriptomics or histopathology alone. This work highlights the potential of combining deep molecular features with interpretable morphometric signatures to improve prognostication in localized PCa, and establishes a broadly applicable strategy for multimodal biomarker development in solid tumors.

#2679 Integrated Bulk and Single-Cell Transcriptomics Reveal Hepatocyte-Like Reprogramming in Metastatic Small Intestinal Neuroendocrine Tumors.

Sunanda Biswas Mukherjee[1], **James P. Madigan**[2], Samira M. Sadowski[1]

[1]Surgical Oncology Program, National Cancer Institute, NIH, Bethesda, MD,[2]Postdoctoral Fellow, National Cancer Institute, Rockville, MD

Liver metastasis is the primary determinant of poor prognosis in small intestinal neuroendocrine tumors (siNETs), yet the molecular mechanisms enabling metastatic adaptation remain largely unknown. Here, we integrate bulk and single-cell transcriptomic analyses to dissect tumor-intrinsic programs underlying this process. Bulk RNA-seq analysis of 44 primary and 37 metastatic siNET patient samples revealed extensive transcriptional remodeling during liver metastasis. Differential expression and pathway enrichment analyses demonstrated upregulation of metabolic and various liver-related pathways, alongside downregulation of intestine-specific programs in metastatic tumors. These results suggest a tumor-intrinsic phenotypic shift toward hepatic functional states. Further, application of the ESTIMATE algorithm, which infers tumor purity from the relative abundance of stromal and immune transcriptional components, demonstrated consistently high purity in metastatic samples, indicating that the observed transcriptional programs reflect tumor-intrinsic alterations rather than contamination from normal liver tissue. To validate these observations at single-cell resolution, we analyzed five matched primary and liver metastatic siNET patient samples using *in-house* single-cell RNA-seq data. Integrative clustering revealed distinct neuroendocrine (NE) and hepatocyte-like tumor populations, reflecting the cellular heterogeneity within the metastatic niche. Pseudotime and trajectory analyses highlighted a continuous progression from primary tumor-enriched NE clusters toward metastasis-enriched hepatocyte-like clusters, suggesting a gradual reprogramming of tumor cells along a liver-adaptive axis. These hepatocyte-like states exhibited activation of biological processes like hepatic functions and xenobiotic metabolisms. Together, these indicate a selective transcriptional plasticity that enables metastatic tumor cells to acquire liver-specific functional traits, thereby facilitating their survival, metabolic integration, and persistence within the liver microenvironment. In conclusion, by integrating bulk and single-cell transcriptomic data, this study reveals that siNET liver metastasis arises through a tumor cell-state transition toward a hepatocyte-like identity, representing a novel paradigm of liver-specific adaptation in neuroendocrine tumor metastasis and highlights liver-adaptive transcriptional programs that may be therapeutically targeted to disrupt siNET metastatic persistence.

#2680 Dosage-dependent adaptations to Complex I mutations in cancer cell lines.

Neil Ruthen[1], Ziad El Bakouny[2], Amy Shepherd[3], Sonia Boscenco[1], Benan Nalbant[2], Caleb Lareau[2], Payam Gammage[4], Ed Reznik[2]

[1]Weill Cornell Grad. School of Medical Sci., New York, NY,[2]Memorial Sloan Kettering Cancer Center, New York, NY,[3]Cancer Research UK Scotland Institute, Glasgow, United Kingdom,[4]Payam Gammage (Individual), Glasgow, United Kingdom

Chemical or genetic perturbations of the electron transport chain can evoke profound changes in cellular state. However, whether heteroplasmic mtDNA mutations, which are positively selected in cancer cells and present only in a fraction of the total mtDNA pool, promote dosage-dependent transcriptional or epigenetic adaptations is unknown. To characterize how such mutations impact cancer cell phenotypes, we performed single-cell DOGMA-seq profiling of nine murine cancer cell lines representing five tissue types engineered with m.12426G>A Complex I mutations using TALE-ddBCEs. Each cell line exhibits a full range of heteroplasies, enabling the application of continuous models to describe the quantitative relationship between gene expression or accessibility and heteroplasmy. Using meta-analysis techniques, we identified genes that show consistent, statistically significant transcriptional adaptation with increasing heteroplasmy across cell lines. Two pathways were particularly enriched for lineage-agnostic transcriptional adaptations: glycolysis and iron-response transcriptional elements. Given that non-monotonic, threshold-triggered gene expression patterns have been reported in cells with large mtDNA deletions, we asked whether gene expressions varied non-linearly with respect to heteroplasmic Complex I mutations and whether threshold-triggered effects were conserved across cell lines. Leveraging segmented regression techniques, we identified hundreds of threshold-triggered genes, of which the overwhelming majority are transcribed more frequently when heteroplasmy levels exceed the inferred threshold. These results imply the existence of conserved adaptations to Complex I mutation heteroplasmy and describe bona fide mitochondrial threshold effects.

#2681 Past exposure to genotoxic cancer therapies is associated with elevated local mutagenesis at CTCF binding sites in metastatic tumors.

Kevin C. L. Cheng[1], Jigyansa Mishra[2], Juri Reimand[2]

[1]Univ. of Toronto Faculty of Medicine, Toronto, ON, Canada,[2]Ontario Institute for Cancer Research, Toronto, ON, Canada

Many cancer therapies are known to have mutagenic effects, but their extent and potential functional implications in surviving cancer cells are incompletely understood. In particular, it is unclear how regulatory elements that are vulnerable to mutations are affected by these therapies. CTCF is a master regulator of chromatin organization; it binds DNA at TAD boundaries and other key regulatory elements. Previous studies have observed that CTCF binding sites (CBS) are enriched in mutations in cancer, but the underlying mechanisms are incompletely understood. We asked whether prior treatments were associated with local mutagenesis at CBS in metastatic tumors.

Utilizing a cohort of 4,870 whole-genome-sequenced metastatic tumors from the Hartwig Medical Foundation, we systematically analyzed associations between mutational processes at CBS across 17 cancer types and 45 types of cancer therapies with our computational method RM2.

We found 21 associations involving 6 cancer types and 14 therapy types. Most notably, past exposure to radiotherapy or trifluridine was associated with increased CBS mutation rates in metastatic colorectal cancer. Both radiotherapy and trifluridine are associated with increased SNV burden without a strong trinucleotide preference, consistent with a generally weaker DNA repair in these sites. Therapy-associated mutation enrichment occurred primarily in subsets that display the canonical CTCF binding DNA motif, relatively late replication timing or association with lower gene expression, suggesting that specific chromatin environments enable treatment-associated mutagenesis in CBS. We further asked whether the presence of known driver mutations influences therapy-associated local mutagenesis at CBS. This revealed that mutations in DNA damage response and chromatin regulation pathway genes, including BRCA2 and FBXW7, further elevate CBS mutation rate in radiotherapy-exposed tumors. This suggests higher vulnerability to radiotherapy-associated mutations when DNA damage response pathways, especially homologous recombination, are compromised.

In conclusion, this study provides, to our knowledge, a first analysis of association between cancer therapies and mutational burden at CTCF binding sites. Our findings highlight a previously unknown side effect of genotoxic cancer therapies on key regulatory elements. This underscores the need for a deeper understanding of therapy-induced mutations in regulatory regions and their potential implications for cancer biology and treatment outcomes.

#2682 Multiomic dissection of HBV-, HCV-, and non-viral HCC reveals distinct proliferation, interferon, and metabolic signatures.

Amerti Guta[1], Daniel O'Brien[2], Aditya V. Bhagwate[3], Jean-Pierre A. Kocher[3], Lewis R. Roberts[4]

[1]Clinical and Translational Sciences, Mayo Clinic, Rochester, MN,[2]Mayo Clinic, Rochester, MN,[3]Mayo Clinic, Rochester, MN,[4]Department Gastroenterology and Hepatology, Mayo Clinic, Rochester, MN

Background: Hepatocellular carcinoma (HCC), the most prevalent primary liver cancer, develops through multiple pathways; however, the extent to which HBV, HCV, and non-viral etiologies shape tumor biology and influence treatment responses remain incompletely understood. The availability of viral detection methods from sequencing data and multiomics workflows give us a new opportunities to study how etiology influences the molecular landscape of HCC. Here, we analyze TCGA's LIHC samples categorized into HBV-, HCV-, and non-viral tumors to compare genomic, transcriptomic and methylation profile of these HCC tumors to identify biological pathways specific to each group.

Methods: Whole-exome, RNA-seq, and clinical data from TCGA-LIHC (n=325) were analyzed. Viral status was assigned using Exogene (≥5 HBV/HCV reads; mixed infections excluded; non-viral = 0 reads). Mutation and clinical comparisons were performed using cBioPortal. RNA-seq data were processed with edgeR for 3-way differential expression (median count ≥25; $|\log_2 FC|>2$; FDR<0.05). Pathway enrichment used ShinyGO. Findings were validated using the GSE62232 microarray cohort analyzed with limma.

Results: Demographic patterns reflected known risk profiles: HBV patients presented younger (mean 53.9 years) and were predominantly male (78.8%) and Asian (92.9%), while HCV and non-viral groups were older and primarily White. Non-viral HCC showed the highest proportion of females (42.7%) and nearly half lacked significant fibrosis, consistent with metabolic disease. In contrast, HCV had the highest cirrhosis burden (47.2%), and HBV tumors showed the greatest proportion of poorly differentiated histology (52.2%).The comparison of the expressed genes between the 3 tumor subtypes revealed distinct etiology-associated pathways. Metabolic and mitochondrial including fatty acid β-oxidation differential expressed in Non-viral HCC. Activation of antiviral and interferon signaling, including type I IFN response and OAS-mediated defense pathways are observed in HCV-HCC. Finally, Cell-cycle and proliferation pathways are differentially expressed in HBV-positive, a finding consistent with effects of viral integration. Clustering analysis separated HBV and non-viral tumors into distinct groups. These signatures were reproduced in a validation cohort.

Conclusion: Our analyses highlight that HBV-, HCV-, and non-viral HCC harbor distinct transcriptional and signaling pathways. These etiology-specific signatures provide a framework for developing more precise biomarkers and for tailoring therapeutic strategies to the molecular biology of each etiology.

Acknowledgement: We acknowledge the late Dr. Sean Cleary, MD, for his invaluable contributions to this project. *Disclosure: AI has been used to trim sentences in order to fit in the word limit.*

#2683 Multi-omic analysis of patient and preclinical data highlights challenges in targeting tumor heterogeneity in glioblastoma.

Ha Dang, Verah Nyarige, Gonzalo Lopez, Ann Forslund, Wei Zhang, Bo Hu, Junfei Zhao, Maria Ortiz-Estevez, Alexandre Alloy, Romain Georges, Elizabeth Tindall, Josh Baughman, Kai Wang, Jorge Benitez-Hernandez, Celia Fontanillo

Bristol Myers Squibb, San Diego, CA

Glioblastoma (GBM) is the most aggressive and lethal primary brain tumor in adults, characterized by extensive tumor heterogeneity and cellular plasticity. A wide range of tumor cell states have been reported that are tightly embedded within neural and glial developmental programs. State transition in response to microenvironmental factors and therapeutic pressures poses a major obstacle to effective treatment. Therefore, understanding GBM heterogeneity and the mechanisms driving it is essential for developing durable therapies. We applied integrative analytical strategies leveraging bulk and single-cell data across large patient cohorts to deeply characterize GBM tumor subtypes and cell states and identify targetable genes that both distinguish tumor cells from normal neuro-glial lineages and remain constitutively activated across tumor states. Our analysis identified ~400 multi-state genes with consistent activity in multiple tumor subtypes and cell states and differentiation from the normal lineages. Interestingly, canonical targets such as *EGFR* and *VEGFA*, while widely studied, lacked consistent activation across all tumor states. *EGFR* was less active in NPC-like state and *VEGFA* was restricted to hypoxia-associated mesenchymal programs. Similarly, *MDM2* showed activation across tumor states but was also broadly expressed in normal lineages, limiting its therapeutic specificity. These suggest these common targets may not address the full spectrum of tumor heterogeneity or differentiate from normal lineages, likely contributing to the challenges in recent clinical trials. Further analysis revealed the enrichment of cell cycle activities and DNA damage responses among multi-state genes suggesting they are the key differentiating factors between GBM tumor and matured normal brain cells. In addition, multi-omic profiling showed that DNA methylation was a major mechanism of gene silencing for multi-state genes and in some cases resulted in complete gene shutdown in normal cells. Finally, integration with DepMap CRISPR viability screen data revealed a subset of genes with strong dependencies in GBM cell lines and neurosphere models across subtypes, consistent with patient data. However, most of these genes also demonstrated dependency across pan lineages, highlighting potential challenges such as peripheral toxicity when targeting multi-state genes. In summary, our study identified cell cycle regulation remains a distinguishing feature of GBM and highlighted the complexity of differentiating and targeting tumor heterogeneity. Overcoming these challenges may require innovative therapeutic modalities capable of selectively targeting multiple tumor states.

#2684 Androgen receptor expression negatively correlates with immune infiltration and response to immune checkpoint inhibitors in ER-positive/HER2-negative breast cancer.

Jun Arima[1], Kohei Chida[2], Rongrong Wu[3], Takafumi Shima[1], Toru Kuramoto[1], Hiroki Hamamoto[1], Kohei Taniguchi[4], Nao Kawaguchi[1], Ryo Tanaka[1], Yoshiro Imai[1], Kosei Kimura[1], Mitsuhiko Iwamoto[1], Kenichi Hakamada[5], Takashi Ishikawa[6], Sang-Woong Lee[1], Kazuaki Takabe[2]

[1]Department of General and Gastroenterological Surgery, Osaka Medical and Pharmaceutical University Hospital, Takatsuki, Japan,[2]Roswell Park Comprehensive Cancer Center, Buffalo, NY,[3]Tokyo Medical University, Tokyo, Japan, Japan,[4]Center for Medical Research & Development, Division of Translational Research, Osaka Medical and Pharmaceutical University Hospital, Takatsuki, Japan,[5]Hirosaki University Graduate School of Medicine, Hirosaki, Japan,[6]Breast Surgery, Tokyo Medical University, Tokyo, Japan

Background: AR plays a pivotal role in a subset of triple-negative BC, particularly the luminal androgen receptor (LAR) subtype, which is known to be resistant to chemotherapy. Notably, enzalutamide, an AR inhibitor, improved the pathological complete response (pCR) rate in ER+/HER2- BC in a randomized clinical trial, although the underlying biological mechanisms remain unclear. Early-phase studies have implicated preliminary clinical benefit when enzalutamide was combined with ICIs in LAR-TNBC. Building on these clinical findings, our study investigated how AR expression affects the tumor microenvironment (TME) and modulates the efficacy of ICIs in ER+/HER2- BC.

Methods: A total of 4070 BC patients from five cohorts with transcriptome of bulk tumors (I-SPY2 [GSE173839], TCGA, METABRIC, SCAN-B [GSE96058], GSE271080[NCT02955395]) and two cohorts with Single-cell transcriptome (GSE246613, GSE167036) were analyzed. High expression of AR was defined as the top two-thirds of expression levels for each cohort. LAR-TNBC was defined as the top two-thirds of AR-expressing tumors within the TNBC/Basal subtype.

Results: ER+/HER2- BC exhibited substantially lower levels of genomic instability compared with LAR-TNBC in TCGA. This low genomic instability is consistent with the immunologically “cold” phenotype characteristic of ER+/HER2- disease.Among ER+/HER2-BC, AR expression was consistently and negatively associated with number of Tumor-Infiltrating Lymphocytes (TILs) consistently in the TCGA, METABRIC, and SCAN-B cohorts (all $p < 0.05$). Further, AR expression was associated with reduced infiltration of CD8+ T cells, dendritic cells (DCs), M1 macrophages in the METABRIC and SCAN-B cohorts (all $p < 0.05$). Moreover, high AR expression was associated with lower pCR rates after neoadjuvant ICI treatment in ER+/HER2- BC in the I-SPY2 trial ($p=0.002$). Single-cell transcriptomic analyses revealed that AR was expressed not only in epithelial cells but also in various stromal and immune cell populations, including fibroblasts, T cells, and myeloid cells. Notably, AR expression in epithelial and endothelial cells were inversely correlated with ICI response. Analyzing the NCT02955395 trial cohort, we found that enzalutamide treatment significantly increased the infiltration of CD8+ T cells, DCs, and M1 macrophages in ER+/HER2- BC, similar to that observed in AR-low tumors (all $p < 0.05$).

Conclusion: We found that AR expression was inversely associated with immune and myeloid cell infiltration as well as ICI response in ER+/HER2- BC. Given that AR suppression with enzalutamide induced a similar immune microenvironmental profile, combining ICIs with this treatment may provide clinical benefit in ER+/HER2- BC.

#2685 Analysis of long-read sequencing data with *vmwhere* reveals variation in microsatellite length and chromatin state in Ewing sarcoma.

Sara K. Peterson[1], A. McCauley Massie[2], Alex Rubinsteyn[3], Jeremy R. Wang[3], Ian J. Davis[4]

[1]Curriculum in Bioinformatics and Computational Biology, University of North Carolina at Chapel Hill, Chapel Hill, NC,[2]Department of Pediatrics, University of North Carolina at Chapel Hill, Chapel Hill, NC,[3]Department of Genetics, University of North Carolina at Chapel Hill, Chapel Hill, NC,[4]Departments of Pediatrics and Genetics, University of North Carolina at Chapel Hill, Chapel Hill, NC

Microsatellites (mSats), or short tandem repeats (STRs), are repeated 1-6 bp DNA motifs that are abundantly distributed across the human genome. Variation in STR length contributes to genetic diversity and structural variation, and expansions beyond a pathogenic threshold underlie nearly 60 genetic disorders. mSat repeats can also serve as non-canonical enhancers for transcriptional regulators, including through binding the EWS::FLI1 fusion oncoprotein of Ewing sarcoma. Genome-wide analysis of mSats has been limited by short-read sequencing constraints, including read length and mapping ambiguity. Long-read sequencing has improved analyses of these regions but requires specialized algorithms. We developed a computational pipeline for genome-wide reference-based detection, length genotyping, sequence decomposition, and visualization of tetrameric mSats using long-read nanopore whole-genome sequencing. We applied this approach to GGAA mSats in five Ewing sarcoma cell lines and 100 diverse normal population genomes. We find both EWS::FLI1 binding to GGAA mSats and chromatin accessibility correlated with repeat length. Comparative analysis revealed a subset of mSats (2 - 3%) that were selectively expanded or contracted in Ewing sarcoma relative to normal genomes. Although we hypothesized that this variation in mSat length would converge towards a similar repeat length, we found that expanded loci tend to fall between 11 and 13 whereas contracted loci are commonly between 4 and 6. Further, expanded mSats demonstrated the highest proportion of mSats with EWS::FLI1 occupancy and accessible chromatin, compared to same and contracted. Finally, we show mSats demonstrating cell line-specific gained or lost chromatin accessibility was associated with expansion and contraction, respectively, in those cells. These results reveal a selective expansion of chromatin accessible mSats in Ewing sarcoma and provide a generalizable framework for resolving the genetic and structural complexity of mSats in human disease using long-read sequencing.

#2686 Extraction of cellular networks and microenvironmental characteristics in liver cancer tissues using geospatial approaches for therapeutic and diagnostic potential.

Kanae Echizen[1], Yoshiki Nonaka[1], Tomonori Kamiya[1], Maho Tsuda[2], Yoshimi Yukawa-Muto[2], Hideki Fujii[2], Kenichi Kohashi[3], Ryo Takahashi[4], Takahiro Kodama[4], Naoko Ohtani[1]

[1]Graduate School of Medicine, Department of Pathophysiology, Osaka Metropolitan University, Osaka, Japan,[2]Graduate School of Medicine, Department of Hepatology, Osaka Metropolitan University, Osaka, Japan,[3]Graduate School of Medicine, Department of Pathology, Osaka Metropolitan University, Osaka, Japan,[4]Graduate School of Medicine, Department of Gastroenterology and Hepatology, Osaka University, Suita, Japan

Liver cancer arising in the context of metabolic dysfunction-associated steatotic liver disease (MASLD) has been increasing in prevalence in recent years. These tumors are characterized by remarkable heterogeneity in both malignant cells and the surrounding stromal and immune compartments, which contributes to therapeutic resistance and disease progression. Understanding the spatial organization and cellular interactions within the tumor microenvironment (TME) is therefore essential for developing more effective therapeutic strategies.

In this study, we performed single-cell RNA sequencing (scRNA-seq) and Visium spatial transcriptomics analyses using human liver cancer specimens derived from MASLD-associated cases to dissect intra-tumoral heterogeneity at both the molecular and spatial levels. We developed a spatial analytical framework that integrates pathway activity scores with geostatistical approaches and distance metrics derived from histopathological landmarks, calculated using a digital unroll method. This approach enabled the identification of region-specific cellular populations and spatial gradients of metabolic and immune activities within tumor tissues.

Furthermore, we employed a cell-cell communication analysis to delineate localized signaling networks and microenvironmental niches that sustain tumor progression. Distinct interaction patterns were observed among hepatocyte-like cancer cells, endothelial cells, and immune infiltrates, suggesting spatially restricted communication hubs. Notably, we identified specific secreted factors from defined cell types that may serve as potential non-invasive biomarkers reflecting intratumoral spatial states.

Collectively, our study provides an integrative geospatial framework to map the cellular architecture and communication networks in MASLD-associated liver cancer. This spatially resolved understanding of tumor ecosystems may contribute to precision stratification of patients and the development of novel therapeutic strategies.

#2687 First single slide spatially resolved multiomic integration of pancreatic cancer: High-plex proteomic and whole transcriptome analysis.

Mari-Claire McGuigan[1], Luke McNickle[1], Assya Legrini[1], Ghazal Latifi[1], Claire Kennedy-Dietrich[1], Hannah Morgan[2], Olivia McCabe[3], Fraser Duthie[3], Tengyu Zhang[1], Michail Doukas[4], Andrea Gonzelz Cisar[1], Yoana Doncheva[1], Josefina Martinez Vasquez[1], Yi Cui[5], Sanghamithra korukonda[5], Ashley Heck[5], Kim Young[5], Joanne Edwards[6], Joseph Beechem[5], Nigel Jamieson[1]

[1]Jamieson Spatial Laboratory, The University of Glasgow, Glasgow, United Kingdom,[2]Glasgow Tissue Research Facility, The University of Glasgow, Glasgow, United Kingdom,[3]Department of Pathology, The Queen Elizabeth University Hospital, Glasgow, United Kingdom,[4]Pathology and Clinical Bioinformatics, Erasmus MC, Rotterdam, Netherlands,[5]R&D, Bruker Spatial Biology, Seattle, WA,[6]Translational Cancer Pathology (Edwards Lab), The University of Glasgow, Glasgow, United Kingdom

The increasing prevalence of incidentally diagnosed pre-malignant pancreatic Intraductal Papillary Mucinous Neoplasms (IPMNs), the cost of surveillance and the low rate of progression to cancer, underscores the importance of identifying IPMNs likely to progress to cancer. Currently available imaging and endoscopic tools cannot assess the complexity of IPMNs in their evolution to cancer. Understanding the spatial and molecular heterogeneity of pancreatic pre-malignant lesions is a critical strategy to enhance biological understanding, improve early detection and inform therapeutic strategies.

Spatial transcriptomics offers the ability to robustly profile the spatial molecular landscape of IPMNs; however, cell type heterogeneity poses challenges. A same slide multiomic approach, combining high-plex proteomic and transcriptomic profiling, overcomes the limitations of transcriptionally defined cell type heterogeneity while preserving the exploration of cellular functionality through transcriptomic pathway and gene module analysis.

A 64 plex protein panel followed by a whole transcriptome RNA panel using CosMx SMI (Bruker) was applied to a Tissue Microarray (TMA) of 40 x 1.5mm cores from patients with pancreatic cancer originating in IPMNs from various histological subtypes. Experimental time was 9 days to first visualisation of the data.

From the RNA analysis 340,069 cells were identified with a mean of 1,545 transcripts and 1,157 unique genes per cell. In the protein 416,766 cells were identified, expression analysis demonstrated a mean fluorescence intensity of 16,287. After alignment of the decoded RNA transcripts to the co-ordinates of the protein data there were 412,680 cells across 335 fields of view, enabling multiomic integration within the same tissue regions.

The analysis pipeline incorporated three distinct approaches for cell typing: RNA: 33 clusters RNA & Protein: 28 clusters Protein : 44 clusters

Cell type annotation of the RNA was performed using a hybrid computational-manual approach. The top 20 most highly expressed genes and top 20 most differentially expressed genes per cluster were identified and provided to a large language model (Claude, Anthropic), generating cell types at three levels of granularity.

All annotations were reviewed to ensure consistency with established pancreatic cell type markers.

Proteins were clustered and cell-typed using differential expression analysis. Protein-based cell typing showed enhanced alignment with multiomic cell typing compared to RNA alone, demonstrating the value of multiomic data in validating RNA-based cell type annotations with protein data.

This multiomic approach provides unprecedented resolution of cellular heterogeneity in IPMNs highlighting the complexity the pre-malignant state and establishes a framework for identifying early markers of malignant progression.

#2688 A unified prostate cancer single-cell atlas reveals molecular subtypes and lineage plasticity across disease progression.

Hanbyul Cho, Yuping Zhang, Jiayi Zhou, Rahul Mannan, Saravana M. Dhanasekaran, Xuhong Cao, Arul M. Chinnaiyan

University of Michigan, Ann Arbor, MI

Introduction: Prostate cancer displays extraordinary cellular and molecular heterogeneity in both localized and metastatic disease settings, reflecting the underlying variation in the tumor programs and cellular states that drive this disease.
Methods: To examine this, we built a harmonized single-cell atlas by integrating 17 human prostate scRNA-seq studies (163 samples, 106 donors) representing various disease stages. We reprocessed the raw FASTQ data to reduce pipeline-driven batch effects. Metadata were standardized to a unified schema for donor identity, tissue site, disease state, and histologic grade. Cell type annotation was performed using a cluster-level pseudobulk correlation framework informed by Tabula Sapiens, Human Protein Atlas, and prostate-specific references.
Results: Our uniform workflow yielded ~756,000 high-quality singlets representing various cell types, including ~267,000 epithelial and ~149,000 luminal cells. Data Integration using BBKNN preserved biological structure while effectively merging studies, resolving stromal (SMC, fibroblast subtypes, endothelial, Schwann), immune (T/NK, B/plasma, myeloid), and epithelial (luminal, basal, hillock, club) compartments.
Within the luminal epithelium, we identified transcriptomic molecular subtypes consistent with canonical prostate cancer drivers. Expression-based scoring of ERG/TDRD1 and ETV1/ETV4 distinguished ERG+, ETV+, and ETS- tumor programs, where ETS fusion-positive tumors form distinct transcriptional neighborhoods. Inferred copy-number burden from RNA-based pseudobulks showed increased CNV burden in high-grade primary and metastatic CRPC relative to benign/normal tissue. In metastatic disease, we further resolved three reproducible phenotypic states, which are AR-driven adenocarcinoma, neuroendocrine PCa (NEPC), and double-negative (AR-/NE-) with occasional intra-tumoral coexistence, reflecting lineage plasticity relevant to treatment resistance. Transcriptional signature and module analysis revealed several additional facets of the different prostate cancer subtypes. This atlas establishes a unified framework for interrogating epithelial lineage states, molecular drivers, and tumor microenvironment programs across the clinical spectrum of prostate cancer.

#2689 Single-cell multiome sequencing reveals distinct transcriptional programs associated with ecDNA amplifications in medulloblastoma.

Hui Hui[1], Yan Yuen Lo[2], Jessica Wang[2], Rishaan Kenkre[3], Jon D. Larson[2], Sunita Sridhar[4], Owen Chapman[5], Lukas Chavez[6]

[1]Sanford Burnham Prebys Med. Discovery Inst., La Jolla, CA,[2]Sanford Burnham Prebys Medical Discovery Institute, San Diego, CA,[3]Sanford Childrens Health Research Center, San Diego, CA,[4]Rady Children's Hospital, San Diego, CA,[5]Nagoya City University, Nagoya, Japan,[6]Sanford Burnham Prebys Medical Discovery Institute, La Jolla, CA

Extrachromosomal DNA (ecDNA) is a key driver of intratumoral heterogeneity and has been linked to therapeutic resistance and poor patient outcomes. However, technical limitations in identifying, isolating, and analyzing ecDNA at the single-cell level have hindered our understanding of its role in tumor development and treatment response. We have previously developed a single-cell multiome(RNA + ATAC) sequencing approach that enables the simultaneous analyses of ecDNA and its gene expression profiles. Initial application of this method in a medulloblastoma tumor of the sonic hedgehog subgroup revealed distinct transcriptional signatures in ecDNA-positive compared to ecDNA-negative and non-malignant cells. Building on these findings, we performed multiome single-cell sequencing in an additional cohort of medulloblastoma specimens harboring ecDNA amplifications. Initial analyses revealed distinct functional characteristics between ecDNA-positive and ecDNA-negative tumor cells. For example, ecDNA-positive tumor cells show up-regulation of DNA replication, recombination, and damage repair pathways, while ecDNA-negative cells demonstrated increased expression of synaptic activity, cell signaling, and morphogenesis pathways. Our ongoing analysis focuses on further defining the transcriptional programs that distinguish ecDNA-positive from ecDNA-negative tumor cells, ultimately informing future functional genetic and pharmacological studies targeting transcriptional dependencies in ecDNA-driven medulloblastoma tumors.

#2690 Leveraging linked-reads to predict extrachromosomal DNA in advanced prostate cancer.

Alexander Fortuna[1], Natalie Fredriksson[1], Mital Bhakta[1], Rahul Mannan[2], Fengyun Su[2], Rui Wang[2], Dan Robinson[2], Yi-Mi Wu[2], Xuhong Cao[2], Arul M. Chinnaiyan[2], Lisa Munding[1], J. Zachary Sanborn[1]

[1]Cantata Bio, LLC, Scotts Valley, CA,[2]University of Michigan, Ann Arbor, MI

Prostate cancer is a complex disease that affects millions of men each year. Recent research has revealed that the hormone-dependent nature of prostate cancer stems from the high expression and genetic amplification of the androgen receptor *(AR)* and may be driven by extrachromosomal DNA (ecDNA). Identifying ecDNA from other modes of amplification (e.g. HSR via breakage-fusion-bridge cycles) using whole-genome sequencing (WGS) data remains challenging due to the complexity of copy number and structural variation in cancer. This is compounded in FFPE where this sample type is often at risk of nucleic acid fragmentation, DNA crosslinks, and deamination further complicating variant discovery.

In this study we investigated if structural variants and linkage patterns derived from two Dovetail linked read chemistries, LinkPrep™ (a Tn5-based method compatible with cells and fresh-frozen tissue) and Dovetail®-FFPE (an MNase-HiC-based method compatible with FFPE), could predict the presence of ecDNA. We benchmarked our approach using four cancer cell lines with known ecDNA or HSR, then applied this technique to clinical metastatic castration-resistant prostate cancer (mCRPC) cases stored in FFPE. We generated libraries at ~30x coverage and utilized BWA for alignment, Hi-C breakfinder for structural variants, DeepSomatic for SNV and InDel detection, Purple for CNVs, and an in-house script for ecDNA detection. AmpliconArchitect was used on orthogonal shotgun WGS to predict ecDNA.

By analyzing the long-range linkage from amplicons to elsewhere in the genome, our method correctly identified the presence (or absence) of ecDNAs in all four cell lines and made ecDNA predictions across the samples with *AR* amplicons among the clinical mCRPC FFPE cohort. Two analytical methods were employed to predict ecDNA presence: a novel Z-score-based method that quantifies the observed difference from expected contact distribution across the amplicon (ecDNA 5.7-fold increase vs. HSR) and a log2-ratio test comparing intra- vs. inter-chromosomal amplicon-linked contacts (ecDNA 3-fold increase vs. HSR). Both methods were found to be robust down to 5x coverage. Finally, for samples with suspected integrated amplicon(s), the percentage of all amplicons integrated at each site is estimated through site-specific vs. total amplicon linkage.

In addition to ecDNA prediction, Dovetail libraries detect variants across the full range of oncogenic driver alterations, including SNVs/InDels, copy number, and structural variants. Comparing against a fresh frozen, WGS-derived truth set for the mCRPC cohort, and Dovetail®-FFPE libraries successfully recalled homozygous *PTEN* deletions, *TMPRSS2::ERG* fusions, and oncogenic mutations to *BRCA2*, *TP53,* and *KMT2C* genes. Our findings show that Dovetail libraries provide researchers with a powerful platform for comprehensive genetic variation discovery in both fresh-frozen and FFPE tissues.

#2691 Logic-gated Switch-DARPin-based immune cell engagers guided by data-driven tumor-antigen profiling: A computational workflow for the development of cancer immunotherapies.

Albulena Toska, **Ana Maria Florescu**, Eleni Tselempi, Alexander Link, Martin Steegmaier, Marcela Guzman Ayala

Molecular Partners AG, Schlieren-Zurich, Switzerland

Precise targeting of tumor-associated antigens (TAAs) and understanding of the tumor microenvironment (TME) are essential for the development of effective and safe immunotherapies. However, the lack of highly specific, clean TAAs remains a challenge for targeted immunotherapy of solid tumors. Switch-DARPins are engineered molecules designed to conditionally activate immune cells based on co-expression of a specific combination of TAAs, enabling localized logic-gated tumor-cell killing while minimizing off-tumor toxicity.
To support the rational design of Switch-DARPins, we developed DARPin Compass, a computational workflow that integrates transcriptomic, proteomic, and structural data to identify optimal TAA pairs for dual-targeting strategies. The workflow evaluates TAA prevalence, tissue specificity, and DARPin compatibility, and identifies suitable models for preclinical validation. Additionally, it incorporates machine learning to identify candidate biomarkers for patient stratification and integrates TME profiling (including single-cell [sc] level) to assess antigen expression across TME cell compartments and evaluate therapeutic applicability. Moreover, the workflow identifies existing clinical data of the TAAs.
DARPin Compass enables us to identify clinically actionable TAA pairs and extend the Switch-DARPin concept by including co-stimulatory signals. The workflow thereby supports the development of next-generation multi-specific immune cell engagers for solid tumors with complex antigenic and microenvironmental landscapes. Our first logic-gated Switch-DARPin immune cell engager, a CD3 T cell engager (TCE) with CD2 co-stimulation, was designed to be selectively active against solid tumors which co-express mesothelin (MSLN) and EpCAM (AND-gate). We found that MSLN and EpCAM show low co-expression in healthy tissues, while both TAAs are expressed in >50 % of ovarian cancer (OC) cells from in-house curated scRNAseq patient samples.
Our DARPin Compass results captured the underlying patient heterogeneity and suggested that combinatorial targeting of both, EpCAM and MSLN, may lower the risk of on-target off-tumor toxicity compared to only targeting one of the TAAs. Our initial preclinical data validated this concept of logic-gated preferential tumor-targeting and supports further investigation.
In summary, our DARPin Compass allows to identify potential novel TAAs, profile their expression patterns and assess their safety regarding expression in healthy human cells. Used to develop our first Switch-DARPin TCE for conditional CD3/CD2 activation in OC by targeting MSLN and EpCAM, this workflow is widely applicable to discover and characterize novel TAA pairs for logic-gated immune cell engagers to treat different solid tumors lacking selective single TAAs.

#2692 EpiGuide: Tracking epigenetic plasticity in circulating tumor DNA to monitor tumor progression.

Edoardo Giuili[1], Renske Imschoot[1], Sam Kint[1], Maisa Renata Ferro dos Santos[1], Lotte Cornelli[1], Jef Haerinck[2], Joachim Taminau[2], Kathleen Schoofs[1], Ruben Van Paemel[3], Leander Meuris[4], Sofie Roelandt[1], Robin Van Belle[1], Sofie Van de Velde[1], Eva De Smet[1], Nicolas Debusschere[1], Celine Everaert[1], Geert Berx[5], Katleen De Preter[6]

[1]VIB-UGent Center for Medical Biotechnology, Gent, Belgium,[2]Center for Inflammation Research, VIB-UGent, Gent, Belgium,[3]Department of Biomolecular Medicine, Gent, Belgium,[4]Department of Biochemistry and Microbiology, University of Ghent, Gent, Belgium,[5]Center for Inflammation Research, VIB-UGent, Ghent, Belgium,[6]VIB-UGent Center for Medical Biotechnology, Ghent, Belgium

Cell state transitions such as epithelial-to-mesenchymal plasticity (EMP) play an important role in the progression of triple-negative breast cancer (TNBC) and are strongly associated with therapy resistance. These transitions are hypothesized to be largely regulated by DNA methylation (DNAm) changes, which are retained in tumor-derived plasma cell-free DNA (cfDNA). Therefore, detecting EMP-related DNAm signatures in cfDNA offers a minimally invasive strategy to monitor tumor dynamics in liquid biopsies. However, estimating the tumoral cfDNA EMP fractions is challenging because liquid biopsy samples contain a mixture of cfDNA originating from both cancer and healthy cells.

As a solution, DNAm deconvolution algorithms can be adopted to estimate tumoral cfDNA fractions in liquid biopsy samples. In the last decade a high number of DNAm deconvolution tools have been developed. However, despite the need to identify the most effective deconvolution tools for tumor fraction estimation, no benchmarking study has specifically focused on this task. Therefore, we developed DecoNFlow, an automated Nextflow pipeline including 12 DNAm deconvolution tools and 3 differential methylation analysis tools. This is the most comprehensive pipeline for DNAm deconvolution to date, which allowed us to perform a benchmarking of 12 deconvolution tools using 3.5K in silico mixtures spanning multiple tumor types, sequencing depths, marker-selection strategies and profiling technologies (paper in review). We show that CelFiE is the overall top-performing tool across multiple evaluation criteria.

In a subsequent proof-of-concept study, we assessed EMP monitoring in vivo using the MMTV-PyMT mouse model, which develops TNBC-like tumors which spontaneously undergo EMP. First, several cell lines have been derived from primary tumors of this model and characterized. These cell lines exhibited distinct EMP states (epithelial or mesenchymal) or stably co-existing EMP states. Following orthotopic injection of these cell lines into mice, we performed methylation profiling on both tumors and plasma cfDNA. Tumor EMP state fractions were estimated using CelFiE and a DNAm EMP atlas of MMTV-PyMT tumors as reference, consisting of both single-cell and bulk EMP DNAm markers. We demonstrated that EMP states can be differentially detected in cfDNA, and that mice injected with mixed cell lines show significantly higher tumoral cfDNA fractions than those injected with epithelial-only lines, suggesting that coexistence of multiple EMP states may promote higher tumor burden.

In summary, this study presents a robust analytical and computational pipeline that allows to monitor EMP in a minimally invasive way through cfDNA DNAm analysis. In future, clinical application of this approach is expected to be instrumental for timely identification of cancer patients at risk for therapy resistance through epigenetic plasticity.

#2693 Elucidating the role of specific cancer testis antigens in the progression and development of hepatocellular carcinoma.

Frida Mariana Delgadillo[1], Barbara Yang[1], Sabrina Stogoski[1], Shrikanth S. Gadad[2], Enrique I. Ramos[1]

[1]The University of Texas at El Paso, El Paso, TX,[2]The University of Texas Rio Grande Valley, McAllen, TX

Hepatocellular carcinoma (HCC) is a primary type of liver cancer and the third leading cause of cancer-related deaths. Non-resolving liver inflammation caused by a variety of etiological factors, such as viral hepatitis infections or alcohol abuse, initiates the transition from fibrosis to cirrhosis, and finally to cancer. Due to poor late-stage survival rates, novel biomarkers and therapeutic targets are desperately needed to improve HCC patient outcomes. Potential candidates include a group of Cancer Testes Antigens (CTAs), a large group of tumor-associated antigens expressed in multiple tumor types. The melanoma-associated antigen (MAGE) subfamily of CTAs is overexpressed in HCC tumors and may drive tumor progression and tumorigenesis. However, little is known about the expression patterns of these CTAs in the multiple precursor liver diseases that contribute to HCC development, such as chronic hepatitis or cirrhosis. Furthermore, the mechanisms regulating the expression of these members in liver tissue prior to and following metastatic development have not been fully elucidated. Initial Enzyme-Linked Immunosorbent Assay (ELISA) results have demonstrated an autoimmune response to these proteins as tumor-associated antigens in serum from patients with precursor liver conditions. Using computational approaches, we have evaluated the expression patterns of these CTAs in publicly available liver disease transcriptomic datasets. The analyzed samples were stratified by disease etiology to provide a comprehensive view of the spectrum of the transition from healthy to diseased liver. Wet-lab approaches, including Immunohistochemistry (IHC), were employed to validate these responses at the protein level. Our findings indicate that MAGE subfamily CTAs are potential biomarkers of HCC development, with the activation of individual members varying during the transition from diseased liver to cancer. By elucidating the molecular mechanisms and pathways by which HCC-specific CTAs function, we will be able to develop them as diagnostic markers and therapeutic targets.

#2694 Dissecting the mechanisms of drug resistance development post neoadjuvant osimertinib treatment in EGFR-mutant non-small lung cancer.

Su-Jin Choi[1], Jii Bum Lee[2], Hyuk Jee[3], Hyo Sup Shim[4], Byung Jo Park[5], Chang Young Lee[5], Min Hee Hong[2], Byoung Chul Cho[6], Sun Min Lim[2]

[1]Dept. of Research Support, Yonsei Biomedical Research Institute, Yonsei University College of Medicine, Seoul, Korea, Republic of,[2]Division of Medical Oncology, Department of Internal Medicine and Yonsei Cancer Center, Severance Ho, Yonsei University College of Medicine, Seoul, Korea, Republic of,[3]DAAN Biotherapeutics, Seoul, Korea, Republic of,[4]Department of Pathology, Yonsei University College of Medicine, Seoul, Korea, Republic of,[5]Department of Thoracic and Cardiovascular Surgery, Yonsei University College of Medicine, Seoul, Korea, Republic of,[6]Division of Medical Oncology, Department of Internal Medicine and Yonsei Cancer Center, Yonsei University College of Medicine, Seoul, Korea, Republic of

Introduction: Despite treatment with osimertinib in *EGFR*-mutant non-small cell lung cancer (NSCLC), drug-tolerant persisters (DTPs) survive through reversible adaptations. Early intervention may be an effective strategy to delay or prevent the emergence of acquired resistance to osimertinib. In this study, we characterized DTPs that survived neoadjuvant osimertinib treatment *via* single-cell RNA sequencing, and identified DTPs at an early transition stage before they acquire resistance.
Methods: Neoadjuvant osimertinib was administered daily for two 28-day cycles followed by surgical resection and adjuvant osimertinib for 3 years. We performed single-cell RNA sequencing on matched pre- and post- treatment samples from 17 patients with NSCLC harboring *EGFR* mutations (E19del, N=7; L858R, N=10). The analysis was performed based on the Python Scanpy package.
Results: Tumor epithelial cells were divided into 11 subclusters. Based on the increase in modules, signatures, and regulon activity, we subclustered and annotated them accordingly. High DTP features included the Multi Adaptive, EMT, Immune Evasion, ERS/UPR, Cycling, AT1, and Hyper Ciliated clusters. The AT2, Chromatin Accessible, Intermediate, and Detox Ciliated clusters exhibited weak DTP features. After neoadjuvant osimertinib, the proportion of Multi Adaptive, ERS/UPR, and EMT clusters were significantly increased. The Multi Adaptive cluster had the highest DTP signature whereas the Immune Evasion cluster expressed genes known for recruiting immunosuppressive cells. The ERS/UPR cluster showed increase in *XBP1* regulon activity as well as endoplasmic reticulum stress and unfolded protein response signature. The Cycling cluster was characterized by increased activity of *E2F* regulons with upregulated proliferation genes. The AT1 cluster had strong *Wnt* signaling and increased *TEAD4* regulon activity. The Hyper Ciliated cluster showed increased expression of ciliogenesis genes. Trajectory analysis revealed that EMT, Immune Evasion, Cycling, and AT1 clusters which commonly express alveolar markers, originated from AT2 and then diverge into three lineages at the Intermediate cluster. Association analysis of gene expression with pseudotime revealed that type I interferon and TGFβ pathways were significantly augmented in all lineages.
Conclusion: Our analysis shows the diversity and heterogeneity of the DTPs population and the evolutionary trajectories of DTPs after neoadjuvant osimertinib treatment in *EGFR*-mutant NSCLC. Targeting these DTPs features may potentially be applied for development of novel therapeutic strategies to overcome resistance to osimertinib.

#2695 HELP-TCR: A harmonized and explainable language processing framework for functional analysis of t-cell receptor repertoires.

Yulyana Kalesnik[1], Dawid Krawczyk[2], **Maciej Pietrzak**[3], Michal Seweryn[4]

[1]Centre for Digital Biology and Biomedical Sciences, Faculty of Biology and Environmental Protection, University of Lodz, Lodz, Poland,[2]University of Lodz Doctoral School of Exact and Natural Sciences, University of Lodz, Lodz, Poland,[3]Department of Biomedical Informatics, The Ohio State University, Columbus, OH,[4]Regional Digital Medicine Center, Copernicus Memorial Hospital and University of Lodz, Lodz, Poland

T cells are essential contributors to anti-tumor immunity, but identifying the specific T-cell receptor (TCR) features that differentiate tumor-reactive responses from background immune activity remain difficult to resolve. Tumors reshape TCR repertoires through neoantigen exposure, chronic stimulation, and immune escape, creating patterns that are biologically relevant not easily quantified with existing computational methods. Current approaches either rely on global repertoire summaries or on deep learning models with limited interpretability, which restricts their translational and clinical applications.To address this gap, we developed HELP-TCR, an explainable machine learning framework that applies concepts from natural language processing to the functional analysis of tumor-associated TCR repertoires. HELP-TCR represents TCR repertoires by the position-specific distributions of features (single amino acids and/or amino acid pairs), transforming sequences into tensor structures. To increase reproducibility, we adapt the principles of ensemble learning and proposed a series of preprocessing steps, among which a consensus grouping method is applied to merge the features with highly similar position-wise distributions opening the venue for explainable dimension reduction. A modified (to the dimensionality of the task) deep learning architecture enables accurate classification, while post-hoc analysis based on saliency map highlights the most informative features contributing to model predictions.Using a dataset of TCR sequences from non–small cell lung cancer, HELP-TCR demonstrated stable and high predictive performance (AUC ~0.96), outperforming DeepTCR (AUC 0.76) and TCR-BERT embeddings, which showed limited class separability. Post-hoc saliency analysis identified positional amino acid motifs and residue-pair interactions that contributed to tumor–normal discrimination, offering mechanistic insights potentially reflecting tumor reactivity, immune pressure, or clonal remodeling within the tumor microenvironment.HELP-TCR offers an interpretable and reproducible framework for analyzing tumor-associated TCR repertoires in settings where sequence-level information is relevant. Its representations align with emerging clinical applications of TCR profiling, such as assessing of response to immunotherapy, identification of neoantigen-reactive or tumor-enriched clonotypes and studying of immune dynamics within the tumor tissue. HELP-TCR provides a practical foundation for generating testable hypotheses and advancing translational efforts aimed at improving patient stratification and informing T-cell–based therapeutic strategies.

#2696 Unlocking novel gene-based biomarkers using an explainable deep learning framework for precision oncology.

Sydney Grant, Aritro Nath

City of Hope Comprehensive Cancer Ctr., Duarte, CA

Somatic genomic alterations are widely profiled in cancer and remain the primary indicator for personalized therapy, yet their clinical utility is limited to a small set of actionable targets benefiting only a fraction of patients. AI/ML offers a transformative path to precision oncology by leveraging large-scale genomic data, but poor interpretability, often reduced to single-gene insights, limits clinical adoption and overlooks cancer's biological complexity. We address this gap with a novel framework combining PhenoMap and PhenoSurv. PhenoMap converts gene-level alterations into a phenotypic feature map using over 9,000 pan-cancer genomes and transcriptomes, trained to emulate enrichment scores for 6,000+ pathways from MSigDB using a combined LASSO-Random Forest approach. This map serves as input to PhenoSurv, a variational autoencoder designed to predict disease-free survival. PhenoSurv employs an innovative architecture that distinctly embeds eleven phenotypes and optimizes reconstruction loss, Kullback-Leibler divergence, and Cox survival loss on the latent space. This yields survival-relevant latent features, enabling discovery of multi-phenotypic vulnerabilities and prognostic biomarkers, which we tested and validated in breast, lung, and brain cancer. PhenoMap pathways that exceeded baseline performance in internal and external validation included 3,382 for lung, 3,772 for brain, and 4,188 for breast cancer. Clustering by PhenoMap scores revealed patient subsets with shared dominant signaling pathways. Notably, PI3K and KRAS signaling-enriched clusters included patients lacking PIK3CA (54%) or KRAS (67%) mutations in breast and lung cancer, respectively, indicating PhenoMap identifies broader cohorts for targeted therapy beyond single-gene biomarkers. PhenoSurv outperformed existing AI/ML models for survival prediction across cancer types while providing multilevel explainability at phenotype, pathway, and gene levels. Using DeepSHAP, we identified key pathways driving predictions across cohorts. Over 50 pathway-level biomarkers showed significant survival differences between high- and low-signaling groups, including NOTCH1 signaling in breast cancer (TCGA: $p = 0.0098$; MSK: $p = 0.003$), the CLEC7A inflammasome pathway in lung (TCGA: $p = 0.0045$; MSK: $p = 0.041$), and inositol phosphate metabolism in brain cancer (both $p < 0.0001$). Survival declined progressively with the number of poor prognostic markers across cancer types. PhenoMap and PhenoSurv bridge a critical gap in precision oncology by delivering interpretable models based on clinical genomic data that reveal clinically actionable biomarkers. These mechanism-based insights enable biologically informed patient stratification, paving the way for more effective personalized treatment strategies.

#2697 Single-cell transcriptomic characterisation reveals pathway determinants of bipolar androgen therapy response in prostate cancer.

Rosalia Quezada Urban[1], Shivakumar Keerthikumar[2], Peter Lau[3], Georgia Cuffe[1], Linda Teng[1], Ashlee K. Clark[4], Gail P. Risbridger[5], Renea A. Taylor[4], Megan Crumbaker[6], ANTHONY JOSHUA[7], Mitchell G. Lawrence[5]

[1]Monash University, Clayton, Victoria, Australia,[2]Peter MacCallum Cancer Centre, Melbourne, Australia,[3]AGRF, Melbourne, Australia,[4]Monash University, Melbourne, Australia,[5]Monash University, Clayton, Australia,[6]Garvan Institute, Sydney, Australia,[7]St Vincents Health Australia, Melbourne, Australia

Purpose: Bipolar androgen therapy (BAT), which alternates between castrate and supraphysiological testosterone levels, represents a promising alternative to continuous androgen suppression in advanced prostate cancer. However, only a subset of patients' tumours respond. Using patient-derived models of metastatic castration-resistant prostate cancer, we aimed to identify molecular programs distinguishing BAT responders from non-responders using single-cell transcriptomics.
Experimental Procedures: We profiled over 60,000 cells from four patient-derived xenografts (PDXs) using the 10x Genomics single-cell RNA-seq platform. Mouse reads were removed with Xenocell, leaving approximately 40,000 human prostate cancer cells for downstream analysis. Samples included two complete responders, one partial responder, and one non-responder, all evaluated 24 hours after BAT exposure, with responders also assessed at a long-term (6-week) timepoint. Differential expression and gene set enrichment (GSEA) analyses were performed using Hallmark, KEGG, and Gene Ontology collections.
Results: BAT triggered robust androgen-responsive transcriptional reprogramming across models, yet the scale and persistence of pathway activation differed by response category. GSEA revealed that responders exhibited suppression of MYC target genes and stress-response pathways, alongside upregulation of metabolic and differentiation programs, including oxidative phosphorylation, cholesterol homeostasis, and cell adhesion. In contrast, the non-responder maintained MYC activation with enrichment of inflammatory, epithelial-mesenchymal transition (EMT), and cell-cycle pathways, suggesting incomplete androgen pathway re-engagement. Over time, complete responders showed reduced proliferative signalling, consistent with stable treatment adaptation.
Conclusions: Our single-cell transcriptomic analyses delineate molecular signatures underlying BAT sensitivity and resistance. MYC activity and inflammatory remodelling emerge as potential drivers of resistance, whereas metabolic and differentiation programs define durable response. These insights provide a foundation for identifying biomarkers and designing rational combination strategies to enhance BAT efficacy.

#2698 MicroRNA expression can detect canine multicentric lymphoma in golden retrievers in serum samples taken pre-diagnosis.

Heather Treleaven[1], Latasha Ludwig[2], Alicia M. Viloria-Petit[3], R. Darren Wood[1], R. Ayesha Ali[4], Geoffrey Wood[1]

[1]Department of Pathobiology, Ontario Veterinary College, University of Guelph, Guelph, ON, Canada,[2]Department of Population Medicine and Diagnostic Sciences, College of Veterinary Medicine, Cornell University, Ithaca, NY,[3]Department of Biomedical Sciences, Ontario Veterinary College, University of Guelph, Guelph, ON, Canada,[4]Department of Mathematics and Statistics, University of Guelph, Guelph, ON, Canada

Canine lymphoma (cL) is one of the most common cancers in dogs, accounting for an estimated 24% of all canine malignancies. Multicentric cL (m-cL) represents 85% of all cL cases and shares many characteristics with human non-Hodgkin's lymphoma (hNHL). Due to these similarities as well as shorter overall lifespans, shared environments, and more homogenous genetics found in purebred dogs, m-cL is a valuable spontaneous animal model for hNHL. Prognosis for m-cL is quite variable, primarily depending on immunophenotype (T or B cell origin) and stage, and has median survival times ranging from 6-12 months after CHOP chemotherapy. Unfortunately, dogs aren't often diagnosed until they have late-stage disease, and relapse following chemotherapy is very common. A biomarker for early diagnosis could help identify patients when their disease is at an earlier stage, leading to better treatment responses and longer survival times. Potential biomarkers for early detection include microRNAs (miRNAs), which are small, non-coding pieces of RNA that control gene expression and are readily isolated from blood. These molecules are dysregulated in several types of cancer, and their sequences are nearly or entirely identical between dogs and humans. This makes them good non-invasive biomarkers with cross-species applications. Given the growing body of literature showing differential expression of miRNAs at the time of diagnosis, we sought to investigate whether any of these miRNAs could detect m-cL patients in samples taken prior to the onset of clinical symptoms and diagnosis. MiRNA expression was measured by real-time quantitative PCR in serum samples from 46 m-cL dogs and 40 control dogs enrolled in the Golden Retriever Lifetime Study. Each dog had a minimum of 3 samples, taken at roughly 1-year intervals for their whole lives. For the m-cL dogs, the samples were taken anywhere from 3 weeks to 5 years prior to diagnosis, with some having a 4^{th} sample taken at the time of diagnosis. We trained 5-fold cross-validated logistic regression models to classify samples as either m-cL or controls on 2 different training data splits. The first used only the samples from each m-cL dog taken between 3 weeks and 1-year pre-diagnosis, as we anticipated this range to be the most predictive of early disease. The second model included a random selection of 2 samples from each m-cL dog, resulting in a mixed-time population. We did this to examine the differences in miRNA selection and performance when the training populations were more or less homogenous, with respect to sampling time. As m-cL has a variety of subtypes, we also repeated our analyses using only the B-cell (n=15) or T-cell (n=26) immunophenotyped patients. We achieved accuracies between 65-88% across the training sets with similar miRNAs included in all models. With further testing, miRNAs offer potential for early diagnosis in both veterinary and human patients.

#2699 Accumulation of somatic mutation and clonal architecture of fallopian tube epithelium.

Seoyihl Kim[1], Wonjune Seo[2], Soyeon Kim[3], Taekeun Park[4], Miso Kim[4], Bhumsuk Keam[5], Tae Min Kim[5], Dong-Wan Kim[5], Se Ik Kim[6], Jeonghwan Youk[4]

[1]Cancer Research Institute, Integrated Major in Innovative Medical Science, Seoul National University College of Medicine, Seoul, Korea, Republic of,[2]Cancer Research Institute, Seoul National University College of Medicine, Seoul, Korea, Republic of,[3]Cancer Research Institute, Biomedical Research Institute, Seoul National University Hospital, Seoul National University College of Medicine, Seoul, Korea, Republic of,[4]Cancer Research Institute, Seoul National University Hospital, Seoul National University College of Medicine, Seoul, Korea, Republic of,[5]Cancer Research Institute, Integrated Major in Innovative Medical Science, Seoul National University Hospital, Seoul National University College of Medicine, Seoul, Korea, Republic of,[6]Department of Obstetrics and Gynecology, Seoul National University College of Medicine, Seoul, Korea, Republic of

Background: High-grade serous ovarian carcinoma (HGSOC) is the most common subtype of epithelial ovarian cancer, characterized by somatic *TP53* mutations (≈ 96 %) and by germline or somatic *BRCA1/2* mutations in 15~20 % of cases. Mounting evidence suggests that the fallopian tube fimbria, rather than the ovary, serves as the predominant cell-of-origin for the majority of HGSOC. Despite this evidence, a direct genomic comparison between ampullary and fimbrial epithelia has been lacking. Although somatic mutations accumulate gradually, it remains poorly defined due to challenges in reconstructing clonal lineages how these processes shape clonal architecture in normal fallopian tube epithelium.

Methods: Fallopian tube epithelial organoids were derived from surgically resected tissues and cultured in 3D matrigel. We established single cell-derived clonal organoids from anatomically distinct fallopian tube epithelial regions (ampulla and fimbria) obtained from *BRCA1/2* germline mutation carriers (*BRCA1* n=3; *BRCA2* n=1) and one *BRCA* wild-type individual. Low-input DNA libraries were sequenced on the Illumina NovaSeqX (~15×) to identify somatic single-base substitutions (SBS), small insertions and deletions (indels), and structural variants (SVs), followed by mutational signature extraction and phylogenetic reconstruction to reveal clonal expansion dynamics.

Results: Across the five patients analyzed, somatic mutation burden showed only a weak and statistically imprecise correlation with age, with point estimates indicating annual increases of 7.12 SBS (95% CI, -9.6 to 23.9) and 0.04 indels (95% CI, -2.65 to 2.73). Total SBS and indels burdens were comparable between ampullary and fimbrial organoids and largely unrelated to germline *BRCA1/2* status, parity, or menopausal age, although these null associations should be interpreted cautiously given the limited sample size. No SVs were detected in either region. *BRCA1/2* germline carriers did not exhibit HRD-associated signatures, suggesting absence of somatic-level haploinsufficiency in normal epithelium. Phylogenetic analyses identified region-specific clonal dynamics: fimbrial organoids frequently showed late clonal expansion events emerging during adolescence or later. Cancer-related variants (e.g., *TP53, MET, CSMD3*) were detected in both regions, though additional clonally expanded samples will be required to evaluate region-specific enrichment.

Conclusions: Somatic mutations accumulate with age in the fallopian tube epithelium, but *BRCA* haploinsufficiency alone does not confer homologous recombination deficiency. Region-specific late clonal expansion in the fimbria, potentially influenced by its constrained, finger-like architecture, may underlie the disproportionately higher incidence of HGSOC originating from this anatomical site. Ongoing sample expansion is underway to refine evolutionary models.

#2700 SpaceMarkers 2.0: A framework for spatially aware cell-cell communication in spatial transcriptomic data.

Orian Stapleton[1], Dmitrijs Lvovs[2], Luciane Tsukamoto Kagohara[1], Elana Judith Fertig[2], Atul Deshpande[1]

[1]Johns Hopkins University, Baltimore, MD,[2]University of Maryland School of Medicine, Baltimore, MD

Background: One key limitation of single cell RNA-sequencing (scRNA-seq) is the loss of spatial resolution due to the dissociation of cells from their tissue. Despite this limitation, current computational approaches infer cell-cell interactions from scRNA-seq and often generalize findings to the tissue context. SpaceMarkers was developed to infer cell-cell communication directly in-situ using 10x Visium. SpaceMarkers 2.0 is extended to leverage both Visium and VisiumHD datasets, as illustrated using samples from colorectal cancer (CRC) patient tumor and normal adjacent tissue.

Method: SpaceMarkers uses spatially varying features as proxies for cellular activity and applies kernel-based smoothing to represent the ‘influence’ from cell populations in their vicinity. We hypothesize that two cell states interact in regions where their cellular weights and influence overlap. A Gaussian mixture model is used to separate background from enriched values to quantify ‘hotspots’ within a given tissue. Previously, SpaceMarkers inferred molecular changes due to cell-cell communication for individual genes in the transcriptome. Here, we added the ability to incorporate prior knowledge of ligand-receptors (LR) in pairs of interacting cell populations by computing ligand overexpression within a cell population under the influence of a spatially overlapping population. We also estimate receptor scores from statistical tests to identify cell type-specificity for each receptor. SpaceMarkers calculates an aggregated LR score based on the geometric mean of the ligand and receptor score enriched in the tissue-defined interaction region. We extend this by computing per-sample and grouped condition hotspot overlaps as well as applying rank statistics to identify molecular programs between cancer and normal tissue.

Results: SpaceMarkers 2.0 identified spatial hotspots where normal samples were enriched for plasma to epithelial cell signaling programs while tumor samples were enriched for stromal and plasma cell interactions. At the plasma-stromal boundary we observed a tumor specific enrichment of fibroblast growth factor (FGF) ligand signaling from plasma cells to stromal cells, with FGF23 emerging as a dominant ligand engaging FGFR4 and FGFR3 on stromal cells.

Conclusion: In CRC Visium and Visium HD datasets, this framework delineates tumor specific interaction boundaries and resolves which cell states drive LR axes in-situ across patients. Beyond CRC, the SpaceMarkers framework can be applied to additional solid tumors, enabling comparisons in cohorts of samples in matched conditions or longitudinal sampling of carcinogenesis. Overall, SpaceMarkers 2.0 proposes a central framework for leveraging spatial information and multi-sample modeling for interpreting cellular communication in the tumor microenvironment.

#2701 A transcriptomic framework to predict response and prioritize indications for p53 restoration therapy.

Hosun Lee, Seunghwan Jung, Boram Kim, Seung-Hyun Shin, Yong Ho Heo, Yu-Yon Kim, Daejin Kim, Haemin Chon, In Young Choi

Hanmi R&D Center, Hanmi Pharm. Co. Ltd., Gyeonggi-do, Korea, Republic of

Introduction: TP53 has been recognized as a promising therapeutic target because of its pivotal role in tumor suppression and the high prevalence of its functional alterations in cancer. However, sensitivity to p53 restoration varies markedly across cancer cell lines and is not determined solely by the presence or absence of intact p53. These findings suggest that additional, pathway-level factors may modulate responsiveness to p53 reactivation. In this study, focusing on p53 restoration therapy, we aimed to (1) elucidate molecular mechanism underlying variable responses, (2) build a transcriptomic prediction model capable of estimating restoration sensitivity, and (3) apply this framework to prioritize clinical indications across tumor types.
Methods: In vitro results of p53 restoration were curated from 28 cell lines (20 sensitive [S], 8 resistant [R]). Transcriptomic differences between S and R were evaluated by Gene set enrichment analysis (GSEA) and gene set variation analysis (GSVA) using p53-related gene sets from MSigDB. RNA expression data were normalized by Non-paranormal (NPN) transformation, and singscore values were computed to quantify pathway activity. A logistic regression model was trained to estimate the probability of S or R classification, with the cutoff (specificity ≥0.9) stabilized through bootstrap resampling and fixed at the median. External datasets - CCLE, TCGA, cBioPortal, and GEO (GSE271757, GSE223463, GSE169321) - were analyzed to explore appropriate clinical indications.
Results: GSEA revealed a distinct downregulation of DNA elongation and Mismatch repair pathways in the S group, indicating reduced baseline DNA repair activity in S cells. Among gene sets tested, Signature A, achieved the strongest discriminatory power between S and R (PR AUC = 0.754). For indication prioritization, integrative analysis combining Signature A-based predictions from CCLE and TCGA, together with TP53 alteration prevalence from cBioPortal, identified lung, head and neck, ovarian cancers as Tier 1 indications. By investigating the biological nature of Signature A, we observed that DNA-damaging therapies may enhance p53 restoration sensitivity. Consistently, analysis of GEO cohorts with pre- and post-treatment RNA-seq data revealed an increased fraction of S from 52% to 96% in ovarian cancer, and 85% to 92% in pancreatic cancer following DNA-damaging therapy.
Conclusion: Signature A, a transcriptomic signature, stratifies p53 restoration responsiveness across cancer types and provides a robust, reproducible framework for indication prioritization and for understanding the mechanistic context of p53 restoration during the patient treatment journey.

#2702 Integrative Computational Pipeline for Tracking Neoantigen Retention Across PDX Passages in Genitourinary Cancers.

Md Imran Khan[1], Tyler Gross[1], Christian Migliarese[2], Ian Shea[3], Jonathan F. Lovell[4], Roberto Pili[3]

[1]Genetics, Genomics and Bioinformatics, University at Buffalo, State University of New York, Buffalo, NY,[2]Pathology and Anatomical Sciences, University at Buffalo, State University of New York, Buffalo, NY,[3]Medicine, University at Buffalo, State University of New York, Buffalo, NY,[4]Biomedical Engineering, University at Buffalo, State University of New York, Buffalo, NY

Cancer neoantigens are highly attractive targets for personalized immunotherapies because they are uniquely expressed on tumor cells and absent from normal tissues. However, validating predicted neoantigens—through immunogenicity testing, HLA characterization, and expression analysis—is often limited by the small amount of tumor tissue obtainable in clinical settings. Patient-derived xenograft (PDX) models therefore serve as valuable systems for expanding tumor material and studying tumor evolution, yet the extent to which PDX models retain patient-specific neoantigens across passages remains insufficiently characterized. In this pilot study, we analyzed neoantigen prediction and retention in five (n=8) genitourinary tumors and their matched PDX passages using paired whole-exome sequencing (WES) and RNA-seq data from the NCI Patient-Derived Models Repository (PDMR). We implemented a reproducible, semi-automated Nextflow workflow combining nf-core pipelines for tumor-normal variant calling (sarek), HLA class I typing (hlatyping), transcript quantification (rnaseq), and in silico HLA-peptide binding prediction (epitopeprediction). Variant clonality was assessed with PureCN, and downstream analyses prioritized expressed, nonsynonymous variants with predicted HLA-binding affinity. Primary tumors contained 14-156 candidate neoantigens per patient. Retention in derived PDX models was generally high: initial engraftment (P0) preserved 50-89% of primary tumor neoantigens, and later passages maintained 46-95%. Although some neoantigens were lost during engraftment or propagation, most remained stable over serial passages, indicating preservation of key features of the tumor-specific immunogenic landscape. By the time of presentation, this analysis will be expanded beyond the initial five cases to include a larger PDMR cohort of genitourinary cancers. We will also incorporate our own PDX and CDX datasets to evaluate neoantigen retention or divergence across passages in an independent system. Together, these results will provide a broader assessment of neoantigen stability in patient-derived models and support the identification of robust, persistent neoantigens for personalized vaccine development.

#2703 PTMax: An AI-enabled platform integrating literature mining and multi-omics for functional interpretation of phosphorylation in cancer.

Yanling Sun, Sara S. Savage, John M. Elizarraras, Eric Jaehnig, Bing Zhang

Lester and Sue Smith Breast Center, Baylor College of Medicine, Houston, TX

Phosphorylation is a central regulator of protein function and oncogenic signaling, and advances in mass spectrometry now enable unbiased, proteome-wide identification of cancer-associated phosphosites. However, the functional relevance of most sites remains poorly understood and scattered across the literature.To address this gap, we developed PTMax, an AI-enabled resource that integrates comprehensive literature mining with systematic multi-omics data to advance functional interpretation of phosphorylation in cancer.To standardize phosphosite information reported across published studies, we enhanced our literature-mining pipeline to efficiently extract site-level evidence and associated functional information from full-text articles and pathway figures. Evidence aggregated from these sources was used to generate functional summaries, which were evaluated through both automated and manual quality assessments. PTMax additionally incorporates dozens of mass spectrometry-based phosphoproteomics datasets and multi-omics data from CPTAC cancer cohorts, including RNA, protein, phosphosite abundance, and phenotype associations. For each phosphosite, we computed two evidence scores that quantify literature-derived information richness and data-driven support, respectively. We also constructed signature sets that group phosphosites by cancer hallmarks, co-mentioned genes or diseases, and pathway figure associations, and generated a co-regulated phosphorylation network to facilitate pathway- and network-level interpretation.PTMax currently contains more than 40,000 literature-derived phosphosites extracted from over 500,000 sentences and 1,400 pathway figures, capturing ~70% of low-throughput-validated and ~80% of regulatory-annotated phosphosites in PhosphoSitePlus. Notably, over 30,000 sites lack prior regulatory evidence, underscoring the value of AI-driven literature mining. Integration with multi-omics resources adds ~200,000 unique phosphosites, including 65,000 sites with quantitative associations and 26,000 linked to cancer phenotypes. The PTMax interface enables users to query individual genes or phosphosites and retrieve comprehensive, context-rich information together with user-friendly visualizations. In addition, pathway and network-based analysis modules help translate phosphosite lists into functional and signaling insights. In summary, PTMax unifies literature and figure mining with large-scale experimental datasets to deliver a comprehensive, multi-dimensional resource that advances the functional study of phosphorylation in cancer.

#2704 NCI's childhood cancer data initiative: Advancing pediatric cancer research.

Subhashini Jagu, Jaime Guidry Auvil, Mark Cunningham, Bahar Sayoldin, Patrick Dunn, Sean Burke, Catherine Bullen, Hayley Dingerdissen, Rebecca Steck, Martin Ferguson, Johanna Lucinda Goderre, Gregory Reaman, Warren A. Kibbe

National Cancer Institute, Rockville, MD

The Childhood Cancer Data Initiative (CCDI) is a transformative effort to accelerate research and improve outcomes for children, adolescents, and young adults (AYAs) with cancer. Data are the cornerstone of cancer research, and CCDI is building a FAIR-aligned data ecosystem that functions as a multi-stakeholder interoperability platform, integrating diverse tools and services to advance pediatric cancer research. All CCDI tools and resources are accessible through the CCDI Hub, the central entry point to the ecosystem. The foundation begins with the CCDI data model, which establishes harmonized data standards to ensure consistency and interoperability across data sets, offering a framework for discovery and analysis.

Building Cohorts: The CCDI Childhood Cancer Data Catalog serves as a comprehensive inventory of pediatric and AYA cancer data resources, including registries, repositories, knowledgebases, and catalogs. It provides study-level summaries and helps users identify where specific data types and studies are located. Once users identify studies of interest, they can move to the CCDI Hub Explore Dashboard to search CCDI data sets. The dashboard indexes data at the file level to facilitate cohort building. Users can build cohorts within the Childhood Cancer Data Commons (C3DC) using clinical data, or within the National Childhood Cancer Registry (NCCR) using real-world data. Cohorts built in C3DC can be exported as manifests containing participant identifiers, which can then be uploaded to the CCDI Hub to locate associated genomic, imaging, or other data. Similarly, users can export cohorts to NCCR to access related real-world data. For cross-institutional discovery, users can query pediatric data sets across participating repositories using the CCDI Federation API, as if querying a single virtual database.All of these resources are interconnected through the CCDI Participant Index, which maps participant identifiers across studies and repositories and allows researchers to connect data from the same participant, supporting data integration and cohort expansion.

Analysis and Visualization: After cohorts are built, researchers can leverage integrated analysis and visualization platforms to further explore, interpret, and derive insights from the data. The Cancer Genomics Cloud provides a cloud-based computational environment where researchers can analyze data using custom workflows and advanced analytical tools. To make data accessible to clinicians and non-bioinformaticians, CCDI offers intuitive visualization platforms like the CCDI cBioPortal Cancer Data Explorer. Together, CCDI's many tools and resources, integrating data from thousands of participants, enable new insights that would not be possible when studied in isolation.

: Integration of Clinical and Research Data
Poster Session

#2708 Revealing fibroblast-mediated impacts to therapy response through spatially resolved drug response prediction in lung cancer.

Robert F. Gruener[1], Weijie Zhang[2], Lilin Wang[2], Adam M. Lee[2], R. Stephanie Huang[3]

[1]University of Minnesota, College of Pharmacy, Minneapolis, MN,[2]University of Minnesota, Minneapolis, MN,[3]Asst. Professor, Dept. of Medicine, University of Minnesota, Minneapolis, MN

The tumor microenvironment (TME) can profoundly impact both the biology and drug sensitivity of surrounding cancer cells. There is currently no way to comprehensively evaluate the impact these interactions have on drug response across multitudes of drugs and patients. In this work, we developed a computational drug prediction approach to interrogate the effects of the TME on cancer drug response, identified fibroblast-mediated drug response associations in non-small cell lung cancer (NSCLC) patients, and validated these associations in co-culture models.

Our approach leveraged information rich single-cell *in situ* RNA sequencing data combined with our previously established single-cell drug response prediction models (scIDUC). We obtained two independent NSCLC datasets - one sequenced using NanoString CosMx (n=8 slides) and the other sequenced using 10X Xenium (n=4 slides). Given cancer-associated fibroblasts (CAFs) make up the majority of the TME and are known to impact drug response for select agents, our primary focus was to examine the influence of local fibroblast density on the drug response of cancer cells. To this end, we identified CAF-drug associations for each patient individually, aggregated the results across patients and nominated consistent findings for validation.

We used spatial windows of 100-nearest-neighbor and quantified the surrounding fibroblast density of every tumor cell. We applied scIDUC, which integrates the single-cell expression profiles with DepMap bulk expression and drug screening data to project drug response. Within each slide, we performed 100 bootstrap iterations of balanced random sampling of CAF-high and CAF-low tumor cells, predicted drug sensitivity for every tumor cell (independently for each of the 493 drugs response models), and then correlated predicted response with continuous fibroblast density. The results were then aggregated across the 100 bootstrap sampling. We observed drug-specific patterns where cancer cells were predicted to be made more sensitive, more resistant, or unchanged with increased fibroblast density. Among the most consistent results across patients were CAF-induced resistance to the HER2 inhibitor lapatinib and 5-fluorouracil as well as CAF-induced sensitization to the BRAF inhibitor dabrafenib. Experimental coculture assays using NSCLC lines (Calu-3, A549) and IMR-90 fibroblasts confirmed the predicted CAF-mediated resistance to lapatinib and 5-FU and CAF-mediated sensitization to dabrafenib.

This work demonstrates a scalable approach for generating therapeutic hypotheses directly from spatial single-cell data and reveals drug-specific, microenvironment-dependent sensitivities that may inform precision treatment strategies and guide functional investigation of tumor-stroma interactions.

#2709 PRECISE: A prognostic thyroid follicular cell-derived gene signature for papillary thyroid carcinoma.

Sophie Li[1], Chia C. Wu[1], Vicente R. Marczyk[1], Matthew A. Loberg[2], Aatish Thennavan[3], Maxime Tarabichi[4], Li Xu[1], Ying C. Henderson[1], Tuan M. Tran[3], Quanhu Sheng[5], George J. Xu[2], Eric C. Huang[6], Marie-Claude Hofmann[7], Xiao Zhao[1], Stephen Y. Lai[1], Michelle D. Williams[8], Wenyi Wang[9], Sarah Hamidi[7], Mark E. Zafereo[1], Maria E. Cabanillas[7], Nicholas E. Navin[3], Vivian L. Weiss[2], **Jennifer R. Wang**[1]

[1]Department of Head and Neck Surgery, The University of Texas MD Anderson Cancer, Houston, TX,[2]Department of Pathology, Microbiology, and Immunology, Vanderbilt University Medical Center, Nashville, TN,[3]Department of Systems Biology, The University of Texas MD Anderson Cancer, Houston, TX,[4]Institute for Interdisciplinary Research (IRIBHM) - Jacques E. Dumont, Universite Libre de Bruxelles, Brussels, Belgium,[5]Department of Biostatistics, Vanderbilt University Medical Center, Nashville, TN,[6]Department of Laboratory Medicine and Pathology, University of Washington School of Medicine, Seattle, WA,[7]Department of Endocrine Neoplasia and Hormonal Disorders, The University of Texas MD Anderson Cancer, Houston, TX,[8]Department of Pathology, The University of Texas MD Anderson Cancer, Houston, TX,[9]Department of Bioinformatics and Computational Biology, The University of Texas MD Anderson Cancer, Houston, TX

Purpose: Papillary thyroid carcinoma (PTC) exhibits heterogeneous behavior. There is a need for effective biomarkers and improved risk stratification methods in PTC. Gene signatures derived from bulk RNA sequencing capture composite transcriptional profiles that are confounded by tumor microenvironment cells. We developed a thyroid follicular cell-derived gene signature, *Prognostic RNA Expression Cell-specific Integrated SignaturE* (PRECISE), using single-cell and nucleus RNA sequencing techniques and evaluated its prognostic utility across independent cohorts.

Experimental Procedures: PRECISE was developed using a discovery cohort of PTC patients (MDACC n=109) with a median follow-up of 14 years. Within the cohort, 11 PTC tumors and 4 normal thyroid samples were successfully sequenced using single-nucleus RNA sequencing. Genes that were significantly downregulated in malignant cells compared to normal thyroid follicular cells were integrated with previously identified differentially expressed genes from single-cell RNA sequencing. Prognostic significance was assessed using bulk RNA sequencing in the discovery cohort and validated in 2 additional cohorts (VUMC n=65; TCGA n=370). A rank-based single-sample method was used for score calculation. Associations between PRECISE score and progression-free (PFS) and disease-specific survival (DSS) were evaluated using multivariate Cox proportional hazards models, and predictive models were compared using Harrell's C-statistic and ANOVA.

Results: PRECISE comprised of 41 genes downregulated in PTC tumor cells and upregulated in normal follicular cells, capturing dysregulation of thyroid function and metabolism pathways. Higher PRECISE score was significantly associated with shorter PFS across all 3 cohorts (MDACC HR=1.64, P=0.002; VUMC HR=2.54, P<0.001; TCGA HR=1.63, P=0.012) and remained significant after TNM stage adjustment in two cohorts with ≥5 years follow-up (MDACC aHR=1.42, P=0.038; VUMC aHR=2.12, P=0.024). PRECISE score was also associated with DSS in these cohorts (MDACC HR=4.16, P<0.001; VUMC HR=2.23, P=0.01), independent of TNM stage in the MDACC cohort (aHR=2.83, P=0.015). Incorporating PRECISE significantly improved predictive performance for PFS (MDACC P=0.031; VUMC P=0.024) and DSS (MDACC P=0.008) beyond stage-based models.

Conclusions: PRECISE is a thyroid epithelial gene-derived signature with independent prognostic value in PTC.

#2710 Single-nuclei multiomic profiling reveals conserved adaptive states in EGFR- and ALK-mutant lung adenocarcinoma.

Naomi Kaste Mfonfu[1], Floriane Braye[1], Galina Boldina[2], Matteo Cesaroni[2], Luc Friboulet[1], Sergey Nikolaev[1], Andrey Yurchenko[1]

[1]INSERM U981 (Gustave Roussy), Villejuif, France,[2]Translation Medicine Unit, Sanofi, Vitry-sur-seine, France

Background: Resistance to EGFR and ALK tyrosine kinase inhibitors (TKIs) in lung adenocarcinoma (LUAD) remains a major clinical challenge. Tumor persistence and relapse arise from dynamic lineage transitions and adaptive signaling rewiring, yet the molecular features defining minimal residual disease (MRD) remain incompletely understood.
Methods: We generated single-nucleus RNA and ATAC sequencing datasets from the longitudinal patient tumor biopsies at baseline, minimal residual disease (MRD), and relapse. In total, we analyzed 38 patient samples (18 baseline, 10 MRD, 10 relapse, including 6 matched samples) across both RNA-seq and ATAC-seq. Moreover, we generated six patient-derived xenograft (PDX) models harboring EGFR or/and ALK mutations, sampled at baseline and during MRD (2 baseline samples and 3-6 MRD samples per model).
Results: Transcriptomic analyses revealed consistent remodeling of regulatory programs associated with differentiation, adhesion, and stress adaptation. Across PDX models, a conserved persister signature emerged, enriched in pathways related to ciliogenesis, neuronal signaling, lipid metabolism, and senescence. In patient samples, MRD and relapse were marked by transcriptional transitions from alveolar to ciliated and neuroendocrine-like states, reflecting a lineage continuum also observed in PDXs, and this shift was supported by 127 significantly altered genes between baseline and MRD (34 downregulated and 93 upregulated), quantifying the extent of transcriptional reprogramming associated with the emergence of drug tolerant persister cells.
Conclusion: Together, these results point to shared adaptive trajectories across preclinical and clinical contexts, capturing the continuum from drug-tolerant persistence to established resistance. These findings define a conserved adaptive landscape across EGFR- and ALK-driven LUAD and lay the groundwork for identifying therapeutic strategies to eradicate residual disease and prevent relapse in TKI-treated lung cancer.

#2711 Large-scale integration of single-nuclei and spatial transcriptomics from the ETOP BEAT-meso trial reveals clinically relevant heterogeneity in malignant pleural mesothelioma.

Daria Buszta[1], Jonathan Bac[1], Maxim Norkin[2], Arsh Shaikh[1], Bernd Illing[1], Adriano Martinelli[1], Isinsu Katircioglu[1], Melissa Ensmenger[1], Sylvie Andre[2], Marina Alexandre-Gaveta[2], Sanjay Popat[3], Anthony Pope[4], Riyaz Shah[5], Toby Talbot[6], Julia Giner[7], Janthur Wold-Dieter[8], Ernst Nadal[9], Annamaria Catino[10], David Gilligan[11], Amy Roy[12], Georgia Dimopoulou[13], Rosita Kammler[14], Stephen P. Finn[15], Zoi Tsourti[13], Enriqueta Felip[16], Patrick Vagenknecht[14], Solange Peters[17], Rolf A. Stahel[18], Marianna Rapsomaniki[1], Raphael Gottardo[1], Krisztian Homicsko[2]

[1]Biomedical Data Science Center, Lausanne University Hospital; University of Lausanne, Lausanne, Switzerland,[2]Department of Oncology, Lausanne University Hospital; Swiss Cancer Center Leman, Lausanne, Switzerland,[3]Department of Medicine, The Royal Marsden Hospital - NHS Foundation Trust, London, United Kingdom,[4]Department of Oncology, Clatterbridge Cancer Centre NHS, Liverpool, United Kingdom,[5]Department of Medical Oncology, Kent Oncology Centre Maidstone, Kent, United Kingdom,[6]Department of Medical Oncology, Royal Cornwall Hospital, Turuto, United Kingdom,[7]Department of Medical Oncology, Parc Tauli Hospital Sabadell, Sabadell, Spain,[8]Department of Medical Oncology, Kantonsspital Aarau, Aarau, Switzerland,[9]Department of Medical Oncology, ICO Hospitalet (Bellvitge), Barcelona, Spain,[10]Department of Medical Oncology, IRCCS Istituto Tumori Giovanni Paolo II, Bari, Italy,[11]Department of Medical Oncology, Addenbrooke's Hospital, Cambridge, United Kingdom,[12]Department of Medical Oncology, University Hospital Plymouth, Plymouth, United Kingdom,[13]ETOP Statistical Center, Frontier Science Foundation - Hellas, Athens, Greece,[14]Translational Research Coordination, ETOP IBCSG Partners Foundation, Bern, Switzerland,[15]Pathologist, University of Dublin and St. James's Hospital, Dublin 8, Ireland,[16]VHIO Vall D'Hebron Institute of Oncology, Barcelona, Spain,[17]CHUV Lausanne University Hospital, Lausanne, Switzerland,[18]University Hospital Zurich, Zurich, Switzerland

Malignant pleural mesothelioma (MPM) is a rare, aggressive cancer of the lung lining, predominantly caused by asbestos exposure (1,2). Despite advancing therapies, 5-year survival remains poor at 10-20% (3,4). A major challenge in managing MPM is its extensive heterogeneity, which contributes to variable treatment response. Comprehensive characterisation of this heterogeneity may help guide more effective therapies. Meeting this need requires large-scale, multimodal datasets that capture the cellular, spatial and molecular landscape of MPM. We analysed FFPE tissues from 159 patients enrolled in the BEAT-meso trial (5), generating the largest multimodal MPM dataset from a single clinical trial. The dataset includes paired single-nuclei FLEX RNA-seq (snRNA-seq; 612,587 cells), spatial Xenium transcriptomics (37,949,307 cells), H&E images, and matched clinical data. We built a high-resolution snRNA-seq atlas through extensive preprocessing, reference integration, and hierarchical cell type annotations. Clinical variables were used to stratify the cohort and assess variation in cellular composition, pathway activity, and molecular patterns. Xenium data were used to contextualise the snRNA-seq-derived annotations, and transcriptomic data of malignant cells were utilised to identify clinically associated programmes. We used foundation models to learn multimodal representations across histology and transcriptomic data, and studied relationships across modalities and their associations with clinical variables.Histology-based stratification revealed differences in cell-type composition, pathway activation, and checkpoint signalling between epithelioid and non-epithelioid tumours. Foundation-model analysis identified patients with sarcomatoid-like molecular signatures, revealing heterogeneity beyond standard classification. Transcriptional programme analysis further refined malignant cell states across histologies. Integration with spatial transcriptomics confirmed the presence and localisation of all snRNA-seq-derived cell types and enabled identification of tertiary lymphoid structures. We present the most extensive multimodal resource for MPM, integrating single-nuclei, spatial and clinical data from 159 BEAT-meso patients. This multimodal framework refines molecular and histological characterisation of MPM, highlighting features associated with aggressive disease, and provides the cancer and computational biology communities with a scalable reference for benchmarking, training next-generation models, and accelerating biomarker and therapeutic discovery.

#2712 MPACT-DPD: An interpretable machine learning classifier for predicting the functional impact of *DPYD* missense variants.

Lulu Jiang[1], Ryan Jonathan Swartz[2], Lauryn Allyn Hahn[2], Brianna Bembenek[3], Hannah Marie Krause[4], Kelly Bouchonville[4], Steven M. Offer[4]

[1]Informatics, University of Iowa, Iowa City, IA,[2]Carver College of Medicine, University of Iowa, Iowa City, IA,[3]Mayo Clinic, Rochester, MN,[4]University of Iowa Holden Comprehensive Cancer Center, Iowa City, IA

5-Fluorouracil (5-FU) is a widely prescribed chemotherapy for colorectal, breast, gastric, and head and neck cancers. The drug inhibits thymidylate synthase, blocking DNA synthesis and causing cytotoxic stress that halts tumor growth. However, patients carrying deleterious variants in *DPYD*, the gene encoding the rate-limiting enzyme in 5-FU metabolism (dihydropyrimidine dehydrogenase, DPD), can experience fatal toxicity due to impaired drug clearance and accumulation of 5-FU metabolites. Current pharmacogenetic screening guidelines in the U.S. recommend testing for few of the >2,000 nonsynonymous variants that have been reported for *DPYD*, leaving patients with rare, uncharacterized mutations at risk. To interpret expanded testing, however, a means to classify *DPYD* variants of unknown significance is needed. To address this, we developed MPACT-DPD, a random-forest-based classifier that accurately predicts the functional impact of *DPYD* missense variants. Our model was trained on *in-vitro* activity of 156 variants and leveraged a feature set of biochemical, evolutionary, and AlphaFold3-derived structural features. We optimized hyperparameters using ten-fold stratified cross-validation and evaluated model performance with Matthews correlation coefficient (MCC) to account for moderate class imbalance (7:3 neutral to deleterious). It achieved exceptional performance, with a Matthews correlation coeffient (MCC) of 0.906 and an accuracy of 95.1% on an independent validation set (n=43). Furthermore, a SHAP (SHapley Additive exPlanations)-based interpretability analysis revealed cofactor proximity and residue conservation as the key drivers of predictions. MPACT-DPD showed superior performance at variant classification against other tools, including a *DPYD* gene-specific variant classifier, and has the potential to expand pre-treatment genetic screening to improve the safety of personalized 5-FU-based chemotherapy.

#2713 Ensemble machine learning using unmatched pre-treated multi-omic data can classify response to immune checkpoint inhibition in non-small cell lung cancer.

Alexander Azizi[1], Arvind Ravi[1], Natalie Vokes[2], Stephen-John Sammut[3], Petar Stojanov[4], Justin Gainor[5], Gad Getz[1]

[1]The Broad Institute of MIT and Harvard, Cambridge, MA,[2]UT MD Anderson Cancer Center, Houston, TX,[3]Institute of Cancer Research, London, United Kingdom,[4]Broad/DFCI, Cambridge, MA,[5]Massachusetts General Hospital, Charlestown, MA

Introduction: Immune checkpoint inhibitors (ICI) improve survival in non-small cell lung cancer (NSCLC), yet predictive biomarkers remain limited. Multi-omic data can improve classification, but incomplete multi-omic overlap poses challenges for integrative analysis. Ensemble methods can leverage partially overlapping multi-omic data for biological insight and predictive power. We developed an ensemble machine learning (ML) framework integrating unmatched exome and transcriptome datasets to classify ICI response, enabling model training when only a single data modality is available for a patient.
Methods: Using the SU2C-Mark Foundation NSCLC dataset (SU2C NSCLC), separate exome- (n=241) and transcriptome-based (n=84) models were trained using cross-validation, and validated via ensemble learning on overlapping multi-omic data (n=68). Models were tested in an independent SU2C NSCLC cohort (MDA), and externally validated in melanoma and urothelial datasets.
Results: In SU2C NSCLC, separate models were trained in the unmatched exome and unmatched transcriptome data, and results were blended to predict response in the 68 matched, multi-omic cases (46% responders). The baseline ensemble model using the clinically assessed PD-L1 tumor proportion score (TPS) achieved an area under the ROC curve (AUC) of 0.60. Incorporating domain knowledge and blending the two model predictions (tumor mutation burden [TMB] & *CXCL9* expression) improved AUC to 0.76, while a simple ensemble including TMB, *CXCL9*, PD-L1, first-line therapy and dual ICI reached AUC 0.80. LASSO models adding Amp5p15.33 (*TERT* locus), SBS7b COSMIC mutational signature, and clonal neoantigens achieved AUC 0.79; non-linear models (RF/XGBoost) reached 0.73. In the MDA cohort (n=22), baseline PD-L1 AUC was 0.68, domain knowledge ensemble was AUC 0.88, simple ensemble AUC was 0.82, and the previously selected test model of LASSO achieved 0.79. The domain knowledge ensemble generalized well on external data: in urothelial cancer (Mariathasan et al. *Nature* 2018; train n=105; val n=45), AUC was 0.94, and in melanoma (Freeman et al., *Cell Rep Med.* 2022; unmatched exome n=99, unmatched RNA n=98, matched multi-omic validation n=55), AUC was 0.65. Differential expression and pathway analysis in misclassified tumors highlighted stromal and histologic heterogeneity as residual error sources. *CXCL9* expression and TMB were not co-linear in TCGA, helping to explain their additive power.
Conclusion: A pragmatic ensemble ML framework can integrate unmatched exome and transcriptome data to classify ICI response in NSCLC. Blending immune (*CXCL9* expression) and genomic (TMB) features yields robust, interpretable, generalizable, and biologically meaningful models. This approach supports translation of clinically actionable, integrative biomarkers for precision immunotherapy.

#2714 Development of a novel Ikaros/Aiolos transcriptional signature and correlation with patient response in multiple myeloma patients treated with CELMoDs.

Saleh Tamim[1], Nicholas Stong[1], Yan Kai[2], Diana Jankeel[2], Bonny Gaffney[2], Antonina Kurtova[3], Alberto R. Perez[4], Celia Fontanillo[2], Tracy T. Chow[3], Patrick R. Hagner[1], Danny Jeyaraju[1], Chad C. Bjorklund[1], Michael Amatangelo[1], Kai Wang[2], Anita Gandhi[1], Maria Ortiz-Estevez[5]

[1]Bristol Myers Squibb, Summit, NJ,[2]Bristol Myers Squibb, San Diego, CA,[3]Bristol Myers Squibb, Brisbane, CA,[4]Bristol Myers Squibb, Lawrenceville, NJ,[5]Bristol Myers Squibb, Sevilla, Spain

Background: Multiple myeloma (MM) is a neoplasm characterized by the clonal proliferation of malignant plasma cells in the bone marrow. Immunomodulatory drugs and distinct CELMoD™ agents modulate Cereblon to induce the degradation of the hematologic transcription factors, Ikaros (Ik) and Aiolos (Ai), resulting in anti-proliferative and pro-apoptotic cell intrinsic effects on multiple myeloma tumor cells. While Ik/Ai degradation in MM cells can be semi-quantified using immunohistochemistry (IHC), clinical responses are not always correlated. Here, we devise a quantitative RNA-seq based Ik/Ai activity score in MM cells utilizing preclinical next-generation sequencing data and validate our approach using clinical data.
Methods: CUT&RUN and ChIP-seq experiments were performed on H929 MM cell line to identify binding targets of Ik. To refine the target list, we investigated transcriptional changes of the Ik targets when exposed to lenalidomide (LEN), pomalidomide (POM), and mezigdomide (MEZI) at 6, 24, and 48-hour timepoints, and iberdomide (IBER) at a 24-hr timepoint. Differential expression (DE) analysis between compound-treated and DMSO-treated samples was performed using DESeq2, and significantly DE genes were determined. Ik binding target results were overlapped with the DE genes to generate a high-confidence Ik regulon: 115 up-regulated and 95 down-regulated targets.
Results: Gene Set Variation Analysis was performed on Ik regulon to derive an Ik activity score. The score was first applied to RNA-seq paired samples (N=7) at screening and at cycle (C) 2 day (D) 15 from patients treated with MEZI in the CC-92480-MM-001 study. On-treatment samples had significantly lower activity score compared to screening. The Ik activity score was then applied to IBER-treated patients from the CC-220-MM-001 study, comparing RNA-seq paired samples (N=41) at screening and at C2D15. On-treatment samples, similarly, had significantly lower activity score compared to screening. Responders (R) of IBER and MEZI showed a slight trend of greater change in activity score.To determine if the change in activity score could be used as a biomarker of response with progression-free survival (PFS), the IBER dataset was investigated. Using an optimal cutpoint, significant association was observed with higher change in activity score favoring longer PFS. Association analysis using IBER IHC paired, at screening and at C2D15 samples (N=55), similarly showed significant association with higher percentage of Ik degradation also favoring longer PFS. Validation using IBER samples (N=22) having both RNA-seq and IHC data resulted in significant association between PFS and RNA-seq based and IHC based scores.
Conclusions: We compiled Ik targets and devised an RNA-seq based Ik activity score that is significantly associated with patient outcome and is comparable with the IHC score.

#2715 A comprehensive single-cell atlas of head and neck squamous cell carcinoma defines malignant cell states and enables deconvolution of legacy bulk transcriptomic cohorts.

Yuanyuan Shen, Tingyi Li, Roger Li, Xuefeng Wang, Xiaoqing Yu

Moffitt Cancer Center, Tampa, FL

Background: Head and neck squamous cell carcinoma (HNSCC) is characterized by intratumor heterogeneity driven by diverse malignant cell states and a complex tumor microenvironment influenced by HPV infection and tobacco exposure. Previous studies have used single-cell RNA sequencing (scRNAseq) to explore this complexity, none has delivered a large-scale, integrated, rigorously curated, and systematically validated atlas with high-resolution cell subtype annotation. Existing scRNAseq resources lack direct links to large legacy bulk transcriptomic cohorts that contain deep clinical characterization and long-term outcomes.
Methods: We curated, annotated,integrated scRNAseq datasets from 7 HNSCC studies, comprising 137 individuals across all disease stages. After stringent quality control and batch correction, cells were classified into major cell type and cell states. Epithelial cells were then subclustered to define transcriptional cell states and associated hallmark pathway activities. Using these atlas-derived malignant and microenvironmental states, we constructed a Bayesian model to predict cellular composition within individual cell types. This model was then applied for deconvolution of 1705 samples in 24 bulk transcriptomic HNSCC cohorts, enabling estimation of cell-state proportions and associations with HPV status, alcohol and tobacco exposure, and clinical outcomes.
Results: Clustering of 368,842 high-quality cells identified 63 cell states across 16 major cell types. Within the malignant epithelial population, we defined 12 distinct states including chromatin remodeling, cilia, E2F targets, EMT-II, cell cycle phases, and stress responses. Deconvolution of bulk cohorts using the BayesPrism approach recapitulated these altas-defined signatures and uncovered reproducible clinical association across datasets. Lower EMT-II ($p=0.02$), higher glutathione ($p=0.038$), increased cDC3 ($p=0.024$), and elevated IFN-TAM ($p=0.0153$) were associated with improved survival. HPV status demonstrated significant associations with distinct cell states including CD4 Tcm, CD8 Temra, proliferative fibroblast, G2M epithelial cells, myofibroblasts, and TNFRSF9+ Treg cells.
Conclusions: This study establishes a comprehensive single-cell atlas for HNSCC and introduces a BayesPrism-powered framework for projecting malignant and microenvironmental cell states onto heterogeneous bulk transcriptomic datasets. By linking high-resolution cellular profiles with large, clinically annotated cohorts, our work provides a scalable and robust strategy to decode the ecosystem heterogeneity of HNSCC.

#2716 Machine learning-based screening tool for multiple myeloma detection in chronic kidney disease patients with limited laboratory testing.

Wen-Chi Wu[1], Muh-Hwa Yang[1], Chih-Yu Yang[2]

[1]Department of Medical Oncology, Taipei Veterans General Hospital, Taipei, Taiwan,[2]Department of Internal Medicine, Division of Nephrology, Taipei Veterans General Hospital, Taipei, Taiwan

Background: Multiple myeloma (MM) and chronic kidney disease (CKD) share similar clinical manifestations including renal impairment and anemia, making MM diagnosis challenging in general and nephrology clinics. Many CKD patients harbor undiagnosed MM, but healthcare insurance restrictions and public health system constraints limit ordering of specialized tests (serum protein electrophoresis, free light chains, immunoglobulins). This diagnostic delay can result in irreversible renal damage and delayed treatment. We developed a machine learning model using routine laboratory parameters to identify CKD patients requiring MM-specific workup or hematology referral.

Methods: We analyzed 4,759 CKD patients (591 MM, 4,168 non-MM controls; 12.4% prevalence) from a tertiary center. Using only routine tests available in general practice, we engineered features including CBC (hemoglobin, WBC, platelets), biochemistry (total protein, albumin, calcium, LDH, creatinine), and urine studies (protein, albumin, creatinine). Three feature sets were tested: RANK1 (20 features), RANK2 (16 features), and RANK3 (4 minimal features). We compared XGBoost, Random Forest, and Logistic Regression using stratified 5-fold cross-validation. with both unbalanced and SMOTEENN-resampled data.

Results: XGBoost achieved optimal performance: accuracy 95.1%, F1-score 0.798, ROC-AUC 0.962, PR-AUC 0.889. The minimal 4-feature model (platelet, WBC, urine protein, LDH) maintained clinically useful performance (F1 0.596, PR-AUC 0.627). SHAP analysis revealed hemoglobin/WBC ratio, platelet count, albumin/total protein ratio, and total protein as top predictors, capturing MM's characteristic hematologic suppression and paraproteinemia without requiring specialized assays. Dimensionality reduction visualization (PCA, UMAP, t-SNE) demonstrated distinct clustering patterns between MM and non-MM CKD patients, confirming inherent feature space separability despite overlapping clinical presentations.

Conclusions: This ML-based screening tool demonstrates potential for identifying high-risk CKD patients warranting MM-specific testing using only routine laboratory data. However, this retrospective single-center study has limitations including potential selection bias and lack of external validation. Prospective multicenter validation studies are needed to assess real-world clinical utility, optimal decision thresholds, and impact on diagnostic timeliness before implementation in clinical practice.

#2717 Prostate cancer risk stratification by polygenic score in diabetic and non-diabetic men.

Gukjin Lee[1], Sang-Hyuk Jung[2], Jonghyun Lee[3], Ki Won Moon[4], Jae-Seung Yun[5], Dokyoon Kim[3]

[1]Bucheon St. Mary's Hospital, The Catholic University of Korea Bucheon, Seoul, Korea, Republic of,[2]Department of Medical Informatics,, Kangwon National University College of Medicine, Chuncheon, Korea, Republic of,[3]Department of Biostatistics, Epidemiology and Informatics, Perelman School of Medicine, University of Pennsylvania, Philadelphia, PA,[4]Division of Rheumatology, Department of Internal Medicine, Kangwon National University College of Medicine, Chuncheon, Korea, Republic of,[5]St. Vincent's Hospital, College of Medicine, the Catholic University of Korea, Seoul, Korea, Republic of

Background: Type 2 diabetes mellitus (T2DM) has been inversely associated with prostate cancer (PrCa) risk. However, it remains unclear whether a polygenic risk score (PRS) for PrCa can effectively stratify risk among men with T2DM. This study aimed to assess whether a PrCa PRS could predicts PrCa risk independently of T2DM status.
Methods: We analyzed data from over 140,000 men in the UK Biobank and Penn Medicine Biobank. A PrCa PRS was constructed using summary statistics from a large-scale genome-wide association study. Cox proportional hazards models were used to evaluate the association between PRS and incident PrCa, adjusting for relevant covariates and testing for interaction by T2DM status. Additionally, sex hormones and insulin-like growth factor-1 (IGF-1) levels were analyzed to explore potential mediators.
Results: T2DM was associated with a reduced incidence of PrCa. IGF-1 levels were positively associated with PrCa risk in both diabetic and non-diabetic men, while sex hormone levels showed no significant association in men with T2DM. PRS was significantly associated with PrCa risk regardless of T2DM status ($P < 0.001$). Men in the very high PRS category had the highest PrCa risk, particularly among those without T2DM. Adjusting for testosterone and IGF-1 levels did not attenuate the association between PRS and PrCa.
Conclusions: PrCa PRS effectively stratifies prostate cancer risk in men both with and without diabetes, underscoring genetic susceptibility as a robust, independent risk factor. Given the significantly lower baseline IGF-1 levels in T2DM patients, IGF-1 might partially explain the reduced PrCa risk observed in this population.

#2718 Liquid biopsy cfDNA methylation predicts lung tumor size and metastatic potential in a single assay.

Kade P. Pettie[1], Shiva Farashahi[1], Jackson Killian[1], Andrew Wong[1], Yifan Wu[1], Dorna Kashef[1], Franziska Michor[2], Jocelyn Charlton[1], Kieran Chacko[1]

[1]Data Science, Harbinger Health, Cambridge, MA,[2]Assoc. Professor, Dept. of Biostatistics & Computational Bio., Dana-Farber Cancer Institute, Boston, MA

Liquid biopsy enables noninvasive assessment of cancer severity and prognosis, informing clinical decisions across the cancer care spectrum. Estimates of the fraction of tumor-derived DNA shed into circulation (tumor content; TC) reflect disease severity, with higher TC more frequently observed in advanced stages and linked to poorer outcomes. However, TC is a product of a complex pathology and is impacted by many factors including tumor type, size, shedding rate, aggressiveness, vascularization, genotype, and metastatic state. We aim to predict two of them, size and metastatic state, using a targeted cell-free DNA (cfDNA) methylation assay.

To assess metastatic potential, we trained models for two binary prediction tasks in lung cancer: distant metastasis (Stage I/II vs IV) and late stage (Stage I/II vs III/IV). Features quantifying region-level methylation patterns were residualized with respect to sample-level TC to capture signals orthogonal to size. TC was evaluated as a single predictor in parallel. We trained on a dataset of 54 true and 324 synthetic lung cancer cfDNA samples to further emphasize size-independent, stage-related features. All models were assessed at 90% target specificity on an independent test set of 30 true cancer samples classified as lung cancer by a multiclass tissue-of-origin model to represent the end-to-end performance of the assay. For size prediction, we developed a lung-specific TC estimator, fit log-linear models linking TC to radiology-derived tumor size metrics, and generated predictions for 57 held-out test samples. All samples were from the CORE-HH clinical study (NCT05435066).

The residual methylation models identified distant metastasis with 87.5% sensitivity (14/16 Stage IV) at 83% specificity (5/6 Stage I/II) and late stage with 67% sensitivity (16/24 Stage III/IV) at 83% specificity (5/6 Stage I/II). These results substantially improved on the TC-only model (19% and 17% sensitivity, respectively, at the same specificities), indicating methylation metrics capture tumor progression-associated signal orthogonal to TC. For size prediction, restricting to Stage I-III cases with PET metrics (N = 19) yielded the strongest fits ($\log_{10}$(total volume) $R^2 > 0.5$, $p < 5\times10^{-4}$). Test set predictions showed moderate explanatory power ($R^2 = 0.24$, $p = 1.3\times10^{-4}$), consistent with factors beyond size (e.g., visceral metastasis) influencing shedding.

These findings highlight the potential for stage and size prediction models to deliver clinically actionable insights from a single blood draw. Late-stage prediction could guide workup prioritization, treatment intensity, and surveillance strategies, while size prediction may support prognosis and therapy selection. These capabilities motivate further model development for complementary prediction tasks (e.g., aggressiveness, genotype) toward a suite of tools for precision oncology.

#2719 Molecularly-informed prediction of treatment efficacy in GDSC cell line data using computational reasoning.

Robert Doczi[1], Akos Takacs[1], Anna Dirner[1], Dora Lakatos[1], Barbara Vodicska[1], Dora Gorog-Tihanyi[1], Reka Szalkai-Denes[1], Eniko Kispeter[1], Andras Makkos[2], Aniko Gorbe[2], Peter Ferdinandy[2], William T. Beck[3], Christophe Le Tourneau[4], Petak Istvan[1]

[1]Genomate Health, Cambridge, MA,[2]Semmelweis University, Budapest, Hungary,[3]University of Illinois at Chicago, Chicago, IL,[4]Gustave Roussy, Villejuif, France

The Digital Drug Assignment (DDA) system is a knowledge-graph-based computational method that automates reasoning at the patient level and scores molecularly targeted agents (MTAs) based on the full tumor genomic data. This approach was predictive of relative benefit of the agents as used in the SHIVA01 trial (DOI: 10.1038/s41698-021-00191-2). Here, we evaluated the predictive power of DDA on a larger scale by analyzing tumor genomic and drug sensitivity data from the GDSC database. Our study was based on data from 659 cell lines derived from a broad spectrum of solid tumors. Corresponding drug sensitivity data were available for 34,713 treatment datapoints involving 87 types of MTAs. All tumor genomic profiles were processed using DDA, which scores MTAs and stratifies them according to predicted efficacy. Consequently, the same MTA can receive different drug scores across tumors, depending on their individual molecular profiles. Treatments were then ranked for each tumor based on their DDA scores, resulting in 72 treatment groups defined by ranking positions (i.e., drugs ranked at the same position across tumors formed one treatment group). Sensitivity to treatment was determined using Z-scores of IC50 values, with treatments showing negative Z-scores classified as sensitive. Among the top-ranked MTAs, 54% of treatments were sensitive, with sensitivity gradually decreasing across lower-ranking groups and reaching 0% in the bottom group. A linear trend across DDA score rank groups from top to bottom was confirmed by the Cochran-Armitage trend test ($Z = -10.42$, $p = 2.08e-25$), indicating a very strong negative trend across ordered groups from the top towards the bottom. Increased confidence in the benchmark drug response classification was achieved by excluding treatments around the median with progressively larger absolute IC50 Z-score thresholds. With IC50 Z-score exclusion thresholds of absolute 1, 2, 2.5, and 3, the sensitivity of cell lines to top-ranked treatments was 59%, 67%, 74%, and 83%, respectively, while remaining 0% in the bottom groups in all cases. Thus, increasing confidence in drug response correlated with higher predictive accuracy. Although group sizes decreased with stricter thresholds - reducing statistical power - the results remained highly significant throughout, the Cochran-Armitage trend test Z-values gradually increased from -8.33 to -4.68 (all $p < 0.001$). These results demonstrate the predictive power of DDA-score-based treatment ranking across solid tumors and MTAs, with top-ranked drugs having the greatest efficacy. The findings strongly support the notion that there is a correlation between aggregated scientific evidence and drug sensitivity. DDA can potentially address challenges with complex molecular profiles in routine clinical settings and clinical trial design.

#2720 A comprehensive LLM-enabled pharmacodynamic biomarker resource to accelerate cancer drug development.

Yuntao Yang, Li Zhao, Seyedmehdi Orouji, Ying Zhu, Rebecca Johnson, David Maxwell, Kaitlyn Brickey, Bissan Al-Lazikani

Genomic Medicine, UT MD Anderson Cancer Center, Houston, TX

Introduction: A major challenge in oncology drug development is confirming target engagement of therapeutics in patient tumors. Pharmacodynamic (PD) biomarkers provide this link, enabling early assessment of target validity, drug activity and rational dose selection. However, systematic resources connecting drug targets to validated PD biomarkers remain limited. To address this, we developed a comprehensive dataset and analytic framework to identify and prioritize target-specific PD biomarkers across nine major target classes implicated in cancer biology.

Materials and Methods: We curated biomarker candidates from multiple genomic and pharmacologic resources for nine target classes: transcription factors/cofactors, kinases, phosphatases, ubiquitin ligases, deubiquitinases, acetyltransferases, deacetylases, methyltransferases, and demethylases. Source databases often apply broad definitions to functional classes such as transcription factors. To improve accuracy and reduce annotation artifacts, we cross-referenced PFAM, Enzyme Classification, and PDB databases to refine protein classifications. Using the canSAR interactome, we identified direct target-biomarker interactions supported by experimental evidence. To capture context-specific transcriptional biomarkers, we computed cohort-specific correlations using TCGA, TARGET, and GTEx datasets. Finally, we employ LLM-based fact-checking agent to extract and harmonize antibody annotations from the Antibody Registry, focusing on enzyme targets with measurable substrate modifications.

Results: From 2,900 targets and 100,000 interactions, we propose 73,000 high-confidence target-biomarker relationships involving over 2,100 potential drug targets. Of these, 67% represent transcription factor-gene interactions and 33% enzyme-substrate interactions. Commercial antibodies were identified for over 2,800 biomarker candidates, supporting experimental validation. The resulting dataset covers more than 60% of the top 20 predicted targets across 19 cancer types. We provide all the data in our canSAR platform and as a download from canSAR-PD.

Discussion: This resource provides a systematic framework for PD biomarker discovery in oncology. By integrating curated molecular interactions with LLM-derived antibody annotations, it enables robust evaluation of target engagement and drug activity. The dataset establishes a foundation for developing PD biomarkers to guide dose selection, monitor response, and accelerate cancer drug development.

#2721 Phenome-wide association study of pre-cancer diagnosis electronic health records identifies risk and protective factors in the All of Us Research Program.

Charles C. D. Rich[1], Alyssa B. Bair[2], Britton E. Richardson[1], Katelyn C. Forbes[1], Blaine A. Bates[3], Mary F. Davis[4], Matthew H. Bailey[5]

[1]Biology, Brigham Young University, Provo, UT,[2]Data Science, Brigham Young University, Provo, UT,[3]Chemical Engineering, Brigham Young University, Provo, UT,[4]Microbiology and Molecular Biology, Brigham Young University, Provo, UT,[5]Simmons Center for Cancer Research, Brigham Young University, Provo, UT

Background: The All of Us Research Program represents a rich resource for cancer epidemiology research, with over 400,000 participants with whole genome sequences linked to electronic health records (EHRs). Large cancer datasets often focus exclusively on cases without controls and neglect pre-diagnosis healthcare occurrences. Here, we perform a phenome-wide association study (PheWAS) of pre-diagnosis EHR data between cancer cases and matched controls, revealing co-occurring and mutually exclusive phenotypes that can be subsequently investigated using All of Us genomic data.
Methods: Using SNOMED CT codes, we identified 48,000+ cancer cases across 23 cancer types in All of Us version 8. To conduct PheWAS while eliminating temporal ascertainment bias, we implemented a matched truncation strategy: for each cancer case diagnosed at age X, we matched control individuals on birth year, sex, and race and truncated their EHR data at age X, ensuring equal opportunity to accrue diagnoses. We tested associations between cancer diagnosis and approximately 2,100 clinical phenotypes using logistic regression adjusted for age, sex, and EHR metrics including length of EHR and total ICD code count, with Bonferroni correction for multiple testing. For coding aspects of this study, Claude by Anthropic was used for debugging and troubleshooting.
Results: Our analysis confirmed established cancer risk factors, validating All of Us as a robust platform for cancer epidemiology research. Notably, we identified unexpected inverse associations with pain-related phenotypes: chronic pain (P-value=7.7×10^{-47}, OR=0.67) and general pain (P-value=2.9×10^{-44}, OR=0.72). Additional inverse associations included sleep disorders (P-value=2.9×10^{-27}, OR=0.79) and mood disorders (P-value=5.2×10^{-32}, OR=0.77), suggesting potentially protective relationships warranting further investigation.
Conclusions: This comprehensive PheWAS of pre-diagnosis EHR data in All of Us reveals a complex landscape of cancer-associated phenotypes extending beyond traditional risk factors. The identification of potentially protective phenotypes, combined with our rigorous approach to temporal bias elimination, establishes a foundation for hypothesis-generating research in precision cancer prevention. These findings underscore the importance of diverse biobanks and rigorous methods for identifying phenotypic relationships. Claude by Anthropic was used to revise text for grammar, clarity, and length optimization. Importantly, all scientific content, hypotheses, analyses, and conclusions remain the original work of the authors.

#2722 Integrated analysis identifies ELF3-CREB1 co-activation as a prognostic driver of high-risk pancreatic cancer.

Poorva Poorva[1], Rimpi Khurana[2], Varunkumar Krishnamoorthy[3], Sudhakar Jinka[3], Yan Guo[2], Vineet Kumar Gupta[3], Nagaraj Nagathihalli[3]

[1]Department of Surgery, University of Miami Miller School of Medicine, Miami, FL,[2]Department of Public Health Sciences, University of Miami Miller School of Medicine, Miami, FL,[3]Department of Surgery, University of Miami Miller School of Medicine, Sylvester Comprehensive Cancer Center, Miami, FL

Background: Patients diagnosed with pancreatic ductal adenocarcinoma (PDAC) face a dismal prognosis, with only about 13% surviving five years. Transcriptional factors play a vital role in PDAC survival and prognosis by defining tumor aggressiveness, therapeutic resistance, and clinical outcome. Key regulators such as CREB1 have previously been linked with tumor progression and shorter survival. While CREB1 signaling driving PDAC is known, the systematic characterization of active Transcription Factor (TF) associated with CREB1, and their clinical relevance is limited. In this study, we aimed to identify critical TF activity associated with CREB1 and assess their combinatorial prognostic impact in PDAC.
Methods: We utilized the VIPER (Virtual Inference of Protein-activity by Enriched Regulon) algorithm with high-confidence DoRothEA regulons (A-C) to infer TF activity across 182 TCGA-PAAD RNA-seq samples (178 Primary Tumors [TP] and 4 Normal Tissues [NT]). Differential Activity Analysis (DAA) using limma identified TFs dysregulated between TP and NT. Survival analyses utilized Kaplan-Meier and Cox Proportional Hazards modeling on the TP cohorts, focusing on the interaction between two key dysregulated TFs, CREB1 and ELF3 (ETS transcription factor 3). R version 4.3.0 was used for all analyses, including GSVA (v1.50.5) and VIPER (v1.36.0). Differential expression and pathway analyses were performed using the R packages limma (v3.58.1), GSVA (v1.50.5), msigdbr, gplots, and ggplot2.
Results: DAA identified 44 significantly dysregulated TFs (FDR < 0.05). The epithelial lineage regulator ELF3 showed the highest activation in tumors, while the lymphoid regulator PAX5 (paired box 5) was highly repressed. Although single-TF prognostic tests were non-significant, combinatorial analysis revealed a strong context-dependent effect. The simultaneous High CREB1 and High ELF3 activity defined a uniquely aggressive subgroup with a markedly shorter median overall survival (272 days) compared to the lowest-risk combination (492 days). Cox modeling confirmed a significant synergistic interaction between the two TFs (HR =2.31, p = 0.049).
Conclusion: This analysis reveals that the highly activated epithelial driver ELF3 acts synergistically with CREB1 to define a high-risk prognostic signature in PDAC. Our findings underscore that TF networks, rather than single factors, are crucial for patient stratification and represent compelling, context-specific therapeutic targets in PDAC.

#2723 Genomic drivers and an immune-cold microenvironment are associated with relapse in Chinese pediatric B-ALL.

Dan Yu[1], Yanni Hu[2], Xue Tang[3], Junlin Wang[1], Junwen Wang[1], Jianwen Xiao[2]

[1]Faculty of Dentistry, The University of Hong Kong, Hong Kong, Hong Kong,[2]Department of Haematology and Oncology, Children's Hospital, Chongqing Medical University, Chongqing, China,[3]Department of Hematology and Oncology, Shenzhen Children's Hospital, Affiliated to Shantou University Medical College, Shenzhen, China

Background: Relapse remains a major challenge in pediatric B-cell Acute Lymphoblastic Leukemia (B-ALL). This study aims to identify the specific genomic and cellular markers that drive treatment failure and are associated with relapse and poor Event-Free Survival (EFS) in Chinese pediatric B-ALL patients.

Methods: We performed an integrated multi-omic analysis on a cohort of 105 Chinese pediatric B-ALL patients, including 13 EFS Event (relapse plus died) cases. The cohort was profiled using ultra-deep gene panel sequencing (N=87), single-cell RNA-sequencing (scRNA-seq, N=52), and VDJ-sequencing (N=40). We integrated genomic, transcriptomic, and immune repertoire data to identify biomarkers associated with relapse and EFS. Associations were tested using Fisher's Exact Test, the Wilcoxon rank-sum test, and Cox regression.

Results: Our scRNA-seq and VDJ-seq analyses revealed the cellular landscape of relapse. We found a positive correlation between B-ALL blast proportion and BCR clonality and a negative correlation between T-cell proportion and TCR clonality ($p=0.041$). Notably, relapsed patients showed a higher BCR clonality but a highly polyclonal TCR repertoire, suggesting immune failure.

We identified that mutations in a curated panel of ALL-Drivers was significantly associated with relapse status ($p=0.033$) and a higher B-ALL blast percentage ($p=0.013$). And the higher ALL-Drivers VAF burden phenotype correlates with relapse status ($p=0.006$).

The non-relapse patients were found exhibited an “immune-hot" phenotype, characterized by significantly higher T-cell exhaustion and cytotoxicity scores ($p<0.001$). This state of active immune engagement is associated with PD-1/PD-L1 pathway. Relapse was associated with an "immune-cold" state, lacking this active T-cell engagement.

Finally, survival analysis and KM plot confirmed the prognostic significance of these findings. The presence of an ALL-Driver is significantly associated with poor Event-Free Survival ($p=0.021$).

Conclusion: Our findings reveal a biological pathway to poor prognosis. ALL-Drivers are linked to a high B-ALL blasts burden. This high-risk state is strongly correlated with patient relapse and is characterized by an "immune-cold" microenvironment, defined by the absence of the PD-L1 mediated T-cell exhaustion and cytotoxicity signature seen in non-relapsed patients.

#2724 A machine learning approach to classify breast cancer receptor subtype using genomic features.

Sandro Satta, Philip Miller, Samuel Rivero-Hinojosa, Ekaterina Kalashnikova, Angel Rodriguez, Minetta C. Liu

Natera, Austin, TX

Risk stratification, treatment course, and prognosis for patients with breast cancer presently rely upon the accurate determination of receptor subtype, ascertained through immunohistochemistry (IHC) for estrogen receptor (ER) and progesterone receptor (PR), and evaluation of HER2 expression (IHC and/or gene amplification via in situ hybridization). While IHC-based subtyping assays are informative, they require high-quality tissue samples and the technical assays can be susceptible to fixation artifacts, variability in antibody staining performance, semi-quantitative and subjective result calling. In cases of diminished sample quality, IHC-based subtype assessment may not agree with gene expression-based classification, and alternative approaches may be needed. This study aimed to develop a machine learning classifier able to predict breast cancer receptor subtypes using genomic features, without relying on immunohistochemistry or gene expression data.

This study included 19,559 patients with primary breast cancer, identified using Natera's proprietary real-world database, linked to a clinical claims database. Hormone receptor (HR) and HER2 subtype was determined from patient treatment codes. We developed a biologically-informed feature set by combining somatic mutations across 19,820 genes, using whole exome sequencing (WES) data from the SignateraTM testing workflow. Each mutation was assigned a composite mutation_score (range 1-12) based on variant class (SNV, insertion, deletion), superclass (SNP/INDEL), predicted impact (VEP annotation impact: MODIFIER to HIGH), and functional consequence (such as frameshift, stop-gain, missense, synonymous). A Random Forest classifier was trained with a stratified 75/25 train-test splitting and hyperparameter optimization.

The model was trained on features from 14,669 patients in the training cohort. In a test cohort of 4,890 patients, the model achieved 80.3% overall agreement with HR/HER2 status as inferred through medication claims data, with balanced performance across four major subtypes. Per-subtype metrics were: for HR+/HER2-, the model showed a precision of 0.935, recall 0.911, and F1 score of 0.923; for HR-/HER2+, precision was 0.714, recall was 0.753, and F1 score was 0.783; for HR+/HER2+, precision was 0.748, recall was 0.734, and F1 score was 0.741; lastly, for the TNBC subtype, precision was 0.730, recall was 0.816, and F1 score was 0.770.

Overall the genomic classifier accurately classifies breast cancer into one of the four major receptor subtypes. After definitive validation against clinically-reported HR/HER2 status, this classifier could be used to guide analyses of de-identified genomic datasets that lack complete clinical annotation.

#2725 Grade-dependent survival and co-mutation landscapes in TP53-mutant gliomas: Biological insights and therapeutic implications.

Harpreet Kaur, Kevin Camphausen, Uma Shankavaram

Radiation Oncology Branch, NIH-NCI, Bethesda, MD

Background: Gliomas display wide heterogeneity across grades, ranging from lower-grade anaplastic tumors (grades 2 and 3) to glioblastoma (GBM, grade 4). TP53 mutations occur frequently, but their prognostic significance depends strongly on co-mutation context and tumor grade. Dissecting these interactions is critical for stratification and therapy.
Methods: We analyzed somatic mutation and survival data from The Cancer Genome Atlas (TCGA) and Memorial Sloan Kettering (MSKCC) cohorts from TCGAbiolinks, and cBioPortal. Mutational profiling and co-mutation network analyses were performed using maftools, Kaplan-Meier and Cox regression models evaluated grade- and context-specific survival effects. Therapeutic associations were curated from OncoKB and NCI-MATCH.
Results: In grade 2 gliomas, TP53-mutant tumors showed a major survival advantage (40.2 vs 19.4 months in WT), enriched for co-mutations in IDH1 and ATRX. Grade-3 TP53-mutant tumors retained this advantage (32.9 vs 15.2 months) with additional mutations in MUC16 and APOB. By contrast, GBM (grade 4) showed only a modest TP53 benefit (14.8 vs 11.5 months), as protective IDH1/ATRX co-mutations were rare and proliferative drivers (EGFR, PTEN, NF1, PI3K) dominated. Within TP53-mutant gliomas, survival diverged by co-mutation profile. Favorable mutations (ATRX, IDH1, COL6A3, LAMA1, HYDIN, ADGRV1, NAV2) were linked to slower growth, immune visibility, or lower-grade biology. Mutations (PTEN, EGFR, RB1, NF1) exerted modest effects. In contrast, deleterious co-mutations (OBSCN, PRDM9, DNAH11, PTPN3) amplified genomic instability, defining a worst-prognosis subgroup.
Conclusions: The prognostic role of TP53 in gliomas is shaped by grade-specific co-mutation context. TP53-mutant tumors with IDH1/ATRX resemble lower-grade gliomas and may benefit from IDH inhibitors, whereas tumors with proliferative or instability drivers may require PI3K/mTOR inhibition or trial enrollment. This integrative framework highlights the need for co-mutation-aware stratification in both prognostication and therapeutic decision-making.

#2726 Clinicopathological and molecular significance of MUC13 in HCC.

Anupam Dhasmana[1], Swati Dhasmana[2], Rajasekhar Baru[1], Abigail Gomez[2], Iris A. Perez[2], Sheema S. Khan[2], Murali M. Yallapu[2], Subhash C. Chauhan[2]

[1]Division of Cancer Immunology and Microbiology, Medicine and Oncology Integrated Service Unit, University of Texas Rio Grande Valley, McAllen, TX,[2]University of Texas Rio Grande Valley, McAllen, TX

Background: Mucin 13 (MUC13), a cell surface glycoprotein aberrantly expressed in multiple epithelial carcinomas. Although in liver cancer MUC13 has not been comprehensively investigated. This study elucidates the clinical and molecular relevance of MUC13 expression in liver cancer samples followed by its role in liver carcinogenesis.
Methods: The significance of MUC13 and its impact on hepatocellular carcinoma (HCC) was investigated in MUC13 positive and negative subsets of HCC samples using an integrated approach combining bioinformatics and molecular biology. We performed proteomics analysis on protein samples extracted from paraffin embedded (FFPE) tissues. Differentially expressed proteins were identified by bioinformatics guided mass spectrometry and functional enrichment analyses. The MUC13 expression status was conformed in HCC tissue before samples selected for proteomics analysis. Later we performed MUC13 IHC expression analysis in HCC, MSLD, MASH, and fibrosis samples. Further, MUC13 expression in serum samples were determined by sandwich ELISA while cytokines profiling analyses were performed using cytokines arrays.
Result: Our deep data mining and bioinformatics analyses demonstrated higher expression of MUC13 in HCC samples as compared to normal liver and a similar pattern was observed in our proteomics analysis. Interestingly, in our proteomics analysis, we observed remarkable molecular level changes in MUC13+ve HCC subset as compared MUC13-ve HCC samples. Some of the key differentially expressed proteins are associated with several important pathways like PTK2 signaling, NF-KB activation, TLR signaling, MAP kinase activation, and AKT signaling. Whereas DNA repair, apoptosis, and TP53 associated pathways were depleted. IHC and ELISA analyses demonstrated strong MUC13 expression in HCC tumors/serum samples as compared to very faint or no expression in normal liver tissues/serum samples. Additionally, we observed a distinct expression pattern of several cytokine (Osteopontin, PDGFs, EMMPRIN/CD147, MIF, ICAM-1, VEGF) in HCC patients versus healthy normal serum samples.
Conclusion: This comprehensive study suggests 1) high expression of MUC13 in HCC, 2) MUC13+ve HCC patients' subset has a remarkable differential molecular profile as compared to MUC13-ve HCC patients' subset and normal liver tissues samples 3) HCC patients represent a relatively differential cytokine profile as compared to healthy normal serum samples. These intriguing findings suggest a crucial role of MUC13 in HCC and can be a useful indicator for therapy response and prognosis.

#2727 A designed live bacterial therapeutic restores responder-like microbiome profiles and improves immune checkpoint inhibitor (ICI) response in a predictive model.

Glen J. Weiss[1], Sonia Timberlake[1], Kinga Zielinska[2], Marina Santiago[3], Johannes Woehrstein[1], Christopher Weidenmaier[3]

[1]mbiomics GmbH, Munich, Germany,[2]Malopolska Centre of Biotechnology, Jagiellonian University, Krakow, Poland,[3]mbiomics Inc., Boston, MA

Background: The gut microbiome has been shown to predict response to ICI, but associations of individual species have not been statistically robust or reproducible. Fecal microbial transplant (FMT) has been reported to improve response probability in melanoma and kidney cancer, but drug development has focused on very simple microbial consortia.
Methods: We sought to replicate the therapeutic benefits of FMT for improving response to ICIs in a model, and design therapeutic microbial consortia that when added to a patient's gut microbiome could improve response rates to ICIs. We trained a machine learning model to predict response to ICI, based on gut microbiome species profiles from baseline samples in patients starting ICI therapy, and used it to evaluate candidate therapeutic consortia intended to improve response to ICI. We trained a machine learning model to predict responders (R) vs. non-responders (NR) to ICI, based on baseline gut microbiome species profiles from patients starting ICI therapy (n=418). Parameters were fixed and called NR vs. R model. We built therapeutic consortia designed around donor FMT and ICI response-related species and mechanisms. ICI patients can be NR for many reasons, so we next focused on patients where the baseline gut microbiome had good predictive value for IO response (n=257) and asked whether FMT and our therapeutic consortia would improve response probabilities.
Results: Publicly-available data from 418 NSCLC patients was analyzed. The median age was 65 years (range 24-92), 260 men, 63% were on at least 2nd line therapy. 19.4% received antibiotics near the start of ICI, and 118 of 271 had tumors with PD-L1 <50%. Our model had mean AUC 0.62 for predicting response in hold-out test sets (patients never seen by the model), and discriminated OS curves ($p<0.0001$). Focusing on patients where the gut microbiome model had good predictive value (n=257), we showed that in agreement with clinical experience, healthy donor FMT improves response rates in our model when added to baseline patient microbiomes and outcomes are exposure-dependent (i.e.modeling increasing fractions of FMT species engrafting and replacing increasing fractions of patient baseline microbiomes). We showed that our candidate therapeutic consortia improve response rates when added to baseline patient microbiomes, and outcomes are again exposure-dependent. Conclusions: Our candidate therapeutic consortia have promise for improving response rates in patients on ICI therapy. We isolated bacteria to culture these consortia, which we are developing to combine with ICI.
Conclusions: Our candidate therapeutic consortia have promise for improving response rates in patients on ICI therapy. We isolated bacteria to culture these consortia, which we are developing to combine with ICI.

#2728 The Cancer Complexity Knowledge Portal: A FAIR-aligned tool for resource discovery.

Orion Banks, Ashley Clayton, Aditi Gopalan, Amber Nelson, Verena Chung, Amy Heiser, Jay Hodgson, Aditya Nath, Adam Hindman, Milen Nikolov, Adam Taylor, Angie Bowen, Susheel Varma, Jineta Banerjee

Sage Bionetworks, Seattle, WA

Enabling discovery of interoperable data and sustainable computational tools can help maximize the value of shared resources, supporting both human- and machine-driven reuse. The Cancer Complexity Knowledge Portal (CCKP), developed by Sage Bionetworks' Multi-Consortia Coordinating (MC^2) Center with support from the NCI Division of Cancer Biology (DCB), serves as a public, NIH-supported, domain-specific repository that consolidates cancer research resources from multiple DCB consortia, including CSBC, PS-ON, TEC, CCBIR, MetNet, and PDMC. The portal provides a unified entry point for discovering and accessing datasets, computational tools, publications, and other outputs generated by the cancer research community. To support sharing and discoverability across diverse resources and data modalities, the CCKP employs versioned metadata models, which are maintained in a public GitHub repository and aligned with NIH Common Data Elements (CDEs). Metadata are curated through the Synapse platform, which functions as the backend repository supporting submission, review, and release via the CCKP. The portal aggregates metadata and links to original records, thereby accommodating materials stored in web-accessible archives. A unified search interface, clickable filters, and related resource links are available to help users navigate to relevant entries. The CCKP includes a number of resource-specific features to improve FAIRness: Croissant metadata is available for datasets, to support reuse in AI and ML contexts; the Cancer Complexity Toolkit provides auto-generated evaluation data, representing the sustainability and reusability of catalogued research software; visitors can access modularized educational resources via integration with the Cancer Complexity Education Program. As of late 2025, the CCKP indexes research outputs from over 160 NCI-funded cancer grants, encompassing 4,178 publications, 1,029 datasets, and 321 computational tools. Curated datasets represent key biological themes, including drug resistance or sensitivity (574), tumor microenvironment (563), metastasis (358), evolution (289), and epigenetics (103). These datasets span multiple species models, including human, mouse, and organoid systems, and data modalities such as sequencing, imaging, and spatial profiling. By surfacing a curated metadata database with intuitive search tools, the CCKP operationalizes FAIR-aligned discovery to amplify reuse of existing resources. This approach serves both experimental and computational research communities, enhancing transparency, interoperability, and secondary use of cancer data to accelerate mechanistic insights and therapeutic innovation. ChatGPT 5.1 was used for initial abstract drafting and refinement. *All content was evaluated and approved by the authors.*

#2729 The selective landscape of somatic mutations encodes histopathological information in breast cancer.

Gift Asefon, Nic Fisk

University of Rhode Island, Kingston, RI

Cancer effect size quantifies the strength of evolutionary selection acting on somatic mutations within tumors, providing insights into which genetic alterations are being actively selected during tumor evolution. While histopathology has long been the gold standard for cancer diagnosis and classification, the relationship between evolutionary selection pressures on specific mutations and observable tumor morphology remains unexplored. We investigated whether combinations of somatic mutations, weighted by their cancer effect sizes, could serve as genomic proxies for pathological features in breast cancer. Using deep learning-based feature extraction from pre-trained histopathology models, we extracted high-dimensional morphological representations from H&E-stained whole slide images and performed cross-modal analysis to identify which mutation-selection profiles correspond to distinct histological patterns. By identifying mutation combinations whose evolutionary selection signatures associate with specific pathological features, we tested whether these genomic profiles could contribute to classifying breast cancer molecular subtypes. Our findings reveal that evolutionary selection patterns acting on specific mutation combinations show measurable correspondence with pathological features and provide contributory predictive value for subtype classification, though they do not fully recapitulate the discriminative power of histopathological assessment. This suggests that the selective landscape of somatic mutations partially encodes morphological information, with cancer effect sizes capturing aspects of the evolutionary processes that shape tumor architecture. These results provide evidence that mutation-selection profiles can complement traditional pathology and advance our understanding of how evolutionary forces influence both the genetic and morphological characteristics of breast cancer. Moreover, because cancer effect sizes capture the directionality and strength of selective pressures, their association with histopathological assessment models may improve prediction of tumor evolutionary trajectories without -omics data, offering insights into likely progression patterns with which to inform treatment strategy.

#2731 Sylvester Data Portal: Population-level characterization of a diverse clinicogenomic cohort.

Oliver Mazariegos[1], Jeronimo Pissinis[1], Pearl Seo[2], Marcin Pilarczyk[1], Lukas Rupprecht[1], Caty Chung[1], Franklin Sotolongo[3], Marcin Blicharz[1], Piotr Smol[1], Michal Pyrkosz[1], Mateusz Jura[1], Vasileios Stathias[3], Stephan Schurer[1]

[1]Univ. of Miami Sylvester Comprehensive Cancer Ctr., Miami, FL,[2]University of Miami, Miami, FL,[3]University of Miami Miller School of Medicine, Miami, FL

The Sylvester Data Portal (SDP), developed at the University of Miami (UM) Sylvester Comprehensive Cancer Center, is an advanced cloud-based multi-omics platform that streamlines the management of real-world and research data. SDP provides an integrated framework for managing and harmonizing the center's clinicogenomic data generated by major genomic profiling vendors, including Caris Life Sciences, Foundation Medicine, NeoGenomics and Guardant Health. SDP now supports population-scale analyses that enable comparative studies across Sylvester's catchment population. To facilitate secure and role-based access to clinical and genomic data, SDP provides three structured interfaces: (1) The Clinical Dashboard, which summarizes aggregated patient demographics and data availability; (2) the Clinical Browser, which supports query and visualization of de-identified subject-level data; and (3) Clinical Collections, which integrate protected health information with next-generation sequencing data under IRB and Data broker approvals. This integrated infrastructure enables standardized and reproducible access to a large, diverse and growing clinicogenomic dataset, supporting translational research and promoting equitable representation in precision oncology. Using this framework, the demographic and molecular profiles of the Sylvester clinicogenomic cohort were systematically evaluated and compared with those of the Cancer Genome Atlas (TCGA). The Sylvester cohort includes over 30,000 samples, almost three times the number of samples reported in TCGA (11,387), and is derived primarily from targeted panel sequencing rather than whole exome sequencing. Notably, close to half of the cases, 45.9%, within this cohort are from patients that self-identify as Hispanic, vs. 3.52% in TCGA, reflecting the distinctive population from the cancer center and contributing to improved genomic representation of an underrepresented group in cancer genomics. Mutational prevalence was also compared, in particular TP53 is more often mutated in the TCGA cohort, 36.99% vs. 26.72%, whereas KRAS mutations are more prevalent in the SDP cohort 7.5% vs. 9.81%.

#2732 Florida Cancer Research (FL CARES) network and the Platform for Accelerating Collaborative Computational Cancer Research (PAC3R).

Jeronimo Pissinis[1], Michael S. Sinclair[1], Marcin Pilarczyk[1], Caty Chung[1], Dusica Vidovic[1], Lukas Rupprecht[1], Franklin Sotolongo[1], Oliver Mazariegos[1], Kathleen M. Jagodnik[1], Carlos Obregon[1], Tingyi Li[2], Ling Cen[3], Jiang Bian[4], Ji-Hyun Lee[4], Qianqian Song[4], Bikhyat Adhikari[5], Till Krenz[1], Ritik Bhandari[1], Umamaheswari Natarajan[6], Gogce C. Crynen[7], Appu Rathinavelu[6], Stuart Chalk[8], Mondal M. Ananda[5], Xuefeng Wang[3], Vasileios Stathias[1], Stephan Schurer[1]

[1]Univ. of Miami Sylvester Comprehensive Cancer Ctr., Miami, FL,[2]H. Lee Moffitt Cancer Center, Tampa, FL,[3]Moffitt Cancer Center, Tampa, FL,[4]UF Health Cancer Center, University of Florida, Gainesville, FL,[5]Florida International University, Miami, FL,[6]Rumbaugh Goodwin Institute for Cancer Research, Nova Southeastern University, Ft. Lauderdale, FL,[7]Bioinformatics and Statistics Core Facility, The Herbert Wertheim UF Scripps Institute for Biomedical Innovation & Technology, Jupiter, FL,[8]University of North Florida, Jacksonville, FL

The Florida Cancer Research (FL CARES) Network (https://floridacancernetwork.org/) is a statewide collaboration advancing cancer research and improving patient outcomes through coordinated research initiatives and a focus on understanding population-health variation across demographic categories. Funded by the State of Florida Department of Health's Bankhead-Coley Cancer Research Program, FL CARES unites six research organizations, including the state's three NCI-designated Cancer Centers. The Network has established a collaborative research consortium with unified policies, coordinated data and metadata standards, and diverse datasets and analysis tools.To accelerate computational research, FL CARES is developing the Platform for Accelerating Collaborative Computational Cancer Research (PAC3R) (https://pac3r.floridacancernetwork.org). This advanced informatics system enables FAIR (findable, accessible, interoperable, reusable) data management, including standardization, harmonization, and integration of multimodal cancer-related datasets. PAC3R is designed to support secure data sharing, deployment of scalable bioinformatics tools, and collaborative analyses across the FL CARES Network.PAC3R builds upon the Sylvester Data Portal (SDP) (https://sdp.miami.edu/), a cloud-based multi-omics platform that manages clinicogenomic and research data for the Sylvester Comprehensive Cancer Center. PAC3R integrates diverse multimodal cancer datasets to support analyses such as transcriptional perturbation signatures, cell sensitivity data, and small-molecule interactions, alongside local cancer panels from Moffitt Cancer Center and Nova Southeastern University. The platform also incorporates large-scale public genomics resources including The Cancer Genome Atlas (TCGA) and the Clinical Proteomic Tumor Analysis Consortium (CPTAC).Overall, the FL CARES Network and its advanced informatics system, the PAC3R platform, demonstrate the power of a unified semantic data model, harmonized datasets, and computational strategies to detect and understand outcome variations across Florida's populations, supporting the long-term goal of advancing effective cancer prevention, diagnosis, and treatment for all.

#2733 An interactive web platform for integrative analysis of drug responses in polyploid giant cancer cells.

Li-Ju Wang, Hsiao-Chun Chen, Chien-Hung Shih, Yuan Zhang, Huikang Ye, Ying-Ju Lai, Yushu Ma, Tiffany Habib, Hsi-Chun Wang, Yu-Chih Chen, Yu-Chiao Chiu

UPMC Hillman Cancer Center, Pittsburgh, PA

Polyploid giant cancer cells (PGCCs), typically arising from whole-genome duplication, are major drivers of therapeutic resistance and tumor recurrence. Building on our recently published high-throughput single-cell drug screening platform and ongoing efforts to profile PGCC responses across multiple cell lines representing diverse cancer lineages, we developed an interactive web-based platform that enables integrative analysis and visualization of these data. The platform integrates high-throughput PGCC drug screening results with multi-omic features curated from public cancer data resources, including somatic mutations, copy number alterations, gene expression profiles, and pathway activity scores. It supports two primary analysis modules: (1) a gene- or pathway-centric module that identifies compounds whose anti-PGCC efficacy is influenced by specific molecular features, and (2) a compound-centric module that identifies genes or pathways associated with the efficacy of a selected compound. Statistical comparisons, interactive visualizations, and annotations from external knowledgebases enable users to explore drug-feature relationships and generate new hypotheses. The platform facilitates systematic investigation of PGCC vulnerabilities through data-driven exploration. Example analyses demonstrate that compounds targeting oxidative stress response and cytoskeletal remodeling pathways preferentially suppress PGCC-enriched cell populations, consistent with their structural plasticity and adaptive signaling. Integration with baseline pharmacogenomic datasets further distinguishes PGCC-selective inhibitors from broadly cytotoxic agents, supporting the prioritization of therapeutic candidates. In summary, this interactive web resource provides an accessible and scalable framework for analyzing the molecular and pharmacologic landscape of PGCCs. By integrating our prior and ongoing high-throughput datasets with multi-omic data, it accelerates the discovery of biomarkers and therapeutic strategies to overcome treatment resistance driven by genome-doubled tumor populations.

: Large Language Models in the Clinic
Poster Session

#2737 Real-world usability of a clinical trial knowledge platform in a community cancer network.

Tony Kin Wai Hung[1], Shriya Amara[2], Paulette Schwartz[1], Aanshi Thumar[1], Zaid Raza[1], Elizabeth O'Brien[1], Gilad Kuperman[3], Barry Stein[1], Peter Yu[1], Jun J. Mao[4]

[1]Hartford HealthCare, Hartford, CT,[2]TeamX Health, Los Angeles, CA,[3]Columbia University, New York, NY,[4]Memorial Sloan Kettering Cancer Center, New York, NY

Background: Clinical trial participation in the United States remains suboptimal, and limited provider awareness contributes to missed opportunities for enrollment. Although public registries are comprehensive, they are not optimized for rapid use during clinical encounters. A clinical trial knowledge platform that consolidates protocol information, surfaces eligibility criteria, and generates concise AI-assisted summaries was previously evaluated at a comprehensive cancer center and demonstrated high feasibility and user engagement. We assessed real-world usability of this platform among oncology providers in a large community cancer network.
Methods: Ten oncology providers completed a standardized 30-minute guided session using the platform, followed by a 30-minute semi-structured interview and a 10-item modified Mobile Health App Usability Questionnaire (mMAUQ; Likert scale, 1-7; score ≥5 defined as favorable). During the guided session, participants were asked to complete standardized trial-search, eligibility-review, and summary-review tasks that reflect typical point-of-care use. Quantitative results were summarized descriptively. Qualitative data were analyzed using grounded-theory and interpreted through the PACMAD usability model.
Results: Usability ratings were consistently high (overall mean score, 6.8). All participants reported favorable usability and indicated willingness to recommend the tool to colleagues. Mean scores were 6.9 for ease of navigation, 6.9 for learnability, and 6.8 for usefulness in supporting trial-referral discussions. Qualitative findings mirrored quantitative results: providers identified rapid access to eligibility criteria for prescreening during time-limited visits as the most clinically valuable feature and described the tool as intuitive, easy to recall, and cognitively light, with minimal technical concerns. Suggested refinements focused on workflow integration, including interoperability with clinical systems and potential ambient support in patient encounters.
Conclusions: In a community oncology setting—where limited access to trial information can exacerbate disparities in enrollment—a clinical trial knowledge platform demonstrated excellent usability and strong perceived clinical utility. Providers reported that rapid access to eligibility criteria supported prescreening and gave them enough information to discuss trials with patients during routine care. These findings suggest that the practical integration of trial knowledge into time-limited clinical encounters—beyond trial matching alone—may be a critical determinant of whether digital clinical trial applications translate into increased participation in research. Evaluation of the platform’s effect on trial accrual and equitable access to research opportunities across diverse care environments is underway.

#2738 From chaos to columns: High-accuracy clinical data extraction with CIDER.

Mate Posta, Aida Figler, Zsofia Dobolyi, **Balazs Gyorffy**

Semmelweis University, Budapest, Hungary

The analysis of unstructured medical records represents a crucial challenge in clinical research and healthcare. Large Language Models (LLMs) offer a transformative opportunity to extract structured information from narrative text; however, their use in medical environments is limited by security, ethical, and reproducibility issues. Here we present CIDER (ClinIcal Data ExtractoR), a locally deployed, open-source LLM-based system designed for the secure analysis of medical documentation.

CIDER operates through an automated pipeline integrating vLLM-based inference, predefined data schemas, and prompt-engineered extraction rules to convert unstructured clinical text into structured variables. The system processes batch uploads, parsed reports using a fine-tuned model, and generates standardized output tables for direct analytical use. We evaluated CIDER's ability to extract structured clinical data from real-world Hungarian-language pathology and histology records. Using the Qwen3-VL-32B-FP8 model as the backbone, we analyzed 2046 pathological records and validated the model's outputs across six key clinical variables: sex, T stage, N stage, primary tumor organ, year of surgery, and tumor size. The extracted data were compared with manually mined data.

When manual data were available, extraction accuracy was very high for sex (99.4%, 1971/1982 identical), T stage (95.34%, 879/922), N stage (92.19%, 437/474), year of surgery (97.94%, 1998/2040), and primary tumor organ (95.52%, 1771/1854). The largest tumor size reached an accuracy of 77.05% (1333/1730 identical). Notably, CIDER was also capable of retrieving clinically relevant information in cases where manual annotations were missing, identifying additional instances for sex (n=64), T stage (n=780), N stage (n=213), tumor size (n=291), year of surgery (n=6), and primary tumor organ (n=15).

In summary, CIDER demonstrated strong performance across the evaluated parameters. These results show that a locally deployed, open-source LLM system can achieve near-expert level accuracy in structured data extraction from complex, non-English medical texts. By operating entirely within institutional infrastructure, CIDER ensures full data sovereignty and provides a scalable solution for automated medical record interpretation, supporting research, registry development, and clinical decision-making in multilingual healthcare environments. The CIDER platform is publicly accessible at https://llm.gyorffylab.com/cider.

#2739 Evaluation of large language models for automated clinical trial matching in oncology.

Aakash Desai, Ellen McNeeley, Sanad Alhuski, Maya Khalil, Matthew Might, Rebecca Arend, Andrew Crouse, Mehmet Akce

University of Alabama at Birmingham, Birmingham, AL

Background: Efficient patient-trial matching remains a critical challenge in oncology, complicated by heterogeneous documentation, missing data, and complex eligibility criteria. Large Language Models (LLMs) offer potential to automate eligibility screening by interpreting unstructured clinical notes and biomarker data.
Methods: We evaluated 6 models: llama3.2:3b, llama3.3:70b, medgemma_27b_text_it, deepseek-r1:8b, gpt-oss20b and gpt-oss120b for clinical trial eligibility determination across 19 key questions reflecting common eligibility criteria from oncology clinical trials. Data were extracted from patient medical records with known trial matches, and models' binary (yes/no) responses, confidence scores, and reasoning excerpts were analyzed. Concordance between models and interpretability of outputs were assessed.
Results: Both gpt-oss20b and gpt-oss120b models demonstrated high agreement on eligibility determinations for well-documented criteria such as measurable disease, ECOG status, age, and tissue availability, with confidence scores commonly above 0.90. Differences emerged in criteria requiring inference or where documentation was incomplete; gpt-oss120b showed greater confidence and nuanced reasoning in ambiguous cases. Both models flagged missing or unclear data, providing reasoning transparency that supports clinical review. Concordance metrics suggested strong reliability (Cohen's kappa >0.8) for explicit criteria, with potential to significantly reduce manual screening burden. The remaining models provided poorer quality responses in general and were unable to respond coherently at all if required to provide that response in a structured format.
Conclusions: LLMs can accurately and transparently automate critical components of oncology trial eligibility screening, augmenting manual review processes. Differences in model confidence with uncertain data underscore the need for ongoing refinement and highlight the value of explainable AI in clinical decision support. These findings support integrating LLMs into clinical trial matching workflows to improve trial access and enrollment efficiency.
Impact: Automated, interpretable LLM-based clinical trial matching represents a promising advancement toward precision oncology by scaling patient access to tailored therapies and optimizing trial throughput.

#2740 Applications of large language models to CAR-T cell therapy clinical data using Google cloud computing.

Emmanuel Contreras Guzman[1], Matthew Jankowski[1], Andre De Menezes Silva Corraes[1], Malvika Gupta[1], Monica L. Shaw[1], Madiha Iqbal[2], Talal Hilal[3], Saurabh Chhabra[4], Ricardo Daniel Parrondo[2], Jody K. Mclean[1], Kim R. Riester[1], Kayla Joseph[1], Melinda Tan[5], Holly Ross[2], Cleyonia Barnett[2], Sylvia Carter[2], Semy Girmay[2], Rachel Wolan[2], Milana Ramsey[6], Christian Downhour[6], Kristy Morgan[6], Shae Sibley[6], Erica Rushing[6], Lucy Holmes[1], Allison Burgstahler[1], Stephen M. Ansell[7], Hassan Alkhateeb[1], Matthew Hathcock[1], Ramona Bruno[1], Allison C. Rosenthal[6], Hemant Murthy[8], Patrick B. Johnston[9], Jonas Paludo[1], Yi Lin[1]

[1]Mayo Clinic, Rochester, MN,[2]Mayo Clinic Florida, Jacksonville, FL,[3]Mayo Clinic Comprehensive Cancer Center, Phoenix, AZ,[4]Mayo Clini, Phoenix, AZ,[5]Mayo Clinic Cancer Center Minnesota, Rochester, MN,[6]Mayo Clinic, Phoenix, AZ,[7]Assistant Professor, Div. of Hematology, Mayo Clinic College of Medicine, Rochester, MN,[8]Mayo Clinic, Jacksonville, FL,[9]Hematology, Mayo Clinic College of Medicine, Rochester, MN

Large Language Models (LLM) are being widely adopted into the medical field for their impressive ability to analyze and summarize large amounts of text data. These models enable clinicians and researchers to extract meaningful insights from complex datasets and may assist with decision making. Here we present our workflows and application of LLM for the interpretation and summarization of clinical data related to CAR-T cell therapy.

Using an LLM (Gemini 2.5 pro) in the Google Cloud Computing (GCP) environment, two applications were developed to analyze CAR-T cell therapy clinical data: 1) extracting and summarizing CRS and ICANS event-related data to streamline the compliance team workflow, and 2) identifying features available at time of CAR-T infusion able to classify patients into high- or low-monitoring needs 14 days post CAR-T. Patient data (vitals, labs, hematology notes, and EKGs) were extracted from the electronic medical record (EMR) using Google BigQuery into SQL tables in GCP. For each application, relevant data fields were retrieved, formatted into JSON objects, and embedded in the LLM prompt for context-aware processing. Both applications have undergone iterative prompt engineering after analyzing the LLM output against ground truth data in the EMR.

For the application extracting and summarizing CRS and ICANS events, the LLM was optimized on Mayo Clinic Rochester data. When compared to the IEC compliance database, the LLM achieved 100% accuracy and F1 score for CRS events, and 96% accuracy and 82% F1 score for ICANS events. The match rate for CRS and ICANS grades were 83% and 89% respectively. We applied the same LLM to Mayo Clinic Arizona (MCA) and Mayo Clinic Florida (MCF) cases, who document clinical notes and toxicity flowsheet differently, and achieved an accuracy (MCA: 93%, MCF:93%) and F1 score (MCA: 96%, MCF: 96%) for CRS and accuracy (MCA: 81%, MCF:82%) and F1 score (MCA: 76%, MCF: 75%) for ICANS. LLM was able to capture events missed by manual reviews. For most of the discrepancies where compliance team final adjudication is needed, LLM will be updated to flag discrepancies for review by the compliance team.

For the application related to the monitoring needs 14 days post CAR-T, the LLM identified 5 categories predictive of high or low monitoring needs post CAR-T infusion (disease status, inflammatory and tumor burden markers, hematologic status, renal function and performance status). Our model achieved a sensitivity of 85.7%, specificity of 23.8%, and F1 score of 65.5% for our first cohort, compared with data extracted by the LLM from the EMR. For our second cohort, with demographics statistically similar to cohort 1 and using the same 5 categories, the LLM achieved a sensitivity of 83.3%, a specificity of 28.6%, and F1 score of 65.4%. Our workflow and applications of LLM's provide examples and guidance to others interested in applying LLM's for clinical and research applications.

#2741 Large language model-based triage of Hematology/Oncology patient messages: Performance, safety, and clinical implications.

Dinh Nguyen, Sinjin Lee, Brett Anwar, Mason Kellogg, Ronil Synghal, Khang Nguyen

SCPMG, Pasadena, CA

Background: Patient portal messages are a major source of real-time symptom reports in Hematology/Oncology, but manual review is labor-intensive and may delay identification of urgent issues. Large language models (LLMs) can process free text at scale, yet their safety and performance for triage in cancer care are uncertain.
Methods: We conducted a retrospective study of adult patients with hematologic malignancies receiving care at a single center within Southern California Permanente Medical Group, the care delivery arm of Kaiser Permanente, from November 2024 to November 2025. All patient-initiated messages to the Hematology/Oncology clinical team were extracted from the electronic health record portal. A stratified sample of messages was annotated by clinicians for urgent and non-urgent categories. Messages labeled as urgent reflected symptoms warranting prioritized clinician review within 24-48 hours. We developed an LLM-based classifier using few-shot learning that generates a label populating the “Topic” column in the receiving clinician’s inbox. Primary outcomes included discriminative performance metrics such AUROC, sensitivity, specificity, and F1 score for classifying urgent messages.
Results: A total of 10,683 messages from 2,287 unique patients were processed by our model; 433 messages were labeled as urgent. For urgent message classification, the few-shot LLM achieved an AUROC, sensitivity, specificity, and F1 score of 91.05% (95% CI, 85.69%-96.42%), 97.62% (95% CI, 92.50%-99.89%), 84.48% (95% CI, 74.60%-93.34%), and 89.13% (95% CI, 81.82%-95.74%) respectively.
Conclusions: An LLM-based triage system reliably categorized patient messages into urgent and non-urgent categories and has the potential to facilitate timelier action for urgent symptoms within a Hematology/Oncology department. The system’s practical utility highlights its relevance for departments seeking to leverage NLP to improve message management in cancer care.

#2742 An artificial intelligence domain-specialized scalable and clinically relevant pipeline to automate standardized O-RADS stratification for imaging reports in ovarian cancer.

Asmi Agarwal[1], Min Ren[2], Jingjing Gong[3], Richard Selinfreund[4], Ruchika Goel[5], Yanhui Guo[6]

[1]SIU School of Medicine, Springfield, IL,[2]Ultrasound Department, Shanghai First Maternity and Infant Hospital, Shanghai, China,[3]Shanghai Changning Maternity and Infant Health Hospital, Shanghai, China,[4]Department of Pathology, SIU School of Medicine, Springfield, IL,[5]Department of Hematology and Oncology, Johns Hopkins University and SIU School of Medicine, Springfield, IL,[6]Department of Computer Science, University of Illinois Springfield, Springfield, IL

Purpose: Despite therapeutic advances, ovarian malignancies continue to carry a disproportionate mortality burden among women worldwide. Timely and accurate assessment of adnexal lesions is critical for improving outcomes, yet the disease is often diagnosed at an advanced stage due to subtle or misinterpreted early findings. The Ovarian-Adnexal Reporting and Data System (O-RADS) provides a standardized framework for malignancy risk stratification; however, in practice, its manual application can be time-consuming and prone to inter-observer variability, creating barriers to consistency and incorporation within clinical workflows. To address this urgent clinical need, we developed an artificial intelligence (AI) pipeline that automates O-RADS classification directly from free-text pelvic ultrasound reports.

Procedures/Methods: By integrating *Lingshu*, a multimodal *Domain-Specialized* large language model (LLM) for medical reports reasoning, with traditional machine learning classifiers, our system transforms unstructured radiology narratives into structured, high-fidelity malignancy risk assessments, eliminating the need for manual scoring. We also compared the performance of this framework with that of an equivalent pipeline using *MedGemma.*

Data/Results: We analyzed 413 de-identified pelvic ultrasound reports and extracted semantic embeddings using Lingshu. These embeddings, representing clinically meaningful linguistic patterns, were used to then train machine learning classifiers via a 5-fold cross-validation. Lingshu and a logistic regression model performed the best, achieving a mean accuracy of 0.773 ± 0.031, weighted precision of 0.777 ± 0.029, recall of 0.767 ± 0.028, F1-score of 0.765 ± 0.032, and a macro-averaged AUROC of 0.929 ± 0.019. Notably, this achieved a lower AUROC of 0.923 ± 0.027.

Conclusion: A foundation model such as Lingshu demonstrates remarkable semantic understanding. We show that this model can be safely and effectively leveraged to standardize O-RADS risk assessment directly from unstructured ultrasound reports, bridging the gap between AI capability and real-world radiology practice. Our approach establishes a *scalable and clinically impactful pathway* for integrating AI into gynecologic oncology workflows, paving the way for broader adoption of LLM-driven tools in early ovarian cancer detection and risk stratification. Importantly, this AI-driven framework is not intended to replace expert radiologic judgment but to augment it by enabling the consistent application of O-RADS criteria, supporting diagnostic confidence, and reducing variability across providers and institutions. In doing so, it has the potential to expedite early identification of high-risk adnexal lesions and ultimately improve clinical decision-making and patient outcomes.

#2743 Deploying artificial intelligence driven digital pathology for real world clinical decision-making in pancreatic cancer.

Ashish Manne[1], Alejandro Leya[1], Abdul Rehman Akbar[1], Upender Manne[2], Anne Noonan[1], Anup Kasi[3], Ashwini Esnakula[1], Ravi Paluri[4], Anil Vasdev Parwani[5], Muhammad Khalid Khan Niazi[1]

[1]The Ohio State University, Columbus, OH,[2]University of Alabama at Birmingham, Birmingham, AL,[3]The University of Kansas Cancer Center,[4]Atrium Health Wake Forest Baptist, Winston Salem, NC,[5]The Ohio State University Wexner Medical Ctr., Columbus, OH

Pancreatic ductal adenocarcinoma (PDAC) remains one of the deadliest malignancies, driven by limited therapeutic options and the absence of widely implemented, clinically actionable biomarkers. Transcriptomic subtyping, particularly the classical (CL) versus basal-like (BL) Moffitt classification, offers prognostic and predictive value: CL tumors show improved outcomes and greater sensitivity to 5 fluorouracil based regimens (e.g., FOLFIRINOX). However, BL tumors exhibit poor outcomes across treatment regimens and may benefit from clinical trial prioritization or intensified oversight. But routine use of RNA-based subtyping is hindered by cost, turnaround time, and restricted access to commercial assays such as Purity Independent Subtyping of Tumors (PurIST). To overcome these barriers, we developed a deep learning model that infers PDAC molecular subtypes directly from hematoxylin and eosin (H&E) whole slide images (WSIs) by integrating with matched RNA-sequencing data for supervised training. In this initial iteration, WSIs from 126 Pancreatic Cancer Action Network (PANCAN) patients with high-quality slides and confirmed CL or BL transcriptomic profiles were curated. Bulk RNA-seq underwent standardized preprocessing, including quality control, alignment, normalization, and quantification of Moffitt-derived gene signatures to generate high-confidence molecular labels for supervised training. These annotations served as ground truth for supervised training. Using five-fold cross-validation, the model classified PDAC tumors into CL and BL subtypes with strong performance (area under curve, AUC: 0.83; accuracy: 77%; specificity: 80%; sensitivity: 72%), comparable to existing image-based PurIST subtyping literature (AUC 0.83-0.86). Our ongoing work with larger multi-institutional datasets aims to further enhance accuracy and generalizability. This proof of concept establishes the feasibility of AI-driven digital pathology for rapid, scalable Moffitt PDAC molecular subtyping directly from WSIs of routine H&E slides. By eliminating the need for RNA-based assays, this approach offers a cost-effective and scalable alternative, particularly valuable for real-world and resource-limited clinical settings. Prospective validation studies will be crucial for refining performance, assessing clinical utility, and enabling integration into precision oncology workflows for PDAC treatment.

#2744 Automating clinical and pathological staging for breast cancer patients.

Arshad Mohammed[1], Umair Ayub[2], Pooja Advani[3], Shakeela W. Bahadur[2], Amye J. Tevaarwerk[4], Tufia C. Haddad[4], Elisabeth I. Heath[4], Brenda J. Ernst[2], Ben Zhou[5], Cui Tao[6], Sara J. Holton[4], Karthik V. Giridhar[4], Irbaz B. Riaz[2]

[1]Mayo Clinic Alix School of Medicine, Phoenix, AZ,[2]Division of Hematology/Oncology, Mayo Clinic, Phoenix, AZ,[3]Division of Hematology/Oncology, Mayo Clinic, Jacksonville, FL,[4]Division of Hematology/Oncology, Mayo Clinic, Rochester, MN,[5]Department of Computing and Augmented Intelligence ASU, Tempe, AZ,[6]Department of Artificial Intelligence and Informatics, Mayo Clinic, Jacksonville, FL

Background: Accurate staging is essential for treatment selection, prognosis assessment, and trial eligibility. While prior studies attempted automating pathological (p) staging, few address clinical (c) staging and no studies have compared LLM-derived staging with clinician staging during clinical visit and retrospective cancer registry staging.
Methods: We developed a multi-agent framework using Gemini-2.0-Flash-001 and GPT-5 to (1) identify reports (2) extract key data, and (3) apply AJCC 8th edition staging criteria. LLM staging was compared with clinician documentation and registry staging in breast cancer patients. Clinician-registry agreement served as the reference standard. Two independent breast oncologists reviewed discordant cases.
Results: We analyzed 122 randomly selected breast cancer patients across all three Mayo Clinic sites from 2018 - 2023. LLM performance matched or exceeded human inter-rater agreement for pathological staging (95-99.2% vs. 95-98.4%). Clinical staging was more challenging, with LLM concordance of 73-77.9% for cT and 87-89.3% for cN versus 87.8% and 91.0% clinician-registry agreement. Among 89 patients with clinician-registry concordance, LLM concordance was 98.9% for pT/pN, 79.8% for cT, and 91.0% for cN. Experts favored LLM staging in 27.8% (5/18) of cT and 25.0% (2/8) of cN discordances. Error analysis revealed LLM challenges in handling non-mass enhancements (6 cases), selecting radiologic measurements (2 cases), identifying discrete masses (2 cases), and miscellaneous (3 cases).
Conclusion: LLMs achieved human-level performance for pathological staging (98%), supporting human-in-the-loop deployment. For clinical staging (79.8% cT, 91.0% cN), future work must enhance multimodal reasoning and integrate physical examination data. Prospective validation is needed to assess real-world impact. With targeted refinements and oversight, automated staging can transform registry workflows while augmenting clinical decision-making.

Clinical-Pathological Staging Concordances

Comparison	pT	pN	cT	cN
LLM vs. Registry	96.7%	99.2%	73.8%	87.8%
LLM vs. Clinician	95.9%	96.7%	77.9%	89.3%
Clinician vs. Registry	95.1%	98.4%	87.8%	91.0%

#2745 Patients prefer ChatGPT to physician responses in cancer communication.

Aaron Segura, Bernard Tawfik, Ben Liem, Zoneddy Dayao, David Y. Lee, Jacklyn M. Nemunaitis, David Savage, Moises Harari-Turquie, Nicole Hill, Charles Foucar, Amy Tarnower, Dulcinea Quintana, Jude Khatib, Thomas Schroeder, Martha Mapalo, Yolanda Sanchez, Ramesh Gopal

University of New Mexico Comprehensive Cancer Center, Albuquerque, NM

Introduction
Large language models like ChatGPT (GPT) are increasingly utilized by patients and physicians yet it is unknown whether either group prefers the output of GPT compared to physician-authored content. This study evaluated how patients and physicians perceive and compare ChatGPT-generated versus physician-authored recommendations.
Methods
We surveyed 51 adult female breast cancer patients and 15 physicians at the University of New Mexico Comprehensive Cancer Center to compare their evaluations of GPT versus physician-authored responses to four cancer scenarios related to treatment, family dynamics and employment. Each scenario included two blinded, responses to the same question—one from GPT and one from a physician. Participants rated each on 7-point Likert scales for helpfulness, empathy, and informativeness and indicated their preferred response (1 = strongly agree, 7 = strongly disagree). The primary outcome was the proportion preferring GPT (binomial test vs 50%); secondary outcomes were within-subject Likert differences (Δ = GPT - physician) analyzed with Wilcoxon signed-rank tests.
Results
Among 66 participants (51 patients; 15 physicians), patients preferred GPT 71/104 (68.3%, $p = 0.00025$), while physicians preferred GPT 31/52 (59.6%, $p = 0.21$), with no significant difference between groups ($p = 0.82$). Preferences varied by scenario: patients showed no significant differences in S1 or S2 (52.6% and 58.6% preferring GPT; both $p > 0.45$), strongly favored GPT in S3 (85.7%, $p = 0.00018$), and significantly favored GPT in S4 (71.4%, $p = 0.036$). Physician preference for GPT was near equipoise for all scenarios (36.4-75.0%, all $p \geq 0.15$). Patient ratings favored GPT for helpfulness ($\Delta = -0.36$, $p = 0.009$), empathy ($\Delta = -0.46$, $p = 0.009$), and informativeness ($\Delta = -0.42$, $p = 0.013$). Physician ratings showed no significant differences for helpfulness ($\Delta = -0.10$, $p = 0.59$) or informativeness ($\Delta = +0.18$, $p = 0.57$), with a trend toward higher empathy for GPT ($\Delta = -0.44$, $p = 0.058$).
Conclusion
Patients showed a strong overall preference for GPT-generated recommendations, with scenario-specific differences. Physicians demonstrated a smaller, nonsignificant preference for GPT. While ratings were numerically close for all domains, patients consistently judged GPT responses as more helpful, empathetic, and informative, whereas physicians rated the two sources similarly. These findings suggest that physicians could combine GPT-generated responses preferred by patients with their own recommendations to improve clinical communication.

#2746 AI vs human abstraction of pain scores and analgesic trends in low-dose radiation therapy for osteoarthritis: A concordance study.

Camille Schwartz[1], Michael Anderson[2], Kelsey Moakler[2], Bradley Newby[2], David Davenport[2], Matthew Schwartz[3]

[1]University of Nevada, Las Vegas, Las Vegas, NV,[2]Comprehensive Cancer Centers of Nevada, Henderson, NV,[3]University of Nevada, Las Vegas (UNLV), Las Vegas, NV

Background / Significance:
Accurate clinical data abstraction underpins outcomes research but remains resource-intensive and variable. Artificial intelligence (AI) offers potential to streamline this process while maintaining accuracy, yet its validation in real-world oncology data is limited. This undergraduate-led study evaluated Microsoft Copilot in replicating human chart abstraction for pain and functional outcomes among osteoarthritis (OA) patients treated with low-dose radiation therapy (LDRT), emphasizing concordance, efficiency, and reproducibility.
Methods:
Clinical notes from 30 patients (55 joints) treated with LDRT (3 Gy in six 0.5 Gy fractions) between August 2024 and August 2025 were analyzed. Human reviewers manually extracted Numeric Rating Scale (NRS, 0-10) and von Pannewitz Score (VPS, 0-4) data at baseline, end-of-treatment (EOT), and one-month follow-up. Microsoft Copilot (HIPAA-compliant) independently extracted identical data. Discrepancies were classified as exact, minor (≤2-point difference), or missed. Concordance was calculated using intraclass correlation coefficient (ICC) for NRS and weighted kappa for VPS. Abstraction time per chart was recorded.
Results:
AI achieved 92 percent exact match for NRS (ICC = 0.96, 95 percent CI 0.93-0.98) and 94 percent for VPS (kappa = 0.91). No fabricated data were produced; one human omission was detected by AI. Mean abstraction time was about 2 minutes per chart versus 30 minutes for humans, a greater than 10-fold efficiency gain.
Conclusions:
AI-assisted abstraction showed near-perfect concordance with human reviewers while reducing time and labor by over 90 percent. This undergraduate-led investigation demonstrates that responsible AI implementation can enhance accuracy, reproducibility, and efficiency in radiation-oncology outcomes research and accelerate evidence generation in oncology.
Disclosure:
No external funding or conflicts of interest. Data abstraction performed using Microsoft Copilot (HIPAA-compliant); no generative AI tools were used for writing.

#2747 Source discipline matters: Guideline anchored large language model outperforms Open Evidence for decision support in acute leukemias.

Peter Palumbo[1], Connor Yost[2], Emilio Del Toro[1], Demetrios Garbis[1], Peter Odutola[3], Yash Kumar[4], Arturo Loaiza[5], Matthew Sullivan[6]

[1]Dartmouth Geisel School of Medicine, Hanover, NH,[2]Department of Internal Medicine, Creighton University School of Medicine, Phoenix, AZ,[3]Department of Molecular Biology, Harvard University, Cambridge, MA,[4]Institutional Liaquat National Medical College Hospital, Karachi, Pakistan,[5]Department of Hematology and Oncology, St. Luke's University Health Network, Bethlehem, PA,[6]Department of Hematology and Oncology, Dartmouth Hitchcock Medical Center, Lebanon, NH

Background

Acute leukemia is one of the most complex and rapidly evolving domains in hematologic oncology, where treatment selection depends on a variety of factors such as molecular subtype and performance status. The National Comprehensive Cancer Network (NCCN) provides updated, lineage-specific algorithms for Acute Myeloid Leukemia (AML) and Acute Lymphoblastic Leukemia (ALL), yet these guidelines are dense and frequently revised. Large language models (LLMs) may assist clinicians in synthesizing this data, but the reliability of their outputs depends critically on their evidence sources. This study compared an NCCN-anchored retrieval-augmented model (RAG GPT-5) with Open Evidence (OE), a model linked to journal-based sources such as *NEJM* and *JAMA*, to assess accuracy, safety, and guideline concordance in acute leukemia decision support.

Methods

Forty de-identified AML and ALL vignettes were independently evaluated by two models: Open Evidence (O_1) and an NCCN-anchored retrieval-augmented GPT-5 model (O_2).). Reviewers were blinded to model identity and rated each response using a modified Generative Performance Score (mGPS = Guideline Concordance - Hallucination Penalty; range –1.0 to + 1.0). Statistical comparison used independent-samples t-tests.

Results

The RAG model (O_2) demonstrated significantly higher overall performance (mean = 0.84, SD = 0.25) compared with Open Evidence (O_1, mean = 0.70, SD = 0.32); $t(\approx 78) = -2.17$, $p = 0.033$. Qualitative review revealed key distinctions in clinical reasoning:

- Open Evidence frequently hallucinated agents (e.g., ipilimumab), omitted prior therapy context, and failed to adjust for infection recovery or cardiac risk before chemotherapy.
- RAG GPT-5 exclusively cited NCCN recommendations, with minor rounding errors (e.g., ATRA dose), and occasionally defaulted to conservative but still guideline-concordant dosing (e.g., daunorubicin).
- Neither model fully addressed dual-tumor or BCR-ABL-positive scenarios, and both under-recognized recent updates such as *menin inhibitors* for MLL-rearranged AML, which are emerging but not yet NCCN-listed. Variance was smaller for the RAG system, indicating more consistent performance across cases.

Conclusions

In acute leukemias, evidence source materially alters LLM behavior and reliability. Guideline-anchored retrieval produced significantly more NCCN-concordant recommendations and fewer hallucinations than OE. While both systems occasionally missed nuanced treatment history or recent investigational agents, only OE introduced clinically unsafe suggestions. These findings support NCCN-anchored RAG as the safer and more consistent foundation for LLM-based decision support in acute leukemias, where precision and patient context are paramount. Future work should expand to relapse and transplant scenarios with prospective clinician validation.

#2748 Arkangel AI, OpenEvidence, ChatGPT, Medisearch: Are they objectively up to medical standards? A real-life assessment of LLMs in healthcare.

Natalia Castano -Villegas[1], Maria Camila Villa[2], Katherine Monsalve[3], Isabella Llano[2], Laura Velasquez[2], **Jose Zea**[2]

[1]Arkangel AI, Bogota, Colombia,[2]Arkangel IA, Bogota, Colombia,[3]Arcangel IA, Bogota, Colombia

Background: Large language models (LLMs) are increasingly used in healthcare, but standardized benchmarks fail to capture their validity and safety in real-world scenarios. Evaluating their quality is critical for safe integration into practice.
Methods: Four fictitious clinical vignettes were developed by independent specialists and tested in four conversational agents: ArkangelAI, OpenEvidence, ChatGPT, and Medisearch. Each vignette included four questions. Responses were evaluated by four external clinicians using an eight-criterion Likert scale: 1-2 = dissatisfaction, 3 = neutral, 4-5 = satisfaction, 6 = not applicable. The criteria considered correctness, consensus, bias, standard of care, updated information, patient safety, real sources in references, and context-awareness. Response times were measured with medians/interquartile ranges (IQR). Results were reported as frequencies. Hypothesis tests were applied ($\alpha = 0.05$).
Results: There were 128 Question-answer pairs. ArkangelAI-Deep had the highest satisfaction (92.9%), followed by OpenEvidence (83.6%), ChatGPT-Deep (80.5%), and Medisearch (71.1%). Most dissatisfaction was for the real-source-of-references criteria: GPT-Personalized 75%, GPT-Regular 97%. Conversely, ArkangelAI-Deep, ChatGPT-Deep, and OpenEvidence obtained 100% satisfaction. All performed well in correctness and agreement with the consensus. ChatGPT was the lowest-scoring in non-biased answers. The safest for patients was GPT-Personalized, followed by Arkagel AI-Deep. Medisearch had the fastest response time (18 s), while GPT-Deep (13 min) and ArkangelAI-Deep (7.4 min) were slowest, showing a trade-off between depth and usability.
Conclusions: ArkangelAI-Deep and OpenEvidence consistently outperformed others, while Medisearch and GPT-Regular had significant limitations. These results underscore the need for standardized frameworks to ensure safe use of LLMs in healthcare.

#2749 Towards a foundation model for treatment-related adverse events in cancer immunotherapy.

Bin Baek[1], Tingyi Li[1], Biwei Cao[2], Xiaqing Yu[1], Xuefeng Wang[1]

[1]Biostatistics and Bioinformatics, H.Lee Moffitt Cancer Center and Research Institute, Tampa, FL,[2]Biostatistics, H.Lee Moffitt Cancer Center and Research Institute, Tampa, FL

Background: Immune-related adverse events (irAEs) provide important clues about immune activation during checkpoint blockade, yet real-world AE reporting is often sparse and fragmented. A further challenge is that FAERS provides unstructured case-level reports, while ClinicalTrials.gov reports arm-level AE tables that differ greatly in completeness and level of detail across trials. These differences make it difficult to study toxicity patterns across data sources in a unified way. To address this gap, we developed a denoising AE foundation model that reconstructs missing Preferred Terms (PTs), learns latent AE co-occurrence structure, and generates biologically interpretable AE embeddings.

Methods: We collected ten years of FAERS reports related to immune checkpoint inhibitors (2015Q1-2025Q2) and curated a vocabulary of 200 treatment-related PTs. The model treats each AE profile as partially observed and performs PT-aware masking, case-level PT dropping, and multi-label reconstruction on a BioBERT backbone. Candidate-set validation was used to evaluate recovery of truly unobserved PTs, and mid-layer pooling was applied to improve stability across diverse AE profiles. For ClinicalTrials.gov, we harmonized arm-level AE tables by standardizing differences in reporting depth and AE granularity. We then generated pooled AE signatures for each treatment arm and evaluated whether these signatures could distinguish immunotherapy arms with known differences in clinical outcomes.

Results: The model recovered intentionally hidden AEs with strong performance (Recall@5 = 0.38; Recall@10 = 0.51). The learned embedding space separated well-known irAEs from non-immune toxicities and formed clusters that aligned with MedDRA SOC patterns. When applied to ClinicalTrials.gov treatment arms, the AE signatures reflected cancer-type-specific patterns, including dermatologic events in melanoma and hepatic or gastrointestinal patterns in hepatocellular carcinoma and GI cancers. Arm-level embedding profiles also differentiated treatment arms with superior outcomes across several ICI trials, suggesting that the representation space captures meaningful biology related to treatment response.

Conclusions: We present a foundation model that integrates FAERS and ClinicalTrials.gov AE data to denoise AE profiles, learn biologically grounded toxicity embeddings, and reveal AE patterns associated with clinical benefit. This framework provides a scalable approach for studying AE biology and may support AE-based biomarker development and arm-level prediction of immunotherapy efficacy.

#2750 Rapid curation of colon cancer cohorts using on-site peta-scale language model for MSI classification from pathology reports.

Joshua Jay Levy, Nathalie Nguyen, Minh-Khang Le, Keluo Yao, Jane Figueiredo

Cedars-Sinai Medical Center, Los Angeles, CA

Background: Pathology reports are highly heterogeneous, making it difficult to extract structured information needed for cohort curation. Earlier machine-learning models had to be trained separately for each specific task, limiting flexibility. Newer large language models (LLMs) can follow written instructions—"prompts"—to identify or summarize information directly from the text, allowing a single model to perform many tasks without retraining. These models were previously too large to run within hospital systems, but compact GPU platforms, such as NVIDIA DGX, now make state-of-the-art LLMs containing hundreds of billions of parameters feasible to deploy locally. This enables rapid prototyping of flexible extraction workflows. Here, we evaluate locally deployed LLMs for rapid cohort curation using mismatch repair (MMR) status extraction from colorectal pathology reports as an example.
Methods: A total of 82 colorectal pathology reports were collected across two study cohorts (ColoCare and SeroNet). Most reports included MLH1, MSH2, MSH6, and PMS2 staining results used to determine MSI (microsatellite instability) status. Two locally deployed LLMs (GPT-OSS 20B and 120B) classified each case as MSI, MSS, or ambiguous based on documented MMR expression or any direct MSI statement, with cases lacking clear MMR information assigned to an ambiguous category. Model predictions were compared with manual MSI annotations. For reports the model classified as ambiguous but annotators judged MSI or MSS, each model was prompted to restate and justify its decision to assess reasoning consistency.
Results: Both models performed well across the 82 reports. The 20B model achieved 96.3% accuracy, while the 120B model achieved 95.1%. For MSI, the 120B model showed higher sensitivity (87.5% vs. 77.8%) and F1 score (87.5% vs. 82.4%), with both models maintaining high precision and specificity (≥ 87.5% and ≥ 98.6%, respectively). For MSS, performance was strong for both models, with the 120B model showing slightly higher precision (97.6% vs. 95.5%) and specificity (97.4% vs. 94.6%). The 20B model perfectly identified all ambiguous cases, whereas the 120B model assigned two MSS reports to "unable to be assessed." In reviewing these discrepancies, the models remained consistent with their original classifications but differed in how they interpreted the phrase "MSI IHC low prob": the 120B model viewed it as indeterminate and returned "unknown," while the 20B model interpreted the same wording as supporting MSS in the context of intact MMR expression.
Conclusion: These findings demonstrate the practical utility of leveraging state-of-the-art LLMs within privacy constrained hospital settings. Further work will assess performance in more technically challenging scenarios and clarify how ambiguous wording impacts quality control when integrating LLMs into clinical workflows.

#2751 Large language model-derived molecular patient similarity from real-world MTB data.

Sophie Lugani[1], Oğuz Serbetci[2], Alexander Reinicke[2], Benedikt Kortum[1], Berkay Ozdin[1], Thomas Debertshauser[1], Dominik Modest[1], Ulrich Keilholz[1], Ulf Leser[2], Manuela Benary[1]

[1]Charite - Berlin University Medicine, Berlin, Germany,[2]Humboldt-Universitat zu Berlin, Berlin, Germany

Background:
Molecular tumor boards (MTBs) frequently evaluate patients with rare molecular profiles where prospective evidence is scarce. To address this challenge, we investigated whether large language models (LLMs) can structure real-world MTB documentation into analyzable representations to identify molecularly similar patients.
Methods:
MTB documentation from 2,788 patients and pathology reports from 506 patients discussed at the Charité MTB (2020-2025) were structured using NVIDIA Nemotron-49B. Textual summaries and structured features on prior targeted therapies, immunohistochemistry (IHC), and molecular alterations (MOL; CiViC-weighted) were extracted, yielding 1,736 textual, binary and numeric features. The LLM output was vector embedded using bge-multilingual-gemma2. Patient similarity was computed using cosine distance for embeddings, and Jaccard (binary) and absolute error (numeric) for structured features. Similarity rankings were ensembled via reciprocal-rank fusion and evaluated using MRR and nDCG, against BM25 and embedding baselines on raw MTB documentation. As a proxy for ground truth, MTB recommendations were structured into course of action, drug, agent class, and clinical trial elements and used as similarity targets.
Results:
LLM-based information extraction achieved F1 scores of 96% for mutation detection and 92% for IHC, evaluated against 30 manually annotated pathology reports. The ensemble similarity method - combining structured-feature similarity, summary-embedding similarity, and BM25 via reciprocal-rank fusion - showed the highest alignment with MTB recommendations (MRR@1000 = 25.8, nDCG@10 = 10.1), outperforming BM25 alone (22.8, 8.6) or text-embedding similarity of MTB documentation (22.2, 8.3), with all improvements statistically significant ($p < 0.01$). Structured features derived from MTB documentation (20.2, 9.2) outperformed those derived from pathology reports (17.9, 8.0). Together, these findings indicate that LLM-derived representation improved therapy-aligned patient similarity over text- and embedding-based baselines. Across all cases, 486 unique therapeutic entities were identified; among 290 drug entities, 163 were recommended to more than one patient, and 65% of patients shared at least one recommendation with another case.
Conclusion:
LLM-derived clinical-molecular representations enabled scalable retrieval of molecularly matched cases in real-world MTB datasets. This approach supports institutional case library formation and systematic case series generation, enhancing evidence generation in precision oncology.
[O.S. and S.L. contributed equally to this work.]

#2752 CancerSTFormer enables multi-scale analysis of spot-resolution spatial transcriptomes and dissects the gene and immune regulatory responses of targeted therapies.

Benjamin Strope[1], Dana Varghese[1], William Bowie[1], Stacy Wang[1], **Qian Zhu**[2]

[1]Lester Sue Smith Breast Center, Baylor College of Medicine, Houston, TX,[2]Lester Sue Smith Breast Center, Molecular and Human Genetics, Dan L. Duncan Cancer Center, Baylor College of Medicine, Houston, TX

Despite the success of immunotherapy, a significant number of cancer patients still do not respond to it. It is important to understand why treatment fails and to find better treatment for them. We believe that achieving the goal of increasing the efficacy of immunotherapy must start with understanding the spatial microenvironment and the mechanisms of immunosuppression, so that biology-driven treatment strategies can be developed. A growing number of studies have placed increasing importance to the concept of niche, a multicellular environment, and recognize that niches are the primary contributor of tumor phenotypes and clinical outcomes rather than individual cells or cell types. Spatial transcriptomics are adept at providing niche-level gene expression measurements. Given the importance of niches, we believe that a spatially aware foundation model for cancer ST data collections will realize the therapeutic and prognostic potential of these datasets. We propose CancerSTFormer, consisting of a pair of spatially aware transcriptomic foundation models at the 50μm-Local and 250μm-Extended scales. The models possess unique capabilities to recover ligand-target gene relationships, niche-specific differentially expressed genes, and revealing the gene and immune regulatory responses of immune-checkpoint blockade therapies, and other targeted cancer therapies, on patients' tumors given ST profiles through perturbation analysis.

In the pre-trained setting, we sought to perturb each gene encoding PD-1, PDL1, and CTLA-4 proteins, respectively PDCD1, CD274, and CTLA4, on TNBC ST profiles to simulate and understand ICB response. In silico perturbations correctly recapitulated anti-tumor immune response in both the long distance (250um Extended model), and short-range settings (50um Local model) according to GSEA. In the fine-tuned setting, we show that the tool can refine anti-PD1, ganitumab, and trebanalib treatment-resistance and sensitivity signatures. From ISPY-2 trial, we derived PD1-responsive and PD1-resistant gene sets, which served as gold standards to train a gene-classifier within for predicting response-associated genes from ST data. We next applied in silico deletion of PDCD1 using this fine-tuned model, and evaluated the results using the PD1-sensitive/resistant gene sets of the Holdout group. When compared against a fine-tuned Geneformer and a norefinement control, both Local and Extended CancerSTFormer variants consistently achieved higher accuracy in predicting resistant and sensitive genes in holdout cohorts across all 3 treatments.

Overall, this tool reuses ST data for understanding how gene perturbation impact spatial niches in cancer, while also providing ST-driven, gene-based refinement of treatment-resistance and sensitivity signatures derived from existing bulk transcriptomics.

#2753 Ontology-guided hierarchical cell typing with large language models for analyzing tumor microenvironment.

Jeongbin Park, Yuchang Seong, Hongyoon Choi

Portrai, Inc., Seoul, Korea, Republic of

Background
Due to the emergence of a vast amount of single-cell RNA sequencing (scRNA-seq) and single-cell resolution spatial transcriptomics (ST), there has been a demand for cell type annotation pipelines that are reproducible, scalable, and capable of functioning as end-to-end solutions. Reference-dependent cell typing may be compromised due to a labor-intensive preparation step for scRNA-seq data matching the data to be labeled and the algorithm. Also, reference-free pipelines couldn't provide appropriate human-interpretable labels for each deconvoluted cell type, limiting their comparison with the existing literature. Furthermore, many algorithms often overlook the hierarchical structure of cell type annotations.
Method
We developed hierarchy-aware LLM-aided cell type annotator using cell type ontology tree. LLM can be any type, but we focused on gpt-4o and gpt-oss-20b. Step 1, we first excluded cell ontologies not relevant to the context, reducing ~2,300 entries to about 400-500. Step 2, terms were processed in batches of 150 using the context and an LLM; the curated list was then reprocessed by the LLM, yielding fewer than 40 cell-type terms. Step 3, we elicited context-specific marker genes with the LLM in five independent runs and aggregated the results into a single list. Step 4, we clustered single cells using highly variable genes to obtain cluster labels, restricted the data to the Step 3 markers, and computed differentially expressed genes (DEGs). Using the top 20 DEGs for each cell, we queried the Step 2 term list to assign a cell-type label. We then retrieved the Cell Ontology tree and performed unsupervised hierarchical clustering on cluster centroids to infer relationships; aligning these with the ontology enabled hierarchical cell-type labeling for each cell.
Results
We applied the agentic workflow using LLM (gpt-oss-20b) to 40,000 lung cancer single-cell samples. A continuous hierarchy was reconstructed from "cell" (level 1) to T follicular helper cell (level 10). To assess performance, we compared Adjusted Rand Index (ARI) values between four ground-truth levels and the 10-level predicted hierarchy. We observed a maximum of 0.86 (Level 2 ground truth vs. Level 5 predicted label). Overall, the pipeline completed annotation efficiently, requiring approximately 40 minutes for ontology filtering and 20 minutes for all subsequent steps, demonstrating scalability for large-scale single-cell datasets.
Conclusion
Our pipeline provides scalable cell-type annotation to meet the recent surge of scRNA-seq data. Moreover, by leveraging the flexibility and memory capabilities of LLMs, it enables typing of minor cell types; by using existing cell-type ontology trees, it supports hierarchy-aware cell typing; and by constraining selections to the established cell ontology, it reduces hallucinations and yields human-interpretable cell typing.

#2754 VGL: Vision-Gene-Language multimodal LLM integrating histopathology and gene expression for cell type classification in lung cancer.

Haenara Shin, Dongjoo Lee, Jeongbin Park, Hongyoon Choi

Portrai, Inc., Seoul, Korea, Republic of

Background
Understanding the tumor microenvironment requires models that resolve cellular heterogeneity across molecular and spatial modalities. With the expansion of spatial transcriptomics, single-cell RNA-seq, and high-resolution histopathology imaging, there is a need for a unified foundation model that jointly interprets gene expression, spatial context, and visual tissue features. We developed a multimodal large language model (LLM) that integrates these modalities into a single adaptive framework handling heterogeneous inputs—including gene expression profiles, spatial transcriptomics spots, single-cell measurements, and histology patches—while generating harmonized outputs such as genes, cell types, and image-derived descriptors.
Method
We built a multimodal LLM within a Vision-Gene-Language (VGL) framework that integrates gene expression, histology images, and biological language representations. The model is based on MedGemma-4b-it and was fine-tuned using QLoRA for parameter-efficient training. Training used 5.2 million multimodal samples of H&E patches paired with highly variable gene expression profiles from non-small cell lung cancer, totaling 1,745,240 cells and spatial spots across scRNA-seq and spatial transcriptomics platforms (Visium, Xenium). The model was trained using multi-task learning across five canonical tasks spanning image-to-gene, gene-to-cell type, and cell type-to-gene objectives with task-specific ratio scheduling on 4 x H100 GPUs. We evaluated performance on cell type classification from gene expression profiles across 12 major immune and stromal cell types.
Results
The trained VGL model achieved 70.07% accuracy on the held-out test set (n=20,764) for predicting cell types from gene expression profiles, compared to 16.32% accuracy for the naive pre-trained model, a 4.3-fold improvement. Validation performance was similar (69.85% accuracy, n=41,529), indicating robust generalization. These gains demonstrate the value of a multimodal LLM that jointly leverages single-cell, spatial transcriptomics, and histology information. Through cross-modal learning and masking, the model learned gene and cell type embeddings that generalized across data platforms and spatial contexts and produced biologically consistent outputs even when only a subset of modalities was available.
Conclusion
We introduce a multimodal LLM-based spatial foundation model, VGL, that unifies single-cell RNA-seq, spatial transcriptomics, and histopathology imaging into a modality-agnostic framework. The improvement in cell type classification highlights the model's ability to capture and reason over cross-modal biological structure. This framework lays the groundwork for spatial AI systems that interpret heterogeneous molecular and imaging data and enable scalable tumor microenvironment profiling.

#2755 Large scale extraction of adverse events by large language models uncovers latent structure of treatment toxicity.

John Lazar[1], Divneet Mandair[2], Catherine C. Smith[2], Travis Zack[3]

[1]UCSF - University of California San Francisco, San Francisco, CA,[2]UCSF, San Francisco, CA,[3]UCSF School of Medicine, San Francisco, CA

Managing treatment toxicity is a major challenge in oncology. Large-scale data on treatment related adverse events (AEs) could help oncologists better understand and predict toxicity. However, most AE datasets are limited to small numbers or restricted types of events due to the labor-intensive manual reporting traditionally required to document AEs. Automated extraction of AEs from the electronic health record (EHR) could enable large-scale analysis but is a challenging task as information about most AEs is in diffuse, unstructured data such as clinical notes.We therefore developed and validated an agentic large language model (LLM) pipeline, *AE-Extract,* to extract and grade AEs from oncologists' progress notes. The pipeline is highly sensitive with a recall of >95% for events in the same organ system and a precision of 67% compared to manual annotation. Lower precision relative to recall reflects uncertainty in the attribution of events to treatment effects as well as design choices to prioritize higher recall over precision. To comprehensively characterize AEs during cancer therapy, we subsequently applied *AE-Extract* to a set of 84,684 progress notes from an academic cancer center. We identified 279,457 total AEs, a mean of 3.3 per note. To identify recurrent patterns of treatment toxicity, we applied non-negative matrix factorization (NMF) to the AE data and identified 85 latent factors that capture patterns of toxicities in the dataset. These latent patterns capture co-occurrence of mechanistically related events such as neuropathy and falls as well as associations in different organ systems without known mechanistic connection such as pruritus and colitis in patients receiving immunotherapy or neuropathy and nail changes in patients receiving cytotoxic chemotherapy. As the latent factors quantify core patterns of AEs, we next studied how they could be used as robust feature sets for analysis of treatment toxicity. First, we found that the latent patterns identified in the first part of a patient's treatment course can predict development of new AEs as well as worsening severity of existing AEs. We also found these patterns of treatment toxicity correlated with patient demographics and comorbidities: we recapitulated known associations such as the link between gender and cancer induced nausea/vomiting as well as novel relationships such as a link between ischemic heart disease and vestibulocochlear symptoms including tinnitus and hearing impairment.Overall, our work demonstrates a new method for accurate, high-throughput extraction of AEs from clinical notes. We show how comprehensive evaluation of treatment toxicity allows for better characterization of patterns of AEs, identifies robust associations between treatment toxicity and patient characteristics, and may serve as a starting point for building personalized models to predict treatment toxicity.

#2756 Development of an LLM framework for analysis of heterogeneous breast cancer patients genomic reports.

Krishna Rani Kalari[1], Xiaojia Tang[2], Thanmayee Boyapati[3], Tanya L. Hoskin[4], Sumathilatha Myla[4], Sumedha G. Penheiter[5], Richard M. Weinshilboum[6], Liewei Wang[5], Hamid R. Tizhoosh[7], Karthik Vikram Giridhar[2], Matthew P. Goetz[8], Judy C. Boughey[9]

[1]Biomedical Informatics, Mayo Clinic College of Medicine, Rochester, MN,[2]Mayo Clinic Cancer Center Minnesota, Rochester, MN,[3]University of Minnesota, Twin cities, Minneapolis, MN,[4]Quantitative Health Sciences, Mayo Clinic, Rochester, MN,[5]Mayo Clinic College of Medicine, Rochester, MN,[6]Professor, Dept. of Pharmacol. & Med., Mayo Clinic College of Medicine, Rochester, MN,[7]Mayo Clinic, Rochester, MN,[8]Mayo Clinic College of Medicine and Science, Rochester, MN,[9]Radiation Oncology, Mayo Clinic, Rochester, MN

Background: The increasing volume and diversity of clinical genomic reports pose a significant challenge across healthcare institutions for the interpretation and proper implementation of precision oncology research. Reports from multiple different vendors (e.g., Invitae, Ambry Genetics, Foundation Medicine) are typically PDFs and exhibit substantial heterogeneity in panel design, gene coverage, and reporting standards, which hinders efficient retrospective data mining and patient cohort identification within the electronic medical records. We sought to develop a framework to interrogate all of these reports.
Methods: We extracted genomic reports from patients with breast cancer treated with neoadjuvant chemotherapy and developed MolHarmonizer, a novel, scalable framework leveraging Python and Gemini LLMs, designed to process and harmonize genomic data from disparate multi-vendor reports. Gemini LLMs are employed explicitly for robust information extraction, normalization, and structuring of key genomic features, transforming unstructured data into a unified, queryable dataset.
Results: Our MolHarmonizer framework successfully processed 1,147 genomic reports from 1703 breast cancer patients (2006-2023) from 23 different companies, demonstrating robust capability to extract and standardize critical actionable biomarkers. Data sources included Invitae (n=554), Ambry Genetics (n=189), Natera (n=95), Mayo Clinic (n=88), Tempus (n=63), Guardant Health (n=47), and Foundation Medicine (n=37), with others contributing less than 20 reports. Of the samples, 827/1147 (72.1%) were germline (blood/saliva). A majority of the patients were tested using the panels due to a personal/family history (n=925). Overall, 413/1147 (36.0%) reports identified at least one mutation. For breast cancer, 75 reports showed BRCA1/2 mutations (37 BRCA1, 37 BRCA2, and one patient with both BRCA1 and 2). Other mutations identified included: PIK3CA (n=40), TP53 (n=96), PTEN (n=21), ESR1 (n=13) and AKT1/2 (n=8).
Conclusion: MolHarmonizer, a powerful framework leveraging Gemini LLMs, effectively addresses genomic data heterogeneity by automating biomarker extraction and harmonization. This enables rapid cohort identification and deep retrospective analyses for clinical insights, biomarker discovery, understanding disease history, facilitating novel pattern discovery, e.g., predicting BRCA1 mutations from WSI, and accelerating research within our neoadjuvant BC cohort. Future plans include expanding to include over 20,000 breast cancer patients, developing a user-friendly chatbot, and ensuring inter-institutional adaptability for a variety of complex diseases.

#2757 Scale meets Speed: A transcriptome-wide spatial analysis that runs a rapid and interactive hypothesis-driven workflow with AtoMx® SIP.

Evelyn R. Metzger[1], Patrick Danaher[1], Nicole Ortogero[1], Sayani Bhattacharjee[1], Prajan Divakar[1], Joseph M. Beechem[2]

[1]Bruker Spatial Biology, Seattle, WA,[2]Bruker Spatial Biology, Piedmont, CA

The potential of whole-transcriptome spatial analysis to answer complex biological questions is often hindered by the sheer weight of its computational and analytical demands. As the number of cells, samples, and plex increases these computational challenges are compounded resulting in bottlenecks that slow the pace of discovery. Moreover, these complex datasets often require specialist data analysis expertise that can further slow "data-to-insight". To bridge this gap, we created a new analysis paradigm that enables biologists and researchers with less analytical expertise to interact with their data directly, performing deep hypothesis-driven analysis in a rapid, conversational and accessible workflow. In this presentation we discuss three advancements arriving in the reimagined AtoMx® Spatial Informatics Platform (SIP) and in development and highlight results found in a publicly available colon adenocarcinoma FFPE WTX sample. First, we have redesigned the architecture with the goal of putting biology front and center, allowing researchers to quickly observe, hypothesize, and learn iteratively. Second, an agile computational engine, leveraging a foundational model trained on >1 billion spatially-resolved single cells, automates cell annotations, reducing analysis time from days to hours. Third, this workflow creates a carefully-curated package of summary tables, thousands of times smaller than a full dataset, but far richer than a human-generated prompt. Once an LLM ingests this package, it stands ready to answer diverse questions about the dataset, *e.g.* "what pathways are spatially variable in tumor cells?", or "what are the spatial contexts T cells inhabit in this tissue?" We applied this approach to the colon sample (412,052 cells). Our foundational model automated cell typing and spatial domain assignment, providing the basis for the analysis. We then applied the LLM chat workflow. An initial query rapidly identified the dominant pro-tumoral signatures (EGFR, TGF-β, MAPK) and reduced pro-apoptotic TRAIL pathway. A follow-up "conversational" query for molecular drivers identified a significant MIF (tumor) to CD74 (TAM) ligand-receptor interaction, providing a direct mechanistic link to the observed MAPK activity. This entire workflow from automated cell typing to mechanistic insight was completed rapidly and generated all reproducible figures, demonstrating a complete analysis-to-visualization pipeline that does not require expert coding abilities. In conclusion, the AtoMx® SIP successfully bridges the gap between complex spatial data and biological insight. This new paradigm democratizes whole-transcriptome analysis, enabling researchers to conduct rapid, iterative, hypothesis-driven discovery without deep computational expertise.

#2758 *PAX3/7::FOXO1* fusion detection and transcriptomic prediction from whole-slide images of rhabdomyosarcoma using attention-based deep learning frameworks: A multi-institutional study.

Dorsa Ziaei[1], **Hyun Jung**[1], Philip J. Lupo[2], Pagna Sok[3], Jack F. Shern[4], Corinne M. Linardic[5], Syed Abbas Bukhari[4], Hsein-Chao Chou[4], Jun S. Wei[4], Curtis Lisle[6], Uma Mudunuri[1], Javed Khan[4]

[1]Frederick National Laboratory for Cancer Research, Frederick, MD,[2]Emory University School of Medicine, Atlanta, GA,[3]Baylor College of Medicine, Houston, TX,[4]National Cancer Institute, Bethesda, MD,[5]Duke University School of Medicine, Durham, NC,[6]KnowledgeVis, LLC, Maitland, FL

Background: Rhabdomyosarcoma (RMS) is a highly malignant pediatric soft-tissue sarcoma where molecular subtyping, particularly *PAX3/7::FOXO1* fusion status, drives prognosis and treatment. However, histology-based diagnostic approaches remain limited by subjectivity and the scarcity of comprehensive molecular annotations. To overcome these challenges, we improved our previously reported convolutional neural network learning models that predict *PAX3/7::FOXO1* fusion status from whole-slide images (WSIs) while additionally trained models to infer gene expression profiles from histology, thereby linking morphology to transcriptomic signatures.**Methods:**A total of 826 independent WSIs from three sources [Children's Oncology Group (COG) biobanking protocols = 322, Kids First (KIDS) = 252, Childhood Cancer Data Initiative/Molecular Characterization Initiative (CCDI/MCI) = 252] were used to train and evaluate an Attention-Based Multiple Instance Learning (ABMIL) model using UNI2-h foundation features for fusion classification. For gene expression prediction, 135 RMS WSIs paired with bulk RNA-seq data were used to fine-tune a SEQUOIA transformer model, which was trained on TCGA UCEC/COAD datasets. Model performance was evaluated using the Matthews Correlation Coefficient (MCC), AUC, and Pearson's r correlation, with biological validation through pathway enrichment analysis.**Results:**The fusion detection model achieved robust and generalizable performance across independent test cohorts (MCC ≥ 0.80, AUC ≥ 0.94), with multi-institutional training improving external generalization (MCC up to 0.84). The gene expression model reliably predicted bulk transcriptomic profiles from WSIs (mean $r > 0.6$, $p < 0.05$), identifying biologically meaningful pathways including cell cycle and muscle development. Together, these models demonstrate the feasibility of integrating morphological imaging data to gain molecular insights that would not be possible with histology alone.**Conclusions:**This work presents the first large-scale validated deep learning framework for simultaneous molecular subtyping and transcriptomic inference in RMS. By combining digital pathology with molecular prediction, our approach offers a scalable, tissue-sparing, and generalizable tool for advancing precision oncology in RMS.

#2759 An innovative AI-based platform for antibody stability improvement and affinity optimization.

Yiran Li, Hao Peng, Xinyu Bian, Hui Zhao, Yang Li, Panpan Zhang, Jinying Ning, **Feng Hao**

Kyinno Biotechnology Co., LTD, Beijing, China

Background: Bispecific antibodies (bsAbs), which simultaneously target two distinct antigens, offer advantages in specificity, efficacy, and resistance management, making them an increasingly important modality in therapeutic antibody development. However, their complex formats impose stringent requirements on affinity and stability. Traditional affinity maturation methods, such as saturation mutagenesis and phage display, are costly, time-consuming, and limited in their ability to improve stability. To overcome these challenges, we developed an AI-based antibody engineering approach that uses deep learning to predict key mutations based on engineering objectives and integrates these predictions with high-throughput expression, enabling greatly reduced screening efforts and rapid identification of optimized antibody variants.

Methods: We developed a deep learning-based AI model to support antibody engineering by simulating antigen-antibody docking and predicting affinity changes, enabling targeted mutation design according to defined optimization goals. For antibodies with poor stability, the model proposes engineered disulfide bonds or CDR/framework mutations to adjust surface hydrophobicity while maintaining affinity. For functional enhancement, it identifies key CDR residues and generates combinatorial multi-site mutations, allowing selection of variants with preserved affinity but improved blocking or functional performance.

Results: As an example using a symmetric scFv bispecific antibody, we applied AI-driven design to generate 50 candidate variants, followed by binding-based screening to eliminate molecules with altered affinity. Then candidate molecules were expressed, purified, and subjected to stability evaluation. This approach effectively find a new mutant reduced aggregation under one-week accelerated thermal stress from 100% to less than 5%, while increasing the melting temperature (Tm) by up to ~10 °C. For functional enhancement of nanobodies, we applied single-point mutagenesis followed by three rounds of combinatorial design, generating a total of 260 variants —representing a ~1000-fold reduction compared with traditional multi-site saturation libraries (10^3-10^5). This process yielded a nine-site mutant (with at least one mutation per CDR) that demonstrated a two-fold improvement in reporter cells blocking tests.

Conclusions: We developed an AI-guided approach to design targeted antibody variants, accelerating the discovery of molecules for bispecific antibody assembly and drug development.

#2761 Large language model-derived re-contextualization reveals functional landscapes across cancers.

Yibing Guo, Yanhao Tan, Chien-Hung Shih, Li-Ju Wang, Yu-Chiao Chiu

University of Pittsburgh, Pittsburgh, PA

The vast heterogeneity of human cancer necessitates a deeper understanding of how fundamental biological pathways are functionally reconfigured across different cancer types in contrast to non-malignant diseases. Conventional pathway analyses based on static, disease-agnostic gene sets often obscure the plasticity and tumor-specific roles of pathways. We address this limitation by leveraging the knowledge integration of large language models (LLMs) to generate and embed context-aware pathway descriptions, enabling a novel framework for quantifying pathway relevance and functional variability across the oncological landscape. We applied this framework to analyze 268 KEGG pathways across 35 cancer types and 7 non-malignant diseases. We performed two complementary analyses of the LLM-generated context-aware pathway descriptions: 1) disease-level analysis by applying unsupervised clustering to the embeddings derived from the context-aware descriptions to map inter-disease functional relationships; and 2) pathway-level analysis that quantifies the functional variability of each pathway across diseases to understand their disease-specific roles. The disease-level analysis revealed a coherent functional atlas of diseases. Within cancers, lineage and cell type drove distinct yet biologically consistent groups, such as hematologic malignancies, gastrointestinal cancers, and hormonal cancers. Non-malignant conditions (e.g., neurodegenerative disorders) formed separate, distinct clusters. Pathway-level analysis showed marked functional variability. Pathways with the lowest variation across diseases mainly involved conserved cellular functions (e.g., *mitophagy, AMPK signaling*), while highly dispersed pathways captured context-specific programs (e.g., *viral carcinogenesis, transcriptional misregulation in cancer*). Independent validation using a literature-derived pathway relevance score across diseases confirmed that the top 20 most dispersed pathways had significantly higher relevance scores than the bottom 20 ($p < 0.01$). Furthermore, the continuous level of dispersion correlated positively with pathway relevance ($p < 0.01$). These observations support that the semantic heterogeneity captured by LLMs across diseases truly reflects biological specificity and functional relevance. In summary, LLM-generated context-aware pathway descriptions and their corresponding embeddings successfully capture disease-specific functional organization and reveal mechanistic coherence across cancers. This represents a significant methodological advance over traditional static approaches, providing a dynamic, biologically relevant map for understanding heterogeneous cancer mechanisms and identifying novel therapeutic strategies.

#2762 LLM-based extraction of immunotherapy toxicities reveals severity-dependent effects on overall survival.

Zeyun Lu[1], Mustafa Saleh[1], Charles Lu[2], Intae Moon[1], Razane El Hajj Chehade[1], Elio Ibrahim[1], Yevgeniy R. Semenov[2], Toni K. Choueiri[1], Alexander Gusev[1]

[1]Dana-Farber Cancer Institute, Boston, MA,[2]Massachusetts General Hospital, Boston, MA

Characterizing immune-related adverse events (irAEs) among patients with cancer receiving immunotherapy remains challenging. Traditional ICD-based identification often misses or misclassifies irAEs, and manual chart review is labor-intensive, error-prone, and not scalable. Existing large language model (LLM)-based approaches often do not fully capture irAE onset dates and severity information, frequently missing mild events and limiting their utility for time-sensitive and severity-stratified analyses.We developed a two-stage prompting strategy to extract irAE type, severity, and onset date from large volumes of unstructured clinical notes for patients receiving immunotherapy. In the first stage, the model summarizes irAE-related information from long and heterogeneous clinical documentation. In the second stage, it extracts structured irAE details. This approach improves extraction accuracy and supports more reliable identification of irAE types and onset timing.

Using expert-curated ground truth, we evaluated multiple reliable and increasingly used large language models, including ChatGPT 4o, Llama 3.1 with 70B and 450B, Llama 3.3 with 70B, and DeepSeek R1. Across models, LLM-based methods achieved higher sensitivity (0.95 vs. 0.57), higher precision (0.69 vs. 0.64), and higher F1 scores (0.77 vs. 0.55) compared with ICD-based extraction. For cases in which both LLM and ICD identified an irAE, LLMs more accurately captured event types (83% vs. 38%) and consistently identified earlier onset dates (on average 27 days earlier). This strategy is model-agnostic and will continue to improve extraction accuracy as the underlying LLM models improve.

We applied our pipeline, which incorporates ChatGPT 4o, to 340,277 notes from 8,768 patients treated with immunotherapy in the Dana-Farber Cancer Institute Profile cohort, covering 21 cancer types. 87% of patients developed at least mild irAEs within two years of treatment initiation. Consistent with prior work, CTLA-4 inhibitors were associated with higher irAE incidence (HR = 3.93; P = 1.94e-19), using Cox models that incorporate irAE onset timing, information typically unavailable in earlier studies. Survival analyses stratified by time-dependent irAE severity showed that mild irAEs were associated with reduced hazard of death (HR = 0.86; P = 5.64e-92), whereas severe irAEs were associated with an increased hazard of death (HR = 1.04; P = 1.15e-3). We also observed system-specific severe irAEs that aligned with underlying cancer type; for example, patients with non-small cell lung cancer had a higher instantaneous risk of severe respiratory irAEs (HR = 2.37; P = 1.29e-9) compared with other cancers.

These findings demonstrate that LLM-based clinical text extraction enables scalable and accurate characterization of irAEs, providing deeper insights into their prognostic implications.

#2763 Leveraging large language models to classify pathology reports into ontological hierarchies.

Brenda Fried, Ali Kamali, Cesar Colorado-Jimenez, Melissa Pulitzer, David Kim, Leonardo Boiocchi, Alexander Chan, Mariko Yabe, Mikhail Roshal, Syed Aijazuddin, Ahmet Dogan, Chad Vanderbilt, Khawaja Hassan Bilal, Gregory Goldgof

Memorial Sloan Kettering Cancer Center, New York, NY

Free-text pathology reports vary in style, terminology, and uniformity, making consistent diagnostic extraction difficult for research cohort development. This issue is amplified in large archives, where evolving classifications and intentional ambiguity hinder standardized, categorical diagnoses. Structured ontologies such as OncoTree address this by enforcing codes. While OncoTree is used here as an example, the approach generalizes to any hierarchical ontology, including current WHO classifications.
Using cutting-edge LLMs, we developed OncoPath, an application that classifies pathology reports within structured ontologies. We tested OncoPath by applying OncoTree hierarchy through a structured tree-walk, progressing from broad anatomic categories to specific subtypes. High-level categories are assessed first, then plausible child nodes, with each node's children displayed so the model can anticipate downstream options. Diagnostic paths are summarized, and the model selects the optimal code with a confidence tier (<50%, 50-90%, >90%). Multiple configurations of LLaMA 3.3 70B Instruct were evaluated. Surgical and hematopathology reports were processed separately, and accuracy was verified by pathologist review against the 10 most prevalent molecular codes, covering 49.6% of surgical and 84.9% of hematopathology cases.
The classifier mapped diagnoses to OncoTree codes with high accuracy. Heme-based coding worked well with the full report, whereas Surg-based coding performed best with a targeted summary because reports often contained multiple parts from different sites and diagnoses. Heme reports reached 90-100% accuracy; Surg codes reached 80-100%, except HGSOC (high grade serous ovarian carcinoma) at 60%, reflecting the inherent difficulty, even for pathologists, of determining the tumor's primary site of origin. Codes were stored with original reports, enabling direct reuse in research and operations. The traversal approach provided auditability, confidence levels, and automatic re-evaluation when diagnoses changed.An LLM-assisted OncoTree traversal provides a scalable method to convert diverse pathology reports into structured codes. By standardizing reports while preserving diagnostic nuance, OncoPath enables retrospective cohort development and analyses of incidence, progression, and practice patterns. This framework can readily extend to other structured disease ontologies, establishing a generalizable approach for transforming unstructured reports into standardized, reusable data.

#2764 Maximizing high-risk incidental pulmonary nodule referrals using artificial intelligence.

Ivan M. Marrufo[1], Raymond Johnson[2], Samuel Newman[3], Paras Patel[4], Kalyani Narra[5]

[1]Texas College of Osteopathic Medicine, University of North Texas Health Sciences Center, Fort Worth, TX,[2]Department of Radiology, JPS Health Network, Fort Worth, TX,[3]Office of Clinical Research, JPS Health Network, Fort Worth, TX,[4]Division of Interventional Pulmonology, JPS Health Network, Fort Worth, TX,[5]JPS Oncology and Infusion Center, JPS Health Network, Fort Worth, TX

Background: Effective lung cancer screening and pulmonary nodule (PN) management programs require timely detection and robust care coordination. We report the initial outcomes of an artificial intelligence (AI) tool for obtaining referrals to pulmonary following the detection of high-risk PN findings.

Methods: JPS Health Network created the Pulmonary Nodule Risk Score (PNRS) classification system using nationally accepted PN guidelines. AI-driven Natural Language Processing (NLP) enabled navigators to identify patients meeting the PNRS 4B criteria (Table 1), the highest risk PN category. PNRS 4B detection and referral rates were compared over 22 months, spanning 11 months pre- and post-NLP implementation. Statistical analysis used Fisher's Exact for categorical variables and Mann-Whitney U or t tests for continuous variables.

Results: From June 1, 2023-April 25, 2024 (pre-NLP), 26,393 chest CTs were performed; 23,396 were obtained post-NLP (April 26, 2024-March 20, 2025). The pre- and post-NLP periods included 76 and 106 PNRS 4B patients, respectively. Post-NLP workflow significantly improved referral within 90 days rates from 55 (72%) to 98 (93%) ($p<0.001$). Appointment completion improved from 68% to 78% ($p=0.17$). Pre- and post-NLP comparisons demonstrated no significant differences in biopsy completion (65% vs 60%), Malignancy was noted in 28 (37%) vs 38 (37%). If pre-NLP referrals had reached 93% with the same 37% malignancy rate, an estimated 6 additional patients would have been diagnosed.

Conclusion: The AI tool significantly increased referral rates and expedited malignancy detection, potentially reducing missed or delayed diagnoses in high-risk nodules.

PNRS 4B Criteria and Recommended Clinical Management Pathways

PNRS:	**Score Description:**	E**quivalent Radiology Findings:**	**Associated Recommendation(s):**
PNRS 4B	Very Suspicious	**Solid Nodule**: Single or Multiple ≥ 15 mm (≥ 1,767 mm^3) nodule(s) at baseline or new or; Growing ≥ 8 (≥ 268 mm^3) nodule. **Part Solid Nodule:** Solid component ≥ 8 mm (268 mm^3) at baseline or new or; Growing solid component ≥ 6 mm (113 mm^3) upon follow-up. **Ground Glass Nodule (GGN)**: Growing ≥ 8 mm (268 mm^3). **Perifissural or Juxtapleural Nodule**: Growing ≥ 10 mm (524 mm^3).	**Pulmonary Referral Recommended** AND **Follow-Up Diagnostic Chest CT** AND/OR; **PET/CT** AND/OR; **Tissue sampling** / **biopsy** AND/OR; **GGN Consider Resection**

#2765 Microbiome foundation modeling of cancer: MiFM-derived continuous trajectories and risk clocks for pan-cancer immunotherapy response prediction.

Hongru Shen, Yajing Bi, Yan Zong, Zhangyan Lyu, Chao Zhang, Kexin Chen, Xiangchun Li

Tianjin Medical Univ. Cancer Inst. & Hospital, Tianjin, China

Background: The human microbiome shapes cancer risk, progression and response to immunotherapy, but most existing microbiome models are task-specific and fail to generalize across cohorts and sequencing platforms. We developed MiFM (Microbiome Foundation Model), a self-supervised Transformer trained on ~2 million human, animal and environmental microbiome profiles. MiFM encodes communities as multi-level tokens (species, genus and functional pathways) and uses masked reconstruction plus contrastive learning to obtain transferable embeddings that capture taxonomic and functional structure. Here, we evaluated whether MiFM embeddings can support continuous, clinically interpretable readouts of cancer trajectories and immunotherapy response.
Methods: From MiFM embeddings we derived two continuous metrics: (1) a disease pseudotime placing each patient along a microbiome-encoded cancer progression trajectory; and (2) a microbiome cancer risk clock estimating microbiome-derived cancer risk and immunotherapy non-response at the individual level. We applied this framework to colorectal cancer (CRC) cohorts spanning normal mucosa, adenoma and carcinoma, and to 12 independent pan-cancer immune checkpoint blockade cohorts (n =1237). We additionally defined a microbiome-based aging acceleration signature and evaluated its association with disease pseudotime, the risk clock and overall survival.
Results: In CRC, disease pseudotime recapitulated the adenoma-carcinoma sequence, with median values of 0.15 (normal), 0.38 (adenoma) and 0.72 (carcinoma; $p < 0.001$), and separated disease states more clearly than conventional stage. The risk clock identified high-risk individuals within histologically normal mucosa whose microbiome embeddings resembled adenomas (AUC = 0.85) or carcinomas (AUC = 0.92), indicating a preclinical window for intervention. Across 15 CRC cohorts (n = 3739), baseline gut microbiome embeddings identified non-responders to immune checkpoint blockade with a median cross-cohort AUC of 0.84 and an AUC of 0.95 in a non-small cell lung cancer cohort. The aging acceleration signature correlated with both disease pseudotime and the risk clock and independently predicted overall survival (HR = 2.52, $p < 0.001$).
Conclusions: To our knowledge, MiFM is the first large-scale microbiome foundation model applied to oncology, yielding continuous microbiome-derived readouts of cancer progression and immunotherapy response. The disease pseudotime and microbiome cancer risk clock capture cancer trajectories beyond conventional staging, enable ultra-early identification of high-risk lesions in normal-appearing mucosa and support robust prediction of immunotherapy resistance across cohorts. This framework delivers concrete microbiome biomarkers and a scalable platform for microbiome-guided precision oncology.

#2766 Self-supervised learning defines a universal biomarker of malignancy in platelet RNA.

Hongru Shen, Yan Zong, Yajing Bi, Jilei Liu, Chen Lyu, Fangyu Shi, Yichen Yang, Meng Yang, Yang Li, Kexin Chen, Xiangchun Li

Tianjin Medical Univ. Cancer Inst. & Hospital, Tianjin, China

Background: Early detection of cancer via liquid biopsy has transformative potential for patient outcomes, yet its clinical translation is limited by the poor generalizability of machine learning models, which often overfit to cohort-specific technical or biological artifacts and fail in independent datasets. Tumor-educated platelets (TEPs) constitute a rich but underexplored source of systemic cancer signals: their RNA profiles integrate tumor-host interactions and may encode biologically generalizable disease information. Conventional supervised approaches, which depend on labeled data, are particularly prone to overfitting, leaving much of the TEP transcriptomic landscape untapped. Here, we investigate whether self-supervised learning (SSL), trained without cancer labels, can extract a robust and biologically interpretable cancer-associated representation from TEP transcriptomes that generalizes across cohorts.
Methods: An SSL framework pretrained on 22.3 million transcriptomes was applied to 2,134 TEP RNA-seq samples spanning eight cancer types across four independent cohorts generated at multiple sequencing centers. The primary output—a single SSL-derived feature—was evaluated for pan-cancer detection in discovery and external validation cohorts. Performance was compared with a conventional supervised Random Forest classifier trained on the same data. Biological interpretability was assessed using transcript-level associations and pathway enrichment analysis.
Results: The SSL feature achieved strong pan-cancer performance in the discovery cohort (AUC 0.903) and consistently generalized across external cohorts (e.g., glioblastoma AUC 0.785; non-small cell lung cancer AUC 0.803). In direct comparison, the supervised classifier demonstrated limited cross-cohort transferability (AUC 0.553 and 0.711, respectively). Across cancer types, the SSL approach yielded a median 0.23 improvement in AUC over supervised learning. At a screening-relevant threshold of 99.9% specificity, the SSL feature achieved a median sensitivity of 47.9%. In an independent colorectal cancer cohort, it detected Stage I disease with an AUC of 0.819 and retained measurable sensitivity (24.1%) at 99.9% specificity. Biological analysis indicated that the SSL feature was reproducibly associated with platelet transcripts involved in epithelial-mesenchymal transition and coagulation pathways (FDR < 1×10^{-6}), including COL6A3, FLNA, PF4, and SPARC, across all cohorts.
Conclusions: A self-supervised representation learned from large-scale transcriptomic data can extract a reproducible, biologically interpretable signal from TEPs that generalizes across cohorts and cancer types. This framework offers a technically and clinically scalable strategy for developing robust liquid biopsy biomarkers for early cancer detection.

: Radiomics and AI in Medical Imaging
Poster Session

#2770 *astril*: Automated segmentation toolkit for radiology image libraries.
Alexander L. Ling[1], C. Zoe Linke[1], Christopher M. Jannotta[1], Data Science Teamlab[2], E. Antonio Chiocca[1]

[1]Mass General Brigham, Boston, MA,[2]Break Through Cancer, Boston, MA

Volumetric tumor segmentation improves patient monitoring vs. standard radiological assessment and is often needed for extracting radiomic features. Despite this, widespread implementation of such analyses into clinical and scientific studies is hindered by the time-intensive nature of scan curation and segmentation, and by the significant computational expertise required to process large imaging datasets. To overcome these barriers, we created a python package (astril - https://github.com/Alexander-Ling/astril) that enables fully automated pre-processing, segmentation, and quantification of radiology images using simple command line arguments, starting from unprocessed DICOM directories. astril also supports the training and application of new segmentation algorithms.The first pipeline implemented in astril is for segmenting recurrent glioblastoma (GBM) MRI images, enabling users to automatically pre-process (verify integrity, parse metadata, select optimal series, de-identify, co-align, skull strip, and normalize) and segment (tumor, peritumoral edema, and necrosis) volumes, starting from raw DICOM directories and ending with tabulated volumetric statistics. The built-in CNN segmentation algorithm was trained on manually segmented images from a recurrent GBM patient cohort, enabling the algorithm to correctly handle artefacts such as resection cavities, scar tissue, and low-enhancing tumor. Automated segmentation volumes with astril are highly correlated with manual segmentations and are associated with patient clinical outcomes.This provides a robust platform for rapid, standardized, and automated processing of radiology imaging libraries, and it enables simplified training and distribution of new segmentation algorithms.

#2771 Integrating image and text-based AI improves identification of metastatic sites from whole-slide pathology images.

Yixin Chen[1], Ziyu Su[1], Muhammad Khalid Niazi[1], Anil Vasdev Parwani[2], Elshad Hasanov[1]

[1]The Ohio State University, Columbus, OH,[2]The Ohio State University Wexner Medical Ctr., Columbus, OH

Metastatic cancer accounts for most cancer-related mortality, and determining the most likely metastatic destination of a tumor is essential for prognosis and treatment planning. Although every tumor arises from a primary site, its biological behavior varies widely: some remain localized, whereas others spread to distant organs following well-recognized patterns of organ-specific tropism. In clinical practice, distinguishing these behaviors relies on whole-slide images (WSIs), immunohistochemistry, and clinical information. However, metastatic lesions often lack distinctive histological features, making it difficult to determine whether a tumor has metastasized and, if so, its site of spread—especially in poorly differentiated biopsies. We hypothesize that tumors retain subtle morphological cues—rooted in metastatic potential and organ-specific tropism—that can help distinguish localized from metastatic phenotypes and, when metastasis is present, indicate the likely site of dissemination. Leveraging computational pathology and AI-based models, these latent features can be uncovered to improve tumor stratification and metastatic site prediction. We propose a novel image-and-text-based AI model that analyzes each region within a WSI to determine metastatic status and site. Our model utilizes medically meaningful textual descriptions—textual prototypes—generated by a pre-trained pathology AI model. In our study of 3,804 metastatic cases across six clinically relevant sites, each WSI was converted into patch-level image features using a pre-trained pathology AI model. After identifying metastatic disease, the model compares each patch with concise text descriptions of metastatic patterns (e.g., lymph node metastasis). A visual-textual similarity matrix quantifies how closely each patch matches these descriptions, guiding attention toward the regions most indicative of the metastatic site. Our model achieves an AUC of 88%, an accuracy of 74%, and a macro-F1 of 60%. These findings demonstrate improved metastatic-site classification by providing metastatic-specific semantic cues that direct attention to diagnostically important regions. We believe our model can suggest the most likely metastatic site using only routine pathology slides and offers a practical, scalable strategy for AI-assisted diagnosis.

#2772 Noninvasive artificial intelligence system for prediction of lenvatinib based therapeutic regimens response and outcome in unresectable hepatocellular carcinoma.

Bo Chen[1], Yuqian Gan[1], Enguang Zou[1], Yi Wang[2], Gang Chen[3]

[1]The First Affiliated Hospital of Wenzhou Medical University, Wenzhou, China,[2]Wenzhou Medical University, Wenzhou, China,[3]The First Affiliated Hospital of Wenzhou Medical University, China

Purpose: Lenvatinib represents a first-line therapeutic option for unresectable hepatocellular carcinoma (uHCC), with four established treatment regimens utilized in clinical practice. However, treatment response rates remain suboptimal, with only a subset of patients achieving meaningful clinical benefit. We hypothesized that radiomics features reflecting tumor vascularization and microenvironmental heterogeneity could enhance treatment response prediction. This multi-center retrospective-prospective hybrid study aimed to develop and validate radiomic deep learning models (VALIANT) for personalized treatment response stratification in uHCC patients.
Methods: This study enrolled 435 uHCC patients (2018-2024) from four institutions with histologically or radiologically confirmed unresectable disease. Radiomic features were extracted from arterial and venous phases of contrast-enhanced CT imaging acquired prior to treatment initiation. Eight VALIANT models were constructed using transfer learning strategies, with performance evaluated by area under the receiver operating characteristic curve (AUC) through five-fold cross-validation and external validation cohorts. Additionally, a prospective validation cohort of 16 patients received treatment recommendations based on the highest-scoring predicted regimen, with subsequent response assessment.
Results: Partial response (PR) was achieved in 159 patients (37% response rate). The eight VALIANT models demonstrated robust performance with a mean AUC of 0.92. The arterial phase-based TPI model exhibited superior discriminative ability (training AUC 0.95; external validation AUC 0.92) with balanced classification metrics (sensitivity 0.90, specificity 0.84, accuracy 0.95), indicating excellent generalizability across institutions. All VALIANT models significantly stratified patients into distinct response/non-response groups with divergent overall survival outcomes (log-rank $P < 0.01$). In the prospective cohort, 13 of 16 patients (81.3%) achieved the predicted response category, with 87.5% concordance between AI-predicted optimal regimen and actual clinical response.
Conclusion: The integration of deep learning radiomics and tumor phenotypic features in VALIANT models significantly enhances treatment response prediction for lenvatinib-based therapy in uHCC. This clinically applicable AI system enables comparative assessment of four lenvatinib-based regimens, facilitating personalized therapeutic selection and potentially improving patient outcomes through precision medicine approaches.

#2773 Multi-regional CT-based radiomics fusion predicts pathological pollutant index associated with lung adenocarcinoma.

Yutong Li[1], Xiaoxi Pan[2], Abishek Balachandra[2], Chingyi Young[3], Maria Esther Salvatierra[4], Carmen Behrens[4], Luisa Maren Solis Soto[4], Yinyin Yuan[2], Chengyue Wu[5]

[1]UT MD Anderson Cancer Center, Houston, TX,[2]Institute for Data Science in Oncology, UT MD Anderson Cancer Center, Houston, TX,[3]Ent Data Engineering and Analytic, UT MD Anderson Cancer Center, Houston, TX,[4]Translational Molecular Pathology Department, UT MD Anderson Cancer Center, Houston, TX,[5]Department of Imaging Physics, UT MD Anderson Cancer Center, Houston, TX

Introduction: Lung adenocarcinoma (LUAD) is the most common non-small cell lung cancer, especially in never-smokers. Environmental pollution, particularly airborne particulates (PM2.5/PM5), is a critical factor driving lung cancer initiation [1]. However, reliable individual-level pollution exposure quantification is challenging. We recently introduced the lung pollutant index (LPI), an AI-derived metric quantifying tissue-resident pollutant burden from pathology images. However, pathology-based LPI is invasive and unsuitable for large-scale application. We propose a machine-learning framework to predict CT-based LPI (CT-LPI) from chest CT, enabling non-invasive pollutant burden quantification for individuals undergoing chest imaging, including high-risk smokers and never-smokers with incidental nodules.

Methods: We retrospectively investigated 153 LUAD patients who received preoperative lung CT at MD Anderson Cancer Center (IRB 2023-0114) with surgical pathology. LPI computed from digitalized H&E images [2] categorized cohorts into LPI-high (n=61) and LPI-low (n=92). Region-wise radiomics features (793 per region) were extracted from 5-mm peritumoral ring, normal lung, and whole lung, including first-order, texture, shape, Laplacian-of-Gaussian, wavelet, and habitat features. We incorporated COPD-associated radiomic markers to enhance biological interpretability. We built a multi-regional ensemble framework with features selected using mutual information and Elastic-Net. Region-specific classifiers (Ridge Logistic, Gradient Boosting, CatBoost) were trained, with final predictions via weighted-average ensemble [3].

Results: In 5-fold cross-validation, the multi-regional ensemble achieved AUC 0.719 and ACC 0.687, improving AUC by 0.048 over the best single-regional model and outperforming simple averaging (0.710), LogisticNet (0.664), and ElasticNet (0.661). Incorporating COPD-associated markers improved AUC to 0.724.

Conclusion: We developed CT-LPI, predicting tissue-resident pollutant burden from routine CT using complementary multi-regional features. This framework non-invasively quantifies individual exposure to environmental carcinogens implicated in lung cancer initiation. By enabling scalable monitoring of pollution-driven biological alterations, CT-LPI may support environmental exposure assessment and personalized risk stratification. Next steps include external validation, application to screening datasets, and integration with other biomarkers. [1] Hill W, et al. Nature. 2023. [2] Pan et al., Nature Cancer, under review. [3] Shaheen A, et al. Front Neurosci. 2022.

#2774 Pulmonary nodule tracking in metastatic Ewing sarcoma enables personalized predictive models.

Kevin A. Murgas[1], Shambhavi Kurup[2], Maureiq Ojwang[2], Rene Malazarte[1], Danh D. Truong[1], Heiko Enderling[2], Joseph A. Ludwig[1]

[1]Sarcoma Medical Oncology, MD Anderson Cancer Center, Houston, TX,[2]Radiation Oncology, MD Anderson Cancer Center, Houston, TX

Metastatic Ewing sarcoma (ES) is a rare, aggressive sarcoma subtype with poor outcomes, especially in the relapsed/refractory setting. Standard response evaluation, typically performed after two chemotherapy cycles, may be too delayed to effectively guide therapy for patients with rapidly progressing disease, limiting opportunities to switch to alternative regimens. Data-driven clinical tools are critically needed to provide earlier, patient-specific predictions of treatment efficacy.

We performed a retrospective analysis of patients with metastatic ES with serial CT imaging. Tracking longitudinal measurements of individual pulmonary nodules within a modified RECIST framework, we calibrated patient-specific "digital twin" models based on ordinary differential equations and predictive simulation. Each digital twin estimates nodule-specific growth and response dynamics to various therapies, providing parameters to predict disease behavior and treatment response. We also evaluated response metrics, specifically the Disease Control Rate (DCR) compared to the Overall Response Rate (ORR), as predictors of Progression-Free Survival (PFS) and Overall Survival.

Using the digital twin framework, we accurately recapitulated observed clinical trajectories, including periods of response, stability, and progression across multiple lines of therapy. Model-derived parameters, including patient-specific tumor growth rates and drug sensitivity rates, demonstrate potential as novel prognostic biomarkers for predicting time to progression and survival outcomes.

Longitudinal surveillance in metastatic ES is a valuable yet underutilized clinical resource. Here, we demonstrate a digital twin model of pulmonary nodule growth as a platform for robust response classification and prognostic prediction. These patient-specific models can adaptively forecast individual treatment responses in silico, allowing prioritization of the most effective therapies. This approach offers a framework to optimize treatment sequencing, accelerate evaluation of novel agents, and ultimately maximize therapeutic opportunities for patients with this aggressive disease.

#2775 Deep-learning CT biomarker improves early efficacy detection in simulated randomized phase II NSCLC trials.

Chiharu Sako[1], Brenda F. Kurland[1], Taly G. Schmidt[1], Dwight H. Owen[2], Arpan A. Patel[3], Nicholas C. Love[3], Olivier Gevaert[4], George R. Simon[5], Ravi B. Parikh[6], Petr Jordan[1]

[1]Onc.AI, San Carlos, CA,[2]OSU Comprehensive Cancer Center, Columbus, OH,[3]University of Rochester Medical Center, Rochester, NY,[4]Stanford University, Stanford, CA,[5]Ohio Health, Columbus, OH,[6]Emory University, Atlanta, GA

Background: Early decision-making in advanced non-small cell lung cancer (NSCLC) phase II trials is limited by the modest ability of objective response and progression-free survival (PFS) to detect early biological activity or predict overall survival (OS). Quantitative deep-learning analysis of routine CT imaging may offer a more sensitive measure that better reflects long-term benefit. We evaluated whether Serial CTRS, a fully automated CT-based deep-learning imaging biomarker, could improve early efficacy detection in simulated randomized phase II NSCLC trials.

Methods: We evaluated the utility of Serial CTRS using data from the randomized phase III trial of cetuximab plus carboplatin/paclitaxel with or without bevacizumab in advanced NSCLC, which did not meet its co-primary endpoints of PFS in patients with EGFR FISH-positive cancer and OS in the entire study population (SWOG S0819; N=1275). Serial CTRS is a convolutional-neural-network pipeline, trained on a large real-world advanced NSCLC dataset, using paired baseline and follow-up thoracic CT scans to generate a continuous imaging score without manual annotation. To quantify OS surrogacy, we repeatedly sampled 1000 pairs of random 50-patient arms from the full cohort, and correlated Serial CTRS differences at 8, 16, and 24 weeks with final OS hazard ratios (HR), comparing results with best overall response (BOR) and PFS. To simulate a positive phase II trial, we constructed a balanced subset (target OS HR≈0.50) using stratified pruning matched on randomization factors. We then simulated 1000 two-arm phase II trials (n=50/arm) with realistic staggered enrollment (averaging 1 patient/day) and interim analyses (IA) at 12-48 weeks from study start. PFS was evaluated via log-rank tests and Serial CTRS differences via Wilcoxon rank-sum tests (α=0.05). False-positive rates were evaluated through null simulations using the full dataset.

Results: Serial CTRS differences showed increasing concordance with OS HR across timepoints (R^2=0.10, 0.23, 0.35 at 8, 16, and 24 weeks), outperforming BOR (R^2 = 0.08) and PFS (R^2=0.09, 0.20, 0.28). In the simulated phase II trials, the biomarker achieved 60% (95% CI 58-62%) power and 66% (63-69%) power at 36 weeks to detect a long-term survival benefit while maintaining a 5-6% false-positive rate. BOR achieved 35% (33-37%) power, and PFS achieved 49% (46-51%) and 50% (48-52%) at the same timepoints.

Conclusions: A fully automated deep-learning CT biomarker provided earlier and more reliable efficacy readouts than BOR and PFS in simulated phase II NSCLC trials. These results suggest that quantitative CT biomarkers using the full thoracic scan can strengthen early drug-development decisions by improving power and reducing uncertainty around early activity signals. Ongoing work is focused on broader evaluation across tumor types, therapeutic modalities, and additional clinical datasets.

#2776 Prognostic value of CT radiomics in patients with *gBRCA1/2* and *PALB2* and advanced pancreas cancer.

Sonal Gandhi[1], Jayasree Chakraborty[2], Hadi Ghahremannezhad[3], Richard Do[2], Natally Horvat[1], Kenneth H. Yu[4], Wungki Park[3], Eileen M. O'Reilly[3]

[1]Medicine, University of Iowa, Iowa City, IA,[2]Memorial Sloan Kettering Cancer Center, New York City, NY,[3]Memorial Sloan Kettering Cancer Center, New York, NY,[4]Gastrointestinal Oncology Service, Memorial Sloan Kettering Cancer Center, New York, NY

Introduction: A phase II trial at Memorial Sloan Kettering Cancer Center (MSK), IRB #12-045 evaluated cisplatin/gemcitabine +/- PARP inhibitor veliparib in patients with *gBRCA*1/2 and *PALB*2 (core homologous repair deficiency; cHRD) and advanced pancreas cancer (PDAC). Although the study found no significant difference in overall survival (OS) between treatment arms, patients receiving veliparib had higher rates of stable disease (SD) or partial response (PR), suggesting heterogeneous treatment benefit within this population (RR 74.1% vs. 65.2%; P = 0.55). Leveraging this trial cohort, the present study aimed to identify CT radiomic signatures predictive of OS and to assess whether changes in radiomic features over time provide additional prognostic value.
Methods: We retrospectively analyzed contrast-enhanced CT scans of patients with cHRD and PDAC that were enrolled in the trial. A trained machine learning specialist processed baseline, 6-week, and 3-month scans using an automated pancreas segmentation workflow, and 134 radiomic features were extracted from each scan. Highly correlated features ($r > 0.9$) were removed. We performed univariate Cox proportional hazards method to identify features associated with OS. Significant top two features were integrated into multivariate Cox models to investigate their predictability using repeated 3-fold cross-validation to avoid overfitting. Kaplan-Meier analysis compared OS between radiomics-defined high- and low-risk groups.
Results: Among the 26 patients enrolled at MSK, baseline (pre-treatment) CT scans were available for 23 (88%), 6-week scans for 25, and 3-month scans for 24 (92%). Twenty-five patients received cisplatin and gemcitabine, and 16 also receiving veliparib. Radiologist-assessed treatment responses were PR (n = 21), SD (n = 2), and progressive disease (n = 3). Several radiomic features were significantly associated with OS across all three time points, with the top 2 features selected for optimal prognostic stratification. Lower gray-level non-uniformity in the baseline pancreas was associated with worse OS, indicating that increased pancreatic textural homogeneity correlates with poorer outcomes. Delta-radiomics analyses demonstrated that longitudinal changes in pancreatic texture also correlated with OS.
Conclusions: CT radiomic features demonstrate prognostic value for overall survival in patients with cHRD and advanced PDAC, supporting radiomics as a promising tool for patient stratification in future trials. Ongoing work is evaluating correlations between radiomic signatures and genomic profiles to further refine predictive models.

#2777 Automatic contrast phase classification of polyphasic CT scans.

Georgia Hughes[1], Mayank Patwari[2], Yi Wei[3], Michael Parker[4], James Parkin[4], Zhenning Zhang[5], Aleksandr Filippov[6]

[1]Astrazenca UK, Cambridge, United Kingdom,[2]Astrazeneca UK Limited, Cambridge, United Kingdom,[3]Astrazeneca UK, Cambridge, United Kingdom,[4]Norfolk and Norwich University Hospital, Norwich, United Kingdom,[5]AstraZeneca US, Gaithersburg, MD,[6]AstraZeneca Oncology, Gaithersburg, MD

Contrast phases refer to the different stages of blood vessel, tissue, or organ enhancement following the administration of an intravenous contrast agent during CT scans. Contrast phases help distinguish abnormal lesions from normal tissue, where lesions appear hypo- or hyper-vascular, depending on the disease. Therefore, selecting the appropriate phase based on the specific pathology is crucial for accurate detection, meaningful diagnostic interpretation, clinical workflows, and robust quantitative analysis. However, in many polyphasic CT scans, information about phases is missing from the metadata.

This study presents a fully automated pipeline to predict the contrast phase of CT scans, using organ-based image features. Our approach has the following novel contributions: (1) Focuses on a limited set of organs (aorta, portal vein, kidney), reducing reliance on extensive organ coverage. This is useful for scans with varying field-of-view where many organs may be absent. (2) Introduces engineered features derived from first-order PyRadiomic statistics, quantifying inter-organ relationships to capture phase-specific intensity patterns.

Our pipeline distinguishes non-contrast scans and all three major contrast phases: arterial, portal venous, delayed. Automated segmentation of the aorta, portal vein/splenic vein, and kidneys is performed using TotalSegmentator, a state-of-the-art deep learning algorithm for CT scan segmentation. For each organ mask, a comprehensive set of first-order statistical features, including mean, median, minimum, maximum, standard deviation, skewness, kurtosis, energy, and entropy, is extracted with PyRadiomics to capture intensity distributions. Engineered features reflecting the mean and maximum intensity differences between organs are created, along with the total mean intensity of all three organs, to better distinguish phases.

The model was trained and validated on the TOPAZ-1 phase 3 biliary tract cancer trial dataset. TOPAZ-1 comprised of 1418 CT baseline scans (447 portal venous, 396 arterial, 323 non-contrast, 252 delayed) annotated by a radiologist with eight years of experience. For classification, a random forest classifier was developed. Classification achieved an overall accuracy of 0.97, with weighted average precision, recall, and f1-score all at 0.97. Per-phase precision, recall and f1-score all exceed 0.93. On analysis, the engineered features indicate the arterial phase is characterized by a brighter aorta, the venous phase by a brighter portal vein, the delayed phase by increased renal intensity, and non-contrast scans by lower overall intensity relative to the other scans. These patterns align with radiologist expectations and support the model's interpretability.

By focusing on organs and features that are most indicative of phase differences, the pipeline yields a simple and interpretable model that achieves accurate polyphasic CT phase identification.

#2778 Learning spatial transcriptomic patterns from whole-slide images with a cancer-scale foundation model.

Minsoo Lee[1], Soonyoung Lee[1], Tae Hyun Hwang[2], Jongseong Jang[1]

[1]LG AI Research, Seoul, Korea, Republic of,[2]Department of Surgery, Vanderbilt University Medical Center, Nashville, TN

Background
Spatial transcriptomics (ST) provides essential insights into tumor microenvironment (TME) organization, but remains costly and limited in clinical scalability. Predicting spatial gene expression directly from routine whole-slide images (WSIs) could enable large-scale molecular phenotyping across diverse cancer types. However, existing approaches rely on self-supervised patch encoders and small gene panels, limiting biological fidelity and cross-cancer generalization.
Methods
To explicitly capture molecular variation underlying tissue morphology, we train a DINOv2-based patch encoder jointly with a spatial transcriptomics prediction head. This design aligns visual representations with gene-expression signals, addressing the morphological ambiguity often encountered in tumor pathology, where cells with similar appearance may exhibit distinct transcriptomic states relevant to tumor progression or immune activity. To model tissue-level biological organization, we introduce a masked transformer that integrates information from neighboring patches. Spatial relationships are crucial in cancer tissues, where gene expression patterns are shaped by tumor-stroma interfaces, immune niches, and gradients across the invasive front. By referencing local spatial context, the model captures these microenvironmental dependencies that conventional patch-level encoders overlook.
Results
We evaluate our framework on the HEST-benchmark, which comprises ten cancer types designed to assess ST prediction from WSIs. Without using the benchmark's training data, our foundation model already achieves comparable performance to state-of-the-art methods that were trained separately for each cancer type in the HEST-benchmark, demonstrating strong cross-cancer generalization. When further fine-tuned on each cancer cohort within the benchmark, our model surpasses prior approaches by a large margin. Qualitatively, the predicted spatial expression maps reproduce tissue features that are clinically and biologically meaningful, including localized expression changes and tumor-associated regions. These patterns closely match ground-truth ST profiles, indicating that the model captures spatial domains shaped by tissue organization.
Conclusion
Our model shows that large-scale pretraining enables reliable prediction of spatial gene expression directly from routine histology. By generating spatial gene expression maps from standard pathology slides, this approach can support biomarker assessment, enhance characterization of the tumor microenvironment, and provide value where spatial transcriptomic assays are not available. Overall, these findings highlight the potential of foundation-model-based pathology to make spatial transcriptomic insights more accessible in both clinical and research settings.

#2779 Development and evaluation of a MIRAI 5-year risk model with a breast cancer polygenic risk score.

Christopher G. Scott[1], Peter Kraft[2], Imon Banerjee[3], Ramon Correa Medero[3], Aaron D. Norman[1], Fergus J. Couch[1], Karla Kerlikowske[4], Stacey J. Winham[1], Celine M. Vachon[1]

[1]Mayo Clinic, Rochester, MN,[2]National Cancer Institute, Rockville, MD,[3]Mayo Clinic, Phoenix, AZ,[4]UCSF, San Francisco, CA

Artificial intelligence (AI)-scores estimated from digital mammograms predict future breast cancer (BC) risk. MIRAI is a deep learning BC risk model that provides a continuous 5-year risk of overall BC from four screening full field digital mammograms. Common germline genetic variation in the form of a polygenic risk score (BC-PRS) is associated with increased BC risk and may improve MIRAI's 5-year risk prediction. Our goal was to develop an updated MIRAI 5-year risk model that incorporates the BC-PRS (MIRAI+PRS) and to evaluate its discriminatory accuracy and calibration for both overall and invasive BC compared to MIRAI alone. We developed the MIRAI+PRS model by multiplying each woman's 5-year MIRAI risk estimate by their relative risk based on their BC-PRS relative to the population mean. We evaluated the models within the Mayo Clinic Biobank mammography cohort, comprised of 12,307 women without a prior history of BC; 176 invasive and 250 overall BC were diagnosed within 5 years. MIRAI was estimated on screening mammograms closest to enrollment but at least 6 months prior to BC. Discriminatory accuracy, assessed by C-statistic, was high and similar for MIRAI+PRS vs. MIRAI models, for overall BC and invasive BC (Table). Calibration assessed by observed to expected (O/E) ratios was also similar for MIRAI+PRS compared to MIRAI predictions for BC outcomes (Table), although there was improvement in decile-specific O/E ratios across the lowest risk deciles (<1.67%) for MIRAI+PRS. Calibration for invasive cancer was poor for MIRAI with or without PRS. In summary, the MIRAI+PRS risk model did not result in significant difference of discriminatory accuracy or overall calibration compared to the MIRAI model, but there was evidence for improved calibration for women with 5-year risk below 1.67%. For invasive BC, the model had poor calibration regardless of whether PRS was included, underscoring the importance of training AI models for BC outcomes that are associated with a clinical intervention.

MIRAI and MIRAI+PRS 5-year risk model performance within the Mayo Clinic Biobank mammography cohort

Model	**HR per SD (95% CI)**	**C-index (95% CI)**	**Obs/Exp Ratio (95% CI)**
Overall BC (Invasive + DCIS), N=250			
MIRAI 5 yr Risk (log)	1.69 (1.55, 1.84)	0.71 (0.68, 0.74)	0.96 (0.84, 1.09)
MIRAI+PRS 5 yr Risk (log)	1.97 (1.78, 2.19)	0.72 (0.69, 0.75)	0.93 (0.82, 1.05)
Invasive BC, N=176			
MIRAI 5 yr Risk (log)	1.68 (1.51, 1.86)	0.71 (0.67, 0.75)	0.68 (0.58, 0.78)
MIRAI+PRS 5 yr Risk (log)	1.99 (1.76, 2.24)	0.73 (0.69, 0.76)	0.66 (0.56, 0.76)

#2781 Investigating feature selection strategies with habitat-based radiomics for oropharyngeal cancer.

Oya Altinok[1], Ghulam Rasool[1], Asim Waqas[1], Matthew B. Schabath[1], Albert Guvenis[2]

[1]Moffitt Cancer Center, Tampa, FL,[2]Biomedical Engineering, Bogazici University, Istanbul, Turkey

Background: Habitat radiomics characterizes intratumoral heterogeneity by partitioning tumors into biologically meaningful and statistically distinct subregions. Because HPV-positive and HPV-negative oropharyngeal cancers (OPC) differ in morphology, intensity distribution, and texture, we evaluated different machine learning methods and habitat feature aggregation strategies to develop an HPV prediction algorithm.

Methods: Radiomic tumor habitats were generated from 192 pretreatment CT scans using a two-level unsupervised clustering approach (K=3). Tumors exhibited one to three habitats of varying prominence. Six aggregation strategies were compared: maximum, largest-volume, sum, mean, minimum, and variance. Each strategy produced a separate feature set and classifier. Support Vector Machine (SVM) models with a radial basis function kernel were trained using 7-fold nested cross-validation. Logistic regression, Gaussian process classification, random forest, naïve Bayes, and extreme gradient boosting (XGBoost) were also evaluated to benchmark model performance. HPV status was defined using p16 immunohistochemistry. SHapley Additive exPlanations (SHAP) analysis was used to interpret model behavior, and Kaplan-Meier curves were generated for the best-performing classifier.

Results: With SVM, maximum aggregation achieved the highest balanced accuracy across all strategies (training 0.906; test 0.896) and was the overall best-performing approach. Other aggregation strategies (largest-volume, sum, mean, minimum, and variance) demonstrated lower performance (test balanced accuracy range: 0.292-0.834). SVM also outperformed all other machine learning algorithms (test balanced accuracy range: 0.572-0.796). SHAP identified shape and texture features—including VolumeDensityConvexHull3D, Compactness2_3D, and InformationCorrelation1Merged3D—as major contributors to HPV-positive predictions, whereas HPV-negative tumors exhibited more heterogeneous habitats. Kaplan-Meier analysis showed that predicted HPV groups closely matched ground truth (p=0.52 HPV-; p=0.75 HPV+).

Conclusions: These results likely imply that the tumor's outcome is not determined by the average properties of its habitats, but rather by the presence and intensity of the most extreme or critical local microenvironmental condition that provides the strongest selective pressure or dictates the dominant biological process. These findings support maximum aggregation as an effective and biologically relevant strategy for HPV prediction in OPC.

#2782 Automated segmentation of hepatocellular carcinoma lesions on contrast-enhanced MRI using an AI model in patients with cirrhosis.

Emma J. Stevenson[1], Nathan Lay[1], Stephanie A. Harmon[1], Haoyue Zhang[1], Fahmida Haque[1], Peter Choyke[1], Theo Heller[2], Ross Filice[3], Baris Turkbey[1], Christine Hsu[2]

[1]Molecular Imaging Branch, National Cancer Institute (NCI), Bethesda, MD,[2]Liver Diseases Branch, National Institute of Diabetes and Digestive and Kidney Diseases (NIDDK), Bethesda, MD,[3]Radiology, MedStar Georgetown University Hospital, Bethesda, MD

Purpose: Develop an automated hepatocellular carcinoma (HCC) detection model on multi-phasic contrast-enhanced T1 MRI images. **Methods:** Multi-phase (pre-contrast, arterial, venous, and delayed phases) contrast-enhanced T1 MRIs were obtained from two institutions (Center 1: n=106; Center 2: n=87) and acquired between 2007 and 2023. An expert radiologist manually contoured 1794 focal liver lesions across 586 scans and assigned each lesion a score using the Liver Imaging Reporting and Data System (LI-RADS). Six 3D full-resolution nnU-Net models were trained on multi-phase (pre-contrast, arterial, venous, and delayed) or only arterial-phase contrast-enhanced T1 images. Lesion size (maximum lesion diameter ≥ 1 cm) and lesion score (LI-RADS ≥ 3) criteria were applied to assess the impact on the training of these nnU-Net models. Model performance was evaluated at a scan and lesion level. Performance metrics included dice similarity coefficient (DSC), sensitivity, specificity, accuracy, and positive predictive value (PPV). **Results:** The arterial phase without lesion criteria was determined to have the best overall performance among the models developed. At the scan level, the arterial phase model achieved 93% (40/43) sensitivity, 46.6% (7/15) specificity, and 81% (47/58) accuracy. At a lesion level for the arterial phase model, the performance dropped slightly, with 65.9% (126/191) sensitivity, 68.1% (126/185) PPV, and 51.8% (133/257) accuracy. In a failure analysis, it was observed that 45.2% (57/126) of true-positive lesions had a LIRADS score ≥ 4, while 9.2% (6/65) of false-negative lesions had a LIRADS score ≥ 4. **Conclusion:** An arterial phase contrast-enhanced MRI nnU-Net model was developed on multi-institutional data to detect HCC in patients with cirrhosis, producing promising results. This study indicates that AI models can improve detection in high-risk patients.

Categorization of Models based on the Inclusion of MRI Phases, Lesion Score, and Size Threshold

Model	MRI Phase(s) Used	Lesion Inclusion	Size Threshold
A	Pre-Contrast, Arterial, Venous, and Delayed	All	None
B	Arterial	All	None
C	Pre-Contrast, Arterial, Venous, and Delayed	LIRADS ≥ 3	None
D	Arterial	LIRADS ≥ 3	None
E	Pre-Contrast, Arterial, Venous, and Delayed	LIRADS ≥ 3	≥ 1.0 cm
F	Arterial	LIRADS ≥ 3	≥ 1.0 cm

#2783 Lung cancer intelligent detection (LUCID) using a universally accessible, cross-platform, AI-powered application.

Gowrishankar Palaniswamy [1], Elangovan Krishnan[2], Jansi R. Sethuraj[3], Muhammad Waqas Khan[4], Aravind Raghavan[1]

[1]MUSC Health Lancaster Medical Center, Medical University of South Carolina, Lancaster, SC,[2]AIM DOCTOR, Chennai, India,[3]The University of Texas Health Science Center at Houston, Houston, TX,[4]Medical University of South Carolina (MUSC), Lancaster, SC

Introduction: Lung cancer represents the leading cause of cancer-related mortality globally. Only 29% achieve 5-year survival, primarily due to late diagnoses. In addition, the economic burden exceeds $3.9 trillion internationally. Only one-third of all lung cancer patients are diagnosed early enough so that effective treatment can be implemented. Deep learning architectures have revolutionized diagnostic imaging, extracting complex imaging patterns beyond human capability. EfficientNetB0, a state-of-the-art convolutional neural network achieves remarkable accuracy and computational efficiency. Its application to computed tomography (CT) imaging offers unprecedented potential for early lung cancer detection and mortality reduction.

Methods: Anonymized CT images of normal, benign, and malignant lung (n = 1190) were proportioned into training (60%), validation (20%), and testing (20%) sets. Preprocessing and augmentation improved data quality and model generalizability. EfficientNetB0 was trained and optimized, with performance evaluated by accuracy, precision-recall, F1-score, F2-score, and area under the receiver operating characteristic curve (AUROC) on validation and test sets. The trained model was deployed in a universally accessible, cross-platform application for independent validation by experts globally.

Results: EfficientNetB0 demonstrated exceptional performance in distinguishing normal, benign, and malignant lung lesions. The model achieved perfect accuracy, precision, and recall for both classes, with F1-scores of 1.00 (training and validation). AUROC values of 1.00 demonstrate outstanding discriminative capacity. The confusion matrix confirmed zero misclassifications across 137 lesions (24 benign, 113 malignant). The model's exemplary performance suggests substantial potential to augment clinical decision-making and advance equitable cancer care.

Conclusion: EfficientNetB0 represents a paradigm-shifting diagnostic tool for lung cancer stratification on CT imaging, demonstrating clinical-grade accuracy that augments expert radiologist interpretation. The model's exceptional discriminative capacity, achieving high sensitivity and specificity, positions it as a transformative adjunct to conventional diagnostic workflows. Deployment via an accessible cross-platform application facilitates dissemination across resource-constrained environments, democratizing precision diagnostics. This deep learning architecture substantially augments early detection capabilities, potentially reducing mortality through timely clinical intervention. These findings establish a robust foundation for prospective validation studies and clinical integration to optimize lung cancer outcomes globally.

#2784 Integrating spatial transcriptomics with MRI reveals distinct radio-spatial genomic profile concordant with prostate cancer clonal heterogeneity.

Thineskrishna Anbarasan[1], Sandy Figiel[1], Max Beesley[2], Wencheng Yin[1], Ruth McPherson[3], Richard Colling[1], Freddie Hamdy[1], Richard J. Bryant[1], Bartlomiej Papiez[1], Alastair D. Lamb[2], Ian Mills[1]

[1]University of Oxford, Oxford, United Kingdom,[2]Barts Cancer Institute, London, United Kingdom,[3]Oxford University Hospitals, Oxford, United Kingdom

Introduction: Prostate cancer (PCa) risk stratification, to precisely identify patients at greatest risk of progression to metastatic disease remains challenging. Integrating clinical data, multiparametric MRI (mpMRI) radiomics, and spatial transcriptomics (ST) may enable identification of imaging features linked to genomic signatures of aggressive PCa.

Methods: Organ-wide spatial transcriptomics (Visium^{TM} v2, 10x Genomics) was performed on formalin-fixed paraffin-embedded prostatectomy sections and metastatic lymph nodes from patients recruited to a trial (ISRCTN10046036). A patient with Gleason 4+4 PCa and pre-operative mpMRI was included. This is a sub-study, part of a larger project mapping prostate cancer clonal dynamics in ten men using inferred clonal genomic analyses (SpatialInferCNV). Image processing involved anatomical segmentation and qualitative correlation with radiologist and pathologists. Image registration was performed using the ProsRegNet deep learning pipeline. Multiple ST sections were mapped to a common coordinate framework using SpatialStitcher (locally developed). Radiomic features were extracted using PyRadiomics.

Results: Eight ST sections representing over 85000 ST spots (55µm diameter) were mapped to T2-axial MRI. Image registration achieved a DICE similarity coefficient of 0.861 for prostate capsule. The landmark deviation for urethra and BPH nodule were 2.17mm and 2.62mm respectively. A total of 93 radiomic features were selected. First-order radiomics significantly correlated with ST spot-level histological annotation according benign vs Gleason grade group (GG2, GG3 and GG5) ($p<0.001$). Inferred clonal phylogenomic analysis revealed a region on the axial sections (X clone) with high concordance with lymph node metastasis. This region, harboured a distinct z-normalised textural (features: GLSZM, GLCM, GLDM, GLRLM, NGTDM) radiomic score compared to other tumour and benign regions ($p<0.001$). No difference in first order radiomics (visible to the eye) was observed between the X clone and other tumour clones ($p = 0.21$).

Conclusion: We show a distinct textural radiomic profile within the prostate that harbours a phylogenetic correlation with lymph node metastases. Further radio-spatial genomic profiling of the cohort and validation analyses are underway. These could offer insights into improving current MRI-based risk stratification for follow-up and lesion targeting for biopsy or focal therapy.

#2785 Assessing the risk of breast cancer recurrence with pre-treatment MRI: A transfer learning study on multicenter data.

Kanika Bhalla[1], Adrian Sanchez[1], Jose Marcio Luna[1], Tabassum Ahmad[1], Debbie L. Bennett[1], Andrew A. Davis[2], Aimilia Gastounioti[1]

[1]Radiology, Washington University School of Medicine in St. Louis, St. Louis, MO,[2]Oncology, Washington University School of Medicine in St. Louis, St. Louis, MO

Background: MRI features have demonstrated prognostic value in predicting future breast cancer recurrence. However, deep learning studies remain limited particularly those evaluating performance across tumor subtypes and different time horizons in large multicenter datasets.
Materials and Methods: We used pretreatment DCE-MRI exams from the multicenter MAMA-MIA dataset (433 breast cancer patients who underwent NAT; 115 with recurrence events, 318 recurrence-free) to evaluate a transfer-learning framework based on DenseNet121 pretrained on ImageNet. Middle tumor-containing slices were bias-field corrected, resampled, cropped to the tumor regions, and resized to 224×224 pixels. The top 10% of DenseNet121 layers were unfrozen for model fine-tuning for recurrence prediction. Five-fold stratified cross-validation preserved site distribution across data splits. Model performance was evaluated using Harrell's C-index and time-dependent AUCs at 3 and 5 year horizons. Correlated C-indices were compared using the two-sided Kang et al. test. We also assessed the added value by our deep-learning risk score to a baseline prognostic model based on the established clinical factors HR and HER2. Model performance was also assessed across tumor subtypes.
Results: Our deep learning model achieved a C-index of 0.67±0.03 with 3 and 5 year AUCs of 0.69±0.04 and 0.67±0.10, respectively. Adding our deep-learning risk score to the baseline model significantly improved performance from 0.64 to 0.71 (p=0.007). Subtype-specific evaluations (Table 1) showed variable performances with the highest performance in HER2-pure and TNBC patients.
Conclusion: Our findings highlight the potential of a transfer-learning-based DenseNet121 MRI model to predict 3 and 5 year recurrences in breast cancer patients, providing added value beyond standard clinical factors. Future optimizations will aim at improving subtype-specific performance in large multicenter datasets.

Table 1. Recurrence-free survival analysis results in multi-center MAMA-MIA dataset (N = 433).

Added prognostic value by our deep learning model			
Model	*C-index*	*p-value**	
DL model	0.67 ± 0.03	0.01	
Baseline model (HR, HER2)	0.64 ± 0.05	N/A	
Baseline + DL	0.71 ± 0.05	0.007	
* p-value for C-index differences with respect to the baseline model.			
Performance of our deep learning model by time horizon			
3-year AUC	0.69 ± 0.04		
5-year AUC	0.67 ± 0.10		
Performance of our deep learning model by breast cancer subtype			
	C-index	*3-year AUC*	*5-year AUC*
Luminal A (N = 121)	0.61±0.02	0.61±0.11	0.64±0.08
Luminal B (N = 50)	0.67±0.13	0.62±0.09	0.57±0.07
TNBC (N = 120)	0.70±0.04	0.72±0.03	0.72±0.15
HER2-enriched (N = 65)	0.65±0.16	0.59±0.19	0.68±0.28
Her2-pure (N = 56)	0.82±0.11	0.86±0.13	0.90±0.20

#2786 CorrectionNet: A lightweight residual refinement framework for improving medical image segmentation.

Antoine Azar[1], **Cally Lin**[2], Naryeong Kim[3]

[1]Computer Science, EPITECH, Paris, France,[2]Biomedical Data Science, Stanford University, Stanford, CA,[3]Biology, Stanford University, Stanford, CA

Accurate and reproducible image segmentation is crucial for oncologic imaging tasks, including tumor delineation, treatment planning, and quantitative response assessment. Despite strong baseline performance from modern deep learning frameworks such as nn-Unet, automated segmentations frequently exhibit systematic boundary errors and under-segmentation of small or infiltrative tumor regions, resulting in costly manual correction efforts. We present CorrectionNet, a lightweight and modular refinement framework designed to work on top of existing segmentation models. The method extracts patch-based regions of interest around the initial segmentation and inputs both multimodal imaging and base-model probability maps to a shallow 3D U-Net. Instead of predicting full masks, CorrectionNet learns residual connections, enabling it to fix high-confidence false positives/negatives and improve boundary regularity while preserving the global tumor structure. Training focuses on voxels where the base model is likely incorrect or uncertain, yielding efficient learning behavior and minimal computational overhead. In current quantitative evaluations, CorrectionNet maintained whole-lesion Dice performance relative to nnU-Net (ΔDice = -0.0002 ± 0.0024, $p = 0.18$) while achieving measurable improvements in boundary accuracy (ΔHD95 = -0.089 ± 0.786 mm; one-sided $p = 0.03$). Nearly half of all local voxel edits (47.7%) represented true error corrections, with the model showing a strong preference for eliminating false-positive boundary over-segmentation (FP fix precision = 81.5%). CorrectionNet hyperparameters further enable researchers or clinicians to tune the balance between false-positive removal and false-negative recovery, accommodating diverse tumor morphologies and clinical priorities. Overall, CorrectionNet provides a practical and scalable refinement layer for oncology segmentation workflows. By improving local boundary fidelity without retraining or replacing base models, it has the potential to reduce manual editing effort and enhance clinical deployment of automated segmentation.

#2787 Evaluation of imaging-based prognostication (IPRO) using artificial intelligence (AI) in stage IV colorectal cancer (CRC) patients treated with first-line (1L) systemic therapy.

Mohammed A. Alvi[1], Ronald Bridges[2], Marina Salluzzi[2], Felipe Soares Torres[3], Kartik Jhaveri[3], Natasha B. Leighl[4], John Riskas[1], Shahid Haider[1], Vignesh Sivan[1], Oleksandra Samodorova[1], Jay Hennesy[1], Duoaud Shah[1], FELIX BALDAUF-LENSCHEN[1], **Omar F. Khan**[5]

[1]Altis Labs, Inc., Toronto, ON, Canada,[2]Cumming School of Medicine, University of Calgary, Calgary, AB, Canada,[3]Department of Medical Imaging, University of Toronto Temerty School of Medicine, Toronto, ON, Canada,[4]University Health Network, Toronto, ON, Canada,[5]Department of Oncology, Univ. of Calgary Faculty of Medicine, Calgary, AB, Canada

INTRODUCTION: Accurate prognostication in stage IV CRC informs treatment decisions and stratifies patients in clinical trials. Tumor, node, metastasis (TNM) staging derived from pre-treatment computed tomography (CT) imaging classifies extent of disease but may not fully characterize prognosis. IPRO-α is an AI-generated prognostic score derived from pre-treatment CT imaging, with higher scores representing improved survival. IPRO-α was trained and validated to predict survival in advanced non-small-cell lung cancer. This study evaluates generalizability and prognostic utility of IPRO-α in real-world stage IV CRC patients receiving 1L systemic therapy, compared to TNM substage.

METHODS: We retrospectively evaluated IPRO-α and TNM substage in a real-world dataset of stage IV CRC patients treated with 1L systemic therapy between 2010-2018 at 17 cancer centers. We evaluated median overall survival (mOS) and hazard ratios (HR) using Cox proportional hazards models across stage IV substages (A, B, C) and matched relative distributions for IPRO-α.

RESULTS: 372 patients had available pre-treatment CT and known TNM substage (IVA=141, IVB=162, IVC=69). The median age was 61 years (IQR 52-69), with 32.8% (n=122) females. TNM substage IVA mOS was significantly better than IVB, with no statistically significant difference between stage IVB and IVC (Table 1). Distribution-matched IPRO-α groups showed significant survival differences across high, intermediate and low scores.

CONCLUSIONS: IPRO-α may stratify survival with greater prognostic discrimination than TNM substage in metastatic CRC patients. IPRO-α, trained on lung cancer data, learned shared prognostic features allowing generalizability of survival predictions to entirely different tumour sites. Future work will evaluate IPRO-α's ability to stratify survival in various CRC treatment subsets.

Median OS for stage IV CRC patients stratified by TNM substage and IPRO-α survival scores.

	N	mOS in months (95% CI)	HR (95% CI)	p-value
IPRO-α High	141	24.0 (19.1-29.6)	0.74 (0.58-0.93)	0.010
IPRO-α Intermediate	162	17.9 (16.2-20.9)	reference	-
IPRO-α Low	69	10.0 (7.4-13.0)	2.28 (1.70-3.06)	< 0.001
Stage IVA	141	20.8 (17.9-27.5)	0.77 (0.61-0.98)	0.032
Stage IVB	162	17.2 (14.4-20.1)	reference	-
Stage IVC	69	13.0 (10.9 - 16.0)	1.14 (0.85-1.53)	0.363

#2788 Multi-site development of automated lesion classification for comprehensive tumor burden assessment: Addressing the RECIST trial-practice disconnect.

Ella Pavlechko[1], Xi Jiang[1], Ravikumar Komandur Elayavilli[2], Eleanor McCabe[2], Jon McDunn[2], **Sean Khozin**[3]

[1]SAS Institure, Cary, NC,[2]Project Data Sphere, Cary, NC,[3]CEO Roundtable on Cancer & Project Data Sphere, Cary, NC

Background: Response Evaluation Criteria in Solid Tumors (RECIST) mandate manual selection of 2-5 target lesions with unidimensional measurements, generating inter-reader discordance beyond 30% while folding 3D tumor dynamics into categorical outcomes with limited biological interpretability. RECIST protocols are rarely used in routine practice, creating a trial-practice disconnect that undermines endpoint validity. Automated volumetric quantification of total tumor burden represents an alternative contingent on reliable autonomous model performance across diverse imaging environments.
Methods: We developed a modular dual-architecture system combining UNet segmentation with ResNet50 classification, trained on 2,464 CT scans from 1,324 patients across three continents (North/South America & Asia) acquired on heterogeneous scanner platforms (GE, Siemens, Philips, Toshiba). The 11,705-lesion dataset had a clinically representative class distribution: 2,125 malignant (18%), 193 benign (2%), and 9,387 other findings (80%). Preprocessing applied Hounsfield windowing (level: -600, width: 1500) and Lungmask segmentation. To improve classification performance and address class imbalance, we augmented minority-class images using flips, rotations, and sharpening.
Results: Segmentation training demonstrated loss reduction of 86% across epochs with parallel convergence in training and validation sets. Classification performance on held-out development data (n=1,332 lesions) yielded 86% accuracy, 91% sensitivity, 17% specificity, 94% positive predictive value (PPV), and 11% negative predictive value at 0.5 probability threshold. Precision-recall area under curve was 0.89. Model performance remained stable across scanner manufacturers without platform-specific recalibration.
Conclusions: High sensitivity (91%) with constrained specificity (17%) exhibits successful optimization for malignancy detection in imbalanced datasets. The 94% PPV confirms reliable malignancy identification, while precision-recall AUC of 0.89 supports effective minority class discrimination despite 11:1 imbalance. Stable cross-platform performance allows for multi-site training to be a viable paradigm for generalized deployment. This initial work provides the foundation for lesion-level classification within a fully autonomous system for volumetric tumor burden quantification. Our development path includes classification refinement, expansion to whole-body CT across organ systems, and integration of autonomous detection and segmentation modules. The next steps in establishing TTB as a regulatory-grade endpoint addressing RECIST's limitations require external confirmation in independent cohorts, prospective clinical-trial evidence, and correlation with clinical outcomes.

#2789 Depth prediction in superficial esophageal cancer using a foundation model from endoscopic images.

Sehun Kim[1], Sohyung Kim[1], Hyosoon Yoo[1], Hyuk Lee[2], Yang Won Min[2]

[1]Samsung Precision Genome Medicine Institute, Samsung Medical Center, Seoul, Korea, Republic of,[2]Department of Medicine, Samsung Medical Center, Sungkyunkwan University School of Medicine, Seoul, Korea, Republic of

Background: For superficial esophageal cancer (SEC) without a risk of lymph node metastasis (LNM), upfront endoscopic submucosal dissection (ESD) is the preferred treatment over surgery. The representative factor for predicting LNM risk is tumor depth, but the insufficient prediction accuracy during pre-procedure evaluation frequently results in unnecessary surgery or the need for salvage surgery after ESD. Accordingly, we propose to predict SEC tumor depth using a foundation model (FM) applied to pre-procedural endoscopic images. Using a foundation model (GastroFM) that was pretrained on approximately 500,000 EGD images, we propose utilizing its knowledge gained from pre-training to provide a reliable, pre-histopathology prediction of invasion depth from endoscopic images.

Methods: We adapted a FM, which is based on a vision transformer architecture and was pretrained on approximately 500,000 upper endoscopic images, for SEC depth prediction. We propose utilizing the knowledge gained from this pre-training to provide a reliable, pre-histopathology prediction of invasion depth from endoscopic images. The model was trained and validated on a retrospective cohort of 839 ESD cases for SEC (April 2007-January 2023) using an 8:1:1 train/validation/test split. For each case, esophageal ESD expert selected tumor-displaying images (median 10, range 4-36) from pre-procedure endoscopy. We applied Attention-based Multiple Instance Learning (AbMIL) to aggregate these variable-length image sequences into a single case-level prediction score for the binary task: mucosal cancer vs submucosal cancer.

Results: The overall cohort distribution was 529 cases (63.1%) with mucosal cancer and 310 cases (36.9%) with submucosal cancer. On the test set, a FM achieved an AUC of 0.821 and an overall accuracy of 0.810. Key metrics for the binary classification were: sensitivity 0.645, specificity 0.906, F1 score 0.714, positive predictive value 0.800, and negative predictive value 0.814.

Conclusion: We developed a FM with a discriminative power for depth prediction in SEC. This model is expected to be a valuable supplementary tool in the pre-procedure workup, assisting endoscopists and surgeons in determining the optimal treatment plan for SEC.

#2790 Foundation model-based gastric cancer staging from complete, uncurated EGD image sequences.

Sehun Kim[1], Hyosoon Yoo[1], Yang Won Min[2], Hyuk Lee[2]

[1]Samsung Precision Genome Medicine Institute, Samsung Medical Center, Seoul, Korea, Republic of,[2]Department of Medicine, Samsung Medical Center, Sungkyunkwan University School of Medicine, Seoul, Korea, Republic of

Background: Histopathologic assessment remains the gold standard for gastric cancer staging but creates significant treatment bottlenecks. While AI-based prediction of pathologic outcomes from endoscopic images shows promise, existing approaches rely on manually selected images, introducing selection bias and missing the case-level context essential for clinical decisions. We present GastroFM, a vision transformer-based foundation model that learns from complete esophagogastroduodenoscopy (EGD) image sequences, enabling case-level predictions aligned with clinical practice.
Methods: GastroFM is pretrained using a modified DINOv3 framework on approximately 500,000 images from 13,515 pathology-confirmed EGD cases at Samsung Medical Center (2019-2023). We then fine-tuned the pretrained model for gastric cancer staging using Attention-based Multiple Instance Learning (AbMIL), which aggregates uncurated, variable-length image sequences (1 to 105 images per case) into case-level predictions. We evaluated the model on gastric cancer staging at multiple granularities using a 75%/10%/15% train-validation-test split (8,121 cases with gastric cancer): (1) early gastric cancer (EGC) vs. advanced gastric cancer (AGC), (2) four-class T-stage (T1-T4), and (3) lymph node metastasis (N0 vs. ≥N1).
Results: On the test set, GastroFM achieved: AUC 0.93 (accuracy 0.91) for AGC classification, substantially exceeding expert endoscopic assessment (76.8% accuracy in our cohort); AUC 0.84 (overall accuracy 0.67) for 4-class T-stage classification; and AUC 0.85 (accuracy 0.87) for lymph node metastasis prediction.
Conclusion: Unlike conventional approaches that rely on manually selected images, GastroFM analyzes complete, uncurated image sequences, providing case-level predictions aligned with clinical practice workflows. Further comparative studies with existing foundation models and large-scale external validation are necessary to fully establish its superiority and clinical utility in diverse settings.

#2791 Deep learning-based survival prediction of post-operative GBM patients via multimodal radiomic phenotypes drawn from Kaniadakis vector embedding in latent space.

Roy Nasr, **Bardia Rodd**

SUNY Upstate Medical University, Syracuse, NY

Purpose: The aim of this study was to use multimodal imaging biomarkers and AI-guided personalized precision survival prediction in improving outcomes for patients with post-operative glioblastoma (GBM).
Method: A cohort of 450 de novo GBM cases from the University of Pennsylvania, each featuring the four standard multimodal MRI sequences (T1, T2, FLAIR, T1-Gadolinium), was analyzed. We extracted 354 radiomic biomarkers per modality (Pyradiomics) and reduced these high-dimensional features to a stable 11-dimensional latent space using Density-Based Isomap (PR-Isomap), with the optimal dimension determined by a gap statistic, which we developed specifically for such projection. These latent biomarkers were then normalized, fused across modalities, and projected into a risk-sensitive feature space via Kappa (Kaniadakis) Vector Embedding. The resulting multimodal features fed into a deep learning-based survival model using the log-hazard ratio, optimized via a survival loss function based on the negative log-likelihood of the Cox proportional hazards model for patient outcome prediction.
Results: The final survival-prediction model achieved a 71.7% accuracy in binary classification via a consensus of multiple machine learning classifiers with 10-fold cross-validation and a C-index of 0.5196, indicating a modest but statistically meaningful predictive capability using the imaging embeddings alone. To assess prognostic separation, a Kaplan-Meier survivorship curve was stratified by hazard-score quartiles. Distinct thresholds were established: the first quartile Q1) hazard score was -0.36 and the third quartile (Q3) score was -0.29. The median hazard score of -0.33 separated the cohort into 225 high-hazard patients and 225 low-hazard patients. The resulting stratified Kaplan-Meier curves demonstrated clear separation between these risk groups, definitively confirming the capacity of the MRI-derived embeddings to differentiate patient survival trajectories.
Conclusion: The integration of deep learning with multimodal MRI embeddings offers a powerful, objective methodology for GBM prognostication. The resulting quantitative hazard scores successfully differentiate high- and low-risk patient survival trajectories. This multimodal imaging biomarker-driven approach provides personalized risk information for post-operative GBM patients, and supporting precision neuro-oncology by informing the selection of personalized adjuvant therapies.

#2792 Leveraging PR-isometric guided deep learning to decode CT-based tumor heterogeneity and enhanced NSCLC prognosis.

Joel Thomas[1], Blake Gilbert[1], Harmen Siezen[2], Lan Ma[1], Jimmy J Azarnoosh[1], **Bardia Rodd**[3]

[1]University of Maryland at College Park, College Park, MD,[2]University of Amsterdam, Amsterdam, Netherlands,[3]SUNY Upstate Medical University, Syracuse, NY

Background: Non-small cell lung cancer (NSCLC), responsible for the majority of lung cancer-related deaths, displays prognostically meaningful intratumoral heterogeneity on CT imaging that is frequently overlooked by qualitative assessment. To advance quantitative risk stratification in precision oncology, we develop a deep learning framework to derive CT-based radiomic phenotypes in EGFR-mutated NSCLC and evaluate their association with overall survival.
Method: A cohort of 130 NSCLC patients with expert-annotated tumor masks from the Stanford Radiogenomics Dataset was analyzed. To improve radiomic stability and reduce sampling variance, 1,300 augmented 2D tumor slices were generated using controlled augmentation protocols. For each patient, slices with maximal tumor burden were selectively curated to emphasize intratumoral heterogeneity in subsequent modeling. High-level morphological descriptors were extracted through a pre-trained ResNet50, and the resulting embeddings were projected into a lower-dimensional manifold via Parzen-Rosenblatt Isometric Mapping (PR-Isomap), preserving nonlinear geometric relationships linked to heterogeneous growth dynamics. Gap statistics determined the optimal latent dimensionality. These low-dimensional vector biomarkers were then used to classify survival outcomes.
Results: PR-Isomap-derived embeddings demonstrated pronounced stratification of patient survival cohorts, underscoring the method's capacity to encode clinically salient heterogeneity within tumor phenotypes. A ResNet50 backbone was optimized over 200+ training epochs using an Adaptive Moment Estimation-based optimizer with a learning rate initialized at *10-4* 10^{-4} and adaptively decayed to ensure stable convergence. Model training employed a cross-entropy loss function to enhance discriminative capability across survival categories. The resulting classifier attained a 97% slice-level accuracy, exhibiting robust generalization across all augmentation regimes. Notably, model discrimination of survival endpoints was attributable to biologically meaningful tumor-intrinsic structural patterns, rather than extraneous anatomical noise, owing to segmentation-informed slice curation that systematically excluded non-tumoral confounders.
Conclusion: Integrating deep learning-based CT-derived heterogeneity signatures with PR-Isomap embeddings enhances survival stratification in NSCLC. These imaging-driven, low-dimensional Deepomics features provide clinically actionable prognostic biomarkers, enabling earlier identification of high-risk patients and informing precision treatment planning.

: Advocates Poster Session 1
Poster Session

#ADV01 Patterns of lung cancer clinical trials in Latin America and their implications for patient treatment access and research equity.

Sofia Jubany

1

Patterns of lung cancer clinical trials in Latin America andtheir implications for patient treatment access and research equityThis project analyzes patterns of lung cancer clinical trialparticipation in Latin America and their impact on patient access to innovativetherapies and research equity. It examines structural barriers limitingregional participation, including the scarcity of early-phase and later-linestudies, disparities in research infrastructure, funding, and molecular testingcapacity. The work also highlights the importance of including Latin America'sdiverse population in oncology research to improve the global representativenessof evidence. Finally, it explores opportunities for patient and researchadvocates to contribute to expanding clinical trial accessibility,strengthening collaboration among stakeholders, and promoting more equitableclinical research participation across the region.

#ADV02 Transforming cancer care together: A regional collaborative model to strengthen oncology systems.
DONJETA Zeqa

Europa Donna Albania, Tirana, Albania

#ADV03 Patient engagement in research: Lessons from the ASH Research Collaborative Patient Collaboration Team.

TODD Kennedy

Advocate, Coto de Caza, CA

In December 2024 I was asked to lead a Patient Engagement Work Group for the ASH Research Collaborative (ASH RC) Multiple Myeloma Research Network. The goal was to ensure meaningful, ongoing patient engagement in core functions of the ASH RC. Under my leadership, over the course of 2025 we met our key deliverables including recruiting a diverse team of patient and care partner advocates, reviewing best practices in patient-centered research and engagement, reviewing and scoring research proposals, collaborating as active members of research teams including co-authorship on abstracts accepted by ASH, and creating a charter to serve as the foundation for a proposed, permanent “Patient Collaboration Team.” The impact of these work group deliverables led to approval by ASH RC senior leaders to approve the creation of the PCT, which I chair. This poster will describe lessons learned in the work group stage as well as plans for the PCT going forward.

#ADV04 Backfilling in early-phase oncology trials: A patient perspective on dose-finding innovation.

Kirstin Spencer

Advocate, Winchcombe, United Kingdom

Early-phase clinical trials aim to identify safe andeffective dosing strategies, balancing anti-tumour activity with acceptabletoxicity from both clinical and patient perspectives. Historically,dose-finding studies have largely focused on identifying the highest dose thatcan be safely tolerated. However, with targeted therapies and immunotherapies,the goal has increasingly shifted toward identifying doses that maintainbiological activity while keeping side effects acceptable. minimisingunnecessary toxicity and keeping side effects acceptable.“Backfilling” refers to the concurrent enrolment ofadditional patients at lower dose levels, which have already shown to be safe,while a higher dose is currently tested. This enables deeper understanding ofdrug behaviour, anti-cancer activity, and interactions with metabolic andbiological markers, supporting more confident selection of the most appropriatedose for later-phase trials. Importantly, many therapies demonstrate differentbiological effects across dose ranges, meaning that collecting data acrossmultiple dose levels may reveal activity that would not be evident ifdose-finding focused only on identifying the highest tolerated dose.Recent regulatory initiatives and guidance supporting doseoptimisation reflect this evolving approach. The United States of America Foodand Drug Administration (FDA, 2024) and the Methodology for the Development ofInnovative Cancer Therapies (MDICT) Taskforce (2022) both encourage dosefinding studies to consider broader information/evidence than toxicity aloneand highlight the value of backfilling in generating richer datasets collectingadditional information that will ultimately help selecting the optimal dose.From a patient-advocate perspective, backfilling is morethan a technical refinement. It is a practical strategy that widens recruitmentopportunities and allows additional information to be gathered earlier in drugdevelopment. This can help identify effective and tolerable dosing sooner andreduce delays caused by needing additional trials to redefine the appropriatedose. By improving understanding of how treatments behave across dose levels,backfilling may help reduce unnecessary toxicity and metabolic stress.Integrating patient perspectives into trial methodology discussions cantherefore help ensure dose-finding strategies are not only scientificallyrobust but also better aligned with tolerability and real-world patientexperience, enabling kinder, better-tolerated treatments for both current andfuture patients.

#ADV05 Analysis of trends in pancreatic cancer clinical trials and barriers to clinical trial enrollment.

Cassadie Moravek

Pancreatic Cancer Action Network, Manhattan Beach

#ADV06 Meeting people where they are: Feasibility and acceptability of an integrated cancer screening program for NYCHA residents.

TANISHA Hill

New York, NY

Cancer disparities are deeply connected to access,especially for communities facing longstanding structural barriers topreventive care. This poster will highlight a current Cancer Health ResearchCenter (CHRC) grant project I am partnering on with Dr. Jamilia Sly toinvestigate the feasibility and acceptability of an integrated cancer screeningprogram designed to better serve New York City Housing Authority (NYCHA)residents. As a co-investigator, I support the project across key phases of theresearch process, including data collection, analysis and interpretation, andknowledge dissemination. The work is grounded in community-informed engagementand is focused on understanding what screening approaches are realistic,respectful, and usable for residents, especially when it comes to trust,communication, and barriers that often prevent people from completing screeningand follow-up care. The poster will share the project's purpose,community-centered design considerations, and early insights related to feasibility(implementation realities, participation, and operational fit) andacceptability (resident perspectives, perceived value, and culturalresponsiveness). Ultimately, this project aims to generate practical evidencethat can strengthen integrated screening approaches and help move cancerprevention and early detection closer to the communities that need it most.

#ADV07 Lung cancer biomarker testing: Driving precision treatment and improved outcomes.

DAVE Bjork

Advocate, Georgetown, MA

Background: Biomarker testing has become a cornerstone ofmodern lung cancer management, enabling precise diagnosis, individualizedtherapy selection, and ongoing monitoring. Comprehensive molecular profilingnow guides treatment decisions for both non-small cell lung cancer (NSCLC) andsmall cell lung cancer (SCLC), transforming outcomes and expanding access totargeted and immune-based therapies. Objective: This poster highlights current biomarker testingstrategies in lung cancer, the clinical relevance of key genomic andimmunologic markers, and emerging technologies that are reshaping real-timedisease assessment. Content Overview: We present an overview of essentialactionable biomarkers—including EGFR, ALK, ROS1, BRAF, MET exon 14 skipping,RET, NTRK, and KRAS G12C—and their associated targeted therapies. We alsodiscuss immunotherapy-related biomarkers such as PD-L1 expression and tumormutational burden (TMB), emphasizing their role in predicting response tocheckpoint inhibitors. The poster outlines recommended testing methodologies,including tissue-based next-generation sequencing (NGS), liquid biopsy approaches(ctDNA), and reflex testing protocols that reduce diagnostic delays. Key Messages: Broad molecular testing improves detection ofactionable alterations. Immunotherapy biomarkers remain essential yet imperfectpredictors of response. Liquid biopsies provide minimally invasive options forinitial testing and resistance monitoring. Integrating multi-omics andAI-supported analytics may enhance future decision-making. Conclusion: Comprehensive biomarker testing is vital todelivering precision oncology in lung cancer. Advances in testing technologies,standardization efforts, and streamlined workflows will further improvediagnostic accuracy, clinical decision-making, and ultimately patient outcomes.

#ADV08 Patient perceptions of mammographic compression: Empowering women to improve mammography outcomes.
Vivian M. Lee

Aqua Partners, Los Altos, CA

Most women are not informed during mammogram procedures thatmammographic compression is critical to improving image quality and reducingradiation exposure. After multiple experiences of delays due to callbacks andre-imaging due to insufficient mammographic compression, I decided to initiatean advocate-led survey to assess the awareness and understanding of theclinical benefits of mammographic compression. I developed a questionnaire thatwas completed voluntarily and anonymously by 100 women undergoing routinescreening mammography about their perceptions of and tolerance for pain,anxiety, fear and discomfort associated with mammograms. Findings reveal asubstantial gap in patient awareness which may contribute to lack of compliancewith mammographic screening recommendations. My preliminary findings show thatpatient education can be effective in making women aware that they DO have thepower to improve the usefulness of their mammogram as well as minimize theirradiation exposure.

#ADV09 Early detection is power.
ETHEL Olomu

Engraced Life Foundation, Lagos, Nigeria

Since 2022, Engraced Life Foundationhas been at the forefront of restoring dignity and saving lives through thePinkRoom School Outreach — an initiative designed to introduce breast healtheducation, menstrual hygiene, and self-esteem restoration to adolescent girlsin secondary schools across Nigeria. PinkRoom creates a safe and engaging spacewhere young girls can learn about their bodies, understand early signs ofbreast changes, and access dignity kits that promote self-care and confidence.It is more than a health program — it’s a movement for awareness, compassion,and empowerment.

#ADV10 Tenacious at such a time as this.
TARAH Green

Tenaciosly Teal, Yukon, OK

Life is made of times when you must be strong because lifeoften feels hard, and also there are times, even in adversity, when life feelsreally great. Despite whether you can describe your life as good or bad at anygiven time, life always requires tenacity - even when we feel lacking. Thedefinition of tenacious is: Keeping a firm hold of something, clinging oradhering closely; determinism, possessing determination.

#ADV11 Beyond informed consent: A social work framework for authentic shared decision-making across the cancer survivorship continuum.

Nicole Normandin Rueda

Patient Empowerment Network, Kyle, TX

The Promise and Reality of Shared Decision-Making Shareddecision-making (SDM) - the process where clinicians and patients collaborateto make healthcare decisions informed by best evidence and patient values - iswidely endorsed as the gold standard for patient-centered cancer care. Yetsignificant gaps persist between SDM as an aspirational concept and SDM aslived reality for patients navigating cancer survivorship. A Social WorkPerspective on Patient Empowerment As a Licensed Master Social Worker who servedas caregiver for my father during his seven-year Stage IV pancreatic NETjourney (2005-2012), worked in pediatric oncology at Texas Children's Hospital(2014-2016), and now leads patient empowerment initiatives nationally throughPatient Empowerment Network, I have witnessed how structural barriers, powerdynamics, and psychosocial factors profoundly shape patients' capacity toparticipate meaningfully in decisions affecting their care and survival. Thisposter presents a social work framework for understanding barriers to authenticSDM across the cancer survivorship continuum and proposes research prioritiesand practice interventions that move beyond rhetoric to genuine patientempowerment.

#ADV12 Community-driven innovation to address breast cancer disparities: The AfroPink Pink Pop-Up Model and the launch of TechPink.

VINA Morris

Advocate, Bayonne, NJ

Breast cancer mortality remains disproportionately highamong Black women and medically underserved populations, often due tostructural barriers to early detection, limited access to preventive care, andlower participation in research. Community-based models that integrateculturally relevant outreach, screening access, and survivor-centered supportare critical to addressing these disparities.AfroPink, a survivor-led nonprofit organization, developedthe Pink Pop-Up Program, a community-embedded initiative that delivers breastcancer education, self-advocacy resources, and screening access directly intotrusted community settings such as churches, parks, small businesses, andcommunity centers. Through partnerships with healthcare institutions, theprogram connects participants to breast screening services, patient navigation,and follow-up care while addressing barriers related to cost, transportation,and medical mistrust.Building on the trust and engagement established throughthis model, AfroPink is launching TechPink, an initiative designed to leveragetechnology to improve survivorship outcomes and expand community participationin innovation. TechPink focuses on increasing digital literacy, expandingaccess to technology training for survivors, and exploring technology-drivenapproaches to improve health data literacy, research participation, andlong-term survivorship support.AfroPink also collaborates with research institutions andpublic health partners to support community-engaged research efforts and ensurethat the lived experiences of survivors from underserved communities informscientific discovery and cancer care innovation.This poster presents the AfroPink model as an integratedcommunity-engaged approach that combines outreach, screening access,survivorship support, and technology empowerment to improve early detection,strengthen research participation, and advance more equitable breast canceroutcomes.

#ADV13 The positive impact of one-to-one peer support on AYA cancer patients and survivors.

MARIELLE Mcleod

Cancer Hope Network, Summerville, SC

One-to-onepeer support through a trained mentor program improves patient reportedoutcomes regarding overall mental health, distress on NCI scale, and hope forthe future in adolescent and young adult cancer patients and caregivers. Whenmatching patients and caregivers in this demographic with mentors who canconnect with life circumstances and age-related issues such as working duringtreatment, caring for young children, fertility preservation, relationshipstress, and financial toxicity, patients report greater positive impact onoutlook and mental health. Methods: When a support seeker contacts ourorganization, our cancer support coordinators complete a thorough intake callwhere they assess the caller's needs and current circumstances, as well as evaluatethe support seeker's current state of mental health. They are then matched with a trained andvetted mentor who has been through a similar evaluation. Through tracking visitlogs submitted by mentors as well as survey feedback from our support seekers,we can evaluate the effectiveness and suitability of the match. If thepatient's circumstances or prognosis change, supplemental matches or outsidereferrals can be made as necessary. The program is offered in a virtualcapacity and free of cost to the participants, so it eliminates barriers tocare for our target demographic and increases participation and positiveoutcomes. Results: Between January 2023 and July 2025, 119 AYA patients orcaregivers were matched with a mentor through Cancer Hope Network. Each matchhad at least 1 phone call visit, and 75% of them completed more than one visitwith a mentor. The survey feedback from this group demonstrates significantimprovement in outlook, distress levels, hope for the future, and feelings ofisolation. Among survey respondents, 77% reported decreased levels of distresson the NCI scale. The averageself-reported score on the scale before connecting with a mentor was 8. Theaverage post-connection score was 5 as self-reported by surveyrespondents. Several respondentsreported significant decreases in distress, by as many as 6 or 7 points on thescale. AYA support seekers report discussing relationships, work or school,parenting, mental health, fertility, isolation, and lack of support with theirmentors. Numerous respondents voiced thepositive impact of mentorship including one young woman diagnosed withmetastatic disease while pregnant with her third child who shared, "My mentorhas been so helpful in giving me HOPE that even with a "poor prognosis" I maystill be around to raise my kids. She has been so kind and supportive, and Ireally appreciate having the perspective of another young mom who has gonethrough the same thing and whose priorities mirror mine. Thank you for matchingme!" These findings underscore the value of accessible, empathetic peer supporttailored to AYA patients and caregivers' life circumstances and psychosocialneeds.

#ADV14 Concept to impact: Creating a research-driven, patient informed research program.

ANGELA Timashenka Geiger

Advocate, Charleston, SC

The Medical University of South Carolina (MUSC)NCI-designated Hollings Cancer Center (HCC) Survivorship and Cancer OutcomesResearch (SCOR) Initiative was founded in 2022 to meet the needs of the growingpopulation of cancer survivors and their caregivers, SCOR provides atransdisciplinary hub for collaboration for clinicians, researchers, andpatients to improve cancer survivorship, care delivery and outcomes. To thatend, SCOR's mission is to: 1. 2. 3. 4. Deliver evidence-based, equitable,accessible and patient-centered care to cancer survivors. Foster transformativeand paradigm-changing research in cancer survivorship, outcomes and caredelivery. Establish a pipeline to inspire, train and retain the next generationof survivorship and cancer care delivery researchers. Engage the South Carolinacommunity to advance awareness of cancer survivorship. This poster will demonstrate how thisinitiative became a formal program with deliberate attention to patient/survivoradvocacy.

#ADV15 Pelotonia from community to discovery: How grassroots philanthropy amplifies Ohio State's cancer research capacity.

JOE Apgar

Pelotonia, Columbus, OH

As a cancer survivor and CEO of Pelotonia, I've witnessedfirsthand how grassroots community engagement creates sustained researchfunding to amplify institutional capacity in ways that transform both researchand outcomes. Over 18 years, Pelotonia's peer-to-peer community fundraisingmodel has raised more than $340 million directed to cancer research at The OhioState Comprehensive Cancer Center. This funding has supported the recruitmentof world-class scientists and their labs, underwritten an annual researchfellowship program, launched institutional programs including the DrugDevelopment Institute and the Pelotonia Institute for Immuno-Oncology, and manymore key research initiatives. This case study explores the history and impactof Pelotonia and how grassroots engagement creates a social movement in supportof cancer research. It also makes the case that this model, scaled andreplicated, holds the potential to transform how the world funds andaccelerates the science that will save lives.

#ADV16 Care and treatment of the LGBTQ+ community in the present hostile political environment?.

JOEL Pointon

SWOG, San Diego, CA

Historically, members of the LGBTQ+ community have facedincreased challenges in securing quality, equitable healthcare in the US. In a hostile political environment, how canwe support this community in obtaining equitable care and treatment?It takes both systemic change and individual action toprotect and advance LGBTQ+ healthcare equity, especially when facing politicalhostility. Advocacy, education, inclusive practices, and strong partnershipsare all key to ensuring that LGBTQ+ individuals receive the care they deserve.

#ADV17 Ethics and access in pediatric CAR T-cell therapy.

VICTORIA Lee

Advocate, Chapel Hill, NC

Advanced gene and cell therapies, including CAR T-celltreatments such as tisagenlecleucel (also known as Kymriah), have significantlyimproved outcomes for pediatric patients with relapsed or refractory B-cellAcute Lymphoblastic Leukemia (ALL). However, access, in the form of clinicaleligibility criteria, institutional capacity, and financial barriers, continuesto impede families and patients from pursuing these options. Currentqualifications require refractory disease or multiple relapses following theexhaustion of conventional treatment options before a patient becomes eligiblefor CAR T-cell therapy, delaying access to treatments with demonstratedefficacy. While designed to save lives, health policy implementations andprotocols limit the maximum impact of these therapies, while potentiallycontributing to disease progression for patients and higher financial burdenson families. This poster applies a bioethical approach to the currentaccessibility standards of pediatric CAR T-cell therapy, addressing the fourmain bioethical imperatives: autonomy, beneficence, non-maleficence, andjustice. From a patient advocacy perspective, this poster highlightsopportunities for improvement specifically aligned with patient-centered needsin advanced gene cell therapy development, implementation, and practice.

#ADV18 Survivorship and peer support: Outcomes from youth leadership initiatives.

Max Penzer

MIB Agents, Medford, MA

MIB Agents is a nonprofit organization dedicated toproviding support for patients and families affected by Osteosarcoma (OS), amalignancy that primarily affects children and AYAs. Over the past decade, MIBhas implemented youth-led initiatives to inform OS research, lobby forpertinent legislation, and connect with current patients affected by OS. Oneprogram, called Ambassador Agents, connects OS survivors with current patientsand families affected by OS. Another program, called the Junior Advisory Board,is a panel of AYAs who are responsible for informing OS research, lobbying forpediatric cancer legislation, and producing podcasts to spread their voiceacross the OS community. Additionally, the osTEAo podcast, run by OS survivors,aims to discuss post-treatment roadblocks that OS survivors face. One of thelargest indirect benefits of these programs is the creation of a peer supportcommunity between different OS survivors. Participation in these youth-ledinitiatives has facilitated coping among AYAs by fostering structuredopportunities for peer-to-peer connection and mutual support. Engagement inprograms such as the Ambassador Agents and Junior Advisory Board has beenassociated with reduced isolation, enhanced resilience, and a strengthened senseof identity within the osteosarcoma survivorship community.

#ADV19 From survivor to partner: integrating patient voice across the cancer research continuum.

JACQUELINE Smith

Ovarian Cancer Alliance of San Diego, Rancho Santa Fe, CA

From bench to bedside, cancer research translates scientificinnovation into patient care — yet integrating the patient voice across thatcontinuum requires a shift in research culture. For those who choose to movebeyond survivorship into advocacy, the role of *patient partner* transformslived experience into a scientific asset, amplifying impact from discovery tocare.Clinical outcomes are the cornerstone of cancer research —yet treatment carries costs that extend far beyond — physical, psychological,economic, and caregiver burden. Patient partners bring these dimensions to theforefront, ensuring research reflects the full human cost of cancer treatment.Their contributions span the research process — from study design and grantapplications to clinical trial recruitment and dissemination of findings —while extending beyond into policy and legislative advocacy and fundraising.Realizing the full potential of this partnership demandsconfronting real barriers: communication gaps, structural exclusion, anddiffering priorities. Bridging these requires shared commitment — researcherscommunicating in lay terms; patient partners deepening their understanding ofthe scientific process. Ultimately, this produces research that reflectsreal-world needs, earns public trust, and drives meaningful change for those itis meant to serve.For patient partners, this is more than contribution. It isagency. It is hope.

#ADV20 Man Up to Cancer to men facing cancer.

BILL Minh Thach

Advocate, Katy, TX

This poster presents a comprehensive mental healthinitiative addressing the critical gap in psychological support for men withcancer, who often face cultural stigma around expressing vulnerability andseeking mental health care. Through Man Up to Cancer, we have developedpeer-led support programs that create safe, judgment-free spaces where men canopenly discuss anxiety, depression, grief, identity shifts, body imageconcerns, and the emotional burden of diagnosis and treatment. The poster willoutline our multi-pronged approach: facilitated support groups that provideongoing structured peer connection, in-person meetups that foster localcommunity building and reduce isolation, and an annual retreat that brings mentogether from across regions to deepen relationships, share experiences, andbuild a sustained support network. We will present program participation data,participant testimonials on impact, and lessons learned about what language,formats, and facilitator characteristics most effectively engage men in mentalhealth conversations. Particular emphasis will be placed on addressing barriersspecific to men of color, who face compounded stigma at the intersection ofmasculinity norms and cultural attitudes toward mental health. The poster demonstrateshow community-based advocacy organizations can fill critical gaps inpsychosocial oncology services and provides a replicable model for reducingmental health disparities in cancer care.

: Advocates Poster Session 2
Poster Session

#ADV21 "What's that?" The question that saved my life and fueled "The Big See," a multi-media skin cancer awareness campaign (launched in 2019-present).

Susan Manber

Advocate, Cortlandt Manor, NY

Skin cancer is the #1 most prevalent form ofcancer, but people tend to think it's "just skin cancer" - no big deal comparedto other "more serious" cancers. Most people have no idea that more than 2people an hour die from skin cancer. As a Merkel Cell Carcinoma survivorserving as Chief Patient Officer at a major health care communications agency,together with the Skin Cancer Foundation, we crafted a pro bono campaign thatwould focus on driving early detection to save lives. Methods The campaign tapsinto critical insights from our research, including qualitative interviews withfoundation leadership, survivors, dermatologists, and clinical researchers.Co-creation workshops helped to refine the research insights into the campaignconcept and core messaging platform including television, print, outdoor,digital, and social media. Messaging platform We love the sun but we hate thedamage - we get checked when someone points out something suspicious. Whenpeople get to a dermatologist early enough to save their lives - they, or afamily member would say: "I saw something new, changing, or unusual." Thatbecame our core messaging platform. Our key human insight Cancer is the enemy,not the sun. Our tagline became the two critical words my daughter Sarina saidto me that saved my life: "What's That?" The Big See: the cancer you can see Weshot the campaign on the beach in San Diego, using a comedian hidden behind amirror to engage passersby. People would stop to look and read the engagingfacts displayed as our comedian told jokes - because laughter is the bestmedicine. We wrapped hard hitting messages in humor: · 2 people an hour die ofskin cancer · 5 year melanoma survival = 99% when caught early; drops to 20%when not · 5 sunburns doubles your risk Bringing the campaign to the communityThe campaign continues to run in national and local streaming and digital mediaand is supported by the Big See microsite and social media. We folded theFoundations'Destination Health Skin Program into the Big See brand -giving people access to free screening through a traveling skin cancerscreening program. We are grateful to the dermatologists across the country whovolunteer to help us give free skin checks. Results We were invited to launchthe campaign on the creativity stage at the Cannes Lions festival, adding toour global reach. To date, we have raised over $75 million in donated media,driving thousands of people to get checked. Through our Destination Health Skinprogram, with the help of more than 600 dermatologists, we have provided nearly34,000 free skin cancer screenings. Our volunteer dermatologists haveidentified more than 13,000 suspected skin cancers and skin precancers,including 672 suspected melanomas.65% of Destination Healthy Skin participants have never beenscreened for skin cancer before. Conclusion The program continues to bring skincancer screening to at-risk populations to help detect cases of skin cancer,saving thousands of lives all across the country. We continue to expand effortswith support from our partners to include focused screenings efforts for keypopulations including men and Hispanic people who are less likely to usesunscreen or sun-protective clothing.

#ADV22 The culture of cancer: Breaking down barriers to research.

Daniel G. Garza

Cheeky Charity, Laguna Beach, CA

This poster explores how culture, stigma, and survivorstorytelling shape access to cancer research and prevention, with a focus onanal cancer in Latine and LGBTQ+ communities. Drawing on my work with CheekyCharity and my lived experience as an anal cancer survivor, it highlights howbilingual outreach, creative media, and survivor-led initiatives can dismantlesilence and make cancer education more approachable. The poster will illustratethe interconnected circle formed by culture, religion, and social normsalongside research, studies, and outcomes. By showing how these forcesinteract, the project emphasizes the need for survivor-informed, culturallyresonant approaches that bridge communities and science, breaking down barriersto prevention and care.

#ADV23 Embedding cancer advocates as structural partners in oncology conferences: A scalable implementation model based on RISE UP for Breast Cancer and Women's Health Conference.

DIANE Heditsian

Redwood City, CA

Background: Patient, research and policy cancer advocatesare frequently included in oncology meetings, yet participation often remainssymbolic. We developed and operationalized a full-integration model at the 2026RISE UP for Breast Cancer and Women's Health conference to structurally embedadvocates across all dimensions of a scientific meeting.Methods: As Advocate Lead on the planning committee I hadthe opportunity to implement a multi-level advocate integration frameworkencompassing governance, grant support, programming, and on-site engagement.Advocacy participation included agenda development for the general meeting andindividual sessions, abstract review and speaker and poster selection. Duringthe meeting, advocates were embedded as judges alongside venture capitalists,industry representatives and medical and regulatory experts, to weigh in onpitches at the curated competition that spotlighted high-impact ideas in thewomen's health arena. In the general sessions advocates shared their storiesand their perspectives on topics ranging from pregnancy-related breast cancerto navigating menopause after a breast cancer diagnosis, to inability toconceive due to uterine fibroids. They served as presenters at poster sessions,participated in audience Q/A discussions, and hosted non-profit advocacyorganization information tables throughout the exhibit hall.Results: As a result of a targeted effort to attract adiverse group of advocates, a steeply reduced advocate registration fee, aswell as travel support scholarships, 54 advocates registered for theconference, representing 16.18% of total attendees. At RISE UP, 18 advocatesfrom six states served as speakers or judges, and an advocate presented in 100%of conference general sessions ranging from scientific to clinical to policyrelated. Advocates were integrated into 65 planning meetings over 9-months andreviewed and judged 111 abstracts. All advocate speakers were the invitedguests of RISE UP at a fundraiser awards luncheon as a show of appreciation fortheir participation in the meeting. Qualitative feedback from researchers andphysicians indicated improved discussion of patient-centered endpoints, equityconsiderations, and real-world evidence as well as increased opportunity forcollaboration. The results of the attendee satisfaction Likert Scale surveyquestion: Do you feel that the advocate stories and advocate perspectives ineach session enriched the meeting? are forthcoming.Conclusions: Structural advocate integration is feasible,scalable, and associated with measurable increases in engagement andtranslational relevance. This implementation model provides a replicableframework for oncology conferences seeking to move from symbolic inclusion toauthentic partnership with advocates.

#ADV24 How digital spacial profiling is changing the fight against lung cancer.

MICHEL Itel

Advocate, Stones Corner, Australia

Lung cancer is the leading cause of cancer death globally, and while immunotherapies and targeted therapies have been transformative, they only work in roughly 1 in 5 patients. We have not been able to reliably predict who will respond, until now. Digital Spatial Profiling allows us to read the tumour microenvironment: the complex ecosystem of immune cells, cancer cells, and supporting structures that ultimately determines whether a treatment succeeds or fails.

#ADV25 Thriving in the grey: A patient needs model to balance science and reality.

CARRIE Camino

Neuroendocrine Tumor Research Foundation, Libertyvlle, IL

This poster presents a framework for encouraging the Patient Voice and empowering Patient Agency for neuroendocrine tumor (NET) cancer patients, an uncommon cancer. Utilizing Maslow's hierarchy of needs, it defines a Patient's Matrix of Needs outlining patient education priorities, as well as medical and caregiver engagement and empowerment strategies. In socializing this model with Patients, we seek to accelerate a Patient's understanding of their diagnosis and thrivership mindset, helping Patients develop a personalized action plan towards meeting their individual needs. In socializing this model with the Research community, we help drive a holistic view of patient care and support the intersection of Patient and Researcher engagement to drive improved discovery and treatment outcomes.

NET Research Foundation and other organizations have a wealth of materials and activities that speak to Patient thrivership needs. These materials will benefit from better organization around a Needs Matrix to help Patients more quickly navigate them. Additionally, Research has medical outcome data related to treatments. The poster will include examples of linking research and thrivership educational materials, as well as highlight areas for future development to support true NET Patient Agency.

#ADV26 Henrietta Lacks House social determinants of health.

DAVID Sanders

Henrietta Lacks House of Healing, Dundalk, MD

Henrietta Lacks has been commonly known as the "invitro" miracle but there has been little effort to connect her to theSocial Determinants of Health which concept was non-existent at the time of hersecreted discovery in the era of Professional Autonomy dominated health law.Now that we are in an era of Patient/Health Equity influence on health law itis time to take a look these factors from the perspective of the science hercells helped to create and possibly descientificate the complicated for buildinghealth intelligence for all.

#ADV27 Policy and how it impacts cancer research.

LASHELLE Scott

Advocate, Houston, TX

This poster will demonstrate how policy impacts cancer research by presenting the process of a bill or budget (state or federal) and how it creates policy for researchers to create clinical trials/treatment options.

#ADV28 HEALing The Bronx: A grassroots model for cancer education, health equity, and community engagement through art and literacy.

COLETTE Smith

Advocate, Bronx, NY

HEALing The Bronx is a community-driven initiative designed to address cancer disparities in the Bronx, where outcomes for lung, breast, colorectal, and prostate cancers are disproportionately poor compared to other regions of New York State. The program integrates arts, education, and advocacy to improve health literacy and empower residents. What began with two tree beds has grown to 24 educational tree beds, including four feature beds equipped with interactive QR codes and signage providing cancer prevention and screening information. The initiative also includes outdoor art libraries, blending literacy and creative expression to foster mental well-being and health awareness. Our first art library installation is complete, and our goal is to add two new libraries annually until all 24 Bronx zip codes are represented. HEALing The Bronx demonstrates how grassroots engagement, cultural relevance, and creative strategies can drive measurable impact in underserved communities. Future plans include expanding Care Within Our Reach community events to multiple Bronx neighborhoods, reaching over 1,500 residents in 2026, and increasing participation in screening and clinical trials. This poster will showcase the program's design, outcomes to date, and its potential as a scalable model for reducing cancer disparities through community empowerment.

#ADV29 Lo que no se ve: Indigenous-centered cancer prevention and survivorship equity in California.

ISABELLA Mireles

Advocate, Goleta, CA

This poster examines how culturally grounded cancerprevention and screening programs in Indigenous Latino communities informcancer survivorship research - using California as a well-documented caseexample. California is home to one of the largest Indigenous Mexicanpopulations in the United States, estimated in the hundreds of thousands, yetIndigenous identity is rarely captured in cancer prevention, screening, orsurvivorship research. While Latino populations are often treated as culturallyhomogeneous in cancer research, Indigenous communities experience distinctlinguistic, cultural, and structural barriers that shape engagement with cancerprevention services and long-term survivorship outcomes. Drawing on astructured review of cancer prevention and screening interventions implementedamong Indigenous Mexican communities in California - with comparative insightsfrom Indigenous-focused interventions in Mexico and broader internationalevidence that demonstrate the importance of culturally grounded cancerprevention approaches - this project synthesizes evidence on how factors suchas Indigenous language access, community trust, and culturally specific healtheducation influence participation in cancer prevention and screening. Theposter highlights how survivorship outcomes commonly attributed to “Latinoculture” may depend on whether Indigenous identity is explicitly acknowledgedand centered in intervention design. By placing California-based Indigenouscancer prevention research in direct conversation with cancer survivorshipframeworks, this work identifies gaps in how protective factors and equity arecurrently conceptualized in Latino cancer research. The findings underscore theneed for survivorship research and prevention strategies that account forheterogeneity within Latino populations and offer implications for developingculturally responsive interventions that can support improved survivorshipequity both within California and in other regions with Indigenous Latinocommunities in the U.S..

#ADV30 Bridging gaps in KRAS-mutant lung cancer care: A patient perspective on clinical trial access and community support.

LISA Haines

Advocate, Rockport, MA

Despite significant advances in precision oncology, access to clinical trials remains a significant challenge for patients with KRAS-mutant lung cancer. Once considered “undruggable,” KRAS mutations now have emerging targeted therapies, making clinical trial participation increasingly important. This poster presents a patient-informed perspective from an 11-year stage IV lung cancer survivor, highlighting real-world barriers to clinical trial access and enrollment. Patients frequently encounter substantial obstacles when searching for appropriate clinical trials, including fragmented and difficult-to-interpret information, complex eligibility criteria, and limited guidance through the enrollment process. Additional barriers such as geographic distance to academic cancer centers, financial toxicity related to travel, lodging, childcare, and lost wages, as well as rigid trial schedules, further restrict participation. These challenges disproportionately limit access for many patients and contribute to reduced diversity and representativeness in clinical research. Cancer-focused support communities play a critical role in addressing these gaps by providing education, peer support, shared knowledge, compassion and patient empowerment. Such communities help patients better understand treatment options, navigate clinical trial opportunities, and advocate for themselves within complex healthcare systems. Improving patient-inclusive trial navigation, supportive services, and community engagement is essential to ensuring equitable access to clinical trials. Addressing these barriers can enhance inclusivity, strengthen the generalizability of trial findings, and support the continued advancement of precision cancer care for all patients.

#ADV31 Accelerating gastric cancer research: Programs of the Gastric Cancer Foundation.

Harriet A. Patterson

Gastric Cancer Foundation, Albany, CA

Learn about how a patient advocacy organization is workingto accelerate research and move progress forward while helping educate andsupport patients. Research impact includes creating the firstgastric cancer registry, funding seed grants to support exciting new ideas, andsupporting advanced science with multi-year grant support.

#ADV32 Quantifying patient priorities: Identifying and weighing key non-clinical factors for scalp cooling decision-making in chemotherapy-induced alopecia prevention.

Rebecca Munoz

Advocate, Austin, TX

BACKGROUND: Chemotherapy-Induced Alopecia (CIA)is consistently ranked as one of the most psychologically distressing sideeffects of cancer treatment. Scalp cooling (SC), or cold capping, remains theonly primary preventative strategy, yet its use demands a significantcommitment from the patient: added time at infusion appointments, potentialacute discomfort, and often substantial out-of-pocket financial cost.
While research exists on the clinical efficacy of SC devices and protocols(i.e., what works), there is a critical and unmet need for research focused onpatient values and decisional science (i.e., what matters). Currently, patientslack standardized tools to systematically weigh these complex clinical andnon-clinical trade-offs against their personal priorities, often leading toreliance on anecdotal information and subsequent high rates of decisionalregret when expectations are unmet. The absence of structured supportnecessitates reliance on peer groups, such as the Chemotherapy Cold Cappersnetwork.
The immediate aim of this study, titled The VALUED Study, is to pilota quantitative approach to identify and prioritize the specificpatient-determined factors (including clinical efficacy expectation,psychosocial impact, financial cost, and practical time commitment) that exertthe greatest influence on a patient's decision to utilize scalp cooling duringchemotherapy.

METHODS: This ongoing project utilizes across-sectional, mixed-methods online survey designed to capture a targetedsnapshot of the trade-offs individuals make regarding hair preservation. Thisinitial data collection phase leveraged an existing patient advocacynetwork. The survey was distributed electronically across a target populationof individuals with a history of cancer who considered or used scalpcooling. Data from this interim analysis, including ranking andweighting scores, were analyzed descriptively toestablish preliminary factor prioritization of logistics,utility, and experience. Qualitative data from open responses werereviewed using rapid thematic analysis to enrich the context of thequantitative findings.

CONCLUSION: These preliminary findings representthe foundational data regarding quantified, patient-determined decisionalpriorities currently absent from supportive care literature.The pilot data fromthis ongoing study provides an opportunity for clinicians, patient advocates,and supportive care networks to gain initial, evidence-based insight intowhat truly drives patient decisions, offering a path toward more robust shareddecision-making and reduced decisional regret.

#ADV33 Bridging the communication gap in pancreatic cancer: A stage IV PDAC survivor's perspective on improving research and biotech communication of innovation.

Elise Roth Tedeschi

Advocate, Smyrna, GA

Despite significant advances in pancreatic ductaladenocarcinoma (PDAC) research, survival rates remain low, in part due topersistent gaps in how scientific innovation is communicated to oncologists,patients, and the broader public. As a long-term Stage IV PDAC survivor,patient advisor, and participant in the AACR Scientist↔Survivor Program, I haveobserved that many promising developments, including molecularly targetedtherapies, biomarker-driven trials, and emerging diagnostic technologies,remain inconsistently translated beyond academic research settings. Incommunity oncology settings, care appropriately centers on standardof-carepathways; however, limited access to timely, practical information aboutemerging options can leave patients, particularly those with advanced disease,unaware that additional therapeutic or trial options may exist. This posterpresents a survivor-informed perspective on structural and cultural barriersthat impede effective communication among researchers, biotechnology companies,clinicians, patients, and mass media. Drawing from lived experience, patientadvisory roles, and engagement with scientific, clinical, and patientcommunities, key challenges are identified, including siloed dissemination ofresearch findings, highly technical messaging, time constraints in clinicalpractice, and the absence of trusted, patient-centered translation mechanisms.Based on these observations, the poster proposes a conceptual framework toimprove the communication of PDAC innovation that integrates survivor voicesearly and consistently across research dissemination, clinical education, andpublic engagement. Recommended strategies include concise, clinician-focusedsummaries of emerging data, co-created patient education resources, andresponsible use of mass media and digital platforms to accurately contextualizeinnovation. By positioning communication as a critical component of cancercare, rather than a downstream activity, this survivor-informed frameworkhighlights opportunities to improve awareness of emerging therapies andclinical trials, support shared decision-making, and reduce missedopportunities for patients with pancreatic cancer.

#ADV34 What survivors really need: A patient-centered model for supporting breast cancer patients through education, advocacy, and community connection.

MARSHELLE Harris

Wellness 4 Life, Gardendale, AL

This poster outlines a patient-centered support framework built around what survivors truly need during diagnosis, treatment, and life after cancer. It includes emotional support, evidence-based information, wellness tools, and culturally responsive resources. I show how my programs and advocacy training help survivors better understand treatment options, ask clearer questions, manage side effects, navigate menopause after cancer, and feel empowered in their healthcare journey.

#ADV35 Paths to research advocacy: Webinar education.

SUSUN Livingston

Powell-Drescher, Seattle, WA

The Powell-Drescher Ovarian Cancer Research Foundation is proud to introduce Paths to Research Advocacy, a quarterly educational webinar series created to inform, empower, and inspire ovarian cancer patients, survivors, and their loved ones to engage meaningfully with ovarian cancer research. Grounded in the Foundation's mission to champion collaboration between scientists and survivors, this series brings together leading researchers, clinicians, advocates, and survivor-scientists to share their unique journeys and perspectives. Each session blends personal storytelling with timely, relevant research topics, helping participants understand not only what is happening in ovarian cancer science but how they can play an active role in shaping its future. Through candid conversations and accessible education, the Paths to Research Advocacy series aims to: • Demystify the research process by offering patient-friendly explanations of emerging studies, clinical trials, and scientific innovation. • Highlight diverse advocacy pathways, showing how survivors, patients, and caregivers can contribute to research—whether through sharing experiences, participating in studies, or serving as research partners and advisors. • Strengthen the scientist-survivor partnership, fostering a two-way dialogue that elevates patient voices and accelerates impactful, human-centered research. • Build community and confidence, ensuring every participant walks away better equipped to engage in advocacy that aligns with their skills, interests, and lived experience. By illuminating the many paths to research advocacy, this webinar series empowers ovarian cancer patients and survivors to help drive the discoveries that may transform care for generations to come.

#ADV36 From silence to science: Survivor advocacy and community partnership to advance equity in cancer research.
HARJEET Kaur

Advocate, Calgary, AB, Canada

This poster explores how survivor-led, community-informedadvocacy can strengthen equity and inclusion in cancer research by addressingcultural stigma, silence, and mistrust that limit engagement amongunderrepresented populations. Drawing on lived experience as a blood cancersurvivor and patient partner, this work highlights how meaningful collaborationbetween patients, researchers, clinicians, and community networks can improveresearch relevance, participation, and knowledge translation. Focusing on SouthAsian communities, the poster examines how culturally responsive dialogue andpatient-led engagement can surface barriers to early diagnosis, clinical trialparticipation, and survivorship care that are often overlooked in traditionalresearch settings. It emphasizes the value of patient partners in translatinglived experience into actionable insights that inform research design,recruitment strategies, and communication approaches. By bridging communityadvocacy and cancer research, this work demonstrates how inclusivescientist-survivor partnerships can build trust, enhance diversity in researchparticipation, and support more equitable cancer outcomes across the carecontinuum.

#ADV37 Timely diagnosis and treatment of childhood and adolescent cancer: Challenges and opportunities.

CALLUM Mullen

Advocate, Huntsville, ON, Canada

Timely diagnosis and treatment of cancer are key tenets ofquality care, with important implications for patient outcomes and overallwellbeing. Children and adolescents are particularly vulnerable to delays incare due to patient-, clinical-, and health-system-level factors. We aimed to measure the diagnostic interval in childrendiagnosed with cancer in Québec, Canada, between 2012 and 2022, using adata-driven approach. As a complementary exploratory aim, we reviewed theliterature to identify barriers and enablers to survivorship care amongsurvivors of pediatric cancer. We identified 2927 children and adolescents with cancer inour population-based cohort and observed differences in diagnostic delay byage, cancer type, diagnosis period, and rurality. Barriers and enablers tosurvivorship care also operated at the patient, clinician, and health-systemlevels, although their relative importance likely varies across survivorship.Improving childhood cancer care requires attention not onlyto treatments, but also to the diagnostic and post-treatment phases of care.Identifying barriers across the care continuum may help guide interventions toimprove access and quality in pediatric oncology.

#ADV38 ROS1-positive lung cancer treatment access gap across Canada - A call for equitable, patient-centered care.

K. M. TAHSIN HASSAN Rahit

Advocate, Calgary, AB, Canada

Title: ROS1-Positive Lung Cancer Treatment Access Gap Across Canada - A Call for Equitable, Patient-Centred CareBackground: ROS1-positive non-small cell lung cancer (NSCLC) represents 1-2% of NSCLC cases, yet patients face significant treatment access barriers despite availability of effective targeted tyrosine kinase inhibitors (TKIs). This analysis evaluates provincial coverage disparities for ROS1 TKIs across Canada to inform patient advocacy and policy reform efforts.
Methods: We conducted a comprehensive pan-Canadian analysis of public drug coverage policies for ROS1-targeted therapies as of March 2026, examining first-line through third-line treatment access across all Canadian provinces and territories. Coverage policies, exceptional access programs, and clinical trial availability were systematically reviewed.
Results: While first-line agents (crizotinib, entrectinib) demonstrate universal coverage, profound inequities emerge in advanced-line therapy access in Canada. Second-line coverage requires case-by-case review with documented intolerance rather than progression, creating clinical and ethical challenges. Any advanced-line therapies remain virtually inaccessible through public funding across all provinces, forcing patients toward clinical trials or treatment discontinuation. Next-generation TKIs addressing resistance mutations (repotrectinib, taletrectinib, zidesamtinib) and CNS disease remain accessible only through clinical trials. Critically, coverage termination after exhaustion of first TKI line creates a "therapeutic cliff" for patients who develop resistance, despite availability of potentially effective subsequent therapies.
Conclusions: Canadian patients with ROS1-positive NSCLC face unjustifiable barriers to life-extending therapies beyond first-line treatment. The disconnect between therapeutic availability and public funding perpetuates health inequities and undermines precision oncology principles. Urgent policy reform is needed to: (1) establish consistent pan-Canadian coverage frameworks, (2) enable progression-based (not just intolerance-based) second-line access, (3) create pathways for third-line and resistance-directed therapy funding, and (4) accelerate approval timelines for next-generation TKIs. Patient-centered knowledge dissemination regarding clinical trial opportunities and exceptional access pathways remains critical until systemic coverage improvements are achieved. This analysis provides an evidence-based framework to support patient advocacy, inform healthcare provider counselling, and guide policy reform toward equitable access to ROS1-targeted therapies.

#ADV39 Addressing gaps in colorectal cancer care: Real-world impact of a national clinical navigation program.
JOHN Woerner

Advocate, Minnetonka Beach, MN

#ADV40 Disparities in access to precision oncology drugs across Canada and between Canada and the US, 2009-2025.

Sharon Batt

Advocate, Halifax, NS, Canada

In a unique funding initiative called Patient Voices inResearch, the Marathon of Hope Cancer Centres Network (MOHCCN) asked a group ofpatients from across Canada to develop themes for a research agenda and toselect the successful applicants. One theme was equity and disparities inaccess to precision medicine. I was a survivor-investigator in a study selectedto systematically document the approval process for new cancer drugs in Canadaand disparities in access between Canada and the U.S. and among provinceswithin Canada. Canadian cancer patients often hear about new oncology drugsthrough announcements that the FDA has approved a drug for use in the U.S.Because Canada has its own drug approval process, a drug approved in the U.S.may not be available in Canada. Furthermore, each Canadian province decideswhich drugs to fund under its health plan. Our research team, led by oncologistBishal Gyawali at Queen's University in Kingston Ontario, conducted aretrospective cohort study of adult solid-cancer approvals by the FDA andHealth Canada from 2009 to 2025 to identify where delays happen. Criticalvariables were time to approval, time to funding decision, and availability ofeffective anti-cancer drugs. We calculated the magnitude of clinical benefit foreach drug based on the validated ESMO-Magnitude of Clinical Benefit Scale toassess whether the delays would likely affect patient outcomes. My posterhighlights key research findings and how they can be applied to policies toaddress patients' concerns about inequities in access to cancer drugs.

: Immune Checkpoints
Poster Session

#2796 Translating combined PD1 and LAG3 inhibition from preclinical models to patients with refractory, DNA replication repair deficient (RRD) glioblastoma: An IRRDC study.

Anirban Das[1], Vienna Mazzoli[1], Owen Crump[1], Olha Kos[1], Nuno M. Nunes[1], Lucie Stengs[1], Amanda Li[1], Adrian Levine[1], Yoshiko Nakano[1], Hope Friedman[1], Katharine O'Flaherty[1], Alexander Stein[2], Gadi Abebe-Campino[3], Annika Bronsema[2], Vanessa Bianchi[1], Melissa Edwards[1], Stergios Zacharoulis[4], Birgit Ertl-Wagner[1], Daniel A. Morgenstern[1], Trevor J. Pugh[5], Pamela Ohashi[6], Eric Bouffet[1], Cynthia E. Hawkins[7], Peter B. Dirks[1], Uri Y. Tabori[1]

[1]The Hospital for Sick Children, Toronto, ON, Canada,[2]University Hospital Hamburg-Eppendorf, Hamburg, Germany,[3]Chaim Sheba Medical center, Ramat Gan, Israel,[4]Bristol Myers-Squibb, New Brunswick, NJ,[5]UHN Princess Margaret Cancer Centre, Toronto, ON, Canada,[6]Princess Margaret Cancer Cente, Toronto, ON, Canada,[7]Staff Neuropathologist, Dept. of Pathology, The Hospital for Sick Children, Toronto, ON, Canada

Background and Aims: Glioblastoma driven by DNA Replication Repair Deficiency (RRD) account for 10% of all high-grade glioma in children and young adults, harbour high tumor mutation burden (TMB) and can respond to anti-PD1 immune-checkpoint inhibition (ICI). However, not all respond, and the majority ultimately progress, highlighting the need for combinatorial therapies for sustained immune-surveillance.
Methods: We performed transcriptomic analyses of human RRD-glioblastoma specimens for immune checkpoint expression, and accordingly, tested combined ICI in immunocompetent murine models. Based on these preclinical data, we treated refractory patients using a combination of anti-PD1+anti-LAG3 through single-patient trial/compassionate access. Complimentary immuno-genomic biomarker analyses including circulating tumor DNA (ctDNA) were performed to investigate mechanisms and track responses.
Results: Human RRD-glioblastoma (n=80) demonstrated high LAG3 expression, providing a strong rationale for therapeutic targeting. We tested combined anti-PD1+anti-LAG3 inhibition in three immunocompetent RRD-glioblastoma murine models. In the anti-PD1-responsive (Nestin-CreMSH2$^{LoxP/LoxP}$-POLE$^{S459F/+}$) model, anti-PD1+anti-LAG3 resulted in universal tumor response and superior survival to ICI-monotherapy. In the anti-PD1 resistant models (Mlh1$^{-/-}$/NestinCre+/Trp53$^{LoxP/LoxP}$ and therapy-induced hypermutant ENU/Trp53$^{-/-}$ gliomas), anti-PD1+antiLAG3 improved survival, overcoming the lack of response to ICI-monotherapy. Biologically, high LAG3 expression and immune-exhaustion observed in CD8 T-cells after treatment with anti-PD1 was ablated following the addition of anti-LAG3. Serially transplanted, post-anti-PD1 treated tumors showed response, confirming, in-vivo, that resistance to anti-PD1 could be abrogated by anti-PD1+anti-LAG3. Seven children with refractory RRD-glioblastoma who had progressed after anti-PD1 treatment were treated using anti-PD1+anti-LAG3, resulting in objective radiological responses and prolonged ongoing survival. Tolerability was better than a previous study of combined CTLA4 and PD1 inhibition for similar patients. Paired immuno-genomic tumor analyses, serial blood flow-cytometry, T-cell receptor clonotype, and CSF ctDNA analyses provided novel insights into the mechanisms of immunological invigoration and first-in-human, radiological responses.
Conclusions: LAG3 is an effective target in refractory RRD-glioblastoma. Combined inhibition with anti-PD1 inhibition demonstrated radiological response, prolonged survival and manageable toxicities in patients, and unearthered mechanisms of immune-responses. The combination will now be tested in biomarker-driven clinical trials in RRD-glioblastoma and other immune-inflamed solid tumors.

#2797 A macrophage endocytic checkpoint for PD-1 governs durable vs hyperprogressive response.

Madhubanti Mullick[1], Ella McLaren[1], Suchismita Roy[1], Brandon Biagas[1], Mahitha Anandachar[1], Vanessa Castillo[1], Samuel Williams[1], Celia Espinoza[1], Courtney Tindle[1], Gajanan Katkar[1], Saptarshi Sinha[1], Pradipta Ghosh[2]

[1]University of California, San Diego, San Diego, CA,[2]UC San Diego Health, San Diego, CA

Clinical responses to PD-1 blockade span a wide continuum, from durable regressions to hyperprogressive disease (HPD); yet the macrophage-intrinsic switches that determine these extremes responses remain undefined. Using a macrophage systems model built from >12,500 transcriptomes and calibrated with single-cell transcriptomes from >1,000 anti-PD-1-treated patients, we identified *CCDC88A* (encodes the endocytic adaptor, GIV) as a top responder-linked gene and mechanistic driver of tumor-associated macrophage (TAM)states predictive of clinical benefit versus HPD. Loss of GIV in macrophages increased cell-surface PD-1 across species and platforms (primary cell-line, and organoid co-cultures), impaired phagocytosis, and accelerated tumor progression. In syngeneic models, myeloid-specific GIV deletion converted anti-PD-1 therapy from tumor-controlling (beneficial) to tumor-accelerating (hyperprogressive), without altering T cell targeting; transcriptomic analyses of tumor-infiltrating myeloid cells confirmed a shift towards HPD-associated macrophage signatures. Mechanistically, GIV engages a TIR-like BB-loop (TILL) motif within the PD-1 cytoplasmic tail and functions as an endocytic adaptor, driving dynamin-mediated PD-1 internalization and recycling. A pharmacogenomic perturbation strategy revealed that blocking endocytic trafficking phenocopies GIV loss both *in vitro* and *in vivo*: PD-1 is trapped on the TAM surface, checkpoint blockade fails, and tumors accelerate under therapy. Conversely, preserving GIV•PD-1 coupling enhances response durability. Finally, we uncover a clinically relevant vulnerability: FDA-approved psychotropic and antiemetic drugs that impair receptor internalization (e.g., prochlorperazine) negate anti-PD-1 efficacy and induce HPD-like progression *in vivo*, consistent with pharmacoepidemiologic evidence linking such drugs to increased mortality and immune-related adverse events in patients receiving checkpoint therapy. Collectively, these findings establish GIV-dependent PD-1 routing as a macrophage-encoded checkpoint that dictates whether PD-1 blockade elicits tumor clearance or fuels malignant outgrowth. By repositioning TAMs as active arbiters of immunotherapy fate, this work exposes PD-1 trafficking, and its drug-induced derailment, as a new axis for therapeutic control and precision risk mitigation in solid tumors.

#2798 CD112 drives tumor immune evasion in HER2-positive breast cancer through sphingolipid metabolism-dependent remodeling of CD8+T cell receptor landscapeand consequent dysfunction.

YI ZHANG, Bingqiu Xiu, Jiong Wu, Qi Zhang

Fudan University Shanghai Cancer Center, Shanghai, China

Purpose: HER2-positive breast cancer (HER2+BC) features high TMB and abundant TILs, supporting immunotherapy potential. HER2-targeted therapies also engage the immune system. However, PD-1/PD-L1 inhibitors show limited efficacy, suggesting unique immunosuppressive mechanisms in this subtype.
Methods: Integrated analysis of FUSCC and validation cohorts identified key immune checkpoints. Experimental validation was performed through knockdown of candidate immune checkpoints and in vivo screening. Mouse scRNA-seq revealed CD8+ T cells as the most impaired subset. CD112-high tumor cells were characterized via stable cell lines and multi-omics analysis, with validation by spatial transcriptomics. TurboID proximity labeling identified CD112-UGCG interaction. CD8+ T cell function was assessed using conditioned medium co-culture and exogenous GlcCer supplementation. To demonstrate that CD112-driven sphingolipid metabolism exerts its function through CD112-CD112R axis, we utilized Cd112r-KO mice.
Results: We revealed that non-pCR HER2-positive patients have a comparable level of TILs but exhibited a more exhausted phenotype, and found significant upregulation of CD112 in residual tumors following HER2-targeted therapy. Moreover, while PD-L1 is highly expressed in TNBC, CD112 shows specific enrichment in HER2+BC, with predominant localization to malignant epithelial cells. These findings suggest that CD112 may hold greater therapeutic potential in HER2+BC. In addition to its canonical immunosuppressive function, our study revealed that CD112 promotes the metabolism of sphingolipid, particularly glycosphingolipid. Mechanistically, through TurboID we uncovered a previously unreported interaction between CD112 and the key enzyme UGCG in Golgi, which prevents UGCG degradation and thereby elevates glycosphingolipid level. Functional experiments demonstrated that CD112-mediated suppression of CD8+T cells is partially dependent on its regulation of sphingolipid metabolism. By altering the glycosphingolipid content of exosomal membranes, CD112-high tumor cells leads to the aberrant aggregation of CD112 key receptor-CD112R in lipid rafts of neighboring CD8+T cells, which increases CD112-CD112R interaction frequency and amplifies suppression effect. For furture in vivo translation, a combination therapy of anti-HER2, anti-CD112R, and a UGCG inhibitor is proposed.
Conclusion: We identified CD112 as a key immunosuppressive regulator in HER2+BC, surpassing PD-L1. We also revealed a metabolism-dependent mechanism of CD112-mediated immunosuppression executed through the CD112-UGCG-GlcCer axis. Inhibition of this axis may further enhances the efficacy of anti-CD112R treatment in HER2+BC, presenting a promising combination strategy.

#2799 Tumoral IL-33/ST2 signaling drives immune escape through reduced antigen presentation.

Alyssa Mauri Cornista[1], Tao Yu[2], Zhuolong Zhou[2], Niksa Roki[1], Alberto Sigler[1], David M. Suissa[1], Haniyeh Eyvani[3], George E. Sandusky[4], Rimpi Khurana[5], Yan Guo[6], Molly Dalzell[1], Shyamananda Singh Mayengbam[7], Prasenjit Dey[7], Christine Rafie[1], Erietta Stelekati[8], Jashodeep Datta[9], Saratchandra S. Khumukcham[10], Jatin Roper[10], Nivedh Paluvoi[11], Sandro Satta[12], Daniel Bilbao Cortes[12], Alejandro Villarino[8], Kevin Van der Jeught[8]

[1]Microbiology and Immunology, University of Miami Miller School of Medicine, Miami, FL,[2]Medical and Molecular Genetics; Melvin and Bren Simon Comprehensive Cancer Center, Indiana University School of Medicine, Indianapolis, IN,[3]Medical and Molecular Genetics, University of Miami Miller School of Medicine, Miami, FL,[4]Pathology and Laboratory Medicine, Indiana University School of Medicine, Indianapolis, IN,[5]Sylvester Comprehensive Cancer Center, University of Miami Miller School of Medicine, Miami, FL,[6]Sylvester Comprehensive Cancer Center; Public Health and Sciences, University of Miami Miller School of Medicine, Miami, FL,[7]Immunology, Roswell Park Comprehensive Cancer Center, Buffalo, NY,[8]Microbiology and Immunology; Sylvester Comprehensive Cancer Center, University of Miami Miller School of Medicine, Miami, FL,[9]Division of Surgical Oncology, Dewitt Daughtry Department of Surgery, University of Miami Miller School of Medicine, Sylvester Comprehensive Cancer Center, Miami, FL,[10]Medicine, Division of Gastroenterology; Pharmacology and Cancer Biology, Duke University Medical Center, Durham, NC,[11]Division of Surgical Oncology, Dewitt Daughtry Department of Surgery, University of Miami Miller School of Medicine, Miami, FL,[12]Sylvester Comprehensive Cancer Center; Pathology and Laboratory Medicine, University of Miami Miller School of Medicine, Miami, FL

The majority (up to 85%) of colorectal cancer (CRC) patients have a microsatellite stable (MSS) tumor phenotype, which is a poor responder to immune checkpoint blockade (ICB). Therefore, there is a need to identify novel checkpoints in the tumor microenvironment, such as ST2 (Stimulation 2, IL33 receptor). We demonstrated ST2 to be prominently expressed on human tumor cells, especially MSS tumors, through multiplex immunofluorescence staining of CRC patient samples and publicly available datasets. Using CRC patient-derived organoids, we established that activation of tumoral IL33/ST2 signaling conferred tumor cell protection from T cell-mediated killing. To investigate the mechanistic basis of how tumor cells escape T cell killing, we used colonoscopy-induced, orthotopic murine tumors. We uncovered that IL33/ST2 signaling reduced antigen presentation, driven by reduced immunoproteasome activity. Removing tumoral ST2 signaling using CRISPR/Cas9-gene editing leads to significant tumor growth control and increased infiltration of T cells with a reduced terminally exhausted phenotype. Altogether, these findings indicate ST2 as a potential, novel checkpoint target on tumor cells to enlarge the pool of patients benefiting from ICB.

#2800 Understanding the mechanism by which CD4$^+$ T cells sensitize mesenchymal CD73-deficient tumors to anti-CTLA4 immune checkpoint blockade therapy.

Brian Hongtao Feng[1], Caitie Hanna Sams[1], Isabel O'Connell[1], Shiney Chandraganti[1], Anushka Dongre[2]

[1]Cornell University, Ithaca, NY,[2]Department of Biomedical Sciences, Cornell University, Ithaca, NY

Triple-Negative Breast Cancer (TNBC) is a highly aggressive disease with poor patient outcomes due to its resistance to chemotherapy and immunotherapy. Despite its efficacy in Melanoma and Lung carcinoma, immune checkpoint blockade (ICB) therapy is only effective in a small minority of TNBC patients. Epithelial-to-Mesenchymal Transition (EMT) is a key driver of malignant progression leading to greater metastatic potential and an immunosuppressive tumor microenvironment, driving resistance to therapies. Our previous results demonstrate that epithelial tumors respond to anti-CTLA4 therapy while mesenchymal tumors are resistant. Strikingly, knockout of CD73 in mesenchymal tumors results in complete sensitization to anti-CTLA4 treatment but not anti-PD1 therapy, the more clinically used treatment. Using our preclinical mouse models together with immunofluorescence staining, we observed that CD73-deficient tumors display increased infiltration of CD4$^+$ and CD8$^+$ T cells upon anti-CTLA4 treatment relative to non-responding controls. Most notably, while CD73 deficient tumors continued to respond to anti-CTLA4 treatment without CD8$^+$ T cells, they failed to respond in the absence of CD4$^+$ T cells. However, the mechanisms by which CD4$^+$ T cells facilitate the elimination of mesenchymal tumors remain unknown. Preliminary results demonstrate that cytotoxic CD4$^+$ T cells play a crucial role in potentiating the response of CD73-deficient tumors to anti-CTLA4. Moreover, tumors contain plastic CD4$^+$ T cell subsets that reduce immune suppression under anti-CTLA4 treatment while promoting immune suppression under anti-PD1 treatment. These results reveal that CD4$^+$ T cells can specifically target lethal mesenchymal cancer cells in response to anti-CTLA4 but not anti-PD1 therapy. Future work is aimed at understanding whether CD4$^+$ T cells eliminate tumors via direct interactions with cancer cells or through indirect activation of other immune cells. Given the inefficacy of anti-PD1 therapy in TNBC clinical trials, characterizing the CD4$^+$ T cell response to anti-CTLA4 provides a mechanistic basis for leveraging its therapeutic potential.

#2801 SRY-mediated upregulation of PD-L1 promotes immune evasion in hepatocellular carcinoma and contributes to sex-specific disparities in immunotherapy response.

Bingyi Ren, Kai Sheng, Yichen Yang

The First Affiliated Hospital of Xi'an Jiao Tong University, Xi'an', China

Background: The impact of sex chromosomes on the tumor microenvironment (TME) is significant, beyond hormonal effects. This study investigates the role of the sex-determining gene SRY in the immune microenvironment of hepatocellular carcinoma (HCC), focusing on how SRY regulates immune checkpoints and contributes to gender disparities in immunotherapy response.

Methods: Multiple HCC mouse models (chemically induced, hydrodynamic, orthotopic, subcutaneous) using SRY transgenic knockout (KO) or knock-in (KI) mice were employed. To eliminate hormonal effects, the mice were castrated. Flow cytometry, immunofluorescence, and ELISA assessed T cell changes in the TME. Cellular models used PCR array, CUT&Tag, qPCR, WB, and luciferase assays to explore SRY's transcriptional regulation. Clinical samples validated correlations between SRY, immune markers, and PD-L1.

Results:•In castrated male SRY-KO mice, increased $CD8^+$ T cells and elevated GZMB, TNF-α, and IFN-γ were observed in the TME.•SRY-KI in castrated males reduced $CD8^+$ T cells and functional markers.•Ectopic SRY in castrated females similarly impaired T cell infiltration and function.•PCR array in SRY-overexpressing HCC cells revealed upregulation of PD-L1.•CUT&Tag and luciferase assays confirmed SRY binds the IRF1 promoter, upregulating IRF1 expression.•IRF1 knockdown abolished PD-L1 upregulation, confirming an SRY-IRF1-PD-L1 axis.•In vivo, PD-L1 knockdown in SRY-overexpressing tumors reversed immune suppression and tumor growth.•Anti-PD-L1 treatment showed enhanced efficacy in SRY-overexpressing tumors.•Clinical HCC samples confirmed positive SRY-PD-L1 correlation and negative SRY-$CD8^+$ T cell correlation.

Conclusions: SRY, a male-specific gene, regulates the immune checkpoint PD-L1 via IRF1, suppressing $CD8^+$ T cell function in the TME. Targeting the SRY-IRF1-PD-L1 axis may improve immunotherapy outcomes, especially in male HCC patients.
The text has been translated and polished using AI.

#2802 *In vitro* antigen-specific T cell exhaustion model for immunomodulators evaluation.

Emilio Cosimo, **Hannah Findlay**, Robert Benson, Agapitos Patakas

RoukenBio, Motherwell, United Kingdom

The identification of novel molecular mechanisms underlying exhausted $CD8^+$ T cells (T_{EX}) represents a critical objective in advancing immunotherapeutic strategies for cancer and other diseases. Nevertheless, high-throughput analysis of *in vitro* T_{EX} remains challenging. We developed a human *in vitro* model of $CD8^+$ T cell exhaustion using antigen-specific or TCR-transgenic T cells subjected to chronic antigen stimulation. Repeated exposure to cognate peptide antigens induced hallmark exhaustion phenotypes, including co-expression of inhibitory receptors (PD-1, TIM-3 and LAG-3) and transcription factor TOX. Exhausted T cells exhibited diminished cytokine secretion (e.g. IFN-γ), reduced proliferation (e.g. Ki-67), and impaired cytotoxicity. These features closely mirror exhaustion observed in tumour-infiltrating lymphocytes and chronic infection settings. Checkpoint blockade was evaluated for functional rescue. Anti-PD-1 restored partial proliferation and modest IFN-γ production. However, neither agent fully reversed exhaustion, as other inhibitory pathways remained active. These findings align with clinical observations where monotherapy yields partial rescue. Our model thus enables quantitative assessment of exhaustion reversal and supports combinatorial checkpoint strategies. To generate sufficient antigen-specific T cells for high-throughput assays, we employed artificial antigen-presenting cells (aAPCs) derived from engineered K562 lines expressing diverse HLA alleles and co-stimulatory ligands. This platform supports expansion of rare endogenous T cells to $>10^8$ cells per donor, preserving native TCR expression. Functional validation included CMV-specific and MART-1-specific T cells, which demonstrated antigen-specific cytotoxicity and cytokine responses. This scalable and physiologically relevant assay system permits precise modelling of T cell exhaustion and facilitates systematic evaluation of immunotherapeutic interventions. It serves as a reliable platform for the quantitative screening of agents that inhibit or reverse T cell exhaustion, thereby supporting the rational development of advanced immunotherapies.

#2803 Ex vivo micro-tumor testing platform to characterize and predict patient-specific immunotherapy drug responses.

Felix M. Behr[1], Esmee Koedoot[1], Timothy J. P. Sijsenaar[1], Lea Le Large[1], Cor D. de Kroon[2], Anne van Altena[3], Farbod Khoraminia[1], Laurie C. Steinbusch[2], Christi M. Steendam[4], Dieudonne J. van der Meer[1], Willemijn Vader[1], Nelleke Ottevanger[3], Judith R. Kroep[5]

[1]VitroScan, Leiden, Netherlands,[2]Leiden University Medical Centre, Leiden, Netherlands,[3]Radboud University Medical Centre, Nijmegen, Netherlands,[4]Catharina Ziekenhuis, Eindhoven, Netherlands,[5]Dept. of Medical Oncology, K1-P, Leiden Univ. Medical Ctr., Leiden

Background. Immunotherapies have shown significant clinical benefit, but upfront identification of patients with therapy-sensitive cancers remains a major challenge. We have previously demonstrated that our ex vivo micro-tumor platform, which preserves the tumor microenvironment (TME), is predictive for clinical responses to platinum-based therapy (Koedoot et al., npj precision oncology, 2025). Here, we show that the platform also enables patient-specific profiling of drug sensitivity and immune activity for immune checkpoint inhibitors (ICIs) and bispecific T cell engagers (BiTEs).

Methods. Fresh tumor tissues were collected from colorectal cancer (CRC, N=6), non-small cell lung cancer (NSCLC, N=23) and ovarian cancer (OC, N=85) patients with primary or recurrent disease. Micro-tumors including the TME were isolated from resections, ascites or pleural fluid, embedded in hydrogel and exposed to chemotherapeutics, six ICIs and/or CD3xMUC16 BiTE ubamatamab. Drug responses were quantified by extracting morphological features from high-throughput 3D imaging. Treatment sensitivity was defined by statistically significant immune cell expansion and micro-tumor killing. Sensitivity profiles were correlated with immune cell populations. Supernatants collected after treatment were analyzed for secreted cytokines, chemokines and cytotoxic mediators using multiplex immune biomarker profiling. PD-L1 tumor proportion scoring (TPS) reported on original patient tumor tissue was used (NSCLC).

Results. Significant ex vivo ICI responses were observed in 50% of OC, 27% of early NSCLC, and 33% of metastatic NSCLC samples, with reproducible results across serial samples. Most OC samples were positive for T-cell, macrophage and NK-cell markers but not for B-cell markers. Stronger immune responses were observed in OC samples with high CD3 ($p=0.01$) or CD68 ($p=0.003$) expression. Importantly, immune sensitivity correlated with PD-L1 TPS ($p=0.13$, NSCLC). Ubamatamab induced significant immune expansion in 42% (8/19) of OC samples, half of which also showed significant tumor killing. When compared to non-responders, ubamatamab responders with effective tumor killing exhibited robust and simultaneous upregulation of T cell effector cytokines (IFN-γ, IL-2), cytotoxic mediators (Granzyme B, Perforin) and pro-inflammatory cytokines (CXCL9, CXCL11).

Conclusions. This study reports classification, characterization and prediction of autologous patient-specific sensitivity to ICIs and BiTEs by characterizing immune populations and reporting correlation with known clinical markers (PD-L1). Our ex vivo micro-tumor platform enables functional profiling of patient-specific immunotherapy responses, supporting biomarker discovery and selection of patients for emerging immunotherapies. The next step is to correlate the ex vivo sensitivity to actual clinical outcome.

#2804 Sialic acid inhibits engager-mediated T cell activation.

Johanna Nimmerfroh[1], Dinah Heiligensetzer[1], Michael Sandholzer[1], Anastasiya Borsch[2], Heinz Laubli[1]

[1]Department of Biomedicine, University Hospital and University of Basel, Basel, Switzerland,[2]Department of Biomedicine, University of Basel, Basel, Switzerland, Basel, Switzerland

Background: Although T cell-based therapies have led to a significant success in certain tumor types, a large proportion of patients receiving cancer immunotherapy still progress with the disease. Thus, there is interest in identifying and blocking alternative pathways mediating immune suppression. Beyond canonical protein-based immune checkpoints, tumor-associated glycosylation—particularly hypersialylation—has emerged as a key modulator of immune suppression. Sialic acid-containing glycans on tumor cells are recognized as glyco-immune checkpoints that engage inhibitory Siglec receptors on immune cells. While the immunosuppressive role of tumor sialylation is well established[1], new evidence indicates that sialylation of the T cells themselves[2] may also contribute to immune dysfunction, suggesting a previously underappreciated layer of glyco-regulation in the tumor microenvironment.
Methods: Human T cells were treated with pan-sialidase to enzymatically remove surface sialic acids. Desialylated T cells were then stimulated with anti-CD3/anti-CD28 or co-cultured with bispecific T cell engagers and tumor target cells, followed by flow cytometry. Primary samples from patients with chronic lymphocytic leukemia (CLL) were analyzed through single-cell RNA sequencing combined with lectin-based glycan profiling.
Results: We discovered that T cells treated with sialidase exhibited enhanced proliferation and activation. In a co-culture system with bispecific T cell engagers and target cells, we demonstrated that sialidase-treated T cells showed enhanced cytotoxicity, including increased cytokine production, T cell proliferation, and tumor cell killing. When studying T cell subsets, we observed that sialidase treatment lowered the activation threshold particularly in naïve T cells. Our findings were validated using primary samples from patients with chronic lymphocytic leukemia (CLL): sialic acid remodeling led to improved immune function.
Conclusion: Sialic acids on T cells significantly modulate their function. Enzymatic removal of these glycans enhances T cell response and may help overcome resistance mechanisms in cancer immunotherapy. Future studies will investigate whether distinct glycan signatures among T cell subtypes correlate with functional heterogeneity.[1]Dobie, C., Skropeta, D. *Br J Cancer* 2021*,124,* 76-90.[2]Edgar, L. J.; Paulson J. C *et al. ACS Cent Sci* 2021*, 7, 1508-1515.*

#2806 Myoglobin expression boosts T-cell metabolism and antitumor effector function.

Julia Werner[1], Haifeng Xu[1], Georgios Theodorakis[1], Ichiro Katahira[1], Mitrajit Ghosh[1], Michal Gorzkiewicz[1], Luisa de Sousa Santos[1], Ann Kathrin Bergmann[1], Max Anstotz[1], Anne Busch[1], Diran Herebian[1], Sascha Dietrich[1], Carsten Berndt[1], Ertan Mayatepek [1], Aleksandra Pandyra[2], Dirk Brenner[3], Philipp Lang[1]

[1]University Hospital of Dusseldorf, Dusseldorf, Germany,[2]University Hospital Bonn, Bonn, Germany,[3]University of Luxembourg, Luxembourg, Luxembourg

The tumor microenvironment is frequently hypoxic and characterized by a scarcity of nutritional resources, including limited glucose availability. As effector T cells have high energy demands, tumor metabolism can contribute to T-cell dysfunction and exhaustion. In this study, we assessed hypoxia in spleen and tumor tissue from tumor-bearing C57BL/6J mice using RT-PCR, histology, and flow cytometry. Next, $CD8^+$ T cells isolated from C57BL/6J or $P14^+$ mice were transduced with a Thy1.1 (control) or Thy1.1-myoglobin (Mb) packaging retrovirus, and Mb expression was confirmed by RT-PCR and Western blot. The metabolism of these cells was analysed using flow cytometry, TEM, FIB-SEM, Seahorse assays, metabolomics, and luminescence-based approaches. Furthermore, effector function was measured in vitro by flow cytometry. $P14^+$ $CD45.1^+$ $CD8^+$ Mb-transduced and control T cells were transferred into B16F10-gp33 or MC38-ova tumor-bearing mice and analysed by flow cytometry and histology. Finally, B16F10-gp33 tumor-bearing mice received additional treatment with an anti-PD-1 checkpoint inhibitor. Here, we demonstrate that expression of the oxygen-binding protein myoglobin in T cells can enhance their mitochondrial and glycolytic metabolic functions. Metabolites and TCA cycle intermediates were markedly increased in the presence of myoglobin and were associated with elevated ATP levels. Myoglobin-expressing T cells exhibited reduced HIF-1α expression after activation and during infiltration into the tumor microenvironment. Accordingly, myoglobin expression increased effector T-cell function against tumor cells in vitro, accompanied by reduced superoxide levels. Following adoptive transfer into tumor-bearing mice, myoglobin expression promoted greater infiltration into the tumor microenvironment. Although myoglobin-expressing T cells showed increased effector cytokine expression, PD-1 remained detectable and targetable by anti-PD-1 monoclonal antibodies, which—when combined with transfer of myoglobin-expressing T cells—achieved maximal efficacy in delaying tumor growth. Taken together, we show that expression of myoglobin in T cells enhances their metabolism, infiltration into tumor tissue, and effector function against cancer cells.

#2807 Immune cell-dependent resistance to LAG3 blockade in SMARCB1-deficient renal medullary carcinoma.

Jing Qian[1], Kai Yu[1], Deepa Bisht[1], Melinda Soeung[2], Pankaj Chauhan[1], Fei Duan[1], Menuka Karki[1], Rong He[1], Nizar M. Tanir[1], Hania Khan[3], Zilong Zhao[1], Luigi Perelli[1], Giannicola Genovese[1], Linghua Wang[1], Jianjun Gao[4], Pavlos Msaouel[5]

[1]UT MD Anderson Cancer Center, Houston, TX,[2]Dana-Farber Cancer Institute, Boston, MA,[3]UT Southwestern, Dallas, TX,[4]Medical Oncology, UT MD Anderson Cancer Center, Houston, TX,[5]Genitourinary Medical Oncology, UT MD Anderson Cancer Center, Houston, TX

Background: Renal medullary carcinoma (RMC) is an exceptionally aggressive kidney cancer of young individuals with sickle cell trait, characterized by SMARCB1 loss, rapid progression, and a median survival of ~13 months. Transcriptomic profiling shows a highly inflamed microenvironment with broad immune-checkpoint upregulation. Among these, PD-1 (log_2 fold-change 1.7; FDR = 0.008) is increased, and LAG-3 (log_2 fold-change 4.6; FDR < 0.0001) shows one of the strongest elevations relative to adjacent kidney tissue. These findings motivated an RMC-specific clinical trial testing anti-PD-1 plus high-dose anti-LAG-3 (NCT05347212), yet mechanisms underlying resistance to LAG-3 blockade remain unknown.

Study Design and Methods: To investigate RMC response to PD-1 and LAG-3 inhibition, we used a somatic-mosaic immunocompetent genetically engineered mouse model (GEMM) of RMC on a sickle-trait background. We compared anti-PD-1 and anti-LAG-3 monotherapy with isotype IgG in immunocompetent mice to assess baseline sensitivity to checkpoint inhibition. To dissect mechanisms of LAG-3 resistance, we evaluated anti-LAG-3 treatment in RAG1-knockout mice lacking mature B and T cells and examined anti-LAG-3 under $CD4^+$ T-cell depletion to identify the immune subsets driving resistance. Tumor weights were assessed at endpoint, and statistical comparisons were performed using the Mann-Whitney test.

Results: Anti-PD-1 monotherapy failed to control tumor growth, confirming intrinsic resistance to PD-1 blockade (mean tumor weight: IgG 0.58 g vs anti-PD-1 0.75 g; p = 0.6682). In contrast, anti-LAG-3 monotherapy exacerbated tumor progression (IgG 0.74 g vs anti-LAG-3 1.27 g; p = 0.0297). Loss of adaptive immunity partially reversed this phenotype: in RAG1-knockout mice, anti-LAG-3 showed a trend toward reduced tumor burden (IgG 1.415 g vs anti-LAG-3 0.61 g; p = 0.127). $CD4^+$ T-cell depletion abrogated resistance, yielding significantly lower tumor weights under anti-LAG-3 (anti-LAG-3 1.39 g vs anti-LAG-3 + CD4 depletion 0.75 g; p = 0.0291).

Conclusions: Our findings identify an immune cell-dependent mechanism limiting the efficacy of LAG-3 blockade in SMARCB1-deficient RMC. Disrupting this axis, alone or alongside PD-1/LAG-3 inhibition, emerges as a testable strategy to blunt immune checkpoint therapy-induced adaptive reprogramming and restore anti-tumor activity.

#2808 A first in class VIP receptor antagonist as an immunotherapeutic for acute myeloid leukemia.

Swapnaa Balaji[1], Antonio Ward[1], Yuou Wang[2], Jian-Ming Li[2], Srijon Sarkar[2], Sonia Mecorapaj[2], Tenzin Kalsang[3], Shuhua Wang[2], Cynthia Giver[2], Edmund Waller[1]

[1]Cambium Oncology, LLC, Atlanta, GA,[2]Emory University, Atlanta, GA,[3]Columbia University Irving Medical Center, New York, NY

Current immune checkpoint therapies targeting PD-1 and PD-L1 are ineffective in treating Acute Myeloid Leukemia (AML). Vasoactive Intestinal Peptide (VIP) is an immunosuppressive 28-amino acid neuropeptide overexpressed in nearly 30% AML patients, suggesting that some AML tumors may be using VIP expression as a mechanism to evade immune surveillance. We hypothesize that AML cells secrete VIP which signals through the VIP-R (receptor) on T cells to limit anti-cancer immunity. Therefore, targeting the VIP signaling with a VIP-R antagonist can reverse immunosuppression and potentiate anti-cancer immunity. Using *in silico* modeling, *in vitro* screening for potentiation of T cell activation, and proof-of-principle screening in mouse leukemia models, we identified a novel VIP-R antagonist, ANT308. ANT308 shows stronger binding affinity to VIP-R as compared to VIP and potentiates activation of human and mouse T cells with an EC_{50} in the range of 200-400 nM. Immunofluorescence assays show that ANT308 colocalizes with the VIP receptor, VPAC1. Co-IP and flow cytometry confirmed ANT308 binding to VPAC1. In addition, ANT308 treatment of leukemic mice induced strong T cell-mediated anti-leukemic activity. To improve the pharmacokinetics of ANT308, we have developed a novel fusion peptide combining ANT308 and Fc fragment of IgG4 named CAMV-01. In a Jurkat T-cell activation assay, CAMV-01 has an EC_{50} of 100-200 nM and reduces T cell exhaustion. Furthermore, CAMV-01 significantly improved survival in multiple murine leukemia models, including those that secrete VIP (C1498) and the VIP negative cell line P815. *In vitro* stability studies show that CAMV-01 remains stable in plasma for > 4 days, whereas the ANT308 peptide is stable for only 15 minutes. PK studies with intravenous (i.v.) or subcutaneous (s.c.) injection of 15mg/kg CAMV-01 show a half-life of 2 weeks in mice, compared to 15 minutes for the ANT308 peptide. Using Sprague-Dawley rats receiving a single i.v. or s.c injection of 5mg/kg CAMV-01, the C_{max} and $t_{1/2}$ were estimated to be 82 nM and 165 hours (i.v.) respectively and 0.7 nM and 235 hours (s.c.) respectively. In a P815 mouse model, s.c. administration of CAMV-01 induced a stronger tetramer-positive CD8+ T-cell response compared to ANT308. In conclusion, CAMV-01 is a novel, first-in-class immunotherapeutic targeting the VIP immune checkpoint, with a robust pharmacokinetic and pharmacodynamic profile and promising potential for the treatment of AML.

#2809 VIP/VPAC signaling as a phagocytosis checkpoint in TP53-mutated acute myeloid leukemia.

Zihan (Clarence) Chen[1], Tuisha Gupta[2], Fanyuan Zeng[2], Yujie Chen[3], Jian Ming Li[2], Cynthia R. Giver[4], Kiranj Chaudagar[2], Edmund K. Waller[5]

[1]College of Computing, School of Chemistry and Biochemistry, Georgia Institute of Technology, Atlanta, GA,[23]Graduate Division of Biological and Biomedical Sciences, Emory University, Atlanta, GA,[4]Hematology and Medical Oncology, Emory University, Winship Cancer Institute, Atlanta, GA,[5]Emory University School of Medicine, Atlanta, GA

Background: Acute myeloid leukemia (AML) remains one of the most lethal hematologic malignancies, especially in TP53-mutated disease where standard chemotherapy provides poor long-term survival. Immune evasion by myeloid cells in the tumor microenvironment is a major barrier to cure. We hypothesized that targeting vasoactive intestinal peptide (VIP)/VIP receptor (VPAC) signaling would overcome myeloid cell-mediated immunosuppression and enhance anti-tumor responses in AML.
Methods: RNA-seq differential expression, survival analyses, and flow cytometry of AML bone marrow and PBMC were used to profile VIP/VPAC expression and myeloid versus blast compartments in TP53-mutated and non-mutated cases. TP53-wildtype and TP53 loss-of-function human and murine AML cell lines were used to measure VIP production by ELISA and macrophage phagocytosis of VIP-producing versus low-VIP cells in M1- and M2-like co-culture assays. In vivo efficacy of the long-acting VIP receptor antagonist ANT308 and its IgG4 Fc fusion ANT308-Fc3 was evaluated in C1498 and WEHI3 AML models, including VIP, VPAC1, and VPAC2 knockout hosts.
Results: VIP expression was elevated in PBMC from ~36% of AML patients compared with healthy donors and was enriched in TP53-mutated cases. High VIP expression and TP53 loss-of-function each associated with inferior survival in cBioPortal datasets. RNA-seq showed that TP53-mutated AML is characterized by increased VIP and immunoregulatory pathway signatures together with reduced apoptosis and effector $CD8^+$ T-cell-associated genes. Secretome analysis of human leukemia cells demonstrated higher VIP secretion from TP53 loss-of-function lines than from TP53-wildtype THP-1, confirming leukemia-intrinsic VIP production. In patient samples, both $CD34^+$ blasts and $CD34^-$ myeloid cells contained VIP^+ cells, but non-blast myeloid cells accounted for most VIP^+ events, indicating they are a major VIP source in the AML microenvironment. ANT308 enhanced phagocytosis of VIP-secreting WEHI3 leukemia cells by both M1- and M2-like macrophages but did not alter phagocytosis of VIP-low C1498 cells, supporting VIP as a phagocytosis checkpoint in AML. Consistent with a host contribution, VIP-, VPAC1-, or VPAC2-knockout mice bearing C1498 leukemia showed improved survival relative to wild-type mice. In vivo treatment of wild-type C1498-bearing mice with ANT308 or the long-acting Fc fusion ANT308-Fc3 eradicated established leukemia in up to 65% of animals.
Conclusions: VIP/VPAC signaling defines a previously unrecognized phagocytosis checkpoint that reinforces myeloid immunosuppression in AML and is linked to TP53-mutated disease. VPAC antagonism with ANT308-Fc3 restores macrophage phagocytosis and produces durable leukemia control in preclinical models, supporting clinical development of VPAC-targeted immunotherapy for high-risk AML.

#2810 Anti-PD-1 efficacy is associated with a clonal trajectory composed of chronic effectors with lymph node homing capacity.

Mingshuang Wang*[1], Guanning Wang*[2], Khushboo Patel[2], Ajeya Nandi[2], Timmy Lai[2], Shira Rosenberg[2], Zhoumu Xiang[2], Stella Park[2], Tara C. Mitchell[2], Alexander C. Huang#[2]

[1]Department of Neurosurgery, Perelman School of Medicine, University of Pennsylvania, Philadelphia, PA,[2]Division of Hematology/Oncology, Department of Medicine, Perelman School of Medicine, University of Pennsylvania, Philadelphia, PA

Introduction: Immune checkpoint blockade (ICB), such as anti-CTLA-4 or anti-PD-1 (αPD-1), drives distinct patterns of T cell differentiation that ultimately influence treatment efficacy. However, it has been challenging to identify and define distinct T cell differentiation states in humans. We apply a novel algorithm *Clonotrace* (Nancy Zhang, UPenn) to define differentiation trajectories by monitoring single clones across differentiation states after αPD-1. We test the hypothesis that certain differentiation trajectories will have unique properties, including cell states and trafficking patterns, that will influence clinical efficacy.

Methods: We performed single cell RNA and paired TCR sequencing on 132,898 CD8+ T cells from 36 stage III melanoma patients treated with neoadjuvant αPD-1, including 12 patients with matched tumor, uninvolved regional lymph node, and blood samples. We applied *Clonotrace* to define differentiation trajectories by grouping clonotypes that have a similar transcriptional footprint across CD8 cell states. We then defined these differentiation trajectories in terms of cell state composition, antigen specificity, tissue distribution, gene regulation, and association with clinical outcomes.

Results: We identified 10 distinct clonal trajectories that differentiate from naïve/stem-like CD8 T cell states to exhausted and/or effector CD8 T cell states. These trajectories largely separated into two sets of clones based on antigen specificity and the expression of pathways associated with chronic stimulation. Further examination of the antigen-specific clones identified one particular trajectory (Traj 5), that was associated with clinical response. Traj 5 included clones with a unique chronic effector cell state that was able to traffic between lymph node and tumor. In contrast, Traj 1 was composed of terminally exhausted CD8 clones that were tumor-resident and associated with αPD-1 resistance.

Conclusion: We identify a unique differentiation trajectory in patients that retains effector T cell differentiation in the setting of chronic stimulation. These chronic effectors retain the ability to traffic between lymph node and tumor and are associated with the efficacy of αPD-1. These findings indicate maintaining trafficking ability is essential for the efficacy of ICB. In contrast, terminal differentiation results in CD8 T cells becoming “locked” in the tissue and terminally exhausted.

#2812 Bhlhe40 shapes distinct T cell reponses to anti PD1 and anti CTLA4 immune checkpoint therapy.

Akata Saha[1], Tomoyuki Minowa[1], Alexander S. Shavkunov[1], Avery J. Salmon[1], Sunita Keshari[1], Kristen E. Pauken[1], Kenneth H. Hu[1], Ken Chen[2], Matthew M. Gubin[1]

[1]Immunology, UT MD Anderson Cancer Center, Houston, TX,[2]Bioinformatics and Computational Biology, UT MD Anderson Cancer Center, Houston, TX

The transcriptional programs that enable CD4 and CD8 T cells to sustain anti-tumor immunity are not fully defined. We investigated the role of the transcriptional regulator Bhlhe40 in shaping CD4 and CD8 T cell responses during anti-PD-1 and anti-CTLA-4 immune checkpoint therapy (ICT). Using conditional knockout mice, we found that anti-PD-1 efficacy depends on CD8 T cell-intrinsic Bhlhe40, with potential contribution from CD4 T cells. In contrast, anti-CTLA-4 relies primarily on CD4 T cell-intrinsic Bhlhe40 and remains effective even without Bhlhe40 in CD8 T cells. Loss of Bhlhe40 skewed CD8 T cells toward TCF-1+ naïve/progenitor exhausted-like states, impairing IFNγ production, glycolysis, and mitochondrial fitness. CD8 T cell-intrinsic Bhlhe40 was also required for ICT-driven macrophage remodeling from suppressive $CX3CR1^{+}$ to $iNOS^{+}$ macrophages. Analysis of human cancer datasets showed that *BHLHE40* is enriched in tumor-reactive and activated/exhausted CD8 T cells, correlating inversely with *TCF7* (TCF-1) and positively with *TOX* and *IFNG*. Importantly, higher *BHLHE40* expression was observed in responders to ICT in a cohort of patients with basal cell cancer. Together, these findings show Bhlhe40 is a subset- and therapy-specific regulator of T cell programs, controlling effector differentiation, metabolism, and ICT efficacy, providing a mechanistic basis for the divergent modes of action of anti-PD-1 versus anti-CTLA-4.

#2813 Targeting AHR overcomes PD-L1-driven resistance to immune checkpoint blockade in triple-negative breast cancer.

Minkyoung Choi[1], Ju Hee Kim[2], Han-Byoel Lee[3], Wonshik Han[3]

[1]Seoul National University, Seoul, Korea, Republic of,[2]Center for Medical Innovation, Seoul National University Hospital, Seoul, Korea, Republic of,[3]Seoul National Univ. College of Medicine, Seoul, Korea, Republic of

Introduction: Triple-negative breast cancer (TNBC) has higher tumor immunogenicity than other subtypes, and immune checkpoint inhibitors (ICIs) targeting the PD-1/PD-L1 axis have been applied in its treatment. However, responses to immune checkpoint blockade (ICB) remain limited by intrinsic and acquired resistance, highlighting the need for predictive biomarkers and new combination strategies to improve anti-PD-L1 efficacy.The aryl hydrocarbon receptor (AHR) regulates immune responses and PD-L1 expression, promoting an immunosuppressive tumor microenvironment (TME). AHR signaling may also interfere with interferon-mediated immune activation and affect ICB response. This study aimed to examine how AHR activation contributes to anti-PD-L1 resistance in PD-L1 overexpressing TNBC and whether AHR blockade enhances therapeutic efficacy.
Methods: PD-L1-overexpressing (PD-L1 OE) and control (Ctl) 4T1 cells were generated. The AHR antagonist (CH-223191) and anti-PD-L1 antibody were applied in vitro and in vivo. Flow cytometry, western blotting, cell proliferation assay, quantitative RT-PCR, immunohistochemistry (IHC), and co-culture of macrophages and cancer cells were performed. An orthotopic syngeneic mouse model was established by injecting 4T1 Ctl or PD-L1 OE cells into the mammary fat pad. Mice were treated with CH-223191 (5 mg/kg, i.p., four times weekly) and anti-PD-L1 antibody (150 μg, i.p., twice weekly), alone or in combination.
Results: PD-L1 OE tumors showed reduced responsiveness to anti-PD-L1 therapy compared with control in vivo, confirming intrinsic resistance to ICB. AHR expression was elevated at both RNA and protein levels in PD-L1 OE tumors after anti-PD-L1 treatment. Combination therapy with CH-223191 and anti-PD-L1 antibody tended to suppress tumor growth compared with monotherapy, suggesting an ability to overcome PD-L1-driven resistance in vivo. In vitro, CH-223191 reduced 4T1 viability in a dose-dependent manner, suggesting a potential tumor-intrinsic role of AHR signaling. Co-culture of PD-L1 OE 4T1 cells with macrophages promoted M2-like polarization, supporting an immunosuppressive microenvironment. Collectively these findings suggest that AHR activation contributes to anti-PD-L1 resistance by promoting an immunosuppressive TME, and that AHR blockade could enhance anti-PD-L1 efficacy in TNBC.
Conclusions: AHR activation was linked to PD-L1-driven anti-PD-L1 resistance, and AHR inhibition enhanced responsiveness in vivo. These findings suggest that AHR mediates PD-L1 axis-driven resistance and that its inhibition may serve as a promising combination strategy in TNBC. Further studies should elucidate the mechanistic link between AHR signaling and PD-L1-mediated immune regulation and validate its therapeutic potential.

#2814 Comprehensive single-cell atlas of immune ecosystem in response to immune checkpoint blockade therapy.

Dayoung Lee[1], Ji Yoon Lee[1], Jiwon Kim[1], You Jin Song[2], Namsung Moon[1], Juyoung Lee[1], Harim Koo[3], Jason K. Sa[1]

[1]Korea University, Seoul, Korea, Republic of,[2]Korea Univ. Medical Center, Seoul,[3]National Cancer Center - Korea, Goyang, Korea, Republic of

Despite the clinical success of immune checkpoint blockade (ICB) in several malignancies, a majority of patients failed to achieve clinical response. A deeper understanding of the cellular and molecular mechanisms underlying ICB resistance is essential for advancing precision immunotherapy. In the present study, we analyzed the complex transcriptional profiles of 663,526 single cell data across eight different cancer types with clinical response to ICB therapy. Through integrative analysis, we delineated the transcriptional heterogeneity of exhausted CD8+ T cells and immunosuppressive macrophages and assessed their contribution to ICB treatment outcomes. Exhausted T cells demonstrated a wide spectrum of exhaustion states that stratified patients by clinical response. Notably, terminally exhausted T cells were particularly enriched in non-responders and exhibited high expressions of TIGIT, HAVCR2, and CTNNB1-driven WNT signaling activity, while responders were marked by activation of cytotoxic effectors and NF-κB transcriptional regulators. Immunosuppressive macrophages were functionally associated with terminal T cell exhaustion via aberrant activation of CD137 signaling axis. Transcriptional regulatory network analysis further revealed key transcriptional factors and immune checkpoint molecules that are differentially expressed across all cell states, offering new therapeutic targets. Our study provides a comprehensive single-cell atlas of immune cell states predictive of ICB response, uncovering substantial cellular and transcriptional heterogeneity and crosstalk between exhausted T cells and macrophage populations. These findings present mechanistic insights into cellular programs that can be therapeutically modulated to overcome ICB resistance.

#2815 Cytoplasmic PD-L1 levels are associated with tumor progression in small cell lung cancer.

Ji Young Lee, Anindita Das, HyeonJoo Cheon

Department of Oncology, Wayne State University, Karmanos Cancer Institute, Detroit, MI

Lung cancer is the leading cause of cancer-related mortality. Small-cell lung cancer (SCLC), accounting for about 10-15% of lung cancer diagnoses, is an exceptionally lethal subtype. Due to rapid growth, early metastasis, and resistance to therapy, SCLC often causes patient death within months. Standard first-line platinum-etoposide (PE) therapy shows significant effects and high response rates. However, recurrence is nearly inevitable, and recurrent tumors are often resistant to further treatment. Recently, combination treatments incorporating an anti-PD-L1 antibody (either atezolizumab or durvalumab) alongside PE therapy have significantly improved survival rates compared to standard PE treatment alone in SCLC patients. However, in contrast to non-small cell lung cancer (NSCLC), other immune checkpoint inhibitors (ICIs), including anti-PD-1 combined with PE, have not shown survival benefits in SCLC. The reason why only anti-PD-L1 demonstrate in SCLC remains unclear and requires further investigation. Furthermore, unlike in other cancers, the efficacy of anti-PD-L1 in SCLC is not correlated with PD-L1 expression on the cell membrane. The selective efficacy of anti-PD-L1 in SCLC suggests that it may function through a distinct mechanism of action, independent of the traditional T cell-dependent pathway. Our previous study found that PD-L1 operates in a cancer cell-intrinsic manner, independent of the interaction with PD-1. Based on these results, we hypothesize that non-membranous intracellular PD-L1 contributes to cancer cell-intrinsic PD-L1 functions and is associated with tumor progression. To test this hypothesis, we performed immunocytochemistry (IHC) and immunofluorescence (ICC) on SCLC specimens from patients at various disease stages and on SCLC cell lines. Our analyses revealed that membranous PD-L1 was rarely detected in SCLC cells in culture or in patient specimens. Instead, PD-L1 expression was predominantly found in the cytoplasm and nucleus of SCLC tumor cells. Among 72 SCLC samples, 59 cases (82%) exhibited cytoplasmic PD-L1, 10 cases (14%) displayed nuclear PD-L1, while only 6 cases (8%) showed membranous PD-L1 expression. We observed a trend toward increased cytoplasmic PD-L1 prevalence and intensity in stage II and III SCLC tumors compared with stage I tumors. In contrast, membranous PD-L1 was readily detected on the cell membrane of most NSCLC tumor cells. Despite the minimal membranous PD-L1 expression, anti-PD-L1 durvalumab significantly increased cisplatin cytotoxicity in SCLC cells independent of T cells. Our findings suggest that intracellular, rather than membranous, PD-L1 plays a key role in SCLC progression. Further studies on its functions and mechanisms may guide the development of more effective SCLC therapies.

#2816 Discovery and preclinical evaluation of novel peptide inhibitors targeting the TIGIT immune checkpoint.

Haozhe Cui, Xinyi Zhang, Wanding Wang, Francesco Zonta, **Eyad Elkord**

Xi'an Jiaotong-Liverpool University, Suzhou, China

Immune checkpoint (IC) receptors negatively regulate immune responses and play crucial roles in maintaining self-tolerance and preventing autoimmunity. However, tumor cells can exploit these pathways to evade immune recognition and destruction. TIGIT has emerged as a key immune checkpoint receptor, which exerts immunosuppressive effects through direct and indirect mechanisms. While preclinical studies with TIGIT-blocking monoclonal antibodies demonstrated encouraging antitumor activity, clinical trials of anti-TIGIT monotherapy showed disappointing outcomes, shifting attention toward alternative strategies. In this study, we identified potential peptide-based inhibitors against TIGIT. Through computational affinity maturation, starting from the anti-TIGIT antibody MG1131, we identified a library of TIGIT-inhibitory peptides. This process integrated sequence sampling, molecular dynamics, and free energy calculations, guided by Monte Carlo selection. Compared with conventional monoclonal antibodies, these peptides are expected to provide superior tissue penetration, reduced immunogenicity, and an improved safety profile. In this study, two mutant peptides (named T-M2 and T-M3) exhibited stronger inhibition of TIGIT-CD155 interactions than the wild-type peptide in hTIGIT-CHO-K1 cell-based blocking assay. Furthermore, these peptides induced higher levels of IFN-γ secretion from both human CD4+ and CD8+ T cells. This enhanced immunostimulatory activity was confirmed in a co-culture system of hTIGIT-Jurkat and hCD155-CHO-K1 cells, where the mutant peptides induced greater IL-2 secretion. The in vivo therapeutic efficacy of these peptides, either as monotherapy or in combination with immune checkpoint inhibitors, is currently being evaluated in MC38 tumor-bearing and humanized HCT116 mouse models. Tumor growth dynamics, as well as the phenotype, cytokine profile and activation status of T cells in the tumor microgovernment, tumor-draining lymph nodes, and spleens will be assessed in the treated groups and compared with control groups. Collectively, this study introduces novel TIGIT-blocking peptides as promising candidates for cancer immunotherapy, offering a potential alternative or complementary approach to antibody-based immune checkpoint blockade.

#2817 Immune checkpoint therapy induces tertiary lymphoid structures in a murine model of triple-negative breast cancer.

Zachary D. Schrank, Benjamin G. Vincent, Jonathan S. Serody

University of North Carolina School of Medicine, Chapel Hill, NC

Background: Though immune checkpoint therapy (ICT) is approved for the treatment of triple-negative breast cancer (TNBC), response rates are low and non-durable. There is thus an urgent need for improved therapeutic biomarkers and deeper understanding of TNBC antitumor immune responses to tailor improved immunotherapies. Tertiary lymphoid structures (TLS) are intra-tumoral lymphoid tissues composed of B cells and T cells that are associated with improved survival and response to ICT. Despite these associations, it is unclear what impact ICT has on these structures and whether they mediate ICT efficacy. We sought to examine if ICT may promote formation of TLS in TNBC.

Methods and Results: In this study, we show induction of TLS following immune checkpoint therapy (anti-PD-1 and anti-CTLA-4) in an orthotopic murine TNBC model. This model, T11-APOBEC, genocopies clinical TNBC and is dependent upon B cells and $CD4^+$ T cells for response to immune checkpoint therapy. Using immunofluorescence, we show that TLS formation is significantly upregulated in the periphery of T11-APOBEC tumors following ICT, whereas tumors treated with vehicle control show little to no TLS formation ($p = 0.0286$). These TLS are composed of B cells coalescing with $CD4^+$ and $CD8^+$ T cells and are also associated with pro-inflammatory macrophages and monocytes. Using spatial transcriptomics and K-nearest neighbor analysis, we show that these TLS are identified as a spatially and transcriptionally distinct niche in an unbiased manner. TLS in this model are significantly enriched for four widely used transcriptional signatures of human cancer-associated TLS, and they also significantly upregulate pathways associated with B cell activation, humoral immunity, and germinal center activity. We then further show that a signature derived from these ICT-induced TLS are focally enriched in a cohort of human TNBC samples by spatial transcriptomics, suggesting the formation of similar structures in TNBC patients.

Conclusions: These data suggest that ICT promotes the formation of TLS in TNBC, which may mediate enhanced anti-tumor adaptive immune responses. This model also provides a platform to further investigate mechanisms of formation and function of these structures in the context of ICT, which will inform predictive biomarkers and improved immunotherapy approaches for this aggressive disease.

#2818 Preclinical Characterization of ALG-094295, a highly potent and orally bioavailable small molecule PD-1/PD-L1 inhibitor targeting dimerization, internalization and degradation of PD-L1.

Heleen Roose[1], Kristina Rekstyte-Matiene[1], Sarah Stevens[2], Kusum Gupta[2], Sandra Chang[2], Nour Fayyad[1], Cheng Liu[2], Vladimir Serebryany[2], Lillian Adame[2], Kha Le[2], Antitsa Stoycheva[2], Dinah Misner[2], Lawrence M. Blatt[2], Sushmita Chanda[2], David B. Smith[2], Julian A. Symons[2], Andreas Jekle[2], **Tongfei Wu**[1]

[1]Aligos Belgium BV, Leuven, Belgium,[2]Aligos Therapeutics, Inc., South San Francisco, CA

Background: PD-1/PD-L1 antibody-based therapies have demonstrated tremendous success in the treatment of a variety of cancers. However, these antibody drugs are associated with several disadvantages, such as weak tumor penetration, immune-related adverse events and emergence of anti-drug antibodies. Here, we report the discovery and characterization of ALG-094295 as a highly potent and orally bioavailable small molecule PD-1/PD-L1 inhibitor that binds to PD-L1 and promotes PD-L1 dimerization, internalization and degradation, offering a different mechanism of action with potential advantages over PD-1/PD-L1 antibody therapeutics.
Methods: The interaction of PD-1/PD-L1 and PD-L1 dimerization were assessed by AlphaLISA®. Cellular activity was measured using PD-1 expressing Jurkat NFAT luciferase T cells and CHO-hPD-L1 cells. *In vivo* PD-L1 target engagement, tumor growth inhibition and tumor infiltration of T-cells were assessed in a humanized-PD-L1 MC38 subcutaneous tumor mouse model. *In vitro* ADME tox profile was established using standard assays. Pharmacokinetic (PK) studies were performed with rat, dog and cynomolgus monkey.
Results: ALG-094295 demonstrated inhibition of PD-1/PD-L1 interaction at sub-nanomolar concentrations and induced PD-L1 dimerization. In vitro studies showed that ALG-094295 activated T cells with approximately ten times greater potency compared to INCB086550, an orally administered small molecule PD-L1 inhibitor that has demonstrated clinical responses in a phase I trial. Furthermore, treatment of CHO-hPD-L1 cells with ALG-094295 resulted in internalization and reduction of PD-L1 protein levels. In ex vivo human PBMC assays, ALG-094295 demonstrated PD-L1 target engagement, T cell activation and immune cell mediated tumor cell killing. In a humanized PD-L1 MC38 mouse model, a single oral dose of ALG-094295 (5 mg/kg) achieved PD-L1 target engagement comparable to INCB086550 (150 mg/kg PO). Daily oral dosing of ALG-094295 (50 or 150 mg/kg) in humanized PD-L1 MC38 mice over 21 days resulted in tumor growth inhibition equivalent to twice-weekly administration of durvalumab (10 mg/kg IV), with tumor size correlating with increased $CD8^+$ T-cell infiltration. ALG-094295 demonstrated no in vitro liabilities for CYP450 inhibition or induction mediated drug-drug interactions, off target toxicity, cardiovascular safety, or genotoxicity. Preclinical *in vivo* PK data suggests once-daily oral dosing is feasible in humans.
Conclusion: ALG-094295 is a highly potent and orally bioavailable small molecule PD-1/PD-L1 inhibitor that promotes PD-L1 dimerization, internalization and degradation. ALG-094295 has the potential to overcome some limitations of antibody-based therapies due to potent PD-L1 blockade, oral delivery and novel mechanism of action.

#2819 Preclinical characterization of ALG-093940, a potent and orally bioavailable small molecule PD-1/PD-L1 inhibitor targeting PD-L1 dimerization, internalization and degradation.

Heleen Roose[1], Kristina Rekstyte-Matien[1], Sarah Stevens[2], Kusum Gupta[2], Sandra Chang[2], Nour Fayyad[1], Cheng Liu[2], Vladimir Serebryany[2], Lillian Adame[2], Kha Le[2], Antitsa Stoycheva[2], Dinah Misner[2], Lawrence M. Blatt[2], Leonid Beigelman[2], Sushmita Chanda[2], David B. Smith[2], Julian A. Symons[2], Andreas Jekle[2], **Tongfei Wu**[1]

[1]Aligos Belgium BV, Leuven, Belgium,[2]Aligos Therapeutics, Inc., South San Francisco, CA

Background: PD-1/PD-L1 antibody-based therapies have demonstrated tremendous success in the treatment of a variety of cancers. However, these antibody drugs are associated with several disadvantages, such as weak tumor penetration, immune-related adverse events and emergence of anti-drug antibodies. Here, we report the characterization of ALG-093940, a potent and orally bioavailable small molecule PD-1/PD-L1 inhibitor that binds to PD-L1 and promotes PD-L1 dimerization, internalization and degradation, offering an alternate mechanism of action with potential advantages over PD-1/PD-L1 antibody therapeutics.

Methods: The interaction of PD-1/PD-L1 and PD-L1 dimerization were assessed by AlphaLISA®. Inhibition of PD-1/PD-L1 in cell culture was measured using PD-1 expressing Jurkat NFAT luciferase T cells and CHO-hPD-L1 cells. *In vivo* PK/PD/Efficacy were assessed in a humanized-PD-L1 MC38 subcutaneous tumor mouse model. *In vitro* ADME tox profile used standard assays. Pharmacokinetic (PK) studies were performed in mice, rat, dog, and cynomolgus monkeys. Safety and tolerability were evaluated by oral administration in rats and cynomolgus monkeys.

Results: ALG-093940 inhibited PD-1/PD-L1 interaction with an IC_{50} of 0.048 nM and induced PD-L1 dimerization with an EC_{50} of 79 nM. ALG-093940 showed comparable T-cell activation potency to INCB086550 an orally dosed small molecule PD-L1 inhibitor which demonstrated clinical responses in a phase I study. Furthermore, treatment of CHO-hPD-L1 cells with ALG-093940 resulted in internalization and reduction of PD-L1 protein levels. In ex vivo human PBMC assays, ALG-093940 demonstrated PD-L1 target engagement, T cell activation and immune cell mediated tumor cell killing. In the *in vivo* humanized-PD-L1 MC38 mouse model, oral once daily dosing of ALG-093940 at 1.5, 15, 50 or 150 mg/kg demonstrated dose-dependent PD-L1 target engagement and tumor growth inhibition, where tumor size correlated with tumor-infiltration of $CD8^+$ T-cells. ALG-093940 demonstrated no in vitro liabilities for CYP-mediated drug-drug interactions, off target toxicity, cardiovascular safety, or genotoxicity. Preclinical *in vivo* PK data suggests once-daily oral dosing is feasible in humans. In addition, ALG-093940 was well tolerated when orally administered in rats for 14 days up the highest dose tested at 150 m/kg/day (up to the saturation of exposure), and in cynomolgus monkeys as a single dose up to 500 mg/kg and multiple doses for 3 days at 300 mg/kg/day.

Conclusions: ALG-093940, an orally available small molecule, is a potent PD-1/PD-L1 inhibitor targeting PD-L1 dimerization, internalization and degradation. ALG-093940 demonstrated excellent efficacy and safety, warranting further evaluation as a potential clinical candidate for the treatment of cancer.

#2820 Spatial mapping of PD1-PD-L2 interactions suggests an additional checkpoint axis in non-small cell lung cancer.

Anna Gorbunova[1], Amanda Lindberg[2], Lars Muhl[3], Ghazal Lessan Toussi[1], Hui Yu[2], Patrick Micke[2], **Carina Strell**[2]

[1]Department of Clinical Medicine, University of Bergen, Bergen, Norway,[2]Department of Immunology, Genetics and Pathology, Uppsala University, Uppsala, Sweden,[3]Department of Medicine, Huddinge, Karolinska Institutet, Stockholm, Sweden

Background: Immune checkpoint inhibitors have transformed non-small cell lung cancer (NSCLC) treatment, yet durable benefit remains limited. Current biomarkers, such as PD-L1 immunohistochemistry (IHC), measure protein abundance rather than functional PD1-ligand engagement and therefore provide limited predictive value. The second PD1 ligand, PD-L2, has often been ignored, but may influence immune regulation in the cellular context. Therefore, the activation of the PD1-PD-L1 axis is not sufficient to explain clinically relevant immune mechanisms.

Methods: We analyzed a tissue microarray of early-stage, surgically resected NSCLC (N=345), a cohort previously extensively immunoprofiled, including PD-L1 IHC and PD1-PD-L1 proximity ligation assay (PLA) [1]. We extended this work using fluorescent PLA (co-stained for CD3 and pan-cytokeratin) to visualize PD1-PD-L2 interactions across tumor, stromal, and T-cell compartments, alongside PD-L2 protein expression by IHC. Image analysis was performed in QuPath.

Results: In normal lung, PD-L2 was primarily expressed on macrophages and occasional granulocytes. Among tumors, squamous cell carcinomas (SqCC) showed higher PD-L2 expression than adenocarcinomas (AD) ($p=0.003$) and increased PD1-PD-L2 interactions ($p=0.047$), consistent with greater immune infiltration. Notably, amplification of 9p24.1, including the PD-L1 and PD-L2 locus, was also observed more frequent in SqCC. PD1-PD-L2 interactions displayed a distinct immune contexture from PD1-PD-L1. Within tumor cell compartment, PD1-PD-L2 correlated only weakly with $CD4^+$, $CD8^+$, $CD163^+$, $FoxP3^+$, PD1, and PD-L1, while PD1-PD-L1 showed strong associations with these immune populations, indicating partly distinct mechanisms of immune regulation. In the stroma, both ligands showed more similar immune-association patterns. Clinically, high PD1-PD-L1 interaction was generally associated with better prognosis. In contrast, PD1-PD-L2 interaction in SqCC showed only a trend toward better survival ($p=0.061$), whereas in AD it demonstrated a trend toward shorter survival ($p=0.092$). Also, compartment-specific PD1-PD-L2 interactions in the tumor stroma were associated with poor prognosis, particularly in SqCC with T cell-rich stroma ($p=0.033$).

Conclusion: Our findings suggest that PD1-PD-L2 represents a spatially and biologically distinct checkpoint axis in NSCLC, differing from PD1-PD-L1 in immune phenotypes and clinical associations. Including PD-L2-specific interaction analyses may enhance understanding of checkpoint biology and support refined patient stratification, particularly in SqCC, where PD-L2 co-amplification and upregulation appear to be more common.

References: [1] Lindberg A, Muhl L, Yu H, et al. *J Thorac Oncol.* 2025;20:625-640.

#2821 TRIB2 regulates immune evasion in antiandrogen-resistant and neuroendocrine prostate cancer.

Sharad K. Suthar[1], Azizur Rahman[2], Sang-Yoon Lee[1], Jitender Monga[3]

[1]Department of Neuroscience, Neuroscience Research Institute, Gachon University, Incheon, Korea, Republic of,[2]Department of Surgery, Louisville University School of Medicine, Louisville, KY,[3]Department of Urology, Henry Ford Health + Michigan State University Health Sciences, Detroit, MI

Background: Enzalutamide resistance remains a major clinical challenge in advanced prostate cancer. We previously identified Tribbles homolog 2 (TRIB2) as highly upregulated in enzalutamide-resistant prostate cancer (ERPC), including neuroendocrine (NE)-type resistant tumors, where it drives tumor cell survival, lineage plasticity, and therapeutic resistance. Targeting TRIB2 suppresses the growth of resistant cells, highlighting its critical role in disease progression. Immune checkpoint molecules, including B7-H3 (CD276) and PD-L1 (CD274), are also elevated in ERPC and NE prostate tumors and contribute to impaired T cell-mediated anti-tumor immunity. These convergent findings led us to hypothesize that TRIB2 promotes immune evasion in treatment-resistant prostate cancer and that its inhibition may enhance T-cell-mediated anti-tumor immunity.

Methods: Enzalutamide-resistant (C4-2B^{ENZR} and LNCaP^{ENZR}) and NE (NCI-H660) prostate cancer cell lines were used to investigate TRIB2-dependent immune regulation. TRIB2 expression was modulated using lentiviral shRNA knockdown, plasmid-mediated overexpression, or pharmacological inhibition using the selective TRIB2 inhibitor TBI-001. B7-H3 and PD-L1 expression was measured using western blot and flow cytometry. Modified cancer cells were co-cultured with activated human CD8$^+$ T-cells, and T-cell activation, cytokine production, and cytotoxicity were evaluated using standard immunological assays.

Results: Both TRIB2 knockdown and TBI-001 treatment markedly reduced B7-H3 and PD-L1 expression in ERPC and NE prostate cancer cells, whereas TRIB2 overexpression increased immune checkpoint levels. TRIB2 inhibition enhanced CD8$^+$ T-cell activation and cytokine secretion (IFN-γ and TNF-α), and improved T cell-mediated cytotoxicity against resistant cancer cells. Conversely, cells with elevated TRIB2 levels strongly suppressed T-cell activation and cytotoxicity. Immune checkpoint blockade partially restored T-cell function against TRIB2-high cells, with combined blockade showing enhanced effects in restoring anti-tumor immunity.

Conclusion: These findings demonstrate that TRIB2 facilitates immune evasion in enzalutamide-resistant and neuroendocrine prostate cancer by upregulating immune checkpoint proteins and suppressing anti-tumor T-cell activity. This represents a dual mechanism by which TRIB2 drives treatment-resistant prostate cancer progression through both tumor-intrinsic effects and modulation of the tumor microenvironment. Therapeutic targeting of the TRIB2-immune checkpoint axis represents a rational strategy to overcome enzalutamide resistance, offering the combined benefit of inhibiting tumor growth while restoring effective anti-tumor immunity.

#2822 Serial transcriptomic analyses capture the effects of neoadjuvant immune checkpoint inhibition in resectable gastroesophageal cancer.

Blair V. Landon[1], Christopher Cherry[1], Rachel Keogh[1], Jaime Wehr[1], Gavin Pereira[1], Noushin Niknafs[1], Richard J. Battafarano[2], Stephen C. Yang[2], Stephen Broderick[2], Jinny Ha[2], Russell K. Hales[3], K. Ranh Voong[3], Kristen A. Marrone[1], Chen Hu[1], Josephine L. Feliciano[1], Ali H. Zaidi[4], Ronan J. Kelly[5], Vincent K. Lam[1], Valsamo (Elsa) K. Anagnostou[1]

[1]The Sidney Kimmel Comprehensive Cancer Center, Johns Hopkins University School of Medicine, Baltimore, MD,[2]Department of Surgery, Johns Hopkins University School of Medicine, Baltimore, MD,[3]Department of Radiation Oncology, Johns Hopkins University School of Medicine, Baltimore, MD,[4]Allegheny Health Network Cancer Institute, Allegheny Health Network, Pittsburgh, PA,[5]The Charles A. Sammons Cancer Center, Baylor University Medical Center, Dallas, TX

Introduction: Immune checkpoint inhibition (ICI) is gaining momentum as peri-operative therapy for resectable cancers, however early changes in the tumor microenvironment (TME) during and after neoadjuvant ICI have yet to be characterized.
Methods: Bulk RNA sequencing (RNAseq) was performed on 71 serial tumors sampled at baseline, post 2 cycles of neoadjuvant ICI (post-ICI), and at the time of resection, in a cohort of 32 patients with resectable gastroesophageal cancer treated with neoadjuvant nivolumab or nivolumab + relatlimab, followed by concurrent ICI and chemoradiation (NCT03044613). We performed gene set enrichment analyses (GSEA) of RNAseq data, stratified by pathological response and clinical outcomes. Complete (pCR) and major pathological response (MPR) were defined as 0% and ≤10% residual tumor at resection.
Results: GSEA revealed an upregulation of interferon alpha, interferon gamma, antigen processing and presentation, and pro-inflammatory M1 macrophage gene sets post-ICI compared to baseline (FDR-adjusted $p < 0.006$). After chemoradiation, resected tumors showed depletion of DNA repair, chromosome maintenance, cell proliferation and cell cycle progression gene sets, reflective of the cytotoxic effect of therapy (FDR-adjusted $p < 10e-06$). Notably, in the nivolumab + relatlimab arm, induction of adaptive immune response gene sets and TNFa signaling through NF-kB was noted in resected specimens (FDR-adjusted $p < 10e-05$). Among patients who attained a pCR, there was an upregulation of interferon alpha, interferon gamma, and antigen processing and presentation gene sets post-ICI (FDR adjusted $p < 10e-06$). Similarly, in those who attained an MPR there was an upregulation of inflammatory response, interferon gamma, and B cell receptor gene sets (FDR adjusted $p < 10e-09$), while cellular metabolism and oxidative phosphorylation gene sets were down regulated post-ICI (FDR adjusted $p < 0.05$). Linking transcriptomic profiles with disease recurrence, we found a downregulation of inflammatory related gene sets post-ICI in recurrent cases (FDR adjusted $p < 0.0006$). Depletion of oxidative phosphorylation, metabolism, and chromatin regulation gene sets was noted in baseline tumors of patients that attained long overall survival (FDR adjusted $p < 10e-05$). In post-ICI tumors, there was an upregulation of inflammatory and adaptive response gene sets in patients with longer overall survival (FDR adjusted $p < 10e-08$), while the oxidative phosphorylation and metabolism gene sets remained suppressed (FDR adjusted $p < 0.003$).
Conclusions: Neoadjuvant ICI induces differential inflammatory and metabolism expression programs that are reflective of pathological responses, recurrence and survival, broadening our understanding of actionable mechanisms of ICI efficacy.

#2823 Single-cell RNA-seq reveals insights into the effects of immune checkpoint inhibitors.

Junting Lu, Jinghui Xiu, **Ce Zhong**, Wentao Li, Wei Yun, Tan Pang, Jingqi Huang

Pharmacology, Pharmaron, Beijing, China

Immune checkpoint inhibitors (ICIs) have demonstrated superior clinical efficacy, significantly prolonging patient survival across various cancers. However, the mechanisms by which ICIs modulate the immune system and memory function require continued exploration. Single-cell RNA sequencing (scRNA-seq) offers a powerful tool for oncology research and development. In this study, we performed scRNA-seq following treatment with an anti-PD-1 antibody in a murine colon adenocarcinoma model. Mice were inoculated with MC38 tumor cells, treated with ICIs, and subsequently re-challenged with the same tumor cells after tumor regression. Tumor-infiltrating lymphocytes (TILs) and peripheral blood mononuclear cells (PBMCs) were isolated and analyzed using scRNA-seq alongside flow cytometry. Single-cell suspensions were processed using the 10x Genomics Chromium platform. Single-cell libraries were constructed, sequenced, and pre-processed, including demultiplexing and mapping to the reference genome. Filtered data underwent dimensionality reduction and clustering, and cells were annotated into distinct populations based on classical markers. Within the tumor microenvironment (TME), we observed notable activation of $CD4^+$ and $CD8^+$ T cells, a reduction in immunosuppressive $CD4^+$ Treg cells, and an increase in Th1 cells. Among $CD8^+$ T cells, cytotoxic effector (Teff) and memory (Tem) subsets were elevated, indicating effective T-cell activation and enhanced anti-tumor immunity. Similarly, PBMC analysis revealed increased naive T cells and Th1 cells within the $CD4^+$ population, while $CD8^+$ T cells exhibited expansion of Tem subsets with a slight increase in Teff cells. Overall, our findings demonstrate that checkpoint blockade promotes durable anti-tumor responses through expansion and differentiation of memory T cells and enhanced immune cell infiltration at both genetic and peripheral levels. Anti-PD-1 therapy directly potentiated the tumor-killing capacity of TILs, promoting a shift toward subtypes favorable to tumor clearance. Concurrently, treatment reprogrammed T-cell subsets in PBMCs, improving differentiation potential and thereby strengthening effective anti-tumor immune responses.

#2824 Intragenic rearrangement burden: A novel biomarker to predict immune checkpoint blockade response in TMB-low cancers.

Akshat Gupta[1], Selena Xiao[1], Hillary Wang[1], Rohit Bhargava[1], Adrian V. Lee[2], Adam M. Brufsky[1], **Xiaosong Wang**[1]

[1]Department of Pathology, University of Pittsburgh, Pittsburgh, PA,[2]University of Pittsburgh, Pittsburgh, PA

Background: Immune checkpoint blockade (ICB) efficacy is limited, and biomarkers like Tumor Mutation Burden (TMB) fail in TMB-low cancers (e.g., breast, ovarian) despite many being immunologically "hot". This paradox suggests an uncharacterized neoantigen source. We investigated intragenic rearrangements (IGRs)—cryptic structural mutations—as this source, hypothesizing IGR burden is a superior biomarker for T-cell inflammation and ICB benefit in these tumors.
Methods: We performed a pan-cancer WGS analysis (ICGC, n=1,033) correlating IGR burden with T-inflamed signatures. We used multivariate regression to compare IGRs against TMB, indels, fusions, and SCNA on immune infiltration, validating in TNBC (n=513), HGSC (n=33), and ESAD cohorts. Predictive power for ICB response was assessed by Kaplan-Meier, Cox regression, and ROC analysis in ESAD (durvalumab), HGSC (NACT + pembrolizumab), and mTNBC trials. We also analyzed a breast cancer immunopeptidomic dataset (n=26) to correlate IGR burden with presented neopeptides.
Results: Pan-cancer analysis showed IGR-high and TMB-high are distinct T-inflamed subsets. In TMB-low cancers, IGR burden was the most significant covariate for T-cell inflammation (p=0.0098), not TMB (p=0.224). In TNBC, IGR burden was the *only* significant genomic marker for the T-inflamed signature (p=0.008). Mechanistically, IGR burden strongly correlated with *presented* IGR-derived neopeptides (Pearson R=0.54) and showed evidence of immunoediting.In clinical trials, IGR burden predicted ICB benefit. In HGSC (NACT+Pembro), high IGR burden predicted superior OS (AUROC=0.80; 5-yr OS ~85% vs ~30%, HR=0.17, p=0.009), outperforming PD-L1 (HR=0.77, p=0.65). In ESAD (durvalumab), IGR burden (AUROC=0.74) also outperformed PD-L1 (AUROC=0.46). Critically, IGR burden was predictive, not just prognostic. High IGR burden predicted improved OS in mTNBC with chemo-IO (HR=0.18, p=0.074) but *poorer* OS with chemo-only (HR=4.29, p=0.032).
Conclusions: IGR burden is a powerful predictive biomarker for ICB response in TMB-low malignancies where TMB and PD-L1 fail. Supported by immunopeptidomic evidence of neoantigen presentation, it outperforms existing markers, distinguishes true ICB benefit from prognosis, and resolves the "hot" TMB-low tumor paradox. IGR burden represents a critical new tool for patient selection.

: Immune Mechanisms Invoked by Other Therapies and Exposures
Poster Session

#2828 Paclitaxel induces colocalization of CXCL9$^+$ tumor-associated macrophages and CD8$^+$ T cells to potentiate antitumor immunity in head and neck squamous cell carcinoma.

Minsu Kwon[1], Jeong Heon Kim[1], Jisu Hong[1], Seo-Won Choi[1], Jung Min Kim[1], Hyo Jung Cho[2], Myungchan Park[3], JI-HYUN SEO[4], Jung Je Park[4]

[1]Otorhinolaryngology Head and Neck Surgery, Asan Medical Center (AMC), Seoul, Korea, Republic of,[2]Gastroenterology, Ajou University School of Medicine, Suwon, Korea, Republic of,[3]Urology, Haeundae Paik Hospital, Inje University College of Medicine, Pusan, Korea, Republic of,[4]Institute of Medical Science, Gyeongsang National University College of Medicine, Jinju, Korea, Republic of

Background: Paclitaxel is a key chemotherapeutic agent for head and neck squamous cell carcinoma (HNSCC). Recent studies have suggested the role of paclitaxel in immune responses, particularly relevant to tumor-associated macrophages (TAMs). This study explores the immunomodulatory role of paclitaxel in the tumor microenvironment (TME), focusing on its interaction with TAMs in HNSCC.
Methods: In vitro and in vivo studies were conducted on murine samples and human samples from our tertiary referral center. The in vitro experiment involved murine bone marrow-derived macrophages (BMDMs) to evaluate phagocytic functions and the expression of MHC-related genes and proteins. Our in vivo study aimed to discriminate the spatial characteristics of SPP1+/CXCL9+ TAMs and their interaction with CD8+ T cells, especially under exposure to paclitaxel, using mouse oral carcinoma (MOC) and HNSCC samples.
Results: Paclitaxel enhanced macrophage phagocytosis and upregulated antigen processing genes. In the murine HNSCC model, paclitaxel combined with anti-PD-1 significantly suppressed tumor growth, whereas either treatment alone was ineffective. This was associated with the redistribution of CXCL9+ TAMs into the tumor core. Consistently, human HNSCC samples demonstrated that paclitaxel-based neoadjuvant chemotherapy (NAC) was linked to improved survival and increased infiltration of CXCL9+ TAMs and CD8+ T cells into the tumor core, indicating a shift from an "immune-excluded" to an "inflamed" microenvironment.
Conclusion: Paclitaxel upregulates the phagocytic and antigen-presenting function of TAMs while spatially redistributing them toward the tumor core and subsequently inducing CD8+ T cell infiltration. Such features suggest that Paclitaxel may reprogram an immune-deserted TME to an anti-tumoral condition, ultimately contributing to immunotherapy responsiveness.

#2829 Afatinib exerts an inhibitory effect on T cell-mediated cytotoxicity.

Masaru Yokomura[1], Seiji Nagano[2], Hiroshi Kawamoto[2], Takahiro Asakage[3], Ryohei Katayama[1]

[1]Division of Experimental Chemotherapy, Cancer Chemotherapy Center, Japanese Foundation for Cancer Research, Tokyo, Japan,[2]Institute for Life and Medical Sciences, Kyoto University, Kyoto, Japan,[3]Department of Head and Neck Surgery, Institute of Science Tokyo, Tokyo, Japan

Immune checkpoint blockade (ICB) has become a cornerstone of cancer therapy by enhancing antitumor immunity, and combinations of targeted therapies with ICB are widely evaluated across malignancies. However, the biological determinants that predict synergistic or antagonistic effects between targeted agents and ICB remain poorly understood. To identify agents that modulate T-cell effector function, we performed an *in vitro* inhibitor library screening using WT1-specific cytotoxic T cells (CTLs) generated from induced pluripotent stem cells (iPSCs) (Maeda T et al, *Cancer Res*. 2016). WT1-specific CTLs were co-cultured with HLA class I matched cancer cells in the presence of exogenous WT1 peptide. In this screening, immunosuppressive agents such as JAK inhibitors (ruxolitinib and tofacitinib) and src inhibitor dasatinib markedly suppressed T cell-mediated killing as expected. We newly identified afatinib, a second-generation EGFR tyrosine kinase inhibitor, as a potent suppressor of T-cell effector function. Afatinib significantly reduced interferon-γ (IFN-γ) secretion and T-cell activation. Notably, this IFN-γ reduction was independent of T-cell proliferation. RNA-seq analysis revealed that afatinib downregulated the T-cell receptor (TCR) pathway signature. RT-qPCR demonstrated a dose-dependent suppression of *IFNG* mRNA expression in afatinib-treated T cells. Furthermore, afatinib impaired tumor rejection in an immunological memory mouse model which mice had been previously cured with anti-PD-L1 therapy, demonstrating functional suppression of T cell mediated antitumor immunity. Collectively, these findings identify afatinib as a negative regulator of T cell effector function and raise the possibility that EGFR-TKI-induced immunosuppression in T cells may contribute to the limited clinical efficacy of EGFR-TKI plus ICI combinations observed in EGFR-mutant NSCLC. Our screen platform provides a useful framework for predicting drug-ICI interactions and guiding rational combination strategies.

#2830 Immunomodulatory response in Dato-DXd-treated non-small cell lung cancer patient-derived organotypic tumor spheroids (pDOTS).

Satoru Yasuda[1], **Patrick Hall Lizotte**[2], Elena Ivanova[2], Zhaorong Li[2], Yui Tanaka[1], Daisuke Okajima[3], Minh Ha[2], David A. Barbie[2], Cloud P. Paweletz[2]

[1]Daiichi Sankyo Inc, Baskin Ridge, NJ,[2]Dana-Farber Cancer Institute, Boston, MA,[3]Daiichi Sankyo Co. Ltd., Tokyo, Japan

Background: Datopotamab deruxtecan (Dato-DXd, DATROWAY) is a TROP2-directed ADC with a highly potent Topo I inhibitor payload, which is approved for HR+ breast cancer and EGFR-mutated NSCLC in the US and is being investigated in several registrational phase 3 trials, including 1L NSCLC, 2L+ TNBC, and urothelial carcinoma. While the cytotoxic payload-induced apoptotic effect of DXd is well investigated, its immunomodulatory effect is less characterized. Here we analyze tumor cell-intrinsic immunological response to Dato-DXd using short-term microfluidic culture of patient-derived organotypic tumor spheroids (pDOTS) in non-small cell lung cancer (NSCLC) samples.

Methods: Four surgical NSCLC cases collected from Brigham and Women's Hospital under an IRB-approved protocol were studied. TROP2 antigen density on EpCAM+ cells was assessed by quantitative flow cytometry and immunofluorescence; baseline immune profile was assessed by flow. *Ex vivo* response to vehicle, unconjugated Datopotamab, IgG-DXd, and Dato-DXd were assessed by live/dead imaging endpoint analysis. Modulation of tumor cell immunogenicity at 24hr and 72hr was analyzed by 10x single cell RNA sequencing (scRNAseq).

Results: Four NSCLC explants with high tumor cell content and high TROP2 expression (3+ by IF) were studied. Response to drug treatment was measured by change in raw live cell area compared to control samples. Unexpectedly, EpCAM+TROP2+ tumor cells from all four samples at both timepoints exhibited negative pathway enrichment scores for Hallmark TNF-α Signaling via NFκB and Inflammatory Response when comparing Dato-DXd to control-treated. Individual gene level analysis revealed significant downregulation of myeloid-associated cytokines (IL-23a, IL-6) and chemokines (CSF1/2, CXCL1/2/3, CCL2, CCL20, IL-8), indicating possible reduced recruitment of myeloid-derived suppressor cells (MDSCs) and tumor-associated macrophages (TAMs). Investigation of tumor cell immunogenic cell death in response to Dato-DXd treatment revealed inconsistent induction of pro-inflammatory signaling.

Conclusions: Our results indicate clear and consistent immunomodulation of NSCLC tumor cells when treated with Dato-DXd, principally downregulation of myeloid-associated inflammation. Statistically significant differential expressions of CSF1/2, CXCL1/2/3, and IL-8 (CXCL8) chemokines reveal a potentially unappreciated mechanism underlying ADC therapeutic efficacy: reduced recruitment of pro-tumoral myeloid cells by tumor cells.

#2831 RAS(ON) inhibition in both cancer and immune cells by daraxonrasib drives anti-tumor immunity.

Nataliya Tovbis Shifrin[1], Mariela Moreno Ayala[1], Cristina Blaj[1], Kevin Chen[2], Felix Mbuga[1], Joaquin Pechuan Jorge[1], Rashi Raghulan[1], Rich Liang[1], Linh Tran[1], Enrico Payson[1], Alice Kumamoto[1], Alexander McNamara[1], Marie Josette Catherine Menard[1], Michael Weiss[1], Lillian Seu[1], Elsa Quintana[1]

[1]Revolution Medicines, Redwood City, CA,[2]Medicine, UCLA, Los Angeles, CA

Daraxonrasib (RMC-6236) is an orally bioavailable, RAS(ON) multi-selective, tri-complex inhibitor of oncogenic mutant and wild-type variants of N, H and KRAS, demonstrating broad activity across RAS-mutant cancers. Preclinical studies have shown that daraxonrasib not only suppresses tumor cell proliferation but also promotes a striking remodeling of the tumor microenvironment (TME), characterized by depletion of immunosuppressive myeloid cells (including M2 macrophages) and increased infiltration of T cells. Collectively these changes sensitize tumors to immune checkpoint blockade. We have reported that the combination of daraxonrasib plus pembrolizumab, with or without chemotherapy, demonstrated encouraging preliminary antitumor activity, and was generally well tolerated, in patients with 1L RAS mutant NSCLC.Given that RAS functions as a key immunosuppressive oncogene, a primary driver for the antitumor immune effects of daraxonrasib is tumor-cell intrinsic inhibition of oncogenic RAS. However, it is well established that the RAS-MAPK signaling pathway regulates critical immune processes, including maintenance of M2 macrophages and T cell receptor signaling. Here, we demonstrate that daraxonrasib has direct effects on immune cell populations and that inhibition of wild-type RAS in these cells contributes to antitumor immunity, highlighting a dual mechanism of action for this RAS(ON) multi-selective inhibitor.To determine the tumor-cell independent contributions of RAS (ON) inhibition to antitumor immunity in vivo, we used a syngeneic tumor model intrinsically resistant to daraxonrasib. Daraxonrasib treatment was initiated at the time of tumor implant. In this model, although daraxonrasib alone did not inhibit cell proliferation in vitro or affect tumor growth in vivo, it promoted favorable TME remodeling, including macrophages depletion and increased T cell infiltration. Importantly, daraxonrasib treatment – when initiated at the time of implant – sensitized these tumors to subsequent checkpoint inhibitor therapy. Together, these and earlier preclinical findings reveal that daraxonrasib acts through coordinated RAS(ON) inhibition in both tumor and immune compartments. The impact of RAS(ON) inhibition in the immune compartment includes depletion of M2 macrophages and prevention of T cell exhaustion (as suggested by in-vitro data), leading to an immune-permissive TME that enhances responsiveness to checkpoint blockade. Collectively these preclinical data support the ongoing clinical evaluation of this combination in RAS-driven cancers.

#2832 Evaluation of Natural Killer cells' contribution to Enhertu toxicity in breast cancer patient derived xenograft-derived 3D models.

Chou Fu-Ju[1], Annamaria Rapisarda[1], Veena Jagannathan[1], Marianna Zipeto[1], Michael Ritchie[1], Markus Hippich[1], Daniel Ciznadija[2], Brandon Walling[1], Stefano Cairo[3], Mara Gilardi[1], BanuPriya Sridharan[4]

[1]Champions Oncology (Rockville, MD), Rockville, MD,[2]Champions Oncology, Hackensack, NJ,[3]Champions Oncology, Inc. (Hackensack, NJ), Rockville, MD,[4]Champions Oncology, Inc. (Hackensack, NJ), Hackensack, NJ

Evaluating the impact of natural killer (NK) cells on antibody-drug conjugate (ADC) activity is essential for understanding and optimizing treatment efficacy. NK cells play a critical role in mediating antibody-dependent cellular cytotoxicity (ADCC), one of the key mechanisms through which ADCs exert their therapeutic effects. By recognizing and eliminating tumor cells via ADC Fc receptor engagement, NK cells can enhance the overall cytotoxic response and influence treatment outcomes. Assessing this interaction provides valuable insights into resistance mechanisms, guides the design of next-generation ADCs with improved immune engagement, and helps identify patient populations most likely to benefit from such therapies.

The primary objective of this study was to evaluate the contribution of NK cells to the cytotoxic activity and potential toxicity of trastuzumab deruxtecan (Enhertu) in breast cancer patient-derived xenograft organoid cultures (TumorGraft3D). A luciferase-tagged TumorGraft3D co-culture system incorporating a BioGlo luminescence endpoint was employed to enable real-time assessment of tumor cell viability and treatment response in the presence or absence of NK cells. A 3D co-culture system was established using breast cancer models that were transduced with luciferase at a multiplicity of infection (MOI) of 10 to allow quantifiable luminescence-based viability measurements. Following successful transduction, NK cells were added at predetermined ratios to the organoid cultures. Imaging and luminescence measurements were conducted at multiple time points to evaluate dynamic changes in cell viability and treatment effects. TumorGraft3D cells were seeded and transduced with luciferase. After confirming signal stability, NK cells, Enhertu or Trastuzumab were introduced into the culture system. Viability and imaging analyses were performed on Day 1 and Day 4 post-seeding, capturing both early and delayed treatment effects. Brightfield microscopy was used to visualize morphological changes, and BioGlo luminescence readings quantified cell survival and treatment response.

In the CTG-0708 model of HER2+ invasive ductal carcinoma, the addition of NK cells resulted in a slight increase in Enhertu-mediated cytotoxicity, suggesting a modest but measurable enhancement of ADC activity in the presence of NK cells. Trastuzumab efficacy demonstrated a clear correlation with antibody concentration, indicating dose-dependent ADCC activity. In contrast, Enhertu toxicity appeared independent of antibody concentration, likely due to the previously shown inefficient release of payload in vitro.

These findings suggest a potential immunomodulatory effect of NK cells on ADC efficacy, and support the use of this platform to more accurately model ADC mechanisms of action.

#2833 Amivantamab restores antitumor immunity in non-small cell lung cancer through EGFR/MET expression-dependent mechanisms.

Takamasa Ishino[1], Ryo Yoshichika[1], Fumiaki Mukohara[2], Ken Suzawa[2], Shinichi Toyooka[3], Yosuke Togashi[1]

[1]Department of Tumor Microenvironment, Okayama University, Okayama, Japan,[2]Department of General Thoracic Surgery and Breast and Endocrinological Surgery, Okayama University, Okayama, Japan,[3]Department of General Thoracic Surgery and Breast and Endocrinological Surgery, Dentistry and Pharma, Okayama University, Okayama, Japan

Introduction: Epidermal growth factor receptor (EGFR) mutations are one of the most common oncogenic drivers in non–small cell lung cancer (NSCLC). Although EGFR tyrosine kinase inhibitors (EGFR-TKIs) have demonstrated clinical benefits, acquired resistance still limits the long-term efficacy, with activation of MNNG HOS Transforming (MET) signaling serving as a representative bypass mechanism. Recently, amivantamab, a bispecific antibody against EGFR and MET, has shown clinical efficacy. However, its immunological role in human tumors has not been directly investigated.

Methods: We analyzed 40 surgically resected fresh NSCLC samples to evaluate EGFR/MET expression and their correlation with immune suppression. Tumor-infiltrating lymphocytes (TILs) were evaluated by flow cytometry and immunohistochemistry. To assess the immunomodulatory effects of amivantamab, tumor digests including viable TILs were cultured *ex vivo* under conditions with or without amivantamab.

Results: *EGFR* mutations and elevated EGFR protein expression showed a tendency for reduced infiltration of $CD8^+$ T cells and dendritic cells (DCs). *Ex vivo* exposure to amivantamab enhanced $CD8^+$ T-cell effector functions and DC maturation in TILs, particularly in tumors with high EGFR/MET expression, independent of *EGFR* mutation status.

Conclusion: This study provides the first direct evidence using fresh human NSCLC samples that amivantamab can restore antitumor immunity through $CD8^+$ T-cell activation and DC maturation. Expression levels of EGFR and MET may serve as predictive biomarkers for amivantamab monotherapy as well as for amivantamab-based combination immunotherapies.

#2834 Identification of CXCL10-CXCR3 axes as mediators of radioresistance in diffuse midline glioma (DMG).

Mostafa M. H. Ibrahim[1], Niloofar Khairkhah[1], Carl Koschmann[2], Yue Zhao[3], Stefanie Galban[1]

[1]Department of Radiology, University of Michigan Medical School, Ann Arbor, MI,[2]Department of Pediatrics, University of Michigan Health System, Ann Arbor, MI,[3]Gilbert S. Omenn Department of Computational Medicine and Bioinformatics, University of Michigan Medical School, Ann Arbor, MI

Diffuse Midline Gliomas (DMGs) are aggressive, universally fatal brain tumors with a 100% recurrence rate driven by therapeutic resistance. Many molecular therapies target epigenetically driven gene expression changes in DMG H3K27M-altered tumors, but whether they target methylation, acetylation, or downstream vulnerabilities, these treatments have failed to prevent recurrence. Since no recent therapies have prompted long-term responses, radiation remains the standard of care; however, radiotherapy often suppresses an immune response, and when tumors recur, an immune suppressive and tumor promoting microenvironment provides a niche for tumor cells to regrow uncontrollably.

In preliminary studies utilizing single-cell RNA sequencing (scRNA-seq) in a murine model of DMG, we uncovered a complex cellular tumor microenvironment that is modulated upon radiotherapy. In fact, radiation therapy significantly increased the expression of pro-tumorigenic genes in both PDGFRA+ DMG cells (e.g., Tgfa, IL133, Fgf2, Pdgfa) and tumor associated-microglial cells (e.g., IL4i1, IL33, Fgf2, Tgfbr1), suggesting a coordinated pro-tumorigenic response. Furthermore, CXCL10 dramatically increased in tumor cells (DMG) in response to radiotherapy, whereas CXCR3 was found to be predominantly expressed in T cells in these tumors. Interestingly, CXCL10 has previously been shown to be associated with macrophage infiltration and cell proliferation, and expression of the chemokine receptor/ligand pair CXCR3/CXCL10 plays an important role in the proliferation of glioma cells (Pessina et al. *Oncoimmunology* 2015). These findings suggest radiotherapy-induced immunosuppression occurs through the CXCL10-CXCR3 axis, and thus, in ongoing studies, we are evaluating whether blockade of CXCL10-CRCR3 axes can prevent radioresistance. Lastly, as previously hypothesized, we detected an increase in stemness gene expression in radiated tumors, which was prevented when mice were treated with a pan-ALDH inhibitor (CVT-10216).

In summary, we have characterized the stromal and immune tumor microenvironment in untreated and radiated DMG and have identified potential targets that may inform future therapeutic strategies to prevent recurrence.

#2835 Leveraging radiation inducible surface protein targets for tumor microenvironment reprogramming.

Courtney M. Tamaki[1], Maxwell Foisey[2], Charlotte Chen[1], Nam Woo Cho[1]

[1]Radiation Oncology, UCSF - University of California San Francisco, San Francisco, CA,[2]Microbiology & Immunology, UCSF - University of California San Francisco, San Francisco, CA

Radiation Therapy (RT) is one of the most common treatments for patients with solid tumors, administered to over 50% of patients. Failure of tumor control following RT, however, is a significant clinical challenge. In the present study, we identify a suite of novel proteins as radiation-inducible surface proteins across a variety of cancers, including breast and non-small cell lung cancers. Specific proteins characterized act as enzymes which deplete metabolic substrates, thus altering both the tumor microenvironment (TME) as well as cell intrinsic function. Using cell-surface capture mass spectrometry, bulk-RNA sequencing, fluorescence spectrometry, and cytometry by time of flight (CyTOF), we comprehensively characterize our target upregulation following RT, both as a surface protein and the enzymatic consequence of perturbation. To increase induction of surface expression, we evaluated combinatorial strategies of RT with small molecules and other soluble factors. These combinations significantly increased expression *in vitro* in both mouse and human non-small cell lung cancer cell lines. Additionally, *in vivo*, tumor-targeted RT/combination treatment significantly upregulated our protein of interest on tumor cells, as well as on a subset of macrophages and fibroblasts. Functional investigation suggests these macrophages and fibroblasts may have an immunosuppressive role within the TME. Leveraging these findings, we developed directed therapies, including antibody-drug conjugates (ADCs) and antigen-specific chimeric antigen receptor (CAR) T cells, to ablate both tumor and immunosuppressive cells with increased levels of the target, providing a more conducive combinatorial therapy to control tumors. In conclusion, we have identified and characterized a radiation-inducible therapeutic target, providing framework for reprogramming the TME and improving treatment efficacy.

#2836 Tumor-derived extracellular vesicles as key messengers of radiotherapy-induced immunogenic cell death to sensitize small cell lung cancer to immunotherapy.

Shanghai Liu[1], Kai Kang[1], Zhuoran Yao[1], Ren Luo[1], Hui Wang[1], Zichong Peng[1], Shuangsi Liao[1], Yilan Zeng[1], Ruizhan Tong[1], Jiaming Zeng[2], Weidi Xiao[2], Jianxin Xue[1], Linglu Yi[1], Chu Wang[2], You Lu[1]

[1]Division of Thoracic Tumor Multimodality Treatment, Cancer Center, West China Hospital, Sichuan University, Chengdu, China,[2]Beijing National Laboratory for Molecular Sciences, Key Laboratory of Bioorganic Chemistry and Molecular Engineering of Ministry of Education, College of Chemistry and Molecular Engineering, Peking University, Beijing, China

Background: We previously showed low-dose radiotherapy (LDRT) exerts immunostimulatory effects in both preclinical models and clinical settings for SCLC, yet its immunogenic cell death (ICD) mechanisms remain unclear. As extracellular vesicles (EVs) mediate intercellular stress signaling, we hypothesized that tumor-derived EVs play a critical role in orchestrating immunogenic signaling in the initial stages of radiotherapy response. This study tracks ICD signals from tumor to DCs via EV monitoring and elucidate their function spectrum throughout this process.

Methods: Plasma EVs from prospective extensive-stage-SCLC cohorts treated with LDRT plus chemo-immunotherapy and PDX/PDO-derived EVs post-irradiation underwent proteomic profiling. Post-irradiation cellular components - cell pellets, debris, and EVs - were used to activate DC-T axis respectively. EV inhibition and live-cell imaging confirmed radiation-induced EVs (RT-EVs) activate the axis versus non-irradiated EVs (NT-EVs). SCLC CDX and PDX models were established, and corresponding homogeneous PBMCs were collected for in vivo EV function evaluation.An ICD tracking system based on stable isotope labeling traced EV-mediated immunogenic transfer from irradiated SCLC and MC-38ova cells to DCs.

Results: Proteomic analysis identified LDRT-EVs were specifically enriched in DC activation pathways and exhibited stronger ICD hallmarks, termed “Spark-EVs”. Spark-EVs significantly enhanced DC and T cell activation more than other cellular components, with efficacy comparable to whole-cell lysates. Spark-EVs potently activated the DC-T cell axis compared to NT-EVs, whereas the EV release inhibitor reversed this effect to control levels. Live-cell imaging confirmed nearly threefold greater DC uptake of Spark-EVs than NT-EVs ($p < 0.0001$). In CDX models, Spark-EV-pulsed DCs + anti-PD-1 enhanced tumor suppression versus NT-EVs + anti-PD-1 or anti-PD-1 alone. Patient T cells primed with Spark-EV-pulsed hDCs showed enhanced stemness and cytotoxicity in vitro. Adoptive transfer of these T cells into PDX models yielded superior tumor control. EV-labeled tracing showed that Spark-EVs were enriched with increased OVA antigens, DAMPs (e.g. HSPD1), which deliver into DCs then. Additionally, Integrated multi-level proteomics and prognostic analysis identified Junction plakoglobin (JUP) as a potential key transmitter of ICD signal.

Conclusion: Using EV-based tracing, we visualized how LDRT triggers tumor cells to generate Spark-EVs, which deliver enhanced immunogenic signals to DCs. Furthermore, we delineate that radiation-responsive EV-borne proteins (e.g. JUP, HSPD1) that mediate the release, transmission, and effector functions of LDRT-induced immunogenic signaling. These findings establish Spark-EVs as key, targetable messengers of LDRT-driven ICD.

#2837 Enhanced tumor immune cell infiltration and antigen presentation after carbon ion radiotherapy correlates with curative outcomes.

Matilde Recusani[1], Sarah Meister[1], Federica Ciamarone[1], Julian Schlegel[1], Ralph Sinn[2], Carmen Klein[3], Jennifer Furkel[1], Aoife Gahlawat[1], Christel Herold-Mende[4], Max Knoll[1], Michael Breckwoldt[2], Dirk Jaeger[5], Juergen Debus[6], Amir Abdollahi[1]

[1]Translational Molecular Radiooncology, DKFZ, Heidelberg, Germany,[2]Neuroradiology Department, University Hospital Heidelberg, Heidelberg, Germany,[3]Translational Radiation Oncology, NCT, Heidelberg, Germany,[4]Neurosurgical Research, University Hospital Heidelberg, Heidelberg, Germany,[5]Dir., Dept. of Medical Onc., Heidelberg University Hospital (UKHD), Heidelberg, Germany,[6]Heidelberg Ion-Beam Therapy Center (HIT), Heidelberg, Germany

Limited immune cell infiltration and deficient presentation of neoepitopes and tumor-associated antigens (TAA) via major histocompatibility complex class I (MHC-I) represent key barriers to effective immunotherapy. This study investigates whether particle radiotherapy (RT) can modulate tumor antigen presentation and T cell recruitment. By evaluating protons, helium, carbon, and oxygen ions, we assessed how distinct biophysical properties—particularly ionization density (linear energy transfer, LET)—influence immune priming. To this end, we evaluated the induction of MHC-I expression in a comprehensive panel of human tumor cell lines (CaSki, SK-MEL-37, A549, PC3, LNCaP), as well as in B16-F1 melanoma, GL261 and 005 genetically engineered glioblastoma models in syngeneic C57BL/6 mouse. Flow cytometry revealed MHC-I upregulation is time-, dose-, and LET-dependent. The role of the cGAS-STING pathway was confirmed using isogenic STING-KO B16 cells, which exhibited reduced RT-induced MHC-I expression. In vivo, high-LET carbon ion irradiation (CIRT) resulted in enhanced tumor MHC-I expression and increased intratumoral infiltration of $CD3^+$ and CD8+ T cells. Adoptive transfer of Superparamagnetic Iron Oxide Nanoparticles (“SPION”)-labeled T cells, followed by high-field MRI tracing, confirmed enhanced intratumoral influx after fractionated (5 × 3 Gy) and single ultra-High Dose Rate (uHDR, FLASH) CIRT. Further characterization of tumor-infiltrating lymphocyte (TIL) composition and immunological memory was performed using single-cell RNA sequencing and mass cytometry (CyTOF). Collectively,
these data indicate that modulating RT quality can improve neoantigen expression, MHC-I presentation, and T cell recruitment, highlighting the potential of particle radiotherapy to reprogram the tumor immune microenvironment.

#2839 Inhibiting both Class IIb HDACs is superior to isoform-specific inhibition for improved antitumor immune response..

Satish Kumar Reddy Noonepalle[1], Manasa Suresh[1], Xintang Li[1], Sonia Sebaoui[1], Bryan Weselman[1], Marie Durr[1], Nithya Gajendran[1], Chiara Ripamonti[2], Gianluca Fossati[2], Christian Steinkuhler[2], Alejandro Villagra[1]

[1]Georgetown Lombardi Comprehensive Cancer Ctr., Washington DC, DC,[2]Italfarmaco S.p.A., Cinisello Balsamo, Italy

Class IIb histone deacetylases, including HDAC6 and HDAC10, have garnered significant interest due to their non-canonical structure, cytoplasmic localization, and their role in immunomodulatory antitumor responses. It is reported that HDAC6 inhibitors, Tubastatin A and Nexturastat A (NextA), inhibit both HDAC6 and HDAC10 isoforms with varying selectivity. In addition, HDAC6 genetic knockout models failed to recapitulate the effects observed with highly selective and isoform-specific HDAC6is, suggesting potential off-target effects. Therefore, it is crucial to discriminate the effect of inhibiting specific isoforms of Class IIb HDACs. We previously reported that dual HDAC6/10 inhibitors significantly suppressed tumor-promoting M2-like macrophage (Mφ) function and phenotype in vitro and in vivo. In this study, we report novel HDAC inhibitors, ITF3756 and ITF6475, referred to as ITF3 and ITF6, respectively, and their effects on macrophage function and phenotype using murine bone marrow-derived Mφs (BMDMs), murine RAW264.7 cells, human PBMC-isolated monocyte-derived Mφs, and Thp1 monocyte-derived human Mφs. We performed several assays, including cytotoxicity, HDAC inhibition profiling, gene expression analysis by qPCR, flow cytometry analysis of phenotypic markers, tumor cell phagocytosis, antigen cross-presentation, and T-cell activation assays to comprehensively characterize the effect of dual HDAC6/10 inhibition vs HDAC6-specific inhibition. As reference molecules, we also used NextA (dual HDAC6/10) and CPD11352 (CPD) (HDAC6-specific) inhibitors to compare the effect on Mφs. Finally, we demonstrated the therapeutic effect of ITF3 in combination with radiation therapy to suppress prostate cancer in an immunocompetent Myc-Cap murine model. The data indicated that both cytotoxicity and HDAC inhibitory activity of ITF3 were similar to NextA, and ITF6 was similar to CPD on both murine and human Mφs. Gene expression analysis of phenotypic markers by qPCR and protein levels by immunoblot indicated that ITF3 significantly suppressed M2-like Mφs, whereas ITF6 did not. In contrast, neither ITF3 nor ITF6 affected M1 Mφs. Furthermore, murine BMDM-derived M1-like Mφs treated with ITF3 and ITF6 significantly increased tumor cell phagocytosis, SIINFEKL antigen cross-presentation, and SIINFEKL-mediated activation of OT-1 CD8 T-cells. These results mirrored the effects observed in murine and human macrophages treated with NextA and CPD. Finally, a combination of ITF3 with radiation therapy significantly suppressed Myc-Cap prostate cancer tumor growth while inducing an immune-stimulatory effect, as evidenced by increased infiltration of antitumor M1 Mφs and CD8 effector T cells. Overall, we demonstrated that dual HDAC6/10 inhibition is superior to HDAC6 inhibition alone for instigating an immunomodulatory antitumor immune response in prostate cancer therapy.

#2840 Modulation of the tumor microenvironment using 5-fluorouracil to increase T cell infiltration in breast cancer bone metastases.

Galilea Chora Hernandez[1], Paloma Almeida Luna[1], Kiomy Esparza Palomares[2], Erasmo Perez Mendez[1], Samanta Jimenez[3], Ricardo Gonzalez Sanchez[3], Candice Internicola[4], Felipe Olvera[5], **Pierrick G.J. Fournier**[3]

[1]Posgrado en Ciencias de la Vida, Centro de Investigacion Cientifica y de Educacion Superior de Ensenada, Ensenada, Mexico,[2]Centro de Nanociencias y Nanotecnologia, UNAM, Ensenada, Mexico,[3]Departamento de Innovacion Biomedica, Centro de Investigacion Cientifica y de Educacion Superior de Ensenada, Ensenada, Mexico,[4]INSERM UMR 1033, Universite de Lyon, Lyon, France,[5]Departamento Biologia Molecular y Bioprocesos, Instituto de Biotecnologia, UNAM, Cuernavaca, Mexico

Bone metastases are a frequent complication of advanced breast cancer, against which immune checkpoint inhibitors are not effective. We previously identified that PD-1$^+$ T cells in a mouse model of bone metastases are inactivated, potentially because of the expansion of PD-L1$^+$ myeloid-derived suppressor cells (MDSC) in bones. 5-Fluorouracil (5-FU) can decrease MDSC in thymoma and colon cancer models. Thus, we aim to determine the efficacy of 5-FU in breast cancer bone metastases as well as its potential side effects.Balb/C mice were inoculated in the left cardiac ventricle with 4T1 breast cancer cells to cause bone metastases within 10 days. A treatment with 4 inoculations of 5-FU (50 mg/kg) prevented splenomegaly and the expansion of PMN- and M-MDSC in bones, as assessed by flow cytometry. Treatments with doses of 10 or 25 mg/kg were not as efficient against MDSC. Also, while these lower doses tended to increase T cell infiltration, 50 mg/kg decreased it, suggesting toxicity. Thus, we modulated the number of inoculations at 50 mg/kg. Two and three inoculations decreased the splenomegaly and histological damage, but also the total number of bone marrow cells. Flow cytometry confirmed these treatments decreased PMN-MDSC, while there was only a trend toward a decrease in M-MDSC in bone metastases. More interestingly, the numbers of CD4$^+$ and CD8$^+$ T cells were increased, especially naïve and central memory T cells. On radiographs, the bone destruction caused by cancer cells was also decreased. However, a single inoculation did not cause any long-lasting effects on MDSC and T cells, and the osteolysis area was not decreased. As 5-FU sharply decreased the number of bone marrow cells in bone metastases, we sought to assess potential side effects. Three inoculations of 5-FU in healthy mice decreased neutrophils, monocytes, B cells, and NK cells in bones 3 days after the last inoculation, while T cells were still increased. However, these effects were transient since a week later, the mice had recovered. We evaluated levels of hematopoietic stem cells (HSC) and myeloid and lymphocytic progenitor cells (MPC, LPC). Surprisingly, in these conditions, 5-FU transiently increased the number of HSC and LPC, which could explain the rapid recovery, while MPC remained stable. Cancer treatments can affect bones and increase the risk of fracture, so we assessed the bone 3D microarchitecture using microCT. Two and three inoculations of 5-FU did not cause any changes in the trabecular bone volume, or the thickness or number of the trabeculae. Surprisingly, histomorphometry analysis did not reveal any changes in the number of osteoclasts, the myeloid cells dedicated to bone resorption. Thus, 5-FU could be used to decrease MDSC and increase T cells in bone metastases, turning them into a hot microenvironment to increase the efficacy of immunotherapies in breast cancer patients.

#2841 PM54 reshapes the tumor microenvironment to potentiate checkpoint blockade.

Eugenio Bustos-Moran, Daniel Torralba, Ismael Fernandez-Miranda, Maria Jose Guillen, Pablo Aviles, **Marcelo L. Ribeiro**, Carmen Cuevas

Pharma Mar, S.A., Madrid, Spain

Background: PM54, a next-generation synthetic ecteinascidin, combines enhanced DNA-minor-groove binding with dual activity: direct cytotoxicity and immune modulation through immunogenic cell death and innate signalling cascades. This study aimed to characterize the immunomodulatory effects of PM54 alone and in combination with PD-1/PD-L1 blockade in in vitro and humanized tumor models.
Methods: PBMCs from healthy donor were pre-stimulated with anti-CD3/CD28 complex and coculture for 96h with MDA-MB-231 (high PD-L1) pre-treated with PM54 and IOs (anti-PD1/PD-L1). Number of resulting target cells was analysed by flow cytometry. NXG mice engrafted with human hematopoietic CD34+ cells (Hu-CD34^{+}) were xenografted with MDA-MB-231 xenografts. Randomly allocated mice (n≥4/group) were treated with placebo, PM54 (0.6 mg/kg, i.v., Days 0, 14) ± atezolizumab (10 mg/kg, i.p., twice weekly). On day 28, animals were euthanized, and tumors weighed and analyzed by multiparametric flow cytometry and RNA-seq.
Results: In vitro coculture experiments showed an increase in the immune mediated cytotoxicity of target cells upon combination of lower doses of PM54 with atezolizumab, sensitizing cells to immunotherapy. On day 28, treatments of Hu-CD34^{+} bearing MDA-MB-231 tumors induced a statistically significant tumor reduction (vs placebo: 988.4 mm^3). The median of tumor volume (mm^3) was 305.8 (p=0.0159) for PM54, 715.6 (p=0.0317) for atezolizumab and 199.7 (p=0.0286) for the combination. Of note, statistically significant tumor reduction was also recorded in the combination vs PM54 or atezolizumab (in both, p=0.0159). In humanized MDA-MB-231, PM54 + atezolizumab expanded CD3^{+} cells (32.2% vs 9.3%), increased CD8^{+} cells (44.7% vs 19.8%), reduced Tregs (10.0% vs 42.8%), modestly increased cytotoxic NK cells, and downregulated PD-L1 on tumor and immune compartments. Transcriptomics analysis demonstrated that the combination arm renders the highest number of deregulated genes (1404 up and 981 down genes vs 537 and 908 up genes or 278 and 552 down genes in PD-L1 o PM54 treatment, respectively). Among them, GSEA showed an increase upon treatment or combination in MHC genes, IFNg and IFNα response, and NK activity and TCR signaling, leading to an enhance inflammatory response. Moreover, CIBERSORT analysis of immune populations complemented cytometry evaluation with an increase in CD8 T cells, Tfh, activated DCs and NK cells and M1/M2 ratio increase upon treatment and combination.
Conclusions: PM54 is a dual action immunochemotherapeutic that drives ICD, increases allogenic immune cytotoxicity of tumoral cells and, in vivo, augments effector CD8^{+} responses, diminishes Tregs, and reprograms suppressive myeloid cells. These immunologic effects synergize with PD-1/PD-L1 blockade, supporting development of PM54-based combinations for transcriptionally driven, immune-cold malignancies.

#2842 Investigating the capability of metformin to increase the efficacy of oncolytic herpesvirus in ovarian cancer.

Emma Sielski[1], Maria C. Courreges[2], Fabian Benencia[2]

[1]Biological Sciences,, Ohio University, Athens, OH,[2]Biomedical Sciences, Ohio University, Athens, OH

Background: Ovarian cancer (OC) is common, and frequently fatal, gynecological malignancy lacking distinct symptoms, resulting in late-stage diagnosis and difficult treatment. Although direct causes of OC are unknown, an association between OC and Type Two Diabetes (T2D) exists. Individuals with T2D, characterized by chronic metabolic dysregulation, are more likely to develop cancer later in life than those without. Recently, the effects established by anti-T2D medications, traditionally used to manage hyperglycemia, have been examined within the scope of metabolically reprogramming cancer cells to sensitize them for further treatment. Metformin is a low-cost medication currently being studied as a chemotherapy adjuvant in numerous types of cancer, given its ability to manipulate cellular glucose metabolism, proliferation pathways, and promote apoptosis. Several preclinical studies have demonstrated metformin's ability to decrease inflammation in diseases other than T2D, suggesting it influences immune responses, thus creating the possibility of a novel treatment option to increase the efficacy of current immunotherapies, such as oncolytic virotherapy. Oncolytic viruses are biological anti-tumor agents capable of selectively infecting cancer cells, eliciting an anti-cancer immune response in patients. We hypothesize that metformin dysregulates glucose metabolism in OC cells, decreasing cell viability and increasing the efficacy of oncolytic virus HSV1716. This hypothesis was tested human and mouse ovarian cancer cell lines.

Methods: Mouse ovarian cancer cells (ID8, BPPNM) or human ovarian cancer cells (A2780, SKOV3) were grown in MEM 10% FBS. For some experiments, high (5 g/l) and normal (1 g/l) glucose MEM was used. Cells were treated with 50, 25, 12.5, and 6.25 mM of metformin in 2D and 3D environments. Scratch assays were used to monitor effects on cell motility. All experiments were monitored at 24-,48- and 72- hours post-treatment. Finally, metformin was administered in conjunction with HSV-1716 at varying concentrations to OC cells.

Results and Conclusions: We observed that metformin decreased cell viability and motility, and spheroid growth as determined by MTS assays, flow cytometry analysis and light microscopy. The effect of the drug was further exacerbated by virus treatment, indicating that a combination of both therapeutic strategies is feasible. Further investigations using in vivo OC mouse models will help determine the effects of metformin on immunosuppressive cell populations in the OC tumor microenvironment and its capacity to increase oncolytic efficacy in vivo.

#2843 Changes in MAVS expression and T-cell infiltration in the tumor microenvironment following platinum-based chemotherapy in high-grade serous ovarian carcinoma.

Yuki Yasui, Erika Nakatsuka, Yusaku Shimizu, Mina Sakata, Yuki Takemoto, Gaku Yamamoto, Aasa Shimizu, Mahiru Kawano, Yasuto Kinose, Kenjiro Sawada, Michiko Kodama

Gynecology, Osaka University, Suita, Japan

Background: High-grade serous ovarian carcinoma (HGSC) exhibits low sensitivity to immune checkpoint inhibitors (ICIs), partly due to limited tumor-infiltrating T cells. Type-I interferons (IFNs) from tumor cells may enhance T-cell infiltration. We investigated MAVS (mitochondrial antiviral-signaling protein) as an inducer of Type-I IFN signaling in HGSC and analyzed its association with immune-cell infiltration in relation to paclitaxel/carboplatin (TC) therapy and prognosis.
Methods: We first included advanced HGSC cases at our institution that underwent interval debulking surgery (IDS) following neoadjuvant TC therapy. Paired pre-treatment biopsies and IDS specimens were collected for immunohistochemistry to evaluate MAVS expression in cancer cells and $CD8^+$/$CD4^+$ T-cell infiltration. Changes in MAVS expression and T-cell infiltration before and after TC therapy were analyzed, along with their correlation with sensitivity to TC. Next, using human HGSC cell lines, we assessed changes in MAVS expression and T-cell infiltration following platinum administration. Finally, we established an ID8 mouse model and divided mise into a cisplatin-treated group and a control group to compare the rate of ascites production and changes in body weight. We also compared immune-cell profiles in ascites (e.g., $CD4^+$ and $CD8^+$ T cells) and MAVS expression in tumor cells between each groups.
Results: We analyzed 45 cases treated from December 1, 2019 to August 31, 2025. MAVS expression increased after TC therapy in most cases, and this increase correlated with enhanced $CD8^+$ T-cell infiltration. In prognostic analyses, decreased MAVS expression after TC therapy was associated with poor prognostic features.
In cell line experiments, MAVS expression was enhanced in platinum-treated cell lines, as demonstrated by Western blotting.
In the ID8 mouse model, the rate of ascites production was faster in the cisplatin-treated group. We also visualized the proportions of immune cells within ascites in this group. Tumor cells derived from this model likewise exhibited increased MAVS expression in the cisplatin-treated group, as demonstrated by Western blotting.
Conclusions: In HGSC, TC therapy-induced changes in MAVS expression may contribute to the induction of $CD8^+$ T-cell infiltration. In vivo, platinum administration similarly suggested potential alterations in MAVS expression and immune-cell infiltration. MAVS may serve as a biomarker for patient selection in ICI therapy for HGSC.

#2844 Cannabis smoking increases systemic inflammation and reduces immunity.

Adele Hammoudi, Mayilvanan Chinnaiyan, Sulfath Thottungal Parambil, Gautham Chengizkhan, Vengatesh Ganapathy, Lurdes Queimado

Otolaryngology, University of Oklahoma Health Sciences, Oklahoma City, OK

Introduction: Cannabis is the most used federally illegal drug in the United States with a percentage increased from 19.0% in 2021 to 22.3% in 2024 among people aged 12 or older. Smoking remains the most common mode of cannabis use, even among cancer patients. Despite the anti-inflammatory potential of certain cannabinoids, cannabis smoke contains numerous carcinogens and toxicants that can potentially disrupt immune homeostasis and heighten inflammation. Understanding these effects is crucial as inflammation and immune function shape cancer development, progression, and therapeutic response. Objective: To characterize systemic inflammation and immune alterations associated with cannabis smoking.

Methods: Following IRB approval, 44 participants were recruited via Redcap, a secure online survey. Demographics, substance use data, and blood samples were collected for a total of 24 non-users (NU) and 20 exclusive cannabis users (CAN) who smoke cannabis at least bi-weekly over the past month. Users of tobacco products, including blunts and e-cigarettes, were excluded. Product use status was biochemically verified using liquid chromatography tandem mass spectrometry (LC-MS) to quantify THC and its metabolite THC-COOH. Complete blood count (CBC) was obtained on each participant and (CBC)-derived inflammatory markers were calculated. A novel 13-antibody multiparametric flow cytometry panel was used to separate 21 immune cell subsets characterizing both myeloid and lymphoid cells. Data was analyzed using Welch's t-tests.

Results: Our CBC data show significantly higher red blood cell distribution width-standard deviation ($p=0.038$) and lower absolute number of monocytes ($p=0.038$) in CAN users compared to NU. We also observed a significant increase in platelet-to-lymphocyte ratio in CAN users vs NU ($p=0.028$). Our myeloid immune cell phenotyping data show that cannabis smokers have significantly higher number of low-density neutrophils (LDNs) than NU ($p=0.035$). Preliminary lymphoid immune cell phenotyping data suggest that cannabis smokers have significantly fewer B cells ($p= 0.014$) and activated B cells ($p= 0.016$) than NU. Our preliminary data also show a non-significant decrease in $CD8^+$ T cells. These findings indicate that cannabis smoking induces systemic inflammation (higher PLR and LDNs) and suppresses immune responses (fewer B and CD8+ T cells).

Conclusions: Our data demonstrate for the first time that cannabis smoking induces a proinflammatory and immunosuppressive state that may promote diverse human diseases, including cancer. We established the first comprehensive framework to evaluate the immunological effects of cannabis smoking. These findings reveal how cannabis use profoundly alters the immune system at both cellular and functional levels. Grant support: NIH/NCI (R01CA242168, Queimado); TSET HPRC (Queimado); PHF Bridge (Queimado); NIH/ NIGMS (U54GM104938-10)

#2845 Human serum proteomics reveals extracellular vesicle-mediated metabolic-adhesive signaling and suppression of adaptive immunity in E-cigarette users.

Rizwana Begum, Shilpa Thota, Shreya Pokharel, Biplov Sapkota, Joseph Francis

Louisiana State University, Baton Rouge, LA

Background: While the toxicological impact of combustible cigarette smoke is well characterized, the systemic biological consequences of electronic cigarette use remain poorly understood. As serum contains secreted and vesicle-associated proteins, it provides a window into early biological responses to vaping. We performed serum proteomics to determine how vaping shapes the biology of extracellular vesicles (EVs), metabolic stress pathways, and immune function in humans.
Methods: Serum from adult e-cigarette users and non-vaper controls underwent LC-MS/MS proteomics followed by Gene Set Enrichment Analysis (GSEA) across GO Biological Process (BP), Cellular Component (CC), Molecular Function (MF), KEGG, and curated MSigDB C2 secretome/EV signatures.
Results: Our results demonstrate that serum from human vapers showed increased expression of glycolytic and oxidative stress-adaptive enzymes (GPI, PKM, IDH1, SOD2), along with significant upregulation of Hypoxia up-regulated protein 1 (HYOU1), indicating engagement of a hypoxia-responsive/ER stress metabolic program. Concordantly, GSEA revealed enrichment of glycolysis, carbon metabolism, ribonucleoside metabolism, and precursor metabolite generation. Cellular component analysis identified strong enrichment of extracellular vesicle, secretory vesicle, membrane-enclosed lumen, and curated secretome signatures, accompanied by upregulation of ECM-cytoskeletal remodeling pathways, including focal adhesion, ECM-receptor interaction, and actin filament organization. These EV-linked pathways were supported by increased abundance of EV-associated adhesion molecules and immunomodulatory factors, including the Neural cell adhesion molecule L1-like protein (CHL1) and the integrins **ITGB1** and **ITGB2**, which are known to be packaged into EVs during epithelial or immune stress. In parallel, immune-related pathways, including adaptive immune response, immunoglobulin-mediated immunity, and antigen binding, were the only processes negatively enriched, indicating selective suppression of humoral immunity.
Conclusions: Chronic e-cigarette use induces a coordinated serum phenotype characterized by hypoxia/ER stress-induced metabolic reprogramming, enhanced extracellular vesicle and adhesion signaling, and downregulation of adaptive immune mechanisms. These findings suggest that metabolic stress-driven EV secretion may contribute to altered immune communication and weakened antibody-mediated responses in e-cigarette users.

#2846 Inflammasome dependent and independent dysregulation associated with periodontal disease and oral cancer risk in people with HIV.

Alejandro Yamil Odeh[1], Juliana Mary Serrano-Rodriguez[2], Jurelis Torres Reyes[1], Oscar Antonio Loperena Gonzalez[1], Jeannette L. Salgado Montilla[1], Ramon F. Gonzalez-Garcia[1], Gabriel Borges Velez[1], Josue Perez-Santiago[1]

[1]University of Puerto Rico Comprehensive Cancer Center, San Juan, PR,[2]University of Puerto Rico - Rio Piedras, San Juan, PR

Introduction: People with HIV (PWH) exhibit immune dysregulation, which can increase their susceptibility to periodontal disease (PD), elevating the risk of chronic oral inflammation, tissue damage, and oncogenesis. Persistent periodontitis may drive the development of oral squamous cell carcinoma (OSCC) through increased prevalence of pathogenic bacteria and elevated levels of inflammatory cytokines. In fact, our preliminary data show dysbiosis of the oral microbiome associated with PD. Furthermore, PD can be associated with inflammasome dysfunction, which can impact downstream production of cytokines. In PWH, these inflammatory processes may be exacerbated, fostering a pro-oncogenic microenvironment. This study aims to quantify levels of inflammasomes and inflammatory markers in PWH and evaluate their association with PD and OSCC risk.

Methods: Saliva and oral rinse samples, along with sociodemographic and clinical data, were collected from 202 virologically suppressed PWH. A comprehensive periodontal assessment was performed, and participants were categorized into four groups based on PD severity: none, mild, moderate, and severe. Protein levels of inflammasomes (NLRP3 and NLRC4) were quantified in saliva using ELISA, while cytokine concentrations (IL-1β, IL-4, IL-6, IL-8, IL-10, IL-17A, and TNF-α) were quantified using ELLA. Statistical analyses were performed using R statistical software. Median values were compared using Mann-whitney or Krukal-wallis tests with post-hoc adjustment.

Results: Participants with PD exhibited significantly higher levels of IL-1β (400 pg/mL vs 235 pg/mL, $p<0.01$), IL-6 (25.4 pg/mL vs 14.2 pg/mL, $p<0.01$), and IL-8 (798 pg/mL vs 549 pg/mL, $p=0.04$) while there was a trend for higher levels of IL-17 (2.01 pg/mL vs 1.50 pg/mL, $p=0.05$). In addition, IL-1β was significantly higher in subjects with moderate (408 pg/mL, $p=0.01$) and severe PD (378 pg/mL, $p=0.01$) when compared to no PD (235 pg/mL). On the other hand, while there was no significant difference in the levels of NLRP3 and NLRC4 by PD status, people with severe PD (3.37 ng/mL) had significantly lower levels of NLRP3 when compared to moderate (5.83 ng/mL, $p<0.01$) or no PD (5.71 ng/mL, $p=0.02$).

Conclusion: There were increased levels of inflammatory cytokines, particularly IL-1B, and alterations to inflammasome levels according to PD severity, supporting the role of pyroptosis in the pathogenesis of PD. Chronic elevation of additional pyroptosis independent inflammatory cytokines and dysbiosis of the oral microbiome may contribute to a persistent inflammatory microenvironment associated with increased OSCC risk in PWH. These results highlight the importance of monitoring oral cytokine profiles as both biomarkers of disease progression and potential indicators of cancer risk in PWH.

#2847 Sweet boost: Sucralose enhances regulatory T cell (Treg) functions *in vitro*.

Sadhana Bom[1], Jessica A. Jana[2], Kelsey M. Ertwine[2], Rachel Cumberland[3], Kristin T. Morder[2], Abigail E. Overacre-Delgoffe[2]

[1]University of Pittsburgh School of Medicine, Pittsburgh, PA,[2]Department of Immunology, University of Pittsburgh School of Medicine, Pittsburgh, PA,[3]UPMC Hillman Cancer Center, Pittsburgh, PA

Non-nutritive sweeteners (NNS) like sucralose, aspartame, and saccharin are widely used as sugar alternatives. While the FDA considers NNS safe, concerns about their long-term effects are growing. Sucralose, derived from sucrose and about 600 times sweeter, has been shown to dampen the efficacy of anti PD-1 in cancer in both mice and human. It lowers the T- cell cytotoxic function and enhances regulatory T cell (Treg) proliferation. Tregs are vital for immune tolerance but potently suppress anti-tumor immunity in the tumor microenvironment. How sucralose enhances Treg function still unknown, representing a critical gap in understanding potential dietary influences on cancer immunotherapy. Therefore, studying the sucralose -Tregs interactions is a novel approach to understand possible resistance mechanisms in cancer. We isolated Tregs from Foxp3-reporter mice and treated them with varying concentrations of sucralose *in vitro*. Cell proliferation was monitored daily via cell counting, while Tregs phenotype and function were evaluated using flow cytometry. A suppression assay was performed by coculturing Tregs (treated with 0 mM, 0.05 mM, or 0.5 mM sucralose) with CD8+ T cells. Sucralose's effect on Treg differentiation and metabolism was assessed using the naïve CD4+ T cell differentiation and Seahorse assays, respectively. Our study showed that sucralose significantly enhances proliferation, suppressive capacity, and differentiation of Treg *in vitro* while also increasing the mitochondrial spare respiratory capacity, suggesting improved metabolic fitness in these cells. These findings highlight the interactions between sucralose and Tregs, which may help us to understand how artificial sweeteners influence immune regulation and resistance mechanisms in cancer, offering insights for future *in vivo* research and informing dietary recommendations and immune modulation strategies in cancer treatment.

#2848 Harnessing SHP2-targeted signaling to reinforce anti-tumor immune responses.

Bayarbat Tsevegjav[1], Hirotake Tsukamoto[2], Osamu Kikuchi[1]

[1]Division of Clinical Pharmacology and Cancer Immunotherapy, Center for Cancer Immunotherapy and Immunobiology, Graduate School of Medicine, Kyoto University, Kyoto, Japan,[2]Division of Clinical Immunology and Cancer Immunotherapy, Center for Cancer Immunotherapy and Immunobiology, Graduate School of Medicine, Kyoto University, Kyoto, Japan

Background: SHP2, a non-receptor protein tyrosine phosphatase, regulates both immune checkpoint signaling via PD-1 and oncogenic RAS/MAPK pathways, making it a promising target for integrated anti-cancer therapy. While SHP2 inhibitors have been primarily investigated for their tumor-intrinsic effects, their immunomodulatory potential remains unclear. Therefore, we investigated whether SHP2 inhibition can simultaneously relieve PD-1-mediated T cell suppression and inhibit tumor-intrinsic MAPK signaling, a dual-action mechanism particularly for tumors driven by RAS/MAPK signaling.
Methods: Primary murine T cells and human Jurkat T cell lines were used to assess the immune cell responses. Flow cytometry was performed to characterize T cell activation, and cell viability was quantified using WST-1 and CellTiter-Glo assays. T cell-mediated cytotoxicity against cancer cells was evaluated by the LDH release assay. qPCR was conducted to analyze the gene expression profiles related to immune activation. To assess the impact on oncogenic signaling, RAS/MAPK pathway activity was measured by western blotting. For in vivo evaluation, mice bearing MC38-OVA syngeneic tumors received oral SHP2 inhibitor TNO155 (10 or 20 mg/kg, BID for 14 days).
Results: Pharmacological inhibition of SHP2 using TNO155 (1 nM-10 μM) did not affect T cell viability, indicating its suitability for in vitro immunological analysis. Despite its minimal cytotoxicity, SHP2 inhibition significantly modulated T cell activation. Flow cytometric analysis revealed the upregulation of activation markers, including CD69 and Granzyme B expression, alongside enhanced T cell-mediated cytotoxicity against tumor cells, as measured by LDH release assay (increase of 20.9% cytotoxicity at 1 μM TNO155; $P < 0.05$). In syngeneic tumor-bearing immunocompetent mice, oral administration of TNO155 (p.o. BID) led to a significant reduction in tumor volume compared to vehicle-treated controls (tumor growth inhibition: 39.6% (10 mg/kg; $P < 0.05$) and 62.4% (20 mg/kg; $P < 0.01$) on day 14. Immunohistochemical and flow cytometric analyses detected the infiltration of $CD8^+$ tumor-infiltrating lymphocytes, and qPCR revealed elevated expression of IFNγ-responsive genes, including *Cd274* (~2.2-fold induction; $P < 0.001$) in tumors. Notably, intratumoral $CD8^+$ T cells exhibited enhanced effector function, with a marked increase in Granzyme B^+ cells (control: 4.46 ± 1.86%; TNO155: 18.94 ± 12.27; $P < 0.05$) and a decrease in exhaustion markers TIM-3 and LAG-3.
Conclusions: These findings demonstrate that SHP2 inhibition enhances anti-tumor immune responses and supports its potential as a dual-function therapeutic strategy in cancer immunotherapy. This study provides a robust preclinical foundation for the translational development of SHP2-targeted approaches in precision oncology.

#2849 Endostatin and prolactin combination trigger PRLR induction and channelize CD1d signaling in TNBC.

Ritis Kumar Shyanti[1], Rajesh Singh[2], **Manoj K. Mishra**[1]

[1]Cancer Research Center, Department of Biological Sciences, Alabama State University, Montgomery, AL,[2]Microbiology, Biochemistry, and Immunology, Cancer Health Equity Institute, Morehouse School of Medicine, Atlanta, GA

Triple-negative breast cancer (TNBC) is a very aggressive breast cancer subtype and therapeutically challenging because of the absence of hormone receptors (ER, PR and HER2). TCGA datasets revealed that prolactin receptor (PRLR) was downregulated in TNBC, associated with poor overall survival. PRLR induction has been shown to reduce tumor proliferation in TNBC. However, no pharmacologically active molecule has been reported that can induce PRLR. In addition, natural killer T (NKT) cells, potent antitumorigenic immune cells activated via CD1d lipid antigen interactions, are diminished in TNBC tumors. Prior studies have demonstrated that CD1d expression is crucial for the progression of breast tumors and regulates antitumor immune responses mediated by NKT cell activation. In this study, we found that treating endostatin (2.5 μM), an anti-angiogenic protein, in combination with prolactin (2.5 nM) significantly reduced the proliferation and colony-forming potential of TNBC cells. The treatment combination was found to induce PRLR and CD1d expression (CD1d A and B isoforms) in the TNBC cell line MDA-MB-468. Further, we observed that the combination reduced epithelial-mesenchymal transition (EMT) markers and oxidative phosphorylation marker COXIV. Human NKT cells were isolated from PBMCs and co-cultured with treated TNBC cells. NKT activation was quantified by IFN-γ secretion using ELISA. Additional analyses using TNBC tissue slides are undergoing to determine PRLR and CD1d co-expression patterns. Our findings identify endostatin-mediated restoration of the PRLR as a novel strategy to restrict TNBC cell growth while simultaneously enhancing CD1d-dependent NKT cell activation, representing a promising therapeutic option for TNBC.

#2850 PHI-501, a novel pan-RAF inhibitor, enhances immunotherapy efficacy by converting cold tumors into hot tumors.

Sung Eun Kim[1], Sue Min Kim[1], Ky-Youb Nam[2], JeongHyeok Yoon[2], Sang Joon Shin[3]

[1]Yonsei University College of Medicine, Seoul, Korea, Republic of,[2]Pharos iBio Co., Ltd., Anyang, Korea, Republic of,[3]Division of Medical Oncology, Department of Internal Medicine, Yonsei Cancer Center, Seoul, Korea, Republic of

Background: Immune checkpoint blockade (ICB) has significantly improved survival outcomes in patients with melanoma; however, a substantial proportion of patients remain non-responsive. Therefore, converting “cold” tumors into “hot” tumors represents a critical therapeutic strategy to enhance responsiveness to ICB therapy. PHI-501, a novel pan-RAF inhibitor, is proposed to enhance immunotherapy responsiveness by promoting immune activation and converting “cold” tumors into “hot,” immune-inflamed tumors. In this study, we sought to characterize the immunomodulatory mechanisms by which PHI-501 primes antitumor immunity in melanoma.

Methods: RNA sequencing was performed on SK-MEL-3 ($BRAF^{V600E}$) melanoma cells treated with PHI-501 (10 μM, 48 h), followed by gene set enrichment analysis (GSEA) to identify immune-related transcriptomic alterations. To validate immune activation, SK-MEL-3 melanoma cells were treated with PHI-501 and analyzed for JAK/STAT signaling and type I interferon (IFN) response using quantitative PCR (qPCR). Additional experiments with IFN-γ (24 h) co-treatment were performed to assess MHC class I induction. Western blotting was performed on cell lysates and culture supernatants to measure intracellular immune markers and the extracellular release of HMGB1 in SK-MEL-3 and SK-MEL-29 ($BRAF^{V600E}$).

Results: GSEA of RNA-seq data from PHI-501-treated SK-MEL-3 cells revealed enrichment of the type I interferon response (NES = 1.17, p = 0.14) and the tissue-specific immune response (NES = 1.64, p = 0.01). PHI-501 treatment downregulated the expression of key MAPK pathway regulators such as DUSP6, SPRY4, ETV4, and ETV5, while upregulating canonical interferon-stimulated genes (ISGs) including IFIT1, IFIT2, IFIT3, and IRF1 ($p<0.05$). Consistent with the transcriptomic results, qPCR analysis demonstrated robust induction of immune-related genes. In SK-MEL-3, STAT2, IFNA1, and IRF1 transcripts were upregulated approximately 12-, 9-, and 7-fold, respectively. Furthermore, IFN-γ co-treatment synergistically enhanced MHC class I expression, increasing levels by more than 7-fold in SK-MEL-3 compared with controls. Additionally, extracellular HMGB1 levels increased in culture supernatants of SK-MEL-3 and SK-MEL-29 cells, accompanied by elevated IRF1 and NLRP3 protein expression in cell lysates.

Conclusion: Taken together, these findings demonstrate that PHI**-**501 activates immune-related signaling pathways, including the type I IFN and downstream JAK/STAT cascades. Overall, these results suggest that PHI-501 may serve as a promising therapeutic agent capable of enhancing ICB responsiveness when used in combination with immunotherapy.

#2851 EGFR-TKI drives the reprogramming of CD8$^+$ T cell immunity in non-small cell lung cancer.

Ssu-Pei Yu[1], Hao-Chen Chi[1], Meng-Yun Lin[1], Chao-Chi Ho[2], Geen-Dong Chang[3], Ming-Shyue Lee[4], Chun-Jung Ko[1]

[1]Graduate Institute of Immunology, National Taiwan University, Taipei City, Taiwan,[2]Department of Internal Medicine, National Taiwan University Hospital, Taipei City, Taiwan,[3]Graduate Institute of Biochemical Sciences, National Taiwan University, Taipei City, Taiwan,[4]Department of Biochemistry and Molecular Biology, National Taiwan University, Taipei City, Taiwan

Non-small cell lung cancer (NSCLC), the most common type of lung cancer, remains the leading cause of cancer-related deaths globally. Although different cancer-driving mutations have been reported in NSCLC, their prevalence varies across ethnic groups. Among Asian patients, EGFR mutations have been reported to be the most prevalent. EGFR tyrosine kinase inhibitors (EGFR-TKI) are applied to NSCLC patients carrying EGFR mutations, although EGFR-TKIs are effective treatments, their potential impact on the immune system remains largely unknown. Understanding the interactions between EGFR-TKIs and immune regulation is crucial for developing combination therapy strategies. In this study, we demonstrated that EGFR-TKI suppresses the activation, proliferation, and effector cytokine production of CD8$^+$ T cells. Moreover, in therapeutic models, EGFR-TKI treatment negatively impacts the antitumor response of CD8+ T cells. Notably, when EGFR-TKIs were combined with anti-PD-1 therapy, tumor growth was increased compared with anti-PD-1 monotherapy, indicating that EGFR-TKIs may diminish the efficacy of immune-checkpoint blockade. In parallel with our findings in mouse models, studies of NSCLC patients who underwent EGFR-TKI also showed decreased CD8$^+$ T cell activation and IFNγ production. Moreover, we identified potential EGFR-TKI-interacting targets in T cells and found that EGFR-TKIs bind to actin-interacting proteins, thereby disrupting cytoskeletal organization and compromising T-cell function. Together, these results reveal an EGFR-independent mechanism through which EGFR-TKIs attenuate CD8$^+$ T-cell antitumor activity. In conclusion, our findings not only suggest a suppression effect of EGFR-TKI on CD8$^+$ T cells but also provide crucial information on developing EGFR-TKI combination strategies with immunotherapies for NSCLC patients.

#2852 Targeting notch signaling in triple negative breast cancer with a novel adeno-associated virus-mediated therapy to enhance immunomodulation.

Mrityunjoy Biswas[1], Md. Manirujjaman[1], Yong Ran[2], Samarpan Majumder[1], Luis Del Valle[1], Jovanny Zabaleta[1], Barbara A. Osborne[3], Lucio Miele[1], Todd Golde[2], **Fokhrul Hossain**[1]

[1]LSU Health New Orleans, New Orleans, LA,[2]Emory University, Atlanta, GA,[3]University of Massachusetts, Amherst, Amherst, MA

Triple-negative breast cancer (TNBC) is a group of aggressive breast cancers with a higher mortality rate. TNBC patients have a higher rate of mortality due to metastasis or local recurrences, which are chemo- and radio-resistant. Notch signaling has emerged as an important factor in TNBC. There is strong evidence for Notch signaling involvement in TNBC. Recent studies suggest that Cancer Stem cells (CSCs) that emerge after chemotherapy or targeted agents in TNBC are often Notch-dependent. Notch inhibitors, including Gamma Secretase Inhibitors (GSIs), are quite effective in preclinical models of TNBC because they eliminate CSCs that are resistant to chemotherapy. Unfortunately, this approach has had minimal success in clinical trials due to its intestinal toxicity and adverse effects on immune cells. To avoid these toxicities, we aim to use a recombinant adeno-associated virus (r-AAV) vector encoding a soluble Notch1 decoy (r-AAV-Notch1D) to block Notch signaling intratumorally in TNBC. r-AAVs are non-replicating viruses and, therefore, are a safe platform for *in vivo* gene delivery. We found that r-AAV-GFP transduced both human and mouse TNBC cells. Our r-AAV constructs contain a C1QTNF3-derived collagen domain (CD) that facilitates the trimerization and stabilization of secreted fusion proteins. We purified these proteins using His-Tag affinity chromatography and found that they significantly reduced mammosphere growth in human TNBC cells and reduced Notch intracellular domain (NICD) expression. Intratumoral injections of the r-AAV-Notch1D virus significantly reduced syngeneic mouse TNBC tumor (C0321) growth and increased the tumor-infiltrating lymphocytes, including CD3 and CD8. Notably, the r-AAV-Notch1D virus significantly enhanced the efficacy of immunotherapy (a-PD1) in mediating the anti-tumor effect in the syngeneic TNBC mouse model. We performed RNA sequencing to identify tentative target(s) for r-AAV-Notch1D. We found that *Hmox1, Timp3, Il33, Adam8, Ero1l,* and *Saa3* genes were upregulated, on the other hand *Gm11408, Gm9844, Gm11407, Gm8430, Rnu3a, and Per1* genes were downregulated upon the treatment. From our Gene Ontology analysis, we found that r-AAV-Notch1D treatment enhanced hexosaminidase activity, carbohydrate catabolic process, covalent chromatin modification, histone modification, and histone acetylation. r-AAV-Notch1D treatment also altered several cellular pathways, including MicroRNAs in cancer, Ferroptosis, Porphyrin metabolism, Mineral absorption, and the Cytosolic DNA-sensing pathway. Given the diverse biological functions of these pathways, further study is warranted to elucidate their roles in TNBC. Overall, our findings indicate that the r-AAV-Notch1D virus is a promising approach for treating TNBC, alone or in combination with immunotherapy, and is a candidate for translational application.

#2853 VPAC antagonism as potential therapeutic for prostate cancer.

YuJie Chen, Tuisha Gupta, Kiranj Chaudagar, Edmund K. Waller

Emory University School of Medicine, Atlanta, GA

Background: Tumor-associated macrophages (TAM) within prostate cancer (PC) microenvironment correlates with poor clinical outcomes and with acquired resistance to androgen-deprivation therapy (ADT). Our preclinical work has established that macrophage phagocytosis can partially restrain PC growth at both castration-sensitive and -resistant stages; however, this response remains incomplete. We therefore hypothesized that activating phagocytosis by targeting androgen-regulated checkpoints on macrophages empowers ADT and provides a combinatorial therapeutic strategy to control PC via anti-tumor immunity.
Methods: Bone marrow-derived macrophages (BMDM) profiled using RNA sequencing and Western blot to identify androgen-regulated immune checkpoints, followed by functional validation in polarization and phagocytosis assays. In vivo anti-tumor efficacy of candidates was tested using syngeneic TrampC1, Myc-CAP, cMyc-Rb-knockout (KO) models in both wildtype (WT) and immune checkpoint-knockout mice. Treatment with androgen receptor (AR) and immune checkpoint blockade alone and the combination arms with relevant untreated controls.
Results: Transcriptomic and proteomic profiling revealed selective upregulation of VIP receptor 1 (VPAC1) on immunosuppressive M2-like BMDM vs anti-tumor M1-like. Functional assays revealed an increased IL-12 expression in BMDM following AR and VPAC co-blockade. Enzalutamide upregulated VPAC1 on both M1/M2-like BMDM. It also increased phagocytosis of PC cells in VIP-KO BMDM relative to untreated control, but not in WT, indicate that VPAC1 serves as an androgen-regulated macrophage-suppressive checkpoint. Bioinformatic analysis showed positive correlations between 1) VPAC1 and AR, and 2) VIP and synaptophysin (SYP) in prostate adenocarcinoma samples. Furthermore, degarelix improved the survival of syngeneic TrampC1 tumor (harboring both adenocarcinoma and neuroendocrine phenotypes)-bearing mice, particularly in VPAC1-KO mice, compared to VIP or VPAC2-KO and WT controls, with corresponding benefits in prostate tumor growth control. In the androgen-sensitive Myc-CAP syngeneic model, a potent VIP receptor antagonist, ANT308, increased degarelix-mediated tumor control. ANT308 treatment yielded similar effects in androgen-independent Myc-Rb-KO PC model, highlighting the synergy of co-blocking VIP/VPAC and AR pathways for controlling PC.
Conclusions: VPAC1 is an androgen-regulated macrophage checkpoint. VPAC inhibition with ANT308 leads to anti-tumor phagocytosis and enhances ADT-mediated control of prostate tumors in both adenocarcinoma and mixed adeno-neuroendocrine diseases. Further mechanistic investigation is needed to elucidate the intrinsic versus extrinsic role of VIP/VPAC at those stages, informing the design of clinical trials for ANT308 in PC patients.

#2854 Antibiotics blunt the innate immune mechanisms underlying HER2+ breast cancer therapy efficacy.

Lily J. Parker[1], Payal Mitra[1], Nofar Erlichman[1], Pavani Chalasani[2], Rong Li[1], Romina E. Araya[1]

[1]Biochemistry and Molecular Medicine, George Washington University School of Medicine and Health Sciences, Washington, DC,[2]George Washington Cancer Center, Washington, DC

Cancer patients are especially vulnerable to infections. About 20-60% of patients may receive antibiotics at some stage during their treatment, including perioperative care and neutropenic periods. Retrospective studies indicate that antibiotics can negatively affect outcomes in various cancers. HER2+ breast cancer (BC) patients often receive targeted treatments such as anti-HER2 antibodies and/or small-molecule tyrosine kinase inhibitors (TKI), which remain understudied in this context. Published work indicates that HER2+ BC patients experience more severe reductions in survival following antibiotic exposure than HER2-negative cases. Although this antibiotic effect is thought to result from host microbiota disruptions, the precise mechanisms remain unclear. To understanding how antibiotics specifically affect HER2 therapies, we examined how antibiotics influence responses to HER2-targeted therapies using an orthotopic HER2+ BC mouse model, administering an oral broad-spectrum antibiotic cocktail (ABX) to deplete the microbiota or water (H2O) as a control, and employing an anti-HER2 antibody (anti-HER2/neu) or the TKI neratinib. While antibiotic treatment alone did not influence tumor growth, it notably impaired responses to HER2 therapies. To simulate clinical scenarios, we administered oral ciprofloxacin (cipro) or amoxicillin/clavulanic acid (am/clav), common antibiotics used for cancer patients, alongside neratinib, which was most affected by ABX. Cipro reproduced the ABX effect, completely blocking neratinib response, while am/clav caused a partial impairment. Next, we characterized immune cells in tumors and the bloodstream after HER2-targeted therapy by spectral flow cytometry. In H2O mice, both HER2 therapies led to immune remodeling of the tumors, with reduced tumor-associated neutrophils and macrophages, and increased NK, CD8+, and CD4+ T cell infiltration. In contrast, NK cells were systemically decreased in untreated ABX mice compared with H2O mice and did not recover after therapy, explaining the failure to recruit these cells to the tumor site in ABX mice. To assess the role of NK cells in therapy efficacy, we depleted NK cells with an anti-asialo-GM1 antibody before and during HER2 therapies. As expected, NK cell depletion abolished the anti-HER2 response but also led to a partial reduction in neratinib efficacy, hinting that neratinib engages tumor-extrinsic innate immune mechanisms influenced by antibiotics. Overall, our findings show that antibiotic-induced disruption of the gut microbiota hampers HER2+ BC therapy by impairing the immune response both systemically and within the tumor microenvironment.

#2855 Evaluation of ^{212}Pb-PSMA radioligand therapy in an immunocompetent prostate cancer model.

Melissa Monterosso[1], Aneesha Jones[1], Kayden Kwah[2], Anna Amiss[1], Didier Boucher[1], Aimee Horsfall[1], Heather Green[1], Johannes Koehbach[1], Ralph Huebner[1], Yaowu He[2], Stephen Rose[1], Gary Li[1], Feifei Liu[1], Joana Brilhante[1], Simon Puttick[1], Anna Karmann[1], John Hooper[2], **Thomas Kryza**[1]

[1]AdvanCell Pty Ltd, Sydney, Australia,[2]Mater Research Institute, Brisbane, Australia

Introduction: Prostate cancer (PC) is the second leading cause of cancer-related death in men, and metastatic castration-resistant prostate cancer (mCRPC) remains incurable. Prostate-specific membrane antigen (PSMA) is a validated therapeutic target. Targeted alpha therapies (TAT) employing radionuclides such as lead-212 (^{212}Pb) and actinium-225 (^{225}Ac) are in development, delivering high-linear-energy-transfer radiation with potent cytotoxic and potentially immunomodulatory effects. However, currently available PSMA-positive preclinical models rely on human xenografts, which do not allow for the study of radioligand therapy-induced immune modulation.

Objective: The immunomodulatory effects of PSMA-targeted alpha therapy are believed to play a key role in the anti-tumor efficacy towards PC. However, the lack of immunocompetent *in vivo* models of PSMA-positive PC has been a major hurdle in mechanistic and translational studies. To overcome this, we established a syngeneic prostate cancer model expressing murine PSMA (mPSMA) and developed a high-affinity PSMA-directed TAT tool compound specific to mPSMA.

Methodology: Murine bone-metastatic prostate cancer cell line, RM1-BM, which recapitulates late-stage TP53-mutant disease, was engineered to express murine FOLH1 (mPSMA) using the PiggyBac transposon system. Expression of mPSMA was confirmed both *in vitro* and *in vivo* by western blotting and immunohistochemistry. The affinity and specificity of the TAT agent ^{212}Pb-PS0001 (AdvanCell) for murine and human PSMA were assessed using inhibition and cytotoxicity assays. Biodistribution and therapeutic efficacy were assessed in immunocompetent C57BL/6 mice bearing mPSMA-RM1-BM tumors. Blood and tissue samples collected from treated animals underwent multiomics analyses to characterize immune response modulation induced by ^{212}Pb-PS0001.

Results: RM1-BM-mFOLH1 cells expressed mPSMA at levels comparable to human PSMA-positive C4-2 cells. ^{212}Pb-PS0001 exhibited high-affinity, selective binding and robust tumor uptake in RM1-BM-mFOLH1 models, with minimal off-target accumulation. Therapeutic evaluation demonstrated that a single administration of ^{212}Pb-PS0001 significantly inhibited RM1-BM-mFOLH1 tumor growth in immunocompetent mice, whereas untreated controls showed progressive disease. Notably, several treated animals achieved durable tumor control, suggesting potential induction of an anti-tumor immune response.

Conclusion: By establishing a syngeneic, mPSMA-positive metastatic prostate cancer model, we enabled the evaluation of PSMA-TAT in an immunocompetent setting. Preliminary studies with ^{212}Pb-PS0001 demonstrated selective PSMA targeting, favorable pharmacokinetics, and potent anti-tumor efficacy, supporting its utility as a PSMA-TAT tool compound for investigating immune-mediated mechanisms of action in prostate cancer.

#2856 Induction of immunogenic cell stress through the inhibition of topoisomerase I.

Douglas E. Kline, Cory Alvey, Adelyn L. Zelaya Lazo, Tanushree Samanta, Amy Neely, Alireza Tafazzol, James Grayczyk, Luke Broses, Erik Ladomersky, Julie Purkal, Ji Huang, Greg Buchanan, Kenneth Bromberg, Relja Popovic, Darren Phillips

AbbVie Inc., North Chicago, IL

When normal tissue homeostasis cannot be maintained, cells initiate distinct pathways of regulated cell death (RCD) to preserve health of the organism. Exploiting RCD pathways to induce tumor cell death is a mainstay of cancer therapy. More recently it has become appreciated that the manner in which cancer cells die can have drastic impacts on local tissue microenvironments and ultimately disease progression. Emerging preclinical and clinical data suggest certain forms of RCD can cause the release of damage-associated molecular patterns (DAMPS) to not only activate innate immunity but also generate antigen-specific adaptive immune responses, a defining feature of immunogenic cell death (ICD). In addition to bona fide ICD, it is recognized that tumor cells paralyzed in a non-replicative senescent state are also highly immunogenic through the release of immunostimulatory soluble factors, upregulation of major histocompatibility complex (MHC) molecules, and altering the array of antigens presented to T cells.
Clinical data with topoisomerase I inhibitor (TOP1i)-ADCs show responses in numerous human cancers with growing evidence that immune system engagement may contribute to their clinical activity. Therefore, we sought to determine the immunogenicity of topoisomerase I inhibition. TOP1i treatment *in vitro* induced a highly immunogenic state of murine tumor cells, which when injected to mice, acted as a cellular vaccine and resulted in the rejection of secondary live tumors. Vaccination with TOP1i treated cells required host type 1 conventional dendritic cells (cDC1) and $CD8^+$ T cells for protection. Interestingly, characterization of cell death kinetics following TOP1 inhibition reveled that the immunogenicity of TOP1i treated cells is largely derived from stressed, living cells rather than dead cells. Treatment with highly immunogenic doses of TOP1i *in vitro* revealed that tumor cells rapidly alter their physiology to exhibit multiple hallmarks of cellular senescence. Following TOP1i treatment, tumor cells were durably arrested in cell cycle (G2M), upregulated p21, exhibited heightened β-galactosidase activity and produced inflammatory senescence associated secretory phenotype (SASP) cytokines, as well as type I IFNs, and became sensitive to senolytic agents. Moreover, TOP1i treated cells were able to induce robust cDC1 activation and promote the acquisition of a mregDC like phenotype which was dependent on tumor expression of the stimulator of interferon genes (STING). Using a human antigen expressing syngeneic tumor model we demonstrated that TOP1i-ADC activity was greatly enhanced in the presence of adaptive immunity and synergizes with anti-PD1 therapy. Together these data highlight the immunogenic nature of topoisomerase I inhibition and provide new insights into the potential mechanism underlying the emerging clinical benefits of TOP1i-ADCs for the treatment of cancer.

#2857 Repeated RFA remodels the PDAC microenvironment and synergizes with CSF1R blockade and checkpoint inhibition to enhance anti-tumor immunity.

Lincoln Strickland[1], Wendao Liu[2], Casey Van Kirk[1], Shwetapadma Dash[1], MacKenzie Demmel[1], Alyssa Waller[1], Nicolette R. Mardik[3], Jesse Cox[1], Curtis J. Wray[4], Zhongming Zhao[5], Nirav Thosani[6], Jennifer Bailey-Lundberg[1]

[1]University of Nebraska Medical Center, Omaha, NE,[2]The University of Texas MD Anderson Cancer Center UTHealth Houston Graduate School of Biomedical Sciences, Houston, TX,[3]The University of Texas Health Science Center, Houston, TX,[4]Assistant Professor, Dept. of Surgery, UT Health Science Ctr. at Houston, Houston, TX,[5]Assoc. Professor, Biomedical Informatics and Cancer Bio., University of Texas Health Science Center at Houston, Houston, TX,[6]University of Texas Health Science Center at Houston, Houston, TX

Background: Pancreatic ductal adenocarcinoma (PDAC) is defined by a profoundly immunosuppressive tumor microenvironment (TME). In the majority of cases, treatment is palliative as there are few effective therapeutic options shown to improve clinical outcomes. We previously demonstrated that a single radiofrequency ablation (RFA) session is safe, induces tumor necrosis, enhances immune cell infiltration, including an abscopal effect, and synergizes with immune checkpoint blockade (ICB) to further suppress tumor growth.

Hypothesis: We proposed that repeated RFA sessions would more effectively restrain tumor progression, amplify immune cell recruitment, and enhance responsiveness to immunotherapy.

Methods: Using a bilateral tumor-bearing *Kras*^{G12D};*Trp53*$^{R172H/+}$;*Pdx1*:Cre syngeneic PDAC model, we compared tumor responses following single versus 3 repeated RFA sessions. Single-cell RNA sequencing and cytokine profiling were used to characterize TME remodeling. Given our prior findings with a single RFA session + ICB, we evaluated repeated RFA in combination with ICB and tested whether adding CSF1R blockade (PLX3397) could counteract RFA-induced myeloid immune suppression.

Results: Repeated RFA significantly reduced tumor growth rates and increased tumor necrosis in both treated and contralateral lesions compared to a single RFA session. scRNA-seq and cytokine analysis revealed that repeated RFA elevated Csf1 levels, promoting differentiation of immune suppressive Csf1r+ M2-like macrophages via the Csf1/Csf1r axis. While repeated RFA combined with ICB improved tumor control compared with either therapy alone, the addition of CSF1R inhibition further enhanced efficacy. The triple combination (repeated RFA + ICB + anti-CSF1R) produced the greatest reduction in tumor volume and weight and yielded the most pronounced remodeling of the TME.

Conclusions: Repeated RFA intensifies tumor necrosis, suppresses tumor progression, and remodels the PDAC TME, but concurrently induces a compensatory Csf1/Csf1r-driven M2-like macrophage response. Macrophage reprogramming through CSF1R blockade enhances both RFA- and ICB-mediated anti-tumor immunity. These findings support integrating repeated local ablative therapy with myeloid-targeting agents and checkpoint blockade to improve immunologic control of pancreatic cancer.

: Microbiome, Inflammation, and Response to Immunotherapy in Cancer
Poster Session

#2861 Comparative genomics of gut commensal *Lachnospiraceae* and their associations with cancer treatment response with immune checkpoint inhibitors.

Shiva Jahanbakhshi, Amna Bibi, Rebecca Hoyd, Caroline Dravillas, Nyelia Williams, Shiqi Zhang, Aaditya Pallerla, Shankar Suman, Joseph Amann, Mounika Goruganthu, Tamio Okimoto, Yangyang Liu, Marisa A. Bittoni, Ni Shi, Alvin Anand, Bailey Conrad, Lane Nevers, Kristen Heitman, Maxine Webb, Elizabeth M. Grainger, Madison Grogan, Christian Quiles, Tong Chen, Carolyn J. Presley, Lang Li, Patrick Bradley, Yael Vodovotz, David P. Carbone, Steven K. Clinton, Jiangjiang Zhu, Daniel Spakowicz

The Ohio State University, Columbus, OH

Immune checkpoint inhibitors (ICIs) are seminal advances in cancer therapeutics, yet response rates are variable. The gut microbiome is increasingly recognized as a modifiable determinant of ICI efficacy. The BEWELL trial delivered a black raspberry (BRB) nectar dietary intervention that significantly enriched the colonic microbiome with members of the *Lachnospiraceae* family. When BRB-modulated microbiomes were transferred into mice, these microbiomes enhanced ICI antitumor activity, implicating specific taxa in shaping therapeutic responsiveness.To investigate the mechanism by which *Lachnospiraceae* altered ICI effectiveness, we individually supplemented the microbiomes of mice with closely related strains enriched by BRB: *Blautia obeum*, *Blautia massiliensis*, and *Agathobacter rectalis*. In a heterotopic mouse model (1×10^6 MC38 cells injected subcutaneously into C57BL/6 mice, treated every 3 days with anti-PD1 or IgG), *B. obeum* and *B. massiliensis* improved ICI effectiveness, whereas *A. rectalis* did not. We compared the genomes of these organisms and identified 177 KEGG orthologs uniquely shared by *B. obeum* and *B. massiliensis* but absent in *A. rectalis*. KO pathway assignments and enrichment analyses were conducted using KEGGREST mapping and clusterProfiler overrepresentation testing, with all genome-encoded KOs as the background.We identified four relevant pathways associated with immunity and ICI response:**(1)** Key genes for the Wood-Ljungdahl pathway, a major route for producing acetate, shown to be a T-cell energy source (acetyl-CoA decarbonylase/synthase (K00194, K00197, K00198) and putative phosphotransacetylase (K01490));**(2)** Genes for synthesizing vitamins essential for T-cell proliferation—folate (B9) (dihydropteroate synthase (K00796), GTP cyclohydrolase I (K022391), methylenetetrahydrofolate reductase (K00297)) and cobalamin (B12) (cob(I)alamin adenosyltransferase (K019221), corrinoid adenosyltransferase (K0174), cobalamin reductase (K0175));**(3)** L-rhamnose synthesis genes whose cell-wall decorations act as microbe-associated molecular patterns, priming innate immunity (dTDP-4-dehydrorhamnose reductase (K00067) and dTDP-glucose 4,6-dehydratase (K00935)); and**(4)** Genes converting bile acids to secondary, iso-bile acids that interact with host receptors (FXR, TGR5) to regulate Th17/Treg balance (3-alpha-hydroxycholanate dehydrogenase (K0164))
Collectively, these processes align with host-relevant metabolic and signaling environments that may impact anti-tumor immunity. Our study suggests that novel food products can be developed for human testing to enhance anticancer immunotherapeutics. Furthermore, BRB-responsive *Lachnospiraceae* possess enriched metabolic and immunomodulatory gene programs that may underlie their association with improved tumor response to ICI treatment.

#2862 Dietary animal protein intake and progression-free survival (PFS) of patients (pts) with advanced urothelial cancer (UC) and renal cell carcinoma (RCC) on immune checkpoint blockade (ICB).

Timothy B. Winslow[1], Ritesh Kotecha[2], Neha Ratna[2], David Gavrilov[2], Cihan Duzgol[2], Mahnoor Akhlaq[2], Min Yuen Teo[2], Ashley M. Regazzi[2], Samuel Funt[2], David H. Aggen[2], Scot Niglio[2], Maria Carlo[2], Daniel Lage[2], Neil Shah[2], Aditi Gupta[2], Darren F. Feldman[2], Martin H. Voss[3], Robert J. Motzer[4], Jonathan E. Rosenberg[2], Gopa Iyer[2], Brendan John Guercio[1]

[1]University of Rochester Wilmot Cancer Institute, Rochester, NY,[2]Memorial Sloan Kettering Cancer Center, New York, NY,[3]Asst. Attending, Dept. of Med. Onc., Memorial Sloan Kettering Cancer Center, New York, NY,[4]Attending Physician, Ball Memorial Hospital, New York, NY

Background: Dietary fiber intake has been associated with longer PFS on ICB in observational studies, putatively due to effects of fiber on the gut microbiome. However, associations in observational studies may be due to confounding rather than causal relationships. Dietary animal protein intake impacts health and can be correlated with fiber intake. We investigated whether animal protein intake is associated with ICB outcomes in UC and RCC and whether confounding by animal protein intake might account for associations of fiber intake with ICB outcomes.
Methods: We conducted a retrospective analysis of a prospectively collected cohort, wherein baseline dietary data were collected using the Willett Food Frequency Questionnaire from pts with advanced UC or RCC initiating ICB at Memorial Sloan Kettering. Associations of diet with clinical outcomes were assessed using univariable and multivariable Cox proportional hazards regression.
Results: From 2/2021-6/2022, 86 pts eligible for this analysis were enrolled (UC n = 38; RCC n = 48; median follow-up 14.6 months). Median animal protein intake was 44 g/day (interquartile range [IQR] 31-54), below the American average of 88 g/day. Median fiber intake was 17.2 g/day (IQR 13-24), similar to the American average of 15 g/day. Intake of animal protein and fiber were correlated (Spearman's rho 0.46, $p < 0.001$). There were no statistically significant associations of animal protein intake above vs below the median with PFS in either univariable or multivariable models (Table 1). Dietary fiber intake was associated with longer PFS even after adjusting for animal protein intake and clinical covariables (Table 1).
Conclusion: Dietary animal protein intake was not associated with PFS among pts with UC and RCC on ICB. The association of dietary fiber with longer PFS could not be attributed to confounding by animal protein intake.

Hazard ratios for progression-free survival by average daily intake of animal protein and fiber

	Animal protein intake at or above the cohort median (44 g/day)		Fiber intake at or above the American average (15 g/day)	
Outcomes	HR (95% CI)	p	HR (95% CI)	p
Univariable	0.74 (0.43-1.26)	0.27	0.45 (0.26-0.77)	**0.004**
Multivariable 1*	0.94 (0.53-1.68)	0.85	0.46 (0.26-0.82)	**0.009**
Multivariable 2**	0.82 (0.45-1.50)	0.53	0.49 (0.26-0.92)	**0.026**
*Multivariable model 1 included animal protein and fiber intake simultaneously. **Multivariable model 2 further adjusted multivariable model 1 for age, performance status, cancer type, and stage (IV vs III).				

#2863 Investigating the impact of metabolic endotoxemia on breast cancer risk and progression.

Lauren M. Moulden[1], Adam S. Wilson[1], Valerie S. Payne[1], Marissa M. Howard-McNatt[2], Katherine L. Cook[1]

[1]Department of Cancer Biology, Wake Forest University School of Medicine, Winston Salem, NC,[2]Department of Surgery, Wake Forest University School of Medicine, Winston Salem, NC

Breast cancer is the most diagnosed cancer in women and the second most deadly, responsible for 670,000 deaths globally each year. Two main risk factors for breast cancer are aging and obesity, both of which are known to cause microbial dysbiosis and alterations in gut barrier function. These changes can result in chronic low levels of circulating lipopolysaccharides (LPS) in the blood, termed metabolic endotoxemia (ME). LPS interacts with toll-like receptor 4 (TLR4) resulting in the release of pro-inflammatory cytokines. Previously, our group has shown in non-cancerous postmenopausal women that obesity increases circulating LPS levels and other biomarkers of ME. However, in breast cancer patients (n=60), menopause status, not obesity, increases plasma LPS binding protein, anti-LPS IgG, and anti-LPS IgA. To investigate the impact of menopause, adiposity, and breast tumor presence on ME, we have employed a C57BL/6 murine study bearing E0771.Bo-ER+ breast tumors. Female 11-week-old C57BL/6 mice were placed on a low-fat control diet (10% kcal from fat, n=24) or a high-fat lard diet (60% kcal from fat, n=24). Subgroups of mice on each diet (n=8) underwent sham or ovariectomy (OVX) surgeries to model menopause. Additionally, we introduced fecal microbiota transplantation (FMT) groups (n=8) to examine the role of the gut microbiome. After 13 weeks of intervention, E0771.Bo-ER+ cells were injected into the mammary fat pad. We show the presence of a breast tumor (~400 mm^3 in tumor volume) significantly increases markers of ME. Furthermore, we show that a low-fat diet-derived FMT into high-fat diet consuming mice reduces breast tumor growth. LPS can vary in structure (displaying varying numbers of fatty acid chains on the lipid A toxin) and can differentially activate downstream TLR4 signaling. We show that various acylated isoforms of LPS can differentially activate NFκB and alter macrophage polarization and function. Overall, we aim to show whether the presence of breast cancer can directly influence ME and determine whether ME can impact breast cancer growth, thereby identifying a novel risk factor for breast cancer.

#2864 Prebiotic fiber supplementation mitigates the effects of maternal obesity on offspring's gut microbiome and mammary tumorigenesis.

Seema Yadav[1], Fabia Andrade[1], Melike Ozgul Onal[1], Sydney Shirk[1], Sercan Kenanogly[1], Christopher Staley[2], Leena Hilakivi-Clarke[1]

[1]The Hormel Institute, University of Minnesota, Austin, MN,[2]University of Minnesota Medical School, Minneapolis, MA

The prevalence of maternal obesity has gradually increased over successive decades, with over 50% of pre-pregnant women in the United States at present time classified as overweight or obese. Maternal obesity exerts deleterious effects on numerous pregnancy outcomes and imparts enduring negative health consequences on offspring, including elevating female offspring's susceptibility to and mortality from breast cancer. Since the gut microbiome contributes to obesity and its adverse effects, and influences breast carcinogenesis, we investigated here whether gut dysbiosis, characterized by reduced fecal short-chain fatty acid (SCFA) levels, in mouse offspring born to diet-induced obese C57BL/6 dams (OB offspring) contributed to their higher E0771 mammary tumor burden, compared with control offspring. Fecal microbiota transplant (FMT) from OB offspring increased E0771 mammary tumor burden in control offspring host, suggesting a causality between gut dysbiosis and increased mammary tumorigenesis in OB offspring. Further, levels of SCFA receptor FFAR2 in CD4+ T cells, CD8+ T cells and Foxp3+ regulatory T cells in Peyer's patches in gut and in CD8+ T cells in tumors were significantly lower in control offspring receiving FMT from OB offspring donor than from control offspring donor. To determine if increased mammary tumorigenesis in OB offspring can be reversed by increasing fecal SCFA production by dietary fiber, we employed the MMTV-PyMT mammary tumor model, in which mammary tumors develop "spontaneously" by 4 months of age. Our results indicated that MMTV-PyMT OB offspring exhibited significantly increased mammary tumor burden compared with controls. Supplementing offspring via drinking water with partially hydrolyzed guar gum (PHGG), a prebiotic fiber, exhibited significantly lower mammary tumorigenesis and higher fecal levels of SCFA propionic acid than OB offspring receiving maltodextrin (MDX) control. In contrast, control offspring receiving PHGG did not show changes in mammary tumorigenesis, although PHGG supplementation increased their fecal butyric acid levels. These results suggest that increased mammary tumorigenesis in OB offspring are linked to their gut dysbiosis. In addition, prebiotic
fiber PHGG, consumed by adult OB offspring, reverses adverse effects of maternal obesity on both their gut microbiome and mammary tumorigenesis.

#2865 Colorectal cancer-infiltrating bacteria promote the proliferation of cytotoxic lymphocyte populations endowed with antitumor properties.

Martina Villa[1], Julija Djordjevic[1], Elisa Sorrenti[2], Pedro Ventura[3], Davide Bressan[4], Antonino Cassotta[3], Caroline Junqueira[3], Fulvio Chiacchiera[4], Federica Sallusto[3], Dimitrios Christoforidis[5], Giandomenica Iezzi[2]

[1]Institute for Translational Research USI-EOC, Ente Ospedaliero Cantonale, Bellinzona, Switzerland,[2]Ente Ospedaliero Cantonale, Bellinzona, Switzerland,[3]Institute for Research in Biomedicine, Bellinzona, Switzerland,[4]Department of Cellular, Computational, and Integrative Biology, University of Trento, Trento, Italy,[5]Department of Surgery, Ente Ospedaliero Cantonale, Lugano, Switzerland

Colorectal cancer (CRC) is the second-leading cause of cancer deaths worldwide. During CRC carcinogenesis alteration of the gut epithelial barrier allows the translocation of commensal bacteria from the gut to the tumor tissue and their interaction with infiltrating immune cells. Infiltration by cytotoxic T lymphocytes is associated with improved survival, but their potential interplay with tumor-infiltrating bacteria has not been fully investigated.We previously identified a panel of bacteria whose abundance in CRC tissues correlates with the extent of lymphocytic infiltration. In this work, we have investigated the capacity of these bacteria to induce lymphocyte-mediated immune responses.Peripheral blood mononuclear cells from healthy donors or patients were cultured with cryopreserved bacteria of interest and assessed for proliferation based on CFSE dilution. Proliferating cells mostly consisted of CD4-CD8- double negative (DN) T cells expressing γδTCRs, and in particular the Vδ2 chain. CD4+ and CD8+ TCRαß+ T cells were also detected among proliferating cells. Following activation, DN Vδ2+ T cells released IFNg, TNFα, perforin, and granzymes suggesting a cytotoxic potential. Their concomitant expression of NKG2D led us to investigate whether they could mediate tumor-cell killing against CRC cell lines. In contrast to CD4+ and CD8+, bacteria-reactive DN T cells showed MHC-independent tumor cell killing.Analysis performed by large-scale flow cytometry and single-cell RNA sequencing of primary CRC samples revealed the presence of DN TCRγδ+ T cells among tumor-infiltrating lymphocytes (TILs). Interestingly, their phenotypes and transcriptomic profiles were found to partially overlap with those of bacteria-reactive DN T cells from peripheral blood. The reactivity of DN TILs to CRC-associated bacteria is currently under investigation.Bacteria-mediated activation of CRC-infiltrating DN T cells may favor a double-sided targeting of the tumor, contributing to an effective antitumor immune response.

#2866 Host-microbe-epigenetic crosstalk: Dissecting the role of microbiome, immune dysregulation, and DNA methylation in squamous cell carcinoma.

Armando G. Licata[1], Cristina Gurizzan[2], Deborah Lenoci[1], Marta Lucchetta[1], Carlo Resteghini[3], Luigi Lorini[2], Rosalba Miceli[4], Paolo Bossi[3], Loris De Cecco[1]

[1]Research department, Fondazione IRCCS Istituto Nazionale dei Tumori, Milan, Italy,[2]Department of Biomedical Sciences, IRCCS Humanitas Research Hospital, Milan, Italy,[3]Department of Biomedical Sciences, Humanitas University IRCCS Humanitas Research Hospital, Milan, Italy,[4]Unit of Biostatistics for Clinical Research, Fondazione IRCCS Istituto Nazionale dei Tumori, Milan, Italy

Squamous carcinomas of the oral cavity and head and neck share molecular, microbial, and immune features. Dysbiosis and intratumoral microbiota are increasingly implicated in epithelial transformation, with taxa such as *Fusobacterium nucleatum* linked to inflammation, hypoxia, immune evasion, and metastasis across squamous sites. Defining how host-microbe-immune interactions evolve from oral premalignant lesions to invasive tumors could reveal early biomarkers and modifiable microbial targets for prevention, risk stratification, and intervention. We analyzed samples from 66 oral potentially malignant diseases (OPMD) and 74 head and neck squamous cell carcinoma (HNSCC) using a multi-omics approach. Cohorts were profiled via RNA-seq, shotgun metagenomics, and multiplex cytokine assays. Epigenetic profiling of 20 HNC samples was performed using Nanopore sequencing to assess genome-wide DNA methylation. In OPMDs, a high-risk hypoxic subtype showed an elevated incidence of malignant transformation ($p < 0.0001$), reduced microbial diversity, and significantly elevated abundance of *Fusobacterium nucleatum* and *Leptotrichia wadei* ($Log_2FC > 1$, $FDR < 0.05$). *F. nucleatum* activity correlated strongly ($R>0.7$) with keratinocytes and pericytes. While HNSCC alpha diversity remained stable, community structure shifted (PERMANOVA $p=0.001$), marked by an enrichment of *Lactobacillus spp.* driving palmitate metabolism, whereas OPMD favored starch degradation and nitrate reduction. Immune profiling revealed a profound dysregulation within head and neck tumors. While OPMD was characterized by high levels of pro-inflammatory mediators (TNF-α, IL-6), these cytokines were markedly downregulated in HNSCC. This suggests a functional shift from an acute inflammatory response in OPMDs toward a chronic, immune-suppressive state in established carcinoma. Finally, our epigenetic analysis linked oral dysbiosis with host metabolism, revealing significant differential methylation in overweight HNC patients. Our analysis revealed significant hypomethylation affecting key oncogenic and immunomodulatory genes, including NOTCH1, STAT3, and the antigen-presenting gene HLA-DRB1. Our findings demonstrate a conserved microbial trajectory in the progression of head/neck carcinomas, characterized by the enrichment of *Fusobacterium* and a functional switch from a pro-inflammatory to an immune-evasive tumor microenvironment. These results point to a shared microbial etiology in squamous cancers, and the ongoing epigenetic analysis will provide deeper mechanistic insights into how these host-microbe interactions drive malignant transformation.

#2867 Interaction between T-cell inflamed gene expression profile score and tumor-associated microbiome on colorectal cancer mortality in a heterogeneous patient population.

Claire Elizabeth Thomas[1], Hang Yin[1], Jeroen Huyghe[1], Nicole Catalina Lorona[2], Scott D. Labrie[1], Keith R. Curtis[1], Orsalem Kahsai[1], Sosun Nayemi[1], Ningxin Ma[3], Timothy Randolph[3], Conghui Qu[1], Sushma Thomas[1], Li Hsu[1], Amanda L. Koehne[4], Heather Green-Mantrana[5], Marc Matrana[5], James J. Tiesinga[6], William M. Grady[1], Diana Redwood[7], Christopher I. Li[1], Li Li[5], Riki (Ulrike) Peters[1], Jane C. Figueiredo[2], Timothy K. Thomas[7], Amanda I. Phipps[8], **Meredith A. Hullar**[1]

[1]Public Health Sciences, Fred Hutchinson Cancer Center, Seattle, WA,[2]Cedars-Sinai Medical Center, Los Angeles, CA,[3]Clinical Research Division, Fred Hutchinson Cancer Center, Seattle, WA,[4]Experimental Histopathology, Fred Hutchinson Cancer Center, Seattle, WA,[5]Ochsner Health System, New Orleans, LA,[6]Alaska Native Medical Center, Anchorage, AK,[7]Alaska Native Tribal Health Consortium, Anchorage, AK,[8]Department of Epidemiology, University of Washington, Seattle, WA

Background: The microbiome and tumor immune response are important and inter-related components that are implicated in colorectal cancer (CRC) prognosis. However, associations between these components and potential joint effects on CRC mortality remain unclear.

Methods: We included 366 participants with CRC (106 African American, 161 Alaska Native, 91 Hispanic, 8 non-Hispanic White) from the Translational Research Program in Cancer Differences across Populations (TRPCDP). 241 participants who did not die of CRC were matched to 125 participants who died of CRC during follow-up by age, sex, tumor site, tumor stage, year of diagnosis, and population group. We sequenced microbial DNA from the V4 region of the 16S rRNA bacterial gene and sequenced RNA using the Illumina TruSeq RNA Exome kit from formalin-fixed paraffin embedded (FFPE) tumor tissue. We calculated the T-cell inflamed gene expression profile (GEP) score as a weighted sum of $\log_2$-transformed transcripts per million of 18 genes: CCL5, CD27, CD274 (PD-L1), CD276 (B7-H3), CD8A, CMKLR1, CXCL9, CXCR6, HLA-DQA1, HLA-DRB1, HLA-E, IDO1, LAG3, NKG7, PDCD1LG2 (PDL2), PSMB10, STAT1, and TIGIT. We dichotomized the T-cell inflamed GEP score into high and low groups using the top tertile as a threshold. Using logistic regression, we estimated odds ratios (OR) and 95% confidence intervals (CI) for associations between bacterial presence and dichotomized T-cell inflamed GEP score, as well as interaction effects of bacteria and dichotomized T-cell inflamed GEP score on CRC-specific mortality, adjusting for matching factors.

Results: Among 48 genera tested, Anaerococcus was associated with lower odds of high T-cell inflamed GEP score (OR=0.34, 95% CI 0.20-0.58) and Leptotrichia was associated with higher odds of high T-cell inflamed GEP score (OR=2.93, 95% CI 1.66-5.22). When combined, the joint effect of tumors being Leptotrichia positive and low T-cell inflamed GEP score was associated with over four times the odds of CRC mortality (OR=4.41, 95% CI 1.86-10.83) compared to tumors that were Leptotrichia negative and high T-cell inflamed GEP score.

Conclusions: The joint effect of Leptotrichia presence and low T-cell inflamed GEP score resulted in markedly higher odds of CRC death. Understanding the influence of this immune-microbiota interaction may improve CRC prognostic stratification and enable the discovery of new treatment targets to improve CRC prognosis.

#2868 MaaT013 pooled fecal microbiotherapy improves gastrointestinal physiology and controls inflammation which delays GvHD in a proof-of-concept humanized mouse study.

Julie Reygner[1], Margaux De Seilhac[2], Cyrielle Gasc[1], Emmanuel Prestat[1], Charlotte Petitjean[1], Sophie Declomesnil[1], Carole Schwintner[1], Nathalie Corvaia[1], Sheri Simmons[1], Ernst Holler[3], Robert R. Jenq[4], **Bastien Laperrousaz**[1]

[1]MaaT Pharma, Lyon, France,[2]Immunology and New Concepts in ImmunoTherapy (INCIT), UMR 1302, University of Nantes, University of Angers, INSERM, CNRS, Nantes, France,[3]Department of Internal Medicine III (Haematology/Oncology), University Hospital Regensburg, Regensburg, Germany,[4]Department of Hematology & Hematopoietic Cell Transplantation, City of Hope, Duarte, CA

Background: Acute graft-versus-host disease (aGvHD) is a life-threatening complication of allogeneic hematopoietic stem cell transplantation (allo-HSCT), where allogeneic donor T cells recognize recipient tissues as foreign and damage them. Gut microbiota disruption following allo-HSCT has been associated with increased aGvHD incidence, severity, and mortality. The gut microbiota plays a key role in the modulation of the immune system, particularly in maintaining immune tolerance. These results prompted the development of fecal microbiotherapies to restore a healthy and diverse gut microbiota and to treat or prevent aGvHD. Growing clinical evidence supports the efficacy of fecal microbiotherapy in aGvHD mortality. MaaT013, a standardized allogeneic fecal microbiotherapy derived from pooled healthy human fecal microbiota, has demonstrated unprecedented efficacy and favorable safety profile as third-line treatment of aGvHD with gastro-intestinal (GI) involvement in the pivotal ARES trial.

Method: In this study, we combined *in vitro*, *in vivo*, metagenomics, metabolomics and transcriptomics studies to elucidate the underlying mechanisms by which MaaT013 influences GvHD.

Results: We demonstrate that MaaT013-derived metabolites control inflammation and prevent inflammation-induced gut barrier alteration in an *in vitro* leaky gut model. We also show that MaaT013 is able to modulate immunity by activating TLR and NOD sensors, stimulating DC-mediated IL-10 production and Tregs amplification *in vitro*. We further demonstrate that beneficial bacteria from MaaT013 safely engraft in the digestive tract of germ-free mice, leading to the production of anti-inflammatory metabolites and restoring healthy gut physiology and immune homeostasis. Transcriptomic analysis of colon tissue from MaaT013-treated germ-free mice provides further evidence that MaaT013 promotes gastrointestinal maturation and restores immune functions. Finally, we demonstrate that MaaT013 delays the appearance of GvHD symptoms in a humanized mouse model of aGvHD using highly immunodeficient mice engrafted with human Peripheral Blood Mononuclear Cells (PBMCs).

Conclusion: Altogether, these results support the potential of MaaT013 to mitigate aGvHD through restoration of microbial diversity, gut barrier integrity, and immune homeostasis, leading to control of inflammation.

#2869 Maternal obesity promotes gut dysbiosis, CD4⁺ T-cell reprogramming and increased prostate cancer in offspring.

Fabia de Oliveira Andrade[1], Lu Jin[1], Melike Ozgul Onal[1], Seema Yadav[1], Sercan Kenanoglu[1], Christopher Staley[2], Leena Hilakivi-Clarke[1]

[1]The Hormel Institute, University of Minnesota, Austin, MN,[2]University of Minnesota Medical School, Minneapolis, MA

Maternal obesity (MO) is a growing global concern linked to long-term disease risk in offspring and may also increase prostate cancer susceptibility, although the mechanisms remain unclear. We tested whether MO-induced gut dysbiosis promotes prostate cancer in male offspring and reprograms immune function. Using a TRAMP-C1 allograft model, we evaluated male offspring from dams fed a control diet or an obesity-inducing diet (OID). Gut microbiota was assessed by 16S rRNA sequencing and SCFA profiling. Causality was tested using antibiotic ablation and fecal microbiota transplantation (FMT), and microbiota modulation was further examined using a prebiotic intervention with partially hydrolyzed guar gum (PHGG). Activated splenic T cells were analyzed with paired RNA-seq and ATAC-seq. MO increased prostate tumor burden in adult offspring and induced gut dysbiosis marked by reduced α-diversity and significantly lower fecal butyric acid. Gut microbiota ablation reversed the MO-induced increase in tumor growth, whereas FMT from MO offspring transferred the pro-tumor phenotype to control mice. MO induced profound immune reprogramming that was specific to CD4⁺ T cells and not observed in CD8⁺ T cells. RNA-seq data revealed activation of Th2 and pro-inflammatory pathways, including Th17 differentiation (NES 1.96, p.adj 0.009) and JAK-STAT signaling (NES 2.1, p.adj 0.0009). We also observed reduced antigen-presentation (NES -2.24, p.adj 0.0007) and interferon-signaling programs (NES -3.4, p.adj 8.39E-06), indicating impaired IFN-driven activation.Twenty-one loci exhibited concordant chromatin (ATACseq) and transcriptional remodeling, including repression of *Zbtb10* and *Ifrd1*, regulators of Th1 differentiation. These molecular changes manifested in vivo as increased Th2 (GATA3⁺) and Th17 (RORγ⁺) cells and reduced Th1 (Tbet⁺) cells in spleen, and impaired CD8⁺IFNγ⁺ cytotoxicity in tumors. Antibiotic ablation partially normalized inflammatory signatures, indicating that gut dysbiosis contributes to—but does not fully explain—MO-driven immune remodeling. These findings suggest a combined effect of long-lasting epigenetic alterations and microbiome-driven signals. Prebiotic PHGG, which increases SCFA production, reduced tumor growth in MO offspring, demonstrating that microbiome-targeted interventions can mitigate MO-induced cancer susceptibility. Overall, our data indicates that MO is associated with a microbiota-dependent increase in prostate cancer risk in offspring, alongside a durable and epigenetically imprinted CD4⁺ T-cell program.

#2870 Amino acid metabolic reprogramming drives doramectin-enhanced CD8⁺ T cell immunity and tumor control.

Sedigheh Taghinezhad-S[1], Amirhossein Mohseni[2], Vincenzo Casolaro[3], Zhongwei Lv[4], Dan Li[5]

[1]Department of Hematology-Oncology, Henry Ford Health, Detroit, MI,[2]Division of Gynecologic Oncology, Department of Women's Health Services, Henry Ford Health, Detroit, MI,[3]Department of Medicine, Surgery and Dentistry "Scuola Medica Salernitana", University of Salerno, Baronissi, Salerno, Italy,[4]Department of Nuclear Medicine, Shanghai Tenth People's Hospital, Tongji University School of Medici, Shanghai, China,[5]Department of Nuclear Medicine, Sun Yat-sen Memorial Hospital, Sun Yat-sen University, Guangzhou, China

CD8⁺ T-cell metabolic programming is a pivotal determinant of antitumor immunity, yet strategies to therapeutically activate these pathways remain limited. Here, we show that doramectin, a clinically available macrocyclic lactone, enhances antitumor immunity by reprogramming amino acid metabolism in CD8⁺ T-cells. In tumor-bearing mice, doramectin promoted amino acid-dependent metabolic engagement, strengthened effector function, supported memory differentiation, and increased CD8⁺ T-cell infiltration into the tumor microenvironment, collectively resulting in durable tumor control. These findings suggest that doramectin induces a metabolically reinforced T-cell state capable of sustaining immunosurveillance. Mechanistically, doramectin enhanced amino acid-linked bioenergetic and biosynthetic pathways, consistent with elevated metabolic fitness and immune competence. A critical requirement for this metabolic reprogramming was revealed through the role of the gut microbiota. Doramectin treatment led to a selective microbial shift, with specific taxa trafficking to lymphoid tissues where they delivered signals required for CD8⁺ T-cell metabolic engagement. When these microbial signals were disrupted, the metabolic reprogramming and corresponding antitumor effects failed to manifest, indicating that the microbiota acts as a permissive metabolic cofactor rather than an autonomous initiator of immunity. Together, these results define a metabolism-centered mechanism by which doramectin enhances antitumor immunity through microbiota-enabled amino acid metabolic reprogramming of CD8⁺ T-cells. This work highlights the therapeutic potential of targeting amino acid metabolism, supported by microbial cues, to improve T-cell mediated immunotherapy in solid tumors and underscores the importance of host-microbe metabolic crosstalk in shaping antitumor immune responses.

#2873 Neurotensin suppresses anti-tumor immunity and is associated with poor prognosis in colorectal cancer.

Haoming Wu, Yang Wang, Dana Napier, Hong Jiang, Dong Li, Jing Li, B. Mark Evers

Markey Cancer Center, University of Kentucky, Lexington, KY

Introduction. Colorectal cancer (CRC) is a leading cause of cancer-related deaths worldwide with substantial heterogeneity in patient outcomes. Neurotensin (NTS) and its high-affinity receptor (NTSR1) have been implicated in CRC progression, particularly in modulating tumor metabolism and immune responses. NTS secretion increases under psychological stress and high-fat intake. Given the widespread expression of NTSR1 on immune cells, we hypothesized that NTS modulates anti-tumor immunity in CRC. The purpose of our current study was to integrate clinical, *in vivo*, and functional evidence to delineate the impact of NTS on immune responses and patient outcomes.

Methods. (i) Clinical survival: Overall survival (OS) was analyzed in a single-institution CRC cohort (University of Kentucky; n=196) stratified by tumor NTS expression, and findings were validated using KMplot (n=1,061). (ii) Transcriptomic correlation: Correlations between NTS and immunosuppressive genes (e.g., IL10, ENTPD1) were assessed utilizing publicly available datasets (GEPIA/TCGA). (iii) *In vivo*: Murine CRC cells (MC38) were implanted subcutaneously into NTS wild-type (NTSWT) and NTS knockout (NTSKO) mice to compare tumor growth. Tumor-infiltrating immune cells and granzyme B (GZMB) expression were quantified by immunohistochemistry (IHC) and flow cytometry. (iv) *In vitro* cytotoxicity: MC38 cells were co-cultured with spleen-derived CD8+ T cells from MC38-primed mice, with or without NTS treatment, and cytotoxicity was measured by LDH release.

Results. (i) High NTS expression was associated with shorter OS in the institutional cohort ($P<0.05$) and was validated in the KMplot dataset (n=1,061; $P<0.001$). (ii) NTS expression showed significant positive correlations with multiple immunosuppressive genes, including IL10 ($P=0.0038$) and ENTPD1 ($P=0.046$). (iii) *In vivo*, NTSKO mice exhibited markedly slower tumor growth, with increased immune-cell infiltration and higher intratumoral GZMB expression. (iv) *In vitro*, NTS treatment significantly reduced CD8+ T-cell cytotoxicity against MC38 cells, as indicated by decreased LDH release, supporting a direct suppressive effect of NTS on effector T-cell function.

Conclusions. High NTS expression identifies CRC patients with poorer prognosis and functionally suppresses anti-tumor immunity by limiting CD8+ T-cell infiltration and cytotoxic activity. Interventions that lower NTS (e.g., stress reduction and dietary optimization) may improve responses to immunotherapy and clinical outcomes. These findings provide a biological rationale for targeting the NTS/NTSR1 axis in combination with immunotherapeutic strategies.

#2874 PPARδ overexpression in villin-positive gastric progenitor cells drive gastric tumorigenesis independent of helicobacter infection in mice.

Daoyan Wei[1], Yi Liu[1], James C. Yao[1], Imad Shureiqi[2], Xiangsheng Zuo[1]

[1]UT MD Anderson Cancer Center, Houston, TX,[2]University of Michigan, Ann Arbor, MI

Background Overexpression of the single gene PPARδ in villin-positive gastric progenitor cells (VGPCs) has been shown to induce gastric adenocarcinoma (GAC) in villin-PPARδ mice. However, PPARδ overexpression alone in colonic epithelial cells or pancreatic progenitor cells in mice fails to initiate tumorigenesis but dramatically accelerated tumor development in the colon and pancreas. These findings raise the question of whether additional factors cooperate with PPARδ to drive GAC. *H. pylori* infection is a strong risk factor for human GAC. In modified SPF barrier where villin-PPARδ mice are housed, *helicobacter* species is not excluded and presumed to be endemic. Whether such *helicobacter* infection contributes to PPARδ-driven GAC remains unknown.

Methods A new villin-PPARδ mouse line was generated via *in vitro* fertilization using frozen sperm of villin-PPARδ mice and housed in helicobacter-free barrier. At 4 weeks of age, half of the mice remained in helicobacter-free barrier (villin-PPARδ-L1), while the other half were transferred to modified SPF barrier, where *helicobacter* species is commonly detected in the gastrointestinal tract of housed mice (villin-PPARδ-L2). These mice, along with the previous villin-PPARδ mouse line that had been maintained in modified SPF barrier for years (villin-PPARδ-L3), were followed for 25, 35, and 55 weeks (n =10-12 mice per group). Wild type (WT) littermates from each line were served as controls. All mice were evaluated for tumor multiplicity and subjected to histologic examination. *Helicobacter* species was assessed by detecting 16S rRNA genes from genomic DNA extracted in mouse stomach contents and stools using qPCR/PCR.

Results *Helicobacter* species was not detectable in villin-PPARδ-L1 mice at all ages and villin-PPARδ-L2 mice at 10 and 25 weeks but were detected in villin-PPARδ-L2 mice at 35 and 55 weeks and villin-PPARδ-L3 mice at all ages. Longitudinal follow-up revealed that gastric tumorigenesis progressed in an age-dependent manner. Gross lesions were initially found in the lesser curvature of the gastric corpus at 25 weeks and eventually expanded to occupy the whole gastric corpus at 55 weeks. All mice examined at ≥ 25 weeks developed at least gastric hyperplasia. At 35 weeks, approximately 60% of mice developed low-grade or high-grade gastric dysplasia, and by 55 weeks, around 70% developed GACs, including 30% with large, locally invasive GACs. Chronic inflammation was present in gastric lesions and positively correlated with tumor progression. No significant differences in gastric inflammation and tumorigenesis were observed among three villin-PPARδ mouse lines. None of WT controls developed gastric tumors.

Conclusions PPARδ overexpression in VGPCs drive gastric tumorigenesis independent of helicobacter infection in mice, suggesting that PPARδ may be a potential therapeutic target for GAC.

#2875 Toll-like receptor 4 deletion promotes bacterial burden and cutaneous tumorigenesis in mice lacking one *Ikkα* allele in keratinocytes.

Deep Kumari Yadav, Amit Kumar Singh, Debra Tross, Yinling Hu

National Cancer Institute Frederick, Frederick, MD

Toll-like receptor 4 (TLR4) is an extracellular pathogen recognition receptor (PRR) that identifies a variety of pathogens and damage-associated molecular patterns. Analysis of human TCGA database reveals many mutations of the *Toll-Like Receptor 4* (*TLR4*) gene in human skin cancers. The exact function of PRRs in response to elevated ambient and commensal bacteria for carcinogenesis is still unknown. Recently, we found a low number of spontaneous skin squamous cell carcinomas (SCCs) in 1-year-old $Ikka^{f/+}$K5 Cre mice with specific *Ikka* reduction in keratinocytes. Interestingly, ablation of *Tlr4* enhanced SCC numbers and sizes but reduced the latency of SCC development in $Ikkα^{\Delta KC/+}; Tlr4^{-/-}$ mice compared to $Ikka^{\Delta KC/+}$ mice. Both spontaneous skin SCCs obtained from $Ikka^{\Delta KC/+}$ and $Ikka^{\Delta KC/+}; Tlr4^{-/-}$ mice showed loss of wild-type (WT) *Ikka* allele. Thus, we hypothesize that *Ikka* reduction in keratinocytes alters skin microbes and *Tlr4* deletion promote this condition, which lead to increased spontaneous skin SCCs. Indeed, the bacterial burden were increased in the skin of $Ikka^{\Delta KC/+}$ and $Ikka^{\Delta KC/+}; Tlr4^{-/-}$ mice compared to the skin of WT and $Tlr4^{-/-}$ mice predominately Gram (+) firmicutes. Further, we explore the interactions between bacteria and their hosts using skin organoids derived from these mice. Organoids are three dimensional structures recapitulating the organ's epithelial layer, linking the gap between *in vitro* and *in vivo* models. Skin organoids infected with heat killed gram positive bacteria reveals more DNA damage in the $Ikka^{\Delta KC/+}; Tlr4^{-/-}$ along with impaired bacteria clearance in these mice. Together, these findings suggest that increased bacteria cause genomic instability which leads to DNA damage. Additionally, we are investigating which bacterial pathways compromise the integrity of the skin genome through Ikka reduction or Ikka reduction/Tlr4 deletion, as well as whether Tlr4 deletion affects immune cell function in combat against bacterial infections.

#2877 The role of oral microbiota in pre-metastatic niche preparation in the brain.

Rene Nicolas Rico, Sarah B. Johnson, Vivian R. Orellana, Ashish V. Damania, Matthew C. Wong, Bharat B. Singh, Lon W. R. Fong, Brenda Melendez, Nadim J. Ajami, Jennifer A. Wargo, Golnaz Morad

UT MD Anderson Cancer Center, Houston, TX

Background: The oral microbiota plays a critical role in maintaining oral health and immune homeostasis. Emerging evidence suggests a link between oral microbiota and the brain, particularly in the context of brain development and neurological diseases. However, its contribution to brain tumors is underexplored. In this study, we investigated the role of oral microbiota dysbiosis (OMD) in brain metastasis (BrM) development. We hypothesized that OMD may alter the brain's physiological state in ways that favor premetastatic niche (PMN) preparation, thereby creating conditions conducive to BrM development.
Methods: Mice with subcutaneous BP melanoma tumors, with no intracranial tumors, were used to model the PMN preparation stage in the brain during melanoma development. To induce OMD, 5 days after primary tumor injection, mice were treated with chlorhexidine gluconate mouthwashes every 12 hours for 10 days. Saliva and stool samples were collected longitudinally and analyzed via 16S rRNA amplicon sequencing. Primary melanoma tumors were measured using a caliper. Brain samples were analyzed by mass spectrometry and immunohistochemistry. Digital spatial profiling was used to determine immune composition and transcriptional signatures in both brain and melanoma samples.
Results: Chlorhexidine treatment led to OMD, as verified by a reduction in alpha diversity and alterations in bacterial composition of the oral microbiota. The gut microbiota remained unchanged. Mice with OMD demonstrated a significant increase in primary tumor growth compared to controls ($p=0.039$), associated with lower immune infiltration. In the brain, OMD resulted in upregulation of proteins associated with acute inflammation and a reduction in peri-vascular extracellular matrix and adhesion proteins, suggestive of blood-brain barrier remodeling.
Conclusion: Our investigation suggests oral microbial imbalance is associated with alterations of the peri-vascular niche and may contribute to PMN preparation in the brain. Ongoing studies in our group investigate the impact of these OMD-induced alterations on BrM development, providing insights for microbiota-targeted translational applications.

#2879 Intra-tumoral microbiota and host genotype cooperatively shape neutrophil antitumor activity in colorectal cancer.

Elisa Sorrenti[1], Valeria Governa[2], Davide Bressan[3], Nicolo' Formaggio[4], Bianca Cali[4], Camilla Basso[5], Martina Villa[6], Giuseppe Sconocchia[7], Klaus-Peter Janssen[8], Milo Frattini[9], Fulvio Chiacchiera[3], Jean-Philippe Theurillat[4], Sara De Dosso[10], Luigi M. Terracciano[11], Lubor Borsig[12], Giulio C. Spagnoli[13], Dimitrios Christoforidis[14], Giandomenica Iezzi[5]

[1]Institute for Translational Research USI-EOC, Ente Ospedaliero Cantonale, Bellinzona, Switzerland,[2]Department of Biomedicine, University of Basel, Basel, Switzerland,[3]Department of Cellular, Computational, and Integrative Biology, University of Trento, Trento, Italy,[4]Institute of Oncology Research, Bellinzona, Switzerland,[5]Faculty of Biomedical Sciences, Universita della Svizzera Italiana, Lugano, Switzerland,[6]Ente Ospedaliero Cantonale, Bellinzona, Switzerland,[7]Institute of Translational Pharmacology, National Research Council, Rome, Italy,[8]Department of Surgery, School of Medicine, Klinikum rechts der Isar, Technical University of Munich (TUM), Munich, Germany,[9]Laboratory of Genetics and Molecular Pathology, Istituto Cantonale di Patologia EOC, Locarno, Switzerland,[10]Medical Oncology Department, Oncology Institute of Southern Switzerland (IOSI) EOC, Bellinzona, Switzerland,[11]Department of Biomedical Sciences, Humanitas University, Milan, Italy,[12]Institute of Physiology, University of Zurich, Zurich, Switzerland,[13]Institute of Translational Pharmacology, National Research Council, Rome, Italy,[14]Department of Surgery, Ente Ospedaliero Cantonale, Lugano, Switzerland

Colorectal cancer (CRC) represents a major cause of cancer related death worldwide. Defined genetic alterations are known to underlie CRC oncogenesis. However, in the last decades a critical role of the composition of tumor microenvironment has also been recognized. While tumor infiltration by T lymphocytes has been consistently recognized to predict improved clinical outcome, the role of tumor-associated neutrophils (TANs) in CRC is still debated.CRC develops in a microbiota-rich environment, and barrier dysfunction allows bacterial translocation into the mucosa. Neutrophils, as first responders to bacteria, may interact with tumor-infiltrating bacteria. However, the functional outcome and prognostic relevance of these interactions have not been thoroughly investigated. Here we unravel that TAN recruitment and functions are modulated by intra-tumoral microbiota and only defined bacterial species are able to unleash TANs' antitumor potential. Fusobacterium nucleatum (Fn) promotes expression of neutrophil-recruiting chemokines in tumor cells and enhances neutrophil migration more efficiently than Bacteroides fragilis (Bf). Importantly, Fn, but not Bf, triggers neutrophils to release cytotoxic proteins showing tumoricidal activity in vitro and in xenograft models. Mechanistically, these antitumor effects are elicited upon Fn binding to an activatory receptor (R-a) expressed on neutrophils but are impaired upon R-a blockade or in neutrophils from donors carrying a R-a loss-of-function polymorphism. Supporting these findings, in human CRCs, elevated Fn loads, high TANs densities, and expression of wild-type, but not polymorphic, R-a allele, correlate with improved patient survival. Our findings identify microbiota composition and host genetic background as critical determinants of TAN functional profiles and offer insights into neutrophil-targeted therapeutic strategies in CRC.

#2880 Antibiotic driven microbiota disruption impairs HER2 targeted therapy efficacy.

Romina Elizabeth Araya[1], Lily Parker[1], Payal Mitra[2], Nofar Erlichman[1], Pavani Chalasani[3], Rong Li[2]

[1]Biochemistry and Molecular Medicine-SMHS, George Washington University, Washington, DC,[2]The George Washington University, Washington,[3]Division of Hematology and Oncology, George Washington Cancer Center- George Washington University, Washington, DC

Up to 60% of cancer patients require antibiotics during therapy, yet retrospective studies indicate that antibiotic exposure can worsen outcomes across cancers. In breast cancer (BC), HER2+ patients show notably reduced survival after antibiotic use, an effect attributed to microbiota disruption, though mechanisms remain unclear. Our previous work demonstrated the role of microbiota signaling in chemo and immunotherapy efficacy. But HER2+ BC relies on targeted therapies, thus the impact of antibiotics on these agents requires further investigation. To address this, we used 16S rRNA sequencing of cecal content from mice bearing HER2+ TUBO tumors to assess whether an anti-HER2 antibody or neratinib, a HER2 tyrosine kinase inhibitor, each induces distinct microbiota shifts. Anti-HER2 increased *Oscillospiraceae*, *Rikenellaceae*, *Ruminococcaceae*, and *Lachnospiraceae*, whereas neratinib increased only the latter two Families. However, alpha diversity metrics remained unchanged. To study how these microbes contribute to treatment, we first depleted the gut microbiota using a broad-spectrum antibiotic cocktail (ABX). We observed the partial and complete loss of anti-HER2 and neratinib efficacy, respectively, on TUBO tumors. A clinically relevant antibiotic, such as ciprofloxacin (cipro), also fully halted neratinib response, whereas amoxicillin/clavulanate (am/clav) caused partial impairment. Because both antibiotics and neratinib were administered orally, we quantified plasma neratinib by LC-MRM mass spectrometry and ruled out antibiotic-induced blockade of neratinib absorption. Cipro and am/clav significantly reduced alpha diversity to a lesser extent than ABX, with cipro showing the most dramatic effect. Families enriched by HER2 therapies, including *Lachnospiraceae* and *Ruminococcaceae,* were targeted by cipro and am/clav. Notably, both antibiotics increased *Akkermansia*, a Family previously linked to favorable immunotherapy outcomes, suggesting that HER2-targeted therapies may rely on microbiota features, like *Lachnospiraceae* or *Ruminococcaceae*, distinct from those supporting checkpoint blockade. Spectral flow cytometry analysis of the tumor immune infiltration revealed that HER2 therapies triggered NK, CD8+, and CD4+ T cell infiltration. Antibiotic-treated tumors showed enrichment of pro-tumor macrophages and neutrophils with no significant NK cell recruitment. Microbiota alpha diversity was positively correlated with tumor NK and CD8+ T cell content, which, in turn, were associated with treatment outcomes. Overall, our findings demonstrate that antibiotic-driven disruption of gut microbiota composition and diversity impairs immune mechanisms linked to the efficacy of HER2+ BC therapy. These results highlight the potential of microbiota-based strategies to mitigate antibiotic-associated therapeutic resistance in HER2+ BC.

#2881 Interleukin-1 upregulates dual oxidase 2 expression and ROS production in human pancreatic cancer cells in a STAT1/STAT3-dependent manner.

David J. Mallick[1], Yongzhong Wu[2], Mariam M. Konate[1], Becky A. Diebold[2], Smitha Antony[1], Jennifer L. Meitzler[2], Goujian Jiang[2], Jiamo Lu[2], Krishnendu K. Roy[1], James H. Doroshow[1]

[1]NCI Division of Cancer Treatment and Diagnosis, Bethesda, MD,[2]NCI Developmental Therapeutics Branch, Bethesda, MD

Chronic pancreatitis and sustained pancreatic inflammation increase the risk of pancreatic ductal adenocarcinoma (PDAC), in part through the release of pro-inflammatory cytokines and excessive generation of reactive oxygen species (ROS). Interleukin-1 (IL-1), a major upstream cytokine secreted by malignant or microenvironmental cells, promotes pancreatic inflammation, tumorigenesis, invasiveness, and intratumoral heterogeneity. Previously, our laboratory has established that dual oxidase 2 (DUOX2), one of seven NADPH oxidase (NOX) family members, plays a critical role in H2O2-mediated host defense and chronic inflammation in the gastrointestinal tract. DUOX2 is upregulated and expressed along with its maturation factor, DUOXA2, in several human pancreatic cancer cell lines following exposure to various pro-inflammatory cytokines, including IFN-γ, IL-4, and IL-17A. In the present study, we show that IL-1α and IL-1β robustly upregulate DUOX2/DUOXA2 mRNA and protein expression in a panel of human PDAC cell lines and patient-derived PDAC organoids. IL-1 exposure triggers transient activation of STAT1 and STAT3, followed by sustained induction of DUOX2/DUOXA2, without increasing expression of other NOX family members. Activation of canonical IL-1 signaling in PDAC cell lines was supported by the observation of IL-1-related upregulation of IL-8 (CXCL8) mRNA, a chemokine essential for neutrophil recruitment and a potent promoter of angiogenesis, in IL-1-treated PDAC cells. Co-administration of Anakinra, an IL-1 receptor antagonist, markedly suppresses IL-1-induced DUOX2/DUOXA2 and CXCL8 expression *in vitro*. Knocking out DUOX2 in BxPC-3 cells established DUOX2 as the predominant source of IL-1-mediated ROS production. Targeted siRNA knockdown of proximal IL-1 pathway nodes, such as IL-1R1, MYD88 and IRAK1/2, significantly decreased expression of DUOX2/DUOXA2 and of CXCL8. We also found that STAT1 and STAT3, two transcription factors involved in downstream transcription in the IL-1 pathway, are crucial for the regulation of DUOX2/DUOXA2 in pancreatic cancer. Collectively, these findings define an IL-1-STAT1/STAT3 axis that drives DUOX2-dependent ROS production in PDAC, reinforcing a pro-oxidant, pro-inflammatory microenvironment.

#2882 The impact of high fat diet on tumor growth is dependent on fatty acid composition and tumor type.

Rebecca C. Simpson[1], Freya E. R. Edge[2], Jordan W. Conway[1], Hsin-Yi Tseng[3], Mirei Okada[2], Inah Camaya[1], Laura Smith[1], Akshaya Ramanathan[1], Oliver K. Fuller[2], Stewart W. C. Masson[2], Jessamy Tiffen[3], Georgina V. Long[1], Erin R. Shanahan[2]

[1]Melanoma Institute Australia, The University of Sydney, Sydney, Australia,[2]School of Life and Environmental Science, The University of Sydney, Sydney, Australia,[3]Centenary Institute, The University of Sydney, Sydney, Australia

Diet is a key factor that shapes the gut microbiome, systemic metabolism and immune function. However, how specific macronutrients alter host physiology and tumor-immune interactions relevant to tumor progression and response to immune checkpoint inhibitor (ICI) immunotherapy remains unclear. We therefore sought to investigate how high fat diets (HFDs) varying in macronutrient source and composition influence metabolism, the gut microbiome and anti-tumor immunity. C57BL/6 mice were fed either a standard chow (CD), high fat (HF)/high sugar (HS)-Copha or HF-Lard diet for 2 or 7 weeks prior to inoculation with a syngeneic cancer cell line. These diets notably have differing fatty acid compositions; the copha-based (plant) HFD has more MCFAs compared to the lard-based (animal) HFD that is dominated by LCFAs. Mice on HF-Lard exhibited impaired glucose tolerance and reduced insulin sensitivity compared to CD and HF/HS-Copha after 2 and 7 weeks on diets. However, only mice on HF-Lard longer term had both elevated fasting glucose and insulin. Profiling the gut microbiomes of mice revealed both HFDs rapidly induced gut dysbiosis characterized by reduced diversity, although HF/HS-Copha compared to HF-Lard were enriched with metabolically beneficial species *Blautia coccoides*, *Parabacteroides merdae* and *Bacteroides acidifaciens*. Notably, HF-Lard accelerated the growth of B16-F10 and YUMM3.3-UVR melanomas while both HFDs accelerated the growth of MC38 colorectal adenocarcinomas. Similar results were observed in the short-term study except for B16-F10 where no differences between diets were observed. This suggests the acceleration is independent of obesity though may be influenced by the immunogenicity or intrinsic insulin sensitivity of the tumor. Spectral flow analysis of immune cells across the mesenteric lymph nodes (MLN), spleen, tumor draining LN (tdLN) and tumor revealed divergent immune profiles across diets. Both HFDs had lower plasma cells, cDC1s and CD8 T cells in the tdLN compared to CD. However, HF-Lard mice had higher frequencies of monocytes, and both Th17 cells and RORgt+ Tregs, indicating polarization towards suppressive phenotypes in addition to impaired anti-tumor priming. This was accompanied by enhanced exhaustion across CD8 T cells in the tumors of HF-Lard mice.Together this suggests that HFDs dominated by LCFAs are associated with metabolic dysfunction, and altered microbiome and immune phenotypes, which could contribute to accelerated tumor growth for melanoma. It also highlights that tumor type/genetics are important factors in how the diet-gut axis influences tumor growth. Ongoing work will focus on understanding how specific fat sources and diet durations impact ICI treatment and ultimately inform the design of more specific dietary interventions to enhance the efficacy of treatment.

#2883 Divergent gut microbial communities are linked to differences in baseline immune profiles, tumor features and ICI outcomes in melanoma.

Rebecca C. Simpson[1], Ines Pires Da Silva[1], Jayden Beckwith[1], Irene L. M. Reijers[2], Judith M. Versluis[2], Camelia Quek[1], Alexander M. Menzies[1], Gonzalez Maria[1], James S. Wilmott[1], Christian U. Blank[2], Richard A. Scolyer[1], Erin R. Shanahan[3], Georgina V. Long[1]

[1]Melanoma Institute Australia, The University of Sydney, Sydney, Australia,[2]Netherlands Cancer Institute, Amsterdam, Netherlands,[3]School of Life and Environmental Science, The University of Sydney, Sydney, Australia

We have previously identified links between gut microbial community assemblages, defined by the ratio of *Ruminococcaceae* to *Bacteroidaceae,* and response to immune checkpoint inhibitor (ICI) immunotherapy, suggesting microbiome-immune interactions may prime patients for treatment outcomes. To investigate how these microbial states shape baseline immune tone and anti-tumor immunity we profiled peripheral immune and tumor-intrinsic features across these stratified patient groups. In 129 Australian and Dutch stage III melanoma patients treated on trial with neo-adjuvant anti-PD-1/anti-CTLA-4 immunotherapy (OpACIN-neo/PRADO), pre-treatment stool (microbiome; 16S rRNA gene sequencing) and PBMCs (immune profiles; mass cytometry) were analyzed. Tumor biopsies were subject to DNA/RNA sequencing, with tumor mutation burden (TMB) and IFN-γ score assessed. Clear differences in baseline peripheral immune profiles were observed upon stratifying patients by microbial community types. *Ruminococcaceae* (Ru)-dominated gut microbiomes were associated with higher ICI response rates, had greater frequencies of circulating memory B and T cell subsets (CD27+ B cells, CD8+ Tem (CD45RA-CCR7-)) and higher ICOS+ Tregs. *Bacteroidaceae* (Ba)-dominated patients had higher frequencies of total B cells and a more naïve immune profile. Further, the pre-treatment tumors of Ru-dominated patients were enriched with pathways involved with immune signalling and antigen presentation while Ba-dominated patient tumors were enriched with pathways associated with dysregulated metabolism and cell proliferation. The distribution of tumor TMB and IFN-γ groups between responders (R) and non-responders (NR) within each microbial community type was also significantly different; 81% of Ba-R had high TMB, compared to only 54% of Ru-R, and 72% of Ba-dominated patients belonged to the IFN-γ low group compared to 48% of Ru-dominated patients, with all Ba-NR being IFN-γ low. Gene ontology enrichment analysis further revealed distinct biological programs associated with response within each microbial community type. Ru-R were enriched for T, B and NK cell differentiation and cytotoxicity, while Ba-R showed enrichment for extracellular matrix remodelling. Together this demonstrates that different microbial community types are associated with altered baseline peripheral immune tone and tumor features. Furthermore, it suggests that ICI response within each microbial community type may be characterised by divergent predictive markers and mechanisms of response. This is highly relevant to optimally targeting the gut microbiome in the clinic and identifying patients who will benefit most from microbiome-modifying interventions.

#2884 Defined bacterial consortium highlights the impact of carcinogenic bacteria on DNA methylation and tumorigenesis.

Siddhi Chitre[1], Claudia Mercado-Rodriguez[1], Anthony Pompetti[2], Pyounghwa Park[2], Raad Z. Gharaibeh[1], Jean-Pierre Issa[2], Christian Jobin[3]

[1]University of Florida, Gainesville, FL,[2]Coriell Institute for Medical Research, Camden, NJ,[3]University of Florida College of Medicine, Gainesville, FL

BACKGROUND: Colorectal cancer (CRC) is second leading cause of deaths in the USA. Bacteria like *E. coli* harboring the carcinogenic island *pks* promote CRC in preclinical models. However, the impact of carcinogenic bacterial DNA methylation and CRC development is unknown.

METHODS: A defined consortia of 13 bacterial isolates (C13) containing either *E. coli* low pks (C13-DSMZ) or *E. coli* high pks (C13-UM149) were used in the study. Mice were administered 10^8 CFU of the bacterial consortia via oral gavage. 2 weeks later, they received 2% Dextran sodium sulfate (DSS) for one week, and tissues were collected at week 7 for analysis. Stools, colonic tumors and matched normal mucosa were collected. Stool samples were subjected to 16S rRNA sequencing. Tumors and normal mucosa were subjected to reduced representation of bisulfite sequencing (RRBS) and RNA-seq analysis for methylation and gene expression analysis respectively. Western Blot (WB) and Immunofluorescence (IF) analysis were used to determine DNA damage and cell proliferation in IEC-6 cells. Immunohistochemistry (IHC) was performed on colonic tissues.

RESULTS: IEC-6 cells exposed to *E. coli* DSMZ exhibited lower DNA damage (γH2AX expression), whereas cells treated with *E. coli* UM149 showed elevated γH2AX. Mice colonized with C13-UM149 developed significantly more tumors than those with C13-DSMZ ($p = 0.046$). IHC of colonic tissues showed that C13-UM149 exhibited higher Ki-67 (cell proliferation), β-catenin (oncogenic signaling), and γH2AX compared with C13-DSMZ ($p < 0.05$). Genome-wide methylation analysis showed broader CpG alterations in C13-DSMZ tumors (247,797 CpGs) than C13-UM149 mice (172,727 CpGs). Compared to C13-DSMZ, C13-UM149 tumors had 70,650 hyper and 65,024 hypomethylated CpGs, and 192 hyper and 220 hypomethylated promoters. These changes were associated with upregulation of *Il5ra* (inflammation), *Galr1* (tumor growth), and *Minar1* (tissue remodeling), and downregulation of *Tmed6* (protein trafficking) and *Pcdhb19* (adhesion) in C13-UM149 tumors. In normal mucosa, C13-UM149 altered 28,316 hyper and 59,780 hypomethylated CpGs with increased *Aldoart1* (glycolysis) and *Palm3* (immune signaling) expression. C13-UM149 tumors also showed promoter hypomethylation driving increased expression of *Sema4c* (tumor invasion) and promoter hypermethylation accompanied by increased *Mmp9* expression (matrix remodeling). C13-DSMZ tumors exhibited promoter hypermethylation with elevated expression of *Mecom* (tumor progression) and promoter hypomethylation with increased *Wnt7b* (oncogenic signaling).

CONCLUSION: Distinct *pks* activities differentially modulate DNA methylation and influence gene expression and tumor development. Our findings suggest that the methylome can shift in two directions depending on the bacterial context, with predominant hypermethylation in tumors and hypomethylation in normal tissues.

#2885 Intron retention marks a myeloid-skewed immune desert and nominates an ICI nonresponse marker in *H. pylori*-positive gastric cancer.

Daisuke Takayanagi[1], Junya Kitadani[2], Masahiro Katsuda[2], Toshiyasu ojima[2], Keiji Hayata[2], Manabu Kawai[2], Sinichi Hashimoto[3], Kazuhiko Tagawa[4], Toru Sugino[4], Satoshi Wada[5], Hiroki Yamaue[6], Takuya Tsunoda[7]

[1]Division of Medical Oncology, Showa Medical University, Tokyo, Japan,[2]Second Department of Surgery, Wakayama Medical University, Wakayama, Japan,[3]Wakayama Medical University, Wakayama, Japan,[4]Zenick.lab Corporation, Tokyo, Japan,[5]Showa Medical University, Tokyo, Japan,[6]Pancreatic Cancer Center, Division of Gastroenterological & General Surgery, Department of Surgery, Showa Medical University, Tokyo, Japan,[7]President & CEO, Showa University, Tokyo, Japan

Background: The benefits of immune checkpoint inhibitors (ICIs) in gastric cancer (GC) vary according to the *Helicobacter pylori* (Hp) status. While profiling transcriptomes, intron retention (IR) emerged as a major distinguishing feature in Hp-positive disease, but its immunologic significance remains unclear.
Methods: We analyzed 66 RNA-seq tumor samples (39 Hp-positive and 27 Hp-negative) from 24 patients. Alternative splicing (AS) were quantified USING PSIsigma, rMATS. AS-derived neoantigens were predicted (SNAF; strict filters), and a quality-weighted neoantigen burden was calculated. Antigen-presentation machinery (APM) was summarized using a purity-adjusted APM score. Tumor microenvironment (TME) features were profiled using ESTIMATE, Hallmark GSEA, ssGSEA, CIBERSORTx, and a four-class subtype (desert/immune-enriched [IE]/IE fibrotic/fibrotic). High IR was defined as three or more IR events. Statistical analysis was performed using the Mann-Whitney test and Spearman correlation, with BH-FDR correction.
Results: Across Hp infection status, Hp-positive tumors harbored more IR/AS events and a higher total neoantigen burden under strict filters; however, IR-specific and quality-weighted burdens were not significantly higher. In Hpnegative tumors, higherquality neoantigen burden correlated with intrinsic APM capacity ($\rho \approx 0.41$, $p=0.034$), indicating preserved antigen-APM coupling. Within Hp-positive tumors, IRhigh (n=12) versus IRlow (n=27) tumors showed higher neoantigen metrics (IRderived 4 vs 1, $p=4.6\times10^{-7}$; weighted 24.1 vs 12.2, $p=3.9\times10^{-4}$), enrichment of G2M/E2F/MYC/mitotic spindle programs (FDR<0.05), higher tumor purity (p=0.022), lower ImmuneScore (p=0.0156) and StromalScore (p=0.017), and uniform classification as the Desert subtype (12/12). NMD and splicing signatures were significantly elevated (p=0.014/0.034), CD8/IFN signatures were reduced (p=0.034), and the APM score favored IRlow tumors (p=0.050). A Myeloid/mastcell-skewed pattern was also evident (MDSC signature, p = 0.037; activated mast cells, p=0.0077; resting mast cells, p=0.0027). In Hp-positive tumors overall, quality-weighted neoantigen burden correlated positively with NMD/splicing ($\rho \approx 0.63$, $p=1.9\times10^{-5}$; $\rho \approx 0.67$, $p=3.7\times10^{-6}$), while IR burden correlated negatively with CD8/IFN activity ($\rho \approx -0.44$, p=0.0056). IR events were not enriched in core APM genes.
Conclusions: In Hp-positive GC, high IR defines a proliferative, NMD/splicing-stressed, myeloid/mastcell-skewed immunedesert microenvironment characterized by neoantigen-APM uncoupling. This phenotype aligns with limited ICI benefit, identifying high IR as a potential predictive marker of ICI nonresponse, supporting prospective validation and hypothesis-driven evaluation of ICI-based regimens that reprogram myeloid-rich TMEs or modulate splicing/NMD pathways.

#2886 Microbiota-driven modulation of tumor growth in Li-Fraumeni Syndrome: Evidence for bile acids as a key mediator.

Noel W. Y. Ong[1], Camilla Giovino[2], Nicholas Fischer[2], Paula Rosanna Quaglietta[2], Ashby Kissoondoyal[2], David Malkin[2]

[1]Medical Biophysics, University of Toronto, Toronto, ON, Canada,[2]The Hospital for Sick Children, Toronto, ON, Canada

Li-Fraumeni Syndrome (LFS) is caused by a germline mutation in *TP53,* which greatly increases the risk of earlier onset malignancies. Microbial communities can regulate the host inflammation and metabolism, linking them to p53 biology. However, we do not fully understand how gut microbiome contributes to this risk. In this study, we looked at how depleting microbiota impacts tumor development in a mouse model of LFS. *Trp53*$^{R172H/WT}$ (LFS) mice and their wildtype (WT) littermates received a broad-spectrum antibiotic cocktail to deplete the gut microbiota. After four days of treatment, mice were injected subcutaneously with MC38 colon adenocarcinoma cells and continued the antibiotic treatment until study endpoint. LFS mice that received antibiotics developed significantly smaller tumors compared to untreated LFS controls, while the tumor growth in WT mice did not change. This suggests that microbial activity promotes tumor growth in mutant p53 mice. To interrogate if microbial metabolites, rather than live organisms, caused this effect, we transferred filtered fecal matter from LFS mice to WT recipients. These filtrates increased tumor size, showing that soluble microbial products can mimic the tumor-promoting effect. Faecal filtrate was analyzed with LC-MS and untreated LFS mice showed higher levels of fecal bile acids compared to WT animals. The presence of these bile acids also positively correlated with subcutaneous tumor mass, and antibiotic treatment reduced bile acid presence. We observed increased NF-κB levels in the intestines of untreated LFS mice. ELISAs further confirmed elevated intestinal pro-inflammatory cytokines expression, including IL-6, TNF-α, IFN-γ, and IL-17A, which decreased after microbiota depletion. In addition to these intestinal changes, untreated LFS mice had higher total levels of circulating plasma pro-inflammatory cytokines, which slightly decreased after antibiotic treatment. FITC-dextran assays demonstrated increased gut permeability in untreated LFS mice, returning to normal after treatment with antibiotics. Mutant p53 has been reported to enhance the mevalonate pathway, leading to increased cholesterol synthesis and an expanded pool of primary bile acids. These bile acids can then be converted by gut microbiota into secondary bile acids that have known inflammatory and NF-κB-activating effects. This combined metabolic and microbial pathway may explain the elevated bile acids and inflammatory signaling seen in LFS mice. Taken together, these data broaden the current understanding of LFS biology by revealing that tumor susceptibility is shaped not only by cell-intrinsic mutant p53 functions but also by microbiota-driven metabolic and inflammatory cues. This integrated view opens new avenues for therapeutic intervention beyond traditional surveillance-based care.

: Modifiers of Inflammation and the Tumor Microenvironment
Poster Session

#2891 Specificity and timing of TREM-1 blockade initiation impact its therapeutic efficacy in cancer.

Alexander B. Sigalov

SignaBlok, Inc., Shrewsbury, MA

Overexpression of triggering receptor expressed on myeloid cells 1 (TREM-1) is associated with the immune-suppressive tumor microenvironment (TME) and unfavorable prognosis in pan-cancer. TREM-1 is mainly expressed on neutrophils, monocytes, and macrophages including monocyte-derived macrophages. These cells can play different or even opposite roles in the pathogenesis of cancer. Despite more than two decades of intensive research in the field, the question whether specificity of TREM-1 inhibitor can impact its antitumor efficacy has never been addressed mostly, due to the lack of cell-restricted approaches to TREM-1 blockade. This study aims to determine whether broad or macrophage-specific TREM-1 blockade demonstrates distinct therapeutic efficacy and superior outcomes in cancer models. Ligand-independent TREM-1 inhibitory peptides GF9 and GA31 (the latter in a form of macrophage-targeted lipopeptide complexes, GA31-LPC) were evaluated in animal models of pancreatic cancer. GF9 inhibits TREM-1 on all TREM-1-expressing cells, while GA31-LPC targets TREM-1 predominantly on macrophages. In the Kras (G12D)/Trp53 null/Pdx1-cre (KPC) mouse allograft tumor model established in fully immunocompetent C57BL/6 mice, GF9 and GA31-LPC alone significantly inhibited pancreatic cancer progression. In combination with anti-PD-L1 therapy, GA31-LPC, but not GF9, overcame cancer resistance to PD-L1 checkpoint blockade and synergized with immunotherapy. In PANC-1 xenograft-bearing athymic nude mice with intact innate immunity but lacking T cells, both GF9 and GA31-LPC increased complete response rate and survival when combined with chemotherapy. The effectiveness of these agents was dependent on the timing of TREM-1 blockade initiation relative to chemotherapy. GF9 was effective only when given with but not after chemotherapy. In contrast, GA31-LPC was effective only when given after but not together with chemotherapy. Unexpectedly, GF9 and GA31-LPC alone or combined with anti-PD-L1 and chemotherapy did not exhibit significant antitumor effects in the orthotopic Pan02 syngeneic pancreas tumor allograft model established in C57BL/6 mice. This suggests that selecting the appropriate animal model is critical when developing antitumor agents that target TME. The detailed mechanisms of this paradoxical finding require further investigation for their potential contribution to the long-standing debate whether to activate or inhibit TREM-1 in cancer. In summary, these findings for the first time demonstrate that both inhibitor specificity and timing of treatment initiation are crucial for therapeutic TREM-1 inhibition. This has significant implications for clinical strategies targeting TREM-1, particularly informing tailored treatment approaches for not only pancreatic cancer but also other hard-to-treat tumors.

#2892 Safety and activity of cLRRC15-IFNa, a conditionally active biologic targeting IFNa specifically to LRRC15+ CAFs.

Justin Killebrew, Linda Liang, Shannon Okada, Aelish Guinn, Alton Etheridge, Brett Robison, David Colby, David Jurchen, Jacqueline Pham, Jamie Nguyen, John Skonier, Kendyl Daniels, Kerri Thomas, Laura Carlucci, Lynn Amon, Megan Sprague, Meri Galindo, Remington Lance, Sam Wrenn, Sandra Notonier, Shannon Fallen, Shea McClain, Wendy Curtis, Zane Kraft, John Mulligan, Diane Hollenbaugh

Bonum Therapeutics, Seattle, WA

While cancer-associated fibroblasts (CAFs) have emerged as a key cell type capable of influencing malignant cell growth, this axis of cancer biology has not yet been exploited for therapeutic benefit. CAFs enable tumor growth through multiple mechanisms including deposition of extracellular matrix, production of soluble factors, and inhibition of the immune response. Recent advancements have revealed how distinct CAF populations correlate with patient prognosis and response to therapies across many solid tumor types. Amongst these CAF subsets, LRRC15 expression has been shown to identify a myofibroblast population with a central functional role in supporting tumor cell growth and inhibiting anti-tumor immune responses. Approaches to reprogram or reduce this LRRC15+ population of CAFs may provide therapeutic benefit in multiple solid tumor indications.

IFN-α signaling directly on tumor-supporting CAFs drives reprogramming, countering the TGF-β signal on which the phenotype depends. IFN-α also effectively promotes both innate and adaptive immune responses, including dendritic cell maturation, repolarization of suppressive myeloid cells, and CD8+ T cell activation. However, the use of systemic IFN-α therapy has been limited by significant dose-limiting toxicities.

We have generated a conditionally active cLRRC15-IFNα therapeutic that targets IFN-α activity to LRRC15+ cells while remaining largely inactive on other cells. Our approach uses a novel dual-binding antibody (DBA) mechanism that takes advantage of the ability of an antibody to bind specifically and competitively to two distinct antigens. With this technology, IFN-α is bound and inactive in circulation and only becomes active when the therapeutic binds to LRRC15.

Once localized to the surface of an LRRC15+ CAF, cLRRC15-IFNα exerts anti-tumor activity both by direct cis-signaling of IFN-α on CAFs and by trans-signaling to adjacent immune cells. In vitro, reporter cell and receptor binding assays demonstrate that cLRRC15-IFNα has >100-fold preferential IFN-α activity in the presence of LRRC15. In primary cells, cLRRC15-IFNα preferentially induces IFN-α signaling in LRRC15-expressing activated human fibroblasts. cLRRC15-IFNα inhibits tumor growth in mouse syngeneic tumor models, avoids clinical signs of IFN-α-mediated toxicity, and demonstrates robust combinatorial activity with anti-PD-1. In the TME, cLRRC15-IFNα drives the activation of CD8+ T cells. Collectively, these results demonstrate the potential of the DBA platform and support the clinical development of cLRRC15-IFNα.

#2893 Selective inhibition of eIF4A targets tumor-associated macrophages to restore lymphoma-specific immunity.

Haley Lynn Klimaszewski[1], A. Douglas Kinghorn[2], Michael R. Grever[3], Robert A. Baiocchi[3], John T. Patton[3]

[1]College of Medicine, The Ohio State University, Columbus, OH,[2]Division of Medicinal Chemistry and Pharmacognosy, College of Pharmacy, The Ohio State University, Columbus, OH,[3]Department of Internal Medicine, Division of Hematology, The Ohio State University, Columbus, OH

Background: Silvestrol is an antineoplastic translation inhibitor targeting eukaryotic translation initiation factor 4 subunit A (eIF4A). Silvestrol's antineoplastic effects are well characterized, with our group reporting anti-tumor activity in Epstein-Barr Virus (EBV)-associated lymphoma. While the direct anti-tumor effect in EBV-associated lymphoma was modest, silvestrol mediated indirect tumor control by preserving $CD8^+$ T-cell viability and cytotoxicity. However, silvestrol's impact on the myeloid compartment remains poorly understood. We hypothesize that silvestrol supports anti-tumor immune activity by suppressing tumor-associated macrophage (TAM) growth in the tumor microenvironment (TME).

Methods: Co-cultures (co-cx) of EBV-transformed lymphoblastoid cell lines (LCL) and autologous peripheral blood mononuclear cells (PBMC) were used to model the lymphoma TME. LCLs were transformed by native virus in SCID mice before ex vivo culturing. Flow cytometry was used to profile immune population frequency and phenotype. Cell proliferation was monitored via MTS assay. Cytokine arrays and trans-well assays were used to explore soluble and contact-dependent features of the model. Magnet bead separation was used to deplete or enrich immune populations. Transcription was analyzed with AmpliSeq.

Results: Depletion of $CD8^+$ T-cells from co-cx led to LCL expansion, whereas $CD14^+$ depletion improved LCL control. Cytokine arrays showed co-cx media (CM) was enriched for cytokines linked to recruitment, differentiation, and activity of immunosuppressive macrophages. Silvestrol-treated co-cx showed reduced $CD14^+$ and $CD206^+$ populations by flow and decreased CCL2, CCL8, CCL7, IL-8 by cytokine array. To assess silvestrol's direct effect on myeloid subsets, $CD14^+$ cells were isolated and incubated in CM. $CD14^+$ cells in CM showed increased proliferation and expression of TAM markers CD206 and CD163. CM-driven proliferation required LCL-PBMC contact and presence of T-cells in initial co-cx. CM-polarized $CD14^+$ cells inhibited proliferation of activated T-cells. Silvestrol treatment of CM-cultured $CD14^+$ cells reduced proliferation, CD206 and PD-L1 expression, and down regulated M2 and TAM transcriptional signatures.

Conclusions: Our co-cx replicates features of a lymphoma TME, exhibiting monocyte polarization toward immunosuppressive TAMs. Silvestrol suppresses TAM proliferation and polarization in co-cx and in monocytes incubated in CM. Planned experiments include Ribo-seq to identify deferentially translated transcripts in silvestrol-treated monocytes, murine studies of silvestrol's effects on TAMs, and synergy studies with other immunotherapies. Overall, these findings, along with previously reported immune effector sparing qualities, support eIF4A inhibition as a therapeutic strategy to target immune escape mechanisms in the lymphoma TME.

#2894 Alphavirus replicon expressing IL-12 reprograms tumor-associated macrophages and neutrophils and induces anti-tumor immunity.

Forrest Bowling[1], Momoko Ishikawa[1], Dhanya Nambiar[2], Jayalaxmi Sastri[1], Keiko Ishimoto[1], Fumiya Tao[1], Koyo Takahashi[1], Ivan Stepanek[2], Hongbin Cao[2], Davis Leitner[1], Kenta Matsuda[1], Fred Baik[2], John Sunwoo[2], Quynh Thu Le[2], Jonathan Smith[1], Wataru Akahata[1]

[1]VLP Therapeutics, Inc., Gaithersburg, MD,[2]Stanford University, Stanford, CA

Immunosuppressive myeloid cells such as tumor-associated macrophages (TAMs) and neutrophils (TANs) contribute to resistance against immune checkpoint therapies by fostering a suppressive tumor microenvironment (TME). To overcome this barrier, we developed a single-cycle alphavirus replicon particle (VRP) vector encapsulating self-amplifying RNA (saRNA) encoding interleukin-12 (IL-12) for intratumoral delivery, leveraging the natural tropism of alphaviruses for myeloid cells. The VRP was engineered with a capsid nuclear localization signal mutation to enhance transgene expression and reduce host cell toxicity. In preclinical studies, single-cell RNA sequencing of treated mouse 4T1 breast carcinoma tumors and draining lymph nodes revealed that IL12-VRP preferentially transduced M2-like TAMs and TANs, reprogramming them toward pro-inflammatory phenotypes via interferon signaling. This effect was further amplified by IL-12 expression, leading to expansion of pro-inflammatory $Nos2^{+}$ macrophage and neutrophil populations. IL12-VRP also activated cytotoxic NK and T cells, inducing IFN-γ expression and enhancing anti-tumor immunity. Compared to lipid nanoparticle-based delivery of the same saRNA replicon, IL12-VRP achieved superior tumor control in the MC38 colorectal model with ~1000-fold lower RNA gene copies in the dose. IL12-VRP suppressed MOC2 head and neck model tumor growth, prevented nodal and lung metastases, and remodeled immune landscapes in both tumors and lymphoid tissues. CT26 colorectal carcinoma model mice treated with IL12-VRP exhibited tumor reduction, durable systemic immune memory and rejected subsequent tumor rechallenge. These findings establish IL12-VRP as a potent immunomodulatory platform capable of reprogramming myeloid cells and enhancing adaptive immunity. This approach may improve outcomes in myeloid-dominant TMEs and augment current immunotherapies. Ongoing clinical evaluation (NCT06736379) will determine its translational potential.

#2895 JAK inhibition enhances virotherapy in gliomas by modulating interferon-driven resistance.

Andres R. Lopez-Rivas[1], Andrew Gregg Gillard[1], Akhila Parthasarathy[1], Dong Ho Shin[1], Angelis Morales-Rivera[1], Claudia Solbes-Godina[1], Alejandra Duran[1], Joy Gumin[1], Christopher A. Alvarez-Breckenridge[1], Marta M Alonso[2], Frederick F. Lang[1], Juan Fueyo[1], Candelaria Gomez-Manzano[1]

[1]MD Anderson Cancer Center, Houston, TX,[2]Universidad de Navarra, Navarra, Spain

Background: Treating glioblastoma remains a therapeutic challenge in oncology. Our laboratory developed an oncolytic adenovirus, termed Delta-24-RGD, which has been tested in clinical trials for recurrent glioblastoma patients with encouraging results (NCT00805376, NCT02798406). Here, we aim to further improve the efficacy of Delta-24-RGD by targeting factors that maintain the immunosuppressive characteristics of gliomas.

Methods: We performed bulk RNA-sequencing of murine gliomas treated with Delta-24-RGD or control (PBS) and analyzed the upstream regulators using Ingenuity Pathway Analysis. A correlation plot of IFNγ and IDO1 transcript levels from 38 glioblastoma patient samples was obtained from the Delta-24-RGD plus Pembrolizumab clinical trial (NCT02798406) and analyzed in R Studio. Western blots, qPCR, and ELISA in glioma cells validated the IFNγ-induced IDO1 expression. To study macrophage polarization, bone marrow-derived macrophages (BMDMs) were stimulated with IFNγ or IL-4 in the presence or absence of JAK inhibitors, and gene expression of immunosuppressive markers was assessed by qPCR. Therapeutic efficacy in vivo was assessed by quantifying brain-infiltrating leukocytes using flow cytometry and evaluating tumor growth and survival.

Results: RNA sequencing revealed IFNγ as the top upstream regulator in murine tumors treated with an oncolytic virus. In addition, we observed upregulation of the tryptophan metabolism and immunoregulator IDO1 network in these treated tumors. We found a significant and positive correlation between IFNγ and IDO1 in glioblastoma tumor biopsies from the clinical trial. In vitro studies demonstrated that IFNγ treatment of glioma cells increased JAKs/STATs phosphorylation levels, IDO1 expression, and the Kyn/Trp metabolite ratio, which were abrogated by concomitant treatment with JAK inhibitors. Additionally, we observed that the JAK inhibitors reduced the expression of anti-inflammatory genes (Retnla, Arg1, Ido1, and Cd274) in polarized BMDMs. In syngeneic glioma models, we demonstrated that combination therapy with Delta-24-RGD and Baricitinib (a JAK inhibitor) yielded better tumor control when compared to monotherapy controls. Moreover, we observed that combination therapy reprograms the myeloid compartment of the tumor microenvironment towards an immunostimulatory phenotype.

Conclusions: Our study highlights the dual role of IFNγ in gliomas treated with oncolytic virotherapy: while it promotes antitumor immunity, it also induces immunosuppressive pathways such as IDO1 activation and tryptophan metabolism. These findings underscore the complexity of immune regulation in the tumor microenvironment and support the therapeutic potential of JAK inhibition in combination with oncolytic viruses for cancer treatment.

#2896 Therapeutic targeting of TGR5 abrogates bile acid driven myeloid cell immunosuppression in cholangiocarcinoma.

Enis Hikmet Ozmert[1], Binbin Li[2], Jingchun Yang[2], Hannah Elizabeth Stumpf[3], Jessica R. Willhite[1], Danielle Carlson[1], Jennifer L. Tomlinson[4], Jon Covel[5], Raghuveer Ramachandra[5], Steven Olson[5], Rory L. Smoot[6], Sumera Ilyas[2]

[1]Gastroenterology and Hepatology, Mayo Clinic, Rochester, MN,[2]Mayo Clinic, Rochester, MN,[3]Mayo Clinic College of Medicine and Science, Rochester, MN,[4]Mayo Clinic Hospital-Rochester, Rochester, MN,[5]Sanford Burnham Prebys, La Jolla, CA,[6]Surgery, Mayo Clinic, Rochester, MN

Background: Cholangiocarcinoma (CCA) is an aggressive hepatobiliary malignancy with limited treatment options. CCA exhibits a distinct desmoplastic and tolerogenic tumor immune microenvironment (TIME) characterized by elevated bile acid concentrations resulting from obstructive cholestasis and dysregulated bile acid metabolism. TGR5 is an essential component of bile acid signaling. We hypothesize that bile acids promote CCA progression by establishing an immunosuppressive TIME through TGR5 signaling, which can be therapeutically targeted using SBI-364, a novel potent small molecule TGR5 inhibitor.

Methods: Single-cell RNA sequencing (scRNA-seq) of immune cells from human intrahepatic (iCCA) and perihilar (pCCA) CCA tumors were conducted. Therapeutic studies were performed using syngeneic murine models of iCCA (PMID: 38458319), a novel syngeneic model of pCCA, and patient-derived xenograft (PDX) models. In collaboration with Sanford Burnham Prebys, SBI-364, a first in-class competitive TGR5 antagonist, was assessed in vivo. Additionally, we performed co-culture experiments with bile acid +/- SBI-364-treated murine bone marrow-derived monocytic myeloid-derived suppressor cells (M-MDSCs) and $CD8^+$ T cells to assess functional immunosuppressive effects.

Results: Human scRNA-seq revealed significantly increased TGR5 (GPBAR1) expression predominantly in myeloid cell populations within the CCA TIME. SBI-364 treatment significantly reduced tumor burden in both syngeneic orthotopic iCCA models and a novel pCCA model that recapitulates the anatomic characteristics of perihilar CCA. In contrast, NOD/SCID mice bearing PDX535 (predicted sensitive) and PDX136 (predicted resistant), SBI-364 treatment did not achieve tumor reduction, suggesting that TGR5 inhibition predominantly attenuates tumor progression through modulation of bile acid-immune cell interactions. SBI-364 treated murine tumors had a significant reduction in immunosuppressive macrophages expressing interleukin-10 and M-MDSCs compared to vehicle treated tumors. Furthermore, bile acid-treated M-MDSCs exhibited enhanced suppression of $CD8^+$ T cell proliferation and function, an effect that was abrogated by SBI-364 co-treatment.

Conclusion: We demonstrate that TGR5 inhibition represents a promising therapeutic strategy across multiple immunocompetent preclinical CCA models. We demonstrate that the bile-acid TGR5 axis promotes CCA progression via immunosuppressive myeloid cells. Specifically, TGR5 signaling potentiates the immunosuppressive capacity of M-MDSCs, contributing to an immunosuppressive niche that facilitates tumor progression. These results establish TGR5 as a rational therapeutic target for overcoming immune evasion in cholangiocarcinoma.

#2897 A patient-derived fragmented tumor assay for detailed evaluation of drug response in the tumor microenvironment (TME) using scRNAseq.

Daniel C. Rabe, Daniel J. Gorski, Shiyuan Zheng, Mary Flaherty, Tommy Trieu, A'Riane Branch, Terykah Hollis, Lovepreet Singh Chahal, Brian Roberts, Richard A. Klinghoffer, Sonal Khare

Tempus AI, Inc., Chicago, IL

Background: Many platforms exist for evaluating drug response in patient-derived tumor models. However, they are limited by their ability to recapitulate the multitude of cell types present in the TME. Additionally, they don't represent physiological ratios of tumor to immune cells and lack many secreted factors present in the TME. Each of these characteristics can have a profound impact on the efficacy of TME-targeting therapeutics. To overcome these limitations, we investigated the use of a fragmented tumor assay to interrogate TME alterations following treatment.

Methods: We developed a method of processing fresh patient tumor specimens into drug penetrable (~1mm^3) fragments, allowing short duration (4 to 48h) drug exposure and evaluation of therapeutic response by measuring cytokine/chemokine secretion using multiplexed ELISA and alterations in cell populations via single cell RNAseq (scRNAseq). To determine how therapies broadly affect the TME, we treated samples with either the multikinase inhibitor, Lenvatinib, immune checkpoint inhibitors (ICIs) Pembrolizumab/Nivolumab, or STING agonist cGAMP.

Results: Endothelial cells of the tumor vasculature are one of the most difficult TME cell components to evaluate by conventional bulk analysis methods. To evaluate responsiveness of endothelial cells we exposed endometrial cancer specimens to Lenvatinib. Following drug exposure, tumor fragments were processed for scRNAseq. Well-defined and expected cell clusters were resolved including endothelial, tumor epithelial, stromal, and multiple immune cell populations. Analysis revealed differential expression across these diverse cell populations in response to drug treatments. Specifically in endothelial cells we observed significant dose-dependent downregulation of transcripts involved in angiogenesis.

To examine immune perturbations, we treated tumor fragments with STING activators and ICIs. We observed activation of Type I Interferon genes and Interferon Stimulated Genes (ISGs), consistent with T-cell activation and proliferation through both ELISA and scRNAseq. Transcriptional changes in macrophages indicated activation of IFNγ and PI3K, consistent with changes from an immune-repressive to immune-activating state. Epithelial cells showed increased MYC and PI3K signatures and decreased signatures involved in hypoxic responses as well as NFκB signaling.

Conclusions: Our results demonstrate that TME-dependent cell-specific responses to drug exposure are observable by combining tumor fragmentation and scRNAseq. This allows the platform to be used for the characterization of responses to new investigational agents, particularly those that target the non-tumor cell components of the TME, evaluate mechanism of action in detail, and assess the promise of such agents for treating solid tumor malignancies.

#2898 Aging-related morphological change in regional lymph nodes promotes an immunosuppressive microenvironment in colorectal cancer.

Kosuke Kanemitsu[1], Rin Yamada[2], Daiki Yoshii[2], Yukio Fujiwara[2], Yoshiyuki Tagayasu[1], Teruki Sako[1], Kota Arima[1], Kohei Yamashita[1], Kazuto Harada[1], Norihisa Hanada[3], Yoshihiro Komohara[2], Masaaki Iwatsuki[1]

[1]Department of Gastroenterological Surgery, Kumamoto University Hospital, Kumamoto, Japan,[2]Department of Cell Pathology, Kumamoto University Hospital, Kumamoto, Japan,[3]Department of Surgery, Izumi General Medical Center, Kagoshima, Japan

Background: Lymph nodes (LNs) play a central role in anti-cancer immunity, yet the influence of aging on LN morphology and function in cancer remains largely unexplored. This study aimed to elucidate the relationship between aging-related LN alterations and the tumor immune microenvironment in colorectal cancer (CRC).
Methods: Mesenteric LNs from 160 CRC patients who underwent curative resection were histologically examined. LN ectasia—defined as sinusoidal dilation with loss of sinus macrophages—was quantified and correlated with clinicopathological factors, systemic inflammatory markers, and immune cell infiltration in the primary tumor (CD3, CD8, Foxp3, Iba1, CD163 by IHC).
Results: LN ectasia was significantly more frequent in elderly patients (≥70 years) and in right-sided colon cancers (p=0.002). Patients with marked LN ectasia showed lower serum albumin and leukocyte counts, indicating systemic immunosenescence. Immunohistochemical analysis revealed significantly reduced infiltration of $CD8^+$ cytotoxic T cells and $Iba1^+/CD163^+$ macrophages in tumors from patients with high LN ectasia, representing a “cold” immune microenvironment. However, LN ectasia was not directly associated with prognosis.
Conclusions: Aging-related LN ectasia reflects functional decline of regional lymphoid structures and correlates with attenuation of local anti-tumor immune activity in CRC. LN ectasia may serve as a histopathological biomarker of LN senescence and systemic immunosuppression in elderly cancer patients.

#2899 Oncolytic virus-chemotherapy combination improves control of PDAC growth and spread.

Biplov Sapkota[1], Naveen Chintala Ramulu[1], Shreya Pokharel[1], Mohammed T. Hussain[2], Brent Stanfield[2], Konstantin Kousoulas[2], Joseph Francis[1]

[1]Department of Comparative Biomedical Sciences, Louisiana State University, Baton Rouge, LA,[2]Department of Pathobiological Sciences, Louisiana State University, Baton Rouge, LA

Pancreatic ductal adenocarcinoma (PDAC) remains one of the deadliest solid tumors. Its progression is driven by KRAS-dependent signaling, a dense desmoplastic stroma, early metastatic spread, and an immunologically ‘cold’ tumor microenvironment (TME). Therapies that combine direct cytotoxic activity with TME reprogramming may improve treatment response. Oncolytic virotherapy offers such a dual mechanism.We hypothesize that a genetically engineered herpes simplex virus (HSV-1) strain, HSV-1(VC2), engineered to express murine GM-CSF, can synergize with gemcitabine by modulating tumor-intrinsic signaling and initiating early steps toward a more immune-responsive TME. *In vitro* studies using murine $KRAS^{G12D}$ $TP53^{R172H}$ Cre (KPC) cells demonstrated a strong synergistic interaction between the proposed oncolytic virus (oV) and gemcitabine, as supported by ZIP synergy modeling. qPCR analysis showed that gemcitabine increased EMT-associated transcripts (TGF-β, fibronectin, TAZ) as well as pro-survival/pro-migratory transcripts (CAV1, AKT, CTNNB1, PI3K). The oV alone activated STING-associated innate immune pathways. The combination treatment suppressed gemcitabine-induced EMT and proliferative signaling while maintaining antiviral and immunostimulatory gene expression, indicating coordinated transcriptional modulation consistent with enhanced cytotoxic and immunogenic activity.To evaluate in vivo relevance, we used an orthotopic immunocompetent PDAC model in which 10^4 KPC cells were surgically implanted into the pancreas of WT C57BL/6 mice. This model reflects PDAC growth kinetics and metastatic behavior. In preliminary studies, oncolytic virotherapy alone did not reduce tumor size but markedly reduced liver metastasis, with 1 of 4 mice showing liver involvement compared to 4 of 4 in the control group at day 38. In another study, the same OV application schedule (administered on days 10 and 24 after tumor implantation) was used together with gemcitabine (given weekly starting on day 11 at 100 mg/kg). This combination further decreased primary tumor burden compared with either monotherapy at the 38-day endpoint (n=8 mice/group). A Panc-1 xenograft model showed similar patterns in primary tumor reduction and metastatic spread.Ongoing work includes flow cytometry, targeted transcriptomics, and proteomic profiling to define immune and molecular contributors to synergy. Additionally, in vitro studies using human PDAC and pancreatic stellate cell 3D co-cultures, as well as human PDAC organoids, are in progress. Together, these findings position HSV-1(VC2) GM-CSF as a clinically relevant partner for gemcitabine and a potential strategy to improve PDAC responsiveness through both cytotoxic and immune-mediated effects.

#2900 Activation of the cGAS-STING signaling pathway as an immunotherapeutic approach to glioblastoma.

Louise Leparc, Judit Sanchez Gil, **Hiroaki Wakimoto**

Massachusetts General Hospital, Boston, MA

Glioblastoma (GBM) is the most aggressive primary brain tumor, characterized by rapid progression, resistance to therapy, and a highly immunosuppressive tumor microenvironment (TME). By sensing and reacting to cytosolic DNA, the cGAS-STING signaling pathway plays a critical role in innate immune defense, producing type I interferons and pro-inflammatory cytokines. In GBM, STING expression is frequently downregulated, contributing to tumor immune evasion. We set out to evaluate the potential of stimulating cGAS-STING signaling as a strategy to modulate the TME and provoke anti-tumor immunity in preclinical models of GBM based on murine GBM stem-like cell lines (005, NF53, C3, RIG) that are driven by TP53 loss and HrasV12. We found heterogeneous baseline expression levels of cGAS-STING components in these murine GBM cells, analogous to our observation in human patient-derived GBM cells. Despite this variability, murine GBM cells consistently responded to exposure to STING agonist ADU-S100 with transient IRF3 phosphorylation and robust induction of type I interferons (IFN-β) and chemokines (CXCL10, CCL5). *In vivo*, intratumoral injection of ADU-S100 (50 micrograms) mediated therapeutic efficacy against murine orthotopic GBM in C57BL/6 mice as it resulted in significant survival extension including long-term survival. This was achieved despite apparent ADU-S100-elicited, acute and transient body weight loss. Rechallenge of the same GBM cells in the contralateral hemisphere in long-term survivors was rejected, indicative of immune memory. These findings support pharmacological cGAS-STING activation as a strategy to counter GBM-driven immune suppression and a promising immunotherapeutic approach to this deadly brain tumor.

#2901 Integrated spatial, single-cell, and in vivo dissection of matrix CAF-driven immune exclusion in colorectal cancer.

Yuki Nakanishi[1], Kosuke Iwane[1], Yu Muta[1], Kento Yasumura[1], Mayuki Omatsu[1], Naoki Aoyama[1], Munehiro Ikeda[1], Yoko Masui[1], Go Yamakawa[1], Yasuhiro Fukui[2], Hiroaki Kasashima[2], Akihisa Fukuda[1], Hiroshi Seno[1]

[1]Kyoto University, Kyoto, Japan,[2]Osaka Metropolitan University Graduate Scholl of Medicine, Osaka, Japan

Background:
Fibrotic colorectal cancers (CRCs) are largely microsatellite stable and characterized by desmoplastic stroma that excludes cytotoxic T cells. Cancer-associated fibroblasts (CAFs) are major stromal constituents, yet how specific CAF subsets regulate immune exclusion remains poorly understood.

Methods:
We integrated orthotopic in vivo tumor models with spatial and single-cell transcriptomic analyses of human and murine CRCs to elucidate the mechanisms by which matrix CAFs modulate the tumor immune microenvironment.

Results:
Matrix CAFs highly expressed *THBS2*, a matricellular protein enriched at the invasive tumor front. In vivo, global or fibroblast-specific *Thbs2* deletion disrupted the fibrotic barrier and markedly increased intratumoral $CD8^+$ T-cell infiltration. Mechanistically, THBS2 restrained CXCL9/10 production by dendritic cells and macrophages, limiting recruitment of $CXCR3^+$ $CD8^+$ T cells. Neutralization of CXCL9/10 or blockade of CXCR3 reversed these effects, confirming the central role of the CXCL9/10-CXCR3 chemokine axis in CAF-mediated immune exclusion. Spatial transcriptomic profiling of human CRC further demonstrated that loss of THBS2 in matrix CAF-rich regions correlated with increased proximity between $CD8^+$ T cells and myeloid cells and elevated chemokine expression. Despite enhanced infiltration, these $CD8^+$ T cells displayed features of exhaustion, rendering tumors more responsive to immune checkpoint blockade.

Conclusion:
This integrated spatial, single-cell, and in vivo dissection reveals that matrix CAF-derived THBS2 orchestrates immune exclusion in fibrotic CRC via suppression of the CXCL9/10-CXCR3 axis. Targeting THBS2 or its downstream stromal pathways may represent a promising therapeutic strategy to overcome stromal-driven immunotherapy resistance in microsatellite-stable colorectal cancer.

#2902 Deciphering the function of lipid-associated macrophages in immunotherapy resistance of hepatocellular carcinoma.

Xiaohang Long[1], Yaxian Wang[1], Siyuan HUANG[1], Joaquim Si Long VONG[1], Joseph Jao-Yiu Sung[2], Lam, Stephen CHAN[3], Alfred Sze-Lok Cheng[1]

[1]School of Biomedical Sciences, The Chinese University of Hong Kong, Hong Kong, Hong Kong,[2]Lee Kong Chian School of Medicine, Nanyang Technological University, Singapore, Singapore, Singapore,[3]Department of Clinical Oncology, The Chinese University of Hong Kong, Hong Kong, Hong Kong

Background: Hepatocellular carcinoma (HCC) is a leading cause of cancer-related mortality globally. While immune-checkpoint blockade (ICB) has transformed oncology, its efficacy in HCC is limited by an immunosuppressive tumor microenvironment (TME) and diverse disease etiologies, yielding response rates below 30%. Our prior work identified several key transcriptional and epigenetic drivers of immune exclusion and myeloid-mediated immunosuppression underlying ICB resistance in preclinical models (*Gut* 2018, 2020, 2023, *Sci Transl Med* 2021). To develop precise immunotherapies, it is critical to identify the central regulatory nodes within the TME of ICB-resistant patients.
Methods: We applied single-cell RNA sequencing (scRNA-seq), single-cell Assay for Transposase-Accessible Chromatin using sequencing (scATAC-seq), and spatial transcriptomics to investigate the TME of HCC patients resistant to ICBs (from trial NCT05873244), with treatment-naïve patients serving as controls.
Results: Multi-omics analysis uncovered a subcluster of tumor-associated macrophages (TAMs) characterized by high levels of lipid-associated genes. Bioinformatics analysis of open chromatin regions identified a transcription factor (MTF) that was significantly up-regulated in TAMs from ICB-resistant HCCs but not in treatment-naïve tumors. Spatial transcriptomic profiling and multiplex immunohistochemistry confirmed the co-localization of MTF with the lipid-associated macrophages (LAMs) in patient tumors. Chromatin immunoprecipitation-sequencing in THP-1 cells revealed that MTF binding was enriched in phagocytosis-related genes. Functional studies in macrophage cell lines demonstrated that knockdown or overexpression of MTF modulated phagocytic capacity. Integrated RNA sequencing and Cut&Tag analysis further delineated its downstream targets and involvement in phagocytic pathways.
Conclusions: This study identifies a novel key transcriptional regulator and provides mechanistic evidence for its role in modulating macrophage phagocytosis and lipid metabolism in HCC ICB resistance. Our findings uncover critical epigenetic and transcriptional alterations within the immunosuppressive myeloid landscape and highlight promising therapeutic targets to overcome ICB resistance. These insights lay the groundwork for targeting the immunometabolic axis as a new strategy to counteract ICB resistance in HCC.
Acknowledgment: This study is supported by the General Research Fund (14120621, 14119023 and 14112525) CUHK Research Committee-Direct Grants (504643107) and the Li Ka Shing Foundation.

#2903 Modulating the tumor microenvironment (TME) to enhance anti tumor immunity using metabolic inhibitors.

Takeshi Ito[1], Shun Kishimoto[1], Kazutoshi Yamamoto[2], Jeffrey Brender[2], Frank Echtenkamp[1], Daniel Crooks[1], Murali Cherukuri Krishna[2], William Marston Linehan[1]

[1]Urologic Oncology Branch, National Institutes of Health, Bethesda, MD,[2]Molecular Imaging Branch, National Institutes of Health, Bethesda, MD

The tumor microenvironment (TME) presents a challenging setting for anti-tumor immunity due to its extreme metabolic features: nutrient deprivation, metabolite accumulation, acidity and hypoxia. Immune cells become dysfunctional under these unfavorable conditions resulting in diminished anti-tumor activity. Thus, strategies to address immunosuppressive conditions in the TME are warranted. We utilized metabolic inhibitors to modulate the TME and enhance anti-tumor immune responses. Neuroendocrine tumors (NETs) and chimeric antigen receptor (CAR)-T cells for somatostatin receptor 2 (SSTR2), a potential therapeutic target for NETs, were utilized as our experimental model. SSTR2 CAR-T cells were prepared from $CD8^+$ T cells of healthy donors. To recapitulate T cell dysfunction in TME, CAR-T cells were cultured under unfavorable metabolic situations: acidic, hypoxic and low glucose conditions. The CAR-T cells exhibited dysfunctional phenotypes including decreased proliferation and viability and impaired cytotoxicity and cytokine production capacity. Additionally, exhaustion-related markers were significantly upregulated on CAR-T cells especially under acidic conditions. To modulate metabolism of NETs, we utilized inhibitors targeting lactate dehydrogenase A (LDHA) and mitochondrial complex I. LDH inhibitor NCI-006 reduced glucose consumption and lactate (Lac) production from NETs by inhibiting lactate fermentation, resulting in reduced extracellular acidification. However, NETs exhibited metabolic rewiring to oxidative phosphorylation (OXPHOS) after NCI-006 treatment. In contrast, Complex I inhibitor IACS-010759 treatment induced OXPHOS inhibition and rewiring to aerobic glycolysis. Combined treatment with these inhibitors successfully interrupted metabolic rewiring of NETs by blocking both aerobic glycolysis and OXPHOS. Hyperpolarized magnetic resonance imaging (HP-MRI) with 1-13C pyruvate (Pyr) and electron paramagnetic resonance (EPR) pO2 imaging were conducted to monitor in vivo metabolic activities in NET-derived xenograft tumors. Consistent to our in vitro findings, NCI-006 suppressed Lac production from Pyr, and IACS-010759 treatment resulted in elevated pO2 level in xenograft tumors. However, metabolic rewiring was also observed in xenograft model; NCI-006 treatment exacerbated hypoxia and IACS-010759 promoted Lac production from Pyr. To overcome the metabolic rewiring, we attempted combination treatment with NCI-006 and IACS-010759 on xenograft mice. The combination treatment effectively abrogated metabolic flexibility of NET-derived xenograft tumors. Metabolic stress resulted in CAR-T cell dysfunction, while NCI-006 and IACS-010759 showed potential to improve the extracellular environment of the TME. Further studies are warranted to test the feasibility and efficacy of metabolic inhibitors in combination with CAR-T therapy.

#2904 Infectious bursal disease virus (IBDV) as a novel virotherapy for stimulating innate and adaptive immune responses in different cancer models.

Vicent Tur Planells[1], Yonina Bykov[1], Gloria Dawodu[1], Leticia Perez Rodriguez[2], Noemi Garcia Romero[3], Angel Ayuso Sacido[3], Jordi Cano Ochando[4], Daniel Lozano Ojalvo[5], Adolfo Garcia Sastre[1], Estanislao Nistal Villan[6], Sara Cuadrado Castano[7]

[1]Microbiology, Icahn School of Medicine at Mount Sinai, New York, NY,[2]Precision Immunology Institute (PRIISM), Icahn School of Medicine at Mount Sinai, New York, NY,[3]Experimental Sciences, Francisco de Vitoria University (UFV), Madrid, Spain,[4]Microbiology, National Center of Microbiology Health Insitute Carlos III, Madrid, Spain,[5]Immunology, Center for Research in Food Sciences CSIC-UAM, Madrid, Spain,[6]Pharmaceutical Sciences, CEU San Pablo University, Madrid, Spain,[7]Microbiology, Ichan School of Medicine at Mount Sinai, New York, NY

Within cancer immunotherapy, oncolytic viruses (OVs) are recognized as a promising and robust treatment approach. This study presents the potential of Infectious Bursal Disease Virus (IBDV), an avian-specific pathogen with no known human zoonosis, as a novel therapeutic agent. We assessed IBDV's efficacy against several cancer types, including glioblastoma (CT-2A, patient-derived glioblastoma stem cells), melanoma (B16-F10), colorectal carcinoma (CT-26), and B-cell lymphoma (A20). We have evaluated the infectivity, cytotoxicity, replication kinetics, and analyzed the expression of pro-inflammatory and anti-viral (IFN-I/IFN-III) cytokine responses in all tumoral models following viral infection, in comparison to those elicited by a very well-known OV, Newcastle disease virus (NDV). We further evaluated IBDV's anti-tumor effects in preclinical glioblastoma, colon, melanoma, and B-cell lymphoma models using immunocompetent mice. Immunological responses to IBDV virotherapy were analyzed locally, in the tumor microenvironment (TME) and systemically (in tumor-draining and distal lymph nodes) via spectral flow cytometry. Results demonstrate that IBDV significantly exhibits oncolytic activity both in vitro and in vivo, effectively infecting, replicating in, and killing all cancer models, while inducing type-I/III IFN responses and enhancing pro-inflammatory (IL-1β and IL-6) responses. Notably, in melanoma (B16-F10) and glioblastoma (CT-2A) in vivo models, IBDV treatment delayed tumor growth and improved overall survival compared to PBS-treated mice, while complete tumor elimination was achieved in 30% of colorectal carcinoma (CT-26) and 60% of B-cell lymphoma (A20) engrafted mice. In the A20 lymphoma model, a bilateral tumor setup was also used to assess abscopal effects. IBDV was injected in only one tumor, and delayed growth was observed in the contralateral, untreated tumor, indicating partial systemic immune activation. Overall, IBDV virotherapy elicited robust innate and adaptive immune responses within the TME, disrupting tumor immunotolerance. This was evidenced by the elevated ratios of M1/M2 and CD8+/Treg immune cell populations upon IBDV treatment compared to PBS-treated mice. In melanoma and colorectal carcinoma models, there was an upregulation of immunosuppressive markers on both CD4+ and CD8+ T cells in the TME and tumor-draining lymph nodes. Conversely, in the A20 lymphoma model, IBDV treatment resulted in a marked reduction of immunosuppressive features, characterized by decreased M2-like monocyte/macrophage populations and reduced expression of immunosuppressive markers on both CD4+ and CD8+ T cells. These findings highlight IBDV’s potential as a robust OV and suggest combining IBDV treatment with therapies targeting co-inhibitory markers to enhance efficacy.

#2905 Pancreatic adenocarcinoma immune tumor microenvironment is shaped by differential miRNA expression.

Maksymilian Jan Pilecki, Shannon M. Wallet, Robert Maile, Gerik Tushoski- Aleman, Song Han, Steven J. Hughes

Department of Surgery, University of Florida College of Medicine, Gainesville, FL

Introduction: Pancreatic ductal adenocarcinoma (PDAC) is a malignancy with poor prognosis and advanced stage at diagnosis. The tumor microenvironment (TME) plays a role in driving aggressive, treatment-resistant PDAC subtypes. This study explores miRNAs' role in modulating the immune cell composition of the PDAC TME.
Methods: The Database of Differentially Expressed microRNAs in Cancer was queried for miRNAs with log2 fold-change ≥3.5 or ≤-3.5 between PDAC and normal pancreas. miRNA and predicted target mRNA expression in neoadjuvant-treated PDAC samples was profiled using Nanostring nCounter. Patient and disease characteristics, miRNA target prediction, biologic pathways, immune infiltration, and survival were analyzed to identify associations with aggressive, treatment-resistant disease.
Results: Differentially expressed miRNAs were analyzed using Nanostring nCounter. Principal component analysis revealed two sample clusters: one with younger patients, high nodal stage, frequent positive surgical margins, and poor neoadjuvant treatment response; the other with less advanced disease features and better neoadjuvant treatment response. 14 differentially expressed miRNAs and 31 mRNA targets were identified. These were predicted to activate cytokine signaling, neutrophil degranulation, phagosome formation, IL-27 signaling, and tumor microenvironment pathways on Qiagen Ingenuity Pathway Analysis. Survival-congruent expression, defined by inverse hazard ratio between miRNAs and target mRNAs, was observed for miR-148a-3p (targets: SLC2A1, ITGA5) and mir-193a/b-5p (target: RORC). Low miR-148a-3p levels and high miR-193a/b-5p levels were linked to short overall survival. TIMER 2.0 analysis demonstrated positive correlation between ITGA5 expression and cancer-associated fibroblasts, M2 macrophages, and regulatory T cell infiltration; global suppressive effect of SLC2A1 on immune cell infiltration; and a mixed effect of RORC on immune cell infiltration, characterized by positive correlation with neutrophil and type 1 macrophages and negative correlation with CAF, natural killer cell, and dendritic cells.
Conclusion: Distinct miRNA expression profiles in neoadjuvant-treated PDAC are linked to increased inflammatory signaling and immunosuppressed TME via effect on predicted mRNA targets. A subset of miRNAs differentially expressed between advanced, treatment-resistant PDAC and treatment-responsive PDAC is predicted to influence the PDAC TME via upregulation of immune pathway signaling and effects on the TME composition. Particularly, we demonstrated that low miR-148a-3p expression in treatment-resistant PDAC facilitates ITGA5-mediated immunosuppressive cell infiltration and predicts worse survival. Together, these findings highlight miRNAs' role as critical modulators of the PDAC immune TME and clinical outcomes in PDAC.

#2906 The iRGD peptide reprograms the tumor microenvironment and potentiates immunotherapy in an advanced humanized PDAC mouse model..

Norio Miyamura[1], Yukihito Kuroda[1], Kodai Suzuki[1], Yuki Kunisada[1], Hotaka Kawai[2], Henri Havia[3], Tero Jarvinen[3], Moriya Tsuji[4], Kazuki N. Sugahara[1]

[1]Columbia Univ. Vagelos College of Physicians & Surgeons, New York, NY,[2]Okayama University, Okayama, Japan,[3]Tampere University, Tampere, Finland,[4]Columbia University, New York, NY

Pancreatic ductal adenocarcinoma (PDAC) presents a desmoplastic, poorly perfused, and immunosuppressive tumor microenvironment (TME) that limits immunotherapy. We recently discovered that the tumor-penetrating peptide iRGD, which binds αv integrins and neuropilin-1 (NRP-1), reprograms this hostile TME by targeting tumor-infiltrating regulatory T cells (Tregs) and inhibiting transforming growth factor-β (TGF-β), a key driver of fibrosis, vascular collapse, and immune suppression. Here, we show that iRGD elicits similar effects in humanized PDAC mice reconstituted with functional human immune cells. PDAC-infiltrating Tregs expressed αvβ5 integrin in addition to NRP-1, enabling iRGD-mediated targeting and depletion in transgenic and syngeneic PDAC models. In contrast, splenic Tregs lacked αvβ5 and remained unaffected. αvβ5$^+$ Tregs represented a highly suppressive CCR8$^+$ Treg subset. These αvβ5$^+$ Tregs were also identified in human PDAC tissue and could be induced from human CD4$^+$ T cells. Beyond Tregs, αvβ5 was broadly expressed on cancer cells, fibroblasts, and endothelial cells in PDAC. Our recent studies showed that the αvβ5-rich TME facilitates integrin-dependent TGF-β activation, which is effectively antagonized by iRGD. Owing to its tumor-penetrating activity, systemic iRGD monotherapy broadly inhibited TGF-β signaling in syngeneic PDAC tumors, improving vascular perfusion, reducing stromal fiber density, and enabling deep infiltration of CD8$^+$ T cells. iRGD also significantly enhanced the response to immune checkpoint blockade. In humanized PDAC mice, iRGD reproduced these TME-modifying effects: it reduced vascular collapse and hypoxia, increased pericyte coverage, decreased stromal fibers, improved the CD8/Treg ratio, and activated human cytotoxic T cells. Early data further suggest that combining iRGD with checkpoint blockade prolongs survival in these mice. These findings indicate that the biological activity of iRGD is preserved across species despite potential differences in its target proteins. Collectively, iRGD orchestrates a coordinated reprogramming of the PDAC TME through αvβ5-dependent Treg targeting and TGF-β suppression, resulting in enhanced anti-tumor immunity in both mouse and humanized models. These results strongly support further clinical development of iRGD-based immunotherapies and highlight αvβ5 as a promising, mechanistically defined target for treating PDAC and other desmoplastic, TGF-β-rich tumors.

#2907 Characterization of tumor microenvironment phenotypes as potential biomarkers for immune infiltration.

Iqra A. Arif, Ruchi Shah, Katherine A. Johnson, Cheri A. Pasch, Dustin Deming

McArdle Laboratory for Cancer Research, Madison, WI

Background: Improved biomarkers are needed to identify immune permissive tumor microenvironment (TME) phenotypes that correlate with tumor infiltrating CD8+ T cells (TILs) and immunotherapy response. Myofibroblastic and inflammatory cancer-associated fibroblasts (myCAFs and iCAFs) are CAF subtypes involved in remodeling extracellular matrix and immunomodulation. Versican (VCAN), a matrix proteoglycan, and its proteolysis product, versikine (Vkine), regulate immune infiltration in the CRC TME. Here, we evaluate VCAN proteolysis and CAF phenotypes together as potential biomarkers for immune infiltration.
Methods: Immunohistochemistry was performed to evaluate the below CAF markers, as well as VCAN and Vkine, in 636 primary and metastatic patient tumor samples. CD8+ TILs were quantified per high-powered field (HPF). All other stains were scored on a scale of 0-3 based on stromal abundance and intensity. MyCAF (αSMA and TAGLN) and iCAF marker (PDPN and ICAM1) scores were averaged and categorized as previous. VCAN status was categorized as previous.
Results: Of the VCAN proteolytic weak (VPW) cancers, 25.9% were myCAF high, 9.6% were iCAF high, 31.9% were neither high, and 32.7% were both high. Of the VCAN proteolytic predominant (VPP) cancers, 31.9% were myCAF high, 16% were iCAF high, and 30.3% were both high. Of the VCAN/Vkine low (VVL) cancers, 18.5% were myCAF high, 14.1% were iCAF high, and 14.1% were both high. In VPW cancers, the mean CD8+ TILs/HPF were relatively low across all CAF phenotypes with the neither high phenotype having the greatest TILs (5.7/HPF). In VVL cancers, the mean CD8+ TILs/HPF in the both high (3.2) and myCAF high (4.5) phenotypes were less than that observed with the iCAF high (7.7) and neither high (12.5) phenotpyes. For VPP cancers, the mean CD8+ TILs/HPF in myCAF high cancers (10) is significantly lower ($p=0.045$) than in all other phenotypes (neither high 24.2, iCAF high 16.5, both high 23.4).
Conclusion: The absence of CAFs or the presence of high iCAF correlates with enhanced T-cell infiltration in VVL and VPW metastatic cancers. For VPP cancers, the presence of a high myCAF phenotype does not suppress T-cell infiltration, though it is reduced relative to cancers with an absence of CAFs or presence of iCAFs. The combination of CAF phenotype and versican status should be further assessed as a biomarker for immune therapy response.

#2908 SR-A antagonism remodels the myeloid population of tumor immune microenvironment, expands CD8-positive T cells, and enhances antitumor efficacy in vivo.

Steven R. Post[1], Fariba Jousheghany[1], Thomas J. Kelly[1], Charles M. Quick[1], **Behjatolah M. Karbassi**[2]

[1]Pathology, University of Arkansas for Medical Sciences, Little Rock, AR,[2]University of Arkansas for Medical Sciences, Little Rock, AR

Introduction: Tumor-associated macrophages (TAMs) are key regulators of the tumor immune microenvironment (TIME). Macrophage class A scavenger receptors (SR-A) modulate macrophage activation and polarization, and increased SR-A-positive TAMs are associated with poor outcomes in several cancers, including breast cancer. We previously showed that SR-A engagement skews macrophages toward an immunosuppressive phenotype, suggesting that SR-A blockade may reprogram the TIME and enhance antitumor immunity. In this study, we tested whether SR-A blockade reprograms the TIME and limits tumor progression in tumor-bearing mice.

Methods: EO771 cancer cells were injected into mammary fat pads of syngeneic mice to establish breast tumors. Tumor-bearing mice were treated with an SR-A antagonist or a control, and then $CD45^+$ tumor-infiltrating cells were isolated for single-cell RNA sequencing. In separate cohorts, SR-A blockade was combined with CD137-targeted activation, and mice were euthanized when tumors reached the predefined tumor endpoint (volume ≥ 1.5 cm^3). In parallel, mice were treated with the appropriate controls for both SR-A antagonist and CD137 activation. Tumor volume, time to the tumor endpoint, and the presence of lung metastases were determined. Mice showing complete tumor regression were rechallenged by assessing tumor growth following the injection of EO771 cells into the contralateral mammary fat pad.

Results: Monotherapy with the SR-A antagonist did not significantly alter primary tumor growth. However, single-cell RNA-seq of $CD45^+$ tumor-infiltrating cells indicated a shift in the polarization of tumor-associated macrophages toward an immunostimulatory, antigen-presenting phenotype, characterized by the upregulation of MHC class II molecules. Further, there was an increase in a cytotoxic T-cell subset characterized by high expression of the CD137 co-stimulatory receptor. Extending these results, we evaluated the effect of combining the SR-A antagonist with targeted CD137 activation. Treating tumor-bearing mice with the combination of SR-A antagonist and CD137 activation significantly inhibited both tumor growth and the proportion of mice that developed lung metastases compared to control-treated mice. Moreover, a subset of treated mice achieved complete tumor regression and rejected subsequent tumor rechallenge, consistent with the generation of durable systemic antitumor immune memory.

Conclusions: Inhibiting SR-A-dependent interactions reprograms macrophages toward a tumor-hostile, antigen-presenting phenotype, enhances cytotoxic T-cell responses, and synergizes with CD137-targeted activation. Thus, SR-A-blocking strategies may improve the efficacy of co-stimulatory receptor agonists by conditioning the TIME.

#2909 Targeting USP22 reprograms the tumor microenvironment and sensitizes KRAS-mutant, TP53-Null Lung cancer to immunotherapy.

Keqiang Zhang, Ching Ouyang, jinhui Wang, Wendong Li, Walter Tsark, Yuanyuan Gao, Mingxiao Yang, Aimin Li, Colt Egelston, Crystal Marconett, Dan Raz

City of Hope National Medical Center, Duarte, CA

Ubiquitin-specific peptidase 22 (USP22), a deubiquitinase and component of the “Death-By-Cancer” gene signature, is overexpressed in many cancers and associated with recurrence, therapy resistance, and poor prognosis. Although USP22 has recently been implicated in tumor immune evasion, its role in KRAS-driven lung cancer and antitumor immunity has remained unclear. Here, we aimed to investigate the role of USP22 in tumor progression and antitumor immunity in KRAS-driven lung cancer.
By immunohistochemistry analysis, USP22 was found to be highly expressed in nearly all human KRAS-mutant lung adenocarcinomas and in early-stage KRAS-induced mouse tumors, where its strong correlation with the proliferation marker Ki67 highlights USP22 as a potentially important mediator of KRAS-driven tumor biology and reinforces its promise as a therapeutic target.
To define USP22’s role in tumor progression and immune regulation, we generated a conditional Usp22 knockout (Usp22-KO) model in $KRAS^{G12D}$; $Tp53^{-/-}$ (KP) mice. Usp22 loss significantly suppressed tumor growth, prolonged survival, and promoted tumor differentiation, accompanied by reduced KRAS pathway activity and partial restoration of p53 signaling. Spatial transcriptomics, RNA sequencing, and multiplex immunofluorescence revealed that Usp22 deletion reprogrammed the tumor microenvironment by decreasing $CD206^{+}$ M2 macrophages, reducing TGF-β1 levels, limiting angiogenesis, increasing $CD8^{+}$ T cell infiltration, and diminishing $FOXP3^{+}$ regulatory T cells. Mechanistically, Usp22-KO altered gene expression and protein stability, reducing c-Myc, PD-L1, TGF-β1, and secreted protein acidic and rich in cysteine (SPARC); disruption of the TGF-β1-SPARC axis led to a marked depletion of immunosuppressive PD-L1^+ M2 macrophages. Functionally, Usp22 deletion substantially enhanced sensitivity to anti-PD-L1 immune checkpoint blockade in KP lung cancer. Collectively, these findings reveal USP22 as a critical driver of tumor progression and immunosuppression in KRAS-mutant, TP53-deficient lung cancer and demonstrate that targeting USP22 has significant therapeutic potential for overcoming resistance to immune checkpoint inhibitor therapy.

#2910 GRN deficiency loosens stromal barriers and enhances MHC-II signaling yet reduces MHC-I driven cytotoxic immunity.

Feng Guo, Boping Jing, Tadahito Yasuda, Mayu Yasuda, Hudie Li, Fabio N. de Mello, Alan Y. Wang

Brown Center for Immunotherapy, Indiana University School of Medicine, Indianapolis, IN

Progranulin (GRN) is a multifunctional regulator of tissue remodeling and myeloid biology. Although neuroprotective in the CNS, increasing evidence indicates that GRN supports a fibrotic and immune suppressive tumor microenvironment.We investigated whether host GRN restrains anti-tumor immunity and whether its inhibition could be therapeutically leveraged. Using C57BL/6J Grn-/- mice across three syngeneic models (KPC pancreatic ductal adenocarcinoma, B16-F10 melanoma, MC38 colorectal carcinoma), GRN loss consistently delayed tumor growth, with the most pronounced effect in KPC subcutaneous tumors, indicating a substantive but incomplete contribution of host GRN to tumor control.Single-cell RNA-seq and cell-cell interaction analyses of KPC tumors revealed coordinated rewiring of antigen presentation and stromal programs in Grn-/- hosts: MHC-II signaling predominantly B to T was increased, whereas MHC-I inputs decreased. Cancer-associated fibroblasts exhibited downregulation of chemokine/GPCR sensing, ER-phagosome and complement pathways. CAF composition shifted toward iCAF expansion with mCAF/vCAF reduction, and fibroblast→tumor ECM adhesion pairs (COL/FN1/LAM→CD44/SDC) were diminished, consistent with a loosened stromal matrix.In T cells, $CD4^+$/$CD8^+$ central or resident memory compartments expanded, while cytotoxic and exhausted $CD8^+$ populations declined; pseudotime analyses demonstrated attenuated progression from memory toward cytotoxic or exhausted endpoints.Collectively, these data indicate that host GRN sustains a myeloid-CAF program that strengthens stromal tension and supports MHC-I driven T-cell terminal differentiation. GRN loss relaxes this circuit, reducing MHC-I availability while enhancing B-T MHC-II engagement, which shifts T cells toward memory states and limits cytotoxic output. These findings identify GRN blockade as a TME reprogramming strategy that should be paired with agents restoring $CD8^+$ signal-1 (MHC-I) to convert enlarged memory pools into durable cytotoxic control in PDAC.

#2911 Versican expression and proteolysis as a biomarker for CD8+ T cell infiltration across cancer types and molecular profiles.

Ruchi Shah[1], Elizabeth L. Field[1], Cheri Pasch[1], Dustin A. Deming[2]

[1]Univ. of Wisconsin Madison Sch. of Med. & Public Health, Madison, WI,[2]University of Wisconsin Carbone Cancer Center, Madison, WI

Background: Current biomarkers for immune checkpoint inhibitor (ICI) response, including tumor mutation burden (TMB) and microsatellite instability (MSI), do not completely identify responsive patient populations. Versican (VCAN), a matrix proteoglycan found in the tumor microenvironment (TME), and its proteolysis product, versikine (Vkine), can regulate immune infiltration. Here we evaluate VCAN status as a biomarker for CD8+ T cell infiltration across cancer types and molecular profiles.

Methods: Patients (n=123) were identified and consented as part of an IRB-approved protocol. Patient characteristics were collected for all patients, and *PIK3CA*, *KRAS*, *TP53*, *BRAF*, *BRCA1/2*, *PTEN*, and *CDKN2A* mutation status were identified in a subset of 45 patients. Cancer samples were collected prior to ICI treatment, and were stained for VCAN, Vkine, and CD8. VCAN and Vkine staining was scored 0-3 based on stromal abundance and intensity. CD8+ tumor infiltrating lymphocytes (TILs) were quantified per high powered field (HPF). Cancers were assigned a VCAN status as previously.

Results: Clinical characteristics: 28 Colorectal , 8 Bladder, 44 Lung, 16 Skin, 6 Esophageal, and 21 other pan-cancer patients. Median CD8+ TIL abundance was higher in MSI-high (MSI-H) cancers (11.33) than in microsatellite stable (MSS) cancers (7.67; p=0.05). A weak positive correlation between TMB and CD8+ TIL abundance was observed (spearman's 0.201). A trend of elevated CD8+ TILs/HPF were observed in VCAN proteolytic predominant (VPP, percent of cancers 5%, mean CD8+ TILs/HPF 13) and VCAN/Vkine low (VVL, 37%, 15) cancers relative to VCAN proteolytic weak (VPW, 58%, 10). This relationship was preserved independent of MSI status, though MSI-H cancers had higher CD8+TIL abundance in VPP (MSI-H median CD8+ TILs/HPF 20, MSS 9), VVL (15, 11), and VPW (10, 5, p = 0.02) cancers compared to MSS cancers. VVL and VPW cancers were most prevalent across mutation profiles. Those cancers that are KRAS mutant were more likely to be VVL. A trend towards increased CD8+ TILs/HPF in VVL/VPP cancers relative to VPW cancers was observed generally across the mutation profile. However, CD8+ TILs/HPF were similar across VPP/VVL and VPW for *KRAS*-mutant cancers.

Conclusion: While TMB and MSI-H status correlate moderately with CD8+ T cell infiltration, VCAN status predicts CD8+ TIL abundance across several cancer types and mutation profiles. Further studies to investigate the impact of VCAN proteolysis on immune infiltration and ICI response are necessary to better identify patient populations which could receive benefit from ICIs.

#2912 SECN-15: Antisense oligonucleotide-mediated Neuropilin-1 suppression enhances anti-tumor immunity and overcomes checkpoint inhibitor resistance in solid tumors.

Andre Maaske, Sven Michel, Anne Sadewasser, Julia Festag, Monika Schell, Janani Sekar, Stefanie Raith, Frank Jaschinski, **Richard Klar**

Secarna Pharmaceuticals GmbH & Co. KG, Planegg, Germany

Background:Immune checkpoint inhibitors (ICIs) have transformed cancer therapy, but their efficacy remains limited in many solid tumors due to suppressive features of the tumor microenvironment (TME). Neuropilin-1 (NRP1), a multifunctional co-receptor, promotes tumor progression through immunosuppressive mechanisms and neoangiogenesis. High NRP1 expression correlates with poor prognosis and ICI resistance in different solid tumors, including gastric cancer. SECN-15 is a locked nucleic acid (LNA)-modified antisense oligonucleotide (ASO) designed to selectively downregulate NRP1 and counteract its protumorigenic functions.
Methods: NRP1-specific ASOs were generated using the OligoCreator™ platform and evaluated *in vitro* and *in vivo* in syngeneic murine tumor models as monotherapy or in combination with anti-PD-(L)1 antibodies. NRP1 knockdown was assessed at RNA and protein levels, including soluble NRP1 as a target engagement biomarker. Tumor cell composition and transcriptomic profiles were analyzed by flow cytometry and RNA sequencing. In silico analyses of publicly available bulk and single-cell RNA-seq datasets from cancer patients informed indication selection for the upcoming Phase I/II clinical trial and elucidated NRP1 biology in human tumors.
Results: Systemic SECN-15 treatment of tumor-bearing mice induced robust NRP1 knockdown in macrophages, T cells, and endothelial cells, leading to tumor growth delay and complete regressions in a subset of animals, both as monotherapy and in combination with anti-PD-1 treatment. Transcriptomic profiling revealed upregulation of pro-inflammatory pathways and downregulation of extracellular matrix and epithelial-to-mesenchymal transition (EMT) genes. Analysis of single-cell RNA-seq datasets from patients with gastric cancer identified endothelial cells and macrophages as major NRP1-expressing populations. NRP1high endothelial cells exhibited activation of TGF-β signaling, while NRP1high macrophages showed an upregulation of hypoxia and EMT pathways and suppressed allograft rejection signatures, in comparison with their NRP1low counterparts. These findings suggest that NRP1 promotes an immunoregulatory, pro-angiogenic TME in gastric cancer, further supporting its selection as a lead indication.
Conclusion: SECN-15 represents a promising therapeutic strategy to enhance anti-tumor immunity and overcome ICI resistance. Integration of preclinical and single-cell data highlights NRP1's role in sustaining an immunosuppressive TME which is currently further investigated in *in vitro* models. IND-enabling studies are underway to advance SECN-15 into clinical development.

#2913 Type I interferon reprograms neutrophil-T cell interactions to enhance antitumor immunity and informs a combinatorial strategy for esophageal cancer.

Tingxuan Gu[1], Kun Yu[1], Zigang Dong[2]

[1]Tianjian Laboratory of Advanced Biomedical Sciences, Academy of Medical Sciences, Zhengzhou University, Zhengzhou, China,[2]Zhengzhou University Medical College, Zhengzhou, Henan, China

Background: Type I interferons (IFN-I) integrate antiviral and antitumor responses by coordinating innate and adaptive immunity. Although their canonical function involves dendritic-cell (DC)-mediated antigen presentation, we identified a DC-independent mechanism whereby IFN-I directly reprograms neutrophils and reshapes the tumor immune microenvironment (TME) in esophageal squamous cell carcinoma (ESCC). This study pursued three aims: (1) to define the cellular compartments required for IFN-I signaling; (2) to dissect how IFN-I-reprogrammed neutrophils potentiate T-cell antitumor function; and (3) to evaluate translational strategies combining IFN-I agonism, TGF-β and PD-1 blockade.

Methods: Differentiated neutrophil-like cells were stimulated with IFN-α or IFN-I inducers (RIG-I-2CARD, STING-CTD ± c-di-GMP). N1/N2 polarization markers (CD54/ICAM-1, CD86, SELL, ARG1) were analyzed by flow cytometry and Western blot. Co-cultures of neutrophils, T cells, and KYSE esophageal carcinoma cells quantified T-cell cytotoxicity. Mechanistic assays used ICAM-1/LFA-1 blockade, metabolic inhibitors (nor-NOHA, DPI, NAC), and Transwell tests. For *in-vivo* validation, Ifnar1 fl/fl with CD4-Cre, Itgax-Cre, and S100a8-CreERT2 mice restricted IFN-I signaling to T cells, DCs, or neutrophils. MC38 tumor (C57BL/6) and KYSE450 xenograft (HSC-NSG) were established. IFN-I activation used Ad5-IFNA4 (10^7-10^8 PFU i.v., weekly) or c-di-GMP (20 μg i.p., q3d). Combination arms received TGF-β-trap and/or anti-PD-1 (10 mg/kg i.p.). Tumor growth, N1/N2 ratio, and $CD8^+$ Teff infiltration were assessed by flow cytometry.

Results: IFN-I signaling acted as the dominant upstream regulator of neutrophil-dependent tumor control. IFN-α and IFN-I inducers consistently polarized neutrophils toward an N1-like phenotype. Only neutrophils pretreated with IFN-α enhanced T-cell-mediated tumor killing; untreated cells failed. Direct addition of IFN-α to the culture had no effect, confirming that neutrophil priming by IFN-I is required. Blocking ICAM-1/LFA-1 or separating cells by Transwell reduced T-cell killing, indicating contact dependence. In vivo, Ad5-IFNA4 and c-di-GMP were well tolerated and increased intratumoral $CD54^+$ N1-like neutrophils. Ongoing studies in Ifnar1 conditional and HSC-NSG models are testing whether sustained IFN-I activation synergizes with PD-1 and TGF-β blockade to enhance $CD8^+$ Teff infiltration and antitumor efficacy.

Conclusions: Type I interferon signaling links neutrophil reprogramming to T-cell activation. IFN-I drives N1 polarization, promotes ICAM-1/LFA-1-dependent contact, and may relieve ARG1/NOX2-mediated suppression to restore T-cell cytotoxicity.These findings support a therapeutic framework combining IFN-I agonists with TGF-β and PD-1 blockade for durable antitumor immunity in ESCC.

#2914 Modulating the tumor microenvironmentwith an engineered oncolytic herpesvirus facilitates potent antitumor response.

Joseph Najjar[1], Geetanjali Geetanjali[2], Chase Kangas[2], Vk Gadi[3], Bin He[2]

[1]Biomedical Engineering, University of Illinois Chicago College of Medicine, Chicago, IL,[2]Microbiology and Immunology, University of Illinois Chicago College of Medicine, Chicago, IL,[3]University of Illinois at Chicago, Chicago, IL

Oncolytic viruses (OV) are a promising approach to cancer treatment, whereby attenuated viruses selectively infect and kill tumors, while sparing healthy cells. Tumor antigens and cytokines released from infected cells prime and activate the immune system to generate durable antitumor responses. This inflames the tumor microenvironment and may complement immune checkpoint inhibitor (ICI) therapy. However, this synergy is yet to be demonstrated: in a randomized, double blind, phase III trial, the HSV based talimogene laherparepvec (TVEC) in combination with anti-PD1 ICI therapy failed to improve both progression free survival and overall survival relative to anti-PD1 therapy alone. This may be attributable to viral factors that promote tumor selective replication in part by suppressing antitumor immune elements. Consequently, there is an unmet need for OVs that overcome the limitations of current therapies. We previously developed a novel oncolytic HSV, DN146, optimized for maximum immune stimulation without compromising tumor selective replication. Re-engineering of the γ_1 34.5 gene in DN146 permits efficient viral replication and tumor cell killing, while robustly activating STING and RIG-I. *In vivo*, DN146 exhibits strong immune stimulation and dendritic cell maturation, and robust clearance of metastatic lesions as compared to clinical analogues in a mouse model of triple negative breast cancer. We armed DN146 with an engineered high affinity SIRPα to further potentiate its antitumor effects by blocking the SIRPα-CD47 immune checkpoint. Antagonists of this checkpoint improve macrophage phagocytosis and T-cell recruitment to the TME. Further, CD47 blockade can improve cross presentation of tumor antigens to CD8+ T-cells. Together, these effects should cooperate with STING activation from DN146 to broadly reprogram the tumor microenvironment. When tested in a bilateral, murine colorectal cancer model, this virus achieves clearance of both locally injected and distal un-injected tumors, indicating strong local and systemic antitumor effects.

#2915 Tumor-intrinsic METTL5 restricts T cell-induced ferroptosis by impairing ATF4 translation in ovarian cancer.

Jiakai Hou[1], Cheng-wei Ju[2], Nicholas A. Egan[1], Yanjun Wei[3], Yunfei Wang[4], Minghao Dang[5], Tianyi Zhou[1], Leilei Shi[6], Ningbo Zheng[1], Si Chen[1], Ashley Guerrero[1], Xiaofang Liang[1], Wanfu Wu[1], Areej Akhtar[1], Chitra Dhiman[1], Debanwita Roy Burman[1], Andro Gerges[1], Mason D. Flores[1], Han Li[2], Li-Sheng Zhang[2], Marleen Kok[7], Xiaobo Mao[8], Linghua Wang[9], Qin Feng[1], Yiwen Chen[3], Sanghoon Lee[10], Daniel McGrail[11], Nidhi Sahni[6], Chuan He[2], Amir A. Jazaeri[10], Weiyi Peng[1]

[1]Biology and Biochemistry, University of Houston, Houston, TX,[2]The University of Chicago, Chicago, IL,[3]Bioinformatics and Computational Biology, The University of Texas MD Anderson Cancer Center, Houston, TX,[4]Clinical Science Lab, H. Lee Moffitt Cancer Center & Research Institute, Tampa, FL,[5]Lymphoma and Myeloma, The University of Texas MD Anderson Cancer Center, Houston, TX,[6]Epigenetics and Molecular Carcinogenesis, The University of Texas MD Anderson Cancer Center, Houston, TX,[7]Netherlands Cancer Institute, Amsterdam, Netherlands,[8]Neurology, Johns Hopkins University School of Medicine, Baltimore, MD,[9]Genomic Medicine, The University of Texas MD Anderson Cancer Center, Houston, TX,[10]Gynecologic Oncology and Reproductive Medicine, The University of Texas MD Anderson Cancer Center, Houston, TX,[11]Cleveland Clinic, Cleveland, OH

To systematically define tumor-intrinsic mechanisms driving immune resistance in ovarian cancer (OC), we integrated an *in vitro* genome-wide CRISPR immune screen, *in vivo* targeted immune screens, and analysis of 16 published ICB patient cohorts. From this pipeline, 693 candidate genes were shortlisted, and METTL5 emerged as a key regulator of tumor-intrinsic immune evasion. Pan-cancer TCGA analysis revealed significant METTL5 upregulation across multiple cancer types, with OC showing the second-highest expression among 34 malignancies. Although METTL5 expression did not correlate with OC stage or overall survival, higher expression was strongly associated with reduced cytolytic activity scores, suggesting suppressed antitumor immunity. In the MDACC HGSOC cohort (NCT03026062), patients with elevated METTL5 expression in baseline tumor samples exhibited significantly poorer responses and shorter overall survival after ICB therapy, supporting its clinical relevance. Mechanistically, METTL5 loss in OC models specifically reduced m^6A methylation at A1832 of 18S rRNA, disrupting helix 44 structure and impairing ribosomal scanning and translation. RiboLace-based active ribosome profiling demonstrated that METTL5 knockout reprograms translation, notably downregulating genes enriched in the “Response of EIF2AK1 to Heme Deficiency” pathway, consistent with defective integrated stress response (ISR). Translation of ATF4 was markedly reduced, accompanied by decreased expression of downstream targets SLC7A11 and SLC3A2, key components of the cystine/glutamate antiporter that suppress lipid peroxidation and ferroptosis. As a result, METTL5-deficient OC cells displayed increased lipid peroxidation and heightened sensitivity to T cell-mediated ferroptosis *in vitro* and *in vivo*. Reintroduction of ATF4 restored SLC7A11/SLC3A2 expression and reversed ferroptosis sensitivity, while pharmacologic inhibition of ferroptosis produced similar effects. These findings identify METTL5 as a central regulator of ATF4 translation, oxidative stress control, and immune resistance in OC. Elevated METTL5 expression may serve as a biomarker for poor ICB response. Therapeutically, METTL5 inhibition, ATF4 translation suppression or ferroptosis induction represent potential strategies to enhance immunotherapy efficacy. This study establishes the METTL5-ATF4-ferroptosis axis as a critical tumor-intrinsic mechanism of immune evasion and provides a generalizable framework for decoding cancer-immune interactions.

#2916 Tumor-intrinsic IRE1α signaling drives immune evasion and resistance to immune checkpoint inhibitor in lung cancer by upregulating PD-L1 and remodeling the tumor microenvironment.

Youngjoo Jeon[1], Hyun Kyung Ahn[1], Hongsoon Kim[1], Sung-Yup Cho[2], Jaemoon Koh[3], Yoon Kyung Jeon[4]

[1]Cancer Research Institute, Seoul National University, Seoul, Korea, Republic of,[2]Seoul National University Cancer Research Institute, Seoul, Korea, Republic of,[3]Seoul National University Hospital, Seoul, Korea, Republic of,[4]Department of Pathology, Seoul National University College of Medicine, Seoul, Korea, Republic of

Tumor cells exploit endoplasmic reticulum (ER) stress pathways for survival. While the role of the unfolded protein response in tumorigenesis is well-established, its specific effect on the tumor microenvironment (TME) and therapeutic resistance in non-small cell lung cancer (NSCLC), particularly via IRE1α signaling, remains poorly understood. Here, we demonstrate that high IRE1α activity correlates with poor prognosis and resistance to immune checkpoint inhibitors in NSCLC patients. IRE1α activation was associated with an immunosuppressive TME, characterized by enriched regulatory T-cell (Treg) and M2-like tumor-associated macrophage (TAM) signatures in patient cohorts. Consistently, genetic ablation of tumor-intrinsic IRE1α (*ERN1* KO) in immunocompetent mice significantly attenuated tumor growth and enhanced CD8+ T-cell infiltration. Mechanistically, IRE1α promoted the expression and secretion of key chemokines, specifically CCL20, which in turn drove M2-like macrophage differentiation in vitro. Notably, this pro-tumorigenic secretome was abrogated by the IRE1α inhibitor MKC8866. Concurrently, IRE1α-XBP1s signaling synergized with IFNγ to directly upregulate tumor-intrinsic PD-L1 expression. This process was mediated by the activation of the RIG-I-IRF1 axis, sustained STAT1 phosphorylation, and direct XBP1s binding to the *CD274* promoter. Collectively, tumor-intrinsic IRE1α orchestrates immune evasion in NSCLC by amplifying tumor-intrinsic PD-L1 expression through the IFNγ-STAT1-XBP1s-IRF1 axis and remodeling the TME via chemokines such as CCL20 that recruit immunosuppressive cell populations. The combination of an IRE1α inhibitor and anti-PD-1 antibody represents a promising strategy to enhance the efficacy of immunotherapy for NSCLC.

#2917 Novel strategies for targeting B7-H3 to empower precision oncology.

Di Zhao

UT MD Anderson Cancer Center, Houston, TX

Immune checkpoint B7-H3 (encoded by CD276) is an emerging immunotherapy target across diverse cancer types. However, our limited understanding of B7-H3 biology, its dysregulation, and its role in modulating immune and stromal components of the tumor microenvironment (TME) hinders the clinical application of B7-H3-targeting therapy. By leveraging genetically engineered mouse models and multi-omics approaches with single-cell resolution, we identified B7-H3 as one of the most promising checkpoint immunotherapy targets in cancers containing *PTEN* and *TP53* defects. In addition to suppressing T cells, we identified non-canonical dual functions of B7-H3 in modulating myeloid and stromal cells in the TME, thereby promoting cancer progression and therapy resistance. In this study, we answered long-standing questions regarding B7-H3 signaling and its cellular counterpart in the TME, uncovered the cellular and molecular basis of resistance to B7-H3 immunotherapy in cancer treatment, and developed innovative biomarker-driven, combinatorial strategies for B7-H3-targeted immunotherapy in malignancies.

#2918 Agonist activation of RIG-I^{+}tumor associated macrophages enhances anti-tumor immunity and therapeutic response in glioblastoma.

Han Xu[1], Sungwoon Lee[1], Felipe Saceanu Leser[2], Olga Federova[3], Peiwen Lu[4], Eric Song[5], Anne Eichmann[2], Akiko Iwasaki[4], Anna Anna Marie Pyle[3], Jean-Leon Thomas[1]

[1]Neurology, Yale School of Medicine, New Haven, CT,[2]Cardiovascular Research Center, Department of Internal Medicine, Yale School of Medicine, New Haven, CT,[3]Molecular, Cellular and Developmental Biology, Yale School of Medicine, New Haven, CT,[4]Immunobiology, Yale School of Medicine, New Haven, CT,[5]Ophthalmology and Visual Science, Yale School of Medicine, New Haven, CT

Glioblastoma (GBM), the most frequent and aggressive primary tumor of the brain, escapes all standard-of-care treatments that are provided after resection, including chemotherapy, radiotherapy or immunotherapy. The GBM tumor microenvironment is regulated by immunosuppressive mechanisms of the innate immune system, thereby contributing to the lack of anti-tumor adaptive immunity. We found that tumor associated macrophages (TAMs) can be repolarized into a M1 anti-tumor phenotype via agonist stimulation of the retinoic acid-inducible gene I (RIG-I), a cytosolic double-stranded RNA pattern recognition receptor (PRR). Innate immunity is governed by PRRs, which act as sensors of foreign and danger-associated molecular patterns and initiate the innate immune response. In silico analysis of adult GBM datasets available in the public domain revealed that *RIGI-I* expression by a subset of activated M1 TAMs positively correlated with patient survival. Studies in syngenic mouse models of GBM showed that intratumoral delivery of stem-loop RNA 14 (SLR14), a RIG-I agonist, improved the efficacy of all standard anti-GBM treatments, beyond the effects of other nuclei acid sensor agonists. We found that the combined activation of M1 TAMs and priming of functional cytotoxic CD8^{+} T lymphocytes and NK cells were accounting for the anti-GBM effect of SLR14, opening a significant new avenue for adult GBM treatment.

#2919 A little STING spices up tertiary lymphoid structures: Therapeutic induction of mature TLS by STING and lymphotoxin-β receptor activation confers immune protection against cancer metastasis.

Yasuhiro Kikuchi, Maxwell Duah, Fumiaki Kanamori, **Masanobu Komatsu**

Johns Hopkins All Children's Hospital, St. Petersburg, FL

Significant clinical evidence demonstrates an association of tertiary lymphoid structure (TLS) formation with cancer survival. Clinically translatable pharmacologic/biologic agents that induce TLS-rich tumor immune environment could provide a breakthrough strategy to treat therapy-resistant cancers. Here, we show that simultaneous activation of innate immune effectors, STING and lymphotoxin-β receptor (LTβR), by their agonists induces the formation of multiple TLS in TLS-free tumors in a manner dependent on $CD4^+$ and $CD8^+$ T cells. Using this approach, functional TLS were induced in all treated mice, in different tumor types and anatomical sites—TLS developed in adenocarcinomas and sarcomas in the pancreas, mammary gland, skeletal muscle, and subcutaneous tissues. TLS also developed in the brain harboring gliomas. STING activation alone was insufficient for inducing B cell-containing TLS or eliciting long-term therapeutic effects. However, when combined with LTβR activation, it improved the fitness of TLS with B cell expansion and maturation to IgG-producing long-lived plasma cells and memory cells, exhibiting lymph node follicle-like germinal center responses within tumors. In addition, the treatment induced high endothelial venule formation, increased $CD4^+$ T cell recruitment, memory $CD8^+$ T cell expansion, and the accumulation of $TCF1^+$ stem-like $CD8^+$ T cells around TLS. These immune responses resulted in strong suppression of tumor growth and metastasis, with excellent survival benefit, demonstrating that the treatment successfully immunized mice against tumor cells. The STING/LTβR combination therapy also substantially improved the efficacy of anti-PD-1 immune checkpoint blockade in resistant tumors. The immediate early response to the combination therapy was mediated mainly by $CD8^+$ T cells. The delayed but prolonged response was mediated by humoral immunity of B cells, which exerted a lasting anti-tumor effect together with the cellular immunity of $CD8^+$ T cells and NK cells. Our finding establishes a foundation for the therapeutic induction of TLS in cancer. Unlike other reported strategies, TLS induction by this method does not require viral antigens or artificial genetic manipulations to boost immune response, making it feasible for clinical applications. The high-affinity tumor-specific IgG-producing long-lived plasma cells and memory B and T cells generated in these TLS could provide lifelong protection against tumor recurrence and metastases. Effective tumor immunization by this strategy is expected to improve other cancer immunotherapies and suggests broad therapeutic applications in cancer. Since STING agonists are clinically available and humanized agonistic antibodies to LTβR can be developed, this strategy is readily translatable to clinical use for cancer treatment.

#2920 Metabolic reprogramming of hepatic macrophages restores CD8⁺ T cell immunity in T cell-desert hepatocellular carcinoma.

Liangliang Ji[1], Delaney Bessel[1], Sophia Brosnan[1], Isha Malik[1], Zijian Xu[1], Jiaxin Li[1], Peng Li[1], Xian Zhang[1], Jing Zhang[1], Ting-Wei Tsu[1], Shengyu Gao[1], Amaia Lujambio[2], Ming Li[1]

[1]Immunology Program, Memorial Sloan Kettering Cancer Center, New York, NY,[2]Icahn School of Medicine at Mount Sinai, New York, NY

CD8⁺ T cell-mediated immunosurveillance relies heavily on the functional integrity of antigen-presenting cells (APCs), particularly dendritic cells (DCs) that prime and activate T cells in secondary lymphoid organs. However, DCs are often defective in certain pathological contexts, such as β-catenin-mutated cancers, disrupting the cancer-immunity cycle and giving rise to “T cell-desert” tumor immunotypes that resist immunotherapy. Besides DCs, macrophages can also act as APCs and modulate CD8⁺ T cell activation, but their antigen-presenting function remains less well understood. Using genetic mouse models, we systematically characterized mice with macrophage-specific deletion of the mTORC1 suppressor *Tsc1* and found a striking increase of CD8⁺ T cells in the liver-but not in other tissues. This tissue specificity likely reflects the unique intravascular niche in which Kupffer cells interact directly with circulating CD8⁺ T cells. Notably, this CD8⁺ T cell expansion occurs independently of DC compartments. In a MYC/β-catenin-driven “T cell-desert” hepatocellular carcinoma (HCC) model, TSC1-deficient hepatic macrophages (hMϕs) reinvigorated antigen-specific CD8⁺ T cell responses and suppressed HCC progression, also in a DC-independent manner. hMϕs from wild-type mice predominantly express T-cell immunoglobulin and mucin domain-containing 4 (TIM-4), while TSC1-deficient hMϕs consist of both TIM-4⁺ and TIM-4⁻ subsets, with the TIM-4⁻ population driving CD8⁺ T cell expansion. Moreover, TSC1-deficient hMϕs exhibited enhanced tumor antigen acquisition and presentation capacity. Combining TSC1 deficiency in hMϕs with anti-PD-L1 immunotherapy significantly improved outcomes in murine “T cell-desert” HCC. Metabolic profiling revealed markedly increased mitochondrial activity in TSC1-deficient hMϕs, and their enhanced APC and anti-tumor functions required malate-aspartate shuttle-mediated oxidative phosphorylation. Together, these preclinical studies reveal a DC-independent role for hMϕs in orchestrating CD8⁺ T cell immunity and suggest that metabolic reprogramming of macrophages may offer a promising strategy to overcome immune evasion in “T cell-desert” tumors caused by defective DC function.

: Cellular Responses to Anticancer Drugs
Poster Session

#2924 ζ-Stat inhibits glioblastoma multiforme progression by targeting PKC-ζ/Cx43 signaling and inducing senescence.

Grazielly Teodoro, Shreejana Rimal, Wishrawana S. Ratnayake, Abigail Olatunji, Mildred Acevedo-Duncan

University of South Florida, Tampa, FL

Glioblastoma multiforme (GBM) is a grade IV astrocytic tumor and the most aggressive form of brain cancer, marked by poor prognosis, complex vascular networks, and genomic heterogeneity. PI3K/AKT (Phosphoinositide 3-kinase/Protein Kinase B) signaling and the atypical protein kinase C isoform PKC-ζ, play essential roles in GBM cell proliferation, migration, and resistance to therapy. In addition, PKC-ζ regulates Connexin 43 (Cx43), a gap junction protein that influences cell communication, cytoskeletal organization, and tumor cell motility. This study investigated the effects of ζ-Stat (8-hydroxy-1,3,6-naphthalenetrisulfonic acid), a selective PKC-ζ inhibitor, on GBM cell lines. Treatment with ζ-Stat significantly reduced proliferation by approximately 40% in T98G cells (80 μM) and 30% in U87MG cells (40 μM) ($p \leq 0.001$). Co-immunoprecipitation confirmed a strong association between PKC-ζ and Cx43 in both cell lines. Western blot analysis demonstrated that treatment with ζ-Stat reduced the levels of PKC-ζ and Cx43. As a result of PKC-ζ/Cx43 inhibition, PI3K/AKT signaling was downregulated in T98G cells. In addition, ζ-Stat induced cell cycle arrest, with increased expression of p21, p27, and PTEN, while inducing cellular senescence, as indicated by elevated β-galactosidase activity. Furthermore, ζ-Stat affected epithelial-mesenchymal transition (EMT), reducing the migratory potential of the cells through inhibition of vimentin expression. These findings highlight ζ-Stat as a promising therapeutic candidate for overcoming chemoresistance and improving treatment outcomes in glioblastoma.

#2925 Monzosertib, a selective CDC7 inhibitor, induces cell death via premature mitosis promoted by the FOXM1-cyclinB1 axis.

Hiroko Endo[1], Yu Nishioka[1], Mariko Hatakeyama[1], Youichi Tajima[2], Sayuri Ito[2], Akinori Arimura[3], Hisao Masai[2], Masaaki Sawa[1]

[1]Carna Biosciences, Inc., Kobe, Japan,[2]Department of Basic Medical Sciences, Tokyo Metropolitan Institute of Medical Science, Setagaya, Japan,[3]CarnaBio USA, Inc., South San Francisco, CA

Introduction: Cell division cycle 7 (CDC7) is a highly conserved serine/threonine kinase that plays a critical role in initiation of DNA replication and in replication stress checkpoint. Aberrant CDC7 expression has been implicated in various malignancies, highlighting its potential as a therapeutic target in cancer treatment. Consequently, CDC7 inhibitors are being explored as a novel class of anticancer agents. However, the mechanisms underlying cancer cell death induced by CDC7 inhibition are not fully elucidated. Monzosertib (AS-0141) is a potent, selective, and orally bioavailable CDC7 inhibitor, currently undergoing Phase I clinical trials in patients with solid and hematologic malignancies. In this study, we investigated the mechanisms of cell death induced by monzosertib in human cervical cancer cell lines by comparing cell lines with differential sensitivity to CDC7 inhibition.
Method: Six human cervical cancer cell lines (HeLa, CaSki, ME-180, SKG-I, SKG-IIIa, and C33-A) were used to evaluate their sensitivity to CDC7 inhibitors including monzosertib and simurosertib (TAK-931). Cell viability was assessed by the resazurin assay. Cell cycle distribution and apoptosis were analyzed by flow cytometry. Protein and gene expression levels related to CDC7 and cell cycle regulation were analyzed by Western blotting and real-time PCR, respectively. FOXM1 knockdown was performed by introducing shRNA via lentiviral transduction.
Result: We evaluated the antiproliferative activity of CDC7 inhibitors in six human cervical cancer cell lines. Among tested cell lines, HeLa cells were the most sensitive to CDC7 inhibition, whereas SKG-I cells exhibited the highest resistance. Treatment with monzosertib led to an increase in the sub-G1 population in these cell lines, depending on their sensitivity. Monzosertib increased the expression of the G2 and M-phase marker, cyclin B1 and phospho-CDK1 in HeLa cells in a dose-dependent manner, but not in SKG-I cells. Cell cycle analysis revealed that monzosertib induced cyclin B1 expression during the S-phase, which is characteristic of premature mitosis. These findings indicate that monzosertib-induced cell death appears to result from impaired mitotic progression. Since cyclin B1 expression was found to be elevated, we next examined the role of FOXM1, a transcription factor which regulates cyclin B1 gene expression. Treatment with monzosertib significantly increased FOXM1 expression in HeLa cells, whereas only a mild increase was observed in SKG-I cells. Knockdown of FOXM1 in HeLa cells resulted in reduced cyclin B1 expression and decreased sensitivity to CDC7 inhibition.
Conclusion: We found that the FOXM1- cyclin B1 axis contributes to cell death in cervical cancer cells induced by the selective CDC7 inhibitor, monzosertib.

#2926 Sonrotoclax (BGB-11417), a selective Bcl-2 inhibitor, demonstrates better efficacy than Venetoclax (Ven) and Lisaftoclax (APG-2575) in hematological cancer cells, xenografts, and human bloods.

Haitao Wang[1], Lin Li[1], Yiwen Wang[1], Hao Wang[1], Weiwei Song[1], Shuang Peng[1], Sijia Zhai[1], Ziyu Jia[1], Peng Chi[1], Xiaoyu Feng[2], Teiko Sumiyoshi[3], Wei Jin[1], Zhirong Shen[2]

[1]BeOne Medicine (Beijing) Co., Ltd., Beijing, China,[2]BeOne Medicines (Shanghai) Co., Ltd., Shanghai, China,[3]BeOne Medicines USA, Inc., San Carlos, CA

Background: Bcl-2 overexpression, a hallmark of hematologic malignancies, is associated with cell death evasion and drug resistance. Bcl-2 inhibitors such as Ven counteract this by disrupting Bcl-2 interaction with pro-apoptotic proteins (e.g., BIM), thereby restoring apoptosis. Despite Ven's clinical success, limitations like tumor lysis syndrome and suboptimal complete remission (CR) rates in CLL (chronic lymphocytic leukemia), underscore the need for improved inhibitors. Lisaftoclax (Lisa) and sonrotoclax (Son), are other two Bcl-2 inhibitors at late-stage of development. However, how are the three Bcl-2 inhibitors different from each other is unknown. This study investigates the difference of Ven, Lisa, and Son in different model systems.

Methods: RS4;11- and KMS-12-PE- Bcl-2-G101V cells were generated by ENU mutagenesis. OCI-LY10 expressing BTK-WT and mutations were engineered using lentiviral transduction. *In vitro* cytotoxicity was assessed via CellTiter-Glo (CTG) assay. Bcl-2:BIM complex disruption were examined by MSD assay.

Results: *In vitro* cytotoxicity assay revealed higher potency of Son compared to Ven and Lisa in Bcl-2-dependent cell lines across different indications. In Bcl-2-G101V mutant cells—a mutation presented in ~30% of Ven-relapsed CLL patients—Son retained >10-fold higher potency than Ven and Lisa. Moreover, Son also presented better efficacy than Ven and Lisa in different xenografts in vivo. Given Bcl-2 inhibitors are often used with/after BTK inhibitors in treating B cell lymphoma like CLL, MCL (mantle cell lymphoma), where BTK mutations contributing to resistance, Bcl-2 inhibitors were also profiled on B lymphoma cancer cells expressing BTK mutations. Intriguingly, Son maintained similar activity in OCI-LY10 cells expressing wildtype BTK as in BTK mutations (C481S, T474I, L528W, A428D), where Ven and Lisa exhibited less potent activity. Mechanistically, Son induced stronger Bcl-2:BIM disruption and caspase-3 activation in cancer cells, consistent with enhanced apoptosis. In human, Bcl-2 inhibitor effect is confounded by plasma protein binding (PPB). To understand potential difference in human under PPB, human whole blood from healthy donors was treated with Son, Ven, Lisa, the Bcl-2:BIM protein complex disruption—the very proximal and direct effect of Bcl-2 inhibitors—was then examined. Human whole blood assays also demonstrated that Son has >10-fold lower IC90 than Ven and Lisa in disrupting Bcl-2:BIM.

Conclusions: Son demonstrates significant advantage over Ven and Lisa in preclinical studies, including better efficacy in Bcl-2-dependent cancers, against Bcl-2-G101V and BTK resistance mutations, and enhanced target engagement in human whole blood. These highlight Son's great potential in addressing unmet needs in hematologic malignancies.

#2927 Synthetic lethality of G6PD deficiency and asparaginase for colorectal cancer therapy.

Yun-Cheol Chae[1], Alan Wong[2], Su Hyun Lee[1], Anais Barthe[3], Meaghan McGuinness[3], Samantha Fitzgerald[4], Sima Jeha[1], Seth Karol[1], Kimmie Ng[4], Marios Giannakis[4], Naama Kanarek[2], Alejandro Gutierrez[1]

[1]St. Jude Children's Research Hospital, Memphis, TN,[2]Boston Children's Hosptal, Boston, MA,[3]Boston Children's Hospital, Boston, MA,[4]Dana-Farber Cancer Institute, Boston, MA

Asparaginase, an enzyme therapeutic that deaminates asparagine to produce aspartate and ammonia, is among the most effective treatments for several cancers. However, the molecular determinants governing asparaginase response and resistance remain poorly defined, limiting its therapeutic potential. We previously demonstrated that asparaginase has potent activity in R-spondin fusion colorectal cancer (CRC), whereas APC-mutant CRCs are resistant (Hinze et al., Cancer Discovery, 2020). To elucidate mechanisms of asparaginase resistance in APC-mutant CRC, we conducted an unbiased genome-wide loss-of-function CRISPR/Cas9 screen, which revealed that loss of G6PD confers marked asparaginase sensitivity. This finding was validated using independent CRISPR/Cas9 and shRNA approaches in multiple human CRC cell lines and mouse intestinal organoid models ($P < 0.0001$ for all comparisons). G6PD, the rate-limiting enzyme of the pentose phosphate pathway (PPP), was found to mediate asparaginase resistance through maintenance of NADPH production, whereas other PPP functions, such as ROS detoxification or ribonucleotide biosynthesis, were not implicated. Untargeted metabolomics indicated that G6PD loss impairs the urea cycle, and we found that G6PD inactivation selectively sensitized cells to ammonia toxicity but not to asparagine deprivation ($P < 0.0001$ for ammonia; P = n.s. for asparagine-free media). In G6PD-deficient cells, the toxicity of asparaginase was rescued by small molecules that enhance ammonia detoxification ($P < 0.0001$) or by knockdown of NMRAL1, a redox sensor that inhibits the urea cycle enzyme ASS under NADPH-limiting conditions ($P < 0.05$). To assess whether G6PD deficiency influences asparaginase toxicity in humans, we analyzed a cohort of 586 children with acute lymphoblastic leukemia (ALL) treated with asparaginase and with available assessments of erythrocyte G6PD activity. Seventeen patients had functional evidence of G6PD deficiency, and we observed no increase in grade ≥3 asparaginase-related toxicities among G6PD-deficient patients, either individually or in combination (P = n.s.). Finally, genetic inhibition of G6PD enhanced asparaginase efficacy in vivo in mouse CRC models ($P < 0.01$ and $P < 0.05$), and a tool G6PD inhibitor induced profound asparaginase sensitivity in patient-derived CRC organoids ($P < 0.0001$). Together, these findings reveal that G6PD deficiency unmasks a tumor-selective vulnerability to ammonia toxicity, which can be therapeutically exploited using asparaginase. This work provides a rationale for clinical testing of asparaginase in G6PD-deficient CRC and for the development of clinical G6PD inhibitors as combination partners for asparaginase therapy.

#2928 KRAS inhibition-induced GSDME-mediated pyroptosis and its augmentation by LAT1 inhibition in KRAS-mutant lung cancer.

Kenji Morimoto, Ju Hwan Cho, Po-Lan Su, Peiran Xu, Andrew Barnes, Rahul Shivahare, Jacob Kaufman, Zihai Li, David Paul Carbone, Kai He

The Ohio State University James Comprehensive Cancer Center and Pelotonia Institute for Immuno-Oncology, Columbus, OH

Introduction: KRAS mutations are the most common oncogenic alterations in non-small cell lung cancer (NSCLC) globally. Although KRAS inhibitors (KRASi) show clinical benefit, their efficacy remains limited. This underscores the need to better understand KRASi-induced cell death mechanisms and to identify rational combination strategies that enhance antitumor activity. Pyroptosis, an inflammatory form of programmed cell death mediated by gasdermin (GSDM) pore-forming proteins, has emerged as a potential key mechanism to enhance therapeutic response and antitumor immunity. Whether KRASi induces pyroptosis in KRAS-mutant NSCLC has not been established. Here, we identify KRASi-induced pyroptosis, define its molecular mechanisms, and explore approaches to potentiate this process.
Methods: Murine and human KRAS G12C or G12D mutant NSCLC cell lines (H23, A427, KXP885, 2695L and others) were treated with mutation-specific KRASi. Pyroptosis and associated mechanisms were evaluated by LDH release, live-cell microscopy, Western blotting, and various siRNA knockdowns. LAT1 involvement was assessed using the LAT1 inhibitor JPH203 and rescue with spermidine.
Results: Mutation-specific KRASi induced pyroptosis in KRAS G12C and G12D mutant NSCLC cell lines, as evidenced by LDH release, characteristic pyroptotic morphology, and GSDM cleavage. This process required GSDME, but not GSDMD, as confirmed by GSDME knockdown. Mechanistically, KRASi activated two complementary GSDME-dependent pathways. First, KRASi triggered mitochondrial apoptosis, resulting in caspase-9 and caspase-3 activation and cleavage of GSDME into its pore-forming active N-terminal fragment (GSDME-NT). Second, KRASi stabilized GSDME-NT by suppressing its degradation. Previous research has shown that LAT1-mediated methionine uptake promotes GSDME-NT degradation. Consistent with this, we found that KRASi reduced c-MYC expression and downregulated its transcriptional target LAT1, the major transporter of methionine, thereby decreasing methionine-dependent GSDME-NT turnover and stabilizing the active fragment. Pharmacologic LAT1 inhibition with JPH203 further enhanced KRASi-induced pyroptosis, and this augmentation was reversed by the methionine-derived metabolite spermidine.
Conclusions: We identify GSDME-mediated pyroptosis as a previously unrecognized mechanism of KRASi-induced cell death in KRAS-mutant NSCLC. KRASi promotes both the generation and stabilization of GSDME-NT, while LAT1 inhibition amplifies this process by increasing metabolic stress and reducing GSDME-NT degradation. These findings support metabolic modulation, specifically LAT1 inhibition, as a promising combination strategy to enhance KRAS-targeted therapy and potentially improve immunogenic tumor cell death in KRAS-mutant NSCLC.

#2929 Immune and pharmacodynamic effects of sotorasib plus panitumumab in *KRAS* G12C-mutant colorectal cancer: Paired biopsy results from CodeBreaK 101.

David Hong[1], Lata Mukundan[2], Abraham Anderson[3], Emily Chan[3], Dorothy French[2], Linnea Haeggblom[2], Daniel Lu[2], Toshiki Masuishi[4], Rona Yaeger[5], Yuliya Katlinskaya[3]

[1]UT MD Anderson Cancer Center, Houston, TX,[2]Amgen Inc., San Francisco, CA,[3]Amgen Inc., Thousand Oaks, CA,[4]Aichi Cancer Center Hospital, Nagoya, Japan,[5]Memorial Sloan Kettering Cancer Center, New York, NY

Background: Sotorasib, a *KRAS* G12C inhibitor, plus panitumumab is approved for use in chemorefractory metastatic colorectal cancer (mCRC) . Yet, early effects on the tumor microenvironment (TME) in clinical samples are not well understood. In preclinical models, sotorasib potently suppresses MAPK signaling and promotes a pro-inflammatory TME characterized by $CD8^+$ T cell infiltration and increased IFN-γ activity, implicating adaptive immunity in tumor control. We investigated if these pharmacodynamic and immunologic effects are observed clinically in patients (pts) treated with sotorasib plus panitumumab.

Methods: Paired biopsies before and after 3-4 weeks of sotorasib plus panitumumab treatment were available from 12 pts in Cohort A of CodeBreaK 101 (NCT04185883). We performed whole-transcriptome RNA sequencing (n=12), pERK immunohistochemistry (n=8), spatial analysis of H&E-stained sections using digital pathology (n=10), and single-cell spatial transcriptomics (n=2). Analyses were primarily descriptive, and Wilcoxon signed-rank tests and summary statistics were used to characterize differences between paired biopsies.

Results: Transcriptomic profiling revealed robust suppression of MAPK signaling, shown by an approximate 4-fold reduction in median MAPK Pathway Activity Score with consistent downregulation of cell cycle-related genes. Key MAPK targets were downregulated, including *ETV4* (–6.9-fold), *EPHA2* (–2.8-fold), and *DUSP6* (–2.0-fold), while *EPHA4* was largely unchanged. pERK immunohistochemistry showed an approximately 1.8-fold reduction in H-score and a 2.0-fold decrease in proportion of $pERK^+$ tumor nuclei among profiled pts, consistent with effective MAPK pathway inhibition. Immune activation was reflected by a 1.9-fold increase in the Tumor Inflammation Signature score and upregulation of chemokines and antigen-presentation genes (CXCL9, CCL5, HLA-DPA1). Digital pathology analysis of H&E images showed increased immune cell clustering in the TME, mirroring immune remodeling observed in RNA-seq data. Single-cell spatial confirmed presence of $CXCR6^+$ $CD8^+$ T cells and macrophage derived CXCL10 in the tumor and associated stroma suggesting cytotoxic T cell recruitment and activation. Comprehensive pathway analysis showed upregulation of PI3K-AKT, HER2, and TGFβ signaling in some pts, suggesting compensatory survival mechanisms and a potential rationale for combinatorial strategies.

Conclusion: Paired biopsy analysis revealed potent MAPK inhibition and immune remodeling, providing mechanistic insight into the role of the immune TME in early response to sotorasib plus panitumumab and underscoring opportunities for rational combination strategies in mCRC.

#2930 Unraveling determinants of drug response: PRISM viability profiling of hundreds of oncology therapeutics reveals mediators of selectivity and mechanism.

Matthew G. Rees, Mustafa Kocak, Matthew J. Emmett, Colleen T. Harrington, Li Wang, Anthony Fazio, Alvin Kalathungal, Dennie T. Frederick, Aydin Golabi, Rachael Barry, Emily Reeves, John Davis, Melissa M. Ronan, Laura Doherty, Jillian N. Eskra, William R. Sellers, Jennifer A. Roth

Broad Institute, Cambridge, MA

Incomplete understanding of drug mechanism, selectivity, and polypharmacology can contribute to failed clinical trials. Drug candidates are generally characterized with limited pre-clinical tools and a narrow indication focus based on expected target biology. Using approaches such as large-scale PRISM profiling of 900 cell lines that have been genomically profiled in the Dependency Map coupled with machine learning analysis can provide a more thorough and agnostic understanding of oncology drugs. Here, we demonstrate that systematic characterization of an Oncology Reference library of over 250 oncology drugs, encompassing biologics (e.g., cytokines, antibody-drug conjugates), targeted protein degraders, and small molecules, of which two-thirds have never been tested with large-scale cell line profiling, enables better understanding of on-target and off-target effects. We developed models to quantify selectivity, on-target activity, and polypharmacology. Surprisingly, in some instances, these measures of cellular specificity can anticipate differential outcomes in clinical trials. Among unexpected findings, we identified a recurrent viability signature predictive of compound lysosomal accumulation, a phenomenon associated with phospholipidosis. In addition, CDK4-selective inhibition emerged as a potential therapeutic vulnerability across a diverse range of cancer types, including CDK6-deficient or CDK4-altered cancer. Our findings establish the Oncology Reference dataset and PRISM as a benchmark for evaluating current and emerging cancer therapies: combining large-scale systematic cell line profiling, genomic characterization, and machine learning analysis enables comprehensive characterization of oncology drugs with potential to inform clinical development.

#2931 RC108, a c-Met-targeting ADC, exhibits differential cytotoxicity between cMet-high and HGF-dependent tumor cells compared with Teliso-V, suggesting a potential safety advantage.

Jiayue Geng, Zhanjiao Yu, Haiqing Zhong, Qingbo Wang, Xiao Lv, Tongyu Xiao, Kailin Wang, Xiaoping Zhang, Xiaoli He, Lili Wang, Ying Jiang, Jianing Liu, Yinghao Xin, Jianmin Fang, **Yuanhao Li**

RemeGen Co., Ltd. (Yantai), Yantai, China

Telisotuzumab vedotin (Teliso-V) is the first c-MET-targeting ADC approved by FDA in May 2025 for the treatment of locally advanced or metastatic non-squamous NSCLC with high c-MET protein expression in patients who have received prior systemic therapy. Aberrant c-MET signaling is frequently observed in lung cancer and many other malignancies. Both c-MET overexpression and its ligand HGF contribute to hyperactivated c-MET signaling, promoting tumor proliferation, metastasis, and therapeutic resistance. Consequently, c-MET-targeted therapies employing various modalities have been actively pursued. RC108 is a novel c-MET-targeting ADC developed by RemeGen. It comprises a humanized antibody linked via a cleavable valine-citrulline/PABC linker to the cytotoxic payload monomethyl auristatin E (MMAE). Comparative in vitro studies were performed to evaluate RC108 versus Teliso-V, focusing on binding characteristics and cytotoxicity profiles. Both antibodies recognize distinct epitopes (bins) on the c-MET protein, and although their antigen-binding affinities and cell-binding properties are broadly comparable, RC108 exhibits faster and more efficient endocytosis than Teliso-V. For cytotoxicity assessment, a panel of cancer cell lines-particularly lung carcinoma cells-was characterized for c-MET signaling status using Western blotting to distinguish HGF-dependent versus HGF-independent (c-MET overexpression-driven) activation. The results revealed a clear pattern that RC108 demonstrated equal or superior potency to Teliso-V in c-MET-overexpressing tumor cells, but showed markedly weaker cytotoxicity in HGF-dependent cells. Although the underlying mechanism is under further investigation, clinical observations with RC108 support the hypothesis that this differential activity may confer a potential safety advantage. Since HGF-dependent c-MET signaling is commonly utilized by normal tissues in physiological repair and homeostasis, the lower cytotoxicity of RC108 in HGF-driven cells may indicate reduced interference with normal tissue signaling while maintaining strong activity against tumors driven by c-MET overexpression. Clinically, RC108 has shown a favorable and manageable safety profile in early monotherapy trials, characterized by a low incidence of TRAEs. In contrast, Teliso-V exhibited notable toxicity in earlier studies, with a relatively high discontinuation rate due to TRAEs. Importantly, RC108 was associated with low rates of peripheral neuropathy, a markedly lower incidence of interstitial lung disease (ILD), and no observed ocular toxicity. In summary, RC108 is a c-MET-targeted ADC with distinct properties to be recognized in further studies and may have potentially improved safety margin.

#2932 Combination of miRNA-379-5p and miRNA-125a-3p for the treatment of platinum resistant ovarian cancer.

Serenade Trevino, Trey Zepeda, Sue Anne Chew

Health & Biomedical Sciences, The University of Texas Rio Grande Valley, Brownsville, TX

Ovarian cancer (OC) is the second most common gynecologic cancer and the leading cause of death from cancers of the female reproductive system. The development of resistance to first-line platinum chemotherapy (e.g., cisplatin, carboplatin) contributes to high recurrence and lethality of OC, with over 50% of patients with advanced-stage OC relapsing due to drug resistance within two years of remission. Therefore, there is a need for alternative methods to treat platinum-resistant OC (PROC). Among several mechanisms, resistance to platinum-based therapy has been linked to upregulation of focal adhesion kinase (FAK), which activates signaling pathways that promote cell migration, invasion, adhesion, proliferation, and survival, and its overexpression is an accurate predictor of poor survival. Because FAK inhibitors have been unsuccessful when tested as single agents, combining them with other therapeutic agents may be more effective. Combination therapies are promising as they can improve treatment response while minimizing resistance and adverse side effects. Furthermore, cancer is often driven by multiple molecular pathways, and thus, a single therapy may not be sufficient. miRNA-379-5p has been shown to act as a tumor suppressor by directly targeting FAK and is downregulated in several OC cell lines and patient tumor samples. Additionally, overexpression of miRNA-125a-3p has been shown to inhibit cell invasion, migration, and proliferation, and induce apoptosis and cell cycle arrest in OC cells. BCL2-related ovarian killer (BOK) is a direct downstream target of miRNA-125a-3p, which acts as a pro-apoptotic regulator, and its protein levels can be increased by miRNA-125a-3p. The objective of this study was to investigate the dual delivery of miRNA-379-5p and miRNA-125a-3p for the treatment of PROC. OVCAR3 cells (i.e., adenocarcinoma ovarian cells shown to be platinum resistant) were transfected with each miRNA individually or in combination using Lipofectamine RNAiMAX, and cell viability was assessed using an MTT assay after 48 and 72 hours. After 48 hours, miRNA-379-5p, miRNA-125a-3p, and a combination of these miRNAs reduced cell viability by ~5, 14, and 21%, respectively, compared to the negative control. After 72 hours of exposure, both individual miRNA treatments significantly reduced cell viability by ~13%, while the treatment with both miRNAs reduced cell viability by ~28% compared to the negative control. The treatment of OVCAR3 with the combination of miRNA-379-5p and miRNA-125a-3p was able to significantly reduce cell viability compared to the treatment with each miRNA alone, suggesting a possible additive effect on cell death. Future studies will evaluate the mechanisms underlying reduced cell viability by investigating protein levels of markers for apoptosis, proliferation, and invasion.

#2933 Itareparib: A potent, selective and non-trapper PARP1 inhibitor for combination therapy with DNA damaging agents in solid tumors.

Alessandro Galbiati[1], Gianluca Papeo[1], Nilla Avanzi[1], Fabio Gasparri[1], Claudia Perrera[1], Gemma Texido[1], Lisa Mahnke[2], Shiho Nakano[3], Kang Jin Jeong[4], Gordon B. Mills[4], Junko Murai[3], **Alessia Montagnoli**[1]

[1]Nerviano Medical Sciences, Nerviano, Italy,[2]Nerviano Medical Sciences, Cambridge, MA,[3]Ehime University, Ehime, Japan,[4]OHSU Knight Cancer Institute, Portland, OR

BACKGROUND: The poly(ADP-ribose) polymerase-1 (PARP1) enzyme is critical to DNA Damage Response. Multiple first generation non-selective, trapping PARP1/2 inhibitors have been successful as single agent cancer treatments in homologous recombination (HR)-deficient malignancies; on the other hand, first-generation PARPi such as olaparib (a strong PARP1 trapper), or veliparib (a PARP1 trapper with medium potency), have not been successful in combination with chemotherapy due to a poor therapeutic window. Recently, second generation trapper PARP1-selective inhibitors (e.g. saruparib, M9466, SNV1521 and palacaparib) have entered clinical development, based on preclinical evidence that PARP2 inhibition is associated with anemia and dispensable for anti-tumor efficacy. However, emerging clinical data suggest that these drugs display hematological effects similar to the first generation PARPi. Indeed, all these inhibitors trap PARP1 on DNA lesions, causing hematological adverse effects that are overlapping with those caused by chemotherapy agents such as temozolomide (TMZ) and topoisomerase I inhibitors (TOP1i), thus limiting their combination potential.
METHODS: We used biochemical and cellular assays to evaluate itareparib potency and selectivity. Additionally, we performed cellular proliferation assays and mechanistic assays such as DNA damage markers assessment by high-content imaging and DNA combing assays, to evaluate itareparib activity in combination with DNA damaging agents (DDA). Finally, we performed in vivo experiments in tumor bearing mice and tumor free rats to assess the combination effects of itareparib plus TMZ on tumor growth inhibition and on the bone marrow.
RESULTS: Itareparib is a non-trapper PARPi and showed synergistic activity in combination with TMZ and TOP1i or Antibody Drug Conjugates (ADCs) with TOP1i payloads on DNA damage markers and in proliferation assays in vitro. The combination efficacy with temozolomide was confirmed in vivo in a small cell lung cancer xenografts model. Additionally, the comparative data with trapper-PARPi suggests that the combination efficacy with TMZ and TOP1i is not dependent on the trapping potency. Importantly, itareparib combination with DDA had lower impact on bone marrow precursors both *in vitro* and *in vivo* compared to PARP1-trapping inhibitors. Consistently with literature data, in vitro studies identify SLFN11 expression as a sensitivity biomarker to the combination of itareparib with chemotherapy.
CONCLUSIONS: Itareparib features are designed to expand the application of PARP1i through combination with chemotherapy, ADCs and radionuclides addressing the unmet need of patients with both HR-deficient and HR-proficient tumors. Itareparib is currently in Phase I/II clinical trials in combination with DNA-damaging agents in brain (high grade gliomas), lung and ovarian cancer.

#2934 Characterizing response to PARP inhibitor treatment combinations in advanced prostate cancer.

Bryan Correa Gonzalez[1], Akshaya Karthikeyan[1], Love A. Moore[1], Ethan Sandoval[1], Anamitra Bhuamik[1], Marion Hardy[2], Alan P. Lombard[1]

[1]UC Davis Comprehensive Cancer Center, Sacramento, CA,[2]UC Davis, Sacramento, CA

Background: Combining poly (ADP-ribose) polymerase inhibitors (PARPi) with androgen receptor pathway inhibitors (ARPi) has improved advanced prostate cancer management but questions remain including 1) where in the clinical treatment paradigm will these combinations fare best? 2) what underlies the efficacy of these combinations? and 3) what else may be more effective in combination with a PARPi? Here, we address these questions to advance the utility of PARP inhibition.
Methods: LNCaP (CSPC), C4-2B (CRPC), MDVR (enzalutamide-resistant C4-2B derivative), and AbiR (abiraterone-resistant C4-2B derivative) served as models of different advanced prostate cancer indications. Viability assays, microscopy, western blots and RNA-sequencing were used to investigate response to treatment.
Results: Data suggest prior exposure to an ARPi does not preclude benefit from combination treatment, but that the effect is greatest in ARPi-naïve cells. Despite a decrease in cellular viability, morphology of treated cells reveals a largely cytostatic response. Transcriptomic analysis and western blots suggest current hypotheses explaining the mechanism of combination efficacy may be incomplete, as findings do not support that ARPis induce significant BRCAness nor that PARPis reduce AR activity. Given that PARPi and ARPi combination may be less effective post ARPi exposure, we sought an alternative which may be more effective in this setting. Our work suggests that PARPis induce a robust, ATM-driven DNA damage response, and that co-targeting ATM elicits a synergistic reduction in cellular viability. Co-inhibition of ATM and PARP is much more effective than ARPi containing combinations in models of ARPi-resistant CRPC.
Conclusions: Current results suggest that 1) PARPi and ARPi combinations may be most effective earlier in the treatment paradigm, 2) more work is needed to understand PARPi and ARPi combination efficacy, and 3) ATM inhibition may be better in combination with a PARPi in more advanced settings. Future efforts will be directed at better understanding how these drugs work together and when best to administer them given the rapidly evolving prostate cancer treatment landscape.

#2935 Establishment of experimental model for measuring antibody-drug conjugate (ADC) bystander effects in breast cancer.

Hyunmyoung Yun[1], Won-Ji Ryu[1], Hyein Jung[1], Tae Yeong Kim[1], Cheol-Hwa Hong[1], Yumi Hwang[1], Hyun Ju Han[1], Geon-Uk Kim[1], Seo Young Lee[1], Kyoo Hyun Kim[2], Min Hwan Kim[2], Gun Min Kim[2], Joo Hyuk Sohn[2]

[1]Avison Biomedical Research Center, Yonsei University College of Medicine SBSI, Seoul, Korea, Republic of,[2]Department of Internal Medicine, Yonsei University College of Medicine SBSI, Seoul, Korea, Republic of

Antibody-drug conjugates (ADCs) targeting HER2 and TROP2 are now a mainstay of breast cancer therapeutics. ADCs equipped with cleavable linker-payload systems can kill non-target-expressing cancer cells through a bystander effect, which is influenced by antibody internalization and lysosomal degradation of the linker-payload complex. We first evaluated the IC_{50} values of the HER2-targeting ADC trastuzumab deruxtecan (T-DXd) across a panel of breast cancer cell lines. HER2 protein expression levels correlated well with sensitivity to T-DXd, confirming that HER2 target expression is a major determinant of individual response. We next assessed the presence of bystander effect by co-culturing of MCF7 (low-HER2) with SK-BR-3 (HER2+) cells in culture. T-DXd successfully induced caspase-3 activation in MCF7. Leveraging observation in the co-culture experiment, we established a quantitative co-culture model to measure the magnitude of ADC-mediated bystander activity. In this model, we engineered the TNBC cell line MDA-MB-231 (HER2-null) to stably express EGFP to be co-cultured with SK-BR3 (HER2+). T-DXd was labeled with pHrodo Red to visualize lysosome-ADC contact in breast cancer cells, and DNA damage was assessed by γ-H2AX staining. We observed internalization and co-localization to lysosome of T-DXd in selectively in SK-BR-3 cells, but not in MDA-MB-231 cells. Whereas, γ-H2AX activation were detected in EGFP-tagged MDA-MB-231 cells, suggesting propagation of payload DXd via bystander effect. Finally, we performed genomic analyses to identify genetic factors potentially associated with bystander activity in 50 breast cancer patients treated with ADCs using targeted-panel NGS data. Alterations in NOTCH1, NOTCH2, and NF1 were associated with poor progression-free survival under ADC treatment by Cox regression analysis, and these genes are implicated in lysosomal and autophagy regulation. Collectively, these findings highlight that the anticancer efficacy of ADCs is substantially influenced by the bystander effect and underscore the need for deeper investigation into how genetic factors modulate this process.

#2936 NAMPT inhibition enhances the efficacy of standard chemotherapies and immunomodulation in pancreatic ductal adenocarcinoma.

Purnachandra Nagaraju Ganji[1], Sujith Sarvesh[2], Dhana Sekhar Reddy Bandi[2], Husain Yar Khan[3], Irfana Muqbil[4], Amro Aboukameel[4], Sahar Bannoura[4], Khalil Choucair[4], Walid Sukkari[4], Sunil Jaiman[4], Rafic Beydoun[4], Gergory Dyson[4], Yang Shi[4], N. Vaishampayan[5], Eliza W. Bael[4], Miguel Tobon[4], Steve Kim[4], Herbert Chen[1], Muhammad W. Saif[4], Anthony Frank Shields[6], Philip A. Philip[4], Min Wu[7], Michael Schelle[7], Boris Pasche[4], Asfar S. Azmi[8], Bassel F. El-Rayes[2]

[1]Hematology and Oncology, University of Alabama at Birmingham, Birmingham, AL,[2]University of Alabama at Birmingham, Birmingham, AL,[3]Barbara Ann Karmanos Cancer Institute, Detroit, MI,[4]Wayne State University, Dearborn, MI,[5]Hematology and Oncology, Karmanos Cancer Institute, Detroit, MI,[6]Associate Director for Clinical Research, Barbara Ann Karmanos Cancer Institute, Detroit, MI,[7]Remedy Plan Therapeutics, Gaithersburg, MD,[8]Karmanos Cancer Institute, Detroit, MI

Background: Pancreatic ductal adenocarcinoma (PDAC) is characterized by high metabolic demand and dependency on NAD salvage pathways. NAMPT, the rate-limiting enzyme in NAD biosynthesis, is upregulated in PDAC and supports tumor survival under therapeutic stress. We investigated the preclinical activity of a novel hyperbolic NAMPT inhibitor (NAMPTi) in combination with standard-of-care (SOC) chemotherapy regimens including gemcitabine, paclitaxel, 5-FU, oxaliplatin, hydroxychloroquine, and paricalcitol to determine whether NAMPT blockade enhances cytotoxic and immunomodulatory responses.
Methods: Human and murine PDAC cell lines (PANC-1, MIA PaCa-2, KPC-Luc, and patient-derived 2838c) were treated with NAMPTi (5 μM) alone or with SOC agents at clinically relevant doses. Synergy was assessed in 2D viability and 3D spheroid assays. Olaparib combinations were also tested in BRCA-related models. In vivo, KPC allografts received NAMPTi (20 mg/kg, 5×/week) with gemcitabine, paclitaxel, hydroxychloroquine, 5-FU, oxaliplatin, or paricalcitol for three weeks. Immune infiltrates (CD45+, CD8+, CD4+ subsets), functional markers (GZMB, CD107a, IFNγ, TNFα), and fibroblast subtypes (apCAF, myCAF, iCAF) were quantified by flow cytometry.
Results: Across all PDAC models, NAMPTi alone produced modest growth inhibition, while combination treatment consistently outperformed monotherapies. NAMPTi synergized with gemcitabine-paclitaxel-hydroxychloroquine and gemcitabine-paclitaxel regimens, significantly reducing cell viability in both human and KPC-derived lines. In vivo, NAMPTi combinations markedly suppressed KPC tumor growth compared to SOC alone and reduced metastatic burden to liver and lung (e.g., GPH+NAMPTi: 60% metastasis-negative vs. 20-40% in monotherapy groups). Dual treatment increased CD8+ T-cell infiltration and effector phenotypes, enhanced cytotoxic function (GZMB+, CD107a+), and elevated IFNγ and TNFα production. NAMPTi also shifted fibroblast composition, with significant reductions in myCAFs and apCAFs, suggesting stromal remodeling. In FO and GPH regimens, combining NAMPTi produced superior tumor control, decreased immunosuppressive cell populations, and improved effector memory T-cell signatures.
Conclusions: NAMPT inhibition robustly enhances SOC chemotherapy efficacy in PDAC by simultaneously amplifying cytotoxic responses, remodeling the tumor immune microenvironment, and reducing metastatic spread. These findings support NAMPTi-based combinations as a promising therapeutic strategy and justify further translational development, including biomarker-driven clinical evaluation in PDAC.
"Generative AI was used for improving the language of the abstract".

#2937 Imipridones ONC201, ONC206, and ONC212 show potent killing and colony arrest of small-cell lung cancer cell lines.

Audrey Y. Su, Connor Purcell, Shengliang Zhang, Lanlan Zhou, Ashley S. Uruchurtu, Wafik S. El-Deiry

Brown University, Providence, RI

Introduction: Small cell lung cancer (SCLC) represents about 15% of all lung cancers, with an estimated 5-year survival rate of only 7%. While most SCLC cases initially respond to chemotherapy, a majority (70-80%) of cases recur and become resistant to first-line treatments. As such, further investigation of novel therapeutics is heavily warranted. Imipridones are a class of selective anti-cancer drugs that activate integrated stress response and increase TRAIL expression to lead to cancer cell death. While ONC201 (dordaviprone) has been investigated in small-cell and various other cancers, its derivatives ONC206 and ONC212 have not yet been explored within SCLC. As such, the present study compares ONC201, ONC206, and ONC212 within the context of SCLC.
Methods: Three SCLC cell lines were used: H526, H1048, H1882. For viability assays, cells were plated at 1000 cells/well in a 96-well plate and allowed to adhere overnight before treatment. Viability was assessed 72h after imipridone treatment by Cell-TiterGlo® assay to yield each drug's IC50. Western Blots (WBs) were performed across cell lines at 24h, 48h, and 72h following equitoxic treatments with each imipridone (IC25, IC50, IC75). Colony formation assays (CFAs) were also performed in triplicate for two cell lines (H1048, H1882) after three-day treatment with equitoxic doses of each drug followed by fourteen days of drug-free incubation.
Results: Across cell lines, ONC212 exhibited the lowest IC50, followed by ONC206 and ONC201. By WB, changes in ATF4, cPARP, and ClpX differed by drug, with ONC212 generally inducing the earliest and most significant changes in expression. CFA showed that ONC212 resulted in the greatest decrease in colony formation after 72 hours of treatment, followed by ONC206 and then ONC201.
Conclusions: The present findings suggest that SCLC may be highly sensitive to imipridones, particularly ONC212. Future works will aim to explore combination therapies and potential mechanisms including senescence induction, cell cycle alterations that may lead to reproductive arrest, metabolic changes, and alterations in growth and survival pathways in order to further characterize sensitivity and the colony arrest phenotype.

#2938 KRAS and ERK5 signaling pathways in cancer: Implications for targeted therapy.

Christophe Marcireau[1], Frederic Lacroix[1], Fatima Amor[1], Karine Dobrazix[1], Guillaume Nurit[1], Veronique Jean-Baptiste[1], Eiwen Yang[2], Donald Jackson[2], Colette Dib[1], Gaelle Muzard[1], Franck Slowinski[1], Laurent Debussche[1], Pawel K. Mazur[3]

[1]Sanofi, Paris, France,[2]Sanofi, Boston, MA,[3]PostDoc, UT MD Anderson Cancer Center, Houston, TX

KRAS Signaling in Cancer: KRAS functions as a small GTPase that serves as a molecular switch in cellular signaling, orchestrating proliferation, differentiation, and survival mechanisms. As the central node of the RTK-RAS-RAF-MEK-ERK signaling cascade, KRAS mutations represent the most frequent oncogenic events across human cancers, particularly in pancreatic, colorectal, and lung malignancies. These mutations drive constitutive pathway activation, promoting uncontrolled cellular growth. In lung cancer, KRAS G12C mutations are especially prevalent, leading to the development and approval of targeted therapies such as Sotorasib and Adagrasib. The clinical success of these KRAS G12C inhibitors has established a promising foundation for developing additional molecules targeting various K/N/H RAS isoforms.

ERK5 Signaling and Cancer Progression: ERK5, another member of the MAPK family, is activated by MEK5 in response to mitogenic and stress signals. The MEK5-ERK5 pathway regulates critical physiological and pathological processes, including cell survival and proliferation. Additionally, this signaling axis plays significant roles in metastatic progression and immune modulation within tumor microenvironments. Notably, inhibition of the RAS pathway frequently triggers compensatory upregulation of MEK5-ERK5 signaling, enabling cancer cells to maintain oncogenic signaling despite targeted intervention.

Research Focus: In this investigation, we will establish an ERK5 transcriptional gene signature and demonstrate how broad RAS pathway inhibition leads to ERK5 signaling overactivation through multiple experimental approaches.

#2939 Extrachromosomal DNA plasticity enables novel trajectories of cancer adaptation to drug treatments.

Jingting Chen[1], Joseph M. Dahl[2], Poorya Behnamie[3], Elizabeth Brunk[4]

[1]Department of Biochemistry and Biophysics, University of North Carolina at Chapel Hill, Chapel Hill, NC,[2]Bioskryb Genomics, Inc., Durham, NC,[3]Integrative Program for Biological and Genome Sciences, University of North Carolina at Chapel Hill, Chapel Hill, NC,[4]Department of Pharmacology, University of North Carolina at Chapel Hill, Chapel Hill, NC

Acquired resistance of cancer arises from continual evolution induced by therapeutic pressure. Breaking conventional evolutionary barriers, extrachromosomal DNA (ecDNA) recently emerged as a powerful driver of tumor adaptability and therapeutic failure. Studying ecDNA-driven evolution has largely focused on ecDNA copy number dynamics. However, this perspective overlooks the adaptive potential of ecDNA structural changes. A key mechanism of structural adaptation is ecDNA reintegration into chromosomes to form homogeneously staining regions (HSRs), elongated stretches of chromosomes that store oncogene copies. Prevalent in resistant malignancies, ecDNA-HSR transition is increasingly suspected to underlie therapeutic evasion. Yet how ecDNA reintegration occurs, how it varies across treatment conditions or cell types, and how it enables adaptation and resistance remain unclear. Addressing these gaps will greatly improve our ability to predict resistance progression and counteract ecDNA-driven malignancies, and this requires systematic characterization of ecDNA and HSRs.To fill these gaps, this work provides a systematic, high-resolution characterization of ecDNA drug responses using state-of-the-art single-cell multi-omics sequencing, imaging, and machine learning. We demonstrate that during drug exposure, ecDNA produces distinct adaptive responses in a cell population through complex genomic alterations. First, we consistently see significant ecDNA reduction in the cells that survived treatments. This is tightly correlated with gene expression changes in the same single cells, evidence that ecDNA is subject to selection. Intriguingly, imaging results have uncovered a previously unrecognized type of ecDNA that may represent an intermediate state bridging ecDNA-HSR transition. This observation challenges the traditional two-state view of ecDNA reintegration, suggesting instead a dynamic continuum that may underlie graded adaptation. To dissect this continuum at the functional levels, we are measuring ecDNA, intermediate, HSRs, RNA, and protein configurations in single cells across diverse adaptation models.Integrating innovative single-cell technology development with mechanistic discovery, our findings underscore the remarkable plasticity of ecDNA implicated in resistance acquisition. We show that rather than solely relying on pre-existing pro-survival traits, cancer cells may additionally exploit ecDNA to fast-track genomic changes that enable a wider range of adaptation. Such genomic plasticity may explain the quick relapse after selective therapies, offering new insights into actionable biomarkers that can reverse ecDNA-driven resistance.

#2940 Tumor-selective dimeric and monomeric RAF targeting with a next-generation Type 1 RAF inhibitor.

Mathieu Desaunay[1], Tara L. Peters[2], Evangelia Matenoglou[3], Beau Baars[1], Bijaya Gaire[1], Ana Orive-Ramos[1], Li Ren[2], Joseph P. Lyssikatos[2], Michael R. Burkard[2], Dalton Dacus[2], Matthew J. Sale[4], Stuart A. Aaronson[5], Frank McCormick[6], Evripidis Gavathiotis[7], Stefan D. Gross[2], Poulikos I. Poulikakos[1]

[1]Oncological Sciences, The Tisch Cancer Institute, Icahn School of Medicine at Mount Sinai, New York, NY,[2]Enliven Therapeutics, Boulder, CO,[3]Department of Biochemistry, Albert Einstein College of Medicine, Bronx, NY,[4]UCSF - University of California San Francisco, San Francisco, CA,[5]Icahn School of Medicine at Mount Sinai, New York, NY,[6]UCSF Helen Diller Family Comprehensive Cancer Ctr., San Francisco, CA,[7]Albert Einstein College of Medicine, Bronx, NY

Therapeutically silencing the RAS/MAPK signaling cascade, an oncogenic driver in more than one-third of human cancers, is constrained by a fundamental trade-off: potent pathway inhibition in tumors versus dose-limiting toxicities in normal tissues. BRAF-mutant (BRAF-MUT) cancers are a notable exception, where current clinical RAF inhibitors (RAFis) (Type 1.5 - αC-OUT/DFG-IN) selectively inhibit monomeric BRAF(V600X), while paradoxically activating MAPK signaling pathway in settings where RAF signals as a dimer, including wild-type and RAS-Mutant (RAS-MUT) contexts. While this paradoxical activation limits the broader applicability to BRAF-MUT tumors, it has been therapeutically exploited in vertical MAPK-targeting combinations with MEK or EGFR inhibitors, enhancing antitumor efficacy while restoring physiological MAPK signaling in normal tissues, achieving an improved therapeutic window and enhancing tolerability.To target dimeric RAF-driven tumors, including RAS-MUT tumors, Type 2 (αC-IN/DFG-OUT) RAFis were developed to engage both RAF monomers and dimers. However, as single agents, Type 2 RAFis showed only modest activity. Combining them with MEK inhibitors improved efficacy but also exacerbated toxicities due to MAPK pathway suppression in normal tissues, limiting dosing and ultimately constraining therapeutic benefit.Here, we characterized ELV-3111, a next-generation, highly potent and selective Type 1 RAFi with broad activity across BRAF class I/II/III, CRAF, and RAS-MUT models, including contexts resistant to current MAPK-targeted therapies. Unlike Type 2 RAFis, ELV-3111 induces robust paradoxical MAPK hyperactivation selectively in normal tissues - a phenomenon we successfully modeled in cells. Using complementary biochemical and live-cell assays, alongside molecular dynamics simulations, we demonstrate that this MAPK hyperactivation occurs via a RAS-dependent allosteric mechanism distinct from the paradoxical activation described for Type 1.5 RAFis. This unique property can be therapeutically exploited. Combining ELV-3111 with a MEK inhibitor overcomes the therapeutic ceiling of MAPK pathway targeting by creating a pharmacologically complementary interaction: additive suppression in tumors, where both agents inhibit MAPK signaling, and opposing effects in normal tissues, where MEK inhibition counteracts RAFi-driven hyperactivation. This configuration produced profound and durable regressions across RAS- and BRAF-MUT models, including a RAS-MUT model refractory to current therapies, while maintaining favorable tolerability. This tumor-selective mechanism, previously exploited in BRAF-MUT cancers, can now be extended to RAS-MUT and other dimeric RAF-driven tumors, offering a renewed therapeutic opportunity and the potential to reshape combination strategies across a broader spectrum of MAPK-driven cancers.

#2941 Pharmacologic ascorbate exerts anticancer activity through ROS-dependent metabolic vulnerability in MYCN-amplified neuroblastoma.

Tasfia Farah, Qi Chen

Pharmacology, Toxicology & Therapeutics, KUMC, Kansas City, KS

Background: Neuroblastoma (NB) is an aggressive pediatric cancer with poor prognosis, particularly in patients with MYCN amplification (MNA). MYCN-driven metabolic plasticity allows NB cell survival even under therapeutic stress. Pharmacologic ascorbate (Asc) has emerged as a potential low-toxicity anticancer agent that generates hydrogen peroxide (H_2O_2) and induces oxidative stress, selectively killing cancer cells. This study investigated the ROS-mediated metabolic vulnerability of MYCN-amplified and non-amplified NB cells in response to ascorbate.

Method: Patient-derived MYCN-amplified (MNA) (COG-N-415) and non-amplified (COG-N-618) neuroblastoma cells were treated with 0-20 mM ascorbate for 24 hours. Cell viability was measured using the CellTiter-Glo® assay. Intracellular ATP levels were quantified by HPLC. H_2O_2 and catalase were used to assess ROS dependence. Mitochondrial respiration and glycolytic activity were assessed by Seahorse XF analysis after 1-10 mM ascorbate treatment.

Result: Ascorbate induced a dose-dependent decrease in cell viability in both MNA and non-MNA neuroblastoma cells, with approximately 90% cell death at 10 mM. COG-N-618 (non-MNA) cells exhibited greater sensitivity than COG-N-415 (MNA), showing significant viability loss at 5 mM ascorbate. ATP levels decreased in both cells upon 5 mM ascorbate treatment. Catalase rescued ascorbate-induced ATP depletion, confirming an H_2O_2-mediated mechanism. Seahorse analysis demonstrated progressive inhibition in mitochondrial respiration and glycolysis, with COG-N-618 cells showing dose dependent Oxidative Phosphorylation (OCR) and Glycolysis (ECAR) inhibition at 1-10 mM. For the COG-N-415 cells (MNA), both OCR and ECAR decreased at 1 mM of ascorbate, but 5 mM and 10 mM did not cause further decrease, indicating an adaptive mechanism in the MYCN-amplified cells.

Conclusion: Pharmacologic ascorbate induces cytotoxicity in neuroblastoma cells and triggers ROS-dependent metabolic disruption and MYCN downregulation.

#2942 Inhibition of stearoyl-CoA desaturase 1 (SCD1) by SSI-4 as a therapeutic strategy in non-small cell lung cancer.

Valeria Romina Salerno Gonzales[1], Lauren Antal[2], Tamiel Nichole Turley[3], John A. Copland III[4]

[1]Mayo Clinic Graduate School of Biomedical Sciences, Mayo Clinic, Jacksonville, FL,[2]Research, Mayo Clinic, Jacksonville, FL,[3]Mayo Clinic, Rochester, MN,[4]Mayo Clinic, Jacksonville, FL

Lipid metabolism plays an important role in lung cancer growth, survival, and therapeutic resistance. Stearoyl-CoA desaturase 1 (SCD1), the enzyme that converts saturated fatty acids (SFAs) into monounsaturated fatty acids (MUFAs), represents a metabolic vulnerability since cancer cells depend on MUFAs for membrane biosynthesis, ER homeostasis, and alternative energy to glucose. SSI-4 (a.k.a MTI-301) is a selective SCD1 inhibitor currently in Phase I clinical evaluation for metastatic, unresectable, or refractory solid cancers, but its activity in non-small cell lung cancer (NSCLC) has not yet been characterized. To evaluate how NSCLC models respond to SCD1 blockade, we performed an initial screen of a panel of 17 human non-small cell lung cancer cell lines treated with 100 nM SSI-4 under defined serum conditions. Cell viability assays identified 9 responding cell lines, and dose-response studies confirmed IC50 values ranging from approximately 0.65 to 45.5 nM. Rescue experiments showed that adding oleic acid, an SCD1 regulated MUFA, reversed SSI-4-mediated growth inhibition, confirming mechanistically that this effect occurs through SCD1 blockade. Western blot analysis confirmed that SSI-4 treatment increased markers of endoplasmic reticulum (ER) stress and apoptosis in sensitive lines, consistent with disruption of lipid homeostasis. In contrast, non-responsive lines exhibited minimal induction of these stress pathways and retained viability despite treatment. Soft agar assays further showed that SSI-4 reduced anchorage-independent colony formation in responsive lines, indicating that SCD1 inhibition suppresses a key malignant growth property in these NSCLC models. Collectively, these findings demonstrate that SSI-4 selectively inhibits proliferation in a subset of NSCLC cells through an SCD1-dependent mechanism by reducing MUFA availability and activating stress and apoptotic signaling. This work establishes a framework for subsequent in vivo studies and lays the foundation for exploring SCD1 inhibition as a potential therapeutic strategy for patients with limited treatment options in NSCLC, while also advancing understanding of the mechanisms by which SCD1 supports tumor survival.

#2943 Antitumor effect of TROP2-targeted antibody drug conjugate, datopotamab deruxtecan (Dato-DXd), in association with DNA damage response in breast cancer cell lines.

Seohyeon Lim[1], **Sujin Ham**[1], Hae Min Hwang[1], Youlim Noh[1], Jiwon Koh[2], Chaeyoung Lee[1], Minyoung Jeong[1], Yu-Jin Kim[3], Minyoung Lee[4], Sohyeon Kim[4], Changhee Park[5], Dae-Won Lee[5], Kyung-Hun Lee[5], Seock-Ah Im[5]

[1]Cancer Biology, Graduate School of Interdisciplinary Graduate Program & Cancer Research Institute, Seoul National University, Seoul, Korea, Republic of,[2]Department of Pathology & Cancer Research Institute, Seoul National University Hospital & Seoul National University, Seoul, Korea, Republic of,[3]Cancer Research Institute, Seoul National University, Seoul, Korea, Republic of,[4]Cancer Biology, Graduate School of Interdisciplinary Graduate Program, Seoul National University, Seoul, Korea, Republic of,[5]Department of Internal Medicine & Cancer Research Institute, Seoul National University Hospital & Seoul National University, Seoul, Korea, Republic of

Background: Trophoblast cell surface antigen-2 (TROP2), Tumor-associated calcium signal transducer 2 (TACSTD2) is a transmembrane glycoprotein expressed in various cancer types. Datopotamab deruxtecan (Dato-DXd) is an antibody-drug conjugate (ADC) composed of an anti-TROP2 antibody (Datopotamab) linked via a cleavable peptide linker to DXd, a Topoisomerase-I inhibitor. Topoisomerase-I maintains DNA topological stress by resolving DNA supercoils during replication and transcription. We sought to determine whether this DNA damage mechanism classically induced by topoisomerase I inhibitors emerges when delivered through an ADC, and to further elucidate the previously uncharacterized molecular mechanisms of DNA damage response (DDR) and cell death by Dato-DXd.

Methods: Five established human breast cancer cell lines and one patient-derived breast cancer (PDC) cell line (SNU-3171) were used in this study. MCF7 and SNU-3171 were luminal breast cancer cell lines, and the others were triple-negative breast cancer (TNBC) cell lines. Sensitivity of each cell to Dato-DXd was assessed by colony formation assay (CFA) for 14 days (0.25-5 nM). Internalization and cell cycle analysis were performed by flow cytometry. Apoptosis was detected by Annexin V assay. The protein expression of TROP2, DNA damage, and repair molecules was analyzed by Western blotting and immunofluorescence.

Results: Based on CFA results, HCC1806, HCC70, and SNU-3171 were identified as sensitive cells (IC_{50}<0.5 nM), whereas MCF7, MDA-MB-157, and HCC1395 as less sensitive cells (IC_{50}>2.5 nM) to Dato-DXd. Dato-DXd was internalized within 2 hours in TROP2-positive cells. Following internalization, topoisomerase-I cleavage complexes (Top1ccs) were formed in all TROP2-positive cells; however, co-localization of Top1ccs and ɣ-H2AX was observed only in sensitive cells. Dato-DXd induced G2/M arrest in all TROP2-positive cells. In sensitive cells, the expression of TDP1, XRCC1, DNA Ligase III, and PNKP was decreased, while phospho-Chk1 (S345) and ɣ-H2AX were increased, indicating a reduction in single-strand DNA damage repair capacity and activation of DDR. Moreover, increased doses of Dato-DXd were associated with higher number of Annexin V-positive cells and sub-G1 populations, as well as higher expression of cleaved PARP, caspase-3, and caspase-7 in sensitive cells.

Conclusion: Dato-DXd demonstrated efficient internalization in TROP2-positive breast cancer cells including PDC, and impaired DNA single-strand break (SSB) repair, which consequently induce apoptosis in sensitive breast cancer cells. In particular, formation of Top1ccs and G2/M phase accumulation are induced in most of TROP2-positive cells. Further experiments are required to elucidate how impaired SSB repair contributes to the induction of DNA double-strand breaks and apoptosis.

#2944 Uncovering the zinc-dependent pathways of response and resistance to THZ1 in clear cell ovarian cancer.

Maya Modak[1], Soledad Ochoa[2], Forough Abbasi[3], Dandi Huang[3], Robbin Nameki[3], BJ Rimel[4], Kate Lawrenson[2]

[1]Center for Inherited Oncogenesis, Cedars-Sinai Health Sciences University/ University of Texas at San Antonio, Los Angeles/ San Antonio, CA,[2]Center for Inherited Oncogenesis, University of Texas at San Antonio, San Antonio, TX,[3]Cedars-Sinai Health Sciences University, Los Angeles, CA,[4]University of Washington, Seattle, WA

Ovarian cancer (OC) ranks as the fifth most lethal form of cancer for women and in the US causes the most deaths of any reproductive system malignancies. The current lack of clinical tools for effective early detection results in predominantly late-stage diagnosis. Clear cell ovarian cancer (CCOC), one of the five subtypes of OC, has low rates amongst Western demographics but makes up 25-30% of all cases of OC in Eastern countries such as Japan. A key characteristic of CCOC is its high rates of resistance to standard platinum therapy, with only 20-50% of patients showing response. Thus there is an urgent need for new treatment options for CCOC that can elicit sustained responses. An exciting new area of cancer therapeutics is focused on targeting the epigenetic drivers of cancer. New epigenetic cancer therapies include drugs that target transcription-associated cyclin dependent kinases (CDKs), CDK7/12/13, which promote transcription initiation and elongation by RNA polymerase II (RNAp2). Drugs targeting these proteins, such as THZ1, induce preferential depletion of key transcripts controlling cell survival and oncogenic pathways, and therefore have potent anticancer activity. However the efficacy of targeting transcriptional CDKs in CCOC, and the pathways involved is currently unknown. CCOC lines are sensitive to THZ1 in vitro. In high-grade serous tumor cell lines, transcriptional responses to THZ1 could be largely explained by downregulated expression of master transcription factors (MTFs) SOX17 and PAX8. However, downregulation of CCOC MTFs PAX8, HNF1B and ETS2 did not explain transcriptional responses to THZ1 in the CCOC models. Instead, exposing CCOC cell line RMG1 to THZ1 showed differential enrichment of pathways related to causes and consequences of modified intracellular zinc levels. Previous findings in OC connect intracellular zinc levels with oncogenic processes including metastasis and epithelial-to-mesenchymal transition. However, the role of zinc homeostasis in response to epigenetic drugs in OC is completely novel. Treating CCOC models with zinc chelator TPEN reduced intracellular free zinc by 63-70%. Co-treating CCOC cells with TPEN and THZ1 showed a significant 23% increase in sensitivity to THZ1. THZ1 resistant CCOC models were developed by exposing CCOC lines to increasing doses of THZ1 over a period of 300 days. Surprisingly, pharmacologic reduction of intracellular zinc increased growth of THZ1-resistant cells in the presence of THZ1, suggesting that fine-tuned control of free intracellular zinc dictates cellular responses to THZ1. In addition, THZ1-resistant lines had a 25% reduction in intracellular zinc compared to THZ1-sensitive parental lines. Our ongoing work is focussed on dissecting the impact of zinc on the activity of RNAp2 in the presence of THZ1, and will define the genes and regulatory elements involved in zinc-dependent responses to THZ1.

#2945 Target actin-microtubule network integrity to enhance taxane drug-target engagement and chemosensitivity in prostate cancer.

Felipe Carvolho[1], Tanvi Desai[2], Keira Ly[3], Joubin Jebelli[3], Ajay Bommareddy[1], Jianning Wei[3], **Michael L. Lu**[2]

[1]Biomedical Sciences, Florida Atlantic University, Boca Raton, FL,[2]Florida Atlantic University, Boca Raton, FL,[3]BioMedical Sciences, Florida Atlantic University, Boca Raton, FL

Taxanes exert anticancer activity by binding beta-tubulin on the luminal surface of microtubules, stabilizing protofilaments, suppressing GTP hydrolysis, and thereby promoting drug-target engagement (DTE) and apoptotic cell death. Access of taxanes to luminal binding sites depends on protofilament organization and microtubule lattice integrity, including entry via plus-end openings, small lattice pores, and stress-induced lattice defects. Because microtubules are tightly coupled to the actin cytoskeleton through crosslinking and mechanical support, we hypothesized that kinases controlling actin-microtubule architecture modulate taxane DTE and sensitivity. We investigated the PAK6-LIMK1 signaling axis in human prostate cancer PC3 and DU145 cells using CRISPR/Cas9 PAK6 knockout and small-molecule inhibitors of PAK6 or LIMK1. Taxane chemosensitivity was quantified by cell viability assays, and cytoskeletal organization and DTE were assessed by immunofluorescence microscopy of F-actin, alpha-tubulin, and the +TIP protein CLIP170. Consistent with prior shRNA data, genetic ablation of PAK6 markedly increased taxane sensitivity in both cell lines. PAK6 loss or pharmacologic inhibition produced concordant, distinctive remodeling of the actin-microtubule network, characterized by loss of dorsal, ventral, and transverse stress fibers and the emergence of crooked, banded microtubule cables, indicating compromised cytoskeletal integrity. These structural changes were accompanied by enhanced taxane-induced microtubule bundling and a robust increase in CLIP170 comet number and size, identifying a novel cytoskeletal signature associated with heightened taxane responsiveness. Similar phenotypes and chemosensitization were observed following LIMK1 inhibition, supporting a shared PAK6-LIMK1 pathway that dually regulates actin and microtubule dynamics. Together, these data suggest that disruption of PAK6-LIMK1 signaling weakens cytoskeletal resilience, facilitates taxane access to intraluminal binding sites, and thereby amplifies DTE and cell killing in prostate cancer cells, nominating this axis as a tractable target to overcome taxane resistance in advanced disease.

#2946 RQ43: A quinoline derivative that inhibits pancreatic cancer cell EMT and migration.

Sreyoshi Das, Qi Chen

Pharmacology, Toxicology and Therapeutics, The University of Kansas Medical Center, Kansas City, KS

Background: Pancreatic ductal adenocarcinoma (PDAC) is one of the deadliest cancers due to early metastasis and therapeutic resistance. The epithelial-to-mesenchymal transition (EMT) drives PDAC invasiveness and poor prognosis. RQ-43, a novel quinoline derivative, has shown antiproliferative activity in other cancer models previously with unclear mechanisms. This study investigated its cytotoxic, anti-migratory/invasive effects, and mechanisms of action in PDAC.
Methods: Human (PANC1) and murine (PAN02) PDAC cell lines were treated with RQ-43 (0.625-20 µM) for 48 h, and cell viability measured by MTT assay. Migration and invasion were assessed using wound-healing and Boyden chamber assays at sub-cytotoxic drug concentrations. EMT-related genes and transcription factors were assessed by qPCR. A syngeneic orthotopic PDAC mouse model was used to assess the in vivo effects of RQ-43 in C57/BL/6 mice.
Results: RQ-43 selectively decreased PDAC cell viability in a dose-dependent manner with IC_{50} values of 3.61 µM (PANC1) and 8.24 µM (PAN02). At concentrations of 2.5 µM for PANC1 and 5-20 µM for PAN02, RQ-43 significantly inhibited migration, reducing wound closure by 27.5% in PANC1 and 78% in PAN02 ($p < 0.05$ compared to controls). Invasion through Matrigel-coated Boyden chamber was also significantly suppressed in both cell lines ($p < 0.01$). EMT-related transcription factors Snail and B-catenin were downregulated ($p < 0.05$). In the orthotopic model, RQ-43 treatment (80 mg/kg, daily IP) significantly reduced tumour weight by 62.95% compared with controls. Metastasis rate was 80% in the control group and 25% in the treated group.
Conclusions: RQ-43 demonstrates cytotoxic, anti-migratory/invasive effects in vitro and effectively reduces tumour growth and metastasis in vivo. EMT-related transcription factors were downregulated. Further efficacy and mechanistic evaluation are warranted.

#2947 Inhibition of NRF2 driven antioxidant defence and EMT underlies brusatol induced cytotoxicity in cervical cancer cells.

Gunjan Dagar[1], Mohd Umar Rehmani[1], Teena Haritwal[1], Ajaz A. Bhat[2], Mayank Singh[3]

[1]Medical Oncology, All India Institute of Medical Sciences (AIIMS), New Delhi, India,[2]Translational Medicine, Sidra Medicine, Doha, Qatar,[3]All India Institute of Medical Sciences (AIIMS) New Delhi, New Delhi, India

Cervical cancer remains a major global health burden, and its therapeutic resistance is strongly influenced by redox adaptation, epithelial-mesenchymal transition (EMT), and metabolic reprogramming. Brusatol, a natural quassinoid compound, is known for its ability to suppress NRF2-driven antioxidant defense mechanisms. However, its mechanistic impact on cervical cancer has not been fully characterized.In this study, we first employed quantitative proteomic profiling to obtain an unbiased overview of Brusatol-induced molecular alterations. Proteomics analysis revealed extensive downregulation of proteins associated with antioxidant defense, glycolysis, cytoskeletal organization, and EMT regulation. Conversely, proteins linked to oxidative stress responses, mitochondrial dysfunction, and apoptotic signalling were significantly upregulated. Pathway enrichment analysis confirmed inhibition of glycolytic and redox-regulatory pathways, suppression of cell motility networks, and activation of oxidative stress driven cytotoxic processes.These global proteomic signatures were further substantiated through western blot validation, which demonstrated reduced expression of key components involved in antioxidant defense and EMT regulation following Brusatol treatment. Western blot analysis also showed suppression of glycolytic markers, supporting the proteomics-predicted metabolic disruption.Functionally, Brusatol significantly reduced proliferation, induced apoptosis, suppressed migration, and reversed EMT characteristics in cervical cancer cell lines. Treated cells exhibited decreased mesenchymal marker expression, restoration of epithelial traits, reduced glucose uptake, and impaired glycolytic activity. Importantly, a non-tumorigenic epithelial cell line showed substantially lower sensitivity, indicating selective cytotoxicity toward cancer cells.

Together, these findings demonstrate that Brusatol exerts potent anti-tumor effects in cervical cancer by initiating widespread proteomic reprogramming, suppressing NRF2-linked antioxidant pathways, reversing EMT, and disrupting glycolytic metabolism. The integration of proteomic profiling with biochemical validation and functional assays provides strong mechanistic evidence supporting brusatol as a promising therapeutic candidate for overcoming treatment resistance in cervical cancer.

#2948 A spatial-trapping mechanism of RAF by RAF/MEK glue enables full-dose combination with a pan-RAF inhibitor and drives potent, RAS-mutant tumor-selective MAPK and growth inhibition.

Bijaya Gaire[1], Ana Orive-Ramos[1], Christos Adamopoulos[1], Beau Baars[1], Mathieu Desaunay[1], Evangelia Matenoglou[2], Silvia Coma[3], Nayeli Gutierrez-Trejo[1], Kevin Mohammed[1], Stuart A. Aaronson[1], Jian Jin[1], Tiphaine Martin[1], Ernesto Guccione[1], Evripidis Gavathiotis[4], Jonathan A. Pachter[3], Poulikos I. Poulikakos[1]

[1]The Tisch Cancer Institute, Icahn School of Medicine at Mount Sinai, New York, NY,[2]Albert Einstein College of Medicine, New York, NY,[3]Verastem Oncology, Needham, MA,[4]Albert Einstein College of Medicine, Bronx, NY

The therapeutic benefits of MAPK pathway inhibitors depend on achieving more potent pathway inhibition in tumors over normal tissues, maintaining a broad therapeutic index. In BRAF-mutant cancers, selective BRAF inhibitors (BRAFi) achieve this balance, and their combination with MEK inhibitors (MEKi) at full doses resulted in significant clinical benefit. In contrast, next-generation Type 2 dimeric RAF, also known as pan-RAF inhibitors (pan-RAFi), which target wild-type BRAF and CRAF and demonstrate single-agent activity in RAS-mutant (RAS-MUT) tumors, have failed to achieve comparable therapeutic impact in combination with MEKi, owing to toxicity-driven dose reductions that constrain clinical efficacy. In preclinical and clinical studies, these combinations have reached a therapeutic ceiling, yielding predominantly stable disease and only rare tumor regressions. We show that dose-limiting toxicity in pan-RAFi + MEKi combinations stems from relief of negative feedback by MEK inhibition, which amplifies RAF activation and pan-RAFi engagement in normal tissues, oversuppressing MAPK signaling and limiting the therapeutic index. RAF/MEK glues constitute a distinct category of MEK inhibitors that stabilize RAF-MEK complexes and functionally suppress RAF. Although structural studies have captured these glues bound to both active and inactive RAF conformations, we show that their inhibitory activity stems from a spatial-trapping mechanism: we found that MEK is constitutively cytosolic, RAF/MEK glues sequester RAF in the cytosol, blocking its membrane recruitment and dimerization, steps essential for activation. In line with this mechanism, the RAF/MEK glue avutometinib, when combined with a pan-RAFi, was well tolerated at full dose and, critically, drove tumor regressions across multiple RAS-MUT models, achieving a 90% ORR compared with 0% using a conventional pan-RAFi + MEKi regimen in an insensitive RAS-MUT model. Tumor regressions corresponded with deeper MAPK pathway suppression by both pharmacodynamic and transcriptional metrics, without increased toxicity. Together, these findings reveal an unrecognized mechanism of RAF inactivation by RAF/MEK glues and show that substituting the MEKi with a RAF/MEK glue can overcome the therapeutic ceiling of current MAPK-targeting regimens, shifting outcomes from mostly stable disease to frequent tumor regressions. More broadly, this work establishes drug-induced proximity as a means to increase tumor selectivity by reprogramming the spatial and biochemical state of wild-type signaling effectors, thereby widening the therapeutic window for oncogenic pathway inhibition and providing a new paradigm for precision oncology.

#2949 Palazestrant, a CERAN, in combination with OP-3136, a KAT6 inhibitor, synergistically downregulates cell proliferation and metastasis related gene signatures.

Susanna A. Barratt, Gopinath S. Palanisamy, Azita Ghodssi, Chelsea Hope, Guadelupe Pena, Srinivasan Jayaraman, Raymond A. Ng, David C. Myles

Olema Oncology, San Francisco, CA

Histone lysine acetyltransferases KAT6A and KAT6B are epigenetic enzymes involved in regulating transcription of oncogenic genes, including ERα, MYC, and cell cycle drivers. We previously reported that OP-3136, a KAT6 inhibitor, shows enhanced efficacy in vitro and in vivo in ER+/HER2– breast cancer models when combined with the complete estrogen receptor antagonist (CERAN) palazestrant (OP-1250) (Palanisamy et al., 2024). Here, we further investigate the mechanisms of this synergy by characterizing treatment-dependent transcriptional changes.We used T47D, an ER+/HER2– ESR1–wild-type breast cancer cell line overexpressing KAT6A, as an in vivo xenograft model. We evaluated the impact of OP-3136, palazestrant, and the combination in comparison to monotherapy and OP-3136 combination with the approved antiestrogen, fulvestrant. Xenografts were treated for 28 days, and bulk RNA sequencing was performed on isolated tumors.Palazestrant and OP-3136 combination resulted in greater suppression of genes associated with cell proliferation and cell-cycle progression (Hallmark E2F and G2M gene sets) than monotherapy treatment. While the fulvestrant–OP-3136 combination also reduced these gene sets, the palazestrant combination caused stronger downregulation, consistent with observed efficacy responses. The palazestrant-OP-3136 combination also showed the most potent suppression of key transcriptional regulators of ER+ breast cancer, including PGR, E2F1, MYC, GATA3, and FOXA1.Palazestrant plus OP-3136 further suppressed expression of MTORC1 and TNF-α via NFκB signaling pathways. These pathways were also downregulated by the fulvestrant–OP-3136 combination but to a lesser extent. The observed effects exceeded expected additive responses, indicating that CERAN plus KAT6 inhibition synergistically regulate these pathways at the transcriptional level. Because inhibition of the PI3K/mTOR/AKT axis mitigates endocrine resistance and TNF-α/NFκB signaling promotes metastasis and invasion, these findings suggest that combining a KAT6 inhibitor with palazestrant may represent a promising strategy to overcome resistance in metastatic ER+ breast cancer.Collectively, these data demonstrate that palazestrant and OP-3136 synergize to suppress genes associated with proliferation, survival, and metastasis. The transcriptional changes align with enhanced anti-tumor efficacy and establish a mechanistic rationale for this combination over fulvestrant in ER+ breast cancer. The palazestrant–OP-3136 combination is currently being evaluated in a phase I clinical trial in ER+/HER2– metastatic breast cancer patients.

#2950 Palazestrant directly recruits the corepressor protein NCoR1 *in vitro* leading to complete antagonism of estrogen receptor alpha.

Susanna A. Barratt, Guadelupe Pena, Chelsea Hope, Gopinath S. Palanisamy, Raymond A. Ng, David C. Myles

Olema Oncology, San Francisco, CA

The estrogen receptor (ER) is a well-established driver of breast cancer with approximately 80% of patients presenting as ER-positive (ER+). The current treatment paradigm relies on endocrine therapies; however, there are pharmacokinetic, efficacy and tolerability issues with approved agents indicating a clear unmet need for better treatments for patients. Palazestrant, a complete estrogen receptor antagonist (CERAN), has demonstrated favorable tolerability and efficacy in a heavily pre-treated patient population and is currently being evaluated in two Phase III clinical trials (OPERA-01 and OPERA-02) for the treatment of ER+/HER2-metastatic breast cancer. We previously described preclinical characterization of this molecule (Parisan et al., 2023; Ng et al., 2025) where we demonstrated that palazestrant is a novel, orally bioavailable complete ER antagonist and selective ER degrader that completely blocks estrogen-induced transcriptional activity and demonstrates impressive in vitro and in vivo antitumor activity. As a CERAN, palazestrant can inactivate both the AF-2 and AF-1 domains of ER-alpha resulting in complete antagonism that does not demonstrate any agonist activity. Here we show for the first time that palazestrant and other CERANs completely and potently recruit the corepressor protein NCoR1 to ERα as part of their mechanism of action. Contrarily, selective estrogen receptor modulators (SERMs) such as 4-OH-tamoxifen and vepdegestrant either do not induce recruitment or are incomplete recruiters, in line with previous data indicating that SERMs are not complete antagonists. At the transcriptional level, palazestrant more potently suppresses the transcription of key E2 and cell cycle related genes such as PGR and GREB1 in ER+ breast cancer models as compared to 4-OH-tamoxifen, with strong downregulation observed at concentrations of 5 nM and lower. CERAN molecules palazestrant and fulvestrant consistently demonstrate greater suppression of GREB1 and PGR as compared to SERMs in both ESR1 wildtype and mutant ER+ breast cancer models.Functionally, treatment with palazestrant leads to antiproliferative activity in ER+ breast cancer models comparable or superior to investigational and approved anti-estrogens. All molecules that demonstrate complete antagonism of ER demonstrate a greater total inhibition of proliferation (Emax %). Importantly, in the CAMA-1 ER+/HER2 model, palazestrant demonstrates a complete suppression of cell proliferation where tamoxifen does not. When cells are not stimulated with E2, SERMs like tamoxifen demonstrate induction of cell proliferation where CERANs do not. Palazestrant is a promising therapeutic strategy for treating ER+/HER2- breast cancer patients and is being evaluated clinically, both as monotherapy and combination.

#2951 Adaptive and acquired mechanisms underlying RAS-mutant tumor response to mutant and state selective RAS inhibitors.

Ziyue Kou, Bijaya Gaire, Beau Baars, Mathieu Desaunay, Poulikos I. Poulikakos

Icahn School of Medicine at Mount Sinai, New York, NY

RAS mutations drive over 20% of human cancers and often correlate with poor clinical outcomes. Mutant RAS (RAS-MUT) maintains elevated GTP binding, biasing the protein toward its active (ON) state and driving hyperactivated signaling through effector pathways (MAPK and PI3K, among others), leading to uncontrolled cell growth and resistance to apoptosis. Thus, targeting RAS with small-molecule inhibitors presents a promising therapeutic strategy for RAS-MUT cancers. Recent advances in drug discovery have enabled the development of the pan-RAS(ON) inhibitor RMC6236, which uses a tricomplex strategy, as well as several KRAS-MUT-specific inhibitors (such as Adagrasib, Sotorasib, and MRTX1133) that target the OFF state. However, the antitumor efficacy of these direct RAS inhibitors varies across cancer types and is limited by a “therapeutic ceiling,” marked by stable disease and transient responses for most patients. Thus, a deeper understanding of mechanisms underlying variability in response and development of acquired resistance in RAS-MUT cancers is urgently needed. By analyzing signaling and cell growth inhibition in response to distinct direct RAS inhibitors, we observed similar sensitivity patterns across cell line models, suggesting that the antitumor activity of these drugs is largely confined to a shared subset of RAS-MUT cancers. Notably, we found that a subset of insensitive cells could regain sensitivity to direct RAS inhibitors through serum starvation or cotreatment with an SHP2 inhibitor, indicating hyperactive upstream Receptor Tyrosine Kinase (RTK) signaling contributing to RAS inhibitor resistance. Moreover, we found that resistant cell lines show a greater contribution of wild-type RAS (RAS-WT) to overall RAS activity than sensitive lines, suggesting that resistance may arise from RAS-WT-dependent compensation upon RAS-MUT inhibition. To model acquired resistance, we exposed KRAS-MUT cell line models to high concentrations of various RAS inhibitors individually and derived resistant models that displayed markedly reduced sensitivity compared with parental lines. No evidence of acquired secondary KRAS mutations was observed. However, we detected upregulation of the RTK-RAS-MAPK pathway along with elevated KRAS-MUT protein expression in resistant models. This increased RAS-MUT expression reduced inhibitor effectiveness and impaired suppression of RAS-GTP cycling. We also identified multiple cross-resistance patterns across different direct RAS inhibitors, highlighting the need for better mechanistic understanding to optimize RAS-inhibitor treatments for maximal therapeutic benefit. Together, our results provide mechanistic insight into resistance to direct RAS inhibitors in RAS-MUT cancers and emphasize the urgent need for improved strategies to treat patients who do not respond to current RAS-targeted therapies.

: Drug Resistance 1: Antibodies and ADCs
Poster Session

#2955 Systematic mechanistic profiling of ADC-resistant cancer cell lines.

Tingting Yuan, Yanqiu Bai, Lehua Cheng, **Yanan Xu**, Wenzhang Chen, Yan Gao, Zhuo Wen, Qiangqiang Fan, Zhengang Peng

WuXi AppTec Co., Ltd., Shanghai, China

In recent years, antibody–drug conjugate (ADC) discovery has become one of the hottest areas for targeted therapy development of diverse cancer types. Regardless of its superiority to other therapeutic modalities, resistance remains one of the major and most common challenges, thereby severely hindering its clinical efficacy. ADC-resistant cell lines have been well demonstrated to be valuable and reliable models to help interrogate ADC-relevant resistance, hence facilitating development of therapies overcoming resistance. To this end, we have successfully developed over a dozen of ADC-resistant cancer cell lines by chronically challenging parental cancer cells with escalating dosages of ADCs for several months. We validated such a gain of resistance by a full-dosage drug sensitivity profiling at the endpoint, demonstrating >10 fold of drug IC50 increase in most of the established resistant cell models compared to their respective parental counterparts. To further unravel the underlying drug resistance mechanisms, we applied RNA-Seq and global proteomics profiling on several resistant models paired with their parental controls, including HCC1954 and NCI-N87 Enhertu-resistant, HCC1806 and Colo-205 Trodelvy-resistant cells. Promisingly, we observed that HER2 expression was dramatically and concordantly (~30-fold) reduced at both mRNA and protein levels according to RNA-Seq and global proteomics profiling, which was further validated by flowcytometry and Western blot analysis. Subsequent cross-drug sensitivity profiling revealed that HCC1954 Enhertu-resistant cells were resistant to the other two HER2-targeting ADCs, T-DM1 and RC48 rather than their respective payloads, which further consolidated that reduction of HER2 expression other than any adaptive resistance to payload plays a pivotal role in the HCC1954 Enhertu-resistant model. Interestingly, we didn’t observe any robust reduction of antibody target expression in the other three ADC resistant models, implying diverse resistance mechanisms across different ADCs and cancer cell lines. We will continue to do datamining and validation on these models in the near future, aiming to shed light on more ADC resistance mechanisms.

#2956 Determinants of sacituzumab govitecan therapeutic response in breast cancer models.

Carson J. Walker[1], Nina Dashti-Gibson[1], Julia E. Altman[2], Rachel K. Myrick[2], Emily K. Zboril[1], Oniya M. Smith[2], David C. Boyd[2], Bin Hu[1], Mikhail G. Dozmorov[3], Joshua C. Harrell[4]

[1]VCU Massey Comprehensive Cancer Center, Richmond, VA,[2]Virginia Commonwealth University, Richmond, VA,[3]Biostatistics, Virginia Commonwealth University, Richmond, VA,[4]Pathology, Virginia Commonwealth University, Richmond, VA

This study identifies markers of Sacituzumab Govitecan (SG) response in triple-negative breast cancer (TNBC) models and introduces new SG acquired resistance patient derived xenografts (PDXs) that can serve as examples of patient-acquired mutations or gene regulation changes that confer resistance to this targeted therapy. SG is an antibody drug conjugate (ADC) that has been approved for treating TNBC and estrogen receptor positive breast cancers that have progressed on initial treatments. SG binds to TROP2 and delivers SN-38 as its payload; resistance to SG could be due to inefficient antibody internalization or lack of payload efficacy. We hypothesize that individual intrinsic and acquired SG resistance mechanisms will uncover features that can be targeted to extend the duration of response to SG. Using a linear mixed effects model, we mapped PDX responses to SG *in vivo* to their RNA expression in order to identify differences in gene expression that stratify SG response; developing an initial SG response predictor in this process. By administering suboptimal and continuous SG treatments to formerly SG-sensitive PDXs, we created acquired SG resistant (SGR) models. We then compared the RNA expression between these syngeneic pairs of PDXs to identify acquired resistance mechanisms and common pathways of resistance in patients. Performing antibody internalization assays on the paired sets allowed us to investigate if antibody or encapsulation mediated resistance was responsible for the continued tumor growth. Short-term SN38 testing was used to define the extent of payload resistance in paired models. Through these efforts, we identified 9 SG-sensitive and 3 intrinsically resistant TNBC PDXs whose differential expression led us to focus on 13 genes that predict SG response. Three of the most sensitive models were used to create acquired resistance models and analysis is underway to compare these to the intrinsic resistance models utilizing bulk and single-cell RNA-sequencing, proteomics, and cytotoxic compound screens. RNA sequencing of PDXs with innate SG resistance defined differences in gene expression related to extracellular matrix, angiogenesis, and metal ion trafficking. Conversely, acquired resistance models show diversity in resistance mechanisms including notably heightened extracellular matrix protein synthesis. Ongoing studies aim to define these mechanisms so that candidate therapeutics can be prioritized to overcome SG resistance. In conclusion, a preliminary SG resistance signature has been developed, which we will refine for clinical selection of patients to be treated with SG. Additionally, several biological processes are activated during acquired SG resistance and may be targetable.

#2957 Retinoic acid pathway regulates NECTIN4 expression and enhances NECTIN4-directed chimeric antigen receptor (CAR) T and antibody-drug conjugate therapies in bladder cancer.

Tamilla Nechiporuk[1], Sha Zhu[1], Yuxin Yang[1], Shivani Saxena[2], Jun Zhu[3], Rosalie Nolley[3], Imene Boukhalfa Ep Hanafi[3], Rhea Master[1], Elizabeth Yip[2], Kevin Chang[1], William Dougherty[2], Terence Friedlander[3], Vadim S. Koshkin[1], David Quigley[4], Jonathan Chou[2], Carissa E. Chu[1]

[1]Urology, University of California at San Francisco, San Francisco, CA,[2]Division of Hematology/Oncology, Department of Medicine, University of California at San Francisco, San Francisco, CA,[3]Radiation Oncology, University of California at San Francisco, San Francisco, CA,[4]Urology, Epidemiology and Biostatistics, University of California at San Francisco, San Francisco, CA

Urothelial carcinoma (UC) is the sixth most common malignancy in the United States, with 83,000 new cases and 17,000 deaths annually. Prognosis for metastatic UC remains poor, underscoring the need for new targeted therapies. NECTIN4, a cell adhesion molecule highly expressed in UC, is a target of an FDA-approved antibody-drug conjugate (ADC) enfortumab vedotin (EV) with 40% response rates. NECTIN4 genomic amplifications and expression levels correlate with response to NECTIN4-targeted therapies like EV, but regulators of NECTIN4 remain poorly defined. To identify regulators of NECTIN4 surface expression, we performed a CRISPR interference (CRISPRi) FACS-based screen in bladder cancer cell lines, followed by validation across multiple UC models and use of pharmacological modulators of genetic hits to assess effects on NECTIN4 expression and sensitivity to NECTIN4-directed ADCs and CAR T cells. Our screen revealed both positive and negative regulators of NECTIN4 expression, especially factors linked to luminal differentiation and epithelial-to-mesenchymal transition (EMT), which exert opposing effects. We found that activating retinoic acid (RA) signaling, alone or with PPARγ modulation, transcriptionally induces NECTIN4 as part of the luminal program. Pharmacologic RA activation increased NECTIN4 surface levels and sensitized bladder cancer cells to both EV and NECTIN4-targeted CAR T cells. This RA-driven regulation reinforces luminal identity, acting alongside PPARγ and counteracting EMT-driven therapeutic escape. Modulating RA signaling offers a promising strategy to overcome both, primary resistance due to low NECTIN4 levels and acquired resistance from NECTIN4 downregulation.

#2958 P-glycoprotein (ABCB1) overexpression confers resistance to the antibody-drug conjugate Enfortumab vedotin in EV-resistant organoid and PDX models.

Emilie Decaup[1], Claire Beraud[1], Isabelle Bernard-Pierrot[2], Guerric Gilbert[2], Clementine Krucker[2], Xavier Game[3], Philippe Lluel[1], **Nadege Bidan**[1]

[1]Urosphere, Toulouse, France,[2]Institut Curie, Paris, France,[3]CHU Toulouse, Paris, France

Background: Resistance to Enfortumab vedotin (EV) remains a major clinical challenge in bladder cancer (BC). The resistance can emerge through diverse mechanisms such as alterations in Nectin-4 expression, defects in ADC internalization and trafficking, or changes in downstream processing and payload response. We previously developed EV-resistant BC PDX and organoid models (poster 50, AACR 2025), providing validated preclinical tools to investigate the molecular basis of EV resistance. These models were designed both to elucidate resistance mechanisms and to enable direct comparison with patterns of resistance observed in the clinic.
Methods: F659 PDX model was selected based on its high Nectin-4 mRNA expression and its strong response to EV treatment. Acquired resistance was generated by repeated EV administrations until tumors ceased to regress. From the resulting EV-resistant PDX (F659rP2), a matched organoid model was subsequently established. Both resistant and parental models were profiled using whole-exome sequencing, RNA-sequencing, and immunohistochemistry (IHC), and functionally characterized to assess EV activity and identify resistance mechanisms. Validation of these mechanisms was performed using pharmacological inhibition assays.
Results: Resistance to EV was confirmed in both organoid and PDX models, as evidenced by a marked loss of sensitivity compared with their parental counterparts. Then, Nectin-4 expression was evaluated in resistant and parental models to investigate the underlying mechanisms, Flow cytometry and IHC analyses revealed a decreased cell surface expression of Nectin-4 in resistant models. Transcriptomic profiling identified significant changes in the expression of drug efflux transporters, FGFR3 and PPARγ pathways. Notably, the ABCB1 gene was markedly upregulated in resistant models, and corresponding P-glycoprotein (P-gp) overexpression was confirmed by flow cytometry and IHC.Given that ABC transporters promote drug efflux, reducing intracellular drug accumulation and therapeutic efficacy, we assessed the impact of P-gp inhibition. Our results demonstrate that co-treatment with the P-gp inhibitor tariquidar (XR9576) partially restored EV sensitivity in both resistant organoid and PDX models.
Conclusion: We successfully generated paired in vitro and in vivo EV resistant models. Our findings highlight the role of ABC transporter upregulation in EV resistance associated with a reduction of Nectin4 expression consistent with clinical observations. Other pathways seem to be involved and will need further investigations. Importantly, these EV-resistant preclinical models provide powerful tools for evaluating innovative therapeutic strategies against resistant tumors.

#2959 Improving the efficacy of B7-H3 targeting antibody-drug conjugates in TP53-deficient prostate cancer.

Javier Leo, Di Zhao

UT MD Anderson Cancer Center, Houston, TX

Prostate cancer is the most diagnosed malignancy and the second leading cause of cancer-related death among men in the United States. Treatment options for advanced prostate cancers remain limited, and *TP53* alterations occur in approximately 60% of prostate cancer cases and are associated with higher metastasis rates and worse overall outcomes. Effective therapies are urgently needed for advanced prostate cancers with TP53 defects. Immune checkpoint B7H3 is overexpressed in prostate cancer, and its overexpression correlates with increased risks of clinical recurrence and disease spread. DS-7300a is one of the most advanced B7H3-targeting antibody-drug conjugates (ADC) and has demonstrated clinical activity across multiple refractory malignancies. DS-7300a comprises a humanized anti-B7H3 monoclonal antibody warhead with topoisomerase I inhibitor, Dxd. In this study, we evaluated the efficacy of DS-7300a in prostate cancer that contains TP53 defects. Our results showed that the anti-tumor efficacy of DS-7300a is highly dependent on functional p53 in prostate cancer cells. Mechanistically, we found that DS-7300a and its payload Dxd induce DNA damage and activate the ATM/ATR/CHK signaling cascade, leading to p53 stabilization and transcriptional activation of pro-apoptotic and senescence-associated genes. In contrast, *TP53*-deficient cells fail to sense DNA damage adequately and exhibit a high proliferation rate and low levels of apoptosis and senescence, leading to resistance to DS-7300a. Ferroptosis is an iron-dependent form of regulated cell death triggered by lipid peroxidation. Interestingly, we found that DS-7300a treatment induces lipid peroxidation as well as the expression of glutathione peroxidase 4 (GPX4), an antioxidant that mitigates lipid peroxidation, in TP53-deficient cancer cells. Taking advantage of our isogeneic xenograft models and a newly developed humanized B7H3 mouse model, we demonstrate that inducing ferroptosis by pharmacological inhibition of GPX4 enhanced the anti-tumor effects of DS-7300a in *TP53*-deficient prostate cancer. Collectively, our studies indicate that p53 status dictates anti-tumor responses to DS-7300a in prostate cancer, and ferroptosis induction represents a promising therapeutic approach to overcome resistance to Dxd-based ADCs in malignancies harboring TP53 defects. Our studies will accelerate the development of effective therapies for prostate cancer patients with TP53 defects and provide a strong rationale for using TP53 status as a molecular biomarker to guide patient selection for clinical application of DS-7300a. This novel biomarker-driven combination strategy will also provide insights into the clinical trial design of Dxd-based ADCs and ferroptosis inducers in advanced prostate cancer and other malignancies.

#2960 Overcoming acquired and intrinsic resistance with an integrated ADC platform.

Jie Wen[1], Hao Cheng[2], Cheng Zhang[2], Bingrui Han[2]

[1]Oncology Pharmacology, PharmaLegacy Laboratories, Shanghai, China,[2]PharmaLegacy Laboratories, Shanghai, China

Antibody-drug conjugates (ADCs) emerged as a transformative class of targeted therapeutics, reforming the treatment landscape for a growing number of malignancies by integrating benefits from the specificity of antibodies and the potent cytotoxicity of payloads. Despite the remarkable clinical successes, development of acquired and intrinsic resistance poses a fundamental challenge limiting the long-term potential in a considerable proportion of patients. Various mechanisms have been reported to cause ADC resistance, including alterations in target antigen, impaired ADC internalization, efflux of the cytotoxic payload, dysregulation of lysosomal function and insensitivity to payload *etc.* Elucidating this complex biology is crucial for developing novel ADCs, identifying biomarkers for patient stratification and exploring strategies to overcome resistance. This is not only a scientific need but also an important clinical imperative.
The current study describes an integrated platform recapitulating different clinical scenarios of ADC resistance. Models with acquired resistance were developed by either long-term *in vivo* induction on responsive CDX models or by establishing PDX from post-treatment relapsed patient tumors. Models with intrinsic resistance were first identified by screening ADC responses across a panel of target-positive models, followed by subsequent mechanism studies, such as PD examination, sequencing and *ex vivo* analysis. An Her2- and Trop2-positive gastric PDX shown clear resistance (TGI < 10%) to trastuzumab deruxtecan and sacituzumab govitecan, two clinically used Her2 and Trop2 ADCs respectively, limited response (TGI 10-30%) to Herceptin and no response to Dxd treatment. This result suggests its intrinsic resistance is largely due to the unresponsiveness to payload end. Further study on double-humanized PDX (PDX established on humanized mice) shown significant tumor growth inhibition (TGI > 65%) when treated with anti-PD1 antibody, implicating the clinical benefit of combining immune checkpoint inhibitors with ADCs.
In addition to *in vivo* models featuring ADC resistance, multiple *in vitro* platforms were established to enable rapid assessment of ADC in terms of sensitivity and toxicity. A tissue culture assay using clinical samples allows ADC evaluation and comparative screening of combination strategies over a panel of patient tumors. In addition, the well-known ocular toxicity associated with multiple clinically used ADCs can be recapitulated by a cell-based assay using human corneal epithelial cells. On this platform, belantamab mafodotin, trodelvy and T-DM1 demonstrated consistent high, medium and low cytotoxicity respectively.
The integration of above-mentioned platforms facilitates a deep understanding of resistance mechanisms and promotes the development of ADCs that are better aligned with clinical needs, with the ultimate goal of overcoming resistance.

#2961 Developing ADC-resistant tumor models for efficacy evaluation of next-generation anticancer therapies.

Jian Feng, Fuyin Zhao, Xinlong Dong, Aaron Li Hua, Chenpan Nie, Dorrith Verstegen, Caitlyn Hulsebosch, Wubin Qian, Sheng Guo, Jessie (Jingjing) Wang, Lenno Krenning, Marrit Putker, Ludovic Bourre, Peng Wang, Jun Zhou

Crown Bioscience, Inc., San Diego, CA, United States, San Diego, CA

Introduction: Antibody-drug conjugates (ADCs) pair monoclonal antibodies with cytotoxic payloads. Trastuzumab deruxtecan (DS8201) targets HER2, and datopotamab deruxtecan (DS1062) targets TROP2. Both use a topoisomerase I inhibitor (Dxd) via a cleavable linker. After target-mediated internalization, proteases release the payload, causing DNA damage, apoptosis, and bystander killing. However, resistance may stem from antigen loss, altered internalization, impaired payload release, efflux pumps, or apoptosis regulation. We developed ADC-resistant cell and organoid models via chronic dosing, lentivirus transduction, and Cas9 mediated knock out.

Methods: First, efflux pump proteins (ABCB1, ABCG2) were introduced into HER2+ HCC1954 cells via lentiviral transduction (HCC1954-ABCB1, HCC1954-ABCG2); overexpression was confirmed by Western blot. Cytotoxicity to Dxd/ADC was evaluated by CellTiterGlo (CTG)--assay. Second, chronic *in vitro* exposure generated HCC1954-DS8201R and HCC1954-DxdR. HER2 expression was assessed by flow cytometry (FACS), and ADC binding/internalization by IncuCyte imaging. RNA-seq investigates the resistance mechanisms. Finally, TROP2 was knocked out using CRISPR in two DS1062 responsive organoids. Loss of TROP2 was confirmed using immunofluorescence, and ADC sensitivity was tested using CTG assay. Xenograft models of ADC-resistant cells are in development for further *in vivo* studies.

Results: HCC1954-ABCB1 showed remarkable resistance to MMAE (IC_{50}: 85.8 nM vs 0.3 nM parental) but showed no change to Dxd. While, HCC1954-ABCG2 is resistant to Dxd (IC_{50}: >10 µM vs 0.509 µM parental), with minimal MMAE impact. The RC48 (Her2-targeting ADC with MMAE) and DS8201 are confirmed payload-based resistances. HCC1954-ABCB1 is resistant to RC48 (IC_{50}: >100 nM vs 0.288 nM parental), while HCC1954-ABCG2 is resistant to DS8201 (IC_{50}: >100 nM vs 5.2434 nM parental). These findings suggest that efflux pump proteins preferentially transport distinct cytotoxic payloads. Chronic exposure to Dxd generated HCC1954-DxdR cells reduced sensitivity to both Dxd (IC_{50}: >10 µM vs 0.2023 µM parental) and DS8201 (IC_{50}: >100 nM vs 2.1695 nM). Similarly, chronic exposure to DS8201 produced the HCC1954-DS8201R, showing significant resistance (IC_{50}: >70 nM vs 2.1695 nM). In HCC1954-DS8201R with reduced HER2, confirmed by FACS and RNA seq, showed a decrease in HER2 binding/internalization, whereas HCC1954-DxdR exhibited ABCG2 amplification. TROP2 KO efficiency was 30% (LU11786B) and 5% (BR9465B). Cytoxicity of TROP2 KO models resistant to DS1062. with loss of DS1062 uptake and absence of the DNA damage marker yH2AX. Xenograft models of ADC-resistant cells are able to grow *in vivo*.

Conclusion: We developed a panel of ADC-resistant tumor models to study mechanisms of acquired resistance. These models provide a valuable preclinical platform for advancing ADC therapy.

#2962 HER2 ADC resistance driven by IL-17 signaling and ROR1 upregulation: Overcoming DS-8201 resistance with BRY812 and BR111.

Qianqian Tao[1], Qinqin Zhuang[1], Qizhe Wu[1], Lei Nie[1], Gang Chen[2], Haibin Wang[1], Jingtao Lu[1]

[1]Bioray Pharmaceutical Co., Ltd.,, Hangzhou, China,[2]Bioray Pharmaceutical Corp., San Diego, CA

DS-8201 (Trastuzumab Deruxtecan), a milestone antibody-drug conjugate, has demonstrated reputable efficacy in various solid tumors, particularly in patients with HER2-low and HER2-ultralow expression. However, its widespread application has been accompanied by increasingly prominent drug resistance. To investigate the resistance mechanism towards DS-8201, we successfully established DS-8201-resistant cell lines in breast cancer and in lung cancer, and performed mechanistic investigations on HER2 expression change, DS-8201 internalization efficiency, cross-resistance to DXd as well as ABC transporters expression. Results revealed that these mechanism were observed in both resistant cell lines expect for DXd-resistance, which was only found in breast cancer. Furthermore, we selected lung cancer resistant cell line to perform RNA-seq analysis and found IL-17 signaling as major contributing pathway, with CXCL1 and LCN2 being the mostly affected genes. Literature research revealed possible mechanism includes tumor microenvironment remodeling, enhanced cell survival, and immune evasion.BRY812 (an anti-LIV1 ADC conjugated to MMAE) and BR111 (an anti-ROR1 ADC conjugated to eribulin) are novel ADCs that have shown potent antitumor activity in various solid tumors. Ours studies with both resistant cell lines and corresponding CDX models demonstrated that both BRY812 and BR111 can effectively overcome DS-8201 resistance. Further investigation revealed that treatment with HER2-targeting ADCs (DS-8201 and T-DM1) dose-dependently upregulated ROR1 expression, providing a potential mechanism for BR111's efficacy in this resistant setting. In conclusion, our research findings collectively revealed DS-8201 resistance mechanism and provided evidence that BRY812 and BR111 can overcome DS-8201 resistance.

#2963 Development and characterization of a novel *in vivo* JIMT-1 DS8201a resistant model and its efficacy evaluation.

Qikuan Chen, Longyun Zhang, Ya Xu, Jingjing Zhang, Li Li, Greg Liang, Mingqi Shao, Fan Feng, Yinfei Yin

Shanghai ChemPartner Co., Ltd., Shanghai, China

Trastuzumab deruxtecan, marketed as Enhertu (DS-8201a) is a next generation HER-2 targeted Antibody-Drug Conjugate (ADC), that releases a topoisomerase inhibitor payload. As the Deruxtecan is membrane permeable it exhibits a strong bystander effect as it can diffuse into neighboring cells, killing antigen negative cells. Despite clinical success and reinvigorating ADC interest, acquired and primary resistance driven by tumor heterogeneity and genomic alterations remain a major consideration. To investigate tumor resistance mechanisms, we have established in house a DS8201a resistant JIMT-1 cell line and the corresponding *in vivo* tumor model. We have also acquired a primary resistant gastric cancer PDX model (GAX227M), and we have derived an organoid model (PDXO) from this PDX. Based on *in vitro* and *in vivo* screening, we have demonstrated significant resistance to DS8201a in all models. Furthermore, we have comprehensive whole-exome sequencing (WES) and RNA sequencing (RNA-seq) for the JIMT-1 DS8201a-resistant model that is currently undergoing bioinformatic analysis. Our preclinical toolbox is designed to help decipher resistance mechanisms and guide rational strategies to overcome ADC resistance. These insights will inform the development of next-generation ADC's and improve outcomes in HER-2 positive heterogenous tumors.

#2964 Identification of synergistic dual payload combinations for antibody-drug conjugates to overcome resistance through resistance modeling.

Lili Chai, Yue Zhai, Yan Zhang, Ying Bi, Xue Yang, Zhengtai Li, **Tiejun Bing**

ICE Bioscience, Beijing, China

Background: Antibody-Drug Conjugates (ADCs) are potent cancer therapeutics, but resistance to ADCs or their single payloads remains a critical clinical barrier. Dual payload ADCs—co-delivering two distinct payloads via a single antibody—offer a promising solution by leveraging complementary mechanisms. Clinical progress and pipeline candidates validate this approach. However, a systematic framework to identify resistance-tailored synergistic payload combinations and decipher their mechanisms is underdeveloped.
Methods: We established 10+ drug-resistant cell lines against clinical ADCs/payloads via long-term selection. To elucidate resistance mechanisms and predict synergistic combinations, we performed RNA-seq and WES on resistant/parental pairs, followed by pathway enrichment and synthetic lethality prediction. We screened 100+ dual payload combinations (resistant/parental cell panel, viability assay) to identify hits. Mechanisms of hit combinations were investigated via bioinformatics analysis and validated by Western blotting/immunofluorescence (DDR markers and cell cycle markers).
Results: bioinformatics analysis identified key resistance mechanisms including elevated P-gp transporter and reduced antigen expression. We screened 100+ combinations (TOPO1 inhibitors paired with DDR inhibitors, CDK inhibitors, TYR kinase inhibitors, toxins) and identified three synergistic hits including TOPO1 inhibitor combined with DDR related targets and cell cycle targets. All hits showed significant synergistic effect (IC50 shifts >3 folds and CI<0.9) in resistant cells, while single payloads had minimal efficacy. Bioinformatics implicated enhanced DNA damage and cell cycle dysregulation as core mechanisms, validated by pathway assays.
Conclusions: Our study establishes a systematic framework (resistance modeling, bioinformatics, high-throughput screening) to identify synergistic dual payload combinations for ADCs. The three TOPO1-based hit combinations potently overcome resistance via validated DDR/cell cycle mechanisms. This work provides a rational basis for next-generation dual-payload ADC development and a generalizable strategy to accelerate resistance-overcoming regimen discovery across cancer therapies

#2965 Identification of TROP2 as an adaptive resistance mechanism in KRAS G12C inhibition and its therapeutic targeting.

Masahiro Kashima[1], Hidenori Kitai[1], Yukiko Yoshida[1], Yuriko Ishida[1], Yuma Sato[1], Daisuke Morinaga[1], Kosuke Tsuji[1], Shotaro Ito[1], Kanako C. Hatanaka[2], Takuma Kobayashi[3], Yoshiki Shinomiya[2], Teppei Konishi[3], Yutaka Hatanaka[2], Jun Sakakibara-Konishi[1], Satoshi Konno[1]

[1]Department of Respiratory Medicine, Faculty of Medicine, Hokkaido University, Sapporo, Japan,[2]Center for Development of Advanced Diagnostics, Hokkaido University Hospital, Sapporo, Japan,[3]Biomy Inc., Tokyo, Japan

Background: KRAS mutations occur in up to 30% of non-small cell lung cancer (NSCLC), predominantly at codons 12 and 13. KRAS G12C, the most frequent variant, accounts for approximately 40% of KRAS-mutated NSCLC. The KRAS G12C inhibitors sotorasib and adagrasib have been introduced into clinical practice for KRAS G12C-mutated NSCLC, but their clinical benefit remains limited. One important mechanism for this limited efficacy is adaptive resistance, linked to activation of membrane-associated signaling molecules such as receptor tyrosine kinases, which in turn reactivate KRAS downstream signaling and reduce drug durability. Identifying factors driving adaptive resistance is critical for developing effective combination strategies.
Objective: To identify molecular targets mediating adaptive resistance to KRAS G12C inhibitors in NSCLC and evaluate novel therapeutic approaches to overcome resistance.
Methods and Results: To elucidate the mechanism of adaptive resistance to KRAS G12C inhibitors, we performed RNA sequencing after short-term sotorasib exposure in H1373 cells and found TACSTD2 (TROP2) was a gene with early upregulation of its mRNA expression. To test its functional relevance, we silenced TROP2 by siRNA in H358, H2122, and H1373 cells and found that TROP2 knockdown increased sotorasib-induced apoptosis by flow cytometry and enhanced suppression of PI3K-AKT signaling. Consistent with the in vitro findings, sotorasib increased TROP2 expression in H1373 xenograft tumors. Furthermore, TROP2 suppression by shRNA enhanced the antitumor effect of sotorasib in vivo. In addition, in LU65 xenograft model, the combination of sotorasib with the anti-TROP2 antibody-drug conjugate datopotamab deruxtecan achieved more durable tumor shrinkage compared with sotorasib monotherapy. Finally, we utilized an artificial intelligence (AI) model to analyze TROP2 immunohistochemistry scores in clinical specimens from patients with non-small cell lung cancer (NSCLC) and investigated the association with prognosis.
Conclusion: TROP2-targeted therapy represents a promising strategy to overcome adaptive resistance to KRAS G12C inhibitors in NSCLC and warrants further clinical investigation.

#2966 Zongertinib-tolerant cells enhanced sensitivity to Topo1 inhibition in Her2-positive NCSLC.

Kohei Maruyama, Ryohei Katayama

Japanese Foundation for Cancer Research, Tokyo, Japan

Her2 aberration is found in approximately 2-4% of patients with non-small cell lung cancer (NSCLC). For the treatment of Her2 mutated/amplified NSCLC, the antibody-drug conjugate Trastuzumab deruxtecan, several Her2-selective inhibitors, such as zongertinib and sevabertinib, have shown beneficial efficacy in clinical settings. Although these Her2 inhibitors have exhibited durable clinical benefits, drug resistance is not inevitable, and tumor eventually relapse. To date, numerous resistance mechanisms to pan-ERBB family inhibitors have been identified, and combination strategies to overcome the resistance have been proposed. However, resistance mechanisms to Her2-selective inhibitor zongertinib have not been fully elucidated. In this study, we established zongertinib-tolerant Her2-positive NSCLC cells (zongerR) and investigated their therapeutic vulnerability. To establish the zongerR cells in vitro, Her2-amplified or Her2-mutated patient-derived cells were sequentially cultured with 100 nM zongertinib for 9 days, followed by a drug holiday. After 2-4 cycles, established zongerR cells demonstrated a more than 2-fold increase in cell viability at 100 nM zongertinib in vitro. Immunoblot analysis revealed that zongertinib suppressed Her2 phosphorylation, indicating that resistance mechanisms were related to bypass signaling. To assess the activating bypass signaling in zongerR cells, we performed inhibitor library screening with or without zongertinib. Drug screening revealed that zongerR cells exhibited sensitivity to the multi-tyrosine kinase inhibitor ponatinib and foretinib. Additionally, PI3K/AKT pathway inhibitors (PI3Ki) such as GDC0941 and mTOR inhibitor PP242 also markedly suppressed the survival of zongerR cells in combination with zongertinib. Notably, we identified a single treatment with the TopoI inhibitor SN38 suppressed cell viability in a zongerR cell derived from Her2-amplified H2170 cells (H2170zongerR), compared with H2170 parental cells. From the analysis of immunoblot and cell cycle, TopoI inhibitors induce DNA damage, leading to G2/M arrest and apoptosis, in H2170zongerR. These findings suggested that sequential treatment with zongertinib, followed by T-Dxd, might have been effective. Therefore, we evaluated the treatment efficacy in vivo. In a preliminary result, administration of zongertinib regressed tumor growth for several weeks, whereas tumor regrowth was observed. Subsequently, T-Dxd treatment showed tumor regression in contrast to the continuous treatment of the zongertinib group. Currently, zongertinib and T-Dxd have been approved for Her2-positive NSCLC, whereas treatment strategies to prolong the durable response have not been well-established. Further investigations were needed, but our findings suggested that T-DXd treatment after zongertinib may be a potential therapeutic strategy in a subset of Her2-positive NSCLC.

#2967 Evolution of TOP1 variants under selective pressure from topoisomerase-based therapeutics.

Tejaswini Reddy[1], Lei Kang[2], Hung Le[2], Senthil Damodaran[3], Kanwal Pratap Singh Raghav[2], Scott Kopetz[3], Jordi Rodon Ahnert[3], Ecaterina Elena Dumbrava[3], Timothy A. Yap[3], Stephen Williams[2], Mark J. Routbort[2], Keyur P. Patel[2], Funda Meric-Bernstam[3]

[1]Baylor College of Medicine, Houston, TX,[2]The University of Texas MD Anderson Cancer Center, Houston, TX,[3]UT MD Anderson Cancer Center, Houston, TX

Background: Antibody-drug conjugates (ADCs) that incorporate topoisomerase I inhibitor payloads, including sacituzumab govitecan (SG) and trastuzumab deruxtecan (T-DXd), have demonstrated activity across multiple solid tumors. SG is approved for previously treated triple-negative and hormone receptor-positive breast cancers, while T-DXd is approved for HER2-expressing malignancies. Despite broad clinical use, the mechanisms underlying resistance to topoisomerase-based ADCs remain insufficiently defined. Recent reports indicate that acquired TOP1 mutations may contribute to therapeutic failure. We evaluated the frequency and characteristics of *TOP1* alterations in patients who progressed on ADCs carrying topoisomerase payloads or on camptothecin-based chemotherapy.

Methods: We reviewed 17,092 solid tumor samples profiled by tumor and/or liquid biopsy next-generation sequencing (NGS) through the MDA MAPP platform at The University of Texas MD Anderson Cancer Center from January 2019 to January 2025. Patients exposed to topoisomerase inhibitor-based ADCs (SG, T-DXd, or datopotamab deruxtecan [Dato-DXd]) or irinotecan/topotecan-containing chemotherapy were identified (n = 1,807). Those with available paired pre- and post-treatment NGS formed the analytic cohort (n = 343). We assessed the emergence of *TOP1* variants at progression, changes in variant allele frequency (VAF), and annotated mutations using ClinVar, InterVar, and literature review.

Results: *TOP1* mutations were detected in 160 of 17,092 patients (0.94%). This included 14 of 2,040 patients (0.68%) with liquid-biopsy NGS only, 18 of 1,324 (1.35%) with both liquid biopsy and tumor NGS, and 128 of 13,728 (0.93%) with tumor-only NGS. Nine unique *TOP1* variants, *G363S*, *G365V*, *G365S*, *R364C*, *K333fs*, *R434Q*, *R84K*, *A670G*, and *R364H*, arose at progression. Emergent alterations occurred in 3.4% (5/145) of patients treated with topoisomerase-payload ADCs and 2.1% (4/193) of those receiving irinotecan-based chemotherapy. *G365S* and *R364H* were previously described as pathogenic variants associated with camptothecin resistance, with *R364H* also linked to ADC resistance. One SG-treated breast cancer patient developed three concurrent alterations, *G365V* (VAF 23%), *G365S* (12%), and *R364C* (8%), at progression. Four colorectal cancer patients receiving FOLFIRI plus bevacizumab or panitumumab exhibited distinct emergent *TOP1* mutations at disease progression.

Conclusions: *TOP1* alterations can appear after exposure to topoisomerase-payload ADCs or irinotecan-containing regimens, suggesting a potential resistance mechanism in a subset of patients. The functional impact of these variants and their relevance to therapeutic response remain undefined, warranting further mechanistic and clinical investigation.

#2968 EGFR S442 mutation confers cetuximab resistance that can be overcome by ERBB2 blockade by trastuzumab-deruxtecan.

Neeraj Joshi[1], Sarah J. Harmych[2], Hidenori Tanaka[1], Galina Bogatcheva[1], Marisol A. Ramirez[1], Ramona Graves-Deal[1], Claiborne W. Tydings[2], Claudia C. Wahoski[2], Chelsie K. Sievers[1], Maria Johnson Irudayam[1], James N. Higginbotham[1], Frank L. Revetta[1], Zhiguo Zhao[1], Jeffrey L. Franklin[1], Binyam Yilma[3], Tina M. O'Grady[3], Stamatina Fragkogianni[3], Metamia Ciampricotti[3], M Kay Washington[1], Xingyi Guo[1], Allison S. Walker[2], Jens Meiler[2], Qi Liu[1], Robert J. Coffey[1], Eben L. Rosenthal[4], **Bhuminder Singh**[1]

[1]Vanderbilt University Medical Center, Nashville, TN,[2]Vanderbilt University, Nashville, TN,[3]Tempus AI Inc, Chicago, IL,[4]Professor of Surgery, Vanderbilt University School of Medicine, Nashville, TN

Epidermal growth factor receptor (EGFR) is a critical oncogenic driver in multiple cancers and a therapeutic target of tyrosine kinase inhibitors and neutralizing monoclonal antibodies. However, resistance to EGFR-targeted therapies, particularly the anti-EGFR antibody cetuximab, remains a clinical challenge in colorectal (CRC) and head and neck (HNSCC) cancers. To investigate cetuximab resistance mechanisms, we cultured the cetuximab-sensitive CRC cell line DiFi in 3D in type I collagen with cetuximab, generating cetuximab-resistant derivatives (DiFi-CR). Genomic and transcriptomic profiling revealed that DiFi-CR cells have a mutation of the S442 residue in the EGFR extracellular domain. Patient samples revealed EGFR S442 mutations following anti-EGFR therapy, indicating S442 as a potential resistance hotspot. For an in-depth mechanistic analysis, we reconstituted the EGFR S442I mutation, using a doxycycline-inducible system, and showed that it was necessary and sufficient to induce cetuximab resistance in CRC and HNSCC cells using *in vitro* (2D and 3D) cultures and *in vivo* mouse experiments. *In silico* structural studies, live-cell binding assays, and antibody enrichment in nude mice xenografts revealed that the S442I mutation leads to weaker EGFR-cetuximab binding. Weaker cetuximab binding was also predicted *in silico* for other S442 patient mutations. Importantly, we found that mutant EGFR-driven cetuximab resistance could be overcome by targeting EGFR family member ERBB2 with trastuzumab-deruxtecan. Notably, this combinatorial response was contingent upon a physical interaction between EGFR and ERBB2, as determined by co-immunoprecipitation. Overall, our study establishes EGFR S442 mutations as drivers of cetuximab resistance and highlights co-targeting ERBB2 as a promising therapeutic strategy to restore anti-EGFR efficacy.

#2969 B836: A novel bispecific antibody-drug conjugate (ADC) as a clinical candidate to overcome trastuzumab deruxtecan resistance.

Yi Zhao, Huahua Hao, Xin Yang, Weiwei Pan, XinxinLiang, Quanai Zhang, Xiaoxia Liu, Jingting Cui, Elizabeth Wu, **Zhican Qu**

Nanolattix, Taiyuan, China

Resistance to single-antigen HER2-targeted ADCs, such as Enhertu (trastuzumab deruxtecan, DS-8201) and Kadcyla (trastuzumab emtansine, T-DM1), poses a significant challenge in HER2-positive cancers, often due to tumor heterogeneity and antigen downregulation. To address this unmet medical need, we developed B836, a first-in-class bispecific ADC leveraging the Nanolattix Biolattix technology platform. B836 is engineered to target both HER2 and Tissue Factor (TF). TF is an attractive therapeutic target and is overexpressed in various tumor types. Results from in vitro experiments demonstrated that B836 achieved significantly enhanced cancer cell binding and internalization compared to single-target ADCs. In vivo studies of B836 showed superior anti-tumor efficacy over Enhertu, particularly in animal models characterized by low HER2 expression, suggesting its potential for overcoming primary or acquired resistance mechanisms. GLP safety and toxicokinetic (TK) studies were conducted in cynomolgus monkeys. No drug-related ocular toxicity or abnormalities in body temperature, blood pressure, or electrocardiogram (ECG) were observed. Furthermore, no systemic toxicity was detected at doses up to 5 mg/kg. These collective findings support the continued clinical development of B836, promising therapeutic potential in oncology.

#2970 Limited efficacy of HER3-DXd in colorectal cancer PDX models reveals molecular resistance mechanisms and informs rational combinatorial strategies.

Preeti Kanikarla[1], Alexey Sorokin[2], Alisha Bent[1], Kelly Gale[1], Fengqin Gao[1], Zhensheng Liu[1], Kanwal Pratap Singh Raghav[1], Scott Kopetz[1]

[1]UT MD Anderson Cancer Center, Houston, TX,[2]GI Medical Oncology, UT MD Anderson Cancer Center, Houston, TX

HER3 (ERBB3), a member of the EGFR family, activates PI3K/AKT signaling through dimerization with other ERBB receptors and is frequently implicated in resistance to targeted therapies. Patritumab deruxtecan, a HER3-directed antibody-drug conjugate (ADC), has shown clinical activity in non-small cell lung and breast cancers, and has been recently evaluated in metastatic colorectal cancer (mCRC). Despite frequent HER3 expression in mCRC, its therapeutic relevance in chemotherapy-refractory disease is not well defined. We evaluated HER3-DXd in a panel of 17 molecularly characterized mCRC patient-derived xenograft (PDX) models, the majority of which were derived from patients previously treated with and resistant to irinotecan. Tumor growth inhibition was used to assess response. Molecular profiling (including whole-exome sequencing, RNA sequencing, and Reverse Phase Protein Array) was conducted to elucidate resistance mechanisms and direct rational combination strategies. Single-agent HER3-DXd showed variable activity across models, with limited responses in those exhibiting irinotecan resistance. HER3 expression did not consistently predict response. Interpretation of this association might be limited by the absence of a standardized cutoff for HER3 positivity. The results of the relative weight analysis indicated that 86% of the response was attributable to the payload sensitivity, while only 13% was associated with HER3 expression as determined by IHC. Molecular analyses revealed persistent PI3K/AKT and MAPK signaling in non-responders, along with upregulated receptor tyrosine kinase (RTK) signaling and a correlation with increased expression of drug efflux transporters. Functional studies demonstrated that combining HER3-DXd with MEK, WEE1, or PLK1 inhibitors produced synergistic antitumor effects. Phospho-proteomic data supported adaptive pathway rewiring following HER3 blockade. These findings highlight the complexity of HER3 signaling in chemotherapy-refractory mCRC and support the development of biomarker-driven combination strategies to enhance therapeutic efficacy of HER3-targeted ADCs (and conceivably other ADCs with topoisomerase inhibitor payload) in this setting.

#2971 In-depth profiling of SCLC models of acquired chemoresistance reveals SLFN11-dependent antibody-drug conjugate payload sensitivity and ATR inhibitor synergy.

Buesra Ernhofer[1], Lisa Glatt[1], Benjamin Morris[2], Beata Szeitz[3], Zsolt Megyesfalvi[1], Abigail Deloria[1], Diana Piesel[1], Laura Schnell[1], Kristiina Boettiger[1], Amirali Karimi[2], Monique Nilsson[2], Melinda Rezeli[4], Simon Heeke[2], John Victor Heymach[2], Clemens Aigner[1], Balazs Dome[1], Karin Schelch[1]

[1]Department of Thoracic Surgery, Comprehensive Cancer Center, Medical University of Vienna, Vienna, Austria,[2]Department of Thoracic and Head and Neck Medical Oncology, MD Anderson Cancer Center, Houston, TX,[3]Department of Biochemistry & Molecular Pharmacology, New York University Grossman School of Medicine, New York, NY,[4]Department of Biomedical Engineering, Lund University, Lund, Sweden

Introduction: Small cell lung cancer (SCLC) represents an aggressive malignancy that initially responds well to frontline platinum-based chemotherapy. However, most patients relapse quickly due to rapid development of chemoresistance, emphasizing the urgent need for novel therapeutic strategies to achieve durable clinical benefit.

Methods: To elucidate the mechanisms driving treatment failure, we established *in vitro* SCLC models that acquired cisplatin resistance across distinct molecular subtypes. These models were characterized by proliferation, cell cycle, and proteomic assays. Drug screens were conducted to identify therapeutic vulnerabilities, including responses to unconjugated antibody-drug conjugate (ADC) payloads and targeted pathway inhibitors.

Results: Cisplatin-resistant (CR) SCLC models exhibited broad cross-resistance to clinically relevant cytotoxic drugs such as carboplatin, lurbinectedin, and topoisomerase I and II (TOP1 and TOP2) inhibitors. Resistance was associated with diminished intracellular platinum accumulation, reduced proliferation, and altered cell cycle distribution with G2/M arrest or senescent-like features compared to the corresponding sensitive parental lines. Proteomic analysis of CR models, together with patient-derived samples at treatment relapse, revealed extensive metabolic reprogramming and downregulation of DNA repair and checkpoint control pathways, highlighting shared adaptive signatures. Screening of unconjugated ADC payloads uncovered mechanism-specific vulnerabilities. While CR models were resistant to DNA-damaging payloads such as calicheamicin, microtubule-disrupting ADC payloads (MMAE and DM1) retained sensitivity across all CR models. Responses to TOP1-directed ADC payloads varied and were associated with SLFN11 expression levels. Importantly, inhibition of ATR with ceralasertib synergized with DNA-damaging ADC payloads, re-sensitizing SLFN11-low resistant models by increasing DNA damage and inducing apoptosis.

Conclusion: Our findings demonstrate shared adaptive mechanisms of acquired cisplatin resistance in SCLC, including checkpoint rewiring and metabolic flexibility. SLFN11 was identified as a key determinant of TOP1-directed ADC efficacy. Combining ATR inhibition with DNA-damaging ADC payloads represents a promising strategy to restore DNA damage-induced cell death in resistant SCLC. These insights provide a translational framework for developing rational ADC-based combination therapies to overcome chemoresistance in relapsed SCLC.

#2972 TROP2 upregulation and interaction with HER2 mediate trastuzumab resistance.

Yuan-Liang Wang, Chi-Huan Lu, Cheng-Yen Wei, Jye-Yu Huang, Woan-Eng Chan, Lu-Tzu Chen, Ya-Chi Chen

Biological Discovery, OBI Pharma, Inc, Taipei City, Taiwan

Trastuzumab (Herceptin) remains a cornerstone therapy for HER2-positive gastric cancer, yet acquired resistance severely limits its long-term efficacy. Identifying resistance mechanisms is critical for developing next-generation treatment strategies. We investigated the role of TROP2, a known oncogenic protein, in mediating resistance to trastuzumab. Trastuzumab-resistant HER2-positive gastric cancer (GC) cell lines were developed, characterized, and compared to parental cells. The functional impact of TROP2 on sensitivity was assessed using cytotoxicity assays following genetic knockdown (siRNA) of TROP2. The molecular interaction between TROP2 and HER2 was definitively evaluated using several assays, including co-immunoprecipitation (Co-IP), immunofluorescence (IF) co-localization, blue native PAGE (BN-PAGE), and label transfer binding assays. To define the specific heterodimer interface, site-directed mutagenesis was performed targeting predicted residues.

Trastuzumab-resistant gastric cancer cells exhibited a significant increase in IC_{50} (>5-fold) and displayed markedly higher TROP2 expression compared to sensitive parental cells. Knockdown of TROP2 expression transiently can restore trastuzumab sensitivity in resistant cell lines, confirming TROP2's direct role as a mediator of therapy evasion. HER2/TROP2 heterodimerization was confirmed by Co-IP (co-immunoprecipitation), IF (immunofluorescence), and BN-PAGE provided strong evidence for the direct interaction of HER2 and TROP2 heterodimerization. Binding Interface determination in mutagenesis targeting TROP2-Asp99 and the HER2-Val308/Lys333 interface successfully disrupted the physical interaction between HER2 and TROP2.

TROP2 upregulation and its subsequent physical heterodimerization with HER2 constitutes targetable mechanism of acquired resistance to trastuzumab in HER2-positive gastric cancer. This interaction suggests that TROP2 may sustain critical oncogenic signaling even when HER2 is pharmacologically inhibited. These findings provide a strong molecular rationale for developing strategies aimed at disrupting the TROP2-HER2 complex to enhance and restore therapeutic efficacy.

#2974 The anticancer effect of TROP2-targeted antibody-drug conjugates (ADC) is potentially attenuated by dysregulated cholesterol metabolism in cancer cells.

Kimio Yonesaka[1], Yusuke Kawanaka[1], Takashi Kurosaki[1], Satomi Watanabe[1], Junko Tanizaki[1], Kazuko Sakai[2], Takeshi Teramura[3], Kazuto Nishio[2], Hidetoshi Hayashi[1]

[1]Medical Oncology, Kindai University Faculty of Medicine, Sakai, Osaka, Japan,[2]Genome Biology, Kindai University Faculty of Medicine, Sakai, Osaka, Japan,[3]Cell Biology for Regenerative Medicine, Kindai University Faculty of Medicine, Sakai, Osaka, Japan

Background: Trop-2 is a widely expressed glycoprotein on a variety of different tumors. Datopotamab deruxtecan (Dato-DXd) is a Trop-2-targeted ADC that has demonstrated anticancer efficacy in patients with *EGFR*-mutated non-small cell lung cancer (NSCLC). However, their efficacy is inconsistent. In cancer cells, cholesterol synthesis is promoted, and cholesterol localizes to the cell membrane, playing a crucial role in the endocytosis of various receptors on the cell membrane. The current study aimed to explore the mechanisms underlying the limited efficacy of Dato-DXd using *EGFR*-mutated NSCLC cells.

Materials and methods: We established a Dato-DXd-resistant PC9DR cell line by long-term exposure of *EGFR*-mutated NSCLC PC9 cells to Dato-DXd. A colony formation assay was performed to evaluate anticancer effects. Trop-2 expression on the cell membrane was measured immunologically. Intracellular uptake of Dato-DXd was measured using a pH-Rhod method. Microarray data were analyzed using Transcriptome Analysis Console Software to examine differentially expressed genes and related-pathways.

Result: According to the colony formation assay, 1μg/mL Dato-DXd inhibited 89% colony formation in PC9 cells, but inhibited 5% colony formation in PC9DR cells. In PC9DR cells, cell surface Trop-2 expression was greater than PC9 cells (434,338 vs 400,722 molecules per cell, $p = 0.0012$). However, intracellular uptake of Dato-DXd was significantly reduced in PC9DR cells compared to PC9 cells (two-way ANOVA, $p < 0.0001$). These results suggested that reduced internalization of Trop-2 protein on the cell membrane is hypothetically associated with resistance to Dato-DXd. Second, pathway analysis revealed that the cholesterol metabolism pathway showed the most significant change in PC9DR cells compared to PC9 cells. Specifically, compared to PC9 cells, PC9DR cells showed a marked decrease in the expression of cholesterol synthesis-related enzymes, including HMGCR, MVD, and SQLE, while conversely exhibiting increased expression of the cholesterol transporter ABCA1 (ANOVA $p<0.001$, greater than two-fold change). Therefore, we hypothesized that impaired cholesterol metabolism cause resistance to Dato-DXd. Finally, we exposed the Dato-DXd-sensitive cells including PC9 and HCC827 to the HMGCoA reductase inhibitor, 1μM mevastatin, and evaluated anticancer effect of 1μg/mL Dato-DXd using a colony formation assay. In PC9 cells, Dato-DXd potently inhibited colony formation (relative colony formation area, Control; 100%, Dato-DXd; 3.6%). However, PC9 cells treated with mevastatin, Dato-DXd minimally inhibited colony formation (Control; 100%, Dato-DXd; 77.4%). Similar trend was observed in HCC827 cells.

Conclusion: These results suggest that impaired cholesterol metabolism may cause resistance to Dato-DXd in *EGFR*-mutated NSCLC.

#2975 Q702 enhances trastuzumab efficacy for HER2 + gastric cancer cells.

Mi Young Kim[1], Yoonji Lee[2], Kiyean Nam[2], **Jin-Soo Kim**[1]

[1]Seoul Metropolitan Government Seoul National University Boramae Medical Center, Seoul, Korea, Republic of,[2]Qurient Co., Ltd., Seongnam, Korea, Republic of

Background: Trastuzumab (Tmab) is an effective monoclonal antibody against advanced esophago-gastric cancers (GCs) with HER2 amplification. Unfortunately, the efficacy of Tmab is limited due to primary and acquired resistance to this agent. Q702 is a novel, orally available small molecule that selectively inhibits three receptor tyrosine kinases: Axl, Mer, and CSF1R. Here, we describe a therapeutic synergism between Tmab and Q702 in HER2+ GC cells.
Material and Methods: After screening 37 GC cell lines (J-S Kim et al Int. J. Mol. Sci. 2024, 25(11), 5975), the following GC cells were evaluated: HER2 amplification -positive (HER2+) and Tmab-sensitive NCI-N87 and OE19, HER2+ Tmab-resistant OE33, ESO26, SNU-216, MKN7, YCC19, YCC33, and YCC38 and HER2 negative AGS and SNU638. We assessed the cytotoxic response of these GC cells to trastuzumab alone or in combination with Q702 by 3-(4,5-dimethylthiazol-2-yl)-2,5-diphenyltetrazolium (MTT) assay, and clonogenic cell survival assays. Western blots were performed to assess biochemical changes, especially those related with HER2 signaling components. The statistical significance of differences of colony numbers were determined by using the Kruskal-Wallis test.
Results: HER2+ Tmab-resistant GC cells showed relatively higher expression of AXL than HER2+ Tmab-sensitive GC cells. Q702 significantly decreased the number of colonies in clonogenc assays and exerted dose-dependent effects in HER2+ GC cells. Additionally, we observed that treatment with trastuzumab in combination with Q702 induced a statistically significant decrease of the colonies in HER2 + GC cells, both Tmab-sensitive and Tmab-resistant. Combination with Q702 resulted in decreased phosphorylation of HER2 and its downstream targets, AKT and ERK, in Tmab-resistant HER2+ cells. No growth inhibition was detected in HER2-GC cells treated with Tmab alone or combination.
Conclusion: Collectively, these data support that Q702 could overcome primary resistance to Tmab in HER2+ GC cells.

: Molecular Targets 1
Poster Session

#2979 MAPK driven kinetochore instability as a biomarker and therapeutic vulnerability in glioblastoma.

Jennifer DeLuca[1], **Patrick J. Paddison**[2]

[1]Colorado State University, Fort Collins, CO,[2]Fred Hutchinson Cancer Center, Seattle, WA

Chromosome segregation fidelity relies on stable attachments between kinetochores (KTs) and spindle microtubules during mitosis. We recently identified a previously unrecognized form of KT dysfunction that is prevalent in human glioblastoma (GBM) isolates and is triggered by aberrant activation of mitogen-activated protein kinase (MAPK) signaling during mitosis. This phenotype—termed MAPK-stressed kinetochores (MaSKs)—arises when hyperactive Ras-Raf-MEK-ERK signaling drives excessive phosphorylation of KT components by a network of KT-associated kinases. As a result, MT-binding affinity is reduced and KT-MT turnover becomes abnormally high, producing a lethal mitotic stress state. MaSKs provide a direct mechanistic link between oncogenic Ras/MAPK pathway activity and the generation of chromosome instability, filling a key gap in our understanding of how mitogenic oncogenes disrupt mitosis. Notably, MaSKs appear to be restricted to cancer and transformed cells, where they create unique genetic and molecular dependencies. MaSK-positive cells rely specifically on two non-essential domains of the mitotic checkpoint protein BubR1/BUB1B to recruit PP2A phosphatase and suppress MaSK-induced KT-MT instability. These dependencies suggest new opportunities for tumor-selective therapeutic targeting. In this presentation, we will describe the molecular basis of MaSK formation, the assays enabling their discovery, and evidence supporting their utility as biomarkers for a subset of MAPK-driven tumors. We further discuss how MaSKs can be exploited to identify novel therapeutic strategies and define a patient responder population.

#2980 SMARCA2 and SMARCA4 expression in cancer: A tissue microarray study on 14,966 tumors from 134 different tumor types.

Nina Schraps[1], Anne Menz[1], Florian Lutz[1], Viktoria Chirico[1], Florian Viehweger[1], David Dum[1], Ria Schlichter[1], Andrea Hinsch[1], Fiete Gehrisch[1], Christoph Fraune[1], Christian Bernreuther[1], Seyma Buyucek[1], Martina Kluth[1], Claudia Hube-Magg[1], Katharina Moller[1], Viktor Reiswich[1], Andreas M. Luebke[1], Patrick Lebok[1], Baris Mercanoglu[2], Nathaniel Melling[2], Thilo Hackert[2], Guido Sauter[1], Maximilian Lennartz[1], Till S. Cauditz[1], Andreas H Marx[1], Ronald Simon[1], Stefan Steurer[1], Eike Burandt[1], Natalia Gorbokon[1], Maria Christina Tsourlakis[1], Sarah Minner[1], Till Krech[1], Morton Freytag[1]

[1]Institute of Pathology, University Medical Center Hamburg-Eppendorf, Hamburg, Germany,[2]General, Visceral and Thoracic Surgery Department and Clinic, University Medical Center Hamburg-Eppendorf, Hamburg, Germany

The two mutually exchangeable ATPases SMARCA2 and SMARCA4 form the two catalytic subunits of a polymorphic family of SWI/SNF complexes. In both normal and malignant cells, they play a regulatory role in numerous essential cellular processes. For example, SWI/SNF affects the regulation of cell differentiation, programmed cell death, DNA repair, chromosome stability, signaling pathway crosstalk and cell metabolism. Topical interest in SMARCA4/SMARCA2 is due to the observation of their synthetic lethal relationship, potentially offering new therapeutic approaches. Targeting SMARCA4 deficient cancer cells with SMARCA2 inhibitors or degraders has resulted in significant growth inhibition in experimental systems and further agents are being tested in early clinical trials. To determine the prevalence of SMARCA2/SMARCA4 expression in cancer, a tissue microarray containing 14,966 samples from 134 different tumor entities and 608 samples of 76 different normal tissue types was analyzed by immunohistochemistry. SMARCA2 immunostaining was absent in 6.9%, weak in 8.0%, moderate in 18.3%, and strong in 66.8% of 12,253 interpretable tumors. SMARCA4 staining was absent in 0.7%, weak in 1.9%, moderate in 5.9%, and strong in 91.5% of 13,093 interpretable tumors. Remarkably, losses of SMARCA2 and SMARCA4 were strongly correlated. Of 91 SMARCA4 deficient tumors for which SMARCA2 data were also available, 28 (30.8%) did also show a complete loss of SMARCA2 expression. SMARCA2 deficiency was most commonly seen in Burkitt lymphoma (66.7%), endometrial carcinomas (up to 57.1%), rhabdoid tumors (50.0%) and ovarian carcinomas (up to 37.8%). SMARCA4 staining was predominantly lost in in neuroendocrine carcinomas (up to 25.0%), endometrioid carcinomas (up to 7.7%) and adenocarcinomas of the lung (7.5%). Absent or low SMARCA2 expression was significantly linked to unfavorable tumor phenotype in clear cell renal cell carcinoma, bladder cancer, and breast cancer while weak or absent SMARCA4 staining was linked to unfavorable tumor features in colorectal and clear cell renal cell carcinoma ($p \leq 0.05$). It is concluded, that SMARCA4 deficiency is a rather rare event in tumors, whereas SMARCA2 deficiency is much more common in many different tumor entities and is associated with unfavourable cancer characteristics in several tumor types. The frequent co-deficiency of SMARCA2 and SMARCA4 challenges the concept of a synthetic lethal relationship of these proteins in vivo.

#2981 PM54 targets oncogenic transcriptional networks across multiple cancer types.

Ismael Fernandez-Miranda, Javier Robles, Maria Jose Guillen, Pablo Aviles, **Marcelo L. Ribeiro**, Carmen Cuevas

Pharma Mar, S.A., Madrid, Spain

Background: PM54, a synthetic ecteinascidin analog derived from lurbinectedin, binds GC-rich promoter regions to block transcription, induce DNA double-strand breaks, and trigger S-phase arrest and apoptosis. We aimed to define PM54 transcriptional mechanisms across tumor types and to identify transcriptomic features associated with heightened sensitivity.
Methods: Comprehensive transcriptomic profiling (RNA-seq) was performed following acute PM54 exposure (50 nM, 6 h) in a panel of 32 cancer cell lines representing six tumor types: 12 small-cell lung cancers (SCLC), 8 gastric cancers, 6 prostate cancers, 4 breast cancers, 1 ovarian cancer, and 1 melanoma. Hierarchical clustering, differential expression, GSEA, and GO analyses were used to define temporal transcriptional response clusters. In vivo validation was conducted in four CDX models (SCLC DMS-53, ovarian A2780, melanoma WM-266-4, and TNBC MDA-MB-231) after a single PM54 dose, with RNA-seq performed on day 7.
Results: PM54 induced a rapid, broad transcriptional repression in all models, with >2,000 downregulated genes per line and a conserved core of 1,170 commonly repressed genes (versus 226 commonly induced). Repressed programs included cell cycle, RNA Pol II transcription, chromatin organization, DNA repair and MYC targets; early upregulated signatures implicated metabolism, PARP signaling and stress responses. Unsupervised clustering based on PM54 transcriptional effect identified a “primed” responder cluster (characterized by high baseline transcription and rapid transcriptional shutdown after treatment) and an “adaptive” responder cluster. Curiously, all three POU2F3 SCLC lines and prostate cancer models were into the primed responder cluster. Consistently, in vivo transcriptomic analyses recapitulated these clusters, demonstrating enhanced transcriptional repression, MYC/mTOR signaling suppression, and markedly improved survival outcomes in primed (+192%, +345% and +412% in ovarian, melanoma and SCLC, respectively) compared to adaptive responders (+185% in breast cancer and +240% in gastric cancer).
Conclusions: PM54 rapidly suppresses proliferative/MYC-driven programs and elicits adaptive metabolic/immune responses. Baseline transcriptional state predicts response and may guide patient selection and combination strategies.

#2982 Role of high mobility group nucleosome-binding domain-containing protein 3 (HMGN3) in prostate cancer progression a novel target for therapeutic intervention.

Vikkram Venkatesan[1], Jeffrey Mathew[2], Janani Harikrishnan[1], Gnanasekar Munirathinam[1]

[1]Biomedical Sciences, University of Illinois College of Medicine (Rockford), Rockford, IL,[2]Biology, John Hopkins University, Baltimore, MD

Prostate cancer (PCa) accounts for more than one million new cases globally each year. Standard therapeutic approaches such as chemotherapy, radiotherapy, prostatectomy, and androgen deprivation therapy often yield only temporary benefits and are associated with substantial toxicity. Neuroendocrine prostate cancer (NEPC) represents a rare, highly aggressive subtype of PCa that may develop de novo or emerge as a treatment-resistant form of adenocarcinoma. NEPC is particularly challenging to manage because it is androgen receptor (AR) independent and responds poorly to conventional therapies. Chromatin modulators such as EZH2, BRD4, and NKX2-1 have been shown to promote the development of NEPC. One such novel chromatin regulator namely High Mobility Group Nucleosome-Binding Domain-Containing Protein 3 (HMGN3), a member of the HMGN protein family, binds nucleosomes and modulates chromatin structure, thereby influencing transcription, replication, and DNA repair may also have a role in the progression of NEPC. Previous research has demonstrated that HMGN3 promotes metastasis in cholangiocarcinoma by binding to the transcription factor SNAI2 and interacting with histone deacetylases (HDACs), leading to repression of epithelial-regulatory genes and induction of epithelial-mesenchymal transition (EMT). However, its role in PCa has not been previously explored. Bioinformatic analyses using PCA Tools and Betastasis indicate that AR-negative and neuroendocrine cell lines—such as NCI-H660 and LASCPC—exhibit the highest mRNA expression levels of HMGN3. This suggests that HMGN3 may contribute to EMT-associated metastatic pathways in PCa. To explore this, western blotting and RT-PCR were performed to analyze HMGN3 protein and mRNA levels in NEPC cell lines. Both NCI-H660 and LASCPC showed high protein expression, with LASCPC displaying the highest mRNA expression. Functional assays were carried out by treating BPH-1 cells with *r*HMGN3 in colony formation assays (CFA), while TRAMP-C1 cells were used for wound healing and Transwell migration assays. In these assays, treated groups demonstrated increased colony formation, accelerated wound closure, and higher migratory activity compared to controls. Additionally, a preliminary MTT cell viability assay performed in NCI-H660 cells treated with varying concentrations of monoclonal antibody targeted to HMGN3 showed reduced cell viability relative to untreated controls. Collectively, these findings suggest that HMGN3 as a significant enhancer of tumor growth and metastatic spread, being especially abundantly expressed in aggressive NEPC. In conclusion, our data supports that targeting HMGN3 could serve as an innovative therapeutic approach for advanced, treatment-resistant forms of PCa.

#2983 Genome-wide CRISPRi screen identifies RPS27 as a novel synthetic lethal target for TP53 mutant cancers.

Stephen Paik, Yi Yu, Ashley H. Choi, Samuel R. Meier, Shangtao Liu, Binzhang Shen, Shanchuan Zhao, Xuewen Pan, Jannik N. Andersen, **Teng Teng**

Tango Therapeutics, Boston, MA

TP53 is a master tumor suppressor that regulates diverse cellular functions, including cell cycle progression, apoptosis, DNA damage repair and genome stability. Due to its critical role, TP53 is the most frequently mutated gene across human cancer and its loss often represent an early event in tumorigenesis. However, therapeutic strategies that specifically target TP53-mutant cancers remain limited. To identify novel synthetic lethal targets for TP53 mutant cancers, we engineered and validated isogenic cell lines differing only in TP53 status and performed a genome wide CRISPR interference (CRISPRi) screen in paired A549 cells. The screen identified the small ribosome subunit protein RPS27 as the top dependency unique to TP53 knockout cells. Interestingly, this dependency was specific to the CRISPRi platform, as RPS27 did not score in a parallel CRISPR knockout (CRISPRko) screen. Further examination revealed that most CRISPRko gRNAs targeting RPS27 have multiple off-target sites with less than 3 mismatches. This likely causes general DNA-cutting-induced cytotoxicity that confounds true gene dependencies, which is avoided with the CRISPRi platform. Supporting this conclusion, re-analysis of the public DepMap/Achilles dataset showed that a single mismatch-free gRNA also demonstrate RPS27 dependency in TP53 mutant cell lines. Mechanistically, TP53 drives the expression of RPS27L, a close paralog of RPS27. While TP53 wildtype cells express both RPS27L and RPS27, allowing for functional redundancy in ribosome assembly, TP53 mutant cells lack RPS27L expression and become largely dependent on RPS27 for ribosomal integrity and survival. Single gene validation confirmed that TP53 KO A549 cells are exquisitely sensitive to RPS27 knockdown and this dependency can be rescued by re-expression of either TP53, RPS27 or RPS27L. Together, these findings identify RPS27 as a novel synthetic lethal target for TP53 mutant cancers, revealing a previously unrecognized paralog-dependency within the ribosome and highlighting a potential therapeutic vulnerability.

#2984 *In situ* and functional analysis of Integrin-alpha 5 reveals its role in tumor progression in non-small cell lung cancer.

Mirei Ka[1], Takahiro Ando[2], Munetoshi Hinata[3], Kousuke Watanabe[4], Akiko Kunita[4], Masanori Kawakami[2], Masaaki Sato[5], Hiroyuki Okada[6], Hironori Hojo[7], Tetsuo Ushiku[3], Cecilia C. Krona[8], Patrick Micke[8], Katsutoshi Oda[1], Hidenori Kage[2]

[1]Division of Integrative Genomics, Graduate School of Medicine, The University of Tokyo, Bunkyo City, Japan,[2]Department of Respiratory Medicine, Graduate School of Medicine, The University of Tokyo, Bunkyo City, Japan,[3]Department of Pathology, Graduate School of Medicine, The University of Tokyo, Bunkyo City, Japan,[4]Next-Generation Precision Medicine Development Laboratory, Graduate School of Medicine, The University of Tokyo, Bunkyo City, Japan,[5]Department of Thoracic Surgery, Graduate School of Medicine, The University of Tokyo, Bunkyo City, Japan,[6]Center for Disease Biology and Integrative Medicine, Graduate School of Medicine, The University of Tokyo, Bunkyo City, Japan,[7]Bioinformatics Research Unit, Graduate School of Dentistry, The University of Osaka, Suita City, Japan,[8]Department of Immunology, Genetics, and Pathology, Uppsala University, Uppsala, Sweden

[Background] Integrins are transmembrane receptors that mediate cell adhesion to adjacent cells and the extracellular matrix, thereby regulating fundamental cellular processes. Abnormal integrin expression has been linked to tumor progression and metastasis across multiple cancer types, primarily through their interactions with components of the tumor microenvironment. Integrin alpha-5 (ITGA5) typically forms a heterodimer with the commonly shared beta-1 subunit and functions as a receptor for fibronectin and fibrinogen. This study aimed to investigate the clinical and biological significance of ITGA5 in non-small cell lung cancer (NSCLC).
[Methods] Survival analysis was based on RNA-seq data sets from NSCLC patient cohorts of the University of Tokyo Hospital (n = 100) and The Cancer Genome Atlas (TCGA; n = 986). Protein expression was analyzed by immunohistochemistry (IHC) in diagnostic tissue samples from NSCLC patients from The University of Tokyo Hospital (n = 20) and from the Uppsala University Hospital (Sweden; n = 312), which also included extensive mutation data. The biological relevance of ITGA5 was experimentally evaluated in a xenograft model with Calu-1 cells using an ITGA5 inhibitor (GLPG0187), and the effect of ITGA5 knockdown derived from the same cell line was analyzed by bulk RNA-seq analysis.
[Results] Both RNA and protein-level survival analyses consistently revealed that high ITGA5 expression was associated with shorter survival across multiple cohorts (TCGA RNA: p=0.011; University of Tokyo Hospital RNA: p=0.025; University of Tokyo Hospital protein: p=0.038; Uppsala University Hospital protein: p=0.013). Notably, protein IHC analysis indicated a greater impact of ITGA5 in tumors than in stromal cells. ITGA5 inhibition suppressed tumor growth in vivo compared to controls. Bulk-RNA seq data showed that ITGA5 knockdown altered the expression of genes involved in integrin-mediated signaling. Genes such as FERMT2, SEMA7A, and CCN1/CCN2 showed decreased expression following knockdown, consistent with their roles in integrin activation, ECM remodeling, and pro-invasive signaling. In addition, this analysis showed downregulation of pathways related to inflammation and tumor immunity (e.g., CSF3, CXCL8, IL6ST), EMT (e.g., TGFBR1, CDH2, PXN), and mTOR signaling (e.g., PIK3R2, STAT3, HRAS).
[Conclusion] Our study provides a comprehensive analysis of ITGA5 expression on RNA and protein levels in the clinical context. The results indicate an essential role of ITGA5 in promoting tumor progression and poor prognosis in lung cancer, providing the rationale for further studying ITGA5 as a target with biomarker and therapeutic potential for NSCLC patients with elevated ITGA5 expression.

#2985 TRIB2 as a therapeutic vulnerability in ALK-rearranged non-small cell lung cancer.

Jitender Monga[1], Sudha Sadasivan[2], Sang-Yoon Lee[3], Sharad K. Suthar[3], Craig Rogers[1], Shirish Gadgeel[2]

[1]Department of Urology, Henry Ford Health + Michigan State University Health Sciences, Detroit, MI,[2]Division of Hematology & Oncology, Henry Ford Health + Michigan State University Health Sciences, Detroit, MI,[3]Department of Neuroscience, Neuroscience Research Institute, Gachon University, Incheon, Korea, Republic of

Background: Lung cancer remains the leading cause of cancer-related deaths worldwide. Among its molecularly defined subsets, EML4-ALK rearranged non-small cell lung cancer (NSCLC) is a distinct subtype (3-5% of NSCLC), occurring disproportionately in younger, non-smoking patients. Despite the clinical success of next-generation ALK tyrosine kinase inhibitors (TKIs), including alectinib and lorlatinib, most patients eventually experience disease relapse due to adaptive signaling and bypass mechanisms. The prognosis of relapsed ALK-positive NSCLC is poor, underscoring the critical need to identify novel therapeutic targets that drive tumor growth and survival. We have previously demonstrated that TRIB2, a pseudokinase, promotes tumor growth and therapy resistance in tumors treated with targeted therapy. We therefore evaluated TRIB2 expression in ALK-rearranged lung cancer cell lines and assessed the effects of TRIB2 downregulation on tumor cell growth and viability.
Methods: TRIB2 expression was assessed, and its functional role was tested using shRNA and CRISPR-Cas9-mediated depletion, and pharmacologic inhibition approaches. Cell viability, apoptosis, and downstream signaling changes were analyzed in vitro, while xenograft studies evaluated tumor growth *in vivo*. Synergy studies were performed combining TRIB2 inhibition with ALK inhibitors.
Results: TRIB2 was found to be highly expressed in ALK-positive cell lines and lung tumors. Genetic inhibition of TRIB2 using shRNA significantly suppressed proliferation and induced apoptosis in ALK-positive NSCLC cells. *In vivo*, Dox-induced CRISPR-Cas9-mediated depletion of TRIB2 resulted in significant tumor regression in xenograft models, highlighting its critical role in tumor maintenance. Combination studies revealed that TRIB2 inhibition synergized with ALK-TKIs such as alectinib or lorlatinib to more effectively suppress cancer cell growth than either approach alone. Mechanistic studies demonstrated that TRIB2 loss attenuated ALK signaling, reducing phosphorylation of key survival effectors including STAT3, thereby impairing downstream pathways essential for cell survival and tumor progression.
Conclusions: This study identifies TRIB2 as a critical survival factor in ALK-rearranged NSCLC and establishes its inhibition as a promising therapeutic strategy. TRIB2 targeting not only disrupts tumor maintenance but also enhances sensitivity to ALK TKIs, offering a potential approach to extend the durability of therapeutic responses. These findings provide strong translational rationale for developing TRIB2-targeted therapies to improve outcomes for patients with ALK-positive lung cancer.

#2986 Vertical inhibition of the autophagy pathway promotes growth arrest and apoptotic cell death in pancreatic ductal adenocarcinoma.

Mallory K. Roach[1], Jonathan M. DeLiberty[1], Seamus Degan[2], Lily M. Pita[2], Elyse G. Schechter[2], Noah L. Pieper[2], Runying Yang[2], Mariaelena Pieronon[3], Clint A. Stalnecker[2], Emanuel Frank Petricoin[3], Kirsten L. Bryant[2]

[1]Department of Pharmacology, University of North Carolina at Chapel Hill, Chapel Hill, NC,[2]Lineberger Comprehensive Cancer Center, University of North Carolina at Chapel Hill, Chapel Hill, NC,[3]Center for Applied Proteomics and Molecular Medicine, George Mason University, Manassas, VA

Pancreatic ductal adenocarcinoma (PDAC) is dependent on autophagy for growth. The sole FDA approved inhibitor of autophagy, chloroquine/hydroxychloroquine (CQ/HCQ), inhibited the growth of multiple preclinical models of PDAC. However, clinical trials using CQ alone or in combination with standards of care have shown that CQ has limited clinical efficacy. To identify genes to target as sensitizers to CQ treatment, we performed a CQ-anchored CRISPR-Cas9 mediated loss-of-function screen. We identified multiple autophagy-related genes. This result led us to hypothesize that concurrent inhibition of two nodes (i.e. vertical inhibition) of the autophagy pathway is a more effective method of inhibiting cell growth. Specifically, loss of *PIK3C3*, the gene that encodes VPS34, a protein essential for autophagosome nucleation, sensitized PDAC cells to CQ treatment. We validated this finding via both genetic depletion and pharmacological inhibition with the compound SAR405. Additionally, pharmacological inhibition of ULK1/2, the serine/threonine kinases critical for autophagy initiation, further reduced CQ-mediated anti-proliferative effects. We recently demonstrated that inhibition of the lipid kinase PIKfyve with apilimod potently suppressed autophagy in PDAC. We found that both ULK1/2 and VPS34 inhibitor treatment sensitized cells to PIKfyve inhibition.To elucidate the mechanisms driving decreased cellular proliferation following combination treatment, we explored both autophagy-dependent and -independent pathways using reverse phase protein array (RPPA) based protein pathway activation mapping. We determined that vertical autophagy inhibition resulted in metabolic rewiring including enhanced receptor tyrosine kinase and PI3K-AKT-mTORC1 signaling. Furthermore, by monitoring levels of the autophagy-related protein LC3B following CQ or apilimod treatment alone or in combination with ULK1/2 inhibition, we demonstrated that vertical autophagy inhibition impairs both autophagosome formation and autophagosome processing, simultaneously. We also found that cleaved caspases accumulated more in the presence of two autophagy inhibitors. We validated this finding using Annexin V apoptosis assays and demonstrated that growth suppression was due in part to enhanced apoptotic cell death. In summary, our findings demonstrate that vertical inhibition of the autophagy pathway more effectively suppresses autophagy and increases cell death in PDAC and provides rationale for a vertical inhibition strategy to enhance the therapeutic efficacy of autophagy inhibition.

#2987 Cordycepin inhibits Intrahepatic cholangiocarcinoma progression by targeting NAT10-mediated ac4C RNA modification of VCAN.

Yuting Zhao[1], Yinzhao Chen[1], Yuhan Fang[1], Kai Luo[2], Jialin Qu[3], Dong Shang[3], **Caiming Xu**[4], Guixin Zhang[2]

[1]Dalian Medical University, Dalian, China,[2]The Second Hospital of Dalian Medical University, Dalian, China,[3]The First Affiliated Hospital of Dalian Medical University, Dalian, China,[4]Beckman Research Institute of The City of Hope, Monrovia, CA

Background: Intrahepatic cholangiocarcinoma (ICC) is an aggressive malignancy with poor prognosis. Among RNA modifications that drive tumor progression, N4-acetylcytidine (ac4C) mediated by NAT10 is crucial for RNA stability and translation. Cordycepin, a bioactive compound from Cordyceps sinensis, has known antitumor activity, yet its impact on ICC via RNA-modification pathways remains unclear. This study examines how cordycepin targets the NAT10-ac4C axis to inhibit ICC, providing mechanistic support for RNA-modification-based therapy.

Methods: The antiproliferative effects of cordycepin on HUCCT1 and RBE cells were quantified using CCK-8 assays to determine IC_{50} values. Western blotting was employed to profile RNA-modifying enzymes and identify ac4C/NAT10 as potential targets. The effects of cordycepin on cellular phenotypes were systematically assessed via CCK-8, EdU incorporation, colony formation, flow cytometry, Transwell migration and invasion, and wound-healing assays. Direct cordycepin-NAT10 interaction was validated by molecular docking, cellular thermal shift assay (CETSA) and drug affinity responsive target stability (DARTS) analysis. Global ac4C levels were examined by dot blotting. RNA-seq combined with acRIP-seq was used to define downstream ac4C-regulated genes. Antitumor efficacy was further evaluated in C57BL/6 mouse subcutaneous ICC xenograft models.

Results: Cordycepin exhibited IC_{50} values of 67.18 μM in HUCCT1 cells and 75.50 μM in RBE cells. It markedly suppressed proliferation, migration, and invasion while inducing apoptosis in a dose-dependent manner ($P < 0.05$). Cordycepin significantly reduced NAT10 protein abundance and global ac4C modification levels ($P < 0.05$). Docking analysis predicted a binding energy of −7.0 kcal/mol, and CETSA together with DARTS confirmed direct target engagement. Integrative RNA-seq and acRIP-seq analyses identified VCAN, an extracellular matrix-associated gene, as a principal ac4C-regulated downstream effector. Cordycepin decreased both ac4C enrichment and expression of VCAN, whereas NAT10 overexpression reversed these effects. In vivo, cordycepin substantially suppressed tumor growth, reflected by reduced tumor volume and weight ($P < 0.05$). Correspondingly, NAT10 and VCAN expression in tumor tissues were significantly downregulated.

Conclusion: This study demonstrates that cordycepin directly targets NAT10, attenuating its expression and global ac4C modification, thereby suppressing the downstream oncogenic effector VCAN and restraining ICC progression. These findings underscore the central role of the NAT10-ac4C axis in cordycepin's antitumor activity and identify this pathway as a promising therapeutic target in ICC.

#2988 A druggable genome screen identifies b-catenin transcription targets as desmoid cell vulnerabilities.

Jia Hu[1], Tianjie Pu[1], Vladislav Tsiperson[1], Lakshana Senthilkumar[1], Katherine Prendergast[2], Narasimhan P. Agaram[1], Marco Russo[1], Sameul Singer[1], Ralph Garippa[1], Meera Hameed[1], Aimee Crago[1]

[1]Memorial Sloan Kettering Cancer Center, New York, NY,[2]NYU Langone Health, New York, NY

Background: Desmoid-type fibromatosis (DT) is a rare mesenchymal neoplasm associated with *CTNNB1* activating. DT have variable biologic behavior not explained by secondary genomic events, and in aggressive tumors, local progression can cause significant morbidity. We performed a druggable genome screen to better understand β-catenin function in DT and nominate potential therapies for DT treatment.

Experimental design: A lentiviral shRNA screen (LT3GEPIR backbone) was performed in a primary DT cell line overexpressing TERT (DES9525T). Cell proliferation, cell cycle, gene expression and protein accumulation/localization after pharmacologic inhibition or gene silencing were assessed by CyQuant, Guava Cell Cycle reagent, RNA-seq, and immunoblot in whole cells or after subcellular fractionation (NE-PER extraction), respectively.

Results: 75 significantly enriched and 20 significantly depleted genes were identified in DT cells. Among the genes that had the most significant effects on proliferation were *MDM2*, *BRD4* ($p<0.001$, FC=0.25, 0.31) and *XPO1* (encoding exportin-1; $p<0.002$, FC=0.26) while shRNA targeting *TP53* and *CDKN1A* induced proliferation. Inhibition of exportin-1 with selinexor or shRNA directed at *XPO1* inhibited proliferation (by 51%, $p<0.05$), but failed to affect β-catenin subcellular localization as in other systems. It did have canonical effects on p53/p21 signaling with increased protein levels observed in treated DT cells. Inhibition of MDM2 with milademetan or shRNA similarly increased p53 and p21 and reduced proliferation (by 60%, $p<0.05$). In both cases, p53 induction was associated with G_1 cell cycle arrest. BRD4 inhibition via shRNA or treatment with birabresib reduced proliferation (85%, $p<0.01$) but did not affect p53/p21 signaling. Instead BRD4 inhibition decreased transcription of genes indirectly regulated by β-catenin including potential oncogenes *TNC*, *TGFBI*, and *PITX2*. RNA-seq, ChIP-seq and ChIP-PCR showed that *BRD4* transcription was directly regulated by β-catenin binding to the gene. *MDM2* transcription was also directly modulated by β-catenin, but in its case β-catenin binding to the gene appeared to result in transcriptional repression.

Conclusion: BRD4, MDM2 and XPO1 were identified as potential therapeutic targets in DT with gene products modulating p53/p21 or β-catenin activity. Both *BRD4* and *MDM2* represent direct transcriptional targets of β-catenin though negative regulation of *MDM2* in the context of DT cell dependency on its protein product suggest secondary genetic events or environmental signaling may be necessary to counteract this potential tumor suppressive effect of β-catenin.

#2989 ONCO Prime platform enables discovery of synthetic lethal targets for genetically stratified cancers.

Andrzej Mazan[1], Eliza Zimolag[1], Joanna Szuszkiewicz[1], Marcin Serocki[1], Oleksii Bryzghalov[1], Izabella Wieckowska[1], Marcelina Chmiel[1], Katarzyna Sarad[1], Julia Wirkijowska[1], Wiktoria Luczak[1], Szymon Woroszylo[1], Dariusz Klonski[1], Kamil Kus[1], Andrew Thomason[1], Michal Mikula[2], Rafal Dziadziuszko[3], Krzysztof Brzozka[1]

[1]Ryvu Therapeutics, Krakow, Poland,[2]Maria Skłodowska-Curie Institute of Oncology, Warsaw, Poland,[3]Medical University of Gdansk, Gdansk, Poland

Colorectal cancer (CRC) remains a leading cause of cancer mortality, underscoring the need for new, mechanism-based therapeutic strategies. Using the ONCO Prime discovery and validation platform, based on genome wide CRISPR/Cas9 screenings across clinically relevant models, we identified novel treatment options for genetically stratified CRC patients The ONCO Prime platform integrates healthy human intestinal stem cells (hISCs), isogenic CRC models carrying key driver mutations (*APC*, *KRAS*), and patient-derived primary cultures. All types of models can be genetically manipulated or used in the high-throughput setting for the drug testing. Transcriptomic and machine learning analyses confirmed that these models faithfully recapitulate CRC molecular diversity and clinical behavior. Systematic CRISPR/Cas9 loss-of-function screenings revealed multiple synthetic lethal (SL) interactions, uncovering target genes with first-in-class therapeutic potential. Additionally, using a clinical grade drug that is FDA-approved in other indications, we achieved proof of concept in genetically stratified CRC models, demonstrating strong efficacy as monotherapy in vitro. These data validate ONCO Prime's translational capability to uncover clinically actionable vulnerabilities and deliver tangible therapeutic candidates. This work provides a robust foundation for drug discovery programs and strategic partnerships built on ONCO Prime's ability to bridge functional genomics with therapeutic development. Our first proof of concept establishes ONCO Prime as a scalable platform to drive the next generation of precision, first-in-class oncology therapies.

#2990 PSMA expression in neoplastic cells and tumor-associated vasculature: A tissue microarray study evaluating 12,409 cancers from 135 different tumor types.

Fiete Gehrisch[1], Alexandra Malinowski[1], Anne Menz[1], Florian Lutz[1], Viktoria Chirico[1], Florian Viehweger[1], David Dum[1], Ria Schlichter[1], Andrea Hinsch[1], Christoph Fraune[1], Christian Bernreuther[1], Seyma Buyucek[1], Martina Kluth[1], Claudia Hube-Magg[1], Georgia Makrypidi-Fraune[1], Nina Schraps[1], Katharina Moller[1], Andreas M. Luebke[1], Patrick Lebok[1], Guido Sauter[1], Maximilian Lennartz[1], Frank Jacobsen[1], Till S. Clauditz[1], Andreas H. Marx[2], Ronald Simon[1], Stefan Steurer[1], Eike Burandt[1], Nathalia Gorbokon[1], Maria C. Tsourlakis[1], Sarah Minner[1], Till Krech[1], Morton Freytag[1], Viktor Reiswich[1]

[1]Institute of Pathology, University Medical Center Hamburg-Eppendorf, Hamburg, Germany,[2]Department of Pathology, Academic Hospital Fuerth, Fuerth, Germany

Prostate-specific membrane antigen (PSMA) is a transmembraneous glycoprotein that serves as a diagnostic and therapeutic target in prostate cancer. Beyond prostate malignancies, PSMA expression can also be detected in tumor cells and in endothelial cells (ECs) of newly formed, tumor-associated blood vessels across various other malignancies. To evaluate the prevalence of PSMA expression in both tumor cells and tumor-associated neovasculature, 12,409 tumors from 135 different tumor types, were analyzed by immunohistochemistry in a tissue microarray format. PSMA positivity in tumor cells was detected in 46 tumor entities, including 13 with at least one strongly positive case. Tumor cell PSMA positivity was frequently observed in prostatic adenocarcinoma (84.2-98.7%), granular cell tumor (76.5%), basal cell adenoma of the salivary gland (64.3%), as well as in endometrial (up to 60.7%) and ovarian carcinomas (up to 13.8%). In prostate cancer, PSMA expression was higher in Gleason 4+4 and 5+5 cancers (96.4-98.7%) compared to Gleason 3+3 cancers (94.7%), while it was lowest in recurrent cancers after hormonal therapy (84.2%; p<0.0001). In breast cancer of no special type, PSMA positivity was linked to high grade (p=0.0451), ER- (p=0.0279), and PR-negativity (p=0.0135). PSMA positivity in ECs of tumor-associated vasculature occurred in 4,888 of 10,658 (45.9%) tumors. 123 tumor entities had at least one case with PSMA positive ECs, 106 included at least one sample with many PSMA-positive vessels and 102 had at least one case with strong vessel positivity. EC PSMA positivity was most frequent in renal cell carcinoma (RCC) (88.7-88.9%), adenocarcinoma of the uterine cervix (82.4%) endometrioid endometrial carcinoma (76.7%), colorectal adenocarcinoma (70.5%), cholangiocarcinoma (66.7%), chondrosarcoma (63.5%), HCC (62.5%), and squamous cell carcinomas from different sites (up to 88.2%). The number of positive vessels tightly correlated with their staining intensity (<0.0001) and both parameters were often associated with features of cancer aggressiveness. PSMA staining quantity and intensity in vessels were associated with tumor stage (p=0.0343), tumor grade (p<0.0001), ER- (p=0.0002) and PR-negativity (p=0.0351) in invasive breast carcinoma, multiple grading and staging systems (p=0.0022-0.0388) in clear cell RCC, Fuhrman grade (p=0.0091) and metastatic disease (p=0.0175) in papillary RCC, pT stage (p<0.0001) in urothelial carcinoma, pT stage (p=0.0459), nodal positivity (p=0.0089) and lymphatic invasion (p=0.0023), mismatch repair (MMR) deficiency (p=0.0178) and *BRAF* mutations (p=0.0026) in colorectal adenocarcinoma, and MMR deficiency (p=0.0089) in gastric adenocarcinoma. It is concluded that PSMA expression in tumor cells is largely limited to few cancer entities while EC positivity is common in a broad range of cancer types.

#2991 Superior detection of NTRK fusions across Chinese solid tumors using amplicon-based DNA and RNA NGS co-detection compared with hybrid-capture DNA-NGS.

Mingqian Lu

Yichang Central People's Hospital, Yichang City, China

Background: NTRK fusions are clinically actionable drivers across many solid tumors, with several tumor-agnostic targeted therapies approved. Traditional DNA-based assays often lack sensitivity for NTRK rearrangements. Although RNA-NGS improves fusion detection, the relative performance of amplicon-based DNA+RNA NGS co-detection versus hybrid-capture DNA-NGS for identifying NTRK fusions in pan-solid tumors remains unclear.
Methods: This study analyzed NTRK fusion detection across 16,546 tumors using a 35-gene amplicon-based DNA+RNA NGS co-detection and 4,709 tumors using hybrid-capture DNA-NGS. Tumor types included BRCA, COAD, HNSC, melanoma, NSCLC, PAAD, SARC, THCA, BTC, and STAD. Specifically, the co-detection cohort consisted of BRCA (27), COAD (3,839), HNSC (39), melanoma (111), NSCLC (11,242), PAAD (89), SARC (61), THCA (62), BTC (310), and STAD (766), whereas the DNA-NGS cohort included BRCA (126), COAD (857), HNSC (79), melanoma (42), NSCLC (2,504), PAAD (184), SARC (67), THCA (62), BTC (398), and STAD (446).
Results: Amplicon-based DNA+RNA NGS co-detection demonstrated higher NTRK fusion positivity across multiple solid tumors, including BRCA (2/27, 7.41%), COAD (7/3,839, 0.19%), HNSC (1/39, 2.56%), melanoma (1/111, 0.90%), NSCLC (18/11,242, 0.16%), PAAD (2/89, 2.25%), SARC (1/61, 1.64%), and THCA (1/62, 1.61%), with no NTRK fusions detected in BTC or STAD. All 33 fusions detected by Amplicon-based DNA+RNA NGS were classical 5′-3′ events, with predominant fusion partners including TPM3-NTRK1(42.42%), SQSTM1-NTRK3(12.12%), CD74-NTRK1(9.09%), and several rare forms involving LMNA-NTRK1(3.03%), KIF5B-NTRK2(3.03%), ETV6-NTRK3(21.21%), AKAP13-NTRK3(3.03%), CD74-NTRK3(3.03%), EML4-NTRK3(3.03%). In contrast, hybrid-capture DNA-NGS showed generally lower detection rates across the same tumor types, identifying only sporadic NTRK-positive cases in COAD (1/857, 0.12%), NSCLC (4/2,504, 0.16%), BTC (1/398, 0.25%, NTRK1), and STAD (1/446, 0.22%), and none in BRCA, HNSC, melanoma, PAAD, SARC, or THCA. Among the fusions detected by hybrid-capture DNA-NGS, all but one were classical 5′-3′ rearrangements; a single NSCLC case harbored a non-canonical 5′-5′ ETV6-NTRK3 fusion. Fusion partners detected by this method included PIGR-NTRK1, NTRK1-RHBG, NTRK1-HAPLN2, NTRK1-S100A12, NTRK2-TMPRSS2, and ETV6-NTRK3. Collectively, co-detection demonstrated a markedly broader fusion spectrum and substantially improved sensitivity, particularly in BRCA, COAD, HNSC, and PAAD.
Conclusion: Amplicon-based DNA+RNA NGS outperformed hybrid-capture DNA-NGS in sensitivity and fusion-partner breadth, highlighting the importance of RNA analysis in routine testing for NTRK-guided tumor-agnostic therapy.

#2992 The role of FOXD1 in the anaplastic transformation of thyroid cancer.

Aki Inase[1], Mitsuyoshi Hirokawa[2], Miyoko Higuchi[2], Naoyoshi Onoda[3], Takuya Higashiyama[3], Taiji Koyama[1], Shiro Kimbara[1], Masanori Teshima[4], Hironobu Minami[1], Ken-Ichi Nibu[4], Mitch A. Phelps[5], Naomi Kiyota[1]

[1]Department of Medical Oncology and Hematology, Kobe University Graduate School of Medicine, Kobe, Japan,[2]Department of Diagnostic Pathology and Cytology, Kuma Hospital, Kobe, Japan,[3]Department of Surgery, Kuma Hospital, Kobe, Japan,[4]Department of Otorhinolaryngology-Head and Neck Surgery, Kobe University Graduate School of Medicine,, Kobe, Japan,[5]Ohio State University College of Pharmacy, Columbus, OH

Background: Anaplastic thyroid carcinoma (ATC) is a rare and highly aggressive malignancy. ATC can occur *de novo*, but accumulating pathological and genomic evidence suggests that a subset may arise through progressive dedifferentiation of pre-existing differentiated thyroid carcinoma (DTC), most commonly papillary thyroid carcinoma (PTC). Supporting this concept, coexistent PTC has been reported in approximately 20-30% of ATC cases, and genomic studies indicate that additional somatic alterations—such as TERT promoter and TP53 mutations—may drive this transition. However, the molecular mechanisms underlying this dedifferentiation process remain poorly understood. To address this gap, we compared gene expression profiles between well-differentiated PTC regions and undifferentiated ATC regions within the same tumors.
Methods: RNA was extracted from well-differentiated and undifferentiated regions of the same tumor specimens (FFPE) obtained from six ATC cases. After RNA extraction, RNA libraries were prepared and sequenced using the Illumina NovaSeq 6000 platform, and comparative gene expression analysis was performed. To evaluate the impact of FOXD1 (Forkhead Box D1) on chemosensitivity, siRNA-mediated knockdown was performed, and cell viability after doxorubicin or paclitaxel treatment was assessed using the CCK-8 assay in two ATC cell lines (OCUT-1C and OCUT-1F). To investigate the regulatory mechanism of FOXD1 expression, methylation analysis of the FOXD1 promoter region was performed by bisulfite sequencing in a PTC cell line (KTC-1), OCUT-1C, and OCUT-1F.
Results: Gene expression and KEGG pathway analyses showed EMT activation in ATC. Among transcription factors upregulated in the undifferentiated regions, FOXD1 was consistently overexpressed and therefore selected for further investigation. TGF-β-induced EMT of KTC-1 cells increased the expression of FOXD1 and the EMT-related transcription factors SNAI1 and SNAI2. qRT-PCR analysis revealed that siRNA suppression of FOXD1 altered the expression of EMT-related genes (CDH1, CDH2, SNAI1, SNAI2), whereas knockdown of SNAI1/2 did not affect FOXD1 expression. In both OCUT-1C and OCUT-1F cell lines, FOXD1 suppression restored sensitivity to doxorubicin and paclitaxel. Bisulfite sequencing revealed that the FOXD1 promoter was demethylated in OCUT-1C and OCUT-1F compared to KTC-1.
Conclusions: These findings suggest that FOXD1 contributes to the dedifferentiation process from PTC to ATC. Moreover, restoration of chemosensitivity upon FOXD1 knockdown indicates that FOXD1 could be a promising therapeutic target for ATC. Future studies will further validate FOXD1 expression in additional clinical samples and perform functional analyses using FOXD1-knockout cell lines.

#2993 Deciphering the key role of the glycosyltransferase GALNT14 in osteosarcoma tumorigenesis.

D. Isabel Petrescu[1], Tajhal D. Patel[2], Shoshana Leeds[3], Jeffrey Ritzenthaler[4], Heath Bradley[4], Juan Dou[4], Jason T. Yustein[4]

[1]Graduate Program in Genetics and Molecular Biology, Emory University, Atlanta, GA,[2]Dept of Pediatric Oncology, Baylor College of Medicine, Houston, TX,[3]College of Arts and Sciences, Emory University, Atlanta, GA,[4]Aflac Cancer and Blood Disorders Center, Emory University, Atlanta, GA

Osteosarcoma (OS) is the most common primary malignant bone tumor with bimodal incidence by predominantly affecting adolescents and adults 60 years of age and older. Current treatment of OS commonly involves surgical resection and neoadjuvant and adjuvant chemotherapy, which remains insufficient to improve survival for patients with refractory or relapsed OS. We have identified the glycosyltransferase GALNT14 as a potential therapeutic target for OS by incorporating gene expression data from the NIH TARGET database and transcriptomic analysis of institutional patient-derived xenografts (PDXs) from patient tumors demonstrating chemoresistance. High expression of *GALNT14* in patient tumors is associated with reduced survival likelihood and chemosensitivity compared to patient tumors with low *GALNT14* expression. By comparing samples based on percent necrosis, we determined that *GALNT14* is significantly upregulated in patient samples with low (<90%) necrosis, which is associated with reduced overall and relapse-free survival. To gain further insights into the role of *GALNT14* in OS tumorigenesis and chemosensitivity, we have established *in vitro* and *in vivo* OS models of altered *GALNT14* expression either by knock-out (KO) models in high-expressing *GALNT14* OS cell lines or *GALNT14* overexpression (OE) models in low-expressing *GALNT14* OS cell lines. KO models were established by using CRISPR-Cas9 gRNA targets against *GALNT14* in human OS cell lines. OE models were established using lentiviral transduction of human OS cell lines using a vector expressing *GALNT14*. *In vitro* studies demonstrated that loss of *GALNT14* increased chemosensitivity and decreased metastatic potential, assessed through transwell invasion and migration assays. Furthermore, sarcosphere assays demonstrated decreased stem cell properties in our *GALNT14* KO models. We observed reverse effects by *in vitro* studies of cell lines with overexpression of *GALNT14*, suggesting a specific role for *GALNT14* in OS tumorigenesis. In addition, orthotopic *in vivo* studies using immunodeficient mice injected with *GALNT14* KO cell lines displayed decreased tumor growth and metastasis. RNA sequencing comparing *GALNT14* KO and OE models revealed gene signatures and biological pathways related to immune function, leading us to develop syngeneic models of *GALNT14* OE in murine OS cell lines derived from genetically-engineering murine models (GEMMs). We have validated these models at the protein level and are currently assessing their *in vitro* and *in vivo* characteristics. Our results suggest a role for *GALNT14* in contributing to OS tumorigenesis by mechanisms related to therapeutic resistance, metastatic potential, stem cell properties, and/or immune function. Further studies are ongoing to strengthen our mechanistic understanding of the downstream effects dependent on *GALNT14* expression.

#2994 Integrative pathway analysis of I-SPY2 HER2+ breast cancers reveals drug-repurposing opportunities.

Kingsley V. Chow[1], Tam Binh Bui[1], Denise M. Wolf[2], Annuska Glas[3], Zheyun Xu[4], Gillian L. Hirst[5], I-SPY2 investigators, Amy Clark[6], Julia Wulfkhule[7], Angie DeMichele[8], Emanuel Frank Petricoin[7], Laura J. Esserman[5], Jennifer Rosenbluth[9], Laura van 't Veer[1], Rosalyn W. Sayaman[1]

[1]UCSF - University of California San Francisco, San Francisco, CA,[2]UCSF - University of California San Francisco, Berkeley, CA,[3]Quantum Leap Healthcare Collaborative, San Francisco, CA,[4]Yale University, New Haven, CT,[5]UCSF Helen Diller Family Comprehensive Cancer Ctr., San Francisco, CA,[6]University of Pennsylvania-Penn Presbyterian, Philadelphia, PA,[7]George Mason University, Manassas, VA,[8]University of Pennsylvania, Philadelphia, PA,[9]UCSF - University of California San Francisco, Boston, MA

Background: HER2-positive breast cancer (HER2+) accounts for approximately 20% of all breast cancers. Major advances in HER2-targeted therapy have improved outcomes; however, substantial room for response improvement remains. Molecular subtyping by BluePrint (BP) stratifies HER2+ disease into HER2 and Luminal types. While BP-HER2 tumors achieve up to 78% pathologic complete response (pCR) with standard therapy, BP-Luminal tumors exhibit persistently low pCR rates (<15%). To address this unmet need, we profiled pretreatment molecular features distinguishing responders from non-responders across all HER2+ tumors and within BP subtypes to identify druggable pathways for rational combination or repurposing strategies.
Methods: Baseline microarray profiles from 305 pretreatment HER2+ tumors (87 BP-Luminal, 218 BP-HER2) enrolled across five investigational agents or standard of care in the I-SPY2 trial were analyzed using Gene Set Variation Analysis (GSVA) across 2,265 canonical pathway gene sets. Differential pathway enrichment was assessed using linear models adjusting for treatment arm and false-discovery rate. Two comparisons were performed: (1) pCR vs. no pCR overall and within subtypes, and (2) BP-HER2 vs. BP-Luminal. Shared response- and subtype-specific pathways were grouped by functional similarity and cross-referenced with drug-target databases to identify FDA-approved or investigational compounds.
Results: Across HER2+ tumors and within BP-HER2, we identified 42 pathways enriched in non-responders that were also elevated in BP-Luminal relative to BP-HER2, suggesting a luminal-linked resistance program even in non-luminal tumors. These pathways converged into eight metabolic and signaling themes. Growth-factor/RTK bypass (PI3K/AKT) and DNA repair & oxidative stress defense were strongly upregulated in non-responders within BP-HER2, revealing actionable nodes involving PI3K/AKT (alpelisib, capivasertib), IGF1R (linsitinib), MET (crizotinib, capmatinib), and DNA repair (PARP inhibitors). Notably, metabolic rewiring and lipid homeostasis—targetable by vismodegib and sonidegib—were upregulated in non-responders across both BP subtypes, reflecting a shared metabolic vulnerability.
Conclusions: Luminal biology-linked transcriptional programs may persist within the HER2+ BP-HER2 subtype and contribute to resistance. BP-HER2 non-responders exhibit coordinated activation of RTK-bypass and DNA repair pathways, exposing therapeutic vulnerabilities targetable by existing agents. Furthermore, targeting lipid metabolic reprogramming alongside anti-HER2 therapy may enhance efficacy and overcome resistance across both BP subtypes. Our future directions include testing these drug combinations in patient-derived HER2+ organoid models.

#2995 ATRX in-frame fusions promote endogenous chemoresistance programs but yield immunotherapeutic vulnerabilities in neuroblastoma.

Mohammad Ali Mohammad Nezhady[1], Sheetal Bhatara[1], Siarhei Hladyshau[1], Estevez Prado Daniel[1], Vernon Ebegboni[1], Alja Kozulic-Pirher[2], Arnav Barpujari[3], Bo Wang[1], Yuan Feng[1], Qiqi Jin[1], Xueying Liu[1], Paul Geeleher[1], Xiaotu Ma[1], Jiyang Yu[1], Emily Bernstein[2], Kelly Goldsmith[3], Hunter Jonus[3], Adam D. Durbin[1]

[1]St. Jude Children's Research Hospital, Memphis, TN,[2]Icahn School of Medicine at Mount Sinai, New York, NY,[3]Emory University, Atlanta, GA

High-risk Neuroblastomas (NB) carrying in-frame fusion mutations in the ATRX chromatin remodeler("ATRX-IFF") are chemoresistant, and children with these mutations display poor overall survival. There are no specific agents to target these tumors, and the mechanisms driving chemoresistance remain unknown. To gain insight into the mechanisms of chemoresistance, we used scRNAseq in combination with cisplatin to study if cellular plasticity drives chemoresistance. In contrast to non-ATRX-IFF-bearing NBs, *ATRX*-IFF NBs did not appear to display transcriptionally plastic subpopulations, suggesting that the *ATRX*-IFF promotes an inherent chemoresistance program. To this end, CRISPR-mediated engineering of *ATRX*-IFF into the endogenous locus in wildtype cells, results in enhanced chemoresistance to multiple clinically-used agents. Next, to identify potential targetable proteins directly regulated by the ATRX-IFF, we combined chromatin binding assays with cell surface proteomics. Using cell lines and orthotopic PDXs, we identified that the ATRX-IFF binds to, and nucleates a super-enhancer at the *PTK7* locus, thereby driving extremely high level cell surface expression of PTK7. PTK7 is a pseudokinase receptor that is targeted by experimental CAR-T cell therapies in active preclinical development. Ongoing work is aimed at understanding the dependency of PTK7 on the ATRX-IFF, and using preclinical CAR-T cell models to target PTK7 in *ATRX*-IFF NB.

#2996 Internalization of B7-H3 is enhanced by cholesterol disruption in esophageal cancer cells.

Takashi Imajima, Kenji Tsuchihashi, Takafumi Kitazono, Wataru Kusano, Eishi Baba

Kyushu University, Fukuoka, Japan

B7-H3, a member of the B7-family protein, is highly expressed on cancer cells. An antibody-drug conjugate (ADC) targeting B7-H3 showed potential efficacy in early-phase clinical trials. As endocytosis and subsequent degradation of the ADC drugs are the key processes to release the payload and demonstrate cellular toxicity, alteration in the endocytosis pathway could play a role in the resistance mechanisms or synergistic therapeutic effects. As for HER2-targeted ADCs, one of the most developed ADC targets, some preclinical trials reported a synergistic effect of HER2-targeted ADCs and modulators on the dynamics of HER2 on the cellular membrane, such as membrane cholesterol and HSP90. However, such machinery for B7-H3 and the targeting antibody remains unclear. Thus, we hypothesized that modulating the stability of the membrane B7-H3 could have a synergistic effect with B7-H3 ADC. Using flow cytometry, we evaluated the decrease of surface expression of the targeted antigens as a surrogate marker of their internalization efficacy in TE4, an esophageal squamous cell carcinoma cell line, which showed high expression of both B7-H3 and HER2. Trastuzumab and enoblituzumab, anti-HER2 and -B7-H3 antibodies, respectively, were used to induce endocytosis of target antigens. We validated that there was no epitope interference between therapeutic antibodies, trastuzumab or enoblituzumab, and fluorescent-labelled antibody to detect HER2 or B7-H3. Internalization efficacy was evaluated by comparing surface expression of HER2/B7-H3, between trastuzumab/enoblituzumab and an isotype antibody. The stability at the membrane was modulated by two drugs, pimitespib, an inhibitor of HSP90, and methyl-beta-cyclodextrin (MbCD), a cholesterol disruptor. In flow cytometry analysis, neither pimitespib nor MbCD did not affect the cell surface expression of HER2 and B7-H3. While the pimitespib enhanced trastuzumab-mediated HER2 internalization, enoblituzumab-mediated B7-H3 internalization was not affected. Under MbCD treatment, surface expression of both HER2 and B7-H3 was markedly decreased after administration of targeted antibodies. Additionally, fluorescent immunocytochemistry showed the enhanced internalization of HER2 and B7-H3 molecules at the cell membrane into the cytoplasm. These results suggest that membrane cholesterol, rather than HSP90, might affect the stability of B7-H3 on the cell membrane. In conclusion, membrane cholesterol disruption could enhance the internalization efficacy of HER2 and B7-H3 molecules.

#2997 LTA4H promotes intrahepatic cholangiocarcinoma progression via mTOR activation and T-cell exhaustion.

Ganglian Lin[1], Jinhui Wang[1], Yizhuo He[2], Fangkai Feng[2], **Chongming Zheng**[2], Yi Wang[2]

[1]The First Affiliated Hospital of Wenzhou Medical University, Wenzhou, China,[2]Wenzhou Medical University, Wenzhou, China

Introduction: Intrahepatic cholangiocarcinoma (ICC) is a highly aggressive liver cancer with a poor prognosis. Immune evasion plays a critical role in ICC progression. Leukotriene A4 hydrolase (LTA4H), a key enzyme in eicosanoid metabolism, is overexpressed in multiple cancer types; however, its role and mechanism in ICC remain entirely unexplored.

Methods: LTA4H expression and its prognostic significance were assessed in two independent ICC cohorts (n=130) and cell lines using bioinformatics, immunohistochemistry (IHC), and western blot (WB). LTA4H was genetically modulated in ICC cell lines via lentiviral transduction. Functional impacts on proliferation, migration, and invasion were evaluated by colony formation, real-time cellular analysis, wound healing, and Transwell assays. Spontaneous ICC was modeled in mice via hydrodynamic tail vein injection of a plasmid combination comprising pT3-EF1α-myr-AKT, pT3-EF1α-myr-NICD, and pCMV-SB. Mechanistic insights were investigated through RNA sequencing, metabolomics, and WB. Tumor immune microenvironment was profiled by flow cytometry. The therapeutic efficacy of the LTA4H-specific inhibitor LYS006 was tested in vivo and in patient-derived organoids.

Results: LTA4H was significantly overexpressed in ICC tissues and correlated with poor patient survival. LTA4H overexpression enhanced ICC cell proliferation, migration, and invasion in vitro, and accelerated tumor progression in vivo. Conversely, LTA4H knockdown suppressed these malignant phenotypes. Mechanistically, LTA4H activated the mTOR signaling pathway and induced T-cell exhaustion in the tumor microenvironment. Therapeutic inhibition of LTA4H with LYS006 significantly suppressed tumor growth in mouse models and organoids.

Conclusions: Our study identifies LTA4H as a novel oncoprotein in ICC that drives tumor progression by activating the mTOR pathway and fostering an immunosuppressive microenvironment via T-cell exhaustion. Targeting LTA4H represents a promising therapeutic strategy for ICC.

Clinical Significance: This work unveils the dual pro-tumorigenic functions of LTA4H in ICC and provides a strong rationale for targeting LTA4H, potentially alone or in combination with immunotherapy, for the treatment of this lethal disease.

#2998 Disrupted clock pathway during lineage plasticity and prostate cancer progression.

Nishat Manzar, Himisha Beltran

Department of Medical Oncology, Dana-Farber Cancer Institute, Boston, MA

Most treatment resistant prostate cancers are driven by androgen receptor (AR) signaling. However, AR-negative prostate cancer has been increasingly recognized as the mechanism of resistance, particularly as potent AR-targeted therapies have been introduced earlier in the treatment paradigm. Lineage plasticity and histologic transformation of AR-driven prostate adenocarcinoma to AR-negative neuroendocrine prostate cancer (NEPC) represents one of the most lethal forms of prostate cancer. Here, we explored how the circadian clock pathway changes occur during lineage plasticity and prostate cancer progression. We identified loss of rhythmicity in the expression of clock regulated genes. Clock pathway regulators RORα, BMAL1, and CLOCK are highly expressed in NEPC compared to prostate adenocarcinoma. *RORA* displays marked upregulation in prostate tumors after AR targeted therapy relative to matched pre-therapy tumors. *RORA* overexpression in prostate adenocarcinoma models led to increased cell proliferation and enriched cell cycle pathway. Importantly, we noted that clock pathway is reprogrammed differently in AR-dependent and AR-independent prostate tumors. For instance, *RORA* overexpression in AR-dependent adenocarcinoma cells resulted in enriched androgen response and enhanced sensitivity towards AR-targeted pathway inhibitors. *RORA* knockout in AR-independent models resulted in increased expression of mitochondrial genes and increased sensitivity towards oxidative phosphorylation (OXPHOS) inhibitors. Moreover, targeting RORα in NEPC patient-derived organoids and mouse xenograft models abrogated tumor growth and downregulated the NEPC phenotype. Altogether, our findings point to a mechanistic regulation of clock genes including RORα during prostate cancer progression and nominates potential new strategies to target lineage plasticity.

#2999 Targeting cholesterol pathways in p53 deficient head and neck cancers.

Jovanka Gencel-Augusto[1], Nuo Tian[1], Akshat Singhal[2], Hua Li[3], Liam Woerner[3], Arthur Goldberg[1], Daniel E. Johnson[4], Jennifer Rubin Grandis[5]

[1]Otolaryngology - Head and Neck Surgery, UCSF - University of California San Francisco, San Francisco, CA,[2]UCSD Medical Ctr., San Diego, CA,[3]The University of California, San Francisco, San Francisco, CA,[4]Associate Professor, Dept. of Med. & Pharmacology, UCSF Helen Diller Family Comp. Cancer Center, San Francisco, CA,[5]UCSF - University of California San Francisco, San Francisco, CA

Loss of p53 function is a major driver of poor outcomes in HNSCC, with over 70% of tumors harboring deactivating *TP53* mutations. Despite decades of effort, mutant p53 remains “undruggable”. Cholesterol is essential for membrane integrity and oncogenic signaling, and elevated cholesterol levels correlate with aggressiveness across many cancers. In HNSCC, patients whose tumors express high levels of cholesterol-upregulating genes have a 50% higher risk of death, highlighting this pathway as a clinically relevant therapeutic target. We previously showed that HPV+ HNSCC cells retain wild-type (WT) p53 activity and that p53 transcriptionally regulates multiple metabolic pathways, including cholesterol-regulating genes. These observations led us to investigate how p53 loss rewires cholesterol metabolism and whether this metabolic shift creates a targetable vulnerability in p53-deficient HNSCC. Silencing WT p53 in HPV+ HNSCC cells (siRNA or CRISPRi) increased intracellular cholesterol and proliferation - an effect reversed by cholesterol deprivation. This p53 deficiency also elevated expression and maturation of SREBP1/2, master transcriptional regulators of cholesterol metabolism, along with multiple downstream SREBP targets. Elevated cholesterol and activated SREBP1/2 were similarly observed in HPV-negative p53-mutant HNSCC lines, indicating that p53-dependent cholesterol metabolism is a broader function independent of HPV status. In HNSCC patient-derived xenografts (PDXs), p53-mutant tumors exhibited higher expression and preferential nuclear localization of SREBP1 compared to p53-WT tumors, confirming cholesterol pathway reprogramming *in vivo*. To test pathway dependency, we examined the effects of SREBP1 genetic ablation (via siRNA or in CRISPR knock-out datasets) in HNSCC and other squamous carcinoma lines. SREBP1 loss selectively reduced viability in p53-deficient cells compared with WT counterparts. Pharmacologic inhibition of SREBP1/2 with the small molecule fatostatin also produced an average 2.7-fold greater cytotoxic response in p53-deficient versus p53-proficient HNSCC lines. In isogenic cell line-derived xenograft (CDX) models, fatostatin treatment (315 mg/kg over 32 days) significantly suppressed growth of p53-deficient tumors. A pan-cancer pharmacogenomic screen of >900 cell lines further identified p53 deficiency as a determinant of fatostatin sensitivity. Together, these findings demonstrate that p53 loss confers dependency on SREBP-driven cholesterol metabolism and support therapeutic targeting of this pathway in a genomically defined subset of HNSCC.

#3000 Tumor Treating Fields (TTFields) may weaken glioblastoma network connectivity, with implications for malignancy.

Julius Beichert[1], Jonas A. Kretz[2], Jena Kim[1], Xiaoyu Ma[3], Daniel Dominguez Azorin[2], Andreas E. Moor[2], Haikun Liu[3], **Miriam Ratliff**[1]

[1]Department of Neurosurgery, University Hospital Mannheim, Medical Faculty Mannheim, University of Heidelberg and German Cancer Research Center (DKFZ), Mannheim, Heidelberg, Germany,[2]Department of Biosystems Science and Engineering, ETH Zurich, Basel, Switzerland,[3]Molecular Neurogenetics, German Cancer Research Center (DKFZ), Heidelberg, Germany

Background: Glioblastoma malignancy is strongly driven by the formation of tumor microtubes (TMs), which promote intercellular connectivity and calcium (Ca^{2+}) wave propagation. The mechanisms by which Tumor Treating Fields (TTFields) influence these TM-mediated processes remain incompletely understood.
This study aims to elucidate the effects of TTFields on the structural and functional organization of tumor cell networks and to assess potential frequency-dependent modulation of signaling pathways, including NF-κB.
Methods: A comprehensive set of biological model systems is being utilized, including 2D glioblastoma cell monolayers, 3D brain organoids, and *in vivo*, awake, head-fixed mouse models with chronic cranial windows for longitudinal imaging. Live-cell imaging with confocal and multiphoton microscopy enables real-time observation of morphological and functional tumor dynamics. Quantification of Ca^{2+} signaling is being performed using Cellpose-based segmentation and custom Python analysis pipelines. Immunohistochemistry and spatial transcriptomics (Visium HD) are currently employed to dissect molecular mechanisms; COMET-based immunofluorescence and RNAscope FISH are planned to enable spatially resolved multi-omics.
Results: TTFields induced a marked disruption of glioblastoma network architecture and function. Specifically, treatment resulted in >50% reduction in global GCaMP8s-mediated Ca^{2+} activity, a decrease in pacemaker-like cell populations, and significant reductions in synchronization and Ca^{2+} co-activity within S24 glioblastoma cells in both 2D and 3D models.
Conclusion & Outlook: TTFields disrupt glioblastoma network integrity and Ca^{2+} signaling, potentially reducing tumor aggressiveness. Preliminary data from 3D brain tumor organoids and *in vivo* models support our previous *in vitro* results regarding TTFields-induced activity changes. Parallel studies in patient-derived organoids explore frequency-dependent signaling effects - including NF-κB and MAPK pathways - via spatial transcriptomic profiling. Together, these efforts aim to further elucidate the mechanistic underpinnings of TTFields action and their impact on glioblastoma plasticity and network organization.

#3001 Therapeutic inhibition of oncogenic miR-181a processing for cancer therapy.

Grace McIntyre[1], Jessica Mathew[2], Zoe Jackson[3], Meghana Choragudi[4], Madison Uyemura[1], Aaron Robida[5], Renju Jacob[5], Jose Colina[1], Jiaming Yao[6], Hang Yang Wong[7], Rachel Offenheim[8], Mark Kunkel[9], Sriram Chandrasekaran[3], Peter Toogood[7], Analisa DiFeo[1]

[1]Department of Pathology, University of Michigan, Ann Arbor, MI,[2]Chemistry, College of Literature, Science, and the Arts, University of Michigan, Ann Arbor, MI,[3]Biomedical Engineering, University of Michigan, Ann Arbor, MI,[4]School of Public Health, University of Michigan, Ann Arbor, MI,[5]Center for Chemical Genomics, University of Michigan, Ann Arbor, MI,[6]College of Literature, Science, and the Arts, University of Michigan, Ann Arbor, MI,[7]College of Pharmacy, University of Michigan, Ann Arbor, MI,[8]Medical School, Queens University, Kingston, ON, Canada,[9]Frederick National Laboratory of Cancer Research, National Cancer Institute, Frederick, MD

Background: Oncogenic microRNA-181a (miR-181a) is a master regulator of tumor pathogenesis, driving cancer initiation, progression, metastasis, and immune evasion across diverse cancer lineages by suppressing critical pathways such as STING, WNT, and TGFβ signaling. While genetic ablation of miR-181a is potently anti-tumorigenic and well tolerated, no therapies currently exist targeting miR-181a, presenting a critical therapeutic gap. Targeting miR-181a offers a promising strategy as it regulates multiple oncogenic pathways simultaneously, unlike existing therapies that act on a single target. Nucleotide-based miRNA-targeting therapies have made significant advances with more than 1,300 clinical trials having been conducted to target miRNAs; yet challenges remain in bioavailability, stability, and effective delivery. Therefore, a small molecule pharmacological strategy targeting miR-181a processing represents an attractive alternative with superior pharmacokinetic properties, improved stability, and enhanced delivery potential. Here, we report the discovery and characterization of SMIR-181s (Small Molecule Inhibitors of miR-181a), a novel class of compounds that alter miR-181a biogenesis and suppress cancer properties.

Results: Using a high-throughput biosensor-based screening platform in miR-181a dependent cancer lines, we identified a novel small molecule inhibitor of miR-181a biogenesis. Screening identified a class of seven SMIR-181s, that impair miR-181a maturation, resulting in the accumulation of precursor miR-181a accumulation and depletion of mature. Mechanistic studies reveal that SMIR-181s mediate this depletion by inducing degradation of TARBP2 (Trans-Activating Responsive Binding Protein 2), an RNA-binding protein that acts as a rheostat for stress-induced miRNAs such as miR-181a. Importantly, SMIR-181s display broad cytotoxicity across the NCI-60 cancer cell line panel, with enhanced efficacy in miR-181a high tumor cells while sparing normal cells. Furthermore, these compounds trigger apoptosis and exhibit a novel mechanism of action distinct from all known agents in the NCI-60 database.

Conclusions: Collectively, this work emphasizes miR-181a's potential as a predictive biomarker, establishes proof-of-concept for small molecules that target miRNA processing, and nominates the SMIR-181 class as first-in-class candidates for the treatment of a broad spectrum of miR-181a-driven malignancies.

#3002 Aneuploidy as a metabolic liability: Exploiting novel therapeutic targets in squamous cell carcinomas.

Nadja Zhakula[1], Sejal Jain[2], Zeinab Amini-Farsani[1], Jiankang Zhang[1], Mari Nakamura[1], Laura Byron[3], Joan J. Castellano-Perez[1], Tannishtha Reya[1], Matthew L. Meyerson[2], Alison M. Taylor[4]

[1]Columbia University Irving Medical Center, New York, NY,[2]Dana-Farber Cancer Institute, Boston, MA,[3]Rutgers University, New Brunswick, NJ,[4]Columbia University, New York, NY

Squamous cell carcinomas (SCCs) across epithelial tissues of the lung, head and neck, and esophagus lack canonical oncogenic mutations and urgently require therapeutic strategies. Aneuploidy—chromosomal gains or losses, is detrimental in normal cells yet occurs in >90% of solid tumors in tissue-specific patterns. SCCs exhibit near-universal chromosome 3q gain, which associates with progression, metastasis, and therapy resistance; however, the mechanisms linking aneuploidies to tumorigenesis remain unclear. To investigate aneuploidy-driven dependencies, we engineered isogenic human lung epithelial cells modeling chromosome 3 disomy and 3q gain and performed genome-wide CRISPRi and drug-repurposing screens. Both screens converged on a lipid metabolism dependency specific to 3q gain, with heightened sensitivity to disruption of the sterol regulatory element-binding protein (SREBP) pathway. *SREBF1* emerged as the top genetic hit, while statins (HMGCR inhibitors), were the strongest chemical hits and preferentially induced apoptosis in 3q gain cells. Rescue with mevalonate confirmed on-target effects and additional cholesterol-lowering drugs also induced increased cytotoxicity. Transcriptomic and lipidomic profiling revealed altered cholesterol and fatty acid biosynthesis programs and distinct lipid composition in 3q gain cells. Protein and immunofluorescence analyses further demonstrated impaired SREBP1 activation in 3q gain cells. To identify potential causal gene drivers, we performed a chromosome 3q-focused CRISPRi screen alongside SREBP/HMGCR inhibition. This screen revealed multiple gene candidates—including *TFG*, *SEC62*, *SERP1*, and *RAB43*—whose knockdown rescued drug-induced loss of viability, implicating ER-to-Golgi transport and cellular stress pathways in altered SREBP1 activation. Ongoing studies are determining whether these mechanisms directly explain reduced pathway activation in 3q gain cells. To assess translational relevance, we validated these dependencies in isogenic organoids and SCC cell lines. *In vivo* xenograft studies demonstrated that 3q gain SCC tumors exhibit increased sensitivity to suppression of SREBF1 and HMGCR, leading to reduced tumor volume and weight. These findings support chromosome 3q gain as a biomarker of pathway inhibitor response. Together, our results define an aneuploidy-driven, targetable metabolic vulnerability in SCC. Chromosome 3q gain imposes a metabolic cost that creates actionable therapeutic dependencies, nominating lipid metabolism and mevalonate pathway regulators as precision therapy targets for aneuploid SCC.

#3003 Impact of sequencing technology on actionable fusion detection in precision oncology for lung cancer.

Gabriel Bandeira do Carmo[1], Rafael Canfield Brianese[1], Karina Miranda Santiago[1], Adriano Bonaldi[2], Marina De Brot Andrade[3], Giovana Tardin Torrezan[1], Dirce Maria Carraro[1]

[1]Clinical and Functional Genomics Group, A.C.Camargo Cancer Center, Sao Paulo, Brazil,[2]Laboratory of Genomic Diagnostics, A.C.Camargo Cancer Center, Sao Paulo, Brazil,[3]Department of Anatomic Pathology, A.C.Camargo Cancer Center, Sao Paulo, Brazil

Precision oncology has transformed the management of non-small cell lung cancer (NSCLC), where identifying targetable genomic alterations is central to selecting targeted therapies and improving outcomes. Among these relevant biomarkers, gene fusions represent key actionable events in NSCLC. Because many fusions generate chimeric transcripts rather than recurrent DNA-level breakpoints, RNA-based next-generation sequencing (NGS) has become essential in the molecular evaluation of lung cancer. These assays may differ substantially in gene content and sequencing technology, factors that influence fusion detection and the identification of clinically actionable biomarkers. Understanding how sequencing strategies affect diagnostic yield is therefore crucial for implementing precision oncology in NSCLC. This study compared two RNA-based NGS assays, TruSight Oncology 500 (TSO-500)-RNA (Illumina) and Oncomine Focus Assay (OFA)-RNA (Thermo Fisher), to evaluate their performance in detecting actionable fusions in NSCLC. RNA extracted from 35 NSCLC tumors (IRB: 2496/18) was analyzed in both platforms. TSO-500-RNA uses a hybrid-capture strategy, interrogating 55 genes and enabling the detection of both known and novel partners, requiring at least 80 ng of RNA input. OFA-RNA employs AmpliSeq amplicon-based technology, targeting 23 predefined genes and requiring only 10 ng of RNA. Fifteen fusions were identified in 13 of 35 tumors (37.2%): thirteen were identified uniquely by TSO-500-RNA, while two (*CD74::ROS1* and *KIF5B::RET*) were detected by both panels. Among the 23 genes included in both assays, one actionable fusion (*TRIM33::RET*) was exclusively detected by TSO-500-RNA. Overall, OFA-RNA detected actionable events in 6% of tumors, whereas TSO-500-RNA detected 9%. Most discrepancies were a result of hybrid-capture's greater flexibility to detect novel or noncanonical fusion partners. TSO-500-RNA also detected *YAP1::KMT2A*, an oncogenic fusion with approved therapies in other cancer types, but outside OFA-RNA's target list. Importantly, no discordances were observed when both assays covered the same gene regions, demonstrating technical robustness of both assays within their designed scope. In conclusion, the sequencing strategy is a major determinant of fusion detection in NSCLC. The hybrid-capture-based TSO-500-RNA enables broader gene coverage and discovery of novel fusion partners, resulting in a higher detection rate. Conversely, the amplicon-based OFA-RNA offers reliable detection of predefined fusions with lower RNA input, a critical advantage when working with limited tumor samples. Both features, comprehensive fusion discovery and compatibility with low-input, are essential to fully support precision oncology. Therefore, panel selection should balance tissue availability with the need for broad fusion detection to guide therapeutic decisions in NSCLC.

#3004 OXTR targeted local therapy could be a promising strategy for pleural mesothelioma.

Ichidai Tanaka[1], Hideyuki Itoigawa[1], Kazumi Hori[1], Shoichiro Fukuda[2], Heng Huang[1], Haruka Takata[2], Taketo Kato[1], Mitsuo Sato[1], Yoshitaka Sekido[3], Shinobu Shimizu[1], Tatsuhiro Ishida[2], Toyofumi Fengshi Yoshikawa[1], Makoto Ishii[1]

[1]Nagoya University Graduate School of Medicine, Nagoya, Japan,[2]Tokushima University, Tokushima, Japan,[3]Aichi Cancer Center, Nagoya, Japan

Introduction

Mesothelioma is one of the most aggressive neoplasms worldwide and has an extremely poor prognosis. We have previously discovered that oxytocin receptors (OXTR) are highly expressed in mesothelioma and *OXTR* knockdown significantly decreases the proliferation of mesothelioma cells with high-*OXTR* expression by disturbing the tumor cell cycle. Furthermore, the OXTR inhibitor, cligosiban, demonstrated antitumor efficacy in vivo. However, systemic administration required high doses, raising concerns about systemic toxicity. Therefore, we explored a local treatment strategy using intrathoracic drug delivery, and developed a dissolved formulation of cligosiban to enhance drug accumulation.

Methods

To establish a treatment method for localized control via trans-thoracic administration against pleural mesothelioma, the antitumor effect of a dissolved cligosiban in levulinic acid was evaluated in several mesothelioma cell lines. For *in vivo* analysis, an intrathoracic mesothelioma xenograft model was established with nude mice, and the therapeutic efficacy of intrathoracic administration of the dissolved cligosiban was examined.

Results

In vitro, dose-response experiments in two mesothelioma cell lines with high-*OXTR* expression demonstrated significant concentration-dependent changes in cell viability at micromolar concentrations. In parallel, the dissolved cligosiban significantly decreased the expression of cell-cycle-regulatory genes, including *Cyclin-dependent kinase 1* and *Cyclin E2* in the two mesothelioma cell lines with *OXTR*-high expression. In an orthotopic Y-MESO-27 model established by intrathoracic injection of mesothelioma cells with high-*OXTR* expression into nude mice, intrathoracic administration of the dissolved cligosiban at 50-400 µM was performed. Administration at 100 µM every other day clearly suppressed tumor growth and demonstrated a statistically significant prolongation of survival. Similar trends were observed in an intrathoracic MSTO-211H model, which is mesothelioma cells with low-*OXTR* expression. Next, we implanted the Alzet osmotic pump into the mice subcutaneous tissue and continuously administered total 400 µL (100 µM) of the dissolved cligosiban into the mice thoracic cavity. With injection rate at 1µl/hr, the dissolved cligosiban significantly prolonged mice survival.

Conclusion

Intrathoracic administration of the dissolved cligosiban effectively suppresses mesothelioma progression, representing the first demonstration of OXTR-targeted local therapy as a promising strategy for pleural mesothelioma.

#3005 *Ex vivo* trial of ODM-212, a novel pan-TEAD inhibitor, in patients with primary and metastatic solid tumors.

Juha K. Rantala[1], Eetu Valimaki[2], Janne Suhonen[1], Reetta Riikonen[3], Anu-Maarit Moilanen[3]

[1]Orion Corporation, Espoo, Finland,[2]Misvik Biology, Turku, Finland,[3]Orion Corporation, Turku, Finland

BACKGROUND: The Hippo signaling pathway is a highly conserved signaling cascade that controls the activation or inactivation of YAP/TAZ proteins. In cancer cells, genomic alterations can result in deactivation of the Hippo pathway and consequent hyperactivation of the YAP/TAZ to promote oncogenesis. Since YAP/TAZ induce the oncogenic effects by binding to TEAD transcription factors, TEAD targeting has emerged as a therapeutic opportunity in various solid cancers. ODM-212 is a novel small molecule that binds specifically to all TEAD/TEF transcription factors (TEAD1-4). ODM-212 effectively inhibits growth and viability of patient-derived solid tumor models with or without hippo pathway genetic alterations. Here we present pan-cancer *ex vivo* efficacy and biomarker discovery results of ODM-212 in primary and advanced solid tumors.

METHODS: Parallel to an ongoing multi-site, open-label, first-in-human study of ODM-212 in advanced solid tumor (TEADES, NCT06725758), ODM-212 therapy efficacy was studied using *ex vivo* drug screening in patient-derived functional tumor models. Vital tumor cells dissociated from excess tissues obtained in context of patients´ standard therapy were used to assess ODM-212 and 150 other therapies while DNA sequencing was used for exploratory biomarker evaluation. To assess predictive value of *ex vivo* drug screening, the results will be correlated with observed responses in eligible patients upon completion of the TEADES study.

RESULTS: 395 (n=46 solid cancer types) patient-derived tumor samples were included in the *ex vivo* study of ODM-212 efficacy. 83/395 samples were derived from primary untreated tumors and rest from recurrent metastatic tumors. Largest individual indications included, bladder cancer (n=45), brain tumors (n=61), HNSCC (n=93), lung cancer (n=20), melanoma (n=21) and sarcoma (n=27). ODM-212 demonstrated potent anti-tumor activity in select patient samples across all included main anatomical sites supporting genomic medicine approaches for patient stratification. Highest therapeutic efficacy was seen in Hippo pathway altered, KRAS and YAP driven solid tumors.

CONCLUSIONS: ODM-212 shows potent pan-cancer *ex vivo* efficacy in both primary untreated and heavily pre-treated metastatic tumors. Single agent efficacy correlates with Hippo pathway alterations while encouraging anti-tumor activity is seen also in select patient samples with no known Hippo alterations. This confirms ODM-212 as a potent novel therapeutic to target TEAD transcription factors in solid tumors supporting further clinical development.

#3006 Genomic determinants of PIK3CA mutation driven breast cancer initiation.

Snehal B. Bhandare[1], Ruizhong Wang[1], Poornima Bhat-Nakshatri[1], Stephanie Adama[2], Sarah R. Spivak[1], Farzaneh Behzadnia[3], Cihat Erdogan[3], Hongyu Gao[3], Yunlong Liu[3], Lylah H. Hutson[4], Xin Dauterman[4], George Sandusky[4], Harikrishna Nakshatri[1]

[1]Surgery, Indiana University School of Medicine, Indianapolis, IN,[2]Translational Cancer Biology, Indiana University School of Medicine, Indianapolis, IN,[3]Medical & Molecular Genetics, Indiana University School of Medicine, Indianapolis, IN,[4]Pathology and Laboratory Medicine, Indiana University School of Medicine, Indianapolis, IN

PIK3CA is the second most mutated and/or amplified gene in breast cancer after *p53*. The PIK3CA-specific inhibitor Alpelisib is an FDA approved treatment for breast cancer. Toxicity and rapid development of resistance limit its clinical utility. Mutations in PIK3CA are found in many normal organs including the breast suggesting that additional genomic aberrations are needed for mutant PIK3CA to initiate breast cancer, and those aberrations can be exploited for therapy. Consistent with this possibility, our previous studies have demonstrated that immortalized breast epithelial cells derived from *BRCA1/2* mutation carriers are susceptible to transformation by the *PIK3CA* mutant, whereas transformation of immortalized breast epithelial cells from healthy donors required combinations of mutant *PIK3CA* and SV40-T/t antigens. These results suggest that transformation of breast epithelial cells by *PIK3CA* mutants requires additional genomic aberrations like those induced by SV40-T/t antigens or *BRCA1/2* mutations. To decipher genomic aberrations required for *PIK3CA* mutant driven breast epithelial transformation, we used model system of immortalized breast luminal epithelial cell lines from healthy donors. We show that mutations that activate MEK/ERK pathway such as NF-1 mutation in parallel with *PIK3CA* mutations initiate ductal carcinoma- *in situ* (DCIS)-like breast tumors with accompanying reduction in BRCA2 protein, whereas mutant PIK3CA plus SV40-T/t antigens generate invasive ductal adenocarcinoma (IDC). DCIS and IDC cells differed significantly in the expression of extracellular matrix components including reduced expression of LAMC2 and COL17A1 and upregulation of drivers of aneuploidy in IDC cells. Consistent with the possibility of mutant PIK3CA and MEK/ERK pathway collaboration in breast cancer initiation, Estrogen Receptor-positive/*PIK3CA* mutation-positive breast tumors contained higher levels of activated ERK compared to Estrogen Receptor-positive/PIK3CA-wild type breast cancers.

Significance: To our knowledge, this is the first study to generate DCIS like lesions from breast epithelial cells from healthy women using combinations of breast cancer-enriched genomic aberrations and without the use of viral proteins such as SV40-T/t antigens or HPV E6. In this process, we have developed an isogenic DCIS and IDC model to study breast cancer progression. These results also suggest that mutant PIK3CA is a weaker oncogene and the effective therapy for mutant PIK3CA driven breast cancers needs to include inhibitors of PIK3CA as well as drugs that target genomic aberrations that cooperate with mutant PIK3CA.

: Nanocarriers and Drug Delivery Systems
Poster Session

#3010 LIN-T (lipid integrated tag): An optimized tag-lipid nanoparticle design for targeted therapeutic mRNA delivery.

Tommy Lidstrom[1], Alexandros Kostakis[2], Rosanne Veerman[3], Venera Emruli[3], Safia Guleed[3], Tina Furebring[3], Jonas A. Nilsson[1], Sara Mangsbo[2]

[1]Umea University, Umea, Sweden,[2]Uppsala University, Uppsala, Sweden,[3]Strike Pharma AB, Lund, Sweden

Background: Lipid nanoparticles (LNPs) are the leading platform for mRNA delivery, but targeted delivery remains challenging. Factors such as lipid composition, particle size, charge, and ionizable lipid selection influence biodistribution, cellular uptake, and mRNA translation. Antibody-decorated LNPs offer a strategy to expand therapeutic applications.
Approach: Conventional antibody decoration methods, such as post-formulation conjugation (click or maleimide chemistry), fusion proteins, or site-specific lipid conjugation, require chemical modification of antibodies. Modifications that can compromise stability and increase aggregation risk. To address this, we developed a modular system using a short peptide tag integrated into the LNP surface, enabling rapid antibody attachment via a bispecific antibody design without chemical conjugation.
Innovation: Our 9-amino-acid tag (optimized in our recent Nature com. publication: PMID 39500897) binds an scFv (single-chain variable fragment) domain with picomolar affinity. The tag shows minimal immunogenicity risk in vitro and in vivo, likely as the tag is shielded upon binding. We demonstrate two complementary strategies for tag incorporation on the LNP:
1. Protein-based: Recombinant inert ApoE (ApoEi)-fusion tag for rapid coating of preformed LNPs.2. Synthetic lipid-based: DSPE-PEG-tag conjugate integrated during LNP assembly.
Both approaches preserve tag accessibility and enable efficient antibody decoration. The ApoEi-tag design uniquely also blocks ApoE-LDL receptor interactions, and we can display that this reduces liver tropism.
Results: Using this platform, we achieved targeted mRNA delivery and translation in Her2+, CD40+, CD3+, and CD20+ cells. The synthetic DSPE-PEG-tag supports scalable, GMP-compatible production, and the ApoEi-based method enables a rapid tool for research purposes. Our human scFv can be formatted into a classical Morrison bispecific design and expressed in CHO cells at titers >8 g/L.
Conclusion: These strategies provide a versatile framework for precision-targeted mRNA delivery, supporting customizable LNP therapeutics within for example oncology and autoimmune diseases.

#3011 A STING-boosted lipid nanoparticle mRNA vaccine for therapeutic cancer vaccination.

Alessia Marrocu[1], Osama W. M. Hassuneh[2], Victor M. Moreno Zafra[2], Alaa Zam[2], Emre Demirel[1], Meriem Bahri[1], Adam Walters[2], James N. Arnold[1], Khuloud T. Al-Jamal[2]

[1]School of Cancer and Pharmaceutical Sciences, Faculty of Life Sciences and Medicine, King's College London, London, United Kingdom,[2]Institute of Pharmaceutical Sciences, Faculty of Life Sciences and Medicine, King's College London, London, United Kingdom

Despite the success of immunotherapies and preventative vaccines in virus-associated cancers, the translation of therapeutic vaccination has been limited, often by limited immunogenicity and inability to overcome the immunosuppressive ‘cold’ tumor microenvironment. Recent advances in mRNA vectors for viral immunization, and optimized nanoparticle delivery, have renewed promise for cancer vaccination. In this study, we developed an ionizable stable nucleic acid lipid nanoparticle (SNALP) nanovaccine for the delivery of mRNA-encoded model antigen, ovalbumin (OVA). To counter tumor-associated immunosuppression, we harnessed the innate anti-viral stimulator of interferon genes (STING) pathway by co-encapsulating cyclic dinucleotide STING agonist 2’3’-cGAMP. SNALP formulations were optimized for biocompatibility and cell uptake, with small particle size, near-neutral surface charge, and high encapsulation efficiency of both mRNA and 2’3’-cGAMP within a single platform. SNALP-mediated co-delivery achieved effective mRNA transfection and antigen presentation in primary dendritic cells (DCs) *in vitro*, whilst addition of 2’3’-cGAMP enhanced DC maturation and activation, noted by increased co-stimulatory (CD80, CD86) and MHC-I (H-2Db, H-2Kb) marker expression. Nanovaccine-activated DCs efficiently primed naïve primary $CD8^+$ T cells to elicit effector function and replicate in co-culture. *In vivo*, immunization with 2’3’-cGAMP-boosted OVA-SNALPs elicited a robust immunological T cell response, evidenced by circulating antigen-specific $CD8^+$ T cell populations with central memory phenotypes, and effector splenic $CD8^+$ T cells capable of TCR-mediated cytokine production upon challenge. Therapeutic relevance of 2’3’-cGAMP-OVA-SNALPs was assessed in murine models of melanoma expressing OVA (B16F10-OVA) under different vaccination protocols. The nanovaccine consistently delayed tumor onset and extended survival, completely preventing tumor formation when given prophylactically, or driving total tumor regression when given therapeutically by local (intra-tumoral) or systemic (intra-muscular) routes, in a subset of animals, which was not found in non-adjuvanted controls. Some tumor control was also noted upon therapeutic administration of SNALPs containing irrelevant mRNA, highlighting potentially beneficial innate adjuvancy of the platform itself. Altogether, this work shows that SNALP-based nanovaccines are a versatile and translatable platform for next-generation cancer immunotherapy. The nanovaccine showed potential as a monotherapy, converting immunologically ‘cold’ tumors into responsive microenvironments. This adaptable system enables co-delivery of antigens and immune modulators to target immunosuppressive and induce durable anti-tumor responses. Future studies will explore combining it with additional immunotherapies to improve clinical efficacy.

#3012 Lipid nanoparticles enable high efficiency CRISPR HDR mediated gene insertions in primary human T cells.

Reka Geczy[1], Meenakshi Swaminathan[1], Hannah Ly[1], Mana Novin[1], Bernice Thommandru[2], **Sijo Chemmannur**[1], Sadik Kassim[3], Samuel Clarke[1]

[1]Cytiva, Vancouver, BC, Canada,[2]Integrated DNA Technologies, Coralville, IA,[3]Danaher Corporation, Washington, DC

Stable gene insertion using non-viral delivery is essential to unlocking the next generation of safe and accessible cell and gene therapies. Currently, viral vectors carry high manufacturing costs and insertional mutagenesis concerns, while electroporation (EP) affects cell yield and viability. Lipid nanoparticles (LNPs) can be a promising alternative option for engineering cells for persistent expression of target genes, as they offer a favorable safety profile and are both cost-effective and scalable. In this work, we mapped out the critical parameters governing homology-directed repair (HDR) in primary T cells using LNP-mediated cargo delivery. Cas9 mRNA, a chemically synthesized guide RNA (sgRNA), and an ~100 nt single-stranded donor oligonucleotide (ssODN) were encapsulated within a novel LNP composition using a scalable production platform. A haemagglutinin (HA) epitope tag was knocked in at the CD5 locus as an easily quantified read-out for parameter optimization. CD3+ primary T cells from healthy donors were cultured in well-plates and the CRISPR LNPs added to the media in a one-step process, without further cell manipulation. Various parameters were identified and systematically varied, including (and not limited to) the length of cell activation, cell density, nucleic acid dose and the RNA/DNA molar ratios. Through multiple rounds of optimization, LNPs achieved on average 31 ± 7% HDR in n=5 T cell donors, detected through dual CD5/HA flow cytometry 4 days post-LNP administration. Viability of the cells remained high at 96 ± 5% at the time of HDR detection, relative to untreated controls. The aforementioned results reflect no added enhancers; however, when we tested various small molecules, such as NHEJ inhibitors, HDR rates further improved to over 50% in primary T cells. Finally, we compared the optimized LNP protocol to EP which resulted in similar HA+ frequencies. However, most notably, the yield of viable edited cells by LNP was an order of magnitude higher than EP owing to improved cell viability and proliferation. All together, this data demonstrates how LNPs can achieve clinically relevant knock-in frequencies and showcases the benefits of LNPs as a non-viral alternative for gene insertion. This approach for parameter optimization is applicable for a diverse set of therapeutic loci, providing a framework for the rapid application of LNPs to enable the next generation of T cell therapies.

#3013 Biomimetic exosome-delivered STAT3 inhibitor for radiosensitization in oral squamous cell carcinoma cells.

Kehua Hu[1], Sisi Yan[1], Xiaowan Guo[1], Rurui Xue[1], Yunli Mo[1], Hui Qiu[1], Linlin Bu[2], **Qiuji Wu**[1]

[1]Zhongnan Hospital of Wuhan University, Wuhan, China,[2]Hospital of Stomatology, Wuhan University, Wuhan, China

Background: Signal transducer and activator of transcription 3 (STAT3) is a key driver of resistance to radiotherapy in advanced oral squamous cell carcinoma (OSCC), promoting an immunosuppressive microenvironment via upregulation of immune checkpoints including PD-L1. Although STAT3 inhibition represents a promising radiosensitizing strategy, its clinical application is limited by poor drug delivery. Exosomes, as natural nanocarriers, present an ideal solution with their excellent biocompatibility, low immunogenicity, and inherent targeting capabilities. This study aimed to develop an exosome-based targeted delivery system for a STAT3 inhibitor to improve the efficacy of radiotherapy in OSCC.

Methods: We constructed a biomimetic delivery system (Exo@S3I-201) by loading the STAT3 inhibitor (S3I-201) into exosomes derived from mouse oral squamous cell carcinoma (MOC2) cells via sonication. The system was characterized by transmission electron microscopy (TEM), nanoparticle tracking analysis (NTA), and Western Blot. Drug loading efficiency and pH-dependent release profile were determined by ultraviolet spectroscopy. Cellular uptake and targeting were visualized by fluorescence microscopy. The radiosensitizing effect of Exo@S3I-201 on MOC2 cells were evaluated in vitro through CCK-8 assay, colony formation assay, flow cytometry, live-dead staining.

Results: The successfully constructed Exo@S3I-201 exhibited similar size, dispersion, and stability to plain exosomes. UV absorption confirmed that Exo@S3I-201 retained the characteristic absorption peak of S3I-201, exhibited high drug loading efficiency, and displayed pH-responsive drug release behavior, with maximal release under acidic conditions (pH=5.5) mimicking the tumor microenvironment. Fluorescence microscopy revealed efficient cellular uptake of Exo@S3I-201 into MOC2 cells. Western Blot analysis revealed that Exo@S3I-201 combined with radiotherapy more effectively suppressed STAT3 phosphorylation and expression of its downstream target genes, compared with free S3I-201. Functionally, compared to radiotherapy alone or free S3I-201, the combined treatment markedly inhibited MOC2 cell proliferation and colony-forming ability and induced higher levels of cellular apoptosis.

Conclusion: Our study presented an autologous exosome-based system for targeted STAT3 inhibitor delivery. Exo@S3I-201 significantly enhanced radiosensitivity in OSCC by inhibiting the STAT3 pathway, demonstrating its potential as a novel combination therapy to overcome radioresistance.

#3014 Targeting PLXND1 using RNA bioengineering technologies and customized lipid nanoparticles in advanced prostate cancer.

Huan Qu[1], Menghuan Tang[2], Qiufang Zong[2], Sohaib Mahri[2], Pengfei Xu[1], Joy C. Yang[1], Fan Wei[1], Junwei Zhao[2], Meijuan Tu[2], Neelu Bartra[2], Leyi Wang[1], Allen C. Gao[3], Kit Lam[2], Marc A. Dall'Era[1], Aiming Yu[4], Yuanpei Li[2], Chengfei Liu[3]

[1]Urologic Surgery, UC Davis, Sacramento, CA,[2]UC Davis Comprehensive Cancer Center, Sacramento, CA,[3]Urologic Surgery, UC Davis Comprehensive Cancer Center, Sacramento, CA,[4]UC Davis, Sacramento, CA

Background: PLXND1 (Plexin D1) is a transmembrane receptor that plays critical roles in promoting neural lineage plasticity and driving resistance to enzalutamide therapy in prostate cancer. Despite its significance, PLXND1 has been considered "undruggable." siRNA-based therapeutics offer a strategy to silence disease-driving genes like PLXND1 but face limitations, including instability, poor cellular uptake, and off-target effects.
Methods: We employed an RNA bioengineering approach using a tRNA/pre-miRNA-mir-34a scaffold to stabilize and express siRNAs targeting PLXND1 (BioRNA-siPLXND1). BioRNA/PLXND1-siRNA expression plasmids were constructed via molecular cloning, and the resulting BioRNA was purified and analyzed for quality, yield, and endotoxin levels. We tested BioRNA-siPLXND1 function in vitro and formulated it into lipid nanoparticles (LNPs) using two lipid components: DOPE and DOTAP. The stability, transfection efficiency, and safety of each formulation were evaluated in vitro and in vivo using prostate cancer cell lines and neuroendocrine prostate cancer (NEPC) patient-derived xenograft (PDX) organoids.
Results: BioRNA-siPLXND1 achieved high yield and purity with low endotoxin levels. It efficiently silenced PLXND1 at the mRNA and protein levels, significantly inhibiting cell proliferation, colony formation, and organoid growth in vitro. Among the LNP formulations, LNP-DOTAP demonstrated higher transfection efficiency but greater cytotoxicity in normal cells, whereas LNP-DOPE showed a favorable safety profile and effective delivery. LNP-DOPE-loaded BioRNA-siPLXND1 remained stable for at least 7 days in vitro and suppressed tumor growth in NEPC PDX organoids. In vivo, LNP-DOPE accumulated in tumors within 2 hours, persisted for up to 4 days, and was predominantly retained in tumor tissue by day 7.
Conclusions: Our study demonstrates the feasibility and therapeutic potential of a tRNA-based BioRNA platform for delivering PLXND1-targeting siRNAs in prostate cancer. LNP-DOPE serves as a safe and effective delivery system, offering a promising strategy for targeting "undruggable" oncogenes like PLXND1 in therapy-resistant prostate cancer.
Financial support: This work was supported in part by grants from NIH/NCI R37CA249108 (Liu), R01CA251253 (Liu), R21CA277171 (Liu), Department of Defense HT9425-23-1-0144 (Liu), HT9425-23-1-0325 (Liu), HT9425-23-1-0324 (Dall'Era), and UC Davis Comprehensive Cancer Center Support Grant (CCSG) awarded by the National Cancer Institute (NCI P30CA093373).

#3015 Advancing mRNA therapeutics towards immuno-oncology applications: Lipid nanoparticles demonstrate favorable safety and efficacy profile with repeated mRNA administration in normal and tumor-bearing mice.

Sams MA Sadat[1], **Avisek Deyati**[1], Leanna Yee[1], Zhengyu Chen[1], Kalyan Golla[1], Tony Wu[1], Richard Jiang[1], Jay Paquette[1], Malathi Anantha[1], Noorjahan Aibani[1], Nikita Jain[1], Anitha Thomas[2]

[1]Cytiva, Vancouver, BC, Canada,[2]Cytiva, Marlborough, MA

Lipid nanoparticles (LNPs) have revolutionized mRNA delivery, offering a promising approach for advancing cancer immunotherapy. Effective and safe delivery of tumor antigen-encoding mRNA can stimulate robust anti-tumor immune responses. Here, we developed LNP formulations for immuno-oncology applications and tested its fit-for-use by delivering ovalbumin (OVA)-encoded mRNA as a surrogate payload and evaluated the safety, efficacy, and therapeutic potential in the B16-F10-OVA xenograft melanoma mouse model.Novel ionizable lipids were selected for formulating LNPs by rational screening of pKa, encapsulation efficiency, hydrodynamic size, and biodistribution properties. OVA-encoded mRNA was encapsulated in LNPs using NxGen™ microfluidic mixing technology on the NanoAssemblr™ platform. The LNPs were characterized for hydrodynamic size, polydispersity index (PDI), loading, and encapsulation efficiency. To assess long-term safety and stability, healthy mice received multiple intramuscular (IM) injections of the LNP formulations at 21-day intervals. Physicochemical stability and toxicity were evaluated through the standard assays and clinical observations. Following this series, B16-F10-OVA tumor-bearing mice were vaccinated intramuscularly with OVA mRNA-loaded LNPs. Clinical symptoms and survival outcomes were monitored and compared to untreated controls.OVA mRNA-loaded LNPs were in the desired size range of 60 to 80 nm with a PDI value below 0.2 and an encapsulation efficiency greater than 95%. Long-term stability studies indicated retention of critical quality attributes (CQAs). Repeated IM administration of the proprietary LNPs over an extended period demonstrated stability and tolerability with no detectable toxicity or adverse effects observed in treated animals. Treatment with the OVA mRNA-LNP vaccine improved survival in tumor-bearing mice, significantly extending median survival compared to controls.By retaining the CQAs of the drug products, our novel LNP platform efficiently delivers OVA mRNA as a model for delivering therapeutic or immune modulating nucleic acid payloads. Additionally, repeated IM administrations of these LNPs over an extended period resulted in no detectable adverse events and OVA mRNA LNPs induced potent anti-tumor effects in the B16-F10-OVA model. This favorable safety profile and stability upon repeated dosing underscore LNP suitability for long-term immune modulation or therapeutic strategies for immuno-oncology applications.

#3016 Enhancing CX-5461 therapy in TNBC through liposomal delivery and ATR inhibitor combination.

Henos S. Negash[1], Rachel K. Myrick[2], Sandro R.P. da Rocha[2], J. Chuck Harrell[2]

[1]Virginia Commonwealth University - VCU, Richmond, VA,[2]Virginia Commonwealth University, Richmond, VA

Background: Breast cancer (BC) is the second leading cause of cancer death in women. Triple-negative breast cancers (TNBCs), an aggressive subtype, account for 15-20% of cases and disproportionately contribute to BC mortality. For patients with metastatic TNBC, the current standard of care is chemotherapy; although initially effective, overall survival remains poor. Thus, novel therapeutic strategies are urgently needed to improve TNBC outcomes.

Aims: We aim to evaluate the novel DNA-damaging agent CX-5461 (Pidnarulex), which has shown promising preclinical activity in TNBC patient-derived xenograft (PDX) models with homologous recombination deficiency (HRD), derived from metastatic patients resistant to standard-of-care chemotherapy. CX-5461 is currently in clinical trial and holds FDA Fast Track designation for breast and ovarian cancers with HRD. To enhance efficacy and improve survival, we are exploring liposomal delivery and rational combination with the ATR inhibitor, Berzosertib. As CX-5461 is most effective in DNA repair-deficient backgrounds, we focused on models with HR or other DNA repair pathway deficiencies.

Methods: Human TNBC cell lines and PDX-derived cultures were screened in vitro for single-agent CX-5461 activity. PDX models with $IC_{50} \leq 5$ μM were prioritized for in vivo testing to determine sensitivity (defined as ≥50% tumor volume reduction compared to control). One PDX model (BCM-3887) has been tested in vivo to date. CX-5461 liposomes were prepared using thin-film hydration method with copper complexation-based gradient loading. In vitro responsive cell lines and BCM-3887 were screened for single-agent activity of Berzosertib. Cell lines and BCM-3887 with $IC_{50} \leq 10$ μM for Berzosertib were selected for in vitro combination studies to evaluate synergistic interactions with CX-5461.

Results: CX-5461 has demonstrated potent in vitro single-agent activity. In a pilot in vivo study using BCM-3887 model, strong tumor growth inhibition was observed. Liposomes were prepared with favorable physical characteristics. In vitro combination studies with Berzosertib showed synergy.

Conclusion: CX-5461 is a promising agent for DNA repair-deficient TNBC, with strong single-agent activity demonstrated in vitro and in vivo. Preliminary combination studies with Berzosertib revealed synergistic potential. Future in vivo studies will evaluate whether liposomal delivery and combination therapy can improve survival in TNBC.

#3017 Combination effect of vinorelbine and doxorubicin in free solutions and liposomes in a multicellular spheroids model.

Yong Zhu, Zizhao Xu, Yifan Lu, Shen Zhao, Md Delowar Hossain, Xin Guo

Department of Pharmaceutics & Medicinal Chemistry, University of the Pacific, Stockton, CA

Purpose: Combination drug therapy is a cornerstone approach to treat cancers, yet strategies of delivering drug combinations, including optimal drug ratios and drug formulations, remain challenging. Doxorubicin (DOX) and vinorelbine (VNR) are well established anticancer drugs that inhibit different phases of cell division, thus making them promising candidates for combination therapy. This study evaluated the combination effect of DOX and VNR in various formulations (free solution, pH-sensitive liposomes, and non-pH-sensitive liposomes) at various drug ratios against multicellular spheroids (MCSs) of A549 cells (NSCLC) by cell viability assay and mathematical modeling.

Methods: Non-pH-sensitive liposomes (NonFlip) are composed of cholesterol, POPC and PEG-Ceramide. pH sensitive liposomes (Flip) are composed of POPC, PEG-Ceramide and lipids with a pH-sensitive conformational switch (flipids). A549 MCSs were constructed in 96-well ultra-low attachment microplates with RPMI-1640 and 0.3% collagen. MCSs (~500 μm) were treated with free or formulated DOX, VNR, or DOX:VNR combinations at various ratios. Cell viability was assessed using CellTiter-Glo 3D assay. The effects of drug combination were evaluated by three mathematical models (Greco's, unified theory, and Bliss independent) using the GraphPad Prism 10.6.0 software.

Results: For individual drugs, free DOX, NonFlip DOX, and Flip DOX exhibited similar IC50 values around 5 μM. Free VNR and Flip VNR showed IC50 around 44 μM, while NonFlip VNR displayed IC50 exceeding 200 μM. For combinations, DOX:VNR ratios of 5:1, 1:1, and 1:5 yielded IC50 values of approximately 5, 8, and 16 μM, respectively, in free drug and Flip groups. NonFlip groups at 5:1 and 1:1 showed IC50 values of approximately 5 and 8 μM, but the IC50 of NonFlip DOX:VNR 1:5 exceeded 200 μM. Compared to individual drugs, most of the DOX:VNR combinations in Free drug solution, Flip formulations, and NonFlip formulations demonstrated synergism in Greco's and unified theory models (R^2>0.95). To optimize the synergism, Greco's model favored the DOX:VNR ratio of 5:1 while unified theory favored 1:5. In contrast, the Bliss independent model fitted the cell viability data poorly (R^2<0.9) and did not show synergistic effects.

Conclusions: Greco's and unified theory modeling of the dose dependent cell viability data demonstrated the synergistic effect of combining DOX and VNR in various formulations. The poor fitting of the cell viability data by the Bliss independent model suggests DOX and VNR may not suppress the cancer cell growth independently. Further studies are needed to confirm these findings.

#3018 Lipopolymer-mediated delivery of fusion oncogene-targeting siRNAs attenuates leukemia burden and improves survival in preclinical models of hematologic malignancies.

Mohammad Nasrullah[1], Remant KC[2], Spencer B. Gibson[3], Xiaoyan Jiang[4], Olaf Heidenreich[5], Joseph Brandwein[6], Hasan Uludag[2]

[1]Pharmacy & Pharmaceutical Sciences, University of Alberta, Edmonton, AB, Canada,[2]Chemical & Materials Engineering, University of Alberta, Edmonton, AB, Canada,[3]University of Alberta, Edmonton, AB, Canada,[4]BC Cancer, part of the Provincial Health Services Authority, Vancouver, BC, Canada,[5]Princess Maxima Center for Pediatric Oncology, Utrecht, Netherlands,[6]Faculty of Medicine & Dentistry - Medicine Dept, University of Alberta, Edmonton, AB, Canada

Hematologic malignancies are genetically heterogeneous cancers marked by a range of chromosomal translocations, among which fusion oncogenes, e.g., *KMT2A::AFF1* in acute lymphoblastic leukemia (ALL), *KMT2A::MLLT3* in acute myeloid leukemia (AML), and *BCR::ABL1* in chronic myeloid leukemia (CML), are particularly aggressive and clinically intractable. These fusion-driven hematologic malignancies are associated with poor prognosis and resistance to conventional therapies, emphasizing the need for fusion targeted, personalized treatment strategies. Small interfering RNAs (siRNAs) offer a promising approach due to their capacity for precise gene silencing. However, clinical translation is hindered by delivery challenges, including rapid degradation, off-target effects, hepatic accumulation, and inefficient uptake by hematopoietic cells, largely due to their negative charge, size, and the limited cytoplasmic volume of blood cells.

To address these limitations, we developed a novel lipopolymer-based siRNA delivery platform by conjugating aliphatic lipids onto low-molecular-weight polyethyleneimine (PEI, 1.2 kDa). This modification yielded a series of lipopolymers capable of forming stable nanocomplexes with siRNAs, colloquially known as lipopolymer/siRNA nanoparticles (LPNPs). These LPNPs leverage the cationic nature of PEI for siRNA binding and lipid-mediated mechanisms to enhance cellular uptake. We evaluated the efficacy of LPNPs in delivering siRNAs targeting *KMT2A::AFF1*, *KMT2A::MLLT3*, and *BCR::ABL1* in preclinical models of ALL, AML, and CML, respectively. LPNP-mediated delivery attained efficient intracellular siRNA uptake and robust gene silencing in all three forms of leukemia cell lines, which resulted significant downregulation of fusion oncogene expression. This silencing induced apoptosis and markedly reduced colony-forming potential *in vitro*. *In vivo* biodistribution studies demonstrated enhanced biodistribution of LPNPs in leukemia-accompanying tissues, including bone marrow and spleen, with reduced hepatic sequestration. Particularly, systemic administration of LPNPs led to a substantial reduction in leukemia burden and significantly improved survival in xenograft models of ALL, AML, and CML.

Our findings highlight the therapeutic potential of lipopolymer-mediated siRNA delivery for targeting fusion oncogenes in hematologic malignancies. This platform offers a promising strategy for overcoming current delivery barriers and advancing RNA interference-based therapies toward clinical application.

#3019 The first coacervate based delivery system for efficient and safe genetic engineering in stem cells.

Peipei Zhu[1], Manman Lu[2], Qing Zhang[1], Renxia Zhang[1], Lihong Jiang[2], Xiaowen Fei[2], Xiaofei Gao[1]

[1]Westlake University, Hangzhou, China,[2]Nanoportal Biotech, Hangzhou, China

Stem cell biology, which orchestrates embryogenesis, influences aging, and holds promise for revolutionary therapies, represents a central thread in human health. This underscores the pressing need for advanced delivery technologies to facilitate both research progress and clinical translation. Here, we harness coacervates-regarded as protocells during evolution-to develop a pioneering delivery platform. We identified a mammalian endogenous protein that encapsulates diverse nucleic acids through liquid-liquid phase separation (LLPS), forming protein-based coacervates. These coacervates exhibit superior mRNA encapsulation capacity, efficient cellular internalization, robust cytoplasmic cargo release, and broad compatibility across multiple cell types -including primary immune cells and stem cells. The resulting platform, named ProteanFect, supports diverse genetic cargoes for versatile gene manipulation strategies. ProteanFect demonstrated high versatility and efficiency across key stem cell types, including hematopoietic stem cells (HSCs), human embryonic stem cells (ESCs), and induced pluripotent stem cells (iPSCs) derived from diverse somatic sources such as PBMCs, urine, and adipocytes. It efficiently enabled gene overexpression and knockout through the delivery of mRNA or Cas9 RNP complexes. In a key demonstration of its therapeutic potential for hematological disorders, ProteanFect achieved approximately 80% allele modification at the *BCL11A* locus in HSCs, a strategy aimed at reactivating fetal hemoglobin to treat hemoglobinopathies, with no detectable off-target editing. Furthermore, the platform facilitated precise genetic correction by delivering prime editing tools into PBMC-derived iPSCs, achieving approximately 55% precise base substitution with high cell viability. In summary, ProteanFect constitutes a versatile, safe, and efficient non-viral platform that operates without synthetic lipids or electroporation. By enabling robust transient expression of reprogramming and gene-editing cargo without genomic integration, it provides a safer and more controllable pathway for cellular reprogramming, iPSC generation, and the development of next-generation cell therapies.

#3020 Lymphocyte-mimetic drug carriers enable targeted therapeutic delivery to lymph nodes for enhanced immunomodulation.

Michael J. Donzanti[1], Luisa A. Fink[2], Bahar Bahramimeimandi[2], Kayla Katz[2], Dylan T. Ngo[2], Ana Obradovic[2], Ryan Zurakowski[1], Jason P. Gleghorn[1]

[1]Navicyte Biotechnologies LLC, Newark, DE,[2]University of Delaware, Newark, DE

Introduction: Immunotherapy efficacy in solid tumors is often limited by immune tolerance within tumor-draining lymph nodes (TDLNs), where antigen presentation and T-cell priming originate. Immune activators, such as STING agonists, are capable of reversing local immunosuppression, however their clinical translation has been hindered by rapid systemic clearance, dose-limiting toxicity, and poor lymph node bioavailability. Effective targeting of TDLNs could overcome these translational barriers by reprogramming local immune environments and amplifying durable antitumor immunity. To address this, we have developed a novel delivery platform T-Lymphocyte Mimetic Membrane-wrapped Microparticles (T3MPs).

Methods: T3MPs were fabricated using a flow-focusing microfluidic device to generate uniform, cell-sized alginate microparticles (10-20 μm). Multiple payloads, including cyclic-di-GMP (STING agonist) and cisplatin, were encapsulated within the alginate matrix during particle formation. Drug-loaded T3MPs were cloaked with allogenic T-cell membranes to preserve trafficking proteins, confirmed via flow cytometry. Drug encapsulation and release kinetics were quantified via spectrofluorometry. *In vitro* payload functionality was assessed with THP-1 culture, and *in vivo* biodistribution and efficacy were evaluated following intravenous administration in BALB/c mice.

Results: T3MPs exhibited uniform size distribution and retained key lymphocyte surface proteins (L-selectin, LFA-1) critical for LN trafficking and demonstrated tunable, sustained drug release, achieving ~50% release over 10 days *in vitro*. Following intravenous administration, drug-loaded T3MPs achieved ~700% greater LN-specific delivery than free drug controls and extended the therapeutic index >500-fold by reducing systemic exposure. Delivery of c-di-GMP via T3MPs induced potent activation of lymph node resident antigen presenting cells (elevated IFN-β and IL-12), while co-delivery of c-di-GMP and model tumor antigen (SIINFEKL) enhanced antigen-specific $CD8^+$ T-cell priming.

Conclusions: T3MPs represent a novel lymphocyte-mimetic platform that overcomes pharmacological barriers to lymph node drug delivery, enabling safe, localized immunomodulation for reprogramming immune niches. By combining lymphocyte-inspired targeting with tunable release, this technology offers a broadly applicable strategy to enhance the efficacy of immunotherapies and vaccines. Ongoing work through Navicyte Biotechnologies is advancing the T3MP platform toward IND-enabling studies and strategic pharmaceutical partnerships.

#3021 ONM-421, a pH-responsive polymer-drug conjugate nanoparticle, delivers MMAE to solid tumors and shows antigen-independent antitumor efficacy in mice.

Jason B. Miller, Stephen Gutowski, Qingtai Su, Bhargavi Allu, Austin Burcham, Zirong Chen, Ruolan Han, Tian Zhao

OncoNano Medicine, Inc., Dallas, TX

Introduction: Strategies that enable precise tumor delivery of cytotoxic agents such as monomethyl auristatin E (MMAE) and reduce off-tumor toxicity would profoundly improve cancer treatment outcomes. Though antibody-drug conjugates (ADCs) have been approved for several indications, the efficacy of ADCs can be limited by multiple factors including heterogenous antigen expression and target downregulation which restrict effective treatment in many patients. We have developed ON-BOARD™, an ultra-pH sensitive nanoparticle technology, which shields payloads from systemic exposure during circulation but responds to the acidic tumor microenvironment (TME), to deliver therapeutics in an antigen-independent and histology-independent manner. Herein, we report the preclinical characterization of ONM-421, an ON-BOARD™ polymer-drug conjugate covalently linked to MMAE via a protease-cleavable linker, showing favorable tolerability and anti-tumor efficacy in multiple xenograft models.
Methods: Properties and storage stability of ONM-421 were characterized by dynamic light scattering and HPLC. Linker cleavage was investigated *in vitro* while cytotoxicity assays were performed in human cancer cell lines and primary cells (keratinocytes, corneal epithelial cells) with free MMAE and MMAE-ADCs. Efficacy and tolerability of ONM-421 was studied *in vivo* in multiple human xenograft models, HT-29, HCT-116, and FaDu compared to docetaxel (DTX) and a tissue factor targeting MMAE-ADC tisotumab vedotin (TV).
Results: ONM-421 showed stable uniformly distributed size (D_h<50nm), <1% free MMAE, and consistent pH-responsiveness over a 6-month ongoing storage stability study. ONM-421 showed >1,000-fold payload protection compared to free MMAE *in vitro*, while MMAE payload activity was confirmed after cathepsin B enzymatic cleavage from ONM-421. Incubation of ONM-421 in mouse plasma showed improved stability compared to TV as measured by LC-MS and a cancer cell cytotoxicity assay. ONM-421 also showed markedly reduced toxicity compared to free MMAE and TV in human primary corneal epithelial cell and keratinocytes. In repeat-dose studies, ONM-421 demonstrated potent antitumor efficacy in multiple xenograft models in an antigen independent manner with significantly improved tolerability compared to DTX in all models. ONM-421 resulted in 100% tumor free survival in HT-29 and FaDu, and 82% TGI in HCT-116 while TV was only efficacious in TF^{Hi} FaDu (100% tumor free) but not in TF^{Lo} HCT-116 (20% TGI). ONM-421 also showed better tumor inhibition than TV in large established FaDu and HCT-116 xenografts after a single injection.
Conclusion: ONM-421 demonstrated potent antigen-independent antitumor efficacy in multiple xenograft tumors with good tolerability in mice. The data justifies further development of ONM-421 towards IND-enabling studies.

#3022 A peptide-based drug delivery system to target metastatic prostate cancer.

Yukihito Kuroda[1], Norio Miyamura[1], Chisato M. Yamazaki[2], Erkki Ruoslahti[3], Tambet Teesalu[4], Kazuki Sugahara[1]

[1]Columbia Univ. Vagelos College of Physicians & Surgeons, New York, NY,[2]The University of Texas Health Center at Houston, Houston, TX,[3]Distinguished Professor, Sanford Burnham Prebys Medical Discovery Institute, La Jolla, CA,[4]Univ. of Tartu, Tartu, Estonia

While effective treatments for prostate cancer (PC) such as androgen deprivation therapy (ADT) have been developed, it is still a challenge to treat advanced PC, which has become resistant to ADT or has metastasized. Lately, therapeutic agents that selectively target PCs such as [177Lu]Lu-PSMA-617 have shown promise, suggesting that tumor-specific drug delivery may greatly improve the management of metastatic castration-resistant PC. Here, we report a novel peptide, MHP1 (metastasis homing peptide 1), which effectively homes to metastatic PC in vivo.MHP1 was identified by phage display using experimental metastasis mouse models using the androgen-independent PC-3 human cancer cell line. The mouse models were prepared by either directly injecting the cells into the tibia and/or the brain or through intracardiac or intravenous injections to produce disseminated tumors. Phage display was performed using a cyclic CX7C peptide library expressed on T7 phage. To enrich for peptides that effectively home to metastatic PCs, the phage display was performed in mice by first performing 1 round of ex vivo phage panning using cell suspensions prepared from PC-3 tibia xenografts, followed by 3-4 rounds of in vivo selections in disseminated metastasis mice. DNA sequencing of the enriched phage clones yielded 150 candidate peptides. Phage clones that expressed each peptide on the coat protein were then mixed at an equimolar ratio to produce champion phage pools. “Play-off” in vivo phage display studies were performed by systemically injecting the phage pools into disseminated PC-3 tumor mice. A phage clone that expressed the MHP1 peptide showed the highest tumor-specificity by homing to tumors in various organs without accumulating into corresponding normal tissues. The MHP1 peptide chemically synthesized with a fluorescent tag (FAM-MHP1) effectively homed to tibia and brain xenograft PC-3 tumors. It also homed to disseminated metastatic PC-3 tumors in various organs, such as the jaw, femur, lymph nodes, and eye. Of note, in a spontaneous metastasis model prepared with 22Rv1 human PC cells, FAM-MHP1 homed more effectively to metastatic tumors than to the primary tumor. To identify the receptor of MHP1, affinity chromatography was performed by passing tissue lysates of PC-3 tibia tumors over MHP1-coated beads. A protein was eluted with the MHP1 peptide (but not by a control peptide). Mass spectrometry analysis revealed a list of candidate proteins. Preliminary data suggest that one of the candidates appears promising for being highly expressed in PC tissues. Interestingly, while the protein is intracellular in normal cells, it is misplaced onto the surface of some PC cells making it available for affinity-based targeting. These results suggest that the MHP1 peptide may serve as a promising platform to target metastatic PC. Characterization of the receptor may also lead to additional PC-specific therapies and deeper understanding of PC biology.

#3023 Capsaicin nanoparticles display robust growth-inhibitory activity in human NSCLC.

Kushal Jignesh Modi, Reagan S. Light, Kaitlyn B. Conley, Sarah L. Miles, Piyali Dasgupta

Joan C. Edwards School of Medicine, Huntington, WV

Purpose of the study: The dietary compound Capsaicin is the hot and pungent ingredient of chili peppers. Preliminary data in our laboratory have found that capsaicin displays robust growth-inhibitory activity in human lung cancers. However, the clinical applications of capsaicin as a viable anti-cancer drug are hindered by its adverse side effects, such as gastric irritation, nausea, stomach cramps and a burning sensation in the gut. Clinical trials which explored the pain-relieving activity of capsaicin found that patients who orally ingested capsaicin discontinued taking the drug due to its unpleasant side effects. One strategy to circumvent this drawback is to encapsulate capsaicin in long-acting formulations (like polymeric nanoparticles). Once capsaicin is entrapped in these polymeric nanoparticles, it is released at a very slow rate, so it does not produce any “heat-sensation” and adverse side effects in patients
Experimental procedures: Capsaicin [poly(lactic-co-glycolic acid)] nanoparticles (hereby called CAP-PLGA-NPs] were custom synthesized by a biotech company. The physicochemical properties of these nanoparticles were provided by the vendor. We tested the pro-apoptotic activity of these CAP-PLGA-NPs in a panel of human NSCLC cell lines. We also measured the impact of these CAP-PLGA-NPs on the growth of normal human lung, liver and kidney cells. We also performed soft agar assays to evaluate the ability of CAP-PLGA-NP to inhibit anchorage independent-growth on soft agar. Finally, we tested the anti-neoplastic activity of CAP-PLGA-NPs in SCID mice xenografted with human NSCLC tumors.
Results: The CAP-PLGA-NP displayed greater pro-apoptotic activity than capsaicin in human NSCLCs. CAP-PLGA-NP inhibited colony-formation in soft agar assays. Most interestingly, CAP-PLGA-NP did not impact the growth of normal human lung, liver and kidney cells. The intravenous administration of CAP-PLGA-NPs decreased the rate of human NSCLC tumors xenografted in SCID mice
Conclusions: The long-acting capsaicin drug formulation, namely CAP-PLGA-NP, may be a promising nutrition-based drug in human NSCLCs.
Support or Funding InformationFunding for our study was supported by the NIH R15-AREA Grant (2R15CA161491-02 and 2R15CA161491-03), the Women's Health T3: 3P20GM103434-23W1 (PI: Dr. G Rankin) to PD and MAV and the NIAID-AI151970 grant to TEL. This study was supported in part by the West Virginia IDeA Network of Biomedical Research Excellence (WV-INBRE) grant (NIH grant P20GM103434; PI: Dr. G. Rankin), the National Institute of General Medical Sciences of the National Institutes of Health under the award number P30GM122733.

#3024 Enhancing targeted delivery in multiple myeloma via novel NCI-H929 lipid-extracted-modified nanoliposomes.

Kenny D. Pham, Shivmani Barve, Robert B. Campbell

School of Pharmacy, Department of Pharmaceutical Sciences, Massachusetts College of Pharmacy & Health Sciences, Worcester, MA

Background: Multiple myeloma (MM) is an incurable hematological malignancy characterized by the aberrant proliferation of plasma cells in the bone marrow. Current first line goals of therapy for newly diagnosed symptomatic MM aim to achieve minimal residual disease prior to transplant, a key predictor of overall survival. However, toxicities remain a rate limiting step during induction therapy. Cell membrane lipid-extracted nanoliposomes (CLENs) are a novel drug delivery system that can be optimized to preferentially target MM cells. Prior research involving the use of the multiple myeloma cell line, RPMI-8226, supports the use of lipid extracts (LE) to enhance targeting. This study aims to evaluate whether the inclusion of LE derived from an additional MM cell line, NCI-H929, will also enhance targeting, while decreasing nanoliposome uptake by model off-target and non-target cells.
Methods: The MM (target) cell line explored in this study was NCI-H929. K562-GFP was used as the non-target cell line, and normal healthy peripheral blood mononuclear cells (PBMCs) served as the off-target cell control. Cells were seeded at a concentration of 20,000 cells/mL in vented centrifuge tubes and exposed for 1 hour to varying compositions of nanoliposome preparations including: DOPC, NCI-H929 lipid extract (LE), cholesterol (Chol), and DPPE-rhodamine for fluorescence studies. Nanoliposomes were prepared using a modified thin film method. Relative fluorescence intensity was determined using a fluorescence microplate reader.
Results: Mean liposome diameters (± deviation) for DOPC formulations containing NCI-H929 LE were: DOPC (100%)- 188.6 ± 2 nm, DOPC/LE- 95/5 212.3 ± 2 nm, 90/10- 230.4 ± 2 nm, 85/15- 200 ± 4 nm, and 80/20- 142 ± 1 nm. For formulations including cholesterol, diameters were: DOPC/Chol 90/10- 235 ± 2 nm and DOPC/Chol/LE 80/10/10- 227.4 ± 2 nm. Following 1 hour exposure of the target cell line to different concentrations of DOPC/LE, a statistically significant increase in uptake was observed in DOPC/LE preparations compared to DOPC alone: 95/5 and 90/10 ($p < 0.0001$), 85/15 ($p < 0.001$), and 80/20 ($p < 0.05$), with the highest uptake observed for 90/10. The addition of cholesterol did not further enhance uptake, and no significant uptake was observed in non-target or off-target cells compared to controls.
Conclusions: Our preliminary findings support that cellular uptake in MM cells may be increased via NCI-H929-LE modified nanoliposomes, with diminished uptake by non-target and off-target cell populations. Confirmation studies are currently underway, including cytotoxicity studies comparing conventional chemotherapy against NCI-H929 LE-modified nanoliposomal formulations.

#3025 Self-synergizing mutual prodrug liposomes co-targeting redox homeostasis and PIN1 for cancer therapy.

Nuri Kim, Dongwon Lee

Jeonbuk National Univ., Jeonju-si, Korea, Republic of

PIN1 is a prolyl isomerase that catalyzes the cis-trans isomerization of phosphorylated Ser/Thr-Pro motifs and is overexpressed in various cancer types, where it functions as a key regulator that amplifies oncogenic signaling. PIN1 promotes cancer cell proliferation, survival, and metastasis by stabilizing diverse oncoproteins and disrupting tumor-suppressive pathways such as p53, and its activity is highly sensitive to the intracellular redox state, becoming inactivated in a redox-dependent manner in response to changes in oxidative stress levels. In this study, we developed a mutual prodrug in which all-trans retinoic acid (atRA) is integrated into a single molecule with a quinone methide (QM) precursor that amplifies oxidative stress via glutathione (GSH) depletion, to simultaneously maximize atRA-mediated PIN1 inhibition and reactive oxygen species (ROS)-mediated anticancer activity. We first evaluated the synergistic cytotoxicity of atRA and the QM precursor in MCF-7 breast cancer cells by calculating the combination index and assessing changes in PIN1 and its downstream effector cyclin D1 by Western blotting. To exploit this synergy, we designed and synthesized a mutual prodrug in which atRA is covalently linked to the QM precursor, and confirmed its structure by ^{1}H NMR and LC-MS/MS analysis. Owing to its amphiphilic molecular structure, the mutual prodrug could be stably incorporated into the lipid bilayer at a high loading (~40%) together with DPPC, which enabled the formulation of prodrug-based liposomes. The liposomal surface was subsequently coated with γ-poly(glutamic acid) (γPGA) targeting γ-glutamyl transferase (GGT), yielding particles with a mean diameter of approximately 150 nm. We then examined esterase-triggered release of atRA and QM and evaluated intracellular GSH depletion and ROS amplification, as well as mitochondrial dysfunction, in MCF-7 cells. We further analyzed redox-responsive, PIN1-related, and apoptosis-related signaling by qPCR and Western blotting. Targeting and in vivo antitumor efficacy of the γPGA-coated prodrug liposomes were assessed in an MCF-7 xenograft mouse model, and additional biosafety evaluation revealed no apparent systematic toxicity. Collectively, the mutual prodrug liposomal formulation integrating atRA and the QM precursor disrupted intracellular redox homeostasis and suppressed PIN1-dependent oncogenic signaling, resulting in enhanced anticancer efficacy and reduced systematic toxicity. Thus, this platform offers a next-generation precision nanomedicine candidate that unifies high drug loading, tumor-selective delivery, and self-synergistic mechanisms within a single, clinically translatable system.

#3026 A polymer-drug conjugate platform for tumor specific drug delivery: Advancement of a clinically validated ultra pH-sensitive micelle technology.

Qingtai Su, Stephen Gutowski, Bhargavi Allu, Austin Burcham, Zirong Chen, Ruolan Han, Jason B. Miller, Tian Zhao

OncoNano Medicine, Inc., Dallas, TX

Background: Antibody-drug conjugates (ADCs) have been developed to deliver anti-tumor therapeutics directly to tumors, and have demonstrated some impressive clinical benefits. Challenges with ADCs, however, persist, including necessary identification of exclusively or highly expressed tumor targets, emergence of resistance due to target downregulation, and systemic toxicities from both off-tumor/on-target deployment of payload or unplanned payload release. Herein, we report a polymer-drug conjugate (PDC) platform based on a clinically-validated, ultra-pH sensitive micelle technology - ON-BOARD™. This novel technology enables delivery of cytotoxic compounds through targeting the acidic tumor microenvironment (TME), independent of tumor target expression, offering a differentiated approach from existing therapeutics.

Methods: A pilot library of pH sensitive ON-BOARD™ PDCs was synthesized, connecting clinically utilized warheads (DM1, MMAE, SN-38) via cleavable or non-cleavable linkers. Purity and drug-to-polymer ratio (DPR) were characterized by HPLC and ^{1}H NMR. PDC micelles were characterized for purity, particle size, and pH-responsiveness. Linker reactivities were confirmed by treating formulations under cleavage-inducing conditions. *In vitro* cytotoxicity was evaluated by incubation with different cancer cell lines. *In vivo* anti-tumor efficacy and tolerability were demonstrated in mice bearing human colon cancer xenografts (HCT-116, HT-29) and compared with a standard chemotherapy and/or the corresponding free drug.

Results: The PDC polymers were synthesized with high purities (>95%) and DPR ranging from 2 to 4. The formulated micelles showed sharp pH responsiveness with particle size < 60 nm and an expected > 1,000 drug per micelle ratio. *In vitro* treatment of the cleavable PDC micelles confirmed the reactivity according to their respective linker cleavage mechanisms. Cytotoxicity assays in multiple cancer cell lines showed directed payload release with PDCs containing certain cleavable linkers showing strong potency upon triggering of drug release. DM1 and SN38 PDCs with a cleavable linker demonstrated stronger antitumor activity compared to the ones with a non-cleavable linker in HCT-116 and HT-29 tumors in mice, respectively, while a cleavable SN-38 PDC showed superior efficacy to irinotecan (76% vs 48% TGI) at 21-fold lower SN-38 equivalent dose. MMAE PDCs with cleavable linkers achieved strong efficacy in HT-29 model (99% TGI, 88-100% tumor free) with favorable tolerability compared to the docetaxel control.

Conclusion: A variety of PDCs with different linker drug combinations were generated with ON-BOARD™ pH sensitive micelle technology. The resultant formulations demonstrated strong potency *in vitro* and *in vivo*, offering a promising platform for delivery of therapeutics to the TME with high specificity.

#3027 Cellular uptake of nanoliposomes with optimized cholesterol concentration and lipid extract derived from a model low grade serous ovarian carcinoma cell line.

Sofia Orlando, Krishna Panchal, Heer Patel, Robert B. Campbell

Massachusetts College of Pharmacy and Health Sciences, Worcester, MA

Introduction: Low-grade serous ovarian carcinoma (LGSOC) represents a rare subtype of epithelial ovarian cancer, accounting for less than 10% of all cases and typically diagnosed in younger women. The disease is characterized by tumor growth driven by activating mutations in the MAPK pathway, including *KRAS*, *BRAF*, and *NRAS*. Despite its slow progression, LGSOC remains challenging to treat due to limited responsiveness to conventional chemotherapy. The objective of this study was to isolate cellular lipid extract (LE) material from a model LGSOC cell line, and to utilize the newly acquired LE material to develop a relatively target specific nanoliposomal system. Early formulation and in vitro studies include optimization for cholesterol and LE content.
Methods: Low-grade serous ovarian carcinoma cell line (PM-LGSOC-01, Cytion) was cultured and expanded in EMEM growth medium supplemented with 10% FBS. The PM-LGSOC-01-lipid extract (LE) material was extracted from PM-LGSOC-01 when the cells reached ~90% confluency. Lipid extraction was performed as described previously (Alharbi & Campbell, AAPS Open, number: 5(2018)). Nanoliposomal preparations consisted of DOPC, cholesterol, and LE at various ratios and wereformed by thin film method using a Buchi R-80 rotary evaporator. DPPE-Rhodamine was included in the preparations for cellular studies. Following sonication, particle size and zeta potential values weredetermined using ZetaPals. Fluorescence detection was performed using a fluorescence microplate reader.
Results: Three preparations (1) DOPC (100%), (2) DOPC/Chol (95/5), and (3) DOPC/Chol (90/10) wereprepared with an average particle size of 221 ± 3 nm, 250 ± 5 nm, and 139 ± 0.3 nm, respectively. Preliminary results suggest that the additional inclusion of cholesterol in the nanoliposomal preparations increased their uptake by the target (PM-LGSOC-01) cells. Studies investigating the influence of PM-LGSOC-01-LE on the uptake of nanoliposomes by the target cells are currently underway.
Conclusion: To date, the influence of cholesterol on the uptake of nanoliposomes by LGSOC cells has been investigated. Future studies will evaluate the effect of optimized cholesterol and LE contenton targeting low-grade serous ovarian carcinoma.

#3028 Investigating phosphatidylcholine and phosphoethanolamine phospholipids in conventional and novel cationic nanoliposomes for interactions with chronic myeloid leukemia cells *in vitro*.

Shivmani Y. Barve, Robert B. Campbell

Department of Pharmaceutical Sciences, Massachusetts College of Pharmacy & Health Sciences, Worcester, MA

Background: Lipid Nanoparticles (LNPs) have been established as excellent vehicles for drug/nucleotide delivery for Chronic Myeloid Leukemia (CML). The optimization of lipid ratios of cationic and helper lipids, such as phosphatidylcholine (PC) and phosphoethanolamine (PE)- based lipids, governs the selectivity of LNPs. Furthermore, the incorporation of LE (lipid extracts) derived from target cell membranes has been used to develop CLENs (cell membrane lipid-extracted nanoliposomes) for superior targeting. However, the behavior of PE- and PC-based lipids in the presence of LE is not well understood. In this study, we investigate the cellular interactions of LNPs consisting of PE or PC phospholipids employed in different combinations of cationic lipids and/or lipid extract ingredients using a model CML (K562-GFP) cell line.
Methods: The K562-GFP human CML cell line (CCL-243-GFP) was cultured in RPMI-1640 medium supplemented with 10% fetal bovine serum (FBS). LNPs were prepared using the thin film hydration method and characterized for size and zeta potential. Phase I of the study compared the cellular uptake of LNPs, substituting four cationic lipids (DOTAP, EPC, DOTMA, DODMA) at varying concentrations (0-50 mol%) with the helper lipid DOPC. Phase II involved comparing the PC versus PE helper lipid at a fixed cationic lipid concentration determined in Phase I. Phase III of the study aims to investigate the cellular uptake of LNPs after the inclusion of LE at various concentrations by target and non-target cell lines.
Results: We identified the cellular uptake to be about 250% higher for LNPs containing 25 mol% of DOTAP or EPC compared to the control (DOPC 100 mol%) from Phase I. Phase II revealed that LNPs with helper lipid DOPC performed significantly better at all time points (0 to 120 min) with an increase in cellular uptake compared to helper lipid DOPE. In phase III, the inclusion of LE derived from the target cell in the cationic LNPs led to a selective uptake by the target cell line and decreased uptake by the non-target cell lines.
Conclusion: Results to date revealed that the cellular uptake of LNPs depends largely on the optimum ratio of the cationic lipid to the helper lipid type employed in the development of the nanoparticles, and that inclusion of LE leads to superior targeting.

#3029 A modular lipid-based oral drug delivery system for precision combination chemotherapy in breast cancer.

Shailvi Soni[1], Terrick Andey[2]

[1]Department of Pharmaceutical Science, Massachusetts College of Pharmacy & Health Sciences, Boston, MA,[2]Department of Pharmaceutical Science, Massachusetts College of Pharmacy and Health Science, Worcester, MA

Breast cancer is the third leading cause of cancer-related deaths among women in the United States. Treatment options often include chemotherapy, which involves the use of highly potent but toxic medications that can cause severe adverse reactions, further worsening the patient's condition and, in some cases, leading to fatal outcomes. Additionally, oral delivery of chemotherapeutic agents is limited by poor bioavailability, arising from the harsh acidic and enzymatic environment of the gastrointestinal tract, low oral absorption, and extensive hepatic first pass metabolism, which contribute to the significant toxicity and reduce therapeutic efficiency associated with conventional chemotherapies. This study aimed to develop and evaluate a mannosamine modified, freeze-dried self-emulsifying drug delivery system (SEDDS) capable of co-delivering chemotherapeutic agents to enhance oral absorption and improve targeted delivery for breast cancer treatment

Methods: Four SEDDS formulations were optimized and prepared using varying ratios of Labrasol, Capryol 90, Labrafac PG, and Gellucire 44/14. Primary water-in-oil emulsions containing doxorubicin and ellipticine were dispersed into an external aqueous phase containing mannosamine to form water-in-oil-in-water double emulsions under passive mixing. Formulations were subsequently freeze dried to yield solid, dispersible SEDDS. The formulations were characterized for particle size, polydispersity index, stability, and morphology (SEM). Thermal behavior (DSC, XRD), drug release profile (In vitro Dissolution), permeation (MDCK cell line), and cellular uptake (MDA MB-231 and MDA MB-468 cell lines) were also assessed.

Results: Optimized surfactant-to-oil ratios (1:9 and 2:8 aqueous: oil phase ratios) produced stable primary and double emulsions suitable for SEDDS development. Microscopy confirmed triphasic w/o/w structures with internal aqueous droplets encapsulated within a lipid phase and surrounded by an external aqueous phase. SEDDS demonstrated particle sizes between 190-587 nm and PDI values of 0.005-0.336. Thermal analyses of freeze dried SEDDS indicated the formation of amorphous mixtures with sustained release kinetics. Fluorescence imaging showed efficient cellular uptake of the dual drug loaded formulations.

Conclusion: A mannosamine modified SEDDS was successfully developed, enabling dual loading of doxorubicin and ellipticine with favorable stability, sustained release, and efficient cellular uptake. This work demonstrates the potential of this lipid-based, modular oral delivery platform to enable mono and combination chemotherapy with improved bioavailability and reduced toxicity. By integrating innovative formulation science with targeted drug delivery, this work contributes to broader efforts at designing safe and effective treatments for cancer.

#3030 SU-CCS-1 lipid extract-modified nanoliposomes and characteristic growth profile of a model clear cell sarcoma target cell line.

Ashley Silva[1], **Abigail Chan**[1], Simoun Banoud[1], Charloote Bouchard[1], Robert B. Campbell[2]

[1]Pharmacy, Massachusetts College of Pharmacy & Health Sciences, Worcester, MA,[2]Massachusetts College of Pharmacy & Health Sci., Worcester, MA

Background: Sarcomas account for approximately 1% of adult cancers and 15% of childhood cancers in the United States. Conventional treatment strategies are somewhat effective during early disease, but once metastasized, treatment success significantly declines. Nanomedicine presents an alternative approach to increase current treatment efficacy and prolong survival. Optimization of liposomal preparations is essential to ensure the most selective targeting. The objective of the study was to develop a novel nanoliposomal drug delivery system using a cellular model of human clear cell sarcoma in vitro.
Methods: The SU-CCS-1 cell line was selected as the cellular model for clear cell sarcoma and used for the drug selectivity studies. SU-CCS-1 cells were cultured and expanded in vitro for cellular extraction purposes. Cellular lipid extract (LE) material was derived from a clear cell sarcoma target (SU-CCS-1) cell line. Nanoliposomes were optimized for LE and cholesterol content. DPPE-Rhodamine (used as a fluorescence indicator) for cellular uptake studies, and a fluorescence microplate reader was used to assess relative fluorescence intensity values. Phase I of evaluation included characterization of cells and cellular uptake properties of nanoliposomal preparations of DOPC and cholesterol consisting of 0, 5, and 10 mol% cholesterol content. To characterize the cellular growth characteristics, separate flasks were prepared with either 100% adherent or 100% suspension cells acquired from a mature mixed cell population. The percentage of adherent and suspension cells was determined on Day 0 and Day 5.
Results: An evaluation of growth profile characteristics of the SU-CCS-1 target cell line revealed a substantial transformation of suspension cells to adherent cells over time. While the flask of 100% adherent cells remained 72% adherent after 5 days, the flask of 100% suspension cells transformed to become 59% adherent after 5 days. The particle size for nanoliposomes containing 0, 5, and 10 mol% cholesterol was 283 nm, 139.9 nm, and 247 nm, respectively. Additionally, the inclusion of 10 mol% SU-CCS-1-LE increased uptake of nanoliposomes compared to 0% LE control preparations (without SU-CCS-1-LE).
Conclusion: Preliminary findings suggest that the DOPC:cholesterol ratio affects nanoliposome uptake by SU-CCS-1 cells. The inclusion of SU-CCS-1-LE in nanoliposomes enhances their targeting efficiency. Ongoing studies will investigate the effect of dual incorporation of optimized cholesterol and SU-CCS-1-LE content on the targeting of clear cell sarcoma.

#3031 Enhanced delivery of doxorubicin via milk-derived extracellular vesicles in lung cancer cells.

Cayden Xuanzhang Xia[1], Elise Copeland[2], Akhil Srivastava[3]

[1]Emory University, Atlanta, GA,[2]College of Arts & Sciences, Department of Chemistry, Georgia State University, Atlanta, GA,[3]Departments of Pathology and Anatomical Sciences, Ellis Fischel Cancer Center, University of Missouri School of Medicine, Columbia, MO

Introduction:
Extracellular vesicles (EVs) are nano-sized particles that mediate intercellular communication by transporting proteins, lipids, and nucleic acids. Due to their natural origin and biocompatibility, EVs have gained attention as potential drug delivery systems. However, their clinical use has been limited by low delivery efficiency and potential cytotoxicity. Milk-derived EVs, especially from skim milk and milk powder, offer advantages such as resistance to digestive enzymes and minimal toxicity. Our previous studies demonstrated their effective encapsulation and delivery of doxorubicin, a widely used chemotherapeutic agent.
Materials and Methods:
EVs were isolated from skim milk and milk powder and characterized using nanoparticle tracking analysis (NTA) for size and concentration, and protein content was measured via BCA assay. Doxorubicin was loaded into EVs, and the EV-doxorubicin formulation was tested in A549 and H1299 lung cancer cell lines. Cells were treated with either free doxorubicin or EV-doxorubicin, and apoptosis and viability were assessed at 24, 48, and 72 hours. Apoptosis-related proteins PARP-1, Caspase-9, and Caspase-3 were analyzed using Western blotting.
Results:
The EV-doxorubicin complex demonstrated superior uptake and significantly reduced cell viability in both cell lines compared to free doxorubicin. Apoptosis levels were consistently higher in the EV-doxorubicin-treated groups across all time points. Western blot analysis revealed reduced levels of total PARP-1, Caspase-9, and Caspase-3, supporting enhanced apoptotic activity. EVs alone did not exhibit cytotoxic effects, confirming their safety.
Discussion:
Milk-derived EVs can efficiently encapsulate and deliver doxorubicin, enhancing its therapeutic effects in lung cancer cells while minimizing toxicity. These results highlight the potential of milk EVs as safe and effective drug delivery vehicles for chemotherapeutics.

#3032 Electroporation-enhanced targeted bleomycin delivery for the treatment of canine perianal tumors.

Sergio Fernando Salgado[1], Josmell David Mestanza[2], Andrea Hatsumi Bazan[2], Micaela Vizquerra[2], Mitzi Westreicher[2], Nandi Ken Candela[2]

[1]Universidad Peruana Cayetano Heredia, Lima, Peru,[2]Creo Vet, Lima, Peru

Introduction: Perianal tumors are common in middle-aged to older male dogs. Treatment of these tumors remains a clinical challenge due to the complex anatomy of the region and limited surgical margins, which increase the risk of local recurrence. In this context, electrochemotherapy (ECT) emerges as a promising non-surgical alternative that combines chemotherapeutic agents, such as bleomycin, with high-intensity and short-duration electric pulses, enhancing cell membrane permeability and potentiating the antitumor effect. The objective of this study was to evaluate the efficacy and safety of ECT as a non-surgical treatment for perianal tumors.

Materials and methods: Medical records of dogs of various breeds diagnosed with perianal neoplasms confirmed by histopathology were reviewed. Both benign and malignant lesions of variable size and number were included, excluding apocrine gland anal sac carcinomas. For each patient, the number of treatment sessions, type of clinical response, and recurrence were recorded. All animals underwent ECT consisting of eight monophasic pulses at 5 kHz and an electric field strength of 1,000 V/cm using a long needle electrode. The first pulse was delivered 8 minutes after the administration of intravenous bleomycin (15,000 IU/m2).

Results and discussion: Thirty-three dogs with perianal tumors were treated with ECT. The most frequent diagnoses were adenocarcinoma (57.6%), adenoma (36.4%), and hemangiosarcoma (6.1%). Most lesions were solitary (75.8%) and varied in size: <1cm (30.3%), 1-3 cm (48.5%), and >3cm (30.3%). A single ECT session was sufficient in 87.9% of cases, while 12.1% required two sessions. A complete response (CR) was achieved in 87.9% of patients, and a partial response (PR) was 12.1%. No cases of progressive or stable disease were reported in this study. Regarding tumor type, adenomas showed a 90.9% complete response rate, adenocaricnomas 84.2%, and hemangiosarcomas 100%. The recurrence rate was low (9.1%) with an overall treatment efficacy of 90.9%. Adverse effects were mild and self-limiting, consisting mainly of local inflammation (100%) and transient pain. However, one case presented with mild post-procedural constriction and constipation.

Conclusions: Electrochemotherapy represents an effective option for managing canine perianal tumors, particularly when complete surgical excision is not feasible or when preservation of anal function is desired.

#3033 Electrochemotherapy for rectal adenocarcinoma: Advancing drug delivery through electroporation.

Sergio Fernando Salgado[1], Josmell David Mestanza[2], Micaela Vizquerra[2], Mitzi Westreicher[2], Nandi Ken Candela[2], Andrea Hatsumi Bazan[2]

[1]Universidad Peruana Cayetano Heredia, Lima, Peru,[2]Creo Vet, Lima, Peru

Introduction: Rectal adenocarcinoma is the most common tumor of the lower digestive tract of the dogs, affecting the quality of life. Electrochemotherapy (ECT) is a novel drug delivery system that enhances the intracellular delivery of low-permeability cytostatic drug through the transient permeabilization of the cell membrane. This study aimed to evaluate ECT as a treatment for colorectal adenocarcinoma in dogs

Experimental procedure: Twelve dogs diagnosed with rectal adenocarcinoma were included. For each patient, data recorded included, breed, sex, tumor size, number of treatment sessions, clinical response, recurrence, disease-free interval and post treatment complications. The therapeutic protocol consisted in intravenous administration of Bleomycin (15,000 IU/m2). Traction points were placed in the rectal mucosa to facilitate exposure of the lesion to be treated. Eight minutes after drug administration, electric pulses were delivered using a Biotex EPV200 electroporator (Argentina). A train of eight monophasic pulses (1000V/cm, 5000Hz) was applied using needle and plate electrodes.

Results: This is the first study in dogs evaluating ECT for rectal adenocarcinoma. Most tumors were pedunculated and smaller than 1cm (9/12).; the remaining were broad-based, with one case involving nearly the entire rectal circumference. All lesions were located within 3cm of the anus. All dogs (12/12) underwent a single treatment session, achieving a 100% complete response rate. Ten of twelve dogs remained disease-free at the end of the study; one died of unrelated causes after two years, and two showed local recurrence (at 308 and 688 days, respectively), the latter successfully retreated and disease-free to date, with survival exceeding 1350 days. Observed complications included local inflammation and tenesmus; pain and constipation were reported in two cases.

Conclusion: Bleomycin delivered by electroporation for rectal adenocarcinoma in dogs proved to be effective and can be considered a first-line alternative to surgery. A comprehensive medical management plan is recommended to address post treatment complications.

#3034 Feasibility and safety of electroporation-enhanced bleomycin delivery for the treatment of parenchymal tumors in dogs and cats.

Sergio Fernando Salgado[1], Andrea Hatsumi Bazan[2], Josmell David Mestanza[2], Nandi Ken Candela[2], Mitzi Westreicher[2], Micaela Vizquerra[2]

[1]Universidad Peruana Cayetano Heredia, Lima, Peru,[2]Creo Vet, Lima, Peru

Introduction: Cancer affecting parenchymal organs in dogs and cats present a therapeutic challenge, particularly in cases of multiple lesions or locally advanced disease where surgery is not indicated and medical therapies offer limited response. Electrochemotherapy (ECT) facilitates bleomycin entry into cells through the formation of transient membrane pores, providing a precise drug delivery that enhances cytotoxic efficacy. The aim of this study was to report the safety and feasibility of ECT for the management of parenchymal tumors in both species.

Materials and methods: Five patients (four dogs and one cat) diagnosed with hepatic or pancreatic cancer, for whom no therapeutic option was feasible, were included. Recorded variables included diagnosed pathology, clinical presentation, treatment duration, clinical response, and short-and long-term adverse effects. Bleomycin (15,000 IU/m2) was administered intravenously, followed by electric pulse application using a Biotex EPV200 electroporator (Argentina). Electric pulses (eight pulses of 100 µs, 1.000 V/cm, 5 kHz) were delivered to all lesions, planned preoperatively via computer tomography. Response was evaluated by ultrasonography at 30 and 60 days post-treatment.

Results: Among the four dogs, three were diagnosed with multifocal hepatocellular carcinoma and one with insulinoma. Additionally, a cat was diagnosed with pancreatic adenocarcinoma. All cases were treated. Hepatic lesions were ≤3 cm, located in different lobes, with 2-3 nodules treated per patient. The insulinoma (2.66 x 0.88 cm) was located in the right pancreatic lobe, and the feline adenocarcinoma (2.15 x 1.63 x 1.89cm) was found i the pancreatic body in contact with the duodenum and the pancreaticoduodenal vein. All treatments were performed via laparotomy. A foldable needle electrode was used for hepatic lesions due to deeper access, while plate electrodes were selected for pancreatic tumors to ensure complete coverage. The mean treatment duration was 15 minutes from bleomycin infusion, with longer times for hepatic cases. All patients achieved a complete response: hepatic tumors by day 60, the feline pancreatic tumor showed a partial response at day 30, and a complete response by 6 months. Among hepatic cases, one showed transient liver enzyme elevation, and another case showed normalization of liver enzymes. For pancreatic cases, the specific pancreatic lipase was elevated post-treatment. All animals experienced mild to moderate pain, slightly prolonged in the cat. The dog with insulinoma resolved hypoglycemia but later developed diabetes mellitus requiring medical management, the only long-term adverse outcome observed.

Conclusions: Electroporation-mediated bleomycin delivery represents a viable and safe option for the treatment of malignant parenchymal tumors. Further studies are needed to confirm these preliminary findings.

#3035 Electrochemotherapy as an innovative drug delivery modality for local control of canine acanthomatous ameloblastoma.

Sergio Fernando Salgado[1], Andrea Hatsumi Bazan[2], Josmell David Mestanza[2], Micaela Vizquerra[2], Nandi Ken Candela[2], Mitzi Westreicher[2]

[1]Universidad Peruana Cayetano Heredia, Lima, Peru,[2]Creo Vet, Lima, Peru

Introduction: Acanthomatous ameloblastoma is the most common odontogenic epithelial tumor in dogs. Block excision is the treatment of choice since marginal removal has a recurrence rate exceeding 90% within one year. Electrochemotherapy (ECT) enables intracellular delivery of bleomycin, inducing apoptotic cell death. The aim of this study was to evaluate efficacy, response and complications of ECT in canine ameloblastomas.

Materials and Methods: Twelve dogs with histopathologically confirmed oral ameloblastoma were included. Of the lesions analyzed, nine were smaller than 2 cm and three were larger than 2 cm. All patients were treated with ECT in one or two sessions. In 11 of 12 cases, tooth extraction was required to optimize tumor access. Treatment was performed using an EPV-200 electroporator (Biotex, Argentina) with needle electrodes. Bleomycin was administered intravenously at a dose of 15000 IU/m^2, eight minutes prior to delivering the electric pulses (train of eight 100 µs pulses, 1000 V/cm, 5000 Hz). Tumor response, recurrence and post treatment complications were recorded.

Results: Seventy-five percent (9/12) of the lesions were smaller than 2 cm. A single ECT session was performed in 10 patients (8.3.3%), while the remaining two required a second session- one at 30 days and another at 95 days- based on the initial treatment response. Smaller lesion (<2cm) showed better response when the entire tumor was covered by the electric field. In 11 of 12 cases (91.6%) partial tooth removal was necessary to ensure complete exposure of the tumor and its origin. Clinical responses were complete in 83.3% (10/12), partial in 8.3% (1/12), and stable disease in 8.3% (1/12), with no cases of tumor progression during the follow- up. The main postoperative complications were local inflammation (100%) and mild to moderate pain (33.3%), both managed successfully with analgesic and anti-inflammatory therapy.

Conclusions: Electrochemotherapy represents an effective and safe therapeutic alternative for the conservative management of canine ameloblastoma. Early detection and treatment are associated with higher complete response rates. Extraction of adjacent teeth improves treatment efficacy by enhancing electric field contact with the tumor tissue. Post treatment pain and inflammation control are essential to minimize complications and optimize recovery.

#3036 Intellipulse platform for efficient and effective delivery of therapeutics to solid tumors.

Richard Heller[1], Loree Heller[2], Jody Synowiec[2], Julie Singh[2], Alex Otten[2], Mark J. Jaroszeski[2]

[1]USF Health Morsani College of Medicine, Tampa, FL,[2]University of South Florida, Tampa, FL

The Intellipulse® system is a next generation user-friendly platform for safe and controlled delivery of therapeutics to solid tumors. One issue with delivering therapeutics is being able to get the agent where it is needed without unwanted adverse effects related to clearance of a carrier or off-target events. The second issue with any nucleic acid delivery is having confidence that delivery has occurred. We have demonstrated the utility of this platform by delivering two plasmids encoding immune modifiers directly to melanoma tumors to induce a robust immune response. We previously demonstrated that the intratumor delivery of a plasmid encoding interleukin-12 (pIL-12) resulted in a significant increase in T effector cells and a reduction in T regulatory cells and myeloid derived suppressor cells within the TME, inducing a robust systemic immune response that was amplified when combined with ICIs. The key to make this an effective therapy is to deliver these agents in a manner that has minimal adverse and off target effects while still inducing the desired response. We have designed a novel approach to efficiently deliver multiple plasmids directly to solid tumors. The rationale was based on the premise that by performing intratumor delivery, stimulation would be directed against the specific antigens within the TME to produce an effective local response while stimulating a systemic response, resulting in an abscopal effect. This delivery utilizes a next generation electrotransfer device that enables the use of significantly reduced voltages and includes a means to monitor when successful delivery has occurred. We tested this concept in the B16.F10 mouse melanoma model. Intratumor delivery of pIL-12 resulted in effective control of the treated tumor in over 90% of the mice and generated resistance to challenge. To fully test this approach, we next evaluated a combination therapy delivering both pIL-12 combined with a plasmid encoding the extracellular domain of the PD1 protein, as an alternative form of checkpoint inhibitor. The therapy was tested in a multi-tumor model which included a subcutaneous tumor and intraperitoneal injection of tumor cells. The plasmids were delivered to the subcutaneous tumor; tumors generated by intraperitoneal injection were untreated. Peritoneal tumor growth was not affected by single plasmid delivery or when both plasmids were delivered using other delivery approaches or older electrotransfer technology. Delivery of the plasmids with the Intellipulse® platform resulted in two significant results. Binding of the expressed PD1 peptide to PDL1 on tumor cells was observed by immunohistochemistry and flow cytometry. In addition, complete regression in 90% of the treated mice of the subcutaneous tumor and blockage of peritoneal tumor growth as assessed via in vivo imaging was observed. Work is continuing to explore the treatment of other tumor types.

#3037 Investigating the therapeutic potential of a nanocrystal PRMT5 inhibitor in pancreatic ductal adenocarcinoma.

Faranak Alipourgivi[1], Zhongyue (Claire) Yuan[2], Rahaf Habboub[3], Yoon Yeo[4], Tao Lu[5]

[1]Translational Cancer Biology, Indiana University Melvin and Bren Simon Comprehensive Cancer Center, Indianapolis, IN,[2]Department of Industrial and Molecular Pharmaceutics, Purdue University, West Lafayette, IN,[3]Biochemistry, Molecular Biology and Pharmacology, Indiana University School of Medicine, Indianapolis, IN,[4]Industrial and Molecular Pharmaceutics, Purdue University, West Lafayette, IN,[5]Department of Biochemistry, Molecular Biology and Pharmacology, Indiana University School of Medicine, Indianapolis, IN

Persistent inflammation is a defining feature of pancreatic ductal adenocarcinoma (PDAC), largely driven by sustained activation of the NF-κB signaling pathway. Disruption of NF-κB regulatory mechanisms contributes significantly to this chronic activation. Protein arginine methyltransferase 5 (PRMT5), a known promoter of tumorigenesis in several cancers, including PDAC, colorectal, and breast, has emerged as a promising therapeutic target. Clinical data reveal that PDAC patients with high PRMT5 expression have significantly shorter median survival, underscoring its prognostic and therapeutic relevance. Our lab has been developing small-molecule inhibitors targeting PRMT5. Among these, our patented compound, PR5-LL-CM01 (CM01), has shown superior anti-tumor efficacy and reduced toxicity in PDAC models compared to the commercially available PRMT5 inhibitor EPZ015666. However, CM01's poor water solubility poses a challenge for clinical translation. To address this, we aim to enhance its water dispersibility and bioavailability by formulating CM01 as an albumin-coated nanocrystal (NC) (Abxtal). Preliminary studies confirmed successful production and physicochemical characterization of CM01 NCs, which have an optimized particle size (Z-average ~87 nm) and can be stored at -20ºC as lyophilized solid for at least three months. In this project, we assess the therapeutic potential of CM01 NC in vitro and in vivo. We hypothesize that CM01 NC more effectively inhibits PRMT5-mediated NF-κB signaling and associated oncogenic processes than unformulated CM01, and that it synergizes with gemcitabine (Gem) to suppress PDAC progression. Supporting this hypothesis, CM01 NC showed equal or greater inhibition of PDAC PANC1 and MIA PaCa2 cell growth compared to CM01, and more effectively suppressed 3D spheroid growth and cell migration in vitro. CM01 NC also outperformed CM01 in reducing NF-κB transcriptional activity, with comparable reductions in NF-κB target genes (TNF-α and IL-8) per qPCR assays. Additionally, Chou-Talalay analysis demonstrated that CM01 NC exhibits synergistic activity with Gem. We are now transitioning to in vivo studies to evaluate the pharmacokinetics and therapeutic efficacy of CM01 NC, both as a monotherapy and in combination with Gem, using PDAC models. This study may establish CM01 NC, alone or with Gem, as a promising therapeutic strategy, and could lay the foundation for clinical development of CM01 NC-based treatments for PDAC.

: Novel Targets and Pathways
Poster Session

#3040 FOXM1 as a drug target in NF1-associated malignant peripheral nerve sheath tumors.

Ellen M. Voigt[1], Quinn Hanigan[2], Joshua J. Lingo[2], Altay Koyas[2], Rebecca D. Dodd[3], Benjamin W. Darbro[4], Dragana Kopanja[5], Sung Hoon Kim[6], Benita S. Katzenellenbogen[7], John A. Katzenellenbogen[6], Dawn E. Quelle[2]

[1]Medical Scientist Training Program, University of Iowa, Iowa City, IA,[2]Neuroscience and Pharmacology, University of Iowa, Iowa City, IA,[3]University of Iowa College of Medicine, Iowa City, IA,[4]Pediatrics, University of Iowa, Iowa City, IA,[5]Biochemistry & Molec. Genetics, University of Illinois at Chicago, Chicago, IL,[6]Dept. of Chemistry, University of Illinois at Urbana-Champaign, Urbana, IL,[7]Dept of Physiology and Cancer Center, University of Illinois at Urbana-Champaign, Urbana, IL

Purpose: Malignant peripheral nerve sheath tumors (MPNSTs) are deadly sarcomas that arise spontaneously or via transformation of benign tumors, called plexiform neurofibromas (PNFs) and atypical neurofibromatous neoplasms of uncertain biologic potential (ANNUBPs), in patients with Neurofibromatosis Type 1 (NF1). Understanding molecular events that cooperate to promote malignancy is a priority in the field. One putative driver, FOXM1, is a powerful transcription factor that heightens the activities of kinases, MEK and CDK4/6, known to drive MPNST growth. We sought to understand the role of FOXM1 in these deadly sarcomas and *hypothesized it is a new druggable target that is essential for MPNST pathogenesis.*
Methods: FOXM1 mRNA and protein expression were evaluated in patient-matched PNFs, ANNUBPs, and MPNSTs via RNA-Seq and IHC. For *in vitro* studies, knockdown (KD) of FOXM1 was performed in MPNST cell lines (S462, sNF96.2, JH2-002). Proliferation, survival, and cell cycle progression were measured in response to FOXM1 inhibitors, including newly developed NB-55, NB-73 and NB-115 drugs. To directly test the *in vivo* role of FOXM1 in MPNST initiation and progression, *de novo* MPNSTs were initiated by *Nf1/Ink4a/Arf* editing in the sciatic nerve of $Nf1^{+/-}$, DhhCre, *Foxm1* floxed mice relative to $Nf1^{+/-}$;DhhCre controls.
Results: In patient-matched tumor sets, *FOXM1* mRNA was significantly elevated in MPNSTs relative to PNF/ANNUBP precursor lesions. FOXM1 protein expression rose dramatically in a stepwise manner from normal nerve to PNFs, ANNUBPs, and MPNSTs. FOXM1 KD slowed MPNST cell growth. FOXM1 inhibitors (thiostrepton, FDI-6, and multiple NB drugs) effectively inhibited MPNST proliferation and induced apoptosis. Synergistic killing of MPNST cells was obtained by combining thiostrepton with a MEK inhibitor (mirdametinib), CDK4/6 inhibitor (palbociclib), or EGFR inhibitor (gefitinib), while NB drugs synergized best with gefitinib. Excitingly, targeted *in vivo* deletion of *Foxm1* in the sciatic nerve significantly slowed tumor progression.
Conclusion: Our data demonstrate FOXM1 is an important driver of MPNST pathogenesis. FOXM1 expression and transcriptional activity are greatly increased in MPNSTs compared to benign precursors from the same patients. In agreement, genetic and therapeutic inactivation of FOXM1 promoted MPNST cell arrest and death. Synergistic killing of MPNSTs was achieved by combined inhibition of FOXM1 with MEK, CDK4/6, or EGFR while *Foxm1* ablation in the sciatic nerve significantly slowed tumor progression *in vivo*. Together, these findings reveal that FOXM1 inhibition in specific combination therapies represents a new treatment strategy for MPNST patients.

#3041 Selective PARP2 inhibitor disrupting PARP2-FOXA1 interaction to inhibit androgen receptor signaling in prostate cancer.

Fu Gui[1], Wenfei Hu[2], Qi Miao[3], Zhi Tan[4], Mingxing Teng[3], Adam S. Kibel[1], Wei Zhang[2], Li Jia[1]

[1]Department of Urology, Brigham and Women's Hospital, Harvard Medical School, Boston, MA,[2]Department of Chemistry, University of Massachusetts Boston, Boston, MA,[3]Department of Pathology & Immunology, Center for Drug Discovery, Baylor College of Medicine, Huston, TX,[4]Department of Pharmacology & Chemical Biology, Center for Drug Discovery, Baylor College of Medicine, Huston, TX

Currently targeting androgen receptor (AR) pathways is the primary treatments for advanced prostate cancer (PCa). However, resistance to AR pathway inhibitors and emergence of castration-resistant prostate cancer (CRPC) remain a significant clinical challenge. We previously found that PARP2 interacts with FOXA1 to facilitate the recruitment of AR to genome-wide prostate-specific enhancer regions. Selective disruption of the PARP2-FOXA1 interaction inhibited AR signaling and PCa growth. However, lack of selectivity and potency of existing PARP2/FOXA1-targeting agents and uncertainty of the functional importance of PARP2-FOXA1 binding have limited our study. To address these gaps, we developed a potent small molecule inhibitor UMB-J17 that disrupts PARP2-FOXA1 interaction. In this study, we demonstrated that UMB-J17 competes with FOXA1 for the same PARP2 binding sites, and significantly suppresses AR signaling and PCa cell growth without involving AR-ligand binding. Preclinical studies demonstrated that UMB-J17 exerts potent anti-tumor effects in both in vitro and in vivo CRPC models. UMB-17 also exhibits potent synthetic effect with AR pathway inhibitors in enzalutamide-resistant CRPC models. Furthermore, UMB-J17 enhanced the synthetic lethality of PARP inhibition through AR signaling suppression in PCa. These findings identify UMB-J17 as a promising therapeutic agent that targets PARP2/FOXA1/AR axis for AR signaling inhibition, which is urgently needed to improve CRPC patient outcomes.

#3042 Inhibition of *de novo* purine biosynthesis via PPAT targeting by cucurbitacin B restrains esophageal squamous cell carcinoma growth.

Mengqiu Song[1], Jing Guo[1], Huajie Jia[1], Jie Tian[2], Pan Li[2], Zigang Dong[3]

[1]Department of Pathophysiology, School of Basic Medical Sciences, Henan Medical College, Zhengzhou University, Zhengzhou, China,[2]China-US (Henan) Hormel Cancer Institute, Zhengzhou, China,[3]Henan Medical College, Zhengzhou University, Zhengzhou, China

Background: The *de novo* purine biosynthesis (DNPB) pathway plays a critical role in the malignant progression of tumors. However, its specific contribution to esophageal squamous cell carcinoma (ESCC) growth, radioresistance, and response to targeted therapies remains poorly understood.
Methods: In this study, the underlying metabolic change of ESCC were analyzed by untargeted metabolomics and single-cell RNA sequencing data analyses. The expression and function of PPAT were further evaluated through immunohistochemistry (IHC) and lentivirus-mediated gene manipulation. Additionally, patient-derived xenograft (PDX) and cell-derived xenograft (CDX) models were utilized to assess the role of PPAT and its inhibitor in ESCC tumor growth and radioresistance.
Results: In this study, we identified phosphoribosyl pyrophosphate amidotransferase (PPAT), a key rate-limiting enzyme in the DNPB pathway, as a critical modulator of ESCC malignancy. We demonstrated that PPAT promotes the production of energy-related nucleotides, including AMP, GMP, ADP, GDP, ATP, and GTP, thereby fueling ESCC tumor growth in vitro and in vivo. Moreover, we found that Cucurbitacin B (CuB) specifically targets PPAT and induces its polyubiquitin-mediated degradation via the E3 ligase TRIM38, leading to suppression of the DNPB pathway and inhibition of tumor growth. Importantly, CuB also functions as a radiosensitizer, significantly enhancing the therapeutic efficacy of radiotherapy in ESCC.
Conclusions: Our findings reveal that targeting PPAT represents a promising therapeutic strategy to suppress ESCC progression and enhance the efficacy of radiotherapy.

#3043 CKAP2 modulation with a novel small molecule results in excellent *in-vitro* and *in-vivo* anti tumor activity.

Deepa M. Sridharan, Vignesh Viswanathan, Dmitry Kuchenov, Quynh Mai, Yerem Yeghiazarians, Kurosh Ameri

Soley Therapeutics, South San Francisco, CA

Cytoskeleton-Associated Protein 2 (CKAP2) is an intrinsically disordered protein, considered undruggable, and the most potent microtubule growth factor identified to date. It is associated with malignant progression, modulating multiple cancer-associated processes including cell proliferation, migration, metastasis and angiogenesis, and may act as a functional oncogene by targeting FAK-ERK2 signaling pathway. CKAP2 has been reported to be an important prognostic marker and potential therapeutic target in certain cancers (e.g. non-small cell lung cancer). We have discovered and are developing an oral CKAP2 small molecule modulator as a potential treatment for cancer. Bioinformatics analysis of a 300 tumor cell line panel treated with the CKAP2 modulator demonstrated a strong correlation between CKAP2 protein abundance and drug sensitivity across cancer types, with large B cell lymphoma and acute myeloid leukemia showing the highest drug sensitivity. Additionally, analysis in the TCGA cohort indicated that CKAP2 RNA expression was significantly elevated in patient tumors compared to normal tissues and strongly correlated with their predicted sensitivity to the CKAP2 modulator. Protein array analysis revealed that proteins associated with predicted sensitivity are involved in downstream pathways of CKAP2 such as cell migration and focal adhesion signaling. Functional studies indicated down-stream pathways of CKAP2 to be affected upon treatment. Treatment of cells with either the CKAP2 modulator, or with CKAP2 targeting siRNA, similarly decreased FAK protein level, reduced migration and diminished cell viability/count. Immunofluorescence-based assays confirmed altered CKAP2 phenotype and disruption of microtubule network upon treatment, resulting in G2/M cell cycle arrest. Furthermore, CKAP2 modulation significantly inhibited angiogenesis in tube formation assays using HUVECs and maintained activity in hypoxia, which is a driver of angiogenesis and associated with resistance to many therapies. In-vivo efficacy was demonstrated in a mouse xenograft model of non-small cell lung cancer and three different models of colon cancer with up to 79% tumor volume reduction noted at the highest dose tested and was well tolerated. In conclusion, we have discovered a first-in-class, oral small molecule which modulates CKAP2 and its downstream pathways indicating very good anti-tumor activity both in-vitro and in-vivo. This novel therapy is being considered as a promising therapeutic candidate for the treatment of CKAP2 expressing cancers.

#3044 PKMYT1 inhibition is synthetically lethal with CCNE1 overexpression and synergizes with standard of care chemotherapy.

Natalie Hill, Jeremy Fournier, Srijita Bhowmik, Jenny Zhu, Saranya Chandrasekar, Ester Fernandez-Salas, **Samantha S. Hodge**

Arcus Biosciences, Inc., Hayward, CA

BACKGROUND: CCNE1 is frequently overexpressed in ovarian, endometrial, and colorectal cancers due to gene amplification, reduced degradation (via FBXW7 mut/del), or increased gene transcription. High levels of CCNE1 dysregulate the G1/S checkpoint, increase replication stress, and amplify dependence on the G2/M checkpoint to ensure proper DNA damage repair before mitosis. Additionally, high CCNE1 levels are associated with poor prognosis and response to therapy, highlighting the need for improved treatments for CCNE1 high cancers. PKMYT1 is a protein kinase that regulates the G2/M checkpoint. The data presented here demonstrate that PKMYT1 inhibition, which inactivates the G2/M checkpoint and pushes cells into mitosis, is both synthetically lethal in CCNE1-high cancer cells and synergizes with standard of care chemotherapy *in vitro* and *in vivo*.
METHODS: CCNE1-high cell lines were selected based on CCNE1 gene amplification or FBXW7 LOF. Sensitivity of CCNE1-high cell lines to single agent PKMYT1 inhibition was assessed by measuring the cell cycle, DNA damage, apoptosis, and cell viability. CCNE1-high cancer cell viability was also measured after combined treatment of PKMYT1 inhibition and standard of care chemotherapy. Bliss synergy scores were used to determine synergy. *In vivo* efficacy of PKMYT1 inhibition alone and in combination with chemotherapy was assessed using CCNE1-high human xenograft models.
RESULTS: In CCNE1-high cancer cells, PKMYT1 inhibition disrupts the cell cycle by increasing entry into mitosis, thereby inducing DNA damage and apoptosis. Non-tumorigenic cells are insensitive to PKMYT1 inhibition. In CCNE1-high xenograft models, PKMYT1 inhibition exhibits significant single agent tumor growth inhibition, and its efficacy correlates with increased mitotic entry. Importantly, PKMYT1 inhibition synergizes with standard of care chemotherapies, namely those targeting the S and G2 phases of the cell cycle, in CCNE1-high cancers both *in vitro* and *in vivo*.
CONCLUSION: The data presented here strongly support targeting CCNE1-high cancer cells with a combination of PKMYT1 inhibition and chemotherapy. CCNE1-high cancer cells, which accumulate DNA damage in S phase due to a dysregulated G1/S checkpoint, are highly susceptible to PKMYT1 inhibition due to the propagation of this increased DNA damage into mitosis. Additionally, chemotherapies targeting S/G2 phases, including nucleoside analogs and topoisomerase inhibitors, combine with PKMYT1 inhibition by further enhancing replication stress. Importantly, non-tumorigenic cells are insensitive to PKMYT1 inhibition due to intact G1/S checkpoint and DNA damage repair pathways. In summary, these data highlight PKMYT1 inhibition as a promising approach to selectivity target CCNE1-high cancer cells and enhance the effectiveness of standard of care chemotherapies while sparing non-tumorigenic cells.

#3045 TM4SF20 scaffolds DDR1-IRS4 signaling to drive PDAC metastasis and represents a druggable therapeutic target.

Xinyue Liu[1], Weishuai Liu[2], Antao Chang[1], Jihui Hao[1]

[1]Department of Pancreatic Cancer, Tianjin Medical University Cancer Institute and Hospital, National Clinical Research Center for Cancer, State Key Laboratory of Draggability Evaluation and Systematic Translational Medicine, Tianjin, China,[2]Department of Pain Management, Tianjin Medical University Cancer Institute & Hospital, National Clinical Research Center for Cancer, Tianjin Key Laboratory of Digestive Cancer, Tianjin's Clinical Research Center for Cancer, Tianjin, China

Pancreatic ductal adenocarcinoma (PDAC) exhibits an exceptionally high propensity for liver metastasis, which critically contributes to its poor clinical outcomes. However, therapeutic strategies specifically targeting metastatic progression remain limited. In this study, we investigated the molecular mechanisms driving PDAC liver metastasis and explored therapeutic approaches capable of suppressing metastatic dissemination. Leveraging single-cell sequencing data from pancreatic cancer samples collected at our center, we identified transmembrane 4 L six family member 20 (TM4SF20), a tetraspanin-like transmembrane protein, as a previously unrecognized driver of metastatic progression. TM4SF20 is markedly upregulated in PDAC and highly enriched within liver metastatic lesions. Through integrative analyses combining clinical pathological data, TM4SF20-knockout mouse models, organoid systems, and multiple experimental platforms—including small-animal PET-CT, ultrasonography, immunoprecipitation-mass spectrometry, and in vitro kinase assays—we systematically validated the functional role of TM4SF20 in promoting PDAC liver metastasis. Mechanistically, TM4SF20 acts as a membrane “bridge molecule”: its extracellular domain binds discoidin domain receptor 1 (DDR1), while its intracellular domain interacts with insulin receptor substrate 4 (IRS4). This scaffolding enables DDR1-dependent phosphorylation of IRS4 at T208, thereby activating the AKT signaling cascade and enhancing invasive and metastatic phenotypes. Therapeutic blockade of TM4SF20 with a monoclonal antibody (αTM4SF20) disrupted DDR1-IRS4 complex formation, suppressed downstream signaling, and attenuated PDAC cell migration and invasion. Guided by this mechanistic insight, we developed a TM4SF20-directed antibody-drug conjugate (TM4SF20-ADC) by conjugating αTM4SF20 with the topoisomerase I inhibitor deruxtecan (DXD). TM4SF20-ADC retained high target specificity and exhibited potent antitumor activity, inducing apoptosis, depleting metastatic TM4SF20-positive cells, and markedly inhibiting tumor growth and liver metastasis. In orthotopic PDAC models with established liver metastases, TM4SF20-ADC simultaneously eliminated primary and metastatic lesions, significantly reducing tumor burden and extending survival without detectable systemic toxicity. Collectively, this study identifies TM4SF20 as a key metastatic driver and establishes TM4SF20-targeted ADC therapy as a promising translational strategy for PDAC liver metastasis.

#3046 Robust and durable antitumor activity of a novel PDE10 inhibitor, ADT-030, that enhances the efficacy of chemotherapy and immunotherapy by blocking RAS and β-catenin signaling and overcoming resistance to RAS-selective inhibitors.

Gary A. Piazza[1], Dhana Sekhar Reddy Bandi[2], Veronica Ramirez Alcantara[3], Ganji Purnachandra Nagaraju[2], Junwei Wang[1], Sindhu Ramesh[1], Kristy Berry[1], Khalda Fadlalla[1], Elmar Nurmemmedov[4], Ivan Babic[4], Md Yeashin Gazi[5], Xi Chen[1], Jeremy B Foote[2], Adam B Keeton[1], Yulia Y. Maxuitenko[1], Donald Buchsbaum[2], Fokhrul Hossain[6], Gang Zhou[5], Bassel F. El-Rayes[2]

[1]Auburn University, Auburn, AL,[2]University of Alabama at Birmingham, Birmingham, AL,[3]University of South Alabama, Mobile, AL,[4]CellarisBio LLC, San Diego, CA,[5]Augusta University Medical Center, Augusta, GA,[6]Louisiana State University Health Sciences Center, New Orleans, LA

Resistance to mutant or isoform-specific KRAS inhibitors from compensatory activation of MAPK/AKT signaling by unchecked non-mutant RAS isoforms supports the development of pan-RAS inhibitors. However, secondary mutations or aberrant activation of other oncogenic pathways (e.g., Wnt/APC/β-catenin) may cause resistance to pan-RAS inhibitors. We and others have reported that the cyclic nucleotide-phosphodiesterase 10A (PDE10) isozyme is overexpressed in cancer cell lines and tumors but has low expression and no known function in tissues outside the CNS. PDE10-specific inhibitors and gene silencing were found to selectively inhibit the growth of cancer cells. PDE10 inhibitors developed to treat CNS disorders achieve high brain levels but low levels in peripheral tissues. Thus, we designed a novel, orally bioavailable PDE10 inhibitor, ADT-030, that achieves high systemic levels exceeding those required to inhibit recombinant PDE10 but lacks the major side effect (sedation) caused by conventional PDE10 inhibitors. ADT-030 bound to PDE10 and activated protein kinase G in cancer cells within the same concentration range that inhibited proliferation and induced apoptosis of a large panel of histologically diverse cancer cell lines. These effects also occurred within the same concentration range at which ADT-030 inhibited RAS-mediated MAPK/AKT signaling and selectively degraded the oncogenic (transcriptionally active) pool of β-catenin. Notably, cancer cell lines that developed resistance to pan-RAS, pan-KRAS, or mutant-specific KRAS inhibitors retained full sensitivity to ADT-030. ADT-030 strongly inhibited tumor growth in mouse models of colon, lung, breast, and pancreatic cancer at dosages that were well tolerated. Pancreatic cancer models were particularly sensitive to ADT-030, resulting in tumor regression, inhibition of metastasis, and prolonged survival. ADT-030 also increased survival and inhibited metastasis in mouse models of lung cancer with a durable response that persisted well beyond the treatment period, resulting in cures. ADT-030 also enhanced the antitumor activity of chemotherapy (paclitaxel) and immune checkpoint inhibitors in mouse models of lung, colon, and breast cancer. Deep immunophenotyping studies revealed a significant impact of ADT-030 treatment on the tumor immune microenvironment, characterized by the selective induction of apoptosis in myeloid-derived suppressor cells (MDSC), while increasing tumor infiltration by CD8+ T cells and natural killer cells. These results show that ADT-030 has potential advantages over direct-acting RAS inhibitors, supporting clinical trials of ADT-030 as a monotherapy or in combination with chemotherapy or immunotherapy for a broad range of RAS-driven cancers.

#3047 A small molecule inhibitor of NVL suppresses tumor growth by blocking ribosome biogenesis.

Arin B. Aurora[1], Holly H. Guo[1], Ye Tao[1], Victor E. Cruz[2], Min Fang[1], Vlshal Khivansara[1], Shanhai Xie[1], Ashley Leach[1], Divya Reddy[1], Johann Peterson[1], Jiwoong Kim[3], Noelle S. Williams[4], Jan P. Erzberger[2], Jef K. De Brabander[1], Deepak Nijhawan[1]

[1]Department of Radiation Oncology, Section in Molecular Medicine, UT Southwestern Medical Center, Dallas, TX,[2]Department of Biophysics, UT Southwestern Medical Center, Dallas, TX,[3]Quantitative Biomedical Research Center, Department of Clinical Sciences, UT Southwestern Medical Center, Dallas, TX,[4]Department of Biochemistry, UT Southwestern Medical Center, Dallas, TX

Our research program integrates phenotypic screening with a tunable forward-genetics platform engineered to identify anticancer small molecules and their novel molecular targets. Using this approach, we identified nuclear valosin-containing protein-like (NVL), a hexameric AAA+ ATPase required for large ribosomal subunit (60S) assembly, as the target of a dibenzothiazepinone, MM17. Cryo-EM reconstructions of NVL bound to a substrate analog mimic reveal two MM17 docking sites within the hexameric assembly, with resistance mutations clustering around the ligand binding site. NVL inhibition disrupts 60S biogenesis and stabilizes p53 through MDM2, leading to cell cycle arrest or apoptosis, in the absence of DNA damage. Cancer cells upregulate ribosome production to sustain the high protein synthesis demands of unchecked proliferation, making ribosome biogenesis an attractive therapeutic target. Notably, inhibition of ribosome biogenesis—rather than induction of DNA damage—has recently been identified as a major mechanism underlying widely used chemotherapies such as 5-FU and oxaliplatin. To assess the therapeutic potential of selectively targeting ribosome biogenesis by blocking NVL, we engineered a degron system (NVL-AID) in which administration of 5-Phenyl-indole-3-acetic acid (Ph-IAA) dose dependently degrades the endogenous NVL protein in a colorectal cancer cell line. Degradation of NVL phenocopied the effects of MM17 treatment on the induction of p53, the blockade of ribosome assembly, and on the inhibition of cell growth. Moreover, daily Ph-IAA administration for two weeks effectively suppressed the growth of established NVL-AID xenograft tumors. A more potent and bioavailable MM17 analog, MM927, suppressed tumor growth in mouse models of colorectal cancer through direct NVL targeting, supporting the pharmacological inhibition of ribosome assembly as a cancer vulnerability. Together, these findings validate NVL as a therapeutic target and set a benchmark for the efficacy of small-molecule NVL inhibitors. Current efforts are focused on lead optimization to nominate advanced, orally bioavailable NVL inhibitors that are tested head-to-head with target degradation (NVL-AID) to maximize efficacy. To characterize the on-target toxicities of candidate leads, we developed a CRISPR-engineered, compound-resistant mouse model. Collectively, these tools will enable us to characterize the consequences of inhibiting this novel cancer target in normal tissues and to establish the therapeutic index of optimized NVL inhibitors to support their clinical development.

#3048 Nesuparib enhances anti-tumor efficacy with gemcitabine and nab-paclitaxel in BRCA wild type pancreatic cancer xenograft model.

Banyoon Cheon, Jung-young Shin, Geon Kang, Dae In Park, John Kim, Hyunju Cha

Onconic Therapeutics Inc., Seoul, Korea, Republic of

Pancreatic ductal adenocarcinoma is one of the most aggressive and fatal cancer with limited treatment options. The combination of gemcitabine and nab-paclitaxel (GnP) is the first-line treatment for pancreatic cancer, but the median overall survival remains less than a year, and high toxicity limits its use.
To address this limitation, we explored whether Nesuparib, a dual inhibitor for poly-ADP-ribosyl transferase 1/2 and tankyrase 1/2, enhances anti-tumor efficacy with GnP in BRCA wild-type pancreatic preclinical models.
We first conducted a cell viability assay in BRCA wild-type Mia Paca-2 cells to determine whether Nesuparib increases the cytotoxicity of gemcitabine-based chemotherapy. Combination of Nesuparib with GnP decreased viability by more than 70% compared to GnP treatment alone. In Mia Paca-2 *in vivo* xenograft model, GnP treatment resulted in 31% tumor growth inhibition (TGI) compared to the control group, while Nesuparib with GnP elicited TGI by 79%. At the end of the *in vivo* experiment, changes in various molecules at protein levels were investigated in the separated tumors to characterize plausible mechanisms underlying the significant tumor reduction in Nesuparib with GnP-treated group compared to other treatment groups. Interestingly, c-Myc and MYBL2 levels were increased in the GnP treated one compared to the vehicle control speculating that compensatory mechanisms might be activated after the drug treatment, while these upregulations were restrained by Nesuparib with GnP treatment. We also observed that cyclinD1, β-Catenin, and RAD51 were decreased in Nesuparib with GnP treatment compared to the control or GnP treatment. Collectively, the data suggests that those molecular modulations are closely associated with the tankyrase inhibition by Nesuparib in BRCA wild-type model, and that combining Nesuparib with the standard chemotherapy further reduces cell proliferation and delays DNA repair compared to chemotherapy alone.
Overall, our results suggest that combination with Nesuparib with GnP chemotherapy could be a novel and rational therapeutic option for pancreatic cancer treatment.

#3049 Atamparib: First-in-class PARP7 inhibitor for treatment of NSCLC adenocarcinoma in monotherapy and in combination with standards of care.

Genny Degani[1], Federica Carbone[1], Patrizia Banfi[1], Laura Gianellini[1], Nilla Avanzi[1], Elena Casale[1], Marina Fasolini[1], Laura Riva[1], Gianluca Papeo[1], Francesca Quartieri[1], Fabio Gasparri[1], Michael O. Hottiger[2], Claudia Perrera[1], Alessia Montagnoli[1]

[1]Nerviano Medical Sciences, Nerviano, Italy,[2]Department of Molecular Mechanisms of Disease, University of Zurich, Zurich, Switzerland

PARP7 is a relevant target in cancer cells and is involved in several cellular processes, including type I interferon (IFN-I), aryl hydrocarbon receptor, estrogen receptor, and androgen receptor signaling, and stabilization of the oncogenic RAS-MAPK effector FRA1. Atamparib is the first PARP7 inhibitor in the clinic, with high potency and selectivity. It is orally bioavailable, with favorable safety profile in PhI/II trials both as single agent and in combination with anti-PD1 antibodies. Recent better understanding of PARP7 biology shed light on a unique atamparib dual mechanism of action, that combines direct cancer cell killing with innate immune activation via restoration of IFN-I signaling to assist adaptive response. This insight, along with new preclinical and clinical data, points to new indications and opportunity for combination.

Atamparib biochemical and cellular characterization was conducted by HTRF, SPR and Nanobret. PARP7 crystal structure was determined by X-ray crystallography. In investigating atamparib antiproliferative activity, cancer cell lines from multiple indications have been treated with 0-10 µM of atamparib single agent for 144 hours. Combination with various standards of cares approved in each setting have been evaluated in 7x7 or 7x11 matrix.

Atamparib subnamolar potency and long residence time on PARP7, selectivity versus other members of PARP family, and PARP7 target engagement in cell, were corroborated using biochemical and biophysical assays. The unprecedented crystal structure of PARP7 bound to atamparib was solved by X-ray crystallography at 2 Å resolution, confirming the proposed binding mode. Atamparib was proven to be efficacious in multiple high-unmet-need indications, demonstrating a remarkable anti-tumor activity in NSCLC adenocarcinoma at clinically achievable concentrations, particularly when oncogenic pathways are activated, due to KRAS or other oncogene drivers' mutations. These findings were validated through both *in vitro* and *in vivo* studies. Interestingly, atamparib sensitivity in NSCLC adenocarcinoma KRAS mutant is observed irrespective of the specific KRAS mutation involved. These data support the mechanistic link that connect PARP7 to RAS-MAPK pathway through FRA1, a potent oncogene frequently overexpressed in tumors, where it promotes proliferation, survival, and immune evasion. By inhibiting PARP7, atamparib induces FRA1 degradation, reactivates IFN-I signaling, and triggers tumor cell death and immune-mediated tumor clearance. Moreover, atamparib increases the activity of several standards of care and targeted drugs in late development in NSCLC when combined with them.

Overall, our data shed light on a PARP7 dependency in NSCLC adenocarcinoma context and support atamparib development in this setting, both in monotherapy and in combination with multiple standards of care.

#3050 RPT1G, a novel hyperbolic NAMPT inhibitor, effectively synergizes with PARP inhibitors in solid tumors *in vitro* and in a xenograft breast cancer model.

Michael Schelle, Min Wu, Francis Roushar, Banumathi Cole, Dennise A. De Jesus-Diaz, Gregory Thomas Crimmins

Remedy Plan Therapeutics, Gaithersburg, MD

Background: Poly-ADP ribose polymerase (PARP) inhibitors are key drugs in treating solid tumor patients with defects in homologous DNA repair (HR) pathways. The substrate for PARP enzyme activity, nicotinamide adenine dinucleotide (NAD), is regulated by nicotinamide phosphoribosyltransferase (NAMPT), the rate limiting enzyme in NAD recycling. NAMPT is upregulated in many cancers, in part to supply the NAD consumed by PARP enzymes. RPT1G is a novel hyperbolic NAMPT inhibitor that eliminates NAD in cancer cells while allowing NAD production in healthy tissues. The safety, tolerability, and NAMPT inhibition of RPT1G was recently demonstrated in a first-in-human Phase 1 study (NCT06667765, Crimmins et al., ASH 2025). Here we show that RPT1G synergizes with PARP inhibitors in solid tumor cells and in a xenograft breast cancer model.
Methods: Cells were incubated with RPT1G, olaparib, or in combination for 96 hours then assessed for viability using CellTiter Glo. MDA-MB-436 mouse xenograft studies testing RTP1G, olaparib, or combination were initiated when the average tumor size reached 150-200 mm^3.
Results: RPT1G in combination with the PARP inhibitor olaparib was synergistic across a spectrum of solid tumor cell lines, including breast, pancreatic, and ovarian cancers. Several solid tumor cell lines that are resistant to either RPT1G or olaparib monotherapy showed increased sensitivity to RPT1G and olaparib combinations, including Cal51 (breast) and Mia Paca-2 (pancreatic). Similarly, the MDA-MB-436 triple negative HR-deficient breast cancer xenograft model was insensitive to RPT1G monotherapy, while combination of RPT1G with olaparib synergistically inhibited tumor growth, with complete tumor elimination in 40% of the mice versus <15% with olaparib monotherapy. Furthermore, 80% of mice treated with olaparib monotherapy rebounded despite continuous treatment, compared with <40% of mice showing tumor rebound when treated with RPT1G and olaparib.
Conclusion: Therapeutic inhibition of NAD synthesis with NAMPT inhibitors has been challenging to achieve clinically due to severe on-target toxicity stemming from the critical role of NAD in living systems. RPT1G is the first NAMPT inhibitor that is well-tolerated in people. The high tolerability of RPT1G is especially critical when combining with PARP inhibitors that have known toxicities. We demonstrate that RPT1G in combination with olaparib is efficacious and synergistic in breast, pancreatic, and ovarian solid tumors *in vitro*, and enhances the extent and duration of efficacy in an HR-deficient mouse xenograft breast cancer model. Thus, we present a novel combination strategy to overcome the challenges seen with approved monotherapies in solid tumors.

#3051 Enhancing matchmaking in targeted therapy (TT) for cancer (ca): Beyond the 'arranged' criteria.

Farah Mazahreh, Liyan Mazahreh, Ahmad Mazin Safar

University of Arkansas for Medical Sciences, Little Rock, AR

Cancer is a unique cellular condition marked by constant activation of oncogenes. Heritable DNA changes (mutations, translocations and copy number alterations) can produce this 'constant' state. Theoretically, however, static changes are not limited to DNA alterations in the gene body, but can result from DNA amplification of oncogene's transcription factors (TF) or ligands (for receptor Oncogenes), at a minimum. Constant activation depends on identifying clonal events in oncogenes, but may be also inferred from functional activation of oncogenic pathways in multiple sites of a biopsy as a maneuver to identify the pivotal cancer driver for therapeutic targeting. Targeted therapies have produced major therapeutic benefits especially when drugging pivotal oncogenes. Accordingly, efforts to identify such targets are rational, justifiable and desirable. Standard oncology practice includes next generation sequencing (NGS) for this very purpose. NGS criteria are almost entirely based on DNA variance in the gene body of an expanded lists of cancer genes. NGS, as reported in the literature, identifies targets only in 25% of cases sequenced. We hypothesized that extending DNA criteria to assess TF/Ligand amplification of an extended set of oncogenes will identify rational, but hitherto unrecognized targets increasing the ability to match tumors with relevant Targeted Therapies.
Methods: We examined 1,731 tumor samples in The Cancer Genome Atlas agnostic to histology or stage using an extensive list of wild-type (WT) but over-expressed (2 fold) proto-oncogenes. We recorded amplification of canonical TFs, or ligands (for receptor oncogenes). We also assessed the transcriptional activity of the oncogenes examined. The genes identified are used routinely in a major commercial vendor for NGS.
Results: 31.7% of cases show gene amplification of ligands or TFs of the list of wild type Oncogenes; 4.7% harbor TF/ligand mutations. ~60%of cases demonstrate activation of an oncogenic signaling pathways (without DNA changes) despite wild type oncogenes reflected by transcriptional activity at z-score >2.
Conclusions: Our method outperforms NGS identifying 'targets' to pair tumors with effective Therapies. Many druggable oncogenes are potential targets in unexpected histologies (e.g., Abl in breast cancer). Our method should be integrated in future diagnostic interrogation of cancers. Additionally, the algorithms should change to 'call' these TFs and ligands events as 'actionable'. In doing so, we will be extending beyond the classic oncogene-specific NGS. Assessment of translocations and extrachromosomal DNA mechanisms (among many other proposals) may provide further answers for the remaining cases that cannot be classified using the above. This would allow oncologists to introduce Targeted Therapies to a many patients who currently won't receive such effective and desperately needed treatments.

#3052 RK-582, a tankyrase inhibitor, attacks Wnt-driven colorectal cancer cells with short-type APC mutations and high β-catenin expression.

Hiroyuki Seimiya[1], Mingjue Chen[1], Taichi Oishi[1], Yukiko Muramatsu[1], Manabu Takamatsu[2], Naomi Kawata[1], Ayane Nakamura[1], Saori Inaba[1], Satoshi Nagayama[3], Ryohei Katayama[4], Kensei Yamaguchi[5], Fumiyuki Shirai[6], Tetsuo Mashima[1]

[1]Division of Molecular Biotherapy, Cancer Chemotherapy Center, Japanese Foundation for Cancer Research, Tokyo, Japan,[2]Division of Pathology, The Cancer Institute, Japanese Foundation for Cancer Research, Tokyo, Japan,[3]Gastroenterological Surgery, Cancer Institute Hospital, Japanese Foundation for Cancer Research, Tokyo, Japan,[4]Division of Experimental Chemotherapy, Cancer Chemotherapy Center, Japanese Foundation for Cancer Research, Tokyo, Japan,[5]Gastroenterological Chemotherapy, Cancer Institute Hospital, Japanese Foundation for Cancer Research, Tokyo, Japan,[6]Drug Discovery Chemistry Platform Unit, RIKEN Center for Sustainable Resource Science, Saitama, Japan

Colorectal cancer (CRC) is one of the three major cancers, causing over 90,000 deaths worldwide annually. For unresectable metastatic CRC, cytotoxic, targeted, and immuno-oncology drugs are used, but these therapies only extend survival by about 30 months or less. Approximately 80% of CRCs carry *APC* mutations that upregulate Wnt/β-catenin signaling, yet this pathway has long been considered difficult to target due to the lack of druggable molecules. Tankyrase poly(ADP-ribosyl)ates (PARylates) AXIN, a negative regulator of β-catenin, promoting its ubiquitin-dependent degradation and β-catenin accumulation. Accordingly, tankyrase inhibitors have been proposed as potential therapeutics for Wnt-driven cancer. To establish a targeted therapy for Wnt-driven CRC, we developed an orally available tankyrase inhibitor, RK-582, and investigated its predictive biomarkers. In *APC*-mutated CRC cells, RK-582 inhibited tankyrase-mediated AXIN PARylation, resulting in AXIN accumulation and β-catenin degradation. RK-582 exhibited excellent bioavailability and suppressed Wnt-driven CRC growth in mouse xenograft models. Under approval of the JFCR Institutional Review Board and with patients' informed consent, *APC*-mutated CRC patient-derived cells were analyzed, revealing that *APC* mutations lacking all seven 20-amino acid repeat domains and β-catenin accumulation are predictive biomarkers for sensitivity to tankyrase inhibitors. In original tumor tissues of inhibitor-sensitive cells, β-catenin expression was significantly higher than in inhibitor-resistant cells. Analysis of primary tumor location indicated that left-sided tumors were more common in the inhibitor-sensitive group, with elevated β-catenin levels. Ectopic expression of a gain-of-function *CTNNB1* allele conferred resistance in drug-sensitive CRC cells. *PIK3CA* gain-of-function mutations were associated with inhibitor resistance, whereas *KRAS*, *BRAF*, or *TP53* mutations were not. GLP-compliant toxicity studies, safety pharmacology assessments, and drug metabolism/pharmacokinetic evaluations were completed to generate the preclinical dataset required for clinical trials. Additionally, a large-scale synthesis method for RK-582 was developed, and a GMP-grade active pharmaceutical ingredient was produced, subsequently used to prepare the capsule formulation for the clinical trial. In summary, RK-582 targets the Wnt/β-catenin pathway, a key cancer pathway previously considered undruggable. An investigator-initiated first-in-human clinical trial of this drug is currently ongoing, and these findings are expected to contribute to the development of an innovative therapy for unresectable advanced and recurrent CRC.

#3053 Combination of the MDM2 antagonist ASTX295 and Olaparib as a novel treatment option for *BRCA2* mutant, *TP53* wild-type solid tumors.

Antonio Morales[1], Joanna Obacz[1], Bryn Hardwick[1], Adam Jackson[1], Liam Davis[1], Zoe Haines[1], Patrick Herr[1], Paula Martinez Sanz[2], Violetta Serra[2], Judit Espana-Agusti[3], Gianni Chessari[3], Maria Ahn[3], John F. Lyons[4], Amy Emery[1], **Sarah Holt**[1], Stephen Shuttleworth[1], Barry R. Davies[1]

[1]Mosaic Therapeutics, Cambridge, United Kingdom,[2]VHIO, Barcelona, Spain,[3]Astex Therapeutics Ltd., Cambridge, United Kingdom,[4]Astex Therapeutics Ltd., Cambridge

p53, encoded by the TP53 tumor suppressor gene, is a critical regulator of the cellular response to stress such as DNA damage and oncogenic signaling. p53 triggers the transcriptional program that dictates cell-fate decisions, including cell cycle checkpoint activation, senescence, and apoptosis. In tumors with functional p53, reactivation of TP53 transcriptional activity has emerged as an attractive therapeutic approach to promote cancer cell death. Therefore, inhibition of MDM2, the key negative regulator of p53, has been an attractive target to achieve this strategy. ASTX295 is a selective small molecule antagonist of the p53/MDM2 interaction, resulting in p53 stabilisation. Whilst the efficacy of MDM2 antagonists as monotherapy has been modest, there is a strong rationale for MDM2-combination therapies blocking DNA repair or inducing DNA damage to potentiate p53-mediated apoptosis. We identified components of DNA repair pathways including PARP1 as strong sensitizers to ASTX295 in a genome-wide drug-CRISPR screen. PARP inhibition results in DNA damage when single strand breaks are converted into double strand breaks during S-phase, leading to the accumulation of unresolved DNA damage and triggering checkpoint activation. PARP inhibitors have been shown to induce p53 activation and, in turn, promote p21-mediated cell cycle arrest. In the presence of an MDM2 antagonist, this excessive genotoxic stress combined with sustained p53 activation leads to increased apoptosis, offering a more durable response than PARP inhibition alone. We demonstrated the combinatorial interaction of ASTX295 with Olaparib in drug combination screens, and our proprietary biomarker discovery pipeline, PRIME, identified significantly enriched combination synergy and reduced viability in BRCA2-mutant solid tumor cell lines. We established that synergistic cell death is driven by elevated p53 activity for the combinatorial administration of ASTX295 with Olaparib, particularly in BRCA2-mutant/TP53-wild-type solid cancer cell lines. In vivo, using both cell line- and patient-derived BRCA2-mutant/TP53 wild-type xenograft models, we showed superior anti-tumor activity for the combination compared to single agents, resulting in prolonged control of tumor growth and regressions at well tolerated doses. Taken together, our data provide a strong rationale for combining ASTX295 with PARP inhibitors such as Olaparib in patients with TP53-wild-type/BRCA2-mutant solid tumors.

#3054 Inhibition of ARNT suppresses growth of primary human kidney cancer cells.

Shengchen Su, Yanping Wang, Yanchun Zhang, Patrick Tamukong, Hyung L. Kim

Urology, Cedars-Sinai Medical Center, Los Angeles, CA

Background: Hypoxia-inducible factor (HIF) signaling drives clear cell renal cell carcinoma (ccRCC). ARNT (HIF-1β) dimerizes with HIF-1α and HIF-2α to enable gene transcription. Belzutifan is a small-molecule drug that blocks HIF-2α, which is approved for clinical use. It's been proposed that increased signaling through HIF-1α represents a belzutifan-resistance mechanism. Blocking ARNT should attenuate both HIF programs. We assessed an ARNT-selective small-molecule inhibitor (ARNTi) in renal cancer models.
Methods: 786-O cells were cultured under hypoxia. Cells received belzutifan, ARNTi, or vehicle control (DMSO). After treatment, cells were fixed, and the interaction between HIF-2α and ARNT was quantified using a proximity ligation assay. Primary cultures were generated from patients who underwent nephrectomy. Under hypoxia, both normal and ccRCC primary cell cultures were exposed to ARNTi or vehicle and then processed for proliferation assessment and qPCR of HIF target genes. Primary papillary renal cell carcinoma cultures were evaluated using the same workflow.
Results: ARNTi lowered the proximity ligation signal between HIF-2α and ARNT. The extent of inhibition matched the effect of belzutifan. In patient-derived ccRCC cultures (n=5), ARNTi produced significant growth inhibition under hypoxia compared with vehicle. The magnitude of the effect was similar to belzutifan. Expression of hypoxia-responsive target genes, such as GLUT1, NDRG1, and VEGFa, decreased after ARNTi treatment. ARNTi also suppressed growth in papillary renal cell carcinoma cultures (n=3), indicating activity across histologic subtypes.
Conclusions: Inhibition of ARNT reduces the formation of the HIF-2α and ARNT complex and suppresses proliferation in primary human kidney cancer cells. These effects coincide with reduced expression of HIF target genes under hypoxia. These results support the development of ARNT-directed candidates for the treatment of kidney cancer.

#3055 Targeting the MKK3/MYC protein-protein interaction to overcome drug resistance in MYC-driven cancers.

Payton Fleming, Elsa Bildtsen, Zhen Chen, Eric J. Miller, Yuhong Du, Shi-Yong Sun, Haian Fu, Andrey A. Ivanov

Emory University, Atlanta, GA

MYC is a central oncogenic transcription factor that drives tumor progression in multiple cancer types, including triple-negative breast cancer (TNBC) and non-small cell lung cancer (NSCLC). However, direct MYC inhibition remains highly challenging due to its intrinsically disordered structure and lack of defined drug-binding pockets. We uncovered a novel mechanism of MYC activation through a direct protein-protein interaction (PPI) with mitogen-activated protein kinase kinase 3 (MKK3). Integrative bioinformatics analyses using our AVERON platform revealed that elevated levels of the MKK3/MYC complex significantly correlate with poor clinical outcomes in TNBC and lung cancer, particularly in patient subsets with high MYC dependency.

To define the functional consequences of the PPI, we combined genetic perturbation, chemical biology, and clinical genomics analyses. MKK3 silencing reduced the viability of TNBC and NSCLC cells, and these effects were recapitulated with small-molecule MKK3/MYC PPI inhibitors (MMPins), identified through our TR-FRET ultra-high-throughput screening campaign. Disruption of the MKK3/MYC PPI destabilized MYC and suppressed MYC-driven transcriptional programs. Furthermore, MKK3/MYC PPI inhibition is correlated with the downregulation of lactate dehydrogenase A (LDHA), a key mediator of glycolytic reprogramming and a well-established driver of drug resistance. In TNBC models, MKK3/MYC PPI inhibition reduced LDHA expression and blocked the glycolytic flux that fuels MYC-dependent growth. In NSCLC, MMPins restored apoptotic sensitivity in EGFR TKI-resistant cells and, when combined with osimertinib, significantly suppressed tumor growth in vivo.

Together, these findings define the MKK3/MYC PPI as a mechanistic driver of LDHA-mediated metabolic adaptation and drug resistance. Pharmacological disruption of this interaction offers a promising therapeutic strategy to suppress MYC-dependent oncogenic networks, reverse resistance phenotypes, and improve outcomes in MYC-driven cancers.

Acknowledgments: This work was supported in part by the Emory Center for New Medicines Therapeutic Advancement Award (A.A.I), Mary Kay Foundation Grant for Cancer Research (A.A.I), the NCI's Informatics Technology for Cancer Research (ITCR) Program (R21CA274620, A.A.I.), NCI Emory Lung Cancer SPORE (P50CA217691, H.F.), NCI P01CA257906 (H.F.), Career Enhancement Program (A.A.I., P50CA217691), Winship Cancer Institute (NIH 5P30CA138292). We thank the Emory University Undergraduate Research Program in Biology.

#3056 Inhibition of oncogenic phenotypes by hexanoate in triple-negative breast cancer.

Nahara Yupe-Muniz[1], **Samira B.F. Abdullah-Vargas**[2], Oscar A. Loperena-Gonzalez[1], Ariana S. Garcia- Lopez[1], Gabriel Borges-Velez[1], Josue Perez-Santiago[1]

[1]University of Puerto Rico Comprehensive Cancer Center, San Juan, PR,[2]University of Puerto Rico, Rio Piedras Campus, San Juan, PR

Background: Triple-Negative Breast Cancer (TNBC) is an invasive molecular subtype of breast cancer defined by the lack of estrogen and progesterone receptors, and the absence of HER2 amplification. This molecular profile limits current treatment options contributing to poor patient outcomes. Recent evidence features the microbiome as a key factor in cancer biology, modulating tumor progression through metabolites and bacterial products. Among these products, medium-chain fatty acids (MCFAs), such as hexanoate, are produced by microbial fermentation within the microbiome. Previous studies from our laboratory demonstrated that hexanoate reduces the viability and proliferative capacity in oral cancer cells, which may suggest hexanoate as a promising candidate target for alternative cancer treatments. Therefore, the aim of this study was to evaluate the impact of hexanoate on oncogenic phenotypes including cell viability, proliferation, and migration of the TNBC cell line MDA-MB-231.
Methods: MDA-MB-231 cells were cultured at 37°C, 5% CO_2 in RPMI-media. Cell viability was measured using AlamarBlue after 24, 48 and 72 hours (h) of treatment with sodium hexanoate at 9 different concentrations starting at 800mM (1:2 serial dilution) to measure the half-minimal inhibitory concentration (IC50). Cell proliferation was measured by seeding 100,000 cells per well and counting with TrypanBlue the change in cell number after treatment with hexanoate at 5mM for 24h, 48h and 72h. Cell migration was evaluated using a scratch assay; after inflicting a wound, its width was measured at 0h, 24h, and 48h to calculate the percentage of wound closure.
Results: Hexanoate reduced cell viability at 24h, 48h, and 72h with a consistent IC50 of 29mM. Additionally, no significant effects on the proliferation rate were observed at 24h and 48h when treated with hexanoate, whereas it decreased significantly at 72h ($p=0.004$). Furthermore, hexanoate showed a decreased percentage of wound closure at both time points, showing significance at 48h ($p = 0.002$).
Conclusions: Overall, hexanoate exhibited inhibitory effects on viability, proliferation, and migration in TNBC cells. As a microbiome-associated compound, hexanoate may modulate cancer cell behavior in a time-dependent manner and represent a potential alternative target for TNBC treatment, although additional studies are required for validation.

#3058 A first-in-class orally bioavailable small molecule tumor suppressor activator for the treatment of a wide range of cancers.

Hee-Sung Park, Chakrapani Subramanyam, Kyu-kwang Cho, Se Hee Hyun, Yeonjee Kahm

Promedigen, Daejeon, Korea, Republic of

Novel therapeutic agents capable of restoring the function of key tumor suppressors, frequently inactivated across a wide spectrum of cancers, represent a powerful strategy to address the limitations of current treatments and mitigate resistance to existing therapies. Using colorectal cancer (CRC) as a primary indication, we developed an orally bioavailable small-molecule agent, PMG-A9, that restores the activity of a key tumor suppressor and suppresses the oncogenic transcription factor FoxM1, a major driver of therapeutic resistance. Notably, 5-fluorouracil (5-FU), a widely used first-line CRC therapy, is known to induce substantial upregulation of FoxM1. In this study, we demonstrate that PMG-A9 induces a robust, dose-dependent reduction of 5-FU-driven FoxM1 expression in colorectal cancer cells. Exposure of 5-FU-treated cells to PMG-A9 promotes apoptosis through pro-apoptotic mediators, including PUMA. In preclinical CRC xenograft models, PMG-A9 exhibits robust single-agent antitumor efficacy and shows pronounced synergy when combined with multiple chemotherapeutic agents, including 5-FU, while effectively downregulating FoxM1 in vivo. These findings highlight tumor-suppressor reactivation as a promising, broadly applicable therapeutic strategy to improve treatment outcomes for CRC and, potentially, overcome drug resistance across diverse tumor types.

*Corresponding authors: Hee-Sung Park; hee-sung.park@promedigen.com, Chakrapani Subramanyam; subramanyam@promedigen.com

#3059 Targeting metabolic dependencies in MYC-driven osteosarcoma through Lp-PLA2 inhibition.

Katherine Shelmidine[1], Juan Dou[1], Tajhal Patel[2], Jason Yustein[1]

[1]School of Medicine Pediatrics, Emory University, Atlanta, GA,[2]Pediatrics, Baylor College of Medicine, Houston, TX

Osteosarcoma (OS) is the most prevalent pediatric bone cancer and treatment outcomes and survival rates have remained largely unchanged for decades. Patients with metastatic or relapsed/refractory disease face five-year survival rates below 30%, with no salvage therapies available after standard of care failure. Overexpression of the oncogene MYC contributes to aggressive tumor progression, therapeutic resistance, and metabolic reprogramming in OS, yet direct targeting of MYC remains challenging. Lipoprotein-associated phospholipase A2 (Lp-PLA2), an inflammatory enzyme, regulates phospholipid remodeling and inflammatory lipid signaling that may be exploited by MYC-high tumors. Targeting this pathway with the small-molecule Lp-PLA2 inhibitor Darapladib could reveal metabolic dependencies on phospholipid and fatty acid metabolism that supports growth and survival in MYC-driven OS. A 3D spheroid high-throughput drug screen of 2,036 FDA-approved and bioactive compounds was performed on a high-MYC patient-derived xenograft (PDX) OS cell line and a murine Myc knock-in OS cell line. Darapladib was identified as a candidate compound and IC_{50} values were determined in both 2D and 3D models. High MYC-expressing PDX and murine OS cells were treated in 2D for 72 hours based on IC_{50} values, followed by spheroid formation assays post-treatment. CellTiter-Glo viability was assessed after a 72-hour growth period. Migration capacity was examined via wound healing assays using the same treatment strategy. *In vivo* efficacy of Darapladib was evaluated in NSG mice using two high MYC-expressing PDX models. Darapladib exhibited IC_{50} values below 5 µM in both PDX and murine OS lines, indicating sensitivity to Lp-PLA2 inhibition. Low-MYC expressing OS lines showed relatively higher IC_{50} values compared to high-MYC lines. In 3D spheroids, Darapladib pre-treatment decreased cellular ATP levels and demonstrated significant spheroid size reduction. Darapladib-treated cells exhibited impaired migration in wound healing assays. *In vivo* studies revealed decreased average primary tumor volume in both high-MYC PDX models. Darapladib demonstrates *in vitro* and *in vivo* efficacy in high-MYC OS models, establishing Lp-PLA2 as a novel therapeutic target that potentially exploits MYC-dependent metabolic vulnerabilities. The selective sensitivity of high-MYC expressing lines to Darapladib suggests that MYC status may serve as a predictive biomarker. As Darapladib has an established safety profile from previous cardiovascular clinical trials, these findings support its clinical translation for high-risk OS patients lacking effective therapies. Further studies are warranted to elucidate mechanisms by which Lp-PLA2 inhibition disrupts MYC-driven lipid metabolism and evaluate Darapladib in combination with other targeted therapies.

#3060 Periplocin restores HTR1E signaling by CTCF to inhibit proliferation and dissemination of ovarian cancer.

Rong Xiang, Haojie Chen, Yi Shi, Huimin Liu, Kejia Xu

Nankai University, Tianjin, China

Ovarian cancer (OC) is one of the three malignant tumors threatening women's health, ranking third in incidence and second in mortality among all the gynaecological malignancies. The high mortality of OC is due to the lack of typical symptoms and effective early screening methods in the early stage. In the rapid progression of ovarian cancer, a risk factor that cannot be ignored and is currently a hot topic of cancer research is psychological stress. It is largely unknown about the key and robust factors directly linking psychological stress to the dissemination of cancer cells, causing the lack of effective intervening method. The dysregulation of the neurotransmitter 5-Hydroxytryptamine (5-HT) and its receptor HTR1E-mediated dissemination-suppressing function played an essential role in the growth and peritoneal dissemination of OC, indicating HTR1E to be a potential target for the prevention of the malignant progression of OC. In a previous systematic study screening Periplocin as monomer molecule isolated from the traditional Chinese medicine, it can effectivly restore the HTR1E expression and its anti-tumor signaling against the malignant growth and peritoneal disseminated metastasis of OC. We next found CTCF as insulator enforces TAD boundary between HTR1E and ZNF292 in cancer. CTCF is released from the boundary through competitive binding by Periplocin. In summary, we the first time identified Periplocin to be an effective natural small molecule that was able to restore the HTR1E expression and its anti-tumor signaling against the malignant growth and peritoneal disseminated metastasis of OC. We also clarified the molecular mechanism of the anti-tumor effects of Periplocin. This provides new evidence for the clinical treatment of ovarian cancer.

#3061 CS231295, a novel AURKB-biased multi-kinase inhibitor, demonstrates synthetic lethality in RB1-deficient tumors and potent intracranial efficacy.

You Zhou, Qianjiao Yang, Qinyi Xia, Yu Zhang, **Zhijian Li**, Desi Pan, Song Shan

Shenzhen Chipscreen Bioscience Co.,Ltd., Shenzhen, China

Background: The clinical development of multi-kinase inhibitors targeting Aurora kinase B (AURKB) is often limited by dose-limiting toxicities from concurrent VEGFR inhibition, preventing optimal AURKB target suppression. CS231295 was designed as an AURKB-biased inhibitor to overcome this challenge.
Methods: Kinase profiling was performed using biochemical and cellular assays. RB1 biomarker validation employed an isogenic NCI-H1048-tet-on-RB1 model. In vivo efficacy and pharmacokinetics were assessed in RB1-deficient SCLC cell-derived and patient-derived xenograft models. Brain penetration and intracranial efficacy were evaluated in orthotopic brain tumor models.
Results: CS231295 potently inhibits AURKB (IC_{50} = 1.32 nM) with a balanced multi-kinase profile. Crucially, its direct antitumor activity—evidenced by caspase-3/9 cleavage at 0.3-3 μM—occurs at concentrations overlapping with or below those needed for anti-angiogenic effects (HUVEC tube inhibition at 3-6 μM), indicating a potential synergistic therapeutic window. CS231295 also demonstrated a synthetic lethal relationship with RB1 deficiency, exhibiting heightened cytotoxicity in RB1-deficient compared to RB1-wildtype small cell lung cancer (SCLC) cells. RB1 overexpression in NCI-H1048 cells increased the IC_{50} from 0.671 μM to 8.389 μM, confirming RB1 deficiency as a key sensitivity marker. Oral administration induced significant tumor regression in RB1-deficient SCLC models. Prominent brain penetration (brain-to-plasma ratio ≈1) correlated with robust efficacy in an intracranial tumor model.
Conclusion: CS231295 achieves effective AURKB inhibition at doses concurrently modulating angiogenesis, overcoming a key limitation of prior agents. Its synthetic lethality with RB1 deficiency and marked intracranial efficacy support its therapeutic potential for RB1-deficient malignancies and brain-involved tumors. IND approvals have been obtained in China and the U.S., facilitating global clinical development.

#3062 TRIM7 inhibition blocks RTK/RAS pathway driven tumor proliferation independent of mutation and in the setting of KRASi resistance.

Yuhui Chen[1], Marc Morra[1], Haru Kato[2], Kevin Li[3], Ulhas Bhatt[3], Kevin Gayler[4], Grace Elliott-Fromm[2], Nathan Oien[2], Julio Medina[3], Taylor H. Schreiber[5], **George Fromm**[1]

[1]Kayak Therapeutics, Inc., Durham, NC,[2]Shattuck Labs, Inc., Durham, NC,[3]R2M Pharma, Inc., South San Francisco, CA,[4]R2M Pharma, Inc., South San Fransico, CA,[5]Shattuck Labs, Durham, NC

Most cancer patients experiencing clinical benefit from targeted therapies in RTK-KRAS driven cancers develop acquired resistance (AR) and relapse. The mechanism of resistance in patients who initially respond to monoallelic KRAS G12C/G12D inhibitors is dominated by the accumulation of new mutations in KRAS itself, followed by mutations downstream in the MAP kinase pathway. Therapeutics that more broadly target this pathway, like the multi-KRAS isoform inhibitor daraxonrasib, offer promise in less common mutations (e.g., KRAS G12X/Q61X). However, the tolerability of KRASi combinations has been a concern, and it is unclear whether similar resistance mechanisms will arise in multi-KRASi treated patients, as has been seen in monoallelic-KRASi treated patients. To identify novel approaches for complex or resistant RTK-KRAS driven cancers, we generated a murine CRC KRAS(G12D) AR model and through transcriptional/proteomic analysis, identified the E3 ubiquitin ligase TRIM7 as a putative driver of resistance. TRIM7 is downstream in the RTK-KRAS pathway and is upregulated in KRAS mutant and MSI-high tumors, resulting in (1) aberrant cell proliferation through ubiquitination and stabilization of RACO-1 and activated cJun/AP1 transcription, and (2) dysregulated IFN responsiveness through ubiquitination and degradation of MAVS and STING. TRIM7 is not a known mutated oncogene; rather, its hyperactivation is a byproduct of increased RTK-KRAS signaling due to upstream amplifications or mutations. We developed a highly potent and selective TRIM7 small-molecule inhibitor (KT-300) and showed it directly disrupts the ubiquitination and stability of RACO-1, resulting in decreased phosphorylation of cJun and STAT3, and altered transcription of cJun/AP1 targets. KT-300 reduced ubiquitination of MAVS, resulting in MAVS accumulation, and restored STING signaling in tumor cells where STING was impaired due to TRIM7 overexpression. KT-300 induced significant TGI in a range of KRAS/NRAS mutant tumor models (G12X, G13X, and Q61X) and in cell lines with amplification or mutation of EGFR or MAP kinase. TRIM7 specificity was confirmed using inactive enantiomers, which did not induce TGI. *In vivo*, monotherapy KT-300 delayed the growth of human KRAS-mutant NSCLC, CRC, and PDAC tumor xenograft and PDX models. TRIM7i-induced anti-tumor activity was enhanced in combination with concurrent KRAS inhibition, and KT-300 monotherapy delayed tumor growth in mice that developed resistance and progressed on KRAS inhibitors. TRIM7 inhibition via KT-300 may offer broad, mutation-agnostic activity in RTK-KRAS driven cancers. This represents a novel “pan-RTK-KRAS pathway inhibition” strategy that could extend efficacy to complex mutational backgrounds not addressed by current KRAS inhibitors, including in patients who have developed resistance to existing RTK-KRAS targeted therapies.

#3063 Selective cytotoxicity of butyrate highlights its potential as a targeted anti-cancer agent.

Nahara Yupe-Muniz[1], Josue Perez-Santiago[1], Gabriel Borges-Velez[1], Esther A. Peterson-Peguero[2], Ariana Garcia-Lopez[1], Amanda Prats-Marrero[2], Samira B.F. Abdullah-Vargas[2]

[1]University of Puerto Rico Comprehensive Cancer Center, San Juan, PR,[2]University of Puerto Rico Rio Piedras campus, San Juan, PR

Background: Within the marked heterogeneity of breast cancer, the triple-negative subtype stands out for its highly aggressive nature. Its absence of hormonal receptors prevents the use of targeted treatments, pointing the need to uncover improved therapeutic strategies. Nevertheless, recent studies have recognized butyrate as a potential agent for intervention. Butyrate is a microbial-derived short chain fatty acid that exerts anti-cancer effects. Our preliminary data showed that butyrate treatment can significantly reduce cell viability, migration, and proliferation at concentrations of 5 mM in the triple-negative cell line MDA-MB-231. While butyrate has proven its potential as a treatment option, its safety towards healthy mammary cells remains unclear. Therefore, in this study, we evaluated the effects of butyrate in a non-tumorigenic mammary epithelial cell model (MCF10A).
Methods: Cells were cultured in 1:1 DMEM/F12 supplemented with 20ng/mL EGF, 0.5 ug/mL hydrocortisone, 10ug/mL insulin, 100ng/mL cholera toxin, and 5% horse serum. Cell viability was measured using AlamarBlue assay, and butyrate treatment was given in serial dilutions (1:2) starting at 800 mM for 24, 48, and 72 hours. The half-minimal inhibitory values (IC-50) were assessed via fluorescence (590nm). Cell proliferation was evaluated by treating MCF10A with 5mM of butyrate and then quantifying for 24, 48, and 72 hours using an automated cell counter.
Results: No IC-50 was reached, yet there was a reduction in cell viability with concentrations from 100 mM and higher. In fact, MCF10A cells continued to be viable at 24, 48, and 72 hours at 5mM. There was no significant change in cell proliferation at 5mM in all time points.
Conclusions: These results suggest that butyrate reduced viability in triple-negative breast cancer cells while having no meaningful effect on the viability of MCF10A cell line, indicating a selective cytotoxic response. Proliferation results show that MCF10A presents no significant change in cell growth upon butyrate exposure in comparison to untreated controls. These results show the potential of butyrate as a selective anti-cancer agent and raise interest in the mechanism of which butyrate modulates cancer cell behavior.

#3064 Synergistic combinations of novel small molecule CtBP inhibitors with DR5 agonists or BH3-mimetic PROTACs targeting chemoresistant high grade serous ovarian carcinoma.

Kranthi Kumar Chougoni[1], Nicholette St. Martin[2], Diana T. Dcona[3], Nari Kim[3], Boxiao Ding[4], Ronny I. Drapkin[5], Keith C. Ellis[2], Steven R. Grossman[1]

[1]Hoag Memorial Hospital Presbyterian, Newport Beach, CA,[2]Department of Medicinal Chemistry, School of Pharmacy, Virginia Commonwealth University, Richmond, VA,[3]USC Norris Comprehensive Cancer Center, University of Southern California, Los Angeles, CA,[4]Virginia Commonwealth University, Richmond, VA,[5]University of Pennsylvania, Merion Station, PA

Background: High Grade Serous Ovarian Carcinoma (HGSOC) is especially lethal due to frequent diagnosis at advanced stage and development of chemoresistance. The oncogenic transcription factors C-terminal binding proteins 1 and 2 (CtBP1/2; or “CtBP”) are transcriptional scaffolds/coregulators that drive tumor progression and metastasis in many solid tumors and are amplified in ~10% of HGSOC, with their frequent protein overexpression correlated with poor prognosis.

Results: We have previously reported that CtBP transcriptionally represses the proapoptotic Death Receptors (DR) 4/5 in HGSOC cells, preventing activation of caspase 8-dependent apoptosis. Aside from its role as an oncogenic dependency in HGSOC, CtBP is a therapeutic target encoding an NAD-dependent dehydrogenase domain against which we have developed small molecule CtBP inhibitors (CtBPi) which exhibit significant anti-tumor activity in various solid tumor models without toxicity. Our current lead CtBPi’s, NAS-2-133/134, which are naphthyl derivatives of the 1st generation CtBP inhibitor scaffold 2-hydroxyimino-3-phenylpropanoic acid, exhibit IC_{50} values of 4-17 µM in multiple HGSOC cell lines, while A2780 cells with homozygous deletion of CtBP1/2 (A2780/DKO) were resistant to NAS-2-134 relative to parental A2780 cells (IC_{50}s = >>25 µM [beyond titration] vs. 20 µM, respectively), demonstrating that NAS-2-134 exhibits potent on target cytotoxic selectivity. In addition, NAS-2-134 induced caspase-8 dependent apoptosis in HGSOC cells via upregulation of DR5 and exhibited synergistic cytotoxicity when combined with the DR5 agonists MD5.1 or Biomyifi using Bliss methodology (Bliss synergy scores: MD5.1=15.8, BIOYMIFI=15.3). Further mechanistic studies revealed NAS-2-134 decreased Bcl-2 levels, which prompted evaluation of potential synergy of NAS-2-134 with BH3-mimetics venetoclax (ABT-199) and navitoclax (ABT-263), which target Bcl-2 and Bcl-2/X_L, respectively. Though NAS-2-134 and ABT-199 did not exhibit synergistic cell killing in HGSOC cells, NAS-2-134 and ABT-263 exhibited strong synergy with a Bliss score of 47. Importantly, both NAS-2-134 and the closely related CtBPi NAS-2-133 demonstrated potent in vivo antitumor activity, abrogating growth of OVCAR3 xenografts in immune deficient mice.

Conclusion: We demonstrate that NAS-2-134 exhibits target selective cytotoxicity in HGSOC cells via induction of caspase-8/DR5 dependent apoptosis *in vitro* and both NAS-2-134 and NAS-2-133 exhibit potent anti-HGSOC tumor activity *in vivo;* and 2) concerted targeting of CtBP and DR5 or Bcl-2/X_L is synergistically cytotoxic in HGSOC cells and this strategy may lead to a future low toxicity precision therapy for chemoresistant HGSOC.

#3065 Therapeutic efficacy of CK2 inhibitor in patient-derived lung metastatic model of Ewing sarcoma.

Muhammad Danial[1], Chandrika Gowda[1], Rajesh Rajaiah[1], Marudhu Pandiyan Shanmugam[1], Upendar Golla[1], Sholler Chloe[1], Jeremey Hengst[1], Abhinav Beeravally Nagulapally[1], Yasin Uzun[1], Hannah Valensi[2], Matthew Lanza[1], Giselle L. Saulnier Sholler[1]

[1]Penn State College of Medicine, HERSHEY, PA,[2]Penn State College of Medicine, Hershey, PA

Introduction: Metastatic Ewing sarcoma (ES), a highly aggressive bone cancer, has an extremely poor 5-year overall survival rate of <25%. EWS-FLI oncogenic fusion protein drives tumor progression in nearly all cases. Casein kinase II (CK2) is a serine/threonine kinase that is essential for normal cellular processes and is overactive in cancer. CK2 high-expressing ES patients have a high relapse rate and worse 5-year overall survival. CX-4945 (silmitasertib) is an orally bioavailable, CK2-selective small molecule inhibitor in clinical trial for the treatment of pediatric cancers.

Methods: Patient-derived xenograft (PDX) cell lines derived from relapsed refractory metastatic EWS-FLI1 fusion-positive ES (n=15) were treated with CX-4945 and analyzed. We generated metastatic models of EWS-FLI fusion-positive ES following subcutaneous implant in athymic nude mice. After 4 weeks of treatment with CX-4945, mice were analyzed for the presence of lung and bone metastasis using histology, immunohistochemistry (IHC), and pathology review. We scored the lung metastasis burden. The number and area of tumor cell foci within the lung tissue were noted. Tumor cells and inflammatory cells in the extra-parenchymal space and tumor cells circulating within the blood vessels were confirmed using IHC. Using flow cytometry with a human CD99 antibody, we confirmed tumor cells in the lung tissue. Tumor size and survival (time to reach endpoint) were noted. We then assess the effect of CX-4945 treatment on the occurrence and severity of lung metastasis.

Results: Four weeks of treatment with CX-4945 alone showed slow tumor progression and significantly prolonged survival in two xenograft models. More importantly, treated mice showed significantly less tumor burden in lungs and bone marrow.

Conclusions: These results support further preclinical characterization and mechanistic investigation of CX-4945 for treating ES. A phase 1 clinical trial is evaluating the safety of CX-4945 in pediatric solid tumors, including ES (NCT06541262). Patient derived lung metastasis model of Ewing sarcoma development and assessment for effect of treatment is feasible and essential to determine clinically meaningful therapeutic effect of anti-cancer agent.

#3066 A novel class of allosteric CDK8/19 inhibitors induces synthetic lethality through concurrent mTOR and c-MYC suppression and activation of p53-mediated G2/M arrest.

Hui Chen, Zihan Xu, Erpei Wang, Jason Rivera, Judith Varner

UCSD, San Diego, CA

Cancer cells exhibit dysregulated signal transduction and cell cycle control pathways that drive unchecked proliferation. Both uncontrolled tumor cell growth and the expansion of immunosuppressive macrophages contribute to tumor progression. Although PI3K and MEK inhibitors can initially suppress tumor growth, resistance frequently develops through compensatory activation of alternative signaling pathways. We have identified a novel class of allosteric tyrosine kinase receptor inhibitors that induce synthetic lethality in acute myeloid leukemia (AML), lung carcinoma, pancreatic carcinoma, and other cancers. These compounds target both tumor cells and proliferating macrophages in vitro and in vivo by concurrently inhibiting c-Myc and mTOR, while activating the stress-activated kinase JNK, leading to p53-mediated G2/M cell cycle arrest. Mechanistically, selective inhibitors containing a uniquely positioned single side chain suppress CDK8/19 activation, resulting in Myc degradation, mTOR inhibition, and phosphorylation of JNK and p38. JNK activation drives sustained ATF-2 and c-Jun signaling, leading to activation of p53, Chk1/Chk2, G2/M arrest, and apoptosis. These compounds markedly suppress tumor growth in vivo by blocking both tumor and macrophage proliferation and exhibit strong synergy with anti-PD-1 and anti-CTLA-4 immunotherapies, resulting in tumor eradication and durable immunological memory. Collectively, these findings define a new class of allosteric CDK8/19 inhibitors with potent, synthetically lethal, and immunologically synergistic anti-tumor activity, revealing a promising therapeutic avenue for overcoming resistance in cancer treatment.

#3067 Short-chain fatty acids suppress invasion and clonogenic survival in triple-negative breast cancer cells.

Amanda Prats-Marrero[1], Ariana S. Garcia-Lopez[2], Liah M. Roman-Calderon[2], Samira B. F. Abdullah-Vargas[1], Gabriel Borges-Velez[2], Esther Peterson-Peguero[2], Josue Perez-Santiago[2]

[1]University of Puerto Rico, Rio Piedras Campus, San Juan, PR,[2]University of Puerto Rico Comprehensive Cancer Center, San Juan, PR

Background: Triple-negative breast cancer (TNBC) accounts for 15-20% of all breast cancers. Defined by the absence of estrogen receptors, progesterone receptors, and HER2 expression, this subtype is highly aggressive and has limited therapeutic options, resulting in a five-year survival rate of 78% compared to over 90% for other subtypes. Previous data from our laboratory demonstrated that short-chain fatty acids (SCFAs), microbiota derived metabolites, reduce TNBC cell viability, proliferation, and migration, with butyrate showing the strongest inhibitory effects. However, the impact of SCFAs on invasion and long-term survival remains unclear.
Objective: This study aimed to investigate the effects of SCFAs on invasion and clonogenic potential in a TNBC cell line (MDA-MB-231) as indicators of metastatic behavior and sustained proliferative capacity.
Methods: MDA-MB-231 cells were treated with SCFAs butyrate, acetate, and propionate at 5 mM and invasion was assessed using Boyden chambers coated with Matrigel. Cells were seeded in the upper chamber in serum-free medium, while the lower chamber contained complete medium as a chemoattractant. After 24 hours, cells that passed through the Matrigel layer were fixed, stained, and quantified using ImageJ. To evaluate long-term proliferative potential, clonogenic assays were performed with butyrate-treated cells, chosen for its strong inhibitory effects on TNBC growth and migration. MDA-MB-231 cells were seeded at a density of 1,000 cells per well of a six-well plate and treated with butyrate at 1 mM and 5 mM for 9-10 days. Colonies were fixed, stained, photographed, and quantified using ImageJ.
Results: Butyrate and propionate treatment significantly suppressed invasion compared to control ($p<0.0001$ and $p=0.0031$, respectively), while acetate had no significant effect in invasion ($p=0.4084$). Clonogenic assays showed complete inhibition of colony formation in cells treated with 1 mM and 5 mM butyrate, while control cells formed a mean of 429 colonies per well. Morphologically, treated cells displayed loss of adherence and rounded shapes consistent with cytotoxicity.
Conclusion: Butyrate and propionate significantly inhibited invasion of MDA-MB-231 cells, while butyrate also completely suppressed clonogenic survival. These findings align with our previous transcriptomic data indicating SCFA modulation of pathways involved in oncogenic processes such as migration and cell adhesion. SCFAs demonstrate potent inhibitory effects on metastatic behavior and long-term proliferation, supporting further investigation into their therapeutic potential.

#3068 Targeting ornithine aminotransferase as a promising therapeutic strategy for hepatocellular carcinoma.

Wenan Qiang[1], Yi Yang[2], Tommy Ouyang[2], Vivian Chen[2], Alice Qiu[2], Richard B. Silverman[3]

[1]Chemistry of Life Processes Institute, Department of Obstetrics and Gynecology, Pathology, Northwestern University, Evanston, IL,[2]Chemistry of Life Processes Institute, Northwestern University, Evanston, IL,[3]Department of Chemistry, Northwestern University, Evanston, IL

Comprising 90% of all liver cancers, hepatocellular carcinoma (HCC) is the second leading cause of cancer-related death worldwide. Despite decades of research, prognosis remains poor: approximately 800,000 people are diagnosed with HCC each year, and ~80% die within five years. Therapeutically, there is a critical unmet need for more effective treatments. Resistance to sorafenib, the current first-line multi-target tyrosine kinase inhibitor, has become increasingly common. Moreover, more than 150 clinical trials evaluating targeted agents, immunotherapies, and combination regimens have failed due to insufficient efficacy, underscoring the urgent need for novel, mechanism-based therapeutic strategies. Emerging evidence highlights the central role of metabolic reprogramming in carcinogenesis, treatment resistance, and recurrence across multiple cancers, including HCC. Ornithine aminotransferase (OAT) is a key enzyme in this process, linking amino acid metabolism, particularly glutamine and proline, to polyamine biosynthesis and cancer cell proliferation. OAT is overexpressed in HCC and validated as a therapeutic target in preclinical models. We previously demonstrated that the OAT inactivator LHJ-2-79 effectively inhibits tumor growth in HepG2 and Hep3B xenografts and significantly suppresses alpha-fetoprotein (AFP) secretion, a key HCC biomarker, in Hep3B and HepG2 cells. However, no OAT inactivators have yet advanced to clinical trials. To address this gap, our laboratory recently synthesized SS-1-148, a novel OAT inactivator. Here, we report the effects of SS-1-148 on HCC using IC50 profiling, enzyme expression assays, xenograft survival studies, RNA-seq analysis, and metabolomic data. Our findings reveal cell line-dependent differences in SS-1-148 potency, OAT activity inhibition, tumor growth suppression, metabolic gene expression, and alterations in proline and polyamine levels. In vivo, SS-1-148 inhibited Huh-7 xenograft growth but not Huh-6 tumors. Metabolomic analyses of LHJ-2-79 and SS-1-148 in Huh-6 and Huh-7 cells further demonstrated distinct effects on proline and putrescine levels, suggesting different mechanisms of action between the two inactivators. Collectively, these results support OAT as a promising therapeutic target in HCC and lay the foundation for further development of OAT-based treatment strategies.

#3069 Involvement of ROS species in amiloride derivative-induced lysosome-dependent cell death in triple-negative breast cancer cells.

Noemi Castro[1], Michelle Hu[1], Anastasia Berg[1], Ruiwu Liu[2], KIT LAM[2], Kermit Carraway III[2]

[1]Biochemistry and Molecular Medicine, UC Davis, Davis, CA,[2]UC Davis, Sacramento, CA

Drug resistance leading to cancer recurrence poses a particularly challenging barrier to clinical disease management. Since tumor cells commonly activate anti-apoptotic pathways that cause caspase-dependent pathways to malfunction, cellular resistance to apoptosis is perhaps the most critical factor contributing to the therapeutic failure of conventional and targeted therapeutic agents. Consequently, subpopulations of apoptosis-resistant cells, such as cancer stem cells (CSCs), persist after therapy to seed primary tumor recurrence and metastatic lesions, even after complete remission. The overarching goal of this project is to develop novel drugs that exploit the process of lysosome-dependent cell death, a programmed necrotic cell death mechanism, in suppressing CSC-mediated triple-negative breast cancer. We have previously observed that hexamethylene amiloride (HMA), a derivative of the FDA-approved diuretic amiloride, is cytotoxic in vitro and ex vivo toward cultured cells from a variety of tumor types but not non-transformed cells. HMA also suppresses primary and metastatic tumor outgrowth in vivo. HMA acts on breast tumor cells regardless of subtype, proliferative status, or species of origin. It engages a potent caspase- and autophagy-independent programmed necrotic death mechanism in tumor cells that alters lysosome structure, dysregulates lipid synthesis, leads to lysosomal membrane permeabilization, and acts efficiently toward therapy-resistant CSC-related subpopulations. Although some specifics of the mechanism remain unknown, we examine how the formation of reactive oxygen species is crucial to the induction of necrosis and the potency of HMA and other amiloride derivatives.

: Novel Therapeutics and Drug Targets 2
Poster Session

#3073 Dickkopf1 as a potential therapeutic target in highly aggressive breast cancers.

Mohd Mughees[1], Jian Wang[2], Wendy A. Woodward[3], Megumi Kai[1], MDACC IBC Team[1], Sharon H. Giordano[1], Chandra Bartholomeusz[1]

[1]UT MD Anderson Cancer Center, Houston, TX,[2]Biostatistics, UT MD Anderson Cancer Center, Houston, TX,[3]Associate Professor, Radiation Oncology, UT MD Anderson Cancer Center, Houston, TX

Background: Triple-negative breast cancer (TNBC) and inflammatory breast cancer (IBC) are aggressive and lethal breast cancer subtypes, largely due to the absence of targeted therapies and insufficient understanding of the mechanisms driving metastasis and immune evasion. The glycoprotein Dickkopf-1 (DKK1) inhibits the WNT pathway and has been reported to enhance angiogenesis, metastasis, and invasion in breast cancer. We hypothesized that elevated serum DKK1 expression in IBC patients correlates with poor patient outcomes and that inhibiting DKK1 expression reduces proliferation and stemness in breast cancer cell lines.
Methods: We used the GOBO online tool (http://co.bmc.lu.se/gobo) to analyze gene expressions in breast cancer patients and performed a western blot to check the expression of DKK1 in a panel of TNBC and IBC cell lines. Next, as DKK1 is a secreted protein, we quantified its levels in serum samples from 176 IBC patients from MD Anderson using ELISA. To investigate DKK1's biological role in TNBC and IBC, we performed in vitro cell viability, clonogenic, mammosphere formation, $CD44^{+}/CD24^{-/low}$ flow cytometry, and Western blot analyses.
Results: Using the GOBO datasets, we retrospectively analyzed DKK1 expression in breast tumors and observed that the mean *DKK1* expression was higher in basal tumors (most likely to be TNBC) and HER2+ subtypes than in the other subtypes or normal tissue and cell lines. The DKK1 expression was higher in most of the TNBC and IBC cell lines as compared to the normal breast MCF-7 cells. For serum samples, the median age of patients was 52.5 years (range, 23-78 years), 75.0% were non-TNBC, and 25.0% were TNBC. The disease stage was III in 71.6% and IV in 28.4%, and the nuclear grade was 1 or 2 in 30.5% and 3 in 69.5%. High DKK1-expressing patients (categorized using median expression) showed a high risk of developing metastases (p=0.039), breast cancer-specific mortality (p=0.0183), and shorter overall survival (p=0.0267) compared to low DKK1-expressing patients, confirming literature findings and suggesting that DKK1 is likely to act as a metastasis or tumor promoter in breast cancer. shRNA- and CRISPR-based knockdown/knockout of DKK1 significantly reduced viability, clonogenic capability, mammosphere formation capability, and $CD44^{+}$ and $CD24^{-/low}$ subpopulations in the MDA-MB-231 and SUM149 TNBC/IBC cell lines. DKK1 knockout showed loss of AKT S473 phosphorylation but no effect on beta-catenin expression in SUM149 IBC cells, suggesting beta-catenin-independent signaling.
Conclusions and future prospects: DKK1 could be a clinically significant biomarker with implications for diagnosis and therapeutic targeting in TNBC and IBC. We are now assessing DKK1 inhibition in a high DKK1-expressing genetically engineered mouse model. Additional studies may clarify how DKK1 regulates stemness and metastasis in TNBC and IBC at the molecular level.

#3074 A first-in-class ER stress modulator selectively induces regulated cell death of STK11/TP53-deficient cancer cells.

Ying-Jie Wang[1], Xiaobing Zhang[1], Wei Jia[1], Bo Kang[2], Zhao Xu[1], Mingxing Yin[1], Hongban Zhong[1]

[1]Nain Biotech Co., Ltd., Hangzhou, China,[2]First Affiliated Hospital, School of Medicine, Zhejiang University, Hangzhou, China

Background: The tumor suppressor gene STK11 encodes LKB1 kinase that is a key regulator for cell metabolism, and TP53 gene encoding p53, a transcription factor known as the “Guardian of the genome”, critically protects the DNA integrity of the cell. STK11/TP53-deficient cancers are vulnerable to metabolic stress, redox stress, etc. and resistant to most therapies including immunotherapy, but there is no therapy so far that can specifically target this population of cancer patients. Notably, somatic mutations in KRAS, TP53 etc. are the major drivers, while germline mutations in STK11 and TP53 are the major inherited risk factors for pancreatic cancer that has no efficacious therapies yet.

Methods: The IC50s of our first-in-class PDIA6/IRE1 modulator NAI003, singly or in combination with a variety of marketed anticancer drugs, against multiple cancer cell lines and patient-derived primary cancer cells, were determined by CCK-8 cell viability assay or CellTiter-Glo® luminescent cell viability assay.

Results: NAI003 series compounds selectively kill or inhibit the proliferation of 20 out of 170 human cancer cell lines (with at least one compound having IC50 < 10 μM) via regulated cell death, 11 and 16 out of the 20 cells harbor STK11 and TP53 genetic and functional defects, respectively, and 8 out of the 20 cells carry defects of both genes. Further, NAI003 series compounds, particularly NAI003-7 (that dually targets PDIA6/IRE1 and HDACs), potently kill patient-derived primary cancer cells harboring STK11/TP53 genetic and functional defects. For patient-derived primary pancreatic cancer cells in vitro, NAI003-7 outperformed the current standard of care (SOC) therapy. In contrast, up to a concentration of 50 μM, NAI003 compounds exhibit no cytotoxicity to normal human cells (PBMCs, Jurkat T cells, HCerEpiC cells, etc.), consistent with their good in vivo safety profiles. Their in vivo efficacies in PDX models are currently under investigation.

Conclusion: PDIA6/IRE1-regulated ER stress is a target of vulnerability in STK11/TP53-deficient cancers, and NAI003 is a potential first-in-class small-molecule ER stress modulator that can specifically treat cancer patients harboring STK11/TP53 genetic and functional defects. This compound holds great promise in tackling hard-to-treat cancers such as pancreatic cancer, and in overcoming cancer drug resistance by various mechanisms.

#3075 FGFR2b is a highly prevalent and actionable cell surface target in intrahepatic cholangiocarcinoma.

Nakul M. Shah, Beatriz Alvarado-Hernandez, Xinyue Chen, Quentin Kimana, Felicity Namayanja, Wei Lu, Khaja B Khan, Juan Gallegos, Sangeeta Goswami, Lawrence N. Kwong, Luisa M. Solis Soto, Milind M. Javle, Sachet A. Shukla

The University of Texas MD Anderson Cancer Center, Houston, TX

Intrahepatic cholangiocarcinoma (iCCA) is an aggressive type of biliary tract cancer (BTC) with a rising incidence and limited treatment options. Previously established cell-surface targets of antibody-based therapies are not common in iCCA; for example, HER2 amplification occurs in <5% of patients. Knowledge of targetable membrane-bound proteins is a critical bottleneck in the field. Here, we performed a proteogenomic analysis that revealed FGFR2b as a dominant cell-surface isoform in iCCA and explored the association of its expression with genomic alterations, expression pathways, and splicing regulation.

We developed a comprehensive end-to-end platform to search for cell surface targets, including alternative splicing variants. Briefly, we perform *de novo* assembly of RNA-sequencing data from BTC samples (n=79), the majority iCCA (n=67), to include unannotated alternative isoforms using *stringtie*. Using *fragpipe*, we searched for novel proteins from *in silico* translation of these assembled transcripts in cell surface protein enriched mass spectrometry data from 15 cancer cell lines. Splice junction expression from detected isoforms was normalized and compared. Using *recount3*, we also assessed expression of these splice junctions across 10,415 TCGA samples and 19,081 GTEx samples. An optimized IHC protocol was established using the Roche anti-FGFR2b mouse monoclonal antibody (FPR2-D).

A unique glycosylated peptide from a FGFR2 alternative transcript was detected in the cell-surface mass spectrometry data, and we identified this alternative isoform to be FGFR2b. In our institutional cohort of 79 BTC samples, FGFR2b was the predominant FGFR2 isoform for 88.6% (70/79) of patients, which was further confirmed in 34 BTC samples from TCGA (88.2%; 30/34). Across 33 TCGA tumor types, BTC had the highest average expression of FGFR2b. FGFR2b had limited expression in normal tissues from GTEx. Patients with FGFR2 fusions had significantly higher FGFR2b expression than FGFR2c (p=0.025). FGFR2b expression negatively correlated with epithelial-to-mesenchymal transition and positively correlated with the epithelial splicing factor ESRP1, suggesting that ESRP1-driven FGFR2b expression is a hallmark of a more differentiated subtype of iCCA. In our institutional iCCA samples, 31.6% (6/19) of patients had >10% 2+/3+ staining. Strikingly, all patients with FGFR2 fusions (4/4; 100%) were positive for FGFR2b.

These results indicate that FGFR2b is highly expressed in iCCA, especially in patients with FGFR2 fusions, and highlight it as a compelling therapeutic target. Notably, the positivity rate of 31.6% is higher than that reported for gastric cancer (~16%), a setting in which multiple FGFRb-targeted therapeutic campaigns are currently underway. Our findings provide a strong rationale for the repurposing and evaluation of these FGFR2b-targeting agents in iCCA in prospective clinical trials.

#3076 Development of a SIX1-specific PROTAC for the treatment of esophageal adenocarcinoma.

Asad Faili, Vic Scharfenberger, Ellen Weber, Samaneh Heydarzadeh, Reinhard Buettner, Tristan Lerbs

Pathology, University Hospital of Cologne, Cologne, Germany

Esophageal adenocarcinoma belong to the cancer entities with a sharply increasing incidence. Though multimodal therapies have improved outcomes, prognoses remain poor in advanced stages and the 5-year survival rate is only between 20 to 25%. For this purpose, new therapeutic options are urgently necessary. In this context, this project investigated a SIX1-specific PROTAC (ELX19) in EAC - including potential adverse effects on the immune system. SIX1 is an embryonic transcription factor, which is required during embryogenesis for the development of various organs and tissues. In contrast, it is no longer or only weakly expressed in adult tissue. However, many cancers show a reactivation of cancer, which leads to different pro-tumorigenic features, making SIX1 a potentially therapeutic target. We first tested the efficiency of ELX19 in degrading SIX1 via WB and ELISA. Thereby, a higher SIX1 expression correlated with a better degradation efficiency, leading to a DC50 of below 1 µM in FLO-1 cells. ELX19 also reduced proliferation and increased apoptosis in FLO-1 cells. Importantly, ELX19 did not affect proliferation and apoptosis in a cell line with low SIX1 expression (OE19) suggesting that the effects caused by ELX19 are SIX1-specific. As adverse effects on the immune system can be a major impediment for further clinical development, we tested the effect of ELX19 on primary T helper and cytotoxic T cells. Thereby, unspecific effects only started 3 µM which is common for VHL-based PROTACs. In conclusion, these preliminary results show the potential of a SIX1-targeting PROTAC for the treatment of esophageal adenocarcinoma.

#3077 A novel MMP-targeting peptide suppresses glioblastoma metastasis by reducing MSI1 activity.

Xian Liu, Liang-Ting Lin

Department of Health Technology and Informatics, The Hong Kong Polytechnic University, Hong Kong, Hong Kong

Glioblastoma (GBM) remains the most lethal primary brain tumor, with a median survival of under 15 months, underscoring the critical need for novel therapies. The RNA-binding protein Musashi-1 (MSI1) is a pivotal oncoprotein that drives tumorigenesis and is associated with a poor prognosis. However, direct targeting of MSI1 is hampered by its high homology with MSI2, a lack of specific inhibitors, and the biochemical challenges posed by its C-terminal intrinsically disordered region (IDR), which has obscured key regulatory mechanisms. We employed a comprehensive strategy using GBM cell lines, orthotopic mouse models, and patient-derived tissues. A custom phospho-specific antibody detected MSI1 phosphorylation at Serine 347 (pS347). Functional roles were delineated using tetracycline-inducible shRNA and site-directed mutagenesis. Metastatic potential was assessed via multiplex immunohistochemistry, gelatin zymography for MMP activity, and invasion assays. A cell-penetrating decoy peptide was synthesized by fusing the S347-mimic sequence to the TAT protein transduction domain. We identified Serine 347 as a novel, functionally critical phosphorylation switch within the C-terminal IDR of MSI1. Clinically, pS347-MSI1 levels were significantly elevated in GBM patient samples and correlated with reduced survival in preclinical models. Mechanistically, preventing S347 phosphorylation via the S347A mutation profoundly suppressed GBM tumor formation and invasive potential. For the signaling axis, phosphorylation at S347 is essential for the expression and pericellular localization of key metalloproteinases MMP-2 and MMP-9 in vivo. The subsequent MMP activity drives an Epithelial-Mesenchymal Transition (EMT), as evidenced by the upregulation of vimentin, Twist, Slug, and Snail, which in turn facilitates the F-actin reorganization necessary for effective motility. Based on this mechanism, we engineered a strategic, cell-penetrating decoy peptide that mimics the S347 epitope. This peptide acts as a highly specific competitive inhibitor, selectively reducing MSI1 phosphorylation because MSI2 lacks a homologous serine. Treatment with this decoy peptide successfully recapitulated the anti-tumor effects of genetic dephosphorylation, significantly reducing MMP-2/9 levels, suppressing EMT markers, inducing disruptive morphological changes, and potently inhibiting cellular invasion. Our work establishes MSI1-S347 phosphorylation as a previously unrecognized druggable master switch that drives GBM metastasis via an MMP-EMT signaling axis. The development of a first-in-class MSI1-S347 decoy peptide that effectively neutralizes this switch and curbs invasion offers a highly specific, mechanistically grounded therapeutic strategy with significant potential to combat GBM progression.

#3078 Targeting the non-canonical neddylation of TGRBR2 suppresses the metastatic potentials of oral squamous cell carcinoma.

Yuan-Feng Lin

Taipei Medical University, Taipei, Taiwan

Background: Oral squamous cell carcinoma (OSCC) is the most common malignant tumor in the head and neck region and is characterized by rapid growth, strong invasiveness, early cervical lymph node metastasis, and a high overall metastatic rate. Primary surgery followed by adjuvant concurrent chemoradiotherapy is currently the preferred treatment strategy for most patients with advanced OSCC. Cetuximab, an epidermal growth factor receptor (EGFR) tyrosine kinase inhibitor (TKI), in combination with radiotherapy, has recently been approved by the U.S. Food and Drug Administration (FDA) for the treatment of recurrent or metastatic OSCC. However, TKI resistance mediated by alternative activation of the transforming growth factor-β (TGF-β) signaling axis has been reported in non-small cell lung cancer. Therefore, elucidating the crosstalk between TGF-β receptor signaling and EGFR-mediated signal transduction may be critical for the future precision management of OSCC.
Methods: Gene set enrichment analysis (GSEA) was applied to predict the potential mechanisms through which the protein neddylation inhibitor MLN4924 (Pevonedistat) suppresses cellular migration and lymph node metastasis in OSCC. Site-directed mutagenesis was performed to confirm the requirement of TGFBR2 neddylation in promoting OSCC metastatic potential. A pulldown assay was used to validate TGFBR2 neddylation, and a cycloheximide chase assay was employed to evaluate TGFBR2 protein degradation upon MLN4924 treatment in HSC3 cells.
Results: We found that MLN4924 treatment effectively suppresses the metastatic potential of OSCC cells both in vitro and in vivo. Site-directed mutagenesis targeting residues K1667 and K1700 (Lys→Arg) confirmed that TGFBR2 neddylation is essential for OSCC metastatic progression. GSEA predicted that MLN4924 mainly suppresses the TGF-β signaling axis in treated cells. Pulldown assays further demonstrated that MLN4924 markedly reduces neddylated TGFBR2 levels in HSC3 cells. Consistently, MLN4924 treatment accelerated TGFBR2 degradation, as shown by cycloheximide chase analysis. In rescue experiments, re-expression of wild-type TGFBR2—but not the K1667R/K1700R neddylation-defective mutant—significantly restored migration in TGFBR2-silenced HSC3 cells. Moreover, knockdown of the E3 ligase c-Cbl substantially decreased TGFBR2 neddylation and impaired cell migration.
Conclusion: This study is the first to demonstrate that non-canonical c-Cbl-mediated neddylation of TGFBR2 plays a decisive role in driving OSCC metastatic progression.

#3079 Discovery of a novel, covalent and heterobifunctional thioredoxin reductase inhibitor with antitumor activity.

Yanyan Han, Nicholas Blazanin, Sasi Kotagiri, Md Qudratullah, Xiaobing Liang, **Yonathan Lissanu**

The University of Texas MD Anderson Cancer Center, Houston, TX

Reactive oxygen species (ROS) play a central role in cellular signaling and homeostasis. However, imbalances in ROS levels contribute to various pathologies, including cancer. Tumor cells often upregulate antioxidant systems, such as the thioredoxin reductase (TrxR) and glutathione (GSH) pathways, to buffer against oxidative stress. The identification of aberrant metabolism and ROS has generated excitement and promise as a hallmark targetable vulnerability of tumors. Unfortunately, despite tremendous academic and industry efforts, this promise remains unfulfilled. Here, we report the discovery of YS207, a first-in-class covalent heterobifunctional inhibitor of TrxR1 using the deubiquitinase-targeting chimera (DUBTAC) technology. YS207 is composed of TrxR1 recruiting moiety coupled to deubiquitinase recruiting moiety via a novel chemical linker resulting in stabilization of covalently inhibited TrxR1 for profound generation of therapeutic levels of ROS. YS207 treatment potently inhibited TrxR1 enzymatic activity in vitro and in vivo (IC_{50} of 40nM & 700nM respectively). Mechanistically, YS207 elevated ROS levels, induced lipid peroxidation, and decreased intracellular GSH. Additionally, we observed profound alterations of the mitochondria including swelling, loss of cristae, increased electron density and prominent mitophagy, all characteristic of oxidative damage by using transmission electron microscopy (TEM). Rescue experiments with the ROS scavenger N-acetyl cysteine (NAC) confirmed that YS207-induced cell death was ROS-dependent. Large-scale PRISM profiling across 885 cancer cell lines revealed that sensitivity to YS207 strongly correlates with TrxR1 dependency, NADPH metabolism, and selenoprotein biosynthesis pathways. Notably, dual knockout of TrxR1 and GPX4 partially rescued YS207-induced cytotoxicity, underscoring a cooperative role in redox regulation. Further, we showed promising anti-tumor growth inhibitory activity of YS207 in xenograft models of lung cancer. Taken together, our results demonstrate that YS207 is a potent ROS modulator with potential antitumor activities through novel mechanism of action. We aim to pursue further development of this class of molecules in tumors with enhanced vulnerability to redox imbalance.

#3080 Site-specific conjugation of CPL976H-MMAE enables stable and selective dual targeting of PD-L1 and AXL.

Delfina Popiel[1], Filip Mitula[1], Anna Jablonska[1], Krzysztof Lacek[1], Natalia Czerwinska[1], Tomasz Kornatowski[1], Magdalena Langowska[1], Sylwia Wieczorek[1], Bartosz Wiernicki[1], Damian Kolakowski[1], Adam Zmyslowski[1], Tomasz Banach[1], Joanna Deshayes[1], Michal Mroczkiewicz[2], Marcin Zagozda[2], Joanna Hucz-Kalitowska[1], Emilia Mroz[1], Malgorzata Choros[1], Maciej Wieczorek[3], Olga Abramczyk[1]

[1]Preclinical Research Department, Celon Pharma S.A., Lomianki, Poland,[2]Medicinal Chemistry Department, Celon Pharma S.A., Lomianki, Poland,[3]Clinical Development Department, Celon Pharma S.A., Lomianki, Poland

Background: Combining immune checkpoint blockade with cytotoxic chemotherapy has improved survival in multiple solid tumors; however, systemic toxicity and limited response durability remain key limitations. To overcome these barriers, we developed CPL976H-MMAE, a next-generation bispecific antibody-drug conjugate (ADC) that simultaneously targets PD-L1 and AXL. This dual-target approach aims to suppress immune escape and tumor progression pathways while ensuring efficient and precise delivery of Monomethyl Auristatin E (MMAE) directly to the cancer cells.
Materials and Methods: CPL976H-MMAE was created with Fc-glycan remodeling and click-chemistry conjugation, resulting in an enhanced molecular stability and a standardized drug-to-antibody ratio (DAR). Target binding and stability of CPL975H-MMAE in serum were assessed by Surface Plasmon Resonance (SPR) after incubation in human, cynomolgus, mouse, and rat sera (7 days at 37°C). Pharmacokinetic and biodistribution studies were performed in MDA-MB-231 cell line xenograft models using LC-MS. Efficacy of CPL976H-MMAE was validated ex vivo in patient-derived xenografts (PDX) representing distinct PD-L1/AXL expression profiles. Potential binding to red-blood-cells (RBCs), MMAE release and its partitioning to RBCs were quantified by LC-MS in rat and cynomolgus species.
Results: CPL976H-MMAE retained strong and stable dual-target binding across different species sera, showing highest stability in human and cynomolgus, moderate in mouse, and lowest, but still satisfactory, in rat. ADC binding and MMAE level in RBCs of mouse and cynomolgus species was negligible, even though free MMAE exhibits partial association, further indicating conjugate stability in circulation. Pharmacokinetic analyses revealed a favorable plasma clearance profile and evident, dose-dependent tumor accumulation at 0.8-6 mg/kg, with minimal off-target MMAE exposure. Ex vivo studies confirmed potent cytotoxic activity of CPL976H-MAME in PDXs expressing both high and moderate PD-L1/AXL levels.
Conclusions: CPL976H-MMAE effectively merges immune checkpoint blockade with targeted cytotoxicity, addressing both primary and acquired resistance to PD-1/PD-L1 therapies. High serum stability, sustained tumor accumulation, and limited systemic exposure presents CPL976H-MMAE as a formidable and robust bifunctional ADC. Presented data highlight CPL976H-MMAE translational potential for future therapies, especially for patients unresponsive to current immunotherapies.
This study was supported by The National Centre for Research and Development (POIR.01.01.01-00-0429/19)

#3081 TEAD inhibition by IAG933 as a novel therapeutic strategy for cholangiocarcinoma.

Hidemi Nishi[1], Erik Jessen[2], Danielle M. Carlson[1], Amro M. Abdelrahman[1], Enis H. Ozmert[1], J. Pedro Fincatto Safi[1], Brandon A. Wilbanks[1], Shelby K. Yee[1], Jack W. Sample[1], Nathan W. Werneburg[1], Rory L. Smoot[1]

[1]Surgery, Mayo Clinic, Rochester, MN,[2]Biochemistry and Molecular Biology, Mayo Clinic, Rochester, MN

Background: Cholangiocarcinoma (CCA) is an aggressive hepatobiliary malignancy with marked molecular heterogeneity, limited systemic treatment options, and poor prognosis. Chemoresistance and KRAS mutations remain major therapeutic challenges. Dysregulation of the Hippo pathway, particularly YAP/TAZ hyperactivation, drives CCA progression and resistance. TEAD, the essential transcriptional partner of YAP/TAZ, represents a promising target. IAG933 is a novel oral pan-TEAD inhibitor designed to disrupt YAP/TAZ-TEAD interactions. RMC-6236, a pan-KRAS inhibitor, has also gained attention. Combined TEAD and KRAS inhibition may overcome resistance and improve efficacy in CCA.

Methods: We evaluated IAG933 in human (HuCCT1, RBE) and murine (SB1, FAC) CCA cell lines. Cells were treated with IAG933 alone or in combination with GemCis or RMC-6236. Cell viability assays were used to determine IC_{50} values and calculate combination *indexes* (CI). TEAD activity was assessed by luciferase reporter and qRT-PCR of YAP/TAZ target genes (CTGF, CYR61, NUAK2). Transcriptomic alterations were analyzed by RNA sequencing. In vivo efficacy was evaluated in syngeneic orthotopic and patient-derived xenograft (PDX) models.

Results: IAG933 suppressed TEAD-dependent transcription ($IC_{50} \approx 500$ nM) and downregulated YAP/TAZ target genes. Combination with GemCis or RMC-6236 produced synergistic effects ($CI < 1$) in all CCA lines. Transcriptomic analysis revealed activation of oxidative stress response pathways, particularly SOD2 upregulation. MitoSOX staining confirmed increased mitochondrial ROS after treatment. In vivo, IAG933 monotherapy suppressed tumor growth similarly to GemCis. Dual TEAD and KRAS inhibition achieved marked tumor regression and significantly delayed tumor regrowth after treatment cessation in KRAS-mutant PDX models.

Conclusion: IAG933 effectively suppresses YAP/TAZ-TEAD signaling and inhibits CCA growth. While the combination with GemCis showed limited additional benefit due to strong single-agent efficacy, synergy with RMC-6236 produced durable antitumor effects, particularly in run-out studies, delaying regrowth in KRAS-mutant models. These findings highlight IAG933 as a promising therapeutic candidate targeting the Hippo-TEAD pathway, with potential benefit in KRAS-mutant CCA.

#3082 A novel iNOS inhibitor as a targeted therapeutic approach for inflammatory breast cancer.

Karina Ortega Martinez[1], Maria Florencia Chervo[1], Feng Li[1], Jenying Deng[1], Liliana Guzman-Rojas[1], Wei Qian[2], Jianying Zhou[2], Recep Bayraktar[1], Aireana Phillips[1], Ivonne Uzair[1], Mailin Li[1], Aijun Zhang[1], Spencer Hankins[1], Dale Hamilton[1], Zhonglin Liu[1], Christopher Lincoln[1], Christoforos Thomas[3], Jenny C. Chang[4]

[1]Houston Methodist Research Institute, Houston, TX,[2]Houston Methodist Research Institute, houston, TX,[3]Houston Methodist Research Institute, Houston, Houston, TX,[4]Houston Methodist Hospital, Houston, TX

Nitric oxide (NO), generated by inducible nitric oxide synthase (iNOS), has been implicated in tumor progression, metastasis, and therapy resistance. Our completed phase Ib/II clinical trial in metastatic and locally advanced triple negative breast cancer showed that combination therapy with the pan NOS inhibitor LNMMA and standard chemotherapy elicits potent antitumor activity. Mechanistically, LNMMA targets the breast cancer stem cell (BCSCs) population enhancing their susceptibility to chemotherapy. We have developed a new iNOS inhibitor TDIMER co formulated with a calcium channel antagonist to mitigate the hemodynamic effects associated with systemic iNOS inhibition. We hypothesize that TDIMER can be effective for the treatment of inflammatory breast cancer (IBC), a rare and highly aggressive subtype with high recurrence rates and poor prognosis. In vitro studies were performed using SUM149 IBC cells. iNOS expression was confirmed by RT-qPCR and western blot. TDIMER efficacy was assessed, alone or with docetaxel, and compared to LNMMA, through cell proliferation, apoptosis and cell migration assays. BCSCs ($CD44^{+}/CD24^{-/low}$) were identified by flow cytometry after treatment with TDIMER or LNMMA in combination with docetaxel. In vivo studies using non-tumor bearing NSG mice were conducted to determine TDIMER dose toxicity and effect on blood pressure (BP). Mice received TDIMER (40 mg/kg oral gavage on day 1, 20 mg/kg oral gavage on days 2-5) or in combination with the calcium channel blocker amlodipine (10 mg/kg IP injection on days 1-5). Mice treated with PBS were used as control. BP was measured daily with BP-2000 (Visitech Systems). Animals were euthanized on day 5 for histopathological analysis and assessment of biochemical markers (ALT, AST, BUN) in serum samples. TDIMER treatment demonstrated superior efficacy over LNMMA, with a markedly lower IC_{50} in SUM149 cells. TDIMER more effectively reduced cell viability, and delayed migration relative to LNMMA. Combination therapy with TDIMER and docetaxel induced the highest levels of apoptosis and reduced BCSCs, suggesting potent activity against chemo resistant tumor-initiating cells. In vivo toxicity studies demonstrated that TDIMER treatment did not produce histopathological alterations or significant elevations in serum ALT, AST, or BUN levels, confirming a favorable safety profile. Furthermore, no significant changes in BP were observed across experimental groups, underscoring TDIMER's advantage in achieving potent iNOS inhibition without the need for coadministration of antihypertensive agents. Ongoing studies are aimed to elucidate the antitumor efficacy of TDIMER in xenograft mouse models of IBC. Overall, our findings support continued preclinical development of TDIMER as a novel iNOS targeted therapy for IBC patients.

#3083 YT-DP: A glyco-conjugation-based dual-payloads ADC platform.

Yi Yang, Zhentao Song, Rui Yu, Jiangping Hu, Zhouyang Qian, Xinyue He, Guoli Yang, Ji Chen, Juntao Yu

Glyco-therapy Biotechnology Co. Ltd., Hangzhou, China

Dual-payloads antibody-drug conjugates (ADCs) represent a promising next-generation modality to enhance antitumor efficacy, achieve synergistic effects, and overcome tumor heterogeneity and therapeutic resistance. However, their development faces several key challenges, including: (i) identifying payload combinations that maintain efficacy within a shared safety window without single-agent dominance; (ii) achieving precise and efficient assembly of distinct payloads into antibodies with controlled drug-to-antibody ratios (DARs); and (iii) ensuring robust stability, in vivo efficacy, and favorable safety profiles. To address these challenges, we developed YT-DP, a glyco-conjugation-based dual-payloads ADC platform that enables the incorporation of two distinct mechanism-of-action (MOA) payloads into a single antibody molecule through a one-step glyco-conjugation strategy. This system allows flexible DAR configurations (e.g., DAR 2+2 or DAR 2+4). The YT-DP platform integrates our proprietary cleavable-linker-topoisomerase I inhibitor payload (CLTp) technology (YT-CLTp) with a microtubule inhibitor (MTI) via the YTConju glyco-conjugation system. The YT-CLTp series comprises tunable payload candidates with adjustable target and bystander killing activities, demonstrating superior anti-tumor potency compared with “GGFG-Dxd” in multiple CDX models when conjugated to antibodies. We generated trastuzumab-based dual-payloads ADCs (Tras-DPs) containing an MTI and distinct CLTps at different DARs (DAR 2+2 and DAR 2+4). Tras-DPs exhibited high homogeneity, excellent thermal and plasma stability, and potent synergistic antitumor activity with strong by-stander effects. Notably, Tras-DPs demonstrated markedly superior antitumor activity compared with DS-8201, as well as the corresponding single-payload ADCs or their combinations, in CDX models. In addition, the dual-payloads ADCs showed favorable pharmacokinetic (PK) properties and safety profiles in rat studies. In summary, the YT-DP platform provides a robust and versatile strategy for constructing homogeneous, stable, and synergistic dual-payloads ADCs with tunable DARs. Its broad compatibility with various antibody formats, including Fc-containing bispecific antibodies, underscores its potential to enable next-generation ADCs with an enhanced therapeutic index.

#3084 Network-based discovery of tumor-checkpoint inverter drugs targeting pancreatic ductal adenocarcinoma cell states and macrophage reprogramming.

Yining Chen[1], Alvaro Curiel-Garcia[1], Alex Piacentini[2], Zhouzerui Liu[2], Tim Olsen[2], Richard Yau[3], Praveer Sharma[3], Liz Murray[3], Gaetano Viscido[1], Ken Olive[1], Andrea Califano[1]

[1]Herbert Irving Comprehensive Cancer Ctr., New York, NY,[2]Chan Zuckerberg Biohub, New York, NY,[3]Cellanome, Foster City, CA

Pancreatic ductal adenocarcinoma (PDAC) remains one of the most lethal malignancies, driven by extreme tumor heterogeneity and a profoundly immunosuppressive tumor microenvironment (TME). Distinct PDAC cell states—Gastrointestinal-like (GLS), Morphogenic (MOS), and Primitive (PLS)—coexist within individual tumors and are further stratified by MAPK activity (M^+/M^-), reflecting dynamic transcriptional programs sustained by Master Regulator (MR) proteins. These cell states are hypothesized to differentially modulate the tumor-associated macrophages in the TME. To investigate this, we established a co-culture system of THP-1-derived macrophages with PDAC cell lines representing each state and profiled macrophage transcriptional reprogramming. Macrophages co-cultured with distinct PDAC states exhibited differential activation of M2-like and $TREM2^+/APOE^+/C1Q^+$ immunosuppressive phenotype, suggesting that PDAC cell states may uniquely influence macrophage phenotypes and immune evasion.To identify compounds capable of reprogramming these malignant states, we applied a network-based systems biology framework integrating ARACNe and VIPER to infer MR activity across PDAC states, OncoMatch to identify representative cell line models, and OncoTreat to predict small molecules capable of inverting tumor checkpoint-module activity. Cross-model validation identified state-specific candidate drugs, including Leuprolide, Vinblastine, and Mercaptopurine for GLS; Vindesine, Gossypol, and Binimetinib for MOS; and AT9283, Crizotinib, and Afatinib for PLS. Predicted MR-inversion scores correlated with experimental dose-response profiles in cell lines selected via OncoMatch.Together, these results establish a mechanistic link between tumor-intrinsic transcriptional states and macrophage immunosuppression, while identifying mutation-agnostic, state-specific drugs capable of reprogramming both tumor and immune compartments. This work provides a generalizable framework for network-based drug repurposing to overcome transcriptional plasticity and immune resistance in PDAC.

#3085 Molecular characterization of inhibition of the DNA repair protein RAD51 by the small molecule JKYN-1.

Peter Ferguson[1], Mark Vincent[1], Yousef Najajreh[2], Morgan Black[3], Sweta Sharma Saha[4], Melissa Thomas[5], Olivier Lord[6], Stephen Ritter[7], Jean-Yves Masson[5], Brian Shilton[7], James Koropatnick[7]

[1]London Health Sciences Centre, London, ON, Canada,[2]Faculty of Pharmacy, Al-Quds University, Abu-Dies, Jerusalem, Palestinian Territory,[3]London Health Sciences Ctr., London, ON, Canada,[4]Teesside University, Middlesbrough, United Kingdom,[5]CHU de Quebec-Universite Laval, Quebec, QC, Canada,[6]Universite Laval, Quebec, QC, Canada,[7]Western University, London, ON, Canada

The ability of cancer cells to form large tumors and rapidly adapt to changing environmental conditions results from inherent genetic instability that also confers upon them sensitivity to cytotoxic agents. Cancer cells rely heavily on the action of the protein RAD51, overexpressed in many tumors, to survive DNA damage and replication stress (RS) (Cells 12: 1169-1189, 2023. https://doi.org/10.3390/cells12081169). The IBR-family RAD51 inhibitors not only inhibit tumor cell proliferation as single agents at low micromolar concentrations, but also work synergistically with a variety of established anticancer agents to stop growth and induce cell death (J Pharmacol Expt Ther, 364: 46-54, 2018. doi.org/10.1124/jpet.117.241661). To better understand the synergistic interaction and help improve selectivity against cancer cells, and thus potential for clinical use, we have characterized the activity of IBR2, IBR120, and JKYN-1 using a variety of methods. JKYN-1, the structure of which is a modification of IBR120, is 5-fold stronger as a single-agent inhibitor of proliferation. As demonstrated previously for IBR2 and IBR120, JKYN-1 synergistically inhibited proliferation of cell lines representative of numerous tumor sources in combination with established anticancer drugs. In hydroxyurea-treated human breast carcinoma MCF-7 cells, B02, an established RAD51 inhibitor (Mol Cancer Ther 20:1257-1269, 2021. doi: 10.1158/1535-7163.MCT-20-0252), and JKYN-1 markedly suppressed formation of RAD51 foci while increasing pRPA foci formation, a marker of RS. In human osteosarcoma U2OS cells exposed to ionizing radiation, JKYN-1 alone reduced RAD51 foci formation. Mechanistically, JKYN-1 impaired RAD51-dependent D-loop formation. JKYN-1 inhibited multimerization of RAD51 as well as its ATPase activity, responsible for normal dissociation of RAD51 from DNA following completion of repair. Therefore, JKYN-1 acts as expected in inhibiting RAD51 function. How this contributes to the synergy observed with anticancer agents is being investigated. Derivatives of JKYN-1 are currently being studied for improvements to pharmacokinetic properties. *Funded by Sarissa, Inc., Breast Cancer Canada, and London Health Sciences Foundation.*

#3086 ART1 as an immune modulating therapeutic target in EGFR-mutated lung cancer.

Mimansa .[1], Rajika Jindani[1], Mukherjee Sumit[1], Jorge Quintero[1], Naresh Regmi[1], Grace Ha[1], Justin Olivera[1], Justin Rosario[1], Melissa Tracy[1], Brendan Mullaley[1], Victor Gray[2], Erik Wennerberg[2], Lindsay M. LaFave[1], Brendon Stiles[3]

[1]Albert Einstein College of Medicine, Bronx, NY,[2]The Institute of Cancer Research, London, United Kingdom,[3]Montefiore Einstein Comprehensive Cancer Center, The Bronx, NY

Purpose: Epidermal growth factor receptor (EGFR) mutations drive non-small cell lung cancer (NSCLC). Tyrosine kinase inhibitors (TKIs) provide clinical benefit but are limited by resistance. We investigated the role of mono-ADP-ribosyltransferase-1 (ART1) in mediating EGFR signaling, immune suppression, and therapeutic resistance.
Methods: ART1 expression was assessed in a human tissue microarray. ART1 function was assessed in vitro in HCC827 and other EGFRmu lines using immunoprecipitation, immunofluorescence, and RNA-seq to define MARylation events and transcriptional changes. In vivo studies tested ART1 blockade with the fully humanized anti-ART1 monoclonal antibody, 22C12, alone or in combination with osimertinib in EGFR-mutant NSCLC GEMMs. These approaches enabled integrated assessment of ART1's biochemical, transcriptional, and immunologic functions.
Results: ART1 protein expression was higher in EGFRmu than EGFRwt human tumors. In vitro, ART1 was increased by osimertinib treatment. ART1 enhanced EGFR signaling through NAD^+-dependent mono-ADP-ribosylation (MARylation). ART1 blockade with 22C12 abrogated EGFR MARylation and reduced downstream oncogenic signaling. RNA-seq revealed ART1-dependent regulation of EGFR-related transcriptional programs. In vivo, 22C12 osimertinib and 22C12 each demonstrated single agent efficacy, however small tumors persisted in GEMM models. However, combination therapy with Osimertinib and 22C12 reduced macrophage infiltration, increased tumor-infiltrating $CD8^+$ tissue-resident memory (TRM) T cells, and rendered treated mice tumor-free. This synergy highlighted complementary tumor-intrinsic and immune-modulatory roles of ART1. These dual tumor-intrinsic and immune-modulatory effects identify ART1 as a driver of therapeutic resistance and potential therapeutic target.
Conclusions: ART1 promotes EGFR pathway activation and suppresses antitumor immunity in EGFR-mutant NSCLC. Targeting ART1 enhances efficacy of TKIs while decreasing macrophage infiltration and reinvigorating $CD8^+$ T-cell responses. ART1 inhibition represents a promising therapeutic strategy for overcoming resistance, warranting further investigation including ADP-ribosylome mapping and studies on ART1 blockade in modulating receptor signaling and bispecific antibody or antibody-drug conjugate interactions. Overall, these results support ART1 as a targetable mediator of EGFR-driven tumor progression and immune dysfunction in EGFR-mutant lung cancer. 22C12 is being developed to enter phase 1 clinical trials across multiple tumor types.

#3087 Targeting AURKA and TRIP13 exploits mitotic vulnerability and enhances antitumor immunity in Rb-deficient immunocompetent lung cancer models.

Soma Ghosh[1], Jennifer L. Anderson[2], Andrew G. Sikora[3], Faye M. Johnson[1]

[1]UT MD Anderson Cancer Center, Houston, TX,[2]The University of Texas MD Anderson Cancer Center, Texas, TX,[3]Department of Head and Neck Surgery, The University of Texas MD Anderson Cancer Center, Texas, TX

Rb loss is a common event in multiple cancers and creates vulnerabilities that can be therapeutically exploited. We previously reported that HPV-positive, Rb-deficient cancers depend on two mitotic checkpoint regulators, Aurora kinase A (AURKA) and TRIP13, for proper mitotic exit. Dual inhibition of these proteins induces mitotic catastrophe and cell death. To determine whether this dependency extends beyond HPV-driven tumors and affects the tumor immune microenvironment, we evaluated the combination of AURKA and TRIP13 inhibition in Rb-deficient lung cancer models. To test the combination, we used the TRIP13 inhibitor DCZ0415 and the AURKA inhibitor alisertib. We first assessed the ability of DCZ0415 to inhibit TRIP13. Consistent with previous reports, DCZ0415 binds to TRIP13 as confirmed by CETSA and affinity chromatography assays. Treatment of cancer cells with 10μM DCZ0415 reduced MAD2 association with CDC20 in pull-down assays, indicating that DCZ0415 selectively interferes with TRIP13-mediated MAD2 conversion. TRIP13 ATPase activity was largely unaffected, suggesting a kinase-independent inhibitory mechanism. The IC_{50} values for DCZ0415 in murine non-small cell lung cancer (NSCLC) cell lines were 20μM for 344SQ and 16μM for 344P, as determined by CellTiter-Glo assays. In apoptosis assays (Annexin V), DCZ0415 alone did not induce measurable cell death, while alisertib (200 nM) resulted in ~25% apoptosis after 72 hours. In contrast, the combination treatment produced significantly greater apoptosis. In 344SQ cells, the combination induced ~40% cell death, compared with 4.6% for DCZ0415 and 25% for alisertib alone. Similar findings were observed in 344P cells, with combination treatment inducing ~55% apoptosis. We next evaluated the combination in a PD1-resistant, Rb-deficient immunocompetent mouse model. The combination produced a marked reduction in tumor growth compared with either agent, with significant differences apparent by day 14. Preliminary immunoprofiling of tumor-infiltrating immune cells (TILs) revealed several combination-specific effects. Dendritic cell abundance increased, suggesting enhanced antigen presentation within the tumor. The combination also reduced myeloid-derived suppressor cell (MDSC) levels in the tumor, indicating a shift toward a less suppressive tumor immune microenvironment. Additionally, TIL analysis showed increased overall T-cell infiltration, with both $CD4^+$ and $CD8^+$ T-cell populations elevated relative to single agents. T-cell polyfunctionality was also enhanced, as indicated by higher frequencies of $GZMB^+$ and $IFN\gamma^+$ effector T cells. Together, these findings identify combined AURKA and TRIP13 inhibition as a promising therapeutic approach for Rb-deficient cancers and provide the first *in vivo* evidence of its efficacy and immune-modulating potential in NSCLC.

#3088 Targeting NONO as a therapeutic strategy for metastatic castration-resistant prostate cancer (mCRPC).

Brian McEllin, **Gaelle Mercenne**, Daniele Canzani, Gavin Hirst, Lindsay Pino, Alexander Joel Federation

Talus Bio, Seattle, WA

Prostate cancer is among the most prevalent cancers among men, with approximately 300,000 new cases diagnosed annually. While androgen deprivation therapy (ADT) is effective in controlling early-stage prostate cancer, treatment options are limited once the disease advances to metastatic castration-resistant prostate cancer (mCRPC). This progression underscores the critical need for innovative therapeutic strategies to address this difficult-to-treat stage. Resistance to ADT arises when androgen receptor (AR) signaling becomes active even in the absence of ligands. This resistance is often driven by mutations in the ligand-binding domain (LBD) of AR or the expression of AR variants (AR-Vs) that lack the LBD. Uncovering new strategies to inhibit these constitutively active AR-Vs could provide significant clinical benefit for patients with mCRPC.

Talus Bio has developed a groundbreaking technology, TF-Scan, the first cell-based global screening platform specifically designed to target transcription factors (TF) and other regulome proteins. TF-Scan integrates functional proteomics, automated cell processing, and machine learning to evaluate a drug's ability to modulate the activity of DNA-bound proteins in live human cells. This is an ideal system to identify and optimize compounds that suppress AR through direct or indirect mechanisms.

Building on this mechanistic insight, we applied TF-Scan to systematically identify covalent modulators of NONO (non-POU domain-containing octamer-binding protein) that disrupt AR expression and protein binding. We then initiated an iterative hit-to-lead optimization campaign leveraging TF-Scan to optimize NONO binding, AR disruption and proteome-wide selectivity.. Our chemical series engages NONO at C145 with high selectivity in intact prostate cancer cells and produces a consistent reduction in chromatin-bound AR. Lead compounds suppress both full-length AR and AR-V7 protein levels, downregulate multiple downstream AR/AR-V target genes, and achieve sub-micromolar EC50 values for blocking the accumulation of AR mRNA isoforms. These effects translate into concordant anti-proliferative activity in AR-dependent prostate cancer models. Several advanced analogs exhibit improved solubility, enhanced microsomal stability, and overall favorable ADME/PK profiles. Based on these results, we are advancing our most promising candidates into proof-of-concept in vivo efficacy studies to evaluate their potential as first-in-class NONO/AR-targeting therapeutics for mCRPC.

#3089 Characterization of a novel inhibitor of asparagine synthetase that activates the integrated stress response.

Nicholas T. Walda[1], Lucciano A. Pearce[2], Nigel Richards[3], Wen Zhu[2], Yuichiro Takagi[1], Ronald C. Wek[1], **Kirk A. Staschke**[1]

[1]Biochemistry, Molecular Biology, and Pharmacology, Indiana University School of Medicine, Indianapolis, IN,[2]Chemistry and Biochemistry, Florida State University, Tallahassee, FL,[3]Foundation for Applied Molecular Evolution (FfAME), Alachua, FL

Asparagine synthetase (ASNS) catalyzes the biosynthesis of L-asparagine (L-Asn) from L-aspartate, L-glutamine, and ATP, and plays a central role in anticancer therapies such as L-asparaginase treatment of acute lymphoblastic leukemia. In response to L-Asn depletion, ASNS induction is a key effector of the GCN2-ATF4 arm of the integrated stress response (ISR), enabling tumor cells to maintain amino acid homeostasis under limiting nutrient conditions. However, direct ASNS targeting has long been hindered by the poor cellular potency of existing inhibitors. Here, we delineate the molecular and cellular mechanism of ASX-173, a cell-penetrant ASNS inhibitor with potent biochemical and cellular activity with the potential to starve tumors of asparagine and enhance the impact of combination therapies targeting tumor metabolism.

Using HEK293A cells cultured without exogenous L-Asn, ASX-173 markedly reduced intracellular L-Asn levels, activated the ISR, and stimulated ATF4 transcriptional activity. ISR induction was reversed by physiological levels of L-Asn, confirming on-target activity. Deletion of GCN2 lowered basal ASNS expression, impaired ATF4 induction, and sensitized cells to ASX-173. Similarly, the GCN2 inhibitor GCN2iB suppressed ASX-173-induced ATF4 transcriptional activity and synergized to inhibit the growth of multiple cancer lines, including renal (RENCA) and prostate (Myc-CaP) models. Cell-based thermal protein profiling experiments confirmed direct ASNS binding, shifting its melting temperature from 45 °C to 54 °C. Using recombinant ASNS, ASX-173 inhibited L-Asn production without affecting L-glutamate and showed reduced activity at the Km for Mg^{2+}-ATP. Differential scanning fluorimetry experiments demonstrated that binding of ASX-173 to ASNS requires Mg^{2+}-ATP. Moreover, a 2.58 Å cryo-EM structure revealed ASX-173 bound in the C-terminal synthetase subdomain alongside AMP, PPi, and two Mg^{2+} ions, stabilized by hydrophobic, π-interactions, and hydrogen bonding with AMP to form a composite pocket. The structure indicates that ASX-173 promotes ATP hydrolysis and blocks ammonia transfer, supporting an uncompetitive mechanism.

These findings establish ASX-173 as a potent ASNS inhibitor with strong cellular target engagement and ISR-inducing activity. The heightened sensitivity of GCN2-deficient cells and the synergy with GCN2 inhibition highlight the therapeutic potential of dual ISR targeting and support ASNS inhibition—alone or in combination with ISR-modulating strategies—as a promising approach for cancers dependent on asparagine metabolism.

#3090 VRK1 inhibition leverages paralog synthetic lethality to selectively target VRK2-deficient cancer cells.

Kiera M. Vassallo, Kevin M. Cottrell, Katarzyna B. Handing, Mu-Sen Liu, Alvin Lu, Alice Tsai, Maria Dam Ferdinez, Patrick McCarren, Sirimas Sudsakorn, Jannik N. Andersen, **Kimberly J. Briggs**

Tango Therapeutics, Inc., Boston, MA

Vaccinia-related kinases (VRKs) are a family of serine/threonine kinases involved in a variety of cellular processes, including cell signaling, chromatin modification, nuclear envelope dynamics, and cell cycle progression. More than 60% of glioblastomas and nearly all neuroblastomas have low expression of the *VRK2* gene resulting in deficient VRK2 activity. VRK1 has been identified as a paralog synthetic lethal target in these VRK2-deficient cancers, with the potential for indication expansion into additional cancer types. Here, we show that inhibition of VRK1 leads to a concomitant loss of Barrier to Autointegration Nuclear Assembly Factor 1 (BANF1 or BAF) phosphorylation leading to aberrant nuclear envelope formation and downstream loss of cellular viability. As a target, VRK1 is both tractable and structurally-enabled, with chemical series capable of achieving >4000-fold biochemical selectivity against its paralog VRK2 and >70-fold viability selectivity in VRK2 isogenic cell line pairs. Compounds show strong correlations between biochemical, cellular target engagement, pharmacodynamic, and functional viability assays. Furthermore, in vivo tolerability studies suggest that VRK1 inhibitors are well-tolerated in immunocompromised mice. Preclinical validation studies support the development of VRK1 inhibitors for the treatment of patients with VRK2-deficient tumors such as glioblastoma and neuroblastoma.

#3091 Exploring the anti-tumor potential of HLA-G-targeted therapeutics through diverse preclinical approaches.

Hyeonju Kang, **Inyoung Lee**, Sungyeon Park, Yoo jin Kim, Kyueun Cho, Hongjai Lee, Yiyoung Choi, Jiyeon Hong, Chihye Park, Chungmin Lee, Gyongsik Ha

IMBiologics Corp., Suwon, Korea, Republic of

HLA-G, a non-classical MHC class I molecule with potent immunosuppressive properties, is aberrantly expressed in various solid tumors and plays a critical role in immune evasion. This immune suppression is primarily mediated through its interaction with inhibitory receptors such as ILT-2 on immune cells, which dampens anti-tumor responses and facilitates tumor progression. As such, HLA-G functions as an immune checkpoint molecule, making it a promising target for cancer immunotherapy. Monoclonal antibodies and CAR-T therapies targeting HLA-G have been previously explored; however, further optimization of therapeutic formats, incorporation of novel modalities such as antibody-drug conjugates (ADCs) and multi-specific antibodies, and preclinical validation are needed to advance their clinical potential. In this study, we present a preclinical evaluation of HLA-G-targeting biologics, including ADCs and bispecific antibodies, with emphasis on pharmacokinetics, efficacy, and biomarker-guided tumor selectivity. Notably, in a choriocarcinoma xenograft model, one complete response was observed following ADC monotherapy, suggesting the therapeutic potential of HLA-G-targeted ADCs in specific tumor contexts. To further assess clinical relevance, MiniPDX platforms derived from patient tumors were employed for target validation and biomarker correlation. These studies indicate HLA-G expression may serve as a predictive marker for therapeutic response and revealed differential efficacy across tumor types. In parallel, bispecific antibodies targeting HLA-G and co-expressed tumor antigens were evaluated for binding affinity and cytotoxicity. Bispecific formats demonstrated enhanced tumor cell engagement and potent anti-tumor activity, suggesting their utility in overcoming antigen heterogeneity and resistance mechanisms. Collectively, these findings provide preclinical evidence supporting the development of HLA-G-targeting therapeutics using diverse modalities. ADCs are particularly appealing as they can enhance potency through cytotoxic payloads while minimizing off-target toxicity due to the tumor-specific antigen nature of HLA-G. In addition, bispecific antibodies may offer further tumor selectivity and augment immune activation. This study presents additional efficacy data from in vivo xenograft and MiniPDX models, contributing to the ongoing preclinical evaluation of HLA-G-targeting strategies. Importantly, HLA-G has emerged as a potential therapeutic target capable of delivering robust efficacy through diverse therapeutic modalities and may serve as a predictive biomarker. These findings underscore the potential of HLA-G-targeted therapeutics, particularly ADCs and bispecific formats, as investigational treatment options for cancers with limited effective therapies, such as ovarian cancer.

#3092 Epiregulin and amphiregulin as dual targets in colorectal cancer.

Cara Biddle-Guernsey[1], Joan Jacob[2], Zhengdong Liang[1], Kendra S. Carmon[1]

[1]Center for Translational Cancer Research, The Brown Foundation Institute for Molecular Medicine, University of Texas Health Science Center at Houston, Houston, TX,[2]Pediatrics Oncology-AICT, Baylor College of Medicine, Houston, TX

Advanced-stage metastatic colorectal cancer is associated with high mortality. Current therapies have shown limited survival benefit and are often constrained by dose-limiting toxicity or drug resistance, including constitutively activating mutations (i.e., *KRAS*) limiting epidermal growth factor receptor (EGFR)-targeted therapy efficacy. Thus, novel targeted therapeutic strategies are needed. Antibody-drug conjugates (ADCs) act as guided missiles where a monoclonal antibody (mAb) conjugated to cytotoxic payloads binds its tumor-specific target, internalizes, and traffics to lysosomes for payload release, inducing tumor cell death while sparing normal tissues. We previously developed ADCs targeting the EGFR ligand epiregulin (EREG), which is overexpressed in *KRAS* wildtype and mutant (MUT) colorectal tumors, that were effective at inhibiting tumor growth in CRC cell line- and patient-derived xenograft models. Yet, tumor regrowth was observed upon treatment termination, and residual tumors showed target downregulation as a potential mechanism of ADC resistance. This indicates EREG ADC monotherapy may not be sufficient to eliminate colorectal tumors. Co-targeting of additional cell-surface antigens may enhance intratumoral payload delivery and address potential resistance mechanisms. Previous studies and our analyses of RNA-seq expression data from The Cancer Genome Atlas (TCGA) colorectal adenocarcinoma cohort show EREG is often co-overexpressed with the related EGFR ligand amphiregulin (AREG) in CRC patients, with their expression predominant of all seven EGFR ligands, suggesting potential functional importance. Therefore, we hypothesize that targeting EREG and AREG with ADCs simultaneously will inhibit tumor growth and enhance ADC efficacy compared to single-target ADC monotherapy. We generated EREG knockout (KO), *KRAS*-MUT CRC cell lines via lentiviral transduction using CRISPR-Cas9, which show significantly reduced proliferation and tumor growth compared to the parental and vector cells. These results indicate that EREG actively promotes CRC growth, despite oncogenic mutations downstream of EGFR. We are also generating AREG KO and EREG/AREG-double KOs using CRISPR-Cas9 for characterization. Additionally, we have cloned, produced, and purified human AREG-targeted mAbs for the development of novel AREG-targeted ADCs. AREG overexpression cell lines were generated for mAb validation. Our data demonstrate the AREG mAbs bind AREG with high specificity and promote internalization and lysosomal trafficking in CRC cells. These results suggest AREG to be a suitable therapeutic target in CRC, and we are currently in the process of generating AREG-targeted ADCs. Future work will test whether co-targeting EREG and AREG provides additional therapeutic benefit.

#3093 *SLC25A28* is a synthetic lethal target in nucleotide excision repair-deficient cancer.

Nan Yang[1], Vijai Joseph[1], Lisa Hoeg[2], Xuechun Bai[1], Sizhi Gao[1], Ouathek Ouerfelli[1], David B. Solit[1], Jian Carrot-Zhang[1], Gopa Iyer[1], Daniel Durocher[2], Kent W. Mouw[3], Kenneth Offit[1], Steven M. Lipkin[4]

[1]Memorial Sloan Kettering Cancer Center, New York, NY,[2]Lunenfeld-Tanenbaum Research Institute, Toronto, ON, Canada,[3]Radiation Oncology, Dana Farber Cancer Institute, Boston, MA,[4]Weill Cornell Medical College, New York, NY

Background: Nucleotide excision repair-deficient (NER-D) cancers comprise approximately 10% of bladder urinary tract and uterine cancers. Platinum-based chemotherapy is the current standard of care for NER-D cancers; however, its nephrotoxicity limits applicability in patients with compromised renal function. No druggable targets have been identified for NER-D tumors. Genome-wide CRISPR screening offers a powerful strategy to identify synthetic lethal interactions. We performed a genome-wide screen to identify potential synthetic lethal targets in NER-deficient cells.

Methods: An RT112/84 *ERCC4* knockout (*ERCC4*$^{-/-}$) cell line was generated. ERCC4 status was examined by Sanger sequencing and Western blotting, and nucleotide excision repair activity was assessed using the Host Cell Reactivation Assay (HCRA). A genome-wide CRISPR screen was performed in RT112/84 wild-type (WT) and *ERCC4*$^{-/-}$ cells to identify candidate synthetic lethal targets. Colony formation assays validated candidate interactions, and *SLC25A28* was further tested for synthetic lethality with *ERCC2*, *ERCC3*, and *ERCC5*. RNA sequencing was conducted to investigate the mechanism underlying *SLC25A28-ERCC4* synthetic lethality.

Results: Sanger sequencing and Western blot confirmed *ERCC4* knockout in RT112/84 cells. HCRA demonstrated markedly reduced NER activity in *ERCC4*$^{-/-}$ cells. Genome-wide CRISPR screening identified *SLC25A28* as a top synthetic lethal candidate with *ERCC4*. Colony assays validated the synthetic lethality between *SLC25A28* and *ERCC2*, *ERCC3*, *ERCC4* and *ERCC5*.

Conclusions: Our findings identify *SLC25A28* as a novel synthetic lethal target in NER-deficient cancers, suggesting that inhibition of *SLC25A28* may represent a potential therapeutic strategy for tumors harboring NER pathway mutations. This study was supported by STTR 1 R41 CA275627-01, the Niehaus Center for Inherited Cancer Genomics, and the Breast Cancer Research Foundation.

#3094 Targeting TUBB2B: Exploiting brain metastatic vulnerabilities in triple-negative breast cancer.

Qingling He[1], Jianyang Hu[1], Gary M. Tse[2], Julia Y. Tsang[2], Pui-Chi Lo[1], C Geoffrey Lau[3], **Y Rebecca Chin**[4]

[1]City University of Hong Kong, City University of Hong Kong Shenzhen Futian Research Institute, Hong Kong, Hong Kong,[2]Department of Anatomical and Cellular Pathology, Prince of Wales Hospital, The Chinese University of Hong Kong, Hong Kong, Hong Kong,[3]Department of Neuroscience, City University of Hong Kong, Hong Kong, Hong Kong,[4]Dept Biomedical Sciences and Tung Bio Sci Centre, Dept Precision Diagnostic and Therapeutic Tech, City University of Hong Kong, City University of Hong Kong Shenzhen Futian Research Institute, Hong Kong, Hong Kong

Breast cancer remains a leading cause of cancer-related mortality, with brain metastasis contributing significantly to poor outcomes. Triple-negative breast cancer (TNBC) exhibits aggressive behavior, a high incidence of brain metastasis, and limited therapeutic options, underscoring the urgent need for novel strategies targeting brain metastatic vulnerabilities.

We recently established an in vivo brain metastasis model using an optimized intracarotid injection method and integrated bioinformatics to identify drivers of metastatic colonization. TUBB2B, a β-tubulin isoform involved in axon guidance during neural development, was identified as a novel TNBC gene promoting brain metastatic outgrowth (He et. al. J Exp & Clin Can Res, 2025). In line with its neural-related functions, TUBB2B overexpression in TNBC cells activates astrocytes, which in turn upregulate TUBB2B in tumor cells, suggesting a feed-forward interaction that promotes brain metastatic colonization. Here, we further evaluated the therapeutic potential of targeting TUBB2B and investigated its role in mediating TNBC-stromal cell interactions in the brain niche.

Methods: Patient-derived organoid (PDO) models were established to evaluate TUBB2B knockdown effects on tumor growth and survival. 3D co-culture models were employed to examine carcinoma-astrocyte/neuron gap junctions and dye transfer assays were used to assess intercellular communication. Preclinical studies were performed to test the effect of TUBB2B inhibition alone and in combination with the brain-penetrant Akt inhibitor (Akti) GDC-0068 (Ipatasertib), currently in Phase 3 trials.

Results: TUBB2B knockdown significantly inhibited PDO growth in two independent models and reduced dye transfer between TNBC cells and astrocytes, suggesting impaired gap junction communication. Combining TUBB2B depletion with Akti markedly reduced TNBC cell viability compared to single-agent treatment. Ongoing studies are testing the combination effects of siTUBB2B-gold nanoparticles with Akti (GDC-0068 and Capivasertib) in preclinical animal models.

Conclusions: TUBB2B plays a critical role in TNBC brain metastasis and represents a promising therapeutic target, particularly in combination with Akt pathway inhibition. These findings may inform future clinical strategies for TNBC patients with brain metastases.

This work is supported by National Natural Science Foundation of China (81972781, 82273470) and City University of Hong Kong (9609316, 9680348). This abstract was proofread using AI-assisted tools.

#3095 Optimizing targeting molecule density on drug carriers to improve cellular uptake.

Maria Lambros, Manjot Kaur

Biotechnology and Pharmaceutical Sciences, Western University of Health Sciences, Pomona, CA

Purpose: The purpose of this work is to determine whether the number of targeting molecules on a carrier correlates with improved cell uptake. The xCT transporter is a cell-surface facilitative transporter that imports cystine into the cell and exports glutamate. Using liposomes as the carrier, we conjugated varying amounts of cystine, the targeting agent, to their surfaces to harness the xCT transporter. We evaluated the cellular uptake of liposomal formulations with different levels of the targeting molecule conjugated to the liposomal surface (A: medium, B: low, C: high) in several cell lines.
Methods: Liposomes with different levels of the targeting molecule were formulated, and sulforhodamine B (SRB), a fluorescent dye, was encapsulated in the liposomes. The formulations tested were: three targeted formulations with varying levels of the targeting molecule (A: medium, B: low, C: high), one non-targeted formulation (NT), and an untreated control. These formulations were incubated for 6 hours with five human cancer cell lines (BxPC-3, MIA PaCa-2, A549, OVCAR-8, and PANC-1). After incubation, the cell lines were washed three times, and liposome uptake was quantified by measuring the mean fluorescence intensity of SRB using flow cytometry (Attune NxT, Acoustic Focusing Cytometer, Thermo Fisher Scientific, MA).
Results: Targeted liposomes consistently demonstrated significantly higher uptake than the non-targeted formulation across all five cell lines tested. However, the correlation between targeting-molecule density and uptake was cell-line-dependent. The formulation with the highest targeting molecule density (Formulation C) showed the highest uptake in three of the five cell lines (BxPC-3, MIA PaCa-2, and A549). In contrast, varying the targeting molecule density did not result in a statistically significant difference in uptake among the targeted formulations in the OVCAR-8 and PANC-1 cell lines.
Conclusion: The data suggest that cells' ability to internalize liposomes depends on whether the liposomes carry a targeting molecule. However, the extent of internalization is cell line dependent.

#3096 The anti-cancer effects of silibinin through the modulation of JAK1/STAT3 signaling and inhibition of MMPs levels in triple-negative breast cancer cells.

Shubham D. Mishra, Patricia Mendonca, Sukhmandeep Kaur, **Karam F. a. Soliman**

Pharmaceutical Sciences, Florida A&M University College of Pharmacy & Pharmaceutical Sciences, Tallahassee, FL

Breast cancer is the second most common type of cancer in US women. The most aggressive subtype is triple-negative breast cancer, which corresponds to 10% and 20% and affects African American women disproportionally. Various natural compounds have been identified as having potential therapeutic applications in breast cancer by targeting the tumor microenvironment. Among these compounds, silibinin, a natural compound found in Silybum marianum, has been shown to exhibit anticancer properties against several cancer types. This work examined the anticancer activity of silibinin in MDA-MB-231 (Caucasian) and MDA-MB-468 (African American) TNBC cells by targeting the JAK/STAT signaling pathways and by measuring matrix metalloproteinase (MMP) levels. The approaches included cytotoxicity analyses, 2D and 3D cell culture assays, RT-PCR, Western analyses, and ELISA to evaluate MMP-2 and MMP-9 protein levels in IFN-γ- and TNF-α-stimulated TNBC cells. Silibinin (0.78-400 μM) caused a decrease in cell viability in both cells, with higher sensitivity in MDA-MB-231 cells (IC_{50} = 154.23 ± 4.15 μM) compared to MDA-MB-468 cells (IC_{50} = 175.43 ± 5.87 μM). Antiproliferative activity was observed in both cell lines, with MDA-MB-468 cells exhibiting greater sensitivity over time. Additionally, 3D cellular assays demonstrated silibinin's potency in inhibiting spheroid growth and viability, consistent with the cytotoxicity observed in 2D culture. RT-PCR results show reduced levels of JAK1 mRNA after 6, 12, or 24 hours of silibinin treatment in both cell lines. STAT3 mRNA levels were decreased only in MDA-MB-231 cells (after 6 hours), with no effect in MDA-MB-468 cells. Reduced levels of phosphorylated JAK1 and STAT3 proteins were observed in both cell types. Moreover, using ELISA assays, silibinin significantly reduced TNF-α-induced MMP-2 and MMP-9 protein levels in MDA-MB-231 and MDA-MB-468 cells. In conclusion, the data demonstrate that silibinin exerts anticancer activity against TNBC cells by inhibiting the JAK/STAT signaling pathway and reducing MMP-2 and MMP-9 levels, which play pivotal roles in tumor growth, invasion, and metastasis. Notably, this study underscores differences among distinct TNBC cellular lines with distinct genetic backgrounds, reinforcing silibinin's role as a promising adjuvant treatment for aggressive forms of human breast cancer.

#3097 Preclinical characterization of MBS309, a PD-1-targeted and α-biased IL-2, demonstrating robust anti-tumor activity and a favorable safety profile.

Jiangmei Li[1], Guangzhong Lin[1], Lunfeng Zhang[2], Shuo Huang[2], Shuang Qing[1], Feng Li[1], Mingze Sun[1], Hong Chen[1]

[1]Beijing Mabworks Biotech Co Ltd, Beijing, China,[2]Beijing Mabworks Biotech Co. Ltd, Beijing, China

The clinical impact of PD-1/PD-L1 inhibitors remains limited, as the vastmajority of cancer patients ultimately experience relapse or lack a durable response.Conversely, the therapeutic potential of IL-2, a pioneering immunotherapy cytokine,has been historically overshadowed by its severe toxicity and narrow therapeuticwindow. While past efforts to develop safer IL-2 variants with reduced Treg bias(non-α IL-2) have seen scant clinical success, they have spurred the development of anew class of PD-1/IL-2 bispecific molecules. These agents are engineered to achievecis-engagement and deliver α biased IL-2 signal specifically to PD-1-high andCD25-high CD8+ T cells within the tumor microenvironment.MBS309 was engineered to enhance the safety of IL-2 in cancers relapsed orresistant to PD-1/PD-L1 therapy. It consists of an α-biased IL-2 variant fused to theC-terminus of pembrolizumab (Keytruda). This design retains IL-2's binding toIL-2Rα while significantly reducing its interaction with IL-2Rβγ. In vitro studiesdemonstrated that MBS309 exhibits activity restricted to PD-1 targets. As amonotherapy, MBS309 elicited robust anti-tumor responses across a range ofpreclinical xenograft models, regardless of their intrinsic sensitivity to PD-1 inhibition.In mice, MBS309 showed a favorable safety profile, characterized by a longerhalf-life compared to a clinical-stage benchmark and significantly reduced systemictoxicity. At a dose of 20 mg/kg, it exhibited less toxicity. Pharmacodynamic
investigations revealed the mechanistic basis for this improved therapeutic window:MBS309 induced dampened T cell activation in normal tissues while achieving potentintra-tumoral CD8+ T cell expansion comparable to the benchmark.The compelling preclinical profile of MBS309, characterized by robustanti-tumor efficacy and a favorable safety window, warrants its further clinicalinvestigation as a promising therapeutic candidate for oncology.Disclosures: All the authors are employees from Beijing Mabworks Biotech Co. Ltd

#3098 Discovery of the RAD51 inhibitor JKYN-1 and characterization of its anticancer activity in preclinical models of non-small cell lung cancer.

Yifan Yu[1], Morgan Black[2], Nikolina Radulovich[1], Peter Ferguson[2], James Koropatnick[3], Ming Sound Tsao[1], Mark D. Vincent[3], Geoffrey Liu[1], Samir H. Barghout[1]

[1]Princess Margaret Cancer Center, Toronto, ON, Canada,[2]London Health Sciences Center, London, ON, Canada,[3]Western University, London, ON, Canada

BACKGROUND: RAD51 is a recombinase that plays a central role in homologous recombination-mediated double-strand DNA break repair and is required for the maintenance of genome stability. In addition to this canonical function, RAD51 contributes to the tolerance of replication stress, a phenotype frequently observed in tumor cells, thereby establishing RAD51 as a potential pharmacologic target in multiple malignancies including non-small cell lung cancer (NSCLC). The development of direct small-molecule RAD51 inhibitors has been limited by suboptimal potency and solubility. Here, we report the discovery of JKYN-1, an optimized RAD51 inhibitor, and the characterization of its single-agent and combinatorial antitumor activity in preclinical models of NSCLC.
METHODS: Using molecular docking, JKYN-1 was discovered through virtual chemical modifications of the previously reported RAD51 inhibitor IBR120. Target engagement in cells was evaluated by the cellular thermal shift assay (CETSA) and immunoblotting. CellTiter-Glo assay was used to measure cytotoxicity in cell lines and patient-derived organoids (PDOs) of NSCLC after 6-day treatment.
RESULTS: JKYN-1 (patent application # CA3204011A1) is a derivative of IBR120, with improved solubility and potency. As assessed by CETSA, JKYN-1 bound to and destabilized RAD51 in H1975. Using immunoblotting, we demonstrated downregulation of RAD51 in response to JKYN-1 treatment in a concentration-dependent manner. Compared to the classical RAD51 inhibitor B02, JKYN-1 demonstrated higher cytotoxicity in A549 and H1975 cell lines with over 50% reduction in the IC_{50} values (H1975, 3.2 vs 8.3 μM; A549, 4.9 vs >10 μM). In a panel of 8 *EGFR*-mutated NSCLC PDOs, JKYN-1 and its more soluble mesylate salt displayed sub-micromolar IC_{50} values (0.1-0.88 μM) as opposed to B02 (2.4 to >10 μM). We subsequently evaluated the synergistic potential of JKYN-1 in combination with the EGFR inhibitor osimertinib in osimertinib-resistant models. Combination with JKYN-1 resulted in > 4-fold reduction in the IC_{50} of osimertinib in the laboratory-evolved osimertinib-resistant H1975 cells, and > 2-fold reduction in the LPTO357 PDO. Mechanistically, both JKYN-1 and osimertinib induced downregulation of RAD51 in cell lines and PDOs in a concentration-dependent manner as assessed by immunoblotting, explaining in part the synergistic combinatorial activity.
CONCLUSIONS: Our data identify JKYN-1 and its mesylate salt as promising RAD51 inhibitors with superior anticancer activity compared to existing inhibitors in preclinical models of NSCLC. Moreover, JKYN-1 can potentially overcome resistance to osimertinib in a subset of NSCLC models.

#3099 Selective CDK2 inhibition with ECI830: preclinical characterization, efficacy, and on-target mechanism supported by biomarker and gene signature analysis.

Ophelia Maertens[1], Bradley French[1], Eric Fang[2], Imad Hanna[3], Ying Huang[1], Sajan Joseph[1], Fallon Lin[1], Neil Umbreit[1], Anna Uvarova[1], Vivek Rauniyar[1], Samuel Ho[1]

[1]Novartis BioMedical Research, Cambridge, MA,[2]Novartis BioMedical Research, Emeryville, CA,[3]Novartis BioMedical Research, East Hanover, NJ

Dysregulation of the cell cycle pathway is a hallmark of many human cancers, enabling uncontrolled cell growth. Cyclin-dependent kinases, exemplified by CDK2, CDK4, and CDK6, play crucial roles in regulating cell cycle progression. While CDK4/6 inhibitors such as ribociclib have transformed the treatment landscape for HR+/HER2− breast cancer, selectively targeting CDK2 has remained challenging due to the high degree of structural similarity to other essential CDK family members, such as CDK1. Genetic and pharmacological studies have shown that CCNE1-amplified cancer models have a dependency on CDK2 and that combined inhibition of CDK2 and CDK4 enhances tumor suppression in HR+/HER2− breast cancer models. Here, we describe the preclinical activity of ECI830, an orally bioavailable and potent adenosine triphosphate-competitive CDK2 inhibitor with high selectivity over other CDK family members. ECI830 demonstrated substantial antiproliferative activity in CCNE1-amplified ovarian (OVCAR3) and lung (H810) cancer cell lines. In an HR+/HER2− breast cancer cell line (MCF7) and several patient-derived xenograft models resistant to standard-of-care treatment, the combination of ECI830 and ribociclib resulted in synergistic activity with deeper pathway suppression, enhanced biomarker modulation, and stronger tumor growth inhibition compared with either agent alone. Mechanistic studies demonstrated that the activity of ECI830, alone or in combination with ribociclib, was on-target. Moreover, ECI830 showed a favorable pharmacokinetics and tolerability profile in preclinical mouse models. Taken together, these promising preclinical data support ECI830 as a selective and potent CDK2 inhibitor for the treatment of HR+/HER2- breast cancer and other CCNE1-dysregulated advanced solid tumors, which is currently being investigated in clinical trials.

: Overcoming Chemotherapy Resistance
Poster Session

#3101 Identification and characterization of novel peptide binders against platinum resistant epithelial ovarian cancer.

Pritha Ray[1], Sreyashi Nath[1], Pranita Uttamrao Patil[2], Parijat Das[2], Prasenjit Bhaumik[2]

[1]Imaging Cell Signalling and Therapeutics Lab, ACTREC, Tata Memorial Centre, Navi Mumbai, India,[2]BioScience and Bioengineering, IIT Bombay, Mumbai, India

Background: Acquirement of Platinum-resistance leads to recurrence and poor survival outcomes in epithelial ovarian cancer (EOC) patients with inadequate second-line treatment options. Moreover, the current therapeutic strategies lack the precision to target the chemoresistant cells *in vivo* limiting treatment efficacy. Identification and validation of unique targeting moieties are critical to develop effective therapeutic strategies for this dreadful disease.
Methods: Phage Display peptide library screening, ELISA and FACS were used to identify novel peptide binders using platinum resistant EOC cells (both intrinsic and acquired). MTT, cell cycle analysis, confocal microscopy, scratch assay and adhesion assays used to delineate the peptide properties. Clinical relevance was determined using primary tumor cells derived from high grade serous ovarian cancer (HGSOC) patients and subsequent PDX models. In-silico analysis and molecular docking were employed to identify the putative receptor/s.
Results: Two novel heptapeptides (A and B) exhibiting higher binding capabilities to platinum-resistant cells were identified by phage peptide display screening and further validated using multiple EOC cell lines, primary cells isolated from malignant ascites of high-grade serous ovarian cancer patients, and patient-derived xenograft (PDX) models. Peptide A showed ~2-fold increased binding in intrinsically cisplatin-resistant cells (TOV112D, OVCAR3) while peptide B demonstrated ~3 fold higher binding to $A2780^{Ptres}$ cells compared to platinum-sensitive A2780 cells. Peptide A showed a 5-fold increased binding in chemoresistant patient-derived cells and a 3-fold higher binding towards chemoresistant PDX models compared to chemonaïve counterparts, suggesting the presence of unique surface receptor(s) enriched in resistant populations. Peptide A did not induce toxicity, cell cycle alteration or proliferation but reduced adhesion and invasion of the resistant cells. Intraperitoneal injection of peptide A led to reduced secondary metastasis in platinum-resistant PDX mice. In silico docking identified GPCR proteins, particularly Endothelin Type A/B receptors (ETAR/ETBR), as putative receptors for peptide A. Functional characterization and receptor identification for peptide B are in progress.
Conclusions: With higher affinity towards platinum-resistant cells and ability to impede adhesion, these novel peptide/s have promising potential to be developed as scaffolds for imaging or as therapeutic conjugates for the targeted treatment of platinum-resistant ovarian cancer cells.

#3102 YB-1 small-molecule inhibitor improves chemotherapy success in treating high-grade serous ovarian carcinoma.

Dhanir Tailor[1], Fernando J. Garcia-Marques[2], Abel Bermudez[2], Wenqi Li[3], Annah Rolig[4], Chia-Feng Tsai[5], Tao Liu[5], Tanja Pejovic[6], Sharon Pitteri[7], Sanjay V. Malhotra[1]

[1]Knight Cancer Institute, Oregon Health & Science University, Portland, OR,[2]Stanford University, Stanford, CA,[3]Oregon Health & Science University, Portland, OR,[4]OHSU Knight Cancer Institute, Portland, OR,[5]Pacific Northwest National Laboratory, Richland, WA,[6]Providence OB/GYN Health Center, Medford, OR,[7]Stanford University, Palo Alto, CA

Ovarian cancer is the most lethal gynecological malignancy. The primary treatment regimen—surgery followed by platinum- or taxane-based chemotherapy—offers limited long-term success, as 85-90% of women diagnosed with late-stage disease will recur post adjuvant combination chemotherapy, an unfortunate outcome largely driven by treatment resistance. Thus, once ovarian cancer recurs, available treatments are palliative only. Clinically, the lack of treatment options for these patients is a critical unmet need, which we propose can be addressed with a novel therapeutic approach that directly addresses treatment resistance—therapeutic inhibition of Y-Box Binding Protein 1 (YB-1), a stress-responsive, multifunctional protein. To test this hypothesis, we collected tumor samples and nearby normal tissues from patients whose high grade serous ovarian cancer (HGSOC) relapsed after four to six treatments. These samples underwent proteomic analysis and were used to develop HGSOC treatment-resistant patient-derived xenograft (PDX) models. Using proteomics to profile these samples revealed that, in comparison to nearby normal tissue, malignant tissues significantly overexpressed YB-1 along with the related mRNA-processing pathways. Similar proteomic profiling of mouse HGSC cells exposed to SU056 confirmed that inhibiting YB-1 activated mRNA processing pathways, consistent with the findings from patient tissues. We subsequently employed mouse studies using PDX models from the HGSOC patient samples to determine whether inhibiting YB-1 with the small molecule SU056 significantly delayed tumor progression. These studies demonstrated that HGSOC tumors are susceptible to YB-1 inhibition. To test whether YB-1 inhibition additionally sensitizes tumors to chemotherapy, we combined SU056 with cisplatin and paclitaxel in the HGSC syngeneic mouse model (HGS1) and the treatment-resistant PDX model, finding that SU056 enhanced chemotherapeutic efficacy and extended overall survival. Proteomic analysis performed on mouse cell lines and tumors from syngeneic and PDX studies indicated that SU056 treatment significantly suppresses YB-1 and mRNA processing pathways in both *in vitro* and *in vivo* settings. Overall, these studies indicate that combining a YB-1 inhibitor with chemotherapy could overcome treatment resistance to improve responses in HGSC patients.

#3103 Spatial proteomics reveals vasculature and immune modulation for overcoming doxorubicin resistance in breast cancer.

Gautami Gaidhani, Juraj Jakubik, Leoni Moldaner, Yishu Xu, Zuzana Tatarova

German Cancer Consortium (DKTK), Heidelberg, Germany

Therapeutic resistance hinders the efficacy of single-agent cancer treatments, often mediated by the tumor microenvironment. Significant endothelial cell enrichment following local doxorubicin treatment has been proposed as a resistance mechanism in breast cancer. Here, we apply the tumor vasculature normalization principle using an anti-angiogenic drug combination delivered locally using the high-throughput multiplex implantable microdevice assay in mouse models of breast cancer. Spatial single-cell proteomic profiling paired with unsupervised learning methods confirmed doxorubicin-mediated pro-angiogenic changes, including pericyte detachment and sprouting angiogenesis. A combination with cabozantinib depleted endothelial cells and increased tumor antigenicity by inducing immunogenic cell death with recruitment of leukocytes including neutrophils, and T cells. Leveraging this immune modulatory activity, we tested a systemic triple combination with anti-PD1 immunotherapy, which led to a significant and complete tumor regression. Our study demonstrates a rational drug combination that improves doxorubicin efficacy to overcome microenvironment-driven resistance for long-term breast cancer control.

#3104 Characterization of high plasticity cell states in cutaneous squamous cell carcinoma in response to chemotherapy and immune checkpoint inhibitor treatments.

Ramin Farhad[1], Di Wu[1], Mark A. Taylor[1], Allan Balmain[2], Rosemary J. Akhurst[3]

[1]Helen Diller Family Comprehensive Cancer Center, University of California, San Francisco, San Francisco, CA,[2]Department of Biochemistry and Biophysics, University of California, San Francisco, San Francisco, CA,[3]Department of Anatomy, University of California, San Francisco, San Francisco, CA

Therapeutic resistance and cancer recurrence in cutaneous squamous cell carcinoma (cSCC) are strongly driven by genetic heterogeneity and phenotypic plasticity. Tumor cells that enter high-plasticity, low-proliferative states often evade cytotoxic therapies, including mitotic-targeting chemotherapeutics, yet the molecular mechanisms enabling these transitions and maintaining these states under therapeutic pressure remain poorly defined. Here, we seek to identify, characterize, and ultimately destabilize these therapy-refractory cell states across multiple treatment modalities.

We developed a chemically induced cSCC model in FVB mice using a single initiating dose of DMBA followed by 20 weeks of biweekly TPA promotion. Once tumors reached approximately one cubic centimeter, cohorts were assigned to distinct therapeutic regimens, including anti-PD1 immune checkpoint blockade, cisplatin, paclitaxel, and combination strategies incorporating the Pp2a inhibitor LB100 to test whether pharmacologic perturbation can drive mitotically silent tumor cells back into a proliferative, therapy-responsive state.

Normal skin, papillomas, lymph nodes, and carcinomas were collected and approximately 900,000 cells were profiled using the 10x Genomics single-cell RNA-sequencing platform to map the full spectrum of malignant, stromal, and immune programs across various treatment groups. Ongoing analysis aims to resolve transcriptional signatures associated with high-plasticity states, identify treatment-induced and treatment-specific state transitions, and define potential therapy-evading intermediates that arise under drug pressure. A major focus is the discovery of metagene signatures that correlate with high-plasticity phenotypes and the evaluation of whether these molecular programs can be modulated or therapeutically targeted to re-sensitize tumors to conventional or immune-based therapies. In parallel, we are also examining how immune cell abundance, activation states, and lineage-specific gene expression profiles shift across treatment arms, particularly in response to anti-PD1 therapy, to uncover how the tumor immune microenvironment contributes to or counteracts the emergence of resistant high-plasticity cell states.

This work seeks to establish a unified mechanistic framework describing how plasticity-driven resistance emerges in cSCC and to identify points of therapeutic vulnerability that may improve responses to chemotherapy and immunotherapy both within and beyond this disease context.

#3105 MalforminA1 reverts cisplatin resistance by modulating oncogenic signaling pathways in ovarian cancer.

Yahya Tamimi[1], Aikou Okamoto[2], Ikram Burney[3]

[1]Biochemistry, SQU, Muscat, Oman,[2]Associate Professor, Dept. of Ob/Gyn, Jikei Univ. School of Medicine, Tokyo, Japan,[3]Sultan Qaboos Comprehensive Cancer Care and Research Centre (SQCCCRC), Muscat, Oman

Ovarian cancer is a highly lethal gynecological malignancy, largely due to its late-stage diagnosis, frequent recurrence, and the development of chemoresistance. Standard treatment typically involves surgical debulking followed by chemotherapy, most commonly with platinum-based agents such as cisplatin. Unfortunately, many patients eventually develop resistance to these therapies, reducing treatment effectiveness and contributing to poor overall survival. These clinical challenges underscore the urgent need for novel therapeutic strategies that can overcome or prevent chemoresistance. Marine-derived compounds have recently emerged as a valuable source of potential anticancer agents, with several demonstrating potent biological activity. In our previous work, we identified multiple marine-derived molecules with promising anti-cancer properties, including Malformin A1 (MA1). MA1, a cyclic pentapeptide isolated from the marine fungus *Aspergillus niger*, exhibits cytotoxic activity against both cisplatin-sensitive (A2780S) and cisplatin-resistant (A2780CP) ovarian cancer cell lines. Building on these findings, the present study sought to elucidate the molecular pathways through which MA1 may reverse cisplatin resistance in ovarian cancer. In this study, we assessed the molecular pathways through which MA1 modulates cisplatin resistance in A2780CP cells, using the cisplatin-sensitive A2780S cell line as a reference. The expression of key cancer-related proteins, including ERK1/2 and NF-κβ, was analyzed by Western blot to evaluate the modulatory effects of MA1 on these signaling pathways. MA1 treatment resulted in a significant reduction of total MEK1/2, ERK1/2, and NF-κβ protein levels in A2780S cells, whereas in A2780CP cells, only NF-κβ expression was increased. Furthermore, phosphorylated ERK1/2 and NF-κβ levels were elevated, particularly in A2780CP cells, indicating activation of ERK1/2 and NF-κβ pathways, which play central roles in regulating cell survival and apoptosis. The cytotoxic effects of MA1 were more pronounced in cisplatin-resistant A2780CP cells, supporting the compound’s potential role in reversing cisplatin resistance. Activation of these signaling pathways following MA1 treatment may resensitize resistant cells to apoptosis or other cytotoxic mechanisms, thereby contributing to the overcoming of chemoresistance.In conclusion, our findings demonstrate that MA1 can reverse cisplatin resistance through the modulation of key oncogenic signaling pathways, highlighting its promise as a therapeutic candidate to improve treatment outcomes in ovarian cancer.

#3106 OC201 and OC202e, an AI-driven drug combination, enhance the susceptibility of pancreatic cancer to FOLFIRINOX by modulating HIF-1α.

Yongjin Kim, Sewon Kim, Dong Sub Jung, So Jung Sung, Yenny Kim, Ki Sung Song, Hyemin Won, Yi Rang Kim, **Jihoon Kang**

Oncocross Co., Ltd, Seoul, Korea, Republic of

Objective: Pancreatic cancer remains highly lethal, with a five-year survival rate of ~13%, largely due to late-stage diagnosis, aggressive progression, and resistance to standard therapies. Although FOLFIRINOX is the current first-line regimen, therapeutic resistance limits its durability. Our previous work showed that the AI-derived combination OC201 and OC202e suppresses EMT and metastasis. This study investigated whether OC201/OC202e enhances the response to FOLFIRINOX by modulating multidrug-resistance mechanisms.
Methods: Panc-1 and MIA PaCa-2 cells were treated with OC201 and/or OC202e followed by FOLFIRINOX. Cell viability and clonogenic potential were assessed using MTT and colony-formation assays. Multidrug-resistance determinants—including hypoxia, extracellular matrix factors, dysregulated signaling, genetic alterations, stemness, and ABC transporters were analyzed by Western blotting and RT-qPCR. Stemness was further evaluated using sphere-formation assays. An in vivo hepatic metastasis model was established via intrasplenic injection of Panc-1 cells, followed by 10 weeks of treatment with OC201, OC202e, and/or FOLFIRINOX beginning two weeks post-injection. Metastatic burden was quantified histologically.
Results: OC201/OC202e significantly enhanced FOLFIRINOX efficacy, as shown by reduced colony formation in both cell lines, while MTT assays indicated limited short-term synergy, suggesting a primarily long-term effect. In vivo, the combination further reduced hepatic metastatic lesions compared with FOLFIRINOX alone. Mechanistic analyses revealed decreased HIF-1α and stemness markers (CD44, Flotillin2) following combination treatment. HIF-1α expression correlated with stemness and FOLFIRINOX responsiveness, supporting its role in resistance. These findings align with the known EMT-stemness link and provide mechanistic insight into the observed synergy.
Conclusion: The AI-derived OC201/OC202e combination enhances sensitivity to FOLFIRINOX and suppresses metastasis by targeting HIF-1α and the EMT-stemness axis. Reductions in clonogenicity and resistance-related markers highlight its potential as an adjuvant to standard chemotherapy and underscore the promise of AI-guided strategies for developing synergistic therapeutic combinations.

#3107 CWH43 emerges as a novel therapeutic target linked to chemoresistance in colorectal cancer.

Yu-Jia Chang[1], Chien-Yu Huang[2], Po-Li Wei[3], Cheng-Chin Lee[4]

[1]Graduate Institute of Clinical Medicine, Taipei Medical University, Taipei, Taiwan,[2]School of Medicine, National Tsing Hua University, Hsinchu, Taiwan,[3]Department of Surgery, School of Medicine, College of Medicine, Taipei Medical University,, Taipei, Taiwan,[4]Graduate Institute of Clinical Medicine, College of Medicine, Taipei Medical University, Taipei, Taiwan

Background: Chemoresistance remains a key barrier to effective colorectal cancer (CRC) treatment. CWH43, a regulator of membrane-associated protein processing, has been implicated in CRC progression, but its relevance to therapy response and ferroptosis-related vulnerability is unclear.
Methods: Public CRC datasets were analyzed to examine associations between CWH43 expression, treatment response patterns, and patient outcomes. CRC cell models with altered CWH43 expression were used to assess responses to chemotherapeutic agents and oxidative-stress-related phenotypes. Enrichment analyses were performed to explore biological processes linked to CWH43 dysregulation.
Results: High CWH43 expression correlated with reduced sensitivity to standard chemotherapy and poorer outcomes in advanced CRC. In vitro, CWH43 overexpression promoted a resistant phenotype accompanied by changes in oxidative-stress handling and ferroptosis-associated features. Reducing CWH43 expression increased susceptibility to chemotherapeutic challenge.
Conclusions: CWH43 may serve as a previously unrecognized contributor to chemoresistance in CRC, potentially through modulation of redox and ferroptosis-related processes. These findings support CWH43 as a candidate biomarker of therapeutic response and a target for future mechanistic investigation.

#3108 LEDGF/p75 drives chemoresistance in CML via JAK/STAT pathway modulation.

Thatcher Akele[1], Cecilia Iglesias-Herrero[2], Frauke Christ[1], Zeger Debyser[1]

[1]Catholic Univ. of Leuven Faculty of Medicine, Leuven, Belgium,[2]Laboratory for Molecular Virology and Gene Therapy, Department of Pharmaceutical and Pharmacological, KU Leuven, Leuven, Belgium

Lens Epithelium Derived Growth Factor/p75 (LEDGF/p75,PSIP1) is a H3K36me2/3 reader implicated in several malignancies. Within the MLL/KMT2A fusion complex, it tethers the fusion protein to chromatin. KMT2A rearrangement (KMT2A-r) occurs in ~10% of acute leukemia patients and is associated with poor prognosis due to relapse and chemoresistance. Our lab has shown that LEDGF/p75 is essential for KMT2A-r leukemogenesis but dispensable for hematopoiesis. High LEDGF/p75 levels have been linked to drug resistance in AML blasts, prostate and breast cancer. As a dependency factor in KMT2A-r leukemia, LEDGF/p75 is an attractive therapeutic target and a potential component of combinatorial strategies for LEDGF/p75 driven chemoresistance cancers. However, the leukemic subtypes dependent on LEDGF/p75 remains unclear. We previously showed that LEDGF/p75 depletion sensitizes KMT2A-r AML cells to cytarabine via the sphingosine-1 pathway. Here, we aimed to assess the role of LEDGF/p75 in therapy resistance across multiple leukemia models. Stable LEDGF/p75 knockdown (LEDGF/p75 KD) cell lines were generated using miRNA-expressing vectors, and more than ten leukemia cell lines were screened for LEDGF/p75 dependent chemoresistance. In KMT2A-wild-type (WT) AML cell lines U-937 and Kasumi-1, LEDGF/p75 depletion did not alter cytarabine sensitivity and the same trend was observed in WT T-ALL cell lines Jurkat and SupT-1. However, in the KMT2A-r T-ALL cell line, Karpas-45, LEDGF/p75 KD significantly sensitized the cells to cytarabine (IC_{50} Karpas Mock/KD: 76.32 ± 8.32 µM / 53.75 ± 12.46 µM). Unexpectedly, LEDGF/p75 KD in SEM cells (B-ALL, KMT2A-AF4) increased proliferation and reduced apoptosis upon cytarabine treatment (IC_{50} SEM Mock/KD: 0.12 ± 0.02 µM / 0.53 ± 0.06 µM). The latter was accompanied by a lower level of caspase3. Interestingly, LEDGF/p75 KD in two WT KMT2A CML cell lines, K-562 and JUR-MK1, led to a significant reduction in proliferation upon vincristine treatment (IC_{50} K-562 Mock/KD: 2.61 ± 0.10 nM / 0.81 ± 0.09 nM and IC_{50} JUR-MK1 Mock/KD: 3.93 ± 0.35 nM / 2.37 ± 0.30 nM) and increased apoptosis with elevated caspase3. Treatment of K-562 cells with BCR-ABL inhibitors Imatinib and Ponatinib also showed decreased proliferation upon LEDGF/p75 depletion. RNA-seq analysis of LEDGF/p75 KD K-562 and JUR-MK1 cells showed that LEDGF/p75 loss affects pathways associated with hematopoietic cell differentiation and immune response regulation. Anti apoptotic genes such as BCL-XL and BCL2A1 were downregulated, along with STAT5 and STAT2, key players in the JAK/STAT pathway. Western blotting confirmed reduced total and activated STAT5 in LEDGF/p75 depleted CML cells. Taken together, our result indicates that the role of LEDGF/p75 in therapy resistance is context dependent and varies across leukemic subtypes. We identify a previously unknown function of LEDGF/p75 in mediating drug resistance in CML cells acting through the JAK/STAT Pathway.

#3109 Extracellular matrix glycan signatures predict chemotherapy response in ovarian cancer.

Erica J. Peterson[1], Ryan J. Weiss[2], James D. Hampton[1], Ava R. S. Beaudin[1], Thomas M. Clausen[3], Joseph B. M. Turner[1], Amrita Basu[2], Bin Hu[1], Jennifer E. Koblenski[1], Nicholas P. Farrell[1], Larisa Litovchick[1]

[1]Virginia Commonwealth University, Richmond, VA,[2]University of Georgia, Athens, GA,[3]University of Hawaii, Honolulu, HI

Background: Ovarian cancer (OC) is a highly lethal gynecologic malignancy, most often diagnosed at advanced stages and prone to recurrence after platinum-based chemotherapy. Nearly 30% of patients exhibit platinum-resistant or refractory disease, with aggressive tumors recurring within six months. Emerging evidence implicates glycosaminoglycans (GAGs) as regulators of tumor progression and treatment response, yet their structural complexity limits accurate assessment by transcriptomic or proteomic methods alone.
Methods: To define how GAGs influence OC biology and platinum sensitivity, we analyzed single-cell RNA sequencing and spatial transcriptomic datasets from normal ovary, primary ovarian/fallopian tube tumors, and metastatic abdominal and colonic lesions. CRISPR/Cas9 XYLT1/2 knockout was used to deplete GAGs in ovarian cancer cells, which were evaluated for morphology, proliferation, migration/invasion, and in vivo tumor behavior. To directly quantify tumor GAG composition, glycan reductive isotope labeling mass spectrometry was performed on OC patient-derived xenografts (with known carboplatin response profiles. Complementary pharmacology studies evaluated efficacy and drug distribution of carboplatin and Triplatin, a GAG-targeting platinum agent.
Results: Single-cell analysis revealed that fibroblasts are the predominant source of proteoglycan gene expression within the tumor microenvironment. Spatial transcriptomics analysis of precursor and invasive lesions showed these changes occur in the later stages of ovarian cancer development. XYLT1/2 knockout cells showed a shift from mesenchymal to epithelial morphology, decreased migration/invasion potential, reduced tumor dissemination and absence of ascites, and increased sensitivity to carboplatin associated with higher drug penetration into the tumor. GRIL-MS profiling of four OC PDX models identified chondroitin-4-sulfate (C4S) as the dominant tumor-associated GAG motif, with high C4S strongly correlating with carboplatin resistance. Importantly, elevated C4S reduced carboplatin efficacy but enhanced Triplatin uptake and antitumor activity. A C4S expression threshold stratified tumors by predicted response, and analysis of patient tissue microarrays showed that 40-83% of OC tumors exceed this cut-off depending on subtype.
Conclusions: GAGs play a central role in ovarian cancer progression, dissemination, and platinum resistance. C4S is a mechanistically grounded biomarker capable of predicting differential sensitivity to carboplatin and Triplatin, supporting its integration into precision-medicine strategies and the clinical evaluation of Triplatin for patients with C4S-high, platinum-resistant ovarian cancer.

#3110 Targeting LIF/LIFR signaling with EC359 overcomes chemoresistance and enhances chemotherapy efficacy in ovarian cancer.

Sonal R. Chaudhari[1], Baskaran Subramani[2], Gaurav Sharma[3], William Cole Arnold[1], Durga Meenakshi Panneerdoss[1], Edward R. Kost[1], Bindhu Santhamma[4], Hareesh B. Nair[4], Suryavathi Viswanadhapalli[2], Ratna K. Vadlamudi[1]

[1]ObGyn, UTHSA, San Antonio, TX,[2]UTHSA, San Antonio, TX,[3]ObGyn, UT Health Science Center at San Antonio, San Antonio, TX,[4]Evestra, San Antonio, TX

Background: Ovarian cancer (OCa) is the deadliest gynecologic malignancy, with nearly 90% of patients experiencing disease recurrence following standard treatments. Leukemia inhibitory factor (LIF) and its receptor (LIFR) are implicated in OCa progression, chemoresistance, and recurrence. The TCGA data indicated a negative correlation between the expression of LIFR and LIF and the survival of OCa. Elevated expressions of LIF and LIFR in recurrent OCa underscores the need for innovative therapeutic strategies targeting this pathway. In this study, we tested the hypothesis that the progression of OCa to therapy resistance is dependent on LIF/LIFR signaling and that the standard of care interventions will be enhanced by the disruption of LIF/LIFR signaling with the small molecule inhibitor EC359.

Methods: The effectiveness of the LIFR inhibitor EC359, in combination with paclitaxel and/or carboplatin, was evaluated in both established and chemotherapy-resistant OCa cell lines, as well as in patient-derived xenograft (PDX) models. Paclitaxel-resistant cell lines were developed and characterized through RNA sequencing. To assess therapeutic impact, cell viability, colony formation, and apoptosis were measured using MTT assays, colony formation assays, and apoptosis assays, respectively. Mechanistic insights into the combination therapy were obtained via Western blot analysis to identify modulated signaling pathways. Additionally, 3D organoids derived from xenografts were employed to examine the *ex vivo* effects of EC359 combined with chemotherapy. The efficacy of the combination treatment was further validated *in vivo* using both CDX and PDX models.

Results: Utilizing long term culture of OCa cells with increasing concentrations of chemotherapy, we have successfully established several chemotherapy-resistant OCa model cell lines. EC359 significantly enhanced the anti-tumor efficacy of chemotherapy in reducing cell viability and suppressing colony formation in clonogenicity assays. Further, EC359 treatment enhanced apoptosis in OCa cells by promoting ferroptosis pathway. Remarkably, the combination therapy demonstrated increased effectiveness of chemotherapy in paclitaxel-resistant and carboplatin-resistant OCa cells, underscoring its potential to overcome chemotherapy resistance. The results from the CDX model demonstrated the effectiveness of EC359 as a monotherapy for resistant OCa. Further, the results from PDX model studies demonstrated the efficacy of EC359 in conjunction with carboplatin and as a maintenance therapy for OCa. These findings suggest EC359 as a potent combination agent with chemotherapy for improved therapeutic outcomes in OCa.

Conclusions: These findings provide compelling preclinical evidence that LIFR inhibition with EC359 is a promising strategy to enhance chemotherapy efficacy in OCa. Supported by NIH R01 CA266970.

#3111 Pancreatic cancer cells elevate NAD+production in response to nutrient limitation and chemotherapeutic stress.

Faith Nakazzi[1], Mehrdad Zarei[2], Mariana Lopes[3], Hallie J. Graor[2], William C. Beegan[1], Eric Gu[1], Sakineh Rezaei[1], Peder J. Lund[3], Jordan M. Winter[4]

[1]Biochemistry, Case Western Reserve University, Cleveland, OH,[2]Surgery, Case Western Reserve University, Cleveland, OH,[3]Nutrition, Case Western Reserve University, Cleveland, OH,[4]UH Cleveland Medical Center, Cleveland, OH

Introduction: Pancreatic cancer (PC) cells are consistently in a state of aneuploidy, nutrient deficiency, and hypoxia-induced stress, which may necessitate increased NAD^+ levels to maintain critical survival functions such as antioxidant defense, mitochondrial activity, and DNA repair. Therefore, we hypothesized that PC cells adapt to chemotherapy and nutrient deprivation in their microenvironment by elevating NAD+ levels.

Methods: We used liquid chromatography-mass spectrometry (LC-MS) to measure NAD^+ and its precursors in cancer versus non-cancer cells under stress (nutrient deprivation and chemotherapy). Western blot and qPCR were used to assess enzyme expression in NAD+ synthesis pathways following chemotherapy. Athymic nude mice and C57BL/6 mice were injected with MIA PaCa-2, respectively. Once palpable tumors formed, the mice received treatments with either vehicle or oxaliplatin (5 mg/kg, administered twice weekly) for 21 days, and tumors were collected and tested for NAD+ and its precursors.

Results: Baseline intracellular NAD^+ and NAM levels were higher in PC cells (PANC-1, MIA PaCa-2, and BxPC-3) compared to non-cancer cells (HPDE and HPNE) and stayed elevated after 72 hours of treatment with complete media. During increased cellular stress, such as glucose limitation, NAD^+ and NAM levels rose more significantly in MIA PaCa-2 cells than in HPNE cells, demonstrating pancreatic cancer cells' ability to adapt to the increased NAD^+ demand required to counteract oxidative and energy stress caused by glucose withdrawal. Intracellular NAD^+ levels consistently remained higher in PANC-1 and MIA PaCa-2 cells than in HPNE cells during four days of growth. Interestingly, NAM concentrations in the media declined by ~ 40% over 72 hours across all cell lines, regardless of glucose level, indicating strong utilization of external NAD+ precursors. Both Oxaliplatin and 5-fluorouracil (5FU) significantly increased NAD^+ and NAM levels in MIA PaCa-2 and PANC-1 cells, supporting the model that NAD^+ is necessary for fueling survival mechanisms under stress. Oxaliplatin treatment increased mRNA levels of NMNAT1 and protein levels of NAPRT, NRK, and NMNAT1, the main enzymes in the Preiss-Handler and NAD^+ salvage pathways. Although chemotherapy did not change intracellular NAMPT (iNAMPT) mRNA levels, it increased iNAMPT protein levels, whereas extracellular NAMPT (eNAMPT) protein levels remained unchanged. Chemotherapy also increased NAD+ levels in both MIA PaCa-2 and KPC mouse xenograft models in vivo.

Conclusion: These findings suggest that PC cells actively prioritize NAD^+ synthesis as an adaptive mechanism to survive the harsh microenvironment and develop chemoresistance. Therefore, targeting NAD+ synthesis pathways offers a therapeutic vulnerability to enhance chemotherapy susceptibility in pancreatic cancer.

#3112 Targeting chemoresistance in ovarian cancer.

Dhanamjai Penta[1], Vishal Chandra[1], Lauren Dockery[2], Rajani Rai[1]

[1]OUHSC, Oklahoma, OK,[2]Obstetrics and Gynecology, OU Health Stephenson Cancer Center Gynecologic Cancer Clinic, Oklahoma, OK

Introduction: Ovarian cancer (OvCa) is a highly aggressive malignancy characterized by frequent relapse and metastasis, both of which contribute to its high mortality rate. Although most patients initially respond to platinum-based chemotherapy, up to 80% eventually develop resistance, rendering OvCa largely incurable. Therefore, there is an urgent need to identify new therapeutic targets and develop strategies to overcome chemoresistance. This study identifies integrin β4 (ITGB4) as a key molecular driver associated with cisplatin resistance and explores its potential as a therapeutic target in ovarian cancer.
Methods: Transcriptomic profiling of cisplatin-sensitive (WT) and cisplatin-resistant (CPR) OVCAR8 OvCa spheroids was performed using RNA sequencing to identify differentially expressed genes associated with chemoresistance. Selected candidates were validated by qRT-PCR, and western blotting. The clinical significance of ITGB4 was assessed using publicly available datasets (GSE133859, TCGA-OV) and immunofluorescence analysis of tissue microarray from primary and recurrent OvCa patient samples. Functional roles of ITGB4 were examined using genetic manipulations (overexpression and CRISPR-mediated knockout) followed by migration, invasion, and cisplatin sensitivity assays. Co-immunoprecipitation (Co-IP) was performed to examine the interaction between ITGB4 and TGFβ receptor 2 (TGFβR2).
Results: Transcriptomic profiling revealed ITGB4 overexpression and SERPINB2 downregulation in CPR spheroids, findings that were consistent with GEO, TCGA-OV datasets as well as TMA analysis of patient samples. High ITGB4 expression in platinum-resistant OvCa patients was significantly associated with worse overall and progression-free survival. Functionally, ITGB4 overexpression enhanced cell invasion, migration, and cisplatin resistance, while ITGB4 knockout resensitized resistant cells to cisplatin and suppressed their invasive phenotype. Mechanistically, ITGB4 activated FAK and TGFβ/SMAD signaling pathways, both of which are known mediators of EMT and chemoresistance. CO-IP assays demonstrated a direct interaction between ITGB4 and TGFβR, supporting a cooperative role in promoting SMAD3 activation.
Conclusion: This study identifies ITGB4 as a central regulator of cisplatin resistance and aggressiveness in ovarian cancer and highlights ITGB4 as a promising therapeutic target to overcome chemoresistance and improve treatment outcomes in OvCa patients.
Acknowledgment of Funding: The work is supported by COBRE P20GM135009, SCC CT Pilot Grant, PHF-Seed and PHF CTGA Grant Program.

#3113 Chronic type 1 interferon exposure phenocopies chronic cisplatin exposure in high grade serous ovarian cancer.

Ashlyn Conant[1], Kiera McGivney[2], Tise Suzuki[3], Sharon Asariah[4], Brigitte Vazquez[1], Jay Deng[5], HyeonJoo Cheon[6], Juli Unternaehrer[1]

[1]Loma Linda University, Loma Linda, CA,[2]Whitworth University, Spokane, WA,[3]Southern Adventist University, Collegedale, TN,[4]California University of Science and Medicine , Colton, CA,[5]University of Redlands, Redlands, CA,[6]Wayne State University, Detroit, MI

Despite initial response to platinum-based therapeutics, high grade serous ovarian carcinoma (HGSOC) remains one of the deadliest gynecologic malignancies, due to high molecular and genetic heterogeneity that contributes to acquired drug resistance mechanisms and rapid recurrence. Frontline treatment for the disease has remained largely unchanged for 30 years, with CA125 serving as the only established biomarker for the past 4 decades and PARP inhibitors representing one of the few available targeted therapies. There is an urgent need for improved understanding of factors that may predict therapy response and tumor aggression, thus contributing to recurrence and resistance. We previously published on the dissociation of stemness and therapy resistance in an isogenic pair of therapy sensitive and resistant patient-derived HGSOC cells. RNA sequencing revealed enrichment of JAK/STAT signaling and an upregulation of gene signatures associated with type 1 interferon production and signaling in the chemo-resistant (CR) cells. We hypothesize that chronic, low-level IFN-1 signaling promotes the development of therapy resistance in HGSOC, via the priming of a DNA damage associated IFN-1 response. RT-qPCR and flow cytometry were used to validate the pathways and targets of interest. IFN-1 and pro-tumor interferon-related DNA damage signature (IRDS) genes were found to be significantly upregulated in the CR cells. Acute cisplatin treatment enriched IFN-1-related protein expression in all cells. CR and SE cells exhibited different temporal expression patterns of IFN-1 and IRDS RNA in response to acute cisplatin exposure, with SE cells displaying an acute IFN-1 response to cisplatin and CR cells responding with delayed IFN-1 induction. To determine if IFN-β is a driving factor in the development of resistance, cells were treated with chronic, low-level IFN-β for several weeks. Chronic, low-level IFN-β did not induce anti-viral ISG expression when compared to high dose cytokine after 24 hours. However, after 6 passages the treatment blunted ISG expression in both CR and SE cells. IFN-β treatment phenocopied several aspects of chronic cisplatin exposure: increased resistance to cisplatin, epithelial-like morphology changes, and reduced proliferation. Despite these changes, IFN response was dampened. Future studies aim to explore strategies for surmounting chemotherapy resistance by impacting IFN-I signaling.

#3115 RTF2 drives oxaliplatin resistance in colorectal cancer by promoting phase separation-mediated homologous recombination repair.

Yiran Bie, Chong Chen, Haiqin Jiang, Zhizhong Xiong, Bin Zhong, Haoyang Xv, Yufeng Chen, Lei Lian, Xiaojian Wu, Peishan Hu

The Sixth Affiliated Hospital of Sun Yat-sen University, Guangzhou, China

Colorectal cancer (CRC) is one of the most common malignant tumors worldwide. Current treatment options for CRC include surgery, chemotherapy, and radiotherapy. Chemoresistance is a major factor contributing to poor prognosis in CRC patients. Oxaliplatin is recommended as a first-line chemotherapeutic agent for CRC, and overcoming oxaliplatin resistance holds great clinical significance. In this study, multi-omics cohort analysis using the ARGO database revealed for the first time that Replication Termination Factor 2 (RTF2) exhibits high-frequency mutations in CRC and shows elevated RNA and protein expression levels. We established 42 CRC organoids and performed sequencing and drug-sensitivity assays; RTF2 expression was markedly higher in the oxaliplatin-resistant organoid cohort. As a conserved replication-termination factor, RTF2 prevents DNA degradation during replication-fork stalling, maintains genome stability, and plays a critical role in replication-fork restart. Its high expression is significantly correlated with poor patient prognosis. We found that RTF2 is substantially upregulated in CRC cells compared with normal intestinal epithelial cells, and its expression is also elevated in oxaliplatin-resistant cell lines. Therefore, we generated RTF2-overexpression and RTF2-knockdown CRC cell models, as well as a subcutaneous xenograft nude-mouse model. Using the RTF2 inhibitor Aphidicolin in combination with oxaliplatin, we verified that targeting RTF2 enhances the cytotoxic effect of oxaliplatin on CRC cells. In recent years, increasing evidence has shown that many transcription factors exert biological functions through phase separation. RTF2, which contains an intrinsically disordered region (IDR), may also possess this property. We observed that fluorescently tagged RTF2 formed liquid-like droplets in the nucleus, suggesting potential phase separation, which was further confirmed by FRAP assays. Treatment of CRC cells with the phase-separation inhibitor 1,6-hexanediol reduced their oxaliplatin resistance. Results from comet assays and γH2AX immunofluorescence indicated that the mechanism by which RTF2 regulates resistance may be related to DNA double-strand break repair. Using DR-GFP and EJ5-GFP reporter systems, we found that 1,6-hexanediol significantly inhibited homologous recombination (HR) repair efficiency. These findings suggest that in CRC, RTF2 may enhance oxaliplatin resistance by undergoing phase separation and promoting HR-mediated DNA damage repair. In summary, our study reveals for the first time that RTF2 enhances oxaliplatin resistance in colorectal cancer by undergoing phase separation and promoting HR-mediated DNA repair. This discovery provides new mechanistic insights and potential therapeutic targets for overcoming chemoresistance and improving patient prognosis in CRC.

#3116 CDK4/6 inhibition overcomes 5-FU resistance by suppressing TYMS-driven R-loop-associated DNA damage in colorectal cancer.

Lingling Xu[1], jiabei zhu[1], Jinghua Sun[2], Man Li[2], Ajay Goel[3]

[1]Beckman Research Institute of City of Hope, Monrovia, CA,[2]The Second Affiliated Hospital of Dalian Medical University, Dalian, China,[3]City of Hope, Duarte, CA

Background: Resistance to 5-fluorouracil (5-FU) remains a significant obstacle in colorectal cancer (CRC) therapy. As an antimetabolite, 5-FU induces cytotoxicity by inhibiting thymidylate synthase (TYMS), thereby impairing DNA synthesis and repair. However, CRC cells frequently adapt through TYMS upregulation, thereby strengthening their DNA repair capacity and reducing the efficacy of drugs. R-loops, three-stranded nucleic acid structures formed by hybridization of RNA to its DNA template, are key contributors to replication stress and DNA damage. Since TYMS regulates nucleotide synthesis, it may influence R-loop-associated DNA damage. Cyclin-dependent kinases 4 and 6 (CDK4/6), which control G1-S cell cycle progression via E2F activation, also regulate TYMS transcription. Therefore, we hypothesized that CDK4/6 inhibition may downregulate TYMS and enhance R-loop-related DNA damage, restoring 5-FU sensitivity.

Methods: We established 5-FU-resistant CRC cell lines (HCT116-5FUR and SW480-5FUR). Cell viability was assessed using the MTT assay, and protein and mRNA levels were quantified by Western blot and RT-PCR, respectively. Flow cytometry was used for cell cycle profiling. DNA damage was assessed by γH2AX immunofluorescence, and R-loop formation was detected via S9.6 and anti-nucleolin immunostaining. A luciferase reporter assay was used to monitor the efficiency of double-strand break (DSB) repair. Synergistic effects of 5-FU and the CDK4/6 inhibitor abemaciclib were also evaluated.

Results: TYMS expression was markedly upregulated in HCT116 5FUR ($p<0.001$) and SW480 5FUR ($p<0.01$) compared to parental lines. CDK4 expression was upregulated in HCT116 5FUR and SW480 5FUR ($p<0.01$) compared to parental lines. CDK6 expression was also upregulated in HCT116 5FUR and SW480 5FUR ($p<0.01$) compared to their parental cell lines. Abemaciclib downregulated TYMS expression in HCT116 5 FUR ($p = 0.011$) and SW480 5FUR ($p = 0.0002$) compared to untreated 5-FU-resistant CRC cell lines. TYMS downregulation promoted R-loop-associated DNA damage, indicating a mechanistic link between nucleotide metabolism and genomic instability. Combination treatment with 5-FU and abemaciclib synergistically reduced the viability of resistant cells by inducing G1 arrest and enhancing DNA damage. Abemaciclib alone induced R-loop formation and DNA damage signaling, consistent with TYMS suppression and the amplification of replication stress.

Conclusions: TYMS modulates R-loop-associated DNA damage, contributing to 5-FU resistance in CRC. CDK4/6 inhibition restores chemosensitivity by repressing TYMS and enhancing R-loop-driven genomic stress. Combining CDK4/6 inhibitors with 5-FU represents a promising therapeutic strategy to overcome drug resistance in colorectal cancer.

#3117 Defining the role of nucleolar stress in mediating DDB2 induced oxaliplatin resistance in colorectal cancer.

Vinod Kumar[1], Dennis Hsu[2], Orlando D. Scharer[1], Matthew A. Schaich[1], Katherine E. Helfrich[3], Simon C. Watkins[3], Bennett Van Houten[1]

[1]Pharmacology and Chemical Biology, University of Pittsburgh School of Medicine, Pittsburgh, PA,[2]Medicine, UPMC-Hillman Cancer Center, Pittsburgh, Pennsylvania, Pittsburgh, PA,[3]Center for Biologic Imaging, University of Pittsburgh, Pittsburgh, PA

Background: Colorectal cancer (CRC) is the second most common cause of cancer deaths in the USA. Oxaliplatin containing regimens are generally considered first line therapy for fit patients, either in the form of FOLFIRINOX or NALIRIFOX. However, acquired resistance is inevitable and a significant percentage of patients treated with adjuvant FOLFOX (5-FU/leucovorin/oxaliplatin) fail to respond. Furthermore, oxaliplatin treatment has toxic side effects. Recent studies have shown that oxaliplatin kill cells by inducing stress to nucleolus. We and others have shown that oxaliplatin, but not cisplatin resistance in tumor cells is dependent upon the levels of DDB2, a DNA repair protein involved in damage recognition in chromatin during global genome nucleotide excision repair (GG-NER). However, the role of DDB2 in suppressing oxaliplatin induced nucleolar stress is not known. Therefore, defining the molecular roles of DDB2 in oxaliplatin response, to assess CRC response rates correlate with low DDB2 levels and the mechanisms of how DDB2 acts to remove these DNA lesions will fill an urgent gap in our knowledge.
Methods: DDB2 protein levels were measured by western blot and IHC assay in CRC tissue microarrays. The IC50s for oxaliplatin and cisplatin was obtained by performing cell titer glo (CTG) cell viability and clonogenic assay. The accumulation of DDB2 in nucleolus after oxaliplatin treatment was imaged by confocal microscopy. We used our newly developed SMADNE assay to calculate DDB2 binding kinetics and equilibrium dissociation constant (KD).
Results: We found that high DDB2 expressing CRC cell lines have higher IC50 for oxaliplatin and DDB2 KO cells are more sensitive to oxaliplatin than cisplatin therapy. Our IHC data suggests that DDB2 is differentially expressed in CRC patient's tumor. Interestingly, single molecule analysis by C-trap, reveals that DDB2 binds to oxaliplatin and cisplatin adducts with similar affinities, indicating that while DDB2 recognizes cisplatin lesions loss of DDB2 does not increase cisplatin sensitivity. Confocal microscopic imaging demonstrates that oxaliplatin treatment dramatically facilitated DDB2 accumulation in nucleolus with mutual colocalization of NPM1 (a marker for nucleolar stress). The combination of DDB2 inhibitors (NAEi or CSN5i-3) and oxaliplatin kills HCT116 CRC cells synergistically.
Conclusions: Our studies demonstrate that DDB2 is a potential biomarker for response to oxaliplatin and a new clinically targetable protein in the treatment of CRC. These studies will lay the foundation for clinical trials of combination therapy of Pevonedistat or CSN5i with oxaliplatin and 5FU.

#3118 Dichloroacetate reprograms metabolism and disrupts ROS adaptation, attenuating stemness to reverse chemoresistance in ovarian cancer.

Yen Thi Do[1], **Seungmee Lee**[2], Shin-Wha Lee[3], Eun Ji Nam[4], Jin-Young Kim[5], Sojin Shin[2], Ji Hae Seo[6]

[1]1Department of Gynecology and Obstetrics and Institute for Cancer Research, Keimyung University School of Medicine, Daegu, Korea, Republic of,[2]Gynecologic Oncology, Keimyung University School of Medicine, Daegu, Korea, Republic of,[3]Asan Medical Center, University of Ulsan, Seoul, Korea, Republic of,[4]Yonsei University College of Medicine, Seoul, Korea, Republic of,[5]Department of Internal Medicine, Keimyung University School of Medicine, Daegu, Korea, Republic of,[6]Department of Biochemistry, Keimyung University School of Medicine, Daegu, Korea, Republic of

Chemotherapy resistance and the associated high rates of relapse represent critical barriers in the effective management of ovarian cancer, contributing significantly to poor patient prognosis and mortality. In this study, we investigated the therapeutic potential of Dichloroacetate (DCA), a pan-pyruvate dehydrogenase kinase (PDK) inhibitor, as a strategy to overcome Cisplatin (CP) resistance. We initially identified that CP-resistant ovarian cancer cells exhibit elevated phosphorylation of pyruvate dehydrogenase (pPDH). Treatment with DCA effectively blocked pPDH, leading to a marked suppression of cell migration and invasion through the reversion of motile mesenchymal phenotypes to epithelial characteristics. Furthermore, DCA treatment significantly attenuated stem cell-like properties, as evidenced by reduced sphere formation capacity. When combined with CP, DCA exerted a synergistic anti-proliferative effect by triggering apoptosis in chemoresistant cells. Mechanistic investigations revealed a distinct metabolic adaptation: while CP induces cell death via Reactive Oxygen Species (ROS) generation in sensitive cells, resistant cells display high basal ROS levels and fail to generate further ROS upon CP exposure. Crucially, DCA treatment disrupted this ROS adaptation, inducing a lethal accumulation of ROS specifically in the resistant cells. Collectively, our findings indicate that DCA restores CP sensitivity by targeting ROS metabolism and inhibiting stemness, suggesting it is a promising therapeutic candidate for treating refractory ovarian cancer.

#3119 Modeling chemotherapy persistence in colorectal cancer using patient-derived organoids.

Yasmine Abouleila, Timo Voskuilen, Mayke Doorn, Roel Verkerk, Jasmin Pourfarzad, Joris Maas, Robert G. J. Vries, **Sylvia F. Boj**

HUB Organoids B.V., Utrecht, Netherlands

Therapy resistance in colorectal cancer remains a major clinical challenge. Despite standard-of-care chemotherapies such as FOLFOX and FOLFIRI, tumors frequently develop resistance, leading to treatment failure. A growing body of research implicates drug-tolerant persister (DTP) cells—a reversible, slow-growing population that survives initial therapy—as a critical step in resistance development. These persister cells create a window for cancer to acquire additional adaptations—such as mutations and alternative signaling pathway activation—ultimately leading to irreversible resistance. Understanding this transition from persistence to full resistance is essential for developing therapies that can prevent relapse. To investigate these mechanisms in a clinically relevant context, we developed patient-derived organoid (PDO) models of colorectal cancer capable of surviving FOLFOX or FOLFIRI treatment. These organoids retain the heterogeneity and architecture of the original tumors, providing a physiologically faithful system to study persistence. Because chemotherapy impact varies by mechanism of action, standard assays may not fully capture response diversity. We therefore optimized viability readouts to measure treatment effects across the entire organoid population, capturing both cytotoxicity and partial survival. Using these persistent PDOs, we performed whole-exome sequencing alongside bulk and single-cell RNA sequencing to map the molecular features associated with the DTP state and subsequent resistance. This approach revealed pathways and cellular programs that enable tumor cells to tolerate chemotherapy, highlighting potential targets for overcoming resistance. By modeling clinically relevant persistence, these PDOs offer a platform to test interventions that eliminate persister populations before they evolve into fully resistant tumors.

#3120 Using genome wide CRISPR screening to identify synthetic lethal targets for overcoming chemoresistance in rhabdomyosarcoma.

Aqsa Mazhar[1], Qian Wang[1], Satyanarayana Gadde[1], Daenikka Ravindraraja[1], Belamy B. Cheung[1], Glenn Marshall[2]

[1]Faculty of Medicine and Health, School of Clinical Medicine, Children's Cancer Institute Australia, Children's Cancer Institute, UNSW Sydney, Australia,[2]Kids Cancer Centre, Sydney Children's Hospital, Children's Cancer Institute, UNSW, New South Wales, Australia

Chemotherapy resistance in Rhabdomyosarcoma (RMS), the most common pediatric soft tissue sarcoma, remains a major obstacle to improve survival outcomes, particularly in high-risk alveolar RMS (ARMS), which accounts for approximately one-third of all RMS cases and is clinically more aggressive due to its strong propensity for metastasis, with survival rates fall below 24% after relapse. Drug resistance is a primary driver of treatment failure, contributing to nearly 80-90% of cancer-related mortality. Although irinotecan remains one of the most effective chemotherapeutic agents in RMS, the emergence of irinotecan-related chemoresistance highlights the urgent need to develop rational combination therapies to target the genetic robustness and functional redundancy of RMS cells. To overcome the stagnation in survival outcomes and intrinsic drug resistance, a genome wide Clustered Regularly Interspaced Short Palindromic Repeats (CRISPR) Knockout screening was performed to develop and identify novel therapeutic vulnerabilities and effective combination strategies specifically tailored to overcome irinotecan resistance in ARMS cells. For the first time, our study identified 47 candidate prognostic genes whose deletion potentially sensitizes RMS cells to irinotecan treatment. Along with several druggable targets, pathway enrichment analysis revealed that the DNA damage repair pathway is the most significantly downregulated in irinotecan-resistance in RMS cells, suggesting that targeting this pathway could induce a synthetic lethal interaction with irinotecan. Among the top hits, we validated FGFR4 and PARP1 as key modulators of resistance, and siRNA-mediated silencing of these genes sensitizes RMS cells to irinotecan treatment. Most importantly, FGFR4 was significantly enriched as a gene dependency in ARMS. In addition, pharmacological inhibition of these genes using available small-molecule inhibitors markedly enhanced irinotecan sensitivity and further reduced cell viability, both as single agents and in combination, with a favorable therapeutic window, supporting their potential for clinical translation. We are currently investigating the mechanistic basis and *in vivo* efficacy of these drug combinations in RMS models. This study provides a promising framework for developing personalized and targeted therapeutic strategies to improve outcomes for RMS patients.

#3121 METTL7B-driven m6A RNA methylation promotes gemcitabine resistance and tumor progression in pancreatic ductal adenocarcinoma.

Tung-Wei Hsu[1], Wan-Yu Wang[1], Yen-Hao Su[1], Chih-Ming Su[1], Po-Chen Tseng[2], Hsin-An Chen[1]

[1]Department of Surgery, Division of General Surgery, Taipei Medical University-Shuang Ho Hospital, Ministry of Health and Welfare, New Taipei City, Taiwan,[2]Department of Ophthalmology, Taipei City Hospital, Renai Branch, Taipei, Taiwan

Pancreatic ductal adenocarcinoma (PDAC) remains one of the most lethal malignancies, with a five-year survival rate below 12%, primarily due to rapid development of chemoresistance. To identify molecular drivers of drug resistance, we performed integrated transcriptomic, proteomic, and methylation analyses on gemcitabine-resistant PANC-1 GR cells. We identified the methyltransferase-like protein METTL7B as a novel regulator of RNA methylation-mediated resistance in PDAC. Global m6A profiling revealed hypermethylation in resistant cells that correlated with elevated METTL7B expression. Analysis of TCGA and UALCAN datasets confirmed METTL7B upregulation in PDAC tissues, particularly in KRAS-mutant tumors, and its association with poor overall and disease-free survival. Functional assays demonstrated that METTL7B knockdown suppressed proliferation, migration, invasion, and colony formation while restoring gemcitabine sensitivity. Mechanistically, m6A-seq and RNA-seq analyses revealed that METTL7B methylates oncogenic transcripts such as CSF2, CDKN1A, and FoxM1, enhancing their mRNA stability and translation to promote cell-cycle progression and stress adaptation. Network and pathway analyses further linked METTL7B activity to activation of KRAS and STAT3 signaling, indicating its role in PDAC aggressiveness. Collectively, these results identify METTL7B as a key epitranscriptomic regulator of gemcitabine resistance through m6A-dependent stabilization of oncogenic mRNAs and activation of pro-survival pathways. Targeting METTL7B-mediated RNA methylation offers a promising therapeutic strategy to overcome chemoresistance and improve clinical outcomes in PDAC.

#3122 Integrative multi-omic investigation of gene regulatory networks associated with chemotherapy response in acute lymphoblastic leukemia.

Kelly R. Barnett, Robert J. Mobley, Wenjian Yang, Landon Choi, Kami Chauncy, Kristine R. Crews, Samuel W. Brady, Jun J. Yang, **Daniel Savic**

St. Jude Children's Research Hospital, Memphis, TN

Acute lymphoblastic leukemia (ALL) is the most common pediatric cancer. While treatment outcomes have improved, drug resistance remains a major clinical concern and the primary cause of relapse in patients, with relapsed patient survival rates at approximately 40%. Although changes in gene expression are known to impact drug resistance in ALL, the gene regulatory elements that control and modulate these genes are frequently undefined, and the role of these elements in anti-leukemic drug resistance remains largely unknown. As a result, a more comprehensive epigenetic effort is needed to profile and validate gene regulatory networks linked to anti-leukemic drug response in ALL. We therefore generated matched B-cell origin ALL patient chromatin accessibility and *ex vivo* drug sensitivity (pharmacotyping) datasets covering 16 anti-leukemia drugs in primary ALL cells from over 150 patients to generate a compendium of gene regulatory elements associated with *ex vivo* chemotherapy response. Importantly, *ex vivo* measurements of chemotherapy response are known to associate with clinical outcomes in ALL patients. We further integrated these data with transcriptomics, tumor-normal whole genome sequencing and three-dimensional chromatin conformation results obtained from a subset of these patient biospecimens. We identified 74,307 drug response elements (DREs) and 2,854 drug response genes (DRGs) using a combination of linear modeling and feature selection techniques (p-adj < 0.05, s-value < 0.005). For this analysis, LC50 drug sensitivity was modeled in both continuous and categorical modes against chromatin accessibility and transcriptomic sequence counts. Although many DREs were specific to a singular drug or common drug family, a subset was associated with response to multiple drugs. DREs harbored 868 somatic mutations, many of which overlapped transcription factor (TF) footprints, with PU.1 among the most common overlapping TF sites. TF footprinting identified 148,732 TF binding events associated with drug response. Common TF footprints that correlated with drug response included EBF family TFs for inotuzumab ozogamicin response and STAT family TFs for trametinib response. On average, 74% of these drug response TF footprints mapped to DREs. Subsequent multi-omic integration of gene expression, chromatin accessibility and TF footprinting with three-dimensional chromatin conformation maps identified over 9000 gene regulatory networks linked to altered drug response. Collectively, this work represents the largest study of chromatin accessibility and TF occupancy impacting ALL chemotherapy drug response and supports an important functional role for many DREs in anti-leukemic drug resistance.

#3123 Metabolic reprogramming via statin repurposing: A strategy to reverse the Warburg effect and overcome gemcitabine resistance in pancreatic ductal adenocarcinoma.

Takayuki Noma[1], Mitsuo Shimada[2], Ajay Goel[3]

[1]Beckman Research Institute of The City of Hope, Duarte, CA,[2]Dept. of Surgery, University of Tokushima, Tokushima, Japan,[3]City of Hope, Duarte, CA

Background: Pancreatic ductal adenocarcinoma (PDAC) remains among the deadliest cancers, with mortality projected to rank second in cancer-related deaths by 2030. Gemcitabine is a first-line chemotherapy, but resistance frequently develops, leading to poor prognosis. Metabolic reprogramming, particularly enhanced glycolysis driven by hypoxia and HIF-1α activation, is a key mechanism of gemcitabine resistance. Statins, commonly used cholesterol-lowering drugs that inhibit HMG-CoA reductase, have demonstrated potential metabolic and anti-cancer effects with an established safety profile. This study investigated whether statins could overcome gemcitabine resistance in PDAC by targeting glycolytic adaptation.
Methods: Gemcitabine-resistant PDAC cell lines (MIA PaCa-2 and BxPC-3) and patient-derived 3D organoids were treated with simvastatin alone or combined with gemcitabine. Outcomes included cell viability, apoptosis, migration, invasion, and glycolytic activity (measured by extracellular acidification rate [ECAR] and lactate production). Expression of glycolysis-related genes HIF-1α, HK2, and LDHA was measured by RT-qPCR and Western blotting. Pharmacological modulation of HIF-1α was used to validate the mechanism. Clinical significance was assessed via EUS-FNA samples from 50 patients with PDAC treated with Gemcitabine and transcriptomic data from The Cancer Genome Atlas (TCGA).
Results: Simvastatin reduced the viability of Gemcitabine-resistant PDAC cells compared with parental cell lines (IC50: 20-21 μM vs. 37-39 μM in parental cells; $p<0.01$) and showed synergy with Gemcitabine (Bliss scores: 5.5 and 4.29) and markedly enhanced anti-tumor activity, reducing viability by 41.7% and 44.4%, respectively. The combination significantly suppressed migration and invasion and increased apoptosis ($p<0.001$), accompanied by increased cleaved PARP and caspase-3. Resistant cells exhibited elevated glycolysis, and simvastatin, especially in combination with Gemcitabine, reduced lactate, ECAR, and expression of HIF-1α, HK2, and LDHA at both mRNA and protein levels ($p<0.01$), mimicking HIF-1α inhibition. In two PDAC organoids, combination therapy disrupted structure and reduced viability while downregulating glycolytic genes. Clinically, high HIF-1α/HK2/LDHA expression correlated with Gemcitabine nonresponse and worse PFS/OS in both our gemcitabine-treated cohort and TCGA dataset.
Conclusion: Statins restore gemcitabine sensitivity in PDAC by suppressing HIF-1α-driven glycolytic reprogramming, reversing the metabolic adaptations responsible for chemoresistance. With their proven safety, affordability, and wide availability, statins offer a promising, immediately translatable approach to improve outcomes in gemcitabine-resistant PDAC.

#3124 SRSF1 orchestrates splicing-directed dual-engine glucose metabolism driving chemoresistance in diabetes-associated pancreatic cancer.

Zu-Wei Wang[1], Yi-Ting Chen[2], Jin-Peng Lu[3], Shun-Can Zhu[3], Hong-Yi Lin[1], Yin-Hao Chen[3], Hao-Xiang Zhang[1], Shi Chen[1]

[1]Department of Hepatobiliary Pancreatic Surgery, Fuzhou University Affiliated Provincial Hospital, Fuzhou, China,[2]Fuzhou University, Fuzhou, China,[3]Fujian Medical University, Fuzhou, China

Background: Pancreatic ductal adenocarcinoma (PDAC) patients with concurrent type 2 diabetes mellitus (T2DM) exhibit significantly worse treatment responses and shorter survival rates. However, the molecular mechanisms underlying diabetes-driven chemoresistance and immune suppression remain poorly understood. This study aims to elucidate how the diabetic microenvironment promotes PDAC chemoresistance through the splicing-metabolism axis.
Methods: We investigated SRSF1-mediated splicing regulation using clinical samples from 28 advanced PDAC patients receiving AG chemotherapy, T2DM-associated PDAC mouse models (KPC, KPSC), patient-derived organoids, and multiple in vivo models. Mechanistic studies included scRNA-seq, eCLIP-seq, ATAC-seq, RIP, ChIP-qPCR, and metabolic flux analysis.
Results: This study revealed that pancreatic cancer with concurrent diabetes is prone to chemoresistance, accompanied by SRSF1-driven elevated back-splicing ratios and altered pyruvate metabolism. Mechanistic investigation found that lactate accumulation in the diabetic microenvironment induced K48 lactylation of SRSF1 protein, enhancing its stability and promoting back-splicing events. SRSF1 regulated the linear-to-back splicing conversion of PSMA3-AS1 to circ-PSMA3-AS1, ultimately promoting transcriptional upregulation of metabolic enzymes DLAT and LDHA. DLAT/LDHA provided metabolic resilience through enhanced mitochondrial fusion and glycolysis, enabling cells to activate both TCA cycle and glycolytic energy-producing systems to acquire chemoresistance. Additionally, this metabolic remodeling profoundly impacted the tumor immune microenvironment through upregulated PD-L1 and sustained lactate production, causing immune evasion, suppressing CD8+ T cell function, and promoting Treg expansion. This process constituted a self-reinforcing positive feedback loop, resulting in the intractability of diabetes-associated pancreatic cancer. Based on these mechanistic discoveries, we developed a triple combination therapy (Berberine + anti-PD1 + AG) targeting SRSF1, DLAT, and LDHA while reducing glucose and tumor lactate levels, significantly improving treatment efficacy in diabetic PDAC models.
Conclusions: This study reveals the mechanistic framework underlying poor outcomes in diabetes-associated PDAC and provides a clinically translatable therapeutic strategy. The discovery of the splicing-metabolism-immunity axis opens new avenues for targeting metabolic vulnerabilities in cancer treatment, with particular significance for the growing population of diabetic cancer patients.

#3125 Transcriptomic analysis of glycosylation genes in chemotherapeutic-resistant glioma cells.

Vi P. Dang, Nicole S. Lav, Alan Y. L. Jiang, Jaclyn N. Hanamoto, Daniela A. Bota, Lisa A. Flanagan

University of California, Irvine, Irvine, CA

The purpose of this study was to characterize the glycosylation gene signature of chemotherapeutic-resistant glioma cells derived from dielectrophoresis-based sorting. Glioblastoma, astrocytoma, and oligodendroglioma comprise a class of aggressive and deadly brain tumors called diffuse gliomas. Around 20,000 glioma cases are diagnosed yearly in the US alone. The current standard chemotherapy treatment, temozolomide (TMZ), is insufficient as the 5-year survival rate of glioblastoma patients is as low as 8%. This is due to the presence of TMZ-resistant cells within tumors that lead to chemotherapeutic resistance and tumor recurrence. Thus, it is critical to characterize the molecular profile of TMZ-resistant cells to determine means of targeting them for more effective treatment. Preliminary data from our lab show that glycosylation could be an important dynamic regulator of TMZ resistance. Glycosylation, the post-translational addition of glycans (sugars) to proteins and lipids, regulates the function of many membrane proteins including drug transporters, growth factor receptors, and adhesion proteins. Our lab has developed an innovative dielectrophoresis-based method to sort cells based on electrophysiological membrane properties that are influenced by glycosylation. We used this method to successfully enrich TMZ-resistant populations from various glioma types and patient-derived tumors for downstream transcriptomic characterization using glycosylation gene microarrays, qRT-PCR, and single-cell and bulk RNA sequencing. Our study concluded that TMZ-resistant glioma cells exhibit transcriptomic differences in glycosylation genes, suggesting that these cell-surface sugars may serve as novel biomarkers or targets for glioma treatment. These results could enable the development of effective treatment strategies through targeting glioma cell glycosylation to ultimately improve patient outcomes.

#3127 Overcoming chemoresistance: Restoring doxorubicin sensitivity and natural killer cell immunity in resistant DLBCL cells through reduction of endoplasmic reticulum stress.

Yi-Cheng Lin[1], Chih-Chi Andrew Hu[2], Chih-Hang A. Tang[2], Chun-Yu Cheryl Chuang[1], Chiung-Tong Chen[3]

[1]National Tsing Hua University, Hsinchu, Taiwan,[2]Houston Methodist Research Institute, Houston, TX,[3]National Health Research Institutes, Miaoli, Taiwan

The recurrence of diffuse large B-cell lymphoma (DLBCL) is commonly attributed to its resistance to doxorubicin (DOX), which presents a significant therapeutic challenge and contributes to poor prognosis. Endoplasmic reticulum (ER) stress, pivotal in DOX resistance, is governed by regulating the survival of tumor cells and immune evasion. This study developed DOX-resistant DLBCL cell lines using murine xenografts to investigate the underlying mechanisms and potential therapeutic strategies. Comprehensive analyses were performed, focusing on stress-response pathways, oncogene-driven immunomodulatory signaling, and the cytotoxic activity of natural killer (NK) cells. Resistant cells exhibited elevated IRE1-XBP1s activation and c-MYC expression, which compromised NK cell-mediated tumor killing and reinforced immune evasion. Inhibition of XBP1s through ER stress inhibitor BI09 effectively dismantled this compensatory resistance strategy, reinstated NK cell sensitivity, and substantially increased tumor cell apoptosis. Notably, the combination of BI09 with DOX resulted in substantial anti-lymphoma activity at reduced DOX concentrations, thereby overcoming chemoresistance. These findings indicated that BI09 operated through a dual approach, simultaneously restoring chemosensitivity in refractory DLBCL and counteracting c-MYC-mediated immune evasion. Consequently, this study underscored the IRE1-XBP1s-c-MYC axis as a pivotal pathway in chemoresistance and immune suppression in DLBCL cells, and identified BI09 as a viable therapeutic candidate capable of disrupting chemoresistance and enhancing the efficacy of immunochemotherapy in aggressive lymphoma.

#3128 IDH1 inhibition potentiates gemcitabine efficacy in pancreatic ductal adenocarcinoma.

Yuan Li[1], Wenhao Weng[2], Ajay Goel[1]

[1]Beckman Research Institute of City of Hope, Monrovia, CA,[2]Shanghai Children's Hospital, School of Medicine, Shanghai, China

Background: Pancreatic ductal adenocarcinoma (PDAC) is the most aggressive cancers, with a 5-year survival rate of approximately 13%. Gemcitabine remains standard first-line chemotherapy, over 80% of patients develop resistance, limiting its clinical benefit. Wild-type isocitrate dehydrogenase 1 (wt-IDH1) is highly expressed in PDAC, catalyzing the conversion of isocitrate to α-ketoglutarate and NADPH to support mitochondrial metabolism. Ivosidenib (AG-120) is an FDA-approved oral allosteric inhibitor originally developed for mutant IDH1, but it also effectively inhibits wt-IDH1 under nutrient-deprived and low-magnesium conditions typical of PDAC. This inhibition reduces NADPH, increases chemotherapy-induced reactive oxygen species (ROS), and markedly impairs the survival of resistant cells, providing a mechanistic rationale for combining AG-120 with gemcitabine to overcome chemoresistance.
Methods: The synergistic effect of AG-120 and gemcitabine was evaluated in gemcitabine-resistant PDAC cell lines (MIA PaCa-2 and BxPC-3) using the PicoGreen dsDNA assay. Optimal drug doses were applied in functional assays, including wound healing, migration/invasion, and colony formation, to evaluate effects on cell growth and motility. Mechanistically, wt-IDH1 inhibition reduces NADPH and impairs mitochondrial metabolism, intracellular ROS levels were measured following treatment to evaluate oxidative stress. Mitochondrial function was further examined using Seahorse assays. Transcriptomic profiling via RNA sequencing, combined with qRT-PCR and Western blot validation, was performed to identify key pathways driving the synergistic response. The efficacy of the combination therapy was further confirmed in vivo using a PDAC xenograft model.
Results: The combination of AG-120 and gemcitabine exhibited synergistic anticancer effects on cell proliferation, migration, invasion, and colony formation in gemcitabine-resistant PDAC cell lines. Transcriptomic analysis of genes downregulated by IDH1 inhibition revealed significant enrichment of OXPHOS pathways (enrich score = 2.32, $P<0.01$), supported by Seahorse assays showing suppression of mitochondrial OXPHOS. Mechanistically, gemcitabine-resistant cells exhibited a marked upregulation of the magnesium influx transporter TRPM7, an essential regulator of magnesium homeostasis in mammalian cells, suggesting increased sensitivity and dependency on magnesium. These findings suggest that low-magnesium conditions enhance the responsiveness of resistant PDAC cells to wt-IDH1 inhibition, contributing to the observed synergistic anticancer effect of the combination therapy.
Conclusion: This study provides mechanistic insight into how AG-120 overcomes gemcitabine resistance in PDAC cells by targeting wt-IDH1 and modulating the OXPHOS pathway, highlighting a potential therapeutic strategy to improve treatment outcomes.

#3129 Proteasome-associated DUB inhibition by VLX1570 targets UCHL5/USP14 and enhances cisplatin efficacy in neuroblastoma.

Yi Ju Kao[1], Kuan-Lin Kuo[2], Chen-Hsun Hsu[3], Shih-Ming Liao[3], Po-Ming Chow[3], Kuo-How Huang[3]

[1]National Taiwan University Hospital and National Taiwan University College of Medicine, Taipei, Taiwan,[2]National Taiwan University College of Medicine, Taipei, Taiwan,[3]National Taiwan University Hospital, Taipei, Taiwan

Neuroblastoma is the most common extracranial solid tumor in children, and high-risk disease still carries an unfavorable prognosis despite intensive multimodality therapy. Deubiquitinating enzymes (DUBs) associated with the 19S proteasome, such as ubiquitin C-terminal hydrolase L5 (UCHL5) and ubiquitin-specific protease 14 (USP14), are key regulators of protein homeostasis and have attracted interest as potential therapeutic targets. In this study, we examined UCHL5 and USP14 expression in clinical neuroblastoma specimens compared with normal peripheral nerve tissue by immunohistochemistry, and investigated the effects of pharmacologic inhibition of proteasome-associated DUB activity using the small-molecule inhibitor VLX1570 in a panel of human neuroblastoma cell lines by assessing cell viability, cell-cycle distribution, apoptosis, clonogenic growth, and markers of proteasome stress, endoplasmic reticulum stress, and autophagy, as well as in a xenograft mouse model. Cisplatin remains a cornerstone of induction and consolidation chemotherapy for high-risk neuroblastoma, and resistance or intolerance to cisplatin-based regimens represents a major barrier to cure; therefore, we specifically evaluated whether VLX1570 could potentiate cisplatin-induced cytotoxicity in vitro and in vivo. UCHL5 and USP14 were markedly upregulated in neuroblastoma tissues relative to normal peripheral nerve, and VLX1570 treatment significantly reduced neuroblastoma cell growth, induced G2/M arrest and caspase-dependent apoptosis, promoted accumulation of polyubiquitinated proteins, activated unfolded protein response signaling, and modulated autophagy-related proteins. Notably, combining VLX1570 with cisplatin produced greater suppression of cell viability and clonogenic survival, and enhanced apoptotic signaling, than either treatment alone in vitro. Consistently, VLX1570 significantly suppressed tumor growth in xenograft models, while co-treatment with cisplatin further delayed tumor progression and reduced proliferative indices without overt systemic toxicity. Taken together, these data demonstrate that UCHL5 and USP14 are overexpressed in neuroblastoma and that pharmacologic inhibition of proteasome-associated DUB activity with VLX1570 exerts antitumor effects and enhances the efficacy of cisplatin, supporting further evaluation of DUB inhibitor-cisplatin combination strategies in neuroblastoma.

: Pharmacogenomics and Translational Biomarkers for Precision Cancer Therapy
Poster Session

#3133 A pharmacogenetic interaction analysis of second-line chemotherapy with bevacizumab in metastatic colorectal cancer patients: Results from the randomized BEBYP trial.

Arianna Bandini[1], Paola Orlandi[2], Marco Scalese[3], Gianluca Masi[4], Federica Marmorino[1], Chiara Cremolini[5], Guido Bocci[1]

[1]Department of Translational Research and New Technologies in Medicine and Surgery, University of Pisa, Pisa, Italy,[2]Department of Clinical and Experimental Medicine, University of Pisa, Pisa, Italy,[3]Institute of Clinical Physiology, Italian National Research Council - CNR, Pisa, Italy,[4]Department of Translational Research and New Technologies in Medicine and Surgery, University Of Pisa, Pisa, Italy,[5]Polo Oncologico - AOUP, Pisa, Italy

Metastatic colorectal cancer (mCRC) remains a major therapeutic challenge, and although bevacizumab combined with chemotherapy has demonstrated clinical benefit, validated predictive biomarkers of its activity are still missing. Moreover, pharmacogenetic analyses of angiogenesis-related genes in mCRC patients have failed to predict treatment efficacy and survival outcomes. Based on this rationale, we conducted a pharmacogenetic study on a different approach, investigating the potential combined effect of *EPAS-1, IL-8, VEGF-A,* and *VEGFR-2* single nucleotide polymorphisms (SNPs) on progression-free survival (PFS) and overall survival (OS) in mCRC patients treated with second-line mFOLFOX-6 or FOLFIRI (CHT) with or without bevacizumab. Germline DNA was obtained from peripheral blood samples, and SNPs were genotyped by Real-Time PCR. Pharmacogenetic interaction analysis was performed using the Multifactor Dimensionality Reduction (MDR) approach to explore potential statistical interactions between SNPs associated with treatment outcomes. This analysis included mCRC patients enrolled in the randomized phase III BEBYP trial (clinicaltrials.gov: NCT00720512) at the University Hospital of Pisa, who received second-line mFOLFOX-6 or FOLFIRI with (n=66) or without (n=66) bevacizumab. In the bevacizumab+CHT group, the MDR analysis identified two pharmacogenetic interaction profiles based on specific combinations of *VEGF-A* rs1570360 and *VEGFR-2* rs11133360 genotypes. Patients carrying the favorable genetic profile showed a median PFS of 8.89 months compared with 5.23 months for those with the unfavorable profile (p=0.001), with a multivariable Cox hazard ratio (HR) of 0.49 (95% CI, 0.25-0.96; p=0.039). Median OS was 20.69 vs. 9.28 months (p=0.04) for favorable vs. unfavorable profiles, respectively, with an adjusted HR of 0.54 (95% CI, 0.3-0.98; p=0.042). In contrast, among patients treated with CHT alone, no significant differences were observed in PFS (5.52 vs. 4.85 months, p=0.642) or OS (16.31 vs. 16.34 months, p=0.969) between the two genetic profiles. Overall, the interaction between *VEGF-A* rs1570360 and *VEGFR-2* rs11133360 genotypes identified a favorable pharmacogenetic profile associated with improved PFS and OS in patients receiving bevacizumab, whereas no association was observed in the CHT-alone group. These findings suggest that MDR analysis of angiogenesis-related genes identifies patients who benefit from bevacizumab-based therapy and strengthens the rationale for a pharmacogenetic selection of candidate patients for anti-angiogenic strategies in mCRC.

#3135 Comparative analysis of phenotypic markers of DPD activity as biomarkers of 5-FU toxicity.

Brianna Bembenek[1], Kelly Bouchonville[2], Carlo Largiader[3], Steven M. Offer[2]

[1]Molecular Pharmacology and Experimental Therapeutics, Mayo Clinic Graduate School of Biomedical Sciences, Rochester, MN,[2]Pathology, Carver College of Medicine, University of Iowa, Iowa City, IA,[3]Clinical Chemistry, University of Bern, Bern Center for Precision Medicine, Bern, Switzerland

Nearly 300,000 cancer patients are treated with fluoropyrimidine chemotherapy in the U.S. annually. Approximately one-third of patients experience severe and life-threatening toxicities, which can result in death. Deleterious genetic variants in *DPYD*, which encodes the rate-limiting enzyme of fluoropyrimidine catabolism (dihydropyrimidine dehydrogenase, DPD), have been correlated with severe toxicity in clinical studies. However, these variants explain only 10-30% of toxicity cases. Phenotypic measures of DPD function are attractive biomarkers of fluoropyrimidine toxicity risk with the potential to identify unknown causes of DPD deficiency. In this study, we compared two measures of DPD enzyme activity, blood plasma dihydrouracil to uracil ratio (UH_2:U) and direct measurement of DPD activity in peripheral blood mononuclear cells (PBMCs) using 204 subjects with comprehensive *DPYD* genotype data. DPD PBMC measurements showed higher overall inter-individual variation compared to UH_2:U ratios. Low correlation between UH_2:U and PBMC measurements were noted for matched samples taken from the same subject. As expected, DPD metabolites (U and UH_2) correlated with UH_2:U ratio; however, no correlation was noted between U or UH_2 levels and the PBMC DPD activity. Furthermore, when data were analyzed by genotype, no correlations were noted between UH_2:U and PBMC DPD activity. We observed the expected decrease in UH_2:U ratio for carriers of the four clinically tested *DPYD* variants and identified two novel variants associated with a significantly decreased UH_2:U ratio. To further investigate the impact of rare genotypes and previously identified *DPYD* haplotypes on the UH_2:U ratio, additional cohorts of 1994 and 500 subjects, enriched for specific genotypes, were utilized. Our results suggest that phenotyping may have limited validity as a single test when predicting DPD deficiency at an individual level and call into question the often-reported belief that PBMC DPD activity represents the "gold standard" for identifying DPD deficiency. Additional studies are needed to investigate correlations between phenotypic measures and 5-FU toxicity in patients, potentially as secondary biomarkers in conjunction with genetic tests.

#3136 Pharmacogenetic assays for personalized cancer treatment.

Abhishek Chadha[1], Jarvis Law[2], Zhiwei Wang[1], Max Mamroth[1], Zhenhua Shen[2], Khairuzzaman Bashar Mullah[2], Alexandre Vlassov[1], Anna Chikova[1]

[1]One Lambda Inc., part of Thermo Fisher Scientific, Canoga Park, CA,[2]Life Sciences Solutions, Thermo Fisher Scientific, Pleasanton, CA

Pharmacogenomics is increasingly utilized in various areas of medicine for personalization of drug selection and dosing. Nevertheless, the cost of large pharmacogenomic panels may be prohibitive for some practices due to reimbursement and utility limitations. Smaller, cancer treatment-specific pharmacogenetic panels that are currently available as services provide a limited number of gene targets and do not include important HLA alleles associated in published studies with adverse effects for specific cancer drugs (note that this work does not establish diagnostic capability). We evaluated the feasibility of developing a targeted pharmacogenetic test for cancer related drugs, which includes HLA along with other critical gene targets not captured by commonly available panels. The number of individual qPCR reactions in a given reaction mix is known as the plex level. Standard genotyping assays are designed as 2-plex mixtures, which are provided as an array of multiple reactions per sample present on a single qPCR plate. Increasing the qPCR plex level reduces the number of reactions required per sample, potentially reducing operational cost, reducing operator error rates and improving turn-around time for pharmacogenetic testing. We evaluated the feasibility of implementing maximal multiplexing in our targeted pharmacogenetic panel. We have designed 50 individual qPCR assays and optimized multiplex mixes into fewer than 8 individual reactions. Our assay targets include single nucleotide polymorphisms (SNPs) in HLA-A, HLA-B, HLA-DRB1, HLA-DQA1, UGT1A1, DPYD and CYP2C9. Based on multiple publications, certain polymorphisms in these genes are associated with increased risk of adverse effects for specific cancer drugs. Our new data analysis method allows derivation of genotyping results from up to 9-plex qPCR reactions performed on a standard qPCR instrument. Assays were tested using a combination of synthetic DNAs and human DNA samples, from Terasaki collection of well-characterized DNA samples and the Coriell repository. Our multiplex reactions included assays for detection of HLA and non-HLA alleles in single reactions using a combination of standard qPCR dyes (i.e; ABY, JUN, etc.) as well as FRET and long-stoke shift dyes. Future development of such pharmacogenetic panels may contribute to further advancement in precision medicine.

#3137 Partial alternative splicing in carriers of *DPYD* rs75017182 explains modest association with severe 5-FU toxicity to 5-FU.

Lauryn Allyn Hahn[1], Ryan Schwartz[1], Hannah Marie Krause[2], Lulu Jiang[1], Brianna Bembenek[3], Kelly Bouchonville[1], Steven M. Offer[1]

[1]Carver College of Medicine, University of Iowa, Iowa City, IA,[2]University of Iowa Holden Comprehensive Cancer Center, Iowa City, IA,[3]Mayo Clinic, Rochester, MN

Dihydropyrimidine dehydrogenase (DPD, encoded by the *DPYD* gene) is the rate-limiting enzyme in the catabolism of the widely used chemotherapeutic drug 5-fluorouracil (5-FU). Genetic variations in *DPYD* are predictive biomarkers of 5-FU toxicity. One such biomarker, rs75017182 (the causal allele linked to the “HapB3” haplotype), has been suggested to promote alternative splicing of *DPYD*, leading to expression of an inactive proteoform. However, carriers of rs75017182 exhibit only moderately increased risk of 5-FU toxicity and modestly decreased *ex vivo* DPD activity compared to carriers of another well-studied splice variant, rs3918290 (**2A*). We hypothesized that, unlike *2A, the rs75017182 variant does not cause obligate alternative splicing but instead promotes partial alternative splicing. To test this, we generated dual-fluorescent minigene reporter constructs containing either the G (wildtype) or C (variant) allele. In our minigene system, alternative splicing was elevated in cells transfected with C-containing vectors via flow cytometry, though levels were lower than those observed in a parallel *2A model. To investigate contributions of other variants in LD with rs75017182, we expanded the reporter to include additional relevant genomic regions. The analyses were complemented by the study of *in vivo* splicing in cells engineered to harbor various combinations of variants and in lymphoblastoid lines carrying specific genotype combinations. Overall, our findings demonstrate that rs75017182-C promotes only partial alternative splicing, eliciting a modest decrease in DPD activity and explaining its comparatively weak association with severe 5-FU toxicity. Additional variants in LD have a minimal impact on splicing and 5-FU sensitivity.

#3138 CellMiner Cross-Database (CellMinerCDB) for Exploration of Patient-Derived Cancer Cell Line Pharmacogenomics.

Fathi Elloumi[1], William C. Reinhold[2], Sudhir Varma[3], Yanghsin Wang[1], Meric Kinali[4], Yashuhiro Arakawa[5], Yoshitaka Inoue[6], Mirit Aladjem[1], Yves Pommier[1], Augustin Luna[7]

[1]National Cancer Institute, Bethesda, MD,[2]National Cancer Institute, Rockville, MD,[3]HiThru Analytics LLC, Princeton, NJ,[4]University of Massachusetts-Boston, Boston, MA,[5]Jikei University, Tokyo, Japan,[6]National Library of Medicine,, Bethesda, MD,[7]National Library of Medicine, Bethesda, MD

CellMiner Cross-Database (CellMinerCDB) (https://discover.nci.nih.gov/cellminercdb/) is an established interactive application providing direct access and enabling exploration of cancer cell line pharmacogenomics without extensive programming experience. Data are compiled from many sources, including the National Cancer Institute (NCI), Broad Institute DepMap, Sanger/MGH GDSC, MD Anderson Cancer Center (MDACC) MCLP, and National Center for Advancing Translational Sciences (NCATS) cell line projects. In the version 2.2 update, our collection has expanded to pharmacogenomics data for 1,916 cancer cell lines and over 25,000 drugs. Drug screening data include many additional compounds for potential drug repurposing from the Broad PRISM, NCATS, and NCI. The user interface facilitates uncovering specific samples of interest and identifying drug and cell lines across databases. We also expanded the annotations for cross-referencing other databases and downloading our data for further cancer biology and drug discovery studies. Herein, we provide use cases for CellMinerCDB including (i) data reproducibility given overlaps of cell lines, genes, and drugs across databases; (ii) candidate biomarker discovery; and (iii) cross-dataset analyses.

#3139 drGT: Attention-guided gene assessment of drug response utilizing a drug-cell-gene heterogeneous network.

Yoshitaka Inoue[1], Hunmin Lee[2], Tianfan Fu[3], Rui Kuang[2], **Augustin Luna**[4]

[1]National Library of Medicine, Bethesda, MD,[2]University of Minnesota, Minneapolis, MN,[3]Nanjing University, Nanjing, China,[4]National Library of Medicine, Rockville, MD

Background: Accurate drug response prediction alone is insufficient for translational impact; computational models must also generate biologically plausible hypotheses. We present drGT, a heterogeneous graph neural network (GNN) model over drugs, genes, and cell lines that couples prediction with mechanism-oriented interpretability via attention coefficients (ACs).
Results: drGT encodes a drug-gene-cell line graph and uses ACs to describe drug-gene associations. We assess both predictive generalization (random, unseen-drug, unseen-cell, and zero-shot splits) and biological credibility (text-mined PubMed co-mentions and comparison to a structure-based DTI predictor) on GDSC1, GDSC2, NCI60, and CTRP datasets. Here, we evaluate both regression (IC50 values) and binary classification (cell-line sensitivity) settings to reflect typical pharmacogenomic experiments; we report R^2 for regression and AUROC for classification tasks. Across benchmarks, drGT consistently delivers top regression performance while maintaining competitive classification accuracy. Under random 5-fold cross-validation, where 20% of samples are randomly masked for testing in each fold, drGT attains an R^2 of up to 0.690 (1st overall against similar methods) and an AUROC of up to 0.945 (3rd overall). In leave-one-out generalization tests, where either all samples from one cell line or all samples of one drug are excluded during training, drGT achieves R^2 values of 0.692 (1st) and 0.022 (1st) and AUROCs of 0.706 (3rd) and 0.844 (2nd), respectively. In the zero-shot prediction test, trained on GDSC1 and evaluated on GDSC2, drGT achieves an R^2 of 0.334 (1st) and an AUROC of 0.786 (1st), both of which represent the highest scores among all models. For interpretability, AC-derived drug-gene links recover known biology: among 976 drugs from the NCI60 dataset with known DTIs, 36.9% of predicted links match established DTIs, and 63.7% are supported by either PubMed abstracts or a state-of-the-art (SOTA) structure-based DTI prediction model. Moreover, an over-representation analysis of AC-ranked genes identifies mechanism of action (MoA)-consistent pathways, such as KRAS signaling, for relevant kinase inhibitors, providing pathway-level explanations for the model predictions.
Conclusions: drGT advances predictive generalization and mechanism-centered interpretability with AC-derived drug-gene links, offering SOTA regression accuracy and literature-supported biological hypotheses, demonstrating how interpretable graph learning can bridge AI prediction and biological discovery. Code: https://github.com/sciluna/drGT

#3140 Characterizing the critical role of enhancer-gene regulation in 5-fluorouracil toxicity and resistance.

Hannah Marie Krause[1], Julia Magee[2], Kelly Bouchonville[1], Lauryn Allyn Hahn[1], Ryan Jonathan Swartz[1], Brianna Bembenek[3], Lulu Jiang[1], Steven M. Offer[1]

[1]University of Iowa Carver College of Medicine, Iowa City, IA,[2]University of Iowa, Iowa City, IA,[3]Mayo Clinic, Rochester, MN

5-Fluorouracil (5FU)-based chemotherapy remains a front-line treatment for most patients with colorectal cancer. However, approximately 30% of patients who receive 5FU experience severe, life-threatening toxicity. Dihydropyrimidine dehydrogenase (DPD, *DPYD* gene) mediates the rate determining step in 5FU catabolism. Deleterious genetic variations in *DPYD* have been associated with elevated concentrations of circulating 5FU and significantly increased risk for 5FU toxicity. Five deleterious variants in *DPYD* have been identified as clinical biomarkers of toxicity and have led to prospective genotyping and differential dosing recommendations for carriers of these variants, as noted on recent updates to the FDA label for the 5-FU prodrug capecitabine. Our previous studies also established the importance of epigenetic control of DPD expression. In this study, we used existing epigenetic repositories to identify candidate enhancer elements for *DPYD*. We selected 20 novel high-priority putative enhancers for further study using a combination of reporter assays and CRISPRi applied across multiple cell models. Further studies will investigate means to target these regulatory mechanisms as a means to increase localized efficacy of 5-FU-based therapies in colorectal cancer.

#3141 Integrative genomic analysis reveals pharmacogenomic determinants of chemotherapy response.

Djuraev Farrukh[1], yashodhara Bhattacharya[2], Mohan Uttarwar[2], Sandhya Iyer[2], Hrishita Kothavade[2], Mina Darooei[3], Madhura Basavalingegowda[2], Hetakshi Kurani[3], Bharat Bhosale[4], Aarthi Ramesh[2], Gowhar Shafi[3]

[1]Tashkent Medical Park LLC, Tashkent, Uzbekistan,[23]OneCell Diagnostics India Private Limited, Pune, India,[4]BD Precision Oncology Clinic, Mumabi, India

Background: Pharmacogenomic (PGx)markers are critical in understanding patient responses to chemotherapeutic agents. They influence how patients metabolize popular chemotherapeutic agents like fluoropyrimidines and irinotecan, thereby impacting efficacy and risk of severe toxicity. Although PGx testing significance is well established, their genomic profiling and clinical interpretation involves challenges including limited clinical evidence for many variants, incomplete capture of pharmacogenomic-relevant regions, tumor heterogeneity and sampling bias, and variant interpretation. Many cohort studies among the Uzbek population have also highlighted the challenges including the one among 99 Uzbek cancer patients (breast, gastric, colorectal) identified the clinically significant DPYD IVS14+1G>A splice-site variant, also known as the DPYD *2A allele in a significant fraction of individuals indicating that DPD-related 5-FU risk is present in the population and merits pretreatment consideration. Our current study presents the significance of a comprehensive genomic profiling (CGP) and interpretation of pharmacogenomic markers for effective chemotherapeutic performance in clinical scenario.

Methods: A total of 124 patients who were genomically profiled using our CGP assay was retrospectively investigated for pharmacogenomic variants. The cohort included cancer types including breast, colon, lung, melanoma, pancreatic, stomach, ovarian, rectal, and hepatobiliary tract. CGP was performed on these patients using next-generation sequencing (NGS) with the OncoIndx® panel.

Results: From the CGP results of the 124 profiled patients, three critical pharmacogenomic markers were detected. The DPYD wildtype genotype was detected in 92% (n=114) of patients which was interpreted to be associated with reduced risk of adverse events when treated with 5-FU/ fluoropyrimidine-based chemotherapy. Another 2.4% (n=3) of patients were detected with DPYD c.1129-5923C (HapB3) variant which was interpreted to impact DPYD function and can affect treatment outcomes leading to increased toxicity when treated with standard dosage of 5- FU / fluoropyrimidine-based- based chemotherapy. Further, 4% (n=5) were detected with wildtype genotype of TYMS, and 0.8% (n=1) heterozygous, and 4.8% (n=6) patients detected with 6bp deletion interpreted to cause increased toxicity/ADR. In addition, 9.7% (n=12) of patients were detected with UGT1A1 wildtype which determines response o irinotecan-based chemotherapy.

Conclusion: This study, highlights the significance of profiling and effective interpretation of a patient's PGx phenotype from the profiled genotype as a critical measure to lower risk of debilitating adverse events and guide towards safer, more effective dosing of chemotherapy.

#3142 Genomic determinants of response to the Wnt/Beta-catenin condensate modulator DPTX3186 in gastric cancer PDX models and implications for clinical development.

Francis Carpenter[1], Kip West[2], Doug Baumann[2], Adam Talbot[2], Thomas Durand-Reville[1], Karl Hsu[1], Ann Boija[1], **Isaac Klein**[1]

[1]Dewpoint Therapeutics, Inc., Boston, MA,[2]Dewpoint Therapeutics, Boston, MA

DPTX3186 is a first-in-class small molecule oral condensate modulator (c-mod) designed to disrupt oncogenic wnt/beta-catenin signaling in tumors selectively. DPTX3186 forces beta-catenin to concentrate within an inactive condensate inside tumor cells, resulting in malignant cell death *in vitro* and robust single-agent anti-tumor activity in wnt-driven tumor models *in vivo*. DPTX3186 has an open IND, has been granted Orphan Drug and Fast Track Designations, and is being tested in a combined Phase 1/2 trial focused on gastric cancer. To assess the therapeutic potential of DPTX3186 across gastric cancer and identify biomarkers predictive of high response, we tested DPTX3186 in a diverse panel of well-characterized gastric cancer patient-derived xenograft (PDX) models. Mice implanted with PDX-based tumors were treated with either DPTX3186 or vehicle, with tumor volume and body weight measured for up to 70 days following treatment initiation. Across models, treatment with DPTX3186 resulted in a statistically significant decrease in tumor volume growth, including stasis and regression (as measured by tumor growth inhibition, TGI), and a statistically significant increase in survival, without affecting body weight. Each of the PDX models implanted were characterized in terms of the patients' clinical, genomic, and transcriptomic profiles, enabling analysis of biomarkers that were predictive of increased TGI or survival when comparing DPTX3186 treated mice to vehicle mice. Through these analyses, we identify prevalent and clinically actionable genomic characteristics that predict an increased response to DPTX3186. Specifically, mutations in oncogenes that are associated with greater beta-catenin activity confer greater response to DPTX3186, reinforcing the specificity of the condensate mechanism for wnt-driven tumors. These results demonstrate the promising therapeutic potential of DPTX3186 in gastric cancer, outline our patient selection strategy for the ongoing clinical trial, and provide a roadmap for the clinical selection of high responders to condensate-modulating anti-cancer agents.

#3143 Co-targeting of two distinct androgen receptor-regulated signaling pathways as a therapeutic approach in prostate cancer.

Min-Yu Ko, Rachid Safi, Suzanne E. Wardell, Paige Watkinson, Isabel Jones, Brianna Richardson, John D. Norris, Donald P. McDonnell

Duke University School of Medicine, Durham, NC

Prostate cancer (PCa) is the most frequently diagnosed cancer in men and the second leading cause of cancer-related deaths in the United States. Androgen deprivation therapy (ADT) is initially effective; however, most patients eventually relapse and progress to castration-resistant prostate cancer (CRPC), where tumor growth persists despite being exposed to extremely low levels of androgens. In probing the molecular determinants of androgen receptor (AR) pharmacology in PCa, we made the unexpected observation that PCa cells can recognize and respond differently to different levels of androgens. Notably, we demonstrated that low levels of androgens, functioning through an AR monomer, facilitate a non-genomic activation of the mammalian target of rapamycin (mTOR) signaling pathway to drive proliferation. Conversely, we found that eugonadal levels of androgens (high dose; HD) promote AR dimer formation, which actively suppress c-MYC expression, inhibit proliferation, and drive a transcriptional program associated with a differentiated phenotype.

To elucidate the mechanism(s) by which AR activates mTOR signaling, we dissected the molecular events initiated by androgens in validated cellular models of PCa. These studies revealed that androgens, acting through AR, induce AKT phosphorylation at S473, an early and previously unrecognized regulatory node in AR-driven pathways. Prior studies have established that AKT S473 phosphorylation is mediated by mTOR complex 2 (mTORC2) and can be stimulated by insulin-like growth factor-1 (IGF-1). Indeed, we demonstrated that IGF-1 signaling was absolutely required for androgen-dependent mTOR activation and cell proliferation. These results suggest that androgens/AR act upstream of mTOR to amplify the activity of the IGF-1-AKT signaling axis rather than directly engaging mTOR pathway components.

While we have established that AR-driven mTOR activation occurs through the IGF-1-AKT axis, our data also revealed a distinct AR-regulated growth program centered on c-MYC. Notably, inhibition of the IGF-1-AKT-mTOR pathway suppresses PCa cell proliferation *in vitro* but fails to reduce c-MYC expression, indicating that targeting this axis alone is unlikely to achieve durable control of the disease. It is significant, therefore, that we determined that HD androgens downregulate c-MYC expression while maintaining mTOR activation. Leveraging these insights, we evaluated the utility of combining AKT inhibition with HD androgen treatment in a xenograft model of PCa. This combination strategy was superior to either treatment alone, resulting in robust suppression of tumor growth. Together, these findings establish a mechanistic framework for the dose-dependent effects of androgens on PCa biology and highlight the potential clinical utility of dual-targeting approaches to overcome resistance to standard of care treatments in PCa.

#3144 Targeting AR-SREBP crosstalk in prostate adenocarcinoma.

Sirisha Devarakonda, Prashanth Parupathi, Ekniel Francois, Avinash Kumar

Long Island University, Brooklyn, NY

Androgen receptor (AR) is a well-studied nuclear transcription factor responsible for the progression of prostate cancer. Prostate Cancer (PCa) is the most commonly diagnosed cancer and the second leading cause of cancer-related deaths among men in the United States, despite the availability of advanced AR inhibitors. Hence, there is an urgent need to identify alternative therapeutic targets and agents to supplement AR-based therapy. Sterol regulatory element-binding proteins (SREBPs) are a family of transcription factors, consisting of SREBP-1 and SREBP-2, that are responsible for de novo lipogenesis and cholesterol biosynthesis. Recent studies show that crosstalk between AR and SREBP promotes PCa progression. Consistent with this, we have observed that SREBP is overexpressed in the presence of AR. Therefore, we hypothesized that pharmacological inhibition of SREBPs might be a promising therapeutic approach in androgen receptor-positive PCa. In our study, we evaluated the anticancer activity of fatostatin, an SREBP inhibitor, in AR-positive PCa cell lines (LNCaP and C4) and AR-negative PCa cell lines (PC3 and Du145). We observed inhibition of viability, proliferation, migration, and invasion in all PCa cell lines. Additionally, we observed decreased protein and mRNA expression of SREBPs and AR in the fatostatin treatment group. Notably, fatostatin showed significantly more potent inhibition in AR-positive PCa cell lines compared to AR-negative PCa cell lines. To further understand the molecular mechanism of fatostatin in AR-positive PCa cell lines, we performed RNA-Seq, which revealed inhibition of AR signaling and cholesterol homeostasis. It was also observed that genes involved in mitotic spindle assembly and the mTORC1 pathway have been downregulated. Altogether, our data show that pharmacological inhibition of SREBP may be a potential therapeutic target in AR-positive prostate cancer.

#3145 Pharmacologic inhibition of SREBP-driven lipogenesis suppresses metastatic progression in prostate cancer.

Prashanth Reddy Parupathi[1], Sirisha Devarakonda[2], Ekniel Francois[3], Avinash Kumar[3]

[1]Department of Pharmaceutical Sciences, Long Island University, Greenvale, NY,[2]Long Island University, Greenvale, NY,[3]Long Island University, Brooklyn, NY

Prostate cancer (PCa) progression is increasingly recognized as a metabolically driven process, particularly through alterations in lipid metabolism. Sterol regulatory element-binding proteins (SREBPs) are master transcription factors that regulate genes involved in lipogenesis and are often upregulated in advanced prostate cancer, leading to aberrant lipid accumulation, and are associated with poor prognosis and disease progression. Despite advances in characterizing the metabolic phenotype of PCa, a critical gap remains in understanding how SREBP-driven lipid remodeling mechanistically contributes to the metastatic dissemination of PCa. Our analysis of publicly available patient datasets revealed increased gene expression of SREBPs in prostate tumors compared to normal prostate tissue. Furthermore, we observed substantially higher SREBP gene expression in metastatic samples compared to primary tumors. We also found notably higher levels of SREBPs in the more invasive PC3M and C4-2B cell lines than in their less invasive counterparts, PC3 and LNCaP. Based on these findings, we hypothesize that inhibition of SREBPs by fatostatin could be an effective therapeutic strategy against lethal metastatic prostate cancer. We found that fatostatin inhibited the viability, proliferation, clonogenic survival, migration, and invasion of the more invasive PCa cell lines, with significantly greater potency than in less invasive lines. Immunoblotting confirmed that fatostatin inhibited both SREBPs and their downstream targets more effectively in more invasive PCa cell lines than in less invasive ones. We then performed RNA-Seq and pathway analysis on all cell lines treated with fatostatin. We found that pathways related to EMT and mTORC1 are significantly downregulated in the more invasive prostate cancer cell lines compared to their less invasive counterparts. Overall, our results demonstrate that SREBP-driven lipid metabolism mechanistically contributes to PCa invasiveness and pharmacological inhibition of SREBPs may improve outcomes in lethal metastatic prostate cancer.

#3146 Targeting KMT2D enhances sensitivity to AKT inhibition in treatment resistant prostate cancer.

Abbas Jawadwala[1], Remi M. Adelaiye-Ogala[1], Surendra Gulla[1], Tej K. Sharma[2], Ephraim Jeremiah Gardner[1], Maddie Aust[2]

[1]University at Buffalo, State University of New York, Buffalo, NY,[2]University at Buffalo, Buffalo, NY

Prostate cancer (PCa) is the leading cause of cancer-related deaths in men, with over 299,000 new cases expected in the U.S. in 2024 alone. A loss-of-function mutation in the PTEN gene activates the PI3K-Akt-mTOR pathway, driving increased cell proliferation and metastasis. Prior studies from our group and others have shown that the AKT signaling pathway remains an attractive target in advanced prostate cancers and other solid tumors. In breast cancer, inhibition of the PI3K pathway has been shown to activate KMT2D, a histone lysine dimethyltransferase. Activation of KMT2D enhanced hormone-regulated gene expression and, in turn, enhanced the response to hormone-targeted therapies. We modified treatment-resistant human PCa cell lines (C4-2B ER, LREX) to suppress AKT isoforms using shRNAs. Using these models, we observed increased KMT2D expression and activity, as indicated by increased H3K4 dimethylation, with suppression of AKT2 and AKT3, but not AKT1, isoforms. In addition, we observed increased androgen receptor (AR) expression. Conversely, knocking down KMT2D in the C42B cell line resulted in a significant decrease in proliferation and increased sensitivity to the Akt inhibitor (Ipatasertib). Although preliminary, these findings suggest that KMT2D may be involved in cross-talk with the PI3K-AKT signaling pathway with implications for AR signaling.

#3147 Pinostilbene exhibits anticancer activity in advanced prostate cancer.

Ekniel Francois[1], Prashanth Reddy Parupathi[1], Sirisha Devarakonda[1], Avinash Kumar[2]

[1]Long Island University, Greenvale, NY,[2]Long Island University, Brooklyn, NY

Prostate cancer is the foremost incident cancer and the second major cause of cancer-associated mortality among men in the U.S. Although current therapies, involving androgen receptor (AR) pathway inhibitors have improved survival rates, advanced prostate cancer remains a lethal disease. Therefore, new therapeutic approaches should continue to be investigated. Previous studies from our group as well as others have widely demonstrated the anticancer activity of resveratrol and its analogs. However, pinostilbene, a monomethylated resveratrol analog, is less well studied and reports on its anticancer activity in prostate cancer is limited. In this study, we investigated the anticancer activity of pinostilbene in prostate cancer. We found that pinostilbene inhibited the viability, proliferation, and metastatic potential of all prostate cancer cell lines tested. Of note, pinostilbene exhibited significantly higher potency as an anticancer agent in more invasive compared to less invasive prostate cancer cell lines. Overall, our results demonstrate that pinostilbene shows tremendous potential as an anticancer agent for improved management of prostate cancer.

#3148 Human blood micronucleated reticulocytes: Application as a pharmacodynamic biomarker for DNA double strand breaks in oncology drug development.

Jeffrey C. Bemis[1], Colette Baxter[2], Gillian Langford[2], Timothy A. Yap[3], Susanna Varkey Ulahannan[4], Nehal Lakhani[5], Babar Bashir[6], Kathleen N. Moore[7], Payal Shah[8], Svetlana Avlasevich[1], Dorothea Torous[1], Stephen Dertinger[1]

[1]Litron Laboratories, Rochester, NY,[2]Artios Pharma Limited, Cambridge, United Kingdom,[3]UT MD Anderson Cancer Center, Houston, TX,[4]University of Oklahoma Health Sciences Center, OKC, OK,[5]START Midwest, Grand Rapids, MI,[6]Thomas Jefferson University Hospital, Philadelphia, PA,[7]OU Health Stephenson Cancer Center, Oklahoma City, OK,[8]Perelman Center for Advanced Medicine, Philadelphia, PA

Introduction: Micronucleated reticulocytes (MN-RET) are a well-established biomarker of chromosomal damage, and their assessment is traditionally included as part of regulatory-based, product safety testing during preclinical development. Adaptation of the methodology to high-throughput flow cytometric analysis broadened the utility of the assay and enabled practical translation to human subjects. Most recently, this methodology has been used to demonstrate target engagement via the induction of MN-RET as a biomarker of efficacy during the development of therapies targeting DNA double strand break-repair pathways.
Methods: To support this application, we have conducted studies in clinical models to define basic methodological parameters. In an effort to better understand baseline values over time/between subjects and reproducibility, we evaluated technical replicate variability in MN-RET frequencies based on blood specimens from 14 subjects. Intra-subject variability was based on serial blood draws from 6 subjects, and inter-subject variation was based on up to 344 subjects age 0 to 73 years.
Results: Human models demonstrate increased MN-RET frequencies following exposure to known DNA damaging agents. Inter-subject variation (≥77%) was much greater than intra-subject and technical replicate variability. The relatively large inter-subject variation is apparent from mean and standard deviation values for MN-RET (0.15 ± 0.10%). Neither age nor sex affected inter-subject variation of the MN-RET frequency. In a clinical setting, patients treated with PARP inhibitors at a labelled dose showed elevated MN-RETs, demonstrating the increased unrepaired DNA damage as an indicator of target engagement induced by treatment.
Summary: This translational biomarker of chromosomal damage represents a unique and powerful tool for use in the development of cancer therapies that elicit DNA double strand breaks.

#3149 Micronuclei (MN) dynamics in preclinical models and in patient reticulocytes as a pharmacodynamic biomarker for the first in class DNA polymerase theta (PolΘ) inhibitor ART6043.

Colette L. Baxter[1], Timothy A. Yap[2], Susanna V. Ulahannan[3], Nehal Lakhani[4], Minal Barve[5], Erika P. Hamilton[6], Babar Bashir[7], Helen M. R. Robinson[1], Jayesh B. Majithiya[1], Paula Costales[1], Sarah V. Holt[1], Samantha C. Skelton[1], Marina Roy-Luzarraga[1], Jeff C. Bemis[8], Dorothea Torous[8], Svetlana Avlasevich[8], Susana Barriga[1], Bryony Harrop[1], Gillian A. Langford[1], Ian Smith[1], Graeme C. M. Smith[1]

[1]Artios Pharma Ltd, Cambridge, United Kingdom,[2]UT MD Anderson Cancer Center, Houston, TX,[3]University of Oklahoma Health Sciences Center, OKC, OK,[4]START Midwest, Grand Rapids, MI,[5]SCRI at Mary Crowley, Dallas, TX,[6]Sarah Cannon Research Institute, Brentwood, TN,[7]Thomas Jefferson University Hospital, Philadelphia, PA,[8]Litron Laboratories, Rochester, NY

Introduction: ART6043 is a first in class, potent and selective polymerase domain inhibitor of DNA Polθ, a central mediator of the microhomology-mediated end joining (MMEJ) DNA double strand break (DSB) repair pathway. Novel biomarkers are important to demonstrate target engagement of ART6043. Polθ knock out mouse studies highlighted increased levels of MN in mouse reticulocytes (RETs) and normochromatic erythrocytes since MN are a common hallmark of genome instability. Here we describe the utility of an assay designed to monitor MN induction in reticulocytes from both preclinical models and patient samples to evaluate Polθ inhibition.
Methods: This analysis builds on the MN-RETs assay, which is traditionally used as a preclinical toxicology assessment (Tometsko et al., 1995). This assay involves fixing whole blood, isolating reticulocytes (specifically in the human assay), and labelling them for nucleic acids to stain any MN. High throughput flow cytometry is then used to quantify the number of reticulocytes with MN.
Results: These data demonstrated the utility of MN-RET as a target engagement biomarker for ART6043 in preclinical studies and in the subsequent clinical study (NCT05898399). In preclinical xenograft models ART6043 monotherapy and ART6043 in combination with olaparib induces MN-RET at doses where tumor regressions occurred. The MN-RET data evaluated in the phase 1 trial of ART6043 mirrored the preclinical data. Patients treated with the highest dose of ART6043 evaluated as monotherapy had elevated MN-RETs, while patients treated with ART6043 in combination with olaparib had statistically higher MN-RET levels. This suggests that the combination of two DNA repair pathway inhibitors, targeting separate mechanisms, leads to a synergistic increase in DNA damage.
Summary: The increase in MN-RETs observed in patients dosed with ART6043 has demonstrated target engagement of a Polθ inhibitor for the first time in humans. MN-RETs has demonstrated potential utility as a mechanism of action target engagement biomarker for a range of therapeutics targeting different DNA damage repair pathways.
References: Tometsko, A. M., Dertinger, S. D., & Torous, D. K. (1995). Analysis of micronucleated cells by flow cytometry. 4. Kinetic analysis of cytogenetic damage in blood. *Mutation Research/Environmental Mutagenesis and Related Subjects*, *334*(1). https://doi.org/10.1016/0165-1161(95)90025-X

#3150 InVEST44™ is a cost-effective *in vitro* safety panel that identifies off-target effects in early-stage drug discovery.

Julian R. Wooltorton, Afsara Ahona, Nicole Barbacane, Alex D'Andrea, Justin Lansberry, Cindy Lay, Paige Miller, John Ries, Jamin Steffen, Patricia Valentine

Reaction Biology Corporation, Malvern, PA

Drug development costs exceed $172m and increase to over $500m when clinical trial failures are considered (Sertkaya 2024, DOI: 10.1001/jamanetworkopen.2024.15445). It can take 20 years to bring a drug to market so it is critical to identify safety liabilities early in the discovery process to ensure valuable time and money are not invested in preclinical and clinical trials. In vitro safety panels, such as InVEST44™, can identify potential toxicities of drugs cost-effectively during early-stage drug development. This is particularly relevant as, between 2006 and 2023, the proportion of venture capital investments in early-stage drug discovery has decreased from 50% to 16% while increasing for later stage from 20 to 54% (*The Biopharma Industry Investment Report 2015*. Biotechnology Innovation Organization; Larka 2024, *Trends in Venture Capital Funding for Biopharma Startups*. GlobalData). This highlights a trend towards expensive, high-risk but potentially lucrative, clinical trials and away from early drug discovery. The goal is to demonstrate that early-stage in vitro safety panels are fiscally and scientifically critical steps in drug development to identify off-target effects before advancing drugs to animal testing and clinical trials. InVEST44™ is an in vitro safety panel designed to identify off-target effects of lead compounds for oncology and other therapeutic areas in early-stage drug development, ensuring a more efficient path from discovery to clinical trials. It comprises 44 industry standard, high risk targets based on Bowes et al. (2012; DOI: 10.1038/nrd3845), including GPCRs, transporters, ion channels, nuclear receptors and enzymes. Various assay types are utilized, including radioligand binding, fluorescence polarization, enzymatic activity, cell reporter, calcium mobilization and electrophysiology assays. We identified 20 drug candidates from 17 failed clinical oncology trials between 2001 and 2025, all terminated because of reported severe adverse effects (clinicaltrials.org). These were screened at 10 µM in InVEST44™: 17 drugs elicited >50% effect on at least 1 target, including 8 with 4+ target interactions and one interacting with 15 safety targets. This study demonstrates the importance of in vitro safety panels, such as InVEST44™, by identifying off-targets effect of lead compounds before pursuing time-consuming and expensive animal testing and potentially failed clinical trials. Data from such panels are increasingly being provided to enhance IND applications (Scott, 2022, DOI: 10.1016/j.vascn.2022.107205). In summary, by providing cost-efficient, early-stage identification of off-target effects by lead compounds, in vitro safety panels, such as InVEST44™, have become integral components of drug discovery and warrant increased early-stage consideration and investment in the future.

#3151 High-throughput high-plex proteomic profiling of hepatocyte toxicity to oncologic drug compounds: A platform for toxicity assessment, immune risk prediction, and drug development acceleration.

Nicole Paul, Alyssa Rosenbloom, Nathaniel Robichaud, Kiran Edwardson, **Nathan Chang**, Narges Rashidi, Milad Dagher

Nomic Bio Inc, Montreal, QC, Canada

The rapid and necessary expansion of cancer drug development requires accessible and scalable strategies for early toxicity screening and immune risk profiling. Liver plays a central role in drug metabolism, detoxification, and immune modulation. Robust detection of liver-specific responses to oncologic therapeutics is essential to identify and mitigate hepatotoxicity and immune-related adverse events (irAEs) which could limit clinical development. Here, we demonstrate a high-throughput, high-plex proteomic platform as a powerful approach to evaluate functional perturbations of hepatocytes across a spectrum of cancer drugs.Utilizing the novel Omni 1000 proteomic solution, based on nELISA technology, we profiled 1,000 proteins in >6500 samples of primary human hepatocytes following exposure to a diverse panel of over 550 distinct drug compounds at 3 doses per compound. Omni 1000 protein target content enables simultaneous quantification of stress response markers, inflammatory cytokines, metabolic enzymes, and signaling pathway effectors. This allows for evaluation of both cytotoxic and immunomodulatory signatures. Perturbation with tripolide, doxorubicin, and cobimetinib resulted in dose dependent cell toxicity, detected via increased levels of intracellular proteins such as GAPDH and Casp3 released into the supernatant, consistent with clinically observed hepatotoxicity. We also detect increased Galectin-3, Galectin-1, and VEGFA at non-toxic perturbation doses, indicative of cell stress and potential toxicity at higher doses. In addition, we concurrently observe loss of proteins associated with protection against apoptosis, such as ST6GAL1, a potent inhibitor of FAS-mediated apoptosis. Across the 510 compounds screened, 68 showed similar signs of toxicity, including compounds with dose-limiting liver toxicity in the clinic. Of particular note is PHA-793887, a potential therapeutic candidate, which failed clinically due to unexpected hepatotoxicity, which here was captured in a pre-clinical *in vitro* model.We further demonstrated the platform's ability to identify likely irAEs through detection of dose dependent increases in key cytokines. Hepatocytes perturbed with Imatinib and Pomalidomide demonstrated increases in IL-6, IL-10, and IL-2, indicative of potential irAE and consistent with published literature for these drugs.High-throughput high-plex proteomic analysis of hepatocyte responses offers a significant advance in preclinical toxicology and immune safety, and enables an early stage indication of drug-induced liver injury (DILI) risk and immunotoxic potential, two major barriers in oncology drug development.

#3152 Development of iPSC-derived human liver organoids for preclinical drug testing and toxicology studies.

Fong Cheng Pan[1], Mahi Rahman[1], David Austin[2], Stephan Krieg[3], Luisa Marie A. Pfeifer[3], Anthony Saporita[1], Philip Hewitt[4], Steven Johnston[5], Laura Braeuninger-Weimer[4], Willem Kools[6], Vi Chu[1]

[1]MIlliporeSigma, Temecula, CA,[2]R&D, MIlliporeSigma, Temecula, CA,[3]Discovery Toxicology, Merck KGaA Darmstadt, Darmstadt, Germany,[4]Merck KGaA Darmstadt, Darmstadt, Germany,[5]Merck KGaA Darmstadt, Tempe, AZ,[6]MIlliporeSigma, Burlington, MA

Background and Purpose: Over 90% of drug candidates fail during clinical trials, often due to insufficient efficacy and unmanageable toxicity. Drug-induced liver injury (DILI) is frequently missed in preclinical testing due to a lack of robust and predictive liver models. We report the de novo development of iPSC-derived human liver organoids as scalable, reliable, and physiologically relevant preclinical toxicology models.

Methods: Using an efficient and reproducible iPSC-differentiation protocol, we generated long term expandable, cryopreservable bipotential 3dGRO^{TM} Human iPSC-derived Liver Progenitor Organoids, which differentiate into mature liver organoids (MLOs) containing multiple liver cell types.

Results: The iPSC-derived mature liver organoids display long-term stability, secrete albumin and urea, and express key biomarkers of mature hepatocytes (albumin, CYP3A4, HNF4a, PCK2) and cholangiocytes (Sox17, Sox9, CK7, MRP2). They also exhibit functional Phase I/II liver enzymes (CYP3A4, CYP2C9, CYP1A2, ALT, AST, GST) and active bile salt/drug transporters. Compared to primary hepatocytes, our 3dGRO^{TM} Human iPSC-derived Mature Liver Organoids demonstrate comparable functionality and outperform HepG2 cells and liver spheroids. In DILI assays, MLOs responded to drug treatment with elevated liver enzymes, confirming their potential for toxicology screening.

Conclusion: These liver organoids represent a powerful tool for high-throughput drug screening, DMPK and toxicological studies, with future applications including disease modeling of hepatocellular carcinoma, MASLD, and NASH.

#3153 An integrated *in vitro* profiling platform for the simultaneous assessment of anti cancer efficacy and multi organ toxicity.

Xia Tu, Hao Wen, Dawei Yan, Jingna Ren, Qin Guo, **Peichuan Zhang**, Haiheng Dong

WuXi AppTec, Shanghai, China

The high attrition rate of oncology drug candidates is frequently driven by an insufficient understanding of a compound's therapeutic index early in development. Many promising molecules advance based on potent efficacy, only to fail later due to unanticipated safety concerns. To address this, there is a critical need for a comprehensive *in vitro* strategy that can simultaneously and systematically evaluate anti-cancer activity and organ-specific toxicity risks in the preclinical phase, enabling more informed and de-risked candidate selection.

To address this gap, we developed an integrated *in vitro* profiling platform that synergizes a robust Efficacy & Mechanism Module with an extensive Early Safety & Toxicity Module. The efficacy module delivers a multi-faceted assessment of anti-tumor potential, beginning with high-throughput viability screening across a diverse panel of human cancer cell lines to determine potency and selectivity. It can be further implemented by functional phenotyping assays including angiogenesis, migration, and invasion to evaluate anti-metastatic potential. Furthermore, downstream molecular investigations via qPCR and Western Blot analysis elucidate mechanisms of action and target engagement. The safety module employs a battery of specialized assays in relevant normal cell models to proactively identify a broad spectrum of adverse effects, encompassing organ-specific toxicities such as hepatotoxicity, nephrotoxicity, cardiotoxicity, and neurotoxicity, alongside general toxicological concerns including mitochondrial toxicity, genotoxicity, and phototoxicity. By integrating these rich datasets, our platform empowering the selection of safer and more effective lead compounds for successful translational development.

#3154 Novel inhibitors of BCRP and P-gp found among drugs used in the treatment of cancer.

Martina Timonen, Feng Deng, Mikko Niemi

Clinical Pharmacology, University of Helsinki, Helsinki, Finland

Breast cancer resistance protein (BCRP) and P-glycoprotein (P-gp) are ATP-binding cassette transporters involved in clinically relevant drug-drug interactions (DDI). This study aimed to identify new BCRP and P-gp inhibitors among used in the treatment of cancer, as the inhibition by many commonly used anticancer and supportive care drugs remains unclear. A total of 133 drugs were screened at 50 µM for inhibition of BCRP and P-gp using a transport assay with BCRP or P-gp-expressing membrane vesicles. Following initial screening, 50% inhibitory concentrations (IC_{50}) were predicted, and the most potent inhibitors were selected for experimental IC_{50} determination. The risks of intestinal and systemic inhibition of BCRP and P-gp were assessed by comparing the estimated intestinal concentration (I_2; dose/250 ml) and maximum plasma concentration (I_1) to the IC_{50} values. If the I_2/IC_{50} ratio surpassed 10 or the I_1/IC_{50} ratio exceeded 0.1, in vivo inhibition was considered possible. Mechanistic static modelling was then utilized to assess the risk of a pharmacokinetic DDI in humans. Following initial screening, 24 and 23 drugs were selected for the determination of IC_{50} values for BCRP and P-gp, respectively. Of the investigated compounds, cabozantinib (IC_{50} of 0.65 µM), midostaurin (0.69 µM), and entrectinib (5.8 µM) showed the strongest inhibition of BCRP. Nilotinib (1.0 µM), osimertinib (2.0 µM), and abemaciclib (2.4 µM) showed the strongest inhibition of the P-gp. The highest I_2/IC_{50} ratios for BCRP were observed for mitotane (6190), cabozantinib (1730), and abiraterone (831). For P-gp, the highest I_2/IC_{50} ratios were observed for nilotinib (2880), pazopanib (1580), and mitotane (1480). These compounds might therefore inhibit BCRP or P-gp in the intestine. The highest I_1/IC_{50} ratios for BCRP were observed for doxorubicin (8.2), etoposide (2.8), and fosaprepitant (0.84). For P-gp, the highest I_1/IC_{50} ratios were observed for amscarine (1.6), vinorelbine (0.55), and fosaprepitant (0.50). These compounds might therefore inhibit systemic BCRP or P-gp. Mechanistic static model for BCRP inhibitors suggested that cabozantinib, midostaurin, and apalutamide could almost fully inhibit intestinal BCRP, increasing the exposure to concomitantly administered rosuvastatin by 94%, 89%, and 83%, respectively. Similarly, mechanistic static model for P-gp inhibitors suggested that sorafenib, cabozantinib, and nilotinib could almost fully inhibit intestinal P-gp, increasing the exposure to concomitantly administered dabigatran etexilate by 124%, 123%, and 115%, respectively. Our findings identified multiple novel BCRP and P-gp inhibitors, which may cause transporter-mediated DDIs in cancer treatment. Clinical DDI studies are warranted to investigate the potential interactions in humans.

#3155 Pharmacokinetic/pharmacodynamic correlation and biodistribution of Re (CO)3-phenformin compared with phenformin in murine PDAC model following equimolar intravenous dosing.

Amir Mohammad Gholizadeh[1], Fatima Dagher[1], Mikayla Skillman[1], Airong Li[1], Chun Li[2], Diana S-L Chow[1]

[1]University of Houston, Houston, TX,[2]UT MD Anderson Cancer Center, Houston, TX

Re (CO)3-phenformin (Re-phen) is a newly synthesized rhenium biguanide complex recently reported and structurally characterized as a potential anticancer agent. However, a comprehensive evaluation of its *in vivo* pharmacokinetics (PK), biodistribution (BD), metabolic fate, and PK/pharmacodynamic (PK/PD) properties has not yet been characterized. In this study, we conducted an integrated PK, BD, and PK/PD analysis of Re-phen compared with Phenformin (Phen) following three consecutive equimolar intravenous doses (26.26 µmol/kg per dose) in PDAC-bearing mice, with additional quantification of *in vivo* biotransformation of Re-phen to Phen to support parent metabolite exposure modeling. Blood collected after the final dose and major organs (tumor, pancreas, liver, kidney, spleen, lung) were analyzed using a rigorously validated LC-MS/MS assay. Re-phen achieved markedly higher tissue deposition than Phen across all organs, including tumor (3.05 ± 1.86 vs 0.05 ± 0.02 nmol/g, **p<0.01), pancreas (61.64 ± 36.24 vs 0.08 ± 0.05 nmol/g, **p<0.01), liver (38.27 ± 20.08 vs 0.16 ± 0.06 nmol/g, ***p<0.001), kidney (22.27 ± 5.80 vs 0.08 ± 0.03 nmol/g, ****p<0.0001), spleen (4.60 ± 1.36 vs 0.29 ± 0.07 nmol/g, ****p<0.0001), and lung (4.51 ± 1.40 vs 0.13 ± 0.04 nmol/g, ****p<0.0001), demonstrating extensive distribution and preferential tissue retention. Re-phen also exhibited measurable *in vivo* conversion to Phen, with a fraction metabolized (Fm) of ~11% and an AUC Ratio (Phen/Re-phen) of 0.22, indicating that both the parent compound and its converted Phen contribute to systemic exposure. 3D PK/PD analysis demonstrated a statistically significant inverse correlation between the AUCs of Re-Phen and its metabolite Phenformin and terminal tumor weight. By comparison, Phenformin exhibited only a moderate, non-significant 2D correlation with tumor weight ($r = -0.800$, $p = 0.1333$), supporting the superior antitumor efficacy of Re-Phen. These results indicate that Re-phen displayed a clear exposure-efficacy relationship and that systemic exposure is a key driver of its anti-tumor response. Collectively, this study provides the first comprehensive *in vivo* evidence defining the PK, biodistribution, metabolic conversion, and PK/PD behavior of Re-phen, highlighting its superior tumor delivery, measurable parent-metabolite interplay, and strong exposure-driven antitumor effect. These findings support further development of Re-phen as a rhenium-based therapeutic and as a core component of the Re/99mTc-phen theranostic platform for pancreatic cancer.

#3156 Pharmacokinetics of a series of anticancer agents in immunodeficient female NOD scid gamma mice.

Mohd Beshr Chama[1], Emily J. Koubek[2], Sarah A. Buhrow[3], Renee A. Schoon[1], Joel M. Reid[3]

[1]Oncology Department, Division of Oncology Research, Mayo Clinic, Rochester, MN,[2]University of Michigan, Ann Arbor, MI,[3]Mayo Clinic, Rochester, MN

Introduction: We aimed to characterize the preclinical pharmacokinetics (PK) of a series of 20 anticancer agents in highly immunodeficient female NOD scid gamma (NSG) mice to provide clearance and exposure data for agents under investigation by the NCI PDX Development and Trial Centers Research Network (PDXNet).
Methods: The series of 20 anticancer agents (inhibitors of CDK4/6, PI3K-β/PI3K-δ, ATR, MEK1/2, PI3K, microtubule, EZH2, BCL-2, PARP, histone deacetylase, γ-secretase, FGFR, SHP2, and ERK1/2, as well as a SMAC mimetic) were administered to female NSG mice via IV, PO, or IP routes to characterize plasma exposures under conditions used for PDX efficacy testing. Serial plasma samples were collected 15, 30, 60, 120, 240, 360, 480, and 1440 minutes after dosing. Drug concentrations were quantified using validated LC-MS/MS assays. PK parameters were calculated using non-compartmental analysis.
Results: The PK for each agent was determined, and the clearance and half-life values are listed in the table below. The PK metrics for Navitoclax could not be calculated. Due to higher metabolic rates, mice show faster PK processes. They generally had shorter half-lives and higher weight-normalized clearance than humans. Copanlisib, Navitoclax, and Trametinib were exceptions.
Conclusion: These PK data are critical for understanding the antitumor activities of agents studied by the PDXNet and will aid investigators in developing new approach methodologies for preclinical safety studies in preparation for human clinical trials.

Pharmacokinetic Analysis

Agent	Clearance (L/hr*kg)	Half-life (Hours)
abemaciclib	1.32	10.99
AZD8186	4	2.42
BAY-1895344	1.77	4.72
birinapant	4.19	8.47
cobimetinib	0.76	21.9
copanlisib	9.42	2.78
docetaxel	1.71	1.17
EPZ-011989	1.13	2.06
niraparib	1.25	10.11
olaparib	4.63	3.44
panobinostat	241.55	3.80
RO4929097	1.01	4.2
rogaratinib	0.46	3.86
romidepsin	6.2	14.38
selumetinib	0.77	5.91
SHP099	0.35	55.12
talozoparib	0.295	4.26
trametinib	0.31	37.47
ulixertinib	0.32	2.48

#3157 Pharmacokinetic/pharmacodynamic correlation and biodistribution of paclitaxel and cyclopamine from M-CPA/PTX in HCC mice following multiple dosing.

Emanuel R. Baltrip[1], Lu Dai[2], Qiu-Xu Teng[3], Defeng Deng[3], Guodong Zhang[3], Chun Li[3], Diana S.-L. Chow[2]

[1]Pharmacological and Pharmaceutical Sciences, University of Houston, Houston, TX,[2]University of Houston, Houston, TX,[3]UT MD Anderson Cancer Center, Houston, TX

Hepatocellular Carcinoma (HCC) is the most common form of liver cancer, highly aggressive and heterogenous. Due to lack of effective diagnostic techniques, HCC is often detected when surgical and chemotherapeutic interventions are inadequate. To address this, we developed a polymeric micelle containing Paclitaxel (PTX), a microtubule-stabilizer, and Cyclopamine (CPA), a Hedgehog pathway inhibitor, termed M-CPA/PTX. The M-CPA/PTX contained 2.5 mg each of PTX and CPA, with size of 70.6 ± 3.4 nm, PDI of 0.12 ± 0.04 (n = 3), and encapsulation efficiency of ≥ 80% for both agents. The biodistribution (BD) of PTX and CPA in tumor, liver, lung, spleen and kidney were characterized following IV dosing of 5 mg/kg M-CPA/PTX in C-MYC expressing transgenic mice which were randomized into four groups: vehicle (n = 10), 1 dose (n = 8), 2 doses (n = 7), and 3 doses (n = 9). ANOVA with Tukey's post hoc test was for statistical analysis with p-value < 0.05 for significance. The BD data were compiled in Table 1. The blood concentrations for each agent were substantially lower than those in tumor and organs at 24 hours post the last dose. The BD patterns were distinct between PTX and CPA. The PTX concentrations were the highest in tumor, 369-443 ng/g, followed by liver >> lungs> kidney >> spleen, 11-15 ng/g. The CPA concentrations were high in lungs, 537-751 ng/g, and kidney, 305-339 ng/g, followed by tumor, 218-300 ng/g, and liver, 206-328 ng/g. The BD levels were not significantly altered among the dosing groups. The 3D PK/PD correlation was established for tumor growth inhibition (%), with tumor concentrations of PTX and CPA in individual mice. In conclusion, the biodistributions of PTX and CPA following multiple IV dosing in an HCC mouse model were characterized, and a 3D PK/PD correlation was established with PX and CPA uptakes in tumor, potentially enabling future efficacy projection.Table 1: Biodistribution of PTX and CPA from M-CPA/PTX

#3158 Pharmacokinetic and biodistribution evaluation of nebivolol and dasatinib in the 4T1 triple-negative breast cancer model: Implications for drug-drug interaction.

Airong Li[1], Mikayla Skillman[2], Junhyoung Park[3], Fatima Dagher[2], Amir M. Gholizadeh[2], Emanuel Baltrip[2], Meghana Trivedi[2], Benny A. Kaipparettu[3], Diana S.-L. Chow[2]

[1]College of Pharmacy, University of Houston, Houston, TX,[2]University of Houston, College of Pharmacy, Houston, TX,[3]Department of Molecular and Human Genetics, Baylor College of Medicine, Houston, TX

Background: In our recent *in-vitro* study, nebivolol (NEB) and dasatinib (DAS) synergistically inhibited the growth of 4T1 cell line, which is a murine mammary carcinoma cell line used to study triple-negative breast cancer (TNBC). However, the in vivo disposition and potential for drug-drug interactions (DDI) are not well defined. This study aimed to characterize the pharmacokinetics (PK) and biodistribution of NEB and DAS in 4T1 tumor-bearing mice and evaluate whether co-administration modifies plasma or tissue concentrations.

Methods: Female BALB/c mice (7-8 weeks) were implanted with 4T1 cells orthotopically and treated with NEB (n=5), DAS (n=5), or NEB+DAS (n=6). The regimen was NEB 10 mg/kg once a day and DAS 20 mg/kg twice a day, 5 days/week for 3 weeks. After the last dose, blood was collected at multiple time points and tissues (tumor, liver, kidney, lung, spleen, heart, pancreas, and brain) were harvested at the end. Drug concentration was quantified using a validated LC-MS/MS method. PK parameters were generated by Phoenix (8.5.1) and GraphPad 10 was used to generate the PK profile and statistical analysis.

Results: Co-administration significantly increased NEB exposure in blood, of which the area under curve (AUC normalized by dose) was 229.45±150.98 hr*ng/mL/(mg/kg), compared to 44.51±10.21 hr*ng/mL/(mg/kg) in the NEB alone group ($p<0.05$). The NEB clearance was decreased from 24.06±7.13 to 5.59±2.88 L/(kg*hr) ($p<0.05$). DAS concentration and parameters were not changed significantly in combination group vs. DAS alone group. Biodistribution analysis modified tissue partitioning in the combination group. NEB concentrations in all tissues were higher in combination group than NEB alone group ($p>0.05$ due to the large variance). Tissue-to-blood (T/B) ratios interpreted the tissue uptake of drugs. T/B ratios of both drugs in tumor, liver, lung, spleen, kidney and pancreas were over 1, indicating preferential tissue accumulation. Even though the T/B ratios in tumor were higher in NEB (32.27±61.87) and DAS (99.45±179.53) alone groups than the combination group (2.53±2.25, 3.73±2.41, respectively), no significant difference was observed due to the large variance, suggesting that co-administration can influence intratumoral delivery. The ratio (T/B) of DAS in the kidney was significantly elevated under combination dosing compared with DAS alone, which indicated more DAS accumulation in combination treatment.

Conclusions: Combination dosing led to a higher exposure of NEB in blood with a lower clearance, and an increased renal distribution of DAS. Distribution shifts indicated a drug-drug interaction. These findings provide a foundational framework for mechanistic PK/PD modeling and support further investigation of NEB+DAS combination for TNBC treatment.

#3160 Synergistic preclinical activity of dual CDK4/6 and mTORC1 inhibition in translocation renal cell carcinoma.

Shikha Gupta[1], Prateek Khanna[1], Eddy Saad[1], Renee Maria Saliby[2], Shatha AbuHammad[3], Jiao Li[1], Bingchen Li[1], Prathyusha Konda[1], Usman Ali Ahmed[1], Ananthan Sadagopan[1], Qingru Xu[1], Ziad El Bakouny[4], Wenxin Xu[1], Ramaprasad Srinivasan[5], Toni K. Choueiri[1], Srinivas R. Viswanathan[1]

[1]Department of Medical Oncology, Dana Farber Cancer Institute, Boston, MA,[2]Yale University, New Haven, CT,[3]Krantz Family Center for Cancer Research, Mass General Hospital, Boston, MA,[4]Memorial Sloan Kettering Cancer Center, New York, NY,[5]National Cancer Institute, Bethesda, MD

Background- Translocation renal cell carcinoma (tRCC) is an aggressive subtype of RCC driven by a gene fusion involving a transcription factor in the MiT/TFE gene family, most commonly TFE3. There are currently no approved therapeutic agents specific to tRCC and this subtype of kidney cancer represents a major unmet medical need.
Methods- We utilized integrative genomic approaches associated with activation of the cyclin- dependent kinase 4/6 (CDK4/6) and mammalian target of rapamycin complex 1 (mTORC1) signaling in tRCC. We tested the activity of CDK4/6 inhibitors (CDK4/6i), alone or in combination with mTORC1-selective inhibition, using *in vitro* and *in vivo* models of tRCC.
Results- Our work shows that tRCC tumors harbor multiple genomic and transcriptional features associated with activation of the CDK4/6 and mTORC1 signaling pathways. Pharmacological inhibition of CDK4/6 activity using palbociclib or abemaciclib, causes cell cycle arrest which was also recapitulated upon genetic knockout of CDK4/6 using CRISPR-Cas9. This was further accompanied by impaired cell growth in long-term culture in presence of palbociclib with a rapid cell regrowth observed upon drug withdrawal. CDK4/6 proteins regulate G1-S cell cycle progression by combining with CyclinD1, the expression of which is significantly reduced upon treatment with mTORC1-selective inhibitor, RMC-5552. Combined treatment with the CDK4/6 inhibitor, palbociclib, and RMC-5552 resulted in synergistic suppression of tRCC cell viability and increased markers of apoptosis *in vitro*. The combination of palbociclib and RMC-5552 in a tRCC xenograft model showed greater efficacy than either single agent while also being well-tolerated.
Conclusions- Our work suggests that combined inhibition of CDK4/6 and mTORC1 activity has therapeutic potential in tRCC. This work may offer rationale for molecularly directed therapies in tRCC, which currently lacks any standard of care.

#3162 Assessing statin sensitivity and hypoxia regulation in aggressive metastatic cancers.

Jimin Kim[1], Shannon Shams[1], Diana Vaca[1], Junhui Hu[1], Moe Ishihara[1], Khiara Threets[2], Robert Damoiseaux[1], Lily Wu[1]

[1]UCLA, Los Angeles, CA,[2]Clark Atlanta University, Atlanta, GA

Statins are a class of small molecule, FDA approved drugs that are widely used to combat cardiovascular disease due to their cholesterol lowering effects. Traditionally, they are competitive inhibitors of HMG-CoA Reductase (HMGCR), a critical enzyme involved in cholesterol synthesis. Previous studies in our lab highlighted that various kinds of statins can effectively kill metastasis-driving clear cell renal cell carcinoma (ccRCC) cells that are von Hippel-Lindau gene (VHL) negative, hypoxia inducible factor (HIF)-1α dominant, while sparing the less aggressive VHL positive, HIF-2α dominant cells. Similar to this metastasis driving ccRCC subpopulation, other aggressive cancers such as triple negative breast cancer (TNBC), and neuroendocrine prostate cancer (NEPC) share the same features of HIF-1α dominance and statin sensitivity. While statins' cytotoxicity for cancer is well documented, there is still no consensus on their mechanism of action nor is there a rationale explaining why statins are better at killing aggressive cancers. Our findings suggest that HIF-1α could be the target in statin metastasis-blocking mechanism, rather than its known cholesterol-lowering action. This project uses a multi-pronged approach involving qRT-PCR, western blot, and Clustered Regularly Interspaced Short Palindromic Repeats (CRISPR) knockouts to rule out the role of HMGCR and the cholesterol pathway in statin cytotoxicity in all three cancer models (ccRCC, TNBC, and NEPC). By understanding the possible role that the HIF-1α proteins play in mediating statin sensitivity, we aim to further clarify their mechanism of action in aggressive metastatic cancers and make a step forward in developing a new safe and effective drug that can both prevent and treat these cancers.

: Targeting Cell Surface Vulnerabilities to Overcome Therapeutic Resistance
Poster Session

#3166 TKI adaptive resistance in HER2-driven non-small cell lung cancer at minimal residual disease stage can be targeted using cell surface-directed therapies.

Manale El Kharbili[1], Daniel Wilkinson[2], Lauren Giesy[3], Sharon R. Pine[4], Peter Fecci[2], Kyle Concannon[1]

[1]Medical Oncology, The University of Colorado Anschutz Medical Campus, Aurora, CO,[2]Neurosurgery, The University of Colorado Anschutz Medical Campus, Aurora, CO,[3]University of Colorado Anschutz Medical Campus, Aurora, CO,[4]University of Colorado-Anschutz Medical Campus, Aurora, CO

Background: HER2 mutations drive 1-2% of non-small cell lung cancers (NSCLCs), and recent HER2-directed antibody-drug conjugates and tyrosine kinase inhibitors (TKIs) such as trastuzumab-deruxtecan and zongertinib have significantly improved outcomes. However, these approaches remain non-curative, and nearly all patients develop progressive disease. Novel strategies capable of eliminating minimal residual disease (MRD) are urgently needed. Generating cell-surface-directed therapies that recognize cell membrane proteins present or upregulated upon TKI adaptation remain underdeveloped in the HER2 space due to lack of cell surface dynamic characterization.
Methods: HER2-mutant NSCLC cell lines were treated with zongertinib at varying doses to establish sensitivity values (CellTiter-Glo). A HER2-mutant, zongertinib-insensitive small cell lung cancer line (H446) served as a negative control. Total and cell surface expression of targetable receptors and markers amplified in lung cancers were quantified by western blot and flow cytometry in both, TKI-naïve and TKI-tolerant states (IC50 and IC90 zongertinib exposure). HER2-driven (TKI sensitive and resistant) and control lines were then treated with cell-surface-directed therapies for 24 hours and evaluated for their toxicity.
Results: We demonstrate that HER2-mutant NSCLC cell lines retained demonstrated dynamic changes in cell surface protein expression in treatment-naïve versus zongertinib-induced MRD states. TKI-sensitive and TKI-resistant HER2-driven lines demonstrated high sensitivity to therapies targeting surface proteins, which correlated with their level of expression.
Conclusions: HER2-driven NSCLC cell lines present dynamic changes in cell surface proteins when undergoing TKI treatment. These proteins can be successfully targeted to eradicate residual NSCLC after TKI treatment, supporting this avenue as a rational therapeutic strategy for eradicating MRD and preventing relapse in HER2-mutant NSCLC. Ongoing studies will inform advancement toward early-phase clinical trials with curative intent.

#3167 Preclinical efficacy of a first-in-class anti-ALCAM ADC in hard-to-treat solid and hematologic malignancies.

Qinhong Ma, Daizong Li, Kewei Zhao, Mary Q. Xu, Mason Lu

MedAbome, Inc., Fremont, CA

ALCAM (CD166) is a type I transmembrane glycoprotein that mediates cell-cell adhesion through homophilic ALCAM-ALCAM and heterophilic ALCAM-CD6 interactions. ALCAM is aberrantly overexpressed across a variety of solid and hematologic malignancies. Using our proprietary live-cell immunization (LC-I) and high-throughput screening (LC-HTS) platforms, we developed MAb52-29.1, an anti-ALCAM monoclonal antibody that selectively recognizes a tumor-restricted conformational epitope of ALCAM, exhibiting minimal or no cross-reactivity with normal cells or tissues. Both the chimeric and humanized versions of MAb52-29.1 exhibited high binding affinities to recombinant ALCAM-ECD ($K_D \approx 1.1$ nM). MAb52-29.1 cAb, containing two point-mutations in each Fc, was conjugated to MMAE through an MC-Vc-PAB linker to produce MAb52-29.1-ADC (DAR4). MAb52-29.1-ADC demonstrated potent antiproliferative effects *in vitro*, with cytotoxicity correlating with its high antibody internalization efficiency in various cancer cell lines. Anti-tumor efficacy was demonstrated by a single intraperitoneal (*i.p.*) dose of MAb52-29.1-ADC at 4, 7, or 10 mg/kg using cell line-derived xenograft (CDX) mouse models of triple-negative breast cancer (TNBC), non-small cell lung cancer (NSCLC), gastric cancer (GC), and other tumor types, with subcutaneously inoculated tumors disappearing within 27~30 days after treatment. Preliminary toxicology studies indicated that MAb52-29.1-ADC did not raise any safety concerns. These findings support MAb52-29.1-ADC as a promising therapeutic candidate for treating solid and hematologic malignancies, and potentially mitigating toxicity concerns. Ongoing studies aiming to support further clinical investigation include MAb52-29.1-ADC in patient-derived xenograft (PDX) gastrointestinal (GI) cancer models, along with retrospective analyses of its target expression in clinical tumor samples.

#3168 Fully human anti-HER-2 antibodies to HER-2 domains distinct from trastuzumab as antibody drug conjugates for tumor growth inhibition.

Ginette Serrero[1], Jianping Dong[2], Jun Hayashi[3]

[1]A&G Pharmaceutical, Inc., Columbia, MD,[2]A&G Pharmaceutical, Columbia, MD,[3]Precision Antibody, A&G Pharmaceutical, Columbia, MD

HER2 is a receptor overexpressed in several cancers with prognostic and predictive implications as it is associated with shorter disease-free and overall survivals, resistance to hormonal agents and increased risk of brain metastasis. Trastuzumab is a humanized anti-HER2 neutralizing monoclonal antibody binding to domain IV of HER2 extracellular region. While first FDA approved as a naked antibody, it is at the basis of the development of several antibody drug conjugates bearing different linker and payloads such Ado-Trastuzumab-Emtansine (Kadcyla) and fam-trastuzumab-deruxtecan-nhki (Enhertu). Thus, it would be interesting to develop antibodies to different domains of Her2 which could be used as ADCs as an alternative or even potentiators of trastuzumab based ADCs. We are reporting here the development of fully human internalizing anti-Her2 antibodies that bind to HER2 domain distinct from domain IV, the trastuzumab binding site. These antibodies have been developed by immunizing humanized transgenic mice with recombinant Her2 protein. The screening process included inhibition of binding of trastuzumab to Her2 by enzyme linked immunoassay and by Octet epitope binning as well as internalization assay. Several internalizing antibodies not competing with trastuzumab and with high affinity (Kd ranging from 10^{-9} M to 10^{-12} M) were selected. Their applications as antibody drug conjugates were examined with several HER2 overexpressing breast and gastric cancer cells. Two trastuzumab noncompeting antibodies were further characterized for their ability to inhibit proliferation in vitro and in vivo in mouse xenografts studies and to potentiate trastuzumab effect. Our data also demonstrates that the use of fully human mice constitutes a powerful approach to develop fully human monoclonal antibodies against cancer targets allowing to by-pass the need for humanization and affinity maturation of antibodies.

#3169 Development of conformation selective ITGB6 ADC.

Xiaofei Zhou, Huijie Zhao, Liuge Gu, Guoping Jiang, Wenkai Zhao, Jiangbo Song, Teddy Yang, Ying Lei, Li Tong, **Fei Peng**

Hongcheng Biopharma, Shanghai, China

Integrin β6 (ITGB6), an epithelial receptor upregulated in fibrotic diseases and epithelial-derived cancers, drives tumor progression by regulating immunosuppression, therapeutic resistance, and metastatic processes. Conventional antibodies lack conformational specificity, often resulting in on-target, off-tumor toxicity. To address this, we developed HC029, a novel activation-state-selective anti-ITGB6 monoclonal antibody and antibody-drug conjugate (ADC) designed to specifically target disease-specific ITGB6 conformation while sparing physiological state ITGB6 unaffected. HC029 binds to a unique conformational epitope exposed on activated ITGB6, achieving 100-fold selectivity for disease-specific ITGB6. Binding affinity increases proportionally with disease severity, as demonstrated by enhanced HC029 ITGB6 engagement in the presence of cancer associated fibroblast (CAF) and latency-associated peptide (LAP) predominantly present in tumor microenvironment. HC029 demonstrated weak and partial inhibition on pathological ITGB6 signaling pathway while preserving physiological ITGB6 function. Furthermore, HC029 incorporates an Fc-silenced human IgG1 which further mitigates off target toxicity. HC029 conjugated with camptothecin derivatives (HC029-CPT) retains ITGB6 conformation-dependent binding, selectively kills cancer cells in the presence of CAF and LAP while sparing cells under physiological conditions. In vivo, HC029-CPT demonstrated potent antitumor activity across multiple PDX and CDX *in vivo* models including NSCLC, HNSCC, and BLCA, with no significant weight loss or severe toxicity observed. Exploratory pharmacokinetic and toxicology studies in non-human primate demonstrated that HC029-CPT has a maximum tolerated dose (MTD) exceeding 60 mg/kg, with no drug-related mortality observed. Comprehensive evaluations revealed no significant hematological, biochemical, coagulation, or histopathological abnormalities in potential target organs. HC029-CPT exhibited typical ADC pharmacokinetics in cynomolgus monkeys, with dose-proportional exposure of the intact ADC, total antibody, and payload. The linker-payload was highly stable in both *in vitro* and *in vivo* studies, with minimal payload release (<0.0001%) from the ADC in plasma. Combining ITGB6 disease state selectivity, unique conformational epitope, effector null Fc, extra stable linker payload and safety profile, HC029-CPT expects to achieve a much broader therapeutic window compared to conventional ITGB6 ADC targeting therapeutics.

#3170 Combination of CDK4/6 inhibitory and anti-hypoxia miRNA-6883 lipid nanoparticles with ferroptosis inducers or MEK inhibitors in preclinical breast and colorectal cancer models.

Connor Purcell[1], Leiqing Zhang[1], Maryam Ghandali[1], Shulan Holmes-Farley[1], Audrey Yimin Su[1], Anais Sidonia[1], Ameen Raissi[1], Mackenzie Barrette[1], Emile Youssef[2], Theresa M. Raimondo[1], Wafik S. El-Deiry[1]

[1]Brown University, Providence, RI,[2]SMURF Therpeutics, Providence, RI

Introduction

MicroRNA 6883-5p (miR-6883) inhibits cancer proliferation and hypoxia signaling by silencing the cyclin-dependent kinases CDK4/6, inducing downstream degradation of Hypoxia-Inducible Factor 1α (HIF1α). Prior work demonstrated that CDK4/6 inhibition (CDK4/6i) induces HIF1α degradation through a VHL-independent mechanism via the E3 ubiquitin ligase SMURF2. Notably, several preclinical studies have reported synergy between CDK4/6i and MEK inhibition (MEKi). Others have reported that CDK4/6i sensitizes cancer cells to ferroptosis inducing agents, though this observation is not unequivocally supported and may be context-dependent. Here, we investigate combinations of miR-6883 lipid nanoparticles (LNPs) with MEKi or ferroptosis inducers using in vitro assays and in vivo murine xenograft models.

Methods

A hypoxia response element (HRE)-driven reporter (Addgene #118706) was transduced into HCT116 colorectal carcinoma and SK-BR-3 HER2+ breast cancer (BC) cells. For in vivo experiments, 2 million HCT116-HRE cells were injected subcutaneously into nude mice and tumors ≥150mm3 were treated with 0, 1, or 10μg LNP-encapsulated miRNA. For viability assays, 4,000 cells/well were plated and allowed to adhere overnight. 48-72h after treatment, viability was assessed by CellTiter-Glo®. In vitro hypoxia experiments were conducted in a 0.5% O2 hypoxia workstation.

Results

As a single agent, miR-6883 LNPs significantly attenuated HIF signal in the HCT116-HRE xenograft model, with a 94.3% reduction in luminescence observed 3 days post-treatment with 1μg miR-6883 compared to baseline. Ki67 was significantly reduced with a 10μg dose, supporting the antiproliferative activity of miR-6883. In vitro, the SK-BR-3-HRE model demonstrated a significant reduction in HIF activity with miR-6883 treatment under 0.5% O_2, suggesting that the anti-hypoxia effect of miR-6883 extends to BC. In vitro viability assays were conducted in HCT116 (colorectal), SK-BR-3 (HER2+), MCF-7 (ER+), MDA-MB-231 (triple-negative), and MDA-MB-468 (triple-negative). Combination of small-molecule CDK4/6i and ferroptosis inducers (RSL3 or erastin) or MEKi (trametinib) revealed largely positive synergy scores. Accordingly, miR-6883 LNPs sensitized cells to doses of RSL3, erastin, or trametinib that were ineffective as monotherapies.

Conclusions

Our data support the anti-hypoxia and antiproliferative activity of miR-6883, and provide a basis for combination therapies with ferroptosis inducers or MEKi. Future experiments will employ BC xenografts and assess long-term tumor growth inhibition of combination therapies.

#3171 Multitargeted kinase inhibitor LCI139 overcomes chemotherapy resistance in patient-derived non small cell lung cancer organoids by harnessing intrinsic and extrinsic apoptosis.

Anna Ivanina Foureau[1], Nadeem Wajih[2], Cody C. McHale[3], Hailey L. Dryden[4], Sara Muhiczukic[2], Dhananjaya Pal[1], Bharath Yada[1], David Foureau[1], Fei Guo[1], Raj Dhupar[5], Donald Durden[1], Konstantinos Votanopoulos[4], Shay Soker[6], Eleftherios Markis[2], Kathryn Mileham[3]

[1]Atrium Health, Charlotte, NC,[2]Wake Forest Organoid Research Center, Wake Forest Institute of Regenerative Medicine, Wake Forest School of Medicine, Winston Salem, NC,[3]Levine Cancer Institute, Charlotte, NC,[4]Wake Forest University, Winston-Salem, NC,[5]Wake Forest Institute of Regenerative Medicine, Wake Forest School of Medicine, Winston Salem, NC,[6]Wake Forest Organoid Research Center, Wake Forest Institute of Regenerative Medicine,, Wake Forest School of Medicine, Winston Salem, NC

Introduction: In-silico designed multitarget inhibitor LCI139 (PI3K-CDK4/6-CDK9-AURKA/B) was engineered to overcome resistance inherent to single-target agents by simultaneously targeting tumor metabolism and inducing robust apoptosis. This compound demonstrated nanomolar potency against NSCLC in vitro. We evaluated efficacy in NSCLC cell lines and patient-derived tumor organoids (PTOs)—biofabricated spherical constructs recapitulating cellular matrix of native tumor tissue.
Methods: NSCLC cell lines (NCI-H1703, NCI-H1781) and PTOs generated from unsorted lung tumor suspensions in PEPGEL matrix (n=7) were utilized under IRB-approved protocol. Treatments included LCI139 (0.25-1μM), chemotherapeutics (carboplatin, gemcitabine, pemetrexed, cisplatin), and single-agent inhibitors: PI3K (Buparlisib), CDK4/6 (Ribociclib), CDK9 (AZD4573), AURKA (Barasertib), AURKB (Alisertib). Cell lines were co-treated with inhibitors of (carbenoxolone), Caspase (Casp)-8 (Z-IETD-FMK), Casp-9 (Z-LEHD-FMK), or AMPK activator (PF-06409577). Viability (propidium iodide, CellTiter-Glo), cell cycle (DNA dye) and apoptosis (Annexin-V/7-AAD, Casp-3/7/8/9 activity) were measured. Target inhibition was evaluated immunoblotting for pAkt, pRb, pRNA Pol II, MCL-1, pAMPK, pFOXO3, and p53.
Results: LCI139 achieved nanomolar IC_{50} against H1703 cells (48hr) and demonstrated dose-dependent PTO cytotoxicity: 49% reduction at 0.25μM, 62% at 0.5μM, 78.4% at 1μM (all $p<0.0001$). By comparison, 1 μM single-agent inhibitors reduced PTO viability by: AURKA (34%), AURKB (24%), PI3K (29%), CDK9 (50.9%) all $p<0.0001$; CDK4/6 (6.9%, $p=0.43$). LCI139 overcame significant carboplatin resistance (IC_{50}: 10.25-11.69μM) and outperformed standard chemotherapeutics: gemcitabine (29.2%), cisplatin (28.2%), pemetrexed (no activity). LCI139 activated caspases 8, 9, 3/7 in cells and PTOs. Selective Casp-8 or Casp-9 inhibition diminished but didn't abrogate cytotoxicity. Western blotting confirmed dose-dependent target inhibition: decreased pAKT, pRb, MCL-1, pRNAPol II, and p53 modulation. LCI139 induced metabolic stress via pAMPK-pFoxO3 activation. FoxO3 inhibition diminished LCI139 potency against sensitive H1703 cells. AMPK activation enhanced potency in p53-proficient H1703 and sensitized p53-deficient H1781 cells.
Conclusions: LCI139 demonstrates superior anti-tumor activity versus standard chemotherapeutics in resistant NSCLC through dual activation of intrinsic (cell cycle arrest-induced) and extrinsic (metabolic stress-induced) apoptotic pathways. Efficacy in both cell lines and PTOs validates this micro-physiological platform for drug development, supporting translational potential of multitargeted kinase inhibition for overcoming therapeutic resistance, as aligned with FDA guidance.

#3172 XYD-8006: A novel ADAM9-targeting dual-payload ADC demonstrates superior preclinical efficacy in gastrointestinal and lung cancer models.

Weng Hang Ho, Pengfei Rong, Mengrui Zhao, Jun Li, Xidong Zhang, Hui Ding, Fangxing Ouyang

FDC Biotech, Kunshan, China

Background: A Disintegrin And Metalloproteinase 9 (ADAM9) is a cell surface protease implicated in growth factor shedding, integrin binding, and cell migration, processes critical for tumor progression, metastasis, and neovascularization. Its overexpression is correlated with poor prognosis in multiple solid tumors, and overexpressed in GI and lung cancers but limited in normal tissues, highlighting its potential as a therapeutic target. While Antibody-Drug Conjugates (ADCs) represent a transformative oncology modality, single-payload ADCs face limitations including, tumor heterogenecity, the emergence of payload resistance such as DXD/SN38. To address this, we developed XYD-8006, a ADAM9-targeting ADC equipped with dual-payload platform designed to enhance efficacy and overcome tumor heterogenecity and DXD/SN38 resistance.
Methods: XYD-8006, a humanized anti-ADAM9 IgG1 monoclonal antibody conjugated with high hydrophilic linker to two distinct potent payloads: a microtubule inhibitor and a topoisomerase I inhibitor, with a controlled and specific Drug-to-Antibody Ratio (DAR). The molecule was evaluated for specificity, internalization efficiency, and in vitro/in vivo efficacy across a panel of ADAM9-high, -medium, and -low expressing tumor models.
Results: XYD-8006 exhibited high specificity for ADAM9 with no observed cross-reactivity to paralog family members and demonstrated superior internalization efficiency. In vitro and in vivo study showed, XYD-8006 induced potent, synergistic tumor cell killing, significantly outperforming single-payload ADC controls. Notably, it achieved robust tumor growth inhibition and regression not only in ADAM9-high models but also in models with medium and low ADAM9 expression. XYD-8006 exhibited potent ADAM9-targeted cytotoxicity and tumor suppression, with a favorable pharmacokinetic and safety profile.
Conclusion: XYD-8006 was designed to overcome key limitations of current ADC therapies. Its promising preclinical efficacy across gastrointestinal and lung cancers supports its further development, with an expected entry into clinical study in 2026.

#3173 XYD-295 and XYD-338: Novel hydrophilic site specific linker platform enables next generation dual payload ADCs with enhanced efficacy and safety.

Weng Hang HO[1], Pengfei Rong[1], Mengrui Zhao[1], Jun Li[1], Xidong Zhang[1], Hui Ding[1], Fangxing Ouyang[1], Jun Wang[2], Jiangcheng Xu[2], Yang Liu[2], Jiawang Liu[2], Kyoungwoo Lee[2]

[1]FDC Biotech, Kunshan, China,[2]Beijing Hanmi Pharm. Co., Ltd., Beijing, China

Background: The therapeutic potential of Antibody-Drug Conjugates (ADCs) is often limited by linker technology. Conventional hydrophobic linkers usually lead to ADC aggregation, rapid plasma clearance, and undesired cleavage in blood and normal tissues. We have developed a novel linker platform to overcome these challenges, enabling the construction of more stable, homogenous, and efficacious ADCs, including dual-payload formats.

Methods: Our ADC platform was designed to have: 1) High stability to minimize undesired payload release; 2) High hydrophilicity to improve solubility, and reduce the formation of aggregates; and 3) Efficient enzymatic cleavage and release of potent payload within the tumor. This linker was site-specifically conjugated to antibodies targeting diverse antigens (including DLL3, PD-L1, ADAM9, B7H3, EGFR, and cMET) and equipped with potent payloads such as microtubule inhibitor and a topoisomerase I inhibitor, individually or in dual-payload formats.

Results: ADCs generated with this novel linker demonstrated superior stability in plasma and significantly slower clearance rates compared with ADCs with conventional linkers. These improved pharmacokinetic profiles were translated into stronger anti-tumor efficacy in multiple animal models. XYD-295 with TOP1 inhibitor payload, XYD-338 with microtubule inhibitor payload and the dual-payload format, all showed enhanced and synergistic tumor killing in vitro and in vivo. Furthermore, this designed linker supported a higher drug load with reduced aggregation, and improved safety profile in preclinical studies, suggesting a higher therapeutic index. Several ADCs based on XYD-295, XYD-338 and the dual-payload format were expected entry into clinical study in 2026.

Conclusion: XYD-295 and XYD-338 facilitates the construction of more stable, homogenous, and efficacious ADCs, including dual-payload formats

#3174 Nuvisertib (TP-3654) and Dordaviprone (ONC201) synergize to reduce renal cell carcinoma cell viability.

Kimberly S. Meza[1], Sheldon L. Holder[2], Wafik S. Deiry[1]

[1]Legorreta Cancer Center, Brown University, Providence, RI,[2]Hematology/Oncology, Trinity Health Grand Rapids, Grand Rapids, MI

The Incidence of renal cell carcinoma (RCC) continues to increase in the United States, ranking among the ten most frequently diagnosed cancers in men and women. Unfortunately, resistance to existing treatments remain a major obstacle, driving the need for identification of clinically relevant biomarkers and therapeutic targets. TNF-related apoptosis inducing ligand (TRAIL) is a promising cancer therapy that selectively induces apoptosis in malignant cells while sparing normal cells. TRAIL exerts its cytotoxic effects through binding death receptors DR4 and DR5, initiating caspase dependent programmed cell death. However, intrinsic and acquired resistance mechanisms have limited TRAIL's efficacy as anti-cancer strategy. We have identified a link between the overexpression of oncogenic PIM kinases and regulation of DR5 expression and sensitivity to TRAIL apoptosis in RCC. PIM1 is emerging as a clinically relevant biomarker and therapeutic target in RCC. Nuvisertib (TP-3654) is a selective PIM1 kinase inhibitor currently being evaluated in Phase 1/2 clinical trials for patients with myelofibrosis and has received FDA fast track designation. We find that treatment of RCC cells with low dose (2.5 μM) of Nuvisertinib over 24 hours induces a 5.75-fold ($p<0.01$) increased mean membrane expression of DR5 compared to vehicle control assessed by flow cytometry. We also investigated synergism between Nuvisertib and Dordaviprone, a newly FDA approved imipridone and TRAIL inducer. We evaluated combinations of Nuvisertib and Dordaviprone via Cell Titer Glo in RCC cells and find that combination indices indicate synergism which significantly reduce RCC cell viability more potently than either agent alone. Our findings highlight actionable novel candidate targets and strategies for therapeutic intervention in RCC. Ongoing studies are aimed to uncover mechanistic insights of these treatments in RCC and guide the development of optimal treatment strategies.

#3175 Comparative efficacy of MUC1-C (XYA02) and MUC1-N (PankoMab, DS-3939a analog) antibody-drug conjugates in preclinical NSCLC.

Surender Kharbanda[1], Rehan Ahmad[1], Changchuin Mao[1], Sourav Choudhary[2], Brian Lawney[1], Govind Panchamoorthy[1], Ravi Jasuja[1]

[1]R&D, Xyone Therapeutics Inc., Canton, MA,[2]Birla Institute of Technology and Science, Hyderabad, India

Background: Aberrant glycosylation and elevated expression of MUC1 are common in non-small cell lung cancer (NSCLC), in which the two domains of the MUC1 heterodimer—MUC1-N, the shed extracellular subunit, and MUC1-C, the membrane-anchored oncogenic subunit—serve as therapeutically relevant yet biologically distinct targets. PankoMab-Dxd (DS-3939a analog) is an antibody-drug conjugate (ADC) directed against MUC1-N glycoepitopes, whereas XYA02 is a next-generation ADC targeting the transmembrane MUC1-C subunit that remains tumor anchored and is involved in numerous tumor survival signaling pathways. A direct comparison of these two targeting strategies reveals unique insights into the relative potency of drugs aimed at different MUC1 domains.
Methods: We assessed antigen density, internalization, in vitro cytotoxicity and in-vivo antitumor efficacy of NSCLC cell lines. ADCs (XYA02 and DS-3939a analog) were evaluated using proliferation assays, apoptosis induction, and in vivo tumor growth inhibition studies. Safety of XYA02 in nude mice was assessed by monitoring the body weight, CBC, hematologic parameters and vital organ histology.
Results: High-affinity binding of anti-MUC1-C monoclonal antibody (MAb)* was observed across multiple NSCLC cell lines endogenously expressing MUC1. At 4°C, robust cell-surface binding was detected, and shifting to 37°C resulted in efficient receptor internalization, consistent with productive ADC trafficking. Incubation of NSCLC cell lines with increasing concentrations of the MUC1-C-targeting ADC (XYA02) produced potent, dose-dependent cytotoxicity with low-nanomolar IC_{50} values. In contrast, treatment of the same models with a DS-3939a analog, which targets the shed MUC1-N subunit, resulted in markedly higher IC_{50} values.In vivo, XYA02 achieved durable tumor regressions in both NSCLC CDX and PDX models, whereas the DS-3939a analog produced variable responses. Both ADCs were well tolerated; however, XYA02 demonstrated a superior therapeutic index, with greater efficacy at comparable administered doses.
Conclusions: Our findings demonstrate that targeting the membrane-tethered MUC1-C subunit with XYA02 provides superior antitumor efficacy compared with MUC1-N-directed DS-3939a analog in preclinical NSCLC models. Enhanced efficacy appears to be driven by uniform antigen binding and potential avoidance of MUC1-N-mediated antigen sink effects. These data support prioritizing MUC1-C-selective ADCs for clinical development in NSCLC and other MUC1-driven malignancies.*
https://patents.google.com/patent/US20230265208A1/en

#3176 Tumor-selective regression through MUC16-guided DR5 (TNFRSF10B) clustering by the bispecific anti-MUC16×anti-DR5 antibody IMV-M™.

Iosif M. Gershteyn[1], Viktor Goldmakher[2]

[1]ImmuVia Inc., Cambridge, MA,[2]

Background

IMV-M, a bispecific anti-MUC16×anti-DR5 antibody, previously showed potent MUC16-selective antitumor activity *in vitro* and in xenograft models without requiring secondary crosslinking. In a pilot non-human-primate study, repeated 10 and 20 mg/kg dosing produced no detectable toxicity. Here, we demonstrate that IMV-M induces clustering of death receptor 5 (DR5; TNFRSF10B) through a novel MUC16-dependent mechanism: assembly of multiple IMV-M molecules on a single MUC16 molecule. IMV-M also lacked cytotoxicity toward hepatic cell lines.

Methods

Three bispecific antibodies sharing identical anti-DR5 arms were generated: Sofituzumab (h5A3)×Lexatumumab scFv, 11D10/DR5×Lexatumumab scFv, and (anti-fluorescein)×Lexatumumab scFv. Sofituzumab recognizes multiple tandem repeats within human MUC16, whereas 11D10 binds a single non-repetitive epitope. The anti-fluorescein construct, which does not bind human cells, served as a negative control. Binding to MUC16 was evaluated by (i) ELISA with shed MUC16 and (ii) flow cytometry using MUC16-positive cells. Cytotoxicity was assessed by CellTiter-Glo after 48h exposure.

Results

IMV-M bound shed MUC16 ≈11-fold and cell-surface MUC16 ≈8-fold more strongly than 11D10/DR5 at saturation, while apparent affinities were similar. Only IMV-M induced cytotoxicity in MUC16-positive PK-59 cells, demonstrating that MUC16-mediated clustering of DR5 is required for apoptosis. In hepatocyte-derived HepG2 and Hep3B cells ($MUC16^{-}/DR5^{+}$), IMV-M showed no cytotoxicity, whereas $MUC16^{+}/DR5^{+}$ OVCAR-3 cells were highly sensitive across all concentrations. Secondary crosslinking did not elicit killing in MUC16-negative cells. These findings indicate a low risk of off-target hepatic toxicity, consistent with the benign safety profile of earlier anti-DR5 antibodies.

Conclusions

Effective DR5 agonism by bispecific antibodies requires high-order receptor clustering. IMV-M achieves this through MUC16-mediated assembly of multiple antibody molecules on a single MUC16 molecule, enabling potent, tumor-selective apoptosis without hepatotoxicity.

#3177 JM.

Jeong-Yeon Mun[1], Chang Shu[1], Emily Hsia[2], Mike-Andrew Westhoff[3], Georg Karpel-Massler[4], Markus David Siegelin[1]

[1]Department of Pathology and Cell Biology, Columbia University Irving Medical Center, New York, NY,[2]The Cooper Union for the Advancement of Science and Art, New York, NY,[3]Department of Pediatrics and Adolescent Medicine, Ulm University Medical Center, Ulm, Germany,[4]Department of Neurosurgery, Ulm University Medical Center, Ulm, Germany

Background: Resistance to mitochondrial apoptosis contributes to treatment failure in IDH-wildtype glioblastoma (GBM). Cyclin-dependent kinase 12 (CDK12) regulates transcriptional programs that sustain tumor survival, but its role in apoptotic control is largely unclear.
Methods: CDK12 was inhibited in GBM patient-derived xenografts, stem-like cells, and established lines by genetic depletion or the small-molecule SR-4835. Bcl-xL was targeted using the BH3 mimetic ABT-263 (navitoclax). Viability, apoptosis, and mechanistic endpoints were assessed by combination index analysis, caspase activity, immunoblotting, and gene silencing.
Results: Co-treatment with SR-4835 and ABT-263 produced a synergistic loss of viability across GBM models (combination index <0.5), whereas either agent alone had minimal effects. This synergy was associated with enhanced cleavage of initiator and effector caspases and was fully rescued by the pan-caspase inhibitor zVAD-fmk, confirming caspase-dependent apoptosis. Mechanistically, CDK12 blockade downregulated the anti-apoptotic protein Mcl-1 and induced the pro-apoptotic BH3-only protein Noxa through activation of an ATF4-driven integrated stress response (ISR). Silencing ATF4 blunted SR-4835-induced Noxa expression, and Noxa knockdown significantly reduced apoptosis triggered by the combination, demonstrating its essential role in the response.
Conclusions: CDK12 inhibition activates an ISR-ATF4-Noxa signaling axis that lowers the apoptotic threshold and sensitizes GBM cells to Bcl-xL inhibition. Dual targeting of CDK12 and Bcl-xL represents a mechanistically defined strategy to overcome apoptosis resistance in GBM and may have broader therapeutic relevance across malignancies driven by Mcl-1-mediated survival.

#3178 Antifolate ADCs, a novel linker-drug platform for targeted therapy with a clear differentiating mechanism of action.

Ronald C. Elgersma, Renier C. Heijkants, Eline M. Loosveld, Noortje Veen, Chiel A. J. van der Horst, Iris van de Wetering, Arne J. Bramer, Erik Swiers, Tijl Huijbregts, Mike M. Ruth, Monique van der Vleuten, Gerard J. A. Rouwendal, Miranda M. C. Van der Lee, Benno Ingelse, Patrick H. Beusker, **Wim H. A. Dokter**

Byondis B.V., Nijmegen, Netherlands

Background: Clinical resistance to dominant ADC payloads - topoisomerase-I inhibitors and tubulin inhibitors - is increasing, underscoring the need for novel payloads with a differentiated mechanism of action (MoA). Methotrexate (MTX), a pioneering antifolate, revolutionized oncology and autoimmune disease treatment but suffers from poor tumor selectivity and systemic toxicity. Despite its clinical validation, MTX and related antifolates have not been successfully adapted into targeted therapies. Byondis revisited the class of antifolates and optimized these to a proprietary novel linker-drug platform currently in IND-enabling studies.
Results: Byondis developed a first-in-class antifolate linker-drug platform, featuring optimized payloads with a low- to sub-nanomolar potency and suitable for linker coupling. The resulting optimized payload demonstrates potent inhibition of dihydrofolate reductase (DHFR), *in vitro* cytotoxicity in a broad panel of cell lines, minimal affinity for resistance-associated transporters (BCRP, PGP), and favorable physicochemical properties allowing for the ongoing GMP-scale up of the linker-drug (LD) and good ADC manufacturability. The selected optimized linker contains a glucuronide moiety with the aim to improve the therapeutic index. The PhysChem properties of the LD demonstrates / ensures minimal impact on ADC hydrophobicity after conjugation and perfectly allows its use in a future dual payload approach. The Byondis' lead antifolate ADC is based on the novel antifolate LD platform. This antifolate ADC is based on a yet undisclosed tumor antigen targeting antibody. It shows strong *in vitro* cytotoxicity across a broad tumor cell-line panel and in a deruxtecan insensitive cell-line. Robust *in vivo* efficacy in NSCLC and HNSCC patient-derived xenograft models is demonstrated, with no significant toxicity at doses resulting in tumor regressions. The antifolate ADC delivers optimal pharmacokinetics and anti-tumor activity. GMP manufacturing of the linker-drug is underway.
Conclusions: The antifolate platform reintroduces a clinically validated MoA into the ADC landscape with enhanced selectivity, potency, and manufacturability. Its orthogonal MoA offers potential across different tumor types including an advantage in overcoming resistance to existing ADCs and supports sequential ADC therapy. With broad applicability across tumor types, antifolate-based ADCs are poised to address unmet clinical needs and are ready for clinical translation.

#3179 Rationale for the development of a differentiated Trop2 ADC in solid tumors of the bladder, lung, and breast.

Satyajit K. Mitra[1], Mastewal Abuhay[1], Mary Do[2]

[1]Akari Therapeutics, Tampa, FL,[2]Mercor, San Francisco, CA

Background: Trop2 is a transmembrane protein that is overexpressed in several solid tumor cancers and is a validated target. Trop2 ADCs are approved in TNBC, Her2- HR+ metastatic breast cancer, and 2nd line EGFR-mutated NSCLC in US, China, or Japan. PH1 is a unique immunomodulatory payload targeting the spliceosome and has been used as a platform to generate a Trop2 PH1 ADC and other pipeline ADCs with differentiated preclinical efficacy and safety profiles[1,2,3]. Following significant characterization and derisking of the Akari Trop2 ADC program, the clinical candidate, AKTX-101, is progressing for IND-enabling studies.

Results: Previously, a 75-cell line screen was performed and Trop2 PH1 ADC demonstrated single digit nanomolar (nM) IC50 potency in 8 solid tumor indications *in vitro*[2]. In follow-up experiments, AKTX-101 was tested alongside first-in-class approved Trop2 ADCs and compared with Standard-of-care targeted therapy in these models to identify an advantageous niche for the clinical development of AKTX-101 (Table 1). As AKTX-101 exhibited nM IC50 potency in all urothelial models tested (5/5), and since the PH1 payload is known to synergize with anti-PD-1, the ADC was tested plus/ minus checkpoint inhibitor in a syngeneic MB49 mouse model of urothelial cancer overexpressing human Trop2. Sequential dosing of ADC followed by mPD-1 demonstrated synergy whereas concomitant dosing was associated with additive anti-tumor efficacy.

Conclusion: Our results support the clinical development of AKTX-101 in bladder cancer and in other solid tumor niches. These niches will be explored further in planned translational studies.

References:

1. Mitra SK. 951 A novel splicing-targeted ADC payload drives immune activation, synergy with checkpoint inhibitors, and enhanced therapeutic potential beyond cytotoxicity. Journal for ImmunoTherapy of Cancer. 2025; 13:.

2. *Cancer Res* (2023) 83 (7_Supplement): 6297 3. AACR; Cancer Res 2021;81(13_Suppl): Abstract nr 1832

Table 1:

Table 1: AKTX-101 vs SOC, where a=Enfortumab vedotin, b= Daraxonrasib, c=Trastuzumab deruxtecan

Indication	Driver mutation	Cell line	Metric	AKTX-101	Standard of care
Bladder	FGFR3 fusions	RT112/84	IC50 (nM)	0.30	19.47[a]
		RT112/84	Maximum kill (%)	93.6	94.3[a]
Bladder	FGFR3 fusions	RT4	IC50 (nM)	1.10	68.76[a]
		RT4	Maximum kill (%)	83.5	53.7[a]
Bladder	FGFR3 fusions	SW-780	IC50 (nM)	0.26	61.76[a]
		SW-780	Maximum kill (%)	87.0	61.9[a]
Lung	Kras G12V	NCI-H441	IC50 (nM)	0.43	13.12[b]
		NCI-H441	Maximum kill (%)	69.8	56.4[b]
Lung	BRAF G466V	NCI-H1666	IC50 (nM)	0.07	
		NCI-H1666	Maximum kill (%)	90.0	
Lung	SMARCA4 deletion	NCI-H2126	IC50 (nM)	0.43	
		NCI-H2126	Maximum kill (%)	75.1	
Breast	Different sensitivity to Top1 agents, Her2 amplification	HCC 1954	IC50 (nM)	0.39	3.06[c]
		HCC 1954	Maximum kill (%)	80.2	52.5[c]
Breast	Trastuzumab resistant, Her2 amplification, HR- negative, PIK3CA, TP53 mutations	JIMT-1	IC50 (nM)	0.35	N.A.[c]
		JIMT-1	Maximum kill (%)	89.6	11.8[c]

#3180 ATL-024, a novel topoisomerase I-based ADC targeting the tumor-specific glycopepitope CA242 (CanAg), demonstrates potent activity in colorectal and pancreatic cancer models, and excellent safety profile.

Warren Viricel, Edouard Leroy

Antelope Therapeutics, Lyon, France

CA242 (also known as CanAg) is a tumor-associated carbohydrate antigen that is aberrantly expressed by gastrointestinal solid tumors but is virtually absent from normal tissue. In particular, this glycopepitope is highly expressed in colorectal, pancreatic and gastric tumors (high prevalence and elevated number of copies per tumor cell). Previous clinical trials in the early 2000s showed that CA242 can be safely targeted with an antibody-drug conjugate (ADC), as no significant CA242-related off-tumor toxicities were reported. The modest clinical benefit seen with microtubule inhibitor payloads indicates that alternative payloads, such as topoisomerase-I inhibitors, may enhance therapeutic outcomes in CA242-positive tumors.To exploit CA242 differential expression, we developed a novel CA242-targeting ADC called ATL-024, which is comprised of an anti-CA242 humanized Fc-silenced monoclonal antibody conjugated to the topoisomerase I inhibitor exatecan via a dipeptide cleavable linker. This ADC is a homogeneous construct with a drug-to-antibody ratio (DAR) of 4.ATL-024 demonstrated potent antitumor efficacy in multiple colorectal and pancreatic cancer PDX models showing homogeneous or heterogeneous CA242 expression patterns (as determined by IHC), being effective at doses as low as 3-6mg/kg. Compared to previous cantuzumab-DM4 based ADC (microtubule inhibitor payload), ATL-024 exhibits significantly stronger in vivo anti-tumor activity in colorectal PDX models.In a pilot toxicology study in cynomolgus monkeys, ATL-024 was well tolerated up to 80 mg/kg (Q3W), which was established as the highest non-severely toxic dose (HNSTD). At this dose, findings were limited to mild and reversible hematologic changes in one animal, with normal clinical chemistry parameters, no severe clinical signs and no observed organ toxicities. Pharmacokinetic profiling showed linear dose-dependent exposure and is consistent with systemic stability of the conjugate.Overall, the preclinical characterization of ATL-024 shows a very favorable therapeutic index and support human clinical evaluation for patients with CA242-expressing gastrointestinal tumors such as colorectal or pancreatic tumors. ATL-024 is currently undergoing IND-enabling development.

#3181 Mutant p53-specific TAZ/TEAD pathway dependency as a therapeutic opportunity for triple-negative breast cancer.

Lydia Sakala, Yining Zhang, Jin G. Park, Joshua LaBaer

Arizona State University, Tempe, AZ

Background: Missense mutations in the TP53 tumor suppressor gene lead to gain-of-function (GOF) properties that affect differently tumor growth, metastasis, and resistance to therapies, but targeting mutant p53 is still a major clinical challenge. Using MCF10A cells expressing 10 prevalent TP53 mutations, we performed integrated phenotypic and molecular analyses to identify targetable genes and pathways in Triple-Negative Breast Cancer (TNBC) harboring specific p53 mutations and discovered TAZ/TEAD dysregulation as the key determinants of cell invasion and drug resistance.
Methods: Based on our previous findings, we measured activation status of TEAD in drug-sensitive and resistant mutant p53-expressing cells and evaluated the differential drug response against single or combination treatment of the TEAD inhibitor GNE-7883 and the standard-of-care, doxorubicin. The TEAD activity was verified with a luciferase reporter, and cell viability was measured with phosphatase assays.
Results: The TEAD-luciferase reporter assay showed that p53 G245S and R273H mutants but not R175H or Y163C had elevated activity of the Hippo pathway effector, TEAD. Treatment of GNE-7883 robustly inhibited the hyper-activation of TEAD specifically in the G245S and R273H cells. In viability assays, these "TEAD-addicted" cells uniquely displayed sensitivity to high dose of GNE-7883 monotherapy (IC_{50} ~2.5 μM). Moreover, they also showed hypersensitivity to doxorubicin (IC_{50} = 14 nM), compared to the cells with wild-type p53 (IC_{50} = 250 nM). We were able to develop a synergistic, low-dose combination regimen (3.5 nM doxorubicin + 0.625-1.25 μM GNE-7883) that was cytotoxic for the cells with G245S and R273H mutants yet had minimal to no activity in the wild-type cells. In contrast, R175H and Y163C mutants were resistant to TEAD inhibition, requiring higher doses of GNE-7883 to observe an anti-cancer activity, emphasizing the selectivity of this vulnerability.
Conclusion: We have established a synthetic lethal interaction between TEAD inhibition for a defined chemo-sensitive subgroup of GOF p53 mutants, G245S and R273H, for which the Hippo/TEAD pathway states appear to be a key dependency. We propose a precision approach to therapeutic strategy of combining low, non-toxic dose doxorubicin with TEAD inhibition to increase efficacy while decreasing toxicity. Our ongoing work is to validate these findings in more physiologically relevant models.

#3182 The FLT3 inhibitor quizartinib suppresses the WT1-driven activation of the KIT-STAT5-PIM signaling pathway and induces apoptosis in FLT3-wild type HL-60 cells.

Hideaki Yamauchi, Naoko Hosono, Takahiro Yamauchi

Department of Hematology and Oncology, Faculty of Medical Sciences, University of Fukui, Fukui, Japan

Background: WT1 (Wilms' tumor 1) is a key transcription factor regulating hematopoietic stem cell self-renewal and differentiation. In acute myeloid leukemia (AML), WT1 overexpression promotes leukemogenesis by blocking differentiation and conferring apoptosis resistance. Although several WT1 targets (*BCL2, c-MYC, IGF2, VEGF*) have been identified, its downstream mechanisms remain unclear. Interestingly, although parental HL-60 cells are FLT3-unmutated and resistant to the FLT3 inhibitor quizartinib, WT1-overexpressing HL-60 cells (HL-60/WT1) exhibited increased sensitivity, suggesting that WT1-induced KIT expression may mediate this effect.

Methods: HL-60/WT1 cells were generated via lentiviral transduction, resulting in a 7.5-fold increase in WT1 mRNA expression compared with parental HL-60 cells. To evaluate drug sensitivity, two complementary assays were employed: apoptosis was assessed after quizartinib treatment (700 nM, 48 h) using Annexin V/PI flow cytometry, while dose-dependent cytotoxicity was quantified by XTT assay following 72-hour exposure to graded concentrations of quizartinib. Expression of *KIT* was measured by RT-PCR, and RNA sequencing was performed to obtain transcriptome-wide profiles and fold-change-based comparisons across conditions, enabling identification of WT1-dependent signaling alterations.

Results: Cell growth was comparable between HL-60 and HL-60/WT1 cells (doubling times: 27.3 h and 23.9 h, respectively). HL-60 cells were unresponsive to quizartinib (IC_{50}, not reached), whereas HL-60/WT1 cells exhibited increased sensitivity (IC_{50} = 665 nM). RT-PCR confirmed KIT expression in HL-60/WT1 but not in parental cells, supporting WT1-driven activation of a *KIT*-mediated signaling pathway. Quizartinib markedly increased apoptosis in HL-60/WT1 cells (30.0 ± 10.1%) but not in parental HL-60 cells (7.0 ± 1.6%; Mann-Whitney U, $p < 0.05$). RNA-seq analysis using fold change revealed that WT1 overexpression increased the expression of KIT (1.2-fold), AKT1 (1.4-fold), STAT5A (5.0-fold), and PIM1 (6.2-fold). Notably, quizartinib treatment reduced these transcripts in HL-60/WT1 cells, indicating suppression of a WT1-induced, KIT-driven survival program independent of FLT3.

Conclusion: These findings demonstrate that WT1 overexpression establishes a previously unrecognized KIT-STAT5-PIM signaling pathway that promotes AML cell survival. Importantly, this pathway creates a therapeutically exploitable vulnerability: HL-60 cells that are normally resistant to quizartinib become sensitized through WT1-induced *KIT* activation. Our study provides mechanistic insight into WT1-mediated leukemogenesis and suggests that KIT-targeted strategies may be effective in subsets of WT1-high, FLT3-unmutated AML.

#3183 NEK7 overexpression contributes to stemness of hepatocellular carcinoma.

Hun-Mo Ryoo[1], Eun-Hye Jeon[2], Taehun Kim[3], Ilseon Hwang[4], Keon Uk Park[3], Yun-Han Lee[2]

[1]Internal Medicine, Daegu Catholic University School of Medicine, Daegu, Korea, Republic of,[2]Molecular Medicine, Keimyung University School of Medicine, Daegu, Korea, Republic of,[3]Internal Medicine, Keimyung University School of Medicine, Daegu, Korea, Republic of,[4]Pathology, Keimyung University School of Medicine, Daegu, Korea, Republic of

Hepatocellular carcinoma (HCC) is one of the cancers with the highest mortality rates worldwide, being the sixth most commonly diagnosed cancer globally and the third leading cause of cancer-related deaths. Growing evidence suggests that tumor initiation can be driven by a cancer stem cell (CSC) subset, which is responsible for tumor persistence, relapse, metastasis, chemo-resistance, and radio-resistance, establishing CSCs as important therapeutic targets. Identification and characterization of functional pathways and biomarkers associated with CSC biology will provide useful information for developing novel treatment strategies against HCC. NIMA Related Kinase 7 (NEK7) is a serine/threonine kinase that plays an important role in regulating gene transcription or protein expression of the NLRP3 inflammasome signaling pathway. We have observed that the expression level of NEK7 is significantly elevated in HCC tissues compared to surrounding normal tissues, therefore, we initially investigated whether NEK7 targeting could suppress HCC proliferation. As expected, siRNA silencing of NEK7 effectively inhibited the growth of HCC cell lines such as Huh7, HepG2, and PLC/PRF/5. Based on the previous report that the treatment of vitamin D suppressed stemness of $CD133^{+}/CD44^{+}$ CSCs by reducing NLRP3 expression in triple-negative breast cancer, we next determined to observe if targeting of NEK7 could suppress the metastatic potential of HCC as well. Inhibition of NEK7 expression reduced the abilities of migration, invasion, and sphere formation of both parental HCC cell populations (of Huh7, HepG2, and PLC/PRF/5) and $CD133^{+}$ liver CSCs (isolated from PLC/PRF/5). Our findings suggest that NEK7 contributes HCC stemness, indicating its potential as a therapeutic target for treating primary HCC and preventing metastasis and/or recurrence.

#3184 HMGB1 mediates chemoresistance and tumor progression in glioblastoma: Implications for targeted therapy.

Sucharita Patra, Shreya Banerjee, Mahitosh Mandal

School of Medical Science and Technology, Indian Institute of Technology Kharagpur, Kharagpur, India

Glioblastoma (GBM) is the most prevalent and lethal primary brain tumor, characterized by rapid progression, high recurrence rates, and a median survival of less than 15 months despite current therapeutic interventions. Standard treatments such as surgical resection, radiotherapy, and temozolomide (TMZ) chemotherapy offer limited benefit due to the infiltrative nature of the tumor and the blood-brain barrier. Moreover, GBM frequently develops resistance to TMZ through O6-methylguanine-DNA methyltransferase (MGMT)-mediated repair of chemotherapy-induced DNA damage, significantly reducing treatment effectiveness. During treatment, GBM cells and the surrounding tumor microenvironment (TME) undergo significant physiological stress, including hypoxia, inflammation, and DNA damage. These stressors induce the release of damage-associated molecular patterns (DAMPs), among which High Mobility Group Box 1 (HMGB1) plays a pivotal role. HMGB1 is a multifunctional nuclear protein that, depending on its redox state and subcellular localization, can regulate tumor proliferation, invasion, angiogenesis, and immune modulation. Accumulating evidence suggests that extracellular HMGB1 contributes to tumor progression and therapeutic resistance through complex interactions with immune and stromal components of the TME. In our present study, we aim to validate the protumorigenic functions of HMGB1 using integrated bioinformatic approaches and in vitro analyses to substantiate its relevance in GBM pathology and therapy resistance. Specifically, we explored the correlation between HMGB1 expression and TMZ resistance, examining its association with MGMT expression and the activation of downstream signaling pathways, such as MEK1/2-ERK1/2. By elucidating these molecular interactions, we aim to clarify the mechanisms through which HMGB1 promotes therapy resistance. Additionally, we performed in-silico screening to identify HMGB1-targeting inhibitory compounds with the potential to concurrently suppress MGMT expression and other crucial components involved in TMZ resistance. Collectively, our findings aim to reinforce the significance of HMGB1 as a prognostic biomarker and therapeutic target, offering new opportunities for more effective and personalized treatment strategies for GBM patients.

#3185 SCR-A019, a first-in-class biparatopic ADC targeting MSLN, with a novel topoisomerase I inhibitor demonstrates encouraging efficacy in preclinical models.

Qiong Wang, Yayuan Fu, Qi Deng, Chunlei Xia, Hui Zheng, Youfu Chu, Renhong Tang

Simcere Zaiming, State Key Laboratory of Neurology and Oncology Drug Development. Simcere Pharmaceutical Group, Shanghai, China

Background: Mesothelin (MSLN) is a GPI-anchored glycoprotein that is expressed on many cancers but limited in normal tissues, which makes it an attractive target for antibody-based cancer therapy. However, MSLN is shed from surface of cells at high levels via proteases that cleave at its membrane-proximal C-terminal region. Shed MSLN accumulates in patient fluids and tumors and can block anti-MSLN antibodies from killing cancer cells. To overcome the challenge of MSLN shedding, we developed a novel biparatopic ADC which prefers binding to membrane MSLN rather than soluble MSLN.
Method & Results: The biparatopic ADC SCR-A019 is conjugated with novel topoisomerase 1 inhibitor (CPT116) via a hydrophilic cleavable linker at DAR 6. SCR-A019 specifically recognizes human MSLN with high affinity and showed enhanced internalization and binding capacity compared to parental monoclonal antibody ADC and benchmark ADC in multiple tumor cell lines. In vitro cytotoxicity experiment demonstrated that SCR-A019 induced tumor cell lysis. Compared to benchmark ADC, SCR-A019 drived potent cytotoxicity in the presence of soluble MSLN. In vivo, SCR-A019 showed specific, dose-dependent anti-tumor efficacy toward MSLN positive tumor xenografts including lung and ovary cancer cells. Besides, SCR-A019 exhibited stronger anti-tumor activity than their parental monoclonal-ADC or benchmark ADC. SCR-A019 also have very good stability and favorable developability.
Conclusion: These preclinical data demonstrated SCR-A019 could be a potential first-in-class biparatopic BsADC to overcome the obstacles in antibody-based MSLN-targeting cancer therapy.

#3186 MDM2 Knockdown Enhances Phosphorylation of MCM2 during Cell Cycle Progression.

Nikita Meghani[1], Viola Ellison[2], Jill Bargonetti[1]

[1]Departments of Biology and Biochemistry, The Graduate Center, City University of New York, New York, NY,[2]The Department of Biological Sciences, Hunter College, City University of New York, New York, NY

MDM2 is an oncogenic E3 ubiquitin ligase that forms heterodimers with the homolog MDMX (also known as MDM4) and is classically known for targeting wild-type p53 for proteasomal degradation. However, in breast cancer harboring mutant p53, MDM2 and MDMX have oncogenic roles independent of p53. The MDM2-MDMX complex interacts with mutant p53 without actively degrading it. In breast cancer models that co-express high levels of mutant p53, MDM2, and MDMX, we identified a tripartite complex that regulates DNA repair protein recruitment of 53BP2 and MDC1. Additionally, mutant p53 colocalizes with replication-associated Mini Chromosome Maintenance2-7 (MCM2-7) helicase and Poly (ADP-ribose) polymerase 1(PARP1), forming what we refer to as the mutant p53-PARP-MCM axis. We are using isogenic estrogen receptor-positive T47D cells expressing missense mutant p53 L194F either with and without MDM2 or MDMX knockdown to dissect if the helicase component MCM2 is regulated by these protein scaffolds. We employed western blotting, immunofluorescence, and proximity ligation assays (PLA) to assess their influences on of MDM family member protein expression on MCM2 phenotype. Preliminary result showed that MDM2 knockdown correlated with increased phosphorylation of MCM2 at serine 108, a marker of replication stress, indicating that the presence of MDM2 mitigates replication stress. Using Proximity Ligation Assay, we observed that MDM2 and MCM2 were in close nuclear proximity. However, co-immunoprecipitation did not detect a direct MDM2-MCM2 protein-protein interaction. Future experiments will address whether the directional interaction between MDM2 and mutant p53 facilitates the role of MDM2 in mitigating replication stress signaling. These evaluations may allow for the mutant p53 and MDM2 overexpression biomarkers to serve as a targetable scaffolding hub for drug targeting.

#3187 A patient-derived organoid screening platform for evaluating KRAS inhibitor efficacy.

Merel Derksen, Yasmine Abouleila, Mariana Martins Costa Silva, Gerben ten Hag, Rene Overmeer, Farzin Pourfarzad, Fabian Stavenuiter, Robert G. J. Vries, Sylvia F. Boj

HUB Organoids B.V., Utrecht, Netherlands

The Kirsten rat sarcoma (KRAS) gene is a proto-oncogene frequently mutated in colorectal cancer (CRC), pancreatic ductal adenocarcinoma (PDAC), and non-small cell lung cancer (NSCLC), and is often associated with poor clinical outcomes. KRAS has long been considered an elusive and historically “undruggable” target in cancer therapy. However, recent breakthroughs, including the clinical approval of KRAS^G12C inhibitors such as Sotorasib and Adagrasib, have paved the way for novel compounds targeting KRAS^G12C and other KRAS mutations. The development of KRAS inhibitors can be accelerated and de-risked by using patient-relevant preclinical models that enable efficacy screening and safety assessment. Patient-derived organoids (PDOs), or HUB Organoids®, are advanced 3D models derived from adult stem cells of normal and malignant epithelial tissues, including colon, pancreas, and lung. They recapitulate the molecular heterogeneity, morphology, and functionality of the original tissue, accurately reflecting patient-specific responses HUB Organoids support high-throughput screening, providing a powerful, scalable platform for testing drug efficacy, safety, and resistance mechanisms. Their characterized genomic and transcriptomic profiles allow drug responses to be linked to molecular features, enabling patient stratification. In this study We demonstrate the suitability of our PDO-based platform for KRAS inhibitor screening within six weeks. Eight KRAS inhibitors at various clinical development stages were tested on a panel of over 20 PDOs (CRC, PDAC, and NSCLC) harbouring KRAS mutations (G12C, G12D, Q61R, G13C, G12V, and G12S) using an ATP-based viability assay. Responses varied across PDOs. Notably, G12C and G12D mutants showed selective sensitivity to KRAS^G12C and KRAS^G12D inhibitors, respectively. Resistance to these inhibitors was mitigated by combining them with an EGFR inhibitor, consistent with EGF-driven resistance mechanisms. Additionally, KRAS PDO screening enables assessment of drug synergy and safety in normal tissue-derived PDOs. In conclusion, HUB’s KRAS PDO screening platform offers a time-efficient, mutation-specific approach for evaluating compound specificity, potency, and combination strategies for KRAS-targeted therapies.

: Epigenetic Changes as Molecular Markers of Cancer
Poster Session

#3191 Loss of SMYD5 downregulates proliferative signaling pathways in B cell acute lymphoblasticleukemia.

Brunna Leticia Oliveira Santana[1], Mariana Braccialli de Loyola[1], Brenno Vinicius Martins Henrique[2], Ana Cristina Moura Gualberto[1], **Fabio Pittella-Silva**[1]

[1]Laboratory of Molecular Pathology of Cancer, Faculty of Health Sciences, University of Brasilia, Brasilia, Brazil,[2]Brasilia Children?s Hospital, Brasilia, Brazil

Acute lymphoblastic leukemia (ALL) is characterized by the uncontrolled proliferation of immature lymphoblasts, leading to impaired normal hematopoiesis and potential infiltration of extramedullary tissues. B-cell acute lymphoblastic leukemia (B-ALL) predominantly affects children aged 1 to 4 years, with a progressive decline in incidence in older age groups. Histone methyltransferases (HMTs) act as key epigenetic regulators, and their dysregulation has been associated with tumor initiation and progression. The *SMYD5* gene, a member of the HMT family, is found to be overexpressed in ALL patients and has been linked to hematopoietic, inflammatory processes, genomic stability and regulation of protein synthesis. However, its specific role in ALL remains poorly understood. Therefore, investigating the function of *SMYD5* in this context may provide insights that contribute to the development of more effective diagnostic and therapeutic strategies. We performed a combination of *in silico* and *in vitro* analyses. *In silico* analyses using public databases were conducted to evaluate *SMYD5* mRNA expression in B-cell acute lymphoblastic leukemia (B-ALL). Subsequently, *in vitro* experiments were performed using a CRISPR-Cas9-mediated knockout (KO) approach in the REH leukemic cell line. Following confirmation of SMYD5 loss at the protein level, transcriptomic profiling was carried out to identify differentially expressed genes and to investigate their involvement in relevant biological pathways. *In silico* analysis revealed that *SMYD5* mRNA expression was significantly higher in B-ALL samples compared with healthy bone marrow samples ($p = 0.0022$). In the in *vitro analysis*, *SMYD5* mRNA expression was compared across B-ALL cell lines, and the REH cell line was selected because it displayed the highest expression level. Subsequently, gene knockout (KO) was performed, resulting in the generation of two clones with reduced SMYD5 protein levels. RNA sequencing revealed substantial transcriptional changes in the KO clones compared with the wild-type cell line. GSEA analysis revealed positive enrichment in clones C52 and C78 for the E2F Targets (NES = 3.08, FDR < 0.001; NES = 2.93, FDR < 0.001), Myc Targets V1 (NES = 2.88, FDR < 0.001; NES = 2.86, FDR < 0.001), and Myc Targets V2 (NES = 2.31, FDR < 0.001; NES = 2.33, FDR < 0.001). The reduction of *SMYD5* in knockout clones was associated with downregulation of key proliferative pathways, suggesting its involvement in maintaining proliferative capacity and leukemogenesis. Literature evidence indicates that the E2F and Myc Targets (V1 and V2) pathways regulate pro-proliferative transcriptional programs in B-ALL. Accordingly, our findings suggest that SMYD5 loss dampens these transcriptional programs, potentially reducing the proliferative rate of leukemic cells and highlighting this gene as a potential therapeutic target.

#3192 Genome-wide DNA methylation profiling reveals distinct epigenetic landscapes and novel biomarkers in estrogen receptor-positive and -negative breast cancers.

Dalma Muller, **Balazs Gyorffy**

Semmelweis University, Budapest, Hungary

BACKGROUND: Breast cancer is a molecularly heterogeneous disease driven partly by subtype-specific DNA methylation patterns with diagnostic and prognostic potential. We aimed to construct a comprehensive methylation dataset to identify novel differentially methylated regions, define the global methylation patterns distinguishing breast carcinomas from normal tissue, and characterize differences between estrogen receptor (ER)-positive and ER-negative tumors.
METHODS: We curated a large-scale methylation dataset by processing raw data from HumanMethylation450 and EPIC array platforms (GEO accessions GPL13534, GPL21145) from GEO and GDC. The cohort included solid tissue samples from untreated breast cancer patients and healthy cases. Data preprocessing, BMIQ normalization, and quality control were performed using minfi and wateRmelon in R. Probes were annotated into functional gene regions (TSS1500, TSS200, 5'UTR, first exon, gene body and 3'UTR). Differential methylation analysis ($\Delta\beta > 0.2$) between normal, ER+, and ER- groups was conducted using Kruskal-Wallis and Mann-Whitney tests with Bonferroni correction. Biomarker potential was evaluated using receiver operating characteristic (ROC) analysis with 5-fold cross-validation (cvAUC). Gene Ontology (GO) enrichment was performed with clusterProfiler.
RESULTS: Based on HM450K and EPIC arrays, tumors exhibited significant, location-specific methylation shifts versus normal tissue, with distinct ER-positive and ER-negative patterns. ER-positive tumors showed pervasive promoter hypermethylation (455 hyper-, and 43 hypomethylated gene regions; $\Delta\beta>0.2$, $p<0.05$), enriched for pattern specification (HM450K: 4.7 fold enrichment (FE), $p<0.001$; EPIC: 9.3 FE, $p<0.05$) and appetite regulation (HM450K: 17.2, $p<0.001$; EPIC: 34.3 FE, $p<0.001$). ER-negative tumors (354 hyper-, and 23 hypomethylated gene regions shared by platforms with $\Delta\beta>0.2$, $p<0.05$), and were enriched for homophilic cell adhesion (EPIC: 16.2 FE, $p<0.001$) and olfactory receptor genes (EPIC: FE 12.2, $p>0.001$). Both platforms consistently identified high-confidence, differentially methylated regions, such as hypermethylation in the NEURL2 gene body in ER-positive (cvAUC: 0.99 HM450K, 0.99 EPIC; $\Delta\beta$ HM450K: 0.43, EPIC: 0.3) and the NKAPL 5'UTR in ER-negative tumors (cvAUC: 0.99 HM450K, 0.99 EPIC; $\Delta\beta$ HM450K: 0.47, EPIC: 0.44).
CONCLUSIONS: This study mapped the methylomes of ER+ and ER- breast cancers, identifying subtype-specific patterns of epigenetic dysregulation. The dataset and interactive visualization tools are available at epigenplot.com.

#3193 Secreted BRAF V600E drives ADAR1-dependent RNA editing and defines a therapeutic vulnerability in colorectal cancer.

Toshiaki Takahashi[1], Kunitoshi Shigeyasu[2], Kazuya Moriwake[2], Masashi Kayano[2], Hibiki Umeda[2], Kazuhiro Yoshida[2], Sho Takeda[2], Yuki Matsumi[2], Hiroyuki Kishimoto[2], Tomokazu Fuji[2], Kazuya Yasui[2], Hideki Yamamoto[3], Kosei Takagi[2], Hiroyuki Michiue[4], Yoshiko Mori[5], Fuminori Teraishi[2], Hiroshi Tazawa[2], Yuzo Umeda[6], Ajay Goel[1], Toshiyoshi Fujiwara[2]

[1]Beckman Research Institute of The City of Hope, Duarte, CA,[2]Department of Gastroenterological Surgery, Okayama University, Okayama, Japan,[3]Department of Clinical Genomic Medicine, Okayama University, Okayama, Japan,[4]Neutron Therapy Research Center, Okayama University, Okayama, Japan,[5]Department of Clinical Genetics, Saitama Medical University, Saitama, Japan,[6]Department of Hepatobiliary Pancreatic and Transplantation Surgery, Ehime University, Ehime, Japan

Background & Aims:The BRAF V600E mutation occurs in approximately 8-12% of colorectal cancers (CRC) and confers poor prognosis and therapeutic resistance. Despite the clinical success of combined BRAF and EGFR inhibition in the BEACON trial, resistance rapidly develops. Adenosine-to-inosine RNA editing, which is a post-transcriptional modification driven by adenosine deaminase acting on RNA (ADAR), promotes tumor malignancy and the acquisition of metastatic potential. We previously reported that ADAR1-high macrophages act as mediators of drug resistance and proposed ADAR1-targeted therapy as a potential new approach (Molecular Cancer, 2025). However, the specific patient population likely to benefit from ADAR1-targeted therapy remains unclear. This study investigated whether secreted BRAF V600E protein induces ADAR1-dependent RNA editing to promote tumor progression and therapeutic resistance, and whether JAK inhibition can enhance the efficacy of BRAF/EGFR-targeted therapy.
Methods:We combined analysis of clinical CRC tissues, spatial transcriptomics, and RNA sequencing with functional in vitro and in vivo models to characterize BRAF V600E secretion, intracellular distribution, and downstream molecular effects. Pharmacologic inhibition using JAK, EGFR, and BRAF inhibitors was used to evaluate their effects on the ADAR1-RNA editing pathway and associated tumor phenotypes.
Results:BRAF V600E-mutant CRC cells secreted the mutant BRAF protein through extracellular vesicles and soluble forms that were detectable in systemic circulation and distant tissues. ADAR1 expression was significantly higher in BRAF-mutant vs. BRAF-wild CRC ($p<0.001$). Stromal macrophages and fibroblasts internalizing extracellular BRAF V600E exhibited robust ADAR1 induction and hyper-RNA editing via type I interferon-JAK/STAT signaling, promoting immunosuppressive and tumor-supportive phenotypes. Wild-type tumor cells exposed to BRAF V600E protein upregulated ADAR1 and displayed enhanced proliferation and invasion, suggesting horizontal transfer of malignant traits. While combined BRAF/EGFR inhibition in HT29 and Colo205 cells suppressed direct oncogenic signaling, it paradoxically activated the JAK/STAT-ADAR1 axis, increasing RNA editing and resistance. Co-treatment with JAK inhibitors mitigated this effect, restored sensitivity, and suppressed tumor growth in preclinical models.
Conclusions:Our findings define a novel circulating ‘BRAF-ADAR1-RNA editing’ axis that contributes to immune evasion and resistance in BRAF-mutant CRC. Dual targeting of this pathway, through JAK or ADAR1 inhibition in combination with BRAF/EGFR blockade, represents a rational therapeutic strategy to overcome refractory, mutation-driven colorectal cancer.

#3194 *SETD4* regulates cell proliferation and methotrexate response in pediatric acute lymphoblastic leukemia.

Mariana B. de Loyola, Ana Cristina Moura Gualberto, Brunna Santana, Fabio Pittella-Silva

University of Brasilia, Brasilia, Brazil

Acute lymphoblastic leukemia (ALL) is the most common malignancy in the pediatric population and presents high remission rates. However, relapse persists as a major concern and the disease remains a leading cause of mortality among children and adolescents. Methotrexate (MTX) is widely used in ALL treatment, although resistance is frequently observed in relapsed patients. Leukemogenesis and treatment response are influenced by alterations in gene expression and epigenetic regulation. *SETD4* is a histone lysine methyltransferase that modulates chromatin structure and transcriptional programs linked to oncogenesis. In this study, we investigated its role in leukemogenesis. In our cohort of 83 Brazilian pediatric ALL patients, we observed *SETD4* overexpression, a finding supported by the BloodSpot Leukemia MILE Study cohort, in which *SETD4* upregulation was particularly evident among patients with the t(12;21) translocation. We further analyzed TCGA RNA-seq data from the TARGET-ALL Phase II study, stratifying patients by *SETD4* expression levels. High *SETD4* was associated with enrichment of proliferation-related pathways, including E2F, MYC, G2M checkpoint and DNA repair, which drive accelerated cell-cycle progression and increased leukemic cell survival. To validate these findings, we upregulated *SETD4* in the low-expressing Nalm-6 cell line and knocked down *SETD4* in the high-expressing REH line using siRNA. *SETD4* overexpression increased proliferation in Nalm-6 at 24h (FC= 1.7, $p < 0.01$), 48h (FC= 1.6, $p < 0.01$) and 72h (FC= 2.0, $p < 0.001$), whereas *SETD4* silencing reduced proliferation in REH at 24h (FC= 0.8, $p < 0.05$) and 48h (FC= 0.7, $p < 0.05$). Both systems demonstrated direct association between *SETD4* levels and leukemic cell proliferation. Since methotrexate targets proliferative processes, we investigated whether *SETD4* also influences treatment sensitivity. Higher *SETD4* levels increased sensitivity to MTX (FC= 1.4, $p < 0.0001$), whereas *SETD4* silencing reduced sensitivity (FC= 0.7, $p < 0.001$). Together, these results highlight *SETD4* as a promising biomarker candidate for leukemic burden and treatment response in pediatric ALL.

#3196 MPP8 inhibits PRKN signaling through interactions with SIRT1 and ZEB1 to promote bladder cancer proliferation and metastasis.

Stephany Gonzalez Tineo, Ryan M. Kemper, Surya K. Tripathi, Daniel J. Crona

Division of Pharmacotherapy and Experimental Therapeutics, UNC Eshelman School of Pharmacy, University of North Carolina, North Carolina, NC

Background: Metastatic bladder cancer (mBC) remains incurable, and epigenetic dysregulation is associated with disease progression. We hypothesize that the H3K9me3 reader protein MPP8 complexes with class III histone deacetylase SIRT1 and transcription factor ZEB1 to drive proliferation and metastasis. Here, we explore how MPP8 knockdown ($MPP8^{KD}$) disrupts MPP8-SIRT1-ZEB1 interactions, thereby altering differentially expressed genes (DEGs) and gene networks and abrogating proliferation and metastasis.
Methods: UM-UC-3 mBC cells were used to compare $MPP8^{KD}$ and untransfected ($MPP8^{WT}$) cells. RNA-seq quantified differential expression. DEGs were analyzed in R v4.1.1 using DESeq2.3. Gene enrichment was assessed with GSEA v4.2.3 (Hallmark sets) and IPA pathway analyses (Qiagen). Co-IP WBs evaluated MPP8-SIRT1-ZEB1 protein complexes. CellTiter-Glo™ evaluated differences in viability. Clonogenic assays assessed proliferation while migration/invasion assays evaluated metastatic potential. $MPP8^{KD}$ and $MPP8^{WT}$ cells were injected into NSG mouse flanks, and changes to both tumor volume and TBW were measured until tumors were ≥ 2 cm^3.
Results: Over-representation analysis of DEGs indicated $MPP8^{KD}$ reduced mBC cell growth and DNA replication, as well as increased inhibition of cell migration. GSEA identified downregulated E2F (NES=-1.9, q=0.02) and enrichment of TNFα signaling via NFKB gene sets (NES=1.71, q=0.01). IPA revealed activation of the Parkinson's signaling pathway (z-score=1.54, P=1.1E-03), and consistent with GSEA analyses, predicted reduced proliferation and cellular stress responses. A custom IPA gene network of top DEGs included Parkinson's signaling pathway genes (e.g., PRKN) and demonstrated that MPP8, SIRT1, ZEB1 all act upstream of pathway genes. Moreover, SIRT1 and PRKN were predicted to interact through protein-protein interactions, while $MPP8^{KD}$ directly increased PRKN expression (LFC=1.658, q=2.39E-03). Functionally, we demonstrated MPP8 forms a complex with SIRT1 and ZEB1 in $MPP8^{WT}$ cells, while the MPP8-SIRT1-ZEB1 interactions were lost in $MPP8^{KD}$ cells. $MPP8^{KD}$ reduced viability (44% vs. 84% after 48 h; P=0.0001), colony growth (13% vs. 36% plate covered with colonies at 10 d; P=0.0001), number of migrated cells (97 vs. 470 cells after 18 h; P<0.0001), and number of invading cells (44 vs. 130 cells after 18 h; P=0.02). By D+32 post-injection, all mice with $MPP8^{WT}$ cells were sacrificed (mean vol. 2,859 ± 761 mm^3; n=8). At D+32, tumor volume was significantly smaller in $MPP8^{KD1}$ (mean vol. 234 ± 447 mm^3, P<0.0001; n=8) and $MPP8^{KD2}$ mice (mean vol. 1,341 ± 785 mm^3, P=0.002; n=8). At D+32, changes in TBW were not observed.
Conclusions: Our data suggest the MPP8-SIRT1-ZEB1 axis is a key driver of mBC, and $MPP8^{KD}$ results in PRKN activation that could halt mBC proliferation and metastasis.

#3197 PROMISE, a clonal promoter methylation signature capturing early epigenetic evolution and prognostic programs across epithelial cancers.

Francisco Gimeno-Valiente[1], Constantino De La Vega[2], Yun-Hsin Liu[1], Carla Castignani[3], Ieva Usaite[1], Martin Arana Jorge[1], Elrick Hillary[1], Stephan Beck[4], Miljana Tanic[5], Jonas Demeulemeester[6], Peter Van Loo[7], Charles Swanton[3], Mariam Jamal-Hanjani[8], Nnennaya Kanu[1]

[1]University College London (UCL), London, United Kingdom,[2]University of Cambridge, Cambridge, United Kingdom,[3]The Francis Crick Institute, London, United Kingdom,[4]UCL Cancer Institute, London, United Kingdom,[5]Institute for Oncology and Radiology of Serbia, Belgrade, Serbia,[6]Integrative Cancer Genomics Laboratory, Department of Oncology, KU Leuven, Leuven, Belgium,[7]The University of Texas MD Anderson Cancer Center, Houston, TX,[8]University College London (UCL) Cancer Institute, London, United Kingdom

Epigenetic remodeling is a hallmark of tumor evolution, yet the timing and clonality of promoter methylation events remain poorly defined. We investigated the spatial architecture of promoter DNA methylation in multiregion lung adenocarcinoma (LUAD) to identify clonal epigenetic alterations and evaluate their prognostic and translational relevance across cancers. Reduced representation bisulfite sequencing (RRBS) was performed on 151 tumor regions from 32 TRACERx LUAD patients with matched normal tissue. Differentially methylated regions (DMRs) were quantified for intratumor (ITH) and intertumor (ITeH) heterogeneity. Clonality was evaluated through three complementary metrics of methylation ubiquity, followed by univariate and LASSO Cox modeling. The resulting 30DMR panel, termed PROMISE, was derived through clustering concordance with TCGA LUAD and independently validated in CPTAC 3. PROMISE was subsequently tested for pancancer specificity across 18 tumor types from several publicly available sources.We identified 21,358 promoter DMRs showing a continuum of ITH and ITeH patterns. Promoters with low ITH but high ITeH, ubiquitously hypermethylated within tumors yet variable across patients, represented early clonal events significantly associated with poor survival. LASSO Cox selection yielded a 30-DMR signature encompassing genes involved in immune regulation, epithelial polarity, and TGFβ signaling. PROMISE robustly stratified patients into high and low risk groups in both TCGA LUAD and CPTAC 3 cohorts (logrank $P < 0.01$) and remained independent of clinicopathologic variables. Cross-cancer analyses revealed strong prognostic associations in kidney, thyroid, liver, and colorectal cancers, but minimal signal in squamous, stromal rich, or hematologic malignancies.PROMISE captures a panepithelial program of early, clonal promoter hypermethylation recurrent across multiple carcinomas and predictive of outcome in selected epithelial tumors. These findings highlight clonal methylation remodeling as an early determinant of tumor evolution and nominate PROMISE as a clinically actionable biomarker for cancer risk stratification.

#3198 BAP1 loss rewires chromatin and lineage identity in uveal melanoma.

Daulet Aitymbayev[1], Emma Hammes[1], Lucinda Innes[2], Holy Mary Zaher[3], Juan Martinez Villalobos[4], Arnaud Augert[1], Mathieu Bakhoum[3]

[1]Pathology and Molecular Medicine, Yale University, New Haven, CT,[2]Cornell University, New York, NY,[3]Ophthalmology and Visual Sciences, Yale University, New Haven, CT,[4]University of Connecticut Health Center, Farmington, CT

Background: BAP1 is a chromatin-associated deubiquitinase that antagonizes Polycomb Repressive Complex 1 (PRC1)-mediated ubiquitination, thereby stabilizing chromatin accessibility and genomic integrity. Uveal melanoma is the most common intraocular cancer in adults and loss of BAP1 tracks with a high-risk, metastatic phenotype. However, how BAP1 loss reprograms the epigenetic landscape to drive these lineage and phenotypic changes remains unknown. Our objective is to define the chromatin and transcriptional consequences of BAP1 loss in uveal melanoma.

Description of experimental procedures: To identify regulatory mechanisms altered secondary to BAP1 loss, we profiled the epigenome upon BAP1 loss using ATAC-seq, RNA-seq, and CUT&RUN for repressive marks such as H2AK119Ub and H3K27me3. Differential chromatin accessibility was identified using DiffBind, and motif enrichment was performed with HOMER, to infer changes in lineage-defining transcriptional circuits. Multi-omic integration with RNA-seq and public UM datasets (including TCGA) was used to align BAP1-dependent epigenetic states with low and high-risk tumor classes and to connect epigenetic remodeling to lineage states (melanocytic vs neural crest-like).

Summary of new results: BAP1 loss induced widespread changes in chromatin accessibility and repressive histone marks, including a global reduction in H2AK119Ub and redistribution of H3K27me3. These alterations were not uniform across the genome: distal elements, particularly on chromosome 8, preferentially lost repressive marks and gained accessibility in BAP1-deficient cells, consistent with enhancer remodeling at loci associated with high-risk uveal melanoma. CUTnRUN and ATAC analyses separated genomic regions into two major subsets: 1) melanocytic-lineage regulatory elements that gained repressive marks and lost accessibility, and 2) regions associated with neural crest-like and invasive programs that became more accessible and enhancer-like. AP-2 motifs were strongly enriched within ATAC-seq peaks that gained accessibility in BAP1-deficient UM, and displayed lower H3K27me3 and H2AK119Ub peaks, reflecting a more permissive chromatin state at these regions relative to indolent UM. Together, these data link BAP1 loss to a coordinated epigenetic shift from a melanocytic toward a neural crest-like epigenetic state.

Conclusions: Loss of BAP1 in uveal melanoma is associated with epigenetic remodeling, characterized by redistribution of repressive histone marks, and enhancer reorganization. This epigenetic reprogramming aligns with loss of melanocytic identity and emergence of a neural crest-like invasive state, providing a mechanistic link between BAP1 loss and aggressive tumor behavior.

#3199 Investigating gene regulatory mechanisms associated with B-cell acute lymphoblastic leukemia incidence in Hispanic/Latino populations.

Clarissa Garcia, Julian Grandvallet Contreras, Tzu Phang, Matthew T. Witkowski

The University of Colorado-Anschutz Medical Campus, Aurora, CO

B-cell acute lymphoblastic leukemia (B-ALL) is the most common childhood cancer. In the United States, Hispanic/Latino children exhibit a higher incidence and lower overall survival than non-Hispanic White patients, independent of social determinants. Genome-wide association studies have identified several single-nucleotide polymorphisms (SNPs) associated with B-ALL risk, including a recurrent variant, rs7090445, located in intron 3 of the *ARID5B gene locus*. The rs7090445 risk allele (C) is ~36% more common in Latino/Admixed-American individuals than in non-Latino Whites and rises with Indigenous-American ancestry, highlighting its potential role in B-ALL incidence disparities. The rs7090445 SNP resides within a lymphoid-specific enhancer that physically interacts with the *ARID5B* promoter. However, the role of this non-coding variant in B-cell transformation remains unclear. In humans, *ARID5B* mRNA expression increases at the pro-B cell stage, subsequently peaking at the pre-B stage. In mice, *Arid5b* deletion causes a differentiation delay at the pre-B stage, highlighting the importance of *Arid5b* dosage in B cell progenitor maturation. We hypothesize the B-ALL-associated ARID5B SNP rs7090445 perturbs enhancer function and disrupts normal B-cell development by reshaping the epigenetic landscape governing ARID5B transcription. To investigate this, we analyzed primary B-ALL patient and healthy bone marrow donor ATAC-Seq and RNA-seq datasets to define how the SNP influences chromatin accessibility, transcription factor occupancy, and gene expression across specific lymphoid subpopulations. These analyses revealed the rs7090445 risk allele elicited pro-B cell-specific reductions in *ARID5B* intronic enhancer accessibility and *ARID5B* transcription, with ongoing analysis dissecting genome-wide chromatin accessibility footprints. To functionally dissect these observations, we generated isogenic B-ALL cell clones harboring the rs7090445 risk and non-risk allele. Analyses of these engineered lines recapitulate allele-specific differences observed in patient samples, supporting a direct role for rs7090445 in modulating enhancer function and *ARID5B* gene activation. Ongoing studies aim to map SNP-altered transcription factor footprints and validate candidate regulators in B-ALL cell lines and patient-derived xenograft models. These findings provide a rationale for investigating how rs7090445 may perturb gene-regulatory networks influencing B-cell development and B-ALL.

#3200 WREm6A Prism: Single-cell sequencing of m6A methylation expression signatures and its clinical translation in esophageal squamous cell carcinoma.

Yuan Li, Zhuya Xiao, Qian Mo, Qian Wang, Caiyutian Zhang, Tian Tang

RenMin Hospital of Wuhan University, Wuhan, Hubei, China

Single-cell sequencing and m6A methylation have emerged as focal points in the life sciences. Their convergence—single-cell m6A methylation sequencing—has opened a fresh vantage point, yet comprehensive characterization and translational exploitation remain limited. Leveraging existing platforms, we have devised an integrative strategy that translates the dynamic m6A circuitry into disease-oriented research. m6A methylation is catalyzed by Writers, interpreted by Readers and erased by Erasers. The steady-state abundance of the modification is therefore dictated by the balanced expression of these three determinants. We have translated this ternary logic into a visualization framework—the WREm6A Prism—by projecting Writer/Reader/Eraser transcriptomes onto a ternary phase diagram. Analogous to a prism that disperses white light into a spectrum, the Prism has decomposed single-cell m6A landscapes into interpretable, color-coded maps that integrate multi-omics dimensions. In the context of esophageal squamous-cell carcinoma (ESCC), we have generated and mapped >68 000 malignant and 21 000 micro-environmental cells onto the WREm6A Prism. Primarily, identified three conserved m6A-modulation archetypes: W-high (stem-like), R-high (differentiated), E-high (inflamed/stressed). These archetypes have been independently validated in two external cohorts using both bulk and single-cell data. Prism coordinates have proven more predictive of response to treatment than conventional expression signatures, showing promising application in the prospective selection of patients for targeted or immune combination therapy. Thus, the WREm6A Prism has been established as an intuitive, quantitative and clinically actionable model for interrogating ternary regulatory systems. It has provided a fresh perspective on ESCC biology and has offered immediate translational utilities that are now being extended to other tumour types.

#3201 Chromatin accessibility differentiates cancer associated fibroblast subtypes in pancreatic cancer.

Minh Duc Pham, Chang-Il Hwang, Kedi Huang

University of California, Davis, Davis, CA

Pancreatic ductal adenocarcinoma (PDAC) remains the deadliest cancer with only 13% of five-year survival rate in patients. However, effective drug delivery and administration of immunotherapy have been limited due to the dense fibrotic stroma in PDAC tumor microenvironment, majorly contributed by cancer-associated fibroblasts (CAFs). Unfortunately, targeting CAFs to enhance PDAC treatment has not yet been successful due to the lack of understanding in CAF activation, heterogeneity, and plasticity. Previous scRNA-seq studies revealed different CAF subtypes with diverse phenotypes and functions but the underlying mechanisms of CAF activation remain unclear. Of note, CAFs do not genetically differ from their origins, and they are interconvertible depending on external factors and signaling cues. This plasticity feature suggests that CAFs are characterized by their cellular states rather than an end-of-point differentiation. Therefore, we hypothesized that CAFs activation is regulated by epigenetic reprogramming. Using ATAC-seq and innovative PDAC organoid-CAF co-culture models, we revealed distinct chromatin accessibility profiles of two major CAF subtypes, myofibroblasts and inflammatory fibroblasts *in vitro*. Gained differentially accessible regions were identified across genomes, located not only at promoters but also at enhancers, and they were highly associated with transcriptional signatures of each subtype. In line with this, analysis on snATAC-seq of the fibroblast population within PDAC tumor tissues of both human patients and mouse models also confirmed the distinct chromatin accessibility profiles of different CAF subtypes. Interestingly, by overlaying with snRNA-seq, we discovered that chromatin structure of CAF was primed to be accessible towards late-stage myofibroblast subtype during tumorigenesis. Overall, our study demonstrates the epigenetic basis of CAF plasticity both *in vitro* and *in vivo*, suggesting a novel therapeutic strategy of epigenetically targeting CAF to remodel the stroma and improve treatment outcomes in PDAC patients.

#3202 RNA editing is the potential biomarker for carcinogenesis of Crohn's disease.

Kazuya Moriwake, Kunitoshi Shigeyasu, Masashi Kayano, Eiki Miyake, Yuhei Kondo, Yuya Sakurai, Shunsuke Nakamura, Masafumi Takahashi, Kaori Nitta, Nobuhiko Kanaya, Yoshitaka Kondo, Hiroshi Tazawa, Toshiyoushi Fujiwara

Okayama Univ. Graduate School of Med., Dentistry & Pharm. Sci., Okayama, Japan

Background: Crohn's disease is one of inflammatory bowel disease alongside ulcerative colitis. In Crohn's disease, the major clinical concerns include fibrotic strictures of the ileum and carcinogenesis in the lower rectum and anus. Crohn's disease is associated with higher risk of carcinogenesis than the general population. However, the mechanisms driving carcinogenesis in Crohn's disease remain poorly understood. We recently reported that ADAR1-mediated RNA editing can mark carcinogenesis in ulcerative colitis. In this study, we therefore examine the potential role of ADAR1 in Crohn's disease-associated cancer.
Methods: A single-center retrospective study was conducted on 51 Crohn's disease patients who underwent colorectal resection of at our hospital in 2008-2023. There were 46 non-cancer tissue and five rectal cancer tissue. The expression level of ADAR1 protein was analyzed by immunohistochemistry (IHC) in FFPE samples with immunoreactive score. In vivo, we established AOM/DSS carcinogenesis model mouse. ADAR1 expression and RNA editing level were analyzed by IHC and RT-qPCR.
Results: ADAR1 expression levels were significantly elevated in cancer tissues compared to non-cancer tissues ($p < 0.05$) in colorectal epithelial cells. In addition, ADAR1 expression was upregulated at both the transcriptomic levels ($p = 0.0308$) and protein levels ($p < 0.05$) in the colorectal epithelial tissues of model mouse. Furthermore, the AZIN1 RNA editing ratio was significantly increased in colorectal tissues of model mouse as determined by RESSq-PCR ($p = 0.043$).
Conclusion: In this study, elevated expression of RNA editing enzymes has been observed in cancer tissues of Crohn's disease. A similar result was also observed in colorectal epithelial cells of colitis and carcinogenesis model mouse. These findings suggest that continued research may help establish ADAR1 as a potential biomarker and treatment target in inflammatory bowel disease.

#3203 Deciphering gene regulatory network and spatial heterogeneity underlying cutaneous T cell lymphoma large cell transformation.

Xiaofei Song[1], Jennifer M. Garbarino[2], COLIN NG[2], Lucia Seminario-Vidal[3], Carly M. Harro[4], Jodi A. Balasi[1], Chaomei Zhang[1], Nan Sun[1], Douglas C. Marchion[1], Sean J. Yoder[1], Jose R. Conejo-Garcia[5], Pei-Ling Chen[1]

[1]Moffitt Cancer Center, Tampa, FL,[2]AtlasXomics Inc, New Haven, CT,[3]Eli Lilly, Indianapolis, IN,[4]University of Pennsylvania, Philadelphia, PA,[5]Duke University School of Medicine, Durham, NC

Cutaneous T cell lymphoma (CTCL) is a rare malignancy of skin-homing T cells, with Mycosis Fungoides (MF) representing 50-70% of all cases. Although MF typically follows an indolent clinical course, a subset of MF patients progresses to develop large cell transformation (LCT) that is associated with a worse outcome. Disease progression from patch/plaque (PP) lesions to transformed tumor (TT) is accompanied by profound genetic and transcriptional alterations across multiple signaling pathways, including oxidative phosphorylation and MYC, posing a significant challenge for single-agent therapeutic strategies. Epigenetic therapies such as HDAC inhibitors have shown limited efficacy, underscoring the need to identify key transcription factors (TFs) and novel gene regulatory networks (GRNs) that drive CTCL disease progression and may serve as targeted vulnerabilities. In this study, we first performed joint profiling of gene expression and chromatin accessibility using scMultiome on six MF samples (2 PP and 4 TT). By integrating TF expression, chromatin accessibility at targeting regions, and expression of nearby genes, we inferred cell-type specific GRNs across the tumor microenvironment cell types, including the malignant T cells in PP and TT lesions, and other benign immune and non-immune cells. Importantly, this analysis identified JUND-associated GRNs enriched in B cells and ATF6 networks in myeloid cells, demonstrating robust regulatory signal recovery. Applying the same framework, we identified RUNX2 and ATF2 as putative regulators of PP malignant T cells, and LEF1, IKZF2, and TCF7 as key drivers of transformed CTCL cells. We further validated the critical roles of these transcription factors in in-house and publicly available scRNAseq datasets. To investigate the spatially resolved chromatin accessibility landscape in CTCL, we generated the first spatial ATACseq dataset for this rare cancer and profiled paired PP and TT lesions from the same patient. Spatial clustering and inferred copy number analysis revealed distinct epigenetic clone structures, including PP-dominant clones, TT-dominant clones, and shared clones between PP and TT. Notably, GRNs enriched in PP or TT by scMultiome were recapitulated within PP-dominant and TT-dominant spatial ATAC clones, respectively, highlighting consistent regulatory programs across modalities. Together, these results uncover previously unrecognized GRNs associated with MF progression and provide the first spatially resolved epigenetic map of CTCL. Our findings demonstrated potential regulators and clonal heterogeneity that may inform the development of novel therapeutic strategies, including precision epigenetic or combination therapies.

#3204 DNA methylation profiling in ethnically diverse prostate tissues to identify novel biomarkers predicting prostate cancer progression.

Claire A. Stevens[1], Leonardo Gonzalez-Smith[1], Colton Stensrud[1], Divya Ranjith[1], Jenaye Mack[2], Sarah Buxbaum[3], Sara Falzarano[2], Suhn K. Rhie[1]

[1]Keck School of Medicine of USC, Los Angeles, CA,[2]University of Florida, Gainesville, FL,[3]Florida A&M University, Tallahassee, FL

Prostate cancer (PCa) is the most common non-dermatological malignancy and the second leading cause of cancer-related deaths among men in the United States. Disparate clinical outcomes are especially observed between patients of African American (AA) and European American (EA) ancestry. This difference may reflect the long-term biological consequences of systemic racism, including differential environmental exposures and unequal access to healthcare. Additionally, these factors, along with genetic variation across ancestries, can contribute to epigenetic changes in PCa, including DNA methylation. To date, whole-DNA-methylome data has overrepresented EA individuals, and was used to develop DNA methylation-based biomarkers for PCa. In this study, we comprehensively characterize the genome-wide DNA methylome of PCa in a cohort of ethnically diverse individuals to identify new PCa-specific epigenetic features and a novel set of DNA methylation biomarkers. We obtained formalin-fixed paraffin-embedded (FFPE) prostate tissues from AA and EA PCa patients and generated DNA methylation profiles across normal controls and tumors spanning multiple Gleason grades, molecular subtypes, and pathological features. FFPE tissue regions were macrodissected based on pathologic annotations, allowing for recovery of Gleason grade-specific DNA. DNA methylation assays included both the Illumina Infinium Methylation EPIC array and Whole-Genome Bisulfite Sequencing (WGBS). We identified thousands of hypomethylated and hypermethylated CpG sites between normal and tumor samples across prostate tissue samples first profiled by both the EPIC array that were also covered by WGBS. Based on the most variable differentially methylated regions (DMRs), we identified clusters of tumor samples exhibiting distinct DNA methylation patterns. When we developed a model to identify DMRs that are predictive of tumor grade and other clinicopathological features; interestingly, we found that some DMRs were located within intergenic regions, including enhancers of genes that are typically upregulated in PCa. Additionally, we identified PCa-specific partially methylated domains, which are progressively hypomethylated throughout tumor progression. The average methylation levels at these regions predicted tumor grade. Overall, this study identifies PCa-specific epigenetic features, revealing potential new biomarkers that predict PCa severity and progression, with the inclusion of an ethnically diverse cohort.

#3205 Single cell DNA methylation of early breast cancer reveals epigenomic response to driver mutations and unique signatures of progression and invasion.

Ryan Mulqueen[1], Xiang Li[2], Mariam Mosaad[3], Shanshan Bai[1], Jianzhuo Li[1], Emi Sei[1], Savitri Krishnamurthy[1], Alastair Thompson[4], Nicholas E. Navin[1]

[1]UT MD Anderson Cancer Center, Houston, TX,[2]Department of Bioengineering, Rice University, Houston, TX,[3]Department of Systems Biology, UT MD Anderson Cancer Center, Houston, TX,[4]Baylor College of Medicine, Dan L. Duncan Cancer Center, Houston, TX

The pre-cancerous stage of invasive breast ductal carcinoma (IDC), termed ductal carcinoma *in situ* (DCIS) is a noninvasive neoplasm of the breast duct and is treated by surgical resection and radiation as standard of care. Pathology grading and mutational profiling do not sufficiently predict DCIS progression or recurrence; this uncertainty leads to overtreatment of an estimated 60% of possibly indolent lesions, via invasive surgical interventions and aggressive neoadjuvant therapies. Recent multicancer screening through DNA methylation markers of cell-free DNA show success in identifying staging and type of multiple cancers but fall short on DCIS and early-stage IDC, and do not predict progression nor recurrence. Further, since the methyl- group is covalently linked to DNA it is stable in FFPE-stored clinical samples for decades, allowing retrospective studies on progression and recurrence in a disease which can take decades to progress.

We leverage this promising modality to expand upon our knowledge of DNA methylation in normal, DCIS and synchronous (DCIS+IDC) breast samples using our high-throughput single cell methylation (scMET) method. We profiled 23,692 cells across 13 normal, 10 DCIS, and 18 synchronous samples, equating to >650X coverage of the methylome in total. We paired single cell RNA (scRNA) profiles for all samples, resulting in 154,695 scRNA profiles. As a first-of-its-kind data set, we define methylation-based markers for all expected cell types, including cancer-associated fibroblasts and tumor endothelial cells, enriched in the tumor microenvironment and absent in the normal tissue samples. Through paired copy number calling on scRNA and scMET we match transcriptomes and methylomes to 74 subclonal populations across our DCIS and synchronous samples. In addition to patient and subclone specific mutational events, dozens of these subclones share stereotyped early breast cancer driver events such as 1q amplification and 16q loss. Through these shared events we characterize methylome response to gene dosage changes. Through lineage tracing of inherited methylation changes, known as “epimutations”, we track subclonal populations back to their diploid cell of origin: luminal hormone-responsive epithelial cells. Finally, through our whole methylome capture per cell, we match cell types and subclones to telomere lengths. This reveals signatures of aging with cell type specificity and marked decrease in telomere length through cancer progression. In sum, this study measures the the breast methylome as it progresses from a normal to neoplastic to invasive phenotypes through an epigenetic modality that shows great promise as a biomarker. This work will inform clinically viable approaches to patient stratification to better determine DCIS risk of progression and recurrence.

#3206 Unraveling novel epigenetic therapies for the treatment of TP53^{WT}glioblastoma.

Laurence Haddadin, Shuo Zhang, Mansi Solanki, Bin Lu, Xueqin (Sherine) Sun

Cancer Genome and Epigenetics Program, Sanford Burnham Prebys Medical Discovery Institute, San Diego, CA

Glioblastoma (GBM) remains the most aggressive and treatment-resistant primary brain tumor in adults, with median patient survival of only 12-15 months despite current standard-of-care therapies. To identify new therapeutic strategies, we investigated how chromatin remodeling regulates cell-state transitions in TP53 wild-type (TP53^{WT}) GBM, which represents the majority of cases. We found that the chromatin regulator BRD8, a component of the EP400 complex, acts as a key suppressor of p53 activity. BRD8 maintains H2A.Z occupancy at p53 target loci to repress its tumor-suppressive paradigm. Depletion of BRD8 disrupts this interaction, increases chromatin accessibility, and reactivates p53-dependent transcriptional programs, resulting in a stable cell cycle arrest and a senescent phenotype accompanied by widespread transcriptomic reprogramming. Through small-molecule screening, we identified compounds that selectively impair the survival of BRD8-deficient cells, revealing specific vulnerabilities associated with this arrested state. We further discovered that the histone variant, macroH2A (mH2A), enforces the changes in chromatin accessibility and transcriptional output following BRD8 perturbation, functioning as epigenetic switches that stabilize this altered cell state. Together, these findings reveal a chromatin-based mechanism governing proliferative control in GBM and highlight actionable vulnerabilities that could be exploited through targeted pharmacologic intervention.

#3207 SNP rs4381241 promotes renal cell carcinoma progression via the *FAF1-HDAC3-PDGFB* axis.

Haodong Liu, Xinru Yu, Zeyun Mi, **Kexin Chen**

Tianjin Medical Univ. Cancer Inst. & Hospital, Tianjin, China, Tianjin, China

BackgroundRenal cell carcinoma (RCC) is a highly lethal cancer with limited therapeutic options. Genetic heterogeneity, driven by genomic alterations, plays a key role in tumor progression and resistance to treatment. Genome-wide association studies (GWAS) have identified single nucleotide polymorphisms (SNPs) linked to cancer susceptibility and prognosis. However, the functional mechanisms of these SNPs in regulating RCC development remain unclear. Investigating these SNPs could reveal new therapeutic targets.
MethodsThe functional relevance of the SNP was assessed using EMSA, dual-luciferase reporter assays, and CRISPRa/i to confirm its impact on FAF1 expression. 3C/4C analyses confirmed physical interaction with the FAF1 enhancer region. FAF1 expression was measured in TCGA datasets and RCC tissues using qPCR and Western blot. Gene set enrichment analysis (GSEA) identified PDGFB as a downstream target. Gain- and loss-of-function assays were conducted in RCC cell lines, including CCK-8, wound healing, transwell migration, and colony formation assays, along with in vivo subcutaneous xenograft models. Co-IP, CUT&Tag, and ChIP-qPCR were used to study FAF1's interaction with HDAC3 and its role in PDGFB transcription.
ResultsThe SNP rs4381241, in the intronic region of FAF1, acts as an enhancer that regulates FAF1 transcription. The T>C substitution reduces FAF1 expression. In both TCGA data and RCC tissues, FAF1 mRNA and protein levels were lower in tumors compared to adjacent normal tissues, with higher FAF1 levels linked to better prognosis. Functional assays showed that FAF1 overexpression suppressed cell proliferation and migration in vitro, and tumor growth in vivo, confirming its tumor-suppressive role. Mechanistically, FAF1 interacts with HDAC3 to recruit it to the PDGFB promoter, leading to histone deacetylation at H3K9ac and H3K27ac, suppressing PDGFB transcription and inhibiting PDGFRB/PI3K-AKT signaling.
ConclusionThe intronic SNP rs4381241 is a functional enhancer variant regulating FAF1 expression in RCC. FAF1 suppresses RCC cell proliferation and migration and interacts with HDAC3 to repress PDGFB transcription, inhibiting the PDGFRB/PI3K-AKT pathway. These findings highlight rs4381241 as a key modulator of RCC progression through the FAF1-HDAC3-PDGFB axis.
Keywordsrenal cell carcinoma, rs4381241, FAF1, HDAC3, PDGFB

#3209 Enzymatic enrichment of unmethylated cell-free DNA improves the sensitivity of fragmentomic analysis for the diagnosis of patients with lung cancer.

Valentina Miano[1], Paulina Siejka-Zielińska[1], Calum Mould[1], Sean Knight[2], Seamus Grundy[3], **Robert K. Neely**[1]

[1]Tagomics Ltd, Cambridge, United Kingdom,[2]Lydia Becker Institute of Immunology and Inflammation, University of Manchester, Manchester, United Kingdom,[3]Northern Care Alliance NHS Foundation Trust, Salford, United Kingdom

Global loss of genomic DNA methylation is associated with the progression of cancer. This genome-wide hypomethylation is thought to result from increased rates of genome replication in rapidly dividing cancer cells. We leveraged this aspect of cancer biology to address the challenge of early disease detection in cell-free DNA from a cohort of lung cancer patients. We combined Tagomics' Activace platform, which enriches unmethylated CpG sites of the genome for sequencing, with genome-wide, fragmentomic analysis on this hypomethylated DNA fraction. Using a single sample input (>5 ng of cell free DNA) Activace enables a multiomic (epigenomic and fragmentomic) read-out with only 70 M sequencing reads. We tested the utility of this approach on a small cohort of 36 patients, who presented at the clinic with symptoms of lung cancer, had a blood sample taken and went on to receive a diagnosis using gold-standard testing (imaging, pathology). The cohort contained 14 cancer-free patients, 12 patients with an early-stage (Stage I & II) diagnosis of non-small cell lung cancer and 10 patients with a late-stage (Stage III & IV) diagnosis of non-small cell lung cancer. We sequenced the cfDNA obtained from the plasma of these patients; and enriched and sequenced the unmethylated DNA fraction from the same patients, using Tagomics' Activace platform. We compared the fragmentomics profiles of both the enriched, unmethylated DNA and the whole cfDNA and evaluated the impact of the enrichment on our ability to classify the cohort. Using a leave-one-out approach, a logistic regression classifier, trained on the end motif profiles of the Activace dataset (enriched for unmethylated CpG sites), we correctly classified all but two of the early-stage lung cancer cases (91% sensitivity, 100% specificity). By contrast, using an analogous approach in the WGS dataset (whole cfDNA) eight lung cancer cases (seven early-stage and one late-stage) were misclassified (64% sensitivity, 100% specificity). Multiomics tools, such as the Tagomics' Activace platform enable information-rich insight into disease biology and will likely outperform single analyte-based tests, in the future. The enrichment of DNA containing unmethylated CpG sites improves sensitivity of fragmentomic analysis, relative to analogous analysis of the whole genome, likely due to the enrichment of tumour-derived, hypomethylated DNA fragments in patients with cancer.

#3210 Epigenomic liquid biopsy molecular lung subtyping and real-world (RW) patient outcomes in advanced NSCLC (aNSCLC).

Jayati Saha, Nicole Zhang, Sheila R. Solomon, Shaun Forbes, Matthew Ellis

Guardant Health, Palo Alto, CA

Introduction: NSCLC subtypes include adenocarcinoma (LUAD), squamous cell (LUSC), and small cell (SCLC). Mixed histology, limited sampling, and discordant interpretations often delay treatment. To address this, a plasma-based Molecular Lung Subtype Predictor (MLSP) was developed to quantify LUAD, LUSC, and SCLC from circulating hypermethylated DNA (Guardant360 Liquid, Guardant Health). We report concordance between MLSP and histology from test requisition forms (TRF), real-world (RW) outcomes by therapy type, and subtype-specific genomic profiles.

Methods: The InfinityAI Data Library links de-identified genomic/epigenomic results with longitudinal claims data. Samples were considered “pure” when ≥90% signal was from one subtype. Cohorts were stratified by MLSP-TRF concordance and first-line therapy post-Guardant360 Liquid: chemotherapy (chemo), immunotherapy (IO), chemo-IO, or targeted therapy. RW time to treatment discontinuation (RW-TTD) and time to next treatment (RW-TTNT) were analyzed using Kaplan-Meier and log-rank tests.

Results: Among 8,559 MLSP results, 69.4% were LUAD, 12.4% LUSC, 3.7% SCLC, and 14.6% mixed. Concordance with TRF was 91.6% (LUAD), 75.1% (LUSC), and 56.1% (SCLC). In MLSP-LUAD, Tier 1 mutations included *KRAS G12C* (11.9%), *EGFR* ex19del (9.5%), and *BRAF V600E* (2.1%); *PIK3CA E545K* (6%) was common in MLSP-LUSC, and *RB1* (19%) in MLSP-SCLC. Targetable biomarkers occurred in 43.5% of MLSP-LUAD vs 3.4% LUSC and 2.6% SCLC. In discordant MLSP-TRF cases, genomic profiles favored MLSP predictions. KRAS G12C (7%), PIK3CA E545K (5%), and RB1 (39%) were the most frequent subtype-specific alterations. Targeted therapy improved RW outcomes in MLSP-LUAD; chemo-IO yielded best outcomes in MLSP-LUSC, and IO benefited MLSP-SCLC. Discordant cases treated with IO or targeted therapy showed extended RW-TTNT and RW-TTD, aligning with MLSP-predicted biology.

Conclusion: This study demonstrated high concordance between MLS and TRF, which is consistent with previous analyses. The genomics and RW outcomes of discordant cases were more consistent with MLSP-predicted subtype vs. TRF-reported histology. Discordant pts exhibited genomic patterns and RW outcomes more aligned closely with the MLSP-predictions, suggesting MLSP may more accurately represent underlying tumor biology than standard histology.

#3211 A novel workflow for ultra short cfDNA fragmentomics and multiomic profiling in liquid biopsies.

Xiaojing Yang[1], Madison Valle[1], Duang Ratanachan[1], Kaitlyn Lee[1], Neeti Swarup[2], Irene Choi[2], Hanjun Kim[1], David T. Wong[2]

[1]Zymo Research Corp., Irvine, CA,[2]University of California, Los Angeles, Los Angeles, CA

Background: Liquid biopsy matrices—including plasma, serum, saliva, and urine—are increasingly used for non-invasive cancer detection, companion diagnostics, and recurrence monitoring. However, conventional column-based purification and double-stranded DNA library preparation fail to capture the full cfDNA landscape, particularly ultra-short fragments and single-stranded DNA (ssDNA). We evaluated a novel nucleic acid purification method paired with an ssDNA-compatible library preparation workflow to enable more comprehensive cfDNA profiling, serum and saliva samples as model systems.

Results: We compared several commercially available bead-based cfDNA extraction methods. The MAGicBead cfDNA Isolation Kit, which incorporates a novel nucleic-acid-binding surface, yielded the highest cfDNA recovery. Recovered cfDNA was processed using a library preparation workflow derived from the original Splinted Ligation Adapter Tagging (SPLAT) chemistry, enabling capture of both dsDNA and ssDNA. A distinct population of ultra-short DNA fragments (35-75 bp) was observed in the mapped reads and was detected only with MAGicBead purification, while the dominant nucleosome-associated peak was retained.To determine whether these ultra-short fragments were single-stranded, isolated cfDNA was treated with a single-strand-specific nuclease prior to library preparation. Following digestion, the short-fragment signal was no longer detectable, confirming their ssDNA nature and underscoring the need for an ssDNA-compatible SPLAT-derived workflow.We next applied the optimized workflow to plasma from lung cancer patients and observed differences in the proportion of ultra-short cfDNA fragments relative to healthy controls, suggesting potential fragmentomic utility.Because saliva is an emerging but technically challenging liquid biopsy matrix due to mixed human-microbial content and heterogeneous fragmentation, we further evaluated the workflow in saliva. The ssDNA fragment population was again recovered, and sequencing simultaneously revealed microbial signatures, demonstrating that the workflow captures both host and microbial DNA in a single run and supports a multi-omic approach that may enhance diagnostic performance.

Conclusions: The MAGicBead cfDNA Isolation Kit, combined with SPLAT DNA library preparation, enables robust recovery of ultra-short cfDNA fragments that are routinely lost with conventional workflows. This approach supports comprehensive cfDNA profiling across and below the nucleosome-size range. Our pilot studies reveal previously unrecognized cfDNA features and point toward more sensitive strategies for cancer diagnostics and biomarker discovery.

#3212 Enhancing the detection of circulating tumor DNA by combining Interlace™ global methylation discovery with next-generation sequencing test Labcorp Plasma Complete™.

Kimberly A. Holden[1], Cynthia Maddox[2], Calum Mould[3], Nana Mensah[3], Luca Tosti[3], Iwo Pieniak[3], Paulina Siejka-Zielinska[3], Stephen Evans[3], Debora Lucarelli[3], Robert Neely[3], Anthony Smith[3], Kenneth C. Valkenburg[2], Marcia Eisenberg[4], Brian Caveney[4], Eric Severson[4], Taylor J. Jensen[4], Shakti Ramkissoon[4], Jonathan Williams[1]

[1]Labcorp, San Diego, CA,[2]Labcorp, Baltimore, MD,[3]Tagomics, Ltd., Cambridge, United Kingdom,[4]Labcorp, Durham, NC

Genome-wide methylation patterns are a powerful biomarker. The detection of aberrant methylation has many oncological applications, including using tumor DNA for cancer detection and therapy selection. In liquid biopsies, the ability to detect small amounts of circulating tumor DNA (ctDNA) is crucial to enable earlier diagnosis, monitor minimal residual disease, and assess treatment response. This study evaluated Interlace, an enzymatic technology that enriches unmethylated DNA molecules, to detect ctDNA. This methodology uses an engineered methyltransferase enzyme to target and tag unmethylated CpG sites across the genome. Libraries are then prepared from these tagged regions and sequenced while simultaneously allowing unenriched product to be utilized for downstream molecular applications such as hybrid capture. Interlace was run in parallel with Labcorp Plasma Complete (LPC), a 521-gene next-generation sequencing (NGS) hybrid capture assay that detects genetic alterations in cell free DNA (cfDNA) from the plasma of cancer patients. LPC reports single nucleotide variants (SNVs), insertions and deletions (indels), translocations, copy number amplifications, microsatellite instability (MSI), and blood tumor mutation burden (bTMB). To evaluate the analytical performance of the two tests in parallel, a sample cohort (n=45) including cfDNA reference samples, noncancerous wild-type controls, cancer cell lines, and cfDNA from cancer patients was processed. A head-to-head comparison of LPC results for samples processed with and without the Interlace assay demonstrated 96.7% positive percent agreement and 99.5% positive predictive value. Interlace was able to detect tumor DNA down to 0.1% tumor content in a dilution series created by mixing sheared tumor and wild-type cell line DNA, representative of ctDNA, at target concentrations from 0% to 10%. Using identified differentially methylated regions as input into unsupervised clustering or a proprietary machine learning model, Interlace was able to differentiate blinded cancer cfDNA from cancer cell lines from wild-type samples. Multiomics platforms that evaluate multiple analytes from a single sample, as described here, are powerful tools to provide a more comprehensive view of patient samples. The combination of LPC for somatic variant reporting with Interlace methylation-based ctDNA detection may allow for increased sensitivity in reporting circulating tumor DNA in plasma samples from cancer patients.

#3213 Utility of TAPS+: a positive-readout methylation sequencing approach for high-fidelity epigenetic profiling.

Kimberly A. Holden[1], Kerry D. Fitzgerald[1], Adib Shafi[1], Ashraf Shabaneh[1], Dennis D. Krutkin[1], Tong Liu[1], Eyad Almasri[1], Graham McLennan[1], Nathan Faulkner[1], Craig Marshall[2], Travis Sanders[2], Thomas Harrison[2], Eduard Casas[2], Kristina Giorda[2], Doug Wendel[2], Brian Kudlow[2], Shakti Ramkissoon[3], Marcia Eisenberg[3], Brian Caveney[3], Eric Severson[3], Taylor J. Jensen[3], Jonathan Williams[1]

[1]Labcorp, San Diego, CA,[2]Watchmaker Genomics, Boulder, CO,[3]Labcorp, Durham, NC

Accurate methylation sequencing from clinical samples is challenging due to DNA-damaging chemistries that reduce sequence diversity, limiting data quality and reproducibility—particularly for fragmented or low-input materials such as cfDNA. The objective of this study was to evaluate a new positive-readout methylation method (TAPS+) in a clinically relevant cohort and compare its performance to an enzymatic methylation conversion method employing a negative-readout approach. TAPS+ is a non-damaging chemistry that converts methylated cytosines to thymines while preserving unmethylated cytosines, maintaining full sequence complexity and enabling direct methylation detection. This method was applied to a 24-sample cohort comprising invasive breast carcinoma patients, healthy donors, and control samples spanning a range of methylation states. Libraries were sequenced in parallel with those from an enzymatic negative-readout method to assess conversion efficiency, background, and biological concordance of differentially methylated regions (DMRs). The R package methylKit was used for DMR analysis, and biomarker candidates were identified based on statistically significant methylation differences within annotated genomic regions. Compared to the negative-readout method, TAPS+ achieved a shorter turnaround time and higher library yields across all sample types. In cfDNA samples, TAPS+ produced significantly higher methylation ratios than the negative-readout method ($p = 8.6e-10$). A methylated control showed an 88.8% 5mC rate with TAPS+, versus 76.8% with the negative-readout method, suggesting greater accuracy. CpG island methylation was strongly correlated across methods, though the negative-readout method had greater noise at low coverage sites. Both breast cancer patients and healthy individuals exhibited a characteristic dip in average DNA methylation levels around transcription start sites, consistent with promoter hypomethylation, with no significant differences observed between cohorts. DMR analysis with TAPS+ identified significant biomarker candidates, including *SHH* hypermethylation ($q = 3.15e-5$), associated with cancer development and progression. Additional biomarkers were associated with developmental pathways, cancer signaling, transcriptional regulation, and immune response. The negative-readout dataset did not demonstrate strong biomarker candidates indicative of disease status. TAPS+ enables high-fidelity methylation sequencing from diverse and challenging clinical materials, supporting robust epigenetic analysis within a streamlined workflow. The positive-readout approach demonstrated superior data quality and biological relevance compared to an enzymatic negative-readout method, highlighting its potential utility for translational research, early detection, and clinical assay development.

#3214 Dysregulation of the RNA modification m6A promotes cancer progression and provides therapeutic opportunities.

Gudrun Stengel, Zachary Miles, Eric Davis, Byron Purse

Alida Biosciences Inc, San Diego, CA

The objective of this study is to determine how sensitive detection and quantitation of the RNA modification *N*6-methyladenosine (m6A) can enable cancer detection, mechanistic insights into tumor biology, and improved monitoring of treatment responses. RNA modifications, which are co- and post-transcriptional alterations to nucleobases or ribose, are key regulators of nearly all aspects of RNA metabolism, including transcription, splicing, localization, translation, stability, and interactions with RNA-binding proteins. Among these, m6A is the most abundant modification in human mRNA and long noncoding RNA and is frequently dysregulated in cancer. To enable comprehensive analysis of RNA modifications, we applied a multiplexed proximity-barcoding assay that enriches for modified RNA fragments, encodes modification sites during cDNA synthesis, and quantifies their abundance at each locus using synthetic spike-in controls for calibration. This approach allows concurrent detection of m6A, inosine, and pseudouridine, providing a multidimensional, high-sensitivity view of the cancer epitranscriptome. Application of this assay to neuroblastoma samples and cell line-derived xenograft tumor models revealed consistent increases in m6A abundance across all tumor types examined. Notably, m6A peak patterns also distinguished MYCN-amplified (MNA^+) from ALT-activated (ALT^+) and low-risk neuroblastomas, demonstrating that the method can resolve biologically and clinically distinct subgroups. Treatment of neuroblastoma cell lines and xenograft-derived samples with STC-15, a small-molecule inhibitor targeting the primary m6A writer enzyme METTL3, led to a dose-dependent reduction in m6A levels measurable by this assay. METTL3 inhibition was associated with decreased tumor cell viability and increased sensitivity to chemotherapeutics such as doxorubicin. Sensitive, quantitative measurement of m6A and related RNA modifications provides a powerful strategy to detect cancer-associated epitranscriptomic dysregulation, to dissect molecular heterogeneity in neuroblastoma, and to monitor therapeutic responses to METTL3-targeted interventions.

: Epigenomics
Poster Session

#3219 Arid1a directs lineage specification in mammary epithelial cells.

Erik Ladewig[1], Amaia Arruabarrena-Aristorena[2], Estelle Deby[3], Srushti Kittane[4], Fresia Pareja[5], Ryan Blawski[6], Yangzhenyu Gao[7], Laura Baldino[1], Vito Rebecca[4], Emiliano Cocco[8], Hongkai Ji[4], Pau Castel[9], Christina Leslie[1], Wouter Karthaus[10], Eneda Toska[11]

[1]Memorial Sloan Kettering Cancer Center, New York, NY,[2]Department of Genetics, Physical Anthropology and Animal Physiology, University of the Basque Country UPV/EHU, Bilbao, Spain,[3]School of Life Sciences, Swiss Institute for Experimental Cancer Research (ISREC), Lausanne, Switzerland,[4]Johns Hopkins University, Baltimore, MD,[5]Memorial Sloan Kettering Cancer Center, New York, NY,[6]Johns Hopkins Medicine, Baltimore, MD,[7]Biochemistry and Molecular Biology, Johns Hopkins University, Baltimore, MD,[8]University of Miami, Miami, FL,[9]NYU Grossman School of Medicine, San Francisco, CA,[10]The Ecole polytechnique federale de Lausanne, Lausanne, Switzerland,[11]Johns Hopkins University School of Medicine, Baltimore, MD

Epigenetic regulation is essential for mammary gland development, yet the specific chromatin remodelers that govern mammary epithelial cell fate remain poorly defined. Mutations in SWI/SNF chromatin remodeling complex subunits occur in more than 20% of human cancers, with ARID1A being the most frequently altered. In breast cancer, ARID1A loss of function mutations are enriched in metastatic estrogen receptor-positive (ER^+) disease and associated with endocrine therapy resistance. To define the developmental role of Arid1a in vivo, we generated mice with mammary epithelium specific Arid1a deletion. These animals displayed disrupted ductal branching and aberrant terminal end bud formation. Mammary organoids derived from Arid1a deficient tissue further revealed abnormal cystic morphology and impaired differentiation. To dissect the molecular consequences of Arid1a loss, we performed single cell multiomic profiling that combine single nucleus RNA and chromatin accessibility sequencing from the same cells, together with H3K27ac and BRG1 CUT&RUN-seq. Arid1a loss caused a collapse of normal mammary epithelial lineage architecture, with single cell analyses showing failure to maintain basal, luminal progenitor, and alveolar identities. Instead, Arid1a deficient cells were restricted to an undifferentiated luminal hormonal like state characterized by reduced estrogen receptor signaling competence. Chromatin profiling revealed profound remodeling, including decreased accessibility and impaired SWI/SNF targeting at lineage defining transcription factors (TF) such as Foxa1, Gata3, and Sox9. A CRISPR/Cas9 pooled loss of function screen identified Foxa1 and Meis1 as essential regulators whose deletion recapitulated the Arid1a null phenotype, positioning them as downstream effectors required for mammary cell fate specification. Notably, Meis1 emerged as a previously unrecognized regulator of luminal hormonal identity. Our work provides a framework for understanding how Arid1a rewires the chromatin landscape and transcriptional network in normal mammary development. By identifying lineage specific TF motifs and critical regulators like Meis1, we identify new opportunities for targeted therapeutic intervention.

#3220 Integrated epigenomic profiling reveals distinct transcription factor networks driving therapy resistance in estrogen receptor positive metastatic breast cancer.

Gizem Yayli-Vokshi[1], Sandra Cohen[2], Weiling Li[1], Hong Shao[3], Sydney Bowker[4], Elisa de Stanchina[4], Pedram Razavi[5], Sarat Chandarlapaty[5], Ekta Khurana[6]

[1]Systems and Computational Biomedicine, Weill Cornell Medicine, New York, NY,[2]Sandra and Edward Meyer Cancer Center, Weill Cornell Medicine, New York, NY,[3]Human Oncology and Pathogenesis Program, Memorial Sloan Kettering Cancer Center, New York, NY,[4]Anti-Tumor Assessment Core, Memorial Sloan Kettering Cancer Center, New York, NY,[5]Memorial Sloan Kettering Cancer Center, New York, NY,[6]Weill Cornell Medicine, New York, NY

Background: Endocrine therapy resistance in estrogen receptor positive metastatic breast cancer remains poorly understood, with many resistant tumors lacking actionable genomic alterations. Emerging evidence suggests epigenetic reprogramming drives resistance through transcription factor regulatory network rewiring, yet comprehensive epigenomic characterization of resistant tumors remains limited.
Methods: We performed integrated ATAC-seq and RNA-seq profiling in clinically relevant models of therapy-resistant and sensitive estrogen receptor positive metastatic breast cancer, including patient-derived xenografts harboring diverse genomic alterations, along with sensitive breast cancer cell lines. We applied unsupervised clustering to chromatin accessibility and gene expression data to identify non-genomic clusters. Master regulators were identified by integrating transcription factor binding motif enrichment in accessible chromatin regions with downstream target gene expression networks.
Results: We identified five distinct epigenomic clusters of therapy-resistant estrogen receptor positive metastatic breast cancer, each driven by unique master transcription factor regulatory programs. Cluster 1, comprising all sensitive models such as patient-derived xenografts and cell lines, retained luminal hormone-responsive identity. Therapy resistant tumors segregated into four distinct programs: Cluster 2 showed pioneer factor dominance with enhanced chromatin remodeling while maintaining partial luminal features. Cluster 5 represented an *ESR1*-mutant luminal HER2 hybrid state with *ERBB2* amplification, combining altered estrogen receptor signaling with receptor tyrosine kinase activation. Cluster 4 displayed mesenchymal resistance via epithelial-mesenchymal transition. Cluster 3 represented the most dedifferentiated phenotype, an inflammatory cancer stem cell state with FOXA1 loss.
Conclusion: Our integrated epigenomic approach reveals that therapy-resistance in estrogen receptor positive metastatic breast cancer is orchestrated by four distinct transcription factor-driven regulatory programs that emerge through non-genetic rewiring rather than genomic alterations alone. These clusters span a spectrum from pioneer factor-mediated chromatin remodeling and hybrid luminal-HER2 states to mesenchymal plasticity and inflammatory stem-like networks. Importantly, these epigenetic clusters may explain mutation-negative resistance and reveal subtype-specific therapeutic vulnerabilities. This molecular framework provides a roadmap for precision medicine approaches tailored to the epigenomic state of resistant metastatic breast cancer.

#3221 Profiling histone modifications in single cells to gain insight into the effects of epigenetic drug treatment on tumor cells.

Shuwen Chen[1], Lisa Welter[1], Gilma Sevilla[1], Ploy Setthasap[1], Yana Ryan[1], Shiyi Yin[1], Alan Du[1], Jackson Peterson[1], Mike Covington[1], Mohammad Fallahi[1], Kazuo Tori[1], Bryan Bell[1], Bria Graham[2], Matt J. Meiners[2], Andrea L. Johnstone[2], Keith E. Maier[2], Martis W. Cowles[2], Bryan J. Venters[2], Michael Keogh[2], Xuan Qu[3], Colin McCornack[3], Ting Wang[3], Yue Yun[1], Andrew Farmer[1]

[1]Takara Bio USA, Inc., San Jose, CA,[2]EpiCypher, Inc., Durham, NC,[3]Washington University School of Medicine in St. Louis, St. Louis, MO

Epigenomic remodeling, such as changes in chromatin state, plays a crucial role in cancer biology by regulating gene expression changes that drive tumor progression, immune evasion, and the evolution of therapeutic resistance. Popular methods to study the epigenome include assay for transposase-accessible chromatin with sequencing (ATAC-seq) and chromatin immunoprecipitation sequencing (ChIP-seq). ATAC-seq only profiles open chromatin, missing critical details about the nature of accessible regions or silenced chromatin. ChIP-seq and its newer relative, cleavage under targets and tagmentation (CUT&Tag), provide more detailed information on chromatin states by targeting histone modifications with specific antibodies. ChIP-seq requires 10^6 cells to generate meaningful data—too high for precious samples. CUT&Tag offers higher sensitivity with 10-100x lower input and a significantly simplified workflow. When studying epigenetic changes in cancer, it is widely accepted that single-cell resolution is essential, given the complexity and heterogeneity of tumors and their microenvironment. Hence, there is a high demand to convert current epigenetic assays from bulk to single-cell resolution. In CUT&Tag, DNA is tagmented with a protein A/G-Tn5 fusion enzyme, which inserts sequencing adapters in situ for cell-specific labeling—enabling single-cell resolution. Some labs have experimented with single-cell CUT&Tag (scCUT&Tag), but here we present a novel, ready-to-use, validated method for automated, high-throughput scCUT&Tag. To assess drug induced changes in acetylation, we profiled H3K27ac patterns in thousands of single cells from a lung cancer cell line (A549 WT and A549 p53 KO) before and after epigenetic treatment (decitabine + panabinistat vs DMSO control).We observed global cell-type-specific acetylation in response to epigenetic therapy in both A549 WT and A549 p53 KO cells. When comparing scCUT&Tag data with single-cell total RNA-seq data we found that increased acetylation at gene promoters and enhancers correlated with increased gene expression, corroborating the observed changes in histone modification. In summary, the validated scCUT&Tag method provides a high-throughput, automated approach to identify genes regulated in response to epigenetic drug treatment of tumor cells at the single-cell level. Integrating this single-cell expression data provides deeper insight into cellular regulation, particularly in the context of drug responses in tumor cells.

#3222 Identifying novel biomarkers for Saudi glioblastoma multiform using multi-omics approach.

Abdulmonem A. Alsaleh[1], Ahmed Aloraidi[2], Bahauddeen M. Alrfaei[1]

[1]Blood and Cancer Research, King Abdullah International Medical Research Center, Riyadh, Saudi Arabia,[2]Neurosurgery, , King Abdulaziz Medical City (KAMC), Riyadh, Saudi Arabia

Background: Glioblastoma Multiform (GBM) is a high grade aggressive glioma of the brain and it accounts for almost half of malignant tumours of the central nervous system. As per the latest Saudi Cancer Incidence Report, GBM is the most common central nervous system tumour nationally with about 15 months survival following diagnosis.
Aims: There is a need to identify new molecular biomarkers that can improve diagnostic accuracy and provide a more reliable prognostic prediction, especially for Saudi GBM patients.
Methods: The study recruited 30 consented GBM patients from King Abdulaziz Medical City, Ministry of National Guard Health Affairs (MNGHA) hospitals, Riyadh, under protocol No. RC13/258/R. Resected brain tumour tissues were collected on surgery day and immediately were snap-frozen. DNA and RNA extraction were conducted as per standard protocols. Libraries for Illumina Whole Genome Sequencing, Illumina RNA Sequencing and MGI Whole Genome Bisulfite Sequencing were prepared as per manufacturer's protocols. Analysis pipeline included: 1) quality check of sequence reads, 2) trimming, 3) mapping to reference genome (annotation), 4) generating hit counts, 5) pairwise comparison/enrichment analysis, and 6) pathway analysis.
Results: Preliminary RNA sequencing data of two trial GBM samples has generated 19k and 21k paired end 2 x 150 sequence reads. Majority of the sequence reads (87%) had good quality (Phred Score > 30) and majority had a unique genome mapping (70% of sequence reads). The analysis revealed 19,007 normalised counts and the two samples had high correlation (Spearman's correlation $r = 0.787$, $P < 0.001$). Additionally, the analysis identified 904 Differentially Expressed Genes (DEG), of which 434 and 470 upregulated and downregulated genes, respectively. Additional sequencing data are expected to be generated with full multi-omics integration analysis to be done.
Conclusion: This study marks the first to investigate the GBM multi-omics profile of the untapped Saudi GBM and to further identify and validate novel biomarkers that are population-specific to guide clinical diagnosis and prognosis for GBM.

#3223 Chromatin profiling from formalin-fixed paraffin-embedded samples for biomarker discovery.

Andrea Lynn Johnstone, Eva Brill, Vishnu U. Kumary, Morgan Oatley, Martis W. Cowles, Michael-Christopher Keogh, Bryan J. Venters

EpiCypher, Inc, Durham, NC

As the oncology field moves towards a precision medicine model of patient care, understanding and profiling the epigenetic landscape is increasingly important. Gene expression and cell function are regulated by epigenomic features, including histone post-translational modifications (PTMs), transcription factors, and other chromatin proteins. Mapping the location of these features provides a powerful approach to study chromatin mechanisms driving disease and can be leveraged for biomarker and drug development. Formalin-fixed paraffin-embedded (FFPE) tissues banked from cancer clinical trials could be a rich resource for retrospective biomarker studies, due to their association with drug response and disease progression data. However, using FFPE tissues for genomic mapping assays has been technically challenging for multiple reasons. For instance, the removal of paraffin, heavy cross-linking conditions, and degraded nucleic acids can make FFPE samples unsuitable for standard transcriptomic and epigenomic mapping assays (RNA-seq, ATAC-seq, ChIP-seq). To better leverage chromatin profiling for translational research, we developed a modified CUT&Tag workflow that is compatible with FFPE samples (CUT&Tag-FFPE). CUT&Tag (Cleavage Under Targets and Tagmentation) is an immunotethering-based strategy that uses pAG-Tn5 to selectively cleave and ligate sequencing adapters at antibody-bound chromatin. The entire assay takes place on-slide with intact cells or nuclei extracted from scrolls, enabling a highly streamlined workflow. In this study, we optimized every major step of the workflow, including paraffin removal, *in situ* tissue permeability or nuclei extraction, crosslink removal, antibody selection, and tagmentation. We have applied these modifications to successfully map transcription-linked open chromatin across a variety of FFPE sample tissue types from mouse and human. We find that CUT&Tag-FFPE correlates with RNA-seq and ATAC-seq from corresponding fresh, frozen material. Additionally, we observed open chromatin at tissue specific promoters and at distal elements, such as enhancers. By enabling insights into genomic regulatory mechanisms from FFPE biorepositories, CUT&Tag-FFPE has the potential to accelerate biomarker discovery and drug development research for precision oncology.

#3224 Loss of PIWIL4-piRNA interaction reveals uncertain somatic epigenomic evolution.

Yu-Wei Leu, Shu-Huei Hsiao

National Chung Cheng Univ., Chiayi County, Taiwan

Analyzing genomic and epigenomic changes that are either randomly or causally induced enhances precision medicine. Knockout (KO) of the Piwi-interacting RNAs (piRNA)-interacting genes *PIWIL4* or *L1TD1* in cancer and normal cells may unleash the oncogenic evolution to produce genomic alterations and subsequent alternations. Our findings show that whereas the binding motifs of important epigenetic markers (CTCF, acetylated histone H3 at lysine 27, and trimethylated histone H3 at lysine 9) were maintained in KOs, their global binding sites were markedly changed. Changes in transposable element abundance, chromatin conformation, transcript variations, and gene expression profiles were all found at the same time. Additionally, we discovered new oncogenic insertions and deletions (indels) in the coding sequences of the KOs, indicating separate gene evolution. Our findings also show an unanticipated epigenomic evolution through altered chromatin locations and evolutionary rates. Significantly, we discovered similar patterns of altered transcript variants, increased indels, and transposable element shifts in a number of models, including models of myeloproliferative neoplasm (MPN) expressed by JAK2V617, aged mesenchymal stem cells, *SARS-CoV-2* replicon-expressed cells, and a fetal alcohol syndrome rat model. Genetic reversion was unable to restore these modified transcript variants or transposable element abundances, according to a convincing finding from an MPN model. These results offer strong support for piRNAs' role in somatic genome protection and a potential uncertainty law in epigenomic evolution. (Supported by NSTC 114-2320-B-194 -001, Taiwan)

#3225 Resolving genome regulatory complexity with new multiomic long-read sequencing tools for chromatin state and genetic variation.

Lu Sun[1], James T. Anderson[1], Connor P. Frasier[1], Allison R. Hickman[1], Sabrina R. Hunt[1], Emily A. Madden[1], Keith E. Maier[1], Andrea L. Johnstone[1], Zu-Wen Sun[1], Martis W. Cowles[1], Andrew B. Stergachis[2], Bryan J. Venters[1], Michael-Christopher Keogh[1]

[1]Epicypher Inc, Durham, NC,[2]Devision of Medical Genetics, Department of Medicine, University of Washington, Seattle, WA

High-resolution epigenomic insights are vital to inform the discovery of biomarkers and mechanisms in cancer research. Modern short-read sequencing (SRS) methods such as ATAC-seq, WGBS, and CUT&RUN/ChIP-seq have served as workhorses for studying chromatin architecture, but they are fundamentally limited. These methods lack multiomic insights, requiring labor-intensitve, costly, and sample-consuming parallel assays. Moreover, these assays fragment DNA, losing critical information about coordinated regulatory effects, and are blind to repetitive and structurally complex regions of the genome. These limitations constrain progress in understanding gene regulation and translating genetic discoveries into clinical insights. To overcome these limitations, EpiCypher is developing multiomic long-read sequencing (LRS) technologies that enable single-molecule epigenomic profiling. These approaches directly record chromatin features onto native DNA, preserving the intrinsic relationships between chromatin states and genetic variation across individual DNA molecules. Fiber-seq employs an N6-adenine (6mA) methyltransferase (Hia5) to record chromatin accessibility directly onto DNA, while retaining endogenous DNA methylation (5mC). We have streamlined Hia5 manufacturing and labeling workflows, enabling robust single-molecule chromatin accessibility profiling with near base-pair resolution, readily adopted at the bench. Fiber-seq reveals precise transcription factor (TF) binding footprints and cis-regulatory haplotypes as demonstrated in a genetic disease diagnosis (PMID: 40166185), highlighting its potential for variant-to-function discovery in diseases. DAF-seq (Deaminase-Assisted single-molecule chromatin Fiber sequencing), complements this approach by using a dsDNA cytosine deaminase (SsDddA) to encode chromatin accessibility as a mutation maintained through PCR amplification. As a result, DAF-seq can deliver high-resolution chromatin profiles and TF footprints from low-inputs or even single-cells (bioRxiv DOI: 10.1101/2024.11.06.622310). Remarkably, DAF-seq delivers nearly a 7,000-fold improvement in genome coverage compared to leading single-cell ATAC-seq technologies, while operating at a fraction of the cost.Together, Fiber-seq and DAF-seq represent a versatile toolkit: Fiber-seq provides an unbiased multiomic discovery to simultaneously assess chromatin accessibility, DNA methylation, and inferred TF binding genome-wide; while DAF-seq enables targeted chromatin accessibility mapping from low-input samples, resolving heterogeneity at single-molecule resolution. These LRS technologies bridge genetic and chromatin regulatory information on single molecules to reveal disease mechanisms, define drug responses, and drive precision medicine.

#3226 FOXA1 alterations drive endocrine therapy resistance through unique transcriptional and epigenomic programs in breast cancer.

Srushti Kittane[1], Subhiksha Nandakumar[2], Enrico Moiso[2], Walid Khaled Chatila[2], Yangzhenyu Gao[3], Elza C. de Bruin[4], Claudette Falato[5], Ji Li[6], Hongkai Ji[7], Nikolaus Schultz[2], Maurizio Scaltriti[8], Pedram Razavi[2], Eneda Toska[9]

[1]Johns Hopkins University, Baltimore, MD,[2]Memorial Sloan Kettering Cancer Center, New York, NY,[3]University of North Carolina, Chapel Hill, MD,[4]AstraZeneca Oncology R&D, Cambridge, United Kingdom,[5]AstraZeneca Oncology R&D, Barcelona, Spain,[6]AstraZeneca Oncology R&D, Boston, MA,[7]Johns Hopkins Bloomberg School of Public Health, Baltimore, MD,[8]AstraZeneca Oncology R&D - MedImmune, LLC, Gaitherburg, MD,[9]Johns Hopkins University School of Medicine, Baltimore, MD

Breast cancer is histologically classified into invasive ductal carcinoma (IDC, ~70-80% of cases) and invasive lobular carcinoma (ILC, 10-15%). Both are predominantly estrogen receptor-positive (ER+) and treated with endocrine therapy, yet resistance inevitably develops, driving metastasis and poor outcomes. ILC exhibits hallmark E-cadherin loss, distinct metastatic patterns, and reduced endocrine therapy response compared with stage-matched IDC. However, treatment remains uniform across histologies, underscoring the need to define shared and subtype-specific drivers of resistance. Clinicogenomic analyses of >8,500 MSK-IMPACT tumors revealed recurrent FOXA1 mutations in ER+ disease, enriched in ILC (8% vs 4% in IDC). As a pioneer transcription factor that licenses ER chromatin binding, FOXA1 alterations may reshape ER signaling to promote therapy resistance. To investigate this, we functionally characterized recurrent FOXA1 Helix 1 (H1), Wing2 (W2), and betastrand3 (S3) mutations in IDC (MCF7, T47D), and H1, W2 variants in ILC (MDA-MB-134VI). We assessed treatment response under estrogen deprivation, fulvestrant or oral SERDs ± CDK4/6i and profiled transcriptional and chromatin changes using RNA-seq, ER CUT&RUN, ATAC-seq, and qPLEX-RIME. Across both histologies, FOXA1 mutations conferred a selective growth advantage under estrogen deprivation modeling AI therapy, while retaining sensitivity to SERDs and SERD+CDK4/6i. Mechanistically, H1 mutants were hypermorphic in IDC and ILC, increasing ER recruitment and chromatin accessibility to strengthen canonical estrogen-responsive programs. W2 variants exhibited histology-specific consequences: in IDC they increased ER chromatin binding without pioneering, consistent with enhanced EP300/NCOA3 co-activator engagement, whereas in ILC they also increased accessibility, displaying lineage-restricted pioneer function. Ductal-specific S3 mutants were neomorphic, redirecting FOXA1 to an alternative DNA motif, reprogramming accessibility, and activating proliferation, metabolic, and endocrine-resistant gene networks. Interactome profiling supported enrichment of stemness-linked chromatin remodeling networks.Together, these findings demonstrate that recurrent FOXA1 mutations establish mechanistically distinct oncogenic classes that promote endocrine resistance in ER+ breast cancer with their distribution differing by histology. ILC is enriched for hypermorphic H1 and W2 variants that enhance pioneering and chromatin opening, whereas IDC harbors W2 mutants lacking pioneer activity and neomorphic S3 variants that rewire chromatin. These insights support FOXA1 mutation status as a biomarker of aromatase inhibitor resistance and highlight the need for histology-tailored therapeutic strategies.

#3227 Defining neural molecular features and their functional significance in lung cancer.

Reshmee Bhattacharya, Daphni van Rinsum, Anna Dykhno, Hideo Watanabe

Division of Pulmonary, Critical Care and Sleep Medicine, Department of Medicine, Icahn School of Medicine at Mount Sinai, New York, NY

Background: Lung cancer remains the leading cause of cancer-related mortality, accounting for over 150,000 deaths annually in the US. Although genomic characterization and immunotherapy have significantly reshaped the treatment landscape, overall 5-year survival remains low at ~29.7%, partially due to the heterogeneity across and within histologic subtypes. Lung cancers with neuroendocrine (NE) features exhibit particularly aggressive clinical behavior, including high rates of brain metastasis and poor responsiveness to immunotherapy. Emerging evidence suggests that a subset of LUAD acquires neural traits independent of NE identity. Acquisition of intrinsic neuron-like electrical activity in NE-SCLC drives tumorigenic capability and metastatic potential has been also reported. These neural features may represent an unrecognized biological axis associated with lineage plasticity, metastasis, and immune escape.

Rationale and hypothesis: Our previous epigenomic studies identified neural-like lineage subclasses within LUSC (nLUSC) signified by SOX2/BRN2 circuitry in contrast to classical subset signified by SOX2/TP63 circuitry. Neural factors were unexpectedly co-opted in lung cancer to establish enhancer landscapes consistent with neural developmental pathways. We hypothesize that co-opted neural circuitries establish neural-like epigenomic programs in lung cancers, conferring enhanced neural affinity and intrinsic immune privilege that facilitate metastasis and resistance to immunotherapy.

Experimental procedures: First, we cultured nLUSC cell lines with or without ectopic dNp63 expression that suppresses neural program and quantified migration toward differentiated human glutamatergic neurons in transwell, along with profiling transcriptomic and epigenomic remodeling upon interaction with neurons. Second, we stimulated a panel of classical and neural LUSC cells with IFN-γ to measure the antigen presentation activity. We co-cultured T cells with LUSC lines and measured intracellular and released Granzyme B and perforin levels to quantify T cell-mediated cytotoxicity, along with profiling transcriptomes and enhancer landscapes to identify enrichment of neural signatures.

Results: nLUSC exhibits functionally distinct behaviors compared to their classical counterparts. nLUSC cells demonstrated enhanced migratory capacity towards neurons. Classical cells maintained stronger antigen-presenting potential by both MHC-I and MHC-II markers at baseline and predominantly upregulated APM and enhanced their immunogenicity, whereas nLUSC cells exhibited a more immunosuppressive response; e.g., upregulation of PD-L1**,** CD95 and HLA-E upon IFNγ stimulation.

Conclusions: The study reveals that neural and classical lung cancer subtypes are not only transcriptionally divergent but also functionally distinct in behaviors relevant to neural affinity and immune escape.

#3228 Spatial epigenomic landscape of NF-PanNETs defines tumor progression and microenvironmental niches.

Yang Liu, Dejiang Wang, Xiangjun Di, Jing Du

Yale University, New Haven, CT

Non-functional pancreatic neuroendocrine tumors (NF-PanNETs) display substantial clinical and biological heterogeneity, yet the epigenetic mechanisms and spatial contexts that shape this diversity remain poorly defined. To address this gap, we performed an integrated analysis combining single-nucleus ATAC-seq (snATAC-seq) with spatial ATAC-seq across tumors of varying grades. snATAC-seq resolves chromatin accessibility landscapes for distinct tumor subtypes, immune populations, and cancer-associated fibroblasts (CAFs), uncovering transcription factor (TF) programs that underpin tumor progression and modulate microenvironmental interactions. Spatial ATAC-seq adds a critical layer of context, revealing two major tumor-stroma ecological niches: a proliferative niche characterized by E2F, MYC, and mTORC1 signaling, and an invasive niche enriched for Snail family TFs and KRAS pathway activation. These spatially anchored regulatory circuits highlight how NF-PanNET cell states emerge from the interplay between intrinsic epigenetic programs and local tissue environments. Collectively, our study establishes a spatially resolved epigenomic framework for dissecting NF-PanNET heterogeneity and evolution, providing new biomarkers, regulatory axes, and mechanistic insights with implications for molecular stratification and precision therapy.

#3229 The chromatin remodeler SMARCA5 displays ancestry-specific functions in African American prostate cancer.

Shahid Hussain[1], Khalid Mir[2], Sajad A. Wani[3], Solomon Rotimi[4], Lara Sucheston-Campbell[2], Clayton C. Yates[5], **Moray J. Campbell**[1]

[1]Cedars-Sinai Medical Center, Los Angeles, CA,[2]Karmanos Cancer Institute, Detroit, MI,[3]University of Cincinnati, Cincinnati, OH,[4]Covenant University, Ota, Ogun State, Nigeria,[5]Sidney Kimmel Comprehensive Cancer Center, Baltimore, MD

Previously, we identified that BAZ1A and SMARCA5 were significantly downregulated in in African American (AA) prostate cancer (PCa), and that BAZ1A altered vitamin D receptor (VDR)-dependent transcriptional sensitivity. SMARCA5 is the ATPase core of different chromatin remodeling complexes, including WICH that promotes accessible chromatin at developmental enhancers, and NoRC, which mediated repression of rDNA transcription and contributes to nucleolar stress pathways. In the current study we tested how ancestry shaped the composition and impact of the SMARCA5 complex. Integrative ATAC-Seq, and H3K27ac and AR CUT&RUN in AA (RC43T and RC77T) and European American (EA, LNCaP) PCa cell models revealed AA-specific H3K27ac marked accessible chromatin. These regions were enriched for motifs including the basic leucine zipper/AP-1 motifs such as BATF and significantly intersected AA PCa enhancer landscapes. Likewise, the AR cistrome from AA PCa cell lines significantly intersected with the AR cistrome derived from AA primary tumors. To test whether SMARCA5 complex composition and function differed by ancestry, we performed CRISPR activation of SMARCA5 in AA and EA PCa models. RIME revealed selective assembly of SMARCA5 with WICH and NoRC subunits in AA, but not in EA cells. CUT&RUN demonstrated that AA-enriched SMARCA5 complexes targeted distinct enhancers and promoters compared to LNCaP cells and mirrored the basal H3K27ac cistromes. Reflecting lineage- and stress response-specific roles the AA SMARCA5 cistrome was enriched BATF, VDR, and p53/p73 motifs. Transcriptomic analysis demonstrated that SMARCA5 activation induced a strong luminal differentiation program unique to AA PCa, supported by GSEA. SMARCA5 controlled VDR target genes in AA cells included VDR governed miRNA (e.g. miR-200c) that also related to differentiation. Integrated ATAC- and RNA-Seq analyses demonstrated that luminal genes were the dominant contributors to active enhancer-transcriptome correlations in AA PCa, confirmed using random forest approaches. Finally, ancestry-stratified clinical cohorts from Africa, AA, and EA PCa showed significant clinical associations between vitamin D levels, SMARCA5-dependent gene signatures and tumor grade. Together, these findings suggest that reduced SMARCA5 expression impacts both the availability of lineage-defining active enhancers and the establishment of heterochromatin boundaries, potentially in response to stress (and mediated by p53/p73 pathways). In this manner, ancestry selectively disrupts the SMARCA5 complex, and shapes transcriptional outputs. SMARCA5 complex composition and its chromatin outputs represent ancestry-stratified features with potential biomarker and therapeutic relevance in AA PCa.

#3230 Epigenomic rewiring driven by BAP1 loss in uveal melanoma.

Gulum Yenisehirli[1], Aristeidis G. Telonis[1], Renata L. Volonterio[1], Monica Lopez[1], Jeffim N. Kuznetsoff[1], Ashley N. Zuniga[1], J. William Harbour[2], Zelia M. Correa[1], Stefan Kurtenbach[1]

[1]University of Miami Miller School of Medicine, Miami, FL,[2]Ophthalmology, UT Southwestern Medical Center, Dallas, TX

Loss-of-function mutations of the epigenetic regulator BAP1, the catalytic subunit of the PR-DUB complex, are among the strongest predictors of metastasis in uveal melanoma (UM). Although BAP1 loss is known to disrupt chromatin organization, the specific epigenetic mechanisms that reshape cell identity and promote tumor progression remain poorly defined. Here, we investigated the epigenomic rewiring driven by BAP1 loss using ATAC-seq, reduced-representation bisulfite sequencing, histone modification profiling, and RNA-seq across three BAP1-wildtype and three BAP1-mutant UM cell lines, as well as a normal human uveal melanocyte (UMC) cell line and its isogenic BAP1-knockout counterpart. This design enabled us to isolate the BAP1-dependent chromatin and transcriptional changes in both normal and transformed uveal cells. BAP1-mutant UM displayed coordinated activation of angiogenic and neuronal-mimicry gene programs, accompanied by suppression of immune and inflammatory signaling. Chromatin accessibility analyses revealed a broad reduction of SOX family activity in both UM and melanocyte models lacking BAP1, suggesting that BAP1 maintains lineage-defining SOX programs. In parallel, we identified a distinct set of transcription factors consistently enriched across all UM lines, independent of BAP1 status, highlighting conserved regulatory networks underlying UM biology. DNA methylation profiling uncovered an unexpected global hypomethylation phenotype in BAP1-mutant UM, further highlighting a broader role for BAP1 in maintaining epigenomic organization. Together, these data reveal the multilayered epigenomic consequences of BAP1 mutations and identify regulatory circuits driven by BAP1 loss that drive tumor progression and metastasis in uveal melanoma.

#3231 Chromatin profiling reveals the impact of fulvestrant on estrogen receptor-driven chromatin dynamics in breast cancer cells.

Celine Barlier[1], Mathias Simplicien[1], Ana Hermoso[1], Anais Pourrat[1], Elsa Moreau[1], Celia Fontana[2], Aurelia Delherme[2], Natalie Daluege[3], Gurpreet Bharaj[3], Cibele de Oliveira[3], Alexander Vogt[3], Vincent Piras[1], Coralie Hoareau-Aveilla[1], **Francisco Cruzalegui**[1], Gaylor Boulay[1], Isabel Paiva[1]

[1]Evotec SE, Toulouse, France,[2]Evotec ID, Lyon, France,[3]Evotec, Hamburg, Germany

Background: Epigenetic dysregulations are linked to various diseases, including cancer. Among them, breast cancer is the second leading cause of cancer-related deaths in women with 50% of mortalities attributable to estrogen receptor-positive (ER+) tumors. Endocrine therapies targeting the ER such as Tamoxifen, Fulvestrant (FULV) and Aromatase inhibitors, are widely used in the clinic. Among these therapeutic agents, FULV has been shown to fully antagonize ER activity, primarily through the rapid degradation and elimination of ER from target tissues. However, recent findings indicate that ER, when engaged with FULV, retains the ability to translocate to the nucleus and bind DNA whereas appearing transcriptionally inert.

Results: In this study, we aimed to further investigate the effects of FULV and Estradiol (E2), the natural ER ligand, on ER cistrome, chromatin accessibility, gene transcription, and H3K27ac genome-wide patterns in ER+ breast cancer cell lines. Using the innovative CUT&Tag technology, we first confirmed that both FULV and E2 promote ER binding to DNA. Our findings revealed that E2 not only enhances chromatin accessibility and gene expression but also increases H3K27ac levels at ER binding sites. In contrast, FULV does not significantly alter chromatin accessibility or transcription but is not completely inert, as it induces increases in H3K27ac at a subset of ER binding sites. These observations indicate a decoupling between histone acetylation and transcriptional output under FULV treatment.

Conclusions: This study provides new insights into the mechanistic impact of FULV on ER activity, highlighting its ability to modulate H3K27ac dynamics even in the absence of transcriptional changes. These findings underscore the complexity of ER signaling and suggest that FULV's therapeutic effects may extend beyond simple antagonism of ER activity.

#3232 NOP16 is a histone mimetic that regulates histone H3K27 methylation and gene repression.

Aamir Khan*[1], Ken Takashima*[2], Dian-Jang Lee[3], Maria Fernanda Trovero[4], Xing Wang[1], M. Hafiz Rothi[4], Ying Zhang[3], Zilan Li[5], Sarah Niesen[1], Julia Natale[5], Ernst Schmid[3], Joseph Al Haddad[5], Sabine Dietmann[6], Sumio Ohtsuki[7], Shannan Ho Sui[8], Hiroyuki Oshiumi[2], Judy Lieberman[9], Eric Lieberman Greer[1]

[1]Department of Pediatrics, Washington University School of Medicine in St. Louis, St. Louis, MO,[2]Department of Immunology, Kumamoto University, Kumamoto, Japan,[3]Department of Pediatrics, Boston Children's Hospital, Boston, MA,[4]Department of Pediatrics, Harvard Medical School, Boston, MA,[5]Division of Newborn Medicine, Boston Children's Hospital, Boston, MA,[6]Department of Developmental Biology and Center of Regenerative Medicine, Washington University School of Medicine in St. Louis, St. Louis, MO,[7]Department of Pharmaceutical Microbiology, Kumamoto University, Kumamoto, Japan,[8]Bioinformatics Core, Department of Biostatistics, Harvard T.H. Chan School of Public Health, Boston, MA,[9]Professor of Pediatrics, Dana-Farber Cancer Institute, Harvard Cancer Center, Boston, MA

Post-translational modifications of histone tails alter chromatin accessibility to regulate gene expression. Some viruses exploit the importance of histone modifications by expressing histone mimetic proteins that contain histone-like sequences to sequester complexes that recognize modified histones. Here we identify an evolutionarily conserved and ubiquitously expressed, endogenous mammalian protein Nucleolar protein 16 (NOP16) that functions as a H3K27 mimic. NOP16 binds to EED in the H3K27 trimethylation PRC2 complex and to the H3K27 demethylase JMJD3. NOP16 competitively inhibits the interaction between EED and H3K27me3 and causes EED to translocate from the nucleoplasm to the nucleolus, thereby negatively regulating H3K27me3 modification in the nucleoplasm. NOP16 is overexpressed and linked to poor prognosis in breast cancer. Depletion of NOP16 in breast cancer cell lines causes cell cycle arrest, decreases cell proliferation and selectively decreases expression of E2F target genes and of genes involved in cell cycle, growth and apoptosis. Conversely, ectopic NOP16 expression in triple negative breast cancer cell lines increases cell proliferation, cell migration and invasivity *in vitro* and tumor growth *in vivo*, while NOP16 knockout or knockdown has the opposite effect. Thus, NOP16 is a histone mimic that competes with Histone H3 for H3K27 methylation and demethylation. When it is overexpressed in cancer, it derepresses genes that promote cell cycle progression to augment breast cancer growth**.**

: Genomic Profiling to Understand Cancer Biology
Poster Session

#3236 Genomic landscape of bladder cancer in a turkish cohort: Unveiling the unique mutational spectrum with clinical insights.

Burcu Yucel[1], Fatma Zehra Sarı[2], Dine Guner Mercan[2], Huseyin Ozgur Kazan[1], Ceren Sumer[2], Melike Akman[2], Demet Akdeniz Odemiş[2], Mehmet Baysan[3], Asıf Yıldırım[1], Mahmut Gumuş[1]

[1]Istanbul Medeniyet University, Istanbul, Turkey,[2]Health Institutes of Turkiye, Istanbul, Turkey,[3]Istanbul Technical University, Istanbul, Turkey

Introduction: Bladder cancer is predominantly urothelial carcinoma, and the majority of patients present with non-muscle-invasive bladder cancer (NMIBC), which has a high recurrence rate, or muscle-invasive bladder cancer (MIBC), which is less common but has a high risk of metastasis. Tumor heterogeneity is a characteristic feature of bladder cancer and is associated with a high mutational burden. While chemotherapy is an important treatment modality, tumor heterogeneity ultimately leads to drug resistance and post-treatment recurrence. Identifying the molecular mechanisms underlying both NMIBC and MIBC tumors and identifying biomarkers and therapeutic targets is crucial for disease treatment. Advances in next-generation sequencing technology have enabled advances in understanding the molecular mechanisms of bladder cancer, defining tumor heterogeneity at the genomic levels, and enabling more clinically relevant targeted therapies and effective immunotherapies. This first project, initiated within the National Cancer Genome Project in Turkiye, aimed to discover novel cancer-specific variants through whole genome and transcriptome analyses of bladder cancer tumors.
Methods: Sixty patients diagnosed with bladder cancer were included in the study. DNA was isolated from tumor tissue and blood samples taken from patients with a mass measuring 2 cm or larger on imaging and/or diagnostic cystoscopy who gave informed consent. Two patients were excluded from the study due to different diagnosis. Library preparation from the patients' genetic and somatic DNA samples was performed as recommended by the Illumina PCR-free tagmentation kit. Whole genome sequencing was performed on an Illumina Novaseq 6000 instrument. Somatic and germline variant calling analyses were performed using Illumina Dragen software.
Results: Tumor and blood samples from 48 male (82.75%) and 10 female (17.25%) patients were analyzed. Of the patients, 24.13% (14 patients) reported non-smoking, while 31.03% reported a history of cancer in a first-degree relative. Clinic evaluation revealed 19 (32.75%) of the patients had MIBC, and 39 (67.24%) had NMIBC. The mean age was 67.4±10.54. Of the pathogenic variants obtained through filtering, 45.40% were determined missense mutations, and 22.95% were stop-gained. Most frequently mutated genes detected in our study population were TERT (52.54%), PTPRG (40.67%), and FGFR2/FGFR3 (38.98%), respectively. In previous studies, frequently mutated TP53 and KRAS mutations were observed at a rate of 37.28%, while MYC mutations were observed at a rate of 33.89% in our analysis.
Conclusion: Despite the limited number of patients enrolled in the study, our results unveiled a unique mutational spectrum of bladder cancer in Turkiye. The resulting data will be a valuable resource for understanding drug resistance in bladder cancer and developing therapeutic approaches.

#3237 A multimodal sequencing framework to define viral and host genomic heterogeneity in HPV associated head and neck cancer.

Ella P. Jackert, Shu-Yun Cheng, Swar Vimawala, Liyang Tang, Daniel Kwon, Niels C. Kokot, Uttam Sinha, Albert Y. Han

Caruso Department of Otolaryngology Head and Neck Surgery, University of Southern California, Los Angeles, CA

Background: This study aims to integrate viral and host genomic analyses with social determinants of health (SDOH) to improve biologic risk stratification in patients with human papillomavirus-associated head and neck cancer (HPV+ HNC).
Methods: Patients with biopsy-proven, p16-positive HPV+ HNC were enrolled. Archived or fresh tumor tissue underwent DNA extraction followed by HPV consensus-primer genotyping targeted to the L1 locus (MY09/MY11 primer sequences) to determine viral type. Samples with confirmed HPV infection proceed to short-read sequencing for viral genotype characterization and host mutational profiling, and long-read sequencing to define HPV integration architecture, HPV-host fusion events, and larger structural variants. Demographic, clinical, and SDOH variables were collected to explore associations between patient context and genomic heterogeneity.
Results: To date, 10 patients have provided informed consent and have been enrolled in this study. Additionally, eights archived tumor specimens have been analyzed. The cohort consists of seven White male, two Hispanic or Latino male, and one White female patients. Archived specimens were derived from three White, two Asian, two Black, and one Hispanic patient. Preliminary HPV genotyping demonstrates a distribution of high-risk HPV types, including HPV16, HPV18, HPV33, HPV35, and HPV59. These early results suggest a potential variation across ancestry and SDOH-defined clusters, with White patients predominantly demonstrating the HPV16 genotype, while there is a higher prevalence of non-16 types amongst other racial and ethnic groups.
Conclusions: These early findings highlight the value of broadening HPV genotype characterization and capturing patient diversity to uncover the full spectrum of viral and host genomic variation in HPV+ HNC. Ongoing expansion of the cohort and completion of sequencing analyses will be critical next steps toward defining clinically meaningful genomic subgroups and developing future frameworks for precision risk stratification, surveillance, and treatment personalization in HPV-associated head and neck cancer.

#3238 Integrity of high-molecular-weight DNA is essential for accurate long-read sequencing and comprehensive cancer genomics.

Susan M. Magdaleno[1], Juili Kelvekar[1], Monica K. Campbell[2], Alexis Tapanes-Castillo[3], Hannah E. Saunders[1]

[1]Research and Development, Thermo Fisher Scientific, Austin, TX,[2]Research and Development, Galatea Biotech, Miami Lakes, FL,[3]St. Thomas University, Miami Gardens, FL

Accurate genomic characterization in oncology and cancer research depends on the quality and integrity of input DNA. Conventional genomic DNA (gDNA) extraction kits often produce short or degraded fragments due to excessive mechanical or chemical disruption during lysis, multiple manual transfer steps, and prolonged elution conditions, which limit the utility of extracted DNA for long-read sequencing and structural variant analysis. Short-read sequencing (50-600 bp) further compounds these limitations by providing incomplete assemblies and reduced ability to resolve large-scale rearrangements. Long-read technologies such as Oxford Nanopore and PacBio overcome these issues but require intact, high molecular weight (HMW) DNA fragments (>10 kb). To address these challenges, genomic DNA was extracted from whole blood, cultured cells, and tissue using the Applied Biosystems™ MagMAX™ High Molecular Weight (HMW) DNA Kit on the Thermo Scientific™ KingFisher™ Flex system. The fully automated workflow—comprising cell lysis, magnetic-bead-based DNA binding, sequential washing, and low-salt elution—reduces manual intervention and potential shearing events while improving consistency across users and sample types. An optional brief enzymatic digestion (<15 min) was included for tissue samples to optimize recovery of long fragments. DNA yield and integrity were quantified using Qubit™ fluorometry, Agilent TapeStation, and pulsed-field electrophoresis, and performance was compared against commonly used silica column- and precipitation-based kits. Long-read sequencing was used to assess read length distribution, coverage uniformity, and structural variant detection. Legacy manual and semi-automated gDNA kits exhibited substantial variability in yield (coefficient of variation (CV) >15%) and produced fragmented DNA with median fragment sizes typically below 20 kb, resulting in truncated reads and reduced sensitivity for detecting large deletions and rearrangements. In contrast, the MagMAX™ HMW automated workflow consistently produced DNA fragments >100 kb, with an average yield of 5 µg per sample and CV <1 across replicates; across sample types, 85% of fragments exceeded 40 kb and 75% exceeded 100 kb, enabling longer read lengths and higher variant concordance. The automated process supported batch processing of up to 96 samples in under two hours with less than 30 minutes of hands-on time, substantially reducing operator bias and inter-run variability. Overall, automating the MagMAX™ HMW DNA kit on the KingFisher™ instrument proved essential for preserving DNA integrity, improving reproducibility, and increasing throughput, enabling generation of high-quality HMW DNA that enhances read continuity, structural variant resolution, and data reliability—supporting more complete genomic profiling and accelerating translational oncology research.

#3239 Single assay, tumor-only, somatic SNVs, SVs, and CNVs profiling using nanopore adaptive sampling.

Sergey Aganezov[1], Philipp Rescheneder[2], Rory Sinnott[3], Sissel Juul[1]

[1]Oxford Nanopore Technologies, Inc, New York, NY,[2]Oxford Nanopore Technologies GmbH, Munich, Germany,[3]Oxford Nanopore Technologies plc, Oxford, United Kingdom

Background.
Tumor-only (T-only) testing often trades high sensitivity at low allele fraction (AF) - when using amplicon or hybrid-capture based enrichment - against comprehensive structural and copy-number profiling and overall ease of use, when using whole genome sequencing. Nanopore adaptive sampling (AS) enriches targets by rejecting reads during sequencing if they don't overlap with user-defined targets, yielding high-depth (100-200X) long read (8-15kb) data on target and shallow (5-15X and 500bp) sequencing off-target. As a result, AS simplifies experimental setup by not requiring PCR or pulldown-based enrichment, while at the same time enabling the detection of single nucleotide variants (SNVs), structural variants (SVs), and copy number variations (CNVs) in a single assay.
Methods.
Here, we evaluated variant calling accuracy for T-only AS on a highly aberrant genome (COLO829) and on a "synthetic," less-aberrant genome constructed in silico from COLO829 and its matched normal, retaining only a small number of large-scale CNV events. Performance was assessed across coverage/purity ladders that emulate common conditions. Sequencing targeted a generic multi-region, 700+ cancer-gene-aware panel augmented to cover a range of SV types present in COLO829. SNVs and SVs were inferred with long-read tumor-only pipelines. SVs included translocations, deletions, duplications, and insertions. Genome-wide CNV profiles were derived from the same AS datasets by leveraging off-target reads.
Results.
SNVs.
High (100-200X) on-target depth enabled confident recovery of somatic SNVs at relevant AFs, with high recall down to 0.05 AF and high precision down to 0.1-0.2 AF. These results were consistent across coverage/purity ladders.
SVs.
Long-read on-target data supported robust detection of inter- and intra-chromosomal rearrangements. Notably, events were recovered even when only partially overlapping with the target regions.
CNVs.
The high number of short off-target reads generated stable, genome-wide CNV segmentations from the same runs. Inferred CNV profiles demonstrated expected broad gains and losses on the highly aberrant genome as well as on the synthetic, less-aberrant construct across coverage/purity ladders.
Conclusions.
A single T-only nanopore AS run can (1) deliver sensitive SNV detection via high on-target coverage, (2) provide robust SV discovery, including one-breakend-on-target cases, and (3) yield genome-wide CNV profiles from off-target signal. By avoiding laborious panel-specific hybrid capture assays through simple software-defined targeting, AS offers a practical, streamlined, and highly flexible approach to single-assay tumor-only characterization that covers the full breadth of genomic variation found in cancer.

#3240 Altering is easy, engineering is hard: An automated platform for reproducible, high-fidelity genome engineering.

Travis J. Maures, Montse Morell

EditCo Bio, Redwood City, CA

CRISPR has enabled routine genome editing, but the lack of reproducibility across experiments, cell types, and laboratories remains a major barrier to translational applications. To address this, we developed an automated, industrial-scale gene-editing platform designed to minimize edit-to-edit variability and preserve genomic integrity across diverse cell types. The system performs thousands of concurrent genome-editing reactions under fully tracked and standardized conditions, minimizing batch effects, and ensuring consistent reagent handling and cell maintenance. This environment enables quantitative assessment of editing efficiency and quality across immortalized, primary, and induced pluripotent stem (iPS) cells, generating large-scale datasets that inform both product development and process improvement. Beyond the products and services created on this platform, EditCo Bio applies analytics generated from each project to learn from every edit. The resulting data guide the continuous evolution of our editing strategies and cell-maintenance processes. To demonstrate the analytical power of this approach, we applied the platform in a large-scale study of site-dependent homology-directed repair (HDR) efficiency across several hundred genomic safe-harbor sites in human iPSCs. By systematically varying donor design and chemical modifiers, we identified discrete genomic loci that reproducibly support high knock-in efficiency while maintaining cell viability. Expanded studies further revealed experimental conditions that promote recurrent structural genomic variations, including large deletions and rearrangements, which are undetectable by conventional short-read QC. The results of this work established methods, to (1) accurately measure these structural variations and (2), reduce their occurrence through optimized design and process control. Together, these findings describe an automated cell-engineering platform that transforms genome editing from an empirical procedure into a controlled engineering process.

#3241 High-fidelity whole genome sequencing from low-input FFPE samples: Enabling accurate tumor-informed MRD assay design through superior variant detection and uniform coverage.

Vanessa Process, Sushant Khanal, Madan Ambavaram, Sameer Vasantgadkar, Luca Beker, Alaina Villarreal, Jose Gil, Andrew Laneville, Martina Werner, Greg Endress, Ulrich Thomann, **Eugenio Daviso**

Covaris, LLC, Woburn, MA

Introduction: Tumor-informed Minimal Residual Disease (MRD) monitoring relies on the precise identification of patient-specific somatic variants from primary tumor tissue. However, these samples are frequently archived as Formalin-Fixed Paraffin-Embedded (FFPE) blocks, where DNA damage, fragmentation, and chemical modifications (e.g., cytosine deamination) compromise sequencing quality. Inaccurate baseline profiling can lead to the selection of artifacts as tracking targets or the omission of critical sub-clonal mutations, ultimately reducing MRD assay sensitivity. Here, we present a high-fidelity Whole Genome Sequencing (WGS) workflow optimized for low-input FFPE samples that minimizes amplification bias and artifacts, ensuring the generation of reliable genomic maps necessary for robust MRD target selection.

Methods: Genomic DNA was extracted from FFPE-processed NA12878 cells (FF12878) using the Covaris truXTRAC® FFPE SMART Kit with Adaptive Focused Acoustics (AFA®) technology to ensure active paraffin removal and rehydration. WGS libraries were constructed using the truCOVER® WGS Library Prep Kit with Amplification. The workflow was evaluated using DNA inputs ranging from 1 ng to 50 ng. Library performance was benchmarked against high-quality genomic DNA (NA12878) inputs (0.1 ng - 50 ng). Libraries were sequenced on an Illumina NovaSeq™ X Plus. Data was analyzed for coverage uniformity, duplication rates, and variant calling accuracy (F1 scores) for SNPs and INDELs using the GIAB truth set.

Results: The optimized workflow demonstrated exceptional sensitivity, generating high-complexity libraries from as little as 1 ng of FFPE DNA. Critical for MRD design, the method exhibited minimized GC bias, maintaining normalized coverage centered around 1.0 across 504 clinically relevant cancer genes (TSO500 panel), irrespective of input amount. This uniformity ensures that potential tracking mutations in difficult-to-sequence regions are not missed. Variant calling analysis revealed that the workflow effectively overcomes FFPE-induced damage; F1 scores for SNPs and INDELs in FFPE samples (5 ng) were comparable to those of high-quality gDNA (>0.91 for INDELs and >0.97 for SNPs). Furthermore, duplication rates were significantly controlled (~19% for 5 ng FFPE), maximizing the unique read depth required to validate low-frequency truncal mutations essential for longitudinal tracking.

Conclusions: We have validated a robust WGS workflow that unlocks archival FFPE tissues for high-fidelity genomic profiling, overcoming traditional barriers of low input and DNA damage. By delivering superior coverage uniformity and high variant calling accuracy, this solution provides the precise genomic baseline required for designing highly specific tumor-informed MRD assays

#3242 Integrated long-read target enrichment and comprehensive genomic profiling for hematologic malignancies using the SureSelect Cancer Pan Heme assay.

Brandyn Clark, Adam Janssen, Jeff Fox, Nedda Saremi, Kristi Stephenson, Kelle Hammock, Bahram Arezi

Agilent Technologies, Inc., Santa Clara, CA

Next-generation sequencing (NGS) has transformed cancer research, yet its effectiveness is often constrained by sample quality, tumor fraction, and limitations inherent to short-read sequencing—particularly in detecting structural variants, complex rearrangements, and alterations in repetitive or polymorphic regions. Long-read sequencing offers a solution, but cost and throughput challenges persist. To address these limitations, we developed a flexible, automation-compatible library preparation and target enrichment workflow that supports DNA inputs down to 200 ng, accommodates both enzymatic and mechanical shearing, and enables fast hybridization (90 minutes). Coupled with long-read sequencing and the SureSelect Cancer Pan Heme assay, this platform enables detection of main genomic alterations—including SNVs, indels, CNVs, and gene fusions—within a single assay. The SureSelect Cancer Pan Heme panel, codeveloped with Roswell Park Comprehensive Cancer Center, interrogates 359 DNA and 124 RNA genes, delivering integrated DNA/RNA analysis and overcoming the limitations of conventional single-analyte methods such as karyotyping, FISH, and PCR. Although in this study, we only focus on DNA as the substrate. We demonstrate high enrichment efficiency using a novel fast hybridization buffer, achieving on-target rates >80% for libraries with insert sizes up to 4-5 kb. Comparative analysis versus short-read approaches reveals superior coverage in challenging genomic regions using enriched long-read sequencing as well as allowing to phase variants. This solution offers a cost-effective, scalable, and rapid-turnaround workflow for molecular laboratories, advancing precision oncology in hematologic malignancies. For Research Use Only. Not for use in diagnostic procedures.

#3243 Investigating the value of testing for actionable alterations and circulating tumor DNA in breast and colorectal cancers.

Gargi D. Basu, Nick Johnson, Angela Deem, Judith Frederick, Terence Wong, Janine R. LoBello, Szabolcs Szelinger, Nishitha Therala, Mark Evans, Miriam Walker, Jean-Paul De La O

Exact Sciences Corporation, Madison, WI

Tumor molecular profiling may reveal distinct biological behaviors by identifying actionable alterations (AAs), informing precision oncology. However, the effect of molecular characteristics on ctDNA detection and monitoring is not well studied. Here, we evaluated patients with breast cancer (BC; all subtypes) or colorectal cancer (CRC) who received whole transcriptome and whole exome profiling with the OncoExTra® assay and assessment of circulating tumor DNA (ctDNA) status using the Oncodetect™ assay. The primary objective was to describe the frequency of AAs in BC and CRC overall and stratified by ctDNA status, tumor subtype, and clinical stage. In total, 88 patients were evaluated (42 BC and 46 CRC). All CRC patients and 41 BC patients (97.6%) had an AA identified, and 52.3% had an AA associated with FDA-approved therapy. All stage II-IV tumors (80 samples) and 6 of 7 stage I tumors (85.7%) had an AA. HR+/HER2- BC samples had AAs associated with approved matched therapy in 13 (54.2%) samples , which included *PIK3CA* mutations associated with alpelisib, capivasertib, and/or inavolisib (7 samples; 16.7%) and 1 *ESR1* alteration. *PIK3CA* mutations were present in 9 of 34 (26.5%) stage II/III CRCs, where aspirin therapy has been shown to improve survival. Within our limited cohort, AAs with approved matched therapies were found in 81.8% of stage I-II and 65.7% of stage III-IV CRC and were found in 31.3% and 36.0% of stage I-II vs III-IV BCs, respectively. Among ctDNA-positive BC samples, 27.6% had an AA associated with approved matched therapy vs. 46.2% in ctDNA-negative samples. For CRC, these frequencies were 62.1% and 82.4%, respectively. No association was found between any AA and ctDNA detection. Other AAs associated with FDA-approved therapies are listed in the table. Detection of AAs associated with FDA-approved matched therapy in approximately half of samples tested for ctDNA suggests it may influence therapy selection and disease management.

#3244 Rapid, one-tube sub 10-minute whole genome library prep for cfDNA.

Ben Krajacich, Seana Lymer, Kevin Green, Xiaodong Qi, Kyle Donohoe, June (Junhua) Zhao, Michael Previte

Element Biosciences, Inc., San Diego, CA

As next-generation sequencing (NGS) costs have decreased, it is increasingly more feasible to perform whole genome sequencing instead of a targeted approach to obtain more comprehensive genome information, better cover difficult regions, and provide insights for rare diseases. With increasing adoption of NGS, there is an emphasis on optimizing and streamlining the entire process, particularly library preparation and sequencing steps to reduce turnaround times and simplify workflows. Standard library prep has many complex and time-consuming steps such as end-repair, A-tailing, and PCR that increase barrier to entry for users, require specialized equipment, and can also induce unique errors to the final library. Additionally, each of these steps can also have impacts to the efficiency in which you convert input material into sequenceable library which may be critically limiting in material-limited applications. We have developed a new methodology for a rapid, one-tube, whole genome library prep prior to sequencing on the AVITI ™ platform. Through DNA fragmentation and single-adapter addition, this approach allows for highly efficient PCR-free library creation in under 10 minutes of total time, while maintaining the ability for paired-end sequencing chemistry through circularization on-instrument. We demonstrate the library prep workflow's efficiency on extracted gDNA (Coriell and *E.* coli, *H. influenzae*, and *R. palustris* bacteria to span content across GC ranges) and Horizon cfDNA material (Mimix Multiplex I cfDNA reference at 1-5% VAF). We found high conversion efficiency with <80ng of gDNA allowing for full AVITI24 ™ output of up to 1.5B reads, with high estimated library complexity. Additionally, when more depth per target is needed, we show compatibility of the fast, clean-up free workflow with our Trinity ™ technology which removes need for off-board washing and QC steps, allowing for library prep and enrichment within the timeframe of a standard NGS library prep (<2 hours). These techniques hold promise to streamline and integrate NGS preparation and sequencing while maintaining quality and reducing workflow burden.

#3245 Scaling liquid biopsy biomarker discovery: Multi-center, analytical validation of high resolution ctDNA profiling using TSO500 v2 on NovaSeq X Plus.

Gabriela Edwards Faret[1], Emmanuel Riviere[1], Silvie Franck[1], **Bart Tegenbos**[1], Lisa Van den Bossche[1], Joke Verbist[1], Lien Heyrman[1], Magdalena Lesnicki[2], Rachel Raz[2], Brian Chapman[2], Eric Harness[2], Jan Van de Velde[1], Dirk Goossens[1], Jurgen Del Favero[1]

[1]CellCarta, Antwerp, Belgium,[2]CellCarta, Naperville, IL

Illumina's TruSight™ Oncology 500 (TSO500) ctDNA v2 assay, enables comprehensive genomic profiling from plasma, allowing non-invasive, repeatable monitoring of tumor evolution during clinical studies. The assay covers a broad panel of 523 clinically relevant cancer genes and provides sensitive detection of key biomarkers such as SNVs, indels, CNVs, gene fusions, MSI, and TMB, all from a simple blood draw. Therefore, this RUO assay is well-suited for exploratory biomarker discovery, response monitoring, and mechanistic insights during immunotherapy and targeted therapy development without the need for fresh tissue biopsies.

A validation study was performed to characterize the analytical performance of TSO500 ctDNA v2 assay on the NovaSeq™ X Plus platform for comprehensive genomic profiling of 523 cancer-related genes in ctDNA. The assay was evaluated at two CellCarta laboratories (Antwerp, Belgium and Naperville, USA). Accuracy was assessed using reference materials with a variant allele frequency (VAF) threshold of 0.5% for SNVs and indels. Across both sites, the assay demonstrated >95% overall percent agreement for SNV, indel, CNV, MSI, and TMB results, with positive percent agreement >93.5% and negative percent agreement >95% for SNV, indel, and CNV (no negative reference materials were available for MSI and TMB). Precision assessments showed >97% concordance for intra-run, inter-run, and inter-operator comparisons across all variant classes.

Limit of detection verification confirmed 100% detection of SNVs down to 0.25% VAF, indels down to 0.5% VAF, and CNVs at >1.0 fold change. The optimal input for the assay was determined to be 20 ng ctDNA; however, evaluation of lower inputs (10 ng and 5 ng) demonstrated that while these samples did not consistently meet QC thresholds, SNV and indel detection remained robust, with >98% concordance for SNVs and >95% for indels. Lower input material may therefore be used for exploratory analyses, with the understanding that reduced coverage may limit detection sensitivity (potential false negatives) but does not introduce false-positive variant calls.

These results confirm that the TSO500 ctDNA v2 assay delivers reproducible, high-resolution genomic profiling across sites, supporting its applicability for exploratory biomarker analyses and longitudinal response monitoring in clinical studies.

#3246 SeqF™: evaluation of an affordable nanopore-based assay for decentralized tumor profiling.

Kimberly A. Holden[1], Roi Feingersch[2], Dvir Dahary[2], Margalit Feiger[2], Tal Havkin-Solomon[2], Benjamin M. Cohen[2], George Way[1], Shakti Ramkissoon[3], Marcia Eisenberg[3], Brian Caveney[3], Eric Severson[3], Taylor J. Jensen[3], Jonathan Williams[1]

[1]Labcorp, San Diego, CA,[2]Foresee Genomics, Bar Lev, Israel,[3]Labcorp, Durham, NC

Comprehensive genomic profiling (CGP) guides precision oncology, yet access remains limited in community and regional laboratories. SeqF is a Nanopore-based targeted sequencing workflow for low-throughput assays, utilizing the MinION™ device with standard molecular biology equipment and dedicated bioinformatic analysis software. SeqF was evaluated using 40 DNA samples, derived from clinical and reference specimens, with 20 samples analyzed in each of two targeted panels: EGFR-pathway (commercial off-the-shelf amplicon panel; 12 amplicons across 4 genes; ~1.5 kb total) and MPN (custom amplicon panel; 80 amplicons across 20 genes; ~35 kb total). Testing was performed in a clinical research and development laboratory. The wet-lab workflow comprises PCR-based target enrichment, sample indexing/barcoding, and incorporation of unique molecular identifiers (UMIs) for the EGFR panel only. Indexed libraries then undergo rolling-circle amplification followed by adapter ligation for Nanopore sequencing. Library preparation spans two days, followed by ~12-24 hours of sequencing (runs may be stopped early once coverage targets are met). The analysis pipeline is run via a user interface and involves base calling from raw sequencing reads (HAC in MinKNOW), followed by an automated pipeline that includes demultiplexing, consensus (error correction), alignment, variant calling, annotation, and QC. When compared to sequencing performed on Illumina instruments, and using paired tumor specimens, SeqF achieved >99.7% concordance for single-nucleotide variants at ≥5% variant allele frequency (VAF). Correlations between the measured VAFs (5-40%) in clinical samples and reference standards were ≥95% in both panels tested. The workflow demonstrated feasibility for small batch sizes and delivered robust analytical performance. The process was completed in under 72 hours, from extracted sample to VCF file and sequencing run QC report generation. SeqF enables decentralized tumor profiling with low infrastructure requirements and rapid results, potentially expanding access to precision oncology in community laboratory settings. The streamlined workflow and analysis pipeline may help democratize access to molecular diagnostics, ultimately improving patient outcomes through more timely and personalized treatment decisions. Future enhancements such as expanded panel content, broader UMI integration, and real-time variant interpretation will significantly increase the platform’s utility. This increased utility will enable scalable precision oncology across a wider range of cancer types and healthcare environments.

#3247 Origins of structural variant junctional insertions across >8,000 TCGA whole genomes.

Youyun Zheng[1], Gregory Raskind[1], Sophie Webster[1], Narmen Azazmeh[1], Haruna Tomono[1], Andrew Cherniack[1], David Lehotzky[1], Ron Solan[1], Antonia Kowalewski[1], Xavi Loinaz[1], Hansol Park[2], Vasuki N. Swamy[1], David Heiman[1], Samantha Van Seters[1], Saveliy Belkin[1], Sam Wiseman[1], Chunyang Bao[2], Luis A. Corchete Sanchez[1], Zachary Everton[1], Ryul Kim[2], Beomki Lee[2], Won-Chul Lee[2], Chip Stewart[1], Gengchao Wang[1], Brian P. Danysh[1], Young Seok Ju[2], Esther Rheinbay[1], Gad Getz[3], Rameen Beroukhim[1]

[1]Cancer Program, Broad Institute, Cambridge, MA,[2]Inocras, San Diego, CA,[3]Massachusetts General Hospital, Charlestown, MA

Double-strand break repair leaves recognizable footprints in the genome. Among the most specific are short sequences inserted at structural-variant (SV) junctions—templated insertions often attributed to polymerase-θ-mediated end joining (TMEJ). Yet common readouts based on exact string matches overlook sequence background, distance from the break, and the topological context of candidate templates, inflating false positives and blurring mechanistic interpretation. We present a scalable statistical framework that infers templated insertions with controlled specificity by modeling alignment-score distributions against a distance-adjusted, genome-wide empirical null. The approach explicitly accommodates imperfect copying and partitions candidate templates into four breakpoint-proximal configurations, capturing positional and strand relationships that are informative of mechanisms. Applied to large somatic and germline whole-genome cohorts, the method reveals that template usage spans all configurations but differs systematically across cellular contexts. A notable fraction of events reflect imperfect copying, consistent with error-prone synthesis, whereas one configuration shows comparatively higher apparent fidelity—suggesting distinct biochemical routes within a broader TMEJ-like landscape. Configuration calls also stratify SV architecture: some are enriched in simple rearrangements while others localize to clustered, complex regions, indicating that local topology and repair pathway choice are linked. Beyond structure, configuration-specific burdens align with DNA-repair states and selected genotypes: contexts consistent with homologous-recombination deficiency show enrichment in particular configurations, while others display the opposite directionality, underscoring that “templated insertion” is not a single phenomenon but a family of related processes with diverging determinants. To enable cohort-scale analysis, we optimized the core alignment to produce full score matrices in a single pass and packaged the workflow into a containerized pipeline, yielding order-of-magnitude speedups and portable reproducibility. Together, these results establish a configuration-aware, statistically principled readout of templated insertions that is robust to sequence confounders and informative about mechanisms. Practically, the framework provides (i) a sharper lens for studying double-strand break repair in human samples, (ii) leads for repair-state biomarkers, and (iii) hypotheses connecting SV topology to polymerase usage. In doing so, it aims to move the field from anecdotal sequence sketches toward reproducible, cohort-scale inferences about double-strand break repair involving junctional insertions.

#3248 Characterization of multiple myeloma genomes with LinkPrep assay enables detection of somatic variation and SV-driven interactions of the 3D genome.

Lisa Munding[1], Nathan Becker[2], Enze Liu[2], Alexander Fortuna[1], Jonathan Torchia[1], Aneta Mikulasova[3], J. Zachary Sanborn[1], Brian Walker[2]

[1]Dovetail Genomics, part of CantataBio, Scotts Valley, CA,[2]Myeloma Institute, Sylvester Comprehensive Cancer Center, University of Miami, Miami, FL,[3]University of Edenburgh, Edenburgh, United Kingdom

Multiple myeloma (MM) is characterized by its genomic complexity that includes recurrent driver single nucleotide variation (SNVs) alongside a high burden of structural variation (SV). Complete characterization of somatic variation in a MM genome is dependent on a technology that can accurately and sensitively detect both small and large variants. Here, we demonstrate performance of a novel linked-read approach, called LinkPrep™ technology, for high accuracy detection of both small and large somatic variants in four separate relapse MM genomes.Four MM patient-derived xenografts were profiled with Dovetail® LinkPrep™ kit and sequenced to ~30X on an Illumina platform. Data was analyzed through the Dovetail Analysis Portal to detect SNVs/Indels (DeepSomatic), CNVs (Purple), and SVs (HiC-breakfinder and proprietary tools). Call sets were compared against other genomics technologies including WGS (80X tumor/ 30X normal), PacBio (15X), and OGM (400X).LinkPrep + Dovetail Analysis Portal returned high quality variant results for the four MM samples. LinkPrep data recalled all pathogenic SNV/Indels detected by 80X WGS (notable pathogenic variants were detected in NRAS, KRAS, TP53). LinkPrep data further detected SVs involving the *IGH* locus (inversions and translocations) in all four samples. Deeper analysis of one sample (M24) highlights that LinkPrep data detects genetic alterations common in MM including SNV mutations in NRAS and TP53 (both occurring at 100% VAF), *IGH* rearrangements, chr 1q gain, chr 1p loss of heterozygosity, trisomy of chr 5,7, and 15, and complex rearrangements involving chromosomes 2, 3, 4, 16, and 19. With the exception of a confident subclonal (1% SV-VAF) unbalanced translocation detected by LinkPrep, the remaining LinkPrep large SV calls were validated by other genomics methods. Underscoring the capability of LinkPrep for SV detection, LinkPrep calls at 30X contain >10-100 times more read support for every SV call over other technologies. Using the linked-read feature of LinkPrep data along with CNV segment calls and SV calls provided through the Dovetail Analysis Portal a candidate solution is derived for the complex rearrangement involving chromosomes 2, 3, 4, 16, and 19. This LinkPrep solution, refined down to base pair resolution for every breakpoint, is verified by 400X OGM data. Uniquely, LinkPrep data further enables visualization of the SV-reconstructed 3D genome and reveals neo-loops connecting enhancers with promoters to suggest enhancer hijacking mechanisms associated with the complex rearrangement.Together, these data demonstrate that LinkPrep linked-reads enable improved characterization of somatic variation in highly rearranged genomes, while simultaneously detecting epigenetic states -- all enabled with the accuracy and cost-effectiveness of short read sequencing.

#3249 Extending a cfDNA-optimized library preparation workflow to mechanically sheared FFPE DNA for high-quality NGS data.

Sean Tighe, Owen Smith, Tiffany Truong, Tong Liu, **Elian Lee**, Esteban Toro, Siyuan Chen

Twist Bioscience, South San Francisco, CA

Formalin-fixed, paraffin-embedded (FFPE) tissues are a foundation of retrospective oncology studies but FFPE samples remain challenging for next-generation sequencing (NGS) due to DNA fragmentation, cross-linking, base damage, and highly variable yield. These factors impact library conversion and complexity and can introduce artifactual variants that confound low-frequency mutation detection. To address similar challenges in liquid biopsy, the Twist cfDNA Library Preparation Kit was engineered to deliver high conversion, high-complexity libraries from low-input cell-free DNA, leveraging an optimized end-repair/ligation chemistry with a Twist-engineered T4 DNA ligase. We demonstrate that this chemistry is well-suited for FFPE DNA that has been mechanically fragmented. Here, we evaluated the performance of the Twist cfDNA Library Preparation Kit on mechanically sheared FFPE control standards as well as FFPE DNA extracted from solid tumor blocks.

FFPE samples were processed and extracted, followed by acoustic mechanical shearing. Libraries were prepared with the Twist cfDNA Library Preparation Kit and Twist UMI adapter system followed by target enrichment with oncology-focused capture panels, before sequencing on Illumina instruments. Across FFPE samples of various DIN scores, the cfDNA-optimized workflow produced robust libraries at low input, with high adapter-ligation efficiency, improved library complexity, and uniform target coverage. Duplication rates and off-target reads remained low despite variation in FFPE quality. UMI-based consensus calling efficiently suppressed FFPE-associated artifacts, enabling confident detection of low variant allele frequency (VAF) somatic mutations that align with control expectations. Performance trends scaled favorably with decreasing input mass, supporting sequencing applications for limited, archival material.

These results demonstrate that a library preparation chemistry optimized for low-input, fragmented cfDNA can be effectively repurposed for mechanically sheared FFPE DNA. Combining standardized mechanical shearing with the Twist cfDNA Library Preparation Kit and target enrichment provides a unified workflow for liquid biopsy and tissue-based NGS, expanding the utility of Twist's library preparation and target enrichment solutions for sensitive variant detection in challenging oncology samples.

#3250 Comparative study of human and canine nerve sheath tumors in terms of morphology, prognosis, treatment, epigenetics, transcriptomics, and genomics.

Jace P. Landry[1], Angela D. Bhalla[1], Sharon M. Landers[1], Rossana Lazcano[1], Lindsay A. Parker[2], Tasha M. Miller[2], Noelle Niemi[2], Heather G. Lyu[1], Heather A. Lillemoe[1], **Emily Z. Keung**[1], Christopher P. Scally[1], Christina L. Roland[1], Kelly K. Hunt[1], John M. Slopis[1], Ian E. McCutcheon[1], Beth Boudreau[2], Heather Wilson-Robles[2], Alexander J. Lazar[1], Kunal Rai[1], Dominique J. Wiener[2], Brian W. Davis[2], Brandan Wustefeld-Janssens[2], Keila E. Torres[1]

[1]UT MD Anderson Cancer Center, Houston, TX,[2]Texas A&M University, College Station, TX

INTRODUCTION: Malignant peripheral nerve sheath tumors (MPNSTs) are aggressive sarcomas. An obstacle to treating MPNSTs is a lack of effective systemic therapies. Although over 70% of human MPNSTs have lost or inactivated the epigenome regulator polycomb repressive complex 2 (*PRC2*) (DeRaedt *et al*., *Nature*, 2014), its activity and contribution to canine PNST progression remain unclear.
METHODS: This study compared canine peripheral nerve sheath tumors (PNSTs) and human MPNSTs across biological and clinical features, including PRC2 activity. Immunohistochemical analysis was performed for a human tissue microarray of 54 neurofibromas and 139 MPNSTs, and 63 canine PNSTs for H3K27me3, a repressive histone mark deposited by intact PRC2, and H3K27ac, which increases globally upon H3K27me3 loss. To understand the genomic alterations present in canine PNSTs, we analyzed tumor mutation burden, copy number alteration, and transcriptomes of eight canine PNST/normal pairs.
RESULTS: The results suggested that H3K27me3 loss and associated gain of H3K27ac epigenetically drive human and canine tumors. This study provided evidence that human and canine PNSTs are clinicopathologically similar and may also be similarly driven by epigenetic mechanisms.
CONCLUSIONS: Further studies are warranted to evaluate whether these epigenetic deregulations alter similar gene signatures in humans and canine patients. The knowledge gained from this work advances our understanding of the molecular drivers of MPNST and informs potential therapeutics to evaluate in future clinical studies.

#3251 Insights from liquid biopsy testing in clinical settings: Analysis of an Indian dataset.

Urvashi Bahadur, Aarthi Ravichandran, Bhanumathy G, Sreelaksh Raju, Suhasini Narain, Kaushiki K, Kalainanghi Neelagandan, Anusha N J, Aishwarya Ramkumar, Saman Sajjad, Dhanashree A. More, Ramya Raviprakash, Tanvi Mathur, Srivathsan Adimoolam, Mahalakshmi Prakash, Divya Priya A, Anitha N R, Suruchi Aggarwal, Swetha Nayanala, Shanmukh Katragadda, Sameer Phalke, Vamsi Veeramachaneni

Strand Life Sciences, Bengaluru, India

While solid tumor profiling by tissue Next Generation Sequencing(NGS) is now undertaken routinely in the clinical setting, the availability and adoption of cell free (cf) DNA based NGS assays is limited in the Indian context. This retrospective study assesses the utility of liquid biopsy testing using a validated targeted panel in a clinical setting.A total of 495 plasma samples were analyzed for single-nucleotide variants, indels, copy-number variants, and gene fusions using a targeted unique molecular identifier (UMI) based 74-gene liquid biopsy panel. The panel covers all genes with a Tier 1 drug recommendation for therapy,and additional Tier 2 genes for prognosis or added clinical impact. Variants were assessed for clinical significance,and classified using AMP guidelines. Actionability was defined as the presence of Tier 1 or Tier 2 alterations with therapeutic, prognostic or diagnostic relevance.The most common tumor types tested were NSCLC (43.2%), colorectal cancer (12.1%), and breast cancer (10.1%), followed by hepatobiliary, prostate, pancreatic, and ovarian cancers. Overall, 61.4% of samples (304/495) harbored at least one actionable alteration, with Tier 1 variants detected in 26.5% of the cases. The mean number of alterations in actionable cases was 2.0. The overall actionability of 61.4% was comparable to the actionability obtained from a similar cohort of tissue samples analyzed on the solid biopsy version of this panel (68.3% of 621 cases), thus highlighting the sensitivity and high clinical yield of this panel. The actionability for each cancer type was high for certain cancers; NSCLC (62.1%; n=214), colon (56.7%; n=60), breast (70.0%; n=50) , hepatobiliary (57.6%, n=33, and carcinoma of unknown primary (46.4%, n=28). The most frequently mutated gene overall was TP53, detected in 36.36% of the cases.The distribution of the variant allele frequency (VAF) was also examined. Across 617 reportable events, VAFs ranged from 0.15% to 92.0%. The median VAF was 3.97%, and the 75th percentile was at 19.8%, consistent with the clinical settings in which liquid biopsy is used. 2% of cases had variants with VAF >75%, and these were all found to be in EGFR or TP53, suggestive of copy-number gains in these genes in late-stage disease. Additionally, ESR1 resistance mutations were detected in 11 of the 50 breast cases, underscoring the utility of liquid biopsy in detecting markers of acquired resistance.This analysis thus demonstrates that a compact, guideline-aligned ctDNA panel provides robust detection of clinically meaningful alterations across diverse solid tumors. High rates of actionability, together with the identification of resistance-associated events, support the value of liquid biopsy as a practical and informative tool for precision oncology.

#3252 Simplified genomic profiling using Aspyre Lung solves real-life challenges with limited and poor-quality tissue.

Elizabeth Gillon-Zhang[1], Eleanor Gray[2], Candace King[1], Ethan Clark[1], Cory Kiser[1], Mary Beth Rossi[1], Julia Brown[1], Ryan Evans[1], Katherine Knudsen[1], James Schaffernoth[1], Tatiana Yuen[1], **Magdalena Stolarek-Januszkiewicz**[2], Sophie Hackinger[2], Amanda Green[1], Kelly Pitts[1], Honey V. Reddi[1], Shari Brown[1], Barnaby Balmforth[2]

[1]Biofidelity Inc, Morrisville, NC,[2]Biofidelity Ltd, Cambridge, United Kingdom

Advanced NSCLC treatment guidelines recommend testing patients for genomic biomarkers to access over 30 FDA-approved targeted therapies. Challenges in NSCLC molecular testing include the need for assessment of multiple variants in both DNA and RNA, sample quality and quantity, cost, and clinical need for rapid turn-around time for timely treatment initiation (recommended <14 days). Aspyre Clinical Test for Lung (Tissue or Blood) is a targeted genomic profiling assay which informs on 114 actionable and prognostic biomarkers across 11 first-line genes (*ALK*, *BRAF*, *EGFR*, *ERBB2*, *KRAS*, *MET*, *RET*, *ROS1*, *NTRK1*/*2*/*3*) in patients with NSCLC. The novel assay uses standard PCR and real-time PCR equipment and interrogates nucleic acid directly without a capture step in a highly sensitive and cost-effective manner, enabling rapid and accurate clinical decision making. We present results from an initial cohort of clinical samples sent to Biofidelity Inc. Laboratory (a CAP/CLIA site). De-identified demographic and clinical data were analyzed including biopsy type, pathology diagnosis, tumor content, % necrosis, turnaround time, and variant identified. 177 clinical samples were analyzed, with retrospective, research and non-NSCLC samples excluded prior to analysis. 177 samples were eligible for inclusion. Diagnoses included adenocarcinoma (n=90), squamous cell carcinoma (n=34), unspecified NSCLC (n=49) and other (n=4). 20/177 samples were quantity not sufficient for one or more of tumor (n=11), DNA (n=6) or RNA (n=9); however, 177/177 samples passed internal assay performance checks for both DNA and RNA analysis (100%). Median tumor content was 40% (range 2-95%). Overall, 85 (47.8 %) of samples were positive for a variant, including SNV in *BRAF*, *EGFR*, and *KRAS*, *EGFR* exon 19 deletions and exon 20 insertions, insertions in *ERBB2*, *MET* exon 14 skipping and gene fusions involving *ALK*, *RET* and *ROS1*. QNS samples yielded nine variant calls of which seven were actionable. Of the samples with associated staging information, 32 were Stages I-IIIA (with 22 variant calls, 68.8%) and 30 were IIIB-IV (with 18 variant calls, 60.0%). 93.2% of samples were reported within the target two-day turnaround time (median 2, range 1-4). Aspyre Lung (Tissue) has a high assay success rate and proven rapid 2-day turnaround time, suitable as a cost-effective method for first-line or at relapse testing option, or for samples that are scant, of low quality, and can provide a large fraction of NSCLC patients with actionable biomarker information. Aspyre Lung Tissue simplified genomic profiling offers a new paradigm for informing cancer care management and enables more patients with NSCLC to benefit from effective and better tolerated targeted therapies.

#3253 A new workflow for FFPE tumor samples enables a streamlined solution for structural variant detection and phasing of somatic mutations through long read sequencing.

Camille Conner[1], Ian McLaughlin[1], Juniper Lake[1], Davy Lee[1], Heather Ferrao[1], Greg Endress[2], Ulrich Thomann[2], Martina Werner[2], Luca Beker[2]

[1]PacBio, Menlo Park, CA,[2]Covaris, Woburn, MA

INTRODUCTION: HiFi long-read sequencing provides highly accurate reads of fragments from 500 bp to 25,000 bp in length. These long reads offer an agnostic measure of sequence length and enable structural variant detection, phasing, and direct methylation analysis. However, FFPE tissue has been difficult for HiFi sequencing because extraction often yields short, damaged fragments and fixation crosslinks DNA which disrupts long-read sequencing.
METHODS: We applied the Covaris truXTRAC FFPE extraction by Adaptive Focused Acoustics (AFA) to recover long DNA fragments from FFPE blocks, including molecules up to 5000 bp. To maximize sequencing efficiency, we developed a Kinnex-based library preparation that concatenates multiple FFPE fragments into longer molecules. Kinnex involves PCR, which removes methylation information but preserves sequence quality and contiguity. The Kinnex for FFPE workflow requires 50 ng of input DNA per sample.
RESULTS: Brain, kidney, and uterine tumor FFPE samples were sequenced using this approach, generating more than 100 million HiFi reads per sample with mean read lengths of 750-1,500 bp. The resulting data showed high-quality reads and consistent variant detection across the genome. Variant calling detects >11,000 structural variants and >5.1M small variants per sample, with 60% of variants phased into haplotypes.
CONCLUSIONS: Combining Covaris long-fragment extraction with Kinnex library concatenation makes FFPE samples compatible with HiFi long-read sequencing. Using HiFi sequencing on samples prepared from Covaris-extracted DNA generated high yield sequencing libraries from FFPE samples across diverse tissue types demonstrating consistent performance across varying DNA quality and tissue cellularity. This workflow enables comprehensive analysis of archived tumor genomes, offering a more complete view of genomic variation and fragment characteristics from clinically relevant samples.

#3254 Gene profiling using whole genome analysis of bile tract cancer and its association with clinical factors.

Toshio Kokuryo, Masaki Sunagawa, Junpei Yamaguchi, Taisuke Baba, Takashi Mizuno, Shunsuke Onoe, Nobuyuki Watanabe, Mihoko Yamada, Shoji Kawakatsu, Tomoki Ebata

Division of Surgical Oncology, Nagoya University Graduate School of Medicine, Nagoya, Japan

Background: Bile tract cancer (BTC) is a malignant tumor with poor prognosis. The genetic background and molecular profiles of BTC remain poorly understood. Objective: To clarify the genetic diversity of BTC using whole-genome analysis and identify gene mutations as targets for novel diagnostic and therapeutic approaches.
Methods: Whole-genome sequencing was performed using paired tumor and normal tissue samples from 7 patients with BTC who underwent surgery at our institution. Somatic mutations were detected and annotated using snpEff. Oncoplot analysis visualized mutation accumulation patterns, and associations with clinical factors including lymph node metastasis, vascular invasion, neural invasion, portal vein invasion, and IPNB.
Results: On classification of detected somatic mutations, annotation revealed that intergenic region mutations (mean: 31,085, range: 26,588-39,135) were most frequent. Frameshift variants (mean: 16.7, range: 11-25), splice donor/acceptor variants (mean: 34.3, range: 17-45), and stop gained mutations (mean: 7.4, range: 2-10) were identified as important functional mutations. In addition, missense variants (mean: 529.4, range: 363-647) were also identified. Regarding nonsynonymous mutations, missense mutations were most common in variant classification, and SNPs (single nucleotide polymorphisms) were most frequent in variant type. Among SNV classes, T to G and C to T transitions were highly identified. Thirty genes, including MUC16 and MUC6, were identified with mutations in 3 or more of the 7 cases. Oncoplot analysis of these genes suggested that mutations accumulated more extensively and were associated with tumor mutation burden (TMB) in samples without vascular invasion. In contrast, no accumulation patterns of mutations were observed concerning lymph node metastasis, neural invasion, portal vein invasion, or IPNB. Among the genes (331 mutations, 321 genes) registered in The Cancer Genome Atlas (TCGA) bile duct cancer database, our study identified MUC16, OBSCN, and TP53. However, no overlap in their mutations was observed. It suggests extremely high genetic heterogeneity in BTC.
Conclusion: BTC is characterized by a high mutational burden and genetic diversity. An association between vascular invasion status and mutation accumulation was suggested. Gene profiling is considered important for personalized medicine, and the identified gene mutations may serve as potential targets for novel diagnostic and therapeutic approaches.

#3255 Long-read hybrid-capture based targeting of 95 known cancer genes detects large structural and complex variants with a simple bioinformatics workflow and an AI-based clinical interpretation solution..

Nathan H. Blewett, Megan Zais, Jingxiao Zhang, Jixin Deng, John DiCarlo, Jamie Hill, Christa Haldrup, Matthew Fosbrink, Jonathan Shaffer

Research & Development, QIAGEN Sciences, LLC, Frederick, MD

Short read sequencing has driven progress in identifying cancer-causing mutations ranging from SNPs to small indels. However, the ability to define complex mutations that span multiple kilobases is limited with traditional NGS approaches due to short read lengths. Targeted long-read sequencing, on the other hand, enables characterization of novel, complex mutations as long reads can span and be phased across large genomic regions. Long-read hybrid capture offers probe design flexibility for capturing targeted regions with unresolved structural variants. Here we describe the development of QIAseq xHYB Long Read Hereditary Cancer Panel and chemistry for detection of large structural variants in 95 known cancer driver genes.QIAseq xHYB Long Read Hereditary Cancer Panel and analysis pipelines were used to identify large structural variants in genes involved in cancer progression that human reference DNA were known to harbor. Libraries were prepared using enzymatic long-read fragmentation, after which targeted regions were captured with probes optimized for long DNA fragments. Captured DNA was amplified with chemistry developed for long, fast PCR and sequenced on both PacBio and Oxford Nanopore platforms. Real-time adaptive sampling was also used on the Oxford Nanopore platform to increase sequencing depth and improve uniformity. The resulting long-read sequencing data was mapped and large structural variants detected with CLC Genomics Workbench Lightspeed Module and Franklin by QIAGEN, a cloud-based, AI-powered platform that integrates the world's first open genomic community to power precision medicine at scale.The QIAseq xHYB Long Read probe design targets entire genes, including introns and UTR's, capturing extended regions of genes in an unbiased manner. Enzymatic fragmentation produced libraries with average read lengths of 4.5 kb. Sequencing eight QIAseq xHYB Hereditary Cancer Panel libraries from one capture pool on a Revio SMRTcell yields 30X average coverage, and uniformity greater than 95% of reads > 0.2X of the mean. Sequencing the same libraries on the Oxford Nanopore Minion platform resulted in 12X average coverage, and uniformity greater than 90% of reads > 0.2X of the mean. To increase Minion sequencing depth, we used real-time adaptive sampling to enrich for our target regions, which resulted in average of 30X coverage, and 93% of reads > 0.2X of the mean for 8 libraries on the Nanopore platform. Downstream analysis with CLC Genomics Workbench Lightspeed Module clearly identified the expected large structural variants in Coriell reference DNA, and subsequent clinical interpretation performed by AI-powered Franklin produced informative actionable conclusions from the structural variant reference DNA investigated.

#3256 Identification of germline variants associated with somatic mutational profiles in triple-negative breast cancer among African American women.

Guochong Jia[1], Jie Ping[1], Christine B. Ambrosone[2], John D. Carpten[3], Julie R. Palmer[4], Song Yao[5], Wei Zheng[1]

[1]Vanderbilt University Medical Center, Nashville, TN,[2]Roswell Park Cancer Institute, Buffalo, NY,[3]City of Hope, Duarte, CA,[4]Professor of Epidemiology, Boston University, Boston, MA,[5]Postdoctoral Res. Associate, Dept. of Cancer Prev. & Control, Roswell Park Cancer Institute, Buffalo, NY

African American (AA) women have a higher incidence of triple-negative breast cancer (TNBC) and are diagnosed at an earlier age than women of European ancestry, yet remain underrepresented in cancer genomic studies. We recently charted the mutational landscape of TNBC in 426 AA women. Here, we investigated the associations between germline variants and somatic mutational profiles in those patients.

Whole-exome sequencing was performed on germline and tumor DNA from 426 patients; 402 also had germline whole-genome sequencing or array data. We analyzed somatic mutation status of 49 TNBC or other cancer genes (>2% frequency) and mutational signatures present in>20% samples (SBS1, SBS2, SBS3, SBS5, SBS13, ID6, ID8, and a new indel signature characterized by longer indels ≥5 bp). Germline factors included 1) pathogenic variants at TNBC genes, 2) cis-variants within 500kb of somatic mutated genes, 3) polygenic risk scores (PRS) for TNBC and overall breast cancer in AA women, and 4) credible causal variants (CCVs) with posterior inclusion probability >0.8 at breast cancer risk loci. Pathogenic variants included 34 germline mutations identified in *BRCA1, BRCA2, PALB2,* and *CDH1*, which were classified as pathogenic or likely pathogenic by ClinVar (n=25) or nonsense/frameshift variants (n=9). Firth logistic regression and zero-inflated negative binomial regression were used, adjusting for age at diagnosis, mutation rate, tumor purity, stage, grade, carrier of pathogenic variant (in analyses for other germline factors), and top five germline genotype principal components.

There was no significant association of somatic mutations in the 49 genes with pathogenic variants, cis-variants, or CCVs at risk loci. Patients carrying pathogenic variants in *BRCA1, BRCA2, PALB2,* and *CDH1* were substantially more likely to exhibit SBS3 and ID6, two homologous recombination deficiency (HRD)-related signatures, with 15% (incidence relative ratio, IRR 1.15, 95% CI 1.03-1.28) and 48% (IRR 1.48, 95% CI 1.18-1.87) higher counts, respectively. PRS for TNBC showed no significant associations with mutational signatures. The PRS for overall breast cancer showed a nominally significant inverse association with SBS2 and SBS5 (P=0.01 and 0.02), which may be attributable to potential collider bias inherent to the case-only design. Although no CCVs reached significance after Bonferroni correction, the risk allele of rs6482189, a variant included in the PRS for overall breast cancer but not for TNBC, was associated with the new ID signature (IRR 1.33, 1.17-1.50, $P=7.93\times10^{-6}$).

In summary, this study this study examined germline-somatic relationships in TNBC among AA women, confirmed enrichment of HRD-related signatures in pathogenic variant carriers, and identified a breast cancer risk variant associated with a novel indel signature, offering insights into TNBC biology in AA women.

#3257 Improved Variantplex workflow reduces assay time and enhances sensitivity for acute myeloid leukemia targets.

David Knupp, Michael Washburn

Integrated DNA Technologies, Boulder, CO

Introduction: Acute myeloid leukemia (AML) is a hematologic malignancy with high mortality. Detecting AML minimal residual disease (MRD) throughout the patient's care continuum can be challenging. Anchored Multiplex PCR (AMP™) VARIANT*Plex* assay solutions have been previously used to assess mutations in AML samples; however, the need for faster and more sensitive assay solutions warrants the development of new chemistry workflows to deliver on the need to identify mutations at low variant allele frequencies (≤0.01% VAF) in AML MRD samples. To meet this need, we developed an optimized VARIANT*Plex* workflow to reduce assay turnaround time and increase sensitivity for AML-relevant targets.

Methods: Seraseq Myeloid Mutation Mix was spiked into Genome-in-a-Bottle DNA at frequencies of 1-0.01% and processed using the standard low allele frequency (AF) VARIANT*Plex* workflow and the new optimized workflow. The Archer panel utilized for prepping all samples was designed to target hotspots within 8 genes relevant to AML. Libraries were pooled and sequenced on multiple sequencing platforms. Data were analyzed with Archer Analysis v7.4 using targeted mutation files and customized filters to enhance variant identification in analytical sensitivity.

Results: The new VARIANT*Plex* chemistry workflow reduced total assay time from ~1.5 days to ~7 hours and decreased the number of required bead cleanups from five to three. Workflow improvements increased DNA-to-library conversion resulting in substantial increases to Unique On-Target reads that yielded >100% increase in unique base coverage across AML panel targets. Utilizing tailored PCR conditions for low variant identification also boosted assay performance. The newly developed VARIANT*Plex* assay solution identified the expected (7/7) AML-relevant SNVs/indels and FLT3-ITDs down to 0.01%, with full target space powered to at least 0.1% variant identification.

Conclusions: This improved VARIANT*Plex* workflow enables rapid, highly sensitive identification of AML mutations, supporting MRD identification applications.

#3258 Metatranscriptomic signatures in triple negative breast cancer.

Roshan Kumar[1], Golya Shahrokhi[1], Shafiq Shaikh[1], Sunday Negedu[1], Nicole He[1], Clayton C. Yates[2], Upender Manne[3], Akinyemi I. Ojesina[1]

[1]Medical College of Wisconsin, Milwaukee, WI,[2]Sidney Kimmel Comprehensive Cancer Center, Baltimore, MD,[3]University of Alabama at Birmingham, Birmingham, AL

Triple-negative breast cancer (TNBC) exhibits racial disparities, with women of African ancestry (AA) experiencing higher incidence rates compared to women of European ancestry (EA). To investigate these differences, we performed a comprehensive meta-transcriptomic analysis on TNBC tumor tissues from 17 AA and 19 EA women, using microbial transcript, gene expression and microRNA expression datasets. Hierarchical clustering revealed two distinct groups primarily separated by racial ancestry, with AA tumors exhibiting higher abundance of *Hafnia* and elevated MIR4707 expression, while EA tumors showed increased *Erwinia* levels and MIR1248 expression. Cellular composition analysis using xCell demonstrated that AA tumors had higher Th1 cell abundance, whereas EA tumors contained higher M2 macrophage abundance; particularly, AA women with high M2 macrophage levels experienced poorer disease-free survival (DFS) compared to EA women. Furthermore, we identified a significant association between elevated *SPDYE2B* gene expression, increased *Hafnia* abundance, and reduced DFS, highlighting complex host-microbe interactions. These findings reveal distinct microbial and immune profiles in TNBC tumors between AA and EA patients, with specific bacterial genera and immune cell populations showing ancestry-associated patterns that may contribute to observed disparities in disease outcomes.

#3259 Detection and functional assessment of extrachromosomal DNA amplifications in FFPE lung tumor specimens using Hi-C sequencing.

Kristin Sikkink, Blake Skrable, Alex Hastie, Anthony Schmitt

Arima Genomics, Carlsbad, CA

INTRO: Accurate detection of extrachromosomal DNA (ecDNA) has become increasingly important in oncology diagnostics, as ecDNA-mediated oncogene amplification drives aggressive tumor behavior, therapeutic resistance, and is associated with poor clinical outcomes. As the significance of ecDNA in tumor biology becomes clearer, sensitive methods for identifying and characterizing these structures are essential. Hi-C sequencing has emerged as a powerful approach for ecDNA detection, with our group first demonstrating accurate ecDNA identification from FFPE tumor specimens while others have developed Hi-C based tools for ecDNA detection, sequence reconstruction, and regulatory landscape analysis. Here, we leverage Hi-C to characterize the ecDNA landscape in advanced non-small cell lung cancer (NSCLC) tumors lacking other identifiable drivers by prior CGP analysis.
METHODS: FFPE samples from NSCLC tumors (n=97) were retrospectively selected from patients with Stage III/IV disease whose prior CGP showed no EGFR/RAS mutations or gene fusions (“driver-negative”). Hi-C sequencing was performed by Arima Genomics, and rearrangements, gene fusions, and CNVs (including ecDNAs and other amplifications) were identified with Arima-SV pipeline. Functional characterization of oncogenes on ecDNAs was assessed by IHC. FISH studies are ongoing to corroborate Hi-C based predictions of ecDNAs and other chromosomal amplifications (e.g. homogeneously staining regions (HSRs)).
RESULTS: 95/97 (98%) Hi-C libraries passed QC and were deeply sequenced and analyzed. 33/95 (35%) tumors had amplifications containing at least one oncogene. 13/95 (14%) tumors carried oncogene amplifications predicted to be extra-chromosomal, including those involving MYCL (1), NFIB (1), PDGFD (1), CCND1 (1), CCND3(1), CCNE1 (1), EGFR (2), ERBB2 (1), KRAS (1), FGFR1 (1), and MYC (2). The remaining 20/95 (21%) were predicted to be chromosomally integrated amplifications including CCND1 (1), FGFR1 (12), KIT (2), MDM2 (1), MET (1), MYC (1), NTRK1 (1), and NRG1 (1). Twenty-six tumors had sufficient tissue remaining for functional characterization and a corresponding commercially available IHC test for protein expression. Of these, 7/7 (100%) amplifications predicted to be extra-chromosomal were expressed at the protein level, whereas only 8/19 (42%) not predicted to be extra-chromosomal were expressed at the protein level.
CONCLUSIONS: These data demonstrate that Hi-C can detect ecDNA amplifications from routine FFPE lung tumor specimens and distinguish them from their chromosomally integrated amplification counterparts. This distinction is important because it correlates with amplified oncogene expression patterns and is necessary to inform clinical and translational research programs requiring precise understanding of underlying amplification mechanisms.

#3260 Development of multimodal comprehensive genomic profiling panel with on-flow cell hybrid capture.

Mariam Ashraf[1], Michelle Baird[1], Markus Storbeck[1], Xiaodong Qi[2], June (Junhua) Zhao[2], **Helene Bauby**[1], Zhong Wu[3], Jonathan M. Shaffer[1]

[1]QIAGEN, Inc., Germantown, MD,[2]Element Biosciences, Inc., San Diego, CA,[3]QIAGEN, Inc., Frederick, MD

Hybrid capture is a widely used technique for comprehensive genomic profiling (CGP) due to its ability to target large number of regions and allows for the simultaneous detection of multiple types of genomic alterations. Traditional hybrid capture workflows, however, are often time-intensive and technically demanding, requiring long hybridization time, multiple wash steps, and tightly controlled thermal conditions, all of which limit throughput and turnaround time.

The Element Biosciences AVITI^{TM} sequencer, featuring its Trinity^{TM} flow cell, introduces an integrated hybrid capture system that performs on-flow cell target capture, washing and eliminates post-capture amplification. This innovation reduces total workflow time and improves capture specificity, but also introduces new challenges for the relatively small CGP panel application due to the higher input requirements and lack of post-capture amplification.

To address this limitation, a hybrid capture-based, multimodal library preparation workflow with the QIAseq xHYB CGP panel was optimized for compatibility with the AVITI system and Trinity flow cell. This involved designing AVITI-specific adapters and index primers, as well as modification of hybrid capture and library preparation protocols to suit the Trinity platform.

Our study revealed that multimodal libraries prepared with AVITI-specific adapter and index are fully compatible with Trinity workflow. In addition, optimal CGP panel performance can be achieved by using a newly developed hybrid capture buffer at 71 °C for as low as 0.5 hour compared to traditional hybridization conditions of 60 °C for 16 hours. Furthermore, this workflow is compatible with both fresh DNA and FFPE DNA. Additionally, to achieve optimal Trinity output, we increased the yield of the standard multimodal workflow by implementing an enhanced amplification module. This involved increased amounts of primers and high-fidelity polymerase, along with optimized cycling conditions, resulting in a four-fold increase in library yield for both whole genome and whole transcriptome libraries. This optimized workflow enables robust CGP panel hybrid capture sequencing on the Trinity flow cell from low-input DNA, supporting small sample sets and expanding access to hybrid capture sequencing for low-throughput laboratories.

#3261 Evaluation of FFPE-extracted nucleic acid quality and performance from various commercial extraction kits using contrived multiplexed reference materials.

Dana J. Ruminski Lowe, Richard Howard, Serene Roque, Praveena Kamineni, Edward S. Davis, Andrew Anfora, Yves Konigshofer, Catherine Huang, Russell K. Garlick

LGC, Gaithersburg, MD

Next generation sequencing (NGS) assays and other advanced genomic techniques for tumor profiling require sufficient and high-quality nucleic acid input. Formalin fixed and paraffin embedded (FFPE) samples are a common, yet challenging type of patient sample often used in these tests. Often in clinical labs, the patient specimen is limited, so pre-analytical handling is critical; maximizing nucleic acid yield from the sample is important, but quality and performance in downstream assays cannot be sacrificed. Furthermore, labs must consider the workflow of the extraction system, ease of use, and processing time. Highly consistent, whole process reference materials can greatly facilitate method evaluation. Here we assess the yield, quality, and performance of nucleic acids obtained with industry leading FFPE extraction kits using various Seraseq FFPE standards. Normal human cells were engineered to carry DNA and/or RNA variants. Variant allele frequency (VAF) and concentration in the cells were verified using the Bio-Rad QX-200 Droplet Digital PCR (ddPCR) System. The cells were formalin fixed, embedded in paraffin blocks and sectioned at 10-micron thickness. Extraction was performed with various commercially available kits from QIAGEN, Promega, Beckman Coulter, and AutoGen. Yields were analyzed using Qubit kits and ddPCR. TapeStation assays were used to assess fragment size and quality. VAF and concentration were again measured by ddPCR as well as several NGS assays. Yields, quality, and fragment size were variable between extraction kits. Interestingly, yields determined using Qubit did not always correlate with those measured by ddPCR. Similarly, for some DNA variants, there was a discrepancy between VAFs measured by different extraction kits, which seemed to be related to the GC content of nearby sequences. Increasing the salt concentration of buffer used in the extraction process rescued coverage of variants with lower nearby GC% regions indicating some extraction conditions can be detrimental to accurate variant quantification. Assessing performance of all steps of a tumor profiling workflow, from extraction to variant calling, is imperative to ensure high sensitivity and specificity. Extraction of nucleic acids from FFPE is a critical step that can affect the ability of the assay to accurately detect all variants in a patient sample. As shown here, a consistent standard that is readily available and contains many variants of varying complexity can be an invaluable tool in extraction assessment and optimization.

#3262 Characterization of NGS reference standards for genetic and epigenetic content.

Jayanthi Ramprakash, Matthew G. Butler, Ojaswee Dahal, Colt W. Nash, Andrew T. Anfora, **Yves Konigshofer**

LGC, Gaithersburg, MD

Here, we provide a deeper genetic and epigenetic analysis of cell lines used in reference standards. Blends of tumor and donor-matched normal cell lines can be used to create reference standards for the development and analytical validation of diagnostics in oncology. The normal component is often used as the source of germline single nucleotide polymorphisms (SNPs) to assess copy number variation (CNV), allelic ratios, and loss of heterozygosity (LOH) in the tumor component, to identify additional somatic mutations, and to enumerate these somatic mutations to determine tumor mutational burden (TMB). By adjusting the ratio of tumor and normal components, it is possible to simulate different tumor fractions to establish limits of detection. In order to better characterize the cell lines that are used in TMB and homologous recombination deficiency (HRD) reference standards, we carried out shallow whole genome shotgun (WGS) sequencing to determine CNV and supplemented that with whole exome sequencing to assess allelic ratios and LOH. Epigenetic analyses were carried out to evaluate CpG methylation. Through this characterization, several of the cell lines used for TMB were found to harbor deletions in the region containing the genes MTAP, CDKN2A, and CDKN2B. In a HRD low-positive cell line, PTEN was found to be fully deleted and surrounded by a larger LOH region. In a HRD high-positive cell line, BRCA1 showed signs of CpG methylation in its promoter. In conclusion, these characterizations provide additional utility to existing reference standards.

#3263 Where sensitivity meets complexity: Electrophoretic assessment of genomic DNA integrity at low concentrations and for FFPE samples using DIN-based analysis.

Solange Borg[1], Isabell Priester[2], Annika Dorn[2], Tim Butler[3]

[1]Agilent Technologies, Inc., La Jolla, CA,[2]Agilent Technologies, Inc., Waldbronn, Germany,[3]Agilent Technologies, Inc., Santa Clara, CA

DNA quality is a critical metric of success in downstream applications such as next-generation sequencing (NGS). However, formalin-fixed paraffin-embedded (FFPE) tissues and low-input sources like dried blood spots and buccal swabs often yield fragmented or chemically modified DNA, complicating quality control and subsequent analysis. To evaluate the impact of various sample sources on sample quality and integrity, genomic DNA (gDNA) was extracted from whole blood, dried blood spots, buccal swabs, saliva, and two FFPE tissue types using various commercial kits. Samples were analyzed on an automated electrophoresis platform and a high-sensitivity assay providing a DNA Integrity Number (DIN) to quantify DNA quality. For all samples DIN values across a broad concentration range were successfully generated showing the varying levels of degradation patterns. DIN values were reproducible across replicates and concentrations, confirming assay robustness, however FFPE samples showed significant DIN variability depending on the extraction method. DIN-based electrophoretic analysis offers a reproducible and objective measure of gDNA integrity, making it suitable for low-concentration and degraded samples in genomics workflows requiring stringent quality control, such as NGS.

#3264 Epidemiology meets novel transcriptomics in poorly differentiated endometrial carcinomas.

Thulo Molefi[1], Motshedisi Sebitloane[2], **Zodwa Dlamini**[3]

[1]Medical Oncology, University of Pretoria, Pretoria, South Africa,[2]Discipline of Obstetrics and Gynecology, School of Clinical Medicine, University of Pretoria, Pretoria, South Africa,[3]Pan African Cancer Research Institute (PACRI), University of Pretoria, Pretoria, South Africa

Background: Endometrial cancer (EC) is the commonest gynecological malignancy in high-income settings and is traditionally divided into estrogen-related Type I and non-estrogenic Type II diseases. Type II histologies carry a poorer prognosis and have been under-characterized molecularly in African populations. South African EC data are sparse and largely extrapolated from international cohorts. This study addresses epidemiologic and transcriptomic gaps by profiling clinical outcomes and RNA-level alterations in South African women with epithelial EC, with emphasis on Black females and comparison to African American datasets.
Materials and Methods: Retrospective review of 290 electronic health records (2009-2019) from Inkosi Albert Luthuli Central Hospital to determine incidence, FIGO stage distribution, and survival for epithelial EC. Molecular profiling of 76 poorly differentiated FFPE tumor specimens: total RNA extraction, short-read RNA sequencing, alignment with STAR, quantification with featureCounts/StringTie. Analyses included differential gene expression ($|\log2FC| \geq 1.0$), alternative-splicing (ΔPSI), novel-isoform discovery, and Reactome pathway enrichment to define dysregulated pathways. Publicly available African American datasets were used for cross-population comparisons.
Results: Type II histologies comprised 47.9% of cases and aligned with advanced FIGO stage and median overall survival of 3.7 months. Transcriptome analysis revealed a dual signature: upregulation of MAPK/ERK and retinoic-acid pathways (e.g., MKNK2 +2.03 $\log_2$FC, RARA +2.14) alongside repression of RNA-Pol II transcription and cell-cycle regulators (e.g., ZNF793 −5.26, MYC −4.50). Exon-skipping in GJA1 and widespread intron retention marked splicing rewiring. StringTie uncovered novel lncRNA and zinc-finger isoforms (e.g., LINC01605), two layers absent from existing annotations. Cross-population analysis confirmed key shared drivers of the copy-number-high/p53-abnormal subtype, while novel splicing variants emerged as population-specific.
Conclusion: These findings validate the predominance and aggressiveness of Type II endometrial carcinoma in South African women. The study reveals unique transcriptomic and splicing landscapes in Black females that extend TCGA subtyping. Novel kinase and lncRNA targets (MKNK2, SRPK1, LINC01605) hold promise for tailored therapeutics. Integrating molecular classification into national guidelines, bolstering diagnostic infrastructure, and launching precision-medicine trials will be essential to narrow survival disparities and deliver equitable, biomarker-driven care.

#3265 An optimized WGS workflow for FFPE samples: Enabling high-confidence variant detection for MRD surveillance.

Bella Pfeiffer, Gabrie l Lipof, Alaina Villareal, Kristopher Amirault, Sameer Vasantgadkar, **Madan Ambavaram**, Vanessa Process, Sushant Khanal, Martina Werner, Greg Endress, Ulrich Thomann, Eugenio Daviso

Covaris, LLC, Woburn, MA

This study aimed to define a robust and synergistic workflow for FFPE-based whole genome sequencing (WGS) by evaluating how different extraction and library preparation methods impact coverage uniformity and the reliable detection of complex, actionable variants.Despite representing the vast majority of tumor specimens, formalin-fixed paraffin-embedded (FFPE) samples present significant DNA quality issues that challenge variant calling accuracy and limit their potential for whole genome sequencing (WGS) in precision oncology. Optimizing DNA extraction and library preparation is therefore essential to maximize WGS data quality from FFPE samples, particularly for sensitive applications like tissue-informed Minimal Residual Disease (MRD) monitoring. In this study, we evaluated the impact of different workflow combinations on WGS data quality. We compared libraries from four GIAB FFPE control samples (HG002/3/4/5) prepared using two extraction methods and two library preparation kits. This work expands on previous findings by including bioinformatic analysis of complex variants, coverage uniformity, and clinically relevant variant calling. Performance was assessed via: 1) precision and accuracy of large insertion-deletions (INDELs >16 bp), 2) genome-wide coverage uniformity, and 3) SNP/INDEL variant calling in clinically actionable Tier 1A gene variants. Our analysis of large INDELs (>16 bp) confirmed trends observed in small variant data. The combined Covaris extraction and library prep workflow demonstrated significantly higher precision and accuracy compared to other combinations. Analysis of genome-wide coverage distribution showed that the workflow produced superior coverage uniformity, with a lower coefficient of variation (CV) and a higher percentage of the genome covered. Regarding the calling of clinically actionable Tier 1A variants, the Covaris workflow again achieved the highest F1, precision, and recall. These analyses demonstrate that a workflow optimized for both extraction and library preparation provides a robust solution for FFPE-based WGS. This approach ensures higher data quality, more uniform genome coverage, and more reliable detection of complex and clinically actionable variants. This high-fidelity variant calling directly addresses a central challenge in FFPE-based precision oncology, providing the confident variant detection essential for applications including tumor profiling and MRD surveillance.

: Metabolic Studies in Brain, Pediatric, and Hematologic Cancers
Poster Session

#3269 Rebalancing systemic and cellular energy dysmetabolism in Chronic Lymphocytic Leukemia through exercise training.

Uzma Zaheer[1], Ellie Miles[1], Angela Avramovska[1], Vithushan Srikumaran[1], Andrew Hulton[1], Long Li[1], Caitlin Jeary[1], Andrea Sitlinger[2], Renata Walewska[3], Barbara Fielding[1], David Bartlett[1]

[1]University of Surrey, Guildford, United Kingdom,[2]Duke University Medical Centre, Durham, NC,[3]University Hospitals Dorset NHS Foundation Trust, Dorset, United Kingdom

Introduction: Chronic lymphocytic leukaemia (CLL) cells abnormally express lipoprotein lipase (LPL), an enzyme typically restricted to adipocytes and myocytes for lipid-mediated energy utilisation. This enables CLL cells to store and utilise lipids, potentially competing with or diverting resources from healthy tissues. *In vitro* studies suggest that reducing fatty acid availability may limit CLL proliferation; however, little is known about how patients can modulate this process *in vivo*. Exercise training offers a systemic, non-pharmacological approach to counter metabolic dysregulation, with potential benefits for tumour control and overall health.
Methods: We conducted a 12-week exercise trial involving five treatment-naive (TN-CLL) and five previously treated (Td-CLL) patients. We assessed the metabolic fate of ingested lipids before (Baseline) and after (Post-Intervention) the program. Patients consumed a meal containing 200mg palmitic acid tracer (^{13}CPA), and blood samples were collected hourly for 3 hours (T_{0h}-T_{3h}). We assessed ^{13}CPA enrichment in plasma triacylglycerol (TAG) and non-esterified fatty acids (NEFA), and total fatty acids in immune cells (PBMC) using mass spectrometry, and data were analysed using RM-ANOVA.
Results: Post-meal ingestion, ^{13}CPA enrichment in plasma TAG and NEFA increased steadily from T_{1h}-T_{3h} ($p<0.001$). At Baseline T_{3h}, TN-CLL exhibited higher plasma ^{13}CPA-TAG and unlabelled PA-TAG incorporation than Td-CLL ($p<0.001$). Post-Intervention T_{3h}, TN-CLL ^{13}CPA-TAG levels decreased ($p<0.05$) and were no longer significantly different than Td-CLL. TN-CLL ^{13}CPA-NEFA enrichment increased post-Intervention compared to Td-CLL ($p<0.05$), suggesting enhanced ^{13}CPA-TAG hydrolysis. Similarly, ^{13}CPA uptake into PBMCs, which was higher in TN-CLL at Baseline T_{3h} ($p<0.05$), reduced Post-intervention.
Conclusion: This pilot study demonstrates the feasibility of stable isotope tracing to assess *in vivo* lipid uptake in CLL. Exercise training in TN-CLL patients reduced lipid uptake, suggesting a shift towards a more balanced and healthier metabolic profile. Further research is needed to determine whether exercise can disrupt the lipid dependence of CLL cells.

#3270 Leukemia induced cachexia is driven by dysregulated tryptophan metabolism resulting in inhibition of muscle regenerative capacity.

Alyssa Nicole Polski-Delve[1], Charlotte Hellmich[1], Paul Lonsdale[2], Trey Koev[3], Rebecca Maynard[1], Gwenaelle Le Gall[1], Timothy Pearson[2], Ulrike Mayer[2], Kristian Bowles[4], Stuart Rushworth[1]

[1]Metabolic Health, University of East Anglia, Norwich, United Kingdom,[2]Biological Sciences, University of East Anglia, Norwich, United Kingdom,[3]Chemistry, University of East Anglia, Norwich, United Kingdom,[4]Department of Haematology, Norfolk and Norwich University Hospitals NHS Foundation Trust, University of East Anglia, Norwich, United Kingdom

Cachectic muscle wasting occurs in many cancers but remains poorly defined in hematological malignancies. Leukaemia associated muscle loss is often exacerbated by chemotherapy, limiting treatment efficacy and presenting a poor prognosis, yet its mechanisms remain unclear. We aim to define drivers of leukaemia induced muscle atrophy, focusing on metabolic dysregulation. Using a syngeneic acute myeloid leukaemia mouse model in which C57/Bl6 mice received MN1-overexpressing cells intravenously, we observed significant weight loss independent of food intake. Gastrocnemius mass was significantly reduced in tumor-bearing mice compared to non-tumor bearing controls. H&E staining identified structural abnormalities and reduced fiber area. RNA seq followed by confirmation with RT-qPCR showed strong induction of atrophy genes TRIM63 and FBXO32, consolidating atrophy within our model. To assess muscle regeneration, we used a Pax7-CreERT2 reporter mouse model expressing tdTomato, allowing visualization of the satellite cells. Despite similar satellite-cell numbers in AML and controls, AML muscles displayed higher overall integrated density, indicating increased Pax7 expression and therefore satellite cell activation. However, centrally located nuclei were absent, revealing impaired regenerative activity. To define metabolic contributors, we performed NMR on serum. Tumor-bearing mice showed broad depletion of amino acids, however kynurenine pathway metabolites were strongly elevated. Metabolites of this pathway such as kynurenate and quinolinate have been linked to enhanced oxidative stress and aryl hydrocarbon receptor signaling that can impair muscle stem cell function and promote catabolism (Grishanova A. and Perepechaeva M. 2024). Due to altered amino acid levels and the RNA seq data, we examined transporter mRNA expression in the muscles and found significant upregulation of LAT1 during disease progression, which exchanges intracellular glutamine for branched-chain amino acids and tryptophan, the initial metabolite of the kynurenine pathway. Furthermore, cytokine profiling revealed multiple elevated atrophy-associated mediators, including GDF-15, IL-6, CXCL2, and CD14. IL17A was most elevated (7-fold), consistent with its reported role in lung cancer cachexia via JAK2/STAT3 signaling (Ying L. *et al* 2022). In summary, we have used a multi-omic approach to elucidate metabolic and cytokine changes that occur during leukaemia to drive cachexia. Future work will investigate the mechanism that drives these leukaemia-induced alterations to identify potential therapeutic interventions.

#3271 Integrated metabolic and cell-health profiling as a framework for defining cellular state.

Kayla Sylvester, Anthony C. Lauer, Gediminas Vidugiris, Donna Leippe, Jolanta Vidugiriene

Promega, Madison, WI

Defining cellular state requires understanding how multiple metabolic features change together, yet most assays capture only single parameters. We developed an integrated bioluminescent profiling strategy that measures coordinated metabolic and cell-health indicators from the same low-input sample, providing a practical way to resolve early pathway activity and cellular condition across immune and cancer systems. The approach uses a suite of luminescent assays to quantify ATP, NAD, total NADP(H), metabolic activity, and nutrient utilization including glucose consumption, lactate secretion, and malate accumulation. Together, these features report on glycolytic engagement, mitochondrial contribution, and redox balance, generating compact multiparametric profiles not achievable with isolated assays. In primary T cells, the integrated profiles distinguished early glycolytic, NAD-rich states linked to rapid expansion from more oxidative states associated with memory-biased phenotypes. These early metabolic patterns emerged within the first 72 hours of activation and aligned with later differences in proliferation and T cell-subset composition, demonstrating that early metabolic signatures capture functional trajectories beyond initial activation markers. In cancer-cell models, the same measurements resolved nutrient-dependent shifts in metabolic balance and stress adaptation, illustrating how environmental composition shapes pathway use and overall cellular fitness. The workflow uses standard luminescent instrumentation, minimal material, and is adaptable to additional metabolic markers as the platform evolves. By capturing coordinated metabolic and cell-health features within a scalable framework, this approach provides a practical way to define cellular state and relate early metabolic patterns to later functional behavior across diverse experimental contexts.

#3273 The mitochondrial protease YME1L regulates type 1 interferon signaling via the STING pathway in AML.

Yihe Zhang, Geethu Thomas, Rose Hurren, Yongran Yan, Marcela Gronda, Dakai Ling, Andrea Arruda, Mark David Minden, Aaron D. Schimmer

UHN Princess Margaret Cancer Centre, Toronto, ON, Canada

Yeast mitochondrial escape 1-like 1 (YME1L) is one of four mitochondrial ATP-dependent proteases responsible for maintaining mitochondrial proteostasis and is the sole ATP-dependent protease acting on substrates in the intermembrane space. Here, we investigated the expression and functional importance of YME1L in acute myeloid leukemia (AML).

YME1L protein was upregulated in 6 out of 7 AML cell lines and 17 of 23 primary AML patient samples compared to normal hematopoietic stem cells. Overexpression occurred equally across cytogenetic risk groups of AML. Moreover, high YME1L mRNA expression correlated with inferior 5-year overall survival in AML patients.

To evaluate the essentiality of YME1L in AML, we knocked down the protease in AML cell lines (OCI-AML2, NB4, TEX, and THP-1) with shRNA. YME1L knockdown decreased cell proliferation and clonogenic growth in all tested cell lines. Interestingly, YME1L knockdown did not induce cell death as measured by Annexin V/PI staining. Rather, YME1L knockdown induced AML differentiation as evidenced by increased expression of CD14, a marker of monocytic differentiation.

Depletion of YME1L with shRNA also reduced the engraftment of TEX cells and primary AML cells in the marrow of NSG immunodeficient mice.

To investigate the functional importance of YME1L depletion, we performed RNA sequencing of AML cells after YME1L depletion. Knockdown of YME1L upregulated genes associated with type I interferon (IFN) signaling, defense response to virus, and viral mimicry. We validated the results by real-time PCR and ELISA, confirming the upregulation of IFN-β, IFN-γ, ISG15, IFI44, and IFIT2 following YME1L knockdown. We demonstrated that activation of IFN signaling was secondary to activation of the cGAS-STING pathway as pharmacological inhibition of STING abolished the upregulation of IFN signaling after YME1L depletion. cGAS-STING signalling can be activated by the accumulation of double-stranded DNA (dsDNA) in the cytosol. We showed that YME1L knockdown promoted the leakage of dsDNA from the mitochondria into the cytosol. We also demonstrated that dsDNA leaked into the cytosol via the mitochondrial VDAC channel as treatment of AML cells with the VDAC channel inhibitor, VBIT-4, prevented the accumulation of cytosolic dsDNA and the upregulation of IFN signaling after YME1L knockdown in AML cells.

In summary, we demonstrated that YME1L is overexpressed in a subset of AML cell lines and primary patient samples and is required for AML proliferation and clonogenic growth. YME1L regulates the leakage of mtDNA into the cytoplasm, activation of the cGAS-STING-IFN axis, and controls AML differentiation. Thus, we have uncovered novel functions for the mitochondrial protease YME1L and suggest that targeting YME1L may be a novel strategy in the case of some AML patients.

#3274 Low-protein diet limits liver melanoma metastasis by enhancing natural killer cell function.

Anastasios Bampalis[1], Annalisa Altera[1], Katherine Hampton[1], Alyssa Polski-Delve[1], Charlotte Hellmich[1], Tabitha Barlett[1], Nilda Ilker[1], Matthew Markham[1], Catherine Chinnery[2], Gwenaelle Le Gall[1], Naiara Beraza[3], Stuart Rushworth[1]

[1]Norwich Medical School, University of East Anglia, Norwich, United Kingdom,[2]Haematology department, Norfolk and Norwich University Hospitals, Norwich, United Kingdom,[3]Quadram Institute, Norwich, United Kingdom

Liver metastasis represents a major clinical challenge across multiple cancer types, contributing significantly to patient morbidity and mortality due to the liver's unique immunometabolic environment that supports tumour growth. Low-protein diet (LPD) has been shown to reshape the immunological landscape of the liver and provide a protective phenotype against inflammation and infection. Here, we investigate the impact of LPD on the progression of metastatic melanoma. C57BL/6 female mice were fed *ad libitum* with an isocaloric control diet (22% protein) or with LPD (6% protein) for a duration of two or six weeks before experimental endpoints. Mice were injected with B16F10 melanoma cells intravenously two weeks before experimental endpoints. Nuclear magnetic resonance was used for the detection of metabolites in the liver, lungs and blood serum. Transcriptome analysis was performed on mRNA sequencing data obtained from lung and liver RNA. Flow cytometry was used to screen immune cell populations in the liver. LPD-fed mice showed an 87.5% reduction in melanoma metastatic modules in the liver ($p = 0.021$, Mann-Whitney U (MWU) test), while no reduction was observed in the lungs. Metabolite analysis in the liver identified 15 differentially abundant metabolites ($p.adj < 0.05$, MWU test) and pathway impact analysis (False Discovery Rate (FDR) < 0.05) with MetaboAnalyst identified 14 enriched pathways between the control diet and LPD. Tryptophan catabolism was down-regulated by LPD. Transcriptome analysis in the liver with DESeq2 identified 240 significantly upregulated and 244 downregulated genes in LPD ($|log2FC| > 1$ and $p.adj < 0.05$, Wald test). Gene-set enrichment analysis identified several pathways deregulated in LPD, including downregulation of Tryptophan metabolism, which confirmed our metabolite analysis. These results indicate a shift in immune cell function in the liver, with the Kynurenine pathway heavily impacted. We therefore examined liver immune cells by flow cytometry. Isolated immune cells from the liver showed a 25.2% ($p.adj = 0.012$, MWU test) increase in the Natural Killer (NK) cell ($CD45^+$, $CD3^-$, $NK1.1^+$) population between the control diet and LPD mice. These results suggest an immunological shift toward enhanced NK cell activity in the livers of LPD mice, potentially driven by reduced Tryptophan metabolism and consequently lower downstream Kynurenine levels. Because Kynurenine can result in downregulation of genes encoding NK-activating receptors, its reduction may help sustain NK cell activation. This heightened NK activity could contribute to the decreased number of metastatic melanoma nodules observed in LPD mice. Future work will focus on elucidating the mechanisms underlying this NK cell-mediated protective effect.

#3275 Dietary fiber intake modifies the bile acid metabolic profile in the DIET trial - A randomized double blinded dietary intervention study in melanoma patients receiving immunotherapy.

Yan Jiang, Yufan Qiu, Johannes Fahrmann, Ehsan Irajizad, Satabdi Saha, Nazli Dizman, Christine B. Peterson, Elizabeth M. Burton, Michael A. Davies, Nadim J. Ajami, Jennifer A. Wargo, Jennifer L. McQuade, Carrie R. Daniel-MacDougall

UT MD Anderson Cancer Center, Houston, TX

Background: Dietary fiber is associated with response to immune checkpoint blockade (ICB) in melanoma. We previously conducted the DIET trial (NCT04645680) which was a fully controlled feeding study comparing a high fiber versus a healthy control diet in melanoma patients receiving ICB. The trial revealed that high fiber diet is feasible and safe, and patients on high fiber diet demonstrated a numerically higher response rate. Herein, we report a secondary objective of the effects of dietary intervention on systemic metabolism.
Methods: Melanoma patients (n=45) initiating ICB were randomized (2:1), following a 1-week equilibration, to either a high fiber (30 g/d fiber ramped-up biweekly via whole foods to 50 g/d) or a healthy control diet (20 g/d fiber) for the study duration (up to 10 weeks). Longitudinal blood specimens were collected at baseline and at each infusion (when treated locally) for up to three cycles during the study. Sera from 43 patients were processed for untargeted metabolomics and bile acid (BA) profiling using LC-MS/MS methods. Current analysis focuses on comparison of paired samples from patients in the high fiber (n=6) and the control arm (n=8) collected during equilibration vs week 1-4, reflecting a dietary fiber 30-40 g/day in the high fiber arm.
Results: The untargeted metabolomics analyses revealed changes in BAs and glycine- and taurine- conjugated derivates to be reduced in the high fiber arm compared to control (Wilcoxon rank sum test $p<0.05$). Targeted BA profiling confirmed a decrease in unconjugated secondary BAs and secondary-to-primary BA ratios, which may influence anti-tumor immunity. Specifically, our findings suggest that dietary fiber reduced gut microbiota mediated biotransformation of secondary BAs (deoxycholic acid, lithocholic acid and ursodeoxycholic acid) from primary BAs (cholic acid and chenodeoxycholic acid). Conjugated to unconjugated BA ratios were also decreased in the high fiber arm, suggesting potentially reduced hepatic BA conjugation. Furthermore, in mouse avatar models of melanoma, fecal microbiota transplant was performed using paired fecal specimens (pre vs post high fiber diet) from participants in the DIET trial. Post-high fiber diet recipients showed improved ICB response and decreased secondary-to-primary BA ratios in the circulation (n=5) compared to pre-high fiber diet recipients.
Conclusion: Consistent with prior controlled feeding studies in other settings, our collective findings from circulating metabolites suggested that dietary fiber intervention modulates microbiome mediated secondary BA synthesis and conjugation linked to ICB response. These findings warrant further mechanistic studies in preclinical models and in larger cohort of patients.

#3276 Tracing and modeling lipid homeostasis to understand keratinocyte biology.

Zoya Y. Chih, Michael S. M. Mah, Matthew J. Kolar, Christian M. Metallo

Salk Institute for Biological Studies, La Jolla, CA

Dysregulation of metabolism contributes to the development and progression of many diseases, including cancer. Sphingolipids are bioactive lipids that mediate key cellular functions, such as signaling, apoptosis, and cell proliferation. Previously, we showed the role of serine metabolism in sensitizing tumors through altered sphingolipid biosynthesis to induce metabolic stress, thereby constraining tumor growth. Given the importance of serine, and other nonessential amino acids, in oncogenesis and lipid metabolism, our focus is to explore the tricarboxylic acid (TCA) cycle and sphingolipid metabolic flux in keratinocytes and how these may be dysregulated in cancer. To first evaluate sphingolipid biosynthesis in human keratinocytes, we performed flux measurements in media containing ^{13}C-serine and ^{13}C-glycine, which revealed decreased synthesis of ceramides and sphingomyelins in differentiated keratinocytes compared with undifferentiated keratinocytes. Stable isotope tracing with uniformly-labeled ^{13}C-glucose showed increased flux through the TCA cycle upon differentiation. These data highlight the distinct metabolic changes induced by differentiation and serve as a benchmark for future studies in defining TCA metabolic flux and acyl chain specific alterations to sphingolipid pools in non-melanoma skin cancer models.

#3277 Targeting cytosolic mutant IDH1 by hyperactivation to induce cancer cytotoxicity.

ZIQI Yu, Andrew Intlekofer

Weill Cornell Grad. School of Medical Sci., New York, NY

Somatic mutations in isocitrate dehydrogenase (IDH) enzymes are hallmarks of acute myeloid leukemia (AML), glioma, and several other cancers. Mutant IDH enzymes lose their normal function of catalyzing NADP(H)-dependent conversion of isocitrate to α-ketoglutarate (α-KG) and instead gain an abnormal new activity that reduces α-KG to 2-hydroxyglutarate (2HG), an oncometabolite that drives chromatin hypermethylation and blocks differentiation. Although FDA-approved inhibitors such as ivosidenib and enasidenib effectively suppress 2HG, fewer than half of patients respond, and resistance invariably develops. We discovered that genetic or pharmacologic hyperactivation, rather than inhibition, of mitochondrial mutant IDH2 triggers lethal metabolic toxicity that selectively eliminates IDH2-mutant cancer cells. Building on these findings, we hypothesized that hyperactivation of cytosolic mutant IDH1 could similarly cause toxic 2HG accumulation, redox imbalance, and selective death of IDH1-mutant cancer cells. To test this hypothesis, we engineered human cancer cell lines with inducible expression of hyperactive IDH1 mutants, which resulted in excessive 2HG production, metabolic dysfunction, and impaired cell fitness. In parallel, we found that activation of mitochondrial 2HG production in IDH1-mutant cancer cells triggers profound metabolic collapse, leading to impaired cell growth in vitro and in vivo. Together, these results suggest that direct or indirect hyperactivation of the mutant IDH1 pathway may represent a new therapeutic strategy --- targeting cytosolic IDH1 mutations by driving cancer cells beyond their metabolic limits.

#3278 Metabolic pathway signatures defining response to CD19 CAR T-Cell therapy in aggressive B-cell non-hodgkin lymphoma.

Melinda S.Y. Tan[1], Panwen Wang[2], Patrizia Mondello[1], Jacqueline Turner[1], Andre de Menezes Silva Corraes[1], Chen Wu[1], Zuoyi Shao[1], Kevin Regan[1], Ma Audrey[1], Arushi Khurana[1], Nora N. Benanni[1], Yucai Wang[1], Paul Hampel[1], Jonas Paludo[1], Saad J. Kenderian[1], Urshila Durani[1], Patrick B. Johnston[3], Jose Caetano Villasboas[1], Stephen M. Ansell[4], Ying Li[5], Haidong Dong[6], Hu Zeng[1], Yi Lin[7]

[1]Mayo Clinic, Rochester, MN,[2]Mayo Clinic, Scottsdale, AZ,[3]Hematology, Mayo Clinic, Rochester, MN,[4]Assistant Professor, Div. of Hematology, Mayo Clinic College of Medicine, Rochester, MN,[5]Mayo clinic, Jacksonville, FL,[6]Mayo Clinic College of Medicine and Science, Rochester, MN,[7]Asst. Professor, Div. of Hemat., Mayo Clinic, Rochester, MN

Chimeric antigen receptor (CAR) T-cell therapy achieves high response rates in relapsed/refractory aggressive B-cell non-Hodgkin lymphoma, yet only 40% of patients achieve durable remission. Identifying biological programs linked to long-term response remains critical. As metabolic fitness underlies T-cell persistence and effector function, we profiled metabolic pathways associated with clinical outcomes following commercial CD19 CAR T-cell therapy.

Single-cell RNA sequencing of peripheral blood mononuclear cells collected at baseline (BL), peak CAR-T expansion (PK), and one-month post-infusion (M1) was analyzed using CellRanger v7.0.1, immunopipe. Seurat v4.3.0 was applied for unsupervised clustering to delineate cell subsets based on top differentially expressed genes. Patients were categorized as durable complete remission (CR ≥6 months; n = 16), primary refractory (PD1; n = 4), or relapse after initial response (PD2; n = 12). Gene-set enrichment analysis defined metabolic pathway activity across T-cell, monocyte, dendritic cell (DC), and natural killer (NK) subsets.

Oxidative phosphorylation (OXPHOS) emerged as the dominant metabolic program distinguishing clinical outcomes. At BL and PK, OXPHOS was consistently enriched in PD1 relative to CR across T-cell, monocyte, and DC subsets, suggesting early oxidative activation in non-responders. By M1, this pattern inverted, with higher OXPHOS activity in CR. PD2 largely paralleled PD1, but several subsets including CD8 T central memory, classical monocytes TGFβ, intermediate monocytes CD38, monocytic myeloid-derived suppressor cell (mMDSC) HIF1A, and mMDSC SIRPA, showed OXPHOS enrichment in CR at BL and/or PK that persisted through M1. In contrast, DC and NK subsets exhibited the opposite pattern: OXPHOS was enriched in CR at PK (conventional DC 2 (cDC2), plasmacytoid DC (pDC), NK, proliferating NK), but shifted toward enrichment in PD2 at M1 (cDC2, NK, NK CD56bright).

Glycolysis (GLY) followed a similar trajectory in monocytes and NK cells, with enrichment in PD1/PD2 at BL and PK, followed by enrichment in CR at M1. In T-cells, PD1 maintained GLY enrichment from BL through PK, with no significant differences observed at M1.

The inositol-phosphate metabolism pathway showed a more static pattern and was consistently enriched in multiple PD2 effector and memory T-cell subsets without reversal at M1.

Taken together, these data reveal distinct, lineage-specific metabolic signatures that differentiate durable remission from early and late progression. Dynamic OXPHOS and GLY programming, characterized by lower activity early and enhanced activity at M1 in CR, may reflect adaptive metabolic programming that supports sustained antitumor immunity. Immune-metabolic profiling may therefore serve as a biomarker of response and highlight actionable metabolic pathways to enhance CAR T-cell durability.

#3279 Metabolomic profiling reveals plasma LPC as an indicator of systemic inflammation and immunotherapy response in squamous cell carcinoma.

Tomoyuki Iwasaki[1], Hidekazu Shirota[1], Eiji Hishinuma[2], Naomi Matsukawa[2], Yuki Kasahara[1], Hisato Kawakami[1]

[1]Department of Medical Oncology, Tohoku University Hospital, Sendai, Japan,[2]Tohoku Medical Megabank Organization, Tohoku University, Sendai, Japan

Cancer is increasingly recognized as a systemic disease characterized not only by local tumor growth but also by widespread metabolic and immunologic disturbances that shape disease progression and treatment response. To clarify systemic metabolic alterations associated with prognosis and immune checkpoint inhibitor (ICI) efficacy in squamous cell carcinoma (SCC), we conducted an integrated multi-omics analysis of plasma from 149 patients with advanced or recurrent esophageal or head and neck SCC. Targeted metabolomics quantified 635 metabolites, which were combined with detailed clinical, proteomic, and cytokine datasets. Weighted gene correlation network analysis revealed a single metabolite group—lysophosphatidylcholines (LPCs)—as most strongly associated with the Glasgow Prognostic Score, a marker of systemic inflammation and patient survival. Across nearly all measurable LPC species, plasma levels were markedly reduced in patients with elevated inflammatory burden and poor prognosis. LPC concentrations showed minimal correlation with tumor size, treatment line, or performance status, indicating that LPC reduction reflects host systemic conditions rather than tumor burden or treatment exposure. Survival analysis demonstrated that patients with low LPC levels had significantly shorter overall survival, with the strongest association observed in those receiving ICIs. Among ICI-treated patients, especially those treated in the first-line setting, low LPC levels identified individuals with minimal therapeutic benefit, whereas LPC levels were not prognostic in patients never exposed to ICIs. To explore the biological context of LPC loss, we analyzed plasma proteomic and cytokine profiles. Proteomic signatures in the low-LPC group revealed enrichment of pathways related to inflammation, innate immunity, and coagulation activation; levels of CRP, serum amyloid A, and other acute-phase reactants were substantially increased. Cytokine profiling demonstrated that low LPC levels were accompanied by elevated IL-6, IL-10, and TNF-α, further supporting the presence of systemic chronic inflammation. Conversely, chemokines such as CCL2 and CXCL8 were higher in patients with preserved LPC levels. Together, these multi-omics findings indicate that decreased LPC marks a systemic pro-inflammatory and immunosuppressive state that undermines antitumor immunity and reduces responsiveness to PD-1 blockade.

#3280 Rewiring glutamine metabolism restores osteoblast differentiation in multiple myeloma.

Mumtaz Shirin, Natalya N. Pavlova

Oncological Sciences, University of Utah, Huntsman Cancer Institute, Salt Lake City, UT

More than 80% of multiple myeloma (MM) patients are diagnosed with pathological bone fractures or osteolysis. Currently, no therapeutic strategies focus on restoring bone-building osteoblast cells in patients with MM osteolytic lesions. Metabolic rewiring in MM displays high glutamine dependence or “addiction”, leading to glutamine depletion from the local niche, the bone. Notably, glutamine is essential for driving commitment and differentiation into bone-building osteoblasts to meet the high anabolic demands. The mechanism by which the glutamine-dependent osteoblast progenitor cells sense and respond to glutamine depletion by MM is unexplored. In this study, we demonstrate that the polyglutamine tract of the key osteoblast-differentiation transcription factor, Runt-related transcription factor 2 (RUNX2), serves as the molecular sensor that is exquisitely sensitive to glutamine depletion and consequently inhibits osteoblast differentiation in a glutamine-deprived bone niche developed by MM. We assessed osteoblast differentiation using growth assay, gene expression analysis, and differentiation staining assays. Nascent mRNA translation was measured using a fluorescent reporter-based assay and an on-membrane assay. These systems were analyzed under glutamine depletion, rerouting, or with MM cells. Our findings demonstrate that the polyglutamine tract senses a glutamine deficit resulting from the uncharging of glutamine tRNAs, leading to the suppression of translation of nascent RUNX2 mRNA and, consequently, osteoblast differentiation. Deletion or shortening of the polyglutamine tract renders RUNX2 insensitive to glutamine depletion. Supraphysiological RUNX2 in glutamine-depleted osteoblast progenitors compromises cell fitness, suggesting an adaptive function for this sensing mechanism. Furthermore, in osteoblast progenitors, rerouting glutamine towards anabolic pathways restores nascent RUNX2 translation and osteoblast differentiation under glutamine depletion. We found that MM cells suppress osteoblast differentiation, which can be restored by rerouting glutamine in osteoblast progenitors. These findings demonstrate that the critical transcription factor RUNX2 possesses an in-built glutamine sensor, the polyglutamine tract, which enables it to adapt and make cell fate decisions in response to glutamine deficit. Rerouting glutamine in osteoblast progenitors to make glutamine available for differentiation represents a novel therapeutic strategy to restore bone formation in the MM bone niche.

#3281 Cardiolipin acyl chain remodeling is a therapeutic target in aggressive infantile embryonal brain tumors.

Evangelos Liapis[1], Allison Maas[1], Lea Maristela[1], Adele Ponzoni[1], Kelly O'Neill[1], Annupurna Pamreddy[1], Francesca M. Cozzi[1], Brent Harris[2], Tara Lozy[1], Derek Hanson[3], **Claire L. Carter**[4]

[1]Hackensack Meridian Center for Discovery and Innovation, Nutley, NJ,[2]Georgetown University, Washington, DC,[3]Hackensack Meridian School of Medicine, Hackensack, NJ,[4]Hackensack Meridian School of Medicine, Nutley, NJ

Background: Pediatric embryonal brain tumors that impact infants are highly aggressive CNS WHO grade 4 neoplasms with no standard-of-care. These encompass embryonal tumor with multilayered rosettes (ETMR), atypical teratoid rhabdoid tumor (AT/RT), group 3 medulloblastoma (MB-G3) and recurrent/metastatic sonic hedgehog medulloblastoma (MB-SHH). These tumors have low inter-tumoral genetic heterogeneity yet present with diverse histological features and developmental locations within the brain, which makes identifying therapeutic targets a challenge. The mechanisms driving therapeutic resistance for currently used treatment regimens are unknown. New and more effective treatments are urgently needed. Cardiolipins are mitochondrial-specific lipids, and their fatty acid composition has been shown to regulate mitochondrial structure and function. Despite the known functional significance of cardiolipins, their structure-specific accumulation in relation to mitochondrial phenotypes and cellular function in aggressive pediatric embryonal brain tumors remain ill-defined. Methods: Spatial lipidomic profiles in patient samples and 3D models were determined using mass spectrometry imaging. Cell proliferation and mitochondrial bioenergetics and dynamics were characterized using multiplex immunofluorescence (mIF), transmission electron microscopy, western blotting and metabolic assays. LCLAT1 KD was carried out using siRNA and inducible shRNA. Results: We detected a structure-specific accumulation of cardiolipins and increased expression of the cardiolipin acyl chain remodeling enzyme, LCLAT1 within proliferating tumor cells in patient samples and the 3D tumorspheres. The mitochondria in the proliferating tumor cells were fragmented and displayed a tubular cristae architecture. LCLAT1 KD in ETMR altered cardiolipin profiles, significantly reduced 3D tumorsphere growth, decreased Sox2 and N-Myc expression, increased p53 and p21 expression, and significantly increased LIN28A expression with a parallel increase in the early neuronal marker, doublecortin. Conclusions: Our findings provide novel insight into aggressive infantile embryonal brain tumor biology based on mitochondrial phenotypes and the fatty acid composition of the multifunctional mitochondrial-specific lipid, cardiolipin. We additionally showed evidence of a switch from a stem cell phenotype to upregulated neuronal differentiation pathways following CL fatty acyl chain remodeling in ETMR. Our findings underscore the intimate relationship between CL structure, mitochondrial phenotypes and embryonal brain tumor cell fate. On-going studies: Determine the *in vivo* and *in vitro* functional significance of cardiolipin acyl chain remodeling in ETMR and AT/RT, with a focus on LIN28A and differentiation pathways.

#3282 Metabolic reprogramming in Li-Fraumeni Syndrome underlies the pre-cancer niche and cancer predisposition.

Paula Rosanna Quaglietta, Ashby Kissoondoyal, Noel Wei Yang Ong, Nicholas Fischer, David Malkin

The Hospital for Sick Children, Toronto, ON, Canada

Li-Fraumeni Syndrome (LFS) is a hereditary cancer predisposition syndrome associated with germline mutations in *TP53* (mutp53). Mutp53 abrogates normal tumor-suppressive functions, including DNA repair, metabolism, and apoptosis. The accumulation of these effects, along with clonal expansion of metabolically reprogrammed cells, can enhance cell survival and adaptation to stress conditions, priming a pre-cancerous niche. We hypothesize that germline *TP53* mutations alter metabolism to promote a pre-cancerous primed state. Moreover, metabolic interventions can reverse this state to reduce cancer onset in LFS. LFS (*Trp53*$^{+/R172H}$) mice and wild-type (WT) littermates were followed across four age cohorts (60, 120, 210, 300 days) and treated with metformin-supplemented drinking water (1mg/mL) or left untreated. At endpoint, plasma, muscle, liver, kidney, spleen, thymus, and brain tissues were collected. Flow cytometry immune profiling was performed on spleen and thymus. All tissues were analyzed by LC-MS/MS untargeted proteomics and Seahorse metabolic assays. All statistics were performed in R. Splenic lymphocyte proportions did not differ between LFS and WT mice across development, however we did observe significantly different metabolic states ($p<0.05$). LFS mice expressed significantly higher metabolism-associated functional exhaustion markers KLRG1 and PD1 on NK cells and CD4+ T cells, respectively. Metformin treatment rescued this phenotype by significantly reduced PD1 expression on exhausted T cells (CD4+, CD8+, and CD4+CD8+ double-positive; $p<0.05$) in LFS mice. Tissue proteomics revealed key metabolic and developmental pathway differences in LFS mice, and the effect of longitudinal metformin on the pre-cancer niche. These pathways are being further validated through *in vitro* assays with patient-derived cells to help delineate the role of various cell types in LFS pre-cancer priming. We demonstrated that metabolic reprogramming occurs systemically in LFS to promote a cancer-primed state. Moreover, treatment with a metabolic modulator can aid in rescuing these changes, suggesting potential a potential cancer interception or treatment for LFS patients to revert the cancer priming phenotype.

#3283 Metabolic crosstalk between fatty acid oxidation and glycolysis underlies glioblastoma viability.

Lola Martinez Ibarguren[1], Fiorella Orsini Zanetti[1], Sofia Paz Osorio Rencoret[1], Maria Florencia Arbe[1], Marina Perona[2], Gabriela Salamone[3], Gerardo Martin Oresti[4], Pablo J Saez[5], Catalina Lodillinsky[6], **Marcela Solange Villaverde**[7]

[1]Universidad de Buenos Aires, Facultad de Medicina, Instituto de Oncologia Angel H. Roffo, Buenos Aires, Argentina,[2]Comision Nacional de Energia Atomica, Buenos Aires, Argentina,[3]Academia Nacional de Medicina, Instituto de Medicina Experimental, CONICET, Buenos Aires, Argentina,[4]Instituto de Investigaciones Bioquimicas de Bahia Blanca (INIBIBB, CONICET-UNS), Bahia Blanca, Argentina,[5]Universitatsklinikum Hamburg-Eppendorf (UKE), Hamburg, Germany,[6]Universidad de Buenos Aires, Facultad de Medicina, Instituto de Oncologia Angel H Roffo, Buenos Aires, Argentina,[7]Universidad de Buenos Aires, Facultad de Medicina, Instituto de Oncologia Angel H. Roffo, CONICET, Buenos Aires, Argentina

Metabolic rewiring supports glioblastoma (GB) progression, yet the contribution of fatty acid oxidation (FAO) to GB metabolic plasticity remains poorly defined. GB tumors display elevated expression of FAO-related genes, including carnitine palmitoyltransferase 1A (CPT1A), suggesting a potential reliance on this pathway. Here, we evaluated the functional relevance of FAO in U251 GB cells using etomoxir (ETO), a CPT1A inhibitor. ETO markedly reduced cell viability in monolayers (5-day exposure) and 3D spheroids (9-day exposure; IC50=118 µM) and rapidly disrupted spheroid architecture within 48 hours. Short-term treatment with 200 µM ETO did not alter cell size or granularity, but FAO inhibition induced a clear metabolic shift characterized by increased glucose consumption, elevated lactate release, and enhanced extracellular acidification, consistent with compensatory glycolytic upregulation. To test whether this adaptive response creates a metabolic vulnerability, we inhibited glycolysis with 2-deoxyglucose (2DG). Combined ETO+2DG treatment significantly potentiated cytotoxicity compared with either agent alone after 72 hours. These findings indicate that FAO serves as a relevant energy source in GB cells and that its inhibition triggers increased glycolytic flux as a compensatory mechanism. Together, our data reveal a targetable FAO-glycolysis crosstalk in GB and support the therapeutic potential of dual metabolic pathway inhibition to exploit GB metabolic flexibility.

#3284 CSF metabolomics reveals alterations in one-carbon metabolism and phosphatidylcholine abundance in a methotrexate-treated juvenile rat model.

Jeremy Willekens[1], Chadni Patel[1], Frank Diglio[2], Peter D. Cole[3]

[1]Pediatric Hematology/Oncology, Rutgers Cancer Institute of New Jersey, New Brunswick, NJ,[2]Rutgers Cancer Institute of New Jersey, New Brunswick, NJ,[3]Rutgers Cancer Institute of New Jersey, Montclair, NJ

Background:Although typically curative, treatment for pediatric acute lymphoblastic leukemia (ALL) is associated with neurotoxicity and leads to chemotherapy-related cognitive impairment (CRCI) in 40-70% of survivors, significantly impacting their quality of life. Methotrexate (MTX), a key component of ALL chemotherapy regimens, is a major contributor to CRCI. Using cerebrospinal fluid (CSF) metabolomics, our previous work showed that pediatric patients undergoing chemotherapy exhibited alterations in lipid metabolism, particularly phosphatidylcholines (PC). However, because ALL chemotherapy involves multiple agents, the specific contribution of MTX to these metabolic alterations remains unclear.
Experimental procedures:Using a juvenile rat model designed to isolate MTX-specific effects within a pediatric-relevant context, we administered six intraperitoneal (0.5 mg/kg per dose) and four intrathecal (1 mg/kg per dose) MTX injections between 3 and 8 weeks of age. To characterize MTX-induced metabolic changes, we performed CSF metabolomics at the time of the first intraperitoneal injection and at the fourth. Five weeks after the last injection, we assessed whether MTX exposure impaired spatial and visual memory using Object Placement (OP) and novel Object Recognition (OR) behavioral tests, respectively, in comparison to PBS-treated controls.
Results:MTX-treated rats exhibited spatial and visual memory impairments compared with controls. In accordance with our previous results and MTX's mechanism of action, determinants of one-carbon metabolism were downregulated in the CSF of MTX-treated animals over time. This includes S-adenosylmethionine (SAM, FC = 0.36, p-adj = 0.02) and methionine (FC = 3.24E-06, p-adj = 6.41E-06). In contrast, transsulfuration pathway metabolites such as cystathionine (FC = 3.98, p-adj = 0.001) and cysteine (FC = 2.81, p-adj = 0.02) were upregulated. Last, MTX treatment also induced alterations in lipid metabolism compared to controls, with a significant over-representation of 8 plasmalogens and 9 PC, consistent with our findings in the CSF of pediatric ALL patients undergoing chemotherapy.
Conclusion:Although in use for more than eight decades, neither the mechanism of action nor the side effects of MTX are fully understood. Preclinical models therefore remain instrumental for defining MTX's contribution to chemotherapy-related neurotoxicity. This work, together with our recent findings in humans, demonstrates that CSF metabolomics may enable the early identification of patients at risk for CRCI through predictive biomarkers and guide future neuroprotective interventions.

#3285 Itaconate acts as an oncometabolite to drive lethal pediatric ependymomas.

Siva Kumar Natarajan[1], Joanna Lum[2], James Haggerty-Skeans[3], Minal Nenwani[2], Sanjana Eyunni[2], Mateus Mota[3], Jill Bayliss[3], Akash Deogharkar[1], Erin Hamanishi[1], Simon Hoffman[1], Eleanor Young[2], Qiuyang Zhang[2], Rijul Mehta[1], Abhijit Parolia[1], Peter Sajjakulnukit[2], Robert Doherty[1], Carl Koschmann[4], Arul M. Chinnaiyan[2], Costas Andreas Lyssiotis[2], Deepak Nagrath[2], Sriram Venneti[3]

[1]Pathology, University of Michigan Medical School, Ann Arbor, MI,[2]University of Michigan, Ann Arbor, MI,[3]University of Michigan Medical School, Ann Arbor, MI,[4]Univ. of Michigan Health System, Ann Arbor, MI

ZFTA-RELA ependymomas are highly aggressive brain tumors with significant mortality. These tumors are characterized by the oncogenic fusion of a putative chromatin remodeler ZFTA and the NFκB effector RELA. Using a comprehensive metabolic screen, we discovered that ZFTA-RELA cells generate itaconate, a metabolite linked to the TCA cycle. Although itaconate is a well-known immunomodulatory metabolite produced by macrophages, its production and function within tumor cells have been unclear. We found that itaconate is synthesized by Aconitate Decarboxylase-1 (ACOD1), and that ZFTA-RELA induces ACOD1 expression in an NFκB-dependent manner. Itaconate production in turn supports a coupled metabolic-epigenetic feed-forward loop that sustains pathogenic ZFTA-RELA fusion expression through H3K4me3-dependent, epigenetic activation. To provide the metabolic input required for itaconate synthesis, ZFTA-RELA tumors suppress *PTEN* expression to activate PI3K/AKT signaling pathway. The increased glutaminolysis in these tumors supplied the carbon needed for itaconate generation. As a result, inhibiting glutamine metabolism reduces pathogenic ZFTA-RELA levels and shows strong therapeutic efficacy in multiple in vivo models. Moreover, combining glutamine antagonists with PI3K/mTOR inhibitors prevents spinal metastasis. Overall, our findings show that ZFTA-RELA ependymomas hijack the macrophage-associated itaconate metabolic pathway to epigenetically reinforce expression of the ZFTA-RELA fusion driver, identifying itaconate as an oncometabolite. These results highlight itaconate upregulation as an unrecognized driver of ZFTA-RELA ependymoma and point to new therapeutic avenues for children affected by this devastating disease, while broadening our understanding of oncometabolites as a distinct class of cancer dependencies.

#3286 The Warburg hijack of myeloid immunity via mitochondrial dysregulation in glioblastoma.

Chun Wai Aeon Kwok, Karrie Mei Yee Kiang, Gilberto Ka Kit Leung

Department of Surgery, The University of Hong Kong, Pokfulam, Hong Kong

This study aims to illustrate how the Warburg effect drives glioblastoma (GBM) growth and development by dysregulating myeloid mitochondrial dynamics and evading myeloid immunity in the lactate-rich environment. The myeloid immunity is often reprogrammed and suppressed by GBM. A major driver is the lactate-rich, glycolysis-preferred metabolic tumor microenvironment (TME) established by the Warburg effect. Recent studies suggest that the Warburg metabolism shifts tumor-associated myeloid cells (macrophages and microglia) towards an anti-inflammatory, pro-tumorigenic phenotype and promotes glioblastoma growth by immunosuppressing local myeloid defence. Here, we investigate the interplay between the high-lactate acidic TME and myeloid evasion, with a specific focus on lactate-induced disruption of mitochondrial dynamics. We re-analyzed publicly available bulk RNA-sequencing data (GSE216070) from four GBM samples with and without pharmacological lactate inhibition. Glycolytic activity and M2-like myeloid polarization scores were calculated as the mean $\log_2(CPM+1)$ expression of curated hallmark gene sets. The Warburg signatures were then correlated with gene sets reflecting reactive oxygen species regulation and inter- and intra-cellular mitochondrial dynamics. The analysis deciphers how lactate-driven metabolic rewiring of myeloid mitochondria contributes to GBM invasion and immune escape. To further understand how the Warburg effect orchestrates myeloid evasion in GBM, we propose to perform lactate pre-treated, vitamin C (lactate inhibitor) pre-treated and control myeloid cell cultures, then compare their pro-tumorigenic ability via conditioned medium in GBM proliferation and temozolomide chemoresistance assessment. In addition, the pre-treated myeloid cells will be seeded on the opposite side of μ-Dishes with GBM cells in between, to observe if there is any preferential growth or invasion towards either side under live-cell confocal imaging. The mitochondrial dynamics of the pre-treated cells will also be studied through Western blot and flow cytometry. Preliminary results showed high levels of M2-like immunosuppression, reactive oxygen species mechanism and mitochondrial dynamics and surveillance under the Warburg glycolysis environment. With the poor overall survival rate of high-LDHA patients from the Kaplan-Meier curve, the Warburg metabolism serves as a promising therapeutic target. Our study elucidates how Warburg metabolism promotes GBM immune evasion and invasion by inducing mitochondrial dysregulation in brain myeloid cells via the lactate-rich tumor microenvironment.

#3287 Mitochondrial biogenesis fuels the energetic demands of grade 2 meningiomas.

Stella G. Cavalcante[1], Benedito J. A. Pereira[1], Antonio M. Lerario[2], **Sueli M. Oba-Shinjo**[1], Suely Kazue Nagahashi Marie[3]

[1]Neurology, University of Sao Paulo, Faculty of Medicine, Sao Paulo, Brazil,[2]Internal Medicine, University of Michigan, Ann Arbor, MI,[3]University of Sao Paulo, Sao Paulo, Brazil

Meningioma is the most common primary intracranial tumor, accounting for 37.6% of all brain tumors, and is predominantly classified as grade 1 (G1) or 2 (G2). While G1 tumors typically follow a benign clinical course, G2 meningiomas are more aggressive and exhibit higher recurrence rates. Despite their clinical relevance, the metabolic features of G2 meningiomas - particularly the contribution of mitochondrial function - remain poorly defined. Mitochondria, the cellular powerhouses responsible for ATP production, are essential for meeting the elevated metabolic demands of tumor growth. Prior transcriptomic studies suggest that G2 meningiomas exhibit enhanced oxidative metabolism, cell division, and motility. The objective of this study was to identify mitochondrial components that support the bioenergetic requirements of G2 tumors. Transcriptomic analysis revealed elevated expression of TFAM, the master regulator and protector of mitochondrial DNA (mtDNA), in G2 compared to G1 meningiomas. Its transcriptional coactivator PGC1-α (encoded by *PPARGC1A*) was also upregulated, and both genes demonstrated a strong positive correlation, suggesting that the TFAM/PGC1-α axis may drive increased mtDNA copy number in G2 tumors. Immunostaining confirmed grade-specific TFAM localization, with G2 tumors displaying more diffuse cytosolic distribution. Furthermore, G2 meningiomas showed increased mitochondrial activity, evidenced by upregulated mitoribosomal gene expression and activation of oxidative phosphorylation and tricarboxylic acid cycle pathways. Collectively, these findings indicate that the TFAM/PGC1-α/mtDNA axis is activated in G2 meningiomas, potentially enabling the elevated energy production needed to sustain their increased proliferative and migratory capacity.

#3288 Spermine enhances oxidative phosphorylation independently of translation in glioblastoma.

Alexandra Carbone, Tim Horton, Ayush Rana, Scott Welford

Cancer Biology, University of Miami Miller School of Medicine, Miami, FL

Glioblastoma (GBM) is the most aggressive and lethal primary malignant brain tumor, with a mean survival of only 15 months, emphasizing the need for novel therapeutic strategies. Polyamines, small positively charged molecules necessary for cell proliferation, are frequently dysregulated in multiple cancer types, including GBM. Despite this, their distinct role in tumorigenesis has not been well characterized. There are three major polyamines: putrescine, spermidine, and spermine. Putrescine is converted into spermidine, which is further converted into spermine. The role of spermidine has been well defined, as it serves as a precursor for eIF5a-deoxyhypusine, which undergoes hypusination to promote translation of growth factors. Spermine Synthase (SMS), the enzyme that catalyzes the conversion of spermidine to spermine, is upregulated in high-grade gliomas. Preliminary data suggests that SMS is necessary for GBM tumor development and growth, supporting the idea that polyamine metabolism can be a targetable vulnerability in GBM. However, the specific role of spermine, the product of SMS, in GBM remains unknown. We hypothesize that spermine has distinct, non-redundant cellular functions in GBM and aim to elucidate its role using a CRISPR-mediated autochthonous mouse model of GBM. In this model, a plasmid encoding Cas9 and guide RNAs targeting the tumor suppressors PTEN, P53, and NF1 along with polyamine-related genes of interest are introduced into mouse embryos via intrauterine electroporation (IUE), leading to GBM tumor development. Utilizing this system, we have found that SMS knockout (KO) significantly inhibits GBM growth *in vitro* and *in vivo*. Interestingly, supplementing physiological concentrations of spermine failed to restore cell viability and oxidative phosphorylation (OCR) in SMS KO cells, while wild-type cells exhibited a robust increase in OCR upon spermine supplementation. Further investigation revealed spermine enhances OCR independently of translation, suggesting that it may function through a post-translational modification (PTM) mechanism. Ongoing studies aim to further characterize the role of SMS and spermine in GBM metabolism and tumor growth. These findings suggest that spermine is a critical regulator of GBM development and progression and may offer a novel metabolic target for therapeutic intervention.

#3289 Lipid metabolic rewiring in cancer: A proteomic insight into new axis of therapeutic vulnerability.

Sivasubramani Narayanan, Poorvi Subramanian, Afsana Parveen Jahir Hussain, Natarajan Aravindan

Oklahoma State University, Stillwater, OK

Lipid metabolism plays a pivotal role in cancer progression, influencing cellular energy balance, membrane synthesis, and signaling pathways that drive proliferation and survival. Our previous findings state that in neuroblastoma (NB), a lethal pediatric tumor, loss of retinal degeneration protein 3 (RD3) leads to increased lipid droplet accumulation. Importantly, our studies also found out that RD3 loss in NB results in increased tumor aggressiveness and metastasis, consequent poor clinical outcome of patients. However, the molecular mechanisms underlying the metabolic shift and tumor progression in NB remain unclear. Herein, we investigated the mechanism behind the RD3-dependent metabolic reprogramming in NB by assessing the directed proteomics shift. Proteomic profiling was performed using NB patient-derived clones during diagnosis (CHLA-15, CHLA-42) those harbor high RD3, and in their reverse-engineered (RD3 stably knockdown) counterparts. Global proteomics was performed using DIA on an Orbitrap Exploris 480 (Ideaproteomics) applying statistical (log_2 fold change, $-log_{10}$(Padj) FDR correction) considerations. Functional mapping was performed, and differential expression was realized using Omics Playground V4 (BigOmics analytics). Our findings demonstrate that RD3 knockdown induces a pronounced adipogenic signature in NB. Among the proteins altered, 71 were strongly linked to lipid metabolic pathways, including 47 that were upregulated and 24 that were downregulated. Notably, the upregulation of GPAT1 reflects RD3-dependent control of glycerophospholipid synthesis; increased levels of ACOX1, ECH1 and ACADM indicate RD3-mediated fatty acid β-oxidation; and elevated GPAT4 and DGAT1 expression supports a role for RD3 in modulating triglyceride biosynthesis. In addition, ESYT1 upregulation highlights RD3 involvement in lipid trafficking. PLIN2 downregulation underscores RD3-dependent regulation of lipid droplet dynamics, while reduced SCP2 and APOE expression points to RD3-associated control of cholesterol transport. Our study for the first time recognized that RD3 deficiency dysregulates lipid metabolic activity. This RD3-dependent metabolic disruption of lipid homeostasis leads to the aggressiveness of NB tumors, resulting in poor patient survival. Therefore, harnessing the mechanism of this unrecognized axis of metabolic reprogramming in NB could lead to promising avenues for novel targeted interventions and improve patient survival. Funding: Kerr Foundation 28-34200; Department of Defense, DoD CA-210339; OCAST-HR19-045; NIH P20GM103639; and supported by P30CA225520, P30GM154635 and R23-03.

#3290 Rewiring of pyruvate metabolism in neonatal CD8$^+$ T cells alters functionality and antitumor immunity.

Elinor DeCleene[1], Amy Reynolds[1], Daniela Vega-Mendoza[1], Rebeca Rodriguez[1], Mingkee Achom[1], Naomei Lidman[1], Jose Almeida-Santos[1], Grace Rish[1], Samuel Markson[2], Jared H. Rowe[1]

[1]Dana-Farber Cancer Institute, Boston, MA,[2]Harvard Medical School, Boston, MA

Neuroblastoma (NBL) is the most common extracranial solid tumor in children, accounting for ~15% of pediatric cancer-related deaths. Despite these relatively poor outcomes in high-risk disease, children under 18 months of age often demonstrate spontaneous tumor regression. The mechanisms leading to spontaneous NBL regression are incompletely described and likely consist of both cell intrinsic and extrinsic features. In contrast to the relatively poor immunogenicity of high-risk NBL, regressing tumors have a distinct immunological “signature” suggesting the immune system may play a critical role in this process. The function of individual immune cells is dynamic in early life as the immune system develops. We posited that functional differences in the infant immune system could provide inherent advantages for antitumor immunity against NBL. In particular, neonatal CD8$^+$ T cells have increased proliferative potential, enhanced cytokine production, and may resist exhaustion relative to their adult counterparts. We hypothesized the enhanced functionality of neonatal T cells is controlled by the utilization of distinct pathways of cellular metabolism. We identified that following *in vitro* activation, neonatal CD8$^+$ T cells have distinct RNA expression profiles of genes related to cell metabolism compared to adult T cells. The expression of pathways associated with central carbon metabolism were markedly different between neonatal and adult T cells. Pyruvate serves as the central metabolite hub for these processes, and isotopomer tracing revealed that neonatal T cells process pyruvate differently than adult cells. Extracellular pyruvate supplementation was essential for the proliferation and effector cytokine production in neonatal CD8$^+$ T cells. Neonatal T cells had a preferential conversion of pyruvate to alanine indicating an enhanced use of the glutamic pyruvate transaminase (GPT) reaction. Ongoing studies will identify the subcellular compartmentalization (i.e. cytoplasmic, mitochondrial) and impact of NBL-imposed metabolic constraints in the tumor microenvironment on this newly identified metabolic feature of neonatal T cells.

: RTK-ERBB-PI3K and New Targets in Therapeutic Resistance
Poster Session

#3294 Cell-Autonomous EPHB2 signaling sustains neuroendocrine prostate cancer.

Xinyao Pang[1], Mingchen Shi[2], Dong Lin[2], Adam Classen[1], Hui Xue[3], Xin Dong[3], Rebecca Wu[3], Zoe Maylin[1], Ning Kang[3], Yen-Yi Lin[1], Yu Wang[1], Wei Dong[1], Martin E. Gleave[4], Colin Collins[1], Christopher J. Ong[5], Yuzhuo Wang[3]

[1]University of British Columbia, Vancouver, BC, Canada,[2]Vancouver Prostate Center, Vancouver, BC, Canada,[3]BC Cancer Research Centre, Vancouver, BC, Canada,[4]Distinguised Professor, Dept. of Urological Sciences, University of British Columbia, Vancouver, BC, Canada,[5]Surgery, University of British Columbia, Vancouver, BC, Canada

Neuroendocrine prostate cancer (NEPC) is a lethal subtype of prostate cancer that commonly develops from prostatic adenocarcinoma after long-term androgen deprivation therapy (ADT). Its incidence has risen markedly over the past decade with the widespread use of potent AR pathway inhibitors (ARPIs), yet no effective, approved therapies exist. Most studies focus on terminal NEPC, while the early drivers and transitional cellular states remain poorly defined. To address this gap, we used the LTL331/LTL331R patient-derived xenograft (PDX) model, the only available PDX system that faithfully recapitulate ADT-induced adenocarcinoma-to-NEPC transdifferentiation. Through longitudinal single cell transcriptomic sequencing across the entire process of adenocarcinoma-to-NEPC transdifferentiation of human prostate cancer, we identified a distinct intermediate, transitional cell state in the lineage shift. Within this state, EPHB2 emerged as a potential lineage-determining receptor activated at the onset of NE transdifferentiation. Mechanistically, we found that endothelial cells (ECs) in the tumor microenvironment (TME) initiate NE transdifferentiation by activating an EFNB2-EFNA5-EPHB2 axis in cancer cells. EC-derived EFNB2 upregulates EFNA5, which subsequently activates EPHB2 in a cell-autonomous manner. This signaling pair suppresses AR signaling and luminal lineage programs while promoting NE lineage initiation. In terminal NEPC, sustained EFNA5-driven EPHB2 activation maintains NE identity and enhances aggressiveness through a self-reinforcing loop. Functionally, EPHB2 inhibitor significantly reduced NEPC cell proliferation and NE marker expression. Importantly, combining an EPHB2 inhibitor with an EZH2 inhibitor partially reversed the NE phenotype, restored AR signaling, and resensitized NEPC cells to ARPIs.In conclusion, EPHB2 functions as a dual-phase regulator in NEPC, initially activated by TME-derived ephrin ligands to trigger NE transdifferentiation and later sustained through cell-autonomous signaling to maintain terminal NEPC. These findings position EPHB2 as a promising therapeutic target in intercepting NEPC development and progression.

#3295 Pi3k autoinhibition dictates rras2 dependency across HER2-amplified and PI3K-mutant cancers.

Miranda R. Cabanski-Dunning[1], Matthew J. Sale[2], Lucy C. Young[1], Maria Tarazona-Guzman[1], Dylan Aguinaldo[1], Madeleine Sitton[1], Rony Andre Francois[1], Frank McCormick[1]

[1]UCSF Helen Diller Family Comprehensive Cancer Ctr., San Francisco, CA,[2]UCSF - University of California San Francisco, San Francisco, CA

Aberrant PI3K signaling drives cancer growth, yet tumors activate p110α through distinct mechanisms. In normal cells, the regulatory subunit p85 restrains p110α until activated receptors recruit the complex to membranes. HER2-amplified tumors intensify this route through phosphorylated HER3, which provides multiple phospho-sites that both recruit PI3K and relieve autoinhibition. PIK3CA mutations found in various cancer types, including those with HER2 amplification, can weaken the restraint of p85 and bypass receptor control while preserving the requirement for membrane localization. Given that p110α still requires membrane localization even after autoinhibition is relieved, tumors often use oncogenic KRAS to provide this input. However, most HER2-amplified and many PIK3CA-mutant cancers lack KRAS mutations, suggesting alternative RAS-family proteins may fill this role.To define the contribution of RAS to PI3K signaling in a HER2-amplified context with wild-type p110α, we used KRAS G12C KYSE-410 cells. Through targeted siRNA knockdown, we identified RRAS2, not KRAS G12C, as the dominant PI3K driver, resulting in a ~60% reduction in pAKT. Replacing endogenous p110α with a RAS-binding-defective mutant produced the same effect, demonstrating that RRAS2 exclusively engages this site. Exogenous expression of oncogenic RRAS2 failed to restore pAKT in the presence of the HER2 kinase inhibitor tucatinib, even though RRAS2 remained GTP-loaded, membrane-localized, and bound to p110α. These results show that RRAS2 alone is insufficient to activate PI3K in the absence of phospho-HER3.To test whether p85 restraint prevents RRAS2 from activating PI3K, we expressed p110α mutants that destabilize the helical (E545K) or C2 (C420R) interface with p85. Both mutants restored RRAS2-driven signaling after tucatinib treatment, demonstrating that RRAS2 activates PI3K only when autoinhibition is relieved. To test the model in a physiological context, we used JIMT1 cells, which endogenously co-amplify HER2 and RRAS2 and carry the C420R mutation in p110α. Tucatininb treatment did not affect pAKT, indicating that RRAS2 can sustain PI3K activity when p110α autoinhibition is relieved. RRAS2 knockdown or re-expression of wild-type p110α restored tucatinib sensitivity, confirming that RRAS2 engagement and p110α–p85 regulation form key regulatory nodes.Further, DepMap analyses reveal increased RRAS2 dependency in cells with destabilizing p110α–p85 mutations in the absence of RTK amplification, supporting a model in which RRAS2-driven PI3K signaling requires both relief of autoinhibition and membrane localization.Together, our findings demonstrate that RRAS2 can drive PI3K signaling in contexts previously seen as RAS-independent and where recruitment mechanisms were unclear. Thus, highlighting an additional regulatory node of PI3K activation in HER2-amplified and PI3K-destabilized contexts.

#3296 The receptor-like protein tyrosine phosphatase PTPRH modulates dephosphorylation of the tyrosine kinases EPHA2 and EGFR, alters cell morphology and adhesion, and behaves as a tumor-suppressor in non-small cell lung cancer cell.

Mylena Ortiz[1], Deeya Patel[1], Jesus Garcia-Lerena[1], Andrew C. Nelson[2], Matthew Swiatnicki[1], Eran Andrechek[3]

[1]Michigan State University, East Lansing, MI,[2]University of Minnesota, Minneapolis, MN,[3]Asst. Professor, Dept. of Physiology, Michigan State University, East Lansing, MI

Introduction: The delicate balance of protein phosphorylation is often disrupted in cancers, with hyperactivity of kinases and inactivation of phosphatases driving cell proliferation and survival pathways. PTPRH, a protein tyrosine phosphatase, is found to be mutated in ~5% of non-small cell lung cancer (NSCLC) cases. However, the biological processes in which PTPRH is involved and how they may contribute to tumorigenesis are unknown.
Methods: We uncovered PTPRH's candidate interactors and associated pathways by applying a proximity-dependent biotinylation assay (BioID) and generating a signature transcriptomics in two NSCLC cell lines derived from the primary tumor (NCI-H23) or a metastatic site (NCI-H2023). Spatial subcellular localization, morphological analysis, and cell signaling alteration induced by PTPRH gain or loss were evaluated by confocal microscopy, image analysis, western blot, and cell adhesion assays under basal or stimulated conditions. Functional effects on migration and tumor suppression were assessed using *in vitro* assays and tail-vein or flank injections of PTPRH-overexpressing NSCLC cells in NOD-SCID mice.
Results: PTPRH candidate interactors include signaling molecules and structural proteins linked to integrins and focal adhesions, adherens junctions, migration, and the cytoskeleton, besides stable or transient interactions with the receptor tyrosine kinases (RTK) EGFR, EPHA2, and ROR2, and the phosphatases PTPN3 and PTPRJ. Considering the importance of EGFR in driving lung cancers and the role of EPHA2 in regulating cell adhesion, we delved deeper into understanding how PTPRH regulates RTKs signaling. Overexpression of PTPRH decreased phosphorylation levels of EGFR at the tyrosine residue 1173 (1197) and EPHA2 at tyrosine residue 588 in the primary site-derived cell line following EGF or ephrin-A1/collagen I stimulation. Imaging revealed that the phosphatase and EPHA2 colocalize subcellularly, with PTPRH gain inducing morphological alterations, such as increased eccentricity and smaller size, besides changes in the cytoskeleton organization. These changes are accompanied by increased FAK Y397 phosphorylation, but reduced cell adhesion to the ECM. Additionally, pathway enrichment analysis revealed downregulation of multiple oncogenic, metabolic, and cell adhesion signaling pathways, with increased levels of the phosphatase leading to reduced migration *in vitro*, suppressed tumor growth, reduced cell colonization to the lungs, prolonged tumor latency, and tumor differentiation *in vivo*.
Conclusion: PTPRH regulates key signaling and structural networks, modulating RTK activity, morphology, adhesion, and tumor behavior. Its loss may facilitate NSCLC progression.

#3297 HER2 overexpression confers osimertinib resistance in EGFR-mutant lung cancer.

Gaku Yamamoto, Yu Tanaka, Miku Tsukuda, Sato Sayaka, Saori Matsui, Tetsuya Sakai, Hiroki Izumi, Eri Sugiyama, Yoshitaka Zenke, Shigeki Umemura, Kiyotaka Yoh, Koichi Goto, Hibiki Udagawa

National Cancer Center Hospital East, Kashiwa, Japan

HER2 amplification has been identified in 2-5% of patients with EGFR-mutant lung cancer who have acquired resistance to osimertinib; however, its precise mechanisms in mediating resistance remain unclear. This study aims to elucidate how HER2 aberration contributes to acquired resistance to osimertinib through multiple preclinical approaches. EGFR-mutant cell lines stably overexpressing HER2 were generated by lentiviral transduction using PC9 (EGFR exon 19 deletion) and H1975 (EGFR L858R). Although HER2-overexpressing cells displayed comparable short-term (3-day) sensitivity to osimertinib *in vitro* relative to empty-vector controls, long-term assays (>7 days) revealed a remarkable increase in resistant colony formation across both HER2-overexpressing models. Next, xenograft models bearing HER2-overexpressing cells were established in nude mice to evaluate *in vivo* responses to osimertinib. Continuous oral administration of osimertinib induced initial tumor shrinkage in HER2-overexpressing xenografts; however, these tumors subsequently demonstrated pronounced regrowth, whereas parental tumors exhibited more durable responses. Finally, the combination of a HER2-targeted tyrosine kinase inhibitor and osimertinib synergistically suppressed tumor cell growth in HER2-overexpressing EGFR-mutant cells. In conclusion, HER2 overexpression induced acquired resistance to osimertinib, whereas dual HER2/EGFR blockade overcame this resistance, highlighting this approach as a promising therapeutic strategy for EGFR-mutant lung cancer.

#3298 Preclinical development of TJ106, a potent biparatopic dual payload ADC targeting HER2 for the treatment of Enhertu-resistant tumors.

Siyi Hu, Mao Huang, Xiaobo Cai, Shugaku Takeda, Li Qi, Yangxin Zhang, Haiyan Wu, Yan Zhang, Yanli Mao, Zhaoyuan Chen

Phrontline Biopharma Co., Ltd., Shanghai, China

Background: HER2 overexpression is associated with increased metastatic potential and poor clinical outcomes across multiple tumor types, including breast, gastric, gastroesophageal junction, and lung cancers. Enhertu (trastuzumab deruxtecan, DS-8201a) has transformed HER2-targeted therapy by demonstrating efficacy in HER2-expressing and previously refractory tumors through delivery of a potent topoisomerase I inhibitor payload (DXd) with bystander effect. However, clinical resistance to Enhertu has emerged, driven by mechanisms such as reduced payload sensitivity, HER2 downregulation or heterogeneity, and adaptations within the tumor microenvironment. To address this unmet need, we developed TJ106, a novel biparatopic, dual-payload HER2-targeting antibody-drug conjugate (ADC) designed to enhance tumor cell internalization, overcome resistance mechanisms, and improve the therapeutic window.

Methods: Antibody internalization was evaluated by flow cytometry (FACS). The CellCounting-Lite 2.0 luminescent viability assay was used to assess the in vitro cytotoxicity of TJ106. In vivo antitumor activity was investigated in cell-derived xenograft (CDX) and patient-derived xenograft (PDX) models with high, moderate, or low HER2 expression.

Results: TJ106 consists of a biparotopic antibody, generated from trastuzumab and pertuzumab using knob-into-hole technology, conjugated in a site-specific manner (DAR 4) to the dual-linker payload DLP1, which combines a topoisomerase I inhibitor and a microtubule inhibitor. TJ106 showed superior internalization compared with trastuzumab or pertuzumab in HER2-moderate JIMT-1 (IHC 2+) breast cancer cells and HER2-low Colo-205 (IHC 1+) colorectal cancer cells. TJ106 also exhibited enhanced in vitro cytotoxicity across HER2-expressing tumor cell lines, including NCI-N87 (HER2 3+) gastric cancer, JIMT-1, and Colo-205, compared with trastuzumab-DLP1, pertuzumab-DLP1, and DS-8201a. In the JIMT-1 CDX model, TJ106 demonstrated superior antitumor efficacy versus comparators: TJ106 at 3.0 mg/kg achieved 81.8% tumor growth inhibition (TGI), compared with 69.0%, 71.0%, and 53.0% TGI for trastuzumab-DLP1, pertuzumab-DLP1, and DS-8201a, respectively. TJ106 was well tolerated in mice with no observed treatment-related body weight loss. Furthermore, TJ106 effectively inhibited tumor growth in two Enhertu-resistant PDX models (LD1-0017 and LU9681-R1P12) and one Enhertu-resistant NCI-N87 CDX model.

Conclusion: TJ106, a novel biparatopic dual-payload HER2-targeting ADC, demonstrates robust in vitro and in vivo antitumor activity, including in Enhertu-resistant models, supporting its further clinical development for patients with advanced HER2-expressing tumors.

#3299 Autocrine lymphotoxin signalling promotes ovarian tumor growth through CD74.

Tat San Lau[1], Yi Shun Wong[1], Maciej Jakub Trybull[2], Kit Ying Loucia Chan[1], Ho Sze Jacqueline Lee[1], Chi Chiu Wang[1], Joseph Kwong[2]

[1]Department of Obstetrics and Gynaecology, The Chinese University of Hong Kong, Hong Kong, Hong Kong,[2]School of Medicine, Keele University, Keele, United Kingdom

Background: Ovarian cancer is the eighth most common cause of cancer and cancer death in women worldwide. The 5-year overall survival rate for advanced-stage ovarian cancer is 10-40%. A new therapy for advanced ovarian cancer is urgently needed. Identifying signalling pathways which promote tumor growth is crucial to developing targeted therapy. Lymphotoxin is overexpressed in ovarian cancer cells and mediates tumor-stromal interaction in ovarian tumor. However, the transcription regulation of lymphotoxin and the role of autocrine lymphotoxin signalling in ovarian cancer cells are still unclear.
Methods: To investigate transcriptional regulation of lymphotoxin, correlation analysis and pharmacologic inhibitions was performed in human ovarian cancer cell lines. To investigate autocrine lymphotoxin signalling, lymphotoxin-beta (LTB) was edited in human ovarian cancer cells by CRISPR-cas9 knockout. On the contrary, lymphotoxin genes (Lta and Ltb) were overexpressed in mouse ovarian cancer cells by stable transfection. Tumor growth was examined by cancer spheroid in vitro model and preclinical metastatic tumor in vivo model. Involvement of lymphotoxin-beta receptor (LTBR) and noncanonical NF-κB pathway (RelB and p52) were investigated by pharmacological inhibitions. To identify NF-κB target genes, differentially expressed genes were analysed by NanoString nCounter pan-cancer pathways panel. Relationships between lymphotoxin, NF-κB and CD74 in ovarian tumor samples (TCGA and CUHK) were performed by correlation analysis. Function of CD74 was investigated by CRISPR-cas9 knockout in human ovarian cancer cells.
Results: Positive correlations between IL33 and LTB expression, and between ST2 and LTA expression, are found in human ovarian cancer cell lines. Inhibition of IL33 and ST2 downregulates LTA transcription in human ovarian cancer cells. LTB knockout in human ovarian cancer cells induces cell cycle G2/M arrest and reduces tumor growth in vitro, whereas lymphotoxin overexpression in mouse ovarian cancer cells increases tumor growth in vitro and in vivo. Inhibition of LTBR and p52 reduces lymphotoxin-mediated ovarian tumor growth in vitro and in vivo. Cd74 is upregulated in mouse ovarian cancer cells after lymphotoxin overexpression and LTBR activation. In human ovarian cancer cells, CD74 transcription is regulated by lymphotoxin-LTBR-noncanonical-NF-κB pathway. Positive correlations between lymphotoxin, NFKB2, RELB and CD74 mRNA expressions are found in ovarian tumor samples. CD74 knockout in human ovarian cancer cells induces G2/M cell cycle arrest and reduces tumor growth in vitro.
Conclusion: Our results demonstrated that IL33-ST2 pathway positively regulates lymphotoxin expression in ovarian cancer, and autocrine lymphotoxin signalling promotes ovarian tumor growth through CD74. These results are a foundation for developing targeted therapy for advanced ovarian cancer.

#3300 Targeting OSMR signaling networks for precision oncology.

Pradeep Chaluvally-Raghavan

Medical College of Wisconsin, Milwaukee, WI

Oncostatin M (OSM) is a member of the IL-6 cytokine subfamily that binds to the Oncostatin M receptor (OSMR) and activates JAK/STAT-mediated oncogenic signaling**.** Our single-cell RNA sequencing (scRNA-seq) revealed that OSMR is highly expressed in tumor epithelial cells, whereas its ligand, OSM, is predominantly produced by tumor-associated macrophages. Our data established that OSM-induced STAT3 activation was markedly more robust than that induced by other IL-6 family ligands, leading to enhanced OSMR-driven cellular invasion, migration, and tumor growth**.** Overall, our findings highlight OSMR signaling as a promising therapeutic vulnerability in ovarian cancer. To address the lack of OSMR-targeted treatments, this study aims to develop a monoclonal antibody that blocks OSMR signaling in cancer cells without harming normal epithelial, stromal, or immune cells. We employed sc-RNA seq, clinical samples and signaling pathway analysis to characterize how OSMR serves as a signaling addiction mechanism in cancer cells. To elucidate the mechanism of actions, we performed live-cell image analysis, receptor dimerization assays, in-cell Western analyses and *in vivo* tumor growth assays.Our data shows that anti-OSMR antibody effectively blocked the binding of the ligand OSM to OSMR and subsequently inhibited OSMR dimerization with IL6ST. We also observed that OSMR antibody induced internalization and cytoplasmic degradation of OSMR, resulting in a marked reduction in STAT3 activation, tumor cell invasion, tumor growth, and metastasis. Transcriptome-based analyses, along with *in vitro* and functional assays, further revealed that cisplatin-resistant ovarian cancer cells express significantly higher levels of OSMR compared to cisplatin-sensitive cells, and that these resistant cells depend on OSMR signaling for aggressive tumor growth. Consistently, the treatment of anti-OSMR antibodies sensitized cancer cells to cisplatin therapy both *in vitro* and *in vivo*.In sum, our studies demonstrate that OSMR represents a therapeutically targetable driver of highly aggressive and chemo-resistant ovarian cancers. We also observed an elevated expression of OSMR in pancreatic cancer, glioblastoma, and stomach adenocarcinoma, suggesting a broader clinical applicability of OSMR therapy. Based on the promise of our anti-OSMR therapy *in vivo*, we are actively developing antibody-drug conjugates (ADCs) and bispecific T-cell engagers (BiTEs) of OSMR antibody to further enhance its antitumor efficacy.

#3301 TAK1 is a key regulator of oncogenic signaling and differentiation blockade in rhabdomyosarcoma.

Anh Tuan Vuong[1], Aniket S. Joshi[1], Anirban Roy[1], Kavya Mathukumalli[1], Phuong T. Ho[1], Raksha Bhat[1], Meiricris Tomaz da Silva[1], Tagari Samanta[2], Meghana Trivedi[3], Bin Guo[1], Benny A. Kaipparettu[4], Ashok Kumar[1]

[1]University of Houston, College of Pharmacy, Houston, TX,[2]Baylor College of Medicine, Houston, TX,[3]University of Houston, Houston, TX,[4]Lester and Sue Smith Breast Center, Baylor College of Medicine, Dan L. Duncan Cancer Center, Houston, TX

Rhabdomyosarcoma (RMS) is a malignant soft tissue sarcoma with a skeletal muscle phenotype, accounting for approximately 50% of all pediatric soft tissue sarcomas and 8% of all childhood cancers. Although RMS cells express myogenic regulatory factors, they fail to undergo terminal differentiation into mature muscle cells. Transforming growth factor β-activated kinase 1 (TAK1) is a major signaling protein that activates multiple intracellular pathways in response to growth factors, cytokines, and microbial products. Emerging evidence suggests that TAK1 is also an important regulator of self-renewal, proliferation, and differentiation of muscle progenitor cells. However, the role and mechanisms of action of TAK1 in RMS remain completely unknown. In this study, we demonstrate that TAK1 expression and activity are markedly elevated in a panel of RMS cell lines and in patient tumor specimens. Reverse phase protein array (RPPA) analyses revealed that TAK1 regulates the expression and activity of many molecules involved in cell cycle control, cell proliferation, and oncogenic signaling. Genetic knockdown or pharmacological inhibition of TAK1 suppresses RMS cell proliferation, migration, and invasiveness, while also promoting terminal myogenic differentiation. TAK1 inhibits differentiation in RMS, at least in part, through up-regulating YAP1 signaling. Our results also demonstrate that inducible knockdown of TAK1 in human RMS xenografts retards tumor growth and enhances myogenic differentiation *in vivo*. Collectively, these findings uncover a previously unrecognized role for TAK1 in RMS growth and differentiation, and suggest that TAK1 can be a potential therapeutic target for the treatment of RMS.

#3302 Phosphorylation of StarD10 regulates ErbB2-mediated alcohol-induced breast cancer progression.

Manisha Dagar, Youngyi Lim, Swati Chandla, Monica Justo, Nirmala Mavela, Komal Ramani, Maria Lauda Tomasi

Cedars-Sinai Medical Center, Los Angeles, CA

Introduction: Breast cancer remains the second most common cancer among women worldwide. Excessive alcohol consumption significantly increases breast cancer risk, with even moderate drinking (one drink per day) raising the risk by about 10% compared to non-drinkers. STAR-related lipid transfer domain-containing protein 10 (StarD10), a phosphoprotein overexpressed in 35-40% of primary human breast cancers, interacts with the ErbB2 signaling pathway to promote tumor growth. Our previous studies showed that ethanol exposure causes StarD10 dephosphorylation and enhances ErbB2 expression, leading to increased malignancy and aggressiveness. However, the mechanistic role of StarD10 as a subcellular lipid transporter in regulating ErbB2-driven signaling is still not well understood. This study investigates how ethanol affects StarD10 activity and the ErbB2 signaling pathway using three-dimensional breast cancer organoid models.
Materials and Methods: Lipid overlay assays and co-immunostaining were performed to assess StarD10's lipid-binding specificity in breast cancer cells (MCF-7, SKBR-3, and BT-474) and three-dimensional breast cancer organoid models (PDxO). Additionally, organoids were CRISPR gene-edited to validate the functional outcome of pre-identified StarD10 phospho-sites. Activation of the ErbB2-regulated AKT-mTOR pathway was analyzed by Western blot. Cell viability and migration were analyzed in CRISPR gene-edited breast cancer cells.
Results: A significant decrease in StarD10 phosphorylation was observed in breast cancer cells (MCF-7, SKBR-3, BT-474) and breast cancer organoids (PDxO) in the presence of ethanol. Lipid overlay assay showed that StarD10 interacts with multiple phosphoinositides, including PI(3)P, PI(4)P, PI(5)P, PI(3,4)P_2, PI(4,5)P_2, and PI(3,4,5)P_3. Co-immunostaining further demonstrated an ethanol-induced increase in the interaction between StarD10 and PIP2/PIP3. Inhibition of PP2A activity by CRISPR-mediated gene editing prevented ethanol-induced StarD10 dephosphorylation and the ErbB2-mediated AKT-mTOR pathway, indicating that these phosphatases act as positive regulators of StarD10 function in the organoid model. Moreover, PP2A gene editing significantly reduced cell viability and migration compared to ethanol-treated cells, suggesting a critical role for PP2A-mediated dephosphorylation of StarD10 in promoting ethanol-induced breast cancer cell aggressiveness.
Conclusions: Our findings show that ethanol promotes breast cancer progression by causing dephosphorylation of StarD10 at the T288 residue. Using organoid models, we demonstrate that PP2A phosphatase positively regulates StarD10 activity. Targeting the phosphorylation pathway of StarD10 may serve as a potential therapeutic strategy to reduce alcohol-related breast cancer progression.

#3303 Investigating the impact of HER4 mutations on HER2 signaling.

Denis M. Collins[1], Marta Valenti[2], Johanna Gaubatz[2], Debbie O'Reilly[2], Birgit Bossenmaier[3], Bryan Hennessy[4], John Paul Crown[5]

[1]Cancer Biotherapeutics Research Group, Dublin City University, Dublin, Ireland,[2]Dublin City University, Dublin, Ireland,[3]Bossenmaier Consulting, Munich, Germany,[4]Beaumont Hospital, Dublin, Ireland,[5]St. Vincent's University Hospital - Dublin, Dublin 4, Ireland

Background: HER2 is amplified in ~20% of breast cancers (BCs) and is a member of the HER/ErbB receptor tyrosine kinase family that also includes EGFR, HER2 and HER3. HER4 is mutated in 7% of HER2+ BCs but there are limited data on the impact of HER4 point mutations (MUTs) on HER2 signaling. Previous work has identified EGFR, p38 MAPK, Src and STAT3 as targets impacted by HER4 overexpression. HEK293 cells express wild type (WT) EGFR and negligible levels of HER2, HER3 and HER4. Using plasmid-based overexpression in HEK293 cells, this study examines the co-expression of WT HER2 with WT HER4 or HER4 point MUTs (2 extracellular domain (ECD) and 6 intracellular domain (ICD)).

Methods: Eight HER4 MUTs identified from the COSMIC database were investigated. Four were predicted to be deleterious/damaging and four neutral/tolerated (Provean/SIFT). MUT1 (p.E202D) and MUT2 (p.P224R) are in the ECD; MUT3-MUT8 (p.T1036I, p.Y1242C, p.H1245N, p.S1246R, p.L1247M, p.H1255N) are in the ICD. Mutant primers (Sigma Aldrich) were used for site-directed mutagenesis (QuikChange Lightning) with pRK5 HER4 WT used as a template to generate eight validated HER4 MUT plasmids (SequiServe). HEK293 cells were transfected (Fugene) with either empty vector, GFP control, WT HER2 plasmid, WT HER4, WT HER2/WT HER4, or WT HER2 combined with each HER4 MUT. Transfection was confirmed by Western blot. Protein lysates were analyzed in triplicate by reverse phase protein array (RPPA) to quantify 50 total and 34 phospho-proteins (84 targets). Significant changes ($p < 0.05$) were determined by Student's t-test.

Results: Total EGFR levels were unchanged in response to transfection with WT HER2 or WT HER4, however EGFR phosphorylation at Y992 and Y1068 increased significantly ($p<0.05$) for WT HER2 and WT HER4 individually or in combination. Unlike WT HER4, WT HER2 did not increase phosphorylated levels of p38 MAPK, Src or STAT3. When co-transfected with WT HER2, changes induced by WT HER4 were maintained for Src (Y416) ($p=0.02$) and STAT3 (Y705) ($p<0.01$) but not p38 MAPK (T180/Y182) ($p=0.11$). In the presence of WT HER2, HER4 MUT6 increased phosphorylated HER2 (Y1248) levels ($p=0.01$), and MUTs 2, 6, 7 and 8 significantly increased levels of phosphorylated EGFR (Y1173). In addition, HER4 MUT6 reduced Src (Y527) phosphorylation ($p=0.01$).

Conclusions: Our data reports HER4-activated intracellular signaling pathways distinct from HER2, and HER4 MUTs that can alter EGFR and HER2 activity. These results provide preliminary evidence for the phenotypic impact of the HER4 MUTs examined on HER2 signaling.

#3304 *β,β*-dimethylacrylalkannin inhibits colorectal cancer growth *in vitro* and *in vivo* by targeted FGFR1.

Ran Zhao[1], Fanxiang Yin[1], Kangdong Liu[1], MeeHyun Lee[2], Zigang Dong[1]

[1]Zhengzhou University Medical College, Zhengzhou, Henan, China,[2]Post-Doc, Cellular And Molecular Biology, China-US (Henan) Hormel Cancer Institute, Zhengzhou, China

Background: Colorectal cancer (CRC) continues to be a major global heaith challenge, ranking as a top cause of cancer-related death fatalities. Alarmingly, the five-year survival rate for CRC patients hovers around a mere 10-30%. The disruption of fibroblast growth factor receptor (FGFRs) signaling pathways is significantly implicated in the onset and advancement of colorectal cancer (CRC), presenting a promising target for therapeutic intervention in CRC management. Further investigation is essential to comprehensively elucidate the role of FGFR1 in CRC and to develop effective FGFR1-targeted therapies.

Purpose: This study aims to demonstrate the oncogenic role of FGFR1 in colorectal cancer and investigate the potential therapeutic benefits of inhibiting FGFR1 activity using *β, β*-dimethylacrylalkannin (*β,β*-DMAA) as an FGFR1 inhibitor.

Methods: In the present study, we performed tissue array, kinase profiling analysis assay, computational docking model, knockdown assay to predict and explore the inhibitor of FGFR1. Furthermore, we utilized kinase assay, pull-down, cell proliferation and Patient derived xenograft (PDX) mouse model assays to discover an FGFR1 inhibitor and assess its effects on colorectal cancer growth.

Results: In this study, we found that FGFR1 protein is significantly overexpressed in colorectal cancer and plays a pivotal role in regulated cell growth, particularly in colorectal cancer patients. Furthermore, we conducted a computational docking, kinase profiling analysis, simulation and identified that *β,β*-DMAA could directly bind with FGFR1 within ATP binding pocket domain. Cell-based assays confirmed that *β,β*-DMAA not only inhibited the growth of colon cancer cells but also induced cell cycle arrest, apoptosis, and the modulation of FGFR1-mediated signaling pathways. Moreover, *β,β*-DMAA effectively attenuated the growth of PDX tumors in mice that were FGFR1-positive, all without causing significant toxicity. In summary, our study highlights the pivotal role of FGFR1 in colorectal cancer, suggesting that inhibiting FGFR1 activity could be a promising strategy for therapeutic intervention. We present strong evidence that targeting FGFR1 with *β,β*-DMAA is a viable approach for the management of colorectal cancer. Given its low toxicity and high efficacy, *β,β*-DMAA, as an FGFR1 inhibitor, warrants further investigation in clinical settings for the treatment of FGFR1-positive tumors.

#3305 Biochemical and cellular evaluation of HUNK inhibition by an FDA approved drug as potential therapeutic strategy for HER2+ breast cancer.

Safnas Farwin AbdulSalam[1], Mia M. Eason[2], Shuguang Liang[1], Alison Goupil[3], Anthony Acinapura[1], Maia Dominguez[4], Peter Gallagher[1], Yuan Wang[1], Jianghong Wu[5], Haiching Ma[1]

[1]Reaction Biology Corp., Malvern, PA,[2]Reaction Biology Corp., West Chester, PA,[3]Reaction Biology Corp., Pottstown, PA,[4]Reaction Biology Corp., Media, PA,[5]Reaction Biology Europe GmbH, Freiburg im Breisgau, Germany

Kinase inhibitors have been on spotlight for cancer drug discovery ever since the approval of Imatinib and recently the 100th small molecule kinase inhibitor was approved by the FDA showing the potential of kinase inhibitors for cancer therapeutics and beyond. HER2 kinase is an established drug target in breast cancer therapeutics with multiple inhibitors developed against this target over time. However, cancer developing drug resistance to these inhibitors over time remain as a prognostic challenge for aggressive breast cancer treatment. Recent studies investigating the HER2 resistance mechanism of breast cancers identify HUNK (hormonally upregulated neu-associated Kinase) playing a crucial role in promoting HER2+ breast cancer cell survival and inhibitors resistance via phosphorylation of Rubicon. Recently a first in class HUNK targeted inhibitor HSL119 has been identified and characterized to demonstrate potential of targeting HUNK as a treatment strategy for HER2 resistant breast cancers, but more potent inhibitors for this target are yet to be identified. To address this, we screened 145 FDA approved compounds in HUNK biochemical kinase assay in Reaction Biology's HotSpot assay platform and identified Momelotinib, an orally available JAK1/JAK2/ACVR1 inhibitor used to treat myelofibrosis, inhibiting HUNK with 7.9 nM IC_{50}. NanoBRET target engagement assay confirmed Momelotinib binds cellular HUNK in live HEK293 cells. Furthermore, CellTiter-Glo assays demonstrated Momelotinib inhibits proliferation of HER2+ JIMT1 cells and triple-negative 4T1 breast cancer cells, while caspase-3/7 activation assays indicated Momelotinib induces apoptotic cell death in both lines. These findings highlight Momelotinib as a potential therapeutic candidate for overcoming HER2 inhibitor resistance in breast cancer.

#3306 The role of DDR1 ectodomain shedding in glioblastoma radiation resistance.

Sophia Dunlap[1], Caitlin A. Harvey[1], Christopher D. Willey[2], Ahn Erin[2]

[1]University of Alabama at Birmingham, Birmingham, AL,[2]O'Neal Comprehensive Cancer Center at UAB, Birmingham, AL

Introduction: Glioblastoma (GBM) is the most common malignant brain tumor in adults, and resistance to radiation therapy remains a major therapeutic obstacle. Although genetic alterations contribute to GBM progression, they do not fully explain the emergence of radiation resistance, suggesting contributions from non-genetic mechanisms. Notably, radiation-resistant GBM exhibits elevated collagen deposition. Discoidin domain receptor tyrosine kinase 1 (DDR1), a collagen-binding receptor regulated by ectodomain shedding, is highly expressed in GBM. Here, we demonstrate that radiation-resistant GBM alters DDR1 activity and shedding in response to collagen to promote tumor cell proliferation.

Methods and Results: To investigate DDR1 regulation, we utilized a GBM patient-derived xenoline pair, JX39P (radiation-sensitive) and JX39P-RT (radiation-resistant). JX39P-RT displayed significantly higher DDR1 mRNA and protein expression. When cells were embedded in collagen I to mimic the extracellular environment, DDR1 phosphorylation at Y792 increased more rapidly and to a greater extent in JX39P-RT than in JX39P. Collagen embedment also led to the accumulation of a short DDR1 fragment in JX39P-RT, indicating enhanced ectodomain shedding. Western blotting of conditioned media confirmed increased release of the DDR1 N-terminal fragment and confirmed that ectodomain shedding occurred only in JX39P-RT in response to collagen. Treatment of JX39P-RT cells with marimastat, a broad-spectrum MMP inhibitor, diminished both the N-terminal fragment shed in the media and the short C-terminal fragment in cell lysates. Consistent with elevated DDR1 expression and activation, JX39P-RT exhibited increased phospho-ERK1/2 levels when embedded in collagen I, indicating enhanced downstream signaling pathways. Furthermore, cell proliferation assays and Ki67 staining showed that JX39P cells proliferate more rapidly than JX39P-RT in liquid culture; however, when embedded in collagen I, JX39P showed no significant change in Ki67 staining, whereas JX39P-RT demonstrated a time-dependent increase, indicating that radiation-resistant GBM cells proliferate in response to collagen- and DDR1-mediated signaling.

Conclusions: Together, our results identify DDR1 upregulation and ectodomain shedding as key adaptive mechanisms that promote proliferation and survival of radiation-resistant GBM cells. These regulatory processes enable resistant cells to sustain growth under therapeutic stress, providing a potential mechanism of therapeutic evasion. Future studies will investigate how DDR1 shedding and downstream signaling integrate to maintain radiation resistance and explore strategies to sensitize GBM to radiation therapy.

#3307 CD99 homophilic signaling between tumor-associated macrophages and glioblastoma cells regulates response to immunotherapy.

Tongchao Jiang[1], Zilu Huang[2], Nan Li[3], Haishuang Sun[4], **Tongcui Jiang**[5]

[1]Robert H. Lurie Comprehensive Cancer Ctr. of Northwestern Univ., Chicago, IL,[2]Sun Yat-sen University Cancer Center, Guangzhou, China,[3]Department of Neurosurgery, The First Affiliated Hospital of USTC, Division of Life Sciences and Medicine, University of Science and Technology of China, Hefei, China,[4]Department of Medical Oncology, Sun Yat-sen University Cancer Center, Guangzhou, China,[5]Department of Biochemistry & Molecular Biology, School of Basic Medical Sciences, Anhui Medical University, Hefei, China

Background: Glioblastoma (GBM) is characterized by inevitable recurrence and profound therapy resistance, particularly to immunotherapy, and effective options for recurrent disease remain extremely limited. An immunosuppressive tumor microenvironment dominated by tumor-associated macrophages (TAMs) plays a central role in attenuating antitumor immunity and sustaining therapy resistance. However, the contact-dependent signaling mechanisms linking GBM cells and TAMs to tumor recurrence and treatment failure remain poorly defined.
Methods: We integrated publicly available scRNA-seq datasets from primary and recurrent GBM, as well as from immunotherapy responders and non-responders to map tumor-immune cell communication. Bulk transcriptomic data from TCGA-GBM and two CGGA cohorts (CGGA-693 and CGGA-325) were analyzed to determine the association of CD99 expression with patient survival, activation of signaling pathways, and oncogenic hallmark gene signatures. Spatial transcriptomics were used to assess the spatial proximity of CD99-high tumor cells and macrophages and the local signaling activity. For experimental validation, we performed in vitro and in vivo studies to assess whether CD99 blockade enhances the efficacy of anti-tumor immunotherapy.
Results: Single-cell communication analysis revealed that macrophage populations were enriched and transcriptionally activated in recurrent GBM and immunotherapy non-responders, with CD99 homophilic-mediated interactions between macrophages and tumor cells specifically enriched in these settings. Across TCGA and CGGA cohorts, high CD99 expression was associated with worse overall survival (TCGA-GBM, $p = 0.017$; CGGA-693, $p = 0.047$; CGGA-325, $p = 0.0039$), enhanced JAK/STAT signaling, higher EMT pathway scores, and elevated expression of TGF-β, IL-10, and M2-related gene signatures. Spatial transcriptomics confirmed that CD99-high tumor cells were preferentially neighbored by macrophages, and these niches displayed elevated JAK2/STAT3 activity. Experimentally, under immunotherapy-mimicking conditions, CD99 blockade reduced JAK2/STAT3 signaling and EMT marker expression in GBM cells, lowered TGF-β/IL-10 secretion, and diminished M2 polarization of macrophages in co-culture. In mouse models, combining CD99 inhibition with anti-PD-L1 further suppressed tumor growth and attenuated the tumor-promoting effect of co-injected macrophages.
Conclusions: These findings suggest CD99 homophilic engagement between GBM cells and macrophages as a critical amplifier of a JAK2/STAT3-EMT-M2 polarization loop that drives therapy resistance. Targeting CD99-mediated tumor-macrophage crosstalk may represent a promising strategy to overcome resistance and improve outcomes in GBM.

#3308 NRG1/HER3 axis drives therapy resistance in head and neck squamous cell carcinoma: Evidence from patient-derived xenografts.

Anna Francia[1], Cinzia Girone[1], Boobash-Raj Selvadurai[2], Daria Maria Filippini[3], Giulia Querzoli[4], Matteo Fermi[5], Achille Tarsitano[6], Federica Pagano[1], Davide Zilio[1], Paola Cecchi[1], Andrea Ardizzoni[3], Yosef Yarden[7], Mattia Lauriola[1], **Donatella Romaniello**[1]

[1]Department of Medical and Surgical Sciences, Alma Mater Studiorum Universita di Bologna, Bologna, Italy,[2]Department of Immunology and Regenerative Biology, Systems immunology, Weizmann Institute of Science, Rehovot, Israel,[3]Medical Oncology Unit, IRCCS Azienda Ospedaliero-Universitaria di Bologna, Bologna, Italy,[4]Pathology Unit, IRCCS Azienda Ospedaliero-Universitaria di Bologna, Bologna, Italy,[5]Department of Otorhinolaryngology-Head and Neck Surgery, IRCCS Azienda Ospedaliero-Universitaria di Bologna, Bologna, Italy,[6]Oral and Maxillofacial Surgery Unit, IRCCS Azienda Ospedaliero-Universitaria Di Bologna, Bologna, Italy,[7]Weizmann Institute of Science, Rehovot, Israel

Epidermal Growth Factor Receptor (EGFR) is commonly overexpressed and associated with poor clinical outcomes in Head and Neck Squamous Cell Carcinoma (HNSCC). Indeed, the EGFR monoclonal antibody, Cetuximab (CTX) has been the first FDA-approved targeted drug but demonstrating limited (10-30%) and not durable response due to both intrinsic and acquired resistance mechanisms. Data from our *in vitro* experiments, and confirmed by the literature, showed an increased HER3 protein level after cetuximab treatment in HNSCC 2D cell lines, suggesting that this receptor may represent a bypass pathway to anti-EGFR therapy.However, given the complexity of HNSCC, characterized by different etiology, anatomical sites and high inter- and intratumoral heterogeneity, we focused our research study on a more representative model establishing a small set of characterized patient-derived xenografts (PDXs). Palpable tumors were cryopreserved and expanded for drug testing and ex vivo characterization. Immunohistochemistry analysis revealed that all the established PDX models recapitulate morphological and functional traits of the corresponding patient tumors. While, NGS, Western Blots and QF-PRO®, a FRET-FLIM based technic, identified distinct EGFR signature, protein expression and heterodimers distribution across samples. These results reflected a differential response to anti-EGFR blockade *in vivo*. Moreover, analysis conducted in one PDX model, derived from HPV negative sample, showed high expression of EGFR family members, HER2 and HER3, when tumors are no more responding to CTX treatment.In conclusion, characterized PDX models will help to identify HNSCC subgroups that may benefit to a combinatorial approach using anti-HER3 innovative drugs, like bispecific antibodies, antibody-drug conjugates or aptamers, to bypass compensatory signaling pathway and improve CTX sensitivity.

#3309 Daple-FLT3 gene fusion activates and localizes through a distinct mechanism from FLT3-ITD.

Darren Kao[1], Michael Acquazzino[1], Arnel Ibarra[1], Elena Valenzuela[1], Haley Mai[1], Kimberly Aguilar[1], Elliot Stieglitz[2], Jason Ear[1]

[1]California Polytechnic University, Pomona, Pomona, CA,[2]Pediatrics, UCSF, San Francisco, CA

Gene fusions are stable protein products often occurring from chromosomal rearrangements. These chimeric proteins typically contain distinct molecular entities from each parent gene, and thus, create a product with altered or aberrant function. Gene fusions are frequently found in cancers, including Leukemia. Here, we characterize the kinase activity and subcellular distribution of the Daple-FLT3 (CCDC88C-FLT3) fusion oncoprotein—a rare, but recurrent gene fusion found in patients with hematological malignancies. The protein contains the FLT3 kinase domain and is activated without ligand stimulation. This leads to activation in STAT5a, AKT, and MAPK signaling, which can be modulated by the tyrosine kinase inhibitor (TKIs) sorafenib and to the most specific FLT3 inhibitor quizartinib. The fusions localize to the pericentrosomal space, a unique subcellular localization pattern that is different compared to the well-known FLT3-ITD mutation. We further demonstrate that localization and maximal kinase activation is dependent on the Daple coiled-coil domain. These findings provide evidence that targeting Daple-FLT3 outside of its kinase domain (i.e. the coiled-coil region) may be a complementary approach with TKI therapy.

#3310 UCHL1 deubiquitinates CIP2A to promote tumor progression in gastric cancer.

Lee Ga-ye[1], In-ho Jeong[2], Peter CW Lee[2]

[1]Department of Biochemistry & Molecular Biology, Brain Korea 21 Project, University of Ulsan College of Medicine, Asan Medical Center, Seoul, Korea, Republic of,[2]Department of Biomedical Sciences, University of Ulsan College of Medicine, Seoul, Korea, Republic of

Gastric cancer is one of the most prevalent malignancies worldwide and the fourth leading cause of cancer-related mortality. The intracellular protein degradation mechanisms, both Ubiquitination and Deubiquitination are called proteostasis, which regulate protein stability and play essential roles in tumorigenesis. Among deubiquitinases, UCHL1 has been implicated in the progression of numerous types of cancers, but its functional role in gastric cancer remains to be fully understood. In this study, we found that UCHL1 expression is markedly upregulated in gastric cancer tissues compared to adjacent normal tissues. Also, elevated UCHL1 expression is associated with poor patient's prognosis, supporting its potential role as an oncogenic factor and knockdown of UCHL1 suppressed cell proliferation, migration and invasion in gastric cancer cells. We sought to identify novel binding partners of UCHL1 and revealed that CIP2A is a substrate of UCHL1. Furthermore, UCHL1 downregulation led to reduced expression of the c-Myc protein, a downstream target of CIP2A, followed by suppression of the cell cycle, particularly through the regulation of Cyclin D1. These findings demonstrate that UCHL1 promotes cell growth via the CIP2A-c-Myc-Cyclin D1 axis, underscoring its potential as a therapeutic target in gastric cancer.

#3311 Autologous colorectal cancer-mesothelial co-culture model identifies stromal FGFR3 dependency driving peritoneal dissemination.

Hiroaki Kasashima[1], Yasuhiro Fukui[1], Iguru Omori[1], Zizhou Wang[1], Nobuhiro Naito[1], Yukina Kusunoki[1], Kenji Kuroda[1], Yuichiro Miki[1], Mami Yoshii[1], Tatsuro Tamura[1], Masatsune Shibutani[1], Takahiro Toyokawa[1], Masakazu Yashiro[1], Yuki Nakanishi[2], Naoko Ohtani[1], Kiyoshi Maeda[1]

[1]Osaka Metropolitan University, Osaka, Japan,[2]Kyoto Univ. Graduate School of Medicine, Kyoto, Japan

Background: Peritoneal dissemination of colorectal cancer (CRC) remains a fatal disease with limited therapeutic options. Mesothelial cells, which line the peritoneal cavity, play critical roles in metastatic implantation and stromal remodeling, yet the mechanisms governing tumor-stroma interactions in this setting remain poorly understood. We aimed to establish a physiologically relevant model to elucidate these interactions and identify stromal vulnerabilities.
Methods: We simultaneously derived a novel CRC cell line (OMUCR-1) and cancer-associated mesothelial cells (CAmeso) from the malignant ascites of a single patient with metastatic CRC. As a control, normal mesothelial cells (Nmeso) were established from a patient without dissemination. Cell morphology, growth kinetics, STR profile, and mutational status were characterized. The effects of CAmeso on CRC migration and invasion were evaluated using wound-healing and Matrigel assays. In vivo, OMUCR-1 cells were implanted alone or co-transplanted with CAmeso into nude mice. RNA sequencing was performed to analyze host stromal gene expression, and FGFR inhibition (BGJ398) was tested therapeutically.
Results:OMUCR-1 cells exhibited robust tumorigenicity and harbored KRAS (G12D) and TP53 (R306) mutations. CAmeso significantly enhanced CRC cell migration and invasion in vitro. In xenografts, co-transplantation with CAmeso yielded markedly larger tumors enriched in αSMA-positive stroma compared with OMUCR-1 alone. Bulk RNA-seq revealed upregulation of murine Fgfr3 in tumors containing CAmeso. Pharmacologic FGFR blockade with BGJ398 reduced tumor size and depleted FGFR3-positive stromal components, indicating stromal FGFR3 dependency.
Conclusions: We report the first concurrent establishment of CRC and mesothelial cell lines from the same patient, providing an autologous system for dissecting tumor-stroma crosstalk during peritoneal metastasis. Our findings highlight stromal FGFR3 signaling as a potential mediator of CRC progression and a promising target for therapeutic intervention. This unique platform offers a valuable resource for mechanistic and translational studies on the peritoneal microenvironment in advanced colorectal cancer.

#3312 FLT4-mediated ferroptosis resistance in renal cell carcinoma.

Djazia Haferssas[1], Nathalie Henley[2], Jonatan Barrera Chimal[2], Casimiro Gerarduzzi[1]

[1]University of Montreal, Montreal, QC, Canada,[2]Centre de Recherche de l'Hopital Maisonneuve Rosemont, Montreal, QC, Canada

Background: Renal Cell Carcinoma (RCC) is one of the ten most frequently diagnosed cancers worldwide and constitutes 2-3% of all adult cancers. Tyrosine Kinase Inhibitors (TKIs) are commonly used to treat RCC and have been shown to induce tumor cell ferroptosis, a non-apoptotic form of cell death triggered by lipid peroxidation. However, many patients develop resistance, leading to poor outcomes. FLT4, a receptor tyrosine kinase frequently deregulated in RCC, has been associated with poor survival, yet its contribution to ferroptosis resistance remains unclear.
Hypothesis: We hypothesized that FLT4-driven signaling contributes to a cellular state that reduces ferroptosis sensitivity and promotes RCC progression.
Methods: 1) FLT4 expression and clinical correlations were assessed using The Cancer Genome Atlas (TCGA) RCC RNAseq datasets. 2) ACHN and Caki-2 RCC cell lines were used to examine how FLT4 signaling influences proliferation, survival, stress-response pathways, lipid-associated gene expression, and ferroptosis sensitivity. 3) Luciferase- and FLT4 ovrexpressing RCC cells were implanted into NOD/SCID immunodeficient mice to evaluate tumor growth and ferroptosis-related markers in vivo.
Results: FLT4 was significantly upregulated in RCC and associated with reduced patient survival. In vitro, enhanced FLT4 signaling promoted RCC cell proliferation and survival, was accompanied by reduced activity of stress-response pathways, and led to lower lipid peroxidation and decreased ferroptosis sensitivity. In vivo, FLT4 overexpression accelerated tumor growth and was associated with reduced expression of ferroptosis-related markers.
Conclusion: FLT4 expression is associated with increased RCC cell growth and reduced ferroptosis sensitivity in our models. These findings describe the phenotypic consequences of altered FLT4 signaling in RCC and highlight FLT4 as a potential target for improving RCC outcomes.

#3313 BAP1 stabilizes BIRC5 to promote chemoresistance in gastric cancer.

Park Yu-Jin[1], In-ho Jeong[2], Peter CW Lee[2]

[1]Department of Biochemistry & Molecular Biology, Brain Korea 21 Project, University of Ulsan College of Medicine, Asan Medical Center, Seoul, Korea, Republic of,[2]Department of Biomedical Sciences, University of Ulsan College of Medicine, Seoul, Korea, Republic of

Gastric cancer is a highly aggressive malignancy associated with poor prognosis. 5-Fluorouracil (5FU) is an anticancer drug widely used to treat gastric cancer, however, the development of drug resistance during treatment remains a major clinical challenge. Therefore, understanding the molecular mechanisms underlying 5-FU resistance is essential for improving chemotherapeutic efficacy. The ubiquitin-proteasome system (UPS) is a key regulatory mechanism that controls the stability and function of intracellular proteins, with deubiquitinases (DUBs) serving as important modulators within this pathway. BRCA1-associated protein-1 (BAP1) is a representative DUB that has been implicated in tumorigenesis across various cancers; however, its role in gastric cancer and drug resistance remains poorly understood. In this study, we found that not only BAP1 but also anti-apoptotic protein BIRC5 is expressed at higher levels in 5FU-resistant gastric cancer cells compared to normal gastric cancer cells. We confirmed that BAP1 stabilizes BIRC5, a known anti-apoptotic protein, through deubiquitination. And we identified that knockdown of BAP1 reduced viability, migration, and invasion of gastric cancer cells. Furthermore, reduced BAP1 expression decreased BIRC5 protein expression, and induced apoptosis through the cleavage of PARP and Caspase-3. Notably, treatment with the selective BAP1 inhibitor iBAP-II increased the sensitivity of gastric cancer cells to 5-FU. Our findings revealed that BAP1 enhances 5-FU resistance and promotes gastric cancer progression by stabilizing BIRC5 and highlight BAP1 as a potential therapeutic target to enhance the efficacy of chemotherapy in gastric cancer.

#3314 RIPK2 promotes metastatic behavior in inflammatory breast cancer and is an attractive therapeutic target.

Innocent Ojobile[1], Alaa Zare[2], John M. Githaka[2], Einav Renert[1], Lynne-Marie Postovit[1]

[1]Queen's University, Kingston, ON, Canada,[2]University of Alberta, Edmonton, AB, Canada

Inflammatory breast cancer (IBC) is a rare but aggressive type of breast cancer characterized by early and rapid metastasis leading to poor clinical outcomes. The tumor microenvironment (TME), including immune cells, fibroblasts and endothelial cells, has emerged as a major regulator of IBC aggressiveness, however little is known about how IBC cells may orchestrate this pro-tumorigenic milieu. Inflammatory pathways such as NF-kB, concomitant with cytokine-induced signalling, are upregulated in IBC; however, the mechanisms underpinning these pathways are poorly understood. Receptor Interacting Protein Kinase 2 (RIPK2) mediates nucleotide-binding oligomerization domain (NOD) cell signaling that has been shown to activate NF-kB and to mediate chronic inflammation in a variety of diseases. Herein, we demonstrate that RIPK2 mediates the metastatic behavior in IBC by regulating NF-kB signaling and cytokine production. Specifically, using gain and loss of function strategies, including shRNAs, CRISPR gene editing and a small molecule inhibitor, we show that RIPK2 promotes an inflammatory transcriptome in IBC cells leading to the secretion of factors such as IL-8, IL-6 and Activin-A. As a corollary, RIPK2 enhances key IBC phenotypes, including angiogenic potential, emboli (sphere) formation, 3D invasion, a hybrid-EMT phenotype and metastatic growth in the lung. Collectively, we provide pioneering evidence that RIPK2 regulates the pro-inflammatory phenotype of IBC cells, making it an attractive target for the treatment of this disease.

#3315 CYLD regulates thrombin-induced p38-p65 signaling to inhibit breast cancer progression.

Julio Macias Pimentel, Naa-Oye Bosompra, JoAnn Trejo

Pharmacology, University of California San Diego - UCSD, San Diego, CA

G-protein coupled receptors (GPCRs) are a large and diverse family of cell surface receptors that regulate various physiological responses. Dysregulation of GPCR signaling is associated with multiple diseases, making this receptor family the largest target class of FDA-approved drugs. However, the mechanisms that regulate GPCR signaling are not well defined, and thus important to understand for improving the development of GPCR-targeted drugs. While phosphorylation is recognized as a key mechanism in GPCR regulation, GPCRs are also subject to ubiquitination, which is best known to promote lysosomal degradation. However, we showed that protease-activated receptor 1 (PAR1), which, upon thrombin stimulation undergoes ubiquitination and promotes non-canonical TAB1/TAB2 dependent activation of the p38 MAPK pathway on endosomes. This paradigm underscores a critical limitation of current therapeutic strategies, which predominantly target plasma membrane-initiated signaling while overlooking the contributions of endosomal signaling pathways. Although several E3 ligases have been identified to ubiquitinate GPCRs, the deubiquitinases that reverse this modification remain poorly defined, leaving a major gap in our ability to modulate GPCR signaling with precision in inflammatory diseases. Thrombin-activated PAR1 coupling to endosomal p38 signaling axis provides a powerful model to study how ubiquitination and deubiquitination regulate GPCR signaling. We identified the deubiquitinase CYLD as a key regulator of thrombin-induced PAR1-p38 signaling in endothelial and HeLa cells. Extending these findings to cancer, I demonstrated that thrombin activates p38 in multiple triple-negative breast cancer (TNBC) cell lines where PAR1 is highly expressed. In TNBC cells, CYLD knockdown increased both basal/thrombin-induced phosphorylation of p38 MAPK and p65. Using siRNA and pharmacological inhibitors, I further demonstrated that thrombin-induced p38 signaling functions upstream of NF-κB/p65, with co-immunoprecipitation confirming that p38 directly co-associates and phosphorylates p65 rather than other NF-κB pathway components. Downstream, this pathway drives nuclear translocation of phosphorylated p65, revealed by immunofluorescence and shown to be p38-dependent, as nuclear localization was abrogated by the p38 inhibitor BIRB 796. Functionally, thrombin-p38-p65 signaling upregulated pro-inflammatory cytokines including IL-6, IL-8, IL-1α, and IL-1β, as detected by human cytokine arrays and validated by RT-PCR. Finally, CYLD knockdown enhanced TNBC cell proliferation and migration, demonstrating that CYLD suppresses TNBC growth by inhibiting thrombin-p38-p65-signaling. Collectively, these findings reveal a novel mechanism by which CYLD inhibits TNBC progression through regulation of thrombin-p38-p65 signaling.

#3316 The mystery behind mSin1 phosphorylation.

Samira Mahmoudi, Bing Cheng, Yan Luo, Lei Liu, Shile Huang

Department of Biochemistry and Molecular Biology, LSU Health Shreveport, Shreveport, LA

Mammalian stress-activated protein kinase-interacting protein 1 (mSin1), a core component of the mechanistic target of rapamycin complex 2 (mTORC2), is less well characterized than other mTOR subunits. In particular, the mechanisms regulating its phosphorylation and its functional contribution to mTOR signaling remain poorly defined. Conflicting reports suggest that phosphorylation of mSin1 at T86 is mediated either by Akt or by ribosomal protein S6 kinase 1 (S6K1), highlighting uncertainty regarding its upstream regulation. These discrepancies underscore the need for deeper investigation into the kinases and pathways governing mSin1 phosphorylation. We found that rapamycin treatment decreases overall phosphorylation while paradoxically increasing T86 phosphorylation of mSin1 across multiple normal and cancer cell lines. These effects are independent of mTORC1/mTORC2 and downstream effectors (S6K1 and Akt) yet requires mTOR kinase activity and the subunit mLST8 (mammalian lethal with SEC13 protein 8). Since mTOR acts as a nutrient sensor, we also examined the effect of nutrient availability on mSin1 phosphorylation. Prolonged glucose deprivation, but not amino acid deprivation, markedly decreased mSin1 phosphorylation in HeLa cells, which was restored upon glucose repletion. These effects were not observed in Rh30, VSMC, and MEF cells. Collectively, our findings suggest that that rapamycin inhibits mSin1 phosphorylation by targeting a novel mTOR complex and might be associated with glucose metabolism in some contexts. Further research is needed to define the exact phosphorylation sites and their significance as well as the new mTOR complex regulating these phosphorylation sites.

#3317 ICA-1S and Selinexor decreases atypical teratoid rhabdoid tumor (ATRT) survival and proliferation.

Nuzhat Nowshin Oishee[1], Abigail Oluwafisayo Olatunji[2], Abiral Hasib Shourav[3], Grazielly Teodoro[3], Anna Kharitonova[3], Mildred Acevedo-Duncan[3]

[1]Chemistry, University of South Florida - Upward Bound, Tampa, FL,[2]University of South Florida - Upward Bound, Tampa, FL,[3]University of South Florida, Tampa, FL

Atypical teratoid rhabdoid tumor (ATRT) is a rare, aggressive and rapidly growing cancerous brain and spinal cord tumor mainly affecting young children, less than 3 years of age. ATRT consists of less than 5% of all pediatric CNS tumors. Abnormalities in chromosome 22q11, which includes the putative tumor suppressor gene SMARCB1 are frequently seen in ATRT. SMARCB1is a component of an SWI/SNF ATP-dependent chromatin-remodeling complex that controls the expression of certain target genes involved in cell cycle regulation. Approximately, 75% of ATRTs contains the homozygous deletions of SMARCB1, or loss of one allele and mutation of the other copy for the gene. Due to the rare and complex nature of the disease, ATRT is under researched. It is crucial to understand the signaling pathways that operate in the cell proliferation and survival of the ATRT tumors, and to establish a targeted therapy for this disease. One promising area that can be explored is the atypical Protein Kinase Cs (aPKCs). Protein Kinase C-iota (PKC-ι), an aPKCs isozyme, is over-expressed in many types of cancers. PKC-ι plays a major role in tumorigenesis because it is over-expressed and impacted by PI3K, PTEN and other signaling pathways. However, the role of aPKCs is yet to be discovered in the cell proliferation and survival of the ATRT cells. Therefore, in this study we aim to use, a novel PKC-ι inhibitor ICA-1S, alone or in-combination with Selinexor, and observe the subsequent effects on the ATRT cell proliferation and survival. The central hypothesis is that a PKC-ι inhibitor (ICA-1S) alone or in combination with Selinexor can restrain pediatric ATRT cell proliferation and cell survival by intercepting the PKC-ι/Cdk7/Cdk2 and PKC-ι/Bad pathways cascade in-vivo. To validate the hypothesis, we examined the effects of ICA-1S alone or in combination with Selinexor on the proliferation of ATRT cells. The results of a proliferation assay after a four-day treatment period with ICA-1S, Selinexor and combination helped us achieve the inhibitory concentration of the drugs that reduced the cancer cell proliferation to approximately 50%, which was at 20μM with ICA-1S alone for both the ATRT cells. We also tested various concentrations of Selinexor ranging from 400nM to 1.5μM, which showed more than 50% reduction in ATRT cell proliferation at 400nM, which was the lowest concentration used for both the cell lines. For the CHLA-05 cells, ICA-1S and Selinexor combination treatments caused significant reductions at 20μM ICA-1S+800nM Selinexor. For the CHLA06 cells, ICA-1S and Selinexor combination treatments caused significant reductions at 20μM ICA-1S+400nM Selinexor. These cell proliferation data suggest that ICA-1S and Selinexor have a synergistic effect on the ATRT cells. Furthermore, we plan on observing the effect the combination treatment on PKC-ι/Cdk7/Cdk2 and PKC-ι/Bad pathways both *in-vitro* and *in-vivo.*

#3318 The regulation of IL-6/gp130 signaling by PTPRF in colon cancer.

Haley Stanczyk[1], Carolina Galeano-Naranjo[1], Tianyan Gao[2]

[1]Molecular and Cellular Biochemistry, University of Kentucky, Lexington, KY,[2]Markey Cancer Center, University of Kentucky, Lexington, KY

Elevated Interleukin 6 (IL-6) levels and the activation of IL6/JAK/STAT3 signaling play an important role in promoting tumor growth and progression in colorectal cancer, making the IL-6 pathway a potential therapeutic target. Binding of IL-6 stimulates the formation of a receptor complex consisting of the IL-6 receptor and its co-receptor, gp130, which triggers the activation of JAK family kinases to phosphorylate tyrosine residues on the intracellular domain of gp130. The phosphorylated tyrosine residues act as docking sites for key signaling components, including transcription factor STAT3. Docking of STAT3 to gp130 allows for the phosphorylation of Tyr705 on STAT3 by JAK, the residue necessary for dimerization and nuclear translocation of STAT3 to promote gene transcription. While the phosphorylation-dependent activation of the IL-6 pathway has been intensively investigated, the regulation of signaling inactivation by protein phosphatases remains largely unexplored. Here we determined the role of protein tyrosine phosphatase receptor type F (PTPRF) in negatively regulating the tyrosine phosphorylation steps that control IL-6/gp130 signaling. The expression of PTPRF was depleted by CRISPR-mediated knockout or doxycycline inducible RNAi in 293T and colon cancer cells. We found that PTPRF downregulation resulted in an increase in total protein expression as well as tyrosine phosphorylation of gp130 basally. Additionally, IL-6 stimulation-induced activation of Jak family kinases, as indicated by Tyr1007/1008 phosphorylation, was largely increased and more sustained in PTPRF knockout cells compared to control. Furthermore, results from co-immunoprecipitation experiments showed that the association of STAT3 with gp130 was increased in PTPRF knockout cells, consistent with increased JAK activation. Functionally, the expression of SOCS3, a STAT3 target gene, was significantly elevated upon IL-6 stimulation as determined by RT-qPCR in PTPRF knockdown colon cancer cells. Taken together, this study identifies PTPRF as a novel regulator of the IL-6/gp130 signaling pathway in colon cancer.

#3319 IL-1 beta/ IL-6 co-stimulation synergistically mediates DUOX2/DUOXA2 complex up-regulation via JAK/STAT and p38 signaling events.

Jennifer L. Meitzler[1], Becky A. Diebold[1], David J. Mallick[2], Yongzhong Wu[1], Smitha Antony[2], Mariam M. Konate[2], Krishnendu Roy[2], James H. Doroshow[2]

[1]Developmental Therapeutic Branch, NCI, Bethesda, MD,[2]NCI Division of Cancer Treatment and Diagnosis, Bethesda, MD

Chronic inflammation increases the susceptibility of the colon to neoplasia and cancer through establishment of an inflammatory microenvironment and persistent release of reactive oxygen species (ROS), inducing genome damage. Interleukin -1beta (IL-1beta), a pro-inflammatory cytokine, plays a pivotal role in the pathogenesis of acute and chronic intestinal inflammation, regulating both innate and adaptive immune responses. IL-1beta has been shown to promote accumulation of IL-17A through lymphoid and Th17 infiltration in the colon tumor microenvironment, supporting increased inflammation and correlating directly with poor patient prognosis. New insights into the signaling pathways supported by IL-1beta in the pathogenesis of colon cancer, including angiogenesis and metastasis, may provide downstream targets for treatments that minimally perturb intestinal immunity. Prior studies from our group have demonstrated significant up-regulation of IL-1, dual oxidase 2 (DUOX2) and its partner maturation factor, DUOXA2, in surgically resected colon cancer specimens compared with adjacent normal colonic epithelium. To elucidate a direct link between IL-1 family cytokines, DUOX2/DUOXA2 derived ROS, and colorectal cancer, we examined human colon cancer cells (HT29, Ls513, T84 and Colo205) stimulated with IL-1beta, in cooperation with IL-6. Co-stimulation resulted in a dramatic, synergistic up-regulation of a hydrogen peroxide producing (Amplex Red oxidizing) DUOX2 enzyme complex and was directly associated with enhanced histone H2AX phosphorylation (γH2AX), a marker of DNA double strand breaks. Interestingly, this concentration- and time-dependent induction of expression and oxidative response was not mediated by other IL-1 family members (IL-18, IL-33 or IL-37). Investigations with the interleukin-1 receptor antagonist anakinra established that signaling for IL-1beta/IL-6 co-treatments proceeded through the IL-1 receptor for all cell lines, though minimal receptor expression is present in T84 and Ls513 cells. Similarly, exposure to tocilizumab, an IL-6R antagonist, demonstrated that the IL-1beta/IL-6 synergistic increase in DUOX2/DUOXA2 complex expression is IL-6 receptor dependent. Perturbation of the IL-1 and IL-6 signaling pathway elements MYD88, IRAK1, STAT1, and STAT3 by siRNA knockdown demonstrated their significant contribution to DUOX2/DUOXA2 up-regulation, while dependence on RELA was absent. Knockdown facilitated by MAPK14 siRNA and SB203580 p38 alpha/beta inhibition also demonstrated a role for p38alpha in the regulation of DUOX2/DUOXA2 expression by the IL-1beta/IL-6 signaling axis. Current studies are focused on elucidating the DUOX2 promoter transcription factor binding site(s) responsible for DUOX2 up-regulation through chromatin immunoprecipitation.

#3321 Validating upstream kinase predictions by linking activity to drug target proximity.

Dora Schuller, **Gitanjali Dharmadhikari**, Monique Mommersteeg, Liesbeth Houkes, Simar Pal Singh, Rik de Wijn

PamGene International B.V., 's-Hertogenbosch, Netherlands

Introduction: Sustained cell signaling is one of the hallmarks of tumor growth. Deregulation of kinase signaling can be studied by methods such as peptide microarrays or phospho-proteomics. For this, the prediction of kinases from phosphorylation signatures is a critical and complex. The aim of our study is to validate the biological relevance of kinase predictions, which we evaluate by the integration of kinase activity profiles with sensitivity data from the Genomics of Drug Sensitivity in Cancer (GDSC). A fundamental sensitivity mechanism involves repressing the activity of the drug's target kinase and its downstream survival pathways. We can test this mechanism through network analysis, hypothesizing that the signaling networks of active kinases and drug targets show high connectivity in sensitive cells, that should reflect the biological relevance of the kinase predictions.

Methods: Serine/Threonine Kinase (STK) activity profiling of 11 B-cell lymphoma cell lines was performed via the KinomePro platform (PamGene International B.V.). Kinases were predicted for 10 cell lines generally sensitive to multiple drugs (IC_{50} < 1 µm) compared to one relatively resistant control line (showing sensitivity to a smaller number of drugs). Cell line specific networks were generated from the top kinases and the target kinases of drugs the cells were most sensitive to, using the STRING protein-protein interaction database and Prize-Collecting Steiner Forest algorithm.

Results: To quantify signaling proximity of kinases and drug targets, we developed the network connectivity score. For each cell line, we calculated network connectivity using the median of the shortest paths between each kinase and drug target. This was then tested for statistical significance against a reference set of 50 random networks, generated using the original drug targets and randomized kinase data. Kinase predictions for 5 out of 10 B-cell lymphoma cell lines resulted in significant network connectivity score ($p < 0.07$), depending on the parameters used in the prediction algorithm. These results demonstrate the method’s utility to identify optimal parameter settings for the prediction algorithm.

Conclusion: We developed a validation method for the biological relevance of kinase predictions from phosphorylation signatures obtained in a cellular context. Future work will focus on applying this method to improve studies of the role of kinases in signal transduction by evaluating and optimizing the performance of kinase prediction methods and their potential biases.

#3322 Next-Generation FemtoQuest™ system enables dual-analyte ultrasensitive quantitation of active and total HGF in melanoma plasma samples.

Joseph B. Hwang[1], Raad Gitan[2], Matthew Lippold[2], Brooke Gilliam[2], Rick Wiese[2]

[1]R&D, MilliporeSigma, St. Louis, MO,[2]MilliporeSigma, St. Louis, MO

Hepatic growth factor (HGF) binds to the HGF receptor tyrosine kinase, also known as c-Met. Autophosphorylation of the HGF receptor leads to recruitment and activation of multiple downstream signaling molecules involved in MAPK, Akt/PI3K, STAT and NF-kB pathways. Activation of HGF receptor by HGF can lead to cell growth, cell motility, angiogenesis and cell survival. Upregulation of this pathway can lead to tumorigenesis of different types of cancer. Various approaches to inhibiting this HGF/c-Met axis have been explored, including c-Met neutralizing antibodies and small molecule inhibitors without much success. It is critical to understand the mechanisms of the HGF/c-Met axis to facilitate novel therapies. It is important to differentiate between the active versus total HGF concentration in the blood. Pro-HGF peptide is secreted by liver cells into extracellular matrix, where it can be cleaved by proteases into alpha and beta subunits, which form the active tetramer of 2 alpha and 2 beta subunits. It is the active form of HGF that binds and activate c-Met. We developed an ultrasensitive immunoassay platform utilizing SMC® technology to address the challenge of quantifying low-abundance proteins in blood. Our next-generation FemtoQuest™ system enables detection of two analytes in a single assay well, maximizing sample efficiency. For this study, we developed a novel 2-plex immunoassay that can detect active HGF and total HGF (active HGF plus pro-HGF) simultaneously in a single well. This kit was able to achieve the sensitivity needed to quantitate both apparently healthy and melanoma plasma samples. Statistical difference for both Active HGF and Total HGF were observed in healthy versus melanoma samples. This high sensitivity immunoassay kit can differentiate between active HGF versus total HGF and allow measurement of low abundance proteins, demonstrating the platform's capability to detect differential HGF expression patterns in cancer samples.

: Tumorigenesis Drivers
Poster Session

#3326 C-myc driven by differentiation factors in early-onset colorectal cancer (EOCRC).

Kazuaki Okamoto[1], Yalda Naeini[2], Anton Bilchik[3], Dave Hoon[1]

[1]Department of Translational Molecular Medicine, St. John's Cancer Institute (SJCI), Providence St. John's Health Center (PSJHC), Santa Monica, CA,[2]Department of Surgical Pathology, PSJHC, Santa Monica, CA,[3]Department of Gastrointestinal and Hepatobiliary Surgery, PSJHC, Santa Monica, CA

Background: Early-onset colorectal cancer (EOCRC), patients diagnosed with CRC <50 yrs has become a rapidly increasing global threat in recent years. Generally, EOCRC is known for its high malignancy, characterized by advanced stages at diagnosis and often undifferentiated histological types. Despite numerous previous studies, its molecular pathological characteristics remain largely unexplored. The purpose of this study is to elucidate the progression mechanisms of EOCRC versus Late-onset CRC (LOCRC).

Methods: To identify genes characteristic of EOCRC, an *in silico* analysis was conducted by comparing RNA-seq data from CRC patients aged aged ≤45 with those aged ≥ 60 and using TCGA COAD/READ and GSE39582 CRC database. At the PSJHC, among patients who underwent primary tumor resection for CRC between 2018 and 2021, we then divided 30 patients into two groups using the cutoffs of 45 and 60 yrs of age, respectively. We then performed single-cell level spatial transcriptome analysis using Xenium(10X). Pathways were validated through these analyses using multiplex immunofluorescence (Akoya) staining and *in vitro* analysis with colon cancer cell lines.

Results: In the *in silico* analysis, regulatory gene of cell differentiation exhibited significantly higher RNA expression in EOCRC patients compared to those with LOCRC. The expression levels of these genes are associated with poor overall survival. Furthermore, *in vitro* analysis demonstrated a significant increase in c-myc expression through the NF-κB pathway and the promotion of tumor growth induced by the upregulation of the downstream differentiation factors. Additionally, it was demonstrated that the expression of differentiation factors and respective receptors are higher at the protein level in the EOCRC patients than the LOCRC patients ($p<0.001$). In multiplex immunofluorescence, significant correlation between the expression of differentiation factors and c-myc was observed.

Conclusions: In EOCRC, differentiation factors were expressed at higher levels compared to LOCRC, suggesting that they upregulate c-Myc through the NF-κB pathway. These differentiation factors may contribute to the poor prognosis observed in EOCRC versus LOCRC.

#3327 Structure and function of the L-MYC N-terminus impacts strategies to inhibit the MYC family of oncoproteins.

Tristan M. Kenney[1], Scott Houliston[1], Peter Chien-feng Lin[2], Nikan Movahedi[1], Cheryl Arrowsmith[1], **Linda Z. Penn**[1]

[1]UHN Princess Margaret Cancer Centre, Toronto, ON, Canada,[2]University of Toronto, Toronto, ON, Canada

The *MYC* family of transforming oncogenes function as regulators of gene transcription and is composed of three members, *MYC*, *MYCN* and *MYCL*. As the c-MYC (MYC) protein is deregulated in >50% of human cancers, the role, regulation and structural features of MYC have been well-studied. By contrast, the L-MYC protein has been relatively understudied as historically, oncogenic deregulation was evident only in a subset of small cell lung carcinomas (SCLCs). However, with recent deep genomic analyses of primary patient samples, L-MYC has been shown to be deregulated in numerous human cancers. With this revelation it is important to understand how the L-MYC protein compares to MYC at the structural level, particularly for the development of broad-spectrum inhibitors of the MYC family.

Here we first show that L-MYC expression is anti-correlated with MYC expression and is elevated in several primary patient tumor samples compared to normal, providing further evidence for L-MYC as a driver oncoprotein in primary human cancers. Next, we provide new insights into the biophysical features of an N-terminal region within the transactivation domain of L-MYC, which harbors two regions conserved amongst the MYC family: MYC box 0 (MB0) and MYC box I (MBI). NMR spectroscopy of residues 1-80 of L-MYC confirms that, similar to MYC, it is largely intrinsically disordered and interacts with the known MYC MB0-interacting protein, PNUTS (Phosphatase 1 NUclear Targeting Subunit). On the other hand, L-MYC does not interact with the MYC MB1-interacting protein Bin1 (Bridging integrator 1), suggesting a potential mechanism by which L-MYC evades this tumor suppressor. Together, these results further substantiate the oncogenic role of L-MYC in human cancer and deeply enhance our understanding of the biophysical nature of L-MYC to better inform strategies for the development of anti-cancer therapeutics targeting the MYC family of oncoproteins.

#3328 Investigating resistance to beta-catenin degradation in a colorectal cancer cell line.

Reiss Clifford[1], Christopher I. Milton[1], Jasjot Singh[2], Marc Krenkel[2], Pradeep Ramagiri[1], Konstantinos Mitsopoulos[1], Frank Fischer[2], Marissa V. Powers[1], Dirk Wienke[2], Paul A. Clarke[1]

[1]The Institute of Cancer Research, London, London, United Kingdom,[2]The Healthcare Business of Merck KGaA, Darmstadt, Germany

Oncogenic mutations to the Wnt pathway are present in approximately 80% of colorectal cancer (CRC) patients. In mouse CRC models, Beta-Catenin (BC) loss inhibits tumour growth reinforcing BC as a promising anticancer target. Small molecules or peptides targeting BC have been reported but these generally lack features of high-quality chemical probes. To date there are no reports of these tool compounds progressing to chemical series with more drug-like physiochemical and pharmaceutical characteristics, yet interest in developing BC inhibitors or degraders remains. To explore potential fragment-binding pockets on BC we established a BC-degron model for genetic rescue experiments using the dTAG system to degrade FKBP12^{F36V}-tagged BC. Based on literature and in-house date we selected the APC-mutant, BC-dependent SW480 human CRC cell line as our model of choice. During the characterisation of multiple dTAG single cell clones we identified two resistant SW480 cell clones which proliferated despite BC degradation. One line (Res1) contained no detectable BC protein following treatment with the dTAG^{V}-1 heterobifunctional degrader molecule. Whereas the other, Res2, retained expression of an internally truncated species of BC,that was sufficient to rescue WT-BC function. Genetic and proteomic profiling were used to define the response of resistant populations to BC degradation. Res2 exhibited a similar molecular profile to cells expressing full length BC. Res1 exhibited a proteomic profile distinct from sensitive cells after BC degradation. BC-driven oncogenic gene expression profile was degraded in resistant cells, similarly to sensitive cells. But metabolic pathways, including autophagy, were markedly altered in resistant cells. Additionally, we found a region of chromosome 19 lost only in Res1. Res1 exhibited distinct morphological features to sensitive cells and an increased migratory capacity. Multiple patient-like cancer stem cell subtypes have been classified within the SW480 CRC cell line population, with different invasive and Wnt signalling capacities. But their responses to BC inhibition or loss are unknown. Molecular and cellular characterisation of Res-1 is on-going to identify key SW480 subtype features and mechanism of resistance to BC loss as potential biomarkers to predict patients with resistance to BC inhibition and suggest novel pathway dependencies which can be exploited for combination therapies alongside BC inhibition or degradation.

#3330 Spatial and molecular profiling of tumor initiation in ccRCC.

Omar Bouricha[1], Daqi Deng[1], Anne-Laure Cattin[1], Matous Elphick[1], Scott Shepherd[1], Cathy D. Vocke[2], W. Marston Linehan[3], Samra Turajlic[4]

[1]Cancer Dynamics Laboratory, The Francis Crick Institute, London, United Kingdom,[2]National Cancer Institute, Bethesda, MD,[3]Chief, Urologic Onc. Branch, National Cancer Institute, Bethesda, MD,[4]CRUK Manchester Institute, Manchester, United Kingdom

Clear Cell Renal Cell Carcinoma (ccRCC) is the most common and aggressive type of kidney cancer. ccRCC originates from proximal tubule (PT) epithelial cells in the nephron. Its initiation is characterised by a linear evolution from the loss of one copy of chromosome 3p to the inactivation of the second VHL allele on the remaining copy of 3p. Computational studies established that 3p loss occurs several decades before diagnosis. This offers an unprecedented window of opportunity for early detection, cancer prevention and for broader pan-cancer learning. However, the biological mechanisms driving the pre-cancerous expansion of PT cells harboring these events remain elusive. One of the major unmet needs in ccRCC initiation is the identification of molecular biomarkers for the initially quiescent tumor-initiating cell. Previous studies established that the putative ccRCC cell of origin (COO) is a subtype of PT cells characterized by VCAM1 expression, a marker of tubular injury in human kidneys. Therefore, we hypothesized that VCAM1 can be used as a marker to enrich for cells that have lost a copy of chromosome 3p. Preliminary single-cell whole genome sequencing (WGS) of VCAM1+ PT cells revealed a high incidence of aneuploidies, including chromosome 3-related aneuploidies, indicating that these cells represent a chromosomally unstable epithelial subpopulation within morphologically normal kidney tissue. Therefore, this data supports VCAM1 as a candidate marker for the study of ccRCC initiation in human kidneys.Despite its quasi-ubiquitous role in ccRCC initiation, several studies show that VHL inactivation is insufficient for tumorigenesis in mammalian kidneys. To study this, we used histological analysis of VHL patient-derived normal kidney tissues, where 3p loss occurs on the background of a germline VHL mutation. We demonstrated that VHL inactivation (marked by CAIX expression) occurs in all major cortical epithelial cell types. Surprisingly, only the proportion of CAIX+ distal tubule (DT) cells showed a significant correlation with the age of the patient at the time of tissue collection. In addition, there is a significantly higher proportion of multicellular DT CAIX+ foci compared to CAIX+ PT foci, suggesting clonal expansion after VHL inactivation is favored in DT cells. Only a minority of CAIX+ PT foci were multicellular, indicating that unknown cell-intrinsic or extrinsic factors are necessary for clonal expansion. Results from our cohort show a positive association between the density of VCAM1+ PT cells and CAIX+ PT in VHL patient-derived normal kidney tissues, indicating that tissue stress levels may potentiate the selection and expansion of VHL inactivation in the human kidney. Our data offers novel insight in the putative COO of ccRCC and the mechanisms driving the earliest stages of ccRCC. Moving forward, we plan to expand our cohort and molecularly profile VCAM1+ and CAIX+ cells using multi-omic approaches.

#3331 NanoGlio recapitulates *IDH*-mutant glioma biology and therapeutic response to vorasidenib.

Uijin Kim[1], Satoru Kawakita[1], Emily Miller[1], Wei Huang[1], Francisco Bustamante[1], Lauren Vanderpool[1], Chongming Jiang[1], Albert Lai[2], Zhaohui Wang[1]

[1]Terasaki Institute for Biomedical Innovation, Woodland Hills, CA,[2]Department of Neurology, UCLA Health, Los Angeles, CA

IDH-mutant gliomas are a biologically and clinically distinct subset of diffuse gliomas that remain challenging to model *in vitro*. Vorasidenib, a brain-penetrant dual IDH1/2 inhibitor, is the first FDA-approved targeted therapy for grade 2 non-enhancing gliomas in 2024. Here, we present NanoGlio, a nanoliter-scale organoid platform that enables rapid, passage-zero functional drug testing using minimal patient-derived material. NanoGlio supports the formation of uniform, viable tumor organoids that preserve the cytoarchitecture and cellular heterogeneity of the parental tumors. We established NanoGlio models from 13 cases of grade 2, 5 cases of grade 3, and 9 cases of grade 4 *IDH*-mutant gliomas, including spatially distinct enhancing and non-enhancing regions from 4 patients. Single-cell RNA sequencing confirmed that NanoGlio retains tumor-intrinsic heterogeneity and myeloid lineages present in the original tissue. High-content phenotypic screening revealed heterogeneous responses to Vorasidenib, with NanoGlio sensitivity correlating with tumor grade and molecular subtype. Notably, Vorasidenib induced differentiation-like morphologic changes in grade 2 models but paradoxically enhanced proliferation in a subset of high-grade models. Bulk RNA sequencing showed that NanoGlio captures *in vivo*-like drug response programs, particularly in immune-related and glial differentiation pathways that overlap with molecular changes reported in clinical trials. Furthermore, NanoGlio-derived conditioned media, when applied to co-cultures of HER2-specific chimeric antigen receptor (CAR) T cells and HER2-positive SKOV3 tumor cells, enabled functional assessment of soluble factor-mediated immune suppression. Together, these data establish NanoGlio as a scalable, patient-relevant organoid platform for modeling IDH-mutant glioma biology and therapeutic response, with direct applications to drug-response prediction and rational combination strategies in precision oncology.

#3332 Functional role of PHLDA1 down regulation leads to morphological changes and increased proliferation in MCF-7 breast cancer cells.

Ana Carolina Pavanelli[1], Flavia Rotea Mangone[1], Fernando M. Simabuco[2], Maria Aparecida Nagai[3]

[1]Center for Translational Research in Oncology, Instituto do Cancer do Estado de Sao Paulo and Comprehensive Center for Precision Oncology, Sao Paulo, Brazil,[2]Departamento de Bioquimica, Universidade Federal de Sao Paulo, Sao Paulo, Brazil,[3]Center for Translational Research in Oncology, Instituto do Cancer do Estado de Sao Paulo and Comprehensive Center for Precision Oncology/Disciplina de Oncologia do Departamento de Radiologia e Oncologia, Sao Paulo, Brazil

The PHLDA1 (pleckstrin homology-like domain Family A, member 1) belongs to a family of genes that encode phosphatidylinositol (PIP) binding proteins and function as inhibitors of Akt activation. Previously, we have shown that PHLDA1 down-regulation is a strong predictor of poor prognosis for breast cancer (BC) patients. We have also demonstrated that decreased PHLDA1 expression is associated with more aggressive behavior in non-malignant mammary cells and is linked to a more aggressive BC phenotype and a worse prognosis. Additionally, we demonstrated that PHLDA1 expression is regulated by estrogen via ER. Here, we sought to investigate the effects of PHLDA1 knockdown on cell proliferation, migration, and colony formation, and further assess its involvement in the response to endocrine therapies. The MCF-7 cells were transfected using a CRISPR/Cas9 vector (p5pCas(BB)-2A-Puro (PX459) V2.0) that included guide RNAs (gRNAs) designed to silence the PHLDA1 gene, as well as a control vector with scrambled gRNAs. PHLDA1 knockdown clones (MCF-7koPHLDA1) were confirmed by western blot and qRT-PCR. MCF-7koPHLDA1 clones displayed morphological changes, including loss of regular angular and spindle shapes and a more dispersed cell arrangement. We performed the colorimetric MTT reduction assay to evaluate the effect of PHLDA1 knockdown on the proliferation. MCF-7koPHLDA1 has significantly higher proliferation rates than MCF-7 transfected with the vector containing a scramble (MCF-7-SC). In addition, a clonogenic assay followed by crystal violet staining showed that MCF-7koPHLDA1 also exhibited higher colony-forming ability, with a dispersed organization and limited cell-cell contact, compared with MCF-7-SC. Our data suggest that decreased PHLDA1 expression enhances the proliferation and colony-forming ability of MCF7 cells. Additionally, the obtained clones will be assessed for how PHLDA1 expression influences their response to tamoxifen and fulvestrant treatments. Supported by FAPESP.

#3333 CHAF1A phosphorylation by PLK1 promotes AR-driven enzalutamide resistance in prostate cancer.

Sai Wu[1], Chaohao Li[1], Jia Peng[2], Xiaoqi Liu[1]

[1]University of Kentucky, Lexington, KY,[2]Department of Toxicology and Cancer Biology, University of Kentucky, Lexington, KY

Prostate cancer (PCa) remains a major global health challenge, ranking as the second most frequently diagnosed malignancy and the fifth leading cause of cancer-related mortality among men. Although androgen deprivation therapy and next-generation androgen receptor (AR) pathway inhibitors, such as enzalutamide, have improved clinical outcomes, the inevitable emergence of castration-resistant prostate cancer (CRPC) and treatment resistance underscores the need to elucidate the underlying molecular mechanisms. Polo-like kinase 1 (PLK1), a conserved serine/threonine kinase essential for mitosis, has been implicated in promoting enzalutamide resistance; however, the mechanistic basis of this phenomenon remains insufficiently understood. In this study, we identify Chromatin Assembly Factor 1 subunit A (CHAF1A) as a previously unrecognized modulator of AR signaling and a critical contributor to enzalutamide resistance. Analysis of the clinical database revealed that CHAF1A is significantly overexpressed in PCa compared with benign prostate tissues, and elevated CHAF1A levels correlate with poor patient prognosis. Functional assays demonstrated that CHAF1A knockdown in C4-2 and 22Rv1 cells suppresses cell proliferation, decreases PSA expression, and restores sensitivity to enzalutamide. Conversely, CHAF1A overexpression in C4-2 and LNCaP cells enhances proliferation and upregulates AR downstream effectors. Mechanistic studies revealed that CHAF1A is a potential substrate of PLK1 and undergoes phosphorylation at threonine 591 (T591). Introduction of a phosphorylation-deficient mutant, CHAF1A-T591A, into C4-2 cells attenuated AR signaling and significantly increased their responsiveness to enzalutamide. RNA sequencing further demonstrated pronounced downregulation of AR signaling in CHAF1A-T591A-expressing cells compared with wild-type controls. Using ChIP-qPCR, we show that CHAF1A enhances AR binding to promoter regions of key downstream targets, thereby elevating AR transcriptional activity. Importantly, the T591A mutation markedly diminished AR chromatin occupancy, indicating that PLK1-mediated phosphorylation at T591 is required for CHAF1A-dependent AR activation. Collectively, these findings identify CHAF1A as a novel enhancer of AR chromatin binding and transcriptional output, acting through a PLK1-dependent phosphorylation mechanism. We propose that elevated CHAF1A expression drives enzalutamide resistance by sustaining AR pathway activation, and that disruption of PLK1-mediated CHAF1A phosphorylation represents a promising therapeutic strategy to overcome resistance in CRPC.

#3334 The human Flower isoform hFWE4 facilitates cornification in cutaneous squamous cell carcinoma.

Justin C. Rudd, Patrick T. Kuwong, Rachel E. Johnson, Louise N. Monga-Wells, Meghan Vo, Julia Russolillo, Shreya Reddy, Mallory Jacob, Hunter Litz, Changzhao Li, Andrew Siref, James A. Grunkemeyer, Laura A. Hansen

Creighton University, Omaha, NE

Background: Cutaneous squamous cell carcinoma (cSCC) arises from transformed keratinocytes that often retain partial differentiation potential. Because differentiation status correlates with prognosis, molecular markers that distinguish well- from poorly-differentiated (WD vs PD) tumors are of clinical value. Flower (FWE), a four-transmembrane protein that regulates lamellar body (LB) trafficking during epidermal barrier formation, was examined here as a candidate marker and regulator of terminal differentiation in cSCC.

Methods: FWE expression was analyzed in human cSCC cell lines, xenografts, and clinical tumors. CRISPR/Cas9 was used to generate hFWE knockout (KO) SCC-13 cells for xenografting in NCG mice (n=12). RNA-seq, immunoblotting, and immunofluorescence quantified differentiation-associated changes in KO tumors. Lentiviral EGFP-2A-hFWE4 constructs were used to assess impact of hFWE4 overexpression on proliferation and differentiation outcomes.

Results: FWE was induced during Ca^{2+}-driven differentiation of cultured SCC cells and localized to suprabasal keratinocytes in SCC-13 xenografts. *hFWE* KO tumors exhibited a slight reduction in average mass (0.33 to 0.19g, $p<0.05$) and showed altered keratinization characterized by reduced keratohyalin granule-containing cells and solid parakeratosis. Immunofluorescence of KO tumors revealed 63% and 82% reductions in filaggrin- and loricrin-positive areas, respectively ($p<0.01$-0.0001), while RNA-seq identified 73 downregulated genes (FDR<0.05, $|\log_2 FC|>1$)—enriched for LB and cornification pathways—including *KLK5*, *KLK7*, *SLURP1*, and *LORICRIN*. Ectopic hFWE4 expression induced G1 arrest (↑G1 by 5-17%, ↓S-phase by 6-10%; $p < 0.0001$) in SCC-13, COLO 16 and SCC-12b.2 cells, and reduced the fraction of cells that were $Ki67^+$ (0.57% to 0.13%, $p<0.05$) and $ITGB1^+$ (11.3% to 2.4%, $p<0.05$) while increasing the fraction that were filaggrin$<^+$ (34.6% to 57.2%; $p<0.01$) in SCC-13 xenografts. In human tumors (WD n=9, PD n=5), FWE-positive area was significantly higher in WD than PD regions (6.2-fold increase; $p<0.0001$).

Conclusions: In cSCC, loss of FWE disrupts LB-dependent cornification, while ectopic expression elicits G1-arrest and differentiation. As high FWE-positive area correlates with increased differentiation grade in human cSCC, we propose that FWE represents both a mechanistic regulator of cornification and a promising molecular marker for objective grading of cSCC differentiation.

#3335 Trop-1/EpCAM Thr115 is a novel inducer of cancer cell proliferation and drives hyperproliferative lung damage in COVID-19.

Saverio Alberti[1], Milena Baldassarri[2], Marco Trerotola[3], Giulia Brunelli[2], Laura Bergantini[2], Benedetta tella[2], Giulia Rollo[2], Emanuela Guerra[3], martina ceci[3], Ludovica Pantalone[3], Elena Bargagli[2], Rossano Lattanzio[3], Antonino Moschella[1], Federica M. Previtera[1], Cristiana Bellan[2], Nicola La Francesca[2], Cristoforo Pomara[4], Network for Italian Genomes, GEN-COVID Multicenter Study, Alessandra Renieri[2], Chiara Fallerini[2]

[1]University of Messina, MESSINA, Italy,[2]University of Siena, Siena, Italy,[3]University of Chieti, Chieti, Italy,[4]University of Catania, Catania, Italy

SARS-CoV-2 infection triggers an acute reaction that can severely impair lung function. However, the underlying molecular processes are poorly understood. Our findings showed that the pM115T polymorphism of TROP1/EPCAM associates with COVID-19 severity. The p.M115T polymorphism of TROP1/EPCAM gene had been associated with higher frequency of early-onset breast cancer. However, the functional role of Thr115 Trop-1/EpCAM remained essentially unknown. We explored whether the Thr115 Trop-1/EpCAM acts as a driver of cell proliferation and whether this can play a role in lung pathology / lesion repair in COVID-19 patients. TROP1/EPCAM knockout embryonic stem cells showed altered proliferation. The Trop-1/EpCAM Thr115 allele was found to drive hyperproliferative capacity in murine fibrosarcoma cells, whereas the Met115 allele did not. A corresponding role was assessed in human colon cancer cells, through CRISPR-Cas9 ablation of the endogenous TROP1/EPCAM and comparative transfection of Trop-1/EpCAM Thr115 or Met115 alleles. The Trop-1/EpCAM Thr115 was shown to induce colon cancer cell hyperproliferation, whereas the Met115 allele was devoid of cell growth-driving capacity. Trop-1/EpCAM Thr115 was correspondingly shown to drive the main pathological mechanisms that lead to oxygen-exchange impairment in COVID-19. Morphometric analysis of autoptic lung samples, immunohistochemistry analysis for Trop-1/EpCAM expression, Ki67 proliferation index and comparative computational image analysis were utilized to analyze SARS-CoV-2-infected lungs at autopsy. This showed hyperproliferation of Thr115 Trop-1/EpCAM+ epithelial cells over the alveolar epithelium damaged by the infection. This correlated with Thr115 Trop-1/EpCAM+ inflammatory cells hyperproliferation and alveolar hyaline membrane formation. These multi-layered barriers were computed to reduce oxygen diffusion by up to 100-fold versus normal alveolar structures, with a critical pathological impact. Our findings identify a novel mechanism of induction of cancer cell proliferation by a polymorphic, wild-type Trop-1/EpCAM. A corresponding process was shown to operate in COVID-19 patients, causing an aberrant lung repair, via Trop-1/EpCAM Thr115-induced cell overproliferation. These findings indicate unexpected parallels between inflammation-driven wound-repair in the lungs and cancer cell hyperproliferation as driven by via Trop-1/EpCAM Thr115. Novel diagnostic/ prognostic/ therapeutic opportunities are suggested in Thr115 Trop-1/EpCAM+ COVID-19 patients, and in Thr115 Trop-1/EpCAM+ cancer patients. Acknowledgments: Grant PNRR - Tuscany Health Ecosystem (THE), Next Generation EU, Missione 4, Componente 2, Inv. 1.5, CUP B63C22000680007.

#3336 cGAS/STING-activated macrophages form lipophagosomes to regulate TME and promote progression in obesity-associated pancreatic cancer.

Yi-ting Chen[1], **Zu-Wei Wang**[2], Jin-peng Lu[3], Hao-xiang Zhang[2], Shun-cang Zhu[3], Hong-yi Lin[2], Shi Chen[2]

[1]Fuzhou University, Fuzhou, China,[2]Fuzhou University Affiliated Provincial Hospital, Fuzhou, China,[3]Fujian Medical University, Fuzhou, China

Background: Obesity significantly accelerates pancreatic cancer progression and worsens patient prognosis. However, the specific mechanisms by which macrophages regulate the tumor microenvironment (TME) in obese pancreatic cancer patients remain unclear. Understanding how macrophage-mediated TME remodeling contributes to accelerated disease progression in obesity-associated pancreatic cancer is crucial for developing targeted therapeutic strategies.
Methods: We investigated macrophage phenotypic changes and TME regulation in obesity-associated pancreatic cancer progression. We analyzed cGAS/STING pathway activation in tumor-associated macrophages, characterized mediating lipophagosome formation through lipid engulfment, and examined the resulting immunosuppressive TME. The study evaluated T cell dysfunction, regulatory T cell expansion, and the mechanistic role of tumor-derived mitochondrial DNA in macrophage activation.
Results: We identified a comprehensive mechanism whereby macrophages promote obese pancreatic cancer patient progression through cGAS/STING-mediated lipophagosome formation and TME regulation. Obesity-associated pancreatic cancer develops within a characteristic immunosuppressive environment where macrophages undergo cGAS/STING pathway activation, leading to their differentiation into foam macrophages. These STING-activated macrophages simultaneously cause CD8+ T cell exhaustion and promote regulatory T cell proliferation while competitively uptaking lipids, thereby depleting metabolic resources essential for CD8+ T cell function. Through this lipid engulfment process, STING-activated macrophages form specialized organelles called lipophagosomes, which further enhance Treg proliferation and amplify immunosuppression within the TME. Mechanistically, tumor cells in the obesity environment release mitochondrial DNA that serves as the primary trigger for macrophage cGAS/STING activation, establishing a feed-forward loop that maintains and intensifies the obesity-induced immunosuppressive environment, ultimately driving accelerated tumor progression.
Conclusions: Our findings demonstrate that macrophages promote obese pancreatic cancer patient progression through cGAS/STING-activated lipophagosome formation, which remodels the TME into an immunosuppressive state. This macrophage-centric mechanism provides novel therapeutic targets for treating obesity-associated pancreatic cancer progression.

: Extracellular Vesicles and Long-Range Tumor-Host Communication
Poster Session

#3340 Toward large-scale clinical implementation of extracellular vesicle profiling for precision oncology.
Antonia Schubert[1], Nadine Winkler[1], Robert Ihnatko[2], Joscha Kraske[3], Sunanjay Bajaj[3], Michelle Ne?ling[4], Karsten Richter[4], Dirk Jager[3], Guy Ungerechts[3], Oliver Sedlaczek[5], Jeroen Krijgsveld[2], Thomas Walle[3], Michael Boutros[1]

[1]Signaling and Functional Genomics, German Cancer Research Center (DKFZ), Heidelberg, Germany,[2]Proteomics of Stem Cells and Cancer, German Cancer Research Center (DKFZ), Heidelberg, Germany,[3]Medical Oncology, University Hospital and Medical Faculty Heidelberg, Heidelberg, Germany,[4]Central Unit Electron Microscopy, German Cancer Research Center (DKFZ), Heidelberg, Germany,[5]Department of Radiology, German Cancer Research Center (DKFZ), Heidelberg, Germany

Extracellular vesicles (EVs) are nanosized, membrane-bound particles released by all cell types. They carry proteins, nucleic acids, and lipids reflective of their cellular origin and have emerged as promising non-invasive biomarkers for cancer diagnosis and monitoring of therapy response. However, the clinical translation of EV-based assays remains limited by heterogeneous isolation methods, a lack of standardization of the clinical workflows, and insufficient validation in large patient cohorts.
To address these challenges, our group at the National Center for Tumor Diseases in Heidelberg, Germany, has developed an EV profiling framework compliant with MISEV2023 recommendations. We systematically benchmark isolation and pre-processing procedures to ensure reproducibility and compatibility with high-throughput liquid biopsy workflows within the prospective *EValuate* study (S-773/2021). Blood samples are collected *via* the NCT Cell and Liquid Biobank, processed within 30 minutes, and stored as serum and plasma aliquots at -80 °C for longitudinal analyses. To enable large-cohort EV analyses, we also characterized a miniaturized size-exclusion chromatography protocol using low-volume serum or plasma, which requires no specialized equipment and complements conventional differential centrifugation workflows.
To demonstrate the feasibility of the pipeline, we collected and analyzed a total of 125 serum samples - 109 from 24 patients with hepatocellular carcinoma (HCC) undergoing immune checkpoint inhibitor therapy and 16 quality-control samples from four healthy donors. EVs were isolated and characterized by transmission electron microscopy, nanoparticle tracking analysis, Western blotting, quantitative protein assays, and subsequently profiled proteomically to identify EV-derived protein signatures associated with disease course, radiological treatment response (RECIST), and survival.
This standardized, high-throughput EV workflow bridges biobanking, analytical validation, and clinical correlation, providing a robust and scalable framework for integrating EV-based liquid biopsy assays into precision oncology.

#3341 Focused ultrasound BBB opening yields distinct, tissue-specific extracellular vesicle profiles for glioblastoma liquid biopsy.

Andrew Thede[1], Zehra Demir[1], Khondamir Imomnazarov[2], Stefanyda Maslova[1], Rachel Short-Miller[3], Sean Lodmell[3], Kelley VanVaerenberghe[3], Claire Seibold[3], Adam LaBonte[3], Katie Havranek[3], **Natasha D. Sheybani**[1]

[1]Department of Biomedical Engineering, University of Virginia, Charlottesville, VA,[2]Department of Neuroscience, University of Virginia, Charlottesville, VA,[3]FYR, Missoula, MT

Introduction: Extracellular vesicles (EVs) are highly information-dense liquid biopsy reservoirs carrying proteins, RNAs, lipids, and metabolites that reflect the real-time state of their parent cells. In glioblastoma (GBM), EVs offer a uniquely accessible window into an otherwise sequestered compartment, yet the blood brain barrier (BBB) restricts their enrichment and profile within the circulation. Focused ultrasound (FUS) with microbubbles is now a clinically burgeoning method for transient and precise local opening of the BBB, creating an opportunity to interrogate EV flux from tumor and surrounding brain. While FUS-mediated BBB opening (BBBO) has been shown to augment circulating nucleic acids via “sonobiopsy,” its effects on EV release and cargo remain poorly defined. Here, we evaluate how FUS-BBBO alters the abundance and composition of tumor- versus brain-derived EVs enriched from blood plasma in a high-fidelity GBM model.

Methods: Orthotopic GBMs were established via intracranial SB28 implantation (n=24). Tumors were screened by contrast-enhanced MRI and randomized into volume-matched sham or FUS treatment groups. BBBO was performed using a neuronavigation-guided preclinical FUS system. Plasma was collected 30 min or 24 h post-treatment. EVs were isolated by ion-exchange chromatography and characterized by NTA and Western blot. Tumor- and brain-derived EVs were enriched using Tumor SPARCs™ and Neuro SPARCs™, respectively, and subjected to DIA-MS proteomic analysis.

Results: FUS-BBBO did not significantly alter total plasma EV concentrations associated with either compartment; rather, it induced substantial remodeling of EV cargo. Across samples, >5,000 proteins were identified. Approximately 80% of differentially abundant proteins were unique to either the tumor- or brain-derived EV panel, indicating compartment-specific responses to FUS. Strikingly, FUS exposure yielded 222 and 290 unique proteins within brain-derived and tumor-derived circulating EV populations, respectively. Pathway analysis revealed enrichment in vesicle trafficking, neurovascular stress signaling, cytoskeletal remodeling, and immune regulatory pathways - potentially reflecting FUS-induced alterations in tumor microenvironmental stress, BBB dynamics, and neuro-immune cross-talk.

Conclusions: FUS-BBBO drives robust, compartment-specific reprogramming of EV proteomes in GBM, revealing biomarker candidates absent under sham conditions. These findings position EV profiling as a sensitive approach for capturing FUS-induced tissue remodeling and may expand the biomarker repertoire available for spatially selective GBM liquid biopsy. Ongoing studies are assessing temporal dynamics and correspondence with parental tissue proteomes.

#3342 Mito-EV-driven mitochondrial transfer: A trigger for ferroptosis in glioblastoma.

Junbo Liao, Shuhan Cao, Ka Kit Gilberto Leung, Karrie. M Kiang

Department of Surgery, The University of Hong Kong, Pokfulam, Hong Kong

Background: Glioblastoma (GBM) is the most aggressive primary brain tumor, with limited therapeutic options due to metabolic adaptability and resistance to cell death. Ferroptosis, an iron-dependent pathway involving lipid peroxidation, offers a promising GBM target. Extracellular vesicle (EV)-based mitochondrial transfer enables intercellular shuttling of damaged mitochondria, modulating recipient cell metabolism in cancer microenvironments. During adipocyte thermogenesis, damaged mitochondria are released as Mito-EVs under stress conditions like obesity. This study explores how Mito-EV-mediated transfer from stressed adipocytes activates ferroptosis in GBM cells.
Methods: Mito-EVs containing stressed mitochondria were isolated from adipocytes via centrifugation and characterized by microscopy and protein analysis. GBM cells were exposed to Mito-EVs for mitochondrial transfer, compared to free mitochondria, and confirmed by imaging. Ferroptosis was induced with activators and evaluated through cell death and stress markers. In vivo, circulating Mito-EVs from an obese mouse model were injected into GBM tumor models, alone or with ferroptosis agents, with tumor response assessed by imaging and tissue analysis.
Results: Mito-EV transfer enhanced mitochondrial uptake in GBM cells over free mitochondria, integrating into networks and inducing oxidative stress. This increased ferroptosis sensitivity, with reduced activator requirements and altered cell death regulators. In vivo, Mito-EV treatment promoted ferroptosis and, when combined with activators, reduced tumor growth with ferroptosis evidence and low toxicity.
Conclusions: Mito-EV-mediated mitochondrial transfer from stressed adipocytes boosts ferroptosis in GBM via oxidative stress, proposing a new strategy using circulating Mito-EVs for anticancer effects in obesity-linked contexts.

#3343 ATP6V1C1 in cancer-associated fibroblast-derived extracellular vesicles affects the metastasis and therapeutic sensitivity of lung adenocarcinoma.

Xuanming Chen, Jue Li, **Kai Xiao**

Laboratory of Precision Therapeutics, Department of Pulmonary and Critical Care Medicine, West China hospital, Sichuan University, Chengdu, China

Cancer-associated fibroblast (CAF)-derived extracellular vesicles (EVs) are known to promote lung adenocarcinoma (LUAD) progression, yet the specific protein cargos responsible for this effect remain poorly defined. In this study, we generated a library of patient-derived fibroblasts (PDFs) from paired LUAD tumor and adjacent noncancerous tissues. Through integrated transcriptomic analysis and surface marker identification, we characterized CAFs and normal fibroblasts (NFs), subsequently isolating a distinct CAF subset with high pro-migratory activity using transwell assays. Quantitative proteomic profiling of EVs from 30 matched CAF-NF pairs revealed a high-quality dataset of 2,492 proteins and identified ATP6V1C1, a subunit of the V-ATPase complex, as a highly enriched protein in pro-migratory CAF-EVs. We further demonstrated that CAF-EV-mediated transfer of ATP6V1C1 drove LUAD cell migration and metastasis, a finding robustly validated in cell lines, patient-derived cells (PDCs), and an orthotopic patient-derived xenograft (PDX) model. At the molecular level, EV-delivered ATP6V1C1 suppressed insulin-like growth factor binding protein 3 (IGFBP3) by downregulating the transcription factor ID1. This suppression of IGFBP3 not only triggered epithelial-mesenchymal transition (EMT) but also amplified the IGF1/IGF1R/Akt/ERK oncogenic pathway driven by CAF-secreted IGF1. This dual action creates a self-reinforcing feed-forward loop that exacerbates metastasis. A high-throughput screen using PDCs and patient-derived organoids (PDOs) identified dronedarone as a promising drug repurposing candidate; its therapeutic efficacy was inversely correlated with ATP6V1C1 expression. Targeting ATP6V1C1 disrupted cholesterol homeostasis and synergized with dronedarone to overcome resistance to EGFR tyrosine kinase inhibitors (EGFR-TKIs) in preclinical models. In conclusion, our findings unveil ATP6V1C1 as a dual regulator of LUAD metastasis and propose a novel stroma-targeted combination therapy to suppress tumor progression and combat drug resistance.

#3344 Pyk2 controls rab proteins by vesicle trafficking in glioblastoma cells.

Neisha Marie Ramirez Serrano, Lilia Kucheryavykh

Biochemistry, Universidad Central del Caribe, Bayamon, PR

Glioblastoma (GBM) is the most aggressive primary brain tumor, with a median survival of less than one year. GBM progression depends on constant communication between tumor cells and their microenvironment, primarily mediated through extracellular vesicles (EVs). These vesicles often contain chemokines such as CCL2, CCL12, and CCL5, which attract immune cells. Once recruited, these immune cells can be reprogrammed by tumor-derived signals to support tumor growth. Pyk2 regulates the trafficking and release of EVs by interacting with Rab GTPases, regulators of intracellular vesicle transport. Through activation of RhoA and reorganization of actin, Pyk2 facilitates vesicle movement toward the plasma membrane and their subsequent secretion. We hypothesized that Pyk2 regulates EV trafficking and secretion in GBM cells by coordinating Rab GTPase activity and actin cytoskeletal remodelling.Primary human GBM cell lines with and without CRISPR/Cas9-mediated Pyk2 knockout (Pyk2KO) were analysed. EVs were isolated and characterized by flow cytometry, MEK/ERK signaling was inhibited using Avutometinib(1μM). Confocal immunofluorescent revealed that Pyk2 promotes Rab27a association with $CD63^{+}$ vesicles, consistent with its role in regulating multivesicular body docking and exosome release. Pyk2 regulates actin dependent trafficking of Rab27a thereby controlling vesicle transport and secretion. Quantitative analysis showed that Pyk2KO shifted the EV population toward larger vesicles. Pyk2KO reduced EV cargo levels of CCL2, CCL5, TNF, and VEGF, mediators of TAM activation and angiogenesis. These data indicate that Pyk2 regulates Rab27a-dependent endosomal vesicle docking and release, whereas MEK/ERK signaling enhances plasma membrane-derived EV shedding. Together, these pathways shape the size and immune regulatory cargo of EVs.

Pyk2 controls Rab proteins by vesicle trafficking in glioblastoma cells

#3345 Horizontal transfer of functional extrachromosomal DNA via extracellular vesicles in FGFR2-amplified cancer.

Irene Salamon[1], Giulia Gallerani[2], Jens Luebeck[3], Gianluca Storci[1], Simone Spandau[3], Beatrice Fontana[2], Alessia Soru[2], Mattia Riefolo[1], Marco Pagano Mariano[4], Ilaria Pace[2], Andrea Cavazzoni[4], Vineet Bafna[3], Massimiliano Bonafe'[2], **Manuela Ferracin**[2]

[1]IRCCS Azienda Ospedaliero-Universitaria di Bologna, Bologna, Italy,[2]Alma Mater Studiorum Universita di Bologna, Bologna, Italy,[3]UC San Diego, Tacoma, WA,[4]Department of Medicine and Surgery, University of Parma, Parma, Italy

Cancer cells actively release extracellular vesicles (EVs) into the tumor microenvironment, where they interact with both malignant and non-malignant cells, activating signaling pathways and reshaping the microenvironment. In this study, we investigated EVs secreted by *FGFR2*-amplified cancers of unknown primary (CUPs), which generate extrachromosomal circular DNA (ecDNA) as a mechanism of oncogene amplification. We found that *FGFR2*-containing ecDNA is packaged into both small and large EVs, horizontally transferred to recipient cells, and remains functionally active. Upon exposure to CUP-derived EVs—either by direct administration or co-culture—cancer (NCI-N87, THP1) and non-cancer (HUVEC, fibroblasts) cells internalized *FGFR2* ecDNA, which was subsequently transcribed and translated to some extent. Functionally, CUP-derived EVs polarized THP1 cells toward an M2-like phenotype and promoted HUVEC proliferation. *In vivo*, xenografts generated from CUP cell lines released circulating FGFR2$^+$ EVs, which mediated the systemic transfer of *FGFR2* ecDNA to distant organs. Collectively, these findings demonstrate that tumor-derived EVs can propagate and horizontally transfer oncogenic ecDNA both *in vitro* and *in vivo*, providing a possible mechanistic basis for the high metastatic potential of this tumor type.

#3346 Modeling breast cancer extracellular vesicle-mediated degradation of the lymphatic glycocalyx using a 3D organ-on-chip platform.

Justin Lau[1], Issahy Cano[2], Esak Lee[1]

[1]Biomedical Engineering, Cornell University, Ithaca, NY,[2]Cornell University, Ithaca, NY

Triple-negative breast cancer (TNBC) relies primarily on lymphatic vessels for early metastatic spread, and tumor-secreted factors—including extracellular vesicles (EVs)—can condition the lymphatic microenvironment to facilitate dissemination. The lymphatic endothelial glycocalyx (eGCX) is a sugar-rich barrier that regulates permeability and cell adhesion, yet its susceptibility to tumor-driven remodeling remains poorly understood.

Using a transwell coculture model of LECs and TNBCs, we found that TNBC-conditioned environments markedly disrupt the lymphatic eGCX. MDA-MB-231 conditioned media reduced wheat germ agglutinin (WGA, total glycocalyx) staining by 45.41 ± 9.37 percent, heparan sulfate (HS), one of the most abundant glycocalyx components, by 38.87 ± 8.84 percent, and overall eGCX thickness by 49.37 ± 3.93 percent. SUM-149 conditioned media similarly reduced glycocalyx thickness by 36.80 ± 5.11 percent. TNBC exposure also induced morphological changes in lymphatic endothelial cells (LECs) consistent with impaired barrier function and active glycocalyx remodeling.

To identify specific drivers of this disruption, EVs from TNBC and non-tumorigenic control cells were isolated using a membrane-affinity method and characterized by nanoparticle tracking analysis. LECs exposed to TNBC EVs exhibited reduced WGA and HS staining, and altered VE-cadherin junctions. Protease profiling revealed enrichment of ADAM9, Cathepsin X/Z/P, and MMP-8 in TNBC EVs, suggesting that EV-associated proteases mediate eGCX degradation.

To establish a physiologically relevant baseline, human LECs were cultured in collagen-filled PDMS microfluidic chips under luminal shear (~4 dynes/cm^2). This 3D system produced a significantly thicker eGCX than 2D monolayers (WGA staining intensity in 3D relative to 2D: 1.311 ± 0.096; $p \leq 0.01$), validating its use for assessing tumor- and EV-induced glycocalyx remodeling. This 3D lymphatic organ-on-chip model provides a physiologically relevant platform to study eGCX dynamics and EV-mediated vascular remodeling.

Together, these findings demonstrate that TNBC-derived EVs carry proteolytic cargo capable of degrading the lymphatic eGCX, linking tumor secretome signaling to early lymphatic metastasis. We are now using this organ-on-chip system to investigate the effects of individual EV-associated proteases on glycocalyx remodeling, as well as the potential of targeted therapeutics to preserve eGCX integrity under TNBC conditioning, with the goal of preventing the creation of a metastatic-permissive lymphatic microenvironment.

#3347 Proteomic and functional divergence of small and large extracellular vesicles reveal subtype-specific drivers of ovarian cancer progression.

Kalpana Deepa Priya Dorayappan[1], Fries Brian[2], Wei Fu[3], Ganesh Yadaigiri[1], Lakshmi Narasimhan Chakrapani[1], Sydney Wiggins[4], Shyam Sundaram[5], Thangavel Muthusamy[6], Sudhiksha Anbu Chelian[7], Gabriela S. Vendrell[2], Qi-En Wang[8], David E. Cohn[1], Lianbo Yu[9], David O'Malley[1], Colin Hisey[4], Selvendiran Karuppaiyah[1]

[1]OB/GYN, The Ohio State University, Columbus, OH,[2]The Ohio State University, Columbus, OH,[3]Biomedical Engineering, The Ohio State University, Columbus, OH,[4]Biomedical Engineering, Northwestern University, Evanston, IL,[5]University of Southern California, Los Angeles, CA,[6]Sree Balaji Medical College and Hospital, Chennai, India,[7]Health & Rehabilitation Sciences, The Ohio State University, Columbus, OH,[8]Radiation Oncology, The Ohio State University, Columbus, OH,[9]Medical Bioinformatics, The Ohio State University, Columbus, OH

Objective: High-grade serous ovarian cancer (HGSOC) progression and therapeutic resistance are increasingly attributed to extracellular vesicle (EV) mediated communication. While small EVs (SEVs) are widely studied, the proteome and biological contributions of large EVs (LEVs) remain poorly defined. This study aimed to (i) establish long-term bioreactor-based production of extracellular vesicles (SEVs and LEVs) from ovarian cancer cell lines, (ii) define subtype-specific proteomic cargo, and (iii) compare the functional roles of SEVs and LEVs in tumor growth, metastasis, and immune modulation.
Methods: OVCAR4, CaOV3, and SKOV3 ovarian cancer cell lines were expanded in T-175 flasks and gradually transitioned to serum-free CDM-HD media in Bioreactors. Cell lines were maintained for eight weeks in bioreactors to measure EV secretion. SEVs and LEVs were isolated by ultracentrifugation followed by size-exclusion chromatography (SEC). Particle number and size were quantified by nanoparticle tracking analysis (NTA), and protein concentration was measured by Nano Drop. EV identity and purity were confirmed by Western blotting (CD9, CD63, CD81, LAMP1), Imaging Flow Cytometry (ISF), and transmission electron microscopy (TEM). Proteomic profiling of SEVs and LEVs was performed for each cell line, with downstream pathway analysis using Ingenuity Pathway Analysis. Functional assays included: (i) EdU proliferation assays, (ii) migration and invasion assays, (iii) splenocyte co-culture to evaluate immune modulation, and (iv) mouse xenograft models to assess EV-dependent tumor growth and metastatic dissemination.
Results: Bioreactors supported stable EV production in OVCAR4 and CaOV3 cells, while SKOV3 adapted poorly. NTA and ISF confirmed consistent EV output across eight weeks. SEVs were enriched for CD9, CD63, and CD81, whereas LEVs showed strong LAMP1 expression. Proteomics revealed distinct cargo profiles: SEVs contained proteins linked to cytoskeletal remodeling, migration, and metastatic signaling, while LEVs carried proteins involved in proliferation, metabolism, and stress responses. Functionally, SEVs enhanced migration, invasion, metastatic burden, and immune suppression, whereas LEVs promoted cell proliferation and larger primary tumors in-vivo.
Conclusion: SEVs and LEVs derived from ovarian cancer cells exhibit distinct proteomic signature and exert divergent effects on tumor progression. SEVs predominantly drive metastatic potential, whereas LEVs enhance proliferative tumor growth. EV subtype specific characterization provides new opportunities for biomarker discovery and targeted therapeutic strategies in HGSOC.

#3348 Liposarcoma-derived extracellular vesicles suppress STING signaling and impair innate immune activation in macrophages.

Qi Zhang, Patricia Sarchet, Fernanda C. C. de Faria, Priya Dhawale, Sydney Rentsch, Roma Karna, Valerie Grignol, Jing Wang, Raphael Pollock, Federica Calore

The Ohio State University Comprehensive Cancer Center, Columbus, OH

Purpose: Macrophages are the most abundant immune population in the liposarcoma tumor microenvironment (TME). We previously showed that extracellular vesicles (EVs) released by de-differentiated liposarcoma (DDLPS) promote tumor progression by inducing IL6 secretion from macrophages. Here, we investigated whether DDLPS-derived EVs also disrupt macrophages innate immune signaling.
Methods: U937 cells were differentiated into macrophages with PMA. CD14+ monocytes isolated from PBMCs were differentiated into monocyte-derived macrophages (MDMs) using M-CSF, and macrophage identity was confirmed by flow cytometry. EVs were isolated from Lipo141 and Lipo246 conditioned medium via ultracentrifugation, and from patient serum using ExoQuick. Differentiated macrophages were treated with EVs for 24h, followed by cGAMP stimulation. Gene expression of ifnb1 and innate immunity-related chemokines were assessed by qRT-PCR, while IFNβ secretion was determined by ELISA assay. STING pathway activation was investigated by western blot analysis.
Results: DDLPS-derived EVs markedly suppressed macrophage responses to cGAMP. In U937-derived macrophages, EVs exposure significantly reduced ifnb1 induction ($p=0.044$) and IFNβ secretion in response to cGAMP. EVs isolated from the serum of healthy donors or DDLPS patients ($n=12$) confirmed these findings, with patient-derived EVs leading to a stronger inhibition of ifnb1 ($p=0.0012$) and reduced IFNβ protein levels compared to healthy donor group. Western blot analysis showed decreased phosphorylation of IRF3 and STING, with total protein levels unchanged, indicating selective impairment of STING pathway activation. Consistent with these data, MDMs exhibited similar functional suppression: EV-treated cells displayed reduced induction of ccl5, cxcl9, cxcl10, ifnb1 and ISG15 in response to cGAMP stimulation.
Conclusion: DDLPS-derived EVs impair macrophage responsiveness to cGAMP by suppressing STING pathway activation. These findings reveal an EV-mediated mechanism of immune evasion in liposarcoma and highlight the STING axis as a potential therapeutic target to restore antitumor immune function.

#3350 Isolation and characterization of prostate-specific extracellular vesicles from prostate cancer patients.

Shashi Anand[1], Emily Ridden[2], Ty W. Turner[2], Kunwar Somesh Vikramdeo[1], Ramya Krishna Velagapudi[3], Denise C. Cornelius[2], Ajay Pratap Singh[1], Xinchun Zhou[3]

[1]Department of Cell and Molecular Biology, Cancer Center and Research Institute, University of Mississippi Medical Center, Jackson, MS,[2]Department of Pharmacology and Toxicology, University of Mississippi Medical Center, Jackson, MS,[3]Department of Pathology, Cancer Center and Research Institute, University of Mississippi Medical Center, Jackson, MS

Background: Plasma-derived extracellular vesicles (EV) represent a complex mixture of vesicles originating from diverse tissues. The selective isolation of prostate-specific extracellular vesicles (PSEV) can offer improved specificity for diagnostic and prognostic biomarker development as well as monitoring therapeutic response of prostate cancer (PCa). This study aimed to compare the yield and quality of PSEV enriched from total EV preparations with those isolated directly from plasma.
Materials and methods: Twelve (12) plasma samples (6 from patients with PCa, and 6 from non-cancer subjects) were used in this study. The total EV were isolated with SmartSEC^{TM} columns following the manufacturer's instructions. The PSEV were enriched with anti-PSMA-conjugated magnetic beads from isolated total EV and also directly from plasma samples. Nanoparticle tracking analysis (NTA) was performed to examine the concentration (particles/mL), average diameter (nm), and volume (nm^3) for total EV and PSEV. The ultrastructure of isolated PSEV was imaged under a JOEL JEM1400 transmission electron microscope. The mean values were subjected to an unpaired t-test analysis, and a p-value of less than 0.05 was considered statistically significant.
Results: NTA analysis showed that 1) Total extracellular vesicles isolated with the column resulted in a significant yield from each plasma sample (1.4E+11 to 7.52E+11 particles/ml, 149.8 to 182 nm in diameter, and 752 to 1,360 nm^3 in volume); 2) PSEV concentration was higher in plasma from African American (AA) population ($178.9x10^9$/ml) than in plasma from Caucasian American (CA) population ($166.6x10^9$/ml); 3) the PSEV concentration was higher in method using anti-PSMA-conjugated magnetic beads from plasma directly ($13.4x10^9$/ml) as compared to that enriched from total extracellular vesicles obtained via column ($10.98x10^9$/ml); 4) the average PSEV diameter was greater in method using anti-PSMA-conjugated magnetic beads directly from plasma (198.7nm) as compared to that from total extracellular vesicles obtained via column (149.3nm, p=0.002); and 5) PSEV was about 3.1% of total EV in non-cancer subjects, and 4.7% of total extracellular vesicles in PCa. The TEM analysis demonstrated the existence of electron-dense oval or round particles in diameters ranging from 30-258 nm. However, PSEV showed some spikes on the particle surface.
Conclusion: PSEV enrichment using anti-PSMA-conjugated magnetic beads is a feasible approach that could enhance the specificity of potential EV-associated biomarkers, aiding in improved diagnosis, prognosis, risk prediction, and monitoring therapeutic responses in prostate cancer.

#3351 Exploring the effects of extracellular vesicles secreted by cofilin-1 overexpressing cells on the migration and invasion ability of human lung cancer cells.

Huang Bo-Han, Yi-Jang Lee

Biomedical Imaging and Radiological Sciences, National Yang Ming Chiao Tung University, Taipei, Taiwan

Object: Type I actin-severing protein cofilin-1 (CFL-1) is a widely expressed regulator of the microfilament cytoskeleton in non-muscle cells. It plays a crucial role in actin cytoskeleton construction and influences cell motility. Overexpression of CFL-1 has been observed in various cancers and is related to tumor migration, invasion, and metastasis. In addition, studies have shown that the cytoskeleton plays a key role in exocytosis, implicating that CFL-1 may be a potential regulator of this process. Cancer cells secrete abundant extracellular vesicles (EVs) to mediate intercellular communication, and exosomes are one of the subtypes. Tumor-derived exosomes can promote tumor invasion and metastasis. Recent studies showed that CFL-1 is highly expressed in exosomes from advanced cancer, but its potential mechanisms in tumor-related exosomes remain unclear. Therefore, this study aims to explore the effects of CFL-1 on exosome secretion and whether CFL-1 influences lung cancer cells via exosome-mediated mechanisms.
Methods: This study used H1299/tet-on-cofilin-1 (HCOXP) cells, a tetracycline-inducible cell line, which can induce cofilin-1 overexpression. First, conditioned medium was collected from HCOXP cells overexpressing cofilin-1, and exosomes were isolated by ultracentrifugation. Second, the purity of the isolated exosomes was verified by nanoparticle tracking analysis, transmission electron microscopy, and western blotting. To evaluate the impact on cell migration and invasion, exosomes derived from HCOXP cells were added to H1299, CL1-0, and BEAS2-B cells. Furthermore, the expression levels of matrix metalloproteinases (MMPs) in exosomes from HCOXP cells with and without cofilin-1 overexpression were compared.
Results: The results showed that overexpression of CFL-1 stimulated cells to secrete more exosomes. It is also found that these exosomes may contain more contents. When these exosomes were applied to lung cancer and normal cells, exosomes derived from CFL-1 overexpressing HCOXP cells significantly accelerated the migration and invasion of H1299 cells. However, no increase in migration and invasion ability was observed in CL1-0 or BEAS-2B cells following treatment with these exosomes. In addition, elevated levels of matrix metalloproteinases (MMPs) were detected in exosomes from CFL-1-overexpressing HCOXP cells.
Conclusion: Overexpression of CFL-1 in HCOXP cells was found to promote exosome secretion. These exosomes appear to exhibit homing specificity, potentially influencing their effects on target cells. Overall, this study found the critical role of CFL-1 in regulating the release and the potential impact of exosomes in the tumor microenvironment.

#3353 Pyroptosis-derived extracellular vesicles as key immunoactivators in near-infrared photoimmunotherapy.

Fan Chen[1], Yuxuan Li[1], Ye Lu[1], Peng Guo[1], Weifeng Qian[2], Wei-Hong Tan[1]

[1]Hangzhou Institute of Medicine, Chinese Academy of Sciences, Hangzhou, China,[2]The Affiliated Suzhou Hospital of Nanjing Medical University, Gusu School, Nanjing Medical University, Suzhou, China

Background: Pyroptosis, a lytic and highly inflammatory form of programmed cell death, has emerged as a powerful mechanism for augmenting anti-tumor immunity. Although antibody drug conjugate (ADC)-mediated near-infrared photoimmunotherapy (NIR-PIT) can induce tumor-specific pyroptosis and enhance immune responses, the downstream mediators that bridge pyroptotic cell death to immune activation remain undefined. Here, we investigated whether pyroptosis-derived extracellular vesicles (Pyro-EVs) constitute a key immunostimulatory output of tumor pyroptosis and sought to define their molecular composition and immune-activating functions.
Methods: Pyroptosis was induced in SCC7 murine carcinoma cells using Cetuximab-IR700, a clinically-approved NIR-PIT ADC. EVs released during pyroptosis were isolated by ultracentrifugation and characterized by NTA and nano-flow cytometry. Deep proteomic profiling with organelle-origin mapping, GO enrichment, and nuclear-cytoplasmic signature scoring was performed to define Pyro-EV identity. DNA cargo was examined by nano-flow cytometry, DNase-protection assays, and confocal microscopy. Immunological activity was evaluated by exposing macrophages to Pyro-EVs, followed by RNA-seq, ELISA, and Western blot assessment of nucleic-acid sensing pathways.
Results: NIR-triggered pyroptosis induced rapid release of a distinct EV population, generating Pyro-EVs at 2-3x the abundance of basal EVs. Proteomics identified a pyroptosis-specific signature with 726 emergent proteins enriched for ribosomal subunits, chromatin components, and DNA-binding regulators, absent in apoptotic or necrotic EVs. These molecular hallmarks indicate nuclear rupture and cytoplasmic mixing, establishing Pyro-EVs as a unique class of lytic cell-death-derived vesicles. Pyro-EVs carried elevated levels of double-stranded nuclear DNA, confirmed by DNase resistance and colocalization with chromatin-binding proteins. Functionally, Pyro-EVs were strong activators of innate immunity, inducing broad M1-polarizing programs in macrophages. RNA-seq showed induction of TLR7/9, MyD88, IRAK1/4, and NF-κB-related genes; Western blot validated activation of the TLR7/9-MyD88-IRAK-p65 axis, and ELISA demonstrated increased secretion of TNF-α, IL-6, and other cytokines, confirming DNA-sensing-dependent innate immune activation.
Conclusions: This study identifies Pyro-EVs as a previously unrecognized, immunogenic vesicle class that emerges during NIR-PIT. Pyro-EVs are rich in nuclear DNA and chromatin-associated factors and serve as high-potency activators of macrophage TLR7/9 signaling, establishing them as a central mediator connecting pyroptotic tumor death to innate immune amplification. These findings redefine the immunobiology of pyroptosis and uncover Pyro-EVs as a mechanistic driver of pyroptosis-induced anti-tumor immunity.

#3354 Chemoradiation treatment increases extracellular vesicle release causing treatment resistance in rectal cancer cell lines.

Vivek Somasundaram, Jeremie M. P. Lever, Regina Irwin, Teresa C. Beamon, Karin M. Hardiman

Surgery, University of Alabama at Birmingham, Birmingham, AL

Introduction: Colorectal cancer (CRC) is the 3rd most prevalent form of cancer in the U.S., with younger Americans comprising an increasing fraction of case numbers. Current treatment includes chemoradiation treatment (CRT) followed by surgical resection in incomplete responders. Only about 25% of patients have a complete response to CRT due to the presence of treatment resistance in most patients. ST6GAL1 is a sialyltransferase, that has been shown to be upregulated in various cancer types, including CRC. Our group has previously shown that it confers treatment resistance to CRT *in vitro* and *in vivo*. We have also shown that ST6GAL1 is packaged into extracellular vesicles (ECVs) by human CRC cel lines, and that these ECVs can transfer treatment resistance between cells. We hypothesized that CRT would increase ECV release, thereby, spreading treatment resistance and that these ECVs could be measured in the plasma of a patient derived xenograft model of rectal cancer.

Methods: We cultured SW620 CRC cells, treated with or without 5-Flourouracil and 5 Gy of radiation (CRT), and isolated ECVs from the cells' conditioned medium using differential centrifugation. ECV size and concentration were determined using a Nanosight with NTA software. Our previously validated SW620 ST6GAL1 Control vector (CV) and knockdown (KD) cell line was used to assess transfer of resistance to apoptosis after CRT. We added ECVs isolated from untreated or CRT treated SW620 cells to ST6GAL1 KD cells, treated with 5 Gy of CRT, and performed immunofluorescence for cleaved caspase-3 (CC3). We also co-cultured KD cells with CV cells (+/- CRT) and assessed CC33 staining after CRT. We assessed tumor and plasma ECV levels of ST6GAL1 before, during, and after CRT in a PDX model of rectal cancer.

Results: SW620 cells undergoing CRT had a greater than twofold higher release of ECVs/cell compared to untreated cells (*2.57* ± 0.84 *p=0.033, n=4)*. No significant differences were detected in mean ECV size between CRT(+) and CRT(-) emitting cells. ST6GAL KD cells directly treated with SW620 ECVs cells from either CRT treated or untreated donor cells showed a significantly reduced CC3 production after CRT compared to untreated KD cells. Co-culture of KD cells with radiated CV cells reduced CC3 levels after CRT (1.59± 0.32, n=2). ST6GAL1 could be measured in ECVs isolated from the plasma of the PDX model and the number of ECVs and amount of ST6GAL1 both increased during CRT.

Conclusion: We have shown that exogenously added ECVs containing ST6GAL1 confer treatment resistance *in vitro.* Our co-culture data additionally validates this finding by showing that ST6GAL1 containing cells can transfer ECVs to neighboring cells and confer treatment resistance. Our data reveals that ECV release is increased in response to CRT *in vitro* and *in vivo*. If seen in patients, this increase could be spreading resistance, potentially worsening treatment outcomes.

#3355 Exosomal genetic cargo shift dictated by RD3 deficiency steers progressive neuroblastoma evolution.

Afsana Parveen Jahir Hussain[1], Sreenidhi Mohanvelu[1], Loganayaki Periyasamy[1], Poorvi Subramanian[1], Sheeja Aravindan[2], Natarajan Aravindan[1]

[1]Oklahoma State University, Stillwater, OK,[2]OU Health Stephenson Cancer Center, Oklahoma City, OK

Exosomes are central mediators of systemic cellular communication, directing tumor evolution through the dynamic exchange of genetic and molecular cargo. Neuroblastoma (NB), a lethal pediatric tumor of embryonal origin, where selection and enrichment of treatment-resistant cancer stem cell clones have decisive impact. Recently, we identified acquired RD3 deficiency prompts tumor cell plasticity and regulates tumor progression. Herein, we investigated whether RD3 controls delivery of exosomal genetic cargo. For this we utilized our custom archived Neural crest cell specific Cre conditional LoxP-directed RD3-Knockout (KO, *Tg* mice) driven human syntenic spontaneous NB. Serum exosomes were isolated, from RD3-KO mice and compared with their wild-type counterparts. Exosomal RNA was isolated using the Total Exosome RNA and Protein Isolation kit, characterized by nanoparticle tracking analysis, flow cytometry, transmission electron microscopy, and was then analyzed by paired-end Illumina RNA sequencing. Differential gene expression (DEG) was computed using $\log_2$ fold change with $\log_2$ FDR. DEG analysis identified an animal-independent signature of 53 upregulated and another 1,396 downregulated genes. Functional annotation in Ingenuity Pathway Analysis revealed enrichment in therapy-resistance pathways, including angiogenesis signaling by VEGF (*VEGFA, KDR, FLT1*), NAD^+ salvage pathway II mediated DNA damage response (*NMRK1, NT5C2, NT5C1A*), cell cycle control (*CDK6, CDC7, SIN3A*), pro-survival CXCR4 signaling (*HSP90AA1, RAB11FIP3*), extracellular matrix remodeling (*COL1A1, ADAM12, HSPG2, CD31*), and immune/inflammatory signaling (CD27, IL-1) pathways. Furthermore, oncogenic cell signaling pathways, including RhoGDI signaling (*CDC42, PAK1, ARHGEF2),* regulating migration, invasion, and WNT/β-catenin signaling (*SOX17, MAP3K7, WNT9A*), regulating stemness maintenance, were decisively reprogrammed. These results, for the first time, distinctly demonstrate that RD3 deficiency drives molecular rearrangements that promote therapy resistance, underscoring its central function in exosome-mediated cancer cell signaling that survives intensive multimodal clinical therapy. Crucially, our findings position RD3-regulated exosomal genetic cargo as a promising biomarker and therapeutic target for better clinical management of progressive NB. **FUNDING:** DOD-CA-210339; OCAST-HR19-04; NIH-P20GM103639

#3356 Tumor-derived exosomes promote renal cancer progression via reprogramming of tumor-associated macrophages.

Jinlu Dai[1], Suguru Kadomoto[1], Tyler Robinson[1], Evan T. Keller[2]

[1]University of Michigan, Ann Arbor, MI,[2]Professor, University of Michigan, Ann Arbor, MI

Renal cell carcinoma (RCC), the most common type of kidney cancer, relies heavily on the complex ecosystem of the Tumor Microenvironment (TME) for its progression. A critical cellular component within the TME is the Tumor-Associated Macrophage (TAM), which often adopts a pro-tumor, M2-like phenotype that supports angiogenesis, invasion, and immune suppression. This study investigates the role of tumor-derived exosomes (TDEs) in mediating this critical reprogramming event. In vitro experiments utilized human (786-O renal cancer cell line and THP-1 monocytes) and mouse (Renca RCC and RAW 264.7 monocytes/macrophage) cell lines. The macrophages were treated with RCC-derived exosomes, and the conditioned medium (CM) was used to treat parental RCC cells. Functional assays demonstrated that exosome-educated macrophage CM significantly increased the proliferation, migration, and invasion of both human and mouse RCC cells. Furthermore, Western blot and ELISA analysis confirmed that TDE treatment successfully reprogrammed macrophages, leading to altered cytokine profiles indicative of polarization toward a pro-tumor phenotype. In vivo, the impact of the TDE-educated macrophage CM was assessed in SCID and BALB/c mouse models using intracardial and intrarenal RCC injections. Bioluminescence imaging (BLI) confirmed that CM from exosome-treated macrophages significantly enhanced tumor progression and distant metastasis compared to controls. In conclusion, this research identifies tumor-derived exosomes as critical signaling vectors that effectively reprogram TAMs into pro-tumorigenic cells. This exosome-mediated communication promotes a highly permissive TME, leading to accelerated renal cancer progression and metastasis. These findings highlight the TDE-TAM axis as a potent therapeutic target for mitigating RCC malignancy.

#3358 The consequences of progenitor neutrophil evacuation into the periphery during breast cancer.

Mariah Branson[1], Carolyn Schroeder[2], Melissa Meyer[1]

[1]Microbiology, Immunology, and Pathology, Des Moines University Medicine and Health Sciences, West Des Moines, IA,[2]Office of Research, Des Moines University Medicine and Health Sciences, West Des Moines, IA

Recent results suggest neutrophil progenitors and immature neutrophils are appearing in the periphery in response to cancer and pathogens. The tumor microenvironment (TME) may take advantage of neutrophil progenitor susceptibility by signaling for the neutrophil to support tumor growth. This project tests the hypothesis that neutrophil progenitors experiencing the periphery during cancer will take on unique phenotypic and functional states depending on which tissue they are transferred into, and to which tissues they transit to post-transfer. In mice bearing PyMT B6 orthotopic tumors, congenically marked $CD45.2^+$ neutrophil progenitors were transferred into $CD45.1^+$ recipient mice. Two neutrophil progenitor populations were transferred: total bone marrow neutrophils ($Ly6G^+$), and pre-neus ($CD117^+Ly6G^+$). Cells were transferred into the blood of tumor and non-tumor bearing mice, and into the tumor of tumor bearing mice. After 1 day, tissues were isolated to quantitate adoptively transferred cells in the following tissues: bone marrow, blood, spleen, tumor and lymph nodes. Adoptively transferred cells were also measured for changes in phenotype using spectral flow cytometry and changes in function, including their ability to produce Reactive Oxygen Species (ROS), an anti-microbial function of neutrophils. Preliminary results show that the site of adoptive transfer affects the accumulation of adoptively transferred cells in tissues. Together, these data will help us further understand how tissue environments directly shape neutrophil phenotype and function. If we identify tissue environments influencing neutrophil functionality and expression, especially if promoting pro-tumoral functions, we can further identify pathways and signals to block therapeutically. This method may depress tumor progression, increasing patient survival rates.

#3359 Distinct profile of peritoneal lavage fluid extracellular vesicles in gastrointestinal carcinomatosis.

Fatemeh Tajik, Vinodh Kumar Radhakrishnan, Alex N. Dang, Aaqil M. Khan, Melanie Roman, Shaun Daly, Areg Grigorian, Cristobal Barrios, Sigrid Burruss, Maheswari Senthil

Department of Surgery, University of California, Irvine Medical Center, Orange, CA

Introduction: Gastrointestinal peritoneal carcinomatosis (GI PC) poses significant diagnostic and therapeutic challenges. The commonly used diagnostic tools such as circulating tumor DNA have poor sensitivity in PC. Recent evidence suggests that peritoneal cavity small extracellular vesicles (EV) play a critical role in peritoneal metastasis development and progression. We sought to compare the peritoneal lavage fluid (PL) EV profile (quantity and gene expression) to non-cancer PL to identify the potential of PL EV testing as a liquid biopsy in PC.

Methods: PL samples were collected from GI PC patients and non-cancer patients. The inclusion criteria for the non-cancer cohort were BMI 18-30, no cancer/autoimmune history, and had a non-inflammatory indication for surgery (ex. hernia repair). EVs were isolated by precipitation and characterized via nanoparticle tracking analysis (NTA), cryo-electron microscopy (cryo-EM), and western blot. Size distribution (0.5-199.5nm, 200.5-500.5nm) and concentration were quantified by NTA. EV RNA was profiled using NanoString PanCancer Panel (770 genes). Differential expression used $\log_2$ fold change ≥1.5 or ≤-1.5 and p≤0.05.

Results: A total of 66 PL samples were collected (35 cancer and 31 non-cancer). Of the 31 non-cancer PL, only 19 samples had EV pellets, indicating that in the rest of the samples there were too few EVs to result in an EV pellet. However, all cancer PL had an EV pellet. NTA of the samples that had adequate EV showed that the total quantity of EV (as $\times 10^5$ particles/mL) was approximately two-fold higher in cancer samples compared to the non-cancer cohort (10.9×10^5 vs. 4.5×10^5; p=0.0005). The difference between the cancer and non-cancer PL EV quantity was retained even after systemic therapy (9.7×10^5 vs. 4.5×10^5; p=0.0002). Cryo-EM demonstrated distinct structural differences of EV between the groups, with cancer-derived EVs exhibiting multilayered, multicompartment, and cargo-dense structures, whereas non-cancer samples predominantly contained simple monolayer vesicles. Gene expression profiling demonstrated significant overexpression of genes involved in epithelial-mesenchymal transition, metastasis, cell-cycle regulation, angiogenesis, and extracellular matrix organization (STAB1, PRF1, CCDC80, SPARCL1, VHL, RHOA) in the cancer cohort compared to the non-cancer cohort.

Conclusion: Our study represents one of the largest studies of PL comparison of GI PC to non-cancer. In GI PC the amount of EV and the biophysical and molecular signatures are distinctly different from the non-cancer group. PL EV can be developed into a liquid biopsy in GI PC to fill a critical clinical need.

#3360 Environmental impact on the secretion of tumor-derived exosomes.

Haylie Pullan

Brigham Young University, Provo, UT

Cancer continues to be one of the most prominent and devastating health issues in the world. In the year 2024, an estimated 2,001,140 new cases of cancer were be diagnosed in the United States alone. Of those over 2 million cases, 611,720 people will die from the disease (National Cancer Institute). Our goal is to utilize the basic progression and anatomy of a cancer tumor to help address this horrible disease that takes the lives of so many. Exosomal research is a new field that utilizes proteins, DNA, and RNA from secreted extracellular vesicles to determine tumor characteristics and optimize treatment strategies. While this innovative technique holds promise, the relationship between exosomes and their associated parent cells remains inadequately understood. This research intends to bridge the gap in knowledge by investigating the relationship between the environmental conditions of the parent cell and the secreted exosome characteristics. These characteristics include protein content, types, and the exosome-to-cell ratio. It has been stated in previous literature that cells under more stressful environmental conditions, such as serum starvation and hypoxia, will secrete more exosomes. However, we believe the secretion of exosomes is dependent on cell line and environment. A variety of cell lines that make up a gastrointestinal tumor, including Jurkat, THP-1, MRC5, HUVEC, and AGS cells, were grown and put under these conditions to have their associated exosomes analyzed. This approach enabled us to investigate the impact of serum starvation and hypoxia, showing that low nutrition from media led to a decrease in the number of exosomes, while increased hypoxic conditions led to an increase in secretion. This knowledge can have broad implications for cancer diagnosis and innovative treatment strategies. Our research holds the potential to unveil insights into the intricate interplay between exosomes and cancer, contributing to more effective therapeutic approaches.

#3361 Precise isolation of tumor-relevant EV sub-populations using the Kairos cLDEP particle sorter.

Boyang Su[1], Shujun Xu[2], Reese Wunsche[1], Dennis Lee[1], Hon Leong[1]

[1]Biological Sciences Platform, Sunnybrook Research Institute, Toronto, ON, Canada,[2]Molecular Genetics, University of Toronto, Toronto, ON, Canada

Extracellular vesicles (EVs) are cell-derived fragments released by all cell types and are promising platforms for cancer detection and nanomedicine. Isolating and enriching ultra-pure EV sub-populations from patient biofluids based on cell- or cancer-specific biomarkers can reveal tumor-derived molecular signatures with diagnostic and therapeutic implications. However, most existing EV isolation methods rely on size and density, lacking specificity for defined EV subtypes. Existing nano flow cytometry (nFC) platforms (e.g., Astrios EQ) for EV sub-population sorting are also unsatisfactory due to lengthy preparation, limited specificity, and unknown recovery of target sub-populations. To overcome these limitations, we utilized the Apogee Kairos particle sorter, which applies centripetal liquid dielectrophoretic (cLDEP) force to redirect fluids around optically identified EVs, enabling high-speed, high-precision EV sub-population sorting. Operational protocols were optimized using polystyrene beads of defined sizes, achieving 97% purity and 40% recovery. EVs were isolated from cell culture conditioned media (CM) and prostate cancer patient plasma based on size (200-300 nm, 300-400 nm, 600-900 nm, >900 nm), and further sorted post nucleic acid staining, immunolabeling for EV membrane biomarkers (CD9, CD63, etc.) and cancer-associated biomarkers (PSMA, EpCAM, etc.), achieving 83.5-89.4% purity of target EV sub-populations. Transmission electron microscopy confirmed preserved EV vesicular integrity post-sorting. Protein and RNA analyses revealed the presence of molecular cargo in sorted sub-populations consistent with EV identity and disease relevance. We established a robust standard operating protocol (SOP) for the Kairos cLDEP sorter, providing a powerful approach for isolating cancer-derived EV sub-populations with high precision. This platform advances the utility of EV-based liquid biopsies by enabling tumor-selective EV capture for downstream molecular profiling.

#3362 Lipid nanoprobe magnetic beads enable high-purity plasma EV isolation for broad-spectrum cancer biomarker detection.

Qiuyan Ma, Dehe Kong, Sidhant Narula, Jin-Qiu (Jessie) Chen

OriGene Technologies, Inc., Rockville, MD

Introduction: Extracellular Vesicles (EVs) carry tumor-derived biomolecules and represent a promising source for liquid biopsy-based cancer detection. Many recent studies have revealed critical biomarkers from plasma EV, establish potential diagnostic targets for pancreatic cancers, ovarian cancers and other hard-to-diagnose cancers[1]. Unlike circulating free DNA (cfDNA) or soluble proteins, EVs are actively secreted by viable tumor cells and encapsulate proteins, nucleic acids, and lipids within a protective bilayer that preserves molecular integrity. This stability and cell specificity make EVs ideal for minimally invasive disease monitoring. However, plasma EV isolation remains challenged by abundant protein contaminants that compromise downstream molecular analysis. A simple, high-purity, automation-compatible isolation method is essential to improve EV-based biomarker profiling, particularly from heterogeneous blood derived samples.

Methods: A lipid nanoprobe (LNP)-based magnetic bead system (Captis Diagnostics Inc) was optimized for rapid, high-specificity enrichment of plasma EVs [2]. EVs post enrichment were assessed by cargo DNA, RNA and core tetraspanin abundance compared with pre-enrichment samples. Depletion of albumin and lipoprotein contaminants were confirmed by immunoassays. Comparative recovery efficiency and purity metrics were benchmarked against leading commercial EV isolation reagents. To assess broad biomarker compatibility, EVs from multiple cancer cell lines were spiked into healthy plasma and isolated using LNP beads. Enriched EVs were analyzed using OriGene multiplexed immunoassay panels covering cancer-relevant protein classes, including adhesion molecules, oncogenic receptors, and immune-modulatory factors. These markers represent key tumor hallmarks such as invasion, migration, immune evasion, and therapeutic resistance—commonly represented in EVs from solid tumors.

Results: LNP-based EV enrichment achieved very high EV recovery (>85%) with substantially reduced albumin and lipoprotein carryover compared with benchmark reagents. The immunoassay panels demonstrated robust detection of key cancer-associated biomarkers across diverse cell-line-derived EVs. The results demonstrating strong EV-specific signals and substantial reduction of nonspecific background These findings indicate that LNP isolation provides superior purity and robust compatibility with downstream quantitative analyses.

Conclusion: LNP-mediated EV enrichment provides a rapid, high-purity, and sample-efficient platform for capturing cancer-derived biomarkers directly from plasma. When integrated with omic-assays, this approach enables broad phenotypic characterization of tumor-derived EVs and supports development of minimally invasive diagnostic and treatment-monitoring strategies.

#3363 Fibroblast exosomes induce stromal matrix assembly and breast tumor growth and metastasis.

Bong Hwan Sung[1], Merlyn Emmanuel[2], Metti Gari[3], Jorge Guerrero[4], Maria Virumbrales-Munoz[5], David Inman[3], Evan Krystofiak[1], Alan Rapraeger[6], Suzanne M. Ponik[7], Alissa M. Weaver[1]

[1]Cell & Developmental Biology, Vanderbilt University School of Medicine, Nashville, TN,[2]University of British Columbia, Vancouver, BC, Canada,[3]Cell and Regenerative Biology, University of Wisconsin-Madison School of Medicine and Public Health, Madison, WI,[4]McArdle Laboratory for Cancer Research, University of Wisconsin-Madison School of Medicine and Public Health, Madison, WI,[5]Department of Obstetrics and Gynecology, University of Wisconsin-Madison School of Medicine and Public Health, Madison, WI,[6]Human Oncology, University of Wisconsin-Madison School of Medicine and Public Health, Madison, WI,[7]University of Wisconsin-Madison, Madison, WI

Stromal matrix assembly is a key feature of aggressive tumors and is associated with poor prognosis of breast cancer patients. Fibronectin is a key stromal matrix molecule whose assembly into fibrils is thought to require cells and which serves as a template for stromal matrix assembly. Fibroblasts are the major cell type that secretes and assembles fibronectin and stromal matrix. Here, we identify that small exosome-type small EVs secreted by fibroblasts are critical initiators of fibronectin assembly, revealing a previously unrecognized mechanism of stromal matrix formation. Fibroblasts engineered to be deficient in exosome secretion showed greatly reduced assembly of fibronectin and other stromal matrix molecules in 2D, 3D, and *in vivo* environments, and led to reduced tumor growth and lung metastasis by triple-negative breast cancer cells. Furthermore, transgenic mice with defects in exosome secretion had greatly reduced lung fibrosis after treatment with bleomycin. In a direct test of exosome function on fibronectin assembly, we find that the addition of purified small EVs to purified soluble fibronectin in a cell-free system is sufficient to induce fibronectin assembly. The EV-induced fibronectin assembly requires the presence of fibronectin-binding integrins and syndecan-1 in the EVs. We propose a new model in which secreted exosomes directly drive stromal matrix assembly and tissue fibrosis.

#3364 Exosomes derived from tumor cells in acidic extracellular environment inhibit liver metastasis.

Bei Jin, Weijia Peng, Jingxuan Pan

Sun Yat-sen University, Guangzhou, China

Distant metastasis is the leading cause of cancer-related mortality in patients with solid tumor. Tumor cells tend to colonize specific target organs, exhibiting organ tropism. For instance, ~85% of patients with metastatic uveal melanoma (UM) metastasize to sole organ liver; up to 50% of patients with colorectal carcinoma (CRC) develop liver metastasis. Liver-organotropic metastasis is the consequence of reciprocal cross talk between tumor cells and host microenvironment within the liver. Tumor microenvironment (TME), characterized by acidity and hypoxia, represents a hostile milieu that favors tumor cells over non-tumor cells which cannot adapt. Exosomes, small membranous vesicles encompassing biologically active components (namely proteins, miRNAs, and lipids, etc.), are pivotal in mediating intercellular communication. We aimed at exploring the mechanism by which exosomes mediating the intercellular communication in liver colonization. We found that hepatic metastasis in CRC was significantly facilitated by exosomes derived from tumor cells in normal extracellular environment (normal exosomes), which was, however, remarkably diminished by those derived from tumor cells in normal extracellular environment (acidic exosomes). Further study revealed that exosomes derived from tumor cells in acidic extracellular environment were enriched with the metastasis-suppressor NME1. Acidic exosomal NME1 were uptaken by adjacent tumor cells, resulting in degradation of DDR1 and CD155 via chaperone-mediated autophagy. The decreased DDR1 abolished cancer stem-like cells in UM and CRC. Decline of CD155 in tumor cells enhanced the infiltration of $CD8^+$ T cells in metastatic colonization in liver. These results indicated a novel mechanism whereby tumor cell-derived exosomes mediating intercellular communication to regulate hepatic metastasis.

#3365 Novel mechanism of tumor fibrosis mediated by interorgan crosstalk.

Akiho Nishimura, Takatsugu Ishimoto, Takashi Semba, Atsuko Yonemura

Japanese Foundation for Cancer Research, Tokyo, Japan

Diffuse-type gastric cancer (DGC) shows strong interactions between cancer-associated fibroblasts (CAFs) and cancer cells through PDGF/PDGFR signaling. While PDGFR is expressed in CAFs, PDGF ligands were believed to be mainly secreted by cancer cells. However, DGC cohort analysis revealed a correlation between stromal fibrosis and platelet aggregation, suggesting that platelets may serve as an alternative PDGF source. This study aims to elucidate the mechanisms of interorgan crosstalk through GC fibrosis-bone marrow (BM) hematopoiesis-platelet axis. IL6 was particularly upregulated in DGC and correlated with fibrosis. We established an orthotopic model using IL6-overexpressing murine GC cells, which developed fibrotic tumors. Notably, platelets in peripheral blood of these mice showed increased count, size, and PDGFD concentration. Cell population analysis in BM revealed increased megakaryocyte progenitors and decreased erythroid progenitors, indicating IL6-induced hematopoietic imbalance. These findings suggest that IL6 promotes PDGFD-rich platelet production, contributing to tumor fibrosis. This study highlights a key role of BM-derived platelets to enhance tumor fibrosis in DGC.

#3366 Muscle iron overload contributes to cancer cachexia-induced muscle wasting.

Subin Pyo[1], Yichi Zhang[1], Anna Barbeau[1], ChiHin Feng[1], Amit Roopan[1], Ning Liu[2], Eric N. Olson[2], Matthew G. Vander Heiden[1]

[1]Biology, Koch Inst. for Integrative Cancer Research at MIT, Cambridge, MA,[2]Molecular Biology, University of Texas Southwestern Medical Center, Dallas, TX

Cancer cachexia is a prevalent and often fatal systemic metabolic condition that is characterized by muscle wasting with or without fat wasting. Muscle wasting is therefore the central component of cancer cachexia but the mechanisms whereby cancer leads to skeletal muscle wasting are not well understood. We used several different mouse models of pancreatic ductal adenocarcinoma (PDAC) as well as C26 allograft, one of the most commonly studied models of cancer cachexia, to study the mechanisms underlying cancer cachexia-induced muscle wasting. Transcriptome analyses on cachexic muscle revealed the upregulation of genes related to iron metabolism. To interrogate whether perturbations to muscle iron metabolism can contribute to muscle wasting, we identified that muscle iron levels are elevated in cachexic muscle. Secondly, mice fed low, medium, and high iron diets and showed a positive correlation between dietary iron intake and the severity of muscle wasting. We further demonstrated that increased muscle iron contributes to muscle wasting by generating muscle-specific transgenic mice overexpressing the transferrin receptor (TFRC), which is the primary method of iron intake into the cell. TFRC transgenic mice exhibited decreased muscle mass and myofiber areas compared to mice not overexpressing TFRC. TFRC transgenic mice injected with C26 cancer cells also showed increased muscle wasting compared to control mice with C26 cells. Furthermore, muscle-specific deletion of TFRC in muscle using a muscle-specific tamoxifen-inducible Cre mouse line bred to a conditional TFRC floxed mouse line rescued C26-induced muscle wasting. Our work rigorously demonstrates that elevated muscle iron leads to muscle wasting, and this elevated muscle iron in cancer cachexic muscle contributes to cancer cachexia-induced muscle wasting. Current work is being done to test whether elevated muscle iron is seen in human samples and to decipher the mechanisms by which muscle iron overload leads to muscle wasting.

#3367 Mitochondrial calcium uniporter drives cancer cachexia in pancreatic ductal adenocarcinoma through NETosis-mediated skeletal muscle atrophy.

Xiuchao Wang, Jihui Hao

Tianjin Medical Univ. Cancer Inst. & Hospital, Tianjin, China

Purpose: Cancer cachexia, characterized by persistent weight loss, skeletal muscle atrophy, and adipose tissue reduction—with progressive skeletal muscle wasting being the predominant manifestation—represents a major cause of mortality in pancreatic ductal adenocarcinoma (PDAC) patients. Cachexia is a common and severe complication in PDAC, significantly impacting patients' quality of life and prognosis. This study investigates the role of the mitochondrial calcium uniporter (MCU) in PDAC-associated cachexia, potentially offering novel interventional strategies for its prevention.
Experimental Design: MCU expression was analyzed in PDAC patient tissues and correlated with cachexia incidence. Spontaneous tumor models and orthotopic PDAC models using MCU-overexpressing and control stable cell lines were established to evaluate tumor progression and muscle atrophy. Neutrophil extracellular traps (NETs) formation was detected by H3cit/MPO/DAPI multiplex immunofluorescence. NETs function was examined through anti-Ly6G-mediated neutrophil depletion, DNase I treatment, and $Pad4^{-/-}$ mice. Secretome analysis identified MCU-regulated mechanisms in NETs formation, validated through recombinant protein treatment and receptor inhibition. The role of CCDC25 was investigated using genetic knockout models and AAV9-mediated skeletal muscle-specific silencing.
Results: MCU overexpression significantly correlated with cachexia incidence and reduced skeletal muscle mass in PDAC patients. Compared to the MCU-overexpression group, control mice demonstrated attenuated tumor growth and preserved muscle mass independent of tumor burden. MCU-overexpressing PDAC models showed significantly elevated NETs infiltration in skeletal muscle, while NETs clearance prevented muscle atrophy. MCU overexpression induced cellular senescence and senescence-associated secretory phenotype (SASP) secretion (particularly C3 and CXCL1), promoting NETosis through C3aR and CXCR2 signaling. CCDC25 was identified as a critical NET DNA receptor in skeletal muscle, mediating muscle atrophy through RAC1-dependent ROS production.
Conclusion: Our study reveals a novel signaling pathway wherein tumor MCU overexpression promotes cellular senescence and SASP secretion, driving NETs formation through C3/CXCL1 signaling. NETs engage CCDC25 receptors on muscle cells, activating the RAC1-ROS signaling pathway that ultimately leads to muscle atrophy.
Impact: These findings establish the MCU-NETs-CCDC25 axis as a key mechanism in PDAC-associated cachexia and suggest multiple therapeutic strategies—including MCU inhibition, NETs degradation, and CCDC25 blockade—providing new directions for alleviating cachexia and preserving muscle mass in cancer patients.

#3368 Metabolite-driven post-translational modifications regulate mitochondrial homeostasis in the glioblastoma microenvironment.

Zhongsheng You, Karrie Kiang, Gilberto Leung

The University of Hong Kong, Hong Kong, Hong Kong

Glioblastoma (GBM) is a highly aggressive brain tumor with a dismal prognosis, demanding new therapeutic strategies. A key challenge in treating GBM is the complex communication between tumor cells and the surrounding tumor microenvironment (TME), which enhances tumor resilience. This study investigated how metabolites, abundant in the TME due to altered cancer metabolism, influence intercellular communication and mitochondrial dynamics in GBM. We hypothesized that specific post-translational modifications (PTMs), driven by these metabolites, regulate mitochondrial homeostasis and function, thereby promoting tumor progression. To test this hypothesis, we employed a range of experimental procedures. Co-culture systems were established to model the interaction between GBM cells and stromal cells within the TME. We utilized flow cytometry to analyze cellular characteristics and interactions, while Western blotting and immunofluorescence were used to examine protein expression, localization, and PTMs. Functional assays, including various commercial kits, were performed to assess mitochondrial biology. Bioinformatics analyses were conducted to identify potential molecular pathways involved, and these findings were validated in vivo using animal models. Our unpublished data reveal that an abnormal increase in a specific tumor metabolite leads to the PTM of key proteins. This modification alters the function and expression of these proteins, resulting in heightened interaction between GBM cells and stromal cells. Consequently, we observed an enhancement of mitochondrial-related biological functions within the GBM cells, which ultimately fuels tumor progression. In conclusion, our findings demonstrate that metabolic byproducts in the GBM microenvironment act as signaling molecules, effectively "hijacking" normal stromal cells to support the mitochondrial homeostasis and growth of the tumor. This novel mechanism of intercellular communication presents a potential new axis in GBM pathophysiology, offering promising therapeutic targets to disrupt tumor progression and improve patient outcomes.

#7149 The paradoxical role of SIRT1 in glioblastoma mediated by the tumor microenvironment.

Anza Mnahal, Wanjun Tang, Bo Chen, Karrie Mei Yee Kiang, Gilberto Ka Kit Leung

Department of Surgery, The University of Hong Kong, Hong Kong, Hong Kong

SIRT1, a NAD+-dependent deacetylase, plays a complex role in glioblastoma (GBM), with debates surrounding its function as either a promoter or suppressor of tumorigenesis. This study aims to understand the double roles of SIRT1 in GBM incorporating in vivo and in vitro models. We conducted a series of experimentation to understand the role of SIRT1 starting with comprehensive analysis of SIRT1 expression in patient datasets, followed by SIRT1 knockdown studies in various GBM cell lines (U87, U251, and patient-derived cells) and in orthotopic, subcutaneous and intracranial tumor induction in animal models. Pharmacological interventions using SIRT1 inhibitors were also employed. Our studies uncovered that higher the SIRT 1 expression level, better is the survival in low grade glioblastomas. On the other hand, knockdown of SIRT1 did not affect the in vitro cell proliferation or migration. However, there was significant effect of SIRT1 knockdown on tumor growth. The tumor growth decreased in both intracranial and subcutaneous models. Furthermore, we observed an altered interaction dynamics between tumor cells and the surrounding neurons, caused by SIRT1 knockdown. This indicates that the influence of tumor microenvironment on SIRT1's functional role. This study reveals the dual role of SIRT1 in GBM, highlighting it as a potential therapeutic target. The paradoxical role of SIRT1 inhibition in various models proves the importance of the tumor microenvironment in shaping GBM biology also providing a future target to study.

: Humanized Mouse Models
Poster Session

#3371 genO-BRGSF-HIS mice: A humanized mouse model for assessment of Treg-targeting therapies.

Gaelle H. Martin, Florent Creusat, Siham Hedir, Amelie Marguier, **Fabiane Sonego**, Kader Thiam

genOway, Lyon, France

Therapies targeting regulatory T cells (Tregs) have emerged as a promising strategy to overcome immune suppression and enhance anti-tumor immunity. Tregs maintain immune tolerance under physiological conditions, but within the tumor microenvironment they promote immune evasion and resistance to immunotherapy. Selective depletion or functional modulation of Tregs can restore effector T-cell activity and improve responses to checkpoint inhibitors and other immunotherapies. However, the development of Treg-targeting approaches requires preclinical models that accurately recapitulate human Treg biology, including phenotype, activation status, and distribution in peripheral tissues and tumors. Conventional mouse models often fail to reflect these human-specific features, limiting their predictive value for safety and efficacy. Humanized models that support the development and long-term engraftment of functional Tregs and mimic human immune-tumor interactions are therefore essential to bridge the translational gap and guide clinical development of next-generation immunotherapies. genO-BRGSF-HIS mice, engrafted with human hematopoietic stem cells, enable long-term reconstitution of diverse human T-cell subsets, including $CD4^+$, $CD8^+$, γδ T cells, and Tregs. Among emerging targets expressed by Treg, CCR8, a chemokine receptor expressed on Tregs, has gained attention for its potential in selective Treg depletion to enhance anti-tumor immunity. Importantly, CCR8 expression differs between species—restricted to tumor-infiltrating Tregs in mice but present on both infiltrating and peripheral Tregs in humans. We assessed CCR8 expression in genO-BRGSF-HIS mice and found a pattern consistent with human biology. Treatment of naïve genO-BRGSF-HIS mice with a CCR8-depleting antibody resulted in Treg depletion in spleen and blood. While efficacy of CCR8-targeting compounds remains to be investigated in genO-BRGSF-HIS mice, it is key to first investigate whether Treg cells are recruited into the tumor microenvironment (TME). Thus, we evaluated human immune cell infiltration in the TME of cell derived xenografts. Tumor infiltration by human immune cells varied by tumor type and burden, with Tregs ($CD4^+FoxP3^+CD127^-$) displaying dynamic activation profiles, including PD-1, GARP, and TIM-3 expression in the TME of A549 lung carcinoma xenografts. Notably, subsets resembling induced Tregs (iTregs) were identified, suggesting adaptive regulatory mechanisms within the TME. These findings support the use of genO-BRGSF-HIS mice as a translational platform for investigating Treg biology and evaluating therapeutic strategies in oncology.

#3372 Predictive in vitro assays and PBMC donor banking: reducing variability in humanized mouse studies.

Matthias Bleisch, Philipp Meyer, Ina Rohleff, Eva Oswald, Anna Edinger, **Julia B. Schueler**

Charles River Laboratories, Freiburg, Germany

Humanized mouse models are an essential tool for evaluating immunotherapies in vivo. The use of peripheral blood mononuclear cells (PBMCs) from healthy donors is common as they provide a functional human immune compartment capable of mediating responses such as T-cell activation and tumor clearance. However, donor variability introduces a significant challenge: PBMCs from different individuals differ in their immune cell composition, and alloreactivity. To address this, we established a PBMC donor bank. Each of the currently six donors are characterized for major phenotypic markers by flow cytometry, as well as HLA-type. In addition to the PBMCs itself we created a bank of expanded T cells as source for in vitro and in vivo assays. The phenotypic characterization of the PBMC revealed differences in all major cell types (T, B, NK, NK T cells and monocytes). However, all data were in physiological range. To deeper analyze the immune cells from different donors, we executed in vitro co-culture assays with a representative tumor cell line MDA-MB-231 to screen for killing potential. Solitumab, a CD3/EPCAM bispecific antibody was tested in the presence of expanded T cells from all donors in five independent runs against MDAMB-231. Efficacy was determined by CTG, oneGlo and flow cytometry in parallel to identify the optimal assay read-out. All three assay read-outs displayed acceptable run to run variability. However, flow cytometry was best suited to discriminate between cell viability of immune and tumor cells. The killing activity of the expanded T cells in vitro was predictive for the onset of GvHD in PBMC engrafted immune compromised NSG mice in vivo. Not only induced donors with higher killing efficiency in vitro an earlier onset of GvHD (day 18 post engraftment for donor 6 vs day 40 for donor 2) it also impacted overall survival (29 days vs 36 days, n.s. Kruskall-Wallis). The engraftment of human PBMC in vivo was characterized by analyzing human immune cells in peripheral blood of engrafted mice over the course of the experiment, GvHD scoring and body weight. Each donor displayed a specific pharmacokinetic of engraftment and different immune cell subtyping. These data are donor immanent, as they could be reproduced using the same donor in multiple independent experiments. The ability to induce antitumoral activity for immune modulating compounds was proven in different experimental set-ups for all six donors. A side-by-side comparison testing Solitumab against MDAMB-231 in vivo is currently under way. This approach enables the reduction of variability in tumor growth and treatment response for PBMC based in vivo studies. By banking PBMCs from multiple donors, researchers can pre-screen immune functionality using in vitro T cell killing assays before committing to in vivo studies. This ensures that only PBMC donors with the desired immune characteristics are selected for humanization in vivo thereby supporting the 3Rs.

#3373 Metabolism and carcinogenic potential of inorganic arsenic in humanized-liver mice.

Arpamas Vachiraarunwong[1], Shugo Suzuki[2], Masaki Fujioka[2], Runjie Guo[1], Guiyu Qiu[1], Yurina Kawamura[1], Ikue Noura[2], Anna Kakehashi[2], Hideki Wanibuchi[1], Min Gi[1]

[1]Environmental Risk Assessment, Osaka Metropolitan University, Graduate School of Medicine, Osaka, Japan,[2]Molecular Pathology, Osaka Metropolitan University, Graduate School of Medicine, Osaka, Japan

Inorganic arsenic is a known human carcinogen associated with liver and bladder cancer. Among its species, sodium arsenite (iAs^{III}) undergoes complex hepatic biotransformation, producing methylated metabolites such as monomethylated (MMA) and dimethylated (DMA) forms. However, its human-relevant mechanisms of metabolism and carcinogenicity remain unclear due to species differences in arsenic biotransformation. To clarify these differences, we employed a humanized-liver (HL) mouse model, in which mouse hepatocytes are replaced with human hepatocytes, to investigate the metabolism and carcinogenic potential of iAs^{III}. HL and wild type (WT) mice were administrated 50 ppm of iAs^{III} in drinking water for 4 weeks. Urine, liver, and bladder samples were collected for analysis. Urinary arsenic speciation was determined using high-performance liquid chromatography coupled with inductively coupled plasma mass spectrometry (HPLC-ICP-MS). Histopathology and immunohistochemistry were performed on both liver and bladder tissue, and gene expression profiles were analyzed using RNA sequencing and microarray, respectively. Urinary arsenic speciation revealed distinct species-dependent differences. Dimethylarsinic acid (DMA^{V}) was the predominant urinary arsenic metabolite in both HL and WT mice. Total urinary arsenic in HL mice was lower than in WT mice, but the distribution of metabolites differed markedly. The proportion of MMA^{V} in HL mice (26.4%) was substantially higher than in WT mice (4.7%), whereas DMA^{V} accounted for 58.5% in HL and 80.7% in WT mice. This urinary metabolite pattern more closely resembled that observed in humans exposed to inorganic arsenic. Hepatic arsenic methyltransferase (As3MT) expression was significantly elevated in WT mice treated with iAs^{III} but tended to decrease in HL mice. Gene expression profiles of liver and bladder tissues of HL mice also differed from those of WT mice. Immunohistochemical analysis of proliferation markers is currently underway to evaluate whether iAs^{III} promotes hepatocellular and urothelial proliferative response. Arsenic content in the liver is also currently under investigation, and pathway analysis of the transcriptomic data using Ingenuity Pathway Analysis (IPA) is ongoing to identify key molecular alterations for further validation. In conclusion, these findings indicate that human hepatocytes exhibit lower methylation capacity, resulting in higher proportions of toxic MMA species, suggesting that humans may be more susceptible to arsenic than mice. Furthermore, the HL mouse model effectively reflects human arsenic metabolism and provides a valuable *in vivo* platform for elucidating human-relevant metabolic, toxicological, and molecular mechanisms underlying arsenic-induced hepatotoxicity and carcinogenicity.

#3374 *In vivo* evaluation of immune checkpoint inhibitors using PBMC-humanized NOG-ΔMHC mice engrafted with PDX tumors.

Asami Hanazawa[1], Seinosuke Sakai[1], Masayuki Komatsu[1], Chiyoko Nishime[1], Naohisa Ogo[2], Masami Suzuki[1], Jun-ichi Hata[1], Akira Asai[2], Taichi Yamamoto[1]

[1]Central Institute for Experimental Medicine and Life Science (CIEM), Kawasaki, Japan,[2]Graduate School of Pharmaceutical Societies, University of Shizuoka, Shizuoka, Japan

Immunotherapy has emerged as the “fourth pillar” of cancer treatment, complementing surgery as well as chemo- and radiotherapies. Among these modalities, immune checkpoint inhibitors (ICIs), particularly anti-PD-1 antibodies, are key tools. Ongoing efforts are focused on identifying novel therapeutic targets and optimizing combination regimens using existing agents. Animal models are indispensable for evaluating the therapeutic efficacy and safety of preclinical drug development. However, conventional syngeneic mouse models often fail to recapitulate human pharmacodynamics and toxicity profiles, especially in molecularly targeted therapeutic contexts, where interspecies differences are pronounced, which underscores the urgent need for translationally relevant platforms.To address this gap, we established mouse models by engrafting human peripheral blood mononuclear cells (PBMCs) into NOG-ΔMHC mice, followed by the transplantation of patient-derived xenografts (PDXs) or PDX-derived cell lines (PDXCs). These models partially reconstitute human immune components, while PDX/PDXC tumors preserve critical features (e.g., histological architecture, cellular heterogeneity, and tumor microenvironment), thereby allowing for a more faithful modeling of human cancer, including immune-tumor cell interactions. We developed two distinct lung adenocarcinoma-derived PDX/PDXC models and optimized testing schedules tailored to each strain. Using these models, we assessed the antitumor efficacy of an anti-PD-1 antibody (KEYTRUDA®) and a novel IDO1/TDO2 dual inhibitor (KYPS-80), both applied as monotherapies and in combination. Both models exhibited tumor growth suppression across the treatment groups, accompanied by enhanced $CD8^+$ T cell activation. Histopathological analyses revealed tumor nest regression, single-cell necrosis, and fibrosis, indicating a therapeutic response. In conclusion, we developed a robust and translationally relevant platform for evaluating ICIs and combination immunotherapies, which recapitulates key aspects of human immune tumor dynamics and holds promise for advancing preclinical immuno-oncology research.

#3375 Novelapproaches fororthotopic tumor engraftment in humanized immune system mice.

Audrey Wetzel, Emilie Bayon, Anais Meynet-Cordonnier, Cecilia Mendez, Charline Boulout, Sebastien Tarbuyn, **Dan Georgess**

TransCure bioServices, Archamps, France

Humanized immune system (HIS) mice support engraftment with human tumors, thereby allowing the assessment of drug candidates in preclinical oncology without needing to develop mouse-specific analogs. The site most often used for tumor engraftment in mice is the subcutaneous flank, which leads to imperfect vascularization, prevents metastasis, and does not capture organ-specific biology. We therefore set to develop and validate five protocols for orthotopic engraftment of cancer cell lines that can be reproducibly utilized in HIS mice. The five orthotopic engraftment sites include the femoral bone marrow (via knee-cap surgery), mammary fat pad, liver (via injection in the spleen), pancreas, and lung. All protocols led to an engraftment rate of 100% and were amenable to tumor monitoring via caliper measurements or bioluminescence imaging. Focusing on the orthotopic lung model, we found that 85% of engrafted mice developed liver metastases. The peripheries of both primary (lung) and metastatic (liver) tumors we marked by strong fibrogenesis depicted by picrosirius red staining) and were infiltrated by human T and myeloid cells. In the lungs of engrafted mice, CD4+ T and NK cells upregulated CD25 and CD16 expression, respectively, indicating significant activation compared to non-engrafted mice. Altogether, our results demonstrate that HIS mice can be orthotopically engrafted as robustly and reproducibly as syngeneic models. We also showed that lung orthotopic engraftment leads to an organ specific immune response and distant metastasis, thereby representing a valuable platform for the assessment of novel oncology therapies.

#3376 Developing the next generation of customized human immune system mice for preclinical oncology.

Audrey Wetzel, Emilie Bayon, Sebastien Tabruyn, **Dan Georgess**

TransCure bioServices, Archamps, France

Humanized immune system (HIS) mice, which can be engrafted with human cell line-derived or patient-derived tumors, have become essential tools for preclinical and IND-enabling development of cell therapies and biologics in oncology. However, selecting the appropriate HIS model remains challenging given the diversity of humanizable mouse strains and immune-engraftment protocols. We first compared immune profiles, clinical symptoms, body weight, and survival in severely immunodeficient mice engrafted with either cord blood-derived $CD34^+$ hematopoietic stem cells (HSCs) or peripheral blood mononuclear cells (PBMCs). PBMC-engrafted mice demonstrated poor survival associated with early graft-versus-host disease (GvHD) and exhibited amplification of human T cells with a partially exhausted phenotype ($Lag\text{-}3^+$, $TIM\text{-}3^+$). In contrast, CD34-engrafted mice showed no health deterioration over 30 weeks and developed a complete human immune system comprising T, B, NK, and myeloid cells.These results place the CD34+ HSC engrafted HIS mice as overall superior model for drug assessment as it allows a longer, GvHD-free treatment window and a more complete immune system. We next implemented a universal, irradiation-free, chemoablation-based $CD34^+$ HSC-engraftment protocol to compare the extent of immune humanization across several severely immunodeficient strains, including foundational models (NOG, NCG, BNDG, BRG, and next-generation strains (NOG-EXL, which overexpresses human GM-CSF and IL-3; and FcResolv NOG, which lacks murine Fcγ receptors). For each strain, we measured survival, overall humanization rate (percentage of human among total immune cells), and human immune-subset frequencies in blood. Finally, we demonstrate how hydrodynamic gene delivery of one or more human cytokines into HIS mice can boost certain immune populations when a transgenic strain overexpressing these cytokines is unavailable. Altogether, our findings provide a knowledge base for the selection of the humanized immune system mouse model with the most suitable immune reconstitution profile for assessing any drug candidate based on its mechanisms of action.

#3378 Short telomeres limit braf^{V600E} driven melanomagenesis in humanized telomere (HuT) mice.

Md Hazzaz Bin Kabir[1], Jiawei Liu[1], Fan Zhang[1], Kenneth I Porter[1], Gavin P. Robertson[2], Jiyue Zhu[1]

[1]Pharmaceutical Sciences, Washington State Univ. College of Pharmacy, Spokane, WA,[2]Professor, Dept. of Pharmacology, Penn State University College of Medicine, Hershey, PA

Telomere length influences genomic stability, immune function, and cancer susceptibility. Although mice are widely used to model tumorigenesis, their telomeres are much longer than humans and generally do not impose telomere-dependent proliferative limits. To determine how human-like telomeres affects melanoma development, we used humanized telomere (HuT) mice (*Tert$^{h/h}$* and *Tert$^{h/-}$*) with short, human-range telomeres (7-9 kb) and compared them to wildtype C57BL/6 (*Tert$^{+/+}$*) mice (~50 kb). Oncogenic Braf^{V600E} was activated in *Braf$^{+/LSL\text{-}V600E}$*;*Tyr::CreERT$^{+/o}$* transgenic mice at 2 months of age via tamoxifen, followed by weekly UV exposure to model chronic sunlight-driven melanoma. Tumor initiation, growth, and burden were monitored for 40-60 weeks. Histology, immunohistochemistry, qRT-PCR, Tissues and tumors were analyzed by H&E, IHC, qRT-PCR, γH2AX, TRF2, and telomere analysis assessed tumor biology and genomic integrity. Immune cell populations in peripheral blood, bone marrow, spleen, and tumors were analyzed by flow cytometry. Primary melanoma cell cultures were established and evaluated for Tert mRNA expression, telomerase activity, and somatic mutation analysis. Kaplan-Meier analysis showed significantly delayed melanoma onset in HuT mice compared to wild-type controls (*Tert$^{h/h}$*, $p = 0.0053$; *Tert$^{h/-}$*, $p = 0.0001$; Log-rank test). *Tert$^{h/-}$* mice developed fewer tumors per animal than both *Tert$^{h/h}$* and wildtype mice. Interestingly, male *Tert$^{h/h}$* mice, but not wildtype or *Tert$^{h/-}$* mice, exhibited more rapid melanoma development than female littermates ($p = 0.0005$), mirroring the higher melanoma incidence observed in men. Histological analysis confirmed nevi and pigmented cells. These findings demonstrate that short, humanized telomeres suppress Braf^{V600E}-driven melanomagenesis in a genotype-, age-, and sex-dependent manner. The HuT mouse model provides a physiologically relevant platform to investigate telomere-regulated melanoma biology, immune-tumor interactions, and genomic instability, offering valuable insights for preclinical cancer research.

#3379 Small cell lung cancer humanized mouse models identifies unique T cell infiltration immune phenotypes in response to combination immune-radiation therapies..

Bell Wu[1], Xiaozhuo Ran[2], Olivia Huang[1], Lifang Song[2], Vivek Phillip[2], Adrian Sacher[3], Ming Sound Tsao[3], Benjamin Lok[1]

[1]Medical Biophysics, University of Toronto, Toronto, ON, Canada,[2]Princess Margaret Cancer Centre, Toronto, ON, Canada,[3]UHN Princess Margaret Cancer Centre, Toronto, ON, Canada

Background: Molecular classification of SCLC into subtypes (SCLC-*ASCL1*, SCLC-*NEUROD1*, SCLC-*POU2F3*, and SCLC-Inflamed) has revealed distinct immune contextures; however, preclinical research of the tumor-immune microenvironment is constrained by limited models that poorly capture POU2F3 and inflamed subtypes. To address this, we investigated peripheral blood mononuclear cell (PBMC) humanized mice (hu-mice) as a complement to conventional murine systems to broaden available tumor-immune models. We further characterized SCLC hu-mice for their ability to model therapeutic sensitivity, focusing on a novel triplet regimen, AZD1390 (ATM inhibitor) with radiotherapy (RT) and durvalumab (aPDL1), to investigate how DNA damage repair inhibition plus RT can reshape the immune microenvironment and sensitize SCLC subtypes to aPDL1.

Methods: Immunodeficient mice were intravenously injected with human PBMCs and subcutaneously engrafted with a panel of human SCLC cell-lines corresponding to all subtypes. Peripheral and infiltrating immunity were profiled with multiparameter flow cytometry to assess cytokine, exhaustion, and activation of subtype-specific tumour-immune interactions. Tumor infiltration kinetics and antitumor effects were evaluated following durvalumab monotherapy and combination therapy.

Results: T cell tumor infiltration varied by subtype with SCLC-Inflamed subtypes exhibiting the highest level of infiltration in an HLA-independent fashion. Infiltrating $CD8^+$ T cells rapidly acquired an exhaustion phenotype upregulating PD1, CD39, TOX and downregulating Ki67, IFNG, and TCF1, consistent with impaired effector function. aPDL1 monotherapy revealed subtype-specific sensitivity of engrafted cell-lines, with tumour control across multiple donors seen only in the SCLC-Inflamed cell-line, SBC5. AZD1390 and RT was selected as a candidate combination with aPDL1 as it stimulated increased chemokine (CCL5, CXCL10) expression via a cGAS-STING-mediated mechanism and increased surface PDL1 expression across multiple cell-lines *in vitro*. AZD1390 and RT sensitized otherwise non-responsive xenografts to aPDL1 *in vivo*. Treatment response was associated with higher proportions of $CD39^+CD103^+$ tumor-reactive T cells and reduced terminal exhaustion ($TCF1^-TOX^+$) suggesting a shift towards a more functional T cell repertoire.

Conclusions: Our preclinical observations demonstrate PBMC hu-mice as a viable platform to model intrinsic immune-tumor characteristics of engrafted human SCLC cell-lines. Combinatory radiation therapy enhanced anti-PDL1 efficacy in select models. Future studies will aim to identify response-defining features of treated models to improve patient selection in clinical trials.

#3380 Enhancing preclinical insights in immuno-oncology with humanized mice.

Caroline Mignard, Zoe Perin, Estelle Verronese, Damien France, Vincent Faugeroux, **Marc Hillairet de Boisferon**

Oncodesign Services, Dijon, France

Immune cells within the tumor microenvironment are increasingly recognized as critical targets for cancer therapy. However, findings from conventional animal models often fail to translate effectively to humans due to fundamental interspecies differences. This limitation has driven the development of humanized mouse models capable of more accurately recapitulating human immune biology and supporting the preclinical evaluation of emerging immunotherapeutic strategies.

To recreate a functional human immune system in immunodeficient mice, researchers commonly engraft either human peripheral blood mononuclear cells (PBMCs) or hematopoietic stem cells (HSCs). These humanized mouse models enable the study of human immune cell development, activation, and tumor–immune interactions in vivo, addressing key gaps that traditional syngeneic models cannot. When coupled with the implantation of human tumor cell lines or patient-derived xenografts, humanized mice provide a uniquely relevant platform for assessing a broad spectrum of oncological therapeutic strategies, including adoptive immune cell therapies, immune checkpoint inhibitors, and oncolytic viruses.

In this work, we present tumor growth dynamics and immune profiling outcomes across both subcutaneous and disseminated intravenous humanized tumor models. Randomization strategies incorporating tumor burden and immune cell engraftment are outlined to enhance experimental robustness. Key readouts capturing immune modulation and antitumor efficacy are detailed.

Illustrative datasets and case studies demonstrate the versatility and translational value of these platforms for preclinical assessment of immune-oncology drug candidates. Overall, the findings highlight humanized mice as a powerful bridge between discovery research and clinical development.

#3381 ImmunoPET reveals tumor-associated macrophages in humanized MDA-MB-231 models.

Pin Yi Lee[1], Ayla Vaughn Embs[1], Catesby Mallard[1], Chloe La Prairie[1], Jonathan Mallard[1], Masakazu Kamata[1], Harriet M. Kluger[2], Ping Zhang[1], Bernadette V. Marquez-Nostra[1]

[1]University of Alabama at Birmingham, Birmingham, AL,[2]Yale University, New Haven, CT

Background: Tumor-associated macrophages (TAMs) represent a major component of the tumor immune microenvironment and are associated with tumor progression and therapeutic resistance. Noninvasive detection of TAMs can provide valuable insight into immune infiltration and guide immunotherapy development. However, current macrophage imaging agents lack specificity for human pan-macrophages. In this study, we aim to image human macrophages in a humanized mouse model using our specific macrophage-targeted probe.

Methods: We developed a human-specific CD68-Fab fragment (Fab14) and radiolabeled it with zirconium-89 to obtain [^{89}Zr]Zr-DFO-Fab14. Humanized NSG-SGM3 and control NSG-SGM3 mice were implanted with MDA-MB-231 triple-negative breast cancer cells into the mammary fat pad. When tumors were palpable, mice were injected intravenously with 6.25 µg of human-specific, macrophage-selective [^{89}Zr]Zr-DFO-Fab14 (~30 µCi per mouse). PET imaging was performed at 2-, 24- and 48-hours post-injection (p.i.), and radiotracer uptake was quantified using SUVmean. Ex vivo biodistribution at 48 hours was assessed by gamma counting to evaluate radiotracer specificity and retention. Tumors were harvested for immunofluorescence (IF) analysis of human CD68 expression.

Results: At 2 hours p.i., quantitative analysis of [^{89}Zr]Zr-DFO-Fab14 uptake was similar in both humanized and control tumors, indicating comparable early distribution. By 24 hours, uptake of the immunoPET tracer was significantly higher and more sustained in humanized NSG-SGM3 mice (SUVmean = 0.29 ± 0.04) compared to control mice (SUVmean = 0.20 ± 0.03; ***p =0.0002). Biodistribution studies at 48 hours further validated the imaging specificity, showing markedly higher tumor retention in humanized NSG-SGM3 (4.66± 1.61 %ID/g) than in control NSG-SGM3 mice (1.71 ± 0.63 %ID/g). IF analysis confirmed abundant human CD68^{+} macrophage infiltration in humanized NSG-SGM3 tumors but not in NSG-SGM3 tumors, confirming the specificity of [^{89}Zr]Zr-DFO-Fab14 for human macrophages.

Conclusions: The human-specific [^{89}Zr]Zr-DFO-Fab14 demonstrates macrophage-specific retention in humanized tumors, enabling noninvasive visualization of human TAMs in vivo. This radiotracer represents a promising tool for studying macrophage dynamics in human immune-reconstituted systems and evaluating efficacy of macrophage-targeted therapies in cancer.

#3382 Characterization and preclinical efficacy of a CD3×CD20 bispecific T cell engager in a humanized PBMC mouse model.

Qikuan Chen, Longyun Zhang, Haixia Chen, Xiaowen Gong, Yanjie Chen, Mingqi Shao, Qi Zhu, Bobo Wang, Jingjing Zhu, Yinfei Yin

Shanghai ChemPartner Co., Ltd., Shanghai, China

Immuno-oncology (IO) therapies aim to harness and amplify the body's immune system to recognize, control, and destroy cancer cells. One key therapeutic goal in IO is to enhance T cell-mediated tumor killing. Currently established strategies include immune checkpoint inhibitors (ICIs), which release inhibitory brakes on T cells; T cell receptor-engineered T cell (TCR-T) therapies, which improve surface and intracellular antigen recognition; and chimeric antigen receptor (CAR) T cell therapies, which provide synthetic tumor antigen specificity. While these approaches have achieved success, they also face challenges such as T cell exhaustion, antigen escape, and safety and toxicity concerns, including cytokine release syndrome. Another emerging class of T cell-redirecting therapies are T cell engagers (TCEs); bi- or tri-specific antibodies that physically link T cells to tumor-associated antigens (TAAs). This interaction triggers robust T cell activation and a cascade of cytotoxic events culminating in tumor cell apoptosis. FDA-approved TCEs, such as Epcoritamab (CD3xCD20) for relapsed or refractory diffuse large B-cell lymphoma (DLBCL), Blinatumomab (CD3×CD19) for acute lymphoblastic leukemia (ALL) and Teclistamab (CD3×BCMA) for multiple myeloma, have demonstrated significant clinical efficacy in these respective diseases. While TCEs have shown success in treating hematologic malignancies, their role in Burkitt's lymphoma, an aggressive B-cell non-Hodgkin lymphoma linked to Epstein-Barr virus and MYC dysregulation, remains unexplored. Burkitt's lymphoma is generally considered highly curable using CD20 antibody-based immunotherapy, however resistance to anti-CD20 therapy is emerging, potentially linked to immune effector depletion and exhaustion from continuous intensive treatment. To investigate the efficacy of TCEs in Burkitt's lymphoma, we characterized a CD3×CD20 TCE using *in vitro* binding and cytotoxicity assays, and evaluated its therapeutic activity using an *in vivo* Raji xenograft model (cell line of Burkitt's lymphoma origin, expressing CD19/CD20) in humanized PBMC NOG mice. The CD3×CD20 TCE showed the most potent binding to Raji cells *in vitro*. Furthermore, in the humanized Raji model, the CD3×CD20 TCE achieved significant tumor regression in the high-dose group, and a partial response was observed in the low-dose group. Furthermore, both low and high doses of TCE resulted in a greater reduction in tumor volume compared to the ICI Toripalimab, a humanized PD-1 monoclonal antibody. Evidence of body weight loss (BWL) was observed in the groups that had PBMCs administered (tumour bearing animals), suggesting that the BWL is linked to the model and PBMC rather that the treatment. These findings highlight the potential of CD3×CD20 TCEs as an alternative strategy for treatment of Burkitt's lymphoma.

#3383 Robust multiplex cytokine profiling in second-generation humanized NOG mice using a 41-plex humanized mouse immune panel: Cross-donor validation and implications for translational oncology studies.

Philip Dube[1], Brooke Gilliam[2], Adam Bell[1], Nicholas Smith[1], Janell Richardson[1], Tina Raeber[2], Shane Curran[2], Monika Buczek[1]

[1]Taconic Biosciences, Inc., Rensselaer, NY,[2]MilliporeSigma, St Louis, MO

Background: Second-generation humanized NOG mice (HIS mice) enable evaluation of immune-oncology mechanisms within a physiologically relevant human immune microenvironment. However, translational interpretation of preclinical efficacy studies requires highly specific and reproducible quantification of human cytokines. To support robust immune monitoring, we co-evaluated a 41-plex humanized mouse cytokine/chemokine Luminex panel for performance across diverse human CD34+ donor sources and multiple HIS NOG model variants.

Study Aims/Hypothesis: We hypothesized that the human-specific analytes in the MILLIPLEX® 41-plex humanized mouse multiplex assay would show (i) high specificity for human cytokines with minimal cross-reactivity to host murine analytes, (ii) reproducible quantification across donor-to-donor variation, and (iii) consistent detection sensitivity across advanced HIS NOG models supporting translational oncology applications.

Results: Plasma samples were collected from HIS NOG cohorts reconstituted with ≥3 unrelated CD34+ donor pools and representing multiple second-generation humanized platforms. Across all donors and models, human-restricted analytes yielded quantifiable signals above background. Murine-only control samples confirmed negligible cross-reactivity. Inter-assay and intra-assay CVs demonstrated technical reproducibility. Donor-specific cytokine patterns (e.g., Th1/Th2 balance, myeloid-associated chemokines) were preserved across models, indicating biological fidelity rather than assay drift. Baseline cytokine architecture correlated with reconstitution kinetics and human immune cell subset frequencies, supporting biological coherence.

Conclusions: These validation data demonstrate that the MILLIPLEX® 41-plex Luminex assay provides reproducible, donor-consistent, and human-specific cytokine quantification in second-generation HIS NOG mice. These data support the assay's suitability for mechanistic and pharmacodynamic readouts in oncology studies requiring high-resolution human cytokine/chemokine profiling. Reliable multiplex cytokine measurement strengthens the translational bridge between HIS mouse studies and human immuno-oncology responses, enabling improved interpretation of therapeutic mechanisms, biomarkers, and treatment-induced immune modulation.

#3384 Innovative preclinical mouse models support development of CD3/EPCAM-targeting T-cell engagers.

Jay Zhang, Linlin Wang, Xiaojing Quan, Xiaofei Zhou, Jing Guo

Biocytogen, Waltham, MA

CD3, an essential subunit of the T-cell receptor (TCR) complex, delivers potent activation signals that induce T-cell cytotoxic activity upon engagement. EPCAM (epithelial cell adhesion molecule) is broadly expressed on normal epithelial cells and frequently overexpressed in epithelial-derived malignancies—such as colorectal, gastric, pancreatic, hepatic, breast, and ovarian cancers—making it a compelling target for immunotherapy. CD3 × EPCAM bispecific T-cell engagers (TCEs) function as molecular bridges that connect T cells with tumor cells, resulting in potent and specific tumor cell lysis. Despite their therapeutic promise, CD3 × EPCAM TCEs, particularly in solid tumors, encounter challenges including on-target/off-tumor toxicity, antigen heterogeneity, immunosuppressive tumor microenvironments, and cytokine release syndrome (CRS).

To support preclinical evaluation of CD3 × EPCAM bispecific antibodies, Biocytogen developed double humanized mice expressing humanized CD3E/D/G and EPCAM genes (B-hCD3EDG/hEPCAM mice) on a C57BL/6 background. Humanized *CD3E, CD3D,* and *CD3G* mRNA expression was confirmed by RT-PCR, and human CD3E protein expression on splenic T cells was validated by flow cytometry. Immunohistochemistry confirmed human EPCAM expression in the kidney, lung, skin, small intestine, and large intestine, but not in the heart, liver, or spleen. Flow cytometric analysis of leukocyte subpopulations in spleen, blood, and lymph nodes indicated that humanization did not alter immune cell frequency or distribution.

In a syngeneic tumor model, B-hCD3EDG/hEPCAM mice bearing EPCAM-humanized MC38 tumors exhibited significant tumor growth inhibition following solitomab treatment. This was accompanied by increased proportions of cytotoxic $CD8^+$ T cells and effector $CD4^+$ T cells at the tumor site, elevated cytotoxic $CD8^+$ T cells in the spleen, and enhanced T-cell proliferation in the blood. However, drug-related toxicity was observed in the ileum, characterized by focal epithelial cell necrosis in crypts, goblet cell hyperplasia, and eosinophilic infiltration.

A single-dose toxicity study further demonstrated transient cytokine release, with elevated serum levels of TNFα, IL-6, IL-10, and IFNγ within 24 hours post-dose, returning to baseline within 72 hours.

Collectively, these results validate the B-hCD3EDG/hEPCAM mouse model as a robust and physiologically relevant platform for pharmacological efficacy and safety assessment of CD3 × EPCAM bispecific antibodies in oncology research.

#3385 Humanized mouse models 2.0 - Improved preclinical evaluation of novel immune cell therapies, check point inhibitors, and immune cell engagers by excluding false positive or negative results.

Maria Stecklum[1], Philip Dube[2], Ditte Olsen[3], Jens Hoffmann[4]

[1]EPO GmbH, Berlin, Germany,[2]Taconic Biosciences, Inc., Rensselaer, NY,[3]Taconic, Tornbjergvej, Denmark,[4]Experimental Pharmacology and Oncology Berlin-Buch GmbH, Berlin, Germany

Background
The preclinical evaluation of novel immune therapies require mouse models with a humanized immune system. We previously demonstrated that either peripheral blood mononuclear cells (PBMC), subsets of PBMCs like T and NK cells or CD34+ hematopoietic stem cells (HSC) can be used to establish such models. With the development of next-generation NOG mice, lineage-specific differentiation of immune cell sub-populations of interest can be supported and Fc gamma receptor knock-out mice can exclude false positive or false negative results in studies with antibody-based therapies.
Methods
HSC-humanized mice were generated by i.v. transplantation of CD34+ stem cells using single donors or mixed HSC donor pools. HSC were transplanted to immunodeficient NOG mice and next-generation NOG strains as: NOG-EXL, hIL-2 NOG, hIL-6 NOG, and FcResolv™ NOG. Engraftment and lineage-specific differentiation were compared between the strains. Long-term survival was monitored and human immune cells counts in blood were analyzed by FACS every four weeks.
Breast cancer PDX were established on humanized FcResolv™ NOG mice and treated with different targeted antibodies, like Herceptin or check point inhibitors. Response to treatment was compared with PDX growing on NOG mice to evaluate whether murine FcγRs are confounding the study, leading to false positive or negative results.
Results
Humanized hIL-2 NOG mice showed significantly decreased survival after HSC transplantation in comparison to the other mouse strains. Mice had to be sacrificed within 6-8 weeks after HSC transplantation. In the other mouse strains, transplanted HSCs engrafted and differentiated mainly into B and T cells. NOG-EXL mice displayed the highest engraftment, with up to 80% of human cells in the blood, including a higher portion of myeloid cells after 8 to 12 weeks. Humanized NOG, hIL-6 NOG and FcResolv™ NOG mice showed the longest survival rate with over 400 days.
We have shown that breast cancer PDX models engraft on humanized FcResolv™ NOG and FcResolv™ NOG-EXL and removing murine FcγRs can improve accuracy for efficacy assessment of antibody-based therapies which include an Fc domain.
Conclusions
Next-generation NOG mouse strains, transgenic for human cytokines, can further improve the humanization of mouse models by inducing a lineage-specific differentiation of transplanted hematopoietic stem cells. Engraftment of human tumor cells or PDX seems not to be impaired on mice transgenic for human cytokines.
These improved human tumor-immune cell models allow more predictive preclinical translational studies on tumor immune biology as well as evaluation of new therapies.

#3386 MESHCAP (exogenous microbiota and humanized mice for lung cancer): Towards an innovative preclinical model for testing immunotherapies.

Pierre Montagne[1], Ulrich Jarry[1], Mathilde Harel[1], Laetitia Martinetti[2], Anna Le Mee[2], Charles Ricordel[3], Ahmad FAILI[2], Samer Kayal[4], Remy Pedeux[5], Marwan Touati[6], Valentin Quiniou[6], Hang-Phuong Pham[6]

[1]Biotrial, Rennes, France,[2]OSS - UMR 1242, Univ Rennes, INSERM, OSS, Rennes, France,[3]Pneumologie, Service de Pneumologie CHU Pontchaillou, Rennes, France,[4]Bacteriologie, Service de Bacteriologie CHU Pontchaillou, Rennes, France,[5]Oncotrial, Univ Rennes CNRS INSERM BIOSIT UAR 3480, Rennes, France,[6]PAREAN biotechnologies, St Malo, France

Small cell lung cancer (SCLC) is the most aggressive subtype of lung cancer. The recent combination of chemotherapy with immune checkpoint inhibitors shows a response in only 10 to 15% of patients. At the same time, numerous studies highlight the impact of gut microbiota composition on the response to immunotherapy. To address these current challenges, we are developing a xenograft model called "MESHCAP." This model involves grafting circulating tumor cells (CTCs) from SCLC patients onto mice that have been humanized for both their immune system and their gut microbiota. With its unique dual humanization, this model will allow us to take into account the influence of the microbiota when testing new therapeutic strategies. Based on the literature, we have identified a bacterial consortium hypothesized to be beneficial for the response to immunotherapy. This consortium is cultured in the laboratory and then inoculated into immunodeficient mice whose endogenous microbiota has been previously depleted by antibiotic treatment. We are able to detect the presence of these bacteria in the feces by 16S sequencing more than a month after inoculation. In parallel, we have humanized the immune system of immunodeficient mice by injecting human CD34+ hematopoietic stem cells. This engraftment results in chimerism of the mouse immune system. Currently, we are developing the generation of doubly humanized mice for both the microbiota and the immune system. Preliminary data suggest a cross-talk between the humanized microbiota and the human immune system. In our laboratory, we routinely isolate CTCs from patients diagnosed with CTC. We then inject them subcutaneously to generate CDXs (CTC-derived xenografts). It is these CDXs that we will implant into our doubly humanized mouse model to investigate the impact of the microbiota and immune system on therapies (e.g. immunotherapy).

#3387 Enhancing the predictability of human pharmacokinetics for antibody-drug conjugates (ADCs) using human FcRn transgenic mice.

Xinhe Feng[1], Kefeng Gong[1], Weifang Wang[1], Xinhua Ding[1], Ludovic Bourre[2], Xiaolong Tu[1], Luke Yu[2]

[1]Crown Bioscience, Taicang, China,[2]Crown Bioscience, Inc., San Diego, CA

Introduction Accurate human pharmacokinetic (PK) prediction for antibody-drug conjugates (ADCs) remains a pivotal challenge in early discovery and preclinical stages. Wild-type (WT) mouse models poorly predict human PK due to species-specific FcRn interactions. While hFcRn transgenic models improve mAb PK prediction, their value for complex ADCs requires further validation. This study evaluates hFcRn and HSA/hFcRn transgenic mice using marketed ADCs to establish their role in translational DMPK assessment.

Methods Four ADCs (T-DXd, T-DM1, SG, EV) were administered intravenously (10 mg/kg) to C57BL/6 WT, hFcRn, and HSA/hFcRn mice. Serial blood samples were collected over 28 days. Total antibody and ADC concentrations were measured by ELISA, free payloads by LC-MS/MS. PK parameters were derived via non-compartmental analysis.

Results WT mice consistently overestimated ADC half-lives, while hFcRn transgenic models showed human-relevant values. HSA/hFcRn mouse half-lives correlated strongly with human (r^2=0.95, $p<0.05$) and NHP (r^2=0.98, $p<0.01$). Please find the comparison of PK parameters in the table 1.

Furthermore, the platform successfully differentiated the stability characteristics between ADCs with stable (T-DXd) and more labile (EV) linkers, providing insights into ADC structure complexity and PK relationships.

Conclusion This study demonstrates that hFcRn transgenic mouse model accurately recapitulates human-relevant PK profiles that directly address a major limitation of conventional WT mouse models. The implementation of this platform enables more reliable human PK predictions and informs FIH trial design, and also provides a strategic approach to de-risking ADC development through data-driven candidate selection, reducing early discovery and late-stage dependency on NHP studies, and accelerating the translation of promising ADC therapeutics into clinical evaluation.

#3388 One-stop solution for preclinical evaluation of bispecific T-cell engagers targeting STEAP1.

Hongyan Sun, Yuqing Han, Fang Zhu, Yujing Zhang, Huixin Yang, Xiang Gao

GemPharmatech Co., Ltd., Nanjing, China

STEAP1 (Six-Transmembrane Epithelial Antigen of the Prostate 1) is a membrane protein highly expressed in prostate and other epithelial cancers, making it an attractive target for immune-based therapeutics. To support the development of STEAP1-directed agents, GemPharmatech established a comprehensive in vitro-in vivo evaluation platform designed to characterize STEAP1 expression, functional relevance, and T-cell engager (TCE)-mediated pharmacology. AMG509 (Xaluritamig), a Phase III STEAP1×CD3 TCE currently in clinical development, was used as a benchmark molecule to validate platform performance. Methods: In vitro assays were developed to quantify endogenous STEAP1 expression across prostate cancer cell lines (e.g., LNCaP, 22Rv1) using flow cytometry, followed by evaluation of T-cell dependent cytotoxicity (TDCC) with both luciferase-based and flow-based readouts. T-cell activation markers (CD69, CD25) and cell conjugation frequency were analyzed to characterize the efficiency of T-cell recruitment to STEAP1-positive tumor cells. Cytokine profiling (IL-2, IFN-γ, TNF-α, IL-6) was performed via Cytometric Bead Array (CBA) to monitor T-cell activation and cytokine release potential. Additionally, GemPharmatech engineered 22Rv1-hSTEAP1 and RM-1-hSTEAP1 cell lines to expand the translational scope of the STEAP1 platform across human and murine tumor contexts. In vivo, a panel of humanized immune mouse models (PBMC-NCG, NCG-MHC-dKO, and HSC-NCG) were employed to evaluate STEAP1-targeted TCE pharmacology under distinct immune settings. AMG509 treatment led to potent, antigen-dependent tumor suppression in STEAP1-positive xenografts, achieving >90% tumor growth inhibition and, in several cases, complete regression. Tumor analyses revealed robust infiltration of human CD3+ T-cells and increased local IFN-γ expression, consistent with effective STEAP1-directed immune engagement. Treated mice maintained stable body weight and displayed no signs of cytokine release syndrome (CRS) or graft-versus-host disease (GVHD), confirming the models' suitability for translational safety assessment. Collectively, these results demonstrate the establishment of a robust and modular evaluation workflow for STEAP1-targeted immunotherapies. By integrating antigen quantification, immune functional assays, and humanized in vivo systems, GemPharmatech's platform enables comprehensive and reproducible assessment of emerging TCE modalities. This work provides valuable preclinical insight into STEAP1 biology and establishes an experimental foundation for future therapeutic programs targeting this clinically relevant antigen.

#3389 Preclinical models for evaluating bispecific antibodies targeting PD-1 and VEGF.

Hongyan Sun, Chenyang Liu, Yunlong Jiang, Yujing Zhang, Huixin Yang, Xiang Gao

GemPharmatech Co., Ltd., Nanjing, China

Immune checkpoint inhibitors have transformed oncology treatment, yet primary and acquired resistance remain a significant clinical challenge. Bispecific antibodies targeting both PD-1 and VEGF have achieved remarkable success in clinical trials and have attracted widespread attention by concurrently modulating T-cell immunity while remodeling vasculature within the tumor microenvironment. Physiologically relevant preclinical models that accurately recapitulate human immune and target interactions are essential for evaluating novel therapeutics targeting PD-1 and VEGF. We established an integrated preclinical platform utilizing complementary humanized models. First, we developed BALB/c-hPD1/hPDL1 dual-humanized mice using CRISPR/Cas9 technology and engineered a CT26-hPDL1-hVEGFA dual-humanized colon carcinoma cell line. Implantation of these cells into BALB/c-hPD1/hPDL1 mice created an in vivo system simultaneously modeling the human PD-1/PD-L1 checkpoint and VEGFA signaling pathways. In this target-humanized model, the PD-1/VEGF bispecific antibody Ivonescimab demonstrated significant tumor growth inhibition, and showed superior efficacy compared to combination therapy with anti-PD-1 and anti-VEGFA antibodies, thereby validating the model's capability for assessing the synergistic effects of bispecific antibodies. To assess human T-cell-mediated responses to PD-1/VEGF bispecific antibody treatment, we established a dual-humanized model by engrafting the human tumor cell line LS174T into human peripheral blood mononuclear cell (PBMC) immune system humanized NCG mice. This model demonstrated robust human T-cell reconstitution suitable for evaluating mono- and combination therapies. In efficacy experiments using this model, Ivonescimab similarly exhibited potent antitumor activity with no observed treatment-related hemorrhagic complications, providing preliminary evidence for the safety profile of this combination strategy. These two models used together provide an integrated and translationally relevant preclinical platform for assessing efficacy and potential safety liabilities of PD-1/VEGF-targeted therapies. Using this comprehensive platform will effectively support the discovery and development of novel immunotherapies for complex indications, enabling preclinical risk assessment and accelerating candidate drug translation.

#3390 Enhanced human immune system engraftment in a novel triple-engineered NCG-hIL6-mTSLP-mFlt3-KOmouse model.

Hongyan Sun, Jun Xing, Shiying Guo, Yujing Zhang, Huixin Yang, Xiang Gao

GemPharmatech Co., Ltd., Nanjing, China

Robust humanized mouse models are critical for evaluating human hematopoietic stem cell (HSC) biology, immune system development, and therapeutic efficacy. The NCG strain provides a superior platform for human HSC engraftment due to severe immunodeficiency. To further enhance human immune system reconstitution, we engineered a next generation strain NCG-mTSLP-hIL6-mFlt3 KO by: 1. knocking in human IL6 (hIL6) to support human myeloid cell survival and inflammation, 2. transgenic (Tg) expression of mouse TSLP (mTSLP) to enhance human T and B cell development and lymphoid organogenesis, and 3. knocked-out (KO) mouse Flt3 (mFlt3) to eliminate cytokine competition for FLT3 ligand (FLT3L) and promote the expansion of FLT3-expressing human dendritic cells (DCs) and natural killer (NK) cells. Human CD34+ HSCs were transplanted into NCG and NCG-mTSLP-hIL6-mFlt3 KO mice. Human immune cell reconstitution was longitudinally monitored in the peripheral blood of mice by flow cytometry (up to 18 weeks post-transplantation). Human immunoglobulin (IgG and IgM) levels were quantified by ELISA. Selected cohorts of HSC-NCG-mTSLP-hIL6-mFlt3 KO mice received repeated intraperitoneal injections of recombinant human FLT3L protein at 18 weeks post-transplantation. Lymphoid tissue development was assessed anatomically. HSC-NCG-mTSLP-hIL6-mFlt3 KO mice exhibited improved engraftment and reconstitution of human immune cells compared to HSC-NCG controls. Flow cytometry revealed significantly higher levels of human T cells, NK cells, plasmacytoid DCs (pDCs), and conventional DCs (cDCs) in peripheral blood at multiple time points. Furthermore, functional human B cell maturation was confirmed by elevated serum levels of human IgG and IgM. Anatomical analysis revealed advanced development of various lymph nodes, which are key sites for antigen presentation and the initiation of adaptive immunity. Administration of exogenous human FLT3L further amplified reconstitution levels of human NK cells, pDCs, and cDCs, validating the responsiveness to human cytokine signaling. The NCG-mTSLP-hIL6-mFlt3 KO mouse model offers a powerful platform for human HSC engraftment and development of a functional, multi-lineage human immune system, including lymphoid (T, B), myeloid (DC subsets), and NK cells. Together with enhanced lymphoid organ development, this model is positioned to be a valuable tool for translational immunology and preclinical evaluation of immunotherapies.

#3391 The humanized FcRn mouse model: A superior platform for predicting human PK of therapeutic antibodies.

Hongyan Sun, Yujing Zhang, Yuansheng Yi, Huixin Yang, Xiang Gao

GemPharmatech Co., Ltd., Nanjing, China

Monoclonal antibodies (mAbs) are a rapidly expanding class of biotherapeutics with broad applications spanning oncology, autoimmune disorders, and infectious diseases. A key factor driving their clinical efficacy and dosing strategy is their pharmacokinetic (PK) profile, particularly serum half-life. While mice remain the preferred in vivo model for preclinical PK studies assessing absorption, distribution, metabolism, and excretion, conventional inbred and outbred strains fall short when it comes to accurately modeling the PK behavior of human mAbs and other human-derived biologics. The neonatal Fc receptor (FcRn) plays a pivotal role in regulating the extended half-life and homeostasis of immunoglobulin G (IgG) in vivo. By binding to IgG in a pH-dependent manner within acidic endosomes, FcRn rescues it from lysosomal degradation and recycles it back to the systemic circulation. This salvage pathway is a critical determinant of the PK profile of therapeutic mAbs. However, significant differences in the FcRn-IgG interaction exist between species, often leading to poor translatability of PK data from conventional mouse models, such as C57BL/6, to humans. To bridge this translational gap, we have developed a novel humanized FcRn mouse model, which expresses the human FcRn transgene while being deficient in the murine counterpart, providing a more reliable platform for evaluating the PK properties of human mAbs. In vivo PK studies comparing IgG1 and Keytruda in the humanized FcRn model versus wild-type C57BL/6 mice demonstrated a significantly improved correlation with known human PK profiles. The humanized FcRn model accurately recapitulated the expected serum half-life observed in patients, whereas wild-type mice exhibited artificially prolonged clearance due to murine FcRn-mediated recycling. To date, this FcRn humanized mouse model is the only validated rodent system capable of predicting the serum half-life of human IgG-based therapeutics. It serves as an essential tool for the non-clinical screening of mAb candidates to optimize half-life, reliably forecast human pharmacokinetics, and strategically guide clinical development plans.

#3392 Development of novel NCG-hIL15 and hIL-2 mouse models for preclinical assessment of human NK cell function.

Hongyan Sun, Yinlian Zhang, Yunlong Jiang, Yujing Zhang, Huixin Yang, Xiang Gao

GemPharmatech Co., Ltd., Nanjing, China

Natural Killer (NK) cells are critical mediators of antitumor immunity, exerting direct cytotoxicity and secreting immunoregulatory cytokines. They play a particularly important role in antibody-dependent cellular cytotoxicity (ADCC), a key mechanism harnessed by many therapeutic antibodies. To study these mechanisms, humanized mouse models have been employed, however; conventional human immune cell transplanted immunodeficient mouse models poorly support NK cell engraftment, limiting their translational utility. To address this gap, we developed two human cytokine-expressing mouse models on the NCG triple-immunodeficient mouse model that lacks functional T cells, B cells, and NK cells. TheNCG-hIL2 and NCG-hIL15, were engineered to constitutively express human IL-2 and human IL-15, respectively. These models were assessed for their ability to sustain human NK cell development and function after reconstitution with human hematopoietic stem cells (HSCs). The NCG-hIL2 model showed enhanced human NK cell reconstitution, underscoring the essential role of IL-2 in NK cell maturation and survival. In contrast, the NCG-hIL15 model supported robust co-engraftment of human T and NK cells, making it particularly suitable for evaluating combination T and NK cell-directed immunotherapies. Both models were evaluated in preclinical immunotherapy studies. The NCG-hIL2 model proved highly effective for assessing ADCC-mediated antibodies such as Trastuzumab, Margetuximab, Rituximab, and Blinatumomab. Together, the NCG-hIL2 and NCG-hIL15 models provide powerful and complementary platforms for studying human NK cell biology, cytokine-driven immunity, and anticancer immunotherapy.

: In Vitro Models 1: 2D and 3D
Poster Session

#3396 Triple negative breast cancer organoids derived from circulating tumor cells to advance metastatic cancer research and drug resistance studies.

Shian-Jiun (SJ) Shih[1], David HSIEH[1], Felix Hsieh[1], Hsiang-Yun Lin[1], Hui Ren[2]

[1]Cellentia Inc., San Carlos, CA,[2]Precision AI, Foster City, CA

Triple-negative breast cancer (TNBC) remains challenging to treat due to a lack of effective targeted therapies, and a higher rate of metastasis compared to other breast cancer subtypes. Circulating tumor cells (CTCs) are a subset of cancer cells that shed from the primary tumor, survive in the circulatory system, and then form new metastatic tumors in new environments (s). We believe that a clinically relevant model of metastatic TNBC could be built from cultivation of functional CTCs in vitro, as we have done so for several solid tumors. To better represent the physiology of metastatic tumors, we aimed to culture these cells into 3D tumor organoids to mimic the establishment of early metastasis from CTCs. These CTC-derived tumor organoids would be a valuable platform for identifying novel drugs or drug combinations capable of effectively treating metastatic TNBC. We successfully established a TNBC CTC organoid line from the blood of a treatment-naïve stage 4 TNBC patient. From whole blood, we isolated CTC-containing PBMC, lysing residual red blood cells and seeding them into a proprietary media and plate system. To evaluate whether PBMC depletion would improve the cultivation of CTC organoids, we tested the use of anti-CD45 magnetic beads to deplete immune cells from the PBMC fraction. The cultures were closely monitored and replenished with fresh media every 2-3 days, and passaged to fresh plates every 2-3 weeks, enabling the steady removal of dead cells. This CTC organoid line of TNBC has been continuously passaged for four months now, consistently forms organoids of various sizes and as large as 200 microns, and slightly increases its growth rate over time. Morphology shows loose and irregular aggregates, similar to other breast cancer organoids, but unlike the spherical and densely packed organoids observed from CTC organoids from colon, renal, and other solid tumors. Due to the looser structure of these organoids, we found that cell health was best maintained during passaging by dissociating mechanically using a P1000 pipette, as opposed to enzymatic dissociation. This organoid line expresses EpCAM and cytokeratin, but not CD45, confirming an epithelial origin. Following our previous success in generating drug-resistant colonies from treating CTC organoid lines from colon and renal cancers with standard of care chemotherapy drugs, we are performing in vitro drug resistance colony selection on this TNBC CTC organoid line and applying RNA-Seq on these drug-resistant clones. Gene expression data are analyzed against public domain data from real patients and their treatment outcomes using an in-house AI algorithm to identify mechanisms of drug resistance. We intend to culture TNBC CTCs from new patient samples to increase our bank size, to improve our representation of the diversity of TNBC and validate the identified drug resistance mechanisms

#3397 Modeling cervical cancer heterogeneity using patient-derived organoids for precision treatment development.

Oda Floetre[1], Hege Fredriksen Berg[1], Dominika Aleksandra Hawryluk[1], Marta Espevold Hjelmeland[1], Stefania Bellone[2], Alessandro D. Santin[3], Camilla Krakstad[1], Mari Kylleso Halle[1]

[1]University of Bergen, Bergen, Norway,[2]Yale UNIV. School Of Med, New Haven, CT,[3]Yale University, New Haven, CT

Background: Cervical cancer encompasses diverse histologic and molecular subtypes, yet robust preclinical models that capture this heterogeneity remain limited. This gap continues to hinder the development of precision treatment strategies. **Objectives**: To establish and characterize a cervical cancer organoid library that reflects intertumoral heterogeneity and supports drug screening and functional genomic approaches.

Methods: Organoids were derived from resected cervical cancer tissue from 15 patients and embedded in Cultrex® to support 3D growth. Early- and late-passage organoids, alongside matched patient tumor tissue, underwent morphological evaluation, immunohistochemical profiling, and whole-exome sequencing. Matched 2D cultures were established to compare genomic features and treatment responses between 2D and 3D systems. Drug sensitivity assays including cisplatin, carboplatin, and antibody-drug conjugates (ADCs) are ongoing. Essential genes and therapeutic vulnerabilities will be identified by CRISPR/Cas screens in selected models.

Results: Organoids were successfully established from 40% of tumor samples, representing multiple histologic subtypes. These organoids preserved key morphological features of their corresponding tumors. Early drug response assays revealed heterogeneous sensitivity to platinum-based chemotherapy. Consistency in mutational and copy-number profiles between tumors and organoids at both early and late time points is being evaluated to determine genomic stability.

Conclusions: This organoid library provides a patient-relevant platform for studying tumor heterogeneity and therapeutic response. Ongoing genomic profiling combined with functional assays across this organoid library may reveal targetable vulnerabilities and ultimately advance precision medicine for cervical cancer patients.

#3398 Macrophage phagocytosis and efferocytosis: Implications for therapeutic modulation in the tumor microenvironment.

Veronica Bergo[1], Carla N. Castro[1], Arianna Bandini[2], Tamara Sahner[1], Sarah Huber[1], Sandra Moor[1], Philipp Metzger[1], Cynthia Obodozie[1], **Holger Weber**[1]

[1]Reaction Biology Europe GmbH, Freiburg, Germany,[2]Department of Translational Research and New Technologies in Medicine and Surgery, University of Pisa, Pisa, Italy

Macrophages play a central role in the tumor microenvironment. Depending on their activation state and local signals, they can exert both pro- and anti-tumorigenic effects. Tumor-associated macrophages (TAMs) often exhibit an immunosuppressive, pro-tumoral phenotype that promotes tumor growth, angiogenesis, metastasis, and therapy resistance. Due to their plasticity and abundance in solid tumors, TAMs are attractive therapeutic targets: either by reprogramming them toward an anti-tumoral state or depleting their tumor-supportive functions. Understanding macrophage behavior in cancer is critical for developing effective immunotherapies, given their dual roles. This requires reliable, physiologically relevant in vitro assays modeling key functions, such as phagocytosis, efferocytosis, cytokine secretion, and tumor cell interaction.

Macrophage phagocytosis and efferocytosis assays assess the impact of test compounds on the uptake activity of human M0, M1, and M2 macrophages. CD14+ monocytes are isolated from cryopreserved PBMCs and differentiated into M0 macrophages using M-CSF for six days, then polarized into M1 (IFN-γ + LPS), M2 (IL-4 + IL-13) or TAM-like (IL-4 + IL-10 + TGF-β) phenotypes. After polarization, cells are treated with test compounds at defined concentrations and time points, followed by incubation with either pHrodo™ bioparticles or apoptotic pHrodo™ labelled tumor cells (camptothecin-treated Raji cells) to assess phagocytosis or efferocytosis, respectively. Quantification is performed by measuring red fluorescence over 12 - 24 hours using a Cytation 5 reader.

Our experiments indicate that M0, M2 and TAM-like macrophages have a strong capacity for phagocytosis and efferocytosis, while M1 macrophages have minimal particle or apoptotic tumor cell uptake. Time-resolved analysis reveals distinct uptake kinetics. M0 and M2 macrophages rapidly internalize targets within 2-4 hours. However, M0 cells subsequently decline in activity, while M2 macrophages maintain a sustained plateau for up to 12 hours with an overall higher uptake. Repolarizing M2 macrophages to an M1 phenotype using LPS and IFN-γ markedly reduces their phagocytic capacity. Blocking the "don't eat me" signal with an anti-CD47 antibody significantly enhances the efferocytosis of Raji cells. We anticipate that cytokine profiling will reveal mechanistic differences between phagocytosis mediated by pattern recognition receptors and efferocytosis, which is critical for tissue homeostasis.

These findings suggest that the phenotype of macrophages strongly influences their phagocytic and efferocytic behavior, with M2 cells exhibiting the highest capacity. Strategies that modulate macrophage polarization or relieve inhibitory signals could enhance these functions and support further investigation into their therapeutic potential.

#3399 Highly multiplexed imaging allows for spatial characterization of tumor organoid models.

Anton Luis Villamejor, Joseph Lownik, Daria Mandel, Sinthia Kabir Mumu, Haley Norwood, Madhura Subba Rao, Joshua J. Breunig, Akil A. Merchant

Cedars-Sinai Medical Center, Los Angeles, CA

The emergence of 3D organoid models bridged the gap between 2D cell culture models and complex animal models. Its ability to accurately recapitulate the structure and function of organs and tumors made it a suitable system to perform mechanistic and perturbation studies with more complexities than a 2D cell culture but without the inconsistencies of animal models mimicking human diseases. One of the advantages of organoid models is it accurately represents a tissues structural environment. However, methods to image and spatially characterize organoid models have typically been limited to H&E staining which only gives a qualitative aspect of the structure. While single-plex immunohistochemical analysis is also possible, these tissues are limited and can be exhausted before full evaluation on multiple slides. Having the ability to image and characterize these structures in an efficient way not only validates the organoid's effectiveness to recapitulates the environment of the original tissue but also highlights spatial changes in these models throughout an experiment using only a single tissue slide. For this study, we produced patient-derived lymphoma and glioblastoma (GBM) cell line derived organoids. Organoids were fixed in hydroxyethyl agarose gel and embedded in paraffin. To spatially characterize the organoids produced, we utilized an automated sequential immunofluorescence imaging platform for its ability to detect up to 80 different proteins in a single protocol run. We selected 50 markers to develop the multiplex panel for organoid profiling. The panel consists of markers targeting extracellular matrix, cell phenotypes (GBM and lymphoma), and metabolic state. We believe that these set of markers can characterize and confirm the recapitulation of the two different organoids. In the patient derived lymphoma organoid, we observed cell type frequencies of T-cell subsets and B-cells which recapitulated flow cytometric analysis of the same organoid, confirming its ability to find relevant cell populations. This was additionally true for the GBM organoid, which contained a mixture of different neural cell states, similar to low-complexity single-plex assays performed on the same organoid. In addition, proliferative T-cells in the lymphoma organoid system also had higher levels of glycolytic and mitochondrial enzyme expression compared to non-proliferative subsets. This preliminary proof of principle demonstrates the utility of highly multiplexed imaging for the evaluation of organoid models with broad implications for pre-clinical and translational studies.

#3400 A 3D bioprinted hydrogel-based tumor model of non-small cell lung cancer for preclinical drug testing.

Jan A. Schlegel[1], Julia Thiel[1], Kanstantsin Lashuk[2], Schueler Julia[2], Thomas E. Murdter[1], Matthias Schwab[1], Meng Dong[1]

[1]Dr. Margarete Fischer-Bosch Institute of Clinical Pharmacology, Stuttgart, Germany,[2]Charles River Germany GmbH, Freiburg, Germany

Lung cancer is the most frequently diagnosed malignancy and remains the leading cause of cancer-related deaths worldwide. Non-small cell lung cancer (NSCLC) is the most prevalent subtype, accounting for the majority of these fatalities. Despite numerous approved therapies, the five-year survival rate for NSCLC patients remains poor, largely due to drug resistance and early relapse. Three-dimensional (3D) tumor models that better recapitulate the in vivo conditions of primary NSCLC hold significant potential for advancing both drug discovery and development. In this study, we developed a hydrogel-based, 3D-bioprinted NSCLC model in a tumor-slice format, in which tumor spheroids or organoids of NSCLC and primary CAFs were directly assembled to create a model that mimics the structure and biochemical properties of the tumor microenvironment (TME). Within this bioprinted approach the spatial distribution and compartment ratios can be defined, enhancing reproducibility and enabling a customizable TME reconstruction. A composite bioink consisting of alginate, collagen, and Matrigel was developed to generate a bio-functionalized hydrogel matrix that supports the structural stability and enables the co-culture of different cell types. Several drugs used for first-line treatment of NSCLC were applied to the system to evaluate the treatment efficiency. The printed 3D tumor slices can be cultured for up to 14 days while maintaining their architecture and proliferative capacity. The process is highly reproducible and supports consistent generation of tumor-like constructs suitable for downstream analyses and drug testing. Functional assays including cytotoxicity assays, live imaging, multiplex immunofluorescence staining and 3D imaging were established to assess cell viability, tumor-stromal cell interaction, and treatment response within the printed 3D tumor slices. The culture can also be expanded to include PBMCs to investigate immune cell behavior within the TME, making the model suitable for evaluating immunotherapies. In conclusion, we established a standardized 3D hydrogel-printed model incorporating NSCLC tumor spheroids or organoids and primary CAFs. By reconstructing the TME, this system provides a reproducible and physiologically relevant platform for preclinical drug screening and cancer research. Together with the established analytical methods, this platform serves as a valuable tool for drug discovery and development.

#3401 Modeling the multicellular blood-brain barrier with a PDX-derived glioblastoma microenvironment: comparing human and mouse biochip systems for tumor heterogeneity and drug response.

Michelle Zimmer[1], **Amelie Paillereau**[2], Thomas Sommermann[2], Lars Winkler[1], Joshua Alcaniz[1], Jens Hoffmann[1], Knut Rennert[2]

[1]Experimental Pharmacology and Oncology Berlin-Buch GmbH, Berlin, Germany,[2]Dynamic42 GmbH, Jena, Germany

Glioblastoma (GBM) is a highly malignant primary brain tumor whose therapeutic management is hindered by its invasive behavior and the restrictive properties of the blood-brain barrier (BBB). The BBB tightly regulates molecular transport between the circulatory system and the brain, limiting penetration of therapeutic agents. Widely used 2D *in vitro* systems offer little predictive value, as they lack key physiological features such as barrier integrity, multicellular complexity, and flow-dependent influences. As treatment efficacy depends on both, BBB permeability and direct tumor response, there is a critical need for advanced *in vitro* platforms that more accurately reproduce BBB function to support more reliable preclinical evaluation. To build a physiologically relevant BBB model, we assembled mouse or human brain capillary endothelial cells together with primary astrocytes and pericytes and tested their barrier formation both in static transwell systems and in a microfluidic chip platform. Different combinations and sources of BBB building cells were compared for junctional organization and barrier tightness. The addition of flow further reinforced barrier structure through shear-dependent junctional remodeling. These human and mouse BBB-on-chip models were then combined with patient-derived xenograft (PDX) GBM cell lines, generating a set of mouse PDX/GBM-on-chip and human GBM-on-chip models, that allow evaluation of tumor-heterogeneity under a human or mouse barrier. Initially, we compared treatment responses across conventional 2D cultures, static BBB constructs, the flow-based microfluidic model, and *in vivo* assays. Although 2D and *in vivo* studies demonstrated sensitivity towards cobimetinib, the compound was ineffective at inhibiting growth in the flow-integrated BBB chip. This is consistent with its inability to penetrate an intact barrier. In contrast, the BBB-permeable agent afatinib effectively reduced GBM growth *in vivo* and within the biochip, indicating that the chip reliably reflects whether therapeutic activity depends on BBB penetration. In summary, GBM-on-chip systems unite critical vascular barrier characteristics with GBM co-culture, offering a translational framework to examine tumor-barrier dynamics and determine compound passage across the BBB, thus more effectively connecting *in vitro* assays with PDX and human outcomes.

#3402 *THSD7B* loss is associated with oxaliplatin resistance in colorectal cancer patient-derived tumor organoids.

Graziana Spoto, Luca Falzone, Marco Fichera, Massimo Libra

Department of Biomedical and Biotechnological Sciences, University of Catania, Catania, Italy

Despite significant advances in systemic therapies for colorectal cancer (CRC), this tumor remains the second leading cause of cancer-related mortality worldwide. Among the chemotherapeutic agents most widely used in CRC, oxaliplatin (OX) represents a cornerstone of both single-agent and combination regimens. However, the acquisition of drug resistance mechanisms leads to the failure of these treatments, underscoring the need to elucidate the molecular determinants underlying chemoresistance. Therefore, this study aimed to identify the molecular determinants associated with resistance to OX-based therapies through integrated genomic and transcriptomic approaches performed on drug-sensitive and OX-resistant CRC patient-derived tumor organoids (PDTOs). OX- and FOLFOX-resistant CRC PDTOs (5.24-fold increment of drug resistance) were generated through the administration of increasing and sublethal doses of the drug for at least 90 days and integrated transcriptomic and exomic profiling were performed to characterize the molecular mechanisms sustaining chemoresistance. RNA-sequencing analyses revealed profound dysregulation of pathways involved in cytoskeletal regulation, extracellular space and cell death in both OX and FOLFOX-resistant models, while whole-exome sequencing identified newly acquired variants affecting genes related primarily to cell adhesion and extracellular matrix organization, with notable alterations affecting *LARGE1* and Thrombospondin Type-1 Domain-Containing Protein 7B (*THSD7B*), both genes potentially implicated in OX resistance. Particularly, the presence of the *THSD7B* NM_001080427.1:c.465dup, p.(Pro156ThrfsTer6) frameshift variant was first confirmed in OX-resistant PDTOs by droplet digital PCR (VAF=20.9%). RT-qPCR analyses performed in drug-sensitive and OX and FOLFOX-resistant PDTOs revealed markedly reduced *THSD7B* transcript levels in resistant models. Functional silencing of *THSD7B* using small interfering RNAs performed on Caco2, HT29, and HCT116 CRC cell lines led to a significant downregulation of *THSD7B* expression (from 27% to 90% reduction) and resulted in increased OX resistance, particularly in the more differentiated lines (Caco2 and HT29), whereas no substantial effect was observed in the undifferentiated HCT116 line. Overall, our data show for the first time that *THSD7B* loss mediates OX resistance in CRC. Intriguingly, this evidence has been recently associated with platinum resistance also in lung cancer; therefore, the evaluation of *THSD7B* status may represent a valuable strategy for the early identification of platinum-resistant patients to avoid the administration of ineffective and potentially harmful treatments.

#3403 High content imaging of patient cells to identify CLL and AML patient cohorts that predict drug responses.

David W. Andrews[1], Mark X. Li[1], Alla Buzina[1], Glauber C. Brito[2], Sila Usta[1], Brian Leber[3], Hubert Tsui[1], David Spaner[1]

[1]Sunnybrook Research Institute, Toronto, ON, Canada,[2]Federal University of Sergipe, Sao Cristovao, Brazil,[3]McMaster University, Hamilton, ON, Canada

Biomarkers that predict therapy response greatly facilitate applying precision medicine to patient treatment decisions. However, within populations of Chronic Lymphocytic Leukemia (CLL) and Acute Myelogenous Leukemia (AML) patients there is heterogeneity that is inherent to the disease and also between patients. This heterogeneity, obscures conventional potential biomarkers. As an alternative, we are applying confocal microscopy of live primary patient samples in 2D and 3D microenvironment models that mimic the bone marrow niche to identify cellular phenotypes that can be used as alternative biomarkers. For CLL, live cell painting using non-toxic dyes of cells from 133 patient samples that were grown in 2D niche mimetic cultures enabled machine learning from images. Feature reduction followed by unbiased image clustering revealed five cohorts of patients each with unique drug responses. The results of these studies suggest that high content imaging combined with machine learning and automated image analysis can be used to predict drug responses in a patient specific manner. For AML live cell painting revealed that a novel 3D microenvironmental model was required to inhibit differentiation and enable monitoring the growth of cells from bone marrow aspirates. We are currently applying machine learning to micrographs of AML patient samples stained for CD34 and CD45 to identify putative cancer stem cells within the 3D cultures and for image analysis of staining with a nuclear dye and Annexin V to assess cell-type specific responses to drugs targeting apoptosis proteins. Our results suggest that cellular phenotyping by high content imaging of patient cells grown in microenvironmental models may provide the biomarkers needed to enable precision patient treatment.

#3404 TR-107, a novel mitochondrial ClpP activator, exhibits potent antitumor activity in adrenocortical carcinoma models.

George Karadimov[1], Suresh Kumar[2], Yoo Sun Kim[1], Haiqing Fu[1], Edwin Iwanowicz[3], Lee M. Graves[4], Mirit Aladjem[1], Myriem Boufraqech[2], Jaydira Del Rivero[1]

[1]National Cancer Institute, Bethesda, MD,[2]National Cancer Institute, National Institiutes of Health, Bethesda, MD,[3]Madera Therapeutics, Cary, NC,[4]University of North Carolina School of Medicine, Chapel Hill, NC

Adrenocortical carcinoma (ACC) is a rare, aggressive malignancy arising from the adrenal cortex with limited effective treatment options. The pathophysiology of ACC is characterized by aberrant steroidogenesis and mitochondrial enrichment, reflecting the central role of mitochondria in adrenal steroid hormone synthesis and tumor metabolism. We hypothesized that therapeutically targeting mitochondrial function could yield enhanced antitumor activity in ACC. To test this, we evaluated TR-107, a novel small-molecule agonist of the mitochondrial protease ClpP, which disrupts mitochondrial proteostasis and bioenergetics. TR-107 exhibited potent cytotoxicity at low nanomolar concentrations in NCI-H295R cells (IC_{50} ≈ 24 nM) and in ACC patient-derived organoids (PDOs) (IC_{50} ≈ 15 nM), significantly reducing cell viability and confluency *in vitro*. EdU-based flow cytometry demonstrated reduced S-phase populations and cell size following 48-hour TR-107 treatment, consistent with G1 and G2 arrest. Annexin V/PI assays revealed increased early and late apoptotic fractions in treated ACC cells, confirming apoptotic cell death. Similarly, ACC PDOs and patient-derived xenograft organoids (PDXOs) exhibited substantial decreases in viability upon ClpP activation. Given the high expression of IGF-2 and IGF-1R signaling in ACC, we next examined the combinatorial potential of TR-107 with IGF-1R inhibition. Co-treatment produced synergistic reductions in viability across NCI-H295R cells and PDOs. Collectively, these findings identify mitochondrial ClpP activation as a promising therapeutic strategy for ACC and demonstrate that TR-107 exerts potent antitumor activity as a monotherapy or in combination with IGF-1R blockade. These results provide strong preclinical support for advancing ClpP agonists toward clinical development for the treatment of ACC.

#3405 ATCC's patient-derived 2-D & 3-D cancer models make translational oncology a reality for the scientific community.

Abhay Andar, Ajeet Singh, Changsuk Moon, Stephen Friend, Matthew Graziano, Ruby E. Thamert, Fernanda Ventura, Utsav Sharma, Jonathan Jacobs, **Carolina Lucchesi**

Microphysiological Systems, American Type Culture Collection (ATCC), Manassas, VA

Background: The Human Cancer Models Initiative (HCMI) is a global effort led by the National Cancer Institute (NCI) to advance translational oncology through patient-derived cancer models. Traditional cell lines often fail to capture the complexity of human tumors, limiting their relevance in drug discovery. HCMI addresses this by generating biologically relevant 2-D and 3-D models from patient samples, emphasizing genomic fidelity and clinical relevance. ATCC contributes to the initiative by developing, manufacturing, and distributing these models worldwide. Over 300 models have been released across 28 tissue types, including colorectal, pancreas, brain, and esophagus as well as rare cancers such as Wilms tumor and Ewing's sarcoma. These models span diverse diagnoses, age groups, and racial backgrounds, supporting research into tumor heterogeneity and health disparities. Comparative analyses show strong alignment with The Cancer Genome Atlas (TCGA), retaining over 80% of oncogenic drivers and preserving key transcriptional and epigenetic features. HCMI models offer a robust platform for precision oncology, enabling drug screening, biomarker discovery, and personalized medicine.

Results and discussion: To date, the portfolio includes 329 models spanning common and rare cancers, comprising 91 colon, 54 pancreas, 50 brain, and 37 esophagus. Diversity includes clinical stage, age, and racial representation, enhancing translational relevance. Genomic profiling confirms strong fidelity to patient tumors. TCGA comparisons show >80% retention of oncogenic drivers and high concordance for mutations like BRAF (SKCM), KRAS (PAAD), APC (COAD/READ), and TP53 (ESCA). Concordance exceeds 90% for several cancer types. Additionally, 95% of tumor-model pairs show significant similarity in DNA methylation, and >80% align transcriptionally, preserving epigenetic and transcriptomic features. Models include primary (61%), metastatic (31%), and recurrent (7%) tumors, with samples from varied racial and age groups. This heterogeneity supports research into tumor evolution, drug response variability, and disparities in cancer care.

Conclusion: HCMI offers a next-generation resource for oncology research. By providing clinically relevant, patient-derived models with rich molecular annotation, it enables drug discovery, biomarker validation, and personalized therapy development, bridging the gap between preclinical studies and clinical outcomes.

#3406 Establishing an osteosarcoma organoid model reflecting the bone microenvironment.

Xin Li, Zhi Yang, Ba xuan Hoang, Bo Han

Keck School of Medicine of USC, Los Angeles, CA

Osteosarcoma is the most common primary malignant bone tumor in children and young adults and usually arises in the metaphyses of long bones during periods of rapid skeletal growth. Survival for metastatic or relapsed disease remains poor, and most in vitro studies still rely on two-dimensional plastic cultures that do not reproduce the mineralized matrix, stromal cells, and matrix-bound growth factors that shape osteosarcoma behavior in bone.To address this gap, we established a stepwise bone-mimetic system using Saos-2 osteoblastic osteosarcoma cells. Demineralized bone matrix (DBM) serves as a defined source of bone-matrix-derived growth factors (DBM-DGF), including growth factors such as TGF-β, BMPs, and IGF-1, which act together in a combined effect. Fresh human bone chips provide a more complete bone surrogate with native mineralized matrix, matrix-derived factors, and resident bone cells. In tier 1, Saos-2 cells were treated with matrix-derived growth factor preparations that had been prescreened and grouped by osteoinductive activity. Proliferation was measured by MTT assay. Saos-2 cells showed a graded increase in proliferation across DBM-DGF groups, with the highest-activity preparations producing the strongest proliferative response. These findings indicate that DBM potency directly influences the growth-promoting strength of bone-matrix-derived signals and can be used to approximate “young,” more proliferative, growth-factor-rich bone versus more “aged,” growth-factor-poor bone.In tier 2, conditioned medium from bone-matrix-derived stromal cells is applied to Saos-2 cultures to model paracrine co-culture and test how stromal secreted factors regulate proliferation, differentiation, and migration. In tier 3, fresh human bone chips are combined with Saos-2 cells in three dimensions so that tumor cells experience intact mineralized matrix, matrix-bound growth factors, and resident bone cells at the same time, creating a bone-like microenvironment. This tiered platform directly compares isolated matrix-derived signals with a structurally and cellularly complex bone surrogate and provides a practical, more physiologically relevant model for studying tumor-bone interactions, age-related changes in the bone environment, and for preclinical testing of candidate therapies in osteosarcoma.

#3407 Ensuring diverse *in vitro* lung cancer models: Development of alveolar epithelial cell lines, patient-derived xenografts, and lung adenocarcinoma cell lines from individuals of African ancestry.

Karla E. Gonzalez[1], Bianca Dal Bo[1], Chunli Yan[1], Donna Loza[2], Matthew A. Gladstone[1], Anthony W. Kim[3], Scott M. Atay[3], Takashi Harano[3], W. Dean Wallace[4], Ben Y. Tew[5], Bodour Salhia[5], Beiyun Zhou[6], Kweku Ofosu-Asante[7], Kyle R. Philips[8], Benjamin J. Ryder[8], Desmond Kwakye[7], Chase A. Lilly[7], Yong Huang[8], Nazarius S. Lamango[7], Ite A. Offringa[1]

[1]Surgery, Cancer Biology, USC Norris Comprehensive Cancer Center, Los Angeles, CA,[2]Surgery, USC Norris Comprehensive Cancer Center, Los Angeles, CA,[3]Surgery, USC Keck School of Medicine, Los Angeles, CA,[4]Pathology, USC Norris Comprehensive Cancer Center, Los Angeles, CA,[5]Cancer Biology, USC Norris Comprehensive Cancer Center, Los Angeles, CA,[6]Medicine, USC Keck School of Medicine, Los Angeles, CA,[7]Florida Agricultural and Mechanical University, Tallahassee, FL,[8]University of Florida, Gainesville, FL

Lung cancer disproportionately affects individuals of African ancestry (AA), particularly men, who experience 12% higher incidence and 15% higher death rates than European ancestry men. The causes of this disparity remain unclear; while smoking is the most substantial risk factor for lung cancer, AA men do not smoke more than other groups. Despite the lack of understanding of the increased lung cancer risk and death rates of the AA population, the tools to study lung cancer in this group lag far behind; there are very limited *in vitro* models to study lung cancer in AA individuals. Lung adenocarcinoma (LUAD), which originates in the alveolar epithelium, is the most common histological subtype of lung cancer in all population groups. Immortalized human alveolar epithelial cells (ihAEC) are therefore key tools for studying the etiology and development of LUAD, as well as effects of environmental exposures. In addition to ihAECs, patient-derived xenografts (PDXs), in which human tumors are implanted and grown in immunodeficient mice, and *in vitro* cultured LUAD cell lines, are valuable tools to study lung adenocarcinoma. To address the shortage of these models developed from AA patients, we are taking a 3-pronged approach. We are collecting non-tumor and LUAD tissues from AA lung cancer patients with full consent. When sufficient non-tumor tissue is available, we isolate alveolar epithelial cells and use a CRISPR/Cas9-based gene-delivery approach to generate ihAEC lines. We direct genomic integration of simian virus 40 large-tumor antigen (SV40 LgT) and human telomerase reverse transcriptase (*TERT*) genes into the adeno-associated virus integration site 1 (AAVS1), a safe harbor region that prevents inserted genes from being silenced. When sufficient LUAD tumor tissue is available, we implant tumor sections subcutaneously in immunodeficient mice. Tumors that grow are explanted for a new round of propagation in mice as well as *in vitro* culture. To date one PDX has been established, and cells are in culture from non-tumor and tumor tissue; further characterization is in progress. The development of new ihAEC lines, PDXs, and LUAD cell lines will provide valuable tools for studying responses to environmental exposures, carcinogen detoxification processes, oncogenic transformation, and for testing novel therapies in ancestry-appropriate models. This work is an important step towards minimizing lung cancer health disparities caused by the absence of diverse model systems.

Supported by grants U54CA233396, U54CA233444, and U54CA233465 from the National Institutes of Health (NIH)/National Cancer Institute (NCI), and the Norris Comprehensive Cancer Center core grant, award number P30CA014089 from the NIH/NCI.

#3408 Patient-derived tumor models of tyrosine kinase inhibitor-induced neuroendocrine-transformed lung carcinoma.

Matthew Djan[1], Sebastiao N. Martins-Filho[2], Nhu-An Pham[3], Nikolina Radulovich[3], Quan Li[3], Ming Li[3], Geoffrey Liu[3], Ming Sound Tsao[3]

[1]Medical Biophysics, University of Toronto, Toronto, ON, Canada,[2]Laboratory Medicine and Pathology, University of Alberta, Edmonton, AB, Canada,[3]UHN Princess Margaret Cancer Centre, Toronto, ON, Canada

Background: Lung cancer is the leading cause of cancer-related deaths worldwide, with non-small cell lung cancer (NSCLC) comprising 85% of cases and small cell lung cancer (SCLC) 15%. Tyrosine kinase inhibitors (TKIs) are the frontline therapy for *EGFR*-mutant and *ALK*-fusion adenocarcinomas, yet most patients develop resistance. In 5-10% of TKI-resistant cases, adenocarcinomas (ADC) undergo lineage switching to aggressive neuroendocrine (NE) carcinomas, including LCNEC and SCLC; these patients lack effective therapies and have poor clinical outcomes. To better study NE-transformed tumors, we established clinically relevant patient-derived xenograft (PDX) and xenograft-derived organoid (XDO) models to identify novel therapeutic vulnerabilities and elucidate mechanisms underlying NE transformation.

Methods: Patient biopsy tissues were subcutaneously engrafted into NOD-SCID mice to generate nine NE-transformed PDX models, and six matched long-term XDOs (>10 passages) were established using organoid culture protocol. PDXs/XDOs were characterized by H&E and immunohistochemistry, whole-exome sequencing, and bulk RNA-sequencing. For *in vivo* therapeutic profiling, donor PDX tumors were expanded and randomized into four arms: vehicle, Osimertinib (25 mg/kg, QDx5), chemotherapy [Cisplatin (3 mg/kg, QW) + Etoposide (8 mg/kg, TIW)], or combination. For *in vitro* drug testing, XDOs were dissociated into single cells, seeded into 384-well plates, and treated with Osimertinib, Cisplatin, or Etoposide across a 21-point dilution series (1 nM-10 μM), with viability measured on Day 7 using CellTiter-Glo 3D.

Results: Paired PDXs/XDOs retained key genetic drivers, including *EGFR, TP53,* and *RB1* mutations, along with recurrent alterations in the NOTCH signaling pathway. Histologically, the models recapitulated patient tumor phenotypes, including three SCLC-transformed, two LCNEC-transformed (one ADC-like, one NE-like), and one mixed ADC/SCLC case. Notably, the mixed-histology model maintained both ADC and SCLC components in long-term XDO culture, preserving intratumoral heterogeneity. *In vivo* therapeutic testing revealed minimal response to Osimertinib, chemotherapy, or combination therapy in NE-high tumors, whereas an ADC-like LCNEC PDX exhibited sensitivity to these treatment arms, consistent with clinical observations. XDO drug responses were highly concordant with their matched PDXs, demonstrating resistance to Osimertinib and chemotherapy (IC_{50} > 1 μM). Preliminary high-throughput screening of XDOs with a 58-compound epigenetic probe library identified a candidate therapeutic target to be presented.

Conclusion: Our NE-transformed models preserve patient tumor molecular features, histopathology, and therapeutic response, providing robust platforms to identify novel therapeutic strategies and dissect mechanisms driving lung NE transformation.

#3409 A vascularized 3D microfluidic breast tumor platform for characterizing lymphovascular space invasion among inflammatory breast cancer cell lines.

Melika Mehrabi Dehdezi[1], **Ali Moghaddaszadeh**[1], Zoe Apsel[1], Surbhi Shivhare[2], Xiaoding Hu[2], Bisrat G. Debeb[2], Wendy A. Woodward[3], Marissa Nichole Rylander[1]

[1]University of Texas at Austin, Austin, TX,[2]UT MD Anderson Cancer Center, Houston, TX,[3]Associate Professor, Radiation Oncology, UT MD Anderson Cancer Center, Houston, TX

Highly aggressive cancers such as inflammatory breast cancer (IBC) are characterized by the presence of tumor cell emboli within lymphatic and blood vessels, a phenomenon known as lymphovascular space invasion (LVSI). In this study, we developed a vascularized 3D in vitro tumor microfluidic platform to evaluate LVSI mechanisms including tumor invasion, cancer cells intravasation, vascular and Extracellular Matrix (ECM) remodeling, and emboli formation in IBC cell lines (MDA-IBC3, A3250, and SUM149).Initially, various collagen concentrations (2,3,4,5and 6 mg/mL) were evaluated using optical fiber-based interferometry nanoindentation to measure collagen hydrogel stiffness and identify a concentration representative of normal breast tissue (0.5-1 kPa). A 4 mg/mL collagen concentration was selected, yielding an average stiffness of approximately 0.7 kPa, and was used to assess how the incorporation of cancer cells alters ECM stiffness. Platforms were fabricated by polymerizing a 4 mg/mL collagen type I solution containing cancer cells (2 million cells/mL) around two 22G needles to form vascular channels. These channels were seeded with mKate-tagged telomerase-immortalized endothelial (TIME) cells at 10 million cells/mL, and a shear stress of 4 dyn/cm² was applied to establish aligned, functional endothelium. Confocal microscopy was used to monitor vessel sprouting, permeability, emboli formation, and tumor cell intravasation for one week. Effluent media was collected on Days 3 and 7 for cytokine analysis. By day 7, vessel coverage was significantly reduced in TIME+A3250 and TIME+SUM149 platforms compared to TIME-only and TIME+IBC3 platforms ($p < 0.001$). Although the number of endothelial sprouts was significantly higher in TIME+A3250 platforms compared to TIME+IBC3, the average sprout length did not differ significantly. A3250 cells also exhibited a higher frequency of invadopodia-positive tumor cells compared to MDA-IBC3, indicating a greater invasive phenotype. Consistent with this, the number of intravasated A3250 cells was approximately 15-fold higher than that of MDA-IBC3 cells. Spatial analyses of the platforms' midplanes images further revealed that A3250 cells accumulated around the vessel to a much greater extent than the area farther from the vessel over time. Notably, platforms containing A3250 cells showed an extreme hydrogel deformation, including central separation, suggesting profound collagen remodeling driven by this cell line. This trend was not observed with the other IBC lines (MDA-IBC3 and SUM149).In conclusion, our results indicate that the A3250 IBC cell line shows a more aggressive phenotype compared to the other IBC cell lines. We observed significantly higher intravasation relative to MDA-IBC3, greater disruption of endothelial vessel coverage, and a higher frequency of invadopodia-positive cells.

#3410 Engineering prostate tumor microenvironments via the granular environment for lattice self-assembly (GELS) system.

Alia Starman, Cris Angeles, Ally Freidholm, Ethan Lin, Gabriel Leonard Galahad Declercq, Hunain Khawaja, Cynthia Miranti, Alexander McGhee

University of Arizona Cancer Center, Tucson, AZ

Developing physiologically relevant in vitro tumor microenvironment models demands faithful reproduction of tissue architecture, mechanical properties, and vascularization. To meet these requirements, I have developed a technique called Granular Environment for Lattice Self-assembly (GELS), which leverages granular hydrogel as modular building blocks that both support and constrain cell adhesion, migration, and collective remodeling. GELS is particularly well suited to prostate cancer engineering due to its emergent architecture resembling branching glands and ducts. In GELS, cells remodel their surroundings in proportion to the energy landscape required to displace neighboring granules. When nearby energy barriers are low, cells drive extensive reorganization, whereas high barriers restrict them to localized adjustments. By tuning the spatial distribution and magnitude of these barriers through granule size, surface chemistry, and connectivity, we can implement broad patterns, while allowing cells to contribute fine structural detail by adaptively responding to native chemical cues that guide tissue formation. Preliminary results demonstrate that altering granule size and composition induces a transition from disconnected, organoid-like aggregates to continuous, tissue-like arrangements with interconnected microchannels. We aim to use these insights to derive predictive design rules for tissue self-assembly, enabling the creation of in vitro models for specific tumor microenvironments, including the prostate. By seeding fibroblasts in well-defined patterns within GELS, first we established a healthy stromal environment into which prostate cancer spheroids can be introduced. The subsequent transition of fibroblasts into cancer-associated fibroblasts (CAFs) will be monitored through traction force microscopy for changes in alignment and ELISA readouts of TGF-β levels and localization. These measurements will link mechanical remodeling to biochemical signaling in a dynamically evolving TME. This method holds the potential to significantly advance the field of cancer engineering by enabling the creation of more complex and viable TME models with live readouts of key signals.

#3411 Mechanochemical effects of growth factor gradients in colorectal cancer organoids.

Gabriel L. G. Declercq, Alex Borowiec, Alejandro Moncada, Alia Starman, Surajinder Bharaj, Kevin Pond, Alexander McGhee

University of Arizona Cancer Center, Tucson, AZ

Understanding how colorectal cancer (CRC) cells respond to growth factor (GF) cues in addition to mechanical forces is essential for defining the mechanisms that regulate tissue organization and tumor progression. Here, we used a platform that co-registers mechanical outputs with biochemical readouts to investigate CRC organoid responses to well-defined spatiotemporal GF gradients produced by GF-loaded beads. Embedding the beads within a liquid-like solid microenvironment creates a diffusion-limited system, enabling stable and quantifiable gradient formation. GF-loaded beads were positioned at defined locations within the *in vitro* model to establish local concentration fields, measured through spatially distributed ELISA beads operating under non-depleting Langmuir adsorption conditions. Concurrently, 2D CRC organoids expressing Erk and Akt kinase translocation reporters were cultured on ECM-functionalized hydrogels embedded with fiduciary traction beads, enabling reconstruction of traction stress maps via particle-tracking-based traction force microscopy. Preliminary data shows that organoids exposed to steep GF gradients will exhibit elevated Erk activity along gradient-facing edges, while regions experiencing lower concentrations will display reduced Akt activation. This spatiotemporal response further demonstrates that traction forces will increase in regions with high local GF concentration, indicating a gradient-dependent mechanochemical response. These projected spatial correlations will reveal discrete concentration thresholds above which CRC cells transition from apical to focal contractility, a shift that reflects loss of epithelial organization, increased ECM engagement, and acquisition of a more motile, invasion-prone phenotype relevant to tumor progression. Collectively, these outcomes demonstrate that localized GF release from GF-loaded beads can be quantitatively mapped and directly linked to force generation and kinase dynamics within CRC organoids. This integrated approach will establish a unified framework for probing how GF gradients and mechanical cues interact to shape CRC cell behavior, providing a platform for subtype-specific studies and enabling engineering-driven strategies for targeted therapeutic intervention.

#3412 Next-generation cancer organoids 2.0 in precision cancer medicine: Patient-derived pancreatic ductal adenocarcinoma organoids model tells not only drug sensitivity but also complexity of tumor biology.

Hyemin Kim, Younghoon Choi, Eun Mi Lee, Jungmyoung Han, Se-Hoon Lee, Kwang Hyuck Lee, Jong Kyun Lee, Kyu Taek Lee, So Jeong Yoon, Hongbeom Kim, Sang Hyun Shin, Jin Seok Heo, In Woong Han, Joo Kyung Park

Samsung Medical Center, Sungkyunkwan University School of Medicine, Seoul, Korea, Republic of

Introduction : Organotypic models of patient-specific tumors are revolutionizing our understanding of cancer heterogeneity and its implications for personalized medicine. The study's aims were as follows: 1) to establish a PDAC patient-derived organoid (PDO) model obtained from various PDAC specimens. 2) to find out clinicogenomic factors affecting patients' outcomes.
Methods : The SMC PDAC Cohort Patients were prospectively enrolled and underwent EUS-guided FNB, metastatic sites (such as liver, ascites, lung, and bone), and surgical resection. PDAC PDOs were comprehensively analyzed for histology, next generation sequencing (NGS), and high-throughput screening (HTS) drug sensitivity tests.
Results : The 735 PDAC patients were prospectively enrolled in this study. PDAC PDO platform has been trying to establish from the following cancer specimens: ascites, biopsies from bone, liver, lung, and pancreas, or surgical resection. The success rate was as follows according to the source of obtaining site; ascites due to peritoneal seeding (3/3: 100%), bone mets (1/1: 100%), EUS-FNB (195/183: 87.8%), liver mets (7/8: 87.5%), lung mets (1/1: 100%), surgical specimens (394/500: 78.8%) and PDO was successfully established within 8.2±2.6 days. It took approximately 3 weeks to acquire each specimen and generate sufficient PDAC PDOs for the simultaneous HTS drug sensitivity test and NGS. Whole exome or genome sequencing (WES/WGS, n=302) showed an almost identical concordance between original PDAC tissues and matched PDOs and the increased frequency of genetic alterations in PDOs. The HTS drug sensitivity test (n=151) revealed the clinical correlation between the PDO response and the actual chemotherapeutic response of the study patients in both palliative and adjuvant in real-world settings (ranging from 84.0~ to 91.2%). In addition, whole transcriptome sequencing (n=308) identified nab-paclitaxel resistance-associated genes such as ITGB7, ANPEP, and ST3GAL1, and also found early recurrence-related genes including COL2A1, CALB1, and CYP24A1 in the extracellular matrix, calcium signaling, and vitamin D metabolism.
Conclusions : The PDAC PDO platform may become a valuable tool for personalized medicine and may give us insights into tumor biology.

#3413 Generation of a distal lung cancer organoid model using oncogenic ret-expressing induced pluripotent stem cells.

Jinwook Hwang[1], Christophe Desterke[2], Paul Marcoux[1], Mohamed Amin Bani[3], Frank Griscelli[1], Annelise Bennaceur Griscelli[1], **Ali G. Turhan**[1]

[1]INSERM U1310, Villejuif, France,[2]Universite Paris Saclay, INSERM U1310, Villejuif, France,[3]Gustave Roussy Cancer Center, Villejuif, France

3D-lung organoids generated from normal iPSCs represent a powerful tool to study human lung development and disease. The tyrosine kinase receptor RET is altered by genetic fusions in a subset non-small cell lung cancers (NSCLC). To determine if we can generate lung cancer organoids in this context, we used two iPSC lines harboring RET with oncogenic M918T and C634Y mutations and evaluated their ability to give rose to distal lung organoid structures. NKX2-1+ lung progenitor cells (LPC) were generated after 14 days of culture followed by air-liquid interface cultures giving rise to alveolar structures by day +38. These cells expressed alveolar differentiation markers (such as SFTPC) as well as PD-L1, TTF-1, MUC1, and CK5/6. Transplantation of day+14 LPCs into NOD/SCID mice generated tumors in RET-expressing organoids only whose immunostaining also revealed presence of bronchial structures, ciliated cells, goblet cells and the well-established squamous cell carcinoma marker p40. Single-cell RNA sequencing analyses revealed the presence of fetal neuroendocrine cells, goblet cells as well as alveolar type 2 cells. This single cell RNAseq signature allowed to determine the major genes involved with response or resistance to Selpercatinib, the major inhibitor targeting RET-altered lung cancers.

Significance : These findings show for the first time to our knowledge that iPSC-derived distal lung organoids with oncogenic RET overexpression can recapitulate the characteristics of RET-Driven non-small cell lung cancer (NSCLC). This experimental tool has significant potential as a preclinical model for identifying new therapeutic targets in RET-inhibitor-refractory lung cancers.

#3414 PDO as Translational Model for Biomarker Discovery in NSCLC.

Maria C. Speranza[1], Anna Pasto[2], Halh Al-Serori[2], Elisavet Chatzopoulou[2], Veronika Yankova[2], Henrik Hammaren[3], Patricia Sauer[3], Kathrin Uhrig[3], Helena Rannikmae[2], Lena Eismann[3], Edward Curry[2], Tony NG[2], Kenneth W. Hance[4]

[1]GlaxoSmithKline plc, Boston, MA,[2]GlaxoSmithKline plc, Stevenage, United Kingdom,[3]GlaxoSmithKline plc, Heidelberg, Germany,[4]GlaxoSmithKline plc, Malvern, PA

This study leverages treatment-naïve patient-derived organoids (PDOs) as a powerful translational model to drive biomarker discovery in non-small cell lung cancer (NSCLC). Current biomarker discovery efforts rely predominantly on publicly available datasets that predict cell surface localization at the RNA level. By focusing on the proteomic characterization of the cell surface, specifically targeting N-glycosylated proteins, we aim to capture the dynamic landscape of membrane proteins that play key roles in tumor biology.We performed a surfaceome screening on a cohort of 15 NSCLC organoids and 5 matched normal lung organoids after in vitro treatment with saline, cisplatin and B7H3 ADC. Live-cell biotin labeling followed by enrichment enabled isolation of glycosylated cell surface proteins. Downstream LC-MS/MS-based proteomics allowed quantitative profiling of both enriched and total protein fractions. Concurrently, transcriptomic profiling via RNA-seq and WGS will enable cross-comparative analysis. This proteogenomic approach will be critical given that transcript-level data do not always reflect actual protein expression, particularly for membrane proteins that may be subject to complex post-translational modifications and regulation. Comprehensive multiomic in silico analyses are currently ongoing to integrate our experimental data with external databases, including CPTAC, TCGA, TEMPUS, and GTEx. These computational analyses are designed to refine our list of candidate biomarkers based on high protein expression and differential expression pre- and post-treatment.Our approach underscores the potential of utilizing advanced proteomic and transcriptomic methodologies in tandem with cutting-edge in silico analyses to better understand tumor biology. Further analysis and validation studies will be needed to ensure that the biomarkers we identify have the highest translational potential and can be used as effective diagnostic tools.

#3415 Establishment and characterization of novel patient-derived esophageal tumoroids with long term cultivability.

Takashi Urano[1], Etsuko Yokota[1], Miki Iwai[1], Takuro Yukawa[1], Nagio Takigawa[2], Hideyo Fujiwara[1], Takashi Akiyama[1], Minoru Haisa[1], Takuya Fukazawa[1], Yoshio Naomoto[3], Tomoki Yamatsuji[3]

[1]Kawasaki Medical School, Kurashiki, Japan,[2]General Internal Medicine 4, Kawasaki Medical School, Kurashiki, Japan,[3]General Surgery, Kawasaki Medical School, Kurashiki, Japan

Esophageal cancer, which includes esophageal squamous cell carcinoma (ESCC) and esophageal adenocarcinoma (EAC), is a highly aggressive malignancy and ranks as the eleventh most prevalent cancer worldwide. Despite therapeutic progress, the 5-year survival rate remains poor. To enable the development of new treatment strategies, robust preclinical models of esophageal carcinoma are essential. Recent progress has enabled three-dimensional (3D) organoid systems generated from adult or pluripotent stem cells. Such organoids faithfully reproduce the architecture and functions of the tissue of origin and have been established from multiple human sources, including patient-derived tumors of the colon, prostate, breast, pancreas, esophagus, bladder, and liver. In this study, we generated three human esophageal cancer organoids from surgical specimens and maintained long-term cultures exceeding 12 months. All lines also met a practical durability benchmark—continuous growth for ≥3 months or ≥10 serial passages—thereby enabling consistent pharmacologic testing and cross-batch reproducibility. Two organoids originated from ESCC, and one from EAC that arose in Barrett's esophagus. Whole-exome sequencing showed that these organoids preserved the genetic alterations present in the corresponding primary tumors. In parallel, patient-derived xenografts recapitulated the histopathology of the original esophageal cancers. Comprehensive assessments, including copy-number profiling and immunohistochemistry, demonstrated HER2 expression with amplification and HER3 expression with mutation in the EAC-derived organoid. Notably, HER2-directed antibody-drug conjugates (ADCs), including trastuzumab deruxtecan (T-DXd) and pertuzumab deruxtecan (P-DXd), effectively reduced tumor cell viability in these organoids. The successful creation of esophageal organoids with durable cultivability enables reproducible foundational studies, including drug-sensitivity testing, which are critical for advancing personalized therapy and rational treatment design. This work provides actionable resources for clinicians and researchers seeking to improve therapeutic approaches for esophageal cancer.

#3416 Functional heterogeneity of the human blood-tumor barrier phenotype induced by patient-derived glioblastoma spheroids.

Srishti Kala[1], Luke M. Markowski[2], Moriah E. Katt[2]

[1]Cancer Cell Biology, West Virginia Univ. School of Medicine, Morgantown, WV,[2]Department of Chemical and Biomedical Engineering, West Virginia University, Morgantown, WV

The fundamental limitation to effective chemotherapy in Glioblastoma Multiforme (GBM) is the highly restrictive nature of the Blood-Tumor Barrier (BTB). The BTB functions as a robust regulatory interface, tightly controlling the efflux and influx of compounds and greatly restricting therapeutic access to the tumor microenvironment. We hypothesize that the BTB's functional phenotype is not static but is dynamically modulated by tumor characteristics. This observed heterogeneity is clinically actionable: tailoring drug delivery strategies to match individual tumor profiles is essential for improving prognosis. Thus, compiling a comprehensive database correlating BTB transport characteristics with molecular profiles is necessary to inform rational drug delivery design and optimize clinical outcomes. This study was designed to systematically outline the functional heterogeneity inherent in BTB transport mechanisms, comparing phenotypes induced by two separate Patient-Derived GBM Spheroid (PDS) *in vitro* transwell system. Our human model utilized iPSC-derived Brain Microvascular Endothelial-like Cells (hiPSC-BMECs) co-cultured with the two PDS samples to accurately model the complex neurovascular unit. We utilized a multi-modal functional assessment evaluating barrier integrity, paracellular transport, transcellular permeability, and efflux profile, to comprehensively characterize both the passive "leakiness" and active "tightness" of the BTB. These findings confirm that patient-specific GBM spheroids induce demonstrably heterogeneous BTB functional phenotypes. Junctional integrity is modulated by PDS co-culture, with heterogenous responses corresponding with GBM molecular profile. With limited paracellular “leakiness” and dysregulated active transport seen in both pinocytotic and efflux mechanisms. Current clinical assessment of BTB disruption relies primarily on Gadolinium enhancement on MRI, which only detects gross barrier breakdown. It fails to characterize the subtle, active, and heterogeneous transport mechanisms that significantly impede drug concentration in the tumor mass. Our *in vitro* approach provides a necessary, precise translational tool capable of characterizing the BTB's function from a patient's tumor sample, facilitating the development of truly personalized and effective drug delivery strategies in GBM therapy.

#3417 Development of a patient-derived pancreatic cancer organoid-CAF coculture model to study tumor microenvironment influence on radiotherapy response.

Diego Munoz-Salazar[1], Carolina Bizama[1], Paola Caprile[2], Fernanda Cabrera[1], Angel Castillo[1], Victor Manriquez[1], Macarena Medina[1], Pablo Munoz-Schuffenegger[3], Juan Carlos Roa[1], **Patricia Garcia**[1]

[1]Department of Pathology, Faculty of Medicine, Pontificia Universidad Catolica de Chile, Santiago, Chile,[2]Institute of Physics, Faculty of Physics, Pontificia Universidad Catolica de Chile, Santiago, Chile,[3]Radiation Oncology Unit, Department of Hematology - Oncology, Faculty of Medicine, Pontificia Universidad Catolica de Chile, Santiago, Chile

Introduction: Radiotherapy (RT) is a fundamental treatment modality for pancreatic ductal adenocarcinoma (PDAC) at all disease stages. However, local relapse, driven by treatment resistance, remains a critical issue for improving patient outcomes. While tumor cell-intrinsic factors contribute to resistance, evidence indicates that the tumor microenvironment (TME), particularly cancer-associated fibroblasts (CAFs), plays a crucial role through different mechanisms. Current patient-derived organoid (PDO) models fail to authentically recapitulate CAF-tumor interactions and their influence on RT response, limiting their translational relevance. We developed a coculture system to better mimic these interactions and enable physiologically relevant radiobiological studies.
Methods: PDOs of PDAC and primary CAFs were cocultured in 3D suspension in ultra-low attachment plates with 300ug/mL of Matrigel. The structural integrity and composition of the resulting aggregates were characterized using H&E, Masson's trichrome, PAS-Alcian blue staining, and immunofluorescence (IF) for vimentin, pan-cytokeratin, phalloidin, and DAPI. To test the utility of this model for RT studies, cocultures were exposed to a single radiation dose of 8 Gy. Radiobiological effects were evaluated 12 days post-treatment using H&E, immunohistochemistry for Ki-67 and p16, IF (γ-H2AX), and calcein-AM/propidium iodide viability assay.
Results: The established protocol generated aggregates with organized epithelial-stromal compartmentalization, confirmed by IF and histological analysis. Following a single 8 Gy radiation dose, cocultures exhibited reduced aggregate size and decreased cellular density within the first 12 days post-treatment, with significantly impaired growth kinetics compared to untreated controls. Histological analysis of irradiated samples showed disrupted matrix integrity and increased cellular fragmentation. Elevated γ-H2AX foci indicated DNA double-strand breaks, while reduced Ki-67 and increased p16 staining reflected decreased proliferation and increased senescence.
Conclusion: This work establishes a direct coculture model of patient-derived PDAC organoids with CAFs, providing a platform to characterize RT response in a compartmentalized tumor-stroma context. Our findings reveal compartment-specific responses and differential growth dynamics, highlighting the utility of integrated tumor-stromal models for investigating the effects of RT and advancing toward more physiologically relevant preclinical approaches.
Funding: ANID/FONDECYT Grants #1241269 and 1221253, ANID/FONDAP Grant #152220002.

#3418 Pre-treatment patient-derived esophageal squamous cell carcinoma organoids as a predictive platform for docetaxel, cisplatin and fluorouracil neoadjuvant chemotherapy.

Hajime Kashima[1], Kazuhiro Noma[1], Akito Shimizu[1], Yasushige Takeda[1], Yohei Mizusawa[1], Tasuku Matsumoto[1], Hijiri Matsumoto[1], Tomoyoshi Kunitomo[1], Masashi Hashimoto[1], Naoaki Maeda[1], Satoru Kikuchi[1], Shunsuke Tanabe[1], Hotaka Kawai[2], Toshiaki Ohara[3], Hiroshi Tazawa[1], Hiroshi Nakagawa[4], Toshiyoshi Fujiwara[1]

[1]Gastroenterological Surgery, Okayama University Hospital, Okayama, Japan,[2]Oral Pathology and Medicine, Okayama University Graduate School of Medicine, Dentistry and Pharmaceutical Sciences, Okayama, Japan,[3]Pathology, Okayama University Graduate School of Medicine, Dentistry and Pharmaceutical Sciences, Okayama, Japan,[4]Columbia University, New York, NY

Background: Patient-derived organoids (PDOs) are a promising platform for functional precision oncology. In esophageal squamous cell carcinoma (ESCC), docetaxel/cisplatin/fluorouracil (DCF) is a standard neoadjuvant regimen, yet some patients show poor pathological response, underscoring the need for treatment-naïve biopsy-derived PDO models to predict individual benefit.

Methods: Treatment-naïve endoscopic biopsies from ESCC patients were used to generate three-dimensional PDOs in Matrigel-based, growth factor-supplemented culture. We analyzed 48 consecutive cases collected after technical standardization. Successful establishment was defined as organoid formation after the first cell seeding, and long-term maintenance as ≥5 passages. Long-term PDOs from patients who received DCF followed by esophagectomy were subjected to 72-hour dose-response assays; IC_{50} values were compared with pathological response and clinical course.

Results: PDOs were successfully established in 45/48 cases, and long-term maintenance was achieved in 10/48. Three long-term PDO cases received preoperative DCF alone and underwent esophagectomy (Cases A-C). Case A (pT2N2M0, Ryan grade 1, Ly0, V0) showed low IC_{50} values for all three drugs, indicating broad in vitro sensitivity concordant with good pathological response without lymphovascular invasion. Case B (pT3N0M0, Ryan grade 2, Ly0, V0, positive margin) exhibited markedly elevated IC_{50} values for all drugs, consistent with global drug resistance and suboptimal local control. Case C (pT3N1M0, Ryan grade 2, Ly1b, V1b) showed selective resistance to docetaxel but low IC_{50} values for cisplatin and 5-fluorouracil, paralleling an intermediate pathological response with persistent lymphovascular invasion. PDO drug sensitivity patterns qualitatively paralleled the degree of pathological response, with triple-sensitive PDOs associated with more favorable regression.

Conclusions: Although the current long-term maintenance rate of ESCC PDOs remains modest, PDOs derived from pre-treatment biopsies showed concordance between in vitro DCF sensitivity and clinical response, supporting their potential as a platform to predict neoadjuvant efficacy. Further case accrual and refinement of culture conditions may enable individualized perioperative treatment strategies guided by PDO-derived drug sensitivity.

#3419 Structural heterogeneity of tumor spheroids using quantitative assessment of autofluorescence.

Prabhat Suman, Sooraj Kakkat, Joel F. Andrews, Chandrani Sarkar, Dhananjay T. Tambe, **Debanjan Chakroborty**

University of South Alabama, Mobile, AL

Introduction: Intratumor heterogeneity is a well-recognized contributor to tumor progression and the development of treatment resistance. Procedures like traditional sampling and bulk sequencing often fall short of capturing the vascular intratumoral landscape. Here, we introduce a novel analytical workflow that uses quantitative 3D autofluorescence imaging to examine the structure and cellular organization of breast cancer cells (BCC) spheroids generated from BCCs and fibroblasts (MEFs and CAFs). This innovative approach enables characterization of structure in multicellular tumor spheroids via fluorescence-based volumetric imaging and computational tools.

Methods: Tumor spheroids were created by co-culturing 4T1 (mouse BCC) with MEFs or CAFs in a 2:1 ratio. The spheroids were generated using 24-well AggreWell plates (STEMCELL Technologies), and Z-stack images were taken using a confocal microscope. Custom software was developed using the Google Colab cloud platform and various Python libraries, including OpenCV and scikit-image. Z-stack images were acquired with the EGFP green and red fluorescence channels, and combined at each z-level using the maximum intensity of the two channels. To focus on large-scale objects, the image was filtered using a Gaussian filter and converted to a binary image using the Otsu algorithm. The fluorescent-intensity-weighted centroid of the spheroid was then estimated. With respect to this centroid, three radial functions were computed: mean intensity, standard deviation, and coefficient of variation. Using a log-log regression fit, the power-law relationship between the mean and standard deviation was computed, and Taylor's exponent for each type of spheroid was determined.

Results and Conclusion: Our results identify a significant difference in intra-spheroidal heterogeneity between spheroids grown with MEFs, CAFs, or BCCs. The Taylor's exponent, b, for group A (4T1 and MEFs) spheroids was about 1, indicating a Poisson-like distribution. However, for Group B spheroids (4T1 and CAFs), the exponent was larger, suggesting a super-Poisson aggregation. The fitted exponents (mean ± SD) were $b = 1.12 \pm 0.05$ for the A group and $b = 1.38 \pm 0.04$ for the B group. These higher-exponent spheroids indicate greater radial heterogeneity and uneven distribution of the fluorescent signal. A Taylor's exponent $b > 1$ signifies that the standard deviation grows faster than the mean. i.e., the greater the mean intensity, the more extreme were the denser and rarer regions of the spheroid, potentially creating drug-resistance niches within the spheroid. Our findings are significant and indicate that this label-free, noninvasive method can be used to detect intertumoral heterogeneity in the near future. These insights can inspire future studies to explore changes within the tumor microenvironment and design new strategies targeting treatment-resistant niches in solid tumors.

#3420 DoE-based optimization of transposon-based gene insertion using the Harbor-IN system.

Kanstantsin Lashuk[1], Corey Brizzee[2], Ina Rohleff[1], **Julia B. Schueler**[1]

[1]Charles River Laboratories, Freiburg, Germany,[2]Demeetra, Lexington, KY

Efficient and safe genetic labeling of mammalian cells is essential for applications in cell tracking, functional assays, and high-throughput screening. In this study, we developed and optimized a biosafety level 1 (BSL-1) protocol for stable integration of fluorescent and luminescent reporter genes using a transposon-based system. A Design of Experiments (DoE) approach was employed to systematically optimize co-transfection conditions of plasmid DNA encoding the reporter gene and in vitro-transcribed RNA encoding the transposase. Four commonly used transfection reagents—Lipofectamine 3000, PEI, ViaFect, and jetPRIME—were evaluated for their efficiency and compatibility with the system. Key factors such as nucleic acid ratios, total cargo amount, and reagent concentration were varied to maximize integration efficiency while maintaining cell viability. The optimized protocol achieved robust and reproducible reporter expression across multiple cell types without requiring viral vectors or higher biosafety containment. This work provides a scalable, non-viral strategy for generating stably labeled cell populations, enabling downstream applications in imaging, functional genomics, and assay development under standard laboratory conditions.

#3421 Bioprinted colorectal cancer organoids as a platform for large-scale therapeutic screening.

Taehee Kim, Jonathan Levi, Catherine Chen, Lindsay Ng, Alice Soragni

UCLA - University of California Los Angeles, Los Angeles, CA

Colorectal cancer is the fourth leading cause of cancer-related deaths in the United States. Among patients with metastatic colorectal cancer, approximately 70-75% survive more than 1 year after diagnosis, 30-35% survive more than 3 years, and fewer than 20% survive beyond 5 years. The main treatment options for unresectable metastatic colorectal cancer include cytotoxic chemotherapy, biologics, immunotherapy, and combinations thereof. Therapeutic options for unresectable metastatic disease remain limited, and more predictive preclinical platforms are urgently needed. To address this need, we developed a high-throughput mini-ring screening platform using patient-derived colorectal cancer organoids generated through 3D bioprinting. We generated and screened more than 28,000 bioprinted organoid mini-rings to ensure uniform size, architecture, and reproducibility across models.Screens incorporated standard colorectal cancer agents, including 5-fluorouracil, capecitabine, irinotecan, leucovorin, and oxaliplatin, along with a targeted 100-compound targeted panel spanning diverse pathways. Dose-response profiling enabled robust IC50 determination and revealed distinct sensitivity and resistance patterns across organoid models representing multiple disease stages. Transcriptomic analyses for each model were integrated to contextualize these functional profiles and identify pathway-level features associated with therapeutic vulnerability.This work shows how bioprinted colorectal cancer organoids provide a scalable and biologically relevant platform for high-throughput drug screening to support the development of more precise and effective therapeutic strategies for colorectal cancer.

#3422 Live, label free 3D virtual HE imaging of small intestinal organoids using holotomography and generative cross-modality artificial intelligence.

Jimin Cho[1], **Juyeon Park**[1], Hyun-Seok Min[2], YongKeun Park[1]

[1]KAIST, Daejeon-si, Korea, Republic of,[2]Tomocube, Daejeon, Korea, Republic of

Organoids provide physiologically relevant 3D models of tumor biology, but current imaging depends on fluorescence labeling, clearing, or destructive sectioning, limiting longitudinal analysis and perturbing native states. Holotomography (HT) enables long-term, high-resolution, label-free 3D imaging of live intestinal organoids, capturing crypt budding, mitosis, apoptosis, and drug-induced cytotoxicity. Generative frameworks that translate refractive index (RI) tomography into multiplexed fluorescence or H&E-like contrast, including RI2FL and 3D virtual H&E, have shown accurate cross-modality prediction. Here, we integrate these technologies to achieve live, label-free 3D virtual H&E visualization of growing intestinal organoids.Mouse small intestinal organoids were imaged continuously for 120 hours using low-coherence HT. 3D RI tomograms covering whole organoids were reconstructed and stitched. A 3D generative translation model—trained on paired RI–H&E data from human colon cancer tissues and extended using RI2FL's generalizable strategy—was adapted to predict 3D virtual H&E volumes directly from RI stacks, without staining, fixation, or sectioning. Resulting images were evaluated for epithelial architecture, crypt–villus organization, nuclear morphology, luminal topology, and drug-induced injury. Cisplatin-treated organoids were monitored over days.Label-free HT revealed morphogenesis including symmetry breaking, crypt budding, epithelial migration, extrusion, and luminal remodeling. Applying the model to live RI volumes produced artifact-free 3D virtual H&E with hallmark features: basophilic nuclei, eosinophilic cytoplasm, apical organization, Paneth-like granularity, and mucin-rich domains. Depth-resolved virtual H&E preserved axial continuity of crypt–villus structures. In drug-response assays, cisplatin induced early nuclear condensation, crypt collapse, and epithelial fragmentation; virtual H&E highlighted these patterns more clearly than raw RI, while HT-derived metrics showed decreases in protein density and dry mass. The model maintained stable inference across dynamic, unlabeled, live samples, extending RI2FL's cross-system generalizability to complex multicellular organoids.This work establishes the first long-term, fully label-free 3D virtual H&E imaging of live organoids, enabling multi-day, non-destructive histology with subcellular contrast. The approach quantitatively captures pharmacodynamic injury and viability and offers a scalable platform for preclinical oncology, drug screening, and organoid pathology, introducing a new paradigm of live virtual histopathology.

#3423 Integrating PDX and PDX-derived organoid platforms to enhance translational drug discovery in breast cancer.

Erin E. Trachet[1], Liqiang Zhang[2], Kari Kotlarczyk[3], Gregg Hirschfeld[4], Damaris Diaz[5], Paul Gonzales[5]

[1]Scientific Engagement, TD2 Oncology, Scottsdale, AZ,[2]Preclinical Bioanalysis, TD2 Oncology, Scottsdale, AZ,[3]Preclinical In Vitro, TD2 Oncology, Scottsdale, AZ,[4]Preclinical In Vivo, TD2 Oncology, Scottsdale, AZ,[5]Preclinical, TD2 Oncology, Scottsdale, AZ

Breast cancer remains a leading cause of mortality among women, underscoring the need for translational models that more accurately predict clinical response. Traditional immortalized cancer cell lines lack the genetic diversity, three-dimensional architecture, and stromal microenvironmental context of patient tumors, thereby limiting their translational relevance. Patient-derived xenograft (PDX) models preserve the histologic and molecular features of primary breast tumors across passages and have become powerful systems for evaluating therapeutic response, mechanisms of resistance, and biomarker discovery across subtypes including triple-negative, HER2-positive, and hormone receptor-positive cancers. Despite their translational relevance, PDX studies are resource intensive and low throughput. To address these constraints, patient-derived organoids (PDxO) generated from PDX tumors provide an efficient ex vivo platform for early screening and mechanistic assessment. PDxO models preserve genomic fidelity and phenotypic heterogeneity, enabling direct comparison of drug responses between in vitro and in vivo systems. This integrated workflow supports rapid, iterative evaluation in which compounds are first screened in PDxO cultures to assess efficacy, cytotoxicity, and mechanism of action, followed by validation in matched PDX models to confirm pharmacodynamic performance and in vivo antitumor activity. We have established an advanced organoid-based drug discovery platform by leveraging our breast cancer PDX collection to generate robust PDxO models. We developed and validated high-quality organoid drug-screening assays using CellTiter-Glo 3D and real-time live-cell imaging with the Incucyte system, enabling quantitative assessment of viability, growth kinetics, and treatment responses. Using models such as HCI-015 and HCI-032, we demonstrated consistent organoid formation, reproducible drug sensitivity profiling, and applicability across diverse therapeutic modalities, including agents under evaluation for immunotherapy combinations. Collectively, the integrated use of PDX and PDxO platforms enable a more comprehensive understanding of breast cancer biology and therapeutic vulnerabilities. Correlating drug response data across systems reveals model-specific and subtype-dependent differences, facilitating rational treatment selection and biomarker identification. This complementary approach advances precision oncology by linking high-throughput ex vivo screening with biologically relevant in vivo validation, thereby accelerating the translation of preclinical discoveries into actionable clinical strategies.

#3424 Comparative analysis of 2D and 3D cell culture methods on DNA methylation patterns in medulloblastoma.

Karen Sperle[1], Laurel Stell[2], Micheal Avoseh[3], Aderonke Ajongbolo[1], Haozhe Zheng[4], Darrin Pochan[4], **Sigrid Langhans**[1]

[1]Neurology, Nemours Children's Hospital, Wilmington, DE,[2]Stanford University, Palo Alto, CA,[3]Nemours Children's Hospital, Wilmington, DE,[4]Materials Science and Engineering, University of Delaware, Newark, DE

Epigenetic processes including histone modifications, DNA methylation, chromatin remodeling, and regulatory non-coding RNAs such as microRNAs regulate gene expression without direct alterations to the genome. Among these, DNA methylation which involves the addition of a methyl group to the fifth carbon of cytosine (C), forming 5-methylcytosine (5mC) most frequently in CpG dinucleotides (CpGs), is one of the most studied epigenetic modifications. DNA methylation has been shown to influence tumor development, tumor progression and therapy response in various cancers, including medulloblastoma, the most common malignant brain tumor in children. Due to the extensive genome-wide profiling done by several international consortia and independent groups, extensive genomic databases, including DNA methylation profiles, are publicly available for medulloblastoma making it suitable as a model system to study whether different cell culture techniques influence DNA methylation patterns. Here we sought to investigate whether 3D cell culture systems, commonly referred to as more closely recapitulating in vivo tumor microenvironments, promote DNA methylation patterns in tumor cell lines that are more closely aligned with those of patient tumors. Most commonly used human medulloblastoma cell lines, traditionally cultured as 2D monolayers, were subjected to both anchorage-independent (spheroids) and scaffold-based (collagen, Matrigel, synthetic peptide hydrogel) 3D cell culture methods. Genome-wide methylation profiles were generated using the Infinium MethylationEPIC BeadChip Arrays and compared to the Molecular Neuropathology group/Deutsches Krebsforschungszentrum (DKFZ) brain classifier database. Surprisingly, none of the human medulloblastoma cell lines was considered a match (score equal to or higher than 0.9) and three out of the five cell lines initially tested had values of less than 0.3 and did not meet the study criterion. Moreover, there was considerable differences in scores between cell lines but not between culture condition (2D versus 3D) for a given cell line even when applying different normalization methods to reduce non-biological artifacts. Thus, spheroid- or scaffold-based 3D cell culture methods did not translate into better alignment with patient-derived methylation profiles and suggests limited potential for these models to replicate patient tumor profiles. Furthermore, our data reveal that even in conjunction with advanced cell culture technology, the choice of biological model is a crucial component in engineering accurate disease models.

#3425 Leveraging bioconvergence to enhance organ-on-a-chip technology and revolutionize drug discovery and development.

Shashi K. Tiwari[1], Stephan Krieg[2], Fong Cheng Pan[1], David Austin[1], Kevin Su[3], Luisa Marie Pfeifer[2], Mathab Asadian[4], Xiaoping Song[4], Laura Chacon Orellana[4], Rashmi Ramesh[4], Alessandra Venz[4], Bastien Duckert[4], Mara Lucchetti[4], Joseph Lento[1], Sophie Roth[4], Olivier Henry[4], Dries Braeken[4], Laura Braeuninger-Weimer[5], Philip Hewitt[2], Steven Johnston[6], Vi Chu[1]

[1]MilliporeSigma, Temecula, CA,[2]Merck Healthcare, Darmstadt, Germany,[3]R&D, MilliporeSigma, Temecula, CA,[4]iMEC, Leuven, Belgium,[5]Merck Ventures, Frankfurt, Germany,[6]EMD Group, Darmstadt, Germany

Background: Bioconvergence combines materials science, microelectronics with organoid biology to revolutionize organ-on-a-chip (OOC) technology, facilitating effective translational drug discovery. Our initiative aims to develop new generation of in vitro platforms by integrating human 3D cell cultures with a semiconductor-based, sensor-integrated microfluidic silicon chip, enabling the simulation of interconnected multi-organ physiology.
Methods: We developed human gut and liver organoids from induced pluripotent stem cells (iPSCs) and patient-derived organoid (PDO). The organoids were validated for lineage identity and functionality through immunofluorescence for key markers, RT-qPCR for gene panels, and functional assays such as transepithelial electrical resistance (TEER) and enzyme activity. This validated biology was integrated by connecting it to fluidic and electrical interfaces in sterile conditions.
Results: Duodenal PDO-derived gut organoids exhibited well-defined epithelial architecture and barrier integrity, along with the expression of essential transporters (BCRP) and metabolic enzymes (CYP3A4, UGT1A1). They also displayed lineage markers, including brush border (Villin), goblet (MUC2), Paneth (LYZ), and enteroendocrine (CHGA) cells. iPSC-derived mature liver organoids expressed markers for hepatocytes and cholangiocytes, including albumin, Sox9, CK7, and CK19, demonstrating Phase I/II metabolic competence and relevant drug transporters (CYP3A4, GST, MDR1/P-gp, MRP2). These organoid systems establish a solid foundation for exploring the viability and functionality of the platform.
Conclusions: Integrating validated human organoid biology with scalable semiconductor microfluidics creates a microphysiological platform that significantly enhances translational relevance for toxicology, drug metabolism and pharmacokinetics (DMPK), and disease modeling. It supports the development of safer, more effective therapies while minimizing reliance on animal studies.

: Microenvironmental Determinants of Therapy Response and Resistance 1
Poster Session

#3429 Macrophages promote immunotherapy resistance of hepatocellular carcinoma through increasing tumor cell lipid availability.

Zhixian Liang, Xiaohang LONG, ZHEWEN XIONG, PATRICK WONG, Siyuan HUANG, Siyun Chen, Yiling Zhang, Lingyun ZHANG, Chunning Leung, Saiming Ngai, Stephen Lam CHAN, Alfred S. L. Cheng

The Chinese University of HONG KONG, HONG KONG, China

Hepatocellular carcinoma (HCC) is the most common type of liver cancer. Although increasing immune checkpoint blockade (ICB) inhibitors have been applied in HCC clinical trials, the immunosuppressive tumor microenvironment (TME) restricts therapeutic responses to a small subset of patients. The triggering receptor expressed on myeloid cells-2 (TREM2) plays a critical role in counteracting inflammation and maintaining metabolic fitness in myeloid cells. Recently, we performed single-cell RNA sequencing (scRNA-seq) on tumor biopsies from a phase II clinical trial of pembrolizumab on advanced hepatitis B virus (HBV)-related HCC patients (NCT03419481) and identified a subset of tumor-associated macrophages (TAMs) over-expressing TREM2, which were enriched in non-responders following therapy. Consistently, our syngeneic ICB-sensitive and resistant HCC mouse models verified that $Trem2^+$ TAMs were adaptively increased after anti-PD-1 treatment in resistant tumors. We observed that $TREM2^+$ TAMs enriched in lipid-laden TME and transferred fatty acids to tumor cells. *Trem2* deficiency in myeloid cells reduced the lipid level of tumor cells and re-sensitized them to anti-PD-1 therapy.

#3430 NR4A3 functions as an immuno-metabolic checkpoint in tumor-associated macrophages to mediate radiotherapy sensitivity in rectal cancer.

Xiaowan Guo[1], Gan Tao[2], Xiuli Guo[1], Kehua Hu[1], Rurui Xue[1], Yunli Mo[1], Hui Qiu[1], **Qiuji Wu**[1]

[1]Zhongnan Hospital of Wuhan University, Wuhan, China,[2]The First Affiliated Hospital of Anhui Medical University, Hefei, China

Background: Radiotherapy resistance remains a major therapeutic challenge in rectal cancer. Tumor-associated macrophages (TAMs) are pivotal components of the tumor immune microenvironment. The nuclear receptor NR4A3 is a key regulator of TAM activation. This study aimed to investigate the role of macrophage-expressing NR4A3 in radiotherapy sensitivity in rectal cancer.
Methods: Transcriptomic RNA sequencing analyses were used to identify key differential genes and pathways. Interfering RNAs were applied to modulate NR4A3 expression in macrophages. Signaling pathways and metabolic alterations were assessed by Western blot, qPCR, ELISA. Functional effects were evaluated in macrophage-colorectal cancer cell co-culture models.
Results: High NR4A3 expression in TAMs correlated with improved pathological response and prolonged survival in rectal cancer patients receiving neoadjuvant radiotherapy. Transcriptomic analysis revealed marked alterations in NR4A3 expression and lipid metabolism pathways in post-radiation cells. NR4A3 expression was induced in macrophages following radiotherapy, which was consistently validated in vitro (THP-1, RAW264.7), in murine MC-38 xenograft models, and human rectal cancer samples. NR4A3 knockdown promoted an M2-like polarization state (evidenced by elevated CD163, IL-10) and enhanced expression of immune checkpoint molecules (PD-L1, siglec-15), while suppressing M1 markers (CD86, IL-1β, TNFα). Functional assays revealed that NR4A3-deficient macrophages lost tumor-suppressive capacity in co-culture systems. On the other hand, NR4A3 promoted cholesterol synthesis and efflux in macrophages, with ABCG1 identified as a critical downstream cholesterol exporter. Macrophage-derived cholesterol contributed to tumor cell proliferation. Inhibiting ABCG1 rescued tumor suppressive effect of radiation-activated macrophages.
Conclusion: NR4A3 acts as a radiation-induced "immuno-metabolic checkpoint" in TAMs, enhancing M1 polarization and antitumor immunity, while concurrently driving ABCG1-dependent cholesterol efflux and a pro-tumor metabolic milieu. These results illuminate the dual role of NR4A3 in mediating the paradoxical effects of radiotherapy on the immune microenvironment and underscore its potential as a therapeutic target for overcoming radiotherapy resistance in rectal cancer.

#3431 Neutrophil-like monocytes (NeuMos) with high levels of CXCL2 expression orchestrate systemic granulopoiesis and drive immunotherapy resistance in TNBC.

Fulya Alkan[1], Hilmi K. Alkan[1], Ahmet Caglayan[2], Aysun Caglayan[2], Aminah Lawal[3], Neva Celiker[3], Huidong Shi[4], Thomas Vogl[5], Nouri Neamati[6], Wicha Max[7], Hasan Korkaya[3]

[1]Oncology, Wayne State University, Detroit, MI,[2]University of Michigan, Ann Arbor, MI,[3]Wayne State University, Detroit, MI,[4]Medical College of Georgia, Augusta, GA,[5]Institute of Immunology, Muenster, Germany,[6]Univ. of Michigan College of Pharmacy, Ann Arbor, MI,[7]Department of Internal Medicine, University of Michigan, Ann Arbor, MI

Triple-negative breast cancer (TNBC) is characterized by early metastatic spread and poor response to immunotherapy, yet the systemic immune mechanisms underlying this aggressive behavior remain poorly defined. Using a comprehensive multi-omics approach that integrates single-cell RNA sequencing (scRNA-seq), high-dimensional mass cytometry (CyTOF), flow cytometry analyses, in vivo genetic perturbations, and multiple syngeneic TNBC models, our preliminary data suggested that recently introduced neutrophil-like monocyte population (NeuMo) emerges selectively within highly metastatic tumors. NeuMos exhibit a dynamic monocyte–granulocyte transcriptional profile and initiate a pro-inflammatory cascade driven by CXCL2, and G-CSF signaling. This axis induces robust emergency granulopoiesis in the spleen, markedly expanding immature $CD11b^{+}Ly6G^{+}CXCR2^{+}$ granulocytic cells that infiltrate tumors and peripheral tissues establishing systemic immunosuppression. In contrast, non-metastatic EMT6 tumors maintain balanced adaptive and innate immune compartments with minimal granulocytic activation, highlighting the specificity of NeuMo-driven inflammation to aggressive TNBC states. Functional experiments demonstrate that deletion of S100A9, an upstream amplifier of this inflammatory circuit, disrupts granulocytic expansion, reduces splenic hypertrophy, diminishes lung metastasis, and significantly enhances the therapeutic efficacy of PD-L1 blockade in both AT3 and E0771 TNBC models. These findings put S100A9 as a critical mediator of immunotherapy resistance. Analysis of human TNBC datasets, including TCGA, reveals early induction of S100A8/A9, G-CSF, and CXCL1/2 gene programs associated with high-grade tumors and poor survival, underscoring the clinical relevance of this pathway. Collectively, our work identifies NeuMo-driven inflammatory mediator as a central mechanism linking TNBC tumor-intrinsic programs to systemic immune remodeling, metastasis, and checkpoint resistance. These results not only define a novel myeloid-based biomarker signature for aggressive TNBC but also nominate the S100A9/CXCL2/G-CSF axis as an actionable therapeutic target to improve immunotherapy outcomes.

#3432 Role of M2 macrophages in chemoresistance about the tumor microenvironment of epithelial ovarian cancer.

Jaesung Ryu[1], Baek MooJun[2], HyoWook Gil[3], Eunjung Yang[3], Kwangseock Kim[2], Taewan Kim[4], Kong Hyejeong[5], Beamjun Park[5], **Seob Jeon**[2]

[1]Korea Research Institute of Bioscience and Biotechnology, Daejeon, Korea, Republic of,[2]Soonchunhyang University Cheonan Hospital, Cheonan, Korea, Republic of,[3]Soonchunhyang Cheonan Hospital Medical Center, Cheonan, Korea, Republic of,[4]Soonchunhyang University, Cheonan, Korea, Republic of,[5]Soonchunhyang University, Asan, Korea, Republic of

OBJECTIVE One of the hallmark characteristics of ovarian cancer is the development of resistance to chemotherapeutics. The mutual interactions with tumor cells and stromal microenvironment contribute to phenotypically polarization of tumor associated macrophages. Macrophages consist of at least two subgroups, M1 and M2. M2 macrophages are endowed with a repertoire of tumor-promoting capabilities involving immuno-suppression, angiogenesis and neovascularization, as well as stromal activation and remodeling. Therefore, there is a need for more practical targets to inhibit chemotherapeutic drug resistance and cancer progression due to ovarian cancer-macrophage interactions. To better understand the mechanism of chemoresistance in ovarian cancer cells, we aimed to investigate the influence of macrophages on the tumor cell response to carboplatin and identify the genes associated with chemoresistance.

METHODS Macrophages were differentiated into M1 and M2 macrophages by cytokine treatment of monocytes. The tumor microenvironment (TME) was modified by transwell co-culture assay. We treated the carboplatin and tested chemoresistance. We also examined expression of key genes associated with EMT (Epithelial-Mesenchymal Transition), PD-L1 and chemoresistance. Nanostring analysis identified gene expression changes in tumor signaling pathways in ovarian cancer cells co-cultured with M2 macrophages compared to single-cultures. Functional study (proliferation, migration, invasion, wound healing) were performed to determine the role of the M2 macrophage in ovarian cancer.

RESULTS Compared to single-cultured ovarian cancer cells, iNOS was downregulated in co-cultured with M2 macrophages, while PD-L1,CD206,TGF-b,MDR1,CSF-1 and Arg1 were upregulated. PD-L1 was also upregulated in M2 macrophages. Ovarian cancer cells co-cultured with M2 macrophages showed higher carboplatin resistance compared to single-cultured ovarian cancer cells. EMT-promoting related genes CD2,VIM, ZEB1 and SNAIL1 were upregulated in ovarian cancer cells co-cultured with M2 macrophages. Nanostring analysis revealed changes in the expression levels of genes associated with tumor signaling pathway activation and EMT. Ovarian cancer cells co-cultured with M2 macrophages performed functional study, we found that the functional abilities of the cancer cells were all significantly increased.

CONCLUSION We identified changes in the expression of various genes in ovarian cancer cells which were co-cultured with M2 macrophages, and identified upregulation of PD-L1 as a key factor in chemoresistance. We have also conducted additional nanostrings to refine the impact of M2 macrophage and ovarian cancer cell interactions on tumour signalling pathways as well as chemoresistance in the tumour microenvironment, and will be analysing these data and conducting further experiments.

#3433 A new classification of tumor-associated macrophages and their roles in resistance to immune checkpoint therapy.

Bryan T. Weselman, Satish Kumar Reddy Noonepalle, Manasa Suresh, Alexandra Singh, Isabella Duchovny, Xintang Li, Mackenna Ward, Alejandro Villagra

Georgetown Lombardi Comprehensive Cancer Ctr., Washington, DC

Tumor-associated macrophages (TAMs) perform a wide range of functions in the tumor microenvironment (TME), several of which contribute to resistance to immune checkpoint therapy. Given their high abundance and diverse functions, altering TAM activity is a promising supplement to immune checkpoint therapy. We demonstrate the potential of a new classification of TAMs, characterized by functional distinctions in gene expression, cell-cell interactions, and spatial localization. We validate the functions suggested by gene expression using *ex vivo* functional assays with primary TAMs. We compare markers of the eight functional TAM subpopulations in murine melanoma data with those in human data to develop a translatable gene signature for each functional subtype. We demonstrate that treating bone marrow-derived macrophages with different cytokine combinations can replicate TAM subtypes *in vitro*, advancing the field beyond the conventional M1-M2 model and enabling a more comprehensive approach. To demonstrate the importance of TAM subpopulations in response to immune checkpoint therapy, we show differences in the abundance of each subtype in untreated murine tumor models that are responsive or non-responsive to anti-PD-1 therapy. At the single-cell RNA-seq level, we find changes in the TAM landscape of murine SM1 melanoma tumors after systemic treatment with epigenetic-modifying agents, with or without anti-PD-1 therapy, and compare these changes with those observed in publicly available human melanoma data. Anti-PD-1 therapy in murine tumors results in a clear enrichment of APC-TAMs (an antigen-presenting, phagocytic, and complement-driven subpopulation), which is further enhanced by systemic HDAC inhibitors. The IFN-TAMs, which reflect a more conventional “M1” macrophage, are less strongly associated with response to immune checkpoint therapy. We see a reduction in angiogenic, hypoxia-driven “AFH-TAMs” in response to multiple anti-cancer therapies. In future studies, we will harness the APC-TAM population to overcome resistance to immune checkpoint therapy in multiple murine tumor types. Compared with melanoma tumors, murine breast cancers have a significantly higher proportion of ECM-TAMs, macrophages involved in extracellular matrix remodeling and homeostasis. We will aim to pharmacologically alter the abundance of other tumor-supporting macrophage populations, depending on the characteristics of different tumor types.

#3434 Spatially resolved multi-omic profiling reveals BRCA-dependent immune remodeling during PARP inhibition and PD-L1 blockade.

Kenichi Shimada[1], Filipa Lynce[2], Claudine Isaacs[3], Xue Geng[3], Edward T. Richardson[4], Candace Mainor[3], Mei Wei[5], Julie M. Collins[3], Paula R. Pohlmann[6], Arielle L. Heeke[7], Kelly F. Zheng[4], Madeline Townsend[4], Lauren M. Sloat[1], Jane Staunton[1], Stuart J. Schnitt[4], Hongkun Wang[3], Joan S. Brugge[1], Geoffrey I. Shapiro[2], Jennifer L. Guerriero[4]

[1]Harvard Medical School, Boston, MA,[2]Dana-Farber Cancer Institute, Boston, MA,[3]Georgetown University, Washington, DC,[4]Brigham and Women's Hospital, Boston, MA,[5]University of Utah, Salt Lake City, UT,[6]The University of Texas MD Anderson Cancer Center, Houston, TX,[7]Atrium Health, Charlotte, NC

Background

PARP inhibitors (PARPi) induce synthetic lethality in BRCA1/2-mutant (BRCA-MUT) tumors and can activate DNA-damage-linked immune pathways. The TALAVE study (NCT03964532) examined the combination of the PARPi (talazoparib) with PD-L1 blockade (avelumab). Here we evaluated spatially resolved immune signaling and remodeling in response to talazoparib alone and with avelumab.

Methods

24 patients with advanced HER2-negative breast cancer (12 BRCA-MUT, 12 BRCA-WT) received talazoparib then talazoparib + avelumab. Serial biopsies (baseline, post-PARPi [BX2], post-combination [BX3]) underwent transcriptomic, spatial protein, and multiplex IF. BRCA-dependent TME remodeling and cellular neighborhood (CN) shifts were assessed.

Results

BRCA-MUT tumors showed 83% objective response and 100% clinical benefit, whereas BRCA-WT tumors exhibited minimal activity. BRCA-MUT tumors became fragmented with increased immune activity, while BRCA-WT tumors remained compact and immunosuppressed. γH2AX and pTBK1 were spatially co-expressed and sustained in BRCA-MUT tumors during treatment but declined in BRCA-WT tumors. BRCA-MUT tumors displayed enrichment of $CD8^+$ T cells and $CD163^+$ macrophages after PARPi, whereas $CD4^+$ T cells and $CD68^+CD163^+$ macrophages were depleted in BRCA-WT tumors. PD-1^+ $CD8^+$ T cells were strongly linked to local $CD4^+$ T cell density, and PD-1^+ frequency in $CD8^+$ T cells correlated with longer PFS at baseline and BX3 in BRCA-MUT but not BRCA-WT tumors.

CN analysis revealed $CD4^+$ and $CD8^+$ enriched neighborhoods with intermediate PD-1 expression that expanded after therapy in BRCA-MUT but not BRCA-WT tumors, and these CNs lacked PD-$L1^+$ cells. Between BX2 and BX3, BRCA-MUT tumors sustained immune activity but showed no further T cell activation or infiltration. Spatial mapping identified three PD-$L1^+$ CN types: (1) T cell-dense niches with high PD-1/PD-L1 and γH2AX-pTBK1 activity enriched only at baseline, largely lost after PARPi; (2) macrophage-T cell mixtures that were depleted during therapy; and (3) PD-$L1^+$ dying tumor cells lacking pTBK1 activity and T cell engagement. Across contexts, PD-L1 was either lost before PD-L1 blockade or confined to regions isolated from T cells, leaving little opportunity to reinvigorate T cells.

Conclusions

PARP inhibition reshaped the TME of BRCA-MUT tumors by inducing tumor fragmentation, sustaining γH2AX-pTBK1 signaling, and restoring $CD4^+$ and $CD163^+$ immune cells, whereas BRCA-WT tumors remained structurally intact and immunosuppressed. PD-1^+ T cells localized to PD-L1-negative neighborhoods, and PD-$L1^+$ tumor/myeloid cells were rapidly lost or confined to dying, immune-excluded regions, limiting the impact of PD-L1 blockade. Although PARPi re-engaged T cell programs in BRCA-MUT tumors, strategies beyond PD-L1 inhibition will be required to further enhance T cell infiltration and activation.

#3435 Spatial transcriptomic profiling reveals distinct tumor microenvironment remodeling patterns associated with immune checkpoint blockade response in lung adenocarcinoma.

Heesoo Yoon[1], Jin-Wook Choi[2], Sejoon Lee[2], Jin-Haeng Chung[1], Hyojin Kim[1]

[1]Department of Pathology, Seoul National University Bundang Hospital, Seongnam-si, Korea, Republic of,[2]Precision Medicine Center, Seoul National University Bundang Hospital, Seongnam-si, Korea, Republic of

Although immune checkpoint blockade (ICB) has improved clinical outcomes in non-small cell lung cancer (NSCLC), many patients remain resistant, underscoring the need to understand how the tumor microenvironment (TME) evolves during therapy. Therefore, this study aims to characterize spatial TME remodeling associated with ICB. We performed 10x Genomics Visium spatial transcriptomic profiling on paired pre- and post-treatment tumor samples from seven patients with lung adenocarcinoma. Three patients were classified as responders based on immune Response Evaluation Criteria In Solid Tumors criteria (all stable disease) and were compared with four non-responders. The responder group received a mean of 13 ICB cycles, whereas non-responders received 2 cycles. Pre-treatment samples were obtained from lung (n = 4) and lymph node (n = 3), while post-treatment samples were collected from lung (n = 2), lymph node (n = 2), bone (n = 2), and brain (n = 1). After quality control, the mean number of spots was 2212, with a minimum of 266 spots, a maximum of 4715 spots, for a total of 30,968 spots. Spatial profiling demonstrated that responders exhibited consistently higher infiltration of plasma cells and B cells in both pre- and post-treatment samples. In contrast, non-responders showed increased proportions of cancer-associated fibroblasts (CAFs) at both time points. In the pre-treatment samples, responders showed upregulation of HLA-DMA and HLA-C, suggesting preservation of antigen presentation pathways. Additionally, IGKC, IGHG2, and IGHG1 were upregulated, indicating B-cell activation. Non-responders showed upregulation of extracellular matrix (ECM)-remodeling genes (TMSB4X, ACTB) and ferritin metabolism genes (FTL). In the post-treatment samples, non-responders also showed upregulation of ECM-remodeling genes (COL5A1, COL5A2, COL6A2, COL6A1, FN1, TIMP2, MMP2, MMP14), indicating enhanced tumor cell adaptation to a hostile microenvironment and a potential link to M2-like macrophage polarization. In summary, our findings demonstrate that ICB responders exhibit plasma/B-cell-enriched TMEs, whereas non-responders are characterized by increased CAF infiltration along with ECM remodeling and ferritin metabolism gene upregulation, suggesting a potential mechanism of immune resistance. We are currently validating the impact of this ferritin-associated ECM remodeling signature on ICB therapy outcomes in an independent cohort.

#3436 Emerging evidence of cellular dormancy programs in non-small cell lung cancer (NSCLC).

Grace Ha, Melissa Tracy, Anthony Griffen, Daniel Bravo, Dior Dedushi, Terence Li, David Schecter, Neel Chudgar, Chaoyuan Kuang, Julio Aguirre-Ghiso, Brendon Stiles, Lindsay M. LaFave

Montefiore Medical Center / Albert Einstein College of Medicine, Bronx, NY

Despite the practice-changing incorporation of neoadjuvant chemoimmunotherapy (nCI) into the management of clinical stage II-III NSCLC, lung cancer recurrence remains a clinical challenge. At our institution, long-term follow-up has revealed individuals with evidence of recurrence after curative-intent therapy despite demonstrating initial response to nICI and surgery. One potential explanation is cellular dormancy, a state of reversible growth arrest characterized by reduced metabolism and therapeutic resistance, a process well described in breast and head and neck cancers. To investigate lung cancer dormancy, our group has begun collecting lung tumor bed tissue from resected NSCLC patients following nCI. Using these tissues and downstream patient derived organoid (PDO) generation as our primary model, we aimed to characterize dormancy associated gene expression in NSCLC and determine whether chemotherapy and/or immunotherapy induce these programs. We used complementary approaches to address this question. First, to investigate the impact of nCI on tumor heterogeneity and dormancy programs, single-cell Assay for Transposase-Accessible Chromatin (scATAC) sequencing was performed on surgically resected clinical stage II-III NSCLC specimens representing a range of responses to nCI (untreated, 50%, 85%, and 100% regression). We examined gene activity scores across these samples using chromatin accessibility. Our analyses indicated that untreated patient samples exhibited known intratumoral heterogeneity, including cell states with chromatin features similar to alveolar differentiation intermediates, which have been observed as important precursors to lung cancer evolution. Additionally, scATAC-seq from four resected tumors revealed a distinct EPCAM-positive cell population with high gene scores for numerous known cellular dormancy markers, including NR2F1, BHLHE41, SOX9, SOX2, p21, p27, and RARβ. These cells were enriched in untreated samples, suggesting a pre-existing dormant-like subpopulation, but were also present in tumors across all nICI response categories, suggesting the persistence or induction of dormancy following treatment. In parallel, we examined the expression of canonical dormancy markers using quantitative polymerase chain reaction (qPCR), which demonstrated that Cisplatin exposure to PDOs increased the expression of NR2F1, SOX9, p21, and p27 and decreased Ki67, consistent with treatment-induced dormancy. These studies serve as the foundation for dormancy modeling in NSCLC PDOs. Ongoing efforts include cytokine profiling of patient blood samples with the goal of identifying inflammatory signatures that distinguish complete responders from partial responders to nICI.

#3437 Dynamic waves of anti-and pro-tumoral myeloid and Treg cells are generated in response to cyclophosphamide.

Andrea Franceschini[1], Giovanna Talarico[1], Davide Lombardi[1], Stefania Orecchioni[1], Giulia Bravetti[1], Iros Barozzi[2], Paolo Falvo[1], **Francesco Bertolini**[1]

[1]IEO - European Institute of Oncology, Milan, Italy,[2]Center for Cancer Research, Medical University of Vienna, Vienna, Austria

In addition to its direct cytotoxic effects on cancer cells, chemotherapy exerts profound influences on immune cells. These immunological effects must be carefully considered when designing clinically effective combination regimens that include both chemotherapeutic and immunotherapeutic agents. Cyclophosphamide (Cy), a widely used alkylating chemotherapeutic agent, is known to affect various components of the adaptive immune system and natural killer (NK) cells. Based on the observation that a single dose of Cy can lead to increased tumor growth in EMT6 triple-negative breast cancer-bearing mice with predominant myeloid infiltration (but not in 4T1- bearing mice with predominant lymphoid infiltrate), we investigated the immune transcriptional programs triggered by Cy. Using flow cytometry and single-cell transcriptome analysis in tumor-free, tumor-bearing, and Cy-treated mice, we identify novel effects of Cy on neutrophils—innate immune cells increasingly recognized for their roles in both cancer immune tolerance and rejection. One day after Cy administration, a subset of neutrophils expressing an interferon (IFN) signature and associated with anti-tumor activity is expanded, while neutrophils displaying a potentially pro-tumoral Il1b/TNF inflammatory signature and immunosuppressive regulatory T (Treg) cells are reduced. However, in the absence of additional Cy treatment, these effects are reversed by day 10, with the re-emergence of the pro-tumoral neutrophil population. To functionally validate these single-cell findings and directly test the role of myeloid cells in mediating tumor rebound, we performed in vivo immune cell depletion experiments in the EMT6 model. Mice were injected intraperitoneally with neutralizing antibodies against CD11b or Ly6G, targeting myeloid cells and (more selectively) neutrophils, respectively. Depletion efficiency was confirmed by flow cytometry analysis of peripheral blood. Following depletion, mice were orthotopically transplanted with EMT6 cells and treated with a single dose of Cy. Tumor growth in mice receiving either Cy alone or neutralizing antibodies alone was comparable to that of untreated controls, indicating that neither intervention alone was sufficient to control tumor progression. In contrast, the combination of Cy with broad myeloid-cell and selective neutrophil depletion produced a marked anti-tumor effect, resulting in a significant reduction in tumor size compared with all other groups. This experiment represents the functional validation of our single-cell transcriptomic data, suggesting that neutrophils actively drive tumor rebound following transient Cy exposure. These findings highlight the dynamic and time-dependent nature of Cy's immunomodulatory effects and have implications for the design of effective combinatorial anti-cancer therapies.

#3438 DNA damaging therapies induce a pro-tumorigenic fibroblast phenotype.

Emily Lay[1], Mikal Negasi[2], Ben Flynn[3], Tressan Grant[1], Ioanna Kontou[1], Gernot Walko[3], **Ute Jungwirth**[2]

[1]University of Bath, Bath, United Kingdom,[2]Newcastle University, Newcastle upon Tyne, United Kingdom,[3]Queen Mary University of London, London, United Kingdom

There is growing evidence that anticancer therapies not only target tumour cells but also reshape the tumour microenvironment, paradoxically enabling fibroblasts to acquire a pro-tumorigenic phenotype. These fibroblasts are characterised by an altered secretome and extensive extracellular matrix (ECM) remodelling, which promote therapy resistance and tumour progression.
In this study, we demonstrate that DNA damage-inducing anticancer drugs drive normal fibroblasts towards a fibrosis- and cancer-associated fibroblast (CAF)-like phenotype. Using 3D cell-derived ECM deposition assays, we show that treatment of both normal fibroblasts and CAFs stimulates the formation of a more anisotropic ECM with enlarged pores. This remodelled ECM enhances cancer cell adhesion and proliferation, while unexpectedly reducing migration across the matrix. In contrast, the soluble secretome does not affect cancer cell proliferation but significantly increases chemotactic migration towards the therapy-exposed fibroblasts.
Gene expression profiling by RNA sequencing combined with 2D and 3D *in vitro* analyses, reveals that prolonged drug exposure induces fibroblast senescence, marked by upregulation of β-galactosidase, IL6, CDKN1A, and CDKN2A expression. The therapy-induced senescent fibroblasts also display features of a myofibroblast-like CAF (myCAF) phenotype, including enhanced contractility and increased expression of ACTA2, PDGFRA, MMPs, TIMPs, and extracellular matrix components such as collagens, vitronectin, and VCAM. We have previously shown that myCAFs can promote *in vivo* growth and metastasis, underscoring their critical role in tumour progression.
Our findings suggest that therapy-induced senescence in fibroblasts may create a permissive microenvironment for tumour progression.

#3439 Albumin-bound paclitaxel induced stromal reprogramming drives PDAC resistance to AG neoadjuvant chemotherapy.

Haorui Li, Tiansuo Zhao, Xi Ma, Xiang He, Hongji Dai, Bin Wang

Tianjin Medical University Cancer Institute & Hospital, Tianjin, China

Pancreatic ductal adenocarcinoma (PDAC) is a highly lethal malignancy for which neoadjuvant chemotherapy with albumin-bound paclitaxel plus gemcitabine (AG) is a standard first-line approach. However, secondary resistance to AG therapy is common and its underlying mechanisms remain poorly defined. In this study, we investigated how neoadjuvant AG therapy shapes the tumor stroma in PDAC. Single-cell transcriptomics of patient tumors revealed that AG treatment induces a phenotypic switch of cancer-associated fibroblasts (CAFs) from myCAFs to iCAFs states and identified a previously unrecognized TMEM100^{+}CAFs subset enriched in non-responders. Mechanistic studies showed that albumin-bound paclitaxel activates IL-2-STAT5 signaling to drive TMEM100 expression, and that TMEM100^{+}CAFs promote chemoresistance through paracrine secretion of amphiregulin (AREG) and activation of tumor EGFR signaling. Genetic ablation or antibody blockade of TMEM100^{+}CAFs in mouse models reversed CAFs switching and significantly enhanced the antitumor efficacy of AG therapy. These findings map chemotherapy-induced CAFs plasticity, reveal a TMEM100-AREG axis of resistance, and highlight TMEM100^{+}CAFs as a promising target to sensitize PDAC to neoadjuvant treatment.

#3441 Androgen-driven sexual dimorphism reshapes immune crosstalk and limits immunotherapy response in PDAC.

Sonia Mecorapaj[1], Tenzin Passang[2], Fanyuan Zeng[2], Zihan Chen[1], Shuhua Wang[2], Tuisha Gupta[1], Shayna Jankowski[2], Jian-Ming Li[1], Cynthia R. Giver[3], Swapnaa Balaji[4], Kiranj Chaudagar[2], Edmund K. Waller[5]

[1]Hematology & Oncology, Emory Winship Cancer Institute, Atlanta, GA,[2]Emory Winship Cancer Institute, Atlanta, GA,[3]Hematology and Medical Oncology, Emory Winship Cancer Institute, Atlanta, GA,[4]Cambium Oncology, Atlanta, GA,[5]Emory University School of Medicine, Atlanta, GA

Pancreatic ductal adenocarcinoma (PDAC) remains a lethal cancer, with only 13% of patients surviving 5 years. The limited efficacy of anti-PD-1/PD-L1 therapies indicates that additional immunoregulatory pathways sustain the immunosuppressive tumor microenvironment (TME) that restricts T-cell infiltration. Our recent studies (Ravindranathan Nat Com 2022) demonstrated that combined blockade of vasoactive intestinal peptide (VIP) receptor (VPAC) and PD-1 signaling eradicated PDAC in ~50% of mice, although the underlying mechanism of VPAC inhibition remains undefined. Therefore, we hypothesized that VPAC blockade reshapes the immune microenvironment to enhance antigen presentation and T cell responses to anti-PD1 immunotherapy in PDAC.To address this, we characterized the expression of VIP and VPAC on cancer cells, immune cells, and stromal cells in the PDAC TME. We studied the impact of VPAC signaling on the immune functions of myeloid/lymphoid cells and on the architecture of the TME using PDAC patient specimens, murine models, and relevant *in vitro/ex vivo* systems. Tumor growth kinetics were performed to assess the anti-tumor potential of VPAC blockade.*In vitro* secretome analysis showed that murine MT5 PDAC cells secrete more VIP than KPC-luc, consistent with their faster tumor-growth kinetics. To assess host-intrinsic VIP effects in TME we compared tumor progression in WT and *vip*-knockout (*vip-ko*) mice and found markedly slower growth in *vip-ko* mice, especially in females vs. males. To explore the cellular basis of the anti-tumor response, we depleted immune cell subsets and compared tumor growth kinetics in both female and male *vip-ko* mice. Depletion of CD8+ or CD4+ T cells and of CSF1R+ myeloid cells accelerated tumor growth in *vip-ko* mice, whereas clodronate depletion of phagocytic macrophages attenuated anti-tumor responses only in females. Androgen blockade (ARB) with degarelix restored male responsiveness to VPAC inhibition, highlighting androgen-driven resistance in male against VPAC blockade. Mechanistically, VIP from $CD29^{+}PD\text{-}L1^{+}$ fibroblasts suppressed macrophage phagocytosis of PDAC cells, while VIP loss restored this activity. Strikingly, AR activation further suppressed macrophage phagocytosis selectively in males. Mechanistically, TNF-α and MIF secreted from γδ-T cells and $GZMK^{+}CD8^{+}$ T cells, respectively, enhanced anti-tumor phagocytosis in female *vip-ko* mice. Combined AR blockade, anti-PD-1, VPAC antagonism, and taxotere markedly extended survival in WT male mice bearing orthotopic MT5 PDAC (MST 54 vs. 18 days for untreated control).These findings show that VPAC signaling restrains TNF-α– and MIF-dependent immune crosstalk and limits phagocytic PDAC clearance. These data also reveal androgen-suppressed phagocytosis as a driver of sexual dimorphism in response to VPAC antagonism and suggest translatable approaches for PDAC treatment.

#3442 TiME evolution in the context of diffuse astrocytoma post-therapy relapse and progression.

Aliisa Tiihonen[1], Iida Salonen[1], Ella Raulamo[1], Eelis Mikkonen[1], Emilia Maki[1], Maria Annala[1], Tomi Hoikka[1], Ismail Hermelo[1], Anna Denes[2], Thomas Olsson Bontell[3], Helena Caren[4], Asgeir Jakola[2], Hannu Haapasalo[5], Kirsi Rautajoki[1]

[1]Tampere University and TAYS Cancer Center, Tampere, Finland,[2]Institute of Neuroscience and Physiology, Department of Clinical Neuroscience, Sahlgrenska Academy, University of Gothenburg, Gothenburg, Sweden,[3]Department of Clinical Pathology, Sahlgrenska University Hospital, Gothenburg, Sweden,[4]Sahlgrenska Center for Cancer Research, Department of Medical Biochemistry and Cell biology, University of Gothenburg, Gothenburg, Sweden,[5]Department of Pathology, Fimlab Laboratories PLC., Tampere University Hospital, Tampere, Finland

Tumor recurrence and progression are common in IDH-mutant diffuse astrocytomas, which are typically diagnosed as low-grade central nervous system tumors, but frequently progress to grade 4 after conventional therapy, leading to worsened patient prognosis. The biological mechanisms underlying this pattern of recurrence, particularly the contribution of the tumor immune microenvironment (TiME) to treatment resistance and post-therapy progression, remain poorly understood.

To investigate the evolution of the TiME in these tumors, we analyzed a cohort of more than 80 patients with IDH-mutant astrocytoma. For most patients, longitudinal tumor samples were available from both pre-treatment and post-therapy relapse or progression. Using advanced spatial profiling approaches, including highly multiplex immunohistochemistry (mIHC), we characterized immune and cancer cell subtype populations and assessed how their abundance and spatial organization change as tumors recur and progress to higher grade. All findings are being evaluated in the context of patient treatment history and overall survival.

Our preliminary analyses, based on a subset of the full cohort, reveal differences in overall tumor composition both across patients and within matched primary and relapse tumor pairs, highlighting inter- and intra-patient heterogeneity in the TiME. When examining progression-related changes in recurrent tumors, we observe a marked accumulation of $CD163^+$ macrophages and microglia, accompanied by a decrease in $CD163^-$ myeloid phenotypes after chemotherapy. Relapse tumors also show increased infiltration of both $CD4^+$ and $CD8^+$ T cells, suggesting enhanced lymphocytic response during recurrence.

Treatment-specific differences were similarly apparent. Tumors from patients who received combined radiation and chemotherapy showed a higher overall accumulation of immune cells compared to those treated with radiation therapy alone, indicating a potential additive impact on immune cell recruitment. Furthermore, tumor grade appeared to influence overall myeloid composition, with low-grade tumors (WHO grade 2 to 3) exhibiting a higher proportion of microglia compared to high-grade (grade 4) tumors.

Together, this longitudinal dataset provides insights into both recurrent and patient-specific alterations in the TiME that accompany tumor relapse and progression. As these observations are derived from preliminary analyses of a partial cohort, they will be validated in the complete dataset. Ultimately, this work aims to improve our understanding of treatment failure mechanisms and arising opportunities in diffuse astrocytomas.

#3443 Tumor and microenvironmental co-evolution in metastatic triple-negative breast cancer during immunotherapy.

Seongyeol Park[1], Manon de Graaf[2], Artem Lomakin[1], Zhicheng Ma[1], Noah F. Greenwald[1], Lise Mangiante[1], Clemens L. Weiss[1], Brennan Geti Simon[1], Michael Angelo[3], Marleen Kok[2], Christina Curtis[1]

[1]Stanford University School of Medicine, Stanford, CA,[2]The Netherlands Cancer Institute, Amsterdam, Netherlands,[3]Stanford University, Palo Alto, CA

Cancer cells are constantly shaped by the immune system and the dynamic microenvironment surrounding them. Decoding this co-evolution is essential for uncovering the forces that drive tumor progression and determine therapeutic response. Metastatic triple-negative breast cancer (mTNBC) is the most aggressive subtype of breast cancer with a clear need for better treatment options. While recent immunotherapy trials for mTNBC have shown promise in some PD-L1-positive tumors, the reasons for limited and inconsistent responses remain unclear. To investigate these dynamics, we established a multimodal, longitudinal dataset that combines spatial proteomics (MIBI, 40-plex protein) and spatial transcriptomics (CosMx, 6k-plex) from patients with mTNBC enrolled in the phase II TONIC trial in which nivolumab was given to patients regardless of PD-L1 status (NCT02499367). We collected 400 tissue samples from 110 patients, including both pre- and on-treatment biopsies, enabling detailed analysis of tumor-microenvironment interactions and evolution during immunotherapy. Patients with a complete or partial response, or with stable disease lasting longer than 24 weeks, were classified as responders. Using the SpaTopic algorithm, we extracted ten spatial niches (cellular neighborhoods) in our dataset, six of which were dominated by cancer cells. Comparing these with gene expression-based cell clusters revealed a significant link between tumor cell states and their spatial niches. For instance, tumor inflammatory response gene sets are associated with the immune infiltration niche, while hypoxia and epithelial-mesenchymal transition (EMT) gene sets are related to the tumor core. We also defined genomic clusters based on copy-number alterations inferred from spatial transcriptomics data. Within the same genomic cluster, diverse cellular states and spatial niches were observed, indicating that cancer can adapt non-genetically to different niches. Notably, responders exhibited more organized and consistent changes in cellular states and spatial niches before and after immunotherapy, in contrast to non-responders. For example, cancer cells from responders showed increased expression in inflammatory response genes, while non-responders exhibited patient-specific cellular states. This multi-dimensional approach advances our understanding of tumor-immune interactions in mTNBC and offers potential strategies to enhance immunotherapy response.

#3444 Spatial profiling of recurrent glioblastoma in a Phase I clinical trial reveals favorable immune remodeling induced by intracerebroventricular CAR T therapy.

Wesley V. Wilson[1], MacLean P. Nasrallah[2], Nakial Cross[3], Yael A. Day[2], Vanessa Gonzalez[2], Rachel M. Leskowitz[2], Amy Marshall[2], Julie K. Jadlowsky[4], Gabriela Plesa[2], Donald L. Siegel[2], Elizabeth O. Hexner[2], Joseph A. Fraietta[5], Carl H. June[6], Stephen J. Bagley[2], Donald O'Rourke[2], Zev Binder[5], Andrew J. Rech[5]

[1]Princess Margaret Cancer Centre, University Health Network, Toronto, ON, Canada,[2]Penn Medicine, Philadelphia, PA,[3]Perelman School of Medicine Univ. of Pennsylvania, Philadelphia, PA,[4]CCI, Penn Medicine, Philadelphia, PA,[5]University of Pennsylvania, Philadelphia, PA,[6]Program Director of Translational Research, Abramson Family Cancer Research Inst, University of Pennsylvania, Philadelphia, PA

Recurrent glioblastoma (rGBM) is an aggressive brain tumor with median survival under one year after standard chemoradiation. Antigen heterogeneity, immune exclusion, and a suppressive tumor microenvironment (TME) limit responses to immunotherapy. A first-in-human phase 1 trial of intracerebroventricular EGFR/IL13Rα2 CAR T cells (CART-EGFR-IL13Rα2) in EGFR-amplified rGBM was feasible, produced manageable neurotoxicity, and induced radiographic tumor regressions in a subset of patients (NCT05168423).
To understand how this therapy reshapes the local TME, we analyzed paired tumor resections from 6 patients enrolled in the phase 1 trial, with specimens obtained from the primary intracranial disease site at trial enrollment (pre-treatment) and at radiographic progression after CART-EGFR-IL13Rα2 infusion. Multimodal spatial profiling included regional transcriptomic and protein mapping (GeoMx), single-cell whole-transcriptome imaging (CosMx), and high-resolution spatial transcriptomics (Visium HD). We annotated tumor, myeloid, lymphoid, and stromal compartments and derived composite scores for stemness, invasion, cell death, and immune regulation. Neighborhood- and interaction-based analyses were used to compare cellular states and cell-cell communication.
Across patients, post-treatment samples showed reduced expression of CAR target antigen and a shift in tumor-intrinsic programs toward less stem-like, less migratory, and more apoptotic states, despite radiographic progression. The post-treatment TME was remodeled, with fewer suppressive myeloid- and B-cell-rich niches and increases in interferon-responsive and T cell-associated activation programs. Spatial interaction analyses indicated that pre-treatment rGBM contained dense networks of myeloid-tumor and myeloid-T-cell contacts consistent with impaired antigen presentation and effector function. Post-treatment specimens, in contrast, showed partial disruption of these suppressive circuits and the emergence of microenvironments more permissive to T-cell infiltration and activity.
In the parent phase 1 trial, CART-EGFR-IL13Rα2 was feasible & induced radiographic tumor regressions in a subset of patients. This correlative spatial analysis suggests that prior EGFR/IL13Rα2 CAR T exposure can leave a less suppressive, more immunologically engaged TME at the primary site, even in resections obtained at radiographic progression. Together, these data support the idea that intracerebroventricular CAR T therapy may condition rGBM for subsequent immunotherapy. Myeloid and B-cell interactions are highlighted as candidate targets for armoring next-generation CAR T cells and for designing rational combination and sequencing strategies.

#3445 Astrocytes reprogram radiation-resistant glioblastoma to reveal new therapeutic vulnerabilities.

Rana Abdelgawad[1], Andrew Dhawan[2]

[1]Pharmacology, Cwru, Cleveland, OH,[2]Department of Cancer Sciences, Cleveland Clinic Research, Cleveland, OH

Glioblastoma (GBM) is a highly aggressive and therapy-resistant brain tumor, with limited treatment options and poor patient prognosis. One major barrier to effective treatment is the tumor's interaction with the surrounding brain microenvironment, particularly astrocytes, which can modulate therapeutic responses and contribute to resistance. To investigate how astrocytes influence resistance and uncover exploitable vulnerabilities, we developed direct and transwell co-cultures using patient-derived (HW1) GBM cells and primary human astrocytes plated across multiple ratios (10:90, 50:50, and 90:10). This novel co-culture system enabled us to model both contact-dependent and paracrine astrocyte signaling. We tested whether astrocytes at different densities were able to modulate tumor response to a panel of clinical and pre-clinical drugs, in the post-radiation setting. GBM-astrocyte cocultures were exposed to a clinically relevant radiation protocol (three cycles of 2 Gy daily x 5 days) and screened against 12 drugs, encompassing DNA-damaging agents, multi-kinase inhibitors, and nuclear transport inhibitors. Notably in direct co-cultures, even low concentrations of astrocytes (as few as 10%) significantly altered GBM sensitivity to multiple compounds. Additionally, radiation induced a therapeutic vulnerability in GBM cells when co-cultured with astrocytes, not present in GBM monocultures, to selinexor, afatinib, altiratinib, and crenolanib, with strongest effects at intermediate astrocyte:GBM ratios (10:90, 50:50). Transwell experiments demonstrated similar shifts in sensitivity, supporting the hypothesis that astrocyte-secreted paracrine factors alone are sufficient to reprogram GBM drug response. These observations imply that astrocytes reprogram resistance-associated pathways in GBM cell lines post-radiation treatment, potentially hijacking saturated DNA repair mechanisms, cell cycle checkpoints, stress signaling, and transporter activity, all of which invites further mechanistic investigation. Building upon these findings, ongoing studies include genetic validation of candidate pathways, expanded transwell assays to further separate contact-dependent and paracrine mechanisms, and live-cell imaging to define the temporal resistance dynamics. In conclusion, our study demonstrates that the presence of astrocytes alone significantly influences GBM response to therapy, and radiation therapy can further expose collateral sensitivities driven by astrocyte signaling. Modeling and mechanistically dissecting these microenvironmental interactions is essential for identifying new avenues for combination therapies that may improve outcomes in a cancer type where innovation is urgently needed.

#3446 Loxl2 drives neutrophil-mediated immune evasion and resistance to anti PD-1 therapy in murine melanoma.

Jiah Yang[1], Emre Arslan[2], Veena Kochat[3], Suresh Satpati[3], Kunal Rai[3]

[1]Graduate School of Biomedical Science, UT MD Anderson Cancer Center, Houston, TX,[2]UT MD Anderson Cancer Center, College Station, TX,[3]UT MD Anderson Cancer Center, Houston, TX

Immune checkpoint blockade (ICB) therapy with anti-PD-1 (αPD-1) has revolutionized melanoma treatment; however, response rates remain suboptimal due to innate or adaptive resistance mechanisms. Although substantial efforts have focused on enlightening resistance mechanism and improving the efficacy, the role of epigenetic regulation within tumor remains insufficiently explored.scRNA-seq and scATAC-seq analysis of pre- and post-treatment samples from non-responding melanoma patients revealed upregulation of H3K4 oxidase LOXL2 following nivolumab treatment. LOXL2 expression was enriched in an uncharacterized tumor subcluster, distinct from hypoxic tumor and fibroblast clusters. These findings led us to hypothesize that LOXL2 contributes to immune evasion and promotes αPD-1 resistant tumor microenvironment.To test this, we evaluated the impact of LOXL2 knockdown (KD) in a murine subcutaneous (SQ) melanoma model treated with αPD-1. Tumors were profiled using scRNA-seq to assess cell-type-specific transcriptional changes and immune composition. LOXL2 KD significantly improved a-PD-1 efficacy in B6 SQ tumors, reducing N2 pro-tumorigenic neutrophils and increasing cytotoxic CD8+ T cell infiltration.To investigate how LOXL2 influences tumor-associated neutrophils (TANs) polarization, we examined epigenomic alterations and downstream gene regulation upon LOXL2 KD. We identified SOCS1-mediated NF- κB transcriptional attenuation, along with reduced secretion of pro-inflammatory cytokines (i.e. IL-1β, TGFβ) which favors N1 rather than N2 polarization.Collectively, our findings suggest that LOXL2-driven tumors secrete cytokines that promote N2 neutrophil polarization, leading to CD8+ T cell exclusion and resistance to αPD-1 therapy. Targeting LOXL2 may reprogram the tumor immune microenvironment toward an immune-responsive state, offering a potential strategy to enhance ICB response in melanoma.

#3447 Type III collagen regulated by stress signaling drives chemoresistance in pancreatic cancer by inducing tumor dormancy and remodeling the immunosuppressive niche.

Haiyan Xu, Yicheng Zhou, Shengbai Xue, Siming Wu, Liwei Wang

State Key Laboratory of Systems Medicine for Cancer, Shanghai Cancer Institute, Department of Oncology, Renji Hospital, School of Medicine, Shanghai Jiao Tong University, Shanghai, China

Chemotherapy resistance remains the primary cause of treatment failure in pancreatic ductal adenocarcinoma (PDAC). Therapy induced tumor dormancy enables tumor cells escape from chemotherapy cytotoxicity. Our study reveals that gemcitabine treatment triggers extracellular matrix (ECM) fibrosis and collagen rearrangement, with significant accumulation of type III Collagen (COL3). Crucially, exogenous COL3 supplementation in subcutaneous and orthotopic PDAC models could induce tumor cell dormancy accompanied by p21/p27 upregulation and promote chemoresistance. Meanwhile, COL3 enrich tumor-associated macrophages (TAMs) within chemoresistant niches. Mechanistically, COL3 induction was driven by CREB3L1-activated unfolded protein response (UPR) during chemotherapy stress. CREB3L1 regulated dormancy associated molecules like COL3, p21 and p27 and remodeled the stromal microenvironment. These findings establish COL3 as a central mediator of PDAC chemoresistance by orchestrating dormancy and immunosuppressive niche formation. Targeting the CREB3L1-COL3 axis represents a promising strategy to overcome acquired resistance in pancreatic cancer.

#3448 Sequential senescence-escape cycles drive genomic heterogeneity and osimertinib resistance in EGFR-mutant NSCLC.

Nazia Jamil[1], Hayley McDaid[2], Howard D. Hosgood[3], Qualia Hooker[4], Nadjet Cornejal[2]

[1]Institute for Clinical and Translational Research at Einstein and Montefiore, Albert Einstein College of Medicine, Bronx, NY,[2]Molecular Pharmacology, Albert Einstein College of Medicine, Bronx, NY,[3]Epidemiology, Albert Einstein College of Medicine, Bronx, NY,[4]Van Andel Institute (VAI), Grand Rapids, MI

Acquired resistance to osimertinib remains a critical challenge in the management of EGFR-mutant (EGFR$^+$) NSCLC. Although most patients initially respond, relapse is universal, even after prolonged remissions, suggesting that this interval reflects a durable drug-induced proliferative arrest consistent with cellular senescence. We demonstrate Osimertinib-Induced Senescence (OsIS) in EGFR$^+$ NSCLC cells and show that, several weeks after drug withdrawal, senescent cells resume proliferation. To determine how repeated senescence and escape influence therapeutic response and genomic evolution, we generated isogenic cell lines expanded through four sequential rounds of OsIS over approximately six months. Four distinct evolutionary trajectories were selected, each exhibiting varying degrees of resistance to EGFR inhibitors. Although OsIS-derived lines retained sensitivity to cisplatin, they displayed heterogeneous responses to pemetrexed, while sensitivity to tubulin-interacting drugs and navitoclax was preserved. Genomic analyses confirmed that resistance did not arise from *de novo* single nucleotide mutations or copy number amplification in EGFR or MET. Instead, all OsIS-derived lines had increased tumor mutational burden and acquired mutational signatures associated with base-excision repair defects, replication stress, and, in the most resistant line, oxidative stress. Despite these signatures, therapies directed at DNA repair or replication stress were uniformly ineffective, indicating that resistance was not driven by discrete genomic lesions but rather by age-associated mutational drift. These findings support a model in which OsIS functions as an evolutionary bottleneck whose escape promotes genomic heterogeneity and promotes resistance to EGFR inhibition.

#3449 Heterogeneity in outcomes of cytokine blockade identifies plausible role for SPP1+macrophages in colorectal liver metastasis immune suppression.

Kristin Goodsell[1], Jason Carter[1], Sheela Damle[2], Xiuyun Jiang[1], Heidi Kenerson[1], Ian N. Crispe[1], Venu G. Pillarisetty[1]

[1]Surgery, University of Washington, Seattle, WA,[2]Hematology/Oncology, University of Washington, Seattle, WA

The failure of immunotherapy to demonstrate a benefit in patients with colorectal cancer liver metastases (CRLM) is likely due to both liver-specific immune tolerance and cancer-specific immune evasion mediated by tumor associated macrophages (TAMs), suppressive cytokines (e.g., interleukin-10/IL-10), and immune checkpoints, such as PD-1-PD-L1. We previously demonstrated that IL-10 blockade can activate antitumor immunity in tumor slice cultures (TSC) of CRLM, while PD-1 blockade failed to do so. We hypothesized that immunosuppressive TAMs in the tumor immune microenvironment (TIME) contributed to treatement failure.

Cases were classified as responders or non-responders to IL-10 blockade. Clinical characteristics were analyzed. Bulk and single cell RNA sequencing (RNAseq) and multiplexed immunofluorescence (mIF) were performed on subsets of treated samples. RNAseq data were analyzed in R (Seurat) and Python (Scanpy). AIVIA software was used to quantify SPP1 staining on mIF.

IL-10 blockade increased apoptosis (29% to 45%, $p<0.05$) across all TSC (n=59). Using two tailed t-test, cases were classified by percent apoptosis in anti-IL-10 treatment versus control as responders (53% vs 23%, $p<0.05$) and non-responders (25% vs 24%, $p=0.67$).

Clinical characteristics including primary site, metachronous/synchronous metastasis, mutation status, and prior therapy were not significantly different between groups. BulkRNAseq demonstrated no difference in baseline IL-10 or IL-10 receptor gene expression between groups. scRNAseq identified TAMs as the major source and both T cells and TAMs as recipients of IL-10 signaling.

While non-responders had higher baseline expression of genes related to CD8+ T cell activation ($p=0.03$) and cytotoxicity ($p=0.03$), they also had a higher abundance of M2-macrophage related genes ($p=0.02$) and CD8+ T cell exhaustion ($p=0.04$). Further interrogation of immunosuppressive signaling pathways showed that *SPP1* (encoding osteopontin/OPN) is largely expressed by TAMs within CRLM, while T cells and TAMs express OPN receptors (CD44, ITGB1). mIF demonstrates colocalization of macrophage markers (CD68/CD163) and OPN/SPP1. Preliminary analysis showed that non-responders had significantly more OPN/SPP1+ cells on baseline mIF (4.3 vs 0.1%, $P=0.01$).

Importantly, we determined that OPN secretion is significantly reduced in responders but unchanged in non-responders. The results suggest a role for TAM-related OPN-mediated immunosuppression in the failure of immunomodulatory treatment.

We identify *SPP1+* TAMs as a potentially critical immunosuppressive population in the TIME of liver metastases. Future work will leverage both orthotopic CRLM models and spatial transcriptomics of human tumors to explore the role of osteopontin signaling in CRLM.

#3450 Tumor mass dormancy - a potential driver of long-term persistent melanoma after immunotherapy?.

Yingxiao Shi[1], Zoltan Maliga[2], Tuulia Vallius[3], Shishir Pant[3], Roxanne Pelletier[3], Brigette Kobs[2], Priyanka Solanky[3], Yiwen He[1], Eliezer M. Van Allen[4], Sandro Santagata[5], Patrick Ott[4], Christine G. Lian[6], Elizabeth I. Buchbinder[4], David Liu[4], Peter Karl Sorger[7]

[1]DFCI/Harvard Medical School, Boston, MA,[2]Laboratory of Systems Pharmacology, Harvard Medical School, Boston, MA,[3]Harvard Medical School, Boston, MA,[4]Dana-Farber Cancer Institute, Boston, MA,[5]Brigham and Women's Hospital, Boston, MA,[6]Brigham and Women's Hospital, Harvard Medical School, Boston, MA,[7]DFCI/Harvard Medical School

Introduction - Persistent residual lesions represent a common yet ambiguous outcome in melanoma patients treated with immune checkpoint inhibitors (ICIs). These lesions can reflect either (i) disease eradication with fibrosis and necrosis, or multiple modes of tumor dormancy, including (ii) residual disease characterized by cellular dormancy or quiescence, and (iii) macroscopic tumor mass dormancy, in which overall stability emerges from a dynamic balance between tumor proliferation and loss. Because these lesions are infrequently biopsied, the biological mechanisms that sustain these forms of dormancy remain poorly defined. This study aimed to characterize the cellular and microenvironmental states underlying persistent residual disease following ICI therapy.
Methods - We performed multi-omics spatial profiling on persistent residual lesions resected from six ICI-treated melanoma patients. For comparison, we included lymph node metastases from patients who progressed after ICIs.
Results - In 4 of 6 patients, persistent residual lesions consisted largely of immune cells and scar tissue, suggesting that the PET signal may arise primarily from non-tumor components rather than residual viable tumor. In contrast, one patient with a large residual lymph node lesion harbored viable, proliferating tumor cells at levels comparable to — or exceeding — those in lymph node lesions from patients with active clinical progression after ICI therapy. Extensive cytotoxic T-cell infiltration and high levels of programmed cell death were observed within this lesion. Although some tumor cells expressed cellular dormancy-associated markers (e.g., p27), this was not the dominant tumor state. Strikingly, in another patient, a persistent residual lesion that was pathologically negative for tumor cells by H&E contained discrete nests of tumor cells identified by multiplex IF, with approximately half of them proliferating in close proximity to immune cells.
Conclusion - Together, these findings demonstrate that post-ICI residual disease can arise from persistent, viable tumor cells and that the phenotype is more consistent with tumor mass dormancy rather than the classical cellular dormancy concept. Furthermore, the persistent residual lesion can harbor viable and proliferative tumor cells despite appearing clinically stable, underscoring that such lesions may act as reservoirs with potential for late progression. This dormancy-like state has important implications for patient monitoring, clinical interpretation of stability, and long-term management following ICI therapy.

#3451 Single-cell transcriptomic insights into tumor and immune dynamics driving resistance to ixazomib combined with gemcitabine and doxorubicin in SMARCB1-deficient renal medullary carcinoma.

Kai Yu, Rebecca Tidwell, Tharakeswara Bathala, Rahul Sheth, Menuka Karki, Jianfeng Chen, Jing Qian, Fei Duan, Luigi Perelli, Melinda Soeung, Priya Rao, Arlene Siefker-Radtke, Najat Daw, Davis Ingram, Diana Shamsutdinova, Khalida Wani, Wei-Lien Wang, Alexander Lazar, Zilong Zhao, Sabitha Prabhakaran, Neus Bota, Andrew Futreal, Rare Tumor Initiative Team, Patient Mosaic Team, Liuqing Yang, Chunru Lin, Giannicola Genovese, Jianjun Gao, Linghua Wang, Nizar Tannir, Pavlos Msaouel

UT MD Anderson Cancer Center, Houston, TX

SMARCB1-deficient renal medullary carcinoma (RMC) is a highly aggressive kidney cancer characterized by replication stress and proteotoxic vulnerabilities, yet the molecular determinants of therapy response remain poorly understood. To delineate the mechanisms of response and resistance, we performed integrative single-cell and bulk multi-omic profiling of tumor samples from patients with RMC treated with a combination of the proteasome inhibitor ixazomib, gemcitabine, and doxorubicin. Analysis of 33,410 single cells from 11 patients revealed pronounced intratumoral and microenvironmental heterogeneity. Responding tumors displayed immune-inflamed microenvironments enriched for $CD8^+$ cytotoxic T cells, effector-like and Tfh $CD4^+$ T cells, NK cells, plasmacytoid (pDC) and conventional dendritic cells (cDC1/cDC2), and *S100A8*$^+$ monocytes, consistent with enhanced antigen presentation and effector activation. In contrast, non-responders exhibited abundant macrophages, regulatory T cells, plasma cells, and inflammatory and myofibroblastic cancer-associated fibroblasts (iCAFs/mCAFs), forming immunosuppressive stromal-myeloid circuits that impeded cytotoxic infiltration and response. Malignant cells segregated into six transcriptional states, including proliferative, hypoxia-responsive, epithelial-mesenchymal, and neuroendocrine-squamous hybrid lineages. A proliferative state marked by replication stress, unfolded-protein-response activation, and proteasome component upregulation was enriched in non-responders and persisted at progression, suggesting adaptive proteostasis-driven resistance. Copy-number analyses identified focal gains in *BAG4*, *UBE4B*, and *UBE2W* that may enhance apoptosis evasion and p53 degradation, reinforcing proteotoxic resilience. In contrast, well-differentiated and immune-mimicry tumor states correlated with improved survival. Integrative cell-cell communication analysis highlighted stromal-immune signaling through *BMP4/5* and *WNT4/6* as a hallmark of resistant tumors, whereas *BMP6* expression associated with dendritic-cell activation and favorable immune remodeling. Together, these findings define molecular and cellular programs underlying therapeutic response in RMC and nominate actionable stress-adaptation and stromal-immune circuits as potential targets for future biomarker-guided combination strategies.

#3452 Exploiting stromal vulnerabilities: NFATC2-expressing CAFs enhance chemotherapy sensitivity and reveal a targetable ERBB axis in pancreatic cancer.

Jiahao Guo[1], Samuele Cancellieri[1], **Biswajyoti Sahu**[2]

[1]NCMBM, University of Oslo, Dept. of Medical Genetics, Institute for Cancer Research, Oslo, Norway,[2]Applied Tumor Genomics Research Program, University of Helsinki, Finland, NCMBM, University of Oslo, Dept. of Medical Genetics, Institute for Cancer Research, Oslo, Norway

Pancreatic ductal adenocarcinoma (PDAC) persists as one of the most therapeutically recalcitrant solid tumors, driven in part by an extensive desmoplastic stroma dominated by cancer-associated fibroblasts (CAFs). CAF heterogeneity and transcriptional plasticity are increasingly recognized as key determinants of tumor evolution and treatment response, yet how neoadjuvant therapy reshapes CAF states in human PDAC remains poorly defined. We applied gene regulatory network analysis to single-cell RNA sequencing data from 43 PDAC tumors collected following neoadjuvant therapy. This analysis uncovered a previously undescribed CAF subpopulation defined by expression of the transcription factor NFATC2, classically associated with T-cell signaling. NFATC2-expressing CAFs were significantly enriched in patients exhibiting robust treatment response and extended progression-free survival. Tumors containing this CAF state displayed reduced lymph-node metastasis and a distinct stromal transcriptional program characterized by enhanced pro-apoptotic signaling and suppression of ERBB pathway activity. Functional co-culture assays revealed that NFATC2-expressing CAFs potentiate FOLFIRINOX-induced apoptosis in PDAC cells. Moreover, ERBB inhibition produced strong synergistic cytotoxicity when combined with either FOLFIRINOX or gemcitabine/nab-paclitaxel, suggesting a mechanistically grounded combination strategy for overcoming stromal-mediated resistance. These findings identify NFATC2-expressing CAFs as a predictive stromal biomarker of therapeutic responsiveness and define a tumor-restraining CAF state with actionable molecular features. This work reveals a previously unrecognized vulnerability within the PDAC microenvironment and supports rational integration of ERBB-targeted agents with current neoadjuvant regimens to enhance treatment efficacy in PDAC.

#3453 Macrophage polarization in ALK+ non-small cell lung cancer: Implications for treatment targeting.

Marisa E. Aikins[1], Abdullah Saeed[2], Derek Nancarrow[1], Peter J. Ulintz[3], Peggy Hsu[3], Yusoo Lee[4], Sofia Merajver[5], Kiran H. Lagisetty[5]

[1]Internal Medicine, University of Michigan, Ann Arbor, MI,[2]Thoracic Surgery, University of Michigan, Ann Arbor, MI,[3]University of Michigan, Ann Arbor, MI,[4]University of Michigan Medical School, Ann Arbor, MI,[5]University of Michigan Health System, Ann Arbor, MI

Background: Anaplastic lymphoma kinase-positive non-small cell lung cancer (ALK+ NSCLC) comprises 5-6% of all lung cancers with a median survival rate of 6.8 years. The primary treatment is tyrosine kinase inhibitors (TKI) which have a 30-80% response rate but acquired resistance is inevitable. One area of potential intervention is within the tumor-immune microenvironment (TIME) but the standard immunotherapies, such as immune checkpoint inhibitors, have resulted in low overall response rate (10-15%), toxicity, or inconclusive therapeutic effects in ALK+ NSCLC as a single agent or combined with TKIs in clinical trials. Therefore, it is imperative to gain a more in-depth understanding of the TIME evolution. In particular, there has been increasing evidence showing that macrophage polarization is involved in NSCLC tumorigenesis and drug resistance. The timing, phenotype, and functional state of macrophages within ALK+ NSCLC may offer opportunities for therapeutic targeting.
Methods:Three investigations were carried out to investigate ALK+ NSCLC macrophage evolution: (1) a de novo and treatment-naïve study setting where intratracheal instillation of a CRISPR/Cas9 adenoviral system was administered in C57BL/6 mice for chromosomal rearrangement of *alk* and *eml4* leading to spontaneous formation of tumors in the lungs, (2) a heterotopic TKI treatment study setting where ALK+ NSCLC cells syngeneic to C57BL/6 mice were injected subcutaneously, and (3) analysis of ALK+ NSCLC patient legacy and local cohorts. Tumors from the animal studies were harvested at early, intermediate, and late time points for analysis of macrophage phenotypes. Legacy and local patient cohorts were analyzed to investigate and validate macrophage results in a broad and heterogenous population of ALK+ NSCLC patients.
Results:Macrophage frequency in ALK+ NSCLC increased during tumor progression with localization occurring primarily at the periphery of the tumor. The addition of Lorlatinib further increased macrophage frequency. Macrophage polarization was also altered by specific TKI treatments. Alectinib increased pro-inflammatory:anti-inflammatory macrophage ratios over time, reaching 0.55 at the late time point, which was significantly higher than Lorlatinib at 0.13. Compared with other oncogene-driven NSCLC, ALK+ patients in legacy and local RNAseq datasets demonstrated a lower frequency of pro-inflammatory macrophages.
Conclusions:Differential macrophage polarization was demonstrated using de novo untreated and subcutaneous TKI treated ALK+ NSCLC animal models. Macrophage polarization appears to be TKI-specific with Alectinib treatment increasing pro-inflammatory macrophage subsets and decreasing anti-inflammatory subsets while Lorlatinib shows the opposite despite a smaller tumor size. Macrophage polarization has potential to be a promising avenue for therapeutic intervention.

#3454 Dynamic alteration of ANXA2 expression as a predictor of response to neoadjuvant bevacizumab in newly diagnosed glioblastoma.

Taketo Ezaki[1], Ryota Tamura[1], Yohei Yamamoto[2], Jun Takei[2], Akihiko Teshigawara[2], Kyoichi Tomoto[2], Yasuharu Akasaki[2], Masahiro Toda[1], Yuichi Murayama[2], Hikaru Sasaki[3], Keisuke Miyake[4], Toshihide Tanaka[2]

[1]Department of Neurosurgery, Keio University School of Medcine, Shinjuku-ku, Japan,[2]Department of Neurosurgery, The Jikei University School of Medicine, Minato-ku, Japan,[3]Department of Neurosurgery, Tokyo Dental College Ichikawa General Hospital, Ichikawa-shi, Japan,[4]Department of Neurosurgery, Kagawa University School of Medcine, Miki-cho, Japan

Background: Bevacizumab (Bev) provides only modest and transient benefit in glioblastoma (GBM), and the molecular mechanisms underlying Bev resistance remain insufficiently characterized. Annexin A2 (ANXA2) plays a key role in angiogenesis, extracellular matrix remodeling, and invasive tumor phenotypes, and has emerged as a potential mediator of Bev resistance biology. This study aimed to elucidate the clinical significance of ANXA2 expression dynamics in newly diagnosed GBM by analyzing paired tumor samples obtained pre- and post-Bev therapy, with a focus on their association with treatment response and survival outcomes.
Method: We analyzed 65 samples obtained from 33 patients with GBM, including newly diagnosed GBM without Bev treatment (Naïve Bev; n=15), neoadjuvant Bev treated (NeoBev; n=18), and recurrent GBM after Bev therapy (Refractory Bev) comprising paired pre- and post-Bev samples in same patients. ANXA2 expression was evaluated by qPCR and immunohistochemistry. Progression-free survival (PFS) and overall survival (OS) were also evaluated according to *ANXA2* expression levels, and recurrence patterns on MRI were compared.
Results: Paired analyses showed *ANXA2* expression tended to be higher in Refractory Bev compared with initial surgery specimens, regardless of prior Bev exposure. Immunohistochemistry demonstrated comparable ANXA2 expression across Naïve Bev, NeoBev, and Refractory Bev cohorts. *ANXA2* expression was not associated with prognosis in Naïlve Bev; however, lower expression correlated with favorable PFS in NeoBev (p=0.1062) and significantly longer OS (p=0.0025). Patients receiving ≥ 10 Bev cycles showed significantly lower ANXA2 expression than those with < 10 cycles (p=0.0168), and lower expression in NeoBev resulted in prolonged OS. T1Gd responders showed a trend toward longer PFS (p=0.1037), with a similar trend in T2/FLAIR poor responders (p=0.0688). No significant association was found between *ANXA2* expression and recurrence patterns on MRI.
Conclusion: ANXA2 may represent a key molecular determinant of angiogenesis and invasion and could serve as both a prognostic and predictive biomarker for neoadjuvant Bev response.

#3455 POSTN-driven mechanotransduction sustains β-catenin activity in CAFs to promote melanoma progression and drug resistance.

Jie Wang[1], Bruna DA SILVA SOLEY[2], Linli Zhou[1], Yuhang Zhang[2]

[1]University of Cincinnati College of Pharmacy, Cincinnati, OH,[2]University of Cincinnati, Cincinnati, OH

Cancer-associated fibroblasts (CAFs) are pivotal modulators of the tumor microenvironment, orchestrating extracellular matrix (ECM) remodeling, inflammation, and therapeutic resistance. However, the mechanisms governing their dynamic response to targeted therapies, particularly in melanoma, remain incompletely understood. Our previous work identified β-catenin as a central driver of CAF activation in melanoma. Building on this, we recently discovered that periostin (POSTN), a matricellular protein primarily secreted by CAFs, acts as a major downstream effector of β-catenin-mediated transcriptional reprogramming.In this study, we uncover a novel β-catenin-TCF-POSTN regulatory axis that underlies CAF-mediated resistance to BRAF inhibition in melanoma. Specifically, we show that nuclear β-catenin interacts with TCF4 to drive POSTN expression and secretion in CAFs. Disrupting this interaction, using a dominant-negative TCF4 mutant or the pharmacological inhibitor PNU74654, significantly reduced POSTN expression, mimicking the effects of β-catenin inhibition. Phenotypically, POSTN depletion impaired CAF proliferation, cytoskeletal dynamics, and their ability to promote melanoma cell proliferation and resistance to BRAF inhibition *in vitro*.Mechanistically, we identified a POSTN-driven outside-in mechanotransduction loop in which POSTN activates integrin-focal adhesion signaling to promote actin stress fiber assembly. The resulting cytoskeletal tension induced nuclear deformation, facilitating β-catenin nuclear translocation, thereby sustaining POSTN expression and reinforcing a self-amplifying feedback loop. Interruption of this loop via POSTN knockdown or using actin polymerization inhibitor Cytochalasin D reduced nuclear β-catenin levels, confirming the existence of a POSTN-driven outside-in signaling cascade.Using BRAF-mutant melanoma xenograft models, in which either POSTN expression was ablated or β-catenin-TCF4 interaction was blocked in CAFs, suppressed tumor progression and sensitized melanoma cells to BRAF inhibition. Conversely, POSTN overexpression in CAFs enhanced tumor progression, ECM deposition, including collagen and fibronectin, and resistance to BRAF inhibitors. Importantly, both preclinical models and melanoma patient samples revealed a strong correlation between POSTN expression and nuclear β-catenin accumulation in CAFs.Together, our findings define an important POSTN-mediated feedback loop that sustains nuclear β-catenin signaling and reinforces CAF activation. This axis promotes ECM remodeling and contributes to melanoma progression and targeted therapy resistance. Targeting the β-catenin-TCF4-POSTN circuit represents a promising stroma-targeting strategy to advance targeted therapies against melanoma and improve clinical outcomes.

#3456 Spatial evolution of the tumor immune microenvironment between primary and recurrent serous ovarian cancer using a sixty plex multiplex immuno oncology panel.

Hayeon Shin, Jue young Kim, Yoon Joo Kim, Yookyung Lee, Jae-Hoon Kim

Gangnam Severance Hospital, Seoul, Korea, Republic of

Background: Despite advances in treatment, recurrent ovarian cancer continues to exhibit high recurrence rates, and immune checkpoint inhibitors (ICIs) demonstrate limited response (10-15%) due to a strongly immunosuppressive tumor immune microenvironment (TIME). The mechanisms of immune escape during recurrence remain insufficiently understood, highlighting the need for spatial characterization of TIME remodeling to optimize biomarker-guided combination immunotherapy.
Methods: Formalin-fixed paraffin-embedded (FFPE) primary and recurrent tumor tissues from patients with recurrent serous ovarian cancer were used to construct matched tissue microarrays (TMAs). Multiplex immunofluorescence staining was performed using the Akoya IO60 immuno-oncology panel. Quantitative spatial image analysis was conducted using the Qupath workflow to assess immune cell composition, phenotypes, and tumor-immune architecture changes associated with recurrence.
Results: A total of 58 patients were included, of whom 35 had matched primary and recurrent tumor specimens available. Based on chemotherapy response classification, 41 patients were categorized as platinum-sensitive and 8 as platinum-resistant. Spatial profiling analysis is ongoing. Preliminary observations suggest heterogeneous shifts in T-cell subsets (CD3, CD4, CD8), regulatory T cells (FOXP3+), and immunosuppressive myeloid populations (CD163+, CD206+), along with altered immune checkpoint pathways (PD-1, PD-L1, LAG-3, VISTA) and tumor phenotypes (PanCK, EpCAM) between primary and recurrent tumors.
Conclusion: This study aims to characterize spatial evolution of TIME during recurrence and identify immune escape mechanisms contributing to treatment resistance. The findings are expected to guide the development of precision immunotherapy strategies and improve clinical outcomes for patients with recurrent ovarian cancer.

#3457 Myeloid-derived suppressor cells mediate ferroptosis resistance in HR+/HER2- breast cancer via the ARID1A/AKR1C2 axis.

Guidong Chen, Jinpu Yu

Tianjin Medical Univ. Cancer Inst. & Hospital, Tianjin, China

Breast cancer is the most common malignancy in women, with approximately 70% of cases classified as the HR+/HER2- subtype. Recurrence and metastasis remain the leading causes of mortality in breast cancer patients. Resistance to ferroptosis has been recognized as a key factor in breast cancer progression, yet its relationship with myeloid-derived suppressor cells (MDSCs)-a critical component of the tumor microenvironment-has remained largely unexplored. In this study, we demonstrated that co-incubation of HR+/HER2- breast cancer cells with MDSCs significantly reduced their sensitivity to ferroptosis inducers and this process was closely associated with the downregulation of ARID1A expression. Further bioinformatic analysis and functional cellular experiments indicated that ARID1A loss drived the marked upregulation of the ferroptosis-suppressive gene AKR1C2 through epigenetic regulation. Overall, our findings reveal that MDSCs modulate AKR1C2 transcription by regulating ARID1A expression in HR+/HER2- breast cancer cells, thereby providing a promising strategy for the development of novel therapeutic targets against breast cancer.

#3458 Targeting the CD44-SPP1 axis to overcome therapy resistance in bladder cancer.

Hiba Siddiqui[1], Yuzhen Zhou[1], Jihyun Lee[2], Kevin Bi[3], Jacqueline T. Ochoa[3], Martin Egger[1], Eliezer M. Van Allen[1], Filipe L. De Carvalho[2], Kent W. Mouw[1]

[1]Dana-Farber Cancer Institute, Boston, MA,[2]Brigham and Women's Hospital, Boston, MA,[3]Broad Institute, Cambridge, MA

Introduction: Cisplatin-based chemotherapy remains a mainstay of treatment for muscle-invasive bladder cancer (MIBC), and the recent approval of antibody-drug conjugates (ADCs) enfortumab vedotin (EV) combined with pembrolizumab (P) as the first-line treatment has expanded therapeutic options. However, primary non-response and acquired resistance to these treatments result in poor clinical outcomes. Tumor cells interact with the tumor microenvironment (TME), where tumor-associated macrophages (TAMs) comprise 50-80% of non-tumors cells and can promote an immunosuppresive TME that drives therapeutic resistance. However, the mechanisms underlying tumor-macrophage crosstalk in cisplatin- and EV-based therapeutic settings remain poorly defined.
Methods: We employed snRNA-seq to analyze human samples and performed combined analyses with publicly available datasets. Spatial transcriptomics were used to characterize the distribution of TAM subtypes. CRISPR-Cas9 was used to generate CD44-deficient bladder cancer cell lines and SPP1-deficient macrophages. A series of *in vitro* functional assays including flow cytometry-based macrophage phenotype profiling, phagocytosis assays, immunoblots, and viability assays were performed across cisplatin and MMAE treatment conditions. Direct and indirect co-culturing systems were used to model tumor cell-macrophage interactions. Immunocompetent murine bladder cancer models were used to evaluate therapeutic responses when combining CD44-SPP1 blockade with cisplatin or EV. RNA sequencing was performed to profile gene expression changes in tumor cells and macrophages following CD44-SPP1 axis modulation.
Results: Tumor cell CD44 expression and macrophage SPP1 expression are positively correlated with cisplatin resistance and poor clinical outcomes in bladder cancer patients. SPP1-expressing macrophages were spatially localized near CD44-positive tumor cells in resistant tumors. Cisplatin and EV treatment increased CD44 and SPP1 expression in tumor cells and macrophages, respectively, and recombinant SPP1 was sufficient to induce tumor cell CD44 expression. CD44 deletion enhanced tumor cell response to cisplatin and EV, and flow cytometry and immunoblots showed that SPP1-deficient macrophages exhibit altered polarization states and enhanced phagocytic potential. Co-implantation of CD44-expressing tumor cells with SPP1-deficient macrophages reduced tumor growth. Comprehensive immune profiling of TME changes under various genetic and treatment conditions is underway.
Conclusion: Disrupting the CD44-SPP1 interaction sensitizes bladder tumors to cisplatin and EV. By defining macrophage phenotypes and polarization states within the CD44-SPP1 axis, this work supports therapeutic approaches such as engineered macrophage-based immunotherapies to overcome therapeutic resistance in MIBC.

: Migration and Invasion
Poster Session

#3462 The scaffold protein CNK3 mediates pro-invasive signalling in glioblastoma.

Guillaume Serwe, David Kachaner, Thomas Perreault, Marc K. Saba-El-Leil, Driss Lajoie, Genevieve Arseneault, Vincent Quoc-Huy Trinh, Marc Therrien

Institute for Research in Immunology and Cancer (IRIC), Montreal, QC, Canada

Glioblastoma (GBM) is the deadliest brain cancer with a five-year survival rate of 7% and a lack of targeted therapies for its treatment. One of the main factors limiting better treatment outcomes is the invasiveness of GBM cells, a property which reduces the efficacy of surgical resection and makes recurrence almost inevitable. The development of therapeutics for restraining cell invasion is therefore a crucial goal in the biomedical community. The invasive capacity of GBM cells is largely driven by a rewiring of signal transduction networks which results in abnormal activity of the motility-regulating RHO family GTPases, and activation of pro-invasive gene expression programs. However, the molecular mechanisms controlling this signalling switch are not fully understood, and their elucidation represents a significant challenge in biomedical research.
Our goal is to improve the understanding of rewired signalling in GBM cells by studying the functions of the CNK scaffold protein family. Through genetic knockdown/knockout and in vitro cell migration and invasion assays with GBM cell lines we identified the CNK3 member as a new pro-invasive factor. Crucially, this is also the case in vivo, as loss of CNK3 expression greatly reduced tumour volume in an orthotopic mouse xenograft model. Using GTPase pulldown assays, we then determined that CNK3 supports cell motility by promoting the activation of the RHO GTPases RAC1 and CDC42, while inhibiting the activity of RHOA. Consistent with these findings, CNK3 is required for normal actin-based protrusion formation at the leading-edge of migrating cells, and limits cell contractility and cell-substrate adhesion. To determine the molecular mechanism of action by which CNK3 functions as a scaffold protein, we then identified its proximal interactome by TurboID and validated its functional binding partners through co-immunoprecipitation and functional rescue experiments. These include the RAC1/CDC42 GTPase-activating protein ARHGAP39, and the MAP4K kinases MAP4K4, TNIK, and MINK1. Finally, we identified upstream growth factors and receptor tyrosine kinases (RTKs) that regulate CNK3-dependent motility and RHO GTPase activity. Thus, CNK3 functions by linking signalling by upstream RTKs to downstream regulation of RHO GTPases. Current efforts focus on the identification of pro-motility transcription programs regulated by this signalling axis.
Our research identifies the CNK3 scaffold protein as a new driver of motility in GBM cells and advances our understanding of the molecular mechanisms underlying their invasive behaviour. Ultimately, CNK3 and its binding partners could be new therapeutic targets for limiting the spread of GBM and improving patient survival.

#3463 Exploiting mechanisms of glioblastoma invasion to induce vulnerabilities that promote synergistic lethality.

Rifat S. Sajid[1], Lennart J. van Winden[2], Okty Abbasi Borhani[1], Evelyn R. Kamski-Hennekam[1], Ameesha Paliwal[1], Nakita E. K. Gopal[1], Lauren Omoto[1], Olaf van Tellingen[2], Phedias Diamandis[1]

[1]Princess Margaret Cancer Centre, University Health Network, Toronto, ON, Canada,[2]Department of Pharmacology, Netherlands Cancer Institute, Amsterdam, Netherlands

Glioblastoma (GBM) is the most common and aggressive form of adult brain cancer. Diffuse infiltration of tumor cells into surrounding vital brain tissue prevents complete surgical removal and poses a significant challenge to treatment. Therefore, a better understanding of the molecular programs that drive GBM invasion is crucial to designing more effective therapies. We hypothesized that GBM invasion is mediated by generalizable molecular mechanisms and that disrupting these programs induced vulnerabilities that could be exploited by combination therapies. In this study, we used a clinically diverse cohort of 17 patient-derived GBM cell lines and advanced experimental conditions to develop more controlled models of GBM invasion. Since hypoxia is a known driver of tumor invasion, we cultured GBM cells under 20%, 1%, and 0.2% oxygen concentrations and performed mass spectrometry-based profiling to investigate the invasive signaling pathways promoted by hypoxia. Additionally, we also performed mass spectrometry-based profiling of GBM cells cultured in the glioma cerebral organoid (GLICO) model of brain infiltration to investigate hypoxia-independent invasion mechanisms. These analyses identified the enrichment of several integrin-related signaling signatures as a general mediator of GBM invasion across cell lines, in both hypoxia-induced invasion conditions and in brain infiltration. To identify downstream targets of the integrin signaling pathway that could impair tumor cell migration, we performed a chemical screen using a MAPK compound library (*n*=802 compounds), which identified MAP4K4 as a top invasion-specific kinase. Pharmacological inhibition of MAP4K4 significantly impaired migration across multiple cell lines in live imaging experiments and reduced tumor infiltration in GLICOs, supporting its broad generalizability as a target to disrupt GBM invasion. By performing phospho-proteomic profiling, we then mechanistically determined that MAP4K4 inhibition led to the dysregulation of focal adhesion dynamics and cytoskeletal remodeling, which was validated through live fluorescent imaging experiments. Lastly, to explore if MAP4K4 inhibition induced vulnerabilities that could be exploited by sequential treatment with a second compound, we performed a combination screen using an FDA approved drug library (*n*=3196 compounds). We identified three compounds with a synergistic effect dependent on MAP4K4 inhibition that reduced tumor cell viability by 35-40% compared to single agent treatment. As the therapeutic strategies to treat GBM have remained unchanged for decades, the administration of synergistic drug combinations that exploit the characteristic infiltrative nature of GBM may therefore represent a promising treatment avenue for this devastating disease.

#3464 Defining the role of CRK and CRKL in glioblastoma invasiveness: from cell culture to mouse models.

Piyanka Hettiarachchi, Neka Large, Taeju Peter Park

Children's Mercy Kansas City, Kansas City, MO

Glioblastoma is the most aggressive primary malignant brain tumor affecting both adults and children, with a median survival of only about 15 months despite the standard treatments of surgery, radiation, and chemotherapy. Complete surgical resection is hindered by the highly infiltrative nature of glioblastoma cells, making tumor invasion the most significant cause of recurrence. Dysregulation of CT10 regulator of kinase (CRK) and CRK-like (CRKL) proteins has been implicated in multiple cancers, including glioblastoma, in which their overexpression correlates with poor prognosis. We hypothesized that CRK and CRKL are essential in glioblastoma cell invasion and that their inhibition suppresses tumor infiltration and enhances treatment efficacy. To test this hypothesis, we performed transient and stable knockdown of CRK, CRKL, or both in glioblastoma cell lines (U118-MG and LN-229) using siRNA transfection and shRNA lentiviral transduction. Western blot analyses confirmed significant reductions in target protein levels. Using the xCELLigence real-time cell analysis system, we assessed the impact of CRK and CRKL knockdown on glioblastoma cell adhesion, migration, and invasion. CRKL knockdown substantially reduced all three processes, whereas combined CRK/CRKL knockdown completely abolished adhesion, migration, and invasion. These consistent results across three glioblastoma lines highlight essential, overlapping roles of CRK and CRKL in regulating glioblastoma cell motility. To examine the dependence of in vivo glioblastoma growth and invasion on CRK and CRKL, we transplanted LN-229 glioblastoma cells expressing luciferase and GFP into immunodeficient (NSG) mouse brains using stereotactic surgery. Luciferase and GFP enabled us to monitor in vivo tumor growth through IVIS imaging and identify infiltrating tumor cells by GFP immunohistochemistry. Histological analysis of the xenografted brains revealed diffuse invasion of glioblastoma cells into surrounding brain regions. Currently, we transplant glioblastoma cells with CRK/CRKL knockdown to determine the requirement of CRK/CRKL in glioblastoma invasion in vivo. Then, we plan to test the effects of CRK/CRKL-antagonist peptides we developed on glioblastoma invasion in the mouse brain. Our study highlights the promise of targeting CRK and CRKL as a therapeutic strategy to mitigate glioblastoma invasion and improve the efficacy of standard care for glioblastoma.

#3465 An investigation into the role of AVIL, an actin-binding protein, in glioblastoma metabolism.

Summer Johnson, Robbie Cornelison, Adelaide Fierti, Martyna Glowczyk, Hui Li

University of Virginia School of Medicine, Charlottesville, VA

Glioblastoma (GBM) is one of the deadliest cancers characterized, is highly aggressive, invasive, and incurable, with an average survival of 15 months. The Li Lab identified *AVIL* as a novel proto-oncogene, which is aberrantly expressed in the tissue of cancers like glioblastoma. AVIL is a calcium dependent actin binding protein, implicated in cytoskeletal dynamics. Under physiological conditions, the expression of *AVIL* is limited to a handful of cell types: tuft cells, kidney podocytes, and sensory neurons, suggesting a tightly regulated role. In addition, our lab generated an *AVIL* KO mouse model that has no side effects and are fertile with viable offspring. Previous work has led to the development of a first-in-class small molecule inhibitor against AVIL (C1). While the upregulation of *AVIL* is observed in GBM, the molecular mechanisms involved are still unknown. This project aims to define the interactions and pathways involving AVIL with the goal of determining a molecular mechanism regarding alterations in metabolic phenotype. To elucidate the molecular mechanism of AVIL, we used a comprehensive bioinformatic analysis to pinpoint pathways and downstream targets. We conducted an unbiased screen of the protein using mass spectrometry on glioblastoma (U87) cells treated with C1 over a period of 72 hours. We also utilized RNA sequencing of GBM cells treated with C1 and astrocytes transduced with AVIL. Furthermore, we utilized Seahorse Mitochondrial Stress Tests as a screen for metabolism and mitochondrial function to validate our bioinformatic observations. One candidate mechanism we observed in the MS data suggested that treatment with the inhibitor induced a proteomic change from a glycolytic to an oxidative-phosphorylation profile, indicating a potential metabolic modulatory role of AVIL. This is particularly interesting because actin-glycolytic enzyme interactions are linked to the cytoskeletal regulation of metabolism. In addition, RNA sequencing data presented glycolysis as a top gene set that is differentially expressed after treatment with C1. After exogenous expression of AVIL in human astrocytes, there is an increase in basal metabolic rate and maximal respiration. Defining the metabolic interactions of AVIL will help determine the signaling pathways that are perturbed by *AVIL* expression and reveal downstream effectors. I hypothesize that *AVIL* expression regulates glycolysis via interactions with glycolytic enzymes offering a potential therapeutic strategy for GBM.

#3466 CTNNA1 promotes invasion and migration in clear cell renal cell carcinoma via N-cadherin-dependent adhesion and RhoA modulation.

Shinta Suenaga, Sei Naito, Hiromi Ito, Yuki Takai, Takafumi Narisawa, Mayu Yagi, Atsushi Yamagishi, Hayato Nishida, Norihiko Tsuchiya

Yamagata University Hospital, Yamagata city, Japan

Background and Objectives Clear cell renal cell carcinoma (ccRCC) frequently exhibits amplification of chromosome 5q31.2; however, the biological impact of this alteration remains unclear. CTNNA1, which is located in this region, regulates cell-cell adhesion, but its function in ccRCC has not been fully characterized. This study aimed to clarify the role CTNNA1 in ccRCC progression and its association with cadherin-mediated adhesion and invasive potential.
Methods Whole-transcriptome data from 57 metastatic ccRCC cases treated at Yamagata University were analyzed to assess CTNNA1 expression and its correlation with 5q copy number variation. TCGA data were used to compare cadherin expression profiles. Human ccRCC cell lines (A-498, 786-O, 769-P) underwent CTNNA knockdown using small interfering RNA (siRNA). Expression levels were verified by quantitative real-time PCR (qRT-PCR) and western blotting. Cell invasion and migration were measured by trans well assays, and protein localization was examined by immunofluorescence microscopy.
Results CTNNA1 expression was elevated in ccRCC cases with 5q amplification and correlated with increased invasive potential. Despite low E-cadherin expression, CTNNA1 formed a complex and co-localized with N-cadherin, contributing to intercellular adhesion. CTNNA1 silencing significantly reduced invasion, while overexpression enhanced it. Immunofluorescence revealed αE-catenin localization at cell-cell junctions in adherent cells and a perinuclear redistribution in isolated cells. RhoA localization mirrored CTNNA1 and was disrupted following CTNNA1 knockdown, suggesting its involvement in regulating polarity and migration through RhoA signaling.
Conclusions CTNNA1 promotes ccRCC cell invasion and migration through N-cadherin-mediated adhesion and modulation of RhoA signaling regulation. CTNNA1 may represent a potential therapeutic target for metastasis prevention in ccRCC.

#3467 SUMOylation regulates GATA2 stability to control uterine serous carcinoma invasion.

Anuoluwapo A. Mattix[1], Peng Liu[2], Molly A. Accola[3], William M. Rehrauer[3], Daniel R. Matson[1]

[1]Department of Pathology and Laboratory Medicine, University of Wisconsin-Madison, Madison, WI,[2]Department of Biostatistics and Medical Informatics, University of Wisconsin-Madison, Madison, WI,[3]University of Wisconsin Hospitals and Clinics, Madison, WI

Background: Uterine serous carcinoma (USC) is an aggressive uterine cancer subtype that is responsible for 40% of uterine cancer deaths. We recently demonstrated that USCs lose expression of the zinc-finger transcription factor GATA2 which drives USC invasion, predicts USC recurrence, and is closely correlated with poor cancer-related and overall survival. However, the mechanistic basis of GATA2 downregulation in USC remains unknown.

Methods: *GATA2* RNA transcripts were correlated to patient outcomes derived from The Cancer Genome Atlas (TCGA). *GATA2* gene methylation was assessed in isolated genomic DNA from patient USC tumors by bisulfite sequencing. Ark1 and Ark2 USC cell lines were utilized for *in vitro* studies. GATA2 half-life was measured using cycloheximide chase experiments paired with inhibitors of phosphorylation (staurosporine), acetylation (C646), SUMOylation (ML792), cysteine peptidase activity (N-Ethylmaleimide/NEM), and proteasome-dependent degradation (MG132). Anti-GATA2 immunoprecipitations were performed with custom anti-GATA2 antibodies (Im et al, 2005). Depletion of PIAS2, SENP1, and SUMO2/3 was performed using commercially available siRNAs. Levels of GAPDH, GATA2, PIAS2, SENP1, and SUMO2/3 were measured by western blotting. USC invasion was assessed using Matrigel-coated membrane transwell inserts.

Results: GATA2 IHC protein levels showed no correlation with *GATA2* gene body or proximal promoter DNA methylation, and *GATA2* transcript levels did not predict patient outcome across TCGA USC cases. Post-translationally, USC GATA2 protein half-life was approximately 60 minutes after cycloheximide treatment. Co-treatment with the SUMOylation inhibitor ML792 or the proteasome inhibitor MG132 prolonged GATA2 half-life compared with vehicle, whereas NEM treatment, which inhibits de-SUMOylation and de-ubiquitination, shortened GATA2 half-life. Direct GATA2 SUMOylation was confirmed by anti-GATA2 immunoprecipitation and SUMO2/3 western blot. A candidate siRNA-based approach found that depletion of the E3 SUMO ligase PIAS2 elevated GATA2 levels, while depletion of the SUMO peptidase SENP1 reduced GATA2 levels. siRNA-mediated SUMO2/3 depletion significantly increased GATA2 levels in USC cells and suppressed USC invasion *in vitro* compared to siScramble controls.

Conclusion: USC GATA2 levels are determined by post-translational mechanisms. GATA2 protein has a rapid 60-minute half-life determined by SUMOylation and proteasome-mediated degradation. Depletion experiments support PIAS2 as the GATA2-targeting E3 SUMO ligase and SENP1 as the GATA2-targeting SUMO peptidase. SUMO inhibition increased USC GATA2 levels and suppressed USC invasion, suggesting that SUMO-targeting agents may suppress USC spread through upregulation of GATA2 levels.

#3468 Adrenergic signaling in adipocytes drives ovarian cancer cell invasion.

Monica A. Haughan[1], Carlismari Grundmann[2], Hannah J. Lusk[2], Laura M. Sanchez[2], Joanna E. Burdette[1]

[1]Department of Pharmaceutical Sciences, University of Illinois at Chicago, Chicago, IL,[2]Department of Chemistry and Biochemistry, University of California Santa Cruz, Santa Cruz, CA

High grade serous cancer (HGSC) is the most common and lethal ovarian cancer subtype. HGSC can arise from the fallopian tube and habitually metastasizes to the omentum; consequently, we seek to further elucidate the metabolic crosstalk involved in HGSC colonization of omentum. By applying imaging mass spectrometry (IMS) to co-cultures of HGSC cells and omental explants we are able spatially resolve the chemistry produced and identify molecules unique to the HGSC + omentum cultures as compared to non-tumorigenic co-cultures or monocultures. One such molecule is epinephrine which IMS reveals to be produced by the omentum. From this we hypothesize autocrine epinephrine signaling in omental adipocytes liberates fatty acids driving tumor progression. To aid in more mechanistic investigation a human, pre-adipocyte line which forms spheroids and differentiates to mature adipocytes in culture is employed. Analyzed by IMS adipocyte spheroids and co-cultures with HGSC produced epinephrine confirming an omental cell type responsible to be adipocytes. Omental explants and adipocyte spheroids were subjected to treatment with epinephrine (10μM) or propranolol (1μM) and the resulting conditioned media collected. Three HGSC models -MOE PTEN^{shRNA}, OVCAR4, and OVCAR8- were treated with conditioned media and their invasive potential measured by Matrigel coated Boyden chamber. Propranolol treated conditioned media from either adipocyte source resulted in significantly decreased invasion compared to control while epinephrine treated omental conditioned media significantly increased MOE PTEN^{shRNA} invasion. Untargeted lipidomics performed on treated adipocyte spheroid conditioned media has uncovered lipid species differentially regulated between the epinephrine and propranolol treated conditioned medias including fatty acyls, sterols, and N-acylethanolamides. Current work seeks to explore the impact of epinephrine on sterol biosynthesis, determine if any identified lipid species is sufficient to drive HGSC cell invasion, and identify an upstream HGSC signal inducing epinephrine production in the adipocytes. Overall, we seek to expand our understanding of signaling critical in colonization of the omental metastatic niche and the role of the epinephrine therein.

#3469 A novel mTORC2 signaling pathway defines the pro-metastatic invadopodia network in urothelial carcinoma.

Donna Elizabeth Hansel, Jianya Huan, Francis Anthony San Lucas

UT MD Anderson Cancer Center, Houston, TX

BackgroundUrothelial carcinoma (UC), the most common form of bladder cancer, remains a leading cause of cancer-related mortality worldwide. UC outcomes are driven primarily by stage and grade of the tumor, with highlyinvasive and metastatic tumors showing significantly reduced treatment outcomes. Despite ongoing research,mechanisms that define this behavior in UC remain poorly understood. Our laboratory has identifiedmammalian target of rapamycin complex 2 (mTORC2) as a key regulator of invasive behavior in UC and anassociation between increased mTORC2 activity and higher UC stage.
MethodsGene and protein analyses were performed using Gene Set Enrichment Analysis (GSEA) andphosphoproteomic profiling. Immunohistochemistry and multi-Immunol fluorescence (mIF) assays were used todetermine expression and co-localization of proteins within invadopodia. Targeting of pathway componentswas performed using RNA silencing and inhibitor application, with functional outputs assayed using gelatindegradation assay, transwell invasion, and cell migration assessments.
ResultsOur study identified that mTORC2 can interact with TKS5α, an invadopodial scaffold protein, through putativemTOR phosphorylation. Furthermore, mTORC2 and TKS5α appear co-localize within cells and to the invasiveedge of tumors. Silencing of either mTORC2 or TKS5α results in similar phenotypes in cell invasion and matrixdegradation. Analysis of the Cancer Genome Atlas UC cohort showed high TKS5α expression was associatedwith reduced survival, and GSEA analysis showed PI3K/AKT/mTOR signaling was significantly enriched intumors with high TKS5α expression. These findings suggest that mTORC2 may promote pro-invasive andpro-metastatic activities through invadopodia formation and via a novel, and actionable, signaling cascade thatincludes TKS5α.
SummaryOur studies support a critical role for mTORC2 in driving invasion and metastasis in UC, as demonstrated byboth in vitro and human bladder cancer sample analysis. The study introduces a previously unrecognizedsignaling axis involving mTORC2 and TKS5α in invadopodia formation and metastasis in UC. The results fromthese studies have the potential to define a novel signaling axis in UC invadopodia that broadens ourmechanistic understanding of bladder

#3470 The role of LAP1 isoform balance in regulating nuclear plasticity during confined cancer cell migration.

Alicja Katarzyna Skwara[1], Victoria Sanz-Moreno[2], Jeremy G. Carlton[3]

[1]Cancer Research UK London Research Inst., London, United Kingdom,[2]ICR, London, United Kingdom,[3]King's College London, London, United Kingdom

Metastasis, which accounts for the majority of cancer-related deaths, requires cells to squeeze through narrow extracellular spaces, where the stiffness of the nucleus becomes a major physical barrier. This nuclear deformability is largely governed by nuclear envelope (NE) proteins, including lamina-associated polypeptide 1 (LAP1). LAP1, encoded by *TOR1AIP1*, exists as two isoforms generated from alternative translation start sites: the longer LAP1B, which binds tightly to the nuclear lamina and stabilizes the nucleus, and the shorter LAP1C, which interacts more loosely and promotes nuclear flexibility. Transcriptomic profiling of patient-derived melanoma cell line pairs revealed elevated LAP1 expression in more metastatic cells, with a higher LAP1C:LAP1B ratio associated with increased migratory potential.To dissect the functional consequences of this ratio, we generated stable melanoma cell lines overexpressing mRuby-tagged LAP1B, LAP1C, or wild-type LAP1 via retroviral transduction. Expression and localization were confirmed by immunofluorescence and Western blotting. We then assessed cell motility using transwell migration assays to mimic the mechanical constraints of tissue invasion. We demonstrated that LAP1C overexpression significantly enhanced migration, while LAP1B reduced it, without affecting nuclear morphology or actomyosin contractility. These findings suggest that LAP1 directly regulates nuclear plasticity to enable movement through confined environments.Preliminary data indicate that cellular stress can alter the LAP1C:LAP1B ratio, suggesting that isoform switching may be a regulated adaptive mechanism. This suggests that changes in the tumour microenvironment such as metabolic stress could influence nuclear mechanics through differential LAP1 expression.Strikingly, we found that primary immune and leukemia cells exclusively express the shorter LAP1C isoform, implying that the absence of LAP1B may facilitate their rapid amoeboid migration through dense tissues. Future work will explore how LAP1 isoform regulation supports leukemia cell motility in confined migration, providing broader insight into how nuclear envelope composition shapes cancer cell invasiveness.

#3471 Double-pillar co-culture (DPC) platform for evaluating cancer invasion and immunotherapy efficacy.

Seung Joon Kim[1], Sung Jae Chang[2], Sang-Yun Lee[3], Sang Hyo Kim[2], Bosung Ku[4], Dong Woo Lee[2]

[1]The Catholic University of Korea, Seoul, Korea, Republic of,[2]Gachon University, Seongnam-si, Korea, Republic of,[3]Chungnam National University, Daejeon, Korea, Republic of,[4]Medical & Bio Decision (MBD) Co., Ltd, Suwon-si, Korea, Republic of

Background: Co-culture is an essential in vitro technique for evaluating cancer invasion and immunotherapy efficacy, as tumor-stroma and tumor-immune interactions critically influence cancer progression and therapeutic response. Conventional assays, such as Transwell-based migration or invasion systems, are limited because they cannot simultaneously quantify cell invasion and viability, reducing physiological relevance. To address this, we developed a double-pillar co-culture (DPC) platform enabling high-throughput screening while culturing two distinct cell types in a spatially defined 3D architecture. Cancer cells embedded in Matrigel are seeded onto a central pillar to form a 3D tumor-like spot, while stromal cells, including fibroblasts or immune cells, are embedded in Matrigel on an outer, slightly lower pillar surrounding the core. This configuration allows direct visualization of invasion from the central mass and concurrent monitoring of cell viability.
Methods: A549 lung cancer cells and stromal cells (fibroblasts or lymphocytes) were co-cultured using the DPC platform. For drug screening, compounds including immune checkpoint-targeting drugs were applied to assess their effects on invasion and viability. To evaluate immune cytotoxicity, A549 cells were stabilized in the central pillar for three days, followed by addition of Jurkat cells to the outer pillar at a 1:5 ratio and co-cultured for an extended period. Invasion and viability were quantified using live-cell imaging and fluorescence-based assays and compared to monoculture or vehicle-treated controls.
Results: Co-culture of A549 cells with fibroblasts increased invasion over time. High-throughput screening using multiple compounds showed inhibitory effects on cancer cell invasion. Among them, the EGFR inhibitor Dacomitinib reduced invasion by <40% while maintaining >95% viability, demonstrating anti-invasive activity independent of cytotoxicity. Co-culture with Jurkat cells decreased cancer cell viability by ~55% compared to monoculture, confirming significant immune-mediated cytotoxicity.
Conclusions: The DPC platform provides a physiologically relevant, high-throughput system for simultaneous assessment of cancer invasion and immune cytotoxicity. It enables identification of compounds with selective anti-invasive effects and evaluation of immunotherapy efficacy, offering a versatile tool for preclinical cancer research.

#3472 Targeting a novel secreted protein to modulate MMP activity and restrain lung adenocarcinoma metastasis.

Chi-Ya Shen[1], Wen-Hsin Chang[2], Fan-Ni Hsing[1], Yi-Jing Hsiao[3], Yu-Wen Liao[1], Kang-Yi Su[1], Yu-Ju Chen[3], Ching-Ying Kuo[1], Sung-Liang Yu[1]

[1]Department of Clinical Laboratory Sciences and Medical Biotechnology, College of Medicine, National Taiwan University, Taipei, Taiwan,[2]Graduate Institute of Medical Science, College of Medicine, Taipei Medical University, Taipei, Taiwan,[3]Institute of Chemistry, Academia Sinica, Taipei, Taiwan

Metastasis remains one of the major causes of mortality in lung adenocarcinoma, whereas effective therapies to prevent tumor dissemination remain limited. In our study, we identified complement 1q and tumor necrosis factor-related protein 7 (C1QTNF7), a poorly characterized and dysregulated protein in lung adenocarcinoma, as a potential regulator of metastatic progression. Across six independent proteomic cohorts, we observed a consistent downregulation of C1QTNF7 in tumor tissues compared with paired normal tissues adjacent to the tumor (NAT). Lung adenocarcinoma patients with higher C1QTNF7 expression exhibited earlier-stage disease, better pathological differentiation, and prolonged survival, suggesting that C1QTNF7 may exert a biological function beyond serving as a prognostic marker. Transcriptomic profiling revealed that C1QTNF7-low tumors were enriched for metastasis-related signatures. In contrast, overexpression of C1QTNF7 in cell models significantly suppressed these pathways. Functional assays validated that C1QTNF7 suppressed cell migration and invasion *in vitro*, and further restrained metastatic growth in mouse orthotopic models. Subsequent analysis revealed that matrix metalloproteinases (MMPs), including MMP1, MMP9, and MMP15, were negatively regulated by C1QTNF7 at both the expression and activity levels. Notably, this suppression was consistent across clinical samples and cell models, suggesting that these MMPs may act as key downstream effectors modulating the anti-invasive function of C1QTNF7. Treatment with conditioned medium or recombinant C1QTNF7 protein recapitulated the anti-invasive effects, indicating an extracellular, receptor-mediated mechanism. Furthermore, experiments using the truncated mutant protein demonstrated that the C1q globular domain primarily mediates this activity. Together, our findings unveil C1QTNF7 as a novel secreted protein with potent anti-metastatic activity in lung adenocarcinoma. By suppressing MMP-driven invasion, C1QTNF7 contributes to a favorable clinical outcome. Given its secretory nature and functional domain specificity, C1QTNF7 represents a promising therapeutic candidate for targeting tumor metastasis in lung adenocarcinoma.

#3473 Hypoxia reveals a polyaneuploid cancer cell phenotype with features implicated in tumor escape and early metastasis.

Noreen Hosny[1], Shengkai Li[2], Sarah R. Amend[3], Arwa Abdelshafy[1], Robert A. Gatenby[4], Kenneth J. Pienta[3], Joel Brown[4], Junle Qu[5], Robert H. Austin[2]

[1]Department of Molecular Biology, Princeton University, Princeton, NJ,[2]Department of Physics, Princeton University, Princeton, NJ,[3]Johns Hopkins School of Medicine, Baltimore, MD,[4]Moffitt Cancer Center, Tampa, FL,[5]Shenzhen University, Shenzhen, China

Ten million people die every year globally due to metastasis, as metastatic disease remains largely incurable with existing therapies. Polyaneuploid cancer cells (PACCs), which are large, endoreplicated cells that arise in response to environmental stressors, have recently been shown to possess an increased capacity for metastatic behavior. Prior studies have enriched for PACCs using high doses of chemotherapy and have demonstrated their altered nutrient-sensing capabilities, yet the dynamics of PACCs within a native, tumor-like hypoxic microenvironment remain poorly defined.

In this study, we use our previously established *in vitro* membrane-based culture system that allows cancer cells to self-generate physiologically relevant oxygen gradients. Prostate cancer cells rest beneath an acrylic plug and consume the limited oxygen available directly beneath it, while oxygen diffuses inward from the plug periphery to generate a stable radial gradient. This is coupled with a phosphorescent oxygen-sensing film, whose signal increases in the absence of oxygen, enabling real-time spatial visualization and quantification of hypoxia.

Prostate cancer-derived PACCs emerged in response to the hypoxic stress and were identified in real time using morphology-based criteria (≥1500 μm^2 area and ≥3-fold growth over 16 hours). Similar to previous reports in normoxia, long-term single-cell tracking under hypoxia revealed that PACCs exhibited significantly greater net displacement than non-PACCs, suggesting a heightened capacity to invade surrounding tissue during metastatic progression. PACCs also demonstrated a stronger directional bias toward higher oxygen regions within the gradient. This aerotactic behavior suggests two possible roles in PACC dynamics: (1) escape from severely hypoxic tumor regions for survival, and (2) migration toward oxygen-rich vasculature for intravasation during metastasis. Preliminary work in ovarian cancer cells demonstrates similarly enhanced motility of PACCs, suggesting that this phenotype may extend beyond prostate cancer.

Altogether, these findings suggest that hypoxia shapes a PACC phenotype with enhanced motility and oxygen-directed migration, which may confer increased metastatic potential. Future work will incorporate hanging-drop tumor spheroids in this system to enable 3D modeling of hypoxic PACC behavior and determine whether aerotaxis facilitates outward migration toward oxygen-rich regions.

#3474 Effect of Piezo1 activation and CYRI-B loss in melanoma cell membrane dynamics.

Advait Raja, Sayantika Ghosh, Laura Machesky

Department of Biochemistry, Sanger Building, 80 Tennis Court Road, University of Cambridge, Cambridge, United Kingdom

Background

Cancer cell migration is a critical step in metastasis, driven by cytoskeletal remodelling in response to extracellular mechanical cues. Piezo1, a mechanosensitive ion channel, has been known to promote cell motility through calcium-dependent activation of actin-regulatory pathways. In parallel, CYRI-B acts as a local inhibitor of lamellipodial protrusion by binding Rac1 to prevent activation of the Scar/WAVE complex. However, whether these two pathways interact to regulate cancer cell motility remains unexplored.

Methods

Using B16F1 mouse melanoma cells, we investigated how Piezo1 activation (via the small molecule agonist Yoda1) and CYRI-B knockout influence collective cell migration and membrane fluctuations during cell spreading. Scratch-wound healing assays quantified collective migration, and phase-contract live-cell imaging with kymograph analysis assessed spreading and protrusion behaviour in both wild-type and CYRI-B knockout cells with and without treatment with Yoda1.

Results

Piezo1 activation significantly increased collective cell migration by approximately 35%, cell area by approximately 30%, and membrane fluctuations by approximately two-fold in wild-type cells. However, none of these changes were observed after Piezo1 activation in CYRI-B knockout cells. Kymograph analysis showed that protrusion length increased along with protrusion angle after Piezo1 activation in the presence of CYRI-B. However, these increases were also not observed in CYRI-B knockout cells.

Conclusion

Our findings show that CYRI-B may influence the Piezo1-mediated increase in cancer cell migration and membrane dynamics. This raises the possibility of a previously unrecognized connection between mechanosensitive Piezo1 activation and CYRI-B-mediated membrane fluctuations, adding a new dimension to membrane dynamics in cancer cell motility and spreading.

#3475 Pseudopodia coordinate environmental sensing with nuclear signaling through localized gene regulatory machinery.

Kourosh Kouhmareh[1], Thi Hoa Le[1], Richard L. Klemke[2]

[1]UC San Diego School of Medicine, La Jolla, CA,[2]UCSD Moores Cancer Center, La Jolla, CA

Cells dynamically extend membrane protrusions known as pseudopodia to explore their local microenvironment, facilitating interactions with neighboring cells and extracellular matrix (ECM) components. These structures are implicated in regulating fundamental cellular processes, including migration, differentiation, proliferation, and mechanotransduction. While pseudopodia have long been proposed to function as sensory organelles that relay external cues to the nucleus, the molecular mechanisms underlying this spatial signaling remain incompletely understood. Here, we utilized a microporous membrane-based purification strategy that enables the selective isolation of pseudopodia in response to chemotactic gradients. Using paired transcriptomic and proteomic profiling, we compared isolated pseudopodia and their corresponding cell bodies from highly migratory cells. We identify a distinct enrichment of nuclear transport proteins, RNA splicing enzymes, chromatin remodelers, and components of the translational machinery within pseudopodia, supporting a model in which these structures act as early relay sites for gene regulatory signaling. Extending these findings to human cancer, we applied a pseudopodia-specific gene signature to single-cell RNA sequencing datasets from primary breast, bladder, and pancreatic tumors. Malignant epithelial cells highly enriched for our pseudopodium-associated gene set exhibited coordinated upregulation of chromatin remodeling, intracellular signaling and transport, ECM adhesion, and RNA regulatory pathways, mirroring the protrusion-associated programs identified *in vitro*. Collectively, our findings establish pseudopodia as spatially compartmentalized signaling hubs that couple environmental sensing to chromatin regulation and transcriptional reprogramming. This work uncovers a previously unappreciated mechanism by which cellular architecture directs gene expression changes relevant to both normal physiology and disease.

#3476 Bioenergetic pathways regulate distinct patterns of invasion and matrix remodeling in breast cancer cells upon YAP/TAZ activation.

Adil Khan, Haider Abbas Ali, Bishant Karki, **Jacopo Ferruzzi**

University of Texas at Dallas, Richardson, TX

Breast cancer invasion relies on complex interactions between intracellular signals and microenvironmental factors. Central to this process are the transcription factors YAP and TAZ, two key regulators of the Hippo signaling pathway. YAP/TAZ respond to mechanical and metabolic cues by translocating to the nucleus, where they regulate genetic programs that promote tumor progression. Within the tumor milieu, extracellular matrix (ECM) densification, alignment, and altered cell metabolism modulate the invasive phenotype of breast tumors. However, the role of YAP/TAZ activation in regulating ECM mechanics and cancer cell metabolism during invasion remains poorly understood. To address this gap, we utilized breast cancer spheroids to investigate how inhibition of either glycolysis or oxidative phosphorylation (OxPhos) influences invasion dynamics and ECM remodeling under inducible YAP/TAZ activation. MCF-10A breast cancer epithelial cells and doxycycline inducible nuclear mutants MCF-10A YAP(5SA) and TAZ(4SA) were used to generate spheroids and to conduct invasion assays in 3D collagen I. Control MCF-10A spheroids exhibited limited ECM remodeling and invaded collectively. In contrast, YAP/TAZ-activated spheroids displayed increased proliferation and invaded aggressively through a combination of collective protrusions and single cell migration. Structural and mechanical changes in collagen were monitored using 3D Magnetic Twisting Rheometry, a novel technique to assess heterogeneous stiffening of the tumor microenvironment. We found that YAP/TAZ activated spheroids aligned peritumoral collagen radially and stiffened the matrix. A Seahorse assay revealed that TAZ activation upregulates both glycolysis and OxPhos, while YAP activation primarily increases glycolysis. To explore metabolic heterogeneities during invasion, we used Fluorescence Lifetime Imaging Microscopy (FLIM) of the metabolic cofactor NAD(P)H. FLIM showed that, upon YAP/TAZ activation, the spheroid core exhibited an optical signature consistent with glycolysis, while the periphery adopted a mix of glycolysis and OxPhos. Pharmacological inhibition of metabolic pathways further elucidated the role of metabolism in spheroid invasion. In control spheroids, inhibiting either glycolysis or OxPhos hindered invasion. In contrast, in YAP/TAZ activated spheroids, inhibition of OxPhos shifted invasion from collective to single cell modality. Conversely, inhibition of glycolysis reduced single cell migration, shifting invasion towards collective migration. Taken together, our findings suggest that YAP/TAZ activation confers metabolic adaptability to invading spheroids, highlighting the crucial role of YAP/TAZ-mediated metabolic reprogramming in regulating breast cancer cell invasion modalities, as well as the associated changes in contractility and ECM remodeling.

#3477 Multi-scale modeling to predict cancer cell mechanics and migration based on transcriptional state and microenvironment.

Esra Tiftik Karabay[1], Stephanie I. Fraley[2], Parag Katira[1]

[1]Mechanical Engineering, San Diego State University, San Diego, CA,[2]Bioengineering, University of California, San Diego, San Diego, CA

Cancer is a disease characterized by increasing heterogeneity as it progresses. Single-cell RNA sequencing has shed light on the variety of states that cancer cells can adopt, but connecting transcriptional signatures to functional outcomes remains a major challenge. Here, we have taken a multi-scale modeling approach to connect heterogeneous cytoskeletal gene expression programs exhibited by breast cancer cells to biochemical signaling networks and extracellular matrix conditions that regulate the cellular mechanical state. Our model, G-BoHyM-3D, comprises three key components: transcriptomic data, Boolean-Hybrid-Modular Model (BoHyM), and 3D stochastic cell simulations. We identified multiple signaling nodes that connect various extracellular and gene expression signals to key cytoskeletal proteins. The signaling network is solved using a Boolean Hybrid Modular (BoHyM) approach specifically developed to deal with the distinct timescales and complexities of biochemical signaling processes. This integrated framework predicted differences in cell migration behavior of MDA-MB-231 breast cancer cells based on single-cell transcriptional differences. Further development will offer a versatile and user-modifiable tool for investigating how both extracellular and intracellular signaling mechanisms regulate cellular cytoskeleton components, which in turn influence cell-substrate interactions, force generation, invasion, migration, and emergent phenomena such as collective rotational and invasive cell migration.

#3478 The role of *Shroom3* downstream of Wnt/planar cell polarity signaling in breast cancer cell migration.

Julie A. Learn[1], Kacey VanderVorst[1], Kwabena A. Badu-Nkansah[2], Kermit L. Carraway[1], Sean R. Collins[2]

[1]Biochemistry and Molecular Medicine, University of California, Davis, Davis, CA,[2]Microbiology and Molecular Genetics, University of California, Davis, Davis, CA

The 5-year survival rate for patients diagnosed with metastatic breast cancer (BC) remains below 30%, highlighting the need to better understand the molecular mechanisms driving BC metastasis in order to reveal novel opportunities for therapeutic intervention. Wnt/planar cell polarity (Wnt/PCP) is a non-canonical Wnt signaling pathway that regulates epithelial tissue organization and cell migration during embryonic development. Core Wnt/PCP components are upregulated in more aggressive BCs, and their expression is associated with poor patient outcomes. Our group has demonstrated a role for Wnt/PCP in promoting BC cell dissemination; however, the mechanistic details linking core Wnt/PCP components to downstream actin cytoskeletal rearrangements that drive migration and invasion are not well understood. We therefore performed a phosphoproteomics screen using MDA-MB-231 triple negative BC cells to identify proteins differentially phosphorylated in response to pathway activation by the non-canonical Wnt ligand Wnt5a. Among the proteins identified was Shroom3 (Shrm3), in which two serine residues were significantly phosphorylated in response to Wnt5a treatment. Shrm3 is an F-actin-binding scaffolding protein known to recruit Rho kinase (ROCK), actin, and myosin to the apex of apically constricting cells to drive tissue morphogenesis during development and has previously been shown to function downstream of the Wnt/PCP pathway and to bind the effector Dvl2. Given its described functions, Shrm3 is a promising candidate to serve as a direct link between core Wnt/PCP components and the actin cytoskeleton. Knockdown (KD) of Shrm3 reduces both basal and Wnt/PCP-mediated BC cell migration, as well as the formation of actin-rich protrusions at the leading edge of migrating cells. Live-cell imaging confirms reduced lamellipodia formation and reveals that Shrm3 KD cell protrusions are shorter-lived, retract more quickly, and are less polarized to the leading edge. Additionally, loss of Shrm3 reduces activation of myosin light chain and myosin recruitment to the leading edge of BC cells. Co-localization of Shrm3, ROCK, and core Wnt/PCP component Vangl1 is observed at migratory protrusions, and we also observe Shrm3 localizing to focal adhesions (FAs). Loss of Shrm3 reduces FA number and size and may reduce cell–substrate adhesion. Whether phosphorylation of Shrm3 downstream of Wnt/PCP activation regulates these functions is currently under investigation. Based on these findings, we suggest a model in which core Wnt/PCP components recruit Shrm3 to the leading edge of migrating BC cells, where Shrm3 recruits ROCK, actin, and myosin to promote properly localized contractility that supports lamellipodia stabilization and focal adhesion maturation.

#3479 Estrogen promotes structural memory in breast cancer.

Makena Manes, Samantha Hill, Robert Shaw, Yanqing Zhu, Marco Padilla-Rodriguez, Ghassan Mouneimne

Univ. of Arizona, Tucson, AZ

Mechanobiology investigates how cells sense and respond to physical cues such as stiffness, tension, and shear that shape cytoskeletal architecture, transcriptional programs, and cell behavior. In breast tumors, matrix stiffening and altered tensile forces strongly influence invasion and metastatic potential, and recent data show that invasive estrogen receptor (ER) positive tumors are unexpectedly stiffer and exhibit sharper stiffness gradients than ER-negative disease. Mechanical inputs remodel cytoskeletal and adhesion networks and activate signaling pathways that stabilize long-term behaviors, giving rise to mechanical memory. Although mechanical memory has been linked to durotaxis and poor outcomes, how estrogen intersects with stiffness to establish these structural states remains unclear. Here, we show that estrogen signaling directly enhances structural mechanical memory in breast cancer cells. Estrogen reorganizes focal adhesions and cortical actin architecture in a stiffness-dependent manner, increasing mechanosensing, traction generation, and durotactic migration on stiff substrates while stabilizing suppressive cortical actin bundles on soft substrates. These mechanically encoded states persist even after cells leave their original environment, and their magnitude correlates with estrogen receptor activity, aligning with emerging evidence that ER-positive tumors with strong stiffness-response signatures have worse clinical outcomes and show selective benefit from antifibrotic therapy. Together, these findings reveal that estrogen does not simply modulate gene expression but actively shapes the mechanical states that sustain invasion, identifying hormone-mechanics interactions as tractable targets for limiting progression in ER-positive breast cancer.

#3480 The HER2Δ16 splice variant fuels breast cancer metastasis through integrin-driven signaling.

Guillaume de Lhoneux, Jonathan Boucher, Genevieve Lavoie, Laure Voisin, Marc K. Saba-El-Leil, Sylvain Meloche, Philippe P. Roux

Institute for Research in Immunology and Cancer (IRIC), Montreal, QC, Canada

The HER2Δ16 splice variant, generated by exclusion of exon 16 from *ERBB2*, is frequently detected in aggressive HER2-positive breast tumors and has been linked to enhanced tumorigenicity and therapy resistance. Unlike full-length HER2, HER2Δ16 forms constitutively active homodimers, yet the mechanisms driving its aggressive behavior remain poorly defined.

Using isogenic models expressing full-length HER2 or HER2Δ16, we integrated cell surface proteomics with transcriptomic profiling to identify pathways uniquely altered by the splice variant. HER2Δ16 expression induced a wide range of cell-surface changes, including a striking enrichment of RGD-binding integrins. This remodeling was validated in HER2-positive patient tumors stratified for high *versus* low HER2Δ16 expression. HER2Δ16 cells displayed robust activation of the focal adhesion kinase (FAK) pathway and exhibited enhanced migration, invasion, and anchorage-independent growth. Functional perturbation studies demonstrated that HER2Δ16-driven aggressiveness requires integrin signaling. Integrin depletion or pharmacological inhibition of FAK significantly impaired motility, invasion, and growth in soft agar. *In vivo*, systemic FAK inhibition markedly reduced HER2Δ16 tumor growth and metastatic dissemination in immunodeficient mice, establishing integrin-FAK signaling as a therapeutic vulnerability associated with HER2Δ16 expression.

These findings identify integrin-FAK signaling as a central effector of HER2Δ16-induced metastasis and reveal a previously unrecognized mechanism by which this splice variant rewires the adhesion landscape to promote invasive progression. Targeting integrin-driven signaling may provide a promising strategy to counteract metastatic dissemination in HER2Δ16-positive breast cancer.

#3481 Investigating Frizzled7-driven regulation of Vangl1 in Wnt/PCP signaling in breast cancer.

Savannah R. Free, Kermit L. Carraway, Courtney Dreyer

Biochemistry and Molecular Medicine, UC Davis Medical Center, Sacramento, CA

Wnt/Planar Cell Polarity (Wnt/PCP) signaling is a non-canonical developmental pathway reactivated during tumorigenesis in many cancers, where it promotes tumor aggressiveness and correlates with poor prognosis (Hatakeyama et al., 2014). Vangl1, a transmembrane scaffolding protein specific to Wnt/PCP signaling, is an important site for assembly of protein complexes which drive cytoskeletal rearrangement at the leading edge of migratory cells, thereby supporting metastasis (Dreyer et al., 2023). Vangl1 interacts with the Wnt/PCP transmembrane receptor Frizzled7 both intercellularly—to promote polarity and establish epithelial organization—and intracellularly—to drive localized signaling events that promote migration. However, the regulatory relationship between Vangl1 and Frizzled7 is not fully understood.We recently found that Vangl1 undergoes a Frizzled7-dependent post-translational modification, evident from a mobility shift on SDS-PAGE upon Frizzled7 overexpression. Biochemical assays revealed this is a phosphorylation event that: (1) requires Vangl1's C-terminal PDZ-binding motif, (2) occurs independently of Wnt5a (the presumed Wnt/PCP ligand), and (3) persists despite mutation of two candidate phosphorylation sites—leaving the true sites undetermined.To identify key players and investigate functional consequences of this phosphorylation event, we performed Vangl1 immunoprecipitation-mass spectrometry (IP-MS) with and without Frizzled7 expression. The results identified several Vangl1 interactors, both known and novel, whose binding is altered by Frizzled7. These findings suggest that Frizzled7 may regulate Vangl1 function through phosphorylation-dependent modulation of its protein interactions and provide a foundation for future studies on how these interactions influence cancer cell migration and metastatic behavior.

#3482 NOVA1 regulates alternative splicing of CD44 to suppress breast cancer invasion and metastasis.

Jiefeng Huang, Hong Hu

Department of Breast Surgery, Shenzhen People's Hospital, Shenzhen, China

Background: Aberrant alternative splicing (AS) promotes breast cancer progression by enhancing cellular plasticity, invasion, and metastasis. NOVA1, a neuron-specific RNA-binding protein and splicing regulator, has been implicated in multiple diseases, but its role in breast cancer remains unclear.
Methods:NOVA1 expression and clinicopathologic relevance were analyzed using TCGA and GSEA datasets and validated in patient samples by RT-qPCR, Western blotting, and immunohistochemistry. Functional assays (wound healing, transwell invasion, and mouse metastasis models) were performed following NOVA1 overexpression or knockdown. Transcriptomic sequencing and AS analyses identified NOVA1-regulated splicing events, followed by validation and rescue experiments focusing on CD44 isoforms.
Results: Analysis of 89 paired primary breast carcinomas and matched adjacent normal tissues from the TCGA dataset revealed that NOVA1 is among the most differentially expressed splicing factors. NOVA1 expression was reduced in breast cancer and associated with favorable prognosis. NOVA1 overexpression inhibited migration, invasion, and metastasis and suppressed epithelial-mesenchymal transition (EMT). Transcriptome profiling indicated that NOVA1 regulates extracellular matrix organization and alternative splicing of *CD44*, leading to reduced expression of the pro-metastatic isoform CD44v6. Conversely, NOVA1 silencing increased CD44v6 expression and enhanced metastatic potential. Rosiglitazone treatment restored NOVA1 expression and reduced cancer cell invasiveness.
Conclusions:NOVA1 functions as a metastasis suppressor by repressing CD44v6-mediated EMT, establishing a novel NOVA1-CD44v6 splicing axis in breast cancer. Pharmacologic induction of NOVA1 may represent a promising strategy to limit metastatic progression.

#3483 LRRC15-Integrin β1 connection in osteosarcoma cells: Linking adhesion to invasion.

Sanjit Mukherjee[1], Wei-Dong Chen[1], Lisa M. Jenkins[2], Yuelin Zhu[1], Marbin Pineda[1], Robert Walker[1], Paul S. Meltzer[1]

[1]Molecular Genetics Section, Genetics Branch, Center for Cancer Research, National Cancer Institute, National Institutes of Health, Bethesda, MD,[2]Mass Spectrometry Section, Laboratory of Cell Biology, Center for Cancer Research, National Cancer, National Institutes of Health, Bethesda, MD

Osteosarcoma (OSA) is the most common primary bone cancer in children and adolescents, typically arising during rapid skeletal growth. A frequent feature of OSA is an osteoblastic phenotype with abnormal bone formation. Leucine-rich repeat containing 15 (LRRC15) is a cell-surface protein highly expressed in several solid tumors, particularly OSA. Our previous work identified LRRC15 as a key adhesion molecule regulating migration, invasion, and cell–extracellular matrix (ECM) interactions in OSA cells. Time-course single-cell transcriptomics of LRRC15 knockdown revealed dysregulation of several integrins. Integrins are αβ heterodimeric transmembrane receptors essential for cell–ECM adhesion and bidirectional signaling. The β1 subunit (ITGB1) is especially important in cancer, pairing with several α subunits to bind collagen, fibronectin, and laminin. LRRC15 depletion modestly reduced ITGB1 at both gene and protein levels. Collagen-binding integrins (ITGA1, ITGA10) and RGD-binding integrins (ITGAV, ITGB5) were similarly downregulated. Given the overlap between pathways affected by LRRC15 loss and integrin biology, we hypothesized that LRRC15 and ITGB1 may functionally interact to regulate OSA cell adhesion and migration.

We generated CRISPR-Cas9 knockouts (KO) of LRRC15 and ITGB1 in OSA cell lines. Both LRRC15 and ITGB1 KO cells exhibited comparable defects in proliferation, migration, and spheroid invasion, suggesting a strong functional connection between these molecules. Quantitative mass spectrometry and western blots demonstrated decreased LRRC15 expression in ITGB1 KO cells, and reduced ITGB1 expression in LRRC15 KO cells. Notably, rescue of LRRC15 in KO cells resulted in elevated ITGB1 expression. Furthermore, to detect physical interaction, we performed immunoprecipitation with LRRC15 using extracts from parental and LRRC15 KO cells, followed by immunoblotting with an ITGB1 antibody. A significantly lower ITGB1 signal was detected in LRRC15 KO cells. Similarly, when immunoprecipitation was performed with an ITGB1 antibody and detected by immunoblotting with an LRRC15 antibody, we observed reduced LRRC15 expression in ITGB1 KO cells. These findings indicate that ITGB1 and LRRC15 may physically interact with each other. Taken together, our findings indicate that LRRC15 may modulate integrin-mediated adhesion and signaling in OSA. Specifically, the interaction between LRRC15 and integrin β1 appears critical for maintaining integrin-dependent pathways that drive cell proliferation, migration, and invasion. Further mechanistic studies will be required to delineate the molecular basis of this interaction and its contribution to tumor progression and metastasis

: Pediatric Cancer Genomics and Epigenomics
Poster Session

#3486 Elucidating the role of ecDNA in treatment resistance and immune evasion within pediatric medulloblastoma.

Meenakshi Singhal[1], Joy Ku[1], Kun Wang[2], Rohit Bhargava[3]

[1]Carle Illinois College of Medicine, Urbana, IL,[2]Department of Comparative Biosciences, University of Illinois, Urbana-Champaign, Urbana, IL,[3]Department of Bioengineering, University of Illinois at Urbana-Champaign, Urbana, IL

PurposeExtrachromosomal DNA (ecDNA) has been identified as a key driver of cancer evolution and poor clinical prognosis, with emerging research describing its utility for risk stratification. Coupled with current investigations in immunotherapy-based strategies for pediatric medulloblastoma (MBL), we conducted a data-driven pathway analysis to elicit the mechanisms by which ecDNA oncogenes might be implicated in disease pathogenesis. These insights could inform robust molecular subtyping for improved understanding and outcomes in MBL.
IntroductionThere are four major molecular subtypes of MBL: WNT, G4, SHH, and G3, in order of best to worst prognosis. While greater ecDNA counts have been reported to be associated with worse outcomes, we qualitatively evaluated the pathways involved, with a focus on immune evasion and drug resistance. Within the Childhood Cancer Data Initiative (CCDI) database, oncogenes amplified on ecDNA are denoted as either canonical or non-canonical, with the former referring to established drivers of malignant transformation through dysregulated pathways in apoptosis, cell proliferation, etc. Compared to these well-established direct drivers of oncogenesis, we hypothesized that “non-canonical” oncogenes may serve as an undertapped source of pharmacological insights.
MethodsPatient cohorts were generated using the CCDI database by filtering MBL subclasses for cases with both available survival data and ecDNA presence: SHH (n=33 patients; 787 unique genes on ecDNA); G3 (n=19; 161); G4 (n=25; 291); WNT (n=0; 0). Genes identified in more than three patients per subtype were selected for our pathway analysis.
ResultsWhile ecDNA genes were often related to cell cycle dynamics and adhesion proteins, a primarily non-canonical subset is involved in immune dysregulation through various mechanisms. For SHH patients, GLI2 (n=6 patients) upregulates Wnt signaling, reducing natural killer (NK) and CD8+ T cell activity. In G3 patients, both RAD21 and UTP23 (n=3) are implicated in immune evasion, the former by inhibiting interferon signaling and CD8+ T cell function and the latter through reduced dendritic cell activity. In the G4 subclass, NBAS (n=5) is associated with reduced NK cell function and immunodeficiency disorders, while high CDK6 (n=4) is correlated with T cell suppression. Meanwhile, FZD1 (n=4) promotes Wnt signaling-based chemoresistance, and FAM49A (n=3) is a negative regulator of T cell activation. Although these genes have been previously shown to confer worse prognosis across other cancer types, their role in mediating MBL outcomes has not been established.
ConclusionThere are no approved immunotherapeutic strategies for pediatric MBL, despite evidence of immunomodulatory mechanisms. Our preliminary computational results provide guidance to developing ecDNA screenings that could inform personalized therapies and redefine the standard of care.

#3487 XPO1 as a therapeutic vulnerability in atypical teratoid rhabdoid tumors.

Tessa O. House[1], Irina Alimova[2], Shawna Larsen[1], Gillian Murdock[2], Angela Pierce[2], Breauna Brunt[2], Stefania Tocci[1], Sofia Krykunenko[1], Marissa Coppola[1], Anat Erdreich-Epstein[1], Ron Firestein[3], Natalie Serkova[4], Rajeev Vibhakar[2], **Jessica W. Tsai**[1]

[1]Children's Hospital Los Angeles, Los Angeles, CA,[2]The Morgan Adams Foundation Pediatric Brain Tumor Research Program, Children's Hospital Colorado, Aurora, CO,[3]Hudson Institute of Medical Research, Clayton, Australia,[4]Radiology, University of Colorado Anschutz Medical Campus, Aurora, CO

Background: Atypical teratoid rhabdoid tumor (ATRT) is an aggressive central nervous system tumor that mostly affects infants and children under the age of 3. While there have been some improvements in clinical outcomes with multimodal therapy, there remains significant morbidity and toxicities associated with intensive therapy. Therefore, there is a dire need for less toxic and improved therapies for children with ATRT. The identification of cancer dependencies can be utilized to determine novel therapeutic approaches. We identified exportin-1 (XPO1), a nuclear export protein that transports cargo proteins from the nucleus to the cytoplasm, as a novel dependency in ATRT. In other cancers, elevated XPO1 expression has been associated with poor prognosis.

Methods: We utilized an integrative approach harnessing *in vitro* ATRT models, functional genomics, drug assays, flow cytometry, transcriptomics, and *in vivo* intracranial xenograft models to systematically test the hypothesis that XPO1 is a therapeutic vulnerability in ATRT.

Results: RNA-sequencing data across pediatric brain tumor cell lines reveals that XPO1 is highly expressed in ATRT cells. We utilized CRIPSR-Cas9 to knockout XPO1 expression in a panel of patient-derived ATRT cells and found significant defects in cell viability and proliferation. Pharmacologic inhibition of XPO1 using six different selective inhibitors of nuclear export (SINEs) in multiple ATRT cell lines showed sub-10 nM IC50 values. We found that XPO1 inhibition led to on target degradation of XPO1 protein levels. In ATRT cells treated with an XPO1 inhibitor selinexor, Annexin V flow cytometry showed increased apoptosis relative to DMSO. In addition, ATRT cells treated with selinexor demonstrated G1 cell cycle arrest. Western blotting revealed a significant increase in cleaved caspase-3 levels and activation of TP53 with pharmacologic XPO1 inhibition. Transcriptomic analysis of ATRT cells with genetic and pharmacologic inhibition of XPO1 showed significant upregulation of apoptosis and TP53 signaling pathways, with concurrent depletion of cell cycle gene sets. Lastly, using *in vivo* intracranial xenograft models, the combination of selinexor with radiation and cyclophosphamide led to a reduction of tumor size and significant increase in animal survival.

Conclusion: We demonstrate that XPO1 is a dependency in ATRT, and targeting XPO1 in combination with cytotoxic chemotherapy shows high translational potential.

#3488 Advancing pediatric tumor subtype classification on the pediatric cancer (PeCan) knowledge base by integrating molecular and morphology data.

Stephanie Sandor[1], Delaram Rahbarinia[1], Yuan Feng[1], Ramzi Alsallaq[1], Van L. Nguyen[1], Daniel K. Putnam[1], David Finkelstein[1], Jinman Park[1], Bo Wang[1], Jobin Sunny[1], Jian Wang[1], Sue Qiu[1], Michael Edmonson[1], Robert Greenhalgh[1], Meghann Kirk[1], Ira Baranova[1], Stephen V. Rice[1], Abbas Shirinifard[2], Hoaran Chen[2], Ali F. Pour[2], Clay McLeod[1], Lu Wang[3], Jeffery Klco[3], Brent Orr[3], Michael Dyer[2], Xiang Chen[1], Xiaotu Ma[1], Michael Rusch[1], Jinghui Zhang[1]

[1]Computational Biology, St. Jude Children's Research Hospital, Memphis, TN,[2]Developmental Neurobiology, St. Jude Children's Research Hospital, Memphis, TN,[3]Pathology, St. Jude Children's Research Hospital, Memphis, TN

Recent advances in multi-omics profiling have accelerated the discovery of molecular targets in pediatric cancers. However, clinical interpretation remains constrained by evolving diagnostic standards and limited representation of rare subtypes. To address this, we developed the Cancer Classifications for Kids (CC4K) - a harmonized, molecular classification-driven framework aligned with WHO tumor classification and recent publication standards for pediatric tumors. Using pathogenic variant data hosted on St. Jude Cloud PeCan Knowledge Base (https://pecan.stjude.cloud), we classified 230 subtypes for hematological malignancies (n=70), solid tumors (n=97), and brain tumors (n=63). Most recently, the pathogenic point mutations, CNVs, and gene fusions from ~1,511 paired tumor-normal samples, profiled by the ongoing NCI's Childhood Cancer Data Initiative (CCDI), were integrated into PeCan, extending the subtype repertoire by ~53% (80 new subtypes). Importantly, classification of additional subtypes required aligning molecular data with clinical features, which revealed 16 evidence categories, including "biomarker-confirmed" (n=440) and "rescued" (n=353). Furthermore, the integration of additional multi-modal approaches provided clarity on existing classifications with ambiguous or conflicting data. For example, integrating the data from the Molecular Characterization Initiative (MCI) improved our definition of several previously ambiguous cases including a small round blue cell tumor redefined as Ewing sarcoma following identification of a novel *EWSR1::FUS* reciprocal fusion event, reclassification of an ependymoma as intracranial mesenchymal tumor, *FET::CREB*-fusion positive, and validation of an atypical *NRAS*-positive alveolar rhabdomyosarcoma. Additionally, the integration of CCDI data fine-tuned our knowledgebase on the therapy-relevant molecular drivers such as activation of the Hedgehog signaling pathway in embryonal rhabdomyosarcoma and activation of the PI-3K pathway by recurrent *AKT* hotspot mutations in multiple cancer types. Distribution of tumor mutation burdens from each cancer subtype revealed hypermutators with distinct etiologies as identified through subsequent mutational signature analyses. Collectively, these results demonstrate the importance of a harmonized framework for systematic cross-cohort integration that advances diagnostic precision through molecular-pathologic consensus, helps unravel the complex landscape of rare pediatric tumor subtypes, and lays the groundwork for future therapeutic and classification refinements across the pediatric oncology ecosystem.

#3489 EWSR1::WT1 fusion oncoprotein and the androgen receptor shape the biology of desmoplastic small round cell tumors.

Danh Truong[1], Emre Arslan[1], Veena Kochat[1], Jiaqian Fan[1], Diana Shamsutdinova[1], Davis Ingram[1], Kevin Murgas[1], Clement Agyemang[1], Roberto Cardenas-Zuniga[1], Asmaa G. Ahmed[1], Justin Magrath[2], Alexander Lazar[1], Najat Daw Bitar[1], Sean B. Lee[2], Andrea Hayes-Dixon[3], Kunal Rai[1], Joseph A. Ludwig[1]

[1]UT MD Anderson Cancer Center, Houston, TX,[2]Tulane University School of Medicine, New Orleans, LA,[3]Howard University, Washington, DC

Desmoplastic small round cell tumors (DSRCTs) are rare, aggressive sarcomas driven by the EWSR1::WT1 fusion oncoprotein (FP) and marked by poor long-term survival. Despite a relatively quiet genome with a single known oncogenic driver, DSRCTs display striking transcriptional heterogeneity and express markers from multiple lineages, epithelial, mesenchymal, myogenic, and neural. DSRCTs show a strong male predominance, suggesting a potential role for sex-specific regulatory mechanisms, including androgen receptor (AR) signaling. To investigate the molecular basis of this complexity, we generated a comprehensive, multi-modal atlas of DSRCT, integrating transcriptomic, epigenomic, and spatial omics data (10x Genomics). We focused on dissecting the regulatory architecture shaped by the EWSR1::WT1 fusion and transcription factors such as AR, aiming to uncover mechanisms of lineage specification and therapeutic vulnerabilities. We hypothesized that epigenetic regulation of the EWSR1::WT1 FP contributes to this lineage divergence. To explore FP activity, we found that neogenes (non-coding RNA FP targets) and known FP-regulated genes were more highly expressed in NE-lineage tumors, suggesting that FP affects lineage type. Spatial transcriptomic analysis revealed intratumoral heterogeneity, with distinct clusters of epithelial (AR+, cytokeratin+) and non-epithelial tumor cells. Despite phenotypic differences, all tumor cells expressed neogenes, as confirmed by RNA in situ hybridization (RNAScope). Epigenetic profiling showed enrichment of Forkhead TFs (FOXA1/2). FOXA2 was associated with NE, and AR/GRHL2 were associated with epithelial lineages. CUT&RUN analysis of AR after DHT stimulation revealed co-occupancy of FOXA1/2 and WT1 at AR-bound regions, suggesting interaction between AR signaling, FP, and FOXA1/2. FP knockdown in DSRCT cell lines induced a shift toward an epithelial-like state, increased FOXA1, and decreased FOXA2 expression. Tumor cells exhibit both inter- and intra-tumoral heterogeneity, adopting epithelial and NE phenotypes. We find that the high FP levels favor a NE-lineage state mediated by chromatin accessibility and transcriptional regulation. Spatial analyses revealed co-existing epithelial and non-epithelial tumor cells within the same nests, underscoring the intratumoral heterogeneity. The interaction between FP, AR, and Forkhead transcription factors (FOXA1/2) suggests a potential mechanism by which oncogenic FPs and lineage-defining transcription factors converge to regulate tumor phenotype.

#3490 Preservation and clonal behavior of extrachromosomal DNA in patient-derived xenograft models of childhood cancers.

Rishaan Kenkre[1], Jon D. Larson[1], Owen Chapman[2], Jens Luebeck[3], Yan Yeun Lo[1], Paul Megan[4], Wenshu Zhang[5], Vineet Bafna[3], Robert Wechsler-Reya[6], Lukas Chavez[1]

[1]Sanford Burnham Prebys Medical Discovery Institute, La Jolla, CA,[2]Department of Neuro-oncology, Nagoya City University Graduate School of Medical Sciences, Nagoya, Japan,[3]Department of Computer Science and Engineering, University of California San Diego, San Diego, CA,[4]Rady Children's Hospital, San Diego, CA,[5]University of California San Diego, San Diego, CA,[6]Department of Neurology, Columbia University Irving Medical Center, New York, NY

Background: Extrachromosomal DNA (ecDNA) is a class of structural variants linked to poor prognosis in pediatric cancers. Patient-derived xenograft (PDX) models are crucial tools for basic and translational cancer research, as they are believed to recapitulate the molecular features and intratumoral heterogeneity present in patient tumors. However, ecDNA demonstrates unique evolutionary dynamics under selective pressure, and the behavior of ecDNA during PDX model development and propagation remains largely uncharacterized. This study investigates the fidelity of PDX models in representing ecDNA from primary tumors. By analyzing ecDNA sequence composition and copy number conservation across a variety of pediatric solid cancers, we evaluate the extent to which PDX models recapitulate the ecDNA landscape observed in human tumors.

Methods: Amplicon Architect, a tool that reconstructs focally amplified DNA regions to understand cancer genome architecture, was used to analyze the whole-genome sequencing (WGS) of 338 PDX models and 127 corresponding primary tumors. ecDNA status, sequence, copy number, and associated genes were compared between PDX models and their matched human tumors. Additionally, multiome RNA and ATAC single-cell sequencing of a PDX tumor enabled comparison of ecDNA intratumoral heterogeneity relative to similar data previously obtained from the primary tumor.

Results: ecDNA in PDX models largely recapitulated the spectrum of oncogene amplifications observed in human tumors, with MYCN being the most frequently amplified. ecDNA status remained unchanged for a majority of the PDX models (106/127, 83%) compared to the primary tumors, with 20% of previously ecDNA-negative cases acquiring ecDNA during PDX development. Consequently, ecDNA was more prevalent in the PDX models than in their corresponding human tumors (McNemar's test, $p = 0.0014$). Detailed examination of ecDNA sequences in tumor-PDX pairs showed substantial conservation (67% with >90% sequence overlap) but variable breakpoint concordance. Single-cell analysis demonstrated that rare ecDNA-positive cells from the primary tumor preferentially drive PDX tumor development.

Conclusion: This study highlights the prevalence, oncogenic content, and conservation of ecDNA in PDX models relative to pediatric patient tumors. We observed that ecDNA frequently recapitulates oncogene amplifications found in human cancers, is generally preserved during PDX establishment, and reflects subtype-specific patterns across tumor types. These findings support the utility of PDX models in studying ecDNA biology and their implications for the study of pediatric cancer progression and treatment. Longitudinal sampling during PDX tumor growth and under therapeutic pressure could provide valuable insights into the dynamics of molecular evolution, clonal selection, and ecDNA-driven therapy resistance.

#3491 Epigenetic regulation of the RAB5B GTPase expression in B-cell acute lymphoblastic leukemia.

Katarina Dovat, Yali Ding, Daniel Bogush, Rabab Husain, Ryan Chingakham, Dhimant Desai, Sinisa Dovat

Penn State College of Medicine, Hershey, PA

Ras analog in brain (Rab) proteins are important parts of small GTPase signaling pathways in human malignancies. RAB5B is the GTPase, which promotes cellular proliferation and is overexpressed in a large number of human cancers, including leukemia. Regulation of RAB5B transcription in human hematological malignancies is mostly unknown. Here, we analyze regulation of RAB5B transcription in human B-cell acute lymphoblastic leukemia (B-ALL). The use of global chromatin immunoprecipitation coupled with next generation sequencing (ChIP-seq), showed increased occupancy of IKAROS tumor suppressor protein at the promoter of RAB5B gene in several B-ALL cell lines and primary B-ALL cells. IKAROS direct binding to promoter of RAB5B was confirmed by quantitative chromatin immunoprecipitation (qChIP). The role of IKAROS in transcriptional regulation of RAB5BB in B-ALL was assessed by gain-of-function and loss-of-function experiments. Luciferase reporter assay showed that IKAROS directly represses transcription of RAB5B. Overexpression of IKAROS in B-ALL cells via retroviral transduction resulted in increased IKAROS binding to the RAB5B promoter and decreased RAB5B transcription. This was associated with enrichment in constitutive heterochromatin marker, H3K9me3 and the loss of active chromatin markers, H3K4me3 and H3K27ac. In contrast, shRNA-mediated knockdown of IKAROS inhibited IKAROS binding to the RAB5B promoter and resulted in increased RAB5B expression, along with increased enrichment of H3K4me3 and H3K27ac active chromatin markers, and the loss of H3K9me3 marker at RAB5B promoter. Primary B-ALL cells that carry deletion of one IKAROS allele have increased expression of RAB5B, associated with strong enrichment of H3K4me3 and H3K27ac, as well as the absence of H3K9me3 at RAB5B promoter. In conclusion, presented data suggest that IKAROS functions as a direct transcriptional repressor of RAB5B in B-ALL and that the mechanism of RAB5B repression by IKAROS involves formation of heterochromatin at the RAB5B promoter. Results uncovered a novel mechanism through which IKAROS exerts its tumor suppressor effect and regulate transcription and cellular proliferation in leukemia. Supported by NIH/NCI R01 CA278226 grant.

#3492 Targeting ALKBH5 mediated ChREBP signaling impairs cancer stem cell metabolism and tumor growth in medulloblastoma.

Panneerdoss Subbarayalu[1], Daisy Medina[1], Prabhakar Pitta Venkata[1], Shahad Abdulsahib[1], Saif Nirzhor[1], Santosh Timilsina[1], Deepika Singh[1], Phat Do[1], Desiree Denman[1], Krishna Priya Evani[2], Dhiya Billa[3], Meera Nair[1], Esha Reddy[4], Yogesh Gupta[1], Peter Houghton[1], Yidong Chen[1], Suryavathi Viswanadhapalli[1], Gangadhara R. Sareddy[1], Andrew Brenner[1], Ratna K. Vadlamudi[1], Manjeet Rao[1]

[1]UT Health San Antonio, San Antonio, TX,[2]UT San Antonio, San Antonio, TX,[3]Trinity University, San Antonio, TX,[4]Southern Methodist University, Dallas, TX

Background: Medulloblastoma (MB) is the most common malignant pediatric brain tumor and a major cause of childhood cancer mortality. It comprises four molecular subgroups: WNT, SHH, Group 3, and Group 4. Group 3 MB, often marked by c-MYC amplification, has the worst prognosis. Despite surgery, radiation, and chemotherapy, high-risk patients face low 5-year survival and frequent relapse. Current treatments cause severe side effects. Cancer stem cells (CSCs) drive MB aggressiveness, therapy resistance, and recurrence. This project aims to uncover mechanisms sustaining CSCs and MB progression.
Methods: MB cell lines (HD-MB03, D556, D425, DAOY) with ALKBH5 overexpression, knockdown (siRNA), or knockout (CRISPR), along with controls, were analyzed using viability, migration, invasion, colony formation, cell cycle, and apoptosis assays. RNA sequencing identified ALKBH5-regulated genes, validated by RT-qPCR, western blot, and RNA immunoprecipitation. An orthotopic intracranial xenograft model assessed ALKBH5's tumor-promoting role in vivo.
Results: To explore the role of m6A RNA methylation in medulloblastoma (MB), we silenced key regulators (writers: METTL3, METTL14; erasers: ALKBH5, FTO) in MB cell lines. ALKBH5 depletion caused the greatest reduction in proliferation, suggesting its therapeutic potential. Analysis of pediatric cancer datasets and tissue microarrays confirmed ALKBH5 overexpression and amplification in MB. Knockdown of ALKBH5 increased global m6A levels and reduced MB cell viability, migration, invasion, and stemness (medullosphere formation and NANOG, OCT4, SOX9 expression). Apoptosis assays showed elevated Annexin V-positive cells, and in vivo studies demonstrated suppressed tumor growth in orthotopic xenografts. ALKBH5 loss also increased DNA damage markers (γH2AX, 53BP1). RNA-seq and IPA revealed downregulation of genes involved in glycolysis, lipogenesis, and c-MYC targets, including ChREBP. Western blot confirmed decreased protein levels in these pathways.
Conclusion: ALKBH5 is a critical regulator of MB tumorigenesis and CSC maintenance via m6A RNA demethylation. Targeting ALKBH5 may offer a promising therapeutic strategy to inhibit MB progression, overcome therapy resistance, and improve outcomes for high-risk MB patients.

#3493 UltraFast whole genome sequencing enables personalized treatments in childhood cancers.

Aditi Vedi[1], Jamie Trotman[2], Joao Dias[1], Martina Mijuskovic[3], Sera Choi[3], Laura Kingham[2], Rachel Moore[4], Sarah M. Leiter[1], Rowena Guermech[2], Amanda Semerene[2], Aviva Grisby[2], Sophie Wool[2], Victoria Joslin[2], Zoya Kingsbury[3], Mark Ross[3], David Bentley[5], Sam Behjati[1], Sean Humphray[3], Patrick Tarpey[4], David Rowitch[1]

[1]University of Cambridge, Cambridge, United Kingdom,[2]Cambridge University Hospitals NHS Foundation Trust, Cambridge, United Kingdom,[3]Illumina Inc, Cambridge, United Kingdom,[4]National Health Services (England), Leeds, United Kingdom,[5]Solexa, Inc. (Illumina Cambridge), Essex, United Kingdom

Background: Whole genome sequencing (WGS) improves childhood cancer management by detecting clinically actionable variants beyond the scope of standard assays. However, current turnaround times (TAT) are well beyond clinical decision-making windows. We developed a novel 'Ultra-Fast Whole Genome Sequencing' (UF-WGS) technology to deliver comprehensive genomic results within days, and evaluated its feasibility, accuracy, and clinical impact in real-world pediatric hematology/oncology.**Methods:** Children with suspected or confirmed malignancy in Cambridge were recruited between 2023–2025. Tumor, bone marrow, and/or blood samples were analysed with UF-WGS and standard genomic medicine service (GMS-WGS) concurrently. UF-WGS deploys Constellation mapped read technology, eliminating library preparation by applying crude lysate or DNA directly onto the flowcell surface providing enhanced genome coverage, variant calling and phasing. Variant calls and TAT were benchmarked against GMS-WGS. Only clinically actionable variants as per the UK national genomics test directory were reported. Clinical utility was assessed by multidisciplinary review.**Results:** Fifty-four patients representing the expected range of childhood malignancies were recruited. UF-WGS reduced mean TAT of clinically actionable WGS reports from 37 to 3 days. It recalled 95% of somatic and germline variants and detected 19 additional variants, leading to alterations in clinical management. Discrepancies were due to tissue heterogeneity or low variant allele frequency. Median sequencing depth of UF-WGS (137× tumor; 84× germline) was superior to GMS-WGS (97x tumor; 42x germline).UF-WGS enabled demonstrable clinical benefit including risk stratification, target identification and pharmacogenomic guidance in 18/35 (51%) of prospectively recruited patients. UF-WGS supported de-escalation of therapy, earlier initiation of targeted treatments and optimization of surgical timing. For one patient, rapid identification of a germline *ACVR1* mutation allowed a diagnosis of fibrodysplasia ossificans progressiva, avoiding harmful interventions. In 9/19 (47%) retrospective cases, independent reviewers judged that real-time UF-WGS would have improved management.UF-WGS was particularly advantageous in leukemia, where tumor-only analysis avoided delays associated with obtaining germline DNA. The clinical value of delivering comprehensive cytogenetic, minimal residual disease, and pharmacogenomic data within 72 hours is particularly great in this disease setting. **Conclusions:** UF-WGS is feasible, accurate and clinically impactful in pediatric cancer, delivering real-time WGS to inform management decisions. It offers a scalable framework to consolidate multiple molecular assays into a single, rapid test, supporting ambitions for faster genomic diagnosis and equitable precision medicine delivery internationally.

#3494 Epigenetic landscape and gene regulation in embryonal brain tumors with multilayered rosettes.

Shanzheng Wang[1], Sander Lambo[1], Monika Mauermann[1], Phylicia Stathi[2], Robert Autry[1], Natalie Jager[1], Stefan M. Pfister[1], Marcel Kool[1]

[1]Hopp Children's Cancer Center Heidelberg (KiTZ), Heidelberg, Germany,[2]Princess Maxima Center for Pediatric Oncology, Utrecht, Netherlands

Embryonal tumors with multilayered rosettes (ETMRs) are relatively rare but highly aggressive pediatric brain tumors that mainly affect children under four years of age and are generally associated with poor clinical outcomes. Around 90% of ETMRs harbor amplification of the chromosome 19 miRNA cluster (*C19MC*), in most cases fused to the *TTHY1* gene. The second most recurrent aberration, present in about half of the *C19MC*-negative cases, are bi-allelic mutations in *DICER1*. *C19MC* amplification and positive LIN28A immunostaining are key diagnostic markers for ETMRs. ETMRs also exhibited a distinct DNA methylation profile compared with other embryonal brain tumors such as medulloblastomas (MBs) and atypical teratoid/rhabdoid tumors (ATRTs). However, the detailed epigenetic landscape defined by DNA methylation and histone modifications, its effects on transcriptional regulation in ETMRs, and how these associations differ from MBs, ATRTs, and normal brain tissues remain largely unexplored.

To decode the ETMR epigenome, we generated, collected, and integrated whole genome bisulfite sequencing (WGBS), chromatin immunoprecipitation sequencing (ChIP-seq) of various histone marks and epigenetic regulators, RNA sequencing (RNA-seq), and ribosome profiling (Ribo-seq) data from a series of ETMRs, similar data from a series of MBs and ATRTs covering all molecular subtypes, and normal brain tissues for comparison reasons.

Through integrative multi-omics analyses, we delineated chromatin states and DNA methylation-defined genomic segments of ETMRs for the first time. ETMR genomes are globally hypomethylated, with wider distributions of unmethylated regions (UMRs) and DNA methylation valleys (DMVs) on its genome compared with MBs, ATRTs, and normal brain tissues. These regions are associated with genes involved in embryonal brain development, essential cellular processes, and oncogenic pathways. Low methylated regions (LMRs) are enriched for transcription factor binding motifs such as CTCF and SOX2, and also act as potential enhancers that modulate several transcriptional and epigenetic regulators. Partially methylated domains are correlated with transcriptional repression in ETMRs, consistent with observations in other biological systems. Moreover, TET enzymes are highly expressed in ETMRs, potentially regulated by BET family proteins such as BRD4. Pharmacological inhibition of TETs and BRDs reduced ETMR cell viability.

In summary, our study provides a comprehensive epigenetic landscape of ETMR and its relationship to transcriptional regulation, revealing distinct regulatory mechanisms that enhance understanding of ETMR biology, and identifying potential therapeutic targets for experimental and preclinical validations in this lethal tumor type.

#3495 Characterizing the MYC-induced immunopeptidome.

Jack Faulkner, Anwesha Dasgupta, John R. Prensner

University of Michigan, Ann Arbor, MI

Medulloblastoma, the most common malignant brain tumor typically found in children ages 0-9, comprises four subgroups, each with distinct molecular characteristics. Children with MYC or MYCN amplifications, which occur in Group 3 and Sonic Hedgehog subgroups, respectively, face poor survival rates and high metastasis. MYC and MYCN, both DNA-binding transcription factors, drive oncogenesis by promoting rapid cell division. This study investigates how MYC(N) upregulation stimulates the production of immunogenic neoantigens from non-canonical peptides, which may serve as novel targets for immunotherapy. Prior work shows post-transcriptional control is a critical component of MYC biology, with Group 3 tumors exhibiting significant protein-RNA dyssynchrony. Intriguingly, MYC preferentially drives the translation of upstream open reading frames (uORFs), which are non-canonical peptides that are largely unstable but exhibit robust presentation on the MHC-I antigen system.To test this, we engineered UW228 and ONS76 medulloblastoma cell lines to express MYC or MYCN cDNAs using GFP as a control and verified overexpression via western blotting and qPCR. We assessed HLA-I protein uniformity via flow cytometry. Ribosome and RNA sequencing were used to identify actively translated genomic regions and mRNA transcript levels. HLA-I immunopeptidomics was completed to identify non-canonical peptides with increased surface presence due to MYC(N) expression.We successfully verified MYC(N) overexpression and demonstrated the required HLA-I expression for immunopeptidomic analysis. The sequencing data confirmed that MYC(N) drives the translation of specific non-canonical peptides uORFs, showing increased immunopeptidome complexity in high-risk medulloblastoma models. These results are broadly supportive of MYC(N)'s role in driving the flux of non-productive peptides.Completion of this research will identify novel antigens linked to MYC(N), offering critical information for the development of medulloblastoma-specific immunotherapies to improve outcomes for affected patients. Future research will investigate MYC(N)’s impact on proteasome function and the BAG6 complex, which is responsible for regulating proteasomal degradation of non-canonical translation products. Pathway analyses will also be conducted to compare gene family expression and identify upregulated and downregulated biological functions.

#3496 Epigenetic repurposing by CBFA2T3-GLIS2 reveals a druggable DNA methylation axis in high-risk pediatric AML vulnerability in pediatric AML.

Samrat Roy Choudhury[1], Arundhati Chavan[1], Rhonda E. Ries[2], Giselle Almeida Gonzalez[1], Soheil Meshinchi[2], Jason E. Farrar[1]

[1]Arkansas Children's Research Institute, University of Arkansas for Medical Sciences, Little Rock, AR,[2]Translational Science and Therapeutics Division, Fred Hutchinson Cancer Center, Seattle, WA

The CBFA2T3-GLIS2 (C/G) fusion defines an infant-restricted, clinically devastating subtype of pediatric AML with relapse rates exceeding 90%. While C/G is known to remodel the enhancer landscape, the epigenetic mechanisms that sustain leukemic identity and enforce apoptotic resistance remain undefined.To resolve this, we performed integrative multi-omic epigenetic profiling across primary patient samples, C/G$^+$ AML lines, and a developmentally faithful cord blood CD34$^+$ HSPC model. Genome-wide DNAm mapping (meEM-seq), chromatin profiling (CUT&RUN, ATAC-seq), and transcriptomics uncovered a promoter-biased hypermethylation program unique to C/G$^+$ AML, with ~50% of altered CpGs localized to promoters ($\Delta\beta \geq 0.2$ vs NBM). Despite unaltered global 5mC levels, C/G bound and transcriptionally activated DNMT3B, which imposed focal promoter hypermethylation specifically at transcriptionally active, enhancer-connected loci. Strikingly, these hypermethylated promoters did not silence gene expression; instead, they stabilized expression of CRE-linked genes enriched for apoptotic regulation, EMT, KRAS signaling, and heme metabolism—revealing that C/G converts DNA methylation into a stabilizing rather than repressive epigenetic signal.CRISPR-mediated DNMT3B knockout validated this mechanism: DNMT3B loss reduced locus-specific 5mC and downregulated C/G-dependent targets but induced compensatory DNMT1 and UHRF1 upregulation, forming a maintenance shunt that preserved DNAm at apoptotic effector loci and sustained an elevated apoptotic threshold. Targeted dCas9-TET1 demethylation of the pro-apoptotic gene PMAIP1 (NOXA) restored transcriptional inducibility and apoptotic signaling, directly confirming that DNAm constrains activation of death pathways. In vivo, DNMT3B-deficient xenografts regained Venetoclax sensitivity and extended survival, phenocopying DNMT inhibition and validating the therapeutic relevance of this epigenetic axis. Collectively, these findings establish C/G as a developmental epigenetic architect that repurposes DNA methylation to stabilize oncogenic transcriptional circuits and maintain apoptosis resistance. By defining the C/G-DNMT3B-DNMT1/UHRF1 axis and its enhancer-linked promoter hypermethylation signature, this work identifies aberrant DNAm as a structural and druggable vulnerability, providing the mechanistic rationale for integrating DNMT inhibition with BCL-2 blockade in high-risk pediatric AML.

#3497 Comprehensive analysis of genomic landscape of ultra-rare pediatric malignant rhabdoid tumors.

Elizabeth Rasmussen[1], Elena Mironova[1], Dias Kurmashev[1], Kendra Maa?[2], Stefanie Volz[3], Zhao Lai[1], Stefan M. Pfister[2], Yidong Chen[1], Raushan Kurmasheva[1]

[1]UT San Antonio Greehey Children's Cancer Res. Inst., San Antonio, TX,[2]Hopp Children's Cancer Center Heidelberg (KiTZ), Heidelberg, Germany,[3]Division of Pediatric Neurooncology, German Cancer Consortium (DKTK) and German Cancer Research Center (DKFZ), Heidelberg, Germany

Malignant rhabdoid tumors (MRTs) are ultra-rare, highly aggressive pediatric tumors that occur predominantly in infants, with the highest incidence in children under one year of age. MRTs exhibit high metastatic potential and poor prognosis, with 5-year event-free survival rates below 20%. There are currently no effective therapies for these patients. To better elucidate the molecular mechanisms driving MRT and identify potential therapeutic vulnerabilities, we constructed a comprehensive genomic landscape of 16 MRT xenograft models using whole-genome sequencing (WGS), transcriptome profiling (RNAseq), and DNA methylation analysis (EM-seq), representing intracranial (AT/RT; n=6), extracranial (RTK; n=5), and soft tissue subtypes (n=5). This work builds on our previous studies investigating the *in-vivo* activity of the combination of the PARP1 inhibitor, PEGylated talazoparib (PEG~TLZ), and the DNA alkalyating agent, temozolomide (TMZ), in MRTs, as well as the associated transcriptional changes underlying therapeutic response. WGS analysis revealed recurrent mutations in *TP53*, *BRCA1*, and *BRCA2* genes across tumors, regardless of tumor demographics. All 16 MRT tumors harbored *SMARCB1* alterations, including single-nucleotide variants, whole or partial gene deletion, and/or loss of heterozygosity (LOH). Consistently, LOH was confirmed in 15 of 16 tumors. Differential expression analyses identified elevated activity of Receptor Tyrosine Kinase (RTK), Ephrin, and Epidermal Growth Factor Receptor (EGFR) signaling pathways in good responders (maintained/complete response) compared with poor responders (partial response or progressive disease) across treatment groups (PEG~TLZ, TMZ, and the combination), as reported previously. RNAseq further detected several gene fusions, one of which was experimentally validated. Supervised clustering of EM-seq data revealed a characteristic binary methylation pattern independent of tissue origin. Differential methylation analysis of promoter CpG islands identified 5 genes exhibiting a strong inverse correlation between DNA methylation and mRNA expression, highlighting potential therapeutic targets whose activity may be modulated *via* epigenetic mechanisms. Overall, our comprehensive multi-omics characterization of these ultra-rare MRTs establishes a foundational and enduring resource for the pediatric cancer research community. By providing deeply annotated genomic, transcriptomic, and epigenomic profiles across diverse MRT subtypes, this dataset will support long-term mechanistic studies, enable identification of therapeutic vulnerabilities, and help guide the development of future clinical strategies for this highly aggressive pediatric cancer.

#3498 Improving the utility of the single-cell pediatric cancer atlas through updated cell type annotations, CNV inference, and visualization tools.

Allegra G. Hawkins[1], Joshua A. Shapiro[1], Stephanie J. Spielman[1], David S. Mejia[1], Deepashree Venkatesh Prasad[1], Nozomi Ichihara[1], Arkadii Yakovets[1], Avrohom M. Gottlieb[1], Kurt G. Wheeler[2], Chante J. Bethell[3], Steven M. Foltz[4], Jennifer O'Malley[1], Casey S. Greene[5], Jaclyn N. Taroni[1]

[1]Alex's Lemonade Stand Foundation, Bala Cynwyd, PA,[2]Reify Health, Boston, MA,[3]The University of Texas MD Anderson Cancer Center, Houston, TX,[4]Multiple Myeloma Research Foundation, Boston, MA,[5]University of Colorado Anschutz Medical Campus, Aurora, CO

The Single-cell Pediatric Cancer Atlas (ScPCA) Portal (https://scpca.alexslemonade.org/), developed and maintained by the Childhood Cancer Data Lab, is a data resource for uniformly processed single-cell and single-nuclei RNA sequencing data, as well as de-identified metadata from pediatric tumor samples. Originally comprised of data from 10 projects funded by Alex's Lemonade Stand Foundation (ALSF), the Portal currently contains summarized gene expression data for over 700 samples across more than 50 cancer types drawn from ALSF-funded and community-contributed datasets. Downloads include gene expression data as SingleCellExperiment or AnnData objects containing raw and normalized counts, PCA and UMAP coordinates, and summary reports. Some samples have additional data from bulk RNA-seq, spatial transcriptomics, and/or feature barcoding (e.g., CITE-seq and cell hashing) included in the download. All data on the Portal were uniformly processed using scpca-nf, an efficient and open-source Nextflow workflow written and maintained by the Data Lab, which utilizes alevin-fry to quantify gene expression.

Since presenting the ScPCA Portal at the 2024 AACR Annual Meeting, several new features have been added to the available data. Automated cell type annotation is now performed using three unique methods: SingleR, CellAssign, and SCimilarity. If two of the three methods agree, an ontology-aware consensus cell type label is assigned. The individual annotations and the consensus cell types are included in the cell metadata of the downloaded objects. Some projects also include manually-curated cell type annotations generated as part of the OpenScPCA project (https://openscpca.readthedocs.io).

In addition, copy-number variation (CNV) inference is now performed on each sample using the InferCNV package, specifying the i6 HMM to quantify specific CNV events. Since InferCNV quantifies CNV events using a designated set of normal, or non-malignant, reference cells, consensus cell types are used to identify a diagnosis-appropriate normal cell reference for each sample. The total CNVs observed and the full HMM metadata table are stored in the processed SingleCellExperiment and AnnData objects. The updated cell type annotation and implementation of InferCNV are included as part of the open-source workflow, scpca-nf. The workflow and associated documentation are freely available at https://github.com/AlexsLemonade/scpca-nf.

Finally, the ScPCA Portal hosts an instance of the UCSC Cell Browser, enabling users to visualize and interact with the gene expression data for all samples without needing to download the data. Comprehensive documentation about data processing and the contents of files on the portal, including a guide to getting started working with an ScPCA dataset, can be found at https://scpca.readthedocs.io.

#3499 BRD9 functions as a negative regulator of GBAF in synovial sarcoma.

Jinxiu Li[1], Mary Nelson[1], Li Li[1], Xiaobo Xia[2], Christine Stephan[2], Katarzyna Modzelewska[1], Gary Yu[2], Iain Mulford[2], Honnappa Srinivas[2], Xinyi Ge[1], Sarah McCollum[1], Ewin R Jones[1], Yixuan Guo[1], Xi Chen[2], Thomas Zoller[2], Gregory Hollingworth[2], Ensar Halilovic[3], Tinya J. Abrams[4], Edmund Harrington[2], Sofia Gkountela[5], Giorgio Galli[5], Hans Voshol[6], Nathalie Carte[2], Jason Thomas[2], Xiaoyang Zhang[7], David Lum[7], Martin Hirst[8], Jeffery Yap[7], William Forrester[2], Bradley R. Cairns[7], Kevin Bruce Jones[7]

[1]University of Utah, Salt Lake City, UT,[2]Novartis Biomedical Research, Cambridge, MA,[3]Oncology Translational Medicine, Novartis Insts. for BioMedical Research, Cambridge, MA,[4]Novartis (Cambridge, MA), Acton, MA,[5]Novartis Institutes for Biomedical Research, Basel, Switzerland,[6]Novartis Biomedical Research, Basel, Switzerland,[7]University of Utah Huntsman Cancer Institute, Salt Lake City, UT,[8]Canada's Michael Smith Genome Sciences Centre, Vancouver, BC, Canada

Synovial sarcoma (SyS) incorporates the SS18::SSX fusion oncoprotein into GLTSCR1-containing BRG1/BRM and associated factors (GBAF) complexes, and demonstrated a dependency on GBAF subunit, BRD9. However, SyS clinical trials with multiple BRD9 degraders failed to achieve clinically impactful remissions. Here, we provide a mechanistic framework to explain these results. BRD9 depletion serves to blunt proliferation in SySs harboring minimal genomic alterations, rare in trial participants. In cultured cells, xenografts, and recombinant purified complexes, BRD9 loss does not impact GBAF assembly. Although BRD9 degradation in SyS reduces GBAF enrichment at target loci, BRD9-less complexes maintain or increase chromatin accessibility and associated gene transcription. Biochemical assays with purified recombinant GBAF demonstrate markedly increased nucleosome sliding in the absence of BRD9. Thus, BRD9 restrains GBAF activity, with BRD9 degradation increasing enzymatic remodeling and target gene expression by fusion oncoprotein-distributed GBAFs in SyS. This subtle epigenetic disturbance creates a low hurdle for SyS to surpass.

#3500 Synergistic targeting of EP300/CBP and EYA co-activators collapses the rhabdomyosarcoma core regulatory circuit.

Annika Gustafson[1], Stephanie Nance[2], Berkley Gryder[3], Noha A. Shendy[2], Lars Wick[1], Grace McKay-Corkum[2], K. Elaine Ritter[2], Stephen Connor Purdy[1], Arthur R. Wolin[1], Sheera R. Rosenbaum[1], Sabateeshan Mathavarajah[4], Nickerson A. Demelfi[4], Yueyang Wang[4], Yang Zhang[2], Mark W. W. Zimmerman[5], Anoop M. Kavirayani[2], John Hardin[1], Alexander LaVeck[6], Xiang Wang[6], Neekesh V. Dharia[7], Andrew Hong[8], Guillaume Kugener[7], Jesse S. Boehm[9], Jennifer Roth[7], Javed Khan[10], Francisca Vasquez[7], Kristin B. Artinger[11], Rui Zhao[1], David M. Langenau[12], Jun Qi[5], Kimberly Stegmaier[5], Heide L. Ford[1], Adam D. Durbin[2], **Brian J. Abraham**[2]

[1]University of Colorado Anschutz, Anschutz, CO,[2]St. Jude Children's Research Hospital, Memphis, TN,[3]Case Western Reserve University School of Medicine, Cleveland, OH,[4]Massachusetts General Hospital, Boston, MA,[5]Dana-Farber Cancer Institute, Boston, MA,[6]University of Colorado Boulder, Boulder, CO,[7]Broad Institute of MIT and Harvard, Cambridge, MA,[8]Emory University, Atlanta, GA,[9]Koch Inst. for Integrative Cancer Research at MIT, Cambridge, MA,[10]National Cancer Institute, Bethesda, MD,[11]University of Minnesota, Minneapolis, MN,[12]MGH/Harvard Medical School, Stoneham, MA

Rhabdomyosarcoma (RMS) is a high-risk and lethal pediatric sarcoma that resembles developing skeletal muscle. RMS tumors have low mutation burdens, but these scant mutations often alter genes involved in transcriptional control. Transcriptional dysregulation is critical to RMS pathogenesis, supported by studies in both RMS tumors carrying mutationally derived chimeric transcription factors (“fusion positive (FP)”), or those without (“fusion negative” (FN)). However, mechanisms to selectively target dysregulated transcription in RMS remain outstanding. Here, we develop a novel approach targeting RMS transcription comprising simultaneous targeting of two distinctly acting transcriptional co-activators. We discover a common cell identity-controlling pan-RMS core regulatory circuit (CRC) composed of oncogenic and lineage-specific myogenic master transcription factors (mTFs). These mTFs are regulated by super-enhancers, and they co-bind genome-wide to control the malignant transcriptome of both FP- and FN-RMS. Using a super-enhancer-based reporter screen, we identify the EP300/CBP inhibitor A485 as a potent inhibitor of the pan-RMS CRC, though efficacy of this compound was limited by toxicity. To enhance on-target specificity, we identify the protein EYA2 as a co-factor that binds directly to SIX1, a member of the pan-RMS CRC and exploit a recently developed second-generation EYA1/2 tyrosine phosphatase inhibitor, LG1-34, to inactivate its function. While A485 and LG1-34 independently reduce mTF transcription and drive RMS cell death, in combination, these agents function synergistically to reduce RMS growth in vitro and in vivo. These results demonstrate that combined targeting of enhancer maintenance and CRC cofactors is a powerful strategy to suppress the RMS transcriptome and enforce RMS cell death.

#3501 A critical dependency in Ewing sarcoma: PAX7 attenuates EWS::FLI1 activity at de novo microsatellite enhancers to maintain oncogenesis.

Caroline Fraser, Alex Belt, Andrew McFadden, Ian Davis

UNC Lineberger Comprehensive Cancer Center, Chapel Hill, NC

The pediatric cancer Ewing sarcoma is driven by the fusion oncoprotein EWS::FLI1, which retains the DNA-binding domain of FLI1. Rather than canonical ETS sites, EWS::FLI1 is retargeted to GGAA-microsatellite loci, where it remodels chromatin to establish de novo enhancer elements that drive oncogenic transcription. Because EWS::FLI1 lacks intrinsic chromatin-remodeling activity, it depends on recruited proteins to regulate chromatin. Furthermore, precise regulation of EWS::FLI1 activity is critical: both over and under expression of EWS::FLI1 result in cell cycle arrest. However, mechanisms of EWS::FLI1 regulation at non-canonical GGAA-mSats remain unknown. We used a proximity-labelling proteomic approach to identify EWS::FLI1-associated proteins in a native chromatin context. We discovered that the myogenic transcription factor PAX7 selectively interacts with EWS::FLI1 but not wild-type FLI1. PAX7 silencing impaired cell proliferation, indicating an essential role. We found that *PAX7* is itself a direct target gene of EWS::FLI1, associated with high, ubiquitous PAX7 expression in EwS tumors. Mechanistically, EWS::FLI1 drives the relocalization of PAX7 to GGAA-mSats and ETS-sites, where PAX7 modulates chromatin accessibility and attenuates EWS::FLI1-driven transcription. At GGAA-mSats, PAX7 depletion results in chromatin opening, whereas at ETS sites, chromatin accessibility is deregulated. PAX7 depletion results in and an exaggerated EWS::FLI1 transcriptional response. Mutational analysis of PAX7 revealed that its Paired DNA binding domain and OAR-domain are required for interaction with EWS::FLI1 and that interaction between the two transcription factors is required for cell proliferation. These findings define PAX7 as a context-specific regulator of EWS::FLI1 activity at non-canonical GGAA-microsatellite enhancers and identify a previously unrecognized vulnerability in Ewing sarcoma that could be exploited for future therapeutic intervention.

#3502 Loss of histone 3 lysine 9 trimethylation drives recurrence in high-risk pediatric medulloblastoma.

John DeSisto, Andrew M. Donson, Bethany Veo, Rajeev Vibhakar

The University of Colorado School of Medicine, Aurora, CO

Background: Pediatric Group 3 medulloblastoma (G3 MB) recurs in more than 40% of cases. Initial treatment typically includes surgical resection followed by craniospinal irradiation (RT) and chemotherapy with cisplatin and cyclophosphamide. Recurrent G3 MB is usually metastatic, has poor long-term survival, and no survival-altering treatment. Treatment of recurrent G3 MB impacts only a portion of tumor cells, or worse, may facilitate the emergence of treatment resistant cell clones. G3 MB's cells of origin correspond to neural stem or progenitor cells that originate early in normal development. This suggests that pluripotency genes whose expression is normally epigenetically silenced are reactivated in G3 MB oncogenesis and recurrence. Histone 3 post-translational modifications, particularly trimethylation of histone 3 lysine 9 (H3K9me3), silence expression of pluripotency genes when no longer needed during development. We hypothesize that loss of H3K9me3 at key pluripotency genes facilitates G3 MB recurrence. **Methods:** To model recurrence, we developed treatment-resistant cell lines, tumoroids and orthotopic patient-derived xenograft (PDX) mouse models of G3 MB. Using single cell RNA-Seq and multiomics we analyzed gene accessibility and expression changes between primary-recurrent patient sample pairs. To define cell and tumor micro-environment changes during recurrence, we conducted spatial transcriptomics of primary-recurrent patient sample pairs using a customized gene list. **Results:** Analysis of primary-recurrent patient sample pairs revealed that most cell types are conserved during recurrence, mesenchymal cells begin to outnumber angiogenic populations, hypoxic populations increase, and neural stemlike cells replace progenitor-like populations. Treatment of G3 MB cells with near-IC_{50} levels of cisplatin or RT + cisplatin produces a treatment resistant / recurrent phenotype with enriched DNA repair capability, enriched MAPK and autophagy pathways, and depleted p53 activity. Cisplatin + cyclophosphamide treatment of mice with PDX tumors extends survival but ultimately results in aggressive treatment resistant tumors with divergent stemlike populations as compared to the primary tumors. Expression of *SETDB1,* a demethylase (DM) that removes H3K9me3, decreased upon G3 MB recurrence, while expression of *EHMT2*, a methyltransferase (MT) that places H3K9me2, increased. Similar trends were not observed in non-G3 MB samples. **Conclusions and ongoing work:** H3K9 MT and DM alterations suggest the loss of H3K9me3 leads to emergence of pluripotent gene expression during G3 MB recurrence. We are analyzing CUT & RUN data to verify whether H3K9me3 occupancy is altered through changes in expression of H3K9 MTs and DMs. Longer term, we plan to evaluate whether inhibiting the loss of H3K9me3 diminishes the frequency or severity of recurrence in G3 MB models.

#3503 Somatic changes in Y chromosome copy number are associated with clinical and molecular features in neuroblastoma.

Teodoro Rivera-Wills, Preshita Dave, Esther Rheinbay

Mass General Cancer Center, Boston, MA

Introduction: Neuroblastoma survival is decreased in males, and loss of the Y chromosome (LOY) has been recently shown to affect cancer incidence, survival, and response to therapy in certain tumor types; therefore, we set out to test whether LOY is linked to clinical and molecular features in neuroblastoma.
Methods: Using publicly available allele-specific copy number from next-generation sequencing of neuroblastoma (Korber et al. 2023), we identified areas of duplication or deletion in regions of the Y chromosome. Y chromosome copy number was compared to molecular and clinical variables.
Results: There were 64 tumors from male patients in the cohort, of whom 15 (23.4%) had loss of the Y chromosome and 12 (18.8%) had duplication of the Y chromosome. There was a significant survival advantage in patients with duplications of the Y chromosome, while there was no difference in survival in patients with LOY compared to wild type. We also tested whether LOY is associated with specific molecular features in neuroblastoma. We found that 17q gain ($p=0.01$) and 11q loss ($p<0.001$) were strongly associated with LOY, while MYCN amplification ($p=0.003$) was inversely associated. We also found a significant association with Alternative Lengthening of Telomeres ($p<0.001$).
Conclusions: Our analysis shows that there are significant associations between LOY and specific molecular mechanisms in pediatric neuroblastoma. While we did not observe an association between LOY and survival, we did detect improved survival in patients with a gain of Y. This observation may be linked to other features, such as genome doubling, and merits further analysis.

#3504 Mithramycin analogues trap the EWS-FLI1 transcriptional complex, evict ETV6, and disable oncogenic condensate function in Ewing sarcoma.

Srijan Acharya[1], Rajesh Yetirajam[1], Yasuda Kazuto[1], Suhas Bhosale[2], Jurgen Rohr[2], Markos Leggas[1]

[1]Pharmaceutical Sciences, St. Jude Children's Research Hospital, Memphis, TN,[2]Pharmaceutical Sciences, University of Kentucky, Lexington, KY

Background: Ewing sarcoma is an aggressive pediatric cancer driven by the EWS-FLI1 fusion oncoprotein, which assembles into nuclear transcriptional condensates essential for oncogenic gene regulation. MTMSA-Trp is a synthetic mithramycin (MTM) analogue with improved pharmacokinetics and in vivo efficacy in Ewing sarcoma. MTMSA-Trp binds to the minor groove of DNA and interacts with the major groove-bound EWS-FLI1, but the mechanistic details of these interactions are not well understood.
Methods and Results: Using luciferase reporter assays, we show that MTMSA-Trp selectively inhibits EWS-FLI1-dependent transcription at nanomolar potency, with weaker effects on Sp1-driven transcription. MTMSA-Trp activity is attenuated in EWS-FLI1 knockdown cells, indicating functional dependence. Western blotting confirmed MTMSA-Trp-mediated suppression of EWS-FLI1-regulated targets in multiple Ewing sarcoma cell lines, while non-Ewing lines exhibited minimal response. qRT-PCR analyses revealed that MTMSA-Trp downregulates EWS-FLI1 mRNA, while paradoxically stabilizing its protein and shifting downstream transcriptional programs consistent with EWS-FLI1 antagonism. Biophysical assays demonstrated increased thermal and proteolytic stability of EWS-FLI1 upon MTMSA-Trp treatment, suggesting drug-induced stabilization of the EWS-FLI1 complex. Protein stability assays further showed that MTMSA-Trp prolongs the half-life of EWS-FLI1 in an EWS-FLI1-dependent manner, whereas ETV6, though functionally linked, was not stabilized but essentially evicted from the nucleus. Subcellular fractionation revealed that MTMSA-Trp increases nuclear retention of EWS-FLI1 while dynamically redistributing ETV6 in an EWS-FLI1-dependent manner. These effects extended to chromatin-associated partners of EWS-FLI1 condensates, including BAF155, BAF60a, and ARID1a. Immunofluorescence confirmed that MTMSA-Trp preserved ARID1a-containing nuclear condensates, protecting them from degradation by cycloheximide, and did so only in the presence of EWS-FLI1. At the transcriptional level, MTMSA-Trp downregulated CDK7 and hyperphosphorylated RNA Pol II CTD accompanied by accelerated RPB1 degradation. These effects were abolished when EWS-FLI1 was silenced.
Conclusions: Our results show that MTMSA-Trp binds to and stabilizes the EWS-FLI1 transcriptional complex, maintains its associated condensates, and alters gene expression by disrupting RNA Pol II activity. These findings reveal a previously overlooked mechanism of action for MTM analogues in their interaction with the transcriptional complex, ETV6, and phase-separated oncogenic complexes. They further support the potential of these compounds as a therapeutic approach for Ewing sarcoma.

#3505 DNA methylation signatures of diet quality and treatment-related cardiotoxicity in childhood cancer survivors.

Yoonji Kim[1], Xiaoxi Meng[1], Kwangyeon Oh[1], Tuo Lan[2], Tiffany Eulalio[1], Heather L. Mulder[3], John B. Easton[3], Jinghui Zhang[3], Emily Walker[4], Geoffrey A. Neale[4], Deo Kumar Srivastava[5], Min Ni[6], I-Chan Huang[1], Stephanie B. Dixon[6], Gregory T. Armstrong[1], Melissa M. Hudson[1], Kirsten K. Ness[1], Yikyung Park[2], Zhaoming Wang[1]

[1]St. Jude Children's Research Hospital, Memphis, TN,[2]Washington University in St. Louis, St. Louis, MO,[3]Computational Biology, St. Jude Children's Research Hospital, Memphis, TN,[4]Hartwell Center, St. Jude Children's Research Hospital, Memphis, TN,[5]Biostatistics, St. Jude Children's Research Hospital, Memphis, TN,[6]Oncology, St. Jude Children's Research Hospital, Memphis, TN

Background: Childhood cancer survivors are at increased risk of cardiometabolic risk factors (CMRF) and cardiovascular disease (CVD) due to cancer treatment exposures. Whether DNA methylation (DNAm) signature of diet quality can remediate these risks remains unclear.
Methods: We examined blood DNAm signatures of diet quality and their associations with CMRF/CVD among 2,191 adult survivors of childhood cancer and 283 community controls from the St. Jude Lifetime Cohort. Diet quality was assessed using the Healthy Eating Index (HEI)-2015 and alternate Mediterranean Diet Score (aMED), respectively. Genome-wide DNAm was profiled using the Illumina EPIC BeadChip V1. We identified differentially methylated positions (DMPs), genes (DMGs) and regions (DMRs) for diet quality-associated DNAm signatures in blood, from which DNAm-based scores for a healthy diet (DNAmDiet) were further derived. Multivariable logistic regression examined associations between DNAmDiet and seven outcomes: abnormal glucose metabolism, hypertension, hypertriglyceridemia, hypercholesterolemia, obesity, cardiomyopathy, and myocardial infarction. We also compared diet- and treatment-related methylation effects, focusing on CpGs where healthy diet-associated methylation changes occurred in the opposite direction of treatment-induced alterations, suggesting potential remediation of treatment-related DNAm alterations.
Results: We identified 29 DMPs, 113 DMRs, and 53 DMGs significantly associated with HEI-2015, and 9 DMPs, 16 DMRs, and 16 DMGs associated with aMED ($P<9\times10^{-8}$ for DMPs; FDR<0.05 for DMRs or DMGs). Diet-associated DNAm signatures mapped to key genes including AHRR, CPOX, CLDND1, GPR15, LY9, and MAP4K4, many of which are involved in immune regulation, cellular signaling, nutrient-sensing, suggesting that healthy diet may influence epigenetic regulation of immune and metabolic pathways. A DNAmDiet score based on aMED signatures was associated with lower risk of cardiomyopathy (Odds Ratio [OR]=0.76; 95% CI, 0.65-0.92), hypercholesterolemia (OR=0.65; 95% CI, 0.50-0.84), and hypertriglyceridemia (OR=0.78; 95% CI, 0.63-0.97). Effect sizes for diet-associated DMPs were, on average, twice as large in survivors as in community controls ($|\beta survivor|/|\beta control|=2.02$; P<0.001), despite strong correlations between populations (r=0.85; P<0.001). We found that up to 87.5% of treatment-associated DMPs showed opposite associations with HEI-2015 or aMED scores, with up to 8.9% reaching statistical significance.
Conclusions: DNAm signatures of healthy diet were associated with lower risks of specific cardiometabolic and cardiovascular outcomes. Importantly, healthy diet-related DNAm changes were in the opposite direction of treatment-induced DNAm alterations, suggesting potential for epigenetic recovery through dietary interventions.

: Therapeutic Modulation of the Tumor Microenvironment: New Targets and Approaches 1
Poster Session

#3508 Glioblastoma treatment with multifunctional nanodrug inhibiting laminin-411 activates local immune response, increases survival of mice and reveals AI-selected immune molecular pathways.

Alexander V. Ljubimov[1], Rameshwar Patil[2], Vladimir A. Ljubimov[3], Hui Ding[3], Yizhou Wang[4], Sarah Song[4], Andrei A. Kramerov[1], Oksana Chepurna[1], Vanessa Borges[1], Jessica Dos Santos[1], Eggehard Holler[5], Julia Y. Ljubimova[5], Keith L. Black[3]

[1]Biomedical Sciences, Cedars-Sinai Health Sciences University, Los Angeles, CA,[2]Neurosurgery, Loma Linda University, Loma Linda, CA,[3]Neurosurgery, Cedars-Sinai Health Sciences University, Los Angeles, CA,[4]Computational Biomedicine, Cedars-Sinai Health Sciences University, Los Angeles, CA,[5]Terasaki Institute for Biomedical Innovation, Los Angeles, CA

Introduction: Cancer microenvironment influences tumor growth, invasion, and escape from immune surveillance. Glioblastoma (GBM) extracellular matrix (ECM) especially laminins play an important role in tumor progression. We previously observed a correlation in GBM samples from 130 patients between increased expression of ECM laminin-411 (α4β1γ1) and faster tumor recurrence with decreased patient survival. Laminin-411 is a basement membrane component that can also modulate immune response through Notch signaling. We developed novel nanoconjugate (NC) blocking laminin-411 that can activate GBM local immune system after brain delivery.
Methods: NC was based on non-toxic poly (β-L-malic acid, P) with covalently attached antisense oligonucleotides (AON) against laminin-411 α4 and β1 chains, as well as trileucine (LLL) peptide for endosomal escape, AP-2 peptide for blood-brain barrier (BBB) crossing and GBM cell targeting. The NC was thoroughly characterized and was intravenously administered to mice (5 injections) with intracranial syngeneic GL261 GBM. The NC selected for treatment had the structure [P/mPEG5000(2%)/LLL(40%)/AON(α4β1)(2.0%)/AP-2(2%)]. Tumor RNA sequencing (RNA-seq) was analyzed by bioinformatics with artificial intelligence and validated for select genes by immunohistochemistry. Immune cell populations were analyzed by flow cytometry.
Results: NC treatment in vivo suppressed GBM growth and significantly prolonged animal survival. RNA-sec analysis after treatment with NC suppressing tumor laminin-411 suggested anti-tumor effect with upregulation of apoptotic Casp3, Ifng, Tnf, Il1a, and Il1b genes and reduction of glioma proliferation markers and oncogenes EGFR, c-Myc, Klf4, Irf4, and Ki-67, as well as Notch ligand Dll3. Ingenuity pathway analysis artificial intelligence module AI interpret predicted activation of inflammatory pathways involved in cell signaling during immune responses, pathways related to adhesion and migration of immune cells, and general immune response. In agreement with these data, protein validation showed decreased Ki-67 and Dll3, and increased T cell marker CD4, inflammatory markers IFNγ and TNFα, and anti-tumor M1 macrophage marker NOS2/iNOS. Interestingly, the immunostaining for markers of GBM stem cells, CD133 and nestin, was markedly decreased upon treatment. Flow cytometry also suggested activation of immune response after NC administration.
Conclusion: We describe a novel GBM treatment strategy via NC crossing BBB and targeting critical ECM and immune components of tumor microenvironment that are largely independent of heterogeneous genetic mutations in glioblastoma. Support: NIH grants R01 CA284247, R01 CA188743, R01 CA206220, R01 CA209921, R01 EY013431

#3509 Targeting Spns2 induces immunogenic cell death and systemic anti-tumor immunity to suppress metastasis.

Han Gyul Lee[1], Wyatt Wofford[1], Alhaji H. Janneh[2], Paramita Chakarborty[1], Natalia Oleinik[1], Mohamed Faisal Kassir[1], Odai Darawshi[1], Neil Parikh[3], Stefano Berto[1], Kevin R. Lynch[3], Webster L. Santos[4], Ozgur Şahin[1], Shikhar Mehrotra[1], Besim Ogretmen[1]

[1]The Medical University of South Carolina (MUSC), Charleston, SC,[2]Memorial Sloan Kettering Cancer Center, New York, NY,[3]The University of Virginia, Charlottesville, VA,[4]The Virginia Polytechnic Institute and State University, Blacksburg, VA

Background: Spinster homolog 2 (SPNS2) exports sphingosine-1-phosphate (S1P) to promote oncogenic signaling. Although SPNS2 is associated with metastatic progression, its tumor-intrinsic role in regulating immunogenic cell death (ICD) and anti-tumor immunity remains unclear. We examined how genetic or pharmacologic inhibition of SPNS2 influences metastasis, ICD induction, and systemic immune activation.
Methods: Patient datasets were analyzed in conjunction with breast (4T1, EMT6) and melanoma (B16) models. SPNS2 was ablated using CRISPR or inhibited using a first-in-class small-molecule SPNS2 inhibitor. S1P export, migration, and S1PR1-AKT signaling were assessed in vitro. Orthotopic, tail-vein, co-injection, and vaccination models were used to evaluate tumor growth, metastatic spread, ICD signatures, and systemic immunity. Individual DAMP pathways were disrupted to test mechanistic requirements.
Results: High SPNS2 expression correlated with poor survival across multiple cancer types. SPNS2 promoted S1P export, S1PR1-AKT activation, epithelial-mesenchymal transition, stemness, and lung colonization, whereas SPNS2 loss impaired migration and markedly reduced spontaneous and experimental metastases. SPNS2 inhibition elicited hallmark ICD features—including eIF2α phosphorylation, calreticulin exposure, and ATP/HMGB1 release—enhancing antigen presentation, expanding $CD4^+$ and $CD8^+$ T cells, and limiting primary tumor growth, metastasis, and postsurgical relapse. Vaccination with SPNS2-deficient or inhibitor-treated tumor cells protected against rechallenge with 4T1 or antigenically distinct EMT6 tumors. Disruption of individual DAMP pathways attenuated these responses, demonstrating ICD dependence. **Conclusions:** SPNS2-mediated S1P transport drives metastasis and immune evasion, whereas SPNS2 inhibition induces ICD and potent systemic T-cell immunity. Targeting SPNS2 represents a therapeutic strategy to suppress metastatic progression and generate durable anti-tumor immunity.
Disclosure: Generative AI was used to assist in editing this abstract.

#3510 High-dose FcRH5xCD3 T-cell-engaging bispecific antibody (TCB) overcomes Treg-mediated suppression in-vitro in multiple myeloma.

Kai Lu[1], Darya Khantakova[2], Rin Nakamura[1], Kerstin Trunzer[3], Hyun Yong Jin[1], Elizabeth Punnoose[1], Elizabeth Germino[1], Katerina Hatzi[1]

[1]Genentech, South San Francisco, CA,[2]Washington University School of Medicine, St. Louis, MO,[3]Roche, Basel, Switzerland

T-cell-engaging bispecific antibody (TCB) redirect cytotoxic T-cells to recognize and eliminate multiple myeloma (MM) cells, yet their activity may be influenced by the immunosuppressive tumor microenvironment, including regulatory T-cells (Tregs). Previous studies have suggested that Tregs may influence TCB-mediated cytotoxicity. To test this directly, we developed a human in-vitro co-culture model consisting of healthy donor-derived primary PBMCs, MM cell lines, and ex-vivo activated autologous Tregs, treated with a FcRH5×CD3 T-cell-engaging bispecific antibody analogous to cevostamab which is currently in clinical development. Myeloma cell killing was quantified by multiparametric flow cytometry across a dose range of TCB concentrations. At low FcRH5×CD3 doses, addition of Tregs significantly reduced MM cell killing, T-cell proliferation (Ki-67), and cytokine production (Granzyme B), consistent with Treg-mediated suppression. However, at higher TCB concentrations, cytotoxicity, cytokine production, and T-cell activation were restored, consistent with the idea that higher FcRH5×CD3 levels can overcome Treg-induced inhibition. Importantly, depletion of the added Tregs using an anti-CD25 depleting monoclonal antibody (analogous to CD25-targeting Treg depleters under clinical investigation) reversed the reduction in MM cell killing observed at low TCB concentrations, confirming that the inhibitory effect was Treg-dependent. This dose-dependent pattern was consistent across multiple donors, demonstrating that potent TCB activity effectively overrides Treg suppression. These findings suggest that achieving sufficient T-cell activation through optimal FcRH5 TCB dosing could counteract Treg-mediated immunosuppression in patients, supporting dose selection strategies that maximize efficacy within the immunoregulatory landscape of multiple myeloma.

#3511 Reprogramming the tumor microenviroment to halt metastasis: Akos targets metastatic cancer-associated fibroblast in solid tumors.

Valentina Cerda I[1], Benjamin Prieto[2], Muriel Nunez[2], Daniela Barrera[2], Alexis Salas[3], Patricia Garcia[4], Enrique Brandan[1], Javier Cerda-Infante[2]

[1]Universidad San Sebastian, Santiago, Chile,[2]Environ SpA, Santiago, Chile,[3]Universidad de Concepcion, Concepcion, Chile,[4]Pontificia Universidad Catolica de Chile, Santiago, Chile

Background: Metastasis accounts for ~90% of cancer-related deaths and remains poorly controlled by therapies that primarily target cancer cells. Metastatic cancer–associated fibroblasts (mCAF) are key orchestrators of the tumor microenvironment, driving extracellular matrix remodeling, epithelial–mesenchymal transition, immune evasion, and metastatic dissemination. We identified in mCAF a proteoglycan-modified receptor that integrates these programs and developed Akos, a first-in-class small-molecule inhibitor that selectively blocks its formation and signaling. Here we extend those findings by defining the mechanism of action of Akos on tumor–stroma crosstalk and its molecular specificity toward a proteoglycan-modified stromal receptor in mCAF.
Methods: Primary stromal cultures were established from core biopsies of patients with metastatic cancer (mCAF), non-metastatic cancer (CAF), and non-malignant tissue (BAF). Target expression and Akos modulation were evaluated by gene profiling, IHC, and western blot. Co-cultures measured mCAF-driven invasion, proliferation, and EMT with/without Akos. Prostate, breast, colorectal, and pancreatic xenografts assessed tumor growth and metastasis after Akos treatment. Systemic toxicity, PK, and stromal proteoglycan selectivity were determined. Mechanistic studies examined how Akos-modulated changes in the proteoglycan-modified receptor in mCAF translated into alterations in pro-migratory and invasive signaling in tumor cells.
Results: Akos potently inhibited mCAF-induced tumor cell invasion and proliferation and reduced epithelial–mesenchymal transition markers in tumor cells. Mechanistic analyses showed that Akos selectively blocked formation of the proteoglycan-modified stromal receptor in mCAF, without affecting the expression of other stromal proteoglycans, and downregulated downstream mediators of migration, invasion, and extracellular matrix remodeling. These changes were associated with decreased activation of pro-metastatic signaling in tumor cells in co-culture. In xenograft models, Akos reduced tumor volume by up to 50-fold and tumor weight by up to 30-fold compared with vehicle and completely abrogated spontaneous metastatic foci in all evaluated models, while maintaining stable systemic exposure and no meaningful off-target toxicity.
Discussion: Akos is a highly specific stromal-directed therapy that reprograms metastatic CAF by inhibiting a defined proteoglycan-dependent receptor, disrupts tumor–stroma signaling to tumor cells, and completely blocks spontaneous metastasis across multiple solid tumor models. The combination of mechanistic specificity, robust antimetastatic activity, and favorable safety profile supports the clinical development of Akos as a first-in-class antimetastatic therapy targeting the tumor microenvironment.

#3512 High-precision carbon ion radiotherapy elicits effective in-situ tumor vaccination and durable antitumor immunity.

Sarah Meister[1], Matilde Recusani[1], Maximilian Knoll[1], Ralph Sinn[2], Aoife Gahlawat[1], Jennifer Furkel[1], Michael Breckwoldt[2], Dirk Jager[3], Jurgen Debus[4], Amir Abdollahi[1]

[1]Clinical Cooperation Unit Translational Radiation Oncology, National Center for Tumor Diseases (NCT), German Cancer Research Center (DKFZ), Heidelberg University Hospital (UKHD), Heidelberg Ion-Beam Therapy Center (HIT), Heidelberg, Germany,[2]Clinical Cooperation Unit Translational Radiation Oncology, Neuroradiology Department, National Center for Tumor Diseases (NCT), German Cancer Research Center (DKFZ), Heidelberg University Hospital (UKHD), Heidelberg, Germany,[3]Medical Oncology, National Center for Tumor Diseases (NCT), Heidelberg University Hospital (UKHD), Heidelberg, Germany,[4]Heidelberg University Hospital (UKHD), Heidelberg Ion-Beam Therapy Center (HIT), Heidelberg, Germany

With advent of carbon ion radiotherapy (CIRT) the spatio-temporal precision of external-beam radiotherapy has nearly reached the physical limits. We sought to investigate the potential of CIRT in reprograming the tumor immune microenvironment (TIME). To this end, three syngeneic tumor models were systematically investigated for their response to fractionated (5 x 3 Gy) CIRT vs. standard photon irradiation (XIRT). The models included the paradigmatic C57BL/6 tumor models of colorectal carcinoma (MC-38) and prostate cancer (RM1) as well as genetically engineered non-small cell lung cancer model (Pik3ca+, p53+/–, Y856). We observed substantially augmented antitumoral activity and relative biological effectiveness (RBE) of CIRT vs. XIRT in all three models. Intriguingly, CIRT achieved 100% cure rates in MC-38 and 67% in the Y856 model and increased the median overall survival (OS) three-fold vs. XIRT in the RM1 model. Immunohistological, single-cell transcriptome, and CyTOF analyses revealed enhanced immune cell infiltration in CIRT-treated tumors compared to controls. Moreover, enhanced infiltration of intravenously transferred Superparamagnetic Iron Oxide Nanoparticle (SPION) labelled T cells after CIRT was traced by MRI. The antitumoral responses elicited by CIRT could be significantly reduced in all three tumor models by abrogating the adaptive immune response via depletion of cytotoxic T cells using anti-CD8a antibodies. Additional experiments in immunocompromised athymic nude mice (Foxn1nu/nu) confirmed the significant impact of adaptive immunity in CIRT-elicited antitumoral effects with marked reduction of OS and zero cure rates across all three models. To examine the durability of CIRT-induced in-situ tumor vaccination, cured mice were rechallenged on abscopal sites at day 77 post-CIRT. In the MC-38 model, 100% of the abscopal tumors were rejected within 14 days after implantation indicating that CIRT induces a robust and durable systemic antitumor immunity. Together, our findings highlight the pivotal contribution of adaptive immunity to effective CIRT-induced TIME reprogramming for curative treatments. CIRT may provide novel and effective means of high-precision spatio-temporally controlled in-situ tumor vaccination.

#3513 The novel lncRNA *SEAL1* - key regulator of the pan-cancer myCAF cell state dictating prognosis ans immunotherapy response - is a promising new therapeutic target for solid cancers.

Emely Moller[1], Baroj Abdulkarim[1], Venkatesh Kancherla[1], Soumitra Ghosh[2], Sanne Schrevens[1], Rene Dreos[1], Kristen Gentry[3], Claire Roberts[3], Marco Mina[1], Rudi Micheletti[3], G. Paolo Dotto[4], Daniel Blessing[5], Samir Ounzain[5]

[1]HAYA Therapeutics SA, Epalinges, Lausanne, Switzerland,[2]Department of Immunobiology, University of Lausanne (UNIL), Lausanne, Switzerland,[3]HAYA Therapeutics INC, San Diego, CA,[4]University of Lausanne (UNIL), Epalinges, Switzerland,[5]HAYA Therapeutics SA, HAYA Therapeutics INC, Epalinges, Lausanne, Switzerland

A desmoplastic reaction in the solid tumor microenvironment (TME), typically characterized by extracellular matrix (ECM) dysregulation and an immune suppressive milieu, is a key factor contributing to tumor aggression, therapeutic resistance, metastasis and inevitably poor patient prognosis. Cancer-associated fibroblasts (CAFs), in particular myofibroblast-like CAFs (myCAFs), are central players in the development of TME desmoplasia in the most common and aggressive solid cancers such as breast, lung, head & neck and pancreatic. The contribution of myCAFs to standard-of-care treatment resistance and immunotherapy failure has raised their attraction as therapeutic targets. However, myCAF-targeting therapies have not yet proven to be effective for clinical use and is still a largely unexplored area of solid cancer therapeutics. Long non-coding RNAs (lncRNAs) are increasingly recognized as key regulators of epigenomic and transcriptomic cellular processes and characterized by highly cell-state and disease-specific expression. Targeting myCAF-specific regulatory lncRNAs constitutes a novel therapeutic approach to reduce myCAF-driven detrimental changes in the TME, coupled to an increased susceptibility to combination treatments. Here we identified a novel lncRNA *SEAL1* which is restrictively expressed in the pan-cancer myCAF cell state associated with poor patient prognosis and treatment response. Independent analyses of breast, head & neck and pancreatic cancer patient datasets demonstrated *SEAL1* as a key component of disease-driving myCAF co-regulatory networks. By antisense oligonucleotide (ASO)-mediated targeting of *SEAL1,* and of the murine functional analog *Seal1*, we demonstrated that the myCAF identity was potently reduced in *in vitro* cellular models. In contrast, ASO- or CRISPRi-mediated targeting of *LRRC15/Lrrc15*, a *SEAL1* downstream marker associated with the myCAF cell identity, had no effect on the disease-driving myCAF cell state. *LRRC15* has previously been associated with poor prognosis and an unfavorable response to immunotherapy, being actively pursued as a potential CAF therapeutic target. Moreover, by utilizing a xenograft co-injection *in vivo* model, *SEAL1* targeting in patient-derived myCAFs reduced tumor volume whereas *LRRC15* targeting had no effect. Taken together, this study emphasizes that the Regulatory Genome is still largely under explored and that novel discoveries such as *SEAL1* may uncover previously unknown biological mechanisms. By leveraging regulatory lncRNAs as potent modifiers of specific disease-states, we conclude that the *SEAL1* lncRNA is a major determinant of myCAF pro-tumorigenic transcriptional programs of therapeutic value.

#3514 Histone deacetylase 9 (HDAC9) mediates therapy resistance by regulating tumor-neutrophil interaction in advanced hepatocellular carcinoma.

Yunong Xie[1], Minghe Zhang[1], Linglin Liu[1], Yimiao He[1], Jiahuan Cai[1], Clive Yik-Sham Chung[2], Leung Hoi Wing[1], Terence Kin-Wah Lee[3], Stephanie Ma[2], Ka-Fai To[1], Jingying Zhou[1], Carol Man Carol Tong[1]

[1]The Chinese University of Hong Kong, Hong Kong, Hong Kong,[2]The University of Hong Kong, Hong Kong, Hong Kong,[3]Hong Kong Polytechnic University, Hong Kong

Tyrosine kinase inhibitors (TKIs) and immune checkpoint blockade (ICB) therapies are standard treatments for advanced hepatocellular carcinoma (HCC), but their efficacy is limited by therapy resistance. This study investigates the mechanisms underlying resistance, focusing on the role of tumor-immune interaction. Using single-cell RNA sequencing (scRNA-seq) in a TKI-treated immunocompetent mouse model, we identified an expansion of poorly differentiated tumor cells with significant upregulation of histone deacetylase 9 (HDAC9). Elevated HDAC9 enhanced cancer stemness and reduced the efficacy of TKI therapy. Beyond TKIs, HDAC9 also contributed to ICB resistance by suppressing $CD8^+$ T cell infiltration and cytotoxicity, partly through interactions with immunosuppressive neutrophils exhibiting a neutrophil extracellular trap (NET) phenotype. Neutrophil depletion reversed ICB resistance, restoring $CD8^+$ T cell infiltration and function. Mechanistically, HDAC9 deacetylates translation initiation factor 4 gamma 2 (eIF4G2), enhancing its interaction with YTHDF3 to promote m6A-dependent protein translation, including signaling molecules that mediate tumor-neutrophil crosstalk. Clinicopathological analysis confirmed that HDAC9 correlates with increased neutrophil infiltration and reduced cytotoxic immune activity in HCC patients. These findings identify HDAC9 as a key immunoregulator driving therapy resistance and suggest that targeting the HDAC9/eIF4G2/YTHDF3 axis may improve the efficacy of TKI and ICB therapies in advanced HCC.

#3515 Modulating pancreatic juice ENPP1-STING crosstalk to reprogram the tumor immune landscape in pancreatic cancer.

Sadaaki Nishimura, Jun Tauchi, Ryota Tanaka, Shigeaki Kurihara, Masahiko Kinoshita, Kohei Nishio, HIroji Shinkawa, Takeaki Ishizawa

Hepatobiliary-pancreatic surgery, Osaka Metropolitan Univ. Graduate School of Med., Osaka, Japan

Background:
Pancreatic cancer is among the deadliest solid tumors, primarily due to its profoundly immunosuppressive tumor microenvironment (TME) characterized by poor T-cell infiltration and resistance to immunotherapy. We previously demonstrated that modulation of the STING (Stimulator of Interferon Genes) pathway in hepatic stellate cells, controlled by the autophagy adaptors NBR1 and p62, can convert hepatocellular carcinoma from a “cold” to a “hot” immune phenotype (Molecular Cell, Nishimura S., 2024). These findings highlight the therapeutic potential of precise STING pathway regulation within the stromal compartment.
Objective:
This study aims to elucidate how ENPP1 (ecto-nucleotide pyrophosphatase/phosphodiesterase 1), an enzyme highly enriched in pancreatic juice, shapes the pancreatic TME by modulating extracellular cGAMP availability and STING activation. Because ENPP1 degrades cGAMP—the essential second messenger driving STING signaling—we hypothesize that elevated ENPP1 activity suppresses innate immune sensing and promotes a cold TME in pancreatic cancer.
Methods:
We will analyze pancreatic juice and matched tumor tissues from patients undergoing pancreatic surgery. ENPP1 enzymatic activity, cGAMP degradation capacity, and STING pathway activation (TBK1/IRF3 phosphorylation, type I interferon signatures) will be quantified. Immune profiling will be performed to assess correlations with T-cell infiltration, myeloid composition, and markers of immune exclusion. We will further evaluate whether ENPP1 levels are associated with treatment resistance or clinical outcomes.
Results and Significance:
We anticipate that high ENPP1 activity will correlate with suppressed STING signaling and reduced immune infiltration, defining a mechanism by which pancreatic tumors maintain an immunologically cold TME. This work has the potential to establish ENPP1 as a biomarker for therapeutic resistance and to support the development of ENPP1-STING-targeted strategies—such as ENPP1 inhibition or cGAMP stabilization—to convert pancreatic tumors into a more immune-responsive state. Pancreatic juice-based immune monitoring may provide a minimally invasive tool for real-time assessment of TME immune status.

#3518 Role of sialic acid-siglec axis in pancreatic cancer immune evasion.

Barnita Haldar[1], Karin Hardiman[2], Susan Bellis[1]

[1]Cell Developmental and Integrative Biology, University of Alabama at Birmingham, Birmingham, AL,[2]Department of Surgery, University of Alabama at Birmingham, Birmingham, AL

Pancreatic ductal adenocarcinoma (PDAC) is an aggressive malignancy. A key factor contributing to the lethality of PDAC is immune evasion. Tumor cells suppress anti-tumor immunity by activating immune checkpoint proteins on immune cells including macrophages. Siglec receptors are one of the main checkpoint molecules on macrophages. The ligand for Siglecs is sialic acid. To effectuate immune suppression via Siglecs, PDAC cells increase their surface sialylation by upregulating the expression of sialyltransferases such as ST6GAL1. ST6GAL1 adds an α2,6-linked sialic acid to N-glycans. Both α2,6 sialylation and ST6GAL1 expression are markedly increased in PDAC cells. Our prior studies revealed potent tumor-autonomous functions for ST6GAL1. Our new unpublished results suggest that the tumorigenic effects of ST6GAL1 are also driven by its role in creating sialoglycan ligands for macrophage Siglecs. Macrophages that are polarized to an immunosuppressive M2 phenotype are key contributors to PDAC progression. The goal of our study is to determine whether macrophage Siglecs are promising therapeutic targets for preventing M2 polarization, thus restoring anti-tumor immunity and preventing PDAC progression. We investigated macrophage polarization in our genetically engineered mouse models of PDAC, utilizing either pancreas-specific knock-in of oncogenic K-ras (KC mouse) or K-ras in combination with ST6GAL1 knock-in (KSC mouse). Single-cell RNA sequencing, flow cytometry, and immunohistochemistry showed an increased number of M2 macrophages in KSC vs. KC pancreata. Macrophages co-cultured with ST6GAL1-overexpressed PDAC cells showed increased expression of M2 markers. But adding Siglec-blocking antibodies reversed the ST6GAL1-mediated M2 polarization, indicating that the ST6GAL-mediated M2 polarization of macrophages is mediated through Siglec signaling. Additionally, we determined the phagocytotic capacity of macrophages, which is an established functional readout for anti-tumor behavior of macrophages. Immunofluorescence microscopy and flow cytometry showed that the phagocytotic capability of macrophages was suppressed by ST6GAL1-overexpressed PDAC cells but recovered by Siglec blocking antibody. Overall, our data demonstrate that α2,6 sialic acids on PDAC cells engage with Siglecs on macrophages to induce polarization of macrophages into an immunosuppressive M2 phenotype. Collectively, these results reveal a potential mechanism for targeting Siglecs as a promising immune checkpoint therapy for PDAC patients with high levels of ST6GAL1. Traditional T cell-based checkpoint therapies have limited effectiveness in PDAC. Targeting Siglec checkpoints presents an opportunity to enhance the anti-tumor activity of macrophages, the primary immune cell type within the PDAC tumor microenvironment.

#3519 PD-L2-RGMb interaction modulates anti-cancer immunity through swinging the shift of Th1/Th2 cell balance.

Siyi He[1], Xiaoyi Chong[1], Fangli Jiang[2], Xinru Hua[1], Chenlin Cao[1], Cheng Zhang[3], Xiaotian Zhang[4], Lin Shen[1]

[1]Peking University Cancer Hospital & Institute, Beijing, China,[2]Jiangsu Province Hospital, Nanjing, China,[3]Department of Gastrointestinal Oncology, Peking University Cancer Hospital & Institute, Beijing, China,[4]Affiliated Cancer Hospital of Inner Mongolia Medical University,Peking University Cancer Hospital Inner Mongolia Hospital, Hohhot, China

Immune checkpoint blockade has revolutionized gastric cancer (GC) treatment, yet primary and acquired resistance remain major clinical challenges. Here, we identified extracellular vesicles (EVs) expressing programmed death-ligand 2 (PD-L2-EVs) as a key determinant of anti-PD1 response in GC. Through profiling the extracellular vesicle protein expression profiles in plasma samples from a retrospective cohort of 76 patients, we demonstrated that high baseline PD-L2-EV levels correlate with improved immunotherapy response and survival. Using multiple immunocompetent murine models, we showed that PD-L2-EVs synergize with anti-PD1 to suppress tumor growth by remodeling the tumor immune microenvironment, enhancing $CD8^+$ T cell and NK cell infiltration while reducing immunosuppressive cell populations. Mechanistically, PD-L2 possesses differential binding dynamics between PD1 and repulsive guidance molecule b (RGMb), its binding to the latter mediates Th1 differentiation through promoting STAT4-signaling and augments $CD8^+$ T cell's anti-tumor immunity. On the other hand, AFP reduces cancer cell's expression of PD-L2 and impaired Th1 differentiation, which explained the resistance to immunotherapy for the subtype of AFP-GC. Importantly, through shifting T helper 1/2 cells' balance towards Th1 under PD1 blockade, PD-L2-EV enhances the efficacy of anti-PD1 but not for anti-PD-L1 therapy. Our work nominated PD-L2-EVs as a predictive biomarker in guiding the selection of different types of immunotherapy and potentiates engineered PD-L2-EV as a candidate for therapeutic combination, particularly in AFP-positive patients.

#3520 New role for CDK6 activation in tumor-induced monocyte and platelet reprogramming in breast cancer.

Karen Norek[1], Jacob Kennard[1], Kenneth Fu[1], Robert Shepherd[1], Kristina Rinker[2], **Olesya Kharenko**[1]

[1]Syantra Inc, Calgary, AB, Canada,[2]Schulich School of Engineering, Department of Biomedical Engineering, Syantra Inc; University of Calgary, Calgary, AB, Canada

Background: Tumor-derived signals can reprogram immune cells and platelets to support cancer progression. However, the regulatory mechanisms underlying this systemic education are not well understood.
Methods: RNA sequencing was performed on isolated platelet and white blood cell fractions from breast cancer patients and on THP-1 monocytes exposed to triple-negative breast cancer (TNBC) MDA-MB-231 cells. Transcriptomic data was analyzed using Ingenuity Pathway Analysis (IPA) and Gene Set Enrichment Analysis (GSEA) to identify upstream regulators and enriched pathways.
Results: In both clinical and in-vitro datasets, CDK6 emerged as a key upstream regulator. In patient-derived platelets, CDK6 was identified as a major activated regulator in cancer versus non-cancer samples suggesting a role in tumor-driven systemic remodeling. The CDK6 regulatory network included upregulated and downregulated genes that were significantly modulated. In THP-1 monocytes following contact with TNBC cells, CDK6 activation was confirmed by IPA and accompanied by GSEA enrichment of cell cycle-related pathways such as “regulation of cell cycle process.” Functionally, THP-1 cells exposed to TNBC cells or conditioned media displayed increased proliferation, indicating tumor-induced monocyte reprogramming. This effect was reversed by CDK4/6 inhibitors, highlighting a new immunomodulatory mechanism of these standard-of-care drugs.
Conclusions and Translational Relevance: CDK4/6 activation represents a shared hallmark of tumor education across immune and platelet compartments. These findings reveal a novel mechanism of systemic immune modulation and suggest that CDK4/6 inhibitors can reverse oncogenic activation in monocytes and platelets. This study extends the relevance of these agents beyond tumor cell-intrinsic effects. Targeting CDK6-dependent immune reprogramming may offer a novel strategy to disrupt systemic tumor-immune crosstalk and improve therapeutic responses in breast cancer.

#3521 Studying the mechanism of action and bystander effect of the GSK5764227 antibody-drug conjugate in patient-derived cancer organoids.

Maria Fankhaenel[1], Priya Narayanan[1], Halh Al-Serori[1], Veronika Yankova[1], Mint Htun[1], Elias Sulaiman[1], Barbara Seller[2], Irina Piven[2], Lena Wedeken[2], **Anna Pasto**[1], Tony NG[1]

[1]GlaxoSmithKline plc, Stevenage, United Kingdom,[2]GlaxoSmithKline plc, Berlin, Germany

B7-H3, a member of the B7 family of proteins, is expressed in a variety of tumour types and has emerged as a novel target for cancer therapies due to its specific expression in tumour cells and minimal expression in normal tissues. One potential therapy route comprises of an antibody-drug conjugate (ADC) that specifically binds to B7-H3 and delivers a topoisomerase inhibitor (TOPOi) as its cytotoxic payload. The GSK clinical-stage B7-H3 ADC (GSK5764227) has shown promising results in cancer patients where other treatment options have been exhausted. However, the precise mechanism underlying its therapeutic efficacy remains unclear. We utilised patient-derived organoids (PDOs) generated from different tumour types to investigate the mechanism of action of GSK5764227, from target binding and internalisation to trafficking through endosomal and autophagy pathways to treatment response. By leveraging a partially knockout PDO model, containing a mixture of B7-H3 positive and negative cells, we explored the potential bystander effect of the compound using spatial multiplex and real time imaging at multiple timepoints. In parallel, we analysed the cargo of extracellular vesicles to assess their role in delivering the payload to neighbouring B7-H3 negative cells and enhancing the overall treatment response. Our findings shows that GSK5764227 after binding to B7-H3 within minutes of treatment initiation, is internalised, and trafficked from early endosomes to lysosomes within 24 hours, where the cytotoxic payload is likely cleaved and released. The cleaved payload induces DNA damage, cell cycle arrest and apoptosis through Topoisomerase I inhibition. Furthermore, we observed that payload is trafficking into neighbouring cells through extracellular vesicles derived from treated PDOs, inducing treatment effects, including DNA damage in B7-H3 negative cells, further supporting the drug's bystander effect. Altogether, this work characterises how GSK5764227 induces cell cycle arrest and tumour apoptosis directly in B7-H3 positive cells and indirectly in neighbouring B7-H3 negative cells via bystander effect. Combining clinical, molecular and imaging data, this study enhances our understanding of the drug's mechanism of action and provides a foundation for optimising its use in difficult-to-treat-cancers, ultimately guiding personalised therapeutic strategies for patients.

#3522 Vitamin D (calcitriol) potentiates CB2-mediated anti-tumor responses in prostate cancer cell lines: Molecular mechanisms and therapeutic potential.

William B. Speed[1], Cimona Vaughn Hinton[2], Nakea Pennant[2]

[1]Microbiology, Biochemistry and Immunology, Morehouse School of Medicine, Atlanta, GA,[2]Morehouse School of Medicine, Atlanta, GA

Prostate cancer (PCa) is the most frequently diagnosed non-skin cancer among U.S. men and remains the second leading cause of cancer-related mortality. Vitamin D receptor (VDR) signaling exerts antiproliferative and pro-differentiation effects in prostate tumors, while Cannabinoid Receptor 2 (CB2) has been implicated in immune modulation and antitumor activity. Emerging evidence suggests potential crosstalk between CB2 activation and VDR pathways. We hypothesize that CB2 activation induces VDR expression in prostate cancer cells. DU145 and PC3 cells were plated in complete RPMI for 24 hours, serum-starved for 24 hours, and treated with 10 nM calcitriol, 1 nM AM1241 (CB2 agonist), or starvation media alone. In PC3 cells, AM1241 induced VDR expression at levels comparable to calcitriol, whereas DU145 cells showed minimal induction relative to controls. These preliminary findings suggest a cell line–dependent effect whereby CB2 agonism may enhance VDR expression. Ongoing studies are evaluating whether CB2 activation further augments VDR signaling and modulates its tumor-suppressive functions in prostate cancer.

#3523 Immunological roles of antigen-presenting cancer-associated fibroblasts and mesothelial cells in colorectal cancer.

Yasuhiro Fukui[1], Hiroaki Kasashima[1], Yukina Kusunoki[2], Nobuhiro Naito[1], Zizhou Wang[1], Iguru Omori[1], Yuki Seki[1], Kenji Kuroda[1], Yuichirou Miki[1], Mami Yoshii[1], Tatsurou Tamura[1], Masatsune Shibutani[1], Takahiro Toyokawa[1], Masakazu Yashiro[3], Yuki Nakanishi[4], Naoko Ohtani[2], Kiyoshi Maeda[1]

[1]Department of Gastroenterological Surgery, Graduate School of Medicine, Osaka Metropolitan University, Osaka, Japan,[2]Pathophysiology, Osaka Metropolitan University, Osaka, Japan,[3]Molecular Oncology and Therapeutics, Osaka Metropolitan University, Osaka, Japan,[4]Gastroenterology and Hepatology, Kyoto University, Kyoto, Japan

Cancer-associated fibroblasts (CAFs) play crucial roles in tumor progression and metastasis through their interactions with cancer and immune cells in the tumor microenvironment. Among CAF subsets, antigen-presenting CAFs (apCAFs), characterized by their expression of MHC class II molecules and antigen-presenting ability, have been shown to exert immunosuppressive effects and are thought to originate from mesothelial cells. In this study, we investigated the immune-related functions of apCAFs and mesothelial cells in colorectal cancer (CRC). Using an orthotopic transplantation mouse model, human CRC surgical specimens, and established CAF and mesothelial cell lines, we analyzed their interactions with colorectal cancer cells. Immunohistochemical analysis of CRC tissues revealed that patients with HLA-DR-positive stromal cells had significantly poorer recurrence-free survival compared to HLA-DR-negative patients. The proportion of apCAF marker-positive stromal cells increased with tumor stage. In orthotopically transplanted CRC tumors, flow cytometric analysis demonstrated that the proportion of apCAFs peaked six weeks after transplantation, followed by an increase in myofibroblastic CAFs (myCAFs). Gene expression analysis of mesothelial cells, which are proposed to give rise to apCAFs, showed elevated expression of apCAF-related genes in cancer-associated mesothelial cells (CAmeso) compared with normal mesothelial cells. In an allogeneic mixed lymphocyte reaction using human mesothelial cells, the proliferation of $CD4^+$ T cells was significantly reduced when co-cultured with CAmeso compared to dendritic cells alone, indicating that CAmeso exert immunosuppressive effects despite their antigen-presenting potential. In addition, single-cell RNA sequencing identified CAF subsets with high SLPI expression, suggesting the existence of immunomodulatory CAF populations within the tumor stroma. Furthermore, immunofluorescence staining confirmed the presence of stromal cells co-expressing αSMA and SLPI, and patients with αSMA^+SLPI^+ stromal cells had significantly worse prognosis. Notably, αSMA^+SLPI^+ stromal cells were more abundant in liver metastases and peritoneal dissemination lesions than in primary colorectal cancer tissues, suggesting that these cells may be involved in metastatic progression. Taken together, these findings demonstrate that apCAFs are associated with poor clinical outcomes in CRC, and that cancer-associated mesothelial cells acquire antigen-presenting but immunosuppressive properties under the influence of cancer cells, thereby contributing to tumor progression and unfavorable prognosis.

#3524 Exploring both targeted and untargeted (bystander) effects of GSK5764227 antibody-drug conjugate in patient-derived tumor explants (PDEs).

Debayan Mukherjee[1], Jenny Wade[1], Morgan Heycock[1], Mint Htun[1], Benjamin Miller[2], Zeinab Mokhtari[3], Diana Munera[1], Anna Pasto[1], Paul Barber[1], Tony NG[1], Sue Griffin[1]

[1]Oncology Translational Research, GSK, Stevenage, United Kingdom,[2]Development Biostatistics, GSK, Stevenage, United Kingdom,[3]Oncology Translational Research, GSK, Heidelberg, Germany

Background: B7-H3, a member of the B7 family of immune checkpoint molecules, is emerging as a promising therapeutic target due to its overexpression in several cancers and association with poor clinical outcome. GSK5764227 is a fully humanized IgG-1 monoclonal antibody against B7-H3 conjugated to a topoisomerase 1 (TOP1) inhibitor. GSK5764227 is predicted to selectively target the tumor cells by delivering potent payload, however the role of direct killing vs effects on bystander tumor cells is unknown.
Methods: In this study by using spatial imaging endpoints, we evaluate the expression of B7-H3 and associated genes/ proteins in surgically resected NSCLC tumors samples (Stage IB-IIIB). We then establish a NSCLC patient derived tumor explants (PDE) model, which re-capitulates the pathological tumor microenvironment (TME), and treat the PDE fragments with anti-B7-H3 ADC (GSK5764227), naked anti-B7-H3mAb (GSK5764224), and human-IgG1 control mAb in culture for 72hrs. Using multiplex imaging endpoints, we assess the spatial distribution and binding of GSK5764227 and payload (TOP1 inhibitor) in key cellular subsets and evaluate cell killing (Cleaved Caspase-3) within the TME.
Results: In NSCLC tumor tissues, the B7-H3 protein is abundantly expressed in proliferative tumor epithelial and cancer associated fibroblast (CAFs) cells, but at low-levels in adjacent normal tissue. TOP1 and TOP1 inhibitor sensitivity genes are abundantly expressed in proliferative tumor epithelial and fibroblasts, suggesting that these cells maybe be sensitive to ADC. In PDE models, GSK5764227 and payload showed preferential binding to B7-H3 positive epithelial (EpCam+), fibroblast (aSMA+) and macrophage (CD68+) subsets. In a subset of B7-H3 negative cells, the payload was also detected, suggestive of either downregulation/degradation via internalization of B7-H3 receptor after binding to the ADC, or payload diffusion in B7-H3 negative cells (bystander-effect). This correlated with significant increase in cleaved caspase-3+ staining in payload+ tumor epithelial, macrophages and fibroblast, suggestive that the cell killing could be driven by direct payload deposition in the target population and that all 3-cell types are sensitive to killing by the TOP1 inhibitor payload.
Conclusions: Our results potentially aid in mechanistic understanding of the inter-play between ADC binding and payload deposition, bystander effect and heterogeneity of tumor response, which will support the future design of clinical trials with GSK5764227.

: Tumor Evolution
Poster Session

#3525 Structural variation shapes clonal evolution in pediatric cancer.

Robert Greenhalgh[1], Bensheng Ju[1], Samuel W. Brady[2], John Easton[1], Sivaraman Natarajan[1], Jinghui Zhang[1]

[1]Computational Biology, St. Jude Children's Research Hospital, Memphis, TN,[2]Pharmacy and Pharmaceutical Sciences, St. Jude Children's Research Hospital, Memphis, TN

Tumor clonal evolution is driven by the selection or acquisition of mutations that confer an advantage under the pressures of therapeutic intervention. Much of the knowledge of clonal evolutionary trajectories is based upon single nucleotide variants (SNVs), a mutation type well-suited for detecting subclones and estimating their cancer cell fraction by deep sequencing. To explore the role of structural variants (SVs) in the evolutionary process, we analyzed 13 pediatric cancer patients with multiple spatiotemporally distinct tumor samples and patient-derived xenografts (PDXs) profiled by whole-genome sequencing (WGS). In addition to *de novo* SV calling, the SV presence across all tumor samples from the same patient was analyzed by Fuzzion2, which uses pattern matching to find SVs at a sensitivity as low as a single read pair. We found that clonal architectures defined by SVs largely mirrored those of SNVs, although the branch lengths could differ if SV formation was not affected by therapy-related mutagenesis (e.g. cisplatin). SV-based mutational processes, such as RAG-mediated recombination in leukemia, can be active from diagnosis to relapse, and complex SVs caused by chromothripsis may not be selected for despite their predominant presence at diagnosis. A trio of diagnosis-relapsed rhabdomyosarcoma samples exhibited an intriguing pattern of sharing an ancestral extrachromosomal amplicon of *MDM2*, which co-existed with a second amplicon distinct at diagnosis and relapse. RNA sequencing confirmed each amplicon led to overexpression of different subsets of genes, and SVs derived from WGS indicated that the amplicon private to relapse may have merged with the ancestral *MDM2* amplicon. Validation of this finding is currently underway, leveraging long-read sequencing and cells derived from PDX models of these tumors. Our study emphasizes the importance of examining SVs to gain perspective on the dynamic changes that impact driver genes and amplicon architecture during therapy and may offer new insights on strategies to overcome therapeutic resistance.

#3526 Dynamic evolution of oncogene amplification across 80,000 cancer cell genomes.

Jake June-Koo Lee[1], Sohrab Salehi[1], Matthew Myers[1], Melissa Yao[1], Seongmin Choi[1], Duaa Hassan Al-Rawi[1], Ignacio Vazquez-Garcia[1], Eliyahu Havasov[1], Michelle Wu[1], Jin Lee[1], Fathema Uddin[1], Parvathy Manoj[1], Pedram Razavi[1], Samuel Aparicio[2], Natasha Rekhtman[1], Kenny Kwok Hei Yu[1], Helena A. Yu[1], Charles M. Rudin[1], Andrea Ventura[3], Andrew William McPherson[1], Marc Williams[1], Sohrab Shah[1]

[1]Memorial Sloan Kettering Cancer Center, New York, NY,[2]BC Cancer Research, Vancouver, BC, Canada,[3]Memorial Sloan Kettering Cancer Center, Mamaroneck, NY

Copy-number (CN) amplification is a major mechanism of oncogene activation and a therapeutic target, yet its evolution in human cancers is incompletely understood. We analyzed single-cell whole-genome sequencing (scWGS) data from >80,000 cancer cells in 100 tumors from major cancer types (ovary, breast, lung, and brain) and experimental models to resolve mechanisms and evolution of oncogene amplification. CN distributions across cells revealed two patterns: narrow, uniform peaks from symmetric segregation, consistent with intrachromosomal amplifications (ICamps), and broad, heavy-tailed variation with extreme outliers (>100 copies/cell) indicative of extrachromosomal circular DNA (ecDNA). A probabilistic mixture model of these distributions classified 74 (15%) of 503 amplified regions as ecDNA. These ecDNAs most frequently involved *MYC*, *EGFR*, and *MDM2*, and were enriched in glioblastoma and lung cancers, whereas ovarian and triple-negative breast cancers predominantly showed ICamps. Notably, ICamp events showed significant subclonal specificity, with 227 (53%) of 429 events displaying multiple modes in the CN distribution. These modes were congruent with other genomic features from phylogenetic analysis, suggesting lineage inheritance patterns of symmetric division and clonal expansion. Diversification arose via numeric mechanisms (aneuploidy or genome doubling) and subclone-specific structural variants (e.g., breakage-fusion-bridge cycles or chromothripsis). CN modulation was bidirectional, including loss of amplified derivative chromosome via subclone-specific aneuploidy. Joint analysis of copy-number and structural variants at single-cell resolution uncovered several mechanisms of ecDNA-driven cancer evolution. First, remodeling of ecDNAs through internal rearrangements and recombination between distinct species was often observed, leading to oncogene co-selection. Second, convergent evolution via acquisition of distinct *EGFR*-containing ecDNAs was observed in a glioblastoma, suggesting the potential role of ecDNA loss in shaping subsequent evolution. Third, scWGS of isogenic cell lines distinguished present ecDNAs from historical ecDNAs that underwent genomic rearrangements resulting in chromosomal re-integration. Finally, we show that comparison between circular genome graph-based prediction versus the CN distribution-based prediction of ecDNAs revealed substantial discrepancy with notable tissue-type specificity. In conclusion, this study reveals interpretable distributions of oncogene amplifications consistent with distinct ICamp and ecDNA generative processes. This approach, refining ecDNA identification beyond standard genome graphs, further elucidates how distinct mechanisms of oncogene amplification diversify cancer cell populations. We suggest these new insights will inform patient selection for emerging ecDNA-directed therapies.

#3527 Clonal evolutionary trajectory of HER2-positive breast cancer with ERBB2 or PIK3CA mutations under neoadjuvant treatment.

Kang Wang, Ioannis Zerdes, Emmanouil G. Sifakis, Dimitrios Salgkamis, Jonas Bergh, Thomas Hatschek, Alexios Matikas, Theodoros Foukakis

Karolinska Institutet, Stockholm, Sweden

Background: ERBB2 and PIK3CA are among the most commonly mutated genes in HER2-positive breast cancer and are known mediators of resistance to HER2-targeted therapies. However, the molecular evolution of these mutant tumors under treatment remains poorly understood. In this study, we profiled the multi-omics landscape of ERBB2- and PIK3CA-mutant tumors from the randomized PREDIX HER2 trial, which compared neoadjuvant trastuzumab emtansine (T-DM1) with dual HER2 blockade plus chemotherapy in early-stage HER2-positive disease.
Methods: Fresh-frozen tumor biopsies were used for RNA sequencing and whole-exome sequencing (WES), while FFPE biopsies were used for Xenium 5K spatial transcriptomics. Longitudinal differential gene expressions were analyzed using Gaussian mixed-effects models. Tumor subtypes were assigned with a five-subtype single-sample predictor (SSP.Subtype). Somatic mutations and copy number alterations were profiled using GATK4 Mutect2 and GISTIC2. Somatic mutations were filtered and curated using a 5% variant allele frequency (VAF) cut-off.
Results: Of the 190 patients with available WES data, 7 (3.7%) and 49 (25.8%) patients carried non-synonymous ERBB2 mutations (median VAF = 0.28) and PIK3CA mutations (median VAF = 0.21), respectively. In those patients who did not achieve pathological complete response (pCR) (63%), we identified two ERBB2 mutations (S310Y and R143*) that were consistently detected prior to, during, and after treatment, all located in the extracellular domain. Notably, both tumors maintained the HER2-enriched subtype and ERBB2 amplification during treatment, suggesting mutations may influence trastuzumab binding and blocking HER2 signals. Similarly, we identified 10 patients with persistent PIK3CA mutations during treatment, all of which were known gain-of-function alterations. Only one out of four tumors retained the HER2-enriched subtype, suggesting a potential shift in molecular phenotype under therapeutic selective pressure. Phylogenetic analysis further revealed recurrent clonal expansion involving PIK3CA and acquired KLB mutations, the latter implicated in the regulation of cholesterol metabolism. Further *in vitro* validation of KLB-FGF21 signaling is ongoing.
Conclusion: This longitudinal evolutionary analysis of ERBB2- or PIK3CA-mutant, HER2+ breast cancer suggests that tumors evolve heterogeneously under HER2-targeted therapies, revealing the positive selection of pathogenic ERBB2 and PIK3CA mutations.

#3528 EED drives the small cell lung cancer neuroendocrine phenotype in lung cancer histological transformation.

Yixiang Li[1], Yasmin N. Laimon[2], Hyeonseo Cho[1], Marina Vivero[2], Gabriel R. De Oliveira[2], Andrew Delcea[2], Varunika Savla[2], Yuting Chen[3], Yavuz Durmaz[1], Xintao Qiu[1], Shweta Kukreja[1], Rong Li[1], Talal El Zarif[4], Wesley S. Lu[1], McKayla Van Orden[1], Jacob E Berchuck[5], Roderick Bronson[6], Shuqiang Li[7], Hongbin Ji[3], Katerina A. Politi[8], Matthew L. Freedman[1], Henry Long[1], Sabina Signoretti[2], Matthew Gilbert Oser[1]

[1]DFCI/Harvard Medical School, Boston, MA,[2]Department of Pathology, Brigham and Women's Hospital, Boston, MA,[3]Shanghai Institute of Biochemistry and Cell Biology, Shanghai, China,[4]Dana-Farber Cancer Institute, Boston, MA,[5]Winship Cancer Institute/Emory University School of Medicine, Atlanta, GA,[6]Harvard Medical School, Boston, MA,[7]Broad Institute of MIT and Harvard, Cambridge, MA,[8]Yale Cancer Center, New Haven, CT

Lung cancer histological transformation from lung adenocarcinoma (LUAD) to small cell lung cancer (SCLC) can occur as a resistance mechanism to targeted therapies, particularly in *EGFR*-mutant LUADs with concurrent *RB1* and *TP53* mutations. SCLC transformation has a poor prognosis and there are no targeted therapies to block SCLC transformation. Increased PRC2 complex expression is correlated with SCLC transformation, but it is unknown whether PRC2 complex is functionally necessary for SCLC transformation. In this study, we investigated the functional role of EED, a scaffolding component of the PRC2 complex, in SCLC tumorigenesis and in LUAD to SCLC transformation utilizing two state-of-the-art CRISPR-based, autochthonous immunocompetent genetically engineered mouse models (GEMMs) with comprehensive genomic, transcriptomic, and epigenomic analyses. In a *de novo* SCLC GEMM, we show that loss of EED hinders SCLC development and selects for the formation of LUAD through a NEUROD1-positive intermediate cell state. Mechanistically, EED loss de-represses bivalent genes co-marked by H3K27me3 and H3K4me3, including LUAD oncogenic RAS, PI3K, and MAPK pathway genes, to promote transformation to LUAD. Consistently, these same signaling pathway genes are bivalently marked and silenced in human SCLC patient-derived xenografts, indicating a conserved PRC2-mediated mechanism to repress LUAD oncogenic signaling to maintain the SCLC neuroendocrine identity. In a novel CRISPR-based *EGFR*-mutant LUAD GEMM with *RB1/TP53* loss, we found EED is necessary for LUAD to SCLC transformation and metastatic progression following EGFR withdrawal. Altogether, these findings identify the PRC2 complex as an epigenetic regulator that maintains the SCLC neuroendocrine identity and highlights EED inhibition as a potential therapeutic approach to prevent SCLC transformation in high-risk LUAD.

#3529 Identification of the clonal origin of endometriosis-associated ovarian cancer in normal endometrium.

Koichi Watanabe, Nobuyuki Kakiuchi, Kosuke Ieiri, Hirona Maeda, Tomonori Hirano, Mana Taki, Koji Yamanoi, Ryusuke Murakami, Masaki Mandai, Seishi Ogawa

Kyoto University, Kyoto, Japan

[Introduction]Recent studies have revealed pervasive mutations in cancer-related genes within many normal tissues, including the endometrium. Endometriosis-associated ovarian cancer (EAOC) is hypothesized to arise from endometriotic lesions seeded from the endometrium to the ovary, although direct evidence supporting this origin has been lacking. This study aimed to identify the clonal origin of EAOC in the endometrium by detecting shared somatic mutations between EAOC tumors and endometrial clones.
[Methods]We performed high-density sampling of histologically normal endometrial tissues from 6 patients diagnosed with EAOC (5-32 sample/patient, 84 samples in total) and conducted whole-exome sequencing. The resulting somatic mutation profiles were compared with those of the matched EAOC tumors from the same patients.
[Results]Endometrial samples harbored a median of 28.5 (range 6-74) somatic mutations. In 78 of 84 histologically normal endometrial samples (93%), one or more of known driver gene mutations involving *PIK3CA, PIK3R1, KRAS, PPP2R1A, ARHGAP35* and *FBXW7* were identified, with an average of 2.4 mutations/sample (range 0-7). *PIK3CA* mutations were the most common, detected in 44 of 84 samples (52%), followed by *ARHGAP35* mutations (25/84, 30%). Notably, in two cases, we identified an endometrial sample sharing multiple somatic mutations with the EAOC tumors. In Case 1 (74 y/o, ovarian clear cell carcinoma), one of 32 endometrial samples shared 16 mutations with the tumor, including alterations in *PTEN*, *PIK3CA*, and *KRAS*. In Case 2 (31 y/o, bilateral ovarian endometrioid carcinoma), one of 6 endometrial samples shared 11 mutations with the tumor, including in *PIK3CA, AKT1, PPP2R1A* and *CTNNB1*. Phylogenetic analysis using whole-genome sequencing estimated that the most recent common ancestor of the cancer diverged from the normal endometrial clone in their early 20s in both cases. In Case 1, the tumor acquired additional copy number alterations not present in the endometrial ancestor, suggesting their potential role in carcinogenesis. By contrast, in Case 2 no clear genetic differences were detected between the ancestral endometrial clone and the ovarian tumor, suggesting that the transition from normal tissue to cancer may be driven by non-genetic events.
[Conclusion]We demonstrated that at least some EAOC tumors originate from an ancestral clone in the histologically normal endometrium. This ancestral clone had already acquired multiple driver
events contributing to carcinogenesis. Our findings provide new insights into the early events underlying EAOC development.

#3530 Drug pressure driven evolution upregulates CIDEA to reprogram lipid metabolism and promote chemoresistance in colorectal cancer.

Haigui Wan[1], Yao Shang[2], Dongwen Chen[2], Chuling Hu[2], Yiran Bie[2], Zhengran Zhou[1], Zhengyu Wei[2], Chong Chen[1], Yifan Zheng[2], Peishan Hu[2], Xiaojian Wu[2]

[1]The Sixth Affiliated Hospital of Sun Yat-sen University, Guangzhou, China,[2]Sun Yat-sen University, Guangzhou, China

ABSTRACT

BACKGROUND: Chemoresistance remains a major challenge to long-term survival in colorectal cancer (CRC). Although lipid metabolic reprogramming is a key adaptation under sustained drug pressure, its dynamic changes and core regulators remain unclear. Defining the clonal evolution and metabolic drivers of acquired resistance is essential for identifying therapeutic targets.

METHODS: Forty-six CRC PDOs were established and subjected to long-term, dose-escalating FOLFOX induction to generate resistance models. Whole-exome sequencing (WES) and RNA-seq were performed before and after induction to assess genomic stability, clonal evolution, and transcriptional remodeling. Multi-cohort validation used TCGA, ICGC-ARGO, and recurrent tumor samples from our institution. Functional assays—including lipid metabolic activity, stemness phenotype, and chemosensitivity analyses—were performed for candidate genes, followed by overexpression and knockdown PDO models to evaluate in vivo effects using xenografts.

RESULTS: Resistant PDOs exhibited denser and more irregular structures with reduced gland-like morphology. Early-stage PDOs retained ~80% of the mutational landscape of primary tumors; with prolonged induction, drug pressure drove clonal selection and genomic drift, with ~60% of mutations retained in late stages, indicating PDOs maintain tumor representativeness during long-term culture. Copy-number alterations of dominant clones correlated with gene expression, suggesting a gene-dosage effect. Multi-omics analyses revealed marked upregulation of CIDEA in resistant PDOs, accompanied by lipid metabolic remodeling and increased expression of FASN, ACACB, FABP1, CD36, along with activation of MAPK and PI3K-Akt pathways. Across TCGA, ICGC-ARGO, and recurrent cohorts, high CIDEA expression was associated with advanced stage and higher recurrence. Functionally, CIDEA overexpression promoted lipid droplet accumulation and enhanced fatty acid oxidation (FAO), driving chemoresistance, whereas CIDEA knockdown reduced FAO, downregulated lipid metabolic genes, and restored chemosensitivity. FAO inhibition reversed resistance in CIDEA-overexpressing cells. In vivo xenografts confirmed that CIDEA knockdown improved chemosensitivity, while CIDEA-driven resistance was reversed by FAO inhibition.

CONCLUSIONS: This study delineates the clonal evolution and lipid metabolic remodeling underlying acquired chemoresistance in CRC and identifies CIDEA as a key driver that promotes resistance through lipid droplet accumulation and enhanced FAO, highlighting its therapeutic potential.

Key words: Colorectal cancer; Chemoresistance; Patient-derived organoids; Clonal evolution; Lipid metabolic reprogramming

#3531 Temporal ordering of genomic events reveals distinct evolutionary trajectories in early-onset breast cancer.

Sejung Lee[1], Jeonghyeok Lim[2], Hyeji Kim[3], Min-Chae Kang[4], Eun-Gyeong Lee[3], Sun-Young Kong[5], Jinhyuk Bhin[1]

[1]Biomedical Systems Informatics, Yonsei University College of Medicine SBSI, Seoul, Korea, Republic of,[2]Graduate School of Medical Science, Brain Korea 21 Project, Yonsei University College of Medicine SBSI, Seoul, Korea, Republic of,[3]Cancer Biomedical Science, Graduate School of Cancer Science and Policy, National Cancer Center, Goyang, Korea, Republic of,[4]Targeted Therapy Branch, Research Institute, National Cancer Center, Goyang, Korea, Republic of,[5]Department of Laboratory Medicine, Hospital, National Cancer Center, Goyang, Korea, Republic of

Introduction:
Early-onset breast cancer (EOBC), diagnosed in women under 40, exhibits more aggressive behavior than later onset breast cancer (LOBC), with a higher recurrence rate and poorer prognosis. Despite these clinical differences, the genomic basis of EOBC remains poorly understood, making it crucial to explore these distinctions in order to elucidate age-associated genetic and tumor evolutionary features of EOBC.

Methods:
We performed whole-genome sequencing on 169 Korean breast cancer patients (97 EOBC, 72 LOBC) to comprehensively characterize their genomic landscapes, including single-nucleotide variants (SNVs), copy-number variants (CNVs), and structural variants (SVs). We analyzed germline & somatic driver mutations and mutational signatures to compare the etiological mechanisms between EOBC and LOBC, and reconstructed clonal architectures to determine the molecular timing and temporal ordering of key driver events in both age groups.

Results:
In EOBC, we observed a higher frequency of GATA3, PPM1D, and MYC alterations. The structural rearrangement landscape was characterized by enrichment of intra-chromosomal rearrangements on chromosomes 1q and 8, as well as inter-chromosomal rearrangements involving chromosomes 17 and 8. Copy-number and mutational signature analyses further showed increased prevalence of chromosomal LOH (CN13), chromothripsis-associated amplifications (CN8), and DNA damage-repair-related signatures, including D8 (replication stress) and M2 (base excision repair errors), indicating that EOBC is driven by oncogene activation and replication stress-associated genomic instability. In terms of tumor evolution, EOBC follows a rapid, oncogene-driven trajectory initiated by early TP53-inactivating mutations and PIK3CA-activating mutations, which promote tumor cell survival and proliferation. Whole-genome duplication (WGD) arises subsequently and occurs relatively early in the evolutionary course of EOBC compared with LOBC, further buffering and amplifying pre-existing genomic instability and accelerating tumor progression. In contrast, LOBC exhibited a higher frequency of PTEN mutations and WGD, which underpinned large-scale genomic alterations, including extensive tumor suppressor losses and copy-number signatures related to chromothripsis and WGD (CN25, CN6, CN7), collectively contributing to sustained genomic instability. Evolutionarily, LOBC appears to progress more gradually, beginning with 1q gains (MDM4, MCL1) and early loss of tumor suppressors that support tumor survival and invasion, with WGD typically occurring at a later stage and adding further genomic instability after prolonged tumor development.

Conclusion:
EOBC follows a rapid, oncogene-driven evolutionary trajectory with early genomic instability and WGD, whereas LOBC progresses more gradually with later tumor suppressor loss and WGD.

#3532 Genetic insights into clonal evolution from normal prostate epithelium to cancer via HighGradePIN.

Kohsuke Hishiki[1], Nobuyuki Kakiuchi[2], Yuki Teramoto[3], Koichi Watanabe[4], Kosuke Ieiri[5], Hirona Maeda[4], Tomonori Hirano[6], Yuki Kita[7], Takashi Kobayashi[8], Seishi Ogawa[4]

[1]Urology, Kyoto Univ. Graduate School of Medicine, Kyoto, Japan,[2]Kyoto University Graduate School of Medicine, Kyoto, Japan,[3]Kyoto University Hospital, Kyoto, Japan,[4]Kyoto University, Kyoto, Japan,[5]Kyushu Univ. Graduate School of Medical Sci., Fukuoka, Japan,[6]Kyoto Universtiy Hospital, Kyoto, Japan,[7]Institute for Virus Research, Kyoto Univ., Kyoto, Japan,[8]Postdoctral Research Fellow, Dept. of Urology, Kyoto University Graduate School of Medicine, Kyoto, Japan

Background Prostate cancer (PC) is one of the most prevalent cancers in the developed world, where its incidence is still increasing. Most PCs are thought to arise from high-grade prostatic intraepithelial neoplasia (HGPIN), a well-recognized precursor lesion. However, the genetic landscape of HGPIN and its relationship with normal prostate epithelium (NPE) and PC remains to be fully explored. To clarify the early genetic events and clonal dynamics underlying PC development, we performed comprehensive genomic profiling of NPE, HGPIN, and PC.

Methods We performed laser-capture microdissection (LMD) to obtain samples from PC (n = 49), HGPIN (n = 77), and NEP (n =393), which were subjected to whole-exome sequencing (WES). We measured genome-wide mutation burdens in normal prostate epithelium from 5 patients using a highly accurate sequencing platform, Nanoseq.

Results In NanoSeq, a total of 10,047 SNVs & indels were detected across 393 NPE samples, based on which the mutation accumulation rate in NPE was estimated to be 0.205 mutations/year/exon. Several mutations were shared between NPE and HGPIN as well as between HGPIN and PC, suggesting a common clonal origin. Pathogenic FOXA1 mutations were frequently detected in both HGPIN and PC. Although pathogenic FOXA1 mutations were also found in NPE, they did not overlapped with those in HGPIN or PC and therefore, likely represent independent mutational events. In one case, spatially distinct multifocal cancers exhibited multiple FOXA1 mutations, each of which was shared with corresponding adjacent HGPIN. In additional cases, 12 mutations were shared across PCa, HGPIN, and NPE samples, although no known driver mutations were detected therein. These findings suggest that PCa may arise from clones with apparently normal histology, which progress through HGPIN to PC. Phylogenetic analysis of these samples revealed that PC and HGPIN diverged from a common normal ancestor approximately 45 years earlier.

Conclusions We successfully characterized somatic mutations and CNVs in apparently normal prostate epithelium, which were shared between HGPIN and adjacent PC in some cases. The presence of shared somatic mutations supports a clonal continuum from normal epithelium to precursor lesions and invasive carcinoma. These insights enhance our understanding of early prostate carcinogenesis and highlight potential avenues for early detection and intervention.

#3533 Integrative spatial profiling of protein and chromosomal alterations across normal, precancer, and cancer revealed the presence of aneuploidy in the normal fallopian tube.

Tanjina Kader[1], Yu-An Chen[1], Clemens Hug[1], Jia-Ren Lin[1], Jeremy Muhlich[1], Euihye Jung[2], Charles Drescher[3], Ronny I. Drapkin[4], Peter Karl Sorger[5], Sandro Santagata[6]

[1]Harvard Medical School, Boston, MA,[2]Perelman School of Med. Univ. of Pennsylvania, Philadelphia,[3]Fred Hutchinson Cancer Center, Seattle, WA,[4]University of Pennsylvania, Merion Station, PA,[5]DFCI/Harvard Medical School,[6]Brigham and Women's Hospital, Boston, MA

Introduction: Simultaneous measurement of protein expression and chromosomal alterations within the same FFPE section enables direct analysis of clonal selection and disease progression from normal epithelium through precancerous to cancerous states. We developed a unified workflow based on the one-shot Orion multiplexed imaging platform (Lin et al., Nature Cancer 2023) that integrates high-dimensional protein imaging with a conventional DNA-FISH assay for in situ detection of chromosomal copy number alterations (CNAs). Traditional DNA-FISH, although widely used in diagnostic practice, requires protease digestion and permeabilization steps that destroy antigen epitopes and distort nuclear morphology, preventing reliable protein detection and limiting integration with immunofluorescence. The challenge spans both normal precursor and malignant tissues, where densely packed or overlapping nuclei complicate single-cell CNA scoring - an issue that is now particularly relevant, given the growing recognition that aneuploidy can arise even in morphologically normal epithelia.
Method: Recent advances in multiplexed imaging now enable phenotypic characterization of individual cells harboring CNAs, a capability previously unattainable with conventional immunofluorescence. To realize this potential, we optimized fixation, hybridization, and imaging parameters to preserve both antigenicity and nuclear architecture while maintaining robust CNA detection. The resulting ORION-FISH workflow enables simultaneous visualization and quantification of protein states and chromosomal alterations within the same section.
Results: We have found that normal fallopian tube epithelium harbors MYC and/or CCNE1, both of which are common CNAs in High Grade Serous Ovarian Cancer (HGSOC) and its precursor lesion, Serous Tubal Intraepithelial Carcinoma (STIC). We have also found that these aneuploid cells may have been under strong negative selection pressure, partially due to strong immune surveillance. Currently, we are analyzing in depth precursor samples and HGSOC specimens that will be presented at the meeting. Conclusion: We applied ORION-FISH approach to HGSOC and its precursors to generate spatial maps of aneuploidy and cell states across the normal-precancer-cancer continuum, establishing a foundation for our studies in the HGSOC Pre-Cancer Atlas 2.0.

#3534 Forecasting oncogene amplification and tumor suppressor deletion.

Barbara Hernando[1], Angel Fernandez-Sanroman[1], Alice Cadiz[1], Patricia Santamaria[1], David Gomez Sanchez[2], Maria Escobar-Rey[1], Blas Chaves-Urbano[1], Joe Thompson[1], Marina Torres[1], Gorka Ruiz de Garibay[3], Vera Adradas[4], Eva Alvarez[5], The Pan Prostate Cancer Group, Maxime Tarabichi[6], Tom Lesluyes[7], Juan Manuel Coya[8], Jon Zugazagoitia[9], Luis G. Paz-Ares[8], **Geoff Macintyre**[1]

[1]Spanish National Cancer Research Ctr. (CNIO), Madrid, Spain,[2]Memorial Sloan Kettering Cancer Center, New York, NY,[3]University of Bergen, Bergen, Norway,[4]Universidad de Navarra, Pamplona, Spain,[5]University of Vigo, Vigo, Spain,[6]Universite Libre de Bruxelles, Brussels, Belgium,[7]Institut Universitaire du Cancer de Toulouse-Oncopole, Toulouse, France,[8]CNIO-H12o Lung Cancer Unit, Hospital Universitario 12 de Octubre, Madrid, Spain,[9]Hospital Universitario 12 de Octubre, Madrid, Spain

Oncogene amplification and tumor suppressor deletion can drive tumor initiation, progression and treatment resistance. Detection at diagnosis often signals poor prognosis, but it can also enable opportunities for treatment with highly effective targeted therapies. Predicting the likelihood that a patient will acquire these driver alterations in the future using a genomic test represents an opportunity to realize the benefits of interventions earlier, potentially with preventative intent. Here, we present a forecasting framework that takes as input a DNA copy number profile and predicts whether the tumor will acquire an oncogene amplification or tumor suppressor deletion in the future. This framework leverages mutation rate estimates from the input tumor, alongside gene-specific selection coefficients derived from a large cohort of 7,880 tumors. We demonstrate feasibility using 7,042 single-time-point samples and longitudinally collected tumor pairs from 44 prostate and 100 lung cancers, identifying tumors that went on to acquire amplifications at a later time point with an average AUC of 0.87. We show potential clinical utility by forecasting poor prognosis in low-grade gliomas via CDK4/PDGFRA amplification or CDKN2A deletion, and osimertinib resistance in lung cancers via MET amplification. This study serves as a proof-of-concept for a new class of biomarker, wherein selective pressures and mutation-generating processes can be harnessed to anticipate future genomic alterations.

#3535 Multi-omics analysis of longitudinal melanoma samples reveals evolutionary transitions and therapy-associated cell-state switching.

Yourong Bao[1], Anne Zaremba[2], Giuseppe Tarantino[3], Tuulia Vallius[4], Mark Woodnorth[3], Mariana Lopez Leon[5], Yingxiao Shi[5], Zoltan Maliga[5], Samira Makhzami[6], Tyler Aprati[3], Bojan Karlas[7], Valerie Glutsch[8], Bastian Schilling[9], Jessica Cecile Hassel[10], Carola Berking[11], Jochen Utikal[12], Friedegund Meier[13], Frank Meiss[14], Lucie Heinzerling[11], Katharina Kahler[15], Jiajia Chen[3], Lisa Zimmer[2], Antje Sucker[2], Elisabeth Livingstone[2], Eva Hadaschik[2], Christine G. Lian[16], George F. Murphy[17], Yevgeniy R. Semenov[4], Genevieve Boland[18], Peter Karl Sorger[1], Florian Rambow[19], David Liu[3], Dirk Schadendorf[2]

[1]DFCI/Harvard Medical School, Boston, MA,[2]Department of Dermatology, University Hospital Essen, Essen, Germany,[3]Dana-Farber Cancer Institute, Boston, MA,[4]Harvard Medical School, Boston, MA,[5]Laboratory of Systems Pharmacology, Harvard Medical School, Boston, MA,[6]Department of Applied Computational Cancer Research, University Hospital Essen, Essen, Germany,[7]MGH/Harvard Medical School, Boston, MA,[8]University Medical Center Hamburg-Eppendorf, Hamburg, Germany,[9]Department of Dermatology, University Hospital Frankfurt, Frankfurt, Germany,[10]Department of Dermatology, National Center for Tumor Diseases, University Hospital Heidelberg, Heidelberg, Germany,[11]Department of Dermatology, Venerology and Allergology, University Hospital Erlangen, Erlangen, Germany,[12]Skin Cancer Unit, German Cancer Research Center (DKFZ), Heidelberg, Germany,[13]Skin Cancer Center at the University Cancer Centre Dresden, National Center for Tumor Diseases, Depa, University Hospital Carl Gustav Carus, Dresden, Germany,[14]Department of Dermatology, University of Freiburg, Freiburg, Germany,[15]Department of Dermatology, Venerology and Allergology, University Hospital Schleswig-Holstein, Campus Kiel, Germany,[16]Brigham and Women's Hospital, Harvard Medical School, Boston, MA,[17]Department of Pathology, Brigham and Women's Hospital, Boston, MA,[18]Massachusetts General Hospital, Boston, MA,[19]Department of Applied Computational Cancer Research, Institute for AI in Medicine (IKIM), University Hospital Essen, Essen, Germany

Background: In-transit metastasis (ITM) in melanoma is associated with poor prognosis, yet patients show widely variable clinical outcomes from rapid progression to durable responses. To investigate the mechanisms underlying these variations, we performed multi-omics profiling of sequential tumor biopsies from an ITM melanoma patient who progressed to stage IV over 4 years.
Methods: Whole-exome sequencing (WES) from 14 tumors was analyzed using ABSOLUTE for purity-adjusted variant and CNA calling. Pyclone and PhylogicNDT defined mutational clusters based on cancer cell fraction (CCF) and inferred tumor lineages. The phylogenetic map was then integrated with clinical metadata. Gene set enrichment analysis (GSEA) on bulk RNA-seq assessed lineage- and time-associated melanoma signatures and transcriptional programs.
Results: Phylogenetic reconstruction captured 3 major lineages (L1: ITM; L2: ITM + distant subcutaneous metastases; L3: distant skin metastases) from a common ancestral clone. Combination of anti-PD1 and intralesional T-VEC therapy reshaped the genomic landscape of tumor clones, selectively favoring L3, which expanded into clonality while L1 became undetectable, consistent with therapy-associated selection. L2, branched off L1, also exhibited persistent survival and immune resistance. RNA-seq showed evidence for a coordinated shift from a highly differentiated state towards an AXL-high state following clinical immune intervention. Transcriptional tumor state heterogeneity increased over time, independent of lineages. Both ITM (L2) and distant (L3) lineages initially displayed more invasive, mesenchymal-like cell state profiles immediately following the clone formation, but transitioned towards more differentiated tumor states, benefiting cell proliferation and clonal expansion. By the end of the clinical course, all distant lesions across anatomical sites converged on an MITF-driven, melanocytic-like proliferative state.
Conclusion: This study reconstructed a phylogenetic map for tumor evolution through multi-omics, longitudinal data from an ITM patient to reveal key pathways and tumor state changes associated with metastatic events and heterogeneity in clinical responses. In the next step, the individual phylogenetic trees will be compared with other patients in the cohort to explore intra-tumoral, inter-tumoral, and inter-patient heterogeneity in tumor progression, metastasis sites, and resistance to therapy.

#3536 Quantifying evolutionary dynamics and tumor heterogeneity in oncogene-addicted advanced non-small cell lung cancer.

Lyns C. Etienne[1], Elizabeth E. Martin[2], Pinar Eser[2], Kiara Pontious[2], Junko Tsuji[2], Natalie Lytell[2], Nicholas Chevalier[3], Mandeep Banwait[3], Jennifer L. Peterson[3], Michael S. Lawrence[3], Mari Mino-Kenudsen[3], Jessica J. Lin[3], Zofia Piotrowska[3], Aaron N. Hata[4], Rebecca Heist[3], Dejan Juric[3], Justin Gainor[3], Gad Getz[4]

[1]Chemical Biology, Harvard University, Cambridge, MA,[2]Cancer Program, Broad Institute of MIT and Harvard, Cambridge, MA,[3]Cancer Center, Massachussetts General Hospital, Boston, MA,[4]Massachusetts General Hospital, Charlestown, MA

Non-small cell lung cancer (NSCLC) is characterized by oncogene addiction, where unique genetic, epigenetic, and transcriptomic alterations drive tumor initiation, growth, and survival. Tyrosine kinase inhibitors (TKIs) against actionable oncogenes showed initial promise, but acquired resistance remain significant clinical challenges. To define the evolutionary dynamics underlying resistance and tumor heterogeneity, we integrated WES/WGS and RNA sequencing data from 1,253 longitudinal biopsies and multi-site rapid autopsies from 104 patients, including an ALK-rearranged cohort. We developed a unified framework combining cutting-edge computational tools and novel statistical methods to characterize and quantify tumor heterogeneity under TKI selective pressure. In 2 ALK-rearranged cases with acquired resistance to TKIs, we identified subclones with multiple compound ALK mutations. In pt062, 2 ALK double-mutant subclones shared an ancestral resistance mutation C1156Y, and independently developed secondary hits L1198F and I1171S, where I1171S retains partial sensitivity to Lorlatinib, potentially revealing a transient therapeutic window before full resistance. In pt992, 3 ALK double-mutant subclones shared an original mutation F1193Y, and independently acquired secondary hits G1269A, E1210K, and G1210R, driving differential resistance to Crizotinib and Lorlatinib. In pt992, F1193Y may be a rare activating mutation that is insufficient to confer resistance to ALK TKIs alone, but promoted resistance in combination with secondary hits. Phylogenetic analysis revealed predominantly monoclonal seeding early in disease in pt062 vs polyclonal reseeding after the emergence of resistance in pt992. Metastatic route inference in pt992 suggests that a mix of distinct subclones result in lesions with triple ALK mutations. Intra-tumor heterogeneity (ITH) calculated from the clonal diversity index revealed that TKI exposure increased ITH, resulting in lesion-specific subclones. In pt992, divergent clonal dynamics in G1202R+ clones showed lower ITH than E1210K+ clones. The founding clones persisted at ~50% (pt992) and 85% (pt062) tumor fraction post-TKI, indicating inadequate selective pressure. Copy number alteration- and transcriptomic-based ITH suggest possible structural differences in clonal populations between primary and metastatic tumors. Bray-Curtis dissimilarity scores of inter-tumor heterogeneity revealed 3 clusters in both cases, suggesting that metastatic lesions evolved from specific subclones. RNA-seq immune deconvolution via CIBERSORT showed variable immune cell infiltration patterns without correlation to clinical outcome. These results demonstrate that TKIs drive clonal diversification and evolution of resistance in oncogene-addicted NSCLC, and offer a quantitative framework for lineage-informed therapeutic strategies.

#3537 *Rb1* loss defines distinct migration histories in metastatic prostate cancer subtypes.

Dawid G. Nowak[1], **Ryan N. Serio**[1], Lise M. Brault[1], Domenic V. Gargiulo[1], Rebecca Hassett[2], Ryan J. Chaffee[1], Stephen J. Staklinski[2], Billy Lu[1], Adam C. Siepel[2]

[1]Meyer Cancer Center, Weill Cornell Medicine, New York, NY,[2]Cold Spring Harbor Laboratory, New York, NY

Rb1 loss is a hallmark of lethal castration-resistant prostate cancer (CRPC), yet its role in shaping metastatic dissemination patterns remains poorly understood. Using our EvoCaP somatically engineered mouse model (SEMM), we generated *Pten*/*Trp53*/*Rb1*-deficient (*2PR*) mice and compared them to *Pten*/*Trp53*-deficient (*2P*) controls. Loss of *Rb1* dramatically increased metastatic burden, particularly to visceral organs, and promoted neuroendocrine (NE) differentiation. Lineage tracing revealed that *2PR* tumors establish metastatic hub organs that seed cascade dissemination to multiple secondary sites. Histologically, *2PR* tumors displayed distinct NE and mesenchymal-like (ML) compartments, with NE regions showing elevated β-catenin and EZH2 expression, markers of aggressive castration-resistant prostate cancers including: CRPC-WNT (Wnt signaling driven) and CRPC-NE (EZH2-high) subtypes. Organoids derived from *2PR* tumors confirmed these transcriptional changes and showed enhanced sensitivity to EZH2 and WNT inhibitors. These findings reveal how *Rb1* loss drives lineage plasticity and metastatic evolution in prostate cancer, identifying therapeutic vulnerabilities in this lethal disease subtype.

#3538 Clonal landscape of human nephrons.

Kosuke Ieiri[1], Nobuyuki Kakiuchi[2], Koichi Watananbe[1], Tomonori Hirano[1], Shun Kawaguchi[1], Hirona Maeda[1], Yoshikage Inoue[1], Tatsuki R. Kataoka[3], Hiroko Tanaka[4], Satoru Miyano[4], Masaki Shiota[5], Eto Masatoshi[5], Seishi Ogawa[1]

[1]Department of Pathology and Tumor Biology, Kyoto University, Kyoto, Japan,[2]The Hakubi Center for Advanced Research, Kyoto University, Kyoto, Japan,[3]Department of Pathology, Iwate Medical University, 1-1-1 Idaidori, Yahaba, Shiwa District, Iwate, Japan,[4]Department of Integrated Analytics, M&D Data Science Center, Tokyo Medical and Dental University, Tokyo, Japan,[5]Department of Urology, Graduate School of Medical Science, Kyushu University, Fukuoka, Japan

Background: Renal cell carcinoma (RCC) subtypes are believed to arise from distinct nephron segments, suggesting that the accumulation and patterns of genetic alterations in normal nephron may also vary by segment. However, due to the intricate architecture and the technical challenges in isolating each nephron segment separately, the mutational landscape within the nephrons remains poorly understood.
Methods: We used laser-capture microdissection (LCM) to isolate five distinct nephron segments, including proximal convoluted and straight tubules (PCT and PST), distal convoluted and straight tubules (DCT and DST), and collecting ducts (CD), which were then analyzed using a highly accurate sequencing platform (NanoSeq) and whole exome sequencing (WES).
Results: NanoSeq analysis of the 175 LCM samples from 12 patients revealed that single nucleotide variants (SNVs) linearly increased with aging. However, the accumulation rate markedly varied across segments: PCT and PST showed notably higher rates (123 and 132 SNVs per genome/year, respectively), compared with DST (28), DCT (27), and the lowest in CDs (18). Seven SBS signatures (SBS1,5,8,12,40a-c) were detected. The age-related SBS5 was similar across all segments and accounted for most of the mutations in the distal compartments. In contrast, SBS12, SBS40b and SBS40c were largely confined to the proximal segments, mostly explaining their higher mutational burdens. Furthermore, the SBS12 signature was significantly enriched in PCT, showing a strong transcriptional strand bias. WES analyses on the 683 LCM samples from 6 patients showed frequent monoclonal expansion in the proximal tubules and CDs of aged donors, which were rarely seen in distal tubules. Notably, an extensively expanded clone in the PCT harboring a 3p loss and a mutation affecting PBRM1, a common driver gene in clear cell RCC, was observed in morphologically normal PCTs. In total, 11.7% of all LCM samples harbored ≥1 non-synonymous mutations affecting known RCC driver genes. Most of these mutations were detected in proximal tubules, while rarely found in distal tubules and CDs. Copy number alterations were quite common, found in 35.1% of the samples and strongly correlated with donor age. The most frequent alterations included gains of Chromosomes 10 and 7 and losses of Chromosomes 18 and 22. Of note, chromosome 10 gain was mostly confined to proximal nephrons, while Chromosome 18 loss was almost exclusively found in CD.
Conclusion: Aging kidney nephrons undergo pronounced remodeling characterized by segment-specific accumulation of mutations and clonal expansions. Proximal tubules exhibit the highest mutation rates and accumulate RCC driver alterations. The strong enrichment of the SBS12 signature in the PCT confirmed the previous view that PCT is the origin of this RCC subtype. The strong strand bias for SBS12 suggests the influence of exogenous mutagens absorbed from PCTs, and identifying the causative agent could be important for RCC prevention.

#3539 Spatial profiling of prostate cancer clonal evolution linked to nodal metastases.

Alastair David Lamb[1], Joakim Lundeberg[2], Sandy Figiel[3], Max Beesley[1], Mengxiao He[2]

[1]Queen Mary University of London, London, United Kingdom,[2]Science for Life Laboratory, KTH Royal Institute of Technology, Stockholm, Sweden,[3]University of Oxford, Oxford, United Kingdom

The progression of prostate cancer (PCa) to metastatic disease remains a critical clinical challenge, making it essential to gain a detailed understanding of the factors that enable certain subclones to invade and spread. Building on our previous study, which examined genomic variations in benign and malignant prostate tissues by inferring copy number alterations (CNA) from spatial transcriptomics data[1], this study aims to trace the spatial evolutionary trajectories of PCa subclones within the prostate and to draining lymph nodes and to identify alterations in associated microenvironments features of the metastatic transition.

To achieve this, we performed spatial transcriptomics on entire prostate axial disks and patient-matched lymph node metastases from 10 individuals. Standard spatial transcriptomics (55 µm) was used for tissue profiling; from the spatial transcriptomics data, copy number alterations (CNAs) were inferred to identify distinct tumor subclones, and phylogenetic trees constructed to describe their evolutionary relationships. Additionally, high-resolution spatial transcriptomics (2 µm) technology was employed to gain a cellular-level view of the immediate tumor-microenvironment (TME) surrounding specific subclones in two selected patients.

Analysis of over 1,000,000 barcoded regions identified many distinct tumor subclones, enabling us to trace their evolutionary trajectories spatially. We observed notable subclonal events within the lymph nodes, including polyclonal colonization, indicating multiple origin events during the evolution of the primary disease. Exploration of the immediate TME revealed significant cellular heterogeneity and upregulation of genes related to antigen presentation and inflammatory pathways concentrated near ancestral tumor clones, specifically at the tumor border. By focusing on the inferred CNA profiles of the metastasizing clone across patients, we identified several common features defining the metastatic transition. Additionally, we were able to identify these metastasizing clones in matched diagnostic biopsies taken several months before prostatectomy was performed, raising the possibility of identifying potentially lethal disease at presentation.

In summary, our study provides a detailed spatial map of PCa clonal evolution and dissemination, linking primary tumors to nodal metastases and revealing altered cell composition and gene expression around tumor clone borders. Importantly, it demonstrates subclonal events within lymph nodes, polyclonal colonization, and the potential to identify metastasizing clones at diagnosis, with implications for risk-stratification and treatment decisions in PCa.

1. Erickson, A., He, M., Berglund, E. *et al.* Spatially resolved clonal copy number alterations in benign and malignant tissue. *Nature* **608**, 360-367 (2022). https://doi.org/10.1038/s41586-022-05023-2

#3540 *KRAS*allelic imbalance reshapes tumor evolution through selective clonal outgrowth and chromosomal instability in NSCLC.

Li Zhang, Angeliki Bania, Enrico Gurreri, Alessia Savarese, Roberta Rinaldi, Calogero Carlino, Luigi Perelli, Giannicola Genovese

UT MD Anderson Cancer Center, Houston, TX

KRAS-mutant non-small cell lung cancer (NSCLC), which accounts ~25% of all NSCLC cases, remains one of the most refractory solid tumors due to its pronounced evolutionary adaptability and propensity to develop resistance. *KRAS* allelic imbalance, including loss of heterozygosity (LOH), is recurrently observed in patient tumors, its functional role in shaping clonal selection and tumor evolution remains unclear.We hypothesize that distinct subpopulations harbors LOH of *KRAS* driven by competitive fitness and acquire unique genomic events. To investigate how KRAS allelic imbalance influences tumor evolutionary trajectories, we developed a somatic mosaic genetically engineered mouse model (smGEMM) that integrates a 200-gene CRISPR-Cas9-GFP perturbation library with an allele-resolving fluorescent reporter (Tdtomato) embedded on murine chromosome 6, ~30 Mb from *Kras*^WT and in trans with *Kras*^LSL-G12D. Each perturbation is encoded by an sgRNA coupled to a unique capture sequence, allowing the combined sgRNA-capture element to serve as a recoverable molecular barcode for clonal tracing. This platform allows simultaneous readout of allelic configuration and competitive fitness, facilitating in vivo tracking of both *Kras*-heterozygous (TdT^+/GFP^+) and *Kras*-LOH (TdT^-/GFP^+) subclones.Preliminary lineage-resolved analyses revealed a consistent and reproducible selective expansion of *Kras*-LOH subclones across biological replicates. LOH subclones consistently formed larger tumors and overtook heterozygous populations, demonstrating that allelic imbalance confers a potential competitive advantage rather than representing neutral drift. We performed whole-genome profiling of reporter-mapped subclones showed that *Kras*-LOH tumors undergo extensive genomic rearrangements, including broad copy-number alterations, structural variations, and chromothripsis events. Our findings indicate that genome-scale instability emerges as a positively selected trait during the competitive expansion of LOH subclones.Our study identifies *Kras* allelic imbalance as an active driver of clonal evolution, linking selective advantage, clonal expansion, and increasing genomic complexity. By coupling allele-specific fluorescent tracing with a focused, CRISPR perturbation library, we uncover mechanistic insights into *Kras*-mutant NSCLC evolution and reveal evolutionary vulnerabilities that may be leveraged to prevent or overcome resistance in *KRAS*-driven lung cancer.

#3541 Dynamics of clonal hematopoiesis in ovarian cancer survivors: Correlation with carboplatin and PARP inhibitor exposure.

Elizabeth M. Swisher[1], Marc R. Radke[1], Nithisha Khasnavis[1], Jennifer Lopez Ochoa[1], Mayumi Rubin-Saika[1], Enna Manhardt[1], Emiko Oshima[1], Alexandra Bachmann[1], Roseanne Gamboa[1], David Wu[1], Sioban Keel[1], Sergei Doulatov[2]

[1]University of Washington, Seattle, WA,[2]Columbia University, NYC, NY

Ovarian cancer (OC) survivors may develop therapy-related myeloid neoplasia (TMN), and risk is increased by PARP inhibitor (PARPi) exposure. We characterized clonal hematopoiesis (CH), which may pre-date TMN, in blood from OC survivors, and its relationship to therapeutic exposures in the CHANCES (Clonal Hematopoiesis in cANCEr Survivors) study. We sequenced blood cell DNA using BROCA-MY, our custom next-generation sequencing (NGS) panel with 72 genes associated with OC, bone marrow failure, and leukemia and CH and identified pathogenic variants (CHVs) at ≥1% variant allele frequency (VAF).We sequenced blood from 170 OC patients treated with carboplatin-based chemotherapy (OC chemo), 24 OC patients on a PARPi trial collected prior to subsequent diagnosis of TMN (pre-TMN), and 180 control subjects including OC patients without chemotherapy exposure (N=57) and age-matched cancer-free females (N=123). CHVs were common across all sample groups but were significantly more frequent in OC chemo (88/170, 52%) than controls (68/180, 38%, p=0.01). Within OC chemo cases, PARPi exposure was significantly associated with CHV detection: 39 (34.2%) had 0 CHV, 20 (17.5%) had 1 CHV and 55 (48.2%) had ≥2 CHVs, versus no PARPi exposure: 51 (51%) had 0 CHV, 29 (29%) had 1 CHV, and 20 (20%) had ≥2 CHVs (P<0.0001, chi-squared test for trend). CHVs were significantly more common in OC chemo cases than controls for *TP53* (7.6% vs 1.7%, p=0.009), *CHEK2* (11.2% vs 0.6%, p<0.0001) and *PPM1D* (21.8% vs 0.6%, p<0.0001) while CHVs in *DNMT3A* (21.8% vs 20.6%) and *TET2* (10% vs 7.2%) were identified at similar frequency. OC chemo and pre-TMN cases receiving more >1 platinum regimen had greater frequency of *TP53*-mutated CH (19/96, 19.8%), compared to ≤1 platinum regimens (4/81, 4.9%, p=0.003) We calculated the CH risk score (CHRS) for samples with available complete blood count results; the CHRS stratifies the risk of progression from CH to overt malignancy. OC chemo cases with CH were more likely to be categorized as high risk (7/23, 30.4%, CHRS≥1.0 predicting a >50% 10-year risk of progression to myeloid neoplasia) versus controls with CH (2/43, 4.7%, p=0.007). In serial samples collected from 41 participants in the CHANCES study, 83/88 (94.4%) CHVs were detectable in all samples. CH is frequent in both OC chemo cases and controls, but the number of mutations and involved genes vary by exposures, with chemotherapy selecting CHV in *CHEK2, PPM1D,* and *TP53*. *DNMT3A* and *TET2* CHVs, known to be associated with aging, were not impacted by chemotherapy exposure, while *TP53*-mutated CH was directly associated with platinum exposure, consistent with an increased risk for TMN development. We continue to collect serial samples via the CHANCES study to characterize CH dynamics and TMN risks in cancer survivors with the goal to generate a risk calculator specific for TMN and establish recommendations for surveillance of CH in cancer survivors.

#3542 Evolving toward precision oncology: Leveraging collateral drug responses for personalized second-line osteosarcoma treatment.

Elizabeth Nowak[1], **Jarrell Imamura**[2], Arda Durmaz[1], Masahiro Hitomi[3], Zachary Burke[1], Jacob G. Scott[4]

[1]The Cleveland Clinic, Cleveland, OH,[2]Cleveland Clinic Lerner College of Medicine, Cleveland, OH,[3]Project Staff, Dept. of Stem Cell Biology and Regenerative Medicine, The Cleveland Clinic, Cleveland, OH,[4]Case Comprehensive Cancer Center, Cleveland, OH

Objective: We aimed to model the evolution of chemoresistance to methotrexate, doxorubicin, and cisplatin (MAP) in vitro and to characterize collateral drug sensitivity and resistance patterns over time, potentially informing second-line treatment strategies in chemo resistant primary or recurrent disease.
Methods: Five evolutionary replicates of MG63.3 osteosarcoma cells were treated with six complete cycles of pulsed, clinically relevant doses of cisplatin and doxorubicin, alternating with methotrexate. Dose-response curves were performed after each chemotherapy cycle to assess resistance to MAP and collateral responses to 16 drugs and combinations. RNA sequencing and transcription factor activity inference were performed across treatment timepoints to temporally explore transcriptional correlates of drug response.
Results: Cells developed resistance to doxorubicin (1.49-2.59 fold) and methotrexate (0.92-2.87 fold) but remained sensitive to cisplatin. Collateral resistance emerged to etoposide, vincristine, and topotecan, while sensitivity increased to gemcitabine, cabozantinib, and palifosfamide. Collateral responses varied temporally, with some increasing linearly with evolution of MAP resistance, and some appearing transient or stochastic. Transcriptional profiling revealed increased activity of E2F and ERG and context-dependent roles for interferon signaling. Resistance phenotypes persisted after drug withdrawal and cryopreservation.
Conclusion: Our model reveals temporally dynamic, heterogeneous collateral responses during the development of chemoresistance to MAP in osteosarcoma. While cross-resistance to several agents emerged, collateral sensitivity to gemcitabine and cabozantinib supports a second line use for these agents. These data may inform rational sequencing of therapies to preempt or exploit resistance evolution.

#3544 Single-cell multi-omics uncovers coordinated epigenetic and transcriptomic evolution in IDH-mutant glioma.

Masashi Nomura[1], Ramya Raviram[2], Joshua S. Schiffman[2], Lillian Bussema[1], Vivian Lu[2], Noelle Wheeler[2], John Lee[1], Yilin Fan[1], Mian Hua Zheng[2], Florian Ruiz[1], Husain Danish[2], Sorcha Kellett[3], Labeeba Nusrat[3], Ronan Chaligne[4], Jason T. Huse[5], W. K. Alfred Yung[5], Shota Tanaka[6], Nobuhito Saito[7], Sunit Das[3], Catherine Potenski[2], Dan Landau[2], Mario L. Suva[1]

[1]Massachusetts General Hospital, Boston, MA,[2]Weill Cornell Medical College, New York, NY,[3]University of Toronto, Toronto, ON, Canada,[4]New York Genome Center, New York, NY,[5]MD Anderson Cancer Center, Houston, TX,[6]Okayama University, Okayama, Japan,[7]University of Tokyo, Tokyo, Japan

IDH-mutant gliomas (IDH-G) typically present as low-grade slow-growing tumors at diagnosis, but invariably progress to high-grade and incurable tumors despite maximal treatment. While previous bulk sequencing studies have shown that IDH-mutant gliomas undergo unique changes in DNA methylation and transcriptional programs during the tumor progression, how these jointly facilitate IDH-G evolution at cellular level has been poorly understood. To address this question, we profiled a longitudinal cohort of IDH-G (36 samples from 19 patients) by multi-omics single-nucleus sequencing, co-capturing full-length transcriptional (by Smart-Seq2) and DNA methylation (by extended-representation bisulfite sequencing (XRBS)) from the same single-nuclei. Compared to reduced-representation bisulfite sequencing (RRBS) used for single-cell DNA methylation profiling in our prior multi-omic single-cell study (Chaligne, et al, Nature Genetics, 2021), the XRBS adopted in this study provided higher coverage of CpG islands (mean of 378,888 vs 198,345, $P = 2.2 \times 10^{-16}$), especially in non-promoter regions. Single-nucleus RNA-sequencing analysis showed a longitudinal increase in the fraction of stem-like state and a reciprocal decrease in that of differentiated state after recurrence. Single-nucleus DNA methylation analysis revealed that in both IDH-G subsets (astrocytoma and oligodendroglioma), IDH-G progression was associated with methylation loss, which marks tumors with worse clinical outcome. This methylation loss was uniformly observed across malignant cells within the same individual tumors and was correlated with the increase in the fraction of stem-like population. This suggests that lower DNA methylation is not due to a change in cell state composition, but rather that it may underlie. Differentially methylated and expressed gene analyses of malignant cells with versus without methylation loss identified hypomethylation of PRC2 targets and increased expression of glioma stem-cell genes as potential mechanisms underlying the expansion of stem-like states. Leveraging our quantitative framework that directly measure cell state heritability and transition dynamics based on high-resolution lineage trees build by DNA methylation information suggested that decreased methylation reshapes cellular transitions to increased heritability of stem-like states and decreased differentiation. This study integrating single-cell methylation and transcription within an evolutionary framework shows how DNA methylation loss drives stem-like transcriptional states and altered cell-state dynamics in IDH-G, offering a blueprint for dissecting evolution in human cancers.

#3545 Integrated genomic and transcriptomic profiling uncovers spatial and evolutionary dynamics in astrocytoma.

Serafiina Jaatinen[1], Sonja Mantyla[1], Reetta Natkin[1], Ismail Hermelo[1], Anssi Nurminen[1], Aliisa Tiihonen[1], Iida Salonen[1], Elisa M. Vuorinen[1], Kristiina Nordfors[2], Hannu Haapasalo[3], Kirsi Rautajoki[1], Joonas Haapasalo[4], Matti Nykter[1]

[1]Tampere University, Faculty of Medicine and Health Technology, Tampere, Finland,[2]Tampere University Hospital, Unit of Pediatric Haematology and Oncology, Tampere, Finland,[3]Fimlab Laboratories ltd. and Tampere University, Tampere, Finland,[4]Tampere University Hospital and Tampere University, Department of Neurosurgery, Tampere, Finland

Intratumoral genomic heterogeneity in glioblastoma arises through clonal evolution and may contribute to treatment resistance and poor outcomes, yet the interplay between subclonal diversity and transcriptional states remains incompletely understood. We utilized multi-sampled whole-genome sequencing (WGS), bulk RNA sequencing, and single-cell RNA sequencing (scRNA-seq) to comprehensively map the layers of intratumoral transcriptomic and genomic heterogeneity and trace the evolutionary lineages across twelve spatially distinct tumor regions in two glioblastoma and one IDH mutant high-grade astrocytoma patients. In the IDH mutant astrocytoma, tumor evolution was characterized by early whole-genome duplication followed by a rare chromothripsis between chromosomes 2 and X, as well as region-specific hypermutation enriched for short insertions and deletions. In contrast, both glioblastomas exhibited linear evolution facilitated by early clonal copy number alterations and single-nucleotide variants, and in one patient, extensive loss of heterozygosity, extrachromosomal DNA structures, and high ploidy. Single-cell copy number analysis validated WGS-defined clones in this patient and uncovered additional subclones with distinct copy number alterations undetectable in bulk sequencing, refining the tumor's phylogenetic tree. Transcriptomic profiling revealed region- and clone-specific differences in glioblastoma cell states, while IDH mutant tumor regions generally exhibited neural progenitor-like activity in addition to astrocytoma-like programs. Glioblastoma samples were dominated by astrocytoma-like states but frequently displayed mesenchymal and endothelial-like transcriptional activity, with rarer and more heterogeneous niches of neural progenitor-like or oligodendrocyte precursor-like cells along with elevated proliferation and distinct maturation signatures. Moreover, scRNA-seq-derived subclones showed differences in mesenchymal-like expression and similar transcriptional branching with state differences observed in bulk RNA-seq, reflecting WGS-based clones. Together, these results demonstrate that intratumoral heterogeneity in adult diffuse astrocytomas arises from both genomic divergence and substantial transcriptional plasticity, while inter-patient diversity remains high across these aggressive tumors. By linking single-cell and bulk transcriptional profiles to evolutionary lineages, our multi-omic framework provides detailed insight into diffuse astrocytoma evolution and malignant cell-state organization.

#3546 Quantifying metabolic and clonal dynamics of evolving cancer cells.

Yi Zhong, Malak Aziz, Gabriel Hemighaus, Richa Mandrekar, **Alvin Makohon-Moore**

Center for Discovery and Innovation (Hackensack Meridian Health), Nutley, NJ

Scientists and clinicians have known for decades that cancer evolves within each patient as new clones emerge and the tumor progresses and spreads. Nonetheless, the molecular adaptations of clones evolving in dynamic environments remain difficult to define. Further, clones evolve for years prior to diagnosis and treatment, yet we know relatively little about cancer evolution before therapy. To directly quantify subclonal dynamics, we combined several novel methodologies to rigorously and comprehensively quantify human cancer cell dynamics by 1) evolving cancer cell populations that are comparable in size to clinically detectable human tumors (billions of cells) in highly controlled experimental conditions over extended periods, 2) analyzing cellular phenotypes and environmental parameters in real-time, 3) imposing precisely defined selective pressures such as treatment or metabolite depletion, 4) and enabling longitudinal sampling and characterization of cancer cells and their respective microenvironments. In combination with bioreactor culturing, we used genetic barcoding to quantify clonal dynamics occurring within each population and track the evolutionary fate of subclonal lineages. The size and duration of these cultures allowed us to consistently generate many samples from the same population over time, which is critical for modeling subclonal evolution occurring in patients and to identify adaptive mechanisms that are convergent or heterogeneous across clones. Thus far, we have successfully barcoded 14 human cell lines across solid and hematologic tumor types - including pancreatic, colorectal, leukemia, and others - and cultured these lines to evolve and expand unique clones from each population. We hypothesized that the survival of cancer cells under environmental constraints, including treatment-induced stress or nutrient-depleted microenvironments, is driven by intrinsic adaptive mechanisms that enable treatment resistance and continued evolution. Our results showed that cancer cells established highly dense and proliferative populations, with clones distinctly evolving across evolutionary pressures, including glucose limiting conditions and chemotherapy, while exhibiting ongoing reprogramming of gene and protein expression. Despite maintaining the media flow, oxygen level, and pH of each culture, cancer cells nonetheless depleted select metabolites, thereby fostering an imbalanced nutrient environment that is analogous to human tumors. In addition, we isolated clones from various timepoints across experiments to validate barcodes, quantify phenotypes, and enable experiments with defined subclone proportions. The impact of this work is to directly quantify the evolution of subclones under defined selective pressures, which is significant because the adaptive mechanisms we discover are expected to reveal novel therapeutic targets for enhancing treatments.

: Cancer Surveillance: Emerging Cancer Trends and Population Differences
Poster Session

#3551 Longitudinal changes in marital status, residence, and income among over 450,000 cancer patients: A SEER-based analysis.

Larry Mingda Zhao

BASIS Independent Silicon Valley Upper School, San Jose, CA

Background: The impact of cancer extends beyond clinical outcomes, often disrupting interpersonal relationships, residential stability, and financial security. However, longitudinal evidence on such changes and associated disparities remains limited.
Methods: A total of 457,058 adults diagnosed with multiple primary cancers in SEER-17 (2000-2021) were analyzed and changes in marital status, urbanicity, and household income between the first and last recorded diagnoses were assessed. Analyses were stratified by follow-up interval (short: 2-5 and long: >5 years). Logistic regression models adjusted for multiple demographic and clinical factors were used to estimate odds ratios (ORs) and 95% confidence intervals (CIs) for these changes.
Results: Among patients who were married at first diagnosis (n=255,939), 5% became not married (divorced/separated/single) and 11% were widowed; percentages were higher in women (6% not married; 16% widowed) than men (4%; 7%). Non-Hispanic Black (NHB) women and Hispanic women had the highest proportions becoming not married in both short- (8-11%) and long- (11-13%) intervals. Among patients who remained married from first to last diagnosis (n=214,956), 5% changed urbanicity (1.5% more rural; 3.4% more urban) and 26% changed income (15% increase; 10% decrease). In multivariate models, NHB patients had >2-fold higher odds of being unmarried (not married or widowed, adjusted OR=2.47, 95% CI 2.24-2.74 for short- and 2.19, 2.05-2.34 for long- intervals) and higher odds of income decrease (OR=1.22, 1.10-1.36 for short- and 1.44, 1.36-1.53 for long- interval) compared to non-Hispanic White patients. Hispanic patients also had elevated odds of becoming unmarried (OR=1.73,1.56-1.92 for short- and 1.56, 1.46-1.67 for long- interval), while Non-Hispanic Asian/Pacific Islander patients had lower odds of income decrease (OR=0.68, 0.59-0.78 for short- and 0.52, 0.48-0.57 for long- interval).
Conclusions: Cancer diagnoses are associated with considerable social-economic disturbances for patients, especially impacting women and vulnerable racial/ethnic populations. These findings emphasize the importance of implementing equity-focused interventions in susceptible demographics to address relationship strain, housing stability, and financial hardship.

#3552 Geographic and sociocultural disparities in breast cancer incidence and mortality in Latin America: Joinpoint trend analysis with a focus on regional variations within Colombia.

Oscar Marino Vidal

Medicine, Universidad del Norte, Barranquilla, Colombia

Background: Breast cancer (BC) remains the leading cause of cancer-related mortality among females worldwide. BC is the most common malignancy and cancer-related death among women in Latin America and the Caribbean (LAC), with substantial heterogeneity across the region. While overall BC burden continues to rise, geographic, demographic, and sociocultural disparities shape outcomes. Subnational analysis within countries such as Colombia is essential to identify context-specific challenges and opportunities for targeted interventions.

Methodology: We analyzed data from some of the most burdened countries in Latin America and compared them to the United States to quantify temporal trends in breast cancer (BC) incidence and mortality. Particular attention was given to subnational regions within Colombia. Using national and regional cancer registry sources and Joinpoint regression analysis to estimate annual (APC) and average annual percent change (AAPC) in incidence and mortality, Age-block analyses were performed to compare incidence by country and age group (Early adult, Adult, Later adult). Descriptive and ecological multivariable analyses explored associations with geographic, demographic, and sociocultural variables. We sought to relate these epidemiological trends to geographic, demographic (population structure), cultural, and lifestyle determinants, aiming to identify key correlations that may explain the variability in BC burden observed both between and within countries.

Results: Incidence and mortality rates increased with age across all countries. USA and Argentina exhibited the highest incidence among older adults, while Colombia had the lowest rates. Statistically significant differences in BC incidence were observed among countries in the adult and later adult age blocks (Kruskal-Wallis $p < 0.001$), but not among early adults. Joinpoint regression identified variation in the timing and magnitude of trend changes (joinpoints) between countries and within Colombian cities, with divergent patterns often corresponding to urbanization, socioeconomic status, and access to screening. Multivariable analyses revealed that regional disparities in incidence and mortality correlated more strongly with geographic, demographic, and lifestyle factors than with genetic ancestry.

Conclusions: Marked international and subnational disparities in BC incidence and mortality underscore the influence of geography, population structure, and sociocultural context in Latin America. Findings support the need for tailored public health strategies, emphasizing targeted screening and equitable access to care.

#3553 Geospatial clustering of socioeconomic deprivation and its impact on major cancers in Puerto Rico: 2014-2022..

Liliana Marie Castro-Jimenez[1], Yoel Velazquez Oliver[1], **Hilmaris Centeno-Girona**[1], Carlos R. Torres-Cintron[2], Elba V. Caraballo[1]

[1]Division of Shared Resources and Scientific Operations, University of Puerto Rico Comprehensive Cancer Center, San Juan, Puerto Rico,[2]Puerto Rico Central Cancer Registry, University of Puerto Rico Comprehensive Cancer Center, San Juan, Puerto Rico

Cancer incidence and mortality rates, as well as socioeconomic characteristics, can vary widely across the geographical landscape, challenging the common assumption of uniform risk throughout the population. A Deprivation Index for Puerto Rico was recently published by the Puerto Rico Institute of Statistics measuring economic mobility and demography to identify multidimensional poverty at the municipality level. Leveraging on this new index, this study aims to analyze the top five major cancers in Puerto Rico by sex and to examine their spatial correlation with the index during the period 2014-2022. Deprivation Index data at municipality level (n=78) was obtained using available data for 2014-2018 and 2019-2023 periods. Age-adjusted incidence (AAIRs) and mortality rates (AAMRs) for each top five female and male cancers were obtained from the Puerto Rico Central Cancer Registry. Global spatial autocorrelation for each period was assessed using Moran's index. Getis-Ord Gi* analysis identified high-deprivation (hot spots) and low-deprivation areas (cold spots) for each period. Municipalities identified as hot (n=15) and cold spots (n=19) in both periods were used to compare incidence and mortality using the Wilcoxon rank sum test. Analyses were conducted using R, version 4.4.1. The Deprivation Index of 2014-2018 demonstrated significant positive spatial autocorrelation for both periods: 2014-2018 (Moran index 0.59, $p<0.001$) and 2019-2023 (Moran index 0.44, $p<0.001$). A total of 34 municipalities were consistently classified as hot or cold spots in both periods. There is a notable difference in geographic deprivations areas. High-deprivation areas are concentrated in the southwestern part of the island, whereas cold spots are concentrated in the San Juan Metropolitan area of Puerto Rico. Differences were found across some cancer types with the Deprivation Index. Uterine cancer exhibited significantly higher AAIR in high-deprivation areas ($p<0.05$). Similarly, colorectal cancer in males showed a trend toward higher AAIR in high-deprivation areas ($p=0.107$). Lung and thyroid cancer for both sexes and prostate cancer had significantly lower AAIRs in high-deprivation areas ($p<0.05$). Lastly, ovarian cancer exhibited significantly higher AAMR in high-deprivation areas, while prostate cancer had higher AAMR in low-deprivation areas ($p<0.05$). Deprivation Index showed significant spatial autocorrelation over time, creating a distinct sociodemographic environment between areas. High-deprivation areas exhibited higher incidence for cancers like uterine, but lower incidence for lung, thyroid, and prostate cancer, which requires further analysis. Mortality is higher in high-deprivation areas for ovarian cancer, highlighting that socioeconomic barriers can worsen overall survival. These results emphasize the need for geographically targeted public health planning.

#3554 An entire-population analysis of nationwide trends in cancer incidence and mortality in hungary.

Zsolt Nagy, Balint Laszlo Balint, **Balazs Gyorffy**

Semmelweis University, Budapest, Hungary

BACKGROUND: Hungary faces a persistently high cancer burden, yet detailed, longitudinal assessments of population-level trends across major tumor types remain limited. Understanding shifts in incidence, mortality, and prevalence is essential for refining screening strategies and healthcare-system planning.
METHODS: Nationwide oncology records from the Hungarian National Health Insurance Fund (NEAK), completely covering the entire population of appr. 10 million, were analyzed for the five most common cancer types: breast (C50), colorectal (C18), lung (C34), prostate (C61), and stomach (C16). Annual incidence and mortality were calculated separately, while prevalence values represent two-year aggregated national counts. All metrics were summarized across both sexes and all age groups. Data were validated against established statistics from the Hungarian National Cancer Registry. Temporal changes represent differences between national baseline figures from 2018 and recent data through 2024.
RESULTS: The five tumor types exhibited consistent directional shifts nationwide. Breast cancer incidence increased 4.98%, mortality rose 42.69%, and crude prevalence increased from 37,887 to 39,773. Lung cancer incidence declined 10.61%, mortality decreased 3.02%, and crude prevalence fell from 31,829 to 28,452. Colorectal cancer incidence decreased 2.29%, mortality increased 21.24%, and crude prevalence declined from 27,589 to 26,956. Prostate cancer incidence rose 9.51%, mortality increased 32.55%, and crude prevalence increased from 19,046 to 20,858. Stomach cancer incidence increased 16.45%, mortality decreased 16.57%, and crude prevalence fell from 5,770 to 4,814. These patterns were observed across both sexes and all age groups, indicating broad population-level shifts rather than age- or sex-specific effects. A web tool was established to visualize these trends and is available at www.epidemplot.com.
CONCLUSIONS: Hungarian nationwide data reveal substantial mortality increases for breast, prostate, and colorectal cancers despite divergent incidence trends, indicating critical gaps in early detection and treatment pathways. Lung cancer demonstrated coordinated declines in both incidence and mortality. These findings highlight the need for targeted improvements in screening programs and care coordination for specific tumor types. This standardized framework enables ongoing national surveillance and expansion to additional malignancies.

#3555 Epidemiological characteristics of cancer patients at Ayder Comprehensive Specialized Hospital in Northern Ethiopia.

Meley Atakilti[1], Desta Mulu[2], Amanuel Asefa[2], Dawit Zenebe[3], Gebretsadik Lema[4], Engda Hagos[5]

[1]Medicine, Patriots Healing Medical Center, Mekelle, Ethiopia,[2]Oncology, College of Health Science, Mekelle University, Mekelle, Ethiopia,[3]Epidemiology, College of Health Science, Mekelle University, Mekelle, Ethiopia,[4]Public Health, College of Health Science, Mekelle University, Mekelle, Ethiopia,[5]Biology, Colgate University, Hamilton, NY

Cancer is a critical global public health issue, contributing to high rates of hospitalization and mortality worldwide yet limited research address population-based cancer data in East Africa particularly Northern Ethiopia. This study describes the epidemiology characteristics of cancer by demography, cancer type, and asses the risk factors and evaluates treatment and prevention modalities in Ayder Comprehensive Specialized Hospital, Tigray, Ethiopia filling a crucial information gap in the region. A retrospective descriptive cross-sectional study was employed, and data were extracted from hospital cancer registry and confirmed cancer patient's medical records spanning from September 2017 to September 2025. Key variables include age, sex, location, cancer type, treatment received and survival status. Statistical descriptive analysis was done across the data. The analysis includes 4229 cancer patients. Median age at diagnosis was 46 years and 63.2% of the patients were females. Nearly 44 % were aged 35 to 54. We found that the most common cancer was Breast (12.7%), Cervical (12.3%), Chronic Myeloid Leukemia (8.7%), colorectal cancer (7.5%), ovarian cancer (7%) and Non-Hodgkin Lymphoma (6.9%). While Cervical, Breast and Ovarian Cancer were the leading cancer types in females Chronic Myeloid Leukemia, Non-Hodgkin Lymphoma and Small/Chronic lymphocytic leukemia were among males. In a comprehensive analysis of female Breast cancer patients 25 % were under 40 years, the youngest being 19 and nearly half (45.3 %) of colonic cancer cases were diagnosed under 50 years of age, as young as 8 years old. In addition, a significant proportion of cancer cases (two third) were found in areas with ongoing conflict suggesting exposure to potential environmental risk factors. Significant variation in age and sex was noticed in this study**.** This study calls for expansion of cancer registry sites in the region. These unusual findings among these age groups suggest the need to screen the risk factors among young individuals for genetic predisposition and early environmental and lifestyle exposure in this population (Tigray is a conflict affected region with exposure to environmental contaminants for decades). The absence of molecular testing (BRCA 1 and 2, TP53, MLH1, and MSH2) and genetic risk assessment in those high-risk individuals in the region may be one contributing factor. In collaboration with laboratory research teams' genetic risk assessment is planned to further evaluate risk factors. Targeted earlier screening and management strategies are urgently needed to minimize cancer burden in this region.

#3556 Pediatric cancer in Puerto Rico: Epidemiologic trends and environmental risk context.

Celines Rodriguez Acevedo, Gabriela Pardo, Lenulisy Rosado, MiaSara Perez, Carolyn Ruiz, Karen Ortiz-Ortiz, Carlos R. Torres-Cintron, Ana Patricia Ortiz, Nancy Raquel Cardona, Rocio K. Rivera

University of Puerto Rico Comprehensive Cancer Center, San Juan, Puerto Rico

Background: Pediatric cancer in Puerto Rico shows distinct patterns compared to the U.S., with Hispanic children experiencing disproportionate burdens. Previous observations indicate high rates of malignant epithelial neoplasms, most of which are thyroid cancers. Puerto Rico also contains numerous EPA Superfund and Toxic Release Inventory (TRI) sites that release IARC-classified carcinogens. This study integrates pediatric cancer epidemiology with regional environmental contamination to contextualize risk patterns.

Methods: Pediatric cancer cases ages 0 to 18 diagnosed from 2009 to 2020 and pediatric thyroid cancer cases ages 0 to 20 diagnosed from 2000 to 2022, were obtained from the Puerto Rico Central Cancer Registry. Incidence, staging, and mortality patterns were described. Thyroid cancer case distribution was compared with the geographic placement of EPA Superfund and TRI facilities, and contaminant profiles were classified using IARC rankings.

Results: Among 1,666 pediatric cancer cases diagnosed from 2009 to 2020, the most common cancers were leukemias (24.25%), malignant epithelial neoplasms (predominantly thyroid cancers) & melanomas (18.19%), and lymphomas (15.85%). CNS tumors (5.2 %) and leukemias (4.5%) had the highest mortality. Neuroblastoma and malignant bone tumors showed high rates of local and distant metastatic disease at diagnosis. Several cancer groups demonstrated positive annual percentage changes. From 2000 to 2022, 380 pediatric thyroid cancer cases were identified, with the highest proportions in the Northeast, North, and Central regions, which also contain clusters of Superfund and TRI facilities that release IARC Group 1 carcinogens such as PCBs and cadmium.

Conclusion: Puerto Rico presents a distinct pediatric cancer profile, with thyroid cancer driving the high burden of malignant epithelial neoplasms and showing regional clustering near contaminated areas. These findings underscore the need to evaluate environmental exposures, diagnostic pathways, and structural determinants of pediatric cancer risk to support targeted interventions and enhanced surveillance.

#3557 Pediatric central nervous system tumors: An analysis of patients treated at Children's Nebraska over a 10-year period.

Amelia Nichols[1], Shinobu Watanabe-Galloway[1], Grace Lai[2]

[1]Department of Epidemiology, University of Nebraska Medical Center, Omaha, NE,[2]Department of Neurosurgery, University of Nebraska Medical Center, Omaha, NE

Nebraska has consistently had rates of pediatric Central Nervous System Neoplasms (CNS) above the national average. The study was an exploratory analysis using clinical data to characterize pediatric CNS tumors treated at Children's Nebraska or Nebraska Medicine over a 10-year period. Electronic health records were reviewed to identify patients diagnosed with a CNS tumor, aged 0 to 18 years, and treated at Children's Nebraska or Nebraska Medicine from 2013 to 2023. Data collected included demographics, clinical characteristics, and genetic testing information. ICD-0-3 codes were used to identify patients with a CNS tumor diagnosis. Diagnoses were classified according to the 2016 World Health Organization (WHO) Classification of Tumors. Zip codes were used to identify the Rural Urban Continuum Code (RUCC) of the patient's county of residence to determine urbanicity. The study population characteristics were summarized and descriptively compared by urbanicity, with chi-squared testing to determine significance. A total of 172 patients aged 0 to 18 years were identified as being diagnosed with a primary central nervous system tumor between 2013 to 2023. A greater proportion of patients were diagnosed at a younger age, with a median age at diagnosis of 7 years. The study population was predominantly female (55.81%; n=96), alive (77.33%; n=133), non-Hispanic White (72.09%; n=124), and from a metropolitan area (70.93%; n=122). Considering tumor characteristics, most diagnoses were malignant (87.21%; n=150) and made at the local stage (96.49%; n=165). Gliomas were the most diagnosed (65.12%; n=112) followed by embryonal tumors (16.86%; n=29). Tumor locations were predominantly reported as the brain stem (22.67%; n=39) or cerebellum (21.51%; n=37). Genetic testing data was available for 40 patients. The most affected gene was KIAA1549-BRAF (14.29%; n=6) and the most common gene effect was fusion (28.13%; n=9). Stratification by RUCC revealed minimal variations in the demographic and clinical characteristics between metropolitan and non-metropolitan areas. The proportion of malignant diagnoses, however, was higher non-metropolitan areas than metropolitan areas ($p = 0.0271$). Given the relative rarity of pediatric CNS tumors, data over an extended time period are required to accurately describe the disease and the population in which it occurs. In this analysis, we described the population of pediatric CNS tumor patients treated at Children's Nebraska and Nebraska Medicine. These methods can be expanded to include additional diagnostic years, clinical characteristics, or predictors, such as environmental exposures to gain a better understanding of the trends in pediatric CNS tumors.

#3558 Oral cancer incidence in British Columbia, Canada since the start of the COVID-19 pandemic.

Ilena S. Yim[1], Lewei Zhang[1], Rachel Murphy[2], Miriam P. Rosin[3], Denise M. Laronde[1]

[1]Oral Biological & Medical Sciences, University of British Columbia, Vancouver, BC, Canada,[2]School of Population and Public Health, University of British Columbia, Vancouver, BC, Canada,[3]BC Cancer Research Institute, Vancouver, BC, Canada

Objectives: Since the beginning of the COVID-19 pandemic, there have been notable disruptions to cancer services worldwide. With interruptions to the opportunistic screening of oral lesions at routine dental visits, an initial decrease in the diagnosis and thus incidence of concerning oral diseases, including oral cancer, is expected at the pandemic's onset. Following this, an increase in the diagnosis and incidence of oral cancer in the early years after the start of the pandemic is anticipated due to the recovery of diagnostic delays. However, it is possible that changes observed in the incidence are also related to contributing factors. While there is literature on the impacts of the COVID-19 pandemic on head and neck cancer incidence, minimal research considers temporal trends, which if not considered, it can bias results. Currently, there is no research on the pandemic's impact on oral cancer incidence beyond 2021, while taking into account temporal trends. This project will determine if the incidence of oral cancer in British Columbia, Canada has changed after the start of the COVID-19 pandemic when considering trends.

Methods: Data on the diagnosis of new oral cancers, from January 2010 to December 2022, in British Columbia, were retrieved from the BC Cancer Registry. Cancers of the lip and oral cavity, excluding skin and bone lesions, were included. Salivary gland and pharyngeal cancers were excluded. An interrupted time series design was used to determine differences in oral cancer incidence post-pandemic (2020 and after) by comparing the post-COVID-19 observed incidence to the expected (counterfactual) post-COVID-19 incidence. The expected post-COVID-19 incidence was based on the pre-COVID-19 trend (2010 to 2019). The pre-COVID-19 trend was calculated as the annual percentage change of age-standardized incidence rates using joinpoint regression. Ratios and 95% confidence intervals of observed versus counterfactual post-pandemic age-standardized incidence rates for 2020, 2021, and 2022 were used to determine differences in pre-and post-pandemic incidence.

Results: From 2010 to 2022, there were 3039 new cases of oral cancers in the oral epithelium of the lip and oral cavity diagnosed in British Columbia. There were no significant differences between the expected and observed post-COVID-19 oral cancer incidence overall and by sex-specific analysis. Although not significant, there were much fewer observed compared to expected cases of tongue cancers overall and for females. Age category- and site-specific analysis is to be completed.

Conclusion: Preliminary results suggest no differences in oral cancer incidence since the onset of the COVID-19 pandemic. Data beyond 2022 should be assessed to continue to determine for differences in oral cancer incidence post-pandemic.

#3559 Genetic and clinical profiles of early-onset prostate cancer in Puerto Rican men: A preliminary characterization.

Gustavo Alayon[1], Sebastian Bernaschina-Rivera[2], Natalia Yordan-Fernandez[3], Juliana Melendez-Ojeda[3], Gabriela Castro[4], Lenin Godoy[1], Fabiola Benitez-Rios[5], Laura F. Rodriguez-Fernandez[3], Carmen M. Ortiz-Sanchez[1], Gilberto Ruiz-Deya[1]

[1]Ponce Health Sciences University, Ponce, Puerto Rico,[2]Maimonides Medical Center, Brooklyn, NY,[3]Universidad de Puerto Rico Recinto de Ciencias Medicas, San Juan, Puerto Rico,[4]Pontificia Universidad Catolica de Puerto Rico, Ponce, Puerto Rico,[5]Boston Children's Hospital, Harvard Medical School, Boston, MA

Background: Prostate cancer (PCA) is the second leading cause of cancer-related death among men in the US. Early-onset prostate cancer (EOPCa) accounts for ~10% of all PCA diagnoses, with an ~58,694 new cases reported worldwide in 2021. Although EOPCa accounts for a growing proportion of cases, it remains underexplored. Younger patients often present with distinct clinical features, hereditary predispositions, and long-term survivorship challenges. Hispanic/Latino men, particularly those from Puerto Rico, experience disparities in incidence and outcomes, yet remain underrepresented in PCA research. A better understanding of the epidemiological, clinical, and germline genetic profile of Puerto Rican men with EOPCa is essential to guide risk stratification and inform precision medicine strategies.
Methods: This study retrospectively identified 80 cases of EOPCa of 9,393 patients treated for PCA between 2020-2025 in a tertiary hospital in southern PR. Demographic, clinicopathological variables were collected, including age, PSA, BMI, Gleason score (GS), tumor stage, family history, lifestyle factors, and treatments. Germline genetic testing results were analyzed and variants classified as pathogenic, variants of uncertain significance (VUS), or benign. Frequencies of recurrent alterations were calculated.
Results: Eighty patients were identified; 39 met the inclusion criteria. Age ranged 37-49 years (mean 45.7). PSA at diagnosis ranged 1.7-25.4 ng/mL (mean 6.2). Nearly half (48.7%) were obese (BMI ≥30). At biopsy, GS 6 was most frequent (56.4%); following prostatectomy (87.2% of cases), GS 6 remained most common (50.0%), followed by GS 8 (23.5%). Stage T2 (55.9%) and T3 (23.5%) predominated. Family history of PCA was reported by 38.0%. Most patients consumed alcohol (76.9%) but denied smoking (71.8%). Germline testing identified 10.3% pathogenic variants, 35.9% VUS, and 5.1% carriers, with the remainder negative. In total, 21 alterations were detected: 15 VUS, 5 pathogenic, and 1 benign. Alterations were distributed across 15 genes, with recurrent findings in RECQL4 (n=3), POLD1 (n=3), ATM (n=2), and TMEM127 (n=2).
Conclusions: This study provides the first characterization of the epidemiological, clinical, and germline genetic profile of EOPCa in Puerto Rico. Findings highlight a notable burden of germline alterations and underscore the importance of incorporating genetic testing into clinical management. Expanding research among underrepresented populations is critical to guide early detection, refine prognostication, and reduce PCA disparities.

#3560 Adult T-cell leukemia/lymphoma in America: Unmasking a preventable cancer in Caribbean-born communities.

Paulo S. Pinheiro[1], Amber N. Balda[2], Tabassum Z. Insaf[3], Baozhen Qiao[3], Sophia Hl George[1], Juan C. Ramos[1]

[1]University of Miami Sylvester Comprehensive Cancer Center, Miami, FL,[2]University of Miami Miller School of Medicine, Miami, FL,[3]Bureau of Cancer Epidemiology, New York State Department of Health, Albany, NY

BackgroundAdult T-cell leukemia/lymphoma (ATLL), caused by human T-lymphotropic virus type 1 (HTLV-1), is rare in the United States but endemic in the Caribbean, Japan, and West Africa. The burden of ATLL among Caribbean-born U.S. residents has not been quantified at the population level.

MethodsWe analyzed 2005-2022 data from the Cancer in North America (CiNA) registry to estimate ATLL incidence by race/ethnicity and nativity. Country-specific analyses were restricted to 13 states with <20% missing birthplace data. Sensitivity analyses addressed possible misclassification with peripheral T-cell lymphoma, not otherwise specified (PTCL-NOS). Cause-specific survival was assessed for Florida and New York using multivariable Cox regression and Kaplan-Meier methods.

ResultsATLL incidence was several dozen-fold higher among non-Hispanic Caribbean-born adults compared with U.S./Canada-born populations, with rates in some Caribbean-origin groups approaching those reported in southwestern Japan. Nearly half of all U.S. ATLL cases occurred in New York and Florida, which had the highest national incidence. Within the Caribbean diaspora, risk varied widely by country of birth, with the highest rates in the eastern Caribbean, while Hispanic Caribbean-born populations exhibited lower incidence overall.

Among more than one thousand patients from New York and Florida, five-year survival remained poor. Cutaneous and marrow-dominant forms showed better outcomes than nodal disease. After adjustment for age and sex, non-Hispanic Caribbean-born Black patients had roughly 2½-fold higher mortality than non-Hispanic White patients.

ConclusionsATLL among Caribbean-born U.S. populations represents one of the most concentrated yet preventable cancer disparities in the country. Because vertical HTLV-1 transmission drives lifetime risk, targeted surveillance, maternal screening, and culturally informed prevention programs are urgently warranted. These findings underscore the need for public-health recognition of ATLL as a preventable infection-associated malignancy in Caribbean-origin communities.

#3561 Breast cancer characteristics in relation to age at diagnosis, in a leading oncology institution in Cartagena, Colombia.

Elias Ferreira, Laura Suarez, Maria P. Valera, Jose Aldana, Juan S. Diaz, **Ines Benedetti**

School of Medicine, Histopathology Research group, Universidad de Cartagena, Cartagena, Colombia

Background: Breast cancer is a major public health problem, it is the most commonly diagnosed malignant neoplasia, and the leading cause of cancer deaths in women, worlwide and also in Colombia. .Women living in transitioned countries have considerably higher incidence rates compared with those in transitioning countries, this reflects a higher prevalence of some reproductive risk factors, including early age at menarche. There is scarce knowledge about the clinical characteristics of breast cancer patients living in developing countries. This study, evaluated and compared the characteristics of breast cancer cases in older, middle aged, and young women, treated at an oncology center in Colombia.Objective: To describe the characteristics of breast cancer cases treated in a leading oncology institution in Cartagena, Colombia, and their association with the age at the time of diagnosis.
Methods: A database of women treated for breast cancer at a leading oncology institution in Cartagena, Colombia, between January 2010 and December 2024, was retrospectively analyzed. Were compared clinical and histopathological characteristics between women aged 20 to <40, 40 to <65, and ≥65 years. Clinical information was collected: age at menarche, parity, stage at diagnosis and histological type.
Results: Were included 698 patients with a mean age at diagnosis of 56.06 years (SD=±13.16, 95%CI= 55.08-57.04). Most of cases were middle-aged women (40 to 65 years= 63.33%) with a high proportion of cases in older women (>65 years= 24.21%), and a smaller number of young women (20 to 39 years=10.45%). Were observed significant associations between age at diagnosis and age of menarche (mean=12.09 years, SD=±1.69, 95%CI= 12.74-13.03), (p=0.0001, t test); and, between age at diagnosis and number of pregnancies (mean=3.25, SD=±2.13, 95%CI= 3.08-3.42), (p=0.0001, t test). Most of the tumors (84.45%) were ductal carcinomas, followed by lobular carcinomas (6.3%), and other histological types in small proportion, a statistically significant difference was found between histological type and age (p=0.041, Fisher´s test). Of the patients, 57.11% presented with locally advanced disease (stage II), only 5% presented with metastatic disease, and there was a significant association between age and clinical stage at diagnosis (p=0.0099, X2).
Conclusion: These findings highlight significant associations between age at diagnosis, reproductive factors, and stage at presentation, suggesting different risk patterns across age groups. Most of the cases in this study cohort presented locally advanced disease at the moment of diagnosis, supporting the need for screening and care strategies adapted to age and individual risk in this setting. Future studies incorporating molecular profiling and survival outcomes will be essential to refine risk stratification and inform breast cancer control policies.

#3562 Sex-specific survival patterns in korean breast cancer: Explainable AI insights from K-CURE Cohort.

Seohyun Ahn[1], Juyeon Hwang[1], Sun-Young Kong[1], Jin Ho Park[2], So-Youn Jung[1], Hyun-Jin Kim[1]

[1]National Cancer Center - Korea, Goyang-si, Korea, Republic of,[2]Seoul National University Hospital, Seoul, Korea, Republic of

Background: Male breast cancer (MBC) is rare, but its incidence is increasing worldwide. Evidence regarding survival differences compared with female breast cancer (FBC) is limited. This study aimed to characterize sex-specific survival patterns in Korean breast cancer and to identify key contributing factors using explainable artificial intelligence (XAI) methods.

Methods: This study utilized data from the Korean Clinical Data Utilization for Research Excellence (K-CURE), a nationwide registry of all breast cancer cases in Korea. Patients diagnosed between 2012 and 2021 were analyzed by sex. Overall survival (OS) and breast cancer-specific survival (BCSS) were assessed using multivariable Cox proportional hazards models. XAI techniques, including SHAP and LIME, were applied to identify sex-specific contributors to survival.

Results: Among 200,222 patients (846 males, 199,376 females), males showed significantly poorer OS and BCSS than females (p<.001). This disparity persisted after adjustment (male OS HR ≈1.30-1.40; BCSS HR ≈1.40-1.50). Distant stage was associated with the highest mortality risk in both sexes (male HR ≈9-12; female HR ≈10-24). Distinct sex-specific patterns were observed. In males, metabolic indicators showed opposite associations with survival: higher hemoglobin was linked to lower mortality (HR ≈0.88), whereas higher fasting blood sugar was associated with increased mortality risk (HR ≈1.04). In females, hormone and targeted therapies were associated with reduced mortality (HR ≈0.30-0.55). XGBoost models achieved moderate predictive performance for both outcomes (OS AUC ≈0.85; BCSS AUC ≈0.87). SHAP and LIME analyses consistently supported these patterns, suggesting that metabolic profiles contributed more to risk estimation in males, whereas tumor stage and treatment factors were relatively more influential in females.

Conclusion: These findings indicate that sex differences in breast cancer survival arise not only from differences in overall risk profiles but also from distinct prognostic factors specific to each sex. In males, metabolic indicators were more closely associated with survival, whereas in females, tumor stage and treatment factors had greater relevance. Overall, these results reflect differing underlying mechanisms by sex and highlight the need for tailored, sex-specific management strategies in breast cancer care.

#3563 Survival differences after diagnosis of breast cancer as second primary cancer vs as first primary cancer.

Chun R. Chao[1], Hui Zhou[1], Cody Ramin[2], Lanfang Xu[1], Kimberly Cannavale[1], Hyuna Sung[3]

[1]Department of Research and Evaluation, Kaiser Permanente - Southern California, Pasadena, CA,[2]Department of Computational Biomedicine, Cedar-Sinai Medical Center, Los Angeles, CA,[3]American Cancer Society, Atlanta, GA

Introduction: The incidence of second primary cancer (SPC) is on the rise. In the United States, about 20% of all new cancers diagnosed annually are estimated to be SPC. Prior studies of the SEER registries suggested that survival was inferior in SPC compared with that in the first primary cancer (FPC) of the same type. However, these studies did not account for prognostic factors such as comorbidity, obesity, smoking, and insurance status. We examined survival after breast cancer diagnosis as a SPC vs. as a FPC in a large integrated health care delivery system.

Methods: We identified female members of Kaiser Permanente Southern California (KPSC) aged 18-84 years diagnosed with an invasive breast cancer as a FPC (for the FPC cohort) or SPC (for the SPC cohort) between 2000-2022 using KPSC's cancer registry. Women were followed until the earliest occurrence of death, diagnosis of a subsequent primary cancer, KPSC disenrollment, or 12/31/2023. All-cause and breast cancer-specific mortality were ascertained. Fine and Gray subdistribution hazard regression was used to estimate survival differences in the SPC and the FPC cohort accounting for competing risks. Multivariable models adjusted for age at diagnosis, stage, breast cancer subtype (luminal A, luminal B, HER2-enriched, and triple negative), race/ethnicity, year of diagnosis, Charlson's comorbidity index, body mass index, and smoking. Stratified analyses were performed by age at diagnosis (<50 yrs and ≥50 yrs), stage, and subtype.

Results: A total of 42,972 and 6,363 women were included in the breast FPC and SPC cohort (the mean age at diagnosis: 59.8 yr vs. 66.0 yr), respectively. About half of participants in both cohorts were racial/ethnic minorities. Sixty-five percent of the FPC cohort and 71% of the SPC cohort were diagnosed at localized stage. During a mean follow-up of 7 years, a total of 7,148 (17%) and 1,647 (26%) deaths were observed, including 4,035 (9%) and 838 (13%) breast cancer-specific deaths in the FPC and SPC cohort, respectively. In multivariable-adjusted models, there was an elevated overall mortality in the SPC cohort compared with the FPC [adjusted hazard ratio (aHR) = 1.35 (1.27-1.43)]. Elevated breast cancer-specific mortality was also noted in the SPC cohort: aHR=1.27 (1.17-1.38). Similar findings were observed when stratified by age, stage, or subtype (aHRs range between 1.33-1.40), with the exception that breast cancer-specific mortality was not elevated in SPC for triple-negative breast cancer [aHR=1.04 (0.85-1.27)].

Conclusion: Overall and breast cancer-specific mortality were higher after a breast SPC diagnosis compared to that after a breast FPC diagnosis among an insured population adjusting for prognostic factors. Further research is needed to shed light on the reasons underly the survival difference to inform management for the breast SPC.

#3564 Gastric cancer disparities across generations of Latino populations in the United States: Insights from the Multiethnic Cohort study.

Katherine De la Torre-Cisneros[1], Haejin In[1], Alexandra Adams[1], Chunxia Chen[1], Brijesh Rana[1], Lynne R. Wilkens[2], Meira Epplein[3]

[1]Rutgers Cancer Institute of New Jersey, New Brunswick, NJ,[2]University of Hawaii, Manoa, HI,[3]Duke University Medical Center, Durham, NC

Background: Individuals of Latin American origin in the United States (US) have higher incidence of gastric cancer (GC) than the general population. The contribution of immigration history to this disparity remains inadequately characterized. This study assessed the association between generational immigration status and GC risk among Latino populations.
Methods: We analyzed data from the population-based Multiethnic Cohort Study (MEC), which enrolled residents of Hawaii and California between 1993-1996. Participants who self-identified as Latino of Mexican, Central or South American descent were included, with non-Hispanic Whites (NHWs) as reference group. Cox proportional hazards models were used to estimate hazard ratios (HRs) and 95% confidence intervals (CIs) for GC overall and by anatomical subtype.
Results: Among 79,963 participants (median age 59 yr; 48% male), 377 incident GC cases were identified. Latino participants had around twice the risk of GC compared with NHWs. The risk remained stable across generations: first-generation (born in Mexico, Central/South America) had an HR of 2.17 (95%CI, 1.61-2.92); second-generation (US-born with one or both parents born in Mexico, Central/South America), HR 2.09 (95%CI, 1.56-2.80); and third-generation, HR 2.67 (95%CI, 1.87-3.82). No notable differences were observed across Mexican and Central/South American subgroups. Associations were stronger for non-cardia GC (HRs, 2.78, 2.62, and 3.42 for first-, second-, and third-generation, respectively) but were not significant for cardia GC.
Conclusions: Latino descendants showed more than twofold higher GC risk compared to NHWs, with elevated risk persisting across generations. No attenuation among US-born individuals suggests lasting ancestral or biological susceptibilities beyond immigration-related exposures. These findings underscore the need to identify at-risk populations and guide targeted prevention strategies.

Table 1. HRs of gastric cancer by generation status among Latino descendants

Descendants	NHW	First Generation	Second Generation	Third Generation
Latino				
Participants	39779	18720	14614	6850
Cases	103	123	104	47
HR (95%CI)	1.00	2.17(1.61-2.92)	2.09(1.56-2.80)	2.67(1.87-3.82)
Mexico				
Participants	39779	13703	14156	6850
Cases	103	78	102	47
HR (95%CI)	1.00	1.77(1.27-2.48)	2.03(1.51-2.73)	2.63(1.84-3.77
Central/South America				
Participants	39779	5005	139	6850
Cases	103	45	1	47
HR (95%CI)	1.00	2.78(1.90-4.06)	1.92(0.27-13.76)	2.52(1.75-3.63)

#3565 Epithelial ovarian cancer histotype distributions by race/ethnicity in Kaiser Permanente Northern California, 2000-2022.

Jennifer Anne Doherty[1], Martin Koebel[2], Jia Li[3], Laurie Grieshober[1], Valerie S. Lee[4], Lisa Moy[3], Juraj Kavecansky[5], Lindsay Jane Collin[6], Scarlett L. Gomez[7], Elisa V. Bandera[8], Lawrence H. Kushi[9]

[1]University of Utah Huntsman Cancer Institute, Salt Lake City, UT,[2]Alberta Precision Laboratories, Edmonton, AB, Canada,[3]Kaiser Permanente Northern California, Pleasanton, CA,[4]Kaiser Permanente Northern California Division of Research, Oakland, CA,[5]Kaiser Permanente, Antioch, CA,[6]Emory University, Rollins School of Public Health, Salt Lake City, UT,[7]University of Califonia San Francisco, San Francisco, CA,[8]Rutgers Cancer Institute of New Jersey, New Brunswick, NJ,[9]Director of Scientific Policy, Division of Research, Kaiser Permanente, Oakland, CA

Background: The 2014 and 2020 World Health Organization (WHO) diagnostic classification guidelines for epithelial ovarian cancer (EOC) standardized histotype classification, improved reproducibility across pathologists, and revealed distinct survival differences by histotype. EOC histotype distributions have not been characterized by racial/ethnic groups on a population level using these updated guidelines. We performed centralized pathology review using the WHO 2020 guidelines to characterize distributions of EOC histotypes across Black, Hispanic, non-Hispanic (NH) Asian and Pacific Islander (API), and NH white groups.
Methods: The Kaiser Permanente Research on Ovarian Cancer Survival study includes 6,067 EOC cases ages 18 years and older diagnosed in 2000-2022 who received care for their EOC at Kaiser Permanente Northern California. Original diagnostic slides were centrally reviewed using 2020 WHO guidelines for a subset of 2,470 cases (median 8 slides/patient, range 1-80). Slides for 20 cases did not contain tumor, and 109 were determined not to be EOC, leaving 2,341 cases for analysis. We assessed concordance of the distribution of EOC histotypes before (original diagnosis) and after re-review by calculating unweighted Cohen's Kappa for the cohort overall, and separately for racial/ethnic groups.
Results: Overall there was substantial agreement of histotype assignment between the original diagnosis and the pathologist's review (Kappa = 0.67). Agreement varied across racial/ethnic groups, with substantial agreement for NH API (n=640), Hispanic (n=522), and NH white groups (n=928; Kappas 0.73, 0.67, and 0.61, respectively), but moderate agreement for Black individuals (n=242; Kappa 0.59). Overall, proportions of the histotypes before and after study review increased for high grade serous (HGSC) from 58% to 62%; 14% to 17% for endometrioid; 2% to 3% for low grade serous; decreased for carcinoma, NOS from 5% to 0.6% and for grouped rare EOC histotypes including mixed from 4% to 2%; and were unchanged for clear cell, mucinous, and carcinosarcoma (9%, 4%, and 3%, respectively). The highest proportion of HGSC was among Black individuals (73%), and the lowest among NH API individuals (50%), with similar prevalences for Hispanic and NH white individuals (64% and 66%, respectively). Endometrioid, clear cell, and mucinous histotypes were more common among NH API individuals (23%, 14%, and 6%, respectively) compared with the other groups (ranges of 12-16%, 6-8%, and 2-3%, respectively).
Conclusions: Improved histotype assignment using WHO 2020 refined distinct differences in histotype distributions by race/ethnicity. Specifically, Black individuals are more likely to be diagnosed with the aggressive HGSC histotype, whereas among NH API individuals non-HGSC histotypes were more common, specifically clear cell, endometrioid, and mucinous histotypes.

#3566 Ovarian cancer survival in the era of targeted treatment: A nationwide study in Germany.

Silvia Mignozzi, Victoria Cooley, Lieke Lanjouw, **Renee Turzanski Fortner**

DKFZ German Cancer Research Center, Heidelberg, Germany

Ovarian cancer treatment has changed substantially over time, through the introduction of bevacizumab and PARP (poly[ADP]-ribose polymerase) (PARP) inhibitors for subsets of cases, added to platinum-based chemotherapies, together with improvements in outcomes of cytoreductive surgery. Population-based studies evaluating survival trends in the context of modern treatment are sparse. Nationwide data from the Center for Cancer Registry Data at the Robert Koch Institute and the Federal Statistical Office of Germany were used. Cases were diagnosed between 2010-2021. Results are presented for cases diagnosed through 2019 to allow for mortality follow-up.Flexible parametric models were used to evaluate three- and five-year relative survival in categories of calendar year from 2010-2012 (largely pre-targeted treatment period), 2013-2016, and 2017-2019 (targeted treatment period). Expected mortality rates were derived from German life tables, stratified by age, calendar year and federal state. A core flexible parametric model was adjusted by age at diagnosis and federal state. We further adjusted for histology and stage. Relative survival was predicted from models for females with a median age at diagnosis (63.5 years), diagnosed in the most common federal state (North Rhine-Westphalia) and for each calendar period, each histological subtype and stage group (I–II, III–IV).A total of 51,985 ovarian cancer cases were included. A total of 75% of cases were of high-grade serous histology. Overall, relative survival improved from the earliest evaluated period to the most recently evaluated period (three-year, 2010-2012=65%, 2017-2019=68%; five-year, 2010-2012=51%, 2017-2019=55%). This difference was evident in particular for stage III and IV disease (three-year, 2010-2012=54%, 2017-2019=58%; five-year, 2010-2012=36%, 2017-2019=40%), with improvements observed across histotype. Three-year relative survival for the predominant stage III and IV high-grade serous histotype increased from 54% to 57% across the study period, with a corresponding increase in five-year net survival of 36% to 40%.Ovarian cancer survival improved across the evaluated periods. These improvements are likely related to advancements in achieving minimal residual disease during cytoreductive surgery, given the improvements observed across histotype, together with the introduction of targeted therapies for select disease subgroups.

#3567 Projecting the future cancer burden in Singapore: National incidence and direct medical cost estimates to 2050.

Ian JY Wee[1], Hui Miao[2], Dawn Q. Chong[3], Evelyn YT Wong[3], Grace Yang[3], Kelvin Bryan Tan[4], Cheng Ean Chee[5], Iain B. Tan[3]

[1]Singapore General Hospital, Singapore, Singapore,[2]Saw Swee Hock School of Public Health, National University of Singapore, Singapore, Singapore,[3]National Cancer Centre Singapore, Singapore, Singapore,[4]Ministry of Health, Singapore, Singapore,[5]National University Cancer Institute, Singapore, Singapore

Introduction: Singapore's rapidly ageing population and lifestyle transitions have contributed to a rising cancer burden, placing increasing pressure on healthcare resources. Robust estimates of future cancer incidence and costs are essential to inform national capacity planning, financing strategies, and cancer care policy. Singapore Translational Cancer Consortium (STCC) sanctioned this study to use population estimates and cancer incidence to provide projections of cancer incidence and direct medical costs to the health system through 2050 for the top 15 cancers.

Methods: This population-based study used the National Trusted Research and Real-World Data Utilisation and Sharing Tech (TRUST) platform and included 268,189 incident cancer cases diagnosed from 2000-2021 in the Singapore Cancer Registry. Historical incidence trends were estimated using joinpoint regression. Future cancer incidence to 2050 was projected using generalized additive models stratified by age and sex. National medical claims from 2005-2016 were analyzed to estimate first-year and five-year post-diagnosis costs with a minimum follow-up of five years. Generalized linear models (gamma distribution, log link) were used to project per-patient costs, which were multiplied by projected incidence to obtain national-level expenditure till 2050.

Results: From 2000 to 2021, cancer cases in Singapore nearly doubled. The age-standardized incidence rate surged from 200.8 to 246.4 per 100,000 in women, while remaining stable in men (232.5 to 235.6 per 100,000). Annual percent increases were 0.88% (95% CI: 0.62-1.21) for women and 0.19% (95% CI: 0.06-0.35) for men. The overall annual cancer incidence is projected to soar 3.3-fold from 2.35 to 7.59 per 1,000 population by 2050. The incidence of cancer in females will increase by 3.5-fold (2.39→8.39 per 1,000), and in males nearly 3-fold (2.30→6.79 per 1,000). Adults aged ≥80 years will account for 37.1% of all cases in 2050, which is three times higher than 13.30% in 2000. Financial impact is large: first-year direct medical costs escalated by approximately three fold from US 104.4 million in 2005 to US 308.5 million in 2016. Five-year cumulative costs rose 3.5 fold from US 150.7 million to US 517.0 million during the same period. By 2050, national expenditure is expected to reach US 1.3 billion for cases in the first year post-diagnosis and US 23.6 billion over five years to the health system.

Conclusion: Our study showed that Singapore may face a dramatic escalation in cancer incidence and healthcare costs by 2050. These findings underscore an urgent imperative for early detection, robust prevention strategies, and sustainable financing models to address the mounting clinical and economic burden of cancer.

#3568 Differences in male breast cancer outcomes by race/ethnicity in Florida and the United States: A population-based comparison of FCDS and SEER.

Maurice Chery[1], Alex Sanchez[1], Jovanka Ravix[1], Olusanya Joshua Oluwole[1], Priscila Barreto Coelho[1], Kristy Samaroo[1], Fatima Rasheed[1], Ayodele Omotoso[1], Osmaray Morales Casanova[1], Matthew Schlumbrecht[2], Sophia Hl George[3]

[1]University of Miami, Miller School of Medicine, Miami, FL,[2]Division of Gynecology Oncology, Department of Obstetrics, Gynecology and Reproductive Sciences, University of Miami, Miller School of Medicine, Miami, FL,[3]Univ. of Miami Sylvester Comprehensive Cancer Ctr., Miami, FL

Introduction Male breast cancer (MBC) is rare (<1% of U.S. cases) yet clinically important. Evidence on racial/ethnic differences is limited and often comes from single registries. We characterize sociodemographic, clinical, and treatment features of MBC and evaluate factors associated with overall survival (OS) in Florida and the broader United States in relation to race/ethnicity and nativity.
Methods We performed a retrospective cohort study of the Florida Cancer Data System (FCDS, 1981-2020; N=1,878) and SEER 8 registries (1975-2022; N=4,754), including primary MBC (ICD-O-C56XX). We described sociodemographic variables (age, race/ethnicity; plus insurance/smoking in FCDS; marital status/area-level income in SEER), clinical features (grade, stage, ER/PR/HER2), and treatment types (surgery, chemotherapy, radiation). Registry-specific Cox models shared the same adjustment set (age, grade, stage, ER/PR/HER2, surgery, chemotherapy, radiation). Race/ethnicity was categorized as non-Hispanic White (NHW), non-Hispanic Black (NHB), and Hispanic. In FCDS, we also tested the moderating effect of nativity (U.S.-born vs non-U.S.-born) and the joint effect of race and nativity.
Results In FCDS (n=1,878; 80% NHW, 12% NHB, 8% Hispanic; mean age 67.5 years), NHB men vs NHW and Hispanic were younger at diagnosis (61 vs 69 vs 67 years), had shorter OS (38 vs 59 vs 49 months), more high-grade tumors (56% vs 37% vs 38%), more distant stage (15% vs 7% vs 11%), and lower surgery rates (77% vs 90% vs 86%; all $p<0.01$); ER/PR/HER2 status did not differ by race/ethnicity. In SEER (n=4,754; 84% NHW, 11% NHB, 5% Hispanic; mean age 67.0 years), NHB men were younger (62 vs 68 vs 64 years), had shorter OS (54 vs 70 vs 63 months), more distant stage (14% vs 7% vs 11%), and lower surgery rates (84% vs 91% vs 89%; all $p<0.01$). NHB men had fewer ER-positive (92% vs 96% vs 94%) and PR-positive tumors (80% vs 89% vs 85%; $p<0.01$), while HER2 status did not vary by race/ethnicity. In multivariable models, race/ethnicity was not associated with OS in FCDS; however, among NHB men, non-U.S.-born had lower mortality than U.S.-born (HR 0.54; 95% CI 0.34-0.86; interaction $p=0.01$). In SEER, NHB men had higher mortality than NHW (HR 1.22; 95% CI 1.07-1.38). In both registries, older age, high grade, distant stage, and omission of surgery were independently associated with higher mortality (all $p<0.01$).
Conclusion Across Florida and the United States, MBC OS is chiefly determined by age, grade, stage, and surgery. In SEER, NHB have higher adjusted mortality than NHW, an effect not seen in FCDS. In FCDS, nativity modifies risk among Black men: non-USB have lower mortality than USB. These findings support nativity-stratified surveillance and equity efforts to promote earlier diagnosis and consistent access to definitive surgery.

#3569 Incidence of early-onset solid cancers in Hungary in the first two decades of the 21st century based on a population-based registry.

Istvan Kenessey, Andras Weber, Maria Dobozi, Istvan Szatmari, Petra Parrag, Peter Nagy, Magdolna Dank

National Cancer Registry, National Institute of Oncology Hungary, Budapest, Hungary

Background: Newly discovered malignancies at a relatively younger age (<50) are of great scientific interest. Previous studies found that the incidence of these early-onset cancers showed a global increase, although the pattern varied by cancer type. However, analysis of the Hungarian data has not yet been published.
Methods: The Hungarian National Cancer Registry (HNCR) is responsible for data collection of the Hungarian cancer patients. Its operation is population-based in accordance with international standards and covers the entire country. Based on the 10th Revision of International Statistical Classification of Diseases and Related Health Problems, newly discovered cancer cases were extracted from the HNCR's database. The query focused on patients between the ages of 20 and 49 and period from 2001 to 2019. Next to absolute case numbers, age-standardized values were also analyzed (reference: European Standard Population 2013). Spearman's correlation test was performed to identify gender- and disease-specific trends.
Results: During the studied period, the incidence of early-onset cancers showed decrease among males, while it did not change among females. It should be noted that compared to the total number of newly discovered cancer cases, the proportion of early-onset cancers showed decreasing trend in both genders. Categorization by cancer type revealed that among younger age the incidence of female breast and uterine corpus cancer elevated, while cervical cancer showed a decrease - the latter trend exceeded that of the general population. The incidence of colorectal cancer did not change among females, but decreased among males. The incidence of tobacco-related lung cancer and head and neck region decreased.
Conclusion: Compared to analyses enrolled global trends, the Hungarian situation of early-onset cancers seemed to be more complex. On one hand, activities in the past few years such as introduction of HPV vaccination and restrictions on smoking resulted a decrease in the number of related cancers. On the other hand, new mechanisms underlying the increasing types of cancers (e.g. breast cancer) need to be identified.

#3570 Long-term mortality trends in hairy cell leukemia: A comprehensive U.S. population analysis (1999-2023).

Aqsa Z. Sorathia[1], Basel Aldroubi[1], **Disha Patel**[1], Safa S. Afridi[2], Michael Patrick[1]

[1]St. Joseph University Medical Center, Paterson, NJ,[2]SUNY Upstate University Hospital, Syracuse, NY

Hairy cell leukemia (HCL) is a rare indolent B-cell neoplasm with excellent survival outcomes following purine analog therapy. However, long-term national mortality trends remain underreported. This study aims to evaluate long-term patterns of HCL-related mortality and temporal changes in the United States. Methods:We analyzed CDC WONDER mortality records from 1999 to 2023 for individuals with HCL (ICD-10: C91.4). Age-adjusted mortality rates (AAMR) per 100,000 were calculated and stratified by age, sex, race, Hispanic origin, and place of death. Joinpoint regression (NCI Joinpoint v5.4.0, weighted BIC) identified annual percent changes (APC) and inflection points with 95% confidence intervals (CI). Results:A total of 4,496 HCL-related deaths occurred from 1999 to 2023. The overall AAMR declined from 0.056 in 1999 to 0.040 in 2018 (APC: -2.21; 95% CI: -6.37 to -1.29), followed by a nonsignificant increase to 0.043 in 2023 (APC: 5.07; 95% CI: -0.69 to 21.32). Among males, the AAMR decreased from 0.10 in 1999 to 0.07 in 2015 (APC: -2.22; 95% CI: -2.99 to -1.44), then significantly increased to 0.096 in 2023 (APC: 2.23; 95% CI: 0.69 to 3.80). Females demonstrated a continuous decline from 0.02 to 0.012 (APC: -2.35; 95% CI: -3.51 to -1.18). Mortality was concentrated in adults ≥65 years, with the highest rates in those ≥75 years (0.41-1.24 per 100,000). White individuals had the highest AAMR (0.061), followed by Black (0.020) and Asian or Pacific Islander (0.008). Non-Hispanic individuals accounted for 96% of deaths. Most deaths occurred in inpatient facilities (44%) or at home (26%). Conclusion: HCL-related mortality declined for nearly two decades but has begun to plateau, with a recent increase observed among males. Persistent declines among females contrast with increasing mortality in males, suggesting a widening difference in outcomes between the two groups. Mortality continues to be concentrated in older adults, reflecting the influence of age, comorbid illness, and treatment-related immunosuppression. Continued surveillance is needed to understand the factors driving these changes, including relapse patterns, treatment selection, and the challenges faced by an aging survivor population, to sustain progress and reduce emerging disparities.

#3571 Rising mortality from malignant pleural Effusion in the United States, 1999-2020: Population-level trends and disparities.

Aqsa Z. Sorathia, **Disha Patel**, Basel Aldroubi, Michael Patrick

St Joseph's University Medical Center, Paterson, NJ

Malignant pleural effusion (MPE) indicates extensive tumor involvement of the pleural space and often reflects aggressive disease characteristics and advanced cancer progression. Despite its clinical and prognostic importance across multiple solid tumors, national mortality patterns attributable to MPE remain poorly characterized. We performed a population-based analysis to define demographic and temporal trends in MPE-related deaths in the United States.Methods: Using CDC WONDER Multiple Cause-of-Death data (1999-2020), we identified U.S. deaths listing MPE (ICD-10 C78.2) as a contributing cause. Age-adjusted mortality rates (AAMR; per 100,000; 2000 U.S. standard population) were calculated overall and by sex, race, ethnicity, age, region, and urbanization level. Temporal trends were assessed with Joinpoint regression using log-linear modeling and Weighted BIC for model selection. Annual percent change (APC) estimates and 95% confidence intervals were reported for each segment.Results: A total of 68,700 MPE-related deaths occurred from 1999-2020. The national AAMR increased from 0.68 to 1.40 per 100,000. The optimal model identified two joinpoints (2001, 2007). A modest early increase (APC 1999-2001: +6.7%, 95% CI -2.9 to 15.4) was followed by a transient decline (2001-2007: -4.1%, -9.8 to 8.9). From 2007-2020, mortality rose significantly with an APC of +6.4% (95% CI 5.2-7.8; p<0.01). Females accounted for 58% of deaths; female AAMR rose from 0.68 to 1.44 per 100,000 with three trend segments (APC 1999-2001: +9.6%; 2001-2007: -4.2%; 2007-2020: +6.3%, p<0.01). Male AAMR increased from 0.66 to 1.33 per 100,000, with a single joinpoint at 2007 (APC 1999-2007: –3.1%; 2007-2020: +6.3%, both p<0.01). Most decedents were ≥65 years (70%). Across the study period, racial distribution included White (83%), Black (12%), and Asian/Pacific Islander (4%); 6% were Hispanic. Mortality rates were highest in medium and small metropolitan regions. 50% of all deaths occurred in hospitals, 28% at home, and 8% in hospice facilities. Conclusions: MPE-associated mortality in the U.S. has increased markedly over two decades, with a sustained rise after 2007. Persistent disparities by age, race, and urbanization highlight vulnerable populations and ongoing inequities in early cancer detection, access to systemic therapy, and palliative resources. These findings illustrate a growing burden of advanced malignant disease and support the need for earlier oncologic intervention, improved metastatic surveillance, and therapies that address both tumor control and pleural fluid accumulation. The escalation of MPE mortality further supports the development of disease-modifying interventions beyond conventional drainage-centered management.

#3572 Narrowing of sex and racial/ethnic ratios for hepatocellular carcinoma incidence in the United States, 1992 - 2022.

Samantha Sarlin, Aaron P. Thrift, Hyeyeun Lim

Baylor College of Medicine, Houston, TX

Background: Temporal trends in hepatocellular carcinoma (HCC) incidence in the U.S. have not been uniform across all adult populations. Most national analyses have focused on absolute rates within demographic groups rather than changes in incidence rate ratios (IRRs) over time. Because IRRs directly quantify relative disparities, evaluating their temporal trends can clarify how sex- and race/ethnicity-specific differences are evolving. We examined long-term trends in HCC incidence and IRRs using three decades of SEER data.

Methods: We analyzed HCC cases diagnosed from 1992 to 2022 in the SEER 12 registry. Age-adjusted incidence rates (per 100,000; 2000 U.S. standard) were calculated overall and by sex, race/ethnicity, and age group (<50 vs ≥50 years). Sex ratios were estimated with women as the reference group, while race/ethnicity ratios were estimated with non-Hispanic White (NHW) individuals as the reference group. Temporal trends were evaluated using Joinpoint regression to estimate annual percent change (APC) and average APC (AAPC) with 95% confidence intervals (CIs).

Results: 68,023 total HCC cases were identified. Annual cases increased from 840 in 1992 to 2,846 in 2022. Age-adjusted incidence rose from 4.27 to 7.84 per 100,000 (AAPC, 2.03%). Incidence increased during 1992-2009 (APC, 4.72%), was stable from 2009-2015, and declined during 2015-2022 (APC, 3.41%). Incidence remained higher in men, increasing from 6.97 to 12.24 per 100,000 (AAPC, 2.38%), compared with 2.13 to 3.95 per 100,000 in women (AAPC, 2.45%). However, the male-to-female IRR declined from 3.29 to 3.11, with an inflection in 2012; the IRR increased before 2012 (APC, 0.51%) and decreased thereafter (APC, -1.64%). Across racial/ethnic groups, incidence was highest among NH Asian or Pacific Islander (NHAPI) (14.27 per 100,000), followed by Hispanic (12.12), NH Black (NHB) (9.30), and NHW (4.37). AAPCs were highest for NHW (3.12%) and Hispanic (2.54%), intermediate for NHB (2.37%), and negative for NHAPI (-0.93%). Segment-specific APCs differed by group: NHW rates increased during 1992-2013 and declined thereafter; NHB and Hispanic rates increased during early periods and declined or stabilized in later years; NHAPI incidence increased modestly until 2007 and decreased thereafter. Similarly, the NHAPI:NHW IRR declined from 5.8 to 1.9 (AAPC, -3.93%); the NHB:NHW IRR declined from 2.0 to 1.4 (AAPC, -0.73%); and the Hispanic:NHW IRR decreased slightly from 2.7 to 2.4 (AAPC, -0.57%).

Conclusion: HCC incidence increased through the early 2010s but has declined since 2015. Sex- and race/ethnicity-specific IRRs narrowed across the study period, driven by declining rates among NHAPI and NHB populations and slower increases among Hispanic individuals relative to NHW. These 30-year trends demonstrate substantial shifts in the demographic distribution of HCC incidence in the U.S. and may reflect changes in etiology.

#3574 Epidemiology, survival, and prognostic factors of malignant eyelid tumors: A 17-year population-based study .

said yaseen[1], Bashar I. Almaraziq[2], Shaimaa A. Abdelmoneim[3], Ahmad S. Al Sakini[4], Hamza Khoursheed[1], Joud K. Alhousani[1], Alhareth Alhusban[5], Leen Abu Rabi[1], Ahmad Farouk Alzein[6], Issam Khourshid[7], Mohammad Almajali[1], Hashem Abu Serhan[8]

[1]Jordan University of Science and Technology, Irbid, Jordan,[2]School of Medicine,, Hashemite University, Zarqa, Jordan,[3]Egyptian Ministry of Health and Population, Alexandria, Egypt,[4]University of Baghdad, Baghdad, Iraq,[5]University of Jordan, Amman, Jordan,[6]University of Illinois Chicago, Chicago, IL,[7]Victoria Hospital, Scotland, Kirkcaldy, United Kingdom,[8]Hamad Medical Corporation, Doha, Qatar

Purpose: This study aimed to characterize the epidemiology, survival outcomes, and prognostic factors of primary malignant eyelid tumors, specifically sebaceous adenocarcinoma, malignant melanoma, and Merkel cell carcinoma (MCC).
Methods: We conducted a retrospective analysis of 3,082 cases of primary eyelid malignancies diagnosed between 2004-2021 from the Surveillance, Epidemiology, and End Results (SEER) database. Patients were categorized by histological subtype, age, race, tumor stage, and treatment modality. Kaplan-Meier survival analysis, log-rank tests, and Cox proportional hazards regression were employed to evaluate survival and identify prognostic factors.
Results: Sebaceous adenocarcinoma was the most prevalent subtype (26.57%), followed by malignant melanoma and MCC. Most patients (77.28%) were over 60 years old. While White individuals constituted the majority (86.9%), sebaceous adenocarcinoma showed a higher prevalence in Asian or Pacific Islander populations (11.8%). MCC exhibited the highest rate of distant metastases at diagnosis (19.4%). Surgery was the primary treatment (81.6%). Survival outcomes varied significantly by histology: MCC had the worst prognosis (5-year survival: 43.1%; median: 48 months), whereas melanoma had the best (5-year survival: 71.7%; median: 164 months). Cox regression identified age >60 years (HR: 4.25) and radiation therapy (HR: 2.01) as significant predictors of poor survival.
Conclusion: Malignant eyelid tumors exhibit significant heterogeneity in survival. MCC is associated with the highest mortality, and advanced age and radiation therapy are key prognostic factors, underscoring the need for histology-specific management strategies.

#3575 Early-onset colorectal and pancreatic cancer in the United States: Incidence and mortality projections through 2040.

Woo Joo Lee[1], Sumbal Aziz[1], Seon Hye Won[2], Muhammad Sohaib Asghar[1], Robin Park[3], Thomas Shimshak[1]

[1]Internal Medicine, AdventHealth Sebring, Sebring, FL,[2]Department of Family Medicine, Dongguk University Ilsan Hospital, Goyang-si, Korea, Republic of,[3]Department of Head and Neck-Endocrine Oncology, Moffitt Cancer Center, Tampa, FL

Background Incidence of early-onset colorectal cancer (CRC) and pancreatic cancer (PC) has been rising in many high-income countries, including the United States, but medium-term projections for young adults remain limited. Health-care systems need age-specific forecasts to plan screening, prevention, and survivorship services for adults younger than 50 years.
Methods We used population-based U.S. incidence data for CRC and PC from 1999-2022 and mortality data from 1999-2023, aggregated into 13 five-year age groups (20-24 to 80-84 years). Age-period-cohort (APC) models were fitted with Poisson likelihoods using natural cubic splines for descriptive analyses and a Bayesian APC (BAPC) framework with integrated nested Laplace approximation (INLA) and second-order random-walk priors for projections to 2040. For each cancer and endpoint (incidence or mortality), age-specific posterior means and 95% credible intervals (CrIs) were obtained and then summed over ages 20-49 years to derive projected case counts and rates per 100,000 persons using U.S. population projections.
Results In 2020, the modeled incidence of CRC among adults aged 20-49 years was 12.9 cases per 100,000 persons (95% CrI, 12.3-13.5), corresponding to 16,854 cases (16,092-17,616), and is projected to increase to 21.6 (10.9-32.3) per 100,000 in 2030 and 52.2 (0-162) per 100,000 in 2040, or approximately fourfold higher than the 2020 mean estimate with very wide uncertainty. PC incidence in this age group was 2.08 (1.89-2.27) per 100,000 in 2020, corresponding to 2,707 cases (2,460-2,953), and is projected to rise to 2.83 (2.23-3.43) in 2030 and 4.98 (2.02-7.94) in 2040, roughly a 2.4-fold increase. In contrast, CRC mortality among adults aged 20-49 years is projected to increase more modestly, from 2.81 (2.64-2.97) deaths per 100,000 in 2020 to 3.25 (2.45-4.06) in 2030 and 3.41 (0.51-6.31) in 2040. PC mortality projections are highly uncertain: the mean rate decreases from 2.29 (2.11-2.47) per 100,000 in 2020 to 0.76 (0.33-1.19) in 2030 and 0.38 (0-1.08) in 2040, but CrIs include near-zero and values close to the 2020 baseline.
Conclusions Our APC modeling suggests that, if recent trends persist, early-onset CRC incidence in U.S. adults aged 20-49 years might increase substantially through 2040, with more moderate but still meaningful increases in PC incidence. Projected mortality trends are less pronounced for CRC and highly uncertain for PC, underscoring that these estimates should be interpreted as scenario-based projections rather than precise forecasts. These findings support intensified prevention and early-detection strategies in younger adults while highlighting the need to update projections as additional data accrue.

#3576 Cross-cancer mortality trends in the era of immune checkpoint inhibition: A synthetic control analysis of U.S. cancer statistics.

Woo Joo Lee[1], Sumbal Aziz[1], Seon Hye Won[2], Muhammad Sohaib Asghar[1], Robin Park[3], Thomas Shimshak[1]

[1]Internal Medicine, AdventHealth Sebring, Sebring, FL,[2]Family Medicine, Dongguk University Ilsan Hospital, Goyang-si, Korea, Republic of,[3]Department of Head and Neck/Endocrine Oncology, Moffitt Cancer Center, Tampa, FL

Background: Immune checkpoint inhibitors (ICIs) improve survival in several advanced cancers, especially melanoma and non-small-cell lung cancer. Their overall impact on population-level cancer mortality is unclear.
Methods: We used U.S. Cancer Statistics mortality data from CDC WONDER, 1999-2019. Deaths by cancer site and year were age-standardized to the 2000 U.S. population. We defined an “early-ICI” cancer cluster (cutaneous melanoma; lung and bronchus; kidney and renal pelvis; urinary bladder; Hodgkin lymphoma) and constructed a synthetic control from all other sites with complete data. Synthetic-control models treated 1999-2013 as the pre-intervention period and 2014-2019 as the ICI era. We compared age-adjusted mortality and translated differences into “deaths averted” by multiplying the mortality gap by population size. Robustness was assessed with placebo-in-space and placebo-in-time analyses and site-specific controls. As a cross-check, we applied staggered-adoption difference-in-differences using year of first ICI approval by site.
Results: The early-ICI cluster had a modestly greater decline in age-adjusted mortality than its synthetic control after 2014. From 2014-2019, mortality averaged 0.41 deaths per 100,000 lower than the synthetic control, corresponding to an estimated 27,394 deaths averted versus the counterfactual trend. Pre-intervention fit was close (root-mean-square prediction error [RMSPE] 0.18), with higher post-intervention RMSPE (0.47; post/pre ratio 2.58). In placebo-in-space analyses, several non-ICI cancers had larger RMSPE ratios, indicating that the divergence was not unique. Placebo-in-time analyses using earlier hypothetical intervention years (2006-2010) produced smaller RMSPE ratios (1.39-1.81) than the 2014 specification. Site-level synthetic controls suggested deaths averted for melanoma, lung cancer, and Hodgkin lymphoma but excess deaths for kidney and bladder cancers, indicating heterogeneity. Staggered-adoption difference-in-differences estimated an average treatment effect of −0.96 deaths per 100,000 (95% CI −3.22 to 1.31), consistent with modest benefit or no effect.
Conclusions: In this national synthetic-control analysis, cancers with early ICI approvals had slightly greater mortality declines than other cancers, translating to tens of thousands of potentially averted deaths. However, placebo analyses and difference-in-differences indicate that these gains are modest, heterogeneous, and compatible with residual confounding or concurrent advances in care. ICIs thus appear to be an important contributor, but not the sole driver, of recent improvements in cancer mortality.

#3577 The persistence of racial disparities in prostate cancer survival: A time-varying conditional survival and mortality analysis.

Brendon Wang[1], Andrew Chen[2], Irene Wang[3], Candice Johnstone[1]

[1]Medical College of Wisconsin, Milwaukee, WI,[2]Northwestern Univ. Feinberg School of Medicine, Chicago, IL,[3]Einstein College of Medicine, Bronx, NY

Background: Racial disparities in prostate cancer survival are well-documented, but it is less clear how these mortality risks evolve as patients survive longer. Conditional survival (CS) provides a more dynamic and accurate prognosis for survivors by updating survival estimates over time.
Objective: To investigate racial differences in cancer-specific survival (CSS) and 5-year conditional survival (CS) among men with prostate cancer. We also assessed how the multivariable-adjusted hazard of cancer-specific mortality (CSM) by race changes conditional on time already survived.
Methods: We conducted a retrospective cohort study of 235,972 men diagnosed with prostate cancer (2004-2015) from the SEER database, limited to patients with known PSA and Gleason scores. We used Kaplan-Meier methods to estimate 5-year CSS at diagnosis and 5-year CS for men who had already survived 1-5 years. A series of time-varying multivariable Cox proportional hazards models were fit to calculate Hazard Ratios (HRs) for CSM, adjusting for age, sociodemographics, tumor characteristics (stage, grade, PSA, Gleason), and treatment.
Results: At diagnosis (0 years survived), 5-year CSS was 95.9% for White men, 96.2% for Asian/Pacific Islander (API) men, 94.6% for Black men, and 92.8% for American Indian/Alaska Native (AI/AN) men. While 5-year CS improved for all groups who survived 5 years, the gap between Black (95.5%) and White (96.1%) men narrowed but persisted. In multivariable Cox models at diagnosis, Black men had a significantly higher hazard of CSM compared to White men (HR: 1.07; 95% CI: 1.03-1.11, $P < 0.001$). This elevated mortality risk did not attenuate over time. Conversely, API men had a persistent survival advantage (HR at Year 0: 0.72; 95% CI: 0.68-0.77, $P < 0.001$). The mortality hazard for AI/AN men was not statistically different from White men (HR at Year 0: 1.06; 95% CI: 0.87-1.29, $P=0.54$).
Conclusion: Racial disparities in prostate cancer survival are established at diagnosis and, for Black and API men, persist for at least 5 years, even after adjusting for a comprehensive set of clinical and sociodemographic factors. The persistently higher mortality hazard for Black men highlights that survival gaps are not limited to factors at diagnosis. The lack of a significant difference for AI/AN men, despite lower initial CSS, warrants further investigation. These findings are critical for providing a more accurate, dynamic prognosis in long-term patient counseling.

#3578 Conditional overall survival analysis of HPV-positive oropharyngeal squamous cell carcinoma.

Andrew Chen[1], Irene Wang[2], Brendon Wang[3], Adin-Christian Andrei[1], Latifa Bazzi[1], Coyin Oh[1]

[1]Northwestern Univ. Feinberg School of Medicine, Chicago, IL,[2]Albert Einstein College of Medicine, Bronx, NY,[3]Medical College of Wisconsin, Milwaukee, WI

Background: The incidence of HPV-positive (HPV+) oropharyngeal squamous cell carcinoma (OPSCC) has risen drastically in recent years. Conditional overall survival (cOS) provides useful prognostic information for patients who have survived a certain time period following initial treatment, and can inform surveillance guidelines for HPV+ OPSCC. However, cOS for HPV+ OPSCC has not been evaluated in recent years. We sought to characterize residual survivorship among patients who remained alive at 1, 2, or 3 years after diagnosis by evaluating cOS, stratified by tumor staging and associated risk factors, in HPV+ OPSCC based on a large national cancer database.

Methods: We identified patients diagnosed with HPV+ OPSCC confirmed by p16 immunohistochemistry from 2018 to 2022 using the Surveillance, Epidemiology, and End Results (SEER) database. Demographics (race, gender, age), treatment modality (radiation, chemotherapy, surgery), and clinicopathological variables (overall staging, tumor size, number of positive regional nodes) were collected. Conditional Kaplan-Meier curves were used to summarize cOS stratified by overall stage and Cox regression models were generated to evaluate if tumor size, age, and performed surgery are associated with cOS.

Results: Of the 5298 patients included in the study cohort, 86% were male, 91% were white, 44% had undergone surgery, 84% received radiotherapy, and 64% received chemotherapy. The median age at diagnosis was 61 years old. Increased age (per-year hazard ratio, HR=1.052, 95% CI: 1.042-1.061, $p<0.0001$) and increased tumor size (for every 10mm increase, HR=1.053, 95% CI: 1.045-1.061, $p<0.0001$) were associated with increased mortality. Surgery was associated with lower mortality (HR=0.3023, 95% CI: 0.2478-0.3688, $p<0.0001$). The 4-year overall survival at diagnosis for the study cohort was 83.6% but the cOS increased to 93.5% among patients who had already survived the first two years. Higher disease stage was associated with larger gains in conditional survival. For Stage I patients, 4-year overall survival increased from 90.9% at diagnosis to a cOS of 98.2% among survivors at three years post-diagnosis. Similarly, these increases were from 77.9% to 95.7% for Stage II, 62.7% to 95.2% for Stage III, and 31.7% to 90% for Stage IV patients. Following three years of survival, conditional survival estimates across all stages converged to a high range of 90%-98.2%.

Conclusions: For each tumor stage, survival beyond each subsequent year is associated with a higher survival probability to Year 4. Patients with more advanced stage disease saw the largest gains in conditional survival probability over time. These results suggest that the clinical stage of HPV+ OPSCC may have less impact on continued survival after 3 years, which may have implications for prognostication and long-term surveillance. Further work is needed to evaluate these trends over a longer period of time.

#3579 Racial disparities in conditional survival among patients with oral cavity squamous cell carcinoma: A surveillance, epidemiology, and end results-based analysis.

Irene Wang[1], Brendon Wang[2], Andrew Chen[3], Noah Kornblum[1]

[1]Albert Einstein College of Medicine, Bronx, NY,[2]Medical College of Wisconsin, Milwaukee, WI,[3]Northwestern Univ. Feinberg School of Medicine, Chicago, IL

Background: Oral cavity squamous cell carcinoma (OCSCC) accounts for a substantial proportion of head and neck cancer–related morbidity and mortality in the United States. Persistent racial disparities in incidence, stage at diagnosis, access to surgical care, and overall survival have been well documented. Traditional survival estimates, however, do not reflect how prognosis evolves after patients survive the initial years following diagnosis. Conditional survival (CS) offers a dynamic estimate of prognosis over time and may better characterize the attenuation of racial survival gaps.

Methods: Using the SEER database, we conducted a population-based retrospective analysis of 24632 individuals diagnosed with OCSCC between 2004-2015. 5-year cancer-specific CS was calculated using the Kaplan-Meier method. Information including race, age, various socioeconomic demographics, tumor grade and stage, subsite, and treatment modality was used to perform multivariable Cox regression analysis and obtain hazard ratios (HRs) of 5-year mortality for race. All analyses were conducted using R (version 4.5.1).

Results: Of the OCSCC patients analyzed, 80.6% were White, 8.7% Black, and 10.7% Asian/Pacific Islander (API). Initial 5-year CS revealed marked disparities: Black patients (43.2%) had substantially lower survival than White (62.4%) and API patients (63.1%). However, conditional survival demonstrated a dynamic convergence pattern. By year 5 post-treatment, survivors showed narrowed differences: Black patients reached 84.7%, White patients 87.8%, and API patients 88.9% 5-year conditional survival. Time-varying multivariable Cox regression revealed evolving mortality patterns. Black patients faced increased death risk early (Year 0 HR: 1.15, 95% CI: 1.06-1.24; Year 1 HR: 1.22, 95% CI: 1.09-1.36), but this excess risk disappeared among long-term survivors (Year 4 HR: 1.05, $P = 0.651$; Year 5 HR: 1.08, $P = 0.589$). API patients consistently showed comparable outcomes to White patients across all timepoints (HRs: 0.87-1.02, all $P > 0.05$).

Conclusion: OCSCC racial survival disparities follow a convergence trajectory. While Black patients experience significantly worse outcomes initially, this gap contracts to just 3 percentage points among 5-year survivors, accompanied by complete resolution of excess mortality risk in adjusted models. This temporal concentration of disparities within the first three post-treatment years may implicate early-phase factors in treatment (e.g., diagnostic delays, treatment barriers) as drivers in early mortality. There was no statistically significant difference in API compared to White patients.

: Genetic Epidemiology 1: GxE, GWAS, Polygenic Risk Scores, and Post-GWAS
Poster Session

#3583 Distinct breast cancer gene signatures by estrogen receptor status associated with psychological distress.

Shipra Gandhi[1], Sayeeda Yasmeen[2], Spencer Rosario[2], Wiam Bshara[2], Thaer Khoury[2], Hans Minderman[2], Orla Maguire[2], Zhihong Gong[2], Ayana T. Ruffin[1], Megan Meek Wyatt[1], Mahmoud Abdelbary[1], Chrystal Mary Paulos[1], Elizabeth Repasky[2], Pawel Kalinski[3], Christine Ambrosone[2], Song Yao[2], Chi-Chen Hong[2]

[1]Winship Cancer Institute of Emory University, Atlanta, GA,[2]Roswell Park Comphrehensive Cancer center, Buffalo, NY,[3]University of Pittsburgh, Pittsburgh, PA

Background: Chronic psychosocial distress may accelerate breast cancer progression by altering immune, and inflammatory pathways, yet its genome-wide transcriptional effects in breast tumors remain unclear. This study uses RNA sequencing (RNA-seq) to characterize how distress influences transcriptional programs within the breast tumor microenvironment (TME).
Methods: Tumor samples from the Women's Health after Breast Cancer Study were analyzed for genome-wide transcriptional effects of distress. Participants completed the Perceived Stress Scale (PSS) and the Center for Epidemiologic Studies Depression Scale (CES-D) at diagnosis, including total scores and subscales (somatic symptoms, depressive affect, interpersonal problems, and positive affect). RNA-seq was performed on FFPE tumors from 195 women (152 ER+, 43 ER–). Principal component analysis (PCA) identified distress domains contributing to transcriptional variability. Participants were classified using PSS (>14 vs 0-14) and CES-D somatic symptoms (>3 vs ≤3). Differential gene-expression and gene-set enrichment analyses evaluated high-stress/low-somatic symptoms and low-stress/high-somatic symptoms groups vs a common low-stress/low-somatic symptoms reference, adjusting for age and education. Statistical significance was defined as FDR<0.05.
Results: PCA indicated subtype-specific distress signatures, with CES-D somatic symptoms explaining the most transcriptional variance in ER+ tumors and PSS explaining more variance in ER– tumors. In ER+ tumors, high stress with low somatic symptoms upregulated immune-activation pathways, including B-cell signaling, interferon responses, complement, and antigen presentation (top NES ~2.1-2.7, FDR<0.05). Key genes (*FLG, IGLV3-16, IGKV3D-15, RPS7P3*) mapped to immune-activation and interferon pathways. In ER– tumors, high stress showed enrichment of PD-1 co-inhibition and MHC-I antigen-presentation (NES=2.36 and 2.15, respectively, FDR<0.03), with suppression of neuronal, metabolic, mitochondrial, and protein-synthesis signaling (NES –1.4 to –2.1, FDR<0.05). High somatic symptoms in ER+ tumors enriched translational and ribosomal pathways (NES=3.0, FDR<0.01). In ER– tumors, high somatic symptoms were associated with increased keratinization, leptin, WNT, and IGF signaling (NES~1.8-2.7, FDR<0.02), and reduced chromatin-regulation, DNA replication, RNA-processing, translation pathways, and MHC-I antigen presentation (NES ~1.8 to -1.9, FDR<0.006).
Conclusions: Psychological distress shapes breast-tumor transcriptional programs in a subtype-specific manner. Stress and depressive domains map to distinct immune, metabolic, and biosynthetic pathways in ER+ vs ER– disease, suggesting that different forms of distress engage different processes in the TME. This information could be leveraged to design new treatments for patients.

#3584 Characterizing polygenic risk scores for cancer in prospective cohorts: Considering PRS method construction, age of diagnosis, genetic ancestry, and sample overlap.

Julie-Alexia Dias[1], Gillian King[2], David Bogumil[2], Brian Huang[2], Fei Chen[2], David V. Conti[2]

[1]Department of Biostatistics, Harvard University, Boston, MA,[2]University of Southern California, Los Angeles, CA

Well-established prospective cancer cohorts provide a unique opportunity to investigate the combined use of polygenic risk scores (PRSs) and non-genetic factors for personalized disease risk prediction. However, their application can vary depending on cohort-specific characteristics. We compared four PRS weighting strategies: PRS-CSx, Lassosum, a multi-ethnic joint analysis of marginal summary statistics (mJAM) forward selection procedure, and standard genome-wide association study (GWAS) derived weights, across eight large, prospective cohorts, totaling over a million subjects from the Multiethnic Cohort (MEC, n=73,139), the Genetic Epidemiology Research on Aging (GERA, n=103,358), the Women's Health Initiative (WHI, n=46,794), the Nurses' Health Studies I (NHS, n=20,195) and II (NHS2, n=16,082), the Health Professionals Follow-up Study (HPFS, n=12,649), the UK Biobank (UKB, n=474,775) and All of Us (AoU, n=317,956).

Together, these cohorts represent a uniquely diverse study population spanning multiple racial and ethnic groups, broad age distributions, and both overlapping and non-overlapping samples with discovery GWAS populations. We evaluated PRS performance for four major cancers (breast, prostate, colorectal, and lung) across all weighting methods and contexts. Our findings show that both the choice of PRS construction method and the characteristics of the target cohort substantially influence the characterization of disease risk.

By integrating four distinct PRS approaches across eight large and diverse prospective cohorts, this study provides one of the most comprehensive evaluations to date of context-dependent variation and provides guidance for ongoing development of risk prediction models that combine genetic and non-genetic factors.

#3585 A body mass index polygenic risk score (PRS_{BMI}) and obesity-related cancer risk among women in the Hispanic Community Health Study/Study of Latinos.

Humberto Parada[1], Tamar Sofer[2], Margaret Pichardo[3], Krista M. Perreira[4], Laura Zhou[5], Frank J. Penedo[6], Amber Pirzada[7], Martha Daviglus[8], Gregory A. Talavera[9], Linda C. Gallo[9]

[1]School of Public Health, San Diego State University, San Diego, CA,[2]Department of Biostatistics, Harvard Medical School, Boston, MA,[3]Department of Surgery, Hospital of the University of Pennsylvania, Philadelphia, PA,[4]Department of Social Medicine, University of North Carolina at Chapel Hill, Chapel Hill, NC,[5]Department of Biostatistics, University of North Carolina at Chapel Hill, Chapel Hill, NC,[6]Department of Psychology, University of Miami, Coral Gables, FL,[7]College of Medicine, University of Illinois, Chicago, IL,[8]Department of Medicine, University of Illinois Chicago, Chicago, IL,[9]Department of Psychology, San Diego State University, San Diego, CA

Background. Obesity is associated with an increased risk of cancer including cancers of the colon and rectum, endometrium, and breast among women. Polygenic risk scores (PRS), which sum the effects of risk variants, estimate an individual's genetic predisposition to complex phenotypic traits, such as obesity. We constructed a PRS for body mass index (PRS_{BMI}) and examined whether the PRS_{BMI} was associated with the risk of obesity-related cancers (ORCs) among Hispanic/Latina women. We also examined whether BMI moderated or mediated the association between PRS_{BMI} and ORC risk.

Methods. This prospective cohort study included 8,380 Hispanic/Latina women (mean age at baseline=41.8±0.3 years) from the Hispanic Community Health Study/Study of Latinos (HCHS/SOL). At baseline in 2008-2011, height and weight were measured and used to compute BMI, and participants provided blood samples for genotyping. The PRS_{BMI} was constructed using previously published weights downloaded from the polygenic score (PGS) catalog. The incidence of 13 obesity-related cancers diagnosed from baseline through 2021 was ascertained through linkages with four state cancer registries (n=223 incident ORCs were diagnosed over a mean follow-up of 10.8 years). Survey multivariable Cox regression models estimated the associations (hazard ratios, HRs, and 95% confidence intervals, CIs) between the PRS_{BMI} (per standard deviation, SD) and ORC risk overall and by BMI (<25 vs. ≥25 kg/m^2). Survey multivariable Cox regression and linear regression models tested the mediating effect of BMI (continuous, kg/m^2) on the association between PRS_{BMI} (per SD) and ORC risk.

Results. In stratified analyses, a 1-SD increase in the PRS_{BMI} was associated with an ORC HR of 0.74 (95%CI=0.56-0.97) among women with BMI<30 kg/m^2, but not among women with a BMI≥30 kg/m^2 (HR=0.95; 95%CI=0.68-1.33; $P_{Interaction}$=0.15). In mediation analyses, PRS_{BMI} was significantly associated with BMI (β_a=1.86; 95%CI=1.66-2.06); BMI was significantly associated with ORC risk, adjusting for PRS_{BMI} (β_b=0.07; SE=0.01; HR=1.07; 95%CI=1.05-0.19); and BMI significantly mediated the association between PRS_{BMI} and ORC risk (indirect effect, β_a*β_b=0.13; 95%CI=0.07-0.19).

Conclusion. Genes predisposing women to a higher BMI may primarily impact ORC risk through BMI. These results highlight the importance of weight management for cancer prevention among Hispanic/Latina women.

#3586 Validation and population projection of multi-cancer risk incorporating polygenic risk scores and non-genetic factors.

Emily L. Norton[1], Thomas Ahearn[2], Srijon Mukhopadhyay[3], Jeya Balasubramanian[2], Elle Kim[4], Sara Li[5], Parichoy Pal Choudhury[6], Montserrat Garcia-Closas[7], Nilanjan Chatterjee[1]

[1]Biostatistics, Johns Hopkins Bloomberg School of Public Health, Baltimore, MD,[2]National Cancer Inst. Div. of Cancer Epidemiology & Genetics, Bethesda, MD,[3]University of North Carolina, Chapel Hill, NC,[4]Johns Hopkins School of Medicine, Baltimore, MD,[5]Johns Hopkins University, Baltimore, MD,[6]American Cancer Society, Atlanta, GA,[7]The Institute of Cancer Research, United Kingdom

Background: Multiple risk factors are shared across different cancers, yet risk assessment and prevention strategies remain largely site-specific. Meanwhile, multi-cancer detection tests are emerging as complementary approaches to site-specific screening strategies such as mammography, colonoscopy, and low-dose CT lung scans. Multi-cancer risk prediction could provide a more holistic understanding of an individual's cancer risk, with the potential to improve risk-stratified prevention and screening strategies across multiple cancer types.

Methods: We developed absolute risk models for 14 cancer sites using published non-genetic risk models incorporating 26 risk factors, together with established polygenic risk score (PRS) for each cancer site, using the Individualized Coherent Absolute Risk Estimator (iCARE) tool to integrate relative risk parameters, risk-factor distributions, population incidence rates, and mortality rates. We extended iCARE to estimate risk across multiple cancer sites over specified time intervals. Calibration (expected/observed (E/O) risk) and discrimination (area under the curve (AUC)) of site-specific and combined multi-cancer risk predictions were prospectively evaluated in the non-Hispanic White population in the Prostate, Lung, Colorectal, and Ovarian (PLCO) Cancer Screening Trial. Multi-cancer risk stratification for the US non-Hispanic White population was projected by applying our model with age specific incidence and mortality rates to a reference population derived from the National Health and Nutrition Examination Survey, the National Health Interview Survey, and the Breast Cancer Surveillance Consortium.

Results: Validation in PLCO showed comparable risk stratification between the sexes but better calibration for females (multi-cancer 10-yr risk E/O = 1.05 (95% CI: 1.03-1.07), AUC = 0.60) than males (E/O = 0.76 (95% CI: 0.75-0.77), AUC = 0.61). Between the first and last decile of predicted 10-year risk, the corresponding observed risk ranges 3-20% in females and 7-30% in males. Multi-cancer risk projections for the non-Hispanic White US reference population showed that 24% of males and 23% of females aged 18-74 are at moderate to high risk (10-year absolute risk ≥10%).

Conclusion: Multi-cancer risk prediction models combining non-genetic risk factors and PRS demonstrate meaningful risk stratification. Future studies will include calibration, validation, and projection of these models in US non-White populations. Such models may support counseling on lifestyle interventions that influence multiple cancer risks and help identify high-risk individuals for emerging multi-cancer screening approaches such as liquid biopsy tests. However, further model development and evaluation is needed to ensure optimal performance across population groups.

#3587 Independent validation of polygenic risk scores for overall and triple-negative breast cancer among high-risk African American women.

Yijia Sun[1], Timothy Simmons[2], James L. Li[3], Armaan Jamal[1], Achille V.C. Manirakiza[4], Dmitry Pruss[2], Sarah Ratzel[2], Olufunmilayo I. Olopade[4], Alexander Gutin[2], Elisha Hughes[2], Dezheng Huo[1]

[1]Public Health Sciences, University of Chicago, Chicago, IL,[2]Myriad Genetics, Inc., Salt Lake City, UT,[3]Interdisciplinary Scientist Training Program, University of Chicago, Chicago, IL,[4]Center for Innovation in Global Health, University of Chicago, Chicago, IL

Background: Polygenic risk scores (PRSs) are emerging tools for stratifying breast cancer (BC) risk. We developed PRSs of overall BC and triple-negative BC (TNBC) risk in women of African ancestry, using case-control data from studies unselected for family history. PRS could be part of comprehensive breast cancer risk assessment for women at higher risk due to cancer family history. Here we aimed to evaluate the performance of these PRSs in women with elevated cancer risk.
Methods: We included samples from African American women who underwent multigene hereditary genetic testing between 2016 and 2024 and who tested negative for pathogenic or likely pathogenic variants in known BC genes. Genotyping was performed using custom Axiom PMRA arrays (ThermoFisher) and imputation based on TOPMed reference data. We evaluated two PRS models for overall BC with 2,324,063 variants ("Overall BC Model 1") and 175,173 variants ("Overall BC Model 2"), and three PRS models for TNBC with 554,959 variants ("TNBC Model 1"), 37,226 variants ("TNBC Model 2"), and 162 variants ("PRS-162"). The 313-variant PRS developed in women of European ancestry (PRS-313) served as a benchmark. Only variants with imputation $R^2 \geq 0.7$ were included. Associations between PRSs and BC status were examined using multivariable logistic regression, adjusting for age at diagnosis or testing, the top ten principal components, and weighted family history of BC. Adjusted odds ratio (OR) per standard deviation and area under the curve (AUC) were calculated.
Results: The study included 19,455 unaffected and 12,067 women with BC (2,311 TNBC). Mean age at BC diagnosis was 55.2 years in BC cases vs. 42.1 years at testing in unaffected women. More unaffected women had a family history of BC in first-degree (32.8% vs. 28.0%) and second-degree relatives (55.7% vs. 35.0%) than affected women. Over 95% of African PRS variants and 82% of the PRS-313 variants had an imputation $R^2 \geq 0.7$. For overall BC, PRS-313 showed an AUC of 0.567 (95% confidence interval [CI]: 0.560, 0.574) and an OR of 1.28 (95% CI: 1.25, 1.31). In comparison, the African overall BC Models 1 and 2 performed better, with AUCs of 0.588 (95% CI: 0.580, 0.595) and 0.584 (95% CI: 0.576, 0.591) and ORs of 1.39 (95% CI: 1.35, 1.43) and 1.37 (95% CI: 1.34, 1.41), respectively. For TNBC, Models 1 and 2 yielded similar performance, with AUCs of 0.579 and 0.574, respectively. Notably, the TNBC PRS-162 showed very good performance with an AUC of 0.609 (95% CI: 0.596, 0.622) and an OR of 1.47 (95% CI: 1.40, 1.55).
Conclusion: The PRSs demonstrated good performance among women with a strong family history of BC, reflecting real-world populations where early PRS testing is most relevant for those at elevated risk. The high predictive accuracy of the 162-variant TNBC PRS supports its potential as a cost-effective risk assessment tool to promote equitable care.

#3589 Ancestry-driven transcriptional regulation of breast cancer genes through cis- and trans-eQTLs in colombian populations.

Laura Rey-Vargas, Lina Maria Bejarano, Patricia Lopez, Diego Felipe Ballen-Lozano, Silvia Juliana Serrano-Gomez

Instituto Nacional de Cancerologia, Bogota, D.C, Colombia

Introduction: Significant disparities in breast cancer phenotypes have been observed across population groups. Latina women show a higher prevalence of aggressive tumor subtypes and increased mortality compared to non-Hispanic White women. Genetic ancestry differences have been proposed as a potential mechanism influencing baseline tissue biology and tumor behavior. Specifically, ancestry-specific expression quantitative trait loci (eQTLs) may mediate these effects. This study aimed to identify ancestry-specific eQTLs associated with clinically relevant breast cancer genes.
Methods: RNA-seq data from tumor and adjacent non-tumoral breast tissue of 183 patients from the NCI of Colombia were analyzed to obtain genotypes using a GATK4 variant-calling pipeline and the TOPMed imputation server. Normalized gene expression matrices were generated with STAR and DESeq2, and eQTLs were identified using MatrixEQTL in R. Local ancestry was inferred with RFMix to filter eQTLs within regions enriched for specific ancestries.
Results: In non-tumor breast tissue, 234 Indigenous ancestry-specific cis-eQTLs associated with 18 eGenes were identified, with MACC1 being the only COSMIC-listed gene. Additionally, 1,371 Indigenous ancestry-specific trans-eQTLs were linked to 1,001 eGenes. After prioritization, 164 significant associations were identified, involving 31 COSMIC eGenes regulated by 76 trans-eQTLs. These included oncogenes such as ERBB2, CDK6, FGFR4, LASP1, and MDM2, and tumor suppressor genes like BRCA2, RB1, CDH1, and ATM. Conversely, 26 European ancestry-specific cis-eQTLs associated with four proximal eGenes (ST7L, SLC35E2A, PRPF38A, and ODR4) were identified. Moreover, 160 European ancestry-specific trans-eQTLs were linked to 194 eGenes showing enrichment in membrane-related processes, including oncogenes such as PRKCB and JAK3, and tumor suppressors like ATM and RB1. Due to low African ancestry representation among Colombian patients, this component was not analyzed. For Indigenous ancestry-specific eQTLs, trans associations between 12 variants located in 5q13.3 and tumor-relevant genes in 19q13.1, 11p15.5, and 1p34.2 were validated in cancer tissue, including MUC6, MED29, and PDCD5.
Conclusion: These findings suggest that in non-tumoral breast tissue, transcriptional regulation can be mediated by Indigenous and European ancestry-specific variants influencing the expression of genes with key roles in tumor-related pathways. Validation analyses in tumor tissue indicated that only a subset of Indigenous ancestry-specific eQTLs may retain trans-regulatory effects and contribute to breast cancer biology.

#3590 Genetic and immune signaling divergence underlies the inverse associationbetween asthma and cancer.

Kinsey Garofalo[1], Yinqiao Wang[2], Peyton Cook[1], Yujuan Guo[1], Yong Zhu[1]

[1]University of Arkansas for Medical Sciences, Little Rock, AR,[2]University of Southern California, Los Angeles, CA

An inverse association between asthma and several cancer types has been consistently observed across epidemiologic studies, yet the molecular mechanisms underlying this relationship remain unclear. To address this gap, we conducted a comprehensive genetic and functional analysis to identify variants, genes, and immune signaling pathways that may contribute to this protective association. From literature-validated genome-wide association studies, we compiled 246 asthma-associated SNPs and identified 14 variants that were also significantly associated with cancer risk. Notably, 11 of these SNPs demonstrated reversal directionality, where the asthma risk allele was associated with reduced cancer risk, particularly in glioma and colorectal cancer. Haplotype analysis further revealed 19 genes exhibiting diametric effects on asthma and cancer susceptibility. Among these, IL-9, TLR1, SMAD7, LPP, IL-7R, and HLA-DQB1 also showed inverse gene expression patterns between asthma tissues and multiple cancer types, indicating functional opposition at the transcriptional level. Pathway enrichment using Ingenuity Pathway Analysis identified Th1/Th2 immune axis regulation and glucocorticoid receptor signaling as central networks driving this biological divergence. Specifically, genes upregulated in asthma that elevate Th2-dominant IgE-mediated immune responses were linked to enhanced immunosurveillance and T-cell cytotoxic activation in cancer contexts, suggesting a mechanistic basis for reduced tumor initiation and progression. Meanwhile, glucocorticoid receptor isoform regulation emerged as a potential modulator linking asthma treatment to cancer vulnerability. Together, these results provide the first integrated genetic, transcriptomic, and pathway-level evidence supporting a causal immunologic framework for the inverse asthma-cancer association. This work highlights new molecular targets at the interface of allergic inflammation and tumor immunity and suggests opportunities for therapeutic repurposing of immune-modulating strategies used in asthma to inform cancer prevention and treatment.

#3591 Incorporation of polygenic risk scores with PSA testing for prostate cancer risk stratification in men undergoing prostate biopsy.

Daniel Sabater Minarim[1], Roshan Karunamuni[1], Kylie M. Morgan[1], Tyler Nelson[1], Craig Teerlink[2], Julie Lynch[2], Isla P. Garraway[3], Anna M. Dornisch[1], Tyler M. Seibert[1], Jason L. Vassy[4], Brent S. Rose[1]

[1]Radiation Medicine and Applied Sciences, UCSD Health, San Diego, CA,[2]VA Informatics and Computing Infrastructure, Salt Lake, UT,[3]Urology, UCLA Health, Los Angeles, CA,[4]Harvard Medical Scool, Boston, MA

Purpose: While prostate-specific antigen (PSA) screening reduces prostate cancer (PC) mortality, limited discriminatory ability leads to overdiagnosis of indolent disease and missed clinically significant PC. Genetically informed screening strategies utilizing polygenic scores may improve early PC detection. We hypothesized that incorporating polygenic scores for PC risk (PHS601) and benign elevated PSA (PRS447) with traditional risk factors would improve prediction of clinically significant PC on prostate biopsy in a diverse population.

Methods: We identified veterans who underwent their first prostate biopsy from October 1999 to September 2021 using the VA Corporate Data Warehouse, with genetic data from the Million Veteran Program. We excluded patients with prior PC diagnosis, those without pre-biopsy PSA within 90 days, and PSA levels >50 ng/mL. The cohort included 25,222 men: 19,376 (76.8%) White, 4,891 (19.4%) Black or African American, and 955 (3.8%) other race/ethnicities. The primary outcome was clinically significant PC (Gleason score ≥7). We evaluated two genetic scores (PHS601 and PSA447, both standardized to z-scores) along with pre-biopsy PSA, age at first biopsy, race/ethnicity, and smoking status. We performed multivariable logistic regression using three progressive models: clinical features alone, clinical features plus PHS601, and clinical features plus both genetic scores.

Results: Among 25,222 patients, 8,319 (32.9%) were diagnosed with clinically significant PC. Both genetic scores showed strong independent associations: elevated PHS601 increased risk (OR=1.73, 95% CI: 1.68-1.79, P<0.001), while higher PSA447 decreased risk (OR=0.69, 95% CI: 0.67-0.72, P<0.001). At PSA of 4 ng/mL, predicted probabilities of clinically significant cancer ranged from 9.1% to 56.9% across PHS601 percentile groups (≤2nd to ≥98th). Model discrimination improved from 0.635 (clinical features alone) to 0.714 (plus PHS601) to 0.737 (both genetic scores, p<0.001).

Conclusion: Polygenic scores for PC risk and benign PSA elevation significantly improve prediction of clinically significant PC on biopsy compared to traditional risk factors alone. These findings support genetically informed PC screening strategies. Men with low genetic PC risk could defer biopsy until higher PSA values, reducing overdiagnosis, while those with high genetic risk could undergo biopsy at lower PSA thresholds, reducing missed clinically significant PC.

#3592 Mitochondrial DNA breaks and copy number and the risk of lung cancer in never-smoking women.

Batel Blechter[1], Xiao-Ou Shu[2], Wei Hu[3], Elizabeth Francies[1], Wei Zheng[2], Yu-Tang Gao[4], Qiuyin Cai[2], Hui Cai[5], Gong Yang[6], H. Dean Hosgood[7], Richard Cawthon[8], Qing Lan[3]

[1]National Cancer Institute, Rockville, MD,[2]Vanderbilt University, Nashville, TN,[3]NCI Div. of Cancer Epidemiology & Genetics, Rockville, MD,[4]Chief, Dept. of Epidemiology, Shanghai Cancer Institute, Shanghai, China,[5]Vanderbilt University Medical Center, Nashville, TN,[6]Vanderbilt University School of Medicine, Nashville, TN,[7]Einstein University, New York City, NY,[8]University of Utah, Salt Lake City, UT

Introduction Lung cancer is the leading cause of cancer-related mortality worldwide, with approximately 25% of cases occurring in never-smokers, particularly East Asian women. Mitochondria are critical regulators of cellular energy production and oxidative stress responses, and mitochondrial DNA (mtDNA) is especially susceptible to damage from environmental exposures. While findings from previous studies on mtDNA copy number (mtDNAcn) and lung cancer risk have been mixed, mtDNA fraction with breaks (mtDNAfb) has recently emerged as a potential marker of oxidative stress and mitochondrial integrity. We investigated associations between prediagnostic mtDNAfb, mtDNAcn, and lung cancer risk in never-smoking women in the prospective Shanghai Women's Health Study (SWHS). **Methods** This nested case-control study included 789 incident lung cancer cases and 789 controls individually matched on birth year and blood collection date from the SWHS, a prospective cohort of 74,942 women enrolled between 1996 and 2000. DNA was extracted from white blood cells or buccal cells, and mtDNAfb was quantified using a high-throughput qPCR assay comparing amplification signals from TaqI-treated (digested) and untreated samples. Relative mtDNAcn was derived from qPCR measurements normalized to a reference gene. Conditional logistic regression was used to estimate odds ratios (ORs) and 95% confidence intervals (CIs) for the associations of mtDNAfb and mtDNAcn with lung cancer risk, adjusting for age, body mass index, and assay plate. Sensitivity analyses further controlled for education, environmental tobacco smoke exposure, family history of lung cancer, and mutual adjustment for mtDNAfb and mtDNAcn. Interaction between mtDNAfb and mtDNAcn was tested on a multiplicative scale. **Results** We observed higher mtDNAfb was associated with lower risk of lung cancer with participants in the highest mtDNAfb tertile having 34% lower odds compared with those in the lowest tertile (p trend = 0.026). No independent association was observed for mtDNAcn; however, a multiplicative interaction between mtDNAfb and mtDNAcn was identified (p interaction = 8.3×10^{-6}) where the association between mtDNAfb and lung cancer was more pronounced among participants with low mtDNAcn (OR = 0.47, 95% CI: 0.29-0.78) than those with high mtDNAcn (OR = 1.02, 95% CI: 0.58-1.79). **Conclusions** Lower mtDNAfb was associated with increased lung cancer risk among never-smoking women, particularly among women with low mtDNAcn, suggesting possible pathologic reductions in mitochondrial biogenesis and functioning, and consequently, reduced innate immune activation. These findings provide novel insights into mitochondrial dysfunction as a potential mechanism underlying lung cancer in never-smokers and warrant replication and mechanistic investigation in future studies.

#3593 Associations of BRCA1/2 mutations and polygenic risk score with prostate cancer risk and mortality in a founder population.

Ilir Agalliu[1], Mykhaylo Usyk[2], Michael D`Angelo[2], Victor Kamensky[1], Robert Burk[2]

[1]Epidemiology and Population Health, Albert Einstein College of Medicine, Bronx, NY,[2]Microbiology and Immunology, Pediatrics, Albert Einstein College of Medicine, Bronx, NY

Introduction: Prostate cancer (PrCa) is the most common solid tumor and the second-leading cause of cancer deaths among U.S. men. Although the multi-factorial etiology of this cancer indicates the involvement of several biological pathways, to date the role of rare vs common genetic variants (SNPs) in risk prediction of more aggressive or fatal PrCa remains unclear. The goal of this project is to examine the associations of rare germline *BRCA1/2* mutations and a polygenic risk score (PRS) with risks of total and aggressive PrCa as well as with overall and cancer-specific mortality in a founder population.

Methods: Epidemiological and germline genotype data collected from 943 PrCa cases and 1,199 controls of Ashkenazim Jewish descent were used in this analysis. We evaluated associations of *BRCA1* (185delAG) and *BRCA2* (6174delT) founder mutations and a PRS generated from 77 SNPs with risks of total PrCa and high-grade cancer (defined as Gleason score 7-10) using logistic and multinomial regression models, respectively, and adjusted for age and family history of PrCa. All men were followed for mortality via linkage with the U.S. National Death Index from recruitment into the study (between 1999 and 2003) through 12/31/2022. Cox regression models and competing risk analyses were used to examine associations of *BRCA1/2* mutations and PRS with overall and PrCa-specific mortality after adjustment for age, Charlson comorbidity index as well as clinical factors and PrCa treatment.

Results: The prevalence of *BRCA1 (185delAG:* 1.2% vs 0.7%*)* and *BRCA2 (6174delT:* 1.3% vs 0.9%*)* were higher in cases vs controls. Mutation carriers of either *BRCA1* or *BRCA2* mutations had ORs of 1.92 (95%CI 1.00-3.67) for total PrCa and 3.38 (95%CI 1.63-7.04) for high-grade PrCa compared to non-mutation carriers. The PRS score was also independently associated with a statistically significant 2.2 to 2.3-fold higher risk for total PrCa and aggressive cancer. During a median follow-up of 19.7 years a total of 712 out of 943 (76%) men diagnosed with PrCa had died, of whom 124 (17.4%) were PrCa-specific deaths. *BRCA2* mutation carriers had hazard ratios (HR) of 1.92 (p=0.008) and 2.88 (p=0.01) for overall and PrCa-specific mortality compared to non-mutation carriers. However, there was no association of the PRS score with PrCa-specific mortality (HR=0.98, p=0.89) and a borderline significant 9% lower risk (HR=0.91, p=0.05) with overall mortality.

Conclusion: Carriers of *BRCA1* and particularly *BRCA2* mutations have increased risks of more aggressive and fatal PrCa. Although the PRS score was associated with overall risk, it did not confer any elevated risk for higher Gleason score tumors or fatal PrCa. Evaluation for *BRCA2* mutations might be helpful for risk-stratification of men for PrCa screening and potentially targeted therapy.

#3594 Adrenal-permissive *HSD3B1* genotype and prostate cancer-specific mortality among patients: Insights from the multiethnic cohort Study.

Wei Xiong[1], Xin Sheng[1], Peggy Wan[1], Lynne R. Wilkens[2], Loic Le Marchand[2], David V. Conti[1], Christopher A. Haiman[1], Fei Chen[1]

[1]University of Southern California, Los Angeles, CA,[2]University of Hawaii Cancer Center, Honolulu, HI

Background: The *HSD3B1* gene encodes an androgen synthesis enzyme critical for prostate cancer (PCa) progression. The CC genotype of a common missense variant in *HSD3B1* (rs1047303) is considered adrenal-permissive, resulting in increased androgen synthesis, resistance to androgen deprivation therapy (ADT), and accelerated PCa progression. However, epidemiologic evidence linking this variant to prostate cancer-specific mortality (PCSM), particularly in diverse patient populations, remains limited.
Methods: We investigated the recessive effect of the C allele (CC vs. AA or AC) on PCSM among incident PCa cases in the Multiethnic Cohort (MEC). Cause-specific Cox proportional hazards regression models were used to estimate the hazard ratios (HRs) and 95% CI confidence intervals (CIs), with age since PCa diagnosis as the time scale. Covariates included tumor stage (localized, regional, or distant), Gleason grade (high: ≥8 or low: <8), first-degree family history of PCa, the first ten principal components, and initial course of treatment (chemotherapy, radiation therapy, hormone therapy, or surgery). Analyses were conducted overall and in cases stratified by tumor stage, grade, and metastatic status. A sensitivity analysis was conducted, restricted to men who underwent hormone therapy as part of the initial treatment. Statistical significance was defined as a two-sided p-value <0.05.
Results: Among the 3,216 incident PCa cases (34.7% Japanese Americans, 20.4% Latinos, 19.5% African Americans, 19.1% Whites, and 6.4% Native Hawaiians), 295 (9.2%) died due to PCa over a median follow-up of 5.9 years, and 115 (3.6%) carried the CC genotype. Compared to the AA/AC genotype, the CC genotype was associated with a suggestive 57% increased risk of PCSM (95% CI: 0.80-3.09, P=0.19). The association was stronger among patients with metastatic (HR=5.24, 95% CI: 1.01-8.48, P=0.01), advanced (HR=2.33, 95% CI: 0.67-8.08, P=0.18), or high-grade (HR=2.15, 95% CI: 0.80-5.79, P=0.13) PCa. In the hormone therapy subgroup, the CC genotype was significantly associated with increased PCSM among patients with metastatic (HR=6.79, 95% CI: 2.03-17.2, P<0.001) and advanced (HR=3.29, 95% CI: 1.10-11.7, P=0.03) disease.
Conclusion: In this multiethnic population of PCa cases, the adrenal-permissive CC genotype of *HSD3B1* rs1047303 variant was associated with a markedly increased risk of PCSM, particularly among patients with aggressive disease and those treated with hormone therapy. These findings suggest that *HSD3B1* genotyping may have clinical utility in identifying patients at higher risk of poor outcomes and guiding personalized treatment strategies. Further studies with larger sample sizes are needed to confirm these associations and explore their implications for clinical decision-making.

#3596 Characterizing BRCA1 and BRCA2 mutations in Cameroonian breast cancer patients: Efforts towards bridging the genomic gap in Africa.

Kenn Chi Ndi[1], Berthe Sabine Esson Mapoko[2], Vanessa Mouaye[3], Carmen Vanvolkenburgh[4], Bonaventure Dzekem[4], Paul Ndom[2], Dezheng Huo[4], Olufunmilayo I. Olopade[4]

[1]Medical Oncology, Centre Hospitalier Regional d'Ebolowa, Ebolowa, Cameroon,[2]Medical Oncology, Faculty of Medicine and Biomedical Sciences, University of Yaounde 1, Yaounde, Cameroon,[3]Cancer Control Committee, Yaounde, Cameroon,[4]University of Chicago Medical Center, Chicago, IL

Background: There are profound global inequities cancer genomics research, with publications focusing on cancer genetics from Africa representing only 0.016% of the global total. This genomic underrepresentation creates significant barriers to equitable cancer care and precision medicine for African populations. BRCA1/2 mutations remain critically understudied in these communities, limiting our understanding of hereditary breast cancer patterns. This pioneering study characterizes BRCA1/2 mutations among Cameroonian patients to lay the foundation for future genomic research and address critical knowledge gaps.
Methods: This hospital-based study recruited 82 breast cancer patients from 2 major treatment centers in Cameroon, an underserved population with limited access to genetic services. Following pre-test genetic counseling, saliva samples were collected and analyzed using next-generation sequencing for 29 cancer-associated genes. AI was used to improve the clarity of the language of this abstract.
Results: Pathogenic mutations were identified in 23 patients (28%), with BRCA1 (15) and BRCA2 (2) accounting for 73.9% of all mutations (18.3% and 2.4% of the total population, respectively). The most frequent BRCA1 mutation was *c.4484G>T(p.Arg1495Met)*, present in 7 patients (46.7% of BRCA1 mutations, 8.5% of total population), followed by *c.5155dup(p.Val1719Glyfs6)* in 3 (including 1 with bilateral breast cancer) patients (20% of BRCA1 mutations). *BRCA2* mutations included *c.1813dup(p.Ile605Asnfs*11) and *c.5572del(p.Thr1858Glnfs*5)*. Family history of cancer was reported in 73.9% of mutation carriers compared to 62.2% overall. Variants of uncertain significance were detected in 25.6% of patients. Two of those with the *c.4484G>T* BRCA1 mutation had an associated VUS in the PALB2 gene *(c.365A>G(p.Asp122Gly))*. They were both under 30 and had at least 4 first- and second-degree relatives with breast and ovarian cancer. Two other patients had the same VUS in APC *(c.3760A>G(p.Ile1254Val)*), all with at least 2 relatives with cancer and 1 had the BRCA1 c.4484G>T mutation and the other had no pathologic mutation identified.
Conclusions: This pioneering study reveals striking cancer health disparities, with BRCA1/BRCA2 mutation frequencies exceeding rates in well-studied populations. The predominance of specific mutations and VUSs suggests population-specific genetic architecture requiring tailored approaches. Our work provides a foundation for developing culturally-appropriate cancer prevention strategies, reducing genetic testing disparities, and advancing precision medicine accessibility in vulnerable populations, ultimately contributing to the global effort to eliminate cancer health disparities.

#3597 Defining cancer risk germline variants in shelterin complex genes - a genome-first analysis.

Hasset Nurelegne, Akanksha Nagarkar, Jung Kim, Douglas Stewart, Sharon Savage, Kelvin C. De Andrade

National Cancer Institute, Bethesda, MD

Background: The shelterin complex (encoded by ACD, POT1, TERF1, TERF2, TERF2IP, andTINF2) is essential for telomere maintenance and chromosome stability. Pathogenic or likelypathogenic (P/LP) germline variants in some shelterin genes cause telomere biology disorders aswell as cancer predisposition with long telomeres. To date, studies have focused on clinicallyascertained families. Genome-first approaches identify individuals with rare P/LP variants frompopulation-scale sequencing databases linked to electronic health records, enabling better estimates of variant prevalence and cancer risk.
Methods: We assessed rare (minor allele frequency<1%) P/LP germline variants in ACD,TERF1, TERF2, TERF2IP, and TINF2. Exome and phenotype data were analyzed from UKBiobank (UKB) (N=469,578) and Geisinger DiscovEHR cohort (N=216,361). Variants wereclassified using AutoGVP and literature review. Cancer prevalence and risk in carriers versusnoncarriers were evaluated using logistic regression models, respectively, adjusted for year ofbirth, sex, smoking status, alcohol intake, body mass index, and genetically determined ancestry.
Results: We identified 1,200 individuals (784 in UKB and 416 in Geisinger) with P/LP germlinevariants in shelterin complex genes. The prevalence of shelterin variants ranged from 1:1,886 to1:39,132 in UKB and 1:1,157 to 1:24,040 in Geisinger, ACD and TINF2 had the highestestimates and TERF2 the lowest. In ACD, a variant previously associated with cancer(c.488A>G, p.Asn163Ser) accounted for 49.3% of all ACD carriers. In UKB, TINF2 carriers hadsignificantly increased risk for melanoma (OR 5.33 (1.93-14.70); p=0.015), endocrine cancers(OR 25.30 (9.16-69.87); p<0.001), and mesothelioma (OR 18.38 (2.47-137.02); p=0.036) anddemonstrated overall earlier ages at cancer onset than noncarriers (p=0.0036). In Geisinger,TINF2 was associated with increased risk of cancers of soft tissue including heart (OR 6.76 (1.65-27.60); p=0.01), liver/ bile duct (OR 3.28 (1.03-10.50); p=0.05), and brain/nervous system(OR 5.19 (1.89-14.20); p<0.001). In Geisinger, ACD carriers with c.488A>G had an increasedrisk of eye and orbit cancers (OR 15.27 (2.10-111.00); p=0.007), although there was only onecarrier. The number of cancer events among individuals with TERF1, TERF2, and TERF2IPvariants was insufficient for statistical analyses.
Conclusion: In Geisinger, prevalence of rare P/LP shelterin gene variants was generally higherthan in UKB, reflecting the clinically enriched nature of that cohort. TINF2 had variants with thestrongest cancer associations. Longitudinal studies of younger cohorts are warranted to refineprevalence estimates and cancer risk associated with shelterin complex genes.

#3598 Investigating divergent ER$^+$and ER$^-$breast cancer subtype risks by using oppositely associated genetic variants.

Phillip Schofield[1], Meghana Pagadala[2], Timothy Sears[2], Hannah K. Carter[2]

[1]UC San Diego School of Medicine, La Jolla, CA,[2]UC San Diego, La Jolla, CA

Breast cancer is the second most common cause of cancer-related deaths among women in the United States, with its incidence increasing each year. Estrogen receptor-negative (ER$^-$) breast cancers are particularly aggressive and less responsive to conventional treatments compared to estrogen receptor-positive (ER$^+$) types, though they exhibit higher immunogenicity and better responses to immunotherapies. This study focuses on identifying single nucleotide polymorphisms (SNPs) that are oppositely associated between ER$^+$ and ER$^-$ breast cancers, meaning that the presence of a SNP increases the risk of one subtype while decreasing the risk of the other subtype. We identified 481 SNPs from the Breast Cancer Association Consortium (BCAC) that were oppositely associated between subtypes ($p < 0.1$) and cross-validated these associations using data from breast cancer patients in The Cancer Genome Atlas (TCGA), imputed using the TOPMED imputation server. Our findings revealed 45 SNPs associated with increased ER$^+$ risk but decreased ER$^-$ risk and 2 SNPs associated with increased ER$^-$ risk but decreased ER$^+$ risk that were concordant between the BCAC and TCGA datasets. Of the concordant SNPs that increased ER$^+$ risk, the majority mapped to a region of chromosome 11 near the known tumor suppressor gene *ATM;* however, one SNP on chromosome 10 (10:21471086:C/T) has been previously shown to increase circulating IGF-1 and decrease colorectal cancer risk to a greater extent in women than men. Further analysis using the CIBERSORTx tool showed that this SNP was associated with increased infiltration of perivascular-like immature cells in the tumor microenvironment. Of the SNPs that increased ER$^-$ risk, one localized to a poorly described antisense non-coding transcript of the *DLX2* gene which has been implicated in breast cancer, while the other localized to an intron of the *PTPRN2* gene that is implicated in type 1 diabetes mellitus and many cancers. While this study is limited by its focus on European women and the small sample size of ER$^-$ cases, the results offer preliminary insight into inherited variants that may differentially influence ER$^+$ and ER$^-$ disease, supporting future work aimed at clarifying the pathways that contribute to subtype-specific risk, immune infiltration, and treatment response.

#3599 MYC exon 3 DNA methylation in peripheral blood and the risk of aggressive prostate cancer in the prostate, lung, colorectal, and ovarian cancer screening trial.

Patricia A. Erickson[1], Lauren M. Hurwitz[2], Soren M. Bentzen[3], Stella Koutros[2], Liying Yan[4], Matthew L. Poulin[4], Ann Meyer[4], Allen Burke[3], Arif Hussain[3], Sonja I. Berndt[2], **Kathryn Hughes Barry**[3]

[1]Huntsman Cancer Institute, Salt Lake City, UT,[2]National Cancer Institute, Rockville, MD,[3]University of Maryland School of Medicine, Baltimore, MD,[4]EpigenDx, Inc., Hopkinton, MA

Introduction*:* Our group previously reported that higher DNA methylation at two CpG sites in *MYC* exon 3 in peripheral blood was associated with a higher risk of aggressive prostate cancer (Barry et al, *Br J Cancer* 2017). Here we aimed to assess if our findings for these CpG sites would replicate in an independent group of men.

Methods*:* Using pre-diagnostic blood samples, we conducted a nested prostate cancer case-control study among non-Hispanic White men in the Prostate, Lung, Colorectal, and Ovarian (PLCO) Cancer Screening Trial who were not included in our previous study in PLCO. Cases comprised 251 men who were diagnosed with incident aggressive prostate cancer (stage III or IV or a total Gleason score>=8), and controls comprised 497 men without a previous history of prostate cancer. The controls were individually matched to the cases on several factors, including age at blood draw (+/- 3 yrs), calendar year of blood draw (+/- 3 years), study year of blood draw, sample type (i.e., whole blood or buffy coat), and the source of the DNA (i.e., available DNA from previous genotyping efforts in PLCO or new extractions). Percent DNA methylation at the CpG sites of interest in the exon 3 region of *MYC*, denoted as CpG 214 (GRCh37/hg19 coordinate: Chr8:128753154) and CpG 215 (Chr8:128753187), was quantified using pyrosequencing on bisulfite-treated DNA. We used conditional logistic regression to estimate odds ratios (OR) and 95% confidence intervals (95% CI) for DNA methylation levels, modeled as a continuous variable, in relation to aggressive prostate cancer. We also conducted a meta-analysis to combine the results from our two studies (total of 423 aggressive prostate cancer cases).

Results*:* For both CpG 214 and 215, we observed an elevated risk of aggressive prostate cancer with each unit increase of DNA methylation (for CpG 214, OR=1.05, 95% CI: 0.99-1.12, and for CpG 215, OR=1.03, 95% CI: 0.97-1.09). We observed similar patterns that were statistically significant for both CpG sites when meta-analyzing these results with our previous study (for CpG 214, OR=1.06, 95% CI: 1.02-1.10, and for CpG 215, OR=1.05, 95% CI: 1.01-1.10).

Conclusions: Adding to the literature on the role of *MYC* in prostate carcinogenesis, findings support that higher pre-diagnostic DNA methylation levels in *MYC* exon 3 in peripheral blood are associated with a higher risk of aggressive prostate cancer among non-Hispanic White men. Further study is needed in more diverse populations.

#3600 Pan-cancer genome-wide study reveals shared genetic architecture and novel pleiotropic variants across seven solid cancers.

Xunxuan Chen[1], Gamaliel T. Taengwa[2], Brandon J. Coombes[2], Stacey J. Winham[2]

[1]Cancer Biology, Keck School of Medicine, University of Southern California, Los Angeles, CA,[2]Quantitative Health Sciences, Mayo Clinic, Rochester, MN

Genome-wide association studies (GWAS) have identified thousands of genetic variants associated with individual cancer risk, and polygenic risk scores (PRS) are typically derived from these cancer-specific variants. Although previous pan-cancer studies revealed shared genetic architectures across cancer types, latent factors contributing to cancer risk have not been explored. This may allow for improved prediction of cancer risk based on a latent cancer factor which leverages shared variants across cancers. Here, we conducted an integrative pan-cancer GWAS across seven solid tumors (breast, ovarian, endometrial, pancreatic, lung, colorectal, melanoma) to identify shared latent genetic factors and novel pleiotropic variants. We curated the most recent and large-scale GWAS summary statistics to maximize statistical power, comprising 398,917 cases and 1,501,715 controls of European ancestry. Shared genetic structures among 6,346,960 common variants were evaluated using Genomic Structural Equation Modeling (GenomicSEM). Three latent factors (Common Cancer Factor, Female-Specific Cancer Factor and Non-Sex Specific Cancer Factor) were constructed, and associations of individual variants with each latent factor were estimated. Genome-wide significant loci ($p < 5x10^{-8}$) were functionally annotated and subjected to pathway enrichment analysis. Models capturing shared genetic risk across cancers fit the data well. A single “Common Cancer Factor” explained much of the shared risk (SRMR = 0.064 [lower is better], CFI = 0.938 [closer to 1 is better]), and a correlated two-factor model—distinguishing female-specific from other cancers—showed even stronger fit and biological relevance (SRMR = 0.055, CFI = 0.988). The one-factor (Common Cancer Factor; SRMR: 0.064, CFI: 0.938, AIC: 54.7, p_chisq: 0.021) and the two-factor (Female-Specific Cancer Factor and Non-Sex Specific Cancer Factor; SRMR: 0.055, CFI: 0.988, AIC: 45.4, p_chisq: 0.281) models demonstrated robust model fit and biological relevance. Factor-specific GWAS identified 233 genome-wide significant loci ($p < 5x10^{-8}$) with 24 distinct loci showing shared susceptibility across cancers. More importantly, we identified eight novel variants that were not previously reported or related with any cancer risk, potentially regulating cancer-related genes such as *PRC1*, *CEBPB*, *SMC2*, *KLF5* and *ATXN2*. Further analyses are needed to elucidate their roles in tumorigenesis. Our findings reveal a shared genetic architecture across major solid tumors and uncover novel pleiotropic variants with potential regulatory roles in oncogenesis. This study provides novel insights into the genetic basis of cancer susceptibility and supports the development of multi-cancer PRS to improve prediction in cancer prevention and prognosis.

#3601 Multi-population GWAS meta-analysis identifies novel bladder cancer susceptibility loci and highlights the genetic regulation of smoking-related risk.

Ludmila Prokunina-Olsson[1], Oscar Florez-Vargas[1], Michael G. Levin[2], Diptavo Dutta[1], Charles Breeze[1], Lauren M. Hurwitz[1], Wusheng Yan[1], Philippe Lamy[3], Brenen Papenberg[1], Kevin Wang[1], Chia-Han Lee[1], Roger L. Milne[4], Jian Gu[5], Caroline Y. Um[6], Vijai Joseph[7], Helena Furberg[7], Florence Le Calvez-Kelm[8], Chikashi Terao[9], Koichi Matsuda[10], Francisco X. Real[11], Lambertus A. Kiemeney[12], Stephen J. Chanock[1], Nuria Malats[11], Debra T. Silverman[1], Lars Dyrskjot[3], Nathaniel Rothman[1], Scott M. Damrauer[2], Stella Koutros[1], Jeffrey S. Damrauer[13]

[1]National Cancer Institute, Rockville, MD,[2]University of Pennsylvania, Philadelphia, PA,[3]Aarhus University, Aarhus, Denmark,[4]Cancer Council Victoria, Melbourne, Australia,[5]University of Texas MD Anderson Cancer Center, Houston, TX,[6]American Cancer Society, Atlanta, GA,[7]Memorial Sloan Kettering Cancer Center, New York, NY,[8]International Agency for Research on Cancer, Lyon, France,[9]Riken, Yokohama, Japan,[10]University of Tokyo, Tokyo, Japan,[11]Spanish National Cancer Research Center (CNIO), Madrid, Spain,[12]Professor, Dept. of Epidemiology, Radboud University Nijmegen Medical Center, Nijmegen, Netherlands,[13]UNC Lineberger Comprehensive Cancer Center, Chapel Hill, NC

Urinary bladder cancer (BC) is the ninth most common malignancy worldwide. We conducted a meta-analysis of genome-wide association studies for BC risk in 32,470 cases and 1,753,462 controls, identifying 70 independent genome-wide significant loci, including 43 novel signals. A 70-marker polygenic risk score was strongly associated with BC risk (hazard ratio=1.61 (1.50-1.73) per standard deviation), substantially improving the area under the curve (AUC) when added to a model with age, sex, and smoking status (AUC=0.75 vs. 0.70, p=4.49E-20). BC risk variants (n=4,196 at p<5.0E-8) were enriched in regions of open chromatin in bladder tissue. Integrated germline, transcriptomic, and proteomic analyses nominated additional susceptibility genes and pathways, particularly related to xenobiotic metabolism. We detected a novel BC signal within a known smoking-related locus at 15q25.1 (rs7173514-C, OR=1.07, p=9.64E-10 for BC risk overall, $OR_{Never\text{-}Smoker}$=1.00 and $OR_{Ever\text{-}Smoker}$=1.14). This signal was primarily driven by an insertion/deletion variant within *CHRNA3*-3'UTR rs71581744/rs10637216 (A/ACCCC, r^2=0.78 with rs7173514 in Europeans) linked with smoking cessation, with an additional contribution from a known lead variant for smoking intensity (rs16969968-G/A, D398N within *CHRNA5*). Further analyses revealed significant heterogeneity for rs71581744 by BC subtype (muscle-invasiveness), particularly among current smokers ($OR_{Muscle\ Invasive}$=1.42 vs. $OR_{Non\text{-}muscle\ Invasive}$=1.11, $p_{heterogeneity}$=1.84E-02), consistent with epidemiologic observations that current smokers have a higher risk of muscle-invasive bladder cancer. Our *in-vitro* reporter assays for rs71581744-A/ACCCC demonstrated allele-specific effects on mRNA stability in several cell lines. Since neuronally expressed *CHRNA5* and *CHRNA3* encode subunits of the nicotinic acetylcholine receptors (nAChR) that regulate smoking behavior, we investigated their expression in normal brain tissues in GTEx. The BC risk signal colocalized with a top CHRNA3 eQTL in one brain area, with variable allelic expression imbalance for *CHRNA3* in several brain areas from the same donors. Our results implicate rs71581744-A/ACCCC as a functional variant contributing to BC risk via regulation of *CHRNA3* mRNA stability in specific brain areas, affecting nicotine reward/aversion circuits and possibly bladder function. Overall, our study provides new insights into BC genetics and etiology with relevant clinical implications.

#3602 Genome-wide association study of mantle cell lymphoma identifies novel loci suggesting a critical role for B-cell chromatin readers and DNA repair mechanisms.

Charles E. Breeze[1], Alyssa Clay-Gilmour[2], Hanla A. Park[3], Olafur B. Davi?sson[4], Angelica Macauda[5], Brenda M. Birmann[6], Elizabeth E. Brown[7], Murat Guler[8], Michelle A. T. Hildebrandt[9], Alexandra Nieters[10], Krystle Ong[11], Jojo Biel-Nielsen Dietz[12], Karin E. Smedby[13], Karl Smith-Byrne[14], Rosalie Griffin[15], Sophia S. Wang[16], Susan Slager[5], James R. Cerhan[5], Jonathan N. Hofmann[1], Qing Lan[1], Nathaniel Rothman[1], Ingrid Glimelius[17], Henrik Hjalgrim[12], James Mckay[3], Sonja I. Berndt[1]

[1]National Cancer Inst. Div. of Cancer Epidemiology & Genetics, Bethesda, MD,[2]University of South Carolina Arnold School of Public Health, Columbia, SC,[3]International Agency for Research on Cancer, Lyon, France,[4]Danish Cancer Society, Copenhagen, Denmark,[5]Mayo Clinic, Rochester, MN,[6]Dept of Medicine, Brigham and Women's Hospital, Boston, MA,[7]University of Alabama at Birmingham, O'Neal Comprehensive Cancer Center, Birmingham, AL,[8]German Cancer Research Center DKFZ, Heidelberg, Germany,[9]UT MD Anderson Cancer Center, Houston, TX,[10]Universitatsklinikum Freiburg, Freiburg, Germany,[11]University of Alabama at Birmingham, Birmingham, AL,[12]Danish Cancer Institute, Copenhagen, Denmark,[13]Karolinska Institutet, Stockholm, Sweden,[14]University of Oxford Nuffield Department of Population Health, Oxford, United Kingdom,[15]MD Anderson Cancer Center, Houston, TX,[16]City of Hope National Medical Center, Duarte, CA,[17]Uppsala University, Uppsala, Sweden

Background: Mantle cell lymphoma (MCL) is an aggressive and rare B-cell non-Hodgkin lymphoma with poor prognosis, even with treatment. Despite its clinical importance, the etiology of MCL remains largely unknown. Some studies have reported a positive association with family history, suggesting that genetic factors could contribute to risk. **Methods:** To identify germline genetic variants associated with risk, we conducted the first genome-wide association studies (GWAS) and GWAS meta-analysis for MCL, comprising 1,163 cases and 61,271 controls. The most significant loci were taken forward for replication in three independent studies, including 576 cases and 771,773 controls. To identify potential target genes and pathways of discovered loci, we conducted F-MAGMA, colocalization, and transcriptome-wide association study (TWAS) analyses. To gain insight into underlying regulatory mechanisms, we performed integrative epigenomic analyses using DNase I hotspots and histone mark ChIP-seq data across diverse cell types applying the FORGE2 framework. **Results:** In the joint analyses, we identified eight genome-wide significant loci ($P<5x10^{-8}$) associated with MCL risk, several of which were located near genes with known DNA repair (ATM), telomere (TERT), or RNA-binding functions (RBM20). Further analyses using F-MAGMA, which uses DNase-seq data to prioritize genes from GWAS, identified genes that were significantly associated with risk, including SP140, a chromatin reader and immune regulator of pathogen response. This gene also displayed strong colocalization with our lead variant in whole blood (COLOC posterior probability PP4=0.97). TWAS demonstrated significant associations with SP140 and ACTA2, which has been linked to cell proliferation ($P<3x10^{-6}$). Enrichment for DNase I hotspots was observed in B and T lymphocytes (q-value<0.05), providing evidence for a role in immune cell-specific regulatory regions. Enrichment for enhancer-associated histone mark H3K4me1 was observed in B cells (q-value<0.01), highlighting a role for immune cell-specific enhancers. Transcription factor (TF) motif enrichment analysis pointed to TFs critical for B-cell development and differentiation, notably TCF3 and EP300 (q<0.01 for both), suggesting an association between B-cell lineage regulation and MCL risk. Finally, genome-wide SNP-based heritability was estimated to be 17%, underscoring the importance of common variants in MCL risk. **Conclusion:** Our study provides novel insight into the inherited susceptibility of MCL by identifying eight significant loci and estimating substantial common variant heritability. These findings highlight a role for several distinct biological pathways -specifically DNA repair, telomerase function, and B-cell differentiation- in the etiology of MCL, offering new targets for mechanistic investigation.

#3603 Implications of multiple myeloma polygenic risk scores (PRS) for MGUS.

Alyssa Ione Clay-Gilmour[1], Angelica Macauda[2], Cristine Allmer[2], Danelle Moonen[2], Aaron D. Norman[2], Nicholas Boddicker[2], Janet E. Olson[2], Elizabeth E. Brown[3], Vincent S. Rajkumar[2], Esteban Braggio[4], David Murray[2], Susan Slager[2], Shaji Kunnathu Kumar[5], Celine Vachon[6]

[1]University of South Carolina, Columbia, SC,[2]Mayo Clinic, Rochester, MN,[3]University Alabama Birmingham, Birmingham, AL,[4]Mayo Clinic Arizona, Scottsdale, AZ,[5]Professor of Medicine, Dept. of Hematology, Mayo Clinic, Rochester, MN,[6]Mayo Clinic College of Medicine and Science, Rochester, MN

Background. Genome-wide association studies (GWAS) have identified 35 genetic susceptibility single-nucleotide polymorphisms (SNPs) for multiple myeloma (MM) in individuals of European ancestry (EA) and shown strong genetic correlation between MM and its precursor, monoclonal gammopathy of undetermined significance (MGUS). We evaluate the contribution of the 35 MM variants to MGUS susceptibility overall and by prognostic subgroups.

Methods. The study included 20,756 participants (14,486 controls, 1,883 with MGUS, and 2,163 with MM) from the Mayo Clinic. Logistic regression assuming an additive model estimated odds ratios (ORs) and 95% confidence intervals (CIs) for individual SNPs and for the MM-PRS, adjusted for age, sex, study, and principal components. The PRS was a weighted sum of 35 SNPs with effect estimates from the largest MM GWAS and was modeled continuously (per SD) and by quintiles (Q1-Q5). SNPnexus annotated variants that replicated in MGUS ($P < 0.05$ and $OR > 1.01$) versus those that did not ($P > 0.05$ and $OR < 1.01$).

Results. The 35-SNP MM-PRS was strongly associated with MM risk and modestly with MGUS. Compared with the middle quintile (Q3), MM odds rose from OR=0.55 (CI=0.46-0.65, $P=2.2e^{-11}$) in Q1 to OR = 1.82 (CI=1.59-2.09, $P=6.2e^{-18}$) in Q5. MGUS showed a similar, attenuated pattern (Q1 OR = 0.74, CI=0.64-0.84, $P=6.4e^{-6}$ / Q5 OR=1.36, CI=1.21-1.53, $P=3.4e^{-7}$). Each SD increase in PRS corresponded to OR=1.52 (CI=1.45-1.59, $P=1.3e^{-66}$) for MM and OR = 1.22 (CI=1.18-1.27, $P=1.0e^{-23}$) for MGUS. Higher PRS values were linked to larger M-protein ((0.1-1.5 g/dL: OR=1.40, CI=1.18-1.65, $P=5.8e^{-12}$) vs <0.1 g/dL: OR = 1.19, CI=1.13-1.24, $P=5.8e^{-12}$)) and abnormal free light chain (FLC) ratio ((OR = 1.33, CI=1.21-1.46, $P=1.0e^{-9}$) vs normal ratio (OR=1.19, CI=1.14-1.25, $P=1.4e^{-13}$)). Ten risk loci replicated in MGUS, mapping to genes involved in plasma-cell function, immune regulation, and DNA repair and enriched for Rho GTPase signaling, NF-κB-mediated apoptosis, and RNA polymerase II transcription, implicating early plasma-cell activation and transcriptional control. The 12 non-replicating loci, including *PHC3*, *ATG5*, and *NFIC*, mapped to genes involved in chromatin remodeling, autophagy, and SUMOylation, suggesting roles in stress response and genomic maintenance.

Conclusions. The MM-PRS captures shared heritability between MM and MGUS and correlates with MGUS subtype and severity. Replicating variants highlight immune and cell-cycle pathways relevant to MGUS onset, whereas non-replicating loci cluster in DNA-repair and stress-response processes, underscoring their potential role in progression.

#3604 Prostate cancer risk variants regulate oncogenes by activating enhancers and forming multi-connected enhancer-promoter hubs at different stages of prostate cancer.

Zexun Wu[1], Andrew Vu[2], Matthew Salcedo[1], Suhn K. Rhie[2]

[1]Keck School of Medicine, USC, Los Angeles, CA,[2]USC, Los Angeles, CA

Prostate cancer (PCa) is a complex disease and the second leading cause of cancer death in the US men. Clinical outcomes vary among PCa stages. PCa becomes increasingly aggressive, progressing from localized disease to metastatic PCa, then to metastatic castration-resistant PCa and ultimately to neuroendocrine PCa. Multi-ethnic genome-wide association studies have identified over a thousand of genetic variants associated with PCa risk, including variants linked to aggressive forms of the disease. Considering population-specific linkage disequilibrium patterns, we identified over 40,000 highly linked variants to PCa risk variants. However, most of these variants reside in non-coding regions, making it challenging to elucidate their roles in disease development and progression. Non-coding regions often include functional elements called regulatory elements such as promoters, enhancers, and insulators. Among regulatory elements, enhancer activities, which can be assessed by the histone modification mark H3K27ac, are tightly associated with cell fate. We therefore hypothesized that PCa risk variants affect enhancer activities at distinct disease stages, contributing to disease development and progression, and ultimately influencing clinical outcomes. In this study, we integrated over 200 H3K27ac ChIP-seq and over 550 RNA-seq datasets from prostate tissues and cell lines across PCa progression stages and found stage-specific enhancers and transcription factors (TFs) that are distinctly activated at different stages. Moreover, we found over 5,500 PCa risk variants located in enhancers containing motifs of the identified TFs. To evaluate the PCa risk variants associated with enhancer activities, we integrated patient tissue-derived H3K27ac ChIP-seq data and performed chromatin quantitative trait loci and allelic imbalance analyses. We identified over 700 variants associated with enhancer activities, including those affected by TF binding. Moreover, to identify target genes of these enhancer variants, we analyzed over 100 genome-wide chromatin interaction datasets. By integrating chromatin interaction data with epigenomic and transcriptomic data, we identified enhancer variants involved in chromatin looping to regulate transcription. Furthermore, we found over 1,700 enhancer variants located in multi-connected enhancer-promoter (E-P) hubs, including those potentially regulated by stage-specific TFs. Overall, these findings support a model in which genetic and epigenetic reprogramming converge on E-P hubs to drive transcription of oncogenes and promote disease initiation and progression in PCa.

#3605 Genetic insights into metabolic traits and prostate cancer susceptibility: A two sample Mendelian Randomization study.

HWA SUN KIM, Chung-woo Lee

VHS Medical Center, Seoul, Korea, Republic of

Background: Metabolic syndrome (MetS) and its components have been implicated in prostate cancer, but observational associations remain inconsistent and vulnerable to confounding. We conducted a two-sample Mendelian randomization (MR) study to clarify whether major MetS traits causally influence prostate cancer risk.

Methods: Genetic instruments for body mass index (BMI), waist circumference, systolic/diastolic blood pressure, fasting glucose, and lipid components such as triglycerides (TG), LDL-cholesterol, HDL-cholesterol, and total cholesterol were obtained from male-only large genome-wide association studies (UK Biobank) and MetS from multiple cohorts as exposure sets. Prostate cancer data set was derived from the FinnGen GWAS. Genome-wide significant variants ($p<5\times10^{-8}$) were clumped at $r^2<0.001$. Causal estimates were calculated using inverse-variance weighted (IVW), weighted median, and MR-Egger methods. Heterogeneity (Cochran's Q), horizontal pleiotropy (MR-Egger intercept, MR-PRESSO), and sensitivity analyses were performed.

Results: Higher genetically predicted fasting glucose was associated with reduced prostate cancer risk (OR 0.82, P=0.02). HDL-cholesterol (OR 1.52, P=0.052) and LDL-cholesterol (OR 0.87, P=0.07) showed suggestive effects. BMI, waist circumference, blood pressure, total cholesterol, and triglycerides showed no evidence of causal association.

Conclusions: Our findings implicate glucose and lipid metabolism pathways in prostate cancer susceptibility. Given the exploratory nature and the predominantly European ancestry of the datasets, large scale studies including diverse multiple-ethnic populations are required to confirm these associations and clarify the role of metabolic traits across different ancestries in prostate cancer epidemiology.

#3606 Identification of survival-associated germline variants in hepatocellular carcinoma.

Younghun Han[1], Jinyoung Byun[1], Lewis R. Roberts[2], Katherine A. McGlynn[3], Manal M. Hassan[4], Christopher I. Amos[1]

[1]University of New Mexico Comprehensive Cancer Center, Albuquerque, NM,[2]Mayo Clinic College of Medicine and Science, Rochester, MN,[3]National Cancer Institute - Cancer Genomics Research Laboratory (CGR), Rockville, MD,[4]Assistant Professor, Dept. of Gastrointestinal Medical Oncology, UT MD Anderson Cancer Center, Houston, TX

Background: Hepatocellular carcinoma (HCC) remains a leading cause of cancer-related mortality worldwide. Prognostic models for HCC primarily rely on tumor burden and liver function, with limited consideration of inherited genetic contributions to survival variability. Identifying germline variants associated with survival could refine prognosis and reveal biological mechanisms underlying disease progression.

Methods: We conducted a genome-wide association study (GWAS) of overall survival among 864 patients with HCC from the M.D. Anderson Cancer Center cohort. Genotyping, quality control, and imputation procedures followed previously described protocols (PMID: 38381705). Associations between genetic variants and overall survival were assessed using Cox proportional hazards models adjusted for age, sex, and the first five principal components. Genome-wide significance was defined as $P < 5\times10^{-8}$. Functional annotation and pathway enrichment analyses (MAGMA) were employed to investigate the biological relevance of the identified loci.

Results: After quality control, 8,525,017 single-nucleotide polymorphisms (SNPs) were analyzed. We identified seven new loci associated with HCC survival at the genome-wide significance level. Five out of seven loci are associated with anthropometric traits and hematological measurement traits, reflecting metabolism, hematopoiesis, immune function, and inflammation. A variant in the 3′ untranslated region (UTR3) of *STX7* showed a genome-wide significant association with overall survival (HR = 3.23; $P = 2.56 \times10^{-8}$). Carriers of the risk allele had significantly shorter survival times compared with noncarriers. Pathway analysis revealed enrichment in biologically relevant processes, including liver growth and regeneration (growth hormone and Interleukin-6 (IL-6) signaling pathway), implicating hepatocyte proliferation and IL-6/STAT3-mediated inflammatory signaling. Immune-related pathways, such as regulation of T cell activation and myeloid leukocyte migration, highlight the role of germline variation in immune surveillance. Moreover, pathways governing vascular remodeling and metabolic stress response (e.g., JAK activation, mitochondrial dynamics) suggest that inherited determinants of microenvironmental structure and hepatocyte resilience influence patient outcomes.

Conclusion: This germline GWAS of HCC survival identifies seven new genome-wide significant loci and implicates pathways involved in liver regeneration, inflammation, and tissue remodeling. These findings support a role for inherited genetic variation in shaping HCC prognosis and underscore the potential of integrating germline genetics into prognostic modelling and therapeutic target discovery.

#3607 Tissue-based proteome-wide association study identifies novel risk proteins and candidate drug targets for colorectal cancer.

Qing Li[1], Timothy Su[1], Chao Li[2], Quanhu Sheng[3], Shuai Xu[2], Wanqing Wen[4], Qi Dai[4], Martha J. Shrubsole[4], Jirong Long[4], Qiuyin Cai[1], Bing Zhang[5], Xioa-Ou Shu[1], Bhuminder Singh[1], Ken S. Lau[1], You Chen[6], Yuankai Huo[7], Zhijun Yin[1], Stephen B. Gruber[8], Riki (Ulrike) Peters[9], Victor R. Moreno[10], Wei Zheng[1], Xingyi Guo[1]

[1]Vanderbilt University Medical Center, Nashville, TN,[2]Vanderbilt University, Nashville, TN,[3]Department of Biostatistics, Vanderbilt University Medical Center,, Nashville, TN,[4]Department of Medicine, Vanderbilt University Medical Center, Nashville, TN,[5]Baylor College of Medicine, Houston, TX,[6]Department of Biomedical Informatics, Vanderbilt University Medical Center, Nashville, TN,[7]Department of Computer Science, Vanderbilt University, Nashville, TN,[8]City of Hope National Medical Center, Los Angeles, CA,[9]Fred Hutchinson Cancer Center, Seattle, WA,[10]Cancer Prevention Program, Catalan Institute of Oncology, Hopitalet de Llobregat, Spain

Background Colorectal cancer (CRC) is the second leading cause of cancer-related death worldwide. To date, ~250 genetic risk loci have been identified through genome-wide association studies (GWAS), and transcriptome-wide association studies (TWAS) has implicated ~500 putative CRC risk genes. However, proteins, the primary effectors of cellular function and drug response, remain underexplored. Thus, proteome-wide association studies (PWAS) linking genetic variation to protein abundance in colorectal tissue are essential for identifying causal proteins, clarifying disease mechanisms, and discovering therapeutic targets.

Methods We performed unbiased data-independent acquisition mass spectrometry on 323 normal colon tissues from the Tennessee Colorectal Polyp Study and BarcUVa-seq studies, quantifying >9,000 proteins, and generated matched blood genotypes. Protein preprocessing included low-abundance filtering, $\log_2$ transformation, and PEER adjustment. We conducted PWAS using our previously developed approach which integrates susceptible TF occupied cis-regulatory elements (PMID: 36402776) to build genetically predicted protein expression models and applied to two CRC GWAS datasets separately: (1) European ancestry (80,774 cases, 105,298 controls) and (2) a trans-ancestry meta-analysis (104,346 cases, 153,998 controls). Risk proteins were identified by combining results from both datasets. We performed pQTL analyses of known CRC lead variants (PMID: 38670944), followed by Bayesian colocalization, and evaluated therapeutic relevance by mapping CRC-associated proteins to drug-target interactions using DrugBank, ChEMBL, TTD, and Open Targets.

Results At a Bonferroni-corrected threshold of $P < 0.05$, our PWAS identified 41 proteins significantly associated with CRC risk, including 12 not previously linked to CRC. pQTL analyses identified 14 risk proteins, five with strong colocalization (PP.H4 > 0.8). We also found support for 76 previously reported CRC risk genes based on PWAS or pQTL signals at nominal $P < 0.05$. Among all risk proteins, 13 were potentially druggable, linked to 235 candidate therapeutic compounds. We provided the genetic evidence supporting multiple potential therapeutic drug targets for CRC prevention, with drug-protein interactions mapped to key CRC-relevant pathways such as PGE_2-EP4 signaling (e.g., PTGER4 protein inhibitor E7046, Phase I/II), redox homeostasis (TXN protein inhibitor PX-12, Phase II; ALDH2 approved inhibitor Disulfiram), and BET signaling (BD2-selective inhibitor ABBV-744, Phase I).

Conclusion This study provides the first large-scale tissue-based PWAS in CRC, identifying novel risk proteins and multiple potential druggable targets. These findings advance our understanding of CRC etiology and highlight new opportunities for therapeutic development and CRC prevention.

#3608 Multi-ancestry methylation-wide association analyses identifies putative risk methylation markers for breast cancer.

Shuai Xu[1], Jiajun Shi[2], Y-Thanh Lu[1], Guochong Damon Jia[2], Fei Ye[3], Qiuyin Cai[2], Jirong Long[4]

[1]Vanderbilt University, Nashville, TN,[2]Vanderbilt University Medical Center, Nashville, TN,[3]Vanderbilt University School of Medicine, Nashville, TN,[4]Asst. Professor, Dept. of Epidemiology, Vanderbilt University, Nashville, TN

Introduction: Aberrant DNA methylation is a hallmark of cancer. Identifying methylation sites (CpGs) associated with breast cancer risk may help to elucidate disease mechanisms and inform precision prevention. We conducted a multi-ancestry breast tissue-based methylome-wide association study (MeWAS) to discover breast cancer susceptibility CpGs.
Methods: We profiled DNA methylation in normal breast tissue from 152 African ancestry and 267 European ancestry women using the Illumina MethylationEPIC array, with matched genotype data. We trained ancestry-specific genetic prediction models for each methylation marker, and then tested associations with breast cancer risk by applying S-PrediXcan to ancestry-matched breast cancer GWAS summary statistics (European:133,384 cases and 113,789 controls; African :18,044 cases and 22,187 controls)). We also performed stratified analyses by estrogen receptor status (ER+, ER–) and triple-negative breast cancer (TNBC). Then fixed effect inverse variance weighted meta-analysis was conducted using METAL. Methylation set enrichment analysis was evaluated using R missMethyl.
Results: We successfully built 160,204 African ancestry and 166,069 European ancestry methylation imputation models ($R > 0.1$ and $P < 0.05$). Meta-analysis across ancestries identified 625 CpGs whose genetically predicted methylation levels were significantly associated with overall breast cancer risk (Bonferroni-adjusted $P < 0.05$), 458 (73.3%) of which have not been reported in prior breast tissue MeWAS. Notably, the significant association between genetically proxied methylation levels of cg23766285 and overall breast cancer risk were only observed among African Ancestry. Among 308 CpGs with valid prediction models in both ancestries, 265 (86.0%) showed concordant directions of association. We additionally identified 32, 11, and 11 CpGs that were exclusively associated with risk of ER+ and ER- breast cancer and TNBC at Bonferroni corrected $P <0.05$, respectively. CpGs associated with overall risk (odds ratio [OR], 1.19; 95% confidence interval [CI], 1.02-1.39), ER- breast cancer (OR, 1.97; 95% CI, 1.29-3.05), and TNBC (OR, 2.12; 95% CI, 1.27-3.61) were enriched in promoter regions, whereas ER+-associated CpGs were not. The identified CpGs are involved in various biological processes, including hormone, p53, and KRAS signaling pathways.
Discussion: This is the first multi-ancestry, large-scale, tissue-based MeWAS in breast cancer. Our findings offer novel insight into breast carcinogenesis and breast cancer disparities.

#3609 Identification of miRNA-related SNPs associated with kidney cancer in the Korean population.

Jung-Hee Lee[1], Minsun Jung[1], Sun Ha Jee[2]

[1]Yonsei University College of Medicine, Seoul, Korea, Republic of,[2]Department of Epidemiology and Health Promotion, Institute for Health Promotion, Graduate School of Public Health, Yonsei University, Seoul, Korea, Republic of

Background: MicroRNAs (miRNAs) are small non-coding RNAs that regulate gene expression post-transcriptionally and play critical roles in tumor development. Genetic variants located within miRNA precursor, mature, or seed regions may influence miRNA maturation or target binding, thereby affecting cancer susceptibility. This study aimed to identify miRNA-related single nucleotide polymorphisms (SNPs) associated with kidney cancer in a Korean population.

Methods: We performed genome-wide association analyses of kidney cancer in the Korean population using datasets from the Korean Cancer Prevention Study-II (KCPS-II) and the Korean Genome and Epidemiology Study (KOGES). A subsequent meta-analysis identified three miRNA-related single nucleotide polymorphisms (SNPs) significantly associated with kidney cancer. miRNA-related variants were annotated based on their location within pre-miRNA, mature miRNA sequences, or seed regions using the miRNASNP-v4 database. Functional relevance was interpreted according to predicted effects on miRNA biogenesis and target-binding specificity.

Results: miRNA-related SNPs showed genome-wide significant associations with kidney cancer. The pre-miRNA variant **rs1414273**, located in the hairpin of hsa-mir-548ac, demonstrated a strong association (effect = -1.1112, SE = 0.0498, P = 3.46×10^{-110}). This variant may alter Drosha processing efficiency, thereby affecting the production of miR-548ac. Because miR-548ac regulates genes involved in inflammatory signaling and protein quality-control pathways, disruption of its maturation may influence cellular stress responses relevant to renal tumorigenesis. The mature miRNA variant **rs73239138**, positioned within hsa-miR-1269a, showed a similarly robust association (effect = 1.076, SE = 0.0491, P = 1.71×10^{-106}). miR-1269a is an oncogenic miRNA overexpressed in at least nine cancers and regulates key targets (CXCL9, SOX6, FOXO1, ATRX, RASSF9, SMAD7, HOXD10, VASH1) through pathways such as TGF-β, PI3K/AKT, p53, and caspase-9 signaling; thus, a sequence alteration within its mature strand may affect RISC loading, target recognition, and amplify oncogenic post-transcriptional regulation in kidney cancer. The seed-region variant **rs2925980** in hsa-miR-7854-3p also reached genome-wide significance (effect = -1.0276, SE = 0.0494, P = 5.1×10^{-96}). Seed mutations can reprogram target specificity by creating or disrupting binding sites, suggesting that altered miR-7854-3p targeting contributes to renal cancer susceptibility.

Conclusions: These findings indicate that pre-miRNA, mature miRNA, and seed-region variants contribute to kidney cancer susceptibility in the Korean population. The identified SNPs provide a basis for functional validation and the development of miRNA-based biomarkers in kidney cancer.

#3610 Estrogen receptor-mediated pharmacogenomic eQTLs as predictors of endocrine therapy response in breast cancer.

Martin Meng, Huanyao Gao, August John, Arnab Ghosh, Shreya Indulkar, Liewei Wang

Mayo Clinic College of Medicine, Rochester, MN

Background: Approximately 70% of breast cancers are estrogen receptor-positive (ER+), and endocrine therapies, including selective estrogen receptor modulators (SERMs) and aromatase inhibitors (AIs), are standard-of-care. However, interpatient variability in treatment response and relapse remains substantial, suggesting underlying germline pharmacogenomic factors that modify ER signaling. Here, we mapped ER pharmacogenomic eQTLs to identify germline variants that modulate transcriptional responses to estradiol (E2) and tamoxifen (Tam).
Methods: We treated 30 genotyped lymphoblastoid cell lines (LCLs) with vehicle, E2, Tam, or E2+Tam and performed RNA-seq to quantify ligand-induced expression fold changes. Using MatrixEQTL, we identified SNP-gene PGx-eQTLs (cis, ±200 kb), requiring evidence of ER transcriptional specificity via (i) reversal by dual treatment, and (ii) overlap with ER ChIP-seq binding annotations. Clinical relevance was assessed by linkage to breast cancer GWAS datasets, including NSABP, MA.27, and M3. Chromatin regulatory states were annotated (ChromHMM), and transcription factor motif enrichment was performed from SNP-centered ±200 bp regions.
Results: Distinct PGx-eQTL architectures were identified for E2 and Tam, with partial overlap in ligand-responsive loci. ER PGx-eQTL variants were predominantly enriched in enhancer chromatin and co-localized with canonical ER-binding motifs. Integrative analysis with GWAS of breast cancer outcomes highlighted multiple drug-response-associated loci, including rs311392-MRPL15 and rs7953325-SYCP3. High MRPL15 expression was linked to shorter relapse-free survival, whereas high SYCP3 expression correlated with improved outcomes. Additional loci derived from a GWAS catalog for cancer and hormone phenotypes included rs2850247-SIK2 and rs11673604-LSM4, where higher SIK2 expression was associated with improved relapse-free survival and higher LSM4 expression with poorer outcomes.
Conclusions: We identified ligand-dependent ER PGx-eQTLs that mechanistically connect germline regulatory variants to transcriptional response heterogeneity and clinical endocrine therapy outcomes. These SNP-gene relationships represent potential biomarkers for precision endocrine therapy selection and may reveal endocrine-dependent therapeutic vulnerabilities.

#3611 Cell-type aware transcriptome-wide association study of mammographic density phenotypes.

Joseph H. Rothstein[1], Adriana Sistig[2], Sinan Zhu[3], Tejomay Gadgil[4], Li Shen[2], Stacey E. Alexeeff[4], Ninah Achacoso[4], Lori C. Sakoda[4], Vignesh A. Arasu[4], Laurie R. Margolies[2], Robert J. Klein[2], Laurel A. Habel[4], Xiaoyu Song[3], Pei Wang[2], Weiva Sieh[1]

[1]UT MD Anderson Cancer Center, Houston, TX,[2]Icahn School of Medicine at Mount Sinai, New York, NY,[3]Duke-NUS Medical School, Singapore, Singapore,[4]Kaiser Permanente, Oakland, CA

Background: Mammographic density (MD) phenotypes are highly heritable and strongly associated with breast cancer risk. Genetic variants identified by genome-wide association studies (GWAS) explain only a small fraction of the heritability, and the responsible genes remain largely unknown. Transcriptome-wide association studies (TWAS) can improve power and identify genes associated with MD through their genetically regulated gene expression (GReX) levels. However, cell type heterogeneity in bulk tissue samples can obscure disease associations. Here, we conduct TWAS of MD phenotypes using standard approaches and a new cell-type-aware framework.

Methods: The study population included 24,158 women of European ancestry who underwent screening with Hologic (n=20,282) or GE (n=3,876) digital mammography and participated in Kaiser's Research Program on Genes Environment and Health. Dense area (DA), nondense area (NDA), and percent density (PD) were measured centrally using Cumulus6. Tissue-level gene expression was estimated using standard elastic-net models. Cell-type-specific expression in mammary epithelial, fibroblast, and adipocyte cells was estimated using MiXcan. Linear regression was used to assess associations of GReX levels with MD phenotypes, adjusted for age, BMI, and other covariates. Significance was determined by controlling the false-discovery rate at 0.05.

Results: A total of 20 unique genes at 16 loci were significantly associated with MD phenotypes, including 10 genes at 7 loci for DA and 8 different genes at 7 loci for NDA. Of the 7 genes for PD, 2 also were associated with DA and 3 with NDA. Standard TWAS methods identified 8 genes whose tissue-level expression was significantly associated with MD phenotypes. In contrast, cell-type-aware analyses using MiXcan identified 10, 12, and 7 genes, respectively, using epithelial, fibroblast, or adipocyte models. Among the 12 genes identified by MiXcan but not standard methods, 2 showed opposite directions of association between different cell types.

Conclusion: This TWAS identified novel genes for MD phenotypes, and prioritized genes at known GWAS loci that are likely to be causally associated through their expression levels in mammary epithelial, fibroblast, or adipocyte cells. Disentangling the distinct effects of gene expression in different mammary cell types through cell-type-aware analysis can yield new gene discoveries and insights into the biological basis of dense vs. nondense breast tissue.

: Metabolism and Microbiome in Cancer Initiation and Prevention
Poster Session

#3616 BXQ-350 reduces incidence, severity, and time to on-set of chemotherapy induced peripheral neuropathy via modulation of sphingolipid metabolism.

Gilles H. Tapolsky, Tariq Arshad, Michael Gazda, Nikhil Wilkins, Jackson Bond, James Beach

Bexion Pharmaceuticals, Covington, KY

Background: Chemotherapy Induced Peripheral Neuropathy (CIPN) is a debilitating side effect associated with many chemotherapeutic agents including cytotoxic and targeted agents. Damages to nerve cells are believed to be directly resulting from the antineoplastic agents' cytotoxicity, however, inflammation and the immune system are also involved and contribute to chronic CIPN. Increasing evidence also suggests that specific species of sphingolipids, including gangliosides (GM), lactosyl ceramides (LacCer), glucosyl ceramides (GluCer) and sphingosine-1-phosphate (S1P), may be involved as altered neuronal sphingolipid metabolism has been linked to neuropathic pain and development of CIPN. BXQ-350 is a nanovesicle of Saposin C, an allosteric activator of multiple enzymes controlling sphingolipid metabolism, that lowers systemic GM, LacCer, GlucCer and S1P. Method: BXQ-350 has been investigated preclinically in CIPN models. Clinically, BXQ-350 was investigated in an adult Phase 1 dose-escalation safety study in heavily pretreated all-comer cancer patients with advanced solid malignancies (NCT02859857), in a Phase 1 Proof of Concept (PoC) study in patients with established chronic CIPN from prior cancer treatments (NCT05291286) and is being investigated in a Phase 1b/2a study in combination with FOLFOX7+ Bevacizumab in newly diagnosed first line mCRC patients (NCT05322590). Results: Preclinical results revealed that BXQ-350 is neuroprotective against chemotherapeutic agents known to induce CIPN. Clinically, in the Phase 1 single agent study, several patients spontaneously reported a significant improvement of their neuropathic symptoms shortly after receiving BXQ-350. In the PoC phase 1 study, BXQ-350 treatment arm showed clinically meaningful and statistically significant improvement over placebo. In the combination study in 1L mCRC patients, BXQ-350 seems to delay the onset, severity and frequency of CIPN while enabling the administration of a higher cumulative dose of oxaliplatin. Longitudinal analyses of biomarkers (plasma cytokines, Neurofilament Light (NfL) chains, sphingolipids), and results from CIPN 20 questionnaires, and physician assessments, revealed there were positive correlations between physician assessments, CIPN 20 questionnaire results, NfL and sphingolipid profile changes. A strong correlation was noted between LacCer, a sphingolipid known to induce neurodegeneration and inflammation, in patients developing CIPN and with established chronic CIPN. Conclusions: Preclinical and clinical results suggest that BXQ-350 protects cancer patients from antineoplastic agents known to induce CIPN enabling the administration of higher cumulative doses of oxaliplatin in mCRC patients. A strong correlation was noted between CIPN and LacCer plasma levels and other CIPN biomarkers.

#3617 Immunogenomic alterations driving premalignant lesions to invasive lesions of the head and neck.

Foram Ujjvalkumar Vaidya[1], Alvaro Gutierrez[2], Abberly Lott Limbach[3], Bhavna Kumar[4], Martin P. Alphonse[5], James W. Rocco[4], Mariana Brait[1], Amanda Ewart Toland[6], David Sidransky[1]

[1]The Sidney Kimmel Comprehensive Cancer Center, Johns Hopkins University School of Medicine, Baltimore, MD,[2]Centro de Excelencia en Medicina Traslacional, Universidad de La Frontera, Temuco, Chile,[3]Department of Pathology, College of Medicine, The Ohio State University Wexner Medical Center, Columbus, OH,[4]Department of Otolaryngology-Head and Neck Surgery, OSU Comprehensive Cancer Center, The Ohio State University, Columbus, OH,[5]Department of Dermatology, Johns Hopkins University School of Medicine, Baltimore, MD,[6]Department of Cancer Biology and Genetics, OSU Comprehensive Cancer Center, The Ohio State University, Columbus, OH

Head and neck squamous cell carcinoma (HNSCC) is the seventh most prevalent type of cancer globally with 940,000 new cases and 480,000 fatalities yearly. Oral squamous cell carcinoma (OSCC) is characterized by molecular alterations that drive progression of some preneoplastic lesions to invasive cancer. Not all dysplastic premalignant lesions evolve into carcinoma *in situ* or full-blown carcinoma. Moreover, this transition may occur as these lesions evolve over years. Identifying precancerous lesions likely to progress to invasive cancer remains challenging. Comprehensive immunogenomic profiling may reveal whether immune tolerance is a hallmark of early dysplasia and/or an acquired prerequisite for malignant transformation. We thus conducted a longitudinal study with matched dysplastic and invasive lesions to uncover early molecular drivers, reveal clonal relationships, and to identify genomic and immune mechanisms underlying SCC progression. Samples were obtained from The Ohio State University (OSU) and The Johns Hopkins University (JH). RNA was extracted from a total of 111 FFPE samples from 34 patients with precursor lesions and/or HNSCC across different stages (OSU) and submitted for RNA sequencing. Differential gene expression analysis was performed in invasive versus dysplastic lesions. Immune-related transcripts were annotated by curated immune gene sets to characterize microenvironmental remodelling. To investigate the interactions between tumor and immune cells at the subcellular resolution, spatial transcriptomics of matched dysplasia and invasive SCC was performed in a subset of patients using 10X Genomics Visium HD platform followed by Seurat based downstream analysis. For tumor-immune interaction analysis, we integrated spatial data with a single-cell reference atlas containing annotated immune cell subtypes and tumor cell states. Bulk RNA-seq revealed 164 differentially expressed genes in invasive versus dysplastic lesion, with enrichment in extracellular matrix remodelling, epithelial-mesenchymal transition and cytokine signalling pathways. Moreover, 80% of immune genes (e.g. CXCL9/10, CCL5, STAT1) are upregulated in invasive SCC. Preliminary spatial transcriptomics data revealed distinct immune microenvironments between invasive and dysplastic regions, with enrichment of immune cells at the tumor-stroma interface. The current comparative analysis revealed distinct immune infiltration patterns between dysplastic and invasive lesions, suggesting the spatial evolution of immune evasion mechanisms during cancer progression. Our cohort of samples is unique with paired patient samples that progressed from a biopsy proven premalignant state to invasive cancer over time. Our preliminary data suggest that we can identify premalignant lesions likely to progress and targetable immunogenomic drivers to intercept cancer progression at an earliest stage.

#3618 Obesity-mediated extracellular vesicle secretion as a targetable driver of endometrial cancer initiation and progression.

Lakshmi Narasimhan Chakrapani[1], Kalapana Deepa Priya Dorayappan[1], Ganesh Yadagiri[1], Shyam Sundaram[1], Gabriela S. Vendrell[1], Takahiko Sakaue[2], Jessica Velasquez[1], Xavier Ryon Washington Ramesh[3], Thangavel Muthusamy[4], Casey M. Cosgrove[1], David E. Cohn[1], David M. O'Malley[1], Selvendiran Karuppaiyah[1]

[1]Obstetrics and Gynecology, The Ohio State University, Columbus, OH,[2]Obstetrics and Gynecology, Kurume University, Kurume, Japan,[3]Pathology, Sree Balaji Medical College and Hospital (SBMCH) - Bharath Institute of Higher Education and Research (BIHER), Chennai, India,[4]Cellular and Molecular Biochemistry, Sree Balaji Medical College and Hospital (SBMCH) - Bharath Institute of Higher Education and Research (BIHER), Chennai, India

Introduction: Endometrial cancer (EC) is the most common gynecologic malignancy in the United States, with obesity accounting for approximately 57% of cases. The molecular mechanisms linking obesity to EC initiation remain poorly defined. Emerging evidence suggests that obesity enhances extracellular vesicle (EV) secretion and alters EV-associated oncogenic signaling. This study investigates obesity-mediated EV dysregulation in adipose, uterine, and EC tissues and explores its role in early EC pathogenesis, biomarker development, and therapeutic intervention.

Methods: Endometrial hyperplasia and EC were induced in immunocompetent mice using high-fat diets (HFD; 45% or 60% kcal fat) for 25 weeks. Molecular profiling was conducted using LC-MS/MS. EV concentration and size were quantified by nanoparticle tracking analysis (NTA) and visualized by transmission electron microscopy (TEM). Expression of TMEM205, STAT5, FAS, and the tumor suppressor PIAS3 was assessed by immunohistochemistry, ELISA, and RT-PCR in tissues from HFD-treated mice and obese EC patients. Additional studies evaluated EV-mediated tumor progression and treatment response in xenograft models receiving chemotherapy or immunotherapy.

Results: Obese EC patient samples exhibited significantly increased EV secretion and upregulation of oncogenic proteins in adipose and uterine tissues compared to non-obese controls. In HFD-treated mice, elevated body weight, abdominal adiposity, uterine horn enlargement, and chronic inflammation correlated with endometrial hyperplasia and EC initiation. These phenotypes were associated with increased EV secretion, upregulation of TMEM205, FAS, and STAT5, and marked downregulation of PIAS3. HFD-induced EVs carried oncogenic proteins linked to elevated serum glucose and lipid levels and altered immune profiles. EVs from obese conditions also promoted aggressive EC progression and resistance to chemotherapy and immunotherapy. Treatment with the small-molecule EV secretion inhibitor DAP-5 significantly reduced body weight, adipose accumulation, and EV output in HFD-fed mice and restored normal uterine morphology while suppressing EV-associated oncogenic signaling.

Conclusion: Obesity-mediated EV secretion is a major driver of EC initiation and progression. Targeting EV biogenesis represents a promising preventive and therapeutic strategy for obesity-associated EC. These preclinical findings provide a strong rationale for advancing EV-targeted interventions, including first-in-human trials aimed at preventing obesity-driven EC development.

#3619 Red cabbage juice reprograms the gut microbiome and enhances butyrate production to prevent colorectal cancer.

Bineet Narayan[1], Yariswamy Manjunath[2], Nagabhhishek Sirpu Natesh[2], Chayanee Chanpanich[3], Parsa Ghadermazi[4], BLAKE ARCIGA[5], Samarth Kansara[6], Ajay Tosh[7], John Ulbrich[6], Mary Kate Grossmann[6], Hwang Jiwon[6], Van Nguyen[8], Vikas Satyananda[9], Jussuf T. Kaifi[9], Joshua Chan[4], **Satyanarayana Rachagani**[6]

[1]University of Missouri, Columbia, MO,[2]University of Missouri - Columbia, Columbia, MO,[3]Biomedical engineering, Colorado State University, Fort collins, CO,[4]Biomedical Engineering, Colorado State University, Fort Collins, CO,[5]Nextgen PHI, University of Missouri, Columbia, Columbia, MO,[6]Dept. Veterinary Medicine and Surgery, University of Missouri - Columbia, Columbia, MO,[7]Nextgen PHI, University of Missouri, Columbia, MO,[8]Pathology, University of Missouri, Columbia, MO,[9]Surgery, University of Missouri, Columbia, MO

Background Colorectal cancer (CRC) remains the second leading cause of cancer-related mortality in the United States, with Western diet-induced gut dysbiosis implicated in its pathogenesis. Early interventions targeting the gut microbiome offer a promising prevention strategy. Dietary approaches that enhance short-chain fatty acid (SCFA) production like butyrate, have emerged as potential chemopreventive measures. This study investigated the preventive efficacy of red cabbage juice (RCJ) in a genetically engineered mouse model of CRC by examining its effects on microbial composition, butyrate production and its translational relevance using CRC patient-derived organoids (PDOs).

Methods Tamoxifen inducible $APC^{fl/fl}$;$Cdx\text{-}Cre^{ER}$ (AC) mice for CRC were randomized to receive either phosphate-buffered saline (PBS) or RCJ as oral gavage for 10 weeks. Then, mice were injected with tamoxifen to induce CRC and monitored for weight loss and diarrhea. At the endpoint, colon tissues and cecal contents were collected for immunohistochemistry (IHC), metagenomic profiling, and fecal SCFA quantification by GC-MS/MS. In parallel, PDOs from CRC patients were developed and treated with RCJ alone or in combination with chemotherapeutic agents oxaliplatin or 5-fluorouracil (5-FU) and monitored in real-time on an IncuCyte platform and therapy responses (proliferation and apoptosis) were evaluated by IHC.

Results RCJ significantly reduced polyps and tumor progression in AC mice and improved survival compared to PBS group. Enhanced expression of mucosal protective mucins Muc2 and Muc4 in the colonic epithelium of RCJ-treated mice. Shotgun sequencing revealed enrichment of succinate-to-butyrate metabolic pathways, elevated fecal succinate, butyrate and abundance of butyrate-producing *Clostridia* etc. Treatment of PDOs with 6% RCJ inhibited PDO growth, number, size as analyzed by IncuCyte provided us with its translational relevance for CRC prevention. Further, RCJ and oxaliplatin combination therapy significantly reduced organoid number, size, area vs. RCJ alone, RCJ + 5-FU, or media control, suggesting that RCJ may enhance the therapeutic response of chemotherapy to combat CRC organoids growth. IHC images confirmed these effects, showing decreased proliferation, and increased apoptosis upon the treatment.

Conclusions RCJ modulates the gut microbiome and enhances butyrate production, correlating with reduced tumor burden in a preclinical CRC model. It also exerts inhibitory effect on CRC PDO growth, number, size. Notably, RCJ enhances the efficacy of oxaliplatin in PDOs, suggesting its potential to overcome chemoresistance. These findings underscore the translational potential of RCJ as a dietary intervention targeting gut microbiome-SCFA interactions and an adjunctive chemopreventive agent in CRC prevention, particularly in at-risk surgical populations.

#3620 The human virome and its association with clinical benefit of immune checkpoint inhibitor therapy among patients with advanced non-small cell lung cancer.

Anna E. Coghill[1], Jin Xu[1], Aleksandr Lazaryan[1], Doratha Armenthus Byrd[1], YOUNGCHUL KIM[2], Richard Pollenz[3], Lary A. Robinson[1]

[1]Moffitt Cancer Center, Tampa, FL,[2]Moffitt Cancer Center, TAMPA, FL,[3]University of South Florida, Tampa, FL

Background. The goal of this study was to examine the human gut virome in advanced lung cancer patients being treated with immune checkpoint inhibitor (ICI) therapy to determine whether patterns of viral detection could predict clinical benefit.

Methods. This cohort of 66 patients with stage III-IV lung cancer patients was recruited between June and February 2019. Eligibility was limited to treatment-naïve individuals who were scheduled to receive ICI therapy at Moffitt Cancer Center. DNA was extracted from stool collected within 24-72 hours prior to each patient's first ICI cycle. To generate the mammalian virus and bacterial virus (phage) taxonomic profiles, reads were aligned to publicly available databases using program Bowtie2 version 2.3.5.1. Multivariable logistic regression was used to estimate the association between the relative abundance of viral taxonomic units (OTUs) and ICI clinical benefit. Random forest machine learning analysis was used to select a set of viral OTUs whose relative abundance most accurately classified patients as yes/no for clinical benefit of ICI therapy.

Results. We observed clinical benefit in 34 lung cancer patients treated with ICI therapy. We observed differences in the relative abundance of multiple components of the human gut virome between lung cancer patients according to ICI clinical benefit. Most marked were the differences observed in the relative abundance of phages (bacterial viruses). We observed that 239 phages were abundant at different frequencies in lung cancer patients with versus without clinical benefit of ICI therapy at the $q<0.05$ level (multiple testing corrected p-value). In addition, an area under the curve (AUC) for discrimination of ICI clinical benefit of 91% could be achieved using a 15-phage combination. This included 10 OTUs from the family *Siphoviridae*, 2 from the family *Myoviridae*, 2 from *Podoviridae*, and 1 from family *Caudoviridales.* For all but one of these 15 phages, we were able to identify a consensus bacterial genus as the phage target with high confidence. Two of these bacteria - *Ruminococcus* and *Bacteroides* - have consistently been identified in microbiome studies as being associated with ICI response.

Conclusion. Implications of our research include not just the elucidation of a further component of the human gut environment - phages - that impacts human health and disease, but also the identification of its specific role in potentially altering response to cancer-directed immune checkpoint inhibitor therapy.

#3621 Fecal microbiome signatures for early detection of colorectal cancer and precursor lesions.

Mariana Bisarro Dos Reis[1], Monise Tadin Reis[1], Ana Flavia Peres[1], Claudio Lyoiti Hashimoto[1], Denise Peixoto Guimaraes[1], Jeremy Wang[2], Rui Manuel Reis[1]

[1]Barretos Cancer Hospital, Barretos, Brazil,[2]UNC School of Medicine, NC

Background: Colorectal cancer (CRC) remains a major global health burden, and the development of non-invasive biomarkers for early detection is a critical unmet need. Growing evidence indicates that intestinal microbiome dysbiosis contributes to the adenoma-carcinoma sequence and may support CRC risk stratification.
Aim: To investigate whether intestinal microbiome profiling from residual material of Fecal Immunochemical Test (FIT) samples can serve as a biomarker for CRC screening.
Methods: Residual stool samples from Brazilian FIT-positive individuals (n=133) were classified according to colonoscopy as no lesions (N=30), non-advanced adenoma (NAA=46), advanced adenoma (AA=13), or colorectal cancer (CA=44). In three individuals, the microbiome profile was compared on three collection tubes (two FIT tubes and Omnigut). Bacterial DNA from FIT samples underwent 16S rRNA sequencing on Oxford Nanopore MinION (R10.4.1 flow cells, for 48 hours). Reads were processed using Dorado, aligned with Emu to a curated full-length 16S database, and analyzed in QIIME2 using Python. Alpha diversity (25 different metrics), beta diversity (Jaccard, Bray-Curtis), and differential abundance (ANCOMBC) were assessed.
Results: Alpha diversity was significantly higher in CA samples compared with N and NAA patients (Chao 1, $p < 0.001$ and $p=0.006$; Observed features, $p < 0.001$ and $p=0.007$), with no difference compared to AA. Beta diversity (PERMANOVA, $p = 0.001$ for both metrics) showed significant compositional separation among CA and AA (Jaccard, $p=0.001$, Bray Curtis, $p=0.001$), NAA (Jaccard, $p=0.001$, Bray Curtis, $p=0.001$), and N (Jaccard, $p=0.001$, Bray Curtis, $p=0.003$). Differential abundance indicated increasing dysbiosis as lesions progressed. Compared with N samples, NAA exhibited 42 differentially abundant species (9 decreased, 33 increased), AA showed 65 species (15 decreased, 50 increased), and CRC showed pronounced dysbiosis with 179 species (28 decreased, 151 increased). Preliminary inspection highlights enrichment of *Fusobacterium nucleatum* in CA samples. Analysis of the taxonomic profiles revealed no differences in species composition among the three collection tubes analyzed.
Conclusion: Microbiome profiling using routine residual FIT samples is feasible and reveals a marked diversity shift along the adenoma-carcinoma spectrum. These findings
support the potential of FIT-derived microbiome signatures as non-invasive biomarkers for CRC early detection in Brazilian screening populations.

#3622 Precision therapy against CRC associated *Fusobacterium nucleatum* using bioengineered probiotics expressing guided antimicrobial peptides (gAMPs).

Ankan Choudhury, Colin Scano, Allison Barton, Leigh Greathouse

Baylor University, Waco, TX

Colorectal cancer (CRC) is a leading cause of cancer-related mortality, with Fusobacterium nucleatum (F. nucleatum) identified as a key contributor to its progression. This study explores a novel therapy that targets this pathogen by using a bioengineered probiotic that expresses guided antimicrobial peptides (gAMPs) to selectively inhibit F. nucleatum. in this study, Lactococcus lactis MG1363 was engineered to express gAMPs derived from Ovispirin and Cathelin-related peptide SCF, linked to a Statherin-derived guide peptide that binds specifically to the F. nucleatum membrane porin FomA. The bacteria expressed the AMP/gAMP under the induction of the PNisA promoter by nisin and secreted it via the extracellular secretion signal usp45. The resultant synthetic peptides and probiotics were assayed for antimicrobial activity against the targeted F. nucleatum and other non-target bacteria. Biofilm inhibition and growth kinetic assays were performed with synthetic peptides in vitro or the probiotic in co-culture with a polymicrobial community. We saw that statherin-derived guide peptide enhanced the binding affinity to F. nucleatum, significantly increasing attachment compared to control peptides. In vitro assays revealed that both unguided and guided AMPs effectively inhibited biofilm formation in F. nucleatum, with gAMPs showing reduced toxicity against non-target bacteria. The gAMPs were more effective in modulating growth kinetics, exhibiting selective toxicity towards F. nucleatum at lower concentrations. Co-culture experiments in a simulated human gut microbiome showed the gAMP probiotic maintained microbial diversity while effectively reducing F. nucleatum abundance. Quantitative PCR and 16S rRNA sequencing confirmed that gAMP treatment preserved the richness of the microbiota, contrasting with significant dysbiosis observed in control samples. These findings support the potential of engineered probiotics as a therapeutic approach that targets CRC-associated F. nucleatum.

#3623 Effects of the anti-obesity medication tirzepatide on the tumor microenvironment in a mouse model of obesity-associated, hormone-dependent breast cancer..

Charlotte E. Gibson[1], Amanda L. Kucinskas[2], Emma G. Bailey[1], Flora Tao[3], Katherine E. Sanchez[1], Katherine L. Cook[4], Erin D. Giles[1]

[1]Kinesiology, University of Michigan, Ann Arbor, MI,[2]University of Michigan Medical School, Ann Arbor, MI,[3]Johns Hopkins University, Baltimore, MD,[4]Wake Forest University School of Medicine, Winston Salem, NC

Numerous anti-obesity agents have been approved for obesity/diabetes treatment, but their impact on obesity-related breast cancer is not clear. Our pilot data supported a trend for reduced growth of estrogen-receptor positive (ER+) tumors with tirzepatide (TZP), an FDA-approved incretin mimetic targeting both GLP-1 and GIP receptors. Here, our goal was to determine if TZP-induced changes in the mammary tumor microenvironment contributed to the anti-cancer effects of TZP. Female C57/BL6 mice were fed a 46% high-fat diet to induce obesity. They were then randomized to receive tirzepatide (15-week dose escalation to 75nM) or vehicle for the duration of the study. Three weeks after starting TZP, tumors were initiated by injection of estrogen-receptor positive Py230 cells, and tumor volumes were measured twice weekly. Mice were terminated when tumor volumes reached humane endpoints, or after 16 weeks of treatment. Mammary adipose tissue was collected at the end of the study and processed for histological examination. Adipocyte size was assessed in H&E stained tissues using the Adiposoft plugin for ImageJ, and number of macrophages in the tumor microenvironment was assessed using Mac2 immunofluorescence staining. As expected, TZP induced ~20% weight loss, which was reflected in both an increase in the proportion of small adipocytes and a reduction in the number of large adipocytes in the tumor microenvironment (mammary gland). This suggests that changes in macrophage infiltration are not likely to contribute to the potential anti-cancer effects of TZP in our pilot studies. Ongoing studies will address additional mechanisms by which TZP affects tumors and/or the obese tumor microenvironment.

#3624 Long-term running and risk of colorectal adenoma and cancer.

Yiwen Zhang[1], Edward L. Giovannucci[2]

[1]Harvard School of Public Health, Boston, MA,[2]Professor of Nutrition & Epidem., Harvard TH Chan School of Public Health, Boston, MA

Introduction: Although physical activity is associated with lower risk of colorectal cancer, it was hypothesized that high levels of long-distance running may induce gastrointestinal ischemia and injury, raising concern about potential increased risk of colorectal carcinogenesis. Currently only a small cross-sectional study of 100 participants suggested intensive long-distance running is a risk factor for advanced colon adenomas. No large prospective study has comprehensively evaluated long-term running in relation to risk of colorectal adenoma and cancer.

Methods: We used data from three prospective cohorts: Health Professionals Follow-up Study, Nurses' Health Study (NHS), and NHSII. Running was assessed with biennial validated questionnaires and calculated as cumulative average over the past 8-year period to reflect long-term patterns. Colorectal adenoma risk was evaluated among 160,367 participants with at least one lower gastrointestinal endoscopy during follow-up with logistic regression models accounting for repeated observations. Colorectal cancer risk was analyzed with Cox proportional hazard models among 238,491 participants followed up to 32 years. Multivariable models were adjusted for potential confounders and total physical activity other than running. We also examined associations between running with resting heart rate and cardiometabolic biomarkers.

Results: We documented 12,426 conventional adenomas, 11,251 serrated polyps, and 3583 colorectal cancers during the follow-up period. Running was inversely associated with risk of conventional adenoma and serrated polyps. For high-risk adenoma, compared to participants who reported no running, the ORs (95% CIs) across >0-<1, 1-<2, 2-<3, 3-<4, and ≥4 h/week of running were 0.86 (0.76-0.98), 0.75 (0.55-1.00), 0.83 (0.56-1.23), 0.94 (0.52-1.66), and 0.51 (0.29-0.91), respectively. For colorectal cancer, compared to no running, the HRs (95% CIs) were 0.86 (0.76-0.97) for >0-<1 h/week, 0.60 (0.41-0.87) for 1-<2 h/week, and 0.81 (0.58-1.12) for ≥2 h/week. Results remained similar when further adjusted for body mass index. Biomarker analysis showed higher levels of running were associated with significant lower resting heart rate, lower inflammation status (lower CRP and IL-6), better insulinemic (lower C-peptide) and lipid profile (higher HDL-cholesterol and lower triglycerides), providing biologic support of our assessment of running.

Conclusion: In three large cohorts, long-term running was not associated with an increased risk of colorectal adenoma, serrated polyps, or colorectal cancer. Moderate running levels (approximately up to 2 h/week) were associated with lower risk of colorectal cancer and levels ≥4 h/week were associated with a lower risk of high-risk adenoma. These findings provide reassurance that habitual running, at levels up to at least 4 h/week, is safe and potentially beneficial with respect to colorectal neoplasia risk.

#3625 Central and peripheral adiposity and breast cancer risk in postmenopausal women: A pooled analysis of 11 cohort studies.

Isaias Leon-Cepeda[1], Craigg Pickett[2], Stephanie A. Smith-Warner[3], Robert J. MacInnis[4], Jeanine M. Genkinger[1]

[1]Epidemiology, Columbia University Mailman School of Public Health, New York, NY,[2]Department of Epidemiology and Preventive Medicine, School of Public Health & Preventive Medicine Monash University, Melbourne, Australia,[3]Departments of Nutrition and Epidemiology, Harvard T. H. Chan School of Public Health, Boston, MA,[4]Centre for Epidemiology and Biostatistics, Melbourne School of Population and Global Health, The University of Melbourne, Melbourne, Australia

Background: Central and peripheral adiposity, measured by waist circumference (WC), hip circumference (HC), and waist-to-hip ratio (WHR), has been positively associated with postmenopausal breast cancer (BC) risk, but results are inconsistent after adjustment for body mass index (BMI). Using pooled individual-level data from 11 prospective cohorts, we evaluated associations between WC, HC, WHR, and a body shape index (ABSI; based on waist, height, and weight) and risk of postmenopausal BC overall and BC subtypes defined by receptor status.
Methods: These preliminary analyses evaluated associations between WC, HC, WHR, and ABSI using consortium-wide quintiles and overall BC and tumor negative breast cancer (TNBC) in 402,682 postmenopausal women. Cox proportional hazards regression models were used to calculate hazard ratios (HRs) and 95% confidence intervals (95% CI), adjusting for age, year of questionnaire, study, family history of BC, and reproductive and lifestyle factors. Analyses were performed with and without adjustment for BMI.
Results: During a median follow-up of 2.9-27.5 years across studies, 20,752 incident invasive BC were documented (N=998 TNBC). The pooled multivariable BMI-adjusted HRs (95% CIs) for postmenopausal BC comparing quintile 5 to 2 were 1.14 (1.08-1.21) for WC; 1.06 (0.99-1.14) for HC; 1.10 (1.05-1.15) for WHR, and 1.03 (0.98-1.08) for ABSI. Similar associations were observed among never-users of menopausal hormone therapy. The pooled multivariable BMI-adjusted HRs (95% CIs) for postmenopausal TNBC comparing quintile 5 to 2 were 1.13 (0.87-1.46) for WC; 0.74 (0.45-1.21) for HC; 1.45 (1.15-1.84) for WHR, and 1.18 (0.95-1.47) for ABSI.
Conclusion: Higher compared to lower WC and WHR were associated with increased risk of postmenopausal BC, independent of BMI. Our findings suggest that individual and population-level strategies to prevent central adiposity could help reduce the risk of postmenopausal BC.

Pooled Multivariable (MV) Hazard Ratios (HR) and 95% Confidence Intervals (CI)

Consortium-wide quintiles	**Overall**	**TNBC**
WC (cm)		
<74	0.97 (0.92-1.02)	0.92 (0.74-1.15)
74-<80	REF	REF
80-<86	1.0 (0.95-1.04)	0.89 (0.73-1.1)
86-<95	1.06 (1.02-1.12)	0.94 (0.76-1.17)
≥95	1.14 (1.08-1.21)	1.13 (0.87-1.46)
HC (cm)		
<95	0.91 (0.87-0.96)	0.91 (0.60-1.36)
95-<100	REF	REF
100-<105	1.03 (0.98-1.08)	1.15 (0.82-1.65)
105-<112	1.03 (0.98-1.09)	0.92 (0.60-1.4)
≥112	1.06 (0.99-1.14)	0.74 (0.45-1.21)
WHR		
<75	1.02 (0.97-1.07)	1.37 (1.1-1.69)
75-<79	REF	REF
79-<83	1.04 (1.0-1.09)	1.27 (1.01-1.59)
83-<87	1.03 (0.98-1.08)	1.29 (1.02-1.62)
≥87	1.1 (1.05-1.15)	1.45 (1.15-1.84)
ABSI		
<71	0.97 (0.93-1.01)	1.09 (0.91-1.32)
71-74	REF	REF
74-77	1.01 (0.97-1.05)	1.09 (0.89-1.33)
77-81	1.02 (0.98-1.07)	1.17 (0.95-1.43)
≥81	1.03 (0.98-1.08)	1.18 (0.95-1.47)

#3626 Early life exposures and cancer in adulthood: World Cancer Research Fund International's lifecourse research in cancer.

Vanessa Lani Zarya Gordon-Dseagu[1], Helen Croker[1], **Panagiota Mitrou**[1], Christelle Clary[1], John Krebs[2], Matty P. Weijenberg[3], Monica Baskin[4], Ellen Kampman[5], Laure Dossus[6], Franzel J. Van Duijnhoven[7], Dieuwertje E. Kok[8], Moniek van Zutphen[8]

[1]World Cancer Research Fund International, London, United Kingdom,[2]University of Oxford, Oxford, United Kingdom,[3]Associate Professor, Dept. of Epidem., Maastricht University, Maastricht, Netherlands,[4]VCU Massey Comprehensive Cancer Center, Richmond, VA,[5]Div. of Human Nutrition, Wageningen Univ., Wageningen, Netherlands,[6]IARC-WHO, Lyon, France,[7]Postdoctoral Researcher, Wageningen University, Wageningen, Netherlands,[8]Wageningen University & Research, Wageningen, Netherlands

Background There is increasing recognition that exposure to certain risk factors in early life (defined as birth, childhood, adolescence, and young adulthood) impacts disease risk (including cancer) in adulthood. The identification of age-specific "windows of opportunity" also enables the development of refined cancer prevention recommendations tailored to different life stages. Despite this, there is a paucity of evidence related to how body size and weight, diet, nutrition, and physical activity in early life influences adult cancer risk. The strength of the available evidence-base has also not been assessed in a systematic way.

Methods WCRF International's Global Cancer Update Programme (CUP Global) undertook a collaboration with Wageningen University and Research (WUR) to conduct systematic literature reviews and meta-analyses focused on early-life exposures (birth size, body weight, and alcohol consumption) and risk of colorectal and breast cancer in adulthood. A 2nd collaboration with the International Agency for Research on Cancer (IARC) reviewed relevant biological mechanisms. The Global CUP Global Panel of Experts then interpreted and graded the evidence using pre-defined criteria to determine likely causal associations.

Results Key exposures during early life related to birthweight, body size and alcohol, as well as the biological mechanisms that underpin them, that impact future cancer risk were identified. For colorectal cancer, birthweight was associated with a 9% (95% confidence interval: 1.01-1.16) increased risk, increased BMI during childhood, adolescence and young adulthood were also associated with increased risk. For breast cancer, greater birth weight, length and taller height in childhood inferred an increased risk. Higher BMI in childhood, adolescence and young adulthood were associated with lower risk. Our Panel of Experts concluded that the evidence for several of the associations was strong enough to suggest a likely causal association. In the future, WCRF International will use these results and further discussions with experts in the field of lifecourse research, public health, and policy to develop guidance and recommendations for researchers, policy makers and the public.

Conclusion The current reviews of the epidemiological and mechanistic evidence demonstrate how exposures related to diet, nutrition, and bodyweight can impact cancer risk in adulthood. Understanding the associations between our early years and cancer risk in adulthood enables a better understanding of the aetiology of cancer, how risk factors impact cancer risk as we age, whether there are critical timepoints/windows for cancer risk, and how our environment impacts cancer risk. These findings, alongside a growing evidence-base, enable the development of cancer prevention policy and public health recommendations.

#3627 Metabolomic signatures of physical activity in treatment-naive patients with early-onset vs. late-onset colorectal cancer: Results from the ColoCare Study.

Victoria Maria Bandera[1], Tengda Lin[1], Patricia Erickson[1], Caroline Himbert[1], Aik Choon Tan[1], Mary C. Playdon[1], Alan Maschek[2], Paul Stewart[1], Sheetal Hardikar[1], Elaine M. Glenny[3], Jennifer Ose[4], Victoria Damerell[5], Christy A. Warby[1], Olena Aksonova[1], Oliver Fiehn[6], Kenneth Boucher[2], Peter Schirmacher[5], Ildiko Strehli[1], Megan Mclaws[1], Alejandro Sanchez[1], Jolanta Jedrzkiewicz[1], Lyen C. Huang[1], Vaia Florou[1], Jessica N. Cohan[1], Alexander Brobeil[5], Hans-Ulrich Kauczor[5], Christoph Kahlert[5], Meghana Karchi[7], Elizabeth H. Wood[7], Doratha A. Byrd[8], Erin M. Siegel[8], Adetunji T. Toriola[9], David Shibata[10], Christopher I. Li[11], Jane C. Figueiredo[12], Biljana Gigic[5], Jatin Roper[13], Stephen Hursting[3], Cornelia M. Ulrich[1]

[1]University of Utah Huntsman Cancer Institute, Salt Lake City, UT,[2]University of Utah, Salt Lake City, UT,[3]University of North Carolina at Chapel Hill, Chapel Hill, NC,[4]University of Applied Sciences and Arts, Hannover, Germany,[5]Heidelberg University Hospital (UKHD), Heidelberg, Germany,[6]Professor, University of California, Davis, Davis, CA,[7]University of Tennessee Health Science Center, Memphis, TN,[8]Moffitt Cancer Center, Tampa, FL,[9]Washington University School of Medicine in St. Louis, St. Louis, MO,[10]Assoc. Professor of Surgical Onc., Div. of Interdiscipl. Onc., University of Tennessee Health Science Center - Memphis, Memphis, TN,[11]Fred Hutchinson Cancer Center, Seattle, WA,[12]Samuel Oschin Comprehensive Cancer Institute, Los Angeles, CA,[13]Duke University, Durham, NC

Introduction: Emerging studies link physical inactivity to early-onset colorectal cancer (EOCRC), but most rely on subjective measures of physical activity (PA). Metabolite signatures may offer an objective measure of PA that also captures the systemic metabolic response to activity. We assessed a previously validated PA metabolomic signature in patients with recently diagnosed colorectal cancer (CRC) and compared profile scores between patients with EOCRC (<50 yrs) vs. non-EOCRC (≥50 yrs).

Methods: We examined baseline (pre-surgery) data from 122 stage I-III patients with CRC in the ColoCare Study at Huntsman Cancer Institute (Utah) and Heidelberg University Hospital (Germany). PA for the previous year was measured with the International Physical Activity Questionnaire-Short Form. Untargeted serum metabolites and complex lipids were profiled at the West Coast Metabolomics Center. We calculated a 24-metabolite PA signature developed in >6,000 cancer-free individuals (Papadimitriou et al., CEBP, 2025) consisting of acylcarnitines, glycerophospholipids, monosaccharides, amino acids, and sphingolipids. Following metabolite pre-processing, normalization, and scaling, we performed multivariable linear regression on 20 metabolites available in our dataset, adjusting for age, sex, tumor stage, and body mass index (BMI). Metabolite scores were calculated for each participant by multiplying normalized metabolite concentrations by the previously developed PA metabolite signature coefficients and were then compared between EOCRC vs. non-EOCRC survivors.

Results: Compared to patients with non-EOCRC (67±9 years, N=102), those with EOCRC (39±10 years, N=20) were diagnosed with higher stages (55% vs. 43% stage III), had lower prevalence of obese BMI (25% vs. 37%), and were more physically active (16±17 metabolic equivalent (MET) hrs/week vs. 11±17 MET hrs/week), p>0.05. Patients with EOCRC were more likely to meet PA guidelines (≥150 min/week of moderate to vigorous PA; 60% vs. 38%) compared to those with non-EOCRC, p>0.05. Among the 20 metabolites investigated in our data, 15 showed a consistent direction of association with the previously developed PA signature. Patients with EOCRC had higher scores of the PA metabolite signature (0.04±0.09) than older patients (-0.01±0.10), t=2.3, p=0.03. This modest association remained significant after adjustment for stage, sex, and BMI (β=0.05, p=0.048).

Conclusions: A PA metabolite signature showed comparable associations to questionnaire-derived PA measures in our CRC survivor cohort, consistent with findings in healthy individuals. Patients with EOCRC reported a higher level of PA compared to those with non-EOCRC and had a significantly higher PA metabolite signature score. The metabolite response to PA may clarify how physical inactivity influences EOCRC risk and outcomes.

#3628 Obesity, metabolic dysfunction, and cancer risk: Uncovering the metabolic landscape.

Liza Makowski[1], Mary Playdon[2], Bing Li[3], Sonia L. Sugg[3], Scott A. Summers[2], Cornelia M. Ulrich[2], Deirdre Tobias[4], Edward L. Giovannucci[5], Xuehong Zhang[6], James R. Hebert[7], E. Angela Murphy[8], Joeseph F. Pierre[9], Loretta DiPietro[10], Lorne J. Hofseth[11], **Marinella Temprosa**[12]

[1]University of Tennessee Health Science Center - Memphis, Memphis, TN,[2]University of Utah Huntsman Cancer Institute, Salt Lake City, UT,[3]University of Iowa, Iowa City, IA,[4]Brigham and Women's Hospital and Harvard Medical School, Boston, MA,[5]Professor of Nutrition & Epidem., Harvard TH Chan School of Public Health, Boston, MA,[6]Yale University, New Haven, CT,[7]Professor, Dept. of Epidemiology & Biostatistics, University of South Carolina School of Medicine, Columbia, SC,[8]Asst. Prof., Dept. of Path., Microbiology, & Immunology, University of South Carolina School of Medicine, Columbia, SC,[9]University of Wisconsin-Madison, Madison, WI,[10]George Washington University, Washington, DC,[11]Assistant Professor, Univ. of South Carolina College of Pharmacy, Columbia, SC,[12]Biostatistics and Bioinformatics, George Washington University, Washington, DC

As smoking rates decline, obesity has emerged as the leading modifiable risk factor for cancer in the United States. With obesity rates rising, especially in younger populations, its association with increased cancer risk is becoming more evident. There is an urgent need to understand the mechanisms underlying the relationship between obesity related metabolic dysregulation and cancer risk. This session highlights transdisciplinary research from the NCI-sponsored *Metabolic Dysregulation and Obesity Cancer Risk (MeDOC)* Consortium, which applies integrative methods across basic science, translational models, and clinical research. The MeDOC Consortium aims to discover mechanisms linking obesity and cancer to define markers that will enhance cancer risk prediction and identify targets for intervention. Metabolic alterations include immune dysfunction, metabolite signaling, hormonal imbalance, gut microbiome and adipocyte metabolism which can disrupt several downstream signaling pathways related to cancer initiation and progression. In our novel triangulation approach, we synthesize evidence from randomized controlled trials, mechanistic animal studies, and large-scale secondary data analyses establishing population-level patterns with clinical relevance to build a comprehensive metabolic atlas of cancer risk factors. Our research topics include the gut microbiome, lipid signaling, circulating metabolites, and local and systemic immune landscape, with a focus on how these processes influence the development of colorectal, breast, and liver cancers. We will highlight complementary research projects that bridge animal studies, human cohorts, and data science across diet, inflammation, microbiome, immunity, and obesity and weight loss. We will review current evidence and describe novel applications of systems biology with big data analytics featured as tools to integrate mechanistic insights and population-level patterns to establish robust causal frameworks. Early-career investigators will participate in an open discussion on emerging challenges and opportunities in obesity and cancer research. Specifically, we will report on the role of fatty acid binding protein, ceramides, bile acids, hormones, inflammation, and gut microbiome metabolites in cancers of the colon, breast, and liver, Through a translational lens, the session will emphasize how combining data science, bench studies, and interventional trials can accelerate the discovery of biomarkers, risk stratification tools, and actionable targets for cancer prevention or interception.

#3629 The association between obesity, diabetes and prostate cancer aggressiveness in Louisiana Cohort..

Hari K. Koul, Denise danos, Yong yi, Augusto Ochoa, Lucio Miele, Xio-Cheng Wu

LSU-LCMC Cancer Center, LSUHSC-School of Medicine, New Orleans, LA

Introduction Prostate cancer is the most common cancer in men the United States and Louisiana ranks third for prostate cancer mortality rates in the US. With over 40 % adult obesity rates, Louisiana ranks fourth among states for obesity rates. There is conflicting literature on the association between obesity, diabetes and PCa development. We aim to assess if there is an association between obesity, diabetes and PCa aggressiveness at the time of diagnosis, and if this association is modified by race or obesity status.
Methods Cases of primary invasive locoregional prostate cancer diagnosed in 2011-2020 were obtained from Louisiana Tumor Registry. PCa aggressiveness was defined in accordance with the TNM stage and Gleason score. Obesity was defined as BMI of 30 or higher, and type 2 diabetes was identified using ICD-10 codes. Linear trends were assessed with Cochran-Armitage Trend tests and highly aggressive disease at diagnosis was modeled using logistic regression. Analyses were performed overall and stratified by race.
Results The study included 22,554 cases. Most cases were white (62%), while 35% were Black, and 2% were Hispanic. The overall distribution of PCa aggressiveness was low (23%), intermediate (47%), and high (30%). PCa aggressiveness was significantly associated with older age, Black race, obesity, and diabetes ($p<.001$). Stratified by race, the relationship between diabetes and aggressiveness was significant among whites ($p<.001$) and Hispanics ($p=0.037$) but not Blacks ($p=0.398$). In multivariable models controlling for age and obesity, diabetes was significantly associated with high PCa aggressiveness among lean white (OR=1.40 (1.18,1.66)) and Hispanic (OR = 2.68 (1.13,6.36)) men, but not among lean (OR=1.08 (0.90,1.29)) or obese (OR= 0.94 (0.78,1.12)) Black men.
Conclusion We found that obesity is associated with increased risk of aggressive PCa in both Caucasian and Black men, and Obesity and Diabetes are risk factors that interact in PCa patients. Our ongoing research studies are aimed at assessing the contribution of social, environmental, behavioral, dietary and metabolic risk factors with a special emphasis on epigenetic and metabolic reprogramming for aggressive PCa within the Louisiana Cohort.

#3630 Physical activity, smoking and breast cancer risk: A prospective cohort study in the UK biobank.

Hannach Harsanyi[1], Andrew Harper[1], Heinz Freisling[2], Sasha Lupichuk[3], Adetunji T. Toriola[4], **Lin Yang**[3]

[1]Cancer Care Alberta, Calgary, AB, Canada,[2]International Agency for Research on Cancer,[3]University of Calgary, Calgary, AB, Canada,[4]Washington University School of Medicine in St. Louis, St. Louis, MO

Background: Physical activity and smoking are modifiable breast cancer risk factors that operate through partially shared biological pathways, such as hormone regulation and inflammation. However, their potential interactions, especially across menopausal groups, remain largely unexplored. This study aimed to assess whether smoking status modifies the association between physical activity and breast cancer risk.

Methods: Females ≥40 years without prior cancer in the UK Biobank (2007-2010) provided self-reported lifestyle factors. Physical activity was categorized using metabolic equivalent hours per week (MET-hrs/week): high (≥50), moderate (10-50), and low (<10). Incident cancers were ascertained through May 2022. Interaction between physical activity and smoking status (never, past, current) was evaluated using Cox proportional hazards models with product terms. Multivariable models were adjusted for anthropometrics, reproductive, lifestyle, socioeconomic and screening factors.

Results: Among 242 721 participants followed for a mean of 12.53 years (SD: 2.55), 773 premenopausal and 7989 postmenopausal breast cancer cases occurred. High physical activity was associated with lower risk of both premenopausal (HR=0.78, 95%CI: 0.62-0.97) and postmenopausal (HR=0.88, 95%CI: 0.83-0.94) breast cancer. Smoking status was not associated with premenopausal breast cancer risk (past smoker: HR=0.95, 95%CI:0.79-1.13; current: HR=0.89, 95%CI: 0.70-1.15) but was associated with a higher postmenopausal breast cancer risk (past smoker: HR=1.05, 95%CI:1.00-1.11; current: HR=1.13, 95%CI: 1.03-1.23). When evaluating the joint association between physical activity and smoking, current smoking appeard to attenuate the protective association of physical activity with both premenopausal (HR=1.61, 95%CI: 0.74-3.51) and postmenopausal (HR=1.29, 95%CI:1.02 to 1.62) breast cancer risk, although multiplicative interaction terms were not statistically significant.

Conclusions: Smoking status was not independently associated with premenopausal but associated with higher postmenopausal breast cancer risk. Nevertheless, current smokers appeared to derive less protective benefits from physical activity than never smokers. These findings highlight the importance of evaluating joint lifestyle effects rather than single exposure alone in breast cancer prevention.

#3631 Early BMI increase as a predictive biomarker for immune checkpoint inhibitor ±chemotherapy efficacyin advanced NSCLC: Integrating clinical, genomic, and circulating proteomic data.

Xinan Wang[1], Federica Pecci[2], Valentina Santo[2], Eleonora Gariazzo[2], Edoardo Garbo[2], Alessandro Di Federico[2], Joao Alessi[2], Yi Li[3], Biagio Ricciuti[2], David C. Christiani[4]

[1]Harvard School of Public Health, Boston, MA,[2]Dana-Farber Cancer Institute, Boston, MA,[3]Biostatistics, University of Michigan, Boston, MI,[4]Harvard Medical School, Boston, MA

Background: Baseline body mass index (BMI) has emerged as a prognostic factor for immune checkpoint inhibitor (ICI) in advanced NSCLC. However, with chemo-immunotherapy becoming standard of care, whether early BMI changes predict efficacy and differ by treatment regimen remains unclear. Identifying early predictive changes could inform timely interventions to improve treatment efficacy.
Methods: This retrospective study included patients with advanced NSCLC treated with ICI +/- chemotherapy. Baseline and longitudinal BMI were collected. Baseline covariates included age, sex, histology, smoking status, ECOG PS, TMB, PD-L1 TPS, and therapy line. Multivariable logistic and Cox models assessed early BMI changes at 3, 6, and 9 weeks and objective response rate (ORR), progression-free survival (PFS), and overall survival (OS), adjusting for baseline BMI and covariates. Time-dependent analyses verified temporal associations. To understand molecular profiles associated with baseline BMI (≥25 vs. <25 kg/m²), we assessed circulating proteins (Olink, 2700 proteins) in 141 patients and genomic alterations (OncoPanel) in 728 patients, adjusting for age, sex, and smoking.
Results: Among 1,110 patients (303 chemo-immunotherapy, 797 ICI monotherapy), early BMI increase independently predicted improved outcomes in both regimens, with stronger effects in chemo-immunotherapy. In chemo-immunotherapy, 1% BMI increase at 3 weeks predicted higher ORR (OR 1.48, 95% CI 1.15-2.03), PFS (HR 0.78, 95% CI 0.71-0.86), and OS (HR 0.77, 95% CI 0.69-0.86). Predictive value decreased over time (3, 6, 9 weeks), particularly in chemo-immunotherapy. Older patients with smoking history, lower TMB receiving chemo-immunotherapy were more likely to lose weight within 3 weeks. Genomically, KRAS, KMT2A, RASA1, FANCA, CTNNB1, and ATM mutations were enriched in higher BMI patients, while EGFR, PMS1, FH, TP53, and BAP1 mutations were more common in lower BMI patients. Circulating proteins (SSC4D, LEP, CDHR2 in higher BMI; FSHB, GHRL in lower BMI) showed sex-specific patterns and metabolic regulatory roles.
Conclusions: Early BMI increase predicts improved ICI outcomes in advanced NSCLC, with weight monitoring offering opportunities to optimize efficacy. Baseline BMI-associated genomic and proteomic profiles provide complementary insights: circulating proteins establish chronic metabolic selective environments, while tumor mutations represent evolutionary outcomes.

#3632 Adiposity and cancer: Updated meta-analysis incorporating the largest evidence base to date.

Eleanor Watts[1], Amparo Gonzalez-Feliciano[1], Marc Gunter[2], Nilanjan Chatterjee[3], Steven Moore[1]

[1]National Cancer Inst. Div. of Cancer Epidemiology & Genetics, Bethesda, MD,[2]Imperial College London, London, United Kingdom,[3]Johns Hopkins Kimmel Comp. Cancer Ctr., Baltimore, MD

Background: Global increases in body mass index (BMI) have made obesity a major public health challenge worldwide. Between 2016 and 2018, landmark reviews by the WCRF and IARC established elevated BMI as a risk factor for at least 12 cancers, yet uncertainties remain regarding generalizability beyond Europe and North America, associations with less common or smoking-related cancers, and the relevance of other adiposity measures such as waist circumference. Since these reviews, new large-scale cohorts, particularly in East Asia, and Mendelian randomization studies have greatly expanded available evidence, enabling reassessment of obesity-cancer associations.

Methods: We conducted a systematic review and meta-analysis of prospective cohorts examining BMI and risk of 25 common cancers, searching PubMed, EMBASE, and Scopus through April 23, 2025. Summary risk estimates were calculated using random-effects meta-analysis. We also meta-analysed Mendelian randomization studies, compared associations for BMI and waist circumference, and reviewed emerging imaging-based evidence.

Results: Across 226 articles comprising 1.5 million cancer data points, most cases originated from Europe (59.0%), followed by East Asia (30.1%) and North America (10.6%). BMI was positively associated with 19 cancer types and inversely associated with three. Positive associations for leukaemia (RR per 5 kg/m^2 = 1.09, 95% CI 1.05-1.13), non-Hodgkin lymphoma (1.05, 1.01-1.08), bladder cancer among never-smokers (1.04, 1.01-1.07), and glioma (1.03, 1.01-1.05) represent novel findings not reported in previous WCRF or IARC reviews, suggesting obesity may be linked to a broader range of cancers than previously recognised. For cancers where smoking is a dominant risk factor, we observed increased risks for head and neck cancer (1.07, 1.02-1.13) and bladder cancer, and decreased risks for oesophageal squamous cell carcinoma (0.72, 0.60-0.86) and lung cancer (0.92, 0.86-0.99) among never-smokers. Regional variation was evident, including stronger associations for postmenopausal breast and ovarian cancers in East Asia and weaker associations for gallbladder cancer, although many populations remain unrepresented. Mendelian randomization analyses were broadly consistent with a causal effect. Associations for BMI and waist circumference were highly similar, and available imaging data were limited.

Conclusions: This updated meta-analysis, representing the largest synthesis of evidence to date, highlights the substantial and expanding impact of obesity on cancer risk and underscores the urgent need to address this modifiable risk factor worldwide.

#3633 Synergistic effects of HIV and HPV coinfection in dysregulation of the oral mycobiome in Puerto Rican people with HIV.

Juliana M. Serrano-Rodriguez[1], Jurelis Torres-Reyes[2], Yakshi N. Ortiz-Maldonado[2], Gabriel Borges-Velez[2], Jeannette L. Salgado Montilla[2], Maria M. Sanchez-Vazquez[2], Magaly Martinez-Ferrer[3], Ramon F. Gonzalez-Garcia[4], Josue Perez-Santiago[2]

[1]University of Puerto Rico - Rio Piedras, San Juan, PR,[2]University of Puerto Rico Comprehensive Cancer Center, San Juan, PR,[3]University of Puerto Rico School of Medicine, San Juan, PR,[4]University of Puerto Rico School of Dental Medicine, San Juan, PR

Background: Despite advances in suppressive antiretroviral therapy, people with HIV (PWH) have a higher prevalence of HPV infection than people without HIV (PWOH), suggesting that other factors independent of HIV may be contributing to increased susceptibility of HPV infections in PWH. The human mycobiome (fungal communities of the microbiome) can play an important role in immune modulation, promoting activation of inflammatory pathways and the production of carcinogenic organic compounds. Non-medical factors such as oral HPV infections, can induce oral mycobiome community-level shifts which may facilitate oncogenesis, but it has not been evaluated in the context of HIV in PR. In this study, we evaluated the prevalence of oral HPV infection and chracterized the oral mycobiome in Puerto Rican PWH and PWOH with and without coinfection with oral HPV (HPV+ vs HPV-).
Methods: Saliva and oral rinse samples were collected from 132 sexually active individuals (PWH vs PWOH). Oral rinse samples were analyzed for HPV infection and genotype using the DNA ELISA kit HPV SPF10 and RHA kit HPV SPF10-LiPA25. Extracted DNA from saliva was used to sequence the ITS and characterize the oral mycobiome. Oral mycobiome was analyzed using Shannon index for diversity and Pielou index for evenness using QIIME2 and R-statistical software.
Results: The overall prevalence of oral HPV infection among participants of the study was 33%. The prevalence of oral HPV infection was 3x higher in PWH (44%) compared to PWOH (14%). Considering all HPV+ genotypes 47% were high-risk for cancer development (PWH= 95% vs PWOH= 5%). On the other hand, fungal diversity was significantly lower in PWH compared to PWOH (p= 0.038), while fungal diversity (p= 0.020) and evenness (p= 0.088) was lower in HPV+ individuals compared to HPV- individuals. Furthermore, HPV+ PWH showed significantly lower fungal diversity (p= 0.048) and evenness (p= 0.087) compared to HPV- PWOH. Moreover, PWH had significantly higher abundance of genus *Candida* than PWOH (p= 0.048). HPV+ PWH had significantly higher relative abundance of *Candida* in saliva (p= 0.007).
Conclusion: Higher prevalence of oral HPV infection was observed in PWH in comparison to PWOH in PR. Dysbiosis of the oral mycobiome was observed in both HIV and oral HPV infection, however independent of HIV status, HPV+ individuals had lower oral fungal species evenness. Moreover, *Candida* abundance levels were significantly higher in coinfection of HIV and HPV, indicating that the oral mycobiome may be potentially influenced by a synergistic effect caused by the coinfection. Overall, these findings suggest that HPV status greatly impacts oral mycobiome homeostasis that can potentially contribute to the natural history of HPV and increased cancer risk. Understanding the interplay between viral infections and the oral mycobiome may explain clinical disparities regarding the natural history of HPV in PR.

#3634 Effects of olive oil byproducts polyphenol reach extract on muscle function, sarcopenia-related parameters and skin health.

Adriana Albini[1], Sara Nofri[2], Danilo Morelli[3], Paola Corradino[1], Gianni Lo Franco[4], Calogero Caruso[5], Anna Aiello[5]

[1]IEO - European Institute of Oncology, Milan, Italy,[2]University of Florence, Firenze, Italy,[3]Fondazione IRCCS Istituto Tumori di Milano, Milan, Italy,[4]Fattoria la Vialla, Castiglion Fibocchi (AR), Italy,[5]Biomedicine, Neuroscience and Advanced Diagnostics, University of Palermo, Palermo, Italy

Sarcopenia, the age-related loss of skeletal muscle mass, strength, and function, represents a major determinant of frailty and disability in older adults. Nutraceutical strategies targeting inflammation and oxidative stress have been proposed as adjunctive countermeasures. Olive mill wastewater (OMWW), a byproduct of olive oil production, is rich in hydroxytyrosol and other polyphenols with potent antioxidant and anti-inflammatory effects. Results from a 30-day, single-arm pilot trial to evaluate several biometric and anthropometric parameters, after assumption of the OMWW extract, OMWW-OL (Oliphenolia®), revealed a positive trends to ameliorate sarcopenia-related values in adults with metabolic syndrome, a population at elevated risk for muscle decline. Twenty-nine participants were enrolled, and 23 (15 men, 8 women) completed the study. Assessments included bioimpedance-derived indices of muscle mass, anthropometry, handgrip strength, calf circumference, hydration, and inflammatory/metabolic markers at baseline (T0), after supplementation (T1), and 30 days post-intervention (T2). OMWW-OL was well tolerated. Participants showed modest but consistent trends toward improved fat-free mass index (FFMI), appendicular skeletal muscle mass (ASMM), and handgrip strength at T1, with partial persistence at T2. Calf circumference increased steadily across the observation period. Among biochemical markers, oxidized LDL (oxLDL), a lipid peroxidation indicator linked to muscle catabolism, showed a small but progressive reduction from T0 to T2, consistent with the antioxidant profile of OMWW polyphenols, whereas CRP exhibited a transient rise at T1 before returning near baseline at T2.Although statistical significance was limited by small sample size and study design, the observed trends align with preclinical evidence that OMWW polyphenols mitigate oxidative stress, suppress pro-inflammatory cytokines, and promote muscle protein homeostasis. These exploratory findings justify larger randomized trials to evaluate OMWW as a nutraceutical strategy for sarcopenia prevention and management. Sarcopenia has been also associated with cancer, is higher in oncology patients with metabolic syndrome and worsens response to therapy. Cosmeceutical preparations using OMWW-OL also reveal protective properties for the skin. One of the major polyphenols in OMWW-Ol is hydroxytyrosol, and investigations are ongoing oh the role of the purified substance.

#3635 Interim results of the BEFIT exercise intervention pilot study to assess the microbiome and immune function in a high-risk cohort for lung cancer.

Marisa Bittoni, Zachary Chaplow, Daniel Spakowicz

The Ohio State University, Columbus, OH

Background/Objective: Modifiable lifestyle risk factors, such as diet and exercise, have shown to be associated with reduced lung cancer risk. We recently launched a randomized controlled pilot trial, the BEFIT exercise intervention study, whose overall objectives are to: a) confirm the feasibility of an exercise intervention in high-risk smokers, and b) assess the intervention impact on the microbiome and inflammatory biomarkers**.** This report will describe interim study results, including participant characteristics, recruitment challenges and adherence in this ongoing study.
Methods: Participants from The Ohio State University Lung Cancer Screening Clinic (OSULCSC) and social media were randomized into one of two arms: (a) Exercise/Behavioral Support Intervention - an ACSM-approved 12-week virtual resistance training plus aerobic program, or (b) Standard of Care - an information-only, control condition (e.g. light walking). Eligibility criteria included: ages 40-80 years, exercise<150 minutes/week, 20 pack-year smoking history and computer/internet access. Blood draws, stool samples, physical activity measures and behavior change predictors will be evaluated at baseline and intervention completion, with 1-year follow-up to assess adherence.
Results: Individuals were primarily recruited through the OSULCSC and social media ads. Our goal was to recruit 40 participants (20 per arm), but due to dropout we had 20 in the intervention group and 16 in the control group. Common reasons for withdrawal include too busy, changed mind and no longer interested. Participant characteristics include mean age 63 years, 64% female, 89% white, 52% current smokers and mean BMI of 35 (obese) and 39% body fat. The intervention group showed significantly greater weight loss and increased lean muscle mass after the intervention. Adherence to the intervention was high with almost 90% of sessions attended with no adverse events reported. Biospecimen analyses and social cognitive intermediates are currently underway.
Discussion: We successfully launched the BEFIT exercise intervention study for long-time smokers at high risk for lung cancer with high adherence and no adverse events reported. Despite recruiting challenges and dropout, we successfully recruited and conducted the intervention, with significant improvements in weight loss and lean muscle mass after the intervention. We continue to analyze biospecimen data for changes in the gut microbiome and inflammation, and look forward to reporting these when completed.

#3636 Evaluation of a clinically integrated mHealth intervention to reduce sedentary time in adolescents and young adults with ALL during maintenance therapy.

Brittany J. Ivory[1], Yueh-Yun Chi[1], Jeannie M. Shin[1], Britni R. Belcher[2], David R. Freyer[1]

[1]Cancer and Blood Disease Institute, Children's Hospital Los Angeles, Los Angeles, CA,[2]Department of Population and Public Health Sciences, University of Southern California Keck School of Medicine, Los Angeles, CA

Background: Sedentary behavior (SB) is prevalent in early adolescents and young adults (eAYAs, 12-21 years) during acute lymphoblastic leukemia (ALL) treatment and contributes to cardiometabolic complications. Intervention during therapy can be challenging, but the maintenance phase may be opportune for SB intervention as toxicity from intensive therapy subsides and monthly visits allow for regular study contact.
Purpose: To evaluate the feasibility and acceptability of a clinically integrated, multi-component mobile health (mHealth) SB intervention in eAYAs during ALL maintenance phase; and assess effects on SB and health-related quality of life (HRQoL).
Methods: This ongoing 12-week, single-arm pilot trial includes a Fitbit with inactivity-triggered prompts, three in-clinic or virtual coaching sessions, and an app-based peer chat group. The intervention is aligned with one 12-week cycle of maintenance therapy, and in-person procedures coincide with monthly clinic visits. Feasibility is defined as ≥70% retention, N=20 enrolled, and Fitbit wear time ≥10 h/day on ≥70% days for ≥50% of sample. Acceptability is evaluated via exit surveys. At baseline and week 12, SB is assessed using the activPAL micro4 device and IPAQ questionnaire, and HRQoL is assessed via validated surveys. Outcome differences were compared by number of maintenance cycles completed at enrollment (≤ 2 [early] vs > 2 [late]).
Results: To date, N=20 are enrolled and N=16 have completed the study (median age=16.2 yrs; 69% male; 69% Hispanic; median BMI=23.3kg/m^2; 56% in early maintenance). Retention among completers is 94% (N=15) and 38% (N=6) met Fitbit wear time criteria, the majority of whom were in early maintenance (83% [N = 5] vs 14% [N = 1] in late maintenance). Acceptability is high: 93% (N=14) reported the intervention helped reduce SB and 100% would recommend it to peers. A greater proportion of participants in early vs late maintenance strongly agreed the intervention reduced SB (helpful: 88% vs 29%, p = 0.05; recommend: 88% vs 0%; p = 0.001). Overall, device-measured sedentary and sitting time decreased (−10.4 min/day and −26.3 min/day, respectively) and steps increased (+1,993/day) (all p>0.05); self-reported sitting time also decreased (−154 min/day, p=0.002). Participants in early maintenance showed similar trends to those in later cycles. There were no significant changes in HRQoL.
Conclusions: Preliminary findings indicate this mHealth SB intervention is feasible, acceptable, and can be clinically integrated during active maintenance therapy for eAYAs with ALL. Participants in early maintenance showed high adherence and engagement, suggesting the feasibility and benefit of SB intervention during active treatment for ALL and potential scalability to other types of cancer.

#3637 Improving therapeutic efficacy by targeting adenosine signaling in obese breast cancers.

Yueming Zhu, Amad Uddin, Xin Cui, Yong Wan

Emory Winship Cancer Institute, Atlanta, GA

Accumulated adipocytes in obese cancer patients significantly compromise therapeutic efficacy,yet the underlying mechanisms remain largely undefined. Here, we identify an OTUD4-driven proteolyticaxis as a critical regulator of immune suppression in obesity-associated triple-negative breast cancer(TNBC). Hyperactivation of OTUD4 enhances CD73-mediated adenosinergic signaling in cooperationwith TGF-β, establishing an immunosuppressive tumor microenvironment (TME) enriched with $TREM2^{+}APOE^{+}$ lipid-laden tumor-associated macrophages (LL-TAMs). This adenosine-rich niche promotes LL-TAM polarization toward a $CCL2^{+}$ $IL6^{+}$ efferocytic phenotype, collectively dampening cytotoxic T-cellactivity. Spatial and histologic analyses reveal regional co-expression of TGF-β, OTUD4, and CD73 withinimmune-suppressed tumor zones that spatially align with LL-TAM clusters. To therapeutically target thispathway, we developed W-DB53, a selective small-molecule inhibitor that disrupts the OTUD4-CD73interaction, depletes LL-TAMs, restores T-cell infiltration, and synergizes with immune checkpointinhibitors (ICIs) in obese TNBC models. These findings establish W-DB53 as a macrophage-remodelingprotein-protein interaction (PPI) inhibitor that reprograms efferocytosis and overcomes obesity-drivenimmune resistance in TNBC.

: Natural Products
Poster Session

#3642 Capsaicin-nanoparticles sensitize human squamous cell lung cancer towards the growth-inhibitory activity of paclitaxel.

Amanda M. Sugrue, Kushal J. Modi, Reagan S. Light, Kaitlyn B. Conley, Sarah L. Miles, Piyali Dasgupta

Marshall University, Huntington, WV

Purpose of the Study: Squamous cell carcinoma of the lung (LUSC) develops in the central part of the lung, from cells lining the airways. It is characterized by rapid doubling time, aggressive clinical progression, and a dismal five-year survival rate. The first line treatment for LUSC includes a taxane with carboplatin and immunotherapy. The acquisition of resistance to paclitaxel is a major therapeutic challenge in human LUSCs. Several convergent studies show that nutritional phytochemicals can often improve the therapeutic response of chemotherapeutic drugs. The long-term objective of our laboratory is to identify dietary chemicals that may improve the anti-cancer activity of chemotherapeutic drugs. Our published data show that capsaicin (the spicy component of chili peppers) enhanced the pro-apoptotic activity of the chemotherapy drug camptothecin in human small-cell lung cancers. However, the feasibility of capsaicin as a potential anti-cancer drug is limited by its side effect profile. The administration of capsaicin produces heat sensation, GI irritation, stomach cramps, and nausea. A way to overcome these hurdles is to encapsulate capsaicin into sustained release polymeric systems. The objective of the present research project was to explore the combinatorial activity of Capsaicin [poly(lactic-co-glycolic acid)] nanoparticles (hereby called CAP-PLGA-NPs] and paclitaxel in human LUSCs.
Experimental Procedures: The pro-apoptotic activity of the combination of paclitaxel and CAP-PLGA-NPs was evaluated by Caspase-3 Activity Assays and Cell Death ELISA assays. We also determined the ability of the combination of paclitaxel and CAP-PLGA-NPs to inhibit anchorage-dependent growth using soft agar assay. Chou-Talalay isobologram analysis was used to determine whether the interaction between the two drugs was additive or synergistic.
Results: CAP-PLGA-NPs sensitized human LUSC cells towards the growth-inhibitory activity of paclitaxel
Conclusions: The administration of CAP-PLGA-NPs may enhance the growth-suppressive activity of paclitaxel in human LUSCs.

#3643 The combination of actinomycin D and resveratrol induces synergistic anticancer activities against aerodigestive tract cancers.

Raji M. Lukmon[1], Jihan F. Amin[2], **A.R.M. Ruhul Amin**[1]

[1]Pharmaceutical Sciences, Marshall University, Huntington, WV,[2]The Ohio State University, Columbus, OH

The practice of combining multiple drugs to increase pharmacological efficacy or reduce toxicity is widely adopted in cancer chemotherapeutics. Actinomycin D (Act D) is the first FDA-approved anticancer antibiotic. However, it's widespread application was hindered by severe dose-related toxicities. In the current study, we investigated the *in vitro* and *in vivo* anticancer efficacy of the combination of Act D with resveratrol, a natural dietary compound abundant in red grapes and wines. We found that the combination of Act D and resveratrol synergistically inhibited cancer cell growth *in vitro*. We also explored the underlying mechanism of this synergistic efficacy by investigating the activation of p53 pathway including the expression of p53 target genes *p21*, *PUMA* and *GDF15*. Consistent with the cell growth inhibition, Act D, resveratrol and their combination activated p53 and induced the expression of p21, PUMA and GDF15 mRNA and proteins. The combination had better effects than any of the single agent. Ablation of p53 expression by shRNA almost completely abolished the expression of p21, PUMA and GDF15 suggesting p53-dependent expression of these genes. Finally, we investigated the *in vivo* efficacy of these agents and their combination using MDA686TU (686TU) xenografts in nude mice. Although both Act D, resveratrol and their combination significantly inhibited the growth of xenografts, the combination did not have better effects when compared to single agent. The *in vivo* efficacy of these compounds was further supported by Ki-67 expression in tumor tissues. Taken together, our findings demonstrated that although the combination of Act D and resveratrol showed synergistic effects *in vitro*, the *in vivo* efficacy was not. Supported by P20GM103434 and R15DE032063.

#3644 Chromomycin A2 disrupts leukemia cell viability via integrated autophagic and apoptotic programs.

Keli Lima[1], Emilly O. Vieira[2], Rita C. Cavaglieri[1], Frederico L. Nogueira[1], Glaucia M. Machado-Santelli[2], Leticia V. Costa-Lotufo[2], Eduardo M. Rego[1], Joao A. Machado-Neto[2]

[1]Department of Internal Medicine, University of Sao Paulo, Sao Paulo, Brazil,[2]Department of Pharmacology, University of Sao Paulo, Sao Paulo, Brazil

Acute leukemias urgently require new therapeutic approaches due to high relapse rates and frequent resistance to standard treatments. Advances in molecular profiling have enabled more selective and less toxic strategies, especially for patients with poor prognosis. Chromomycins have emerged as potential agents because they bind GC-rich DNA regions, alter chromatin architecture, inhibit RNA polymerase, and suppress transcriptional programs essential for leukemic cell survival. Among them, chromomycin A2 remains largely unexplored in hematologic cancers despite reported activity in some solid tumors. We investigated chromomycin A2 in a broad panel of leukemia models. Twenty-two human blood cancer cell lines were analyzed (14 myeloid, 17 lymphoid), including resistant variants to venetoclax (n=2), quizartinib (n=1), and ATRA (n=1). Viability (MTT), apoptosis (annexin V/PI), and autonomous clonal growth in cytokine-free methylcellulose were evaluated. Ex vivo assays used primary AML (n=3) and ALL (n=3) samples. Molecular analyses included PCR arrays covering genes related to autophagy, apoptosis, DNA damage, and cell-cycle control, together with Western blotting. Statistical significance was defined as $p<0.05$. Chromomycin A2 reduced viability in all models in a dose-dependent manner (IC50: 0.40 - 4.42 nM). Resistant derivatives showed slightly higher IC_{50} values but remained sensitive. The compound induced time- and dose-dependent apoptosis and fully suppressed autonomous clonal growth at ≥5 nM. Early responses involved autophagy markers (LC3B-II accumulation, SQSTM1/p62 reduction), compatible with decreased transcriptional output and weakened survival signaling. With longer exposure, apoptotic markers (cleaved PARP1) and DNA damage (γH2AX) predominated. Gene expression data indicated a temporal sequence: activation of autophagy and cell-cycle arrest at 6 h, followed by apoptosis-related genes at 12 h. Enrichment analyses highlighted macroautophagy, mitochondrial apoptosis, and G1 DNA damage checkpoint pathways. In ex vivo assays, IC_{50} values ranged from 1.6 to 31.8 nM, with 81-92% efficacy in primary AML and ALL cells. Chromomycin A2 displayed strong antileukemic activity across in vitro and ex vivo models, including resistant subtypes. Its sequential induction of autophagy, apoptosis, and DNA damage suggests a multitarget mechanism. The inhibition of clonal growth indicates potential activity against leukemic stem/progenitor cells. These results support further preclinical development. Supported by FAPESP, CAPES, and CNPq.

#3646 Differential mechanisms of MCF-7 cytotoxicity by oleuropein and punicic acid and the role of oxidative stress and peroxiredoxin antioxidants.

Samantha Diiorio[1], Braden Quitmeyer[2], Shelley A. Phelan[1]

[1]Fairfield University, Fairfield, CT,[2]Histogenetics LLC, Ossining, NY

Many natural compounds have been shown to possess anticancer properties against breast cancer cells in vitro and/or in vivo, and there is increased interest in understanding the effects and mechanisms of action of such products as an alternative to traditional chemotherapy. Oleuropein is a polyphenolic compound derived from olive leaves that has demonstrated antioxidant and anticancer properties in breast cancer and other cancers. Punicic acid is a poly-5-unsaturated fatty acid found in pomegranate seeds that has also shown antioxidant and anticancer effects in various cancers. The MCF-7 cell line is an important model for estrogen receptor-positive (ER+) breast cancer which is useful for studying the effects and mechanisms of these natural products. We sought to compare oleuropein and punicic acid in this model and hypothesized that both would induce cytotoxicity in MCF-7 cells by increasing the oxidative stress and disrupting mitochondrial function. Cells were treated with 50 or 200 ug/ml oleuropein, 10 or 50 ug/ml punicic acid, or 70% ethanol as a control for 72 hours. Cytotoxicity was measured using an lactate dehydrogenase (LDH) release assay, and oxidative stress was assessed using the MitoSOX assay for mitochondrial ROS and malondialdehyde (MDA) quantification for lipid peroxidation. We found that oleuropein induced a significant increase in LDH release, and morphological changes consistent with apoptosis, but no significant increase in ROS. Punicic acid induced a dose-dependent increase in LDH release, and additionally led to an increase in mitochondrial ROS and lipid peroxidation. Since we previously reported significant induction of expression of the Peroxiredoxin antioxidant genes by both oleuropein and punicic acid in these cells, we also set out to examine the effects of Prdx suppression on susceptibility to these compounds. Using transient siRNA transfections targeting each of the six Prdx genes, we found that suppression of Prdx2, Prdx3, Prdx4 and Prdx5 significantly increased MCF-7 susceptibility to punicic acid, but not to oleuropein. Together, our data suggest that these compounds induce cytotoxicity through different mechanisms, with oxidative stress playing a major role in punicic acid-induced toxicity. Targeting peroxiredoxins may be an effective strategy for increasing breast cancer cell susceptibility to these compounds in future therapeutic applications.

#3647 Combining optimally synthesized quercetin analogs with BRAF inhibitors as a novel synergistic approach to treat melanoma.

Ahlam Armaly[1], Paige Toran[1], **Victoria Del Gaizo Moore**[2]

[1]Chemistry, Elon University, Elon, NC,[2]Pharmaceutical Sciences, High Point University, Fred Wilson School of Pharmacy, High Point, NC

The purpose of this research is to generate novel quercetin analogs to use in combination with vemurafenib as a more effective treatment for BRAF-mutated melanoma. Mutations that activate BRAF signaling are found in approximately half of melanoma patients and current clinical use of BRAF inhibitors are not considered curative as recurrence rates are still high. Furthermore, resistance to BRAF inhibitors can occur making the drug no longer effective. Quercetin is a common flavonoid small molecule found in many foods with known antitumorigenic activity. While quercetin has been heavily studied in various cancers, its clinical use is limited by its low bioavailability, most likely due to the presence of numerous phenol groups. We hypothesize that quercetin analogs with higher bioavailability would enhance its antitumorigenic properties, thereby increasing its synergistic potential with BRAF inhibitors.
There are two major stages of this research: 1. Making quercetin analogs, generation of BRAF-resistant melanoma cells, and analysis of base-line drug sensitivity and 2. Evaluation of synergistic drug combinations. First, we are using bio isosteric replacement to alter quercetin while maintaining desired biological functions. Numerous studies have focused on altering the phenol groups on quercetin to improve functionality, including methods to convert the phenol to less polar groups that can improve bioavailability and anticancer properties of the analogs. The novelty of these proposed analogs is introducing fluorinated phenol bio isosteres. Initial small-scale synthesis reactions have been run using a diethyl (bromodifluoromethyl)phosphonate reaction with commercially bought quercetin followed by column chromatography, which generated 2-3 products with several phenols functionalized with fluorine. Currently, those fractions are being further purified via additional chromatography, and then specific compounds will be identified using IR-spectroscopy, mass spectrometry, and H1-NMR. Drug sensitivity methods have also been established using CellTitre Glo 2.0 (Promega). Consistent with previously published results, the IC_{50} for Doxorubicin-HCl on SK-Mel28 cells is ~1uM. Resistance cells are currently being generated through short-term exposure of SK-Mel28 cells to 20uM vemurafenib. Next, cells will be chronically grown in a low concentration drug.
During stage 2, the synthesized quercetin analogs +/- vemurafenib will be tested on both untreated and vemurafenib-resistant melanoma cells. These experiments will examine the potential synergetic effects of these novel combinations while maximizing the clinical relevance to patients with BRAF-mutated melanoma by potentially mitigating the risk of high doses and prolonged use of vemurafenib.

#3648 Luteolin inhibits DNA methyltransferase 1 and alpha 6-integrin gene expression to suppress proliferation and stemness in breast cancer cells from patients of West African ancestry.

Michael H. Hall[1], Mya St. Louis[2], Ozichi Amobi[1], John Olanrewaju[3], Shawneee Angeloni[1], Ubaldo Soto[1], Eileen Brantley[1]

[1]Loma Linda University, Loma Linda, CA,[2]Oakwood University, Huntsville, AL,[3]Babcock University, Ilishan-Remo, Nigeria

Breast cancer mortality remains disproportionately high among women of West African (WA) ancestry, a disparity influenced in part by biological differences that shape how tumors behave and respond to treatment. We evaluated the ability of luteolin (a naturally occurring flavonoid) to confer anticancer actions in breast cancer cell lines from patients of WA and European ancestries. In estrogen receptor-positive (ER+) breast cancer cells, including those resistant to the anti-estrogen fulvestrant and triple-negative breast cancer (TNBC) models, luteolin reduced proliferation and impaired mammosphere formation. Our data suggest that luteolin can provide an alternative or complementary approach to treat breast cancer, irrespective of subtype. Notably, breast cancer cells from patients of WA ancestry demonstrated heightened sensitivity to luteolin's antiproliferative and anti-stemness effects, suggesting potential ancestry-related therapeutic vulnerabilities. Because the elevated stemness-associated molecules DNA methyltransferase 1 (DNMT1) and alpha-6 integrin (ITGA6) are both linked to poor outcomes and disease aggressiveness, we examined their regulation following luteolin treatment. Luteolin decreased the expression levels of DNMT1 and ITGA6. These findings suggest that luteolin and other natural products have the potential to help thwart drivers of aggressive breast cancer and improve breast cancer survival among patients of West African ancestry.

#3649 High-throughput screening of natural products discovers inhibitors of ribosome biogenesis.

Garrett Kimble[1], Michael Buszczak[2], Mark J. Henderson[3], Vincent Tagliabracci[2], Monagna Jarajapu[1], Bruce Posner[2], Barry R. O'Keefe[4], Sara Sanders[3]

[1]UTSW, Dallas, TX,[2]UT Southwestern Medical Center, Dallas, TX,[3]National Center for Advancing Translational Sciences(NCATS), Rockville, MD,[4]National Cancer Institute, Bethesda, MD

Cells must double their ribosome abundance every cell cycle. Thus, cancer cells have a high demand for ribosomes to match their high proliferation rate. For this reason, ribosome biogenesis has become an alluring target for cancer interventions. As the result of an evolutionary arms race, nature has produced a rich source of bioactive molecules and thus screening natural product fractions presents an opportunity to discover novel compounds that target ribosome biogenesis. In collaboration with the NIH's National Center for Advancing Translational Science (NCATS) we have screened the NCI's natural products library for inhibitors of ribosome biogenesis using a ribosome biogenesis reporter system called RiboSNAP. The RiboSNAP reporter incorporates a SNAP tag on an endogenous ribosomal protein that can be covalently labeled with fluorescent substrates in live cells. Substrates can then be washed out leaving newly synthesized SNAP tagged protein free for subsequent labeling with different substrates to distinguish between old and new ribosomes. This allows for the tracking of newly produced ribosomes from the nucleolus to the cytoplasm as a readout for ribosome biogenesis. Inhibitor discovery is predicated on the finding that inhibition of ribosome biogenesis throughout the pathway results in retention of newly translated SNAP tagged RPL28 protein in the nucleolus and/or nucleus. Previous work by our group and others has determined that nucleolar morphology serves as an indicator of ribosome biogenesis inhibitor mechanism of action and therefore different puncta morphologies indicate the inhibition of different targets. This image-based analysis suggests our screening efforts have identified not only inhibitors of rRNA transcription, but also rRNA processing and ribosome maturation. Once screening is complete, our efforts will shift towards purification of the active compounds and target identification to further our understanding of how ribosome biogenesis responds to perturbations and to develop cancer interventions. (This work was supported by 5UG3CA290312-01)

#3650 Evaluating the immunomodulatory role of celastrol in murine acute graft versus host disease after allogeneic hematopoietic stem cell transplantation.

Tara Chand Yadav[1], Yogamaya Divakar Prabhu[1], Vasantharaja Raguraman[1], Shanid Mohiyuddin[1], Venkatesh Rajamanickam[2], Ibrahim Mohammed[3], Deepthi Rao[3], Gerhard C. Hildebrandt[1], **Senthilnathan Palaniyandi**[1]

[1]Department of Medicine, Hematology and Medical Oncology, University of Missouri - Columbia, Columbia, MO,[2]Earle A. Chiles Research Institute, Providence Cancer Institute, Portland, OR,[3]Department of Pathology and Anatomical Sciences, University of Missouri - Columbia, Columbia, MO

Introduction: Allogenic hematopoietic stem cell transplantation (HSCT) is used to treat various hematological malignancies. Graft versus host disease (GVHD) is a serious complication arising after HSCT and acts as a major limiting factor of bone-marrow transplantation. Acute GVHD (aGVHD) primarily targets the gastrointestinal tract, skin, and liver, driven by alloreactive T-cells. We hypothesize that Celastrol, a bioactive triperpenoid possessing anti-inflammatory and anticancer properties, can mitigate aGVHD symptoms.

Methods: A well-defined murine aGVHD MHC-mismatched model was used, recipient (C57BL/6) mice received total body irradiation of 850 cGy and received bone marrow and splenocytes from either C57BL/6 (syngeneic) or BALB/c (allogeneic). They were then treated with Celastrol (2mg/kg) or vehicle control from day 1. On day 7, the animals were scored for clinical GVHD, euthanized, and their organs were collected for further analysis. The gut and colon pathology score was evaluated to assess inflammation, apoptosis, and disease severity.

Results: The clinical GVHD score showed a significant reduction in disease burden ($p < 0.0001$) in celastrol-treated mice compared to the allogenic control. The colon pathology scores also showed a significant decrease in gut injury in celastrol-treated ($p < 0.01$) mice compared to allogenic control. To assess the anti-inflammatory effect of Celastrol, we performed CD3+ staining of colon tissue, which showed significantly reduced ($p < 0.05$) T-cell infiltration in Celastrol-treated mice compared to allogenic control. A significant reduction in TUNEL-positive apoptotic cells ($p < 0.01$) was observed in the Celastrol-treated mice compared to allogenic recipients. To further validate and identify the pathways involved in pathophysiology, we performed RNASeq analysis. RNA-seq analysis of the colon identified differentially expressed genes (972 upregulated; 536 downregulated) between the Celastrol-treated and allogenic control group. Furthermore, gene set enrichment analysis revealed significant downregulation of genes Mpeg1, Lyz2, CX3CR1, Laptm5, and Pld4, which are relevant to the involvement of GM-CSF in the Celastrol-treated group. This suggests that GM-CSF-driven alloantigen presentation in the gut is reduced, thereby alleviating GVHD symptoms.

Conclusion: Celastrol acts as an anti-inflammatory immunomodulator, attenuating alloreactive immune cell-mediated injuries and protecting gut barrier integrity in aGVHD after hematopoietic stem cell transplantation.

#3651 Carnosic acid induces ROS and activates ASK1 signalling in NSCLC cells.

Eric J. O'Neill, Evangelia Tsiani

Health Sciences, Brock University, St. Catharines, ON, Canada

Carnosic acid (CA), a phenolic diterpene found in rosemary (*Rosmarinus officinalis*), has demonstrated anticancer activity in multiple tumor models; however, its mechanisms in non-small cell lung cancer (NSCLC) remain poorly defined. Many polyphenols exert biological effects through reactive oxygen species (ROS) generation and activation of apoptosis signal-regulating kinase 1 (ASK1)-mediated signalling, prompting this investigation into the role of ROS and ASK1 in the actions of CA. Cell viability was measured in NSCLC cells (H1299, A549, H460), and normal lung fibroblasts (MRC-5) following 48-hour CA treatment using the MTT assay. Migration of H1299 cells was assessed by scratch assay. ROS generation was quantified using dichlorodihydrofluorescin diacetate (DCFDA) fluorescence, and protein expression and activation were evaluated by western blotting and immunocytochemistry. CA decreased cell viability in a dose-dependent manner across NSCLC cell lines with IC_{50} in the micromolar range; H1299 showed the greatest sensitivity. In MRC-5 fibroblasts, maximal inhibition reached only ~50% of control compared with complete inhibition of growth observed in the NSCLC cell lines. In H1299 cells, CA significantly impaired wound closure after 24 hours, comparable to inhibition by paclitaxel. CA increased intracellular ROS levels and activated the antioxidant response pathway, evidenced by nuclear accumulation of nuclear factor erythroid 2-related factor 2 (Nrf2) and upregulation of heme oxygenase-1 (HO-1). Western blotting demonstrated activation of ASK1 and downstream mitogen-activated protein kinases (MAPK), including extracellular signal-regulated kinase (ERK), c-Jun N-terminal kinase (JNK), and p38. Pretreatment with N-acetylcysteine (NAC) attenuated CA-induced cytotoxicity, supporting a role for ROS in mediating these effects. In summary, carnosic acid inhibits viability and migration of NSCLC cells while partially sparing normal lung fibroblasts. Its effects involve ROS generation and activation of ASK1-dependent MAPK signaling. These findings provide mechanistic insight into the anticancer potential of CA in lung cancer. Future work will evaluate CA using an *in vivo* tumor xenograft model.

#3652 Thymoquinone blocks pancreatic ductal adenocarcinoma growth by altering novel circRNAs and miRNAs.

Bin Bao[1], Irfana Muqbil[2], Md Hafiz Uddin[1], Yang Shi[1], Yin Wan[1], Adeeb Aboukameel[1], Ramzi M. Mohammad[1]

[1]Oncology, Barbara Ann Karmanos Cancer Institute, Detroit, MI,[2]Lawrence Tech University, Southfield, MI

Pancreatic ductal adenocarcinoma (PDAC) is projected to become the second leading cause of cancer-related deaths worldwide underscoring the urgent need for the identification of novel therapeutical strategies. Circular RNAs (circRNAs) are a sub-group of small non-coding RNAs with a closed loop structure generated by back splicing of RNAs which play a significant role in the regulation of transcriptional and post-transcriptional processes of many genes. Altered regulations of circRNAs result in tumorigenesis and progression of a wide variety of tumors. To date there are no studies that have evaluated whether circRNAs could be modulated using natural agent derivatives for therapeutic benefit. The objective of this study is to identify tumor associated circRNAs and miRNAs modulated by black seed derivative *Nigella sativa* thymoquinone (TQ) in PDAC models. Methods: circRNA-seq, RNA pull-down, cell viability, RT-qPCR, CSC sphere formation, colony formation assays and miRNA transfection technique. TQ treatment resulted in the downregulation of PDAC-oncogenic circRNAs, along with the inhibition of cell growth, CSC self-renewal capacity, and clonogenic capacity. RT-qPCR showed that TQ suppressed the expression of 5 of the sequencing identified circRNAs (hsa_circ_0054853, hsa_circ_0012152, hsa_circ_0001495, hsa_circ_0006877, and hsa_circ_0000567) that were inherently elevated in PDAC and not in normal cells. CircR-0054853 was found to bind to specific tumor suppressor miRNAs, miR-1248 and miR-1287. The forced-expressions of these miRNAs result not only in the inhibition of cell growth but increased the sensitivity to TQ in PDAC cells as TQ treatment increased expressions of these miRNAs. These findings suggest that circR-0054853 may act as an oncogenic circRNA by sponging tumor-suppressive miRNAs, thereby promoting PDAC growth, a process that can be reversed by TQ. Notably, circR-0054853 contains 22 binding sites for AGO2, and RNA immunoprecipitation assays confirmed that its binding to AGO2 was downregulated by TQ. We also found that TQ significantly increased the efficacy of gemcitabine/nap-paclitaxel or pan Kras inhibitor RMC6236 in Kras mutant PDAC in vitro and animal models. The co-treatment of TQ with RMC6236 showed a remarkable combination effect on EZH2 and REK/MEK pathway in Kras mutant cells. In conclusion, for the first time we report that TQ has anti-tumor activity and exerts its inhibitory effects on tumor-associated cell signaling through the regulations of circRNAs, miRNAs and RBP interactions that warrants further pre-clinical and clinical investigations.

#3653 Screening of natural products library against 5-lipoxygenase (5-LOX) and mPGES1 proinflammatory targets for CRC interception.

Krishnendu Goswami[1], Nataliya Smith[2], Ravi Manjhi[2], Gopal Pathuri[1], Brandon Somerville[3], Yurong Song[3], Venkateshwar Madka[1], Kajal Biswas[4], Altaf Mohammed[4], Robert H. Shoemaker[4], Matthew J. Hart[2], **Chinthalapally V. Rao**[1]

[1]Center for Cancer Prevention and Drug Development, Stephenson Cancer Center, Department of Medicine, University of Oklahoma HSC, Oklahoma City, OK,[2]Center for Therapeutic Science, Department of Biochemistry and Physiology, University of Oklahoma HSC, Oklahoma City, OK,[3]Frederick National Laboratory for Cancer Research, Frederick, MD,[4]Division of Cancer Prevention, Chemopreventive Agent Development Research Group, National Cancer Institute, Rockville, MD

Colorectal Cancer (CRC) remains the leading cause of cancer-related mortality worldwide. Inflammation is a key hallmark of many cancers, including CRC. Pro-inflammatory lipid mediators play a key role, while COX-2 inhibiting NSAIDs are promising, their chronic use is linked with unwanted side-effects. In this context, mechanistic studies suggest that targeting microsomal prostaglandin synthase-1 (mPGES-1) and 5-lipoxygenase (5-LOX) with natural products (NP) presents a valuable opportunity to intercept CRC and mitigate those side effects. Here we aimed to perform high-throughput screening (HTS) of NCI NPs library (~500,000 semi-purified fractions) to identify potential inhibitors of 5-LOX and mPGES1; and further validate the purified compounds using secondary assays. To establish the enzyme activity inhibitory assays, first we developed a stable Human Embryonic Kidney (HEK) 293 cell lines with mPGES-1 and 5-LOX overexpression as well as 5-LOX overexpressing insect cells. Proteins expression was confirmed using western blotting. Lysates from human 5-LOX expressed in Sf9 insect cells and HEK-293 cells, were used to generate an assay format in 384-well microplates suitable for HTS. In this assay format, lysates are preincubated with inhibitors for 20 minutes, stimulated with arachidonic acid (AA) for 5 minutes. The production of free radicals, as a result of the conversion of AA to 5HPETE and LTA4 by 5-LOX activity, is detected upon the addition of 2',7'-dichlorodihydrofluorescein diacetate (H2DCFDA). The non-fluorescent H2DCFDA when oxidized by the free radicals, generates a highly fluorescent compound, which can be measured to quantify enzyme activity. The reaction was stopped after 15 minutes upon the addition of acetonitrile. Finally, enzyme activity was calculated by measuring "total relative fluorescence units (RFU) at 485-nm excitation and 530-nm emission spectra. The assay has been optimized using a final volume of 15ul and has a Z' Factor score of 0.65 and a S/B of 3.5 in 384-well microplates. The 5-LOX activity was completely inhibited by 20uM NDGA, a known inhibitor of 5-LOX. Additionally, a pre-plated NCI library of semi-purified NP fractions (5mg/ml stock in DMSO) has been assessed to validate the assay and identify potential fractions that demonstrate 5-LOX inhibitory activity. The fractions with the most promising activity based on this evaluation will be presented at the meeting. We have also optimized the mPGES1 activity assay using HEK293 cell line overexpressing COX2 and mPGES-1. In this assay format, treatment with AA results in elevated levels of PGE2, as detected in a PGE2 HTRF assay. In summary, these optimized assays will be employed for large scale robotic HTS of NCI NP library to discover and develop safer inhibitors of proinflammatory targets mPGES1 and 5-LOX for intercepting inflammation associated cancers. (Funded by NCI-UG3CA290310-01).

#3654 Plant-derived exosomes from black soybeans for combatting pancreatic and colon cancer cells.

Zhangzhu Ruixian[1], Makiko Nakahana[1], Yasuyuki Shimizu[1], Mohammed Salah[2], Hiroaki Akasaka[1], Hiroki Kawaguchi[1], Tomoya Ishida[1], Qin Qin[3], Qu Zhang[4], Takeaki Ishihara[1], Daisuke Miyawaki[1], Ryohei Sasaki[1]

[1]Radiation Oncology, Kobe University Graduate School of Medicine, Kobe, Japan,[2]Biochemistry, Faculty of Veterinary Medicine, Qena University, Qena, Egypt,[3]Radiation Oncology, Nanjing Medical University First Affiliated Hospital, Jiangsu Province Hospital, Nanjing, China,[4]Radiotherapy Center, Tongji Medical College, Hubei Cancer Hospital, Huazhong University of Science and Technology, Wuhan, China

Background: Plant-derived dietary exosomes are biocompatible granular vesicles that are considered safe and have been increasingly reported to exert beneficial effects on the human body. We independently developed a novel method for isolating food-derived exosomes from black soybeans and demonstrated their therapeutic efficacy against pancreatic and colon cancer cells.
Materials and methods: We developed a technique to efficiently isolate exosomes from freshly harvested black soybean pods. The size and morphology of the exosomes were evaluated using nanoparticle tracking analysis and transmission electron microscopy (TEM). The antitumor effects were evaluated by assessing the cell proliferation inhibitory effects using WST/MTT assays with human pancreatic cancer MIAPaca-2 and human colon cancer HCT116 cells. The efficacies of different exosome conditioning methods, such as freezing, boiling, boiling in salt, or immediate extraction, were compared in terms of their cell proliferation inhibitory effects. The radiosensitizing effects were also investigated using a colony-forming assay. The extent and frequency of DNA damage were determined using γH2AX staining, a marker for DNA damage, between four groups: control, black soybean exosomes alone, radiation alone, and a combination of both.
Results: The mean size of the exosomes was less than 200 nm. Absorption of the exosome were observed in very high frequency in MIApaca-2 cells. The exosomes obtained from approximately 20 black soybeans exhibited much higher tumor growth inhibitory effects than the solution of black soybeans without exosomes. The exosomes also showed radiosensitizing effect in response to 6 Gy of ionizing radiation.
Conclusions: These findings together represent that the plant-derived dietary exosomes from black soybeans may have potential to be a novel strategy for cancer cell growth inhibition and radiosensitization.

#3655 Dose-dependent anti-proliferative activity of a bioactive hemp-derived extract REPYR-SC1 against prostate cancer.

Joel Costoya[1], Joaquin J. Jimenez[2]

[1]Department of Biochemistry and Molecular Biology, University of Miami Miller School of Medicine, Miami, FL,[2]Dr. Phillip Frost Department of Dermatology and Cutaneous Surgery, University of Miami Miller School of Medicine, Miami, FL

In the US approximately 1 in 8 men are diagnosed with prostate cancer, and metastatic cases account for the majority of prostate cancer-related mortality. Prostatic cancer is the second leading cause of cancer death in men, harboring a 32% 5-year survival rate. Current treatments utilize a combination of androgen deprivation therapy, androgen signaling receptor inhibitors and chemotherapy. Despite these improvements, castration-resistance and chemotherapy resistance remain a significant obstacle to sustained remission and signify a need for novel therapeutic approaches. Immunotherapies and the discovery of new anti-neoplastic agents are current modalities of considerable interest. We explore the use of REPYR-SC1, a novel hemp extract, as an anti-cancer, immunomodulatory agent following the pre-clinical evidence demonstrating anti-neoplastic efficacy of cannabinoid derivatives and their potential immunoactivity. C4 cells were used to model prostate cancer, HPrEC prostate epithelial cells as a non-cancerous control, and CTLL-2 cytotoxic T lymphocytes were chosen as a quantifiable measure of immunomodulatory capability. REPYR-SC1 was administered at 0, 0.1, 0.5, 1, and 5 µL/mL and cultured with C4, HPrEC and CTLL-2 cells for 24 and 48 hours. Morphological assessment was performed by light microscopy, pre- and post-treatment. Subsequent to this manual cell counts were performed pre-and post-treatment, followed by trypan blue exclusion assay. Only viable cells were included in the cell count. REPYR-SC1 produced a significant dose- and time-dependent reduction in proliferation ($p<0.001$) in prostate cancer C4 cells and CTLL-2 cells. At a dose of 1 and 5 µL/mL at the 24- and 48-hour mark, full inhibition of proliferation was observed in C4 cells. HPrEC cells showed minimal susceptibility with 20% inhibition observed for 5 µL/mL at 48 hours. CTLL-2 cells showed significant susceptibility with complete inhibition of proliferation observed at a dose of 1 and 5 µL/mL at 48 hours. REPYR-SC1 exhibited measurable immunomodulatory effects against T-lymphocytes in vitro, and selective anti-neoplastic activity versus prostate cancer cells. In conclusion, REPYR-SC1 demonstrated evidence of potential for prostate cancer inhibition and warrants further investigation.

#3656 A-ring analogs of Andrographolide inhibit wnt1 signaling and exhibit potent anticancer activity in breast and colorectal cancer models.

Rushika Raval[1], Selina Xi[1], Ruirui Liu[1], Abigail Yee[1], Aileen Pak[1], **Edward Njoo**[1], Gary Johanning[2], Feng Wang-Johanning[2]

[1]Chemistry, Aspiring Scholars Directed Research Program (ASDRP), Fremont, CA,[2]SunnyBay Biotech, Fremont, CA

The natural product andrographolide, a labdane diterpenoid extracted from the plant Andrographis paniculata, has been extensively studied as an anticancer therapeutic, and is putatively known to function through covalent inhibition of NF-kB: a transcription factor at the crossroad of a myriad of cell signaling pathways that modulate tumor survival and metastasis. Functionalization of the C-19 hydroxyl has been shown to alter the primary mode of action from inhibition of NF-kB to modulation of the Wnt/β-catenin signaling pathway. With a systematic series of 12 silyl and trityl ether analogs of Andrographolide, we evaluated their antiproliferative activity in MDA-MB-231 (triple-negative breast cancer), MCF-7 (metastatic breast adenocarcinoma), HCT-116 (human colorectal carcinoma), and HT-29 (colorectal adenocarcinoma) cell lines. These compounds displayed greater potency than the parent compound, andrographolide. We observe unique potency in HCT-116 with the chloro butyl analog (IC 50 = 0.32μM; 24 hr), and the chloro trityl analog (IC50 = 7.32μM; 24 hr). In MDA-MB-231, the chloro butyl analog exhibits an IC50 of 10.11 μM, and chloro trityl exhibits an IC50 of 2.88 μM. Trityl ether analogs in an NF-kB SEAP reporter cell experiment show inhibition of SEAP expression in a dose dependent fashion. Additionally, upon administration of trityl ether analogs, in a Wnt/β-catenin reporter cell assay, we observe decreased luciferase expression at 10 μM. After investigating the activities of this series of compounds in connection to NF-κB and β-catenin inhibition, two putative mechanisms of action previously reported as the cellular targets of andrographolide or its analogs, we find that subtle modifications to C-19 functionalization can greatly affect the in vitro biological profile of these compounds. Notably, the trityl analog displayed significant inhibition of SEAP-coupled NF-κB activity, and diminished antiproliferative activity with coadministration of CHIR99021 compared to the TPS (triphenylsilyl) analog with the only difference being the single substitution of a carbon to a silicon atom. This study underscores the potentially complex polypharmacology of andrographolide and its analogs and highlights the importance of further examination of the lead compounds from this work in other analogous *in vitro* and *in vivo* cancer cell models.

#3657 Preclinical discovery of proscillaridin A glycan analogs for the *in vitro* and *in vivo* treatment of solid tumors.

Shreya Somani[1], Lekhya Menta[1], Gary Johanning[2], Feng Wang-Johanning[2], **Edward Njoo**[1]

[1]Aspiring Scholars Directed Research Program (ASDRP), Fremont, CA,[2]SunnyBay Biotech, Fremont, CA

Cancer persists as one of the leading causes of mortality in the US, accounting for over 2 million new cases and 611,000 deaths in 2024. In parallel, several small-molecule drugs are currently in development for the treatment of malignancies. Within those, natural products, their synthetic analogs, or other derivatives, account for about 50% of all FDA-approved anticancer small molecules. Several naturally-derived cardiac glycosides, including digoxin, digitoxin, and proscillaridin A, have been originally identified as cardiomyocyte modulators and are currently being investigated for their anti-cancer properties. These cardiac glycosides are generally classified into cardenolides and bufadienolides, which bear butenolide and pyrone D-ring functionality, respectively, and have exhibited remarkable in vitro toxicity in various cancerous cell lines. As simple modifications on steroidal small molecules have demonstrated success in augmenting bioavailability or enhancing downstream biological activities, we sought to prepare synthetic analogs of proscillaridin A, a bufadienolide isolated from the genus Scilla. We synthesized five analogs of proscillaridin A bearing acetate esters, silyl ethers, or dimethyl ketals to investigate how ketalization, acetylation, and/or silylation of the A-ring allylic glycoside might alter its anti-cancer properties. The antiproliferative activity of these compounds was evaluated alongside proscillaridin A and two model cardiac glycosides — digoxin and digitoxin — across several breast, colorectal, liver, and ovarian cancer cell lines. Through a diverse panel of cell viability and cytotoxicity experiments, reporter assays, and cell cycle and protein marker analysis by flow cytometry, we find that ketalization of the glycan of proscillaridin A provides similar, and in some cases enhanced, in vitro potency. Subsequently, to evaluate the preclinical applicability of these compounds in inhibiting solid tumor growth, we found that direct, intraperitoneal injection of proscillaridin A and its analogs demonstrated reasonably potent antitumor activity in a murine mammary cancer model, albeit with dose-limiting ADMET properties. This study establishes the foundation for further in vitro and in vivo evaluations of cardiac glycosides for the treatment of cancer.

#3658 C-4 analogs of podophyllotoxin inhibit tubulin polymerization: A generalizable platform for the discovery of antimitotic therapeutics for cancer.

Shreya Somani[1], Stella Yang[1], Lekhya Menta[2], Yining Xie[1], Anna Gribok[1], Evy Hsen[1], **Edward Njoo**[1], Gary Johanning[3], Feng Wang-Johanning[3]

[1]Chemistry, Aspiring Scholars Directed Research Program (ASDRP), Fremont, CA,[2]Aspiring Scholars Directed Research Program (ASDRP), Fremont, CA,[3]SunnyBay Biotech, Fremont, CA

Antimitotic agents, such as podophyllotoxin and its derivatives, act through a ubiquitous mechanism of action by targeting the most fundamental mechanisms of cell division, and have demonstrated broad clinical potential as anticancer therapeutics. Given the pharmacological importance of the C-4 hydroxyl on podophyllotoxin, we sought to establish a structure-activity relationship between chemical modification and in vitro potency. We previously reported that increased C-4 sterics of podophyllotoxin esters have minimal effect on cell-free tubulin polymerization, yet decrease in vitro potency against human colon cancer cells. In this study, the antiproliferative activity of 26 novel carbonate, carbamate, and silyl ether podophyllotoxin analogs was evaluated for inhibition of in vitro cell viability, cell cycle arrest, cell-free tubulin polymerization, immunofluorescence imaging, and docking models. In human and murine colorectal cancer (HCT-116, HT-29, CT-26), lung cancer (A549, Calu-1), triple-negative breast cancer (MDA-MB-231 P), liver carcinoma (Hep G2), ovarian adenocarcinoma (SK-OV-3), and embryonic kidney cells (HEK-293), the carbonate analogs exhibited greater antiproliferative activity when compared to their carbamate counterparts, while the silyl ether analogs performed the poorest. Most notably, the t-butyl carbonate exhibited the most potent activity with IC50 at or below single digit nanomolar ranges, while the carbamates exhibited IC50 values greater than 42 nM. Correspondingly, the most potent analogs also exhibited potent cell cycle G2/M arrest by flow cytometry, with t-butyl carbonate causing arrest to the greatest percentage (69.2%), affirming tubulin inhibition as the primary mechanism of action. However, those differences were not reflected in the cell-free biochemical assay, where the best carbonates and carbamates showed similar percentages of tubulin inhibition (85.78% and 85.28% respectively), and no correlation was observed between C-4 substituent and tubulin inhibition. Additionally, in silico modeling revealed a minimal difference in each analog's binding affinity, providing further evidence that C-4 functionalization does not directly alter a compound's ability to bind to tubulin. Collectively, our results suggest that absolute binding to tubulin is not the primary determinant of biological activity for C-4 analogs of podophyllotoxin across a broad panel of cancer cell lines, and that the impact of structural changes at C-4 on biological potency is agnostic to logP and steric bulk. Altogether, the structure-activity relationship described enables future development of podophyllotoxin-based antimitotic agents for cancer.

#3659 Heterogeneous expression and cancer-selective regulation of endogenous membrane TRAIL by quercetin across various human cancer cell lines.

Erin Marie Thorpe[1], Candece L. Gladson[2], Michael Kalafatis[1], Center for Gene Regulation in Health and Disease (GRHD), Cleveland State University, Cleveland, OH,

[1]Chemistry, Cleveland State University, Cleveland, OH,[2]Department of Cancer Biology, Cleveland Clinic, Cleveland, OH

We have recently shown that several human glioblastoma cell lines (M059K, T98G, A172), as well as normal human astrocytes, possess endogenous tumor necrosis factor-related apoptosis-inducing ligand (TRAIL). In addition, we demonstrated that the flavonoid quercetin promotes the trafficking of endogenous membrane TRAIL (mTRAIL) to the plasma membrane in glioblastoma cells, where it can interact with death receptors already present on the surface of neighboring cancer cells and trigger apoptosis through both the extrinsic and intrinsic pathways. In contrast, although normal human astrocytes also express endogenous mTRAIL, quercetin treatment did not enhance its trafficking to the plasma membrane or induce apoptosis. Together, these observations suggest that quercetin selectively activates mTRAIL-mediated apoptosis in cancer cells but not in normal cells (*Thorpe et al., Cancers* 2025, 17, 3197; https://doi.org/10.3390/cancers17193197). The present study explores whether mTRAIL expression and responsiveness to quercetin extend across a broader spectrum of human cancer and non-malignant cell lines. Western blotting and flow cytometry were used to evaluate mTRAIL expression in a panel of human cancer and normal cell lines, including breast cancer (MCF-7, BT-20, HCC1937), melanoma (A375, MeWo, WM164), Burkitt lymphoma (RA-1, DG-75, Daudi), normal fibroblasts (08398), and additional models currently under investigation. Endogenous mTRAIL was detected in several malignant and non-malignant lines, including MCF-7, HCC1937, A375, RA-1, Daudi, and 08398 fibroblasts, but was absent in BT-20, MeWo, WM164, and DG-75. In RA-1 and A375 cancer cells, flow cytometry further confirmed that quercetin treatment increased cell-surface mTRAIL in a concentration-dependent manner, resulting in apoptosis. Collectively, including data from our previously published findings, endogenous mTRAIL expression was detected in 8 of 12 human cancer cell lines (67%) and in all 3 non-transformed cell lines (100%), indicating that expression may vary among cancer cell lines but appears to be consistent in normal cells. Overall, these findings support a role for quercetin in promoting mTRAIL trafficking and presentation at the plasma membrane, ultimately resulting in the demise of neighboring cancer cells. Ongoing studies aim to elucidate the functional significance of endogenous mTRAIL expression across various cell types and to define the molecular mechanism by which quercetin promotes mTRAIL trafficking to the plasma membrane of malignant but not normal cells, with the goal of establishing its potential therapeutic relevance across different cancer types.

#3660 Network pharmacology reveals functional components and molecular mechanisms of andrographis combined with lactoferrin in pancreatic cancer treatment.

Yuan Li[1], Wenhao Weng[2], Ajay Goel[1]

[1]Beckman Research Institute of City of Hope, Monrovia, CA,[2]Shanghai Children's Hospital, School of Medicine, Shanghai, China

Background: Pancreatic cancer (PC) remains the most lethal malignancies, underscoring the need for novel therapeutic strategies. Natural plant-derived bioactive compounds have garnered increasing attention as potential anticancer agents due to their safety, affordability, and ability to target multiple pathways regulating cellular growth. Network pharmacology has emerged as a powerful approach to elucidate the multi-target and multi-pathway mechanisms of various bioactive compounds, offering theoretical insights into their synergistic therapeutic potential in complex diseases. Among natural agents, Andrographis (Andro) and Lactoferrin (Lf) have shown potent anticarcinogenic properties. However, their potential synergistic interactions and the underlying mechanisms remain largely unexplored.

Methods: In this study, we investigated the synergistic anticancer effects of Andro and Lf on PC cell lines (MIA-PaCa-2 and BxPC-3), and explored growth-regulatory pathways underlying their combined activities. Cell viability, migration, and invasion assays were performed to evaluate the antiproliferative and anti-invasive activities. Using Network pharmacology and pathway enrichment analyses, we further identified key targets and signaling pathways associated with the synergistic effects of these two compounds in PC. Subsequently, the findings from cell-culture experiments were validated using patient-derived 3D tumor organoids.

Results: The combined treatment with Andro and Lf demonstrated marked synergistic anti-tumor activity, significantly suppressing cell viability, proliferation, migration, and invasion in PC cells. Network pharmacology identified 13,778 disease-related targets and 164 putative drug targets, with 148 overlapping targets between PC and the combination treatment were deciphered. Notably, AKT1 emerged as a central node, indicating strong associations between PC progression and the pharmacological activity of Andro and Lf. Pathway enrichment analyses further indicated that the synergistic effects of the combination were predominantly linked to the PI3K-AKT signaling pathway (P<0.05) and accompanied by a significant reduction in intracellular calcium levels. Consistently, AKT1 expression was significantly higher in PC tissues compared with normal tissues in the TCGA dataset (FC = 1.24, P<0.05). Finally, in 3D organoid models, the combined treatment showed stronger anticancer activity, significantly reducing organoid number and size (P<0.05), highlighting its therapeutic potential.

Conclusion: Our study provides evidence that the synergistic anticancer effects of Andro and Lf in PC are mediated via the PI3K-AKT signaling pathway and modulation of intracellular calcium levels, highlighting their promise as a combinatorial therapeutic strategy.

#3661 Discovery of Spondias mombin flavonoid rutin as a novel DNA methyltransferase 1 inhibitor and potential agent to treat triple negative breast cancer in patients of West African ancestry.

Afees John Olanrewaju[1], Elyssa Fraser[2], Joseph Enya[3], Leviticus Arietarhire[3], Ezekiel Olugbogi[4], Toluwanimi Afolabi[5], Oladimeji Soremekun[1], Michael Hall[2], Ozichi Amobi[2], Victor Chinedu[2], John Khalaf[6], Jonathan De Anda[7], Shawnee Angeloni[2], Ubaldo Soto[6], Eileen J. Brantley[8]

[1]Anatomy, (Eureka Research Lab), Babcock University, Ilishan-Remo, Nigeria,[2]Basic Science, Loma Linda University Health, Loma Linda, CA,[3]Anatomy, Babcock University, Ilishan-Remo, Nigeria,[4]Biochemistry, Babcock University, Ilishan-Remo, Nigeria,[5]Anatomy, Olabisi Onabanjo University, Ilishan-Remo, Nigeria,[6]Department of Basic Sciences, Loma Linda University Health, Loma Linda, CA,[7]Department of Pharmaceutical and Administrative Sciences, Loma Linda University Health, Loma Linda, CA,[8]Loma Linda University Health, Loma Linda, CA

Women of West African (WA) ancestry disproportionately experience poor breast cancer outcomes, even when diagnosed with the estrogen receptor (ER)-positive subtype. Recent chromatin accessibility analyses reveal ancestry-specific upregulation of DNA methyltransferase1 (DNMT1), with elevated DNMT1 levels in WA patients correlating with worse survival. Given the traditional use of *Spondias mombin* in WA populations for breast cancer, and the known epigenetic activity of flavonoids, we investigated the therapeutic potential of its major flavonoid, rutin and sought to delineate a probable mechanism of anticancer action. Seventeen breast cancer-related molecular targets were screened using molecular docking and Molecular Mechanics/Generalized Born Surface Area binding energy calculations. Rutin's binding interactions were analyzed in detail using 2D/3D interaction mapping, hydrogen-bond profiling, and stability metrics. Rutin demonstrated strong potential binding affinity to 10 of 17 breast cancer targets, with the most favorable interaction observed with DNMT1, surpassing those with HER2, mTOR, AKT1, and EGFR. Docking analyses identified multiple stabilizing hydrogen-bond interactions within the DNMT1 catalytic pocket, suggesting direct inhibition of enzymatic activity. Rutin also engaged key regulators of proliferation (CDK4, Cyclin D1), angiogenesis (VEGF-A), and DNA repair (BRCA1/2), indicating a multi-targeted anticancer profile. The strong DNMT1binding supports a mechanism in which rutin may relieve methylation-dependent silencing of tumor suppressor genes, whose reduced expression associates with poor survival, particularly among patients of WA ancestry. Colony-forming assays reveal that rutin exhibits potent antiproliferative activity in breast cancer cells, particularly those derived from patients of WA ancestry. Quantitative PCR analyses show that rutin inhibits DNMT1 gene expression in cells derived from patients of WA ancestry. Our in-silico findings identify rutin as a high-affinity DNMT1inhibitor with multi-pathway anticancer potential, supporting a role for flavonoid-mediated epigenetic reprogramming in reducing breast cancer disparities. Our in vitro findings suggest that rutin inhibits DNMT1 to ultimately suppress TNBC cell proliferation. These results justify further mechanistic validation in ancestry-derived breast cancer models and support the development of *S. mombin*-derived flavonoids as low-toxicity, ancestry-relevant therapeutic candidates.

#3662 Activity profiling of natural compounds identifies potent chemotypes active in parental and drug-resistant lymphoma models.

Filippo Spriano[1], Francesca Ghirga[2], Deborah Quaglio[2], Mattia Mori[3], Alberto J. Arribas[1], Bruno Botta[2], Francesco Bertoni[1]

[1]Institute of Oncology Research, Universita della Svizzera italiana, Bellinzona, Switzerland,[2]Department of Chemistry and Technology of Drugs, Sapienza University of Rome, Rome, Italy,[3]Department of Biotechnology, Chemistry and Pharmacy, University of Siena, Siena, Italy

Background. Despite the big improvements achieved during the years, too many patients affected by lymphomas still succumb to their disease. Plants represent an extremely rich source of structurally diverse secondary metabolites, which can provide novel active compounds. Thus, we screened a curated library of 37 natural (mostly plant-derived) and nature-derived compounds in cell lines derived from marginal zone lymphoma (MZL), including those with acquired resistance to targeted agents. The library consisted of molecules selected through a cheminformatics approach for their diversity, and spanned 16 chemical classes, including anthranoids, flavonoids, chalcones, triterpenes, alkaloids, acetophenones, benzophenones, coumarins, and a dibenzofuran derivative.
Methods. The library was screened for anti-proliferative activity in 6 MZL lymphoma-derived models (VL51, and 3 BTK/PI3K/BCL2 inhibitors (i) resistant; Karpas1718, and BTKi/PI3Ki resistant). Cells were treated with each compound at 0.4 µM, 4 µM, and 40 µM for 72 hours. Cell viability was assessed using an MTT assay, normalized to DMSO controls. Data were analyzed by class and by individual compound across doses and cell-line subgroups, using a ≥30% reduction in proliferation as the threshold for activity.
Results. At 0.4 µM, most compounds displayed minimal inhibition, with only vismione B (anthranoid) showing partial activity. At 4 µM, modest reductions were observed in selected chalcones and in usnic acid (dibenzofuran). At 40 µM, clear class- and compound-dependent effects emerged. The most active compounds, osajin (flavonoid), ursolic acid (triterpene), usnic acid (dibenzofuran), cordoin, and 4,4′-O-methoxy-chalcone, reduced viability to <25% across all models. These compounds were also validated in a dose-dependent study. By class, chalcones, flavonoids and anthranoids were among the most active chemical classes. A comparison between parental and resistant sublines revealed that most active compounds retained their activity in both settings, indicating resistance-independent mechanisms of action. Some of the tested flavonoids showed preferential activity in VL51 rather than Karpas1718. Finally, selected compounds were tested against the CB-33 lymphoblastoid cell line, with a particular focus on usnic acid (benzofuran), which demonstrated more cytotoxicity in lymphoma cells than in the non-lymphoma cell line.
Conclusions. This screen of structurally diverse natural compounds identified chalcones, flavonoids, and anthranoids as the most active classes in lymphoma models. The reproducible, dose-dependent activity of osajin, ursolic acid, usnic acid, cordoin, and 4,4′-O-methoxy-chalcone across all models highlights them as promising lead scaffolds for further mechanistic studies and medicinal chemistry optimization toward novel anti-lymphoma agents.

#3663 Antiproliferative screening in B cell lymphoma: Ghanaian medicinal plants and their phytochemical correlates.

Filippo Spriano[1], Alberto J. Arribas[1], Alberto Furlan[2], Johnson Nketiah[3], Barbara Z. Anibea[3], Andrea Cavalli[2], Afua A. Mensah[1], Dorcas Osei-Safo[3], Francesco Bertoni[1]

[1]Institute of Oncology Research, Universita della Svizzera italiana, Bellinzona, Switzerland,[2]Institute of Research in Biomedicine, Universita della Svizzera italiana, Bellinzona, Switzerland,[3]Department of Chemistry, University of Ghana, Accra, Ghana

Background. Lymphomas remain a major cause of morbidity and mortality, with patients relapsing due to resistance to treatment and cumulative toxicity. Over 60% of anticancer drugs are derived from plant-derived natural products (NPs) or their derivatives. NPs add 3D-rich scaffolds that broaden chemical space and engage “hard” targets. Semi-synthesis around NP cores can enhance potency, selectivity, and pharmacokinetics, preserving novel mechanisms orthogonal to current agents, which help bypass or delay resistance. Here, we have studied NPs derived from 10 Ghanaian individual plant species and 2 defined mixtures for their anti-tumor activity in marginal zone lymphoma (MZL) models, including derivatives with secondary resistance to BTK, BCL2, and PI3K inhibition.
Methods. We screened 48 samples (single species, mixtures, purified compounds, fractions, extracts) in VL51, SSK41, Karpas1718parental and their resistant derivatives (VL51 ibrutinib resistant, SSK41 venetoclax resistant, and Karpas1718 idelalisib resistant) at 10 and 1 µg/mL for 72 h (MTT). Activity was defined as ≥30% inhibition of proliferation. Selected chemotypes were assigned by LC/MS-guided isolation and NMR.
Results. The samples’ activity was heterogeneous, with 7% of all readouts active at 1 µg/mL and 30% at 10 µg/mL. The most consistent and potent inhibition was observed for *Dichapetalum heudelotii* root fractions (DOS-19/20/21/22) and *Xylopia aethiopica* fruit fractions (DOS-34/45/47). DOS-20 contained stilbenoids including (E)-combretastatin A-1, combretastatin B-1, and heudelotols, and produced a strong and broad inhibition of proliferation at 10 µg/mL. DOS-34 and -47, enriched in ent-kaurane diterpenoids, exerted strong inhibition of proliferation at 10 µg/mL, with a clear loss of activity at 1 µg/mL, indicating a steep dose-response behavior. The single compound hexyl-9-oxodecanoate (DOS-8) exhibited higher activity at both 10 and 1 µg/mL in SSK41 venetoclax-resistant cells than in parental cells. Similarly, the single compound isomeranzin, derived from *Clausena anisata*, and the *Xylopia* + *Bambusa* precipitate showed higher activity in SSK41 venetoclax-resistant cells. Subfractions from column chromatography of a mixture of *Aloe vera* and *T. officinale* showed preferential activity in SSK41 cells and Karpas1718, with higher activity in Karpas1718 idelalisib-resistant cells than in parental cells.
Discussion. We observed a strong chemotype-activity pattern: stilbenoids and ent-kaurane diterpenoids were the most potent profiles, while alkaloids exhibited narrower, context-specific effects; fatty ester-rich samples were mostly inactive. The sharp dose dependence of *Dichapetalum* and *Xylopia* fractions with activity in resistant and TP53-defective models suggests that they are priority leads for mechanism-of-action studies and optimization against drug-resistant B-cell lymphomas.

#3664 A novel 4-herb traditional Chinese medicine formula inhibits metastasis of triple-negative breast cancer.

Longling Wang[1], Julia K.M. Lee[2], Judy Y.W. Chan[2], Zhong Zuo[1], Kenneth K.W. To[1]

[1]School of Pharmacy, The Chinese University of Hong Kong, Hong Kong, China,[2]Institute of Chinese Medicine, The Chinese University of Hong Kong, Hong Kong, China

Background and Aim: Breast cancer is the most common cancer in women worldwide. Triple-negative breast cancer (TNBC) is the most aggressive breast cancer subtype with high metastatic capacity and dismal prognosis. Accumulating evidence suggests that Traditional Chinese Medicine (TCM) is a promising strategy for cancer treatment. Our team previously reported that a TCM formula consisting of *H. diffusa, A. paniculata, A. senticosus,* and *C. sinensis* exhibited a potent antitumor effect in a metastatic breast cancer mouse model. The formula was shown to reduce metastatic lesions in the lungs and livers of experimental mice. Recently, we modified this herbal formula by substituting *C. sinensis* with *G. lucidum* (a potent immunostimulatory herb) with an aim to improve the antitumor and antimetastatic efficacy. This study aimed to (i) investigate this modified formula (hereafter called GHAA) systematically both *in vitro* and *in vivo*, and (ii) elucidate its mechanism of action by bioinformatics analysis.
Method: Morphological and chemical authentications of the herbs were accomplished in accordance with the Chinese Pharmacopoeia. The anticancer effect of GHAA or its 4 individual herb extracts was evaluated in the TNBC cell line by MTT assay. The synergistic anticancer effect was analyzed by the SynergyFinder software. Anti-migration and -invasion effects were evaluated by wound healing and invasion assays, as well as in the zebrafish xenograft model. RNA sequencing was conducted in TNBC cells treated with GHAA or its individual herbs to elucidate the differentially expressed genes and altered pathways following treatment. The transcriptomic signatures induced by GHAA or its individual herbs were queried against the Connectivity Map database to elucidate their possible mechanism of action. The antitumor and anti-metastatic efficacy of GHAA was also investigated in nude mice bearing TNBC tumor xenografts *in vivo*.
Results: GHAA inhibited TNBC proliferation in a concentration-dependent manner *in vitro* (IC_{50} ~ 1 mg/mL). Simultaneous combination of GHAA and doxorubicin was mildly synergistic. GHAA induced apoptosis, but it had no effect on cell cycle regulation. Also, GHAA was shown to significantly inhibit TNBC migration and invasion, and metastasis in the zebrafish model. RNA-seq analysis revealed that ribosomal biogenesis is the top altered biological process by GHAA. Using the connectivity mapping approach, the most potent herb (*A. paniculata*; IC_{50} ~ 0.2 mg/mL*)* within GHAA was found to share a highly similar transcriptomic signature as cathepsin inhibitors, implying its mechanism of action. Finally, GHAA also displayed significant antitumor and anti-metastatic efficacy in TNBC-inoculated nude mice without inducing notable toxicity.
Conclusion: The findings advocate clinical evaluation of GHAA for the treatment of metastatic TNBC.

#3665 Oleuropein, a phenolic compound from olive leaves, exerts cytotoxicity and peroxiredoxin induction in MDA-MB-231 breast cancer cells.

Giovanna Kalin, Adam Vaz, Shelley A. Phelan

Biology, Fairfield University, Fairfield, CT

Extra virgin olive oil, a foundational element of the Mediterranean cuisine, has been widely associated with numerous health benefits, including the prevention of degenerative diseases and the promotion of longevity. A major bioactive component of the olive tree is oleuropein, a phenolic compound predominantly found in olive leaves and fruit. Oleuropein has been well-characterized for its potent antioxidant and anti-inflammatory properties, as well as its potential anticancer effects demonstrated in both animal and cell-based models. In this study, we investigated the effects of oleuropein on the human triple-negative breast cancer cell line MDA-MB-231. Cells were treated with oleuropein at concentrations of 50, 200, and 400 µg/mL, or 70% ethanol control. We assessed cell viability using the MTS assay, and cytotoxicity and apoptosis using a Caspase 3/7 activity. We found the highest concentration of oleuropein to induce a 3-fold decrease in viable cell density and an 8-fold increase in apoptosis. We also examined the effect of oleuropein on the expression of the peroxiredoxin (Prdx) gene family, which encodes thiol-specific antioxidant proteins known to protect cells from oxidative damage and that we previously demonstrated to be induced by oleuropein in MCF-7 cells. We found significant induction of Prdx gene expression in MDA-MB-231 cells by oleuropein, with a marked induction of Prdx1 with the 400 ug/ml treatment. Current research is aimed at measuring Prdx protein expression in oleuropein-treated cells, as well as the effect of Prdx suppression on oleuropein susceptibility. Together, these findings suggest that oleuropein exerts dose-dependent anticancer effects in MDA-MB-231 cells that result in a robust peroxiredoxin antioxidant protein response. Further exploration of the mechanism of action of oleuropein in MDA-MB-231 cells will provide important insights into its pro-oxidant effects and potential therapeutic applications.

#3666 Antitumor effects of coffee diterpenes, kahweol acetate and cafestol, on taxane-resistant and neuroendocrine prostate cancer cells.

Tomohiro Hori, Hiroaki Iwamoto, Taiki Kamjima, Hiroshi Kano, Makino Tomoyuki, Renato Naito, Hiroshi Yaegashi, Kazuyoshi Shigehara, Takahiro Nohara, Kouji Izumi, Atsushi Mizokami

Department of Integrative Cancer Therapy and Urology, Kanazawa University Graduate School of Medical Science, Kanazawa, Japan

Background: Epidemiological studies have reported that higher coffee consumption is associated with a reduced risk of prostate cancer. Kahweol acetate and cafestol, major diterpenes found in unfiltered coffee, have shown antitumor activity in prostate cancer cells. However, their effects on treatment-resistant subtypes, including taxane-resistant castration-resistant prostate cancer (CRPC) and neuroendocrine prostate cancer (NEPC), remain unclear. Therapeutic options for these aggressive variants remain extremely limited, highlighting the need for novel agents. We aimed to investigate the antitumor potential and underlying mechanisms of kahweol acetate and cafestol in these refractory prostate cancer models.
Methods: We used docetaxel-resistant (DU145-TxR, PC-3-TxR) and cabazitaxel-resistant (DU145-TxR/CxR, PC-3-TxR/CxR) prostate cancer cell lines, which were established from their respective parental DU145 and PC-3 cells. In addition, the neuroendocrine prostate cancer cell line NCI-H660 was included. Cells were treated with kahweol acetate and/or cafestol (10-100 μM). Cell proliferation and migration were evaluated. Synergistic effects were analyzed using the combination index-isobologram method. Apoptosis induction and cell cycle distribution were evaluated by flow cytometry. Expression of apoptosis-related (cleaved-caspase-3, cleaved-PARP, Bcl-2, Bcl-xL) and EMT-related (Snail, Slug) proteins was examined by western blotting.
Results: Both kahweol acetate and cafestol significantly inhibited proliferation and migration in all resistant and NEPC cell lines in a dose-dependent manner. Combined treatment (30 μM each) produced synergistic inhibition. Flow cytometry demonstrated an increased sub-G1 population and a reduced G2 phase, suggesting apoptosis induction. Western blotting revealed increased cleaved-caspase-3 and cleaved-PARP expression, along with decreased anti-apoptotic Bcl-2 and Bcl-xL levels. EMT markers Snail and Slug were also downregulated, indicating suppression of migratory potential.
Conclusions: Kahweol acetate and cafestol exert strong antitumor effects in taxane-resistant and neuroendocrine prostate cancer cells through synergistic induction of apoptosis and inhibition of EMT. Given their efficacy at clinically achievable concentrations, these coffee-derived diterpenes represent promising candidates for novel therapeutic approaches in treatment-resistant prostate cancer.

#3667 Neohesperidin dihydrochalcone: A novel natural inhibitor of ferroptosis.

Bomi Han, Yi-Xi Gong, Seonghye Son, Eui Man Jeong

Jeju National University, Jeju, Korea, Republic of

Ferroptosis, a form of regulated cell death characterized by the iron-dependent accumulation of lipid peroxides, is increasingly recognized as a critical pathogenic mechanism in various human diseases. Given the significant implication of ferroptosis in pathology, there is an urgent need to identify novel chemotypes with anti-ferroptotic activity. Recently, natural products have garnered attention as safe and effective sources for ferroptosis regulators. In this study, we identified Neohesperidin dihydrochalcone (NHDC), a flavonoid sweetener derived from citrus fruits, as a potent inhibitor of ferroptosis. We demonstrated that NHDC significantly restored cell viability in HT-1080 cells treated with Erastin, a System Xc– inhibitor. Mechanistically, NHDC treatment effectively mitigated the accumulation of lipid reactive oxygen species (ROS) and modulated the expression of ferroptosis-related proteins, including SLC3A2, SLC7A11, and PTGS2. Furthermore, NHDC exhibited a protective effect against ferroptosis induced by Sulfasalazine (SAS), another System Xc– inhibitor, by reverting SAS-induced lipid ROS levels. Interestingly, NHDC showed selectivity in its protective mechanism, distinguishing its activity from RSL3-induced ferroptosis pathways. Collectively, our findings demonstrate that NHDC acts as an effective anti-ferroptotic agent by targeting System Xc– inhibition. This study provides valuable insights into the therapeutic potential of NHDC as a natural candidate for the treatment of ferroptosis-related diseases.

#3668 Targeting apoptotic machinery using methanolic extracts of *Carpobrotus edulis* to suppress pancreatic cancer growth.

Lesetja Motadi[1], Ronald Makalapetlo[2]

[1]University of Johannesburg, Johannesburg, South Africa,[2]Biochemistry, University of Johannesburg, Johannesburg, South Africa

Pancreatic cancer remains a formidable global health challenge. Current cancer treatments, such as chemotherapy are expensive and limited. Consequently, investigating alternative anticancer treatments, such as medicinal plants, is crucial. This study aimed to investigate the potential anticancer properties of a crude methanolic extract and isolated compounds from *Carpobrotus edulis* by targeting apoptotic machinery in pancreatic cancer cells (MIA PaCa2). Multiple assays, including Alamar blue, ATP, Hoechst staining, Caspase 3/7 activity, DNA fragmentation, and RT-qPCR, were conducted to assess apoptosis induction. The crude methanol and isolated compounds did not affect the MRC-5 non-cancerous cell line. Mechanistic investigations confirmed that the crude extract activated the extrinsic TNF-mediated apoptosis pathway, evidenced by a significant increase in TNF expression and caspase 3/7 activity, leading to DNA and nuclear fragmentation, chromatin condensation, and the formation of apoptotic bodies. The loss of cell confluence, supported by non-significant(p>0,05) downregulation of STAT3, further suggested inhibited cell growth. While some changes were observed in the expression of p53, Bak1, and Fas for both the crude extract and isolated compounds, these were not statistically significant (p>0,05). Protein-ligand docking studies of the identified 7,9-Ditert-butyl-oxaspiro [4.5] deca-6,9-diene-2,8-dione and 1-octadecanol proved the compounds as having high affinity for the selected ligands: TNFR, FADD, p53, Bak1, and STAT3. Future research will focus on the further purification and investigation of the most potent isolated compound.

#3669 Oleuropein downregulates MITF via direct PKA inhibition and ERK-mediated turnover in melanoma.

Ingyu Lee, Jihye Kim, Yi-Xi Gong, Eui Man Jeong

Jeju National University, Jeju, Korea, Republic of

The Microphthalmia-associated Transcription Factor (MITF) acts as a molecular rheostat in melanoma, governing the switch between proliferative and invasive phenotypic states. Since constitutive activation of the PKA-CREB axis drives high MITF levels to sustain tumor proliferation, targeting this pathway offers a promising therapeutic strategy. Here, we elucidate the mechanism by which oleuropein modulates MITF stability and expression in melanoma and normal melanocyte models. In B16F10 melanoma cells characterized by aberrant PKA signaling, oleuropein directly inhibited PKA catalytic activity, leading to reduced CREB phosphorylation and subsequent transcriptional suppression of MITF. Furthermore, oleuropein triggered ERK1/2 activation, accelerating MITF protein turnover. Consequently, oleuropein dismantled the hyper-proliferative transcriptional program through dual upstream and downstream regulatory mechanisms. Crucially, oleuropein reduced basal MITF levels in normal human melanocytes and effectively blunted MITF spikes induced by α-MSH or forskolin. This suggests that oleuropein functions as a potent inhibitor of the PKA-CREB axis, preventing pathological signaling amplification under both basal and hyperactivated conditions. In conclusion, by targeting PKA catalytic activity and promoting ERK-dependent degradation, oleuropein effectively attenuates aberrant MITF expression. These findings position oleuropein as a promising modulator of melanoma phenotypic plasticity with potential therapeutic applications.

#3670 Beta-lactams, structural mimics of natural products, as anti-pancreatic cancer agents: A pilot study.

Debasish Bandyopadhyay[1], Tushar Debnath[1], Attrayo Mukherjee[2], Jonathan Rock[1], Omar Espino[1], Vivek Kumar Kashyap[3], Subhash C. Chauhan[4]

[1]Sch. Integr. Bio. Chem. Sc., The University of Texas Rio Grande Valley, Edinburg, TX,[2]School of Biotechnology, Kalinga Institute of Industrial Technology (KIIT), Bhubaneswar, India,[3]The University of Texas Rio Grande Valley, McAllen, TX,[4]The University of Texas Rio Grande Valley, Mc Allen, TX

Around 95% of pancreatic tumors harbor mutations in codons G12, G13, and Q61 of the *KRAS* gene. Thus, there is a significant unmet need for the development of selective KRAS inhibitors. Alternatively, the four-membered cyclic amides, commonly known as β-lactams, are found in nature. Since their discovery, beta-lactam antibiotics have played a central role in fighting against bacterial infections. However, the 'upgradation' of β-lactams from one generation to another is required for drug resistance, which is predominantly due to bacterially produced β-lactamase enzymes that hydrolyze the highly strained β-lactam ring because of tremendous angular strain. We hypothesize that, as cancer cells do not produce β-lactamase enzymes, the β-lactam ring's stability should be higher in tumor environments. With appropriate chemical modifications, β-lactams should inhibit proteins responsible for the proliferation, angiogenesis, and metastasis of various cancers, including hepatobiliary-pancreatic carcinomas (HPCs). HPCs include hepatocellular carcinoma (HCC), biliary tract cancers (BTCs), and pancreatic cancer (PanCa), which are highly challenging to treat and manage. As a part of our ongoing research in developing small molecule inhibitors from natural sources through chemical modifications (semi-synthetic) and/or by appropriate structure-based design and synthesis of structural mimics of natural products, we have successfully carried out computer-assisted design, multi-step synthesis, and *in vitro* anti-pancreatic cancer evaluation of a small series of β-lactams as KRAS inhibitors. There are a few methods for synthesizing the beta-lactam core unit, and we used the [2+2] ketene-imine cycloaddition (Staudinger) reaction followed by derivatization to synthesize the target 2-azetidinones. Further, MTT and apoptosis assays, cell cycle analysis, gamma-H2AX (phospho-Ser139) staining, and BrdU incorporation studies were conducted. Most of the products in this series demonstrated excellent (*in vitro*) activity in pancreatic cancer cell lines. The newly synthesized β-lactams demonstrated hundreds- to thousands-fold higher activity than the positive control, gemcitabine, in PANC-1 cells. Comparison of IC_{50} values in pancreatic cancer cells (PANC-1) and normal pancreatic epithelial cells (NPC) shows that almost all compounds exhibit 3-359 times greater selectivity for PANC-1 than for NPC. The *in silico*, and *in vitro* validated β-lactams could successfully serve as an entry point for clinical trials after appropriate *in vivo* evaluation. The work will significantly strengthen the fight against pancreatic cancer and undoubtedly foster a collaborative environment for future research.

: Science and Health Policy 1
Poster Session

#3674 The impact of race/ethnicity on survival in secondary triple negative breast cancer.

Ana Isabel Jacinto, Theresa Keegan, Qian Li, Fran Maguire, Candice Sauder

UC Davis Comprehensive Cancer Center, Sacramento, CA

Objective: To identify if treatments used for secondary triple negative breast cancer are associated with survival differences by race/ethnicity.
Background: Survival in women with secondary breast cancer, and those with triple negative breast cancer (TNBC), is worse for young women, especially non-Hispanic (nH) Black women. We hypothesize this is related to treatment received.
Methods: Females, aged 15-50 years, diagnosed with a TNBC during 2003-2019 were identified using the California Cancer Registry. Multivariable logistic regression compared characteristics of secondary vs primary TNBC. Multivariable Cox proportional hazards regression models evaluated associations of secondary vs primary TNBC on overall survival (OS) and breast cancer specific survival (BCSS). Analyses were stratified by race/ethnicity.
Results: Of 682 women with a secondary TNBC, 48.5% were nH White, 11.3% were nH Black, and 31% were Hispanic. All women with a secondary TNBC (vs primary TNBC) were more likely to receive a mastectomy and non-anthracycline based chemotherapy. NH White women were less likely than women of other races/ethnicities to have axillary lymph node dissections. Hispanic and nH White women with a secondary (vs primary) TNBC experienced worse OS and BCSS, which was not seen in nH Black and Asian/Pacific Islander women (Figure 1).
Conclusion: While treatments were similar for secondary vs primary TNBCs by race/ethnicity, Hispanic and nH White women with secondary TNBC experienced worse survival. Our findings suggest that tumor biology, rather than treatment, differs in secondary TNBC, warranting different treatment algorithms to improve outcomes.

Figure 1: Multivariable Adjusted Cox Proportional Hazard Ratios for Overall Survival and Breast Cancer Specific Survival for Secondary compared to Primary Triple Negative Breast Cancer by Race/Ethnicity

Overall Survival	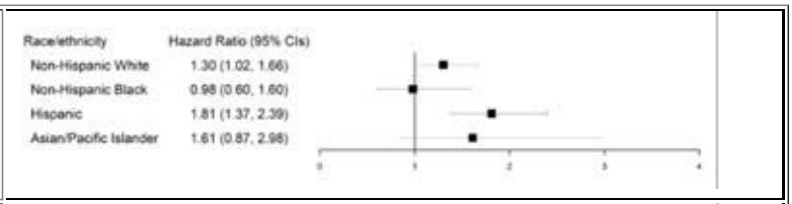
Breast Cancer Specific Survival	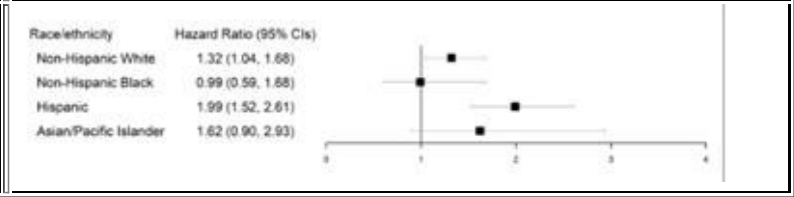

#3675 Identifying determinants of molecular testing for advanced non-small cell lung cancer in the rural United States.

Dena Rhinehart, Amanda L. Blackford, Kristen Marrone, Craig Pollack, Josephine Feliciano

Sidney Kimmel Comprehensive Cancer Center at Johns Hopkins University, Baltimore, MD

Background: Targeted therapies for non-small cell lung cancer (NSCLC) have led to population level improvements in mortality and can double overall survival for some patients with sensitizing mutations. Up to 60% of patients with advanced NSCLC may be eligible for these treatments, and US national oncology guidelines recommend molecular testing for patients with advanced disease. However, patients in the rural US are less likely than urban counterparts to receive molecular testing to determine eligibility for targeted therapies. The most rural populations also face twice the NSCLC mortality rate than the most urban populations, in part due to reduced access to guideline concordant care. Understanding the determinants of and processes involved in testing in the rural US is critical to develop strategies to deliver this care to this population with disproportionately high NSCLC mortality rates. In this study, we are examining patient level and systems level determinants of molecular testing in the rural US.

Methods: Utilizing the SEER-Medicare database linked to federal housing assistance, we have identified a cohort of patients diagnosed with advanced NSCLC between 2014-2019 using the Surveillance, Epidemiology, and End Results (SEER) cancer registry program and Medicare database linked with data from the US Department of Housing and Urban Development. Individuals were 66 to 95 years old at diagnosis and continuously enrolled in fee-for-service Medicare for at least 12 months before diagnosis and either to death or six months after diagnosis. Molecular testing, as evidenced by epidermal growth factor receptor (EGFR) testing was identified via claims using HCPCS codes 81235, 81275, 81276, 81400-8, 81415, 81455, 81504, and 81540. We are also surveying multidisciplinary providers (pathologists, proceduralists, oncologists, nursing) to identify health system barriers and facilitators to molecular testing in the rural Mid-Atlantic. The survey questions were developed using the Consolidated Framework for Implementation Sciences (CFIR) 14-question survey as a guide.

Results: We identified 8713 individuals with advanced NSCLC residing in a rural area at the time of diagnosis in the SEER-Medicare database. The overall rate of EGFR testing was 21.1%. Individuals tested were younger (75.1 v 76.3 years), more likely to be married (36.6% v 32.8%), did not originally qualify for Medicare due to disability (12.1% v 18.6%), did not have concurrent Medicaid coverage (13.9% v 23.3%) and had fewer comorbidities (Charlson score of 0, 46.2% v 40.6%), compared to those who did not have EGFR testing ($p < 0.001$ for all). Provider survey responses are ongoing.

Conclusions: This ongoing study is identifying specific rural US populations in greatest need of efforts to expand molecular testing for NSCLC as well as implementation barriers and facilitators to testing from a multidisciplinary perspective.

#3676 Social disparities in the extension of endocrine therapy among premenopausal breast cancer survivors in Denmark.

Kirsten M. Woolpert[1], Lene Mellemkjar[2], Soren Friis[3], Mette Norgaard[1], Bent Ejlertsen[4], Deirdre Cronin-Fenton[1]

[1]Department of Clinical Epidemiology, Aarhus University and Aarhus University Hospital, Aarhus N, Denmark,[2]Institute of Cancer Epidemiology, Danish Cancer Society, Copenhagen, Denmark,[3]Danish Cancer Institute, Danish Cancer Society, Copenhagen, Denmark,[4]Danish Breast Cancer Group, Rigshospitalet, Copenhagen University Hospital, Copenhagen, Denmark

Introduction Despite universal access to oncology care, social disparities in cancer survivorship persist in Denmark. For premenopausal women with estrogen receptor-positive breast cancer, decisions regarding extending endocrine therapy beyond five years often depend on estimated individual recurrence risk and treatment tolerance. We examined whether social disparities are associated with the initiation of extended endocrine therapy among Danish breast cancer survivors who were recurrence-free at five years post-diagnosis.

Methods We included all women registered in the Danish Breast Cancer Group clinical database who were premenopausal at diagnosis with a first primary, estrogen receptor-positive, stage I-III invasive breast cancer diagnosed during 2008-2011. We further restricted the population to those who initiated adjuvant endocrine therapy and were alive, recurrence-free, and residing in Denmark five years after diagnosis. Extended endocrine therapy was defined as cumulative coverage with endocrine therapy for at least one year beyond the initial five years of treatment. Using the unique personal registration number assigned to all Danish residents, we linked patients across nationwide registries to obtain information on cohabitation, marital status, employment, income, and education, measured at or before endocrine therapy initiation. Associations between social characteristics and treatment extension were estimated using logistic regression, adjusted for patient age at diagnosis, and reported as odds ratios (ORs) with 95% confidence intervals (CIs).

Results Among 1,911 premenopausal patients diagnosed during the study period, 1,136 (57%) continued endocrine therapy beyond five years. Treatment extension varied across all assessed social characteristics. Women living alone at endocrine therapy initiation were less likely to extend (OR = 0.64; 95% CI, 0.51-0.79) compared with those cohabiting with a partner. Similarly, unmarried women (OR = 0.70; 95% CI, 0.55-0.90) and those who were divorced or widowed (OR = 0.67; 95% CI, 0.52-0.87) had lower rates of extension compared with married women. Survivors who were unemployed (vs employed; OR = 0.66; 95% CI, 0.52-0.83) or in the lowest quartile of household income (vs highest; OR = 0.72; 95% CI, 0.55-0.94) also had reduced odds of treatment extension. Finally, women with short education had 0.79 (95% CI, 0.61-1.02) times the odds of extension compared with those with long education.

Conclusions Our study suggested differences in the uptake of extended endocrine therapy according to social characteristics. Future work will build on these findings to evaluate how social and clinical factors together influence long-term treatment adherence and recurrence outcomes, with the aim of informing more equitable survivorship care.

#3677 Supporting communities through open dialogue on cancer care and addressing food insecurity: Partnerships with local YMCAs.

Rosa Barahona[1], Elena Nieves[2], Marya Shegog[3], Brenda Hernandez[4], Letech Caldera-Huerta[1], Lourdes Baezconde-Garbanati[5]

[1]USC Keck School Medicine, Los Angeles, CA,[2]USC Norris Comprehensive Cancer Center, Los Angeles, CA,[3]Lazarex Cancer Foundation, Danville, CA,[4]Weingart YMCA, Los Angeles, CA,[5]USC Keck School of Medicine, Los Angeles, CA

Background: A December 2024 USC Dornsife study found ~25% of LA County households faced food insecurity. The Lazarex Cancer Foundation, in partnership with USC NCCC and local YMCAs, supports communities experiencing cancer disparities and food insecurity. We provide welcoming, culturally responsive spaces for diverse and vulnerable groups to discuss cancer concerns and receive food support. Our goal is to advance cancer knowledge and offer free food by meeting individuals where they are with linguistically appropriate, culturally aligned information. Through YMCA partnerships, we've expanded access to cancer programs, resources, and services that improve outcomes across the cancer disparities continuum.

Methods: From October 2021 to October 2025, Lazarex Cancer Wellness HUBs conduct ongoing outreach across multiple LA County YMCAs and community and faith-based partners. This partnership enables extensive outreach through wellness hubs, giving community members access to food, education, and connections to cancer support services that address key social determinants of health. Content includes screening guidelines, the importance of diverse clinical trial participation, self-advocacy strategies, trustworthy health information, and food access.

Results: Over 8.6 million pounds of free food have been provided. We continue offering this service alongside cancer prevention information and connections to local resources. Food is also delivered to seniors and families lacking transportation or who feel unsafe in public spaces. More than 12,000 individuals across 148 zip codes have been served, with WELA Y completing 2,600+ safe deliveries. The Weingart YMCA has become a model for similar efforts across LA County.

Conclusion: We developed a community outreach model that enables consistent engagement in diverse, vulnerable communities, offering culturally tailored cancer information. These efforts aim to reduce cancer disparities and food insecurity by increasing awareness, knowledge, and access to quality care and trustworthy resources. The Lazarex Cancer Wellness HUB demonstrates an effective approach to empowering individuals as informed advocates for cancer prevention, navigation, advanced care options, and food access.

#3678 Capturing Latino health disparities: Lessons from mail and community-based population health surveys in California.

April P. Vang[1], Juanita E. Quino[2], Angelica M. Rolon[1], Alexa Morales Arana[1], Julie H. T. Dang[3], Moon S. Chen[3], Primo N. Lara[3], Laura Fejerman[4], Luis G. Carvajal-Carmona[1]

[1]The Health Equity Science and Community Research Laboratory (THE LCC Lab), Genome Center, UC Davis, Davis, CA,[2]University of Southern California, Los Angeles, CA,[3]University of California Davis Comprehensive Cancer Center, UC Davis, Sacramento, CA,[4]Public Health Sciences, UC Davis, Davis, CA

Background: Latinos face significant cancer health disparities and remain underrepresented in research. To address regional needs, the University of California Davis Comprehensive Cancer Center (UCDCCC) conducts regular Catchment Area Population Assessments (CAPAs) to inform outreach and engagement strategies. Our purpose was to understand best approaches for capturing Latino health needs responses and to understand breast and cervical cancer screening rates and risk factors.
Methods: This cross-sectional study compared two CAPA survey methodologies used from July 2019 to March 2020: a mail-based approach using probabilistic sampling of residential addresses versus a community-based approach using bilingual coordinators for in-person interviews. Comparisons were made on catchment population representativeness and breast and cervical cancer screening outcomes.
Results: The study included 361 Latino participants (255 community-based, 106 mail-based) across 16 of 19 UCDCCC catchment counties. Mail-based participants were significantly older, more educated, and had higher household incomes than community-based participants. Despite the differences in key demographics of participants in the two survey modalities, our results were inconclusive on whether up-to-date breast and cervical cancer screening rates differed between the two groups. Time since the last routine check-up, primarily among community-based participants, emerged as a key predictor of screening adherence.
Conclusions: Mail-based methods captured more affluent Latinos, whereas community-based methods reached more underserved populations. Each method introduced distinct sampling biases, but together they provided a more balanced representation of the catchment area. **Impact**: Mail- and community-based survey methods enhances the representativeness of Latino health data and supports more equitable research recruitment strategies.

#3679 Trends and disparities in hepatitis C virus-associated hepatocellular carcinoma mortality in the United States, 1999-2023.

Sophia Ahmed[1], **Fareed Baksh**[2], Elangovan Krishnan[3], Arfa Assad[1], Muhammad Uzair[4], Areesha Nawaz[5], Oshaz Fatima[6], Subhan Saleem[1]

[1]Medicine, Allama Iqbal Medical College, Lahore, Pakistan,[2]Internal Medicine, Community Health Systems - Flowers Hospital: Dothan, Alabama, US, Dothan, AL,[3]AIM DOCTOR, Thiruverkadu, India,[4]Medicine, Liaquat Univeristy of Medical & Health Sciences, Jamshoro, Pakistan,[5]Medicine, Dow Medical College, Karachi, Pakistan,[6]Medicine, King Edward Medical University, Lahore, Pakistan

Chronic hepatitis C virus (HCV) infection is a major driver of hepatocellular carcinoma (HCC) in the United States, where HCC incidence and mortality have doubled over the past 25 years. Despite the effectiveness of direct-acting antivirals, HCV-related HCC remains substantial, reinforcing the need for sustained surveillance and early detection. This study, adhering to STROBE guidelines, analyzed deaths related to HCV-associated HCC from 1999 to 2023 using CDC-WONDER data. Deaths were identified via ICD-10 codes (B17.1, B18.2, C22.0), with demographic categorization by place of death, age, gender, race, census region, and urbanization. Age-adjusted mortality rates (AAMRs) were calculated per 100,000 population. Joinpoint regression assessed trend changes, reporting Average Annual Percent Change (AAPCs) with 95% CIs. Statistical analyses were performed using Joinpoint software, Microsoft Excel, and CDC-WONDER mapping tools. From 1999 to 2023, 50,760 U.S. deaths were attributed to HCV-associated HCC. AAMRs increased from 0.19 in 1999 to 0.43 in 2023. Among deaths with place-of-death data, most occurred in medical facilities (38.7%) or at home (35.0%). Joinpoint analysis showed increasing mortality from 1999 to 2012, stable rates through 2016, and a decline to 2023 (AAPC 2.52%). Female AAMRs rose from 0.07 to 0.17, peaking in 2013 before declining (AAPC 2.57%). Male AAMRs increased from 0.31 to 0.73, with early surges, peaking through 2016, then declining (AAPC 3.29%). Mortality was highest in NH Whites, followed by NH Blacks. NH Whites rose until 2013, then declined (AAPC 5.00%), while NH Blacks showed early sharp increases and declined after 2016 (AAPC 4.30%). Metropolitan areas had higher AAMRs than non-metropolitan areas, with both rising until the mid-2010s followed by declines (AAPC: 4.46% and 6.03%, respectively). Across regions, AAMRs rose until the mid-2010s, driven by sharp early increases in the Northeast (32.1%) and steady growth in the Midwest, South, and West (8-10%). Mortality was highest in ages 55-64 and 65-74, both showing sharp increases from 2013 to 2017 followed by declines (AAPC –3.94%). HCV-related HCC mortality has declined since the early 2010s but remains uneven across sex, race, and geography. Males, Black individuals, and urban areas bear the highest burden. These findings underscore the need to strengthen HCV testing, antiviral treatment uptake, and timely HCC surveillance in the high-risk populations.

#3680 Attitudes, beliefs, and perceptions of clinicians on AI-assisted digital health interventions for oncofertility education.

Bhakthi Sahgal, Alvaro Rivera-Andrade, John F. Russell, Ornsiree Junchaya, Pavani Chalasani, Naomi Seiler

George Washington University, Washington, DC

Background: Fertility preservation counseling is a critical component of cancer care, yet patients often face disparities and barriers to timely, comprehensible information. Digital and AI-enabled educational tools may help expand access and standardize communication, but little is known about how frontline clinical staff perceive their acceptability, utility, trustworthiness, or appropriateness. Understanding these perspectives is essential to ensure emerging technologies promote, rather than exacerbate, inequities in oncofertility care.
Methods: This prospective qualitative study will be conducted at two cancer centers representing different tiers of institutions, an NCI-designated and a non-NCI-designated, to capture diverse organizational contexts and care delivery environments. Semi-structured interviews will be completed with multidisciplinary clinical leadership and staff, including directors, oncologists, reproductive endocrinologists, advanced practice providers, oncology nurses, and oncology social workers involved in oncofertility-related communication. Interview guides will draw on patient-centered communication frameworks, human-centered design principles, and implementation-science constructs related to acceptability, utility, trustworthiness, and appropriateness. Sessions will be audio-recorded, transcribed, and analyzed in NVivo using a hybrid deductive-inductive thematic approach to identify patterns related to trust, usability, privacy, accessibility, cultural relevance, and perceived clinical value.
Expected Outcomes: This study will generate insights into how clinical teams perceive and would engage with digital and AI-enabled fertility preservation education tools within onco-fertility settings. Findings will underline the factors influencing their acceptability, perceived utility, and trustworthiness across different institutional contexts. The analysis will highlight key design and implementation considerations that can inform the responsible development and deployment of digital tools supporting oncofertility communication across both NCI-designated and non-NCI cancer centers.
Implications: Findings will inform the equitable design and implementation of patient-centered, clinician-endorsed, culturally responsive digital health interventions for fertility preservation. Results will guide responsible digital tool adoption in oncology communication workflows and support improvements in patient engagement, care quality, and equity across diverse cancer care settings.

#3681 Optimizing genetic/genomic health communication in cancer prevention through video development.

Elena B. Taylor[1], Charite N. Ricker[2], Daisy Hernandez[2], Itzya Ulloa[2], Rosa Barahona[3], Lourdes Baezconde-Garbanati[2]

[1]USC Norris Comprehensive Cancer Center, Los Angeles, CA,[2]Keck School of Medicine of USC, Los Angeles, CA,[3]USC, Los Angeles, CA

Introduction: The Engagement Optimization Unit (EOU) of the USC Center for Optimizing Engagement in Colorectal Cancer Patients (COPECC), in partnership with the Patient Engagement Unit (PEU) and the Community Genetics Navigation Specialists (CoGENES) program, sought to improve educational materials for Hispanic participants in the ENLACE study before they received genetic testing results. Because colorectal cancer (CRC) incidence is rising in adults under 50 and is a leading cause of cancer death among Hispanic men, the team aimed to reduce disparities by providing clearer, more engaging information. Early listening groups (n=25) indicated a strong preference for video-based education, prompting development of a short film explaining the purpose and importance of genetic testing.

Methods: The film was created in collaboration with the USC School of Cinema. The team identified four Key Messages to be woven into the film that outlines the purpose and meaning of genetic testing and design. A film visual outline was produced with patient interviews, content and order of graphic animations. Production work included preparation and actual filming of participants that provided relatable testimonials and cancer team clinicians that provide professional credibility about the purpose and meaning of genetic testing.

Results: Focus groups had previously been conducted to better understand the preferred modality for presenting education materials. Individual comments specifically regarding the video revealed that there was a preference for the video format (5 focus groups 6/8 ,1/3, 3/3, 6/12/ and 3/3 comments specifically stated this preference). Based on this data as well as the literature, an 8-minute film was produced as an optimized format to present the information. The film content included testimonials by three participants, medical professionals (genetic counselor and physician) further explaining the importance of genetic testing, and animated graphics supporting the key messages being delivered. The film was assessed for logical information and content flow, and identification of key messages within the film, and relatability. Two language specific videos were created, one in Spanish and one in English - adding captions, animation, narration, and dubbing in both languages. The film is to be used in an education intervention comparing materials provided to cancer patients prior to receiving their genetic testing results.

Conclusion: Based on previous research, this video will improve our understanding and retention of key genetic messages in colorectal cancer. The video has incorporated elements including information with visual movement, supported by captions and narration to deliver this information on genetic testing to the ENLACE participants. The creation of this video provides, at the very least, an alternative to education delivery mechanism (besides static written information).

#3682 Nationwide epidemiologic and economic burden analysis of neurologic disorders associated with cancer treatment.

Ilaha Huseynli[1], Yiran Xu[2], Russell C. Jeter[2], Stephen N. Housley[1]

[1]School of Biological Sciences, Georgia Institute of Technology, Atlanta, GA,[2]Department of Mathematics & Statistics, Georgia State University, Atlanta, GA

Background: Neurologic disorders associated with cancer treatment (CIND) are common dose-limiting toxicities of many chemotherapies. They can persist long after treatment, impair function, and quality of life. Despite their import, large scale data on incidence, dose-response, and health care utilization and economic burden is limited. Objective: Quantify the epidemiology of CIND, stratified by cancer status, agent, and route of administration, evaluate clinical and treatment-related risk factors, measure health care utilization and economic cost burden, all in a nationwide cohort.
Methods: Using longitudinal IBM Marketscan claims data, we applied multi-tier drug matching to identify adults with incident chemotherapy and classify cancer and neurologic status using ICD 9 neoplasm and neurologic codes. Patients were categorized as having same day or incident neuropathy relative to the cancer diagnosis or first chemotherapy dispensing date. CIND cumulative incidence and time to first event were assessed at 3-month intervals. We modeled adjusted odds and hazards of CIND by cancer status and chemotherapy route and evaluated dose-response in multivariable Cox model adjusted for age, sex, and comorbidities.
Results: Across three cohorts (totaling ~ 3.1M patients), CIND incidence was highest in cancer patients receiving chemotherapy (40.4%) compared to cancer patients alone (34.1%) which was higher still relative to the general population (12%). Higher mean incremental daily dose was significantly associated with increased CIND hazard, with oral agents showing HRs per 1-SD from 1.09-2.23 (bexarotene, capecitabine, hydroxyurea, mercaptopurine, tretinoin; all $p \leq 0.046$) and IV methotrexate showing HR 1.34 (95% CI 1.00-1.79; $p=0.048$). Most CIND events occurred within one year of the last dose, indicating substantial on treatment and delayed CIND risk. Compared with IV administration, oral chemotherapy was associated with a modestly lower hazard of CIND (HR 0.862). Older age and comorbidities (hypertension, peptic ulcer, depression, chronic pulmonary disease, diabetes, and coagulopathy) provide additional independent risk. Healthcare burden analyses revealed opioid dispensing, CIND-directed pharmacotherapy, and rehabilitative services were more frequently used in chemotherapy recipients, accompanied by 51-fold higher per-patient costs (~$53k) relative to general population.
Conclusion: In this nationwide cohort, CIND is common, often delayed, and shaped by route of administration, indication, dose intensity, and patient comorbidity. CIND care concentrates substantial utilization and financial burden in chemotherapy exposed populations, underscoring the need for dose optimized regimens, proactive surveillance, and better supportive care strategies.

#3683 The breast cancer survivorship experience of Korean American women: A qualitative study.

Seulgi Ryu[1], Dongmi Kim[1], Yeeun Kim[1], Wonshik Chee[2], Eun-Ok Im[1]

[1]School of Nursing, The University of Texas at Austin, Austin, TX,[2]Department of Kinesiology and Health Education, College of Education, The University of Texas at Austin, Austin, TX

Background Breast cancer is the most frequently diagnosed cancer among women in the United States. A recent sharp increase in breast cancer was observed among Asian American women, and breast cancer is the most prevalent cancer among Korean American women. There remains a significant gap in research exploring the breast cancer survivorship experience of Korean American women. This study aims to explore the survivorship experiences of Korean American breast cancer survivors.

Methods This is a part of a larger study that evaluated a technology-based coaching/support program among Asian American breast cancer survivors. Only the qualitative data from 10 Korean American breast cancer survivors over the 3-month interventions were included in this analysis. Data were collected through online logs, where all interactions between participants and interventionists were recorded. The online logs included an average of 1,029 lines (range: 428-2149) of text per participant. The data were analyzed using a thematic analysis.

Results Five prominent themes were identified. First, “self-directed coping strategies with pain” were identified; the participants reported several ways to manage pain, such as medication or gaining support through assistive methods (e.g., cuffing therapy, sauna, and acupuncture), which were relevant to Asian cultural aspects. Second, “resilience in survivorship” was enhanced through participation in the culturally tailored intervention. While the participants were motivated to contribute meaningfully to the research, they experienced less pain and were encouraged to exercise more to reduce pain. Third, “challenges of living with and beyond cancer” were noted; the participants reported challenges related to physical or emotional symptoms, a language barrier, being obliged to be filial to their parents, being stigmatized for their illness, lacking time for themselves, and an unsupportive family. Fourth, “resilience and growth through illness” were identified; the participants reported that their families became stronger after the diagnosis, and they became more proactive, finding meaning in their lives. They provided support to other cancer patients or those in need and were grateful to their peers or family for their support. Finally, “positive adaptation and empowerment” were identified; the participants were actively seeking behaviors/strategies to improve their physical or emotional challenges, such as changing their diet, exercising, and focusing on other activities (e.g., travel or finding a new hobby).

Conclusions Even though Korean American breast cancer survivors faced multiple challenges, they had more proactive attitudes and were resilient in their survivorship journey. This study also contributes to the evidence that culturally tailored interventions can empower survivors to cope with illness and enhance their ability to navigate their survivorship journey.

#3684 Socioeconomic and clinical predictors of survival in patients with squamous cell tonsillar cancer.

Shama Karanth[1], Pamela Sandow[2], Mihika Shinde[1], Nimish Valvi[3], Kathryn Hitchcock[1], Cesar Migliorati[2], Dejana Braithwaite[1]

[1]University of Florida, Gainesville, FL,[2]University of Florida College of Dentistry, Gainesville, FL,[3]Ball State University, Muncie, IN

Background: Tonsillar cancer represents a distinct and understudied subset of head and neck malignancies with rising incidence, largely driven by human papillomavirus (HPV), associated oropharyngeal cancer. Understanding the roles of clinical characteristics and socioeconomic factors is critical for optimizing early detection and improving outcomes in this population. This study aimed to identify key demographic, clinical, and socioeconomic predictors of treatment delay and overall survival (OS) among patients with tonsillar cancer.

Methods: We conducted a population-based retrospective cohort study using the Surveillance, Epidemiology, and End Results (SEER) database (2010-2021), including individuals aged 20-85+ years with primary tonsil cancer. Data were extracted using SEER*Stat version. The primary endpoint was OS. Multivariable Cox proportional hazards regression and machine learning models enhanced with Shapley additive explanations (SHAP) were used to assess prognostic factors and model interpretability. Model performance was compared with random survival forest (RSF) analyses.

Results: Among 6,148 patients with Stage I-IV tonsillar squamous cell carcinoma, 1,457 (23.7%) deaths occurred during follow-up (median overall survival [OS], 46 months; interquartile range [IQR], 18-85 months). Nearly half (47.5%) presented with stage IV disease, and most were male (84.3%). Regarding treatment, 2,574 (42%) received chemoradiation alone, while 1,381 (22.5%) underwent combined chemoradiation and surgery. The cohort was predominantly non-Hispanic (NH) White (81%), followed by Hispanic (7.1%), NH Black (6.6%), and Other/Unknown (5.3%). In adjusted Cox models, poorer survival was independently associated with stage IV (HR, 2.21; 95% CI, 1.72-2.47), tumor size >40 mm (HR, 2.09; 95% CI, 1.73-2.54), older age (HR, 2.71; 95% CI, 2.22-3.31), distant metastases (HR, 3.47; 95% CI, 2.78-4.32), rural residence (HR, 1.28; 95% CI, 1.10-1.50), low household income (HR, 1.17; 95% CI, 1.04-1.33), and NH Black race (HR, 1.57; 95% CI, 1.33-1.88). The random survival forest demonstrated good discrimination (C-index 0.715), comparable to that of the Cox model (0.759). SHAP analysis identified metastasis, stage, nodal involvement, income, rurality, and race/ethnicity as key predictors.

Conclusion: In this large, population-based study of squamous cell carcinoma of the tonsil, nearly half of the patients presented with advanced disease, and socioeconomic disadvantage was strongly associated with poorer survival. Machine learning analysis identified metastasis, disease stage, nodal involvement, and social factors as key predictors, suggesting that integrating clinical and social context into prognostic models may guide targeted early detection and precision survivorship strategies to reduce disparities.

#3685 A case of rapid progression from Stage I to Stage IV in an MSI-H/EMAST African American colorectal patient.

Mudasir Rashid[1], Hassan Brim[1], Rabia Zafar[1], Christine Nembhard,[1], Sudhir Varma[2], Hassan Ashktorab[1]

[1]Howard University Hospital, Washington, DC,[2]Hithru, New Jersey, NJ

Colorectal cancer (CRC) remains a leading cause of cancer mortality. While most cases arise sporadically, familial risk contributes to about 30%, underscoring the need to assess family history during screening. Microsatellite instability (MSI) is a well-established diagnostic and prognostic biomarker, but elevated microsatellite alterations at selected tetranucleotide repeats (EMAST) remain poorly characterized, particularly among African American patients.We report a 59-year-old African American female with hypertension, hyperlipidemia, and congenital hearing and speech impairment who presented with rectal bleeding. Colonoscopy revealed a 7 cm mass in the transverse colon and a 15 mm sigmoid adenoma. Pathology confirmed a stage I (pT2N0M0) adenocarcinoma that rapidly progressed to stage IV with liver metastasis within one year. Immunohistochemistry showed loss of MLH1 and PMS2 with retained MSH2 and MSH6; MSI testing was MSI-high (BAT26), and EMAST was positive for RBM47.Whole-genome sequencing revealed dense intronic indel clusters in **MSH3**, suggesting MutSβ dysfunction consistent with EMAST. We also identified 21 deleterious missense variants across DNA-repair, immune, and transcriptional pathways (e.g., **ZAP70, MSH4, ESR1, ACVR1B, LMNA**). CNV gains were enriched in duplication-rich loci such as 11p15.5, 11q14, 13q31-q22, and 20q11-q13, overlapping oncogenic clusters (**IGF2/H19, DNMT3B, SRC, BCL2L1, E2F1**). Additionally, 19 frameshift and stop-gain mutations (e.g., **GRIK2, NOS3, WNT16**) introduced premature termination codons.STR profiling demonstrated bidirectional instability—18 expansions and 28 contractions across 46 intronic loci—confirming a pervasive EMAST pattern driven by MSH3 deficiency. This case illustrates a rare, aggressive MSI-H/EMAST CRC with rapid progression, extensive genomic instability, and dual MSI-EMAST features. Findings highlight the biological aggressiveness of combined MSI-H/EMAST tumors and emphasize the need for genetic counseling, molecular surveillance, and targeted precision strategies in underrepresented populations.

#3686 Insights into smoking cessation support for lung cancer patients: A multi-site survey of patient perspectives post-diagnosis.

Lyric R. Li[1], Jo-Ann Persson[2], Aahna Shah[3], Krishna S. Gunturu[4]

[1]Frank H. Netter M.D. School of Medicine at Quinnipiac University, North Haven, CT,[2]Center for Cancer Care, Griffin Hospital, Derby, CT,[3]The Loomis Chaffee School, Windsor, CT,[4]Hartford Healthcare Medical Group Specialists, LLC, Hartford, CT

Background: Although extensive research demonstrates that quitting smoking after a cancer diagnosis—regardless of stage—improves treatment outcomes and quality of life, 30% of patients continue smoking. This study explored differences between lung cancer patients who smoke post-diagnosis and the general smoker population and examined the gap between evidence and patient perspectives by surveying perceived benefits, barriers, and views on cessation support across two community oncology sites in Connecticut.

Methods: We conducted a cross-sectional survey at two clinical sites, recruiting participants during routine visits. The survey assessed demographics, smoking history, perceived benefits and barriers, prior cessation resource effectiveness, comfort and priorities for clinician discussion, concerns about stigma or financial influence, and knowledge and confidence. Most items used 5-point Likert scales and were summarized descriptively. Items were dichotomized (1-3 vs. 4-5) per prespecified rules; items where “1” indicated highest importance/challenge were inverted for consistency. Data was managed in REDCap.

Results: Sample: N=40; age 68.1±6.9; 55.0% female; 40.4±11.6 years smoking; 13.3±8.7 cigarettes/day; 27.9±22.4 pack-years. Only 7.5% rated current cessation resources as effective.

While 55% felt comfortable discussing cessation, 35% wanted more frequent discussions, and 32.5% wanted oncology teams to address cessation even without explicit survival framing. Concerns included fear that disclosure could affect treatment/resources (37.5%) and finances (27.5%). Knowledge and confidence were moderate (67.5% felt informed and confident).

Top internal barriers were withdrawal (52.5%) and reliance on smoking for stress relief (42.5%); external barriers were less common (17.5% lacked knowledge of resources; 17.5% felt rushed/unsupported). Leading motivators: preventing other smoking-related diseases (80%), improving cancer treatment effectiveness (75%), and enhancing daily comfort (62.5%). Additional drivers included a sense of control (40%) and being a role model (42.5%). *Percentages reflect item-level endorsement (agree/strongly agree); totals do not sum to 100% because multiple selections were allowed.*

Conclusions: Patients reported reasonable knowledge and confidence but low perceived effectiveness of current resources, with many desiring more frequent, nonjudgmental discussions. Stigma and fear of negative consequences may suppress disclosure, limiting support. Internal barriers—especially withdrawal and stress coping—predominated. Future implementation priorities include routine, stigma-aware oncology conversations emphasizing ongoing benefits of quitting; proactive withdrawal management with evidence-based pharmacotherapy; and clear messaging to reduce disclosure fears and foster engagement.

#3687 Establishing a data-driven oncology research ecosystem in sub-Saharan Africa: The Medserve-LUTH Cancer Centre (MLCC) research unit experience.

Adedayo Joseph[1], Anthonia Sowunmi[2], Muhammad Habeebu[2], Bolanle Adegboyega[2], Adewumi Alabi[2], Eben A. Aje[2], Temitope Andero[2], Godwin Uwagba[2], Chidiebere Agbakwuru[2], Bukola Oshikanlu[2], Ayodeji O. Ojetunde[2], Samuel Adeneye[2], Nusirat Adedewe[2], Michelle Mangongolo[2]

[1]Lagos University Teaching Hospital, Nigeria, Nigeria,[2]Medserve-LUTH Cancer Centre, Lagos University Teaching Hospital, Lagos, Nigeria

Background: Sustainable cancer research capacity is critical to advancing evidence-based oncology in low- and middle-income countries (LMICs). Historically, Africa has contributed less than 2% of global cancer research output, largely due to inadequate infrastructure, fragmented data systems, and limited clinical research training. The Medserve-LUTH Cancer Centre (MLCC) Research Unit, established in 2020 in Lagos, Nigeria, was designed as a translational research hub within a high-volume clinical environment to bridge this gap through coordinated clinical studies, data science integration, and workforce development.
Methods: The MLCC Research Unit implements a hybrid academic-industry model incorporating electronic data capture, protocol-driven registries, and cross-disciplinary training. The unit supports investigator-initiated and multicentre studies across all oncologic speciality areas, with a common focus on radiation oncology. Emerging areas of innovation have included pediatric radiation oncology, hypofractionated radiotherapy and financial navigation. Key operational metrics including active studies, research personnel, partnerships, and outputs were analysed to assess growth and impact between 2020 and 2025.
Results: Since inception, the MLCC Research Unit has supported 73 ongoing or completed studies spanning clinical, operational, and implementation research. The team has expanded from 2 to 14 trained personnel, including 5 research associates, 7 research assistants and 2 interns. Collaborative partnerships were established with institutions in over 18 countries, and passive collaborations with 207+ international academic partners, facilitating data sharing and joint publications. 127 peer-reviewed manuscripts and 118 conference abstracts have been produced. Research data generated at MLCC have contributed to regional literature, radiotherapy policy discussions, regional clinical trials (e.g., HYPOAfrica, ARETTA), and national and regional pediatric oncology protocols. Integration of internal quality-assurance audits was initiated in 2021 to improve data completeness.
Conclusion: The MLCC Research Unit demonstrates that structured, locally led oncology research ecosystems can thrive in LMIC contexts when aligned with clinical workflow and supported by digital infrastructure and capacity-building programs. This model offers a replicable framework for developing sustainable cancer research capacity across sub-Saharan Africa, linking local data generation to global cancer control priorities.

#3688 Use of targeted therapies in lung cancer following medicare's national coverage determination for next-generation sequencing.

So-Yeon Kang[1], Patrick Roney[2], Jaeil Ahn[2], Tania Lobo[2], Carole Gresenz[3], Arnold Potosky[2], Anita Kinney[4], Marc D. Schwartz[5]

[1]Georgetown University, Washington, DC,[2]Georgetown University Medical Center, Washington, DC,[3]Georgetown University McCourt School of Public Policy, Washington, DC,[4]Rutgers University School of Public Health, Piscataway, NJ,[5]Lombardi Cancer Center, Washington, DC

Background: Despite its clinical importance and growing utilization, access to genomic testing remains uneven, with insurance coverage emerging as a persistent barrier. The Centers for Medicare & Medicaid Services (CMS) implemented a National Coverage Determination (NCD) in March 2018 for genetic testing using next-generation sequencing (NGS). Implementing nationally standardized coverage policy is expected to promote the use of targeted anticancer therapies with proven efficacy. However, whether this policy change increased the use of genomically targeted therapies, which often require testing results for reimbursement, remains unclear. We evaluated the association between the NCD and the use of oral targeted anticancer therapies among Medicare beneficiaries with lung cancer, a disease characterized by a high prevalence of actionable mutations.

Methods: We conducted a retrospective cohort study using SEER-Medicare Part D claims from 2016-2020. Medicare beneficiaries aged ≥65 with lung cancer were followed for up to 12 months after diagnosis. The primary outcome was initiation of Medicare Part D-covered oral targeted therapies. Key exposures included (1) diagnosis before vs. after the NCD and (2) whether the beneficiary lived in a region whose Medicare Administrative Contractor (MAC) had NCD-equivalent NGS coverage before 2018. Multivariable logistic regression models adjusted for demographics (age, sex, race/ethnicity), clinical factors (stage, comorbidity, and initial cancer therapy), geographic region, urbanicity, and neighborhood socioeconomic indicators.

Results: The cohort included 30,855 beneficiaries with a diagnosis of lung cancer. Overall use of targeted therapies declined over time (7.3% before vs. 6.8% after the NCD). The NCD was not significantly associated with targeted therapy use (p=0.78). However, regional variation was substantial. Compared with beneficiaries in regions with pre-existing NCD-equivalent NGS coverage, those in regions without such coverage had lower baseline targeted therapy use (OR=0.77; 95% CI: 0.62-0.97; p=0.02). Following the NCD, regions that previously lacked NGS coverage experienced a greater increase in targeted therapy use relative to regions with prior coverage (interaction OR=1.24; 95% CI: 1.03-1.51; p=0.03).

Conclusions: Medicare's NCD for NGS was not associated with an overall increase in targeted therapy use among beneficiaries with lung cancer, but it reduced regional disparities linked to earlier differences in NGS coverage standards. These findings highlight how pre-existing local coverage policies can shape downstream access to precision oncology treatments even after national policy changes.

#3689 Lurbinectedin plus atezolizumab vs durvalumab maintenance in ES-SCLC: A comparative clinical and economic analysis.

Manaswini Krishnakumar[1], Suma Sri Chennapragada[2], Arpana Ashok[2], Aswanth Reddy[2]

[1]Saint Vincent Hospital, Worcester, MA,[2]Mercy Hospital, Fort Smtih, AR

Background Extensive-stage small cell lung cancer (ES-SCLC) treatment has evolved with improving survival with addition of immunotherapy treatment. Recently, the IMforte trial reported better survival outcomes by adding lurbectindin maintenance with atezolizumab after induction therapy. This approach challenges the current widely used durvalumab-based regimen (CASPIAN trial) for treatment of ES-SCLC. We aim to analyze the survival outcomes, toxicity, tolerability, and cost-effectiveness of these regimens.
Methods: Data from IMforte and CASPIAN trials were directly extracted from published primary manuscripts and associated supplementary materials and synthesized descriptively. Survival outcomes, including overall survival (OS) and progression-free survival (PFS), were analyzed from trial data. Adverse events (AEs), tolerability, and cost-effectiveness using the incremental cost-effectiveness ratio (ICER) per quality-adjusted life-year (QALY) were compared.
Results: In IMforte maintenance lurbinectedin plus atezolizumab yielded a median OS of 13.2 months vs. 10.6 months for atezolizumab (HR 0.73, p=0.017) and PFS of 5.4 months vs. 2.1 months (HR 0.54, p<0.0001). CASPIAN reported a median OS of 12.9 months with durvalumab (vs. 10.5 months for EP; HR 0.75, p=0.0032) and PFS of 5.1 months (vs. 5.4 months; HR 0.80). Patients in both trials received induction with a chemotherapy immunotherapy combination. Grade 3/4 AEs were higher in IMforte's combination (38% vs. 22%), and the CASPIAN trial reported similar grade 3/4 AEs between treatment arms. IMforte trial showed more myelosuppression (e.g., anemia 8%, neutropenia 7%) and CASPIAN more immune-related AEs (20% vs. 3%). Cost analysis revealed IMforte's ICER at $1,071,238/QALY versus CASPIAN durvalumab at $165,182/QALY, both exceeding the $150,000/QALY threshold but with durvalumab closer to cost-effectiveness. Our institutional drug acquisition cost was calculated to be $319,735 for atezolizumab plus lurbectinidin (12 months) vs $111,312 for duvalumab(12 months) maintenance, approximately.
Conclusions: The IMforte combination offers superior PFS and potentially longer OS than CASPIAN's durvalimab-based regimen, but with increased bone marrow toxicity and significantly higher costs. CASPIAN's regimen is more cost-effective, making it a viable option in resource-constrained settings, and lurbenectin can be used as a following line of treatment after progression on durvalumab. The IMforte trial did not allow a crossover; hence, it is unknown if early introduction of lurbecnectin for ES-SCLC will better survival rather than when used as a subsequent line treatment. These findings inform treatment selection for ES-SCLC, balancing efficacy, safety, and economic considerations.

#3690 The impacts of prior authorization policy reforms on breast cancer treatment.

Margot Eliza Hutchins[1], Alyce Adams[1], Lin Ma[1], Alison Kurian[2], Mina Satoyshi[2]

[1]Department of Health Policy, Stanford Cancer Institute, Stanford, CA,[2]Stanford Cancer Institute, Stanford, CA

Prior authorization (PA) is a widely used cost-containment tool that requires third-party approval for coverage of medical tests and treatments. This process is time-intensive for physicians and is frequently associated with delays in patient care; in cancer care, almost 80% of oral chemotherapies require PA, and most cancer patients undergoing PA report delays of two or more weeks. The burden of prior authorization is a growing concern, and major recent changes in state and federal policy aim to streamline and expedite PA. However, the impact of these policies on cancer care remains unclear. Using data from the Oncoshare database (2012-2020), we evaluate how two California laws (SB 866 and SB 282, passed in 2012 and 2014) affect medication utilization and time to treatment among breast cancer patients using a quasi-experimental design. While we observed no significant changes in medication utilization, both laws were associated with reductions in time to treatment. These findings suggest that PA reform improves timely access to cancer therapies.

#3691 Comparing perspectives on HPV vaccination strategies across jurisdictions with and without school-entry requirements: A qualitative study of key informants in the U.S. and territories.

Erika Escabi-Wojna[1], Natalie M. Alamo[1], Mariola Acosta-Rullan[2], Grace Velez-Crespo[3], Pamela C. Hull[4], Maria E. Fernandez[5], Vivian Colon Lopez[1]

[1]University of Puerto Rico Comprehensive Cancer Center, San Juan, Puerto Rico,[2]Icahn School of Medicine, New York, NY,[3]Puerto Rico Science, Technology and Research Trust, San Juan, Puerto Rico,[4]UK Markey Cancer Center, Lexington, KY,[5]UTHealth Houston School of Public Health, Houston, TX

Introduction: HPV is the most common sexually transmitted infection in the United States (U.S.) and the leading cause of cervical and other HPV-related cancers. Despite an FDA-approved HPV vaccine available for over two decades, vaccination rates remain suboptimal, varying by state and ethnicity. While some jurisdictions require HPV vaccination for school entry, most rely on non-mandatory approaches. This study explored how policy contexts, specifically the presence or absence of school-entry requirements, shape strategies, barriers, and facilitators to HPV vaccination.
Methods: We conducted semi-structured interviews with nine key informants (KIs) from six U.S. jurisdictions between May and August 2024. KIs had at least three years of experience in health or vaccination policy and knowledge of HPV vaccination strategies. Seven participants represented jurisdictions with HPV school-entry requirements, and two represented jurisdictions without. Interviews were audio-recorded, transcribed, and coded using a mixed deductive-inductive approach. Verbal data were compared by theme in Dedoose.
Results: KIs from jurisdictions with school-entry requirements emphasized provider recommendation and reframing HPV vaccination as cancer prevention as effective strategies. Those without school-entry requirements highlighted starting vaccination at age nine and using educational materials. Participants from jurisdictions with school-entry requirements reported that the policy increased vaccination rates, improved access, and convinced hesitant parents. KIs from jurisdictions without this policy described resistance that has prevented its adoption, noting that opposition was often aimed at requirements themselves rather than the vaccine, reflecting opposition to government involvement in health decisions. In both policy contexts, misinformation fueled by social media was a major barrier. KIs described the COVID-19 pandemic as a setback that contributed to ongoing vaccine fatigue and skepticism. They noted general exhaustion with vaccine discussions, while some observed that the pandemic polarized attitudes. All KIs emphasized community engagement through trusted messengers and culturally appropriate outreach in building vaccine confidence.
Conclusions: Policy context shapes HPV vaccination framing, delivery, and accessibility. Jurisdictions with school-entry requirements reported better uptake, attitudes, and access, while those without requirements relied on non-mandatory approaches to navigate cultural and political sensitivities. Comparative insights can guide context-specific implementation approaches to enhance HPV vaccination and reduce cancer outcomes. Funding: NCI grant #R01CA232743. Declaration of Generative AI: The authors used AI for editing suggestions.

#3692 Accelerating global impact in translational cancer research: Lessons from 15 years of the EU TRANSCAN initiative.

Valentina Trapani[1], Katarina Bibova[2], Estela Cepeda[3], Giusi Condorelli[4], Liron Even-Faitelson[5], Charlotte Gudewicz[6], Sebastian Hueckesfeld[7], Anabela Isidro[8], Emma Ito[9], Fei-Fei Liu[9], Hubert Misslisch[7], Elisa Nannicini[10], Floriane Nguyen[11], Martin NovaK[2], Silvia Paradisi[12], Giulia Piaggio[13], Ines Rey Hidalgo[11], Maria Romero[14], Hugo Soares[8], **Giandomenico Russo**[15]

[1]Alliance Against Cancer, UniCamillus-Saint Camillus International University of Health and Medical Sciences, Roma, Italy,[2]Slovak Academy of Science, Bratislava, Slovakia,[3]Fundacion Cientifica de la Asociacion Espanola Contra el Cancer, Madrid, Spain,[4]Italian Ministry of Health, Roma, Italy,[5]Chief Scientist Office, Ministry of Health, Jerusalem, Israel,[6]Institut National du Cancer, Boulogne-Billancourt, France,[7]DLR Projekttrager, Bonn, Germany,[8]Agencia De Investigacao Clinica E Inovacao Biomedica, Lisbon, Portugal,[9]Canadian Institutes of Health Research - Institute of Cancer Research, Toronto, ON, Canada,[10]Regione Toscana, Firenze, Italy,[11]FICYT - Fundacion para el Fomento en Asturias de la Investigacion Cientifica y la tecnologia, Oviedo, Spain,[12]Istituto Superiore di Sanita, Roma, Italy,[13]Alliance Against Cancer (Alleanza Contro Il Cancro), Istituto Nazionale Tumori Regina Elena, Roma, Italy,[14]Alliance Against Cancer, Italian Ministry of Health, Roma, Italy,[15]Alliance Against Cancer, Roma, Italy

Efficient and sustainable collaboration among cancer research funders is critical to addressing the growing complexity of cancer prevention, diagnosis, and treatment. Over the past 15 years, the TRANSCAN initiative, encompassing TRANSCAN, TRANSCAN-2, and TRANSCAN-3, has built a mature and flexible model for aligning translational cancer research funding across Europe and beyond. Supported in its last two phases by the EU ERA-NET co-funding scheme, TRANSCAN promotes convergence between national and regional priorities, and EU-level strategic goals. Since 2011, TRANSCAN has pioneered two innovative features: the integration of public and private funders into a single coordinated framework, and the targeted support of small investigator-driven research consortia. Each participating organization contributes in line with its national strategies and available resources to jointly launch Transnational Calls (JTCs) covering a broad range of translational cancer research topics. The current phase, TRANSCAN-3, coordinated by the Italian Ministry of Health, brings together 31 funding agencies from 20 different countries, including non-European partners such as Canada and Taiwan. The initiative also places strong emphasis on engaging early-career researchers and patient representatives, fostering inclusiveness and shared ownership of the research agenda. A new phase, TRANSCAN-4, is currently being planned, reflecting the continued strategic importance of transnational coordination in cancer research. Between 2011 and 2025, TRANSCAN received approximately €8 million from the European Commission to support its activities and management. During this period, the network successfully implemented 11 JTCs that mobilized a total of €148 million in national and regional funding. In addition, the European Commission co-funded two of these calls, directly supporting research projects with a further €12 million. Altogether, 141 small- to mid-sized consortia, involving 723 research groups, have been funded. These focused, transnational collaborations complemented larger EU-funded cancer consortia and contributed to high-impact translational results. Beyond financial coordination, TRANSCAN has strengthened capacity building, cross-border networking, stakeholder engagement, and long-term strategic alignment among funders. The TRANSCAN initiative demonstrates the value of sustained transnational cooperation in cancer research funding. Its bottom-up, inclusive, and mixed public-private model has significantly advanced the EU and international cancer research landscape in line with the EU Mission on Cancer and Europe’s Beating Cancer Plan. This long-term cooperation model offers a blueprint for future alignment of national and regional, public and private programs to achieve collective impact. More information is available at: www.transcan.eu.

#3693 Barriers and challenges to women leadership in medical research and how to overcome them.

Adriana Albini[1], Elisabetta Vercesi[2], Eva Negri[3], Giovanni Corso[1], Sonia Levi[4], **Douglas McClain Noonan**[5]

[1]IEO - European Institute of Oncology, Milan, Italy,[2]Fondazione Onda, Osservatorio nazionale sulla salute della donna e di genere ETS, Milan, Italy,[3]Department of Medical and Surgical Sciences, Universita di Bologna, Bologna, Italy,[4]Vita-Salute San Raffaele University, Milan, Italy,[5]IRCCS MultiMedica, Sesto San Giovanni, Italy

Women in leading positions in medical research remain underrepresented and face systemic barriers to career advancement, including implicit biases and stereotypes. To explore these issues, and envisage feasible solutions, we conducted a cross-sectional qualitative study using a 33-item questionnaire. The survey was completed by 82 Italian senior academic female researches with an h-index higher than 60 in biomedical research. Major fields of study were biology, neurosciences, immunology, metabolism, genomics, pharmacology and oncology/cancer biology. This cohort offers insights into the experiences, struggles, and achievements of highly successful women in medical research. Findings reveal persistent gender biases and societal expectations slowing or hindering women's career progression, with only 17% of respondents expressing satisfaction with gender parity in opportunities within the field Almost all (91%) reported challenges with work-life balance and lack of institutional support, many respondents emphasized the underrepresentation of women in leadership, with 74% highlighting the need to increase female participation in decision-making roles. Additionally, 61% advocated for promoting more women to senior positions toward achieving gender equality in the field. 89%, experienced at least one gender-related obstacle during their career while 42% were tempted to resign from their professional role. These results highlight the persistent structural and cultural obstacles that even top-performing women face in the field. Targeted strategies such as mentorship, education to counteract bias, flexible work policies, and equitable promotion policies are required for empowerment and to foster a more inclusive environment for current and future generations of women scientists. The study also highlights the resilience, dedication, and motivation of women academic medical researchers. Their sense of responsibility, passion for science, and the search of both personal and social support systems are crucial factors contributing to their persistence in the field, encouraging younger women to pursue a career in medical research.

#3694 Development of a DCE-based classification tree to enhance shared decision-making in patients with advanced prostate cancer.

Pranav Prakash[1], Jennifer A. Wenzel[2], Winter M. Thayer[3]

[1]Johns Hopkins University, Baltimore, MD,[2]Johns Hopkins University School of Nursing, Baltimore, MD,[3]School of Nursing, Johns Hopkins University School of Nursing, Baltimore, MD

Prostate cancer remains one of the most prevalent cancer types in the United States. The extensive range of available treatment options and diverse care pathways often creates significant uncertainty and anxiety for patients navigating the decision-making process. Each patient, along with their support network, tends to have unique priorities regarding treatment, such as financial stability, alleviating symptoms, or extending survival. There is a need for effective tools to help shared decision-making. The Cancer Health Aid to Manage Preferences and Improve Outcome through Navigation (CHAMPION) trial is a randomized controlled study designed to evaluate whether Community Patient Navigators (CPNs), equipped with mobile health tools, can improve patient confidence and satisfaction during cancer treatment decision-making, and enhance collaboration between patients and healthcare practitioners. Within the CHAMPION trial, a nested study, Cancer Preference Reflection and Elicitation for Family Support (C PREFS), utilizes discrete choice experiments (DCEs) to examine and quantify patient preferences when considering treatment options for advanced prostate cancer. DCEs involve presenting participants with hypothetical scenarios and asking them to indicate their preferred choices. The primary objective of this project is to develop a classification tree, which serves as a model for decision-making, informed by interview data collected from patient-supporter dyads. Advanced prostate cancer patient-supporter dyads were interviewed about disease and treatment history, beliefs about medical treatment, and symptomatic characteristics of the cancer. Patients continue to be recruited at the Johns Hopkins Sidney Kimmel Comprehensive Cancer Center. Eligible patients who consent to participate in the study will complete future visit surveys and DCEs that will be used to validate the classification tree. This study is thus contributing towards development of a classification tree capable of accurately predicting the treatment preferences of advanced prostate cancer patients. The resulting tool has the potential to serve clinicians and patients by supporting shared decision-making processes and ensuring that treatment recommendations are closely aligned with individual patient values and preferences.

#3695 The Artemis Project: A patient-led global research consortium advancing prevention-focused breast cancer innovation.

Fran M. Visco[1], Jayanta Debnath[2], Daniel Douek[3], Stephen J. Elledge[4], Silvia C. Formenti[5], Michele S. Garfinkel[1], Cyrus M. Ghajar[6], Patricia K. Haugen[7], Christopher I. Li[6], Herbert Kim Lyerly[8], **Michelle Tregear**[1], Alana L. Welm[9], Frank J. Calzone[10]

[1]National Breast Cancer Coalition, Washington, DC,[2]UCSF - University of California San Francisco, San Francisco, CA,[3]Human Immunology Section, NIAID, NIH, Bethesda, MD,[4]Harvard Medical School, Boston, MA,[5]Weill Cornell Medicine, New York, NY,[6]Fred Hutchinson Cancer Research Center, Seattle, WA,[7]Independent advocate, Sioux Falls, SD,[8]Professor, Duke University (Columbus, OH), Durham, NC,[9]University of Utah Huntsman Cancer Institute, Salt Lake City, UT,[10]Self-employed consultant, Westlake Village, CA

Purpose: The National Breast Cancer Coalition (NBCC), established in 1991, is a collaboration of activists, survivors, grassroots groups and national organizations united to end breast cancer through action and advocacy. Despite progress in certain areas, neither breast cancer incidence nor global mortality have significantly declined. In response, NBCC launched the Artemis Project in 2010, an advocate-led initiative focused on primary prevention of breast cancer and prevention of metastasis, designed to foster new collaborations among researchers and advocates. The project is a response to the fact that despite billions of dollars invested in research that has led to some effective treatments, we still do not know how to prevent or cure breast cancer.
Artemis process: The Artemis Project is a collaboration to identify urgent gaps, set milestones, and co-develop research solutions to primary and metastasis prevention. Unlike traditional research development pipelines, Artemis integrates trained patient advocates as equal partners in priority setting, research design and oversight. Advocates identify the participants and choose the issues. Collaborations form at the annual meeting among researchers and advocates who often would not have met otherwise.The annual Artemis meeting brings participants together to explore new ideas, develop innovative projects towards Artemis's goals, and outline work plans for 12-18 months after the meeting. Online meetings are held throughout the year for the groups to interact and to report progress. Seed funding for some projects has been provided by NBCC. NBCC schedules webinars throughout the year on relevant topics for Artemis participants.
Selected Artemis outcomes: The first Artemis project led to an ongoing initiative to develop a breast cancer prevention vaccine, with a plan in place to move to a Phase I trial by mid-2026. The vaccine, consisting of 6 self-antigens overexpressed in breast cancer, is being developed under a contract with the NCI Prevent Program. DNA Land, an effort stemming from another Artemis project, has recruited over 33,000 individuals who have consented and contributed genomic and matched phenotypic data to underpin bioinformatics studies supporting prevention-focused breast cancer research.Additionally, researchers participating in Artemis have formed many collaborations that have grown into externally funded research efforts, including a project to eliminate disseminated tumor cells.
Conclusions: Now 15 years in, the Artemis Project has created a durable, advocate-led ecosystem that unites researchers, clinicians, and advocates to pursue transformative prevention solutions rather than incremental advances. This model is adaptable across disease research areas.

: Adoptive Cell Therapy 1
Poster Session

#3699 The "Preservation & Expansion" process: A key milestone for enhancing accessibility of autologous tumor-infiltrating lymphocyte therapy by enabling long-term cryopreservation of seed cells.

Zhou He, Xingming Ma, Feng Yin, Shanshan Liang, Wenjia Zhuang, Hui Yan, Huajun Jin

Shanghai Juncell Therapeutics Co., Ltd, Shanghai, China

Background: Tumor-infiltrating lymphocyte (TIL) therapy has shown promising efficacy in advanced solid tumors. However, its autologous nature poses a major limitation due to the ineligibility of many patients with advanced disease for repeated tumor resections, leading to a loss of potential treatment opportunities. To overcome this challenge, we developed a “Preservation & Expansion” strategy, in which TIL seed cells are generated from initial tumor tissue and cryopreserved for on-demand expansion into final products (FP) upon treatment need.
Objective: This study aimed to validate the feasibility of expanding FPs from cryopreserved TIL seed cells after various storage durations.
Methods: Tumor tissues were processed and initially cultured to generate seed cells. Seed cells generated from tumor tissues were either immediately expanded (G0) or cryopreserved for 3 days (G3D), 1, 2, 3, or 6 months (G1M-G6M), or 1 or 2 years (G1Y, G2Y) prior to expansion. Cell viability was assessed at the seed, intermediate, and FP stages. Phenotypic analysis (CD3+, CD8+, CD4+, CD56+) was performed on both seed cells and FPs, while functional analyses, including IFN-γ secretion and cytotoxicity via real-time cell analysis (RTCA), were conducted on the FPs.
Results: Viability of cells derived from various tumor tissues post-thaw was comparable across different cryopreservation durations, with the following results (%): G0: 79.7±6.4; G3D: 80.9±5.1; G1M: 81.0±5.8; G2M: 80.2±3.9; G3M: 81.3±4.7; G6M: 81.0±5.3; G1Y: 80.4±5.6; G2Y: 80.8±4.8. Moreover, no significant differences in cell viability were observed during the REP culture phase at various time points. Phenotypic characterization by flow cytometry revealed similar profiles among seed cells cryopreserved for different durations and their corresponding final cellular products. Furthermore, cryopreservation duration had minimal impact on the effector functions of the final products, as evidenced by well-maintained levels of IFN-γ secretion and cytotoxic activity across all groups. IFN-γ secretion levels (ng/ml) were: G0: 14.5±7.0; G3D: 15.0±4.2; G1M: 13.4±5.0; G2M: 14.8±5.0; G3M: 16.5±5.0; G6M: 16.5±5.0; G1Y: 16.9±5.0; G2Y: 20.4±5.0. Cytotoxicity assessed by RTCA (%) was as follows: G0: 76.8±7.9; G3D: 78.1±4.3; G1M: 78.3±8.9; G2M: 77.4±9.0; G3M: 79.2±8.3; G6M: 79.9±3.7; G1Y: 77.2±8.7; G2Y: 83.2±3.6.
Conclusion: TIL seed cells can be effectively expanded into functional FPs with consistent viability, phenotype, cytokine secretion, and cytotoxicity after long-term cryopreservation up to two years. These results validate the "Preservation & Expansion" process as a robust and feasible approach to improve the accessibility and practicality of autologous TIL therapy by decoupling tumor resection from treatment timing.

#3700 Engineering iPSC-derived NK cells with autocrine feeder signaling to enhance cytotoxic function.

Yi-Chen Sun[1], Zhi-Qian Lin[2], Chieh-Min Wang[2], Yun-Yi Yang[3], Yi-Ping Yang[2], **Kai-Feng Hung**[4]

[1]Taipei Tzu Chi Hospital, The Buddhist Tzu Chi Medical Foundation, New Taipei City, Taiwan,[2]Taipei Veterans General Hospital, Taipei, Taiwan,[3]Kang Chiao International School, New Taipei City, Taiwan,[4]National Yang Ming Chiao Tung University, Taipei, Taiwan

Natural killer (NK) cells are key effectors in cancer immunotherapy, but their clinical translation is hindered by limited cell expansion and persistence. Feeder-based expansion systems using tumor-derived K562 cells achieve robust cell proliferation but raise safety concerns. To address these challenges, we generated human induced pluripotent stem cell (iPSC)-derived NK cells endowed with self-feeder properties and autocrine signaling that promote cell expansion and functional activation while minimizing oncogenic risk. Specifically, iPSCs were differentiated into hematopoietic progenitors (iHPCs) under defined conditions and subsequently matured into NK (iNK) cells. The self-supporting iNK cells were then established by viral transduction to express CD86, 4-1BB ligand (4-1BBL), and interleukin-21 (IL-21) bispecific antibodies engineered in a single-chain variable fragment (scFv) format. We showed that the optimized hybrid differentiation protocol yielded highly pure (92.1% $CD56^+$) NK cells that expressed early activation markers ($CD161^+$) but remained phenotypically immature ($CD94^+$ 2.2%, $CD16^+$ 17.7%), consistent with an early-stage but lineage-committed NK phenotype. The engineered self-supporting iNK cells exhibited robust expression of CD86, 4-1BBL, and IL-21 bispecific scFv. Co-culturing the self-supporting iNK cells with primary NK cells isolated from peripheral blood prolonged the viability of the primary NK cells beyond the typical two-week lifespan, indicating self-feeder supportive function. Importantly, the self-supporting iNK cells exhibited enhanced cytotoxicity against K562 cells and retained their cytolytic function even after repeated re-challenge with K562 targets. In conclusion, the engineered iNK cells demonstrated dual functionality, acting both as feeder cells and as cytotoxic effectors against target cancer cells. These self-supporting iNK cells with autocrine feeder signaling hold potential to advance NK cell-based cancer immunotherapy.

#3701 Safety and efficacy of CAR T-cell therapy in CNS lymphoma: A meta-analysis.

Ahmad Shawabkeh[1], Muaath I. Alsufi[1], Homam AbuHashesh[1], Heba Khreisat[1], Zaid Muhanna[1], Salma Salman[2], Ahmad Obeid[1], Layan AlDaher[1], **Jehad Yasin**[1]

[1]School of Medicine, University of Jordan, Amman, Jordan,[2]School of Medicine, Ain Shams University, Ain Shams, Egypt

Background: The efficacy and safety of Chimeric Antigen Receptor T-cell (CART) therapy in Central Nervous System Lymphoma (CNSL) remain uncertain, given the limited representation of CNS involvement in pivotal CAR T-cell trials. This meta-analysis synthesized data from studies evaluating outcomes in both primary (PCNSL) and secondary CNS lymphoma (SCNSL) cohorts treated with CART.

Methods: A comprehensive search was performed across PubMed, Scopus, Web of Science, and clinical registries up to June 2025. Studies reporting efficacy or toxicity outcomes in CNSL following CART therapy were included. Proportions were stabilized using the Freeman-Tukey double arcsine transformation and pooled using inverse variance weighting. Between-study heterogeneity was estimated with the DerSimonian-Laird method, and τ^2 confidence intervals were calculated via the Jackson approach. Random- or fixed-effects models were applied based on $I^2 \geq 50\%$ or $< 50\%$, respectively. Publication bias was assessed using Egger's regression. Subgroup and multiple meta-regression analyses evaluated moderators including CNS category (PCNSL, SCNSL, or Both) and publication year.

Results: Data from thirty-nine studies encompassing 1,457 participants were meta-analyzed. The pooled overall response rate (ORR) was 0.75 [95% CI: 0.70-0.79; $I^2 = 52.2\%$]. Complete response (CR) rate was 0.52 [95% CI: 0.46-0.58; $I^2 = 63.0\%$], and partial response (PR) rate 0.18 [95% CI: 0.14-0.22; $I^2 = 50.40\%$]. No significant publication bias was detected. Meta-regression indicated no significant effect of publication year or CNS category on ORR. Cytokine Release Syndrome (CRS) occurred in 83.8% [95% CI: 79.1-88.2; $I^2 = 71.4\%$], with grade ≥3 CRS in 5.74% [95% CI: 3.21-8.76; $I^2 = 62.1\%$]. Immune Effector Cell-Associated Neurotoxicity Syndrome (ICANS) was reported in 44.4% [95% CI: 35.9-53.1; $I^2 = 86.5\%$], with severe (grade ≥3) events in 16.8% [95% CI: 11.9-22.4; $I^2 = 74.3\%$].

Conclusions: CART therapy achieves robust response rates in CNS lymphoma, with efficacy comparable between PCNSL and SCNSL. Neurotoxicity remains frequent but manageable, and severe CRS events are infrequent.

#3702 No impact of dexamethasone on CAR-T cell expansion in vitro and in patients with RRMM.

Lelisa Gemta[1], **Lawrence P. Andrews**[1], Matthew J. Frigault[2], Binod Dhakal[3], Jacalyn Rosenblatt[4], Michael R. Bishop[5], Sigal Shachar[1], Jenny Mu[1]

[1]Arcellx, Rockville, MD,[2]Massachusetts General Hospital, Boston, MA,[3]Department of Medicine, Medical College of Wisconsin, Milwaukee, WI,[4]Beth Israel Deaconess Medical Center, Harvard Medical School, Boston, MA,[5]David and Etta Jones Center for Cellular Therapy, University of Chicago, Chicago, IL

Chimeric antigen receptor (CAR)-T cell therapy is an effective treatment for relapsed/refractory multiple myeloma (RRMM). The Phase 1 trial of anitocabtagene autoleucel (anito-cel), an autologous D-Domain BCMA-directed CAR-T cell therapy, demonstrated a 100% overall response rate and a median progression free survival rate of 30.2 months, with a median follow-up of 34 months (Bishop et al., 2024). No delayed neurotoxicities were observed (Kaur et al., 2025), such as parkinsonism or cranial nerve palsies reported in up to 10% of real-world ciltacabtagene autoleucel (cilta-cel)-treated patients and associated with elevated absolute lymphocyte count (ALC) indicative of CAR-T cell hyper-expansion as a major risk factor (Lim et al., 2025). Pre-emptive intervention using dexamethasone (Dex) based on ALC has been proposed to limit uncontrolled expansion and prevent delayed neurotoxicity (Turner et al., 2025). However, in patients with large B-cell lymphoma treated with axicabtagene ciloleucel in ZUMA-1, prophylactic steroids did not hinder CAR-T cell expansion (Cohort 6; Oluwole et al., 2021). Thus, further investigation of the impact of Dex on CAR-T cell expansion and function is warranted.

In the Phase 1 study of anito-cel (n=38), 66% of patients received Dex to treat cytokine release syndrome (CRS) events. Patients requiring Dex intervention showed higher soluble BCMA levels at screen, indicative of greater tumor burden. No patients received prophylactic Dex. Consequent Dex use did not suppress CAR-T cell expansion below levels observed in non-Dex-treated patients (ALCmax: 1.39 [0.82-3.07] vs 1.01 [0.49-1.28] k/ul). Differences in CAR-T cell activation-associated cytokines were observed between Dex and non-Dex-treated patients.

The increase of CAR-T cell expansion in patients with higher tumor burden, who required intervention with steroids, is consistent *in vitro* when CAR-T cells were stimulated with a high BCMA density cell line (H929) compared to a low BCMA density cell line (Raji). For these *in vitro* studies, surrogate versions for anito-cel (D-Domain), cilta-cel (VHH) and idecabtagene vicleucel (scFV) were generated and the impact of Dex on CAR-T cell phenotype and functionality was assessed. Treatment with Dex did not impact CAR-T cell expansion, cytolytic activity, CAR expression, CD4:CD8 ratio or differentiation/activation state. While Dex did not impact CAR-T cell expansion (D-Domain 4.8 vs 4.4; VHH 5.4 vs 4.3; scFV 5.3 vs 4.9 fold expansion), Dex treatment decreased IL-2 production, *in vitro*, making it an effective CRS treatment.

While increased ALC and rapid CAR-T cell expansion within the first 28 days has been identified as a biomarker for delayed neurotoxicities, these data suggest that high dose steroids may not be an efficacious intervention for ALC restraint. Instead, Dex treatment is likely to curb proinflammatory cytokines and thus is an appropriate intervention for CRS management.

#3703 Sentinel lymph node-derived CD45$^+$ cells combined with low-dose radiotherapy and PD-1 blockade as a next-generation adoptive cell therapy in head and neck cancer.

Pardis Mohammadzadeh[1], Tomoya Kurokawa[1], Kelsey Decker[1], Peter Vo[1], Prakriti Sen[1], Riley N. Jones[2], Sayuri Miyauchi[2], Santiago Fassardi[1], Anais Zourelidis[1], Robert Saddawi-Konefka[3], Joseph A. Califano[1]

[1]Gleiberman Head and Neck Cancer Center, Moores Cancer Cencer, University of California San Diego, San Diego, CA,[2]Department of Radiation Medicine & Applied Scienes, and Moores Cancer Center, University of California San Diego, San Diego, CA,[3]Department of Head and Neck Cancer Surgery, University of California San Diego, San Diego, CA

Purpose: Head and neck squamous cell carcinoma (HNSCC) is the seventh most common cancer globally, representing roughly 6% of all malignancies. Each year it accounts for an estimated 660,000 new diagnoses and over 325,000 deaths, with incidence projected to rise by nearly 30% by 2030. Despite advances in surgery, radiation, and immunotherapy, patients with HPV-negative HNSCC continue to face poor outcomes, with five-year overall survival rates often below 55%. Adoptive cell therapy (ACT) in solid tumors remains limited by the scarcity of tumor-reactive T cells and their functional exhaustion after expansion. The sentinel lymph node (SLN), the initial site of tumor antigen presentation and T-cell priming, may provide a rich and minimally exhausted source of tumor-specific lymphocytes. Here, we evaluated the immunologic and therapeutic advantages of SLN-derived leukocytes over those from tumor tissue in an orthotopic model of HPV$^-$ HNSCC.

Methods: CD45$^+$ immune cells isolated from donor SLNs, NSLNs, tumors, or SLNs preconditioned with low-dose tdRT (4 Gy) in the 4MOSC1 murine model were adoptively transferred into syngeneic tumor-bearing recipients to evaluate their therapeutic potential. Recipient groups included untreated controls, preconditioned mice with 4 Gy tdRT, or a single PD-1 blockade (PD1i) dose before ACT. Phenotypic and functional characterization was performed using flow cytometry, multiplex immunofluorescence, ELISA, and CITE-seq to evaluate cell populations, activation, exhaustion, clonal overlap, and tissue distribution.

Results: SLN-CD45$^+$ populations were enriched in activated CD4$^+$/CD8$^+$ T cells with elevated CD69, CD137, and IFN-γ expression compared with tumor-derived counterparts. mIHC confirmed higher densities of activated T cells in SLN and tumor regions after SLN-CD45$^+$ transfer. TCR analysis revealed substantial overlap between SLN and tumor clonotypes, suggesting selective enrichment of tumor-reactive clones. Functionally, ACT with SLN-CD45$^+$ cells induced greater tumor regression and survival benefits than ACT from tumor source, even without lymphodepletion or expansion in culture. Notably, cryopreserved SLN-derived cells retained comparable efficacy to freshly isolated ones. Preconditioning recipients with 4 Gy tdRT or PD1i further improved intratumoral infiltration, activation, and persistence of transferred cells without added toxicity.

Conclusions: The sentinel lymph node provides a potent, readily accessible reservoir of tumor-reactive immune cells for ACT. Combining SLN-derived ACT with tdRT and PD1i significantly enhances therapeutic efficacy in HPV$^-$ HNSCC. These findings highlight the translational potential of leveraging tumor-draining lymphoid niches as tumor-primed immune reservoirs for next-generation ACT in solid tumors.

#3704 Long-term *ex vivo* expansion of functional CAR-T cells using the biomimetic AeroCyte-based artificial antigen-presenting cell platform.

Yu-Tsueng Liu, Mindy Yin, Guixin Shi

AeroCytek, Inc., San Diego, CA

Strategies to sustain CAR-T cell persistence in vivo include enriching stem-like products, repeated infusions of engineered cells, and improving the tumor microenvironment. Peripheral T lymphocytes exhibit remarkable self-renewal, with studies showing up to 10^{41}-fold expansion in syngeneic mice over 10 years (Nature, 2023; 614:762), and similar potential ex vivo, though technical barriers persist. Here, we assessed a biomimetic phospholipid microbubble platform (AeroCyte) designed as artificial antigen-presenting cells (aAPCs) to support long-term ex vivo CAR-T cell expansion. AeroCyte-J, coated with appropriate ligands, mimics natural cell-to-cell (juxtacrine) interactions for T cell stimulation and undergoes spontaneous dissolution in media. We hypothesized this system would enhance ex vivo production of stem-like T cells and enable repeated dosing to overcome hostile in vivo conditions.

$CD4^+$ T cells were isolated from human blood using anti-CD4-conjugated AeroCyte and activated with anti-CD3/CD28-conjugated AeroCyte (AeroCyte-J328) for two weeks, then restimulated biweekly for about 6 months, achieving up to 10^{16}-fold expansion. Notably, expansion was absent without AeroCyte-J328. Next, three CAR-T cell lines targeting GD2, HLA-A2, or CD19, which were generated from a vial of frozen PBMCs from a different donor, were expanded over seven biweekly cycles using AeroCyte-J328. The expanded cells were $CD3^+$ and included both $CD4^+$ and $CD8^+$ subsets. CAR-T cells from each stimulation cycle were evaluated for target-specific cytotoxicity by co-culturing them for three days without IL-2 with GFP-expressing Raji cells ($CD19^+$, HLA-$A2^-$, $GD2^-$) and T98G cells ($CD19^-$, HLA-$A2^+$, $GD2^+$). Using the number of target cells co-cultured with non-transduced PBMCs as the baseline control (set at 100%), all three CAR-T cell types demonstrated target specificity, particularly at lower effector-to-target (E:T) ratios, as determined by flow cytometry or fluorescence microscopy. Reproducibility was confirmed by expanding CAR-T cell lines derived from one of three additional donor PBMC samples across four biweekly cycles, which produced consistent and comparable results.

Long-term expansion depended on continuous aAPC stimulation and is attributed to intrinsic T cell self-renewal rather than malignant transformation, given that expansion is AeroCyte-J328-dependent and the improbability of simultaneous malignant transformation across independent cultures. Additional preclinical and clinical validation of this simple and robust platform could make CAR-T therapy more accessible and affordable, as well as enable improved treatment of solid tumors, for example through repeated dosing.

Supported by NIH grants R44CA265468 & R43CA298530

#3705 Integration of affinity-dependent modulation and CD5/TRAC knockout generates fratricide-resistant and highly cytotoxic anti-CD5 CAR-T cells.

Seojeong Kim[1], Jeong Hoon Jeong[2], Jihyun Park[3], Youngho Lee[2], Hyung Cheol Kim[2], Hyoung Jin Kang[4], Matthew H. Porteus[5], Steven Feldman[5], Youngil Koh[4]

[1]Seoul National University, Seoul, Korea, Republic of,[2]Curocell Inc., Daejeon, Korea, Republic of,[3]Seoul National University Hospital, Seoul,[4]Seoul National University Hospital, Seoul, Korea, Republic of,[5]Stanford University, Stanford, CA

CD5-positive T-cell malignancies, including T-cell acute lymphoblastic leukemia and peripheral T-cell lymphoma, remain challenging to treat due to severe fratricide during CAR-T manufacturing and a lack of effective therapeutic options. Previous work generated two anti-CD5 CAR-T constructs (CAR5) containing unique CD5 binders with distinct affinities, designated A2CAR5 (high affinity) and C7CAR5 (low affinity), to evaluate how binding strength influences CAR-T cell functionality. A2CAR5 exhibited robust antigen engagement but suffered from severe fratricide accompanied by excessive cytokine release, whereas C7CAR5, with lower affinity, largely avoided fratricide while retaining potent cytotoxicity both in vitro and in vivo. However, attempts to improve the functionality of either construct through CD5 knockdown resulted in only limited enhancement. The present study builds upon these findings by applying CD5 and TRAC gene editing to the high-affinity CAR5 to further enhance its efficacy and safety. A comparative evaluation of A2CAR5 and C7CAR5 with CD5 knockout (KO) was conducted to assess affinity-dependent function, while a CD5/TRAC double knockout (dKO) was designed to develop an optimized allogeneic CAR5 platform. Since allogeneic CAR-T cells may exhibit limited persistence following infusion, achieving potent initial activity is critical for therapeutic success. CD5 KO effectively abolished fratricide in A2CAR5 cells, normalizing IFN-γ and TNF-α secretion to levels comparable to those of non-transduced T cells. Surface marker analysis revealed that fratricide led to a progressive increase in the proportion of CAR^+ cells over time, whereas CD5 KO eliminated this abnormal enrichment, reduced exhaustion marker expression, and preserved a favorable memory phenotype. Following CD5 KO, A2CAR5 consistently demonstrated superior functional performance compared to C7CAR5, exhibiting stronger cytotoxic activity specifically against $CD5^+$ target cells and greater functional persistence under repetitive antigen exposure. To achieve efficient disruption of both CD5 and TRAC, a sequential targeting approach was adopted, which proved more effective and consistent than conventional double knockout methods. In conclusion, these findings indicate that CD5 knockout reduces fratricide and limits T-cell exhaustion, supporting the development of optimized allogeneic CAR5 cells through the integration of binder design and gene editing. Future work will incorporate AAV6-mediated CAR knock-in at the TRAC locus to further enhance genomic precision and product consistency.

#3706 Impact of number of IL-2 infusions and product out of specification status on outcomes of tumor infiltrating lymphocyte therapy for melanoma.

Mohamed A. Aboelatta[1], Jeffrey E. Johnson[1], Jabra G. Zarka[1], Matyas Benada[2], James W. Jakub[3], Roxana S. Dronca[3], Ruqin Chen[3], Mahesh Seetharam[4], Deepti Behl[1], Svetomir N. Markovic[1], Lisa A. Kottschade[1], Heather N. Montane[1], Matthew S. Block[1], Anastasios Dimou[1], Robert R. McWilliams[1], Paula Gill[1], Yi Lin[1], **Arkadiusz Z. Dudek**[1]

[1]Mayo Clinic, Rochester, MN,[2]Charles University, Hradec Kralove, Czech Republic,[3]Mayo Clinic, Jacksonville, FL,[4]Mayo Clinic, Scottsdale, AZ

Background: High-dose interleukin-2 (IL-2) is administered after tumor-infiltrating lymphocyte (TIL) infusion to promote in-vivo expansion and persistence, yet optimal dosing and the clinical significance of out-of-specification (OOS) TIL products remain unclear. We investigated the impact of number of infused IL-2 doses and manufacturing OOS status on outcomes in metastatic melanoma treated with commercial TIL therapy.

Methods: We retrospectively analyzed 31 patients treated across three Mayo Clinic sites. Planned IL-2 was 600,000 IU/kg every 12 hours for ≤6 doses; actual dosing varied based on clinical tolerance. Patients were grouped as low (0-2) vs high (≥3) IL-2 doses. TIL products were classified as within-specification or OOS per commercial release criteria. Survival associations were evaluated using Kaplan-Meier and multivariable Cox regression.

Results: In our 31-patient cohort, the median age was 59 years (range 17-77), 58% were male, and 84% had ECOG 0. At TIL infusion, M-stage distribution was M1a 6%, M1b 10%, M1c 61%, and M1d 23%. LDH was elevated above the upper limit of normal in 42%. The median number of IL-2 infusions was 4 (range 0-6); 58% of patients received ≥3 doses, while 2 patients (6%) received none. Out-of-specification (OOS) TIL products occurred in 6 patients (19%). Best responses included complete response (26%) and partial response (23%), for an overall response rate of 48% and a disease-control rate of 61% (CR + PR + SD). Among responders, the median duration of response was 84 days (95% CI 73-95). At data cutoff, the median follow-up was 253 days (95% CI 137-370). The most common grade 3/4 toxicities occurring >14 days after TIL infusion were lymphopenia (39%), anemia (16%), and thrombocytopenia (10%). Median progression-free survival (PFS) was 99 days (95% CI 73-125) with 20 progression events, and median overall survival (OS) was 193 days (95% CI 32-354) with 13 deaths. Number of infused IL-2 doses was dependent on patients tolerability. Receiving ≥3 IL-2 doses was associated with improved overall survival (394 vs 101 days; $p < 0.001$) and a trend toward longer progression-free survival (110 vs 59 days; $p = 0.055$). OOS products predicted inferior PFS (30 vs 110 days; $p = 0.003$) and showed a trend toward worse OS (120 vs 394 days; $p = 0.079$). In multivariate analysis, ≥3 IL-2 doses independently improved PFS (HR 0.20, 95% CI 0.06-0.69; $p = 0.011$) and OS (HR 0.09, 0.02-0.36; $p = 0.001$), while OOS status increased risk of progression (HR 8.10, 2.24-29.25; $p = 0.001$) and death (HR 6.16, 1.35-28.20; $p = 0.019$).

Conclusions: Higher number of infused doses IL-2 and meeting commercial TIL release criteria were independently associated with improved outcomes.

#3707 Durable remission of high-risk and refractory neuroblastoma by PHOX2B derived peptide-HLA directed CAR T cells: An IND enabling study.

Muzamil Y. Want[1], Richa Kapoor[1], David Groff[1], Keelan O'Reilly[1], Liron Grossmann[1], Alvin Farrel[1], Rebeca A. Ventura[2], Peiyao Li[1], Quinlen Marshall[2], Jenny pogoriler[3], Daniel Martinez[3], Matt Beasley[4], Ben Kiefel[4], Mark Yarmarkovich[5], John Maris[1]

[1]Division of Oncology and Center for Childhood Cancer Research, Children's Hospital of Philadelphia, Philadelphia, PA,[2]University of Pennsylvania, Philadelphia, PA,[3]Children's Hospital of Philadelphia, Philadelphia, PA,[4]Myrio Tx, Melbourne, Australia,[5]NYU Langone Health, New York, NY

Effective cellular therapies for solid tumors are limited by the lack of tumor-specific antigens. We previously showed that non-mutated self-peptides from essential intracellular neuroblastoma (NB) oncoproteins are presented by common HLA allotypes, enabling selective targeting (Nature 2023). Here, we report IND-enabling studies of second-generation PHOX2B PC-CAR T cells incorporating a 4-1BB costimulatory domain. A GMP-grade lentiviral vector encoding the PHOX2B peptide-HLA-specific CAR was produced at CHOP and used to transduce healthy donor and patient T cells. PHOX2B expression and epitope heterogeneity were analyzed across solid tumors, NB xenografts, and cell lines by RNA-seq, IHC, and a PHOX2B scFv assembled with klickmer detecting the QYNPIRTTF/HLA complex. Safety was evaluated using the X-scan and sCRAP cross-reactivity algorithms integrated with experimental testing across 25 normal HLA-A24/23 primary cell lines and HLA-matched PHOX2B negative cancers. Functional activity was assessed via IncuCyte based cytotoxicity, multiplex cytokine profiling, and T-cell activation/proliferation by flow cytometry. Efficacy was tested in four HLA-A24/23 NB xenografts (including chemotherapy-resistant models) and one non HLA-A*24:02/23:01 NB control in NSG MHC-I/II deficient mice receiving a single ~7×10^6 PC-CAR T-cell infusion. Longitudinal expansion, immunophenotype, and transcriptional states were characterized by flow cytometry and single-cell RNA-seq. PHOX2B was highly expressed in all neuroblastomas and pheochromocytomas and not expressed in other cancers. Klickmer staining revealed variable epitope density correlating with PC-CAR T cell activation. PHOX2B PC-CAR T cells mediated potent, dose-dependent killing of HLA-A24/23 neuroblastomas, sparing antigen-negative non-HLA-A24/23 cancer cells unless peptide-pulsed. Antigen engagement triggered proliferation, effector cytokine release, and IFN-γ dependent upregulation of HLA-I, significantly increasing antigen density. No cross-reactivity was detected in co-culture assays. A single dose of PC-CAR T cells induced complete regression (>50 days) across all xenografts. One relapse in each of two models either regressed spontaneously with re-emergence of PC-CAR T cells or after re-treatment. Responses were durable >120 days, whereas PHOX2B+ non-HLA-A24:02/23:01 controls showed progressive disease. Expansion peaked at day 14 with $CD8^+$ effector-memory predominance transitioning to central-memory persistence. PHOX2B-directed PC-CAR T cells show stringent specificity, potent cytotoxicity, and curative efficacy in preclinical patient-derived NB models. These IND-enabling data supported the ongoing first-in-human/child Phase 1 trial (NCT07007117), validating PHOX2B as a lineage-restricted immunotherapeutic target in high-risk neuroblastoma.

#3708 Improving antitumor T cell therapy with membrane-tethered engineered cytokine agonists.

Diana Gumber[1], Saul Priceman[2], Christine E. Brown[3], Leo D. Wang[1]

[1]Immuno-oncology, City of Hope National Medical Center, Duarte, CA,[2]Keck School of Medicine of USC, Los Angeles, CA,[3]City of Hope National Medical Center, Duarte, CA

Chimeric antigen receptor (CAR) T cell therapy has demonstrated marked success in the control of hematological malignancies. However, the hostile milieu and chronic antigen exposure in the tumor microenvironment contribute to the induction of exhaustion and loss of efficacy of CAR T cells in the treatment of solid tumors.

Overcoming T cell exhaustion is essential for improving immunotherapeutic efficacy in the treatment of solid tumors. One strategy focuses on engineering CAR T cells that generate a supportive local immune environment through expression of activation and survival-promoting proteins. Specifically, interleukin-2 (IL2) is an attractive candidate as it is a potent stimulator of proliferation and effector function in T cells. However, the therapeutic application of systemic IL2 is associated with life-threatening complications and T cell exhaustion. To address these toxicities, we have developed membrane-tethered engineered cytokine agonists (MECAs), which are cell-surface constrained proteins that transduce a defined subset of cytokine-mediated signals to promote T cell function without toxicity or T cell exhaustion.

Here, we evaluate the influence of MECAs on the proliferation and cytotoxicity of CAR T cells in a glioblastoma-targeting model. IL13Rα2-targeting CAR T cells co-expressing the MECAs demonstrated improved cytotoxic function and proliferation in recursive challenge in in vitro models. Preliminary results demonstrate that MECA-expressing CAR T cells are not toxic in an in vivo orthotopic glioma model. Additionally, the CAR T cells co-expressing MECA had greater anti-tumor activity compared to CAR only T cells.

Exhaustion of antigen-specific T cells is a central challenge across multiple cancer immunotherapy modalities. The proposed MECAs have the potential to revolutionize immunotherapy by providing effective and widely applicable orthogonal signals that improve the proliferation and effector activity of adoptively transferred CAR T cells.

#3709 A first-in-class Erythrocyte-anti-PD-1 conjugate overcomes immunotherapy resistance across pan-solid tumors: A phase I trial.

Xiaoqian Nie[1], Liu Yang[2], Kurban Mattursun[3], Zheling Chen[2], Xiaofei Gao[1]

[1]Westlake University, Hangzhou, China,[2]Zhejiang Provincial People's Hospital, Hangzhou, China,[3]Westlake Therapeutics, Hangzhou, China

Background: Despite the success of immune checkpoint blockade (ICB), most patients fail to respond or eventually develop resistance due to insufficient efficacy or immune-related toxicities. We developed αPD-1-Ery, an erythrocyte-PD-1 antibody conjugate in which anti-PD-1 antibodies are covalently linked to erythrocyte membranes. Unlike conventional antibodies, αPD-1-Ery selectively accumulates in the spleen, where it efficiently engages and activates T cells, leading to reductions in immunosuppressive myeloid cells. These coordinated effects remodel the immune landscape, reprogram the tumor microenvironment, and suppress tumor growth in ICB-resistant models. Based on these findings, we initiated a phase I investigator-initiated trial of αPD-1-Ery in patients with advanced solid tumors that had progressed on prior PD-1/PD-L1 therapy (NCT06026605).

Methods: This first-in-human study evaluated the safety, tolerability, pharmacokinetics (PK), and preliminary efficacy of αPD-1-Ery monotherapy. Eligible patients had histologically confirmed solid tumors progressing on prior PD-1/PD-L1-containing regimens. αPD-1-Ery was administered intravenously every 21 days at dose levels of 2×10^{11} or 3×10^{11} cells per infusion. Safety was assessed per NCI-CTCAE v5.0, and efficacy per RECIST v1.1.

Results: As of October 31, 2025, 14 heavily pretreated patients with 11 tumor types were enrolled. No dose-limiting toxicities or TRAEs > grade 3 occurred, and no severe immunotoxicities were observed. αPD-1-Ery showed encouraging anti-tumor activity, with a DCR of 78.6% (11/14) and an ORR of 42.9% (6/14), including 1 CR and 5 PRs. Responses were more pronounced at the higher dose level (ORR 57.1%, 4/7), supporting a dose-dependent effect. Median PFS was 5.5 months, and the 12-month OS rate was 71.4%, indicating durable benefit. PK analysis demonstrated dose-proportional exposure, with mean Cmax values of 2,711 and 5,107 cells/μL for the low and high doses, respectively. Tmax ranged from 0.5 to 48 hours, and engineered erythrocytes persisted for 7-21 days. Free antibody levels remained <5%, confirming in-vivo stability and spleen-targeted delivery. Biomarker analysis identified a spleen-associated myeloid signature: responders had higher baseline circulating PMN-MDSCs and showed rapid post-treatment declines compared with non-responders, consistent with spleen-mediated myeloid modulation.

Conclusion: αPD-1-Ery is safe, well tolerated, and demonstrates encouraging anti-tumor activity in ICB-resistant solid tumors. Erythrocyte-drug conjugates represent a novel therapeutic class for overcoming resistance to checkpoint blockade, with broad implications for cancer treatment and drug development.

#3710 Adapting and validating a humanized mouse model for testing of immune-shielded genetic modifications in therapeutic cells.

Mino Yakoub, Katrin Ridders, Henning Jelten, Audrey Holtzinger, Matthias Austen, Claudia Wrzos

Evotec International GmbH, Gottingen, Germany

Introduction: Allogeneic transplantation of “off-the-shelf” cell therapies offers a transformative approach for treating a wide range of diseases, including various oncological diseases. However, host-mediated immune rejection ‘’Allogeneic rejection’’ remains a critical barrier to therapeutic success. To address this, immune shielding strategies have been developed to evade immune detection, necessitating robust in vivo models for evaluating their protection from immune cells. Many in vivo models fall short in mimicking the human host immune milieu. We have established a model that incorporates multiple transplantation sites for therapeutic cells, such as under the kidney capsule of the mice. Additionally, we have characterized relevant readouts for the evaluation of the survival of immune-shielded therapeutic cells and monitoring allogeneic rejection.
Methods: We utilized the immunodeficient BRGSF mice. These mice were humanized using CD34+ from distinct human donors, resulting in the BRGSF-HIS mice (purchased from Genoway). We transplanted these mice with therapeutic stem cell-derived cells. Post-transplantation, mice received human FLT3 ligand to enhance human myeloid cell development. At the end of the study, blood, spleen, and kidney tissues are collected for flow cytometry, MSD cytokine profiling, and histology. Other functional readouts were performed during the in-life phase.
Results: The model was validated by transplanting wild-type (non-immune shielded) stem cell-derived therapeutic cells under the kidney capsule of BRGSF-HIS mice. In addition, a subset of BRGSF-HIS mice serves as a control group and does not undergo transplantation. The BRGSF-HIS were tested by flow cytometry of blood and spleen to confirm the presence of all the human immune cells essential for allogeneic rejection, including CD4/CD8 T-cells, NK cells, B-cells, monocytes, and M1/M2 macrophages. A comparative analysis was performed on both transplanted and non-transplanted BRGSF-HIS, focusing on the assessment of immune cells and cytokines in the blood and spleen. The transplanted mice exhibited a pronounced pro-inflammatory phenotype in T-cells, characterized by increased CD4+ and CD8+ TEMRA and CD69+ populations, elevated Th1 subsets, and reduced Th2 cells. We observed a tendency for a shift of splenic M2 to M1 macrophages in the transplanted mice. Systemic immune activation was further demonstrated by increased levels of pro-inflammatory cytokines found in both plasma and spleen samples. Histological assessment of immune infiltration at the transplantation site revealed a high abundance of human T-cells, accompanied by macrophages.
Conclusion: We developed a model to evaluate allogeneic rejection of immune-shielded therapeutic cells, assess their survival, and analyze immunophenotyping resulting from transplantation, as well as human host immune infiltration.

#3711 Enriching CD8+ and CD4+ neoantigen-reactive tumor infiltrating lymphocytes by cell surface marker-based sorting.

Lisa M. Kenney, Nivedita Ratnam, Abraham A. Hakim, Juliette Rault-Wang, Steven A. Rosenberg, Frank J. Lowery

Surgery Branch, National Cancer Institute, Center for Cancer Research, National Institutes of Health, Bethesda, MD

Introduction: Adoptive cell transfer (ACT) of tumor-infiltrating lymphocytes (TIL) is FDA-approved for metastatic melanoma and is under investigation for metastatic epithelial cancers. Identifying neoantigen-reactive TIL currently requires time- and resource-intensive testing against patient-specific neoantigens, enabling selection only at the culture level. Cell-surface markers capable of isolating tumor-relevant $CD8^+$ and $CD4^+$ TIL could eliminate the need for personalized sequencing and screening.
Methods: Single-cell RNA/TCR sequencing of mixed population of neoantigen-specific and bystander TIL derived from pooled cultures from a metastatic GI cancer lesion with known reactivity identified CD103 as the top marker of tumor-relevant $CD8^+$ TIL and CD31 as a bystander marker. Similar analysis of bulk TIL from another GI malignancy lesion derived from a different patient identified PD-1 and ADGRG1 as $CD4^+$ enrichment markers and CD69 and KLRB1 as depletion markers. Markers were tested for their ability to enrich tumor-relevant $CD8^+$ and $CD4^+$ TIL from pooled epithelial cancer fragments (11 retrospective and 5 prospective $CD8^+$ samples; 10 retrospective $CD4^+$ samples). Following culture in IL-2 in GREX100 flasks for 21 days, TIL were sorted based on expression of CD103 and CD31 for the $CD8^+$ TIL and PD1, ADGRG1, CD69 and KLRB1 for the $CD4^+$ TIL. Sorted populations were expanded using rapid expansion protocol (REP) and evaluated for neoantigen reactivity by upregulation of 4-1BB and/or OX40 expression and IFN-γ release via ELISpot. Single-cell TCR sequencing of populations was done to identify and confirm neoantigen specificity. Group comparisons were performed using non-parametric paired t-tests.
Results: Across retrospective and prospective samples, $CD103^+CD31^-$ $CD8^+$ TIL showed mean neoantigen reactivity of 19.3% and 18.3% and median enrichment of 5.7x ($p = 0.0244$*) and 8.1x over bulk $CD8^+$ TIL. Single-cell TCR sequencing confirmed enrichment in retrospective samples ($p = 0.0312$*) and validated 1-3 unique neoantigens per patient. Among 10 patients with $CD4^+$ neoantigen-specific responses, $CD4^+$ bulk TIL showed a mean reactivity of 13.8%, with 1-5 neoantigens validated per patient. $CD4^+CD69^-PD\text{-}1^+$ selection produced a 2.2x median increase in reactivity ($p = 0.0195$*) and superior capture of neoantigen-specific TCRs vs $CD4^+$ Bulk ($p = 0.0039$**). Overall 14 of 16 patient samples studied for $CD8^+$ reactivity showed enrichment by $CD103^+CD31^-$ while 9 of 10 patient samples studied for $CD4^+$ reactivity showed enrichment with $CD4^+$ $CD69^-PD1^+$.
Conclusion: Selection of $CD103^+CD31^-$ cells enriches tumor-relevant $CD8^+$ TIL, while $CD4^+CD69^-PD\text{-}1^+$ most effectively enriches $CD4^+$ TIL. Clinical-scale sorting using these markers could generate neoantigen-enriched TIL without patient-specific screening, expanding treatment feasibility for patients with more rapidly progressing disease.

#3712 Pleiotropic oxidized carbon nanozymes reprogram CAR T cell metabolism to enhance persistence through redox modulation.

Kevin Song[1], Yue Hu[2], Paul Derry[2], Thomas Kent[2], Xiaotong Song[3]

[1]University of Houston, Houston, TX,[2]Texas A&M University, Houston, TX,[3]Texas A&M Univ. Health Science Center (Houston, TX), Houston, TX

Adoptive CAR T cell therapy faces major challenges in solid tumors due to chronic antigen stimulation, oxidative stress, and metabolic exhaustion. We recently developed Pleozymes, pleiotropic oxidized carbon nanozymes that function as synthetic redox mediators with multiple enzymatic activities, including superoxide dismutase-like scavenging and NADH/NAD^+ interconversion. Pleozymes are 3-8 nm oxidized carbon nanoparticles synthesized from coconut-derived activated charcoal and exhibit broad redox potential and mitochondrial localization, enhancing both oxidative phosphorylation and glycolysis in mammalian cells. To investigate their role in T cell metabolic resilience, we treated GPC3-targeted CAR T cells with Pleozymes during chronic co-culture with GPC3-positive HCC Huh7 cells over repeated stimulation cycles. Cell proliferation, apoptosis, exhaustion marker expression, and memory subset differentiation were assessed by flow cytometry and metabolic assays. Pleozymes markedly enhanced CAR T cell expansion and viability across repeated tumor challenges. Apoptotic rates were reduced, and expression of exhaustion markers TIM-3 and LAG-3 decreased significantly. Pleozymes promoted differentiation toward T stem cell memory (TSCM) and central memory (TCM) phenotypes, indicating improved persistence potential. Metabolic profiling indicated elevated total ATP levels and enhanced NAD^+-dependent catabolic activity, consistent with concurrent activation of glycolysis, fatty acid β-oxidation, and tricarboxylic acid (TCA) cycle flux. Collectively, these findings demonstrate that Pleozymes act as metabolic cofactors that restore redox balance and sustain bioenergetic flexibility in CAR T cells. By mitigating exhaustion and enhancing memory differentiation, Pleozymes offer a novel, non-genetic strategy to improve CAR T cell persistence and antitumor efficacy in solid tumor settings.

#3713 Fluorescence potency assays for evaluating HER2 CAR T-cell-mediated killing in cancer cells.

Danny Flanigan, Nathalie Opdam - van de Laar, Denise Sullivan, DANIEL MILLARD, STACIE CHVATAL

Axion BioSystems, Atlanta, GA

Introduction Harnessing the potent cytotoxicity of chimeric antigen receptor T (CAR-T) cells has revolutionized cancer immunotherapy. A key factor influencing CAR-T cell efficacy is target antigen density on cancer cells. Human epidermal growth factor receptor 2 (HER2), overexpressed in various cancers like ovarian and lung carcinomas, is a promising target for CAR-T cell therapy. Traditional cytotoxicity assays generally provide only static endpoint measurements and often rely on 2D cell culture models, which fail to capture the structural complexity of tumors in vivo—a factor crucial to CAR-T cell efficacy. Live-cell imaging offers a solution by enabling non-invasive, real-time monitoring of cytotoxicity. Therefore, this study aims to explore the dynamics of CAR-T cell-mediated cytotoxicity against cancer cells with varying HER2 expression levels, comparing outcomes between 2D and 3D cell culture models using the Omni platform by Axion BioSystems. Methods Monolayers and spheroids of SKOV3 (ovarian carcinoma) and A549 (lung adenocarcinoma) cells, tagged with GFP, were exposed to HER2 CAR-T cells at different Effector:Target (E:T) ratios. Using the Omni platform, hourly brightfield and fluorescent images were captured over 72 hours to assess cancer cell growth and cytotoxicity and quantify the cytolysis of fluorescent target cells. Percent cytolysis of the target cells was calculated by comparing the green fluorescent intensity of treated wells to no treatment control wells. Results As expected, A549 cells treated with CAR T-cells exhibited dose-dependent decrease in fluorescence confluency (%), with near-complete cell lysis observed in the 5:1 E:T ratio group at 160 hours. Immune cell-mediated killing was assessed by applying HER2-targeted CAR T-cells to both SKOV3-GFP and A549-GFP spheroids. SKOV3-GFP spheroids treated with CAR T-cells showed a dose-dependent decrease in fluorescence intensity, with higher E:T ratios (2:1, 5:1, and 10:1) resulting in approximately 75% reduction in fluorescence intensity by 72 hours. In contrast, A549 spheroids only exhibited significant killing at 5:1 and 10:1 E:T ratios, while minimal decreases in intensity were observed at other ratios. Conclusion The Omni platform enables real-time monitoring of CAR T-cell interactions with target cells, providing key insights into the cytotoxic potential of these engineered immune cells. Fluorescent metrics were used to track immune cell-mediated killing, with changes in fluorescence confluency and intensity reflecting the extent of target cell death. Results showed that the potency of CAR T-cell-mediated cytolysis was dose-dependent, with higher E:T ratios leading to greater target cell killing. SKOV3-GFP spheroids, which overexpress HER2, were more susceptible to HER2 CAR T-cell-mediated killing, while A549-GFP spheroids with low HER2 expression required higher E:T ratios for effective cytolysis.

#3714 Immunopeptidomic discovery of fetal WNT-associated antigen NKD1 enables HLA-A2+ restricted TCR-T therapy for MSS mCRC.

Jaeyop Lee, Swara Patel, Inaki Etxeberria, Elizabeth Benitez, Jura Pintar, Andres Rettig, Christopher Cowley, Stefanie Gerstberger, Kathleen Luckett, Asha Saxena, Zita Aretz, Tatyana Korontsvit, Zhuoning Li, Kevin Soares, Emmanouil Pappou, T. Peter Kingham, William Jarnagin, Philip B. Paty, Martin R. Weiser, Michael D'Angelica, Julio Garcia-Aguilar, Jinru Shia, Mara Monetti, Christopher A. Klebanoff, Karuna Ganesh, David A. Scheinberg

Memorial Sloan Kettering Cancer Center, New York, NY

T cell-engaging therapies have achieved limited success in microsatellite stable (MSS) metastatic colorectal cancer (mCRC), in part because of a paucity of truly cancer-specific targets. Systematic interrogation of the immunopeptidome, the repertoire of peptides presented by human leukocyte antigen (HLA) class I molecules, can expand the pool of druggable antigens beyond conventional surface receptors. Nonetheless, both neoantigenic driver mutations and recently described oncofetal peptides are rare or absent in most CRCs. Our recent work shows that mCRC cells adopt a highly stereotyped fetal-like phenotype, characterized by activation of a developmental WNT signaling program that is further enriched in metastasis-initiating cells and conserved across diverse patients. We hypothesized that this transcriptional reprogramming generates a cancer-specific, developmentally fixed HLA-I ligandome that can be exploited for T cell therapy. Using an integrated platform for systematic collection and multimodal profiling of matched normal colon, primary tumor, and metastases from patients undergoing CRC surgery, we established ex vivo patient-derived organoids (PDOs) that faithfully capture patient-specific CRC cell states and provide an effectively inexhaustible source of tumor cells for immunopeptidomic discovery and functional validation. In HLA-$A2^+$ PDOs, representing the most common HLA allele, immunopeptidomic analyses identified recurrent presentation of peptides derived from fetal WNT program genes, in particular NKD1, that are prevalent across mCRC PDOs from HLA-$A2^+$ patients and undetectable in healthy tissues. These peptides were immunogenic in vitro, eliciting robust reactivity from healthy donor T cells and supporting their suitability as therapeutic targets. Moreover, naive $CD8^+$ T cells engineered with NKD1-specific T cell receptors (TCRs) showed strong cytokine activation and potent, antigen-dependent cytotoxicity against mCRC PDOs without detectable off-target activity, consistent with a favorable therapeutic index. Together, these data nominate NKD1 as a conserved antigen in mCRC and support the clinical advancement of an NKD1-directed TCR-T cell product as a first-in-class precision therapy for patients with MSS mCRC.

#3715 Epigenetic and signaling-based engineering enhances CAR-T cell function in oculo-cerebral lymphoma.

Marion Alcantara[1], Jaime Fuentealba[1], Silvia Menegatti[1], Anne-Laure Privat[1], Lisseth Silva[1], Kyle Raymond[1], Daniel De Murat[1], Valentine Pottez Jouatte[1], Lamia Lamrani[1], Zelia Gouveia[1], Denis Malaise[2], Carole Soussain[1], Sebastian Amigorena[2]

[1]Institut Curie, Saint-Cloud, France,[2]Institut Curie, Paris, France

Patients with PCNSL, an aggressive B-cell malignancy confined to the central nervous system (brain, cerebrospinal fluid, spinal cord and/or eye), face poor outcomes, particularly upon relapse. Although CD19-directed CAR-T cell therapies have transformed the treatment of systemic B-cell malignancies, their application in PCNSL has been constrained by neurotoxicity concerns in pivotal studies. Recent data demonstrate feasibility and safety in this setting; however, more than half of patients eventually relapse, highlighting the need for more persistent CAR-T cells capable of functioning within the immunosuppressive CNS microenvironment. To address this, we first evaluated a panel of second-generation CD19 CARs, including ITAM-tuned “1XX” variants, using a 3D spheroid model of PCNSL. T cells expressing the (SJ25C1)1XX-CAR format demonstrated the highest antitumor activity. To further improve their durability, we knocked out SUV39H1, a histone methyltransferase that limits memory T cell differentiation through histone H3 lysine 9 trimethylation (H3K9me3), an epigenetic mark associated with chromatin compaction. The resulting (SJ25C1)1XX-CAR SUV39H1 KO T cells showed enhanced cytotoxicity in vitro, and superior tumor control and survival in an orthotopic PCNSL xenograft model compared to conventional second-generation CAR-T cells. To further test persistence, we established an ocular lymphoma rechallenge model. Following initial tumor clearance by both edited and non-edited 1XX CAR-T cells, only SUV39H1 knockout CAR-T cells maintained long-term protection upon rechallenge in the contralateral eye. Ex vivo spleen analysis confirmed their accumulation and enrichment in memory precursors ($CD27^{+}KLRG1^{-}$) with elevated Ki67 expression, indicating enhanced proliferative potential. Altogether, our study supports the clinical translation of a next-generation cell therapy for PCNSL based on epigenetically reprogrammed, signaling-optimized CAR-T cells. We are currently developing a GMP-compatible manufacturing process incorporating the RQR8 marker/safety switch to enable rituximab-mediated elimination in the event of unexpected toxicity, in preparation for a future phase I/II clinical trial.

#3716 Regulatory immunotherapy utilizing activated natural killer cells and antitumor response for hepatocellular carcinoma.

Ola Sayed Ahmed[1], Refaat Gabre[2], Amr Iamail Abdelraouf[3], Hisham Imam[4], Maha Genhia[2]

[1]Cancer Biology, National Cancer Inst., Cairo, Egypt,[2]Biotecnology, Facutly of Science- Cairo University, Cairo, Egypt,[3]Surgical, National Hepatology and Tropical Medicine Research Institute, Cairo, Egypt,[4]Biomedical, Niles, Cairo, Egypt

Background: Hepatocellular carcinoma (HCC) is among the most prevalent and fatal cancers globally, but viable therapeutic alternatives are scarce. Natural killer (NK) cells are components of the innate immune system that exhibit significant anti-cancer properties. Recent findings indicate that activation with interleukins IL-15 and IL-18 promotes the production of NK cells exhibiting augmented effector capabilities and potential “memory-like” characteristics. This study examined the cytotoxic efficacy of IL-15/18-stimulated NK cells against human HCC tissue in vitro.
Methods: NK cells were collected from healthy donors and patients with HCC, followed by in vitro activation with IL-15 and IL-18. The cytotoxic efficacy of activated NK cells was assessed in co-culture with human HCC cells. This study demonstrated that IL-6 and IL-1α participated in regulating the anti-tumor efficacy of IL-15/18-activated NK cells.
Results: The results indicate that NK cells from patients with HCC and healthy donors exhibited comparable expression levels of both activating and inhibiting NK cell receptors. The expansion of NK cells from HCC patients was inferior compared to that of healthy donors in response to IL15/18 ($p < 0.001$ on day 5). In vitro, NK cells from both groups of persons exhibited significant cytotoxicity against HCC targets, and this was associated with the inhibitory effects of activated NK cells on the production of IL-6 and IL-1alpha. Lower levels of spontaneous HCC formation were observed in a spontaneous model of HCC after IL-15/18 activated NK cells that trafficked to the liver ($p < 0.01$).
Conclusion: IL-15/18-activated NK cells from both healthy donors and HCC patients exhibit comparable levels of anti-tumor efficacy against HCC cells. These results indicate that IL-15/18 activation augments the therapeutic efficacy of NK cells, endorsing their application as a promising immunotherapeutic approach for hepatocellular carcinoma.

#3717 DLL3-targeted *in vivo* CAR-T therapy of small cell lung cancer with lipid nanoparticles and circular RNA.

Yishan Ma[1], Jingsheng Cai[2], Yufei Xia[1], Xiaonan Huang[1], **Mantang Qiu**[2]

[1]Chinese Academy of Sciences, Beijing, China,[2]Peking University People's Hospital, Beijing, China

Background: The survival of small cell lung cancer (SCLC) is discouraging, necessitating the development of novel targets and effective therapeutic approaches. Delta-Like Ligand 3 (DLL3) represents a promising target for the treatment of SCLC, with ongoing vigorous therapeutic strategies, including DLL3-targeted chimeric antigen receptor-T (CAR-T) cell therapy. Here, we report DLL3-targeted in vivo CAR-T therapy constructed by circular RNA (circRNA) and antibody-conjugated lipid nanoparticles (LNP), yielding promising therapeutic potential for treating SCLC.

Methods: Circular RNAs (circRNAs) are covalently closed single-stranded RNAs that are resistant to exonuclease-mediated degradation. Compared with linear mRNA, circular RNA is more stable and efficient as translate templates, thus circRNA has been considered as “the next generation” of mRNA. RNA-LNPs were prepared via microfluidic mixing an aqueous solution of the circRNA and an ethanolic solution of the lipid components at a ratio of 3:1. LNPs were conjugated with purified rat anti-mouse CD5 (CD5-LNP) or IgG (IgG-LNP) via SATA-maleimide chemistry reaction to obtain antibody conjugated LNP-circRNA.

Results: We have previously reported a highly efficient TREM1/DAP12-based novel multiple-chain CAR structure. In current study, we successfully synthesized and validated the feasibility of circRNA encoding DLL3-targeted CAR. To quantify the percentage of CAR-T cell in vivo, LNPs were intravenously injected into 8-week-old mice. CAR T cells in the immune organ and peripheral blood were characterised via flow cytometry 24h post injection. CD5-conjugated LNP showed a significant higher CAR-T percentage in peripheral blood (~15%) and immune organs (~12% in lymph node, ~16% in spleen, and 22% in thymus) compared to non-targeted LNP (unconjugated LNP and IgG-conjugated LNP). We further analysed the CAR-T cell duration in vivo. CD5-targeted LNP were intravenously injected into 8-week-old mice at dose of 30 ug RNA per mice. Immune organ and peripheral blood were isolated and characterised via flow cytometry at each time point. We observed that the CAR expressing T cells reached peak at 24h, then completely diminished after 5days. Lastly, using mice subcutaneous and orthotopic models, we demonstrated the efficacy of circRNA-based CAR-T therapy in SCLC tumor eradication, significantly extending survival. By Day 28 post-injection, 3/4 mice in the experimental group remained alive, whereas all in the control group had perished by Day 21. No significant increase of liver toxicity (indicated by AST and ALT) among the indicated groups, suggested favorable safety profile.

Conclusion: Leveraging antibody-conjugated LNP and circRNA, we have effectively engineered DLL3-targeted CAR-T cells in vivo, which shows effective cytotoxicity against SCLC. This research offers a promising avenue for advancing SCLC and in vivo CAR-T therapeutics.

#3718 CAR Detection Reagents - Pioneering advances in CAR T analytics.

Stephan Wilmes, Desire Missing, Anja Brauchle, Nadine Borgelt, Johanna Mullers, Monika Winkels, Larissa Mockel, Michaela Niemoller, Dagmar Hau?ler-Kuballa, Franziska Antonia Bertram, Olga Goldbach, Dominik Poschen, Astrid Imann, Silvia Ruberg, Anijutta Appelshoffer, Fabio El Yassouri, Marsilius Mues, Volker Nolle, Andreas Bosio, Christian Dose, Anne Richter

Miltenyi Biotec B.V. & Co. KG, Bergisch Gladbach, Germany

Chimeric Antigen Receptor (CAR) T cell therapies have transformed cancer treatment, offering targeted and effective options for patients with hematologic B-cell malignancies, including leukemias, lymphomas and multiple myeloma. Their precision in targeting and eliminating cancer cells has positioned them as a promising approach in cellular immunotherapy. Accurate detection of CAR expression is essential for research, pre-clinical applications, clinical manufacturing, and patient immunomonitoring. To address these needs, we developed CAR Detection Reagents optimized for flow cytometric analysis of CAR-engineered T and NK cells, ensuring exceptional quality and specificity. Our recombinant antigen-based CAR Detection Reagents mimic CAR interactions with tumor cells, targeting key cell surface antigens such as CD19, BCMA, CD22, MSLN, CD123, B7-H3, HER2, and CD33. We also created anti-CAR antibodies for CD19 FMC63 and GD2 14G2a CARs, along with linker-specific antibodies for G4S- and Whitlow-linkers, commonly used in commercial CAR T cell products. All these reagents feature an engineered human IgG1 Fc region to prevent Fcγ receptor binding, ensuring background-free analysis. Available in various conjugates (e.g., fluorophores, biotin), they offer superior performance and flexibility in panel design. Our flow cytometric analysis demonstrated bright and specific staining with low background on primary CAR T/NK cells and model cell lines, crucial for reliable CAR T cell enumeration in product manufacturing and patient monitoring. CAR Detection Reagents are also applicable for magnetic activated cell sorting (MACS). In immunomonitoring post-adoptive cell transfer, rapid isolation of CAR T cells from blood or PBMCs can be critical, as CAR T cells in these samples can be present in very low numbers falling below the detection limit. Magnetic enrichment substantially enhances analytical sensitivity, ensuring long-term monitoring of CAR T cell persistence, vital for assessing treatment efficacy and patient response. Furthermore, MACS-purified CAR T cells can undergo deep phenotyping and functional assays. Detecting CAR T cells in tissue samples is essential for understanding their distribution and activity within the body. This capability allows researchers and clinicians to assess CAR T cell infiltration and therapeutic impact at tumor sites, offering insights into treatment effectiveness and resistance mechanisms. Using fluorescence microscopy, we demonstrate precise detection and enumeration of CD19 FMC63 CAR T cells with a FMC63-targeting anti-CD19 CAR antibody in fresh-frozen and PFA-fixed tissue samples from treated mice. This approach enhances our understanding of CAR T cell dynamics *in vivo*. In summary, these versatile CAR Detection Reagents are invaluable tools for advancing CAR T cell research and clinical therapies. AI tools were used to improve this abstract.

#3719 From gene to bedside: Mayo Clinic's first-in-house BAFF-R CAR-T.

Yan Luo[1], Shaohua Guo[1], Yaqing Qie[2], Martha E. Gadd[2], Tanya Hundal[2], Hemant S. Murthy[3], Mohamed A. Kharfan-Dabaja[3], Hong Qin[4]

[1]Department of Cancer Biology, Mayo Clinic Florida, Jacksonville, FL,[2]Regenerative Immunotherapy and CAR-T Translational Research Program, Mayo Clinic Florida, Jacksonville, FL,[3]Division of Hematology and Medical Oncology, Department of Internal Medicine, Mayo Clinic Florida, Jacksonville, FL,[4]Department of Immunology, Mayo Clinic, Rochester, MN

Chimeric antigen receptor (CAR)-T cell therapy has revolutionized the treatment of B-cell malignancies. Despite the clinical success of CD19-targeted approaches, relapsed/refractory (R/R) disease—often driven by antigen loss or immune escape—remains a major challenge. To overcome this, we developed a novel CAR-T cell therapy targeting BAFF-R, a receptor consistently expressed in chronic lymphocytic leukemia (CLL) and other B-cell malignancies. We developed a new anti-BAFF-R monoclonal antibody and engineered the MC10029 CAR construct using its scFv. Antigen-specific cytotoxicity was validated in both in vitro and in vivo models, including Nalm-6 (leukemia) and Z138 (lymphoma), and CD19-knockout tumor cells to model (R/R) disease. MC10029 CAR-T cells were generated from healthy donors and CLL patients, and their cytotoxicity was evaluated against MEC-1, a CLL cell line, as well as autologous CLL patient tumor samples. These studies demonstrated potent and specific antitumor efficacy. We transitioned to clinical-grade production, using GMP-compliant lentivirus to manufacture MC10029 CAR-T cells under regulatory guidelines. With FDA IND approval, we initiated a Phase 1 clinical trial to evaluate safety and dosing. Our first patient, treated with a low-dose, single infusion, achieved a complete metabolic response within 2 months. The therapy is well tolerated, with no severe advent events such as cytokine release syndrome or neurotoxicity, supporting both the safety and efficacy of the therapy. Conclusion: This study represents Mayo Clinic's first homegrown CAR-T cell therapy, developed entirely in-house—from antibody discovery and CAR design to GMP manufacturing and clinical trial—marking a significant step toward personalized, next-generation immunotherapy for B-cell malignancies.

#3720 Nectin-4-targeted CAR-NK cells exhibit potent antitumor activity against bladder cancer.

Mohammad Mousaei Ghasroldasht, Piyush K. Agarwal

Department of Surgery, Section of Urology, University of Chicago, Chicago, IL

Background: Bladder cancer (BC) remains a major clinical challenge due to frequent recurrence and limited durable responses to current therapies such as Bacillus Calmette-Guérin (BCG) immunotherapy and cisplatin-based chemotherapy. Natural Killer (NK) cell therapy has recently emerged as a promising immunotherapeutic approach, particularly when combined with Chimeric Antigen Receptor (CAR) technology to enhance tumor recognition and cytotoxicity. Nectin-4, an adhesion molecule highly expressed in BC, represents a strong therapeutic target for CAR-engineered NK cells. In this study, we aimed to target bladder cancer using Nectin-4-specific CAR-NK cells.
Methods: Nectin-4-specific CAR-NK cells were generated via lentiviral transduction, and CAR expression was confirmed by fluorescence microscopy. The cytotoxic activity of CAR-NK and unmodified NK cells was evaluated against Nectin-4-positive (SW780) and Nectin-4-negative (T24) bladder cancer cell lines using LDH release and CCK-8 viability assays at early time points. A 3D spheroid model was used to assess CAR-NK cell attachment, infiltration, and long-term cytotoxicity. Gene expression profiling following co-culture was performed to evaluate activation and apoptosis-related pathways. An in vivo xenograft model was used to validate the in vitro findings.
Results: Nectin-4 CAR-NK cells demonstrated significantly enhanced cytotoxicity compared with parental NK cells within 4 hours of co-culture with SW780 cells, as assessed by LDH and CCK-8 assays. In 3D spheroid models, CAR-NK cells showed stronger attachment and affinity for Nectin-4-positive tumor spheroids during short-term co-culture and exhibited higher cytotoxicity after prolonged exposure compared with unmodified NK cells. Gene expression analysis revealed increased activation markers and cytotoxic mediators in CAR-NK cells, along with upregulation of apoptosis-related genes in target tumor cells following treatment.
Conclusions: Engineering NK cells with a Nectin-4-specific CAR markedly enhances their ability to recognize and eliminate Nectin-4-positive bladder cancer cells. These findings support the potential of Nectin-4 CAR-NK therapy as a targeted immunotherapeutic strategy for bladder cancer. Future development of multi-targeted CAR-NK constructs designed to modulate the tumor microenvironment may further improve efficacy and overcome immune resistance.

#3721 Anti-tumor function and long-term persistence of KSQ-001EX, a SOCS1-edited eTIL® therapy, independent of IL-2 co-administration.

Dipen Sangurdekar[1], Erica Tobin[1], Karrie Wong[1], Ashish Yeri[1], Alex Smashnov[1], Kelly Bowen[1], Giorgio Sarkis[1], Violetta Medik[1], Hsinyi Lu[2], Sevinj Isgandarova[2], Michelle Carrasco[1], Patricia Harris[1], Cara L. Haymaker[2], Micah Benson[1], Anna Truppel-Hartmann[1], Rodabe N. Amaria[2]

[1]KSQ Therapeutics, Lexington, MA,[2]UT MD Anderson Cancer Center, Houston, TX

Tumor Infiltrating Lymphocyte (TIL) therapy is an autologous adoptive cell therapy for cancer involving the isolation, *ex vivo* expansion, and infusion of polyclonal T cells from a patient's own tumor. Seeking to improve clinical efficacy and durability of TIL therapy, we developed KSQ-001EX, a CRISPR/Cas9 engineered TIL (eTIL®) therapy with inactivation of the SOCS1 gene to enhance T cell persistence and anti-tumor functionality. KSQ-001EX is being investigated in a phase 1/2 clinical study (NCT06237881) in patients with advanced solid tumors. Metastatic melanoma patients received lymphodepleting chemotherapy followed by KSQ-001EX without IL-2 in Cohort 1 (n=4) or with high-dose IL-2 in Cohort 2 (n=8), at a dose range of 0.5-10e9 cells (median 5.25e9). KSQ-001EX was directly monitored in blood and tissue samples via indel tracking of the SOCS1 gene locus. Correlative analyses were performed by integrating patient baseline characteristics, drug product (DP) manufacturing data, multi-modal and single-cell characterization of tumor starting material, KSQ-001EX DP, post-infusion PBMCs and on-treatment tumor tissue biopsies. All 12 KSQ-001EX DPs were enriched in CD8+ T cells, exhibiting a "Young TIL" phenotype with a median of 39% CD27+ cells and low expression of exhaustion markers. All DPs showed strong polyfunctionality and cytotoxicity against redirected lysis targetcell lines. Infused cell dose, particularly absolute dose of CD27+ KSQ-001EX cells, predicted post-infusion engraftment, expansion, persistence, and infiltration of KSQ-001EX in tumor tissue at day 28, and was the strongest factor associated with clinical activity. Clonal tracking of T cells in post-infusion blood revealed similar expansion of KSQ-001EX clones before day 9 and after day 21 across most patients and between cohorts, with top infiltrating clones in tumor correlating with clonal expansion in blood at day 28. To further understand the contribution of IL-2 to KSQ-001EX engraftment, persistence and function, cytokines and phenotypic characteristics of peripheral blood CD8+ T cells post-infusion were compared between Cohort 1 and Cohort 2. While no differences were observed in the frequency or activation state of CD8+ T cells between Cohorts, elevated expression of TOX in CD8+ T cells and increased frequencies of Treg were observed in Cohort 2 (with IL-2) between day 9-28 post infusion. In conclusion, higher infused CD27+ KSQ-001EX dose is associated with favorable expansion kinetics and persistence. KSQ-001EX engraftment, function and long-term persistence in absence of IL-2 at lower doses than traditionally used with unmodified TIL suggest the beneficial effects of SOCS1 inactivation. Based on these collective data, we confirm the functional enhancement introduced by SOCS1 deletion. Further investigation of eTIL in the absence of IL-2 and higher DP doses is warranted.

#3722 Preclinical development and evaluation of CD87-directed CART for colorectal cancer.

Andrea Feci[1], Trevor Baybutt[1], Robert Carlson[1], Emmett Grover[1], Jagmohan Singh[1], Ross Staudt[1], Miao Cao[1], Edoardo Manca[1], Jasmine Alvarez[1], Scott A. Waldman[2], Adam Snook[3]

[1]Thomas Jefferson University, Philadelphia, PA,[2]Chair, Dept. of Pharm. & Exp. Therapeutics, Thomas Jefferson University, Philadelphia, PA,[3]Sidney Kimmel Cancer Center at Thomas Jefferson University, Philadelphia, PA

Background: Chimeric antigen receptor T-cell (CAR-T) therapy has shown success in hematologic malignancies; however, its efficacy in solid tumors, including colorectal cancer (CRC), remains limited by poor tumor penetration, an immunosuppressive microenvironment, antigen heterogeneity, and a risk of on-target/off-tumor toxicities. CD87, the receptor for the urokinase plasminogen activator (uPAR), has emerged as a promising target, given its near-universal overexpression in CRC, and its near absence in normal tissues, except certain myeloid cells. Recent studies on the elimination of senescent myeloid cells in mice have supported the safety of CD87-directed CAR-T cells *in vivo*. Here, we pursued safety and efficacy studies of human CD87-directed CART (CART87) for use in CRC. We employed a Jurkat NFAT-Lucia reporter platform to functionally screen and optimize human CD87-specific CAR designs, then advanced the top candidates into CARTs for testing against a panel of CRC cell lines. Moreover, we employed bioinformatics to identify potential risks associated with targeting CD87 in humans.

Methods: To assess the potential safety of targeting CD87, we analyzed public bulk and scRNAseq datasets from human and mouse tissues. Furthermore, we quantified CD87 surface expression in human blood leukocyte populations and assessed their susceptibility to CART87. To optimize the CAR87 design, we employed a Jurkat NFAT-Lucia reporter assay, which measured CAR activation upon stimulation with recombinant uPAR and CD87-expressing cells. Constructs with high tonic signaling and non-specific activation by CD87-negative cells were eliminated. We then engineered CD87-directed CAR-T cells (CART87) and assessed their activity against CD87-positive CRC cell lines compared with CD87-negative HEK293 cells and CD87 knockout (KO) cells.

Results: scRNAseq analysis of bone marrow, whole blood leukocytes, and organ tissues revealed that CD87 mRNA expression is restricted to mature monocyte-lineage cells, with murine organs/tissues showing analogous results. Correspondingly, CD87 surface expression by flow cytometry was largely restricted to mature myeloid lineage cells. The Jurkat-NFAT reporter system enabled rapid comparison of single-chain variable fragments (scFv), structural and signaling domain configurations, and identified lead construct #3 (CAR87.3). CART87.3 demonstrated specific and potent cytolytic activity *in vitro* against CD87-positive CRC cell lines T84, SW480, LS174T, and DLD1.

Conclusions: This work identifies CD87 as a safe, selectively-expressed target antigen for the development of CAR-T therapy in CRC. The *in vitro* results support the advancement of human CART87 towards *in vivo* validation. Furthermore, we describe the rational design of a CART87 construct using a high-throughput strategy that could be broadly applied in CAR design for other target antigens.

#3723 Evaluation of *ex vivo* CAR-T cell cytotoxicity and infiltration using multimodal 2-D and 3-D imaging approaches.

Catherine McManus, John G. Foulke, Meghan Sikes, Luping Chen, Hyeyoun Chang, Fang Tian

ATCC, Manassas, VA

Background: Chimeric antigen receptor T (CAR-T) cell therapy has revolutionized cancer treatment, particularly for hematologic malignancies. Beyond CD19 and CD20, BCMA (B-cell maturation antigen)-targeted CAR-T therapies have become a major focus, especially for multiple myeloma. In fact, BCMA is considered one of the most validated targets in plasma cell malignancies. In pursuit of improving the efficacy and number of applications of this therapy, sensitive and robust cytotoxicity assays are required to efficiently evaluate different CAR constructs, effector-to-target cell ratios, and immune effector cells ex vivo. Furthermore, as CAR-T cell therapy is now under active investigation for the treatment of solid tumors, there is an urgent need for models that mimic the complexity of 3-D tumor environments.

Methods and results: In this study, we engineered two luciferase-GFP dual reporter cancer cell lines, Raji-GFP-Luc2 and NCI-H929-GFP-Luc2, and demonstrated their use in a streamlined combined bioluminescence and live imaging assay. Notably, Raji-GFP-Luc2 and NCI-H929-GFP-Luc2 endogenously express high levels of the two FDA-approved CAR-T target antigens, CD19 and BCMA, respectively. Using these lines in co-culture with mock and targeting CAR-T cells, we tracked reporter cancer and CAR-T cell interactions by fluorescence live imaging. Fluorescence quantification clearly demonstrated that CAR-T cells killed cancer cells at higher levels compared to mock controls in both 2- and 3-D co-culture. We then evaluated dose-dependent cancer cell killing by targeting CAR-T cells in 2- and 3-D by luciferase assay. Importantly, we found that quantification of either transgene yields comparative results despite utilizing distinct assays and readouts. Finally, we embedded reporter cancer cell spheroids in 3-D matrices and performed time-lapse imaging of CAR-T cell infiltration. Bioluminescence assay of the embedded spheroids confirmed increased cancer cell killing by targeting CAR-T cells in a solid tumor model.

Conclusions: Overall, our dual reporter cancer cell lines are powerful and effective tools for assaying CAR-T cell cytotoxicity. Furthermore, our multimodal imaging platform integrates bioluminescence and live fluorescence imaging to quantitatively and visually assess CAR-T cell cytotoxicity. With scalability and sensitivity, this assay provides an avenue for standardizing CAR-T cytotoxicity testing and will aid in the expansion and improvement of this promising therapy.

#3724 Exogenous IL-2 administration promotes circulating T-cell levels, persistence and therapeutic efficacy of allogeneic UCART20x22 in a B-cell lymphoma mouse model.

Shipra Das[1], Hana Cho[1], Marco Rotondi[2], Isabelle Chion-Sotinel[2], Margaux Sevin[2], Vivian Dai[1], Jean-Charles Epinat[2], Roman Galetto[2], Laurent Poirot[2], Adrian Kilcoyne[1]

[1]Cellectis, Inc., New York, NY,[2]Cellectis, Paris, France

Background: Non-Hodgkin's lymphoma (NHL) ranks as the sixth most common cancer among women and the seventh among men in the United States, with B-cell lymphomas constituting 80-85% of cases. Diffuse large B-cell lymphoma (DLBCL) is the predominant subtype. Despite significant advances in the treatment of B-NHL, significant unmet need remains for patients who are chemorefractory, relapse following autologous CD19 CAR-T or are unable to access autologous CD19 CAR-T because of supply, cost or other constraints. Off the shelf engineered allogeneic CAR-T offers a potential additional therapeutic option for patients. Advanced editing technology such as TALEN allows TRAC knockout to mitigate the risks of GvHD and also allows for the investigation of multiple alternative targets such as CD20 and CD22, to treat patients who may have antigen escape following previous treatment. While engineering technology can overcome the challenges of allogeneic therapy, efforts must still be made to further enhance expansion and persistence to allow for deep and durable responses. Clinical evidence suggests that the IL-2 cytokine, a potent T-cell growth factor essential for the proliferation of activated T cells, when combined in low-dose with CAR T-cell therapies improves pharmacokinetics and anti-tumor efficacy without compromising safety.

Method: NSG mice were engrafted with Daudi-luc-GFP cells on D-7. UCART20x22 (bi-specific TALEN®-engineered allogeneic T-cells targeting both CD20 and CD22), or vehicle were infused on D0. IL-2 was infused intraperitoneally after UCART20x22 administration as per different test regimens. Bioluminescence imaging was performed at regular intervals during the study to assess tumor control. UCART20x22 expansion and persistence was also measured at different timepoints.

Results: IL-2 administration significantly increased circulating T-cell levels and prolonged T-cell persistence. Increased tumor control was observed when low-dose UCART20x22 was combined with exogenous interleukin 2 (IL-2). No relapse was observed up to day 50 in the concomitant IL-2 treated mice. These responses were observed even when the IL-2 treatment regimens were delayed respect to UCART20x22 infusion, although the intensity of T cell responses were less strong than upon concomitant treatment. No adverse effect were observed, as measured by body weight assessment over time. Additionally, there were no clinical signs of treatment-related morbidities in any of the treatment groups.

Conclusion: The results of the *in vivo* studies support the use of IL-2 to improve the therapeutic outcomes of UCART20x22 in terms of depth and durability of disease response. This is currently being investigated in the NatHaLi-01 clinical study for R/R B-cell lymphomas, aiming to optimize response rates and durability of response in this patient population.

#3725 Stem cell-derived allogeneic anti-CD19 CAR-iNKT cell therapy GT719 for relapsed/refractory B cell malignancies.

Dehui Zou[1], Wei Liu[1], Yan Yu[1], Huimin Liu[1], Yi Wang[1], Sisi Feng[2], Xiaona Xu[2], He Zhang[2], Ershao Zhang[2], Jiang Li[2], Jingman Wang[2], Jing Hao[2], Ning Wang[2], Huipin Zheng[2], Yin Cheng[2], Jun Cui[2], Jingwei Sun[2], **Yarong Liu**[2]

[1]State Key Laboratory of Experimental Hematology, National Clinical Research Center for Blood Diseases, Haihe Laboratory of Cell Ecosystem, Institute of Hematology & Blood Diseases Hospital, Tianjin, China,[2]Grit Biotechnology, Shanghai, China

Background: Adoptive cell therapy, particularly CAR-T therapy, has transformed the treatment of hematologic malignancies, but autologous products remain limited by high cost, long manufacturing, and insufficient functional T cells in heavily pretreated patients. These challenges underscore the need for off-the-shelf allogeneic approaches. Invariant natural killer T (iNKT) cells are an attractive cell platform because they recognize lipid antigens via the non-polymorphic CD1d molecule, avoiding graft-versus-host disease (GvHD). CAR-engineered iNKT cells also provide multimodal tumor killing, tumor microenvironment modulation, enhanced infiltration, and natural bone marrow homing. However, their scarcity in peripheral blood poses manufacturing challenges. To address this, we developed GT719, an allogeneic anti-CD19 CAR-iNKT therapy generated through in vitro differentiation of cord blood-derived $CD34^+$ hematopoietic stem cells. Rational CAR design and optimized manufacturing enable scalable production capable of treating thousands of patients per batch. Extensive preclinical studies show that GT719 eliminates malignant B cells through coordinated CAR-, invariant TCR-, and NK receptor-mediated cytotoxicity and selectively depletes immunosuppressive macrophages and myeloid-derived suppressor cells.

Study Design and Methods: Based on promising preclinical results, a first-in-human investigator-initiated clinical trial (NCT06948981) has been launched to evaluate the safety, toxicity, dose-limiting toxicities (DLTs), and recommended treatment dose of GT719 for patients with relapsed or refractory CD19-positive B cell malignancies, including both B cell non-Hodgkin lymphoma (B-NHL) and B cell acute lymphoblastic leukemia (B-ALL). This open-label *Trial in Progress* begins with two single-patient acceleration cohorts testing doses of 5×10^7 and 1×10^8 cells per patient, followed by a classical 3+3 dose-escalation design testing doses of 5×10^8 and 1×10^9 cells per patient. Enrolled patients undergo a standard lymphodepletion regimen consisting of cyclophosphamide and fludarabine from Day -5 to Day -2, consistent with protocols used for autologous CAR-T therapies. GT719 is administered intravenously on Day 0, and the primary safety observation window for DLTs extends from Day 1 to Day 28. Adverse events are assessed for incidence and severity according to CTCAE version 5.0. Although the trial is ongoing, we anticipate presenting preliminary safety and efficacy data for GT719 at the meeting. Clinical trial registration number: NCT06948981

: Biomarkers Predictive of Therapeutic Benefit 4
Poster Session

#3729 A biologically grounded predictor of neoadjuvant breast cancer therapy response from tumor transcriptomics and histopathology.

Thomas Cantore[1], Danh-Tai Hoang[2], Lipika Ray[1], Amos Stemmer[3], Tiangen Chang[1], Saugato Rahman Dhruba[2], Eldad David Shulman[1], Emma M. Campagnolo[3], Joo Sang Lee[3], Salomon M. Stemmer[4], Stephen-John Sammut[3], Yuan Yuan[5], Stan Lipkowitz[6], Sheila Rajagopal[3], Carlos M. Caldas[7], Nishanth Ulhas Nair[6], Eytan Ruppin[8]

[1]NIH-NCI, Bethesda, MD,[2]National Cancer Institute - Cancer Data Science Laboratory (CDSL), Bethesda, MD,[34]Rabin Medical Ctr. Inst. of Oncology, Petach Tikva, Israel,[5]Cedars-Sinai, Los Angeles, CA,[6]National Cancer Institute, Bethesda, MD,[7]University of Cambridge, London, United Kingdom,[8]National Cancer Institute, Rockville, MD

Background. While expression-based signatures inform adjuvant therapy in breast cancer (BC), no approved molecular biomarkers exist for the neoadjuvant setting, where early prediction of response could guide treatment. Identifying such biomarkers is challenging given the molecular heterogeneity of breast cancer, where multiple malignant subtypes may coexist within a tumor and influence therapy response.

Methods. We developed *BRIDGE*, a computational framework that deconvolves the pretreatment bulk tumor transcriptome to estimate molecular subtype composition and predict pathological complete response (pCR) to neoadjuvant therapy. BRIDGE was trained on 9 transcriptomics datasets and tested on 23 independent ones spanning different subtypes, composing one of the most variable multi-cohort validations to date. Six additional datasets with pre-treatement H&E slides and response data were analyzed to evaluate histology-based predictions.

Results. Analyzing measured BC transcriptomics, BRIDGE outperformed surrogate implementations of established commercial signatures (Oncotype DX, MammaPrint, RORS) in ER+/HER2− tumors, where these assays are clinically approved in the adjuvant setting. It also outperforms other transcriptomic signatures in subtypes where validated predictive biomarkers are limited. In ER+/HER2− patients, it yields an ROC-AUC of 0.79 with a high Odds Ratio (OR = 7.4); in HER2+ disease, an AUC of 0.78 (OR = 7.2); and in TNBC, an AUC of 0.71 (OR = 4.4). We further developed BRIDGE-Slide, which applies BRIDGE to pre-treatment histopathology slides via deep learning-inferred transcriptomics. BRIDGE-Slide outperforms direct slide-to-response models, underscoring its potential as a first-of-its-kind, fast, low-cost biomarker. Finally, spatial transcriptomics shows that BRIDGE-derived subtype assignments form spatially cohesive regions aligned with canonical molecular features, reinforcing its biological interpretability.

Conclusions. BRIDGE is a biologically grounded framework for neoadjuvant BC response prediction, validated on a rich set of diKerent patients cohorts. Its histopathology based version opens the door for fast and low cost prediction in the neoadjuvant setting, upon further prospective testing and validation.

#3730 Spatial determinants of TILs in immunotherapy sensitivity of patients with non-small cell lung cancer (NSCLC).

Miguel Lopez de Rodas Gregorio[1], Ravi Kamble[2], Matthew Blair[1], Yao Nie[2], Marghoob Mohiyuddin[2], Sowmi Utiramerur[2], Kurt Alex Schalper[1]

[1]Pathology, Yale School of Medicine, New Haven, CT,[2]Roche, Pleasanton, CA

Immune checkpoint blockers (ICB) targeting T-cell co-inhibitory receptors such as PD-1 and CTLA-4 provide clinical benefit to a subset of patients with non-small cell lung cancer (NSCLC). The abundance and functional state of tumor-infiltrating lymphocytes (TILs) have been proposed as immunotherapy biomarkers. However, the role of the spatial arrangement and distribution of TILs in immune evasion and immunotherapy sensitivity remains less explored. We used multiplexed quantitative immunofluorescence to measure and spatially map major TIL subpopulations (CK, CD4, CD8 and CD20), candidate tumor-antigen specific T-cells (CK, CD8, CD39 and PD-1) and T-cell functional differentiation states (CD4, CD8, TOX, TCF7) in consecutive tissue microarray sections from baseline NSCLCs in three retrospective cohorts treated with frontline chemotherapy (CTX, n=156), first line ICB (1L-ICB, n=56) or ICB as second or subsequent treatment line (2L+-ICB, n=68). We studied the spatial characteristics of TILs using computational metrics of cell heterogeneity and clustering, and their association with clinicopathologic variables and treatment-specific outcomes. We identified five spatial metrics significantly associated with overall survival (OS) only in the 1L-ICB patient population. A high Morisita-Horn Index (spatial diversity) of CD8+ or CD20+ TILs and CK+ cancer cells in the stromal tissue compartment, and a high Ripley's k (Rk) function (spatial clustering) of CD8+ T-cells in the total tissue area were associated with shorter OS (HR=1.57, CI:1.09-2.28; HR=1.42, CI:1-2.01; HR=1.38, CI: 1.03-1.83; respectively). In contrast, a high Rk function of CD8+ T-cells and the Moran's Index (MI, spatial autocorrelation) of CD20+ TILs measured within the cancer cell nests were significantly associated with longer OS (HR=0.58, CI:0.35-0.95; HR=0.44, CI:0.23-0.84, respectively). Tumors with high Rk values for CD8+ TILs in the cancer cell compartment had a higher density of inactive effector T-cells (CD8+ PD1- CD39-) and bystander-like effector T-cells (CD8+ PD1+ CD39-) than tumors with low CD8+ Rk. Tumors with high MI of CD20+ TILs in the cancer cell area showed higher densities of inactive effector T-cells, progenitor-like effector T-cells (CD8+ TOX+ TCF7+) and lower levels of candidate tumor antigen-specific effector T-cells (CD8+ PD1+ CD39+) than tumors with low MI of CD20+ TILs. There was a significant association between higher MI of CD20+ TILs and advanced age (≥65). The spatial arrangement of TILs in baseline tumor samples is associated with distinct local T-cell responses and frontline immunotherapy outcomes in patients with NSCLC. Increased clustering of CD8+ and CD20+ TILs within the cancer cell nests is independently associated with favorable survival in this population. This supports a strong biomarker potential for the integrated analysis of TILs incorporating spatial features.

#3731 Development of a gene expression predictor for bevacizumab response.

Yi Ren[1], Chee Yit Lim[1], Yaw Chyn Lim[2], Joseph W. Foley[1], Raymond Tsang[1], Wan Qin Chong[3], Boon Cher Goh[3], **Joshua K. Tay**[1]

[1]Department of Otolaryngology, National University of Singapore (NUS), Singapore, Singapore,[2]NUS Centre for Cancer Research (N2CR), National University of Singapore (NUS), Singapore, Singapore,[3]Department of Haematology-Oncology, National University Cancer Institute, Singapore, Singapore

Background: Bevacizumab, an anti-vascular endothelial growth factor (VEGF) monoclonal antibody, inhibits tumor angiogenesis and is used to treat several advanced-stage cancers, such as glioblastoma, ovarian, lung, and colorectal cancers. More recently, it has been incorporated into treatment regimens for locally advanced nasopharyngeal carcinoma (NPC). Despite its widespread adoption, no reliable biomarker has been developed to predict the treatment outcome. Moreover, bevacizumab treatment carries risks such as bleeding, hypertension, and proteinuria. Therefore, selecting patients for bevacizumab addition to already intensive chemotherapy regimens remains a clinical challenge.

Methods: We obtained 19 formalin-fixed paraffin-embedded (FFPE) biopsies from a completed phase 2 clinical trial (NCT01309633) for locally advanced NPC, where patients received bevacizumab prior to standard concurrent chemoradiation. Based on haematoxylin and eosin (H&E) identification, tumor epithelial regions were isolated by laser-capture microdissection, with biological replicates when available. RNAseq libraries were prepared with an in-house RNAseq technique optimized for FFPE tissues. Differential expression between complete response (CR, n=11) and partial response (PR, n= 8) tumors was assessed, and a bevacizumab response gene signature was derived. Gene signature scores were computed using single-sample gene set enrichment analysis (ssGSEA) and gene set variation analysis (GSVA).

Results: After quality control, 37 tumor epithelial libraries were analyzed (21 CR and 16 PR). We identified 58 differentially expressed genes (p.adj<0.05), with 44 upregulated in PR. These genes were related to extracellular matrix remodelling, vascular endothelia, and immune response. GSEA using cell-type signature gene sets or Curated Cancer Cell Atlas gene sets from MSigDB showed enrichment of inflamed fibroblasts, endothelial, and stromal cell types in PR, and cell-cycle programs in CR. Therefore, the 44-gene panel was used as a gene signature to predict reduced response to bevacizumab. Both ssGSEA and GSVA scores robustly separated PR from CR (p<0.001). These findings suggest that stromal/vascular inflammation in the tumor epithelial regions is associated with reduced bevacizumab response.

Conclusions: In this study, we derived a 44-gene tumor epithelial signature that predicts reduced response to bevacizumab in locally advanced NPC and confirmed its performance with ssGSEA and GSVA. The signature captures stromal, endothelial, and immune-inflammatory programs within tumor epithelial regions and informs patient selection for anti-angiogenic therapy. Our current work includes validation in independent patient cohorts across multiple cancer types to improve clinical utility and generalizability.

#3732 Time-series deep learning radiomics for predicting post-radiotherapy rib fractures in non-small cell lung cancer.

Yijun Chen[1], Michael Farris[1], Ariel Choi[1], Nga Thi Thanh Nguyen[1], Amanda Goetz[1], Corbin A. Helis[1], Fei Xing[2], Liang Liu[2], Qing Lyu[3], Christopher T. Whitlow[3], Christina K. Cramer[1], Michael D. Chan[1], Dan Bourland[1], Michael T. Munley[1], Jeffrey S Willey[1], **Yuming Jiang**[1]

[1]Radiation Oncology, Wake Forest University School of Medicine, Winston Salem, NC,[2]Cancer Biology, Wake Forest University School of Medicine, Winston Salem, NC,[3]Radiology, Wake Forest University School of Medicine, Winston Salem, NC

Background and purpose: Rib fracture is a recognized clinical complication in medically inoperable patients with non-small cell lung cancer (NSCLC) undergoing stereotactic body radiotherapy (SBRT), leading to diminished quality of life and delayed recovery. This study aimed to develop and validate a deep learning model for predicting post-radiotherapy rib fracture using time-series CT radiomics.
Material and methods: This study retrospectively collected CT scans from 67 NSCLC patients, comprising 1,605 individual ribs as separate instances. We proposed a novel Knowledge-aware Temporal Mixture of Experts (KA-TMoE) model that integrates radiomics from sequential CT scans to estimate fracture risk for each rib. Model performance was evaluated using area under the curve (AUC), sensitivity, specificity, and F1 score. Model interpretability was achieved using SHapley Additive exPlanations analysis, which attributed predictive value to each input feature.
Results: The KA-TMoE model demonstrated strong predictive performance, achieving favorable AUC in the validation cohort (0.792). The DeLong test confirmed statistically significant improvements over ablation variants, underscoring the importance of integrating temporal data and domain knowledge. High sensitivity (0.85) and specificity (0.78) reflected a well-balanced trade-off, surpassing alternative approaches. Whitney U tests further supported its robustness, which showed significant differences in output distributions across cohorts. Among the top 20 most influential features, half originated from three-month postoperative radiomics, emphasizing the critical role of temporal information.
Conclusion: The KA-TMoE model provides a robust, accurate framework for predicting rib fractures after SBRT in NSCLC patients. Its predictive power enables personalized risk assessment, better patient management, and optimized clinical prognosis.

#3733 Optimizing NGS-based biomarkers for mismatch repair and proofreading deficiency.

Jan Budczies[1], Klaus Kluck[1], Michael Menzel[1], Daniel N. Kazdal[2], Matthias Kloor[3], Albrecht Stenzinger[4]

[1]University Hospital Heidelberg, Heidelberg, Germany,[2]Institute of Pathology, University Hospital Heidelberg, Heidelberg, Germany,[3]Applied Tumor Biology, Heidelberg University Hospital (UKHD), Heidelberg, Germany,[4]Heidelberg University Hospital (UKHD), Heidelberg, Germany

Testing for mismatch repair and proofreading deficiency (MMRD and PRD) in cancer tissues supports the guidance of immunotherapies and the screening for cancer predisposition syndromes. As more and more patients are receiving molecular tumor diagnostics based on broad sequencing approaches, there is an opportunity to integrate MMRD/PRD testing with the testing for clinically actionable mutations. To reach this aim, there is a need to optimize the NGS-based biomarkers and cutpoints. We analyzed whole exome sequencing (WES) of 1487 patients from the TCGA cohorts of colorectal, stomach, and endometrial cancer (COADREAD, STAD, and UCEC). PCR-based testing and detection of deleterious mutations in POLE or POLD1 served as reference for MMRD and PRD status, respectively. MSI scores were derived from paired tumor-normal (T/N) and from tumor-only (T-only) data using MSIsensor and MSIsensor-pro, cutpoints were optimized by maximizing the balanced accuracy. Missense mutation burden, indel burden, and counts for 96 mutation types were determined from the somatic mutation calls. Using a training-test split (70% vs. 30%), elastic net classifiers were trained and validated for the prediction of MMRD and PRD status. With MSI scores from T/N data a close to perfect separation of mismatch repair deficient from proficient tumors was achieved in the pooled COADREAD/STAD/UCEC cohort (AUC=0.99, optimal cutpoint=2.1%), while MSI scores from T-only data performed less perfect (AUC=0.94, optimal cutpoint=6.7%). The performance of MSI scores from T-only data improved when analyzed separately in COADREAD, STAD, and UCEC which can be explained by differing optimal cutpoints of 12.4%, 3.3%, and 5.6%, respectively. Combining missense and indel burden permitted a close to perfect separation of mismatch repair deficient for proficient tumors. Tumors simultaneously exhibiting MMRD and PRD formed a distinct cluster in UCEC, but not in COADREAD and STAD. Both MMRD and PRD were reflected by characteristic signatures in the partition of the mutations to 96 mutation types. We compared the performance of the following three classifier types to separate tumors with respect to MMRD and PRD: (1) based on MSI scores, (2) combining missense mutation and indel burden, and (3) based on the 96 mutation types. Overall, the three classifiers performed similarly and allowed a good separation in almost all comparisons. Separating proofreading-deficient from -proficient tumors when MMRD was present was the only task that was achieved by none of the classifiers. Simulation studies investigating tumor purity showed that classifiers based on missense mutation/indel burden and mutation types outperformed MSI scores for low tumor purities. The study opens new avenues for MMRD and PRD detection in the setting of clinical WES. We are currently investigating which of the NGS-based markers perform satisfactorily when gathered with large sequencing panels instead of WES.

#3734 Early-onset low-grade adverse events as predictive biomarkers in advanced NSCL: A multi-treatment cohort analysis.

Dung-Tsa Chen[1], Andreas N. Saltos[1], Zachary Thompson[1], Junmin Whiting[1], Sebastian Viracacha[1], Timothy I. Shaw[1], Ignacio I. Wistuba[2], Jhanelle E. Gray[1]

[1]Moffitt Cancer Center, Tampa, FL,[2]UT MD Anderson Cancer Center, Houston, TX

Purpose: This study aims to assess whether early-onset, grade 1 (G1) and low-grade (LG) treatment-related adverse events (TrAEs) can serve as predictive markers for favorable survival outcomes in advanced non-small cell lung cancer (NSCLC) across different treatment modalities.

Methods: We analyzed data from 577 NSCLC patients across 11 cohorts treated at Moffitt Cancer Center: 5 immunotherapies (n=383), 3 targeted therapies (n=88), and 3 chemotherapies (n=106). Data for analysis used AE data derived from Common Terminology Criteria for Adverse Events (CTCAE v4-5), treatment response including comparison of responder (complete response (CR) and partial response (PR)) versus non-responder (stable disease (SD) and progressive disease (PD)) and comparison of disease control (DC: CR/PR/SD) versus PD using Wilcoxon two-sample test, progression-free survival (PFS) and overall survival (OS) using Kaplan-Meier survival curve with log-rank test. Our analytic approach leveraged multiple AE parameters to develop a set of innovative AE biomarkers. Early-onset G1/LG TrAEs were defined as those occurring within 30 days of treatment initiation.

Results: Early-onset AE analysis across all treatment types revealed that (a) Immunotherapy had lower frequency of G1 and LG TrAEs compared to chemotherapy and targeted therapy; (b) higher frequency of G1 and LG TrAEs were associated with better treatment response in immunotherapy (responder vs non-responder with p=0.047 (G1) and 0.069 (LG); DC vs PD with p=0.005 (G1) and 0.018 (LG)), but no significant results in chemotherapy and targeted therapy; (c) For patients who did not encounter HG non-treatment related AEs (non-TrAEs), if they frequently experienced G1 and LG TrAEs, their survival outcomes tended to be better compared to the ones with less or no AE experiences in immunotherapy (median PFS: 5.5 vs 3.5 months with p=0.03 for G1 and 5.5 vs 3.3 months with p=0.015 for LG; median OS: 18.2 vs 12.2 months with p=0.008 for G1 and 16.1 vs 12.2 months with p=0.04 for LG). Please note that non-TrAEs represent a strong surrogate for compromised baseline health status. Without proper adjustment, this factor may confound the observed association between early-onset G1 and LG TrAEs and survival outcomes. For in chemotherapy and targeted therapy, both G1 and LG TrAEs did not show significant survival association.

Conclusion: G1 and LG TrAEs within 30 days of therapy initiation were associated with better treatment response and improved survival in advanced NSCLC, especially in immunotherapy-treated patients. These findings support the use of early-onset G1/LG TrAE profiles as potential predictive biomarkers.

#3735 Septin9 isoforms as biomarkers of taxane response in breast cancer.

Jycole E. M. Bush[1], Jacob Essif[1], KATE LATHROP[2], April Risinger[1]

[1]UT Health Science Center at San Antonio, San Antonio, TX,[2]Mays Cancer Center, San Antonio, TX

Microtubule-targeting agents (MTAs), including the taxane paclitaxel, are widely used for the treatment of breast cancer. However, there are no clinically validated biomarkers to predict taxane response. Emerging evidence implicates septins, a conserved family of GTP-binding cytoskeletal proteins, key regulators of growth, migration, invasion, and taxane response of breast cancer cells in vitro. Notably, isoforms of septin9 (SEPT9) have opposing roles with SEPT9_i1 promoting migration, epithelial-mesenchymal transition and paclitaxel resistance whereas SEPT9_i2 is associated with decreased oncogenic phenotypes and may serve a protective role. We tested the hypothesis that septin9 isoform expression in breast tumors correlates with the response of breast cancer patients to taxane chemotherapy regimens in both retrospective and prospective clinical studies. In a retrospective analysis we found a significant increase in post-metastatic survival time of taxane-treated patients whose tumors expressed the highest levels of SEPT9_i2 mRNA. Notably, this correlation was only observed in women diagnosed with triple-negative breast cancer (TNBC) that rely most heavily on response to taxanes as they are not co-administered with targeted therapeutics. In a prospective study of neoadjuvant taxane response, women with a complete pathological response to taxane-based chemotherapy regimens had significantly lower expression of SEPT9_i1 mRNA in their tumors than non-responders. Furthermore, majority of tumors that did not respond fully to taxanes in neoadjuvant settings had increased SEPT9_i1 mRNA expression in the residual tumor after treatment. Finally, we validated a SEPT9_i1 specific antibody for immunohistochemistry and SEPT9_i1 mRNA correlated with protein in breast biopsies. Ongoing experiments in the laboratory are elucidating the mechanism by which expression of septin9 isoforms regulates response to taxane chemotherapy using isogenic cell line and tumor models. This work is uncovering a reciprocal relationship between expression of oncogenic and tumor suppressive isoforms and identifying alternative chemotherapeutic options for treatment of tumors with unfavorable septin expression profiles.

#3736 C3C: A biomarker for extracellular cathepsin activity and ADCs.

Marina Crespo-Bravo, Nicholas Willumsen, Morten Karsdal

Nordic Bioscience, Herlev, Denmark

Background: Antibody-drug conjugates (ADCs) combine the specificity of monoclonal antibodies with the potent cytotoxicity of small-molecules payloads. While classical ADCs rely on antigen binding, internalization and intracellular linker cleavage in the lysosomes recent studies show that certain tumors exhibit extracellular cathepsin activity capable of cleaving ADC linkers in the tumor microenvironment (TME) and creating a peritumoral “drug halo” that enhances bystander killing even in antigen-low or antigen-negative TME. For this reason, identifying tumors with high extracellular cathepsin activity may be critical for optimizing ADC efficacy and patient stratification.
Methods: We developed and investigated the potential of C3C, an ELISA-based biomarker that measures type III collagen fragments generated by cathepsins. Since the same cathepsins responsible for cleavage type III collagen and generating C3C also cleave commonly used peptide ADC linkers, we hypothesize that C3C could provide and non-invasive readout of cathepsin activity in the TME. We measured C3C in serum from patients with colorectal cancer (CRC) (n = 10), pancreatic ductal adenocarcinoma (PDAC) (n = 10) and non-small cell lung cancer (NSCLC) (n = 10) and compared to healthy controls (n = 26). To assess biological specificity, we also measured C3-HNE, a biomarker reflecting neutrophil elastase-driven inflammation.
Results: We found significantly elevated levels of C3C compared to healthy individuals in patients with CRC ($p = 0.03$), PDAC ($p = 0.006$) and NSCLC ($p < 0.001$). In contrast, C3-HNE showed no correlation with C3C in any indication, suggesting that C3C does not simply reflect general inflammation but instead captures cathepsin activity implicated in extracellular ADC linker cleavage.
Conclusion: The results suggest that C3C is a promising biomarker for identifying cathepsin-rich TMEs that may support payload release and potent bystander activity of ADCs. Furthermore, C3C could be used to select patients more likely to benefit from cleavable-linker ADCs representing a potential tool for both drug development and clinical precision oncology.

#3737 BXQ-350: A novel biologic that targets dysregulated sphingolipid metabolism and normalizes key anti-tumoral and pro-tumoral sphingolipids in newly diagnosed metastatic colorectal carcinoma patients (mCRC).

Gilles H. Tapolsky, TARIQ ARSHAD, Michael Gazda, Jackson Bond, Nikhil Wilkins, James Beach

Bexion Pharmaceuticals, Covington, KY

Background: Dysregulated sphingolipid metabolism is common to many cancer types, including mCRC, and leads to elevated concentrations of specific sphingolipids, including pro-tumoral gangliosides (GM3), lactosylceramides (LacCer), glucosylceramides (GluCer) and sphingosine-1-phosphate (S1P) and lower concentration of anti-tumoral ceramides. In mCRC patients, several studies have shown elevated concentrations of the pro-tumoral sphingolipids are associated with a worse prognosis and poor survival. Therefore, targeting dysregulated sphingolipid metabolism and returning sphingolipid metabolism to homeostasis could be a promising therapeutic approach. BXQ-350 is a nanovesicle of Saposin C, an allosteric activator of sphingolipid metabolism, that affects dysregulated sphingolipid metabolism. BXQ-350 lowers GM3, LacCer, GluCer and S1P levels while it also increases ceramide levels promoting a return to homeostasis and an anti-tumoral environment. In a single agent Phase 1 study, BXQ-350 was safe and well-tolerated (no DLT, no MTD) and showed signs of activity. Among patients with PFS > 6 months, there were 4 recurrent CRC patients: 1 patient had a PFS of ~12 months, 2 of ~18 months, and 1 is still on study after 7 years.
Method: BXQ-350 is being investigated in a Phase 1b/2a study in combination with mFOLFOX7 and Bevacizumab as SoC in newly diagnosed mCRC patients (NCT05322590) to assess the efficacy and safety of BXQ-350.The Phase 1b/2a is a safety dose escalation part to establish the RP2D exploring 1.8 and 2.4 mg/kg BXQ-350 in combination with SoC. Primary objectives are to assess safety and preliminary efficacy of BXQ-350 in this combination. Secondary objectives include longitudinal analysis of several biomarkers, including sphingolipid profiling.
Results: A total of 32 evaluable patients were enrolled, and all 32 patients have completed SoC treatment schedule plus BXQ-350. Amongst these 32 patients, 21 (66%) are alive and in active follow-up. The disease control rate was 94% (30 pts had SD, PR or CR). As of September 2025, ORR was 59% and PFS was 10.6 months. Analysis of sphingolipid profiles shows that BXQ-350 significantly (> 50%) and durably lowers plasma levels of GM1-3, LacCer, GluCer and S1P while increasing Cer levels (> 50%); furthermore, statistically significant associations between LacCer, Cer, Cer/S1P and Glu/Cer levels and survival were observed.
Conclusions: BXQ-350 was safe and well tolerated in combination with SoC in 1L mCRC. Ongoing monitoring of patients suggests that BXQ-350 may provide a clinical benefit to 1L mCRC patients in combination with FOLFOX 7 + Bevacizumab. Basal and longitudinal analysis of sphingolipid showed that BXQ-350 impacts plasma levels of critically important sphingolipids and associations between key sphingolipids and survival were noted.

#3738 Characterization of TAG-72, a glycan-based ADC target and its pan-tumor expression profile.

Joseph D. Schonhoft, Martijn H. den Brok, Marleen H. van Stevendaal, Thaddeus J. Unger, Lieke W. Wouters, Luc M. Zijlmans, Renate van Daalen, Raffaella Rossin, Marc Robillard, Keith Orford

Tagworks Pharmaceuticals BV, Nijmegen, Netherlands

Background: Tumor-Associated Glycoprotein 72 (TAG-72) is a cancer-specific glycoepitope displayed on mucins and expressed across epithelial cancers, predominantly adenocarcinomas. Initially studied using the B72.3 and CC49 antibodies, TAG-72-expressing cancers lack optimal therapeutic approaches. TGW101, a novel antibody-drug conjugate (ADC) targeting non-internalizing TAG-72, incorporates a CC49-derived diabody and a DAR4 MMAE payload linked via a trans-cyclooctene-based linker that enables controlled cleavage following administration of a tetrazine small-molecule trigger. This ADC-trigger system is currently in phase I clinical development (NCT06959706) for select solid tumors that frequently express TAG-72. Here we present characterization of the TAG-72 glycoepitope, the development of fit-for-purpose TAG-72 IHC assays for patient selection, estimates of its prevalence across solid tumors, and its overlap with established predictive biomarkers used in standard-of-care settings for populations with unmet need.
Methods: Glycan arrays were set up by GlycoDisplay, using engineered cells transfected with a range of probes containing mucin-like repeats. TAG-72 IHC assays were developed at NeoGenomics.
Results: A cell-based glycan array analysis revealed that the CC49-diabody binding requires clustered Thomsen-nouvelle (Tn) and/or sialylated-Tn (STn) glycans on the tandem repeat domain of specific cancer-associated mucins, including MUC1, 2, 5AC, 6, 13, and 17, suggesting it is co-dependent on macrostructural glycan conformation. Optimized IHC using both B72.3 and CC49 anti-TAG-72 clones revealed highly specific staining, with positive staining of the duodenum luminal mucosa (known to be moderate or low positive) and absent staining in the duodenum submucosa, muscularis, and other normal tissues including kidney. Both B72.3 and CC49 IHC clones demonstrated highly similar staining patterns. Additionally, TAG-72 staining was observed in CDX and PDX xenograft models where tumor regressions occurred following treatment with TGW101. Initial screening of tumor microarrays indicated expression across a wide range of solid tumors, with highest expression in adenocarcinomas and mucinous tumors. Scoring criteria, biomarker overlap, and estimated prevalence for both B72.3 and CC49 clones by indication will be presented.
Conclusions: TAG-72 is a tumor-associated glycoepitope consisting of STn and Tn glycans present on multiple mucin proteins. It is widely expressed in epithelial cancers, while almost entirely absent in normal tissues, making it an attractive therapeutic target. Current commercially available antibodies show excellent specificity using modern IHC techniques and could facilitate biomarker-driven clinical development for TAG-72-targeted therapies.

#3739 Isolation and characterization of pancreatic cancer-derived small extracellular vesicles as a novel liquid biopsy approach.

Ravi Kumar Paluri[1], Ashish Kumar[1], Yixin Su[1], Gregory L. Kucera[2], Ashish Manne[3], Jingyun Lee[1], Sangeeta Sing[1], Susy Kim[1], Cristina Furdui[4], Gagan Deep[5]

[1]Wake Forest Baptist Health, Winston Salem, NC,[2]Associate Professor, Dept. of Internal Med., Wake Forest University School of Medicine, Winston-Salem, NC,[3]Ohio State University, Columbus, OH,[4]Atrium Health Wake Forest Baptist, Winston Salem, NC,[5]Wake Forest University School of Medicine, Winston-Salem, NC

Background: A major challenge in managing pancreatic cancer (PanC) is late detection and the inability to identify non-responders early. Existing liquid biopsy approaches offer limited capacity to rapidly and noninvasively track the tumor's evolving molecular landscape, which is essential for overcoming therapy resistance and guiding targeted treatment. Small extracellular vesicles (sEV; <200 nm) circulate widely and carry cargo reflective of their cells of origin. Using our established methods for isolating tissue-specific sEV, we identified pancreas-specific surface markers, isolated circulating pancreas derived sEV ($sEV^{Pancreas}$), and evaluated their potential as a liquid biopsy platform.

Methods: We analyzed fresh-frozen PanC tissues (n=12) along with matched healthy samples. sEV were isolated from tissues, subjected to surface protein shaving, and analyzed using LC-MS/MS based on published methods. Proteomic data, combined with the Human Protein Atlas, were used to identify $sEV^{Pancreas}$. They were isolated from archived plasma samples of PanC patients (n=10) and healthy individuals (n=5) using biotin-tagged antibodies and streptavidin-coated magnetic beads. Isolated sEV/$sEV^{Pancreas}$ were characterized for size and concentration by nanoparticle tracking analysis (NTA), and for various biomarkers' expression using nano-flow cytometry, RT-PCR, RNA sequencing, and digital PCR.

Results: Prolyl 4-hydroxylase subunit beta (P4HB) and annexin A4 (ANXA4) were identified as pancreas-specific sEV surface markers. Nano-flow cytometry confirmed significantly higher levels of P4HB- and ANXA4-positive sEV in PanC plasma compared to healthy controls ($p<0.01$). Using these markers, we isolated $sEV^{Pancreas}$ from blood plasma samples of PanC patients and controls. NTA confirmed that the isolated vesicles were <200 nm in both groups. Notably, $sEV^{Pancreas}$ from PanC patients exhibited significantly higher expression of the PanC biomarker cholecystokinin A receptor ($p<0.01$) and lower levels of miR-320-5p, a microRNA associated with poor prognosis. RNA sequencing of $sEV^{Pancreas}$ revealed several upregulated (e.g., endosulfine-α, MUC12) and downregulated (e.g., DYNC1I2, POM121C) genes in the PanC group. Finally, KRAS copy number and mutation status was reliably assessed in $sEV^{Pancreas}$, highlighting the potential for KRAS mutational profiling.: we reliably characterized wild type and mutated KRAS status (G12D and G12V).

Conclusions. We demonstrate that pancreas-derived sEV can be selectively isolated from blood using newly identified pancreas-specific markers. These $sEV^{Pancreas}$ harbor distinct molecular signatures and reliably capture KRAS copy number and mutations, supporting their potential as a rapid, minimally invasive liquid biopsy platform. These findings lay the groundwork for sEV-based assays for treatment monitoring and response assessment.

#3740 OncoGraph: A patient-specific blood test using protein markers to monitor cancer recurrence and treatment response.

Mao Mao[1], Wenjian Wang[2], Qingqi Ren[3], Shiyong Li[1], Wei Wu[1]

[1]SeekIn, Shenzhen, Guangdong, China,[2]Sun Yat-sen Memorial Hospital, Sun Yat-sen University, Guangzhou, Guangdong, China,[3]Peking University Shenzhen Hospital, Shenzhen, Guangdong, China

Background: ctDNA-based MRD assays are increasingly used for post-treatment monitoring but remain costly and technically demanding, limiting global accessibility, particularly in low- and middle-income countries (LMICs). Protein tumor markers (PTMs) are inexpensive and clinically effective in select cancers (e.g., PSA for prostate, AFP for liver), but most malignancies lack disease-specific markers, and existing markers have restricted applicability with substantial inter-patient variability, limiting individualized monitoring. We developed OncoGraph, a patient-specific approach that identifies abnormally elevated PTMs and tracks their longitudinal dynamics to monitor recurrence and treatment response. This approach offers an affordable, scalable solution suited for LMIC healthcare systems.
Methods: Baseline blood samples from newly diagnosed cancer patients were analyzed by OncoSeek, a validated multi-cancer early detection assay quantifying a predefined panel of common PTMs (e.g., AFP, CEA). For individuals testing positive, PTMs exceeding internally validated thresholds were designated as patient-specific PTMs. These markers were longitudinally tracked after surgery or during therapy to monitor recurrence, response, or progression. Using OncoGraph, we evaluated postoperative recurrence in 24 liver cancer patients and treatment monitoring in 23 advanced lung cancer and 116 lymphoma patients receiving chemotherapy or targeted therapy.
Results: In liver cancer (n=24), 13 patients had elevated baseline PTMs (all AFP). After surgery, OncoGraph-positive patients had a higher recurrence rate (4/5 vs. 1/8) and shorter median recurrence-free survival compared with OncoGraph-negative patients (385 days vs. not reached; HR 12.8; $P < 0.01$).In advanced lung cancer (n=23), 17 patients carried PTMs elevated at baseline (CEA and/or CYFRA21-1). After a median of 44.5 days after treatment initiation (range, 31-63), patients with significant PTM decrease had longer median progression-free survival (438 vs. 191.5 days; $P < 0.05$).In lymphoma (n=116), only eight patients had baseline-abnormal PTMs (all CA125). After two treatment cycles, all eight showed marked OncoGraph decrease, fully concordant with interim PET/CT responses (partial or complete response) assessed after 2-4 cycles.
Conclusion: OncoGraph provides a patient-specific framework for PTM-based monitoring, addressing limitations of traditional PTMs through patient-specific marker selection. By selecting patient-specific informative PTMs and tracking their longitudinal dynamics, OncoGraph delivers early, clinically actionable signals of recurrence risk and treatment response across multiple cancer types. Its low cost, minimal technical requirements, and broad applicability make it a practical and scalable monitoring solution, particularly for LMIC healthcare settings.

#3741 Radiation-dendritic cell combination therapy drives systemic cellular immune shifts in liver cancer.

Melody Wu[1], Panwen Wang[2], Chen Wu[3], Ying Li[4], Christopher L. Hallemeier[5], Thomas D. Atwell[6], Nguyen H. Tran[7], Andre de Menezes Silva Corraes[7], Kevin Regan[7], Zuoyi Shao[7], Rayaan Kamal[7], Haidong Dong[8], Lewis R. Roberts[9], Sean Park[5], Yi Lin[10], Lionel Aurelien Kankeu Fonkoua[7]

[1]Medical Scientist Training Program, Mayo Clinic College of Medicine and Science, Rochester, MN,[2]Mayo Clinic - Department of Biomedical Informatics, Scottsdale, AZ,[3]Mayo Clinic Graduate School of Biomedical Sciences, Rochester, MN,[4]Mayo Clinic - Department of Quantitative Health Sciences, Jacksonville, FL,[5]Mayo Clinic - Department of Radiation Oncology, Rochester, MN,[6]Mayo Clinic - Department of Radiology, Rochester, MN,[7]Mayo Clinic, Rochester, MN,[8]Mayo Clinic - Department of Immunology, Urology, Rochester, MN,[9]Mayo Clinic - Department of Gastroenterology & Hepatology, Rochester, MN,[10]Mayo Clinic - Department of Hematology & Oncology, Rochester, MN

Introduction: Liver cancer remains a leading cause of cancer mortality globally with limited treatment options for patients (pts) with unresectable hepatocellular carcinoma [HCC] and intrahepatic cholangiocarcinoma [iCCA][1,2,3,4]. We hypothesize that combining the intratumoral dendritic cell (DC) vaccination after external beam radiotherapy (EBRT) without (phase I) and with (phase II) systemic atezolizumab and bevacizumab (atezo/bev for HCC) would enhance tumor-specific immunity and improve clinical outcomes, and present preliminary results from our phase I/II trial (NCT03942328).

Methods: Peripheral blood mononuclear cells (PBMCs) were collected at baseline (PRE), after radiation (EBRT), and after completion of DC without or with atezo/bev (POST). Single-cell RNA sequencing with TCR sequencing were analyzed using CellRanger v7.0.1, Immunopipe, Seurat v5.3.0, & Gene-set enrichment analysis (GSEA). Long EFS (EFS-L) is defined as >=12 months (mo) for phase I and >=18mo for phase II, and short EFS (EFS-S) below that.

Results: Seventeen patients have been analyzed to date (Phase I: n=8 [4 HCC, 4 iCCA]; Phase II: n=9 HCC). 674,106 cells were sequenced (146,843 PRE; 168,838 EBRT; 114,437 POST).

GSEA for EFS-L vs EFS-S were comparable at PRE, EBRT and POST between phase I and phase II. EFS-S was associated with enrichment of interferon alpha (IFNα; B naïve, monocytes, pDC, cDC2, NK, Treg, CD8 Tcm and Tem at PRE and POST; B intermediate, CD4 Tem and NK at EBRT) and reactive oxygen species (ROS; PRE: pDC, CD8 Tcm, Tem. EBRT: CD4 Tem. POST: CD8 T naïve Tem, CD4 Tcm & Tem, cDC2) pathways.

In contrast, EFS-L was associated with enrichment of WNT-β-catenin (WNT; CD14 mono at EBRT & POST, B intermediate at EBRT), TGFb (PRE: NK; EBRT: B intermed, CD4 Tem; POST: monocytes, CD4 naïve & Tem, pDC, cDC2), and angiogenesis (EBRT: NK; POST: monocytes, cDC2) pathways.

Interestingly, enrichment of protein secretion pathway in NK cells was associated with EFS-L, but among other cells were associated with EFS-S (PRE: CD16 mono, Treg; POST: CD16 mono, CD4 & D8 Tem).

Compared to phase I, addition of atezo/bev in phase II pts was associated with a significant increase in Gini coefficient ($p<0.0001$), suggesting expansion of certain TCR clones, along with a trend for increased Gini coefficient from Pre to Post in both phase I and II.

Conclusions: Preliminary analysis of this study combining EBRT with intratumoral DC vaccination +/- PD-L1/VEGF blockade identified distinct treatment-related changes in systemic cellular immune profiles. Enhanced TCR clonal diversity in phase II suggests added immunologic benefit from PD-L1/VEGF blockade. As accrual continues, integrated analyses will identify systemic immune correlates of clinical benefit and resistance to this multimodal immunotherapy approach.

#3742 Immune microenvironment rather than genomic alterations drives hyperprogression-related features in 11q13 amplified Chinese esophageal cancer.

Ling Deng

Guangzhou Medical University Affiliated Qingyuan Hospital (Qingyuan People's Hospital), Qingyuan City, China

Background: Immune checkpoint inhibitors (ICIs) have transformed the therapeutic landscape of esophageal cancer (ESCA), yet a subset of patients experience hyperprogressive disease (HPD) following immunotherapy. Previous studies have suggested that genomic alterations located on chromosome 11q13—including amplification of CCND1, FGF3, FGF4, and FGF19—may contribute to HPD. This study aimed to investigate whether 11q13 amplification in ESCA is associated with genomic features or distinct immune microenvironment characteristics that could help explain resistance to immunotherapy and the development of HPD.
Methods: Tumor samples from 341 ESCA patients were analyzed using a 733-gene next-generation sequencing (NGS) panel to characterize genomic profiles, including DDR pathway alterations, tumor mutation burden (TMB), and intratumor heterogeneity (ITH). Multiplex immunofluorescence (mIF) was also performed to evaluate key immune microenvironment components. Patients with and without 11q13 amplification were compared with respect to genomic alterations and immune cell infiltration.
Results: Among the 341 ESCA patients, 49.3% (168/341) exhibited 11q13 amplification. Genomic analysis revealed no significant differences between the 11q13-amplified and non-amplified groups in DDR pathway gene alterations, TMB, or ITH, suggesting that 11q13-associated immunotherapy resistance is unlikely to be driven by intrinsic genomic instability. In contrast, immune microenvironment profiling demonstrated marked differences: patients with 11q13 amplification exhibited significantly reduced infiltration of $FOXP3^+$ regulatory T cells (P=0.005) and $CD3^+CD4^+FOXP3^+$ T cells (P=0.03) in the tumor stroma, while showing significantly increased infiltration and density of $CD8^+PD\text{-}1^+$ T cells in the tumor parenchyma (P=0.01 for density; P=0.02 for positivity). These immune patterns are consistent with previously reported features associated with HPD, suggesting that immune dysregulation rather than genomic alterations may underlie hyperprogression in 11q13-amplified ESCA.
Conclusion: 11q13 amplification in ESCA does not correlate with DDR gene alterations, TMB, or ITH, but is strongly associated with distinct immune microenvironment features previously linked to HPD, including reduced stromal regulatory T cell infiltration and increased parenchymal $CD8^+PD\text{-}1^+$ T cell presence. These findings highlight the clinical importance of immune microenvironment dysregulation in 11q13-amplified ESCA and underscore the need for tailored therapeutic strategies for this molecular subgroup.

#3743 ddPLEX EGFR/KRAS/BRAF: A highly multiplexed droplet digital PCR (ddPCR) panel for ultra-sensitive NSCLC biomarker detection.

Surbhi Jain[1], Cailin Festog[1], Mai Ho[1], Cindy Li[1], Necip Mehmet[1], Ady Melendez-Molina[1], Toshiro Newsum[1], Prithwish Pal[1], Mina Rostamza[1], Yusuke Ono[2], Leisa Jackson[3], Brittany D'Alessio[3], Gunnar Johnson[3], Gary A. Pestano[3]

[1]Bio-Rad Laboratories, Hercules, CA,[2]Sapporo Higashi Tokushukai Hospital, Sapporo, Japan,[3]Biodesix, Inc., Louisville, CO

Biomarker testing for actionable oncogenic driver mutations is recommended in national and international guidelines based on the improved outcomes observed with use of targeted therapies in eligible patients with metastatic NSCLC. Here, we demonstrate the performance of the ddPLEX EGFR/KRAS/BRAF Mutation Detection Assay Kit, a research use only kit developed for the QX600™ Droplet Digital™ PCR (ddPCR) System. This kit is designed for the detection, discrimination and quantification of 37 actionable variants in the *EGFR*, *KRAS*, and *BRAF* genes in a single ddPCR well. It also has a companion total quantification well that quantifies *EGFR*, *KRAS* and *BRAF* genes in a mutation agnostic manner and allows for variant allele frequency (VAF) calculation. It provides same day results with a streamlined workflow, includes positive and internal controls and is compatible with plasma and formalin-fixed paraffin-embedded (FFPE) samples.

The analytical performance of the ddPLEX EGFR/KRAS/BRAF Mutation Detection Assay Kit was evaluated internally, and the findings are presented here. The results demonstrated an analytical sensitivity of 0.025%-0.1% in a background of 132 ng of human genomic DNA for all targeted variants. The assay had an analytical specificity of 100% when tested with 1000 copies input of each variant, one at a time, in a total of 132 ng of human genomic DNA. The mutant assay did not cross-react with any of the commonly reported mutations located in the same amplicon as *KRAS* G12C and *BRAF* V600E. The mutant assay was linear from 800 copies to 4 copies per reaction with a R^2 in the range of 0.94-0.99. The total quantification assay was also linear in the range of 1.3 ng to 53 ng of total DNA input with a R^2>0.99 for all three targets. With previously extracted and archived cell-free DNA from plasma and FFPE DNA that were tested with alternative PCR based methods, the ddPLEX kit had a concordance of 100% and 96.5%, respectively.

In conclusion, the ddPLEX EGFR/KRAS/BRAF Mutation Detection Assay Kit is sensitive, accurate, and efficient in time and cost for detecting clinically relevant NSCLC variants. Multiplexing maximizes information and reduces sampling bias from specimens with low nucleic acid quantities such as FFPE and plasma.

#3744 Peripheral immune indices predict pathologic complete response and residual cancer burden in inflammatory breast cancers.

Hui Gao[1], Ranjan Upadhyay[1], Angela Alexander[2], Angela N. Marx[3], Megumi Kai[3], Chelain R. Goodman[1], Azadeh Nasrazadani[4], Savitri Krishnamurthy[1], Anthony Lucci[5], Rachel M. Layman[1], Sadia Saleem[3], Vicente Valero[6], Michael C. Stauder[7], Susie X. Sun[8], Gary J. Whitman[9], Miral M. Patel[9], Huong C. Le-Petross[9], Chasity L. Yajima[3], Lily Villarreal[3], Heather Lopez[3], Bora Lim[1]

[1]UT MD Anderson Cancer Center, Houston, TX,[2]TRIUMPH Postdoctoral Fellow, UT MD Anderson Cancer Center, Houston, TX,[3]Breast Medical Oncology, UT MD Anderson Cancer Center, Houston, TX,[4]Azadeh Nasrazadani (Individual),[5]Professor, Dept. of Surgical Oncology, UT MD Anderson Cancer Center, Houston, TX,[6]Professor of Medicine, UT MD Anderson Cancer Center, Houston, TX,[7]Assistant Professor, UT MD Anderson Cancer Ctr., Houston, TX,[8]Breast Surgical Oncology, UT MD Anderson Cancer Center, Houston, TX,[9]Diagnostic Imaging, UT MD Anderson Cancer Center, Houston, TX

Background: Circulating immune profiles offer a noninvasive approach to monitor treatment response in breast cancer. Inflammatory breast cancer (IBC), although clinically distinct, shares resistance and immune evasion features among each other. To identify immune escape mechanisms and early predictors of response in IBC, we profiled longitudinal peripheral immune markers and evaluated their association with pathologic complete response (pCR) and residual cancer burden (RCB) across treatment regimens and subtypes and developed composite immune indices to improve prediction under class imbalance.

Methods: Peripheral blood samples (n=93) from patients treated with neoadjuvant or induction therapy for IBC were analyzed by multiparameter flow cytometry and annotated for subtype, regimen, pCR, and RCB. Group comparisons used Mann-Whitney U (pCR) and Kruskal-Wallis (RCB). Predictive models included logistic regression and random forest classifiers with class-weighting. Composite indices included CD8 Exhaustion, CD8 Memory, NK-ADCC scores derived from z-scaled components. Model performance was assessed using 5-fold cross-validation with AUC, PR-AUC, and calibration. Planned extensions include leave-one-regimen validation, temporal analyses, and external evaluation using a pre-registered pipeline.

Results: Univariate analyses identified significant associations between pCR and the CD8 Exhaustion Index ($p \approx 0.007$) and CD8 Memory Index ($p \approx 0.038$), with NK-ADCC trending ($p \approx 0.078$). Logistic regression and random forest models incorporating combined indices improved AUC from ~0.70 when individually associated, to ~0.92 ± 0.07 (5-fold CV), albeit with wide uncertainty due to only up to 5 pCR events. Individual markers linked to pCR included Stem_Memory_CD8, NKG2A_ADCC, and CTLA4_CD8, while CD56hi NK and NKG2A +CD56hi NK distinguished RCB gradients ($p<0.05$ before correction). No markers remained significant after FDR adjustment given sample size.

Conclusions: Peripheral immune signatures, particularly combined CD8 exhaustion, memory indices, NK ADCC were associate with higher pCR and lower RCB. Composite indices outperform single markers and capture the balance between immune activation and suppression. Ongoing cross-cohort validation will assess generalizability across regimens and subtypes. Severe class imbalance (~5/93 pCR) and small subgroup sizes constrain precision of our analysis. Findings are hypothesis-generating and warrant external validation in larger prospective cohorts.

#3745 Unveiling clear cell renal cell carcinoma heterogeneity associated with locally advanced disease using single nucleus multi-omics.

Pratik Shah[1], Anita Ng[2], Justin Wang[3], Houman Khalili[2], Tony Pham[4], Melissa Neumann[1], Xinhua Zhu[1], Annette Lee[5], Andrew Shih[2]

[1]Northwell Health Cancer Institute, New Hyde Park, NY,[2]The Feinstein Institute for Medical Research, Manhasset, NY,[3]College of Agriculture and Life Sciences, Cornell University, Ithaca, NY,[4]CUNY School of Medicine, Manhattan, NY,[5]ATL Consulting, Wayne, NJ

Clear cell Renal Cell Carcinoma (ccRCC) is the most common type of kidney cancer with diverse clinical courses that are driven by molecular and histological heterogeneity. Overall survival of ccRCC patients has improved significantly with the introduction of adjuvant therapies, including immunotherapy and tyrosine kinase inhibitors (TKI), particularly for patients at higher risk of recurrence post-nephrectomy. However, the response rate to these targeted therapies for those that relapse can vary greatly. To decipher the molecular underpinning of therapy responsiveness associated with advanced stage ccRCC, we performed single nucleus analysis of gene expression and chromatin dynamics on fresh post-nephrectomy tumor samples collected in 8 patients.

Upon comparing different ccRCC subpopulations between stage 3 (n=6) and stage 1 (n=2) patients, we observed large global transcriptional differences with an enrichment of a subset of metabolically active RCC cells with heightened *EDIL3* expression. Besides the increased distribution of this RCC subset in stage 3 patients, we have identified chromosomal regions in these cells that overlapped with 4 genome-wide association study (GWAS) hits for increased risk of ccRCC (Purdue et al., 2024). Among the clusters of ccRCC subsets discovered in this cohort, the gene signatures of *EDIL3*-ccRCC are significantly associated with lower survival time (OR= 4.65; P=1.9E4) in stage I-III TCGA-KIRC (n = 372). Intriguingly, these cells, as well as a *FOS* expressing ccRCC cluster, are also enriched in patients in our cohort that eventually relapsed. Together with the upregulation of ERK and RAS signaling compared to other tumor cells, the increased fatty acid metabolism in *EDIL3*-ccRCC may present an alternative signaling mechanism that can contribute to progression due to metastasis and disease recurrence. In silico prediction of drug responsiveness revealed an overall decrease of therapeutic sensitivity of *EDIL3*-ccRCC toward various EGFR inhibitors. In contrast, while *FOS*-ccRCC signature also appears to be associated with disease recurrence, these cells are highly sensitive to various TKI and Sunitinib in particular. These results suggest the potential to leverage the differential therapeutic vulnerability of ccRCC subpopulations to provide better combination therapies in the clinic.

With the goal of improving the conceptual framework for the design of adjuvant therapies, our study offers an in-depth characterization of ccRCC subpopulations that are associated with higher stages and disease progression, possibly through different druggable oncogenic pathways.

#3746 Single-cell liquid biopsy profiling in mCRPC receiving PSCA-targeted CAR-T cell therapy.

Doanna Minh Pham[1], Stephanie Nicole Shishido[1], Saul J. Priceman[2], Tanya B. Dorff[3], Peter Kuhn[4]

[1]USC - University of Southern California, Los Angeles, CA,[2]University of Southern California, Los Angeles, CA,[3]City of Hope Comprehensive Cancer Ctr., Los Angeles, CA,[4]Assoc. Professor, Dept. of Cell Bio., University of Southern California, Los Angeles, CA

Metastatic castration-resistant prostate cancer (mCRPC) represents an aggressive, treatment-refractory stage of prostate cancer with limited treatment options and poor prognosis. Chimeric antigen receptor (CAR)-T cell therapy has demonstrated success in hematological malignancies, but its efficacy in solid tumors is limited by tumor microenvironment (TME) barriers and tumor cell heterogeneity. In this study, we applied a single-cell enrichment-free liquid biopsy platform to monitor disease progression and CAR-T cell response in mCRPC patients enrolled in a Phase 1 clinical trial (NCT03873805). Using fluorescent whole-slide imaging (fWSI), we analyzed peripheral blood (PB) and bone marrow aspirate (BMA) from eight patients (four responders and four nonresponders) collected longitudinally before, during, and after therapy. Two key findings emerged: 1) lymphodepletion mobilized circulating tumor cells (CTCs) from bone marrow into PB, altering compartment-specific cellularity regardless of response, and 2) clearance of clonal CTCs after CAR-T cell infusion occurred in responders but not in nonresponders. Single-cell analyses further revealed that PB and BMA captured distinct CTC subtypes, underscoring the complementary value of both compartments for monitoring. This multi-omic analysis leverages high-resolution single-cell liquid biopsies to characterize circulating rare cells, such as CTCs and their subtypes, to correlate them with clinically observed responses to CAR-T cell therapy in mCRPC.

#3747 Discovery and functional characterization of enhancer hijacking oncogene rearrangements in NSCLC using Hi-C sequencing of FFPE tumors.

Kristin Sikkink, Blake Skrable, Sid Selvaraj, Alex Hastie, **Anthony Schmitt**

Arima Genomics, Carlsbad, CA

INTRO: Molecular profiling of solid tumors has revealed many targetable biomarkers; in NSCLC, ~50% of patients harbor such biomarkers (EGFR mutations or ALK fusions). However, limited precision therapeutic options exist for the remaining ~50%. To address this need, we aimed to identify and functionally characterize novel tumor-driving genomic mechanisms involving known oncogenes using Hi-C sequencing of FFPE NSCLC tumors.
METHODS: FFPE NSCLC tumors (n=97) were retrospectively selected from Stage III/IV patients whose prior CGP showed no EGFR/RAS mutations or gene fusions (“driver-negative”). Hi-C sequencing was performed by Arima Genomics, and rearrangements, gene fusions, and CNVs were identified with Arima-SV pipeline. Oncogenes within ~1 Mb of a rearrangement (“oncogene rearrangements”) were evaluated for potential enhancer hijacking events by analyzing breakpoint-crossing 3D regulatory interactions with putative enhancers at rearrangement partner loci. Functional characterization of rearranged oncogene activation was assessed by IHC.
RESULTS: 95/97 (98%) Hi-C libraries passed QC and were deeply sequenced and analyzed. 35/95 (37%) of tumors had oncogene rearrangements involving 47 oncogenes. 26/95 (27%) tumors carried 33 rearranged oncogenes linked to response to targeted therapies (Level 1/2 therapeutic response evidence; OncoKb), including BRAF (1), ERBB2 (3), FGFR1 (9), FGFR2 (2), FGFR3 (2), NRG1 (4), NTRK1 (1), NTRK2 (1), RET (5), ROS1 (2), KRAS (2), and PIK3CA (1). 3/95 (3%) tumors had PD-L1 rearrangements. 8/95 (8%) tumors had 11 rearranged oncogenes of lower-level significance, such as PIK3CB (1), CCND1 (3), BCL6 (1), and MYC (2), CLDN18 (3), and HRAS (1). 23 had sufficient tissue remaining for further functional characterization and a corresponding commercially available IHC test for protein expression. 11/23 (48%) were expressed in >10% of the tumor cells, including FGFR1 (2/9, 22%), ERBB2 (2/3, 66%), NTRK1 (0/1, 0%), NTRK2 (1/1, 100%), ROS1 (0/2, 0%), CLDN18 (0/1, 0%), BCL6 (1/1, 100%), MYC (2/2, 100%), and CCND1 (3/3, 100%). Lastly, we observed that 10/11 (91%) rearrangements with both features of enhancer hijacking ((1) strong breakpoint-crossing oncogene 3D interactions and (2) partner locus enhancers) were expressed at the protein level, versus only 1/12 (8%) lacking one or both features.
CONCLUSIONS: These data demonstrate the capability of Hi-C to detect rearranged oncogenes and predict their exogenous expression. Many activated rearranged oncogenes correspond to targets of FDA-approved or standard-of-care therapies, albeit potentially activated by a mechanism different than those well-established (point mutations or gene fusions). Further studies are needed to determine whether such oncogene rearrangements confer therapeutic susceptibility or serve as other predictive biomarkers or drug targets.

#3748 A proportion of shared mutations in lung squamous cell carcinoma provides insights that may guide therapeutic approaches.

Jaewoong Lee[1], Jun Hyeok Lim[2], Lucia Kim[3], Woo Kyung Ryu[4], Hyun-Tae Shin[5], In-Jae Oh[6], Sabin Park[1], Yoo Duk Choi[7], Semin Lee[1], Jeong Seon Ryu[8]

[1]Department of Biomedical Engineering, UNIST, Ulsan, Korea, Republic of,[2]Inha University College of Medicine, Incheon, Korea, Republic of,[3]Department of Pathology, Inha University College of Medicine, Incheon, Korea, Republic of,[4]Division of Pulmonology, Inha University College of Medicine, Incheon, Korea, Republic of,[5]Inha University College of Medicine, Jung-gu,[6]Chonnam National Univ. Hwasun Hospital, Jeonnam, Korea, Republic of,[7]Department of Pathology, Chonnam National University Medical School, Gwangju, Korea, Republic of,[8]Inha Univ. Hospital, Incheon, Korea, Republic of

Lung squamous cell carcinoma (LUSC) frequently arises within a genetically altered epithelium, yet the clinical significance of the cancerized field remains unclear.To investigate its biological and prognostic significance, we performed whole-exome and transcriptome analyses on precancer, primary tumor tissues, and their matched normal tissues from 76 LUSC patients. We defined the proportion of shared mutations (PSM) between precancer and corresponding tumor samples, which negatively correlates with poor recurrence-free survival and overall survival. Interestingly, high PSM was associated with early chromosomal instability, tobacco-related mutational signatures, and upregulation of metabolic and proliferative genes such as *RRM2* and *TIMMDC1*. Furthermore, molecular features of RRM2 and TIMMDC1 were enriched in the independent non-recurrence group. Additionally, copy number variations and gene expression patterns differed significantly between the PSM-low and PSM-high groups, suggesting the presence of clonal evolution within a cancerized field. These results demonstrate that PSM serves as a novel biomarker for prognosis and reveals key early events in the progression of LUSC.

This study was supported by a grant (RS-2022-NR-071926 and RS-2018-NR031072) from the National Research Foundation of Korea (NRF).

#3749 Integrative multiomics and functional studies to identify biomarkers of AOH1996 sensitivity across AML subtypes.

Hamsini Kala[1], Dana Abou Abbas[2], Robert J. Hickey[3], Linda H. Malkas[4], Caroline M. Li[1], Robert G. Lingeman[1], Guido Marcucci[2], Le Xuan Truong Nguyen[2], Brian Ball[5], Amanda Blackmon[5], Melissa Ronan[6], Jennifer Roth[7], Matthew G. Rees[7]

[1]Beckman Research Institute of The City of Hope, Duarte, CA,[2]City of Hope, Duarte, CA,[3]City of Hope National Medical Center, Duarte, CA,[4]City of Hope National Medical Center, Sylmar, CA,[5]PS Hematology, City of Hope National Medical Center, Duarte, CA,[6]Broad Institute of MIT and Harvard, Cambridge, MA,[7]Broad Institute, Cambridge, MA

Acute myeloid leukemia or AML encompasses diverse molecular subtypes driven by distinct transcriptional and genetic programs that influence therapeutic response. AOH1996 which is a PCNA-dependent replication stress pathway inhibitor has demonstrated preclinical activity in AML. However biomarkers that may predict sensitivity across heterogeneous AML subgroups remain undefined. We first applied integrative multiomic analysis to begin defining the molecular contexts in which AOH1996 may be most effective. Transcriptomic, genomic, and proteomic datasets from PRISM, DepMap, and other curated subtype annotations were integrated with AOH1996 response metrics also known as AUC. Initial analyses focused on quantitative assessment of MYC RNA expression relative to AOH1996 sensitivity using a quadrant based visualization framework, and ongoing multi-omic analyses incorporating mutational backgrounds. Pathway activity scores, and protein level features are being used to explore broader biomarker patterns across AML models. Guided by these computational findings we are developing complementary in vitro studies in a panel of molecularly annotated AML models to functionally probe AOH1996 response, with planned readouts broadly focused on cell growth, cell cycle behavior, and stress associated phenotypes consistent with replication stress and innate immune pathway engagement. Preliminary computational results reveal subtype dependent variation in the relationship between MYC expression and AOH1996 response which aligns with MYC's established role in driving transcriptional load and replication stress and nominating MYC expression as a biologically plausible candidate biomarker. Together, this integrated multiomics and emerging experimental framework supports the feasibility of biomarker-guided evaluation of AOH1996 across AML subtypes and provides a foundation for future translational studies aimed at molecularly informed therapeutic stratification.

#3751 QVT Subscore: An interpretable radiomic panel of tumor vascularity reveals treatment-specific mechanisms-of-action (MoA) in NSCLC.

Haojia Li[1], Pushkar Mutha[2], Young Kwang Chae[3], Kai Zhang[1], Liam Il-Young Chung[3], Amogh Hiremath[1], Rhea Chitalia[1], Justin Yau[3], Omid Haji-Maghsoudi[1], Trishan Arul[1], Vamsidhar Velcheti[4], Anant Madabhushi[1], Nathaniel Braman[1]

[1]Picture Health, Cleveland, OH,[2]Wallace H. Coulter Department of Biomedical Engineering,Georgia Institute of Technology and Emory University, Atlanta, GA,[3]Feinberg School of Medicine, Northwestern University, Chicago, IL,[4]Department of Hematology and Oncology, Mayo Clinic, Jacksonville, FL

Table1: Directionality of QVT Score and Subscore change from baseline to first on-treatment CT

Treatment Group	S0819 arm1: mono chemotherapy (chemo)	S0819 arm2: chemo+cetuximab (cet)	S0819 arm3: chemo+bevacizumab(bev)	S0819 arm4: chemo+cet + bev	mono ICI
N	170	157	116	114	147
QVT Score	—	—	⬇	⬇	⬆
Subscore 1: Branching	—	—	⬇	⬇	⬆
Subscore 2: Curvature	—	—	⬇	⬇	⬆
Subscore 3: Torsion	—	—	⬇	⇩	⬆
Subscore 4: Radius	—	—	⬇	—	—
Subscore 5: Vessel Volume	—	—	—	—	⬆
Subscore 6: Inflection Points	—	—	⬇	⇩	⬆
Note: Black Arrow p<=0.05, White Arrow 0.05<p<0.1, — no trend					

Background: Tumor angiogenesis drives treatment resistance by fostering an immunosuppressive microenvironment. VEGF inhibitors (VEGFi) target the vasculature, while immune checkpoint inhibitors (ICI) do not address this mechanism directly. Quantitative Vessel Tortuosity (QVT) Score is a radiomic biomarker of vascularity previously shown to be associated with ICI response. Here, we introduce QVT Subscore, an interpretable panel that isolates distinct vascular attributes (e.g., branching, curvature, radius), enabling treatment-specific insight into vascularity MoA and vascular normalization.

Methods: QVT Subscores are derived by grouping the 910 QVT features comprising QVT Score into six biological categories, summarized by principal component analysis. The panel was evaluated in 557 patients from the phase 3 SWOG S0819 trial and a real-world ICI monotherapy cohort (n=147). QVT score/subscore changes from baseline to first on-treatment CTs were assessed by paired t-test and substratified by objective response (OR).

Results:While the mono-chemotherapy showed no vascularity changes, VEGFi regimens reduced QVT Score, with Branch and Curvature Subscores decreasing significantly but Vessel Volume unchanged. In contrast, ICI recipients exhibited significant increases in QVT Score and 5/6 Subscores, showing opposite changes to VEGFi in four subscores and differing effects on vessel Radius and Volume. VEGFi produced the greatest vascularity decrease in patients achieving OR, with milder decreases in non-OR. For ICI, OR showed negligible QVT change, while vascularity significantly increased in non-OR across all subscores except Radius.

Conclusions: The QVT Subscore panel captures granular tumor vascular remodeling from different treatments, providing mechanistically grounded insights into clinical trial arm performance. Future work will assess the panel’s potential for identifying regimens that benefit from adding VEGFi.

#3752 RNA editing deaminase activation as a dynamic marker to track hematopoietic stem cell fitness and leukemia evolution.

Inge van der Werf[1], Jessica Pham[1], Neha Katragadda[1], Kendale Wirtjes[1], Athena Mohebbi[1], Emma Klacking[1], Thomas Whisenant[2], Ludmil B. Alexandrov[2], Sheldon Morris[1], Catriona Jamieson[1]

[1]Sanford Stem Cell Institute, La Jolla, CA,[2]UC San Diego, La Jolla, CA

Myeloproliferative neoplasms (MPNs) are clonal hematopoietic stem cell-derived disorders that can evolve into acute myeloid leukemia (AML) at variable rates. Although JAK2 inhibitor therapies have improved outcomes, and variant allele frequency (VAF) monitoring informs therapeutic response, predicting if pre-leukemic stem cells will acquire self-renewal and transform into malignant leukemia stem cells (LSCs) remains a critical challenge. Our recent studies identified inflammatory responsive RNA-editing enzymes, ADAR1 and APOBEC3C as contributors of pre-leukemic stem cell (LSC) evolution. Given that MPNs are stem cell-driven disorders, we hypothesize that RNA-editing signatures mediated by these enzymes could serve as real-time indicators to track disease progression. This study aims to integrate driver mutation VAF, ADAR1 and APOBEC3C gene expression, and RNA-editing patterns into a comprehensive biomarker tool to evaluate MPN progression, predict therapeutic response, guide clinical decision making, and prevent transformation to leukemia.

We performed longitudinal 150-gene next-generation sequencing (NGS) analyses for 129 MPN patients with a median follow-up time of 958 days (range 0-4214). From this cohort, we selected four patients who were treated with the JAK2 inhibitors, progressed to sAML, underwent stem cell transplantation, and had cryopreserved peripheral blood and bone marrow mononuclear cells stored in our biorepository. For these patients, we had 15, 17, 24, and 31 sequential time points collected between 2013 and 2025. qPCR was performed on $CD34^+$ immunomagnetic bead-selected cells to measure ADAR1, APOBEC3C, STAT3, and JAK2 expression levels. During treatment, we observed dynamic changes in ADAR1, APOBEC3C, JAK2, and STAT3 expression levels. Notably, while VAF remained stable, both lactate dehydrogenase (LDH) and ADAR1 expression levels increased. Survival and self-renewal assays comparing time points with relatively low versus high ADAR1 expression revealed significantly increased colony counts at the high-expression time points. These findings suggest that ADAR1 expression may serve as a dynamic marker for both disease progression. Further single-cell RNA sequencing studies will delineate differences in HSCs and HPCs at sequential time points for four MPN patients that progressed to sAML.

#3753 Uncovering tumor microbial and immune biomarkers of immunotherapy response in lung cancer.

Lili Ma[1], Chao Cheng[1], Shwetha Vasanth Kumar[1], Spiridon Tsavachidis[1], Aaron P. Thrift[1], Joseph F. Petrosino[1], Hee-Jin Jang[1], Robert Taylor Ripley[1], Christopher I. Amos[2], Hyun-Sung Lee[1], Matthew B. Schabath[3], David C. Christiani[4], Yanhong Liu[1]

[1]Baylor College of Medicine, Houston, TX,[2]University of New Mexico Comprehensive Cancer Center, Albuquerque, NM,[3]Moffitt Cancer Center, Tampa, FL,[4]Harvard Medical School, Boston, MA

Background: Although immune checkpoint inhibitors (ICIs) have shown promise, fewer than half of advanced Non-Small Cell Lung Cancer (NSCLC) patients respond, and biomarkers such as PD-L1 and tumor mutational burden poorly predict response. The intratumoral microbiota directly interacts with cancer and immune cells, yet its relationship with immune subsets in ICI-treated NSCLC is unclear. We hypothesize that integrating tumor microbiota with immune features could improve prediction of response and patient stratification.

Methods: We analyzed total RNA-Seq data from 120 stage IV NSCLC patients whose tumor samples were collected prior to ICI therapy. Patients were classified as 30 responders or 82 non-responders,and progression-free survival was evaluated. A dual RNA-Seq approach profiled both host and microbiota: human reads were removed (Bowtie2), non-human reads classified (Kraken2). Microbial α-diversity (Chao1, Shannon), β-diversity (Bray-Curtis). Host immune profiling included differential expression (DESeq2) and immune infiltration (CIBERSORT), with group differences tested by t-test.

Results: We detected 273 microbial species. α- and β-diversity did not differ between responders and non-responders. Differences between responders and non-responders were mainly driven by Gram-negative taxa. Streptomyces was the only Gram-positive genus enriched in responders. Immune profiling showed that responders had higher expression of antigen-presentation genes, greater $CD8^+$ T-cell cytotoxicity, and upregulation of PD-1 and CTLA-4, whereas non-responders had impaired antigen presentation, reduced effector T cell activity, and a neutrophil-dominant suppressive axis with increased S100A8 and ARG1; GSVA indicated enrichment of neutrophil-mediated Gram-negative killing pathways.

Conclusions: As microbial signals in low-biomass lung tumor RNA-seq are susceptible to contamination, we removed taxa commonly associated with environmental sources. Notably, Streptomyces-a genus producing several anticancer natural products—remained more frequent in responders, suggesting a potential link to favorable outcomes. In addition, our results suggest that responders exhibit antigen presentation and activated effector T cells, yet also display high expression of PD-1 and CTLA-4, placing them in an inflamed but suppressed state that becomes responsive upon checkpoint inhibition. Conversely, non-responders are dominated by innate immune programs with suppressed adaptive immunity, and therefore fail to mount an effective antitumor response even when treated with immune checkpoint inhibitors. Machine learning approaches integrating immune-microbiome crosstalk are ongoing. If validated, these intratumoral microbial and immunological predictors could optimize patient selection for immunotherapy and support precision treatment strategies in NSCLC.

: Circulating Tumor Cells, Metastasis, and Dissemination Biology 2
Poster Session

#3757 Establishment of 3D culture system of circulating tumor cells with immune cell evasion strategy.

Ji Eun Moon, **Jihyun Lee**, Soee Kim, Minseon Hwang, Jung Won Kim

Cytogen, Inc., Seoul, Korea, Republic of

Introduction
Circulating tumor cells (CTCs), are cancer cells shed from primary tumors, travel through the vasculature and give rise to metastatic lesions. CTCs have more advantages as a diagnostic tool compared with other liquid biopsy components such as cell-free DNA, because they contain all cellular components could provide more information of cancer cells. However, the number of CTC in the blood is very small, there are limitations in applying various kinds of analyses. Therefore, we have developed CTC 3D culture system for expanding number of CTCs after the enrichment of CTC with automated Smart Biopsy^{TM} Cell Isolator. In this study, a CTC-mimicking model with the cancer cell lines to establish a 3D culture environment suitable for CTC growth and a pilot test of CTC 3D culture with clinical samples were performed.
Method
To establish the 3D culture system with cancer cell lines, we spiked H358 (lung cancer), HCT116 (colon cancer) with peripheral blood mononuclear cells (PBMCs) (cell:PBMC ratio= 1:10 ~ 1:250) and initiated culture under 3D conditions. To retain only the minimal number of cancer cells required for growth we tested various approaches including dynamic culture and static culture. Then mixed cell suspension was embedded into the matrigel and incubated until growth. A pilot test for CTC 3D culture was performed with clinical samples of prostate cancer after the approval of institutional review board of Ewha Womans University Mokdong Hospital.
Result
We observed that immune cell movement increased both in frequency and speed when higher numbers of PBMCs were present within the gel. As a result, following significant PBMC migration out of the dome, cancer cells progressively expanded and formed small clusters. Starting with 100 cells per dome, cancer cell clusters reached approximately 100-150 μm in diameter by week 2. By recapitulating in vitro the key challenges encountered in clinical samples, such as extremely low number of CTCs and their susceptibility to immune-mediated elimination, our model enables systematic evaluation of these limitations and the identification of strategies to overcome them. Furthermore, pilot application of this system using clinical blood samples yielded promising preliminary results.
Conclusions
We have established the 3D CTC culture system with various kinds of in vitro tests for defining culture conditions that allow CTC-like cells to survive immune pressure and our culture system was validated with successful growth of CTC with ex vivo culture of clinical samples of prostate cancer.

#3758 Pilot study of the clinical correlation of CTC counts and AR-V7 expression with resistance to androgen receptor inhibitors in metastatic prostate cancer.

Jihyun Lee[1], Minseon Hwang[1], Soee Kim[1], Choung-Soo Kim[2], Jung Won Kim[1]

[1]Cytogen, Inc., Seoul, Korea, Republic of,[2]Department of Urology, Ewha Womans University Mokdong Hospital, Ewha Womans University School of Medicine, Seoul, Korea, Republic of

Introduction

Androgen receptor splice variant 7 (AR-V7) is a constitutively active isoform of the androgen receptor and has been associated with resistance to AR-targeting therapies and progression to metastatic prostate cancer (mPCa). However, tissue-based detection of AR-V7 is limited by the poor accessibility of metastatic lesions, particularly before and after treatment. To address this limitation, we developed a CTC-based AR-V7 detection system using CytoGen's Smart Biopsy™ CTC platform and investigated the clinical association of CTC counts and AR-V7 expression androgen receptor inhibitor (ARI).

Method

Peripheral blood samples (20 mL) from 12 mPCa patients were processed using the Smart Biopsy™ Cell Isolator for CTC enrichment. 5 samples from healthy donor were used as negative control of CTC counts by immunofluorescence and the cut-off of AR-V7 expression. CTCs were enumerated by immunofluorescence (IF), and AR-V7 transcripts were analyzed using droplet digital PCR (ddPCR)

Results

To investigate the clinical correlation of CTC counts and AR-V7 expression to the resistance of ARI, blood samples of mPCa patients were collected and CTC enrichment was proceeded with Smart Biopsy™ Cell Isolator. Number of CTC in all of 12 mPCa patients' samples were successfully counted by IF assay. 10 patients showed the high CTC burden (≥10 CTCs per 5mL of blood) and it was statistically significant correlation with the resistance of ARI. AR-V7 expression in CTC were also tested by ddPCR. 5 out of 12 mPCa patients showed AR-V7 positive CTC and 4 out of 5 patients were associated with ARI's resistance.

Conclusions

In this pilot study, CTC counts and/or AR-V7 detection in CTC showed the meaningful correlation to the resistance of ARI, suggesting that they may serve as potential diagnostic tools for predicting the treatment response of ARI.

#3759 Next-generation liquid biopsy for circulating tumor cell detection in metastatic prostate cancer.

Minzhi Sheng[1], Omar Alawamry[2], Shuyang Feng[3], Urban Emmenegger[4], Kristin Cimolini[1], Danny Vesprini[5], Andrew Loblaw[5], Laurence H. Klotz[6], Christopher S. Lim[7], Stanley K. Liu[1], Hon Sing Leong[1]

[1]Sunnybrook Research Institute, Toronto, ON, Canada,[2]Department of Medical Biophysics, University of Toronto, Toronto, ON, Canada,[3]Department of Urology, West China Hospital, Chengdu, China,[4]Department of Hematology and Oncology, Sunnybrook Health Sciences Centre, Toronto, ON, Canada,[5]Department of Radiation Oncology, University of Toronto, Toronto, ON, Canada,[6]Professor, Dept. of Surgery, Univ. of Toronto Sunnybrook HSC, Toronto, ON, Canada,[7]Department of Radiology, University of Toronto, Toronto, ON, Canada

Prostate cancer (PCa) is the most frequently diagnosed malignancy among Canadian men, and metastatic disease (mPCa) carries a poor prognosis. Liquid biopsy that analyzing circulating tumor cells (CTCs) provide a minimally invasive tool for disease assessment, yet commonly used CTC markers such as EpCAM show variable expression in PCa, especially in advanced or treatment-resistant settings. More reliable biomarkers are needed to improve CTC detection and patient stratification. We use monoclonal antibodies against STEAP1, a transmembrane protein highly overexpressed in PCa but minimally present in normal tissues, and integrated them into an imaging flow cytometry (imFC) CTC assay to detect and characterize CTCs. CTCs from localized and metastatic PCa patients were isolated using Ficoll density gradients and stained with DAPI, CD45, EpCAM, and STEAP1 antibodies. High-content images were analyzed through a computational pipeline incorporating machine-learning classification to identify and classify intact CTCs, CTC fragments, and tumor-derived extracellular vesicles (EVs) internalized by immune cells. STEAP1$^+$ CTCs were detected in most metastatic patients, including individuals who lacked detectable EpCAM$^+$ CTCs, highlighting the limitations of EpCAM-only assays. Patients with active disease exhibited higher STEAP1$^+$ CTC counts compared with those with localized or stable disease. Additionally, STEAP1$^+$ extracellular vesicles and CTC fragments were observed within CD45$^+$ immune cells, suggesting broader tumor-immune interactions measurable through this platform. We further extended this workflow to a clinical study evaluating treatment-associated changes in abundance of CTC expressed with different PCa biomarkers, PSMA, STEAP1, and STEAP2 in patients receiving Pluvicto therapy. In this study, CTCs were enriched using the Parsortix microfluidic capture platform. Early results indicate that STEAP-family markers remain detectable in patients with low or fluctuating PSMA expression, supporting their value in monitoring therapeutic response. Together, these findings position STEAP1, STEAP2 and PSMA as robust biomarkers for next-generation CTC-based liquid biopsy assays and demonstrate their potential to enhance diagnostic sensitivity and treatment monitoring in mPCa.

#3760 Spatial immune signatures predict outcomes in HPV-positive oropharyngeal cancer: Results of a clinical trial.

Nader Sadeghi[1], Alex Mlynarek[1], Marco Antonio Mascarella[2], Alan Spatz[3], Khalil Sultanem[4], William D. Foulkes[5], Severine Landais[6], Michael Hier[1], **Sabrina Wurzba**[7]

[1]McGill University, Montreal, QC, Canada,[2]McGill University Health Centre, Montreal, QC, Canada,[3]Director/Pathology, McGill University, Montreal, QC, Canada,[4]McGill University, Monteal, QC, Canada,[5]Professor, Depts. Medicine, Oncology, Human Genetics, & Ob & Gyn, McGill University, Montreal, QC, Canada,[6]Centre de recherche du CHU Sainte-Justine, Montreal, QC, Canada,[7]McGill University, Montreal, QC, Canada

Background: The incidence of Human Papillomavirus (HPV)-associated oropharyngeal cancer (OPC) has been increasing in recent years. While patients with HPV-positive OPC generally demonstrate more favorable outcomes compared to those with HPV-negative disease, a subset still experiences locoregional recurrence and distant metastasis. These clinical challenges underscore the need for a better understanding of the tumor microenvironment (TME) and its role in modulating treatment response. We hypothesized that the composition and spatial dynamics of the TME differ between complete responders and partial/non-responders, and these differences may serve as predictive biomarkers.

Methods: This retrospective study included patients with p16-positive OPC treated at two major cancer centers in Montreal between 2010 and 2023. Formalin-Fixed Paraffin-Embedded (FFPE) tissue blocks were retrieved, and tissue microarrays (TMAs) were constructed for high-dimensional immune profiling using imaging mass cytometry (IMC). Immune cell populations were analyzed across treatment response categories (complete vs. partial responders) and treatment stages (pre- vs. post-treatment). Deep learning-based cell segmentation was applied to quantify immune cell subsets, assess spatial architecture, and perform network and neighborhood analyses of the TME to identify potential predictive and prognostic immune signatures.

Results: Tissue specimens were obtained from HPV-positive (p16+) OPC patients, of whom 79.6% were male, with a mean age of 62.5 years. IMC revealed distinct immune landscapes between response groups. In complete responders, treatment induced a robust recruitment of anti-tumor immune cells (e.g., CD8+ T cells and B cells), suggesting an activated immune phenotype post-treatment. In contrast, non-responders exhibited enrichment of immunosuppressive or tumor-promoting cell types following therapy. Spatial co-localization and cell-cell interaction analyses further indicated that B and T cells interactions may contribute to therapeutic success.

Conclusion and Impact: This study provides novel insights into the spatial and cellular remodeling of the immune microenvironment in HPV-positive OPC before and after treatment. Our findings highlight the prognostic potential of IMC-based immune profiling and support the development of predictive biomarkers to guide the selection of patients who may benefit from neoadjuvant chemotherapy or immunomodulatory interventions.

#3761 Aneuploid primary cancers metastasize as diploid cancer stem cells.

Olufemi Emmanuel Akanni[1], Jerry Thomas Thornthwaite[2]

[1]Osun State University, Osogbo, Nigeria,[2]Cancer Research Institute of West Tennessee, Henderson, TN

The standard cancer treatment modalities have focused on destroying daughter cancer cells while having minimal effect on Cancer Stem Cells (CSCs). The details of the underlying mechanism by which CSCs metastasize in our sarcoma model are presented. To understand the fundamental process of metastatic disease, we used a chemically induced cancer model by painting the shaved distal thigh musculature of DBA/6J mice with 1.0% 3-methylcholanthrene in sesame oil. Approximately 90% of the mice developed an intramuscular tumor *in situ* within six months. The original chemically induced cancer cells were enzymatically dissociated into single cells, and 5×10^4 sarcoma cells in 0.1 ml were injected intramuscularly into new mice. Using our DAPI-Nuclear Isolation Medium and our high-resolution DNA flow cytometry, we generated DNA histograms of the tumor cell populations. When the primary tumors reached 2.0 cm in diameter, metastatic nodes in the lungs were detected using an India ink contrast stain after dissecting about 10 small 1.0 mm metastatic nodules and enzymatically dissociating the metastatic cancer cells into viable populations, as described above. The metastatic tumors were almost exclusively diploid, showing a normal total DNA content. When diploid metastatic tumors were transplanted intramuscularly, they grew as an aneuploid population containing both diploid cancer stem cells and aneuploid daughter cancer cells, with the same DNA Index, which served as a fingerprint of each original tumor. We could repeat this process many times. Our early observations revealed that the diploid population of an aneuploid cancer was the most virulent to metastasis. The diploid metastatic CSCs with their low S-phase would have a good chance of escaping the immune system, as their cell surfaces would appear normal. They would also be less affected by chemotherapy or radiation therapy because of their low S-phase. All excised lung metastases between 2 and 8mm in diameter maintained their diploid DNA histogram pattern, with only 1% aneuploidy. These diploid metastases, after enzymatic single-cell preparations, were either transplanted into the flank of a new mouse or placed in cell culture. Aneuploid cells began to emerge from the diploid cell populations, resulting in a DNA index equivalent to that of the original chemically induced sarcoma. These data indicate that cancer stem cells (CSCs) originate in the diploid portion of the primary aneuploid sarcoma, as only these diploid cells can evade the immune system and establish diploid lung metastases. The diploid CSCs still retained the capacity to transform into daughter aneuploid cells.

#3762 Genetic characterization of disseminated tumor cells of historical cryo-preserved bone marrow samples from primary breast cancer patients.

Anne Rohloff[1], Rui Pedro Lousa Das Neves[1], Christiane Driemel[1], Daniel Doerr[2], Oliver Hoffmann[3], Rainer Kimmig[3], Nikolas Hendrik Stoecklein[1], Sabine Kasimir-Bauer[3]

[1]Department of General, Visceral and Pediatric Surgery, University Hospital Duesseldorf, Duesseldorf, Germany,[2]Department of Endocrinology and Diabetology, University Hospital Duesseldorf, Duesseldorf, Germany,[3]Department of Gynecology and Obstetrics, University Hospital Essen, Essen, Germany

Background: Metastatic relapse is the leading cause of death in patients with hormone receptor-positive, HER2-negative primary breast cancer (BC). While some patients experience late relapse after more than 10 years, others relapse within 3-7 years, yet the biological mechanisms underlying this variability remain poorly understood. Disseminated tumor cells (DTCs) in the bone marrow (BM) are hypothesized to represent a clinically occult reservoir driving metastatic progression. In this study we characterized genomic alterations of DTCs to define their clonal relationship to matched primary tumors (PTs) and distinguish genomic features contributing to early versus late relapse.

Methods: Our study is based on a cohort of cryopreserved BM samples collected at diagnosis from 600 BC patients treated between 2006 and 2012 with more than 12 years of follow-up. From this cohort, we selected BM samples previously diagnosed as DTC-positive using a standardized immunocytochemistry assay. For this study, we established a workflow to detect and isolate DTCs from cryopreserved BM using the CellSearch® system. After thawing, up to 20 Mio mononuclear cells per sample were processed with CellSearch® for the detection of $EpCAM^+/DAPI^+/CK^+/CD45^-$ DTCs (CS-DTCs). Individual CS-DTCs were subsequently isolated, and their whole genomes were amplified using adapter-linker PCR. Low-pass next-generation sequencing (NGS) was performed to assess copy-number alterations (CNAs).

Results: Thus far, we detected and isolated CS-DTCs in 31/35 BM samples previously diagnosed as DTC-positive. In our initial CNA analysis, 75% of CS-DTCs displayed aberrant copy-number profiles characteristic of BC, whereas matched white blood cells showed normal genomic profiles. In one patient analyzed to date, we isolated 16 CS-DTCs demonstrating a shared clonal CNA pattern, however, individual CS-DTCs also harbored private CNAs. Additional BM samples and the corresponding PTs are currently being processed to enable direct comparison of DTCs with their matched primaries.

Conclusions: Our preliminary results demonstrate that this CellSearch®-based workflow enables reliable detection, isolation, and genomic characterization of single DTCs from long-term cryopreserved BM samples. This approach provides a robust platform for exploring clonal relationships between DTCs and PTs. The overall aim is to uncover mechanisms underlying minimal residual disease and relapse in BC.

#3763 CCR7 expression and spatial distribution in inflammatory breast cancer: A baseline characterization for therapeutic targeting.

Surbhi Shivhare[1], Caren Sanchez[1], Richard Larson[1], Lacey Dobrolecki[2], Michael Lewis[2], Jennifer Chen[3], Susanne Lin[4], Anastasiya Evdokimova[5], Daria Goncharova[5], Angela Alexander[6], Azadeh Nasrazadani[6], Rachel Layman[6], Bora Lim[6], Vicente Valero[6], Anthony Lucci[3], The MDACC Inflammatory Breast Cancer Team, Wendy A. Woodward[1]

[1]Department of Breast Radiation Oncology, UT MD Anderson Cancer Center, Houston, TX,[2]Lester and Sue Smith Breast Center, Baylor College of Medicine, Houston, TX,[3]Department of Breast Surgical Oncology, UT MD Anderson Cancer Center, Houston, TX,[4]Department of Veterinary Medicine & Surgery and Department of Translational Molecular Pathology, UT MD Anderson Cancer Center, Houston, TX,[5]BostonGene Corporation, Waltham, MA,[6]Department of Breast Medical Oncology, UT MD Anderson Cancer Center, Houston, TX

Purpose: Inflammatory breast cancer (IBC) is a rare, highly aggressive subtype marked by rapid proliferation, extensive angio-/lymphangiogenesis, and early metastasis. CCR7, a chemokine receptor involved in immune trafficking, promotes tumor migration toward lymphatics via CCL19/CCL21. This study provides an integrated genomic, protein, spatial, and functional evaluation of CCR7 in IBC to assess its therapeutic potential.

Methods: Clinical analysis used genomic data from HR+ HER2- and TNBC IBC compared with subtype-matched non-IBC. CCR7 expression was assessed in IBC and non-IBC cell lines by immunoblotting; ligand secretion (CCL19/CCL21) in tumor and stromal cells was measured by ELISA. CCR7 localization was evaluated using subcellular fractionation and IF, along with testing of a CCR7-blocking antibody. Multiplex IF was performed on BCM PDX models representing distinct CCR7 genomic and protein states. Functional studies included the CCR7 antagonist Navarixin, CCL19/21-induced migration assays, and generation of CCR7 CRISPR knockout clones.

Results: CCR7 CNAs occurred in both IBC and non-IBC but did not correlate with mRNA or protein levels. CCR7 protein was broadly expressed, with strongest membranous expression in A3250 and variable levels in IBC-3, SUM-190, and SUM-149. The blocking antibody reduced membranous CCR7 only in A3250, indicating subtype-specific accessibility. IBC cell lines did not secrete CCL19/CCL21, supporting reliance on stromal ligands, which varied by coculture. Across six BCM PDXs, CCR7 was consistently expressed, whereas ligand levels were heterogeneous; MBI-117 showed high CCL19/CCL21. Spatial profiling revealed $CCR7^+$ tumor cells aligned along $Podoplanin^+$ lymphatics with $CCL21^+$ stromal cells and $CD163^+$ macrophages enriched around $CCR7^+$ emboli. Navarixin reduced proliferation in IBC3 and SUM-190 by 96h, and CCL19/21 enhanced migration in A3250 and SUM-149. CCR7-KO SUM-149 clones were generated, with functional analyses ongoing.

Conclusion: CCR7 expression in IBC is independent of copy number and supported by a ligand-rich microenvironment that positions $CCR7^+$ tumor cells along lymphatics. Integrated genomic, spatial, and functional data support CCR7 as a therapeutic target in IBC, with studies ongoing.

#3764 Dynamic regulation and physical interaction of IGF1 and CYR61 in prostate cancer cells.

Greisha L. Ortiz Hernandez, Carmina Patrick, Jessica Wu, Susan L. Neuhausen

Population Sciences, Beckman Research Institute of The City of Hope, Duarte, CA

Prostate cancer (PCa) remains a leading cause of cancer-related mortality among men, with limited treatment options for advanced disease. Cysteine-rich angiogenic inducer 61 (CYR61), a matricellular protein with an insulin-like growth factor-binding domain, has been implicated in tumorigenesis, yet its role in PCa progression is incompletely understood. Given our published studies validating that silencing CYR61 impaired proliferation, migration, and PI3K/AKT signaling, while PI3K/AKT inhibition abrogated insulin-like growth factor-1 (IGF1)-induced CYR61 expression and proliferation, and the established involvement of IGF1 in PCa and its association with therapy resistance, this study specifically investigated the molecular interplay between IGF1 and CYR61. Our studies by confocal microscopy revealed that IGF1 induces nuclear CYR61 expression and translocation in a time-dependent manner across PC3, 22Rv1, and LNCaP cells, with maximal expression observed at 24 hours post-treatment. Immunoprecipitation assays also demonstrated a physical interaction between IGF1 and CYR61 in PC3 and HEK293T cells, suggesting direct or complex-mediated binding. These findings position CYR61 as a critical effector of IGF1 signaling and raise the possibility of extracellular interactions that modulate PCa progression. Ongoing studies using the AVEXIS system aim to define the IGF1-CYR61 interactome and identify additional binding partners, which may uncover novel therapeutic targets and biomarkers. Future directions include mapping these interactions in tumor microenvironment compartments and exploring combinatorial strategies integrating CYR61 inhibition with IGF1R or PI3K inhibitors to curb aggressive PCa.

#3765 Cost-effective targeted DNA mutation and gene expression change profiling in circulating tumor cells using new Droplet Digital PCR technologies.

Yoon-Tae Kang, Srikanth Perike, Adam Corner, Cynthia Shu, Andrew Prantner, Nathan Knapp, David Coe, Elizabeth Jordan Dreskin

Bio-Rad Laboratories, Hercules, CA

Introduction: Liquid Biopsies provide a less invasive method for cancer diagnosis and prognosis when compared to conventional tissue biopsies. Over the past two decades, fragmented tumor derived DNA (ctDNA) found in blood has been studied extensively and shown to contain tumor-specific gene mutations and distinct fragment patterns compared to non-tumor cfDNA, which are now employed to monitor the molecular status of patients with cancer. Similarly, Circulating tumor cells (CTCs) have recently evolved as promising biomarkers whose existence and quantity in blood have shown a close correlation to disease progression and recurrence potential. While initial studies on CTCs relied on their protein marker expression and enumeration, recent CTC studies at the molecular level revealed genomic mutations in Estrogen receptor 1 (ESR1) for breast cancer, and epidermal growth factor gene (EGFR) across various cancers. Along with ctDNA studies, detection of mutations and gene expression changes in CTCs can offer additional insights into drug efficacy evaluations and prognosis. However, the rarity of CTCs and lack of streamlined protocols utilizing cost-effective technologies for clinics present a crucial challenge.
Methods: For lung cancer, three non-small cell lung cancer cell lines with different EGFR mutations were prepared. For breast cancer, one epithelial breast cancer cell line (MCF7) with/without acquired tamoxifen resistance was prepared. Each CTC sample was prepared by spiking cancer cells into a total of 7.5 ml of whole blood from healthy donor at a concentration of up to 100 cells/ml. The Genesis Cell Isolation System efficiently captured CTCs based on size and deformability and the enriched CTCs were subsequently processed for simultaneous DNA and RNA extraction using the SingleShot Cell Lysis Kit. Either extracted gDNA or total RNA was used for mutation detection using ddPCR or gene expression studies upon cDNA synthesis, respectively. To determine the presence of specific EGFR/ESR1 mutations within the genomic DNA of captured cells, Droplet Digital PCR was performed using assays for EGFR/ESR1 mutation variants as well as known mutations PIK3CA p.E542K and GATA3 p.D336fs*17. For gene expression changes in breast cancer upon tamoxifen resistance, 6/7-multiplex gene expression assays with targeted representative genes were performed using a QX600 or a QX700, respectively.
Results: The streamlined combined protocol using the Genesis System and ddPCR facilitated sensitive detection of specific genomic DNA mutations as well as gene expression changes in CTCs upon drug treatment.Discussion and
Conclusions: ddPCR is a cost-effective approach for unlocking molecular information carried by CTCs in blood for liquid biopsy. Further studies using clinical specimens with larger sample sizes would facilitate the clinical use of the suggested protocol.

#3766 Depletion of circulating tumor cells using an automated device using non-hemolytic affinity based substrates.

Jayant Khandare[1], Yuvraj Patil[1], Prathamesh Jakka[1], Neha Mulye[1], Aditi Wadekar[1], Srusthi Parekh[1], Karan Kulkarni[1], Tulsi Yadav[1], Tanvi Deshpande[1], Harshal Padma[1], Rakshit Kamble[2], Aravindan Vasudevan[1]

[1]Actorius, Pune, India,[2]Actorius, Los Angeles, CA

Background: While 90% cases are associated with metastatic deaths, it is imperative to monitor early stage cancer patients for the presence of systemic disease to improve overall survival (OS) and PFS. In spite of complete remission, upto 25-50 % of CRC stage II-III and early breast cancer cases are known to relapse. Further, the existence of micro-tumors using radio-imaging tools is undetected due to limit of detection. Post curative intent therapies, accounting minimal residual cellular disease (MCRD), is represented by circulating tumour cells (CTCs). CTCs are known for their extravasation and invasiveness from primary sites to distant. Further they could evade immune systems, and thus there is need to design safer extracorporeal devices for the capture and depletion of CTCs especially overexpressing PD-L1. We designed an automated device to capture and remove CTCs from whole blood.
Methods: We designed an automated micro-processor operated fluidic device OncoMetastat, having cartridges for blood, reagent tubes, and a 3D-printed biocompatible spiral channel. The controller unit powers peristaltic pumps for blood circulation through the spiral channel (96 mm diameter × 6 [H] mm). It consisted an antibody and transferrin conjugated 2 mm glass beads. In addition, with 4 vibrators for micro-stirring of blood for enhanced CTC capture from 5 - 10 ml patients blood (n=54). WBC count, hemolysis and protein binding was measured. The beads were scanned for CTCs with $CK18^{+}$ve, DAP^{I+}ve with $CD45^{-}$ve) with an automated scanning ability and compared with OncoDiscover CTC enumeration platform approved by CDSCO India. We analyzed true positives, false negatives and sensitivity, specificity, PPV, NPV and accuracy.
Results: Retrospectively, 54 pan-cancer patients' blood including breast, CRC, prostate, lung were used to capture and deplete CTCs. OncoMetastat platform demonstrated capture efficiency of > 90%, compared to OncoDiscover. Auto-scanning demonstrated 100% efficiency of CTC imaging, compared to manual imaging. Leukocyte adhesion was low with anti-EpCAM and transferrin glass beads (2 ± 1 WBCs/per sample, n = 54). WBCs enumerated showed trends specific to cancer type (mean WBC count/ml of 4.9×10^6 - Breast CA, 3.9×10^6 - Rectal CA, 3.5×10^6- Prostate CA), showed decrease in WBC by 40% compared to healthy controls (mean of 6.9×10^6 WBCs/ml). Clinically insignificant hemolysis (<1%) and protein-binding (~1.5%) was noted. Vibration-assisted showed enhanced CTC sequestration (>90% cell capture efficiency. The sensitivity (94.4%), specificity (92.9%), PPV (94.4%), NPV (92.9%), accuracy (93.8%) was observed for CTC capture.
Conclusions: We showed depletion of CTCs with specificity and efficiency. Automated device demonstrate the ability to remove CTCs from whole blood as an extracorporeal device for enhancing cancer therapy outcome.

#3767 Detection of circulating tumor cells (CTCs) as a next-generation liquid biopsy for neuroendocrine tumors (NETs) by taking advantage of existing theranostic probes.

Michael Greenberg[1], Ezequiel Silva Nigenda[2], Julie Hallet[1], Omar Alawamry[1], Simron Singh[1], John Trant[2], Hon Sing Leong[1]

[1]Sunnybrook Research Institute, Toronto, ON, Canada,[2]University of Windsor, Windsor, ON, Canada

When neuroendocrine cells become cancerous, the resulting Neuroendocrine Tumours (NETs) can be challenging to detect. NETs are often asymptomatic, because they often lead to hormonal imbalances, which are associated with other diseases. In terms of biomarkers, NETs often overexpress Somatostatin Receptor 2 (SSTR2). This biomarker is the primary method of detecting and treating NETs and a specific molecule called DOTATATE is used for clinical PET scans and therapies to detect and combat this cancer in NET patients. DOTATATE compounds consist of two active components. The DOTA component is a metal chelator that carries the component detected by PET scan. The TATE component is a modified octreotate compound which binds to the Somatostatin Receptor 2 (SSTR2).Here, we offer the TATE-Cy5 probe, which takes advantage of the clinical use of DOTATATE for use in a blood test. Similar to DOTATATE, TATE-Cy5 also contains tyrosine-3-octreotate, meaning that it can to bind to SSTRs with equal effectiveness. However, instead of the DOTA chelator, TATE-Cy5 has a fluorescent Cy5 probe, which can be used to detect the presence of NETs because we hypothesize we can detect circulating tumor cells (CTCs) in patient blood samples. We predict that there are high numbers of CTCs that bind the TATE-Cy5 probe in patient whole blood samples according to disease severity.Results show that TATE-Cy5 binds to cell lines overexpressing SSTR2. Moving onto clinical samples, we also observe the presence of CTCs that bind TATE-Cy5 in whole blood samples from NET patients. We further subclassified CTCs as based on a combination of co-expressing biomarkers, CTCS that are positive for SSTR2, and tumours positive for both SSTR2 and EpCAM. With further testing, we will be able to use TATE-Cy5 to monitor patient treatment response over time.In summary, we have developed a novel and cancer specific CTC liquid biopsy that takes advantage of existing imaging probes in the form of DOTATATE. This technology has significant clinical implications because it can be used as a companion liquid biopsy for existing and emerging therapies.

#3768 Spatially resolved lineage and microenvironmental remodeling define metastatic progression in oral squamous cell carcinoma.

Chung Ji Llu[1], Hui-Wen Cheng[2], Li-Han Lin[2], Kuo-Wei Chang[3]

[1]Department of Oral and Maxillofacial Surgery, Mackay Memorial Hospital, Taipei, Taiwan,[2]Department of Medical Research, Mackay Memorial Hospital, Taipei, Taiwan,[3]School of Denstry, National Yang Ming Chiao Tung University, Taipei, Taiwan

Background: Lymph node metastasis is the strongest prognostic factor in oral squamous cell carcinoma (OSCC), yet the spatially coordinated cellular programs that drive metastatic evolution remain insufficiently defined. Conventional bulk and single-cell transcriptomic methods cannot preserve tissue architecture or resolve how malignant, stromal, and immune compartments interact *in situ*.

Methods: We performed Visium spatial transcriptomics on 20 OSCC tissue specimens, including normal epithelium, primary tumors without nodal metastasis (N^-), primary tumors with nodal metastasis (N^+), and metastatic lymph nodes. SpatialCpie was used to estimate intra-spot cellular composition, CellChat to infer intercellular signaling networks, and Monocle3 to reconstruct epithelial lineage trajectories across the metastatic continuum.

Results: Spatial mapping revealed that invasive tumor fronts contained mixed malignant epithelial, fibroblast, and immune populations, distinguishing them from more homogeneous tumor cores. Pseudotime analysis demonstrated a continuous epithelial lineage progression from normal to metastatic states, accompanied by increased epithelial plasticity and downregulation of differentiation-associated markers. Stromal profiling showed a shift toward matrix-remodeling fibroblast phenotypes positioned adjacent to invasive epithelial regions. Metastatic lymph nodes exhibited reduced cytotoxic T-cell signatures and expansion of B-lineage populations, indicating immune suppression within the metastatic niche. Integrated signaling analysis revealed a coordinated communication axis linking epithelial state transition, stromal activation, and immune remodeling during metastatic progression.

Conclusions: This spatially resolved framework identifies metastatic OSCC as a dynamically evolving multicellular ecosystem shaped by epithelial plasticity, stromal reprogramming, and immune adaptation. These findings provide mechanistic insight into the development of nodal metastasis and highlight microenvironmental features with potential biomarker and therapeutic relevance.

#3769 Predicting efficacy of curative-intent surgery in advanced gastric cancer: A biologically informed staging approach.

Yingying Wu, Zhenxin Wang, Hong Zeng, Yihong Sun, Zhaoqing Tang, Xuefei Wang

Zhongshan Hospital Fudan University, Shanghai, China

Background: Treatment strategies for advanced gastric cancer (GC) largely depend on the presence or absence of metastasis. However, a subset of patients with limited metastasis may still derive meaningful benefit from curative-intent surgery, challenging the traditional binary staging paradigm. Current assessments of metastasis rely on lesion volume and anatomical distribution, which oversimplify tumor biology. The degree to which patients with metastatic GC can benefit from surgery remains unclear. We therefore propose a serum-derived staging model that integrates systemic tumor-host interactions to define biological tumor stage and inform surgical decision-making in a biologically informed manner.

Methods: Advanced GC was stratified by metastatic burden into locally advanced GC (LAGC), limited metastatic GC (LMGC), and widely metastatic GC (WMGC). Cohort 1 included 179 patients receiving curative-intent surgery following preoperative systemic therapy (100 LAGC, 48 LMGC, 31 WMGC). Serum samples were obtained at baseline and preoperatively. Cohort 2, an independent dataset collected during a different period, included 149 patients (109 LAGC, 25 LMGC, 15 WMGC) with baseline serum samples. Systemic inflammatory profiles were characterized via Olink platform. Baseline samples from Cohort 1 served as the training set. Feature selection was performed using ordinal logistic regression, XGBoost, and SVM-RFE, followed by Elastic Net regression for model construction. Preoperative samples from Cohort 1 were used for internal validation, and Cohort 2 for external validation.

Results: Three inflammatory proteins, IL-22 RA1, HGF, and 4E-BP1, were significantly associated with metastatic burden and were incorporated into the tumor-induced perturbation score (TIPscore). Baseline TIPscore distinguished WMGC, the subgroup least likely to benefit from surgery, from LAGC and LMGC with an AUC of 0.812. Lower TIPscore was associated with improved overall survival (OS) ($p = 0.049$). In preoperative samples from Cohort 1, TIPscore outperformed conventional M0/M1 staging, increasing 1-year OS prediction AUC from 0.683 to 0.850 in advanced GC overall, and reaching 0.875 in the LMGC subgroup. Among LMGC patients receiving curative surgery, a lower post-treatment TIPscore predicted better OS ($p = 0.034$) and event-free survival (EFS) ($p = 0.015$). TIPscore was further validated in Cohort 2, achieving an AUC of 0.810 for distinguishing WMGC from LAGC and LMGC, and 0.711 for distinguishing WMGC from LMGC.

Conclusions: TIPscore is a biologically informed staging model that reframes metastatic burden as a continuous biological spectrum rather than a categorical variable. By precisely situating individual patients along this spectrum, TIPscore provides prognostic insight to guide surgical decision-making and may be particularly valuable in ambiguous clinical contexts such as LMGC.

#3770 DNA methylation-based model predicts occult lymph nodal metastasis for resectable NSCLC patients.

Long Jiang[1], Xing Li[2], Yanhua Chen[2], Changbin Zhu[2], Ziming Li[1]

[1]Shanghai Lung Cancer Center, Shanghai Chest Hospital, Shanghai Jiao Tong University School of Medicine, Shanghai, China,[2]Amoy Diagnostics Co., Ltd., Xiamen, China

Background: Patients with non-small cell lung cancer (NSCLC) harboring pathologic lymph nodal metastases (LNDM) (pN1-2) have substantially higher recurrence risks. However, 10~15% of patients staged as cN0 via preoperative CT have lymph node involvement confirmed by pathologic evaluation. Endobronchial ultrasound-guided transbronchial needle aspiration (EBUS-TBNA) improves preoperative nodal staging, but extensive sampling of multiple stations increases procedural risk and complexity. Thus, exploring LNDM biomarkers are needed. This was aimed to develop a tumor DNA methylation-based model to predict intrathoracic nodal metastases indicating more precised patient population receiving EBUS-TBNA evaluation.
Methods: Primary tumor tissue and paired preoperative plasma from 68 patients with resectable NSCLC was retrospectively collected (pN0=24, pN1=24, pN2=20, all pN2 were mediastinal nodal metastases). Tumor DNA was extracted and subjected for enzyme conversion and methylation sequencing (EM-Seq). Differentially methylated CpG sites associated with nodal involvement were identified by comparing pN0 vs pN1/2 (Wald test). A lymph-node-metastasis methylation score was constructed using LASSO regression and its performance assessed by ROC analysis. Promoter-localized differentially methylated sites were subjected to Gene Ontology (GO) and pathway enrichment analyses. Further validation of this model on preoperative plasma cell-free DNA is undergoing.
Results: Differentially methylated 6,745 CpG sites between pN0 and pN1/2 tumors ($p<0.05$) were disclosed. An 8-CpG methylation score discriminated patients with and without nodal metastases with an AUC of 0.962 (cut-off 2.0; sensitivity 1.0; specificity 0.841). The methylation score increased with pathologic nodal stage (median pN0=0.76, pN1=2.74, pN2=3.30, pN1 vs pN0 $p<0.01$, pN2 vs pN0 $p<0.01$, pN2 vs pN1 $p=0.26$). No correlation to primary tumor size ($r=-0.08$, $p=0.505$) was found, making it only LNDM relevant. Among differentially methylated loci, 28% (1,872 sites) were located in promoter regions. In node-positive tumors, enriched GO terms included epithelial cell polarity and cell-cell adhesion, whereas node-negative tumors showed enrichment of phenylalanine, tyrosine, and glycine/serine metabolism.
Conclusions: A DNA methylation model strongly associated with the presence and extent of intrathoracic nodal involvement was developed for resectable, cN0 NSCLC. This model has the potential to preoperatively identify patients who most warrant EBUS-TBNA. Its predictive performance in pre-treatment plasma is being validated, and plasma-based results will be presented at the AACR.

#3771 Monitoring tumor dynamics through circulating cancer stem cells in colorectal cancer patients.

Monika Pizon[1], Dorothea Schott[1], Ulrich Pachmann[1], Katharina Pachmann[2]

[1]Laboratory Dr. Pachmann, Bayreuth, Germany,[2]Laboratory Dr Pachmann, Bayreuth, Germany

Background:
Colorectal cancer (CRC) remains one of the most commonly diagnosed and lethal malignancies worldwide. Tumor recurrence and metastasis are major determinants of patient survival. Circulating cancer stem cells (cCSCs), a rare subpopulation of tumor cells present in peripheral blood, are believed to drive tumor growth, metastasis, and therapy resistance. While tumorsphere culture has been used to identify cancer stem cells from primary tumors or cell lines, we have established an effective method for detecting and characterizing circulating cancer stem cells in the blood of CRC patients.
Methods:
Metastatic and non-metastatic CRC patients were included in this study. For the detection of circulating cancer stem cells, we used a functional assay for tumorsphere formation (stemtrac®). Immunofluorescence and qRT-PCR were employed to assess surface marker expression and pluripotency-associated genes. Additionally, we report a case of a 40-year-old man with metastatic KRAS-positive CRC, who was longitudinally monitored using both circulating epithelial tumor cell (CETCs/CTCs) and cCSC analyses in correlation with clinical and imaging findings.
Results:
Patients with metastatic disease exhibited a significantly higher number of tumorspheres compared with non-metastatic patients (median: 48 vs. 15 spheres per 100 µl blood), suggesting a correlation between tumorsphere count and disease stage. Tumorspheres showed high expression of EpCAM and CD133, elevated ALDH1 activity, and upregulation of pluripotency genes such as SOX2, OCT4, and NANOG. No sphere formation was observed in healthy controls (n = 50). In the case study, fluctuations in CETCs/CTCs and cCSC levels reflected treatment response and disease activity, with sustained increases preceding clinical or radiological evidence of progression.
Conclusion:
This study demonstrates that tumor stem cells can be detected in peripheral blood from both metastatic and non-metastatic CRC patients. The number of tumorspheres derived from circulating cancer stem cells serves as an independent indicator of metastatic potential. Serial monitoring of CETCs/CTCs and cCSCs provides a non-invasive and dynamic tool for evaluating treatment efficacy and identifying early disease progression. A deeper understanding of the biology of circulating cancer stem cells may facilitate the development of more effective and personalized therapeutic strategies for colorectal cancer.

#3772 Exploring gene mutations of circulating tumor cells by Oxford nanopore adaptive sequencing implemented with a newly developed bioinformatic pipeline.

Ta-Hsien Lee[1], Jin-Ru Wang[2], Shiuan-Ru Hou[2], Ju-Chien Cheng[3], **Ching-Ping Tseng**[2]

[1]Department of Clinical Laboratory, Tri-Service General Hospital Penghu Branch, Penghu, Taiwan,[2]Department of Medical Biotechnology and Laboratory Science, Chang Gung University, Taoyuan, Taiwan,[3]Department of Medical Laboratory Science and Biotechnology, China Medical University, Taichung, Taiwan

Circulating tumor cells (CTCs) represent an important and easily accessible biological material for monitoring treatment response and early detection of patients with cancer. In this study, we aimed to develop a precision workflow combining immunomagnetic bead- and negative selection-based enrichment of CTCs with the Nanopore adaptive sequencing technology to detect mutations in cancer-relevant genomic regions and to understand the intrinsic properties of CTCs. PowerMag system which we developed in our previous studies was used to deplete leukocytes and enrich CTCs from blood sample followed by whole genome amplification. The amplified DNA was subject to Nanopore adaptive sequencing using the Oxford Nanopore GridIon device and the BED file to define 76 common cancer gene mutation target regions. A bioinformatic analytical platform was also developed in-house for efficient extraction of high-confidence reads. The confidence for the presence of mutated nucleotides was determined by implementing a logistic calculation based on the quality score of the indicated nucleotides. The workflow has been validated by using human peripheral blood leukocytes as the biological source of DNA. In addition, preliminary analysis of OECM-1 oral cancer cells spiked into human peripheral blood also reveals that CTCs enrichment followed by adaptive sequencing and the use of analytical tools developed in-house are applicable to identify cancer-associated gene mutation even with a few numbers of reads spanning the gene mutation regions. Taken together, the combined platform represents a new tool for real-time, cost-effective genomic profiling of rare CTCs, with potential applications in the clinical management of cancer patients.

#3773 ROR1 and PMEPA1 as combined predictive biomarkers for metastasis in triple-negative breast cancer: Multi-omics and clinical validation.

Hao Wang[1], **Linze Xu**[1], Song An[2], Yang Liu[1]

[1]Department of Hepatobiliary Cancer, Liver Cancer Center, Tianjin Medical University Cancer Institute & Hospital, National Clinical Research Center for Cancer, Key Laboratory of Cancer Prevention and Therapy, Tianjin's Clinical Research Center for Cancer, TianJin, China,[2]Department of Breast Oncology Surgery, Tianjin Cancer Hospital Airport Hospital, TianJin, China

Background: Triple-negative breast cancer (TNBC) remains the most aggressive subtype of breast cancer, characterized by high heterogeneity, early metastasis, and lack of effective targeted therapies. Early identification of high-risk patients is crucial for improving outcomes. Previously, we identified receptor tyrosine kinase-like orphan receptor 1 (ROR1) as a TNBC-specific extracellular vesicle (EV) marker capable of capturing tumor-derived EVs (2025 AACR #Abstract 2005). Building on this foundation, we conducted an integrated multi-omics and clinical validation study to uncover novel ROR1-associated molecules that could enhance the prediction of metastatic potential in TNBC.

Methods: EV proteomics were used to confirm TNBC-specific markers. scRNA-seq (GSE176078) and TCGA-BRCA bulk RNA-seq data were analyzed. hdWGCNA identified hub genes in epithelial-mesenchymal transition (EMT)-high invasive TNBC cells. LASSO, support vector machine (SVM), and random forest algorithms were applied to screen EMT-related metastasis genes. TCGA data were split (7:3) into training and validation sets, and AutoGluon machine learning with undersampling constructed the metastasis prediction model. For clinical validation, TNBC patients were categorized by metastatic status, immunofluorescence staining of PMEPA1 and ROR1 was performed on TNBC tumor tissues, with CKpan distinguishing tumor parenchyma from stroma.

Results: Proteomic and computational analyses identified PMEPA1 as a key metastasis-associated gene, showing the highest predictive performance (AUC) in the WeightedEnsemble-L2 model. In clinical samples, patients who later developed distant metastases exhibited significantly higher PMEPA1 and ROR1 expression than those who remained metastasis-free. Co-localization analysis showed both proteins enriched in $CKpan^{+}$ tumor regions. The combination of ROR1 and PMEPA1 improved predictive performance for TNBC metastasis compared to either marker alone, consistent with bioinformatics predictions. These findings suggest cooperative involvement of ROR1 and PMEPA1 in TNBC progression.

Conclusions: PMEPA1 is identified as a novel ROR1-associated molecule involved in TNBC metastasis. Co-expression of PMEPA1 and ROR1 serves as a robust predictor for metastatic progression. Integrating machine learning-based transcriptomic modeling with clinical validation provides a promising framework for early metastasis risk stratification in TNBC. Ongoing studies aim to elucidate the ROR1-PMEPA1 signaling axis as a potential therapeutic target.

Research Sponsor: National Natural Science Foundation of China (No. 82202603).

#3774 Genomic landscape of acute myeloid leukemia in an African ancestry cohort: A pilot study.

Oluyemi Akinloye[1], Olayiwola Akianji Popoola[1], Olatunde Olugbenga Fakoya[1], Stella Samson Rwazuala[2], Nneka Nwanyiaru Osobukola[1], Michael Forster[3]

[1]Center for Genomics of NCDs and Personalized Healthcare (CGNPH), University of Lagos, Lagos, Nigeria,[2]Department of Haematology, Muhimbili University of Health and Allied Sciences, Dr es Salaam, Tanzania, United Republic of,[3]Department of Clinical Molecular Biology, University of Kiel, Kiel, Germany

Introduction: Acute myeloid leukemia (AML) is a diverse hematologic cancer that is distinguished by the uncontrolled growth and improper development of immature clonal myeloid cells. AML patients' age, performance status, comorbidities, genetics, and other clinical characteristics unique to leukemia, such as molecular classification, all influence their prognosis.
Methods: In a pilot mixed African sample (Tanzania and Nigeria), we explore and identify genomic mutations and their possible influence on the clinical outcome of AML in an African Ancestry population. A total of six participants were recruited for the pilot study: n=4 (67%) from Tanzania and n=2 (33%) with an age range of between 14-71 years, and (2)33% female and (4)67% females. Genomic DNA was obtained from blood samples of all participants; a DNA library was prepared with targeted selected genes associated with Leukemia and sequenced on an Illumina Next-generation sequencer.
Results: The study demonstrated numerous and diverse mutations in the African ancestry population. While CEBPA and BTK show 100% mutation, STAG2, CALR, BRAF, NOTCH1, and ZRSR2 demonstrated the lowest mutation (17%) in AML. A missense mutation predominates in
CSF3R, NRAS, BRAF, ASXL1, BTK, and CBL, while CALR and NOTCH1 had only in-frame deletions. In-frame driver mutations were found in FLT3 AML_3, while FLT3 and NOTCH1 were found only in AML_4. All samples had a mutation in SETBP1, CEBPA, and BTK. Pathogenic mutations were detected with a frequency of 67% in FLT3, 33% in NRAS and 17% in BRAF, NOTCH1, and CALR. The NRAS mutations identified in this study have been associated with cancers other than AML and stand out in our cohort, as both genetic modifiers of AML biology and therapeutic targets. BRCA1 and TP53 are the most common pathogenic mutated variants in the TCGA dataset. They both show robust therapeutic targeting potential.
Conclusions: The molecular signature identified in this African Ancestry population demonstrated genomic diversity in the African Ancestry population. Some of the genomic variations identified in this study are rarely documented in AML (NRAS; Gln61His, Gly13Asp: BRAF Val600Glu, Val640Glu). This is an indication of the need to review the genomic criteria for the diagnosis and management of AML, especially with more comprehensive data of the African Ancestry population. We describe various mutated genes with their potential therapeutic targets in AML, including DASATINIB (CBL), which shows promise as a therapeutic target for AML in the African Ancestry population. This study provides a basis for committing resources to a larger cohort and further exploring the genomic diversity and variants in an African Ancestry population.
Keywords: Acute Myeloid Leukemia: African Ancestry Population: Mutations Diversity and Variants: Therapeutic Targets

#3775 Integrated CTC analysis to characterize tumor progression and enable broad multi-omics biomarker platforms for next-generation cancer Therapeutics.

Hyoyong Kim[1], Sehyung Pak[2], Dajeong Lee[3], Seung Hwan Son[3], Giho Seo[3], Kangwon Jang[1], Byung Hee Jeon[2]

[1]Cytogen, Inc., Seoul, Korea, Republic of,[2]CytoGen Inc., Seoul, Korea, Republic of,[3]Humic Inc., Seoul, Korea, Republic of

Background: Circulating tumor cells (CTCs) offer a minimally invasive approach to evaluate tumor progression, metastatic potential, and therapeutic response. CytoGen's SMART BIOPSY™ platform, based on high-definition HDM Chip technology, enables sensitive CTC capture from non-clinical and clinical samples. Establishing the translational value of CTC dynamics in non-clinical efficacy studies is essential for developing biomarkers that can support clinical trial design and IND filing.
Methods: To investigate the relationship between CTCs, tumor burden, and metastasis, xenograft models were generated using both non-metastatic and metastatic human cancer cell lines. Blood samples were collected longitudinally during tumor growth and after therapeutic intervention. CTCs were isolated using the SMART BIOPSY™ platform and evaluated by immunofluorescence (IF) to enumerate total CTCs and quantify target-marker-positive CTC populations. Tumor size and metastatic progression were assessed through imaging and necropsy to determine correlations with CTC dynamics.
Results: IF-based analysis demonstrated a clear correlation between CTC counts and tumor burden, with metastatic models consistently yielding higher CTC numbers than non-metastatic models. Importantly, therapeutic treatment that led to tumor reduction produced a significant decrease in target-marker-positive CTCs, indicating that SMART BIOPSY™ sensitively reflects pharmacodynamic changes. These findings validate the platform's reliability for monitoring tumor progression and early treatment response in non-clinical efficacy studies.
Conclusions: While this study focused on IF-based CTC characterization, the SMART BIOPSY™ platform is fully compatible with a broad multi-omics workflow, including scRNA-seq, FISH, NGS, immunofluorescence panels, and proteomics, enabling comprehensive biomarker discovery for metastasis and drug resistance. The translational insights obtained from non-clinical CTC analyses can be directly leveraged in IND filing, supporting patient stratification strategies and pharmacodynamic monitoring in early-phase clinical trials. Collectively, SMART BIOPSY™ provides a robust bridge that connects non-clinical efficacy studies with clinical drug development, establishing a versatile and expandable platform for next-generation oncology therapeutics.

#3776 Methodology and clinical validation of a centrifugation-free microfluidic isolation platform for circulating tumor cell clusters in cancer patients.

Jason Chia-Hsun Hsieh[1], Pei-Hung Chang[2], Tzu Keng Chiu[3]

[1]Chang Gung Memorial Hospital at Linkou, Taoyuan, Taiwan,[2]Chang Gung Memorial Hospital at Keelung, Taipei City, Taiwan,[3]Chang Gung University, Taoyuan, Taiwan

BACKGROUND: Circulating tumor cell (CTC) clusters are aggregates of tumor cells found in the peripheral blood and are typically linked to unfavorable clinical outcomes. However, current technologies capable of isolating, counting, or culturing these clusters without prior blood processing remain limited.
METHODS: We developed a microfluidic single-cell-picking system that enables isolation of cells without sample preparation or centrifugation, thereby preserving their native morphology and viability. Unlike conventional centrifugation or bead-based enrichment—which often compromises fragile clusters—this platform combines real-time fluorescence-activated droplet extraction with coordinate-guided picking to selectively retrieve single cells and intact clusters for downstream multi-omics investigation.
RESULTS: The system demonstrated a linear recovery efficiency of 93% ($R^2 = 0.9985$) and sustained higher levels of cell viability and metabolic function compared with magnetic bead-based techniques. In clinical testing, it distinguished cancer patients from healthy individuals based on CTC and CTC-cluster counts, underscoring its value for liquid biopsy applications and precision oncology.
CONCLUSION: This proof-of-concept work indicates that a gentle, preprocessing-free microfluidic strategy can effectively isolate and characterize both single cells and intact clusters, offering insights into metastatic biology and enhancing the potential of clinical diagnostic tools.

#3777 Spatial co-elevation of IGF1R and STMN1 associates with metastatic progression in osteosarcoma.

Piaopiao Luo, Xiaoqian Ma, Tairan Wang, Yiqing Wang, Xiang Nan

Anhui Medical University, Hefei, China

Background: Osteosarcoma metastasis remains the leading cause of patient mortality, and current therapeutic strategies offer limited benefit for metastatic disease. Identifying metastasis-associated signaling programs is essential for developing more effective interventions.
Methods: We integrated single-cell RNA sequencing, spatial transcriptomics, ligand-receptor interaction analysis, and functional assays to define molecular programs associated with osteosarcoma progression. Clinical cohorts were used to evaluate associations with metastasis and survival. In vitro and in vivo models were applied to validate mechanistic insights and therapeutic response.
Results: High IGF1R and STMN1 expression strongly correlated with distant metastasis and poor prognosis. Single-cell communication analysis revealed enhanced crosstalk between $STMN1^{+}$ osteosarcoma cells and cancer-associated fibroblasts (CAFs), predominantly driven by IGF-mediated signaling. Spatial transcriptomics confirmed the co-localization and coordinated upregulation of IGF1R and STMN1 in metastatic niches. Functional assays demonstrated that stromal IGF1/IGF2 activation of IGF1R increases STMN1 expression, and stronger spatial co-elevation of these molecules reflects enhanced coordination that facilitates tumor dissemination. Dual targeting of IGF1R and STMN1 significantly suppressed osteosarcoma invasion and metastatic outgrowth in both in vitro and in vivo models.
Conclusions: This study identifies the IGF1R-STMN1 axis as a mechanistically coherent and spatially reinforced driver of osteosarcoma metastasis. The spatial co-elevation of IGF1R and STMN1 marks metastatic niches and represents a promising therapeutic vulnerability, offering new avenues for improving outcomes in osteosarcoma.

#3778 Circulating tumor cell based *ex vivo* platform for characterizing circulating hybrid cell dynamics in multiple cancer types.

Chia-Liang Yen, Wan-Syuan Jian, Ting-Chun Liu, Pei Yu Chen, Shih-Pei Wu, Po-han Chen

CancerFree Biotech, Jersey City, NJ

Circulating hybrid cells (CHCs) arising from tumor-leukocyte fusion may contribute to metastasis and therapy resistance through enhanced DNA repair, immune evasion, and acquired migratory capacity. However, the prevalence, expansion dynamics, and clinical significance of CHCs across cancer types remain poorly characterized.Circulating tumor cells (CTC)-enriched samples from patients with breast cancer, NSCLC, and colorectal cancer were analyzed through extended ex vivo culture. CHCs were identified by dual pan-cytokeratin and CD45 immunofluorescence combined with morphological criteria. An AI-assisted image analysis platform is being developed for automated CHC quantification and characterization. A subset underwent parallel culture with cisplatin to assess chemoresistance and clinical correlations with treatment history and disease status were evaluated. Initial validation demonstrates reliable discrimination between immune cells and non-immune cells (potential CTCs/CHCs), enabling systematic quantification. Dual immunofluorescence staining revealed distinct CHC populations characterized by co-expression of epithelial (pan-CK^+) and hematopoietic ($CD45^+$) markers with large cell size. CHCs were rarely observed in early culture across all cancer types but became prominent by extended culture, indicating progressive enrichment over time. Complete quantitative analysis with statistical validation is ongoing. These findings establish extended ex vivo culture as a platform for investigating CHC biology, assessing drug sensitivity, and determining clinical relevance.

#3779 Plasma exosomes identify metastatic potential in early stage melanoma.

Lauren Emily Miller

Cell Biology & Physiology, Brigham Young University, Provo, UT

Exosomes are emerging as key players in cancer progression, facilitating local and distant interactions that contribute to tumor metastasis. Survival with malignant melanoma rapidly decreases following metastatic spread. Patients with a diagnosis of metastatic melanoma experience a five-year survival rate which decreases from 91.3% (no metastasis) to 16%. It is imperative that early detection of metastatic melanoma is implemented to improve survival rates. Known as “messengers of metastasis”, exosomes provide a reflection of their cell of origin, unveiling critical insights into tumor microenvironment maintenance and metastatic behavior. Using stage I patient samples with metastatic melanoma as well as a mouse model, we isolated exosomes from the local environment, such as the primary tumor, as well as through the bloodstream. From nanoparticle analysis, exosome concentration differed within the localized and systemic environments among stage I patients, further supporting our understanding of the heterogeneity among patient tumors, despite being classified in the same stage of cancer. Proteomic analysis of exosomes with mass spectrometry conveyed stark differences in the expression of proteins found in the localized, tumor environment and those found in the systemic environment of which plasma-derived exosomes were isolated. Eighteen proteins with known metastatic characteristics were statistically found to be uniquely expressed in the bloodstream or in the primary tumor. Interestingly, plasma-derived exosomes containing metastatic proteins were found in the patients with stage I melanoma. These proteins may serve as an early indicator of metastatic melanoma with further studies.

#3780 The role of KRT10 in cancer brain metastasis.

Bo Chen[1], Liyang Zhang[2], Karrie M. Kiang[3], Gilberto Ka Kit Leung[4]

[1]The University of Hong Kong, Hong Kong, Hong Kong,[2]Xiangya Hospital Central South University, Hong Kong, Hong Kong,[3]The University of Hong Kong, Hong Kong, China,[4]Univ. of Hong Kong, Hong Kong, Hong Kong

KRT10 is a keratin family protein that regulates epithelial structure and cellular differentiation. While the role of KRT10 in cancer metastasis has been previously reported, the specific mechanisms underlying its involvement remain unclear. In this study, we applied an integrated multi-omics strategy—including spatial transcriptomics and metabolomics—combined with in vitro assays to investigate the mechanism of KRT10 in non-small cell lung cancer (NSCLC) brain metastasis. We observed elevated KRT10 expression in NSCLC relative to normal tissues. Silencing KRT10 markedly reduced NSCLC cell migration and invasion. We then examined the tumor microenvironment and identified metastatic niches where KRT10 was concentrated. NSCLC cells interacted with pro-metastatic neutrophil extracellular trap (NET) DNA via KRT10, and the specific DNA sequences involved were subsequently confirmed. The predictive ability of KRT10 in metastasis was also explored. Overall, inhibiting KRT10 could serve as a potential therapeutic strategy to inhibit NSCLC cell brain metastasis.

#3782 High-sensitivity CD19⁺ cell enrichment enables rare mutation detection and MRD-focused liquid biopsy in chronic lymphocytic leukemia.

Yasser Abdelrahman, Junmei Wang, Yue Zhang, Pan Du, Binggang Xiang

Predicine, Inc., Hayward, CA

Background: Accurate TP53 mutation detection is critical for clinical trial enrollment and MRD monitoring in chronic lymphocytic leukemia (CLL), as TP53 disruption drives treatment resistance and guides eligibility and stratification in most CLL trials. Patients with TP53-aberrant disease are typically excluded from chemoimmunotherapy-based protocols and redirected to targeted-agent or high-risk studies, making reliable TP53 testing essential. However, targeted therapies can markedly suppress circulating CLL cells, reducing tumor fraction and compromising assay sensitivity. In line with the 2024 ERIC TP53 testing update recommending CD19⁺ B-cell enrichment for low-lymphocyte-count samples (≤10×10^9/L), Predicine developed and validated an immunomagnetic CD19⁺ enrichment workflow optimized to isolate rare CLL circulating tumor cells from whole blood under low-burden conditions.
Methods: Whole-blood samples were processed using an anti-CD19 immunomagnetic capture system. Because bead binding masks CD19 epitopes, enriched cells were quantified by flow cytometry using CD20 as a surrogate marker. Performance was evaluated across key analytical metrics, including cell viability, purity, ambient-temperature stability, intra- and inter-assay precision, and cross-site concordance. The workflow's impact on mutation detection was assessed using MEC-1 spike-in controls and CLL patient samples by comparing TP53 variant allele frequencies (VAFs) before and after enrichment. Refinements were implemented to minimize cell loss and erythrocyte carryover, ensuring scalability for clinical trial environments.
Results: The assay consistently yielded high-quality CLL cells with a median viability of 97.7% and substantially increased the tumor-cell fraction from 10.3% in PBMCs to 79.6% post-enrichment. B-cell enrichment was successful from whole blood stored at room temperature for at least four days. Precision studies demonstrated strong intra- and inter-assay reproducibility, and results were concordant across independent testing sites. Importantly, Enrichment significantly improved the sensitivity of mutation detection. In MEC-1 spike-in samples, the median TP53 VAF increased by 3.6-fold, while the CD19⁺ cell frequency increased by over 4-fold, highlighting robust tumor cell recovery and an enhanced signal-to-background ratio for NGS.
Conclusions: Predicine's validated CD19⁺ enrichment workflow enables efficient, reproducible recovery of rare CLL CTCs and fully aligns with ERIC 2024 recommendations for tumor-cell enrichment at low lymphocyte counts. This approach supports accurate TP53 mutation assessment under low-burden conditions and provides a trial-ready liquid-biopsy solution for MRD monitoring, early relapse detection, and biomarker-guided clinical trial enrollment in CLL.

: Combination Immunotherapies
Poster Session

#3786 Peripheral immune signature of dostarlimab in addition to standard of care definitive radiation in patients with medically inoperable endometrial cancer.

Liyun Chen[1], Rachel Furuya[2], Linda Odibo[2], Lulu Sun[3], David Mutch[2], Carolyn McCourt[2], Matthew A. Powell[2], Julie K. Schwarz[1], Jessika A. Contreras[1], Premal H. Thaker[2], Stephanie Markovina[1]

[1]Department of Radiation Oncology, Washington University in St. Louis, St Louis, MO,[2]Department of Gynecologic Oncology, Washington University in St. Louis, St Louis, MO,[3]Department of Pathology, Washington University in St. Louis, St Louis, MO

Upfront surgical staging is considered standard of care for patients with localized endometrial cancer. However, for patients with significant comorbidities surgery may be high risk or inadvisable. These patients can undergo definitive radiation therapy (RT) delivered with brachytherapy (BT) with or without external beam RT (EBRT). The tolerability and potential benefit of immunotherapy in this patient cohort is unknown. We performed a prospective Phase I trial of dostarlimab in conjunction with definitive RT for patients with medically inoperable endometrial cancer. Ten patients were enrolled. Dostarlimab was administered three weeks prior to the start of RT and then concurrently with RT for three cycles. Here we report the dynamics of circulating immune profiles to identify potential treatment-predictive biomarkers. Longitudinal analysis of paired peripheral blood mass cytometry (CyTOF) and soluble protein analytes (ELISA) was performed at baseline, on- and post-treatment timepoints. One cycle of neoadjuvant dostarlimab prior to RT was associated with increased serum type I interferon-induced chemokines (CXCL9, CXCL10, CXCL11) and IL-2 family cytokines (IL15, IL21), pivotal for immune cell activation and adaptive immune response. While the abundance of T cell populations in PBMCs remained mostly unchanged, effector memory CD4 and CD8 T cells had increased expression of Ki-67 and granzyme B, indicating a proliferative and cytotoxic phenotype. Initiation of RT was associated with multiple changes in plasma protein analytes including further increases in CXCL9/10, upregulation in inflammatory cytokines IL-1 and TNF, as well as cytokines with tumor-promoting potential CCL4, CCL7, and G-CSF. T cells expressing granzyme B and activation markers (CD38, HLA-DR) remained elevated, indicating sustained functional potential. CD11c+ DCs, monocytes, and Treg cells were also increased after RT. Notably, patients treated with BT+EBRT (n=3) compared to those with BT (n=7) had higher increase in DCs and monocytes as well as overall changes in cytokine expression during treatments, such as increased IL4 and IL10 associated with T cell function and decreased CCL2 and CXCL13. At 6-week post-treatment, cytokines elevated from baseline persisted in patients treated with BT+EBRT while less variations in cytokine profiles were observed in the group without EBRT. Lastly, we observed a sustained decrease in PD-1+ T cells after 1 cycle of dostarlimab but an increased frequency of LAG-3+ or Tim-3+ T cells at cycle 2 and 3 of dostarlimab with RT.
Taken together, the circulating immune profile demonstrated an association between the baseline and on-treatment immune activation signature with dostarlimab in addition to RT, highlighting the potential of this combination regimen to enhance therapeutic efficacy in patients with inoperable endometrial cancer.

#3787 The safety of PARP inhibitors combined with immune checkpoint inhibitors versus immune checkpoint inhibitor monotherapy: A systematic review, meta-analysis, and trial sequential analysis of randomized controlled trials.

Mus'ab Theeb Mustafa[1], Aws Khalid Abushanab[2], Ahmad Yousef Alazzam[2], Mahmoud Taysir Mousa[2], Ahmad Sa'ed[3], Noor N. Al-Bzour[4], Osama Wadah Rammaha[2], Zaher Mutaz Ashour[2], Hamza Muneer Alakhras[3], Yihea Mohammad Al-Mashaqbah[2], Ahmad Sami Othman[3], Nour Maher Mustafa[3], Renad Fawwaz Al Banawi[2], Anwaar Saeed[5]

[1]Prince Hamza Hospital, Amman, Jordan,[2]Faculty of medicine, Hashemite University, Zarqa, Jordan,[3]Jordan University Hospital, Amman, Jordan,[4]Jordan University of Science and Technology, Irbid, Jordan,[5]University of Pittsburgh, Pittsburgh, PA

Background: The combination of poly(ADP-ribose) polymerase inhibitors (PARPi) and immune checkpoint inhibitors (ICI) represents a promising strategy with potential synergistic effects. Preclinical studies suggest that PARPi-induced DNA damage may enhance tumor immunogenicity and augment the efficacy of ICI. Currently, this approach is being studied across multiple malignancies. However, the risk of additive adverse events remains a major concern. We conducted the first meta-analysis of randomized controlled trials (RCTs) to assess the safety of PARPi plus ICI versus ICI monotherapy.

Methods: We conducted a PRISMA-compliant systematic review, searching PubMed, Web of Science, and the Cochrane Library for RCTs comparing PARPi+ICI combination therapy against ICI monotherapy. The safety outcomes were serious adverse events (SAEs), immune-mediated adverse events (imAEs), treatment discontinuation, and specific treatment-related adverse events. Risk ratios (RR) and 95% confidence intervals (CI) were pooled using a random-effects model. Heterogeneity was assessed using the I^2 statistic. Finally, Trial Sequential Analysis (TSA) was performed to test the reliability of the pooled results and classify findings as conclusive, inconclusive, or suggestive.

Results: Six RCTs (DUO-E, KEYLYNK-008, ORION, SWOG 1929, MORPHEUS, and BAYOU) encompassing 1537 patients comparing PARPi+ICI with ICI monotherapy were included. The combination was associated with a significantly suggestive higher risk of SAEs (N=5; RR 1.77; 95% CI: 1.29-2.43; I^2=0%) and anemia (N=6; RR 3.27; 95% CI: 2.50-4.29; I^2=16%), neutropenia (N=5; RR 4.13; 95% CI: 2.35-7.27; I^2=18%), and significantly conclusive leukopenia (N=3; RR 3.93; 95% CI: 2.24-6.91; I^2=2%), vomiting (N=6; RR 3.47; 95% CI: 2.20-5.46; I^2=0%). Conversely, the combination led to a significantly inconclusive lower incidence of imAEs (N=3; RR 0.77; 95% CI: 0.61-0.98; I^2=0%). No significant differences were observed in discontinuation of the ICI component (N=5; RR 1.31; 95% CI: 0.85-2.02; I^2=0%, INC), diarrhea (N=6; RR 1.15; 95% CI: 0.81-1.64; I^2=5%), hypothyroidism (N=5; RR 0.77; 95% CI: 0.51-1.16; I^2=0%,), however they all were inconclusive.

Conclusions: The addition of PARPi to ICI therapy conclusively increases the risk of leukopenia and vomiting. Furthermore, our TSA found suggestive evidence for an increased risk of SAEs, anemia, and neutropenia. Conversely, while pooled analysis suggested a reduced risk of imAE, our TSA revealed this finding to be inconclusive and warrants further investigation. Similarly, the current evidence is inconclusive for the risk of ICI discontinuation or diarrhea. Based on these findings, watchful clinical monitoring and risk-benefit assessment are essential when considering this combination.

#3788 Integrated single-cell analysis identifies biomarkers associated with clinical benefit in patients with PD-L1 positive, advanced NSCLC treated with SBRT followed by atezolizumab plus tiragolumab.

Jii Bum Lee[1], Dong Kwon Kim[2], Sang Hoon Lee[2], Kyung Hwan Kim[1], Su-Jin Choi[2], Min Hee Hong[1], Byoung Chul Cho[1], Sun Min Lim[1]

[1]Yonsei Cancer Center, Yonsei University College of Medicine, Seoul, Korea, Republic of,[2]Yonsei University College of Medicine, Seoul, Korea, Republic of

Background: Prior studies have shown that the addition of SBRT to immunotherapy in oligometastatic non-small cell lung cancer (NSCLC) may improve clinical outcomes. SKYROCKET is a single-center, single-arm phase II study that evaluated whether SBRT combined with atezolizumab plus tiragolumab enhances anti-tumor efficacy in PD-L1-positive oligometastatic NSCLC.
Methods: Patients initially received SBRT to all oligometastatic sites, and subsequently received a fixed dose of 1200 mg IV of atezolizumab and 600 mg of tiragolumab every 3 weeks on day 1 of each 21-day cycle within 7 days of SBRT. The primary endpoint was investigator-assessed progression-free survival (PFS) from the start of SBRT. Secondary endpoints included PFS in PD-L1 high subset, objective response rate (ORR), overall survival (OS) and safety profile. Exploratory endpoints included characterization of immune remodeling and stromal dynamics via single-cell RNA sequencing (scRNA-seq) obtained from tumor biopsies at baseline (BL) and on-treatment (OT), and were further characterized as clinical benefit (CB, PR or SD ≥6 months) and no clinical benefit (NCB, PD or SD <6 months).
Results: A total of 41 patients were enrolled. At a median duration of follow-up of 9.8 months (IQR, 6.3-15.8), the median PFS at the start of SBRT was 9.3 months (95% CI, 6.0-NR). In patients with PD-L1 high (≥ 50%), the median PFS was 11.4 months compared to 6.4 months in patients with PD-L1 low (<50%) expression (P = 0.029, HR, 0.39, 95% CI, 0.16-0.95). Of the 39 patients with measurable lesion, the ORR and DCR was 56% and 92%, respectively. No new safety adverse events were seen with the addition of SBRT to atezolizumab plus tiragolumab. ScRNA-seq of paired BL and OT (n=3) and single-time point (n=2) identified CD8 progenitor-exhausted (T_{PEX}) and terminally exhausted (T_{EX}) subsets. CD8 T_{PEX} cells markedly expanded after treatment, with target engagement evidenced by high TIGIT and PD-1 expression in CD8 T_{PEX}/T_{EX} subsets. Pathway analyses showed enhanced T-cell activation and TCR signaling. CD4 Tregs were reduced in the CB group but increased in the NCB group. Pseudotime analysis showed T_{EM} cells in CB preferentially transitioned into $CXCL13^{+}$ helper states, while NCB skewed toward Treg differentiation. The CB group showed reduced Treg suppression and NECTIN-TIGIT signaling, whereas NCB maintained proliferative $CTLA4^{high}$/$TIGIT^{high}$ Tregs supported by ICAM/Galectin-CTLA4 pathways.
Conclusion: In PD-L1 positive oligometastatic NSCLC, atezolizumab plus tiragolumab after completion of SBRT improves PFS with manageable safety profile. Combination therapy boosts cytotoxic/helper T-cell programs in CB, whereas persistent ICAM/Galectin-CTLA4-driven Tregs underlie resistance to treatment.

#3789 Treatment with ACR-2316, a potential first- and best-in-class WEE1/PKMYT1 inhibitor, combined with anti-PD-L1 induces complete tumor regression with durable immune memory.

Taronish Dubash[1], Joelle Baddour-Sousounis[1], Amira Elbakry[1], Jessica Hopkins[1], Subodh Kumar[1], Yingchun Spring Liu[1], Ahmed Youssef[1], Kate Rappard[1], Ignacio Arribas Diez[2], Georgia Mista[2], Marc Isaksson[2], Francisco Santana[1], Luka Romero[1], Zachary Best[1], Nina Lipjankic[2], Anna-Maria Alves[1], Daphne Garcia-Lopez[1], Portia Lombardo[1], Calvin Yang[1], Emma Ahrman[2], Valentina Siino[2], Magnus E. Jakobsson[2], Helen Nilsson[2], Ayesha Murshid[1], Lei Shi[1], Caroline Wigerup[2], Michail Shipitsin[1], Joon Jung[1], David Proia[1], Kristina Masson[1], Peter Blume-Jensen[1]

[1]Acrivon Therapeutics Inc., Watertown, MA,[2]Acrivon AB, Medicon Village, Lund, Sweden

Introduction: ACR-2316 is a potent and selective dual WEE1/PKMYT1 inhibitor rationally designed using Acrivon's generative phosphoprotemics AP3 platform. Currently advancing in a Phase 1 clinical study in AP3-identified solid tumor types, ACR-2316 was engineered for superior single-agent activity and high selectivity resulting in potent DNA damage and complete tumor regression across preclinical *in vivo* models. This study demonstrates that ACR-2316 not only damages the nuclear and mitochondrial genomes, but also stimulates the innate immune system, leading to complete tumor regression and lasting immune memory in mice when combined with PD-L1 blockade.

Results: To investigate the mechanisms of immune activation by ACR-2316, we performed AP3-based proteomic profiling of xenograft tumors from ACR-2316 treated mice and observed strong upregulation of innate immune signaling pathways, including type I interferon. These findings were further validated at the cellular level, where ACR-2316 treatment led to the activation of double stranded RNA and DNA sensing machinery RIG-I, MDA5 and cGAS. Furthermore, we found evidence of mitochondrial DNA fragmentation with ACR-2316 treatment, suggesting that this may serve as an additional immune sensor.In a syngeneic colorectal cancer model, ACR-2316 monotherapy resulted in dose-dependent tumor growth inhibition. In combination with anti-PD-L1, ACR-2316 exhibited striking synergy, leading to complete tumor regression in mice. To assess the durability of this response, tumor cells were re-injected into tumor-free mice that were previously treated with the combination therapy. All animals remained tumor-free for over 200 days through four sequential tumor re-challenges, demonstrating strikingly robust and durable immune memory. To dissect the mechanism of this durable immunity, we systematically depleted key immune cell subsets in tumor re-challenged mice. While depletion of either $CD4^+$ or $CD8^+$ T cells alone did not enable tumor growth, co-depletion of both subsets resulted in tumor formation. This suggests that the immune memory generated by the combination treatment of ACR-2316 and anti-PD-L1 is co-dependent on both $CD4^+$ and $CD8^+$ T cell subsets.

Conclusions: Our findings reveal the dual role of ACR-2316 in inducing tumor intrinsic DNA damage and promoting immune activation through multiple immune sensing mechanisms, resulting in permanent immune memory co-dependent on CD4+ and CD8+ T cell subsets. This provides a strong rationale for combining ACR-2316 with immune checkpoint inhibitors in the clinical setting. ACR-2316 is in a phase 1 monotherapy trial and has already shown initial clinical activity with tumor shrinkage and a confirmed partial response during dose escalation across solid tumors predicted by our AP3 platform to be sensitive to ACR-2316.

#3790 Combined inhibition of myeloid cell PI3Kγ and regulatory T cell integrin αvβ8 promotes durable tumor suppression.

Erpei Wang[1], Giuliana Mognol[2], MOHAMMAD AMJAD[2], Hui Chen[2], Mark Paradise[2], Dean Sheppard[3], judith Varner[2]

[1]University of California, San Diego, San Diego, CA,[2]University of California, San Diego, San diego, CA,[3]University of California, San Francisco, San Francisco, CA

The immunosuppressive tumor microenvironment (TME) remains a critical barrier to effective immunotherapy. Immune suppressive myeloid cells and regulatory T cells can each prevent effective anti-tumor immune responses. The integrin αvβ8 promotes immune evasion by serving as a key activator of latent TGF-β in regulatory T cells, while the lipid kinase PI3Kγ promotes immunosuppressive signaling in myeloid cells. Genetic and pharmacological inhibition of PI3Kγ stimulates integrin αvβ8 expression on regulatory T cells both in mouse models of cancer and in patients enrolled in cancer clinical trials. Inhibition of either αvβ8 or PI3Kγ significantly suppressed head and neck tumor growth, suggesting they each play important roles in modulating anti-tumor immunity. To gain mechanistic insights into the impacts of these therapeutic approaches, we performed single-cell RNA sequencing (scRNA-seq) on HPV+ HNSCC tumors from wild-type (WT) and PI3Kγ knockout (KO) mice, with or without anti-αvβ8 treatment, to investigate the individual and combined impacts of PI3Kγ inhibition and αvβ8 blockade in the TME. RNA velocity and cell-cell communication inference analysis was performed to uncover dynamic regulatory interactions among cell populations. Antagonism of integrin αvβ8 led to increased CD8+ T cell infiltration and a reduction in TGF-β-responsive transcriptional programs. PI3Kγ inhibition promoted a proinflammatory shift in myeloid cells, characterized by diminished M2-like polarization and enhanced antigen presentation, and increased CD8+ T cell recruitment. Together combined inhibition of αvβ8 and PI3Kγ reversed T cell exclusion and promoted durable tumor suppression.

#3791 Cry1 inhibition reverses resistance to T cell-based immunotherapy by promoting anti-tumor immunity.

Tae Woo Kim[1], Oh Se Jin[2]

[1]Department of Convergence Medicine, Korea Univ. College of Medicine, Seoul, Korea, Republic of,[2]Korea university, Seuol, Korea, Republic of

T cell-based immunotherapy, including immune checkpoint blockade (ICB), has dramatically changed the paradigm of cancer treatment. However, many cancer patients do not achieve durable responses to immunotherapy, and resistance to these treatments remains a major clinical challenge. We previously showed that immune pressure imposed by immunotherapy selects for immune-resistant tumors that acquire both tumor cell-intrinsic and tumor cell-extrinsic refractoriness through NANOG-driven transcriptional upregulation of HDAC1. In this study, we identify CRY1 as a pivotal NANOG-dependent effector that integrates these refractory traits. In $NANOG^{high}$ tumor cells, CRY1 stabilizes Cyclin A and MCL1, thereby promoting cancer stem cell-like properties and resistance to cytotoxic T lymphocyte (CTL)-mediated killing, a process that depends on HDAC1-mediated epigenetic silencing of APC3 and TRIM17. In parallel, CRY1 suppresses CXCL10 expression via HDAC1-dependent transcriptional repression, leading to reduced recruitment of $CD8^+$ T cells into the tumor microenvironment (TME). Importantly, pharmacological inhibition of CRY1 synergizes with anti-PD-1 antibody treatment and adoptive CTL transfer to reduce tumor growth by converting immune-resistant tumors into an immune-sensitive state. Thus, our findings implicate CRY1 as a central molecular target for controlling $NANOG^{high}$ tumors and provide a rationale for combining CRY1 inhibitors with T cell-based immunotherapy to reverse the complex refractoriness of tumors.

#3792 EGFR promotes immune evasion and resistance to immunotherapy in *NF1* mutant melanoma.

Milad Ibrahim[1], Irineu Illa-Bochaca[2], Tara Muijlwijk[1], Ines Delclaux[2], KATHERINE VENTRE[2], George Jour[2], Shi Qiu[3], Agrima Dutt[1], Paola Angulo salgado[1], Amanda W. Lund[4], Markus Schober1[2], Iman Osman[2]

[1]NYU Langone Medical Center, New York, NY,[2]NYU Langone Health, New York, NY,[3]NYU Langone Health, NYU Langone Health, NY,[4]NYU Langone Health Perlmutter Cancer Ctr., New York, NY

Background: Immune checkpoint inhibitors (ICIs) have greatly improved survival rates in melanoma patients, including those with melanomas driven by deactivating mutations in the *NF1* tumor suppressor gene. However, primary or secondary resistance occurs in 50-60% of cases. Moreover, *NF1*-mutant melanoma patients with co-occurring *BRAF* or *NRAS* mutations generally do not respond to BRAF and/or MEK inhibitors, leaving them without effective treatment options. Gaining a better understanding of the mechanisms behind ICI resistance in *NF1*-mutant melanomas, along with identifying more effective treatment strategies, remains an unmet clinical need.

Methods: We compared melanoma cells and their surrounding cell types in 22 *NF1*-mutant and 20 *NF1* wild-type human melanoma tissues using single-cell spatial transcriptomics and highly multiplexed immunohistochemistry. We inferred communication networks between melanoma cells and the microenvironment using Cell-Chat. Finally, we tested how EGFR inhibitors affect the tumor growth and the immune microenvironment in syngeneic mouse models using flow cytometry.

Results: *NF1*-mutant melanoma cells are enriched in pathways related to epithelial-to-mesenchymal transition and immune evasion pathways mediated by significantly increased expression of *EGFR, NGFR, VEGFA, TGFB1,* and *TGFB3*. These cells are more closely associated with cancer-associated fibroblasts (CAFs), and their microenvironment contains significantly more inflammatory CAFs that are enriched in EGF signaling. Conversely, there was less CXCL9 signaling from CAFs to T cells in *NF1*-mutant melanoma microenvironment. This *NF1*-mutant immunosuppressed microenvironment results in significantly less infiltration of T cells which were also less proliferative and exhibit lower cytotoxic activity compared to *NF1* wild-type melanoma, possibly due to the reduced expression of HLA antigens on the surface of *NF1*-mutant melanoma cells. Higher levels of EGFR were detected in ICI resistant *NF1*-mutant melanoma patients and correlated with reduced antigen presentation and T cells infiltration. Pharmacological inhibition of EGFR restored antigen presentation and immune cell responses in *NF1*-mutant melanoma syngeneic mouse model, both alone and in combination with anti-PD1 antibodies.

Conclusion: Our results reveal that hyperactive EGFR signaling promotes immune evasion and immunotherapy resistance in *NF1*-mutant melanoma patients and suggest that EGFR inhibitors may improve ICI treatment outcomes in *NF1*-mutant melanomas with increased EGFR activity.

#3793 Preventing nk cell activation in the damaged liver induced by cabozantinib/pd-1 blockade increases survival in hepatocellular carcinoma models.

Satoru Morita[1], Tomofumi Ando[2], Hiroto Kikuchi[2], Atsuyo Morita[2], Tatsuya Kobayashi[2], Grace Birch[3], Ryota Tanaka[4], Aya Matsui[2], Zhiping Ruan[2], Peigen Huang[2], Alexei Hernandez[5], Erin M. Coyne[5], Sarah M. Shin[5], Robin Kate Kelley[6], Mark Yarchoan[5], Stefan Halvorsen[7], Slim Sassi[7], Mari Mino Kenudson[8], Shadmehr Demehri[4], Rizwan Romee[3], Won Jin Ho[5], Dan Duda[2]

[1]Surgery, Keio University School of Medicine, Tokyo, Japan,[2]Radiation Oncology, Harvard Medical School/Massachusetts General Hospital, Boston, MA,[3]Bone Marrow Transplant and Cellular Therapy Program, Dana Farber Cancer Center, Harvard Medical School, Boston, MA,[4]Visiting Staff, MGH/Harvard Medical School, Charlestown, MA,[5]Oncology, Johns Hopkins University School of Medicine, Baltimore, MD,[6]UCSF - University of California San Francisco, San Francisco, CA,[7]Center of Computational and Integrative Biology (CCIB), Massachusetts General Hospital and Harvard Medical School, Boston, MA,[8]Pathology, Harvard Medical School/Massachusetts General Hospital, Boston, MA

The addition of anti-VEGF antibody treatment to immune checkpoint blockade (ICB) has increased the efficacy of immunotherapy in advanced hepatocellular carcinoma (HCC). Despite an initial promise, adding multitargeted kinase inhibitors of VEGFR with ICB has failed to increase survival in HCC. To reveal the mechanisms underlying treatment failure, we studied the effects of cabozantinib/ICB using orthotopic murine HCC models with or without liver damage. We monitored tumor growth and liver function, recorded survival outcomes, and performed immune profiling studies for intra-tumoral and surrounding liver. Cabozantinib/ICB treatment led to tumor regression and significantly improved survival in mice with normal livers. However, consistent with the clinical findings, combination therapy failed to show survival benefits despite similar tumor control when tested in the same models but in mice with liver fibrosis. Moreover, preclinical and clinical data converged, showing that activating immune responses by cabozantinib/ICB treatment induced hepatoxicity. Immune profiling revealed that combination therapy effectively reprogrammed the tumor immune microenvironment and increased NK cell infiltration and activation in the damaged liver tissue. Surprisingly, systemic depletion of NK reduced hepatotoxicity elicited by the combination therapy without compromising its anti-cancer effect, and significantly enhanced the survival benefit even in mice with HCC and underlying liver fibrosis. These findings demonstrate that preventing NK activation allowed for maintaining a favorable therapeutic ratio when combining ICB with cabozantinib in advanced HCC models.

#3794 ACR246, a first-in-class 5T4 antibody-drug conjugate (ADC), showed promising anticancer efficacy in preclinical models and patient with esophageal cancer.

Xi Jiao[1], **Zhenwei Miao**[2], Na Zhuo[1], Panpan Zhang[1], Jifang Gong[1], Feng Wang[2], Yan Dai[3], Li Yang[2], Wu Yao[2], Shanhui Weng[2], Johannes Nippgen[2], Lin Shen[1]

[1]Peking University Cancer Hospital & Institute, Beijing, China,[2]Hangzhou Adcoris Biopharma Co., Ltd., Hangzhou, China,[3]SIP LifeLink Oncology Research Institute, Suzhou, China

Background: Advanced esophageal squamous cell carcinoma (ESCC) poses a significant therapeutic challenge, particularly after progression on first-line immune checkpoint inhibitors. The oncofetal antigen 5T4 represents a promising target due to its high expression in ESCC and limited presence in normal tissues. ACR246 is an investigational anti-5T4 ADC composed of a fully human IgG1 monoclonal antibody conjugated to a topoisomerase I inhibitor via a stable cleavable linker, with a drug-to-antibody ratio of 8.
Methods: Proteomic sequencing of tumor and adjacent tissues from ESCC patients was performed to compare 5T4 protein levels and estimate immune infiltration. The antitumor efficacy of ACR246 was assessed across a panel of preclinical models, including cell lines, patient-derived organoids (PDOs), and xenografts (PDXs) of gastroesophageal cancer. Its efficacy was benchmarked against a 5T4-Deruxtecan (DXd) ADC and chemotherapy in these models. 5T4 expression level in PDX and PDO tissues was assessed by immunohistochemistry (IHC) to correlate with response. The synergistic potential of ACR246 with anti-PD-1 was investigated in 5T4-positive ESCC PDO-PBMC co-cultures and a murine ESCC model expressing human 5T4, with tumor microenvironment changes analyzed by flow cytometry. A clinical case from a heavily pretreated ESCC patient is included.
Results: Proteomics confirmed significantly elevated 5T4 protein levels in ESCC tumors versus adjacent tissues. High 5T4 expression correlated with reduced infiltration of CD4+ T cells, CD8+ effector memory T cells, and dendritic cells, indicating an immunosuppressive milieu. *In vitro* studies showed that ACR246 exhibited high specificity for 5T4-expressing cancer cells and demonstrated superior activity over irinotecan in multiple gastroesophageal cancer PDOs. In PDX models of gastroesophageal cancer (n=9), ACR246 achieved significant tumor growth inhibition, with efficacy positively correlating with 5T4 expression. Remarkably, ACR246 outperformed the 5T4-Dxd ADC across these PDX models. Furthermore, ACR246 combined with anti-PD-1 showed enhanced antitumor activity in ESCC PDO-PBMC co-cultures and murine ESCC models, accompanied by increased IFN-γ+ CD8+ T cells and reduced M2-like macrophages. Finally, a 5T4 positive, anti-PD-1-refractory ESCC patient (NCT06238401) receiving ACR246 (3.6 mg/kg) achieved a confirmed partial response (cycle 4) with 51% reduction in the volume of target liver and lymph node metastatic lesions. No grade ≥ 3 treatment-related adverse events (TRAEs) were observed during the treatment period.
Conclusion: Integrated preclinical and clinical data establish ACR246 as a promising therapeutic for 5T4-positive ESCC and support its broader evaluation in other 5T4-expressing solid tumors.

#3795 Crept-618: First GalNAc-siRNA targeting CREPT reverses HCC immune evasion and synergizes with anti-PD-1.

Jianghua Li[1], **Alex Zou**[2], He Yang[1], Jiayu Wang[1], Weihua Yang[1], Zhijie Chang[3], Jun Li[1]

[1]Tsinghua University, Beijing, China,[2]UC Berkeley, Berkeley, CA,[3]Tsinghua University, Berkeley, China

Purpose: Immune checkpoint inhibitors (ICIs) achieve responses in only approximately ~20% of hepatocellular carcinoma (HCC) patients due to immunologically “cold” tumors characterized by poor T-cell infiltration. We identify CREPT—overexpressed in HCC and linked to worse survival (HR=2.722, P=0.0018) and ICI non-response (higher expression in non-responders; GSE215011, P<0.01)—as a dual driver of tumor proliferation and immune silencing. We present CREPT-618, the first GalNAc-conjugated siRNA targeting CREPT.

Experimental Procedures: CREPT expression was analyzed in TCGA, GEO, CPTAC databases and validated by immunohistochemistry in a 104-patient HCC tissue microarray. Functional roles were tested via CREPT knockdown in HCC cell lines (LM3, Huh7, Hep3B and Hepa1-6) using proliferation, migration, and invasion assays. In vivo efficacy was assessed in humanized orthotopic implantation mouse models with or without anti-PD-1 combination. The underlying mechanism was studied using RNA-seq, ATAC-seq, ChIP-seq, and scRNA-seq. CREPT-618 was tested for potency (no transfection), specificity, PK, biodistribution (Cy5/LC-MS), and GLP toxicology in mice, rats, and monkeys.

New, Unpublished Data: CREPT recruits the SIN3A-HDAC1/2 complex to the CCL5 promoter, leading to chromatin compaction (ATAC-seq) and silencing IFN-γ/IRF1-induced CCL5 transcription (ChIP-seq). CREPT loss increased CCL5 secretion (3.7-fold, P<0.001), driving CD8+ T/NK infiltration (2.8-fold, P<0.01; scRNA-seq)—prevented by CCR5 blockade, confirming CCL5 dependence. CREPT-618 achieved potent, specific silencing (IC_{50} 0.046-1.628 nM; RNA-seq/PCA validated) with liver-focused PK (Cmax ~200 μg/g, T½ ~70 h). In orthotopic HCC, monotherapy modestly suppressed growth across 3 batches (IHC target engagement confirmed), while combination with anti-PD-1 drove synergistic 78.3% tumor regression (P<0.001) and a 5.1-fold increase in cytotoxic CD8+ T cells. CREPT-618 was well-tolerated up to 100 mg/kg (rodents) and 30 mg/kg (monkeys).

Conclusion: CREPT drives HCC growth and immune evasion by repressing CCL5, blocking T-cell recruitment via the CCL5-CCR5 axis. CREPT-618—the first siRNA targeting CREPT—silences this oncogenic hub, restores CCL5 signaling, converts “cold” tumors to “hot”, and synergizes with anti-PD-1. These preclinical data will enable a first-in-human trial; preliminary human safety and CREPT knockdown data will be presented at AACR.

#3796 Targeting midkine with HBS-101 enhances chemotherapy and immunotherapy response in TNBC via immune activation and oncogenic pathway suppression.

Baskaran Subramani[1], Megharani R. Mahajan[1], Panneerdoss Subbarayalu[2], Zhenming Xu[1], Neelam Mukherjee[1], Gangadhara R. Sareddy[1], Hareesh B. Nair[3], Ratna K. Vadlamudi[1], Suryavathi Viswanadhapalli[1]

[1]UTHSA, San Antonio, TX,[2]UT Health San Antonio Greehey Children's Cancer Res. Inst., San Antonio, TX,[3]Texas Tech University Health Science center, El Paso, TX

Background: Triple-negative breast cancer (TNBC) is an aggressive subtype with high recurrence and resistance to standard therapies. Midkine (MDK), a heparin-binding growth factor that functions as a cytokine, is overexpressed in TNBC and promotes tumor progression, immune evasion, and chemoresistance. We recently developed HBS-101, as a first-in-class small-molecule MDK inhibitor and demonstrated its therapeutic efficacy in preclinical TNBC models. This study evaluates whether MDK inhibition enhances chemo and immunotherapy efficacy as well as the mechanistic understanding of combination therapy effects.
Methods: TNBC cell lines were treated with HBS-101 alone or in combination with chemotherapy (doxorubicin and paclitaxel), and assessed for viability, apoptosis, and synergy. 3D organoids derived from patient-derived xenografts (PDX) were employed to examine the ex vivo effects of combination therapy. The efficacy of HBS-101 with chemotherapy and immunotherapy (PD-L1 inhibitor) was evaluated using human and murine cell line-derived xenograft (CDX) models of TNBC respectively. In vivo, orthotopic TNBC tumors were established in immunocompetent mice and treated with combination treatments. Tumor growth, and immune cell infiltration were analyzed using xenograft models. RNA-seq was performed on HBS-101 treated cells to identify changes in immune and apoptotic pathways. Molecular and immunological effects were examined using RT-qPCR, Western blotting, flow cytometry, and immunohistochemistry.
Results: Combination treatment with HBS-101 and chemotherapy produced synergistic anti-tumor activity in TNBC models, significantly reducing 2D and 3D cell viability, stemness, and tumor growth relative to monotherapies. Similarly, combining HBS-101 with immunotherapy also yielded strong synergistic effects in syngeneic TNBC models, outperforming individual treatments. Mechanistic studies revealed that HBS-101 disrupted MDK-mediated signaling pathways, including STAT3, thereby sensitizing tumor cells to treatment and enhancing immune activation. Combination therapy also increased infiltration of CD8 positive T cells and macrophages, accompanied by elevated levels of IFN-gamma and granzyme B. RNA-seq analysis showed upregulation of immune and apoptotic pathways and suppression of immunosuppressive signals. These molecular changes correlated with reduced tumor burden, and increased apoptosis, supporting the mechanistic synergy of MDK inhibition in combination therapy.
Conclusion: MDK inhibition with HBS-101 enhances the efficacy of chemo-immunotherapy in TNBC by disrupting oncogenic signaling and promoting immune activation. These findings support the therapeutic potential of HBS-101 as part of a combination strategy to overcome resistance and improve outcomes in TNBC.

#3797 A novel tritherapy overcoming the immune suppressive tumor microenvironment elicits robust antitumor activity.

Brian G. Morreale[1], Andrea Monell[1], Han Yu[2], David B. Sykes[3], Jonathan F. Lovell[4], Michael J. Nemeth[1], Scott I. Abrams[5]

[1]Department of Immunology, Roswell Park Comprehensive Cancer Center, Buffalo, NY,[2]Department of Biostatistics and Bioinformatics, Roswell Park Comprehensive Cancer Center, Buffalo, NY,[3]Center for Regenerative Medicine, Massachusetts General Hospital, Boston, MA,[4]Department of Biomedical Engineering, University at Buffalo, Buffalo, NY,[5]Roswell Park Cancer Institute, Buffalo, NY

Immune checkpoint inhibitors (ICIs), such as those that engage PD-1 on cytotoxic $CD8^+$ T cells, can improve survival outcomes across multiple solid cancer types. However, in several cancers, such as triple-negative breast cancer (TNBC), the use of these agents is effective in limited subsets of patients. It is thought that this limitation is tied to numerous barriers which inhibit their efficacy, including the immune suppressive tumor microenvironment (TME) and a low infiltration of antigen (Ag)-specific $CD8^+$ T cells. Myeloid-derived suppressor cells (MDSCs) constitute a prominent immune suppressive component of the TME and are produced in response to tumor-derived factors. MDSCs consist of immature myeloid subpopulations that inhibit the proliferation or effector functions of cytotoxic $CD8^+$ T cells. To overcome this obstacle of immune suppression, our laboratory has developed a novel approach to target MDSC 'biogenesis' in the bone marrow to mitigate their production and bolster novel immunotherapies. We identified a metabolic susceptibility in MDSCs, which mitigates MDSC function using agents known as dihydroorotate dehydrogenase (DHODH) inhibitors. DHODH inhibitors block *de novo* pyrimidine metabolism and are being used as an anti-AML therapy to promote the maturation of myeloid progenitors common to both leukemic cells and MDSCs. This anti-MDSC approach boosted ICI activity, which significantly diminished tumor growth and metastasis; however, tumors persisted. To achieve more effective tumor response, we turned to the concept of epitope-specific immunization (ESI). We hypothesized that not only does DHODH blockade 'reprogram' MDSCs, but a peptide-based ESI approach targeting an endogenous tumor Ag in combination with our anti-PD-1/anti-MDSC regimen would result in greater tumor reduction by activating and expanding low frequencies of Ag-specific $CD8^+$ T cells. We optimized a tri-therapy regimen consisting of our anti-PD-1/anti-MDSC regimen with an ESI to boost intra-tumoral T cells. We showed that such a novel tri-therapy regimen caused significant antitumor responses, substantially more so compared with the single- and double-agent controls, which correlated with an increase in intra-tumoral Ag-specific $CD8^+$ T cells. To further demonstrate that this tri-therapy enhanced T cell function, we integrated an 'add-back' approach. We isolated $CD8^+$ T cells from tri-therapy-treated mice and showed following adoptive transfer that they significantly reduced tumor growth compared to $CD8^+$ T cells derived from vehicle or the dual-agent combination controls. Altogether, our results suggest that a novel multi-modal strategy that concurrently reduces MDSCs, overcomes T cell exhaustion, and expands tumor-reactive $CD8^+$ T cells, has important therapeutic implications to improve outcomes against ICI-refractory tumors.

#3798 *In vivo* results of AGX101, a TM4SF1-directed tubulin inhibitor conjugate, in combination with immune checkpoint inhibitors.

Shou-Ching Jaminet, Paul Jaminet, **Glen J. Weiss**

Angiex, Cambridge, MA

Introduction: TM4SF1 (Transmembrane-4 L-Six-Family-Member-1) is an endothelial marker with critical roles in angiogenesis, as well as a tumor cell antigen that contributes significantly to invasion and metastasis. TM4SF1 is upregulated 20-fold in angiogenic tumor vascular endothelium compared to normal vasculature endothelium and exhibits a unique nuclear internalization pathway. AGX101 is a novel tubulin inhibitor conjugate specifically directed against TM4SF1, delivering a potent maytansinoid payload directly to the nucleus of cells within the tumor microenvironment resulting in three mechanisms of action (MoAs): (1) activation of tumor immune surveillance, (2) tumor blood supply deprivation, and (3) direct tumor cell killing.
Methods: TM4SF1 expression was assessed using immunohistochemistry. Safety and pharmacokinetics of AGX101 were evaluated in non-human primates (NHP), with escalating doses to determine the highest non-severely toxic dose (HNSTD). Efficacy studies were also conducted in mouse models, enabling assessment of the minimum effective dose (MED) needed to engage each of the three MoAs. The combination of HNSTD and MED enables calculation of a therapeutic index (TI). The potential for synergy with immune checkpoint inhibitors (ICIs) was also investigated.
Results: Notable cancers with high TM4SF1 scoring intensity include lung cancer, kidney cancer, ovarian cancer, GI cancers, and breast cancer. In NHP, AGX101 exhibited a favorable safety profile.In preclinical efficacy studies, monotherapy demonstrated robust efficacy through each of the three MoAs in mouse syngeneic models including CT26 colon carcinoma and human tumor xenograft models including MIA PaCa-2 pancreatic cancer. Measured by exposure, TI was large. In syngeneic mouse models the effects of ICIs were potentiated by the AGX101 murine surrogate AGXB01, suggesting potential synergy. High response rates (RR) were achieved including CT26 with 71% RR for AGXB01+anti-CTLA-4 antibody vs 13% for anti-CTLA-4 alone; Renca mouse renal cancer model with 80% RR for AGXB01+anti-CTLA-4 antibody vs 20% for anti-CTLA-4 alone. In B16F10 mouse melanoma, a non-responsive model, AGXB01+ anti-PD-1 antibody or anti-CTLA-4 antibody ~doubled survival time vs either monotherapy of AGXB01 or anti-PD-1 antibody or anti-CTLA-4 antibody. In rechallenge experiments, 38 of 39 mice that had been rechallenged after tumor-free responses successfully eradicated new tumors without drug retreatment, demonstrating a durable immune response.
Conclusion: AGX101 represents a promising new approach in cancer therapy. The preclinical data suggest that AGX101 could provide a significant therapeutic benefit by novel and differentiated mechanisms of action, namely selectively targeting the tumor vasculature and potentiating ICIs. Further clinical development of AGX101 is ongoing.

#3799 HER3 inhibition sensitizes metastatic colorectal and pancreatic cancer to immunotherapy.

Chao Wei[1], Moeez Ghani Rathore[2], Elizabeth Bryson[1], Kimberly Curry[3], Jennifer Baek[3], Jordan M. Winter[4], Rui Wang[3]

[1]Case Western Reserve University School of Medicine, Cleveland, OH,[2]Case Comprehensive Cancer Center, Cleveland, OH,[3]Case Western Reserve University, Cleveland, OH,[4]UH Cleveland Medical Center, Cleveland, OH

INTRODUCTION: Metastatic colorectal cancer (mCRC) and pancreatic cancer (mPC) demonstrate 5-year survival rates of 14% and 3%, respectively, with over 70% patients developing distant metastases in the liver. Immune checkpoint inhibitors (ICIs) exhibit significant efficacy in some solid tumors and MSI CRC but have limited therapeutic benefit in MSS mCRC/mPC. This project aims to identify potential novel combination strategies to overcome ICIs resistance in mCRC/mPC. We previously discovered that liver endothelial cells activate HER3 signaling in cancer cells through NRG1 and LRG1 ligands, promoting metastatic growth via distinct AKT/RSK pathways. This study investigates whether inhibiting HER3 pathway can enhance immunotherapy efficacy in mCRC/mPC, especially MSS tumors.

METHODS: Metabolic changes in CRC/PC cells and tumors were first determined by LC-MS and ELISA for key metabolites, and then further assessed by *in vitro* assays, including Seahorse FX and TMRE, in the context of HER3 activation and/or inhibition. Phosphorylation activation of HER3 and downstream metabolic enzymes were evaluated by Western blotting and IHC staining using murine/patient tumor tissues. We developed syngeneic, orthotopic CRC/PC liver metastases by hepatic injection of murine CRC and PC cells (MSI or MSS), and assessed T cell infiltration and activation by IHC staining and flow cytometry. More importantly, therapeutic efficacy was assessed by treating these models with HER3 inhibitor sapitinib and/or anti-PD-1 antibodies.

RESULTS: LC-MS analysis revealed that mCRC/mPC exhibited significantly elevated glycolytic metabolites compared to primary tumors, with HER3 inhibition reversing this metabolic reprogramming. HER3 activation enhanced phosphofructokinase 2 (PFK2)-S483 phosphorylation and increased lactate secretion in CRC/PC cells. In murine CRC/PC liver metastases, *HER3* KO tumors showed decreased lactate, which reduced exhaustion of $CD8^+$ T cells, determined by decreased expression of TOX, and increased cytotoxic $CD8^+$ T cells, determined by increased Granzyme B levels. Most importantly, the combination of HER3 inhibition with anti-PD-1 significantly extended survival in CRC/PC liver metastases (both MSI and MSS), and achieved ~40% complete response rate, which is markedly superior to monotherapies.

CONCLUSIONS: We identify a novel HER3-PFK2-lactate metabolic axis that promotes immunosuppression in CRC/PC liver metastases. Targeting this pathway sensitizes CRC/PC liver metastases to checkpoint blockade, offering a promising strategy to extend immunotherapy benefits beyond the limited patient population currently responsive to ICIs.

#3800 Combinational effects of VC2-GMCSF oncolytic virus and paclitaxel in end-stage breast cancer animal model.

Reza Ghavimi, Leila Rahimian, Vladimir Chouljenko, Harikrishnan Mohan, Ojasvi Dutta, Md Mehedi Hasan, Jeongha Lee, Minori Kojima, Jose Sezar Menk, Konstantin Kousoulas

Louisiana State University, Baton Rouge, LA

Resistance and metastasis continue to make breast cancer a clinical challenge. VC2-GM-CSF drives antitumor immunity; paclitaxel remodels tumor environment to boost immune infiltration. Thus, combined use may yield superior therapeutic benefit over the use of either agent alone. This study investigates the potential synergistic interactions of VC2-GM-CSF with paclitaxel using the murine 4T1 breast cancer model in vitro and in vivo. In vitro, 4T1 cells were treated with paclitaxel alone or in combination with VC2-GM-CSF, and cell viability was assessed by MTT assay. Viral entry was quantified using a flow-cytometric assay. We further explored the in vivo antitumor effect of combined VC2-GM-CSF and paclitaxel in an orthotopic 4T1 stage IV metastatic model of breast cancer. Established 4T1 tumors in BALB/c mice were treated intratumorally with VC2-GM-CSF combined with paclitaxel. On day 31, tumors and lungs were collected for histopathological evaluation. Flow cytometric quantification of lymphocytes infiltrating the tumors was performed for $CD45^+$, $CD3^+$, $CD4^+$, and $CD8^+$ cells. The combined treatment was substantially more effective in inducing dose-dependent decreases in the viability of 4T1 cells and cell death than either single therapy in vitro. Flow cytometric entry assays showed that paclitaxel does not impair the entry of VC2-GM-CSF into cancer cells. In vivo, the combination significantly reduced primary tumor growth compared with the control treatment. Flow cytometry and immunohistochemistry analyses indicated increased T-cell infiltration in tumors after combination therapy. Together, these results demonstrate an enhanced antitumor effect resulting from the complementary cytotoxic and immunomodulatory mechanisms of paclitaxel and oncolytic virotherapy.

#3801 Synergistic therapy by combination of a plant virus immunomodulator and IL-12 against murine ovarian cancer.

Xinyi Deng[1], Jessica Fernanda Affonso de Oliveira[2], Nicole F. Steinmetz[1]

[1]UC San Diego, La Jolla, CA,[2]University of California San Diego - UCSD, San Diego, CA

Cowpea Mosaic Virus (CPMV) is an immunostimulatory agent that can induce antitumor immunity by reversing the immunosuppressive tumor microenvironment (TME) upon intratumoral treatment. In situ injection of CPMV activates and recruits innate immune cells which initiate tumor cell killing and antigen processing, ultimately launching systemic and adaptive antitumoral immunity. IL-12 is a promising proinflammatory cytokine that facilitates antigen processing and promotes T cell proliferation. CPMV primarily activates innate immune cells while IL-12 plays a key role in the adaptive immune response; therefore, we hypothesized that the synergistic combination of CPMV and IL-12 would be beneficial for reducing tumor burden. We tested our study using a murine ovarian carcinoma model. Mice were inoculated with bioluminescent tumor cells. Tumor burden was monitored using bioluminescence, body weight, and circumference. Survival was established based on humane endpoints. Our data show that the combination of CPMV + IL-12 outperforms the single-arm treatment. Robust efficacy is demonstrated for the combination group. In ongoing studies, we are deciphering the mechanism of action through immunological investigation. This work was funded in part through grants from NIH: R01 CA224505 and R01 CA274640.

#3802 Adaptive cd73 upregulation undermines parp inhibitor efficacy and creates a therapeutic opportunity for combined blockade in advanced prostate cancer.

Ping xie[1], Jie Fan[1], Hui Tang[1], Longzhen Song[2], Bin Zhang[1]

[1]Northwestern University Feinberg School of Medicine, Chicago, IL,[2]Department Medicine, Northwestern University Feinberg School of Medicine, Chicago, IL

Metastatic castration-resistant prostate cancer (mCRPC) remains a major cause of cancer-related mortality in the male population. While poly(ADP-ribose) polymeraseinhibitors (PARPi) are approved for selected mCRPC patients with homologous recombination repair (HRR) deficiencies, combinations with PD-1/PD-L1 inhibitors immunotherapy have demonstrated limited efficacy in unselected populations. To investigate the immunomodulatory effects of PARPi in an unbiased manner, we performed bulk RNA sequencing on HRR-proficient MyC-CaP cells treated with PARPi Olaparib or control vehicle. Pathway enrichment analysis revealed a marked upregulation of CD73 (NT5E), an emerging immune checkpoint ectoenzyme that generates extracellular adenosine, suggesting an adaptive mechanism that undermines PARPi efficacy and enables unwanted immunosuppression. CD73 induction by PARPi was confirmed in both human and mouse prostate cancer cell lines, with more pronounced effects in the HRR-compromised PTEN knock-out (KO) cells. Mechanistically, Olaparib-driven CD73 expression was mediated through the DNA damage-activated ATR-CHEK1-IRF1 and TGF-β1-AKT signaling pathways. Concurrently, PARPi enhanced tumor cell immunogenicity by activating the type I interferon pathway and antigen presentation machinery. *In vivo*, combining Olaparib with CD73 blockade therapy delayed tumor growth, improved T-cell infiltration, and augmented antigen-specific $CD8^+$ T-cell effector function across HRR-proficient and PTEN KO prostate cancer models. These findings highlight PARPi-induced CD73 upregulation as a novel resistance mechanism and support PARPi plus CD73 blockade as a promising therapeutic strategy for mCRPC, irrespective of HRR status.

#3803 The unique presentation of four immunotherapy toxicities in a single patient.

Orianna Guarisma-Lugo[1], Roderick Brice[1], Samuel Ramirez[1], Winston W. Tan[2]

[1]Hematology-Oncology, Mayo Clinic Florida, Jacksonville, FL,[2]Assistant Professor, Dept. of Hem./Onc., Mayo Clinic Florida, Jacksonville, FL

Medical advancements with immunotherapy have cured some patients with previously incurable metastatic renal cancer. We present the case of a 74-year-old male metastatic renal cancer patient who received only one dose of the combination of ipilimumab with nivolumab. In response to his treatment, he developed autoimmune hepatitis, myasthenia, myositis, and myocarditis. Although these serious side effects are considered to rarely occur, they can quickly become life-threatening and even fatal. These immune-related adverse events (irAEs) may further develop into secondary life-threatening symptoms such as respiratory failure due to advanced myasthenia; cardiotoxicity of myocarditis with possible cardiogenic shock, cardiac arrest, and severe heart failure; and liver failure consequently from autoimmune hepatitis. Furthermore, the ability for physicians to detect immunotherapy toxicity early is extremely important in intervening in a timely manner to avoid lethal conditions for the patient. With patients receiving immunotherapy, communication, collaboration, and multidisciplinary care are essential. Any subtle or sudden changes in their health status or symptoms should prompt further investigation. It is our purpose to highlight this patient to raise awareness of toxicity to significantly reduce the fatality rates and increase the therapy’s success rate in the years to come.

#3804 Engineering CAR macrophages in combination with anti-tumor therapies to suppress brain metastasis.

Shih-Ying Wu, Abhishek Tyagi, Eleanor Cecile Smith, Ravindra Pramod Deshpande, Jee Won Kim, Kounosuke Watabe

Wake Forest University School of Medicine, Winston Salem, NC

Brain metastases pose a significant clinical challenge for patients with HER2-positive breast cancer, with up to 50% of those with metastatic disease developing CNS involvement. Although HER2-targeted therapies such as trastuzumab deruxtecan (T-DXd) have improved systemic outcomes, their limited penetration across the blood-brain barrier (BBB) leaves the brain as a sanctuary site for recurrence. Innovative strategies are urgently needed to overcome BBB restrictions and effectively treat HER2-positive brain metastases.To address this, we leveraged the unique ability of macrophages to cross the BBB and perform phagocytic and immune-modulatory functions. We engineered chimeric antigen receptor macrophages (CARMA) to express tumor antigen-specific scFv and activate down-stream signaling to enhance anti-tumor immunity. We hypothesize that CARMA can penetrate the BBB, exert potent anti-tumor activity, and synergize with tumor antigen-targeted therapy and T-DXd to improve outcomes in brain metastases. In preclinical models, CARMA demonstrated strong antigen-specific phagocytosis and significant suppression of brain metastases. Notably, CARMA exhibited minimal neurotoxicity compared to CAR-T cells and induced a bystander killing effect mediated by cytokines upregulation upon tumor antigen engagement.To further enhance efficacy, we evaluated a combination strategy of CARMA and T-DXd to synergize antibody-dependent cellular cytotoxicity (ADCC) with macrophage-mediated phagocytosis. Our results showed that this combination dramatically suppressed brain metastases. These findings position CARMA as a promising immunotherapy platform for HER2-positive breast cancer brain metastases, offering potential to overcome BBB limitations and improve patient outcomes through multi-modal synergy.

#3805 Enhancing anti-tumor immunity via *in vivo* LNP delivery of a universal chimeric adapter protein to activate innate immune cells through T cell engagers.

Kevin Carbajal, Warren Anderson, Matthias Schroff, **Maximilian Richter**

Inceptor Bio, Durham, NC

T cell engagers (TCEs) have achieved remarkable successes both in liquid and solid tumors. However, relapses tend to occur in a significant fraction of patients, driven by antigen escape or T cell exhaustion. Currently, TCEs are unable to engage innate immune responses and thereby fail to leverage the innate immune system's crucial support functions, such as inducing a pro-inflammatory environment and promoting antigen spread and T cell licensing against tumor neoantigens.
Here we describe a chimeric adaptor protein that renders innate immune cells engageable by existing T cell engagers. This T cell engager receptor (TCE-R) is comprised of an extracellular domain that is recognized by all CD3-targeting TCEs, and a set of intracellular signaling domains that drive innate cell effector function upon TCE binding. Following initial administration of the TCE alone to induce tumor debulking, TCE-R is delivered in vivo using mRNA encapsulated in a lipid nanoparticle (LNP) allowing trafficking of pro-inflammatory innate immune cells to the tumor, inducing a broader TCE-driven anti-tumor response.
In a monocyte cell line stably expressing TCE-R, we have demonstrated TCE-mediated phagocytosis of target cancer cells as well as TCE-driven induction of pro-inflammatory signaling pathways. Further, TCE-R delivered as an LNP-encapsulated mRNA to primary human macrophages and dendritic cells in vitro resulted in expression of TCE-R on the cell surface, demonstrating the ability to deliver the transgene to relevant lineages of the innate immune system. Lastly, in vivo delivery of TCE-R LNP to innate immune cells in immune competent Balb/c and immunocompromised NSG mice has been demonstrated through surface expression of the human TCE-R on multiple myeloid cell lineages.
Taken together, our data lay the foundation to endow any anti-CD3 TCE with the ability to engage innate immune cells, recruit them to the tumor site, activate them in situ, and to leverage new effector functions to aid, broaden, and expand TCE-driven T cell responses ultimately leading to antigen spread, T cell licensing and durable remission.

#3807 Engineering and preclinical development of a differentiated EGFR/PDL1 bispecific ADC for the targeted therapy of solid tumors.

Liang Zhu, Chen Chuan, Mei Tian, Dandan Liu, Jiyuan Tian, Lisha Dong, Yongxin Shang, Rongmei Yan, Kezhen Ye, Liang Tian, Jian Peng, Zhenping Zhu

Earendil Labs, Wilmington, DE

Both EGFR and PDL1 are well-established therapeutic targets for a broad range of malignancies. Nevertheless, their therapeutic efficacy remain limited, as many patients are either refractory to or develop resistance during the course of treatment. EGFR and PDL1 are frequently co-expressed in multiple tumors, where they play key roles in promoting tumor progression and immune evasion. Notably, PDL1 expression is modulated by EGFR signaling, and the significant crosstalk between EGFR and PDL1 signaling has been reported. In this study, we developed a bispecific antibody (bsAb) targeting both EGFR and PDL1. The bsAb demonstrated enhanced binding avidity towards PDL1+/EGFR+ cancer cells, with higher efficiency of internalization, and more potent EGFR-directed blockade of PD1/PDL1 interaction. Several bsAb ADCs were generated by conjugating with various cytotoxic payloads. *In vitro* data demonstrated that the lead bsADC induced potent antitumor activity and strong bystander killing activity. Importantly, no Immunotoxicity was observed on PDL1+ human antigen-presenting cells. *In vivo* efficacy studies demonstrated that the lead bsADC achieved superior antitumor activity compared with MRG003 analog (an anti-EGFR ADC) and the clinical-stage PDL1V analog (an anti-PDL1 ADC) in multiple CDX models.

#3808 Regulation of PD-L1$^+$ tumor associated macrophages by collagen expressing myCAFs and luminal progenitors in endocrine-resistant breast cancer.

Nirmal Das[1], Cheng-Han Hsieh[2], Rumela Chakrabarti[2]

[1]University of Miami Miller School of Medicine, Miami, FL,[2]Department of surgery, University of Miami Miller School of Medicine, Miami, FL

Endocrine resistance is a major clinical obstacle that undermines the effectiveness of hormone-based therapies and drives disease progression. Around 15-20% of ER+ breast cancers are intrinsically endocrine resistant and an additional 40-50% acquire resistant during treatment, leading to metastatic progression. The five-year survival rate of these patients drops to 20-25%, while many of them progress to TNBC, a very aggressive subset of breast cancer.Recently, we demonstrated that PD-L1$^+$ tumor-associated macrophages (TAMs) are a central mediator for endocrine resistance and are recruited by Dll1-mediated Notch signaling. However, regulation of the PD-L1$^\pm$TAMs in endocrine resistance is not completely understood. Single-cell RNA sequencing (scRNA-seq) followed by cell chat communication analysis depicts that PD-L1$^+$ TAMs are regulated by myCAFs (Myofibroblasts, a type of cancer-associated fibroblasts) and LPs (Luminal progenitors). CD61+ luminal progenitor cells are linked to tumor heterogeneity and enriched with tumorigenic potential, serving as a cell of origin for breast cancers. Mechanistic studies reveal myCAFs are enriched in collagen, which is further corroborated in endocrine-resistant breast cancer patients' samples and ER+ mouse mammary tumors stained with trichrome and SMA staining. Closer investigation also shows that these SMA+ myCAFs are in close proximity to PD-L1$^+$ TAMs, aiding juxtracrine signaling. Further analysis highlights that myCAFs which are high in collagen signaling, are mediating interaction with PD-L1$^+$ TAMs through APP-CD74 and Col1a1/Col4a1/Col4a2/Col6a3 crosstalk. Detailed analysis on CD61$^+$ LPs, on the other hand, by scRNA-seq show that LPs crosstalk to PDL1$^+$ TAM through APP-CD74 signaling as well. APP (Amyloid precursor protein) is a transmembrane protein that is often correlated with worse clinical outcomes. Functionally, PD-L1$^+$ TAMs augments LP activity, as seen by increasing sphere number. Detailed investigation shows that these PD-L1$^+$TAMs are CD74$^+$ and IFN-γ responsive. Moreover, co-culture of PD-L1$^+$ TAMs treated with FDA approved drug Milatuzumab, a CD74 inhibitor, resulted in fewer and smaller tumor spheres, underscoring the crucial function of CD74 in mediating this crosstalk. Analysis of downstream regulators confirm that CD8$^+$ T cells are exhausted, suggesting a strongly immune-suppressive TME. Together, we identified a complex cell signaling network between myCAF-luminal progenitor expressing APP and collagens with CD74$^+$/PD-L1$^+$ TAMs in endocrine resistant tumors, identifying novel actionable vulnerabilities in these breast cancer patients.

#3809 Bax activation promotes immune activity and synergizes with PD-L1 blockade immunotherapy against mutant KRAS-driven lung cancer.

Abu Syed Md Anisuzzaman, **Xingming Deng**

Emory University, Atlanta, GA

The mutant KRAS-driven non-small cell lung cancers (NSCLC) frequently co-occurring mutations of LKB1 or p53 exhibit varying degrees of resistance to conventional treatments and anti-PD-L1 immunotherapy. It is urgently needed to develop new strategies to improve the outcome of these diseases. We have recently discovered that small molecule Bax activator CYD-2-11 targets the S184 structural pocket in the C-terminal tail of Bax, thereby activating its proapoptotic activity with potent antitumor activity against lung cancer. Here we further found that, in addition to apoptotic cell death, CYD-2-11 also induces cytosolic DNA and activation of cGAS-STING-TBK1-IRF3 pathway, thereby upregulating PD-L1 and producing interferons (IFN alpha and IFN beta) and chemokines (CCL5 and CXCL10). The combination of CYD-2-11 with anti-PD-L1 synergistically enhances intratumor CD3+ total T cells, CD8+ cytotoxic T cells and CD44+ memory/effector T-cells in association with reduction of regulatory T cells (Tregs), exhausted $CD8^{+}$T cells and $Gr\text{-}1^{+}$ $CD11b^{+}$ and $CD49d^{+}$ MDSCs, which contribute to increased immunity leading to the synergistic suppression of lung tumor growth and prolonged survival in genetically engineered mutant KRAS-driven lung cancer mouse models that are resistant to anti-PD-L1 immunotherapy. These findings provide preclinical evidence for the mechanism-driven combination of small molecule Bax activator with anti-PD-L1 as an effective strategy for lung cancer therapy, especially for those mutant KRAS-driven lung cancers that are resistant to PD-L1 blockade immunotherapy.

#3810 Intratumoral (IT) ruxotemitide (LTX-315) in combination with pembrolizumab in patients with unresectable advanced melanoma refractory to PD-1/PD-L1 therapy: Final results from the ATLAS-IT-05 study.

Stephane Dalle[1], Adi Diab[2], John M. Kirkwood[3], Miguel F. Sanmamed[4], Laurent Mortier[5], Marta Nyakas[6], Thomas Urban Marron[7], Maciej Gil[8], Oystein Rekdal[8], Karim A. Benhadji[8], Caroline Robert[9]

[1]Centre Hospitalier Universitaire de Lyon, Lyon, France,[2]UT MD Anderson Cancer Center, Houston, TX,[3]Vice Chairman For Clinical Res., Dept. of Medicine, University of Pittsburgh Medical Center, Pittsburgh, PA,[4]Clinica Universidad de Navarra, Pamplona, Spain,[5]Hopital Claude-Huriez, Universite de Lille, Lille, Lille, France,[6]Oncology, Oslo University Hospital, Oslo, Norway,[7]The Tisch Cancer Institute, New York, NY,[8]Lytix Biopharma AS, Oslo, Norway,[9]INSERM U981 (Gustave Roussy), Fontenay aux Roses, France

Background: Advanced unresectable cutaneous melanoma refractory to prior immunotherapy is associated with poor prognosis and limited treatment options. Ruxotemitide, an oncolytic peptide, induces immunogenic cell death and remodels the tumor microenvironment to enhance antitumor immunity. Preclinical and early clinical data support synergistic activity with PD-1 blockade. This Phase 2 study evaluated intratumoral (IT) ruxotemitide in combination with pembrolizumab in patients with unresectable advanced or metastatic melanoma accessible for IT injection after prior checkpoint inhibitor (CPI) failure.
Methods: This was an open-label, single-arm Phase 2 study enrolling adults with stage IIIB-IV (M1b) cutaneous melanoma and at least one injectable lesion (cutaneous, subcutaneous, lymph node, or intramuscular). Patients received IT ruxotemitide (up to seven injections during the first 29 days) in combination with pembrolizumab 200 mg IV every 3 weeks until disease progression or for up to 24 months. The primary endpoint was objective response rate (ORR) per RECIST v1.1. Secondary endpoints included duration of response (DoR), progression-free survival (PFS), and safety.
Results: Twenty-three patients were enrolled, with a median age of 68 years (range, 42-91 years). Over half (52.1%) of pts had received three or more prior lines of therapy, and all had previous CPI treatment. Twenty-two patients were evaluable for efficacy. ORR was 13.6% (80% CI, 5.1-27.9). The clinical benefit rate was 36.4%. All responses were durable, lasting more than 24 months. Median PFS was 6.3 months. The safety profile was consistent with known effects of IT immunotherapy and pembrolizumab. The most common treatment emergent adverse events (TEAEs) were injection-site reactions (95.7%), fatigue (30%), pruritus (26.1%), hypotension (26.1%), and anemia (21.7%). No TEAEs led to treatment discontinuation.
Conclusions: IT ruxotemitide plus pembrolizumab demonstrated durable antitumor activity and manageable safety in heavily pretreated patients with CPI-refractory advanced or metastatic melanoma with injectable disease. These findings support further clinical evaluation of this combination in melanoma.

#3811 Exploring immunomodulatory tumor-derived vaccines targeting triple negative breast cancer cells.

Marcio C. Bajgelman[1], Karina Thomaz[1], Daniela Mizobuti[1], Susana Ramalho[2], Sophie Derchain[1]

[1]Brazilian Biosciences National Laboratory, Brazilian Center for Research in Energy and Materials, Campinas, Brazil,[2]Women's Hospital - CAISM, University of Campinas, Campinas, Brazil

Breast cancer remains a major public health concern and is the leading cause of cancer-related deaths among women. Triple-negative breast cancer (TNBC) is the subtype with the poorest prognosis, and due to its phenotypic characteristics, no effective treatment is currently available for most diagnosed patients. This underscores the urgent need for novel therapeutic strategies. In this project, we explore antitumor vaccines generated from genetically modified TNBC cells expressing the immunomodulatory ligands TNFSF 4-1BBL and OX-40L. TNFSF ligands have the ability to costimulate T cells, enhancing their activation and proliferation. Previous studies from our group demonstrated that such vaccine combinations can increase T-cell proliferation, boost interferon-gamma production, inhibit regulatory T cells, and enhance T cell-mediated antitumor cytotoxicity, leading to a long term antitumor immunity and preventing tumor recurrence in cured and rechallenged animal models. Here, we generated antitumor vaccines derived from human TNBC cells, which were obtained after neoadjuvant chemotherapy from a patient sample provided by the CAISM-UNICAMP biobank. These cells were genetically engineered to express OX-40L and 4-1BBL, and the resulting tumor cell-based vaccines were evaluated in vitro for their antitumor potential. We observed that the vaccines enhanced immune responses in T lymphocytes from both autologous and allogeneic TNBC vaccines. Experimental assays confirmed that these tumor-derived vaccines induced elevated production of immunomodulatory cytokines and improved the antitumor T cell-mediated cytotoxicity. Our findings support the potential of this strategy as a promising immunotherapy approach for TNBC.

Ethical approval CAAE: 08897219.9.0000.5404

Supported by CNPq 308403/2022-3, and FAPESP 2023/12245-0

#3812 A novel 'Seed-and-Boost' immunotherapy drives potent TCR-T cell expansion, tumor infiltration, and durable tumor control.

Kar Wai Tan[1], Kan Xing Wu[1], Jin Wei Tan[1], Melissa Wirawan[1], Yovita Purwanti[1], Ana Dios[2], Fan Zhao[2], Natasha Girgis[2], Alessandra Nardin[1], Evan W. Newell[3], Anish Suri[2], Steven N. Quayle[2], **Michael Fehlings**[1]

[1]ImmunoScape Pte Ltd, Singapore, Singapore,[2]Cue Biopharma Inc., Boston, MA,[3]Fred Hutchinson Cancer Center, Seattle, WA

Background: While TCR-engineered T cell therapies show promise in solid tumors, long-term efficacy is limited by insufficient in vivo expansion and persistence. Current strategies also face significant challenges in manufacturing and clinical management. We present a novel strategy combining low-dose TCR-T cells (Seed) with a TCR-targeted cytokine biologic (Boost) to drive selective in vivo expansion, enhance tumor infiltration, and sustain tumor-specific responses. We demonstrate this by targeting WT1-positive solid tumors using WT1-specific TCR-T cells plus CUE-102, a clinically validated ImmunoSTAT™ fusion protein enabling controlled TCR engagement and delivery of IL-2 to WT1-specific T cells.

Methods: We generated a highly specific dual HLA (HLA-A:02:01 and HLA-A:02:07) targeting TCR against the $WT1_{37-45}$ antigen. Preclinical characterization of this TCR, engineered into human primary T cells, included potency assessment against various WT1-positive cancer cell lines and testing for antigen cross-reactivity and HLA alloreactivity. WT1-specific TCR-T cells were combined with CUE-102 to assess specific TCR-T cell expansion, anti-tumor efficacy, tumor infiltration, and long-term efficacy both in vitro and in various xenograft models using WT1-expressing ovarian and pancreatic cell lines.

Results: WT1-specific TCR-T cells demonstrated potent in vitro cytotoxicity against HLA-A*02:01 and HLA-A*02:07 WT1-positive cancer cell lines. In addition, we observed a favorable safety profile with no antigen cross-reactivity or HLA alloreactivity. In combination with CUE-102, we observed high potency and sustained anti-tumor cell efficacy at very low effector to target cell ratios and a vigorous selective in vivo expansion of WT1-specific TCR-T cells. In xenograft models of WT1-positive ovarian and pancreatic cancers, the combination therapy led to significantly higher numbers of circulating TCR-T cells, enhanced tumor infiltration, and robust tumor control even at very low TCR-T cell doses, compared to TCR-T cell monotherapy. Furthermore, in animals with higher tumor burden, the combined treatment resulted in sustained tumor regression and significantly extended survival.

Conclusion: Our data demonstrate that boosting with CUE-102 triggers robust in vivo expansion and activation of engineered TCR-T cells seed, resulting in effective anti-tumor responses, T cell persistence, and prolonged survival without additional cell engineering. This approach offers a potentially transformative solution for long-term benefits in solid tumor patients and can address cell therapy manufacturing and clinical management challenges by enabling the infusion of fewer seed TCR-T cells, eliminating the need for systemic IL-2 administration, and potentially avoiding toxic conditioning regimens.

#3813 Synergistic immunomodulation by Tumor Treating Fields combined with immunotherapy across solid tumors: A systematic review with translational relevance to pancreatic ductal adenocarcinoma..

Douaa Albelal, Hari Krishnareddy Rachamala, Hani Babiker

Hematology and Oncology, Mayo Clinic Florida, Jacksonville, FL

Background: Pancreatic ductal adenocarcinoma (PDAC) remains highly lethal due to aggressive biology, stromal desmoplasia, and profound immunotherapy resistance. Tumor Treating Fields (TTFields) disrupt mitosis and induce immunogenic cell death (ICD), type I interferon signaling, and microenvironment remodeling, providing a rationale for combining TTFields with immune checkpoint inhibition. This is the first systematic review to comprehensively synthesize mechanistic and clinical evidence for TTFields immunotherapy combinations across solid tumors, with emphasis on their translation relevance to PDAC.
Methods: A systematic search of PubMed, Scopus, Web of Science, Embase, Cochrane Library, and ClinicalTrials.gov was conducted through October 26, 2025, following PRISMA 2020 guidelines. Eligible studies evaluated TTFields combined with immunotherapy. Two reviewers independently screened and extracted data using Covidence. Evidence was summarized narratively by tumor type, study design, and immunotherapeutic approach.
Results: Thirty-seven studies met criteria, including preclinical and clinical investigations across glioblastoma, NSCLC, mesothelioma, PDAC, and other tumors. Preclinical models consistently showed that TTFields trigger ICD hallmarks such as calreticulin exposure, HMGB1 and ATP release, and activate STING/type I interferon pathways, enhancing dendritic-cell maturation and T-cell and NK-cell function. Across in vivo models, TTFields combined with PD-1 or CTLA-4 blockade, vaccines, or other immunotherapies reduced tumor growth and increased lymphocyte infiltration. Clinical evidence, although early-phase and heterogeneous, indicates the combination is feasible, with toxicity dominated by low-grade skin reactions and no excess immune-related adverse events. In glioblastoma, adding TTFields to pembrolizumab and temozolomide showed numerically improved survival. The LUNAR phase 3 trial in metastatic NSCLC demonstrated an overall survival advantage when TTFields were added to systemic therapy, including immunotherapy. Evidence in PDAC remains preliminary, but the ongoing PANOVA-4 study combining TTFields with atezolizumab and chemotherapy highlights emerging translational relevance.
Conclusions: TTFields enhance antitumor immunity when combined with immunotherapy across solid tumors. In PDAC, these mechanisms may help counteract the immunosuppressive microenvironment. Ongoing gastrointestinal trials will clarify optimal combinations, biomarkers of response, and the clinical role of TTFields-based immunomodulation.

: Diagnostic Biomarkers 1
Poster Session

#3817 Fusions and rearrangement detection in gastrointestinal and lung tumors leveraging low-pass whole-genome sequencing based Hi-C chemistry.

Darren S. Sigal[1], David Jacob Hermel[2], Alex R. Hastie[3], Anthony Schmitt[3]

[1]Scripps Clinic and Scripps Cancer Center, La Jolla, CA,[2]Scripps Health, La Jolla, CA,[3]Arima Genomics, San Diego, CA

Introduction: Molecular profiling in solid tumors has enabled the detection of actionable oncogenic drivers that guide targeted therapy. While point mutations in genes such as *EGFR* and *KRAS* are well established, gene fusions that activate key signaling pathways have become increasingly important therapeutic targets. Although RNA sequencing remains the gold standard for fusion detection, clinically relevant events are still missed. This study evaluates the ability of Hi-C whole-genome sequencing to improve detection of actionable fusions and structural rearrangements in solid tumors.
Methods: All cases had molecular testing such as FISH, DNA panel sequencing, and/or RNA transcriptome sequencing as part of clinical care. Hi-C sequencing is a novel whole-genome DNA assay optimized for structural variant detection from FFPE tissues. Its chemistry captures linked read pairs that originate near each other in both three-dimensional and linear genomic space. This increases breakpoint coverage, amplifies rearrangement signals, and allows detection of fusions obscured by non-unique or complex genomic regions.
Results: A total of 60 solid tumor cases were evaluated, the majority of which were gastrointestinal—including pancreatic adenocarcinoma, gastric cancer, and colorectal cancer. Hi-C sequencing was first applied to detect known fusions and rearrangements (12 cases) like *ALK, FGFR2, ROS1, NTRK3,* with 100% concordance with FISH (8 cases), whole transcriptome (1 cases), and DNA panel sequencing (3 cases), and able to detect fusion partner in all cases. Next it was used to successfully identify actionable or potentially actionable structural variants across the cohort (48 cases) which had no targetable driver genes detected by NGS. Hi-C detected targetable gene fusions involving *NRG1* in three cases, and *PRKCB* in another case. Additional rearrangements were detected proximally to genes whose overexpression may be linked to tumor progression like *NRG1, KRAS, NOTCH3*, and *CHST9*.
Conclusions: Hi-C sequencing shows strong potential as a complementary tool for molecular classification of gastrointestinal and other solid tumors. By detecting gene fusions and rearrangements—including those missed by conventional testing—Hi-C may expand the number of patients who can be matched to targeted therapies.

#3818 A robust RNA-seq solution for severely degraded FFPE samples: The PredicineWTS Tissue NGS platform.

Min Wang, Yasser Abdelrahman, Guanglong Jiang, Yong Huang, Pan Du, Binggang Xiang

Predicine, Inc., Hayward, CA

Background: Formalin-fixed, paraffin-embedded (FFPE) tissues remain essential resources for cancer research and the discovery of clinically relevant biomarkers. However, RNA extracted from FFPE samples is often highly degraded, chemically modified, and fragmented, posing major challenges for transcriptomic analyses, including gene expression profiling and RNA fusion detection. To address the need for a robust RNA-seq method capable of handling severely degraded RNA, we developed the PredicineWTS Tissue platform, which integrates optimized extraction chemistry with a proprietary RNA-seq pipeline tailored for FFPE RNA.
Methods: The PredicineWTS Tissue platform employs a proprietary extraction protocol that simultaneously isolates DNA and RNA from a single FFPE section, maximizing material utility for multi-omics applications. The RNA-seq workflow supports inputs as low as 10 ng and tolerates extreme degradation, including DV200 values down to 10%. A customized bioinformatics pipeline enables comprehensive expression profiling and detection of RNA fusions and splicing variants. DNA isolated during extraction is preserved for downstream genomic assays, enabling integrated analyses. Performance validation was performed using commercial reference materials.
Results: The platform showed strong performance on heavily degraded FFPE RNA. High-quality libraries were generated from samples with DV200 values as low as 10%, achieving approximately 93% uniquely mapped reads, 90% exonic reads, and detection of ~19,000 genes. Expression accuracy correlated strongly with an independent third-party company's results (Pearson $r \geq 0.94$). Fusion detection sensitivity was evaluated using titrated Seraseq material (50%, 20%, 10%, and 5% tumor purity), and all expected fusions were detected down to the 10% tumor purity, supporting sensitivity for low-abundance events relevant to cancer biomarker discovery. DNA recovered during extraction showed yield and quality comparable to leading extraction methods, further supporting workflow versatility.
Conclusion: PredicineWTS Tissue assay provides a powerful and reliable RNA-seq solution of severely degraded FFPE samples. By enabling robust expression profiling and sensitive fusion detection at low RNA quality and input, the platform advances biomarker discovery and supports integrated multi-omics studies. Its performance with archival and challenging FFPE material positions it as a valuable technology for precision oncology and translational research.

#3819 Validation of TruSight Oncology Comprehensive for detecting and reporting clinically relevant mutations.

Mauro Chavez, Silvia Chan, Stewart Comer, Gajalakshmi Dakshinamoorthy, Dan Schmidt, Giang Howard, Lisa Tulathimutte, Martin Martchovsky, Carey Davis, Eileen de Feo, Denise Perry

Illumina Lab Services, Illumina, Inc., San Diego, CA

Comprehensive genomic profiling (CGP) is transforming cancer diagnostics by enabling the detection of a wide range of actionable biomarkers and immunotherapy response signatures in a single test. TruSight Oncology Comprehensive (TSO Comp) is a qualitative *in vitro* diagnostic test that evaluates both DNA and RNA from formalin-fixed, paraffin-embedded (FFPE) tissue and analyzes 517 cancer-associated genes with known clinical relevance in one integrated workflow. This study presents the verification and validation of TSO Comp with added laboratory developed test (LDT) claims by conducting accuracy, analytical specificity, and precision (inter and intra run repeatability) studies. Assay performance was assessed using 19 cell lines, contrived and Seraseq® reference materials, and 41 clinical samples to detect the following variant classes: small variants (SNVs, MNVs and indels), fusions/splice variants, Tumor Mutational Burden (TMB), Copy Number Variants (CNVs), and Microsatellite Instability (MSI). The latter two, along with 31 additional fusions and two additional splice variants, were validated as part of the LDT. Overall, the study resulted in 99.4% positive percent agreement (PPA) rates and >99.9% negative percent agreement (NPA) rates for small variants. 100% PPA was estimated across 17 CNVs, 41 fusions/splice variants, and two MSI positives. Furthermore, 100% NPA was estimated for all evaluated samples considered for CNV, fusions/splice variants, and MSI status. TMB scores between reference results and TSO Comp were highly correlated, with R^2 = 0.97. The LoD for CNVs resulted in 100% detection rates for ≥ 2.6 fold change (i.e., 5 copies) in gene amplification when measured across five replicates of four clinical samples. Three contrived cell lines with replicates were used to establish the LoD of 20% tumor content for MSI. In addition, 23 healthy donor samples resulted in 100% analytical specificity for CNV and MSI. All variants and MSI status resulted in ≥ 98.8% inter and intra runs concordance across nine clinical and one Seraseq reference material with replicates.This study demonstrates how TSO Comp can be extended to include additional variant claims with high sensitivity and specificity as an LDT while maintaining clinical interpretation and reporting of cancer mutations central to the CGP of FFPE. Indeed, TSO Comp significantly reduces the burden of validating certain variant classes (e.g. study size was reduced by a minimum factor of two) and allows laboratories to validate and report on additional claims as cancer diagnostics knowledge evolves.

#3820 Concordance analyses of a rapid, targeted, and comprehensive genomic profiling panel for the detection of guideline-recommended biomarkers in non-small cell lung cancer.

Amanda Williamson[1], Hardik Parikh[2], Jon Williams[3], Jie An[2], Erin DeBlasi[2], Alison Roos[4], Leandra Blann[5], Luca Quagliata[6], Mark Tomilo[7], Marcia Eisenberg[8], Brian Caveney[8], Taylor J. Jenson[1], Shakti Ramkissoon[1], Eric Severson[1]

[1]Labcorp, Durham, NC,[2]Labcorp, Buffalo, NY,[3]Labcorp, San Diego, CA,[4]Thermo Fisher Scientific, Phoenix, AZ,[5]Thermo Fisher Scientific, Houston, TX,[6]Thermo Fisher Scientific, Basel, Switzerland,[7]Thermo Fisher Scientific, Ann Arbor, MI,[8]Labcorp, Burlington, NC

Targeted therapies and immunotherapies have improved survival in non-small cell lung cancer (NSCLC). For advanced and early-stage disease, clinical guidelines emphasize timely biomarker results to optimize outcomes. Laboratories face challenges in meeting expanding biomarker demands while conserving tissue and maintaining turnaround times suitable for clinical use and trial enrollment. This study evaluated concordance between the targeted Oncomine™ Precision Assay (OPA), a rapid, low-input NGS panel, and the OmniSeq® INSIGHT (OSI) comprehensive genomic profiling (CGP) assay and assessed OPA's feasibility for expedited biomarker reporting in routine practice. We retrospectively selected 200 advanced NSCLC samples with residual nucleic acid previously tested by OSI. DNA and RNA were re-run using OPA on the Genexus instrument with inter-assay controls. Concordance analyses focused on DNA variants in *BRAF*, *EGFR*, *ERBB2(HER2)*, *KRAS*, and *MET*, and RNA fusions in *ALK*, *MET*, *RET*, *ROS1*, and *NTRK1-NTRK3*. Sensitivity and specificity of OPA relative to OSI were calculated. Workflow metrics including ease-of-use and hands-on time were also evaluated.In a preliminary cohort of 37 samples, OPA showed Assay-QC pass rates of 95% (DNA) and 100% (RNA). Five samples that failed OSI RNA QC passed OPA, though no additional fusions were detected; these were excluded from concordance calculations. Averaged sequencing metrics were 1.07M DNA mapped reads and 125,180 RNA fusion mapped reads. Inter-assay controls were 100% concordant for SNV/Indels (20/20) and fusions (44/44). In the clinical cohort, OPA showed 96.7% for SNV/Indels (29/30), 100% for CNVs (3/3) and fusions (2/2). Specificity was 99.89%, with one potential false positive possibly below OSI's limit of detection (LOD). Turnaround time was 1 day with <1-hour hands-on time. OPA demonstrated high concordance with OSI for a defined set of actionable NSCLC biomarkers. While not all clinically relevant biomarkers (e.g., TMB, MSI, or genes outside the OPA panel) were assessed, results showed strong analytical agreement for overlapping targets. CGP assays like OSI remain the standard for broad biomarker testing in advanced NSCLC, but OPA's rapid turnaround and low-input requirements offer a practical option for timely detection of select actionable biomarkers, making it a useful complement to CGP when time or tissue is limited.

#3821 Clinical utility of a urine-based urothelial cancer test in equivocal upper tract lesions: improving malignancy detection and minimizing unnecessary URS.

Paolo Piatti[1], Yap Ching Chew[1], Farah Toullier-Garcia[1], Ernest Kaufmann[2], Kilian Rothlin[2], Philipp Baumeister[2], Agostino Mattei[2], Christian Fankhauser[2]

[1]Pangea Laboratory, Tustin, CA,[2]Luzerner Kantonsspital, Lucerne, Switzerland

Background and Objective: Upper tract urothelial carcinoma (UTUC) is a rare but aggressive malignancy that often requires diagnostic ureterorenoscopy (URS), an invasive procedure associated with infection, ureteral injury, and potential tumor seeding. In patients with equivocal imaging, deciding whether to perform URS is challenging and may lead to unnecessary procedures. A non-invasive and accurate diagnostic tool is therefore needed to improve risk stratification. Bladder CARE™, a urine-based epigenetic assay with high accuracy for bladder cancer and UTUC, received FDA Breakthrough Device Designation in December 2023. This study evaluated its diagnostic performance in patients with equivocal upper-tract lesions, with the goal of confirming malignancy and reducing unnecessary URS in selected cases.

Material and Methods: Between December 2023 and August 2025, urine samples from 46 patients with suspected UTUC were analyzed using Bladder CARE™. All patients subsequently underwent URS, with nephroureterectomy performed when malignancy was confirmed. Results were classified using the Bladder CARE Index (BCI): positive (> 10), low positive (2.5-10), and negative (< 2.5). Sensitivity, specificity, PPV, and NPV were calculated using histopathology from URS and/or nephroureterectomy as the reference standard. Associations between BCI and tumor grade were also assessed.

Results: Patients had a mean age of 70 years (16 female, 30 male); 24 were UTUC-positive and 22 negative. Mean BCI was significantly higher in UTUC-positive cases vs negatives (85.8 vs 1.7). The positive category showed excellent performance (93% sensitivity, 100% specificity, PPV 100%, NPV 95%), supporting its use to avoid URS in appropriately selected patients. Low-positive results also detected a substantial proportion of cancers but with lower certainty (86% sensitivity, 69% specificity), making URS evaluation appropriate for these cases. Bladder CARE™ detected 88% of low-grade and 100% of high-grade tumors, and 90% of Ta and 100% of T1-T3 tumors. Cytology detected only 2 of 19 UTUC cases. Mean BCI values were higher in high-grade vs low-grade tumors (111.7 vs 54.2) and in T1-T3 vs Ta lesions (136.7 vs 56.0), indicating correlation with tumor aggressiveness.

Conclusion: Bladder CARE™ demonstrated strong diagnostic accuracy with potential to modify the UTUC management pathway. A positive result may allow direct progression to definitive treatment without diagnostic URS, reducing morbidity and expediting care. The correlation between BCI and tumor grade/stage may further support treatment selection, including kidney-sparing approaches or neoadjuvant therapy. While multicenter validation is needed, this non-invasive assay represents a promising advance in UTUC diagnostics and clinical decision-making.

#3822 Enabling multiomic analysis in cell-free DNA tubes by addressing the impact of pre-analytical factors.

Shuting Zhao, Teng-Kuei Hsu, Francis Apolinario, Aurora Martinez-Horta, Yizhen Zhong, Aditya Rao, Jimmy Lin, Richard Bourgon, Tanya Moreno, Ofer Shapira, Kang Li

Freenome, Brisbane, CA

Background: Cell-free DNA (cfDNA) tubes are widely adopted for genomic liquid biopsies because they allow delayed processing after blood collection while ensuring cfDNA stability. However, it remains poorly understood whether other analytes, especially plasma proteins, are stable in cfDNA tubes when subjected to preanalytical stresses during delayed processing. This study investigates the effect of time and temperature variations during transit on protein profiles in samples collected in Streck cfDNA tubes, and a computational method to mitigate the impact.

Methods: We collected blood from 10 healthy donors into Streck cfDNA tubes. Plasma was separated at varying time points and after exposure to different temperature conditions to simulate shipping stress. A total of 2,903 proteins were measured using an immuno-proteomic profiling platform to assess changes in protein abundance. We also assessed a computational regression approach to correct for preanalytical impact on protein levels measured by a bead-based multiplex immunoassay and determine the effect size change of biomarker candidates in a clinical cohort (cancer n=105 vs. control n=538).

Results: Using a 20% abundance change cutoff, we observed that over half of the proteins (1,574) remained stable over prolonged time and temperature exposure. While 351 proteins showed negative bias, the majority of perturbations (978) were concentration increases, with proteins from blood cells overrepresented. Some proteins, such as Macrophage Migration Inhibitory Factor (MIF), were highly correlated with plasma hemoglobin (Hb) level, indicating a red blood cell (RBC) lysis effect. Other proteins, such as Epidermal Growth Factor (EGF), were more correlated with plasma potassium (K) level, suggesting broader lysis effects involving other blood cell types. Using the independent clinical cohort, we confirmed that MIF and EGF levels were highly correlated with Hb and K, respectively. The regression results showed that the Hedges' g effect size for MIF between case and control groups increased from 0.184 to 0.468 after Hb-regression, and the EGF Hedges' g increased from 0.318 to 0.467 after K-regression, demonstrating the power of this computational method to unmask potential protein biomarkers.

Conclusions: Preanalytical variables significantly impact plasma proteomic profiles in cfDNA tubes, especially for proteins that are associated with blood cells. The protein abundance changes in response to preanalytical stresses in cfDNA tubes can confound analyses and lead to false findings. Our results demonstrate that leveraging preanalytical markers like K and Hb allows for computational mitigation of this variability. Implementing robust sample quality control and computational correction strategies is essential to ensure the reliability of plasma proteomic measurements from samples collected in cfDNA tubes.

#3823 Genomic landscape of resectable hepatocellular carcinoma defined by tissue based whole-exome sequencing.

Jie Hu[1], **Haoran Tang**[2], Cancan Jia[2], Feng Xie[2], Yue Zhang[2], Jian Zhou[1]

[1]Liver Cancer Institute, Zhongshan Hospital, Fudan University, Shanghai, China,[2]Huidu (Shanghai) Medical Sciences, Ltd., Shanghai, China

Introduction: Hepatocellular carcinoma (HCC) is the seventh most common malignancy worldwide. Recent advances, including immune checkpoint inhibitors and anti-VEGFR therapies, have improved outcomes for HCC patients, especially in the adjuvant setting after surgical resection. However, many patients still experience disease recurrence and develop treatment resistance, and the molecular biomarkers underlying these events remain poorly defined. Here, we report a retrospective translational study using tissue-based whole-exome sequencing (WES) to investigate molecular biomarkers in patients with resectable HCC.
Methods: In this retrospective study, 88 patients with surgically resected HCC were enrolled. Tumor tissue samples collected at the time of surgery were submitted for molecular profiling using PredicineWES+, a whole-exome sequencing (WES) assay with boosted sequencing in 600 tumor-relevant genes. Matched normal tissue samples also underwent WES to rule out germline variants.
Results: Across 88 patients, PredicineWES+ identified 14,042 somatic mutations and 951 copy number variations. The median tumor mutation burden was 2.41 muts/Mb (range, 0.48-9.74 muts/Mb). The most frequently altered genes were TP53 (70%), TERT (41%), RB1 (25%), and CTNNB1 (22%), with TP53 and RB1 predominantly affected by copy number loss and most TERT variants occurring in the promoter (including 30 C228T events). TP53 alterations were slightly more prevalent in Barcelona Clinic Liver Cancer (BCLC) stage C than in earlier stages, but without statistical significance. No significant associations between TP53, TERT, RB1, or CTNNB1 alterations and prognosis were observed.
Conclusion: Comprehensive tissue-based WES profiling in resectable HCC revealed a characteristic genomic landscape, highlighting the complexity of molecular drivers underlying recurrence and resistance in HCC and underscore the need for integrative biomarker strategies in tumor genomics to refine risk stratification and guide adjuvant therapy.

#3824 Cross-cohort robust detection of colorectal cancer using a minimal junction-based platelet RNA panel.

Jin Sun Choi[1], Ji Won Park[2], Yewon Kim[3], Sangick Park[4], Dahyun Park[3], Eunhye Chai[3], Hyo Jun Kim[2], Seung Chul Heo[1], Seung-Yong Jeong[2], TaeJin Ahn[3], Rumi Shin[1]

[1]SMG-SNU Boramae Medical Center, Seoul, Korea, Republic of,[2]Seoul National University Hospital, Seoul, Korea, Republic of,[3]Foretell My Health, Inc., Seoul, Korea, Republic of,[4]Handong Global University, Pohang, Korea, Republic of

Background:
Tumor-educated platelets (TEPs) incorporate cancer-derived RNA signals and represent a promising minimally invasive platform for early cancer detection. However, gene-level TEP signatures such as the widely used 921-gene panel often exhibit reduced performance across heterogeneous cohorts. Because platelet RNA predominantly reflects regulated splicing events rather than transcriptional abundance, exon-exon junction features may provide higher biological specificity and improved stability against hematologic variability. In this study, we aimed to identify representative exon-exon junction alterations in platelet RNA that distinguish CRC from healthy controls.
Methods:
We analyzed public platelet RNA-seq data (132 CRC and 21 healthy samples; NIH BioProject PRJNA737596) and a prospective clinical cohort (44 CRC and 96 healthy samples), both of which contained a substantial proportion of early-stage CRC (stage I-II, ~52%). Junction-level read counts were quantified, normalized, and filtered based on differential expression, reproducibility, and independence from hematologic indices. A 10-junction panel was selected using logistic regression modeling, and support vector machine (SVM) classifiers were trained and validated using stratified, independent subsets. Performance of the 10-junction model was compared with an identically preprocessed model based on the previously reported 921-gene TEP panel. Functional annotation of the 10 junctions was conducted to assess mechanistic relevance.
Results:
The 10-junction panel demonstrated consistently strong diagnostic performance across cohorts. In the public validation set (n=68), the model achieved a sensitivity of 89.4%, specificity of 85.7%, and an AUC of 0.912. In the clinical validation set (n=75), sensitivity was 87.5%, specificity 93.3%, and AUC 0.959. Detection of early-stage CRC was robust in both datasets (AUC 0.903 and 0.956 in the public and clinical cohorts, respectively). Notably, the junction-based model outperformed the 921-gene panel in the clinical cohort (AUC 0.959 vs. 0.895). Functional enrichment analysis indicated involvement of vesicle trafficking, autophagy, and platelet-immune signaling pathways, consistent with known mechanisms of platelet reprogramming in cancer.
Conclusions:
A compact junction-based TEP RNA panel enables accurate detection of CRC, including early-stage disease, and demonstrates superior cross-cohort robustness compared with conventional gene-level approaches. Its small feature set, strong biological coherence, and consistent performance highlight its potential as a scalable and cost-efficient liquid biopsy for CRC screening. Multi-institutional prospective validation is warranted.

#3825 Integrating CpG-level methylation and transcriptomics for high-resolution cancer epigenetics.

Chao Dai, Guanglong Jiang, Ziqi Zhu, Giancarlo Bonora, Yong Huang, Kemin Zhou, Pan Du

Predicine, Inc., Hayward, CA

Background: Promoter hypermethylation is a key mechanism for silencing tumor suppressor genes in cancer. While whole-transcriptome sequencing (WTS/RNA-seq) is widely used to study cancer biology, high-resolution integration of methylation and expression data remains challenging. Conventional differential methylation region (DMR) approaches aggregate signals across promoters, potentially obscuring fine-scale regulatory effects.
Methods: We analyzed three pairs of parental and sotorasib-resistant NSCLC cell lines using PredicineEpic genome-wide DNA methylation profiling and PredicineWTS RNA-seq. Instead of promoter-level aggregation, we quantified fragment-level methylation changes at individual CpG sites within promoter regions. Correlations between CpG-specific methylation alterations and differential gene expression were evaluated across varying TPM $\log_2$ fold-change thresholds. In addition, more than 50 FFPE tissue biopsies from multiple cancer types were profiled with PredicineEpic and PredicineWTS to systematically assess the relationship between DNA methylation and gene expression.
Results: CpG-level methylation changes showed stronger inverse correlations with gene expression than promoter-level averages. For genes with $\log_2FC \geq 4$, CpG fragment beta differences correlated with expression changes at $R = -0.92$ ($n = 7$, $p = 0.001$). Similar trends were seen at lower thresholds: $\log_2FC \geq 3$ yielded $R = -0.63$ ($n = 22$, $p = 0.001$), whereas promoter-level beta differences showed no significant correlation. Consistent patterns of stronger CpG-level correlations were also observed across all tissue biopsy datasets.
Conclusions: High-resolution CpG-level methylation analysis provides greater sensitivity for linking epigenetic alterations to transcriptional changes than conventional promoter-level approaches. Fragment-level methylation profiling can reveal critical transcriptional regulatory events and may have important applications in liquid biopsy and biomarker discovery.

#3826 Systematic assessment of histomorphologic and immunohistochemical features in metastatic castration-resistant prostate cancer biopsies.

Elnaz Mahmoudabadi[1], Erolcan Sayar[1], Peter S. Nelson[1], Michael Schweizer[2], Funda Vakar-Lopez[3], Lawrence True[3], Jakob Valk[3], Maria Tretiakova[3], Nancy Y. Greenland[4], Deepika Sirohi[4], Bradley A. Stohr[4], Jeffry P. Simko[4], Michael C. Haffner[1], Chien-Kuang Cornelia Ding[4]

[1]Division of Human Biology, Fred Hutchinson Cancer Center, Seattle, WA,[2]Division of Clinical Research, Fred Hutchinson Cancer Center, Seattle, WA,[3]Department of Laboratory Medicine and Pathology, University of Washington, Seattle, WA,[4]Department of Pathology, University of California San Francisco, San Francisco, CA

Background: Metastatic castration-resistant prostate cancer (mCRPC) represents a heterogeneous disease spectrum. While many tumors remain androgen receptor (AR)-driven, others undergo lineage plasticity toward neuroendocrine prostate cancer (NEPC). The significance of intermediate or mixed phenotypes—such as tumors with co-expression of AR and neuroendocrine (NE) markers or lacking all lineage markers—remains poorly defined. We sought to systematically characterize histomorphology and immunohistochemistry (IHC) in real-world mCRPC biopsies.
Methods: 117 mCRPC biopsies from two institutions were retrospectively reviewed and classified by tumor morphology on H&E. IHC was performed for NKX3.1, AR, synaptophysin (SYP), insulinoma-associated protein 1 (INSM1), and Ki-67. Expression was semi-quantitatively scored using H-scores (0-300), and Ki-67 was reported as the percentage of tumor nuclei with positive staining.
Results: Histologic distribution included 44 adenocarcinomas, 53 poorly differentiated carcinomas, 15 NEPC, and 5 mixed subtypes. Using H-score >40 as a cutoff, adenocarcinomas frequently expressed NKX3.1 (93%) and AR (100%), with limited NE marker expression (13% for INSM1 and 46% for SYP). Poorly differentiated carcinomas most often retained NKX3.1 (80%) and AR (84%), while NE marker expression was less common (SYP 27%, INSM1 26%). Mixed tumors demonstrated co-expression across lineages, (AR 100%, NKX3.1 100%, SYP 80%, INSM1 50%). NEPC showed diffuse NE differentiation (SYP 85%, INSM1 75%) with rare NKX3.1 or AR positivity (8% and 0%, respectively). High H-scores (>200) were enriched in NKX3.1 (83%) and AR (92%) positive adenocarcinomas, while majority NEPC showed high SYP expression and high Ki-67 proliferation index. Low H-score (<40) are seen across all four IHC markers in 1 poorly differentiated carcinoma and 2 NEPC.
Conclusions: This study provides one of the first systematic, standardized assessments of mCRPC biopsy morphology and IHC marker expression. NKX3.1 and AR predominated in adenocarcinoma and poorly differentiated carcinomas, whereas SYP and INSM1 reliably identified neuroendocrine carcinomas. Mixed subtypes exhibited overlapping lineage features. Ki-67 indicated differences in tumor proliferation across subtypes. These findings highlight the morphologic and immunophenotypic heterogeneity of mCRPC and emphasize the need for integrated pathologic evaluation to refine diagnosis and support translational research.

#3827 Cyclic immunofluorescence (CyCIF) staining for highly multiplexed circulating tumor cell (CTC) imaging using the Genesis Cell Isolation System with Celselect Slides.

Yoon-Tae Kang[1], Floyd Watkins[2], Dominique Winston[2], Marta Gonzalez-Plasky[2], Adam Corner[1], Nathan Knapp[1], David Coe[1], Elizabeth Jordan Dreskin[1]

[1]Bio-Rad Laboratories, Hercules, CA,[2]Bio-Rad Laboratories, Ann Arbor, MI

Introduction: Blood-based liquid biopsy enables the analysis of CTCs, which is providing a less invasive method for cancer monitoring compared to tissue biopsy methods. Immunofluorescent (IF) staining of CTCs can identify expression of protein markers associated with cancer origin, progression and metastasis. However, conventional IF imaging is limited to 4-5 markers at a time due to the spectral overlap, hindering in-depth insights into disease status and tumor heterogeneity. CyCIF is a method for performing highly multiplexed IF imaging via repeated cycles of imaging and fluorescence inactivation, thus enabling multiple biomarker studies from the same sample, which is crucial for studying extremely rare cells, such as CTCs. Here, we demonstrate on-system CyCIF on CTCs captured using the Genesis Cell Isolation System with Celselect Slides.

Methods: To run a CyCIF, two destaining buffers and a custom Genesis protocol were prepared. Contrived CTC samples were prepared by spiking breast cancer cells (MCF7) into whole blood from a healthy donor. The samples were processed following the Genesis Enumeration protocol with either Indirect Stain Kit or Indirect Stain Kit. The stained Celselect slides were imaged then destained following a two-step-destaining protocol (destaining and stripping) using hydrogen peroxide and low pH stripping buffer. Upon checking the destaining performance, the slide was re-stained and imaged again using the same antibody panel or a new panel. Hydrogen peroxide can deactivate fluorophores through irreversible chemical oxidation and intentionally erase fluorescent signals. Mild stripping buffer works by disrupting antibody-antigen interactions to remove antibodies, allowing the membrane to be re-probed for different proteins.

Results: The slide was stained using a standard CTC panel (CK/CD45/DAPI), destained and restained using the same CTC panel. At each step, the slide was scanned and analyzed using the BioTek Lionheart (Agilent) and its Gen5 software under the same exposure time and conditions (LUTs) Over 82 percent of spiked cancer cells were initially captured and stained using the test panel. Upon destaining with the optimized protocol, 90.32% of these cells were detained. Restaining with the same panel resulted in detection of over 85% of the originally captured CTCs. This demonstrates effective on-system CyCIF demonstration for rare cell studies with minimal cell loss.

Discussion and Conclusions: By combining CTC capture with a custom protocol, we present a cost-effective, efficient, and powerful solution for multiplexed protein marker expression studies on CTCs. This chemistry and protocol can be applied to multiple CTC staining panel applications using one Celselect slide across many sample types, thus maximizing the results with a limited sample type and volume for liquid biopsy.

#3828 Signatera HRD score enables high accuracy classification of homologous recombination deficiency.

Kimberly Zhu, Carly B. Scalise, Rojin Safavi, Annette Angus, Matthew Rabinowitz, Catalin Barbacioru, Ahmet Zehir

Natera, Inc., Austin, TX

Homologous recombination deficiency (HRD) is known to predict patient response to poly (ADP-ribose) polymerase (PARP) inhibitors and platinum agents, yet reliable detection remains difficult in patients who lack pathogenic variants in canonical homologous recombination repair genes. For these cases, HRD status can be assessed by the genomic “scars” caused by genomic instability, such as loss of heterozygosity (LOH), telomeric allelic imbalance (TAI), and large-scale state transitions (LST). However, current approaches have limited sensitivity, especially in specimens with low tumor purity. Here, we describe the development and performance of Signatera HRD score, an algorithm that uses tissue-based whole-exome and -genome sequencing (WES and WGS) data to determine HRD status. The algorithm integrates somatic single nucleotide variant (SNV) and copy number variant (CNV) features within a probabilistic framework to infer genomic scarring with high sensitivity and specificity. The underlying model was trained on WES and WGS data from 1,600 tumors of multiple cancer types. From genome-wide copy-number profiles of these tumors, non-negative matrix factorization identified 22 distinct and recurrent CNV signatures. Of these 22 signatures, 9 correlated with LOH and broader genomic instability and were retained as HRD features. The CNV signatures, combined with established single-base substitution (SBS) and insertion and deletion (ID) mutational signatures adjusted for tumor purity, were then fed into a machine learning classification model to predict HRD status. We retrospectively evaluated the performance of Signatera HRD score model in a cohort of 206 patients who underwent bespoke, mPCR-NGS tumor testing (Signatera^{TM}) with orthogonally determined HRD status. Initial performance (measured as the area under the curve [AUC]) was 0.8, but increased to 0.92 by adjusting the CNV signatures for the ploidy of each sample. Incorporating established SBS and ID mutational signatures further improved the discriminative power of the model to an AUC of 0.97. Using an HRD-status threshold derived from the training set of patients, the model achieved 94.4% sensitivity at 94.2% specificity in the evaluation cohort. Feature-importance analyses indicated that mutational signatures were the dominant contributors to model performance. In conclusion, Signatera HRD score is a tissue-based model that combines ploidy-adjusted CNV signatures with SBS/ID mutational signatures to reliably predict tumor HRD status, achieving performance comparable to or better than established genomic-scar metrics such as LOH, TAI, and LST. By leveraging widely available NGS data, this approach can expand access to HRD assessment and help identify patients more likely to benefit from PARP inhibitors without requiring specialized scar assays.

#3830 Diagnostic potential of salivary miR-300 and miR-340-5p in oral cancer among Pakistani patients.

Muhammad Jawad Khan, Andleeb Zahra, Ghulam Rabia, Syeda Aba Ali, Afraz Ahmad Raja, M. Qaiser Fatmi

Department of Biosciences, COMSATS University Islamabad, Islamabad, Pakistan

Oral cancer is a significant global health concern, ranking as the sixth most common cancer worldwide. The metastasis of oral squamous cell carcinoma (OSCC) is influenced by a combination of environmental, demographic, and genetic factors, including specific genes and miRNAs. Among demographic factors, age, socio-economic status, lifestyle, and pre-existing diseases play important roles, while genetic factors, such as the differential expression of miRNAs and their target genes, are critical in disease progression. Given their differential expression, miRNAs and their target genes hold potential as diagnostic biomarkers. This study aimed to detect and profile the expression of miRNAs and their target genes in the Pakistani population. We conducted a meta-analysis of 318 miRNAs and their differentially expressed target genes. From this pool, significant miRNAs and genes were identified through *in silico* functional enrichment, pathway, and network analyses. Our analyses highlighted a set of differentially expressed genes regulated by miR-300 and miR-340-5p. To further investigate the dysregulation of these target genes, network analysis was performed using Cytoscape. We then assessed the expression of miR-300, miR-340-5p, and their target genes ALB, CDH1, CDKN1A, and BCL2 in saliva samples from oral cancer patients and healthy controls. Receiver operating characteristic (ROC) analysis was conducted to evaluate the diagnostic potential of these miRNAs, and the area under the curve (AUC) was calculated for each. Our expression and network analyses revealed that miR-300 and miR-340-5p were significantly downregulated in cancer patients. These results indicate that miR-300 and miR-340-5p possess strong diagnostic potential for oral cancer, with AUC values of 0.827 and 0.704, respectively. Overall, our findings demonstrate that miRNAs and their target genes exhibit robust discriminatory capacity, supporting their potential as biomarkers for oral cancer.

#3831 Validation of blood tumor mutation burden in Labcorp Plasma Complete.

Vito Caropreso[1], Kenneth C. Valkenburg[1], Robert Summersgill[1], Amy Meltzer[1], James R. White[1], Ellen Verner[1], Jennifer B. Jackson[1], John Pruitt[2], Deborah Boles[2], Eric Severson[2], Marcia Eisenberg[2], Brian Caveney[2], Taylor Jensen[2], Shakti Ramkissoon[2]

[1]Labcorp, Baltimore, MD,[2]Labcorp, Durham, NC

Introduction: Tumor mutation burden (TMB) is an important and clinically relevant genomic signature for guiding physicians towards immunotherapies for their cancer patients. Blood TMB (bTMB) represents a potential method to measure TMB in cancer patients via blood-based liquid biopsy testing. Labcorp Plasma Complete™ (LPC) is a laboratory developed test (LDT) that analyzes circulating tumor DNA (ctDNA) to identify genomic alterations in cancer without the need for an invasive tumor tissue biopsy. In this study, we demonstrate that LPC can successfully and reproducibly report bTMB using a cohort of 84 clinical plasma samples compared to an orthogonal LDT.

Methods: Sequencing libraries were generated using 25ng of cell-free DNA (cfDNA) from 84 unique plasma samples originating from individuals diagnosed with varying solid cancer types. bTMB values from LPC were compared to bTMB values from an orthogonal test. A subset of 6 samples with a range of bTMB values reported by the orthogonal test were processed in triplicate across multiple operators and sequencing instruments to demonstrate reproducibility of the bTMB value reported by LPC. The standard deviation and average positive and negative agreement (APA and ANA) of the bTMB values were assessed based on bTMB-high and bTMB-not high status between all evaluable replicates. Specificity was assessed in 20 non-cancerous plasma samples to determine how many observations had a higher bTMB value than the established limit of blank.

Results: Concordance of bTMB values between LPC and the orthogonal test demonstrated a Pearson correlation coefficient of 0.78. LPC reported bTMB values from 0-37.13 mutations/Mb and samples were categorized as bTMB-high if the value was ≥7 mutations/Mb by LPC and ≥15 mutations/Mb by the orthogonal. Lower bTMB values were categorized as bTMB-not high, resulting in a positive percent agreement (PPA) of 100% and negative percent agreement (NPA) of 97.5%. Samples processed for reproducibility purposes demonstrated a 100% APA and 100% ANA with an average standard deviation of 0.94 mutations/Mb.

Conclusions: Utilizing the highly trained bTMB algorithm, LPC can produce accurate and reproducible bTMB values. The addition of this molecular signature to LPC will help guide physicians towards immunotherapy options, and the added utility will enable a more comprehensive precision oncology strategy for cancer patients.

#3832 Utilization, challenges, and outlook of cell of origin classification by immunohistochemistry in DLBCL: A U.S. survey of oncologists and pathologists.

Anthony Hesser[1], Dorian Cohen[1], **Gary Gustavsen**[1], Barbara Furtado[2], Brad Thomas[2], Shady Gendy[2]

[1]Health Advances LLC, Newton, MA,[2]AstraZeneca Oncology, Gaithersburg, MD

Background: Cell of Origin (COO) classification in treatment-naïve (TN) diffuse large B cell lymphoma (DLBCL) is universally recommended across guidelines as an essential prognostic tool, yet some patients are never tested or receive equivocal results that prohibit classification. We sought to determine what barriers to COO classification exist and what could mitigate these barriers.
Methods: Double-blinded phone interviews with 8 oncologists and 10 pathologists informed current practices, challenges, and survey design. A double-blinded, online survey of 60 oncologists who treat DLBCL and 60 pathologists (26 board-certified in hematopathology) who perform COO classification was conducted from September 29 to October 10, 2025. Respondents were from a mix of academic and community-based settings in the United States.
Results: We found that oncologists view COO as a valuable tool that provides prognostic insight and a more comprehensive diagnosis, with 54% of oncologists incorporating COO classification into treatment decision-making for some patients and an additional 32% of oncologists incorporating COO for all patients. Survey results suggest that 83% of TN DLBCL patients in the US are tested for COO, with 90% of US practices using immunohistochemical (IHC) techniques. Oncologists and pathologists prefer IHC due to its accessibility, fast turnaround time, and relatively low cost. Gene expression profiling (GEP), while offering more granular classification, is less common due to higher costs and taking 4-6 days longer to return results. 89% of US oncologists were confident using IHC results for treatment selection as they consider the IHC-GEP concordance sufficient. Although IHC is routine, 10-15% of samples initially yield equivocal results due to challenges with all three Hans algorithm markers, particularly with CD10 and MUM1, citing variability in staining protocols, ambiguity in scoring weakly positive cells, and difficulty interpreting focal versus diffuse signal. After secondary review, only ~3% of samples remain equivocal and another ~6% are unreportable due to inadequate sample quality or quantity. The potential for oncologists to use pathology results is impeded by missing information in the report, lack of a COO classification in the top-line diagnosis, and variation in report structure, even among pathologists at the same institution.
Conclusion: IHC is a widely used, reliable method for COO classification in TN DLBCL with 86% of oncologists using the results for treatment decisions. Our findings suggest that developing consensus guidelines for standardized pathology reports and developing educational materials to reinforce the clinical implications of COO and guide handling of equivocal results will help mitigate testing barriers and increase the proportion of patients receiving actionable COO classifications.

#3833 Development of a novel extracellular vesicle-based biomarker approach for pediatric high-grade glioma.

Adriana Fernandez Garcia, Poorvi Iyer, Pablo Ashi, Kosuke Funato

Biochemistry and Molecular Biology, University of Georgia, Athens, GA

Pediatric high-grade gliomas (pHGGs) account for 20% of childhood brain tumors and are associated with poor survival rates. Currently, pHGG detection relies on Magnetic Resonance Imaging (MRI), a costly and time-consuming procedure. Extracellular vesicles (EVs) carry molecular markers indicative of their cellular origin and can be isolated from various biofluids, offering an alternative approach. Recent studies showed that pHGGs contain cells that molecularly and morphologically resemble radial glia (RG), a type of neural progenitor. Given that RGs are normally exclusive to the developing brain, we hypothesized that EVs secreted from RG-like glioma cells (RG-EV) serve as a pHGG biomarker. However, there are no established molecular markers to specifically detect RG-derived EVs. To address this, we first identified a combination of surface markers to differentiate EVs derived from RG-like glioma cells from those of non-RG cells. We next validated the expression of these markers in patient-derived cell lines. Our analysis of EVs showed that pHGG cells secrete a significantly higher proportion of RG-EV compared to human astrocytes (88.88 ± 7.69% vs 0.57 ± 0.28%; $p < 0.0001$), along with other tumor-associated markers, including targets of chimeric antigen receptor (CAR) T cell therapy such as disialoganglioside GD2 (73.46 ± 11.75% vs 0.32 ± 0.07%; $p < 0.001$). Taken together, our findings showed that RG-derived EVs can be specifically isolated and detected by the combination of markers, distinguishing pHGG cells from non-malignant astrocytes. This work establishes a basis for developing a novel EV-based diagnostic biomarker approach for pHGGs.

#3834 Performance validation of a next generation sequencing myeloid assay on an integrated nucleic acid purification and sequencing system.

Amanda Weaver, Ubaradka Sathyanarayana, Hayden Tomazin, Gary Pestano

Biodesix, Inc., Louisville, CO

The large diversity of myeloid neoplasms requires in-depth characterization of genetic abnormalities, including single-nucleotide variants (SNVs), small insertions and deletions (INDELs), and fusions and translocations for diagnosis and management. NGS can identify mutations associated with myeloid disorders to diagnose specific subtypes or identify a personalized and patient-specific treatment. We validated a targeted NGS myeloid assay for use in our CAP/CLIA accredited clinical laboratory. The myeloid NGS panel can identify up to 45 key DNA targets and 34 fusion driver genes covering over 800 unique fusions. The assay utilizes an automated purification system and sequencer with an on-board bioinformatics pipeline and report generation capabilities. This automated workflow has a turnaround time of approximately 24 hours from loading of the test specimen on the purification system to results ready for review. All steps were hands-off except for sample loading and transfer of the nucleic acid purification plate to the sequencer. Commercially available reference materials consisting of contrived DNA and RNA from cell lines with SNVs, INDELS, and fusions common to myeloid disorders were used for analytic sensitivity and precision studies. Precision was evaluated in triplicate over 2 instruments, 3 days, 2 operators, and 3 runs. For analytic specificity, ten normal healthy donor DNA and RNA were extracted from blood collection tubes designed to stabilize nucleic acid. For accuracy, 8 peripheral blood lymphocytes specimens from patients with a variety of myeloid disorders were extracted and assayed on both the myeloid panel under validation and a reference NGS myeloid panel. The 8 myeloid specimens' primary diagnosis was chronic myeloid leukemia (n=3) and myelodysplastic syndrome (n=5). For accuracy, the NGS myeloid assay panel had 100% concordance to the reference NGS myeloid panel. All ten normal healthy donors had no variants detected indicating high specificity. Limit of detection was established as ≥5% Variant Allele Frequency (VAF) for DNA and ≥250 fusion mapped reads for RNA fusions. For precision, the %CV between all conditions was 4.8-28.6% for the 23 DNA variants and 17.9-36.0% for the 9 fusion variants. Our data supports the use of this targeted myeloid NGS assay and the integrated purification/sequencer system for the detection of genetic lesions in myeloid neoplasms. The streamlined workflow accelerated result generation, enabling faster treatment decisions. Automation reduces the need for qualified operators and facilitates efficient clinical management of patient samples for disease diagnosis and treatment guidance. Additionally, availability of timely results can benefit patients by enabling earlier treatment decisions. These qualities support the use of this system in clinical settings for more efficient management of patients' disease.

#3835 The expression of Napsin A by immunohistochemistry in colorectal adenocarcinomas: An observational study.

Cawekazi Cingo[1], Rahaba Marima[2], Tebogo Marutha[2], **Zodwa Dlamini**[2], Benny Mosoane[1]

[1]Department of Anatomical Pathology, University of Pretoria, Pretoria, South Africa,[2]Pan African Cancer Research Institute (PACRI), University of Pretoria, Pretoria, South Africa

Background:
Distinguishing primary colorectal adenocarcinoma from metastatic pulmonary adenocarcinoma can be challenging in small biopsies, particularly when tumors are mucin-rich or poorly differentiated. Napsin A is widely used as a marker of pulmonary adenocarcinoma, yet scattered reports suggest it may sometimes be expressed in non-pulmonary primaries, including colorectal cancer. We set out to see how often napsin A is expressed in colorectal adenocarcinomas in our setting and to gauge how much of a diagnostic trap it may pose.
Methods:
We retrospectively reviewed 107 colorectal adenocarcinoma samples using formalin-fixed, paraffin-embedded tissue blocks. Napsin A immunohistochemistry was performed using polyclonal and monoclonal antibodies. Three pathologists independently reviewed the slides; napsin A was considered positive when granular cytoplasmic staining was present in at least 1% of tumor cells. For each case, we recorded tumor differentiation, histological subtype, and CDX2 status.
Results:
Of the 107 tumors, 83 (77.6%) were moderately differentiated, 18 (16.8%) poorly differentiated, and 6 (5.6%) well differentiated. Histological subtypes included not otherwise specified (84.1%), mucinous (6.5%), signet ring (6.5%), and a small number of other variants. All cases were CDX2 positive, supporting a colorectal origin. Napsin A staining was observed in only 1/107 cases (0.9%) of poorly differentiated signet-ring adenocarcinoma, confined to the monoclonal antibody; none showed positivity with the polyclonal antibody.
Conclusion:
In this series, napsin A expression in colorectal adenocarcinoma was uncommon but not absent. Thus, a napsin A-positive metastatic adenocarcinoma could still represent a colorectal primary, especially in unusual histological subtypes. Our findings support cautious use of napsin A, always alongside morphology, a broader immunohistochemical panel, clinical data, and, where possible, molecular work-up. A larger multicenter dataset would help clarify generalizability and whether specific colorectal carcinoma subtypes are more prone to napsin A expression.

#3836 IGF system genes as colorectal cancer biomarkers in Puerto Rico.

Hilmaris Centeno-Girona, Camille Zenon-Melendez, Sheila Natalie Lopez Acevedo, Ingrid Montes-Rodriguez, Elba V. Caraballo-Rivera

University of Puerto Rico Comprehensive Cancer Center, San Juan, Puerto Rico

Introduction: Colorectal cancer (CRC) disproportionately affects Hispanic/Latino (H/L) populations; however molecular biomarkers remain understudied in this population. While individual IGF-axis have been explored as CRC biomarkers, comprehensive transcriptomic evaluation of the complete IGF system, including IGFs, receptors, and binding proteins, for stage-specific detection remains limited, particularly for H/L living in Puerto Rico. This study aimed to characterize transcriptomic dysregulation of the IGF system in CRC and evaluate individual genes and multi-gene signatures as diagnostic biomarkers to discriminate tumor from normal tissue and differentiate early-stage from advanced-stage disease.

Methods: RNA was extracted from 28 tissue samples (15 CRC cases, 13 controls) from the Puerto Rico Familial Colorectal Cancer Registry (PURIFICAR) using QIAGEN RNeasy Kit. RNA sequencing was performed on Illumina NextSeq 550. Differential gene expressions were analyzed using DESeq2 (adjusted $p<0.05$, log2FC>1). Pathway enrichment was analyzed using the Reactome database. Logistic regression models (crude and age and BMI-adjusted) estimated odds ratios for gene associations, overall and by CRC stage. ROC analysis determined diagnostic performance: AUC, sensitivity, and specificity. An IGF system multi-gene signature score was developed using the uncorrelated differentially expressed IGF genes (IGF1, IGF2, IGFL2, IGFL4). Significance was set at $p<0.05$.

Results: Our results show dysregulation of the IGF system across CRC stages, with IGF2 and IGF1R consistently upregulated and stage-specific IGFBP expression patterns. The multi-gene signature demonstrated good CRC discrimination (AUC: 0.831, $p=0.002$), with superior performance in advanced disease (AUC: 0.894, $p=0.002$). Among individual genes, IGFBP5 showed highest crude accuracy (AUC: 0.856, $p=0.020$), which improved when adjusted for age and BMI (AUC: 0.964, 92.3% sensitivity/specificity, $p<0.001$). IGFL4 showed excellent discrimination in advanced-stage models (adjusted AUC: 1.00, OR: 6.03, $p<0.001$). Early-stage detection was particularly strong for IGFBP5 and IGFL2 (adjusted AUC>0.94). Enriched pathways included IGF1R-SHC signaling and platelet activation in advanced disease.

Conclusion: This transcriptomic analysis identifies IGFBP5 and a multi-gene IGF signature as potential stage-specific biomarker candidates for CRC in H/L in Puerto Rico. Further validation in larger cohorts is warranted to determine whether IGF system genes can improve CRC detection.

: Liquid Biopsies: Circulating Nucleic Acids 3
Poster Session

#3840 Detection of minimal residual disease in colorectal cancer patients after surgery through circulating tumor DNA profiling.

Luis Maya Janssen[1], Ekaly Apagnha[1], Flavio de Alencar Teles Barreto[1], Andre Araujo de Medeiros Silva[2], Mayra Veloso Ayrimoraes Soares[1], Joao Batista de Sousa[2], **Fabio Pittella-Silva**[1]

[1]Laboratory of Molecular Pathology of Cancer, Faculty of Health Sciences, University of Brasilia, Brasilia, Brazil,[2]Division of Colorectal Surgery, Brasilia University Hospital, University of Brasilia, Brasilia, Brazil

Accurate identification of minimal residual disease (MRD) after curative-intent resection remains a critical unmet need in colorectal cancer (CRC). Given the narrow postoperative window during which current adjuvant chemotherapy (ACT) improves outcomes, rapid and reliable biomarkers are essential to guide timely treatment decisions. Here, we assess the prognostic performance of a targeted liquid-biopsy mutation panel for postoperative ctDNA detection to identify MRD and support ACT decision-making in CRC. We performed targeted sequencing using a Thermo Fisher Scientific NGS platform (Ion S5 Oncomine based panel) to assess more than 200 hotspot mutations across key CRC-associated genes. All samples were sequenced to a mean depth of ~50,000× using 10-20 ng of cfDNA, enabling detection of variants with a VAF >0.05%. ctDNA was evaluated before and after treatment in 49 patients with resectable stage I-III CRC (32 colon, 17 rectal), with blood samples collected at baseline and again 4 weeks after surgery or neoadjuvant therapy. Baseline ctDNA alterations were detected in 75% of patients (37/49), with higher detection rates in stage III (78%; 21/27) compared with stage II (69%; 11/16) and stage I (67%; 4/6). Across all baseline-positive samples, 76 mutations were identified in 10 genes, predominantly *TP53* (n=26), *APC* (n=14), *KRAS* (n=10), and *PIK3CA* (n=6), with a median VAF of 0.97% (range 0.05-17.9%). Post-treatment ctDNA positivity was observed in 57% of patients (28/49), indicating persistent MRD. A reduction in VAF after treatment occurred in 30% (15/49), including 9 patients with >50% decreases, consistent with a partial molecular response but ongoing subclinical disease. Conversely, 27% (13/49) showed increased VAF, suggesting inadequate treatment response and a higher risk of relapse. Complete ctDNA clearance occurred in 24% of patients (12/49), 8 with colon cancer and 4 with rectal cancer, all of whom remain event-free for at least 12 months. Up to date, one rectal cancer patient remains ctDNA-negative for 18 months. Finally, 18% of patients had no detectable mutations at either time point, underscoring the need for further assay refinement to improve detection sensitivity in this subgroup. In conclusion, postoperative ctDNA positivity identified patients with persistent molecular disease, while ctDNA clearance correlated with short-term event-free outcomes. These findings support the use of ctDNA profiling as a practical tool to guide postoperative treatment decisions.

#3841 Prognostic significance of PI3K-AKT pathway alterations identified by ctDNA sequencing in metastatic castration-resistant prostate cancer.

DongSoo Kyung[1], Yongjun Cha[1], Chang Wook Jeong[2], Seung-hwan Jeong[2], Chel Lee[3], Won Yeong Ko[1], Jee-Soo Lee[4], Moon-Woo Seong[4], Cheol Kwak[2], Tae-You Kim[5]

[1]IMBdx, Seoul, Korea, Republic of,[2]Urology, Seoul National University Hospital, Seoul, Korea, Republic of,[3]Pathology, Seoul National University Hospital, Seoul, Korea, Republic of,[4]Laboratory Medicine, Seoul National University Hospital, Seoul, Korea, Republic of,[5]Internal Medicine, Seoul National University Hospital, Seoul, Korea, Republic of

Background: Aberrations in the PI3K-AKT pathway are key drivers of castration-resistant prostate cancer (CRPC), promoting therapeutic resistance and poor outcomes. As these alterations become increasingly relevant for targeted therapy, defining their prevalence and prognostic value through noninvasive genomic profiling is essential. We therefore assessed PI3K-AKT pathway alterations in metastatic CRPC using high-depth circulating tumor DNA (ctDNA) sequencing.
Methods: A total of 127 patients with mCRPC underwent high-depth ctDNA sequencing using the AlphaLiquid®100 assay, covering PI3K-AKT pathway genes and homologous recombination repair genes. Paired PBMCs were available for 87 patients, while 40 underwent plasma-only profiling with our machine learning-based model applied to remove CHIP-related variants. For orthogonal comparison, PTEN immunohistochemistry (IHC) was performed using a mouse monoclonal antibody (clone 6H2.1, M3627, Dako). ctDNA metrics were evaluated with baseline clinical data and overall survival (OS), and outcomes were compared between PI3K-AKT-altered and wild-type disease.
Results: Among 127 patients (median age, 66 years), high-grade tumors were common (Gleason ≥8 in 71.7%), with advanced clinical T3-T4 disease in 78.7%, nodal involvement in 59.8%, and synchronous metastasis in 58.3%. The median PSA at diagnosis was 53.7 ng/mL, and 33.1% had undergone prior surgery. Somatic ctDNA alterations were detected in 91.3% (median 3; range 0-47), with substantial heterogeneity in variant types and tumor fractions (median 0.98%; range 0.05-79.6%). PTEN pathogenic mutations were found in 9.4% and activating *PIK3CA* and *AKT1* alterations in 7.9% and 0.8%. PTEN loss by IHC was present in 46.9% (30/64), with the overall 54.7% concordance with PTEN pathogenic mutations in cfDNA. Baseline clinical features were similar between PI3K-AKT-altered and wild-type tumors, except for higher T3-T4 disease ($p<0.001$). PTEN IHC loss was not associated with overall survival (OS) in the full cohort (HR 1.47, 95% CI 0.36-6.06) or in synchronous metastasis (HR 2.41, 95% CI 0.37-15.55). In contrast, PTEN pathogenic mutations detected via ctDNA were associated with inferior OS in the overall cohort (HR 3.19, 95% CI 0.90-11.37; $p=0.073$) and showed significant impact in synchronous metastasis (HR 4.91, 95% CI 1.29-18.67; $p=0.019$). A similar trend was seen for PIK3CA and/or AKT1 mutations (HR 3.25, 95% CI 0.95-11.16; $p=0.061$).
Conclusion: PTEN pathogenic mutations identified through ctDNA sequencing were strongly associated with worse overall survival in mCRPC and outperformed PTEN IHC in prognostic value. These results underscore the utility of ctDNA profiling for detecting PI3K-AKT pathway alterations and its potential to inform targeted treatment strategies in mCRPC.

#3842 Non-invasive cfDNA methylation profiling for prediction of PD-L1 tumor proportion score status in NSCLC.

Wei Tian, Anton Valouev, Kunwar Singh, Matthew Ellis, Katie Quinn, Tingting Jiang, Martina Lefterova, Justin Odegaard, Darya Chudova

Guardant Health Laboratory, Redwood City, CA

Background: Programmed death-ligand 1 (PD-L1) expression, measured by tumor proportion score (TPS), guides immunotherapy (IO) selection in NSCLC. However, tissue-based PD-L1 immunohistochemistry (IHC) is often limited by insufficient tissue, sampling bias and intratumoral heterogeneity. cfDNA methylation signatures enable non-invasive measurement of tumor-derived epigenetic signals and may be able to capture PD-L1-associated biology from a simple blood draw. We developed a cfDNA methylation-based predictor to identify patients with low PD-L1 TPS (<50%), a group more likely to benefit from IO combination regimens rather than IO monotherapy.

Methods: cfDNA methylation profiles of >500 plasma clinical patient samples, each with paired tumor PD-L1 IHC data, were analyzed across thousands of regulatory regions. A regularized logistic regression model was trained to predict samples with PD-L1 TPS <50%. Model performance was evaluated on an independent test cohort (N=90) by comparing predicted calls with IHC-based PD-L1 TPS measurements.

Results: The cfDNA methylation predictor for identifying PD-L1 TPS <50% cases achieved >50% sensitivity, 87% specificity, and >90% positive prediction value (PPV). Model performance was consistent across NSCLC histologies (LUAD and LUSC) and remained robust at tumor fractions as low as 0.05%. Approximately 70% of liquid biopsy samples were evaluable, supporting the feasibility of cfDNA methylation analysis for the majority of clinical samples.

Conclusions: Our methylation-based PD-L1 low predictor enables non-invasive detection of NSCLC cases with tissue PD-L1 TPS <50%, offering a potential alternative when tissue is limited or not available. Further investigation is warranted to determine whether an epigenetic PDL1 IHC trained classifier can support treatment decisions by identifying NSCLC patients more likely to require IO chemotherapy combination therapy.

#3843 Sequencing full-length mRNA in whole blood of breast cancer patients for antibody-drug conjugate therapy selection.

Jacob Bradley[1], Gabriel Benitez[1], Mark Barnett[1], Oliver Eve[1], Ivalya Ivanova[1], Katrina Morris[1], Alice Seguret[1], Ahmad Zyoud[1], John Davey[1], Yuanyuan Cheng[1], Amy Robinson[1], Arran Turnbull[2], Mike Dixon[2], Han-Yu Chuang[1], Rick Hockett[1], **Richard Kuo**[1], Pamela N. Munster[3]

[1]Wobble Genomics, Edinburgh, United Kingdom,[2]Western General Hospital, Edinburgh, United Kingdom,[3]UCSF - University of California San Francisco, San Francisco, CA

Identifying biomarkers for selection of therapeutics is a critical unmet need. For many existing treatments, particularly antibody-drug conjugates, there are limited or only partially effective options for determining efficacy. For example, breast cancer therapy selection requires accurate quantification of tumour HER2 expression, but current HER2 testing methods, primarily based on IHC and ISH, lack the precision to distinguish HER2 status in HER2 low and ultra-low patients. When determining HER2 ADC eligibility, the lack of reliable HER2 quantification can lead to under- or over-treatment. Developing an accurate and reliable HER2 quantification method will enable safer and more effective HER2 ADC utilization.We have developed a novel platform that leverages long-read sequencing to capture full-length mRNA and generate isoform-level expression profiles. We processed 30 tumor biopsies and 50 whole blood samples from breast cancer patients, as well as blood samples from 50 control patients. By integrating the tumor and blood transcriptome data, we characterized the expression of 61,537 genes from the Ensembl reference, including 1,223 cancer-related genes, such as HER2 (based on COSMIC Cancer Gene Census, established ADC targets and HER2-expression related gene sets) to identify novel splice junctions and other features with the potential to act as diagnostic biomarkers for ADC targets including HER2. We identified 17,114 novel splice junctions from novel RNA isoforms (not previously reported in the Ensembl reference human transcriptome annotation) across 5,423 genes that were found at 5-50% prevalence within our cancer patient cohort. This included 1,381 novel splice junctions found within 357 of the cancer-related genes, including 12 novel splice junctions in HER2 representing potential alternative receptor structures. Comparative analysis of combined feature sets in samples with different HER2 statuses demonstrate potential for developing a liquid biopsy method of characterising cancer receptor profiles for informing suitable ADC therapies. Our novel approach utilizing full-length RNA sequencing enables more comprehensive characterization and precise quantification of tumor-associated expression of HER2 and other cancer-related genes, providing new insights into transcript diversity and expression patterns that are critical for improving diagnostic accuracy, refining treatment selection, and ultimately enhancing patient outcomes.

#3844 Longitudinal ctDNA monitoring in melanoma using highly multiplexed USE-PCR incorporating bespoke targets enables real-time detection of treatment response and recurrence.

Hunter Miller[1], Annalara Fischer[1], Melissa Hall[2], Michael E. Egger[3], Kavitha Yaddanapudi[4], Lucien Jacky[5], John Alvarado[5], Aaron Aguiar[5], Nathaniel Clark[5], Paul Belitz[5], Jeremy Myslinski[5], **Jerrod Schwartz**[5], Paul Flook[5], Mark Linder[1]

[1]Department of Pathology and Laboratory Medicine, University of Louisville, Louisville, KY,[2]Health Brown Cancer Center, University of Louisville, Louisville, KY,[3]Department of Surgery, Health Brown Cancer Center, University of Louisville, Louisville, KY,[4]Department of Medicine, Department of Microbiology and Immunology, Health Brown Cancer Center, University of Louisville, Louisville, KY,[5]ChromaCode, Inc., Carlsbad, CA

Purpose: Circulating tumor DNA (ctDNA) is a promising biomarker for real-time monitoring of treatment response and recurrence, but current sequencing-based assays are limited by cost, TAT, performance on difficult regions, and sampling frequency. Universal Signal Encoding PCR (USE-PCR) is a highly multiplexed digital PCR chemistry that enables >30 tumor-informed targets to be measured per reaction. We evaluated its performance in a longitudinal melanoma cohort with dense serial sampling.

Methods: Tumor/ctDNA sequencing identified subject-specific variants, including challenging GC-rich loci such as *TERT* c.-124C>T. Multiplexed, tumor-specific USE-PCR panels were designed using Apollo, an automated cloud-based workflow. Panels flexibly incorporated additional targets and were compatible with low-shedding ctDNA. Plasma cfDNA and matching PBMC samples were collected from 8 melanoma subjects at high density (up to 20 timepoints per patient over ~2 years). Plasma ctDNA VAF trajectories, corrected for PBMC, were quantified on a commercial dPCR platform and compared with clinical course and treatment events. Analytical validation included sensitivity, precision, linearity, specificity, cross-platform performance, and robustness with low DNA input (<10 ng).

Results: USE-PCR detected distinct molecular phenotypes including clear treatment response (rapid VAF decline), molecular recurrence (0→5%→15% VAF within ~80 days), stable disease (VAF ~0), and mixed responses with target-specific fluctuations often preceding clinical progression or therapy change. An average of four variants were measurable per subject. Sampling at ~20-day intervals uncovered rapid, low-level shifts in ctDNA, including subclonal SNVs at <0.2% VAF, not achievable with quarterly surveillance. Detection was reliable down to 80 ppm with ≤14 SNV targets, strong precision (CV <15%), and linearity over 4 logs. The platform was robust on GC-rich and historically difficult NGS targets, including the *TERT* promoter, maintained performance with low cfDNA input (<10 ng), and allowed seamless addition of new variants (e.g. *BRAF* V600E/K, *NRAS* Q61) for longitudinal monitoring.

Conclusions: USE-PCR is a rapid (median TAT < 6 hrs), low-cost, and highly scalable platform for tumor-informed ctDNA monitoring, enabling high multiplexing, compatibility with difficult genomic loci, and frequent sampling suitable for real-time clinical management. High-density longitudinal data reveal molecular patterns aligned with disease activity supporting USE-PCR for dynamic treatment response assessment and recurrence monitoring. Processing of a larger cohort is in progress to enable prospective clinical validation.

#3845 Enhancing MRD detection through an ultrasensitive ctDNA test: Insights from real-world clinical data.

Rachel Marty Pyke, Steven Dea, Sherif El-Refai, Fabio C. P. Navarro, Charles W. Abbott, Yi Chen, Janet Lai, Gabor Bartha, John M. Lyle, Jason Harris, Vijay Gunuganti, **Sean M. Boyle**, Richard O. Chen

Personalis, Inc., Fremont, CA

There is a need for more sensitive circulating tumor DNA (ctDNA) tests that can achieve earlier detection of disease. The NeXT Personal Dx (NPDx) ctDNA MRD test utilizes a bespoke panel of up to ~1800 variants to achieve ultrasensitive detection down to ~1 part per million (PPM) of ctDNA with high analytical specificity (>99.9%). Here, we describe the real world performance from more than 5,000 patients profiled using NPDx. In this analysis we examined performance in a variety of real world testing situations and in the ultrasensitive range below 100PPM and 10 PPM, the latter of which has not been previously characterized.

Overall, the median limit of detection (LOD) across all timepoints was 1.90 PPM (IQR:1.53-2.70 PPM) across 15 different cancer types. This performance was achieved with a relatively low median cell free DNA (cfDNA) input of 12ng (range 2-30 ng). 45.3% of tests were ctDNA positive overall. The NPDx tests performed well with challenging FFPE tumor samples (low tumor DIN <=3.4 or tumor fraction <=20%), achieving low LODs (median = 2.38 and 2.33 PPM, respectively). NPDx also achieved a median LOD of 3.78 PPM on low TMB tumors (<=0.98 mutation/MB). With ultra-low cfDNA inputs (<=5ng, 11.98% of cohort), NPDx achieved a median LOD of 2.31 PPM.

Next we looked at performance in the ultrasensitive ranges below 100 PPM and 10 PPM. 40.2% of detections were in the ultrasensitive range below 100 PPM. Notably, 36.6% of all ultrasensitive detections were found to be <10 PPM (14.7% of detections overall), which aligned well with data from published NeXT Personal clinical studies (Lung - 42.5% in RWD, 40.5% in Black et. al 2025; Breast - 37.5% in RWD, 42.2% in Garcia-Murrillas et. al 2025). Detection rates <10 PPM were consistent across cfDNA input amounts down to 2 ng. For those patients who had sustained ctDNA positivity after a ctDNA negative timepoint, 49% had their first MRD+ detection <10 PPM.

Two case studies demonstrate the clinical value of detections below 10 PPM in patient management. A 68-year-old female with squamous NSCLC underwent left upper lobectomy and MRD monitoring with NPDx. After three negative results, two low-level positives (6.2 and 9 PPM) prompted PET imaging that revealed a surgical-site recurrence. ctDNA rose to 80 PPM on the day of imaging, and radiation therapy led to ctDNA clearance. A 67-year-old female with colorectal cancer treated with FOLFOX + Avastin achieved ctDNA clearance and remained negative for over a year. Following a treatment break, low-level ctDNA positivity (1 and 3 PPM) preceded imaging-confirmed recurrence and chemotherapy was resumed. These cases highlight how NeXT Personal detections <10 PPM can guide earlier clinical interventions in real-world practice.

These data demonstrate the consistent performance of NPDx in challenging real world conditions with limited inputs. The data also indicate the importance of detections below both 100 PPM and 10 PPM in the clinical setting.

#3846 Short double-stranded cfDNA: A novel precision biomarker class for cancer diagnostics.

Mirko Sonntag[1], Zhoutao Zhang[1], Denise Leupold[1], Jan Mueller[1], Yevhen Vainshtein[1], Christina Hartwig[1], Georg F. Weber[2], Kai Sohn[1]

[1]In-Vitro Diagnostics, Fraunhofer IGB, Stuttgart, Germany,[2]University Clinics Erlangen, Erlangen, Germany

Background: Cancer diagnostics relies on highly specific and sensitive biomarkers to detect early stages in cancer progression as well as recurrence of disease (MRD). However, current approaches often fail to fulfill these needs, however, liquid biopsy based on cell-free DNA (cfDNA) and in particular short double-stranded cell-free DNA (footprint DNA) holds great promise for improvements. Derived from interaction of regulatory proteins including transcription factors at DNA-binding motifs, footprint DNA comprises genome-wide DNA footprints from plasma samples. Selective enrichment and quantitative analyses of footprint DNA reveal significantly different signatures for complex diseases diagnostics including various cancer types.
Methods: Footprint DNA of more than 200 plasma samples from various tumor types, including colorectal cancer and pancreatic ductal adenocarcinoma, as well as non-cancer controls were analyzed by high-throughput sequencing followed by bioinformatic peak identifications to generate a comprehensive reference annotation for genome-wide liquid footprint sites. Additionally, quantitative evaluation of footprint DNA from individual patient samples was used to differentiate between clinical conditions and benchmarking against standard of care diagnostics.
Results: Peak calling revealed approximately 8.6 million different peaks in about 6.5 million footprint regions. 3.3 million peaks overlap with annotated transcription factor bindings sites (TFBS). Moreover, 33,675 promotor regions, 55,406 CTCF sites and more than 100,000 enhancer binding regions are covered by footprint DNA signals. We also found that footprint DNA at defined genomic loci semi-quantitatively correlated with physiological markers like ALT or urea from major organ systems including liver or kidney. In a proof-of-concept cohort, differential footprint DNA biomarkers distinguished between clinical conditions, notably also closely related cancer types of colorectal cancer and pancreatic ductal adenocarcinoma (PDAC). Even same organ diseases (SOD) like pancreatitis and PDAC could be specifically discriminated using footprint DNA biomarkers.
Conclusion: Footprint DNA bears strong potential for cancer diagnostics, demonstrated by disease and cancer discrimination as well as differentiation between same organ disease. Footprint DNA enrichment sets the groundwork as identification platform of discriminatory footprint DNA biomarkers, which allows panel-based cancer detection for clinical applications. This opens new possibilities in early cancer detection and monitoring of minimal residual disease (MRD). Comprehensive footprint annotation will therefore provide a strong basis for the diagnostic of cancer and other complex diseases.

#3848 Urine cell-free DNA methylation-based deconvolution identifies tumor-specific cell types in localized urinary tract cancers.

Ze Zhang[1], Rashad Nawfal[1], Gunsagar Gulati[1], Damien Vasseur[1], Ji-Heui Seo[1], Hunter Savignano[1], Razane El Hajj Chehade[1], Karl Semaan[1], Tamara Merhej[2], John Canniff[1], Noa Phillips[1], Ning Shen[3], Phillip Adams[1], Ilana Epstein[1], Jack Horst[1], Alexis Zinselmeier[1], Rachel Throwbridge[1], Gwo-Shu Mary Lee[1], Jamil Azzi[4], Michelle S. Hirsch[4], Martin Kathrins[4], Timothy N. Clinton[4], Matthew Mossanen[4], Keegan Korthauer[3], Toni K. Choueiri[5], Matthew L. Freedman[1], Sylvan C. Baca[1]

[1]DFCI/Harvard Medical School, Boston, MA,[2]Harvard Medical School, Boston, MA,[3]Department of Statistics, The University of British Columbia, Vancouver, BC, Canada,[4]Brigham Women's Hospital, Boston, MA,[5]Dana-Farber Cancer Institute, Boston, MA

Background: Urine is a promising liquid biopsy source for non-invasive detection and monitoring of cancers of the urinary system, which currently lack screening tools for early diagnosis. Cell-free DNA methylation immunoprecipitation sequencing (cfMeDIP-seq) is a well-established tool to profile enriched 5-methylcytosine (5mC) signals in cell-free DNA (cfDNA). Recently, the *decemedip* computational framework was developed to enable cell-type deconvolution from cfMeDIP-seq data, providing a strategy to infer tumor- and immune-derived cfDNA contributions.

Methods: We designed a customized urinary cancer cfMeDIP-seq deconvolution panel and integrated it with the *decemedip* framework to estimate the proportions of nine cell types, including immune subsets (B cells, $CD4^+$ T cells, $CD8^+$ T cells, monocytes, neutrophils, and natural killer cells) as well as tumor-specific signatures for prostate, kidney, and urothelial cancers. Urine cfDNA from 54 patients at Dana-Farber Cancer Institute was profiled by cfMeDIP-seq, comprising 19 localized bladder cancers (BLCA), 18 localized renal cell carcinomas (RCC), 9 localized upper tract urothelial carcinomas (UTUC), and 8 non-cancerous kidney disease cases. Deconvolution was applied to infer cell-type composition across these groups.

Results: RCC samples exhibited significantly higher kidney cancer-derived cfDNA signal than BLCA and UTUC ($p = 3e-06$), while urothelial cancers showed significantly higher urothelial cancer-derived signal compared to RCC ($p = 1e-05$). The kidney-to-urothelial cancer cfDNA signal ratio distinguished RCC from urothelial cancers with an AUC of 0.984. In the bladder cancer cohort, five patients with low urothelial cancer signal had received neoadjuvant therapy, suggesting that deconvolution captures treatment-related changes. Excluding these cases further improved the discriminatory performance (AUC = 0.987). RCC patients also demonstrated significantly higher kidney cancer-derived signal than those with non-cancerous kidney disease ($p = 0.03$), supporting the utility of this approach for benign-malignant differentiation.

Conclusions: Urine cfDNA deconvolution via cfMeDIP-seq enables detection of tumor-specific signals and profiling of immune cell composition across localized urinary cancers. This noninvasive liquid biopsy approach demonstrates potential for early detection, disease subtyping, minimal residual disease assessment, and treatment response monitoring and warrants validation in larger prospective cohorts.

#3849 Frequent monitoring of NSCLC immunotherapy using an mDETECT liquid biopsy reveals unexpected complexity and opportunities.

Mihaela Mates[1], Andrew Robinson[1], Harriet Feilotter[2], Sofia Genta[1], Keira Frosst[3], Keira Parr[3], Garrett Baron[1], **Christopher R. Mueller**[3]

[1]Kingston Health Sciences Centre, Kingston, ON, Canada,[2]Toronto General Hospital, University Health Network, Toronto, ON, Canada,[3]Queen's University, Cancer Research Institute, Kingston, ON, Canada

The methylation DETEction of Circulating Tumour DNA (mDETECT) assay is a targeted DNA methylation-based Next Generation Sequencing liquid biopsy designed to detect cancer-specific methylation patterns. We have developed a version of our mDETECT assay that sensitively and quantitatively monitors Non-Small Cell Lung Cancer (NSCLC). This targeted approach assesses 23 differentially methylated genes in NSCLC patients covering 229 CpGs. Our assay has a 95% sensitivity at 95% specificity with an AUC of 0.95.

We conducted a pilot observational study to frequently measure tumour dynamics in patients undergoing first-line pembrolizumab monotherapy for metastatic NSCLC. 19 participants were recruited prior to the initiation of immunotherapy and followed using the mDETECT NSCLC assay. 40 mL of blood was collected pre-treatment then weekly or biweekly after treatment initiation with some patients being followed for up to 2.3 years. In total we collected 226 samples (median 11.8 timepoints per patient). Radiological assessment was performed approximately every three months as per the standard of care.

The primary aim of the study was to determine if overall survival (OS) could be predicted with the mDETECT assay within the first 6 weeks of treatment. Patients were divided by short (< 1 year), medium (1-4 years), and long term (> 4 years) OS. Patients with short OS showed constant or increasing mDETECT levels and never dropped below 80% of their pre-treatment mDETECT level. Patients with long OS showed an immediate decrease within the first 6 weeks of treatment and generally reached undetectable levels. Patients with medium OS showed a slower decline and a higher plateau than the long OS patients. These patterns, while derived from a small pilot cohort, suggest the mDETECT assay can determine within weeks if a patient is responding to immunotherapy. Continued monitoring revealed progression in some initially responding patients, with increasing mDETECT levels detected 4-6 months in advance of radiological progression.

Frequent assessment of tumour burden by a liquid biopsy such as mDETECT offers the opportunity to rapidly determine a patient's response to therapy and potentially modify treatments earlier than with radiology alone and on an ongoing basis. These findings support the feasibility and potential clinical utility of integrating methylation-based ctDNA monitoring into immunotherapy management workflows and justify further prospective validation in a larger study.

#3850 Liquid biopsy-based monitoring of disease status in patients with HPV-positive oropharyngeal carcinoma (OPSCC).

Jens Peter Klussmann[1], Oliver Siefer[1], Zurwa Merrjam Uzun[1], Jannik Johannsen[1], Dustin Firmenich[1], Nora Wuerdemann[2], Ernst J.M. Speel[3], Julie George[4]

[1]Department of Otorhinolaryngology, Head and Neck Surgery, University of Cologne, Cologne, Germany,[2]Medical Oncology, University of Cologne, Cologne, Germany,[3]Department of Pathology and Clinical Bioinformatics, Erasmus Medical Center, Rotterdam, Netherlands,[4]University of Cologne, Cologne, Germany

Introduction: The incidence of HPV-associated oropharyngeal carcinoma (HPV+ OPSCC) is increasing worldwide. In cases of tumor recurrence, distant metastases are often already present, which complicates curative tumor treatment. It is therefore of highly critical to collect molecular parameters to monitor the response of patients to therapy.
Material/Method: The aim of this study is to establish an HPV-specific blood-based analysis (liquid biopsy) to enable both early diagnosis and monitoring of disease progression. To this end, our clinical biobank includes >1800 circulating tumor DNA (ct-DNA) samples from> 300 patients with HPV-associated OPSCC at the time of initial diagnosis, during tumor treatment, as part of clinical follow-up care, and in the event of tumor recurrence.
Results: In a cohort of 434 longitudinally collected ctDNA samples from 53 patients with HPV+ OPSCC quantitative PCR (qPCR) and digital droplet PCR (ddPCR) was performed probing for E6 HPV-16 DNA sequences. In all cases, the HPV status was confirmed by p16-IHC, HPV16 DNA PCR for E6 and L1, and determination of the viral load in the tumor. There was a high concordance between qPCR- and ddPCR-based detection of HPV E6 ($P<0.001$), with ddPCR yielding higher sensitivity and specificity (>80%). HPV-16 ctDNA levels significantly correlated with tumor stage and tumor volume ($P<0.05$). In individual cases, a positive HPV ctDNA signal could be determined months before the diagnosis of tumor recurrence.
Discussion: ddPCR-based quantification of ct-HPV16-E6 DNA in blood is a promising diagnostic method to monitor therapy response and tumor progression in patients with HPV+ OPSCC. Prospective clinical studies are warranted to clinically validate ct-HPV16-E6 DNA as a quantitative biomarker for therapeutic efficacy and longitudinal disease monitoring.

#3851 Ultrasensitive ctDNA monitoring predicts early response of immunotherapy in recurrent metastatic non-small cell lung cancer.

Kishen R. Patel[1], Bailiang Li[2], Charles W. Abbott[2], Cristina Naceur-Lombardelli[1], Sadegh Saghafina[3], Sevasti Galani[1], James R. M. Black[1], Wing Liu[1], Nicola Steele[4], Gillian Price[5], Shobhit Baijal[6], Dean Fennell[7], Matthew G. Krebs[8], Tanya Ahmad[1], Alexandra Pender[9], Siow M. Lee[1], Mariam Jamal-Hanjani[1], Nicholas McGranahan[1], Allan Hackshaw[1], Sean Michael Boyle[2], Richard O. Chen[2], Charles Swanton[3], Crispin T. Hiley[1]

[1]University College London (UCL) Cancer Institute, London, United Kingdom,[2]Personalis, Inc., Menlo Park, CA,[3]The Francis Crick Institute, London, United Kingdom,[4]The Beatson West of Scotland Cancer Centre, Glasgow, United Kingdom,[5]Aberdeen Royal Infirmary, Aberdeen, United Kingdom,[6]The University Hospital Birmingham NHS Trust, Birmingham, United Kingdom,[7]Leicester Cancer Research Centre, Leicester, United Kingdom,[8]The Christie, Manchester, United Kingdom,[9]Royal Free Hospital, London, United Kingdom

Background: Circulating tumor DNA (ctDNA) offers a minimally invasive approach for response monitoring of cancer immunotherapy treatment and early prediction of therapeutic outcomes. However, the clinical utility of ctDNA-based liquid biopsy faces a critical challenge: reliable ctDNA detection in low-shedding tumors and in patients with low molecular residual disease (MRD) following treatment response. We employed an ultrasensitive ctDNA assay to address this technical limitation, enabling precise longitudinal monitoring essential for optimizing IO therapy.

Methods: We analyzed longitudinal plasma samples from 41 patients with non-small cell lung cancer (NSCLC) [adenocarcinoma (n=19), non-adenocarcinoma (n=22)], who received IO monotherapy (n=33) or combined IO and chemotherapy (n=8) in the *Deciphering Anti-tumour Response and Resistance With INtratumour Heterogeneity (DARWIN 2)* trial nested within the TRACERx study. Using NeXT Personal®, an ultra-sensitive personalized liquid biopsy approach, we tracked up to ~1,800 patient-specific somatic variants per case across 233 plasma samples.

Results: The median limit of detection across all tests was 1.52 parts per million (PPM), enabling ctDNA detection across six orders of magnitude (range 2.1-309,673 PPM), with 21% of positive ctDNA detections in the ultrasensitive range (<100 PPM), with that increasing to 28% while on treatment. Histological subtype had no impact on detection with this assay. Early molecular response (mR), defined as either >50% reduction in ctDNA or sustained ctDNA negativity from pre-treatment baseline to the subsequent plasma sample (median interval: 43.5 days), was significantly associated with improved clinical outcomes. Patients achieving early mR exhibited superior progression-free survival (PFS; HR = 0.33, 95% CI 0.14-0.77, $p = 0.010$) and overall survival (OS; HR = 0.31, 95% CI 0.14-0.70, $p = 0.005$). All patients with complete response by RECIST criteria achieved early mR (sensitivity = 100%). Conversely, disease in all patients lacking mR progressed within 15 months. Furthermore, durable molecular complete response (dmCR), defined as ctDNA negativity maintained for ≥180 days, was strongly associated with improved survival outcomes (2-year PFS: 50% vs. 9%, HR = 0.31 95%CI 0.11-0.90, $p = 0.032$; 2-year OS: 86% vs. 13%, HR = 0.06, 95% CI 0.01-0.48, $p = 0.007$ for dmCR vs. non-dmCR, respectively).

Conclusions: Early ctDNA kinetics serve as a robust predictor of long-term immunotherapy outcomes in patients with advanced NSCLC. The ability to detect ultra-low ctDNA levels allowed for accurate assessment of minimal residual disease, irrespective of lung cancer histology. These findings establish ultrasensitive ctDNA monitoring as a valuable tool for precise, real-time evaluation of immunotherapy response, with implications for clinical decision-making.

#3852 Ultrasensitive AI-driven framework for MRD detection based on multidimensional cfDNA features.

Yunfei Shi[1], Hao Zhang[2], Zexiao Lin[3], Ningyou Li[2], Maolong Wang[4], Hua Bao[2], Jinfeng Zhang[2], Zhili Chang[2], Yong Ge[5], Peng Li[6], Pan Wang[7], Liang Huang[8], Xiangming Liu[9], Lu Han[10], Wangming Ji[11], Teng Sun[9], Dujun Hua[2], Xunbiao Liu[2], Mingya Wang[2], Baihan Zhu[2], Dongqin Zhu[2], Xue Wu[2], **Haimeng Tang**[12], Hao Zhang[9], Yang Shao[13]

[1]The First Affiliated Hospital of Kunming Medical University, Kunming, China,[2]Geneseeq Research Institute, Nanjing Geneseeq Technology Inc., Nanjing, China,[3]Department of Medical Oncology, The Third Affiliated Hospital of Sun Yat-sen University, Guangzhou, China,[4]Department of Thoracic Surgery, Qingdao University Affiliated Hospital, Qingdao, China,[5]Department of Thoracic Surgery, Affiliated Hospital of Xuzhou Medical University, Xuzhou, China,[6]Department of General Surgery, The First Medical Centre, Chinese People's Liberation Army (PLA) General Hospital, Beijing, China,[7]Cancer Hospital, Chinese Academy of Medical Sciences and Peking Union Medical College, Beijing, China,[8]Beidahuang Group General Hospital, Branch 1, Harbin, China,[9]Affiliated Hospital of Xuzhou Medical University, Xuzhou, China,[10]The First Medical Centre, Chinese People's Liberation Army (PLA) General Hospital, Beijing, China,[11]PLA Rocket - Force Characteristic Medical Center, Beijing, China,[12]Geneseeq Technology Inc., Toronto, ON, Canada,[13]Nanjing Geneseeq Technology Inc., Nanjing, China

Minimal residual disease (MRD) detection is essential for postoperative risk stratification and recurrence prediction in cancer, yet current fixed-panel assays exhibit limited sensitivity and specificity, particularly in tumor-naïve settings. We developed Shielding Ultra, a pan-cancer MRD assay targeting hotspot mutations across 2,365 cancer-related genes. Leveraging ultra-deep unique molecular identifier-based sequencing and AI-driven bioinformatics, the assay integrates somatic mutations, copy number variations (CNVs), and fragmentomic (Frag) features to enable multidimensional MRD assessment within a unified workflow. Analytical validation established a detection limit of 0.0048% and demonstrated 94% sensitivity in late-stage preoperative plasma, with approximately 99% specificity in healthy controls. Tumor-naïve analysis achieved 98.9% concordance with tumor-informed workflows following multimodal integration, supporting applicability when tumor tissue is unavailable. Clinical validation across colorectal, cholangiocarcinoma, and lung cancer cohorts confirmed strong prognostic performance at early postsurgical timepoints while maintaining high specificity. In colorectal cancer, MRD positivity showed a robust association with relapse, yielding hazard ratios up to 32.47 and achieving longitudinal sensitivity of up to 90.9% during postoperative surveillance. In lung cancer, recurrence detection sensitivity was 51.5% at one week after surgery and increased to 72.7% with the addition of one-month postsurgical sampling. Across cancer types, multimodal cfDNA integration strengthened detection performance and enabled reliable identification of MRD across diverse clinical contexts. These findings demonstrate that Shielding Ultra enables sensitive and specific MRD detection through the integration of multidimensional cfDNA features and AI-based algorithms. Its strong prognostic performance across multiple malignancies and compatibility with tumor-naïve workflows support its utility for postoperative risk stratification and personalized disease management.

#3853 Genomic profiling of circulating tumor DNA in endometrial cancer in Asia: A-TRAIN study.

Hiroki Tamura[1], Yuki Kojima[2], Kazuki Sudo[3], Wan Zamaniah Wan Ishak[4], Marcelo S. Imasa[5], Arb-aroon Lertkhachonsuk[6], Ryoka Miki[7], Hiroshi Yoshida[8], Shinji Kohsaka[2], Yukari Nagasaka[1], Ryunosuke Machida[9], Tetsuya Sasaki[10], Tomomi Hata[9], Kenichi Nakamura[9], Kan Yonemori[9]

[1]National Cancer Center Hospital, Tokyo, Japan,[2]National Cancer Center Japan, Tokyo, Japan,[3]National Cancer Center Hospital - Japan, Tokyo, Japan,[4]University Malaya Medical Centre, Kuala Lumpur, Malaysia,[5]St. Lukes Medical Ctr., Quezon City, Philippines,[6]Faculty of Medicine Ramathibodi Hospital, Bangkok, Thailand,[7]Life Technologies Japan Ltd, Tokyo, Japan,[8]Gastrointestinal Oncology Division, National Cancer Center Hospital, Tokyo, Japan,[9]National Cancer Center Hospital , Tokyo, Japan,[10]Clinical Research Support Office, National Cancer Center Hpspital, Tokyo, Japan

Background: Endometrial cancer affects more than 420,000 women worldwide, with approximately 40% of cases occurring in Asia. Recently, endometrial cancer is now more precisely categorized through molecular subtyping, which has improved prognostic assessment and guided treatment strategies. In this study, we identified molecular subtypes of endometrial cancer in Asian patients using comprehensive genomic profiling of liquid biopsy samples, circulating tumor DNA (ctDNA).
Methods: This is an Asian multicenter prospective observational study conducted by five institutions in Japan, Malaysia, Philippines, Taiwan, and Thailand (NCT05099978, ClinicalTrials.gov). Eligible patients had histological diagnosis of endometrial cancer with metastatic or recurrent disease. Genomic profiling was conducted by AmpliSeq HD custom panel (Thermo Fisher Scientific), targeting 23 genes (752 amplicons), designed using AmpliSeq Designer to cover on genes and hotspot mutation regions associated with endometrial cancer. This panel can identify (1) full-length in following genes: *ARID1A, ARID1B, B2M, CCNE1, CTCF, JAK1, PIK3R1, PTEN, RB1, RPL22, SMARCB1, SMARCA4* and *TP53*, (2) hotspot mutation or region in following genes: *AKT1, BRAF, CTNNB1, ERBB2, KRAS, MET, MYC, PIK3CA, POLE* and *PPP2R1A*.
Results: From August 2022 to March 2024, a total of 60 patients with advanced endometrial cancer were enrolled, including 44 from Japan, 10 from Taiwan, 3 from Malaysia, 2 from Philippines, and 1 from Thailand. The median age was 59 (range, 31 to 79) years. Most cases were at relapse (36; 60.0%) at liquid biopsy. In terms of therapy, 10 (16.7%) of the subjects had received radiation prior to the liquid biopsy, and 33 (55%) of the patients had received chemotherapy prior to the liquid biopsy. Genomic alterations were detected in 75.0% (45/60), with a median number of 2 genomic abnormality per case (range, 0-12). The most frequently altered genes were *PTEN* (n=20, 33.3%), *TP53* (n=19, 31.7%), *PIK3CA* (n=19, 31.7%) and *CTNNB1* (n=14, 23.3%). CNV analysis excluded 18 samples with both low coverage depth and low uniformity, or low uniformity alone, resulting in a total of 42 cases analyzed. CNVs were detected in eight patients: 2 with *ERBB2* amplification, 2 with *PIK3CA* amplification, 2 with *MYC* amplification, and 2 with *CCNE1* amplification.
Conclusion: The comprehensive genomic profiling of liquid-based samples prior to treatment initiation may help guide personalized therapeutic strategies for Asian patients with advanced or recurrent endometrial cancer.

#3854 Plasma cell-free RNA transcriptome analysis reveals transcriptional dysregulation and immune remodeling in pancreatic ductal adenocarcinoma.

Gyuryang Park[1], Hyosil Kim[2], Tae Young Kim[1], Sung Joon Kim[1], Jin-Hwa Park[1], Baeki E. Kang[3], Jung Won Chun[1], Sung-Sik Han[1], Tae Min Kim[3], Sang Myung Woo[1]

[1]National Cancer Center - Korea, Goyang-si, Gyeonggi-do, Korea, Republic of,[2]Cancer Research Institute, College of Medicine, The Catholic University of Korea, Seoul, Korea, Republic of,[3]Department of Medical Informatics, College of Medicine, The Catholic University of Korea, Seoul, Korea, Republic of

Pancreatic ductal adenocarcinoma (PDAC) is a highly lethal cancer due to poor early detection and frequent treatment resistance. Current tumor markers, including carbohydrate antigen 19-9 (CA19-9), show limited diagnostic and prognostic accuracy, underscoring the need for efficient biomarkers. Cell-free RNA (cfRNA), which circulates in body fluids and can be obtained through a minimally invasive approach, reflects tumor- and tissue-specific gene expression, offering strong potential as a biomarker across various cancer types. In brief, whole blood samples were collected from PDAC patients (n=63) and healthy controls (n=8), followed by plasma isolation via centrifugation prior to cfRNA extraction. Cell-free nucleic acids were isolated using a standardized circulating nucleic acid protocol, and cfRNA purity was enhanced through additional DNase treatment and a cleanup step. Complementary DNA (cDNA) libraries were generated using a low-input, strand-specific RNA sequencing method and were paired-end sequenced on a high-throughput next-generation sequencing platform.cfRNA transcriptomic analysis identified 541 differentially expressed genes (adjusted $p < 0.05$, $|\log_2 FC| > 1$), of which 496 were upregulated and 45 were downregulated in PDAC compared with healthy controls. Although most genes were not correlated with tumor stage, a subset displayed progressive, stage-dependent expression changes. Such gradual increases or decreases across tumor stages may reflect tumor burden and disease advancement, suggesting their potential as molecular indicators of PDAC progression. Functional enrichment analysis revealed pathways related to extracellular matrix remodeling, immune regulation, and cell proliferation. Additionally, cfRNA deconvolution analysis inferred shifts in immune cell composition. Notably, the proportion of neutrophils increased from approximately 7-9% in healthy controls to 10-15% across PDAC stages, whereas naïve CD4 T cells showed a marked decline from about 26% to 10-15%, and naïve B cells decreased from roughly 13-14% to 5-10%. In contrast, regulatory T cells exhibited a relative increase across PDAC stages. Together, these alterations reflect an immune landscape progressively skewed toward immunosuppressive features in PDAC. These findings collectively suggest cfRNA transcriptomic profiling captures tumor-derived transcriptional dysregulation and systemic immune remodeling, highlighting its promise as a biomarker source and a longitudinal monitoring tool for PDAC. Funding: This work was supported in part by the National Cancer Center, Korea (No. 2510590).

#3855 Circulating DNA methylation signatures enable early detection of gastrointestinal cancers.

Ruo-Kai Lin, YAO-YU HSIEH

Taipei Medical University, Taipei, Taiwan

Background: Early detection of gastrointestinal cancers remains a major clinical challenge due to their asymptomatic early stages—particularly for pancreatic and liver cancers—combined with the limited sensitivity of current screening modalities, inadequate identification of high-risk populations, and persistent disparities in surveillance access. Given the high mortality associated with pancreatic and liver cancers and the substantial global incidence of colorectal cancer, more effective early diagnostic strategies are urgently needed.

Methods and Findings: We previously identified aberrant DNA methylation of *ZFP30* and *ZNF781* in circulating tumor DNA (ctDNA) from patients with pancreatic cancer, and aberrant methylation of *TMEM240* in patients with colorectal cancer, with *TMEM240* hypermethylation additionally associated with liver metastasis in gastrointestinal malignancies. In this study, we evaluated methylation levels of *ZFP30/ZNF781* and *TMEM240* in hepatocellular carcinoma (HCC) tumor tissues and matched adjacent normal tissues using qMSP, revealing significantly elevated methylation in all tumor samples. Aberrant methylation of these genes was also detected in plasma cell-free DNA (cfDNA) from patients with liver cancer. Analysis of TCGA Western cohorts further confirmed consistently increased methylation of these loci in pancreatic, colorectal, and liver cancers.

Validation: We validated these biomarkers in independent Asian (Taiwan) and Western (U.S.) cohorts comprising 101 gastrointestinal cancer cases—including pancreatic, colon, rectal, and liver cancers—and 350 cancer-free healthy subjects. Aberrant methylation of *ZFP30/ZNF781* and/or *TMEM240* was detectable across all gastrointestinal cancer types analyzed.

Results: Detection sensitivities were 93.8% for early-stage pancreatic cancer, 100% for late-stage pancreatic cancer, 90.62% for colon cancer, 99.0% for rectal cancer, and 90% for liver cancer, with a specificity of 98% in cancer-free controls.

Conclusion: These results demonstrate that circulating DNA methylation signatures of *ZFP30/ZNF781* and *TMEM240*provide a highly sensitive and specific non-invasive approach for detecting a broad spectrum of gastrointestinal cancers, supporting their potential utility as early detection biomarkers.

#3856 Detection of cfDNA shedding from advanced precancerous lesions.

Fei Lu, **Liliana Cerna**, Spenser Alexander, Noura Tbeileh, Esha Atolia, Dina Hafez, Eser Kirkizlar, Matthew Rabinowitz, Alexey Aleshin, Trupti Kawli

Natera, Inc., Austin, TX

Minimally invasive, blood-based tests for the detection of colorectal cancer (CRC) and advanced precancerous lesions (APLs) have emerged as a screening tool to aid in the early detection of cancer. While cell-free (cf)DNA detection of CRC has demonstrated high sensitivity and specificity, APL detection has been less successful. In an effort to understand these limitations, we evaluated the prevalence of APL cfDNA biomarkers from plasma samples. Formalin-fixed, paraffin-embedded (FFPE) or fresh frozen (FF) APL tissue and matched normal blood samples from 61 (FFPE n=27, FF n=34) individuals were obtained through biobanks. Whole-genome sequencing (WGS) data was used to design custom, research-use only, personalized, mPCR-NGS-based circulating tumor (ct)DNA assays. Matched plasma samples collected at the same time as tissue and whole blood collection were evaluated for the presence of circulating APL biomarkers in plasma. Sensitivity was calculated in FFPE and FF for the overall cohorts, by APL subtype, and lesion size. Because the subtype distribution differed from expected prevalence in screening trials (pmids 38477985, 40455622), a distribution was constructed to be representative of the final pivotal study so that a reflective sensitivity estimate could be calculated. Overall at a 90% specificity, APL plasma sensitivity adjusted for subtype incidence was 25% and 37% in matched FFPE and FF tissue samples, respectively. The lower plasma detection rate in FFPE samples could be due to the compromised tissue gDNA integrity and personalized mPCR assay design-ability with FFPE tissue preservation methodology. Median plasma sample variant allele frequencies (VAF) of detected samples was 3.6x10-5 and 1.4x10-5 for FFPE and FF, respectively. APL plasma sensitivity for was calculated for each APL subtype, including high-grade dysplasia (FFPE: 40%, N=10; FF: 38%, N=10), villous growth >25% (FFPE: 25%, N=8; FF: 38%, N=13), tubular adenomas >10 mm (FFPE: 25%, N=4; FF: 33%, N=3), and serrated lesions >10 mm (FFPE: 20%, N=5; FF: 50%, N=8). In general, sensitivity increased as lesion size increased (FFPE: 4-10 mm 20%, 11-20 mm 30%, 21-30 mm 50%, ≥31 mm 50%; FF: 4-10 mm 22%, 11-20 mm 47%, 21-30 mm 67%, ≥31 mm: 33%). In this study, we established a baseline of APL ctDNA shedding using a tissue-informed ctDNA assay that can be used for optimizing assays designed to detect APLs at expected levels in cell-free DNA.

#3857 Comprehensive profiling of circulating tumor DNA in blood enables sensitive detection and genomic characterization of HPV cancer and precancer.

Qin Wang[1], Samuli Eldorfs[1], Sangmi Sandra Lee[2], Yana Al-Inaya[1], Gjystina Lumaj[1], Eliana Epstein[3], Dipon Das[1], Emma Ricart[4], Harsharan Dhillon[5], Juniper Lake[5], Michael G. Drage[3], Shun Hirayama[6], Viktor Adalsteinsson[7], Benjamin T. Davis[3], Doga C. Gulhan[2], Daniel Faden[3]

[1]Otolaryngology-Head and Neck Surgery, Massachusetts Eye and Ear, Boston, MA,[2]Department of Biomedical Informatics, Harvard Medical School, Boston, MA,[3]Mass General Brigham, Boston, MA,[4]Harvard Medical School, Boston, MA,[5]Pacific Biosciences, Menlo Park, CA,[6]Wakayama Medical University, Wakayama, Japan,[7]Broad Institute, Cambridge, MA

Background: Human papillomavirus (HPV) causes six cancer types, yet five lack population-level screening. We have developed HPV-DeepSeek, a blood-based, multi-feature HPV whole-genome sequencing assay targeting circulating tumor HPV DNA (ctHPVDNA). HPV-DeepSeek has detected HPV+ oropharynx cancer years prior to clinical diagnosis, establishing the feasibility of blood-based HPV+ cancer screening. Here we extend testing to HPV+ anal cancer (HPV+AC) with well-defined precancer stages, to comprehensively assess blood-based detection of HPV+ cancer and precancer.
Methods: HPV-DeepSeek was applied to a pre-diagnostic cohort collected 2.8-8.6 years before HPV+AC diagnosis (N=6) and to a prospective cohort (SCAN-LITE, NCT06971276), comprising HPV+AC (N=10), anal intraepithelial neoplasia 3 (AIN3) (N=20), AIN2 (N=20), AIN1 (N=20), anal HPV-infection (N=20), anal HPV-negative with past HPV history (N=14), and healthy controls (N=60). For validation, 78 paired tissue samples were profiled with HPV-DeepSeek and 5 underwent PacBio long-read sequencing.
Results: 4/6 pre-diagnostic samples tested positive, with detection lead time 2.8 to 7.2 years before cancer diagnosis. In the SCAN-LITE study, the sensitivity for HPV+AC was 100% (10/10). Profiling ctHPVDNA detected HPV-human integration in 6/10 cases and HPV-HPV rearrangements in 8/10, which were validated in paired tissue. PIK3CA mutations were found in 2/10 cases, and CNVs were detected in 3/10 cases at the chr3q hotspot. In precancers, ctHPVDNA was detectable with decreasing positivity by disease severity: 32.5% in AIN3/AIN2 and 12.5% in AIN1/infection. 1/14 (7.1%) HPV-negative control tested positive and was later diagnosed with HPV-infection at follow-up. All healthy controls were negative, yielding 100% specificity. No HPV integration, PIK3CA mutations, or CNVs were detected in precancer. While HPV+AC primarily showed HPV16 (10/10) with one case also harboring HPV35, precancer exhibited diverse genotypes. 20 genotypes were detected, including 6 multi-genotype infections found exclusively in high-grade precancers (AIN3/2). Fragmentomics analysis revealed distinct length profiles across stages, particularly di-nucleosome peaks enriched in HPV+AC while depleted in precancer, reflecting HPV epigenetic changes during carcinogenesis.
Conclusions: HPV+AC is detectable in blood at and before clinical diagnosis. We also show, for the first time, that HPV precancer can be detected in blood, with increasing positivity as stages progress. Blood-based detection of HPV+ cancer hallmarks, including HPV integration, PIK3CA mutation, and CNV, differentiates cancer from precancer, while fragmentomics adds to stage-specific signatures. Together, these findings support the feasibility of blood-based HPV+ cancer and precancer screening with the potential of stage differentiation.

#3858 Methylation profiling of cell free DNA using EMSeq whole genome sequencing and a targeted methylome panel for classification of pediatric ocular and brain tumors.

Laura A. T. Kagami[1], David N. Buckley[1], Jesse L. Berry[1], Susan N. Chi[2], Xiaowu Gai[3], Erin Kiehna[4], Katrina O'Hollaran[1], Dejerianne Ostrow[1], Tom Rosenberg[2], Yan Chen Wongworawat[5], Liya Xu[1], Jaclyn Biegel[1]

[1]Children's Hospital Los Angeles, Los Angeles, CA,[2]Dana-Farber Cancer Institute, Boston, MA,[3]Medical College of Wisconsin, Milwaukee, MN,[4]Novant Health, Charlotte, NC,[5]Loma Linda University, Loma Linda, CA

Methylation profiling has become an increasingly valuable tool for brain tumor subclassification, especially when histologic evaluation is ambiguous and standard genetic assays are non-informative. While methylation profiling of tumor tissue is well-described, comparable analysis using cell free DNA is not yet established, especially in pediatric oncology.

We evaluated the feasibility of enzymatic methylation conversion (EMSeq) and either direct whole genome sequencing (WGS) or hybridization with a 123 megabase methylome panel (Twist BioScience). Both methods were performed on 13 samples from 12 patients with central nervous system (CNS) tumors or retinoblastoma (RB), including 10 cerebrospinal fluid (CSF) and three aqueous humor (AH) samples using 5 ng of cfDNA input. All 13 samples classified accurately with an in-house neural network model. To assess sensitivity, six CSF samples from two patients were further diluted for 1 and 2 ng input into each assay. Classification results remained consistent across dilutions, and no appreciable differences were observed between EMSeq WGS and the Twist assay.

We selected EMSeq WGS for further studies due to the ability to generate genome-wide copy number plots, unbiased CpG coverage, and faster turnaround time. Twenty-eight diagnostic and surveillance AH and CSF samples representing 13 embryonal tumors (medulloblastoma, atypical teratoid/rhabdoid tumors, embryonal tumor with multilayered rosettes, RB), five gliomas (low- and high-grade), four ependymomas, and six other CNS tumors were processed using EMSeq WGS. We compared copy number profiles generated from cfDNA EMSeq WGS to our clinically validated LBSeq4Kids platform, which combines low passage WGS (LP-WGS) to detect copy number alterations and a targeted sequencing panel to detect structural variants and fusions. In all cases, copy number profiles generated from EMSeq WGS were concordant with those from LBSeq4Kids LP-WGS.

Diagnostic AH samples, and CSF samples obtained via lumbar puncture, external ventricular drain, or ventriculoperitoneal shunt demonstrated methylation profiles concordant with their expected tumor classes. In contrast, samples obtained intraoperatively or at recurrence showed reduced classification accuracy, with some clustering with non-cancer control references. In our experience, depending on CNS tumor type and anatomic location, CSF samples obtained via intraoperative collections have rendered less reliable cfDNA data.

Herein we demonstrate that methylation profiling of cfDNA using EMSeq WGS is feasible and informative, expanding the diagnostic potential of liquid biopsy approaches to pediatric tumors. Integration of methylation analysis into our current LBSeq4Kids platform will enable comprehensive molecular profiling for diagnosis, subclassification, and disease monitoring.

#3859 Dynamic systemic immune modulation in metastatic neuroendocrine tumor (NET) patients treated with targeted alpha-emitter ^{212}Pb-DOTAMTATE AlphaMedix.

Alessandra Jordano Conforte[1], Izabela Tworowska[2], Sara Fonseca Costa[1], Marta Brzezinska[1], Amaia Martinez Usatorres[1], Noushin Hadadi[1], Sylvain Monnier-Benoit[1], Simona Pavan[1], Rouzbeh Esfandiari[3], Brian Hashemi[1], **Pedro Romero**[1], Ebrahim S. Delpassand[2]

[1]Novigenix SA, Epalinges, Switzerland,[2]RadioMedix, Houston, TX,[3]Excel Diagnostics & Nuclear Oncology Center, Houston, TX

Peptide receptor radionuclide therapy (PRRT) has been increasingly explored as a therapeutic strategy for multiple solid tumors, such as prostate cancer and somatostatin receptor-expressing GEP-NETs. While Lutathera (^{177}Lu-DOTATATE), a β-emitting PRRT, represents the current GEP-NETs standard of care. α-emitting PRRTs such as AlphaMedix (^{212}Pb-DOTAMTATE) are emerging as promising alternatives with distinct radiobiological characteristics. Ionizing radiation from PRRT not only induces DNA damage but also modulate the immune system, contributing to therapeutic response.We sought to identify evidence of systemic immunomodulation associated with α-emitter AlphaMedix treatment and to compare it with that elicited by Lutathera. Whole-blood immunotranscriptomes were analyzed using the LITOSeek platform to characterize immune signatures and pathways differentially activated by α- and β-emitting PRRTs. This approach elucidates the immunological mechanisms underlying α-particle therapy and uncovers potential biomarkers of treatment response.

Methods: Whole blood samples were collected with PAXgene Blood RNA tubes from GEP-NET patients before and throughout AlphaMedix or Lutathera treatment. Differential expression, over-representation analysis, digital cytometry, and trajectory identification were used to characterize treatment-induced regulation of peripheral immunotranscriptomes, immune cell composition, and heterogenous responses within the patient population.

Results: AlphaMedix therapy induced strong peripheral transcriptomic changes in patients achieving complete or partial response, detectable from 8 weeks after first infusion, and up to 6 months after end of treatment. AlphaMedix triggers similar transcriptomic changes throughout the treatment among patients responding to the therapy, which is stronger and different from patients treated with Lutathera. The ^{212}Pb radioligand therapy triggers early generation of ROS, DNA damage, apoptotic responses, inflammation and monocyte recruitment. The results reveal two waves of immunotranscriptome modulation, likely reflecting kinetics heterogeneity of immune activation between early and late responders. Lymphopenia, particularly affecting B cells, was observed in patients treated with either AlphaMedix or Luthatera, with more pronounced lymphopenia among patients treated with Lutathera.

Conclusions: Data-driven characterization of treatment-associated transcriptional changes in peripheral immune cells underscores immune modulation associated with clinical response to radioligand therapy. The translational potential of whole-blood RNA liquid biopsy is demonstrated with Immuno-Pharmacodynamic profiling of patient response to radioligand therapy, and identification of immune-related biomarkers of clinical response.

#3860 A low-cost bioassay for multi-cancer detection in cfDNA using quantitative methylation-specific PCR.

Emily Neaga, Sarah Falotico, Mayur Gurnani, Miguel Williams, Anthony Shuber

Harbinger Health, Cambridge, MA

Liquid biopsy multi-cancer detection tests hold significant promise to improve patient outcomes by enabling earlier intervention. However, emerging sequencing-based assays face practical challenges due to high costs, complex workflows, and long turnaround times. In contrast, quantitative methylation-specific PCR (qMSP) enables rapid turnaround times with low-cost, low-complexity, and scalable workflows, while accommodating flexible batch sizes and decentralized testing. Harbinger Health's proprietary methylation biomarkers were applied to Harbinger Health's proprietary qMSP method to enable low-cost multi-cancer detection. Harbinger Health's biomarkers are associated with the initiation of oncogenesis and are ubiquitously observed across multiple cancer types. This redundancy enabled the selection of six highly pan-cancer-informative methylation patterns, reducing the genomic footprint while largely maintaining cancer detection performance. Despite the informative nature of these biomarkers, background methylation from processes like aging can attenuate disease detection. To address this limitation, Harbinger developed a qMSP method that incorporates locked nucleic acid (LNA) blockers to suppress probe mishybridization to stochastically methylated somatic cell-free DNA (cfDNA), improving selectivity for defined methylation patterns in low abundance circulating tumor DNA (ctDNA). The qMSP panel underwent analytical validation during development and demonstrated high sensitivity, specificity, and reproducibility for detecting cfDNA fragments with defined methylation patterns. The panel was applied to 130 cfDNA samples obtained from the CORE-HH clinical study (NCT05435066), representing 62 non-cancer samples and 68 cancer samples across nine cancer types. Samples were selected to reflect a similar range of methylation signals observed in the CORE-HH study cohort. The cancer samples represented a balanced stage distribution. cfDNA samples were processed into bisulfite libraries and analyzed by qMSP using 5 ng of library per reaction. The cycle threshold (Ct) of each methylation marker was normalized to an internal reference assay and delta Ct values were used to measure methylation. Using target-specific detection thresholds established on 62 non-cancer samples to achieve an equivalent of 97% specificity, qMSP detected at least one positive target for 30 of 68 (44%) cancer samples. This work represents an initial proof of concept for a low-cost multi-cancer detection assay. qMSP reactions in this study cost less than $5 per sample and were completed in under five hours, addressing key barriers to population-scale implementation such as cost and turnaround time. Future refinements, including expansion of the marker panel, optimization of detection thresholds, and improved assay design, are expected to further improve clinical performance.

#3861 Low-cost detection of advanced adenomas in cfDNA using quantitative methylation-specific PCR.

Emily Neaga, Sarah Falotico, Mayur Gurnani, Miguel Williams, Anthony Shuber

Harbinger Health, Cambridge, MA

Removal of advanced adenomas during colonoscopy has been shown to significantly reduce colorectal cancer incidence and mortality. However, many patients recommended for colorectal screening remain unscreened due to the invasive nature of colonoscopy. Liquid biopsy cancer detection tests hold significant promise to improve patient outcomes by broadening access and enabling earlier intervention. However, the cost, complexity, and turnaround times of emerging sequencing-based assays present challenges for population-level adoption. To address these challenges, Harbinger Health applied a refined panel of methylation markers in a methylation-specific quantitative PCR (qMSP) assay. qMSP provides a rapid, low-cost, and scalable approach for advanced adenoma (AA) detection in cell-free DNA (cfDNA). Harbinger Health utilizes proprietary methylation biomarkers associated with the initiation of oncogenesis. Redundancy across these markers enabled the selection of six highly pan-cancer-informative methylation patterns that distinguish cancer from non-cancer cfDNA with a small genomic footprint. Harbinger Health developed a qMSP method that quantifies specific methylation patterns using probes that hybridize to highly methylated variants, combined with locked nucleic acid (LNA) blockers that suppress non-specific signal from partially methylated variants. This improved selectivity enables the detection of rare circulating DNA (ctDNA) variants within a heterogenous cfDNA background. The qMSP panel underwent analytical validation during development and demonstrated high sensitivity, specificity, and reproducibility. The qMSP panel was evaluated in a cohort comprised of 62 cfDNA samples collected from patients with no reported cancer in the CORE-HH clinical study (NCT05435066) and 38 commercially sourced cfDNA samples collected from patients with confirmed advanced colorectal adenomas. cfDNA samples were processed into bisulfite libraries and analyzed by qMSP at 5 ng of library per reaction. The cycle threshold (Ct) of each methylation marker was normalized to an internal reference assay and delta Ct values were used to measure methylation. Using target-specific detection thresholds established on 62 non-cancer samples to achieve an equivalent of 90% specificity, qMSP detected at least one positive target for 18 of 38 (47%) AA samples. This work demonstrates the use of qMSP to quantify highly informative methylation markers for AA detection in cfDNA. A six-marker panel effectively distinguished AA samples from non-cancer samples in a cohort of 100 cfDNA libraries. Notably, marker selection was not optimized for AA detection, and an expanded panel with AA-specific biomarkers is expected to further improve clinical performance. qMSP reactions in this study cost less than $5 per sample and exemplify a rapid, low-cost analytical method for the detection of advanced colorectal adenomas.

#3862 Convergent chromatin remodeling enables pan-aerodigestive detection of advanced malignancies in plasma cfDNA.

Axel Misael Hidalgo, Ayesha Hashmi, Jeff Szymanski, Pradeep Chauhan, Lilli Greiner, Faridi Qaium, Daniel J. Ma, David M. Routman, Katie M. Van Abel, Aadel A. Chaudhuri

Mayo Clinic, Rochester, MN

Background:
Liquid biopsy approaches for cancer detection often rely on tissue-specific methylation or fragmentation features to infer tumor origin. However, a pan-aerodigestive cancer detection strategy is clinically valuable given shared risk exposures, field cancerization, and frequent diagnostic ambiguity among lung, esophageal, and head & neck cancers. We hypothesized that advanced-stage disease exhibits convergent chromatin remodeling, producing a dominant malignancy-associated fragmentomic signal that supersedes subtler tissue-of-origin patterns.
Methods:
Whole-genome EM-seq (~15×) was performed on plasma cfDNA from 120 patients with stage III/IV aerodigestive cancers (lung, esophageal, head & neck; squamous and adenocarcinoma) and 60 age-matched controls. Four fragmentomic modalities were assessed: (1) genome-wide fragmentation in 5-Mb bins (DELFI-like), (2) NMF spectral components, (3) 4-mer end motifs, and (4) promoter-centric nucleosome scores (Griffin). All preprocessing occurred strictly within each training fold of a repeated stratified 10-fold CV (100 repeats) to prevent data leakage. No test-sample information was used in training. Hyperparameters were tuned only within training partitions. Random Forest classifiers were trained under this fully nested scheme.
Results:
The multimodal classifier robustly detected advanced aerodigestive malignancies with a mean AUROC 0.86 and AUPRC 0.94. However, modality dissection revealed a clear performance hierarchy: nucleosome positioning (Griffin) alone achieved AUROC 0.85 and AUPRC 0.93, nearly matching the full integrated model, whereas end motifs performed poorly (AUROC 0.61). Biological interpretation demonstrated prominent nucleosome depletion centered at promoters of proliferation-associated genes, indicating a convergent epigenetic state of promoter opening across late-stage aerodigestive malignancies.
Conclusions:
Advanced aerodigestive cancers exhibit a dominant, convergent chromatin remodeling signature detectable in plasma cfDNA, driven primarily by altered nucleosome positioning. In late-stage disease, this shared malignancy-associated fragmentomic signal outweighs tissue-of-origin-dependent patterns. These findings highlight the utility of nucleosome-based fragmentomics not merely for detection, but for resolving diagnostic ambiguity in patients with indeterminate masses and for monitoring total tumor burden in high-risk aerodigestive malignancies.

#3863 Enhanced cfDNA fragmentation-based treatment monitoring on the Ultima Genomics platform.

Laurel K. Millberg[1], Garrett Graham[1], Zachary Skidmore[1], Jordan Gumm[1], Kevin Jacobs[1], Ariel Jaimovich[2], Elena Helman[2], Bryan Chesnick[1], Roberto Olivares-Amaya[1], Timothy Mcdaniel[1], Sian Jones[1], Amoolya Singh[1], Lorenzo Rinaldi[1]

[1]Delfi Diagnostics, Palo Alto, CA,[2]Ultima Genomics, Freemont, CA

Introduction: Whole-genome analysis of cell-free DNA (cfDNA) fragmentation, such as DELFI-Tumor Fraction (DELFI-TF), has emerged as a powerful tool for monitoring therapeutic response in patients with late-stage cancer. In this study, we assessed the technical feasibility of the Ultima Genomics sequencing platform for a cfDNA fragmentation-based monitoring application.
Methods: The study consisted of two cohorts: 1) 48 longitudinal plasma samples collected from 16 stage IV lung cancer patients and 2) 4 tumor, normal, and matched plasma samples of varying tumor types from treatment-naive stage IV patients. cfDNA was sequenced using three methods: the Illumina NovaSeq6000 (mean depth: 11.8x) and the Ultima UG 100 using the standard approach (8 replicates per sample, 11.0x) or ppmSeq (174.6x). Fragmentation features and DELFI-TF were computed, and DELFI-TF values were compared against somatic variant allele frequencies (VAF) from a 500-gene targeted sequencing panel. WGS somatic variants were identified by filtering ppmSeq variant calls and used to categorize reads into two groups based on their likely origin: tumor or white blood cell (WBC). Fragmentation features were then calculated per group as well as for all reads combined.
Results: Ultima sequences were high quality, with 88.3% of bases >Q30 base quality and 99.0% of reads aligned on average. Fragment length distributions (FLDs) within the 100-220bp range (Pearson $R > 0.998$, $p < 1e\text{-}5$) and genome-wide fragmentation profiles (Pearson $R > 0.939$, $p < 1e\text{-}5$) were highly correlated between platforms. Limits of blank, with overlapping bootstrapped confidence intervals, and ctDNA detection (100% positive, 95.7% negative, and 97.4% overall percent agreement) were also consistent. Ultima-DELFI-TF correlated strongly with VAF (Pearson $R=0.979$, $p<1e\text{-}5$), showed high precision across replicates (median robust CV: 2.6%), and reflected longitudinal ctDNA patterns in treatment response. Classifying read origin by somatic variants from ppmSeq resulted in tumor-derived FLDs that displayed a higher proportion of short fragments than WBC-derived FLDs (p-value < 1e-5, KS test). When compared to a reference FLD derived from samples with undetectable ctDNA, the tumor-derived FLD deviated more from the reference distribution than the WBC-derived and combined FLDs (median KL-divergence of 0.227 [tumor], 0.078 [WBC], and 0.089 [combined]). The relative frequencies of 10 fragment end motifs were consistently elevated in the tumor-derived fragments across the whole cohort (all $p < 1e\text{-}5$, Chi-sq).
Conclusions: These data support the technical feasibility of implementing DELFI-TF on the Ultima platform. Combining DELFI-TF with Ultima ppmSeq enables the detection of tumor-originated reads and provides a path toward more sensitive disease detection.

#3864 Serial ctDNA monitoring in metastatic breast cancer using an ultrasensitive tumor informed structural variant based assay.

Mitchell J. Elliott[1], June Roh[1], Kareena Thakur[1], Sasha Main[2], Karen Howarth[3], Sofia Birkealv[3], Jennifer Yen[3], Volundur Hafstad[3], Wendy Levin[4], Vikash Kumar[1], Long Nguyen[1], Meredith Li[1], Scott Victor Bratman[5], Eitan Amir[1], Philippe L. Bedard[6], Lillian L. Siu[7], Hal Berman[8], David Cescon[9]

[1]Department of Medical Oncology and Hematology, Princess Margaret Cancer Centre, Toronto, ON, Canada,[2]Department of Medical Biophysics, University of Toronto, Toronto, ON, Canada,[3]SAGA Dx, Lund, Sweden,[4]SAGA Dx, Morrisville, NC,[5]The Governing Council of The University of Toronto, Toronto, ON, Canada,[6]UHN-Toronto General Hospital, Toronto, ON, Canada,[7]UHN Princess Margaret Cancer Centre, Toronto, ON, Canada,[8]Department of Pathology, Toronto General Hospital, Toronto, ON, Canada,[9]Princess Margaret Cancer Centre, Toronto, ON, Canada

Background: Circulating tumor DNA (ctDNA) dynamics correlate with treatment response in metastatic breast cancer (mBC), yet evidence generated using tumor-informed, ultrasensitive assays remains limited. In addition, the landscape of serial ctDNA monitoring across different receptor subtypes and through multiple lines of therapy remains poorly characterized. Furthermore, the performance of structural variant (SV) based ctDNA detection has not been established in this setting. Validating ctDNA as a reliable biomarker of response and progression in mBC, particularly across treatment transitions, could provide clinical utility.
Methods: We conducted a single-center retrospective study in patients with mBC receiving standard-of-care systemic therapy. Serial blood samples were collected prospectively at enrollment, radiographic restaging events (+/-30 days), and at disease progression. ctDNA was analyzed retrospectively using an ultrasensitive, whole genome sequencing (WGS)-based, tumor-informed SV digital PCR assay. Clinical data, real-world progression-free survival (rwPFS) across sequential lines of therapy, and overall survival (OS) were obtained from the medical record.
Results: Results were available for 28/100 patients (18 ER+/HER2-, 6 TNBC, 4 HER2+), contributing 120 evaluable timepoints (median 3 per patient, range 1-18) with a median follow-up of 12.2 months (range 2.0-16.3). Patients received a median of 2 lines of metastatic therapy (range 1-8). Orthogonally validated fingerprints contained a median of 13 SVs (range 4-16). ctDNA was detected in 77% (92/120) of all sampled timepoints, with 34% (31/92) of positives falling within the ultrasensitive range (variant allele fraction ≤0.01% or ≤100 ppm). Serial ctDNA monitoring closely mirrored each patient's treatment course. Notably, no radiologist-adjudicated progression occurred without a preceding rise in ctDNA from on-treatment nadir. Four patients (1 ER+/HER2-, 1 TNBC, 2 HER2+) had undetectable ctDNA with a median rwPFS of 27 months (range 20-40) and remain on therapy without rwPFS or OS events. Accrual is ongoing, with continued serial plasma collection and maturing rwPFS/OS data.
Conclusion: These preliminary findings demonstrate the feasibility of ctDNA monitoring in a real-world, heterogeneous mBC cohort using a tumor-informed, ultrasensitive SV-based assay. ctDNA dynamics closely tracked treatment response across sequential lines of therapy, and early signals suggest that ctDNA clearance below the ultrasensitive detection threshold is associated with prolonged disease control. The high proportion of timepoints within the ultrasensitive range underscores the relevance of assay sensitivity for metastatic monitoring. Updated results from the full cohort, including correlation with all matched radiographic restaging events will be presented.

: Molecular Classification and Tumor Biology in Cancer
Poster Session

#3868 Distinct tumor microenvironmental landscapes define molecular subtypes in non-muscle-invasive bladder cancer.

Songjun Xu[1], Matthew H. V. Byrne[2], Jiarui Zhang[1], Ahmad Alalti[2], Devika Agarwal[3], Neil Beeharry[1], Olesya Chornoguz[1], Kyla Dooley[4], Kin Cheung Lee[4], Shuwei Li[1], Guneet Walia[1], Tommaso Mansi[1], Joel Greshock[1], Calliope Dendrou[5], Freddie Hamdy[6], Lisa Browning[7], Dan J. Woodcock[2], Patrick Wilkinson[1], Shibu Thomas[1]

[1]Johnson & Johnson, Spring House, PA,[2]Nuffield Department of Surgical Sciences, University of Oxford, Oxford, United Kingdom,[3]Kennedy Institute, University of Oxford, Oxford, United Kingdom,[4]Centre for Human Genetics, University of Oxford, Oxford, United Kingdom,[5]Kennedy Institute, University of Oxford; Weatherall Institute for Molecular Medicine, John Radcliffe Hospital, Headington, Oxford, United Kingdom,[6]Nuffield Department of Surgical Sciences, University of Oxford, Oxford, United Kingdom, Department of Urology, Oxford University Hospitals NHS Foundation Trust; NIHR Biomedical Research Centre, Oxford, United Kingdom,[7]Department of Cellular Pathology, Oxford University Hospitals NHS Foundation Trust, Oxford, United Kingdom

Background:
Non-muscle-invasive bladder cancer (NMIBC) are biologically heterogeneous tumors that are classified based on stage/grade alone, which does not provide an accurate separation as it misses underlying molecular phenotypes. The UROMOL molecular classification, derived from large-scale transcriptomic profiling of NMIBC (Lindskrog SV, et al. *Nat Commun*. 2021;12:2301), stratifies tumors into prognosis-associated biology with distinct molecular subtypes. The relationship between molecular states and tumor microenvironment (TME) composition remains poorly defined.
Methods:
We performed transcriptomic subtyping and single-cell-level TME profiling of NMIBC tumors (patient n=16, sample n=34, cell n = 108108). Tumors were classified into UROMOL subtypes using NMIBC classifier (Lindskrog SV, et al. *Nat Commun*. 2021;12:2301) based on aggregated gene expression profiles. We quantified epithelial, stromal, and immune populations, and assessed pathway activity using curated immune and stromal gene module scores.
Results:
3 UROMOL subtypes were observed: Class 1 (luminal papillary), Class 2a (basal-inflamed), and Class 2b (luminal-inflamed). Class 1 tumors (n=6, 17.6%) exhibited an epithelial-dominant, immune-cold TME characterized by ~80.1% epithelial cells (95% CI: 74-86.2%) and minimal immune infiltration, including T cells (~1.9%, CI: 0.5-3.3%), macrophages (~1.4%, CI: 0.5-3.3%), and fibroblasts (~8.4%, CI: 4.3-12.5%). This composition is consistent with differentiated luminal biology and may have favorable baseline prognosis. Class 2a tumors (n=9, 26.5%) displayed a distinct TME composition pattern, with an increase in T-cell (~4.8%, CI: 1.7-8.0%) and macrophage (~1.9%, CI: 0.6-3.1%) infiltration compared to Class 1, alongside increased fibroblast (~17.5%, CI: 9.6-25.3%) and endothelial (~8.1%, CI: 4.9-11.4%) content. These tumors showed increased effector and checkpoint activity, reflecting a more active immune microenvironment than class 1. Class 2b tumors (n=19, 55.9%) showed a heterogeneous immune-stromal landscape with pronounced fibroblast enrichment (~27%, CI: 19.7-34.4%) and extracellular matrix remodeling, alongside elevated immune infiltration, including T cells (~17.5%, CI: 15-20.0%) and macrophages (~11.2%, CI: 7.4-14.9%), this reflects an immune-active, fibroblast-rich TME architecture.
Conclusions:
UROMOL subtypes are defined by distinct TME architectures with differences in cellular composition from immune-cold, epithelial-rich Class 1 tumors to highly immune infiltrated Class 2b tumors enriched with T cells and fibroblasts. Given the limited sample size, these observations should be validated in a larger cohort.
This study demonstrates that UROMOL molecular classes of NMIBC are associated with distinct TMEs, revealing biologically meaningful differences in immune infiltration and stromal composition.

#3870 Deep learning-powered morphological analysis of acute myeloid leukemia.

Ezgi June Olgac[1], Meghan Burr[2], Minna Suvela[1], Daniela Mendoza-Ortiz[1], Ella Sinervuori[1], Heikki Kuusanmaki[1], Mika Kontro[1], Caroline Heckman[1]

[1]University of Helsinki, Helsinki, Finland,[2]Deepcell, Inc., Menlo Park, CA

In this study we demonstrate that deep learning-based analysis of single cell images can distinguish acute myeloid leukemia (AML) bone marrow (BM) mononuclear cells (MNCs) from healthy BM MNCs based on morphological features. We further show that differences in *ex vivo* drug responses to BCL2 inhibitor venetoclax links to shifts in morphology of venetoclax-sensitive (ven-sen) and -resistant (ven-res) AML. Our sample cohort consisted of cryopreserved BM MNC samples from 6 healthy donors and 12 donors with AML. The AML samples were selected based on ex vivo sensitvity to venetoclax (6 ven-sen + 6 ven-res). Moreover, 2 longitudinal sample pairs (diagnosis-relapse) from 2 AML patients were included in the cohort. The AML samples were from patients recruited to the NCT04267081 trial and healthy donor samples from patients undergoing hip replacement surgery. Samples were thawed, fixed with 2% paraformaldehyde, and stored at +4°C until the time of imaging. The samples were prepared in a single cell suspension and 25,000-50,000 brightfield images collected per sample using the high-resolution single cell imaging and sorting platform, REM-I (Deepcell). Imaging data were synced to REM-I's data suite Axon. Morphological analysis through Axon was carried out based on 115 dimensions of cell morphology; 51 human-interpretable, and 64 deep-learning features. Analysis parameters were set to random sampling with equal number of data points per sample. Differential morphology analysis on Axon yielded divergence scores (Range: 0-1) as a quantified measure of morphological distinction.Comparison of healthy samples (n=6) against pooled AML samples (n=12) demonstrated that healthy and AML BM cells are distinct in their morphology and map into different clusters in a uniform manifold approximation and projection (UMAP) graph. Differential morphology analysis between these sample groups highlighted deep-learning embeddings in the top 10 differential morphology features, with divergence scores ranging from 0.55-0.65. Additionally, an analysis comparing healthy samples (n=6) to ven-sen (n=6) and ven-res (n=6) AML, revealed that the two different AML sample groups were distinct in morphology from each other as well as from the healthy samples. Finally, in the analysis of two longitudinal AML patient sample pairs for morphological analysis of AML progression, we observed changes in morphology between the diagnosis and relapse samples. This anaysis also revealed a substantial morphological shift in the patient that had a higher change in *ex vivo* ven response between the diagnosis and relapse samples. Our study demonstrates that cutting-edge methods powered by deep learning can facilitate the analysis of morphological features of AML with high-dimensionality that cannot be achieved by methods that depend only on human perception. These results indicate that drug response and disease progression in AML are reflected by changes in cell morphology.

#3871 Molecular correlates of response and survival in a phase II trial of weekly carboplatin/paclitaxel plus cemiplimab (wCP+C) in advanced/metastatic mucosal head and neck squamous cell carcinoma (a/mHNSCC).

Mateus Trinconi Cunha[1], Fahad Rind[2], Priyanka Bhateja[1], Esmerina Tili[3], David Konieczkowski[4], Darrion Mitchell[4], Sujith Baliga[4], Sung Jun Ma[4], Simeng Zhu[4], Gogineni Emile[4], John Grecula[4], Nolan Seim[5], Catherine Harring[5], Lauren Miller[5], Abberly Lott Limbach[6], Kang Stephen[5], James W. Rocco[5], Christian Rolfo[7], Dukagjin Blakaj[4], Marcelo Bonomi[8]

[1]Head and Neck Medical Oncology, The Ohio State University Wexner Medical Center, Columbus, OH,[2]Clinical Trials Department, The Ohio State University Wexner Medical Center, Columbus, OH,[3]Anesthesiology, The Ohio State University Wexner Medical Center, Columbus, OH,[4]Radiation Oncology, The Ohio State University Wexner Medical Center, Columbus, OH,[5]Otolaryngology, The Ohio State University Wexner Medical Center, Columbus, OH,[6]Pathology, The Ohio State University Wexner Medical Center, Columbus, OH,[7]Medical Oncology, The Ohio State University Wexner Medical Center, Columbu, OH,[8]Head and Neck Medical Oncology, The Ohio State Universiy Wexner Medical Center, Columbus, OH

Background: a/mHNSCC exhibits poor prognosis and limited immunotherapy efficacy. Weekly low-dose chemotherapy may enhance immunogenicity while reducing toxicity. We conducted a phase II trial of weekly low-dose chemotherapy plus cemiplimab as first-line treatment in a/mHNSCC, with integrated genomic profiling to explore molecular correlates of outcome. Patients received weekly carboplatin (AUC 1) and paclitaxel (30 mg/m²) plus cemiplimab (350 mg q3w). Forty-two patients were enrolled from Dec 2021-Dec 2024. Median age was 68 (range 42-81); 38/42 were male, and 27 (64%) were HPV-positive. Median OS (27 events) was 16.4 months (95% CI, 12.6-23.9); median PFS (36 events) was 5.62 months (95% CI, 5.0-10.3). Objective response rate (ORR) was 43% (18/42, PR or CR). The treatment was well-tolerated. These results were previously presented at ESMO 2025. We aim to present an exploratory analysis of pathogenic genomic mutations in this cohort and their correlation with ORR, PFS, and OS.
Methods: Of the 42 enrolled patients, genomic analysis (Tempus xT/xF) was performed in 29. The 4 most prevalent pathogenic alterations were analyzed separately, while all genes with detected pathogenic alterations were grouped and analyzed by pathway or functional group, with time-to-event outcomes assessed via Kaplan-Meier and log-rank, and Cox models when appropriate. Prevalence of tumor mutations between responder groups (CR/PR versus PD as ORR) and extreme PFS groups (<3 versus >12 months) was performed with odds ratio. P-values< 0.05 were deemed statistically significant. Due to the hypothesis-generating nature of this report, p-value adjustments for multiple tests were not performed.
Results: Pathogenic alterations included TP53 (N=14), CDKN2A (N=11), TERT promoter (N=8), and FGF3/FGF4 copy number gains (CNG; N=17). Mutations in NOTCH pathway genes (NOTCH1/3, FBXW7; N=7) were enriched in patients with primary progression ($p = 0.02$) and those with PFS <3 months versus >12 months ($p = 0.03$). NOTCH alterations conferred inferior PFS (HR 3.6; 95% CI, 1.4-9.3; $p < 0.01$) and OS (HR 2.9; 95% CI, 1.05-8.0; $p = 0.04$). TERT promoter mutations were associated with worse OS (HR 4.9; 95% CI, 1.7-14.5; $p < 0.01$) and trended toward poor PFS (HR 2.2; 95% CI, 0.9-5.2; $p = 0.08$). FGF3/FGF4 CNGs also trended toward inferior PFS (HR 2.6; 95% CI, 0.9-7.4; $p = 0.08$) and were associated with worse OS (HR 2.5; 95% CI, 1.0-6.6; $p = 0.04$).
Conclusions: Weekly low-dose chemotherapy plus cemiplimab shows promising activity in a/mHNSCC. Exploratory genomic profiling suggests NOTCH pathway mutations may be markers of poor prognosis and resistance. TERT and FGF3/4 alterations may also confer inferior outcomes and warrant further study.

#3873 Molecular heterogeneity in non-muscle invasive bladder cancer reveals clinically divergent subtypes with contrasting Bacillus Calmette-Guérin response and clinical outcomes.

Jee-Woo Seo, Il-San Jeong, Yeo-Gyeong Yoon, Jae-Yoon Kim, Seon-Young Kim, Seung-Woo Baek, Seon-Kyu Kim

Korea Research Institute of Bioscience & Biotechnology (KRIBB), Daejeon, Korea, Republic of

Background: Non-muscle-invasive bladder cancer (NMIBC) is an early-stage, molecularly heterogeneous malignancy with diverse clinical outcomes from frequent recurrence to occasional progression. Unlike muscle-invasive bladder cancer (MIBC), NMIBC lacks a unified molecular subtype. Current classification systems provide biological insights but offer limited prognostic precision. Although recurrence and progression are often treated as a continuum, recurrent tumors commonly exhibit Bacillus Calmette-Guérin (BCG) resistance, whereas progressive tumors tend to respond to BCG, highlighting the need for a precise molecular classification.
Methods: By integrating ten previously established omics-based classifiers of NMIBC, we identified six clinically and molecularly distinct subtypes. Fifty representative genes per subtype (300 total), designated as the Molecular Heterogeneity of NMIBC 300-gene signature (MHN300), were selected to build an AutoML-based prediction model. The model was trained and validated across 11 independent NMIBC cohorts and 7 single-cell RNA-seq datasets. Each subtype underwent comprehensive molecular characterization, including transcriptomic and genomic analyses, and prognostic relevance was assessed using Kaplan-Meier and Cox regression analyses.
Results: Six molecularly and clinically distinct NMIBC subtypes (C1-C6) were defined through integration of ten prior classifiers. C1 exhibited early cell-cycle and uroplakin activity, whereas C2 showed pan-fibroblast TGF-β and EMT signaling. C3 combined strong immune and late cell-cycle programs, while C4 and C5 both featured late cell-cycle activation with opposing clinical behaviors; C4 showing favorable BCG response and prolonged progression-free survival (PFS, $P < 0.001$ by log-rank test), and C5 displayed a high-frequency recurrence NMIBC (24% with ≥2 recurrence per year, HR = 5.12, 95% CI 2.82-9.39, $P < 0.001$ by log-rank test), along with BCG resistance and endothelial enrichment in scRNA-seq. C6 demonstrated FGFR3 and early cell-cycle features. The MHN300 AutoML classifier achieved 0.88 accuracy and was validated across independent cohorts.
Conclusions: The MHN300 classifier refines the current molecular framework for NMIBC by resolving intra-subtype heterogeneity and delineating biologically coherent, clinically meaningful subgroups with distinct risks of recurrence and progression. This refined taxonomy provides a foundation for subtype-guided precision management of NMIBC.
Grant Support: This study was supported by grants from the Korea Research Institute of Bioscience and Biotechnology (KRIBB) Research Initiative Program (KGM5192423).

#3874 Phosphoproteomic subtyping and characterization of colorectal cancer by comprehensive phosphoproteomics of fresh frozen endoscopic biopsy specimens.

Jun Adachi[1], Hirokazu Shoji[2], Hidekazu Hirano[2], Yosui Nojima[3], Satoshi Muraoka[1], Yutaka Saito[2], Ken Kato[2], Narikazu Boku[4], Yukihide Kanemitsu[2]

[1]National Institute of -Biomedical Innovation, Health, and Nutrition, Osaka, Japan,[2]National Cancer Center Hospital, Tokyo, Japan,[3]The University of Osaka, OIsaka, Japan,[4]University of Tokyo, Tokyo, Japan

Background and Aims: Phosphorylation is a key post-translational modification that regulates protein activity, localization, and interactions. By mapping phosphorylation patterns, phosphoproteomics provides real-time insights into how cancer cells reprogram their signaling networks to promote growth, survival, metastasis, and therapy resistance. While conventional deep phosphoproteomics requires a relatively large amount of clinical samples, we have developed a highly sensitive method using endoscopic biopsy samples which can offer excellent quality for hosphoproteomic analysis. In this study we evaluated the phosphoproteomic landscape in fresh-frozen endoscopic biopsies from patients with colorectal cancer (CRC).
Methods: Endoscopic biopsy specimens were obtained from 102 treatment-naïve CRC patients and snap-frozen in liquid nitrogen within 20 seconds of collection. Ultra-deep proteome and phosphoproteome analyses were performed using tandem mass tag (TMT)-based multiplexing. Genomic profiling was conducted with a targeted, high-multiplex PCR-based next-generation sequencing (NGS) panel.
Results: Ultrasensitive mass spectrometry-based proteomics using 204 naïve colorectal cancer specimens and 204 normal tissue adjacent to the tumor (NAT) quantified an average of 23985 phosphorylation sites. Consensus clustering clearly divided colorectal cancer into subtype 1 (proliferative type, 33%), subtype 2 (EMT type, 25%), Subtype 3 (Metabolic type, 20%), and subtype 4 (Abnormal RNA splicing type, 21%). Kinase activity profiles were obtained from phosphoproteome data and kinases that are specifically activated or inactivated in each subtype were identified. While concordance between these phosphoproteomic subtypes and the consensus molecular subtypes (CMS) was low, sidedness was associated with different kinome activity of tumor and NAT.
Conclusions: This proof-of-concept study demonstrates that phosphoproteomic analysis can delineate CRC subtypes independent of CMS classification and provide detailed kinase activity landscapes. Our pioneering approach enables robust clinical phosphoproteomics from small endoscopic biopsies, offering a promising tool for monitoring therapeutic kinase activities and advancing precision oncology.

#3875 Identifying the tumor site of origin using molecular profiling with an AI-based classifier.

Carlos E. Zuazo, Michael J. Demeure, David R. Braxton, **Sourat Darabi**

Hoag Cancer Institute, Newport Beach, CA

Background: Identifying the primary site of origin for tumors in an accurate and timely manner is a critical step in treating cancer in an effective way. In cases of cancers of unknown primary, deep learning-based genomic classifiers that can improve diagnostic workflows and decrease inaccuracies have been validated for clinical use by previous studies, but reports of clinical utility are lacking. Use of molecular profiling for identification of site of origin has shown to be accurate in about 70-95% cases and can reveal actionable targets for treatment. We report our experience of consecutive cases where a commercial AI-based classification tool was used in routine practice at a high-volume community cancer center.

Methods: Patient tumors, initially classified as cancers where the primary site was uncertain, were subjected to molecular profiling and AI-based genomic classification (GPSai) capable of recognizing a set of 90 distinct primary tumor sites and many histological subclasses. Molecular profiling consisted of whole exome and whole transcriptome sequencing of FFPE tumor samples, along with other predictive biomarker assays performed by a commercial laboratory (Caris Life Sciences). The identification of targetable mutations was reported, but variants of unknown significance were excluded when reporting genomic alterations.

Results: We reviewed 320 samples from 313 patients between December 2022 and October 2025 who were profiled using GPSai, 77 (24%) of which were cancers with unknown primary. Those cases which were unable to be classified were further investigated by a molecular pathologist. Of the 243 (76%) samples that received a tumor type assignment by the classifier, non-small cell lung cancer was the most represented, with 41 of 243 (16.9%), followed by pancreatic adenocarcinoma, with 25 of 243 (10.3%), and colon cancer, with 21 of 243 (8.6%). The classifier also assigned classifications of miscellaneous rare cancer types (21 of 243, or 8.6%), including rhabdomyosarcoma, angiosarcoma, and thymic carcinoma. 161 of 313 (51.4%) patients were women, 152 of 313 (48.6%) were men, and 201 of 313 (64%) patients were 65 or older in age. Mutations were found in 173 of 320 (54%) samples, with the most common being in *TP53, KRAS,* and *TERT.* Further, 51 of 320 (16%) of samples analyzed had a high tumor mutational burden (TMB), 10 of 320 (3%) had a mismatch repair deficiency, and 45 of 320 (14%) samples were positive for *PD-L1* (SP142) and 53 of 320 (16.6%) for *PD-L1* (22c3)..

Conclusion: 243 of 330 (76%) patient samples were assigned a cancer diagnosis, which is consistent with the range reported in published studies to date (70-95%). Among those that could not be classified, targetable mutations were commonly found, including *KRAS* and *EGFR*. AI-based genomic classification of tumor site of origin is useful in clinical practice in identifying treatment options for patients.

#3876 Prognostic and predictive value of the Clearseq1-4 tumor microenvironment classification in localized and metastatic clear-cell renal cell carcinoma.

Benoit Beuselinck[1], Lisa Kinget[2], Edward Mctaggart[3], Octavie Demeulenaere[3], Edouard Roussel[4], Bram Boeckx[5], Jessica Zucman-Rossi[6], Gabrielle Couchy[6], Henri Vandermeulen[7], Liesbeth De Wever[7], Marcella Baldewijns[8], Agnieszka Wozniak[9], Diether Lambrechts[10], Stefan Naulaerts[11], Abhishek D. Garg[9], Annelies Verbiest[12], Maarten Albersen[4]

[1]UZ Leuven, Leuven, Flemish Brabant, Belgium,[2]General Medical oncology, UZ Leuven, Leuven, Flemish Brabant, Belgium,[3]Oncology, KULeuven, Leuven, Flemish Brabant, Belgium,[4]Urology, UZ Leuven, Leuven, Flemish Brabant, Belgium,[5]VIB, KULeuven, Leuven, Belgium,[6]INSERM, Paris, France,[7]Radiology, UZ Leuven, Leuven, Flemish Brabant, Belgium,[8]Pathology, UZ Leuven, Leuven, Flemish Brabant, Belgium,[9]KU Leuven, Leuven, Belgium,[10]Catholic University of Leuven, Leuven, Belgium,[11]Oncology, KULeuven, Leuven, Belgium,[12]UZ Antwerpen, Antwerpen, Belgium

PURPOSE: The ccrcc1-4 transcriptomic subtypes were previously identified on fresh frozen clear-cell renal cell carcinoma (ccRCC) samples and have proven their prognostic value post-nephrectomy/metastasectomy and predictive value for first-line vascular endothelial growth factor receptor-tyrosine kinase inhibitors (VEGFR-TKIs). We aimed to extend and validate the ccrcc1-4 classifier on formalin-fixed paraffin-embedded (FFPE) tissues and to validate its prognostic and predictive value across the RCC treatment landscape.

EXPERIMENTAL DESIGN: RNA sequencing of tumoral FFPE tissue was performed. A classifier called Clearseq was designed to determine ccrcc1-4 subtypes. Subtypes were correlated with outcome after surgical and systemic therapies. External validation was pursued as well as characterization at single-cell transcriptomic level.

RESULTS: A total of 668 tumoral samples (337 primary tumors and 331 metastases) from 364 patients were assigned into ccrcc1, ccrcc2, ccrcc3 and ccrcc4-tumors. The angiogenic ccrcc2-subtype had a favorable prognosis after nephrectomy in localized setting, after cytoreductive nephrectomy and upon metastasectomy with curative intent and was correlated with improved outcome on first-line VEGFR-TKIs. Ccrcc4-tumors were enriched for sarcomatoid features and had the largest treatment benefit on immune checkpoint blockade (ICB) treatment in any line, resulting in overall survival outcomes comparable to those of less aggressive subtypes. These findings were corroborated in a post-nephrectomy cohort, and external cohorts of metastatic patients treated with ICB and/or angiogenesis inhibitors.

CONCLUSIONS: We validated the Clearseq classifier to predict ccrcc1-4 molecular subtype on FFPE tissues and confirmed its performance with respect to previous biomarker findings for both surgical and systemic treatment approaches.

#3877 Integrative application of Lymphly reveals shared molecular landscape across B-cell lymphomas.

Dmitrii Snitkin, Pavel Zemskiy, Andrey Suponin, Mark Meerson, Ekaterina Nesterenko, Alexander Bagaev, Alexander Nesmelov, Konstantin Chernyshov, **Nikita Kotlov**

BostonGene Corporation, Waltham, MA

Background: We previously created Lymphly, a hierarchical framework that uses discrete genetic events to enhance diffuse large B-cell lymphoma (DLBCL) classification. However, the molecular relationships between DLBCL subtypes and the broader B-cell lymphoma landscape remain poorly delineated. Here, we evaluated if Lymphly can elucidate molecular patterns across B-cell lymphomas to inform therapeutic development and trial design.

Methods: Lymphly was used to classify a meta-cohort of ~1,500 DLBCL samples and ~2,000 samples with available molecular data across multiple non-DLBCL B-cell lymphoma diagnoses from internal and publicly available datasets. The samples were assigned canonical (EZB, MCD, BN2, N1) and newly identified subtypes (JS3, JS6), as well as TP53+ and MYC+ statuses. Integrative analyses of molecular and clinical parameters highlighted distinct genomic architectures and risk profiles that may constitute potential therapeutic targets.

Results: Lymphly revealed shared genetic and transcriptional features between non-DLBCL lymphomas and specific DLBCL subtypes in the study cohort, indicative of convergent molecular phenotypes between specific Lymphly subtypes and lymphoma diagnoses. Specific Lymphly subtypes dominated certain diagnoses, and samples within each subtype shared similar gene expression profiles. Subtype EZB was enriched among follicular (FL) and Burkitt (BL) lymphoma samples, reflecting their germinal-center origin (GCB). Many of the FL samples also showed BCL2 translocations, which were less common in BL samples. Subtype BN2, featuring mutations affecting *NOTCH2* and NF-κB signaling, was enriched among marginal zone and splenic marginal zone lymphoma samples. Subtype MCD, featuring alterations in MYD88 and CD79B, was enriched in primary central nervous system lymphoma and high-grade B-cell lymphomas. Newly classified subtypes JS6 and JS3 revealed additional links between DLBCL and other B-cell lymphoma entities: JS6, a GCB-like entity, was linked to primary mediastinal B-cell lymphoma, while JS3, an activated B-cell-like entity, overlapped with T-cell/histiocyte-rich large B-cell lymphoma and plasmablastic lymphoma.

Conclusions: Lymphly demonstrated applicability beyond DLBCL, capturing canonical and newly identified subtypes and shared molecular patterns across B-cell malignancies. Applying DLBCL genetic classification to other B-cell lymphomas revealed potential trajectories of transformation into DLBCL, with Lymphly subtypes reflecting their natural molecular counterparts within the DLBCL spectrum. By integrating an interpretable and a rule-based classification with cross-disease molecular insights, Lymphly is poised to translate these insights into data-driven strategies that optimize decision-making across all stages of diagnostic and treatment development.

#3878 ZEB1 expression in NEUROD1-positive and combined YAP1-dominant pulmonary neuroendocrine carcinomas is associated with a locally immunosuppressive microenvironment.

Noriko Takemura-Kobayashi[1], Kei Asayama[1], Rawya Mohamed Salih Ibrahim[1], Masahiro Maki[1], Ryota Matsuoka[1], Aya Shiba-Ishii[1], Ayako Suzuki[2], Yutaka Suzuki[2], Daisuke Matsubara[1]

[1]Department of Diagnostic Pathology, Institute of Medicine, University of Tsukuba, Ibaraki, Japan,[2]Department of Computational Biology and Medical Sciences, the University of Tokyo, Chiba, Japan

Background: Pulmonary neuroendocrine carcinomas (pNECs), comprising small cell lung carcinoma (SCLC) and large cell neuroendocrine carcinoma (LCNEC), are classified into four molecular subtypes based on the expression of ASCL1, NEUROD1, POU2F3, and YAP1. In non-small cell lung cancer, Zinc finger E-box binding homeobox 1 (ZEB1), a key regulator of epithelial-mesenchymal transition (EMT), is more frequently expressed in poorly differentiated carcinoma (large cell and pleomorphic carcinoma) than in adenocarcinoma and squamous cell carcinoma. ZEB1 expression in cancer cells is linked to the decreased CD8+ T-cells and PD-L1 mediated immunosuppression. However, the features of ZEB1-positive SCLC/LCNEC are poorly understood.
Aim: We investigated the expression of ZEB1 in pNECs and its association with tumor microenvironment.Methods: Western blotting was performed on pNEC cell lines (13 SCLC and 1 LCNEC: 8 ASCL1-dominant, 3 NEUROD1-dominant, 1 POU2F3-dominant, and 2 YAP1-domiant). Immunohistochemistry was conducted on surgically resected samples (33 SCLC and 46 LCNEC). Spatial transcriptome analysis was performed on one ZEB1-positive SCLC sample.
Results: Western blotting using pNEC cell lines showed EMT-like phenotype in NEUROD1- and YAP1-dominant cell lines (high ZEB1, E-cadherin loss). Vimentin was absent in NEUROD1-dominant but present in YAP1-dominant cell lines. ASCL1- and POU2F3-dominant cell lines were largely epithelial (low/absent ZEB1, E-cadherin retained), although a part of ASCL1-dominant cell lines expressed ZEB1. In the xenograft from a ZEB1-positive ASCL1-dominant cell line (H2081), the expression of ZEB1 and E-cadherin was mutually exclusive; ZEB1-positive area was NEUROD1-positve, whereas ZEB1-negative area was ASCL1-positive. Immunohistochemistry on whole-slide sections from surgically resected samples revealed that most ZEB1-positive pNECs were NEUROD1-positive or combined YAP1-dominant cases (combined with adenocarcinoma or squamous cell carcinoma), with localized ZEB1 expression, whereas POU2F3-dominant cases showed low or no expression of ZEB1. Vimentin was highly expressed in a few combined YAP1-dominant pNECs but negative in most cases. The ZEB1-positive area exhibited significantly reduced CD3+ and CD8+ T cells infiltration and, in spatial transcriptome analysis, increased tumor-associated macrophages (TAMs) infiltration than in the ZEB1-negative area in the same cases.
Conclusion: Focal expression of ZEB1 was observed in NEUROD1-positive and combined YAP1-dominant pulmonary neuroendocrine carcinomas. ZEB1-positive area was poor in CD3+ and CD8+ T cells and enriched in TAMs, suggesting that ZEB1-mediated EMT is associated with a locally immunosuppressive microenvironment.

#3879 SPP1-driven immunometabolic reprogramming of tumor-associated neutrophils in glioblastoma.

Matthew Alexander Abikenari[1], John Hyunkuk Choi[1], Ravi Medikonda[1], Lily Kim[1], Rohit Verma[2], Justin Liu[1], Adam Sjoholm[1], George Nageeb[1], Brandon Hwa-Lin Bergsneider[2], Caren Yu-Ju Wu[3], Kwang Bog Cho[1], Andrew Tran[1], David Bakalov[4], Matei Banu[1], Michael Lim[1]

[1]Neurosurgery, Stanford University School of Medicine, Stanford, CA,[2]Stanford University School of Medicine, Stanford, CA,[3]Taipei Chang Gung Memorial Hospital, Ghanghua, Taiwan,[4]Medical Scientist Training Program, University of Utah, Salt Lake City, UT

Introduction: Tumor-associated neutrophils (TANs) in glioblastoma (GBM) are heterogeneous and poorly captured by the classical N1/N2 dichotomy. We characterized TAN states relative to peripheral blood neutrophils (PBNs) and wondered if a discrete, targetable program drives their pro-tumoral phenotype.
Methods: Public scRNA-seq datasets were reanalyzed (GSM8380727, GSM8380728: TANs 15,000 cells; PBNs 10,000 cells; 36,601 genes). Standard Seurat workflow was applied (stringent QC; SCTransform; integration; PCA/UMAP; shared-nearest-neighbor clustering). Differential expression used Wilcoxon rank-sum with Bonferroni FDR (adj. $p<0.05$, $|\log2FC|>0.25$). Module scoring examined prespecified programs: antigen presentation/co-stimulation, interferon/cytotoxicity, lipid/stress adaptation. Functional enrichment and protein-protein networks were assessed via GSEA and STRING.
Results: Integration revealed six tumor-associated Neutrophil states beyond the classical N1/N2 paradigm. Among them, an SPP1+ (osteopontin-high) (avg log2FC ~10.7; adj. $p\approx0$) population was particularly transcriptionally associated with lipid processing genes (APOE, APOC1, APOC2) and chemokine master regulators (CCL3, CCL4) of immune cell recruitment and metabolic reprogramming. SPP1+ TANs featured repression of cytotoxicity pathways and induction of oxidative and lipid metabolism modules, pointing toward a shift from antimicrobial to tissue-remodeling and tumor-supporting activities. Network analysis revealed two large hubs: SPP1-APOE/APOC (lipid remodeling) and CCL3/CCL4 (immune signaling) that are bridged by metabolic stress genes (CTSB, EIF1B) into a cohesive immunometabolic circuit.
Conclusion: Single-cell analysis characterizes GBM TAN heterogeneity and implicates an SPP1-centered, APC-like neutrophil axis bridging lipid regulation (APOE/APOCs) and chemokine signaling (CCL3/CCL4). This osteopontin-driven axis establishes a mechanistic basis for TAN-mediated tumor support and nominates SPP1 and its lipid-chemokine network as actionable targets to reprogram TANs for anti-tumor activity.This is among the first studies to define an osteopontin-driven immunometabolic axis in pro-tumoral neutrophils, establishing a mechanistic framework for future neutrophil-targeted immunotherapies in glioblastoma.

#3880 Functional high risk multiple myeloma is unified by a highly proliferative signature on gene expression profiling.

Hashini Thilakaratne, Jessie Zhao, Daniel Wong, Tiffany Khong, Sridurga Mithraprabhu, **Nicholas E. Bingham**, Andrew Spencer

Australian Centre for Blood Diseases, Alfred Health - Monash University, Melbourne, Australia

Background: Multiple myeloma (MM) is a haematological malignancy with globally improving survival rates. Functional high-risk (FHR) MM, defined as progressive disease less than 18 months from diagnosis, has a median overall survival <3 years, but FHR patients are not identified by conventional prognostic scores nor by gene expression (GE) signatures, such as SKY92 (SkylineDx). Additionally, the biology of therapy resistance and aggressive behaviour in FHR myeloma is poorly understood. We sought to define the transcriptional features of FHR MM and identify molecular pathways that unify this aggressive phenotype.

Methods: The MMProfiler microarray was performed on RNA extracted from bone-marrow aspirate samples of consecutive newly diagnosed MM (NDMM) patients. SKY92 risk classification (high- vs standard-risk) and genome-wide expression data (~20,000 genes) was obtained. Data was normalised across all samples prior to dimensionality reduction techniques, differential gene expression (DGE) analysis and pathway analysis. Clinical data and survival outcomes were collected. DGE analysis cutoffs were adj $p<0.01$ and $|log2FC|>1.0$).

Results: Forty-eight patients were included, of whom 13 (27%) patients met criteria for FHR MM. FHR status was associated with inferior survival (3-year overall survival 58.7% versus 88%, p=0.018). Firth logistic regression demonstrated that R-ISS, R2-ISS and SKY92 classification were not significantly associated with FHR status (R-ISS OR 2.62; 95% CI 0.82-9.85; R2-ISS OR 2.08, 95% CI 0.94-5.64; SKY92 OR 3.55, 95% CI 0.96-16.03).

DGE analysis identified a 16-gene proliferative module upregulated in FHR MM (*MCM2, FOXM1, CDCA5, KIF14, UBE2T, TYMS, KIF4A, NCAPH, SAC3D1, FAM72C, KIF15, ZWINT, CDT1, OIP5, TPX2, CDC20*). These genes functionally converge on cell cycle progression and mitosis, and contain a significant *FOXM1*-driven mitotic program. Formal pathway enrichment confirmed activation of E2F targets, G2/M checkpoint, MYC targets, and DNA repair pathways, consistent with a unified high-proliferation phenotype in FHR MM. A 6-gene proliferative signature derived from the DGE set (*FOXM1* and targets *KIF14*, *ZWINT*, as well as *MCM2*, *UBE2T*, and *TYMS*) demonstrated strong discrimination of FHR status (AUC = 0.912; $p = <0.001$).

Conclusion: FHR MM is poorly identified by current prognostic algorithms. Biologically, we show FHR MM is defined by a cell-cycle driving transcriptional program, at the gene expression level suggestive of a *FOXM1*-driven program. This data suggests early progression in MM reflects a distinct biological state with increased cell-cycle and replication stress pathways. The 6-gene proliferative signature described here warrants validation as a diagnostic tool for FHR MM. The proliferative program seen in FHR MM may represent a novel therapeutic vulnerability, suggesting a role for cell-cycle targeting therapeutic approaches.

#3881 Heterogeneity in tumor microenvironment across MMR subtypes of endometrial cancer: Analysis from the ENGOT-EN6-NSGO/GOG-3031/RUBY trial.

Lucy Gilbert[1], Annika Auranen[2], Mitchell I. Edelson[3], Mikalai Pishchyk[4], Joseph Buscema[5], Tamar Safra[6], Nicole S. Nevadunsky[7], Christine Gennigens[8], Kari Ring[9], Line Bjorge[10], Bhavana Pothuri[11], Helen D. Eshed[12], Iwona Podzielinski[13], Noelle G. Cloven[14], Tashanna K. Myers[15], Kathryn P. Pennington[16], Claire Rooney[17], Rumen Kostadinov[18], Robert W. Holloway[19], Trine Nottrup[20]

[1]Division of Gynecologic Oncology, Research Institute, McGill University Health Centre, Gerald Bronfman Department of Oncology, McGill University, Montreal, QC, Canada,[2]Tays Cancer Centre and FICAN Mid, Tampere University and Tampere University Hospital, Tampere, Finland,[3]Hanjani Institute for Gynecologic Oncology, Jefferson Abington Hospital, Willow Grove, PA,[4]Grodno Regional Clinical Hospital, Grodno, Belarus,[5]Gynecologic Oncology, Tucson Medical Center Health Cancer Center - Wilmot, Tucson, AZ,[6]Department of Oncology, Tel Aviv Sourasky Medical Center, Tel Aviv, Israel; and Faculty of Medicine, Tel Aviv University, Tel Aviv, Israel,[7]Department of Obstetrics, Gynecology, and Women's Health, Montefiore Medical Center, Albert Einstein College of Medicine, Bronx, NY,[8]Department of Medical Oncology, CHU of Liege; and Belgium and Luxembourg Gynaecological Oncology Group (BGOG), Leuven, Belgium,[9]University of Virginia Health System, Charlottesville, VA,[10]Haukeland University Hospital and University of Bergen, Bergen, Norway,[11]Departments of Obstetrics/Gynecology and Medicine, Division of Gynecologic Oncology, Laura & Isaac Perlmutter Cancer Center, NYU Langone Health, New York, NY, USA and GOG Foundation, Philadelphia, PA,[12]Texas Oncology, Austin, TX,[13]Department of Gynecologic Oncology, Parkview Health, Fort Wayne, IN,[14]Texas Oncology, Fort Worth, TX,[15]Baystate Medical Center, Springfield, MA,[16]Division of Gynecologic Oncology, Department of Obstetrics and Gynecology, Fred Hutchinson Cancer Center, University of Washington School of Medicine, Seattle, WA,[17]GSK, Cambridge, United Kingdom,[18]GSK, Upper Providence, PA,[19]AdventHealth Cancer Institute, Orlando, FL,[20]Department of Oncology, Copenhagen University Hospital - Rigshospitalet; and Nordic Society of Gynecologic Oncology (NSGO), Copenhagen, Denmark

Background: In RUBY Part 1 (NCT03981796), dostarlimab + carboplatin-paclitaxel (D+CP) significantly improved PFS and OS vs CP alone in pts with primary advanced or recurrent endometrial cancer (EC). Although MMR deficiency (dMMR) is a predictive biomarker for clinical response, benefit is also observed in the MMR proficient (MMRp) subgroup. Additional insights into the underlying biology and heterogeneity of these tumors are needed to inform potential drivers of response to D+CP.
Methods: RNA sequencing (RNASeq) and whole exome sequencing were performed on 400 tumor samples from RUBY Part 1. Tumors were categorized as dMMR or MMRp per the testing method used for study enrollment. Genomic alterations and RNAseq signatures associated with infiltrating cell types or oncogenic processes were analyzed.
Results: Unsupervised clustering of tumor transcriptional profiles revealed two distinct histological subtype-associated clusters. dMMR tumors were predominantly in the endometrioid cluster; MMRp tumors were distributed across both clusters. Gene signature analysis revealed significant enrichment for tumors with high immune cell signature scores in the dMMR subgroup (Table); however, considerable overlap was observed with a subset of MMRp tumors demonstrating similarly high signature scores. Conversely, signatures associated with tumor senescence and interferon-stimulated genes were enriched in the MMRp subgroup. Genomic analysis revealed frequent alterations in *TP53*, *PTEN*, *PIK3CA,* and *ARID1A*, with higher mutation rates of several genes (eg, *JAK1* and *RNF43*) observed in dMMR tumors, concomitant with higher tumor mutational burden.
Conclusions: These results highlight the molecular and transcriptomic heterogeneity of EC, providing hypotheses to explore the impact of tumor characteristics beyond MMR status on response to dostarlimab+CP in EC. Exploration of the association between these biomarkers and outcomes is ongoing.

Table: Gene signatures across MMR subgroups

Signature	***P* value (Wilcoxon)**	**Signature score higher in**	**Median dMMR/MSI-H**	**Median MMRp/MSS**
Tumor senescence_Combes	<0.001	MMRp/MSS	–0.66	0.27
Th1 cells_Danaher	<0.001	dMMR/MSI-H	0.26	–0.28
NK cells_Bagaev	<0.001	dMMR/MSI-H	0.38	–0.22
Cytotoxic cells_Danaher	<0.001	dMMR/MSI-H	0.30	–0.31
T cells_Bagaev	<0.001	dMMR/MSI-H	0.20	–0.22
Myeloid interferon-stimulated genes_Combes	<0.001	MMRp/MSS	–0.61	0.17
Abbreviations: dMMR, mismatch repair deficient; MSI-H, microsatellite instability-high; MSS, microsatellite-stable; NK, natural killer; MMRp, mismatch repair proficient; Th1, T helper type 1				

#3883 Integrated morphometric and molecular classification of central nervous system cancers in 10 seconds using a unified platform with picosecond infrared laser mass spectrometry.

Alexa Nina Fiorante[1], Michael Woolman[1], David Munoz[2], Farshad Nassiri[3], Gelareh Zadeh[4], Sunit Das[2], Howard Ginsberg[2], **Arash Zarrine-Afsar**[3]

[1]University of Toronto, Toronto, ON, Canada,[2]Unity Health, St. Michael's Hospital, Toronto, ON, Canada,[3]UHN Princess Margaret Cancer Centre, Toronto, ON, Canada,[4]UHN Princess Margaret Cancer Centre, Toronto, ON, Canada, Toronto, ON, Canada

The World Health Organization (WHO) now advocates for an integrated approach in the diagnosis of Central Nervous System (CNS) cancers. However, the proposed WHO workflow is complex, relying heavily on multiple instruments—like genetic sequencers and immunohistochemistry scanners—with variable, often lengthy, turnaround times.
Leveraging the link between lipid metabolism and cancer, we demonstrate that Picosecond InfraRed Laser Mass Spectrometry (PIRL-MS) can profile the tissue lipidome in just 10 seconds, achieving over 80% sensitivity and specificity for CNS tumor type prediction. This was validated across a large cohort of 150 pediatric (3 morphometrically distinct types, 7 molecular classes) and 1,142 adult (24 morphometric, 8 molecular classes) brain tumour types. While initial results provided strong classification, falling short of robust diagnostic criteria, the ongoing incorporation of machine learning has increased sensitivity and specificity to over 94% in select cases. The capabilities of PIRL-MS to deliver a 10-second diagnosis—based on downstream phenomic (lipidomic) changes—for both morphologically and molecularly distinct tumor (sub)types (e.g., IDH mutation status, medulloblastoma subgroups) offers a clear path toward a unified diagnostic platform. This approach can integrate morphometric and molecular diagnoses on a single instrument in seconds, drastically reducing the need for tissue manipulation and lengthy preparation steps, a feat unmatched by current methods.

#3884 Multiplex immunofluorescence based spatial analysis of HER2 positive breast cancer patients treated with bintrafusp alfa: A translational pathology study.

Maria Gabriela Raso[1], Elizve N. Barrientos-Toro[1], June Li[1], Renganayaki K. Pandurengan[1], Harsh Batra[2], Ximing Tang[1], Diego Oliva Rico[1], Julia Mendoza Perez[1], Jill Schwartz Gomez[3], Senthil Damodaran[3], Alastair Thompson[4], Andreas W. Machl[5], Natalia Jacob[6], Jennifer Keating Litton[7], Rashmi Krishna Murthy[3], Cara L. Haymaker[1]

[1]Translational Molecular Pathology, UT MD Anderson Cancer Center, Houston, TX,[2]Pathology and Molecular Medicine, McMaster University, Hamilton, ON, Canada,[3]Breast Medical Oncology, UT MD Anderson Cancer Center, Houston, TX,[4]Baylor College of Medicine, Dan L. Duncan Cancer Center, Houston, TX,[5]Senior Scientist II, Translational Oncology, EMD Serono, Inc., Billerica, MA,[6]Merk SA, Buenos Aires, Argentina,[7]Division of Clinical Research, UT MD Anderson Cancer Center, Houston, TX

Purpose: To characterize spatial remodeling of the tumor immune microenvironment and to define therapy associated cellular and architectural changes in stage II and III HER2 positive breast cancer treated with Bintrafusp Alfa, a bifunctional antibody that combines PD-L1 blockade with a TGFβ trap.
Experimental Design: Formalin fixed paraffin embedded baseline and on treatment biopsies (TP2) from patients enrolled in the MD Anderson clinical trial NCT03620201 were analyzed across five Multiplex Immunofluorescence (mIF) panels that captured: (1) PD axis T cell states, (2) cytotoxic, memory, and regulatory T cell subsets, (3) tumor and myeloid checkpoints and metabolic ligands, (4) T cell co-stimulation and exhaustion markers, and (5) myeloid and neutrophil axes. Spatial analysis was performed using the SPIAT R package to quantify cell-type distributions, identify unsupervised spatial clusters, and define neighborhood compositions. Cases were classified as responsive or refractory based on composite TP2 spatial features such as cytokeratin (CK) fragmentation, intratumoral CD8 positive infiltration, checkpoint-rich interfaces, and mixed immune and tumor clustering.
Results: A subset of TP2 specimens showed clear spatial remodeling characterized by(i) fragmentation of CK architecture into smaller epithelial nests separated by broader stromal areas,(ii) increased infiltration of CD8 and CD3 T cells at tumor stroma interfaces and within epithelial nests,(iii) localized PD1, PDL1, OX40 positive, and ICOS positive immune niches with focal TIM3 expression, and(iv) closer proximity of macrophages and neutrophils to fragmented CK borders without widespread activation of myeloid subsets.These features were enriched in responsive tumors, forming mixed tumor and immune clusters and inflamed spatial neighborhoods. In contrast, refractory tumors retained cohesive CK nests, peripheral T cell rims, and limited checkpoint marker expression.
Conclusions: Combined PD-L1 and TGFβ inhibition with Bintrafusp Alfa promotes heterogeneous spatial reprogramming of the breast cancer microenvironment. Beneficial remodeling is characterized by mixed epithelial and immune clusters, intratumoral cytotoxic and memory T cell infiltration, and checkpoint rich interfaces, while refractory cases are defined by persistent epithelial cohesion and suppressive myeloid environments. Overall, spatial compartmentalization, checkpoint expansion, and immune clustering emerged as indicators of response intensity. Our findings stress the need to tailor interventions to the spatial context; immune excluded tumors may benefit from T cell priming or myeloid reprogramming, while inflamed responders might require maintenance of checkpoint inhibition to sustain tumor clearance.

#3885 Application of transcriptomic bladder-cancer subtypes to upper-tract urothelial carcinoma (UTUC) across international cohorts reveals racial differences and translational limitations.

Joshua M. Scurll[1], Henning Bahlburg[1], Tran Anh Thu (Wendy) Phung[1], John Heard[2], Mamoru Hashimoto[3], Kazutoshi Fujita[3], Daniel Luthringer[2], Toru Sakatani[2], Kaoru Murakami[2], Charles J. Rosser[2], Ewan A. Gibb[1], Peter C. Black1[1], **Hideki Furuya**[2]

[1]University of British Columbia, Vancouver, BC, Canada,[2]Cedars-Sinai Medical Center, Los Angeles, CA,[3]Kindai University, Osaka, Japan

Background and Objectives: Management of UTUC follows bladder cancer (BC) guidelines but could be refined. Molecular subtyping has yielded valuable insights into tumor biology and therapy response/resistance for muscle-invasive (MI) and non-MI (NMI) BC and could have similar value for UTUC. Like NMIBC, UTUC is predominantly luminal-papillary (LumP) in subtype, which has spurred more granular UTUC-specific classification schemes. Here, we investigated whether MIBC and NMIBC subtyping could be translated to UTUC.

Methods: Histologically confirmed FFPE UTUC nephroureterectomy specimens were retrospectively collected from Cedars-Sinai Medical Center (Los Angeles, USA) and Kindai University (Osaka, Japan). RNA-seq was performed on 126 tumors, which were classified using consensus-MIBC and UROMOL2021-NMIBC frameworks. Event-free survival (EFS) was estimated by Kaplan-Meier analysis, excluding cases with prior or concurrent BC.

Results: Of 126 UTUCs, 69 (54.8%) were NMI and 55 (47.3%) MI. The LumP subtype was most common (57%), enriched in NMI-UTUC (75%) versus MI-UTUC (36%), mirroring NMIBC vs. MIBC. Cedars-Sinai tumors were mainly NMI (59%), while Kindai tumors were mostly MI (58%), suggesting population differences. LumP enrichment in Cedars-Sinai (80% of NMI vs. 33% of MI) contrasted with more balanced distributions in Kindai (5/10 NMI, 7/15 MI), indicating potential race-specific variation.Within LumP-UTUC, all four UROMOL classes were represented, whereas non-LumP UTUCs were mostly UROMOL 2b. Stratification by LumP vs. other revealed opposing (but not significant) survival trends in NMI- and MI-UTUC: LumP had poorer 5-year EFS in NMI-UTUC but better outcomes in MI-UTUC. Further stratification of LumP NMI-UTUC by UROMOL class showed no significant EFS differences, although Class 2b tumors had comparably poor outcomes to LumP MI-UTUC. Pathologic T stage remained the strongest prognostic factor (EFS: Ta > T1 > T2 > T3/4; $p < 0.05$).

Conclusions: LumP prevalence in UTUC is largely driven by NMI tumors, recapitulating NMIBC biology. Subtype and stage distributions vary between Western and Asian cohorts, implying race-related molecular diversity. While BC-derived classifiers can categorize UTUC, their clinical interpretation does not directly translate. Tumor stage outweighs molecular subtype as the principal determinant of outcome.

#3886 A novel glioblastoma subtype classification using hallmark gene set signatures: Association between poor prognosis and TP53 downstream pathway.

Yu Jin Kim[1], Jeongman Park[2], Woo Young Kwon[3], Jaejoon Lim[4], Sung Hwan Lee[5]

[1]Department of Biomedical Science, College of Life Science, CHA University, Seongnam-si, Korea, Republic of,[2]Department of Medicine, Hallym University, Chuncheon-si, Korea, Republic of,[3]CHA University, Seoul, Korea, Republic of,[4]2Department of Neurosurgery, Bundang CHA Medical Center, Seongnam-si, Korea, Republic of,[5]CHA University, Seongnam-si, Korea, Republic of

Glioblastoma (GBM) is an extremely aggressive and treatment-resistant primary brain tumor with a markedly poor prognosis. Although various molecular subtypes have been proposed to improve diagnostic and therapeutic approaches, their translation into clinical practice remains limited due to ambiguous classification criteria resulting from intra-tumoral heterogeneity and low clinical relevance. In this study, RNA-seq data from GBM cell lines in the DepMap database and bulk RNA-seq datasets from The Cancer Genome Atlas (TCGA), the Chinese Glioma Genome Atlas (CGGA), PRJNA1051047, and in-house cohorts were utilized. Furthermore, GeoMx DSP data paired with matched in-house RNA-seq samples were examined to characterize spatial transcriptomic patterns. Using Hallmark single-sample Gene Set Enrichment Analysis (ssGSEA) module scores, GBM cell lines were divided into two new subtypes by Non-negative Matrix Factorization (NMF) consensus clustering. Differentially expressed gene (DEG) signatures derived from these clusters were then used to classify IDH-wildtype GBM samples from four independent cohorts into two groups—designated as CA (cytokine-active) and GA (growth-active) subtypes—via a Bayesian compound covariate prediction (BCCP) model. The CA subtype exhibited poorer survival outcomes and elevated enrichment of tumor-associated pathways, including IL2-STAT5 signaling, apoptosis, and inflammatory response. Notably, TP53 emerged as a prominent upstream regulator in the CA group, consistent with increased ssGSEA module scores of 10 TP53-related pathways in various curated datasets in four patient cohorts. GeoMx DSP analyses further compared TP53 expression and ssGSEA module scores across α-SMA, CD45, and CD31 annotated regions of interest (AOIs) categorized into CA and GA subtypes. While TP53 expression did not significantly differ between the two groups in any AOI category, the Hallmark TP53 signaling module score was specifically elevated in α-SMA AOIs of CA subtype, particularly around perivascular regions. Collectively, two clinically relevant subtypes were identified, with the CA subtype being strongly associated with poor prognosis and significant dysregulation of TP53 downstream pathways. These findings suggest that TP53 may play a potentially important role in the aggressiveness of GBM.

#3887 Multiple myeloma risk classification of CoMMpass using Consensus Genomic Staging identifies differences between patients with high and low African genetic ancestry.

Steven M. Foltz[1], Chaitanya R. Acharya[1], Alexander Gout[1], Yuxin Jin[2], David E. Avigan[3], Ravi Vij[4], Shaji Kunnathu Kumar[5], Sagar Lonial[6], Hearn Cho[1], Katie Wozniak[1], Jonathan J. Keats[7], Craig Cole[8], John D. Carpten[9], George J. Mulligan[1]

[1]Multiple Myeloma Research Foundation, Norwalk, CT,[2]Beckman Research Institute of The City of Hope, Duarte, CA,[3]Beth Israel Deaconess Medical Center, Boston, MA,[4]Washington University School of Medicine, St. Louis, MO,[5]Mayo Clinic, Rochester, MN,[6]Emory Winship Cancer Institute, Atlanta, GA,[7]TGen (The Translational Genomics Research Institute), Phoenix, AZ,[8]Karmanos Cancer Institute, Detroit, MI,[9]City of Hope, Duarte, CA

Background: Multiple myeloma is the second most common adult blood cancer and remains incurable, despite recent advances. The IMWG/IMS recently published updated risk criteria, Consensus Genomic Staging (CGS), combining genomic events with clinical measures to identify high-risk patients (Avet-Loiseau, et al. JCO 2025). We applied CGS risk criteria to baseline samples from the Multiple Myeloma Research Foundation CoMMpass Study (NCT01454297), a prospective, longitudinal observational study that enrolled more than1100 participants between 2011-2017.

Methods: We assessed patient risk following CGS criteria. Criteria 1: del(17p), with a cutoff of >20% clonal fraction, and/or TP53 mutation. Criteria 2: an IgH translocation including t(4;14), t(14;16), or t(14;20) along with 1q+ and/or del(1p32). Criteria 3: monoallelic del(1p32) along with 1q+ or biallelic del(1p32). Criteria 4: beta-2 microglobulin >= 5.5 mg/L with normal creatinine. Patients meeting one or more criteria were classified as High Risk. To test if risk showed association with genetic ancestry, we grouped patients into those with high African genetic ancestry and those with low African genetic ancestry. Genetic ancestry was measured using ADMIXTURE in comparison to 1000 Genomes.

Results: We evaluated the CGS risk status of 877 CoMMpass patients, finding 69.2% (573/828) to be Standard Risk (SR) and 30.8% (255/828) to be High Risk (HR). HR patients showed worse progression-free survival (median PFS 26.3 months vs. 42.5 months; log rank test, $p < 0.0001$) and overall survival (median OS 63.9 months vs. median not reached; $p < 0.0001$). 10.6% (91/858) of patients met Criteria 1, 10.7% (93/873) met Criteria 2, 5.6% (49/877) met Criteria 3, and 8.7% (73/835) met Criteria 4.

We found 14.2% (123/867) of patients to have high African-like genetic ancestry (AFR-high) and 85.8% (744/867) to have low African-like genetic ancestry (AFR-low). We observed significantly fewer HR patients within the AFR-high group (20%, 23/115) than in the AFR-low group (32.4%, 231/712) (Fisher's exact test, $p = 0.0065$). The AFR-high group met HR criteria at a lower rate across all criteria, but only with Criteria 3 was the difference significant (p-value = 0.03). Higher levels of creatinine in AFR-high patients may have impacted meeting the normal creatinine requirement of Criteria 4.

Conclusions: HR patients comprise 30.8% of CoMMpass subjects and show significantly worse PFS and OS than SR patients. AFR-high patients met HR criteria at a lower rate than AFR-low patients according to the CGS criteria. Clinical trials that utilize CGS criteria to determine patient eligibility may be challenged to enroll a representative patient population, including AFR-high patients. Screening and eligibility criteria should be carefully considered to mitigate potential enrollment disparities.

#3889 Genomic-immunophenotypic landscape of early-stage pulmonary carcinoid tumors and their prognostic implications.

Song Xu[1], Lingling Zu[1], Ning Zhou[1], Jingya Wang[2], Xiongfei Li[3], Haixiang Yu[4], Sibo Peng[1], Chunxia Su[5], Dingzhi Huang[2]

[1]Department of Lung Cancer Surgery, Tianjin Key Laboratory of Lung Cancer Metastasis and Tumor Microenvironment, Lung Cancer Institute, Tianjin Medical University General Hospital, Tianjin, China, Tianjin, China,[2]Tianjin Medical University Cancer Institute and Hospital, National Clinical Research Center for Cancer, Key Laboratory of Cancer Prevention on and Therapy, Tianjin's Clinical Research Center for Cancer, Tianjin, China., Tianjin, China,[3]Department of Thoracic Surgery, Shanghai Chest Hospital, Shanghai Jiao Tong University, Shanghai, China., Shanghai, China,[4]Department of Thoracic Surgery, China-Japan Union Hospital of Jilin University, Changchun, China, Changchun, China,[5]Department of Medical Oncology, Shanghai Pulmonary Hospital and Thoracic Cancer Institute, Tongji University School of Medicine, Shanghai, China, Shanghai, China

Background: Pulmonary carcinoids (PCs), encompassing atypical carcinoids (ACs) and typical carcinoids (TCs), represent a rare category of lung cancer characterized by low to moderate malignancy. However, there is a limited understanding of the genomic and immune characteristics associated with PCs on a global scale.
Methods: This study enrolled 126 surgically resectable PC patients, comprising 44 ACs and 82 TCs. Next-generation sequencing utilizing a 578-gene panel was conducted and immunohistochemical staining for PD-L1 and CD8 was also carried out.
Findings: The most frequently altered genes in PCs were identified as *EGFR* (n=16, 18%), *KMT2C* (n=11, 12%), *LRP1B* (n=10, 11%), *MEN1* (n=10, 11%), and *NOTCH2* (n=9, 10%). Dysregulation of the RTK/RAS, NOTCH, and PI3K pathways was commonly observed in these PCs. Our study unveiled that only 4.6% of the PC patients were identified as PD-L1 positivity, and TMB and CD8+ T cell infiltration were found to be low in early-stage PCs, as manifested by the “immune-excluded” or “immune-desert” microenvironment. We identified age, gender, TNM stage, tumor type, smoking status, TMB, and LRP1B mutation as indicators of poor prognosis. We found that for those surgically resectable early-stage PC patients with *LRP1B* mutation, patients exhibit an increased risk for tumor-related mortality and recurrence, and subsequently further proposed a molecular classification based on the status of LRP1B mutation.
Interpretation: We depicted the genetic and immune landscape of PCs and proposed a LRP1B mutation based molecular classification. Our research offers novel insights into the biological mechanisms of PCs which contributes to the individualized treatment for PC patients.

#3890 HDAC6 as a convergent oncogenic and immunoregulatory hub across multiple cancer types.

Chia-Wei Wu[1], Chia-Yi Hsu[2], Eing-Mei Tsai[2], **Tsung-Hua Hsieh**[1]

[1]Department of Medical Research, E-Da Hospital/E-Da Cancer Hospital, I-Shou University, Kaohsiung, Taiwan,[2]Department of Obstetrics and Gynecology, Kaohsiung Medical University Hospital, Kaohsiung, Taiwan

Histone deacetylase 6 (HDAC6) has emerged as a critical regulator of tumor progression across multiple malignancies. Our integrated analyses reveal that environmental phthalates (BBP, DBP) drive oncogenic processes in breast epithelial stem cells and ER-negative breast cancer by activating ER-EGFR-PKA or AhR-cAMP-PKA-CREB1 signaling, leading to HDAC6 upregulation, β-catenin/LEF1-TCF4 activation, epithelial-mesenchymal transition (EMT), and enhanced metastatic potential. Beyond breast cancer, clinical datasets and functional studies demonstrate that elevated HDAC6 expression correlates with advanced stage, higher tumor grade, and poor survival in lung cancer, oral squamous cell carcinoma (OSCC), and endometriosis-associated ovarian carcinoma (EAOC). Mechanistically, HDAC6 promotes tumor progression by regulating HIF-1α/BNIP3-mediated autophagy in lung cancer, driving AP-1-dependent IL-13 expression and M2 macrophage polarization in OSCC, and mediating ARID1A mutation-associated IL-10-driven immunosuppressive macrophage programming in EAOC. Importantly, pharmacologic HDAC inhibition (TSA, vorinostat) suppresses autophagy, reverses macrophage polarization, reduces EMT, and markedly inhibits tumor growth in relevant in vitro and in vivo models. Together, these findings position HDAC6 as a convergent oncogenic and immunoregulatory hub across environmentally induced, hormone-independent, and mutation-associated cancers, supporting HDAC6-targeted therapies as a promising strategy for limiting tumor progression and reshaping the tumor immune microenvironment.

#3891 Morphologic spectrum of bladder cancer variants and incidental prostate pathology in cystoprostatectomy specimens.

Shannon Carskadon[1], Aryan Joshi[2], Nilesh S. Gupta[3], **Nallasivam Palanisamy**[1]

[1]Urology, Henry Ford Health, Detroit, MI,[2]Biochemistry, Michigan State University, East Lansing, MI,[3]Pathology, Henry Ford Health, Detroit, MI

High-grade bladder cancer exhibits substantial morphologic heterogeneity, and several variant histologies show distinct biological behavior and therapeutic responsiveness. To define the full pathologic spectrum in cystoprostatectomy specimens, we analyzed 44 cases treated between 2010 and 2023.The cohort (mean age 67.1 ± 12.2 years) predominantly presented with advanced disease; pT3a was the most common stage (25%), and one-third showed invasion of≥pT3. High-grade urothelial carcinoma was the primary subtype (14 cases). True variants were frequent and included squamous differentiation (6), sarcomatoid (2), micropapillary (1), nested (1), giant-cell/pleomorphic (1), and small-cell carcinoma (1). Papillary carcinoma and CIS were reclassified into the high-grade urothelial category. Margin positivity occurred in 6 patients (13.6%), especially among aggressive variants such as squamous, sarcomatoid, and micropapillary carcinoma. Lymph-node metastasis was identified in 3 patients (6.8%), all with high-grade invasive disease.Incidental prostate adenocarcinoma was common, spanning Grade Groups 1-4 and often multifocal. These tumors were low-volume, organ-confined, and rarely showed adverse features such as extraprostatic extension, seminal vesicle invasion, or positive margins. Cribriform/glomeruloid patterns were uncommon. Additional findings included HGPIN, chronic inflammation, and treatment-related changes. Actual bladder cancer invasion into prostatic stroma (pT4a) was rare (one case). Significantly, incidental prostate cancer did not correlate with bladder cancer histology or stage, reflecting their biological independence.Variant histologies have direct therapeutic implications: sarcomatoid, micropapillary, and small-cell carcinoma are associated with aggressive behavior, higher positive-margin rates, and may warrant intensified systemic therapy or enrollment in variant-specific clinical trials. Accurate identification prevents under-treatment of high-risk patients. In contrast, the incidental prostate cancers were clinically silent and indolent; recognizing them avoids unnecessary PSA surveillance, misinterpretation of imaging findings, and prevents staging errors, especially in distinguishing incidental cancer from actual prostatic stromal invasion.Overall, integrated bladder-prostate pathologic assessment improves staging accuracy, guides risk-adapted management, and supports multidisciplinary decision-making. These findings underscore the biological and clinical significance of variant histology in bladder cancer, while confirming that incidental prostate cancer in cystoprostatectomy specimens is typically low-risk and does not influence bladder cancer outcomes.

: Molecular Targeted Therapy
Poster Session

#3895 Targeting RET fusions in sarcomas with vepafestinib, a 3rd generation RET inhibitor with superior blood-brain barrier penetration.

Ryan Cheng[1], Allan J. W. Lui[1], Tom Zhang[1], Christopher A. Febres-Aldana[2], Michael Trombetta[1], Qing Chang[1], Inna Khodos[1], Elisa de Stanchina[1], Igor Odintsov[3], Marc Ladanyi[1], Romel Somwar[1]

[1]Memorial Sloan Kettering Cancer Center, New York, NY,[2]National Cancer Institute, Bethesda, MD,[3]Brigham and Women's Hospital, Boston, MA

Background
RET fusions are known drivers across multiple cancer types. While the FDA-approved small-molecule RET inhibitors selpercatinib and pralsetinib yield overall response rates of ~50-80%, on- and off-target resistance mutations and CNS disease progression underscore the need for novel therapies. Vepafestinib is a RET inhibitor with enhanced specificity and potency against RET solvent-front (G810) and gatekeeper (V804) mutations. Preclinical models of brain metastases demonstrate superior CNS penetration and anti-tumor activity compared to selpercatinib. Here, we investigated the therapeutic potential of vepafestinib in RET fusion-driven sarcomas.
Methods
Patient-derived xenograft (PDX) and cell line models of a SPECC1L::RET-driven sarcoma were established from a brain metastasis. Isogenic cell line models expressing SPECC1L::RET were generated via CRISPR-Cas9 genomic editing of human mesenchymal stem cells (HMSC). Xenograft models were developed by implanting either PDX tissue or HMSC-RET cells into the subcutaneous flank of NOD *scid* gamma (NSG) mice. To model brain metastasis, HMSC-RET cells stably expressing a bioluminescent reporter were implanted into the cerebellum of NSG mice. Protein expression and phosphorylation were assessed by Western blotting. Cell growth was measured using a viability dye.
Results
We established a PDX (Sarc-01pdx), a patient-derived cell line (Sarc-01cl), and an HMSC line harboring the SPECCL1::RET fusion (HMSC-RET). Expression of SPECCL1::RET was confirmed by RT-PCR and Western blot. Vepafestinib effectively inhibited the growth of Sarc-01cl (IC50=0.09 μM) and HMSC-RET (IC50=0.21 μM), compared to the isogenic control (HMSC IC50=12.7μM), with dose- and time-dependent reductions in the phosphorylation of RET (Y905 and Y1062) and downstream effectors, including AKT and ERK1/2. While selpercatinib and pralsetinib also inhibited the growth of the RET fusion-driven sarcoma cells, they showed more off-target effects in the control HMSC cells relative to vepafestinib.In both PDX and cell line xenograft models, vepafestinib (50 mg/kg BID) caused tumor growth inhibition comparable to selpercatinib (10 mg/kg BID) and pralsetinib (15 mg/kg BID). Upon cessation of treatment, tumor recurrence was not observed in mice treated with vepafestinib, whereas regrowth was detected in 1/5 and 3/5 mice in the selpercatinib and pralsetinb groups, respectively. Intracranially, vepafestinib was significantly more effective than selpercatinib at blocking tumor growth (p=0.042) and improving survival (median: 56 vs 32 days, p=0.0025).
Conclusions
Our preclinical results support vepafestinib as a promising, CNS-active therapy for RET fusion-driven sarcomas. Vepafestinib is currently being evaluated in the ongoing phase 1/2 margaRET trial for advanced RET-altered solid tumors (NCT04683250).

#3896 MERTK inhibitor MRX-2843 sensitizes AML to venetoclax and azacitidine in preclinical models.

Aashis Thapa[1], Chloe Hope[1], Edward B. Henderson[1], Austre Y. Schiaffino Bustamante[1], Gianna Branella[1], Alejandro De Janon[2], Sunil Raikar[1], Xiaodong Wang[3], Stephen V. Frye[3], H. Shelton Earp[3], Shuichi Takayama[4], Deborah DeRyckere[1], Douglas K. Graham[1]

[1]Emory University, Atlanta, GA,[2]Georgia Institute of Technology & Emory University, Atlanta, GA,[3]University of North Carolina at Chapel Hill, Chapel Hill, NC,[4]Georgia Institute of Technology, Atlanta, GA

While many patients with acute myeloid leukemia (AML) have an initial favorable response to treatment with standard of care venetoclax, a BCL2 inhibitor, and azacitidine, a DNA methyltransferase inhibitor, sustained remissions remain elusive and new therapies are urgently needed. We identified MERTK (MER Receptor Tyrosine Kinase) as a potential therapeutic target in AML and developed MRX-2843, a first-in-class dual MERTK/FLT3 kinase inhibitor that is currently being tested in leukemia patients. Here we describe a novel therapy that combines MRX-2843 with venetoclax and azacitidine to provide enhanced therapeutic effects in preclinical AML models. In human AML cell line cultures (KG-1, OCI-AML5, and NOMO-1), treatment with the 3-drug combination (MRX-2843/venetoclax/azacitidine) reduced cell density compared to venetoclax/azacitidine. Mathematical modeling using the fractional product method revealed a synergistic interaction between MRX-2843 and venetoclax/azacitidine in 2 of the 3 cell lines and an additive interaction in the other. In all 3 cell lines, MRX-2843 synergized with venetoclax/azacitidine to increase induction of cell death compared to venetoclax/azacitidine alone. Furthermore, in all 3 cell lines, the 3-drug combination reduced levels of c-MYC protein compared to venetoclax/azacitidine. These findings reveal a potential mechanism of the enhanced therapeutic effects mediated by the 3-drug combination. The triple combination also provided enhanced therapeutic effects against the KG1 cell line in an AML organoid model system that mimics many features of the bone marrow microenvironment, including chemoprotection. These data support addition of MRX-2843 to current standard of care venetoclax/azacitidine to better target bone marrow disease. Indeed, the 3-drug regimen significantly reduced bone marrow disease burden and prolonged survival in immune-compromised mice inoculated with the KG1 AML cell line. After the first treatment cycle (28 days), the fraction of human CD45+ leukemia cells in the bone marrow was significantly reduced in mice treated with the 3-drug combination (8.5±5%, n=4) compared to vehicle (67±8%, n=5, $p<0.001$), MRX-2843 (41±9%, n=6, $p=0.0451$), or venetoclax/azacitidine (40%±8%, n=6, $p=0.0482$). Moreover, mouse survival was significantly prolonged by the triple combination (median survival > 150 days, 59.1% survival after 150 days of treatment) compared to MRX-2843 (median survival = 76.5 days, 0% survival at 150 days, $p<0.0001$) or venetoclax/azacitidine (median survival = 104.5 days, 4.6% survival at 150 days, $p<0.001$). Together these findings (i) implicate co-administration of MRX-2843, venetoclax and azacitidine as an effective strategy to treat AML, (ii) reveal a potential mechanistic basis for this strategy, and (iii) support evaluation of this novel 3-drug combination in future clinical trials.

#3898 Profiling tumor selectivity of state- and paralog-selective RAS inhibitors through a signaling inhibition index (SII).

Beau Baars[1], Ana Orive-Ramos[1], Matthew Emmett[2], Bijaya Gaire[1], Mathieu Desaunay[1], Ziyue Kou[1], Guangyan Li[2], Christos Adamopoulos[1], Stuart A. Aaronson[3], Shaomeng Wang[4], William R. Sellers[2], Tiphaine Martin[1], Evripidis Gavathiotis[5], Poulikos I. Poulikakos[1]

[1]The Tisch Cancer Institute, Icahn School of Medicine at Mount Sinai, New York, NY,[2]Broad Institute at MIT and Harvard, Cambridge, MA,[3]Icahn School of Medicine at Mount Sinai, New York, NY,[4]Department of Internal Medicine, Department of Pharmacology, University of Michigan, Ann Arbor, MI,[5]Albert Einstein College of Medicine, Bronx, NY

The landscape of RAS-directed therapies has rapidly advanced following the advent of mutant-selective KRAS(G12C) inhibitors, driving the development of additional RAS-targeting agents, including mutant-selective (e.g. KRAS(G12C), KRAS(G12D)), as well as paralog- and state-selective compounds. Non-mutant- specific RAS inhibition can currently be achieved through three strategies: (i) guanine nucleotide exchange-OFF inhibitors (panRAS-GEF(OFF)i) that indirectly inactivate RAS by targeting SHP2 or SOS1, (ii) KRAS-OFF inhibitors (panKRAS(OFF)i) that spare NRAS and HRAS, and (iii) active-state RAS(ON) inhibitors (panRAS(ON)i) that directly block binding of effector RAF. Although these therapeutic modalities have shown promise, their clinical effectiveness and tolerability ultimately depend on achieving a high therapeutic index, defined as potent inhibition of oncogenic signaling in tumor cells with minimal effects on normal cells. To more robustly quantify tumor selectivity in preclinical models, we introduce the signaling inhibition index (SII), which measures the differential suppression of oncogenic signaling between RAS(MUT) and RAS(WT) cells, providing a more structured metric of tumor selectivity that has previously been poorly defined. Here, we evaluated the SII for state- and paralog-selective RAS inhibitors across diverse RAS(MUT) and RAS(WT) models. PanRAS-GEF(OFF)i exhibited neutral or negative SII, reflecting reduced MAPK suppression in KRAS(G12X) cells compared to wild-type cells. KRAS(G13D) models, especially with NF1 loss, showed low sensitivity. Combining SHP2 and MEK inhibition resulted in low tumor-selectivity, while RAS(Q61X) models were resistant due to MEK inhibitor-induced NRAS reactivation and altered SHP2 conformations. Consistent with these findings, analysis of DepMap SHP2-inhibitor sensitivity and dependency datasets showed that RAS(MUT) cell lines are not more sensitive than RAS(WT) cells to SHP2 inhibition, further underscoring the limited tumor selectivity of panRAS-GEF(OFF)-based approaches. In parallel, we assessed panKRAS(OFF)i and panRAS(ON)i potency/selectivity across a panel of RAS(MUT) and RAS(WT) cell line models. KRAS(OFF) inhibitors demonstrated higher selectivity, whereas active-state RAS(ON) inhibitors showed broader activity but narrow selectivity. Comparative analyses of published datasets revealed correlated sensitivity patterns across RAS inhibitor classes, indicating that therapeutic activity is largely restricted to the same subset of RAS(MUT) cancers. These findings highlight the importance of systemic SII quantification for therapeutic selectivity and for guiding the rational design and clinical implementation of next-generation RAS-targeted therapies.

#3900 Tegavivint, a first-in-class TBL1 inhibitor demonstrates potent activity in WNT-driven colorectal cancers.

Raffaella Soldi[1], Tithi Ghosh Halder[1], Jaeger Moore[1], Serina Ng[1], Jamie Cox[2], Taylor Bargenquast[1], Mahtab Youseffi[3], Julissa Simmons[3], Elena Ramirez[3], Aundrietta Duncan[3], Stephen Horrigan[3], Sunil Sharma[1]

[1]Honor Health Research Institute, Phoenix, AZ,[2]Honor Health Research Institute, Scottsdale, AZ,[3]Iterion Therapeutics, Houston, TX

Background. Tegavivint is a clinical phase investigational small molecule that disrupts Wnt/β-catenin signaling by targeting transducing beta-like protein 1 (TBL1), a critical mediator of nuclear β-catenin transcriptional activity. Unlike upstream Wnt inhibitors, tegavivint selectively impairs oncogenic transcriptional programs while sparing physiological Wnt functions, minimizing systemic toxicity. Preclinical studies and early-phase clinical trials have demonstrated that tegavivint suppresses tumor growth and enhances immune infiltration across multiple cancer models, including hepatocellular carcinoma and non-small cell lung cancer. Mechanistically, tegavivint promotes degradation of nuclear β-catenin, downregulates Wnt target gene expression, and modulates the tumor immune microenvironment. This mode of action is particularly relevant in colorectal cancer (CRC), where aberrant Wnt signaling, frequently driven by APC or CTNNB1 mutations, plays a central role in tumorigenesis. The present study investigates the potential therapeutic efficacy of tegavivint in CRC.

Methods. To evaluate the cytotoxic potential of tegavivint in CRC, we conducted the Broad PRISM screen. Annexin V analysis revealed dose- and time-dependent induction of apoptosis. To further elucidate the molecular consequences of treatment, transcriptomic profiling was performed in HCT15 cells. To investigate the influence of the tumor microenvironment on drug sensitivity, dose-response analyses were extended to CRC organoid models, including cell line-derived organoids co-cultured with fibroblasts, as well as patient-derived organoids (PDOs) containing endogenous stromal components. Last, Tegavivint was investigated in a combination drug screen to identify mechanisms of activity and potential synergies in 2D cells and PDOs.

Results. Tegavivint monotherapy exhibited robust antitumor activity across a spectrum of CRC preclinical models, including 2D cell lines, 3D spheroids, PDOs. RNA-seq analysis revealed marked transcriptional repression of Wnt/β-catenin signaling interacting genes along with induction of apoptotic programs, confirming the reprogramming of Wnt/b-catenin signaling and subsequent cell death by tegavivint. Furthermore, Tegavivint treatment induced apoptosis in responsive models, validating our initial mechanistic predictions and supporting its role as a targeted therapeutic agent in WNT-driven CRC. Tegavivint demonstrated synergistic activity when combined with VEGF-TKIs and pan-RAS inhibitors, while combination with other Wnt-inhibitors yielded no added activity.

Conclusion. These findings underscore the translational promise of Tegavivint as a therapeutic strategy in colorectal cancer, supporting its advancement toward clinical development to improve outcomes in WNT-driven disease subsets.

#3901 BGB-58067, a brain-penetrative MTA-cooperative PRMT5 inhibitor, demonstrates promising anti-tumor activity and favorable selectivity in tumors with MTAP-deletion.

Amy Jiang[1], Jinyan Chen[1], Xiaoxin Liu[1], Hongyu Chen[1], Huijun Kang[1], Jie Li[1], Haiying Li[1], Bo Zhang[1], Chenge Zhao[1], Hao Zhu[1], Xin Zhou[1], **Sanjia Xu**[1], Yibin Xu[2], Xing Zhou[1], Shifan Ma[1], Ming Fang[1], Min Xu[1], Lan Hua[1], Chuanxiu Yang[1], Yue Wu[1], Beibei Jiang[1], Xi Wu[1], Fan Wang[1], Ye Liu[1], Zhitao Wan[1], Jing Li[1], Jiyuan Zhang[2], Zhiwei Wang[1], Zhirong Shen[1], Yu Shen[1], Lai Wang[1], Xiaomin Song[1]

[1]BeOne Medicines, Beijing, China,[2]BeOne Medicines, Shanghai, China

PRMT5 was identified as a synthetic lethal target for cancers harboring homozygous deletion of the MTAP gene. MTA was found to accumulate in tumor cells with MTAP-deletion, which inhibited PRMT5 enzymatic activity and increased susceptibility to additional PRMT5 depletion. The homozygous MTAP-deletion was observed in 15% of all tumor types. MTA-cooperative PRMT5 inhibitors have been developed as potential antitumor therapies in tumor types with MTAP-deletion as they selectively bind and stabilize the catalytically inactive PRMT5/MTA complex to inhibit PRMT5 enzymatic activity. BGB-58067 is a highly potent and selective MTA-cooperative PRMT5 inhibitor with good brain penetration potential. BGB-58067 is highly selective for PRMT5 over other methyltransferase family members. It shows strong killing potency and good selectivity (>50-fold) in the cancer cell lines panel with MTAP-deletion over cell lines with MTAP-WT. BGB-58067 very weakly hits on normal hematological cells and demonstrates preferable selectivity (>30-fold) than competitors. BGB-58067 induces robust anti-tumor activity in multiple cell line-derived xenograft models. BGB-58067 demonstrates desirable pharmacokinetics properties and low DDI risk. It exhibits excellent unbound brain-to-plasma partition coefficient to support robust intracranial anti-tumor activity. BGB-58067 shows favorable nonclinical safety profile in the GLP studies, as well as good selectivity in an in vitro SafetyScreen87-off target profiling study. In conclusion, BGB-58067 demonstrates robust potency and selectivity, providing a favorable safety margin for patients, with high potential for the treatment of brain tumors and brain metastases.

#3902 WEE1 inhibition as a therapeutic strategy in triple-negative breast cancer: Evaluating single agent and combination activity of azenosertib in preclinical models.

Catherine Lee, **Alexandra Levy**, Mona Abed, Heekyung Chung, Olivier Harismendy, Doris Kim

Zentalis Pharmaceuticals, San Diego, CA

Background: WEE1 kinase maintains genomic integrity by regulating the G1/S and G2/M cell cycle transitions, allowing cells to repair damaged DNA before progressing to the next phase. Treating tumor cells with azenosertib, a highly selective oral WEE1 inhibitor (WEE1i), promotes premature cell cycle entry, accumulation of DNA damage, and ultimately cell death. While clinically meaningful activity has so far been observed in platinum-resistant ovarian cancer, we sought to explore vulnerability to WEE1 inhibition in other solid tumor types, such as breast. With over 300,000 new cases of breast cancer diagnosed each year in the United States, approximately 15-20% are triple-negative breast cancer (TNBC). TNBC is a particularly aggressive subtype with limited availability of targeted therapies for patients. Although recent approvals of immune checkpoint inhibitors and antibody-drug conjugates (ADCs) have improved outcomes in some patients with TNBC, many eventually experience disease progression, underscoring the continued need for new therapeutic strategies.

Methods: Using results from four *in vitro* pharmacogenomic drug screens in cell lines, we analyzed breast cancer models for sensitivity to WEE1i and potential molecular correlates, including subtype classification, mutation and expression of genes associated with replication stress, and pathway enrichment. *In vivo* efficacy of azenosertib was evaluated in a panel of ~10 TNBC xenograft models implanted subcutaneously in immunocompromised mice. Clinically relevant doses of azenosertib were tested as monotherapy treatments or in combination with current standard-of-care therapies for TNBC.

Results: When compared to non-TNBC breast, TNBC cell lines were significantly more sensitive to WEE1i *in vitro* and tended to have higher Cyclin E1 protein expression, a known marker of replication stress and vulnerability to WEE1i. *In vivo*, single agent azenosertib demonstrated moderate to strong efficacy in a panel of TNBC xenograft models. In models that were less sensitive to single agent azenosertib, combinations with sacituzumab govitecan (SG), trastuzumab deruxtecan (T-DXd), or datopotamab deruxtecan (Dato-DXd) enhanced tumor growth inhibition and prolonged duration of response beyond what was achieved with any of the agents alone.

Conclusions: We demonstrated *in vitro* and *in vivo* evidence that TNBC models are susceptible to WEE1 inhibition. Our findings suggest that azenosertib as a single agent, or in combination with standard-of-care therapies, may be a potential treatment strategy for TNBC and warrants further exploration.

#3903 SPEDOX-6: First-in-human Phase IB/IIA trial on soft tissue sarcomas.

C. J. Yu[1], leslie Wang[1], Kinsley Wang[1], Mengmeng Liu[1], Faqing Huang[2], Warren A. Chow[3], Xiaojiang Cui[4]

[1]Sunstate Biosciences, LLC, Pasadena, CA,[2]University of Southern Mississippi, Hattiesburg, MS,[3]University of California at Irvine, Irvine, CA, CA,[4]Cedars-Sinai Medical Center, Los Angeles, CA

Purpose: Soft tissue sarcomas (STSs) are extremely aggressive & deadly rare tumors with multiple subtypes. Early diagnosis is very difficult & STSs are frequently diagnosed only at advanced stages. DOX has remained the only standard of care in past 45 years with low efficacy and high dose-dependent cardiotoxicity. Better agents are urgently needed.
Methods: Our patented single protein encapsulation (SPE) platform allows encapsulation of small-molecule drugs by a single protein (albumins or globulins) to make new generation nanodrugs that have no artificial nanoparticles, no chemical modifications to drugs and proteins. SPEDOX-6 was successfully prepared by encapsulated 9 doxorubicin (DOX) molecules into the binding pockets of each native HSA molecule, which was confirmed and characterized by UV, fluorescence, membrane dialysis, size-exclusion HPLC and size distribution. SPEDOX-6 provides a novel approach for improving DOX's efficacy and reducing its side effects by targeting cancer cells with low neonatal Fc receptor (FcRn) levels.
Results: In mouse model, heart tissues' DOX was 4 to 8 times lower from SPEDOX-6 than from DOX, indicative of lower cardiotoxicity of SPEDOX-6. PK profiles of same dose for SPEDOX-6 and DOX shown that SPEDOX-6 has shown 48X increase of SPEDOX-6 total exposure upon its encapsulation. In rat model, the total exposure for SPEDOX-6 increases 7-17 times compared to DOX. SPEDOX-6's cardiotoxicity at 50 mg/kg was undetectable, in contrast to observable DOX's cardiotoxicity at 5-10 mg/kg. In mouse model efficacy study on HT-1080 (STS), SPEDOX-6 remarkably suppresses HT-1080 (the lowest FcRn) with 3 out of 10 mice tumor free. SPEDOX-6 at 30 mg/kg is significantly better than Doxil at 4 mg/kg (MTD) and DOX at 3.5 mg/kg (MTD) in inhibiting SK-ES-1 (Ewing sarcoma, with the highest FcRn) tumor growth, but SPEDOX-6 has less efficacy against SK-ES-1, relative to HT-1080. For MB-MDA-231 (TNBC, medium FcRn) model, SPEDOX-6 has shown superior anticancer efficacy in comparison to DOX. Combined with 3 mouse model studies, SPEDOX-6's antitumor efficacy displays an inverse relationship with the FcRn expression level, thereby providing a potential mechanism for SPEDOX-6 to effectively target tumors with low FcRn. IND (IND #: 152154) applications with 8 dosing escalation levels were approved by FDA and first-in-human phase IB was initiated at UCI and Cedar Sinai in June 2025 (NCT07064018). At present, initial dose (20 mg/m^2) with 3 patients (lung/pancreatic/cervical cancer) was completed and dose level 2 (40 mg/m^2) is underway with enrollment of 3 patients (2 STSs/ uterine cancer).
Conclusions: With Orphan Drug Designation of SPEDOX-6, only phase 2A trial is needed for full approval, granted by FDA. Superior clinical antitumor efficacy of SPEDOX-6 on STSs is expected to be achieved because a possible high dose at 310 mg/m^2 (> 4-folds DOX) can be used for treating patients without cardiotoxicity, which will save lots of lives.

#3904 SPOP drives AR-V7-mediated ARPI resistance in prostate cancer.

Joanina K. Gicobi[1], Susanna M. Gregory[2], Nicole A. Becker[2], Elizabeth A. Bering[2], Jacob J. Orme[1]

[1]Medical Oncology, Mayo Clinic, Rochester, MN,[2]Biochemistry and Molecular Biology, Mayo Clinic, Rochester, MN

Approximately 288,000 men are diagnosed with prostate cancer (PCa) in the United States each year, with cases expected to double by 2040. While metastatic PCa can be treated with androgen deprivation therapy (ADT) and AR pathway inhibitors (ARPI), it inevitably develops into treatment resistant, lethal disease. The most common ARPI resistance mechanism in PCa is the expression of AR splice variant AR-V7 that lacks the ligand binding domain and is constitutively active. Patients with PCa expressing AR-V7 experience inferior overall survival. Speckle-type POZ protein (SPOP) is an adaptor protein of the Cullin3-based E3 ubiquitin ligase that facilitates both degradative and non-degradative polyubiquitination of targets such as AR. Loss-of-function SPOP mutations occur in approximately 10-15% of prostate cancers, and *SPOP*-mutant PCa is a unique subtype that has been shown to be exquisitely sensitive to ADT and ARPI treatment. This sensitivity is mediated in part by increased androgen availability via upregulation of hydroxysteroid 17-beta dehydrogenase 4 (HSD17B4) and related steroid synthesis pathways, reduced AR degradation, and enhanced AR cofactor activity. The remarkable efficacy of ARPI in ADT-resistant *SPOP*-mutant prostate cancer is not well understood.We *hypothesized* a novel mechanism by which wild-type SPOP promotes AR-V7-mediated resistance to ARPI in PCa. This mechanism may explain the exceptional ARPI sensitivity of *SPOP*-mutant PCa, distinct from its susceptibility to ADT. We further proposed that clinical SPOP inhibition may broaden this enhanced ARPI susceptibility to the 85-90% of PCa expressing wild-type SPOP.Our *results* show that SPOP drives ARPI resistance in prostate cancer that can be reversed by SPOP inhibitor. Bulk RNA sequencing showed that SPOP inhibitor targets spliceosome machinery and more importantly, abrogated AR-V7 expression both at transcriptional and protein level. Further investigation revealed that wild-type SPOP ubiquitinates spliceosome regulator SFPQ, promoting AR-V7 alternative splicing and ARPI resistance. While SPOP loss is pathogenic in PCa, leveraging the weakness conferred by *SPOP* mutation in the 85% of patients with SPOP-wild type provides an innovative strategy to sensitize ARPI resistant disease to standard of care treatment and save lives.

#3905 A pan-TEAD inhibitor, SIGX2649, blocks Hippo-YAP/TAZ signaling pathway and suppresses solid tumor growth in preclinical studies.

Hualing Peng

Signet Therapeutics Inc, Shenzhen, China

The Hippo-YAP/TAZ signaling cascade is a critical regulator of tissue homeostasis, with TEAD transcription factors (TEAD1-4) serving as essential downstream effectors. Perturbation of Hippo signaling permits YAP/TAZ nuclear accumulation, leading to TEAD-mediated transcriptional programs that drive oncogenic processes such as tumor cell proliferation, resistance to apoptosis, drug resistance, and remodeling of the tumor microenvironment.

Here, we report the discovery of SIGX2649, a potent pan-TEAD inhibitor identified through AI-guided design and organoid-based screening. Leveraging generative AI and predictive AI models significantly accelerated lead identification and optimization during SIGX2649's development. SIGX2649 blocks palmitoylation of TEAD1/2/3/4, disrupts YAP/TAZ-TEAD protein interaction, and suppresses TEAD-dependent transcription. Notably, SIGX2649 displays a superior capacity to enhance the binding of the transcriptional repressor VGLL4 to TEAD relative to other multi-TEAD inhibitors, thereby further strengthening its pharmacological activity. Consequently, it inhibits proliferation across a spectrum of tumor models in vitro, including YAP-activated liver-cancer organoids and mesothelioma cells bearing LATS mutations and NF2 loss. In vivo, SIGX2649 exhibited robust antitumor efficacy in xenograft models, favorable pharmacokinetics, and minimal hepatic- or renal- targeted toxicity compared with other TEAD inhibitors under comparable efficacy. Combined with RAS-pathway inhibitors, SIGX2649 elicits pronounced synergistic responses in KRAS-mutant solid tumors.

The robust efficacy and considerable safety characteristics presented by SIGX2649 in preclinical trials support its potential to serve as a highly promising small-molecule therapeutic in future cancer treatment.

#3906 Small-molecule inhibitors as salvage therapy for CBFB::MYH11-associated acute myeloid leukemia.

Thuy An Nguyen[1], A S M Waliullah[1], Joshua Pei[1], Misha Padigala[1], Malena Nong[1], Nazifa Azam[1], Hien La[2], Nicholas Nguyen[1], Katelyn Do[1], Ramzia Ismailzada[1], Anna Bookstaver[1], Barbara Dziegielewska[1], Ly P. Vu[3], Nam Chu[4], Francine Garrett-Bakelman[5], Hong Zhu[6], Jeffrey W. Craig[1], Bon Q. Trinh[1]

[1]Department of Pathology, University of Virginia, Charlottesville, VA,[2]Biomedical Physics Program, Vietnam National University, Hanoi, Viet Nam,[3]Terry Fox Laboratory, Bristish Columbia Cancer Research Centre, Vancouver, BC, Canada,[4]Department of Cancer Biology and Genetics, Ohio State University, Columbus, OH,[5]Department of Biochemistry and Molecular Genetics, University of Virginia, Charlottesville, VA,[6]Department of Public Health Sciences, University of Virginia, Charlottesville, VA

Acute myeloid leukemia (AML) is an aggressive blood cancer and the most common form of acute leukemia in adults. Although chemotherapy with cytarabine and an anthracycline induces high remission rates, it often causes severe side effects, and relapse is common. These limitations highlight the urgent need for new treatment options, particularly for relapsed disease, where therapeutic resistance remains a significant obstacle. Genetic rearrangements are major drivers of AML, generating fusion proteins that disrupt normal hematopoietic regulation in about 20–40% of cases. Among these, CBFB::MYH11, resulting from chromosome 16 inversion or t(16;16) translocation, occurs in 10–15% of adult AML. This fusion protein sequesters RUNX1 in the cytoplasm, impairing core-binding factor function, blocking myeloid differentiation, and promoting leukemic cell survival. Thus, CBFB::MYH11 represents an attractive therapeutic target in AML, including in the setting of relapsed disease. Using a comprehensive virtual screening pipeline that integrates chemical structures from FDA-approved drugs, natural products, the ZINC22 database, and experimental compounds, we systematically identified lead compounds targeting the CBFB component of the CBFB::MYH11 fusion protein. To experimentally validate our cheminformatics-based predictions, we established multiple cytarabine-resistant AML cell lines, including CBFB::MYH11, to model therapy-induced resistance. In parallel, we isolated mononuclear cells from peripheral blood and bone marrow samples from AML patients with and without CBFB::MYH11 at both diagnosis and relapse, enabling direct comparison between in vitro and patient-derived resistance mechanisms. Treatment with the experimental compound SM1, one of the predicted top-binding candidates, selectively induced cell cycle arrest and apoptotic cell death in chemoresistant and chemosensitive AML cells harboring CBFB::MYH11, while sparing AML cells with other chromosomal aberrations. Both primary and relapsed AML patient cells harboring CBFB::MYH11 were similarly affected. We then established xenograft and patient-derived mouse models of AML to evaluate the therapeutic efficacy of SM1 *in vivo*. Ongoing studies will assess SM1's impact on animal survival and aim to extend both *in vitro* and *in vivo* analyses to additional lead compounds identified in our *in-silico* screening. The success of this study could enable the development of a small-molecule therapeutic toolkit for chemoresistant AML harboring CBFB::MYH11 and support future applications in other AML subtypes with oncogenic fusions.

#3907 Molecular determinants of response in laparoscopically triaged advanced ovarian cancer.

Sara Corvigno[1], Nicholas W. Bateman[2], Amma Asare[1], Chunqiao Tian[2], Jun Yao[3], Sean Cronin[2], Jonathan Ogata[2], Tamara Abulez[2], Kelly A. Conrads[2], Brian L. Hood[2], Joseph Celestino[1], Nicole D. Fleming[1], Kathleen M. Darcy[2], Amir A. Jazaeri[1], Shannon N. Westin[1], Christopher Tarmey[2], Thomas P. Conrads[2], George L. Maxwell[2], Sanghoon Lee[1], Anil K. Sood[1]

[1]Department of Gynecologic Oncology and Reproductive Medicine, UT MD Anderson Cancer Center, Houston, TX,[2]Gynecologic Cancer Center of Excellence, Department of Gynecologic Surgery and Obstetrics, Uniformed Services University of the Health Sciences, Walter Reed National Military Medical Center, Bethesda, MD,[3]Department of Molecular & Cellular Oncology, UT MD Anderson Cancer Center, Houston, TX

BACKGROUND: High-grade serous ovarian cancer (HGSC) is the most lethal gynecologic malignancy, marked by genomic instability, extensive peritoneal spread, and frequent recurrence despite initial chemosensitivity. Complete gross resection (CGR) at primary surgery is the strongest predictor of survival, yet it is not always achievable. Conventional imaging often underestimates disease burden and reliable molecular predictors of surgical and chemotherapeutic response are lacking. To address this, we performed a multi-omic analysis of tumors obtained during laparoscopic scoring procedures that triaged patients to primary tumor reductive surgery (pTRS) or neoadjuvant chemotherapy (NACT) followed by interval tumor reductive surgery (iTRS).

METHODS: Pre-treatment fresh-frozen tumor samples were collected from 40 patients across four groups: pTRS-CGR, pTRS-R1 (gross residual disease), iTRS-CGR, and iTRS-R1. Bulk RNA sequencing and multiplexed quantitative proteomics were performed to characterize transcriptomic and proteomic profiles. Integrative proteogenomic analyses identified concordant molecular signatures associated with treatment outcomes. Findings were validated in an independent multi-omic cohort of 30 HGSC patients treated with identical protocols.

RESULTS: Patients achieving pTRS-CGR had the most favorable overall survival (OS) (87.5 months, median OS), whereas iTRS-R1 had the poorest outcome (22.9 months, median OS). Multi-omic integration revealed distinct expression signatures across response groups. A total of 73 proteins and 229 transcripts were significantly upregulated in iTRS-R1 tumors compared to others, with strong proteomic-transcriptomic concordance (Spearman Rho=0.837, P<1E-4). Pathway analysis showed enrichment for primary cilium formation and cell anchoring in pTRS-CGR tumors, while iTRS-R1 tumors exhibited activation of oxidative phosphorylation, mitochondrial metabolism, and stress-adaptive signaling. Notably, EEF2K (Eukaryotic elongation factor 2 kinase), a key regulator of energy conservation and stress response, was markedly overexpressed in iTRS-R1 tumors. Validation confirmed elevated EEF2K in poor NACT responders with higher residual disease burden.

CONCLUSION: Laparoscopic triage effectively stratifies advanced HGSC for optimal surgical management, with pTRS-CGR achieving the best survival outcome. Multi-omic analyses highlight metabolic reprogramming as a hallmark of poor responders and identify EEF2K as a potential prognostic biomarker and therapeutic target. These data support biomarker-driven approaches to improve outcomes in advanced ovarian cancer.

#3908 Liquid biopsy-informed precision oncology clinical trial to evaluate the utility of ctDNA genomic profiling for therapy optimization in patients with advanced or metastatic solid tumors.

Amna Jamali[1], Jaime Wehr[1], Jenna VanLiere Canzoniero[1], Maria Fatteh[1], Katerina Karaindrou[1], Michael Conroy[1], Ilias Ziakas[1], Mohamed Sherief[1], Timsy Wanchoo[1], Faith Too[1], Lily Scharpf[1], Ruth Moges[1], Dana Petry[1], Kala Visvanathan[1], Ellen Verner[2], Amy Greer[2], Kory Kreimeyer[1], Jonathan Spiker[1], Rachel Karchin[1], Christine L. Hann[1], Vincent K. Lam[1], Joseph Christopher Murray[1], Josephine Feliciano[1], Kristen Marrone[1], Julie R. Brahmer[1], Ming-Tseh Lin[3], Taxiarchis Botsis[1], Hao Wang[1], Mark Sausen[2], Christopher D. Gocke[3], Rena Xian[3], Jessica Tao[1], Valsamo (Elsa) K. Anagnostou[1]

[1]Department of Oncology, Sidney Kimmel Comprehensive Cancer Center, Johns Hopkins School of Medicine, Baltimore, MD,[2]Labcorp, Baltimore, MD,[3]Department of Pathology, Johns Hopkins School of Medicine, Baltimore, MD

Background: Genomic profiling via liquid biopsies (LB) has advanced precision oncology decision-making; however, a major challenge is critically interpreting LB data to improve the selection and order of genotype-specific therapies.
Methods: We present updated results from the first planned analysis of an observational biomarker trial, aimed at assessing the clinical utility of serial LB in patients with advanced or metastatic solid tumors (NCT05585684). Primary endpoints assessed feasibility, prevalence of actionable alterations, and fraction of patients receiving genotype-matched therapies. Secondary endpoints encompassed progression-free survival (PFS), overall survival (OS), and concordance between LB and tumor next-generation sequencing (NGS). Serial LBs at baseline, early (1-3 weeks) on therapy, and at progression, employed a clinically validated 33-gene panel NGS assay (Labcorp Plasma Focus). Matched white blood cell (WBC) NGS was used to identify clonal hematopoiesis (CH)-derived variants. Mutation actionability was evaluated using a multi-resource programmatic approach, and levels of evidence (1-4) were assigned, followed by review at the Johns Hopkins Molecular Tumor Board (JH MTB).
Results: Among 50 patients, 45 baseline and 12 progression LBs were reviewed at MTB. JH MTB classified 72.5% (n=50) of baseline alterations as tumor-derived. In 19 patients with archival tissue NGS, 32 variants were detected in the baseline LB, of which 78.1% were also detected in tissue NGS. Furthermore, 23.2% (n=16) of LB alterations at baseline, 20.0% (n=6) early on-therapy, and 13.0% (n=3) at progression were CH derived. Upon MTB review, 29.2% variants at baseline, 21.9% at early on-therapy and 26.1% at progression were classified as actionable (58.8% level 1, 11.8% level 2, 11.8% level 3 and 17.6% level 4 evidence). Of 45 patients reviewed, 38 received therapeutic recommendations and 57.9% initiated recommended therapy. Patients treated with MTB recommended therapies had significantly longer median PFS and OS compared to those who received standard of care (p=0.027 and p=0.00062 respectively). MTB-recommended therapy selection was independently associated with PFS and OS, in multivariate analyses adjusting for clinical covariates including sex, smoking status, age, and prior lines of systemic therapy (p=0.043 and p=0.006, respectively). Subset of patients treated with genotype-matched MTB recommendations had significantly longer median PFS and OS compared to those who received standard of care (p=0.026 and p=0.0074 respectively).
Conclusion: Our findings emphasize the importance of precision oncology interventions driven by programmatic workflows within a multidisciplinary MTB, supported by comprehensive LB molecular information to guide therapy selection and improve patient outcomes.

#3909 SMARCA4 ablation mitigates distal-less homeobox 1 (*DLX1*)- driven oncogenicity in prostate cancer.

Ankita Bhattacharyya[1], Susanta Samajdar[2], Bushra Ateeq[1]

[1]Department of Biological Sciences and Bioengineering, Indian Institute of Technology Kanpur, Kanpur, India,[2]Aurigene Oncology Limited, Bangalore, India

Prostate cancer (PCa) is a molecularly heterogeneous malignancy with high prevalence and mortality rates in males across the globe. Several enhancer-driven oncogenic programs regulated by transcription factors (TFs) such as AR, FOXA1, MYC, and ERG contribute to PCa progression. Previously, elevated expression of DLX1, a homeobox TF, was reported to be oncogenic in PCa, and was established to be transcriptionally regulated by the AR/ERG/FOXA1 circuitry. While therapeutic inhibition using the BET inhibitor (BETi) and anti-androgen treatment was effective, the activation of alternate signaling cascades and bypass pathways often leads to drug resistance in PCa. To overcome BETi resistance in PCa, we employed a bottom-up approach to identify alternative therapeutic strategies. Given that the SWI/SNF chromatin remodeling complex, specifically SMARCA2/4, is a key regulator of the AR/FOXA1/ERG enhancer circuitry, here we explored the therapeutic efficacy of a dual PROTAC degrader targeting SMARCA2/4, in *DLX1*-high PCa. In silico analysis of a publicly available BRG1 ChIP-seq dataset showed peak enrichment at multiple sites on the *DLX1* promoter and along the *DLX1* gene body, implying its direct transcriptional control. In agreement, we noted the co-expression of *SMARCA4* in *DLX1*-high PCa patients in the TCGA-PRAD cohort as well as in the Indian PCa cohort. Mechanistically, we show that SMARCA2/4 PROTAC degrader treatment mitigates *DLX1* expression in ERG-fusion positive PCa as well as in Castration-Resistant Prostate Cancer (CRPC) models. Furthermore, cell-based functional assays using the PROTAC degrader confirmed a decrease in the proliferative, invasive, and migratory potential of PCa cells along with reduced foci formation capacity. Similarly, PROTAC degrader treatment of isogenic RWPE1 cells overexpressing *DLX1* showed reduced tumorigenicity, suggesting direct inhibition of DLX1 by the PROTAC degrader. Finally, we also observed remarkable inhibition of DLX1 in BETi-resistant PCa cells, suggesting the efficacy of SMARCA4 ablation in bypassing BETi resistance and mitigating DLX1-driven PCa oncogenicity.

#3910 AR copy number amplification and AR/KLK3 expression patterns reveal mechanisms of AR signaling inhibitor (ARSI) resistance and highlight the need for AR-directed therapeutic innovation in metastatic castration resistance prostate cancer (mCRPC).

Celine Robert-Tissot[1], Phuong A. Nguyen[1], Elisabeth A. Murphy[2], Yawei J. Yang[2], Evisa Gjini[1], Michaela Bowden[1]

[1]Flare Therapeutics, Cambridge, MA,[2]Caris Life Sciences, Irving, TX

Metastatic CRPC is predominantly driven by androgen receptor (AR) signaling. Despite second-generation ARSI, resistance remains a challenge and is associated with AR ligand-binding domain (LBD) mutations and AR copy number amplification (CNA). Prostate-specific antigen (PSA), encoded by kallikrein-related peptidase 3 (KLK3), serves as a key marker of AR transcriptional activity. We hypothesized that AR genomic alterations underpin variation in AR expression and activity and that real-world profiling would identify distinct AR/KLK3 expression-defined subgroups. From the Caris Prostate Cancer Database (N=17,429), 511 mCRPC patients treated with ARSI (Abiraterone and/or Enzalutamide) were identified. Whole exome and transcriptome sequencing (Caris Life Sciences) were performed on pre- and post-treatment tumor biopsies to assess AR alterations and RNA expression of AR and KLK3. Patients were stratified by AR CNA (CN>2) and pathogenic AR LBD mutations and categorized into four RNA subgroups: $AR^{hi}/KLK3^{hi}$, $AR^{hi}/KLK3^{lo}$, $AR^{lo}/KLK3^{hi}$, $AR^{lo}/KLK3^{lo}$. Associations with time on treatment (TOT) and overall survival (OS) were evaluated with Kaplan-Meier and log-rank tests. ARSI reduced AR wild-type (WT; mut–/CNA–) tumors and enriched for AR alterations, with AR CNA in 42–51% and AR mut in 3–10% of post-treatment samples. AR CNA+ and AR mut+ tumors showed significantly higher AR RNA and KLK3 RNA versus WT (all $p<0.05$). AR CN correlated with AR RNA ($\rho=0.77$, $p<0.0001$) and was associated with elevated KLK3 RNA ($p<0.0001$); AR RNA correlated with KLK3 RNA ($\rho=0.4$, $p<0.0001$). The dominant RNA subgroups were $AR^{hi}/KLK3^{hi}$ and $AR^{lo}/KLK3^{lo}$ (each 31%), followed by $AR^{lo}/KLK3^{hi}$ and $AR^{hi}/KLK3^{lo}$ (each 19%). AR CNA+ tumors were enriched in $AR^{hi}/KLK3^{hi}$ (55%), AR mut+ in $AR^{lo}/KLK3^{hi}$ (48%), and AR WT in $KLK3^{lo}$ (59%) subgroups. $AR^{lo}/KLK3^{hi}$ patients had the best ARSI response; $AR^{hi}/KLK3^{hi}$ and $AR^{lo}/KLK3^{lo}$ showed intermediate TOT, and $AR^{hi}/KLK3^{lo}$ the shortest. $AR^{hi}/KLK3^{hi}$ patients had worse OS versus $AR^{lo}/KLK3^{hi}$ (HR=2.79, 95% CI 1.05–7.42, $p=0.04$). AR CNA predicted shorter TOT versus AR WT (HR=1.94, 95% CI 1.17–3.22, $p=0.01$). AR CNA is the main driver of elevated AR signaling and reduced ARSI response, while AR mut is associated with lower AR expression and better outcomes. $KLK3^{lo}$ tumors, largely AR WT, show reduced AR dependence with limited benefit from AR-targeted therapies. These findings highlight a high-risk AR-driven subgroup defined by high AR expression and AR CNA. FX-111, a selective degrader of transcriptionally active, hormone-bound AR (AR_{ON}) in IND-enabling studies by Flare Therapeutics, offers a promising strategy to address this resistance. Ongoing analyses of AR/KLK3 subgroups aim to elucidate biological drivers of differential ARSI response.

#3911 Use of ALK inhibitors in patients with non-lung malignancies bearing *ALK* alteration prolongs treatment duration.

Vitor Abreu de Goes[1], Miguel Zugman[1], Koral Shah[1], Ali Moradi[1], Salvador Jaime-Casas[1], Yu Jun Li[1], Daniela V. Castro[1], Benjamin Mercier[1], Jadon Fann[1], JoAnn Hsu[1], George Zhang[1], Vicki Doctor[2], Amber Moran[2], Maurie Markman[2], Alexander Chehrazi-Raffle[1], Charles Nguyen[1], Sumanta Kumar Pal[1]

[1]Beckman Research Institute of The City of Hope, Duarte, CA,[2]Cancer Treatment Centers of America, Philadelphia, PA

Introduction

ALK inhibitors are known to produce deep and durable responses in selected cancer types. However, data on their agnostic use are scarce, and the rarity of *ALK* alterations hinders clinical trial feasibility. We evaluated real-world outcomes of these drugs in tumor types without current FDA approval.

Methods

We collected clinical and genomic data on patients who received off-label ALK inhibitors between January 1st, 2013, and December 31, 2024, through electronic medical records at a single institution. Descriptive analyses were used to summarize patients' characteristics and treatment patterns. We compared the time to treatment failure (TTF) on ALK-targeted therapy and on its prior line of therapy, as well as radiographic response as evaluated by the provider or radiology report.

Results

A total of 19 patients were included. The median age at therapy start was 62 years, with 63% Caucasian and 31% Asian. The most common histologies were sarcomas (5/19), papillary renal cell carcinoma (3/19), and gastric adenocarcinoma (2/19). Most patients (73%) had two or more metastatic sites at treatment start, usually harboring *ALK* fusions (62%) or point mutations (21%). ALK inhibitors were administered as third-line or later in 52% of patients, with alectinib being the most common (52%), followed by crizotinib (36%). Prior treatments often included chemotherapy (58%), other tyrosine kinase inhibitors (32%), and checkpoint inhibitors (21%). The median TTF with ALK therapy was 6.7 months (95% CI, 3.3 - 21.9), compared to 2.6 months (95% CI, 1.6 - 5.5) for the previous line. Among 15 patients on ALK inhibitors with imaging, 7 had partial responses, 4 had stable disease, and 1 achieved a complete response.

Conclusion

ALK inhibitors improved clinical outcomes in comparison with prior therapies across several malignancies. This supports the rationale for its agnostic use for tumors where clinical trials are not feasible.

#3912 NQO1 as a target to overcome therapy resistance in multiple myeloma.

Seungbin Han[1], Christina Verbruggen[1], Lenka Besse[2], Shilpa Kurian[1], Silvia Nerreter[1], Umair Munawar[1], Marietta Truger[3], Elena Gerhard-Hartmann[4], Andrej Besse[2], Ann-Sophie Hainold[1], Cornelia Vogt[1], Emma Besant[1], Nina Rein[1], Max Koppel[1], Xiang Zhou[1], Claudia Haferlach[3], Andreas Rosenwald[4], Christoph Driessen[2], Ondrej Slaby[5], Hermann Einsele[1], Leo Rasche[1], Markus Sauer[6], Johannes Waldschmidt[1], K. Martin Kortum[1]

[1]Department of Internal Medicine II, University Hospital Wuerzburg, Wuerzburg, Germany,[2]Clinics for Medical Oncology and Hematology, Cantonal Hospital St. Gallen, St. Gallen, Switzerland,[3]MLL Munich Leukemia Laboratory, Munich, Germany,[4]Institute of Pathology, University of Wuerzburg, Wuerzburg, Germany,[5]Masaryk University, Brno, Czech Republic,[6]Department of Biotechnology and Biophysics, University of Wuerzburg, Wuerzburg, Germany

Background: Overexpression of NAD(P)H:quinone oxidoreductase 1 (NQO1) has been linked to poor prognosis and therapy resistance in solid tumors, but its role in multiple myeloma (MM) remains unclear. Combination therapies including proteasome inhibitors (PIs), immunomodulatory drugs (IMiDs), and/or immunotherapies have improved outcomes in MM, yet most patients eventually develop resistant and relapse. We recently identified NQO1 overexpression across PI-resistant MM models and that high *NQO1* expression is associated with inferior outcome in PI treated MM patients. Hence, we here extend these findings in an independent MM cohort (n = 93) from our institution and in *NQO1* upregulated MM cell line models to examine how NQO1 affects MM immunotherapy targets and sensitivity to standard treatment regimens.

Methods: RNA-seq was performed on bone marrow-derived $CD138^+$ cells from 24 newly diagnosed MM (NDMM) and 69 relapsed/refractory MM (RRMM) patients, as well as MM cell lines. Surface density of immunotherapy targets was quantified via direct stochastic Optical Reconstruction Microscopy (*d*STORM). Sensitivity to PIs and IMiDs was assessed using AlamarBlue assays.

Results: In the MM RNA-seq cohort, *NQO1* expression was significantly higher in RRMM compared with NDMM ($p = 0.0002$), supporting an association of *NQO1* with treatment-exposed, advanced disease. Furthermore, overexpression of *NQO1* in MM cell lines led to an increased IC_{50} for bortezomib and carfilzomib, whereas IMiDs sensitivity remained intact. No upregulation of PI resistance-related genes was identified by RNA-seq. To test whether NQO1-dependent mechanisms are causative for PI resistance, NQO1-high MM cells were treated with NQO1 inhibitor ES936, which restored the sensitivity to both PIs to the wild type levels. In subsequent dSTORM analysis, no differences were observed in BCMA, SLAMF7, or GPRC5D, whereas CD38 surface density was significantly reduced in both NQO1-High myeloma cell lines. Consistent with the expression data, NQO1-overexpressing cells showed reduced sensitivity to CD38-directed therapies (daratumumab (Dara) and isatuximab (Isa). Notably, NQO1 inhibition with ES936 restored CD38 surface expression and rescued Dara and Isa responses, supporting that NQO1 is directly involved in CD38 downregulation and resistance to anti-CD38 antibodies. Of note, RNA-seq comparison of NQO1-high vs. WT MM models did not reveal changes in CD38 mRNA levels, pointing toward a post-translational mechanism, such as altered protein stability or trafficking.

Conclusions: NQO1 is upregulated in RRMM and functionally induces resistance to PIs and CD38-directed therapies which are widely used in current MM treatment. Inhibition of NQO1 with ES936 rescues CD38 expression, and restores PI sensitivity and anti-CD38 responses, supporting NQO1 as a promising target in treatment-exposed or relapsed MM.

#3913 Inavolisib demonstrates anti-tumorigenic effects in pre-clinical models of serous endometrial cancer.

Miller Singleton[1], Haomeng Zhang[2], Alexandra Diggs[3], Braxton Burnett[4], Kristen N. Taylor[5], Chunxiao Zhou[4], Victoria Lin Bae-Jump[6]

[1]Gynecologic Oncology, University of North Carolina at Chapel Hill, Chapel Hill, NC,[2]Department of Gynecology, Beijing Obstetrics and Gynecology Hospital, Capital Medical University. Beijing Maternal and Child Health Care Hospital, Beijing, China,[3]UNC School of Medicine, Chapel Hill, NC,[4]University of North Carolina at Chapel Hill, Chapel Hill, NC,[5]Swedish Cancer Institute Gynecologic Oncology and Pelvic Surgery, Seattle, WA,[6]Assistant Professor, Dept. of Ob/Gyn, Div. of Gyn. Onc., University of North Carolina at Chapel Hill, Chapel Hill, NC

Objectives: Inavolisib is an oral selective PI3K inhibitor that has shown promising anti-tumorigenic activity in multiple pre-clinical models of cancer as well as breast cancer clinical trials, via promoting the degradation of mutated p110α, the catalytic subunit encoded by PIK3CA. The phosphatidylinositol 3-kinase (PI3K) signaling cascade is critically implicated in the tumorigenesis and progression of uterine serous carcinoma (USC), one of the most aggressive subtypes of endometrial cancer (EC). Given the urgent need to develop more effective treatment interventions for this highly lethal subtype of EC and that PI3Ka alterations are common in USC, we aimed to investigate the anti-tumorigenic and anti-invasive activities of inavolisib in serous EC cell lines.
Methods: The human serous EC cell lines, ARK1 and ARK2, were used in this study and treated with inavolisib (obtained from Genentech). Cell proliferation was evaluated by MTT assay. Cell cycle progression was examined by Cellometer. Cellular stress was evaluated by DCFH-DA assay and change in mitochondrial membrane potential was measured by JC-1 assay. Apoptosis was evaluated using a cleaved caspase-3 assay. Cell adhesion was evaluated using a laminin-1 assay, and cell migration was assessed by wound healing assay. Western immunoblotting was used to measure downstream protein expression related to cell cycle progression, cellular stress, and apoptosis.
Results: After 72 hours of treatment with inavolisib, the proliferation of ARK1 and ARK2 cells was inhibited in a dose-dependent manner (IC50: ARK1 674 nM, ARK2 2969 nM). Treatment of both cell lines with inavolisib significantly arrested the cell cycle at the G1 phase, increased intracellular reactive oxygen species levels, and decreased mitochondrial membrane potential compared with untreated cells ($p<0.05$). Inavolisib also significantly increased the activity of cleaved caspase-3 and reduced the expression of BcL-2 and MCL-1 in both cell lines. Moreover, inavolisib effectively decreased cell adhesion and migration at doses of 100 and 250 nM in the ARK1 and ARK2 cells ($p<0.05$). Western immunoblotting results demonstrated that treatment with inavolisib downregulated the expression of downstream targets of the PIK3CA/mTOR pathway (phosphorylated [p]-AKT, p-S6) and the cell cycle proteins CDK4 and cyclin D1 and upregulated the expression of the pro-apoptotic Bax and PDI proteins in both cells.
Conclusions: Inavolisib exhibits potent anti-tumorigenic and anti-invasive effects in serous EC cell lines, suggesting that this novel agent is a promising therapeutic option worthy of further exploration in the treatment of aggressive serous ECs.

#3914 Inavolisib exhibits anti-proliferative effects in pre-clinical model of endometrioid endometrial cancer.

Alexandra Diggs[1], Haomeng Zhang[2], Miller Singleton[3], Braxton Burnett[1], Kristen N. Taylor[4], Chunxiao Zhou[5], Victoria Lin Bae-Jump[6]

[1]University of North Carolina at Chapel Hill, Chapel Hill, NC,[2]University of North Carolina, Chaple Hill, NC,[3]UNC Lineberger Comprehensive Cancer Center, Chapel Hill, NC,[4]Gynecologic Oncology and Pelvic Surgery, Swedish Cancer Institute, Seattle, WA,[5]University of North Carolina, Chapel Hill, NC,[6]Assistant Professor, Dept. of Ob/Gyn, Div. of Gyn. Onc., University of North Carolina at Chapel Hill, Chapel Hill, NC

Objectives: Phosphoinositide 3-kinase (PI3K) is a key intracellular signaling enzyme that regulates cell growth, survival, and metabolism. Genetic alterations in the PIK3CA pathway are among the most common molecular events in endometrial cancer (EC), occurring in up to 80% of cases. Inavolisib is a highly selective PI3K-alpha inhibitor, and promotes the degradation of mutated p110α, the catalytic subunit encoded by PIK3CA. It has shown promising antitumorigenic activity in preclinical and clinical models of multiple solid tumors including endocrine resistant breast cancer. Endometrioid EC is the most common subtype of EC, one of the only cancers for which both incidence and mortality continue to rise. The backbone of its adjuvant treatment consists of a platinum-doublet, but new therapies are urgently needed. We aimed to investigate the effects of inavolisib on cell proliferation, cellular stress, apoptosis, cellular adhesion and migration in endometrioid EC cell lines.

Methods: The human endometrioid EC cell lines, HEC-1B and EC-023, were treated with inavolisib (supplied by Genentech). Cell proliferation was evaluated by MTT and colony formation assays. Cellular stress was evaluated by measuring levels of reactive oxygen species (ROS) via DCFH-DA assay and change in mitochondrial membrane potential via JC-1 assay. Cell cycle profile was evaluated by Cellometer. Apoptosis was evaluated using cleaved caspace-3 assay. Cell adhesion was evaluated using laminin-1 assay, and cell migration was assessed by wound healing assay. Western immunoblotting (WB) was used to measure downstream protein expression related to cell cycle progression, cellular invasion, and apoptosis.

Results: Inavolisib inhibited the cell proliferation and colony formation of HEC-1B and EC-023 cells, in a dose dependent manner (IC50: HEC-1B 7921 nM, EC-023: 310 nM). After 24 hours of treatment, inavolisib induced G1 cell cycle arrest in both cell lines. Treatment with inavolisib increased intracellular ROS levels and reduced mitochondrial membrane potential compared to control groups (all $p<0.05$). Importantly, inavolisib effectively decreased cell adhesive and migrative abilities in the HEC-1B and EC-023 cell lines (all $p<0.05$). WB supported these results, showing that treatment with inavolisib resulted in downregulation of the cell cycle regulatory proteins cyclin D-1, CDK2 and CDK4, inhibition of downstream targets of the PIK3CA pathway (phosphorylated [p]-AKT, p-44/42, and p-S6), and upregulation of the pro-apoptotic protein Bcl-xl, Bcl-2, and Mcl-1 in both cell lines.

Conclusions: Inavolisib demonstrated potent anti-proliferative and anti-invasive effects in endometrioid EC cell lines. Inavolisib may be a novel treatment strategy in EC, a cancer well-known for alterations in the PIK3CA/mTOR pathway.

#3915 From bench to bedside: A CNS penetrant and Omnipotent EGFR inhibitor, WSD0922-FU targeting primary mutations and the C797S acquired resistance mutation shapes the treatment landscape of EGFR mutant NSCLC.

Wei Zhong[1], Yue Liu[2], Carina Yu[2], Xiaolei Wang[2]

[1]Wayshine Biopharm, Corona, CA,[2]Wayshine Biopharm (Shanghai), Shanghai, China

The molecular landscape of EGFR-mutated non-small cell lung cancer (NSCLC) has evolved substantially with the widespread adoption of the third-generation covalent EGFR tyrosine kinase inhibitor (TKI) osimertinib as first-line therapy for tumors harboring classical EGFR mutations, along with the expanded use of next-generation sequencing (NGS). Consequently, patterns of acquired resistance have shifted: the once-predominant EGFR-T790M resistance mutation associated with first-generation EGFR TKIs has decreased in incidence, while EGFR-C797S has emerged as a major resistance mechanism following front-line third-generation EGFR TKI therapy. In parallel, increasing evidence highlights differential therapeutic responses to first-line third-generation EGFR TKIs between tumors with EGFR-L858R and EGFR-Ex19del mutations. Comprehensive genomic profiling through NGS continues to refine our understanding of the spectrum of classical, non-classical, and bypass resistance alterations, particularly those involving or co-occurring with C797S. Using paired tissue and plasma samples, we provide real-world evidence characterizing the molecular landscape of classical and non-classical EGFR mutations, as well as bypass signaling alterations that include C797S. We further describe the activity profile of WSD0922-FU, a molecule specifically designed to address the evolving EGFR mutational landscape, supported by translational data spanning preclinical to clinical studies. Our data demonstrate that WSD0922-FU exhibits potent activity not only against classical EGFR mutations and on-target resistance mechanisms following osimertinib—including C797S—but also against a range of non-classical EGFR alterations affecting both intracellular and extracellular domains (Q701L, E709X, L718X, G719X, S768I, V769M, L792X, V834X) as well as EGFRvIII. Collectively, these findings inform the clinical development strategy for WSD0922-FU as a potential first-line therapy for classical EGFR mutations, a second-line option for patients with CNS metastases after osimertinib, and a targeted treatment for tumors harboring C797S following osimertinib resistance.

#3916 A potent CDK7 inhibitor TY-2699a has the potential for combination with chemotherapy or immunotherapy in solid tumors.

Shengli Dong*, Apeng Liang*, Zhengfei Guo, Zhiyong He, Meihua Li, Xinlong Yang, Chao Zhou, Yu Yu, Hongqiang Li, Jian Zhu, Chengshan Niu, Shaoqing Chen, Jun Li, Yusheng Wu

TYK Medicines, Inc., Changxing, Zhejiang, China

Introduction: In recent years, PD-1 inhibitors and Trop2-ADC have been approved for the treatment of triple-negative breast cancer (TNBC). However, the efficacy of PD-1 inhibitor monotherapy is modest, benefiting only a small proportion of patients with TNBC. Chemotherapy remains the cornerstone of TNBC treatment; nevertheless, the risk of recurrence with these therapies remains high over time. Consequently, there is an urgent need to enhance the efficacy of immunotherapy and chemotherapy in patients with TNBC. TY-2699a, an orally active and highly selective CDK7 inhibitor developed by TYK Medicines, has shown monotherapy efficacy in TNBC (DCR 50%) and favorable tolerability, with lower gastrointestinal toxicity and manageable hematologic adverse events, supporting its potential for combination therapy in TNBC.

Results: In this study, we discovered that TY-2699a enhanced the efficacy of Gemcitabine and Nab-paclitaxel in TNBC HCC70 CDX mouse models when combined with TY-2699a, respectively. We observed that TY-2699a effectively killed EMT6 cells *in vitro* and improved PD-1 efficacy both *in vitro* and in an EMT6 syngeneic CDX mouse model. These findings warrant further investigation to determine whether TY-2699a enhances PD-1 efficacy in a TNBC 4T1 mouse model. Previously, we reported that TY-2699a is more potent than FDA-approved CDK4/6 inhibitors in head and neck squamous cell carcinoma (HNSCC). T-DXd (DS-8201) treatment achieved an ORR of 58.8% and a PFS of 20.5 months in patients with HER2-expressing salivary gland carcinoma (SGC). Our data suggest that TY-2699a and T-DXd act a synergistically effect on HNSCC Cal33 cells. Cetuximab is the only FDA-approved targeted therapy agent for HNSCC. Interestingly, we found that TY-2699a significantly enhanced the efficacy of Cetuximab in HNSCC FaDu cells both *in vitro* and in a CDX mouse model.

In summary, TY-2699a demonstrated antitumor efficacy as a monotherapy in TNBC, achieving a DCR of 50% with a manageable clinical safety profile. Beyond its role as a monotherapy, TY-2699a holds significant promise for use in combination therapies with chemotherapy or immunotherapy in TNBC and HNSCC. * Correspondence to: Shengli Dong and Apeng Liang.

#3918 *FGFR2* might be a promising therapeutic target for some types of carcinomas: Analysis of 1312 tumors with *FGFR2* abnormalities.

Hinano Nishikubo[1], DONGHENG MA[2], Tomoya Sano[2], Canfeng Fan[2], Daiki Imanishi[2], Takashi Sakuma[2], Yurie Yamamoto[2], Masakazu Yashiro[2]

[1]Molecular Oncology and Therapeutics, Osaka Metropolitan University Graduate School of Medicine, Osaka, Japan,[2]Department of Molecular Oncology and Therapeutics, Osaka Metropolitan University Graduate School of Medicine, Osaka, Japan

Background: Genetic abnormalities of the *fibroblast growth factor receptor 2* (*FGFR2*) gene, including amplification, fusions, and mutations, have been reported in various solid tumors. While molecular targeted therapies against *FGFR2* fusion have been proved to be useful in cholangiocarcinoma, the therapeutic significance of FGFR2 inhibitors remains unclear in other various solid cancers. Genomic and clinical information from solid tumor cancer gene panel testing cases is consolidated in the Center for Cancer Genomics and Advanced Therapeutics (C-CAT) database in Japan. This study aimed to utilize the C-CAT database to clarify the clinical-pathological significance of *FGFR2* abnormalities.

Materials & Methods: A total of 101,231 patients with solid cancer have been registered in the C-CAT database between June 2019 and June 2025. Of the 101,231 cases, 1312 cases with *FGFR2* gene abnormalities were analyzed. Tumor type distribution, co-mutations, and responses to FGFR inhibitors were evaluated. Disease control rate (DCR) was assessed in patients who received FGFR-targeted therapy.

Result: *FGFR2* alterations included amplification in 515 cases, fusion in 280 cases, and mutations in 568 cases. Their abnormalities were detected most frequently in the biliary tract (271 cases), esophagus/stomach (231 cases), and breast (211 cases). Amplification was frequent in the esophagus/stomach (205 cases) and breast (105 cases). *FGFR2* fusions are frequently detected in the biliary tract (163 cases), followed by breast (21 cases), pancreas (13 cases). Mutations were frequent in the uterus (111 cases), breast (89 cases), and biliary tract (86 cases). Among 1312 *FGFR2* alteration cases, *FGFR2* inhibitors were administered in 85 cases. Of the 85 cases, DCR was achieved in 49 cases, 44 cases of which were biliary tract cancer.

Conclusions: *FGFR2* might be a promising therapeutic target not only for cholangiocarcinoma with fusion but also for esophagus/stomach cancer and breast cancer with *FGFR2* alterations.

#3919 The emerging role of claudin 18.2 as a potential driver in gastric cancer progression.

Lisa Negro[1], Elisabetta Puliga[2], Emanuela Boccuni[2], Simona Corso[1], Silvia Giordano[1]

[1]Oncology, University of Turin, Turin, Italy,[2]Candiolo Cancer Institute - IRCCS, Torino, Italy

Gastric cancer (GC) represents one of the most impactful cancers on human health. Because of its strong aggressiveness and lack of resolutive therapies, researches are focusing their efforts on identifying novel molecular targets and new therapeutic strategies. Claudin 18.2 is a tight-junction protein expressed by the normal gastric epithelium. During malignant transformation, it is exposed on the whole tumor cell surface, becoming an accessible and druggable target. However, its role in tumor progression and proliferation is poorly investigated, partly due to the paucity of commercially available CLDN18.2-expressing cell lines. Taking advantage of our precious and molecularly annotated GC Patient-Derived Xenograft (PDX) platform, which includes approximately 200 primary cell lines and organoids, we assessed the Claudin 18.2 expression through RNA-Seq analysis, using the median expression value as the threshold for classification. The RNA-seq results were validated on representative PDXs using Real-Time-qPCR and Immunohistochemistry. Further, CLDN18.2 expression was evaluated in GC primary cell lines derived from low-, median-, and high-expressing PDXs (Real-Time-qPCR, Western Blot, and Immunofluorescence). For our analysis, we focused on four low-expressing (GTR181, GTR031, GTR498, GTR233), three median-expressing (GTR571, GTR797, GTR435), and three high-expressing (GTR789, GTR568, GTR816) CLDN18.2 cell lines. To explore the potential cell-autonomous role of CLDN18.2 as a driver in gastric cancer, we silenced the CLDN18.2 gene in median- and high-expressing cell lines. In high-expressing cells, CLDN18.2 silencing reduced cell proliferation compared with their wild-type counterparts, whereas no significant difference was observed in median-expressing cells, suggesting that high-expressing models are addicted to CLDN18.2. To further support the role of CLDN18.2 as a potential driver in high-expressing GC primary cell lines, we evaluated the cancer cell-autonomous sensitivity to Zolbetuximab - an anti-CLDN18.2 monoclonal antibody capable of inducing, in vivo, Antibody-Dependent Cellular Cytotoxicity (ADCC) and Complement-Dependent Cytotoxicity (CDC) - of low-, median-, and high-expressing models. High-expressing cell lines were highly sensitive, whereas sensitivity progressively decreased in median-expressing and low-expressing cells. These results suggest a potential CLDN18.2 dependency in high expressing GC cell lines, supporting a role for CLDN18.2 as a driver in GC proliferation. From a translational point of view, our preliminary data suggest that the efficacy of the anti-CLDN18.2 monoclonal antibody Zolbetuximab in high CLDN18.2-expressing tumor cells may be enhanced by the cancer cell-autonomous response, in addition to its established ADCC and CDC.

#3920 *PIK3CA* and *ARID1A* co-altered tumors are sensitive to AKT inhibitor, capivasertib.

Rian Engeldinger[1], Shirsa Udgata[1], Jordan Noelle Stoecker[1], Xingqi Shen[1], Ruchi Shah[1], Alexa Schmitz[1], Katherine A. Johnson[1], Cheri Pasch[1], Dustin A. Deming[2]

[1]Univ. of Wisconsin Madison Sch. of Med. & Public Health, Madison, WI,[2]University of Wisconsin Carbone Cancer Center, Madison, WI

Background: PIK3CA (PK) and ARID1A (AD) co-alterations occur in 1% of cancers. These cancers had enhanced sensitivity to PI3K inhibition with copanlisib (cop) in the MATCH trial arm Z1F. Given the recent FDA approval of the AKT inhibitor, capivasertib (capi), here we aim to evaluate the potential benefit of capi treatment in the setting of PK and AD alterations and the mechanism by which enhanced sensitivity might be occurring.
Methods: CRISPR/Cas9 was used to knockout AD from SW48PIK3CA-H1047R (SW48PK), and PIK3CAH1047R mutant locally advanced rectal cancer (LARC) patient-derived cancer organoids (PDCOs). PK or PKAD Colorectal (CRC), ovarian (OC), and renal (RC)PDCOs were obtained from the NCI repository and were treated with 2 μM capi for 48 hrs. Percent relative change in the longest diameter (PRC) was measured prior to and after treatment in(capi or control) and effect size was measured using Glass's delta (GD) . Western blot was used to determine levels of PI3K proteins (RPS6, AKT), apoptotic proteins (MCL-1, BCL-xL, Bax, Bims), and mTORC1 protein, PRAS40. Athymic nude mice were flank injected with SW48PK and SW48PKAD and treated with 100mg/kg capi (10% DMSO in 90% of 20% SBE-β-CD in saline) or vehicle b.i.d for 28 days or until moribund. Ki-67 and cleaved caspase-3 in these tumors were assessed by immunohistochemistry (IHC) and quantified as positive cells/high powered field (HPF).
Results: Capi treatment responses were observed in PKAD co-altered CRC PK (PRC 4.8%, GD 2.0), LARC-PK (0.5%, 0.9), OC-PKAD(10%, 1.03), RC-PKAD (1.52%, 1.52), and LARC-PKAD (2.91%, 1.78) PDCOs, indicating sensitivity across cancer types and enhanced sensitivity in co-altered lines relative to PK alone for LARC. Western blot showed greater reduction in p-RPS6 in LARC-PKAD by 6h compared to LARC-PK, but no significant differences were seen in 2D lines. p-AKT increased upon capi treatment across all 2D and 3D lines. Among apoptotic proteins, BCL-xL steadily increased over time in co-mutant cultures. Bims (cytotoxic isoform of Bim) had a stronger induction in 6h in LARC-PKAD compared to LARC-PK. Levels of p-PRAS40, MCL-1, Bax, and Bak remained largely comparable across lines. In vivo, PKAD tumors showed a significant tumor growth delay ($p = 0.01$) with capi treatment, while PK tumors did not ($p = 0.06$).
Conclusion: PIK3CA and ARID1A co-altered tumors have enhanced sensitivity to capi relative to PIK3CA mutant tumors, potentially through induction of Bims. Capi should be investigated further clinically in PIK3CA and ARID1A co-altered cancers. Additionally, further studies identifying novel drug combinations with capi are warranted to further enhance patient response

#3921 Periostin on tumor stromal cells might be associated with the malignant progression of patients with gastric cancer.

Canfeng Fan[1], Hinano Nishikubo[1], DONGHENG MA[2], Tomoya Sano[2], Daiki Imanishi[2], Takashi Sakuma[2], Yurie Yamamoto[2], Masakazu Yashiro[2]

[1]Osaka Metropolitan University, Osaka, Japan,[2]Osaka metropolitan university, Osaka, Japan

Periostin is one of matrix cellular proteins. It has been reported that the periostin in the tumor microenvironment might regulate the FAK signaling via the interaction with integrins expressed on cancer cells, resulting in the stimulation of proliferation and invasion. In gastric cancer (GC), the periostin has reported to be overexpressed in the tumor stroma, however, the role of periostin and the types of cells remains to be unclear. Then, in this study we examined the significance of periostin on the clinico-pathologic features of GC by immunohistochemical study, using 689 GC samples. Also, 4 GC cell lines were used to examine the effect of periostin on the proliferation and the invasion activity of GC cells by proliferation assay and invasion assay.The immunohistochemical study of periostin confirmed that the expression of periostin was frequently found on stromal fibroblasts in the tumor. High expression of periostin in the tumor stroma is associated with worse survival rates ($p < 0.001$, log-rank), deeper T invasion ($p < 0.001$), frequent lymph node metastasis ($p < 0.001$), distant metastasis ($p = 0.021$), higher recurrence rates ($p < 0.001$), and higher stage ($p < 0.001$). *In vitro* assays using GC cell lines demonstrated that periostin significantly promoted the invasion and migration ability of GC cells, but did not affect the proliferation activity.In conclusion, the periostin, which is mainly expressed on the tumor stromal fibroblasts, might be associated with the malignant progression of GC.

#3922 Polymeric delivery of TRAIL mRNA for inducing apoptosis in non-small cell lung cancer.

Gurkirat Singh Sandhu[1], Hasan Uludag[2]

[1]Faculty of Pharmacy & Pharmaceutical Sciences, University of Alberta, Edmonton, AB, Canada,[2]Department of Chemical and Materials Engineering, University of Alberta, Edmonton, AB, Canada

Tumor necrosis factor-related apoptosis-inducing ligand (TRAIL) activates death-receptor pathways to trigger caspase-dependent apoptosis, yet recombinant TRAIL has demonstrated limited activity in non-small cell lung cancer (NSCLC) because of rapid clearance and apoptotic resistance. Delivering TRAIL as messenger RNA (mRNA) may overcome these limitations, but mRNA therapeutics remain limited in oncology due to delivery inefficiencies, instability, and incomplete cytosolic release. This study evaluated biodegradable cationic lipopolymers for TRAIL mRNA delivery and examined whether combining TRAIL mRNA with small interfering RNAs (siRNAs) targeting anti-apoptotic mediators could strengthen apoptotic responses in resistant NSCLC settings. Biodegradable cationic lipopolymers were screened based on their delivery profiles. Nanoparticles were characterized by hydrodynamic diameter, zeta potential, and transmission electron microscopy (TEM). A549 lung adenocarcinoma cells were used for mechanistic studies, including multi-day viability assays, caspase-3/7 activity using the Caspase-Glo assay (24-72 hours), mitochondrial membrane potential analysis using tetramethylrhodamine ethyl ester (TMRE), nuclear morphology by Hoechst staining and confocal microscopy, DNA damage assessment by alkaline comet assay, and enzyme-linked immunosorbent assay (ELISA) for TRAIL protein detection. Additional NSCLC cell lines: Calu-3, H1975 GFP^+, and H1299 GFP^+ were used for viability-based bioassays to support mRNA-induced TRAIL activity.The selected polymer formed compact nanoparticles with 100-200 nm size and+15-40 mV zeta-potential. In A549 cells, TRAIL mRNA induced a clear time-dependent apoptotic response: viability declined progressively and reached approximately 40-50% at later time points with higher mRNA doses. Caspase-3/7 activity increased by ~2-fold at 24 hours and remained detectable at 48-72 hours. Confocal imaging showed mitochondrial depolarization together with condensed and fragmented nuclei, and comet assay confirmed DNA strand damage. siRNAs alone reduced viability but did not match the effect of TRAIL mRNA. In combination studies, siRNAs allowed lower TRAIL mRNA doses to achieve viability reductions comparable to higher-dose mRNA alone and maintained reduced viability further into the time course, improving both potency and duration of response.The delivery platform evaluated here supported effective TRAIL mRNA activity in A549 cells, and incorporating siRNAs further reinforced and prolonged the apoptotic response at reduced mRNA doses. These findings highlight a practical path toward combination nucleic acid strategies designed to counter apoptotic resistance in NSCLC.Portions of this abstract were drafted with the assistance of AI under the supervision and full scientific verification of the authors.

: Prognostic Biomarkers 2
Poster Session

#3926 Serum soluble TREM2 predicts poor survival, mirrors surface TREM2 level on circulating M-MDSCs, and enhances MDSC-mediated suppression of T-cell proliferation in indolent B-cell lymphoma.

Hao-Yuan Wang[1], Po-Chun Liu[2], Fu-Chen Yang[2], Ching-Fen Yang[3], Chia-Ming Liang[4], Chia-Ying Wu[1], Chun-Kuang Tsai[1], Po-Shen Ko[1], Yao-Chung Liu[1], Nien-Jung Chen[2]

[1]Department of Medicine, Taipei Veterans General Hospital, Taipei, Taiwan,[2]School of Life Sciences, National Yang Ming Chiao Tung University, Taipei, Taiwan,[3]Department of Pathology and Laboratory Medicine, Taipei Veterans General Hospital, Taipei, Taiwan,[4]Department of Surgery, Taoyuan Branch of Taipei Veterans General Hospital, Taoyuan, Taiwan

Triggering receptor expressed on myeloid cells-2 (TREM2) is an anti-inflammatory surface receptor with a soluble isoform (sTREM2). Monocytic myeloid-derived suppressor cells (M-MDSCs) promote tumor growth, and our recent work shows that high surface TREM2 on circulating M-MDSCs predicts poor outcomes in diffuse large B-cell lymphoma. However, its role in indolent B-cell lymphoma remains unclear. This study investigated the clinical significance of serum sTREM2 and surface TREM2 on circulating M-MDSCs in treatment-naïve indolent B-cell lymphoma and explored immunomodulatory effects in murine models.

This prospective study enrolled 93 patients (2019-2025). Diagnoses included follicular lymphoma (*n*=54; 33 low-grade, 21 grade 3A), marginal zone lymphoma (*n*=21), lymphoplasmacytic lymphoma (*n*=6), small lymphocytic lymphoma (*n*=4), and mature B-cell neoplasms (*n*=8). Median age was 68; 46.2% were male; 58.1% had bone marrow (BM) involvement; 66.7% had Lugano stage IV; and 21.5% had high-risk IPI. Fourteen patients received active surveillance, and 79 received first-line therapy. The median serum sTREM2 level was 997 ng/L.

Normalized surface TREM2 on circulating M-MDSCs was calculated relative to paired healthy controls. ROC analysis identified 8.52% as the optimal cut-off. High surface TREM2 (>8.52%) was associated with inferior OS (*P*=0.031; 2-year OS: 84.6% vs 94.5%) and shorter time to next treatment (TTNT) (*P*=0.001; median: 48.69 months vs not reached [NR]). The TTNT disadvantage was observed in both active-surveillance patients (*P*<0.001; median: 16.87 vs 51.06 months) and those receiving first-line therapy (*P*=0.009; median: 48.69 months vs NR).

Serum sTREM2 levels increased across tertiles of normalized surface TREM2 (median: 694, 920, and 2,149 ng/L), with significant differences between lower and higher (*P*<0.001) and intermediate and higher groups (*P*=0.001).

ROC analysis identified 1,371 ng/L as the optimal serum sTREM2 cut-off. Elevated sTREM2 (>1,371 ng/L) predicted inferior TTNT (*P*<0.001; median: 48.69 months vs NR) and worse OS (*P*=0.002; median: 66.25 months vs NR).

To explore the functional roles of sTREM2, CellTrace Violet-labeled murine T cells were cocultured with WT or *Trem2*-knockout BM-derived MDSCs. Across varying MDSC:T-cell ratios, sTREM2 consistently suppressed T-cell proliferation, with stronger inhibitory effects at higher proportions of MDSCs, and the suppressive activity of sTREM2 was more pronounced with *Trem2*KO MDSCs than WT MDSCs.

In conclusion, elevated serum sTREM2 correlates with higher surface TREM2 on circulating M-MDSCs and predicts inferior survival in indolent B-cell lymphoma. Preliminary murine data suggest that sTREM2 augments MDSC-mediated suppression of T-cell proliferation, supporting a functional role for sTREM2 in lymphoma immunopathogenesis.

#3927 Analytical performance of a novel tissue-informed non-bespoke whole genome MRD detection assay.

David Delfosse, Alexander Fine, Daokun Sun, Akshay Kakumanu, Tristen Ross, Devika Singh, Ravin Poudel, Maryam Zand, Brian Reilly, Farzana Ahmed, Liv Parsons, Tuan Nguyen, Ena Shinnishi, Noel Vega, Hanna Tukachinsky, Chang Xu, Alex Robertson, Brett Wallden

Foundation Medicine, Inc., Boston, MA

Background: Detection of circulating tumor DNA (ctDNA) in early-stage cancer offers significant prognostic value and has potential for guiding clinical care decisions. However, achieving sufficient sensitivity for reliable detection at this stage is challenging. Personalized panels can increase turnaround time and operational complexity.To overcome these limitations, we developed a tissue-informed molecular residual disease (TI-MRD) laboratory developed test that does not use custom panels.
Methods: The TI-MRD assay defines a personalized tumor signature from whole genome sequencing (WGS) of tissue FFPE, and scans for this signature in cell-free DNA (cfDNA) from plasma, also sequenced using WGS. TI-MRD employs a novel algorithm using aneuploidy and somatic SNVs to define a tumor signature without requiring a matched normal sample. Samples from patients with early stage lung and colon cancer were used in a study for determining the lower limit of detection (LLoD) of the assay. The precision study also included samples from patients with breast, bladder, melanoma, ovarian, and pancreatic cancers. Analytical specificity of the assay was assessed using cfDNA from donors with no known history of cancer and a tumor signature derived from a panel of cancer FFPE samples.
Results: The LLoD for the TI-MRD assay was established using sample titrations ranging from > 44,000 PPM (> 4.4%) to 5 PPM and was based on a ≥ 95% probability of detecting tumor fraction (TF). LLoD for the TI-MRD assay was also evaluated as a function of tumor mutational burden (TMB), where the lowest TMB value tested was < 1 mut/Mb and the highest TMB value tested was > 9 mut/Mb. The titration data for estimating the analytical sensitivity for the TI-MRD assay demonstrated that the LLoD can be < 10 PPM. Reproducibility was determined by testing 6 replicates from 10 patients with TF values ranging from 380,000 PPM (38%) to 32 PPM. Precision was also evaluated as a function of cfDNA input mass (3.5 - 20ng) and FFPE input mass (10 - 220ng). Detection of ctDNA was highly reproducible across the range of cfDNA and FFPE input masses and was maintained across a 4-log range of TF values. The TI-MRD assay also achieved an empirical specificity of 100% from donors with no known history of cancer.
Conclusion: This TI-MRD assay demonstrated robust analytical performance with high sensitivity, reproducibility, and specificity for detecting ctDNA, highlighting the potential of this assay to guide therapeutic decisions in the early setting across many different cancer types.

#3928 Dynamic inflammatory biomarkers are associated with cancer cachexia in a prospective lung cancer cohort.

Elham Kazemian[1], Carlos David Cruz-Hernandez[2], Karen L. Reckamp[1], Puneeth Iyengar[3], Neil A. Bhowmick[4], Jane C. Figueiredo[5], Kamya Sankar[1]

[1]Cedars-Sinai Medical Center, Los Angeles, CA,[2]Cedars-Sinai Medical Center, Beverly Hills, CA,[3]Memorial Sloan Kettering Cancer Center, New York, NY,[4]Assoc. Professor, Dept. of Medicine, Cedars-Sinai Medical Center, Los Angeles, CA,[5]Samuel Oschin Comprehensive Cancer Institute, Los Angeles, CA

Background: Cancer cachexia is a multifactorial syndrome characterized by progressive skeletal muscle loss that affects approximately 40-50% of patients with non-small cell lung cancer (NSCLC)Despite its clinical impact, reliable biomarkers for early detection and risk stratification remain poorly defined.
Methods: In this prospective longitudinal study,we conducted an analysis of 27 patients with stage IV NSCLC from the SeroNet-CORALE cohort with at least two plasma samples collected between 2020-2023. Cachexia was defined according to international consensus criteria (weight loss >5% or >2% with BMI<20 kg/m2 over 6 months). We quantified 40 biomarkers using MesoScale Discovery platforms, including inflammatory cytokines, chemokines, metabolic hormones, angiogenic factors, and mitochondrial DNA. Firth penalized logistic regression models were used to evaluate associations between log2-transformed biomarker levels and cachexia status, with adjustment for age, sex, race, and treatment exposures.
Results: We enrolled lung cancer patients (65% female, mean age 65±10 years) with predominantly adenocarcinoma histology (89 percent), and the proportion classified as cachectic was 22 percent at diagnosis and 20 percent and 19 percent at the subsequent timepoints. Cachectic patients showed consistently lower BMI (21.0±2.0 vs 27.0±7.0 at T1; 21.8±4.9 vs 25.2±4.9 at T2). At T1, cachexia was strongly associated with elevated GDF15 (OR: 4.29, 95% CI: 1.04-29.74, p=0.044) and IL-15 (OR: 43.83, 95% CI: 2.39->999, p=0.007), while IL-4 demonstrated protective effects (OR: 0.09, 95% CI: 0.00-0.66, p=0.013). By T2, the biomarker profile had shifted, with significant associations emerging for elevated mtDNA (OR: 2.13, 95% CI: 1.07-7.69, p=0.022) and reduced levels of IL-5 (OR: 0.17, p=0.011), IL12/IL23p40 (OR: 0.44, p=0.010), and MDC (OR: 0.26, p=0.006). Longitudinal analysis revealed that baseline inflammatory biomarkers were associated with future cachexia risk. Elevated MCP-1 at baseline showed a strong, though non-significant, trend toward association with increased odds of cachexia at the 6-month follow-up (OR: 3.72, 95% CI: 0.91-42.70, p=0.070). In contrast, higher levels of MDC (OR: 0.19, 95% CI: 0.02-0.77, p=0.016) and TARC (OR: 0.28, 95% CI: 0.04-0.96, p=0.041) at baseline were significantly associated with reduced odds of cachexia at the subsequent timepoint.
Conclusion: This exploratory study reveals temporal variations in inflammatory profiles associated with cancer cachexia. While requiring validation in larger cohorts, the distinct biomarker patterns at different timepoints suggest cachexia biology may evolve from initial cytokine activation to later-stage mitochondrial and immune dysregulation. The association between baseline biomarkers and future cachexia development warrants cautious interpretation but may inform future research directions.

#3929 Prognostic significance of ctDNA in patients with metastatic uveal melanoma.

Andrew David Knight[1], Aleigha Lawless[2], Eric P. Wehrenberg-Klee[3], Genevieve Boland[2], Ryan J. Sullivan[4], Kamaneh Montazeri[2]

[1]Oncology, Mass General Cancer Center, Boston, MA,[2]Mass General Brigham, Boston, MA,[3]Invterventional Radiology, Massachusetts General Hospital, Boston, MA,[4]Harvard Medical School/Massachusetts General Hospital, Boston, MA

Background: Circulating tumor DNA (ctDNA) is an emerging prognostic biomarker in solid tumors. However, the independent prognostic value in metastatic uveal melanoma (mUM) remains incompletely defined. We evaluated the prognostic significance of baseline ctDNA as measured by the Signatera assay, assessed the relationship to known prognostic factors such as LDH and liver metastases, and the impact of ctDNA clearance while on treatment.

Methods: We retrospectively evaluated patients with mUM who had ctDNA collected within 30 days prior to treatment initiation. Kaplan-Meier (KM) and Cox proportional-hazard models were used to evaluate OS and PFS. Baseline ctDNA values were categorized into 3 tiers: Not-detected (ND), Low (<5 MTM/mL), and High (>5 MTM/mL). Multivariate Cox models were used to adjust for LDH (log-transformed) and liver metastases. Clearance of ctDNA was compared to persistently positive ctDNA. Patients treated with front-line tebentafusp were assessed as a prespecified subgroup.

Results: 41 patients had baseline ctDNA measurements taken prior to frontline treatment; 26 received front-line tebentafusp and 66% had detectable ctDNA. Higher ctDNA levels correlated with elevated LDH.

In the full cohort, detectable ctDNA was associated with shorter PFS (HR 3.07, 95% CI 1.14-8.30; p=0.027). In a 3-tiered stratification, high ctDNA (>5 MTM/mL) was predictive of shorter PFS (HR 4.65, 95% CI 1.62-13.4; p=0.004) and approached significance for OS (HR 4.60, 95% CI 0.97-21.8; *p*=0.055). On KM analysis, there was significant separation between the groups for both PFS (p=0.0048) and OS (p=0.011). As a continuous variable, higher ctDNA values (log-transformed) strongly predicted both PFS (HR 2.23, 95% CI 1.54-3.23; p<0.001) and OS (HR 3.26, 95% CI 1.79-5.92; p<0.001). In multivariate analysis, ctDNA remained independently prognostic of PFS (HR 1.75, 95% CI 1.06-2.87; p=0.028).

Clearance of ctDNA was associated with improved PFS (HR 0.25, CI 95% 0.08-0.76; p=0.015) and OS, with no deaths in the clearance group (HR not calculable).

In the tebentafusp-only subgroup, baseline ctDNA remained significant for OS (HR 2.47, 95% CI 1.30-4.66; p=0.005) and PFS (HR 1.83, 95% CI 1.22-2.74l; p=0.003). Clearance in this subgroup remained associated with improved PFS (HR 0.21, CI 95% 0.06-0.79; p=0.021) and OS (no deaths). Multivariate model trends were consistent with the full cohort but were limited by sample size.

Conclusions: Baseline and on treatment ctDNA measured using the Signatera assay are prognostic in patients with mUM. ctDNA results remained prognostic in the tebentafusp subgroup and after adjusting for LDH and liver metastases.

#3930 Developing a prognostic gene expression biomarker for re-irradiation in recurrent glioblastoma.

Brooke C. Braman[1], William C. Chen[1], Radhika Mathur[1], Akshara Vykunta[1], Vivian Tang[1], Nadeem Al-Adli[1], Joseph F. Costello[1], Minesh P. Mehta[2], Kanish Mirchia[1], Jacob S. Young[1], David R. Raleigh[1]

[1]University of California San Francisco, San Francisco, CA,[2]NRG Oncology, Philadelphia, PA

Introduction: Glioblastoma is the most common primary, malignant brain tumor. Despite aggressive treatment, the prognosis remains poor, and recurrence is nearly universal. Radiotherapy improves overall survival (OS) in patients with newly diagnosed glioblastoma (ndGBM). Re-irradiation (reRT) improves progression-free survival (PFS) when added to bevacizumab in recurrent GBM (rGBM), but an OS advantage in unselected populations has not been demonstrated. Here we test the hypothesis that gene expression profiling can identify glioblastomas with better prognosis after re-irradiation delivered at the time of disease recurrence.

Methods: A retrospective cohort of 98 IDH-wildtype, CNS WHO grade 4 GBM tissue samples (n=43 ndGBM, n=55 rGBM) from 83 patients who ultimately underwent reRT at the time of any tumor recurrence was analyzed using a barcode-based RNA hybridization platform with a custom 291-gene panel representing pathways underlying GBM growth and therapeutic response. Univariate analysis identified 60 genes associated with outcomes after reRT. A ridge regression model was trained using gene expression data to predict OS after reRT normalized to OS from diagnosis. Model outputs were mapped to reRT scores, which were dichotomized (high versus low) using the maximally selected rank statistic.

Results: The median time between RT courses was 19.9 mo. Median OS after reRT was 9.74 mo. Median OS after reRT for tumors with high versus low reRT scores was 12.5 versus 8 mo ($p<0.001$). The hazard ratio for death after reRT for tumors with low reRT scores compared to tumors with high reRT scores was 2.47 ([95% CI 1.47-4.16], $p<0.001$). Using only gene expression data from ndGBM, the median OS after reRT for tumors with high versus low reRT scores was 10.5 versus 5.7 mo ($p=0.022$; HR for low reRT scores: 2.20, [95% CI 1.09-4.45], $p=0.027$). Using only gene expression data from rGBM, the median OS after reRT for tumors with high versus low reRT scores was 16.82 versus 9.18 mo ($p=0.0014$; HR for low reRT scores: 3.55, [95% CI 1.55-8.17], $p=0.0028$). There were no differences in MGMT promoter methylation status or demographic characteristics between tumors with low versus high reRT scores. ReRT scores were calculated for a second cohort of 10 patients with spatially sampled ndGBM (n=6-19 samples/patient). By a mean-rating, one-way random effects, absolute agreement model, the intraclass correlation coefficient estimate for the reRT score was 0.89 ([95% CI 0.76-0.97], $p<0.001$), which indicates high score concordance for regionally distinct samples from within individual tumors.

Conclusions: Gene expression data from ndGBM or rGBM should be considered as a stratification variable for reRT clinical trials. The model reported here requires validation in additional cohorts to determine its prognostic value.

#3931 Immune cell profile changes in patients treated with tarlatamab for extensive stage small cell lung cancer in real world practice.

Dhauna Karam Prasad[1], Andre De Menezes Silva Corraes[1], Malvika Gupta[1], Audrey Ma[2], Chen Wu[1], Zuoyi Shao[1], Kevin Reagan[1], Rayaan Kamal[1], Ashley Potter[1], Abdullah Al-Ajmi[1], Syeda Mina[1], Sykler J. Taylor[1], Antonious Hazim[1], Anastasios Dimou[1], Kaushal Parikh[1], Mohammed Shanshal[1], Ailsa Luce[1], Anna Schwecke[1], Julian Molina[1], Aaron Mansfield[1], Katherine Smith[1], Lucy Holmes[1], Haidong Dong[1], Yi Lin[1], Konstantinos Leventakos[1]

[1]Mayo Clinic Cancer Center Minnesota, Rochester, MN,[2]Columbia University, New York, NY

Background: Tarlatamab, a Delta-like ligand (DLL3)/CD3-targeted bispecific T-cell engager (TCE) is FDA approved in patients (pts) with extensive stage small cell lung cancer (ES-SCLC), after progression on frontline chemoimmunotherapy. We aimed to evaluate the immune cell profile in pts who received this therapy in standard-of-care (SOC) practice with progression free survival (PFS) less than and greater than two months (mo).

Methods: Patients who received tarlatamab at Mayo Clinic Rochester and consented to immuno phenotyping of blood are included in the present study. Immune phenotyping was performed on whole blood by flow cytometry and analyzed by Kaluza. Data analysis was performed with Microsoft Excel and PRISM.

Results: Eighteen patients with median age 64 (range 37-79) were included in the study. 66% of our cohort were women and 83% had present or past history of smoking, with an average of 40 pack years (range 26-60). With a median follow-up of 2 months, the median PFS for the cohort was 1.5 mo (range 0.33-2.76 months). 61% (13/18) of patients had PFS <2mo. 39% (5/18) had PFS>2mo and of which, three patients had partial response with one maintaining stable disease and one patient with mixed response. At baseline (BL), there were no difference in T cell, CD4 or CD8 cell count between patients in the PFS<2mo and PFS>2mo groups. Patients with PFS<2mo had higher exhausted CD8 T cells compared to those in the PFS>2mo group (CD8+PD1+TIGIT+CD57+, PFS<3mo vs >3mo, cells/mL: 7.14±4.28, 1.58±1.37, p=0.009). Additionally, when analyzing the B-cell population, the PFS<2mo group had lower percentage of B cells compared to the group with PFS>2mo at baseline (6.0±7.5, 10.4±14, p=0.02). At day 7, the group with PFS<2mo had lower Treg compared to the group with PFS>2mo (2.88±1.38, 4.60±1.47, p=0.02). Also, the PFS<2mo group had an increase of B cells compared to the group with PFS>2mo at day 7(<2mo vs >2mo: 10.0±14, 4.37±3.07, p=0.04). Finally, the group with PFS>2mo had decrease in total monocytes (mono), classical mono, and immunosuppressive cells (PFS<2mo vs >2mo, Mono: 340±347, 253±106, p=0.04. Classical mono: 305±283, 155±109, p=0.02. CD14+HLA-DRneg: 105.8±96, 12±39, p=0.03) compared to the group with PFS<2mo by day 7. While no changes were seen between BL and day 7 for intermediate mono in PFS<2mo group, PFS>2mo group had decreased post treatment intermediate monocytes (BL vs day 7, cells/mL, intermed mono: 32.5±15,17.7±6.2, p=0.03).

Conclusion: In this study investigating the SOC outcomes of tarlatamab, early progression was associated with higher presence of exhausted CD8 T cells, B cells, and immunosuppressive monocytes. Analysis of additional patients will be shared at AACR meeting.

#3932 Spatial immune checkpoint profiling reveals predictive biomarkers of immunotherapy response in oral squamous cell carcinoma.

Shu-Han Yu[1], Chih-Hung Ye[1], Kah Yap Yi[1], Thien-Long Le[1], Le-Bao-Long Nguyen[1], Patrick Chun Theng Chong[1], Huai-Cheng Huang[2], Ruey-Lomg Hong[2]

[1]Institute of Biotechnology, National Taiwan University, Taipei, Taiwan,[2]Department of Oncology, National Taiwan University Hospital and College of Medicine, Taipei, Taiwan

Introduction: Oral squamous cell carcinoma (OSCC) remains a leading cause of cancer-related mortality in Taiwan. Despite the widespread use of surgery, radiotherapy, and chemotherapy, patient prognosis remains poor. Immunotherapy (IO) has demonstrated clinical benefit; however, only 15-20% of patients with recurrent or metastatic OSCC respond favorably. This underscores the urgent need for reliable biomarkers to guide patient selection and personalize treatment strategies.
Methods: To investigate immune checkpoint dynamics associated with IO outcomes, we integrated single-cell RNA sequencing (scRNA-seq) to define immune signatures predictive of treatment response. These findings informed the design of a customized Opal multiplex immunohistochemistry (mIHC) panel to spatially map immune cell populations and checkpoint molecules within the OSCC tumor microenvironment. Paired pre- and post-IO tumor specimens from 18 OSCC patients treated with anti-PD-1 therapy were analyzed using this panel. Spatial data were subsequently processed with AI-assisted computational profiling to quantitatively assess immune cell infiltration and checkpoint expression patterns in situ.
Results: Integrated analysis of scRNA-seq, mIHC, and AI-assisted spatial profiling identified seven immune checkpoint signatures significantly associated with improved survival, all representing distinct expression patterns within $CD8^+$ T-cell subsets. A risk scoring model integrating spatial immune cell densities with survival data successfully stratified patients into low- and high-risk groups, with the low-risk group demonstrating significantly longer overall survival (OS). Notably, the $LAG\text{-}3^-TIM\text{-}3^+PD\text{-}1^+CD8^+$ T-cell population was enriched in high-risk patients and displayed an immune-desert phenotype prior to IO treatment.
Conclusion: These results yield two key insights: (1) immune checkpoint signatures, not only PD-1/PD-L1 can be used to stratify OSCC patients with favorable survival outcomes, and (2) low-risk patients, they already have higher infiltrated T cells with the presence of co-inhibitory checkpoint molecules, whereas, the high-risk patients, post-IO treatment, they will have higher immune infiltation. Overall, our study highlights the prognostic value of integrated immune checkpoint expression profiling and supports the rationale for exploring combination immune checkpoint blockade strategies in OSCC.

#3933 sB7-H3 as a prognostic biomarker in osteosarcoma: Insights into clinical outcomes.

Lu Xie[1], **Yuwei Zhao**[1], Kunkun Sun[2], Yiyang Yu[1], Jie Xu[1], Yuhang Wang[1], Chenchen Yang[1], Hengyue Ma[1], Tingting Ren[1], Xiaodong Tang[1]

[1]Musculoskeletal Tumor Center, Peking University People's Hospital, Beijing, China,[2]Pathology Department, Peking University People's Hospital., Beijing, China

B7 homolog 3 protein (B7-H3), a member of the B7 checkpoint family, is aberrantly and consistently expressed on the membranes of various human cancer cells and is associated with poor prognosis. Emerging evidence also indicates that soluble B7-H3 (sB7-H3) correlates with adverse outcomes in multiple malignancies. In this study, we measured sB7-H3 levels in peripheral blood using an enzyme-linked immunosorbent assay (ELISA) from 100 newly diagnosed osteosarcoma (OTS) patients, both before and after neoadjuvant chemotherapy, and simultaneously assessed B7-H3 tissue expression via immunohistochemistry (IHC) analysis of surgical specimens. Our analysis showed significant associations between B7-H3 tissue expression and histopathological response to chemotherapy, with the H-score threshold >75 identifying patients with particularly poor prognosis ($p < 0.05$). Although no significant correlation was observed between tissue and circulating B7-H3 expression, we found that lower baseline sB7-H3 levels (pre-sB7H3 < 21.2425 ng/mL) predicted poor clinical outcomes. By integrating sB7-H3 levels with established prognostic indicators, including metastatic status and lactate dehydrogenase (LDH) levels, we developed a comprehensive prognostic model that demonstrated strong predictive accuracy for survival outcomes. Notably, pre-sB7-H3 levels were significantly associated with good histological responses ($p < 0.05$). Longitudinal monitoring during treatment revealed that dynamic changes in sB7-H3 levels positively correlated with disease progression ($p < 0.05$) and inversely correlated with good histological responses ($p < 0.05$). These findings highlight serum sB7-H3 as a clinically valuable biomarker in OTS, providing prognostic information both at diagnosis and throughout the course of treatment in a relatively convenient manner.

#3934 Apoptosis-inducing factor mitochondria-associated 2 (AIFM2) functions as an oncogenic driver and prognostic biomarker in oral squamous cell carcinoma.

Chung-Hsien Chou[1], Shu-Chun Lin[1], **Kuo-Wei Chang**[2]

[1]Oral Biology, National Yang Ming Chiao Tung University, Taipei, Taiwan,[2]Dentistry, National Yang Ming Chiao Tung University, Taipei, Taiwan

Head and neck squamous cell carcinoma (HNSCC), including oral squamous cell carcinoma (OSCC), is a prevalent malignancy with limited therapeutic success. Apoptosis-inducing factor mitochondria-associated 2 (AIFM2), also known as ferroptosis suppressor protein 1, has been implicated in ferroptosis regulation and cancer progression, yet its role in HNSCC/OSCC remains unclear. This study investigated the oncogenic functions, clinical relevance, and epigenetic regulation of AIFM2 in OSCC. Transcriptomic data from TCGA-HNSCC and in-house OSCC RNA-Seq datasets were analyzed to assess AIFM2 expression and clinical associations. Functional assays examined the effects of AIFM2 knockdown and overexpression on OSCC cell proliferation, migration, invasion, and drug responses. Bioinformatic prediction, luciferase reporter, and miRNA mimic assays were performed to identify microRNAs regulating AIFM2. A Light Gradient Boosting Machine (LGBM) model was employed to predict patient mortality risk. High AIFM2 expression correlated with advanced stage, poor differentiation, p16 negativity, and worse survival in HNSCC/OSCC. AIFM2 knockdown reduced migration and invasion, while overexpression enhanced proliferation, migration, and invasion but had minimal impact on sensitivity to cisplatin, palbociclib, or cold atmospheric plasma. Bioinformatic and experimental analyses identified miR-32-5p and miR-432-5p as direct suppressors of AIFM2, both downregulated in tumors. AIFM2-associated transcripts were enriched in pathways related to oxidative stress, lipid metabolism, and E2F targets. Furthermore, the AIFM2-associated gene expression signature generated by the LGBM model effectively stratified patients by prognostic risk. Collectively, these findings indicate that AIFM2 functions as an oncogenic driver in OSCC, promoting tumor progression and poor prognosis, and is epigenetically regulated by tumor-suppressive miR-32-5p and miR-432-5p, representing a potential prognostic biomarker and therapeutic target.

#3935 Peripheral T-cell receptor beta repertoire in breast cancer: Implications for prognosis and therapy-associated immune repertoire dynamics.

Ling-Ming Tseng[1], Chi-Cheng Huang[1], Ji-Lin Chen[2], Yi-Fang Tsai[1], Ta-Chung Chao[1], Wen-Chi Wu[1], Pei-Ju Lien[1], Yen-Shu Lin[1], Chin-Jung Feng[1], Yen-Jen Chen[1], Jiun-I Lai[1], Jen-Hwey Chiu[2], Chih-Yi Hsu[1], **Chun-Yu Liu**[1]

[1]Taipei Veterans General Hospital, Taipei, Taiwan,[2]National Yang Ming Chiao Tung University, Taipei, Taiwan

Purpose: Sequencing of the T-cell receptor (TCR) repertoire provides insight into host immune status and can serve as a biomarker of therapeutic response. This study aimed to comprehensively evaluate the relationships between peripheral TCR repertoire characteristics, clinicopathological parameters, survival outcomes, and treatment regimens in breast cancer.
Experimental Design: Peripheral blood from patients with early- or late-stage breast cancer was analyzed using the Oncomine™ TCR Beta-LR Assay, and matched tumor tissues were profiled with the Oncomine™ Comprehensive Assay v3. Patients were classified into three groups: (1) first-line surgery followed by adjuvant therapy, (2) neoadjuvant chemotherapy (NACT) followed by surgery, and (3) de novo or recurrent Stage IV disease. TCR diversity metrics including clonality, convergence, richness, and Shannon diversity were correlated with clinicopathologic features, genomic alterations, and overall survival using Pearson correlation, Kaplan-Meier, and Cox regression analyses.
Results: Among 856 enrolled patients, baseline TCR clonality was inversely correlated with both richness and Shannon diversity, while convergence showed a modest positive association with clonality. Higher clonality correlated weakly but significantly with patient age and tumor stage. Elevated baseline clonality was associated with poorer overall survival and remained an independent prognostic factor in multivariate Cox analysis. Patients harboring ARID1A mutations exhibited reduced TCR richness and lower Shannon diversity compared with wild-type counterparts. Treatment-specific analysis revealed that adjuvant chemotherapy, particularly taxane- or anthracycline-taxane-based regimens, induced peripheral T-cell clonal expansion and loss of diversity, with trastuzumab-associated changes confined to HER2-enriched but not luminal B2 subtypes. Similarly, NACT, especially anthracycline-taxane or platinum-containing regimens, promoted clonal expansion and reduced diversity, with HER2-targeted effects again restricted to HER2-enriched tumors.
Conclusion: Peripheral TCR clonality serves as an independent prognostic biomarker in Stage IV breast cancer. HER2-targeted therapies and specific chemotherapy regimens modulate immune repertoire dynamics in a subtype-dependent manner. These findings highlight that treatment type significantly influences TCR diversity and underscore the potential of integrating repertoire profiling with genomic and clinical data to guide personalized therapy in breast cancer.

#3936 IQGAP3 as a gatekeeper of epithelial integrity and prognostic biomarker in extrahepatic cholangiocarcinoma.

Naoki Rikiyama[1], Daisuke Douchi[1], Ming Zhu[1], Keigo Murakami[2], Mitsuhiro Shimura[1], Takehiko Saijo[1], Shusuke Migita[1], Shuichiro Hayashi[1], Hideaki Sato[1], Koetsu Inoue[1], Shuichi Aoki[1], Masahiro Iseki[1], Takayuki Miura[1], Shimpei Maeda[1], Hideaki Karasawa[1], Masaharu Ishida[1], Hideo Ohtsuka[1], Masamichi Mizuma[1], Kei Nakagawa[3], Shinobu Ohnuma[1], Atsushi Masamune[4], Toru Furukawa[2], Michiaki Unno[1]

[1]Department of Surgery, Tohoku University Graduate School of Medicine, Sendai, Japan,[2]Department of Investigative Pathology, Tohoku University Graduate School of Medicine, Sendai, Japan,[3]Division of Gastroenterological and Hepato-Biliary-Pancreatic Surgery, Department of Surgery, Tohoku Medical and Pharmaceutical University, Sendai, Japan,[4]Division of Gastroenterology, Tohoku University Graduate School of Medicine, Sendai, Japan

Background: Biliary tract cancer (BTC) is an aggressive malignancy for which reliable prognostic biomarkers remain scarce. Although recent efforts have advanced the molecular characterization of intrahepatic cholangiocarcinoma (iCCA), the biology of extrahepatic CCA (eCCA) is still insufficiently understood. IQ motif-containing GTPase-activating protein 3 (IQGAP3) is a scaffold protein involved in cytoskeletal regulation, cell-cycle control, and epithelial junctional stability. Because epithelial-mesenchymal transition (EMT) drives invasion and metastasis in BTC, we hypothesized that IQGAP3 may influence epithelial identity and clinical behavior in eCCA. This study sought to clarify the clinicopathological significance of IQGAP3 and examine its biological role using integrated pathological and functional analyses.

Methods: We retrospectively analyzed 100 patients who underwent curative resection for perihilar or distal CCA between 2016 and 2020. IQGAP3 expression was assessed by immunohistochemistry and quantified using QuPath-based H-scores; tumor regions were manually annotated in QuPath to ensure that H-scores reflected staining intensity exclusively in cancer cells. Associations with clinicopathological factors and overall survival (OS) were evaluated using standard statistical approaches. Functional studies were conducted in HuCCT1 and TFK-1 cells with shRNA-mediated IQGAP3 knockdown. RNA sequencing and gene set enrichment analysis (GSEA) were performed to identify transcriptional changes associated with IQGAP3 loss. Expression of epithelial markers, including E-cadherin (CDH1), was examined in cell models and resected tissues.

Results: High IQGAP3 expression was associated with significantly longer OS than low expression (median 102.7 vs 40.2 months; hazard ratio 0.51; 95% CI 0.30-0.88; $P = 0.017$). Low IQGAP3 levels correlated with lymph-node metastasis, advanced stage, and positive resection margins. Functional assays showed that IQGAP3 knockdown activated EMT-related transcriptional programs in both cell lines (normalized enrichment score 1.43 and 1.44; $P < 0.01$; false discovery rate $q < 0.25$) and reduced CDH1 expression, suggesting impaired epithelial cohesion. In clinical samples, IQGAP3 and CDH1 mRNA levels demonstrated a strong positive correlation ($r = 0.74$), supporting a biological link between IQGAP3 loss and disruption of epithelial integrity.

Conclusions: IQGAP3 plays a key role in maintaining epithelial identity in CCA. Its loss promotes EMT activation and is associated with more aggressive disease features, whereas high expression confers favorable prognosis in eCCA. IQGAP3 may serve as a practical biomarker for risk stratification and represents a potential target for strategies aimed at limiting EMT-driven tumor progression.

#3937 Investigation of inherited genetic variation for predictors of immune mediated colitis following immune checkpoint inhibitor (ICI) therapy of patients (pts) with melanoma.

Ahmad A. Tarhini[1], Zhihua Chen[2], Mohammad Ali Khaksar[1], Sandra J. Lee[3], F. Stephen Hodi[3], Tingyi Li[2], Howard Streicher[4], Vernon K. Sondak[5], John M. Kirkwood[6], Xuefeng Wang[2], Peter A. Kanetsky[7]

[1]Cutaneous Oncology and Immunology, H. Lee Moffitt Cancer Center, Tampa, FL,[2]Biostatistics and Bioinformatics, H. Lee Moffitt Cancer Center, Tampa, FL,[3]Dana-Farber Cancer Institute, Boston, MA,[4]National Cancer Institute, Rockville, MD,[5]Cutaneous Oncology, H. Lee Moffitt Cancer Center, Tampa, FL,[6]University of Pittsburgh Medical Center, Pittsburgh, PA,[7]Cancer Epidemiology, H. Lee Moffitt Cancer Center, Tampa, FL

Background: Immune mediated colitis is a common toxicity following ICI therapy of melanoma and can be life threatening. Therefore, predicting the risk of developing colitis may inform the treatment plan and clinical follow up. We hypothesize that inherited genetic variation is an important factor in predisposing pts to this immune related adverse event (irAE).
Methods: We conducted genome-wide genotyping on samples from 744 consenting pts enrolled in ECOG-ACRIN E1609 trial (NCT01274338) that tested ipilimumab. We used Illumina Infinium Global Screening Array v.3.0 + Multi-Disease BeadChip with 730059 designed loci. Genotypes were quality controlled, harmonized with the 1000 Genomes Phase 3 (1KGP3) genotypes, and imputed against the hrc-r1.1 reference panel using the Michigan Imputation Server 2, pipeline v2.0.6. We used logistic regression implemented in plink (v2.00a4LM glm with firth fallback) to estimate associations between inherited genetic markers and the occurrence of colitis, adjusting for genetic ancestry. We also calculated the value for 5 published polygenic risk scores (PRS) for inflammatory bowel disease (IBD) listed in PGS-Catalog v20240318 and tested the association with colitis in E1609 pts treating irAE grades as categorical (Kruskal-Wallis test) and as dichotomous (Wilcoxon rank-sum test) variables. IrAEs were graded using CTCAE v.4.
Results: There was no significant difference in distribution of the PRS across grade of colitis (Kruskal-Wallis) with any of the 5 PRS. However, all demonstrated stronger differences when irAE grades were dichotomized at >3 vs. other. PRS PGS004253 was most significant in association with grades 4-5 colitis (P = 0.01; AUC 0.73). This PRS (*Medha. Nature Commun 2024*) was trained in a non-melanoma European population that has a genetic ancestry similar to our melanoma study cohort (*Tarhini. AACR 2025*) and for which all markers in the PRS were available in our dataset. From our genome-wide association analysis, we identified 10 independent SNPs that were significantly associated with colitis irAE. When combined using log(OR) as weights, these SNPs were significantly associated with the severity of irAE grades, both across irAE grades (Kruskal-Wallis P = 2.5e-26) and when dichotomized as any colitis irAE vs. none (Wilcoxon P = 8.9e-30). In multivariable survival analysis adjusting for primary status (known, unknown) and sex (male, female), our 10-SNP PGS trended towards an association with survival outcomes.
Conclusion: Our results support an association between inherited genetic variation and the risk of colitis following ICI, including PRS for IBD selected based on inherited genetic similarity with the population used to train the PRS as well as a novel PRS score computed using 10 SNPs identified from our GWAS analysis.

#3938 Scalable AI-driven tumor-stroma ratio quantification for prognostic stratification in stage II-III colorectal cancer.

Wei Kit Tan[1], Marcia Zhang[1], Juha P. Vayrynen[2], Shuji Ogino[3], Mai Chan Lau[1]

[1]Bioinformatics Institute (BII), Agency of Science, Technology and Research (A*STAR), Singapore, Singapore,[2]Translational Medicine Research Unit, University of Oulu, Oulu, Finland,[3]Department of Pathology, Brigham and Women's Hospital, Boston, MA

Introduction: The tumor-stroma ratio (TSR), defined as the proportion of stromal content within the primary tumor, has been proposed as a prognostic histopathologic marker for colorectal cancer (CRC). Higher stromal content is often linked to poorer prognosis in stage II-III disease. However, TSR assessment remains manual and is prone to interobserver variability, while existing AI algorithms - often trained and tested on single-institution datasets - lack independent validation for generalizability. In this study, we developed an AI-driven TSR quantification model trained on the public Cancer Genome Atlas (TCGA) pathologist-annotated regions and validated it using predictions on (i) TCGA whole-slide images (WSI) and (ii) two large independent CRC cohorts (NHS/HPFS tissue microarray (TMA)).

Methods: We trained a SegFormer semantic segmentation model on 99,871 image tiles derived from pathologist-annotated regions (J.V.) from 469 TCGA H&E images spanning stage I-IV CRC. The model was trained to segment three major tissue categories: tumor, stroma, and others. For validation, we applied the model to 375 stage II-III CRC samples within the TCGA cohort (a subset of the 469 training images, evaluated beyond annotated regions) and to 537 NHS/HPFS TMA images. TSR was defined as the area of stroma divided by the sum of stromal and tumor areas. Patients were stratified into TSR-high and TSR-low groups using the cohort median as the cut-off. Prognostic associations were evaluated using Cox proportional hazard model.

Results: Computed TSR values range from 18.17% to 100% with a median of 88.56% for the NHS/HPFS cohort; and range from 11.72% to 99.87% with a median of 70.30% for the TCGA cohort. In the NHS/HPFS cohort, AI-derived TSR-high group showed significantly worse outcomes for overall survival (HR = 1.38; 95% CI = 1.06-1.81; P = 0.017) and CRC-specific survival (HR = 1.49; 95% CI = 1.03-2.15; P = 0.035). However, in the TCGA cohort, TSR stratification showed no significant prognostic value for either pathologist-annotated or WSI-AI-derived TSR for overall survival (HR = 1.12, 95% CI = 0.69-1.82; P = 0.647, and HR = 0.97; 95% CI = 0.59-1.60; P = 0.909, respectively) and CRC-specific survival (HR = 0.79, 95% CI = 0.40-1.58; P = 0.513, and HR = 0.88; 95% CI = 0.43-1.77; P = 0.723, respectively).

Discussion: While AI-derived TSR showed prognostic significance in the NHS/HPFS cohort, the lack of significance in TCGA suggests limited generalizability across cohorts. Notably, this is, to our knowledge, the first study to evaluate TSR using the well-established TCGA CRC dataset. These findings highlight the need to further dissect the stromal composition - through molecular staining or AI-driven profiling of immune populations, stromal subtypes, and tumor-immune spatial interactions - to capture the biological mechanisms underlying TSR and improve its robustness as a prognostic biomarker.

#3939 Circulating tumor cell analysis for early detection of minimal residual disease in oral cancer.

Xi Zhang[1], Sarj Vasani[2], Waqar A. Afridi[1], Danyelle A. Ferreira[1], Omar Breik[2], Gunter Hartel[3], Liz Kenny[2], **Chamindie Punyadeera**[1]

[1]Griffith University, Brisbane, Australia,[2]Royal Brisbane and Women's Hospital, Brisbane, Australia,[3]QIMR Berghofer Medical Research Institute, Brisbane, Australia

Background: The key clinical problem in detecting minimal residual disease (MRD) in oral cancer (OC) patients is the lack of sensitive, standardized tools to identify residual cancer cells that remain after treatment but are undetectable by conventional imaging or pathology. We aim to assess whether circulating tumor cells (CTCs) can serve as a biomarker for early detection of MRD.
Methods: This longitudinal observational study collected blood samples from 50 OC patients at baseline, and at one, three, and twelve months following surgery. CTCs were isolated using a spiral microfluidic device that leverages inertial microfluidic principles for separation. CTC was defined as either pan-cytokeratin (CK+) or cell-surface vimentin (CSV+), DAPI positive and CD45 negative. The presence of CTCs was compared between patients who experienced recurrence and those who remained disease-free.
Results: At one month, patients with recurrence showed significantly higher total CTC counts (mean 2.75 vs 0.61; $p = 0.0021$) and significantly elevated CTC phenotype positivity (cytokeratin positive (CK+) cell surface vimentin positive (CSV+): $p = 0.0001$). At three months, CTC differences further widened (mean 8.0 vs 0.91; $p = 0.0042$), with strong separation across multiple CTC cluster phenotypes, including CK-CSV+ ($p = 0.0001$) and CK+CSV+ ($p = 0.0003$). Significant CTC-based differences persisted at one year ($p = 0.0241$).
Conclusions: CTCs demonstrate strong promise as early biomarkers for MRD and impending recurrence in OC. Multiple markers exhibit statistically significant separation well in advance of conventional clinical detection, highlighting their potential for early intervention, supporting its integration into routine clinical practice for improved patient outcomes.

#3940 Persistent immune microenvironment changes associated with progression risk in Barrett's esophagus.

Hyun Young Park[1], Erin E. Grayhack[1], Ashten Omstead[1], Christopher Sherry[1], Alisha Khan[1], Catherine Lewis[1], Neda Dadgar[1], Kunhong Xiao[1], Gursimran Kochhar[1], Michael Landau[1], Douglas B. Stairs[2], Ali H. Zaidi[1], Patrick L. Wagner[1]

[1]Allegheny Health Network, Pittsburgh, PA,[2]Penn State Cancer Institute, Hershey, PA

Barrett's esophagus (BE) is the principal risk factor for esophageal adenocarcinoma (EAC). Since only a small number of patients with BE progress to high-grade dysplasia (HGD) or EAC, biomarkers of risk are in high demand. Our previous work identified alterations in the relative abundance of lamina propria lymphocyte and macrophage subsets in BE patients at initial diagnosis. In this study, we extended these findings by analyzing serial surveillance samples from these patients to assess the changes of these immune microenvironments over time. Formalin-fixed, paraffin-embedded tissue samples from patients with non-dysplastic BE undergoing endoscopic biopsy were examined. Initial diagnostic samples (n=58) and serial surveillance samples (n=78) from 58 unique patients were examined, among whom 25 were subsequently diagnosed with HGD or EAC ("progressors"), while 33 patients did not progress during at least 5 years of surveillance ("non-progressors"). Immunohistochemical staining was performed with antibodies specific for CD3 and CD8 (lymphocytes), CD68/CD86 co-positive ("M1- like") macrophages, and CD68/CD206 co-positive ("M2-like") macrophages. Regions of interest (ROI) selected from the lamina propria in the region of BE were subjected to digital image analysis, and subgroup comparisons of immune cell densities were carried out using Welch's t-test for the outcome of progression. In total, 3540 ROIs from non-progressors (1526 initial, 2014 follow-up) and 2994 ROIs from progressors (1077 initial, 1917 follow-up) were examined. Relative to non-progressors, progressor biopsies contained a markedly greater density of CD3+ lymphocytes (4586 vs. 2633, $p=0.0019$) and a significantly lower density of CD8+ lymphocytes (798 vs. 1359, $p=0.002$). Concomitantly, M1-like macrophages were significantly elevated in progressors (84.7 vs. 34.6, $p=0.003$), while M2-like macrophages were markedly decreased (35.5 vs. 80.3, $p<0.0001$) relative to non-progressors. The difference persisted at follow-up biopsy, (CD3+:1566 vs. 1228, $p<0.0001$; M1: 244 vs. 48.4, $p<0.0001$), whereas other immune cells changed (CD8+: 350 vs. 396, $p=0.096$ vs. M2: 66.5 vs 37.6, $p=0.0066$). The immune cell density suggests that there is an enduring feature of the BE microenvironment.The BE immune microenvironment demonstrates substantial differences in lamina propria lymphocyte and macrophage populations in patients who are destined to progress to HGD or EAC, relative to those who are not. These findings, which we show here to persist in serial biopsies over time, warrant further investigation to deepen our understanding of this altered immune microenvironment, both as a biomarker of progression risk and a potential target for immunomodulatory prevention strategies.

#3941 A RHO GTPase pathway signature as a potential prognostic biomarker and therapeutic target in bladder cancer.

Weiyi Gong[1], Chongwen Cao[2], Peng Wang[3], Shang-Jui Wang[4], Akshay Sood[5], Lingbin Meng[3], Qingqing Wu[6], Cheryl Lee[5], Anil Vasdev Parwani[6], Jenny Li[6], Xuefeng Liu[7]

[1]Comprehensive Cancer Center, Biomedical Sciences Graduate Program, The Ohio State University, Columbus, OH,[2]Comprehensive Cancer Center, The Ohio State University, Columbus, OH,[3]Department of Medicine, Wexner Medical Center, The Ohio State University, Columbus, OH,[4]Department of Radiation Oncology, Wexner Medical Center, The Ohio State University, Columbus, OH,[5]Department of Urology, Wexner Medical Center, The Ohio State University, Columbus, OH,[6]Department of Pathology, College of Medicine, The Ohio State University, Columbus, OH,[7]Department of Pathology, Urology and Radiation Oncology, Wexner Medical Center, The Ohio State University, Columbus, OH

Background: The RHO GTPase cycle regulates essential cellular processes, including proliferation, differentiation, senescence, and programmed cell death. However, many predicted downstream effectors of this pathway remain poorly characterized, and their prognostic relevance in bladder cancer (BLCA) is not well understood. This study aimed to develop a prognostic model for BLCA based on RHO GTPase cycle effector gene expression and to identify key effectors functionally involved in BLCA progression.
Methods: RNA-seq data and clinical information from The Cancer Genome Atlas (TCGA) and our James institutional cohort were analyzed. LASSO and Cox regression analyses were used to construct a prognostic gene signature associated with the RHO GTPase cycle. Patients were stratified into high- and low-risk groups based on this signature. Pathway enrichment analyses and therapy-response predictions were performed to compare biological features between risk groups. Candidate effector genes were functionally validated in BLCA cell lines using shRNA-mediated knockdown, followed by proliferation and colony-formation assays.
Results: The resulting gene signature reliably stratified patients into high- and low-risk groups, with Kaplan-Meier curves showing significantly reduced survival in the high-risk group. These findings were validated in our independent dataset. Among the signature genes, UACA, CLTC, and SNAP23 emerged as key candidates. Pathway enrichment indicated activation of YAP and EMT signaling in high-risk patients. Bioinformatic drug-prediction analysis identified PI-103 and PLX-4720 as potential therapeutic compounds for the high-risk group. Functional experiments demonstrated that knockdown of each signature gene significantly reduced proliferation and colony formation in BLCA cell lines and consistently induced a senescence-like morphology.
Conclusions: This study establishes a robust prognostic model for BLCA based on RHO GTPase cycle effector genes and highlights UACA, CLTC, and SNAP23 as potential prognostic biomarkers and promising therapeutic targets. Our findings provide a foundation for further investigation into RHO GTPase pathway effectors and their potential role in improving BLCA diagnosis and treatment.

#3942 NRF2 pathway activation predicts poor radiation response in laryngeal cancer: Insights from a large proteogenomic characterization study.

Kelly Gaudian, Harit Panda, Emily Wilkerson Zarbock, Kate Zhao, James Sun, Benjamin Wahle, Paul Zolkind, M. Ben Major

Washington University School of Medicine, St. Louis, MO

Patients with advanced laryngeal cancer often experience poor outcomes, and current clinical guidelines lack reliable predictive biomarkers. Preclinical cancer studies have implicated NRF2, a transcription factor that promotes antioxidant defense and metabolic reprogramming, in resistance to radiation therapy (RT). This study investigates whether activation of the NRF2 pathway influences clinical outcomes in larynx cancer patients receiving RT or surgery. We identified 135 larynx cancer patients who were treated at Siteman Comprehensive Cancer Center with either surgery and RT or surgery alone. Tumor samples were obtained from the WashU Head & Neck Tumor Center tissue bank and characterized using RNA sequencing, targeted exon capture sequencing, and mass spectrometry-based proteomics. Gene and protein expression profiling were used to independently calculate an NRF2 activity score, allowing the classification of tumors along a continuum of NRF2 activity. Kaplan-Meier analysis and Cox proportional hazards modeling were employed to compare disease-free survival (DFS) and locoregional failure (LRF) rates between NRF2-high and NRF2-low groups. In patients treated with surgery and RT, differential gene and protein expression analysis identified numerous NRF2-induced targets that were associated with locoregional failure. In those treated with radiation, NRF2-high patients had significantly worse outcomes than NRF2-low, with 5-year LRF rates of 51.0% and 17.1% (HR = 7.2, 95% CI: 2.0-25.7), and 5-year DFS rates of 25.4% and 50.7% (HR = 2.9, 95% CI: 1.3-6.2), respectively. Notably, NRF2-activity status was not significantly prognostic in the surgery alone cohort, indicating that NRF2 activation is specifically associated with radiation resistance. Ontological enrichment analyses identified upregulation of pathways associated with antioxidant response and dsDNA break repair in NRF2 high tumors, suggesting possible mechanisms of resistance. Discovery-based proteomics aligned closely with the gene expression data. Exon capture sequencing revealed 10 patients harboring driver mutations in NRF2 or KEAP1, 9 of which were categorized as NRF2 high from expression data. Logistic regression identified NRF2 score as the most predictive variable associated with outcomes for radiation-treated patients, followed by nodal involvement. These findings suggest NRF2 activation is associated with worse outcomes in patients receiving surgery and radiation, but not surgery alone. Future implications include validating NRF2 as a biomarker across data sets and the development and testing of NRF2-targeted therapies.

#3943 Morphology-derived spindle-cell gene signature in HPV+ HNSCC is linked to pEMT, molecular subtype, HPV integration, and recurrence-free survival.

Shaomiao Xia[1], Yvonne Xinyi Lim[2], Min Liu[2], Bailey Grab[3], Siddhi Patil[4], Shiting Li[3], Laura Rozek[5], Nisha J. D'silva[2], Maureen A. Sartor[6]

[1]Department of Computational Medicine and Bioinformatics, University of Michigan Medical School, Ann Arbor, MI,[2]University of Michigan School of Dentistry, Ann Arbor, MI,[3]Department of Computational Medicine and Bioinformatics, University of Michigan Medical School, Ann Arbor, MI,[4]Georgetown University, Washington, DC,[5]Oncology Department, School of Medicine, Georgetown University, Washington, DC,[6]Assistant Professor, Dept. of Bioinformatics, University of Michigan Medical School, Ann Arbor, MI

Spindle-shaped epithelial cells are frequently observed in HPV+ head and neck squamous cell carcinoma (HNSCC) cell lines and at invasive fronts in tumors, but how this morphology relates to transcriptional programs, aggressive phenotypes, and spatially organized niches remains unclear. This study aimed to understand the spindle phenotype by deriving a morphology-linked gene signature and testing its association with partial epithelial-mesenchymal transition (pEMT), HPV integration (HPVint) into the host tumor genome, tumor molecular subtypes (immune-strong, IMU vs highly keratinized, KRT), and patient recurrence-free survival (RFS), and by mapping this program *in situ* using spatial transcriptomics. We quantified cell morphology in two HPV+ HNSCC cell lines using cell aspect ratio, roundness, and circularity, and used bulk RNA-seq (n = 12) to identify genes differentially expressed in spindle-enriched conditions. We derived a 45-gene spindle-cell signature (SCS) and computed SCS and pEMT scores in 236 HPV+ HNSCC tumors from four cohorts: UM_FF (18), UM_FFPE (62), HVC (83), and TCGA (73). In parallel, we generated Nanostring CosMx 6k-plex spatial transcriptomics from four HPV+ tonsil tumors, clustered cells into major compartments, and projected SCS/pEMT scores and HPV gene expression onto tissue coordinates to characterize spatial niches. In HNSCC tumors, SCS scores are highly correlated with pEMT scores (Pearson's $r = 0.72$) despite sharing only two genes, indicating this signature robustly captures a pEMT-like program. KRT tumors had markedly higher SCS scores than IMU tumors in the pooled analysis ($p = 1.3 \times 10^{-9}$). Across four cohorts, SCS scores tended to be higher in HPVint+ than HPVint- tumors, with significant differences in three cohorts (p range 0.016-0.045) but not the HVC ($p = 0.21$), suggesting cohort-specific heterogeneity. Taken together, these patterns firmly link the spindle program to molecular subtype and suggest an association with HPVint. Survival analysis of 70 University of Michigan patients shows that patients with low SCS scores have significantly better RFS than those with high scores (Log-rank test, $p = 0.014$). We are incorporating CosMx data with these patterns to test the hypothesis that high SCS epithelial states preferentially occupy tumor-stromal interfaces and cancer-associated fibroblast-rich regions and are associated with distinct local immune architecture, defining a spatially restricted invasive niche. These analyses support that SCS captures an invasive state enriched in KRT and HPVint+ HNSCC and associated with poorer RFS. By connecting cell shape, transcriptional state, viral features, and spatial microenvironment, this study suggests morphology-derived biomarkers and spatial niches that may refine risk stratification and guide targeted therapeutic strategies in HPV-associated HNSCC.

#3944 The impact of diversity on transcriptional heterogeneity of skeletal muscle from pancreatic ductal adenocarcinoma patients.

Praveen Bhoopathi[1], Vignesh Vudatha[2], Arunima Punjala[2], Vashti Bandy[2], Anna Gibson[2], Dongyu Zhang[2], Katarzyna M. Tyc[3], Mikhail Dozmorov[3], Jeremy Ducharme[4], Martin Schonk[4], Brittney Poole[4], Sarah Judge[4], Leopoldo Fernandez[1], Andrew R. Judge[4], Jose G. Trevino[1]

[1]Surgery (Surgical Oncology) and Massey Comprehensive Cancer center, Virginia Commonwealth University - VCU, Richmond, VA,[2]Surgery (Surgical Oncology), Virginia Commonwealth University - VCU, Richmond, VA,[3]Department of Biostatistics, Virginia Commonwealth University - VCU, Richmond, VA,[4]Department of Physical Therapy and Myology Institute, University of Florida, Gainesville, FL

Objective: Cachexia plays a major role in the morbidity and mortality of pancreatic ductal adenocarcinoma (PDAC) patients. The objective of this study is to delineate the molecular pathways of muscle that contribute to cancer cachexia from surgically resected PDAC patients.
Methods: At surgical resection for PDAC, rectus abdominus muscle was sharply divided and shock frozen immediately for RNA-seq. Total RNA was extracted from the frozen tissue using standard protocols, and RNA integrity was confirmed prior to library preparation. The resulting high-quality RNA was then used for RNA sequencing (RNA-seq) analysis to find distinct variants in addition to a core transcriptional signature of roughly 13,007 frequently expressed transcripts, differential transcript expression was evaluated. KEGG pathways and MSigDB collections (Hallmark, Curated, GO signatures) were used in Gene Set Enrichment Analysis (GSEA), which uses both fold change and ranking of differentially expressed genes (DEGs) to find enriched biological pathways.
Results: Significant transcriptome variations in muscle tissue were found to be associated with patient race and survival. MSigDB gene sets comparing Black and White) patients revealed that the AA cohort had higher activation of pathways linked to inflammation, cardiomyopathy, and muscle atrophy/proteostasis. Three overlapping genes were found by cross-referencing these pathways with significant DEGs: CYP4B1, DDIT4 (upregulated in AA, significantly related with muscular atrophy/cachexia), and GINS1 (downregulated in AA, associated with proliferation). Additionally, eight genes including the physiologically significant genes ADAM28, SENCR, and MEG8 (related with muscle differentiation and tumor progression) were found to be substantially associated with overall survival.
Conclusion: RNA-seq and GSEA of muscle tissue provide critical insights into the systemic molecular alterations associated with PDAC. The identified pathways and genes, particularly those demonstrating racial and survival-associated heterogeneity (e.g., DDIT4, GINS1), represent potential biomarkers and therapeutic targets for addressing muscle dysfunction and cachexia in PDAC.

#3945 Serum detection of MUC1 and renin identifies circulating biomarkers for breast cancer prognosis.

Alakesh Bera[1], Hai Hu[2], COL Craig D. Shriver[3], **Meera Srivastava**[4]

[1]USUHS - Uniformed Services University of the Health Sciences, Bethesda, MD,[2]Chan Soon-Shiong Institute of Molecular Medicine at Windber, Windber, PA,[3]Uniformed Services University of the Health Sciences, Bethesda, MD,[4]Uniformed Services University, Potomac, MD

Background: Cytogenetic abnormalities involving multiple loci on the long arm of chromosome 1 are among the most frequent alterations in human breast carcinoma. To define their biological and clinical significance, we conducted a large-scale integrative genomic analysis across diverse breast cancer datasets.
Methods: Data from over 13,000 breast tumors (n = 13,146 samples; 12,229 patients across 30 studies) were analyzed using cBioPortal, including The Cancer Genome Atlas (TCGA). Copy number alterations, mRNA/protein expression, and clinical outcomes were evaluated. Comparative analyses with >100,000 samples across 35 other cancers (n = 105,424) determined specificity. Mutual exclusivity and co-occurrence analyses identified genetic interaction patterns relevant to tumor progression. Serum detectability of top candidates was evaluated.
Results: Eight genes particularly TRIM67, DISC1, REN, DNM3, ATP1B1, VSIG8, SPTA1, and MUC1 from different loci of 1q chromosome showed recurrent amplifications (12-15%) in breast tumors, significantly exceeding frequencies in pan-cancer datasets (~3%). These genes displayed low baseline expression in normal breast tissue but were highly expressed in tumors. Co-occurrence analyses revealed significant genetic interplay, including TP53 with MUC1/SPTA1/VSIG8 and PIK3CA with TRIM67/DISC1/REN, suggesting cooperative gain-of-function driving aggressive phenotypes. Among the eight amplified 1q genes, MUC1 and REN showed the strongest clinical relevance, as both encode secreted or shed proteins that were readily detectable in serum and have established associations with aggressive breast cancer biology. In contrast, DNM3 and ATP1B1 were detectable at lower abundance in serum-derived extracellular vesicles, supporting their potential as emerging but less established circulating markers.
Conclusions: Multi-locus amplifications contribute collectively to breast cancer progression through distinct gene interaction networks. This study identifies a core set of functionally relevant, serum-detectable gene products that may serve as biomarkers for prognosis, recurrence monitoring, and therapeutic targeting in aggressive breast cancer.

#3946 Association between MLK4 expression and colon cancer patient survival.

Nathan Kumar[1], Hitesh Kapoor[1], Piush Srivastava[2], Deepti Srivastava[2], Saket Jha[2], Sunil Kumar Singh[2], David Allison[3], Ajay Rana[2], Gerald Gantt[1]

[1]Division of Colon and Rectal Surgery, Department of Surgery, University of Illinois at Chicago, Chicago, IL,[2]University of Illinois at Chicago, Chicago, IL,[3]Department of Pathology, University of Illinois at Chicago, Chicago, IL

Background: Mixed Lineage Kinase 4 (MLK4) is a protein kinase from the serine/threonine kinase family functioning through the MAPK pathway. The association of MLK4 with colon cancer oncologic outcomes has not been well described. We aimed to investigate the molecular expression of MLK4 at both the protein and mRNA levels, its differential expression across stages, and the association with survival in cases of increased expression using the TCGA databases.

Methods: An *in-silico* analysis of MLK4 in colorectal cancers was performed using the TCGA database for stage-wise expression and overall survival analysis in 288 patients. A TMA of colon cancer and matched adjacent normal colon tissue, annotated with survival data and clinical stage (AJCC 8th edition), was used to investigate differential expressions of MLK4 in colon cancer. Laser Capture microdissection was performed with FFPE samples consisting of normal tissue and tumor. MLK4 RNA was quantified using organic extraction and RT-PCR techniques.

Results: IHC of MLK4 in 74 matched sample pairs revealed a significant ($p < 0.05$) increase in MLK4 expression (mean difference = 0.405, 95% CI = 0.2028 to 0.6080) in colon cancer compared to normal tissue. The correlation coefficient ($r = 0.4721$, $p < 0.0001$) suggested a moderate correlation between MLK4 levels in normal and tumor tissues. RT-PCR analysis in colon cancer specimens revealed a significant ($p<0.05$) increase in mRNA levels of MLK4 (mean difference = 2.139, 95% CI = 0.8789 to 3.400). High MLK4 expression showed a trend toward reduced overall survival compared with low expression (HR = 1.25, log-rank p = 0.079). Similarly, higher MLK4 methylation demonstrated a trend toward poorer overall survival in colon adenocarcinoma patients (HR = 1.54, 95% CI 0.96-2.47; log-rank p = 0.07).

Conclusion: Increased expression of MLK4, both transcriptionally and translationally, in colon cancer suggests involvement in colon tumor pathology. Cellular-level expressions and correlations of MLK4 kinase with survival can help elucidate the complex nature of colon cancer development and identify unknown prognostic markers.

: Spatial Proteomics and Transcriptomics 2
Poster Session

#3950 Spatial transcriptomic dissection of microenvironmental drivers of NMIBC progression.

Jacob Alltucker[1], Yiling Shen[2], Suhyeon Choi[1], Pavithra Nedumaran[1], Andrew Martinez[1], Joseph Lownik[1], Huihui Ye[1], Hideki Furuya[1], Dan Theodorescu[3], Simon Knott[1]

[1]Cedars-Sinai Medical Center, Los Angeles, CA,[2]Tsinghua University, Beijing, China,[3]University of Arizona, Tucson, AZ

Background: High-grade non-muscle invasive bladder cancer (NMIBC) is an aggressive malignancy characterized by a high rate of progression to muscle-invasive bladder cancer (MIBC). Once muscle-invasive, the disease is associated with significantly worse overall survival. Thus, novel strategies for identifying therapeutic targets and biomarkers of progression are urgently needed. We utilized spatial transcriptomics to elucidate the tumor microenvironment states and cellular interactions that underlie progressive NMIBC. We hypothesized that progressive NMIBC is defined by distinct molecular and architectural compositions that converge on an MIBC-like phenotype.
Methods: We constructed tissue microarrays using transurethral resection specimens from 18 high-grade NMIBC patients who progressed to MIBC within 5 years and 27 risk-matched non-progressors, along with 52 MIBC cystectomy specimens. We then performed Xenium in situ expression analysis using a 5,000-gene panel with an additional 100 genes focused on stromal and immune signaling. Data were analyzed using single-cell variational inference with Leiden clustering-based cell typing, custom neighborhood (“niche”) evaluation, and computational workflows to characterize cellular interactions, transcriptional programs, and ligand-receptor signaling across progressor status and disease states.
Results: We generated a single-cell-resolution spatial transcriptomic atlas of over 4 million cells spanning NMIBC and MIBC tissues. Preliminary analysis revealed substantial intra- and inter-patient heterogeneity in both tumor-intrinsic transcriptional programs and microenvironment composition. Non-progressor tumors demonstrated increased immune activation signatures and enrichment of cytotoxic CD8+ T cells, while progressors showed enrichment of tumoral mTOR signaling and other oncogenic pathways. Ongoing work aims to define spatial niches and cellular interaction networks that differentiate progressive versus non-progressive disease and evaluate their alignment with MIBC-like architecture.
Conclusions: This study establishes the first single-cell spatial transcriptomic analysis directly comparing NMIBC progressors and non-progressors, providing a framework to define microenvironmental trajectories underlying progression to invasion. By leveraging high-resolution spatial transcriptomics to identify candidate biomarkers and potential drivers of invasion, this work may inform early risk stratification and microenvironment-targeted therapeutics aimed at preventing transition to MIBC.

#3951 Spatial mapping of B7-H3 mediated cellular plasticity in treatment naive pancreatic cancer.

Assya Legrini[1], Tengyu Zhang[1], Mari-Claire McGuigan[1], Colin Wood[1], Luke McNickle[1], Claire Kennedy-Dietrich[1], Ghazal Latifi[1], Yoana Doncheva[1], Josefina Vasquez[1], Hannah Morgan[2], Pamela McCall[2], Michail Doukas[3], Joanne Edwards[1], Nigel Jamieson[1]

[1]Univ. of Glasgow, Glasgow, United Kingdom,[2]Glasgow Tissue Research Facility, Univ. of Glasgow, Glasgow, United Kingdom,[3]Erasmus MC, Rotterdam, Netherlands

Pancreatic Ductal Adenocarcinoma (PDAC) remains one of the most lethal cancers, with only 20% of patients surviving 5 years post pancreatectomy. Despite rationale for targeting immune pathways, existing immunotherapies have provided minimal benefit to date. The immune checkpoint molecule, B7-H3, has emerged as a promising therapeutic target across solid tumours. However, its cellular origins, spatial context and clinical relevance in PDAC is poorly defined. This study aims to address this unmet need. An integrated spatial multi-omics strategy was applied across two treatment naïve PDAC cohorts. These FFPE tissue microarrays were divided into a test cohort (n=27), and a validation cohort (n=74). GeoMx regional proteomics (Bruker) was applied on section of the test cohort, while GeoMx regional whole transcriptome (Bruker), CosMx single cell 64-plex protein (Bruker) and CosMx 6K RNA (Bruker) assays were applied to serial sections of the validation cohort. Additional CosMx single cell whole transcriptome (WTx) data was generated from an Intraductal Papillary Mucinous Neoplasm (IPMN) whole section cohort (n=6). GeoMx samples were fluorescently stained with Syto13, PanCk, CD45 and αSMA, and masks were selected for PanCk+ve epithelium and tumour microenvironment (TME). CosMx samples were fluorescently stained for DAPI, PanCk, CD298/B2M, CD45 and CD68. Extensive clinicopathological data was available for all samples. Across regional protein and transcriptome profiling, B7-H3 expression was consistently elevated in TME and fibroblast enriched compartments compared to epithelium. Reduced epithelial expression significantly correlated with improved disease specific survival. B7-H3 ranked transcriptomic regional signatures revealed suppression of T-cell activation and antigen presentation pathways, alongside enrichment of fibro-inflammatory, myeloid and stromal signalling pathways. Single-cell spatial proteomics and RNA validated and resolved these signatures to discrete cellular niches. B7-H3 high tumours were characterised by dense clustering of fibroblasts, antigen-presenting macrophages and exhausted T-cell phenotypes, whereas B7-H3 low tumours demonstrated epithelial dominant clustering and increased spatial separation between B7-H3 enriched cell types and cytotoxic lymphocytes. WTx data further demonstrated graded B7-H3 expression variation from normal to dysplasia to IPMN cancer, highlighting spatial-temporal remodelling throughout oncogenesis.

Across all spatial platforms, B7-H3 consistently mapped within fibro-inflammatory and immunosuppressive niches, features strongly associated with aggressive disease and poor prognosis. Collectively, these findings establish B7-H3 as a robust spatial biomarker in PDAC and provide compelling biological rationale for therapeutic targeting of B7-H3 in a malignancy historically resistant to immune-based treatments.

#3952 Spatial multi-omics dissection of follicular lymphoma by GlycoScope-IN-DEPTH reveals a galectin-8L-driven complement-enriched, immune-exhausted microenvironment.

Stephanie P. T. Yiu[1], Ankit Basak[2], Carolina Ortiz-Cordero[2], Alex K. Shalek[2], Laura Kiessling[2], Sizun Jiang[1]

[1]Beth Israel Deaconess Medical Center, Boston, MA,[2]Massachusetts Institute of Technology, Boston, MA

Follicular lymphoma (FL), an indolent malignancy of germinal center B cells, accounts for ~40% of non-Hodgkin lymphomas. Although most patients experience slow progression, a subset undergoes transformation, and CD20-negative relapses pose a therapeutic challenge. FL is characterized by BCL2 overexpression and highly mannosylated surface immunoglobulins that engage lectins on antigen-presenting cells to sustain B-cell receptor signaling and promote immune evasion. Yet, a systematic understanding of glycan-mediated interactions within the FL microenvironment remains limited.

To address this gap, we developed GlycoScope, a multimodal spatial profiling platform that co-detects glycans and proteins at single-cell resolution in situ. Applying GlycoScope to tonsil, follicular hyperplasia (FH), and treatment-naive FL tissues, we identified selective enrichment of Galectin-8L in B cells, with significantly higher expression in FL. In tonsil and FH, Galectin-8L localized to the $BCL2^{+}$ mantle zone, whereas in FL it extended across both follicular center and mantle zones, suggesting its potential as a structural landmark to dissect the organization and local cellular architecture of lymphoid tissues.

Stepwise neighborhood analyses anchored on Galectin-$8L^{+}$ mantle-marginal zone rims revealed localized enrichment of checkpoint-expressing T cells with Galectin-$8L^{High}$ B cells. To further probe the functional states of these niches, we integrated GlycoScope with spatial transcriptomics on the same slide (GlycoScope-IN-DEPTH). Stratifying follicles by Galectin-8L expression showed that Galectin-$8L^{High}$ B cells adopt transcriptional programs enriched for immune synapse formation and complement activation, both positively correlated with Galectin-8L levels. CD4 T cells in the same cores exhibited terminal exhaustion, while macrophages displayed enhanced phagocytic and complement-cascade signatures, together indicating a coordinated, Galectin-8L–associated remodeling of the immune microenvironment.

Additional glycan-lectin imaging demonstrated that the distinct intrafollicular distribution of Galectin-8L potentiates interactions with its cognate lectin Galectin-8, which we found expressed on macrophages and T cells. These observations support a Gal8L-Gal8 interaction axis across B-T-macrophage compartments that orchestrates a complement-enriched, immune-exhausted microenvironment in FL.

Together, this integrated spatial framework highlights glycan-dependent immunoregulatory networks in FL and positions Galectin-8L as a functional landmark for mapping, and potentially targeting, dysregulated immune niches in lymphoid malignancy.

#3953 Assessing the role of immune aggregates as potential biomarkers of immunotherapy response in appendiceal adenocarcinoma (AA) using spatial proteomics.

Matt Lastrapes[1], Eleanor A. Fallon[2], Brenda Melendez[1], Bharat B. Singh[1], Davis Ingram[1], Khalida M. Wani[1], Lon W. Fong[1], Ashish Damania[1], Vivian Orellana[1], Nadim J. Ajami[1], Jillian Losh[1], Alexander Lazar[1], Kanwal Pratap Singh Raghav[1], John P. Shen[1], Melissa Taggart[1], Jennifer A. Wargo[1], Beth A. Helmink[1], Paul A. Scheet[1], Michael Geoffrey White[1]

[1]UT MD Anderson Cancer Center, Houston, TX,[2]Roswell Park Comprehensive Cancer Center, Buffalo, NY

Appendiceal adenocarcinoma is a rare tumor representing less than 1% of all gastrointestinal malignancies. Unfortunately, over 50% of AA patients present with stage IV disease with many patients being unresectable and with few systemic therapy options. Data from a recent clinical trial suggests improved overall survival on atezolizumab and bevacizumab combination therapy for patients with unresectable metastatic AA (NCT03074513). We previously studied general immune effects in a subset of these patients using spatial transcriptomics, suggesting immune aggregates like tertiary lymphoid structures (TLS) could be important biomarkers of response in AA. Here, we aim to characterize the landscape of immune aggregates using single-cell spatial proteomics to further understand potential biomarkers of immunotherapy response in AA. Single-cell spatial proteomics was performed on pre-treatment FFPE biopsies from eight trial participants using nanoString's CosMx Spatial Molecular Imager (SMI) with the 64-plex human IO protein panel. Data processing was done using nanoString's AtoMx platform and exported to the R package Seurat for analysis. Cell type annotations were obtained using CELESTA. Immune aggregates were manually identified and labeled using CosMx staining images and Napari. The profiled trial cohort (n=8) was grouped by clinical response, measured as whether a patient was alive (n=4) or deceased (n=4) at trial follow-up. Peritumoral immune aggregates were manually annotated across all patients using the CD45 staining images from AtoMx and Napari to add labels to cells. Overall, we detected 75 unique immune aggregates across 7 of the 8 patient samples profiled. At the tissue level, we identified higher Treg density ($p=0.085$, t-test) in deceased patients compared to living patients. Among cells in immune aggregates, there was a trend towards higher B cell ($p=0.14$) and fibroblast ($p=0.16$) density in aggregates from living patients. Neighborhood analysis performed within these structures uncovered 9 cellular neighborhoods, representing many components of tertiary lymphoid structures. Unsupervised clustering of immune aggregates according to cellular neighborhood composition resulted in the separation of aggregates with more germinal center B cells from others with more CD4+ and CD8+ T cells. With challenges in tissue collection and sequencing of AA surgical specimens, spatial proteomics provides a meaningful framework for studying the tumor microenvironment and treatment response in such tissues. The presence of mature immune aggregates in AA tumors suggests a potential role in driving response to immunotherapy, and work remains ongoing to further characterize these aggregates to best predict response to immunotherapy in future AA patients.

#3954 Identifying biomarkers of response in BRAF p.V600E mutant colorectal cancers (mCRC).

Gagandeep Brar[1], Brooke Rhead[2], Unnati Jariwala[2], Stamatina Fragkogianni[2], Amit Mahipal[3]

[1]City of Hope Comprehensive Cancer Ctr., Duarte, CA,[2]Tempus, Chicago, IL,[3]Case Comprehensive Cancer Center, Cleveland, OH

Background: *BRAF V600E* mutations occur in 8-12% of patients (pts) with mCRC and are associated with poor response to standard systemic therapies and low survival rates. However, a subset of pts with *BRAF V600E* mCRC have a more indolent course with response and survival rates similar to non-*BRAF* mCRC pts, suggesting that the impact of *BRAF V600E* as an oncogenic driver may be heterogeneous. Here, we explore the genomic and transcriptomic differences between responders (R) vs non-responders (NR) in *BRAF V600E* mCRC pts treated with first line (1L) systemic therapy.

Methods: The Tempus Lens Platform (Tempus AI, Inc., Chicago, IL) was used to query the Tempus multimodal de-identified database and establish and subsequently analyze a cohort of pts diagnosed with *BRAF-V600E* mCRC with xT (DNA) ± xR (RNA) testing prior to 1L chemotherapy ± bevacizumab (n=274). Pts with concomitant MSI-H/dMMR results were excluded. Pts with best response recorded at least 15 days after 1L start were classified as R (complete response/partial response/stable disease) vs NR (progressive disease). RNA expression data was normalized and quantified as transcripts per million (TPM), and compared using Wilcoxon rank-sum tests. Gene set enrichment analysis (GSEA) was performed on a curated collection of 50 gene sets defined by biological states or processes. Adjusted p-values (q-values) were computed for expression analyses using the Benjamini-Hochberg method. Landmark real world overall survival (rwOS) was defined as time from 1L treatment start +90 days until death or loss to follow up. Hazard ratio (HR) was calculated using Cox proportional hazard models and tested using a log-rank test.

Results: Patient demographics and tumor characteristics did not differ by response status, including tumor sidedness, number of metastases, location of metastases and therapy received. Median age was 64 and 59% were female in the overall cohort. The 90 day landmark rwOS analysis was longer in R vs NR (median 15.0 vs 8.8 months given survival to 90 days from 1L treatment start; HR 0.53; 95% CI [0.31-0.89, p=0.016]).Of the genes analyzed, *ARID2* (8.9% vs. 0%, p=0.006) and *FLCN* (5.4% vs. 0%, p=0.048) alterations were significantly enriched in NR (n=56) vs. R (n=96). Rs exhibited significantly higher expression of *STARD9* compared to NRs (q=0.046), as well as positive enrichment expression in the *Wnt* pathway (q=0.02) and negative enrichment in multiple pathways associated with cell proliferation, immune infiltration, angiogenesis and bile acid metabolism (q<=0.05).

Conclusions: Rs with *BRAF V600E* mCRC had improved survival outcomes and had minimal somatic and transcriptomic changes compared to NRs treated with 1L therapy at the gene level. Interestingly, GSEA revealed significant differences in Wnt, cell proliferation, immune infiltration, angiogenesis and bile acid metabolism pathways suggesting therapeutic implications that should be explored.

#3955 Spatial characterization of tumor-immune interactions in MMR-p and MMR-d among African American colorectal cancer patients using attention-based modeling.

Hassan Brim[1], Khushi Desai[2], Shweta Dixi[1], Justin Hong[2], Colles Price[3], Jonathan H. Chen[4], Nicolas Fernandez[5], Sara Sim[5], Sami Farhi[5], Rabia Zafar[1], Elham Azizi[5], **Hassan Ashktorab**[1]

[1]Howard University, Dist. of Columbia, DC,[2]Columbia, New York, NY,[3]Takeda Pharmaceutical Company Ltd., Deerfield, IN,[4]Northwestern University, Chicago, IL,[5]Broad, New York, NY

Background: Colorectal cancer (CRC) disproportionately affects African American individuals, who experience higher incidence and mortality than non-Hispanic White patients. Immune infiltration varies widely across CRC phenotypes, particularly between microsatellite instability (MSI) and microsatellite stable (MSS) tumors. Recent single-cell studies show that MSI tumors demonstrate stronger anti-tumor immunity, with coordinated variation between immune and malignant cell types, highlighting the need for spatial analyses to understand tumor-immune interactions.
Aim: To investigate spatial cellular organization in MSI and MSS tumors from African American patients using advanced computational and machine learning approaches to characterize immunomarker profiles. Methods: Spatially resolved single-cell transcriptomic profiling was performed using 10X Genomics Xenium 5k, which measures up to 5,000 genes in situ. Because such data require sophisticated processing, we employed machine learning innovations—including self-supervised learning—and robust artifact-correction tools to derive biologically meaningful signals. We introduce a pilot dataset of four CRC samples (2 MSI, 2 MSS) and present an analysis pipeline for preprocessing and annotating spatial CRC data using curated marker sets.
Results: Spatial profiling revealed distinct immune-tumor ecologies across phenotypes. MSS tumors showed depleted T/NK and B-cell populations, whereas MSI tumors exhibited higher immune-cell abundance and strong cytotoxic $CD8^+$ T-cell activity marked by elevated CXCL13, GZMA, GZMB, and GZMK expression. MSI samples also demonstrated activated T-cell programs supported by pro-inflammatory myeloid cells expressing CXCL10, consistent with an immune-hot, therapy-responsive microenvironment. In contrast, MSS tumors were fibroblast-driven and metabolically reprogrammed, characterized by high TGFB1, FAP, COL1A1, LDHA, and SLC2A1 expression, reflecting an immune-cold state with minimal T-cell infiltration. To analyze cellular communication, we applied AMICI—an interpretable attention-based model predicting a cell's gene expression from its spatial neighbors. AMICI revealed phenotype-specific interaction patterns, neighborhood length scales, and key genes mediating immune-stromal-tumor signaling.
Conclusion: This pilot study establishes an integrated spatial and computational framework for dissecting MSI-MSS differences in CRC among African American patients. Future work will expand AMICI-based analyses to further resolve neighborhood-driven phenotypes and cell-cell communication networks that shape immune infiltration and therapeutic response.

#3956 Spatial transcriptomic mapping of ER-positive breast tumors reveals immune pathway remodeling and resistance mechanisms following anti-PD-1 therapy.

Oliver J. De Sa[1], Megan Hopkins[1], Angel Arnaout[1], Arif Awan[2], Gregory Pond[3], Jane Bayani[1], Melanie Spears[1]

[1]Ontario Institute for Cancer Research, Toronto, ON, Canada,[2]Ottawa Hospital Research Institute, Ottawa, ON, Canada,[3]Assistant Professor, Dept. of Oncology, Department of Oncology, McMaster University, Hamilton, ON, Canada

Estrogen-receptor-positive (ER+) breast cancers (BCs) make up approximately 70%-80% of BC cases and demonstrate low lymphocyte infiltration, mutational burden, and modest objective response rates to immune checkpoint blockade (ICB), making them attractive candidates for novel immunostimulatory combination therapies. Here, we employ CosMx Single Cell Imaging (SMI) technology to spatially profile the transcriptional landscape of ~6000 targets in 9 ER+ BC patients, both pre- and post-treatment with the anti-PD-1 antibody Cemiplimab, to identify spatially resolved mechanisms of resistance and potential therapeutic targets. After quality control, ~3.1 million cells across 18 unique tissue sections were analyzed, allowing for robust characterization of immune, stromal, and epithelial cell niches with the ability to identify rare immune cell subsets at a high resolution. Comparing relative abundances of cell types of patients pre- and post-therapy, we see a high concordance of cell-types between tissue sections of the same patient. While 8/9 patients were dominated by Luminal A/B cancer epithelial cells, one patient had purely basal cancer epithelial cells, highlighting the value in spatial transcriptomic platforms for molecular subtyping in BC patients. To define metrics of patient response to Cemiplimab therapy, we quantified changes in tumor-intrinsic inflammatory/immune pathways and leveraged spatial information to calculate changes in tumor-infiltrating lymphocytes (TILs). 3/9 patients showed increased levels of type I/II IFN signaling in the tumor epithelium, 5/9 showed no change, and 1/9 showed a sharp decrease, coinciding with a unique increase in TNF-α signaling via NF-κB. 6/9 patients showed increases in TILs following therapy, defined as the fraction of tumor cells ≤ 0.1 mm from the nearest CD8 T-cell. The patient with the most pronounced decrease in TILs was the same patient who showed reduced IFN signaling previously, indicating agreement between response indicators, and suggesting upregulation of TNFa signaling via NFkB as a resistance mechanism to T-cell invasion. Our early work provides a comprehensive spatially resolved analysis of the mechanisms through which ER+ BCs resist ICB, suggesting that spatially mapped transcriptional programs can uncover actionable resistance pathways, and guide the design of next-generation immunotherapeutic combinations for ER+ BC.

#3957 Spatially derived transcriptomic predictors of immune checkpoint blockade outcome in advance gastric cancer.

Changjin Hong[1], Sunho Park[1], Jean R. Clemenceau[1], Minji Kim[1], Inyeop Jang[1], Seock-Jin Chung[1], Sung Hak Lee[2], Sam C. Wang[3], Tae Hyun Hwang[1]

[1]Section Surgical Research, Vanderbilt University Medical Center, Nashville, TN,[2]St. Mary's Hospital Pathology, The Catholic University of Korea, Seoul, Korea, Republic of,[3]Department of Surgery, University of Texas Southwestern Medical Center, Dallas, TX

Background: Advanced gastric cancer (GC) responds poorly to systemic therapy, including Immune Checkpoint Blockade (ICB), yet how the tumor microenvironment (TME) drives resistance remains unknown. We assembled the largest spatial transcriptomic dataset in Immune Checkpoint Blockade (ICB)-treated GC, derived signatures encoding spatial composition and their cellular functions and phenotypes, and validated these as outcome predictors across bulk, single-cell, and independent spatial cohorts.
Methods: Pre-treatment samples from advanced GC patients receiving ICB were profiled using spatial transcriptomics to derive spatial signatures that deconvolve immune, stromal, and tumor compartments and capture TME niches associated with ICB non-response. These spatial signatures were projected onto multiple external datasets, including four bulk RNA-seq cohorts, one single-cell RNA-seq cohort, two 10x Visium cohorts (27 GC samples), and one proteomic cohort, representing the largest integrated validation set for GC immunotherapy biomarkers to date.
Results: Spatial immune signatures in non-responders showed Th2, regulatory Th17, and a homing-lymphocytes program marked by VLA-4 and CXCR4, confirmed in scRNA-seq. Stromal signatures in non-responders included inflammatory CAF programs, complement system activation (C1S, C3, A2M, IL6ST), growth-factor signaling, and MHC-II antigen-presenting states. When projected onto bulk RNA-seq and proteomic cohorts, these spatial immune and stromal modules were consistently enriched in clinical non-responders and associated with inferior survival. In 10x Visium data, non-responder stroma exhibited a strong complement system, aligned with ECM remodeling and myofibroblast properties, and showed reduced neighboring T-cell infiltration. Spatial bivariate analyses localized MHC genes and M2-like $C1q^{+}$ macrophages to inflamed stromal niches. Additional non-responders, including an MSI-H case, retained Th2-dominant profiles, whereas responders revealed higher tumor-antigen expression and dendritic-cell activation.
Conclusion: Spatially derived transcriptomic signatures that incorporate functional states of the GC immune microenvironment robustly distinguish ICB non-responders across bulk, single-cell, and independent spatial datasets. These data nominate the inflammatory stromal niches, $C1q^{+}$ macrophage clusters, and skewed Th2 as actionable features of ICB resistance and potential therapeutic targets. Our results support incorporating spatial transcriptomics into pre-treatment assessment to refine patient selection, prioritize combination strategies that remodel the stromal-immune interface, and advance toward clinically deployable, GC-specific biomarkers for immunotherapy.
AI was used for language editing only; authors are responsible for all content and approved the final version.

#3958 Spatial transcriptomic profiling of peritoneal metastases identifies multicellular programs in patient tumors undergoing pressurized intraperitoneal aerosol chemotherapy (PIPAC).

Heini Maaret Natri[1], Arianna L. Williams-Katek[1], Muhammad Talha Waheed[2], Tiana Li[3], Marwan Fakih[4], Mingye Feng[5], Amit Merchea[6], Sue Chang[7], Richard L. Whelan[8], Danielle Deperalta[8], Thanh H. Dellinger[2], Nicholas Banovich[1], Mustafa Raoof[2]

[1]Division of Bioinnovation and Genome Sciences, TGen (The Translational Genomics Research Institute), Phoenix, AZ,[2]Department of Surgery, City of Hope, Duarte, CA,[3]Department of Cancer Genetics and Epigenetics, City of Hope, Duarte, CA,[4]City of Hope National Medical Center, Duarte, CA,[5]Department of Immuno-Oncology, City of Hope, Duarte, CA,[6]Department of Surgery, Mayo Clinic, Jacksonville, FL,[7]Department of Pathology, City of Hope, Duarte, CA,[8]Department of Surgery, Northwell Health, New York, NY

Peritoneal Carcinomatosis (PC) is a metastatic cancer of the lining of the abdominal cavity, most often originating from the gastrointestinal or gynecological tracts. PC occurs in approximately 20% of colorectal cancer and 60% of ovarian cancer cases, with estimated 5-year survival rates as low as 6%.

Pressurized intraperitoneal aerosolized chemotherapy (PIPAC) is a locoregional drug delivery modality administered via a minimally invasive laparoscopic approach. PIPAC shows promise in the treatment of peritoneal metastasis in early trials on colorectal cancer (CRC) or appendiceal cancer (AC) in patients who cannot undergo cytoreductive surgery.

The spatial organization of the tumor microenvironment (TME) and the complex cellular interactions within profoundly shape biology and treatment response. Spatial transcriptomics offers an opportunity to characterize TME heterogeneity in its native architecture, allowing the identification of biomarkers, interactions, and gene expression programs as well as resistance mechanisms and new potential targets.

We performed image-based spatial transcriptomic profiling of 152 tissue samples, including 50 pre-treatment and 65 post-treatment metastatic tumors and 17 pre-treatment and 20 post-treatment tumor-adjacent normal tissue samples from 19 patients who participated in a Phase I trial on Oxaliplatin PIPAC. Through a comprehensive characterization of transcriptional profiles of a total of 1,249,711 cells, as well as cellular neighborhood and ligand-receptor interactions, we describe the heterogeneity of PC in its spatial context.

We have further characterized treatment-driven changes in pre- and post-treatment tumors of a subset of 7 patients who underwent PIPAC with mitomycin IP. Through cell-based niche and proximity analyses, we identify distinct shifts in the composition and architecture of treated tumors. Most notably, treatment resulted in an 87% decrease in the number of malignant cells, as well as an expansion of the plasma-barrier niche and an increased number of immune infiltrates. Further analysis revealed distinct differences in the abundance of specific cancer-associated fibroblast and immune subsets, demonstrating changes in TME architecture.

Overall, our results provide an invaluable characterization of PC in CRC and AC, garnering new insight into their architecture, cellular composition, and cell-cell interactions at baseline and in response to regional chemotherapy. Further analyses and follow-up studies can identify and validate new, actionable biomarkers to target these hard-to-treat tumors.

#3959 Novel methodology to explore glioma malignant transformation with spatial multi-omics.

Michal Polonsky[1], Jonathan Fox[1], Sheel Shah[2], Noa Hadas[1], Richard Everson[2], Long Cai[1]

[1]Biology and Biological Engineering, CalTech - California Institute of Technology, Pasadena, CA,[2]Neurosurgery, UCLA, Los Angeles, CA

Low-Grade Gliomas (LGG) generally have an indolent course and good prognosis after maximal safe resection; however, these tumors can progress into high grade gliomas through a poorly understood process of Malignant Transformation (MT). We sought to identify molecular drivers and cellular interactions predictive of MT, with the aim of informing early detection and providing new treatment targets. We developed a novel spatial multi-omics approach termed seqFISH+ which allows us to quantify the transcriptional states and DNA profiles of single cells within patient biopsies. With this approach, clones of cancer cells can be identified by shared DNA profiles, and matched with their transcriptional profiles and cellular interactions within the tumor microenvironments. We applied our experimental methodology to biopsies of 19 LGG patients as well as three Glioblastoma patients and compared the transcriptomic and genomic landscape of LGG patients which underwent MT to those that did not. We used a tailored gene panel to measure expression of 1150 genes and identified 12 cell types within the tumor biopsies encompassing malignant cell subtypes, immune cells and normal stromal cells. In addition to transcriptomic data, our novel pipeline allowed us to quantify hundreds of DNA loci within the same cells encompassing the entire genome at 3.3Mb resolution. Our final data set contained transcriptomic data of >600k single cells with matched DNA data for >200k cells. With our transcriptomic data we were able to identify known as well as novel gene markers associated with malignancy of LGG tumors. Our DNA data identified known chromosomal alterations such at 1p/19q deletion within malignant cells. As the location of the cells is left intact, we can now probe the spatial organization of the tumor-microenvironment and identify spatial signatures correlating with MT. DNA information will be used to identify individual cancer clones which contribute to progression. This information will enable us to identify clinically relevant molecular events and cellular interactions, which can be used as biomarkers for progression. With this highly multiplexed data we are constructing a comprehensive dictionary of cell intrinsic changes coupled with changes in the microenvironment to elucidate drivers of the MT process.

#3960 Spatially resolved transcriptomic signatures of gallbladder carcinogenesis from precursor to undifferentiated stages.

Yeseul Kim[1], Yoseob Lee[2], Harim Oh[1], You-Na Sung[1], Yoo Jin Lee[1], Yona Kim[1], Inho Park[3], Jinhyuk Bhin[2], Su-Jin Shin[3]

[1]Department of pathology, Korea University Anam Hospital, Seoul, Korea, Republic of,[2]Department of Biomedical Sciences, Yonsei University College of Medicine, Seoul, Korea, Republic of,[3]Department of pathology, Gangnam Severance Hospital, Seoul, Korea, Republic of

Background: Biliary intraepithelial neoplasia (BilIN) is recognized as a precursor lesion of gallbladder carcinoma. However, the transcriptomic alterations underlying the sequential process of carcinogenesis remain poorly understood. Moreover, the differentiation status of gallbladder carcinoma varies among patients, with some tumors exhibiting both differentiated and undifferentiated components within the same tumor. To elucidate key transcriptomic changes across this histologic spectrum, we performed spatial transcriptomic analysis on gallbladder tumor samples containing coexisting areas of normal epithelium, BilIN, differentiated carcinoma, and undifferentiated carcinoma to understand the molecular differences between lesions within individual patients.
Methods: A total of 59 regions of interest (ROIs) were selected from 13 patients, including normal (n = 11), dysplasia (n = 14), differentiated carcinoma (n = 22), undifferentiated carcinoma (n = 8), and metastatic lesions (n = 4). Spatial transcriptome profiling was performed using GeoMx Digital Spatial Profiling (GeoMx DSP) with EpCAM staining. The maximum size of each ROI was 750 × 625 μm, and each ROI included at least 200 cells. From GeoMx DSP-derived expression profiles, gene-expression dynamics were patterned via A-orthogonal nonnegative matrix factorization (AONMF), and epithelial-stromal crosstalk was inferred via weighted gene co-expression network analysis (WGCNA).
Results: Pathway enrichment analysis revealed bile acid metabolism and fatty acid metabolism were highest in normal spectrum and progressively diminished with histological worsening. From the differentiated spectrum, cell proliferation programs were upregulated, and the undifferentiated spectrum was characterized by EMT signature. Epithelial-stromal interaction analysis showed a TNC-ITGB1 axis in epithelial regions that activates TGF-β signaling in stromal cells within undifferentiated carcinoma. Patients harboring undifferentiated carcinoma exhibited distinct transcriptional patterns within the differentiated regions, showing increased HDGFL3 and decreased MMP1 expression compared with patients without progression to undifferentiated carcinoma, suggesting that HDGFL3 upregulation may represent an early molecular cue preceding dedifferentiation.
Conclusion: This study provides spatial transcriptomic insights into the sequential carcinogenic process of gallbladder tumorigenesis. EMT pathway is elevated in the undifferentiated spectrum in association with the TNC-ITGB1 axis, and HDGFL3 is upregulated in differentiated regions of patients harboring undifferentiated components. Thus, upregulation of HDGFL3 may serve as potential predictive biomarkers for the progression from BilIN to undifferentiated gallbladder carcinoma.

#3961 Identifying the molecular signature of infiltrating edge cells in glioblastoma as drivers of tumour invasion and recurrence.

Alyona Ivanova[1], Shamini Ayyadhury[2], Yanxia Ma[3], Xuehong Gui[3], Akshay V. Basi[3], Megan Yijun Wu[4], Trevor J. Pugh[5], David G. Munoz[6], Sungnam Cho[3], Tosin Oyewale[7], Lucas Schutz[7], Chibawanye I. Ene[3], Jared K. Burks[3], Sunit Das[8]

[1]University of Toronto, Toronto, ON, Canada,[2]PMGC, UHN, Toronto, ON, Canada,[3]MD Anderson, Houston, TX,[4]Lab Research Project Coordinator, The Hospital for Sick Children, Toronto, ON, Canada,[5]UHN Princess Margaret Cancer Centre, Toronto, ON, Canada,[6]St. Michael's Hospital, Toronto, ON, Canada,[7]Ariadne.ai, Heidelberg, Germany,[8]Asst. Professor, Dept. of Surgery, University of Toronto, Toronto, ON, Canada

Glioblastoma (GBM) is the most common malignant brain tumor in adults. Despite extensive research, there haven’t been remarkable gains in resolving the seeds of GBM recurrence, and the outcomes for many patients suffering from this devastating disease remain poor. Our knowledge on GBM heterogeneity is mostly restricted to the surgically resectable tumor core, while functional characterization of tumor cells at the infiltrating edge remains largely elusive due to the presence of normal functional brain tissue in the peritumoral lesion. Edge-derived cells exhibit larger capacity for infiltrative expansion and are the main drivers of treatment failure and tumor recurrence, making them action targets for novel treatment approaches.In this study, we present a first-of-its-kind integrative spatial investigation of GBM, combining two complementary spatial omics modalities high-definition spatial transcriptomics (ST - Visium HD) and spatial proteomics (SP - COMET) to achieve a comprehensive morphological, transcriptomic, and proteomic characterization of invasive tumor edge in situ. This multimodal spatial framework enabled to resolve the complex molecular landscape of the GBM periphery and to identify druggable biomarkers specific to edge-derived malignant cell populations.By integrating pathologically annotated H&E images with high-resolution spatial gene expression, we delineated patterns of tissue architecture and captured continuous gradients of gene expression across tumor-brain interface. Using NicheCompass, we dissected tissue hierarchies and spatially localized cellular processes within the infiltrative compartment of GBM. Through unsupervised phenotyping, we identified top spatially variable genes and active gene programs, revealing modules indicative of tumor cell hijacking of neuronal pathways. These findings align with previously described mechanisms of glioma-neuron synaptic coupling and formation of neurite-like tumor microtubes, consistent with enrichment of OPC- and NPC-like cellular states at tumor margin.Complementing the transcriptomic layer, SP was used to guide single-cell segmentation for ST analysis, infer cell types based on canonical phenotypic markers, and characterize cell state and function through protein-level profiling. This dual-modality approach allowed for precise spatial mapping of highly invasive edge cell populations and their functional states.By integrating multiple spatial omic layers, our study provides an unprecedented multimodal view of GBM invasion and identifies novel, spatially defined biomarkers that distinguish malignant edge-derived cells. These findings hold potential translational value as diagnostic and prognostic tools, enabling early assessment of treatment response and facilitating personalized therapeutic strategies aimed at mitigating GBM progression and recurrence.

#3962 Same-species multiplex IF with HCR™Gold IF: Cross-clone benchmarking using Abcam's oncology-validated primaries.

Wudy Yang[1], Randy Chen[1], Harry Choi[1], Aneesh Acharya[1], Will Howat[2]

[1]Molecular Instruments, Inc., Los Angeles, CA,[2]Abcam, Cambridge, United Kingdom

Background: Spatially resolved, multiplexed immunofluorescence (mIF) is essential for oncology research to profile tumor-immune architecture, track pathway activation, and stratify biomarkers in precious FFPE specimens. Conventional mIF is often limited by species constraints, secondary antibody cross-reactivity, and custom conjugations that slow panel development. Here, we present a plug-and-play workflow that pairs HCR™ Gold IF and Encoder reagents with Abcam's broad portfolio of primary antibodies to deliver robust same-species multiplexing with minimal optimization and rapid turnaround, streamlining setup from antibody order to imaging in about one work week.

Methods: The HCR™ HiFi Encoder binds with high affinity to the Fc domain of unmodified primary antibodies, forming a stable 1:1 complex without compromising antigen recognition. This encoding process is fully compatible with commonly used antibody buffers. Human cancer lines and FFPE tumor sections (e.g., lung, breast, colorectal) were processed using standard fixation/antigen retrieval, permeabilization, and blocking. Off-the-shelf Abcam primary antibodies were HiFi-encoded and detected with fluorophore-labeled HCR™ Gold amplifiers. Multiplexing was achieved by assigning orthogonal HCR™ initiators to each unmodified antibody, allowing simultaneous detection of multiple targets within a single sample. No primary conjugation or iterative stripping steps were required. Panels included oncology-relevant markers for epithelium (panCK), immune subsets (CD3, CD8, CD68), proliferation (Ki67), and stroma (a-SMA).

Results: Same-species multiplexing with Abcam primary antibodies produced high-contrast images that preserved expected subcellular/localization patterns across tumor cells, immune compartments, and stroma. Orthogonal Encoders minimized channel crosstalk and HCR™ Gold amplification yielded bright, linear signals suitable for quantitative comparisons across regions of interest. Replicate runs across tissues showed consistent signal-to-background and spatial patterns. Panel build time was markedly reduced; researchers can purchase Abcam antibodies and generate imaging-ready data in ~5 days, enabling rapid iteration of oncology panels and testing of alternative clones.

Conclusions: HCR™ Gold IF with Encoders provides a practical, cancer-focused solution for standardized, same-species multiplex IF using widely available Abcam primary antibodies. The enzyme-free, isothermal amplification preserves epitopes while delivering sensitive, reproducible signals, supporting robust characterization of the tumor microenvironment, pathway activity, and checkpoint expression from limited clinical material. This streamlined, plug-and-play approach lowers barriers to spatial biomarker studies and accelerates discovery and translational research.

#3963 Spatially Resolved Cell-Cell Communication Reveals Intra-tumoral heterogeneity in Small Cell Lung Cancer.

Tingxiao Gao, Jalal Kazan, Fatema Zohora, Gregory Schwartz, **Benjamin Lok**

Medical Biophysics, University of Toronto, Toronto, ON, Canada

Introduction: Small cell lung cancer (SCLC) is an aggressive neuroendocrine malignancy with a 5-year survival rate of only 7%. Despite ongoing advances, most patients derive limited benefit from existing therapies, underscoring the need to better understand mechanisms of SCLC progression and resistance. Cell-cell communication (CCC) through ligand-receptor (LR) interactions has been studied to have a key role in regulating process that influence tumor cell plasticity and spatial organization. We hypothesize that tumor-tumor CCC mediates heterogeneity within SCLC and contributes to its aggressive phenotype. Method: We generated spatial transcriptomic profiles from two SCLC circulating tumor cell-derived xenograft (CDX) samples at single-cell resolution using VisiumHD. Hematoxylin and eosin (H&E) staining confirmed the neuroendocrine morphology of each sample by an expert pathologist. We inferred CCC using CellNEST, a graph neural network model our lab developed to detect intercellular LR interactions directly from spatial transcriptomic data. Results: Across both CDX samples, we identified 380,790 high-confidence LR interactions at single-cell resolution. The five most frequently observed LR pairs were L1CAM-L1CAM (n=5430), MDK-PTPRZ1(n=5260), NECTIN1-NECTIN1(n=4172), VEGFA-NRP1 (n=2984) and GRN-SORT1 (n=2840). These LR pairs are biologically consistent with known pathways in SCLC, including those regulating cell adhesion, angiogenesis, and neuroendocrine differentiation. By spatially mapping these recurrent LR back to the tissue, we further revealed interesting region-specific communication patterns, suggesting that CCC contributes to transcriptionally and morphologically distinct tumor subregions. Discussion: This study provides spatially resolved characterization of tumor-tumor interactions in SCLC CDX models at single-cell resolution. By identifying highly recurrent LR interactions and mapping their spatial organization, we aim to uncover potential biological mechanisms underlie intra-tumoral heterogeneity. Ongoing work will expand this framework to larger SCLC cohorts to identify CCC-driven transcriptional programs and evaluate their potential as biomarkers and therapeutic targets to shed light on future therapeutic strategies for SCLC.

#3964 Spatial profiling of the neuroblastoma tumor microenvironment using seqFISH.

Christopher Riccardi[1], Michal Polonsky[2], Michael J. Zobel[1], Rebekah Kennedy[1], Melody Khoshneviszadeh[1], Anya Zdanowicz[1], Bruce Pawel[1], James Amatruda[1], Long Cai[2], Shahab Asgharzadeh[1]

[1]Children's Hospital Los Angeles, Los Angeles, CA,[2]California Institute of Technology, Pasadena, CA

Background: Neuroblastoma is the most common extracranial solid tumor of childhood, and high-risk disease remains difficult to treat. Increasing evidence suggests that interactions among tumor cells, immune populations, and stromal elements influence progression and therapeutic response. However, the spatial organization and subtype diversity of these populations within intact tumors remain poorly defined.

Methods: We applied seqFISH, a spatial transcriptomic platform, to eight regions of interest (ROIs) from fresh-frozen tumors of seven patients using a custom 2,514-gene panel, and to three ROIs from two tumors using a commercial 516-gene immuno-oncology panel. Tumor specimens represented a range of clinical risk groups and included primary, metastatic, MYCN-amplified, and post-therapy states. All samples were analyzed and integrated using the scVI Python package, a deep generative model that extracts latent embeddings from high-dimensional data while mitigating batch effects and preserving biologically relevant structure. To assign cell identities, we developed a novel joint-analysis algorithm that integrates seqFISH data with the NBAtlas single-cell RNA-seq reference (362,991 cells across 61 patients), enabling initial mapping of major neuroblastoma, immune, and stromal lineages, followed by refinement through spatial context, proximity relationships, and canonical marker gene expression. CAFs, TAMs, and T-cell populations were re-integrated separately to resolve subtype structure, and spatial statistics methods were used to identify cell-type associations occurring more frequently than expected by chance.

Results: We profiled over 450,000 spatially resolved cells and identified major cell types with high-confidence NBAtlas-guided assignments. Neuroblastoma tumor cells displayed proliferative signatures associated with clinical risk, mirroring patterns observed in NBAtlas. We resolved diverse stromal states - including vascular, inflammatory, interferon-stimulated, myofibroblastic, and tumor-like CAFs - and distinguished M1- and M2-like TAM subsets in situ. Spatial analyses revealed conserved neighborhoods, including enrichment of $CD4^+$ naïve/central-memory T cells adjacent to inflammatory CAFs and strong co-localization between vascular CAFs and endothelial cells.

Conclusion: By integrating seqFISH with a large neuroblastoma single-cell reference, we generate a detailed spatial map of the neuroblastoma tumor microenvironment. This combined approach enables refined identification of cellular subtypes and reveals reproducible microenvironmental structures that may influence tumor behavior and therapeutic vulnerability. Ongoing efforts include expanding sample size, incorporating *spatial* copy-number analysis, and applying this framework to additional pediatric solid tumors.

#3965 Spatialomics detection of neuroendocrine involvement in cancer tissue.

Scott T. Clarke, Chris Vonnegut, Leticia Montoya, Mae Voeun, Wenjun Zhou, Anna Cartier, Aleksey Rukavishnikov

Thermo Fisher Scientific, Waltham, MA

The study of neuroendocrine involvement observed in inflammation, neuronal damage, cancer, and neurodegenerative disease is an emerging field offering new opportunities of intervention and treatment of currently intractable disease. Cancer cells are known to invade the space surrounding neurons (perineuronal invasion) and derive pro-survival and anti-apoptotic benefits from the nerve fibers and their neurotransmitters, secreted amines and peptides. Formation of new neural tissue is a characteristic of cancer with poor prognosis. We present a spatial-omics approach of multiplexing immunohistochemistry (IHC) with mRNA in situ hybridization (ISH) detection to examine the microenvironment of neuroendocrine involvement and the biomarkers relevant to these tissues and infiltrating immune cells. We image both protein and mRNA abundance and distribution in FFPE tissue with neuroendocrine involvement. ISH detection uses single stranded branched DNA amplification scheme (ss-bDNA) for single molecule detection, while IHC detection uses direct antibody labeling for moderate and high abundant targets and enzymatic signal amplification for low abundant targets. We present protocol modifications with significant improvements minimizing incompatibility between IHC and ISH otherwise resulting in diminished or loss of signal. These modifications retain IHC and ISH signal, minimize auto-fluorescence, and shorten protocol time required for multiplexed workflows. We show multiplex IHC labeling of neural biomarkers such as S100B, CD56, glial fibrillary acidic protein (GFAP), chromogranin A (CgA) and synaptophysin in relevant tissue which are often over-expressed in non-endocrine structures and tissues of some tumors, and in neurodegenerative disease models. The presence of neural mRNA expression, combined with immune markers such as FoxP3 and PD-1, PD-L1 and proliferation markers of PCNA and Ki-67 in cancer tissue, reveal the neuroendocrine involvement in the tumor immune microenvironment. For Research Use Only. Not for use in diagnostic procedures.

#3966 *In situ* spatial multiomic profiling of breast cancer tissue utilizing the CosMx Spatial Molecular Imager.

Megan Hopkins[1], Oliver De Sa[1], Dan Dion[2], Vida Talebian[2], Jane Bayani[2], Melanie Spears[2]

[1]Diagnostic Development, Ontario Institute for Cancer Research, Toronto, ON, Canada,[2]Ontario Institute for Cancer Research, Toronto, ON, Canada

Breast cancer is a leading cause of cancer-related death among Canadian women. Advances in treatment have underscored the importance of tumor heterogeneity, and the diverse cellular composition of the tumor microenvironment across molecular subtypes. The evolution of single cell imaging technologies now allows researchers to incorporate spatial context when evaluating these complex cellular interactions, allowing cellular and sub-cellular resolution across the proteome and transcriptome. In this study, a 100-core tissue microarray (TMA) from 25 breast cancer tissue blocks spanning molecular subtypes was utilized. A single 5-micron section was subjected to two consecutive rounds of staining for CosMx SMI proteomic profiling using the 64-plex Immuno-Oncology assay followed by transcriptomic profiling using the 6K RNA assay. In total, 102 fields of view (FOVs) were profiled following the CosMx Multiomic Assay protocol (MAN-10201-04). After quality control of the protein assay, we profiled 175,139 cells identifying a mean of sixty-seven unique proteins per cell. With subsequent staining for the 6K RNA assay, 120,797 cells were profiled, using the overlaid FOV map for downstream data stitching, identifying a total of 6,176 genes, a mean of 365 unique genes per cell, and a mean of 556 transcripts per cell. To check concordance of cell typing, we identified HER2 as a consistent target between the clinically reported data, inclusion in the protein panel and inclusion (ERBB2) in the RNA panel. We found all core HER2 expression measured via the CosMx SMI matched the clinical annotations, and a strong correlation between HER2 protein expression and ERBB2 gene expression across the entire flow cell ($r=0.79$, $p=5.71e-23$). Conversely, Ki67 displayed a weak correlation ($r=0.13$, $p=0.201$), highlighting the importance of evaluating both metrics to discern a full picture of biological processes. CELESTA cell typing identified various structural cells expected to be found in breast tissue within the proteomic profiling (adipose, endothelial, epithelial, and vascular smooth muscle cells), along with various immune populations including B cells, CD4+, CD8+ T-cells, dendritic cells, natural killer cells, neutrophils, macrophages, and fibroblasts. These findings were corroborated in the transcriptomic data, with InSituType supervised clustering (BreastCancer_Wu.RData) revealing populations of cancer associated fibroblasts (CAFs), tumor associated macrophages (TAMs), tumor infiltrating lymphocytes (TILs), both naïve and memory B cells, along with basal, HER2+, Luminal A and Luminal B epithelial cell populations. In ongoing work, we continue to integrate proteomic and transcriptomic data to further investigate unknown cell populations found across the TMA and categorize fundamental differences in tumor epithelium interactions across molecular subtypes of breast cancer.

#3967 Spatial whole transcriptomic profiling of breast cancer tissue with CosMx Spatial Molecular Imager.

Megan Hopkins, Oliver De Sa, Dan Dion, Vida Talebian, Jane Bayani, Melanie Spears

Ontario Institute for Cancer Research, Toronto, ON, Canada

Spatial transcriptomics provides an opportunity to investigate the relationship between gene expression and tissue architecture, revealing new insights into cell-to-cell interactions that promote tumorigenesis, immune evasion, and other disease mechanisms. Here we employ the CosMx SMI Whole Transcriptome assay to profile 87 cores from a tissue microarray (TMA) of 25 breast cancer blocks spanning molecular subtypes. A single 5-micron section was stained following Bruker's published protocol (MAN-10184-06) with the Human Whole Transcriptome Panel (WTX), 19K-plex, utilizing 37,872 imaging barcodes to capture over 18,000 genes in the human protein-coding transcriptome. We analyzed 154,213 cells and identified 18,934 genes overall, with mean transcripts per cell of 926, and in the 90^{th} percentile identifying 2,060 transcripts per cell. Cells were assessed for quality control, normalized and cell-typed using InSituType with a reference profile of well-defined breast epithelial, stromal, and immune cells. We compared molecular subtyping of the cancer epithelium as assigned by InSituType with subtyping by histology, finding a high overall concordance between core-level subtype assignment and spatial single-cell assignments. Strikingly, basal cell types were present at high levels across all cores regardless of subtype, making up 98%, 64%, 50%, and 30% of triple negative, Luminal A, HER2, and Luminal B cores, respectively. HER2 enriched cells were the most unique, making up ~45% of HER2 core cells and <1% of cells in other cores. These results display the heterogeneity of tumor cell composition and emphasize the value of single-cell resolution in molecular subtyping when designing targeted therapeutics. We next investigated immune cell compositions of all cores and found Myeloid lineages to be the most dominant, followed by T and B cells. Immune cells were similar in composition across different subtypes, however, varied by their spatial distribution in the tumor, with the triple negative subtype displaying the highest level of tumor infiltration. In ongoing work, we continue to characterize inter- and intra- core heterogeneity to further understand how local immune niches and the surrounding microenvironment shape the initiation or suppression of tumorigenic programs.

#3968 Spatial transcriptomic features associated with response to neoadjuvant therapy in triple-negative breast cancer.

Shiqing Liao, Teia Noel, Joseph Lownik, Pavithra Nedumaran, Yoona Yang, Richard Mebane, Aagam Shah, Andrew Martinez, Akil A. Merchant, Simon Knott

Cedars-Sinai Medical Center, Los Angeles, CA

Background: The KEYNOTE-522 trial established pembrolizumab plus neoadjuvant chemotherapy as a standard for early-stage triple-negative breast cancer (TNBC) by significantly improving pathologic complete response (pCR) and event-free survival. Yet biomarkers predicting response and the biology underlying residual disease—particularly the divergent outcomes observed among patients with residual cancer burden class 2 (RCB2) from chemotherapy only and chemotherapy plus immunotherapy—remain poorly defined. We hypothesized that spatial cellular architectures at diagnosis, and their longitudinal remodeling with therapy, govern TNBC treatment response and resistance.

Methods: We performed single-cell resolution spatial transcriptomic profiling on 131 diagnostic biopsies, 161 resection specimens, and 38 metastatic lesions from patients treated with neoadjuvant chemotherapy with or without pembrolizumab, including 50 paired pre/post-treatment samples for longitudinal analysis. A 60-marker spatial proteomic panel provided cross-modality validation. Spatial features, including cell-type abundance, co-localization, tumor-immune interface structure, and niche organization, were evaluated across pCR versus non-pCR groups, RCB classes (0-3), and longitudinal transitions within each therapeutic arm.

Results: Across 6 pathologist-annotated histologic regions, we resolved 17 major cell types, 72 gene-defined subtypes, and 96 spatial communities. Early analyses highlight contrasting $CD8^+$ T-cell spatial states: intra-tumoral $CD8^+$ infiltration characterizes responders, whereas stromal-restricted $CD8^+$ localization, together with $CD33^+$ myeloid programs, marks non-response and T-cell exclusion. Additional cohort-specific variation was observed in fibroblast density, stromal architecture, and myeloid-lymphoid proximities. Integrating diagnostic and longitudinal spatial features, we are developing an interpretable spatial risk score to distinguish treatment response and RCB class.

Conclusions: This study represents one of the largest integrated spatial transcriptomic and proteomic analyses of TNBC neoadjuvant therapy to date. Emerging patterns suggest that cytotoxic T-cell access to tumor nests marks effective anti-PD-1 response, whereas fibroblast-driven stroma and myeloid-mediated exclusion underlie resistance. These insights provide a roadmap for designing combination therapies to overcome stromal and myeloid barriers to neoadjuvant immunotherapy.

#3969 Stereoseq spatial transcriptomics reveals cell-type contributions to prostate cancer metastasis.

Jonathan Panzer[1], Shannon Carskadon[2], Albert Levin[1], Sean Huang[3], Vikrant Kumar[3], Indra Adrianto[1], **Nallasivam Palanisamy**[2]

[1]Public Health Sciences, Henry Ford Health, Detroit, MI,[2]Urology, Henry Ford Health, Detroit, MI,[3]MIRXES Lab Private Limited, Singapore, Singapore

Prostate cancer remains a significant cause of morbidity and mortality among men, with African-American (AA) men experiencing a disproportionate disease burden. Although molecular profiling has advanced our understanding, the cellular origins and spatial microenvironmental transitions that drive malignant progression and metastatic potential remain incompletely defined. To characterize these transitions, we performed high-resolution spatial transcriptomic profiling on benign (n = 1) and malignant (n = 2) prostate tissues obtained from three AA men using STEREO-seq (SpaTial Enhanced REsolution Omics-sequencing), generating 83,144 cell-bins across all samples. Data were processed using the STEREO-seq Analysis Workflow (SAW v6.0) and analyzed with Stereopy and Seurat. Cell-type annotation was performed using Azimuth with the Prostate Cell Atlas as a reference, and stringent quality filters (>20% mitochondrial RNA or annotation confidence <0.5) resulted in 63,861 high-confidence annotations. Spatial niche characterization was performed using QUICHE (QUantitative InterCellular nicHe Enrichment) to define microenvironmental structure and cell-cell ecosystems. Compositional analysis revealed a pronounced expansion of club epithelial (CE) cells in malignant tissues, with enrichment correlating with tumor grade, accompanied by a marked reduction in fibroblasts. CE cells in high-grade lesions showed strong upregulation of LTF (avg_log2FC = 6.92, padj = 7.9×10^{-67}), while fibroblasts exhibited widespread loss of actin-associated genes (ACTG2, ACTA2, ACTB), indicating cytoskeletal disruption and microenvironmental remodeling. Basal epithelial cells displayed near-complete loss of KRT15 expression (avg_log2FC = -4.92, padj = 6.1×10^{-281}), suggesting depletion of structural epithelial populations and glandular destabilization. QUICHE analysis revealed distinct tumor-associated spatial niches highly enriched for CE cells, whereas fibroblast-rich niches dominated benign regions. Differential niche-level expression recapitulated global transcriptomic patterns, including loss of tumor suppressor gene activity, architectural breakdown of glandular structures, and activation of pathways implicated in invasion and metastasis. These findings highlight substantial shifts in cellular composition and spatial organization accompanying malignant transformation in prostate cancer. ST profiling identified CE-cell-driven niches and transcriptomic signatures strongly associated with metastatic potential, offering novel biomarkers and spatially defined cellular interactions that improve our understanding of PCa progression in African-American men. This spatially resolved framework provides a foundation for future studies aimed at dissecting microenvironmental drivers of metastasis and developing cell-type-specific therapeutic strategies.

#3970 Genome wide testing of archived ovarian and uterine carcinosarcoma FFPE tissue using FusionPlus Hi-C to determine HRD status.

Amanda Bradshaw[1], Christopher Elms[1], Mia Jeffris[2], Jon Belton[2], Williams Ricketts[2], Alex R. Hastie[2], **Michael Birrer**[1]

[1]Cancer Institute, University of Arkansas for Medical Sciences, Little Rock, AR,[2]Arima Genomics, Carlsbad, CA

Genomic rearrangements such as gene fusions and copy number variation are chromosomal abnormalities important in cancer, including diagnosis and treatment. Approximately 50% of ovarian cancers involve homologous recombination deficiency with characteristic genomic rearrangements. HRD tumors have been shown to respond well to PARPi treatments. PARPi are an approved treatment for cancers known to have abnormalities in DNA repair mechanisms including ovarian cancers. Ovarian and uterine carcinosarcoma is a rare and aggressive form of gynecologic cancer with few diagnostic and treatment options. Genetic testing and HRD assays are invaluable in cancer diagnosis and treatment. Molecular testing in lung and other solid tumors has led to the identification of driver mutations that can be targeted by new therapeutics. Detection of these fusion proteins by RNA sequencing is the current gold standard but evidence suggests that fusions are still missed for various reasons. This study aims to improve detection rate of targetable fusions and rearrangements in solid tumors, ovarian and uterine carcinosarcoma specifically, using a new method called Hi-C sequencing. The Hi-C assay has been promising in locating genomic abnormalities in various types of cancer. Hi-C sequencing is a whole genome DNA-sequencing assay for detection of structural variation based on unique Hi-C chemistry which leverages sequencing of linked pairs of reads which occur nearby one another in 3-dimensional and linear space, from FFPE samples. Linking reads amplifies the rearrangement signal by giving it many more read pairs spanning the breakpoint and also overcoming masked fusions resulting from breakpoints in non-unique sequences. This method is useful for a variety of specimen types and preservation methods as well as archival periods. Hi-C testing works well for formalin fixed paraffin embedded tissue which is important for solid tumor testing such as with carcinosarcoma. We used Hi-C testing on archived FFPE ovarian and uterine carcinosarcoma tissue to determine if it could be beneficial in future cases improving prognosis, and therapeutic choices, particularly in identifying HRD tumors and the use of PARPi treatments. Our data has shown that 7 out of 18 samples tested had aberrations involving genes potentially involved in HRD. These genomic aberrations included significant rearrangements, gene fusions, and loss-of-function in several genes involved in HRD including RAD51B, CHEK2, and FANCA1. These data suggest that Hi-C testing could be a valuable tool in the molecular classification of solid tumor cancers and provide earlier more thorough diagnosis and more precise treatment options for gynecologic carcinosarcoma with the notable benefits of being faster and lower cost, possibly advancing clinical research with the discovery of novel biomarkers and therapeutic targets.

#3971 Rapid antibody drug conjugate markers and RNA biomarkers in solid tumors using a hybrid Ultivue InSituPlex and Protease-Free RNAscope Workflow.

Patrick Savickas[1], AKASH PARVATIKAR[2], Jack Casey[2], Anushka Dikshit[3], AMAN TYAGI[2]

[1]Histowiz, New York, NY,[23]Bio-Techne Corporation, Newark, CA

Introduction: The spatial relationships between tumor cells, immune infiltrates, and the surrounding stroma—characterized by both protein expression and transcriptional activity—are critical determinants of therapeutic response and disease prognosis. Traditional spatial profiling approaches often require serial sections, compromising exact cellular co-localization, or utilize harsh processing steps that degrade target integrity. There is an urgent need for robust, high-throughput, single-slide methods to co-detect protein and RNA with high fidelity.

Methods: We developed and validated a novel, streamlined hybrid workflow combining Ultivue's highly multiplexed InSituPlex technology (protein detection) with Advanced Cell Diagnostics' (ACD) newly developed protease-free capability with RNAscopeTM in situ hybridization (ISH) workflow. This pairing is crucial: the protease-free ISH step prevents the degradation of critical cell surface epitopes required for robust downstream multiplex immunofluorescence (mIF) protein staining. A comprehensive panel was rapidly assembled, including key immuno-oncology protein markers for antibody drug conjugates (ex. HER2) via InSituPlex, co-detected with relevant transcriptional targets (e.g., cytokine mRNA, therapeutic target transcripts) via ISH. The assay was applied to FFPE tissue sections from Non-Small Cell Lung Cancer (NSCLC), Triple-Negative Breast Cancer (TNBC), and Gastric Cancer (GC) to demonstrate broad applicability.

Results: We successfully achieved simultaneous, high-resolution co-localization of up to 5 protein markers and 3 RNA transcripts within a single tissue section across all three heterogeneous cancer types. The protease-free pre-treatment maintained optimal tissue and epitope morphology, enabling exceptional signal-to-noise ratios for both protein and RNA channels. Critically, this combined multi-omic readout allowed for the precise spatial phenotyping of cell populations (e.g., CD8+ T cells co-expressing specific cytokine mRNA) and the assessment of spatial proximity between cells defined by combined protein/transcriptional signatures. The modularity of the Ultivue assay allowed for rapid assembly and substitution of antibody panels, enabling high-speed assay optimization.

Conclusion: This innovative, combined Ultivue InSituPlex and protease-free ACD ISH assay provides a powerful, single-slide platform for spatially resolved multi-omic analysis. It overcomes the technical limitations of traditional sequential staining, offering a high-throughput, high-fidelity tool that can be rapidly deployed for complex biomarker validation, detailed tumor microenvironment characterization, and improved patient stratification strategies in translational oncology and clinical trials.

#3972 Comprehensive immune landscape analysis of solid tumors using a 17-Plex immunofluorescence assay in clinical trials.

Jaspreet Kaur[1], Richard Van Krieken[1], Xun Li[1], Ying Huang[2], Lisa Kattenhorn[2], Naveen Dakappagari[1], Margaret E. McLaughlin[2], Jennifer Bordeaux[1]

[1]Navigate BioPharma Services, Inc., Carlsbad, CA,[2]Novartis BioMedical Research, Cambridge, MA

Background: The tumor micro-environment is highly complex; accumulating evidence indicates that immune cell composition and spatial distribution can contribute to disease progression and inhibition of antitumor immunity. There is a growing effort to leverage new technologies for in-depth analysis of the complexities within the tumor immune microenvironment. We validated a 17-plex, subcellular resolution, pan-immune cell panel to interrogate the immune cell types and their spatial organization in whole tissue sections.
Methods: We co-developed a 17-plex pan-immune cell immunofluorescence (IF) assay with RareCyte® utilizing the Orion™ platform to characterize immune cell populations and their functional states in formalin-fixed paraffin-embedded (FFPE) tissues from melanoma, breast, lung, prostate, and colorectal cancers. A single, 4-micron FFPE section was stained in one-step, using the intelliPATH™ FLX (Biocare Medical) with a cocktail of antibody-fluorophore conjugates targeting Granzyme B, Ki67, CD3e, CD20, CD4, CD163, CD8a, PDL1, NKp46, PD-1, LAG3, FOXP3, CD11b, CD138, SOX10, Cytokeratin, and Hoechst nuclear stain. Imaging was performed on the Orion™ platform, and data were analyzed using HALO® (Indica Labs).
Results: The assay enabled comprehensive spatial profiling of T, B, NK, and myeloid cell distributions within tumor and stromal compartments. Functional states of T cells (cytotoxic, regulatory, exhausted) and macrophage/B-cell niches were distinguished based on immune checkpoint and activation marker expression. Proximity analyses identified immune synapses and organized lymphoid structures, facilitating robust microenvironment characterization.
Conclusions: The Orion™ 17-plex pan-immune cell IF assay will enable comprehensive qualitative and quantitative analysis of the tumor microenvironment in clinical trial specimens. We anticipate that this approach will support the development of next-generation therapies by enabling detailed characterization of immune cell and tumor cell spatial biology across multiple cancer types.

#3973 A framework for antibody validation via spatial proteo-transcriptomics using the CellScape platform.

Tim Schunk[1], Tim Mandelkow[1], Shida Xiong[1], Jonas Raedler[1], Rodler Severin[1], Philipp Nuhn[1], Anne Letsch[1], Marion van Macklenbergh[1], Jan Weitkamp[1], Jakob Kohler[1], Arne Christians[2], Oliver Braubach[3], Steve Lott[3], Micaela Mathiak[1], Gavin Gordon[4], Bjorn Konukiewitz[1], Christoph Rocken[5], **Niclas Christian Blessin**[1]

[1]Universitatsklinikum Schleswig-Holstein, Kiel, Germany,[2]Bruker Spatial Biology,[3]Canopy Biosciences, St. Louis, CA,[4]Bruker Spatial Biology, St. Louis, CA,[5]Professor, Dept. of Pathology, Christian-Albrechts-University, Kiel, Germany

Spatial proteomics depends on antibody reliability, yet many antibodies used in routine diagnostics and research - particularly in conventional brightfield and multiplex fluorescence immunohistochemistry - are only subjectively or insufficiently validated, leading to potential false conclusions and limiting the use of spatial proteomics in large-scale clinical research studies.To address this limitation, we developed a fully automated - thus objective - deep learning-based framework for antibody validation. The in-situ staining patterns and interdependencies of various antibody clones for the same target were compared to the corresponding RNA expression pattern using a network of deep learning algorithms. For this purpose, a tissue microarray (TMA) was constructed from 50 different normal and 50 different neoplastic tissues including carcinoma entities, lymphomas, and other human neoplastic tissues from 1040 patients. All antibody clones were pre-tested in conventional brightfield IHC and assembled in 10- to 30-plex mfIHC assays using the CellScape™ Precise Spatial Proteomics platform (Bruker Spatial Biology, USA)to compare different antibody clones for the same target across 100 different human tissue types. The same TMA slide can then be used for spatial transcriptomics on the CellScape™ via HCR™ Gold (Molecular Instruments, Los Angeles, US) or on the CosMx® Spatial Molecular Imager (Bruker Spatial Biology, USA). A framework of different deep learning models (U-Net and DeepLab3^{+}) was developed for analysing protein and RNA expression. This spatial proteo-transcriptomics approach allows for both (i) the direct deep learning-based comparison of different antibody clones for the same target and (ii) an interpretation in view of the mRNA expression of the corresponding gene on a single-cell level across 100 different healthy and neoplastic tissues across the human body. Through the automatic assessment of every individual antibody clone, objective metrics such as fraction of expression on different tissue-compartments (%), accordance with other antibody clones for the same target (%), as well as correspondence with the RNA expression (%) were computed. Given that linear regression analysis showed an ultra-low signal deterioration across the different cycles (<1 %) - due to the novel EpicIF for gentle bleaching of the fluorochromes on the CellScape platform - a direct comparison of antibodies from different cycles was possible without cumbersome rearrangement of the antibodies for mfIHC panel creation. These findings highlight the potential of using an automated framework for antibody validation in favour of using publicly available non-spatial RNA expression libraries.In conclusion, here we present the first objective, pathologist reviewed, and fully automated deep learning-based framework for antibody validation using spatial proteo-transcriptomics.

#3974 Decoding cancer hallmarks through single-cell whole transcriptome imaging in invasive ductal carcinoma.

Claire Williams, **Patrick Danaher**, Megan Vandenberg, Martin Shelton, Mirko Corselli, Christine Kang, John Lyssand, Joseph Beechem

Bruker Spatial Biology, Seattle, WA

Tumor adaptation to microenvironmental stressors underlies key cancer hallmarks, including immune evasion, altered metabolism, angiogenesis, and uncontrolled proliferation. However, the spatial organization and cell-type specificity of these adaptations remain poorly characterized in intact tissue. To address this, we generated a spatially resolved, single-cell transcriptomic map of a grade II HER2+ invasive ductal carcinoma using the CosMx® Whole Transcriptome assay on the CosMx Spatial Molecular Imager (SMI). We assayed over 600,000 cells within a ~1 cm² FFPE tumor section. Spatial domain mapping and cell classification identified 37 distinct tumor, immune, and other stromal subtypes. Copy number analysis revealed clonal divergence across two tumor lobes and five transcriptionally distinct malignant clusters, suggesting spatially restricted evolutionary trajectories.

To investigate immune evasion, we characterized a robust T-cell infiltrate comprising 7.3% of cells. Spatial and transcriptional analyses revealed cytotoxic CD8+ T cells losing effector function and initiating exhaustion programs upon tumor entry. Tumor cells responded with localized activation of JAK-STAT, MHC-I, and NF-κB signaling, suggesting coordinated resistance to immune attack. These findings highlight spatially organized immune suppression and identify candidate mechanisms that may contribute to T-cell dysfunction in HER2+ breast cancer.

Next, we assessed tumor-induced metabolic reprogramming and angiogenesis, by modeling gene expression relative to vascular proximity. Hypoxia-related genes (e.g., HILPDA, VEGFA) were enriched in vessel-distal regions, while nutrient-associated genes (e.g., AZGP1, PLA2G2A) localized near vasculature. ELF3, a transcription factor associated with poor prognosis in HER2+ cancers, was unexpectedly upregulated in hypoxic zones. Cell cycle analysis revealed low-proliferation regions with stressor-specific transcriptional profiles, indicating localized growth constraints.

This dataset showcases the power of subcellular whole transcriptome imaging in resolving hallmark cancer behaviors directly within tissue context. This same data set could be re-interrogated for any/all of the hallmarks of cancer, even those that haven't been discovered yet. While derived from a single HER2+ breast cancer sample, the analytical framework we present, integrating spatial context with single-cell resolution, serves as a template for future studies investigating patient-specific tumor adaptations to microenvironmental stressors across diverse samples and clinical settings.

#3975 Spatially resolved multi-omics reveal metastatic ecosystem remodeling and immunomodulatory niches in HGSOC.

Yufeng He[1], Ce Luo[2], Yuanguang Meng[3], Zhe Zhang[3], Zexian Zeng[1]

[1]Peking-Tsinghua Center for Life Sciences, Academy for Advanced Interdisciplinary Studies, Peking University, Beijing, China,[2]Center for Quantitative Biology, Academy for Advanced Interdisciplinary Studies, Peking University, Beijing, China,[3]Department of Obstetrics and Gynecology, Seventh Medical Center of Chinese PLA General Hospital, Beijing, China

High-grade serous ovarian carcinoma (HGSOC) is the most lethal gynecologic malignancy. HGSOC spreads within peritoneal cavity via transcoelomic dissemination, and the greater omentum is a frequent site of metastatic tumor deposition. Embedded beneath the omental mesothelium, the fat-associated lymphoid clusters (FALCs, known as milky spots) serve as portals for early peritoneal metastasis. Yet how metastatic ecosystems differ from the primary tumor microenvironment, and are spatially organized around FALCs remains unclear. To address this, we profiled matched primary and metastatic tumor samples from 17 HGSOC patients using single-cell RNA sequencing with paired TCR/BCR profiling and spatial multi-omics including Visium HD spatial transcriptomics, multiplex CODEX imaging and spatial metabolomics. In FALC-rich regions within metastatic lesions, we identify a stereotyped architecture in which small aggregates of B cells and plasma cells are interlaced with $CD4^+$ and $CD8^+$ T cells and dendritic cells. Stromal regions between these FALCs and adjacent tumor border are highly infiltrated by *SPP1*$^+$*C1Q*$^+$ macrophages. We show that the B cells in metastasis mainly consist of IgG^+ and IgA^+ populations, and are class-switched and clonally expanded. Integrating spatial transcriptomics with histology, we found the abundance of the niche enriched for IgA^+ B cells associates with worse overall survival using a deep learning framework. Spatial metabolomics mapped spatial metabolic niches and showed that metastases shift toward glycolytic, lipid and phospholipid metabolism, whereas primary tumors retain more oxidative programs. Collectively, our findings provide a spatially resolved atlas of HGSOC metastasis and a foundation for spatially informed biomarker development.

: Advances in Therapeutic Antibodies
Minisymposium

#4051 BHB299: An AI/ML-optimized high avidity/low affinity CEACAM6-directed T cell engager for diverse solid tumors.
R. Henrici, K. Stephenson, R. Sanyal, M. Montgomery, M. Markova, A. Prater, B. Steurer, T. Park, D. Barreras, N. Huskey, J. Wojciak, J. Corbin, P. Greenside;
BigHat Biosciences, Inc., San Mateo, CA

Background: Solid tumors remain a major cause of global mortality, with millions of new cases annually. Despite a rapidly advancing standard of care, few patients achieve durable responses. CEACAM6 is a cell surface antigen expressed at extremely high levels on CRC (>85%), NSCLC (>50%), Gastric (>30%), Pancreatic (>30%) and a variety of other tumor types where it drives tumor metastasis and immune suppression through heterotypic interactions with adjacent cancer and infiltrating immune cells. CEACAM6 has historically been considered undruggable due to its moderate expression on healthy myeloid cells, which act as a peripheral antigen sink and a source of on-target/off-tumor dose-limiting toxicity.
Methods: A single domain VHH anti-CEACAM6 antibody was discovered and co-optimized alongside a CD3 binding domain for ultra-fast dissociation and developability using BigHat's proprietary AI/ML and cell-free protein synthesis (CFPS)-enabled platform. Comprehensive in vitro and in vivo studies of PK, PD, and safety were performed to support the candidacy of BHB299 for first-in-human evaluation.
Results: The resulting "2+1" T cell engager binds to cell surfaces with high CEACAM6 densities with high avidity and slow dissociation, but dissociates rapidly from myeloid cells with moderate target densities. This dynamic CD3 and CEACAM6 engagement selectively establishes an immunological synapse between tumor cells and T cells but not healthy myeloid cells, with >10,000x differential in IC50 in vitro using relevant models of cancer and whole blood from human donors. This avidity-based or "IF-BETTER" mechanism also eliminates sensitivity to soluble forms of CEACAM6, which may act as a decoy and antigen sink for high-affinity therapeutics. BHB299 also features a pH conditional CD3 agonist, which further enhances cell killing in the tumor microenvironment to reduce the risk of antigen escape due to low target expression. In vivo, BHB299 leads to complete responses or durable partial responses in multiple models of colon, rectal, lung, and pancreatic tumors, including metastatic PDX models of CRC and lung cancers. In safety studies in humanized mouse models and primates, no MTD was reached, consistent with a substantial therapeutic window.
Conclusion: BHB299 is a first-in-class CEACAM6-directed bispecific T cell engager for the treatment of diverse solid tumors, potentially up to 10% of all new cancers in the US each year. The molecule was engineered on BigHat Biosciences's AI/ML-powered antibody design platform to maximise tumor-specific target engagement. First-in-human studies are supported by the preclinical data package and are planned for 2026.

#4052 ENA101: A first-in-class bispecific T cell engager targeting a DARKFOX peptide presented by solid tumors.

T. Cornforth, C. Johnston, D. Howie, H. Adamson, R. Bergin, A. Black, L. Blackholly, E. Border, C. Cox, E. Denham, M. von Essen, V. Jefferson, L. Johnson, E. Lam, J. Lewis, M. Li, T. Lobry, H. McIntyre, I. Mount, J. Senra, M. Simpson, A. Stacey, E. Tye, M. Vologianni, **J. Dukes**;

Enara Bio, Oxford, United Kingdom

Background: Bispecific T cell engagers are an emerging immunotherapy for solid tumors, capable of potently redirecting polyclonal cytotoxic T cells to lyse tumor cells independent of their native specificity. This mechanism enables potent immune activation and has delivered landmark clinical benefit in solid tumors, exemplified by tarlatamab and tebentafusp, which achieved unprecedented efficacy even in immunologically 'cold' settings such as small-cell lung cancer and uveal melanoma. Progress in solid tumors is constrained by the limited availability of antigens with sufficient tumor specificity to ensure efficacy with a robust therapeutic window. To address this, we discovered and validated DARKFOX™, a novel cancer-specific Dark Antigen® encoded by an alternative open reading frame (altORF) of the canonical FOXM1 gene. DARKFOX is highly prevalent, tumor-specific, and homogeneously expressed within tumors, with a robustly presented HLA-A3 peptide (DARKFOX-A3). We have developed TCR-mimic antibodies with picomolar affinity for DARKFOX-A3 and incorporated them into our EnTiCE® T cell engager platform, engineered for best-in-class functional and manufacturability properties.

Methods: Antibodies specific for DARKFOX-A3 were generated from mice immunized with the antigen and subsequently affinity-matured in vitro to achieve high-affinity binding to the peptide-HLA complex. The optimized sequences were reformatted as single-chain variable fragments (scFvs) and engineered into Enara's EnTiCE® T cell engager platform. Proteins were expressed in mammalian systems and purified for use in functional assays, analytical characterization, and in vivo efficacy studies. Expression analyses were performed using RNA in situ hybridization.

Results: DARKFOX-A3-specific binders incorporated into Enara's optimized EnTiCE® half-life-extended T cell engager format achieved robust yields and high purity using a scalable mammalian expression system. ENA101 demonstrated pM binding affinity for DARKFOX-A3 and potently redirected and activated T cells, inducing cancer cell lysis with low-pM EC_{50} values across multiple DARKFOX-A3^{+} targets. In vitro co-culture assays with normal cell models, together with binding motif analyses, confirmed a highly specific pHLA binding profile. In vivo, ENA101 exhibited strong anti-tumor efficacy in xenograft models. Planned first-in-human studies are supported by expression data indicating high prevalence of DARKFOX across major tumor types, such as squamous NSCLC, enabling patient enrolment without antigen pre-screening.

Conclusions: ENA101 exhibits the hallmarks of a best-in-class bispecific T cell engager for solid tumors, including potent and highly specific redirection of T cell activity against antigen-positive cells across multiple tumor types. CMC activities and IND-enabling studies are currently in progress.

#4053 NRP1 drives a novel cross-presentation pathway exploitable by peptide-linked antibodies to redirect viral memory T-cells against solid tumors.

Anne V. Philips, Celine Kerros, Helen He, Lisa St. John, Noah Tubo, Ho Ngai, Qiyang Zhou, Chunhua Shi, Anthony Sump, Gheath Alatrash, **Jeffrey J. Molldrem**

UT MD Anderson Cancer Center, Houston, TX

Background: Although NRP1 is known to regulate tumor angiogenesis [1,2] and immune suppression [3,4], its role in antigen processing has not been defined. We discovered that NRP1 engagement triggers a previously unrecognized pathway enabling cross-presentation of exogenous peptides on MHC-I. We exploited this biology using a peptide-linked anti-NRP1 monoclonal antibody (5D6) to redirect antiviral $CD8^+$ T cells against NRP1-expressing tumors.
Methods: HLA-A2-restricted CMV, SARS-CoV-2, and tumor-associated peptides were chemically conjugated or recombinantly fused to 5D6 through a pH-sensitive cleavable linker. Internalization, trafficking, and antigen processing were evaluated by confocal microscopy and mass spectrometry. Functional cross-presentation was assessed using peptide-specific $CD8^+$ T cells in breast, lung and renal cancer cells *in vitro*, and in NSG mice bearing human carcinoma xenografts dosed with peptide-linked 5D6 followed by adoptive transfer of peptide-specific TCR-T cells.
Results: NRP1 ligation induced rapid antibody internalization into endosomal and lysosomal compartments, enabling efficient liberation of peptide cargo and high-density MHC-I cross-presentation on tumor cells. Pep-5D6-treated tumor cells were selectively killed by cognate $CD8^+$ T cells. *In vivo*, pep-5D6 followed by a single dose of peptide-specific TCR-T cells eradicated established tumors across multiple xenograft models within 1-4 weeks. These data reveal that NRP1 can function as a receptor for antigen delivery and cross-presentation, demonstrating its potential for therapeutic exploitation.
Conclusions: We identify a previously unrecognized NRP1-mediated cross-presentation pathway and introduce a first-in-class strategy that repurposes abundant viral memory T cells for targeted tumor elimination. This mechanistic insight defines new immunobiology for NRP1 and establishes a translational platform for redirecting pre-existing antiviral immunity toward NRP1-expressing cancers.
References: 1.Niland S, Eble JA. Neuropilins in the context of Tumor Vasculature. Int J Mol.Sci. 2019: 20(3) 2.Domingues A, Fantin A. Neuropilin-1 Regulation of Vascular Permeability Signaling. Biomolecules 2021 11(5) 666 3.Roy S, Bag AK, Singh RK, Talmadge JE, Batra SK, Datta K. Multifaceted Role of Neuropilins in the Immune System. Front. Immunol. 2017; Vol 8 4. Kawaguchi K, Suzuki E, Nishie M, Kii I, Kataoka TR, Hirata M, Inoue M, Pu F, Iwaisako K, Tsuda M, Yamaguchi A, Haga H, Hagiwara M, Toi M. Downregulation of Neuropilin-1 on Macrophages modulates Antibody-mediated Tumoricidal Activity. Cancer Immunol Immunother. 2017 Sep:66(9):1131-1142
An AI tool was used for general language editing purposes.

#4054 Tumor-activated PrimeBody biologics platform enables more potent CD47 targeting and superior therapeutic index in preclinical models.

A. Springer, S. Lai, C. Thanos, J. Humphrey, U. Eskiocak;
Voro Therapeutics, San Diego, CA

Systemic toxicities and dose-exposure limitations caused by target expression on normal tissues remain major barriers to effective cancer therapy. Tumor-activated masked biologics are a promising strategy to improve safety and efficacy, as highlighted by evolving clinical data with masked T-cell engagers (TCEs) and masked antibody-drug conjugates (ADCs). However, an optimized platform that balances protease specificity, systemic stability, and tumor release kinetics across diverse tumor types is lacking.VORO's PrimeBody biologics platform employs novel activation linkers that are rapidly cleaved in the tumor microenvironment but are stable in normal tissues, demonstrating substantially improved tumor-selectivity compared to clinical benchmarks. These linkers are coupled with novel, finely tuned affinity-based masking domains to precisely control target affinity and tumor-specific release kinetics. PrimeBody masking is ideal for novel, more potent CD47-targeted biologics to overcome safety limitations caused by ubiquitous CD47 expression in healthy tissues and simultaneously enable enhanced anti-tumor efficacy.VOR-101 is a masked, Fc-enhanced, high-affinity CD47 blocker that remains a latent prodrug until it is activated by proteolytic cleavage in the tumor microenvironment. In vitro, unmasked VOR-101 drives potent phagocytosis (EC_{50} ~20 pM) by primary human macrophages against epithelial cancer cell lines (DLD-1, HCT116, HT29, MCF-7, CAL27), while masked VOR-101 is inert (>2,000-fold higher EC_{50}). Ex vivo, VOR-101 is rapidly activated by human tumor surgical samples across all tested tumor types yet remains stable and intact in serum from healthy volunteers, cancer patients, and non-human primates for >14 days. In contrast, identical constructs engineered with clinical benchmark linkers exhibited significantly slower tumor activation and rapid serum degradation. Consequently, VOR-101 achieves >700-fold tumor-to-serum selectivity, a major improvement over the <25-fold selectivity observed with benchmark linkers currently in clinical development.In a translational hCD47/hSIRPα mouse model, magrolimab induced 50-60% depletion of red blood cells (RBCs) and exhibited poor systemic exposure (~10 nM). By contrast, VOR-101 at equimolar dosing achieved ~1 µM blood concentrations (~100-fold higher systemic concentration) while maintaining normal RBC counts. In xenograft models, VOR-101 induced durable complete responses that persisted well beyond the dosing period.Together, these findings demonstrate that VOR-101 (a tumor-activated, Fc-enhanced, high-affinity CD47 blocker) significantly improves the therapeutic index in preclinical models compared to clinical comparators. VOR-101 is advancing through IND-enabling studies with potential to exhibit single-agent activity in solid tumors.

#4055 Integrated CD2-costimulation on CD3 T cell engager EVOLVE platform yields differentiated and superior T cell effector profile.

E. Stewart, J. Zeiger, D. Ryan, R. Khalil, W. DeMaria, C. Brown, K. Ralph, A. Abduqadir, J. S. Myers, J. S. Fine, O. A. Sergeeva, S. Trombetta, S. Martomo;
EvolveImmune Therapeutics, Inc, Branford, CT

The EVOLVE platform utilizes a CD3 T-cell engager (TCE) with integrated CD2 costimulation to enhance the efficacy and durability of T cell responses. CD2 is a costimulatory receptor expressed on the majority of T cells in the tumor microenvironment (TME). We hypothesize that T cell co-engagement via CD3 and CD2 will result in superior T cell activation in the TME, conferring a greater anti-tumor effect. EVOLVE104, which recently entered the clinic, is a tri-specific molecule targeting CD3, CD2 and tumor antigen ULBP2/5/6. We showed previously that ULBP2/5/6, while minimally expressed on normal human tissues, is upregulated in solid tumors of squamous origin as well as in bladder cancer (1). In xenograft mouse models, EVOLVE104 showed significant tumor growth inhibition compared to bispecific TCE (2). In this study, we use a series of in vitro tests to compare T cell phenotypic and functional profiles after stimulation with EVOLVE104 or with other first generation bispecific TCE formats which lack integrated costimulation. We find that chronic stimulation of human peripheral blood-derived T cells with EVOLVE104 led to greater than a 30-fold increase in CD8+ T cell effector-to-naïve ratios compared to CD3 stimulation alone, demonstrating greater differentiation of T cells after exposure to EVOLVE. These EVOLVE104-stimulated effector cells showed two-fold or greater upregulation of activation markers such as CD25, CD69 and CD137 in a concentration-dependent manner after 24 hours when compared to bispecific TCE-treated T cells, with expression of these markers persisting through multiple rounds of stimulation. EVOLVE104-treated T cells also showed faster and sustained proliferation kinetics in chronic stimulation assays and TDCC assays. In this model, approximately 50% of effector CD8 T cells were proliferating by day 3 with EVOLVE104, compared to 20% with a bispecific TCE, which increased to >80% after multiple rounds of stimulation. Additionally, T cell function was maintained in vitro following chronic stimulation as measured by tumor cell killing of ULBP2/5/6+ tumor cells and by cytokine release in a mixed lymphocyte reaction assay. In conclusion, T cells stimulated with EVOLVE TCE platform with CD2 integrated costimulation shows differentiated and superior T cell phenotype with sustained tumor cell killing and cytokine production in vitro compared to T cells stimulated with TCE bispecific formats lacking CD2 costimulation. This study supports the hypothesis that the EVOLVE platform may provide deeper and more durable anti-tumor responses than first generation bispecific T cell engager formats. A first-in-human clinical dose escalation trial with EVOLVE104 is currently underway (NCT07217171).

#4056 Preclinical evaluation and safety of CBX-250 in acute myeloid leukemia: A bispecific T cell engager targeting Cathepsin-G peptide/HLA complex.

Jennifer Helble[1], Geraldine L. C. Paulus[1], Preethi Sankaran[1], Tanzila Rahman[1], Sarah Jaffe[1], Nga Sze Amanda Mak[1], Chunhua Shi[2], Jun Yan[2], Timothy Heffernan[2], Jeffrey Molldrem[2], Gheath Al-Atrash[2], Dmitri Wiederschain[1], Benjamin Lee[1]

[1]Crossbow Therapeutics, Inc., Cambridge, MA,[2]The University of Texas MD Anderson Cancer Center, Houston, TX

Acute myeloid leukemia (AML) presents a challenge for targeted immunotherapy due to the scarcity of tumor-specific surface antigens. An emerging strategy involves targeting peptide-HLA (pHLA) complexes derived from intracellular proteins. CG1 (FLLPTGAEA), a peptide derived from the Cathepsin G (CG) leader sequence presented by HLA-A*02:01, is selectively expressed on AML cells. CBX-250 has been developed as a TCR-mimetic (TCRm) bispecific T cell engager (TCE) antibody that binds to CG1/HLA-A*02:01 pHLA on AML cells and CD3 on T cells. We previously demonstrated that CBX-250 elicits in vitro killing of leukemia cells at sub-nanomolar EC_{50} levels. To further evaluate CBX-250 potency, we assessed a panel of CG1-positive U937 cell lines with varying levels of HLA-A*02:01 in T cell cytotoxicity assays. We observed comparable cytotoxicity across cell lines with target copy numbers ranging from 383-7930/cell, and notably, still observed robust killing of tumor cells with 33 target copies/cell. We also found that CBX-250 induced dose-dependent bystander killing of CG1/pHLA-negative cells only in the presence of CG1/pHLA-positive cells, highlighting the beneficial potency effects of CBX-250 in a tumor microenvironment with heterogenous target expression. To evaluate the safety of CBX-250, we assessed CBX-250-induced cytokine release in healthy donor HLA-A*02:01+ PBMCs and whole blood. We found no induction of cytokines in either PBMCs or whole blood when exposed to CBX-250, suggesting the risk for off-target adverse cytokine release is low. Although platelets likely do not present CG1, they can express high levels of class I HLA on their surface and may be potential targets for cross-reactivity with CBX-250. We found no increases in platelet activation following treatment with CBX-250, supporting the favorable safety profile of CBX-250. We assessed CBX-250 specificity by screening a library of >6,500 human proteins for off-target binding partners and found the only significant interactions were with CD3, one of its targets, and FCGR2A, an interaction which likely occurs through the Fc domain due to the high concentrations of CBX-250 tested. No other interactions were detected, indicating high specificity of CBX-250. To evaluate the pharmacology of CBX-250, serum pharmacokinetics (PK) and anti-drug antibody (ADA) formation were evaluated in naive male cynomolgus monkeys. The PK profile for IV and SC administration were consistent with IgG-like molecules, and the majority of the animals exhibited no ADA formation, suggesting minimal immunogenicity risks for CBX-250. Overall, our data demonstrate that CBX-250 is effective against a wide range of CG1/pHLA target densities and capable of mediating bystander killing. These features, combined with its encouraging safety profile, support clinical development of CBX-250. Phase 1 trial (NCT06994676) is ongoing.

#4057 Gastrointestinal tumor-associated target: A first-in-class therapeutic monoclonal antibody.

U. Goh[1], S. Kim[1], H. Kim[2], Y.-B. Kim[1];
[1]ReCerise Therapeutics, Seoul, Korea, Republic of, [2]Sungkyunkwan University, Gyeonggi-do, Korea, Republic of

Background:
Immune checkpoint blockade has improved outcomes in several cancers, but tumors with strongly immunosuppressive microenvironments, such as microsatellite-stable colorectal cancer (MSS-CRC), pancreatic cancer, and many hepatocellular carcinomas (HCCs), remain largely unresponsive. These tumors exhibit immune exclusion, impaired innate effector function, and dense tumor-supportive stroma. TM4SF5, a four-pass transmembrane glycoprotein enriched in gastrointestinal cancers, has been implicated in exclusion of effector lymphocytes, NK-cell dysfunction, and recruitment of tumor-associated macrophages (TAMs) and cancer-associated fibroblasts (CAFs), suggesting a central role in establishing an immunosuppressive tumor microenvironment (TME).
Methods:
A first-in-class monoclonal antibody was developed against native TM4SF5, recognizing the conformational extracellular epitope to disrupt TM4SF5-mediated signaling and immune-suppressive functions. Full-length TM4SF5 was reconstituted into a virus-like lipoparticle to maintain its native membrane conformation, enabling selection of TM4SF5-specific antibodies. A lead clone with high-affinity binding to both human and mouse TM4SF5 was Fc-optimized to generate the candidate RCT1213. RCT1213 was evaluated in vitro and in vivo for anti-tumor efficacy using patient-derived xenograft (PDX) tumor samples and TM4SF5-positive MSS-CRC cell line xenograft, respectively. Combination studies with immune checkpoint inhibitors (ICIs) assessed therapeutic interactions.
Results:
RCT1213 bound TM4SF5 with high affinity and attenuated TM4SF5-driven suppressive signaling in vitro PDX-derived tumors. Treatment with RCT1213 restored NK-cell activation and cytotoxic function, consistent with reversal of TM4SF5-mediated innate immune suppression. In MSS-CRC xenograft models, RCT1213 inhibited tumor growth and remodeled the TME, increasing immune-cell infiltration while reducing suppressive stromal and myeloid components. Combination therapy with ICIs yielded superior tumor control compared with either agent alone.
Conclusion:
Targeting TM4SF5 with RCT1213 alleviates TM4SF5-driven immunosuppression and restores innate effector function, resulting in robust anti-tumor activity in MSS-CRC models. These findings position TM4SF5 as an upstream immune-modulatory target and support RCT1213 as a first-in-class therapeutic candidate. IND-enabling studies are underway to advance RCT1213 into clinical development for MSS-CRC and other TM4SF5-expressing solid tumors.

: Advancing Cancer Research Through an International Cancer Registry: AACR Project GENIE® Use Cases Minisymposium

#3988 Beyond G12C: Pan-cancer landscape and co-mutational architecture of rare RAS alleles across 211,526 patients.

N. Coleman[1], D. Hong[2];

[1]Trinity College Dublin, Dublin, Ireland, [2]UT MD Anderson Cancer Center, Houston, TX

Background: KRAS G12C has renewed interest in RAS biology, yet most RAS-mutant cancers harbor non-G12C variants whose therapeutic potential is uncertain and tissue-contextual. We aimed to map the prevalence, co-mutation signatures, and potential actionability of rare RAS alleles to inform next-generation clinical trial design.
Methods: We performed a pan-cancer analysis of AACR Project GENIE v.18, analyzing 250,018 tumor samples from 211,526 patients to quantify the prevalence of rare KRAS alleles (G12D/V/A/R, Q61, G13D), NRAS, and HRAS alleles by lineage, to define co-mutation signatures and assess clinical actionability.
Results: KRAS was altered in 32,946 tumors (16%; 35,614 patients). Rare KRAS alleles demonstrated strong codon-lineage patterns: G12D (9,457) and G12V (7,602) were the most common, each enriched across pancreatic adenocarcinoma (PDAC; 31.8%), colorectal cancer (CRC; 16.7%), and lung cancer (13.2%); G12A (1,542) occurred mainly in LUAD (41.4%) and CRC (20.5%), rarely in PDAC (1.36%); G12R (1,683) was highly pancreas-restricted (69%). G13D (2,596) was dominantly colorectal (55.9%). Q61X (2,279) occurred in PDAC (26%), LUAD (21%), and CRC (16%). HRAS mutations were rare (1,983 tumors <1%; 1,860), most frequently occurring in urothelial carcinoma (12.5%), thyroid cancer (6.3%), and HNSCC (2%). Codon-61 variants (Q61H/K/L/R; 461) accounted for 23.3% of all HRAS mutations, with enrichment in thyroid (22.8%), urothelial (17.4%), melanoma (6.3%), and HNSCC (6.1%); additional recurrent hotspots included G12 (234) and G13 (248). NRAS alterations were detected in 5,882 tumors (3%; 5,715 patients), most frequently in melanoma (1,440; 24.5%), CRC (565; 9.6%), and LUAD (300; 5.1%). Q61X accounted for 51% of all NRAS mutations, most commonly in melanoma (25%), CRC (10%), and LUAD (5%). KRAS-mutant tumors showed significant co-occurrence with TP53, SMAD4, CDKN2A, STK11, KEAP1, and APC (all $p<0.001$); KRAS was mutually exclusive with NF1, RB1, and PTEN (all $p<0.001$). HRAS-mutant tumors significantly co-occurred with NOTCH1, FGFR3, NF1, TERT, AKT1, ARID1A, PIK3CA, CDKN2A, CCND1, CDK4, and CDK6 (all $p\leq0.01$), with weaker associations for STK11, SMAD4, and TP53. NRAS-mutant tumors significantly co-occurred with CDKN2A, APC, BRAF, NF1, and TERT (all $p<0.001$) and were mutually exclusive with TP53, STK11, and PIK3CA.
Conclusions: Rare RAS alleles are common across solid tumors and show distinct codon- and lineage-specific architectures. KRAS alterations are broadly pan-epithelial, whereas HRAS and NRAS cluster within discrete niches. Co-mutation patterns differ, with KRAS linked to PDAC/LUAD/CRC tumor-suppressor pathways, HRAS to NOTCH1-FGFR3-PI3K-AKT-CDK signaling, and NRAS to BRAF, NF1, and TERT. These data support co-mutation-driven combinations and lineage-tailored therapeutic strategies for next-generation RAS-targeted approaches.

#3989 Mutant p53 neomorphic activities drive organ-specific metastatic programs through distinct transcriptional networks.

G. Efe[1], R. Navaridas[1], K. M. Cunningham[1], D. Hasson[2], C. Lu[3], J. J. Manfredi[2], C. L. Prives[4], A. K. Rustgi[1];
[1]Herbert Irving Comprehensive Cancer Center, New York, NY, [2]Icahn School of Medicine at Mount Sinai, New York, NY, [3]Columbia University Irving Medical Center, New York, NY, [4]Columbia University, New York, NY

Mutations in the tumor suppressor p53 correlate with poor prognosis and high metastasis rates, which account for more than 90% of cancer-related mortality worldwide. Our recent work (Cancer Discovery PMC10841313), highlights that mutant p53 may exhibit neomorphic gain-of-function properties, driving squamous cell carcinoma (SCC) metastasis beyond its classic role via wild-type p53 loss. While our previous work and emerging studies have highlighted the neomorphic gain-of-function activities of mutant p53 in promoting metastasis, the tissue-specific transcriptional programs that underlie metastatic organotropism remain underexplored.
To identify mutant p53-dependent mechanisms in facilitating organ-specific metastasis, we performed RNA-sequencing coupled with ChIP-sequencing on esophageal squamous cell carcinoma (ESCC)-derived lung and liver metastases harboring either mutant p53-R172H or p53 deletion. Analyses included differential gene expression (DEG), pathway enrichment, and comparisons between primary tumor and metastatic tumor transcriptomes. These studies were complemented by analyses of aero-digestive squamous cell carcinoma datasets from the AACR Project GENIE, TCGA, and tissue microarrays assessing mutant p53 in relation to patient survival and enriched molecular pathways.
Mutant p53 contributed to distinct transcriptomic shifts in liver versus lung metastases. In lung metastases, 618 genes were upregulated and 667 downregulated dependent upon mutant p53-R172H, with enrichment in distinct immune response programs. By contrast, liver metastases showed 1,320 upregulated and 1,355 downregulated genes, with strong downregulation of interferon and inflammatory response pathways. Our analyses exhibited minimal overlap between up- or downregulated genes across tissues (103 shared downregulated and 77 shared upregulated genes), highlighting organ-specific p53-mediated transcriptional control.
Furthermore, comparisons with primary tumors revealed subsets of DEGs uniquely dependent on p53-R172H across metastatic and primary contexts. Notably, only a small core set of genes (*Acot1*, *Ldhb*, *Bcat1*, *Il18rap*, *Kif6*, *Paqr4*, *Il1rl1 and Cdc20)* were upregulated in all three settings (primary, lung, liver), while most gene expressions were organ-specific.
Overall, our results reveal novel insights into the mechanisms underlying mutant p53-mediated metastatic organotropism. These data highlight the necessity of incorporating the organ specific context metastatic cancers into therapeutic strategies driven by mutant p53.

#3990 Real-world evidence of KMT2C mutation as a biomarker of sensitivity to platinum-based therapy in solid cancers.

Bruno Bockorny[1], Yingying Yu[2], Pedro Danielian[1], Yujing Jan Heng[1], Xiaohui Li[1], Stamatina Fragkogianni[2], Lisa Macera[2], Metamia Ciampricotti[2], Gerburg M. Wulf[1]

[1]Beth Israel Deaconess Medical Center, Boston, MA,[2]Tempus, Chicago, IL

Introduction: Epigenetic dysregulation, driven by alterations in the lysine methyltransferase 2C (*KMT2C*) gene, contributes to tumor growth. *KMT2C* is a putative tumor suppressor mutated in 7%-10% of solid tumors. Loss of *KMT2C* function impairs homologous recombination DNA repair, making tumor cells more susceptible to PARP inhibition. The study used a real-world dataset to assess if *KMT2C* mutations predict platinum-based chemotherapy (PBC) responsiveness and clinical outcomes in solid cancers.
Methods: The Tempus Lens Platform (Tempus AI, Inc., Chicago, IL) was used to query the Tempus multimodal de-identified database and establish and subsequently analyze a cohort of patients (pts) with solid cancers and Tempus xT (DNA) testing. Pts characteristics were compared using Chi-squared/Fisher's exact tests and/or Wilcoxon sum tests. Real-world overall survival (rwOS) and progression-free survival (rwPFS) were compared between *KMT2C*^{mut} vs *KMT2C*^{wt} and defined as the time from PBC initiation to death or loss to follow up (FU) and as the time from PBC initiation to first progression, death, or loss to FU, respectively. Median rwOS and rwPFS were estimated by Kaplan-Meier and compared using log-rank tests. Risk set adjustment was used to avoid immortal time bias due to left truncation. Findings were validated in the AACR Genie dataset for rwOS after PBC and non-PBC.
Results: A total of 143,961 patients were included, and stage IV disease accounted for 76%. GI cancers comprised 36% of the cohort, followed by lung (25%) and breast (11%). *KMT2C* mutations occurred in 5.3% overall, most frequent in cervical (14%), endometrial (11%), urinary tract (8.6%) and breast cancer (8.4%). African American patients showed slightly higher prevalence versus non-AA both overall (5.6% vs 5.2%, p=0.089) and in GI cancers (5.4% vs 4.6%, p=0.013). In PBC-treated patients, median rwOS was longer in *KMT2C*^{mut} vs *KMT2C*^{wt} across all cancers (19.6 vs 16.7 mo, p=0.038), endometrial (42.3 vs 31.9 mo, p=0.03), head and neck (28.4 vs 13.3 mo, p=0.02), and GI (18.9 vs 15.7 mo, p=0.006). Within the GI group, colorectal cancers (CRC) had the largest impact (median rwOS of 51.0 vs 25.3 months, p=0.01). In CRC, rwPFS for *KMT2C*^{mut} vs *KMT2C*^{wt} were Not Reached vs 16.7 months (p=0.001), respectively. AACR Genie was analyzed to validate these results. A total of 1,551 CRC cases were included, with 8% harboring *KMT2C* mutations. CRC *KMT2C*^{mut} had improved rwOS compared to *KMT2C*^{wt} following PBC (Not Reached vs 57.5 months, p=0.005). This effect appeared specific to PBC, with no difference after irinotecan-based therapy.
Conclusion: *KMT2C* mutations are linked to improved survival after platinum chemotherapy, particularly in CRC and other GI cancers, supporting *KMT2C* as a predictive biomarker. Laboratory studies to define the mechanistic basis of this association are underway.

#3991 BRAF N486_P490del and fusions as distinctive gene alterations in pancreatic ductal adenocarcinomas: Analysis of C-CAT and AACR Project GENIE data.

K. Ochi[1], C. Morizane[1], K. Shiraishi[2], T. Koyama[1], K. Sunami[3], R. Kitadai[1], Y. Okuma[1], T. Shiraishi[2], E. So[1], Y. Goto[1], S. Hakui[1], K. Fujisaki[1], K. Onuma[1], Y. Komori[1], D. Yamashige[1], M. Okada[1], S. Harai[1], Y. Maruki[1], Y. Kawamoto[1], Y. Nagashio[1], S. Hijioka[1], H. Ueno[1], T. Okusaka[1];

[1]National Cancer Center Hospital, Tokyo, Japan, [2]National Cancer Center Research Institute, Tokyo, Japan, [3]National Cancer Center Hospital, Department of Laboratory Medicine, Japan

Backgrounds: *BRAF* genomic alterations (GAs) have been identified in various tumors and are categorized into three distinct classes. Based on their impact on RAS-independent kinase activity, class 1 (monomer) and class 2 (dimer) are significant treatment targets and class specific regimens are being developed. However, the distribution of these classes across different primary sites has not yet been clarified. In patients with pancreatic cancer (PC), class 2 *BRAF* GAs have occasionally been encountered in clinical practice. Because precision oncology is limited in PC, *BRAF* GAs are precious target. To elucidate the patterns of *BRAF* GAs in PC, we investigated two extensive databases. Methods: We analyzed the Japanese nationwide C-CAT data and the AACR Project GENIE data. *BRAF* GAs were annotated using OncoKB and AlphaMissense and classified into three classes based on the published literature. Results: In the C-CAT data (N=107,714), as summarized in the table, *BRAF* GAs (n=3559, 3.3%) were frequently observed in thyroid, skin, and colorectal cancers, but these were mainly class 1(mostly V600E). In contrast, PC showed a distinct profile: among 11,959 patients with PC, *BRAF* GAs were detected in 230 (1.92%), Class1 was relatively rare (15.6%) and 60.4% (139/230) were class 2. These were mainly composed of in-frame deletions (n=97), with N486_P490del (n=79) and fusions (n=28). In GENIE data (N=250,018), 1.6% (169/10,730) of patients with PC harbored *BRAF* GAs. Although proportion of V600E was higher than that in C-CAT (19.5%), class 2 was dominant (63%, 108/169), such as fusions(n=48) and N486_P490del (n=28). Among *BRAF* N486_P490del positive solid tumors, pancreas was dominant primary site in both C-CAT (82%, 79/96) and GENIE (52%, 28/53). Conclusions: Class 2 *BRAF* GAs, especially N486_P490del and fusions, are distinctive alterations in patients with PC, and the development of class 2 specific targeted therapies is urgently needed.

Cancer type	Total	BRAF oncogenic	Frequency	Class1		Class2					Class3
					V600E		N486_P490del	fusion	K601E	G469A	
	N	n	%	n/%	N	n/%	n	n	n	n	n/%
Thyroid	880	460	52.2	454/98.6	454	6/1.3	1	3	2	0	0/0
Skin	1507	208	13.8	167/80.2	138	23/11.0	0	8	2	6	10/4.8
CNS/Brain	3181	254	7.9	177/69.6	177	52/20.4	1	43	1	0	12/4.7
Bowel	14909	1174	7.8	758/64.5	759	126/10.7	2	25	22	18	233/19.8
Biliary Tract	7729	341	4.4	58/17.0	54	92/26.9	4	2	18	20	159/46.6
Lung	4577	195	4.2	33/16.9	32	78/40.0	3	13	22	18	54/27.6
Prostate	3865	112	2.8	1/0.8	1	88/78.5	0	30	30	15	3/2.6
Pancreas	11959	230	1.9	36/15.6	34	139/60.4	79	28	2	4	15/6.5

#3992 Leveraging Ultima Genomics ppmSeq WGS-cfDNA to accurately detect clonal evolution over sequential blood biopsies.

Elizabeth E. Martin[1], Julian Hess[1], Carrie Cibulskis[1], Mendy Miller[1], Brian P. Danysh[1], Chip Stewart[1], Elena Helman[2], Ilya Soifer[2], Doga C. Gulhan[3], Dejan Juric[4], Doron Lipson[2], Gad Getz[1]

[1]Broad Institute of MIT and Harvard, Cambridge, MA,[2]Ultima Genomics, Tel Aviv, Israel,[3]Krantz Family Center for Cancer Research and Dept. of Pathology, Massachusetts General Hospital, Boston, MA,[4]Krantz Family Center for Cancer Research and Dept. of Pathology, Massachusetts General Hospital, Cambridge, MA

Comprehensively modeling tumor evolution is important for cancer diagnosis, treatment, and minimal residual disease (MRD) monitoring. Liquid biopsies enable non-invasive sampling of tumor DNA during a patient's cancer treatment. Accurate detection of low allele fraction somatic variants in circulating tumor DNA (ctDNA) has clinical importance for cancer detection and monitoring. Current ctDNA panel sequencing methods lack the breadth of variants captured in whole genome sequencing (WGS) and cannot fully track tumor clones over time. Moreover, deep and accurate cell-free DNA (cfDNA) sequencing is challenging due to constraints of low tumor fraction in the blood and the high cost of WGS sequencing.

Ultima Genomics (UG) developed paired plus-minus sequencing (ppmSeq) technology, a whole-genome duplex sequencing approach that lowers observed error rates and allows for a high yield of duplex molecules. Using UG's deep WGS ppmSeq, we developed our mutation calling algorithms to enable sensitive detection of somatic variants in cfDNA samples, allowing us to track clonal populations over time. To test whether we could identify shared clonal populations in patient sequences between other platforms and ppmSeq technology, we collected post-mortem tissue specimens from 12 patients of various cancer types (breast, cholangiocarcinoma, etc.) and 38 pre-mortem cfDNA samples from the same patients. First, these patients' data were sequenced with existing Illumina sequencing technologies (WES) and then on the UG sequencing platform for both tissue and ppmSeq.

We sequenced the ppmSeq data to an average depth of 135x (range 104x to 208x) and achieved an average duplex proportion of 38% (range 31% to 44%). For all patients' tissue and cfDNA samples that were sequenced with both ppmSeq WGS (UG) and WES (Illumina), we reconstructed phylogenetic trees to determine the life history of the cancer using our PhylogicNDT suite of tools. Phylogenies reconstructed from ppmSeq WGS cfDNA identified many more mutations and richer trees than those reconstructed from WES of the same cfDNA samples. We compared the cfDNA ppmSeq phylogenies with those constructed from WGS of the same patient's tissue samples and identified the same clonal populations, enabling us to match clones from the blood to the tissue and track the progression of individual clones.

The identification of large clonal populations in ctDNA sequenced with Ultima Genomics' ppmSeq approach is an improvement over methods with lower sensitivity and coverage; moreover, this approach can identify clonal populations that change over a given treatment course. This more accurate inference of cancer evolution information could enable us to better guide therapies and identify novel mechanisms of resistance that would have been missed with prior methods.

#3993 Artificial intelligence-integrated analysis of the gut microbiome in early- and late-onset colorectal cancer among populations at increased risk using clinical, genomic, and social determinants data.

S. Manjarrez[1], F. Carranza[1], B. Waldrup[1], X. Qi[1], A. L. Cruz Gomes[1], D. O. Garcia[2], A. Maldonado[2], J. Karmouch[1], R. Jenq[1], PE-CGS Network, E. Velazquez-Villarreal[1];

[1]City of Hope National Medical Center, Duarte, CA, [2]University of Arizona, Tucson, AZ

Early-onset colorectal cancer (EOCRC) is rising globally and disproportionately affects populations at increased risk. The gut microbiome has been implicated in colorectal cancer development, yet its relationship to early- versus late-onset disease within these communities remains unclear. This study aimed to characterize microbiome differences across age-defined CRC subgroups using an AI-enabled, multi-domain analytical framework.We analyzed 2,715 colorectal cancer (CRC) tumor samples from patients in our NIH Cancer Moonshot COPECC PE-CGS Network and public data repositories. Within this cohort, stool samples were collected from 23 patients diagnosed with CRC. Microbial profiling was performed using 16S rRNA sequencing and complemented by whole-exome sequencing, RNA sequencing, clinical variables, and social determinants of health (SDOH). Mutation frequencies across different populations were evaluated using the AACR Project GENIE database. Conversational artificial intelligence platforms (AI-HOPE) were used to integrate and query multi-omics and SDOH data, enabling identification of patterns associated with age at onset.EOCRC cases demonstrated lower microbial richness compared with late-onset CRC. Distinct differences in microbial composition and relative abundance were observed when stratifying by genetic ancestry, mutation frequency, gene fusions, copy number variation, clinical features, and SDOH factors. AI-guided integration further highlighted age-specific microbial profiles that aligned with multi-omic alterations.These findings reveal notable microbiome differences between early- and late-onset CRC in populations at increased risk. This preliminary work underscores the utility of artificial intelligence-supported integrative analysis and highlights the need for larger comparative studies to determine whether specific microbial signatures contribute to variations in CRC onset and outcomes.

#3994 Differences in the mutational landscape across race and sex highlight distinct TP53-associated risk in multiple myeloma.

C. Ugwu[1], N. Ubah[2], M. Megiso[1], A. Uriepero Palma[1], T. Verinumbe[1], A. Chachua[1], S. King[1], A. Neely[1], E. Obomanu[1], A. Taneja[3], A. Turki[4];

[1]Jefferson Einstein Philadelphia Hospital, Philadelphia, PA, [2]Montefiore St Luke Cornwall Hospital, Newburg, NY, [3]Sidney Kimmel Comprehensive Cancer Center, Jefferson Einstein Philadelphia Hospital, Philadelphia, PA, [4]Marienhospital University Hospital, Ruhr-University Bochum, Germany

Background:
Complex health disparities involving race, sex, and genomics have been described in multiple myeloma (MM) (Tebuka E et al. Blood Gl. Hem. 2025). Large genomic studies have highlighted the impact of the mutational landscape (Maura F et al. JCO 2024; Schavgoulidze A et al. Blood 2024); however, the role of gene-gene interactions, including those involving TP53 alterations, has not yet been extensively examined by race and sex.

Methods:
Using a large, multi-institutional targeted sequencing dataset from the AACR GENIE v18 cohort, we analyzed 1,020 patients with MM (White n=839; Black n=181). Patients with at least one successfully profiled gene were included. Co-occurrence analyses were restricted to mutation-bearing patients. Clinical features, mutation burden, and fraction of genome altered were compared using Wilcoxon and Fisher tests. Differences in co-occurrence distributions were evaluated with Mann-Whitney U tests. Overall survival was assessed using multivariate Cox models, including interaction terms for TP53 with race and sex.

Results:
Age differed between Black and White patients (median 63.5 vs 66 years; p=0.002) but not between males and females. Mutation burden and fraction of genome altered were comparable across groups (p>0.16). No individual mutation frequency differences remained significant after correction for multiple testing.

In contrast, the landscape of gene-gene interactions with TP53 varied substantially by race (p=0.027) and sex (p=0.038). White patients showed numerous TP53-associated co-mutations, including TP53-TET2 (11.1% vs 0%), -FAT1 (10.2% vs 0%), -KRAS (8.3% vs 0%), -DNMT3A (7.4% vs 0%), -DIS3 (6.5% vs 0%), -BRAF (5.6% vs 0%), and TP53-TRAF3 (4.6% vs 0%). Black patients exhibited more NRAS-centered co-mutations, including NRAS-KRAS (7.41% vs 1.35%) and NRAS-CYLD (6.17% vs 1.57%). The NRAS-centered pattern was present in both sexes, with females showing slightly higher NRAS frequency and stronger clustering with DNMT3A and TET2. Examination of sex subgroups also showed the highest proportion of TP53 co-mutations among White males (16.6%) compared with White females (10.3%, p=0.009).

Overall survival did not differ by race (p=0.83) or sex (p=0.11). TP53 mutation was associated with significantly shorter survival (p=0.0018), with a significant interaction between TP53 status and sex (p=0.0078). TP53-mutated males had the poorest outcomes.

Conclusions:
These findings underscore the importance of gene-gene interactions in MM and their relevance to understanding health disparities. The absence of TP53 co-mutational patterns among Black patients is notable and may have implications for future trial design and risk-stratification strategies.

: Biomarkers That Change Management: Predicting Therapy Benefit, Progression, and Metastatic Risk Minisymposium

#4015 Whole-genome duplication predicts metastasis risk and timing across human cancers.

J. Xu, H. Walch, M. Perry, C. Fong, J. Jee, K. Pichotta, A. Price, A. L. Richards, C. Bandlamudi, M. Donoghue, N. Schultz, W. K. Chatila;
Memorial Sloan Kettering Cancer Center, New York, NY

Introduction:
Whole-genome duplication (WGD) is a pervasive event in cancer evolution, conferring tolerance to large-scale genomic alterations and reshaping selective pressures. While WGD is linked to aneuploidy and poor prognosis, its impact on metastatic risk across cancer types remains unclear. We evaluated whether WGD detected in the primary tumor predicts subsequent metastasis risk and timing in a pan-cancer cohort.
Methods:
We analyzed 33,349 tumors across 29 cancer types profiled by MSK-IMPACT (2014-2024). Metastatic site and timing were derived from NLP-based annotations integrating pathology and radiology reports. Analyses were restricted to stage I-III primary tumors without prior metastasis. Landmark analyses at 1 and 3 years compared distinct metastatic sites among patients with sufficient follow-up, excluding cancer types with fewer than 50 eligible patients at the 3-year landmark. Within each cancer type, nonparametric cumulative incidence functions were estimated with death as a competing event. WGD was inferred from FACETS allele-specific copy numbers, defining WGD-positive as >50% of autosomes with major copy number ≥2.
Results:
In total, 6,434 primary tumors met inclusion criteria, comprising 5,170 WGD- and 1,264 WGD+ cases. Across cancer types, WGD+ tumors showed a significantly higher likelihood of metastasis within three years compared with WGD- tumors (60.4% vs. 42.0%, $p<0.001$), a pattern consistent within individual cancer types. WGD+ tumors also exhibited a greater metastatic burden, with a higher proportion of patients developing metastases to ≥3 sites (20.4% vs. 11.3%, $p<0.001$). WGD+ tumors were more likely to develop brain metastases overall (4.7% vs. 2.6%, $p=0.003$). One-third (32.2%) of WGD+ tumors lacked TP53 alterations, indicating genome doubling can arise independently of canonical TP53 loss. WGD significantly predicted metastatic progression in both TP53-altered (HR=1.10, $p=0.043$) and TP53-wildtype tumors (HR=1.38, $p<0.001$), with a larger effect size observed in the TP53-wildtype subset.
Conclusions:
In this pan-cancer, primary-only analysis, WGD emerged as an early and consistent predictor of metastatic progression across tumor types, with effects persisting in TP53-wildtype disease. These findings position WGD as a unifying hallmark of cancer progression and highlight how large-scale genomic-clinical integration can reveal key determinants of tumor evolution.

#4016 Tissue-based homologous recombination deficiency status prediction in patients with breast, ovarian, and pancreatic cancers.

P. Safabakhsh, D. Tolkunov, B. Overstreet, M. Lefterova, L. Lawrence;
Guardant Health, Palo Alto, CA

Introduction: Homologous recombination deficiency (HRD) is a predictive biomarker of response to PARP inhibitors and other DNA damage response (DDR)-targeting therapies across cancer types. HRD can be detected by identifying mutations in *BRCA1/2* or other homologous recombination repair (HRR) genes, or through copy number (CN) or single nucleotide variant (SNV)-based signatures associated with genomic instability. While genomic instability status (GIS) is an FDA-approved biomarker for ovarian cancer treatment, comprehensive tissue-based GIS detection across multiple cancers is still limited. We developed and validated a tissue-based GIS predictor integrating CN and SNV signatures for breast, ovarian, and pancreatic cancers.
Methods: We implemented an ensemble model to predict GIS using HRR gene deficiency to infer SNV and CN signatures associated with HRD. The model was trained on clinical samples processed on Guardant360 Tissue (Guardant Health, Palo Alto, CA), incorporating select HRD-associated COSMIC single base substitution (SBS) signatures (v3.4) and genomic scarring features such as loss-of-heterozygosity (LOH). The aggregate model was evaluated on an independent cohort of clinical breast, ovarian, and pancreatic samples with tumor purity ≥ 20%. *BRCA1/2* or *PALB2* biallelic loss and strict wildtype status in 14 HRR genes were used as orthogonal labels to assess sensitivity; while a cohort wildtype for an expanded set of pathogenic or likely pathogenic variants in HRR genes was used to estimate specificity.
Results: The GIS model achieved an overall AUC of 0.98, with sensitivity of GIS detection of 90% in breast cancer, 91% in ovarian cancer, and 80% in pancreatic cancer. GIS detection in HRR-negative samples was < 3% in all three cancer types. Prevalence of GIS detection among clinical samples was 256/803 (32%) in breast cancer, 56/107 (52%) in ovarian cancer, and 40/214 (19%) in pancreatic cancer. Among patients with GIS detected, 75% of breast cancers, 39% of ovarian cancers, and 67% of pancreatic cancers did not harbor pathogenic *BRCA1/2* or *PALB2* mutations.
Conclusions: We present a tissue-based genomic instability detection method demonstrating strong performance in breast, ovarian, and pancreatic cancers. Prostate cancers, which also commonly exhibit HRD, showed a distinct genomic scarring signature and are being actively investigated for future incorporation into the GIS model.This comprehensive biomarker expands HRD testing beyond HRR mutations to capture a broader patient population who may benefit from DDR-targeting therapies.

#4017 Integrated multi-omics approaches in resectable hepatocellular carcinoma with microvascular invasion for revealing therapeutic target.

J. So, I. Kang, W. Kwon, S. Lee;
Omics & Real-world Data-driven AI for Precision Medicine Lab, Seongnam, Korea, Republic of

Introduction: Hepatocellular carcinoma(HCC) with microvascular invasion(MVI) has the traits of aggressive and rapid proliferation rate and penetration along blood vessels. Therefore, MVI is one of the clinical features of liver cancer with a high risk of recurrence and a poor prognosis. There is a need to explore biomarkers and customized drugs for early diagnosis of MVI.
Methods: Using gene expression of resected human HCC samples (Discovery cohort, n=240), we identified a transcriptomic signature predictive of MVI. Subsequently, we performed integrated analyses using data from the cancer dependency map (DepMap) project, including multi-omics based cancer-specific molecular characterization, compound-based drug sensitivity screening, and integrative *in-silico* prediction approaches to investigate determinants of MVI. The resulting MVI-predictive transcriptomic signature was validated across multiple independent cohorts (TCGA-LIHC, n=373; KOREA, n=188; TOKYO, n=183; MODENA, n=78; ZHONGSHAN, n=159).
Results: The MVI 1,028 genes signature was identified in the discovery cohort, and its predictive performance was robustly validated in the independent validation cohort (AUC = 0.889, $p < 0.01$). Multi-omics analyses revealed aggressive tumor biology associated with the MVI signature and highlighted specific biomarkers.
Conclusions: Integrative multi-omics profiling of resectable HCC with MVI reveals biomarkers for the diagnosis of MVI and therapeutic target. This target will increase the therapeutic effect and play a key role in the precision medicine.

#4018 Stromal immune composition significantly contributes to adenomatous polyp recurrence or progression to cancer.

M. Dehankar[1], L. A. Boardman[1], D. O'Brien[2], E. A. Thompson[3], J. M. Kachergus[3], J. Shi[3], A. Abyzov[1], M. Suvakov[1], R. P. Graham[1], C. Wang[1];

[1]Mayo Clinic, Rochester, MN, [2]Ambry Genetics, Aliso Viejo, CA, [3]Mayo Clinic, Jacksonville, FL

Background: Most colorectal cancer (CRC) arises from polyps and is mainly prevented by polypectomy. The most important polyps to manage with colonoscopy are those with highest CRC risk- namely, advanced polyps (> 1cm, villous histology or high-grade dysplasia (HGD). Yet, 48% of advanced polyps recur within 1 to 3 years of removal, and up to 5% of advanced polyps under surveillance still progress to CRC. We performed this pilot study to investigate molecular and microenvironment heterogeneities of polyps and how they might impact their clinical behavior.

Methods: GeoMx spatial transcriptomics was performed on FFPE tissues from three different polyp outcome phenotypes (POPs) including the polyp that does not recur (POP-NR), that recurs following polypectomy but cured by colonoscopy (POP-R) or the polyp despite polypectomy develops CRC at the polypectomy(ies) site (POP-CRC). Normal colon and polyp with low or HGD from the index polyp were assessed from 6 patients with POP-NR, 9 with POP-R and 12 with POP-CRC with a minimum of 2 follow up colonoscopies at 3-year intervals. Epithelium was identified as PanCK positive, and stroma identified as PanCK negative and positive nuclear staining. Cell type deconvolution was implemented using single-cell adult human intestinal tract catalogue (Elmentaite *et al.,* https://www.gutcellatlas.org/). Differential gene expression (DEG), cell type abundance and functional enrichment analyses was performed using linear mixed effects model, and observations with p-value < 0.05 and log2FC >= |1| are reported.

Results: The greatest number of DEGs were identified in stroma of the index POP-CRC compared to POP-NR polyps (n = 17 down and 11 upregulated genes), followed by epithelium of the index POP-CRC vs POP-NR polyps (n = 10 down and one upregulated gene(s)). Between the index POP-CRC and POP-R, epithelium showed downregulation of 7 genes, and upregulation of no genes. In stroma two genes were down and none upregulated. Four genes were downregulated in stroma of the index POP-R vs POP-NR polyp and 3 in epithelium, and one gene was upregulated in stroma and another in epithelium. *MZT2B* was upregulated in stroma of both the index POP-R (log2FC = 1.09, p-value = 0.0014) and POP-CRC (log2FC = 1.29, p-value = 0.0001) and has been implicated as a prognostic marker associated with worse prognosis in certain cancers. IgM and IgA plasma cells, proximal progenitors, MMP9+ inflammatory macrophages and myofibroblasts were found to be downregulated in epithelium of index POP-CRC and POP-R compared to POP-NR polyps; while microfold cells were downregulated in stroma of index POP-CRC and POP-R compared to POP-NR polyps.

Conclusions: The stromal microenvironment and less so, epithelial features present in the index polyp differ based on a polyp's future clinical behavior. The polyp-immune interaction warrants further study as a potential prevention target against polyp progression.

#4019 Clinical validation of WES-based HRD scoring and its prognostic value for PARP inhibitor maintenance therapy in ovarian cancer.

D. Kyung[1], K. Han[2], Y. Cha[1], W. Ko[1], H. Roh[1], N. Park[2], C. Lee[2], S. Kim[2], T.-Y. Kim[2];
[1]IMBDx, Seoul, Korea, Republic of, [2]Seoul National University Hospital, Seoul, Korea, Republic of

Background: Homologous recombination deficiency (HRD) predicts PARP inhibitor (PARPi) sensitivity in ovarian cancer. We evaluated the clinical and analytical performance of a WES-based genomic profiling assay generating HRD scores and BRCA status, and assessed its prognostic value for PARPi maintenance.
Methods: We included 81 consecutive patients with epithelial ovarian cancer (FIGO I-IV) who had received PARPi therapy between 2017-2024 at Seoul National University Hospital. After tumor purity estimation and microdissection, formalin-fixed, paraffin-embedded (FFPE) surgical tumor tissues and matched blood were analyzed using the CancerProfiler™ WES panel. HRD scores were derived from genomic scar metrics (LOH, TAI and LST) following the scarHRD algorithm. Germline and somatic BRCA1/2 variants were profiled concurrently. HRD-high status was defined at ≥42 and ≥50. Tumor purity and fraction were estimated from WES data and incorporated into HRD computation to ensure quantitative stability.
Results: Median age was 56; 96% had high-grade serous carcinoma and 94.8% FIGO III-IV disease. Optimal cytoreduction (<1 cm residual) was achieved in 61%, and 52% received neoadjuvant chemotherapy. By the WES panel assay, a total of 46 patients had germline or somatic BRCA mutations. HRD-high status was observed in 77.8% at ≥42 and 66.7% at ≥50; the ≥50 cutoff showed a stronger association with germline BRCA (OR 3.15; p=0.021). Among 73 PARPi maintenance recipients (52 first-line and 23 second-line), HRD ≥50 showed differential predictive value by NAC. In first-line recipients, PFS was similar between HRD-high and -low after NAC (15.3 vs 11.3 mo, p=0.77) but markedly longer in HRD-high without NAC (median not reached vs 7.66 mo, p=0.001). This pattern persisted in the second-line setting (NAC: 19.48 vs 6.49 mo, p=0.049; no NAC: 17.78 vs 2.43 mo, p<0.001). BRCA mutation predicted benefit only in NAC-treated first-line patients (17.7 vs 4.5 mo, p=0.007) and not elsewhere. HRD-high was an independent predictor of longer PFS (first-line HR=0.26, p=0.02; second-line HR=0.20, p=0.029). In multivariable analyses, the predictive value of PARP inhibitors was BRCA-dependent only in the first-line setting (HR=0.09, p=0.001), with no significant association observed in the second-line (HR=0.28, p=0.226). By contrast, HRD-high status remained a consistent independent predictor in both first- (HR=0.26, p=0.02) and second-line therapy (HR=0.02, p=0.029), emerging as the sole significant determinant after recurrence.
Conclusions: HRD ≥50 is a robust predictor of PARPi benefit—particularly in treatment-naïve tumors—whereas BRCA status shows limited and NAC-dependent predictive value. These findings support prospective multi-center validation of WES-based HRD assays as scalable alternatives to array-based platforms.

#4020 Utility of CA19-9 for prediction of asymptomatic pancreatic cancer among patients with new onset diabetes.

J. Fahrmann[1], C. Lopez[2], E. Irajizad[1], S. Chari[1], J. Vykoukal[1], R. Spencer[1], J. B. Dennison[3], E. J. Koay[3], F. McAllister[3], M. P. Kim[1], J. Rinaudo[4], P. A. Hart[5], W. E. Fisher[6], S. Van Den Eeden[7], B. Wu[1], Z. Feng[8], S. M. Hanash[3], A. Maitra[9];
[1]The University of Texas MD Anderson Cancer Center, Houston, TX, [2]Fred Hutchinson Cancer Center, Seattle, WA, [3]UT MD Anderson Cancer Center, Houston, TX, [4]National Cancer Institute, Bethesda, MD, [5]The Ohio State University Wexner Medical Center, Columbus, OH, [6]Baylor College of Medicine, Houston, TX, [7]Kaiser Permanente Northern California, Oakland, CA, [8]Fred Hutchinson Cancer Research Center, Seattle, WA, [9]NYU Grossman School of Medicine, New York, NY

Purpose: New-onset diabetes (NOD) is an early indicator of pancreatic ductal adenocarcinoma (PDAC). There remains a need to establish biomarkers that can reliably identify NOD patients at risk of having occult PDAC. Here, we assessed the predictive performance of single timepoint CA19-9 as well as an established algorithm that considers repeat CA19-9 testing for risk prediction of PDAC among a prospective cohort of patients with NOD.
Methods: CA19-9 was assayed in 6,516 serially collected pre-diagnostic plasma samples collected from 2,121 NOD patients from the Consortium of Chronic Pancreatitis Diabetes and Pancreatic Cancer (CPDPC)-initiated NOD study who completed the 3-year study follow-up period. The specimen set included 25 pre-diagnostic samples from the 12 PDAC cases diagnosed during study follow-up. We applied a single threshold (ST) method, which considers CA19-9 levels at a single time point, as well as a previously established parametrical empirical Bayes (PEB) algorithm [referred to as $PEB^{CA19\text{-}9}$], which considers prior CA19-9 results, with 'case' calls made based on pre-specified cutoffs corresponding to 1% 1-year risk. Resultant CA19-9 continuous data as well as case calls were provided to the EDRN Data Management and Coordinating Center as part of a Prospective-sample-collection-Retrospective-Blinded-Evaluation (ProBE)-compliant Phase 3 biomarker validation study. Sensitivity, specificity, population-level positive predictive value (PPV), and negative predictive value (NPV) are reported.
Results: The 3-year incidence of PDAC in the NOD cohort was 0.57%. At the patient level, CA19-9 yielded sensitivity of 83.3% at 97.2% specificity, with respective PPV and NPV of 14.7% and 99.9%. Sensitivity for early-stage (I-II) disease was 100%. In a subset of patients, CA19-9 first tested 'positive' at a median (interquartile range [IQR]) of 7 months (4 to 14 months) prior to clinical PDAC diagnosis. Of the two PDAC cases missed by CA19-9 using the ST method, one (diagnosed with stage III PDAC) was detected using the $PEB^{CA19\text{-}9}$ algorithm.
Conclusion and Relevance: In the setting of adult new onset diabetes, CA19-9 is a readily available and promising biomarker that can be leveraged for earlier detection of an underlying pancreatic cancer.

#4021 Precision diagnostics for early melanoma detection using spatial biology and AI guided image analysis.

Y.-C. Kao[1], S. X. Tan[1], X. Tan[2], H. Oey[1], K. J. Lee[1], T. Vallius[3], R. Pelletier[4], A. Causer[5], C. Zhou[1], D. Smit[1], J. O'Neill[1], A. Xiong[6], B. O'Brien[7], A. Collins[7], P. K. Sorger[8], H. Soyer[1], K. Khosrotehrani[1], Q. Nguyen[2], M. S. Stark[1];
[1]Frazer Institute, The University of Queensland, Dermatology Research Centre, Brisbane, Australia, [2]QIMR Berghofer Medical Research Institute, Brisbane, Australia, [3]Harvard Medical School, Brookline, MA, [4]Laboratory of Systems Pharmacology, Harvard Program in Therapeutic Science, Harvard Medical School, Boston, MA, [5]Institute for Molecular Bioscience, the University of Queensland, Brisbane, Australia, [6]QIMR Medical Research Institute, Queensland, Australia, Brisbane, Australia, [7]Sullivan Nicolaides Pathology, Brisbane, Australia, [8]Harvard Medical School, Winchester, MA

Accurate diagnosis of melanoma is particularly challenging, as malignant lesions often resemble benign naevi. The gold standard for diagnosing melanocytic lesions relies on the examination of morphological cell features using hematoxylin and eosin (H&E) stained tissue samples. This process however is often subject to variability, lacking the sensitivity to precisely define cell types with a high degree of accuracy. This project aims to overcome histopathological limitations by accurately defining transcriptional cell states, indicative of invasive potential, in benign and malignant lesions. We propose that this will enable more precise definitions of true melanomas in a sea of benign or indolent lesions, which constitute the bulk of excised lesions sent for diagnosis. To identify these “hidden” cell states, we performed spatially resolved whole transcriptome profiling (Visium CytAssist) of whole lesions using a large progression series of samples (n=75): ranging from healthy skin, naevi (benign and low to high grade dysplastic naevi), melanoma *in situ*, T1a melanomas, and melanoma arising from pre-existing naevi. To enable deconvolution of the Visium ‘spots’, we performed Single Cell RNA sequencing on healthy skin, naevi and thin melanomas, to determine marker genes specific to each cell type present in human skin. This analysis revealed a change of melanocyte cell states along melanoma progression, from conventional naevus to T1a melanomas. We further identified naevus and melanoma-specific signatures which can be spatially resolved, enabling classification of lesions as “benign” or “malignant”, as well as identifying previously hidden regions of malignant potential. We further utilised single cell resolved Xenium (transcriptomic) and Orion (proteomic) platforms to validate the spatial expression of benign and malignant genes and to finely characterise immune cell populations within the tumour microenvironment. Additionally, all specimens have been assessed for a panel of 361 cancer genes, facilitating a comprehensive characterization of the mutational profile driving melanoma progression. By integrating the molecular data with spatial gene expression analysis, we have developed an innovative deep learning model that enhances diagnostic precision for melanoma based on H&E-stained slides. Together, we have defined melanocyte cell states across melanoma progression and uncovered key tumour-microenvironment interactions. We envision that these data will permit AI-guided diagnosis to accurately delineate benign and malignant melanocytic lesions.

: Cracking Adaptive Resistance: AI-Enabled, Screen-Guided Targets in Tumor Plasticity, DNA Damage, Metabolism, and CTC-Associated Immunity
Minisymposium

#4033 Chemical trapping of inactive GRB2 dimer unveils a novel cancer vulnerability by coupling replication stress to anti-tumor immunity.

Z. Ahmed[1], D. E. Jones[2], J. A. Tainer[1];
[1]UT MD Anderson Cancer Center, Houston, TX, [2]University of Arkansas, Little Rock, AR

Growth Factor Receptor-Bound protein 2 (GRB2), a critical signal transduction adaptor, has been an elusive therapeutic target due to its ubiquitous SH2/SH3 domains, despite prior clinical evidence (e.g. a striking 75% complete remission in AML patients using liposomal antisense GRB2 RNA) supporting the high value of its inhibition. We overcame this long-standing "undruggable" challenge by leveraging our discovery that the GRB2 dimer is its auto-inhibited form with a unique druggable interface. We will report the structure-guided discovery and optimization of small molecule GRB2 inhibitors (GRB2i) that act by stabilizing this inactive dimer. Combining experimental structural biochemistry and AI-Machine Learning (AI-ML) refinement across chemical space, we have developed potent clinical leads. Our data reveal GRB2i primarily targets cancer-critical DNA Damage Response (DDR) pathways, rather than canonical GRB2 roles in cell growth and proliferation. Specifically, our GRB2i chemically induces catastrophic Homologous Recombination (HDR) deficiency and replication fork instability. This vulnerability renders cancer cells exquisitely sensitive to PARP inhibitors and other DNA damaging agents. Importantly, we show that GRB2i activates the cGAS/STING pathway, triggering the release of pro-inflammatory cytokines and creating a significant immune destruction liability for cancer cells. These collective results unveil a novel structure-guided strategy for small molecule GRB2 inhibition, demonstrating its potential as a single agent or strategic combination therapy to enhance anti-tumor immunity and exploit a central cancer vulnerability.

#4034 Computational ranking-guided discovery of Plexin-B2 as a driver of circulating tumor cell clusters and AI-facilitated neutralization to prevent and inhibit metastasis.

F. Tong[1], M. Veit Acosta[1], Y. Sun[2], Y. Jia[3], G. Hu[4], H. Liu[1];

[1]Northwestern University - Chicago, Chicago, IL, [2]Northwestern Univ. Feinberg School of Medicine, Chicago, IL, [3]Northwestern University, Chicago, IL, [4]Tufts University, Boston, MA

Our previous studies and other works demonstrate that multicellular circulating tumor cell (CTC) clusters are up to 50 times more efficient than single CTCs in mediating viable metastasis (*Cancer Discovery*, 2018, 2023). Yet, the molecular targets underlying this phenomenon and the CTC cluster interactions with immune cells remain poorly understood. To uncover key mediators of CTC clustering and metastatic progression, we developed a computational ranking pipeline integrating adhesion network analysis and metastasis-free survival modeling. This analysis prioritized Plexin-B2 (PLXNB2) as a top-ranked transmembrane protein associated with poor distant metastasis-free survival and enriched expression in CTC clusters from patients with advanced breast cancer. Functional studies demonstrated that loss of PLXNB2 (Plxnb2) markedly reduces both homotypic tumor-tumor and heterotypic tumor-myeloid (monocyte) cluster formation, thereby suppressing spontaneous metastasis *in vivo*. Mechanistically, PLXNB2 engages SEMA4C on tumor cells and SEMA4A on myeloid cells to drive intercellular adhesion and metastatic colonization. Integrative proteomic and pathway network analysis further identified downstream PLXNB2 signaling effectors regulating cell adhesion and stemness plasticity, corroborating its importance as a central hub for clustering. To therapeutically block PLXNB2 functions in metastasis, we obtained 106 anti-PLXNB2 monoclonal antibodies (mAbs) for functional screening and optimization, both computationally and experimentally. Using artificial intelligence (AI)-driven structural platforms and language models, we assessed the IgG binding and neutralizing possibilities in clustering and proliferation assays. Experimental screen of top candidates revealed that several antibodies effectively disrupted both homotypic tumor-tumor and heterotypic tumor-monocyte clustering. Furthermore, we implemented an AI-guided structural modeling workflow to predict the PLXNB2-IgG complex, identify active binding residues, and optimize antibody-antigen energetics for enhanced affinity and neutralization. Together, these findings identify PLXNB2 as a key molecular regulator of CTC clustering and metastatic seeding and establish a framework for structure-guided antibody engineering to therapeutically target CTC cluster-driven breast cancer metastasis.

#4035 SWELL1 controls epigenetic methylation, mitochondrial metabolism, and anti-tumor immunity in IDH-mutant gliomas.
H. Cheng, J. Chen, J. Huang, W. Liu, Z. Qiu;
Johns Hopkins University, Baltimore, MD

Diffuse gliomas account for the majority of adult brain malignancies with limited therapeutic options. Among them, isocitrate dehydrogenase (IDH)-mutant (mIDH) gliomas occur in the majority of diffuse low-grade gliomas with signatures of epigenetic hypermethylation, disrupted mitochondrial metabolism, and an immunologically “cold” microenvironment. Thus, identifying novel mediator that links these processes is critical for developing new treatments. Here, we identified SWELL1 (also known as LRRC8A) as a critical mediator for the mIDH glioma progression. SWELL1, the essential component of the volume-regulated anion channel (VRAC), has been linked to glucose metabolism, glutamate-mediated neuron toxicity, and ATP-induced microglial activation. In our study, SWELL1 knockout (SKO) in primary mouse mIDH gliomasphere cells resulted in increased epigenetic methylation, together with loss of cellular stemness transcriptional programs. Moreover, metabolomic and Seahorse analyses revealed loss of TCA cycle metabolites and decreased mitochondrial respiration in SKO gliomasphere cells, leading to loss of cell growth activities. These findings were further validated using patient-derived TS603 gliomasphere cells and the analysis of a recently published single-cell RNA-sequencing (scRNA-seq) dataset, in which tumors with low SWELL1 mRNA expression exhibited loss of proliferation and increased inflammation signatures. We further performed orthotopic xenograft model using mouse gliomasphere cells and found that mIDH SKO tumors progress slower with prolonged mouse survival. Within the tumor microenvironment, SKO tumors exhibited a profound immune-reactive phenotypes, with increased microglial and tumor-associated macrophage antigen presenting activation, as well as T cell cytotoxic activation. Importantly, orthotopic tumoral VRAC inhibition with an FDA-approved drug dicumarol phenocopied the genetic knockout, extended survival, and synergized with anti-PD-1 checkpoint blockade, significantly boosting anti-tumor efficacy. Our study identifies SWELL1 as a novel, targetable mediator that couples mitochondrial metabolism and epigenetics to oncogenic progression and immune exclusion in mIDH gliomas, providing a strong preclinical rationale for targeting VRAC as potential IDH-mutant glioma therapeutics.

#4036 Deciphering regulatory drivers of lineage plasticity and resistance to antibody-drug conjugates in urothelial bladder cancer.

Jiaqian Luo, Sizhi P. Gao, Jacob E. Tallman, Fengshen Kuo, Merve Basar, Cansu Yol, Syed M. Alam, Hui Jiang, Xinran Tang, Doris X. T. Zheng, Jordan E. Eichholz, Alejandra Lopez Rojas, Ecenur Turkay, Jonathan E. Rosenberg, Gopakumar Iyer, Eugene J. Pietzak, David B. Solit, Hikmat Al-Ahmadie

Memorial Sloan Kettering Cancer Center, New York, NY

Urothelial bladder cancer (UC) displays significant phenotypic heterogeneity, with ~ 30% of tumors exhibiting variant histologic features such as micropapillary, plasmacytoid, squamous, neuroendocrine, and sarcomatoid differentiation. Many of these histologic variants are often associated with aggressive behavior and reduced response to targeted therapies. Emerging clinical data suggest that lineage plasticity may underlie resistance to antibody-drug conjugates (ADCs), including enfortumab vedotin (EV), a Nectin-4-targeting ADC now standard in advanced UC. However, the mechanistic link between lineage transitions, ADC target expression, and ADC sensitivity remains incompletely understood. To study the regulatory mechanism, we conducted integrative genomic and transcriptomic profiling on 341 macrodissected bladder tumor specimens encompassing conventional UC and diverse histologic variants. A subset of mixed histology tumors was further profiled using spatial transcriptomics (10x Genomics Visium) to evaluate intratumoral heterogeneity. Regulon activity was inferred using transcriptomic data. Functional validation of candidate regulators was conducted in bladder cancer cell lines and patient-derived organoids using CRISPR/Cas9-mediated knockout and overexpression.We identified two dominant transcriptional categories across the histologic subtypes. Tumors with plasmacytoid, micropapillary, or nested histology retained a luminal urothelial signature and consistently expressed ADC targets such as NECTIN4, TACSTD2 (Trop-2), and ERBB2 (HER2). In contrast, tumors with squamous, sarcomatoid, or neuroendocrine features showed loss of urothelial identity, downregulation of these ADC targets, and activation of lineage-alternative transcriptional programs. Spatial transcriptomics confirmed marked intratumoral heterogeneity, showing spatially differential lineage program and ADC target expression. Master regulator analysis discovered a core luminal transcriptional program governed by FOXA1, GATA3, and PPARG, which was progressively silenced in variant histologies. These tumors concurrently activated alternative lineage-specific regulators, including ASCL1 and NEUROD1, consistent with neuroendocrine reprogramming. Perturbation of these regulators in organoid and cell line models modulated Nectin-4 expression and altered sensitivity to EV in vitro. This study establishes lineage reprogramming as a central mechanism regulating ADC target expression and ADC response. Lineage regulators represent tractable modulators of ADC response and support the development of rational combination strategies to overcome plasticity-associated resistance. Ongoing studies using multi-omics and functional modeling aim to further define lineage regulatory networks and inform targeted therapeutic strategies.

#4037 Pharmacological inhibition of eIF4A1 suppresses leukemogenesis via specifically rewiring amino acid biosynthesis.

Xiaoxu Zhang[1], Honghai Zhang[1], Lei Dong[2], Alexandra Huang[3], Xueer Wang[1], Lili Ren[1], Hongjie Bi[4], Sean O'Leary[3], Rui Su[1]

[1]Beckman Research Institute of The City of Hope, Monrovia, CA,[2]UT Southwestern Center, Dallas, TX,[3]University of California Riverside, Riverside, CA,[4]Harbin Medical University, Harbin, China

Acute myeloid leukemia (AML) is an aggressive blood malignancy with a dismal 5-year survival rate below 30%. Dysregulation of mRNA translation is a hallmark and a driver of tumorigenesis, including leukemogenesis. However, the precise contributions of translation factors to AML pathogenesis and their potential as therapeutic targets remain poorly understood. Here, we identify eukaryotic translation initiation factor 4A1 (eIF4A1) as a promising vulnerability of AML; genetic depletion or pharmacological inhibition of eIF4A1 markedly suppresses AML initiation and progression via reprogramming amino acid metabolism. Through unbiased multi-omics analysis, we identified eIF4A1 as the most highly expressed translation factor in AML. Notably, eIF4A1 expression was significantly elevated in AML cells and patient samples compared to healthy controls. eIF4A1 knockout (KO) dramatically inhibited AML cell proliferation, suppressed mitochondrial respiration, and reduced global translation intensity *in vitro* and substantially delayed AML progression *in vivo*. While eIF4A1 is traditionally studied within the cap-binding eIF4F complex, our other findings uncover a novel eIF4F complex-independent mechanism. BioID-MS assays, coupled with the validation of PLA assays and co-IP assays, revealed the robust RNA independent proximity of eIF4A1 and mRNA stabilizer Y-box binding protein 1 (YB-1). Integrative RNA-seq and proteomics demonstrated phosphoglycerate dehydrogenase (PHGDH) as a functionally essential target of eIF4A1. Moreover, metabolic profiling combined with isotope tracing (^{13}C) orthogonally confirmed the crucial role of eIF4A1 in rewiring *de novo serine* metabolism, in which PHGDH serves as the rate-limiting enzyme. Gene specific CLIP-qPCR verified the direct binding of both eIF4A1 and YB-1 to PHGDH mRNA. Furthermore, the KO of either eIF4A1 or YB-1 accelerated *PHGDH* mRNA decay. Collectively, these findings suggest an eIF4F-independent mechanism of eIF4A1: eIF4A1 cooperates with YB-1, stabilized *PHGDH* mRNA and reprogrammed amino acid metabolism in AML. Zotatifin, an FDA-approved eIF4A1 inhibitor, administered intraperitoneally (0.5 mg/kg; twice weekly for five weeks), dramatically reduced the leukemia burden and significantly prolonged survival of AML mouse models *in vivo* (immunodeficient xenograft model: 63 *vs.* 150 days median survival for PBS *vs.* Zotatifin, $P = 0.0006$; immunocompetent bone marrow transplantation model: 40 *vs.* 75 days, $P = 0.001$). Moreover, Zotatifin demonstrated strong synergistic activity with the YB-1 inhibitor SU056 in eradicating AML both *in vitro* and *in vivo* ($P < 0.0001$), primarily by disrupting amino acid biosynthesis. Overall, our findings identify eIF4A1 as a key regulator of AML pathogenesis and metabolic homeostasis. Targeting eIF4A1, particularly with Zotatifin, represents a promising therapeutic strategy for AML.

#4038 Anti-ROR2 therapies target cancer stem cells in triple-negative breast cancer.

E. M. Ghia, C. Huang, R. A. Shatsky, G. F. Widhopf II, D. Elson, J. Xian, S. Zare, A. M. Wallace, B. A. Parker, T. J. Kipps; University of California, San Diego, La Jolla, CA

ROR1 and ROR2 are developmentally restricted, structurally related cell surface proteins expressed during embryogenesis but absent in adult tissues. Many cancers, including breast cancer, aberrantly express ROR1/ROR2. We hypothesize that ROR1 and ROR2 mark triple-negative breast cancer (TNBC) stem cells (CSCs) and mediate cancer stemness, epithelial-mesenchymal transition (EMT), metastasis, and resistance to reactive oxygen species (ROS) triggered by radiation or chemotherapy via ROR1/ROR2 signaling. Patient-derived xenografts (PDX) in immunodeficient NOD-scid gamma (NSG) mice (N=7) enabled direct comparison of TNBC tissue and early-passage (T1) PDX using oligonucleotide-barcoded antibodies and single-cell RNA-seq. PDX retained high proportions of $ROR2^+$ TNBC cells with variable or absent ROR1. $ROR2^+$ cell abundance in T1 PDX matched biopsy and showed enriched stemness, EMT, and upregulated ERK1/2, NF-κB, NRF2 target genes (FDR<0.0001). Extreme limiting dilution assays showed 1,000 or 50,000 $ROR2^+$, but not ROR2-negative, cells, formed secondary PDX tumors ($p<0.0001$). APR-246, an investigational anti-cancer agent, promotes cell death via p53 restoration/ROS generation. We generated a high-affinity, humanized monoclonal antibody (mAb) specific for human ROR2 (h6E6) that could block ROR2 signaling, analogous to the capacity of our previous anti-ROR1 mAb (zilovertamab) to block ROR1 signaling. Observing that the vast majority of $ROR1^+$ TNBC co-express ROR2, we hypothesized that targeting $ROR2^+$ TNBC cells with h6E6 mAb could synergize with APR-246 to reverse CSC properties, inhibit PDX engraftment, and overcome resistance to oxidative stress induced by therapy. *In vitro*, h6E6 treatment enhanced TNBC PDX cell sensitivity to APR-246 versus isotype control (hIgG1) ($p<0.005$). In NSG mice with $ROR2^+$ TNBC PDX, intravenous h6E6, compared to control hIgG1, reduced expression of cancer stemness and EMT genes, as well as ERK1/2, NF-κB, and NRF2 pathway targets (FDR<0.0001), and caused a 5-fold reduction in NQO1, the main NRF2 downstream target, and increased sensitivity to APR-246 ($p<0.001$). By integrating rigorous experimental controls in both *in vitro* and *in vivo* studies using early-passage PDX, our work demonstrates that anti-ROR2 antibody therapy, combined with redox-modulating agents like APR-246, can effectively target CSC-driven disease persistence and therapy resistance in TNBC, supporting future clinical trials of h6E6 targeting $ROR2^+$ TNBC.

#4039 Deletion of peroxiredoxin 3 (PRX3) impairs mitochondrial bioenergetics and tumor growth in mesothelioma, supporting the first in human clinical testing of the PRX3 inhibitor RSO-021.

V. Gibson[1], J. Dzialo[2], C. Poile[2], J. Rogel[2], A. Habibovic[1], K. Butnor[1], S. Duloo[2], J. Spicer[3], D. A. Fennell[2], **B. Cunniff**[1];
[1]University of Vermont, Burlington, VT, [2]University of Leicester, Leicester, United Kingdom, [3]King's College London, London, United Kingdom

Aggressive tumors, including mesothelioma, generate high levels of reactive oxygen species (ROS) to support rapid growth and proliferation. To survive under increased oxidative stress, tumor cells upregulate antioxidant expression and activity, including the mitochondrial hydrogen peroxide (H_2O_2) scavenging enzyme peroxiredoxin 3 (PRX3). PRX3 is overexpressed in many cancers and promotes proliferation, survival and chemoresistance, highlighting it as a promising therapeutic target in oncology. Here we demonstrate that genetic deletion of PRX3 via CRISPR/Cas9 in the H-MESO-1 human mesothelioma cell line impairs mitochondrial bioenergetics and suppress mesothelioma tumor growth. PRX3 knockout (PRX3 KO) cells displayed significantly reduced oxygen consumption rates, extracellular acidification rates, and elevated mitochondrial ROS (mROS), indicating PRX3 deficient cells exist in an energetically compromised state. PRX3 deletion also decreased proliferation, colony formation and 3D spheroid growth in Matrigel. In vivo PRX3 KO cells failed to form tumors in SCID mice, whereas control cells generated substantial tumor burden. RNAseq-based gene set enrichment analysis of PRX3 KO cells supported the observed phenotypes including downregulation of oxidative phosphorylation, glycolysis and E2F and MYC targets. Re-expression of PRX3 in PRX3 KO cells partially rescued these phenotypes, reducing mROS, improving mitochondrial function, and enhancing colony formation. In a first-in-human phase 1 trial treating patients via weekly local intrapleural administration with RSO-021, the clinical formulation of the covalent PRX3 inhibitor thiostrepton (TS), at 90 mgs was well tolerated leading to disease control in 67% of patients at 12 weeks and was associated with tumor reductions (NCT05278975). Functional genomic screening identified SLC7A11, a cystine/glutamate transporter, as a mediator of resistance to PRX3 inhibition. Targeting PRX3, especially in combination with SLC7A11 inhibition, represents a promising approach for treating aggressive and treatment-resistant forms of cancer. Collectively, these findings identify PRX3 as a key regulator of redox metabolism, mitochondrial function, and mesothelioma tumorigenesis, and establish RSO-021 as a novel first-in-class PRX3 inhibitor with significant therapeutic potential in oncology. Phase 2 testing of RSO-021 is ongoing.

: Cutting-Edge Advances in Hematology
Minisymposium

#3979 Targeting nicotinamide metabolism with NAMPT-inhibitor OT-82 potentiates venetoclax in preclinical models of pediatric and adult acute myeloid leukemia.

M. Haber[1], M. Karsa[1], P. Connerty[1], A. Karsa[1], D. Spurling[1], G. Pomilio[2], V. Litalien[2], J. Xie[3], L. C. Cheung[4], R. S. Kotecha[4], O. Chernova[5], A. V. Gudkov[6], R. B. Lock, PhD[1], M. D. Norris[7], A. H. Wei[2], D. Moujalled[2], K. Somers[3];
[1]Children's Cancer Institute Australia, Sydney, Australia, [2]Walter and Eliza Hall Institute, Melbourne, Australia, [3]Children's Cancer Institute, Sydney, Australia, [4]The Kids Research Institute Australia, Perth, Australia, [5]Oncotartis, Inc, Buffalo, NY, [6]Roswell Park Comprehensive Cancer Center, Buffalo, NY, [7]Children's Cancer Institute Australia, Randwick, Australia

This study evaluates whether targeting the heightened dependence of acute myeloid leukemia (AML) on nicotinamide metabolism can be therapeutically exploited to inhibit AML progression and mitigate venetoclax resistance. AML continues to have poor survival outcomes in children and adults. While the BCL-2 inhibitor venetoclax has revolutionised the treatment of adult AML, there are increasing reports of inherent and acquired resistance to venetoclax. Emerging evidence implicates metabolic reprogramming and increased dependence on the activity of nicotinamide phosphoribosyltransferase (NAMPT), the rate limiting enzyme in the cellular nicotinamide biosynthesis pathway, in AML progression and venetoclax resistance. We evaluated the efficacy of the clinical-stage NAMPT inhibitor OT-82 alone and in combination with venetoclax against AML cell lines *in vitro* and primary AML bone marrow patient samples *ex vivo* by resazurin reduction-based viability, synergy, live/dead and apoptosis assays. Xenograft models derived from 7 pediatric and 9 adult AML patients were treated with OT-82 or venetoclax or their combination in a Single Mouse Trial design to assess therapeutic benefit across a diverse AML panel. PDXs encompassed *KMT2A*-rearranged, *FLT3*-mutant, *TP53*-deficient, and epigenetically altered subtypes, reflecting the heterogeneity of human AML and included venetoclax-refractory cases. OT-82 demonstrated potent single-agent activity against AML cell lines *in vitro* and primary patient samples from *de novo* and relapsed/refractory AML patients *ex vivo* with nanomolar IC50s. The drug induced apoptosis in leukemia cells while sparing normal progenitors. Strong synergy was observed between OT-82 and venetoclax. *In vivo*, OT-82 potentiated venetoclax and venetoclax/azacitidine in a venetoclax-resistant pediatric AML cell line xenograft model, significantly extending survival of mice treated with OT-82/venetoclax or OT-82/venetoclax/azacitidine in comparison to the single agents or venetoclax/azacitidine. Extending in vivo efficacy testing to 16 additional AML PDXs in Single Mouse Trial format demonstrated that OT-82 significantly delayed AML progression across the AML PDX panel ($p=0.0051$), as well as the individual adult and pediatric AML PDX panels ($p=0.0185$, $p=0.0009$, respectively). The OT-82 and venetoclax drug combination induced the most pronounced survival extensions, achieving maintained complete responses in 4/7 and 7/9 pediatric and adult AML PDXs, respectively, including high-risk cases and those with resistance to single agent venetoclax. In conclusion, this study establishes NAMPT inhibition by OT-82 as a promising metabolism-targeting strategy to overcome venetoclax resistance and supports clinical translation of OT-82 in combination with venetoclax in adult and pediatric AML.

#3980 Non-canonical CAR T cell states correlate with durable therapeutic responses in multiple myeloma patients.

K. Wu[1], K. Law[1], S. Kwek[2], M. Arias-Badia[2], A. Lyu[1], R. Wolters[2], A. Lea[2], M. Clark[2], C. Liu[2], Y. Li[1], R. Owens[1], L. Trieu[1], A. Tran[1], M. Bridge[1], Z. Fan[2], A. Cheung[2], J. Wolf[2], A. Portuguese[1], J. Gauthier[1], T. Martin[2], J. Eyquem[2], L. Fong[1];
[1]Fred Hutchinson Cancer Center, Seattle, WA, [2]UCSF, San Francisco, CA

Background: Chimeric antigen receptor (CAR) T cells targeting B-cell maturation antigen (BCMA) have exhibited unprecedented efficacy with >70% initial response rate in patients with relapsed/refractory multiple myeloma (RRMM), which led to FDA approval of 2 CAR T products: ciltacabtagene autoleucel (cilta-cel) and idecabtagene vicleucel (ide-cel). However, long-term clinical outcomes vary markedly in RRMM patients. Prior studies have shown that specific states of CAR T cells, immature myeloma phenotype and hostile tumor microenvironment (TME) are associated with rapid relapse, but much remains to be elucidated regarding how CAR T cells evolve, persist and interact with host immunity over time in patients with distinct clinical outcomes.
Methods: We acquired longitudinal bone marrow (BM) and peripheral blood mononuclear cells (PBMC) samples from 22 RRMM patients receiving 4 different anti-BCMA CAR T products, including cilta-cel (n=7), ide-cel (n=5), BB21217 (n=1) and orva-cel (n=9). The frequency and cell states of CAR and non-CAR T cells were assessed using flow cytometry and single-cell multi-omics (scRNA-seq).
Results: At 1-month post-infusion, the frequency of CAR T cells in BM was significantly higher in durable responders (DR, PFS$\geq$12mo) than transient responders (TR, PFS<12mo) (p=0.04). Single-cell transcriptomic profiling further demonstrated CAR T cells in DR patients were significantly enriched in memory-like and proliferative states with less exhaustion phenotype. After 1 month, the frequency of persisting CAR T declined in all patients, but DR patients had significantly higher frequencies of CAR T cells than TR ($p<0.0001$). By 6 months, persisting CAR T cells in DR patients predominantly exhibited a non-canonical state (T persisters) possessing high expression levels of AP1 genes, NF-κB regulators, and effector cytokines as well as low level of exhaustion-related genes. By single-cell TCR tracking, these T persisters transitioned from multiple cell states at early timepoints. In DR patients, classical monocytes within the BM exhibited less immunosuppressive phenotype post CAR T infusion.
Conclusions: Favorable clinical outcomes in RRMM patients are associated with greater expansion and persistence of CAR T. Durable responses are also associated with non-canonical CAR T cell states as well as a less immunosuppressive tumor microenvironment. These results provide insights into the determinants of durable clinical responses with anti-BCMA CAR T cells for RRMM.

#3981 A bivalent molecular glue linking lysine acetyltransferases to oncogene-induced cell death.

M. N. Nix[1], S. Gourisankar[2], S. Nettles[3], K. Bowman[4], H. Yang[4], B. G. Dwyer[5], R. C. Sarott[3], H. Abuzaid[3], M. Martinez[3], A. Krokhotin[3], L. Chen[3], M. M. Davis[3], D. Fernandez[1], T. Zhang[3], M. R. Green[4], S. M. Hinshaw[3], N. S. Gray[3], G. R. Crabtree[3]; [1]Stanford University, Stanford, CA, [2]Stanford Cancer Institute, Stanford, CA, [3]Stanford School of Medicine, Stanford, CA, [4]UT MD Anderson Cancer Center, Houston, TX, [5]Stanford Schoool of Medicine, Stanford, CA

Cancer therapies that activate cell death are critical to avoid relapse. Approximately 30% of diffuse large B cell lymphoma (DLBCL) cases, the most common non-Hodgkin lymphoma, fail standard-of-care treatment regimens, highlighting the need for new death-promoting targeted therapies. Here, we introduce a gain-of-function small molecule modality that kills DLBCL cells at sub-nanomolar potency (IC_{50} = 0.8 nM) through induced proximity. These bivalent compounds, Lysine Acetyltransferase Transcriptional/Epigenetic Chemical Inducers of Proximity (KAT-TCIPs), leverage the endogenous activity of the co-activating KATs E1A Binding Protein p300 (p300) and CREB-Binding Protein (CBP) to drive the transcription of death-promoting genes normally repressed by oncogenes. Specifically, KAT-TCIPs recruit p300/CBP to genomic loci controlled by the master transcriptional repressor BCL6, dysregulated in ~40% of DLBCL cases, and rapidly reprogram the epigenome to promote BCL6-dependent cell cycle arrest and apoptosis. We report the first X-ray co-crystal structure of a TCIP molecule bound to p300 and BCL6, which guided the optimization of our lead KAT-TCIP, TCIP3. Additional biophysical characterization of TCIP3 revealed its function as a molecular glue that cooperatively seeds ternary complexes on chromatin. This compound exhibits robust preclinical efficacy *in vivo*. It ablates germinal center B cells, which are naturally enriched for BCL6 expression, in immunized mice (5 mpk bid dosed intraperitoneally) relative to vehicle controls. Additionally, TCIP3 eliminates tumors in DLBCL cell line-derived xenograft models within 11 days at the same dose. Notably, this molecule spares healthy lymphocytes and fibroblasts in cytotoxicity analyses. Collectively, our findings establish KAT-TCIPs as powerful tools for co-opting the malignant function of oncogenic drivers to activate robust cell death, with implications for precision epigenetic therapies.

#3982 FGFR1+ cancer-associated fibroblasts contribute to the failure of CAR-T cell therapy in B-cell lymphoma through the secretion of TGFβ.

N. Di Siervi, M. Revuelta, G. Medico, G. G. Inghirami, L. Cerchietti;
Weill Cornell Medicine, New York, NY

Despite significant advancements in chimeric antigen receptor (CAR) T-cell therapies targeting CD19 for relapsed B cell malignancies, over 50% of lymphoma patients do not achieve sustained remission. The roles of cancer-associated fibroblasts (CAF) in reprogramming lymphoma microenvironments and their relationship with CAR T-cell response are becoming increasingly evident. Evidence suggests that TGFβ-activated stromal gene signatures are enriched in immunosuppressive lymphoma microenvironments (LME) and in non-responder CAR T-cell patients (Cerchietti. Cancer Discovery 2021, Locke. Nature Medicine 2024). In previous studies using pre-clinical lymphoma models, we demonstrated that FGFR1 inhibition in CAFs can reverse extracellular matrix compositional changes and increase the secretion of several monocyte chemoattractant proteins, thereby promoting the infiltration of anti-lymphoma macrophages and inducing anti-tumor effect in $FGFR1^{neg}$ lymphoma cells (Di Siervi. Cancer Research 2024). We report now that $FGFR1^{+}$ CAF are a consistent source of TGFβ. We discovered that TGFβ secretion in CAF is tightly regulated by FGFR1 activity. Genetic downregulation and pharmacological inhibition of FGFR1 (SSR128129E, FGFR1i) in three different activated fibroblast models led to a significant decrease in TGFβ transcription, expression, and secretion ($p < 0.005$). We developed a patient-derived xenograft (PDX) model from a B-cell lymphoma patient refractory to CD19 CAR T cell therapy, that we use to test the effect of pharmacological FGFR1 inhibition to the anti-tumor effect of human CD19-CAR T cells. Compared to vehicle, FGFR1i significantly reduced circulating tumor cells and increased circulating CAR T-cells ($p < 0.005$). These findings correlated with a reduced tumor burden and increased CAR T cell infiltration in the intrasplenic tumors.To further characterize CART-cell function, we analyzed exhaustion phenotype. We observed a significant reduction in exhausted $CD4^{+}$ and $CD8^{+}$ T-cell populations ($PD1^{+}$ $LAG3^{+}$) in the CART plus FGFR1i group ($p< 0.05$). Moreover, mice treated with the combination exhibited improved overall survival compared to those treated with CAR T cells alone ($p< 0.05$) or FGFR1i alone ($p < 0.05$). To test whether these results were specific for CD19-CAR T cells, we conducted similar experiments using BAFFR-CAR-T cells. Consistently, the combination of BAFFR-CAR T cells and FGFR1i increased CAR T cell expansion ($p < 0.005$), reduced T-cell exhaustion ($p < 0.05$), and improved overall survival compared to FGFR1i ($p < 0.005$) and CAR T cell therapy alone ($p < 0.005$). In conclusion, our findings suggest that the multifactorial changes induced by FGFR1i rewire the immunosuppressive LME, enhancing CAR T-cell infiltration, expansion, and antitumor activity.

#3983 Condensate dynamics drive adaptive METTL3 inhibitor resistance.

X. Yang[1], M. Eleftheriou[2], E. Yankova[2], S. Evans[2], T. M. Nelson[3], I. Wakiro[1], E. Batchelor[1], K. Chang[1], J. M. L. Dias[4], A. Pierson[1], G. Girard[1], R. Raghuraman[1], D. Aspris[5], V. Tandon[2], G. Han[1], L. P. Tsamouri[6], H. Luo[7], J. Russell[2], M. T. Bejar[2], M. P. Alcolea[2], A. Edakkara[2], M. Gu[2], R. Ollinger[8], M. Gozdecka[2], B. J. P. Huntly[2], R. Rad[9], L. Vasiliauskaitė[10], Y. Ofir-Rosenfeld[10], G. S. Vassiliou[2], Y. Cheng[11], M. Arora[12], R. C. Centore[12], C. E. Mason[13], O. Rausch[10], S. Arora[12], K. Tzelepis[2], M. G. Kharas[1];
[1]Molecular Pharmacology Program and Center for Cell Engineering, Memorial Sloan Kettering Cancer Center, New York, NY, [2]Cambridge Stem Cell Institute, University of Cambridge, Cambridge, United Kingdom, [3]Weill Cornell Medicine, New York, NY, [4]Department of Paediatrics, University of Cambridge, Cambridge, United Kingdom, [5]MRC Toxicology Unit, University of Cambridge, Cambridge, United Kingdom, [6]Pharmacology Program of the Weill Cornell Graduate School of Medical Sciences, Memorial Sloan Kettering Cancer Center, New York, NY, [7]Cancer Epigenetics Institute, Fox Chase Cancer Center, Philadelphia, PA, [8]Institute of Molecular Oncology and Functional Genomics, School of Medicine, Technische Universitat Munchen, Munich, Germany, [9]Institute of Molecular Oncology and Functional Genomics,School of Medicine, Technische Universitat Munchen, Munich, Germany, [10]Storm Therapeutics Ltd., Babraham Research Campus, Cambridge, United Kingdom, [11]Institute of Modern Biology, Nanjing University, Nanjing, China, [12]Transition Bio, Inc., Cambridge, MA, [13]Department of Physiology and Biophysics, Weill Cornell Medicine, New York, NY

The RNA methyltransferase METTL3, catalyzing N^6-methyladenosine (m^6A) modification, is implicated in oncogenesis. METTL3 inhibitors have shown potent anti-tumor efficacy across diverse preclinical models and are being tested in early-phase clinical trials. However, how cells fundamentally and dynamically respond to disruption of the m^6A RNA methylation machinery and what drives resistance to the catalytic inhibition of METTL3 remains unknown. Using genome-wide CRISPR sensitization and resistance screens in sensitive and resistant cancer models, we identify the nuclear m^6A-reader YTHDC1 as a critical determinant of METTL3 inhibition response. Genetic depletion of *YTHDC1* markedly sensitizes cells to METTL3 inhibitor (METTL3i) treatment *in vitro* and *in vivo* across solid and hematologic cancers, and its overexpression drives primary resistance.

A YTHDC1-condensate imaging screen identified YTHDC1 interactor PABPN1, a PAXT complex component and a resistance hit from our CRISPR screen, as a negative regulator of YTHDC1 condensate dynamics. PABPN1 overexpression restores METTL3i sensitivity in resistant models, whereas its loss induces resistance, highlighting that the state of YTHDC1 nuclear condensates functionally mediate METTL3i response.

Mechanistically, catalytic blockade of METTL3 remodels YTHDC1 condensates, increasing their intensity, size, and number while reducing their biophysical dynamics in sensitive cancer models and patient samples. In contrast, healthy human blood cells retain dynamic condensates, and resistant cancers display static condensates. Integrating direct RNA nanopore m^6A mapping, bulk-RNAseq and quantitative proteomics in YTHDC1-overexpression model, we find that residual m^6A modification persist on transcripts, and YTHDC1 drives restoration of MYC/BCL-2 programs upon METTL3 inhibition. Furthermore, YTHDC1 enhances binding to *MYC* and *BCL-2* mRNAs under METTL3i treatment, preserving their translation despite global m^6A loss. Accordingly, MYC overexpression phenocopies YTHDC1-mediated resistance to METTL3i, confirming its functional relevance. Therapeutically, co-targeting with a newly developed YTHDC1 inhibitor or the clinically approved BCL-2 inhibitor venetoclax synergistically enhances METTL3i efficacy *in vitro* and *in vivo* in clinically relevant models including AML patient-derived xenografts.

Together, these findings uncover adaptive reorganization of the m^6A machinery across hematologic and solid cancers. The YTHDC1 pathway and its condensate state act as predictive biomarkers and enhancers of therapeutic efficacy in METTL3-targeted cancers. Combinatorial targeting of METTL3 and YTHDC1/BCL-2 as a strategy to overcome therapeutic resistance.

#3984 Lymphotoxin alpha induces myeloid differentiation and programmed cell death in myeloid leukemic stem cells resulting in deep and sustained remission in vivo.

P. J. Jost[1], U. Hockendorf[2], S. Dutta[3], A. Kloos[4], M. Runtsch[5], C. Zotsch[1], S. Vosberg[1], Y. Wang[6], S. Kienreich[1], B. Flasch[1], G. Malovan[1], V. Jager[1], S. Stanzer[1], S. Preis[1], T. Odinius[7], C. Wagner[2], L. Buschhorn[2], V. Dill[2], B. Perfler[1], T. Haferlach[8], K. Dohner[9], K. Gotze[10], J. Ruland[11], F. Bassermann[10], A. Wahida[12], M. Heikenwalder[13], C. Branca[2], J. Schmollerl[14], J. Zuber[14], A.-C. Burk[15], R. Zeiser[16], H. Sill[17], A. Kumar Jayavelu[6], A. Zebisch[18], M. Heuser[19], M. A. Dengler[3];

[1]Medical University of Graz, Graz, Austria, [2]Department of Internal Medicine III, Klinikum rechts der Isar, School of Medicine and Health, Technical University of Munich, Munchen, Germany, [3]Clinical Division of Oncology, Department of Internal Medicine, Medical University of Graz, Graz, Austria, [4]Department of Hematology, Hemostasis, Oncology and Stem Cell Transplantation, Hannover Medical School, Hannover, Germany, [5]Clinical Oncology, Cycuria Therapeutics, Graz, Austria, [6]Proteomics and Cancer Cell Signaling, DKFZ and Hopp Children's Cancer Center (KiTZ), Heidelberg, Germany and Department of Pediatric Oncology, Hematology, and Immunology, University of Heidelberg, Heidelberg, Germany, [7]Department of Internal Medicine III, Klinikum rechts der Isar, School of Medicine and Health, Technical University of Munich & Department of Medical Oncology and Hematology, University Hospital Zurich, Zurich, Switzerland, Munich, Germany, [8]Munich Leukemia Laboratory (MLL), Munich, Germany, Munich, Germany, [9]Ulm University Hospital, Department of Internal Medicine III, Ulm, Germany, [10]Department of Internal Medicine III, Klinikum rechts der Isar, School of Medicine and Health, Technical University of Munich & German Cancer Consortium (DKTK), partner site Munich, a partnership between DKFZ and TUM University Hospital, & Bavarian Ca, Munich, Germany, [11]German Cancer Consortium (DKTK), partner site Munich, a partnership between DKFZ and TUM University Hospital & Institute of Clinical Chemistry and Pathobiochemistry, School of Medicine and Health, Technical University of Munich & TranslaTUM, Munich, Germany, [12]Institute of Metabolism and Cell Death, Helmholtz Centre Munich, Munich, Germany, [13]Division of Chronic Inflammation and Cancer, German Cancer Research Center (DKFZ), Heidelberg, Germany, [14]Research Institute of Molecular Pathology, Vienna BioCenter (VBC), Vienna, Austria, [15]Faculty of Medicine, Clinic for Internal Medicine I, Hematology, Oncology and Stem cell transplantation, University Medical Center Freiburg, Freiburg, Germany, [16]University of Freiburg, Freiburg, Germany, [17]Division of Hematology, Department of Internal Medicine, Medical University of Graz, Graz, Austria, [18]Division of Pharmacology and Division of Hematology, Department of Internal Medicine, Medical University of Graz, Graz, Austria, [19]Martin Luther University of Halle-Wittenberg, Halle, Germany

Frequent relapse driven by resistant leukemic stem or progenitor cells (LSC) represents one of the major challenges in acute myeloid leukemia (AML) therapy. Based on the concept of cytokine-induced myeloid differentiation as observed during emergency granulopoiesis of healthy hematopoeitic progenitors, we dissected individual cytokines for their effect on myeloid differentiation of LSCs.We identified that cytokines from the TNF family potently induced cellular differentiation in LSCs from a range of different genetic backgrounds of AML. The induction of this differentiation program is driven, at least in part, by the activation of programmed inflammatory cell death and subsequent release of pro-inflammatory cytokines such as IL-1beta. Mechanistically, we identified that TNFR receptor 1 (TNFR1)-mediated signaling induces Receptor-interacting protein kinase 3 (RIPK3) dependent cell death of LSCs upon loss of the pro-survival protein TNFR associated factor 2 (TRAF2). TNF family cytokines such as Lymphotoxin alpha (LTα3) efficiently repress leukemia by depleting TRAF2 from the intracellular pool of LSCs via activation of both TNFR1 and TNFR2. Competitive and simultaneous recruitment of TRAF2 to both TNFR1 and TNFR2 results in the failure of LSCs to generate a robust pro-survival signaling complex I at the proximal portion of TNFR1. This results in RIPK3-dependent inflammatory cell death of LSCs.Of note, in contrast to conventional therapies, LTα3 exerted only minimal toxicity on the healthy hematopoiesis but instead promoted hematopoietic progenitors. This cytokine-induced propagation of healthy progenitor cells mimics the process observed during emergency granulopoiesis. Exposure of healthy primary human bone marrow progenitors to LTα3 resulted in propagation of healthy progenitors cells. Co-treatment of malignant and healthy progenitor cells from AML patients within the same culture repressed the malignant LSCs but propagated the healthy progenitors. Accordingly, this tumor-suppressive mechanism can be harnessed to simultaneously clear malignant progenitors cells and promote healthy hematopoiesis.In mouse model systems, genetic deletion of the TNF superfamily member gene lymphotoxin alpha (Lta) blocked cell death and accelerated leukemogenesis. In patient-derived xenograft mouse models, exposure to recombinant LTα3 resulted in deep and sustained remissions. Leveraging this endogenous tumor-suppressive mechanism may de-couple treatment efficacy on malignant cells from undesired bone marrow (BM) suppression.

#3985 MED12L: A novel player in platelet dysfunction in myeloid neoplasms.

M. Brindisi[1], L. Crisafulli[2], M. Zampini[1], M. G. Liturri[1], A. Campagna[1], L. B. Lanino[3], M. Ubezio[1], G. Todisco[4], G. Maggioni[1], A. Russo[1], M. Bacci[1], N. Manes[1], E. Riva[1], D. Ventura[1], N. Pinocchio[1], E. Calvetti[1], D. Strina[2], T. Nageswara Rao[5], M. Della Porta[1], F. Ficara[2];

[1]IRCCS Humanitas Research Hospital, Rozzano (MI), Italy, [2]Institute for Genetic and Biomedical Research, Milan Unit, CNR, Milan (MI), Italy, [3]Yale University, New Haven, CT, [4]Humanitas University, Pieve Emanuele (MI), Italy, [5]HOCH Health Ostschweiz, Cantonal Hospital St. Gallen, St. Gallen, Switzerland

Myeloproliferative neoplasms (MPN) impose substantial clinical burden through thrombotic complications and leukemic progression, representing the main determinants of patient morbidity and mortality. These clonal malignancies arise from somatic mutations in hematopoietic stem cells (HSC), most commonly *JAK2*-V617F. Despite therapeutic advances, molecular mechanisms underlying aberrant megakaryopoiesis and pathologic thrombocytosis remain unmet. This study investigates Mediator complex subunit 12-like (MED12L), a functionally uncharacterized protein, in normal and malignant hematopoiesis, identifying a novel regulatory function in platelet (PLT) turnover dynamics. In *JAK2*^{V617F} mice genetic ablation of the transcription factor *Pbx1* resulted in amelioration of thrombocythemia and erythrocytosis. Transcriptomics analysis of their stem/progenitor cells uncovered downregulation of *Med12l*. Conversely, in *JAK2*^{V617F} mice, *Med12l* was upregulated in common Megakaryocyte (Mk)-Erythroid progenitors and in committed Mk (but not erythroid) precursors, rising the hypothesis that MED12L dysregulation contributes to aberrant PLT homeostasis in myeloid malignancies. To assess the functional significance of MED12L in the hematopoietic system, we studied *Med12l* knockout (KO) mice and performed systematic hematopoietic characterization under steady-state and stress conditions. We also generated *Med12l* KO/*Jak2*^{V617F} compound mutants (JM mice) to assess the impact of MED12L absence in vivo in an MPN setting. Clinical validation utilized MPN and myelodysplastic syndrome cohorts. Our investigations reveal a previously unrecognized role for MED12L in regulating PLT lifespan and turnover. Blood analysis of *Med12l*-KO mice demonstrated an altered PLT compartment, with increased mean PLT volume, distribution width, area, internal complexity, and elevated surface integrin expression with respect to WT. These findings indicate impaired PLT maturation, supported by a higher frequency of reticulated PLT and increased mitochondrial and endoplasmic reticulum content. *In vivo* PLT depletion with anti-GPIbα antibody revealed impaired recovery kinetics in KO mice, with delayed bone marrow Mk-primed HSC and Mk-committed progenitor expansion. Critically, *in vivo* biotinylation studies definitively established accelerated platelet clearance in MED12L absence. Importantly, in *JM* mice the absence of MED12L counteracted thrombocytosis, a hallmark of MPN, without affecting erythrocytosis. Consistently, scRNA-seq from MPN patients showed a higher proportion of MED12L-expressing platelets compared to healthy donors; similarly, in patients affected by myelodysplastic syndrome we observed a strong correlation between the expression of MED12L in CD34^{+} cells and platelet features.This study uncovers MED12L as a novel player in platelet biology, highlighting its potential as a therapeutic target in myeloid neoplasms.

: Digital Pathology
Minisymposium

#3997 Elucidating broad cell-cell interactions via 3D super-cell graphs for prostate cancer risk stratification.

Y. Zhao[1], S. Chow[1], R. Yan[1], R. Serafin[1], E. Baraznenok[1], L. D. True[1], P. Lal[2], A. Madabhushi[3], J. T. Liu[1];
[1]University of Washington, Seattle, WA, [2]University of Pennsylvania, Philadelphia, PA, [3]Emory University, Atlanta, GA

Prostate cancer treatment decisions rely heavily on the examination of 2D histology sections. However, because these sections provide limited sampling of tissue volumes without 3D glandular and cellular context, interpretation can be misleading and ambiguous. We have developed a slide-free 3D pathology method that generates volumetric datasets that mimic the appearance of H&E staining. Using these 3D pathology datasets, we have shown that computational analysis of 3D histomorphometric features describing glandular and nuclear morphology offer better prognostic value than analogous 2D features. However, given that the spatial organization of cells in 3D remains largely unexplored, we investigate whether quantifying 3D cell–cell interactions can further enhance prognostication.
To analyze 3D cell–cell interactions, we first applied a deep-learning segmentation model (Cellpose) to identify all cell nuclei from H&E-analog 3D pathology datasets, and then extracted 3D histomorphometric features from those nuclei, including shape descriptors, texture metrics, and contextual features. Since directly modeling the interactions between millions of cells in 3D is both computationally prohibitive and prone to overfitting, we grouped spatially adjacent and morphologically similar cells into “supercells”, reducing the data to approximately 10% of the original cell count (with exponentially less cell connections) while preserving the overall structure of the cell interactions. Leiden clustering based on nuclear histomorphometric features was used to group these supercells into broad cell types. We then constructed 3D supercell graphs using k-nearest neighbors, where each supercell is represented as a node and edges indicate supercell interactions.
To evaluate the prognostic value of these 3D supercell graphs, we generated graphs for a cohort of 76 archived prostatectomy specimens with known 5-year biochemical recurrence (BCR) outcomes. Quantitative features extracted from the 3D supercell graphs were used as inputs to a LASSO model with 5-fold cross-validation, achieving an AUC of 0.745 ± 0.06 for predicting 5-year BCR. 3D histomorphometric features previously derived from cancer glands and nuclei masks yielded an AUC of 0.751 ± 0.08. Combining all of these features yielded an AUC of 0.837 ± 0.05. In parallel, we are assessing whether end-to-end graph neural network (GNN) learning provides additional prognostic value compared with traditional machine classifiers based on 3D supercell graph features, especially in a low-shot regime with limited cohort sizes.
In summary, based on H&E-analog 3D pathology datasets, we have introduced 3D supercell graphs as a data-efficient method to capture broad cell interactions within the tumor microenvironment, showing that these 3D supercell graph features are of prognostic value.

#3998 AI-driven spatial analysis of 1100 head and neck squamous cell carcinoma patients H&E slides uncovers three subtypes with markedly distinct tumor microenvironments and survival patterns.

S. Biswas[1], A. Stemmer[1], S. Patiyal[1], E. Shulman[1], C.-P. Day[1], T.-H. Chen[2], M.-H. Yang[3], D.-T. Hoang[1], E. Ruppin[4];
[1]Cancer Data Science Laboratory, Center for Cancer Research, National Cancer Institute, Bethesda, MD, [2]Department of Oncology, Taipei Veterinary Hospital, Taipei, Taiwan, [3]Institute of Clinical Medicine, National Yang Ming Chiao Tung University, Taipei, Taiwan, [4]Cedars-Sinai Medical Center, Los Angeles, CA

Background: The spatial organization of the tumor microenvironment (TME) is a critical determinant of tumor progression and patient outcomes in head and neck squamous cell carcinoma (HNSC). However, spatial transcriptomics (ST) technology remains limited by high costs and tissue requirements, which restrict its application to large clinical cohorts and hinder biomarker translation.
Methods: We trained a deep learning model on a HNSC ST cohort comprising 21,466 spots from 10 slides to predict spot-level spatial gene expression directly from *H&E*-stained histology slides. We validated the model's performance and robustness across two independent HNSC ST cohorts consisting of 11,485 spots from 8 slides covering diverse anatomical sites and sample types.
Results: We first demonstrated that our model robustly predicts spatial expression of 2,772 genes (Pearson $r > 0.4$ for predicted vs. actual ST gene expression) across all three ST cohorts. Second, we applied it to infer the spatial gene expression for 1,145 patients from two independent datasets (TCGA-HNSC, n = 445; HANCOCK, n = 700). Third, spatial clustering of inferred TCGA-HNSC profiles identified 11 shared spatial clusters representing TME composition within each patient. Fourth, hierarchical clustering of these TME compositions revealed three distinct patient subgroups, termed *SpatioStates*, each associated with unique biological features and survival patterns. The *Proliferative SpatioState*, dominated by hyperproliferative-hypoxic programs, represents an aggressive tumor niche associated with poor overall survival. In contrast, the *Immune-Activated SpatioState* exhibits strong inflammatory signaling and robust immune-cell engagement, reflecting active antitumor immunity and showing significantly improved prognosis compared with the *Proliferative SpatioState* (HR = 0.66, p = 0.023) after adjustment for age and stage. Meanwhile, the *Metabolic SpatioState* is characterized by high oxidative phosphorylation and stress-response pathways corresponding to metabolically adaptive tumor regions with intermediate survival outcomes. Remarkably, these *SpatioStates* are consistently repeated in the independent HANCOCK cohort, maintaining significant prognostic discrimination between *Proliferative* and *Immune-Activated SpatioStates* (HR = 0.46, p = 0.005), underscoring the robustness and generalizability of our model.
Conclusions: This study establishes the first scalable computational framework for inferring prognostic spatial TME architecture from routine *H&E* slides in HNSC. The identified *SpatioStates* demonstrate robust survival stratification across independent cohorts, thereby facilitating large-scale spatial profiling and establishing a foundation for integrating spatial biology into clinical biomarker development.

#3999 Pan-cancer prediction of response to immune checkpoint blockade from histopathology.

D.-T. Hoang[1], S. Mukherjee[1], S. Patiyal[1], L. R. Pal[1], T. Chang[1], S. Biswas[1], S. Dhruba[1], A. Stemmer[1], A. Singh[1], A. Yousefi-Rad[2], T.-H. Chen[3], B. Wang[1], D. Marino[4], W. Shon[4], Y. Yuan[4], M. Faries[4], O. Hamid[4], K. Reckamp[4], B. Waissengrin[4], B. Ornelas[4], K. Yao[4], P.-Y. Chu[5], L. Ley[2], D. Akbulut[2], N. El Ahmar[6], S. Signoretti[6], D. A. Braun[7], J. Lee[8], H. Joo[9], H. Kim[9], A. Osipov[4], R. A. Figlin[4], J. Bar[10], I. Barshack[10], C.-P. Day[1], S. Hannenhalli[1], K. Sargsyan[4], A. B. Apolo[2], K. D. Aldape[11], M.-H. Yang[12], M. B. Atkins[13], Z. A. Ronai[9], E. Ruppin[1];

[1]National Cancer Institute - Cancer Data Science Laboratory (CDSL), Bethesda, MD, [2]National Cancer Institute - Genitourinary Malignancies Branch, Bethesda, MD, [3]National Yang Ming Chiao Tung University, Hsinchu, Taiwan, [4]Cedars-Sinai Medical Center, Los Angeles, CA, [5]Taipei Veterans General Hospital, Taipei, Taiwan, [6]Brigham and Women's Hospital, Boston, MA, [7]Yale School of Medicine, New Haven, CT, [8]Sungkyunkwan University, Suwon, Korea, Republic of, [9]Cedars-Sinai Medical Center, Jim and Eleanor Randall Department of Surgery, CA, [10]Sheba medical center, Ramat Gan, Israel, [11]National Cancer Institute, Bethesda, MD, [12]National Yang Ming Chiao Tung University, Taipei, Taiwan, [13]Georgetown Lombardi Comp. Cancer Center, Washington

Background: Immune checkpoint blockade (ICB) has transformed cancer therapy, yet only a subset of patients benefit, underscoring the need for robust, generalizable biomarkers capable of identifying tumors with sufficient immune activation. Although numerous immune-related gene signatures and transcriptomic approaches have been proposed, most lack pan-cancer robustness and fail to generalize across independent cohorts. To address this gap, we derived TIME_ACT, an unsupervised 66-gene tumor immune activation (“hotness”) signature that integrates immune infiltration, inflammatory activity, and spatial TIL density. This signature accurately predicts tumor hotness across diverse cancer types, forming a robust pan-cancer measure of immune activation.
Methods: TIME_ACT was evaluated across 22 publicly available pre-treatment ICB transcriptomic cohorts (n=1,416) spanning seven cancer types. To enable prediction from pathology, TIME_ACT scores were inferred from H&E slides using Path2Omics, a recently published deep-learning model trained on TCGA, and validated in nine new histopathology cohorts from different medical centers and populations (n=459).
Results: TIME_ACT accurately identifies immune-hot tumors across eight TCGA cancer types (AUC 0.96-1.00) and two external datasets (AUC 0.96-0.98). TIME_ACT genes were consistently enriched in T cells, B cells, and dendritic cells at single-cell resolution. Spatial analyses shows that TIME_ACT-high regions co-localize with lymphocyte-dense niches adjacent to the tumor epithelium. Across 22 transcriptomic ICB cohorts, TIME_ACT robustly predicted response (mean AUC 0.74; mean OR 5.49). Importantly, histopathology-inferred TIME_ACT scores achieve strong performance across nine multi-centric cohorts (mean AUC 0.73; mean OR 5.07), matching transcriptomic-based prediction levels and importantly, outperforming direct slide-based models.
Conclusions: TIME_ACT is a robust pan-cancer tumor immune activation signature that predicts ICB response directly from the readily available tumor pathology slides. Upon further prospective testing and validation, it offers an exciting new way for further democratizing precision immunotherapy.

#4000 A large-scale, multi-target deep learning model for virtual genomic profiling in colorectal cancer.

E. N. Bergstrom, T. Wu, M. Chatzianastasis, T. Tran, A. Rosenfeld, R. Burns, A. Jurdi, H. Costa, F. Zhang;
Natera, Inc., Austin, TX

Molecular profiling of tumor biopsies is the cornerstone of precision oncology, guiding therapy selection and prognostic assessment. Computational analysis of routine H&E slides offers a complementary approach that can accelerate insights and optimize downstream molecular testing. Recent advances in computational pathology have demonstrated that deep learning models can infer molecular features directly from digital H&E images, termed virtual genomics. However, most studies in colorectal cancer (CRC) have been constrained by limited cohort sizes and single-target prediction frameworks, restricting their clinical relevance and generalizability. Here, we present a transformer-based deep learning framework designed for large-scale, single- and multi-task virtual genomic profiling in CRC. Trained on 45,155 patients with matched digital H&E images, whole-exome sequencing (WES), and circulating tumor DNA sequencing for molecular recurrence monitoring, we validated all results on an external cohort from The Cancer Genome Atlas (TCGA, n=422 CRC patients). We embedded all images using H-optimus-0 and trained a transformer-based multiple instance learning aggregation head for downstream virtual genomic predictions. We trained individual models to predict genes found in the MSK-IMPACT505 cancer gene panel and a single model that predicts all genes simultaneously. Individual models predicted 379 mutated genes with an internal area under the receiver operating curve (AUROC)>0.7. We validated 254 of these genes within TCGA with an AUROC>0.7. Training a multi-task learning model to predict all genes simultaneously improved the AUROC for 85% of the genes. Based on NCCN guidelines in CRC, we further trained individual models to predict MSI status, BRAF V600E, KRAS G12D/V/G13D, and POLE/POLD1 exonuclease mutations with AUROCs of 0.96, 0.92, 0.83, and 0.83, respectively. For the BRAF, KRAS, and POLE/POLD1 mutations, we observed continued benefit from increasing cohort size from as small as 10 mutated cases up to the maximum positivity within our cohort, suggesting that we have not reached the full performance potential for these mutations. Finally, virtually-imputed BRAF mutations stratified minimal residual disease (MRD) risk better than the WES-derived genomic mutation status revealing that the model was capturing MAPK pathway activation rather than single mutation status. The virtual genomic algorithm advances virtual genomic profiling in CRC, demonstrating scalable and potentially generalizable prediction of hundreds of genomic alterations from routine histology. Beyond serving as a low-cost pre-screening tool to guide molecular testing, the virtually imputed biomarkers capture pathway-level activity that better correlates with clinical outcomes such as MRD risk, underscoring its potential to transform precision oncology through image-based genomic insight.

#4001 AI-driven spatial cell classification and tumor-infiltrating lymphocyte (TIL) patch analysis reveal spatial immunoarchitecture in arsenic-associated bladder cancer.

S. Singhal[1], A. Dikshit[2], S. Singhal[1], K. L. Gardner[3];

[1]University of North Dakota, Grand Forks, ND, [2]Bio-Techne Corporation, Newark, CA, [3]Vagelos College of Physicians & Surgeons, New York, NY

The integration of artificial intelligence (AI) with digital pathology provides unprecedented opportunities to decode the spatial complexity of tumor-immune interactions. We developed an AI-driven spatial pathology framework that combines multiplex fluorescence in situ hybridization (mFISH) and deep-learning-based digital histopathology to classify cells and identify tumor-infiltrating lymphocyte (TIL) patches in bladder tumors. Formalin-fixed paraffin-embedded samples were analyzed using RNAscope mFISH targeting three arsenic-responsive genes - *NKIRAS2, AKTIP,* and *HLA-DQA1.* Whole-slide images were co-registered with H&E slides and processed using nuclear segmentation and a convolutional neural network for automated cell-type classification. AI-assisted spatial clustering and TIL patch detection algorithms quantified immune-tumor proximity, heterogeneity, and neighborhood context at micron-level resolution. The AI model achieved >92% accuracy in distinguishing tumor, stromal, and lymphocytic populations. Quantitative mapping revealed that low-grade tumors contained densely packed TIL clusters with a mean inter-TIL distance of <30 µm, reflecting robust immune infiltration. In contrast, high-grade tumors exhibited a >3-fold reduction in TIL patch density and increased spatial separation between lymphocytes and tumor boundaries, consistent with immune exclusion. Spatial co-expression of *NKIRAS2-AKTIP* was enriched in immune-cold regions, while *HLA-DQA1* expression correlated with higher TIL density and active immune interfaces. Pathway enrichment analysis of TIL-proximal regions highlighted upregulation of inflammatory and oxidative stress pathways, whereas immune-depleted zones showed activation of DNA repair and cell proliferation signatures. Gradient-based quantification of TIL patch density and co-expression topology stratified tumors into immune-inflamed, immune-intermediate, and immune-cold phenotypes that correlated with histologic grade and exposure signatures. This integrative approach bridges molecular multiplex imaging with spatial computational pathology, establishing a scalable framework for digital immune landscape mapping. Our findings highlight how environmental exposures reshape tumor-immune architecture and demonstrate the potential of AI-guided pathology for precision immunoprofiling and exposure-related cancer risk assessment.

#4002 Peritumoral collagen microarchitecture is differently prognostic of biochemical recurrence across populations in prostate cancer.

A. Subramanian[1], N. Tokuyama[2], T. Pathak[2], P. Lal[3], A. Madabhushi[2];
[1]Georgia Institute of Technology, Atlanta, GA, [2]Emory University, Atlanta, GA, [3]University of Pennsylvania, Philadelphia, PA

Background
Extracellular matrix remodeling contributes to prostate cancer progression, yet race-associated differences in collagen architecture and their relationship to biochemical recurrence (BCR) remain poorly understood. We investigated whether collagen microstructure features differ between African American (AA) and European American(EA) men who had undergone radical prostatectomy, and whether population-specific collagen signatures carry prognostic value in the post-surgical setting.
Methods
We analyzed H&E-stained whole-slide images from radical prostatectomy specimens representing 101 AA and 101 EA men. Collagen fibers within the peri-tumoral region were computationally extracted using a deep-learning-based image-analysis pipeline, followed by quantification of 19 collagen morphology and texture features spanning structural (orientation, length, curvature, thickness, density, tortuosity, branching, intersection angles), spatial (inter-fiber distance), and textural (texture entropy and Haralick metrics) categories. The dataset was randomly divided into an 80% training set and a 20% independent test set, with equal representation of AA and EA patients in the test subset. Within the training set, population-specific prognostic features were identified using univariate median-threshold survival analysis ($p<0.05$). Multivariate Cox models were then trained separately using AA-derived and EA-derived feature subsets, and model performance was evaluated exclusively on the held-out test set to prevent data leakage.
Results
Nine collagen features were prognostic in AA patients, indicating more irregular collagen texture, greater fiber twisting, and higher variation in fiber orientation and curvature—suggesting a more disrupted stromal environment. In contrast, only five features were prognostic in EA patients, largely corresponding to differences in collagen density, fiber spacing, and overall stromal compactness. Only the collagen orientation variability feature was shared across both groups, underscoring the distinct tumor remodeling patterns in AA versus EA patients. The prognostic value was not retained when each population specific features was applied to the other population. In the full cohort, the AA-specific features demonstrated significant association with BCR (HR = 4.09, 95% CI: 1.09-15.34, p = 0.0243), whereas the EA-specific features did not (HR= 0.96, 95 % CI: 0.31-2.98, p = 0.9408).
Conclusion
Peri-tumoral collagen architecture differed markedly between AA and EA patients, influencing which features predicted BCR. Only AA-derived collagen patterns remained prognostic across groups, highlighting the need for population-aware prognostic approaches.

: Microenvironmental Determinants of Tumor Evolution and Immune Escape
Minisymposium

#4078 Vagal sensory neuronal inflammatory memory promotes gastric tumorigenesis through ILC2-mediated epigenetic signaling and the CGRP/Ramp1 axis.

Yi Zeng[1], Puran Zhang[1], Ruhong Tu[1], Feijing Wu[1], Xiaofei Zhi[2], Jin Qian[1], Biyun Zheng[1], Hualong Zheng[1], Shuang Li[1], Hiroki Kobayashi[1], Yosuke Ochiai[1], Masahiro Hata[1], Juli Lin[1], Junya Arai[1], Leah B. Zamechek[1], Timothy C. Wang[1]

[1]Columbia University Irving Medical Center, New York, NY,[2]Nantong University, Nantong, China

Background: Mammalian tissues can “remember” prior inflammatory or injurious events and respond more rapidly to later stimuli. Whether vagus-derived sensory neurons encode such experiences and convert them into tumor-promoting signals remains unknown. We show that inflammatory memory within vagal sensory neurons drives gastric regeneration and tumorigenesis through ILC2-mediated epigenetic reinforcement and CGRP/RAMP1 signaling.

Methods: Gastric injury was induced by high-dose tamoxifen (HDT) or *Helicobacter pylori* infection/eradication. Orthotopic (ACKP) and spontaneous (Iqgap3-CreERT2; $KRAS^{G12D}$) tumor models assessed memory-driven initiation. Trpv1-Cre; hM3Dq and Trpv1-Cre; DTA mice enabled chemogenetic activation or ablation of nodose ganglion (NG) neurons. An AAV-C-Fos-tTA/TetO-Cre-DTA TRAP system labeled and ablated neurons activated during the first injury. Ramp1 was deleted in gastric stem cells (Iqgap3-CreERT2; $Ramp1^{flox}$), and $IL25R^{+}$ ILC2s were depleted genetically or pharmacologically. Chromatin of sorted NG neurons was analyzed by ChIP-qPCR for H3K4me3 enrichment at memory loci.

Results: Prior injury produced persistent “neuronal memory” marked by expanded $CGRP^{+}$ fibers that accelerated mucosal recovery but enhanced metaplasia and tumorigenesis. Activation of $Trpv1^{+}$ NG neurons was required; activation mimicked memory, while ablation or vagotomy abolished it. TRAP tracing showed reactivated neurons during reinjury overlapped with and exceeded those from the first; ablating the initial cohort erased the phenotype. MRI and c-Fos in the brainstem revealed stronger vagal signals after reinjury, indicating peripheral memory transmission to the central axis. During memory formation, subsets of sensory terminals directly innervated gastric isthmus stem cells; anterograde and retrograde tracing verified bidirectional connectivity, providing a structural basis for rapid signal recall. Memory neurons released CGRP acting on $Ramp1^{+}$ isthmus stem cells; deleting or antagonizing Ramp1 suppressed dysplasia and tumorigenesis. $IL25R^{+}$ ILC2s infiltrated the isthmus and maintained NG memory via IL-5-triggered CGRP release, Wnt5a-guided terminal attraction, and IL-13-induced SMYD4 with enhanced H3K4me3 in NG neurons. These cues reinforced the feedback sustaining the memory state.

Conclusions: We identify a vagal sensory neuronal inflammatory memory circuit linking prior injury to gastric tumor initiation. ILC2-mediated IL-13/SMYD4/H3K4me3 signaling stabilizes memory within NG neurons, while CGRP/RAMP1 and neuro-epithelial contacts transmit it to the mucosa, forming a neuro-epigenetic feedback loop driving inflammation-associated gastric cancer.

#4079 Unique mechanism of MASLD-associated hepatocarcinogenesis: LSEC-derived CXCL9 facilitates T-cell exhaustion in steatotic tumor microenvironment.

N. Ohtani[1], T. Kamiya[1], K. Echizen[1], Y. Nonaka[1], Y. Yukawa-Muto[1], H. Fujii[1], S. Itoh[2], N. Kawada[1];

[1]Graduate School of Medicine, Osaka Metropolitan University, Osaka, Japan, [2]Graduate School of Medical Sciences, Kyushu University, Fukuoka, Japan

In recent years, the incidence of hepatocellular carcinomas (HCC) associated with MASLD (Metabolic dysfunction-associated steatotic liver disease) and MASH (Metabolic dysfunction-associated steato-hepatitis), has continued to rise, although that of viral HCC declines because of the development of anti-viral drugs. However, combination therapy with atezolizumab plus bevacizumab in non-viral liver cancers, including MASLD-related cases, has shown no clear clinical benefit (Cheng et al., J Hepatol 2022), and monotherapy with anti-PD-1/PD-L1 antibodies has even exacerbated disease (Pfister et al., Nature 2021). These findings suggest that mechanisms of HCC development in steatotic MASLD-related liver fundamentally differ from HCCs of other etiologies. In this study, we sought to elucidate the unique mechanisms driving MASLD-associated hepatocarcinogenesis, with a focus on how exhausted T cells arise within the highly steatotic tumor microenvironment. We employed chemical carcinogenesis mouse models of MASLD-associated liver cancer previously established by our group (Yoshimoto et al., *Nature* 2013), alongside patient-derived samples. Multiplex assay for plasma profiling of healthy controls, MASLD/MASH patients, and MASLD/MASH-related liver cancer patients revealed a high level of CXCL9 specifically in the MASLD/MASH-related cancer group. Consistently, CXCL9 levels were increased in samples of our MASLD-related mouse models. Notably, blockade of the CXCL9-CXCR3 axis reduced T-cell trafficking from lymph nodes to the liver and, surprisingly, markedly suppressed tumor formation. Pharmacologic inhibition of lymphocyte migration revealed similar effects. Because CXCL9 expression was predominantly upregulated in liver sinusoidal endothelial cells (LSECs) in the MASLD-HCC model, we generated LSEC-specific CXCL9-knockout mice, which also consistently exhibited reduced tumorigenesis. Although CXCL9 is generally considered a favorable chemokine that recruits cytotoxic T cells to enhance anti-tumor immunity in other cancer types, it plays a detrimental role in MASLD-associated HCC. Our results suggest that LSEC-derived CXCL9 recruits T cells from lymph nodes, but these T cells rapidly undergo exhaustion in the steatotic microenvironment, ultimately promoting cancer progression. To further dissect this process, we performed single-cell TCR sequencing of $CD8^+$ T cells from lymph nodes and liver tissues. We will present the pseudotime analysis of the clonal trajectory, which may suggest the unique mechanisms underlying MASLD-associated HCC development.

#4080 The neural bridge: Stress-remodeled enteric nervous system (ENS) in the colitis-cancer transition.

X. Zhou, C. Chen, H. Choi, J. Liu, S. Chi, N. Tran, M. Ciorba, S. A. Stewart, **X.-Y. He**;
Washington University School of Medicine in St. Louis, St. Louis, MO

Chronic stress, driven by environmental and psychosocial factors, disrupts systemic homeostasis and adversely affects cognitive function, behavior, and the cardiovascular, gastrointestinal (GI), and immune systems. It is closely associated with GI disorders and can exacerbate inflammatory bowel disease (IBD), a known precursor to colorectal cancer (CRC). Effective repair of the colonic epithelium is essential for favorable long-term outcomes in IBD patients, who frequently experience chronic GI injury. Moreover, disruption of gut homeostasis is linked to conditions such as obesity, diabetes, and colitis, all of which may contribute to tumorigenesis. Although multiple mechanisms are implicated in gut homeostasis, a key regulator is the enteric nervous system (ENS), an extensive network of neurons and enteric glial cells (EGCs) that innervates the GI tract. EGCs act as signaling hubs, modulating intestinal motility, immune responses, and epithelial barrier function by releasing factors that influence neighboring cells in response to environmental changes. In Crohn's disease, for example, a reduced glial network is correlated with impaired mucosal healing. Therefore, understanding the mechanisms that facilitate gut homeostasis of significant therapeutic importance, as defective mucosal repair can lead to fibrosis and increased risk of GI adenocarcinoma. To address the role of stress in colitis, a pre-cancer disease, we used a physical restraint model from our previous work, which induces a leaky gut phenotype in mice. In a dextran sodium sulfate (DSS)-induced colitis model, we further found that stress significantly delayed colitis healing, with the accumulation of p16+ senescent enteric glial cells (senEGCs). The senEGCs, which no longer proliferate but remain metabolically active, secrete a diverse array of cytokines, growth factors, and proteases, collectively known as the senescence-associated secretory phenotype (SASP), resulting in inhibiting intestinal organoid outgrowth. Remarkably, either pharmacological intervention with senolytics drug (dasatinib and quercetin) or genetic ablation of senescent cells in INK-ATTAC mice fully reverses stress-impaired colitis recovery. Colitis-associated cancer (CAC), a CRC subtype linked to IBD, carries a high mortality rate: within 30 years of disease onset, over 20% of IBD patients develop CAC, and more than half of these cases result in death. Inflammation also plays a role in the development of sporadic CRCs. In two established CAC models, we found restraint stress increased colorectal tumor number by two-fold relative to controls and enhanced tumor innervation. Given that perineural invasion is a strong and independent prognostic indicator in CRC, our findings provide new insights into the systemic influence of stress on CRC development and open avenues for novel therapeutic strategies to improve CRC treatment outcomes.

#4081 A multimodal single-cell atlas reveals a pathogenic epithelial-myeloid circuit driving HNSCC progression.

C. Nam[1], H. Zhao[2], E. Salman[2], D. Arnaudov[2], U. K. Sinha[2], Y. Park[3], **D.-C. Lin**[2];

[1]Keck School of Medicine of USC, Los Angeles, CA, [2]University of Southern California, Los Angeles, CA, [3]Yonsei University Health System, Seoul, Korea, Republic of

In this study, we performed single-cell RNA sequencing (scRNA-seq) on 167 samples from patients with head and neck squamous cell carcinoma (HNSCC), including distal normal tissues, premalignant lesions, peri-tumor regions, primary tumors, lymph node metastases, and distant metastatic or recurrent tumors. This comprehensive atlas allowed us to profile the full spectrum of immune and stromal populations across the continuum of HNSCC progression. By integrating transcriptional states, cellular compositions, and intercellular communication networks, we uncovered key features of the dynamically evolving tumor microenvironment and identified stage-specific mechanisms that shape tumor development, metastatic competence, and therapeutic resistance.

A central finding was the discovery of a previously unrecognized intratumoral monocytic subset, which we termed Tumor-Reprogrammed Monocyte (TrMo). TrMo cells are markedly enriched in tumor tissues and strongly associated with adverse pathological features and poor patient survival. We also delineated major epithelial heterogeneity programs—including cell-cycle activation, hybrid epithelial-mesenchymal transition (hEMT), and epithelial senescence (EpiSen)—and validated these states in patient-derived organoid models. Notably, normal tissues were dominated by high EpiSen scores, whereas tumors exhibited diverse and spatially organized transcriptional programs.

Using co-association analyses, we identified a robust multicellular module composed of hEMT cancer cells, TrMo cells, myofibroblastic CAFs, regulatory T cells, and Endo_C3-RGCC endothelial cells. Spatial transcriptomic profiling confirmed the physical co-localization of this module in tumor tissues, highlighting a coordinated, tumor-promoting niche.

To investigate its functional relevance, we focused on the bidirectional communication between hEMT tumor cells and TrMo cells. Spatial data demonstrated their intimate juxtaposition in situ, while in vitro co-culture experiments revealed a reciprocal signaling loop. TrMo cells enhanced EMT features in cancer cells by activating the EGFR pathway, whereas hEMT tumor cells induced TrMo activation through CD44-dependent cues. Using patient-derived tumor organoids, we further validated this reciprocal circuit and showed that disrupting either EGFR signaling in tumor cells or CD44 signaling in monocytes attenuated the tumor-promoting phenotypes.

Together, these findings define a pathogenic epithelial-myeloid signaling axis that emerges early in HNSCC progression, becomes reinforced in advanced disease, and represents a promising therapeutic vulnerability. Our work provides a comprehensive multi-modal atlas of the HNSCC microenvironment and establishes a mechanistic framework for targeting multicellular tumor niches that drive aggressive behavior and treatment failure.

#4082 The gut microbiota influences chronic sleep deprivation-induced colorectal cancer progression and treatment response.

M. C. Hernandez[1], Y. Yang[2], C. Jobin[1];

[1]University of Florida College of Medicine, Gainesville, FL, [2]University of Florida Department of Medicine, Gainesville, FL

BACKGROUND: Sleep deprivation (SD) is common among cancer patients and a known disruptor of immune regulation and microbiota balance. We hypothesize that SD-induced bacterial dysbiosis promotes carcinogenesis and reduces 5-Fluorouracil (5-FU) efficacy by creating an immunosuppressive tumor-microenvironment (TME).

METHODS: Chronic SD and fecal microbiota transplant (FMT, $5*10^7$ CFU single oral gavage) mouse models were used to evaluate murine colorectal cancer using MC38 cancer cells. Tumor growth and 5-FU response were assessed. TME immune cell infiltration, tumor gene expression of circadian rhythm (CR) genes, inflammatory, and immune markers were compared between SD and controls.

RESULTS: Chronic SD exposure increased *PER2*, *CRY1*, *CRY2* and decreased *BMAL1* CR gene expression compared to non-SD mice. Chronic SD mice experienced a significant increase in tumor volume (endpoint mean 734 mm^3 SD vs 476 mm^3 non-SD, p=0.0002), remodeled TME via a significant increase in Ly6G+ Neutrophils (0.0366) and CD19+ B cells (0.0163). This was associated with a decrease in *TNFα*, *IL1β* and *IL17A* gene expression. FMT from SD mice to recipient non-SD mice conferred greater MC38 tumor volume (endpoint mean 1086 mm^3 SD vs 618 mm^3 non-SD, p=0.0092) and a pro-inflammatory TME via increase in IL6+ producing Ly6G+ Neutrophils and *IL-6* mRNA accumulation in the tumor ($p < 0.0001$). Interestingly, SD mice exhibited larger tumor volumes (endpoint mean 2241 mm^3 SD vs 1033 mm^3 non-SD, p=0.0059), and fewer cytotoxic and effector immune cells and markers following 5-FU treatment. Gene expression analysis revealed altered *IL17a* (p=0.0195*), IL6* (p<0.0001), *IFNγ* (p=0.0366), and *CD27* (p=0.0228) mRNA accumulation. FMT from SD donor mice to recipient non-SD mice exhibited impaired 5-FU response as seen with higher tumor volume (endpoint mean 1055 mm^3 SD vs 630 mm^3 non-SD, p=0.0033), decreased infiltration of CD4 and CD8+ T cells in the TME along with decreased gene expression of *TNFα* (p= 0.0296) and *IL6* (p=0.0485) in the tumor.

CONCLUSION: Chronic SD promotes carcinogenesis, disrupts circadian rhythm regulation, and weakens chemotherapy efficacy through microbiota-driven immune dysregulation. These findings identify SD as a modifiable factor influencing cancer outcomes and highlight the gut microbiota as an important mediator of this pathology.

#4083 The impact of obesity-induced changes in adipose tissue on ovarian cancer progression.

Sofia Howe, Emily Rodriguez, Mikella Robinson, Carrie Danielle House

San Diego State University, San Diego, CA

Obesity, characterized by excessive accumulation of body fat, is increasingly prevalent and is recognized as a risk factor for ovarian cancer. Omental adipose tissue is the initial metastatic niche for ovarian cancer cells, providing a conducive microenvironment enriched in fatty acids and cytokines that facilitates tumor migration and proliferation. Elevated NF-κB signaling associated with obesity is well-documented to aberrantly influence cancer cell behavior, potentially enhancing the tumor-supportive characteristics of adipose tissue. Despite this established link, the role of specific adipose cell populations in NF-κB-mediated ovarian cancer metastasis, particularly omental preadipocytes which are progenitors to mature adipocytes, remains unclear. Previous studies in our lab identified Insulin-like growth factor-1 (IGF-1), secreted by preadipocytes, as an activator of NF-κB that promotes extracellular matrix (ECM) remodeling and metastasis. Therefore, we hypothesize that preadipocytes from obese omental tissue contribute to ovarian cancer progression through IGF-1 mediated enrichment of NF-κB signaling. To test this, we used in vitro co-culture and in vivo co-injection models with human ovarian cancer cell lines to compare adipocytes and preadipocytes in supporting ovarian cancer during isolation stress-inducing conditions. Our findings revealed that mature adipocytes and preadipocytes generate tumors and activate NF-κB at similar levels. However, when we compared co-injections of GFP labeled cancer cells with isolated omental preadipocytes from high or normal BMI donors, we found that high BMI preadipocytes enhanced early tumor growth and reduced survival of mice. Tumors from high BMI exhibited increased phosphorylation of p65 (Rel A), suggesting that the obese adipose microenvironment may modulate NF-κB signaling dynamics to support tumor growth. We further assessed SOX2 and FN1 expression in GFP positive sorted cells and found a significant decrease in SOX2 expression and increased FN1 levels, suggesting reduced cancer cell stemness and enhanced proliferative, ECM-remodeling programs. To assess IGF-1 secretion, we utilized co-culture studies and found increased IGF-1 levels from high BMI preadipocytes. Our findings highlight the critical role of obesity-induced alterations in omental adipose tissue, particularly in preadipocytes, with IGF-1 signaling as a key factor that may drive metastasis. Ongoing studies aim to interrogate IGF-1 dependent NF-κB activation for ECM-remodeling and metastatic growth using knockdown models. These results will be further validated in an obesity-induced mouse model to assess whether IGF-1 is required to drive ECM remodeling and metastasis. This study provides valuable insight into how obese adipose tissue influences tumor biology, potentially guiding the development of therapeutic strategies for obese ovarian cancer patients.

#4084 Dissecting myeloid-driven mechanisms of immunotherapy resistance in prostate cancer bone metastases.

A. Lyu[1], Z. Fan[2], M. Clark[2], A. Lea[2], R. Wolters[2], L. Qiu[2], K. Tucker[1], L. Trieu[1], Y. Li[1], A. Tran[1], A. Muralidhar[1], E. Van Allen[3], L. Fong[1];

[1]Fred Hutchinson Cancer Center, Seattle, WA, [2]University of California San Francisco, San Francisco, CA, [3]Dana-Farber Cancer Institute, Boston, MA

Background: Patients with metastatic castration-resistant prostate cancer (mCRPC) are generally refractory to immune checkpoint inhibitors (ICIs), particularly those with bone metastases, the most frequent site of disease progression (70-90%). The bone marrow (BM) harbors diverse immune populations, with myeloid cells comprising >70% of its cellular compartment. Among these, neutrophils, known mediators of ICI resistance across multiple malignancies, predominate, whereas macrophages, including *SPP1*-high tumor-associated macrophages (*SPP1*^{hi}-TAMs), are relatively sparse, implicating neutrophils as potential key drivers of ICI resistance. However, their role in human mCRPC bone metastases remains poorly characterized. We hypothesize that single-cell characterization of immunosuppressive neutrophil subsets can find new therapeutic opportunities to enhance immunotherapeutic efficacy.

Methods: We performed single-cell profiling of prostate cancer biopsies across disease stages and tumor sites, including bone metastases, as well as bone samples from tumor-free patients who underwent hip replacement surgery. To validate these findings, we also employed a murine intraosseous CRPC model, combining multi-omic single-cell analyses with functional assays and mechanistic studies.

Results: Single-cell profiling of patients revealed abundant neutrophil populations in the bone compared to other soft tissues, with distinct subsets corresponding to developmental trajectories. Among mature neutrophils, an inflammatory subset expressing elevated *IL1B* expression (*IL1B*^{hi}-mNeu) was significantly enriched in mCRPC bone metastases versus tumor-free bone tissues and expressed elevated immunosuppressive transcriptional programs. Multi-omic analyses of the intraosseous CRPC murine model identified an analogous *Il1b*^{hi}-mNeu population that suppressed CD8^{+} T cell function in co-culture. *In vivo* studies showed that targeting *Il1b*^{hi}-mNeu with a CXCR1/2 antagonist or adoptive transfer of these neutrophils into CRPC-bearing mice demonstrated that *Il1b*^{hi}-mNeu are key drivers of ICI resistance in intraosseous CRPC. Pathway analyses implicated pro-tumor inflammatory signaling as a major mechanism, in particular through IL-1β-mediated pathways. Pharmacologic inhibition of IL-1R diminished *Il1b*^{hi}-mNeu -mediated CD8^{+} T cell suppression *in vitro* and improved ICI responsiveness *in vivo*.

Conclusions: Our studies identify a distinct mediator of immunotherapy resistance in prostate cancer bone metastases. We demonstrate that mature inflammatory neutrophils (*IL1B*^{hi}-mNeu) are enriched in human mCRPC bone metastases and drive ICI resistance through IL-1R signaling. These findings suggest that targeting these cells and their signaling pathways could represent promising therapeutic strategies for overcoming ICI resistance in advanced prostate cancer.

: Novel Molecular Mechanisms Driving Cancer Metastasis
Minisymposium

#4087 Senescent cancer cells facilitate metastasis by adhesion-mediated clustering and immune modulation.

S. Anvar[1], C. Maharjan[1], Z. Chen[2], J. D Somers[2], Z. Jin[1], H. Kates[3], S. H. Ramirez[1], A. M. Andrews[1], B. M. Runyon[1], M. E. Carelock[1], Y. Zhang[2], J. Liu[4], W. Zhang[1], L. Cui[2];
[1]University of Florida, College of Medicine, Gainesville, FL, [2]University of Florida, College of Pharmacy, Gainesville, FL, [3]University of Florida, Health Cancer Institute, Gainesville, FL, [4]University of New Mexico, Alnuquerque, NM

Therapy-induced senescence (TIS) occurs following cytotoxic stress and has previously shown to promote tumor metastasis through senescence-associated secretory phenotype (SASP) of stromal cells in the tumor microenvironment, however, whether senescent cancer cells directly participate in metastatic dissemination remains unclear. Here, we report that therapy-induced senescent breast cancer cells actively promote metastatic seeding by physically adhering to parental breast cancer cells and forming circulating senescent-parental cell clusters. Senescence was induced in MDA-MB-231 cells with doxorubicin (39 nM, 7 days) or in 4T1 cells via irradiation (50 Gy, 7 days) and confirmed by X-gal staining, NIR-BG2 senescence probe activity, and increased p16 and SASP expression. RNA-seq revealed upregulation of migration, motility, and adhesion pathways of senescence cells with specific increases in ICAM1, JUP, CLDN1, and CLDN7. Functionally, senescent cells were able to migrate independently, but the presence of both senescent and parental cells in co-culture significantly enhanced migration of both cell types in trans-well and wound healing assays. Hanging-drop aggregation produced large mixed clusters in co-culture, whereas parental cells alone formed scattered microcolonies. Direct adhesion assays showed parental tumor cells preferentially attached to senescent cells versus the substrate, with individual senescent cells binding multiple parental cells. In vivo, orthotopic co-injection of senescent and parental MDA-MB-231 cells in NSG mice resulted in significantly increased lung metastasis. Early tail-vain tracking revealed greater initial lung seeding when co-injected parental cancer cells with senescent MDA-MB-231 in NSG mice and 4T1 cells in NSG and BALB/c mice models, respectively. Interestingly, in immune competent BALB/c mice, metastatic progression sustained over time. These findings reveal a previously unrecognized mechanism in which senescent cancer cells cooperate with parental cancer cells through cell-cell adhesion mediated clustering to facilitate early metastatic colonization. Ongoing studies examine the functional role of ICAM1 and JUP, and the involvement of the immune system as a second phase of metastasis following dissemination, where senescent cells may reshape the microenvironment to promote tumor cells survival. These results suggest that targeting senescent cell adhesion and immune programs may suppress early dissemination and metastatic relapse following cancer therapy.

#4088 Extracellular matrix rigidity controls breast cancer metastasis via TYK2-mediated mechanotransduction.

Z. Hu[1], H. E. Majeski[1], A. Mestre-Farrera[1], S. Cai[2], A. Lalezarzadeh[1], Y. Zhang[1], K.-I. Arimoto[1], D.-E. Zhang[1], H. M. Piwnica-Worms[2], L. Fattet[3], J. Yang[1];

[1]UC San Diego, La Jolla, CA, [2]UT MD Anderson Cancer Center, Houston, TX, [3]Centre de Recherche en Cancerologie de Lyon, Lyon, France

Mechanical cues from the extracellular matrix (ECM) regulate various cellular processes. In breast cancer, increased tumor stiffness is associated with elevated metastasis risk and poor survival. Whether and how the soft extracellular matrix (ECM) of normal mammary tissues actively suppresses malignant progression is poorly understood. Here, we identify TYK2 as an essential mechanosensitive metastasis suppressor that preserves epithelial integrity specifically under low ECM stiffness. Using human and mouse basal-subtype mammary acini and multiple triple-negative breast cancer (TNBC) patient-derived organoid models, we show that genetic depletion or pharmacologic inhibition of TYK2 potently induces EMT, disrupts basement membrane, and drives multicellular invasion under soft physiological stiffness. Importantly, this mechanotransduction pathway is independent of canonical interferon/JAK/STAT signaling, as neutralizing type I interferons or inhibiting JAK1/2 or STAT3/5 did not alter stiffness-dependent EMT and invasion. Mechanistically, TYK2 localizes to the plasma membrane via IFNAR1 binding under low stiffness, which retains the EMT transcription factor TWIST1 in the cytoplasm. Increasing ECM stiffness causes TYK2 to disperse into the cytoplasm, leading to nuclear translocation of TWIST1 and EMT activation. In vivo, TYK2 knockdown or systemic inhibition with the clinical TYK2 inhibitor deucravacitinib markedly increased local invasion and significantly enhanced lung metastasis in MCF10DCIS and TNBC patient-derived xenografts, while leaving primary tumor growth unchanged. Supporting a mechanosensory role of TYK2, normal human breast epithelium exhibited strong membrane-localized TYK2, whereas invasive breast cancers displayed diffuse cytoplasmic TYK2, mirroring the high-stiffness phenotype observed in vitro. These findings uncover TYK2 as a ECM rigidity-dependent epithelial safeguard that actively suppresses EMT and metastatic progression in basal-subtype breast cancer. By demonstrating that TYK2 blockade or loss unleashes invasion and metastasis in multiple xenograft and patient-derived TNBC models and that normal breast epithelium relies on membrane-anchored TYK2 for mechanotrasnduction, this work reveals a fundamental stiffness-governed epithelial defense mechanism. Given the increasing clinical use of TYK2 inhibitors for autoimmune diseases, these results raise important considerations for patient monitoring and metastasis risk.

#4089 Immunosuppressive cellular topography and genomic adaptations sustain colorectal cancer metastasis to the brain.

A. Sathe[1], M. Zhang[1], X. Bai[1], J. Kang[1], R. Meka[1], H. Sun[1], M. Humayun[2], X. Wang[2], S. M. Grimes[1], A. Khan[1], M. Liu[1], A. S. Luksik[3], M. Lim[1], C. K. Petrisch[1], C. M. Jackson[3], H. Vogel[1], J. Shen[1], R. D. Kamm[2], M. Gephart[1], S. Han[1], H. P. Ji[1];
[1]Stanford University School of Medicine, Stanford, CA, [2]Massachusetts Institute of Technology, Cambridge, MA, [3]Johns Hopkins University School of Medicine, Baltimore, MD

Colorectal cancer metastases to the brain (CRC-BMets) are lethal and resistant to immunotherapy and radiation. The cellular and molecular adaptations that sustain CRC-BMets remain poorly defined. The objective of our study was to identify the tumor-intrinsic and microenvironmental programs that support metastatic growth in the brain. To understand these mechanisms as they operate in the patient's metastatic niche, we performed sequencing and imaging-based spatial transcriptomics on 51 patients, including a subset with paired primary tumors and longitudinal radioresistant tumors. Using patient-derived three-dimensional co-culture systems, microfluidic assays and single-cell sequencing, we experimentally perturbed the intercellular interactions that promote tumor growth in the metastatic niche.Metastatic tumor cells showed significantly elevated chromosomal instability and activation of RNA-processing, stress-response, and junctional remodeling pathways compared with paired primary tumors. After radiation therapy, resistant clones retained their copy-number alterations and displayed increased epithelial-mesenchymal transition and transcriptional plasticity. Spatial mapping revealed that tumor cells proliferated preferentially in endothelial-rich regions. Tumor cells acted as multicellular ligand hubs (*MIF*, *GDF15*, *PRSS3*, *SEMA3C*) reinforcing tumor-supportive interactions with multiple surrounding microenvironmental cell types in the metastatic niche. Adjacent brain parenchyma expressed astrocytic and glial activation, together with angiogenic and matrix-associated pro-tumor features. CRC-BMets reconstructed a stromal microenvironment dominated by macrophages and fibroblasts in proximity to tumor cells, with sparse lymphocytes. This conserved macrophage-fibroblast neighborhood promoted angiogenesis and extracellular matrix remodeling, with increased regulatory T cell and exhaustion gene signatures. Macrophages expressed high levels of *SPP1*, predicted to orchestrate a matrix remodeling immunosuppressive program via interactions with corresponding receptors on neighboring cells. In a microfluidic device, CRISPR deletion of *SPP1* reduced macrophage mobility in the presence of tumor cells. When co-cultured with a CRC-BMet patient-derived spheroid and fibroblasts, *SPP1* knockout led to reduced expression of lipid-metabolism related genes in macrophages and disrupted tumor-promoting interactions. Together, these findings indicate that CRC-BMets are maintained by spatially organized tumor-intrinsic adaptations and multicellular stromal programs that persist after radiotherapy. These tumor genomic adaptations, multicellular ligand hubs, and an SPP1-dependent macrophage-fibroblast axis define targetable vulnerabilities in this aggressive metastatic site.

#4090 ADAR1 acts as a metastatic switch by sustaining survival programs in breast cancer brain metastasis..

T. Sposito, E. Klacking, J. Pham, R. Sasik, I. Van der Werf, N. Kfoury-Beaumont, T. Beaumont, V. Goodwill, A. A. Khalessi, T. Whisenant, C. Jamieson;
University of California San Diego - UCSD, San Diego, CA

Background: Essential for preventing autoinflammation, adenosine deaminase acting on double-stranded RNA (ADAR1) has been widely implicated in tumor progression and immunotherapy resistance. However, its role in the establishment and progression of metastasis remains unexplored. High-grade breast cancer (BC) patients harboring ADAR1 overexpression have been correlated with a worse prognosis and reduced survival, suggesting that ADAR1 activation may also play a role in BC stem cells transformation. This project focused on the brain niche, one of the most aggressive and least studied sites for BC metastasis.
Methods: We investigated ADAR1 dependencies in BC brain metastasis (BC-BrM) using single-cell RNA sequencing (scRNA-seq) of orthotopically derived triple-negative breast cancer (TNBC) BrM. The model was generated by intra-cerebroventricular implantation of TNBC cells carrying a nanoluc-GFP reporter for tracing ADAR1 activity into *Rag2γc*$^{-/-}$mice. Data from this mouse model were compared with scRNA-seq and imaging of metastatic patient samples.
Results: When TNBC cells were implanted into the mouse brain to form BrM, we observed upregulation of the tumor extracellular matrix (ECM) and JAK/STAT-driven inflammatory response, together with the activation of the WNT/β-Catenin pathway and ADAR1, compared to non-implanted TNBC cells. Consistent with these findings, we observed acorrelation between nuclear ADAR1 and WNT/β-Catenin activation in human tumors. As a readout for increased β-Catenin stability, we detected a marked inhibition of its negative regulator, GSK3β, in samples with high nuclear ADAR1/β-Catenin levels.
Sc-RNA seq analysis of patient samples identified a cluster with high ADAR1 level characterized by fast dividing cells and activation of Protein Arginine Methyltransferase 1 (PRMT1), a driver of *de novo* fatty acids synthesis in BC cells. This cluster positively correlated with cancer cell proliferation programs, lipid remodeling and suppression of inflammatory stimuli. ADAR1 downregulation in the mouse model confirmed a decrease in PRMT1 across several clusters and revealed a reduction in the metastatic drive of the tumors, by impairing cell-cycle progression, ECM deposition and lipid remodeling. Finally, we identified a highly stressed cluster, predominantly composed of ADAR1 KD cells, characterized by endoplasmic reticulum stress, a robust unfolded protein response, and an apoptotic signature.
Conclusions: Our findings identify ADAR1 as a critical “metastatic switch” that enables BC cells to coordinate proliferation and stress adaptation programs required for survival in the brain microenvironment. ADAR1 loss destabilizes metastatic proteostasis ultimately leading to programmed cell death. This study uncovers a key dependency of BC-BrM on ADAR1, highlighting it as a promising therapeutic target for disrupting the metastatic niche.

#4091 KPC1 regulates mesenchymal reprogramming in metastatic melanoma through ubiquitin-dependent degradation of ZEB1.

Yusuke Nakano[1], Matias A. Bustos[1], Kelly Chong[1], Yoshinori Hayashi[1], Aaron Ciechanover[2], **Dave S.b. Hoon**[1]

[1]St. John's Cancer Institute, Santa Monica, CA,[2]The Rappaport Faculty of Medicine and Research Institute, Halifa, Israel

Background: Advance stages of metastatic melanoma (MM) transitions reversibly between melanocytic and mesenchymal (MES)-like cell states, enabling invasion, therapeutic resistance, and immune evasion. While transcriptional regulators of this plasticity are well described, the role of post-translational control remains underexplored. The ubiquitin E3 ligase KPC1 (RNF123) regulates NF-κB signaling through p105 processing, but its contribution to melanoma cell-state transitions is unknown. We investigated whether KPC1 regulates MES reprogramming through ubiquitin-dependent modulation of ZEB1, a central MES transcription factor.
Methods: We integrated bulk RNA-seq, single-cell RNA-seq, and proteomic datasets from TCGA-SKCM, GSE115978, and PXD006003. Deconvolution (BayesPrism, CODEFACS) was used to derive melanoma-cell-specific expression profiles, and Monocle3 was applied to reconstruct pseudospatial trajectories. Functional validation included siRNA knockdown, qRT-PCR, Western blotting, cycloheximide chase, MG132 treatment, ubiquitination assays, and wound-healing migration assays. Multiplex immunofluorescence (mIF) on a clinically annotated stage III/IV melanoma FFPE tissue microarray (n = 110) assessed protein-level associations and clinical relevance.
Results: Across TCGA and scRNA-seq datasets, KPC1 expression showed a strong inverse association with MES gene signatures and was lowest in melanoma cells enriched for MES pathways. Trajectory analysis demonstrated that MES progression accompanied a continuous decline in KPC1. KPC1 knockdown did not change ZEB1 mRNA but markedly increased ZEB1 protein, indicating post-transcriptional regulation. Loss of KPC1 delayed ZEB1 degradation in CHX-chase assays, reduced ZEB1 ubiquitination, enhanced CDH2 expression, suppressed CDH1, and increased cell migration. Proteasome inhibition further confirmed that ZEB1 turnover is KPC1-dependent. In melanoma patient samples, low KPC1 protein co-localized with high ZEB1 and CDH2 and predicted significantly shorter overall survival. Combined evaluation of KPC1, ZEB1, and CDH2 improved prognostic resolution beyond individual markers.
Conclusions: KPC1 functions as a post-translational suppressor of MES-like reprogramming in metastatic melanoma by promoting ubiquitin-dependent degradation of ZEB1. Loss of KPC1 stabilizes ZEB1, activates MES transcriptional and phenotypic programs, and correlates with poor clinical outcomes. These findings identify KPC1 as a key regulator of melanoma cell-state plasticity and supports its potential utility as a theragnostic target.

#4092 Tumor cell JAG1 promotes lymph node metastasis and predicts recurrence in lymph node positive breast cancer patients.

B. Gordon[1], S. Youn[1], B. Swaminathan[1], N. Obacz[1], R. Vadakath[1], P. Teneqexhi[1], I. Alvarez-Lopez[2], M. Rezola[2], S. Manzano[2], Z. Telletxea[2], Z. Xu[3], Z. Chen[3], E. Er[1], L. Naiche[1], M. Munoz Caffarel[2], **J. Kitajewski**[3];

[1]University of Illinois Chicago, Chicago, IL, [2]Biogipuzkoa Health Research Institute, Donostia-San Sebastian, Spain, [3]University of Illinois Cancer Center, Chicago, IL

Lymph node metastasis is a “canary in the coal mine” in breast cancer, acting as a distinct prognostic indicator of aggressive disease. In preclinical models, invasion of tumor cells into lymphatics and lymph nodes is promoted by LECs that are active participants in the promotion of tumor cell invasion. It remains unclear how breast tumors interact with LEC cell signaling pathways to transverse lymphatic endothelium. Better understanding of specific and clinically actionable mechanisms that tumor cells use to promote lymphogenous metastasis are needed to reduce disease progression to distant organs. Expression of the Notch ligand JAG1 has long been associated with poor prognosis in patients, and JAG1 has been established to have critical roles in lymphatic specification and development. Using mouse models, we report that JAG1 expression in tumor cells actively promotes lymph node metastasis. JAG1 expression in tumor cells promotes progression through multiple stages of the lymphogenous metastatic cascade, including lymphovascular invasion into peritumoral lymphatic vessels, entry to mammary lymphatic collecting ducts, invasion into the subcapsular sinus of the lymph node, and overt nodal metastasis. To understand the underlying mechanisms of JAG1-driven metastasis, we determined that exposure of LECs to JAG1, either by JAG1-expressing tumor cells or tethered exogenous ligand, disrupted lymphatic barrier integrity and increased tumor cell migration across LEC monolayers in vitro. JAG1-stimulated transendothelial tumor migration could be suppressed with a Notch4-inhibiting antibody, but was not affected by treatment with a canonical Notch inhibitor. We demonstrated that JAG1 expression in tumor cells promotes VEGFR3 activity in LECs. JAG1-dependent lymph node metastasis can be suppressed with two distinct soluble VEGFR3 antagonists in vivo. In human synchronous breast and lymph node samples from node positive patients, we demonstrate that tumor cells in the lymph node are enriched in JAG1 compared to the primary tumor. Enrichment of JAG1 in lymph nodes was clinically meaningful, as JAG1 levels in the node, but not the primary tumor, predicted disease recurrence post-lumpectomy, which suggests that molecular workup of sentinel lymph nodes may be informative in lymph node positive patients. These data provide a novel mechanism by which tumor cells regulate cell behaviors in nearby lymphatic endothelium to promote invasion and lymphogenous metastasis.

#4093 Lipocalin-2 drives brain metastatic progression through reciprocal tumor-microenvironment interactions in lung cancer.

D. He[1], Y. Zhu[2], J. Zhang[1], W. Zhuang[1], H. Bai[1], J. Wang[1];

[1]State Key Laboratory of Molecular Oncology, Department of Medical Oncology, National Cancer Center/National Clinical Research Center for Cancer/Cancer Hospital, Chinese Academy of Medical Sciences & Peking Union Medical College, Beijing, China,

[2]Department of Radiation Oncology, Sichuan Clinical Research Center for Cancer, Sichuan Cancer Hospital & Institute, Sichuan Cancer Center, Affiliated Cancer Hospital of University of Electronic Science and Technology of China, Chengdu, China

Background: Brain metastasis (BM) is a leading cause of death in lung cancer patients, and the brain's unique microenvironment is key to metastatic initiation and progression. However, the molecular mechanisms of tumor microenvironment crosstalk in lung cancer BM remain unclear. Lipocalin-2 (LCN2) is associated with inflammation and cancer, but its specific role in lung cancer BM is undefined.
Methods: Single-cell sequencing analysis was conducted on BM specimens from patients with lung cancer BM, and data mining of public databases was performed to identify key molecules. Cell lines with stable LCN2 knockdown or overexpression were constructed using lentiviral transduction. Transcriptome sequencing and immunofluorescence assays were applied to verify the in vitro functions of LCN2, including its regulatory effects on downstream signaling pathways and cellular behaviors. For in vivo studies, murine models of lung cancer BM were established via brain orthotopic injection and intracardiac injection of tumor cells. Bioluminescence imaging and multiplex immunofluorescence staining was utilized to investigate the role of LCN2 in BM tumor initiation and progression, as well as its interaction with brain microenvironmental components.
Results: LCN2 was upregulated in BM compared to primary tumors, correlating with shorter intracranial disease-free and overall survival and plasma LCN2 was higher in BM patients. LCN2 is dispensable for BBB transmigration but is essential for promoting tumor growth within the brain microenvironment. LCN2 promoted intracranial tumor growth and upregulates VEGF-A via the JAK2/STAT3 signaling pathway to facilitate angiogenesis in lung cancer BM. More importantly, LCN2 bound to SLC22A17 on astrocytes to activate the JAK2/STAT3 signaling pathway and induce CCL2 secretion, which recruited macrophages that secreted IL-1β to upregulate LCN2 in tumor cells via the IL-1R-NF-κB signaling axis. Inhibition of IL-1β-IL-1R and JAK2/STAT3 signaling by IL-1R inhibitor anakinra combined with STAT3 inhibitor SH4-54 an suppress LCN2-driven tumor progression.
Conclusions: Tumor-derived LCN2 orchestrates a brain-specific metastatic program through dual mechanisms: a paracrine loop involving astrocyte activation and macrophage recruitment and a tumor-intrinsic angiogenic pathway via SLC22A17-JAK2-STAT3-VEGF-A signaling. These mechanistic insights suggest that LCN2 may serve as both a therapeutic target and a prognostic biomarker in lung cancer BM.

: Oncogenic Transcriptional Control: From Chromatin to Cell Fate
Minisymposium

#4060 SOX2 is a master regulator of classical squamous cell carcinoma.
R. Falter, Y. Song, X. Zhang;
University of Utah Huntsman Cancer Institute, Salt Lake City, UT

Classical squamous cell carcinoma is defined by recurrent 3q amplification and overexpression of the lineage-specific transcription factor SOX2. However, the extent to which SOX2 contributes this molecular subtype remains incompletely understood. Here, we identify SOX2 as a master regulator of the classical SCC subtype through integrated analysis of chromatin accessibility, transcription factor binding, 3D chromatin interactions, and gene expression. Across TCGA and cell line datasets, classical SCCs exhibit SOX2 copy number gain, focal amplification, and elevated expression. Dependency analyses reveal that classical SCC cell lines are uniquely sensitive to SOX2 loss, which we functionally validate using SOX2 CRISPRi, resulting in impaired proliferation and reduced SOX2 protein levels. ATAC-seq following SOX2 depletion demonstrates that SOX2 is required to maintain chromatin accessibility at thousands of regulatory elements. Regions that lose accessibility upon knockdown show the strongest SOX2 ChIP-seq binding and are enriched for SOX2 motifs. Conversely, SOX2 overexpression in SOX2-low non-classical SCC lines is sufficient to induce chromatin opening at newly bound enhancers, supporting a direct pioneer factor role for SOX2. HiChIP profiling reveals that SOX2 loss disrupts enhancer-promoter chromatin loops, whereas SOX2 overexpression creates new interactions at target genes. SOX2-dependent looping events overlap strongly with SOX2-driven accessibility changes. Finally, transcriptomic analyses show that SOX2-regulated enhancer-promoter interactions activate pathways enriched in classical SCC. Genes associated with SOX2-driven loops and accessibility changes exhibit the strongest expression alterations.Together, these data demonstrate that SOX2 is both necessary and sufficient to activate classical SCC epigenomic and transcriptional programs. By functioning as a pioneer factor that controls chromatin accessibility, chromatin looping, and downstream oncogenic expression, SOX2 emerges as a central regulator of classical SCC.

#4061 Single cell transcriptomic analysis of T-SCLC patients identifies PHOX2B as a factor in NE transformation.

A. Sabet[1], M. Wang[1], S. Rakhade[2], A. Quintanal-Villalonga[1], E. Redin[1], C. M. Rudin[1], J. Chan[1];
[1]Memorial Sloan Kettering Cancer Center, New York, NY, [2]Herbert Irving Comprehensive Cancer Ctr., New York, NY

Lung neuroendocrine (NE) transformation is a molecular process by which non-small cell lung cancers (NSCLCs) transdifferentiate into small-cell lung cancer (SCLC). This transition involves coordinated histological and molecular reprogramming. NE transformation is frequently observed in EGFR-mutant LUAD, occurring in up to 15% of patients treated with EGFR targeted therapies. Whereas LUAD is typically driven by activating oncogenic mutations that hyperactivate the MAPK signaling, SCLC is defined by near-universal inactivation of the tumor suppressor genes *TP53* and *RB1*. Although concurrent loss of *TP53* and *RB1* appears to be a prerequisite for NE transformation, this genetic background alone is insufficient to induce the phenotypic switch. In this project, we aim to identify molecular drivers that promote NE transformation in *TP53/RB1*-deficient LUAD tumors.We conducted single cell transcriptomic profiling on a cohort of 47 tumors and patient-derived xenografts (PDXs) from 24 patients with transformed or combined NE histology. Our analysis identified high levels of *PHOX2B* in transformed SCLC (T-SCLC) cases versus non-transformed SCLC and LUAD. *PHOX2B* is a neural crest transcription factor (TF) and acts a known oncogenic driver in neuroblastoma. In two EGFR-mutant LUAD cell lines with concurrent inactivation of *TP53* and *RB1*, we found that PHOX2B overexpression induced upregulation of NE markers such as SYP. Furthermore, we observed a pronounced decrease in EGFR signaling along with MAPK (ERK) and YAP activity. ChIP-seq analysis revealed *PHOX2B* binding to the EGFR promoter, suggesting that PHOX2B may act as a transcriptional repressor of EGFR. Despite these changes, PHOX2B overexpression did not drive full morphologic NE transformation *in vitro* or *in vivo*. Moreover, PHOX2B knockout in *de novo* as well as T-SCLC cell lines did not substantially reduce NE marker expression. Our research uncovers a previously unidentified role for *PHOX2B* in NE differentiation. They suggest that *PHOX2B* likely primes cells for transformation by shutting down EGFR signaling, which may represent a necessary but insufficient factor for NE transformation. Future work will investigate the molecular mechanism by which PHOX2B contributes to NE differentiation and cooperates with other factors to drive plasticity.

#4062 MBD4 regulates FOXA1 lineage-specific enhancers to promote prostate tumorigenesis and progression.

X. Chen, J. A. Villa-Pulgarin, J. Wu, U. Chan, A. Orgel, J. Owiredu, A. Yadav, A. Sboner, C. E. Barbieri;
Weill Cornell Medicine, New York, NY

BACKGROUND: Like many cancers, prostate cancer (PCa) relies on tissue- and lineage-specific transcription factors essential for normal tissue function and tumor progression. A key master factor is the androgen receptor (AR), which regulates prostate tissue identity and differentiation, maintaining normal, growth-suppressive, prostate-specific luminal programs via androgen response elements (AREs). However, during tumorigenesis, AR is co-opted to drive oncogenic transcription programs, including the reprogramming factors like FOXA1 and HOXB13. Despite AR's critical role, the mechanisms and functional implications of both its oncogenic and growth-suppressive programs in PCa remain incompletely understood. We hypothesized that the previously known methyl-CpG reader and DNA repair protein, MBD4, safeguards these lineage trajectories by restraining pioneer factor engagement.
METHODS: We performed an epigenetic-focused CRISPR screen (2,508 genes) in an LNCaP ARE-activated model to nominate the regulators of AR programs. We engineered MBD4 knockout and inducible overexpression models and profiled chromatin and transcription by ATAC-seq; CUT&RUN (AR, FOXA1, H3K27ac, H3K4me3, H3K27me3); and RNA-seq across AR^+ and AR^- lines. Proliferation and lineage-identity programs were also evaluated in normal mouse prostate organoids. Clinical relevance was assessed using multi-cohort patient transcriptomes and cancer-dependency datasets.
RESULTS: MBD4 emerged as a gatekeeper of the AR/ARE-mediated growth-suppressive program. MBD4 loss increased chromatin accessibility and enhancer acetylation at FOXA1-enriched loci, with FOXA1 binding expanding upon loss and decreasing with MBD4 overexpression. MBD4 localized to AR/FOXA1 enhancers and limited FOXA1 engagement. Functionally, MBD4 knockout accelerated proliferation in AR^+ lines (e.g., LNCaP, MDA-PCa-2b) and slowed growth in AR^- lines (e.g., PC3, DU145). In normal mouse prostate organoids, MBD4 disruption biased luminal epithelial identity programs and reprogrammed enhancer architecture. Across patient cohorts, MBD4 expression and dependency patterns tightly tracked with AR status/lineage, linking lineage context to chromatin plasticity.
CONCLUSIONS: MBD4 acts as a gatekeeper of the AR/ARE-mediated growth-suppressive program by limiting lineage-specific enhancers and restraining FOXA1 engagement. Loss of MBD4 promotes FOXA1-driven reprogramming and lineage plasticity, nominating the MBD4-FOXA1 axis as a potential therapeutic target.
AI DISCLOSURE: Generative AI was used to help draft the wording of this abstract; all content was supplied, reviewed, and approved by the authors.

#4063 Oral small-molecule condensate modulator (c-mod) inhibits MYC activity and demonstrates robust anti-tumor activity across diverse tumor models.

J.-G. Ren, D. Baumann, A. Talbot, T. Durand-Reville, I. Klein, **A. Boija**;
Dewpoint Therapeutics, Inc., Boston, MA

MYC is a key oncogenic driver that is commonly overexpressed or amplified across a wide spectrum of human cancers. Despite its therapeutic relevance, MYC has remained difficult to target pharmacologically due to its intrinsically disordered structure and dependence on dynamic biomolecular interactions. MYC forms transcriptional condensates to drive oncogene expression, suggesting that it might be inhibited by this mechanism. Using a condensate-focused screening approach, we previously identified first-generation MYC condensate modulators (c-mods) capable of disrupting MYC condensates and suppressing MYC-dependent transcription. Here we describe the profile of our orally bioavailable MYC Development Candidate (DC) with improved pharmacological properties, potency, and selectivity. This compound reduces MYC condensates, represses MYC-driven gene expression, and selectively inhibits the growth of MYC-addicted cancer cells by inducing apoptosis and cell-cycle arrest. Broad in vitro activity has been observed across multiple solid tumor types. In animal models, oral administration of our DC produces robust anti-tumor responses with an emerging tolerability profile supportive of continued development. Preclinical biomarker studies further demonstrate modulation of MYC pathway activity in vivo. Together, these findings position MYC condensate modulation as a promising therapeutic strategy for MYC-driven cancers.

#4064 NSD3 is a critical cofactor that enables fusion oncoprotein-driven 3D genome reorganization and activation of oncogenic transcriptional programs.

Y.-H. Chen, K. Sampat, I. D. Yonchev, C. E. Hawkins, C. Ponne, **K. P. Eagen**;
Baylor College of Medicine, Houston, TX

Fusion oncoprotein transcription factors such as BRD4-NUT reprogram chromatin organization to activate oncogenic transcriptional programs, yet the mechanisms by which they reshape gene regulatory architecture remain poorly understood. BRD4-NUT and NUT variant fusions drive NUT carcinoma, an aggressive squamous malignancy with a median survival of only 6.5 months. Although BRD4-NUT induces *de novo* tumor formation by reorganizing chromatin to activate pro-growth transcriptional programs, the chromatin-level mechanisms underlying this process have not been established. Here, we identify the chromatin regulator NSD3—also a recurrent NUT fusion partner—as a critical cofactor required for fusion oncoprotein-mediated chromatin reorganization and transcriptional regulation. Using CUT&RUN chromatin profiling, we show that NSD3 is highly enriched within BRD4-NUT chromatin “megadomains”, where it deposits histone H3K36me2 and stabilizes BRD4-NUT binding to chromatin. NSD3 also promotes the stability of BRD4-NUT nuclear condensates. Hi-C analysis reveals that loss of NSD3 attenuates the long-range chromatin interactions that link BRD4-NUT megadomains both within (*cis*) and between (*trans*) chromosomes, demonstrating that NSD3 is required for 3D genome reorganization by a fusion oncoprotein. Through these chromatin regulatory functions, NSD3 sustains expression of BRD4-NUT target genes, including *MYC* and MYC-regulated transcriptional networks. NSD3 depletion reduces proliferation and promotes differentiation of BRD4-NUT+ cells. Together, these findings identify NSD3 as a mechanistic cofactor co-opted by a fusion oncoprotein to integrate chromatin architecture, 3D genome topology, and transcriptional activation. This work reveals a generalizable model in which wild-type chromatin regulators are hijacked by fusion oncoproteins to establish oncogenic transcriptional and gene regulatory states, and it nominates NSD3 as an actionable vulnerability for therapeutic strategies targeting fusion-driven cancers.

#4065 EcDNA-borne structural variants drive oncogenic fusion transcript amplification.

H. Yi[1], S. Zhang[1], J. Swinderman[2], Y. Wang[1], V. Kanakaveti[1], K. L. Hung[1], I. T. Wong[1], S. Srinivasan[1], E. J. Curtis[1], A. Bhargava-Shah[1], R. Li[1], M. G. Jones[1], J. Luebeck[3], C. Bailey[4], Y. Zhao[1], J. Belk[1], K. Kraft[1], Q. Shi[1], X. Yan[1], S. K. Pritchard[1], K. S. Mahajan[1], F. Liang[1], M. Jamal-Hanjani[5], D. W. Felsher[6], L. Gilbert[2], V. Bafna[3], P. S. Mischel[1], H. Y. Chang[7];
[1]Stanford University School of Medicine, Stanford, CA, [2]Arc Institute, Palo Alto, CA, [3]University of California at San Diego, La Jolla, CA, [4]The Francis Crick Institute, London, United Kingdom, [5]University College London (UCL) Cancer Institute, London, United Kingdom, [6]Stanford Hospital, Stanford, CA, [7]Amgen, Stanford, CA

Extrachromosomal DNA (ecDNA) amplifications are key drivers of human cancers. Here, we show that ecDNAs are major platforms for generating and amplifying oncogene fusion transcripts across diverse cancer types. By integrating analysis of whole genome and transcriptome sequences from tumor samples and cancer cell lines of a wide variety of tissue types, we reveal that ecDNAs have the highest rate of oncogene fusion events of any copy number alteration. Focusing on the most common ecDNA fusion hotspot, we find that fusion of the 5' end of the long noncoding RNA gene, *PVT1*-with exon 1 joined to diverse 3' partners-confers increased RNA stability, potentially via an SRSF1-dependent mechanism, and enhances MYC-dependent transcription and cancer cell survival. These results demonstrate that ecDNA fosters genome instability and frequent oncogene fusion formation in cancer.

#4066 Epidemiology meets epitranscriptomics: Uncovering a novel *TERT*-antisense transcript regulated by RNA methylation and its role in cancer cell growth and proliferation.

B. Papenberg[1], O. Florez-Vargas[1], M. Ho[1], K. Forsythe[1], C.-H. Lee[1], S. M. Mbulaiteye[2], P. J. Batista[3], L. Prokunina-Olsson[1]; [1]National Cancer Inst. Div. of Cancer Epidemiology & Genetics, Bethesda, MD, [2]National Cancer Inst. Div. of Cancer Epidemiology & Genetics, Rockville, MD, [3]National Cancer Inst. Center for Cancer Research, Bethesda, MD

Human telomerase reverse transcriptase (TERT) maintains telomeres at chromosome ends and its dysregulation contributes to human health conditions. Multiple GWAS signals are detected within the *TERT* genomic region at chr 5p15.33. As a potential proxy for these signals, we investigated a highly polymorphic variable number tandem repeat (VNTR)2-1 within intron 2 of *TERT*, with 57-143 copies of a 42 bp repeat unit per allele. Functional annotation predicted an antisense intronic transcript with a variable-length open reading frame (2,505-5,211 bp; 834-2,038 aa).

Within this *TERT*-antisense transcript, we predicted N6-methyladenosine (m6A) consensus motifs in each 42 bp repeat. The consensus repeats and m6A-deficient variants of VNTR2-1 were cloned into a m6A-deficient dual-luciferase reporter vector (m-psiCHECK-2) and expressed in the bladder cancer cell line UMUC3. Transient treatment with STM2457, an inhibitor of the m6A writer METTL3, reduced reporter expression, confirming that m6A motifs within VNTR2-1 are methylated by METTL3.

VNTR2-1 expression was experimentally validated by 5'-RACE/Nanopore-seq in UMUC3. Additionally, RNA-FISH further visualized the transcript, showing co-localization with ribosomes and suggesting translation potential.

We explored potential peptides produced from VNTR2-1 transcript by analysis of public mass spectrometry datasets using PepQuery and identified several unique VNTR2-1 peptide fragments in human tumors. Next, we cloned a synthetic FLAG-tagged gene containing three VNTR2-1 consensus repeats with native Kozak sequence and translation start/stop codons. Western blotting confirmed the translation of the VNTR2-1 peptide that was ablated by start codon mutation, suggesting that the native Kozak sequence is sufficient for VNTR2-1 translation. These results support VNTR2-1 as a peptide-producing transcript.

RNA-seq following VNTR2-1 overexpression revealed upregulation of pathways related to DNA replication and cell cycle, while CRISPR-Cas9 knockout (V2.1KO) produced reciprocal downregulation of these pathways. To determine whether these transcriptional shifts translated to functional differences, we measured proliferation of UMUC3 as well as the lung cancer cell line A549 using xCELLigence Real-Time Cell Analysis. Overexpressing cells exhibited accelerated growth compared with wild type, whereas V2.1KO cells proliferated more slowly, mirroring the pathway-level changes. BrdU incorporation assays further corroborated impaired DNA replication in V2.1KO cells.

In summary, we identified a novel antisense transcript produced by VNTR2-1 within a *TERT* intron that functions as a lncRNA and/or translated peptide to modulate cell proliferation, potentially contributing to cancer and other disease-related phenotypes.

: Pediatric Cancer from Mechanism to Translation
Minisymposium

#4024 Dysregulated AKT signaling reprograms osteosarcoma to drive selective reliance on EP300.

I. Delahunty[1], S. Nance[1], Y. Zhang[1], F. Lamoureux[2], Q. Liu[3], W. C. Wright[1], K. E. Ritter[1], N. A. M. Shendy[1], B. Brounais[2], S. Kietlinska[1], B. De Kegel[4], M. G. Rees[4], M. Kocak[4], A. B. George[4], A. M. Kavirayani[1], P. P. Prinsen[1], Y. Khashana[1], M. M. Ronan[4], J. Roth[4], A. Sweet-Cordero[5], X. Ma[1], L. M. Guenther[1], P. Geeleher[1], B. Ory[2], J. Qi[3], B. Abraham[1], **A. D. Durbin**[1];
[1]St. Jude Children's Research Hospital, Memphis, TN, [2]Universite de Nantes, Nantes, France, [3]Dana-Farber Cancer Institute, Boston, MA, [4]Broad Institute, Cambridge, MA, [5]UCSF - University of California San Francisco, San Francisco, CA

Cancer cells are dependent on the control of transcription for maintenance of the malignant cell state. EP300 and CBP are paralogous, commonly expressed, master epigenetic enzymes, whose activity controls normal and malignant transcription. Here, using a cancer-wide integrative chemical-genetic analysis, we find enhanced dependency on EP300 compared to CBP in most cancer lineages, including osteosarcoma (OS). OS is a highly lethal malignancy of bone and has enhanced dependency on EP300, compared with CBP. To take advantage of selective pharmacology targeting EP300 alone that spares CBP in untransformed cells and thereby reduces toxicity, we used the EP300-targeted degrader JQAD1. We identify a specific genetic subgroup of OS, marked by dysregulation of the PI3K-AKT-mTOR pathway, that is both genetically dependent on EP300 and uniquely sensitive to EP300 degradation. Expression of constitutively active AKT in insensitive OS cells induces sensitivity to JQAD1, driven by physical relocalization of EP300, CBP and H3K27ac to genetic subtype-enriched dependency loci. Mechanistically, combinations of AKT inhibitors and JQAD1 suppress the growth of AKT-dysregulated OS. These observations extend across >850 cancer cell lines, where multiple AKT inhibitors, including the FDA-approved capivasertib, positively combine with EP300 degraders in a manner mechanistically dependent on control of protein synthesis. Finally, combination treatment is synergistic in AKT-dysregulated, orthotopic OS xenografts. These findings reveal genetic and transcriptional determinants of EP300 degrader function in high-risk OS and provide a foundation for biomarker-directed investigation of co-targeting of EP300 and AKT for therapeutic gain across cancers marked by enhanced protein translation.

#4025 Sequential cell free DNA analysis reveals genetic heterogeneity in patients with relapsed neuroblastoma enrolled in the SIOPEN-ITCC BEACON study.

Y. Iddir[1], C. Bobin[1], A. Saint-Charles[1], J. Masliah-Planchon[1], M. Gambart[2], E. Saberi-Ansari[1], A. Colaprico[1], A. Bellini[1], C. Butterworth[1], V. Attignon[3], D. A. Tweddle[4], J. R. Tall[5], D. Hughes[5], R. Weston[6], A. Vilaplana[7], L. Chesler[8], L. Moreno[7], S. George[9], **G. Schleiermacher**[1];

[1]Institut Curie, Paris, France, [2]Toulouse University Hospital, Toulouse, France, [3]Centre Leon Berard, Lyon, France, [4]Newcastle University, Newcastle, United Kingdom, [5]The Institute of Cancer Research, London, United Kingdom, [6]Birmingham University, Birmingham, United Kingdom, [7]Vall d'Hebron Institute of Research, Barcelona, Spain, [8]The Institute of Cancer Research, Sutton, Sutton, United Kingdom, [9]The Institute of Cancer Research, Sutton, United Kingdom

Background: Outcome for high-risk neuroblastoma following relapse remains poor, with an urgent need to increase understanding of the biology to develop effective (combination) therapies.
Aims : To characterize tumor-specific molecular alterations for patients enrolled in the SIOPEN-ITCC BEACON trial (EudraCT 2012-000072-42, evaluating different backbone chemotherapy regimens +/-bevacizumab in high risk refractory/relapsed NB) and to analyze resistance mechanisms based on sequential cfDNA.
Methods: Samples were collected from 191 BEACON patients. Tumor samples were available for 73 patients (2:diagnosis, 24:refractory; 47:relapse), and liquid biopsies for 182 patients (1-6 samples per patient, mean: 3). cfDNA lcWGS (low coverage Whole-genome sequencing), cfDNA WES (Whole-exome sequencing or targeted panel-sequencing was conducted on all plasma samples, with paired germline analyses.
Results: Molecular analysis of 63 tumor samples (41 large NGS-panel and 22 WES), , identified MYCN amplification in 17 cases, and mutations in RAS/MAPK/P53 pathway genes in 24% of patients, with 17.5% harboring an *ALK* mutation. cfDNA quantity at enrollment in BEACON did not correlate with disease burden (SIOPEN score), but showed correlation with outcome (HR p=0.02). From plasma samples obtained at inclusion and analyzed by WES, a mean of 35[5-96] SNVs were shared with tumor samples, while 31[7-73] and 11[2-29] SNVs were unique to tumor and plasma, respectively. cfDNA specific SNVs frequently targeted genes of pathways in cell-to-cell and cell-to-extracellular matrix connections. Sequential cfDNA quantities and ctDNA content evaluated by WES were measured for 139 patients, and showed distinct dynamics correlating with disease status. Notably, cfDNA quantity increases were associated with the emergence of new mutations in all analyzed cases, including alterations in genes of the RAS/MAPK pathway such as *HRAS*. Evidence of clonal hematopoiesis during treatment was observed in 40% of cases. Fragment size and nucleosome footprint analyses for inference of transcription factor and overall expression profiles is ongoing.
Conclusions: In refractory/relapsed high-risk neuroblastoma patients, 1/4 had at least one mutation in RAS/MAPK/p53 pathway genes, which might correlate with poorer survival. 53% of SNVs observed in tumor were detectable in plasma, and plasma-specific SNVs were observed in all cases. This finding underscores the value of plasma sample collection during follow-up to study tumor heterogeneity and clonal evolution.

#4026 Spatial T-cell receptor profiling uncovers barriers to T-cell engagement and shared tumor-reactive clonotypes in high-risk neuroblastoma.

Y. Jiang[1], W. Yu[2], S. Pedersen[1], J. Eagles[1], A. Thadi[2], A. Naranjo[3], N. B. Collins[4], S. DuBois[4], R. Bagatell[2], B. D. Crompton[5], K. Tan[2], T. J. Pugh[1];

[1]UHN Princess Margaret Cancer Centre, Toronto, ON, Canada, [2]Children's Hospital of Philadelphia, Philadelphia, PA, [3]University of Florida, Gainesville, FL, [4]Dana-Farber Cancer Institute, Boston, MA, [5]Dana-Farber Cancer Inst., Boston, MA

Background: Survival for patients with high-risk neuroblastoma (NB) is ~50%. While T-cell infiltration correlates with improved outcomes in some pediatric cancers, T-cell diversity, spatial organization, and antigen specificity remain poorly characterized. We integrated bulk T-cell receptor (TCR) sequencing, spatial transcriptomics, and spatial TCR profiling in NB patients from the Children's Oncology Group phase 3 trial ANBL1531, which evaluated 131I-metaiodobenzylguanidine therapy during frontline induction.
Methods: We applied hybrid-capture TCR sequencing to paired biopsy and resection FFPE tumors (10 samples from 5 patients), longitudinal PBMCs (84 samples from 33 patients), and cfDNA (14 samples from 12 patients). Using shared TCRs across sample types and timepoints, we designed a Xenium panel with 377 genes and 100 TCRα/β/γ/δs, enabling spatial mapping across 1.90 million cells (median 138,742, range 17,175-715,510 cells per tumor). We predicted TCR specificity using MixTCRpred, and inferred sequence convergence using GLIPH2 against a database of reference TCRs (4,146 known specificities, 595,689 controls, 16,888 NB from the Precision oncology for young people cohort).
Results: PBMC TCR repertoires showed biphasic dynamics, with diversity contracting mid-therapy (Shannon mean 476→151) then recovery post-therapy (413; p=0.0006, linear mixed-effects model), likely corresponding to chemotherapy-driven lymphopenia. In tumors, TCR diversity declined between biopsy and resection while hyperexpanded clonotypes increased (mean 30→59%), indicating potential selective clonal enrichment. Spatial profiling of the 10 tumors revealed immune-tumor compartmentalization, with macrophage-enriched barriers segregating immune cells from clusters of tumor cells. Spatial TCR profiling enabled in situ α/β chain pairing, identifying four TCRα/β clonotypes (all $CD8^+$ effector memory) not resolvable by bulk sequencing. One clonotype with predicted NY-ESO-1 specificity expanded from biopsy to resection (2.22→4.92% of all T cells), suggesting antigen-driven clonal proliferation. Despite this expansion, clonotype spatial positioning remained unchanged, indicating that microenvironmental architecture constrains T-cell localization. GLIPH2 identified 8 NB-restricted TCR sequence motifs shared across 3-7 NB patients. These motifs occurred in individuals with convergent MHC alleles, suggesting recognition of common NB-associated antigens.
Conclusions: Integrated TCR and spatial profiling revealed macrophage-mediated compartmentalization and restricted T-cell localization. Clonotypes predicted to be tumor-reactive also expanded during therapy. Shared NB-specific TCR motifs suggest convergent antigen recognition and targets for immunotherapy.

#4027 Co-targeting GPC2 and B7-H3 with CAR T cells achieves durable responses in preclinical high-risk neuroblastoma and medulloblastoma models.

P. M. Schurch[1], B. Draper[2], V. P. Zecchino[1], H. Pan[1], B. Nelson[1], A. M. Giudice[1], J. B. Foster[1], L. K. Donovan[2], K. R. Bosse[1]; [1]Children's Hospital of Philadelphia, Philadelphia, PA, [2]University College London, London, United Kingdom

Glypican 2 (GPC2) is highly expressed in pediatric cancers including high-risk neuroblastomas and medulloblastomas, and GPC2 CAR T cells are now in phase 1 trials (NCT05650749, NCT07087002). However, durable responses are limited by heterogeneous antigen expression, treatment-induced antigen loss, and poor CAR T persistence. In neuroblastoma, interconvertible adrenergic (ADRN) and mesenchymal (MES) states further complicate targeting, as state switching downregulates GPC2 and GD2, whereas B7-H3 remains consistently expressed. B7-H3 is also abundant across other GPC2$^+$ cancers, supporting a dual GPC2.B7-H3 CAR strategy. To approach GPC2.B7-H3 dual CAR T cell targeting, we engineered seven GPC2/B7-H3 co-targeting bicistronic CAR constructs containing CD28, 4-1BB, or OX40 costimulatory domains and either two (dual, d1-3) or one (parallel, p1-4) CD3-ζ signaling domain. Among these, d1 and p2 were prioritized because they drove strong activation of Jurkat NFAT-GFP CAR T cells in co-cultures with isogenic NALM-6 cells expressing either or both antigens and showed superior cytokine secretion in human CAR T co-incubation assays compared with single-antigen B7-H3 (B) or GPC2 (G) CARs. *In vivo*, dual-targeting CAR T cells - double-transduced (B/G) or expressing d1 or p2 - achieved potent clearance of COG-N-453x neuroblastoma PDXs, with 16-week cure rates of 83.3%, 83.3%, and 100%, exceeding single CARs (B, 57.1%; G, 0%). Human CAR T cell persistence was detected in bone marrow and spleen of cured mice at 16 weeks, suggesting a role of enhanced T cell persistence in durable remissions. In the aggressive COG-N-561x model, only bicistronic CARs d1 and p2 achieved durable 14-15-week cures (d1, 100%; p2, 71.4%), surpassing double-transduced (B/G, 33.3%), co-administered (B+G, 20%), or single CARs (B, 20%; G, 0%). Upon rechallenge, only d1 and p2 cohorts rejected tumors and remained tumor-free long-term (d1, 71.4%; p2, 60%), again with persistent CAR T cells in bone marrow and spleen through the 36-week study endpoint. Finally, across *in vitro* medulloblastoma models, repeat tumor-stimulation assays confirmed superior activity of d1 and p2. In an aggressive orthotopic group 3 medulloblastoma 7316-10374 xenograft model where 100% of GPC2 CAR-treated mice relapsed, the p2 CAR outperformed d1 and the single B7-H3 CAR, with 16-week cure rates of 100%, 71.4%, and 60%, respectively, confirming the superiority of dual GPC2.B7-H3 targeting and a potential advantage of parallel CD3ζ-sharing designs. Altogether, GPC2.B7-H3 bicistronic CARs induced durable and curative responses across neuroblastoma and medulloblastoma models, nominating this approach as a next-generation GPC2 CAR T strategy for clinical testing.

#4028 Surface localized nuclear envelope proteins define a therapeuticvulnerability in MYC-driven Group 3 medulloblastoma.

S. K. Singh[1], Y. Suk[1], M. A. Rossotti[2], J. Ibanez-Vega[3], M. Shaikh[1], Y. Chen[4], H. Patel[1], L. Escudero[1], A. Delaidelli[5], A. Khanna[1], S. Slassi[1], C. Barba Bazan[1], E. Apel[1], S. Custers[1], S. Grewal[6], W. Maich[1], L. Asselstine[1], D. McKenna[1], Y. Xiao[7], W. Gwynne[8], J. Moffat[7], H. Suzuki[9], P. H. Sorensen[10], R. Truant[1], K. Henry[11], E. Sotillo-Pineiro[12], C. Venugopal[1], C. L. Mackall[13], G. Krenciute[3]; [1]McMaster University, Hamilton, ON, Canada, [2]NRC, Ottawa, ON, Canada, [3]St Jude Children's Research Hospital, Memphis, TN, [4]Stanford Cancer Institute, Stanford, CA, [5]BC Cancer Agency, Vancouver, BC, Canada, [6]Michael G. DeGroote School of Medicine at McMaster University, Hamilton, ON, Canada, [7]The Hospital for Sick Children, Toronto, ON, Canada, [8]McMaster University, Georgetown, ON, Canada, [9]National Cancer Center Japan, Tokyo, Japan, [10]BC Cancer Research Centre, Vancouver, BC, Canada, [11]University of Ottowa, Ottowa, ON, Canada, [12]Stanford University, Stanford, CA, [13]Stanford Hospital, Stanford, CA

Medulloblastoma (MB) is the most common malignant pediatric brain tumor and is comprised of four molecular subgroups (WNT, SHH, Group 3, and Group 4). Regardless of subgroup, MB patients are treated with the same standard of care (SoC) (surgical resection, chemotherapy, craniospinal irradiation) that can lead to lifelong neurocognitive deficits in survivors. A subset of Group 3 MBs harbors focal amplifications of the MYC oncogene (MYC-G3MB) that invariably lead to disease recurrence which currently remains incurable. Therefore, there is an urgent need for development of therapies that are safe for the vulnerable developing brain while exerting potent anti-tumor efficacy against therapy-resistant subtypes. Here, we identify nuclear envelope (NE) proteins LBR and TMPO to be highly expressed in MYC-G3MBs in contrast to normal tissue and human neural stem cells (hNSCs), and a context-specific mislocalization of NE proteins to the plasma membrane (PM), only in MYC-G3MBs. NE protein expression correlated to worse MB patient prognosis and survival and was significantly enriched in recurrent tissue compared to the patient matched primary samples. High resolution microscopy and transcriptomic analysis implicated hyperproliferative cell states and endogenous chromosomal instability to drive NE deformation and the creation of DNA double strand break-capturing nuclear envelope tubules (dsbNETs), critical recently described factors in genome stability that mediate the repair of rapidly accumulating DNA damage in cancers such as MB. CRISPR Cas9-mediated endogenous tagging of LBR and TMPO revealed exposure of N-termini to the extracellular matrix and linked ER or ER-like vesicles to be directly trafficked to the cell surface in MYC-G3MBs. We developed single domain antibodies (sdAbs) specific to the N-terminus of LBR and TMPO and engineered second generation chimeric antigen receptor (CAR) T cell mono (LBR or TMPO) and bispecific (LBR and TMPO) therapies. We demonstrate the potent anti-tumor efficacy of NE protein-targeted CAR T cell therapies in patient derived xenograft models (PDX) of MYC-G3MBs. We present nuclear envelope proteins aberrantly mislocalized to the plasma membrane exclusively in G3MB as a novel class of cancer-selective therapeutic targets, for the development of a new class of CAR T cell therapies for treatment-refractory childhood MB.

#4029 Neuronal activity-regulated mechanisms promoting growth of diffuse hemispheric glioma, H3G34-mutant.

K. R. Taylor[1], **S. H. Wu**[1], R. Drexler[1], G. A. V. Cruzeiro[2], I. Liu[2], A. E. Ivec[1], L. Ni[1], C. A. O. Biagi, Jr.[2], P. J. Woo[1], M. Su[1], Y. Byun[1], M. Filbin[2], M. Monje[1];

[1]Stanford University, Stanford, CA, [2]Dana Farber Boston Children's Cancer and Blood Disorders Center, Boston, MA

Neuronal activity robustly drives glioma progression, mediated via paracrine and synaptic mechanisms and offering novel therapeutic avenues for a disease with a devastating prognosis. While the activity-dependent regulation of diffuse midline glioma, H3K27-mutant (DMG-H3K27) and IDH-wildtype glioblastoma has been investigated thoroughly, the interaction of neurons with diffuse hemispheric glioma, H3G34-mutant (DHG-H3G34) remains to be elucidated. Recent transcriptomic analyses suggest a distinct cell-of-origin for DHG-H3G34, demonstrating these tumors primarily resemble early interneuron lineage cells. In the healthy context, neuronal progenitor cells are highly responsive to neuronal activity during development. We previously reported a proliferative response of patient-derived DHG-H3G34 cultures to active neurons *in vitro*, yet the key neuronal mechanisms governing the progression of DHG-H3G34 are unknown. Here, we explored the neuronal activity-dependent mechanisms that drive DHG-H3G34 growth. We found that activity-induced DHG-H3G34 proliferation in neuron-glioma co-culture is abrogated in the presence of a voltage-gated sodium channel blocker (tetrodotoxin) that prevents action potentials or an AMPA receptor inhibitor, confirming that activity-dependent mechanisms drive DHG-H3G34 malignant cell proliferation and raising the possibility of AMPAR-mediated synaptic mechanisms. Immuno-electron microscopy in two independent patient-derived models demonstrated multiple types of synaptic structures in DHG-H3G34 xenografts, including neuron-to-glioma synapses. Preliminary electrophysiological recordings of xenografted DHG-H3G34 cultures confirmed the presence of spontaneous and stimulation-evoked inward currents consistent with excitatory postsynaptic currents (EPSCs). Further optogenetic stimulation of both glutamatergic cortical projection neurons and GABAergic neurons promoted the proliferation of DHG-H3G34 xenografted cells within the stimulated circuits *in vivo*. Activity-regulated conditioned media harvested from optogenetically stimulated acute cortical slices induced DHG-H3G34 proliferation in monoculture, thus confirming paracrine signaling as one key mechanism in driving tumor growth. Subsequent proteomic analysis of active conditioned media indicated multiple novel proteins of interest including neuronal cell adhesion molecule (NrCAM) and neurofascin (NFASC). Both paracrine factors increased proliferation and migration in multiple DHG-H3G34 cell lines. Overall, these findings suggest that DHG-H3G34 gliomas integrate into neural circuits and leverage both conserved and tumor-type-specific activity-regulated mechanisms. Continued investigation into these activity-dependent mechanisms of glioma growth aims to identify potential therapeutic strategies for these lethal brain cancers.

#4030 Targeting MYB with REM-422 for the treatment of pediatric T-cell acute lymphoblastic leukemia - A report from the Pediatric Preclinical Testing Consortium (PIVOT).

R. B. Lock[1], K. Evans[1], B. Watts[1], M. Agoncillo[1], C. M. Smith[1], S. Neuhauser[2], T. M. Stearns[2], E. L. Jocoy[3], J. Kwon[4], J. H. Chuang[4], S. Levin-Furtney[5], B. A. Teicher[6], C. Kung[5], C. J. Bult[2], M. A. Smith[6];

[1]Children's Cancer Institute, Lowy Cancer Research Centre, School of Clinical Medicine, UNSW Medicine & Health, UNSW Centre for Childhood Cancer Research, UNSW Sydney, Australia, Sydney, Australia, [2]The Jackson Laboratory for Mammalian Genetics, Bar Harbor, ME, [3]The Jackson Laboratory, Sacramento, CA, [4]The Jackson Laboratory for Genomic Medicine, Farmington, CT, [5]Remix Therapeutics, Watertown, MA, [6]National Cancer Institute, Bethesda, MD

Introduction: While survival rates for pediatric acute lymphoblastic leukemia (ALL) have improved dramatically over the past 60 years, outcomes remain poor for certain patients, particularly those with relapsed/refractory T-cell ALL (T-ALL). MYB is a transcription factor involved in the regulation of hematopoietic stem and progenitor cells, which exhibits strong dependency in lymphohematopoietic neoplasms. REM-422 is an orally available small molecule degrader of *MYB* mRNA that is currently being evaluated in Phase 1 clinical trials (NCT06118086 and NCT06297941). Therefore, it was of interest to test the *in vivo* activity of REM-422 against the PIVOT pediatric ALL patient-derived xenografts (PDXs).

Methods: *MYB* mRNA expression was assessed via RNA sequencing and expressed as fragments per kilobase of transcript per million mapped reads (FPKM, Rokita *et al*., *Cell Rep*., 2019). MYB protein expression was assessed by immunoblotting using a MYB monoclonal antibody (clone D2R4Y). For *in vivo* efficacy testing in NSG mice, REM-422 was administered at 5 mg/kg via oral gavage, daily for 3 weeks. A single mouse trial design (1 vehicle control, 1 drug treated mouse per PDX) was used for testing across pediatric ALL PDXs. Standard PIVOT methods were used to assess event-free survival (EFS). Stringent objective response (OR) measures modeled after the clinical setting were also used to evaluate activity (Houghton *et al*., *Pediatr. Blood Cancer*, 2007).

Results: *MYB* mRNA expression was significantly higher in 90 pediatric ALL PDXs (mean 153 FPKM, range 16.0-321) compared with 154 PDXs derived from pediatric solid tumors (mean 4.0 FPKM, range 0.04-240, $P<0.001$), with no significant differences in expression between pediatric ALL subtypes. *Ex vivo* exposure of 2 PDXs to REM-422 for 6-24h resulted in almost complete ablation of MYB protein levels. REM-422 was well tolerated in NSG mice, with no overt signs of toxicity or weight loss >5%, and with all intended doses administered. In the efficacy study, 28 of 30 planned PDXs were evaluated. REM-422 extended mouse median EFS by 20.7 days compared with vehicle control-treated mice ($P<0.0001$). While REM-422 extended survival in both the T and B-lineage PDXs, the 10 T-lineage PDXs (Treated-Control [T-C] 33.0 days, T/C 3.6, $P<0.0001$) exhibited a better overall response compared with the B-lineage PDXs (T-C 19.4 days, T/C 2.5, $P=0.0004$). Moreover, REM-422 elicited ORs in 8/10 T-lineage (2 Partial Responses [PRs], 3 Complete Responses [CRs] and 3 Maintained CRs [MCRs]) compared with only 2/18 B-lineage (1 PR, 1 MCR) PDXs.

Conclusions: REM-422 exhibited potent single-agent *in vivo* activity against a large panel of pediatric T-ALL PDXs, supporting its potential clinical evaluation in this disease. Future research directions will include efforts to identify effective combinations with targeted and/or standard-of-care drugs.

: Precision Prevention: Advances in Early Detection and Risk Assessment Minisymposium

#4069 Therapy-associated clonal hematopoiesis and risk of hematologic malignancy after primary cancer treatment.

K. M. Barnao[1], R. L. Kelly[1], W. Zhou[2], I. Chan[3], Y. Cao[4], K. L. Bolton[3], M. J. Machiela[1];
[1]National Cancer Institute, Rockville, MD, [2]Leidos Biomedical Research Inc., Frederick, MD, [3]Washington University School of Medicine, St. Louis, MO, [4]Washington University in St. Louis, St Louis, MO

Clonal hematopoiesis (CH) is the age-related expansion of hematopoietic stem cells, driven by single nucleotide variants (SNVs) or insertions and deletions (indels) in driver genes (clonal hematopoiesis of indeterminate potential, CHIP) or large-scale mosaic chromosomal alterations (mCAs). Both CHIP and mCAs are associated with increased hematologic malignancy risk. Prior studies have suggested cancer therapies may select for CH clones with DNA damage response mutations (e.g., CHIP in *TP53)*. While therapy-related CHIP is recognized, the contribution of cancer treatment to mCA prevalence and the relationship of treatment-induced mCAs to subsequent cancer risk remains poorly understood. We investigated how exposure to cancer therapy may promote the acquisition or expansion of mCAs and consequently increase susceptibility to subsequent hematologic malignancies.Using genomic data from UK Biobank participants, we detected CHIP and mCAs in individuals with (N=24,607) and without prior cancer (N=453,763), classified as likely cancer therapy-exposed (hereafter referred to as exposed) or unexposed. We identified 422 exposed individuals who subsequently developed a hematologic malignancy. Logistic regression models, adjusted for age, age^2, sex, smoking status, and genetic similarity, were used to compare CH prevalence between exposed and unexposed groups, and between participants in the exposed group who did and did not develop hematologic malignancies.Autosomal mCAs were detected in 5.2% of therapy-exposed individuals compared to 3.0% of unexposed individuals (OR=1.2, 95% CI=[1.1-1.3], p=9.6×10^{-6}). CHIP was also enriched among therapy-exposed participants (7.6% vs. 4.5%; OR=1.4, 95% CI=(1.3-1.5), p=3.4 ×10^{-40}). 17.5% of therapy-exposed individuals who developed incident hematologic malignancies harbored mCAs, compared with 3.7% who did not develop a hematologic malignancy (OR=4.9, 95% CI=[3.8-6.4], p=1.9×10^{-32}), with notable enrichment of mCAs highly associated with hematologic malignancies (e.g., chromosome 9 p-arm copy-neutral loss of heterozygosity (chr9pCNLOH), chr14qCNLOH, and chr13q Loss). CHIP was observed at a frequency of 18.0%, compared to 6.3% of those who did not progress (OR=2.9, 95% CI=[2.2-3.7], p=8.3×10^{-16}).These findings demonstrate that cancer therapy is associated with increased frequency of detectable CHIP and autosomal mCAs, with enrichment of mutations commonly observed in hematologic malignancies. Importantly, these events were detectable prior to diagnoses of a therapy-related hematologic malignancy, highlighting their potential as early indicators of hematologic malignancy risk in cancer survivors. Identifying high risk autosomal mCAs in this population could inform precision risk stratification and guide targeted surveillance strategies for individuals at risk of subsequent therapy-related hematologic malignancies.

#4070 *APC* mosaicism and colibactin-associated signature as key factors in unexplained colorectal polyposis.

K. Driouch[1], Z. Tariq[1], A. Dardenne[2], M. Dhooge[3], J. Netter-Coti[4], M. Le Mentec[1], S. Farelly[3], M.-C. Gorenstein[4], I. Bieche[1], A. Chansavang[3], E. pasmant[1], C. Colas[1], O. Trabelsi-Grati[1], B. Buecher[1];
[1]Institut Curie, Paris, France, [2]Hopital Saint-Antoine, Paris, France, [3]Hopital Cochin, Paris, France, [4]Hopital Europeen Georges Pompidou, Paris, France

Background: Colorectal adenomatous polyposis is usually linked to genetic predisposition, and affected patients should receive genetic counselling and germline testing. In *APC*-associated polyposis, the absence of a suggestive family history does not exclude the diagnosis, given the frequency of *de novo* mutations. *APC* mutations may arise postzygotically, resulting in a somatic mosaicism in a significant fraction of patients who show no germline *alterations*. However, a substantial proportion of patients remain genetically unexplained, suggesting that additional mechanisms, possibly environmental or microbial, may contribute to disease onset and progression. Growing evidence suggests that gut microbiota (especially *pks*$^+$ *Escherichia coli* that produce the colibactin) may induce characteristic DNA mutations thus contributing to the disease.

Methods: In this study, 125 patients with unexplained colorectal adenomatous polyposis were included. Next-generation sequencing was performed on 337 polyps and 173 healthy tissues. Somatic mosaicism was diagnosed when a same *APC* pathogenic mutation was identified in ≥ 3 neoplastic lesions or in healthy biopsies and in ≥ 1 colonic lesion (n=60 patients). Colibactin-associated *APC* variants were identified and the presence of *pks*$^+$ bacteria was explored by qPCR. Finally, the clonal architecture of each lesion was inferred by classifying all mutations as clonal or subclonal.

Results: APC somatic mosaicism was identified in 22 patients (36.7% of assessed cases). Most mosaic variants were not detectable in blood, except in two patients who showed low-level germline mosaicism. Overall, 94.4% of neoplastic lesions carried a somatic *APC* variant; those without *APC* mutations often harbored alterations in other driver genes such as *KRAS, BRAF, CTNNB1* or *RNF43.* Several *APC* mutations showed patterns characteristic of exposure to colibactin, produced by *pks*$^+$ bacteria, including the recurrent splice-site mutation c.835-8A>G. Nearly 19% of lesions displayed mutations fitting the colibactin-associated signature. PCR testing for pks$^+$ bacteria was positive in 22% of samples, but there was no concordance between pks$^+$ PCR positivity and colibactin-related mutations, suggesting that exposure may be past or transient. The clonal analyses indicated that mosaic and colibactin-associated *APC* mutations are early, clonal events detected in multiple polyps. A rare case of transmission of a mosaic *APC* variant to offspring confirmed the early acquisition and possible involvement of germline cells. In contrast, mutations in other driver genes tend to appear later, as subclonal alterations.

Conclusion: Overall, the findings suggest that somatic *APC* mosaicism explains one third of unexplained colorectal adenomatous polyposis. Moreover, early-life exposure to colibactin-producing bacteria may also contribute to disease initiation and progression in some patients.

#4071 The impact of patient biology on racial disparities in breast cancer outcome.

J. DeWitt, D. Jiminex-Tovar, S. Haricharan, E. Oropeza, M. Raghunathan;
San Diego State University, San Diego, CA

Hormone receptor positive (HR+) breast cancer is the most common subtype of breast cancer diagnosed globally. Despite effective targeted therapies, HR+ breast cancer remains a leading cause of cancer-related death in women. Long-standing epidemiological research identifies significantly worse outcomes for Black women diagnosed with HR+ breast cancer relative to White women. While structural factors such as access to healthcare and education level contribute to this outcome disparity, it persists even in analyses where these factors are controlled. In-depth analyses of the somatic molecular biology that may underlie these outcome disparities are hampered by a lack of datasets that represent Black patient populations. Here, we generate a HR+ breast cancer patient transcriptomic dataset that overrepresents Black women and controls for access to healthcare and education level. We find that signatures relating to the tumor microenvironment, i.e. collagen deposition and prognostically unfavorable T-cell landscapes are enriched in HR+ tumors from Black women. Importantly, we find, using experimental model systems *in vitro* and *in vivo*, that race-aligned collagen deposition patterns are at least partially attributable to tumor cell-intrinsic signaling and critical for Black breast cancer metastasis. We also find that unfavorable T-cell signatures in HR+ tumors from Black women, which have previously been attributed to race and ancestry, are more strongly poverty-aligned. Using multiple independent datasets, we identify STAT4 as a potential master regulator of this poverty-associated tumor immune signature. Together, these findings provide new evidence that somatic molecular biology of breast cancer patients can be modified by multiple structural factors such as self-identified race and poverty burden to promote poor patient outcomes. Integrating an understanding of structural factors into molecular cancer research is critical for implementing truly personalized, and maximally effective, oncology systems.

#4072 Single-cell pathology of the normal breast uncovers occult cytomorphologic signatures that signal future cancer risk and etiologic origins.

M. Abubakar[1], S. M. Lawrence[2], J. D. Hughes[3], S. Fan[1], K. Mutreja[2], R. M. Pfeiffer[1], G. L. Gierach[1], B. Jenkins[3], J. E. Henry[4], M. A. Duggan[5];

[1]National Cancer Institute, Bethesda, MD, [2]Leidos Biomedical Research, Frederick, MD, [3]Johns Hopkins Bloomberg Sch. of Public Health, Baltimore, MD, [4]Indiana University, Indianapolis, IN, [5]University of Calgary, Calgary, AB, Canada

Background: Malignant transformation involves progressive changes in cellular morphology. However, the point along the early carcinogenesis trajectory when these changes first signal cancer risk and etiologic origins remains unknown. **Methods:** In this prospective cohort study of 3,415 healthy women who donated normal breast tissue (NBT) to the US-based Susan G. Komen Tissue Bank (KTB) between 2009-2019, machine learning algorithms were used to characterize 72,237,858 cells in digitized histologic sections of NBTs. Occult alterations in epithelial nuclear area, perimeter, chromasia, nuclear contour irregularity, epithelial nuclear density, and stromal cellular density defined three cytomorphologic signatures that were denoted by their histogenesis i.e., epithelial, stromal, and mixed (epithelial and stromal). Associations of cytomorphologic signatures with subsequent breast cancer (BC) incidence were assessed using multivariable Cox proportional hazard regression with age as timescale and left truncated at study entry. Analyses were performed overall and by tumor subtype (estrogen receptor-positive (ER+) and ER-). **Results:** After a median follow-up of 6 years (range:1-16 years) post-donation, 104 previously healthy women developed BC. Women with the stromal (hazard ratio (HR) and 95% confidence interval (CI) = 3.01 [1.56-5.80]; *P*=0.001), epithelial (HR= 2.28 [1.31-3.96]; *P*=0.003), or mixed (HR= 2.18 [1.18-4.03]; *P*=0.010) signatures in their NBT had more than double the risk of BC than those without any signature. RNA sequencing analyses revealed the stromal signature to be characterized by heightened expression of inflammation, angiogenesis, and epithelial-to-mesenchymal transition genes. Etiologically, the stromal signature was associated with younger age, Black race, multiparity, contraceptive pill use, and BC family history, and in subtype-specific analysis, it was most strongly predictive of aggressive, ER- BC (HR= 9.04 [3.22-25.39]; *P*<0.0001). The epithelial signature (reflecting age-related epithelial functional decline) demonstrated contrasting etiologic profile from the stromal signature, and was most strongly associated with future ER+ BC, particularly when detected in stroma-poor/adipose-rich microenvironments (HR= 7.04 [1.49-33.19]; *P*=0.01). The mixed signature, which was subtype-agnostic in its BC predictive value, was characterized by heightened expression of wound response genes, shorter (-3 years) latency to BC diagnosis than the epithelial and stromal signatures (*P*<0.0001), and by its association with obesity and older age (>25 years) at first childbirth. **Conclusion:** Oncogenic processes may imprint occult cytomorphologic signatures in breast tissues long before cancer diagnosis, with implications for BC risk prediction, targeted prevention, and early interception strategies.

#4073 Deep plasma proteomics for early-stage breast cancer detection.

A. Horrmann[1], Y. Travadi[1], J. Carey[1], K. Mallery[1], E. Boytim[2], G. Schaap[1], C. Rungkittikhun[1], K. Kamalanathan[1], N. R. Bristow[1], C. Galeano-Garces[1], A. Groth[1], A. R. Hesch[1], **P. Advani**[3], J. Hwang[2], B. R. Konety[1], J. M. Drake[1];
[1]Astrin Biosciences, St. Paul, MN, [2]University of Minnesota, Minneapolis, MN, [3]Mayo Clinic, Jacksonville, FL

Annual breast cancer screening is a critical piece of women's health. While mammography remains the gold standard, increased breast density leads to decreased sensitivity, underscoring the need for more sensitive and accessible screening methods. Liquid-based biopsies for early breast cancer detection are emerging but currently remain out of reach for clinical use. Recent data on nucleotide assessment from plasma in breast cancer have been mixed with 87% sensitivity for late-stage disease (stage 3-4) but only 20% sensitivity for early-stage disease (stage 0-2). Proteomics is an exciting area for early cancer screening where improvements in sample preparation and equipment have enabled major advances in early cancer detection. This is particularly true for a deep proteome assay as proteins can be identified which are 8-9 orders of magnitude less abundant than the most common plasma proteins. This study evaluates the presence of breast cancer using label-free shotgun mass spectrometry-based proteomics on less than 1 ml of plasma from 1,259 women classified as either healthy or newly diagnosed treatment naïve breast cancer patients with a focus on early-stage disease. We trained using a cohort of 845 women, comprising of 466 healthy and 379 with breast cancer and validated on 397 women (195 healthy and 202 breast cancer) using a protein-based machine learning classifier to distinguish these groups. All plasma samples were processed in a blinded manner coupled with semi-quantitative, label-free mass spectrometry (MS)-based analysis. The median number of proteins detected per patient across breast cancer and healthy individuals was 7,064 and 7,054, respectively. The validation performance achieved 92.3% specificity for healthy controls and an overall sensitivity of 92.6% with an AUC of 0.975 (95% CI: 0.961-0.987) for breast cancer patients. Sensitivity broken down by clinical stage (0-IV), molecular subtypes (HR+/HER2+, HR-/HER2+, HR+/HER2-, and HR-/HER2-) and pathological subtypes (LCIS, DCIS, ILC, and IDC) were ≥85% and indistinguishable across all stages and subtypes. Gene set enrichment analyses (GSEA) identified pathways including epithelial-to-mesenchymal transition (EMT) and PI3K-AKT signaling as enriched in the breast cancer samples, highlighting that our test can identify cancer-related proteins in early-stage patients. Overall, we have developed a highly sensitive blood-based assay that utilizes deep proteomic profiling to identify distinctive cancer specific signatures in women who are undergoing screening for breast cancer. This work enables us to develop a protein-based classifier from plasma for early detection of breast cancer and enhances screening strategies for women with dense breasts who are at average or high-risk based on family history, specific genetic mutations such as BRCA1/2, race, or other factors.

#4074 Non-invasive early detection of cancer-predisposing liver diseases using genome-wide cfDNA fragmentomes.

Akshaya Vijaya Annapragada[1], Zachariah Foda[1], Hope Orjuela[1], Carter Norton[1], Shashi Koul[1], Noushin Niknafs[1], Sarah Short[1], Keerti Boyapati[1], Adrianna Bartolomucci[1], Dimitrios Mathios[2], Michael Noe[1], Chris Cherry[1], Jacob Carey[3], Alessandro Leal[3], Bryan Chesnick[3], Nic Dracopoli[3], Jamie Medina[3], Nicholas Vulpescu[1], Daniel Bruhm[1], Sarah Bacus[4], Vilmos Adleff[1], Amy Kim[1], Steve Baylin[1], Greg Kirk[1], Andrei Sorop[5], Razvan Iacob[5], Speranta Iacob[5], Liana Gheorghe[5], Simona Dima[5], Katherine McGlynn[6], Manuel Ramirez-Zea[7], Claus Feltoft[8], Julia Johansen[8], John Groopman[1], Jillian Phallen[1], Rob Scharpf[1], Victor Velculescu[1]

[1]Johns Hopkins University School of Medicine, Baltimore, MD,[2]Washington University School of Medicine, St Louis, MO,[3]DELFI Diagnostics, Baltimore, MD,[4]Seqbiomarque, Brea, CA,[5]Fundeni Clinical Institute, Bucharest, Romania,[6]National Cancer Institute, Bethesda, MD,[7]Institute of Nutrition of Central American and Panama, Guatemala City, Guatemala,[8]Copenhagen University Hospital, Copenhagen, Denmark

INTRODUCTION: Liver disease occurs on a continuum from steatosis to fibrosis, cirrhosis and ultimately hepatocellular carcinoma (HCC), with a 30% lifetime risk of HCC among those with cirrhosis (LCr). If identified early, steatosis and fibrosis are potentially reversible, and in LCr, surveillance can reduce cancer morbidity and mortality. Despite these benefits, conventional LCr detection modalities are invasive or have limited performance. We previously demonstrated that cost-effective liquid biopsies of genome-wide cell-free DNA (cfDNA) fragmentomes enable early detection of HCC. Here, we use these technologies to detect liver steatosis, fibrosis, and cirrhosis towards improved pre-cancer intervention and HCC surveillance.

METHODS: We performed low-coverage, whole genome sequencing of plasma cfDNA from separate Discovery (n=423) and Validation (n=221) cohorts including individuals with no known liver disease (n=397), chronic liver disease and early fibrosis (n=91) including viral hepatitis and metabolic associated steatotic liver disease, or advanced fibrosis/cirrhosis (n=156). We computed genome-wide fragment length, coverage, and repeat element features (DELFI and ARTEMIS), cross-validated a machine learning classifier for fibrosis and LCr detection in the Discovery Cohort and evaluated the locked model in the Validation Cohort. We then performed whole methylome sequencing (n=28) and cell-type deconvolution to reveal mechanisms of change to cfDNA fragmentomes in LCr.

RESULTS: Individuals with early liver disease/fibrosis and advanced fibrosis/cirrhosis were detected with high performance (AUC=0.90, 95% CI=0.86-0.95 and AUC=0.95, 95% CI=0.93-0.98, respectively) in the Discovery Cohort. At an 80% specificity locked cutpoint, Validation Cohort sensitivity was 70.8% (90% CI=52.3%-87.5%) for early liver disease/fibrosis and 90.1% (90% CI=84.4%-94.4%) for advanced fibrosis/cirrhosis. The model displayed low cross-reactivity for other fibrotic origin conditions including benign lung nodules or chronic pancreatitis (median scores 0.087 and 0.068 respectively vs. 0.55 for LCr, $p<0.0002$). The approach outperformed the existing fibrosis index FIB-4, detecting 5.07x (95% CI=3.03-17.35) and 1.2x (95% CI=1.18-1.32) more cases of early liver disease/fibrosis and advanced fibrosis/cirrhosis in simulations. cfDNA methylome deconvolution revealed increased contributions of liver endothelium ($p=0.00016$) and blood monocytes ($p=5.2\times10^{-5}$) and decreased contribution of hepatocytes ($p=0.00035$) with shorter fragment lengths in LCr.

CONCLUSIONS: A cfDNA fragmentome biomarker enabled early detection of liver disease including LCr and reflected both liver-derived and immune-cell related changes. These analyses may enable accessible early detection of pre-cancer conditions with potential to improve liver disease management and early detection of HCC.

#4075 Enhanced early detection of pancreatic cancer using a multi-analyte liquid biopsy approach.

A. Bergamaschi[1], D. Haan[1], V. Friedl[1], G. Oliviera[1], M. Cipriano[1], T. Phillips[1], Y. Xue[2], Y. Ning[2], M. Collins[1], M. Kesling[1], M. Riviere[1], N. Nguen[1], V. Lopez[1], A. Leighton[1], R. Malta[1], M. Nabiyouni[1], C. Fraire[1], G. Guler[2], S. Dhillon[1], C. (. Coruh[1], M. Peters[1], S. Chowdhury[1], E. Nilson[1], S. Quake[3], W. Volkmuth[2], S. Levy[1];

[1]ClearNote Health, San Diego, CA, [2]ClearNote Health, San Mateo, CA, [3]Stanford University, Stanford, CA

Background: Pancreatic ductal adenocarcinoma (PDAC) has a 5-year survival rate of less than 12% due to late diagnosis when curative options are limited. Early detection, especially stage I-II disease, could improve survival, but current non-invasive tests lack enough sensitivity. Multi-analyte liquid biopsies that combine genomic, epigenomic, and glycan data show promise for better detection. We developed a prediction model for the early detection of pancreatic cancer by integrating epigenomic and genomic features with haplotype information and CA19-9 biomarker levels, achieved a markedly more sensitive predictor.

Methods:

We employed a training set of 162 pancreatic cancer patients and 983 non-cancer patients. Cell-free DNA was isolated and employed to perform 5-hydroxymethylcytosine (5hmC) profiling, low pass whole-genome sequencing (WGS) and genotyping. CA19-9 biomarker levels were also measured in plasma. The resulting 5hmC gene-based changes, fragment size differences, and genotyping coupled with CA19-9 levels, were used for logistic regression model building. The prediction model performance was validated in an independent validation cohort of 1,445 individuals, consisting of 259 pancreatic cancers and 1,186 non cancer with several high-risk features including diabetes, family history, genetic predisposition and heavy smokers. Cancer performance was measured through sensitivity and specificity metrics and 95% confidence intervals (CIs).

Results:

After training the prediction model to optimize feature selection, the final model was locked at a specificity threshold of 97.75% and used to score an independent clinical cohort in a blinded manner. In the independent validation cohort, the multi-analyte model achieved an overall sensitivity of 82.6% (95% CI: 77.45%-87.04%) and importantly, early-stage sensitivity (n=138) was 76.8% (95% CI: 68.87%-83.57%). These measures point to an increase of sensitivity of > 8-15% compared to an earlier version of the assay. Test specificity was 97.45% (95% CI: 96.41%-98.29%), consistent with the pre-established 97.75% training specificity, highlighting robust performance across datasets.

Conclusions:

The multi-analyte model demonstrated strong early-stage PDAC detection while maintaining high specificity. By integrating orthogonal biological features such as epigenomics, genomics and CA19-9 levels, we have been able to improve PDAC detection performance, ensuring that the breadth of oncogenic development can be detected through an early detection blood test.

: Tumor Microenvironment, Immunomodulation, and Enabling Delivery and Models Minisymposium

#4042 Tumor-tailored ionizable lipid nanoparticles facilitate IL-12 circular RNA delivery for enhanced lung cancer immunotherapy.

Y. Xu[1], S. Xu[2], B. Li[3];
[1]Baylor College of Medicine, Houston, TX, [2]UTSW, Dallas, TX, [3]University of Toronto, Toronto, ON, Canada

mRNA-based immunotherapies are hindered by systemic toxicity and transient expression, necessitating frequent dosing. This is especially problematic for potent cytokines like Interleukin-12 (IL-12), whose use is limited by severe adverse effects.
To address this, we developed a platform using circular RNA (circRNA), which offers more sustained protein expression than linear mRNA. A high-throughput combinatorial method (Ugi reaction) was used to screen for ionizable lipids to deliver circRNA to lung tumors. The lead LNP, H1L1A1B3, showed a fourfold increase in circRNA transfection efficiency over the ALC-0315 standard. H1L1A1B3 LNPs were also dual-functional, acting as an immune adjuvant by potently activating NF-κB and IRF innate immune pathways. This LNP was loaded with circRNA encoding IL-12, providing significantly delayed decay in protein expression.
Therapeutic efficacy was validated in two lung cancer models. In a subcutaneous LLC1 model, a single intratumoral injection of H1L1A1B3-circRNA-IL-12 LNPs delayed tumor progression. Combined with an anti-PD-L1 checkpoint inhibitor, this induced robust tumor regression. Immunological profiling revealed a profound remodeling of the tumor microenvironment (TME), including an eightfold increment in $CD45^+$ leukocytes and enhanced infiltration of $CD8^+$ and $CD4^+$ T cells, increasing the $CD8^+$/Treg ratio.
Second, in an orthotopic HKP1 NSCLC model, a single intratracheal administration of the IL-12 circRNA LNPs effectively suppressed lung tumor growth. This local delivery resulted in sustained serum IL-12 and IFN-γ for at least five days but did not cause systemic liver toxicity (normal AST/ALT levels). The treatment successfully recruited immune cells, including $CD8^+$ T cells, to the lung tumors.
In conclusion, this work presents a tumor-tailored, dual-function LNP (H1L1A1B3) that efficiently delivers stable IL-12 circRNA and provides intrinsic immunostimulatory effects. The platform enables sustained, localized cytokine expression, remodeling the TME to be immunologically "hot." These results highlight the potential of this LNP-circRNA platform to advance RNA drug delivery, offering a potent and safer immunotherapeutic strategy for lung cancer by overcoming systemic toxicity and transient expression hurdles.

#4043 A novel TAM-targeted therapeutic for rare and aggressive solid tumors.

F. H. Barnett[1], J. James[2], S. Premeau[1], R. R. Crum[1], A. Basbaum[1], R. Schmidt[1];
[1]Resolute Science, Inc., San Diego, CA, [2]Corvid LLC, San Diego, CA

A hallmark of aggressive tumors is the dense infiltration of tumor-associated macrophages (TAMs), which often constitute 30-50% or more of the total cells within a tumor. TAMs foster an immunosuppressive microenvironment and promote resistance to chemotherapy, immunotherapy, and radiation. They also facilitate macrophage vascular mimicry, a non-endothelial microcirculation in hypoxic tumor regions as described by Barnett et al., 2016. Resolute Science, Inc. has developed macrophage-targeted conjugates (MAC-TACs), a novel class of synthetic drug conjugates that exploit TAM biology and the TAM microcirculation for targeted delivery of payloads to tumor cells. By targeting TAMs rather than tumor cells, this platform bypasses resistance from tumor heterogeneity and receptor evolution. Our lead candidate, RS-5, an MMAE-conjugated MAC-TAC, has shown near-complete to complete regressions in 22 studies across 10 solid tumor models, including CDX, syngeneic and PDX models. MAC-TACs comprise four components: a receptor targeting ligand, backbone, linker, and payload. This modular design enables the development of therapeutic and imaging molecules, including radiopharmaceuticals. MAC-TACs target an overexpressed receptor found on TAMs. Immunohistochemical analysis reveals a high and relatively uniform expression of the TAM-targeted receptor across a range of metastatic tumor types, including sarcoma, melanoma, bladder, prostate, pancreatic and gastric cancers. In vitro and in vivo studies demonstrate selective uptake by TAMs, which internalize and release the payload to adjacent cancer cells. Receptor expression correlates with therapeutic response. A complete response was observed in a doxorubicin-resistant soft tissue sarcoma (STS) PDX model. In a second PDX STS model, a near-complete response was observed over two months of treatment. In an A375 melanoma CDX model, a near-complete response was also observed. In an intracranial U87MG glioma model, RS-5 demonstrated a 79% increase in median survival, and in an HT1080 luciferase brain metastasis model, a 100% increase in median survival was observed. Across studies, body weight and hematologic/chemical parameters remained within normal ranges. RS-5 exhibits a favorable PK/PD profile; MTD and DRF are complete, and 4-week toxicology studies are underway.These preclinical results support broad clinical utility, particularly for TAM-rich tumors. A first-in-human dose-escalation study is planned for the summer of 2026.

#4044 GPNMB CAR-T cells target both glioblastoma and the tumor microenvironment to relieve immune suppression.

Sheila Kumari Singh[1], Neil Savage[1], Muhammad Vaseem Shaikh[1], Shan Grewal[1], Franz J. Zemp[2], Nick Mikolajewicz[3], Joanna Pyczek[4], Hinda Najem[5], Jeffrey Wei[3], Shawn C. Chafe[1], Kui Zhai[1], William Maich[1], CHIRAYU CHOKSHI[1], Nazanin Tatari[1], Dillon McKenna[1], Mohamed Taleb[1], Lucas Asselstine[1], Hong Han[1], Kevin Brown[6], Chitra Venugopal[1], Thomas Kislinger[7], Amy B. Heimberger[5], Jennifer A. Chan[4], Jason Moffat[6], Douglas J. Mahoney[4]

[1]McMaster University, Hamilton, ON, Canada,[2]Southern Alberta Cancer Research Institute, Calgary, AB, Canada,[3]University of Toronto, Toronto, ON, Canada,[4]University of Calgary, Calgary, AB, Canada,[5]Northwestern University, Chicago, IL,[6]Sick Kids Research Institute, Toronto, ON, Canada,[7]UHN Princess Margaret Cancer Centre, Toronto, ON, Canada

Glioblastoma (GBM) remains uniformly lethal, driven by profound intratumoral heterogeneity, and an immunosuppressive tumor microenvironment (TME) dominated by tumor-associated macrophages (TAMs). The identification of novel therapeutic targets is crucial for advancing promising therapies that address both tumor and TME. Here, we identify glycoprotein non-metastatic melanoma protein B (GPNMB) as a clinically relevant surface marker expressed on both GBM cells and TAMs. Genetic loss of GPNMB in GBM models reduced tumor cell proliferation, delayed intracranial tumor growth, and altered transcriptional programs linked to immune regulation and leukocyte activation, indicating GPNMB sustains both tumor fitness and an immunosuppressive niche. We generated both anti-human and anti-mouse GPNMB CAR-T cells showing potent activity: In orthotopic patient-derived xenografts, GPNMB CAR-T therapy induced complete tumor remission; murinized GPNMB CAR-Ts similarly produced sustained tumor control in syngeneic GBM models. In a humanized mouse model of recurrent GBM, anti-human GPNMB CAR-T therapy drove tumor regression in most animals despite a highly suppressive myeloid-rich TME. An integrated central nervous system myeloid single-cell RNA-sequencing atlas revealed GPNMB$^+$ macrophages are enriched for lipid transport, and GPNMB expression correlates with immunosuppressive gene signatures. Consistent with this, GPNMB was preferentially expressed by immunosuppressive macrophages, and GPNMB CAR-Ts selectively eliminated immunosuppressive over pro-inflammatory macrophages in vitro and in vivo. Collectively, these data establish GPNMB CAR-T therapy as an extremely promising therapy inducing complete GBM remission in PDXs and immunocompetent models by simultaneously targeting GPNMB+ tumor cells and immunosuppressive macrophages.

#4045 Collagen binding enhances anti-CTLA4 therapy in recurrent glioblastoma.

L. Barr[1], J. Takei[1], C. Wang[2], O. Iwaloye[1], K. Furudate[3], H. Ichie[1], S. Tsuzuki[1], J. Ishihara[2], S. Osuka[1];
[1]University of Alabama at Birmingham, Birmingham, AL, [2]Imperial College London, London, United Kingdom, [3]UT MD Anderson Cancer Center, Houston, TX

Recurrent glioblastoma (rGBM) is an aggressive malignant brain tumor, with a median survival of 6 months. rGBM establishes an immunosuppressive tumor microenvironment (TME) driven by regulatory T cells (Treg) and exhausted T cells (Tex). Since both Treg and Tex highly express CTLA4, antagonistic CTLA4 antibodies (αCTLA4) were considered promising therapeutic agents. Despite this rationale, clinical trials showed no survival benefit in rGBM, likely due to poor tumor penetration of αCTLA4. Therefore, technology to enhance αCTLA4 delivery in rGBM tissue is critically needed. rGBM acquires treatment resistance through alteration of extracellular matrix (ECM) proteins in the tumor microenvironment (TME). Our lab proposes utilizing this ECM change as a reservoir to accumulate αCTLA4. We focused on COL I & III, which are minimally expressed in the normal brain but highly upregulated in rGBM. We created CBD-αCTLA4 by fusing αCTLA4 with the collagen-binding domain (CBD) of von Willebrand factor (vWF), leveraging vWF's selective binding to COL I & III at sites of vascular disruption, inflammation, and tumors while sparing normal organs with COLI&III high expression. In syngeneic rGBM murine models, CBD-αCTLA4 showed greater accumulation than αCTLA4 using confocal microscopy and biodistribution assay. Single-cell RNAseq showed CBD-αCTLA4 reduced Treg and Tex populations within rGBM tumors, thereby transforming the immunosuppressive TME and facilitating the recruitment of type 1 conventional dendritic cells (cDC1s) into the tumor. Survival analysis in our models revealed CBD-αCTLA4 treatment (100μg i.v., twice) prolonged survival by 140% with a 14% CR rate in rGBM mice models, while αCTLA4 (non-CBD) treatment showed no survival extension. For clinical translation, we developed a humanized CBD-αCTLA4 (CBD-Ipilimumab) and validated its efficacy in 3D human GBM slice cultures, demonstrating decreased Treg cells in human tumor tissue. Furthermore, CBD-ipilimumab significantly prolonged survival in peripheral blood mononuclear cell (PBMC)-humanized mice bearing human rGBM tumors. Collagen-binding αCTLA4 achieved enhanced intratumoral accumulation, reversed the immunosuppressive profile, and elicited potent antitumor effects in rGBM. Our results suggest that CBD-αCTLA4 holds significant promise as an innovative immunotherapy for rGBM. Moreover, this collagen-targeting platform has broad implications, as it can be extended to other antibody-based therapeutics for brain tumors.

#4046 A novel DLL3 trispecific T cell engager antibody integrating the CD2/CD58 co-stimulatory pathway demonstrates superior antitumor efficacy and balanced safety profile.

Cheng Luo[1], Devin Liu[1], Yingyu Li[1], jingjing Nie[1], Na Li[1], Fan Zhou[1], Xin Wang[1], Yang Xin[1], Mingzhu Shao[1], Tingting Yang[1], Hai Huang[1], Cheng Chen[1], Mingrui Du[1], Jiashun Cai[1], Li Chen[1], **Yu Liang**[2]

[1]Probio, Inc, Nanjing, China,[2]Probio, Inc, Pennington, NJ

As a clinically validated therapeutic modality, T-cell engager (TCE) antibodies showed great success in hematological tumors. However, they still face a number of challenges in effectively treating solid tumors, including a lack of tumor-specific targets, insufficient T cell infiltration of some tumors, and immunosuppressive forces within the tumor microenvironment (TME) leading to T cell anergy and exhaustion. These challenges contribute to the narrow therapeutic window of TCEs in treating solid tumors and partially explain why no solid tumor-targeting TCE received regulatory approval until the DLL3-targeting tarlatamab became the first (and only to date) in 2024. To address the aforementioned challenges, a number of approaches are being explored and tested clinically, including those integrating a co-stimulatory moiety into the TCE to prevent or revert T cell exhaustion and promote sustained proliferation of the infiltrated T cells within the TME. Amongst co-stimulatory pathways, those mediated by CD28 and 4-1BB have been the most extensively explored, even though recent studies have shown that they are often associated with excessive toxicity or paradoxical immunosuppression. In contrast, the CD2-CD58 axis offers a promising alternative based on a few possible modes of actions, including promoting a balanced T cell co-stimulation at both the priming and effector stage, and stabilizing immunological synapse. Therefore, to further enhance the efficacy, persistence, and safety of conventional TCEs targeting DLL3 and other solid tumor targets, we designed a novel class of DLL3xCD3xCD2 trispecific antibodies based on an internally developed CD3 VHH antibody with cyno cross-reactivity. These trispecific TCEs were evaluated in a suite of *in vitro* functional assays whereby they demonstrated superior potency in tumor cell killing and sustaining T cell proliferation compared to the parental bispecific TCE (DLL3xCD3) and tarlatamab, especially at low E/T ratios, which mimics the scarcity of T cell infiltration into the TME of solid tumors. Additionally, this enhanced tumor cytotoxicity was accompanied by an increased, but balanced, cytokine profile with a reduced release of proinflammatory cytokines (TNFa, etc.), and an insignificant level of tumor antigen-independent T cell activation or cytokine release. For *in vivo* studies, these trispecific TCEs demonstrated a favorable IgG-like pharmacokinetics profile and greater antitumor activity than clinical benchmarks in two human PBMC-reconstituted CDX models (SHP77 and NCI-H82). In summary, the incorporation of a CD2 co-stimulatory moiety into a DLL3-targeting TCE leads to a novel, next-generation TCE with improved efficacy and safety profiles in preclinical studies. IND-enabling studies are ongoing with the potential to advance it to clinical studies in the near future.

#4047 CBP/p300 and PARP inhibitor combination treatment synergistically enhances anti-tumor efficacy in models of advanced prostate cancer.

O. I. Richter[1], S. Sardar[1], X. Zhang[2], J. D. Kindrick[2], L. Ravindranath[1], C. H. Chau[3], C. J. Thomas[2], C. McNair[4], X. A. Su[1], A. Sharp[5], J. de Bono[5], K. Frese[6], W. D. Figg[3], K. E. Knudsen[7], A. A. Shafi[1];

[1]Uniformed Services University of the Health Sciences, Bethesda, MD, [2]National Center for Advancing Translational Sciences, Bethesda, MD, [3]National Cancer Institute, Bethesda, MD, [4]Thomas Jefferson University Kimmel Cancer Center, Philadelphia, PA, [5]The Institute of Cancer Research, London, United Kingdom, [6]CellCentric Ltd., Cambridge, United Kingdom, [7]Parker Institute for Cancer Immunotherapy, San Francisco, CA

Metastatic castration-resistant prostate cancer (mCRPC) is a uniformly fatal disease which has displayed resistance to many single-agent therapies, underscoring the need for novel combination therapies. Histone acetyltransferases CBP/p300, which act as androgen receptor (AR) coactivators, are often upregulated in mCRPC. Elevated CBP/p300 levels are associated with reduced progression-free and overall survival in prostate cancer patients. Our recent work has demonstrated that CBP/p300 play important roles in regulating DNA repair, particularly homologous recombination, and that inhibition of CBP/p300 may sensitize mCRPC to existing therapeutics. A Phase 1/2a study investigating a CBP/p300 inhibitor, CCS1477, alone and in combination regimens is currently underway. However, research into CCS1477 combination treatments is highly limited, necessitating further investigation into combination therapies and markers of sensitivity to improve outcomes for mCRPC patients. We hypothesized that combination treatment using CBP/p300 inhibitors (CBP/p300i) with PARP inhibitors (PARPi) would enhance anticancer effects by synergistically impairing DNA damage repair in cancer cells. Using preclinical 2D and 3D models, including patient-derived explants, we evaluated the functional impacts of targeting CBP/p300 and PARP pathways in combination. We found that this combination therapy was significantly more effective than either monotherapy at reducing cell growth both *in vitro* and *ex vivo*. Importantly, a comprehensive screen with clinically relevant PARPi revealed that combination of CBP/300 and PARP inhibition demonstrate synergy across several PCa cell lines. To assess the utility of CBP/p300 and PARP combination therapy in patients, we treated PCa patient-derived explants (PDEs) from a racially diverse cohort with CBP/p300i and PARPi. Ki67 staining revealed decreased proliferation in combination therapy-treated tissue, supporting the findings from 2D models. To investigate genomic alterations that may underlie differential treatment responses, we performed whole-exome sequencing (WES) on tissues from our PDE cohort. This analysis identified distinct germline and somatic variants that segregated with treatment responders versus non-responders. Spatial transcriptomics will identify molecular signatures distinguishing responders from non-responders, advancing precision medicine in diverse populations. Our findings indicate that CBP/p300 inhibition in combination with PARPi may have stronger anti-tumor effects than single-agent therapies. Analysis of patient-derived models provides insight into the patient subsets most likely to benefit from this combination therapy, supporting its potential as a novel therapeutic approach to improve outcomes for mCRPC patients.

#4048 3D bioprinted cancer models for drug screening versus 2D and *in vivo* models: A comparison study.

Aurelie Cadiou[1], Eva-Laure Matera[2], Doriane Mathe[1], Marine Fellmann[1], Jerome Guitton[3], Kamel Chettab[4], Christophe Marquette[4], Charles Dumontet[2]

[1]Antineo, Lyon, France,[2]CRCL, Lyon, France,[3]Hospices Civils de Lyon, Lyon, France,[4]University of Lyon, Lyon, France

3D models are increasingly used to perform preclinical drug screening. 3D bioprinted models offer a promising alternative to better mimic the in vivo setting. In this work we compared molecular characteristics and drug sensitivity of two HER2 positive human cancer lines, the breast cancer model BT-474 and the ovarian cancer model SK-OV-3. Both models were a) cultured in classical 2D systems, with analyses during the exponential growth phase; b) bioprinted using a fibrinogen/alginate/gelatin bioink and characterized at different time points; c) implanted subscutaneously in CB17-SCID mice and treated once tumors were established (median volume #100 mm3). All models were compared using RNA sequencing. Drug sensitivity was evaluated against HER2 specific agents (lapatinib, trastuzumab-emtansine) and paclitaxel in 2D and 3D models and against paclitaxel in tumor models. Tumor bearing mice were treated with different paclitaxel doses ranging between 2.5 mg/kg (ineffective) to 30 mg/kg (T/C ratio of 0.4). Paclitaxel accumulation in tumor cells was quantified in all models exposed to various concentrations of drug. IC50 values were found to be approximately 3 to 10-fold higher in 3D models than in 2D models for all treatments tested. Analysis of 3D models at different time points using non disruptive (Presto Blue) or disruptive (flow cytometry analysis) methods showed active proliferation of tumor cells up to 40 days after bioprinting, as documented by Ki67 staining. In a standard assay objects were printed on day 0, exposed to treatments on day 4 and analyzed up to day 11. Addition of cancer associated fibroblasts (CAFs) in the bioink reduced sensitivity of tumor cells to therapy. Coculture with adipocytes or in the presence of adipocyte conditioned medium also showed reduced sensitivity to therapy. Tumor cell concentrations of paclitaxel was quantified by mass spectrometry at various time points and concentrations in the 2D and 3D settings as well as in in vivo tumor models. RNA profiling of the different models identified a category of genes which were highly expressed in the 2D setting only, while genes specifically expressed in in vivo models tended to be also more highly expressed in 3D models. Differentially expressed genes were confirmed using RT-qPCR and are currently being explored at the proteomic level. Gene Ontology analysis suggested that genes involved in cell adhesion, focal adhesion and extracellular-matrix receptor interactions tended to be less expressed in 2D models. These results suggest that 3D bioprinted models better mimic the in vivo situation than 2D models and should be systematically used in the preclinical drug screening process of novel agents, in order to reduce and better choose relevant murine models.

: Adoptive T Cell Therapy
Minisymposium

#4006 Iterative engineering of GPC-3 targeted synthetic TCR and antigen receptor (STAR) cells in advanced solid tumors.

Changsong Qi[1], Jiarui Li[1], Chang Liu[1], Hongli Zheng[2], Dongmei Yang[2], Dan Liu[1], Panpan Zhang[1], Miao Zhang[1], Ran Xue[1], Jifang Gong[1], Lian Liu[1], Min Tao[1], Siyuan Cheng[1], Jian Li[1], Xiaotian Zhang[1], Jin Yin[2], Xueqiang Zhao[2], Xin Lin[3], Lin Shen[1]

[1]Peking University Cancer Hospital, Beijing, China,[2]Bristar Immunotech Limited, Beijing, China,[3]Tsinghua University School of Medicine, Beijing, China

Background: Glypican-3 (GPC3) is a highly specific and promising tumor-associated antigen. Adoptive cell therapies for solid tumors face significant hurdles including poor T-cell trafficking and limited persistence. To address these challenges, we initiated an iterative design process for GPC3-targeted STAR-T cells (YTS102). Our initial enhanced construct (v2) incorporated the chemokine receptor CXCR2 to improve tumor trafficking. We further optimized the construct to enhance T-cell expansion and persistence, leading to a v3 version armored with membrane-bound IL-15 (mbIL-15).
Methods: The STAR-T platform utilizes a high-affinity GPC3-specific scFv (GC33) fused to TCR constant domains. Preclinical evaluation was conducted through comprehensive in vitro (cytotoxicity, cytokine secretion, migration) and in vivo (Huh-7 and MKN45 xenograft models) assays to validate the functional attributes of each engineered construct. A first-in-human, investigator-initiated phase I trial (NCT05344664) was also conducted to evaluate the safety and preliminary efficacy of both v2 and v3 GPC3 STAR-T cells in patients with heavily pretreated, GPC3-positive advanced solid tumors.
Results: Preclinical studies confirmed the distinct advantages of each design. The CXCR2-armored v2 STAR-T cells showed enhanced chemokine-mediated migration, while the mbIL-15-armored v3 construct demonstrated superior proliferation, persistence, and potent serial killing ability. Both constructs mediated robust anti-tumor efficacy in xenograft models. In the phase I study, 7 evaluable patients (6 gastric cancer, 1 hepatocellular carcinoma) received STAR-T cell therapy (either v2 or v3). The safety profile was manageable; cytokine release syndrome (CRS) occurred in 6/7 patients (3 Grade 1-2; 3 Grade 3), and Grade 2 ICANS was observed in one patient. Encouraging clinical activity was observed, with an objective response rate (ORR) of 42.8% (3/7) and a disease control rate (DCR) of 71.4% (5/7).
Conclusion: Iterative engineering of GPC3-targeted STAR-T cells with functionalities to enhance tumor trafficking (CXCR2) and persistence (mbIL-15) results in potent anti-tumor activity. Early clinical data demonstrate a favorable safety profile and promising efficacy in heavily pretreated patients with GPC3-positive solid tumors. These findings validate our optimization strategy and support the continued clinical development of YTS102 as a promising therapeutic for solid tumors.

#4007 The cellular architecture of the infused T cell predicts efficacy of autologous tumor-infiltrating lymphocyte therapy (LM-103) in acral melanoma.

Chao Zhang[1], Jilong Yang[1], Xiangchun Li[2], Kexin Chen[2], Hongru Shen[2]

[1]Department of Bone and Soft Tissue Tumor, Tianjin Medical Univ. Cancer Inst. & Hosp., Tianjin, China,[2]Department of Epidemiology and Biostatistics, Tianjin Medical University Cancer Institute & Hospital, Tianjin, China

Acral melanoma (AM), the predominant melanoma subtype in Asia, shows poor response to immune checkpoint inhibitors, underscoring the need for alternative immunotherapies. An investigator-initiated trial evaluates autologous tumor-infiltrating lymphocyte (TIL) therapy (LM-103) in four Chinese patients with advanced AM, achieving a 75% disease control rate and one durable complete response. To define determinants of therapeutic outcome, integrated single-cell RNA sequencing (scRNA-seq) and T-cell receptor sequencing (TCR-seq) are performed on infused TIL products, tumors, and longitudinal peripheral blood. Single-cell profiling reveals marked heterogeneity within the infused products, including naïve, regulatory, follicular helper (Tfh), cytotoxic, and multiple exhausted T-cell states. Responders demonstrate striking enrichment of Tfh and intermediate exhausted (TEX_int) $CD8^+$ T cells, whereas the non-responder product is dominated by terminally exhausted subsets. Pseudotime analysis supports a conserved exhaustion continuum in which TEX_int cells occupy a plastic, functionally competent intermediate state.Cell-cell communication modeling shows that responder products contain a densely connected signaling ecosystem driven by Tfh- and TEX_int-mediated costimulatory pathways, such as CD40, CD70, and FASLG. In contrast, non-responder products exhibit sparse, immunosuppressive networks dominated by TGFβ and MIF signaling. TCR integration demonstrates higher clonality within Tfh and TEX_int subsets in responders.Longitudinal tracking reveals that the complete responder maintains stable high clonality after infusion. Notably, a dominant clonotype enriched in the TEX_int population of the infused product persists in peripheral blood and later adopts a progenitor-like exhausted (TEX_prog) state. This finding provides direct in vivo evidence that intermediate exhausted T cells can differentiate into a progenitor-like state after adoptive transfer, establishing a durable, self-renewing reservoir capable of sustaining long-term anti-tumor immunity.These results define the cellular and clonal architecture underlying successful TIL therapy in AM. Durable benefit is determined not by the size of the infused product but by the presence and persistence of coordinated Tfh-TEX_int ecosystems that seed long-lived progenitor-like immunity. These insights offer mechanistic biomarkers and provide a foundation for optimizing TIL manufacturing for melanoma subtypes refractory to current immunotherapies.

#4008 A novel, first in class chimeric antigen receptor dendritic cell platform driving broad and durable antitumor immunity in solid tumors.

S. L. Namen[1], G. Pandey[2], T. Naismith[1], C. Willoughby[1], L. Longtine[1], U. Panni[2], C. F. Lichti[2], K. Singhal[1], M. Griffith[3], **C. DeSelm**[1]; [1]Washington University School of Medicine in St. Louis, St. Louis, MO, [2]Washington University in St. Louis, St. Louis, MO, [3]Washington University, St. Louis, MO

Chimeric Antigen Receptor Dendritic Cells (CAR-DCs) represent a new class of immunotherapy designed to overcome the key limitations of CAR-T and immune checkpoint blockade (ICB) in solid tumors. By engineering conventional dendritic cells (cDCs) with a tumor-targeting CAR delivered via non-integrating mRNA, we have harnessed the intrinsic ability of DCs to cross-prime a broad repertoire of antitumor CD8+ T cells. This approach merges the precision of CAR technology with the natural antigen-presenting potency of DCs, enabling broad immune activation by inducing polyclonal $CD8^+$ T-cell responses that extend beyond CAR-restricted epitopes. To enable clinical advancement, we have developed a scalable human manufacturing process that reliably produces >300 million CAR-DCs, overcoming a longstanding barrier to the translational deployment of DC-based therapies. Immunotherapies such as CAR-T and ICB have transformed hematologic cancer treatment but remain ineffective in many solid tumors due to finite target antigens and dependance on pre-existing tumor-reactive T cells. To overcome these challenges, we engineered type I conventional DCs with a CAR recognizing B7-H3, a clinically relevant solid and liquid tumor antigen. In vitro, B7-H3 CAR-DCs displayed enhanced uptake of diverse tumor antigens, maturation, and superior cross-presentation of tumor derived antigens to $CD8^+$ T cells, driving potent cytotoxic T-cell activation. In vivo, using a C57BL/6 syngeneic 1956 sarcoma model comprised of 75% B7-H3$^+$ and 25% B7-H3$^-$ tumor cells, untreated mice exhibited progressive disease. In contrast, both intratumoral and intravenous administration of B7-H3 CAR-DCs induced complete to almost complete tumor regression and confer durable protection upon rechallenge, demonstrating the establishment of robust, target-independent immunity. Analysis of tumor-draining lymph nodes (tdLNs) revealed that B7-H3 CAR-DCs delivered substantially greater amounts of tumor antigen to tdLNs. Correspondingly, transcriptional profiling of tdLN $CD8^+$ T cells revealed signatures of enhanced activation, increased proliferative potential, and a shift toward memory formation which are hallmarks of efficient cross-priming. Mass spectrometry of MHC-I-cross presented peptides and tetramer analyses demonstrated CAR-DCs generated a broad expansion of endogenous tumor neoantigen-specific $CD8^+$ T cells, confirming strong and effective diversification of the antitumor T-cell response. Together, these results position mRNA-engineered CAR-DCs as a first-in-class, translationally ready cell therapy platform that integrates antigen specificity, broadening of the antitumor T-cell response, durable memory formation, and GMP-compatible large-scale manufacturing thereby supporting rapid advancement toward IND-enabling studies and clinical evaluation in solid tumors.

#4009 Decoding the medulloblastoma surfaceome prioritizes the oncofetal antigen GPC2 for potent CAR-T cell therapy.

D. Usta[1], W. Gwynne[2], Y. Suk[3], Y. Chen[1], M. T. Radosevich[4], D. Chernova[4], Y. Feng[4], E. Nasajpour[4], M. Trissal[5], R. Poetschke[5], A. Delaidelli[6], C. Dunham[7], L. Labanieh[4], J. van der Lugt[8], S. Nierkens[8], M. G. Filbin[9], C. Petrisch[4], P. H. Sorensen[10], K. Ryan[4], C. Venugopal[3], E. Sotillo-Pineiro[4], C. L. Mackall[11], S. K. Singh[3], **S. Heitzeneder**[4];

[1]Stanford Cancer Institute, Stanford, CA, [2]McMaster University, Georgetown, ON, Canada, [3]McMaster University, Hamilton, ON, Canada, [4]Stanford University, Stanford, CA, [5]Dana-Farber Boston Children's Cancer and Blood Disorders Center, Boston, MA, [6]BC Cancer Agency, Vancouver, BC, Canada, [7]BC Children's Hospital, Vancouver, BC, Canada, [8]Princess Maxima Center, Utrecht, Netherlands, [9]Dana-Farber Cancer Institute, Boston, MA, [10]British Columbia Cancer Research Centre, Vancouver, BC, Canada, [11]Stanford Hospital, Stanford, CA

Key determinants for efficacious CAR-T antigens remain near absence in vital tissues and that antigen levels in clinical specimens exceed CAR-T detection thresholds. CAR-T cells meeting these criteria have demonstrated clinical benefit in aggressive pediatric brain tumors, as seen in H3K27M-mutant diffuse midline glioma responding to GD2-directed CAR-T cell therapy. Medulloblastoma (MB) is a devastating childhood brain tumor, for which standard-of-care is fails in 30% of patients, and leaves many survivors with debilitating long-term effects. Survival rates of recurrent disease reside below <10%. Increasing cure rates and diminishing treatment-related morbidity necessitates targeted therapies, but success using CAR-T cells in MB has been limited by a dearth of suitable cell-surface targets. We profiled the CAR-T antigen landscape of MB through integrating unbiased surfaceome analysis from tumor and normal tissue transcriptomes and quantitative antigen density mapping of candidate targets on n= 24 MB tumor biopsies across all molecular subtypes. We found that MB closely resembles prenatal brain and credentialled oncofetal antigens as the predominant target pool in MB. A quantitative flow cytometry-based assay to precisely quantify antigen densities of candidate targets in clinical specimens prioritized GPC2 as the top candidate. GPC2 antigen densities ranged from ~1700-24500 molecules/cell across MB subgroups (mean: 6374 +/-4968). Because antigen density greatly influences CAR-T potency, we previously engineered GPC2-CAR-Ts tuned towards clinical densities on neuroblastoma and demonstrated that cJUN-overexpression (OE) augments their potency by lowering antigen detection thresholds (Heitzeneder et. al, 2022). Here, we employ orthotopic xenograft models and locoregional CAR-T delivery to study the interplay between GPC2 antigen density and CAR potency and to inform a phase-1 trial design. We found that both GPC2-CAR-T constructs (+/-cJUN) achieved durable disease control against GPC2-intermediate GR4-MB (ICB1299: ~9000 mol/cell and MBT375, a newly established PDX: ~6500 mol/cell). In a highly aggressive, MYC-amplified, GPC2-high GR3-MB model (SU_MB002: ~18800 mol/cell), recurrence occurred in 3/5 mice post GPC2-CAR, whereas repeated dosing or cJUN-OE significantly improved persistence and long-term anti-tumor control. In a GPC2-low, GR3-MB model (HDMB03: ~3000 mol/cell) used to further dissect antigen detection limits, only cJUN.GPC2-CAR-T cells maintained anti-tumor responses. This work informed an ongoing phase-1 clinical trial at Stanford (NCT07087002), currently testing repeated, locoregional GPC2-CAR-T infusions and is planned to employ cJUN overexpression in patients with recurrent/refractory MB, aiming to provide a targeted treatment option for this devastating malignancy.

#4010 NK-TCR cells: A next-generation platform expanding NK-cell therapeutic potential.

N. Uprety, B. Liu, R. Basar, R. Shrestha, F. Reyes Silva, M. Daher, K. Rezvani;
UT MD Anderson Cancer Center, Houston, TX

Background: Adoptive transfer of engineered natural killer (NK) cells has emerged as a promising strategy for solid and hematologic malignancies; however, the absence of a physiological T-cell receptor (TCR) limits the spectrum of antigens for targeting and prevents recognition of intracellular targets. To address this challenge, we developed a n NK-TCR platform that enables stable expression of fully functional TCRs in NK cells without inducing alloreactivity or GvHD. Using this system, we generated two lead NK-TCR products targeting the intracellular tumor antigens NY-ESO-1 and PRAME, with additional TCRs in development.
Methods: Primary human NK cells were engineered to express either an NY-ESO-1-specific TCRα/β receptor or a PRAME TCRα/β receptor recognizing target peptides presented on HLA-A*02:01. Both products incorporated the full CD3 signaling complex (ζ, ε, γ, δ) and a chimeric CD28-CD3ζ costimulatory module, and IL-15 to support activation and in vivo persistence. Each NK-TCR cell product was evaluated independently for in vitro for cytotoxicity, cytokine production, proliferation and serial-killing capacity against multiple tumor cell lines, including Saos-2 (osteosarcoma), A375 (melanoma), U266B1 (multiple myeloma), and THP-1 (AML).
Results: NY-ESO-1-TCR NK cells showed potent antigen specific activity, efficiently eliminating Saos-2, A375 and U266B1 cells, with strong cytokine production, sustained serial killing and superior persistence relative to non-transduced NK cells. The PRAME TCR NK cells showed equally strong activity against U266B1, Saos2, and A375 cells. In vivo, NY-ESO-1 TCR NK cells mediated rapid tumor regression and prolonged survival in multiple myeloma xenograft models, with durable persistence and no signs of exhaustion or toxicity. PRAME TCR NK cells achieved similarly superior in vivo activity in a U266B.1 Multiple Myeloma model compared to non-engineered controls. Based on the strength of these findings, NY-ESO-1-TCR NK cells are now under evaluation in multiple myeloma with a separate study in synovial sarcoma, and PRAME TCR NK cells have entered clinical evaluation for AML and melanoma. Together, these data establish NK-TCR platform as a next-generation cellular therapy approach with broad applicability and the capacity to extend NK-cell therapies to intracellular antigen targets.

#4011 Universal T cell therapy screening library in preclinical models of CAR T cell therapy.

A. Eapen, L. Wu, L. Moser, B. Quach, W. Gamal, K. Rodrigues, K. C. Tsui, Z. Good, T. Roth;
Stanford University School of Medicine, Stanford, CA

Currently approved T cell therapies fail to induce a durable remission for many of the patients who receive them, highlighting a pressing need to improve patient outcomes. To comprehensively explore genetic strategies to enhance function of engineered T cells, we have developed CRISPR-All, a combinatorial genetic perturbation language capable of simultaneously inducing natural gene overexpression, gene knockouts, and gene knockdowns, as well as new synthetic sequences such as chimeric antigen receptor (CAR) binders or signaling domains and synthetic gene sequences. Using CRISPR-All, we have created a T cell therapy “meta-library”, termed CRISPR-All Cell Therapy Universal Screening (CACTUS), collated from a comprehensive review of literature on effector function-enhancing genetic modifications in both native and engineered human T cells. In CACTUS2, we also included perturbations informed by clinical dataset analysis of patients receiving CD19-CAR or bispecific CD19/CD22-CAR therapy. We introduced the CACTUS2 library into primary human T cells along with a CD19-28Z CAR (axi-cel) and performed an in vitro assay in which edited CAR T cells are chronically stimulated over the course of 14 days via repetitive co-culture with target human leukemia or lymphoma cell lines (NALM6, Toledo, JeKo-1). Top hits across these screens emerged as synthetic chimeras of overexpressed genes. The large-scale analysis of perturbations relevant to T cell fitness in cancer models empowered by the CRISPR-All screening method is an important step in improving CAR T cell therapeutic designs for enhanced therapeutic outcomes.

#4012 Triple disruption of *CCDC6*, *CBLB*, and *ASB2* promotes the therapeutic efficacy of Glypican 3 targeted T cells.

Azlann Arnett[1], David Steffin[1], Antonino Montalbono[1], Nisha Ghatwai[1], Amy Courtney[1], Gabriel Barragan[1], Magda Magda Esparza Cerda[1], Michael Wood[1], Marie Pouzolles[1], Kshitij Rai[2], Frederic D. Bushman[3], Dimitrios L. Wagner[4], Andras Attila Heczey[5]

[1]Baylor College of Medicine, Houston, TX,[2]Rice University, Houston, TX,[3]Department of Microbiology, University of Pennsylvania, Philadelphia, PA,[4]Center for Cell and Gene Therapy, Baylor College of Medicine, Houston, TX,[5]Seattle Children's Research Institute, Seattle, WA

Viral insertions of chimeric antigen receptor (CAR) cassettes into specific genes can lead to clonal expansion of the resulting CAR T cell population and complete remission of cancer. Viral integration events provide a unique opportunity to study regulators of CAR T proliferation and function. We analyzed the clonal dynamics of twelve patients enrolled in our glypican 3 (GPC3) CAR T cell and IL15 GPC3 CAR T cell clinical trials using VDJ transcripts from single cell RNA sequencing of products and peripheral blood samples. One patient with hepatocellular carcinoma (HCC) treated with IL15 CAR T cells had a remarkably expanded clone. At peak expansion $14.7x10^9$ CAR^+ T cells were circulating in the patient based on flow cytometry. Expansion was accompanied by grade 3 cytokine release syndrome requiring activation of the inducible caspase 9 safety switch which rapidly eliminated all CAR T cells as measured by flow cytometry and completely resolved related symptoms. Response assessment with 3D imaging decreased the primary liver mass and either eliminated or significantly reduced the size all metastatic tumors. Alpha-feto-protein tumor marker (half-life ~ 1 week) decreased from 14500 to 760 over 5 weeks. To determine whether viral integration was associated with this clone we performed whole genome integration analysis. Sonic abundance of intronic integrations in CBLB, CCDC6 and an exonic integration in ASB2 closely mirrored abundance of the expanded clone. We validated these integrations were present in the clonally expanded IL15 CAR T cells using targeted single cell DNA sequencing. Viral integrations can disrupt gene function through the creation of chimeric transcripts. We identified CAR CBLB, CAR ASB2, and IL15 CCDC6 chimeric transcripts in our single cell RNA sequencing. Transcriptomic analysis revealed a unique gene regulatory program. Seurat clustering identified three clusters enriched for the expanded clone. Two clusters were associated with rapidly dividing cells expressing significantly higher levels of TYMS, PCNA, and CDK1. While the last cluster expressed transcription factors associated with T cell function ZNF683 and RUNX2. In a model of HCC, simultaneous knock out of these genes, or combinatorial knockout of CBLB and CCDC6 using base editing led to increased CAR T cell expansion and anti-tumor activity. To our knowledge this is the first report of integration driven clonal expansion seen in solid tumor CAR T therapy. As an integration in CBL was previously associated with clonal expansion, our CBLB finding suggests integration in this gene family may lead to clonal growth. We identified CCDC6 a gene with unknown function in T cells, as a regulator of CAR T proliferation. These results demonstrate the impact of multiple genetic disruptions in CAR T cells resulting in robust expansion and antitumor activity and support the careful implementation of these perturbations to enhance patient outcomes.

Tuesday, April 21, 2026

: AACR Project GENIE: Genomic Characterization
Poster Session

#4096 A pan-pediatric gene-regulatory network analysis reveals druggable dependencies across pediatric solid tumors.
Daniel Lee[1], Abid A. Reza[2], Syed A. Bukhari[2], Jun S. Wei[2], Hsein-Chao Chou[2], Xinyu Wen[3], Andrew S. Brohl[4], Javed Khan[5]

[1]FDA, Silver Spring, MD,[2]NIH, Bethesda, MD,[3]Programmer/Analyst, Dept. of ABCC, NIH, Bethesda, MD,[4]Moffitt Cancer Center, Tampa, FL,[5]National Cancer Institute, Bethesda, MD

Background: Pediatric tumors often co-opt normal developmental gene-regulatory programs, with errors in lineage-restricted progenitors that halt or reverse differentiation. Because these cancers arise within restricted developmental windows, display fetal-like programs, and carry relatively few driver mutations compared to adult tumors, we hypothesized that a pan-pediatric, transcriptome-inferred gene-regulatory network (GRN) analysis will discover lineage-specific regulons that anchor each tumor to a developmentally arrested state, which would identify actionable biomarkers and therapeutic targets.
Methods: We analyzed 2541 bulk RNA-seq from 35 pediatric cranial and extracranial solid-tumor samples, after batch correction. We inferred a pan-pediatric GRN from gene expression data, integrating networks inferred by ARACNe-AP and GENIE3 into a consensus GRN across all tumor types. We used a one-vs-rest strategy to identify tumor-specific differentially expressed genes (DEGs) within the regulons. Using hypergeometric tests, we quantified transcription factor (TF) activity and their regulons across tumors by assessing the enrichment of tumor-specific DEGs within each regulon. To map genes to drugs, we queried drug libraries, including Mechanistic Interrogation PlatE, Profiling Relative Inhibition Simultaneously in Mixtures, ChEMBL, DrugBank, and DrugCentral. We filtered druggable genes among TFs, their regulon members, and their interactors using log fold change and adjusted p-values, and ranked candidates in 19 tumors with DepMap data by using effect size.
Results: We identified 281 enriched TFs across tumors. The functional enrichment analyses showed that TF programs are usually restricted to specific tumor classes, mirroring their developmental cell-of-origin and highlighting candidate tumor-specific biomarkers. Examples include neurodevelopmental and neural-crest-related TFs (e.g., PHOX2B, ASCL1, and SOX10) in neuroblastoma (NB) and muscle-lineage TFs (e.g., MYOG, MYOD1, and PAX3/7) in fusion-positive rhabdomyosarcomas (FP-RMS). Our analysis suggests that TFs behave as robust, tumor-type-specific expression signatures and can distinguish tumors that may be histologically similar but arise from different developmental lineages. Furthermore, we used our TF-centric approach to identify known and new drug targets, such as SIX1, RRM2, AURKA, and BIRC5 in FP-RMS, and ACVR2B & BMPR1B in NB.
Conclusions and Future Directions: A unified GRN framework analysis of pan pediatric solid tumors resolves lineage-specific regulons associated with tumorigenesis and yields a ranked set of druggable genetic dependencies. *In vitro* and *in vivo* validation studies are currently underway.

#4097 cBioPortal for cancer genomics.

Ino de Bruijn[1], Tali Mazor[2], Gaofei Zhao[1], Manda Wilson[1], Avery Wang[1], Floris Vleugels[3], Pim van Nierop[3], Henk-Jan van den Ham[3], S. Onur Sumer[1], Jessica Singh[3], Baby A. Satravada[1], Oleguer Plantalech[3], Angelica Ochoa[1], Zain-ul-Abideen Nasir[1], Ramyasree Madupuri[1], Pieter Lukasse[4], Aaron Lisman[1], James Lindsay[2], Xiang Li[1], Bryan Lai[1], Ritika Kundra[1], Priti Kumari[5], Sowmiyaa Kumar[3], Tim Kuijpers[3], James Ko[1], Zeynep Karagoz[3], Karthik Kalletla[5], Prasanna K Jagannathan[6], Jason Hwee[1], Guizela Huelsz Prince[4], Charles Haynes[7], Benjamin Gross[1], Zhaoyuan Fu[2], Ruslan Forostianov[4], Calla Chennault[1], Rima AlHamad[1], Ugur Dogrusoz[8], Allison Heath[7], Adam C. Resnick[7], Trevor J. Pugh[6], Chris Sander[9], Jianjiong Gao[1], Nikolaus Schultz[1], Ethan Cerami[2]

[1]Memorial Sloan Kettering Cancer Center, New York City, NY,[2]Dana-Farber Cancer Institute, Boston, MA,[3]The Hyve, Utrecht, Netherlands,[4]SE4BIO, Houten, Netherlands,[5]Caris Life Sciences, Irving, TX,[6]University Health Network, Toronto, ON, Canada,[7]Children's Hospital of Philadelphia, Philadelphia, PA,[8]Bilkent University, Ankara, Turkey,[9]Harvard Medical School, Boston, MA

cBioPortal is a widely used platform for interactive visualization and analysis of large-scale multimodal cancer datasets. It provides cohort exploration tools, such as OncoPrint, mutation “lollipop” plots, survival and enrichment analyses, detailed patient-level views, and integrated variant annotations to support interpretation.

The public instance of cBioPortal (https://www.cbioportal.org) serves >40,000 unique visitors globally each month. It hosts data from >500 studies, all also available through the cBioPortal Datahub. In 2025, we added 38 new studies (~35,000 samples). We also added Tumor Break Load (TBL) scores across PCAWG, CCLE, and all 32 TCGA Pan-Cancer Atlas studies. More than 99 cBioPortal instances are deployed at institutions and companies worldwide.

cBioPortal partners with AACR Project GENIE to provide access to the GENIE cohort in a dedicated instance (https://genie.cbioportal.org). Users can explore >268,000 clinically sequenced samples from 20 institutions, as well as GENIE Biopharma Collaborative (BPC) cohorts with detailed clinical annotations, including NSCLC (~2,000 samples), colorectal cancer (~1,500), and breast cancer (~1,200), with more to come.

Over the past year, cBioPortal progressed along two complementary directions. First, we introduced a chat-based interface for natural-language data exploration, reflecting ongoing efforts to utilize AI, specifically large language models, to augment traditional query and visualization workflows in cBioPortal. Second, we released several core platform enhancements: 1) we improved the performance for large cohorts by switching the backend database from MySQL to ClickHouse, an OLAP (Online Analytical Processing) database; 2) the Plots tab can now visualize variant allele frequencies, connect multiple samples from the same patient, and has more flexible categorical sorting; 3) variant interpretation has been strengthened through integration of AlphaMissense predictions; 4) we released a redesigned About page highlighting the year’s accomplishments and future roadmap. It is worth noting that many of these features were developed using AI-assisted technologies, which are increasingly standard practice in software engineering.

cBioPortal is open source (https://github.com/cBioPortal) and developed collaboratively by groups at Memorial Sloan Kettering Cancer Center, Dana-Farber Cancer Institute, Children’s Hospital of Philadelphia, Princess Margaret Cancer Centre, Bilkent University, SE4BIO, and The Hyve. We welcome contributions from the cancer research community.

#4099 Genomic and clinical landscape of 10,000 Korean pan-cancer patients reveals molecular determinants of prognosis and therapeutic response: K-MASTER program.

Ji Yoon Lee[1], Jisoo Hong[2], Kyong Hwa Park[3], Soohyeon Lee[3], Jwa Hoon Kim[3], Ju Won Kim[3], Ji Won Lee[3], Yonghwa Choi[2], Doyoon Kim[2], Yoonji Kim[2], Woo Young Jang[2], Jiwon Kim[1], You Jin Song[1], Dayoung Lee[1], Hyeonmin Jeong[1], Wooseok Lee[1], Yoon Ji Choi[3], Jason K. Sa[1]

[1]Korea Univ. College of Medicine, Seoul, Korea, Republic of,[2]oncoMASTER, Seoul, Korea, Republic of,[3]Korea Univ. Medical Center, Seoul, Korea, Republic of

Precision oncology relies on molecular characterization of the tumors to guide individualized therapy. Although large-scale precision oncology programs have revealed profound insights into the molecular complexity of human cancers, their direct clinical impact remains incompletely defined. Building upon our prior work, we expanded the K-MASTER program, one of the world's largest East Asian pan-cancer cohorts, integrating deep molecular profiling with long-term clinical outcomes. We analyzed 10,000 Korean patients with advanced malignancies, combining molecular aberrations with eight years of survival, treatment modalities, and therapeutic response data. Comparative analyses with the Western cohort, including AACR-GENIE, uncovered ancestry-specific molecular disparities. Furthermore, we developed a unified metric, the Molecular-Prognostic Index (MPI), to systematically quantify and compare the prognostic impact of individual genomic alterations at both pan-cancer and individual tumor levels. Using this framework, we identified key alterations and pathways shaping patient survival and therapeutic sensitivities. Korean cancer patients exhibited distinct molecular features, including frequent *CDKN2A* loss and mismatch repair deficiency-related mutational signatures. Prognostic modeling revealed that actional alterations curated in OncoKB and *APC* mutations conferred favorable clinical outcomes, whereas mutations in *TP53, CDKN2A, KRAS,* and *SMARCB1* were significantly associated with poor survival across multiple tumor types. Machine-learning-based analyses further identified DNA damage repair deficiency and chromosomal instability as robust predictors of response to platinum-based chemotherapy and immune checkpoint blockades. Collectively, these results provide unprecedented insights into the complex molecular and clinical landscape of Korean advanced cancers, establish a population-specific framework for precision oncology therapy, and provide mechanistic and prognostic insights essential for global translation of genomic medicine.

#4100 Large language models for tumor genomic interpretation.

Jennifer Yu[1], Madison Darmofal[2], Michele Waters[2], January Choy[2], Thinh N. Tran[2], Chenlian Fu[1], Leah Morales[1], Kaicheng U[1], Ross L. Levine[2], Nikolaus Schultz[2], Michael F. Berger[2], Quaid Morris[2], Justin Jee[2]

[1]Tri-Institutional Computational Biology & Medicine, Weill Cornell Medicine, New York, NY, [2]Memorial Sloan Kettering Cancer Center, New York, NY

Introduction: Algorithms trained on real-world data aid in tumor genomic prediction tasks, such as identifying cancer driver mutations and inferring cancer type. The extent to which generalist large language models (LLMs) trained on large natural language corpora can replace or supplement such domain-specific algorithms with zero-shot inference is unknown.
Methods: We evaluated the zero-shot performance of proprietary (GPT-5, o3-mini, GPT-4o and Claude 3.7 Sonnet), open weight (DeepSeek and Qwen3) and domain-specialized medical (MedGemma) LLMs on three tasks: (i) Distinguishing tumor-somatic mutations from clonal hematopoietic (CH) variants in patients with matched tumor-whole blood profiling (N=37,179 patients; 54,807 samples), (ii) Classifying oncogenic variants using the OncoKB dataset as a positive control (N=10,489 patients; 10,752 samples; 13,470 variants), and (iii) Predicting cancer type from tumor genomic profiles in the multi-institution AACR GENIE dataset (N=97,074 patients; 102,791 samples).
Results: Multiple LLMs approached the accuracy of MetaCH, a supervised model for distinguishing somatic tumor mutations from CH variants. o3-mini achieved the highest accuracy for distinguishing oncogenic driver from benign passenger mutations. Among patients with non-small cell lung cancer and mutations in *KEAP1*, those with VUSs classified as oncogenic by GPT-5 had worse overall survival than those with VUSs classified as benign. GPT-5, o3-mini, and Claude 3.7 Sonnet had accuracy approaching that of a supervised model, GDD-ENS, at classifying 34 cancer types using tumor genomic profiles. Ensemble approaches combining prediction results from GPT-5 and GDD-ENS improved cross-institutional generalizability and performance by an average of 20%. In their reasoning, LLMs discussed clinically relevant genomic features consistent with feature importances from GDD-ENS.
Conclusion: Without task-specific training, LLMs achieved performance comparable to specialized supervised models across all tasks.

F1 score comparison across three cancer genomics prediction tasks.

	Mutation status(Tumor-somatic vs. CH)	Oncogenic Variants(Benign vs. Oncogenic)	Cancer Type(34 types)
GPT-5	0.94	0.80	0.49
GPT-4o	0.96	0.75	0.32
o3-mini	0.93	0.82	0.43
Claude 3.7 Sonnet	0.95	0.79	0.43
DeepSeek	0.86	0.79	0.23
Qwen3	0.95	0.79	0.26
MedGemma	0.86	0.77	0.19
MetaCH	0.98	n/a	n/a
AlphaMissense	n/a	0.90	n/a
GDD-ENS	n/a	n/a	0.57

#4102 EGFR mutation subtype modifies the clinical impact of TP53 functional loss on brain metastasis and survival in lung cancer.

Lexi Li[1], Yiye Wong[2], Nathan Yan[3], J. Nicholas Bodor[4], **Yunyun Zhou**[4]

[1]Homestead High School, Cupertino, CA,[2]The Kings Academy, Sunnyvale, CA,[3]The Harker School, San Jose, CA,[4]Fox Chase Cancer Center, Philadelphia, PA

Background:
Brain metastasis (BM) is common in EGFR-mutant non-small cell lung cancer (NSCLC). Exon 19 deletion (Ex19del) and L858R, the two predominant EGFR sensitizing mutations, differ in biological behavior, therapeutic response, and CNS relapse patterns. TP53 is the most frequent co-mutation in EGFR-mutant disease, has been associated with increased metastatic potential and CNS progression, but its subtype-specific effects in the BM setting remain unclear. We examined whether TP53 functional loss differentially influences BM risk and post-BM survival in EGFR subtypes.
Methods:
We analyzed NSCLC patients from MSK-IMPACT cohort and GENIE BPC cohort. Aim 1 (BM risk): time-to-BM Cox models evaluated associations of EGFR subtype, TP53 status, and their interaction with BM at presentation and BM during follow-up, adjusting for demographics, smoking, and stage. Aim 2 (post-BM prognosis): Among patients with radiographically confirmed BM or CNS, overall survival (OS) from BM diagnosis was evaluated using multivariable Cox models adjusting for BM timing, local intracranial therapy, systemic treatment generation, and extracranial metastatic burden.
Results:
Among 152 patients, time-to-BM analyses similarly showed shorter BM-free survival for TP53 functional loss (adjusted HR=1.65, P=0.11). Among 836 patients with BM, TP53 functional loss predicted worse OS (adjusted HR=1.97, P=0.05), and this adverse effect differed markedly by EGFR L858R and Ex19del subtype (interaction P=0.047). In Ex19del tumors, TP53 loss had a modest association with poorer OS, whereas in L858R tumors it was strongly associated with worse outcomes (median OS 34.7 vs 48.2 months). Results were consistent across cohorts and robust to exclusion of low-VAF TP53 variants.
Conclusions:
TP53 functional loss has distinct clinical implications across EGFR mutation subtypes, conferring both higher risk of brain metastasis and significantly worse post-BM survival in L858R compared with Ex19del disease. These findings reveal important subtype-specific heterogeneity within EGFR-mutant NSCLC and support integrating TP53 status into BM risk assessment and management strategies.

#4103 Dynamic co-mutation patterns and therapeutic implications in BRAF-altered malignancies: Evidence from AACR Project GENIE.

Mohamed M. Khamis[1], Vivek Subbiah[2], Mohamed Gouda[3]

[1]Mercy Hospital St. Louis, St Louis, MO,[2]Sarah Cannon Research Institute, Nashville, TN,[3]The University of Texas MD Anderson Cancer Center, Houston, TX

Background: BRAF gene alterations result in persistent activation of the MAPK signaling cascade, a well-established oncogenic driver across diverse tumor types. A comprehensive pan-cancer analysis of BRAF alteration types (mutations, CNAs, and fusions), co-mutation landscapes, and actionability in large cohorts remains limited.
Methods: We utilized AACR Project GENIE v18.0-public to characterize BRAF alteration prevalence, co-mutations, and actionability. OncoKB levels (L1-L4) defined actionability, and serial samples were analyzed for clonal evolution.
Results: Among 204,292 samples, BRAF alterations were detected in 23,363. BRAF mutations were identified in 12,860 samples (7,359 with V600 and 5,501 with non-V600 variants). Prevalence was highest in thyroid cancer (44.9%), melanoma (38.0%), and histiocytosis (33.5%). V600 variants predominated in thyroid cancer (97.2%; 98.4% in papillary and 99.2% in anaplastic) and melanoma (76.7%), while non-V600 variants were enriched in NSCLC (73.3%), endometrial (98.5%), and bladder cancer (96.6%). BRAF copy number alterations (CNAs) were present in 10,274 samples, with the highest prevalence in breast (85.9%), esophagogastric (70.3%), and ovarian (69.6%) cancers. BRAF fusions occurred in 1,153 samples, with the highest prevalence in glioma (16.8%) and prostate cancer (14.2%). Tumor-centric actionability was high in histiocytosis (93.5% actionable), thyroid cancer (91.9%), and melanoma (79.3%), and was substantial in colorectal cancer (50.6%) and glioma (31.6%). Alteration-centric analysis confirmed L1 evidence as highest level for V600 alterations across solid tumors and for fusions (e.g., KIAA1549-BRAF in glioma). Non-V600 alterations showed L2-L4 evidence as highest level (e.g., MEK inhibitors in histiocytoses; investigational RAF inhibitors). Non-V600 tumors showed significantly higher co-mutation burden, with 40 genes enriched, including RTK/RAS (KRAS: 18.5% vs 1.3%; NF1: 18.7% vs 3.6%), chromatin remodeling (ARID1A: 20.1% vs 7.3%), and PI3K/AKT (PIK3CA: 19.8% vs 8.8%). Co-mutation analysis revealed a substantial fraction of events with OncoKB evidence, particularly in RTK/RAS, chromatin, and PI3K/AKT pathways, creating opportunities for rational combination strategies. Serial analysis of 2,314 samples from 1,072 patients demonstrated dynamic evolution of co-mutations, supporting serial profiling to identify emerging therapeutic targets.
Conclusions: This study represents the most extensive pan-cancer analysis of BRAF alterations, highlighting their prevalence, co-mutation, and actionability patterns. Non-V600 tumors exhibit higher genomic complexity and actionable co-mutation burden, which could inform combination strategies. The dynamic evolution of co-mutation underscores the need for serial profiling to uncover emerging therapeutic vulnerabilities.

#4104 The genomic landscape of skin adnexal carcinomas in the AACR GENIE database: Implications for precision cancer medicine.

Valbert Oliveira Costa Filho[1], Mariana Macambira Noronha[1], Pedro Robson Costa Passos[1], Carlos Diego Holanda Lopes[2], Giuseppe G. F. Leite[3], Carlos Wagner de Souza Wanderley[4], Sam D. Saibil[5], Danielle Calheiros Campelo Maia[1], Erick F. Saldanha[2]

[1]Universidade Federal do Ceara, Fortaleza, Brazil,[2]Princess Margaret Cancer Centre, University Health Network, Toronto, ON, Canada,[3]Division of Infectious Diseases, Department of Medicine, Escola Paulista de Medicina Universidade Federal de Sao Paulo, Sao Paulo, Brazil,[4]Brigham and Women's Hospital, Harvard Medical School, Boston, MA,[5]Department of Medicine, University of Toronto, Toronto, ON, Canada, Toronto, ON, Canada

Skin adnexal carcinomas (SAC) are rare and heterogeneous malignancies. These group of tumors differentiate from skin appendageal, such as hair follicles and sebaceous glands, and are molecularly and clinically distinct from keratinocyte carcinomas. Recurrent or metastatic SACs are aggressive tumors with poor survival outcomes, and limited available therapeutic options. Here we leveraged the AACR GENIE database to uncover the genomic landscape of SAC. Genomic data from samples classified as SAC according to the World Health Organization classification were selected from the AACR GENIE 1.8 dataset and annotated using the OncoKB^{TM} database. Tumor mutation burden (TMB) values were provided by the AACR team, with classification defined as low (<2 mut/Mb), intermediate (2 to 16 mut/Mb), and high (>16 mut/Mb). Mutational signatures were generated and matched to the COMISC database. A total of 224 samples were retrieved, including primary (73.7%, n=165) and metastatic (26.3%, n=59) tumors. Clinicodemographic analysis revealed 53.6% (n=120) female and identified race distribution as white (73.2%; n=164), Asian (10.3%; n=23), black (5.4%; n=12) and non-specified (11.1%; n=25). Extramammary Paget disease was the most common subtype (48.7%; 109), followed by tumors with apocrine/eccrine (32.6%; n=73), sebaceous (17.4%; n=39), and follicular differentiation (1.3%; n=3). The median number of mutations per sample was 4 (IQR 2-3). The most frequently mutated genes were *TP53* (45%), *PIK3CA* (20%), *KMT2C* (17%), *ERBB2* (17%), and *NOTCH1* (12%). The main altered pathways involved RTK-RAS (54.9%), TP53 (48.7%) and PI3K (37.1%). The most frequent copy number losses were in *CDKN2A* (11.8%) and *CDKN2B* (10.5%). The main copy number gains were observed in *ERBB2* (8.7%) and *MYC* (8.1%). The most frequent actionable mutations annotated by OncoKB^{TM} occurred in *PIK3CA* (Level 1; 17%), *ERBB2* (Level 1; 12%), *CDKN2A* (Level 4, 4.9%), *PTCH1* (Level 3A, 4.5%), and *ARID1A* (Level 4, 4%). Actionable *BRAF* mutations were detected in 2.2% of patients (0.4% Level 1 and 1.8% Level 2), whereas *KRAS* Level 1 mutations were observed in 3.6% of patients. The median TMB was 2.7 mut/Mb (IQR 0.85-6.83), 38.8% (n=87) samples had low TMB, 48.6% (n=109) had intermediate TMB, and 12.5% (n=28) had high TMB. Three COSMIC mutational signatures were matched: SBS2 (activity of APOBEC family of cytidine deaminases), SBS6 (defective DNA mismatch repair), and SBS7b (ultraviolet exposure), dominating 37.4%, 36.9%, and 25.7% of tumors, respectively. Our study profiled the largest cohort of SACs reported to date and identified a subset of patients with high TMB and actionable genomic alterations, including Level 1 alterations per OncoKB. These findings highlight the relevance of genomic profiling in SACs to inform clinical decision making, enable clinical trial matching, and improve the biological understanding of these rare malignancies.

#4105 Distinct age associated genomic landscapes in colorectal, pancreatic, small bowel, and anal cancers: A pan gastrointestinal analysis of 34,000 tumors from AACR Project GENIE v18.0.

Ahmed Abdelhakeem[1], Nency Ganatra[2], Dina Elantably[1], Tayo Adeoye[1], Nayef H. Abdel-Razeq[1], Mosalem M. Osama[3], Hani M. Babiker[1]

[1]Mayo Clinic Florida, Jacksonville, FL,[2]Department of Internal Medicine, Baptist Hospitals of Southeast Texas, Beaumont, TX,[3]Saint Luke`s Cancer Institute, Kansas City, MO

Background: Early-onset gastrointestinal (GI) cancers are increasing globally, yet the genomic basis for age-related differences across multiple tumor types remains poorly defined. We leveraged AACR Project GENIE v18.0 (N≈34,000 GI tumors) to characterize molecular distinctions by age in colorectal, pancreatic, small bowel, and anal cancers with sufficient early-onset representation.
Methods: Clinical and genomic data were extracted and tumors classified into early-onset (<50 years) and late-onset (≥50 years). Mutation frequencies were compared by cancer type and age group, focusing on recurrent drivers, DNA repair, Wnt signaling, RAS/MAPK, chromatin remodeling genes, and targetable alterations.
Results: Early-onset colorectal cancer (N=5,724) showed increased Wnt/β-catenin pathway alterations: APC (+4.9%), TCF7L2 (+4.1%), and TP53 (+5.0%), while late-onset tumors (N=15,807) were enriched for BRAF (−5.4%), RNF43 (−1.9%), and GNAS (−1.1%), indicating divergent tumorigenic pathways. Early-onset pancreatic cancer (N=890) exhibited significantly lower frequencies of canonical drivers—KRAS (−24.7%), TP53 (−15.6%), CDKN2A (−6.9%), SMAD4 (−6.0%)—with enrichment of MEN1 (+3.5%), TSC2 (+3.0%), ATRX (+2.0%), DAXX (+1.9%), and CTNNB1 (+2.4%), consistent with fusion-driven, hereditary, and chromatin remodeling biology. Small bowel cancer (N=99) in early-onset patients demonstrated enrichment in DNA damage response and MAPK/RAS genes including BRCA2 (+7.2%), NF1 (+7.4%), FBXW7 (+8.8%), FLT4 (+6.5%), ARAF (+6.4%), and ALK (+5.1%), whereas late-onset tumors (N=538) were enriched for KDR (−5.1%) and MGA (−5.2%). Early-onset anal cancer (N=62) showed elevated MGA (+7.8%), WHSC1/NSD2 (+6.9%), PBRM1 (+6.2%), FANCA (+5.2%), ERCC5 (+6.2%), and MSH6 (+5.9%), highlighting chromatin remodeling and DNA repair pathways potentially related to HPV biology; late-onset tumors (N=464) had enrichment in ATM (−5.6%), PTEN (−5.5%), STK11 (−5.2%), APC (−5.2%), and KMT2C (−5.0%), reflecting age-associated genomic instability.
Conclusions: This pan-GI age-stratified analysis reveals distinctive oncogenic programs in early-onset GI cancers characterized by Wnt/TP53-driven colorectal, fusion- and chromatin remodeling-driven pancreatic, DNA damage response/MAPK-driven small bowel, and chromatin-immune DDR signatures in anal cancers. These findings underscore the need for age-tailored precision oncology and support routine genomic profiling in early-onset GI malignancies to identify targetable alterations enriched in younger patients.
Citation: AACR Project GENIE Consortium. AACR Project GENIE: Powering Precision Medicine Through an International Consortium. Cancer Discov. 2017;7(8):818-831. (Data: GENIE Release 18.0-public)Acknowledgement: AACR and Project GENIE registry

#4106 Pan cancer enrichment of homologous recombination repair (HRR) gene alterations in 101,240 tumor samples from AACR Project GENIE: Implications for tumor-agnostic PARP inhibitor expansion.

Ahmed Abdelhakeem[1], Nency Ganatra[2], Dina Elantably[1], Tayo Adeoye[1], Nayef H. Abdel-Razeq[1], Osama M. Mosalem[3], Hani M. Babiker[1]

[1]Mayo Clinic Florida, Jacksonville, FL,[2]Baptist Hospitals of Southeast Texas, Beaumont, TX,[3]Saint Luke's Cancer Institute, Kansas City, MO

Background: PARP inhibitors are restricted to a subset of BRCA-associated cancers, but homologous recombination repair (HRR) deficiency signifies a broader genomic vulnerability that may extend therapeutic opportunities across diverse malignancies. We utilized AACR Project GENIE v18.0-public to define the pan-cancer prevalence of HRR gene alterations.
Methods: Somatic mutation and clinical sample data from GENIE v18.0-public were analyzed. HRR genes included BRCA1, BRCA2, ATM, CHEK2, PALB2, RAD51B/C/D, RAD51L1, BARD1, BRIP1, and core FANC genes. HRR alteration rates were calculated by tumor type using unique samples; only de-identified aggregate results are reported.
Results: Among 101,240 tumors, HRR gene alterations were frequent in multiple non-BRCA-associated cancers. Highest rates were seen in sialoblastoma (100%), large cell medulloblastoma (50%), malignant glomus tumor (50%), lung cancer (46.0%), infantile fibrosarcoma (42.9%), liver (40%), kidney (40%), non-melanoma skin (36.9%), colorectal (36.6%), melanocytoma (34.2%), biliary tract (33.3%), bladder (31.5%), and ovarian/fallopian tube (30.2%). Notably, lung, bladder, hepatobiliary, renal, gastrointestinal, and some sarcoma subtypes showed HRR mutation prevalence equal or higher than current PARP indications, yet lack FDA approval.
Conclusions:HRR alterations are widespread across solid tumors, often surpassing rates in cancers eligible for PARP treatment. These findings support expanding tumor-agnostic HRR genomic testing beyond BRCA-linked malignancies and warrant prospective trials of PARP inhibitors in HRR-enriched tumor types such as lung, bladder, hepatobiliary, renal, gastrointestinal, and pediatric/rare cancers. Impact: Large-scale genomic profiling from AACR Project GENIE demonstrates that HRR gene alterations are common across diverse solid tumors, with prevalence in multiple cancer types surpassing those currently eligible for PARP inhibitor therapy. These findings support broad implementation of HRR genomic testing in routine molecular diagnostics and provide a rationale for expanding PARP inhibitor use beyond BRCA-associated malignancies. The data justify prospective tumor-agnostic clinical trials of PARP inhibitors in HRR-enriched cancers such as lung, bladder, hepatobiliary, renal, gastrointestinal, and select pediatric and rare tumors; this could transform therapeutic decision-making and accelerate development of synthetic lethality-based targeted therapies
Citation: AACR Project GENIE Consortium. Cancer Discov. 2017;7(8):818-831
Acknowledgement: AACR and Project GENIE

#4107 Factors associated with early treatment discontinuation in the AACR Project GENIE Biopharma Collaborative (BPC) non-small cell lung cancer (NSCLC) cohort.

Dany Hamze, Sanjay Mishra, Aleenah Mohsin, Sarah Minuit, Ece Gamsiz Uzun, Jeremy L. Warner

Brown University, Providence, RI

Background: Early treatment discontinuation in NSCLC is frequent and is associated with worse outcomes. We sought to identify clinical and genomic factors associated with early discontinuation among patients with NSCLC treated with immune checkpoint inhibitors (ICIs) or tyrosine kinase inhibitors (TKIs), now central to most NSCLC treatment strategies. We used the AACR Project GENIE BPC registry, which captures granular drug exposures along with other clinical and genomic variables.

Methods: Data were obtained from the BPC NSCLC v2.0 cohort on May 19, 2025. Patients receiving ICIs or TKIs were included if the identified drugs had different start and end dates. Early discontinuation thresholds were first clinically estimated, then empirically defined using 1) Gaussian Mixture Models and 2) Classification and Regression Tree analysis, with consensus cutoffs of 3.0 and 4.3 months for TKIs and ICIs, respectively. Multivariable logistic regression (MLR) was applied to evaluate associations between early discontinuation and: sex; stage; drug class; oncogenic driver mutations in *EGFR*, *ALK*, *KRAS*, and *BRAF*; and line of therapy (first-line [1L] vs later-line). Because the cohort predates wider first-line ICI adoption, most ICI exposures in BPC occur in later lines.

Results: 910 of 1846 (49%) treatment episodes were included. By our definition, early discontinuation occurred in 420 (46%) of these. In MLR, TKI exposure (OR 0.17, 95% CI 0.12-0.24) and receiving TKI or ICI as 1L treatment (OR 0.56, 95% CI 0.39-0.78) were inversely associated with early discontinuation. Stage IV was associated with a trend towards early discontinuation (OR 1.56, 95% 0.94-2.65). Conversely, the presence of an *EGFR* mutation trended away from early discontinuation (OR 0.72, 95% CI 0.48-1.07). The final model demonstrated good discrimination with an AUC of 0.74. Calibration analysis showed excellent agreement between predicted and observed probabilities.

Conclusions: Receiving TKIs in any line and ICI treatment in 1L were inversely associated with early discontinuation, suggesting differential tolerability. *EGFR* mutation status demonstrated a trend toward lower discontinuation risk, independent of TKI exposure or line of therapy. Stage IV trended towards a higher early discontinuation risk, which could reflect early progression of disease while on treatment. Limitations include: 1) the exclusion of episodes with a single dose or a clinical trial medication (both are recorded with the same start/end date in BPC); 2) a lack of ground truth for discontinuation reasons; 3) unknown cross-episode interactions in patients with multiple treatment episodes; and 4) unmeasured confounders, such as social determinants of health (SDOH). Despite these limitations, our findings highlight distinct factors that may inform individualized strategies and warrant further investigation.

#4109 Pan-cancer landscape of IDH1/2 mutations with a focus on non-small cell lung cancer: Insights from the AACR GENIE Registry.

Zhaohui L. Arter, Cathleen Park, Misako Nagasaka, Sai-Hong I. Ou

UCI Health, Orange, CA

Background: IDH1 and IDH2 mutations are oncogenic drivers across several tumor types. Their prevalence, mutational spectrum, and co-alteration profiles in Non-Small Cell Lung Cancer (NSCLC) remain incompletely defined. Given the availability of approved IDH1 and IDH2 inhibitors, characterizing these mutations has potential therapeutic relevance.
Methods: We queried the AACR GENIE v18 database (n=250,018 tumor samples) to assess IDH1/2 mutation frequency, subtype distribution, associated histologies, co-mutations and survival outcomes in NSCLC.
Results: IDH1 and IDH2 mutations were identified in 5,380 (2.2%) and 2,761 (1.1%) patients, respectively. IDH1 mutations—primarily R132H (50.4%) and R132C (20.6%)—were enriched in gliomas (42.6%), cholangiocarcinoma (6.0%), lung adenocarcinoma (4.8%), and melanoma (4.4%). IDH2 mutations—mainly R140Q (20%) and R172K (9.8%)—were most frequent in AML (20.3%), colorectal cancer (7.4%), and NSCLC (5.9%). Among 30,454 NSCLC patients, IDH1 and IDH2 mutations occurred in 1.2% and 0.7%, respectively. EGFR co-mutations were found in 83 (21.8%) of IDH1- and 39 (22%) of IDH2-mutant NSCLC. KRAS co-mutations were seen in 170 (44.5%) of IDH1- and 51 (29%) of IDH2-mutant NSCLC (Table). Across major oncogenic subgroups, IDH co-mutations occurred in 1.04% (IDH1) and 0.60% (IDH2) of EGFR L858R, 1.18% and 0.13% of EGFR E746_A750del, and in 2.01% and 0.81% of KRAS G12C, respectively. Among 1,846 patients with available survival data, the median overall survival (OS) was 14.7 months for stage IV KRAS G12C+/IDH1/2- patients compared with 9.7 months for KRAS G12C+/IDH1/2+ (P = 0.02).
Conclusions: In stage IV KRAS G12C-mutant NSCLC, IDH1/2 co-mutations were linked to shorter median OS. These findings, along with the frequent co-alterations of IDH1/2 with EGFR and KRAS, warrant further study of targeted and combination strategies.

Table: IDH1/2 Co-Alterations in NSCLC

Feature	IDH1 (n=366)	IDH2 (n=199)
EGFR co-mutations	83 (21.8%)	39 (22%)
L858R / E746_A750del	19 / 18	11 / 2
KRAS co-mutations	170 (44.5%)	51 (29%)
G12C / G12V / G12D	62 / 28 / 24	25 / 15 / 4
G12A / G12F / G12S / G12R	10 / 2 / 2 / 1	2 / 2 / 1 / 1
Other KRAS variants	41	6

#4110 Genomic vulnerabilities and clinical behavior of metaplastic breast cancer through integrated registry and GENIE analysis.

Ahmed Shatta[1], Diego F. Chamorro[2], Blessie Elizabeth Nelson[1], Bora Lim[1]

[1]UT MD Anderson Cancer Center, Houston, TX,[2]University of Pittsburgh Medical Center, Pittsburgh, PA

Background: Metaplastic breast cancer (MpBC) is a rare and highly heterogeneous subtype of breast cancer, predominantly triple-negative and characterized by chemoresistance, early relapse, and poor survival. Despite its classification within the triple-negative breast cancer (TNBC) spectrum, the clinical behavior and molecular landscape of MpBC remain poorly defined, limiting the development of targeted therapeutic strategies.
Methods: Clinical MpBC cases from MD Anderson Cancer Center (2014-2025) were annotated for subtype, stage, and survival. Genomic data from the AACR GENIE MpBC cohort (v16.1; n=258) were evaluated for pathogenic mutations and copy-number alterations. Variant frequencies, hotspot patterns, and mutual exclusivity were assessed using Fisher's exact test. Analyses were performed in R, with statistical significance defined as $p<0.05$.
Results: Among 105 MpBC cases in the MDACC registry, 92.9% were TNBC, with an overall mortality rate of 34.3%. HER2-positive disease was rare (3.5%) but demonstrated the highest proportional mortality (50%). ER-positive tumors ≥10% (3.5%) had a 25% mortality rate, whereas ER/PR low-positive (<10%) tumors exhibited clinical outcomes similar to TNBC. Notably, mortality was observed even among early-stage patients, underscoring aggressive tumor biology that is independent of stage. Genomic analysis of 258 MpBC cases (267 samples) from GENIE identified recurrent *TP53* mutations (57%), including canonical hotspot variants (R248Q, R175H, R273C), consistent with pervasive genomic instability. *PIK3CA* alterations (34%), driven predominantly by H1047R, were frequently mutually exclusive with *TP53* mutations ($p=0.043$), suggesting distinct molecular subclasses with differential oncogenic drivers. Additional recurrent alterations in chromatin regulators (*KMT2C* 17.1%, *KMT2D* 10.5%) and copy-number gains involving *AGO2* (22.9%), *RAD21* (20.4%), *RECQL4* (19.8%), and *MYC* (19.4%) highlight potential vulnerabilities in DNA repair, replication stress response, and transcriptional regulation. Genomic profiling of the institutional MpBC cohort is ongoing.
Conclusion: These integrated clinical and molecular findings reinforce MpBC as a major contributor to mortality within the TNBC population despite its rarity and nominate PI3K/AKT pathway alterations, genomic instability, and epigenetic deregulation as potential therapeutic targets. These findings further support the need for biomarker-driven precision oncology trials, including basket-style designs and rare-tumor initiatives, to advance targeted therapies for rare, aggressive breast cancer subtypes.

#4111 Comprehensive multi-omics characterization of colorectal cancer in a community catchment population.

Brigette Waldrup[1], Francisco Carranza[1], Yuxin Jin[1], Yonatan Amzaleg[1], Mackenzie Postel[2], David W. Craig[3], John D. Carpten[3], Boudoir Salhia[4], Charite N. Ricker[5], Julie O. Culver[5], Carmen E. Chavez[6], Mariana C. Stern[7], Lourdes Baezconde-Garbanati[7], Heinz-Josef Lenz[5], Enrique I. Velazquez-Villarreal[3]

[1]City of Hope, Beckman Research Institute, Department of Integrative Translational Sciences, Duarte, CA,[2]University of Southern California, Keck School of Medicine of USC, Department of Translational Genomics, Los Angeles, CA,[3]City of Hope Comprehensive Cancer Center & Beckman Research Institute, Department of Integrative Translational Sciences, Duarte, CA,[4]University of Southern California, USC Norris Comprehensive Cancer Center and Keck School of Medicine of USC, Department of Translational Genomics, Los Angeles, CA,[5]University of Southern California, Keck School of Medicine & USC Norris Comprehensive Cancer Center and Keck School of Medicine of USC, Department of Translational Genomics, Los Angeles, CA,[6]University of Southern California, USC Norris Comprehensive Cancer Center, Los Angeles, CA,[7]University of Southern California, USC Norris Comprehensive Cancer Center & Keck School of Medicine of USC, Department of Population and Public Health Sciences, Los Angeles, CA

Introduction: Colorectal cancer (CRC) remains a leading cause of cancer mortality and disproportionately affects Hispanic and Latino populations in the United States, who remain underrepresented in genomic research. To address this gap, we performed a comprehensive multi-omics analysis to identify biological and genetic factors contributing to CRC disparities, including somatic alterations, gene expression programs, and genetic similarity (NASEM terminology for genetic ancestry).

Methods: Through the Cancer Moonshot PE-CGS Network, we analyzed 204 paired primary CRC tumor/normal samples from individuals in the Los Angeles catchment area. For comparison, 3,920 Non-Hispanic White (NHW) CRC samples were evaluated using public datasets, including AACR Project GENIE. DNA exome sequencing was used to assess somatic mutations, copy number alterations, gene fusions, and genetic similarity. RNA sequencing profiled differential gene expression, pathway activity, and immune signatures. Analyses followed NASEM best practices for the use of race, ethnicity, and genetic ancestry in genomics research.

Results: Genetic similarity analysis identified a high prevalence of Peruvian-from-Lima-like (1KG-PEL-like) similarity among Hispanic and Latino patients. Higher 1KG-PEL-like similarity was associated with microsatellite stability status, younger age at diagnosis, and left-sided tumor location. Somatic analysis revealed significant alterations in APC, TP53, KRAS, and other CRC-associated genes, with notable differences in mutation frequencies compared with NHW samples. Copy-number profiling identified amplifications in drug-targetable loci, and fusion analysis detected clinically relevant events including ALK, FGFR1, RAF1, and enriched PTPRK fusions in tumors with the highest 1KG-PEL-like similarity. Transcriptomic analyses demonstrated distinct pathway activation and immune-related expression programs compared with NHW CRCs.

Conclusion: This study provides one of the most comprehensive multi-omics characterizations of CRC in an underrepresented population. By integrating genetic similarity with somatic, structural, and transcriptional features, these findings reveal biologically meaningful patterns that may contribute to CRC disparities. This work establishes a foundational framework for future investigations and supports the development of ancestry-informed precision oncology strategies.

#4112 Identification of NTRK missense mutations in glioblastoma multiforme: Insights from AACR Project GENIE and structural-functional analyses.

Jehad A. Yasin[1], Muaath I. Alsufi[1], Ahmad Shawabkeh[1], Abdallah Al-Ramadi[1], Mohammad Alghaniem[1], Layan AlDaher[1], Reger Mikaeel[2]

[1]School of Medicine, The University of Jordan, Amman, Jordan,[2]Department of Pathology and Immunology, Washington University School of Medicine, Saint Louis, MO

Background: Neurotrophic tyrosine receptor kinase (*NTRK*) alterations are oncogenic drivers in diverse malignancies; however, their relevance in glioblastoma multiforme (GBM) is incompletely defined. While *NTRK* fusions have been well characterized, the prevalence, pathogenicity, and potential clinical impact of *NTRK1/2/3 missense mutations* in GBM remain largely unexplored. Using the AACR Project GENIE registry (v18.0), we profiled *NTRK* missense variants in GBM and integrated survival and structural analyses to evaluate their functional significance.
Methods: Data from 7048 GBM samples (6523 patients) were curated. Post-sequencing overall survival (OS) was assessed by exploratory Kaplan-Meier (KM) and univariate Cox regression. Pathogenicity and structural consequences were evaluated through AlphaMissense, REVEL, LoGoFunc, PROVEAN, MutPred2, and DynaMut on AlphaFold-predicted structures.
Results: Missense mutations in *NTRK1* (1.8%), *NTRK2* (1.3%), and *NTRK3* (1.3%) were rare. Four variants were consistently detected in the extracellular domain: *NTRK2* p.Y359D (0.23%), *NTRK2* p.G344D (0.21%), *NTRK1* p.H298Q (0.25%), and NTRK1 p.P302S (0.23%). In NTRK1, 15/16 patients carried both p.H298Q and p.P302S together, while isolated p.H298Q (n = 1) or p.P302S (n = 0) events were rare. A similar pattern was observed in NTRK2 p.Y359D/p.G344D mutants, where p.Y359D and p.G344D co-occurred in 14/15 patients, indicating co-mutation enrichment. KM analysis suggested a trend toward improved OS for p.Y359D (p = 0.047) and H298Q (p = 0.037). Cox regression pointed to protective effect of p.H298Q (HR = 0.32, 95% CI: 0.103-0.992). AlphaMissense classified p.Y359D and p.G344D as 'likely pathogenic' and p.H298Q/p.P302S as 'likely benign', whereas PROVEAN predicted all four as deleterious. DynaMut suggested destabilization for p.Y359D (ΔΔG –2.48 kcal/mol) and increased flexibility, while it demonstrated stabilization for p.H298Q (ΔΔG +0.261 kcal/mol), consistent with its gain-of-function classification by LoGoFunc, and low REVEL score of 0.104. MutPred2 analysis signaled functional impact for p.Y359D, which showed a high pathogenicity score (0.923; REVEL score = 0.910) with coordinated disruption of regulatory motifs and mechanistic changes, including gain of loop structure, loss of a sulfation site at p.Y359, altered ordered interfaces, and perturbed metal binding.
Conclusions: This analysis suggests that previously underrecognized NTRK missense mutations may be present in GBM and could have functional relevance; however, these findings should be interpreted cautiously given the study's retrospective registry design, reliance on tumor-only sequencing (with potential germline or passenger variants), incomplete clinical and molecular covariates, lack of multiple-testing adjustment, and the absence of experimental validation.

#4113 Distinct clinical, molecular and multi-omics biomarkers in early-onset head and neck squamous cell carcinoma.

Joab O. Odera[1], Rong Jiang[2], Morgan C. Byrd[1], Oyomoare L. Osazuwa-Peters[3], Nosa Osazuwa-Peters[1]

[1]Duke University School of Medicine, Durham, NC,[2]Head and Neck Surgery & Communication Sciences, Duke University School of Medicine, Durham, NC,[3]Department of Population Health Science, Duke University School of Medicine, Durham, NC

Background Early-onset head and neck squamous cell carcinoma (EOHNSCC) incidence is rising globally, often independent of traditional risk factors such as tobacco and alcohol. Whether EOHNSCC harbors distinct molecular and multi-omics signatures compared to typical-onset HNSCC (TOHNSCC) remains poorly understood.

Methods We analyzed The Cancer Genome Atlas (TCGA) Firehose Legacy and AACR GENIE datasets to compare EOHNSCC (18-49 years) and TOHNSCC (>49 years) HNSCC. Features included somatic mutations, copy number alterations (CNAs), structural variants, gene fusions, DNA methylation, mRNA expression, and protein expression. HNSCC onset group differences were assessed for significance using Fisher's exact and Wilcoxon rank sum tests ($p < 0.05$). Pathway enrichment leveraged GO, KEGG, Reactome, and CORUM databases. Multivariable logistic regression evaluated associations between EOHNSCC and clinical covariates.

Results Across both datasets, our study cohort was composed of 2,472 individuals with HNSCC ($N_{AACR\ GENIE}$= 1,961; N_{TCGA}=511). In AACR GENIE, EOHNSCC patients were more likely female (aOR = 1.49, 95% CI: 1.09-2.02), non-white (aOR = 1.99, 95% CI: 1.38-2.83), and had lower mutation burden (aOR = 0.44, 95% CI: 0.29-0.64). However, in TCGA, EO-HNSCC patients had lower histological grade tumors (G3 vs G1 aOR = 0.38, 95% CI: 0.14-1.00), more likely to receive neoadjuvant therapy (aOR = 17.02, 95% CI: 3.32-101.65), and had little to no prior smoking history (reformed vs non-smoker: aOR = 0.28, 95% CI: 0.13-0.57). Molecular markers in TCGA for EOHNSCC was characterized by concurrent mutation and mRNA overexpression in *GDNF, FRYL, KIAA0586, CADPS, MYF5*, and *DCTN1*, enriched in hypoxia-related pathways. Integration of CNAs and expression highlighted *ASH2L* and *SERPIND1*, which are associated with cell cycle regulation signaling. Methylation-driven expression involved motility genes (*SPIPM6, SPAG6, ODAD3, RSPH4A*), enriched in cilium movement and DAP12 signaling. *HSPA2* hypomethylation was correlated with *HSPA2* CNA and upregulated mRNA expression, linked to cancer invasion and metastasis. Genes with mRNA-protein concordance included *NOTCH1, SYK, SERPINE1, IRS1, CHEK2, EIF4E*; associated with translation initiation. In AACR GENIE, EOHNSCC showed higher KCNIP1 mutation, while TOHNSCC was enriched for *NOTCH1, FAT1, KMT2D*, and *PIK3CA*. Of note, *FAT1* was the only gene mutated in both datasets; consistently in TOHNSCC.

Conclusions EOHNSCC exhibits distinct multi-omics signatures involving hypoxia, cell motility, cell cycle regulation, cancer metastasis, and translation initiation. Candidate biomarkers include *GDNF, ASH2L, SPAG6, HSPA2, EIF4E* and *KCNIP1*. Minimal overlap across datasets underscores the need for validation and exploration of prognostic and therapeutic implications.

#4114 Population-based patterns of human papillomavirus infections and cervical cancer incidence, driver mutations and overall survival.

S. Ahmed Hussain[1], Chunqiao Tian[2], Christopher Tarney[1], Thomas Beltran[3], Pouya Javadian[1], Ryan McLaughlin[4], Paulette Mhawech-Fauceglia[5], Doris M. Benbrook[6], Sean Cronin[1], Zachary Kopelman[1], Colin Sitler[3], Leslie M. Randall[7], John Chan[8], Daniel Kapp[9], Chad A. Hamilton[10], Charles A. Leath[11], Christina Washington[12], Kathleen Moore[12], Kristen Bunch[1], Nicholas Bateman[2], Thomas P. Conrads[13], G. Larry Maxwell[13], Kathleen M. Darcy[14]

[1]Walter Reed National Military Medical Center, Bethesda, MD,[2]The Henry M Jackson Foundation for the Advancement of Military Medicine, Bethesda, MD,[3]Womack Army Medical Center, Fort Liberty, NC,[4]Uniformed Services University of the Health Sciences, Bethesda, MD,[5]Aurora Diagnostics, Las Vegas, NV,[6]OU Health Stephenson Cancer Center, Oklahoma City, OK,[7]Mid-Atlantic Gynecologic Oncology and Pelvic Surgery Associates, Falls Church, VA,[8]California Pacific Medical Center, San Fransisco, CA,[9]Stanford University School of Medicine, Stanford, CA,[10]The Ochsner Cancer Institute, New Orleans, LA,[11]University of Alabama at Birmingham, Birmingham, AL,[12]Oklahoma University Health Sciences Center, Oklahoma City, OK,[13]Women's Health Integrated Research Center, Falls Church, VA,[14]Henry M. Jackson Foundation, Bethesda, MD

Background: Human papillomavirus (HPV) infection is the primary cause of cervical carcinoma. Variations in HPV prevalence, tumor genomic alterations, and survival outcomes across population groups remain incompletely characterized. Understanding the interplay of viral and host tumor biology is essential to optimize prevention and treatment in cervical cancer.

Methods: High-risk HPV prevalence was evaluated in non-Hispanic White (NHW), non-Hispanic Black (NHB), and Hispanic (HSP) females aged 18-59 years using the National Health and Nutrition Examination Survey (NHANES, 2005-2016). Age-adjusted incidence of cervical cancer was evaluated using data from 21 regions in SEER (2004-2020). Somatic driver mutations were analyzed in tumors from patients with cervical cancer using the Genomics Evidence Neoplasia Information Exchange (GENIE v16.0). Overall survival was examined using Kaplan-Meier and Cox regression models among stage I-IV cervical cancer cases in the National Cancer Database (NCDB, 2004-2020).

Results: Among 11,033 NHANES participants, high-risk HPV prevalence was similar in White and Hispanic women but higher in Black women (2.1-fold higher odds of any HPV infection; 1.5-fold higher odds of HPV16/18). Fig 1A shows the higher distribution of high-risk HPV genotypes individually and concurrent high-risk infections in NHB patients compared with either HSP or NHW patients. Data from SEER shows that age-adjusted incidence of cervical cancer was higher in both HSP and NHB patients compared with NHW patients. Rates declined in all groups from 2004-2000 (Fig 1B). Fig 1C displays somatic mutations in tumors from 595 cervical cancer patients in GENIE. BRD4, ERBB3, MTOR, and GRM3 mutations were more frequent in NHB than NHW patients. ERBB3, CIC, PIK3R1, and PI3K pathway alterations were enriched in NHB compared with HSP patients, whereas SMARCA4, CIC, KDM5C, and RANBP2 mutations were more common in White than Hispanic patients. In 117,170 NCDB cases, 5-year survival was 76% for HSP, 69% for NHW, and 60% for NHB patients (Fig 1D, $p<0.0001$). Compared with HSP women, mortality risk was 40% worse for NHW and 91% worse for NHB patients ($p<0.001$).

Conclusions: Differences in HPV infection pattern are linked with cervical cancer incidence, somatic mutations, and survival, reflecting biologic and clinical heterogeneity across populations. Integrating viral genotyping with incidence rates and tumor molecular profiling may inform precision prevention, risk assessment, and personalized treatment to improve outcomes for all patients.

Translational Relevance: This study links viral, incidence, genomic and survival data across multiple national datasets to reveal population-level variations in cervical cancer. These insights support efforts to enhance HPV vaccination, early detection, and individualized prevention, screening and therapeutic decision-making.

#4116 Clonal trajectories of chronic lymphocytic leukemia and Richter transformation over the patients' lifespan.

Ian Marquez-Lopez[1], Aleix Real[1], Nuria Russinol[1], Nicholas Williams[2], Romina Royo[3], Markus van Roosmalen[4], Heribert Playa-Albinyana[1], Juan Antonio Pineyroa[1], Melika Bashiri[1], Pablo Mozas[5], Armando Lopez-Guillermo[5], Julio Delgado[5], Dolors Colomer[1], Ruben van Boxtel[4], Jyoti Nangalia[2], Elias Campo[1], Ferran Nadeu[1]

[1]IDIBAPS, Barcelona, Spain,[2]Wellcome Sanger Institute, Cambridge, United Kingdom,[3]Barcelona Supercomputing Center, Barcelona, Spain,[4]Princess Maxima Center for Pediatric Oncology, Utrecht, Netherlands,[5]Department of Hematology, Hospital Clinic, Barcelona, Spain

Richter transformation (RT) is a rare but clinically challenging event in the evolution of chronic lymphocytic leukemia (CLL), characterized by transformation of CLL into an aggressive lymphoma, commonly diffuse large B-cell lymphoma. Although the molecular profiles of CLL and RT are well characterized, their evolutionary trajectories remain uncertain. A better understanding of CLL and RT dynamics could enable earlier identification and intervention in high-risk patients. Thus, our aim was to trace CLL/RT clonal histories over the lifespan of the patients through tumor phylogenies.
To that aim, we applied primary template-directed amplification-based single-cell whole-genome sequencing to 5 patients, analyzing 349 single cells from up to 6 sequential time points spanning up to 19 years from CLL diagnosis to RT. A bioinformatic workflow that integrates existing algorithms with an in-house PTA-artifact filtering strategy was developed to optimize the sensitivity and specificity of the variant calling. A median sensitivity of 87.7% was obtained for point mutations at a sequencing depth of ~20×, with only ~5% of cell-specific artifacts remaining.
Our analyses revealed an increased mutational burden from normal B-cells to CLL and from CLL to RT explained by the combination of therapy-related and cell-intrinsic mutational processes. In addition, a high intratumor heterogeneity was detected both in terms of somatic mutations and copy number alterations, which was not previously captured by bulk sequencing. The phylogenetic reconstruction revealed remarkable intrapatient parallel genomic evolution. This was exemplified by the independent acquisition of multiple del(13q) in 3 cases, del(9p21) in 2 cases, or 7 LOH(17p) in 4 different phylogenetic clades with distinct *TP53* mutations in 1 patient.
Next, we used clock-like mutations to time the acquisition of genetic drivers, the diversification steps between CLL and RT, and their clonal bursts, which are indicative of periods of rapid proliferation. These analyses revealed that initial CLL genetic drivers were acquired up to 30 years before diagnosis. However, abrupt clonal bursts were not triggered by these genetic drivers, suggesting that cell-extrinsic factors such as B-cell receptor stimulation or microenvironmental changes could initiate the expansion of CLL. On the other hand, RT diversifies from the CLL early, including before CLL diagnosis. However, these clones follow a years-long process of clonal evolution in which the acquisition of high genomic complexity at advance stages facilitates their final outgrowth.
Overall, this study provides a roadmap of the origin, early diversification steps, and evolution of CLL and RT with potential clinical implications for early detection and intervention, while providing a framework for the study of the evolution of other hematological and solid tumors.

: Application of Bioinformatics to Cancer Biology 4
Poster Session

#4121 Incorporation of cut-point robustness in the discovery and evaluation of molecular cancer biomarkers using SCRIBE (Survival Cut-point Reporting and Integrative Biomarker Evaluation).

Miguel Lopez de Rodas Gregorio[1], Barani Kumar Rajendran[1], Javier Ramos Paradas[1], Carlos E. de Andrea[2], David L. Rimm[3], Hongyu Zhao[4], Kurt Alex Schalper[1]

[1]Pathology, Yale School of Medicine, New Haven, CT,[2]Pathology, Clinica Universidad de Navarra, Pamplona, Spain,[3]Yale School of Medicine, New Haven, CT,[4]Yale School of Public Health, New Haven, CT

Precision oncology relies on the use of biomarkers for matching cancer patients with specific therapies aiming to maximize efficacy and minimize toxicity. Although a large number of candidate biomarkers are reported, only few of them show adequate performance in independent studies and are implemented clinically. Major limitations of molecular biomarker studies in oncology include the utilization of individual cohorts and the selection of single, and arbitrary cut-points to stratify patients that increase the risk of false discovery and data overfitting. To address this challenge, we introduce a novel concept for biomarker discovery, development, prioritization and validation incorporating the cut-point robustness along ranges of consecutive cut-points as a critical parameter. We also report SCRIBE, a novel and user-friendly automated computational tool for simultaneous analysis, and discovery of biomarkers and their impact along cut-point ranges in independent datasets. To illustrate the performance of our approach, we used SCRIBE to assess the biomarker potential of the mRNA expression levels of 13 HLA class II antigen-presentation machinery genes in baseline tumor samples from three independent cohorts of patients with lung adenocarcinoma. Our analysis identified *HLA-DQB1* as the HLA class-II gene with the most robust prognostic association. The analysis of two cohorts identified the optimal cut-point range between the 44^{th} and 57^{th} percentiles. To define a single cut-point, we selected the percentile with the strongest hazard ratio effect, which corresponded to the 49^{th} percentile. We applied this cut-point to the three cohorts and found that higher levels of *HLA-DQB1* were significantly associated with longer overall survival. Using Cox proportional hazard models including *HLA-DQB1* and stage, both features were significantly and independently associated with survival in the cohorts. Finally, we performed an unsupervised discovery analysis of the whole transcriptome incorporating the cut-point robustness and identified genes with prominent and previously unreported association with prognosis in patients with lung adenocarcinoma. Notably, *AVEN* emerged as the top gene with a dramatic negative survival effect. We provide a novel conceptual framework for biomarker studies incorporating the cut-point robustness as a key property. We also provide a novel integrative computational tool for automated analysis of multiple biomarkers incorporating relevant cut-point ranges and other properties to enhance the impact of biomarker studies. We envision SCRIBE as a valuable tool for researchers and clinicians seeking to improve the reproducibility and applicability of biomarker studies and to support the development and clinical use of existing and novel biologically driven anti-cancer therapies.

#4122 Identification of molecular signatures in pancreatic ductal adenocarcinoma through multiomics.

Benjamin Miao[1], Tung-Shing Mamie Lih[2], Yingwei Hu[2], Hui Zhang[2]

[1]Johns Hopkins Univeristy, Baltimore, MD,[2]Johns Hopkins University School of Medicine, Baltimore, MD

Pancreatic ductal adenocarcinoma (PDAC) is among the deadliest malignancies, with a dismal five-year survival rate. Despite continuous efforts to study its molecular signatures, the high degree of tumor-associated cellular heterogeneity in PDAC introduces extraneous microenvironmental components that complicate analysis. In recent years, multi-omics approaches have shown promise in deconvoluting cellular composition and enabling more specific, comprehensive cancer profiling. To better characterize PDAC, in this study, we analyzed transcriptomic and proteomic data from 140 tumor tissues with 67 paired normal adjacent tissues, along with single-cell RNA sequencing data from 73 tumor tissues. Using this integrative approach, we successfully attributed molecular signatures to distinct cell-type populations. Overall, we found 59 tumor-cell derived PDAC molecular signatures and evaluated them for functional relevance, prognostic value, and potential therapeutic implications. Among these, we identified molecular targets associated with increased tumorigenic activity and immunosuppression. Moreover, survival analysis of protein phosphorylation and overall expression informed prognostic significance for potential targets. Notably, we found that several phosphorylation changes correlate with poor patient survival, suggesting potential paths for therapeutic intervention by targeting protein post-translational modifications. Our study provides a detailed understanding of PDAC through characterization of key tumor-specific signatures that could serve as potential targets to help improve clinical outcomes for this disease.

#4123 Dissecting the baseline tumor microenvironment in mNSCLC by transcriptional profiling identifies tumor microenvironmental conditions predictive for immunotherapy response.

Lilian van Vlerken-Ysla[1], Arash Nabbi[2], Zhou Zhu[3], Ross Stewart[4]

[1]Early Oncology Translational Medicine, AstraZeneca, Gaithersburg, MD,[2]Early Oncology Data Sciences and AI, AstraZeneca, Mississauga, ON, Canada,[3]Early Oncology Data Sciences and AI, Astrazeneca, Gathersburg, MD,[4]Early Oncology Translational Medicine, Astrazeneca, Cambridge, United Kingdom

Background: The MYSTIC trial (NCT02453282), a phase 3 study of durvalumab ± tremelimumab vs. standard of care (SOC) chemotherapy in 1L metastatic NSCLC, did not meet its primary endpoint of overall survival (OS) in the intent-to-treat (ITT) population. This analysis aimed to identify whether baseline tumor-immune microenvironment (TME) features were predictive for either favorable or poor response to durvalumab (D) ± tremelimumab (T) treatment in this patient population.
Methods: RNA sequencing was performed on baseline tumor samples from 185 patients in the MYSTIC biomarker-evaluable population (BEP). Non-negative matrix factorization (NMF) was used to resolve distinct clusters based on the expression of the top 10% most variable protein-coding genes. The resulting clusters were analyzed for differences in clinical outcomes, genomic alterations, immune cell composition, pathway activity, and T-cell and B-cell repertoire.
Results: NMF identified four distinct clusters within the MYSTIC BEP population of which two clusters were notably characterized by tumor immune grouping. Cluster 1 (20% of patients) exhibited hallmarks of a pro-inflammatory TME, with high T-cell signatures, macrophage infiltration, and expression of checkpoint inhibitors. Patients in this cluster treated with D+T experienced a prolonged survival (mOS 19.78 months) compared with patients on this treatment in any of the other three clusters (HR 0.39, 95%CI 0.15-1). Cluster 1 was also enriched for patients with PD-L1≥50%. Cluster 3 (20% of patients) displayed features associated with immune suppression, including high granulocyte and Treg infiltration, low macrophage signature, and enrichment of TGFbeta and stemness pathways. These patients experienced worsened survival outcomes when treated with D+T (mOS 2.17 months), compared to other clusters (HR 3.13, 95%CI 1.48-6.6). Most notably, patients in cluster 3 had significantly worsened survival on D+T compared to patients in cluster 1 (HR 6.15, 95%CI 2.02-18.8). The remaining two clusters could be characterized by histology, with Cluster 2 (35% of patients) characterized by non-squamous histology and enrichment for STK11 and MYC alterations, and Cluster 4 (25% of patients) characterized by squamous histology, aggressive proliferation signatures, and enrichment for TP53, MLL2, PTEN, and PIK3CA alterations. Neither of these two clusters drove notable impact to D+T treatment.
Conclusions: NMF clustering of baseline MYSTIC tumor samples revealed distinct TME profiles linked to divergent immunotherapy responses. A pro-inflammatory cluster predicted benefit with D+T, while a suppressive cluster aligned with poor outcomes. Findings suggest response depends not just on overall immune infiltration but on the specific immune cell composition within the TME.

#4124 Cancer stem cells and where to find them: Their trajectories and implications in cancer evolution.

Zixuan Lan[1], Philip Awadalla[2]

[1]Molecular Genetics, University of Toronto, Toronto, ON, Canada,[2]Molecular Genetics, University of Oxford, Oxford, United Kingdom

Cancer cells are heterogeneous within and among biopsies and can be perceived as a hierarchical structure defined by growth potential, in which more stem-like cells are at the apex. Cancer stem cells (CSCs) thus represent a distinct subset of cancer cells with stemness properties that play a pivotal role in tumour growth, recurrence, and metastasis. How and where CSCs originate remain somewhat controversial as differentiated cells may also regain stemness-like properties through dedifferentiation, and CSC phenotypes can vary among patients and cancer types. To systematically identify and trace potential CSC populations in lung adenocarcinoma (LUAD), we implemented an integrative computational framework that leverages both genomic and transcriptomic features from single-cell RNA sequencing (scRNA-seq) datasets from LUAD patients. By reconstructing developmental trajectories, we defined differentiation states within malignant compartments and detected rare cancer cell subsets as candidate CSCs in each biopsy. We then inferred copy number variations (CNVs) for individual malignant cells and generated phylogenetic trees based on CNV patterns to reconstruct clonal evolution. Our analyses revealed that CSC-like cells not only emerged as early ancestral clones but also arose later during tumour evolution, exhibiting similar stemness programs but undergoing dedifferentiation. We also explored their spatial organization with Visium spatial transcriptomics, and we observed that CSC-like states localized to spatially variable regions and were found near immune and stromal niches, suggesting microenvironmental influences on stemness. Finally, through deconvoluting bulk RNA-seq data and performing survival analysis, we derived a stemness signature capable of stratifying patient disease outcomes. In summary, this integrated multi-modal analysis provides insights into the identity, evolutionary dynamics, spatial distribution, and clinical relevance of CSCs in LUAD. Our approach offers a foundation for identifying CSC-driven mechanisms of tumour progression in LUAD and other cancers, and new biomarkers for prognosis and therapy response.

#4125 Goblet cell appendiceal adenocarcinoma is molecularly distinct from other histologic subtypes: Insights from large-scale genomic, transcriptomic, and organoid modeling.

Saikat Chowdhury[1], Ichiaki Ito[1], Samuel Rivero-Hinojosa[2], Chia-Mei Young[1], Eleanor A. Fallon[3], Beth A. Helmink[1], Taylor Neilson[1], Vasily Aushev[2], Sacha El Khoury[1], Abdelrahman MG Yousef[4], Mahmoud Mohamad Gamal Yousef[5], Shruti Sharma[2], Robert Lentz[2], Adham Jurdi[2], Paul F. Mansfield[1], Keith Fournier[1], Yuan-Hung Lo[1], Michael G. White[1], John Paul Shen[1]

[1]UT MD Anderson Cancer Center, Houston, TX,[2]Natera, Inc., Austin, TX,[3]Roswell Park Comprehensive Cancer Center, Buffalo, NY,[4]University of New Mexico Health Sciences Center, Albuquerque, NM,[5]Upstate Medical University, New York, NY

Background: Appendiceal Adenocarcinoma (AA) is a rare cancer, though recent data indicate a rising incidence, now exceeding 1 per 100,000 individuals annually. Goblet cell adenocarcinoma (GCA) of the appendix, which accounts for ~15% of all AA, is associated with worse survival than non-goblet AA. To elucidate the unique tumor biology of GCA, we systematically compared the genomic and transcriptomic landscapes of GCA versus non-GCA AA, identifying GCA-specific driver mutations and dysregulated pathways that distinguish GCA from other AA histologic subtypes.

Methods: Whole-exome sequencing (WES) data from 1,202 AA tumors were generated as part of the standard workflow for personalized, tumor informed circulating tumor DNA testing (Signatera^{TM}), including 385 patients with GCA, 450 with mucinous, 206 with enteric-type, and 161 with signet ring cell histology. Transcriptomic profiling was available for 63 tumors (n=25 GCA, 38 non-GCA) using Altera^{TM} tumor genomic profiling test (Natera, Inc.). Isogenic organoids with gene knock-out (KO) were generated using CRISPR/Cas9 in a *KRAS/GNAS* co-mutant murine tumor.

Results: There were striking differences in the somatic mutation landscapes between GCA and non-GCA tumors, with frequent *mutations in KRAS (73.4%), TP53 (39.5%), and GNAS (36%)* in non-GCA tumors. In contrast, GCA did not harbor a single gene mutation in more than 20% of the cohort. In GCA, the most commonly mutated gene was *ZFP36L2* (18%), a zinc finger protein that binds and stabilizes mRNA transcripts, and has previously been reported to inhibit cell proliferation. Other commonly mutated genes in GCA included *TP53* (17%) and *SMAD4* (10%), with only 10% of tumors harboring *KRAS* mutations. Transcriptional regulators such as *WTAP* (9%), *SOX9* (8%), *ARID1A* (7%), *MLLT4* (7%), *KMT2D* (7%), and *KMT2B* (4%) were also frequently altered. Performing Gene Set Enrichment Analysis (GSEA) on the differentially expressed genes between GCA and non-GCA tumors revealed that the bile acid and adipogenesis pathways were upregulated in GCA. Survival analysis showed worse OS in GCA vs non-GCA AA (94.7 months vs not reached; HR 3.51, 95% CI 2.67-4.63; $p < 0.0001$). To explore the potential significance of *ZFP36L2,* organoids derived from *ZFP36L2* KO showed decreased doubling time and allowed propagation of the organoid culture without doxycycline-induced expression of GNAS^{R201C}, a known oncogenic driver in AA. Transcriptomic analysis comparing *ZFP36L2* KO to parental lines showed enrichment for androgen response, EMT, TNFα, Wnt, Hedgehog, KRAS, and TGFβ signaling.

Conclusion: Clear molecular differences between GCA and the more common mucinous AA were observed. It is clear that strategies for developing new drugs for AA must treat GCA as a distinct entity and not merge these patients with other histological subtypes, as has frequently been done previously.

#4126 Quantification of step-specific selection reveals ordered acquisition of driver mutations in colon cancer.

Kira A. Glasmacher, Jeffrey Peter Townsend

Yale University, New Haven, CT

Colorectal cancer is a leading cause of cancer mortality worldwide. Colon adenocarcinoma develops through sequential evolutionary steps originating in adenomatous polyps. Many driver mutations of colon cancer and their relations have been hypothesized. However, quantitative timing and strength of selection across specific stages of progression remains unknown. Somatic single nucleotide variants from colon adenomas and adenocarcinomas were analyzed using a step-specific likelihood model that treats adenoma formation and malignant progression as consecutive steps within a shared evolutionary trajectory. Analyses were stratified by *POLE*/*POLD1* mutation and DNA mismatch repair (MMR) status to evaluate background-specific effects. We identified mutations under positive selection during initial formation of adenomas and later in malignant progression to adenocarcinomas, and also quantified how each successive driver changes selection on the next. Many trends of step-specific selection emerged that were consistent across *POLE*/*POLD1*-mutant and MMR-deficient tumors, such as high early selection on *APC* and strong late selection on *CTNNB1* and *TP53*. However, step-specific selection varied across the steps of progression in mutants of other genes, including *KRAS*, *BRAF*, and *FBXW7*. Inferred evolutionary trajectories point to early disruption of WNT and TGF-β signaling, followed by later acquisition of TP53, MAPK, and PI3K pathway mutations. These findings provide a data-driven, high-resolution temporal sequence of the selective pressures shaping tumorigenesis. They identify potential biomarkers for early detection, and reveal how polymerase and mismatch-repair backgrounds alter evolutionary paths by purely altering gene- and site-specific mutation rates. Consistency with experimentally identified early drivers (*APC*, *KRAS*) and late drivers (*TP53*) validates the approach and demonstrates its suitability for extending step-specific analyses to many additional cancer types. Ultimately, such high-resolution evolutionary trajectories enable precision-medicine targeted drug treatments to be exquisitely tailored to individual patients and facilitate treatments that not only target extant variants but also anticipate additional therapies that could be useful to forestall or prevent the next driver mutation and consequent burgeoning tumor burden.

#4127 Inferring transcriptomic programs from circulating tumor DNA methylation signatures in small cell lung cancer using RRBS and EM-seq.

Yuanxin Xi[1], Allison Stewart[2], Lixia Diao[1], Qi Wang[1], Li Shen[1], Runsheng Wang[2], Alberto Duarte[2], Alexa Halliday[2], Kavya Ramkumar[2], Robert Cardnell[2], Bingnan Zhang[2], Carl M. Gay[2], Lauren A. Byers[2], **Jing Wang**[1]

[1]Bioinformatics and Computational Biology, UT MD Anderson Cancer Center, Houston, TX,[2]Thoracic/Head & Neck Medical Oncology, UT MD Anderson Cancer Center, Houston, TX

Background: Small cell lung cancer (SCLC) exhibits profound epigenetic remodeling and transcriptional plasticity, yet tissue scarcity limits multi-omic profiling. Circulating tumor DNA (ctDNA) methylation analysis via reduced representation bisulfite sequencing (RRBS) or enzymatic methyl-seq (EM-seq) provides a minimally invasive window into tumor biology. However, the relationship between ctDNA methylation features and transcriptomic states such as epithelial-mesenchymal transition (EMT) or neuroendocrine (NE) differentiation remains poorly defined but may serve as means to monitor patient therapeutic response.
Methods: We analyzed matched ctDNA methylation RRBS and bulk RNA-seq data from N = 43 SCLC patients collected at baseline. CpG methylation levels were quantified and mapped to gene bodies, promoters, and distal regulatory regions. To capture functional methylation signatures, CpG sites were ranked by their correlation with RNA expression of the corresponding genes and by feature importance predicting expression levels or calculated transcriptomic scores (e.g., EMT, MYC, ASCL1/NEUROD1 subtype indices). High-ranking CpG sites were aggregated into gene-level and pathway-level signatures, followed by GO and KEGG enrichment analyses to identify key regulatory networks. These were further evaluated in SCLC patients treated longitudinally with frontline chemotherapy.
Results: Genome-wide ctDNA methylation profiles predicted bulk RNA-seq-derived gene expression as well as predefined score metrics (such as EMT score, NE score) with high concordance (Wilcoxon $R^2 = 0.63 \pm 0.07$, $p < 0.001$). Ranking analysis revealed that predictive CpG sites were enriched in enhancer and promoter regions associated with EMT regulators and NE lineage genes. Functionally, GSEA further linked high NE scores to activation of Hedgehog signaling, and EMT scores to enrichment of G2/M checkpoint pathways, suggesting distinct regulatory programs underlying SCLC phenotypes.
Conclusions: Integrative analysis of ctDNA methylation and transcriptomic data reveals that ranked, functionally annotated CpG features can accurately infer gene expression programs and biological states in SCLC. These approaches provide a mechanistic framework to interpret ctDNA methylation signatures and enable noninvasive characterization of tumor subtypes and therapeutic resistance in SCLC patients.

#4128 Proteomic signatures of tumorigenicity, immune evasion, and multidrug resistance in a murine T-cell lymphoma with CNS/ocular tropism.

Ori Braitbard[1], Jacob Hochman[2]

[1]The Department of Bioinformatics, Jerusalem College of Technology, Jerusalem, Israel,[2]Alexander Silberman Institute of Life Sciences, The Hebrew University of Jerusalem, Jerusalem, Israel

Background: The S49 T-cell lymphoma and its derivative sublines provide a powerful model to dissect how T cell lymphomas acquire tumorigenicity, evade immune surveillance, develop multidrug resistance, and disseminate to the CNS and eyes. The malignant suspension growing line T-25 contrasts with three derivatives: an immunogenic non-tumorigenic adherent T-25-Adh cell line, a tumorigenic revertant Rev-2-T-6, and a MDR1 overexpressing HU-1 cell line, which is drug-resistant yet non-tumorigenic in adults (derived from T-25-Adh). Rev-2-T-6 and HU-1 cell lines are capable of CNS/ocular metastasis in neonates.
Methods: We used label-free quantitative proteomics to define programs that underlie these divergent phenotypes. Biological triplicates of T-25, T-25-Adh, Rev-2-T-6, and HU-1 cells were analyzed and compared by high-resolution LC-MS/MS, and proteins were quantified using MaxQuant LFQ. We quantified 3,500 proteins across all lines with high reproducibility.
Results: Unsupervised clustering and PCA showed tight triplicate clustering, with T-25 clearly separated from the other variants; HU-1 and T-25-Adh clustered together, and Rev-2-T-6 occupied an intermediate position, consistent with its partial revertant phenotype. Compared to T-25 cells, HU-1, Rev-2-T-6, and T-25-Adh showed 17, 19, and 29 significantly regulated proteins, respectively. HU-1 was enriched for cAMP-related, nuclear envelope, and RNA-processing proteins, together with marked MDR1 overexpression. It showed reduced MHC-I heavy chains and ribosomal components. This is consistent with immune evasion and altered mitochondrial function in a multidrug-resistant yet non-tumorigenic background. Rev-2-T-6 up-regulated cAMP and DNA-replication factors down-regulating MHC-I and mitochondrial enzymes, supporting proliferative, glycolysis-shifted “revertant” state. T-25-Adh displayed down-regulation of cell-cycle and oxidative phosphorylation proteins, defining an adherent, immunogenic, non-tumorigenic program.
Conclusions: The present proteomic atlas of S49-derived lymphoma lines reveals shared and lineage-specific signatures of malignancy, immune escape, and drug resistance. Loss of antigen presentation and mitochondrial metabolism, together with activation of cAMP and proliferative programs, characterizes tumorigenic cells, whereas the immunogenic adherent phenotype is associated with reduced proliferation, metabolic down-shifting, and enhanced adhesion/immune pathways. MDR1 up-regulation in HU-1 decouples drug resistance from tumorigenicity while preserving CNS/ocular tropism. These data nominate antigen-processing machinery, cAMP signaling, mitochondrial metabolism, and ABC transporters as biomarkers and therapeutic targets in CNS-tropic lymphomas and provide a framework for comparative analyses with human T-cell malignancies.

#4129 Spatial single-cell transcriptomic profiling reveals distinct immune and stromal landscapes across TIL/PD-L1-defined TNBC subtypes.

Kyungsoo Kim[1], Soong June Bae[2], Yoonjin Cha[2], Yoonwon Kook[2], Ah Yoon Kim[2], Jee Hung Kim[2], Sung Gwe Ahn[2], Joon Jeong[2]

[1]Yonsei University, Seoul, Korea, Republic of,[2]Gangnam Severance Hospital, Seoul, Korea, Republic of

Purpose:
Triple-negative breast cancer (TNBC) displays marked heterogeneity in immune contexture, influencing response to immune checkpoint blockade. We aimed to characterize spatial and cellular differences among TNBC subtypes stratified by tumor-infiltrating lymphocytes (TILs) and PD-L1 expression using single-cell spatial transcriptomics.
Experimental Procedures:
We analyzed 36 TNBC cores using the Xenium platform (~5,000 genes per cell) and annotated major cell populations, including epithelial, fibroblast, and immune cells. Each core was classified into four TIL/PD-L1 subtypes ($TIL^+PD\text{-}L1^+$, $TIL^+PD\text{-}L1^-$, $TIL^-PD\text{-}L1^+$, and $TIL^-PD\text{-}L1^-$) based on histologic TIL density (≥30%) and PD-L1 CPS (≥10). Pairwise intercellular distances between tumor and stromal/immune cells were computed within a 50-μm radius to quantify spatial immune exclusion and stromal remodeling.
Results:
Distinct spatial and transcriptional profiles were observed among subtypes. $TIL^+PD\text{-}L1^+$ tumors exhibited dense immune infiltration and upregulation of antigen-presentation and T-cell activation genes in both $CD4^+$ and $CD8^+$ subsets. In contrast, $TIL^+PD\text{-}L1^-$ tumors showed prominent desmoplastic stroma and reduced immune-cell proximity, accompanied by fibroblast enrichment of *POSTN*, *FBLN1*, and *SFRP2*, suggesting extracellular-matrix remodeling that may hinder immune infiltration. Epithelial cells in $TIL^+PD\text{-}L1^-$ cores displayed higher expression of *XBP1*, *FOXA1*, and *MLPH*, indicating epithelial plasticity and potential immune evasion. Spatial mapping further revealed that tumor margins in $TIL^+PD\text{-}L1^-$ cores contained more aggressive epithelial phenotypes than corresponding cores in $TIL^+PD\text{-}L1^+$ tumors.
Conclusions:
Single-cell spatial transcriptomics delineated distinct immune and stromal architectures across TIL/PD-L1-based TNBC subtypes. The $TIL^+PD\text{-}L1^+$ subtype represents an immune-active microenvironment, whereas the $TIL^+PD\text{-}L1^-$ subtype demonstrates stromal-driven immune exclusion. These findings provide spatial evidence that combined assessment of TILs and PD-L1 can stratify TNBC patients by their potential responsiveness to immunotherapy.

#4130 Single-cell multi-omic characterization of gastric intestinal metaplasia reveals potential genetic, epigenetic and isoform signatures of lesions at high risk for GC progression.

Dongin Lee[1], Xiangqi Bai[1], Sue Grimes[1], Kyungtae Lee[1], Yan Wang[1], Charlotte Wong[1], Anuja Sathe[1], Ignacio Wichmann[1], Youlim Kim[2], Rithika Meka[1], Renee Long[1], Allison Im[1], Billy Lau[1], Robert Huang[1], Hanlee P. Ji[1]

[1]Medicine, Stanford University School of Medicine, Stanford, CA,[2]Microbiology and Immunology, Stanford University School of Medicine, Stanford, CA

Worldwide, gastric cancer (GC) is the fifth most common malignancy and the third leading cause of cancer-related deaths. Gastric intestinal metaplasia (GIM) is a precursor lesion of GC. However, only a small number of GIM lesions progress to GC. A key challenge is identifying the genomic, molecular and cellular features of GIM that predict their risk of becoming invasive cancer. Once these features are identified, one could “intercept” patients at high risk for developing GC. We conducted a single-cell multi-omic analysis of endoscopic biopsies of GIM lesions. These patients underwent GC risk evaluation using a two-biopsy approach. We used the pathology results to determine a clinical risk stage based on the Operative Link on Gastric Intestinal Metaplasia Assessment (OLGIM). Clinical stages include I and II which are low risk versus III and IV which are high risk. Each biopsy underwent single cell RNA-seq and single cell assay for transposase accessibility of chromatin (ATAC). Therefore, we had both of these genomic readouts for each cell. In addition, we used single cell long read sequencing to identify transcript isoforms and mutations. Overall, we obtained the following single cell cell features of GIM which included: (1) gene expression, (2) chromatin accessibility, (3) copy number aberrations, (4) somatic variants, and (5) isoform expression. We compared the single cell genomics features between high-risk and low-risk groups. For example, we observed that key genes specifically expressed in intestinal-like stem cells, which are linked to potential gastric cancer-initiating cells—such as *CDH17*, *SI* and *CPS1*—were more highly expressed among the high-risk group, which also exhibited increased chromatin accessibility at the same genes. Furthermore, we detected differential isoform usage of gastric-related genes between the two groups, which implies that isoform changes are related to GC progression. These findings provide genomic, molecular and cellular features of GIMs that are associated with high risk of developing GC.

#4131 Multi-omics characterization of PRMT5 inhibition identifies vulnerabilities for combination therapy in MTAP-deleted cancers.

Eliana Destefanis[1], Blanka Bordas[1], Jose C. Martinez[2], Samar Sayedyahossein[1], Samuel Moffitt[1], Enakireru M. Erhumuoghene[1], Daniel Dominguez[2], Kathleen M. Mulvaney[1]

[1]Fralin Biomedical Research Institute, Virginia Tech Cancer Research Center, Washington, DC,[2]University of North Carolina, Chapel Hill, NC

Homozygous deletion of CDKN2A on chromosome 9p21 is the most frequent genomic loss in cancer and often extends into the adjacent MTAP gene. This co-deletion occurs in ~10% of tumors (>200,000 cases annually in the U.S) and is particularly enriched in aggressive malignancies such as glioblastoma (GBM), malignant peripheral nerve sheath tumors (MPNST), pancreatic ductal adenocarcinoma (PDAC), and non-small cell lung cancer (NSCLC). In these tumors, MTAP loss leads to intracellular accumulation of its substrate methylthioadenosine (MTA), which partially inhibits protein arginine methyltransferase 5 (PRMT5) by competing with its methyl donor S-adenosyl-methionine (SAM) at the active site, reducing its ability to symmetrically dimethylate arginine residues (SDMA). This creates a synthetic-lethal dependence on residual PRMT5 activity and has driven the development of MTA-cooperative PRMT5 inhibitors, which show encouraging preclinical activity and single-agent response rates of 21-29% in early clinical trials in the advanced, refractory setting. We therefore hypothesized that defining the molecular consequences of PRMT5 inhibition could guide patient stratification and inform rational combination strategies capable of enhancing therapeutic efficacy and preventing resistance. To test this, we performed multi-omics profiling, including short- and long-read transcriptomics and whole-cell proteome mass spectrometry, across MTAP-deleted NSCLC, GBM, and PDAC models, integrating these data with in-house and publicly available datasets to define PRMT5-dependent methyl events and their downstream molecular consequences. Transcriptomic and proteomic analyses revealed strong and consistent pathway-level alterations across models following PRMT5 inhibition, including activation of MAPK signaling, a compensatory program validated to synergize with PRMT5 inhibitors in vitro and in vivo. Across eight distinct PRMT5 methyl-enrichment mass spectrometry studies, we identified 180 PRMT5 substrates enriched mainly for proteins involved in RNA metabolism and pre-mRNA splicing, including multiple snRNP-associated components of the spliceosome. We therefore examined the splicing consequences of PRMT5 inhibition and observed widespread increases in intron retention and reductions in exon skipping, with enrichment of splicing alterations in transcripts involved in DNA damage repair across models. Overall, this study provides a comprehensive substrate map of PRMT5 and characterizes the transcriptional, proteomic, and splicing programs activated upon its inhibition across MTAP-deleted GBM, NSCLC, and PDAC models. These findings highlight pathway and splicing-associated vulnerabilities as targets for rational combination strategies and establish a mechanistic framework to guide biomarker development and future therapeutic exploration.

#4132 Landscape of allele-specific expression in prostate cancer reveals recurrent, stage-specific events in AR signaling and resistance pathways.

Margaret Tsui[1], Kevin Hu[1], Hanbing Song[2], Sarah Hsu[1], Rebecca Chen[1], Lorraine Nuniz[1], Julia Pham[1], Chih-Hao Chang[1], Keliana Hui[1], David Quigley[3], Jingjing Li[4], Franklin Huang[1]

[1]Division of Hematology and Oncology, Dept. of Medicine, University of California San Francisco, San Francisco, CA,[2]University of California San Francisco, San Francisco, CA,[3]Urology, University of California San Francisco, San Francisco, CA,[4]Neurology, University of California San Francisco, San Francisco, CA

The effects of cis-regulatory alterations in prostate cancer (PCa) are insufficiently characterized, presenting an opportunity to discover driver genes and therapeutic targets. To comprehensively study these effects, we identify genes undergoing allele-specific expression (ASE) in localized PCa and metastatic castration-resistant PCa (mCRPC) samples. By defining recurrent ASE events across prostate tissue and tumor-enriched ASE, we develop CASEDI, a computational framework for prioritizing cancer drivers by integrating ASE and clinical data. CASEDI reveals genes showing recurrent ASE and altered expression in PCa, including AR-regulated and oncogenic ACSM1. mCRPC samples show enrichment of ASE in DNA repair, resistance pathways, and oncogenes and increased frequency of monoallelic expression (MAE) compared to localized tumors. We define an mCRPC gene signature based on MAE status that identifies a subgroup of localized patients with worse prognosis. Using ASE analysis, we expand the landscape of cis-regulatory events in PCa to inform the identification of additional therapeutic targets.

#4133 Single cell multi-omics enables molecular dissection of gastric cancer subtypes.

Junha Cha[1], Anuja Sathe[1], Yan Wang[2], Susan M. Grimes[3], Hanlee P. Ji[2]

[1]Stanford University School of Medicine, Stanford, CA,[2]Stanford University, Stanford, CA,[3]Medicine, Stanford University, Stanford, CA

Gastric cancer (GC) has different histopathological subtypes that include intestinal, diffuse, and mixed. These subtypes are identified based on histologic cell morphology and are clinically informative, more so than molecular subtypes. Namely, histologic subtypes differ in prognosis, rates of metastasis and treatment response. However, many questions remain about the genomic features that distinguish each histologic subtype. Integrating single-cell datasets is particularly challenging at the molecular level due to technical variation. We developed an integrative data set combining in-house and public multi-omics datasets - they include bulk sequencing, scRNA-seq, spatial transcriptomics, and proteomics. The scRNA-seq data included 208 tumors from 118 patients. This single cell data was harmonized to reduce the effects of batch variability. For analysis, we developed a computational pipeline incorporating generalized linear models, non-negative matrix factorization for meta-program identification, sample-level pseudo-aggregation and network-based gene expression analysis. This pipeline enabled gene-wise dissection, pathway-centric interpretation of malignant transcriptional programs and systematic quantification of cell state dynamics across integrated cohorts. We identified distinct tumor-intrinsic gene expression programs across subtypes. The intestinal and mixed tumors expressed immune-associated programs, while the MSI tumors exhibited elevated cell-cycle signaling compared to MSS. In the tumor microenvironment, the diffuse subtype showed reduced B-cell differentiation but increased dendritic cell abundance, whereas intestinal subtype was enriched for T-cell subtypes, including regulatory T cells with immunosuppressive potential. From the single cell results, we determined that TIGIT expression was significantly elevated among CD8 and regulatory T cells. This result was confirmed with multiplexed immunofluorescence staining on an independent set of 142 GCs. Fibroblast-driven interactions dominated diffuse tumors, while intestinal and mixed tumors displayed immune-mediated “hot tumor” phenotypes.

Overall, our study showed that the analysis of an integrated, harmonized single-cell data from GC revealed malignant and microenvironmental programs distinguishing subtypes. Our results provided some subtype-specific vulnerabilities and provides insight into potential future therapeutic targets.

#4134 A long-read sequencing and phylogenetic framework for improved detection and timing of overlapping and repetitive somatic structural variations.

Anton Goretsky[1], Yuelin Liu[1], Ayse Keskus[1], Tanveer Ahmad[1], Chi-Ping Day[2], Erin K. Molloy[3], Mikhail Kolmogorov[1]

[1]Cancer Data Science Laboratory, National Cancer Institute, National Institutes of Health, Bethesda, MD,[2]National Cancer Institute, National Institutes of Health, Bethesda, MD,[3]Department of Computer Science, University of Maryland, College Park, College Park, MD

Despite their accuracy in identifying single nucleotide variants (SNVs), current short-read sequencing technologies struggle to resolve repetitive regions and complex structural variants (SVs), as the reads are simply too short to span such challenging genomic segments. Mapping issues in homologous regions, the high barrier to accurate phasing, and other limitations increasingly point to long-read sequencing as a method to overcome these challenges. Here we develop a computational framework for harmonization and joint analysis of different variant types in the evolutionary context. We particularly focus on structural variants, as they have significant functional consequences and play a large role in driving cancer initiation and progression. As such, we explore the application of long-reads to improve precision breakpoint calling for structural variants in highly repetitive regions, demonstrating their efficacy in resolving complex structural variants. We use this framework to profile 23 subclones of a mouse melanoma cell line, characterized with distinct growth phenotypes and treatment responses. Uniquely, our framework reveals recurrent amplifications of putative driver genes across different lineages caused by independently acquired structural variants, suggesting parallel evolution. In addition, our approach revealed gradual and lineage-specific methylation changes associated with aggressive clonal phenotypes. We show our set of phylogeny-constrained variant calls along with openly released sequencing data can be a valuable resource for the development of new computational methods.

#4135 Site-specific oral microbiome patterns in Puerto Rican head and neck cancer patients.

Gabriela N. Garcia Quinones[1], Jaleniz Suarez Perez[2], Orlando Castro Ortiz[3], Maria Sanchez Vazquez[3], Jonathan Hernandez Agosto[1], Filipa Godoy Vitorino[2], Magaly Martinez Ferrer[1]

[1]Pharmaceutical Sciences, University of Puerto Rico Medical Sciences Campus, San Juan, Puerto Rico,[2]Department of Microbiology and Medical Zoology, University of Puerto Rico Medical Sciences Campus, San Juan, Puerto Rico,[3]Cancer Clinical & Translational Research, University of Puerto Rico Comprehensive Cancer Center, San Juan, Puerto Rico

Introduction: Head and neck cancers (HNCs) are the seventh most common cancer globally and the sixth most prevalent in Puerto Rico. They are also the eighth leading cause of cancer deaths among Puerto Rican men. Understanding HNC development and prognosis in this population is vital. The oral microbiome plays a significant role in HNC, as previous studies have shown that microbial dysbiosis can affect diagnosis and treatment. *However, little is known about the oral microbiome patterns in Puerto Rican HNC patients and their stability in response to clinical factors.* Therefore, the objective of this study is to determine the bacterial communities associated with HNC in Puerto Rican patients.
Methods: Genomic DNA was extracted from 79 histologically confirmed HNC tumor samples from Puerto Rican patients, followed by HPV genotyping and microbiome analyses using 16S rRNA gene amplicon sequencing. Data were deposited in Qiita/Deblur for quality control and bioinformatics analyses. Downstream analyses, including alpha and beta diversity, taxonomic characterization, and biomarker analyses, were conducted using QIIME2, MicrobiomeAnalyst, and Random Forest.
Results: Although beta diversity was similar across different anatomic sites, a significant difference was observed between the larynx and the oropharynx ($P = 0.041$, $FDR = 0.355$). The larynx consistently demonstrated lower richness and Shannon diversity compared to the oropharynx, hypopharynx, and oral cavity. Furthermore, Random Forest models showed weak discriminatory power ($MDA < 0.05$) for all six metadata variables analyzed: anatomic location, surgery, HPV status, radiotherapy, and chemotherapy. This was observed despite the contributions from various phyla, including *Bacillota_A*, *Deinococcota, Pseudomonadota*, and *Bacteroidota*, as well as genera such as *COE1, Duncaniella, Escherichia, Paramuribaculum*, and *Aggregatibacter.*
Conclusions: The oral microbiome of Puerto Rican HNC patients appears highly resilient, with significant variations in richness and diversity primarily linked to the laryngeal anatomical site. To enhance predictive accuracy for overall, cancer-specific, and disease-free survival, future studies will systematically correlate the microbiome's composition with clinical HNC characteristics. This will be accomplished by employing an array of survival-based machine learning methodologies, including penalized Cox regression (Elastic Net), Random Survival Forests, and Gradient Boosted Survival models (XGBoost-Cox). This work promises to unlock the microbiome's potential as a powerful tool for improving patient prognoses.

#4136 Pan-cancer transcriptomic signatures of immune checkpoint blockade response and machine learning-based prediction across TIGER cohorts.

Junqing Zhang[1], Hongru Shen[2], Yajing Bi[2], Xiangchun Li[2]

[1]Tianjin Medical University, Tianjin, China,[2]

Immune checkpoint blockade (ICB) can induce durable remission in a subset of patients with advanced cancer, but accurately identifying responders before treatment is essential to maximize clinical benefit and avoid unnecessary immune-related toxicities. To address this need, we systematically analyzed bulk RNA-seq cohorts from the Tumor Immunotherapy Gene Expression Resource (TIGER) encompassing multiple tumor types treated with ICB, and developed a machine learning-based framework for response prediction in a pan-cancer, multi-cohort setting.

We included cohorts of glioblastoma, head and neck squamous cell carcinoma, non-small cell lung cancer, renal cell carcinoma, gastric cancer, and several melanoma datasets, with all samples annotated as responders or non-responders. Within each cohort, we performed differential gene expression analysis between responders and non-responders and applied Hallmark gene set enrichment to define key biological pathways associated with ICB response. On this basis, we extracted transcriptomic features and trained support vector machine (SVM) classifiers. Model performance was assessed by repeated 10-fold cross-validation within cohorts and further examined using leave-one-dataset-out (LODO) validation and cross-dataset testing among melanoma cohorts.

Across tumor types, responders exhibited a highly consistent immune-activation landscape, including marked up-regulation of interferon-γ/α responses, allograft rejection, and TNF-NF-κB and IL6-JAK-STAT3 inflammatory signaling, together with metabolic reprogramming involving oxidative phosphorylation and cholesterol homeostasis. Non-responders more frequently showed enrichment of cell-cycle and proliferation pathways (G2M checkpoint, E2F targets) and epithelial-mesenchymal transition, with tumor type-specific patterns in melanoma and renal cell carcinoma. SVM models achieved good discrimination, with many within-cohort areas under the ROC curve (AUCs) exceeding 0.7 and some approaching 0.9, while maintaining practically useful performance in cross-cohort evaluations.

Collectively, this study delineates shared immune and metabolic programs associated with ICB benefit and tumor type-dependent resistance features, and proposes a transcriptome-machine learning prediction framework applicable across multiple cancers and cohorts, providing a solid data and methodological foundation for further optimization of immunotherapy response prediction using advanced representation learning approaches.

#4137 The acidic tumor microenvironment facilitates colorectal cancer liver metastasis through LPL lactylation-mediated reprogramming of macrophage cholesterol metabolism.

Yifan Zheng, Zhengyu Wei, Zhengran Zhou, Peishan Hu

The Sixth Affiliated Hospital of Sun Yat-sen University, GuangZhou, China

Colorectal cancer liver metastasis (CRLM) remains a major challenge in clinical treatment, with its recurrence and poor prognosis closely linked to tumor microenvironment (TME) reprogramming and immune cell dysfunction. As core immunoregulatory cells in the CRLM microenvironment, tumor-associated macrophages (TAMs) undergo significant metabolic reprogramming during disease progression; however, the mechanism by which metabolic reprogramming regulates TAM phenotype and promotes tumor metastasis has not been fully elucidated.A multi-omics strategy integrated single-cell RNA sequencing (scRNA-seq) and ICGC-ARGO/GEO transcriptomic data to analyze metabolic dynamics in CRLM lesions. TAMs were stratified into high (HCTAM), medium, and low (LCTAM) subgroups by cholesterol metabolic activity. Spatial transcriptomics (ST) verified spatial gene expression and metabolic activity, and in vitro functional experiments validated gene functions and regulatory relationships.Cholesterol metabolic pathways were abnormally upregulated in CRLM lesions, with TAMs exhibiting the highest cholesterol metabolic activity among immune and stromal cells. HCTAMs had significantly elevated M2 polarization scores, localized to late-stage macrophage differentiation, and co-expressed multiple M2 markers. Five machine learning algorithms identified lipoprotein lipase (LPL) as significantly overexpressed in HCTAMs, with high LPL expression independently associated with advanced CRC stages and poor overall survival. Mechanistically, lactate dehydrogenase A (LDHA) was significantly upregulated in HCTAMs, and TAM cholesterol metabolic was activity positively correlated with TME acidosis scores. ST confirmed LPL enrichment in acidotic regions, and multiplex immunofluorescence showed LPL colocalization with pan-lactylation. Lactate-induced lactylation modification regulated the expression of LPL . Transcriptomic analysis revealed significant EMT pathway enrichment in CRC cells of high-LPL group. In vitro experiments confirmed LPL colocalization with M2 TAM marker CD163; TAM LPL knockdown reduced cholesterol levels and downregulated M2 polarization markers. Co-culture experiments showed LPL-knockdown TAMs inhibited the invasion and migration of CRC cells and downregulated EMT-related marker expression.In conclusion, this study confirms that the acidic microenvironment in CRLM lesions drives LPL overexpression in TAMs through lactate-dependent lactylation modification. This effect maintains high cholesterol metabolic activity in TAMs and promotes their M2 polarization, further enhancing CRC cell EMT progression and invasiveness, ultimately exacerbating CRLM development.

#4138 Integrative computational and experimental analysis identifies carcinogenic effects of 1,4-Phenylenediamine in hepatocellular carcinoma via PI3K/AKT-MAPK and JAK/STAT signaling pathway.

Liuxian Ban[1], Ran Ding[2], ZhiQing Long[2]

[1]University of Hong Kong, Shenzhen Hospital, Shenzhen, China,[2]Sun Yat-sen University Cancer Center, Guangzhou, China

Hepatocellular carcinoma (HCC) is strongly influenced by environmental chemical exposures, among which 1,4-Phenylenediamine dihydrochloride (1,4-PDD) may act as a potential carcinogenic agent. In this study, we employed a network toxicology framework to systematically elucidate the molecular mechanisms linking 1,4-PDD exposure to HCC development. Differentially expressed genes and putative targets associated with 1,4-PDD were identified by integrating toxicogenomic databases, transcriptomic profiles, and protein-protein interaction networks. A multi-algorithm machine learning pipeline-combining random forest, LASSO regression, and support vector machines was implemented to refine and prioritize key targets with high stability. These targets were subsequently used to construct a prognostic model via multivariate Cox regression, which demonstrated robust predictive performance in independent validation cohorts. Mechanistic analyses indicated that the key targets were predominantly enriched in oncogenic signaling pathways, particularly the p-AKT, p-MEK, p-ERK1, and p-STAT3 axes, suggesting that 1,4-PDD exposure may promote malignant progression by activating PI3K/AKT-MAPK and JAK/STAT signaling cascades. Overall, this study delineates system-level toxicological mechanisms of 1,4-PDD in HCC and presents a molecular prognostic model with potential translational value for assessing chemical exposure-related liver cancer risk.

#4139 Resource allocation deconvolution for pathway analysis.

Junhao Wang, Yifei Wang, Tianshu Michael Bao, Yong Li

Baylor College of Medicine, Houston, TX

Background: Traditional pathway analysis mainly focuses on comparing pathway activity among different samples, ignoring how pathways share and compete for a limited transcriptional "budget."
Methods: We present PathwaySpectra, a framework that characterizes the transcriptional budget allocation and competitive landscape of pathways at the single-sample level. It can flexibly integrate standard annotations and user-defined gene sets and can be easily extended to various data types and disease scenarios.
Results: In an immune checkpoint inhibitor (ICI) cohort, PathwaySpectra revealed previously unannotated high-efficiency modules whose budget shares positively tracked clinical response, as well as low-efficiency modules enriched in progressive disease. Using composition-aware models with covariate adjustment, these associations remained robust. Compared to common supervised pathway scores, PathwaySpectra not only demonstrates the ability to distinguish response-related signals but also to identify previously unknown related signals. The competition view further suggested a reallocation of budget from immune-effective to inefficient pathways in non-responders, potentially constraining resources for productive immune activation.
Conclusions: PathwaySpectra offers a complementary perspective beyond standard pathway activity metrics, enabling budget-based, sample-by-sample pathway analysis and supporting custom gene sets for research targeting specific questions, thereby facilitating the discovery of pathway-level therapeutic response biomarkers.

#4140 *In silico* analysis of Lacunae cornuta phytochemical against high-risk HPV targets.

Solomon Owumi[1], Esther M. Pius[1], Oluwaseun M. Owolabi[1], Ifeoluwa O. Alabi[1], Victor O. Eso[1], Sanusi A. Abdullah[1], Hikmah A. Abdulganiyu[1], Jesutosin O. Babalola[1], Chima Amadi[2], Chinedum Udekwu[3], Adegboyega K. Oyelere[4], E. Oluwabunmi Olapade-Olaopa[5], Olorunseun O. Ogunwobi[3]

[1]Biochemistry, University of Ibadan, Ibadan, Nigeria,[2]Dedra Nutraceuticals and Biotechnology Initiative, Abuja, Nigeria,[3]Chemistry and Biochemistry, Michigan State University, Lansing, MI,[4]Chemistry and Biochemistry, Georgia Institute of Technology, Atlanta, GA,[5]Surgery, University of Ibadan, Ibadan, Nigeria

High-risk Human Papillomavirus (hrHPV) particularly HPV 16 and 18 is the primary etiological agent for cervical carcinogenesis, a disease disproportionately impacting women globally and a leading cause of morbidity and mortality. hrHPV encode oncoproteins that disrupt cell cycle regulation, inhibit apoptosis, and facilitate malignant transformation. *Launaea cornuta* (LC) is a medicinal plant known to contain flavonoids, terpenoids, and phenolic acids. Traditionally valued for its anti-inflammatory, antiviral, and anticancer properties, LC has demonstrated bioactivity in various preclinical models, indicating its potential applicability in the management of HPV-related pathologies. We used Network Pharmacology to identify molecular targets in hrHPV-induced cervical cancer. Bioinformatics analyses showed that LC phytochemicals interact with key genes—CASP3 (caspase-3), BCL2 (B-cell lymphoma 2), and HIF1A (hypoxia-inducible factor 1-alpha) —linked to apoptosis and hypoxic response. Molecular docking simulations assessed the binding affinities of LC-derived compounds to hrHPV oncoproteins (E6 and E7) and hub genes. Protein structures were taken from databases, and docking scores were used to estimate inhibitory effects. NP analysis identified CASP3, BCL2, and HIF1A as central genes implicated in the pathogenesis of hrHPV-induced cervical cancer. These genes represent critical nodes linking viral oncogenesis, apoptosis regulation, and cellular adaptation to hypoxia. Several LC phytochemicals exhibited strong binding affinities to hrHPV E6/E7 oncoproteins and the hub genes. MD analysis showed that several LC phytochemicals—such as stigmasteryl methyl ether, Tricyclo(20.8.0.0(7,16))triacontane, 1(22), 7(16)-diepoxy, and tremulone—demonstrated strong binding affinities (-5.9 to -8.4 kcal/mol) with E6, E7 oncoproteins and hub genes, indicating potential for viral inactivation or inhibition of oncogenic function. LC phytochemicals may inhibit oncogenic mechanisms driven by hrHPV through targeted interactions with both viral and host cell proteins, thereby facilitating apoptosis and reducing tumor progression. Their therapeutic potential
is highlighted by the modulation of critical pathways involving CASP3, BCL2, and HIF1A. The in-silico evaluation of LC phytochemicals demonstrates promising inhibitory activity against hrHPV E6 and E7 oncoproteins and key molecular targets involved in cervical cancer. Further research is necessary to translate these findings into clinical applications.

#4141 Multimodal single-cell analysis of systemic immune remodeling induced by cytoreductive nephrectomy combined with immune checkpoint inhibitors in metastatic renal cell carcinoma.

Suebin Park[1], Byungjin Hwang[2]

[1]Department of Clinical Drug Discovery and Development, Yonsei University College of Medicine, Seoul, Korea, Republic of,[2]Department of Biomedical Sciences, Yonsei University College of Medicine, Seoul, Korea, Republic of

Background: The role of cytoreductive nephrectomy (CN) in metastatic renal cell carcinoma (mRCC) remains uncertain in the immuno-oncology era. Ongoing trials such as PROBE (NCT04510597) and NORDICSUN (NCT03977571), focus on deferred CN versus no CN, but neither includes an upfront CN arm. To address this gap, we performed a multimodal single-cell analysis comparing the immunological effects of upfront CN, deferred CN, and no CN in combination with ICIs.
Methods: We performed multimodal single-cell sequencing integrating bulk RNA-seq, scRNA-seq, CITE-seq, and TCR-seq on peripheral blood mononuclear cell (PBMC) samples obtained from five patients undergoing CN and ICI therapy in different treatment orders. Eleven PBMC samples collected across treatment time points were pooled, genotyped, and demultiplexed using SNP-based assignment, followed by normalization and processing with the Seurat workflow. Bulk RNA-seq and genotyping enabled donor identification and transcriptomic profiling, while single-cell transcriptomic, surface proteomic, and TCR clonotype data were jointly analyzed to characterize cellular components, immune activation states, and clonal dynamics associated with CN in combination with ICI therapy.
Results: We analyzed 133,943 cells and identified 16 immune cell types. Immune composition differed by the sequencing of cytoreductive nephrectomy (CN) and ICI therapy. In the upfront CN group, CN increased memory B cells, classical monocytes, and NK cells, and these changes persisted during nivolumab plus ipilimumab treatment. In the deferred CN group, CN also expanded NK cells but additionally increased $CD8^+$ effector memory T cells. Transcriptomic, ADT, and TCR analyses revealed distinct immune states and clonal expansion patterns contributing to systemic immune remodeling.
Conclusions: This study reveals that CN combined with ICIs exerts different immune effects depending on whether CN is performed upfront or deferred. While both approaches increased NK cells, B- and T-cell responses differed between groups. Our multimodal single-cell analysis further identified distinct transcriptional, proteomic, and clonal changes associated with each approach. Although the optimal timing of CN remains uncertain, these findings highlight the need for further investigation to refine patient selection and guide CN integration with ICI therapy in mRCC.

#4142 Metabolic transition analysis from dormancy to awakening in breast cancer.

Javier Villela Castrejon[1], Herbert Levine[2], Jason T. George[3]

[1]Translational Cancer Research, Texas A&M University, Houston, TX,[2]Northeastern University, Boston, MA,[3]Texas A&M University, Houston, TX

Dormancy and late relapse remain pressing challenges in ER+ breast cancer. Mechanistically, dormancy can reflect a cellular quiescence of micrometastatic cells or tumor-mass dormancy constrained by angiogenic or immune bottlenecks. A long-standing hypothesis is that dormant disseminated tumor cells (DTCs) reside in a glycolysis-high, mesenchymal-like state, whereas successful awakening requires a transition toward an epithelial, OXPHOS-dependent phenotype.
Here, we test this hypothesis using a catabolic-anabolic AMPK/HIF-1/MYC regulatory model with four phenotypic states (OXPHOS, Warburg, hybrid W/O, and glutamine-reliant Q), each with distinct metabolic signatures. We integrated these signatures with longitudinal experimental and relevant clinical intervention datasets, including viral infection-induced awakening model, clinical endocrine-therapy time courses, and dormancy models. In addition, three complementary epithelial-mesenchymal transition (EMT) metrics were integrated to assign a consensus epithelial, hybrid, or mesenchymal phenotype to each sample to connect the intrinsic relationship of EMT with metabolic phenotype and dormancy status. Across models, we uncover marked metabolic diversity during cancer awakening, including transitions from quiescent, glycolysis-dependent or mesenchymal-biased states toward hybrid W/O metabolic configurations characterized by coordinated changes of AMPK and HIF-1, altered ROS source balance, and re-engagement of epithelial and proliferative signaling pathways. These metabolic and transcriptional transitions reveal the molecular features associated with dormancy exit and may provide new opportunities to therapeutically prevent awakening and late metastatic relapse.

#4143 Integrative analysis of XPC and VEGFA as risk biomarkers in T-cell lymphoma: A case-control study.

Faten Awwad[1], Lama M. Bani Salameh[1], Laith N. AL-Eitan[2], Nour Abdo[3], Sohaib Al-Khatib[4]

[1]Faculty of Medicine, Jordan University of Science & Technology, Irbid, Jordan,[2]Department of Biotechnology and Genetic Engineering, Faculty of Science and Arts, Jordan University of Science & Technology, Irbid, Jordan,[3]Department of Public Health, Faculty of Medicine, Jordan University of Science & Technology, Irbid, Jordan,[4]Department of Pathology and Laboratory Medicine, Faculty of Medicine, Jordan University of Science & Technology, Irbid, Jordan

Introduction: T-cell lymphoma (TCL) is a rare and aggressive type of non-Hodgkin lymphoma (NHL) that accounts for around 12% of all cases and shows variable clinical and molecular features. Germline single-nucleotide polymorphisms (SNPs) have been increasingly recognized as modulators of cancer risk. However, the role of such genetic variants in TCL in a non-western population remains largely unexplored. Therefore, we aimed to investigate the relationship between XPC, VEGFA and TNFAIP8 SNPs and the risk of developing TCL in an Arab population.
Methods: A total of 31 TCL patients and 289 matched healthy controls were recruited from King Abdullah University Hospital (KAUH), Females represented 32.3% (n=10) of patients and 61.3% (n=146) of controls, with mean ages of 44.1 and 43.2 years, respectively. Genomic DNA was extracted from formalin-fixed paraffin-embedded (FFPE) tissue samples for lymphoma cases and from peripheral blood samples for controls. Selected SNPs were genotyped using a sequencing protocol, and significant ones were identified using adjusted p-values and the Bonferroni false discovery rate (FDR) correction. We validated our findings using the GEO cohort (GSE6338) and performed linear modeling of microarray data to identify differentially expressed genes, applying a cutoff of log2FC > 0.5. All analyses were conducted in R version 4.4.3.
Results: The primary cohort showed that XPC rs2228001G>T was associated with higher TCL risk in both the co-dominant [TT: OR 2.353; 95% CI 1.01-5.59; p=0.0471] and recessive models [TT: OR 2.811; 95% CI 1.29-6.08; p=0.0084]. VEGFA rs3025039C>T also showed a strong association with increased risk in the co-dominant [TT: OR 19.091; 95% CI 4.70-78.99; p=0.00003], dominant [OR 3.227; 95% CI 1.36-7.75; p=0.0076], and recessive [OR 15.333; 95% CI 3.94-60.06; p=0.00006] models. Conversely, TNFAIP8 rs1045241C>T showed a protective effect in the co-dominant [OR 0.158; 95% CI 0.02-0.56; p=0.0141], dominant [OR 0.382; 95% CI 0.14-0.92; p=0.0446], and over dominant models [OR 0.152; 95% CI 0.02-0.53; p=0.0116]. In the validation dataset (GSE6338), VEGFA showed significant upregulation (LogFC=0.598; adj. p=0.000795), while XPC showed no significant change (LogFC=0.090; adj. p=0.457).
Conclusion: This study identifies VEGFA rs3025039 as a potential genetic risk factor for T-cell lymphoma in the Jordanian population. Gene expression analysis further confirmed upregulation of VEGFA in TCL validation cohort, suggesting a possible role in disease progression. These findings provide the first evidence in an Arab population cohort linking specific SNPs and gene expression changes to TCL risk, offering potential targets for population-specific personalized therapies.

#4144 Immunotherapy response predictors in colorectal cancer: A multi-omics approach.

Joaquin Pedro Merlo[1], Marco Adrian Scheidegger[2], Ada G. Blidner[2], Alejandro Cagnoni[2], Gabriel A. Rabinovich[2], Karina Marino[1]

[1]Instituto de Biologia y Medicina Experimental (IBYME) - CONICET. UADE - INTEC, Buenos Aires, Argentina,[2]Instituto de Biologia y Medicina Experimental (IBYME) - CONICET, Buenos Aires, Argentina

Predicting immunotherapy (IT) outcomes remains a clinical challenge as approved biomarkers show limited efficacy. Although aberrant glycosylation has been linked to tumor progression, its role in predicting IT outcomes is underexplored. With the goal of aiding in patient stratification, we integrated genomic, transcriptomic and glycomic data to explore the predictive capacity of glycoimmune genes. Using unsupervised machine-learning methods and cross-validation with two independent cohorts, we developed the GlycoImmune Signature (GIS), an 18-gene expression signature associated with improved response to IT and survival outcomes. We applied the GIS to colorectal cancer (CRC) samples from TCGA-COAD and characterized their immune infiltration and proteomic profiles. MSI-H patients and predicted responders (TIDE algorithm) showed higher GIS scores ($p<0.0001$). High GIS-scoring (GISH) patients exhibited a “hot” tumor microenvironment (TME) and upregulation of immune-related signatures compared to low GIS-scoring (GISL) cases. Interestingly, approximately 40% of MSI-L/MSS patients were GISH, suggesting that the GIS may identify patients who might respond to IT but are not currently considered by clinical guidelines. Single-cell transcriptomics data of CD45+ and tumor cells (GSE200997) of treatment-naïve samples were aggregated per patient to generate pseudobulk profiles and classify them into GISH and GISL. GISH tumors showed an enrichment of effector CD8+ T cells and reduced infiltration of Tregs and Th17 cells, confirming previous findings. Mapping these GISH and GISL-associated cell states onto cells from patients treated with IT (GSE205506) revealed that GISH-associated effector CD8+ T cells were more cytotoxic and prevalent in responders, while those from GISL patients expressed exhaustion markers (*LAG3, PDCD1, CTLA4, EOMES, TOX).* In turn, GISH-associated Tregs showed the loss of regulatory markers (*FOXP3, CTLA4*, *TIGIT*). To translate our transcriptomic marker into a proteomic one, we analyzed proteomic data from GISH patients in TCGA-COAD, finding 29 upregulated proteins associated with immune response and cell killing, and 9 downregulated proteins associated with metabolic reprogramming. Among the former, six proteins present relevant biological roles and are highly expressed in CRC tumors, which could serve as cost-effective clinical readouts. Overall, these findings position the GIS as a multi-omics surrogate of IT response in CRC and highlight its potential to expand patient eligibility for immunotherapy.

#4145 Genome-wide metabolic modeling identifies key modifiers of precancerous LUSC evolution.

Neel Sanghvi, Thomas Cantore, Chi-Ping Day, Sanna Madan, Nishanth Ulhas Nair, Eytan Ruppin

National Cancer Institute, Bethesda, MD

Background: Metabolic alterations drive tumorigenesis, yet few metabolic cancer drivers have been established. The squamous cell carcinoma subtype of lung cancer (LUSC) is particularly underserved, with few, potentially harmful treatment options and overall poor prognosis. Here, we aim to discover actionable modifiers of tumorigenesis through a systematic, genome-scale metabolic analysis of human lung samples. We identify metabolic genes whose knockout (KO) may drive carcinogenesis and, critically, those whose KO may revert (pre)cancerous states back to the healthy lung.

Methods: We analyzed bulk transcriptomes from 122 normal, precancerous, and cancerous samples spanning the LUSC evolutionary spectrum. First, sample-specific metabolic states were modeled in-silico using iMAT (Zur et al., 2010) on the HumanGEM model. Second, gene KOs were simulated with rMTA (Valcárcel et al., 2019) to estimate their oncogenic risk and back-to-normal reversion potential. Third, top scoring genes in both categories were corroborated by independent and orthogonal validations: a mouse gene-null phenotype dataset (KnockOut Mouse Project), differential expression in a separate LUSC precancer progressors vs regressors cohort, the Dependency Map (DepMap), and an LLM/AI-enhanced literature review. Corroborated, top-scoring genes were finally mapped to small molecule inhibitors via the DrugBank database.

Results: Reassuringly, top predicted risk genes (KO → progression) emerging from the metabolic modeling analysis were associated with greater cancer incidence in null allele mice (Wilcoxon $p = 0.02$), downregulated in LUSC precancer lesions that progressed to cancer ($p < 0.0094$), and associated with tumor suppressive activity in literature ($p < 0.01$), compared to background genes. Conversely, top reversion genes (KO → regression) were downregulated in LUSC precancer samples that regressed to normal ($p < 0.04$), overlapped with genes whose KOs lowered cancerous growth in the DepMap (odds-ratio/OR > 1.6, $p < 0.0083$), and were associated with oncogenic activity in literature ($p < 0.01$). Top validated reversion genes were enriched in glutamine and glucose usage pathways (OR > 7, padj < 0.09). Top risk-mitigating inhibitors included antiviral Lamivudine (*CMPK1*), antidepressant Phenelzine (*AOC3, GPT1/2*), and antihyperlipidemic Statins (*ABCB1*).

Conclusions: Genome-scale metabolic modeling analysis of LUSC samples uncovered several gene KOs and drugs that may revert precancerous metabolic states to non-cancerous ones. Although these genes and drugs warrant further experimental testing, top candidates were prioritized through and supported by multiple independent computational analyses. This work paves the way for a new class of treatments that may bring tumors closer to a non-cancerous homeostasis instead of the standard-of-care cell killing that too often leaves resistant residual disease.

#4146 Melanocytic transcriptional state is an independent marker of survival in metastatic melanoma.

Ziyin Huang[1], Kristen E. Rhodin[2], Rami Al-Rohil[3], Viviana Geron[2], Arul M. Chinnaiyan[1], Margaret H. O'Connor[2], Christina Vadala Angeles[1], Smita K. Nair[2], Georgia M. Beasley[2], Matthew K. Iyer[1]

[1]University of Michigan, Ann Arbor, MI,[2]Duke University, Durham, NC,[3]University North Carolina, Chapel Hill, NC

Introduction: Advanced cutaneous melanoma shows substantial heterogeneity in clinical outcomes, even among patients classified within the same clinical stage. Understanding the molecular drivers underlying this heterogeneity is critical for advancing treatment strategies. Previous studies have identified distinct melanoma transcriptomic states - Tirosh *et al.* and Balderson *et al.* have agreed on a four-subtype model defining “Undifferentiated”, “Neural Crest”, “Transitory”, and “Melanocytic” states. However, their biological and clinical relevance remains unclear. Here we profiled in-transit melanoma (ITM) using digital spatial RNA profiling to associate melanoma transcriptomic states with overall survival (OS) and acral melanoma (AM) status.
Methods: Digital spatial profiling (Nanostring GeoMx Whole Transcriptome Atlas) was performed across a tissue microarray constructed from patients with ITM diagnosed from 1990-2020. After filtering poor quality areas of interest (AOIs), we processed the data using noise correction and quantile normalization. We applied Principal Component Analysis (PCA) to define melanoma subtype signatures by ranking genes contributing to each of the first four PCs. We performed gene set enrichment analysis using GSEA with significance defined as an adjusted p-value < 0.05. Association between gene or gene-set expression and OS was evaluated using optimal expression cutoffs to define high and low groups, with a minimum group size of 20%. Cox proportional hazards models were then used to assess survival differences between groups.
Results: We analyzed a cohort of 84 patients (116 AOIs) with ITM passing QC. PCA of transcriptional profiles revealed distinct transcriptional states. The PC1 axis differentiated Transitory from Undifferentiated melanoma, PC2 reflected immune cell infiltration, PC3 corresponded to stromal cells and Neural crest-like melanoma, and PC4 associated with Melanocytic melanoma. We derived gene sets from the PCA results and associated the expression of each gene set with OS. Across a cohort of treatment-naïve ITM, high expression of the melanocytic state conferred a median overall survival difference of 7.59 years (melanocytic ‘high’=5.16 years vs ‘low’=12.75 years, log-rank p=0.0024) and independently associated with poor survival in multivariate analysis. AMs showed higher melanocytic state gene expression compared to non-acral cases. These findings were validated in external datasets, supporting that the melanocytic state predicts poor prognosis.
Conclusion: The melanocytic transcriptional state was independently associated with worse overall survival in patients with metastatic melanoma and was enriched in acral melanoma, suggesting that assessment of the melanocytic state may have value for clinical risk stratification.

#4147 CEDAR: A comprehensive database of curated cancer epitopes and receptors.

Zeynep Kosaloglu-Yalcin[1], Ibel Carri[2], Nina Blazeska[2], Randi Vita[2], Daniel Marrama[2], Hannah K. Carter[3], Morten Nielsen[4], Alessandro Sette[2], Bjoern Peters[2]

[1]La Jolla Institute for Immunology, San Diego, CA,[2]La Jolla Institute for Immunology, La Jolla, CA,[3]UC San Diego, La Jolla, CA,[4]Technical University of Denmark, Lyngby, Denmark

The identification of immunogenic cancer epitopes, including patient-specific neoepitopes and shared tumor-associated antigens (TAAs), is a critical foundation for advancing effective cancer immunotherapies. To provide the community with a centralized data source for this research, the Cancer Epitope Database and Analysis Resource (CEDAR, cedar.iedb.org) offers the most extensive and actively updated collection of experimentally validated cancer epitope and receptor data. Currently, CEDAR hosts data from 6,242 publications, encompassing 152,636 T Cell Assays, 143,715 B Cell Assays, and 4,394,087 MHC Ligand Assays, covering 666 distinct restricting MHC alleles.

CEDAR's comprehensive catalog includes neoepitopes, oncoviral epitopes, and TAAs, storing both positive and negative immune responses across human, mouse, and other species. The central element of the database is the experimental data validating these tumor molecule interactions; assay information is meticulously reported, including the specific assay types (e.g., ELISpot, tetramer staining, mass spectrometry) used to confirm T cell, B cell, and MHC binding/presentation. Furthermore, the database stores T and B cell receptors known to specifically recognize these epitopes.

The strength of the CEDAR lies in its rigorous and transparent curation process. All entries are curated by PhD-level scientists following a publicly available curation manual that outlines specific, consistently applied rules for data extraction, validation, and annotation. Curators use extensively validated workflows that combine automated text-mining with detailed manual review to ensure completeness and accuracy. Data is annotated in a highly structured way using community-supported ontologies, such as Uniprot, the Disease Ontology, and The Ontology for Biomedical Investigations (OBI), among others. This high degree of standardization ensures data accuracy, maximizes interoperability, and enables users to perform highly granular queries, filtering by species, MHC molecules, cancer pathology, antigen type, and specific source antigens.

As an integral and freely accessible companion site to the Immune Epitope Database (IEDB), CEDAR serves as a critical foundation for basic and translational immuno-oncology research. It provides the high-quality, trusted experimental data necessary for validating predictive models, designing targeted therapeutics, and exploring the landscape of tumor immunity.

: Digital Pathology 3
Poster Session

#4151 Phone-based portable slide digitization system for AI-enabled histopathology.

Sergii Domanskyi[1], Todd Sheridan[2], Javad Noorbakhsh[1], Jeffrey H. Chuang[3], **Jill Carol Rubinstein**[4]

[1]The Jackson Laboratory for Genomic Medicine, Farmington, CT,[2]Hartford Healthcare, The Jackson Laboratory for Genomic Medicine, Farmington, CT,[3]The Jackson Laboratory, Farmington, CT,[4]Hartford Healthcare, UCONN School of Medicine, The Jackson Laboratory for Genomic Medicine, Farmington, CT

In traditional histological analysis, pathologists view glass slides using light microscopy. Increasingly, slides are being digitized with high-resolution scanners. Digital pathology has great potential to mitigate disparity in access to specialized cancer care and allows application of artificial intelligence (AI)-based tools for analysis, but digitization costs can be prohibitive. We developed a phone-based system to digitize, visualize, and automate analysis using video capture and image stitching to generate whole slide images, overcoming the innate limitation in phone lens field of view. Our system provides digital pathology capability without need for specialized equipment. A cell phone with attached microscope lens is placed on a custom, 3-D printed rig with light source for smooth video capture across transilluminated slides. We demonstrate system efficacy using Apple iPhone 16 pro + Sandmarc lens. The Telepath is our original app, using 5x optical zoom, locked exposure, fixed white balance, and continuous autofocus to capture video with consistent lighting and color at 60 frames per second. Overlapping images are extracted and aligned with Scale Invariant Feature Transform descriptors and Fast Library for Approximate Nearest Neighbor matcher. After illumination correction, images are stored in TIFF format. Numerical tile-level AI-features are extracted with CTransPath and used to train classification models. The Telepath was used to digitize 24 histology slides prepared from PDX melanoma specimens. Video capture required 0.5 to 2 minutes/slide based on tissue size. Final resolution was 0.57 microns per pixel with average file size of 20 MB. Pathologist review confirms subjective image quality is ample for review. An automatic tumor detection model trained on images digitized on a commercial scanner was tested on images digitized on The Telepath, achieving recall 0.943 ± 0.096, precision 0.763 ± 0.25, accuracy 0.891 ± 0.047, fpp (size-adjusted fpr) 0.094 ± 0.046. We present a portable, affordable, AI-enabled digital pathology system that takes specimens from glass slides to annotated digital images. Given the portability and speed of the system, we envision such applications as direct upload of images to the medical record for secondary or centralized pathology review, automated assessment of prospective donor organs during procurements, and both permanent and frozen section analysis of surgical specimens for such tasks as tumor margin assessment and detection of lymph node metastases. The Telepath dramatically decreases financial and temporal barriers to the implementation of digital pathology, with potential to mitigate disparity in access to specialty care and open the door to broader application of AI-based tools.

#4152 Identification and phenotypical evaluation of androgen receptor indifferent phenotype in treatment-naïve primary prostate cancer cases.

Tessa Tolson[1], Beatrice Knudsen[2], Wei Zhang[3], Mason Hovinga[2], Chance Walker[2], Galaxy Yang[4], Erika Egal[3], Yosep Chong[5], Michael Freeman[4], Yi Qiao[1]

[1]Department of Biomedical Informatics, University of Utah, Salt Lake City, UT,[2]Department of Pathology, University of Utah, Salt Lake City, UT,[3]Huntsman Cancer Institute, Salt Lake City, UT,[4]Cedars Sinai Health System, Los Angeles, CA,[5]The Catholic University of Korea Uijeongbu St. Mary's Hospital, Uijeongbu, Korea, Republic of

INTRODUCTION: High-grade, locally advanced primary prostate cancer (PC) carries an increased risk of metastatic progression. The Androgen Receptor indifferent (ARi) phenotype is characterized by low PSA expression despite high expression of AR and has been noted in CRPC where it is considered to be induced by treatment. We sought to examine primary, treatment-naïve PC cases for evidence of ARi.

METHODS: We applied digital pathology and multiplexed, single-cell resolution tissue staining techniques to a locally advanced PC patient cohort with 27 patients and computational RNA expression analysis to the TCGA prostate cancer dataset (TCGA-PRAD). Thus, we first quantify AR and PSA protein expression levels in cells and then identify tissue regions with >30% AR+ cells and <30% PSA+ cells as ARi cases. The PC regions we analyzed include seminal vesicle invasion (SV), lymph node metastasis (LN), extracapsular extension (ECE), perineural invasion (PNI), cribriform (CRIB), and non-cribriform (HGNC). For computational analysis of the TCGA bulk RNA sequencing data, we stratify patients according to high AR / low PSA (ARi-cohort) and high AR / high PSA (AR responsive, or ARr-cohort) and perform differential expression and gene set enrichment analysis accordingly.

RESULTS: Pathologically, we identified ARi phenotype in one or more tissue samples from 5 out of 27 patients. ARi is more frequent in LN compared to SV; and within the prostate, HGNC exhibited more ARi than CRIB. Computational analysis of the TCGA-PRAD cohort (n=500) revealed that ARi patients, compared to AR-responsive patients, are enriched in epithelial-mesenchymal transition (EMT), stem-like, and ONECUT2-induced gene signatures. Moreover, we demonstrate that ARi phenotype is strongly associated with the Prostate Cancer Subtype 1 (PCS1) and PAM50 Basal subtype, consistent with the aggressiveness of the disease.

CONCLUSION: We identified the ARi phenotype in two cohorts of primary PC patients using both tissue staining with single cell resolution and computational analysis of bulk RNA expression. We further characterized this phenotype using published gene signatures and determined its relationship to PCS and PAM50 subtypes. Furthermore, we propose that the presence of the ARi phenotype can be assessed quickly by clinical immunohistochemistry with AR and PSA antibodies followed by quantification of positive ARi cells (as defined by a high AR:PSA ratio). Moving forward, we will perform single cell RNA expression analysis on the cohort we performed tissue staining to further validate the presence and behavior of ARi phenotype in primary PC, expand into other cohorts, as well as evaluate treatment strategies likely to elicit a response in these cells according to their transcriptomic phenotypes.

#4153 Advancing precision oncology through tumor digital twins: A versatile ViT-determined margin-consistent model for lung adenocarcinoma histopathologic subtyping in hematoxylin-eosin images.

Meghdad Sabouri Rad[1], Mohammad Mehdi Hosseini[1], Muhammad Hassaan Khalid[2], Saverio J. Carello[1], Michel R. Nasr[1], Rossana Kazemimood[3], Ola El-Zammar[1], **Bardia Rodd**[1]

[1]SUNY Upstate Medical University, Syracuse, NY,[2]University of Texas Health Science Center at Houston, Houston, TX,[3]Pathology, University of Texas Health Science Center at Houston, Houston, TX

Background: Digital twin frameworks in oncology require a stable, patient-specific histologic representation of tumor architecture. However, current LUAD subtyping models are vulnerable to stain and scanner variability, domain shift, and poor probability calibration. We investigate whether a state-space/Transformer hybrid with attention and margin-aware training can generate a robust, calibrated “morphology twin” suitable for integration into future tumor digital-twin systems.
Methods: A uniform patch-aggregation WSI pipeline was implemented with identical tiling, Macenko normalization, augmentations, and optimization across all backbones. From 143 FFPE H&E WSIs in BMIRDS-LUAD, we extracted 203,226 tissue patches (224×224 at 20×). Patches were encoded using ResNet50/101, ViT-L, or a state-space/Transformer hybrid (MambaVision). Slide-level predictions were produced via gated-attention MIL and a linear classifier whose logit gaps define decision margins. Training employed cross-entropy combined with a supervised representation term, without handcrafted harmonization or test-time adaptation. Internal development used a WSI-stratified split across five LUAD growth patterns. Zero-shot external evaluation used WSSS4LUAD. Endpoints included accuracy, subtype-specific AUC, feature-margin concordance, internal-to-external performance drop, calibration (ECE/Brier), and run-to-run variability across 10 seeds.
Results: On BMIRDS-LUAD, MambaVision+attention achieved 96.40±3.32% accuracy with ROC-AUC ≥0.99 across all subtypes and strong feature-margin alignment (τ=0.88 train / 0.64 validation). Errors were largely confined to mixed-pattern or low-quality slides. Zero-shot transfer to WSSS4LUAD yielded 83.69±7.76% accuracy—the smallest performance drop (–12.71 points) among all backbones. Calibration improved in-site and out-of-site (ECE/Brier: 0.043/0.098 internal; 0.087/0.154 external), with statistically significant gains over ResNet and ViT baselines. Variability across seeds narrowed (3.32% vs 6.12% for ResNet50), indicating enhanced training stability.
Conclusions: This framework addresses key LUAD subtyping failure modes—cross-site instability, overconfident boundary errors, and limited reproducibility. By integrating state-space modeling, Transformer attention, and margin-consistent learning, it produces a calibrated morphology twin that preserves subtype discriminability under domain shift and provides more trustworthy WSI-derived probabilities. While not a complete cancer digital twin, it forms a robust histologic module for integration into next-generation multimodal and temporal LUAD digital-twin systems.

#4154 Graph theoretic spatial heterogeneity analysis of multiplexed immunofluorescence images enables quantitative differentiation of HGSC precursor lesions in the fallopian tube.

Thomas Jacob[1], T. Rinda Soong[2], Shikhar Uttam[3]

[1]University of Pittsburgh School of Medicine, Pittsburgh, PA,[2]Pathology, University of Pittsburgh, Pittsburgh, PA,[3]Computational and Systems Biology, University of Pittsburgh, Pittsburgh, PA

Background: p53 signatures, serous tubal intraepithelial lesions (STILs), and serous tubal intraepithelial carcinomas (STICs) represent the precursor spectrum of high-grade serous carcinoma (HGSC), with STICs identified in 50-60% of HGSC cases. These lesions harbor TP53 mutations and exhibit similar genomic alterations to invasive HGSC, yet only a subset of these progress to malignancy. Studies suggest a close to a decade long latency period between STIC formation and invasive disease, creating a critical window for intervention. However, the factors determining malignant transformation remain poorly understood and quantified. Critically, the immune microenvironment of these precursors remains quantitatively uncharacterized. Specifically, we lack quantitative metrics associating lymphocytes, immunosuppressive cells, and immune checkpoint expressions in p53 signatures, STIL, and STIC lesions that are concordant with HGSC risk. Quantitative understanding of whether immune escape mechanisms are established early or develop during progression could identify microenvironment biomarkers that predict risk of individual lesions becoming invasive.

Method and Results: Toward this goal, we have developed a spatial heterogeneity analysis (SHEAN) framework for multiplexed immunofluorescence (mIF) that utilizes graph-theoretic representations of fallopian precursor tissue samples to identify quantitative spatial immune signatures that (1) characterize and distinguish normal epithelium (Norm), p53 signatures, STICs, and HGSCs from each other; (2) are sensitive to TP53 mutation status; and (3) can differentiate STICs based on their flat (FLAT) and budding, loosely adherent or detached (BLAD) status. These statistically significant features, confirmed at the image level, include signatures associated with degree of infiltration into, and interaction between T-lymphocytes, M2 polarized macrophages, and epithelial cells. SHEAN also achieved a cross-validated area under the ROC curve (AUROC) of 87.4% in discriminating Norm, p53 signatures, STICs, and HGSCs based on a bootstrapped model that included 53 normal, 68 p53 signatures, 73 STIC, and 32 HGSC regions and used an XGBoost classifier.

Conclusions: SHEAN allows the quantification of immune spatial metrics of the HGSC precursor microenvironment, providing an interpretable, spatially informed model capable of discriminating between lesion categories and enabling the reliable stratification of HGSC risk.

#4155 Development of a virtual Cyclin E1 biomarker using Deep Learning from H&E slides for predicting Cyclin E1 overexpression in gynecological malignancy.

Jeannette Fuchs[1], Kenneth To[2], Christopher Jackson[2], Lawrence Schobs[2], Rohan Lyons[2], Rafay Azhar[2]

[1]Translational Medicine, Debiopharm International S.A., Lausanne, Switzerland,[2]ViewsML, Vancouver, BC, Canada

The purpose of this study was to develop and validate a virtual immunohistochemistry (vIHC) algorithm capable of predicting Cyclin E1 (CCNE1) protein expression from hematoxylin and eosin (H&E)-stained whole-slide images in gynecological malignancy encompassing primarily high-grade serous ovarian carcinoma (HGSOC) and uterine serous carcinoma (USC). CCNE1 is a key cell-cycle regulator whose gene amplification (copy number ≥6) correlates strongly with protein overexpression (H-score >50) and enhanced sensitivity to WEE1 inhibitors. Conventional IHC requires precious tissue and additional laboratory processing; the ViewsML virtual biomarker platform derived from routinely available H&E slides provides a scalable alternative to accelerate patient selection for targeted therapy.

H&E and matched Cyclin E1 IHC whole-slide images were provided by Debiopharm. Sixty paired digital slides (40 HGSOC and 20 USC) were analyzed. The dataset was divided into training (n=45), validation (n=6), and testing (n=9) cohorts. ViewsML utilized neural network models trained to learn morphological and nuclear features predictive of Cyclin E1 expression intensity (0-3+). Model performance was evaluated using per-cell sensitivity, specificity, and concordance with physical IHC intensity and H-score classifications, including ROC AUC metrics. Concordance between predicted and true Cyclin E1 expression was evaluated through nuclear localization distinguishing weak, moderate, and strong staining patterns, allowing quantitative assessment of Cyclin E1-positive tumor fractions across HGSOC and USC.

In conclusion, this study demonstrates the feasibility of an AI-driven virtual biomarker for Cyclin E1 that can predict protein overexpression directly from H&E slides. The virtual IHC approach conserves valuable tissue and accelerates biomarker screening for patient selection, facilitating improved enrichment for Cyclin E1-associated therapeutic trials. Future applications include integration with multiplex virtual markers to further enhance clinical applicability.

#4156 Comprehensive 40-marker cyclic IF panel for spatial profiling of head and neck squamous cell carcinoma.

Danielle Fails, Alyssa Hernandez, Mike Spencer

Bethyl Laboratories, Montgomery, TX

Introduction

Head and neck squamous cell carcinoma (HNSCC) incidence has increased by at least 23 % globally over the last ten years and is predicted to continue to rise by 30 % annually. Treatment for HNSCC often includes a multidisciplinary approach (i.e., chemotherapy + surgery) but success rates are still limited with less than half surviving more than two years post-treatment (Nieszporek et al., 2025). Significant improvements in the number of biomarkers that can be screened at once, while preserving tissue integrity, have been made over the last decade. These staining and imaging improvements have contributed to the identification of novel therapeutic targets while limiting the egregious use of precious tissues. This study aimed to interrogate the tumor microenvironment of head and neck squamous cell carcinoma using the same tissue slice using a fully automated cyclic IF system.

Methods

Two panels of 20 biomarkers each were designed using immune markers, tissue architectural markers, and specific targets of interest in head and neck squamous cell carcinoma. *Panel 1* was comprised of I/O markers (CD3, CD4, CD8, FoxP3, CD56, CD20, CD68, CD11c, aSMA, PD-L1, PD-1, CD45, CD27, CTLA-4, CD19, PCNA, CD14, CD16, SOX10, CD79a) while *Panel 2* was largely comprised of discovery markers (ALDH2, IL-8, CK17, MMP9, MAGE-A4, EpCAM, EGFR, CK14, CK19, CK5/6, p53, CD44, ZEB1, ZEB2, beta-Catenin, E-Cadherin, Vimentin, COL1A1, COL4A1, FAP). Optimization was achieved using FFPE tissue microarrays containing normal and cancerous skin tissues. Pre-processing steps were done in the Epredia© PT Module using Tris-EDTA ph9 solution, at 100°C, for 1 hour. Panel 1 was stained first followed by Panel 2 without removal of the tissue from the instrument. Automated immunofluorescent staining and imaging of the samples was performed on the Lunaphore COMET™ system.

Results

The sequential staining of two 20-plex protein panels on the same tissue demonstrates the COMET's capability of maximizing the number of biomarkers that can be evaluated. This protocol significantly reduces the use of tissue necessary, helps maintain tissue integrity for downstream processing (i.e., H&E staining), and minimizes costs by reducing chip and reagent use.

Conclusions

This comprehensive interrogation of the HNSCC tumor landscape with the use of high-plex, fully automated sequential immunofluorescent staining highlights many of the capabilities of the latest spatial technologies. In using this approach, deeper dives of tumor microenvironments can be achieved with minimal tissue use while keeping reagent and material costs low. References: 1.

Nieszporek, A., Wierzbicka, M., Khan, A., Jeziorny, M., *et al.* Spatial profiling technologies for research and clinical application in head and neck squamous cell cancers. Current Research in Biotechnology. 2025. Vol 10: 100321.

#4157 Spatial immune profiling of solid tumors by complementing H&E with a novel 17-plex immunofluorescence approach.

Richard Van Krieken, Jaspreet Kaur, Xun Li, Naveen Dakappagari, Jennifer Bordeaux

Navigate BioPharma Services, Inc., Carlsbad, CA

Background: Spatial biology has increasingly leveraged “spatial neighborhoods” to integrate how cells are organized and interact, yet standards for defining and identifying these neighborhoods are still developing. Multiplex fluorescence immunohistochemistry (fIHC) offers detailed profiling of immune and tumor cell states, while hematoxylin and eosin (H&E) staining remains a gold standard for visualizing tissue and cellular morphology. We validated a 17-plex fIHC assay on the Orion™ (RareCyte) platform and aligned the fIHC with same slide H&E images to improve fidelity of cellular neighborhoods identification across breast, lung, prostate, melanoma, and colorectal cancers.
Methods: We developed a generalizable workflow to align same-slide H&E and 17-plex fIHC Orion images for assessment of cellular neighborhoods through integration cell phenotyping (via fIHC) with tissue architecture (via H&E). The 17-plex fIHC assay includes antibody-fluorophore conjugates targeting Granzyme B, Ki67, CD3e, CD20, CD4, CD163, CD8a, PD-L1, NKp46, PD-1, LAG3, FOXP3, CD11b, CD138, SOX10, Cytokeratin, and Hoechst nuclear stain. Slides were first stained and imaged by fIHC, followed by H&E staining and imaging on the Orion. Cell phenotyping and slide registration were performed on HALO® (Indica Labs).
Results: Integrating H&E with multiplex fIHC supported identification of spatial themes, including regions with enriched tumor-infiltrating lymphocytes, immune deserts, and mixed/transitional zones populating the tumor/stroma interface. This approach improves interpretability of these patterns by connecting cell phenotypes with tissue architecture morphology, supporting identification of microenvironments with greater consistency.
Conclusions: Combining H&E with multiplex fIHC enables anatomically informed mapping of cellular neighborhoods across multiple tumor types. This discovery-oriented workflow improves interpretability of spatial patterns, is adaptable to diverse datasets and pipelines, and may yield new insights into the immune microenvironment to inform next-generation therapies.

#4158 Cell lines as quality controls for Quantitative Continuous Scoring (QCS) of IHC stained samples.

Ana Hidalgo-Sastre[1], Tze Heng Tan[1], Nicolas Giraldo[2], Nathalie Harder[1], Sophia Varriano[3], Andrew Kunihiro[3], Guenter Schmidt[1], Hadassah Sade[1], Yeoun Jin Kim[3], Marlon Rebelatto[3], **Mark Gustavson**[3]

[1]AstraZeneca, Munich, Germany,[2]AstraZeneca, Barcelona, Spain,[3]AstraZeneca, Gaithersburg, MD

Background: Effectively measuring therapeutic target expression is critical in oncology for precise and accurate patient selection. Target expression is often measured by immunohistochemistry (IHC) using visual pathology scoring; however, digital pathology-based Quantitative Continuous Scoring (QCS) has emerged as a more precise and accurate alternative[1]. Given that IHC assays and whole slide image (WSI) scanners have known variability, we designed a proof-of-concept study to evaluate the applicability of using cell lines as quality controls for QCS scoring of IHC stained samples.
Methods: A panel of cell lines (N=10) were selected to represent a broad range of target expression and cultured as cell pellets into a Formalin-Fixed Paraffin Embedded (FFPE) Cell Micro Array (CMA) for downstream IHC analysis with QCS. The CMA was sectioned (4 µm) and stained with a target antibody according to standard protocols. The stained slides were scanned at 40x, and images were analyzed using a trained QCS deep-learning based QCS model that quantifies membrane staining intensity (SI).
Results: Cell line controls showed highly consistent QCS staining intensity (SI) scores through the entire CMA block (n=40 sections). SI from triplicates run on the same day were compared among each other or across days with a coefficient of variation (CV) <10% for each cell line, demonstrating a high level of precision and reproducibility through the entire cell line pellet. Additionally, cell density was also consistent throughout the FFPE block. Moreover, we observed highly significant correlation (R=0.98) between QCS SI and mass-spectrometry results, thus demonstrating specificity for assessing target expression in cell lines. Finally, early experiments with contrived assay variability showed the ability of cell lines to track the 32% contrived variability observed in tissue and correct that variability to 7%, thus supporting the use of cell lines to potentially improve IHC/QCS precision and reproducibility.
Conclusion: These data support the feasibility of using cell lines as qualitative controls for QCS scoring of IHC stained samples. Given that heterogeneity of expression is not a significant factor like it is in tissue, cell lines provide consistent expression throughout the entire block with a high degree of precision and reproducibility. These data thus support the potential for integrating cell line controls into the quality assurance pipeline for QCS-based IHC measurements in the laboratory setting. Further, cell line quality controls could also be used for bridging and comparability, thus enabling efficient and robust development of QCS assays.[1] Kapil et al. “HER2 quantitative continuous scoring for accurate patient selection in HER2 negative trastuzumab deruxtecan treated breast cancer”. Nature Sci Rep. 2024 May 27;14(1):12129.

#4159 Automated robust normalization and context-aware rescue of TReg cells from multiplex immunofluorescence.

Joao Paulo Oliveira da Costa, Alina Ainbinder, Kenneth Trieu, Henry Reinhart, Yury Sheikin

Pathology, Takeda Pharmaceutical Company Ltd. (U.S.), Cambridge, MA

CCR8^{+}FoxP3^{+} regulatory T cells (Tregs) are a key immunosuppressive subset in solid tumors, but their accurate quantification in multiplex immunofluorescence (mIF) is hindered by slide-to-slide staining variability, dim FoxP3 signal, and background-driven CCR8 false positives. We developed a fully automated, background-aware R pipeline for robust cross-slide calling of CCR8^{+}FoxP3^{+} cells from HALO single-cell data across NSCLC, CRC, GEJ, and HNSCC.Single-cell intensities for CCR8 and FoxP3 were transformed using inverse hyperbolic sine and normalized per slide using robust z-scores (rz) computed from medians and MADs, with fallbacks when FoxP3^{-} or CCR8^{-} reference populations were sparse. FoxP3 positivity was reassessed using a two-stage approach: (i) “soft” FoxP3 calls integrating HALO labels with high-rz outliers, and (ii) a strict rescue rule in which each cell’s FoxP3 rz was evaluated against the empirical FoxP3^{-} distribution, requiring both a minimum rz floor and low FoxP3 background-z, preventing inflation of false positives.
CCR8 calling used a spatially explicit background model: slides were partitioned into fine spatial bins, and CCR8 background medians and dispersions were estimated from local CCR8^{-} cells, with smoothing across sparse regions. This produced a background z-score (bg_z) and a background-adjusted CCR8 rz (rz_bg). From these, we defined a lenient background-aware CCR8 call and a strict CCR8 keeper enforcing strong evidence and artifact filters (cytoplasm completeness, CK negativity, nucleus quality).
Final CCR8^{+}FoxP3^{+} assignments used a FoxP3-aware rule: FoxP3^{+} cells were evaluated with lenient CCR8 criteria to recover dim true positives, whereas FoxP3^{-} cells required the strict CCR8 keeper to prevent spurious double-positive inflation. Agreement analyses showed that the strict CCR8 criteria substantially reduced Halo-only artifacts while adding very few “rescued-only” events. Conversely, FoxP3 soft-rescue recovered dim nuclei primarily in low-background regions.
Processing was optimized using Arrow to avoid loading full datasets into memory, enabling analysis of >10 million cells on a standard workstation. The combined FoxP3 normalization, empirical rescue, and CCR8 background-aware gating produced stable distributions across indications and improved both sensitivity and specificity for CCR8^{+}FoxP3^{+} Treg quantification.

#4160 Ensuring pathologist alignment to safeguard data integrity in multi-centre oncology IVD/CDx clinical trials.

Lindsey Bennie, Bethany Montgomery, David Ribeiro

ARC Regulatory, Belfast, United Kingdom

Background: Multi-centre oncology clinical trials increasingly rely on digital pathology and distributed specialist review, resulting in a heightened risk of inter-pathologist variability. Without robust alignment, differences in tissue interpretation can skew patient inclusion, compromise assay performance, and ultimately threaten the validity of clinical investigations for In Vitro Diagnostic (IVD) and companion diagnostic (CDx) development. Objective: To demonstrate the critical importance of pathologist alignment and the impact of structured interpretation guidance on assay concordance in a multi-reviewer setting.

Methods: ARC Laboratories evaluated the effect of pathologist alignment using a gastric cancer cohort (n=20). FFPE samples were stained with a CLDN18 antibody (Ventana CLDN 18 43-14A) on the BenchMark UltraPlus platform. In Phase 1, two independent, CLDN18-trained gastrointestinal pathologists assessed tumor content, tumor positivity, and percentage tumor involvement without a pathology manual or consensus meeting. In Phase 2, both pathologists underwent an alignment process including a pre-read, defined pathology interpretation manual, and agreement meeting before reassessment.

Results: In the unaligned phase, pathologists agreed on tumor positivity in only 8/20 cases. Tumor content and percentage tumor interpretation differed by up to 50%, resulting in assay performance that would not meet validation acceptance criteria. Following alignment, concordance increased substantially: 18/20 cases met agreement for tumor positivity, and differences in tumor content estimation decreased to ≤20%. Under these conditions, the assay met all required validation parameters and was deemed suitable for use in clinical trials.

Conclusion: This study highlights that even highly trained subspecialist pathologists can exhibit significant variability without structured alignment tools. A defined pathology manual and consensus process markedly improve concordance and are essential for ensuring assay validity in multi-centre or digitally enabled IVD/CDx trials. ARC's findings underscore that systematic pathologist alignment is not optional—it is a foundational requirement for generating reliable, regulatory-ready clinical data.

#4161 Validation of the ViewsML vIHC platform for biomarker classification and intensity binning: A pilot collaboration with Histowiz's PathologyMap platform.

Akash Parvatikar[1], Patrick Savickas[1], Chris Lee[1], Jeffrey Shek[1], Kenneth To[2], Christopher Jackson[2], Lawrence Schobs[2], Rohan Lyons[2], Rafay Azhar[2]

[1]HistoWiz, Long Island City, NY,[2]ViewsML Technologies Inc., Vancouver, BC, Canada

The purpose of this study was to validate ViewsML's Virtual Immunohistochemistry (vIHC) platform, a system that generates virtual biomarker predictions based on H&E whole slide images. This collaboration with Histowiz's PathologyMap platform enables evaluation of vIHC deployment across the PathologyMap database, demonstrating its potential as a scalable and practical alternative for biomarker discovery workflows. Board-certified anatomic pathologists procured 50 lung carcinoma cases for analysis. Formalin fixed paraffin embedded (FFPE) blocks were cut to 4 µm in quadruplicate onto positively charged slides. Each slide was stained with a GLP-regulated H&E stain and digitally scanned on a Leica AT2 onto the Histowiz PathologyMap platform. Slides were then de-stained and re-stained on a Leica BOND Rx platform with CD68, αSMA, and Pan-CK immunohistochemistry markers, and re-scanned. The resulting whole slide images (WSIs) were processed by ViewsML to train AI models to predict IHC expression from H&E images. For each biomarker, paired H&E and IHC WSIs were first spatially registered to ensure precise alignment. The paired data were randomly divided into training (75%), validation (10%), and test (15%) sets. Supervised machine-learning models were trained to predict IHC expression intensity from the corresponding H&E image, using the corresponding physical IHC as supervision. Evaluation was performed on the hold-out test set to verify performance. Once trained, these models enable biomarker predictions directly from a single standard H&E slide. The virtual markers demonstrated high classification performance, with per-cell ROC-AUC values of 0.94 for CD68, 0.92 for PanCK, and 0.95 for SMA. The model predicted per-cell stain intensity across millions of cells, preserving biological variability across expression ranges and tissue compartments.This collaboration validates ViewsML's virtual staining as a reliable computational alternative to physical IHC, capable of both qualitative and quantitative biomarker assessment. Integration with Histowiz's digital pathology infrastructure demonstrates the feasibility of embedding vIHC within scalable workflows for biomarker research, WSI repository annotation, and assay standardization. These findings support further multi-institutional expansion of ViewsML to enable robust, reproducible, and cost-efficient biomarker evaluation.

#4162 AI-based detection and scoring of TROP2 expression in IHC-stained NSCLC specimens.

Jeff Lock, Adam Hsiung, Kevin Gallagher, Harry Nunns, Nam Tran, Ben Ovadia, Arezoo Hanifi, Qingyan Au

Neogenomics Laboratories, Inc., Aliso Viejo, CA

Lung cancer is the leading cause of cancer-related deaths in the United States and non-small cell lung cancer (NSCLC) accounts for approximately 85 percent of all lung cancer cases[1,2]. Trophoblast cell-surface antigen 2 (TROP2), a transmembrane glycoprotein that normally serves as a Ca^{2+} signal transducer linked to cell growth, proliferation, and migration, is frequently observed in NSCLC and elevated expression levels are associated with increased metastatic risks and poor prognostic outcomes. Due to the adverse effects of TROP2 on NSCLC, as well as on many other common cancers, strategies such as antibody-drug conjugates (ADCs) and CAR-NK cells targeting TROP2 expressing tumors have emerged as areas of active investigation and therapeutic development. To serve these efforts, we present an end-to-end workflow for the quantification of TROP2 expression in NSCLC specimens that consists of an IHC staining assay optimized for the detection of TROP2 in FFPE tissue sections together with AI-based image analysis routine for the automated scoring of TROP2 tumor expression in whole-slide image (WSI) specimens. Our analysis algorithms were highly concordant to manual interpretation by pathologists when evaluated using Pearson's correlation coefficient, demonstrating both accurate tumor identification and TROP2 expression scores. By integrating our TROP2 IHC assay with algorithmic image analytics, we offer a comprehensive, scalable solution for discovery-based research efforts and clinical drug trials focused on TROP2 in NSCLC.

References

1) American Cancer Society. Facts & Figures 2025. *American Cancer Society*. Atlanta, Ga. 2025.

2) Siegel, R. L., Kratzer, T. B., Giaquinto, A. N., Sung, H., & Jemal, A. (2025). Cancer statistics. 2025. *CA: A Cancer Journal for Clinicians*, *75*(1). https://doi.org/10.3322/caac.21871

#4163 A general-purpose AI foundation model for spatial proteomics.

Andrew H. Song[1], Anurag Vaidya[2], Muhammad Shaban[1], Yuzhou Chang[1], Huaying Qiu[1], Yao Y. Yeo[1], Guillaume Jaume[1], Wenrui Wu[1], Qin Ma[3], Sizun Jiang[1], Faisal Mahmood[1]

[1]Harvard Medical School, Boston, MA,[2]Massachusetts Institute of Technology, Cambridge, MA,[3]The Ohio State University, Columbus, OH

Standard spatial proteomics (SP) pipelines for biomarker discovery have traditionally relied on cell segmentation followed by single-marker thresholding or rule-based mechanisms to assign cell phenotypes. However, this often suffers from a laborious process of manual annotations and neglects cell states characterized by the coordinated expression of multiple markers as a function of the cellular spatial organization. Moreover, converting the preprocessed cells to actionable biological insights on the cohort level is time-consuming due to its iterative nature of hypothesis generation and testing. We sought to build an AI foundation model trained on a large body of spatial proteomics datasets to address these challenges and further accelerate crucial spatial biology tasks in a platform-agnostic manner.

We present KRONOS, a foundation model for spatial proteomics that operates directly on segmentation-free multiplex image patches. KRONOS extends the self-supervised learning recipe proven to be successful for several pathology foundation models to spatial proteomics, by employing a Vision Transformer architecture that can flexibly handle the variable number of protein markers and simultaneously encode the protein expression levels and the known biological properties of the protein. The training dataset for KRONOS consists of 47 million single-marker patches spanning 175 protein markers, 16 tissue types, eight fluorescence-based imaging platforms, across five different institutions. This diverse and large-scale dataset allows KRONOS to learn rich, low-dimensional image representations that effectively capture spatial protein expressions jointly across different markers.

We evaluate KRONOS across a diverse range of downstream tasks, including cell phenotyping, tissue artifact detection, and patient stratification, and across diverse disease types such as lymphoma, renal cell carcinoma, and skin cancer. Across these tasks, KRONOS consistently outperforms other pathology (UNI) and spatial proteomics foundation model (CA-MAE) baselines, underscoring the importance of a domain-specific model trained on a large corpus of data. Specifically for cell phenotyping, we show that KRONOS is data-efficient and requires only a few cell annotations, addressing a major bottleneck in spatial proteomics where cell-level annotations are expensive to produce, slow to generate, and difficult to reuse across datasets. Furthermore, KRONOS allows “reverse image search” for identifying similar spatial patterns and biological concepts within and across patient cohorts, facilitating the discovery of clinically relevant tumor microenvironments and protein biomarkers.Together, these results position KRONOS as a general-purpose, foundation model for spatial proteomics that streamlines analysis, reduces annotation burden, and unlocks new opportunities for spatial biomarker discovery.

#4164 Implementation of a diffusion-based color checker for histological image batch correction.

Arman Petrosyants[1], Vaagn Chopuryan[2], Vasiliy Minkov[2], Anna Belozerova[2], **Alexander Bagaev**[2], Viktor Svekolkin[2], Aleksandr Sarachakov[2]

[1]Research Center for Digital Engineering and Innovation, Moscow, Russian Federation,[2]BostonGene Corporation, Waltham, MA

Introduction: Inconsistent tissue preparation, staining, and scanning introduce non-biological variations (batch effects) in histological images. These variations cause machine learning models to learn spurious, site-specific features instead of true pathological patterns, leading to inflated internal performance and poor generalizability and hindering clinical adoption. Current stain normalization methods, such as statistical (Reinhard), color deconvolution (Macenko, Vahadane), and generative adversarial networks, rely on relative normalization to an arbitrary "gold standard," a fundamental limitation. Simple methods often distort important morphological details, while advanced techniques still fail to remove all site-specific signatures.
Methods: We introduce a novel generative AI tool for histological image batch correction using a context-aware Stable Diffusion inpainting model to generate a dynamic localized color checker directly on whole slide images (WSIs). The model was trained to inpaint digital representations of a physical color checker (i.e., NIST Traceable Color Transmission Calibration Slide) onto the masked WSI region, preserving the WSI's original color space and establishing a context-aware standard without external references. Trained using 117 Huron and 119 Polaris scanner IHC and H&E WSIs with ground truth scans using the physical NIST color checker, the model enabled subsequent color extraction and image correction to a desired color space. Validation was performed using 78 Huron and 79 Polaris holdout WSIs. The mean-pooled embeddings derived from the Hibou pathology foundational model were used to predict the WSI's original scanner.
Results: The proposed method mitigated batch effects by transforming the task from simple normalization into a sophisticated form of image restoration. The model uses its powerful learned prior to reconstruct the image as it should appear under ideal, standardized conditions, mitigating site-specific batching.Prior to correction, this classifier achieved an AUC-ROC of 0.99, indicating the presence of strong, non-biological scanner-specific patterns (batch effects). After normalization, the performance of the same classifier dropped (AUC-ROC = 0.53), confirming the elimination of scanner-specific artifacts.
Conclusion: The AI image analysis model offers a robust solution to batch effect challenges in computational pathology, eliminating the need for a reference image during IHC and H&E WSI interpretation. Moving beyond relative color matching, this approach delivers color standardization. By improving robustness to technical batch effects and ensuring AI pathology models are trained on true biological signals, this approach is poised to accelerate the deployment of pathology foundational models across preclinical, translational, and clinical trial settings.

#4165 Advancing high-plex spatial proteomics using cleavable fluorophores and automated multiplex cycling.

Alyssa Hernandez, Danielle Fails

Bethyl Laboratories, Inc., Montgomery, TX

Introduction:
Understanding the spatial distribution of proteins within tissue microenvironments is essential for studying immune responses, tissue organization, and disease processes. High-plex spatial proteomics enables detailed mapping of multiple biomarkers on a single tissue section, but traditional methods can be limited by spectral overlap and fluorophore stability. Parahelia's automated staining workflow delivers a gentle heating step designed to maintain tissue structure over multiple staining rounds.
Methods:
Human formalin-fixed paraffin-embedded (FFPE) tissues were used to develop a high-plex workflow integrating Spatomics' CFP technology with automated staining and imaging by using the Parhelia Spatial Station and the Phenoimager HT. Numerous protein targets can be stained using CFPs, which generates strong, localized fluorescence through an HRP-catalyzed reaction between the CFT and nearby residues. After imaging, the fluorescent tags are efficiently cleaved and HRP is deactivated, allowing repeated cycles without compromising tissue quality or antigenicity. The Parhelia Spatial Station enables multiple samples to be processed simultaneously, automating fluid handling and antibody staining through gentle capillary laminar flow to standardize workflow and minimize variability, while the Phenoimager provides high-resolution, quantitative imaging across cycles.
Results:
Iterative staining and cleavage cycles produced clean signal reset between rounds with consistent biomarker detection maintained throughout the workflow. Imaging confirmed distinct signals for all targets, supporting the robustness and reproducibility of the workflow. The combined use of Spatomics' CFP chemistry, the Parhelia Spatial Station, and the Phenoimager HT enabled repeated staining and imaging on the same FFPE section, allowing a diverse set of protein markers to be visualized within a single slide. Consolidating multiple cycles into one tissue section reduced the number of slides required and increased the amount of spatial information obtainable from limited samples.
Conclusion:
This study demonstrates combining Spatomics' CFP patented chemistry with automated staining and high-resolution imaging. This workflow maintains tissue integrity, sensitivity, and reproducibility, offering a robust platform for spatial biomarker discovery and translational oncology research.
References:

1. Pham, T., Nazaroff, C., Labaer, J., & Guo, J.* Ultrasensitive and multiplexed protein imaging with cleavable fluorescent tyramide and antibody stripping. *Int J Mol Sci.* 2021;22:8644.
2. Pham, T., Liao, R., Labaer, J., & Guo, J.* Multiplexed in situ protein profiling with high-performance cleavable fluorescent tyramide. *Molecules.* 2021;26:2206.
3. Nadezhda, N., et al. Validation of an automated PhenoCycler-Fusion slide staining protocol on the Parhelia Spatial Station™. 2024.

#4166 Molecular diagnosis of lung tumors with a history of pancreatic cancer: Spatial profiling-based differential markers and functional insights into invasive mucinous adenocarcinoma.

Ryunosuke Fujii[1], Kousei Ishimura[1], Kazuhiko Shien[1], Shuta Tomida[2], Kenta Manabe[1], Shunsuke Mori[1], Kazuya Hisamatsu[1], Ryota Fujiwara[1], Atsushi Matsuoka[1], Ryo Yoshichika[1], Kazuhiro Okada[1], Yuma Fukumoto[1], Haruchika Yamamoto[1], Kumi Nakajima[1], Shin Tanaka[1], Hidejiro Torigoe[1], Ken Suzawa[1], Kentaroh Miyoshi[1], Mikio Okazaki[1], Seiichiro Sugimoto[1], Hirofumi Inoue[2], Kosei Takagi[3], Hidetaka Yamamoto[4], Shinichi Toyooka[1]

[1]Thoracic, Breast and Endocrinological Surgery, Okayama University Graduate School of Medicine, Dentistry and Pharmaceutical Sciences, Okayama, Japan,[2]Center for Comprehensive Genomic Medicine, Okayama University Hospital, Okayama, Japan,[3]Gastroenterological Surgery, Okayama University Graduate School of Medicine, Dentistry and Pharmaceutical Sciences, Okayama, Japan,[4]Pathology and Oncology, Okayama University Graduate School of Medicine, Dentistry and Pharmaceutical Sciences, Okayama, Japan

Background: Differentiating pancreatic cancer lung metastasis (PCLM) from primary lung cancer, particularly invasive mucinous adenocarcinoma (IMA), sometimes be difficult due to their pathological similarities such as mucin production. This study aimed to identify diagnostic markers for distinguishing IMA from PCLM and to elucidate the molecular pathogenesis of mucinous lung adenocarcinoma using spatial multi-omics analyses.
Methods: We performed spatially resolved transcriptomics by GeoMx digital spatial profiler on surgically resected lung tumors, from nine patients with a history of pancreatic cancer and three patients of IMA without such history. Multiple regions of interest (ROIs) were selected in tumor components from each sample. Based on GeoMx results, validation was performed by immunohistochemistry (IHC) on tissue specimens. Subsequently, functional analysis was conducted using the lung adenocarcinoma cell line.
Results: By spatial transcriptomics profiling, positive UGT2B15 and negative S100A4 were suggested as candidate markers for distinguishing IMA from PCLM. The expression status of these proteins were confirmed by IHC on tissue specimens. Transcription factor analyses suggested that HNF1A was involved in UGT2B15 expression in the IMA, and functional analyses using lung cancer cell lines also demonstrated these associations.
Conclusion: We identified UGT2B15 and S100A4 as potential candidate markers for distinguishing IMA from PCLM. The involvement of the transcription factor HNF1A in the expression of UGT2B15 in the IMA was suggested.

#4167 Virtual inference of collagen architecture from H&E to characterize stromal fiber morphology and organization in colorectal cancer.

Harsimran Kaur[1], Minh-Khang Le[2], Arkadiusz Gertych[2], Maha Guindi[2], Jun Gong[3], Alexandra Gangi[2], Kyle Coleman[2], Jane C. Figueiredo[4], Xiaoying Liu[5], Louis J. Vaickus[5], Keluo Yao[6], Ken S. Lau[7], **Joshua Jay Levy**[2]

[1]Vanderbilt University School of Medicine, Nashville, TN,[2]Cedars-Sinai Medical Center, Los Angeles, CA,[3]Cedars-Sinai Medical Center, Studio City, CA,[4]Samuel Oschin Comprehensive Cancer Institute, Los Angeles, CA,[5]Dartmouth-Hitchcock Medical Center, Lebanon, NH,[6]Cedars-Sinai, Los Angeles, CA,[7]Vanderbilt University Medical Center, Nashville, TN

Background: Collagen architecture is a key determinant of colorectal tumor progression, influencing immune exclusion, fibroblast differentiation, and tumor budding, and plays a central role in shaping the tumor microenvironment. Although image analysis algorithms exist to quantify collagen features such as fiber density, orientation, and organization, but typically require specialized stains like picrosirius red (PSR). Computational methods that infer collagen phenotypes directly from H&E slides could enable larger studies of spatial tumor matrix biology and support development of prognostic imaging biomarkers.

Methods: In this pilot study, four colorectal cancer slides were stained with H&E and imaged, then restained with PSR, and re-imaged. Co-registered stromal patches yielded 40,740 training/validation and 4,528 real PSR and H&E test image patch pairs. Two generative image-to-image translation models, pix2pix and a latent diffusion model were trained to generate virtual PSR (vPSR) patches from the H&E patches. The real PSR test patches paired with the H&E test patches served as reference. The virtual pix2pix (pix2pix-vPSR), diffusion (diffusion-vPSR) and real PSR test patches were processed to obtain collagen fiber masks. Subsequently, 108 collagen fiber density and orientation features were extracted from each mask and correspondence of the features extracted from pix2pix-vPSR and diffusion-vPSR collagen masks were compared with those extracted from real PSR collagen mask using Spearman correlation coefficients.

Results: Both models produced strong correlations with real PSR features, particularly for collagen area fraction ($r > 0.89$), high-density matrix fraction ($r > 0.86$), gap circle count ($r > 0.86$), fiber spine area ($r > 0.83$), coherency/anisotropy ($r > 0.82$), fractal dimension ($r > 0.82$), fiber angle ($r > 0.80$), and fiber length ($r > 0.80$). Diffusion-vPSR correlations ranked among the top 90% and exceeded pix2pix-vPSR correlations by an average $\Delta r > 0.07$, with the gains observed for fiber contour- and thickness-based features, including median length ($\Delta r > 0.20$), thickness variation ($\Delta r = 0.19$), and asymmetry indices ($\Delta r > 0.16$). Smaller improvements were observed for fiber entropy length, variability and for skew/kurtosis/gap statistics (Δr=0.07-0.11). Pix2pix correlations surpassed diffusion correlations in only 10% of features; primarily gap fiber density features ($\Delta r \leq 0.05$).

Discussion: This study demonstrates the feasibility of generating vPSR images from routine H&E slides to infer collagen architecture with high fidelity. Broader application and refinement across larger cohorts will clarify how collagen architecture shapes tumor behavior, recurrence risk, and patient outcomes, supporting further spatial biomarker development.

#4168 All-in-one digital pathology compares and contrasts the tumor microenvironment of renal cell carcinoma tissue with paired, patient derived tumoroids.

Levi Maston, Amber L. Ortiz

Indica Labs, Albuquerque, NM

AI-powered pathology advances translational research by shrinking the gap from discovery to diagnosis through highly performant analytical capabilities. Here, we utilize the HALO®/HALO AI quantitative image analysis platform to compare the tumor microenvironment (TME) of patient tumor samples and corresponding tumoroids. Tumoroids created (in vitro) from primary tumor tissue (in vivo) allow researchers in the field of oncology to more accurately replicate the TME of patient biological specimens. Tumoroids compared to 2-D cell culture are believed to better mimic the physiologically relevant environment by reducing the destruction of native tissue structure and cellular composition. We perform AI-powered image and spatial analysis on multiplexed immunofluorescent tissues incorporating biomarkers for immune subtypes and key features of tumoroids such as TME, cell proliferation, immune profile. The samples have been obtained from the BioStudies BioImage Archive under the study S-BIAD1661 containing samples of clear cell Renal Cell Carcinoma (ccRCC)[1]. By applying digital pathology techniques to these research approaches, we demonstrate a thorough and versatile analysis workflow to address the characterization of tumoroids and their corresponding patient samples and highlight the impact of these tools on research, discovery and diagnostics.

1. Greice Michele Zickuhr, Hazem Abdullah, In Hwa Um, Alexander Laird, Peter Mullen, David J. Harrison and Alison L. Dickson. "Clear Cell Renal Cell Carcinoma Patient-Derived Tumoroids characterisation by Spatial Mass Spectrometry, Histology and Multiplex Immunofluorescence." *BioStudies*, S-BIAD1661, 2025, www.ebi.ac.uk. Accessed 22 September 2025.

#4169 Reading the map: An invitation to the resources of the Human Tumor Atlas Network.

Adam Taylor[1], Ashley Clayton[1], Aditi Gopalan[1], Milen Nikolov[1], Thomas Yu[1], David Gibbs[2], Yamina Katariya[2], Dar'ya Pozhidayeva[1], Ino de Bruijn[3], Seluck Onur Sumer[3], Kristen Anton[4], Jennifer Altreuter[5], Alex Lash[5], Ethan Cerami[5], Nikolaus Schultz[3], Vesteinn Thorsson[2]

[1]Sage Bionetworks, Seattle, WA,[2]Institute for Systems Biology, Seattle, WA,[3]Memorial Sloan Kettering Cancer Center, New York, NY,[4]Dartmouth Health, Lebanon, NH,[5]Dana-Farber Cancer Institute, Boston, MA

Purpose: The Human Tumor Atlas Network (HTAN) sets out to map the cellular and molecular architecture of human tumors over space and time to advance precision oncology. The HTAN Data Coordinating Center (DCC) underpins this mission by standardizing, integrating, and distributing multimodal data; ensuring legacy and impact.
Methods: The DCC developed a scalable cloud ecosystem (Synapse.org, Google BigQuery, custom data portal) for data ingestion, governance, validation, and dissemination. A community-driven process, aligned with NCI standards, produced a consistent metadata schema that ensures interoperability across rich clinical and biospecimen information and all data modalities. The HTAN data portal provides a single landing page for users of HTAN data featuring filter-based search, visualization of imaging and single-cell datasets and detailed documentation. Data are disseminated via a tiered model, with imaging and dbGaP-controlled access sequencing data available from NCI Cancer Research Data Commons General Commons and open-access processed data on Synapse.org. Current work transitions to a modular LinkML data model, adds an AI-assisted curation interface, and includes a streamlined medallion architecture in BigQuery and portal enhancements.
Results: The first five years of HTAN (release v7.0) produced 334 TB of multimodal data (0.23M files) from 2,372 cases and 11,378 biospecimens, spanning >60 disease types and >25 assays. HTAN supports >3,400 unique global users a month. The most frequently accessed data includes scRNA-seq (1075 downloading users), multiplex imaging (197), and spatial transcriptomics (419). Analysis of dbGaP requests to-date (N=127) shows broad academic (75%) and industry use with research themes focused on genome instability (115 requests), immune evasion (52), and metastasis (49), often with multi-omic and AI-driven approaches.
Conclusions: HTAN has established a globally utilized, harmonized foundation for spatially resolved, multimodal cancer research. This enduring platform for community-driven discovery is built on robust data management and transparent access models. The next phase deepens integration of spatial and clinical data, expanding AI-readiness, and strengthening support for reuse and reproducibility. We invite researchers to engage with this resource.
ChatGPT 5, Gemini 2.5 Pro, & Claude Sonnet 4.5 were used to summarize usage metrics, conduct thematic analysis of dbGaP applications, and initial abstract drafting. All content was evaluated and approved by the authors.

#4170 An AI-driven multimodal workflow for enhancing late-phase clinical trial outcome prediction.

Inbal Gazy[1], Assaf Avinoam[1], Reva Basho[2], Jonathan Zalach[1]

[1]Imagene AI LTD, Tel Aviv, Israel,[2]Ellison Medical Institute, Los Angeles, CA

A major challenge in drug development is the gap between early-phase signals and late-stage success. Despite promising early-stage clinical trial readouts, fewer than 10% of drug candidates ultimately progress to regulatory approval, highlighting substantial gaps in predictive fidelity along the development pathway. This gap complicates decision-making, leading to increased development time, costs and risks. Key contributors to this challenge include the small sample sizes inherent to early-phase cohorts and the limited use of patient stratification, shown to be a contributing factor for higher success rates. Recent advances in artificial intelligence (AI) have introduced powerful tools that have the potential to support clinical trial progress evaluation. By integrating multimodal models with real-world data (RWD) within an AI-driven framework, Imagene AI is developing approaches to address the discrepancies between early and late-phase outcomes, and to support better evaluation of late-phase readouts, such as survival outcomes and biomarkers identification, based on early phase cohorts. In this study, we adopted a multimodal foundation-model strategy, built on a diverse set of foundation models. Among them, our digital pathology foundation model, CanvOI, played a central role in enabling prediction of large-cohort outcomes from small-cohort data. Models were trained on a limited sample set of Trastuzumab (Herceptin)-treated breast cancer patients with outcome data. We then generated Kaplan-Meier survival curves for this small cohort with and without an AI-augmented workflow and compared the results with published outcomes from a Phase III trial. Our findings show that the AI-augmented predictions better align with the Phase III clinical trial outcomes, suggesting that this approach has the potential to support more informed decisions using early-phase data. *ChatGPT was used for editing this abstract

: Integrative Computational Approaches 2
Poster Session

#4174 hla2vec: Developing a HLA embedding space using probabilistic cross-reactive groups.

Isabel Quesada, Jordan Tagle, **Kyle Ellrott**

OHSU Knight Cancer Institute, Portland, OR

The genes in the major histocompatibility complex (MHC) that code for the Human Leukocyte Antigen (HLA) protein complex are some of the most diverse genes in the genome. And while some of the alleles such as HLA-A*02:01 are seen in almost 25% of the population, databases such as IMGT/HLA report nearly 20 thousand variants. In cancer populations, this produces a long tail of individuals who are unique within a sampled population. HLA class I typing for The Cancer Genome Atlas (TCGA) covered almost 10K individuals across 33 cancer types, and resulted in over 300 HLA alleles. Within this cohort alleles such as HLA-A*03, HLA-A*33, and HLA-A*2 have been associated with prognosis and immunotherapy response in various cancers. Not all HLA alleles are different, with some alleles observing similar binding patterns that can place them in cross-reactive groups (CREGs). And while this concept has traditionally been documented as a discrete set of documented alleles, from large scale experiments we can start to think of this as a probabilistic space representing probabilistic CREGs (pCREGs). Two alleles in a pCREG may only bind to some fraction, for example 90%, of the same peptides. Using this as a basis we can develop an embedding space where the distance between different HLA alleles is relative to their pCREG association. We have developed a method called HLA2Vec, which has been trained on the 15 million HLA/peptide binding experiments accumulated in the BigMHC dataset. In addition, we developed a benchmark to describe a new model's ability to identify CREGs. We have compared this method to other Protein Modelling Languages (PML), such as Evolutionary Scale Modeling (ESM) in their ability to identify pairs of HLAs that are likely to be in the same pCREG, and found the HLA2Vec to be much more accurate, while using many fewer parameters. With HLA alleles placed in this embedding space, we are able to cluster together smaller groups of individuals with near unique HLA alleles into larger subtypes, based on pCREG status, bringing together patients likely to have similar immune HLA binding patterns for statistical analysis. This analysis has been applied to TCGA data to group rare alleles into larger response groups. The next steps of this research are to see if this method for HLA embedding may also provide insights for developing similar embedding spaces for T Cell Receptor (TCR), and improve HLA pCREG conditional binding prediction.

#4175 Neoantigen-guided TCR discovery pipeline to improve specificity and reduce off-target toxicity in AML.

Pamella Borges[1], Martiela Freitas[1], Samee Ullah[1], Hussein A. Abbas[2], Dinler Antunes[1]

[1]Biology and Biochemistry, University of Houston, Houston, TX,[2]UT MD Anderson Cancer Center, Houston, TX

Identifying and engineering neoantigen-specific T cell receptors (TCRs) remains a major barrier to advancing adoptive immunotherapy for acute myeloid leukemia (AML), a malignancy characterized by a low mutational burden and, consequently, limited neoantigen availability. Recent studies have highlighted recurrent AML-associated mutations as promising sources of therapeutic neoantigens, arising from chromosomal alterations, motivating the development of new strategies to systematically discover and evaluate TCRs targeting antigens while minimizing off-target toxicity. We developed a structure-guided TCR discovery pipeline that designs neoantigen-specific TCRs, determines their presence within AML patient repertoires, and evaluates binding specificity and predicted safety. From the literature, we selected recurrent AML neoantigens restricted by HLA-A*02:01, including the TP53 Y220C peptide (VVPCEPPEV) and the NPM1 mutant peptide (AIQDLCVAV), both of which are among the most common TP53 hot-spot and the most frequent molecular alterations in AML. A melanoma-derived TCR-pHLA structure (PDB: 2BNQ) was used as an unbiased scaffold for inserting each AML neoantigen. ProteinMPNN, a deep learning-based protein sequence design, was then applied to redesign residues within CDR1-3, generating 50,000 candidate TCR sequences predicted to optimize interface complementarity and binding. Single-cell TCR-sequencing (scTCRseq) data were analyzed to extract paired α/β patient TCRs, with high-confidence receptors identified based on barcode redundancy and immune phenotype. Clustering of patient and designed TCRs using GLIPH2 revealed a dominant cluster comprising >90% of TP53-associated patient TCRs and two designed TCRs sharing a CDR3 motif, whereas no convergence was observed for NPM1 sequences. Three designed TCRs (two motif-convergent and one top-ranked by structural confidence) and the 62 patient TCRs from the convergent cluster were structurally modeled using TCRmodel2. All modeled TCRs are now being evaluated with STAG-LLM to predict binding specificity and interface similarity to the TP53-HLA complex. The top candidates will progress to molecular dynamics simulations to characterize contact fingerprints and evaluate potential off-target toxicity using CrossDome, which evaluates TCR cross-reactivity based on biochemical similarity between peptide-HLA ligands and predicts the off-target toxicity risk of T-cell-based immunotherapies. Initial results suggest structural and repertoire-based convergence toward recognition of TP53, supporting its relevance as an immunologic target for AML. By integrating rational TCR design, patient repertoire interrogation, and computational safety screening, this pipeline provides a scalable, reproducible framework for discovering neoantigen-specific, potentially low-toxicity TCR candidates for AML immunotherapy.

#4176 DAG-guided kernel learning framework to mitigate racial disparities in breast cancer.

Min-jeong Baek[1], Jieqiong Wang[2], Vimla Band[1], **Shibiao Wan**[1]

[1]Department of Genetics, Cell Biology and Anatomy, University of Nebraska Medical Center, Omaha, NE,[2]Department of Neurological Sciences, University of Nebraska Medical Center, Omaha, NE

As the second leading cause of cancer death among women in the United States, breast cancer (BC) mortality is disproportionately higher among Black women than among non-Hispanic White women. Artificial intelligence (AI) and machine learning (ML) approaches have been successfully applied to mitigate racial disparities in BC. For instance, previously we developed a multi-modal transfer learning (TL) framework that can help address health disparities by transfer knowledge learned on the majority group (e.g., non-Hispanic White women) to improve performance of AI/ML models for a minority group (e.g., Black women). However, these approaches integrate different omics data in a simplistic manner, but failed to capture the complex cross-omics interaction among them, leading to minor or modest performance improvement for reducing BC health disparities. To address these concerns, we propose a directed acyclic graph (DAG)-guided kernel learning framework to mitigate racial disparities in breast cancer. Specifically, we first encoded the cross-omics interaction knowledge into a DAG graph by a method called non-combinatorial optimization via trace exponential and augmented Lagrangian for structure learning (NOTEARS). Then, we hard-masked the learned graph to retain only biology-consistent projections. From these projections, we computed projection-specific RBF kernels to capture non-linear sample similarity, yielding interpretable, direction-aware kernels used for training a TL model equipped with a data augmentation (DA) method, which were used to reduce breast cancer disparities. By using three omics modalities (i.e., mRNA, miRNA, and DNA methylation) from The Cancer Genome Atlas (TCGA) BRCA cohorts of 1,085 female BC patients, we demonstrated that our proposed framework achieves remarkably better performance (using various performance metrics like ROC-AUC, PR-AUC, Accuracy, and F1-score) compared with state-of-the-art approaches for reducing BC health disparities in terms of time-specific Progression-Free Interval (PFI) predictions. In addition, our framework could quantify and identify multiple key cross-modality interactions to mitigate BC racial disparities. In summary, our proposed framework would provide a novel approach to explore cross-omics interactions for boosting a robust TL model performance to reduce health disparities in BC. We also believe our approach can be extended to mitigate racial disparities for other types of cancer.

#4177 Integrated meta-clustering reveals subtype-specific transcriptomic heterogeneity of pediatric low-grade glioma.

Bulidierxin Tuerhanbayi[1], Jieqiong Wang[2], **Shibiao Wan**[1]

[1]Department of Genetics, Cell Biology and Anatomy, University of Nebraska Medical Center, Omaha, NE,[2]Department of Neurological Sciences, University of Nebraska Medical Center, Omaha, NE

Pediatric low-grade glioma (pLGG) is the most common type of brain tumor in children, accounting for approximately 30% of all central nervous system tumors in children. pLGG has multiple molecular subtypes that differ in disease progression, recurrence patterns, and treatment responses. Conventional wet-lab approaches including molecular profiling and histopathological studies for pLGG characterization are time-consuming, costly, and laborious. Recently, methods based on artificial intelligence (AI) or machine learning (ML) have been widely used for pLGG molecular categorization, but most of them can only identify two or three pLGG subtypes. To more comprehensively characterize the molecular subtypes of pLGG and their potential biological and therapeutic significance, we develop an integrated meta-clustering approach to explore high-resolution molecular subtypes and their transcriptional heterogeneity for pLGG. Specifically, we first performed multiple rounds of random projection (RP) to generate dimension-reduced feature vectors from pLGG transcriptomics data, each of which was subsequently clustered by some conventional clustering algorithms including hierarchical clustering, K-means, and self-organizing maps, as base clustering methods. Then, to yield robust clustering performance, we integrated the clustering results of these RP-based individual clustering algorithms by adopting a weighted meta-clustering (wMetaC) approach. Results based on 543 pLGG patients suggested that our proposed approach demonstrated superior stability and discriminative powers for higher-resolution pLGG subtyping compared to conventional approaches. Based on consensus matrix analysis, we identified two major pLGG subtypes, with one further subdivided into three subgroups and the other into two. Then, we performed cluster-specific differential gene expression analysis, molecular pathway analysis, and gene-drug-disease association analysis. The results showed that the identified five subgroups exhibited significant subtype-specific transcriptomic heterogeneity. In summary, our meta-clustering approach demonstrates higher accuracy and robustness in identifying higher-resolution molecular subtypes of pLGG, revealing the molecular heterogeneity within pLGG and potentially providing new insights for more precise molecular subtyping and precision therapy.

#4178 Mapping the imputation-augmented somatic mutation landscape of 2,551 NSCLC patients highlights contrasting patterns across histologic subtype, smoking status, and ancestry.

Isam Mohd-Ibrahim, Zhuokun Feng, Yu Chen, Lauren Higa, Youping Deng

University of Hawai'i at Manoa, Honolulu, HI

Non-small cell lung cancer (NSCLC) is a genetic disease characterized by an abundance of somatic mutations. Within the many mutations that make up the somatic mutation landscape, a select few actively drive the development of cancer. Mutations in driver genes have gained import as therapeutic targets, biomarkers, and aides in understanding oncogenesis. Recent studies have also shown the preponderance of certain drivers in certain demographics, as is the case for the targetable EGFR mutations in female non-smokers of Asian descent. In this study, we attempt to add further clarity and definition to the somatic mutation landscape of NSCLC using 2,551 secondary DNA-sequencing data aggregated from various cohorts. We also utilized machine learning-based methods to impute smoking status and genetic ancestry to create a broad and deep cohort to identify unique associations between somatic features and specific populations. We aggregated and processed the genomic data into highly granular somatic mutation features and identified 87 significantly mutated genes (SMG), 48 of which are putatively novel driver genes. EAS (patients of East Asian ancestry) patients were found to have fewer SMG per patient and a significantly lower tumor mutation burden than patients of other genetic ancestries. This remained true even after stratifying the populations studied by smoking status and cancer subtype. Besides associations with EGFR, multivariable models also identified more frequent ATM and STK11 mutations in EAS patients. Unsupervised clustering on the 87 SMG and 109 mutational signatures identified 6 distinct clusters, including 2 previously identified distinct KRAS-featuring clusters. Common clinical features were observed within some clusters, for example, female EAS non-smokers were particularly enriched in one cluster. Cox regression models identified better survivability in EAS patients and patients with EGFR mutations, whereas patients with mutations in TP53, KEAP1, and BID had significantly poorer survival. The results from this study identify a clear disparity in the somatic mutation landscape of lung cancer patients of different ancestries, which should be taken into consideration in future studies. The results also highlight the benefits of utilizing large, heterogeneous datasets of a specific cancer type in driver gene discovery and the utility of integrating multiple somatic features. This study also emphasizes the benefits of data imputation, integrating 942 patients with otherwise unknown smoking status.

#4179 Three-dimensional spatial multi-omics of gastric tumor sections reveal hidden features beyond 2D analyses.

Inyeop Jang[1], Soyoung Im[1], Minji Kim[1], Seok-Jin Chung[1], Minsoo Lee[2], Soonyoung Lee[2], Jongseong Jang[2], Tae Hyun Hwang[1]

[1]Vanderbilt University Medical Center, Nashville, TN,[2]LG AI Research, Seoul, Korea, Republic of

Single-section spatial-omics frequently misses microanatomical context and is sensitive to sectioning variability. Recent 3D reconstruction studies highlight substantial heterogeneity within the tumor microenvironment obscuring true biology. Emerging platforms (e.g. Singular Genomics G4X) enable in-situ RNA/protein readouts at subcellular resolution on the same slide with fluorescent H&E, creating serialized spatial multi-omics. This work allows us to map transcript abundance at the subcellular level with x-y-z coordinates, integrating H&E, transcripts, and proteins on the thick tissues, enabling true 3D spatial multimodal tumor modeling.We profiled serial FFPE sections using the G4X system to jointly quantify targeted RNAs and proteins per slice. Across slices, we compared cell types, neighborhood enrichment matrices, and gene-set enrichment to measure inter-slice inconsistency. We then registered the serial sections into a common 3D frame, reconstructed a volumetric atlas, and identified 3D hotspots for exhausted T-cell programs. To directly visualize whether these patterns reflected true 3D structure, we acquired label-free 3D holotomography from the same serial sections, aligned them with the corresponding serial G4X data in a shared 3D space, applied AI-based single-cell segmentation, and mapped cell types defined by G4X RNA and protein expression back to their x-y-z coordinates.Serial 2D slices showed discordant cell-type compositions and neighborhood enrichments, indicating strong variability even within a single tumor block. In contrast, 3D reconstruction revealed a coherent exhausted T-cell domain that failed to reach statistical significance in any individual slice. Holotomography confirmed dense, continuous interfaces among T cells, extracellular matrix, and tumor cells across depth, supporting true biological continuity and demonstrating subcellular localization of transcripts and proteins in 3D.Our 3D spatial multi-omic approach shows that single-section analyses may miss clinically relevant immune niches, whereas integrated 3D RNA-protein-holotomography profiling recovers hidden signals. By mapping and combining the transcripts with proteins and the 3D holotomography at subcellular x-y-z coordinates in thin and thick tissues, we provide a practical workflow for volumetric tumor-immune profiling that can accelerate biomarker discovery and therapeutic targeting in gastric cancer and can be generalized to other cancer types."Generative AI was used only to edit this abstract's language. The authors are responsible for the study concept, data interpretation, and conclusions, and have approved the final version."

#4180 Protocol-specific and coverage-based RNA-seq metrics characterize RNA integrity signatures across cohorts.

Miyeon Yeon[1], Wonyoung Choi[2], Jin Young Lee[2], David Neil Hayes[3], Hyo Young Choi[4]

[1]Preventive Medicine, University of Tennessee Health Science Center, Memphis, TN,[2]University of Tennessee Health Science Center, Memphis, TN,[3]UTHSC Center for Cancer Research, Memphis, TN,[4]Preventive Medicine, University of Tennessee Health Science Center, Memphis, TN

Background: RNA degradation profoundly impacts transcript quantification and downstream biological interpretation. Existing RNA quality assessment methods are largely limited to poly(A)-selected mRNA-seq and do not generalize to total RNA-seq, resulting in inconsistent quality evaluations across sequencing protocols. We hypothesize that base-resolution RNA-seq coverage profiles capture protocol-specific quality signatures. By modeling unexpected variation in these coverage patterns, RNA-seq quality can be accurately assessed for both mRNA-seq and total RNA-seq (including frozen and FFPE samples) within a common analytical framework tailored to each protocol.
Methods: For both mRNA-seq and total RNA-seq, we quantify abnormal variations in per-base coverage by explicitly modeling degradation-related and other low-quality patterns. For mRNA-seq, specifically, we developed the Degradation Score (DS), which estimates the positional decay in read coverage along transcripts. For total RNA-seq, we introduced the window Coefficient of Variation (wCV), a variant of CV metric that captures coverage nonuniformity, reflecting the tendency of degraded samples to show elevated variability across gene bodies. We applied these metrics to over 2,600 RNA-seq profiles spanning multiple sequencing strategies and cohorts, including TCGA (mRNA-seq), CALGB (fresh frozen total RNA-seq), and ALCHEMIST (FFPE total RNA-seq).
Results: Across datasets, our coverage-based metrics showed stronger correlations with conventional QC measures ($|r|$=0.52-0.59 in mRNA-seq, 0.43-0.89 in total RNA-seq; $p<0.001$) than the correlations among themselves ($|r|$=0.24-0.44 in mRNA-seq, 0.44-0.88 in total RNA-seq; $p<0.001$). We also identified a set of samples in which conventional QC flagged high degradation but coverage profiles appeared intact, and vice versa, highlighting protocol-dependent discrepancies. Manual inspection confirmed markedly greater aberrant variability in samples with high DS (mRNA-seq) or high wCV (total RNA-seq). Using standardized within class sum of squares across RNA quality strata, we found that samples classified as high-quality by our metrics consistently preserved known subtype structure across normalization methods.
Conclusions: These protocol-specific, coverage-based measures provide a coherent and reproducible framework for evaluating RNA integrity across sequencing strategies and experimental conditions. Incorporating degradation-aware QC into RNA-seq pipelines improves interpretability, comparability, and biological fidelity of transcriptomic analyses in large cancer genomics studies.

#4181 De-risk targets through mechanism-enabled simulations in the Virtual Lab.

Krishna Bulusu, Katalin Szegner, Laszlo Merő, Eszter Szarka, Ivan Fekete, Maria Victoria Ruiz Perez, Csilla Hegedűs, Imre Gaspar, Gabor Kovacs, Kristof Szalay, Daniel Veres

Turbine Simulated Cell Technologies Ltd., Budapest, Hungary

Minimizing the risk of late-stage failure in drug discovery for novel targets remains a central challenge in translational research. Conventional preclinical perturbation datasets lack mechanistic insight and context specificity. Turbine's Virtual Lab offers access to simulations with mechanistic insights enabled by AI-guided virtual cell modeling to predict phenotypic and transcriptomic outcomes of genetic and pharmacological perturbations in preclinical models representative of patient heterogeneity. This framework enables systematic evaluation of target-disease linkage mechanisms, target liabilities, and combinatorial strategies to enrich preclinical decision-making data packages. We utilized our Simulated Cell technology to construct virtual replicates of more than 1,200 cancer cell lines by integrating large-scale omics data (CCLE) with a curated signaling network as prior knowledge. The virtual cell lines were trained on experimentally observed genetic (DepMap) and pharmacological perturbation data (GDSC2) to accurately represent their phenotypic responses, and on differential gene expression data (LINCS) to describe post-perturbation transcriptomic states. Benchmarking was performed against an unseen set of cell lines across all genes and selective essential genes only. Target assessment reports were generated by merging simulation-derived phenotypic and post-perturbation omics features with curated clinical intelligence, yielding an integrated view of signaling-level mechanisms of action, patient stratification strategies, combination potential, and initial safety assessments. The Simulated Cells accurately reproduced DepMap dependency outcomes, demonstrating a global test-set Pearson correlation of 0.90 across all genes. For selective essential genes only, we measured a cell-line wise 0.55 Pearson correlation. Replicate-level Pearson correlation is 0.78 for the same metric, while baseline (bias) models score only 0.23. Notably, the prospective validation hit rate stands at 70% for dependency predictions, also capturing novel dependencies not identified in DepMap. For a set of 10 in silico-identified targets, we observed a 50% shorter timeline from identification to in vivo validation and a 100% higher rate of in vitro validation compared with industry benchmarks. We have also established a Virtual Lab platform that provides easy, scalable, and interpretable access to these simulations. Turbine's target discovery platform combines mechanistic interpretability with strong concordance to experimental dependencies, bridging computational modeling and translational research. The Virtual Lab interface is user-friendly and optimized for adoption without any data science or AI expertise. This approach enables data-driven, de-risked, and accelerated target selection and portfolio advancement in oncology discovery.

#4182 Pan-cancer landscapes of transcriptional heterogeneity in metastatic tumors.

Ramyar Molania[1], Himisha Beltran[2]

[1]Dana-Farber Cancer Institute, Boston, MA,[2]Dana-Farber Cancer Institute, New York, NY

Metastasis, the spread of cancer from its original site to distant organs, is the leading cause of cancer-related mortality. A deeper understanding of the molecular mechanisms underlying metastatic progression is therefore of critical clinical importance. The availability of large-scale pan-cancer bulk RNA-seq datasets from both primary and metastatic tumors provides a unique opportunity to investigate the shared and distinct transcriptional features of metastasis. Furthermore, this creates an unprecedented opportunity to perform systematic analyses across metastatic tumors from diverse cancer types.However, our initial pan-cancer analysis demonstrated that several major confounding factors,most notably strong tissue background signals in metastatic samples, pose significant challenges for accurately comparing primary and metastatic tumors. We have previously established effective strategies to adjust for immune and stromal components in bulk transcriptomic data. Building on this foundation, we have recently extended our approach to address a key obstacle in studying metastasis: the overwhelming influence of tissue-of-origin signals at metastatic sites.To evaluate our method, we first performed in silico simulations of normal-tissue background correction using TCGA pan-cancer RNA-seq data. We further generated pseudo-bulk profiles from single-cell RNA-seq datasets spanning multiple cancer types, each exhibiting varying degrees of background tissue contamination. Across these datasets, our analyses demonstrate that this approach effectively removes confounding signals, thereby enabling more accurate transcriptomic comparisons between primary and metastatic tumors. Application of this method to large pan-cancer bulk RNA-seq cohorts revealed promising and novel biological insights, including both shared and cancer-type-specific transcriptional programs associated with metastatic progression.Our preliminary analysis indicates that multiple hallmark pathways, including oxidative phosphorylation and epithelial-mesenchymal transition (EMT), are broadly upregulated across metastatic tumors in pan-cancer datasets. In addition, we observe pronounced immunosuppressive signaling within the tumor microenvironment of metastatic lesions, suggesting that metabolic rewiring and immune evasion are coordinated features of metastatic disease.

#4183 Finding Goldilocks: How AI-powered covalent drug discovery removes the “un” from “undruggable”.

Johannes C. Hermann, Robert Everley, Han Wool Yoon, Rohan Varma, Karsten Krug, Daniel Erlanson, Chris Varma, Kevin R. Webster

Frontier Medicines, South San Francisco, CA

Covalent drugs offer a path to drugging hard targets to provide urgently needed novel cancer medications. Starting from small covalent fragments is efficient in principle but difficult in practice due to challenges distinguishing generic from specific reactivity and the influence of the reactive warhead on all other chemical properties. The Frontier™ Platform and covalent AI as a key pillar overcomes these challenges. Focused super large-scale experimental data generation relevant to covalent drug discovery has enabled the development of several powerful covalent AI algorithms. Their application falls into two different fields, firstly the better understanding of the proteome and proteins and potential covalent binding sites and secondly in advancing covalent chemistry. We detail strategic data generation through chemoproteomics experiments, quantum mechanics, experimental chemical property determination, and the leveraging of these data to inform covalent drug discovery for hard-to-drug targets. This includes the AI-driven characterization of covalent binding sites across nearly the complete human proteome. Covalent fragment hits have been identified for multiple difficult cancer targets including KEAP1, ADAR, DHX9, PTPN11, MYC, and many others (>75% of important cancer driver genes). Furthermore, we will highlight several novel AI covalent chemistry applications. We will present an algorithmically designed covalent fragment library for screening, covalent chemical property prediction algorithms, and details of our highly specialized AI-driven covalent drug design engine that autonomously ingests all relevant data for a given project and suggests optimized compounds to be synthesized. We show the impact of this approach for a historically undruggable transcription factor and cancer driver as an example. Undruggable targets across a variety of cancer target classes have become druggable leaning on advanced covalent drug discovery methods.

#4184 Multimodal deep learning framework for predicting clinically significant phenotypes in prostate cancer.

Priyanka Vasanthakumari[1], Mohamed Omar[2]

[1]Computational Biomedicine, Cedars-Sinai Medical Center, Los Angeles, CA,[2]Cedars-Sinai Medical Center, West Hollywood, CA

Prostate cancer is the most common non-cutaneous malignancy and the second leading cause of cancer-related death among men in the United States. Its clinical and biological heterogeneity poses major challenges for accurate outcome prediction and treatment planning. Traditional single-modality models often fail to accurately capture the risk of disease progression. Recent advances in artificial intelligence, particularly foundation models, enable the integration of heterogeneous data into unified representations of tumor biology, which can in turn uncover better predictive and prognostic features than what is possible with unimodal modalities.We develop a multimodal model that integrates histopathology whole-slide images (WSIs), transcriptomics, and clinical data to predict prostate cancer molecular and clinical phenotypes, enhancing both predictive accuracy and interpretability. The framework employs separate encoders for each modality: an image encoder adapted from foundation models CONCHv1.5 and TITAN, a text encoder based on ClinicalBERT for clinical data, and a transcriptomic encoder combining Gene2Vec embeddings with expression-level features projected into a shared latent space. The encoders are contrastively fine-tuned using pairwise alignment, with WSIs serving as the anchor modality based on paired data availability.The multimodal representations are evaluated on several downstream clinically significant prediction tasks, including Gleason grading, metastasis prediction, biochemical recurrence, and molecular alteration status such as TMPRSS2:ERG fusion and PTEN loss. The framework also provides interpretability by quantifying the contribution of each modality and visualizing attention distributions, highlighting joint feature representations that are important to each task.This study uses data from 632 patients with paired data from public and institutional repositories. Inter-modality fine-tuning between WSI and clinical text data yielded promising alignment results, with paired image-text samples achieving significantly higher similarity ranks than unpaired samples (mean p-value $\approx 10^{-29}$). Gleason grade multiclass classification downstream task achieved an overall test accuracy of 81.4% and a weighted F1 score of 79.6%.

#4185 A modular *in silico* triage pipeline for multi omic evaluation of surface protein targets across indications.

Satyajit Rajapurkar, Lena Eismann, Mariana Pereira, Theodore Groth, Mugdha Khaladkar, Kathrin Jansen, Edward Curry, Marica Speranza

GSK, Collegeville, PA

Antibody-Drug Conjugates (ADCs) have revolutionized oncology by coupling cytotoxic payloads with antibodies that selectively target malignant cells. However, balancing efficacy with toxicity continues to be a major challenge, especially when off-target expression in healthy tissues leads to adverse side effects. To address these limitations, we have developed a modular in silico triage pipeline that integrates multi-modal, multi-omic datasets to systematically evaluate candidate surface proteins for targeted bispecific therapy.Our pipeline evaluates candidate antigens based on their MS-based tissue protein expression patterns across diverse cell populations and tissues, enabling the identification of markers that are predominantly upregulated in cancer cells while maintaining low mRNA expression in critical normal tissues. This comprehensive approach supports the rational design of bispecific antibodies that can further enhance specificity by binding to two distinct antigens simultaneously. By streamlining the target selection process, this strategy promises to accelerate the development of more effective and safer therapeutic modalities across a range of cancer indications.Here, we detail the design, implementation, and validation of our *in silico* framework, providing a robust platform for rapid and flexible evaluation of potential surface protein targets for ADCs and beyond.

#4186 A novel integrated AI ML and COSMIC signature profiling approach resolving blast crisis CML heterogeneity into single patient level pan cancer actionable programs enabling repurposable therapies for relapsed refractory and metastasized cancers.

Zafar Iqbal[1], Abdulkareem AlGarni[2], Lubna Alnuaim[3], Sahrish Khan[4], Sohail Rao[5], Yaqob Taleb[6], Nasser Mohammed AlQahtani[7], Muhammad Alshuaibi[7], Essa Al Mansour[8], Mashael AlShuker[8], Azfar Athar Ishaqui[9], Giuseppe Saglio[10], Kaleem Ahmed[11], Rizwan Naeem[12], Masood A. Shammas[13], Muhammad Farooq Sabar[4]

[1]Department of Zoology & SBB, Univ. of the Punjab, Lahore, Pakistan,[2]King Abdulaziz Hospital; Genomic & Experimental Medicine Group (GEM) & QAAA; CLSP, College of Applied Medical Sciences (CoAMS-A), King Saud Bin Abdulaziz University for Health Sciences (KSAU-HS); KAIMRC-ER, NGHA, Al-Ahsa, Saudi Arabia,[3]CLNS, Genomic & Experimental Medicine Group (GEM), College of Applied Medical Sciences (CoAMS-A), King Saud Bin Abdulaziz University for Health Sciences (KSAU-HS); KAIMRC-ER, NGHA, Al-Ahsa, Saudi Arabia,[4]CAMB & SBB, Univ. of the Punjab, Lahore, Pakistan,[5]Department of Zoology & SBB, INNOVACORETM Center for Research & Biotechnology, San Antonio, TX,[6]Department of Basic Medical Sciences, College of Applied Medical Sciences (CoAMS-A), King Saud Bin Abdulaziz University for Health Sciences (KSAU-HS); King Abdullah International Medical Research Centre (KAIMRC-ER), Al-Ahsa, Saudi Arabia,[7]Adult Oncology, Department of Medicine, King Abdulaziz Hospital / KAIMRC-ER, Al-Ahsa, Saudi Arabia,[8]Medical Oncology, Department of Medicine, King Abdulaziz Hospital, Al-Ahsa, Saudi Arabia,[9]Department of Clinical Pharmacy, College of Pharmacy, King Khalid University, Abha, Saudi Arabia,[10]Department of Hematology & Internal Medicine, Orbassano University Hospital,, Department of Clinical and Biological Sciences, University of Turin, Turin, Italy,[11]International Islamic University Islamabad (IIUI), Islamabad, Pakistan,[12]Montefiore Medical Centre & Alberyt Einstein College of Medicine, New York, NY,[13]DFCI, Department of Oncology, Harvard Medical School, Dana-Farber Cancer Institute, University of Harvard, Boston USA., Boston, MA

Blast crisis CML (BC-CML) is a highly refractory and heterogeneous phase. We applied an integrated whole-exome sequencing (WES), COSMIC mutational signature, and machine-learning (ML) pipeline with AI-guided drug mapping to stratify BC-CML at single-patient resolution. In 19 BC-CML cases within 157 patients, WES revealed markedly elevated mutational burden, widespread chromosomal damage, and distinct molecular architectures. ML resolved three BC-CML subtypes enriched for unique COSMIC signatures and targetable pathways. Therapeutic mapping linked each subtype to repurposable FDA-approved agents, supporting a scalable precision-oncology strategy relevant to relapsed, refractory, and metastatic cancers.

Introduction

BC-CML represents a terminal stage where secondary mutations and genomic stress disrupt TKI response [1]. Shared oncogenic programs across myeloid and solid tumors support pan-cancer therapeutic repurposing [2]. A WES-ML-COSMIC strategy enhances molecular stratification beyond conventional staging [3]. We applied this framework to define actionable BC-CML subtypes.

Methods

A total of 157 patients (123 CP, 15 AP, 19 BC) were analyzed under IRB approval [4]. DNA was sequenced on Illumina NovaSeq, aligned to GRCh38 using BWA-MEM [5], processed through GATK and COSMIC/VEP [6]. PCA+scikit-learn enabled ML clustering [7]. COSMIC signatures were generated using SigProfilerExtractor [8]. PanDrugs guided drug repurposing [9].

Results

BC-CML displayed >2,500 somatic mutations and ~54% higher mutational burden than CP/AP with hotspots on chromosomes 1, 7, 17, and 19. ML defined three subtypes:

Cluster 1 (BRCA2/TP53): HR-deficiency; COSMIC S3/S5.

Cluster 2 (IDH1/2, TET2): epigenetic/metabolic dysregulation; S1/S2.

Cluster 3 (JAK2, CSF3R): cytokine/oxidative-stress signaling; S13/S18.

Drug mapping linked them to PARP/MDM2 inhibitors, IDH inhibitors/HMAs, and JAK inhibitors respectively.

Discussion

This integrated WES-ML-COSMIC framework translates BC-CML heterogeneity into discrete, targetable biological programs [2]. The three clusters reflect distinct evolutionary pressures—HR failure, epigenetic drift, and cytokine-driven oxidative stress—each linked to repurposable FDA-approved therapies [3]. This single-patient-level mapping supports a scalable precision-oncology model for relapsed, refractory, and metastatic cancers beyond BC-CML [4,9].

References

1. Kwon HJ Mol Cancer 2025;24:114.
2. Cruz-Rodriguez N Blood 2025;145:931.
3. Herraiz-Gil S Appl Sci 2025;15:2798.
4. Awada H Cancers 2023;15:2248.
5. Li H Bioinformatics 2009;25:1754.
6. DePristo MA Nat Genet 2011;43:491.
7. Pedregosa F JMLR 2011;12:2825.
8. Sondka Z NAR 2023;52:D1210.
9. Mao Y Mol Cancer 2025;24:123.

#4187 scOncoNet: Dual-graph attention network for program-aware *in-silico* gene perturbation in single-cell cancer data.

Tingyi Li, Yuanyuan Shen, Bin Baek, Xiaoqing Yu, Xuefeng Wang

H. Lee Moffitt Cancer Center, Tampa, FL

Identifying genes that functionally drive malignant programs in single-cell tumors remains difficult, particularly when CRISPR or Perturb-seq data are unavailable. Co-expression alone cannot separate correlation from regulatory influence, and existing analyses lack a framework that connects global molecular networks with patient-specific cellular programs. Current single-cell foundation models largely rely on gene-gene relationships while making limited use of the cell-cell structure intrinsic to tumor ecosystems. To address these gaps, we developed scOncoNet, a lightweight dual-graph attention network that integrates gene-gene and cell-cell structure, malignant meta-program supervision, and gene-to-program attribution to enable program-aware estimation of gene influence directly from patient scRNA-seq data. The model incorporates PPI networks to provide global molecular context for the gene encoder and constructs a program-aware cell graph blending local transcriptomic similarity with malignant program similarity. A two-layer architecture jointly learns gene and cell embeddings, with an attention mechanism that adaptively reweights cell-cell edges to highlight biologically meaningful transitions such as EMT or hypoxia. A program-prediction module anchors the cell embedding space to malignant programs, and gene impact scores combine PPI-informed gene embeddings with gradients that quantify each gene's influence on these programs, generating a mechanistic estimate of its potential effect on malignant states. Using an esophageal squamous-cell carcinoma (ESCC) single-cell dataset restricted to epithelial cells, we defined ESCC-specific malignant programs, including proliferation (*MKI67*), EMT (*VIM*), hypoxia (*CA9*), and immune evasion, and applied scOncoNet to prioritize candidate targets. Top-ranked genes were dominated by ESCRT and proteasome components, including multiple *CHMP* family members along with *VPS25, TSG101, PSMD14*, and *PSMC2*, reflecting core survival and vesicle-trafficking functions consistent with their pan-cancer essentiality. Compared with existing scRNA-seq-based approaches, scOncoNet shows stronger alignment between gene embeddings and malignant programs, enabling precise recovery of functional gene-program relationships. Across additional single-cell datasets, the model consistently preserved malignant program structure and generated stable target rankings. In summary, scOncoNet integrates global molecular networks with patient-specific cellular programs to identify functional gene drivers directly from tumor single-cell data. Its ability to reveal core cancer progression machinery and prioritize candidate CRISPR targets without perturbation experiments suggests utility for mechanistic studies and therapeutic target discovery in tumor types lacking perturbation datasets.

#4188 Breaks in the cancer immunity cycle correlate with response-predictive HNSCC immune microenvironment phenotypes.

Sarah R. Harrington[1], Daniel Uralov[1], Sophia Linguiti[1], Hannah Kenny[1], Parvesh Kumar[2], Janvi J. Shukla[1], Marianna Nicodemi[2], Ian Argento[2], Emma J. Anisman[1], Eloise Freitag[2], Adam J. Luginbuhl[1], Larry Harshyne[3], Zhao Lin[3], Alban J. Linnenbach[3], Ubaldo E. Martinez-Outschoorn[3], Joseph M. Curry[1]

[1]Department of Otolaryngology- Head and Neck Surgery, Thomas Jefferson University Hospital, Philadelphia, PA,[2]Sidney Kimmel Medical College, Thomas Jefferson University, Philadelphia, PA,[3]Department of Medical Oncology- Head and Neck Surgery, Thomas Jefferson University Hospital, Philadelphia, PA

Introduction

Head and neck squamous cell carcinoma (HNSCC) displays substantial immune heterogeneity that shapes response and prognosis to immune checkpoint inhibitor (ICI) therapy. Unlike biomarkers for response to ICI therapy, there is still no understanding of resistance mechanisms. To address this need, we performed baseline pathway enrichment analyses across TME subtypes and clinical outcomes. Using pairwise comparisons, we identified reproducible “breakpoints” within the Cancer Immunity Cycle (CIC) that inform future precision-therapeutic strategies.

Methods

Bulk RNA-sequences from TCGA HNSCCs HPV+ (n=94) and HPV- (n=415) and an our neoadjuvant ICI cohorts HPV+ (n=53) and HPV- (n=29) were assigned TME subtypes: Immune Enriched (IE), Immune Enriched Fibrotic (IEF), Fibrotic (F) and Depleted (D) using published signatures. Unbiased and supervised GSEA were performed, contrasting TME subtype pairs to identify enriched pathways mapping to CIC steps. Step activity was defined as Bioprocess Count × mean NES. Connectivity of CIRCOS plot chords, denoting interplay between steps, was quantified by shared processes × mean STRING signal for protein-protein interaction. CIRCOS plots were generated for TCGA and trial cohorts. Survival analyses used Cox and Kaplan-Meier models ($p<0.05$).

Results

HPV+ tumors exhibited a global reduction of stepwise CIC activities compared with HPV-tumors. As expected, CIC mapping revealed consistent low activity in antigen release (step 1) and antigen presentation (step 2), with variable loss of tumor cell killing (step 7) in F/D tumors. IE tumors maintained near-intact steps, IEF showed partial attenuation, whereas F showed breaks in steps 1-2, and D activity was minimal. CIC analysis revealed novel subpopulations within a given TME subtype, differentiated by survival. TCGA survival analyses showed statistically significant higher adaptive immune/TCR activity improved outcomes in IE tumors. In HPV- F tumors, a senescence/autophagy gene set linked to CIC predicted worse progression-free survival (HR=7.06, $p=0.03$). In contrast, HPV+ D tumors exhibited activity of a senescence gene set strongly associated with improved OS (HR=0.209, $p<0.001$). Phenotype-level survival (HPV-agnostic) showed significantly worse outcomes for F vs IE tumors. These patterns were reproducible in our clinical cohort. Future pathologic response to ICI mirrored CIC integrity, with higher response rates in IE/IEF, but did not reach statistical significance.

Conclusion

CIC modeling across independent cohorts reveals recurrent immune breakpoints in HNSCC, particularly in antigen release and presentation. This novel approach to parsing the TME and CIC activity may be valuable for predictive biomarker discovery, pertaining to response to ICI therapy.

#4189 Quantifying uncertainty in virtual spatial transcriptomics using Bayesian neural networks.

Thanosan Prathifkumar[1], Nehan Mohamed[2], Anvith Kakkera[3], Zarif Azher[4], Xiaoying Liu[5], Fred Kolling[3], Laurent Perreard[3], Scott Palisoul[5], Louis J. Vaickus[5], **Joshua Jay Levy**[6]

[1]Central Peel Secondary School, Brampton, ON, Canada,[2]Thomas Jefferson High School for Science and Technology, Alexandria, VA,[3]Dartmouth College Geisel School of Medicine, Hanover, NH,[4]California Institute of Technology, Pasadena, CA,[5]Dartmouth-Hitchcock Medical Center, Lebanon, NH,[6]Cedars-Sinai Medical Center, Los Angeles, CA

Introduction: Spatial transcriptomics (ST) enables whole-transcriptome profiling within intact tissue architecture but remains costly and batch-dependent. Deep-learning-based virtual RNA inference from hematoxylin and eosin (H&E) slides offers a way to collect ST at scale without profiling, yet the reliability of such predictions is unclear. Uncertainty may arise from assay noise, biological limits on what morphology can reveal, or variation in gene abundance across tissue structures. Uncertainty estimation complements accuracy by helping distinguish these sources and clarify why some genes are more challenging to infer. Here, we integrate virtual RNA inference with Bayesian neural networks (BNN) to quantify and characterize uncertainty in spatial transcriptomic predictions.
Methods: An in-house dataset of 65 paired H&E-stained colorectal and triple-negative breast cancer whole-slide images with matched Visium ST data yielded 289,569 spots and corresponding 512×512-pixel H&E patches for 991 spatially variable genes. Using 5-fold patient-level cross-validation, a BNN with Bayesian convolutional and multilayer perceptron layers was trained via variational inference, with Kullback-Leibler divergence regularizing weight distributions. During inference, predictive posterior sampling produced means and log-variances for each gene from image patches, enabling separation of epistemic (uncertainty reducible with more data or improved modelling) and aleatoric (irreducible noise driven by biological variability or assay limits) uncertainty. Gene set enrichment was used to characterize genes ranked by uncertainty.
Results: High epistemic uncertainty genes were enriched for signalling and regulatory pathways such as Histone H4-K12 acetylation and positive regulation of apoptosis. High aleatoric uncertainty mapped to stress-response programs including cellular response to ionizing radiation, medium-chain fatty acid biosynthesis, and myeloid cell activation. Low-uncertainty genes were dominated by stable metabolic and cell-cycle pathways, including aerobic respiration, electron transport, and mitochondrial NADH→ubiquinone transport.
Conclusion: These results suggest that the uncertainty framework highlights gene programs that are more amenable to histology-based inference, with metabolic pathways exhibiting the most reliable morphological association. Further algorithmic refinement and external validation will be key to establishing the utility of uncertainty modelling for cohort design in large-scale ST studies.

#4190 A scalable, proteome-wide protein profiling platform with absolute quantification of 1000 proteins to power oncologic drug discovery pipelines.

Jerid Robinson, Nathaniel Robichaud, Grant Ongo, Kiran Edwardson, Alyssa Rosenbloom, Narges Rashidi, Arya Tavakoli, Jeff Munzar, Milad Dagher

Nomic Bio, Montreal, QC, Canada

Proteomics has been constrained by flexibility, high costs, and inconsistent quantification. We present Omni 1000, a quantitative 1000-plex solution powered by nELISA technology—designed for broad, reproducible, and cost-effective protein measurement. Omni 1000 delivers 0.1 pg/mL sensitivity, 99.99% specificity, and dynamic range spanning 3-6 logs. With <10% CV, Omni 1000 ensures precision for discovery and translational applications.

Omni 1000 content was developed through a rigorous, data-driven strategy to achieve comprehensive proteome-wide coverage while retaining high-value markers. The foundation is built from two sources: (1) a curated set of Most Valuable Proteins (MVPs)—biomarkers selected heuristically based on prevalence in key signaling pathways, translational research, and validated endpoints; and (2) large-scale, high-plex proteomic datasets with disease-association. To optimize, we applied Minimum Redundancy Maximum Relevance (mRMR) to reduce overlap, reconstruction loss minimization to preserve signal from high-dimensional datasets, and prioritized MVPs. Each iteration was validated against key biological ontologies—achieving 92% MVP coverage, 100% Reactome level 0, >80% Reactome level 1, 100% pharma-relevant KEGG signaling pathways, and 100% MeSH disease classes.

For biomarker discovery, Omni 1000 makes large-scale and clinically relevant studies routinely achievable through significant cost-efficiencies and rapid readout with flow cytometry. In a study of plasma biobank samples, use of Omni 1000 successfully demonstrated early insights in detecting active rheumatoid arthritis immune signatures prior to onset of clinical symptoms.

In addition, Omni 1000's high-throughput capabilities were used to support a drug screening platform based on patient-derived tumor organoids. Use of Omni 1000 demonstrated insights on baseline donor heterogeneity and drug compound responses and resistances specific to patient tissue profiles, an effort to advance precision medicine.

Together, we demonstrate a novel 1000-plex solution, Omni 1000, with content balancing critical targets and biological breadth, and demonstrate real-world utility through two key applications: early detection of disease and high throughput drug development.

#4191 TP53 dysfunction drives immunometabolic rewiring via mTORC1 activation and autophagy suppression in colorectal cancer.

Eunseuk Lee, Dana Al-Assi, Randy Rueda-Rivera

RWJ Barnabas Health Community Med. Ctr., Toms River, NJ

The tumor suppressor protein p53 regulates both metabolism and immunity through its control of the mTORC1-autophagy axis; yet the mechanistic consequences of TP53 dysfunction in microsatellite-stable colorectal cancer (MSS CRC) remain unclear. We used an integrative transcriptomic approach that combined bulk RNA-seq (GSE146009), TCGA-COAD/READ (n = 647), and single-cell RNA-seq data (GSE108989), to investigate how TP53 loss alters metabolic-immune coupling in CRC. While p53 and autophagy were activated together in wild-type tumors, mTORC1 signaling remained restrained. This pattern preserved metabolic stability and supported a favorable $CD8^+/FOXP3^+$ immune ratio. In contrast, TP53-mutant and null tumors exhibited a decoupling of p53 from mTORC1, leading to sustained anabolic signaling, autophagy suppression, and upregulation of pro-inflammatory cytokines (IL1B, IFNG), which coincided with enrichment of $FOXP3^+$ regulatory T-cells and immune exclusion. Single-cell profiling confirmed that mTORC1 and autophagy remain co-activated across major T-cell subsets. However, immune-metabolic coordination was weaker in exhausted and regulatory populations. Principal-component and correlation analyses revealed two distinct axes, metabolic intensity and immune polarity, that describe TP53-dependent immunometabolic divergence.Taken together, the results suggest that TP53 dysfunction promotes linked metabolic and immune reprogramming through mTORC1 activation and autophagy suppression, resulting in a FOXP3-dominant, immune-cold tumor microenvironment.. This mechanistic insight provides a rationale for combining mTORC1 and autophagy inhibition with immune-checkpoint blockade in TP53-deficient MSS CRC.

#4192 Coordinated miRNA regulation of AR-PI3K/MAPK crosstalk and EMT in prostate cancer.

Fabiana Buono[1], William Lautert-Dutra[1], Dan Dion[2], Camila Morais Melo[1], Cheryl Crozier[2], Fabiano Pinto Saggioro[3], Rodolfo Borges dos Reis[4], Jeremy Andrew Squire[1], Jane Bayani[5]

[1]Department of Genetics, University of Sao Paulo, Ribeirao Preto Medical School, Ribeirao preto, Brazil,[2]Diagnostic Development, OICR - Ontario Institute for Cancer Research, Toronto, ON, Canada,[3]Department of Pathology and Forensic Medicine, University of Sao Paulo, Ribeirao Preto Medical School, Ribeirao preto, Brazil,[4]Department of Surgery And Anatomy, University of Sao Paulo, Ribeirao Preto Medical School, Ribeirao preto, Brazil,[5]Diagnostic Development / Department of Laboratory Medicine and Pathobiology, OICR - Ontario Institute for Cancer Research, Toronto, ON, Canada

Prostate cancer (PCa) progression and therapeutic resistance are critically dependent on the Androgen Receptor (AR) axis and major survival networks, including PI3K/AKT, MAPK, and epithelial-mesenchymal transition (EMT) programs. While individual microRNAs (miRNAs) have been implicated in these pathways, the broader miRNA-driven regulatory systems controlling these interconnected oncogenic axes remain poorly understood. We performed miRNA expression profiling in a clinically well-annotated PCa cohort and conducted an integrative analysis, identifying functional miRNA clusters through network correlation, pathway enrichment, and mapping to established oncogenic and EMT-related signature scores. Literature-based functional annotation was then combined with our miRNA findings to investigate correlations against key EMT transcription factors and tumour suppressors such as PTEN. We identified distinct miRNA clusters whose targets collectively converge on common oncogenic hubs, including AR-PI3K/MAPK-WNT/NOTCH signalling. With a role in EMT modulation, several miRNAs displayed strong negative correlations with EMT transcription factors, including miR-221-5p and miR-542-3p with SNAI2 (r ~ -0.5), and miR-378d and miR-449b-5p with ZEB2 (r ~ -0.7 and -0.4), supporting their functional involvement in suppressing EMT programs. Additionally, miR-542-3p, miR-449b-5p, and miR-302d-3p correlated inversely with PTEN (-0.7, -0.5, -0.5), suggesting their participation in PI3K/AKT pathway modulation. These findings align with the established tumour-suppressive roles of miR-206, miR-302d-3p, and miR-2110—previously linked to MAPK/ERK, AKT/mTOR, and FGFR/RTK-PTEN regulatory axes (Cancers 2024). Pathway enrichment analyses revealed that targeted pathways, including WNT, NOTCH1, PI3K/AKT, MAPK, ERBB2, and FGFR signalling, form an interconnected oncogenic network. Within this framework, miR-378d and miR-449b-5p exhibited strong negative correlations with ERBB2 (-0.7 and -0.5, respectively). Consistent with these molecular interactions, Correlation with Scote-derived oncogenic signatures, including ERBB2 activation and BRCAness, demonstrated that miRNA clusters strongly associate with genomic instability, proliferation, and therapy resistance phenotypes. Collectively, these findings suggest that the identified miRNA clusters function as integrated regulatory modules that simultaneously coordinate the suppression of AR signalling crosstalk with PI3K/MAPK activation and modulation of EMT. Their strong associations with Scote oncogenic signatures and EMT transcription factors underscore their potential as prognostic biomarkers and as targets for rational combination strategies aimed at disrupting AR-survival network crosstalk and overcoming therapeutic resistance.

#4193 Heterogeneous graph neural network meta-analysis of lung cancer and tuberculosis transcriptomic datasets reveals convergent host response networks.

Andrew Triska[1], Selvakumar Subbian[2], **Natarajan Ganesan**[3]

[1]School of Mathematics and Statistics, The Open University, Milton Keynes, United Kingdom,[2]Public Health Research Institute, Rutgers Health, New Jersey Medical School, Newark, NJ,[3]Biomedical and Anatomical Sciences, New York Institute of Technology, College of Osteopathic Medicine (NYITCOM) at Arkansas State University, Jonesboro, AR

Background: Granulomas, hallmark cellular structures of tuberculosis (TB), have similarities to lung tumors, creating a diagnostic and mechanistic interface between infection and malignancy. However, the comparative, genomewide transcriptional landscape between lung cancer and TB granulomas remains poorly characterized. We hypothesize that the lesions in pulmonary TB and cancer may encode convergent molecular programs that regulate the structure and/or function of cells within the lesions.
Methods: We performed a large-scale integrative meta-analysis of 450 RNA-seq samples from patients with lung cancer, TB patients, and healthy controls. Raw FASTQ files were processed to generate robust count matrices. Differential gene expression (DGE) was assessed using DESeq2, and co-expression networks were constructed via WGCNA with batch correction. To capture complex, non-linear relationships between genes, pathways, and clinical metadata, we developed a Heterogeneous Graph Transformer (HGT), a graph neural network that models multi-type nodes and edges, enabling the discovery of shared and disease-specific regulatory hubs.
Results: Heatmap analysis of the top 100 differentially expressed genes revealed distinct clusters with mixed modules indicative of convergent biology between lung cancer and TB granulomas. KEGG enrichment analysis revealed an overlap between immune and oncogenic signaling pathways, including NF-κB, PI3K-Akt, MAPK, Toll-like receptor, and PD-1/PD-L1 checkpoint pathways. Chromatin remodeling emerged as a common theme, with recurrent histone variants (H2AC, H3C, H4C) suggesting epigenetic plasticity. These shared hub genes implicate chronic inflammation and immune mimicry as mechanistic bridges between granulomas and cancer, making them potential biomarkers to distinguish TB vs lung cancer and/or therapeutic targeting.
Conclusions: This systems-level approach reveals a unique TB granuloma-lung cancer interface rooted in common mechanistic pathways, identifying candidate biomarkers and therapeutic targets for two of the world's most burdensome pulmonary diseases.

#4195 OncoGraphDB: Rapid projections of patient-level multimodal graph database facilitates efficient exploration of tumor subtypes and identifies new combinatorial biomarkers of patient outcomes and gene essentiality.

Jacob Pfeil[1], Amber Tse[2], Severiano Villarruel[1], Emily Rossi[3], Liqian Ma[1], Xi Zhao[1], Josue Samayoa[3], Kyle Halliwill[1]

[1]AbbVie Bay Area, South San Francisco, CA,[2]Former AbbVie Bay Area Employee, South San Francisco, CA,[3]AbbVie Inc., North Chicago, IL

Cancer ‘omics data are often analyzed in isolation of other related data modalities despite the potential for added benefit when analyzing a multimodal model. One strategy is to include all available data, but this approach may obfuscate the underlying signal if data modalities exist in the model that do not significantly contribute to the analysis. To enable efficient exploration of multimodal data, we developed the OncoGraphDB framework to rapidly project subgraphs of a larger, all inclusive, cancer omics knowledge graph. This enabled us to identify subspaces that maximally separate patients of interest using a user-defined metric (i.e. patient survival, drug response, or predicted gene essentiality). We found that across cancer indications, gene expression data provided the most single-mode information, which is consistent with several recently published studies. However, performance was improved when predicting prognosis and shared gene essentiality scores when additional data modalities were included in the analysis, including somatic mutation signatures and DNA methylation profiles. Agentic AI was then applied to the Neo4j graph framework to support interactive interrogation of the cancer -omics knowledge graph providing domain experts an exploratory data portal for hypothesis generation. Finally, we describe the gene expression and image classifiers for projecting new patient samples onto the graph to support N-of-1 reverse translation studies. The OncographDB platform facilitates efficient exploration of complex cancer databases and provides data analysis solutions for precision medicine applications.

All Authors were or are employees of AbbVie. The design, study conduct, and financial support for this research were provided by AbbVie. AbbVie participated in the interpretation of data, review, and approval of the publication. No honoraria or payments were made for authorship.

#4196 Predicting self-antigen recognition of TCRs derived from tumor infiltrating CD8+ T cells via contrastive learning and T cell phenotyping.

Brinda Vijaykumar, Qiaomu Tian, Jack Prazich, Preet Joshi, Neel Patel, John Abel, Anthony Coyle, Daniel Pregibon

Repertoire Immune Medicines, Cambridge, MA

T cell receptor (TCR)-based immunotherapies leverage the ability of a TCR to bind with high specificity and selectivity to peptides derived from intracellular targets, including those overexpressed on tumors. Consequently, TCRs identified from tumor-infiltrating lymphocytes (TILs) that respond to antigens in the tumor microenvironment represent attractive substrates for TCR immunotherapy development. However, de-orphaning TCRs is exceedingly challenging given the diversity of TCR and target sequence space. Although multiplexed peptide-MHC (pMHC) staining assays have improved throughput of direct, *ex vivo* measurement of TCR-pMHC binding, they are limited by TIL sample quality, T cell infiltration, TCR repertoire diversity, and limited pMHC library size. Machine-learning based techniques may overcome these limitations by training models to predict TCR-pMHC interactions and then inferring TCR-pMHC binding on large databases collected in other contexts. Here, we applied a contrastive model of TCR-pMHC binding prediction (1) to 382 tumor samples from 9 indications containing 490,000 T cells. We found that 5,244/490,000 (~1.1%) of TCRs from this dataset were predicted to recognize one of the 4,438 pMHCs in our model training set. Of these, 1,949 were predicted to bind common viral peptides, an observation indicative of bystander recruitment and infiltration. An additional 2,549 TCRs were predicted to bind to Class I onco-antigens, including QLLALLPSL [PRAME], YLEPGPVTA [GP100] and GLYDGMEHLI [MAGEA10]. The model was able to capture TIL TCRs with diverse complementarity-determining regions (CDRs) as well as highly homologous sequences. TCRs predicted to bind self-antigens were phenotyped using Repertoire's DECODE™ platform (2), showing that cancer-specific TCRs tended to have a more cytotoxic and effector like phenotype compared to a memory-like signature on viral specific TCRs (e.g. TCRs specific to cytomegalovirus, Epstein-Barr virus, and influenza). These results demonstrate a way to computationally de-orphan TCR specificities and phenotypically characterize T cells in a high-throughput manner to further our understanding of the TCR landscape in cancer patients. Importantly, this strategy could enable the discovery of TCR sequences suitable for therapeutic development using existing datasets. Future work should focus on increasing the diversity of validated TCR-pMHC specificities and in-vitro validation of predicted TCR-pMHC interactions (as well as reported model performance metrics).1. Abel, John, et al. "REPTRA: Mapping Immune T Cell Receptor Activity from Full Sequences with a Debiased Contrastive Loss." bioRxiv (2025): 2025-10.2. Francis, Joshua M., et al. "Allelic variation in class I HLA determines CD8+ T cell repertoire shape and cross-reactive memory responses to SARS-CoV-2." Science immunology 7.67 (2021): eabk3070.

#4197 Multiomic dissection of KRAS signaling reveals targetable metabolic and DNA repair vulnerabilities in colorectal cancer.

Tom Cohen[1], Ashima Mehta[1], Adam Richardson[1], Monil Gandhi[1], Douglas Guzior[1], Kevin Cho[2], Ethan Stancliffe[1], Gary Patti[2]

[1]Panome Bio, St. Louis, MO,[2]Washington University in St. Louis, St. Louis, MO

Background: KRAS is among the most common oncogenic drivers in colorectal cancer and is historically “undruggable”; yet direct KRAS inhibitors are now entering clinical trials. The systems-level effects of KRAS modulation remain poorly characterized, limiting therapeutic insights. We applied integrated multiomic profiling to reveal mechanistic vulnerabilities that could enhance translational strategies.

Methods: Isogenic HCT-116 colorectal carcinoma cells (homozygous KRAS^G13D mutation vs. partial KRAS loss) were analyzed in biological replicates (n = 3-5) across transcriptomics (15,432 genes), proteomics (6,654 proteins), phosphoproteomics (10,034 phosphopeptides), and metabolomics (3,015 metabolites). Multi-layer data (>30,000 analytes) were integrated via pathway enrichment, correlation networks, and dimensionality reduction to identify core molecular modules downstream of KRAS.

Results: KRAS deletion produced broad molecular reprogramming: 640 transcripts, 74 proteins, 744 phosphopeptides, and 519 metabolites showed significant changes ($q<0.05$). Metabolomics was most perturbed (>17%), revealing increased mitochondrial respiration and branched-chain amino acid catabolism, alongside suppressed glycolysis. Downregulated signaling included collagen biosynthesis, EGFR, IGF transport, and IL-4/IL-13 pathways. Network integration distilled >30,000 features into <100 molecular modules, highlighting metabolic shifts in plasmalogen-associated lipid remodeling and altered phosphorylation of nuclear pore, ribosomal, and DNA repair proteins (ATRX, DAXX). These findings indicate vulnerabilities in oxidative metabolism, lipid metabolism, ribosome biogenesis, and genome stability.

Conclusions: This comprehensive multiomic analysis reveals that KRAS-driven colorectal cancer depends on coordinated control of metabolism, extracellular matrix signaling, and DNA repair pathways. KRAS attenuation shifts cells to oxidative metabolism while exposing vulnerabilities in lipid metabolism and DNA repair machinery. These findings suggest combinatorial therapeutic strategies integrating KRAS inhibition with metabolic or DNA damage-targeted therapies.

#4198 Integrative single-cell transcriptomics and computational docking identify CCL18 as an immunomodulatory target in prostate cancer.

Edwige Flore Gouegni[1], Gebre-Eziagbher Kiros[1], Renee Reams[1], Diana J. Wilke[2], Fredenburg Kristianna[3], Bodour Salhia[4]

[1]College of Pharmacy and Pharmaceutical Sciences, Institute of Public Health, Florida A&M University, Tallahassee, FL,[2]University of Florida, Gainesville, FL,[3]Department of Pathology, Immunology, and Laboratory Medicine, University of Florida, Gainesville, FL,[4]USC Norris Comprehensive Cancer Center, Los Angeles, CA

Background: Prostate adenocarcinoma (PRAD) remains a major cause of cancer morbidity in men, driven by cellular heterogeneity and immune evasion. Single-cell RNA sequencing (scRNA-seq) enables high-resolution profiling of tumor and immune states to uncover cell-specific therapeutic targets. This study integrates scRNA-seq, pathway enrichment, and molecular docking to identify immunomodulatory molecules with therapeutic potential in prostate cancer.
Methods: scRNA-seq data (GSE181294) from 34 PRAD and 5 normal samples (165,905 cells) were processed in Seurat for quality control, clustering, and annotation. Differential expression analyses across tumor, epithelial, and immune compartments were followed by GO/KEGG enrichment and pseudobulk validation. Expression and survival associations were evaluated using TCGA-PRAD via UALCAN. Candidate genes were prioritized through cell-cell communication modeling and validated in silico using structure-based molecular docking with curated ligand libraries.
Results: Seven major cell clusters were identified. Tumor cells showed enrichment of mitotic and chemokine pathways, while T/NK cells exhibited immune-suppressive signatures. CCL18 emerged as a key chemokine overexpressed across tumor and immune compartments and validated in TCGA data. Communication analysis identified CCL18-producing cluster 0 signaling through CCR1, CCR5, and CCR8. Docking revealed high-affinity ligands interacting with residues GLU-9 and ACT-101, supporting the druggability of CCL18.
Conclusions: Integrating single-cell analysis, pathway profiling, and docking highlights CCL18 as a promising therapeutic or vaccine target in PRAD. Its consistent tumor-immune expression and favorable binding properties support further experimental validation.
Keywords: scRNA-seq, prostate cancer, CCL18, immunotherapy, tumor microenvironment, molecular docking.

#4200 Exploring unrestricted antibiotic use gut microbiome imbalance and chemical carcinogens in liver and kidneys toxicity through computer modeling and *in vivo* study.

Solomon Owumi[1], Dooshima A. Bagu[2], Joseph Chimezie[3], Esther M. Pius[1], Uche O. Arunsi[4], Jesutosin O. Babalola[5], Ayomide P. Akomolafe[6], Chima Amadi[7], Chinedum Udekwu[8], Adegboyega K. Oyelere[9], E. Oluwabunmi Olapade-Olaopa[10], Olorunseun O. Ogunwobi[1]

[1]University of Ibadan, Ibadan, Nigeria,[2]Dooshima Bagu, Ibadan, Nigeria,[3]Joseph Chimezie, Ibadan, Nigeria,[4]Chemistry Biochemistry, Georgia Institute of Technology, Georgia Institute of Technology, GA,[5]Biochemistry, University of Ibadan, Ibadan, Nigeria,[6]University of Nebraska, Omaha, NE,[7]Dedra Nutraceuticals and Biotechnology Initiative, ABuja, Nigeria,[8]Chemistry Biochemistry, Michigan State University, East Lansing, MI,[9]Georgia Institute of Technology, Atlanta, GA,[10]Surgery, University of Ibadan, Ibadan, Nigeria

The gut microbiota, vital for human health, can be disrupted by antibiotics, which has been linked to diseases such as cancer. Contamination of food with Aflatoxin B_1 (AFB_1) and Diethylnitrosamine (DEN), both strong liver carcinogens, increases liver cancer risk. This study examines how unrestricted use of common antibiotics (Ampicillin and Ciprofloxacin) affects gut microbes, combined dietary exposure to AFB_1 and DEN, and the development of liver and kidney toxicity in rats. Molecular Docking (MD) and Network Toxicology were used to investigate how AFB_1, DEN, AMP, and CPX cause hepatorenal toxicity by interacting with key hub proteins involved in redox and protective cellular pathways. Ligand orientation and binding energies for STAT3 and EGFR were assessed using molecular docking. Gut microbial analysis shows that AMP and CPX induce antibiotic-driven dysbiosis, suppressing beneficial gram-positive bacteria like Lactobacillus and promoting the growth of opportunistic gram-negative bacteria such as Escherichia coli, Klebsiella pneumoniae, and Pseudomonas aeruginosa. These changes result in toxic metabolite production affecting the hepatic immune system. In the presence of carcinogens, AMP and CPX synergy may contribute to carcinogenesis in co-treated groups. STAT3, EGFR, MAPK8, IKBKB, MMP2, MET, and NOS2 were identified as important hub genes. AFB_1 (–8.5 kcal/mol), CPX (–7.8 kcal/mol), and AMP (–7.6 kcal/mol) showed high affinity for EGFR, indicating a possible synergistic role in EGFR signalling modulation. *In vivo* studies in male Wistar rats showed that co-treatment reduced body, liver, and kidney weights, raised serum hepatic transaminases, creatinine, and urea, decreased antioxidant enzymes, and increased inflammation markers, lipid peroxidation, alpha-fetoprotein, and caspase-3 activity, alongside reduced IL-10 in the liver and kidney. The data indicate that AMP and CPX cause gut dysbiosis and, together with AFB_1 and DEN, have a synergistic hepatorenal toxic effect that may be relevant in the onset of carcinogenesis.

#4201 Simulating trans-endothelial nanoparticle transport via macropinocytosis.

Marvin Skiba[1], **Hae-gyung T. Han**[2], Warren Chan[3]

[1]School of Materials Science and Engineering, Nanyang Technological University, Singapore, Singapore,[2]Harvey Mudd College, Claremont, CA,[3]Nanyang Technological University, Singapore, Singapore

Macropinocytosis is a key mechanism in transendothelial nanoparticle transport into solid tumours. It uses cell membrane ruffles to capture circulating nanoparticles. Endothelial cell ruffles cannot be independently and systematically varied *in vivo*, preventing parameter-specific analysis. We developed an *in silico* model that examines nanoparticle capture by macropinocytosis. We discover that nanoparticle capture rates rise steeply until saturating with ruffle number as well as ruffle turnover time. From our data we derive an equation describing the nanoparticle capture by macropinocytosis. This relationship reveals how ruffle dynamics govern nanoparticle capture efficiency.

: Machine Learning Approaches for Cancer Prediction
Poster Session

#4206 The ancestry-transcriptome link: Machine learning predicts chemotherapy response in breast cancer.

Michelle Guevara-Nieto[1], Maria J. Lopez-Munevar[2], Carlos Orozco-Castano[3], Rafael Parra-Medina[4], Laura Fejerman[5], Valentina Zavala[6], Jone Garai[7], Jovanny Zabaleta[8], Alba L. Combita-Rojas[9], Liliana Lopez-Kleine[2]

[1]Pathology Department, Universidad Nacional de Colombia, Bogota, Colombia,[2]Universidad Nacional de Colombia, Bogota, Colombia,[3]Instituto Nacional de Cancerologia, Colombia, Bogota, Colombia,[4]National Cancer Institute, Bogota, Colombia,[5]UC Davis Comprehensive Cancer Center, Davis, CA,[6]Department of, University of California San Francisco, Santiago, Chile,[7]Stanley S. Scott Cancer Center, Louisiana State University Health Science Center, New Orleans, LA,[8]LSU Health New Orleans, New Orleans, LA,[9]Instituto Nacional de Cancerologia, Bogota, Colombia

Background: Breast cancer resistance to neoadjuvant chemotherapy (NAC) remains a major challenge in Latin America, where limited genomic representation restricts precision-oncology advances. Understanding how genetic ancestry interacts with transcriptomic features may uncover population-specific predictors of treatment response. We investigated the ancestry-transcriptome link using machine-learning models in Colombian breast cancer patients.
Methods: We analyzed 58 women with locally advanced breast cancer treated with NAC (29 responders, 29 non-responders) across five molecular subtypes. RNA-seq identified 339 differentially expressed genes (DEGs); the top 10% most variable DEGs (n=34) were retained following variance-stabilizing normalization. Predictors included clinical variables (tumor size, TNM stage, T-stage, N-stage, grade, clinical stage, treatment regimen, age, BMI, menopause), genetic ancestry fractions (Amerindian-AMR, African-AFR, European-EUR), and 34 DEGs. Recursive Feature Elimination did not improve model performance; therefore, all variables were included. Random Forest (500 trees) and XGBoost models were trained, with hyperparameter optimization via cross-validation.
Results: XGBoost achieved the highest performance (AUC = 0.90) using a learning rate of 0.05, depth 12, and 90% subsample/colsample. Across models, T-stage, age, and Amerindian ancestry consistently emerged as top predictors based on gain, coverage, and split frequency. Among transcriptomic variables, CACNA1D, CLEC3A, TFF1, and TTK showed strongest predictive contribution. Model robustness was confirmed through parameter variation and resampling strategies.
Conclusions: Machine-learning integration of ancestry and transcriptomic features accurately predicts NAC response in Colombian breast cancer patients. Amerindian ancestry, alongside key clinical variables and reproducible gene-expression signatures, influenced prediction performance, underscoring the importance of population-specific factors in treatment resistance. This ancestry-transcriptome framework provides a scalable, data-driven approach for advancing precision oncology in underrepresented Latin American populations.

#4207 Omics-aware patch aggregation via multimodal co-training with a scalable multi-omics encoder for slide-level prediction across an oncology biomarker panel.

Hwanil Choi[1], Tae Hyun Hwang[2], Soonyoung Lee[1], Jongseong Jang[1]

[1]Bio Intelligence Lab, LG AI Research, Seoul, Korea, Republic of,[2]Department of Surgery, Vanderbilt University Medical Center, Nashville, TN

Background: Whole-slide images (WSIs) are widely available, but matched multi-omics profiles are limited, especially when multiple modalities are required. We developed a multimodal learning framework that integrates RNA expression and DNA mutation with H&E WSIs, explicitly modeling partially observed omics to train an omics-aware patch aggregator for slide-level prediction.
Methods: An omics-aware patch aggregator was trained with a slide-level contrastive objective that aligns a Multi-Omics Encoder (MOE) and a Slide Encoder (SE). The MOE is a shared Transformer that tokenizes each omics modality, concatenates modality-specific tokens with omic-type encodings, and uses self-attention to capture cross-omic interactions, allowing new omics to be added without changing the architecture. The SE processes tens of thousands of patches per slide and incorporates patch coordinates via relative positional bias to emphasize spatially proximal regions. Multimodal pretraining used ~20,000 partially paired WSIs and multi-omics profiles from The Cancer Genome Atlas and Genotype-Tissue Expression projects.
Results: After multimodal pretraining, the omics-aware aggregator supported slide-level prediction across an oncology biomarker panel. For gene overexpression, area under the ROC curve (AUC) values were: LAG3 0.84, CLDN6 0.68, CD274 0.98, EGFR 0.74, ERBB2 0.72, ERBB3 0.69, CD276 0.82, VTCN1 0.72, TACSTD2 0.77, FOLR1 0.93, and MET 0.82. By tumor type and task, lung adenocarcinoma achieved AUCs of 0.70 for tumor mutational burden, 0.87 for EGFR mutation, and 0.62 for KRAS mutation; colorectal cancer 0.99 for microsatellite instability; breast cancer 0.95, 0.88, and 0.81 for ER, PR, and HER2 protein subtyping and 0.74 and 0.86 for TP53 and PIK3CA mutations; renal cell carcinoma 0.60 for PBRM1 and 0.74 for BAP1 mutations; and colon adenocarcinoma 0.88 for KRAS and 0.89 for TP53 mutations. Gene overexpression tasks used The Cancer Genome Atlas with five-fold cross-validation across four seeds; lung and colorectal models used Samsung Medical Center cohorts; breast subtyping used the BCNB cohort; and renal and colon tasks used Clinical Proteomic Tumor Analysis Consortium data.
Conclusions: An omics-aware patch aggregation framework co-trained with a scalable multi-omics encoder and WSIs enables accurate slide-level prediction for diverse biomarkers and tumor types and illustrates how partially paired multi-omics data can strengthen digital pathology models. AI was used for language editing only; authors are responsible for all content and approved the final version.

#4208 Machine learning models for predicting prostate cancer risk in Hispanic men.

Ricardo J. Rodriguez-Colon[1], Amaia V. Varela-Parrilla[2], Zinned C. Medina-Nieves[1], Maria M. Sanchez-Vazquez[1], Magaly Martinez-Ferrer[1]

[1]University of Puerto Rico Comprehensive Cancer Center, San Juan, PR,[2]Department of Biology, University of Puerto Rico, Rio Piedras Campus, San Juan, PR

Introduction: Hispanic men in the United States experience a notable prostate cancer (PCa) burden, with studies reporting higher rates of advanced-stage disease at diagnosis compared with non-Hispanic men. However, their genetic and sociodemographic profiles remain untargeted in current risk prediction approaches. These observations highlight gaps in current risk assessment strategies and the need for improved, population-relevant prediction tools. Machine learning (ML) applications in biomedical research have yielded valuable advances in the early detection and prediction of cancer risk. The aim of this study was to develop a ML model to predict PCa risk in Hispanic men leveraging data from the All of Us Research Program.

Methods: The study cohort included 20,172 Hispanic males, 220 PCa cases (1.1%) and 19,952 controls. Predictors included age group (≤40, 41-59, ≥60 years), family history of PCa, smoking status, drinking frequency and the rs10090154 genotype associated with PCa. Data were split 80/20 into training (n= 16, 138) and testing (n= 4,034) sets. To address class imbalance, class weights were applied. Logistic regression, random forest and XGBoost models were trained and evaluated. Models underwent a five-fold cross-validation with sigmoid calibration, and performance was assessed using ROC-AUC, PR-AUC, Brier score, precision recall and F1 score.

Results: Among the three models, the logistic regression model achieved the best balance of discrimination and calibration with a mean ROC-AUC of 0.872 (95% CI: 0.856-0.885), PR-AUC of 0.059 (95% CI: 0.045-0.074), Brier score of 0.0105 and an F1 score of 0.066. The model metrics were accuracy = 0.704, recall = 0.955 and precision = 0.034. Correspondingly, the false negative rate (FNR) was 4.5%, indicating that only 2 out of 44 true PCa cases were misclassified as controls, while the false positive rate (FPR) was 30.6%, meaning roughly one in three non PCa cases were incorrectly flagged as positive. Feature importance and odds ratio analyses identified Age ≥60 and family history of PCa as the most influential predictors for the model, followed by the rs10090154 genotype and former smoking status. Comparatively, the random forest (ROC-AUC= 0.851) and XGBoost (ROC- AUC= 0.858) models demonstrated similar discrimination but exhibited slightly lower calibration and interpretability compared with logistic regression.

Conclusions: A class-weighted, sigmoid-calibrated logistic regression model achieved accurate, interpretable and well calibrated PCa risk predictions. Despite the low observed case prevalence in the All of Us cohort, the model showed strong sensitivity and discrimination, supporting its utility for biomedical and clinical risk stratification in population-based precision health research. These findings highlight the potential of simple and interpretable ML models to improve early PCa risk assessment in Hispanic men.

#4209 A multi-variable machine learning model integrating stage, histology, grade, and treatment to predict mortality in salivary gland cancer: A SEER 2010-2021 population-based study.

Chiugo Okoye[1], Chinemerem Martlin Emeasoba[2], Chidi Obialo-Ibeawuchi[3], Olanipekun Ntukidem[4], Oboseh John Ogedegbe[5], Uchenna Amaechi[6]

[1]Northeast Georgia Health System, Inc., Gainesville, GA,[2]UAMS Northwest, Fayetteville, AR,[3]Walden Univeristy, Minneapolis, MN,[4]Trinity Health Ann Arbor, Yspsilanti, MI,[5]Tirnity Health Ann Arbor, Yspsilanti, MI,[6]Howard University Hospital, DC, WA

Background: Salivary gland cancers are rare, heterogeneous tumors with widely variable clinical outcomes. Current prognostic tools rely on limited clinicopathologic features and do not incorporate complex interactions between tumor biology and treatment patterns. We aimed to develop and validate a machine learning (ML) model integrating stage, histology, grade, tumor size, and treatment modalities to predict all-cause mortality using a large U.S. population-based cohort.

Methods: We identified patients with primary malignant salivary gland tumors in the SEER database (2010-2021). Variables included age, sex, race, AJCC stage, histologic subtype, tumor size, grade, nodal status, surgery, radiation, and chemotherapy. Missing data were imputed using iterative multivariate imputation. Models evaluated included logistic regression, random forest, gradient boosting, and XGBoost. Performance was assessed with 70/30 train-test split and temporal validation using diagnoses from 2010-2017 as training and 2018-2021 as testing. Model interpretability was examined using SHAP values.

Results: A total of 12,678 salivary gland cancer cases met inclusion criteria. XGBoost showed higher performance, with an AUC of 0.87 in the test set and 0.85 in temporal validation, outperforming logistic regression (AUC 0.76). Sensitivity, specificity, and PPV for high-risk classification were 0.81, 0.78, and 0.72, respectively. SHAP analysis identified stage, tumor size, histologic subtype, grade, and receipt of surgery as the most influential predictors of mortality. The model revealed nonlinear interactions between tumor grade and nodal status that were not captured by traditional regression.

Conclusion: We came up with a robust, interpretable machine learning model integrating key clinical, pathologic, and treatment variables to predict mortality in salivary gland cancer with high accuracy. This tool provides a strong framework for individualized risk stratification and may help decision-making regarding treatment intensity, surveillance, and survivorship care. Further prospective validation is warranted to support clinical adoption.

#4210 Transformer and pretraining on external ehr cohort boosts infection risk prediction in hematologic malignancies.

Banafshe Felfeliyan[1], **Natasha Markuzon**[2]

[1]AstraZeneca Canada, Mississauga, ON, Canada,[2]AstraZeneca, Waltham, MA

Infections are a major early driver of morbidity and mortality in hematologic malignancies, particularly in chronic lymphocytic leukemia (CLL), due to intrinsic immune dysfunction and therapy induced immunosuppression. Predicting infection risk and identifying contributors prior to treatment is warranted; meanwhile limited sample size in local EHRs limits our ability to predict them accurately. We demonstrate that an attention-based transformer pretrained on an external cohort (CLL), lymphomas, multiple myeloma (MM)) and finetuned on a local CLL cohort enhances infection risk prediction. We used multimodal genomic and clinical data (EHR, labs, treatment) from two independent datasets, Flatiron CLL Custom Spotlight (FCCS; n=1,725, USA) and DALYCARE (n=3,418; Denmark) that includes CLL, lymphomas, MM. In the absence of standard infection labels prescribed antibiotics served as a proxy; infection prevalence was 33.6% in FCCS and 64.4% in DALY CARE. After schema harmonization and temporal aggregation across four-time windows, we derived 389 features (FCCS) and 688 (DALYCARE), with 249 shared ones including treatment, demographics, labs, vitals, and omics info. Models were trained and evaluated to predict infection risk 24 week post first line treatment with 5fold cross-validation per cohort. Cross cohort generalization was assessed via self-supervised learning (SSL) pretraining on full DALYCARE followed by fine tuning on FCCS. On 249 shared features SSL pretraining on DALY-CARE increased C-index vs training only on FCCS, from 0.63±0.05 to 0.66±0.07, with consistent PR-AUC gain (0.42 ± 0.06 to 0.46 ± 0.1), indicating that knowledge transferred from a larger external cohort, even with mixed lymphoid subtypes, can mitigate performance loss when sample size is limited. Without DALYCARE pretraining and using the full FCCS feature set (389), the transformer reached a higher C-index (0.69 ± 0.02 vs 0.66 ± 0.07), suggesting richer cohort features- still outweigh pretraining benefits. The transformer also outperformed baselines: C-index 0.69 ± 0.02 (FCCS) and 0.68 ± 0.02 (DALYCARE) vs CoxPH 0.59 ± 0.03 and 0.57 ± 0.01; PR-AUC 0.73 ± 0.07 and 0.73 ± 0.04 vs LightGBM 0.60 ± 0.04 and 0.59 ± 0.06. Attention based interpretability scores, and permutation importance are aligned in both cohorts and with known risk factors, including del(17p), renal function markers (eGFR, K+, NA+), and prior infection history. Transformers transfer knowledge across external cohorts, outperform baselines in infection risk prediction, improved interpretability. While focused on CLL, this demonstrates that leveraging external cohorts and other diseases can improve local predictions when samples are limited. Future work will combine transferred prior knowledge with richer cohort features to further enhance performance.

Refs: G. Argoty et al., Pretrained transformers in clinical studies, Nat Commun, 2025.

#4211 AI-driven epigenomic profiling reveals early predictors of cutaneous squamous cell carcinoma risk in hidradenitis suppurativa.

Murali R. Kuracha[1], Sree Naga V. Kuracha[2], Aaren Vedangi[3], Radhakrishna Uppala[4], Lavanya Uppala[5], Venkata Duvvuri[1]

[1]Sirius Mindshare Academy, San Jose, CA,[2]Millard North High School, Omaha, NE,[3]Clinical research, KIMS ICON Hospital, Visakhapatnam, India,[4]Obstetrics and Gynecology, Beaumont Health, Royal Oak, MI,[5]School of Medicine, Creighton University, Omaha, NE

Background: Hidradenitis Suppurativa (HS) is a chronic inflammatory skin disease with a markedly increased risk of cutaneous squamous cell carcinoma (cSCC), including aggressive and often fatal variants. Although cSCC arises through ultraviolet injury, chronic inflammation, impaired wound repair, and smoking, its molecular drivers remain incompletely defined. Emerging evidence implicates epigenetic dysregulation, particularly DNA methylation, as an early indicator of carcinogenic potential. Our HS cohort contained no cSCC cases at recruitment, providing a unique opportunity to identify early epigenomic alterations preceding malignant transformation. Methods: Genome-wide DNA methylation was profiled in blood from 24 HS cases and matched controls using the Illumina MethylationEPIC array. Differentially methylated CpGs were identified through a rigorous bioinformatic pipeline and cross-referenced with cSCC datasets to define overlap with oncogenic pathways. Artificial intelligence approaches, including deep learning, Cox elastic-net survival modeling, random forest, and integrated AI/ML pipelines, were used to prioritize CpGs associated with cSCC risk. Results: We identified significant methylation alterations (FDR ≤ 0.05) at 32 CpG sites across 32 genes in HS, comprising 24 hypomethylated and 8 hypermethylated loci. All are previously implicated in cSCC and converge on canonical oncogenic pathways, including *EGFR/MAPK, p53, TERT, NOTCH* signaling, and DNA repair/chromatin remodeling. The cSCC tumor-trained Cox proportional hazards model (Cox model) demonstrated strong prognostic performance (C-index 0.78-0.84 across cross-validation). Applying this model to HS samples generated a continuous cSCC Epigenetic Prognostic Score (cSCC-EPS) that stratified HS patients into low-, intermediate-, and high-risk methylation phenotypes. SHapley Additive exPlanations (SHAP) analyses highlighted CpGs within *EGFR, DNMT1, TP53, NOTCH3, BRAF,* and *TERT* as the strongest contributors to cSCC predicted risk. This integrative AI-ML epigenetic pipeline identified HS patients with methylation profiles converging on high-risk cSCC tumor biology, suggesting a blood-based molecular window into early carcinogenic processes. Conclusions: HS patients harbor blood-based methylation signatures that mirror early epigenomic alterations seen in cSCC. This AI-integrated framework provides the first evidence that these biomarkers can predict malignant transformation in HS, positioning methylation profiling as a promising tool for early cSCC risk assessment.

#4212 Baseline peripheral blood scRNA-seq AI estimator framework predicts solid-tumor response and adverse events via molecular foundation models and cell-to-patient learning.

Pablo Moreno[1], **Marta Milo**[1], Ricardo Miragaia[1], Alex Proutski[1], Virginia Savova[2], Ikbel Achour[3]

[1]Astrazeneca, Cambridge, United Kingdom,[2]Astrazeneca, Waltham, MA,[3]Astrazeneca, Gaithersburg, MD

Introduction: Accurately identifying patients likely to benefit from therapy and at risk of adverse events from baseline blood samples, is an unmet need in oncology. We developed a translational AI estimator framework that predicts treatment response, adverse events (AEs), and molecular signatures from baseline PBMC single-cell RNA-seq, for solid tumors. We used baseline PBMC scRNA-seq counts (with optional cell-type annotations), pre-trained molecular foundation models (FMs) (scGPT v1.0 [1], scFoundation [2]), cell-to-patient Multi-Instance Learning (MIL) [3] with RECIST labels (CR/PR Responders; SD/PD Non-Responders), to predict responses. We fine-tuned downstream tasks, applied scVI-based data augmentation [4] to improve stability and generalization, with an interpretability layer linking predictions to cell types and gene programs.

Results: Using baseline PBMC scRNA-seq from patients with solid tumor treated with immunotherapy (103 patients, ~12,000 cells/patient), the estimator predicts treatment response from baseline blood across FM backbones and identifies an optimal downstream architecture. We used scFoundation with and without hierarchical attention and scGPT. For scFoundation without hierarchical attention, we observe learning with substantial loss reduction, discrimination of classes with AUC just below 0.8 and F1 scores ≈ 0.78. For scFoundation with hierarchical attention we observe similar performance with slightly worse accuracy with AUC ≈ 0.75 and F1 ≈ 0.70 . For scGPT, we observe learning (loss reduction), good discrimination of classes with AUC ≈ 0.75 and F1 scores just over 0.7. Validation scores are slightly worst in all cases. Results we reported so far are reflecting the ability of our framework to generalize, show competitive performance with differences attributable to hierarchical vs non-hierarchical aggregation. Data augmentation to improve training stability and preliminary AE risk modeling, prioritizing grade ≥3 events, are showing encouraging results. Molecular signatures are used to support mechanistic insight and biomarker explaining predictions.

Conclusions: Baseline blood single-cell signals combined with FM embeddings and cell-to-patient learning can predict treatment response in solid tumors and provide a path to AE stratification and signature discovery. Improvements can be made with larger dataset and interpretable biological rationales can be facilitated by this framework.

References: 1.Cui H. et al. Nature Methods, 21:1470-1480 (2024).2.Hao M. et al. Nature Methods, 21:1481-1491 (2024).3.Do C et al. Bioinformatics, 41: i96-i104 (2025).4.Lopez R. et al. Nature Methods, 15:1053-1058 (2018).

#4213 Generative genomics accurately predicts cancer gene expression.

Gregory Koytiger[1], Alice M. Walsh[1], Vaishali Marar[1], Kayla A. Johnson[1], Max Highsmith[1], **Alexander R. Abbas**[1], Andrew Stirn[2], Ariel Brumbaugh[1], Alex David[1], Darren Hui[1], Jeffrey Kahn[1], Sheng-Yong Niu[1], Liza J. Ray[1], Candace Savonen[1], Stein Setvik[1], Jeffrey T. Leek[1], Robert K. Bradley[1]

[1]Synthesize Bio, Seattle, WA,[2]Variational Bio, Seattle, WA

AI models capable of predicting experimental outcomes could accelerate biomedical research by circumventing fundamental constraints of laboratory experimentation and clinical trials. We developed GEM-1 (Generate Expression Model-1), a generative genomics framework that models the diversity of real-world gene expression experiments and accurately predicts future experimental results.

We trained GEM-1 using 470,691 bulk RNA-seq samples from 24,715 datasets in the NCBI Sequence Read Archive, spanning diverse tissues, diseases, and over 18,000 distinct perturbations. An automated metadata agent harmonized fragmented experimental descriptions using large language models. GEM-1 employs a deep latent variable model that partitions experimental metadata into biological, technical, and perturbational components, using pretrained foundation model embeddings to enable generalization to novel perturbations.

Testing on holdout data deposited after training, GEM-1 achieved pseudoreplicate-level accuracy (pearson correlation of gene rank across samples, r_gene, of 0.65-0.75) for previously observed contexts and maintained strong performance for completely novel genetic (r_gene = 0.58-0.63) and chemical perturbations (r_gene = 0.52-0.68). The model correctly predicted 63% and 70% of enriched gene sets for novel genetic and chemical perturbations, respectively. We extended GEM-1 to single-cell data using 41.5 million cells, achieving comparable performance to established models for cell type annotation while enabling interpretable biological feature inference.

We demonstrated clinical utility by generating synthetic cohorts that accurately recapitulated key biological phenomena: SYNTH-TEx (5,300 healthy tissue samples matching GTEx patterns), SYNTH-interferon (200 samples correctly modeling lupus interferon dysregulation), and SYNTH-cancer (10,523 samples exhibiting known molecular features of cancer). We show that GEM-1 can simulate novel perturbations on specific patient samples, an ability we term "reference conditioning".

This approach represents a significant advance toward AI systems that can predict experimental outcomes before physical experiments are conducted, shortcutting fundamental limitations in experimental speed and clinical trial recruitment and potentially revolutionizing drug development and personalized medicine.

#4215 A comparative assessment of machine learning models for predicting prostate cancer using PVT1 biomarkers and PSA.

Pragyan Kadel[1], Rachel E. Bonacci[2], Emmanuel Owusu Asante-Asamani[3], Olorunseun O. Ogunwobi[4]

[1]Data Science, Clarkson Univ., Potsdam, NY,[2]Biology, Michigan State University, East Lansing, MI,[3]Mathematics, Clarkson Univ., Potsdam, NY,[4]Michigan State University, East Lansing, MI

Prostate cancer (PCa) is one of the leading causes of cancer-related deaths among men, especially in populations of African ancestry. While prostate-specific antigen (PSA) testing is the most common diagnostic tool, its low specificity results in overdiagnosis and overtreatment. Recent studies have shown that specific exons of the PVT1 gene, such as exon 4A, exon 4B and exon 9, may serve as promising biomarkers to improve PCa risk stratification when combined with PSA levels. Building on this work, our study evaluates the predictive accuracy of machine learning techniques in identifying patients with any prostate cancer or high-grade prostate cancer on data from 108 multiracial men with elevated PSA. We explore different combinations of these features using logistic regression and support vector machines (SVMs).We found no single best method across all population groups and endpoints. The optimal classifier varied based on the specific prediction task. For predicting any cancer in the general population, the best performing model was Logistic Regression (F1-score of 0.72) when PSA is combined with PVT1 exon 4a. For cancer grade prediction in the general population, SVM achieved the best performance (F1 score of 0.93) using PSA, PVT1 exon 4a and PVT1 exon 9. For predicting the risk of any cancer among Men of African Ancestry (MoAA) Logistic Regression achieved the best accuracy (F1 score of 0.89) by combining PSA with PVT1 exon 4a.Our results show that combination of PVT1 biomarkers with PSA improves the accuracy of risk prediction across different populations and endpoints. Additionally, Logistic Regression provides more accurate predictions of any cancer whereas SVMs perform better for predicting high grade cancer. Future work will focus on evaluating our models on larger clinical data

#4216 Interpreting PLMs for cancer discovery: High attention hotspots predict pathogenic mutation positions and novel drug binding sites.

Sophia J. Pribus[1], Gowri Nayar[2], Russ Altman[3]

[1]Stanford University School of Medicine, Stanford, CA,[2]Biomedical Informatics, Stanford University, Stanford, CA,[3]Bioengineering, Stanford University, Stanford, CA

Computational proteomics has revolutionized cancer research, guiding targeted experimental exploration to accelerate protein-based mechanistic discovery. Protein Language Models (PLMs) enable scalable, resource-efficient study; through large-scale training on only primary protein sequences, PLMs generate vector representations of protein structure that have been shown to capture biochemical and structural properties. A core component of PLMs is the attention mechanism, which specifically captures long-range interactions across a protein sequence in attention matrices. Using the previously unexplored attention matrices generated by the Evolutionary Scale Modelling 2 (ESM-2) PLM, we developed a novel method to identify High Attention (HA) residues, the specific residues that ESM-2 assigns the most attention to early in training. We found that HA residues had interpretable links to biological function across the human proteome, including proximity to active sites and conservation across protein families. We further used AlphaMissense pathogenicity predictions and TCGA-labeled pathogenic variant positions to determine that HA residues predict protein regions with high pathogenic risk. Finally, we explored the utility of HA residues for novel binding site discovery, an open challenge in cancer research. Using Uniprot and Biolip annotations, we confirmed that HA residues were spatially proximal to previously-known binding sites. We then used SiteMap to predict the bindability of HA residue regions in both annotated and unannotated proteins. We identified multiple cancer protein examples where HA residues identified regions with previously undiscovered high bindability and thus potential novel therapeutic utility. In summary, our work demonstrates the biological interpretability of PLM representations and offers a valuable method to prioritize functionally relevant protein residues for targeted biomedical research.

#4217 Multi-modal modeling of genomic, histopathologic, and lab data predicts survival after hepatectomy in oligometastatic colorectal cancer.

Divya Koyyalagunta, Stefanie Gerstberger, Marion Liu, Chenlian Fu, Simran Chhabria, Madison Darmofal, Kevin Michael Boehm, Justin Jee, Michele Waters, Vinod P. Balachandran, Kevin Soares, Alice C. Wei, Jeffrey A. Drebin, T. Peter Kingham, William R. Jarnagin, Jinru Shia, Francisco Sanchez-Vega, Michael I. D'Angelica, Karuna Ganesh, Quaid Morris

Memorial Sloan Kettering Cancer Center, New York, NY

Background: Oligometastasis is an intermediate stage of metastatic progression with limited spread and organ involvement, where curative treatment remains possible. In colorectal cancer (CRC), ~10% of patients present with liver-limited oligometastatic disease and undergo hepatectomy with curative intent. However, there is an unmet need for pre-operative predictive biomarkers that can distinguish long-term survivors from patients who relapse shortly after hepatectomy and thus did not benefit from surgery. To improve clinical decision-making for oligometastatic CRC, we aimed to develop a machine learning (ML) model to reliably predict post-hepatectomy outcomes using routinely collected clinical data.
Methods: We analyzed 284 CRC patients treated at Memorial Sloan Kettering Cancer Center who had liver-confined oligometastatic disease and underwent metastatic resection via partial hepatectomy. Four data modalities were collected: clinical features; MSK-IMPACT targeted exon sequencing; histopathology features from whole slide images; and laboratory values collected within 30 days pre-hepatectomy. We trained an XGBoost ML model with nested cross-validation to predict which patients would achieve overall survival greater than three years after hepatectomy.
Results: An ML model trained on genomics, histopathology and lab data achieved the highest predictive performance (AUROC = 0.75, SE = 0.03), with comparable performance using only genomics and lab data (AUROC = 0.73, SE = 0.04). Combining ML-predicted risk with the established Clinical Risk Score (CRS) for CRC recurrence showed a modest increase in prognostic discrimination (CRS C-index = 0.606, CRS + ML C-index = 0.635). Lab and histopathology variables contributed most to model predictions, and an elevated systemic inflammation index ((platelets × neutrophils) / lymphocytes) was associated with worse prognosis, consistent with prior work. We further found that deep deletion in dual-specificity phosphatase DUSP4, a regulator of MAPK signaling, was significantly associated with improved long-term survival (log-rank p = 0.016).
Conclusions: A multi-modal ML model using pre-operative genomic, histopathologic, laboratory, and clinical data can predict long-term survival following hepatectomy in oligometastatic CRC. This study offers a strategy for integrating routinely collected data to improve clinical decision making and risk stratification for resection of oligometastatic disease.

#4218 ProteoBridge: Bridging skipped sections via histology-based protein prediction.

Minji Kim[1], Sunho Park[2], Seock-Jin Chung[1], Inyeop Jang[1], Jean R. Clemenceau[1], Soyoung Im[3], Eric Sha[1], Hwanil Choi[4], Soonyoung Lee[4], Jongseong Jang[4], Sam C. Wang[5], Tae Hyun Hwang[1]

[1]Section Surgical Research, Vanderbilt University Medical Center, Nashville, TN,[2]Surgical Section Research, Vanderbilt University Medical Center, Nashville, TN,[3]College of medicine, The Catholic University, Suwon, Korea, Republic of,[4]LG AI Research, Seoul, Korea, Republic of,[5]University of Texas Southwestern Medical Center, Dallas, TX

Background: The progress of spatial multimodal platforms has enabled high-resolution mapping of various types of molecular and morphological characteristics within a tissue. Proteins influence cellular phenotypes and the organization of the tumor microenvironment, with their abundance and patterns highly correlated in adjacent serial sections. Spatial Multimodal platforms such as Singular Genomics G4X, which capture H&E-stained images, multiplexed protein expression, and targeted RNA transcriptomics from the same tissue slide, now create a foundation for three-dimensional (3D) spatial multimodal profiling and 3D tumor microenvironment modeling. However, comprehensive multiplex protein imaging across entire tissue stacks is costly, labor-intensive, and impractical, leading to sparse proteomic sampling that limits accurate 3D reconstruction.Methods: We developed ProteoBridge, a deep learning-based framework that predicts protein expression patterns across serial tissue sections to densify the proteomic information needed for 3D molecular modeling. For each tissue stack, the model was trained on the first section, which contains H&E, multiplex protein images, and RNA transcriptomics. The inputs include H&E tiles and RNA transcriptome data, while the outputs are multi-channel protein maps for the same field of view. The combination of targeted RNA transcriptomics and H&E stained morphology helps define cell types and states, allowing the model to learn morphology-to-protein relationships based on transcriptional programs. The training focused on reducing mean absolute error across protein channels to establish histology-protein correspondences for unmeasured sections.Results: We evaluated ProteoBridge on tissue stacks with multiple profiled sections. Image-level similarity between predicted and measured protein maps was assessed. Using single-slide supervision, ProteoBridge accurately reproduced marker intensities and preserved cross-plane consistency, capturing both intensity values and spatial organization of proteins.. By filling in skipped planes, ProteoBridge generates a more continuous 3D representation of the tumor proteome suitable for downstream 3D molecular modeling and visualization.Conclusion: ProteoBridge requires only routine H&E staining on the remaining sections in a stack to infer protein intensities across serial planes, reducing cost and turnaround time while expanding effective proteomic coverage. Using the G4X platform's multimodal data and extending protein predictions to unmeasured areas allows for cost-effective 3D reconstruction of the tumor proteome, enhancing molecular modeling of the tumor microenvironment and its heterogeneity.Generative AI assisted only with language editing of this abstract. The authors retain sole responsibility for the scientific content and conclusions, having reviewed and approved the final version.

#4219 Predicting immunotherapy response in patients with hepatocellular carcinoma from clinical and textual features using AI techniques.

Anwaar Saeed[1], Meghana Singh[1], Yuming Shi[1], Alireza Tojjari[1], Vaishnavi Balaji[2], Lakshya Sharma[3], Azhar Saeed[4], Thant Hoe[2], Yuxi Zhang[2], **Sola Adeleke**[2]

[1]Department of Medicine, Division of Hematology & Oncology, University of Pittsburgh Medical Cancer & UPMC Hillman Cancer Center, Pittsburgh, PA,[2]Curenetics Ltd, London, United Kingdom,[3]School of Medicine, University of St Andrews, Scotland, United Kingdom,[4]University of Vermont Medical Center, Colchester, VT

Background:
Immunotherapy (IO) improves survival in advanced hepatocellular carcinoma (HCC), yet under 30% of patients respond to treatment. Existing biomarkers have shown limited predictive accuracy. Machine learning (ML) and natural language processing (NLP) techniques could be used to develop prediction models that support personalised treatment. We aimed to develop and evaluate machine learning models that predict response to IO in patients with HCC.
Methods:
We retrospectively analyzed data from 302 patients with HCC treated with immunotherapy at UPMC Hillman Cancer Centre between December 2014 and December 2023. Five machine learning models were developed to predict immunotherapy response including logistic regression, random forest, XGBoost, support vector machine and multi-layer perceptron. Models were initially trained using 20 clinical features, then models were expanded to include 50 combined clinical and text-embedded features. Radiological and clinical notes were processed using a natural language processing (NLP) model to generate text embeddings. Data was split into training (80%) and test (20%) sets. Shapley Additive Explanations (SHAP) was used to interpret the prediction models.
Results:
Of the 302 patients, 215 (71%) had stable disease and 87 (29%) had progression. The best-performing model was the Random Forest classifier incorporating both clinical and NLP-derived features (AUC 0.77, Precision: 0.72, Recall 0.72). Model performance marginally decreased when restricted to clinical variables alone (AUC 0.71, Precision: 0.70, Recall 0.70). Key predictors of response to immunotherapy included lower alpha-fetoprotein (AFP), liver function tests within normal range (AST, ALT, ALP, albumin, bilirubin), higher total protein and lower grade of ECOG performance status. 142 patients had first-line IO treatment with atezolizumab and bevacizumab (Atezo/Bev) and 57 patients had durvalumab and tremelimumab (Durva/Treme). A subgroup analysis showed that model performance for patients receiving Atezo/Bev (test AUC-ROC 0.97) was superior to those receiving Durva/Treme (test AUC-ROC 0.66). However, there was no statistically significant difference in predicted mean response between the two IO regimens (Atezo/Bev 0.55, Durva/Treme 0.64, T-statistic: -1.54, p-value 0.13).
Conclusions:
This study demonstrates that ML models integrating both clinical and NLP-derived features can accurately predict IO response in patients with HCC. Key predictors of disease progression included AFP, liver function blood tests and ECOG performance status. Future work will externally validate these results on larger datasets, with the aim of developing generalizable and clinically useful predictive models.

#4220 Predicting high-risk colorectal polyps using pre-colonoscopy features: Machine learning model development and validation.

Basheer Qolomany, Mrinalini Deverapall, Adeyinka O. Laiyemo, Zaki A. Sherif, Hassan Brim, Hassan Ashktorab

Dept. of Medicine, Howard University College of Medicine, Washington, DC

Background: Advanced colorectal polyp risk stratification typically relies on colonoscopy and/or pathology findings, but there is interest in whether there are non-invasive features visible prior to colonoscopy that can identify which patients are at higher risk. Such a tool could help in clinical decision-making, enabling colonoscopy surveillance to be reserved for those most likely to have high-risk polyps and avoiding unnecessary procedures in those at lower risk.

Methods: We developed machine learning models to predict high-risk polyps using demographic, lifestyle, and comorbidities. Patients with villous/tubulovillous adenoma, high-grade dysplasia, ≥10 mm in size, and/or ≥3 polyps per procedure were considered as having High-risk polyps (HRP), while all others were considered to be Low-risk polyps (LRP). The data set consisted of 4,681 patients from 2014 - 2022 (internal validation; 2018 HRP, 2,658 LRP) and 1,562 patients from 2023-2024 (external validation; 769 HRP, 793 LRP). Models utilized were neural networks, random forest, SVM, Naive Bayes, logistic regression, decision trees, KNN, and XGBoost.

Results: The neural network achieved the best internal performance (ROC-AUC 0.7764, PR-AUC 0.75, accuracy 0.72). However, external cohort performance reduced (ROC-AUC 0.67, accuracy 0.66), suggesting overfitting or feature drift. Less complex models such as Naive Bayes, SVM, and XGBoost, while weaker internally (ROC-AUC 0.54-0.59), demonstrated stronger external performance (ROC-AUC 0.52-0.63, accuracy ~0.53-0.60). This suggests that predictive signal in pre-colonoscopy features exists but is moderate and very sensitive to temporal and cohort variation. Model interpretability analysis using SHAP values revealed that the main variables driving predictions were age, smoking status, sex, occupation, race, and indication for colonoscopy. Additional contributors included family history of colorectal cancer in first-degree relatives, BMI, and several clinical/lifestyle factors such as ASA use, NSAID use, and alcohol use. These results highlight that while traditional clinical risk factors dominate prediction, sociodemographic variables also carry important signal.

Conclusions: HRP prediction based on non-invasive pre-colonoscopy features is feasible but challenging. Performance degradation upon external validation highlights the importance of real-world generalizability and practice or demographic change effects. These findings highlight both clinical utility potential and limitations of pre-colonoscopy risk prediction, and suggest that multimodal data sources (e.g., genomics, microbiomics, imaging, social determinants) may be required to achieve clinically meaningful performance.

#4221 CAPTYN, a six-variable machine-learning model predicting clinical benefit of atezolizumab-bevacizumab in hepatocellular carcinoma: Development and external validation in IMbrave150.

Gae Hoon Jo[1], Sohyun Hwang[2], Bernhard Scheiner[3], Won Suk Lee[4], Beodeul Kang[4], Jung Sun Kim[4], Ho Yeong Lim[4], Chansik An[5], Dong Yun Kim[6], Inyoung Kim[7], Dong-hyuk Heo[7], Matthias Pinter[3], Beom Kyung Kim[6], Chan Kim[4], Hong Jae Chon[4]

[1]Department of Life Science, CHA University, Seongnam, Korea, Republic of,[2]Department of Pathology, CHA Bundang Medical Center, Seongnam, Korea, Republic of,[3]Division of Gastroenterology and Hepatology, Department of Medicine III, Medical University of Vienna, Vienna, Austria,[4]Department of Medical Oncology, CHA Bundang Medical Center, Seongnam, Korea, Republic of,[5]Department of Radiology, CHA Bundang Medical Center, Seongnam, Korea, Republic of,[6]Department of Internal Medicine, Yonsei University College of Medicine, Seoul, Korea, Republic of,[7]Theragen Bio Co., Ltd., Seongnam, Korea, Republic of

Background: Current prognostic models for hepatocellular carcinoma (HCC) treated with atezolizumab plus bevacizumab (AB) rely on limited variables and lack prospective validation. We aimed to develop and externally validate a machine-learning model integrating multiple clinical variables to predict clinical benefit to first-line AB in advanced HCC.
Methods and Results: This multicenter study included 637 patients with unresectable HCC from three hospitals and one phase III prospective trial (IMbrave150), grouped into four AB cohorts. The training set comprised patients from CHA Bundang Medical Center (Korea, n=301) and the Medical University of Vienna (Austria, n=53), while external validation used IMbrave150 (n=99) and Severance Hospital (Korea, n=184) cohort. Clinical benefit (CB) was defined as CR, PR, or SD with PFS ≥6 months by RECIST v1.1; all other cases were classified as non-clinical benefit (NCB). Among 14 candidate variables, nine were identified by univariable Cox regression for OS and PFS. A recursive elimination procedure maximizing five-fold cross-validated AUC for NCB classification identified six optimal predictors—CRP, AFP, platelet, total bilirubin, lymphocyte, and neutrophil—which were used to train an XGBoost classifier, termed CAPTYN. In the training set, CAPTYN achieved an AUC of 0.93. SHAP-based interpretation showed that elevated CRP, AFP, and total bilirubin and reduced lymphocyte counts contributed to NCB, whereas platelet and neutrophil counts exhibited U-shaped associations. In external validation, CAPTYN achieved AUCs of 0.70 (95% CI, 0.59-0.81) in IMbrave150 cohort and 0.67 (0.59-0.75) in Severance cohort, outperforming CRAFITY, ALBI, and CRAPT-M (DeLong's test $p<0.05$). Calibration was acceptable (Brier score=0.22 and 0.24, respectively), and CAPTYN significantly stratified OS and PFS (IMbrave150 cohort: both $p<0.001$; Severance cohort: $p=0.012$ for OS, $p=0.009$ for PFS), whereas comparator models failed to discriminate PFS. Subgroup analyses across demographics and disease features in IMbrave150 consistently showed higher hazard ratios (>1.5) for OS and PFS in CAPTYN-predicted NCB patients.
Conclusion: CAPTYN, a six-variable machine-learning model predicting CB to AB, was externally validated using a prospective trial and a real-world cohort, providing calibrated, interpretable probabilities that may inform individualized treatment decisions.

#4222 Early prediction of engraftment outcomes in hematopoietic cell transplantation using neural ordinary differential equations.

Parham Habibzadeh

Department of Medicine, University of Pittsburgh, Pittsburgh, PA

Background: Engraftment failure after allogeneic hematopoietic cell transplantation (HCT) is a complex event that traditional models struggle to predict due to dynamic interactions among microbiome composition, immune recovery, and clinical risk factors, especially with missing or irregular data. Neural Ordinary Differential Equations (Neural ODEs) address these limitations by treating patient trajectories as continuous-time evolutions, enabling effective learning from such sparse and irregularly sampled measurements where traditional discrete-time networks often fail.
Methods: A synthetic cohort of 1,000 HCT patients over 42 days, modeling dynamic features (e.g. gut bacterial abundance, immune cell numbers) and static risk factors (e.g. age, HHV-6 status, conditioning intensity, initial microbiome diversity) was generated. Microbiome dynamics were governed by Lotka-Volterra equations, capturing predator-prey interactions between beneficial and pathogenic bacteria populations. Literature-derived parameters governed immune trajectories, ensuring biological plausibility. For prediction, a neural ODE framework that learns continuous-time dynamics from discrete, irregularly sampled data, enabling smooth visualization and extrapolation was utilized. The model was trained on only the first 3-7 days of data with class-weighted loss. Feature importance was assessed via permutation analysis.
Results: Validation of the synthetic cohort (N=1,000) confirmed clinically realistic recovery trajectories; for instance, patients receiving myeloablative conditioning engrafted later (mean 20.8 days) than those receiving reduced-intensity conditioning (14.8 days). On this validated cohort, the neural ODE model achieved strong early prediction of Day 42 outcomes using only the first 3 days of data (AUC=0.96; recall=93.8%; precision=88.2%). Permutation feature importance analysis revealed that while early neutrophil dynamics were critical, the dynamics of the abundance of specific beneficial commensals and initial microbiome diversity were dominant predictive signals, outweighing static clinical factors.
Conclusions: Neural ODEs provide a mechanistically grounded framework for learning from sparse, irregularly sampled longitudinal data while maintaining biological interpretability. Beyond HCT, this approach shows promise for dynamic prediction in cancer research where traditional recurrent architectures struggle with irregular time series. The continuous-time parameterization enables smooth trajectory interpolation offering advantages over standard discrete-time neural network models.

#4223 AI-based prescreening of clonal hematopoiesis in patients with liver disease using Sysmex XN hematology analyzer data.

Jeongmin Park[1], Dahyun Kim[1], Ja Min Byun[2], Hyunsoo Cho[2], Eun Ju Cho[2], Youngil Koh[2]

[1]Cancer Research Institute, Seoul National University College of Medicine, Seoul, Korea, Republic of,[2]Seoul National University Hospital, Seoul, Korea, Republic of

Clonal hematopoiesis (CH) is characterized by the clonal expansion of blood cells harboring somatic mutations and is commonly observed with aging. Although CH is known to induce hemogram alterations, differentiating it using standard complete blood count (CBC) metrics alone is challenging, highlighting the need for multidimensional hematologic profiling. To address this, this study leverages expanded CBC parameters from the Sysmex XN analyzer, incorporating broader optical measurements, to explore whether they improve CH detection. Given prior evidence linking CH to liver pathology, this study focuses on the relationship between CH and liver disease. Associations between the two have been demonstrated in large-scale cohorts such as the UK Biobank, and CH-driven macrophage activation has been implicated in the progression of NAFLD, NASH, cirrhosis, and hepatocellular carcinoma. However, liver diseases—including cirrhosis—produce characteristic CBC alterations, making CH discrimination particularly difficult. This motivates evaluating whether an AI model can detect CH-related signals despite liver disease-induced hematologic changes. At Seoul National University Hospital, with support from Sysmex, raw outputs from XN analyzers have been prospectively archived since 2022, covering 146 parameters, including reportable items and research indices. Using these data, 2,173 CBCs from 303 patients with liver diseases were analyzed using diverse machine- and deep-learning methods. Initial models were trained on the first test data per patient. To capture the longitudinal dynamics of CH, features were reconstructed from all repeated tests per patient (mean, standard deviation, maximum, minimum), and a soft-voting ensemble combining logistic regression, LightGBM, and CatBoost was developed, yielding stable performance. A deep-learning MIL model was applied to aggregate repeated CBC measurements across patient time points and capture instance-level contributions, complemented by an autoencoder to compress correlated features into latent clusters and improve model stability. With first-visit data only, logistic regression achieved precision 41.0%, recall 51.6%, F1 0.457; CatBoost achieved precision 39.2%, recall 93.5%, F1 0.552. When summary statistics with soft voting model were used, performance improved to precision 72.2%, recall 80.0%, F1 0.759. Within the MIL framework, analysis of model-weighted instances revealed distinct activation patterns in autoencoder-derived latent clusters associated with liver diseases, offering a novel interpretability perspective beyond traditional feature-importance analysis. This algorithm provides practical guidance to identify CH from CBC data in patients with liver disease, enabling prescreening prior to precision diagnostics and supporting timely diagnosis and improved management.

#4224 Artificial intelligence-derived analysis of wearables-derived biometrics to characterize physiologic response to chemotherapy in solid organ cancers.

Alexander Zhu[1], Lizi Zhang[2], Yuhang Zhang[2], Alexandra Potter[1], Bryan Rettner[1], Alisha Keshwani[1], Alina Keshwani[1], Nicole Hu[1], Anton Melki[1], Zhengyu Fang[2], Meghan McCarthy[1], Jacob Baird[1], Aubrey Pope[1], Samuel Schwartz[1], Quiana Guo[1], Michael Lanuti[1], Xiao Li[2], Chi-Fu Jeffrey Yang[1]

[1]Massachusetts General Hospital, Boston, MA,[2]Case Western Reserve University, Cleveland, OH

Objective: (1) To use wearable-derived biometrics to examine the relationship between physiologic patterns and adverse events during chemotherapy for solid organ cancers. (2) To use machine-learning analysis of these physiologic patterns to predict adverse events.

Methods: Patients with solid organ cancers receiving systemic therapy were enrolled in an ongoing trial evaluating the effects of chemotherapy/ immunotherapy on physiologic patterns. Patients continuously wore a Fitbit for >5 days before and during treatment. We analyzed intra- and inter-personal variation in normalized daily average resting heart rate (RHR) across cycles. We developed a novel, personalized, baseline-referenced statistical framework based on the Change-of-Heart machine learning algorithm, "HeartSense," which standardizes each participant's RHR against their own baseline during sleep and non-sleep periods, generating a score that quantifies daily physiologic stability. Higher scores reflect RHR patterns consistent with pre-treatment baseline and lower scores indicate greater deviation from baseline. We compared lowest HeartSense scores by patients who experienced adverse events vs those who did not in cycle 1. We also examined whether scores from cycle 1 were associated with adverse events in cycle 2.

Results: A total of 54 cancer patients who underwent ≥1 cycle of systemic therapy were included in analysis. Distinct physiologic patterns emerged during therapy. One patient showed cyclic decreases in heart rate after each infusion with recovery to baseline (Figure A), while another exhibited progressive physiologic disruption preceding treatment termination (Figure B). Intrapersonal variation in sleep and non-sleep RHR was significantly smaller than interpersonal variation (Figure C). Lower median HeartSense scores within a cycle were significantly more likely to experience adverse events (Figure D). Lower scores were also associated with adverse events in cycle 2 (Figure E).

Conclusions: Patients exhibit distinct physiologic changes in resting heart rate during systemic therapy and deviation from normal patterns may indicate treatment-related adverse events. Our novel machine learning algorithm identified that lower scores—reflecting abnormal physiologic regulation—were linked to a higher risk of adverse events both during and after the current treatment cycle, suggesting that chemotherapy-related toxicity can be preceded by early physiologic warning signals.

Figure. Evaluating Physiologic Patterns Among All Cancer Patients Undergoing Systemic Therapy. Data from 54 patients undergoing systemic therapy are presented. Figures 1A and 1B show two example patients who underwent adjuvant chemotherapy. Each panel represents a single patient's normalized resting heart rate (RHR). Each panel shows a single patient's normalized resting heart rate (RHR), separated into sleep (blue) and non-sleep (orange) periods. **Figure 1A** is an example of a patient who underwent lobectomy followed by 4 cycles of adjuvant chemotherapy (pemetrexed/cisplatin). The patient wore the watch during the first 3 cycles of adjuvant chemotherapy (the patient did not wear the watch during cycle 4). The blue-shaded regions highlight periods immediately following the date of chemotherapy infusion where the patient exhibited similar decreases in RHR, each lasting approximately 7 days. **Figure 1B** is an example of a patient who underwent lobectomy followed by 2 cycles of chemotherapy (pemetrexed/carboplatin). Eight days after the cycle #1 infusion date, the patient reported worsening neuropathy. After cycle #2, the patient reported further severe worsening of neuropathy, with difficulty pushing buttons and driving their car. The patient discontinued chemotherapy after cycle #2. **Figure 1C.** Boxplot showing intrapersonal and interpersonal variation in resting heart rate (RHR) across systemic therapy cycles. RHR (normalized at the individual level using HeartSense) collected during each systemic therapy cycle was analyzed using dynamic time warping (DTW). The DTW distance, representing the temporal similarity in RHR patterns, was calculated for all pairwise comparisons of cycles, either between individuals or within the same individual, and summarized separately for non-sleep and sleep periods. **Figure 1D.** Boxplot summarizing the worst HeartSense score per cycle calculated by the HeartSense algorithm, stratified by whether the patient experienced adverse event(s) during that cycle. **Figure 1E.** Similar to 1D. However, instead of stratifying by whether adverse event(s) occurred in that cycle, the plot is stratified by whether adverse event(s) occurred in the subsequent cycle. Significance was assessed using a two-sided Wilcoxon rank-sum test (*P<0.05; **P < 0.01; *** P<0.001; **** P<0.0001).

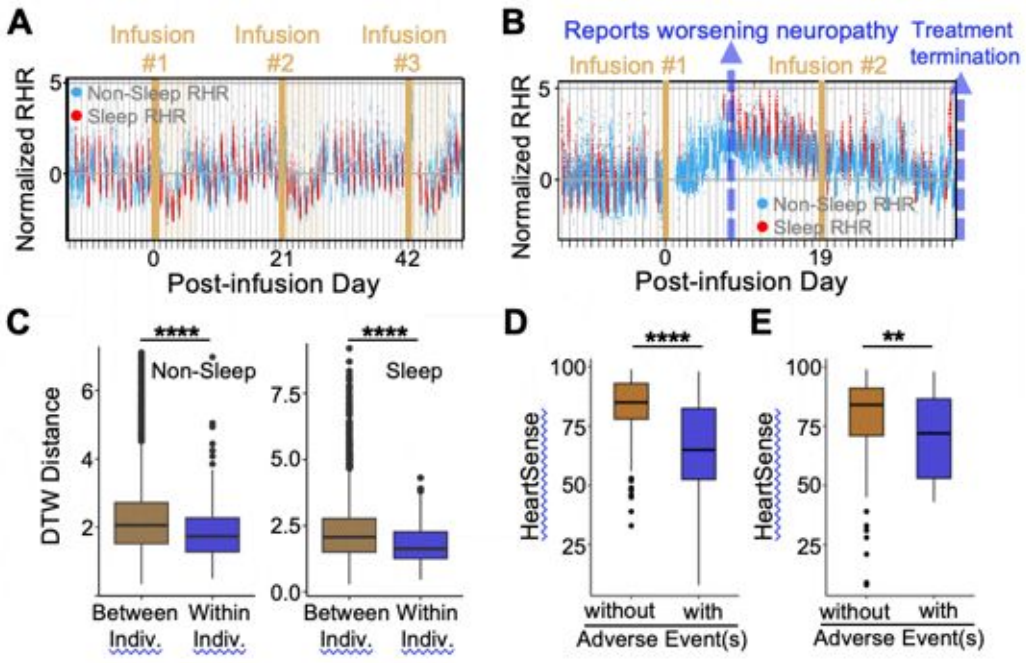

#4225 AI-driven *de novo* design of humanized nanobodies targeting KLK2 for prostate cancer immunotherapy.

Fengze Jin, Puja Singh, Hanyong Chen, Christopher Warlick, **Yibin Deng**

Department of Urology, University of Minnesota Medical School, Minneapolis, MN

Conventional monoclonal antibodies (mAbs) are widely used in cancer therapy but are limited by large size (~150 kDa), structural complexity, and high production costs, motivating the development of alternative antibody formats. Single-chain variable fragments (scFvs), derived from mAbs, retain antigen-binding specificity and affinity while offering a smaller molecular size (~25 kDa), enabling applications such as chimeric antigen receptor (CAR)-T/NK cells and/or bispecific T/NK cell engagers (BiTEs or NKCEs) for immunotherapy. However, scFvs face challenges including structural instability, linker-dependent functionality, and aggregation-prone hydrophobic residues, which limit their therapeutic efficacy. In contrast, single-domain antibodies (sdAbs), derived from the variable antigen-binding domain of heavy-chain-only antibodies (VHHs) and commonly known as nanobodies (~15 kDa), overcome these limitations. Importantly, nanobodies can access cryptic or conformational epitopes—such as deep cavities that are inaccessible to conventional mAbs or scFvs—providing a stable, highly versatile, and clinically attractive biotherapeutic modality for cancer immunotherapy. Traditional methods to develop nanobodies rely on targeting protein-immunized camelids or high-throughput experimental nanobody display systems, including bacteria, phage, ribosome, or yeast display. These approaches are time-consuming, labor-intensive, camelid-derived (with potential immunogenicity), and restricted in library diversity. Moreover, affinity maturation and specificity optimization require multiple iterative rounds of experimental selection—often taking months to years—and may still fail to produce high-affinity nanobodies against difficult targets. To address these challenges, we developed and integrated multiple artificial intelligence (AI) platforms for target-guided humanized nanobody backbone design, soluble protein sequence generation, and enhanced target-nanobody complex prediction and screening. These platforms enable *de novo*, conformational epitope-based nanobody design, generating diverse, high-affinity, and highly specific candidates entirely *in silico,* with experimental validation achievable within weeks to months depending on the target. As a proof-of-principle, we have applied our AI platforms to design humanized nanobodies targeting kallikrein-related peptidase 2 (KLK2), a clinically validated, prostate cancer-specific cell surface protein, and are experimentally engineering the top-designed candidates into T/NK cell engagers and CAR-T/NK cells to evaluate their ability to eliminate KLK2-expressing prostate cancer cells.

#4226 Machine learning based classification of breast cancer using lifestyle and clinical risk factors in Puerto Rican women.

Jorge E. Martinez-Jimenez[1], Sol V. Perez-Martir[1], Doralis de Leon-Vazquez[1], Nelly A. Arroyo[2], Julie Dutil[1]

[1]UPR - Comprehensive Cancer Center, San Juan, PR,[2]Ponce Health Sciences University, Ponce, Puerto Rico

Globally, breast cancer incidence has increased by more than 20 percent and mortality has increased by 14 percent making it a significant public health challenge. Effective prevention and screening strategies require improved early risk assessment tools, especially for understudied populations. Current risk models are predominantly trained on European descent populations, resulting in suboptimal and uneven performance in admixed populations. Our goal was to compare how current machine learning (ML) methods perform to classify breast cancer status in a Puerto Rican population. We used a structured dataset of lifestyle, demographic, reproductive, and established epidemiological risk-factor variables from a Puerto Rican cohort of 1393 woman. Data was preprocessed using systematic data cleaning, removal of outcome-leaking features, normalization of categorical labels, imputation of missing values, and encoding of non-numeric variables. The final dataset was split using a stratified train-test strategy to preserve case-control balance, followed by model development using multiple supervised algorithms. Logistic Regression, Decision Tree, Random Forest, Gradient Boosting, XGBoost, LightGBM, and CatBoost models were trained and compared using stratified 10-fold cross-validation and standardized performance metrics. After hyperparameter tuning with randomized search, the CatBoost classifier achieved the strongest performance on the held-out test set, with a ROC-AUC of 0.8009, PR-AUC of 0.8285, F1-score of 0.7239, and balanced accuracy of 0.7342, outperforming both traditional models and other boosting algorithms. Model interpretability was assessed using SHapley Additive exPlanations (SHAP) and permutation-based feature importance, which consistently identified influential predictors including menopausal status, smoking history, polygenic risk score, age, and number of sisters with breast cancer, among other risk factors. These findings confirm that gradient-boosting approaches, particularly CatBoost, effectively capture nonlinear interactions in multidimensional health data while maintaining interpretability. Overall, this work demonstrates the feasibility and utility of integrating machine learning to predict breast cancer risk using non-genetic and genetic risk factors in a Puerto Rican population.

#4227 Independent validation of the immunotherapy response model using real-world Moffitt Cancer Center cohort.

Isis Yanina Narvaez-Bandera, Alyssa Pybus, Tosin Jolaogun, Paulo C. Morais Lyra, Jeremy Goecks

Machine Learning, Moffitt Cancer Center, Tampa, FL

Immune checkpoint blockade (ICB) has revolutionized cancer therapy, yet many patients derive limited benefit or experience adverse effects. Thus, it becomes crucial to identify when a patient is likely to respond well to ICB treatment, thereby guiding treatment decisions and improving outcomes. Although several studies have applied machine learning (ML) to clinical and laboratory data to predict ICB response, independent validation in large, real-world cohorts remains limited. This gap, driven in part by the small number of available cohorts, restricts model generalizability and hinders broader clinical use. To expand on the most promising model, published as a logistic regression-based immunotherapy-response score (LORIS), we performed external validation using data collected at Moffitt Cancer Center.We analyzed 2,090 patients with advanced melanoma (n=908), non-small cell lung cancer (NSCLC; n=878), and renal cell carcinoma (RCC; n=304) treated with ICB at Moffitt between 2011-2025. The six clinical and laboratory features used in the original LORIS model—age, cancer type, prior systemic therapy, albumin, neutrophil-to-lymphocyte ratio, and tumor mutational burden—were extracted from patient records. Two validation strategies were implemented. First, we evaluated the published LORIS model by directly applying its coefficients to the Moffitt data; no retraining was performed, and all patients were used exclusively for testing, both within each cancer type and in a combined pan-cancer cohort. Second, to assess model reproducibility, we trained a new logistic regression model using an 80/20 train-test split of the Moffitt cohort and compared its performance with LORIS. All evaluations used 1- and 6-month pretreatment windows, with model performance quantified by AUC. Feature contributions were examined to identify predictors driving response.ICB response prediction performance varied substantially across diseases. The highest performance was observed in RCC, where achieved an AUC of 0.85 (1-month pretreatment) and 0.84 (6-month pretreatment). Melanoma showed moderate performance (AUC 0.71-0.74), while NSCLC had lower performance (AUC 0.53-0.55), contributing to the reduced discriminative ability of our pan-cancer model (AUC 0.56-0.61). Incorporating Programmed Death-Ligand 1 (PD-L1) did not consistently improve predictions and in several settings decreased performance. Model performance was similar between 1-month and 6-month pretreatment windows.This large-scale real-world validation confirms partially reproducible predictive signals for RCC and melanoma but highlights limitations in NSCLC and heterogeneous cohorts. Our findings underscore the need for expanded multimodal approaches to improve clinical applicability of ICB response prediction.

#4228 Validation of the CLL treatment infection model (CLL-TIM) in patients with newly diagnosed chronic lymphocytic leukemia (CLL).

Raphael Mwangi[1], Tait D. Shanafelt[2], Soren Basnet[1], Emily L. West[1], Owen Keegan[1], Timothy G. Call[3], Yao Yuan[3], Bryan Alexis Vallejo[3], Paul J. Hampel[3], Lindsey E. Roeker[3], Yucai Wang[4], Saad J. Kenderian[4], Sara J. Achenbach[5], Aaron D. Norman[6], Kari G. Rabe[5], Neil E. Kay[3], James R. Cerhan[6], Curtis A. Hanson[7], Susan L. Slager[3], Sameer A. Parikh[3]

[1]Division of Computational Biology, Mayo Clinic, Rochester, MN,[2]Department of Medicine, Division of Hematology, Stanford University, Stanford, CA,[3]Division of Hematology, Mayo Clinic, Rochester, MN,[4]Mayo Clinic, Rochester, MN,[5]Division of Clinical Trials and Biostatistics, Mayo Clinic, Rochester, MN,[6]Division of Epidemiology, Mayo Clinic, Rochester, MN,[7]Department of Laboratory Medicine and Pathology, Mayo Clinic, Rochester, MN

Prognostic indices such as the CLL International Prognostic Index (CLL-IPI) and the International Prognostic Score for Early-stage CLL (IPS-E) can predict time to first treatment (TTFT) in patients with early-stage CLL. Their ability to predict risk of infection - a leading contributor to morbidity and mortality in CLL - remains uncertain. The CLL-TIM is a machine-learning model developed in Europe that integrates clinical, laboratory, and infection-related data to predict TTFT or infection risk within 2-years of diagnosis, Receiver Operating Characteristic - Area Under the Curve (ROC-AUC) 0.74; Agius et al., *Nat Comm* 11, 363 2020. We conducted the first validation of CLL-TIM in a US cohort of newly diagnosed CLL patients and compared its performance with the CLL-IPI and IPS-E indices. Adults with newly diagnosed CLL (2000-2020) were identified through the Rochester Epidemiology Project using International Classification of Disease (ICD) codes; all diagnoses were confirmed. We replicated the variable selection from the original CLL-TIM model and applied it to our cohort. The primary endpoint was a 2-year composite of either TTFT or incident infection (defined as having blood cultures drawn). Model performance was evaluated using ROC-AUC consistent with the original CLL-TIM methods. CLL-IPI and IPS-E performance was assessed using time-dependent ROC-AUC; pairwise differences in discrimination were tested using DeLong. We identified 454 CLL patients with a median age of 72 years [range, 30-97], 166 (37%) were female, Rai Stage was 0-II in 399 (92%) patients. IGHV genes were unmutated in 130/305 (42%) patients and TP53 disruption (either del17p by FISH or *TP53* mutation) was present in 24/329 (8%) patients. At 2-years, 55 (12%) patients received CLL therapy, and 56 (12%) patients had an infection. The 2-year composite endpoint was observed in 94 (21%) patients. The ROC-AUC was 0.74 (95% CI 0.68-0.80) for CLL-TIM, 0.69 for CLL-IPI (95% CI 0.63-0.75, p=0.11 compared to CLL-TIM) , and 0.68 for IPS-E (95% CI 0.62-0.74, p=0.02 compared to CLL-TIM). We also evaluated the ROC-AUC using all the prognostic models for each individual endpoints. The corresponding ROC-AUC for TTFT at 2 years were 0.79, 0.74, and 0.76 for CLL-TIM, CLL-IPI, and IPS-E, respectively; and for infection at 2 years were 0.68, 0.57, and 0.52, respectively. This is the first validation of the CLL-TIM in a US-based cohort of newly diagnosed CLL patients. Although the CLL-TIM model exceeded the minimally meaningful discrimination threshold (AUC >0.7) for individual patient-level risk prediction, there was no statistical difference in AUC between CLL-TIM and CLL-IPI, suggesting either model can predict the composite endpoint at 2 years. Most of the observed discrimination was driven by prediction of TTFT rather than infection, underscoring the need to develop more infection-specific risk models for newly diagnosed CLL.

#4229 AI based explainable survival modeling for advanced non small cell lung cancer.

Kang Qin[1], An Qin[2], John V. Heymach[1]

[1]MD Anderson cancer center, Houston, TX,[2]Loyola University Chicago, Chicago, IL

Background: Accurate individualized prognostication in advanced non-small cell lung cancer (NSCLC) is hindered by nonlinear interactions among clinical and biological variables. Integrating interpretable artificial intelligence (AI) with classical survival modeling may enhance predictive precision while preserving transparency.
Methods: A real-world cohort of 62 608 advanced NSCLC patients with 52782 observed death events was analyzed. Prognostic variables significantly associated with overall survival (OS) were identified using univariate Cox proportional-hazards regression ($p < 0.05$). Feature refinement was achieved through LASSO-regularized Cox modeling with 5-fold cross-validation ($\lambda = 0.00176$) and stability selection (≥ 0.7), producing a 20-feature prognostic signature. These variables were then used to train and benchmark 18 regression and ensemble machine-learning algorithms for continuous OS prediction. Model performance was evaluated using R^2, RMSE, MAE, calibration plots, and decision-curve analysis (DCA). Feature interpretability was assessed with SHAP (Shapley Additive Explanations) to quantify the direction and magnitude of each predictor's effect.
Results: All 20 variables remained significant in multivariate Cox analysis. Chemotherapy, systemic therapy, and surgery were independent protective factors, whereas age, tumor size, metastatic burden, liver/bone metastasis, regional nodal involvement, and N stage predicted worse outcomes. Ensemble gradient-boosting models outperformed linear baselines ($R^2 \approx 0.15$ vs. 0.10; RMSE ≈ 18 months). LightGBM achieved the highest accuracy ($R^2 = 0.155$; MAE = 11.9 months) with excellent calibration and the greatest net benefit on DCA. SHAP analysis identified chemotherapy, diagnosis year, organ metastatic number, and age as dominant determinants of predicted survival, with strong reproducibility across folds (Spearman $\rho > 0.9$).
Conclusions: A transparent Cox-LASSO-LightGBM-SHAP framework established a robust, biologically consistent 20-factor prognostic signature for advanced NSCLC. The model achieved high predictive accuracy, clinical calibration, and interpretability, revealing treatment modality, metastatic extent, and temporal therapeutic progress as principal survival drivers. This interpretable AI framework enables credible, individualized survival prediction and bridges data-driven modeling with clinical oncology.

: Adaptive Immunity in Cancer
Poster Session

#4233 Transcription factor c-Maf drives Th17-dependent activation of CD8⁺ T cells to sustain anti-tumor immunity.

Ching Tung Wu, Shi-Chuen Miaw

National Taiwan University College of Medicine, Taipei City, Taiwan

Within the tumor microenvironment (TME), Th17 cells exhibit a dual role in tumor progression. Although IL-17A, IL-17F, and IL-21 have been reported to exert anti-tumor effects, the intrinsic mechanisms underlying Th17-mediated tumor suppression remain poorly understood.The transcription factor c-Maf is a known regulator of cytokine production in CD4⁺ T-cell subsets. To investigate its role in tumor immunity, we generated mice with c-Maf-deficient CD4⁺ T cells (). In both subcutaneous tumor models and an orthotopic colorectal cancer model induced by AOM/DSS treatment, mice developed significantly larger tumors than littermate controls, demonstrating that c-Maf expression in CD4⁺ T cell is critical for anti-tumor immunity. Analysis of tumor-infiltrating lymphocytes (TILs) from MC38 tumor-bearing mice showed a marked reduction in Tbet⁺ and IFN-γ⁺ Th1 cells, as well as RORγt⁺, IL-17A⁺, and IL-21⁺ Th17 cells. Although CD8⁺ T cells expressed comparable levels of c-Maf in both genotypes, mice displayed significantly reduced CD8⁺ T-cell cytotoxicity, including lower expression of CD107a, granzyme B, and IFN-γ. These findings indicate that c-Maf deficiency diminishes anti-tumor Th1 and Th17 responses and impairs CD8⁺ T-cell function within the TME. To directly assess the role of c-Maf in Th1 and Th17 cells, we performed adoptive transfers of OT-II⁺ Th1 or Th17 cells. Transfer of c-Maf-deficient Th17 cells resulted in significantly impaired tumor control compared to WT Th17 cells, whereas Th1 cell transfer showed no genotype-dependent differences. This indicates that c-Maf selectively enhances the anti-tumor activity of Th17 cells. Furthermore, transfer of WT OT-II⁺ Th17 cells increased CD8⁺ T-cell cytotoxicity in recipient mice, suggesting that c-Maf ⁺ Th17 cells promote CD8⁺ T-cell activation. Consistent with this, neither WT nor c-Maf-deficient Th17 cells controll tumor growth when transferred into Rag1$^{-/-}$ mice lacking T and B cells, demonstrating that the anti-tumor activity of Th17 cells requires CD8⁺ T cells. Mechanistically, co-culture experiments revealed that the CD8⁺ T-cell cytotoxic enhancement mediated by WT Th17 cells was abolished upon blockade of either IL-17A or IL-21. These results indicate that c-Maf promotes anti-tumor immunity by regulating IL-17A and IL-21 production in Th17 cells, thereby enabling robust CD8⁺ T-cell activation. In summary, our findings identify c-Maf as a critical transcriptional regulator in Th17 cells that sustains anti-tumor immunity through a cytokine-dependent mechanism that augments CD8⁺ T-cell cytotoxic function.

#4234 Glycan-based site specific ADC achieves sustained tumor control through Improved payload delivery and immune activation.

Liu Chih-Chun, Tsai Yi-Chien, Huang Jing-Rong, Lo Fei-Yun, Pei Yu, Hsu Ren-Yu, Tu Tzu-Hsuan, **Chen Ya-Chi**

OBI Pharma Inc,, Taipei, Taiwan

Antibody-drug conjugates (ADCs) achieve potent tumor killing but often limited to induce durable antitumor immunity. The Glycan conjugated platform enables site-specific glycan conjugation, enhancing pharmacokinetics (PK) and intratumoral payload delivery versus conventional cysteine-based ADCs. We hypothesized that this improved payload delivery capability by the Glycan conjugated ADC (OBI-902) would potentiate immunogenic cell death (ICD) and sustains antitumor immune activation relative to a cysteine-conjugated ADC (OBI-992).

Efficacy and immune profiling were evaluated in LL2 syngeneic tumors overexpressing human Trop2. Intratumoral payload, and ICD markers (calreticulin, HSP70, HSP90) were assessed post-treatment. Tumor, lymph node, and blood immune subsets were analyzed by multiparametric flow cytometry, and serum cytokines quantified for systemic immune activation. OBI-902 demonstrated durable tumor growth inhibition and enhanced ICD in the tumor microenvironment, findings that were superior to those observed with OBI-992. Serum IFN-γ, IL-12, and TNF-α elevations indicated systemic immune activation.

In tumors, OBI-902 increased $CD4^+$ and $CD8^+$ T-cell and B-cell infiltration while reducing MDSCs. It also expanded cDC1s and upregulated their MHC-II expression, supporting improved antigen presentation. In tumor-draining lymph nodes, OBI-902 expanded progenitor-exhausted $CD8^+$ T cells yet functional state while limiting terminal exhaustion. Peripheral immune profiling corroborated that OBI-902 increased T-cell proportions and reduced MDSCs. At study endpoint, OBI-902 sustained $CD8^+$ T-cell functionality with higher CX3CR1 and lower CD39 expression, indicating preserved cytotoxicity and T-cell fitness. This readily accessible peripheral immune signatures may serve as pharmacodynamic biomarkers in clinical settings.

The Glycan conjugated platform ADC (OBI-902), enabled by its more stable linker-payload design that delivers greater payload to the tumor, achieved sustained ICD induction and a profound reprogramming of T-cell exhaustion, driving robust innate and adaptive immune activation. These results highlight the Glycan conjugated platform as a next-generation ADC technology and strongly support its combination with immune checkpoint blockade in future clinical studies.

#4235 Cell-level spatial transcriptomics detection of microenvironmental STAT1-expressing plasma cells in colorectal cancer recurrence by G4X.

I-Chuang Liao[1], **Minh-Khang Le**[1], Vivek Pujara[1], Haley Jun[1], Devanshi Pratiher[1], Jane C. Figueiredo[2], Nathalie Nguyen[1], Chintda Santiskulvong[1], Angie Laguna[1], Yi Zhang[1], Keluo Yao[1], Joshua Jay Levy[1]

[1]Cedars-Sinai Medical Center, Los Angeles, CA,[2]Samuel Oschin Comprehensive Cancer Institute, Los Angeles, CA

Introduction: STAT1 mediates interferon signaling and immune responses with diverse roles in cancer. In colorectal cancer (CRC), plasma cells are critical immune mediators, and STAT1 expression in these cells may reflect their functional status. Lower STAT1-expressing plasma cells have been linked to a weakened anti-tumor immune response that facilitates tumor escape. Understanding this relationship could reveal novel prognostic biomarkers and therapeutic targets for CRC.

Materials and Methods: Thirty CRC samples underwent G4X spatial profiling, each with a manually selected 4.5 × 4.5 mm² capture area targeting key histological features, resulting in spatial gene expression profiles for a 360-gene panel for 3,088,252 cells. Tissue sections were processed following the G4X spatial transcriptomics protocol enabling RNA detection at subcellular resolution. Manual pathology annotation was performed by a collaborating pathologist, identifying regions including cancer, dysplasia/cancer in situ, benign epithelium, interface, muscularis, and stroma. Cancer-associated cells were defined by two criteria: (1) spatial localization within annotated cancer regions, and (2) absence of canonical epithelial and malignant epithelial markers (CEACAM5, EPCAM, MUC12). Differential expression analyses identified associated cell markers, and the proportions of cell types expressing these markers were quantified. Cell-level regression models incorporated random patient intercepts and clinical covariates (age, gender, microsatellite status, T and N stage), followed by sample-level univariate analyses across all 30 samples to assess associations between STAT1-positive cell clusters and clinical recurrence.

Results: Differential expression analysis identified STAT1 as the top upregulated gene in cancer-associated cells (log2 fold-change = 2.11; adjusted $p < 0.001$). Clustering of STAT1-positive cancer-associated cells revealed 10 distinct cell clusters, including 5 cancer-associated fibroblast subtypes, tumor-associated macrophages, mixed T cells, 2 epithelial-like cells, and plasma cells. Regression analyses consistently indicated a negative association between proportion of STAT1-positive plasma cells and colorectal cancer recurrence (OR = 0.19; 95% CI = 0.03-1.13; $p = 0.068$).

Conclusion: STAT1-expressing plasma cells in the colorectal cancer microenvironment are significantly associated with recurrence risk. These findings support further validation efforts through immunohistochemistry in a larger study cohort, demonstrating the promise of leveraging spatial transcriptomic insights to inform routine pathology for patient stratification.

#4236 The metabotropic Glutamate receptor-1 is a glutamatergic checkpoint that integrates with TCR to augment anti-tumor CD8⁺ T cell activation, metabolism and effector function.

Salvador Gonzalez Ochoa[1], Maria Teresa P. de Aquino[1], Thomas W. Hodo[1], Thanigaivelan Kanagasabai[1], Muna A. Mohammed[2], Jane Tonello[1], Alla Ivanova[1], Anil Shanker[3]

[1]Department of Biochemistry, Cancer Biology, Neuroscience and Pharmacology, Meharry Medical College, Nashville, TN,[2]Department of Biomedical Sciences, Meharry Medical College School of Graduate Studies, Meharry Medical College, Nashville, TN,[3]The Office for Research and Innovation, Meharry Medical College, Nashville, TN

Background: Glutamate receptors (GluRs), classically linked to neuronal signaling, are also recognized as key immunomodulators. T cell activation requires precise coordination of TCR-driven signaling microclusters and calcium-dependent pathways that shape T cell effector function. Emerging evidence shows that glutamatergic cues influence T cell metabolism, activation, and fate, yet their role within TCR signaling remains poorly defined. Here, we show how GluR-TCR interactions govern CD8⁺ T cell activation and function, particularly within the metabolic and functional constraints of the tumor microenvironment.
Methods: Tumors and lymphoid tissue single-cell suspensions were analyzed for the expression of ionotropic (GluA3, NR1, NR2B) and metabotropic (mGluR1, mGluR5) receptors on CD4⁺ and CD8⁺ TILs by flow cytometry. CD8⁺ T cells were activated with anti-CD3/CD28 or PMA/ionomycin ± IL-2 in the presence or absence of NBQX (GluA3) and CPCCOEt (mGluR1) inhibitors. Expression of glutamate transporters, viability, and extracellular glutamate were assessed by fluorometric assays. CPCCOEt-treated cells were analyzed for mGluR1-TCR colocalization and phosphorylation of TCR-signaling proteins by confocal microscopy and flow cytometry. Metabolic activity was measured by Seahorse XF96 (OCR/ECAR). Intracellular Ca^{2+} dynamics were evaluated using Fura-2 AM ratiometric imaging. CD8⁺ T cell proliferation was assessed by CFSE, and cytotoxicity was tested in vitro and in vivo using a pulmonary metastasis model; activated CD8⁺ T cells ± antagonists were transferred retro-orbitally.
Results: We found that mGluR1 and GluA3 are expressed at higher levels in T cells compared with other immune cell lineages, and their expression increases during CD8⁺ T cell activation. Conversely, pharmacologic inhibition with CPCCOEt significantly impaired CD8⁺ T cell activation, disrupting mGluR1 colocalization with the TCR-Vβ8.1 in the cell membrane and reducing phosphorylation of key proteins involved in TCR-driven signaling, metabolic pathways, inducing a pronounced dysregulation of Ca^{2+} flux. Functionally, CPCCOEt-treated CD8⁺ T cells showed a reduction in proliferation to levels resembling naïve T cells and a marked decrease in cytotoxic activity. In vivo, these impairments translated into an increased burden of secondary metastatic pulmonary nodules, highlighting the essential role of mGluR1 signaling in sustaining effector CD8⁺ T cell function and antitumor immunity.
Conclusion: These findings identify mGluR1 as a critical glutamatergic checkpoint that integrates with the TCR to augment CD8⁺ T cell activation, metabolism, and effector function. Its disruption collapses signaling strength, Ca^{2+} responses, and cytotoxic competence, revealing a potential target to boost T cell potency in solid tumor microenvironments.

#4237 Immunofluorescence-based adaptive immune subtypes in an association with long-term disease-free interval in the Carolina Breast Cancer Study Phase III.

Qichen Wang[1], Timothy Patrick Sheahan[1], Alyssa Joy Cozzo[2], Sarah Christine Van Alsten[2], Ebonee Nicole Butler[1], James Stephen Marron[3], Katherine A. Hoadley[4], Melissa A. Troester[1]

[1]Department of Epidemiology, Gillings School of Public Health, University of North Carolina at Chapel Hill, Chapel Hill, NC,[2]Lineberger Comprehensive Cancer Center, University of North Carolina at Chapel Hill, Chapel Hill, NC,[3]Department of Statistics and Operations Research, College of Arts and Science, University of North Carolina at Chapel Hill, Chapel Hill, NC,[4]Department of Genetics, Lineberger Comprehensive Cancer Center, University of North Carolina at Chapel Hill, Chapel Hill, NC

Adaptive immune subtype defined using bulk RNA expression has been associated with lower risk of breast cancer recurrence. In the context of intralesional heterogeneity, these estimates may not capture relevant localized patterns of immune infiltration. We aimed to 1) compare bulk RNA-based and immunofluorescence (IF)-based immune subtypes to better characterize the tumor immune microenvironment and 2) evaluate associations between spatially-resolved adaptive immunophenotypes defined using IF and breast cancer recurrence. We analyzed 1,665 invasive breast cancer tumors from the population-based Carolina Breast Cancer Study Phase 3, using 5,276 1-mm tumor microarrays cores (up to 4 per tumor). Six adaptive markers (PD-1, CD3, CD4, CD8a, CD8, FOXP3) were quantified by multiplex IF. Core-level adaptive immune subtypes (adaptive-high vs adaptive-low) were defined with k-mean clustering of HALO-estimated percent-positive cells for each marker. Participant-level immune subtypes were defined using k-means clustering on weighted averages of core-level marker values, weighted by total cell count. Tumors were labeled as 'consistent' if all cores matched the participant-level subtypes. As a comparison, we also performed k-mean clustering using only CD8 percent positive (high vs low) on tumor level. Percent agreement was calculated comparing IF (multi-marker) with bulk RNA-based adaptive classifiers (previously defined). We used Cox models to estimate associations between adaptive subtype and 10-year disease-free interval (DFI) stratified by estrogen receptor (ER) status, and adjusted for age, race, and stage. We observed 65% agreement between participant-level IF and RNA adaptive classifiers. Multi-marker IF-defined adaptive-low tumors had worse 10-year DFI [ER+: Hazard Ratio (HR) 1.54, 95% Confidence Interval (CI) 1.07-2.22; ER-: HR 1.72, 95% CI 1.11-2.68]. CD8-low cluster showed a similar association among ER+ tumors [HR 1.52, 95% CI 1.06-2.19], no association among ER- tumors [HR 1.31, 95% CI 0.83-2.06]. RNA-based associations were stronger than those for IF [HR_{RNA} 2.00, 95% CI 1.48-2.70, non-adaptive vs. adaptive, overall]. Exposure misclassification may have attenuated associations because tumors with inconsistent multi-marker adaptive-high IF subtype were significantly associated with worse 10-year DFI compared to those were consistent [HR 1.83, 95% CI 1.18-2.85]. Overall, adaptive immunity is prognostic in breast cancers, but misclassification of adaptive response is a concern for biomarker development. Use of multiple markers reflecting the adaptive immune community may partially overcome intralesional heterogeneity, but bulk profiling masks spatial characteristics. Ideal immune biomarkers for prognosis must be reproducibly measured and sensitive to detect the most impactful immune characteristics.

#4238 Cytokine expression within the different categories of tumor-infiltrating lymphocytes in primary cutaneous melanoma: an immunohistochemical study.

Thato Ntuli[1], Benny Mosoane[1], Tebogo Marutha[2], Rahaba Marima[2], **Zodwa Dlamini**[2], Meshack Bida[1]

[1]Department of Anatomical Pathology, University of Pretoria, Pretoria, South Africa,[2]Pan African Cancer Research Institute (PACRI), University of Pretoria, Pretoria, South Africa

Background:
Melanoma is a highly aggressive skin malignancy with an incidence exceeding 3 per 100 000. Tumor-infiltrating lymphocytes (TILs) are often linked to better prognosis and tumor regression, reflecting an active host immune response. However, melanoma can evade immune attack, so inflammatory cells are not always effective or tumor-directed. This study evaluated tumor necrosis factor (TNF) and interferon-gamma (IFNγ) expression in primary cutaneous melanoma across different TIL categories to determine whether these infiltrates act as active responders or passive bystanders.
Methods: We performed a cross-sectional study using archival primary cutaneous melanoma tissue from the University of Pretoria (2014-2020). Skin punch biopsies, local excisions, and wide excisions were included. Immunohistochemistry for TNF and IFNγ was performed on formalin-fixed, paraffin-embedded sections. Three pathologists independently graded TILs as negative, non-brisk, or brisk and assessed cytokine expression.
Results: Sixty-six patients met inclusion criteria. TIL grades were: negative (39.4%), non-brisk (33.3%), and brisk (27.3%). Overall, 31.8% of melanomas were TNF-positive. TNF expression occurred in 16.7% of brisk TIL cases, 41% of non-brisk cases, and 15% of TIL-negative tumors. IFNγ expression showed a clearer gradient: brisk TILs were IFNγ-positive in 89% of cases, non-brisk in 64%, and TIL-negative in 15%. Extensively pigmented melanomas tended to show low cytokine expression, although numbers were small and firm conclusions could not be drawn.
Conclusion
TNF and IFNγ expression broadly correlated with TIL grade in primary cutaneous melanoma. Brisk TILs were strongly associated with high IFNγ expression, non-brisk TILs showed more modest cytokine levels, and TIL-negative tumors were largely cytokine-poor. These findings suggest functional heterogeneity among inflammatory infiltrates. Larger, ideally multicenter studies including more heavily pigmented melanomas and clinical outcome data are needed to clarify the prognostic and potential therapeutic implications of these cytokine patterns.

#4239 Aging turns B cells into drivers of CD8⁺ cells that weaken tumor defenses.

MONICA BODOGAI[1], Bongsoo Park[2], Fatima-Zohra Braikia[3], Kumaraswami Konda[1], Arya Biragyn[1]

[1]Immunoregulation Section, Laboratory of Molecular Biology and Immunology, National Institute on Aging, Baltimore, MD,[2]Epigenetics and Stem Cell Aging Unit, Translational Gerontology Branch, National Institute on Aging, Baltimore, MD,[3]Gene Regulation Section, Laboratory of Molecular Biology and Immunology, National Institute on Aging, Baltimore, MD

Despite aging being a major risk factor for cancer, the effect of age-induced immune dysregulation in tumor control is poorly understood. While CD8⁺ T cells are central to antitumor immunity, aging changes their phenotype and interactions with other immune cells. Using multiparameter flow cytometry, functional assays. single-cell RNA sequencing, and ATAC-seq, we identify a phenotypically and epigenetically distinct CD8⁺ T cell population (DP8) that accumulates with age in mice and possibly in older humans. DP8 cells exhibit a non-exhausted CD101⁺CXCR6⁺CD39⁺CD73⁺ phenotype. Mechanistically, DP8 differentiation is driven by aging B cells, as aged—but not young—B cells induce DP8 identity and B cell deficiency prevents their emergence. Functionally, DP8 cells suppress CD4⁺ T cell activation and promote tumor progression, and tumors expressing CXCL16 selectively recruit DP8 cells into the tumor microenvironment where they impair antitumor immunity. We propose that DP8 cells are attractive therapeutic targets, as DP8-like cells appear to also increase in older humans, including in late onset breast cancer. In aged mice, the depletion of DP8 cells or their inducer B cells efficiently reverses tumor growth even when anti-PD1 therapy fails.

#4240 Differential impact of short and long-term hypoxia on effector T cell dysfunction.

Maria Villalba-Esparza[1], Ana Lledo-Delgado[2], Shruti S. Desai[1], Adam Aguirre-Ducler[1], Daniel Boiarsky[3], Boyu Huang[1], Samuel M. DeFina[1], Javier Ramos-Paradas[1], Kurt A. Schalper[1]

[1]Pathology, Yale University, New Haven, CT,[2]Immunobiology, Yale University, New Haven, CT,[3]Medical Oncology, Yale University, New Haven, CT

Background: Limiting T cell dysfunction is crucial for improving immunotherapy outcomes in patients with solid tumors, including non-small cell lung cancer (NSCLC). Hypoxia can occur in the tumor microenvironment (TME) and induce tumor infiltrating lymphocytes (TILs) adaptations, yet the impact of sustained hypoxia on human effector T cells remains poorly understood.

Methods: Using Imaging Mass Cytometry (IMC), we simultaneously mapped 36 markers for cancer cells (DNA, H3, CK, Vimentin, PD-L1, PD-L2, FGL1, CD47, β2M), immune cells (CD3, CD4, CD8, CD20, CD56, CD68, CD45RA, CD45RO, FOXP3, DC-Lamp), functional states (LAG-3, PD-1, TIM-3, VISTA, TBET, EOMES, TOX1/2, TCF7, CD25, CD27, CD137, GZB, ARG1, KI67 and CC3) and hypoxia (HIF1α, CA9) in 114 pre-treatment NSCLCs from two independent cohorts of patients treated with chemotherapy (Cohort 1, n=61) or PD-1 axis blockers (Cohort 2, n=53). Single-cell segmentation enabled the study of the relationship between hypoxia and effector T cell states. To assess functional changes, human PBMCs from healthy donors and *in vitro* expanded TILs obtained from primary human NSCLCs were exposed to recurrent TCR stimulation for 6 days under normoxia (21% O_2) or hypoxia (1% O_2). Longitudinal changes in effector T cell phenotype and function were evaluated by flow cytometry, scRNA/ATACseq, migration and cancer cell killing assays.

Results: In primary NSCLCs, hypoxic $CD8^+$ TILs showed heterogeneous distribution, higher activation and dysfunction markers (CD25, PD-1, LAG-3, TIM-3, TOX1/2, GZB, KI67), and distinct association with patient outcomes. Under normoxia, short-term (1 day) stimulation increased activation, cytokine production and cancer cell killing, followed by progressive acquisition of a dysfunctional state during intermediate (3 days) and long-term stimulation (6 days) characterized by increased markers of dysfunction, proliferation, reduced cytokine production, and impaired migration and cytotoxicity. Under hypoxia, short-term stimulation did not alter the T cell phenotype but reduced TNFα production, migration and tumor killing capacity compared to normoxia. However, prolonged T cell stimulation under hypoxia (3-6 days) led to a distinct phenotype with reduced dysfunction markers, increased cytokine production, and improved migration and killing. Differences were noted between PBMCs and TILs. Long-term stimulation under hypoxia showed distinct transcriptomic and epigenetic changes supporting specific mechanisms underlying the observed responses.

Conclusions: Hypoxia modifies the activation and functional profile of effector TILs in NSCLC. Short and long-term hypoxia induces opposite phenotypic, functional and molecular changes on effector T cells during recurrent TCR stimulation. These results expand our understanding of the dynamic role of hypoxia on human T cell dysfunction with prominent biological and translational implications.

#4241 Anti-tumor antigen CD8 T cells infiltrating M3 uveal melanoma metastases are detectable in the blood.

Sol Y. Nunez, Rachele Sintini, Camille Jamet, Setareh Aflaki, Abdoulaye Soumare, Pascale Mariani, Manuel Rodrigues, Marc-Henri Stern, Olivier Lantz, Ana I. Lalanne

Institut Curie, Paris, France

Introduction: Uveal melanoma (UM) is the most common cancer of the eye in adults. 30-40 % of UM become metastatic with preferential tropism to the liver. UMs with loss of one copy of chromosome 3 (M3) are the most prone to metastasize. Current treatments for metastatic UM (mUM) remain largely ineffective. A better understanding of tumor-specific $CD8^+$ T cell responses is essential for the development of new immunotherapies.

Methods: Tumor-infiltrating and blood $CD8^+$ T cells of mUM patients were studied using multicolor tetramer staining and spectral flow cytometry, VDJ single-cell RNA sequencing (VDJ-scRNAseq) and bulk TCR sequencing (TCRseq) for alpha and beta chains.

Results: Analysis of the immune infiltrate of UM metastases revealed the presence of numerous CD8+ T cells in all disomic 3 (D3) (n=15) and M3 (n=22) metastases. In only 12 out of 22 M3 metastases, CD8+ T cells co-expressed CD39 and PD-1 markers, associated with tumor reactivity, as compared to the juxta-tumoral tissue (p=0.0003). VDJ-scRNAseq analysis evidenced increased expression of genes related to chronic activation (*HAVCR2*, *LAG3* and *TOX)* and large clonal expansions of $CD39^+PD1^+CD8^+$ T cells, which were the only proliferating cells in the tumor bed. The tumor antigen (Ag) specificity of $CD39^+PD1^+CD8^+$ T cells was confirmed by staining with tetramers loaded with the tumor associated Ag, Melan-A, while the CMV-specific $CD8^+$ T cells did not co-express CD39 and PD1. A coordinated immune response in the liver and the blood in matched metastasis-blood samples was revealed by a strong positive correlation (Rpea=0.7366, p=0.0017, n=15) between the proportion of memory Melan-A-specific $CD8^+$ T cells in the blood and $CD39^+PD\text{-}1^+CD8^+$ T cells in metastases. Notably, only metastatic patients harbored a significantly higher percentage of memory Melan-A-specific CD8+ T cells as compared to healthy donors (n=9, p=0.0133) and primary UM patients (n=13, p=0.0096), confirming the localized nature of the immune response in the eye, reported by our team (JEM, 2024). To explore if tumor-reactive $CD8^+$ T cells of other tumor-Ag specificities could also recirculate, we performed scRNAseq and scTCRseq analysis of four M3 metastases along with bulk TCRseq for alpha and beta chains in the blood. A large proportion (between 18% and 42%, depending on the patient) of the most expanded $CD39^+PD1^+CD8^+$ TCR clones (≥ 3 cells) from the metastasis were also found in the circulation at the time of liver resection. The stage of the disease when these expanded metastasis-reactive clones appear in the blood and their Ag specificity are currently under investigation.

Conclusions: A subset of M3 mUM patients exhibit an anti-tumor Ag response in liver metastases which was also detectable in the blood. Further characterization of these tumor-Ag specific $CD8^+$ T cells and identifying their Ag specificities may lead to novel biomarkers of metastatic disease as well as novel therapeutic targets.

#4242 IRF8 regulates T cell differentiation and anti-tumor effector function.

Zainab Tiamiyu[1], Dakota Poschel[2], Aaron Behdadnia[1], Kendra Fick[1], Patrick Czabala[3], Yang Zhao[1], Dafeng Yang[3], Sergie BOMBIN[4], Kebin LIU[3]

[1]Biochemistry and Cancer Biology, Augusta University, Augusta, GA,[2]Medical College of Georgia, Augusta, GA,[3]Augusta University, Augusta, GA,[4]Georgia Cancer Center, Augusta, GA

Interferon regulatory factor 8 (IRF8) is a myeloid cell lineage-specific transcription factor that also regulate B cell differentiation under physiological conditions. Under pathological conditions such as cancer, IRF8 acts as a negative regulator of myeloid-derived suppressor cells (MDSCs) to regulate anti-tumor immunity. However, the function of IRF8 in regulation of the adaptive immune response in the tumor microenvironment is incompletely understood. We therefore aimed at building a single cell atlas of IRF8-regulated immune cell differentiation in the tumor microenvironment using genome-wide single-cell multiomics. Unsupervised clustering in combination with maker-based annotation identified 12 major cell subpopulations in tumor-infiltrating leukocytes. IRF8 deficiency resulted in increased myeloid-derived suppressor cells (MDSCs) and memory T cells, but decreased plasmablasts, dendritic cells, and effecter T cells. Pathway enrichment analysis indicates that IRF8 primarily regulates multiple metabolic pathways in plasmablasts. In addition, IRF8 deficiency enhances TCR signaling, MTOC1 signaling, IFNγ signaling, and T cell dysfunction in tumor-infiltrating effector T cells, but not in memory T cells. This hyperactivation is correlated with increased activation of apoptosis pathways in effector T cells. Our findings determine that IRF8 regulates the plasmablasts-effector T cell axis in the tumor microenvironment, and loss of IRF8 expression leads to decreased plasmablasts and hyper activation and dysfunction of effector T cells, resulting in effector T cell elimination and tumor immune escape.

#4243 Mutational-signature adjusted models reveal HLA-mediated depletion of antigenic mutations in non-small cell lung cancer (NSCLC).

Amy Lauren Cummings[1], Andy Han[2], Seung J. Park[3], Sai S. Kollapaneni[3], Daniel Li[3], Arjan Gower[3], Maria Antonia Velez Velez[3], Aaron Lisberg[3], Jonathan W. Goldman[4], Edward B. Garon[5]

[1]UCLA Health, Los Angeles, CA,[2]Department of Medicine, Division of Hematology/Oncology, UCLA - University of California Los Angeles, Los Angeles, CA,[3]UCLA - University of California Los Angeles, Los Angeles, CA,[4]UCLA David Geffen School of Medicine, Santa Monica, CA,[5]Asst. Prof., Dept. of Hem./ Onc., University of California (UCLA), Santa Monica, CA

Background: Quantifying immune editing in human tumors is challenging because observed mutation patterns reflect both mutational processes and selection. Whether HLA class 1 genotypes uniformly influence which somatic mutations persist remains unclear.
Methods: Whole-genome sequencing (WGS) from CPTAC NSCLC tumors with matched blood and adjacent normal lung underwent germline single nucleotide polymorphism (SNP), somatic single nucleotide variant (SNV), HLA typing, neoepitope prediction, and mutational signature decomposition using established pipelines. SNP/SNVs were annotated with codon position, resulting amino acids, and evolutionary similarity metrics (BLOSUM62, PAM250, Miyata, Atchley, Grantham). Four-digit HLA alleles were collapsed into recognized supertypes; neoepitopes with IC50 ≤150 nM were considered high-affinity. Models of expected nonsynonymous mutations were created using the GRCh38 reference, mutational signature, and tumor mutation burden and compared to observed SNP/SNVs using cosine similarity. Statistical significance was assessed using ANOVA and generalized linear models with FDR correction.
Results: 219 cases (111 LUAD, 108 LUSC) were processed successfully. Median SNPs were 862.3, SNVs were 103.8 with an associated median of 62.5 predicted neoepitopes (4.9 high-affinity) per case. Amino acid substitutions arising from the third codon position (N=96) had higher similarity than those from position 1 and 2 (N=226), ($p<0.001$). SBS4 dominated 167 (76.3%) tumors; in blood, SBS5 and SBS58 characterized 152 (69.4%) and 55 (25.1%) cases, respectively. Codon-position biases differed across signatures, with SBS4 showing relative depletion of position-3 substitutions compared to SBS5 and SBS58 ($p<0.001$). Signature-based modeling demonstrated cosine similarity >0.90 with higher cosine similarity in SBS4 compared to SBS5 and SBS58. ANOVA comparisons of amino acid substitutions revealed multiple supertypes (A02, B27, B44) with relative depletion of anchor substitutions and high-affinity neoepitopes with these substitutions (FDR<0.05).
Conclusion: Germline SNPs exhibit strong evolutionary constraint, whereas somatic SNVs show minimal intrinsic codon-position bias, supporting the hypothesis that cancer mutagenesis is a random process. Controlling for mutational signature uncovers HLA-specific immune editing, demonstrating that antigenic mutations are selectively depleted in specific HLA contexts. This signature-conditioned framework provides a clinically actionable platform for improving neoantigen prediction and immuno-oncology translation.

#4244 Investigating the spatial immune tumor microenvironment of dermatofibrosarcoma protuberans.

Maryam Al-Ghezi[1], Malia Rettig[1], Christopher P. Loo[2], Rashi Yadav[2], Wesley Yu[3], Joshua M. Moreau[1]

[1]Cell, Developmental and Cancer Biology, Oregon Health & Science University, Portland, OR,[2]Cancer Early Detection Advanced Research Center, Oregon Health & Science University, Portland, OR,[3]Department of Dermatology, Oregon Health & Science University, Portland, OR

Dermatofibrosarcoma Protuberans (DFSP) is a rare, locally aggressive cutaneous sarcoma driven by the COL1A1-PDGFB fusion. While its molecular drivers are well-defined, the DFSP tumor immune microenvironment remains poorly characterized. Understanding immune-stromal interactions in DFSP may reveal opportunities to complement surgical resection with immunotherapy or targeted approaches. We performed spatial transcriptomics on 16 DFSP patient samples using 10X Genomics Visium v2 (n=12) and Visium HD (n=4), integrated with single-cell RNA sequencing. Our analysis revealed distinct tumor, stromal, and immune populations with high PDGFB-high tumor cells spatially segregated from infiltrating immune compartments. We identified transcriptionally distinct cancer-associated fibroblast (CAF) subsets, including populations enriched for extracellular matrix remodeling and inflammatory signatures that may modulate local immunity. Immune profiling uncovered spatially heterogeneous T cell and macrophage infiltration, with distinct immune-rich and immune-desert zones across patients. Notably, we observed tertiary lymphoid structure (TLS) formation in multiple samples, characterized by elevated TLS signature scores and spatial co-localization of B and T cell markers. CXCL13 and CCL19 emerged as key chemokines defining TLS-associated immune-stromal communication networks. Using cyclic immunofluorescence, we validated the spatial organization of TLS-associated immune niches, confirming co-localization of CD3+ T cells, CD20+ B cells, and CD68+ macrophages within TLS-enriched regions at protein level. This work provides the first spatial immune atlas of DFSP, revealing organized lymphoid structures and CAF-mediated immune regulation that could inform combination strategies targeting PDGFR signaling alongside immune checkpoint or stromal modulation.

#4245 The Immune strategies to convert cold to hot tumors and overcome resistances.

Yang-Xin Fu

tsinghua University, Beijing, China

Cold tumors evade immunotherapy through limiting T cell priming inside draining LN or infiltration into TME. Here, we have developed sequential strategies to overcome the limitation. Firstly, we have developed new mRNA vaccine expressing membrane cytokines with shared or mutated antigens to more and better prime tumor specific T cells (TST) without toxicity. Secondly, we generated tetramer forms of NGR that fusing into Fc-pro-IL2 that selectively targeted CD13 enriched on TME for more IL-2 to rejuvenate dysfunctional T cells. Unexpectedly, cis-delivery of IL-2 on CD13 on tumor vessels can bridge the cross-talk between tumor vessels and TST. Activated T cells can remodel tumor vessels to allow more infiltration. To sustain their anti-tumor activities, we have sequentially delivered tumor-activating cytokines (pro-IL2) guided by anti-PD-1 antibody (anti-PD-1-pro-IL2) or radiation-activating TLR agonists to help DC-T cell interaction inside TME to sustain T-cell effector function. Together, we have sequential strategies converting cold to hot tumors and then simultaneously reinvigorates TIL to overcome the limitations of current immunotherapies.

#4248 Characterization of T-cells in ER$^+$ breast tumors and their matching adjacent tissue reveals that classical exhaustion markers are not indicative of T-cell function.

Diana Savage[1], Edward Buchel[2], Afshin Raouf[1]

[1]Department of Immunology, University of Manitoba, Winnipeg, MB, Canada,[2]Department of Surgery, University of Manitoba, Winnipeg, MB, Canada

The manipulation of patients' tumor-infiltrating T-lymphocytes (TIL) as a form of immunotherapy has shown promising results in the treatment of select cancers; however, limited benefit has been observed in treating invasive estrogen receptor-expressing (ER$^+$) breast tumors. The development of a dysfunctional, exhausted-like T-cell phenotype in the tumor microenvironment has been linked to immunotherapy failure, but the intrinsic and extrinsic factors that result in its development remain poorly understood. We previously showed that breast tumor-adjacent tissue (TAT), located over three centimeters from the primary tumor, contains an inflammatory signature and, therefore, hypothesized that it may be a reservoir of tumor-reactive T-cells. Further, the comparative study of TILs and TAT-T-cells may reveal important information about the mechanisms of TIL exhaustion and how to overcome them. ER$^+$ breast tumor and matching TAT samples were collected from patients undergoing mastectomy procedures, from which the breast cancer cells (BCC), TIL-CD3$^+$ and TAT-CD3$^+$ T-cells were obtained. The cytotoxic CD8$^+$ subset from each CD3$^+$ T-cell sample was isolated and examined for the expression of exhaustion and activation markers and then placed in a three-dimensional co-culture assay with the autologous BCCs. Here, BCC viability and T-cell exhaustion marker expression were assessed and conditioned media was collected for cytokine analysis. Interestingly, the TIL-CD8$^+$ T-cells expanded more rapidly than the TAT-CD8$^+$ T-cells; however, the TAT-CD8$^+$ T-cells were more effective in eliminating autologous BCCs. The enhanced reactivity of the TAT-T-cells was further corroborated with enhanced secretion of activating cytokines such as interferon gamma. T-cells with an increased expression of exhaustion marker TIM-3 (T cell immunoglobulin and mucin-domain containing-3) prior to co-culture were less effective in eliminating BCCs. Further, in co-cultures, up to a 9-fold increase in the expression of exhaustion marker LAG-3 (lymphocyte activation gene 3) was observed in select TIL- and TAT-CD8$^+$ T-cells. Interestingly, the expression of PD-1 (programmed cell death protein 1), the most frequently studied marker in the context of T-cell dysfunction, remained low and unchanged. To our knowledge, this is the first detailed study of the CD8$^+$ T-cells that reside in ER$^+$ breast tumors and their adjacent tissues. We have observed that TAT contains CD8$^+$ T-cells with enhanced reactivity against autologous BCCs despite having a similar exhaustion marker profile as the TIL CD8$^+$ T-cells. Interestingly, our findings also suggest that TIM-3 and LAG-3 may contribute to T-cell exhaustion in ER$^+$ breast tumors and that blocking these receptors might be more effective than blocking PD-1 as immunotherapy.

#4249 High-throughput discovery of MART1-specific TCR-peptide interactions using a Jurkat NFAT Reporter-K562 antigen-presenting cell system and single-cell adaptive immune receptor profiling.

Alex Chenchik[1], Debbie Deng[1], Kitt Paraiso[1], Guido Stadler[2], Ben Yellen[2]

[1]Cellecta, Inc., Mountain View, CA,[2]Celldom, San Carlos, CA

In this study, we developed a high-throughput workflow for identifying MART1-specific T cell receptor (TCR)-peptide interactions relevant to melanoma immunotherapy. Jurkat NFAT-GFP reporter cells expressing individual candidate MART1-TCRs (n=10 to 20) were co-cultured with K562 artificial antigen-presenting cells (APCs) engineered to express a MART1 120-peptide, tumor-associated library in a single-chain trimer (peptide-B2M-HLA-A) format. TCR activation was quantified using the CellDom Microwell EliSpot platform, where GFP expression and IL-2 secretion signaled productive antigen engagement. Cells from positive wells were harvested, and DriverMap adaptive immune receptor (AIR) bulk and single-cell TCR-Seq assays and subsequent NGS analysis were performed to identify the cognate TCR epitopes.To improve epitope presentation, we introduced a G2C substitution in the G4S linker of the single-chain trimer, which enhanced HLA surface expression and increased Jurkat activation compared with the wild-type construct. MART1-TCRs showed differential reactivity across the MART peptide panel, enabling ranking of functional affinity and identification of cross-reactive peptide candidates. Both the bulk AIR DNA and bulk AIR RNA assays show clonotypes that are expanded in MART1 vs Day 0 (control) or DMSO control. On Day 9, approximately 12 clonotypes are expanded at 250x compared to Day 0 in the MART1-stimulated sample. With the single-cell AIR assay, the MART1-stimulated samples showed overrepresentation of clones, whereas there was no clonal overrepresentation in the DMSO control plate.This end-to-end platform shows TCR-peptide interactions with bulk and & single-cell NGS readout, which could enable identification of therapeutic TCR candidates, and provide a scalable method for characterizing antigen specificity for cancer immunotherapy applications.

#4250 Sirt2 dictates TCR activation thresholds through post-translational control of LCK conformational state.

Imene Hamaidi[1], Pingyan Cheng[2], Soo Young Jun[1], Min-Hsuan Wang[3], Min Zhang[4], Odesha Taylor[4], Luis Lopez-bailon[5], Ismail Can[6], Bin Fang[4], Anders Berglund[1], Bradford Perez[7], Ben Creelan[4], Andriy Marusyk[4], Virginia Shapiro[6], Haitao Ji[4], Jose R. Conejo-Garcia[5], Sungjune Kim[1]

[1]Mayo Clinic Florida, Jacksonville, FL,[2]TuHURA Biosciences Inc, Tampa, FL,[3]Taipei Veterans Generation Hospital, Taipei, Taiwan,[4]H. Lee Moffitt Cancer Center, Tampa, FL,[5]Duke University School of Medicine, Durham, NC,[6]Mayo Clinic, Rochester, MN,[7]Florida Cancer Specialists & Research Institute, Trinity Cancer Center, Tampa, FL

BACKGROUND: Tumor-specific T cells are often characterized by reduced TCR signaling due to central and peripheral tolerance pathways that limit their responsiveness. These signals are further weakened by insufficient co-stimulation and active co-inhibitory pathways, collectively establishing a high threshold for activation. The integration of antigen recognition with co-stimulatory and inhibitory cues ultimately determines whether a T cell becomes activated or remains tolerant. Early TCR signaling must therefore be precisely regulated to prevent autoreactivity while still supporting protective immunity. Although phosphorylation and ubiquitination are well-established regulators of proximal TCR signaling, additional post-translational mechanisms remain less defined. SIRT2, a cytosolic NAD^+-dependent deacetylase with emerging roles in immune regulation, has not been examined in the context of TCR signaling.

METHODS: We evaluated proximal TCR signaling events in wild-type and SIRT2-deficient T cells using flow cytometry, immunoblotting, calcium flux assays, and RNA-sequencing. SIRT2-associated pathways were defined by mapping its interactome and acetylated substrates through mass spectrometry and immunoprecipitation. We screened LCK post-translational modifications by mass spectrometry and assessed SIRT2 enzymatic activity using an HPLC-based deacetylase assay. Conformational effects of LCK modification were examined using fluorescence-polarization binding assays and AlphaFold structural modeling. SIRT2 was deleted in human tumor infiltrating lymphocytes (TILs) via CRISPR/Cas9, and the impact of SIRT2 targeting was tested in lung cancer patient-derived xenograft models reconstituted with autologous TILs.

RESULTS: SIRT2 deficiency amplified proximal TCR signaling, leading to elevated phosphorylation of early signaling mediators and increased calcium flux in both naïve and anergic T cells. Loss of SIRT2 also altered thymic selection dynamics and expanded TCR repertoire diversity. Mechanistically, SIRT2 interacted with and deacetylated LCK, the initiating kinase of proximal TCR signaling. Mass spectrometry identified lysine K228 in the LCK linker region as a SIRT2-regulated deacetylation site that governs LCK conformation and kinase activity. Functionally, SIRT2 inhibition in exhausted mouse and human TILs restored TCR signaling capacity and improved anti-tumor responses.

CONCLUSION: Here we identify SIRT2-regulated deacetylation of LCK as a previously unrecognized mechanism that sets the strength and threshold of proximal TCR signaling. Accordingly, SIRT2 targeting reverses the exhausted phenotype of tumor-reactive T cells.

#4251 Th7R cells: CD4⁺ T-cell partners that drive Tpex-mediated antitumor immunity in the tumor microenvironment.

Shota Takei, Ou Yamaguchi, Satoshi Yamasaki, Atsuhito Mouri, Ayako Shiono, Yu Miura, Kosuke Hashimoto, Hisao Imai, Kyoichi Kaira, Ichiki Yoshinobu, Hiroyuki Nitanda, Tomoyuki Hishida, Katsuhisa Horimoto, Hiroshi Kagamu

Saitama Medical University International Medical Center, Hidaka, Japan

Background: Precursor-exhausted CD8⁺ T cells (Tpex) are self-renewing, stem-like CD8⁺ T cells that give rise to terminally exhausted (Tex) cells and maintain long-term antitumor immunity. Within the tumor microenvironment (TME), Tpex localize to tertiary lymphoid structures (TLSs) and high endothelial venules (HEVs) and trigger the CD8⁺ T-cell burst after PD-1 blockade. However, the CD4⁺ T-cell subsets that support Tpex generation and maintenance remain unclear. We previously identified Th7R cells, a Th1-like CD4⁺ T-cell subset (CCR4⁻CCR6⁺, expressing IL7R and TCF7) in lung cancer, associated with immune checkpoint inhibitor (ICI) responsiveness. Th7R and Tpex share stem-like signatures, suggesting a potential partnership.
Objective: To test whether Th7R cells function as CD4⁺ partners sustaining Tpex and long-term antitumor immunity, and to evaluate the antitumor efficacy of Th7R adoptive transfer.
Methods: We analyzed 55 early-stage lung cancer patients undergoing resection and 20 stage II-III patients treated with neoadjuvant anti-PD-1 therapy. Peripheral blood, tumor-infiltrating lymphocytes (TILs), and lymph node T cells were profiled by mass and imaging mass cytometry to assess the spatial and numerical relationship between Th7R and Tpex. In a mouse MCA205 model, CCR4⁻CCR6⁺ Th7R cells sorted and expanded from tumor-draining lymph nodes were adoptively transferred to evaluate antitumor effects and their impact on TILs.
Results: Patients with high preoperative Th7R frequency showed better disease-free survival. Th7R—but not other CD4⁺ subsets—decreased after tumor resection, indicating tumor antigen-driven expansion. In neoadjuvant cases, complete or major pathological responders had higher proportions of Th7R cells. Th7R and Tpex showed a positive correlation in both blood and lymph nodes. Imaging mass cytometry showed Th7R cells located near Tpex within TLSs. In mice, Th7R transfer induced tumor regression and specifically expanded both Tpex and Tex subsets.
Conclusion: Th7R cells are numerically and spatially associated with Tpex and crucial for sustaining long-term antitumor immunity. They may promote asymmetric Tpex division, maintaining renewal and effector supply. Th7R adoptive transfer, alone or with ICIs, represents a promising approach to enhance durable antitumor immunity.

#4252 Tumor extracellular vesicles prime B cells which promote tumor control and epitope spreading to T cell neoantigens.

Georgia Lattanzi[1], Zihan Guo[2], Kendrick Nguyen[1], Ferdinando Pucci[2], Daniel Hollern[1]

[1]Salk Institute For Biological Studies, La Jolla, CA,[2]Oregon Health & Science University, Portland, OR

Advanced solid malignancies are still a major clinical challenge due to their high lethality and limited response to existing therapies. Effective cancer immunotherapy requires T cell recognition of tumor neoantigens, and generation of a durable and robust cytotoxic response Recent studies demonstrate that B cells play a critical and previously underappreciated role in shaping anti-tumor immune responses in neoantigens-rich tumors by coordinating with T cells. However, how B cells respond to tumor neoantigens and regulate T cell responses are still not fully elucidated. By using engineered tumor cell lines expressing neoantigens with different affinity for cognate B cells either on tumor extracellular vesicles (tEVs) or as soluble proteins, we showed that tEVs and neoantigen-specific B cells are required for tumor control. We observed that tEVs-neoantigens are brought into the tumor draining lymph node where they bind and activate B cells. Using single cell RNA-sequencing and flow cytometry we showed that tEVs-neoantigens promote cognate B cells activation either through a germinal center reaction or through extrafollicular response. Notably, activated B cells not only mount direct anti-tumor responses, but also promote epitope spreading to linked T cell neoantigens, thereby broadening the immune response and improving tumor clearance. Epitope spreading consists of the diversification of tumor neoantigens recognized by the immune system and holds significant promise for improving cancer therapies. By co-expressing B and T cell neoantigens on the same tEV we observed extensive and prolonged B-T cells interaction using intravital microscopy, increased activation of CD4 T follicular cells, maintenance of progenitor CD8 T cells and tumor clearance. Thus, B cell response to co-expressed tEV neoantigens enhances the breadth of immune responses by facilitating specific anti-tumor T cell responses. By elucidating how B cells contribute to epitope spreading and tumor control, this research reveals new immunological principles and sets the base for next-generation cancer immunotherapies that harness both humoral and cellular arms of the immune system, offering new strategies to overcome tumor heterogeneity and therapy resistance.

#4253 Integrating neoantigen immunogenicity and tumor clonality for predicting immunotherapy response.

Ko-Han Lee, Timothy Sears, Maurizio Zanetti, Hannah K. Carter

University of California San Diego, La Jolla, CA

Background: Cancer immunotherapy has transformed treatment, yet response rates remain suboptimal. Immunogenic neoantigens—tumor-specific peptides eliciting T-cell responses—represent promising biomarkers, but current predictors have critical limitations: they focus predominantly on MHC-I while neglecting MHC-I/II coordination, and rely on tumor mutation burden (TMB), which lacks immunogenicity specificity and ignores tumor heterogeneity. We developed NeoPrecis, a computational framework integrating immunogenicity prediction with tumor subclonal architecture to improve immunotherapy response prediction.

Methods: NeoPrecis comprises two modules capturing mutation-centric and tumor-centric immunogenic contexts. NeoPrecis-Immuno models wild-type to mutant peptide distance to estimate T-cell recognition likelihood, incorporating amino acid embeddings, MHC-binding motifs, positional factors, and peptide sequences. The model was pre-trained on TCR-binding data for peptide-TCR cross-reactivity discrimination, then fine-tuned on T-cell assay data. NeoPrecis-Landscape integrates MHC-I and MHC-II immunogenicity predictions with PyClone-inferred subclonal structure. For each subclone, immunogenicity is computed as the product of its MHC-I and MHC-II scores. Tumor-level immunogenicity is then calculated as the weighted average of all subclonal scores, with weights determined by subclone prevalence.

Results: NeoPrecis-Immuno outperformed PRIME, ICERFIRE, and DeepNeo on an independent gastrointestinal cancer dataset with validated CD4+/CD8+ T-cell assays. Its interpretable architecture quantifies allele-specific contributions via allele benefit scores, which showed significant prognostic associations in melanoma ($p=0.04$) and NSCLC ($p=0.01$) independent of specific mutations. Across five melanoma and three NSCLC cohorts, NeoPrecis-Landscape outperformed TMB in stratifying ICI responders, particularly in melanoma and heterogeneous NSCLCs. Homogeneous, heavily immunoedited NSCLCs (predominantly smoker tumors) showed reduced neoantigen-based predictive power.

Conclusion: NeoPrecis provides an interpretable framework for neoantigen immunogenicity assessment. By integrating tumor subclonal structure, it outperforms TMB in predicting ICI response, especially in melanoma and heterogeneous NSCLCs with low immunoediting. Poor performance in immunoedited tumors suggests immune evasion mechanisms may dominate ICI response in these contexts.

#4254 Tapasin inhibits MHC I-presentation of a low affinity peptidome which elicits a unique population of highly effective CD8 T cells, in multiple mouse cancers.

Purva Pundeer[1], Joseph Dempsey[1], Adam T. Hagymasi[1], Jeremy Balsbaugh[2], Tatiana Scheglova[1], Ion Mandoiu[2], Pramod K. Srivastava[1]

[1]Immunology, University of Connecticut Health Centre, Farmington, CT,[2]University of Connecticut, Storrs, CT

Neoepitopes are generated from tumor-specific mutations that make tumors targets for CD8 and CD4 T cells. We and others have reported that a significant proportion of neoepitopes which elicit CD8 T cell mediated tumor control in vivo (such as Ccdc85cMUT in the BALB/c Meth A sarcoma and PLK1MUT in the C57BL/6 MC38-FABF colon carcinoma) bind MHC I with low to extremely low affinities (IC_{50} of 500- 50,000 nM) (Srivastava PK 2024 J. Clinical Investigation). The protein Tapasin facilitates the loading the MHCI with peptides that bind MHCI with high affinity. This high affinity immunopeptidome is a key to defense against acute viral infections. We observe that paradoxically, the Tapasin-sculpted immunopeptidome becomes a barrier in control of cancers. Genetic ablation of Tapasin in cancer cells (Meth A fibrosarcoma and 4T1 triple negative breast cancer of BALB/c mice and MC38-FABF colon carcinoma of C57BL/6 mice) leads to highly immunogenic cancer variants that fail to form tumors at challenge doses at which Tapasin-proficient parental tumors readily form tumors. The immune response elicited by Tapasin-deficient tumors is fully active even against the Tapasin-proficient parental tumors. The immunopeptidome of Tapasin-deficient tumors is dominated by low affinity pMHC I complexes. Mass spectrometry analysis of the MHC I presented peptidome shows 760 peptides presented by Tapasin-proficient cells and 1175 peptides by Tapasin-deficient cells. Of this, 500 peptides are shared between the parental and Tapasin-deficient cells. The unique peptidome of Tapasin-deficient cells shows a greater diversity of low affinity peptides (~700 peptide with predicted IC_{50} >2,000 nM in Tapasin deficient cells as compared to ~250 such peptides in Tapasin proficient cells). The low affinity immunopeptidome engages a pool of CD8 T cells with profound anti-cancer activity mediating robust tumor control of Tapasin-proficient parental tumors in adoptive transfer assays. The CD8 T cell repertoire elicited by Tapasin deficient tumors is highly cytotoxic and less exhausted as compared to the CD8 T cells elicited by Tapasin-proficient parental tumors. Lower expression of Tapasin in human cancers is significantly associated with better survival. These observations suggest that ablation of Tapasin can be used for immunotherapy of human cancers.

#4256 Long-read RNA sequencing and immunopeptidomics reveal transcriptomic aberrationneoantigens as targets for T cell immunotherapy in diffuse glioma.

Kenan Zhang[1], Megan Benz[1], Kelly M. Hotchkiss[2], Lin Lin[2], Sarah Quackenbush[2], Aroa Elortza Payros[3], Mark Pieterse[3], Wigard Kloosterman[3], Jeroen Kneppers[3], Mustafa Khasraw[4]

[1]The Preston Robert Tisch Brain Tumor Center, Duke University, Durham, NC,[2]Duke University, Durham, NC,[3]CureVac Netherlands B.V., Amsterdam, Netherlands,[4]Duke Cancer Institute, Durham, NC

Background: Diffuse Glioma (DG) exhibits low tumor mutational burden and limited responsiveness to immunotherapy, suggesting that antigen sources beyond canonical mutation-derived neoantigens are required to support effective antitumor T-cell responses. Transcriptomic aberrations, such as aberrant splicing, fusion transcripts, etc., generate extensive tumor-specific sequences. However, conventional short-read RNA sequencing captures only the sequences overlapping the neojunctions (NJs), thereby substantially underrepresenting this rich source of actionable neoantigens.

Methods: Nanopore long-read RNA sequencing was performed on 11 diffuse glioma tissues. Public data from 6 normal cortices was included as a control. A pipeline was composed to construct the whole-length transcriptome, identify novel transcripts with transcriptomic aberrations, translate peptides, and predict neoantigen candidates. Data-independent acquisition (DIA) proteomics was performed on 4 matched samples to verify the transcription of these novel transcripts and analyzed via DIA-NN. Immunopeptidome data were acquired from 5 matched samples and screened by NeoDisc, a computational pipeline accessing neoantigens based on the functionality of the antigen processing and presentation machinery.

Results: DGs demonstrated a significantly greater burden of both a larger number and higher expression of novel transcripts with transcriptomic aberration compared to normal cortex, indicating transcriptomic aberration as a tumor-enriched source of antigenic diversity. Novel transcripts consist of 8.08% of the total transcriptome in the DG cohort compared to 7.06% in the cortex cohort. Across the 4 DG samples with matched DIA proteomics, hundreds of novel transcripts per sample were identified after filtering for expression and coding probability. Approximately 30-40% of these transcripts showed evidence of translation supported by the DIA proteomics, with ongoing refinement for the high-confidence translated set. Neoantigen prioritization further identified hundreds of high-confidence candidate peptides per tumor with strong predicted HLA binding and immunogenicity features. To verify HLA-mediated peptide presentation as a further validation, DDA and DIA immunopeptidomics spectra for HLA-I and HLA-II have been collected.

Conclusions: Transcriptomic aberration neoantigens represent a biologically authentic and targetable antigen class in diffuse glioma. Integrating whole-length transcriptomics, DIA proteomics, and immunopeptidomics provides a disease-relevant and scalable framework for neoantigen discovery in low-mutation tumors. Cohort expansion and early T-cell functional validation of prioritized neoantigen candidates are undergoing to assess their therapeutic relevance.

#4257 F5446 epigenetically reprograms T cells to boost CEA CAR T cell immunotherapy efficacy in human colorectal cancer metastasis.

Kendra Fick, Patrick Czabala, Zainab Tiamiyu, Dafeng Yang, Kebin Liu

Augusta University, Augusta, GA

Chimeric Antigen Receptor (CAR) T cell therapy emerges as a promising cell-based immunotherapy for human cancer; however, it has shown little efficacy in solid tumors. Recent studies have shown that SUV39H1 decreases CAR T cell persistence and knocking out SUV39H1 increased CAR T efficacy in tumor-bearing mice. Analysis of human colon cancer liver metastases scRNA-seq datasets revealed that histone methyltransferases of H3K9me3 are upregulated in colon tumor and expressed in subsets of T cells in liver metastases of human colon cancer patients. To overcome human colon cancer resistance to CAR T cell immunotherapy, we have developed a SUV39H1-specific small molecule inhibitor F5446. Previously, we found that H3K9me3 promotes differentiation of T_{ex} cells and targeting H3K9me3 is an effective approach to increase $IFN\gamma^{hi}$ $T_{ex\text{-}int}$ cells to reinvigorate CTL functionality to suppress colon cancer liver metastasis. Based on this data, we hypothesize that F5446 is effective in increasing persistence of CAR T cells to suppress metastatic human colon cancer growth in NSG mice. A phase I clinical trial for α-CEA CAR T cell immunotherapy found it is well tolerated in patients with colorectal cancer with modest efficacy. Based on this, we generated second and third generation α-CEA CAR T plasmids for lentivirus transduction of primary T cells. We utilize an experimental liver metastasis model to induce liver metastasis of human colorectal cancer in a humanized mouse model. Mice are then treated with one dose of α-CEA CAR T cells and treated every three days with F5446 until endpoint. Extracted tumors are digested and the CAR T cell phenotypes (memory, effector, naïve, or exhausted) are determined via flow cytometry. We anticipate that F5446 will increase the persistence of CAR T cells in the liver metastases compared to CAR T therapy alone. F5446 is a promising conjunctive treatment with CAR T cell therapy to increase efficacy in solid tumor colon cancer.

#4258 In vivo genome-scale enhancer screen decodes T cell fate decisions in the tumor.

Keely Y. Ji[1], Alex Chang-Yu Chen[1], Laura Hinojosa[2], Bolutito Babatunde[2], Daniela Martinez[1], Thomas J. LaSalle[1], Maria Zschummel[1], Marc A. Schwartz[1], Ferhat Ay[2], Debattama Sen[1]

[1]MGH/Harvard Medical School, Boston, MA,[2]La Jolla Institute for Immunology, La Jolla, CA

During chronic infection and cancer progression, T cells enter a dysfunctional state called exhaustion, posing a significant challenge to disease control and immunotherapy outcomes. Previously, we and others have shown that T cell exhaustion is a differentiation process regulated at the epigenetic level. Exhausted T cells share a conserved program of chromatin accessibility landscapes across chronic infections and tumors (core exhaustion program) that is imprinted in early T cell differentiation. However, it remains unclear whether and which open chromatin regions within the core exhaustion program play a causal role in driving the exhausted state. We hypothesize that the core exhaustion program contains transcriptional enhancers that regulate T cell persistence and differentiation in exhaustion, preventing reinvigoration of function. To test it, we leveraged our novel enhancer editing platform called Systematic Non-coding element Interrogation by Paired sgRNAs (SNIP-R), a pooled CRISPR-based enhancer deletion platform optimized for kilobase-scale perturbation in primary T cells. We performed the first in vivo genome-scale enhancer deletion screen on ova-specific $CD8^+$ T cells (OT-1) in OVA-expressing tumors. We identified networks of regulatory elements in the core exhaustion program that regulate T cell persistence and subset formation in the tumor. Validation studies from the screen showed that deleting one such regulatory element 100kb upstream of the *Klf6* gene (*Klf6-100kb*) in T cells improved tumor control. *Klf6-100kb* perturbed T cells strongly outcompeted control populations and had increased generation of effector-like T cells in the tumor compared to control perturbations. Together, we showed that the core exhaustion program contains causal regulatory elements underlying T cell exhaustion and pinpointed new targets for developing next-generation adoptive T cell therapies.

#4259 Peripheral T cell methylome reveals accelerated systemic immune aging in early lung cancer.

Yu-Ching Wang[1], Shu-Yung Lin[2], Yi-Jhen Huang[3], Sheng-Yao Su[3], Yi-Chieh Wu[3], Jin-Shing Chen[4], Shuenn-Wen Kuo[4], Mong-Wei Lin[4], Chong-Jen Yu[4], Hsing-Chen Tsai[3]

[1]Taiwan International Graduate Program in Molecular Medicine, National Yang Ming Chiao Tung University, Taipei, Taiwan,[2]Department of Internal Medicine, National Taiwan University Hospital, Taipei, Taiwan,[3]Graduate Institute of Toxicology, National Taiwan University, Taipei, Taiwan,[4]Department of Surgery, National Taiwan University Hospital, Taipei, Taiwan

The immune landscape in cancer patients is shaped by dynamic interactions between systemic and local tumor immune responses. While the intratumoral immune microenvironment has been extensively studied, systemic immune alterations, especially in early-stage cancers, remain poorly understood. DNA methylation governs T cell functional and differentiation states, and aberrant patterns have been linked to immune dysfunction. We hypothesized that peripheral blood T cells in early lung cancer exhibit reactive DNA methylation remodeling in response to the presence of cancer. To test this, we profiled circulating CD3+ T cells from 63 patients with early-stage lung cancer (stages I and II) and 70 healthy individuals using Illumina Infinium MethylationEPIC arrays. We identified 824 differentially methylated regions (7373 CpG sites) in T cells from lung cancer patients versus non-cancer controls. Gene ontology analysis revealed promoter hypermethylation in T cell activation and differentiation pathways. Epigenetic clock analysis revealed accelerated biological aging in patient-derived T cells, independent of chronological age. Transcriptomic profiling by RNA-seq further demonstrated enrichment of senescence-associated gene networks. Consistently, deconvolution analysis using MethylCIBERSORT revealed an enrichment of late-differentiated T cell subsets. Similar observations emerged from pseudotime trajectory analysis, which showed peripheral T cells, which shift toward senescent-like states at the in early lung cancer. The extent of senescence correlated with promoter hypermethylation in co-stimulatory gene loci. Furthermore, hypermethylated gene promoters were enriched for binding motifs of the E26 transformation-specific (ETS) transcription factor family, implicating a regulatory role of DNA methylation in T cell state transitions. Finally, using cohort splitting and 10-fold cross-validation, we identified a five-gene immune-derived methylation signature that distinguished early-stage lung cancer from non-cancer subjects with high accuracy (training AUC = 0.953; validation AUC = 0.894). This study reveals previously unrecognized systemic T-cell epigenetic reprogramming in early-stage lung cancer, characterized by senescence features and impaired activation potential, and establishes a framework for developing immune-derived methylation biomarkers for early lung cancer detection.

#4260 Deciphering the dysfunctional immunological synapse in acute myeloid leukemia through microfluidic.

Sofia Titah[1], Clara Lewuillon[1], Faruk Azam Shaik[2], Aurelie Guillemette[1], Eva Gez[1], Nathalie Jouy[3], Laure Goursaud[1], Celine Berthon[1], Salomon Manier[1], Carine Brinster[1], William Langue[4], Tzung Hsuen Khoo[4], Alexandre Poulain[4], Sophie Dabo[4], Dominique Collard[2], Bruno Quesnel[1], Loic Lemonnier[5], Mehmet Cagatay Tarhan[2], Yasmine Touil[1]

[1]Univ. Lille, CNRS, Inserm, CHU Lille, UMR9020-U1277 - Canther - Cancer Heterogeneity, Plasticity and Resistance to Therapies, Lille, France,[2]Univ. Lille, CNRS, Centrale Lille, Junia, Univ. Polytechnique Hauts-de-France, UMR 8520 -IEMN 10 -Institut d'Electronique de Microelectronique et de Nanotechnologie, Lille, France,[3]UMS 2014/US4, Lille, France,[4]Laboratoire Paul Painleve - CNRS UMR 8524, Lille, France,[5]Laboratory of Excellence, Ion Channels Science and Therapeutics, Villeneuve d'Ascq, Lille, France

Minimal residual disease (MRD) in acute myeloid leukemia (AML) arises from residual leukemic cells that resist chemotherapy and evade immune surveillance, notably through the PD-1/PD-L1 immune checkpoint. These persistent cells are the main source of relapse. Our working hypothesis is that alterations in calcium signaling, a key regulator of T-cell activation, contribute to PD-1/PD-L1-mediated immune escape in AML. The project aims to characterize the calcium signaling signature associated with PD-1/PD-L1 axis activation during the formation of the immunological synapse (IS) between T cells and leukemic cells from AML patients, to better understand immune dysfunction and therapy failure.

To facilitate interactions between rare T cells and leukemic cells, we utilize microfluidic devices that enable controlled cell-cell contact and real-time monitoring of calcium dynamics. An AI-based algorithm performs real-time analysis of IS formation, processing about 100 events per image every five seconds. Calcium fluctuation data are extracted and mathematically modeled to quantify responses and classify patient-derived T cells as “responders” or “non-responders” using machine learning.

Immunofluorescence is used to identify key molecular components at the IS, while RT-qPCR quantifies the expression of calcium-regulating genes such as ORAI, STIM, and NFAT isoforms in both T cells and leukemic cells. Our first results reveal altered calcium mobilization in AML-derived $CD8^+$ T cells compared with healthy donors, along with PD-1-dependent inhibition of store-operated calcium entry linked to reduced ORAI1 activity.

Ongoing single-cell RNA sequencing (scRNA-seq) analyses aim to identify transcriptional profiles of T-cell subpopulations, both at rest and during IS formation. By integrating functional calcium signatures and transcriptomic data, we seek to uncover signaling pathways responsible for impaired IS formation in AML. Ultimately, this work will identify molecular targets within the calcium signaling network that could be modulated to restore the cytotoxic activity of exhausted $CD8^+$ T cells against therapy-resistant leukemic cells.

#4261 High-sensitivity HLA-I immunopeptidome profiling from limited clinical PBMC samples.

Anamarija Pfeiffer[1], Lucy Yang[1], Arthur Viode[1], Daniel Redfern[1], **Yuehan Feng**[1], Daniel Green[2], Cheryl McAlpine[2]

[1]Biognosys AG, Schlieren, Switzerland,[2]Greywolf Therapeutics, Oxford, United Kingdom

Background

Human leukocyte antigen (HLA) molecules are central to immune surveillance, presenting antigenic peptides from self and non-self proteins to T cells, and directing adaptive immune responses. Assessment of HLA-presented peptides is increasingly critical in oncology, both for understanding tumor immunogenicity and for guiding immunotherapy strategies. Peripheral blood mononuclear cells (PBMCs) offer a minimally invasive and clinically accessible matrix for such analyses, enabling serial sampling and longitudinal monitoring in clinical trials.

Application of the immunopeptidomics profiling (IMPX) to PBMC samples has demonstrated clinical relevance, as exemplified by its use in the GRWD5769 trial where pharmacodynamic modulation of the immunopeptidome was observed in patients treated with an ERAP1 inhibitor (ESMO 2024, ASCO 2025). Despite these advances, isolating HLA-associated peptides from limited PBMC material remains technically challenging, underscoring the need for more sensitive and robust methods suitable for routine use in clinical settings.

Methods

We developed and optimized an unbiased immunopeptidomics (IMPX) workflow utilizing native lysis and magnetic bead-based immunoprecipitation to isolate HLA class I associated peptides. Lysis and pulldown parameters were systematically refined to maximize recovery and specificity of HLA complexes from limited input material across diverse sample types, including cell lines, tumor tissues, and PBMCs. Downstream liquid chromatography-mass spectrometry (LC-MS) conditions and data processing pipelines were further optimized.

Results

To evaluate the performance of the workflow under clinically relevant conditions, a ramping experiment was conducted using 1 to 10 million PBMCs, reflecting cell yields commonly obtained from trial samples. Incorporation of mild detergent (n-dodecyl β-D-maltoside, DDM) during immunopeptide elution from HLA complexes significantly improved overall recovery, particularly at inputs of ≤5 million PBMCs. Following optimization of both the biochemical and computational pipelines, up to 2,300 HLA class I-associated peptides were confidently quantified from as few as 1 million PBMCs. When 5 million PBMCs were used as input, more than 9,500 unique HLA-bound peptides were identified.

In summary, this high-sensitivity, optimized immunopeptidomics platform enables comprehensive class I HLA profiling from minimal PBMC input, supporting its translational application as a pharmacodynamic readout in clinical studies.

: CAR T Cell Functional Enhancement
Poster Session

#4266 CAR-T-cell monitoring using specific multimers: a fast and specific method allowing uniform evaluation.

Elizabeth Epps[1], Kivin Jacobsen[2], kevin Lenogue[2], Liselotte Brix[2]

[1]Immudex, USA LLC, Philadelphia, PA,[2]Immudex, ApS, Copenhagen, Denmark

CAR-T cell immunotherapy is used successfully against refractory hematological and solid cancer. Cellular Monitoring of CAR-T cells is important both for validating expression of the CAR construct in the transduced T cells prior to infusion, and persistence of the CAR-T cells in the blood of the recipient. CAR expression is often detected by fluorochrome conjugated antibody against a structural part of the CAR construct, and not the specific target for the CAR interaction. We have developed a flexible platform to manufacture direct CAR-T cells detecting multimer reagents, CAR-Dextramer® allowing detection of CAR-T cells of different specificities and affinities Activation of chimeric antigen receptor T (CAR-T) cells are critical for ensuring therapeutic efficacy in adoptive immunotherapy. CAR-T cell activation requires two signals: antigen recognition through the CAR and co-stimulation via intracellular interactions, and by stimulatory molecules such as interleukins. Control of activation and continuous monitoring are essential to optimize potency to improve clinical outcomes in hematologic and solid tumors immunotherapy.
We have developed CAR-T cell activation reagents based on the CAR-Dextramer® scaffold, that contain said stimulatory molecules. These reagents can be used to evaluate the ability of the transduced CAR-T cells to be stimulated or expanded through the specific interaction with its cognate target, and costimulatory signals.

#4267 *In vivo* evaluation of autologous anti-BCMA CAR-T therapy in PBMC-humanized SDKO mice reveals donor-specific immune responses.

Alba Matas-Cespedes[1], Jiwon Yang[2], Kushal Prajapati[3], Destanie Rose[2], Oanh Pham[2], Michael Lehmann[3], Tom McKevitt[1], Georgina Cornish[1], Richard Stebbings[1], James G. Keck[2], **Ilian Radichev**[2]

[1]Clinical Pharmacology and Safety Sciences, AstraZeneca, Cambridge, United Kingdom,[2]Innovation and Product Development, The Jackson Laboratory-West, Sacramento, CA,[3]Clinical Pharmacology and Safety Sciences, AstraZeneca, Gaithersburg, MD

Introduction: Autologous CAR-T therapies targeting B-cell maturation antigen (BCMA) have shown remarkable clinical success in treating multiple myeloma (MM). However, accurate prediction of patient-specific efficacy and adverse events - such as cytokine release syndrome (CRS), immune effector cell-associated neurotoxicity syndrome (ICANS) and Immune effector cell associated hemophagocytic lymphohistiocytosis-like syndrome (IEC-HS) - remains a significant and ongoing challenge. To address the need for personalized screening of CAR-T immunotherapies, we developed and tested a novel humanized mouse model using the NSG-SGM3-IL15-DKO (SDKO) strain, optimized for PBMC engraftment. This model is a new potential preclinical tool to assess individualized CAR-T efficacy and toxicity *in vivo*.

Methods: We evaluated autologous anti-BCMA CAR-T therapy in vivo using five human PBMC donors in the context of an established $BCMA^+$ tumor. For this, SDKO mice were injected intravenously with 1×10^6 MM.1S-luc cells, a model cell line for multiple myeloma. Ten days post-tumor injection, mice were randomized based on their tumor burden and injected with 3×10^6 PBMCs. Four hours later, mice received either PBS, 5×10^6 autologous untransduced T cells (UT), or 5×10^6 autologous anti-BCMA CAR-T cells. Tumor burden and body weight were monitored over 28 days. Blood samples were collected at SD1, SD2, SD5, SD15, SD21 and SD28 to assess human cell engraftment and plasma cytokine levels and tissues retrieved for histopathology.

Results: Autologous CAR-T cells induced rapid and potent tumor regression with low toxicity, whereas UT cells failed to control MM.1S-luc tumors across all donors, with tumor progression even more severe than that observed in the PBS group. However, donor-dependent variability was observed: Donors 0935 and 1295 showed reduced CAR-T expansion, and 0935 failed to achieve complete tumor clearance. Transient tumor resurgence occurred in most CAR-T treated mice, except Donor 5263, where tumors were rapidly and permanently eliminated. In contrast, tumors metastasized to bone marrow in PBMC and UT groups. Cytokine profiling revealed both donor-dependent (IL-9, IL-12p70, IL-12p40) and donor-independent (IL-2, IL-4, IL-5, IFNγ, TNFα, IL-13) secretion patterns. Notably, IL-10 exhibited a unique dynamic: a modest spike at SD1 followed by a CAR-T-dependent decline, while PBS and UT groups showed very high IL-10 levels at SD5, suggesting a link to uncontrolled tumor burden and immune dysregulation.

Conclusion: Our results demonstrate that the SDKO PBMC humanized mouse model has the potential to be a valuable tool for preclinical CAR-T testing, enabling patient-specific evaluation of efficacy and safety, and paving the way for safer CAR-T cells in the clinic.

#4268 Armored allogeneic Epstein-Barr virus specific T cells expressing a multi-functional B7-H3 chimeric antigen receptor exhibit improved persistence, expansion and performance in solid tumor models.

Marvin Chew[1], Pei Yun Teo[1], Joanna Koh[1], Jin Wei Tan[1], Lindsay Kua[1], Richard Ong[1], Fiona Wong[1], Angeline Goh[1], Qingfeng Chen[2], Cliona Rooney[3], Ivan Horak[1], Kar Wai Tan[1], **Lionel Low**[1]

[1]Research and Development, Tikva Allocell Pte. Ltd., Singapore, Singapore,[2]Institute of Cell and Molecular Biology, A*STAR, Singapore, Singapore,[3]Baylor College of Medicine, Houston, TX

Allogeneic chimeric antigen receptor (CAR)-T cells can address the high costs and poor availability associated with autologous CAR-T therapies. However, the development of these “off-the-shelf” are challenged with risks of graft-versus-host disease (GvHD) and allogeneic rejection by the patient’s immune cells. Furthermore, whilst remarkable successes have been achieved in the treatment of hematological malignancies, strategies targeting solid tumors face further challenges including tumor trafficking, antigen heterogeneity, chronic antigen stimulation and an immunosuppressive microenvironment.

To address these challenges, we employed allogeneic Epstein-Barr virus specific T cells (EBVSTs) that have been well tolerated in clinical trials. With a narrowed TCR repertoire, EBVSTs have lower GvHD potential. EBVSTs also express higher levels of CD74 and CXCR4 and can better migrate towards tumors cells. Allogeneic rejection by T/NK cells involves the activation of caspases. We show that armoring CAR-EBVSTs with an engineered serine protease inhibitor, SerpinB9(CAS), increases survival in mixed lymphocyte reactions and humanized mice models. Interestingly, we observed that the armored CAR EBVSTs are also resistant to activation induced cell death induced by chronic antigen stimulation.

B7-H3 is an attractive CAR target due to its overexpression in multiple solid tumors, and tumor stroma, with limited expression in normal tissues. We expressed an engineered V_{HH}-based B7-H3 CAR in our armored EBVSTs (B7H3.CAR-EBVSTs) and observed potent efficacy against various cell-line and patient derived xenografts *in vivo* models. Importantly, we showed that B7-H3 CAR also targets B7H3+ myeloid derived suppressor cells (MDSCs) and alloreactive T cells in co-culture experiments, further enhancing survivability in the presence of these immunological challenges.

Lymphodepletion is an essential preconditioning step prior to CAR-T infusion to ensure efficient engraftment of the cells. However, adverse effects of lymphodepletion include severe cytopenia and increased risks of opportunistic infections. We show that a constitutive IL-7 receptor (IL-7) synergized with SerpinB9(CAS) to boost proliferation in the presence of allogeneic challenge, potentially reducing or removing the need for lymphodepletion.

EBV infection has been associated with epithelial cancers including gastric and has been reported to upregulate B7-H3 in nasopharyngeal cancer (NPC). With partial HLA matching, B7H3.CAR EBVSTs can potentially mediate bispecific targeting of B7-H3+, EBV+ tumors in patients. Thus, our armored B7H3.CAR-EVBSTs present an attractive strategy that can overcome significant challenges and improve efficacy in solid tumors, strongly supporting its future development for evaluation in clinic.

#4269 Structure-guided protein engineering and humanization of GPC1-targeted nanobody CAR T cells for treating pancreatic cancer.

Hsi En Tsao, Mitchell Ho

National Cancer Institute, Bethesda, MD

Glypican-1 (GPC1) is a heparan sulfate proteoglycan that is overexpressed in pancreatic ductal adenocarcinoma (PDAC). We previously developed GPC1 CARs using the dromedary VHH nanobody D4 and the mouse monoclonal IgG antibody HM2, which recognize a membrane-distal epitope and a membrane-proximal epitope, respectively. Here, we integrate structural modeling with CAR functional data and animal experiments to define how epitope position and CAR geometry jointly determine GPC1 CAR efficacy. Modeling of CAR ectodomains incorporating CD8 or IgG4 hinges and CD8 or CD28 transmembrane (TM) domains indicated that only specific combinations yield an intermembrane spacing comparable to that of the TCR-pMHC immune synapse for a given epitope. These geometric predictions aligned with functional data in which D4-IgG4H-CD28TM CAR T cells rapidly regressed tumor bioluminescent in a T3M4 intraperitoneal PDAC model. Together, these results support a model in which epitope spatial location on GPC1 and CAR hinge/TM architecture are key design parameters for GPC1-targeting CAR T cells. To facilitate clinical development of D4 CAR T cells, humanization of the VHH D4 is highly desirable, although humanization of nanobodies such as VHHs is not well established. In addition to the CDR grafting to the nearest germline framework as we described previously for humanization of rabbit and mouse antibodies, we used AI-predicted structural models from multiple platforms to compare both the spatial geometry and sequence similarity of predicted D4 framework and CDR regions with available antibody and nanobody structures. Humanized constructs with the highest humanness scores, geometry, and similarity scores were back-mutated to preserve critical residues in the nanobody framework sequences and were then evaluated for GPC1 binding affinity and cell-surface binding. Using this AI-assisted, structure-guided strategy, we aim to generate clinically suitable humanized VHH nanobody scaffolds for GPC1 CAR T therapy and other nanobody-based clinical applications.

#4270 Enhanced solid tumor rejection using IF-BETTER gated CAR T cells for the treatment of hepatocellular carcinoma.

Leena Halim, Michael Lopez, Michel Sadelain

Columbia Institute for Cell Engineering and Therapy, Vagelos College of Physicians and Surgeons, Columbia University Irving Medical Center, New York, NY

CAR T cell therapy has demonstrated remarkable success in treating hematological malignancies but has been, to date, far less effective against solid tumors. Several common obstacles limiting the activity of CAR T cells in solid tumors have been identified, including low and/or heterogeneous target expression, insufficient T cell functional persistence, T cell exclusion and microenvironmental suppression. We address here the former, focusing on the targeting of glypican-3 (GPC3) in hepatocellular carcinoma (HCC). GPC3 is a GPI-anchored protein that is commonly but heterogeneously expressed in HCC, ranging from of 10^4 to 10^2 molecules per cell in a panel of HCC tumor cell lines. Whereas conventional CARs are efficacious against tumors expressing several thousand GPC3 molecules per cell, they consistently fail in the lower range of GPC3 expression. To overcome this limitation, we adopted an IF-BETTER gating strategy by co-targeting a second antigen that is broadly expressed in order to increase CAR T cell avidity for the tumor and CAR T cell persistence, depending on the structure of the associated chimeric costimulatory receptor (CCR). In contrast to an OR gate, wherein two antigens are targeted by either two CARs or a dual-specific CAR, the second antigen in an IF-BETTER gate does not on its own elicit cytotoxicity and therefore does not have to be as restricted to tumor cells as the CAR target. We identified IL1RAP as a potential CCR target and paired the GPC3 CAR, incorporating the GC33 scFv and the 1XX signaling module to extend CAR T cell persistence, with CCRs providing different costimulatory signals. We investigated the paired GPC3-1XX CAR/IL1RAP CCRs in vitro and in vivo, targeting tumor cell lines with a range of GPC3 expression levels. The GPC3-1XX + IL1RAP-CCR configuration preserved on-target GPC3-restricted cytotoxicity while increasing CAR T cell proliferation and maintaining cytotoxicity after repetitive stimulations, in contrast to control CAR T cells lacking the CCR. In vivo, GPC3-1XX CAR + IL1RAP CCR T cells showed significantly improved tumor control, intratumoral infiltration and survival, most pronounced in the setting of low GPC3 expression. In summary, combining calibrated 1XX CAR signaling with IL1RAP-gated costimulation increases GPC3 CAR T cell persistence and reduces antigen escape. These data support the clinical translation of an IF-BETTER gated strategy targeting GPC3 in hepatocellular carcinoma.

#4272 Glutamic-oxaloacetic transaminase 2 (GOT2) as a dual-functional enhancer for CAR-T cell metabolic fitness.

Xiangyi Fang[1], Shadab Kazmi[2], Andre Kelly[2], Xiaoling Jin[3], Alison Jaccard[4], Nathaniel W. Snyder[5], Alexander A. Shestov[2], Saba Ghassemi[2], Roddy S. O'Connor[2]

[1]Department of Bioengineering, University of Pennsylvania, Philadelphia, PA,[2]Department of Pathology and Laboratory Medicine, University of Pennsylvania, Philadelphia, PA,[3]Center for Cellular Immunotherapy, University of Pennsylvania, Philadelphia, PA,[4]Department of Cancer Biology, University of Pennsylvania, Philadelphia, PA,[5]Lewis Katz School of Medicine, Temple University, Philadelphia, PA

CAR-T cell therapy has transformed the treatment landscape for hematologic malignancies, yet its efficacy in solid tumors remains challenged. Aspartate is one of the most critically depleted metabolites in the solid tumor microenvironment; its deficiency impairs T cell proliferation, redox balance, and mitochondrial fitness. GOT2, a mitochondrial enzyme in the malate-aspartate shuttle, plays a critical role in T cell metabolism, as it catalyzes the conversion of oxaloacetate to aspartate. In doing so, GOT2 also helps maintain redox balance and energy production. In addition to its canonical role in aspartate biosynthesis, recent studies in cancer cells suggest that GOT2 regulates fatty acid metabolism through the activation of the transcription factor PPARδ. In T cells, PPARδ is shown to regulate the formation of central memory phenotype and long-term survival. In this study, we examined whether GOT2 overexpression enhances CAR-T cell metabolic fitness and antitumor activity. We found that GOT2-overexpressing CAR-T cells (CART19-GOT2) exhibit superior cytolytic function in both in vitro hypoxic conditions and in vivo tumor models. In xenograft models of NALM6 leukemia, CART19-GOT2 was able to sustain tumor control and prevented regrowth even after rechallenge. Compared to standard CART19 cells, CART19-GOT2 show enhanced mitochondrial respiration and spare respiratory capacity, indicating better mitochondrial fitness. GOT2 overexpression also elevated intracellular aspartate levels in CAR-T cells in normal growth conditions and under hypoxic stress. Using isotypically labeled nutrients as tracers, we found that aspartate is replenished through a cooperative interplay of fuels in primary human T cells, with glutamine serving as the preferred substrate. Collectively, these findings indicate that GOT2 overexpression is a promising strategy for metabolic enhancement of CAR-T cells for solid tumor immunotherapy.

#4273 Environmental conditioning during CD19-CAR T cell manufacturing impacts antitumor potency in a subcutaneous NALM6 tumor model.

Candy Garcia[1], Anita J. Zaitouna[2], Abriel Czachorowski[3], Lauren Kucharczyk[3], Natalie Czeryba[3], Philip Edward Lapinski[4], Andrea Hodgins-Davis[3], Thomas Sullivan[1], Yelena Bronevetsky[1], NINGCHUN LIU[3], Sheri Barnes[5], Shannon Eaker[6], Scott Wise[3], James Lim[1]

[1]Xcell Biosciences, San Francisco, CA,[2]Covance Inc., Ann Arbor, MI,[3]Labcorp, Ann Arbor, MI,[4]Laboratory Corporation of America, Ann Arbor, MI,[5]Laboratory Corporation of America, Chapel Hill, NC,[6]Xcellbio, SAN FRANCISCO, CA

Chimeric Antigen Receptor (CAR) T cell therapy has transformed outcomes for hematologic malignancies, yet optimizing manufacturing conditions remains critical to improving potency and consistency. We previously demonstrated that culturing CAR-T cells under physiological oxygen and pressurized conditions improved persistence and efficacy in a disseminated NALM6 human ALL model.In this study, we investigated whether these optimized manufacturing conditions similarly improve antitumor activity in a subcutaneous NALM6 xenograft model. CD19-targeted CAR-T cells were expanded under three conditions: standard CO_2 incubation (21% O_2 + 0 PSI), mild hypoxia with hyperbaric pressure (15% O_2 + 5 PSI), reflecting arterial and peripheral blood environments, and hypoxia with hyperbaric pressure (5% O_2 + 5 PSI), modeling the solid tumor and bone marrow microenvironments. After a 10-day tumor stage, a dose of 2.5e6 CAR+ T cells achieved complete tumor clearance in all conditions at 20 days post T cell dose, with faster tumor regression under 5% O_2 + 5 PSI conditions (7 days post T cell dose) compared to normoxia or mild hypoxia (10 days post T cell dose). These *in vivo* outcomes were consistent with enhanced *in vitro* functional activity, characterized by greater cytoxicity at CAR-T-to-effector ratios under 1:30 and increased cytokine production. This consistency mirrors our previous findings in the disseminated model, where CAR-T cells cultured under physiologically relevant conditions demonstrated the *in vitro* characteristics predictive of *in vivo* efficacy. Preliminary findings show enhanced potency and persistence under 5% O_2 + 5 PSI conditions. To determine whether these manufacturing advantages are sustained at lower CAR-T doses, a dose titration study is currently in progress, with complete results forthcoming.These data highlight the potential of physiological manufacturing with the GMP AVATAR Foundry to enhance CAR-T function and lower effective doses, supporting scalable next-generation cell therapies.

#4274 CAR-T cells with GPC3-inducible gene circuits for targeting hepatocellular carcinoma.

Kin Ching Tsang[1], Yuqing Deng[1], Pinghui Zhu[1], Chenzi Zhang[1], Jianwei Ren[2], Bo Feng[1]

[1]School of Biomedical Sciences, The Chinese University of Hong Kong, Hong Kong, China,[2]Centre for Regenerative Medicine and Health, Hong Kong Institute of Science & Innovation, Hong Kong, China

Despite the remarkable success of chimeric antigen receptor (CAR) T-cell therapy in hematologic malignancies, its application to solid tumors such as hepatocellular carcinoma (HCC) remains limited by insufficient tumor-specific activation and systemic toxicity from constitutive immunostimulation. To overcome these challenges, we engineered anti-glypican-3 (GPC3) CAR T cells incorporating inducible gene circuits that enable spatially and temporally controlled activation within the tumor microenvironment. Utilizing a lentiviral delivery system, we generated GPC3-specific CAR T cells exhibiting potent antigen-dependent cytotoxicity against HepG2 cells *in vitro* and significant tumor regression in immunodeficient xenograft models. To achieve precise antigen-gated regulation, we implemented a synthetic Notch (synNotch) receptor system and systematically characterized its induction dynamics and kinetics using a Jurkat T-cell reporter platform. Through single-chain variable fragment (scFv) screening, we identified an optimized anti-GPC3 scFv that conferred high sensitivity and specificity for HCC-associated GPC3. Subsequent engineering refinements, including deletion of the negative regulatory region (NRR) and incorporation of a SyNthetic Intramembrane Proteolysis Receptor (SNIPR) architecture, substantially enhanced receptor responsiveness, yielding robust, GPC3-dependent transgene expression with minimal basal leakage. Functional validation in both two-dimensional co-cultures and three-dimensional tumor spheroids confirmed that the optimized anti-GPC3 SNIPR system drives potent, target antigen-restricted transgene activation exclusively upon engagement with GPC3-positive tumor cells. Collectively, these findings establish a modular and tunable platform for inducible CAR T-cell therapy in HCC, demonstrating that synthetic gene circuits can enforce stringent spatial control over T-cell activation in the anti-GPC3 context. This approach holds significant promise for improving the therapeutic index of CAR T-cell therapy in HCC by simultaneously enhancing antitumor efficacy and mitigating off-tumor toxicity.

#4275 Combining circular RNA and a silicon membrane-based cell engineering approach to create CAR-Ts with membrane bound IL-2 and IL-12.

Armon Sharei[1], Zhihui Song[1], Sophia Hirsch[2], Eleni Rogers[3], Darby Kreienberg[3], Alec Barclay[3], Andrew Larocque[3], Anil Narasimha[3]

[1]Portal Biotechnologies, Inc., Watertown, MA,[2]Portal Biotechnologies, Watertown, MA, MA,[3]Portal Biotechnologies, Watertown, MA

Cell delivery is crucial for cell therapy and drug development, and we have developed a novel mechanoporation technology that allows efficient delivery of a wide range of cargoes to primary cells and cell lines. This technology uses a silicon membrane to temporarily deform cells, creating pores that enable cargo diffusion into the cells. Importantly, this method minimizes disruption to normal gene expression and maintains cellular integrity. It is compatible with various cell types and has been successfully applied in both cell therapy and drug discovery. At Portal, we have successfully delivered CRISPR/Cas9 RNPs, mRNAs, circular RNAs, and siRNAs into T cells, B cells, NK cells, and monocytes. For instance, we achieved over 85% GFP expression and B2M deletion in naive T cells after simultaneous delivery of mRNA and CRIRPR-RNPs. Additionally, we demonstrated the functional expression of a CD19 CAR and membrane-bound IL-2 by delivering two circRNAs. Early data from iPSCs and HSCs show significant potential for stem cell engineering and differentiation. Using a clinical-scale prototype, we have achieved delivery of over $1x10^9$ T cells per minute, resulting in more than 50% knockout efficiency and 90% GFP expression after 7 days of T cell expansion.Our platform also addresses a major barrier to drug development by enabling the delivery of cargoes that are otherwise impermeable to cells, such as small molecules, peptides, PROTACs, DELs, antibodies, and probes. We have successfully delivered a variety of cargos with over 80% efficiency while maintaining high cell viability. The technology has been tested in several cell types, including cancer cell lines, human immune cells, and stem cells. The simplicity of the mechanical delivery method facilitates scalability and integration with liquid handlers for high-throughput applications. This enables rapid and automated screening of molecules previously incompatible with live cell assays, improving drug discovery efficiency. Overall, Portal's technology offers a scalable, cost-effective solution with the potential to significantly advance both cell therapy and drug discovery. By reducing manufacturing time and cost, it seamlessly integrates into existing clinical and industrial equipment, supporting the development of next-generation cell-based treatments that could revolutionize the treatment of diseases with high unmet clinical needs.

#4276 Synecta™ T1 cell-derived nanoparticles and Flowfect® continuous flow transfection enhance non-viral engineering efficiency and manufacturing scalability of CD19-directed CAR-T cells for hematologic malignancies.

Chiquita Hanindya[1], Christopher Abraham[2], Maria Lai[2], Peter Keller[1], Kevin Gutshall[2]

[1]BlueWhale Bio, Philadelphia, PA,[2]Kytopen, Cambridge, MA

Background: Autologous CAR-T cell therapies have transformed outcomes in B-cell lymphomas, leukemias, andother indications, yet manufacturing duration, cost, process variability, and dependence on viralvectors continue to limit broader adoption. Improved processes are essential to deliver moreeffective cell therapies and enable broader adoption. Efficient non-viral gene editing requiresactivation that preserves viability and stem-like phenotypes, unlike CD3/CD28 activators, and adelivery system that achieves high editing efficiency without compromising cell health.BlueWhale Bio's Synecta™ T1 cell-derived nanoparticles (CDNPs) mimic physiologic APC signalingvia membrane-bound OKT-3, CD86, 4-1BBL, IL-7, and IL-15/IL-15RA. Kytopen's Flowfect Tx®continuous flow cell engineering technology maximizes yields of engineered cells, whileprocessing hundreds of billions of cells in minutes. Here we present the synergies of thesetechnologies to enhance CRISPR-mediated knock-in (KI) of a CD19-CAR at the TRAC locus.

Methods: Primary healthy donor (HD) human T cells were activated for 2-3 days with Synecta T1 orcomparator activation technologies and then gene-edited using Flowfect Tx® platform to deliverCas9/sgRNA RNP and a CD19-CAR HDR template. KI and knock-out (KO) efficiency, viability,activation, CD4/CD8 ratio, and expansion were quantified through Day 8. Parallel experimentsevaluated Synecta T1 activation immediately after Flowfect Tx transfection in naïve T cells.

Results: Synecta T1 induced >90% CD69$^+$CD25$^+$ activation while preserving CD3 expression. By Day 8, Tcells activated with Synecta and transfected Flowfect Tx® platform achieved >40% CD19-CAR KIand >90% TRAC KO, exceeding comparator activation technologies (<25% KI) and improving bothKI and KO efficiencies. Synecta T1 supported >80% viability and >5-fold expansion, yielding thehighest CAR-positive cell numbers, while maintaining a favorable CD4/CD8 profile. In the naïveworkflow, delivering RNP with a nanoplasmid HDR donor first and then activating with SynectaT1 increased KI-positive cells and expansion compared with unstimulated control, producingmarkedly higher CAR$^+$ output.

Conclusions: Synecta T1 and Flowfect Tx® platform enable efficient non-viral genome editing and rapidexpansion, supporting a streamlined, non-viral manufacturing approach for CD19-CAR-T cells. Byimproving KI and KO efficiency, Synecta T1 enhances CRISPR-based editing and supports targetedCAR insertion under endogenous promoters. Together, these technologies deliver a scalable workflow that achieves effective therapeutic doses quickly while preserving cell fitness. Futurestudies will evaluate activation strategies aligned with Day-2 or Day-0/1 Flowfect Tx® transfection.

#4277 AQP3 NOT gating mitigates lethal on-target off-tumor pulmonary toxicity of MSLN-directed CAR-T cells in ovarian cancer.

Minghua Xiang[1], Wei Mu[2], Bingbing Zhao[3], Jundong Li[4], Qinglei Gao[1], Huayi Li[4]

[1]Department of Obstetrics and Gynecology, Tongji Hospital, Tongji Medical College, Huazhong University of Science and Technology, Wuhan, China,[2]Department of Hematology, Tongji Hospital, Tongji Medical College, Huazhong University of Science and Technology, Wuhan, China, Wuhan, China,[3]Department of Obstetrics and Gynecology, Guangxi University Cancer Hospital, Nanning, China,[4]Department of Gynecologic Oncology, Sun Yat-sen University Cancer Center, Guangzhou, China, Guangzhou, China

Background: Mesothelin (MSLN) is overexpressed across multiple solid tumors and represents a promising therapeutic target. However, MSLN-directed chimeric antigen receptor (CAR)-T cells have been associated with lethal pulmonary on-target off-tumor toxicity. Here, we implemented a “NOT” logic-gating strategy to engineer dual-input MSLN/AQP3 lung-Specific Attenuated Functionally Engineered (lung-SAFE) CAR-T cells that retained potent antitumor activity against ovarian cancer while preventing fatal pulmonary toxicity.
Methods: A phase I trial (NCT05141253) was ongoing to evaluate the safety of MSLN-directed CAR-T cells in patients with solid tumors. Human MSLN (hMSLN) knock-in NCG mice bearing SKOV3 xenografts received intravenous MSLN-CAR-T cells and were longitudinally monitored for signs of toxicity. Major organs and peripheral blood were collected at moribund stages. MSLN expression, CAR-T cell infiltration, and lung injury were analyzed. Integrated analyses of in-house single-cell ovarian cancer datasets and publicly available single-cell lung datasets were performed to identify candidate inhibitory targets, which were subsequently validated in vitro and in vivo. CAR-T cell activation and cytotoxicity were assessed using flow cytometry, cell lysis assays, and cytokine quantification in co-culture supernatants.
Results: In the phase I trial, two patients with ovarian cancer experienced fatal pulmonary toxicity following MSLN-CAR-T cell infusion. To elucidate the underlying mechanism, we generated hMSLN knock-in NCG mice, which faithfully recapitulated the lethal pulmonary injury observed in patients. This toxicity was mediated by MSLN expression on alveolar cells and CAR-T cell-driven immunopathology. To overcome this limitation, we integrated single-cell transcriptomic analyses of ovarian cancer and healthy lung tissues to identify molecules selectively enriched in alveolar cells but minimally expressed in ovarian cancer cells. Cross-validation in cell lines, organoids, and human tissue specimens identified AQP3 as the most selective target. We then engineered a dual-input MSLN/AQP3 lung-SAFE CAR-T cells, wherein AQP3 delivered an inhibitory signal to suppress MSLN-CAR-T cell activation in the lung. The resulting lung-SAFE CAR-T cells maintained potent cytotoxicity against MSLN+ ovarian cancer cells while sparing AQP3+ alveolar cells in vitro.
Conclusions: This study established hMSLN knock-in NCG mice as a robust preclinical platform to evaluate the safety of MSLN-targeted CAR-T cells, identified AQP3 as a key molecular switch to mitigate their pulmonary toxicity in ovarian cancer, and introduced a generalizable framework that integrated single-cell transcriptomics with “NOT” logic-gating design for precision control of organ-specific CAR-T cell toxicity, advancing the safer translation of CAR-T cell therapies for solid tumors.

#4278 Regulatory T cell inspired engineering of CAR-T cells enhances anti-tumor efficacy in solid tumors.

Avik Chattopadhyay, Erin O'Connor, Leonardo M. R. Ferreira

Department of Pharmacology and Immunology, Medical University of South Carolina, Charleston, SC

Chimeric antigen receptor (CAR)-T cells have revolutionized treatment for hematologic malignancies. Yet, their efficacy against solid tumors remains limited due to the immunosuppressive tumor microenvironment (TME), characterized by nutrient deprivation, hypoxia, and lactate accumulation. Regulatory T cells (Tregs) thrive under such conditions due to expression of the transcription factor FOXP3, which enhances their intratumoral fitness. Leveraging this biology, we engineered effector CAR-T cells to overexpress FOXP3 and evaluated their therapeutic potential in melanoma. *In vitro*, CAR-T cells targeting the melanoma-associated antigen TRP1 efficiently killed B16F10 melanoma cells, with FOXP3 overexpression modestly reducing cytotoxicity. We next tested $CD4^+$, $CD8^+$, or total CAR-T cell subsets in immunocompetent C57BL/6 mice bearing B16F10 melanomas. *In vivo* NanoLuc luciferase imaging revealed superior persistence of FOXP3-expressing CAR-T cells compared to control CAR-T cells. Strikingly, while conventional CAR-T cells exhibited minimal tumor control, FOXP3 overexpression produced divergent outcomes: $CD4^+$ or $CD8^+$ CAR-FOXP3-T cells alone unexpectedly accelerated melanoma growth, whereas total CAR-FOXP3-T cells significantly delayed tumor progression. Mechanistic analyses revealed that FOXP3 overexpression did not alter the extent of CAR-induced T cell activation but did protect CAR-T cells from activation-induced cell death. Further characterization revealed that total CAR-FOXP3-T cells were predominantly $CD8^+$, leading us to hypothesize that supplemental $CD4^+$ CAR-T cells could enhance anti-tumor activity. Indeed, co-administration of $CD4^+$ CAR-T cells and total CAR-FOXP3-T cells resulted in sustained control of melanoma growth *in vivo*, indicating a synergistic interaction between the two cell populations. Our findings provide proof-of-concept for novel CAR-T cell therapy design principles to overcome barriers in solid tumor immunotherapy and inform the development of next-generation cellular therapies.

Funding: This work was supported by Swim Across America Grant 23-1579 to LMRF and an MUSC Specialized Center of Research Excellence (SCORE) 5U54DA016511-18 Pilot Project Award to AC. This study was supported in part by the Flow Cytometry and Cell Sorting Shared Resource, Hollings Cancer Center, Medical University of South Carolina (P30 CA138313).

#4279 A PSMA-targeted CAR-T cell engineered with a CD16A signaling domain mitigates cytokine output while retaining antitumor activity in prostate cancer models.

Parv Barot, Hittu Matta, Sunju Choi, Gong Songjie, Bryant Bravo, Elton Zho, Hsing-Yu Wu, Sam Lin, Zhuoyue Yang, Preet M. Chaudhary

Jane Anne Nohl Division of Hematology and Center for the Study of Blood Diseases, USC Norris Comprehensive Cancer Center, Los Angeles, CA

Introduction: Adoptive transfer of Chimeric Antigen Receptor (CAR) T cells has demonstrated limited efficacy in solid tumors, partially attributable to excessive cytokine release driven by synthetic co-stimulatory domains and functional suppression within the tumor microenvironment. The purpose of this study was to engineer a Prostate-Specific Membrane Antigen (PSMA)-targeted CAR incorporating CD16A, an innate immune receptor with a distinct signaling profile to determine if this alternative architecture supports robust antitumor function while attenuating cytokine output.
Procedures: A lentiviral vector encoding a humanized J591-derived anti-PSMA single-chain variable fragment (scFv) fused to CD16A transmembrane and intracellular signaling domains (PSMA-CD16A CAR) was constructed, omitting canonical co-stimulatory domains (e.g., 4-1BB, CD28). Primary human T cells were transduced and evaluated for in vitro activity using a luciferase-based cytotoxicity assay against $PSMA^+$ LNCaP targets. Cytokine secretion (TNF-α, IFN-γ, IL-2) was quantified by ELISA following co-culture. In vivo antitumor efficacy was assessed in NSG mice bearing subcutaneous LNCaP xenografts (n=5 per group), utilizing untransduced T cells and tumor-only groups as controls.
Results: PSMA-CD16A CAR-T cells demonstrated antigen-dependent cytotoxicity in vitro, mediating efficient lysis of LNCaP cells. Compared with untransduced T cells, CAR-T cells exhibited enhanced killing potency while maintaining an attenuated cytokine secretion profile; levels of TNF-α, IFN-γ, and IL-2 were stable and sufficient to support effector function without supraphysiological spikes. In vivo, PSMA-CD16A CAR-T treatment significantly improved tumor control and prolonged survival. Median overall survival (OS) was 97 days in the CAR-T cohort reaching the study endpoint, compared to 71 days (±8) in untransduced T cells, representing a 36.6% survival increase. Three of five CAR-T treated mice survived to the maximal observation period with observed tumor regression with complete response. While survival was ultimately limited by xeno-reactive graft-versus-host disease (GvHD) inherent to the NSG model, tumor burden was significantly reduced compared to controls.
Conclusions: We report the successful generation of a PSMA-directed CAR relying exclusively on CD16A signaling. This construct preserves potent antitumor function while exhibiting a moderated cytokine profile. These findings support CD16A-based signaling as a viable alternative to conventional co-stimulatory domains. Ongoing work focuses on expanded functional characterization and evaluation in immunocompetent models to further assess safety, efficacy and persistence.

#4280 Restoration of LAT signaling via the ALA-CART platform promotes metabolic resiliency and persistence of AML CAR T cells.

Catherine Danis, Amanda J. Novak, Etienne Danis, Angie Vazquez, Michael Yarnell, Lillie Leach, M. Eric Kohler

University of Colorado Anschutz Medical Campus, Aurora, CO

Despite therapeutic advancements, the majority of patients with relapsed and/or refractory (r/r) acute myeloid leukemia (AML) have very poor prognoses and limited treatment options. While Chimeric Antigen Receptor (CAR) T cell therapy has transformed the treatment of r/r B-cell acute lymphoblastic leukemia (ALL), inducing remissions in up to 90% of patients, yet clinical trials of 2nd generation CAR T cells for patients with r/r AML have not replicated this success. Post-CAR T cell relapses in ALL are common and limit the long term efficacy of this therapy. Mechanisms driving ALL relapses after CAR T cells, such as short duration of activity and antigen modulated escape, have illuminated vulnerabilities of 2nd generation CAR T cells, such as exhaustion, poor persistence, and low antigen sensitivity. The mechanisms underlying AML progression after CAR T cells are not well defined, however, it is likely that similar barriers must be overcome to improve CAR T cell responses in patients with r/r AML.

We recently demonstrated the Linker for Activation of T cells (LAT) is inefficiently engaged in ALL-directed CAR T cells, particularly when antigen levels are low. Through a novel Adjunctive LAT-Activating CAR T (ALA-CART) platform, LAT activity and downstream signaling were restored and ALA-CART cells demonstrated enhanced potency, expansion, and persistence. We hypothesized that CD33-directed ALA-CART cells would similarly show improved potency and persistence in pre-clinical models of AML. Despite exhibiting decreased effector function in vitro, 33ALA-CART cells demonstrated increased efficacy in multiple AML xenograft models. 33ALA-CART cells had greater in vivo expansion and were effective at lower doses than CD33BBz CAR T cells. 33ALA-CART cells showed similar potency as CD33-28z CAR T cells, however, demonstrated enhanced persistence relative to both CD33BBz and CD33-28z CAR T cells. In rechallenge experiments, 33ALA-CART cells demonstrated enhanced expansion and leukemia clearance. Interestingly, the enhanced persistence of 33ALA-CART was strongly correlated with increased mitochondrial activity, a feature associated with long-lived memory T cell subsets and persistence. Consistent with this, RNA-sequencing analysis demonstrates that ALA-CART cells have increased potential for mitochondrial biogenesis and a reduced capacity for glycolysis relative to 2nd generation CAR T cells. Together, these data suggest that increased signaling through LAT results in enhanced metabolic capacity, potentially contributing to the enhanced proliferative, functional, and persistence capacity of 33ALA-CART cells in vivo.

Through restoring LAT activity and downstream signaling, the ALA-CART platform provides a rational strategy to enhance multiple facets of CAR T cell function and represents a promising approach to improve the efficacy of AML-directed CAR T cell therapy.

#4281 Armoring ROR1 CAR T cells with IL18 improves CAR T cell function and cytotoxicity against pancreatic cancer cell-lines *in vitro* and *in vivo*.

Bal Krishna Chand Thakuri, Saule Nurmukhambetova, Tri Tran, Ngoc Tran, Peirong Hu, Pradyot Dash, Rimas J Orentas, Alun Carter

Miltenyi Biotec, Gaithersburg, MD

ROR1 (Receptor tyrosine kinase-like Orphan Receptor 1) is a tumor-associated antigen widely expressed in solid tumors and is a promising target for CAR T cell therapy in pancreatic cancer. Cell-based immunotherapy has met with limited success due in part to the immunosuppressive tumor microenvironment (TME). Here we demonstrate that armoring our previously described[1] ROR1 CAR T cell product with interleukin-18 (IL18) enhanced expansion, persistence, and antitumor efficacy against pancreatic cell lines both *in vitro* and *in vivo*.

ROR-1-specific CAR-T cells were generated in human T cells using lentiviral vectors (LV) expressing a second generation CAR alone, CAR+ constitutive IL-18, or CAR+NFAT-IL18. IL18-ROR1 CAR T cells expanded 1.5 fold more, preserved naïve phenotype, and had reduced LAG3 expression (37% vs 81%) vs CAR. *In vitro* armored CAR cytotoxicity, determined by xCelligence tumor co-culture assays, was equal to or greater than CAR alone against ROR1(+) tumor cell lines. In an AsPC-1 mouse xenograft model, each CAR construct exhibited anti-tumor efficacy, with IL-18 expressing CARs displaying significantly greater tumor control. The constitutive IL18-CAR completely cleared tumor at day 28 post-T cell infusion and showed increased persistence throughout the study when compared to ROR1 CAR-T lacking IL-18 (Fig.1). CAR+NFAT-IL18 similarly controlled tumor growth compared to UTD.

In summary, IL18 armored CAR T cells significantly improved the expansion, persistence, and antitumor efficacy of ROR1 CARs in pancreatic cancer xenograft models. Importantly, NFAT-promoter-based regulation of ROR1 CAR T may offer a viable approach to regulating potential toxicity while retaining boosted IL-18 induced activity. This armoring strategy may offer a promising approach solid tumor indications and warrants further preclinical and translational investigation.

A

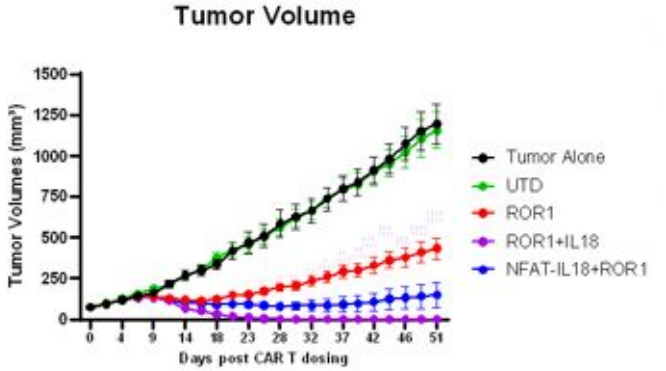

B

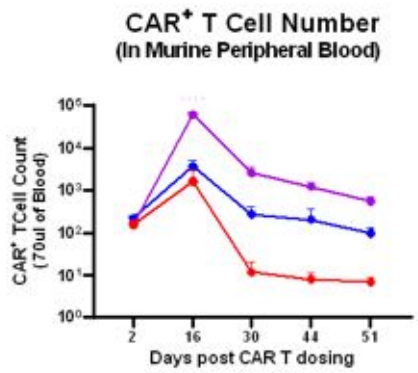

Fig 1. In vivo demonstration of effective constitutive and inducible IL18 armoring of ROR1 CAR T targeting pancreatic cell-lines. $^{*}p<0.05$, $^{**}p<0.01$, $^{***}p<0.001$

Reference:

1. Tran TM et al. J Immunother Cancer 2024;12(4)

#4283 CD3-positive allogeneic CAR T-cells: A novel platform with persistence, BiTE-capture, and no alloreactivity.

Tanya Hundal[1], Yan Luo[2], Yaqing Qie[1], Martha E. Gadd[1], Shaohua Guo[1], Mohamed A. Kharfan-Dabaja[3], Hong Qin[4]

[1]Regenerative Immunotherapy and CAR-T Translational Research Program, Mayo Clinic, Jacksonville, FL,[2]Department of Cancer Biology, Jacksonville, FL,[3]Blood and Marrow Transplantation and Cellular Therapy Program, Mayo Clinic, Jacksonville, FL,[4]Department of Internal Medicine, Mayo Clinic, Jacksonville, FL

Several allogeneic CAR T-cell therapies are in clinical trials to evaluate safety, many of which rely on CRISPR/Cas-based genome editing. However, the Cas enzyme's random repair mechanism elevates the risk of undesired, off-target effects, posing a challenge for safe allogeneic CAR T-cell generation. To mitigate the risk of therapy-related oncogenesis, we sought to pursue an alternative safe strategy to manufacture allogeneic CAR T-cells distinct from the preexisting ones in the clinic. We have developed a CRISPR RNA (crRNA) targeting T-cell receptor beta constant (TRBC) gene, which in conjunction with AsCas12a Ultra enzyme, causes site-specific editing by eliciting a predictable microhomology-mediated end joining (MMEJ) DNA repair pathway, which mitigates off-targeting risk. Targeted amplicon sequencing was employed to evaluate off-targeting and repair mechanisms. Graft versus host alloreactivity as well as CAR T persistence was evaluated using immunocompromised mice. In vivo tumor challenge study was conducted for over 3 months. Engraftment confirmation was done using immunohistochemistry and flow cytometry. Interestingly while evaluating the edited T-cells, we sequestered a unique T-cell population that showed TCR disruption yet remained CD3-positive and did not cause in vivo alloreactivity. These CD3-Retained, Allogeneically Functioning T-cells (CRAFT-cells) showed a similar growth rate as unedited T-cells and were then used as a platform to produce CD19-targeted CAR T-cells and BAFF-R-targeted CAR T-cells. When compared to the standard CD3-disrupted allogeneic CAR T-cells, CRAFT CAR T-cells displayed an equally robust cytotoxicity while possessing a safer genomic profile. CRAFT CAR T-cells could function as effector cells for bispecific T-cell engager (BiTE) and induce CD3-dependent cytotoxicity against tumor cells. Pertinently, CRAFT CAR T-cells as opposed to CD3-disrupted CAR T-cells, were present in mouse xenografts without alloreactivity. Having the onset of MMEJ-directed repair and minimal off-targeting, positions this CRAFT crRNA to generate safer allogeneic CAR T-cells with an overall reduced genotoxic profile in a clinical setting. This unique CRAFT CAR T-cell population displays in vivo persistence. Additionally, CRAFT CAR T can be combined with BiTE therapy, offering a promising and potentially more durable alternative to preexisting ex vivo allogeneic CAR T-cell therapies.

#4284 FT839: A next-generation, off-the-shelf CAR T cell uniquely engineered with a dual CAR system targeting CD19 and CD38 for the treatment of hematological malignancies and autoimmune diseases without conditioning chemotherapy.

Alex J. Garcia[1], Shilpi Chandra[1], Soheila Shirinbak[1], Mark Jelcic[1], Brian Groff[1], Spas Markov[1], Alma Gutierrez[1], Angela Gentile[1], Miguel Meza[1], Karina Palomares[1], Carissa Dege[1], Bjoern Gaertner[1], Ramzey Abujarour[1], John Goulding[1], Tom Lee[1], Karl-Johan Malmberg[2], Maksim Mamonkin[3], Jode Goodridge[1], Martin Hosking[1]

[1]Fate Therapeutics, San Diego, CA,[2]Oslo University Hospital, Oslo, Norway,[3]Vagelos College of Physicians and Surgeons, Columbia Univerisity, New York, NY

Autologous chimeric antigen receptor (CAR) T cell therapies have revolutionized treatment of hematological malignancies and are showing promising results in autoimmune settings. Despite these successes, widespread accessibility to autologous CAR T-cell therapy is challenged by manufacturing complexities, high cost, lack of on-demand drug product availability and the requirement for intensive conditioning-chemotherapy. Moreover, single antigen targeting often fails to address the complex and heterogenous nature of such diseases. FT839 is an off-the-shelf, uniformly engineered, 13-point edited iPSC-derived CAR T cell therapy that overcomes these challenges, delivering potent and flexible multi-antigen targeting with broad patient accessibility.Mediated by its dual CAR system targeting CD19 and CD38 to eliminate malignant and aberrant immune cells, in preclinical studies FT839 exhibited selective elimination of autoimmune disease drivers like B cells, plasma cells and activated T cells as well as hematological cancer cells of lymphoma/leukemia and myeloma origin with profound potency ($p<0.01$). The comprehensive targeting strategy and the depth of activity was further extended when combined with the monoclonal antibody (mAb) rituximab or the T cell engager (TCE) epcoritamab facilitated through the expression of high affinity/non-cleavable Fc receptor (hnCD16) and CD3ε fusion receptor (CD3FR), respectively ($p<0.01$). Furthermore, FT839 features Sword and Shield^{TM} technology, designed to promote functional persistence by directly targeting and evading alloreactive host immune cells. In allogeneic settings with HLA-mismatched donor PBMCs or primed allogeneic T cells designed to quickly eliminate non-host cells, FT839 showed enhanced persistence (21x, $p<0.0001$ vs control), limited alloreactive cell expansion (0.25x, $p<0.0005$ vs control), and durable tumor control (>18x greater cytotoxicity vs control). FT839 has also been engineered with the chemokine receptor CXCR2, and a TGFβ signal redirection receptor to improve trafficking to sites of pathological activity and to counter the suppressive effect of TGFβ, respectively (6.5x greater tissue potency, $p<0.005$). With Sword and Shield^{TM} technology, FT839 obviates the need for conditioning chemotherapy, reducing patient burden and maximizing access. Armed with CD19 and CD38 targeting CARs and the ability to functionally combine with approved therapeutic mAbs and TCEs, FT839 selectively and uniquely eliminates heterogeneously populated disease-driving immune cells. Collectively, FT839 is a scalable, cost-effective, and uniform off-the-shelf CAR T-cell therapy for the broad treatment of hematological malignancies and autoimmune diseases.

#4286 B7-H3 hypoimmune chimeric antigen receptor T cells overcome immune rejection and retain antitumor activity against cholangiocarcinoma.

Chiara Camillo[1], Xiaomeng Hu[1], Giulia Cattaneo[1], Liti Zhang[1], Erica Daniels[1], Luigi Liguori[2], Eduardo Tejeda-Polanco[1], Maoyang Qi[1], Enrica Quattrocchi[1], Francesco Sabbatino[3], Sonja Schrepfer[1], Cristina R. Ferrone[1]

[1]Cedars Sinai Medical Center, Los Angeles, CA,[2]University of Salerno, Fisciano, Italy,[3]University of Salerno, S.Anastasia, Italy

Background. Intrahepatic cholangiocarcinoma (ICC) is a rare, aggressive liver cancer, with limited treatment options and poor survival. Because surgery is the only curative option, but most patients present with advanced disease, novel therapies are urgently needed. CAR-T cell therapy has revolutionized hematologic cancer treatment, but its application in solid tumors is limited.We investigated an allogeneic “off-the-shelf” hypoimmune (HIP) CAR-T platform designed to overcome barriers that hinder CAR-T efficacy in solid tumors. Targeting B7-H3, aberrantly expressed in ICC, the HIP CAR T cells demonstrated promising activity in vitro and in vivo studies. These findings support the potential of allogeneic HIP B7H3 CAR-T cells to improve antitumor responses in advanced ICC.
Methods: Immunohistochemical staining of an ICC tumor vs normal tissue. Generation of HIP T cells with disrupted B2M, CIITA, and TRAC genes using CRISPR-Cas9 editing. In addition, CD47 and anti-B7H3 CAR were expressed using lentiviral transduction. These allogeneic HIP B7H3 CAR T cells were compared to allogeneic WT B7H3 CAR T cells (TCR-/-) that only expressed the anti-B7H3 CAR. HIP phenotype characterization was analyzed by flow cytometry. Killing assay performed with xCELLicence real-time system. BLI for tumor growth.
Results: Immunohistochemistry of human ICC tumors showed strong membrane and cytoplasmic B7-H3 expression compared to normal liver tissue. The B7-H3 epitope recognized by mAb 376.96 was highly expressed in ICC2, ICC3 and hCAF cell lines. B7-H3 CAR T specifically recognized and eliminated ICC targets in vitro. Lentiviral constructs engineering produced both WT and HIP allogeneic CAR T cells with high editing efficiency: TCR knockout in 91% (WT) and 89.8% (HIP) and HLA-I and HLA-II knocked out in 93.3% and 98.7% of HIP B7-H3 cells. CD47 overexpression was restricted to the HIP B7-H3 cells (47.3%). In co-culture assay T cells, NK cells, and macrophages, HIP cells showed protection from adaptive and innate immune clearance. Impedance cytotoxicity assays confirmed that HIP B7-H3 CAR T cells maintained full antitumor activity, matching WT B7-H3 CAR T cell killing rate. HIP CAR-T cells are now validated in in vivo ICC model.
Conclusion: Our findings showed that allogeneic HIP B7-H3 CAR T cells can be efficiently engineered, maintain protection from adaptive and innate immune rejection, and retain full cytotoxic activity against ICC tumors. By combining the tumor-specific activity of B7-H3 CAR-T cells with the immune-evasive properties of HIP cells, this approach offers a promising and widely applicable allogeneic “off-the shelf” therapy for ICC, providing a strong rationale for further preclinical translational studies.

#4287 Cell killing dynamics and heterogeneity in engineered T-cells measured in live CellCage enclosures.

Shawn Levy[1], Richard Yau[1], Shreya Deshmukh[1], JangKeun Kim[2], Jiwoon Park[2], Yanping Yang[3], Makenzie Sacca[1], Shan Sabri[1], Christopher E. Mason[2], Moonsoo M. Jin[3]

[1]Cellanome, Inc., Redwood City, CA,[2]Weill Cornell Medicine, New York, NY,[3]Houston Methodist Research Institute, Houston, TX

Predicting CAR-T clinical efficacy remains a central challenge to the cell therapy field. Existing potency assays generally rely on bulk endpoints and may fail to capture cellular heterogeneity and dynamic interactions governing *in vivo* efficacy. We developed a technology to reveal CAR-T functional heterogeneity at single-cell resolution. Using CellCage Enclosures™, we encapsulated thousands of CAR-T cells at single-cell density with NALM-6, HeLa, and A549 targets across 1:10 and 25:1 E:T ratios in one experiment, enabling parallel cytotoxicity assessment under diverse conditions. Studies with AIC100, a preclinical ICAM1 CAR-T product, revealed striking heterogeneity: individual CAR-T cells exhibited killing at 55% compared to 80% with multiple cells working together. Optimal activity required both CD4+ and CD8+ CAR-T cells within the same microenvironment, suggesting critical cooperative mechanisms, which were product-specific, and impactful to clinical efficacy. A second CD19-targeting CAR-T product against NALM6 targets showed individual cells could kill effectively (50-60%), though cytotoxicity still improved to more than 80% with multiple effectors—but at different E-T ratios. Interestingly, CD8+ CAR-T killing was enhanced ~30% by non-transduced CD4+ T-cells lacking the CAR construct entirely, demonstrating that therapeutic potency can be modulated by cell-extrinsic factors independent of antigen recognition or cytokine secretion. This approach profiles thousands of cellular interactions per experiment, revealing that CAR-T activity emerges from complex cell-intrinsic properties and microenvironment factors unpredictable from bulk measurements. Each product exhibits unique cellular dynamics requiring individual optimization. The CellCage platform enables identification of potent CAR-T subpopulations and quantification of functional heterogeneity, providing a path toward predictive potency assays and rational optimization of cellular therapeutics.

#4288 Use of a 50-marker mass cytometry intracellular cytokine staining panel reveals unforeseen functional diversity within cell therapy products and unmasks potential efficacy 'saboteurs'.

Lauren Tracey[1], Michael Cohen[1], Laura Polanco[2], Erika Smith-Mahoney[3], David King[1], Amedeo Cappione[1], Anna Belkina[2], Christina Loh[1], Jennifer E. Snyder-Cappione[3]

[1]Standard BioTools, Markham, ON, Canada,[2]Boston University Chobanian and Avedisian School of Medicine, Boston, MA,[3]Boston University Chobanian and Avedesian School of Medicine, Boston, MA

Cell-based therapies have proven to be highly effective against certain cancers, yet improvements are needed to extend these successes to a wider variety of malignancies. Single-cell functional assessment of cell therapy products is customarily limited to Th1 cytokines (such as IFN-γ) and the cell survival/proliferative mediator IL-2, overlooking the cellular heterogeneity of CAR T products. This heterogeneity includes diverse antigen-experienced αβ T cells previously differentiated into distinct lineages (for example, Type 1, 2, 17, Treg) and innate T cell populations (iNKT, MAIT, γδ T), with many of the latter pre-programmed to exert immunosuppressive and/or cell repair effector functions. This diversity introduces potential “saboteur” cells with off-target effects that may undermine therapeutic efficacy. Surface marker profiling is insufficient for functional characterization, yet traditional flow cytometry lacks resolution for certain intracellular targets, particularly immunosuppressive cytokines. Mass cytometry (CyTOF™ technology) overcomes this technical limitation, providing superior intracellular signal resolution in the context of large panel analyses, a prerequisite of deep functional assessment of single cells. We hypothesized that there are sizeable proportions of saboteur T cells in cell therapy products that exert functions after stimulation that act in direct opposition to the therapeutic intention of the drug. To assess this, we developed a 50-marker CyTOF intracellular cytokine staining (ICS) panel with 24 functional readouts. This enabled clear detection of individual human T cells producing immunosuppressive cytokines such as IL-10, IL-13 and TGF-β, and measured the composite cytokine responses of both T cells in peripheral blood mononuclear cells (PBMC) and cell therapy products. Our data revealed an unforeseen prevalence of T cells that cross dogmatic lineage paradigms when stimulated. For example, after mitogen stimulation, approximately 30% of T cells from both peripheral blood and a cell therapy product produced the TGF-β-inducing cytokine amphiregulin (AREG), often concurrently with IFN-γ within the same cells. In addition, using the CyTOF ICS panel on TCR-stimulated T cell populations revealed peptide-specific production of AREG, IL-13, IL-4 and MIP-1β by CD8 T cells in PBMC, suggesting CAR T products may release unmeasured cytokines in response to specific CAR antigen binding. From these results, we anticipate application of CyTOF ICS technology to cell therapy testing and modification will transform our understanding of these therapies and ultimately enhance their efficacy.

#4290 Harnessing an optimized cellular therapy platform for ALK-expressing pediatric and adult solid tumors.

Alberto D. Guerra[1], Geoffrey Rouin[1], Patrick Ryan[1], Grant Li[1], David Groff[1], Christina Acholla[1], Matthew Beasley[2], Lauren A. Pitt[2], Kayla Hallac[1], Evan W. Weber[1], Yael P. Mosse[1]

[1]Oncology, Children's Hospital of Philadelphia, Philadelphia, PA,[2]Myrio Therapeutics Pty Ltd, Blackburn North, Australia

Background: Patients with high-risk neuroblastoma and fusion-positive rhabdomyosarcoma face poor survival outcomes and significant treatment-related co-morbidities, necessitating precision targeted therapies. The Anaplastic Lymphoma Kinase (ALK) is a tumor-restricted oncofetal protein highly expressed in these pediatric tumors and select adult malignancies.

Methods: We developed 56 ALK-directed chimeric antigen receptor (CAR) T cell architectures constructed from a library of 11 highly active and specific scFvs produced by Retained Display ™ screen against ALK antigen encompassing the extracellular domain. CAR architectures included varying scFv orientations, CD8 or CD28 transmembrane domains, and CD28 or 41BB co-stimulatory domains. We systematically screened these CAR constructs with multiple T cell donors against neuroblastoma cell lines and spheroid models with a range of ALK surface expression: NB-1 (high), IMR-32 (moderate), NGP (moderate), and CHP134 (low). Lead candidates were tested with two different T cell donors *in vivo* against NB-1 (ALK high) and Felix (ALK moderate) xenograft models with $10x10^6$ CAR+ cells. Peripheral blood was analyzed weekly for CAR+ cells.

Results: Three ALK-directed scFvs significantly increased T cell activation (CD69) and degranulation (CD107a, $p<0.01$) with elevated IL-2, IFNγ and granzyme B production ($p<0.05$) in an ALK-dependent manner after 6 and 24 hours of co-culture. The lead constructs exhibited potent cytotoxicity with tumor clearance in both 2D and spheroid co-cultures confirmed by live imaging of GFP-labeled cell lines and Caspase-3/7 red dye assay across effector-to-target cell ratios of 4:1 to 1:4. Antigen specificity was validated by the absence of activation, cytokine production or cytotoxicity against *ALK* knockout NGP cells. In xenograft models, these CAR T cell constructs achieved complete and durable tumor regression in NB-1 and transient-to-durable responses in Felix tumors. Peak circulating CAR+ T cells occurred at day 14 in NB-1 and day 7 in Felix models with enrichment of central-memory phenotypes (CD62L+ and IL7Rα+, low CD45RA and LAG3). Constructs incorporating CD28 transmembrane and costimulatory domains conferred enhanced activation, cytokine release and efficacy at moderate and low ALK density.

Conclusions: These findings validate ALK as a selective cellular immunotherapy target and highlight novel CAR architectures integrating CD28 transmembrane and costimulatory domains to achieve high antigen sensitivity and sustained functional persistence. These optimized CAR designs enable variable ALK recognition and may improve clearance of minimal residual disease. Next-generation constructs incorporating FOXO1 overexpression and NFAT-inducible IL-15 expression via bicistronic vectors will further address resistance mechanisms within the immunosuppressive solid tumor microenvironment.

#4291 Synecta™ T1 cell-derived nanoparticles enable accelerated, potent T cell expansion for scalable adoptive immunotherapy manufacturing.

Deeksha Muthumani[1], Chiquita Hanindya[1], Gil Joseph[1], Victor Carpio[1], Bakir Valentić[2], Roddy O' Connor[2], Olga Barreiro[3], Ulrich H. Von Andrian[3], Peter Keller[1]

[1]BlueWhale Bio, Philadelphia, PA,[2]Perelman School of Medicine, University of Pennsylvania, Philadelphia, PA,[3]Department of Immunology | Blavatnik Institute, Harvard Medical School, Boston, MA

Background: While Adoptive immunotherapies are expanding clinically, their translation is limited by the lack of scalable, standardized manufacturing. Critical attributes, including T-cell activation and expansion, directly impact yield and product quality. Synecta is a cell-derived nanoparticle (CDNP) platform designed to drive rapid T-cell expansion while streamlining manufacturing. Synecta T1 incorporates membrane-bound stimulatory signals (OKT3-scFv, CD86, 4-1BBL) and cytokines (IL-7, IL-15Rα/IL-15), enabling potent activation and accelerated expansion

Methods: T cells from healthy donor (HD) and patient (PT) samples were isolated, activated, transduced, and expanded using Synecta T1 or a comparator activation system. T-cell functionality was assessed using cytotoxicity assays and repeated antigen-exposure models. Mechanistic studies included CTV proliferation, evaluation of proliferation markers, and inhibitory assays targeting immune-synapse formation. High-resolution live-cell imaging using super-resolution confocal and lattice light-sheet microscopy was used to visualize synapse architecture. Metabolic profiling was performed using Seahorse assays.

Results: Synecta T1-expanded HD and PT T cells exhibited rapid activation (>80% CD69/CD25 by Day 2) and accelerated expansion (2.2-fold HD, 1.4-fold PT samples by Day 3) while maintaining functional fitness under repeated antigen exposure. Rapid T cell expansion, directed by Synecta T1, correlates with early proliferation, as indicated by Cell Trace Violet dilution and the upregulation of proliferation markers.CDNPs express ICAM-1, a crucial adhesion molecule that stabilizes the interaction between Antigen-Presenting Cells (APCs) and T cells via LFA-1. Inhibition of ICAM-1/LFA-1 interaction with small molecules impaired the effective engagement between Synecta and T cells, suggesting that CDNPs' enhanced performance could stem from their ability to mimic the immune synapse. In fact, high-resolution live-cell imaging of CDNP-T cell interactions using F-actin and tubulin probes revealed the assembly and maturation of immune synapses, highlighted by the development of the peripheral supramolecular activation cluster (pSMAC) and the polarized translocation of the Microtubule-Organizing Center (MTOC) toward the CDNP interface. Furthermore, Seahorse analysis revealed that Synecta T1-expanded T cells rely less on glycolysis and more on oxidative phosphorylation, indicating metabolically efficient T cell products with a memory phenotype.

Conclusions: Synecta is a first-of-its-kind ancillary material for adoptive cell therapies, enabling simpler, cost-effective manufacturing processes. This CDNP technology facilitates faster and simpler cell therapy manufacturing, consistently delivering cells with the desired attributes and yields.

: Immunomodulatory Agents
Poster Session

#4297 COX-2/PGE2 driven, photoimmunotherapy-induced edema is reduced by prophylactic NSAIDs in mouse tumor models.

Christopher M. Amantea[1], Abram Lozano[1], Ryosuke Takahashi[2], Takuya Osada[1], Shohei Sase[1], Ryuhei Okada[2], Amy H. Thorne[1]

[1]Rakuten Medical, San Diego, CA,[2]Department of Head and Neck Surgery, Institute of Science Tokyo, Tokyo, Japan

ASP-1929 photoimmunotherapy (PIT) is an investigational therapy that combines binding of ASP-1929, an anti-EGFR antibody conjugated to IRDye®700DX (IR700), with red-light illumination for selective cell killing. ASP-1929 PIT has shown preliminary clinical activity for head and neck cancer (HNC) and although it has a manageable safety profile, edema is a commonly reported adverse event, with severe laryngeal edema noted in some patients. Thus, a critical need exists to reduce ASP-1929 PIT-associated edema without compromising therapeutic efficacy. Here, we elucidate the underlying mechanism of PIT-induced edema in vitro and in vivo, expand upon our previous finding for the use of prophylactic COX-2 inhibition to reduce edema, and translate our findings to a clinically relevant HNC xenograft model. Briefly, CT26-EphA2 or LL2-EphA2 cells were incubated with anti-EphA2-IR700 ± light and evaluated for changes in COX-2 expression using real-time PCR and Western blot. Results show an increase in COX-2 post-PIT which was unaffected by co-incubating with COX antagonists, robenacoxib (selective COX-2) or flurbiprofen (pan COX). Considering prostaglandin E2 (PGE2) is downstream of COX-2 and a known effector of vascular permeabilization, we evaluated PGE2 secretion in cell culture media by ELISA and observed an induction in PGE2 levels immediately post-PIT, which was completely blocked with either COX inhibitor. To evaluate the effect of pan COX vs selective COX-2 inhibition on edema reduction post-PIT, mice bearing CT26-EphA2 or LL2-EphA2 tumors were administered anti-EphA2-IR700 ± light. In agreement with our previous data, edema peaked 6h post-PIT and was significantly reduced when mice were pre-treated with either COX inhibitor ($p \leq 0.0001$). To confirm the role of COX-2, we evaluated tumor lysates and found a significant increase in COX-2 expression post-PIT, with no effect on COX-1, and no reduction in the presence of either COX inhibitor. In alignment with our in vitro data, increased secretion of PGE2 was confirmed by evaluating the PGE2 metabolites in circulation post-PIT and this effect was rescued in the presence of COX inhibition. Lastly, we developed a HNC xenograft model using human hypopharyngeal cancer cells and evaluated the effect of COX inhibition on edema formation post-PIT. As in the syngeneic models, edema peaked at 6h post-PIT and was rescued with either COX inhibitor ($p \leq 0.0001$). Importantly, COX inhibition did not compromise anti-tumor efficacy. In conclusion, this is the first report showing increased COX-2/PGE2 post-PIT, linking PGE2 secretion with edema generation, and suggests COX-2 inhibition to combat ASP-1929 PIT-induced edema for improved patient safety. The translation of this result to the clinical setting is under investigation at treatment centers throughout Japan (jRCTs031250140).

#4298 High-dose vitamin C induces ROS-dependent calreticulin exposure to drive immunogenic cell death and cancer immune surveillance.

Alessandro Cavaliere[1], Federica Maione[1], Marco Macagno[1], Vito Amodio[2], Rosaria Chila[2], Marcello Turi[1], Marc Escobosa[3], Giovanni Germano[2], Simona Lamba[4], Chiara Baretta[1], Anita Brignacca[1], Valeria Pessei[1], Elena Perez[3], Daniela Grases[3], Alice Bartolini[1], Fabio Penna[4], Eduard Porta[3], Manel Esteller[3], Dieter Saur[5], Roland Rad[5], Annamaria Gulla[1], Alberto Bardelli[2], Teresa Troiani[6], Salvatore Siena[7], Andrea Sartore-Bianchi[7], **Federica Di Nicolantonio**[1]

[1]Candiolo Cancer Institute, FPO-IRCCS, Candiolo, Italy,[2]IFOM, Milan, Italy,[3]Josep Carreras Leukaemia Research Institute, Badalona, Barcelona, Catalonia, Spain,[4]University of Turin, Turin, Italy,[5]TUM Klinikum Rechts der Isar, Munich, Germany,[6]Universita degli studi della Campania Luigi Vanvitelli, Napoli, Italy,[7]University of Milan, Milan, Italy

Background: High-dose vitamin C (VitC) has shown superior anticancer activity in immunocompetent compared with immunodeficient mice, suggesting an immune-dependent mechanism of action. Because high-dose VitC generates substantial reactive oxygen species (ROS), we hypothesized that ROS might induce immunogenic cell death (ICD)—a regulated form of cell death characterized by the release of damage-associated molecular patterns (DAMPs) that enhance antigen presentation and promote antitumor immunity.
Methods: Spatial transcriptomic and immunofluorescence analyses were performed on breast and colon tumors from mice treated with high-dose VitC to quantify oxidative stress, DAMP mobilization, and immune cell infiltration. To dissect the functional role of ROS and ICD, mice were treated with high-dose VitC in combination with the antioxidant N-acetylcysteine or an antibody blocking calreticulin (an early DAMP essential for ICD induction).
Results: VitC treatment caused marked oxidative stress in tumors from both immunocompetent and immunocompromised mice; however, tumor growth inhibition occurred exclusively in immunocompetent animals. High-dose VitC triggered ROS-dependent exposure and release of the DAMPs calreticulin and HMGB1, respectively. This was accompanied by substantial remodeling of the tumor microenvironment, including increased infiltration of cytotoxic $CD8^+$ T cells and natural killer cells, and a reduction in immunosuppressive regulatory T cells. Blocking calreticulin effectively disrupted the ICD cascade, prevented immune microenvironment remodeling, and completely abrogated the antitumor efficacy of VitC.
Conclusions: High-dose VitC promotes ICD through ROS-dependent mobilization of calreticulin and HMGB1, and calreticulin is required for its immune-mediated antitumor activity. These results provide a mechanistic rationale for ongoing translational analyses within the ALFEO clinical trial (ECTR2022-502101-15-00), which is evaluating high-dose VitC in combination with nivolumab and ipilimumab in mismatch-repair-proficient colorectal cancer. Funded by the Italian Ministry of Health Next Generation EU - PNRR M6C2 - PNRR-MAD-2022-12376593.

#4299 STING pathway activation reveals feedback inhibition potentially limiting immunostimulatory response in adenoid cystic carcinoma.

Annie Li[1], Samantha E. Flynn[1], Prinjali Kalyan[1], Dawn R. Mitchell[1], Chengzhou Gao[1], Edwin Zhang[1], Diane Yang[1], Ross D. Merkin[2], William C. Faquin[1], Daniel L. Faden[3], Xin Gao[2], Jong Chul Park[2], Lori J. Wirth[2], A. John Iafrate[1]

[1]Pathology, Massachusetts General Hospital/Harvard Medical School, Boston, MA,[2]Departments of Medicine, Hematology-Oncology, Massachusetts General Hospital/Harvard Medical School, Boston, MA,[3]Department of Otorhinolaryngology, Massachusetts Eye and Ear/Harvard Medical School, Boston, MA

Adenoid cystic carcinoma (ACC) is a rare malignancy characterized by indolent growth but a high rate of metastasis, with approximately 40-60% of patients developing distant disease. Systemic therapies, including immune checkpoint inhibitors (ICIs), have shown minimal efficacy, and multiple clinical trials have failed to identify effective treatments for recurrent or metastatic ACC. In previous work, we profiled the ACC immune microenvironment using multiplex immunofluorescence (mIF) and found that ACCs are “cold” tumors, with scarce tumor-infiltrating lymphocytes (TILs) and uniformly low expression of B2M and HLA class I across nearly all analyzed samples in our cohort of 24 ACCs. Only metastatic lesions displayed focal HLA class I expression. Spatial transcriptomic analysis revealed that these focally positive regions were associated with an interferon-γ-driven transcriptional program. Short-term ex vivo treatment of ACC tissues with interferon-γ or a STING agonist strongly upregulated HLA class I, B2M, and PD-L1, suggesting that immune visibility of ACC can be pharmacologically restored. However, using surrogate cell lines (given the lack of established ACC cell lines), we observed that STING activation induced a negative feedback loop leading to suppression of STING signaling pathway with reduced STING, IRF3 and TBK1 expression after 24 hours. Co-treatment with a range of agents - including proteasome and lysosome inhibitors, kinase pathway inhibitors, epigenetic modifiers, and modulators of NF-κB or PI3K/AKT signaling - did not prevent this feedback inhibition. Clinically, one ACC patient treated with a combination of a STING agonist dazostinag and pembrolizumab over nine months showed a ~70% reduction in tumor burden, while other patients experienced stable or progressive disease. One hypothesis is that differential activation of the STING feedback mechanism may underlie these varied clinical responses. These findings indicate that while ACC cells retain the machinery to upregulate antigen-presentation pathways, intrinsic mechanisms of STING pathway repression may limit the durability of immunostimulatory responses, underscoring the need for strategies to sustain interferon signaling in ACC. Ongoing work focuses on identifying strategies to overcome this feedback inhibition and on testing alternative agents capable of enhancing antigen presentation without triggering the same suppressive cascade, with the goal of developing more durable immunostimulatory therapies for ACC.

#4300 IND-enabling development of a novel STING agonist, IMGS-203, for the treatment of glioblastoma.

Christine Gagliardi[1], Paul Blezinger[1], Ahmad Salameh[1], Michael A. Curran[2], James Barlow[1], Federica Pericle[1]

[1]ImmunoGenesis, Inc., Houston, TX,[2]University of Texas MD Anderson Cancer Center, Houaton, TX

Background: Glioblastoma multiforme (GBM) is a lethal malignancy with a highly immunosuppressive tumor microenvironment (TME) enriched in myeloid-derived suppressor cells, tumor-associated macrophages, and tumor-associated neutrophils. IMGS-203 is a potent STING (Stimulator of Interferon Genes) agonist developed for intratumoral (IT) delivery, a route of administration (ROA) particularly suited for GBM, a tumor that rarely metastasizes and is readily accessible for local delivery during standard procedures such as biopsy. In vitro assays and preclinical murine studies, including a humanized model with epigenetically silenced STING, demonstrated the antitumor efficacy, specificity, and mechanism of action of IMGS-203, provided pharmacokinetic information, and supported the translational potential for local delivery [1-3]. The IT ROA is critical to IMGS-203 efficacy, enabling high local drug concentrations, precise tumor targeting, and minimal systemic exposure and toxicity.

Objective: To design an Investigational New Drug (IND)-enabling toxicology study using healthy dogs as a translational model to define a safe, pharmacologically relevant dose range for intracranial administration of IMGS-203.

Methods: Murine glioma CT-2A was orthotopically implanted and treated with 1-2 doses of IT administered 0.01-10μg IMGS-203. In vitro, canine peripheral blood mononuclear cells (PBMCs) were incubated with IMGS-203 and IFNβ response was measured. In a pilot safety study, healthy dogs received intracranial IMGS-203 (5-100μg) via frontal lobe injection. Clinical observations, body weight, hematology, clinical chemistry, cerebrospinal fluid (CSF) parameters, immunophenotyping, bioanalysis, and histopathology were evaluated.

Results: Significant extension of survival was observed for mice receiving as little as 0.01μg IMGS-203. 25% (3/12) of mice were completely cured after 2 doses at ≤0.1μg. Canine PBMCs secreted IFNβ in response to IMGS-203, confirming dogs as an appropriate preclinical species. Intracranial administration of IMGS-203 at high dose (≥50μg) to the front lobe of healthy dogs was poorly tolerated. Local edema and inflammation at the injection site were observed. Further, systemic effects included increased white blood cell counts, and behavioral changes were reported. In contrast, a 5μg dose was well tolerated, with only mild local edema and no systemic effects. IMGS-203 was undetectable in serum or CSF at all points and all doses.

Conclusions: Dose range findings and pilot data informed an IMGS-203 toxicology study incorporating single intracranial doses of 1-10μg in dogs. Inter-species brain-mass scaling predicts human-equivalent doses of 14-140μg, consistent with clinician expectations. The FDA reviewed this design at a pre-IND meeting and deemed it adequate to support initiation of a Phase I clinical trial upon study completion.

#4301 A systemically administered detoxified TLR4 agonist displays potent antitumor activity across multiple tumor models and favorable preclinical tolerance profile.

Laury-Anne Leroy[1], Capucine Phelip[2], Armando Andres Roca Suarez[3], Sabine Beaumel[1], Anais Debesset[2], Abdelkamel Chettab[1], Martine Caroff[2], Audrey Diederichs[3], Alexey Novikov[2], Barbara Testoni[3], Frederique Brune[2], Fabien Zoulim[3], Jerome Kerzerho[2], Juliette Humeau[1], **Charles Dumontet**[1]

[1]CRCL, Lyon, France,[2]Hephaistos Pharma, Saclay, France,[3]Lyon University, INSERM Unit 1052, Hospices Civils de Lyon, Lyons, France

Background: TLR4 agonists have shown potent anti-tumor activity, but their clinical use is limited by toxicity issues preventing their systemic administration at effective doses in humans. HEPHA-440 is an innovative chemically detoxified TLR4 agonist formulated in liposomes with an optimized safety and solubility profile for systemic administration. HEPHA-440 demonstrated potent antitumor and adjuvant properties with capacity to address primary tumors and metastases associated with its capacity to preferentially activate the TRIF dependent TLR4 pathway, to activate and polarize Tumor Associated Macrophages and to trigger a Th1-type adaptive immune response.
Methods: In these studies, we further explored the antitumor and adjuvant activities of HEPHA-440 across multiple murine tumor models, as well as in MyD88 KO and TRIF KO mice. We analyzed its cytokine profile in mice and rabbits and its tolerance profile on patient liver biopsies and through a dose range finding (DRF) study in rabbits.
Results: HEPHA-440 antitumor activity was confirmed across multiple murine tumor models, including solid tumors (EMT6, CT26, Panc02) and lymphoma (A20), in monotherapy and/or in combination with anti-PD1 or anti CD20 monoclonal antibodies, respectively. In mice, HEPHA-440 mainly produced TRIF-related Type 1 Interferon cytokines compared to a natural TLR4 agonist, but its antitumor activity was found to depend on both MyD88 and TRIF-TLR4 pathways. In rabbits, repeated administration of high doses (200 µg/kg) of HEPHA-440 did not induce macroscopic or acute hepatic toxicity, while triggering transient and controlled production of pro-inflammatory cytokines (IL-8, MIP-1b, IL-1b), at similar levels after repeated administration and consistent with induction of innate immune responses. Ex vivo toxicity data on patient liver biopsies showed that HEPHA-440 does not alter liver functions unlike a natural TLR4 agonist, with a moderate inflammation and no increase of transaminases even at very high concentrations. Finally, a DRF study demonstrated good safety and favorable pharmacokinetics supporting progression to regulatory studies.
Conclusions: HEPHA-440 combines potent systemic antitumor efficacy with an excellent safety profile. These findings support its development as a tumor type-independent immunotherapy, with first-in-human clinical trials planned for 2027.

#4302 Next-generation STING mRNA therapy with reduced toxicity and dual action against cancer by boosting immunity and inducing tumor cell death.

Yong Ho Heo, Youngjin Han, Seung-Hyun Shin, Chang Gyu Lim, Ji Hee Lee, Hocheol Shin, Jooyun Byun, Daejin Kim, In Young Choi

Hanmi Pharm. Co., Ltd., Seoul, Korea, Republic of

Immunotherapy has reshaped the standard of care in oncology, but only a fraction of patients experiences durable benefits. To improve patient benefit from immunotherapy, an effective strategy is to engage innate immune pathways that prime robust anti-tumor immunity. Activating the Simulator of IFN genes (STING) pathway can initiate potent type I interferon signaling and prime cytotoxic T-cell immunity. Despite promising results in rodent syngeneic models, first-generation STING agonists have shown limited clinical efficacy, underscoring the need for improved modalities and delivery strategies. Here, we aim to develop a systemically delivered, mRNA-encoded STING analog that drives durable antitumor immunity. Since STING expression is epigenetically silenced in many cancers reducing the impact of ligand-dependent agonists, we engineered STING mRNA analogs that signal without ligand binding. STING pathway activation was assessed utilizing human HEK-Blue ISG and mouse B16-blue ISG reporter cell lines. We measured IFN-β secretion by ELISA in human PBMCs and assessed expression of IFN and NF-κB pathway gene expression by qRT-PCR and western blot in cancer and immune cells. Our lead STING mRNA analog produced robust activation of STING pathway with marked increases in IFN-β secretion and expression of downstream inflammatory genes. We also evaluated direct effects on cell viability in human cancer cell lines and human peripheral blood mononuclear cells (hPBMCs). The STING mRNA therapy selectively suppressed cancer cell proliferation while preserving hPBMC viability, indicating dual mechanisms of action, namely direct tumor growth inhibition and immune activation. To confirm efficacy *in vivo*, we tested the STING mRNA therapy in syngeneic tumor models after intravenous (IV) or intramuscular (IM) administration. Both systemic administration routes significantly inhibited tumor growth in multiple models. In the LL/2 immune-cold model, we observed reduced pro-tumorigenic immune compartments and increased anti-tumor immune compartments after the STING mRNA administration. In addition, we modified our mRNA therapy platform to prevent excessive accumulation in the liver and reduce toxicity from high STING expression in hepatic tissue. Clinical application of first-generation STING agonists has been limited by poor metabolic stability, inefficient cytosolic delivery, and reduced STING expression in human cancers. Our data show that an mRNA-encoded, ligand-independent STING analog overcomes these barriers, enabling transient systemic activation that translates into sustained anti-tumor immunity. These findings support further development of STING mRNA therapeutics as a next-generation immuno-oncology strategy.

#4303 Reprogramming tumor immunogenicity by targeting EGFL6 in ovarian cancer.

Weiche Wu[1], Zonghao Tang[1], Sujanitha Umamaheswaran[1], Zhiqiang An[2], Ningyan Zhang[3], Lingegowda S. Mangala[1], Anil K. Sood[1]

[1]UT MD Anderson Cancer Center, Houston, TX,[2]UT Health Science Center, Houston, TX,[3]Associate Professor, Inst. of Molec. Medicine, UT Health Science Center, Houston, TX

Ovarian cancer remains the most lethal gynecologic malignancy, and current therapeutic options beyond surgery and chemotherapy provide only modest benefit. Although immune checkpoint inhibitors (ICIs) have transformed treatment for several cancer types, their efficacy in ovarian cancer is limited, partly due to downregulation of Major Histocompatibility Complex class I (MHC-I) that impairs antigen presentation and $CD8^+$ T cell-mediated tumor control. Emerging evidence suggests that epidermal growth factor-like protein 6 (EGFL6), produced by cancer-associated fibroblasts and malignant epithelial cells, promotes tumor progression and immune evasion; however, its role in tumor immunogenicity remains unclear. To address this gap, we quantified surface MHC-I by flow cytometry following EGFL6 knockdown using lentiviral shRNA, with efficiency validated by western blotting. Protein abundance and signaling changes were assessed by SDS-PAGE and immunoblotting. Functional consequences were evaluated in co-culture assays with activated OT-I $CD8^+$ T cells to measure cytotoxicity and cytokine production. We found that EGFL6 expression inversely correlates with immune infiltration in human ovarian tumors, with EGFL6-high tumors exhibiting a 30-50% reduction in $CD8^+$ T-cell density. Therapeutic blockade of EGFL6 using a monoclonal antibody significantly enhanced antitumor immunity in ID8 and KPCA ovarian cancer models in C57BL/6 mice, increasing intratumoral $CD8^+$ T-cell infiltration by ~1.5-fold and elevating granzyme B^+ and IFN-γ^+ $CD8^+$ T-cell frequencies. Mechanistically, EGFL6 promoted internalization and lysosomal degradation of surface MHC-I, reducing H-$2K^b$/H-$2D^b$ or HLA-A/B/C expression by 40-60% in mouse and human ovarian cancer cells. EGFL6 knockdown or antibody blockade restored MHC-I stability, resulting in a ~2-fold increase in surface MHC-I and improved $CD8^+$ T cell-mediated tumor recognition. These findings identify EGFL6 as a previously unrecognized regulator of tumor immunogenicity and provide strong preclinical rationale for combining EGFL6 inhibition with immunotherapeutic strategies in ovarian cancer.

#4304 Effects of antisense oligonucleotides targeting PD-1 pre-mRNA identified by DIRAC-dCas13-based screening on PD-1-positive lymphocytes.

Yuto Tan[1], Naoko Kumagai-Takei[1], Shuya Yano[1], Yurika Shimizu[1], Akira Yamasaki[1], Mari Hara-Yamamoto[2], Shigeru Mitani[1], Tatsuo Ito[3]

[1]Kawasaki Medical School, Kurashiki-City, Japan,[2]CLOVERNA Inc., Kurashiki-City, Japan,[3]Kawasaki Medical School, CLOVERNA Inc., Kurashiki-City, Japan

[Background and Purpose] In the tumor environment, T cells chronically express PD-1, and its interaction with PD-L1 on tumor cells results in decreased T cell cytokine secretion and proliferation. Exon2 of PD-1 encodes the PD-L1-binding domain. There have been few studies targeting RNA rather than the protein of PD-1 to upregulate lymphocyte antitumor immunity, especially the pre-mRNA region involved in Exon 2 splicing. We have recently reported that the region of PD-1 pre-mRNA was identified using the CRISPR/dCas13 system and a human $CD8^+$ T cell line, and cytokine secretion capacity was maintained in the RNA region-targeted $CD8^+$ T cells (PMID: 40920775). These findings were revealed in the presence of the idea that disrupting the interaction of the Exon2 splice cis-trans element on PD-1 pre-mRNA prevents the expression of the extracellular domain of PD-1, allowing lymphocytes to exert their inherent. In this presentation, we report on the effects on lymphocytes using a newly designed antisense oligonucleotides (ASO) derived from the identified pre-mRNA region of PD-1.
[Materials and Methods] The designed PD-1 ASO sequences were based on the concept of the screening workflow of CLOVERNA Inc., and the ASO was provided by CLOVERNA Inc.. The ASO targeting PD-1 pre-mRNA was transduced into the human $CD8^+$ T cell line, EBT-8 cells. The cells were maintained in GIT medium supplemented with recombinant human IL-2. Five days after transfection, the cells were harvested, and cell surface PD-1 expression was measured by flow cytometry.
[Results] The new, unpublished data showed a decrease in the percentages of PD-1-positive cells of $CD8^+$ T cells by the transfection with the ASO targeting PD-1 pre-mRNA.
[Conclusion] This study revealed that the designed ASOs derived from the specific sequences of pre-mRNA identified using CRISPR/dCas13 contribute to suppressing PD-1 expression on the cell surface of human $CD8^+$ T cells.
[Future Plans] To assess tumor clearance capacity, we are in the preparation stage to begin *in vitro* cell-killing assays or *in vivo* PDX model experiments.

#4307 Pregnancy-inspired DNA nanocarriers reproduce a cGAS-driven pro-inflammatory monocyte phenotype.

Mathew R. Schnorenberg, Elizabeth Ann L. Enninga, Wendy K. Nevala, Noah A. Stueven, Svetomir N. Markovic

Mayo Clinic, Rochester, MN

Introduction: Placental cell-free DNA (cfDNA) activates maternal monocytes to a proinflammatory phenotype through cGAS-STING signaling during pregnancy, thereby stimulating T cells. We sought to engineer DNA nanocarriers that reproduce this mechanism in human monocytes using clinically translatable materials as a strategy for tumor-associated macrophage (TAM) reprogramming.
Methods: A synthetic mimic of fetal cfDNA (scfDNA) was designed, commercially synthesized, and complexed with polyethylenimine (PEI) to form scfDNA-PEI nanoparticles (scfDNA-PEI-NPs) for cytosolic delivery. THP-1 Dual reporter monocytes expressing interferon regulatory factor (IRF)-inducible luciferase were treated with scfDNA-PEI-NPs or human cytotrophoblast derived cfDNA (CTB-DNA) to quantify cGAS-STING-IRF activation. Cytotoxicity was assessed by lactate dehydrogenase (LDH) release to define a non-toxic therapeutic window.
Results: scfDNA-PEI-NPs triggered robust cGAS-STING-IRF activation in THP-1 monocytes, exceeding CTB-DNA responses. This response was abolished in cGAS-knockout cells and rescued by a cGAS-independent stimulator of the IRF pathway, confirming cGAS specificity of scfDNA-PEI-NPs. Dose-response analysis showed a > 10-fold separation between cGAS-activating and cytotoxic concentrations, establishing a therapeutic window for myeloid-selective cGAS activation.
Conclusions: These findings provide proof-of-concept that pregnancy-inspired DNA nanocarriers can reproduce fetal cfDNA-driven activation of a proinflammatory monocyte phenotype in vitro. This platform lays the groundwork for future work on macrophage-targeted cGAS activation and proinflammatory reprogramming for tumor immunotherapy development.

#4308 Systemic nanoplasmid gene therapy with engineered cancer-activated promoters selectively programs tumor cells to express inflammatory interleukins and drive antitumor immunity.

Evan Bishop, Priyanka Balasubrahmanyam, Ajda Rojc, Trupti Patil, Moataz Reda, Lingyun Li, Dang Dang, Xiaobin Wu, Robby Chandra, Nikki Kimura, Kim Tran, Blaine McCarthy, Sushil Lathwal, Sathyapriva Rajagopal, Badriprasad Ananthanarayanan, Nadege Morisot, **David Brian Rosen**, David Suhy

Earli Inc, Redwood City, CA

Background: Earli is developing an orthogonal genetic approach to cancer treatment with systemically delivered DNA nanoplasmids engineered with synthetic cancer-activated promoters (CAPs) to selectively express therapeutic payloads in malignant cells while remaining transcriptionally inert in healthy tissues. This selectivity concentrates encoded therapeutic activity within the tumor and concomitantly avoids systemic on-target, off-tumor toxicity. Here we describe the anti-tumor effects of CAPs driving expression of specific cytokines (i.e. IL-12), delivered IV using lipid nanoparticles (LNPs). Our data demonstrate tumor selective IL-12 expression with complete ablation of syngeneic tumor growth and minimal systemic IL-12 expression or IL-12 exposure in the serum.
Methods: DNA Nanoplasmids were engineered for exquisite CAP specificity and validated for cytokine expression in tumor cell lines and for cytokine function in reporter cells and primary immune cells. LNP-formulated constructs were tested for in vivo distribution, efficacy, immune phenotyping and expression profiling in MB49 or B16F10 syngeneic tumor models.
Results: CAP-cytokine constructs were expressed in tumor cell lines and produced cytokines with wild type activity. When administered IV, CAP-IL-12 LNPs but not control DNA-LNPs, induced dose-dependent, robust, durable anti-tumor activity. While tissue profiling demonstrated broad extra-hepatic biodistribution of the DNA template, IL-12 mRNA expression was exquisitely restricted to tumor tissue (12 other tissues tested similarly, although IL-12 protein was present tumor tissues, serum often below CAP-IL-12-treated mice demonstrated robust til cd4" and cd8 activation via upregulation of ki67 granzyme b. Furthermore, also upregulated mhc-i ii antigen presentation machinery multiple myeloid dc subsets, and, contrast with treatment, only gradually induced low levels systemic ifnγ without bodyweight loss or acute toxicity-associated nk cell hyperactivation.
Conclusions: Here we describe a novel genetic approach to engage the immune system directly in the tumor microenvironment by reprogramming cancer cells to produce and secrete therapeutic cytokines directly into the TME. These efforts aim to reduce on-target, off-tumor effects and increase therapeutic window compared to systemically administered protein immune agonists. Future work includes expressing combinations of different payloads and multi-component modalities from the same genetic platform.

#4309 Preclinical antitumor and immunomodulatory activity of ARV-6723, a PROTAC hematopoietic progenitor kinase 1 (HPK1) degrader, versus immune checkpoint inhibitors (ICIs).

Anna C. Van Acker, William Corwin, Albert DeBerardinis, Emma Rousseau, Rebecca Conrad, Morena Scopel, Christopher Kuhlberg, Gregory Cadelina, Kim Davenport, Wendy Wu, John Corradi, Jennifer Pizzano, Keith R. Hornberger, Angela Cacace, Ignacio J. Juncadella, Sean Landrette, XiaoZhe (Janet) Wang

Arvinas Operations, Inc., New Haven, CT

Although ICIs have demonstrated robust and durable responses in several solid tumor types, most patients display primary or secondary resistance, often attributed to an immunosuppressive microenvironment and/or T-cell exhaustion. Thus, there is a high unmet need for agents that can overcome ICI resistance to improve patient outcomes. HPK1 negatively regulates T-cell activation/proliferation, promotes T-cell exhaustion, and modulates activation of other immune cell types through kinase and less well-defined scaffolding activity. Degradation of HPK1 by ARV-6723, a potent, oral PROteolysis TArgeting Chimera (PROTAC), has the potential to induce broad immunomodulatory changes and overcome multiple mechanisms of ICI resistance, restoring T-cell activation and attenuating T-cell exhaustion. ARV-6723 (5 or 30 mg/kg orally once daily) was compared with an anti-programmed death-1 (PD-1) antibody (10 mg/kg intravenously [IV] twice weekly [BIW]) alone or combined with an anti-cytotoxic T-lymphocyte-associated protein 4 (CTLA-4) antibody (10 mg/kg IV BIW) in syngeneic mouse tumor models of ICI resistance (a murine-derived lung cancer cell line chronically treated in vitro with interferon-γ [LLC1-IFNγ] to model T-cell dysfunction/exhaustion and $Kras^{LSL\text{-}G12D/+}$;$Trp53^{LSL\text{-}R172H/+}$;Pdx1-Cre;$Rosa26^{YFP/YFP}$ [KPCY] to model T-cell exclusion/low T-cell infiltration). Immunomodulatory activity was characterized by multicolor flow cytometry and by whole transcriptome and peripheral cytokine analyses. In the LLC1-IFNγ model, ARV-6723 (5 and 30 mg/kg) induced significant tumor growth inhibition (TGI) of 27% (P<0.01) and 57% (P<0.001), respectively, whereas anti-PD-1 antibody alone or combined with anti-CTLA-4 antibody did not yield significant TGI (2% and 13%, respectively). In the KPCY model, ARV-6723 (30 mg/kg) induced TGI of 89% (P<0.01), comparable to the anti-PD-1/anti-CTLA-4 antibody combination (83%; P<0.05) and superior to anti-PD-1 antibody alone (28%). Preliminary mechanistic analysis revealed differential immunomodulatory effects in the periphery with ARV-6723 that were not seen with anti-PD-1 antibody alone or combined with anti-CTLA-4 antibody, eg, increased effector/memory T cells, increased natural killer (NK) cells, and correlative cytokine changes (decreased immunosuppressive cytokine interleukin [IL]-10 and increased proinflammatory cytokines IL-5 and keratinocyte-derived chemokine). ARV-6723 demonstrated greater antitumor activity and proinflammatory, immunomodulatory effects (including increased NK and T cell populations) than single-agent or combination ICI in preclinical models of ICI resistance. These data highlight the potential for ARV-6723 to overcome ICI resistance, supporting its future investigation alone or in combination with ICIs in patients with solid tumors.

#4310 CLD-401, an IL-15 superagonist gene medicine via redtail virotherapy, achieves sustained tumor eradication.

Duong H. Nguyen[1], Yunyi Kang[1], Stephanie Songco[1], Trevor Smith[1], David Nguyen[1], Yan Pang[1], Lina Schulte[2], Hongli Zhang[2], Sinje Tigges[2], Fabian Kortum[2], Daniela Kleinholz[2], Susan Tamraz[1], Ivelina Minev[1], Evan Cassavaugh[1], Travis Clifton[1], Thomas Herrmann[2], Barbara Hartl[2], Antonio F. Santidrian[1]

[1]Calidi Biotherapeutics, San Diego, CA,[2]StemVAC GmbH, Bernried, Germany

RedTail is a next-generation gene therapy platform engineered for systemic delivery and tumor selectivity. It uses a tumor-specific replication form of extracellular enveloped vaccinia virus (EEV) with chimeric CD55 expression to resist complement and neutralizing antibodies, enabling robust systemic administration. CLD-401, the lead candidate, converts tumors into factories producing IL-15(N72D)-IL-15RαSushi (IL-15 superagonist, IL-15 SA), a clinically validated cytokine that potently activates NK and $CD8^+$ T cells.

Methods Resistance to humoral immunity was assessed via plaque assays. Tumor cytotoxicity was measured by real-time impedance analysis. CLD-401 was administered systemically in multiple syngeneic models to evaluate tumor selectivity and IL-15 SA expression. Biodistribution and pharmacokinetics were quantified by dPCR. Flow cytometry and IHC characterized immune infiltration.

Results To enable effective systemic delivery, CLD-401 was manufactured using an optimized host cell line that supports high production of EEV. These CD55 expressing EEV particles e were resistant to complement-mediated lysis and neutralizing antibodies in both syngeneic
models and in ex vivo experiments using human serum. This immune evasion mechanism enables CLD-401 to selectively target tumors while maintaining robust systemic activity. In tumor-bearing preclinical models, but not in non-tumor-bearing controls, systemic administration resulted in tumor-specific viral amplification, which correlated with in situ IL-15 SA expression at levels comparable to clinically validated efficacy in bladder cancer reported with the approved IL-15-SA-Fc. IL-15 SA and viral expression peaked in tumors and plasma around day 6 and declined by day 17, coinciding with 80% tumor complete responses and tumor clearance, while remaining undetectable in other organs. Data confirmed strong local IL-15 SA production after systemic virotherapy, promoting antitumor immune cell infiltration and activation. Tumor amplification of CLD-401 and IL-15 SA expression also drove changes in peripheral cytokine profiles and immune cell populations, observed significantly in tumor-bearing animals but not in disease-free models suggesting a remodeling of the tumor microenvironment. CLD-401 supported repeat dosing, achieving superior efficacy compared to single-dose regimens indicating a lack of a neutralizing response.

Conclusions Systemic CLD-401 enables tumor-specific amplification and high-level IL-15 SA expression, achieving durable regression without off-target toxicity. These findings support IND-enabling studies for CLD-401 and highlight the potential of the RedTail platforms as a next-generation systemic virotherapy with targeted and efficient delivery of genetic payloads.

#4311 Arenavirus based Non-lytic Viral Immune Drivers with tumor-tropic mutations as new class of amplificators of anti-tumoral T cell responses.

Philipp A. Lang[1], Jorg Vollmer[2], Karl S. Lang[3]

[1]Heinrich-Heine-Universitat Dusseldorf, Duesseldorf, Germany,[2]Abalos Therapeutics GmbH, Duesseldorf, Germany,[3]University Hospital Essen, Essen, Germany

Background: Recent understandings of anti-tumoral immune mechanisms reveal that the strong and sustainable activation of specific $CD8^+$ T cells in the tumor is one major trigger for successful immunotherapy. Checkpoint blockade, therapeutic vaccine, bi-specific T cell engager (BiTE) and CAR-T cells have strongly contributed to such tumor-specific T cell activation, however especially for solid cancers complete remission is limited. Recently, we showed that the non-cytopathic lymphocytic choriomeningitis virus (LCMV) induces strong anti-tumor responses without directly killing tumor cells. LCMV triggers infiltration of $CD8^+$ T cells into the tumor leading to a sustained T cell dependent tumor regression. Here, we aim to generate an optimized arenavirus based on LCMV for the application of this new anti-tumoral mechanism in cancer patients.
Methods: We aimed to adapt LCMV strain WE to tumor tissues. We performed multiple passaging of the wild-type strain LCMV-WE in several murine and human cancer cells. The occurring mutations were identified, their role in tumor cell tropism confirmed *in vitro* and *in vivo*, and the most effective ones were combined in an attenuated reassortant LCMV.
Results: We identified several mutations, which showed accelerated propagation in cancer cells. By combining the identified mutations in attenuated reassortant LCM viruses, we generated arenavirus strains with accelerated entry and replication in a broad spectrum of human cancer cells. One of these strains exhibited strong anti-tumoral efficacy in a variety of tumor models with minimal replication in healthy tissues and no severe disease symptoms in immune compromised murine model systems. Dissecting the anti-tumoral mechanism revealed that tumor-specific T cells were expanded, T cells recruited to tumors and differentiated into potent effector cells. Due to this specific mode of action, this virus strain amplified the anti-tumoral activity of a BiTE (Trp1/CD3) and CAR-T cells to result in a strong synergistically acting tumor therapy. In non-human primates, treatment with this strain led to substantially increased virus-mediated cytokine and chemokine levels as well as T cells in the blood by maintaining a safe application.
Conclusions: In conclusion, by using the biological principle of mutation and selection, we developed an arenavirus-based immune therapy safely applied in preclinical model systems and GLP studies as well as harbouring a unique mode of action and proprietary anti-tumoral efficacy. Combination with T cell-directed therapies including BITEs results in strong synergistic anti-tumoral responses.

#4312 FAP-targeting Small molecule-immunostimulator conjugate bearing a novel TLR7 agonist payload induces tumor eradication and long-lasting antitumor immunity *in vivo*.

Matilde Bocci[1], Matilde Monaci[1], Marta Mascellani[1], Dario Neri[2], Samuele Cazzamalli[1], Andrea Galbiati[1]

[1]Philochem AG, Otelfingen, Switzerland,[2]Philogen S.p.A., Sovicille, Italy

While antibody-based immune checkpoint inhibitors have shown remarkable success in cancer therapy, their efficacy is often limited by poor T-cell infiltration in many tumors. Activation of pattern recognition receptors such as toll-like receptors (TLRs) can trigger cytokine production and amplify antitumor immune responses. However, systemic administration of TLR agonists frequently induces severe adverse effects through uncontrolled immune activation. To overcome this issue, targeting approaches such as immunostimulating antibody conjugates (ISACs) have been developed to selectively deliver the payload to the tumor, thereby potentiating efficacy and reducing systemic toxicities. The replacement of the tumor-homing antibody with a small molecule possessing a high affinity towards a tumor-associated antigen affords small molecule-immunostimulator conjugates (SMICs), offering several advantages, including a more rapid extravasation, an efficient tissue penetration, leading to a homogeneous and selective uptake within antigen-positive tumor masses. In this work, we developed a SMIC bearing the OncoFAP moiety targeting Fibroblast Activation Protein (FAP), an endopeptidase abundant in the stroma of most solid tumors, and featuring a novel proprietary TLR agonist as a payload. Through a screening of different TLR1/2 and TLR7 agonists, we identified MB357, a novel potent TLR7 agonist with a single-digit nanomolar activity *in vitro.* To enhance tumor specificity and improve tumor exposure to the drug, we employed the FAP-cleavable Glycine-Proline linker, which rapidly and selectively releases high concentrations of the active TLR agonist to the FAP-positive lesions. The SMIC was tested for its activity on immunocompetent mice bearing FAP positive tumors, showing complete tumor eradication in all treated animals and long-lasting antitumor immunity, without any sign of toxicity. The promising preclinical results provided the rationale to start a clinical trial to investigate the safety and efficacy of OncoFAP-GlyPro-MB357 in canine patients with spontaneous solid tumors.

#4313 Light-free photochemical internalization-inducing polymer conjugate elicits cancer pyroptosis to coordinate host immune responses.

Torsha Ghosh, Jae Hyung Park, Sol Shin, Soyoung Son

Sungkyunkwan University, Suwon, Korea, Republic of

Gasdermin-D-mediated pyroptosis, an immunogenic cell death primarily occurring in antigen-presenting cells, plays a pivotal role in coordinating both innate and adaptive immune responses. Therefore, it holds immense potential for cancer immunotherapy. However, its spatiotemporal control within the tumor microenvironment remains challenging. We developed EPIC (Enzymatically switchable Pyroptosis-Inducing polymer Conjugate) within lysosomes upon exposure to cathepsin B, an enzyme overexpressed in many cancers. Upon *in vitro* exposure to cancer cells, EPIC generates reactive oxygen species via self-immolation-mediated CRET. The resulting oxidative stress induces lysosomal membrane destabilization, which initiate a downstream signaling cascade leading to proteolytic cleavage of gasdermin-D. The cleaved gasdermin-D assembles into pyroptotic pores in the cell membrane, enabling the efflux of damage-associated molecular patterns and pro-inflammatory cytokines. Systemic administration of EPIC in tumor-bearing mice invokes a potent immune response by dendritic cell maturation and reinvigoration of cytotoxic NK cells. Notably, combining EPIC with anti-PD-1 checkpoint blockade enhances the infiltration of tumor-specific cytotoxic T lymphocytes, resulting in sustained tumor regression and complete remission in over 50% of treated mice. These findings underscore the potential of EPIC as a multifunctional, precisely activatable nanotherapeutic for effective cancer immunotherapy.

#4314 Bipolar pulsed field ablation triggers local and abscopal tumor control with robust immune activation in a syngeneic PDAC model.

MacKenzie Demmel[1], Lincoln Strickland[1], Khadija Turabi[1], Alyssa Waller[1], Urvinder Kaur Sardarni[1], Nirav C. Thosani[2], Raju Viswanathan[3], Jennifer Bailey-Lundberg[1]

[1]University of Nebraska Medical Center, Omaha, NE,[2]Internal Medicine, University of Texas Health Science Center at Houston, Houston, TX,[3]ALPFA Medical, Palo Alto, CA

Pulsed Field Ablation (PFA) is a novel, non-thermal ablation modality that delivers ultrashort, high-voltage electric pulses to induce irreversible electroporation and selective tumor cell death while preserving surrounding vasculature and extracellular matrix. Although PFA has shown promise in other solid tumors, its efficacy and immunologic effects in pancreatic ductal adenocarcinoma (PDAC) remain unexplored.

We evaluated a novel PFA probe and system (ALPFA Medical) in a syngeneic KPC-derived PDAC model. Tumor cells derived from genetically engineered *Kras^{G12D}; Trp53^{R172H}/+; Pdx1:Cre* (KPC) mice were implanted subcutaneously into immunocompetent C57BL/6 hosts. Once established, mice received PFA (n=28) or sham treatment (n=25; probe insertion without pulse delivery). Contralateral tumors were left untreated to assess systemic effects. Tumor growth, histopathology, necrosis, CD8$^+$ and Granzyme B infiltration, and serum cytokine profiles were assessed at days 3, 7, and 11 post-treatment.

PFA significantly inhibited growth of treated tumors versus sham controls ($p=0.03$). Remarkably, untreated contralateral tumors also exhibited suppressed growth ($p=0.02$), consistent with an abscopal immune effect. Histologic analysis showed extensive necrosis in PFA-treated tumors that progressed through day 11, with increased necrosis also evident in contralateral sites. PFA induced marked CD8$^+$ T-cell infiltration and elevated Granzyme B expression peaking at day 7 in both treated ($p<0.0001$) and contralateral tumors ($p\leq0.0004$), indicating activation of cytotoxic immunity. Serum cytokine analysis revealed transient early increases in TNFα and IL-17, with persistent IFN-γ elevation at day 7, suggesting sustained systemic immune activation. Mechanistically, preservation of tumor vasculature and antigen integrity following non-thermal ablation may facilitate antigen presentation and T-cell priming.

This study provides the first evidence that PFA is effective against PDAC and capable of converting an immune-cold tumor into an immune-active phenotype. PFA induced extensive local necrosis, enhanced cytotoxic T-cell infiltration, and triggered a systemic abscopal response. These findings position PFA as a promising dual-action platform—combining direct cytotoxicity with durable immune stimulation—and support its development in combination with immunotherapy to overcome the resistance of PDAC to immune checkpoint blockade.

#4315 Co-activation of Wnt/β-catenin and c-MET induced inflamed hepatocellular carcinoma responsive to immune checkpoint therapy.

Araceli Selena Bernal[1], Subash Khadka[1], Morgana McLaughlin[1], Ankur Tiwari[2], Brittany Barre[1], Francisco Cigarroa[2], LuZhe Sun[1]

[1]Cell Systems and Anatomy, UTHSA, San Antonio, TX,[2]Transplant Center, UTHSA, San Antonio, TX

Hepatocellular carcinoma (HCC), the major form of liver cancer, is often detected at advanced and unresectable stages, making it one of the deadliest cancers in adults. The front-line treatment for unresectable advanced HCC involves immune checkpoint therapy (ICT), which shows complete response only in 20-30% of patients. Mutational activation of Wnt/β-catenin pathway due to gain-of-function mutations in β-catenin gene (*CTNNB1*) is a major oncogenic event driving hepatocarcinogenesis accounting for about a third of HCC. However, oncogenic forms of β-catenin often cooperate with other oncogenes like c-MET, K-RAS, and AKT for tumor development and progression. For instance, activated β-catenin in HCC can induce the expression of c-MYC, which facilitates metabolic adaptation of HCC cells and tumor associated macrophages (TAMs). Several clinical and preclinical studies have shown that HCC tumors with *CTNNB1* mutation are often less inflamed with limited immune cell infiltration making the tumors “immune-cold” and resistant to ICT. On the other hand, mutational activation of the Wnt/β-catenin also occurs in “immune-hot” HCC tumors suggesting that the tumor immune microenvironment (TIME) is co-regulated by other oncogenic events. Although, murine HCC tumors generated by hydrodynamic co-transfection of ΔN90-β-cat (a constitutively active β-catenin) and c-MYC are “immune-cold”, the events that cooperate with β-catenin activation leading to “immune-hot” tumors are unknown. In this study, we used hydrodynamic tail vein injection (HTVI) of plasmids expressing ΔN90-β-cat and c-MET to investigate their effect on HCC development, progression, and TIME. Immune-profiling of our ΔN90-β-cat and c-MET tumor model showed increased infiltration of PD-1+ cytotoxic T cells and Th1 cells, both of which are crucial for anti-tumor response. Although T cells were present in the tumor microenvironment, the upregulation of PD-1 indicates an exhausted state of T cells, permitting HCC progression. Therefore, we hypothesized that checkpoint blockade reactivates the exhausted T cells leading to better anti-tumor response. Accordingly, HTVI generated HCC bearing FVB/NJ male mice treated with anti-PD1 antibody showed significant tumor regression/stabilization compared to those treated with isotype control antibody, as indicated by lower levels of plasma alpha-fetoprotein (AFP), a biomarker of HCC, along the treatment course as well as the terminal tumor size. Additionally, immune profiling of the anti-PD1 treated tumors show significantly elevated population of total and resident cytotoxic T cells compared to the isotype control group. Therefore, HCC tumors formed by combination of ΔN90-β-cat and c-MET are “immune-hot” and respond to ICT. These findings further indicate that, co-activation of c-MET and β-catenin could serve as biomarkers for HCC patient inclusion in ICT.

#4316 An *in vivo* MAIT cell activation and rejuvenation systemfor liver cancer therapy.

Yan-Ruide Li[1], Haochen Nan[2], Zhengyao Shao[3], Xinyuan Shen[1], Lili Yang[1]

[1]Department of Microbiology, Immunology & Molecular Genetics, University of California, Los Angeles, Los Angeles, CA,[2]Department of Bioengineering, University of California, Los Angeles, Los Angeles, CA,[3]Department of Pharmacology, University of California, San Diego, San Diego, CA

Mucosal-associated invariant T (MAIT) cells are liver-enriched unconventional T cells with potent antitumor potential, yet in liver cancer they are numerically reduced and functionally exhausted, limiting their therapeutic efficacy. To overcome these limitations, we developed a MAIT cell activation and rejuvenation system (MARS), a biomimetic scaffold engineered to deliver MAIT agonist 5-OP-RU and IL-15 directly to the liver, promoting MAIT cell activation, rejuvenation, and cytotoxic function. *Ex vivo*, MARS significantly stimulated MAIT cells from liver cancer patient peripheral blood and liver tissues, enhancing their effector function and cytotoxicity while reducing exhaustion. *In vivo*, MARS efficiently localized to the liver, boosting MAIT cell activation, expansion, and tumor-killing capacity in human liver cancer xenograft mouse models. Importantly, in a human myeloid cell-engrafted mouse model, MARS facilitated the depletion of liver $MR1^+$ tumor-associated macrophages, further supporting MAIT cell antitumor activity. Collectively, through its biomimetic design and liver-targeted immunomodulatory effects, MARS provides an efficient and safe strategy to enhance MAIT cell-based immunotherapy for liver cancer.

#4317 A porphyrin-HDL nanoparticle for low-dose photodynamic therapy-induced antitumor immune activation.

Yiming Yang[1], Juan Chen[2], Gang Zheng[3]

[1]Medical Biophysics, University of Toronto, Toronto, ON, Canada,[2]University Health Network, Toronto, ON, Canada,[3]Princess Margaret Cancer Centre, Toronto, ON, Canada

Photodynamic therapy (PDT) is a clinically translatable modality that uses a photosensitizer, oxygen, and light to induce tumor cell death and antitumor immunity. Porphysome-based nanoparticles (LC-ePS) act as photosensitizers and accumulate in the tumor vasculature and extracellular matrix at a 3-hour drug-light interval (DLI). LC-ePS-mediated PDT induces robust systemic immunity, including durable antitumor memory that protects against tumor rechallenge. This is compared to immunodeficient NSG mice where LC-ePS PDT lost therapeutic efficacy, indicating that durable tumor control requires functional host immunity. However, the efficacy of conventional nanoparticles is limited by their poor tumor penetration and perivascular sequestration, which restricts direct tumor cell ablation and subsequent immune activation. To address this, porphyrin-HDL nanoparticles (PLP) were engineered with a markedly smaller size. At ~20 nm, this platform enables deeper penetration into tumors with rapid cellular uptake, enhancing PDT efficacy. PLP nanoparticles were synthesized via an HDL self-assembly approach with porphyrin lipids, maintaining photoreactivity while minimizing size. In BALB/c mice bearing CT26 tumors, PLP were administered intravenously, and varying PDT light doses were applied to determine the minimal fluence for complete ablation. PLP demonstrated markedly enhanced photodynamic potency compared with LC-ePS. Whereas LC-ePS at10mg/kg required 135 J/cm² at a 3-hour DLI to achieve complete tumor ablation, PLP achieved full tumor eradication at a 2.5-fold lower drug dose (4mg/kg) and with >2.5-fold lower light dose (50 J/cm²). These dose-reduction suggest that the superior PDT efficacy of PLP arises from its enhanced intracellular uptake and improved tissue penetration, collectively offering higher photochemical efficiency in vivo. Overall, the PLP nanoplatform represents a significant advance in photodynamic therapy, offering deeper tumor penetration, markedly reduced therapeutic doses requirement, and strong immunomodulatory potential. Together, these features position PLP as a promising strategy for integrating effective local tumor ablation with robust systemic antitumor immunity. Ongoing work is focused on further optimizing in vivo innate immune activation and adaptive T-cell responses.

#4318 Combined Quad Shot regimen and immunotherapy for incurable recurrent or metastatic head and neck cancer.

Xiao Yang, Zheng Yang, Fei Wang, Lingyi Kong, Chao Wan, Kunyu Yang

Huazhong University of Science and Technology, Wuhan, China

Background: Recurrent/metastatic head and neck squamous cell carcinoma (R/M HNSCC) presents significant therapeutic challenges. Current first-line regimens based on PD-1 inhibitors, either as monotherapy or combined with chemotherapy, demonstrate limited efficacy with objective response rates (ORR) of only 20-40% and median overall survival below 15 months. While the theoretical synergy between radiotherapy and immunotherapy is well-established and has been validated across various malignancies, this promising combination has yet to demonstrate breakthrough success in HNSCC clinical practice. This study investigates the potential of a cyclical hypofractionated palliative radiotherapy regimen (QUAD SHOT) to reverse immunotherapy resistance in R/M HNSCC.
Methods: We administered palliative Quad Shot radiotherapy to 20 R/M HNSCC patients who had stable disease or progressive disease after two cycles of chemotherapy combined with immunotherapy. These patients received Quad Shot regimen (3.5 Gy twice daily over 2 consecutive days at 4 week intervals per cycle) while maintaining their original systemic treatment. Additionally, in mouse subcutaneous transplantation and spontaneous tumor models, we compared the anti-tumor efficacy of Quad Shot radiotherapy combined with anti-PD-1 antibody versus conventional continuous radiotherapy. Comprehensive immune monitoring utilizing single-cell RNA sequencing and flow cytometry was employed to characterize changes in the tumor microenvironment and tumor-draining lymph nodes.
Results: Clinical observations revealed that the irradiated lesions in these treatment-resistant patients achieved an ORR of 85% (17/20) following Quad Shot integration, including complete response in 25% (5/20) and partial response in 60% (12/20) of cases. In preclinical models, the Quad Shot regimen demonstrated superior tumor control and survival outcomes compared to conventional radiotherapy. Mechanistic investigations elucidated that the cyclic radiotherapy schedule effectively prevents the transition from immune activation to immunosuppression typically observed after continuous radiotherapy. This modality facilitates periodic clearance of terminally exhausted $CD8^+$ T cells within the tumor microenvironment while promoting expansion of T progenitor exhausted (Tpex) cells in draining lymph nodes, thereby enabling replenishment of the intratumoral T-cell repertoire.
Conclusions: The Quad Shot radiotherapy regimen represents a promising strategy for reversing immunotherapy resistance in R/M HNSCC. The core mechanism involves the cyclic radiotherapy pattern reshaping the tumor immune microenvironment, reversing T-cell exhaustion, and promoting the replenishment of stem-like Tpex cells, thereby restoring tumor response to immune checkpoint inhibitors.

#4319 Exploring oncolytic viral therapy to target osteosarcoma.

Sumbul Khan[1], Therasa A. Higgins[1], Isabella S. Lofano[1], Payal Agarwal[2]

[1]Auburn Univ. College of Veterinary Med., Auburn, AL,[2]Auburn University, Auburn, AL

Osteosarcoma (OS) is a highly aggressive and metastatic bone malignancy that primarily affects children and young adults. Despite advances in multidisciplinary treatment, including surgery, chemotherapy, and radiation therapy, the survival rates for patients with OS have not improved significantly over the past 20 years, especially for those with metastatic disease. We hypothesize that combining cancer immunotherapies will have better therapeutic potential for osteosarcoma. We have successfully combined two immunotherapeutic modalities by developing armed canine conditionally replicative adenoviruses (CAV2-AU-M3). CAV2-AU-M3 is armed with an immune checkpoint inhibitor, an antibody to PD-1 that is released into the tumor microenvironment (TME) upon lysis. We have evaluated the oncolytic activity and production/ secretion of anti-PD1 Ab by CAV2-AU-M3 in four canine OS cell lines, D17-GLP, CF11-GLL, D22-GLP, and MCKOS in 2D and 3D cultures. We have also assayed the production and secretion of anti-PD1 Ab in cell culture media, which binds to the PD1 receptor and plays a role in inhibiting PD1-PDL1 binding. CAV2-AU-M3 represents a next-gen approach to immunotherapies in solid tumors and creates a blueprint to guide the development of similar treatments in solid tumors such as osteosarcoma.

#4320 Rational design of a repeated-dosing schedule for KNP-101 guided by IFN-γ regulation.

Jihoon Chang, **Byoung Chul Lee**

Kanaph Therapeutics Inc., Seoul, Korea, Republic of

Background: Recombinant IL-12 demonstrated potent antitumor efficacy in early clinical trials; however, its development was hampered by severe systemic toxicities. To overcome these limitations, multiple approaches have been investigated, including strategies to prolong IL-12 half-life while modulating its activity, tumor-localized delivery using an immunocytokine modality, and selective activation through prodrug or masking technologies. While overcoming systemic toxicity has been the central focus in developing cytokines as effective anticancer agents, IL-12 continues to pose unique challenges that require further resolution. IL-12 exerts its antitumor effects primarily through induction of IFN-γ. However, clinical observations indicated that prior exposure to single-injection of IL-12 dramatically regulated toxicity upon subsequent dosing, likely due to negative feedback of IFN-γ expression, known as tachyphylaxis. In addition to tachyphylaxis, due to the delayed induction of IFN-γ following immune activation, pharmacokinetic (PK) and pharmacodynamic (PD) profiles are often uncoupled upon IL-12 treatment, posing additional challenges for clinical development.

Experiments and Unpublished data: We have focused on how IFN-γ is regulated upon repeated-dose of KNP-101, a novel FAP-targeting IL-12-based therapeutic that we have developed. By adjusting dosing intervals and amounts, we characterized IFN-γ dynamics in multiple murine tumor models including CT26, MC38, and EMT6. Repeated dosing of KNP-101 suppressed tumor growth, and analysis of IFN-γ levels revealed that while systemic IFN-γ induction exhibited strong negative feedback, this effect was markedly attenuated within the tumor microenvironment, where IFN-γ function is critical for antitumor immunity. In addition, systemic IFN-γ suppression by repeated KNP-101 treatment could be relieved by anti-PD1 combination. In non-tumor-bearing mice, repeated KNP-101 dosing led to pronounced negative feedback of IFN-γ expression in serum after 3 weeks, which gradually recovered by week 8. In human PBMC systems, recovery occurred more rapidly (~6 weeks). Interestingly, humanized CD34+ mice did not display the same degree of IFN-γ suppression by repeated KNP-101 treatment, suggesting that there is differential regulation of IFN-γ, likely due to differences between mouse and human immune systems such as memory T/NK cell compositions. These findings suggest that optimizing dosing and its frequency in clinical trials will be crucial to achieve sustained efficacy while minimizing cytokine-related toxicity.

Conclusion: Our results demonstrate that the kinetics of IFN-γ regulation differ between systemic and tumor compartments, as well as between species, providing valuable insight for the rational design of IL-12-based immunotherapy.

#4321 Oncolytic virus exhibits potent antitumor and immunomodulatory effects in triple-negative breast cancer using syngeneic and PDX models.

Yelin KIM[1], Jihye B Lee[2], Yoonjin Cha[3], Keunhee Oh[4], Namhee Lee[4], Seoyoung Lee[5], Hei Cheul Jeung[6], Soong June Bae[1], Sung Gwe Ahn[7], Joon JEONG[6], Jee Hung Kim[1]

[1]Gangnam Severance Hospital, Seoul, Korea, Republic of,[2]Institute for Breast Cancer Precision Medicine, Gangnam Severance Hospital, Seoul, Korea, Republic of,[3]Yonsei University College of Medicine, Seoul, Korea, Republic of,[4]Sillajen, Seoul, Korea, Republic of,[5]Gangnam Severance Hospital, Seoul,[6]Yonsei University Health System, Seoul, Korea, Republic of,[7]Yonsei University, Seoul, Korea, Republic of

Triple-negative breast cancer (TNBC), which accounts for 15–20% of breast cancers, is characterized by rapid proliferation and oncogenic pathway activation, creating a permissive environment for oncolytic virus replication. JX-594 (pexastimogene devacirepvec) is a genetically engineered vaccinia virus in which the thymidine kinase gene is replaced with human GM-CSF, enabling selective tumor replication and immune activation. Our in vitro studies demonstrated high sensitivity of TNBC cell lines to JX-594. Based on these findings, we established TNBC syngeneic and patient-derived xenograft (PDX) models to investigate JX-594–induced molecular and immunologic changes within the tumor microenvironment. Syngeneic models were generated by implanting 4T1 and EMT6 cells into the mammary fat pads of BALB/c mice. When tumors reached approximately 30–60 mm^3, mice received intratumoral mJX-594 injections (5×10^7 PFU, three doses every three days). On day 10, tumors were harvested for histopathologic and immunohistochemical (IHC) analyses. For translational validation, TNBC PDX models were established from human breast cancer tissues. When tumors reached approximately 30 mm^3, mice received intratumoral injections of JX-594 (1×10^7 PFU) once weekly for four weeks. After 28 days, tumor samples were examined by IHC for Ki-67, CD31, and vaccinia antigen. Tumor growth and body weight were monitored throughout the treatment period in both models.In syngeneic TNBC models, mJX-594 treatment markedly suppressed tumor growth compared with controls and was associated with increased infiltration of $CD4^+$ and $CD8^+$ T lymphocytes, as well as reduced micro-vessel density as indicated by CD31 staining. In contrast, PD-1/PD-L1 and CD20 expression levels were not significantly altered. In TNBC PDX models, an initial transient increase in tumor size was observed following the first JX-594 administration, followed by pronounced tumor regression and sustained growth suppression after the second treatment. IHC analyses revealed extensive tumor necrosis, decreased Ki-67 and CD31 expression, and positive vaccinia antigen staining, indicating active viral replication and ongoing oncolysis within the tumor microenvironment.This study demonstrates that JX-594 exerts potent anti-tumor activity in TNBC through immune activation, anti-angiogenic effects, and direct oncolytic mechanisms. The consistent therapeutic efficacy observed in both syngeneic and PDX models highlights the translational significance of JX-594. Although several studies have explored oncolytic virus–based therapies for TNBC, preclinical validation using PDX models remains extremely limited. Our findings provide robust *in vivo* evidence supporting the therapeutic potential of JX-594 and establish a translational foundation for advancing oncolytic virotherapy in TNBC.

#4322 Tumor treating fields (TTFields) overcome anti-PD-1 resistance in a murine lung adenocarcinoma model.

Yun Hu[1], Fatemeh Maspourour[1], Qi Wang[2], Ailing Huang[1], Carola Leuschner[1], Jing Wang[2], James W. Welsh[1]

[1]Radiation Oncology, MD Anderson Cancer Center, Houston, TX,[2]Bioinformatics and Computational Biology, MD Anderson Cancer Center, Houston, TX

Tumor Treating Fields (TTFields) are low-intensity, intermediate-frequency alternating electric fields that disrupt mitosis and elicit immunogenic stress. Although TTFields are clinically approved for metastatic non-small-cell lung cancer (mNSCLC) with PD-1/PD-L1 inhibitors or docetaxel, their mechanistic synergy in anti-PD-1-resistant disease remains incompletely understood. We investigated the temporal transcriptomic and functional impact of TTFields using the murine 344SQR lung adenocarcinoma model, which is intrinsically resistant to PD-1 blockade.344SQR cells were exposed to TTFields (150 kHz, 1.62 V/cm) for 24-72 h using the inovitro™ system, and proliferation and clonogenic survival were quantified. RNA-seq with Gene Set Enrichment Analysis (GSEA) defined pathway modulation at 48 h and 72 h. In vivo, 129Sv/Ev mice bearing 344SQR tumors were treated with the inovivo™ system, anti-PD-1, or both treatments together.TTFields significantly inhibited 344SQR proliferation (~60 % reduction at 72 h) and clonogenic survival in vitro. GSEA revealed dynamic, stage-specific transcriptional remodeling. At 48 h, TTFields downregulated mitotic-spindle, DNA-replication, and epithelial-mesenchymal-transition gene sets, indicating early mitotic arrest and replication stress. By 72 h, cells exhibited re-enrichment of G2M-checkpoint, E2F, MYC, and mitotic-spindle programs together with activation of peroxisomal and xenobiotic-metabolism pathways, consistent with sustained mitotic stress and oxidative-damage adaptation. In contrast, marked suppression of glycosyltransferase activity suggested impaired membrane and secretory functions, signifying progression toward metabolic exhaustion and immunogenic cell death.In vivo, TTFields monotherapy delayed tumor progression, while concurrent treatment with TTFields and anti-PD-1 produced significant tumor regression and extended median survival (32 days vs 20-21 days for control or monotherapies). Single-cell transcriptomics revealed that TTFields plus anti-PD-1 increased infiltration of $CD8^+$ cytotoxic T cells and B cells while reducing regulatory T cells, shifting the tumor microenvironment toward an effector-dominant state.These findings demonstrate that TTFields trigger sequential mitotic stress and metabolic collapse, generating an immunogenic tumor phenotype that restores responsiveness to PD-1 blockade. Sustained tumor control requires PD-1 inhibition to capitalize on TTFields-induced immunogenic remodeling and prevent regrowth of metabolically adapted residual cells.

#4323 The SPHK2 inhibitor opaganib potentiates tumor-intrinsic STING activation in triple-negative breast cancer *in vitro*.

Colette R. Worcester[1], Amrita Mitra[2], Harsh B. Pathak[2], Shane R. Stecklein[3]

[1]Cancer Biology, University of Kansas Medical Center, Kansas City, KS,[2]Pathology and Laboratory Medicine, University of Kansas Medical Center, Kansas City, KS,[3]Radiation Oncology, Orlando Health Cancer Institute, Orlando, FL

Triple-negative breast cancer (TNBC) has the poorest prognosis of breast cancer subtypes. Patients with TNBCs that exhibit robust stromal tumor infiltrating lymphocytes and/or gene expression signatures indicative of immune activation have improved response rates to chemotherapy and immunotherapy. DNA damage induces anti-tumor immunity through the stimulator of interferon genes (STING) protein pathway, and STING activation has been associated with better response rates and improved prognosis in TNBC. However, TNBCs also have elevated levels of sphingosine-1-phosphate (S1P), an immunomodulatory biolipid with pleiotropic effects. S1P is produced by sphingosine kinase 1 (SPHK1) and sphingosine kinase 2 (SPHK2). SPHK1 has been shown to lead to cancer cell progression and metastasis, while the role of SPHK2 in TNBC is less well-studied. SPHK2-dependent S1P production has been shown to inhibit STING in an acute lung injury model. Whether tumor-intrinsic STING is inhibited by the SPHK2-S1P axis is not known. We hypothesized that SPHK2 modulates STING pathway activity, and that SPHK2-dependent S1P biogenesis could be targeted to augment anti-tumor immunity in TNBC. We evaluated opaganib, an SPHK2 small molecule inhibitor with FDA orphan drug designation, in *in vitro* TNBC models (BT-549, HCC70, MDA-MB-231, and MDA-MB-468). Opaganib alone did not increase STING activation. However, pre-treatment with opaganib potentiated the synthetic STING agonist diABZI in all cell models. Compared to diABZI alone, western blots of cells treated with the opaganib-diABZI combination had enhanced phosphorylation of STING pathway proteins, such as STING, IRF3, and TBK1. Using BT-549 cells with an interferon stimulated response element (ISRE) luciferase reporter system, we analyzed transcriptional activity downstream of the STING pathway and found that ISRE activity increased in a dose-dependent manner with diABZI-mediated STING stimulation. However, pre-treatment of BT-549 cells with exogenous S1P decreased the diABZI-mediated ISRE activity. Conversely, pre-treatment with opaganib followed by low-dose diABZI treatment potentiated the downstream STING-mediated effects. To further analyze cellular responses to SPHK2 inhibition and STING agonism, we evaluated mRNA expression of 770 immuno-oncology-related genes (NanoString PanCancer IO 360 panel for nCounter) in drug-treated cells. Upregulated pathways in cells treated with the opaganib-diABZI combination compared to cells treated with diABZI alone or opaganib alone included cytokine signaling in immune system and responses to cytokine stimulus. In summary, we show that malignancy-associated production of S1P blunts tumor-intrinsic STING activity and suggest that targeting the SPHK2-S1P axis with opaganib may augment anti-tumor immunity in TNBC.

#4324 Dipeptidyl peptidase 4 restoration facilitates anti-tumor immunity in KRAS-LKB1-mutant lung cancer.

Hiraku Yanada

Asahikawa Medical University, Asahikawa, Hokkaido, Japan

KRAS-liver kinase B1 (LKB1)-mutant (KL) non-small cell lung cancer (NSCLC) represents an aggressive subtype characterized by a profoundly immunosuppressive tumor microenvironment (TME) and poor response to immune checkpoint inhibitors (ICIs). Despite harboring a high tumor mutation burden, KL tumors exhibit reduced immune cell infiltration, low PD-L1 expression, and suppressed interferon and cytotoxic signaling. To elucidate the molecular basis of this immune resistance, we performed multi-omics analyses and found that loss of LKB1 suppresses the mRNA, protein, and enzymatic activity of dipeptidyl peptidase 4 (DPP4), a membrane-bound glycoprotein involved in immune modulation. Restoration of DPP4 expression in KRAS-mutant lung cancer cells reprogrammed the TME and markedly increased immune-related gene signatures associated with T-cell migration and natural killer (NK) cell activation. In three-dimensional microfluidic models, DPP4 overexpression enhanced NK cell chemotaxis and spheroid targeting. In syngeneic KL murine models, DPP4 restoration synergized with anti-PD-1 therapy, leading to significant tumor regression and immune activation. These findings provide the first evidence that LKB1 actively regulates DPP4, establishing DPP4 as a pivotal immune modulator in KRAS-mutated NSCLC. The loss of LKB1 may represent an active mechanism of immune evasion, wherein tumor cells suppress DPP4-mediated immune activation to create an immune-cold TME. Consistent with recent observations linking STK11 and KEAP1 co-mutations to PD-L1-negative or immune desert phenotypes, our data support the concept that DPP4 suppression contributes to immune exclusion in KL-NSCLC. Conversely, DPP4 restoration promoted NK cell migration and enhanced responsiveness to PD-1 blockade, underscoring its role in reprogramming the TME. While DPP4 has context-dependent functions in cancer immunity, our study demonstrates that restoring, rather than inhibiting, DPP4 enhances immune effector recruitment and facilitates antitumor immunity. Collectively, these findings highlight DPP4 as a key immune regulator and promising therapeutic target to overcome ICI resistance and improve immunotherapy outcomes in KRAS-LKB1-mutant lung cancer.

#4326 Dissecting oncolytic virus anti-virus vs anti-tumor immunity in glioma: Insights from a patient derived organoid model.

C. Zoe Linke[1], Ethan Chen[1], Jennifer Gantchev[2], Aanchalika Chauhan[2], Christopher Jannotta[1], Keith L. Ligon[3], Andres Santos[4], Nathalie Agar[2], E Antonio Chiocca[1], Alexander L. Ling[1]

[1]Neurosurgery, Harvey Cushing Neuro-Oncology Laboratories, Boston, MA,[2]Neurosurgery, Surgical Brain Mapping and Molecular Imaging Laboratory, Boston, MA,[3]Pathology, Medical Oncology, Dana-Farber Cancer Institute, Boston, MA,[4]Pathology, Mass General Brigham Cancer Institute and Harvard Medical School, Boston, MA

Introduction. Intratumoral injection of the oncolytic herpes simplex virus (oHSV) CAN-3110 remodels the immunosuppressive microenvironment of recurrent glioblastoma. The immune infiltration triggered by CAN-3110 treatment is correlated with prolonged survival, especially in HSV1-seropositive individuals (Ling et al., 2023). However, it is still unclear if the immune response induced by oHSV therapy is mainly anti-virus or anti-tumor. We aim to dissect this distinction using *ex vivo* patient-derived glioma organoid (pGBO)-immune co-culture models to study the impact of oHSV treatment on anti-tumor immunity.

Methods. pGBOs were generated from surgically resected glioma specimens and characterized by highly multiplexed cyclic immunofluorescence (CycIF), via (up to date) 29 markers. Viral infection kinetics were assessed in these pGBOs using the GFP-expressing oHSV, rQNestin34.5v.1. Following pGBM characterization, we established a co-culture model of several pGBOs clones with rQNestin34.5v.1 and peripheral blood mononuclear cells (PBMCs) from either healthy donors or the pGBO patients. This system was used to assess tumor-immune interaction characteristics and kinetics under viral and non-viral conditions.

Results. Histological and immunofluorescent analyses showed that pGBOs retain tissue microstructures, such as vascular architecture - characterized by endothelial walls containing erythrocytes - for several weeks in culture, even after freezing and thawing the models. The cellular diversity in pGBOs mirrors the heterogeneity found in *in vivo*, comprising neural stem-like, glial, and residual innate immune cell populations. These distinct cell types exhibited metabolic activity, epithelial-to-mesenchymal transition (EMT), and proliferation. Over a three-month culture period, the architecture and phenotype changed to more aggressively glioma, with increased glioma cell expansion and loss of vasculature. Notably, the underlying cellular heterogeneity remained throughout the process. Co-culture of pGBOs with allogeneic PBMCs triggered infiltration of CD3+, CD8+, and CD4+ lymphocytes under viral and non-viral conditions. Staining for cleaved caspase-3 and granzyme B showed active tumor cell killing by granzyme+ CD8 T cells, which appears unrestricted to infected glioma cells. Further, CD20+ lymphocytes were detected in both infected and uninfected pGBOs.

Conclusion. We characterized pGBOs as a physiologically valid *ex vivo* model, observing both vasculature and cellular composition as found in *in situ* gliomas. Immune-mediated tumor cell killing was detected, both with and without virus treatment in PBMC x pGBO co-culture, using imaging and molecular readouts. This model enables investigation of how oncolytic HSV infection modulates immune response and provides a tractable system to dissect anti-tumor vs. anti-virus immune responses.

#4327 Serotonin receptor 5-HT_{2A}as a potential target for HCC immunotherapy.

Rong En Tay[1], Charmaine M. Ho[1], Nicholas D. Z. Ang[1], Hui Chien Tay[1], Daniel Z. Lopez[1], Qiao Rui Na[2], Yi Wen Tan[3], Ser Mei Koh[1], Kim Peng Tan[1], Wendy W. L. Lee[1], Jack Wee Lim[1], Mai Chan Lau[1], Han Chong Toh[4], Olaf Rotzschke[1], Laurent Renia[5]

[1]A*STAR - Singapore Immunology Network (SIgN), Singapore, Singapore,[2]Nanyang Technological University, Singapore, Singapore,[3]National University of Singapore, Singapore, Singapore,[4]National Cancer Centre Singapore, Singapore, Singapore,[5]A*STAR Infectious Disease Labs, Singapore, Singapore

While recent clinical trials of combination immunotherapies for hepatocellular carcinoma (HCC) have shown promising clinical efficacy and survival improvements breakthroughs, there is still much room for further improvement. A key limiting factor for HCC immunotherapy is the intrinsic immunosuppression within the liver microenvironment, resulting in suboptimal priming of tumour-specific CD8 cytotoxic T cells and thus immune evasion by the tumour. Hence, identifying new key molecular pathways suppressing T cell responses within the liver is critical for the rational design of more effective combination immunotherapies for HCC.

Here, we present evidence that targeting 5-HT2A serotonin receptor signalling could be a viable approach for HCC immunotherapy. Disruption of 5-HT2A signalling using either a selective antagonist small molecule, ketanserin, or by knockout of its coding gene Htr2a, augments the cytotoxic effector phenotype of mouse CD8 T cells activated in vitro with immunosuppressive liver NPCs. Similarly, abrogating 5-HT2A signalling in in vitro activated primary human CD8 T cells with ketanserin treatment or CRISPR-mediated disruption of the HTR2A gene also increased expression of the cytotoxic effector molecules Granzyme B and perforin. RNA-seq analysis of 5-HT2A signalling-deficient activated mouse CD8 T cells revealed increased expression of cytotoxicity-related genes such as Granzyme B and reduced expression of transcription factors downstream of MAP kinase signalling pathways. Consistent with these observations, 5-HT2A activation in CD8 T cells rapidly triggered phosphorylation of the p38, ERK, and JNK/SAP MAP kinases.

In vivo, systemic ketanserin treatment significantly prolonged survival of HCC tumour-bearing mice and was non-inferior to αPDL1 + αVEGFA combination antibody treatment. Combining ketanserin with αPDL1 + αVEGFA antibodies also significantly prolonged survival relative to control-treated mice while preserving the occurrence of complete tumour regression observed with αPDL1 + αVEGFA treatment alone. Together, our data describe a role for 5-HT2A as a negative regulator of the cytotoxic effector phenotype in CD8 T cells and highlight the therapeutic potential of targeting 5-HT2A for HCC immunotherapy.

: Monoclonal Antibodies and Antibody-Cytokine Platforms
Poster Session

#4330 AWT038: Dual GDF15-IL-6 neutralization for cancer cachexia.

Fan Ye, Jianing Huang, Fang Huang, Botong Hua, Ella Li, Joyce Kwan, Jenny Jiang, Wen-Chin Huang, Frank Xiao, Hanna Lin, Lili Cheng, Ziyang Zhong

Anwita Biosciences, San Carlos, CA

Cancer cachexia is a multifactorial syndrome marked by involuntary weight loss, anorexia, muscle wasting, and profound fatigue, leading to diminished quality of life and poorer response to therapy. It affects ~50-80% of patients with advanced cancer and contributes to up to ~30% of cancer deaths. Cancer cachexia is driven by overlapping anorexigenic and inflammatory signals. GDF15 engages GFRAL in the hindbrain to suppress appetite and drive weight loss, and clinical GDF15 blockade (e.g., ponsegromab) has increased body weight, appetite, activity, and lean mass in randomized trials. By contrast, IL-6 is a key mediator of inflammation-associated muscle wasting. Phase I/II studies of anti-IL-6 agents (e.g., clazakizumab/ALD518) attenuated lean-mass loss and fatigue.
We engineered AWT038, a novel bispecific fusion protein comprising an engineered high affinity human GFRAL domain fused to an anti-IL-6 antibody. The GFRAL moiety bound GDF15 with KD = 0.11 nM and achieved GDF15 neutralization comparable to ponsegromab in vitro; the anti-IL-6 arm bound IL-6 with KD = 0.13 nM and preventing IL-6 from engaging IL-6R. n a GDF15-secreting HT1080 xenograft cachexia model in SCID mice, AWT038-treated animals showed reduced circulating free GDF15 levels and body-weight gains comparable to ponsegromab. In cynomolgus monkeys, AWT038 was well tolerated at 10 and 30 mg/kg with a terminal half-life of approximately 100 hours and no detectable anti-drug antibodies. AWT038 also exhibits high thermostability (Tm > 65 °C) and favorable developability, being readily manufacturable.
By simultaneously neutralizing GDF15-GFRAL anorexigenic signaling and IL-6 driven inflammatory catabolism, AWT038 addresses two non-redundant drivers of cancer cachexia within a single molecule. This dual blockade supports development as supportive care for patients with advanced cancers and elevated GDF15 and/or IL-6, including those receiving platinum-based chemotherapy where GDF15 rises and weight loss is common. If confirmed in clinical studies, AWT038 could complement or surpass single-axis therapies (e.g., GDF15-only inhibitors) by restoring appetite, attenuating inflammation and fatigue, and preserving muscle mass in a population with major unmet need.

#4331 ZL-1222, a PD-1-targeted potency-reduced IL-12 immunocytokine, overcomes PD-1 resistance and enhances antitumor immunity with an accepted safety profile.

Cathy Wang[1], Lina Wang[1], Xue Wang[1], Xinchuan Dai[1], Qiuping Ye[2], Wilson Peng[2], Ziruo Wen[1], Lei Wang[1], Changwei Lv[1], Min Chen[1], Donghui Li[2], Qidong Hu[2], Bing Wan[1], **Linda N. Liu**[2]

[1]Zai Lab (Shanghai), Co. Ltd, Pudong, China,[2]Zai Lab (US) LLC, Cambridge, MA

Immune checkpoint blockade (ICB) restores T-cell function in the tumor microenvironment (TME), yet many patients with solid tumors exhibit limited response due to resistance. Interleukin-12 (IL-12) is particularly effective at reprogramming the TME and promoting durable, antigen-spreading immunity; however, its clinical use is constrained by systemic toxicity. To address this, ZL-1222, a next-generation IL-12 immunocytokine, is being developed having two single-chain anti-PD-1 antibody fragments that are attached to the N terminus of a knobs-into-holes silenced human IgG_1 Fc domain. An IL-12 mutein engineered to decrease binding to the IL-12 receptor is fused to the C-terminus of one Fc arm. By targeting PD-1$^+$ tumor-infiltrating lymphocytes (TILs), ZL-1222 delivers IL-12 directly to T/NK cells within the TME, enabling cis-activation that enhances antitumor immunity while minimizing systemic exposure and associated toxicities.

In vitro, ZL-1222 demonstrates strong PD-1 antagonist activity. The IL-12 mutein shows a ~1000-fold reduction in IFN-γ production in a human mixed lymphocyte reaction (MLR), a standard functional readout of IL-12 activity. In the presence of PD-1$^+$ cells, ZL-1222 synergistically increases IFN-γ production and tumor-cell killing, outperforming the combination of anti-PD-1 antibody plus IL-12 mutein. In vivo, the ZL-1222 surrogate (m45) shows strong antitumor activity in PD-1-resistant B16F10.OVA and EMT6 syngeneic models. In the CT26 model, depletion of CD8$^+$ T cells or NK cells, but not CD4$^+$ T cells, attenuates the antitumor effects of m45, indicating that tumor-growth-inhibition (TGI) depends on CD8$^+$ T and NK cells. The surrogate also induces antitumor immune memory and inhibits tumor growth in a dose-dependent manner (0.03 to 3 mg/kg) with a strong pharmacokinetics (PK)/TGI correlation. Minimal mouse body-weight loss (<10%) was observed, consistent with the absence of severe treatment-related adverse effects. In a pilot toxicity study, cynomolgus monkeys tolerated single doses of ZL-1222 up to 10 mg/kg without evidence of systemic cytokine storm (IL-6 < 50 pg/mL; TNFα not detectable).

In conclusion, ZL-1222, a PD-1-targeted, potency-reduced IL-12 immunocytokine, achieves potent antitumor activity in PD-1-resistant models via delivery to PD-1$^+$ TILs, engaging CD8$^+$ T and NK cells in the TME while minimizing systemic toxicity. It induces durable immune memory, demonstrates dose-dependent efficacy with robust PK/TGI correlation, and shows favorable tolerability in non-human primates, supporting its potential as a next-generation immunotherapy for solid tumors.

#4332 AR166, a first-in-class PD-1xLAG-3xIL-2v tri-specific immunocytokine delivering *Cis*-acting IL-2v to overcome immune checkpoint inhibitor resistance.

Jaeho Song[1], Seon-mi Yu[1], Jae-Seok Lee[1], Jinkeol Mok[1], WooJeong Lee[1], Seo-Young Koo[1], Ye Rim Gu[1], Min-Young Park[1], Seoyun Yang[1], Juhan Yoon[1], Young Woo Park[1], Wooick Jang[1], Su-Hyung Park[2]

[1]Y-Biologics, Daejeon, Korea, Republic of,[2]Korea Advanced Institute of Science and Technology, Daejeon, Korea, Republic of

Immunocytokines fusing anti-PD-1 antibody with interleukin-2 (IL-2) have demonstrated therapeutic potential in clinical settings in overcoming resistance to PD-(L)1 inhibitors. However, clinical response rates were varied, highlighting the need for improved efficacy, particularly in tumors with primary resistance to PD-1 blockade expressing high levels of LAG-3. Emerging evidence indicates LAG-3, a key immune checkpoint, acts synergistically with PD-1 to promote T cell exhaustion, while dual blockade of LAG-3 and PD-1 can reprogram $CD8^+$ T/Tregs to enhance antitumor immunity. Here, we present AR166, a novel tri-specific immunocytokine engineered with novel Fc-silencing, delivering dual PD-1 and LAG-3 blockade while inducing PD-1-targeted $CD8^+$ T cell activation via an optimized IL-2 variant (IL-2v).

Patient-derived samples were profiled by flow cytometry and IHC. PD-1×LAG-3 bispecific activity and IL-2v *cis*-acting were assessed using PD-1/PD-L1 and LAG-3/MHC II blockade assays, and PD-1 and/or LAG-3-dependent $CD8^+$ T cell pSTAT5 signaling. Fc-silencing was assessed using ADCC, ADCP, and CDC assays. Repeatedly stimulated PBMCs were co-cultured with tumor cells to determine T cell proliferation and activation in the presence of AR166. Patient-derived samples were treated with AR166 followed by immune cell profiling. Antitumor efficacy was evaluated in tumor-bearing (≥300 mm^3) humanized syngeneic mouse models and tumor infiltrating lymphocytes were profiled. Complete responders were rechallenged with tumor cells to assess memory response. Pharmacokinetic and safety profiles were analyzed in hIL-2Rαβγ knock-in mice and cynomolgus monkeys.

Expression of PD-1 and LAG-3 was confirmed in patient-derived tumor samples. AR166 effectively inhibited PD-1/PD-L1 and LAG-3/MHC II pathways while IL-2v showed *cis*-activity only when anchored to PD-1 and/or LAG-3. Assessment of Fc-silencing showed minimal Fc-dependent effector functions. AR166 elicited robust T cell proliferation and activation compared to a PD-1xIL2v competitor in an *in vitro* T cell exhaustion model, with similar results observed in patient-derived $CD8^+$ T cells. AR166 showed remarkable tumor growth inhibition compared to anti-PD-1 and PD-1xIL-2v competitors in humanized mouse models that recapitulate anti-PD1 resistance with high LAG-3 expression, while immune profiling showed rapid expansion of $PD\text{-}1^+TCF1^+CD8^+$ stem-like T cells. AR166 elicited durable tumor regression in a tumor rechallenge model, suggesting tumor-specific immune memory. AR166 achieved favorable safety and pharmacokinetic profiles in both mice and cynomolgus monkeys, supporting its broad therapeutic window.

Our findings show that AR166, a first-in-class PD-1xLAG-3xIL-2v tri-specific, can exceed the efficacy of both PD-1 inhibitors and PD-1xIL-2v with good safety.

#4333 A universal pro-immunocytokine platform using a spatial hindrance strategy to overcome MHC resistance and enhance efficacy.

Chih-Hung Chuang, Shih-Ting Hong, Bo-Cheng Huang

Drug Development and Value Creation Research Center, Kaohsiung Medical University, Kaohsiung City, Taiwan

Immune checkpoint blockade (ICB) drugs are regarded as advanced approaches in cancer immuno-oncology (IO) therapy.
(Background) However, they still face clinical limitations due to insufficient tumor selectivity, which can cause immune-related damage to normal tissues, and limited efficacy, particularly in tumors with major histocompatibility complex (MHC) loss that leads to immunotherapy resistance. While the interferon (IFN) family promotes immune activation and upregulates MHC expression, systemic administration often results in severe toxicities that restrict clinical application.
(Methods) To address these challenges, we developed an innovative pro-immunocytokine (IFN-ICB) platform using a spatial hindrance strategy, in which IFN and ICB are linked via a protease-cleavable linker that mutually masks their activities. Upon protease-mediated cleavage within the tumor microenvironment, both IFN and ICB restore their activities and upregulate tumor MHC expression, thereby enhancing therapeutic efficacy while mitigating systemic toxicity.
(Results) In our project, we initially demonstrated the proof of concept for pro-immunocytokine engineering by fusing IFNs to several ICBs, including anti-CTLA-4, anti-PD-1, and anti-PD-L1 antibodies. To optimize the blocking efficiency of IFN-ICBs, AI-based simulations were employed to predict spatial hindrance structures and calculate relevant blocking parameters. In vitro assessments confirmed that IFN-ICBs enhance tumor MHC expression and increase cytotoxicity. In vivo studies further demonstrated that IFN-ICBs efficiently improve antitumor efficacy in melanoma and colon cancer mouse models, indicating stronger immune responses within the tumor compared with either IFN or ICB monotherapy. Importantly, IFN-ICBs also reduced systemic toxicity and were safer than the combined administration of IFN and ICB drugs.
(Conclusion) Our innovative pro-immunocytokine platform possesses the universal capability to transform any ICB or antibody into a pro-immunocytokine via AI-based prediction, enhancing therapeutic efficacy while improving safety, and thus holds promise to impact the next generation of IO therapeutics.

#4334 AR170, a novel PD-1xVEGFxIL-2v tri-specific immunocytokine to redefine next generation cancer immunotherapy.

Seon-Mi Yu, Jaeho Song, Juhan Yoon, Bum-Chan Park, Wooick Jang, Young woo Park, Chonghun Rhee, Jihye Yoon, Da-Mi Kim, Wanki Park, Yeung-chul Kim

Y-Biologics, Daejeon, Korea, Republic of

Background

Bispecific antibodies that simultaneously target PD-1 and VEGF have shown promise in extending the efficacy of PD-1 inhibition alone, yet despite improved treatment response and prolonged progression-free survival, overall survival advantage over anti-PD-1 monotherapy is so far limited. Interleukin-2 (IL-2) combination can markedly potentiate the efficacy of PD-1xVEGF bispecific antibodies, but challenges remain due to systemic toxicity. To overcome this limitation, AR170 was designed as a novel tri-specific immunocytokine that simultaneously engages PD-1, VEGF, and the IL-2 receptor by incorporating an optimized *cis*-acting IL-2 variant (IL-2v) and complete Fc-silencing.

Methods

VEGF-induced AR170 dimerization was assessed by SE-HPLC. Enhanced PD-1 binding after dimerization was confirmed using bio-layer interferometry (BLI) and flow cytometry. Blockade of PD-1/PD-L1 and VEGF/VEGFR interactions was validated using a luciferase reporter assay. Functional assays were conducted to measure T cell activation, proliferation, cytotoxicity, and cytokine secretion by flow cytometry or ELISA. Fc-silencing was confirmed by ADCC, ADCP, and CDC assays. Antitumor efficacy was evaluated in both hPBMC-engrafted and hPD-1/hPD-L1/hVEGF triple knocked-in mouse models. Safety and pharmacokinetic studies were carried out in hIL-2R knock-in mice and cynomolgus monkeys.

Results

AR170 undergoes VEGF-induced dimerization that synergizes blockade activity of both PD-1 and VEGF. AR170 delivers PD-1-dependent *cis*-acting IL-2v signaling. In addition, Fc-silencing technology effectively minimizes Fc-mediated effector function. AR170 under VEGF-enriched exhaustion conditions induced robust proliferation and activation of $CD8^+$ T cells compared to either PD-1 inhibitor or PD-1xVEGF bispecific antibody *in vitro*. AR170 elicited rapid and durable antitumor responses superior to either PD-1 inhibitor or PD-1xVEGF bispecific antibody in VEGF-expressing tumor-bearing (≥300 mm^3) humanized mouse models, while depletion of $CD8^+$ T cells eliminated antitumor efficacy. Immune cell profiling showed elevated proportion of $TCF1^+PD\text{-}1^+CD8^+$ T cells following AR170 treatment. AR170 demonstrated favorable safety and pharmacokinetic profiles in both mice and cynomolgus monkeys.

Conclusions

AR170 is a next-generation cancer immunotherapy that uses a novel IL-2v fusion approach to surpass the efficacy limitations of PD-1xVEGF bispecific antibodies.

#4335 JMB2403, a potential best-in-class PD-1-dependent IL2Rβγ-targeting tri-specific antibody for safe and potent immunotherapy.

Chunyin Gu, Deyi Wang, Yan Wang, Fangfang Jia, Fu Zhou, Shun Chang, Yu Zhao, Linlin Liu, Huawei Zhang, Peipei Liu, Xiaodan Cao, **Taylor B. Guo**

Shanghai Jeyou Pharmaceutical Co., Ltd., Shanghai, China

Despite the success of PD-1 axis blockade in cancer immunotherapy, it is met with limited efficacy and relapse. Addition of interleukin-2 (IL-2) may enhance treatment efficacy but its use is hampered by a severe toxicity profile. To simultaneously circumvent resistance to checkpoint inhibition and unlock the full therapeutic potential of cytokine-based immunotherapy, numerous groups have sought to engineer an attenuated or biased IL-2 in an anti-PD(L)1/IL2 molecule with limited success thus far. Taking an alternative approach, we screened a naïve alpaca library for weak agonistic nanobodies of IL-2/15Rβ and the common γ chain and attached a potent anti-PD-1 IgG (K_D = 0.18 nM) to generate a tri-specific antibody (JMB2403, also known as 2403T62). JMB2403 retained PD-1 blocking activity and potently activated T cells. JMB2403 did not bind IL2Rα (CD25), but activated STAT5 signaling in an engineered Jurkat cell reporter assay albeit at >500-fold lower levels compared to wild type IL-2. This translated to a JMB2403-induced pSTAT5 increase in NK cells but minimal STAT5 phosphorylation in Treg cells. Notably, JMB2403 concentration-dependently induced phospho-STAT5 only in activated (PD-1$^+$) but not in resting CD8$^+$ T cells, indicating cis-action mediated by PD-1 engagement. In an A375 (melanoma) xenograft model, JMB2403 (4 mg/kg, i.p., twice weekly) exhibited superior anti-tumor efficacy (complete regression in 7 out of 8 animals) than its parental PD-1 antibody as well as pembrolizumab. In contrast, treatment of a clinical-stage PD-1-IL2 fusion protein at equimolar dose failed to elicit any complete responses and caused one death. In an NCI-H292 (lung cancer) model, JMB2403 (4 mg/kg, i.p., twice weekly) strongly inhibited tumor growth with complete response in 6 out of 7 animals. The minimal efficacious dose was 0.13 mg/kg. In a cynomolgus monkey study, treatment of JMB2403 at 4, 12 and 30 mg/kg i.v. on day 1 and day 15 produced a dose-dependent increase in proliferating CD8$^+$ T cells, PD-1$^+$ CD8$^+$ T cells, Treg cells and NK cells were observed after the first dose which returned to baseline before the second dose. Safety wise, no abnormalities were reported in any animals especially known IL-2-related toxicities such as vascular leak syndrome and pulmonary edema. In summary, JMB2403 can induce cis-activation of PD-1$^+$ T cells and display superior anti-tumor efficacy with good tolerability. To our knowledge, this is the first tri-specific antibody of its kind that targets specifically IL2/15 receptor signaling subunits.

#4336 TGI-17a: A potential best-in-class PD-1/IL-2$^{\alpha\text{-bias}}$cytokine fusion protein.

Guoshuai Cao, Yangyang Li, Yuwei Wu, **Haoyu Sun**, Zhigang Tian

Hefei TG ImmunoPharma Co., Ltd., Hefei, China

Background: The limited efficacy of immune checkpoint inhibitors (ICIs) due to resistance remains an unmet medical need, making PD-1/IL-2 a promising therapeutic approach. Many strategies focus on eliminating IL-2's interaction with IL-2Rα to avoid Treg activation. However, such "not-α" IL-2 mutein-based fusion proteins have demonstrated limited clinical success. In contrast, PD-1/IL-2$^{\alpha\text{-bias}}$ approach has shown promising efficacy in patients with ICI-resistant and immunologically "cold" tumors. TGI-17a is a potential best-in-class PD-1/IL-2$^{\alpha\text{-bias}}$ bispecific antibody designed to specifically activate antigen-specific CD8+T cells by synergistically blocking inhibitory PD-1 signaling while enhancing activating IL-2 signaling. It is engineered with an IL-2 variant exhibiting a stronger bias towards IL-2Rα, a strategy anticipated to enhance anti-tumor activity while minimizing IL-2Rβγ-mediated toxicity.
Methods: The binding affinity of TGI-17a for PD-1, IL-2Rα, and IL-2Rβγ was evaluated by Surface Plasmon Resonance (SPR). Its in vitro activity was assessed by measuring STAT5 phosphorylation (pSTAT5) in T cells via flow cytometry. Toxicity of the IL-2 variant was evaluated by intravenous administration of IL-2 variants fused to a surrogate anti-mouse PD-1 antibody in wild-type mice. The anti-tumor efficacy of TGI-17a was investigated in MC38 and B16F10 syngeneic tumor models using humanized PD-1 transgenic mice.
Results: TGI-17a exhibited intermediate affinity for IL-2Rα (KD = 19.2 nM), while its affinity for IL-2Rβγ was over 50-fold lower (KD = 1060 nM), rendering it a more profoundly IL-2Rα-biased molecule compared to the competitor. In functional assays, TGI-17a did not induce pSTAT5 in peripheral T cells even at high concentrations (up to 250 μg/mL), but potently activated PD-1+IL-2Rα+ T cells. Unlike the competitor, whose function was somehow independent of PD-1 binding, TGI-17a's activity was strictly PD-1-dependent (10% pSTAT5 induction: 1.3 μg/mL for TGI-17a vs. 82 μg/mL for IL-2v-Fc). In toxicity studies, TGI-17a was well-tolerated at doses up to 40 mg/kg (IV, twice weekly) in mice, whereas the competitor caused lethality at 5 mg/kg.In the in vivo efficacy studies, TGI-17a demonstrated superior anti-tumor activity compared to the PD-1 antibody pembrolizumab in both MC38 and B16F10 models. It showed comparable efficacy to the competitor in the MC38 model and superior efficacy in the B16F10 model. Furthermore, TGI-17a exhibited significantly better efficacy than a PD-1/VEGF bispecific antibody in the MC38 model.
Conclusions: These results indicate that TGI-17a, a potential best-in-class PD-1/IL-2α-bias bispecific antibody fusion protein, possesses compelling anti-tumor efficacy and a favorable safety profile in preclinical models. This robust evidence supports its further clinical development as a promising therapeutic candidate for pan-cancer applications.

#4337 TGI-17b: A potential first-in-class PD-1/VEGF/IL-2$^{\alpha\text{-bias}}$ trispecific antibody and the potential next generation cornerstone for pan-cancer therapy.

Guoshuai Cao, Yangyang Li, Yuwei Wu, **Haoyu Sun**, Zhigang Tian

Hefei TG ImmunoPharma Co., Ltd., Hefei, China

Background: Immune checkpoint inhibitors (ICIs) have revolutionized the treatment of solid tumors. However, their efficacy is often limited by resistance, remaining a major therapeutic challenge for many patients. Various next-generation immuno-oncology (IO) therapeutics are under extensive investigation. Among these, PD-1/VEGF and PD-1/IL-2$^{\alpha\text{-bias}}$ bispecific antibodies have demonstrated promising efficacy in patients with ICI-resistant and immunologically "cold" tumors.To build upon these advances, we developed TGI-17b, a trispecific antibody combined of PD-1/VEGF/IL-2$^{\alpha\text{-bias}}$. TGI-17b demonstrated superior anti-tumor efficacy compared to either PD-1/VEGF or PD-1/IL-2$^{\alpha\text{-bias}}$ alone in preclinical models, positioning it as a potential next generation cornerstone therapy for pan-cancer applications.

Methods: The binding affinity of TGI-17b for PD-1, VEGF, IL-2Rα, and IL-2Rβγ was evaluated using Surface Plasmon Resonance (SPR). Its in vitro functional activity was assessed by measuring the blockade of PD-1/PD-L1, VEGF/VEGFR1 and VEGF/VEGFR2 interactions. Toxicity was evaluated by intravenous administration of a murine surrogate antibody (mPD-1/VEGF/IL-2$^{\alpha\text{-bias}}$) in wild-type mice, compared with a clinical-stage competitor's murine surrogate (mPD-1/IL-2$^{\alpha\text{-bias}}$). The anti-tumor efficacy of TGI-17b was investigated in MC38 and B16F10 syngeneic tumor models using humanized PD-1 transgenic mice.

Results: TGI-17b exhibited high affinity for VEGF (0.86 nM) and intermediate affinity for IL-2Rα (KD = 24.3 nM), with minimal binding to IL-2Rβγ, confirming its pronounced IL-2R$^{\alpha\text{-bias}}$ character. In functional assays, TGI-17b blocked PD-1/PD-L1 interaction with a slightly higher EC50, and blocked VEGF/VEGFR1 and VEGF/VEGFR2 interactions with significantly lower EC50 values compared to AK112, a PD-1/VEGF bispecific antibody (PD-1/PD-L1 blockade EC50: 0.70 μg/mL for TGI-17b vs. 0.32 μg/mL for AK112; VEGF/VEGFR1 blockade EC50: 0.37 μg/mL vs. 3.53 μg/mL; VEGF/VEGFR2 blockade EC50: 1.29 μg/mL vs. 7.71 μg/mL). In toxicity studies, TGI-17b surrogate demonstrated a favorable safety profile at 40 mg/kg (IV, twice weekly), whereas the competitor's surrogate mPD-1/IL-2$^{\alpha\text{-bias}}$ antibody was lethal at 5 mg/kg.In the in vivo efficacy studies, TGI-17b showed superior anti-tumor activity compared to the PD-1/VEGF bispecific antibody in the MC38 model. In the B16F10 model, its efficacy substantially exceeded that of both the PD-1/VEGF and PD-1/IL-2$^{\alpha\text{-bias}}$ bispecific antibodies.

Conclusions: These results indicate that TGI-17b, a potential first-in-class PD-1/VEGF/IL-2$^{\alpha\text{-bias}}$ trispecific antibody, possesses compelling anti-tumor efficacy and a favorable safety profile in preclinical models. This robust evidence supports its further clinical development as a promising therapeutic candidate for pan-cancer applications.

#4338 Systematic discovery of attenuated IL-2 variants optimized for bispecific antibodies enabling targeted IL-2 delivery to PD-1$^+$T cells.

Jaehyeon Kim, Youngwoo Park, Sangheon Lee, Sooa Choi, Changho Jang, Sunha Yoon, Heebok Lee, Jaebong Yoon, Nayoung Lee, Hyenan Kim

Y-Biologics, Daejeon, Korea, Republic of

Background: Targeted delivery of an interleukin-2 variant (IL-2v) via fusion to an anti-PD-1 antibody has emerged as a promising strategy to overcome resistance to anti-PD-(L)1 therapy. However, unattenuated signaling through the IL-2 receptor β/γ chain (IL-2Rβ/γ), even in the context of *cis*-delivery to PD-1$^+$ cells, can still lead to systemic toxicities. Fusion of IL-2v to bispecific antibodies introduces further challenges associated with dual-antigen targeting and increased risk of adverse events. To address these challenges, we screened IL-2 variants with varying degrees of IL-2Rβ/γ binding that either have IL-2Rα interaction preserved or reduced, for fusion with anti-PD-1-based bispecific antibodies to generate novel tri-specific immunocytokines.
Methods: IL-2 variants were generated and screened for reduced IL-2Rβ/γ binding using random mutagenesis. Variants were evaluated for manufacturability after bispecific antibody fusion via mammalian cell transient expression and affinity purification for both yield and purity. Binding was determined using Octet® and ELISA, while pSTAT5 activity was evaluated on PD-1 negative and PD-1 positive cells to assess PD-1-dependent IL-2 signaling. Variants were classified into non-α, α-biased, or α-masked categories based on the strength of binding to IL-2Rβ/γ for further development. Selected tri-specific immunocytokines fused with various IL-2v configurations underwent safety and efficacy assessment *in vivo* using MC38 syngeneic hPD-1 knock-in mouse tumor models.
Results: We generated a library of IL-2 variants with diverse sequences and, following initial screening, performed additional engineering to further optimize their compatibility with bispecific antibody formats. Selected IL-2 variants were successfully synthesized in a bispecific antibody format with an anti-PD-1 arm, generating fusion proteins that met the acceptable-yield criteria. IL-2 variants showed markedly reduced binding and pSTAT5 activity to both IL-2Rβγ and IL-2Rαβγ compared to wildtype IL-2. The degree of binding attenuation determined whether these variants should be further developed into non-α, α-biased, or α-masked IL-2v. Optimized IL-2v-fused tri-specific immunocytokines showed dramatically attenuated IL-2R which was restored only upon binding to PD-1, demonstrating *cis*-acting PD-1-dependency. This was further verified *in vivo*, where selective PD-1-dependent IL-2v signaling translated into significant tumor growth inhibition with minimal toxicity.
Conclusion: Our approach provides a rational framework to fine-tune IL-2v binding affinity for fusion to bispecific antibodies, which can be replicated for the discovery of other affinity-tuned cytokine variants that exert targeted immune activation and therefore, improve the therapeutic index of tri-specific immunocytokines.

#4339 AI-designed PD-1/IL-18v bispecific antibody overcomes PD-1 resistance and drives potent antitumor responses in refractory models.

DongWon Park[1], Hyeonjin Cha[1], Kyesoo Cho[1], Yeorae Choi[1], Young-Hyun Han[1], Mirim Hong[1], Sohee Kwon[1], Myeong Sup Lee[1], Soyeon Oh[1], Seongchan Park[1], Taeyong Park[1], Jinsol Yang[1], Jonghun Won[1], Mooyoung Song[1], Chaok Seok[1], Yujin Lee[2], Chae-Rim Jung[2], Seung Goo Kang[2]

[1]Galux, Seoul, Korea, Republic of,[2]College of Biomedical Science, KangWon National University, Chuncheon, Korea, Republic of

Cytokines are powerful regulators of antitumor immunity, yet their therapeutic use is limited by short in vivo half-life and systemic inflammatory toxicity. Interleukin-18 (IL-18) is particularly attractive because it strongly activates NK cells and $CD8^+$ T cells, the main tumor-killing lymphocytes. Recent work has shown that antibody-cytokine conjugates such as IL-2 and IL-15 fused to anti-PD-1 antibodies can localize cytokine activity to PD-1-rich tumors and reinvigorate impaired anti-tumor immunity while avoiding systemic exposure. Motivated by this strategy, we applied our AI-driven protein therapeutics design platform, GaluxDesign, to create a next-generation IL-18 variant (IL-18v) optimized for tumor-restricted activity.Using GaluxDesign, we engineered an IL-18v that abolishes IL-18BP binding while preserving attenuated biological activity, even though its affinity for IL-18 receptor alpha (IL-18Rα) was intentionally minimized. IL-18v showed a >10°C increase in thermal stability over wild-type IL-18 and fully escaped IL-18BP-mediated inhibition. To confine IL-18v activity to the tumor microenvironment (TME) and minimize systemic toxicity, we generated a PD-1/IL-18v bispecific antibody for cis-targeted delivery of IL-18v to $PD\text{-}1^+$ T cells. Although free IL-18v has minimal IL-18Rα binding, its potency was restored when conjugated to an anti-PD-1 antibody, enabling PD-1-dependent cytokine activation. The bispecific molecule exhibited minimal activity in $PD\text{-}1^-$ IL-18 reporter cells and NK cells, but showed markedly enhanced signaling activity in $PD\text{-}1^+$ IL-18R reporter cells and, notably, an >800-fold increase in immune activity specifically in $PD\text{-}1^+$ NK92 cells, supporting a mechanism in which IL-18v remains inert peripherally but becomes activated only in PD-1-rich TMEs.In human PD-1 knock-in mice, the PD-1/IL-18v bispecific antibody incorporating a mouse IL-18v surrogate induced >90% tumor regression in the PD-1-responsive MC38 syngeneic model, whereas anti-PD-1 monotherapy showed minimal effect. PD-1/IL-18v also remodeled the TME into a highly inflammatory, antitumor state, as confirmed by immune profiling. In PD-1-less responsive models such as CT26 and in strongly PD-1-refractory tumors like B16-F10, the bispecific surrogate achieved >90% tumor growth inhibition despite complete resistance to PD-1 blockade. Notably, body weight remained stable over repeated treatments, indicating minimal systemic cytokine toxicity.Collectively, these results demonstrate that the AI-engineered PD-1/IL-18v bispecific antibody elicits provides potent PD-1-dependent IL-18 signaling with tumor specificity while limiting systemic adverse effects. The combination of IL-18BP resistance, diminished IL-18Rα affinity and PD-1-restricted activation creates a compelling basis for next-generation cytokine-based cancer immunotherapy.

#4340 AZD6750, a CD8α-guided IL-2 immunocytokine effectively combines with rilvegostomig, a PD-1/TIGIT bispecific antibody, to enhance endogenous immunity.

Matthew J. Elder[1], Aidan H. Riley[1], Sin Lih Tan[1], Jerome Mastio[1], Bruno Frederico[1], Fabien Garcon[1], Hena Khalique[1], Georgina Bowyer[1], Paul Chariou[2], Nicholas M. Durham[2], Maria Broggi[2], Emily Hsiue[3], Simon Rodney[1], Jonathan B. Fitzgerald[3], Nadia Luheshi[1], Mark Cobbold[3], Saso Cemerski[2], Simon J. Dovedi[1]

[1]AstraZeneca, Cambridge, United Kingdom,[2]AstraZeneca, Gaithersburg, MD,[3]AstraZeneca, Waltham, MA

Background: AZD6750 is a CD8α-guided IL-2 immunocytokine engineered to enhance the therapeutic index of IL-2 by reducing aldesleukin-associated toxicities, while preserving the efficacy that has been compromised with recent clinical IL-2 mutein strategies. This should result in a safer, more effective IL-2 with the potential to benefit larger numbers of patients and allow for the utilization of IL-2 in synergistic combinations. Combinations of anti-PD-1 with IL-2 therapies are currently being explored in the clinic with both preliminary clinical and nonclinical evidence that this combination can generate improved responses. As such, a potentially effective therapy is the combination of AZD6750 plus rilvegostomig, a monovalent, Fc-reduced, bispecific IgG1 antibody against PD-1 and TIGIT receptors, to enhance IO activity.

Methods: *In vitro*, antigen-specific tumor cell cytolysis was evaluated after treatment with AZD6750, rilvegostomig, or a combination of both therapies. *Ex vivo*, non-small cell lung cancer (NSCLC) patient-derived tumor samples were treated with AZD6750, rilvegostomig, or a combination of both therapies, and the activity evaluated by IFN-γ secretion. *In vivo*, NSG mice were implanted subcutaneously with antigen-expressing tumors, engrafted with expanded human PBMCs containing enriched antigen-specific $CD8^+$ T cells, and treated with AZD6750, rilvegostomig, a combination of both therapies, or an isotype control and tumor growth was monitored.

Results: *In vitro*, AZD6750 in combination with rilvegostomig improved antigen-specific cytolysis of tumor cells compared with AZD6750 monotherapy (EC_{50} $p<0.01$). In addition, *ex vivo* treatment of primary NSCLC tumors with rilvegostomig plus AZD6750 drove an increase in IFN-γ secretion compared with either AZD6750 (2-fold) or rilvegostomig (6-fold) monotherapies, highlighting the potential of this combination to augment functional responses in tumor infiltrating lymphocytes. *In vivo*, AZD6750 plus rilvegostomig resulted in a statistically significant reduction in tumor growth rate when compared to an isotype IgG (all studies), rilvegostomig (all studies), or AZD6750 (in 2 out of 3 studies) in an antigen-specific humanized mouse tumor model.

Conclusions: These preclinical data demonstrate that AZD6750 combined with rilvegostomig can enhance anti-tumor immune responses, leading to greater tumor cell killing. The Phase 1 study investigating AZD6750 in select advanced or metastatic solid tumors is currently ongoing (NCT07115043).

#4341 A novel αPD-1/αVEGF/IL-21v tri-specific fusion protein exhibits potent antitumor efficacy beyond αPD-1/αVEGF bispecific therapy.

Suna Kim, Sunjung Cho, Hyojoo Bang, So Woon Kim, Yongjun Jung, Seokchan Kang, Suyoon Kim, Mi-Seong Kim, Jun-Eui Park, Young Jin Park, Sungyoub Jung

Mustbio, Suwon-si, Korea, Republic of

Immune checkpoint inhibitors (ICIs) have been widely used for multiple malignancies. Nevertheless, response rates to ICIs remain limited across several tumor types, largely due to insufficient T cell infiltration and the inability to sustain long-term antitumor immunity within the tumor microenvironment (TME). Combinations of αPD-1 with αVEGF monoclonal antibodies (mAbs) or αPD-1/αVEGF bispecific antibodies (bsAbs) have demonstrated improved efficacy relative to αPD-1 monotherapy across multiple cancers. Despite such advances, strategies that not only enhance effector T cell accumulation within the TME but also promote sustained antitumor immune responses are essential to achieve therapeutic benefit in ICI-resistant or -refractory settings. Interleukin-21 (IL-21) enhances $CD8^+$ T cell activation and memory T cell differentiation while limiting Treg expansion, supporting durable antitumor immunity. However, its broad off-target activity and short half-life limit clinical utility, motivating the development of TME-selective IL-21 variants (IL-21v). αPD-1/αVEGF/IL-21v is a tri-specific fusion protein comprising anti-PD-1, anti-VEGF, and an IL-21v engineered to minimize peripheral toxicity while sustaining T cell activation within the TME. This construct was designed to sustain T cell activation via αPD-1, enhance tumor-infiltrating lymphocytes (TILs) via αVEGF, and promote effector/memory T cells via IL-21v. The αPD-1/αVEGF/IL-21v exhibited PD-1/PD-L1 blocking activity comparable to pembrolizumab and VEGF/VEGFR blockade similar to bevacizumab. In $PD\text{-}1^+/PD\text{-}1^-$ HuT78 cells, it induced PD-1-dependent STAT3 activation with ~5,000-fold selectivity for $PD\text{-}1^+$ cells. Consistently, $PD\text{-}1^{high}$ T cells treated with αPD-1/αVEGF/IL-21v secreted markedly higher IFN-γ and granzyme B than with αPD-1/αVEGF. Moreover, αPD-1/αVEGF/IL-21v promoted proliferation of $CD8^+IFN\text{-}\gamma^+Granzyme\ B^+$ effector T cells and improved $CD8^+$T/Treg ratio under *in vitro* TME-mimicking conditions, whereas αPD-1/αVEGF did not produce these effects. Importantly, under resting, peripheral-mimicking conditions, αPD-1/αVEGF/IL-21v induced minimal immune cell proliferation and low cytokine release. In ICI-resistant MC38 tumor model, αPD-1/αVEGF/IL-21v demonstrated superior antitumor efficacy compared with αPD-1 or αPD-1/αVEGF treatment, without adverse effects. Animals achieving complete responses did not relapse upon tumor re-challenge. This long-lasting efficacy was associated with an increased intratumoral $CD8^+$T/Treg ratio and expansion of memory T cell populations within tumors rather than in peripheral blood. In conclusion, αPD-1/αVEGF/IL-21v is a novel TME-selective tri-specific fusion protein that enhances TIL recruitment and amplifies effector/memory T cell populations, offering therapeutic potential beyond αPD-1 or αPD-1/αVEGF therapy.

#4342 MDNA113 is a masked conditionally activated tumor-targeted anti-PD1-IL-2^{SK} with superior safety and therapeutic properties.

Minh D. To, Rosemina Merchant, Aanchal Sharma, Fahar Merchant

Medicenna Therapeutics, Toronto, ON, Canada

Background: MDNA113 comprises of a core anti-PD1-IL-2^{SK} with 'β-enhanced, not-α' receptor selectivity, a removable IL-2 masking domain and an IL-13^{SK} tumor targeting moiety. Anti-PD1-IL-2^{SK} is designed to facilitate cis-binding to maximize synergy between IL-2R signaling and PD1/PDL1 blockade. The IL-2 masking domain blocks binding to IL-2R to minimize systemic toxicity until removal by proteases enriched within the tumor microenvironment (TME). The IL-13^{SK} selectively binds the IL-13Rα2 decoy receptor overexpressed in a broad range tumors but not normal tissues, thereby effectively promoting accumulation at the tumor sites. We present preliminary characterization of MDNA113, designed to enhance systemic tolerability while maximizing therapeutic efficacy within the TME.

Methods: Receptor binding was measured using the Octet Biolayer Interferometry (BLI) platform. IL-2R signaling and PD1/PDL1 blockade were assessed using in vitro cell reporter assays. In vivo pharmacodynamic and efficacy studies were conducted in the MC38 mouse syngeneic colon tumor model.

Results: MDNA113 binds IL-2Rβ with a >150-fold lower affinity than a non-masked anti-PD1-IL-2^{SK} (MDNA223). Binding to IL-13Rα2 and PD1 are not affected. The potency of MDNA113 in IL-2R signaling is reduced by >1000-fold with no change in PD1/PDL1 blockade. Removal of the masking domain by metalloproteases fully restores IL-2R signaling. Mice treated with MDNA113 showed significantly reduced lymphocyte expansion compared to equimolar dose of MDNA223, correlating with enhanced tolerability. In an MC38 colon tumor model, MDNA113 significantly inhibited tumor growth whereas efficacy was compromised when mice were treated with an uncleavable version of MDNA113, indicating that removal of the masking domain activates immune effector cells within the TME. Accordingly, treatment with cleavable MDNA113 resulted in increased tumor infiltration effector CD8^{+} T cells expressing Granzyme B. MDNA113 variants comprising of approved human anti-PD1 antibodies show similar characteristics and studies in non-human primate to evaluate safety, pharmacodynamics and pharmacokinetics are underway.

Conclusions: MDNA113 is a novel Bifunctional SuperKine for Immunotherapy (BiSKIT) with tumor targeting capability to enhance tolerability and maximize therapeutic response by synergizing IL-2R agonism and PD1/PDL1 blockade within the TME.

#4343 A novel anti-PD-1/IL-15 fusion protein JMT108 (SYS6090) with highly selective PD-1$^+$ immune cell activation and potent anti-tumor efficacy.

Ke He, Yushan Kong, Jun Mu, Hongyan Wang, Yisha She, Yanfang Su, Yi Fan, Liping Song

CSPC Pharmaceutical Group Ltd., Shanghai, China

Introduction: PD-1 is a key inhibitory receptor highly expressed on exhausted T cells within the tumor microenvironment (TME). PD-1 blockade has shown durable clinical benefit in a subset of cancer patients. However, its limited efficacy and frequent resistance highlight an unmet clinical need for improved approaches to reinvigorate T cell function. IL-15 supports survival, proliferation, and cytotoxicity of CD8$^+$ T cells and NK cells, yet systemic delivery has shown limited oncology utility due to rapid clearance and inflammatory toxicity. To address these challenges, we developed JMT108, a PD-1 targeted antibody-cytokine fusion protein containing an attenuated IL 15 mutant and IL15Rα sushi domain. This design enables dual immunomodulatory activity: (i) PD-1 checkpoint blockade; and (ii) selective cis-activation of IL-15 signaling in PD-1$^+$ immune cells within the TME, enhancing tumor specific immunity while minimizing systemic toxicity.

Method: Immune cell proliferation was measured *in vitro* in human PBMCs (PD-1$^-$) and pre-activated T cells (PD-1$^+$) using standardized assays. *In vivo* selectivity for PD-1$^+$ versus PD-1$^-$ subsets was assessed in cynomolgus monkeys and human hematopoietic stem cell (hHSC) reconstituted mice. Anti-tumor activity was tested in immune-humanized A375 melanoma and Huh-7 hepatocellular carcinoma xenografts. PK/toxicology were characterized in cynomolgus monkeys, and cytokine release potential was evaluated *ex vivo* in PBMCs.

Results: JMT108 showed markedly higher selectivity for PD-1$^+$ T cell activation versus N-803, with >10,000 fold lower potency in naïve PBMCs. Notably, it reduced PD-1 expression on activated CD8$^+$ T cells, in contrast to the upregulation observed with N-803. In hHSC-mice, JMT108 induced sustained expansion of CD8$^+$ effector cells (PD-1$^+$) without proliferation of naïve T cells. In cynomolgus monkeys, it exerted a long-lasting (>2 weeks) effect on the expansion of PD-1$^+$ immune cells, with PD-1$^-$ subsets showing markedly lower proliferation. JMT108 exhibited superior anti-tumor efficacy versus anti-PD-1 antibodies in both A375 and Huh-7 models, accompanied by robust expansion of tumor-infiltrating immune populations. JMT108 demonstrated a favorable PK profile in monkeys and was well tolerated in a 4-week GLP toxicity study, with minimal inflammatory cytokine induction in hPBMC assays.

Summary: JMT108, a PD-1-targeted IL-15 fusion protein, selectively activates PD-1$^+$ immune cells, downregulates PD-1 on activated/exhausted CD8$^+$ T cells, and drives sustained effector cell expansion with limited off-target proliferation. It achieves greater anti-tumor efficacy than anti -PD-1 antibodies, with favorable PK and safety profile,and low cytokine release risk. JMT108 has been in Phase I clinical trial (NCT06877650).

#4344 Interferon-α and PD-1 blockade mutually mask each other in a tumor-activated manner.

Shi-Wei Chao[1], Chih-Hung Chuang[2]

[1]Graduate Institute of Medicine, Kaohsiung Medical University, Kaohsiung City, Taiwan,[2]Department of Medical Laboratory Science and Biotechnology, Kaohsiung Medical University, Kaohsiung City, Taiwan

(Purpose) Immune checkpoint blockade (ICB) therapies have revolutionized cancer treatment but are often constrained by tumor immune evasion through the loss of MHC I antigen presentation. Type I interferons exert potent antitumor effects that may convert non-responders into responders; however, their systemic administration is limited by severe immune-related adverse events (irAEs). To improve efficacy without compromising safety, we developed a tumor-activated IFNα-PD-1 that uses dual masking to keep both elements inactive systemically.
(Methods) The blocking technology attenuates molecular bioactivity by integrating IFNα into the frameworks of anti-PD-1 antibodies. Through this dual-masking design, both cytokine and antibody functions are sterically constrained, preventing premature activation in circulation. Reactivation occurs upon proteolytic cleavage of a tumor-selective linker, a process termed spatial reclasp, which restores molecular flexibility and releases mutual steric hindrance between IFNα and the antibody. This conformational unmasking enables simultaneous recovery of cytokine signaling and checkpoint blockade exclusively within the tumor microenvironment.
(Results) In ELISA assays, the inactivated lockers exhibited more than 20-fold reductions in antigen-binding activity relative to the parental antibodies, whereas protease activation restored binding to levels comparable with the parental forms. The activated fusion induced marked upregulation of MHC I expression in melanoma cells, confirming spatially restricted IFNα signaling. In vivo, the IFNα-PD1 fusion demonstrated superior tumor suppression and enhanced intratumoral T cell infiltration with minimal systemic toxicity.
(Conclusions) This work establishes IFNα as a tumor-activated checkpoint locker that restores antitumor immunity while mitigating systemic toxicity. The dual-masking architecture provides a generalizable framework for engineering conditionally active immuno-oncology therapeutics, supporting future plug-and-play applications across ICB modalities and enabling safer, more potent next-generation cancer immunotherapies.

#4345 A multi-modal IL-2, SLC-3010, reprograms the tumor immune environment toward antitumor responses.

Junhyeok Heo[1], Daeun Kim[1], Geona Kim[1], Junyoung Lee[1], Sun Young Rha[2]

[1]New Drug Discovery Team, Selecxine Inc., Pohang, Korea, Republic of,[2]Division of Medical Oncology, Department of Internal Medicine, Yonsei University College of Medicine, Seoul, Korea, Republic of

Purpose CD122-biased IL-2 signaling has gained recognition as a refined immunomodulatory strategy for strengthening antitumor T cell responses. However, the modest clinical efficacy of CD122-focused IL-2 approaches, including CD122-biased variants, suggests that targeting CD122 alone does not fully leverage the complexity of endogenous IL-2. We developed SLC-3010, a noncovalent conjugate of human IL-2 and the anti-IL-2 antibody TCB2, designed to reinforce CD122-biased signaling and enable a dynamic interplay among TCB2, IL-2, and IL-2 receptors. This novel structure enables a triple action - CD122-biased IL-2 delivery, prevention of Treg-mediated negative feedback, and restimulation of T cells in conjunction with endogenous IL-2 - while maintaining activation of $CD25^+$CD8 T cells. While the design and primary activity of SLC-3010 have been characterized before, the biological significance of free TCB2 generated through *in vivo* dissociation remains incompletely understood. In this study, we aimed to characterize the multifaceted features of SLC-3010 through a series of studies assessing its pharmacokinetic profile and other drug properties under various experimental settings.

Methods Dynamic interplay between SLC-3010 and free TCB2 was evaluated by ELISA in mouse serum. STAT5 phosphorylation in fresh and activated PBMCs was assessed by flow cytometry. The immunologic role of free TCB2 and transcriptomic alterations in MP CD8 T cells were analyzed in hIL-2 TG and wt mice. Antitumor efficacy was then evaluated in MC38- and EO771-bearing mice of both strains.

Results Free TCB2 persisted longer *in vivo* than SLC-3010 and bound endogenous IL-2, generating additional CD122-biased yet CD25-permissive signaling consistent with enhanced STAT5 phosphorylation in $CD25^+$CD8 T cells. The dynamic interplay between free TCB2 and re-formed SLC-3010 further enhanced CD122-biased IL-2 signaling, leading to suppressed Treg expansion and a 3.65-fold increase in the tumor-infiltrating CD8/Treg ratio in hIL-2 TG mice. Free TCB2-driven signaling promoted a proliferative transcriptional program in MP CD8 T cells. SLC-3010 showed greater antitumor efficacy in hIL-2 TG mice than in wt mice in both MC38 and EO771 tumor models.

Conclusions SLC-3010 functions through a unified triple-action mechanism that combines CD122-biased yet CD25-accessible IL-2 signaling to activate antitumor effector cells, while concurrently disrupting Treg homeostasis and re-amplifying immune stimulation through in vivo complexing between free TCB2 and endogenous IL-2.

#4346 Tumor-localized monoclonal antibody targeting 4-1BB for superior safety and efficacy in cancer treatment.

Yun-Chi Lu[1], Yi-An Cheng[1], Tzu-Yi Liao[2]

[1]PrecisemAb Biotech Co., Ltd., Taipei, Taiwan,[2]Kaohsiung Medical University, Kaohsiung, Taiwan

4-1BB is a potent co-stimulatory receptor that enhances $CD8^+$ T-cell activity and drives robust anti-tumor immunity. However, systemic activation by conventional anti-4-1BB agonist antibodies (Abs) leads to severe toxicities—including hepatotoxicity, thrombocytopenia, and cytokine-mediated inflammation—resulting in multiple terminated clinical trials. To overcome these limitations, we engineered Lock-Urelumab, a tumor-selective pro-agonist form of the clinical anti-4-1BB Ab Urelumab. Lock-Urelumab incorporates an autologous hinge-based antibody lock and an MMP-cleavable peptide linker, enabling spatial hindrance under normal physiological conditions and selective activation within the tumor microenvironment where MMP is overexpressed. Biochemical characterization showed that the antibody lock reduced 4-1BB binding by ~400-fold, suppressing T-cell co-stimulation and preventing pro-inflammatory cytokine secretion. Upon MMP cleavage, Lock-Urelumab fully restored 4-1BB agonist activity. In a human T-cell transfer mouse model, Lock-Urelumab avoided the 4-1BB “antigen sink” effect, exhibited no detectable organ toxicity, and achieved 100% survival, whereas all Urelumab-treated mice succumbed to treatment-related toxicity within 14 days. Importantly, Lock-Urelumab maintained potent anti-tumor activity, inducing 77% tumor growth inhibition (TGI) compared with 45% for Urelumab, and significantly enhanced intra-tumoral T-cell activation. These findings demonstrate that tumor-localized 4-1BB activation can uncouple efficacy from systemic toxicity. Lock-Urelumab represents a next-generation immune checkpoint agonist with strong potential to revitalize 4-1BB-targeted immunotherapy and broaden its clinical applicability.

#4347 A first-in-class bifunctional anti-TRPV6 antibody turns "cold" tumors "hot".

Lindsay B. Alcaraz, Margaux Maurel, Tristan Mangeat, Vincent Roux-Portalez, Jessica Monnic, Marianne Le Gall, Anne Chevrel, Bernard Pau, **Johanna Marines**

Mabqi, Grabels, France

Context : The classification between “hot” and “cold” tumors has emerged as a central paradigm in immuno-oncology. In particular “cold” tumors - including prostate, sarcoma and pancreatic cancers - exhibit poor immune cell infiltration and remain refractory to current immunotherapies. This situation highlights the need of alternative and transformative therapeutic approaches that target underexplored receptors such as ion channels. Among these, TRPV6 calcium channel has emerged as a key oncogenic driver in multiple solid malignancies. While TRPV6-targeting peptides have reached clinical stage, their limitations underscore the potential of a first-in-class antibody that would be able to modulate and reshape the TME.

Methods. We recently identified MQI-201, a fully developable naked anti-TRPV6 antibody. After validating affinity, specificity and safety, we pursued *in vivo* characterization to explore its mode of action and we demonstrated MQI-201 efficacy on 6 cancer models, including 5 classified as “cold”.

Results. Firstly, we validated MQI-201 efficacy in 4 xenografted models: including 2 mPC models (LNCaP and VCaP), 1 pancreatic cancer model (BxPc3) and 1 lymphoma model (L-540). In all models tested, MQI-201 at low dose (1-8 mg/kg) induces a tumor growth inhibition ranging from 71% (VCaP) to 93% (BxPc3 and L-540). Interestingly, in BxPc3 model, MQI-201 proved its superiority over Gemcitabine (TGI 93% vs 45%). Secondly, we evaluated MQI-201 efficacy in 2 syngeneic models described as “cold”: a fibrosarcoma model (MCA-205) and an hormono-resistant prostate cancer model (RM-1). In both aggressive models, we demonstrated that MQI-201 induces potent cytotoxicity (TGI > 80%) and a superiority over SOCs. Interestingly, the efficacy was mediated by paratopic and Fc region with a clear increase of efficacy in Fc-WT as compared to Fc-silent format. Finally, we fully explored the impact of MQI-201 treatment on TME using RM-1 model. MQI-201 induces potent tumor apoptosis and increases the recruitment of T-CD8+ cells, NK cells and Granzyme B+ cells. In addition, total macrophage population was stable whereas M2 pro-tumoral subpopulation decreased by 50% following treatment. The exploration of MQI-201 in afucosylated format is now under exploration.

Conclusion. MQI-201 is a first-in-class anti-TRPV6 antibody able to turn “cold” tumors “hot” by reshaping the tumor microenvironment. These unique properties open new therapeutic avenues for solid cancer treatment to unlock durable responses across immunotherapy-resistant cancers.

#4348 Anticancer activity of a humanized anti-VEGFR-1 monoclonal antibody and its derived antibody-drug conjugates targeting tumor cells and tumor-microenvironment components.

Pedro M. Lacal[1], Maria Grazia Atzori[2], Claudia Ceci[2], Federica Ruffini[1], Sonia Valentini[2], Lauretta Levati[1], **Grazia Graziani**[2]

[1]IDI-IRCCS, Rome, Italy,[2]Systems Medicine, University of Rome Tor Vergata, Rome, Italy

The vascular endothelial growth factor receptor-1 (VEGFR-1) is a tyrosine kinase receptor for VEGF-A and placental growth factor (PlGF), involved in pathological angiogenesis, tumor invasiveness and infiltration by protumoral M2 macrophages. Aim of the study was to investigate the antitumor activity of the humanized anti-VEGFR-1 monoclonal antibody (mAb) hD16F7 and its antibody-drug conjugates (ADCs) derivatives. A unique property of this anti VEGFR-1 mAb is its ability of preserving the decoy/anti-angiogenic function of the soluble VEGFR-1, which sequesters VEGF-A/PlGF in the tumor microenvironment (TME). The humanized anti-VEGFR-1 mAb was initially tested for its ability to hamper migration of human melanoma, glioblastoma (GBM) and endothelial cells in response to PlGF. Thereafter, it was tested in patient-derived tumor xenografts (PDTXs) of melanoma and GBM organoids. Two anti-VEGFR-1 ADCs, derived from hD16F7 mAb by conjugation with monomethyl auristatin E (MMAE) or pyrrolobenzodiazepine (PBD), were also evaluated for their cytotoxic activity on VEGFR-1 expressing melanoma and GBM cells, as well as on cells of the TME (i.e., endothelial cells and M2 polarized macrophages). The hD16F7 mAb inhibited PlGF-induced migration of VEGFR-1 positive human melanoma (CR-Mel) and GBM (U87 and SJ-GBM) cell lines. Moreover, hD16F7 mAb strongly hampered migration of human endothelial cells (HUV-ST) in response to PlGF. Melanoma PDTXs were characterized for VEGFR-1 expression by RT-PCR and for the mutational status of BRAF gene by DNA sequencing. Treatment with hD16F7 mAb (10 mg/kg) significantly inhibited the growth of PDTXs transplanted in immunodeficient mice, both in the case of BRAF wild-type and mutated tumors and regardless of VEGFR-1 expression in melanoma cells. Indeed, hD16F7 mAb can also act on cells of the TME as it recognizes both the human and murine receptors. Moreover, in the case of BRAF mutated PDTXs, hD16F7 mAb also enhanced the efficacy of the BRAF inhibitor vemurafenib. The hD16F7-derived ADCs, hD16F7-MMAE and hD16F7-PBD, exerted a greater cytotoxicity on VEGFR-1 overexpressing melanoma cells (M14-MF5) than on their VEGFR-1 negative counterparts (M14-C2) with the following IC50 values: hD16F7-MMAE 5.84 µg/ml ± 0.59 vs 12.17 µg/ml ± 1.56; hD16F7-PBD 12.4 µg/ml ± 1.9 vs 19.2 µg/ml ± 0.8. The hD16F7-PBD also effectively hampered the viability of M2 macrophages and human endothelial cells (IC50 values: 5.8 µg/ml ± 0.3 and 12.2 µg/ml± 3.9, respectively). The cytotoxic effects of hD16F7-PBD were also demonstrated on GBM organoids by measuring the fluorescence intensity of calcein-AM (viable cells) and propidium iodide (dead cells). In conclusion, the humanized anti-VEGFR-1 mAb hD16F7 and its derived ADCs showed promising antitumor effects on preclinical tumor models that more closely reflect the clinical response.Funding: AIRC IG 2024-ID 30361 and Italian Ministry of Health NRR Plan, grant PNRR-MCNT2-2023-12377670 (CUP F93C24000250007)

#4349 Development of galectin-1 and galectin-7-specific inhibitors: Immunotherapy and molecular imaging in triple-negative breast cancer.

Rita Nehme, David Chatenet, Nicolas Doucet, Yves St-Pierre

INRS - Centre Armand-Frappier, Laval, QC, Canada

Triple-negative breast cancer (TNBC) is the most aggressive subtype of breast cancer, accounting for 12-17% of cases, and is associated with increased metastasis and recurrence. Despite significant advances in recent years, notably the approval of anti-PD-1 immunotherapy as part of the standard treatment for TNBC, current therapeutic options remain limited, are often associated with adverse effects, and are effective for only a minority of patients. Therefore, there is an urgent need to develop new therapeutic strategies. Galectins (GALs) are a family of glycan-binding proteins recognized as glyco-immune checkpoints in cancer. They play key roles in several processes of tumor progression, including immunosuppression, metastatic dissemination, and treatment resistance. In TNBC, GAL-1 and GAL-7 are overexpressed in ~40% of cases and are associated with increased metastasis, poor prognosis, and reduced survival. Despite more than two decades of research, most GAL inhibitors developed have shown limited success, partly due to their lack of specificity. We report the development of novel, specific inhibitors targeting GAL-1 and GAL-7 using camelid antibody-derived nanobodies (Nbs). Lead Nbs were conjugated with the NOTA chelator, labeled with copper-64 (^{64}Cu), and utilized as radiotracers to detect GAL-1 and GAL-7 expression in primary tumors of a TNBC mouse model via positron emission tomography (PET). Additionally, GAL-1 and GAL-7 Nbs were fused to a human IgG1 Fc fragment to generate two novel minibodies (Mbs) homologs, G1M1 and G7M8, to assess the therapeutic potential of galectin inhibition as monotherapies and in combination with anti-PD-1 immunotherapy in a preclinical TNBC model. We identified several high-affinity Nbs specific to GAL-1 and GAL-7, with no detectable cross-reactivity to other galectins. Lead candidates effectively inhibited both GALs binding to T-cell glycoreceptors, preventing T-cell apoptosis in vitro. In PET imaging, ^{64}Cu-labeled Nbs demonstrated specific and optimal accumulation in TNBC 20 h post-administration. Inhibition of GAL-1 and GAL-7 showed therapeutic potential in a TNBC mouse model, reducing lung metastases and modulating both local and systemic immune responses through distinct mechanisms. Notably, G1M1 demonstrated efficacy comparable to anti-PD1 therapy. In summary, we developed highly specific GAL-1 and GAL-7 inhibitors that not only inhibit T-cell apoptosis but also serve as effective diagnostic and therapeutic agents in TNBC. These findings offer a promising strategy to overcome previous limitations in galectin inhibitor development, laying a foundation for novel therapeutic approaches in cancer treatment and for better understanding the role of galectins in cancer and other diseases.

#4350 pH-responsive PEGylated antibodies enables tumor-specific activation and attenuates immune-related adverse events.

Minji Ha, Torsha Ghosh, Sol Shin, Soyoung Son, Jae Hyung Park

Department of Chemical Engineering, Sungkyunkwan University, Suwon, Korea, Republic of

Immune checkpoint blockade using monoclonal antibodies (mAbs) has achieved durable antitumor efficacy but is often limited by immune-related adverse events (irAEs) resulting from systemic immune activation. To decouple antitumor activity from off-target toxicity, a pH-responsive masking approach was developed to suppress mAb function at physiological pH while selectively restoring activity in the mildly acidic tumor microenvironment (TME).

A cleavable poly(ethylene glycol) (PEG) coating was synthesized by reacting carboxy-dimethylmaleic anhydride (CDM) with vacuum-dried PEG-methyl ether in dichloromethane to generate PEG-CDM. Anti-CD47, anti-CTLA-4, and anti-PD-1 antibodies were buffer-exchanged and reacted with a 300-fold molar excess of PEG-CDM to obtain PEG-CDM-modified mAbs. The modified antibodies were characterized for conjugation efficiency, physicochemical stability, and rheological behavior. Their pH-dependent masking and cleavage kinetics were examined under physiological and mildly acidic conditions (pH 7.4 and 6.4-6.8, respectively). Functional recovery was analyzed through in vitro binding and immune cell assays, followed by in vivo evaluation in MC38 and B16F10 tumor-bearing C57BL/6 mice.

PEG-CDM modification effectively masked antibody activity at neutral pH, confirming successful suppression of checkpoint engagement. Under TME-mimicking acidic conditions, PEG-CDM rapidly hydrolyzed, restoring antibody binding and effector functions in a pH-dependent manner. In vivo, PEG-CDM-modified mAbs demonstrated tumor-specific activation and retained antitumor potency comparable to unmodified antibodies while markedly reducing off-tumor immune activation in both MC38 and B16F10 models.

This pH-responsive PEG-CDM masking platform enables conditional activation of immune checkpoint antibodies within the acidic TME while minimizing systemic immune stimulation. The strategy offers a modular and tunable approach to enhance the therapeutic window of checkpoint blockade by balancing efficacy with improved safety, providing a translational path toward next-generation cancer immunotherapies.

AI Disclosure (optional): A generative AI tool was utilized to assist in grammar refinement and structural consistency; all scientific content has been verified by the authors.

#4351 A sex-specific role of CD36 targeting therapy in colorectal cancer.

Huanyu Wang[1], Yi-Ru Yu[2], Yun-Han Lin[2], Jingying Zhou[1]

[1]the Chinese University of Hong Kong, Hong Kong, China,[2]Pilatus Biosciences SA, Epalinges, Switzerland

Colorectal cancer (CRC) is the second leading cause of cancer-related deaths globally. Based on distinct genetic characteristics, CRC can be classified into mismatch repair-deficient (dMMR) and mismatch repair-proficient (pMMR). Unfortunately, current therapies, including immune checkpoint inhibitors (ICIs) and anti-vascular endothelial growth factor (VEGF) antibodies, showed limited efficacy in pMMR CRC patients. CD36, a fatty acid (FA) transporter and scavenger receptor, is broadly upregulated in cancers, and inhibiting CD36-mediated lipid uptake has shown therapeutic promise. We recently developed PLT012, a humanized IgG4 antibody targeting the lipid-binding pockets of CD36, with cross-species reactivity and a superior safety profile in monkeys. Importantly, PLT012 displayed significant therapeutic efficacy in liver cancers, potentially by shifting immunosuppressive tumor microenvironment. Here, we assess the therapeutic efficacy of PLT012 in pMMR CRC. Using the pMMR CRC mouse cell line SL4, our data showed that PLT012 effectively suppressed orthotopic CRC growth in female, but not male mice. This sex-specific effect correlated with higher CD36 expression in female mice, which we also observed in CRC patient samples. Interestingly, our preliminary data further suggested that CD36 was enriched in cancer-associated fibroblasts (CAFs) in a female-biased manner. Taken together, our findings highlight CD36 as a promising therapeutic target for pMMR CRC, particularly in female patients.

#4352 Therapeutic antibody inhibits target-mediated immune migration in advanced in-vitromodelofanimmune suppressive tumormicroenvironment.

Wouter Strijker[1], Iris Voskamp[1], Brian Duggan[1], **Remko Van Vught**[1], Luuk de Haan[1], Ward Celus[2], Linda Gijzen[1]

[1]MIMETAS B.V, Oegstgeest, Netherlands,[2]Montis Biosciences, Leuven, Belgium

It has become increasingly clear that current immune-oncology treatments are inadequate in generating sufficient targeted treatment effects without damaging the surrounding tissue. Rather than focusing on the tumor as the main target, the immune suppressive tumor microenvironment has recently become a novel therapeutic target as it drives tumor growth, therapy resistance and metastasis. However, current in vitro systems often fail to replicate the tumor microenvironment hindering accurate efficacy evaluation. This study used an advanced in-vitro model of an immune suppressive tumor microenvironment to study treatment effects of therapeutic antibodies. Here we report on the use of an organ-on-a-chip based model to study immune cell migration in the context of a subset of immune suppressive macrophages, known as perivascular macrophages (PVM), and on a target protein released by these cells. The model contains an endothelial vessel (HUVEC), macrophages (PVM or M1) and immune cells (PBMCs or T cells) to study the interaction between these cells and determine the effect of target protein and antibodies. The level of immune cell migration showed to be dependent on the activation state of immune cells and pretreatment of the endothelium. PVMs shown to have an inhibitory effect on immune cells migration, in contrast to M1 macrophages that increased the number of migrated immune cells. The released target protein was found to reduce T cell migration, specifically for stimulated T cells. Finally, novel therapeutic antibodies were assessed after addition of the target protein. For one of the antibodies increased migration of stimulated T cells was observed. These findings highlight the potential of targeting PVMs and their released proteins, as important elements of an immune suppressive microenvironment. Additionally, the study shows the utility of the advanced in-vitro model for evaluating therapeutic antibodies. In the future the system will be used for testing additional therapeutics in the context of an immune suppressive tumor microenvironment.

#4353 PHST001, a humanized anti-CD24 hIgG4 antibody, is effective against metastatic tumors and retains its anti-tumor activity in the presence of competing IgG.

Suzana A. Kahn[1], Joseane Sampaio[1], Douglas V. Faget[1], Rachel E. Brewer[1], Giovanni C. Forcina[1], Blacker Grace[1], Priyanka R. Malusare[1], Alexandria Beans[1], Seth D. Ludwig[1], John S. Burg[1], Jennifer Yinuo Cao[1], Raphael F. Rousseau[1], Amira A. Barkal[2], Ravi Majeti[3], Irving L. Weissman[3], Roy L. Maute[1]

[1]Pheast Therapeutics Inc., Redwood City, CA,[2]Brigham & Women's Hospital, Harvard Medical School, Boston, MA,[3]Stanford University School of Medicine, Stanford, CA

Background: CD24 is a highly glycosylated tumor antigen with a restricted expression profile that acts as macrophage “don’t eat me” signal. CD24 is highly expressed by many human cancers and interacts with the macrophage receptor Siglec-10 to protect cancer cells from phagocytosis. PHST001 is a clinical-stage humanized anti-CD24 monoclonal antibody of IgG4 isotype currently in clinical evaluation. In vivo, PHST001 shows significantly greater efficacy against solid tumors than the anti-CD47 antibody Magrolimab. We assessed PHST001's preclinical efficacy against metastatic tumors and the role of Fc receptor engagement in its anti-tumor activity.

Results and Methods: BT474, a human Her2+ breast tumor cell line, metastasizes to the axillary lymph nodes when engrafted in the mammary fat pad of NSG mice. In contrast to control-treated mice, PHST001 treatment inhibited the formation of lymph node metastases in orthotopic xenograft models of BT474. To generate a disseminated metastatic model, BT474 cells were engrafted intracardially. A metastatic model was also generated in a syngeneic system by expressing human CD24 in MC38 cells (MC38-huCD24) and implanting tumor cells intracardially. PHST001 treatment significantly reduced the number and size of metastatic lesions in both xenograft BT474 and immune competent MC38-huCD24 models. To define PHST001’s mechanism of action, a variant antibody bearing a LALAGANA mutation (Fc-inert) was generated. This variant induced phagocytosis of tumor cells to a lesser extent than PHST001 (human IgG4), demonstrating the contribution of Fc receptor engagement to PHST001 efficacy. When combined with a companion agent, such as the anti-Her2 ADC trastuzumab deruxtecan, the Fc-inert version of PHST001 dramatically increased phagocytosis, demonstrating the contribution of CD24 blockade to PHST001 efficacy in absence of direct Fc receptor engagement. In vitro, PHST001 induced phagocytosis of human neutrophils, however this effect was completely inhibited by the IgG present in serum at physiological concentrations (50%). PHST001 anti-tumor efficacy against BT474 in NSG mice was maintained even when mice were supplemented with polyclonal IgG to match levels found in immunocompetent mice.

Conclusions: PHST001 prevents metastatic spread and demonstrates anti-tumor activity against established metastases. In vitro, peripheral blood cells expressing CD24 are protected from PHST001-mediated phagocytosis due to competition for Fc receptors by high levels of endogenous IgG, predicting protection in treated patients. PHST001 retains anti-tumor effects in vivo despite polyclonal IgG presence, indicating that competition for Fc receptors by endogenous IgG is not a barrier for efficacy in the tumor microenvironment.

#4354 Harnessing VLPs and nanodiscs to unlock antibody discovery for challenging membrane proteins.

Hannah Flaherty Duncan, Shicheng Chen, Jia Cui, Tingxu Chen

KACTUS, Waltham, MA

Multi-pass transmembrane proteins (MP-TMPs), including G protein-coupled receptors (GPCRs), ion channels, and transporters, are vital regulators of cellular communication and signaling. They represent over 60% of current drug targets, yet their structural complexity and dependence on lipid environments make recombinant production and antibody discovery extremely difficult. Traditional soluble formats fail to preserve their conformational integrity, limiting immunogenicity and screening relevance. To address these limitations, KACTUS developed a versatile membrane-protein display platform integrating **virus-like particles (VLPs)** and **nanodiscs** to stabilize full-length MP-TMPs in their native conformations. VLPs, composed of self-assembling structural proteins lacking genetic material, provide a natural lipid envelope that supports proper folding and high-density surface display. Using this system, KACTUS successfully presented the full-length **STEAP1** protein (a prostate-cancer-associated antigen) and demonstrated specific binding to the therapeutic antibody Vandortuzumab with an EC_{50} of 89.8 ng/mL. Complementing this, **SMA-based nanodiscs** produced in mammalian cells offer detergent-free solubilization of membrane proteins within native lipid bilayers. The **A2A adenosine receptor (A2AR)** nanodiscs retained structural integrity and exhibited strong binding to anti-A2AR monoclonal antibodies by ELISA (EC_{50} = 0.15 µg/mL) and SPR (K_D = 0.32 nM). In addition, KACTUS developed **CXCR4 VLP immunogens** that generated functional antisera and monoclonal antibodies capable of ligand-blocking comparable to the commercial CXCR4 antibody Ulocuplumab. Further extending this approach, **biotinylated VLPs and nanodiscs** enabled efficient **phage-display antibody panning**, as validated with GPRC5D constructs (EC_{50} = 7.4 ng/mL for VLPs; 0.28 µg/mL for nanodiscs). KACTUS also established the first **TCR-CD3 complex nanodisc**, preserving all native subunits (TCRα/β, CD3ε/γ/δ/ζ) for accurate CD3 antibody screening and binding analysis (SP34 K_D = 0.1 nM). Together, these results demonstrate that the **KACTUS VLP and nanodisc platforms** deliver native-like, bioactive MP-TMPs suitable for antibody generation, ligand binding, and structural interrogation. This integrated technology provides a powerful solution to overcome long-standing challenges in **membrane-protein immunization and screening**, paving the way for next-generation therapeutic antibody discovery.

#4355 Cryo EM-based structural characterization of IMC-002, a next-generation anti-CD47 antibody with a unique binding site and biomarker candidates, supporting evidence of enhanced safety and efficacy.

Hyesun Lee[1], **Jiyea Choi**[1], HyeHyeon Jang[1], Heewook Shin[1], Jiyoung Yoon[1], Woochan Hwang[2], Sung Ho Kim[1], Heung Tae Kim[1]

[1]ImmuneOncia Therapeutics, Inc., Seoul, Korea, Republic of,[2]Lunit Inc., Seoul, Korea, Republic of

CD47 is a ubiquitously expressed transmembrane glycoprotein that interacts with SIRPα on macrophages to deliver a “don’t eat me” signal, thereby inhibiting phagocytosis. Tumor cells upregulate CD47 to evade immune surveillance, which correlates with poor clinical outcomes. Consequently, the CD47-SIRPα axis has emerged as a promising target for cancer immunotherapy. However, clinical development of CD47 blockade has been hampered by hematologic toxicities and rapid drug clearance due to high CD47 expression on normal cells, particularly red blood cells (RBCs). IMC-002 is a fully human IgG4 monoclonal antibody against CD47, developed to achieve an optimized affinity that balances therapeutic efficacy with safety. IMC-002 shows markedly enhanced tumor-cell selectivity with minimal RBC binding, compared with Hu5F9 and 13H3. Moreover, unlike Hu5F9, IMC-002 did not induce RBC phagocytosis and hemagglutination. The tumor selectivity and lack of RBC binding by IMC-002 appear to result from differences in its binding site. Cryo-electron microscopy (cryo-EM) revealed a unique binding interface near residues containing a predicted O-glycosylation site, which is distinct from the binding modes of competitive antibodies. De-glycosylation study also supported this glycosylation-dependent binding selectivity, as reported at AACR 2025. The results from biochemical and structural studies explaining IMC-002’s reduced hematologic toxicity and enhanced tumor selectivity in its clinical trials. Phase 1a data confirmed a favorable safety profile, and a hepatocellular carcinoma (HCC) cohort in phase 1b has been completed. An ongoing Phase 1b trial is evaluating its efficacy in triple-negative breast cancer (TNBC) and biliary tract cancer (BTC) cohorts in combination with standard of care (SoC). IMC-002 in combination with standard-of-care agents enhanced macrophage-mediated phagocytosis and T-cell activation in vitro and showed potent anti-tumor activity in HCC xenograft model, correlating with tumor CD47 expression. In a Phase 1b (NCT05276310), aptamer-based proteomic and AI-assisted IHC analyses of HCC patient samples identified candidate biomarkers associated with IMC-002 efficacy and macrophage-related signatures, suggesting their use in patient selection. In conclusion, the cancer-selective binding of IMC-002 is characterized by binding sites located proximal to a predicted O-glycosylation region, as supported by biochemical and structural studies. Several factors identified through proteomics and AI-based IHC studies showed potential possibilities as predictive biomarker candidates. IMC-002 demonstrated excellent efficacy and safety in clinical trials through its unique binding mechanism, supporting its continued clinical development as a promising cancer therapy.

#4356 Comprehensive characterization of DT-7012, a highly differentiated anti-CCR8 depleting antibody.

Maria Dolores Garcia Fernandez, Christel Franchet, Luc Baron, Solene Rose, Aurelie Janvier, Malaury Schappler, Lelievre Helene, Melanie Frauli, Orphee Blanchard, Thibaut Brugat, **Stephan Schann**, Nathalie Lenne

Domain Therapeutics, Illkirch, France

Background:CCR8 has recently emerged as a promising target in the treatment of solid tumors. DT-7012 is a novel humanized anti-CCR8 IgG1 monoclonal antibody engineered for optimized binding and enhanced effector functions to preferentially deplete tumor-resident Tregs while maintaining peripheral immune integrity.
Objectives: To complete the preclinical characterization of DT-7012, focusing on its binding properties, effector-function potencies, and selectivity compared with clinical-stage CCR8-targeting antibodies.
Methods:A comprehensive series of in vitro assays were conducted to assess DT-7012's binding properties and functional activities. Data were compared against leading clinical-stage anti-CCR8 competitors to elucidate potential clinical advantages. Assays were conducted under tumor-microenvironment-mimicking conditions to evaluate functional robustness.
Results:DT-7012 displayed a unique binding profile, conferring high-affinity interaction and superior FcγR engagement. In cell-based assays, DT-7012 induced potent selective killing activities, including under tumor-microenvironment-mimicking conditions. Collectively, these findings support DT-7012 as a potential best-in-class CCR8-depleting candidate.
Conclusions: With distinct binding and effector characteristics, DT-7012 emerges as a promising therapeutic for selective modulation of the tumor microenvironment. These results provide the preclinical rationale for clinical evaluation in patients with advanced solid tumors.
Keywords:DT-7012, CCR8, Treg depletion, ADCC, ADCP, tumor microenvironment, immuno-oncology.

#4357 Novel monoclonal antibody kills lymphoma cells via LFA-1/ICAM-1 dependent, antibody-mediated cellular cytotoxicity.

Rui Xue Lee[1], Patrick W. Jaynes[2], Edward Kai-Hua Chow[3], Anand Devaprasath Jeyasekharan[1]

[1]National University of Singapore (NUS), Singapore, Singapore,[2]National University of Singapore, Singapore, Singapore,[3]National University of Singapore, National University of Singapore, Singapore

Background: Diffuse large B-cell lymphoma (DLBCL) is an aggressive form of non-Hodgkin's lymphoma. DLBCL patients undergo a first line immunochemotherapy regimen, termed R-CHOP. Unfortunately, approximately 40% of treated patients eventually relapse, or are non-responsive. Thus, there is an urgent need to devise new treatment options. Recently, a novel monoclonal antibody (Antibody X) has been developed as a potential therapeutic strategy.
Methods: CD16 (Fc receptor)-expressing NK92 cells were used as effector cells against target DLCBL cell lines in co-culture assays. A high-content, high-throughput drug screening tool was developed to test the effects of small molecule drugs in combination with immunotherapies.
Results: We observed that instead of direct cytotoxicity or complement-dependent cytotoxicity, Antibody X exerted its anti-tumour effect primarily through antibody-dependent cellular cytotoxicity (ADCC). To understand the regulators of Antibody X-mediated killing, we utilised a newly developed high-content, high-throughput drug screening tool to evaluate the effects of over 1000 FDA approved compounds on Antibody X-mediated ADCC of DLBCL cells. We noted that BCR-Abl inhibitors differentially regulated Antibody X-mediated ADCC through their effects on Src kinases. Cellular contact between lymphoma cells and immune effector cells was also disrupted through the blockade of LFA-1/ICAM-1 immunological synapse formation. This ultimately led to an absence of death in lymphoma cells.
Conclusion: Overall, findings from this study revealed that Antibody X-mediated ADCC is dependent on Src activity and LFA-1/ICAM-1 immunological synapses. We also demonstrated that the novel high-content, high-throughput ADCC platform can be used for immunotherapy-based combinatorial drug screens and mechanistic evaluation of ADCC.
[E.K.C. and A.D.J. are co-corresponding authors for this work.]

: Vaccine Platforms and Target Identification
Poster Session

#4361 Single amino acid residue substitution to improve immunogenicity of HLA peptides targeting p53 neoantigen.

Chi Han Samson Li[1], Hong Wang[1], Kin Tak Chan[1], Genwei Zhang[2], Zhenghui Wang[2], Lipeng Lai[2], Melvin Toh[1]

[1]Sequencio Therapeutics, Hong Kong, Hong Kong,[2]Xtalpi, Inc., Somerville, MA

Background and objective: p53 tumor suppressor gene is frequently mutated in human cancer, which is highly associated with advance malignancy development and poor prognosis. However, there are no effective treatments targeting p53 expressed by mutant p53. Aiming at developing therapeutic vaccines targeting mutant p53, we coupled amino acid residue substitution and HLA peptide prediction using an AI model that we developed. Previously, we reported that modified HLA-A*02:01-specific peptides designed using our approach demonstrated significant immunogenicity in a HLA-A*02:01-humanized mouse model. Here, we further designed modified p53 neo-epitopes specific to HLA-A*03:01 and HLA-A*11:01 using this approach and studied their immunogenicity in HLA-humanized mice.
Methods: The AI model was used to analyze common p53 neoantigens and predict epitopes for HLA-A*03:01 and HLA-A*11:01. The epitopes underwent computer-assisted saturation mutagenesis that simulated single amino acid substitution to obtain the associated presentation score changes. Peptide sequences with improved presentation scores were synthesized. The binding affinity with HLA was determined using surface plasmon resonance (SPR). The immunogenicity was determined by IFNγ ELISpot assay and intracellular cytokine staining (ICS) using splenocytes collected from mice vaccinated with the peptides.
Results: Modified p53 neo-epitopes were analyzed by our AI model after saturation mutagenesis, and twelve of the modified neo-epitopes with at least 5% increase of presentation probability were selected for experimental analyses. Most of these peptides demonstrated high binding affinity with HLA-A*03:01 or HLA-A*11:01 and β2-microglobulin heterodimer as characterized by SPR. Using splenocytes collected from HLA-A*03:01 or HLA-A*11:01-humanized mice vaccinated with pools of these peptides, IFNγ ELISpot assay and IFNγ ICS revealed that all HLA-A*03:01 peptides and 9 out of 10 HLA-A*11:01 peptides effectively induced $CD8^+$ T-cell response. Remarkably, challenging the splenocytes with the respective native neoantigen peptides reactivated the cellular immunity induced by most of AI-designed modified peptides, suggesting that immunization of the AI-designed modified peptides induced $CD8^+$ T-cell response against the native p53 neoantigens.
Conclusion: We have designed multiple peptides derived from common p53 neoantigens and demonstrated that they are strongly immunogenic in HLA-A*02:01, HLA-A*03:01 and HLA-A*11:01 background. These findings further support that the coupling of MHC-I presentation prediction AI model and computer assisted saturation mutagenesis is promising in modifying neo-epitopes to improve anti-tumor immunity via the $CD8^+$ T-cell response.

#4362 Mesenchymal stem cells delivering IL-33 oncolytic vaccinia virus enhance antitumor effects and overcome PD-1 inhibitor resistance in bladder cancerResistance in bladder cancer.

Yong Tang[1], Yingzhao Liu[2], Songlin Li[1], Wenjie Wang[2], Jiahu Wang[3], **Qi Wang**[2]

[1]Department of Urology, Guangxi Medical University Cancer Hospital, Nanning, China,[2]Department of Research, Guangxi Medical University Cancer Hospital, Nanning, China,[3]Genvira Biosciences Inc, Ottawa, ON, Canada

Approximately 80% of patients with advanced bladder cancer (BCa) develop resistance to PD-1 inhibitors, presenting a substantial clinical challenge. This study seeks to develop an innovative therapeutic strategy utilizing mesenchymal stem cells (MSCs) to deliver an oncolytic vaccinia virus engineered to carry interleukin-33 (IL-33), with the objective of overcoming resistance to PD-1 inhibitors and elucidating the associated immune mechanisms. To create the oncolytic vaccinia virus variants OVV-hIL33(GVB-2030)and OVV-mIL33, human or mouse IL-33 cDNA was inserted into the vaccinia virus Copenhagen strain. Integration was confirmed via quantitative PCR and ELISA. The impact on human and mouse bladder cancer cell proliferation was measured using real-time cell analysis. In C57BL/6 mice with the MB49 model, OVV-mIL33's effectiveness with anti-PD-1 therapy was tested. A PD-1 inhibitor-resistant MB49/R cell line was developed, and MSCs were used to deliver OVV-mIL33, forming MSC-OVV-mIL33. Its efficacy with PD-1 inhibitors was evaluated against uncoated OVV-mIL33 by comparing tumor size and survival. Single-cell sequencing, spectral flow cytometry, and multiplex immunofluorescence analyzed cytokines and immune cells in the tumor environment. The findings indicate that OVV-hIL33 (GVB-2030) and OVV-mIL33 demonstrate selective cytotoxicity towards BCa cells in vitro, sparing normal cells. In murine models, intraperitoneal administration of OVV-mIL33 in conjunction with a PD-1 inhibitor effectively inhibited tumor progression and extended survival, although tumor recurrence was observed. Notably, the combination therapy involving MSC-OVV-mIL33 and PD-1 inhibitors demonstrated enhanced efficacy. This regimen not only suppressed both primary and recurrent tumors, achieving a 90% cure rate in mice, but also significantly reduced tumor formation by 60% upon re-challenge with MB49/R, thereby establishing an anti-BCa immune response. The combination therapy effectively remodeled the tumor microenvironment by augmenting the infiltration of cytotoxic CD8+ T cells, memory B cells, and type 2 innate lymphoid cells, while concurrently decreasing the presence of regulatory T cells and terminally exhausted CD8+ T cells. Additionally, the MSC coating conferred protection to the virus against neutralization, thereby ensuring efficient tumor targeting and proliferation. Consequently, we propose that the MSC-mediated delivery of OVV-mIL33, combined with PD-1 blockade therapy, presents significant potential to overcome resistance to PD-1 inhibitors in BCa. This synergistic interaction is principally attributed to the reversal of T cell exhaustion and the enhancement of anti-tumor immune memory formation.

#4363 Viral vector vaccination induces brain resident memory T cells to drive anti-glioblastoma immunity.

Emily Elizabeth Steffke[1], Laila Latifi[1], Taijun Hana[1], Ayaka Hara[1], Morgan Coombs[1], Jo Spurgeon[1], Caitlin Huguely[2], John Hancock[1], Brita Anderson[2], James McAuliffe[3], Vinnycius Pereira-Almeida[3], Amanda Wicki[3], Sara Abdel Malak[3], Laurine Noblecourt[3], Meili Zhang[2], Wei Zhang[2], Dionne Davis[2], Nicole Briceno[2], Hua Song[2], Chen Cam-El Makranz[2], Hideho Okada[4], Mark Gilbert[2], Carol Leung[5], Benoit Van den Eynde[3], Masaki Terabe[1]

[1]LICI, National Cancer Institute, Bethesda, MD,[2]Neuro-Oncology Branch, National Cancer Institute, Bethesda, MD,[3]Ludwig Institute for Cancer Research, University of Oxford, Oxford, United Kingdom,[4]UCSF - University of California San Francisco, Mill Valley, CA,[5]Center for Immuno-Oncology, University of Oxford, Oxford, United Kingdom

Glioblastoma is a lethal brain tumor notable for limited spontaneous induction of $CD8^+$ T cell responses. While viral-vector vaccines can drive particularly high magnitudes of tumor-reactive T cells, they have not been investigated for the treatment of glioblastoma. Here, we demonstrate that heterologous prime-boost vaccination with the simian adenovirus ChAdOx1 and poxvirus modified vaccinia Ankara (MVA) treats the orthotopic, syngeneic, checkpoint-inhibitor refractory SB28 murine model of glioblastoma, both in the context of the murine tumor antigen, P1A, and a newly identified tumor-associated antigen expressed by SB28. Adjuvant anti-PD-1 and anti-CTLA-4 did not further improve outcomes. Vaccination induced immunoediting of tumor antigen expression and tumor-specific recruitment of antigen-specific T cells to challenged brains, the majority of which had a $CD103^+CD69^+CD8^+$ tissue resident memory (TRM)-like phenotype. While induction of TRMs by vaccination has been implicated in superior control of other cancers, their role in mediating anti-glioblastoma immunity was unclear. ChAdOx1/MVA-induced brain TRMs displayed superior polyfunctionality compared to circulating and non-TRM brain antigen-specific $CD8^+$ T cells. Long-term surviving mice maintained consistent levels of antigen-specific TRM cells in their brains at days 70 and 175 post-tumor challenge, despite a three-fold decrease in circulating antigen-specific T cells, indicating durable T cell memory in the brain parenchyma. Furthermore, survivors were protected against a second orthotopic, but not subcutaneous, tumor rechallenge, demonstrating tissue-specific immunological memory. Intracranial adoptive transfer of brain-derived antigen-specific TRMs isolated from vaccinated, tumor-bearing mice was sufficient to prolong the survival of naïve mice challenged with tumors, whereas blood-derived antigen-specific non-TRMs and non-antigen-specific brain-derived $CD8^+$ T cells were not. Despite peripheral administration of the vaccines, antigen-specific $CD8^+$ T cells were induced not only in the brains of tumor-free animals, but in many tissues, including the liver, lung, skin, skull bone marrow, and meninges, with distinct phenotypes observed in different tissues. Overall, we demonstrate that ChAdOx1/MVA vaccination is a potent strategy to induce TRMs to mediate anti-glioblastoma immunity, establishing a basis for further clinical investigation of ChAdOx1/MVA vaccination to treat patients with glioblastoma.

#4364 Next-generation RNA vaccine modalities enable high-fidelity antigen discovery and T-cell immunogenicity screening.

Molly Chilton, Henry Leonard, Elsenoor Klaver, Olivier Reelfs, Lauren Schewitz-Bowers, James Corbett, Rebecca Roberts, Christopher Kirkham, Dan Rocca, **Louise Brackenbury**

Charles River Laboratories, Bristol, United Kingdom

RNA-based cancer vaccines provide exceptional flexibility for encoding tumour-associated antigens (TAAs) or patient-specific neoantigens and recent clinical data show promising efficacy over traditional approaches, yet comparative functional data across RNA formats remain limited. We developed an integrated evaluation workflow to benchmark linear mRNA, circular RNA (circRNA), self-amplifying RNA (saRNA), and 27-mer peptide vaccines for their ability to drive antigen expression and prime functional antigen-specific T-cell responses. Using GFP reporter constructs, expression levels and persistence were assessed across selected RNA formats in primary antigen-presenting cells. Linear mRNA and circRNA robustly produced higher and more durable antigen expression than peptide pulsing, consistent with emerging insights into RNA vaccine potency. Vaccine candidates were subsequently screened using an antigen-specific T-cell expansion workflow, which expands rare tumour-reactive CD8+ T cells via a mature dendritic cell (DC) co-culture system. This platform addresses challenges of low precursor frequency and HLA diversity, enabling de novo priming of T cells against TAAs such as MART-1 or unique neoantigens. In the majority of donors, RNA-encoded antigens elicited stronger T-cell responses than 27-mer peptides, reflected by greater expansion of antigen-specific CD8+ T cells and increased IFNγ release following restimulation. Functional killing was confirmed using peptide-loaded tumour targets and tumour cell lines endogenously expressing relevant-antigen. RNA-encoded antigens produced T cells with higher cytotoxic potential, evidenced by enhanced tumour apoptosis in killing assays. Crucially, the strongest response seen was with a circRNA neoantigen vaccine candidate relative to the same neoantigen encoded in linear mRNA or peptide formats. To support personalised vaccine programs, putative neoantigens were first validated using TAP-deficient MHC-loading assays to confirm direct presentation, then screened in the DC-T-cell co-cultures to generate donor-resolved immunogenicity hierarchies. This enabled rapid identification of high-value epitopes suitable for inclusion in bespoke mRNA or circRNA vaccine constructs. Collectively, these data demonstrate that RNA vaccine modalities can outperform peptide-based vaccination in generating functional tumour-reactive T cells. The integrated platform provides a modality-agnostic, human-relevant workflow spanning antigen selection, RNA vaccine characterisation, and comprehensive functional T-cell assessment, supporting rapid advancement of next-generation cancer vaccine pipelines.

#4365 Pre-existing immunity boosts therapeutic efficacy of oncolytic influenza a virus in the presence and absence of neutralizing antibodies.

Gloria Dawodu, Soner Yildiz, Yonina Bykov, Vicent Tur Planells, Ethan Spodeck, Sara Cuadrado-Castano, Adolfo Garcia-Sastre

Icahn School of Medicine at Mount Sinai, New York, NY

The study of oncolytic viruses that naturally target humans requires models that elucidate the impact of pre-existing immunity on therapeutic efficacy. Recent studies have shown that the presence of anti-viral T cells in the tumor can be associated with potentiation of oncolytic viruses [1,2]. Conversely, the presence of neutralizing antibodies has also been shown to abolish response [1]. Thus, we hypothesized that pre-existing immunity to Influenza A virus (IAV) would lead to abrogation of oncolytic IAV therapy. To study the effect of neutralizing antibodies and IAV-specific T cells on oncolytic virus treatment, we established models of both homosubtypic and heterosubtypic immunity. Mice were infected with either PR8 virus (H1N1) or X-31 virus (H3N2.) 6 weeks post infection, mice were given bilateral CT26 tumors, and one tumor was treated with PR8 deltaNS1. Both tumors were monitored for tumor growth and overall survival. In a single tumor model, flow cytometry was used to define changes in the immune landscape unique to immunized mice. Additionally, anti-viral TILs were analyzed and characterized. Interestingly treated tumors displayed significant delays in tumor growth in PR8 and X-31 mice compared to naïve mice. Additionally, an increased abscopal effect in the contralateral tumor was only observed in X-31 mice. Treatment of X-31 mice resulted in a 20% increase in overall survival compared to PR8 and naïve mice. Rechallenged mice rejected tumor engraftment, indicating a durable anti-tumor memory response.There was an increase in both tumor infiltrating CD8+ and CD4+ T cells in the single tumor model. Amongst CD4s, there was a significant decrease in the presence of T regulatory cells (Treg); corresponding with an increase in CD8:Treg ratio. Immunized tumor bearing mice showed infiltration of anti-viral CD8s prior to treatment with oncolytic virus. X-31 mice had a higher prevalence of anti-IAV CD8s in the tumor and draining lymph node. In both immunization models, CD44+ anti-IAV CD8s were $CD127^{hi}CD69^{hi}$ indicating a central memory phenotype. Further phenotyping TILs in X31-immunized, tumor bearing mice displayed a trends to less T-cell exhaustion and increased cytotoxicity. In models of both homosubtypic and heterosubtypic immunity, therapeutic efficacy is strengthened. This indicates that the presence of neutralizing antibodies does not hinder the therapeutic efficacy of the virus and that the presence of anti-IAV T cells in both models may be responsible for this potentiation. Future studies aim to understand how anti-viral T cells in the TME contribute to anti-tumor response via interaction with anti-tumor T cells and overall myeloid cells.

#4366 Individualized neoantigen vaccine as adjuvant therapy in high-risk esophageal carcinoma: A study with the largest reported cohort and longest follow-up to date.

Ming Wu[1], Hong Shen[1], **Fan Mo**[2], Zixiang Wu[1], Chuanqiang Wu[1], Youping Wang[1], Kailai Wang[1], Shanshan Zhang[2], Ning Han[2], Liqian Wu[2], Wenjin Zhuang[2], Shuqing Chen[3]

[1]The Second Affiliated Hospital of Zhejiang University School of Medicine, Hangzhou, China,[2]Hangzhou Neoantigen Therapeutics Co., Ltd., Hangzhou, China,[3]Zhejiang University, Hangzhou, China

Background: For esophageal carcinoma (EC) patients with residual pathological disease (non-pCR) after neoadjuvant chemoimmunotherapy and surgery, effective adjuvant strategies to reduce recurrence are urgently needed. This study evaluates the safety, efficacy, and immunogenicity of iNeo-Vac-P01, a personalized neoantigen peptide vaccine, in this high-risk setting. To our knowledge, this is the largest and longest-following cohort reported to date for a personalized cancer vaccine in postoperative EC.

Methods: In this single-arm trial (NCT05307835), eligible stage IIA-IIIB EC patients with non-pCR received the vaccine. Tumor and matched normal tissues underwent whole-exome and RNA sequencing. Somatic mutations were identified, and up to 20 individualized long peptides (15-30 aa) encompassing predicted HLA class I and II neoantigens were designed and synthesized for each patient using a proprietary bioinformatics platform (iNeo®). Patients received subcutaneous injections of iNeo-Vac-P01 (300 μg/peptide) co-administered with GM-CSF (40 μg) on Days 1, 4, 8, 15±3, 22±3, 52±7, and 82±7. Primary endpoints were safety and 1-year recurrence-free survival (RFS).

Results: As of November 15, 2025, 26 patients were enrolled, with 23 constituting the efficacy-evaluable population (65.2% were ypT+N+). All patients completed the initial 7-vaccination course. Treatment-related adverse events were primarily Grade 1-2 (fatigue: 39.1%; fever: 30.4%; injection site reactions: 21.7%), with one Grade III acute hypersensitivity event. With a median follow-up of 25.3 months from surgery, the 1-, 2-, and 3-year RFS rates were 91.3%, 85.6%, and 78.5%, respectively. These outcomes compare favorably with the adjuvant nivolumab arm in the CheckMate 577 trial, which reported a 3-year RFS of 43%. The 1-, 2-, and 3-year OS rates were 100%, 95%, and 83.1%, respectively. ELISpot assays confirmed immunogenicity in 100% (23/23) of patients, with 79.5% (233/296) of administered peptides eliciting de novo T-cell responses. TCR sequencing demonstrated durable expansion of neoantigen-specific T-cell clones, detectable during treatment and for six months after the final vaccination.

Conclusion: This study, representing the largest and longest-followed cohort in this context, establishes the individualized neoantigen vaccine iNeo-Vac-P01 as a promising adjuvant strategy for high-risk EC. The compelling survival benefit over historical standards, manageable safety profile, and universal immunogenicity support its potential to change the postoperative management paradigm and warrant further randomized trials.

#4367 Strong therapeutic efficacy of oncolytic virus KLS-3021 in orthotopic head and neck cancer models regardless of PD-L1 expression via tumor microenvironment remodeling.

Sungmin Lee, **Jinwon Seo**, Kiwon Park, Joonsung Kim, Eunjin Lee, Jaeil Shin, Soon-Oh Hong, Sujeong Kim, Sun Jin Kim

Kolon Life Science Inc., Seoul, Korea, Republic of

Treatment of confined or locally advanced head and neck squamous cell carcinoma (HNSCC) remains challenging, even though surgery, radiotherapy, and chemotherapy are standard therapeutic options. High recurrence rates after treatment and limited systemic therapeutic efficacy always meet persistent unmet needs. Recent advances have highlighted the value of neoadjuvant immuno-oncology strategies, which can reduce tumor burden and prime systemic immunity to improve postsurgical outcomes. In recurrent or metastatic HNSCC, first-line therapy is guided by PD-L1 expression, using immune checkpoint inhibitors, chemotherapy, or their combinations; however, clinical benefit remains limited regardless of PD-L1 status. These limitations emphasize the need for new treatment modalities capable of reducing tumor burden and eliciting robust antitumor immunity regardless of PD-L1 levels. KLS-3021 is a genetically engineered oncolytic vaccinia virus encoding PH-20 (hyaluronidase), interleukin-12, and a soluble PD1-Fc. This design enables extracellular matrix (ECM) degradation, intratumoral immune activation, and localized blockade of PD-1/PD-L1 signaling. In this study, the therapeutic activity of KLS-3021 was evaluated in orthotopic HNSCC models. The CAL27 xenograft model was used to investigate antitumor efficacy, viral spread, and apoptotic tumor cell death after a single intratumoral dose of KLS-3021. Syngeneic NOOC1 (PD-L1-high) and MOC2 (PD-L1-low) models were used to study PD-L1-independent tumor control by KLS-3021 and to compare efficacy against standard therapies—anti-PD-1 antibody and cisplatin, respectively—while characterizing TME remodeling and immune activation. In CAL27 model, KLS-3021 produced robust antitumor efficacy, including complete regression with prolonged survival. In NOOC1 model, KLS-3021 outperformed anti-PD-1 therapy in both tumor regression and TME reprogramming. Notably, KLS-3021 markedly degraded the intratumoral ECM, enhancing viral spread and immune cell infiltration, and shifted the TME toward an M1-dominant state with increased CD86 and TNF-α and reduced CD206 levels. This M1-skewed milieu was accompanied by CXCL10 upregulation and increased infiltration of activated T cells. KLS-3021 also induced immunogenic cell death establishing conditions favorable for durable antitumor immunity. In MOC2 model, KLS-3021 provided superior tumor control and survival benefit compared to cisplatin. Collectively, these findings indicate that KLS-3021 elicits potent antitumor immunity and remodels the TME regardless of PD-L1 levels, exceeding current conventional standards. Given its capacity for local tumor debulking and immune activation, KLS-3021 implicates strong translational potential as a next-generation therapeutic, including neoadjuvant applications for HNSCC.

#4368 Vaccine targeting IGF1R induces neutralizing antibody and robust anti-tumor activity in a syngeneic mouse colon cancer model.

Kenneth Nansheng Lin, Melvin Toh, HONG WANG

Sequencio Therapeutics, Hong Kong, Hong Kong

Background Insulin-like growth factors (IGFs) and their receptor (IGF1R) induce important cellular signalling that regulates cell proliferation, survival, and metabolism. Overexpression of IGF1R in cancers is associated with poor prognosis and resistance to conventional therapies, highlighting the need for innovative therapeutic strategy. In this study, we developed IGF1R vaccine candidates and evaluated their anti-tumor activity in a syngeneic mouse colon cancer model.

Methods Recombinant proteins comprising different immune enhancers and computationally-predicted B-cell epitopes in the regions involved in IGF-IGF1R ligand-receptor interaction, intended to induce antibodies to block IGF-IGF1R interaction, were produced. Immunogenicity of the vaccine proteins was assessed in C57BL/6 mice by vaccination 6 times on days 0, 14, 28, 42, 49 and 56 using the proteins adjuvanted with CpG ODN 1826 and AS03. Serum samples were collected at multiple time points for determining anti-IGF1R antibody titers using ELISA as well as *in vitro* neutralization activity via blocking IGF1 binding to IGF1R using competitive ELISA. Anti-tumor efficacy of the vaccines was evaluated in a syngeneic MC38 mouse colon cancer model in C57BL/6 mice, which were vaccinated and inoculated subcutaneously with MC38 cells a week after the last vaccination. Mice administered adjuvant only were used as controls. Tumor growth was recorded twice a week till the end point.

Results IGF1R vaccines induced robust humoral immune response as demonstrated by high titer of anti-IGF1R antibody. Importantly, serum samples collected from vaccinated mice demonstrated strong neutralizing activity, inhibiting IGF1 binding to IGF1R by up to 68% in a competitive ELISA. Two proteins which induced the highest antibody titer (i.e. 1:125,000) were further evaluated for their anti-tumor efficacy. In the anti-tumor study using the MC38 model, these two IGF1R vaccines suppressed the growth of tumors by 62% and 61%, respectively, at the study endpoint compared to controls ($p<0.01$).

Conclusions In summary, these findings establish proof-of-concept that IGF1R-targeting vaccines can elicit neutralizing antibodies that block IGF1 binding to IGF1R, thereby inhibiting the growth of tumors where IGF/IGF1R signalling plays critical roles. This result supports further investigation and optimization to improve these IGF1R vaccines to treat cancers dependent on IGF/IGF1R signalling.

#4369 B7-H3 vaccine induces robust humoral and cellular immunity and inhibits tumor growth in mice.

Kenneth Nansheng Lin, Melvin Toh, HONG WANG

Sequencio Therapeutics, Hong Kong, Hong Kong

Background B7-H3 (CD276) is an immune checkpoint molecule frequently overexpressed in a wide range of cancers, where it plays critical roles in immune evasion, tumor progression, and metastasis, underscoring its potential as a promising target for cancer immunotherapy. Here, we developed a novel protein vaccine to induce humoral and cellular immunity against B7-H3 and evaluated its anti-tumor efficacy in syngeneic mouse colon cancer models.

Methods A recombinant vaccine protein was generated, consisting of tandem repeats of the FG loop fragment of human B7-H3 - a structural motif linking the F and G β-strands of B7 family proteins that is critical for ligand-receptor interactions (though no ligand has yet been identified for B7-H3) - combined with an N-terminal cell-penetrating peptide to enhance immunogenicity. Immunogenicity of this B7-H3 vaccine, adjuvanted with CpG ODN 1826, was studied in BALB/c and C57BL/6 mice vaccinated subcutaneously weekly for 6 weeks. Controls were mice administered adjuvant only. Serum samples was collected at multiple time points to determine anti-B7-H3 antibody titer by ELISA. Splenocytes were harvested to assess cellular immunity using IFNγ ELISPOT assay. Anti-tumor efficacy of vaccine was evaluated in both prophylactic and therapeutic studies using B7-H3-humanized mouse colon cancer cell lines, CT26-hB7-H3 and MC38-hB7-H3, in BABL/c and C57BL/6 mice, respectively. Tumor growth was recorded. Tumor-infiltrating lymphocytes (TILs) were characterized by flow cytometry.

Results The B7-H3 vaccine induced robust humoral and cellular immunity against human B7-H3 in both BALB/c and C57BL/6 mice. In prophylactic studies, the vaccine demonstrated significant anti-tumor activity: 1) in the CT26-hB7-H3 model, tumor growth inhibition (TGI) in vaccinated mice was 99.8%, compared to controls and 90% of vaccinated mice were tumor-free at the endpoint; 2) in the MC38-hB7-H3 model, TGI was 72.4%. Using tumors collected from the MC38-hB7-H3 study, TIL characterization using flow cytometry revealed 1.2-fold and 4.3-fold increases of activated CD4+IFNγ+ and CD8α+IFNγ+ T-cells, respectively. In therapeutic studies, TGI in CT26-hB7-H3 tumor-bearing mice was 91.2%, with 7/12 of mice becoming tumor-free at the end point, and TGI in MC38-hB7-H3 tumor-bearing mice was 85%. In MC38-hB7-H3 tumors, TIL analysis showed a 2.8-fold increase in CD8α+IFNγ+ T cells.

Conclusions Our study demonstrates that the B7-H3 vaccine induces robust humoral and cellular immunity, effectively suppressing the growth of B7-H3-positive tumors in mice. These findings highlight its potential for clinical translation as a therapeutic strategy for B7-H3-overexpressing cancers in humans.

#4370 TROP2-circular RNA vaccine and IL7 synergistically inhibit TROP2+ tumor growth in mouse models.

Zirong He, Yanan Li, Antong Li, Xiaoxuan Liu, Kenneth Nansheng Lin, Fan Yan Meng, Melvin Toh, Hong Wang

Research & Development, Sequencio Therapeutics, Hong Kong, Hong Kong

Human trophoblast cell surface antigen 2 (hTROP2), a transmembrane glycoprotein encoded by the Tumor-Associated Calcium Signal Transducer 2 (TACSTD2) gene, is a promising tumor-associated antigen (TAA) in several types of cancers for targeted immunotherapy. We developed hTROP2 protein and RNA vaccines that effectively suppressed the growth of TROP2-positive tumors in mouse models. However, the efficacy of TAA-targeted vaccines in humans may be limited by self-tolerance and poor tumor infiltration of immune effector cells. Given the critical role of interleukin-7 (IL7) in promoting T-cell proliferation, survival, and repertoire diversity, we hypothesized that IL7 could enhance hTROP2 vaccine efficacy by expanding and diversifying the T-cell pool, thereby improving tumor infiltration and overcoming self-tolerance. To test this, we co-administered an hTROP2-expressing circular RNA-lipid nanoparticle (hTROP2-circRNA-LNP) vaccine with an IL7-expressing circRNA-LNP (IL7-circRNA-LNP) in mouse models. Cellular immune responses were assessed using IFNγ ELISpot assays on splenocytes from vaccinated mice. Co-administration with IL7-circRNA-LNP enhanced the cellular immune response by 2.3- and 2.7-fold for the two predominantly active stimulating peptides compared with the response induced by hTROP2-circRNA-LNP alone. Comparable results were observed when IL7-circRNA-LNP was administered either before or after the hTROP2-circRNA-LNP vaccine. In mice bearing tumors derived from TROP2-humanized cancer cell lines (MC38-hTROP2 and 4T1-hTROP2), co-administration of the hTROP2-circRNA-LNP vaccine with IL7-circRNA-LNP significantly enhanced anti-tumor efficacy compared with hTROP2-circRNA-LNP alone. Tumor growth inhibition increased from 57.4% to 87.0% in the MC38-hTROP2 model and from negligible effect to 63.4% in the 4T1-hTROP2 model. In control mice that received IL7-circRNA-LNP alone, IL7 monotreatment achieved 20% tumor growth inhibition (without statistical significance) in the MC38-hTROP2 model but had no effect in the 4T1-hTROP2 model. Analysis of tumor-infiltrating lymphocytes revealed that co-administration of the hTROP2-circRNA-LNP vaccine with IL7-circRNA-LNP significantly increased the proportions of cytotoxic CD8α+ and helper CD4+ T-cells, as well as their activated subsets (CD8α+IFNγ+ and CD4+IFNγ+ cells). Neither the hTROP2-circRNA-LNP vaccine nor IL7-circRNA-LNP alone significantly altered these T-cell populations. Collectively, our findings demonstrate that IL7 enhances the anti-tumor activity of the hTROP2-circRNA-LNP vaccine by the expansion of cytotoxic and helper T cells. These results suggest that co-administration of IL7-circRNA-LNP with hTROP2-circRNA-LNP represents a promising strategy for human cancer immunotherapy.

#4371 Preclinical potential of γδ T cells in novel virus-like particle vaccines for triple-negative breast cancer.

Arnau Sole Casaramona[1], Anish Ghimire[1], Romano Josi[1], Sanjana Marar[1], Anita Ogriņa-Komarova[2], Simone De Brot[1], Chang Wang[1], David Wiggins[3], Wendao Liu[3], Sarat Kumar Kottarath[3], Martin F. Bachmann[1], Eva M. Sevick[3], Mona O. Mohsen[1]

[1]University of Bern, Bern, Switzerland,[2]Latvian Biomedical Research, Riga, Latvia,[3]University of Texas at Houston, Houston, TX

Triple-negative breast cancer (TNBC) is an aggressive subtype with limited treatment options, high recurrence rates and poor outcomes. The conventional treatment among the standard of care strategies fail to elicit a long-term benefit for these patients. Personalized cancer vaccines using virus-like particles (VLPs), represent a promising strategy with the potential to induce durable immune responses. Recent research has highlighted the innate and adaptive properties of γδ T cells, underscoring their potential in cancer immunotherapy. However, how VLPs interact with γδ T cells, and their clinical efficacy to enhance their antitumor activity remains poorly understood and requires further investigation. We designed and developed novel next-generation VLPs engineered to incorporate cell-adjuvanted innate ligands and present tumor-neoantigens on their surface from a preclinical model of TNBC. We validated them by Cryo-EM and biochemical assays. We evaluated the interaction of VLPs with γδ T cells in wildtype and transgenic mice by transmission imaging techniques. Tumor *in vivo* experimentation was carried out in the 4T1 TNBC model. We compared three subcutaneous (s.c.) administration routes: systemic, targeting tumor-draining lymph nodes (tdLNs), and targeting non-tdLNs. Survival was assessed under different dosing and immune checkpoint inhibitor co-treatment. CD4, CD8, and γδ T cells were depleted to determine their contributions. We performed immunohistochemistry, flow cytometry, and RNA-seq analysis to evaluate the immune response. Our results show that γδ T cells efficiently engulfed VLPs in wild-type mice while this interaction is hindered in transgenic mice lacking key components of innate immune sensing pathways. Our novel VLPs expanded γδ T cells in tdLNs, promoting antitumor subsets and phenotypes. Subtype analysis revealed distinct activation profiles of γδ T cells subsets Vγ-1 and Vγ-4. Evaluation of tdLNs and tumors revealed early expansion of γδ T cells, highlighting innate properties. Depletion of γδ T cells abolished antitumor efficacy of the immunotherapy, suggesting adaptive properties. Furthermore, our personalized vaccine enhanced tumor infiltration of CD4, CD8 and γδ T cells, increased cytotoxic markers, reduced recurrence and metastasis, and improved survival despite low tumor mutational burden. Our findings reveal novel innate and adaptive properties of γδ T cells in response to our next-generation VLPs loaded with diverse innate immune stimuli and presenting tumor-neoantigens from 4T1 cells. These findings have the potential to reshape the field of cancer vaccines by harnessing γδ T cells as key players in anti-tumor immunity.
(*AI tools were used only to improve the clarity of the text in this abstract. All content was reviewed and verified by the authors.*)

#4372 Proteolysis-targeting vaccines, or PROTAX, for robust tumor combination immunotherapy.

Qiyan Wang, wenhua li, Shaomeng Wang, **Guizhi Julian Zhu**

University of Michigan, Ann Arbor, MI

Current peptide vaccines elicit limited antitumor T cell responses, leading to suboptimal tumor therapeutic efficacy. Here, we present proteolysis-targeting vaccines (PROTAX) that facilitate antigen proteolytic processing and cross-presentation to potentiate T cell responses for robust tumor immunotherapy in combination with immune checkpoint blockade (ICB). PROTAX are peptide antigens conjugated with a E3 ligase-binding ligand via linkers. In antigen-presenting cells (APCs), PROTAX bind to E3 ligases to rapidly ubiquitinate PROTAX antigens, facilitating antigen proteolytic processing by proteasome, and thereby promoting antigen cross-presentation to T cells. In mice, PROTAX promoted both the quantity and quality of $CD8^+$ T cell responses against antigens, such as multivalent melanoma-associated antigen Trp2-gp100-Trp1 (TgT) and synthetic long peptide human papillomavirus (HPV)-16 E7. In melanoma-bearing mice, PROTAX-TgT + ICB remodeled the tumor immune microenvironment and enhanced tumor complete regression (CR) rates, in a manner dependent on classic type-1 dendritic cells (cDC1) and $CD8^+$ T cells. PROTAX-TgT + ICB eradicated 100% large $Braf^{V600E}$ SM1 melanomas (~300 mm^3), and promoted the CR rates of M3 melanoma and highly immunosuppressive $Braf^{CA+}$ M2 melanoma with low TgT antigen expression. In an autochthonous $Braf^{V600E}$ melanoma in $Braf^{V600E/Pten-/-}$ mice, PROTAX-TgT + ICB reduced the molecular and cellular immunosuppression in the tumor, inhibited tumor progression and metastasis, and extended mouse median survival from 21 days to 66 days post initial tumor treatment. Similarly, PROTAX-E7 + ICB resulted in 43% CR of large TC-1 tumors (~300 mm^3). In human leukocyte antigen (HLA)-A02:01 human PBMCs from healthy donors and HPV-16^+ Head and Neck Squamous Cell Carcinoma (HNSCC) patients, HLA-A02:01-restricted trivalent $PROTAX^{E6-(E7)2}$ promoted tri-specific $CD8^+$ T cell responses, characterized with enhanced antigen-specific T cell expansion and production of human interferon-γ (IFN-γ) and tumor necrosis factor-α (TNF-α). Therefore, PROTAX hold the potential for robust tumor combination immunotherapy.

#4373 Rational design of immune-cell-homing macroporous hydrogels for enhanced dendritic cell recruitment and cancer vaccination.

Wenhao Xu, Hua Wang

University of Illinois at Urbana-Champaign, Champaign, IL

Macroporous biomaterials have emerged as a promising platform for in situ cancer vaccination because they can create localized immune niches that recruit, activate, and program dendritic cells (DCs) more effectively than traditional soluble vaccines. However, the immune-cell homing profile of these materials remains difficult to rationally control because key physical parameters—stiffness, viscosity, and pore size—are often inherently coupled. To overcome this challenge, we engineered an alginate-based macroporous hydrogel in which these properties were independently tunable, enabling a systematic investigation of how each dimension shapes DC recruitment and downstream antitumor immunity. The resulting design space revealed a striking synergy: hydrogels combining high stiffness, high viscosity, and large interconnected pores generated the most favorable immune microenvironment, recruiting 1.6-fold more DCs and markedly enriching the cDC1 subset associated with efficient cross-presentation. Large-pore hydrogels supported deeper cellular infiltration and increased MHC II expression, while high-viscosity formulations enhanced cell retention within the scaffold. Although softer matrices facilitated early migration in vitro, stiffer gels promoted superior DC proliferation, survival, and release, revealing a two-phase mechanism in which initial recruitment and sustained persistence are governed by distinct material properties. When loaded with GM-CSF, OVA, and CpG, the optimized hydrogel induced the strongest SIINFEKL-specific $CD8^+$ T-cell expansion and achieved significantly delayed tumor progression in prophylactic E.G7-OVA challenge, outperforming all other formulations and soluble controls. These findings establish a mechanistic framework for engineering macroporous hydrogels as programmable immune niches and demonstrate that precise decoupling of material mechanics and pore architecture can amplify vaccine potency in vivo. This work advances the rational design of biomaterial-based cancer vaccines and highlights the importance of material-immune cell crosstalk in generating durable antitumor immunity. AI-assisted text generation (ChatGPT) was used solely for language refinement of this abstract.

#4374 A novel RNA-LNP immunotherapy platform to drive anti-tumor efficacy in solid tumors.

Hailey R. Lee[1], Khalid Rashid[1], Tony Luu[1], Amanda Creech[1], Pu-Lin Teng[1], Emma Lieberman[1], Bridget Vause[1], Catherine Xie[1], Britney Trieu[1], Willy Hugo[1], Ting-Ting Wu[1], Norbert Pardi[2], Caius G. Radu[1]

[1]Molecular and Medical Pharmacology, UCLA Health, Los Angeles, CA,[2]Microbiology, University of Pennsylvania, Philadelphia, PA

Nucleoside-modified RNA vaccines complexed in ionizable lipid nanoparticles (RNA-LNPs) constitute a promising immunotherapy platform for T cell-directed cancer vaccine development. A challenge in generating a proper anti-tumor CD8 T cell response with current RNA vaccine iterations remains, however, in providing optimal activation of antigen-presenting cells. Further, the presence of an immunologically cold tumor microenvironment (TME) presents an additional obstacle in designing an immunotherapeutic strategy to overcome such immunosuppression. To address these challenges, we hypothesized that an optimized RNA-LNP platform which couples an antigen-encoding RNA with a novel RNA-LNP innate immune activator will synergistically activate dendritic cells (DCs) by engaging multiple pattern recognition receptor (PRR) pathways to enhance cross-presentation and drive CD8 T cell responses. To this end, we immunized mice with our novel RNA-LNP platform and demonstrated that multiple DC subsets were activated at both local and distal secondary lymphoid organs respective to the injection site. The DCs from the immunized mice also activated and expanded antigen-specific T cells and resulted in memory T cell formation. Abrogation of these T cell responses in genetic knockout models demonstrate that such T cell activation is mediated by multiple PRRs. Systemic delivery of the novel innate immune activators activated DCs at draining lymph nodes local to the tumor site in an orthotopically implanted murine pancreatic cancer model and subsequently conferred tumor growth suppression. Collectively, these studies establish a new paradigm for RNA-LNP immunotherapy that integrates multifaceted PRR engagement to promote antigen-specific vaccination and facilitate T cell priming and reactivation at the tumor.

#4375 Claudin 6 vaccines effectively inhibit tumor growth in a syngeneic mouse colon cancer model.

Na Wang, Lam Chow, Melvin Toh, Hong Wang

Sequencio Therapeutics, Hong Kong SAR, China

Human Claudin 6 (CLDN6) is a member of the Claudin family of proteins, which plays a crucial role in the structure and function of tight junctions. In humans, CLDN6 is primarily expressed in stem cells and embryonic tissues, with minimal mRNA detected in testis, pancreas, and placenta. Elevated expression of CLDN6 has been found in several types of cancers, suggesting that CLDN6 is an ideal tumor-associated antigen for targeted immunotherapy, albeit its precise role in cancer remains to be defined. Here, we generated recombinant proteins consisting of multiple human CLDN6 B- and T-cell epitopes (CLDN6-B+T) or T-cell epitopes only (CLDN6-T), which were selected based on computationally predicted B/T-cell epitope sequences and fused with the transmembrane domain of diphtheria toxin (DTT) as an immune enhancer. The immunogenicity and anti-tumor activity of these two vaccines were evaluated in mouse models. In both wildtype and HLA*02:01-humanized mice, CLDN6-B+T and CLDN6-T with adjuvant CpG induced robust cellular immune response as assessed by IFNγ ELISpot assay using splenocytes collected from mice vaccinated weekly for 6 weeks. In a syngeneic mouse tumor model using CLDN6-humanized MC38 colon cancer cell line (MC38-CLDN6(K)), both vaccines significantly suppressed the growth of tumor cells inoculated one day after the 6th vaccine dose, compared to control mice that received adjuvant only (n=8 in each group). In this study, 7/8 mice vaccinated with CLDN6-B+T and 8/8 mice vaccinated with CLDN6-T were tumor-free at the endpoint. A replicate study using an independently-derived CLDN6-humanized MC38 cell line, MC38-hCLDN6(C), demonstrated 72.6% and 73.2% tumor growth inhibition by CLDN6-B+T and CLDN6-T vaccines, respectively, compared to adjuvant controls(n=10 in each group). In a therapeutic study in which MC38-hCLDN6(C) cells were inoculated subcutaneously one day before weekly vaccination for 5 times, tumor growth was inhibited by 67.0% and 81.0% in mice vaccinated with CLDN6-T (n=11) and CLDN6-B+T (n=12), respectively, compared to mice that received adjuvant only (n=10). Collectively, our findings demonstrate that CLDN6-targeted vaccines significantly suppressed the growth of CLDN6-positive tumors in mice. These results support CLDN6-targeted vaccines as a promising therapeutic strategy for CLDN6-positive cancers in humans, with their potential to be further validated in upcoming studies.

#4376 Harnessing artificial intelligence to optimize neoantigen prediction and mRNA design for personalized cancer vaccine.

Yang Liu, Qingyi Mao, Wu Xinghan, **Qiu Mantang**

Xinyi Pharma (Hangzhou) Co., Ltd., Hangzhou, China

Background:Neoantigen-based mRNA personalized cancer vaccines (PCV) represent a promising frontier in cancer immunotherapy. However, current neoantigen prediction strategies primarily rely on MHC binding affinity, which leads to limited accuracy in immunogenicity and results in a high false-positive rate. The precise identification of neoantigen epitopes that are efficiently presented by MHC and elicit robust immunogenicity remains a central challenge hindering the clinical application of PCV. Here, we developed EchoNeo 1.0, a multimodal deep learning-driven pipeline that innovatively integrates immunogenicity prediction with mRNA sequence design to accelerate the of application of PCV.
MethodsThe core of pipeline is a multimodal deep learning model for immunogenicity prediction. Trained on publicly available databases (IEDB, TSNAdb v2.0, TESLA) and published immunogenicity data, the model integrates peptide/HLA pseudosequence features with multidimensional biological metrics to achieve accurate immunogenicity scoring. Neoantigen mRNA vaccines were synthesized and formulated with lipid nanoparticles (LNP), and evaluated in mouse models for safety (including toxicology and in vivo biodistribution) and therapeutic efficacy.
Results:Approximately 3,700 peptides (8-11 amino acids) with confirmed experimental immunogenicity data were used to train and validate EchoNeo, which demonstrated superior performance in benchmark tasks against established prediction tools (e.g., DeepImmuno, IEDB Class I Immunogenicity tool) and showed excellent immunogenicity prediction accuracy on independent, clinically validated neoantigen datasets. In C57BL/6 mice intramuscularly administered with vaccine (at a maximum dose of 54 μg, approximately 2.7 mg/kg), no significant adverse changes were observed in body weight, body temperature, blood biochemistry (ALT, AST, DBIL, CREA, UREA, TG, TC, LDL, HDL, LDH, CK), or complete blood count (CBC, DIFF, and RET). In a melanoma model, the vaccine significantly inhibited tumor growth, and enhanced therapeutic effect was achieved when combined with anti-PD-1 antibody.
Conclusion:Superior immunogenicity prediction accuracy was confirmed, as well as the favorable safety and potent antitumor efficacy in mouse models. This work represents a paradigm shift from conventional affinity-based prediction to an end-to-end framework that directly assesses the immunogenicity of neoantigen peptides, holding significant promise for accelerating the development of PCV.

#4377 High affinity receptor bio-selected novel oncolytic RNA virus, IVX055, demonstrates potent anti-tumor activity in human NSCLC, hepatocellular carcinoma and bladder cancer with potential for immunotherapeutic combinations.

Min Quah, Christine Lee, Rebecca Ingham, Oksana Zdanska, **Darren Shafren**

ImmVirX, Newcastle, Australia

Background:
Oncolytic viruses represent a promising therapeutic approach through their dual mechanisms of direct tumor cell lysis and stimulation of anti-tumour immunity. IVX055 is a novel, non-enveloped, single-stranded RNA oncolytic virus developed using a proprietary receptor bio-selection platform, which enables preferential targeting of tumor cells by exploiting overexpressed surface receptors. This platform enhances tumor specificity, efficient viral entry, and replication within the tumor microenvironment. Infection with IVX055 induces cell lysis and potential pro-inflammatory signaling, including PD-L1 upregulation, which may increase immune cell infiltration and sensitize tumors to immune checkpoint inhibitors (ICIs). These immunostimulatory effects position IVX055 as a strong candidate for combination with ICIs, T-cell engagers, antibody-drug conjugates (ADCs), and bispecific antibodies to amplify anti-tumor responses.
Methods:
The oncolytic activity of IVX055 was evaluated *in vitro* using multiple human Non-small cell lung cancer (NSCLC), hepatocellular carcinoma (HCC) and bladder cancer cell lines. Monolayer cultures were infected with varying multiplicities of infection (MOIs). Cell viability was measured using the XTT assay as a surrogate for cytolytic activity and metabolic function. For mouse models, immunocompromized mice were seeded with single flank human tumor cell administrations. Following development of palpable tumors, IVX055 was administered via the i.t route. calliper measurements were employed to assess tumor burden.
Results:
IVX055 demonstrated potent, dose-dependent cytolytic activity in NSCLC, HCC and bladder cancer cell lines. Multiple rounds of viral replication were evident, consistent with high level production of progeny virus coupled with sustained oncolytic activity and induction of a potential pro-inflammatory tumour phenotype. Significant reductions in cell viability were detected shortly after infection, confirming rapid and robust tumor cell killing. Intratumoral administration of IVX055 in human tumor xenograft models using immunocompromized mice was well tolerated and displayed potent anti-tumor activity against NSCLC cancers.
Conclusions:
IVX055 exhibits strong preclinical *in vitro* and *in vivo* oncolytic activity and tumor selectivity, supporting its continued development. Future studies will explore combination strategies with ICIs, T-cell engagers, ADCs, and bispecific antibodies to enhance efficacy in advanced solid tumours. A phase 1 basket study of intratumoral IVX055 in combination with systemic anti-PD1 therapy in pts (n=32) bearing visceral disease from checkpoint refractory NSCLC, HCC and Cholangiocarcinoma is planned to commence in 2026.

#4378 Live attenuated MMR vaccines modulate tumor immune cell infiltration and synergize with standard of care to prolong survival in preclinical HCC models.

Mulu Z. Tesfay[1], Aleksandra Cios[2], Khandoker Usran Ferdous[3], Randal S. Shelton[3], Isabelle Miousse[3], Camila C. Simoes[3], Alexei Basnakian[3], Rangaswamy Govindarajan[3], Martin Cannon[3], Mitesh J. Borad[4], Bolni M Nagalo[2]

[1]UAMS Winthrop P. Rockefeller Cancer Institute, Little Rock, AR,[2]Department of Pharmacology and Physiology, University of Maryland School of Medicine, Baltimore, MD,[3]University of Arkansas for Medical Sciences, Little Rock, AR,[4]Director Phase I Drug Dev, Dept. of Hemat./Onco., Mayo Clinic Arizona, Scottsdale, AZ

Hepatocellular carcinoma (HCC) is a leading cause of cancer-related death worldwide, thus, there is an urgent need to develop more effective therapeutic options for this dismal condition. Tumor-infiltrating lymphocytes (TILs) are associated with improved response to immune checkpoint blockade in HCC, but their low abundance in most cases limits their therapeutic efficacy. Here, we demonstrate, in mice, that low-dose intratumoral immunovirotherapy with the trivalent measles, mumps, and rubella vaccine (MMR) induces superior tumor-growth delay and extended host survival compared to individually administered vaccines for measles, mumps, or rubella viruses. Further, our results show that MMR therapy synergizes with PD-1 and CTLA-4 blockade to reprogram the tumor microenvironment, resulting in increased CD8+ TIL infiltration and reduced PD-1 expression on TILs, among other effects. These changes in the immunological landscape translated into greater survival and more durable tumor-specific and memory immune responses for hosts. Comprehensive toxicology analysis revealed no evidence of MMR-induced liver or kidney toxicity after intrahepatic administration. This work reinforces an unrecognized role of MMR plus ICB in reprogramming the immune landscape in HCC through multimodal immune activation, providing a strong rationale for further development of MMR-based therapies for HCC.

#4379 Enhanced cancer immunotherapy via sPD1-based DNA vaccination targeting epitope-focused TWIST1 antigen.

Zhiwu Tan[1], Mei Sum Chiu[1], Helen Xinyue Yu[2], Xiaoxiao Chang[1], Zhiwei Chen[2]

[1]The Hong Kong Polytechnic University, Hong Kong, China,[2]The University of Hong Kong, Hong Kong, China

TWIST1, a basic helix-loop-helix transcription factor, is overexpressed in a variety of tumors such as melanoma, breast, colon cancer and mesothelioma, and associated with tumorigenesis and metastasis. We have previously shown that full-length TWIST1 vaccine elicited cytotoxic T lymphocytes (CTLs) that recognized TWIST1-expressing tumors and conferred protection against tumor challenge in the form of DNA vaccine and adeno-associated viral vector system, highlighting TWIST1 as a promising target for cancer immunotherapy. In this study, we sought to apply optimization approach on the TWIST1-based vaccine platform in order to enhance T cell immunity and reduce potential toxicity.

We developed a novel soluble PD-1 (sPD1)-based DNA vaccine encoding a truncated version of TWIST1 (sPD1-TruncT1) that includes major T cell epitopes found in both human and mouse proteins. The immunogenicity and antitumor efficacy of the vaccine were evaluated and compared in parallel to full-length TWIST1 vaccine in two murine models of TWIST1-expressing tumors. By doing epitope mapping, we identified immunodominant T cell epitopes within the TWIST1 antigen, showing that majority of T cells recognized a C-terminal conserved region. sPD1-based DNA vaccine encoding epitopes of this conserved region, via in vivo electroporation (EP), elicited more robust TWIST1-specific T cell responses compared to full-length TWIST1 vaccine. Furthermore, these TWIST1-specific T cells were polyfunctional because they produced multiple effector cytokines when encountering TWIST1-expressing tumors. In addition, immunotherapy with the sPD1-TruncT1 vaccine showed a notable enhancement in antitumor efficacy in both preventive and therapeutic scenarios. With the widespread expression of TWIST1 in different cancer types, truncated TWIST1 vaccination has high potential for cancer immunotherapy and warrants investigation in human clinical trials to evaluate its applications as a vaccine for patients with WT1-expressing cancers.

#4380 IRZ-01: A self-adjuvanted outer membrane vesicle vaccine targeting CEA and MUC1 for colorectal cancer immunotherapy.

Kevin Chen[1], Caleigh Fletcher[1], John Cowger[1], James E. Galen[2], Mayukh Das[3], Marcio Chedid[1]

[1]Irazu Oncology, LLC, Baltimore, MD,[2]Center for Vaccine Development and Global Health, University of Maryland, Baltimore, Baltimore, MD,[3]Arcus Biosciences, Hayward, CA

Background: Irazu Oncology developed a tumor vaccine platform using a proprietary, attenuated *Salmonella* Typhi strain engineered to express human tumor antigens and shed antigen-decorated outer membrane vesicles (OMVs). This flexible system enables rapid development of mono- or multi-valent vaccines. IRZ-01 is an OMV-based vaccine displaying epitopes from two well-characterized and validated tumor-associated antigens (TAAs): Mucin-1 (MUC1) and CEACAM5 (CEA). Here we show that IRZ-01 administration to immunocompetent mice triggers potent antigen-specific humoral and cellular immunity and confers single-agent antitumor efficacy in models expressing CEA and/or MUC1.

Methods: *Salmonella* Typhi CVD911Δ*fliC* (pPagL-CEA/MUC1) was cultured in animal-free soytone media to produce IRZ-01 OMVs. OMVs were purified by tangential flow filtration and size-exclusion chromatography. Characterization included DLS (size), TRPS (zeta potential), cryo-EM (morphology), immuno-gold EM, and Western blotting for CEA/MUC1 surface display. Toll-like receptor (TLR) activation was tested using HEK-Blue™ cells expressing human TLR2, 3, 4, 5, 7, 8, or 9 (InvivoGen). Immunogenicity was evaluated in C57BL/6 mice given two doses of IRZ-01 (0.25 µg IV or 2 µg IM, days 0 and 7) or 5×10^9 CFU live bacteria; controls received PBS. Serum IgG was quantified by ELISA (days -1, 6, 20); T-cell responses assessed by IFN-γ ELISPOT on day 21 splenocytes. Antitumor efficacy was assessed in MC38-CEA and MC38-MUC1 syngeneic models by monitoring tumor growth post-challenge with IRZ-01.

Results: Purified IRZ-01 OMVs were 90-100 nm, zeta potential -13.9 mV, with confirmed CEA/MUC1 surface expression by Western blot and immuno-gold EM. IRZ-01 selectively activated TLR2 and TLR4, confirming self-adjuvanting properties due to native microbe-associated molecular patterns (MAMPs) naturally present in their outer membrane.Vaccination elicited rapid, high-titer antigen-specific IgG by day 6, strongly boosted after the second dose, with comparable responses via IV or IM routes and similar to the live vector. IFN-γ ELISPOT showed significant ($p<0.05$ vs PBS) CEA- and MUC1-specific T-cell responses that correlated closely with antibody levels.Encouraged by strong humoral and cellular responses, we conducted efficacy studies using a syngeneic C57BL/6 mouse model implanted with MC38-CEA and MC38-MUC1 cells, IRZ-01 induced marked tumor growth inhibition; volumes receded shortly after treatment and remained significantly lower than untreated PBS control groups for all
experimental groups. Survival data demonstrated >90% survival in groups treated with IRZ-01 regardless of tumor line.

Conclusion: IRZ-01 is a potent, self-adjuvanted OMV vaccine that induces robust CEA/MUC1-specific humoral and cellular immunity and delivers strong single-agent efficacy in syngeneic tumor models.

#4381 Combination therapy with a HIF-1α/c-MET peptide vaccine and carboplatin reprograms the tumor microenvironment to overcome platinum resistance in an intraperitoneal metastasis model of high-grade serous ovarian carcinoma.

Soon Young Lim, JinHwa Hong, DongGeRaMi Moon, Hyeyeon Roh, Ju Won Kim, Ji Won Lee, Kyong Hwa Park

Korea University, Seoul, Korea, Republic of

Ovarian cancer is the most lethal gynecologic malignancy, with most patients diagnosed atadvanced stages (III-IV). Although initially responsive to platinum-based chemotherapy, about60% of patients relapse within a few years due to acquired chemoresistance. Tumor hypoxiahas been implicated as a key driver of aggressive phenotypes and treatment resistance. Ourprevious study showed that a HIF-1α/c-MET-derived peptide vaccine combined with platinumcompounds elicited strong antitumor immunity in a mouse model of ovarian cancer. Here, weinvestigated whether type I immune activation could overcome platinum resistance in anaggressive intraperitoneal metastasis model in vivo. An intraperitoneal metastasis model was established in C57BL/6 mice using a murineplatinum-resistant ID8 ovarian cancer cell line. To evaluate antitumor effects, mice wereassigned to four groups: (1) control, (2) carboplatin, (3) HIF-1α/c-MET vaccine, and (4)combination of carboplatin and vaccine. The vaccine was administered subcutaneously threetimes at one-week intervals prior to tumor inoculation, and carboplatin was administered oneweek after tumor inoculation. Tumor progression and metastatic burden were monitored usingan in vivo imaging system (IVIS). Ascites formation was quantified by measuring abdominalcircumference. Immunohistochemistry (IHC) was used to assess HIF-1α and c-METexpression, intratumoral $CD8^+$/ $CD4^+$ T-cell ratios, and M1/M2 macrophage ratios in the peritoneum. Both monotherapies with either carboplatin or vaccine significantly inhibited intraperitonealmetastasis compared with the control. Furthermore, the combination therapy showedsignificantly better suppression of intraperitoneal metastasis than either monotherapy. Ascitesformation was markedly decreased in both monotherapy groups compared with the control,and it was further decreased in the combination group. IHC revealed that carboplatin aloneincreased HIF-1α and c-MET expression, suggesting activation of tumor-promoting signals,while the vaccine—alone or combined—suppressed expression of these markers. Bothtreatments enhanced intratumoral $CD8^+$ T-cell infiltration and improved the $CD8^+$/ $CD4^+$ ratio($p < 0.0001$) as well as the M1/M2 macrophage ratio ($p < 0.0001$), with the combination therapyshowing the significant effect. These results suggest that immunotherapy with a combination of HIF-1α/c-MET peptidevaccine with carboplatin reversed the tumor hypoxia induced by carboplatin alone andreprogramed the tumor microenvironment toward immune activation, offering a promisingimmunotherapeutic strategy to overcome platinum resistance and prevent recurrence in ovariancancer.

#4382 Bridging *in vitro* screening to *in vivo* efficacy for cancer vaccines.

Hongyan Sun, Jialu Fan, Yujing Zhang, Yunlong Jiang, Huixin Yang, Xiang Gao

GemPharmatech Co., Ltd., Nanjing, China

mRNA cancer vaccines represent a next-generation immunotherapy platform with the potential to elicit robust, antigen specific immune responses. Upon in vivo delivery, mRNA vaccines are taken up by antigen-presenting cells (APCs), translated into the tumor associated antigen and presented via MHC molecules to activate adaptive immunity. However, standard mouse models with murine MHC molecules are not suitable for evaluating these MHC-restricted immune responses. GemPharmatech has developed an in vitro and in vivo mRNA vaccine drug evaluation service platform, including the in vitro and in vivo immunogenicity evaluation, in vivo anti-tumor efficacy and safety evaluation. For in vitro immunogenicity, dendritic cells derived from autologous monocytes (moDCs) are matured and loaded with specific antigen peptides using electroporation or administered with LNP-mRNA. The peptide-pulsed moDCs are then co-cultured with T cells from the same donor. The antigen-specific T-cell response is detected by ELISpot or flow cytometry. In vitro immunogenicity evaluation is applicable to early antigen peptide screening, assessing the affinity of antigen peptides for corresponding HLA molecules and their immunostimulatory capacity. For in vivo evaluation of cancer vaccine, GemPharmatech has developed a series of HLA-humanized mouse models across multiple mouse backgrounds including the immunocompetent mice B6, BALB/c, CB6F1 and the immunodeficient NCG derived mice. These models express human HLA molecules, enabling the accurate evaluation of antigen presentation, immunogenicity, and therapeutic efficacy of mRNA vaccines. The HLA-humanized mice exhibit strain-dependent humoral and cellular immune responses, satisfying various evaluation needs. HLA humanized mice exhibited strain specific humoral and cellular immune responses, but are sufficient to satisfy various evaluation needs. CB6F1 exhibited good combination of humoral and cellular immune response to the same immunogen, making them more suitable for assessing vaccine immunogenicity. In NCG-M-hHLA-A2.1 mice engrafted with hematopoietic stem cells, HLA-A2.1-restricted immune responses were observed, reflecting successful reconstitution of human DCs and functional T cells. Therapeutic studies using TA-1 (mRNA vaccine) or anti-PD1 in a patient derived xenograft (PDX) demonstrated that TA-1 or anti-PD-1 inhibited tumor growth, while combination therapy led to greater tumor inhibition. In conclusion, GemPharmatech has established a comprehensive vaccine evaluation platform that integrates in vitro screening with in vivo models to provide more options for preclinical evaluation of tumor vaccines.

#4383 Utilization of HBV-vaccinated immunity to suppress tumor progression via targeted delivery of HBsAg to CEA-positive colorectal cancer.

Chun-Chia Cheng[1], Zong-Lin Sie[1], Yung-Chin Hsiao[1], Ai-Sheng Ho[2], Chih-Liang Wang[3], Cheng-Liang Peng[4], Chun-I Wang[5], Hong-Zen Yeh[6], Jungshan Chang[7], Chun-Chao Chang[8]

[1]Chang Gung University, Taoyuan, Taiwan,[2]Cheng Hsin General Hospital, Taipei, Taiwan,[3]Chang Gung Memorial Hospital, Taoyuan, Taiwan,[4]National Atomic Research Institute, Taoyuan, Taiwan,[5]China Medical University, Taichung, Taiwan,[6]Taichung Metro Harbor Hospital, Taichung, Taiwan,[7]Taipei Medical University, Taipei, Taiwan,[8]Taipei Medical University Hospital, Taipei, Taiwan

Limited antigen recognition hampers the anti-tumor efficacy of $CD8^+$ T cells. We hypothesized that vaccinated immunity against hepatitis B virus (HBV) in individuals could be harnessed to target hepatitis B surface antigen (HBsAg)-expressed tumor cells, thereby suppressing tumor progression. We aimed to validate the proposed concept and to develop a tumor-targeting agent that delivers HBsAg to colorectal tumor cells via carcinoembryonic antigen (CEA)-targeted antibodies. We generated HBsAg-overexpressed CT26 colorectal tumor cells and utilized HBV-vaccinated BALB/c mice to evaluate the proposed concept. A fusion protein comprising a fragment of HBsAg (fHBs, amino acids 103-170) and a single-chain variable fragment (scFv) against CEACAM5 (CEA), linked to a Fc domain (fHBs-T84scFv-Fc), was constructed to deliver HBsAg into tumor cells for immune recognition and tumor suppression. We found that HBV-vaccinated mice exhibited strong anti-HBsAg responses and significantly suppressed HBsAg-overexpressed CT26 tumor growth, accompanied by increased $CD3^+$ and $CD8^+$ T cell infiltration in tumor tissues. CEACAM5 was identified as a colorectal tumor-specific receptor exhibiting internalization. We consequently demonstrated that the created anti-tumor reagent fHBs-T84scFv-Fc effectively bound tumor cells and inhibited growth of CEACAM5-positive MC38 tumors in the HBV-vaccinated mice. Meanwhile, enhanced infiltration of $CD3^+$ and $CD8^+$ T cells was observed in the tumor tissues under fHBs-T84scFv-Fc treatment. We demonstrated a novel strategy by utilizing HBV-vaccinated immunity for colorectal tumor suppression via CEA-targeted HBsAg delivery. This study suggests that the anti-HBV immunity containing anti-HBsAg $CD8^+$ T cells can be utilized to suppress a range of tumors using HBsAg-antibody conjugates by targeting the tumor-specific internalizing receptors.

#4384 Advancing novel vaccines: Preclinical evaluation in HLA-A2.1/HLA-DRB1*1.1 humanized mice.

Dana Emerson, Zhenlan Niu, Shuaiqiang Zhang, Xiaofei Zhou

Biocytogen, Waltham, MA, MA

The human leukocyte antigen (HLA) system plays a central role in orchestrating adaptive immune responses. While existing single-allele humanized models have been valuable, there is a growing need for preclinical platforms that more fully recapitulate human HLA class I and II restricted immunity to evaluate complex immunotherapies. To address this, we developed a novel MHC I/II dual-humanized mouse model, the B-HLA-A2.1/HLA-DRB1*1.1 mouse.The B-HLA-A2.1/HLA-DRB1*1.1 model was generated by co-integrating the human HLA-A02:01 and HLA-DRB1*01:01 genes into the C57BL/6 background. Human HLA-A2.1 and HLA-DRB1 protein expression was confirmed by flow cytometry on spleen, peripheral blood, and bone marrow leukocytes. Comprehensive immune cell profiling was performed to characterize T and B cell populations. The model's functionality was validated in a therapeutic tumor vaccination study using a human epitope-targeting vaccine.Flow cytometric analysis confirmed stable and robust cell surface expression of both HLA-A2.1 and HLA-DRB1 proteins in homozygous mice. The frequency of CD8+ T cells in the spleen, blood, and lymph node was significantly decreased, while the frequency of CD4+ T cells was significantly increased, demonstrating that the introduction of HLA-A02:01 and HLA-DRB1*01:01 affected the development of T cells. Additional analyses, including hematology, serum biochemistry, and histopathological examination (H&E staining) of major organs, indicated no spontaneous pathology, confirming the overall health and physiological stability of the model. In a vaccine efficacy study, immunization with a human antigen-specific vaccine significantly inhibited tumor growth in the dual-humanized mice compared to controls, demonstrating the model's capability to mount a functional HLA-restricted immune response.We have successfully developed and preliminarily validated the novel B-HLA-A2.1/HLA-DRB1*1.1 dual-humanized mouse model. It represents a powerful and physiologically relevant preclinical tool for investigating combination immunotherapies, including vaccines and immune checkpoint inhibitors, and for studying anti-tumor and infectious disease immunity within a more complete human-like context.

#4385 Engineering durable tumor immunity with a virus-tumor hybrid antigen dendritic cell vaccine.

Jin Muk Kang[1], Eun Hyang Han[2], Jin-kyu Choi[3], Seunghee Youm[2], Tej Pareek[3], Seong-Jin Kim[4], John Letterio[1], **Seunghwan Lim**[3]

[1]University Hospitals, Angie Fowler Adolecent and Young Adult Institute, Cleveland, OH,[2]Case Western Reserve University, School of Medicine, Cleveland, OH,[3]Celloram Inc., Cleveland, OH,[4]MedPacto Inc., Seoul, Korea, Republic of

Introduction: Dendritic cell (DC)-based cancer vaccines have shown limited efficacy in clinical trials, a result that has been partly attributed to poorly immunogenic tumor antigens that fail to induce robust MHC class-II directed CD4+ T cell help. CD4+ T cells 'license' DCs to upregulate key costimulatory molecules (e.g. CD80/86) and cytokines (IL-12) that are essential for the generation of effective, long-lived tumor-directed CD8+ T cells. However, therapeutic approaches that effectively harness both T-cell subsets have been constrained by difficulties in identifying $CD4^+$ T-cell-specific cancer neoepitopes. Here, we introduce , a novel DC-based cancer vaccine platform designed to co-present non-tumor-related $CD4^+$ T helper epitopes from the SARS-CoV-2 Spike protein alongside tumor-specific $CD8^+$ T-cell epitopes derived from tumor-associated antigens (TAAs), leveraging widespread Covid-19 immunity in the context of a cancer vaccine.

Methods: In proof-of-concept studies, PROTEXI was generated by simultaneously loading mature bone marrow-derived DCs (BMDCs) with pMHC-II-$OVA^{323-339}$ and pMHC-I-$Trp2^{180-188}$ complexes. To model the prevalence of SARS-CoV-2 Spike-specific $CD4^+$ T-cell memory, mice were either primed with DC-OVA^{323} or received adoptive transfer of OT-II $CD4^+$ T cells prior to tumor challenge, followed by PROTEXI treatment (weekly for 2 weeks) or PROTEXI in combination with immune modulating agents. The therapeutic potential of PROTEXI in a human immune context was evaluated in humanized mice reconstituted with blood from COVID-19-vaccinated donors. The human version, PROTEXI-Spike/TAA, was designed to co-present $CD4^+$ T-cell-restricted Spike epitopes together with $CD8^+$ T-cell-restricted PRAME and MAGE-A3 antigens.

Results: PROTEXI significantly improved survival and reduced tumor growth, correlating with enhanced T-cell infiltration into immune-cold tumors and induction of gene signatures associated with T-cell cytotoxicity, migration, and memory formation. Combination therapy with either anti-PD-1 immune checkpoint blockade or the ALK5 (TGF-β type I receptor) inhibitor Vactosertib further augmented therapeutic efficacy in therapy-resistant tumor models. Importantly, tumor-specific cytotoxic T-cell memory derived from PROTEXI mice was sufficient to mediate complete tumor rejection upon re-challenge. In humanized models, PROTEXI-Spike/TAA markedly expanded antigen-specific $CD8^+$ T-cell populations and reduced tumor burden, demonstrating translational feasibility and potency.

Conclusion: Collectively, these findings highlight the clinical potential of PROTEXI as an innovative DC vaccine platform that leverages the widespread prevalence of Spike-specific $CD4^+$ T-cell immunity to enhance cancer vaccine efficacy—offering a promising therapeutic strategy for patients with advanced, immune-cold tumors.

#4386 Expanding the therapeutic potential of Bvax: A B-cell-based vaccine for solid tumors.

Hanxiao Wan[1], Joshua L. Katz[1], **Yotam D. Hahn**[1], Si Wang[1], Grace V. Jones[1], Alina R. Murphy[1], Rebecca Du[1], Jeffrey Bacha[2], Roger Stupp[3], Catalina Lee-Chang[3]

[1]Department of Neurological Surgery, Northwestern Univ. Feinberg School of Medicine, Chicago, IL,[2]Sera Biopharma Inc, Chicago, IL,[3]Lou and Jean Malnati Brain Tumor Institute, Robert H. Lurie Comprehensive Cancer Center, Northwestern Univ. Feinberg School of Medicine, Chicago, IL

Glioblastoma (GBM) presents a major clinical challenge due to its highly invasive nature and resistance to treatment. We previously developed Bvax, a novel B-cell-based cancer therapy. In preclinical models of GBM, Bvax elicited robust antitumor immunity by enriching a subpopulation of CD8+ T cells characterized by high TCF1 and low PD-1 expression. Additionally, Bvax differentiated into plasma cells that secreted antibodies targeting tumor-associated proteins involved in motility and matrix remodeling, suggesting the disruption of tumor progression and enhanced immune infiltration. A first-in-human (FIH) Phase I clinical trial at Northwestern University evaluates the safety and feasibility of Bvax in patients with newly diagnosed GBM. Given the encouraging preclinical results in GBM, we explored therapeutic potential of Bvax for other solid tumors, namely lung and prostate cancer. This study aims to characterize the effects of Bvax on tumor growth, survival, and the preferential migration of Bvax in these new models. To assess Bvax in a lung cancer model, we utilized an orthotopic KP (Kras/p53 mutated) lung tumor model that recapitulates KRAS-driven non-small cell lung cancer (NSCLC). Bvax treatment resulted in a marked survival extension (median 39 vs. 17 days) in tumor bearing mice compared to controls (Wilcoxon $p = 0.046$). To further assess biodistribution, we used B cell knockout (muMt) mice and observed enriched Bvax infiltration within the tumor, confirming strong tumor tropism within the lung microenvironment. We next evaluated Bvax in a subcutaneous prostate tumor model known for immune exclusion and poor immunotherapy responsiveness. Twenty one days after tumor induction, Bvax was administered and tumor volumes were measured regularly until they reached the defined size endpoint. At peak treatment response, tumor volumes were reduced by 68% relative to controls, accompanied by a higher percentage of MHC-II tumor-infiltrating B cells. These results suggest Bvax retains efficacy across several tumor types with restricted immune infiltration. Ongoing work is now evaluating Bvax in combination with standard-of-care regimens across both tumor models to determine whether its therapeutic activity can be enhanced. In parallel, we are performing immunophenotyping analyses to define how Bvax reshapes the immune landscape within the tumor and surrounding tissue, and better quantify Bvax infiltration across tumor compartments. Additionally, to support translational relevance, we are extending these investigations into patient-derived samples to assess Bvax function in human disease contexts.

#4387 A clinical-adopted vaccine platform and new immunogenic epitopes combined against prostate cancer.

Elisa Marmocchi[1], Rubens Begaj[1], Marta Cantarelli[1], Davide Bressan[1], Nicole Annesi[1], Martina Cortese[1], Mattia Barbareschi[2], Giovanni Bertalot[2], Francesco Giuseppe Carbone[2], Alessandro Alaimo[1], Marianna Kruithof-de Julio[3], Nicola Ternette[4], Ugo Ala[5], Fulvio Chiacchiera[1], Guido Grandi[1], Andrea Lunardi[1]

[1]CIBIO, University of Trento, Trento, Italy,[2]Pathological Anatomy Unit, Santa Chiara Hospital-APSS, Trento, Italy,[3]University Hospital of Bern, Bern, Switzerland,[4]University of Dundee, Dundee, United Kingdom,[5]Department of Veterinary Sciences, University of Turin, Turin, Italy

Introduction: Prostate cancer (PCa) is the archetype of an immunological “cold” tumour, characterised by a very low mutational burden and neoantigen presentation, and minimal immune infiltration. In line with this, immune therapies turn out to be ineffective in PCa. The project aims at transforming PCa into an immunocompetent tumour through the development of *ad hoc* vaccinal strategies.
Methods and Results: Recruiting adaptive immune cells into the prostate gland: The efficacy of a versatile clinical-adopted vaccine platform (X) to attract the immune system into the prostate tumour is under study in mouse model of advanced PCa. Immunohistochemistry on formalin-fixed paraffin-embedded (FFPE) slides of PCa allografts is defining the tumour microenvironment (TME) composition. $Cd8^+$ T-cells infiltrate PCa tumours, while $Cd4^+$ T-cells and $FoxP3^+$ regulatory T-cells preferentially accumulate in the periphery. A dense network of Collagen VI fibrils might be responsible for the different distribution. Intratumoral injection of X adjuvants does not change T cells behaviour, but it stimulates the formation of tumour abscesses surrounded by tightly packed neutrophils. Identifying immunogenic antigens to instruct effector T cells against PCa: Non-canonical human leukocyte antigen (HLA)-restricted PCa antigens are caught among peptides coming from aberrant splicing events, expression of transposable elements and atypical expression of tissue/development-restricted genes thanks to the integration of in-depth RNA Seq transcriptome with mass spectrometry HLA-I epitome analyses.
Conclusions: We expect that the ability to attract the immune system into the prostate combined with the identification of immunogenic epitopes, will pave the way for the development of tailored and affordable vaccine therapies for the effective treatment of advanced PCa.

#4388 Inducing memory humoral responses using multiple vaccines in PBMC humanized mice.

Destanie Rose, Ilian Radichev, Beau Parry, Leandro Salati D'Abronzo, Zahid Delwar, Jiwon Yang, Li-Chin Yao, James G. Keck

The Jackson Laboratory-West, Sacramento, CA

Humanized mouse models, such as those generated by administering human peripheral blood mononuclear cells (PBMC) into immunodeficient mice, hold great potential for studying immunotherapies and the immunogenicity of biologics and vaccines. Humanized mice are known for their quick engraftment of human cells, strong functional T-cell responses and for their capacity to assess donor-specific responses in vivo. However, these models face several limitations, including partial reconstitution of the human immune system, inadequate human cytokine support, and development of graft-versus-host disease (GvHD). To help address these issues we have developed new immunodeficient mouse strains and here show the potential of hPBMC mice to elicit humoral responses against various antigens. We engrafted human PBMC into NSG-SGM3xIL-15xDKO strain (JAX# 037320) followed by vaccination with formulated vaccines (Tdap, COVID-19 mRNA, or H5N1) or with antigen with or without adjuvant. Elevated levels of human IgG specific for tetanus toxoid, diphtheria, SARS-CoV-2 spike, or H5N1 were found in vaccinated animals compared to unvaccinated controls. Moreover, we also see an increase in total numbers of CD19+ B cells, activated B cells (CD38+) and CD138+ human plasma cells. These findings demonstrate that PBMC humanized mice provide a promising platform for evaluating humoral immunity.

#4389 Establishing a CTC-driven workflow for mRNA-transfected moDC production in personalized cancer immunotherapy.

Giovanna Manga Guimaraes[1], Nadia Bayou[1], Mara Serena Serafini[1], Eleonora Nicolo[1], Letizia Pontolillo[1], Brenno Pasto[1], Nassima Messali[1], Kiran Sahu[1], Paraskevi Giannakakou[1], Gabriela Coeli Menezes Evangelista[2], Olivier Elemento[3], Carolina Reduzzi[1], Jose Alexandre Barbuto[2], Massimo Cristofanilli[1]

[1]Department of Medicine, Weill Cornell Medicine, New York, NY,[2]Biomedical Sciences Institute, University of Sao Paulo, Sao Paulo, Brazil,[3]Systems and Computational Biomedicine, Weill Cornell Medicine, New York, NY

Background: After its success during SARS-CoV-2 pandemic, RNA-based vaccines are now being explored for cancer therapy. One of the strategies is the use of monocyte-derived dendritic cells (moDCs) transfected with tumor mRNA, but access to tumor tissue - especially from metastatic sites - is a limitation. Circulating tumor cells (CTCs) offer an alternative source for tumor material. Here, we developed a workflow integrating CTCs and mRNA technology for personalized cancer therapy.
Methods: Our first aim was to compare the recovery rate (RR) of 3 different CTCs isolation platforms (Parsortix [P], RosetteSep [RS], or ScreenCell [SC]) by spiking fluorescently-labeled breast cancer SKBR3 cells (200, 50, 30; triplicate) into healthy donor (HD) blood and counting the number of recovered CTCs using the Incucyte System. In parallel, moDCs were differentiated from HD monocytes and transfected with 500 ng of GFP-mRNA using Lipofectamine™ MessengerMax™ (LMM) to standardize conditions for CTC-mRNA transfection. GFP expression was assessed at 6, 24, 48, 72, and 96h by confocal microscopy, with non-transfected and mock-transfected moDCs as controls.
Results: Spiking tests showed that P and SC had similar performance and higher RR compared to RS, which yielded the lowest RR (Table 1). Regarding moDCs transfection, GFP expression was detectable at 6h, persisted through 24-48h and declined after 72h, with no signal in the controls. These conditions are currently being tested on SKBR3 cells recovered with SC, to assess the possibility to transfect moDCs with CTC-derived mRNA.
Conclusion: SC and P showed similar RR, but SC's simplicity and lower cost make it more suitable for deployment with our collaborators in Brazil. moDCs transfection was effective and LMM successfully delivered the target sequences for moDC processing and expression, supporting this as an immunotherapeutic approach. Future studies will be performed to validate the workflow also in clinical samples.

Recovery rates (RR) of each enrichment platform

	Parsortix®	ScreenCell®	RosetteSep™
30 spiked cells*	30.0% ± 4	33.3% ± 9	10.8% ± 2
50 spiked cells*	44.0% ± 3	53.5% ± 5	5.0% ± 4
200 spiked cells*	59.4% ± 29	60.75% ± 8	10.9% ± 4
*spiking experiments were conducted in triplicate			

: Antibody Technologies and Platforms 2
Poster Session

#4393 Development of an anti-CD171 (L1CAM) antibody-drug conjugate with high avidity and strong activity in resistant tumor models.

Kyoung-Ho Pyo[1], Hee Su Chae[2], Seong-Hyun Park[1], Younggeun Lee[1], Hojin Yeom[1], Sowon Aum[1], Sun Hee Park[1], Huijo Oh[1], Cheyeon Kim[1], Mi Jin Yoo[2], Min-Jung Shin[2], Hyo Jeong Hong[2], Jong-Soo Kang[2], Ju Hwan Kim[1], Seon-Joo Yoon[2], Taedong Han[1]

[1]AbTis Co., Ltd, Yongin, Korea, Republic of,[2]APITBIO, Inc., Seoul, Korea, Republic of

Background: CD171 (L1CAM) is a cell-adhesion molecule implicated in epithelial-mesenchymal transition (EMT), receptor tyrosine kinase (RTK) activation, and neuroendocrine differentiation across various solid tumors. Spatial transcriptomic profiling of lung and colorectal cancers revealed enrichment of CD171 in EMT- and neuroendocrine-like tumor microenvironments (TMEs), suggesting its involvement in metastasis and therapeutic resistance. Ab612 is a novel anti-CD171 monoclonal antibody developed by APITBIO that demonstrates a favorable developability profile. GLP toxicology studies and GMP manufacturing of Ab612 were completed, providing a robust foundation and enabling accelerated ADC development.
Methods: We characterized Ab612 to evaluate its biochemical stability, binding kinetics, internalization, and antitumor efficacy. Comparative analyses were performed against a benchmarking anti-CD171 antibody. Binding affinity and avidity were measured under both physiological and acidic conditions using surface plasmon resonance (SPR) and flow cytometry, while internalization efficiency was assessed via live-cell imaging. Ab612 was conjugated to MMAE (DAR2) and Exatecan (DAR4) using AbTis's proprietary linker, Abclick® Pro, designed to preserve antibody-FcRn interaction, and thereby support extended half-life. These ADCs were evaluated for *in vivo* efficacy in trastuzumab-resistant breast (JIMT-1) and TKI-resistant lung (Calu-6) xenograft models.
Results: Ab612 maintained strong binding under acidic conditions and demonstrated approximately four-fold higher kinetic affinity relative to internal reference values in SPR assays. In CD171-high ovarian (SNU-840) and breast (JIMT-1) cancer cells, flow cytometry analyses showed 22-23% higher avidity, and live-cell imaging confirmed more than 15% increase in internalization efficiency. Ab612-Abclick® Pro-MMAE and Ab612-Abclick® Pro-Exatecan demonstrated high stability in human plasma. *In vivo*, Ab612-Abclick® Pro-MMAE achieved near-complete tumor regression at ≥3 mpk (minimum effective dose = 3 mpk) and 100% complete responses at 10 mpk in JIMT-1 xenografts without body-weight loss. Ab612-Abclick® Pro-Exatecan induced >100% tumor-growth inhibition in KRAS/TP53-mutant, TKI-resistant Calu-6 models with favorable tolerability.
Conclusion: Ab612-ADCs,generated by conjugation of MMAE or Exatecan to the anti-CD171 monoclonal antibody Ab612 with the high-affinity binding within acidic TMEs using the Abclick® Pro linker, demonstrated highly potent preclinical antitumor efficacy at low effective doses. These findings highlight Ab612-ADCs as a promising therapeutic candidate for CD171-expressing refractory solid tumors characterized by EMT and neuroendocrine phenotypes, offering a potential strategy to overcome resistance in aggressive cancer subtypes.

#4395 A best-in-class HER2xHER2 novel biparatopic antibody-drug conjugate with an efficacious, low-toxicity design that maximizes antibody functionality.

Ge Song, Yushi Chi, Xiansong Xiong, Rui Liu, Xiaoling Yuan, Wan-Jen Yang, Wanli Zhang, Xinwei Wang, Boqi Gu, Qian Zou, Peng Huang, Kuichao Qu, Haixiang Yu, Futang Yang, Qingyu Wang, Chen Hu, Jijun Yuan

Shanghai Henlius Biotech, Inc., Shanghai, China

Introduction: HLX22 is a novel anti-HER2 antibody that binds to a unique site on HER2 subdomain IV, different from trastuzumab. When combined with HLX02 (a trastuzumab biosimilar), HLX22 increases internalization of HER2 homodimers and HER2/EGFR heterodimers, reducing cell proliferation signals. This combination shows stronger antitumor effects than HLX02 plus HLX11 (a pertuzumab biosimilar) both *in vitro* and *in vivo*. Based on the binding sites of HLX22 and HLX02, we developed a biparatopic antibody-drug conjugate (ADC) with an effective, low-toxicity payload, allowing higher dosing and better receptor coverage for improved tumor cell killing.
Methods: Cytotoxicity of HER2xHER2 biparatopic ADC was assessed using the CellTiter-Glo (CTG) assay in tumor cell lines. ADC binding and internalization were evaluated by flow cytometry in cells with varying HER2 expression levels. Pharmacokinetics (PK) of the HER2xHER2 biparatopic ADC were characterized in rats following a single intravenous 5 mg/kg dose. Bystander killing was quantified by co-incubating antigen-positive and -negative (Jurkat) cells, measuring Jurkat viability via the CTG assay. *In vivo* efficacy of HER2xHER2 biparatopic ADC was evaluated in multiple xenograft models (JIMT-1, BT-474 and patient-derive xenografts). Preliminary toxicology in cynomolgus monkeys was assessed at 60 mg/kg, administered every three weeks for three cycles.
Results: The HER2xHER2 biparatopic ADC demonstrated superior internalization efficiency than KN026 (a HER2-targeted bispecific antibody) and trastuzumab deruxtecan in BT474 and NCI-N87 cell lines. The biparatopic ADC showed better anti-tumor efficacy than trastuzumab deruxtecan across multiple cell lines. The ADC induced significant tumor regression at a single 6 mg/kg dose in various xenograft models outperforming trastuzumab deruxtecan head-to-head, including HER2-positive (immunohistochemistry [IHC] 3+, IHC2+ and fluorescence in situ hybridization [FISH]+), HER2-low (IHC2+/FISH- or IHC 1+), and HER2-Ultra low (IHC<1+) models. Preliminary toxicology shows good tolerability in cynomolgus monkeys following 3 doses of the ADC at 60 mg/kg.
Conclusion: We have developed a potential best-in-class HER2xHER2 novel biparatopic ADC that exhibits a superior therapeutic index, antibody-mediated signaling blockade. The preclinical findings support clinical development in breast and gastric cancers, with the hope that the improved therapeutic index of this agent confers survival benefit.

#4396 Selective intratumoral distribution and post-T-DXd activity of K-679, an ultra-high-DAR EGFR-targeted antibody drug-loaded unimicelle conjugate (ADUC).

Hideo Yoshida, Hideyuki Higashi, Masato Mori, Kahori Hosono, Nobuhiro Fujimaki

Kowa Company, Ltd., Tokyo, Japan

Background: K-679 is a compact, 20-nm EGFR-targeted antibody drug-loaded unimicelle (unimer-micelle) conjugate (ADUC) utilizing single-chain polymer nanoparticles that carry DM1 at an ultra-high-drug-to-antibody ratio (DAR, ~50) while maintaining colloidal stability at low antibody mass. This design aims to enhance intratumoral penetration and tumor-selective payload exposure even when antigen density is low and/or heterogeneous. While antibody-drug conjugates (ADCs) have improved cancer therapy, there remains an unmet need for patients progressing after ADC treatment, particularly following trastuzumab deruxtecan (T-DXd). We investigated whether the ADUC design of K-679 enables tumor-selective pharmacokinetics (PK), extensive intratumoral distribution, spatial pharmacodynamics, and activity following prior T-DXd treatment.
Methods: K-679 versus a benchmark ADC (cetuximab-DM1 ADC, cleavable disulfide linker, DAR ~4.5) was evaluated in head-to-head comparisons using EGFR-expressing CDX (HT-29, SK-OV-3, SK-CO-1 [KRAS G13V]) evaluated at DM1-equivalent dosing. Total DM1 (all species, measured after deconjugation) and free DM1 levels in tumor and plasma were quantified by LC-MS/MS. At 48 h, tumor sections were immunostained for human IgG (to map conjugate distribution), CD31 (microvasculature), pHH3 (mitotic arrest), and cleaved PARP (apoptosis). In HT-29 colorectal CDX with HER2-low/EGFR-low expression, animals received T-DXd, then on Day 18 were switched to K-679 or repeat T-DXd for 3 weeks. A parallel arm received K-679 on Day 0 and Day 18. Colorectal PDX harboring KRAS G13D (EGFR IHC score 1+, patchy) were also evaluated.
Results: Across CDX models at DM1-equivalent dosing, K-679 delivered 12.7-13.7-fold higher intratumoral total DM1 and 2.3-3.5-fold higher intratumoral free DM1 while reducing plasma free DM1 by 4.2-8.4-fold versus the benchmark ADC, indicating tumor-selective payload release with reduced systemic deconjugation. At 48 h, K-679's IgG signal exceeded benchmark ADC despite at least an 11-fold lower antibody mass and extended into regions distant from CD31-positive vessels; pHH3 and cleaved PARP increased across the tumor, indicating mitotic arrest/apoptosis. After prior T-DXd in HT-29 xenografts, K-679 induced robust tumor regressions, whereas repeat T-DXd did not. Consistently, two K-679 doses induced complete regressions (6/6) by Day 22, sustained to Day 39. In EGFR-low and heterogeneous colorectal PDX, a single K-679 dose inhibited tumor growth over 3 weeks.
Conclusions: The ultra-high-DAR ADUC design of K-679 confers tumor-selective PK, extensive intratumoral distribution, concordant spatial pharmacodynamics, and activity after prior T-DXd. These data support clinical development for EGFR-expressing solid tumors with low/heterogeneous antigen density and post-T-DXd settings.

#4397 Leveraging patient-derived organoids to investigate bystander effects of antibody-drug conjugates in solid tumor backgrounds.

Oksana Sirenko, **Nikki Carter**

Molecular Devices, LLC (Moldev), San Jose, CA

Background: Antibody-drug conjugates (ADCs) have demonstrated significant clinical benefit, yet their efficacy can be influenced by heterogeneous target expression and bystander killing. Understanding these dynamics in physiologically relevant models is critical for optimizing ADC design and patient selection.
Methods: We established and expanded patient-derived organoids (PDOs) from solid tumor backgrounds using our automated CX.ai platform, enabling high-throughput and standardized culture conditions. Target abundance for HER2 and c-MET was assessed via immunohistochemistry (IHC). Co-culture systems were optimized to include disease and healthy PDOs at defined ratios. Experimental assays incorporated mosaic PDO populations treated with ADCs (trastuzumab deruxtecan, telisotuzumab adizutecan, ADCs) and controls (antibody alone, warhead alone). Readouts included live-cell imaging, fixed-cell labelling, and high-content analysis to quantify PDO shrinkage, cell death, and target expression.
Results: Preliminary data indicate feasibility of generating mosaic PDO systems and detecting differential responses to ADCs. Optimization of co-culture conditions and imaging-based metrics (nuclear count reduction, PDO object shrinkage) are underway to correlate target expression heterogeneity with bystander killing.
Conclusions: PDO-based platforms combined with automated culture and advanced image analysis provide a robust system to study ADC bystander effects in heterogeneous tumor contexts. These findings will inform ADC development strategies and biomarker-driven patient selection.

#4398 Developing 3D cell models for high-throughput antibody-drug conjugate screening in cancer.

Peilin Tian[1], **Morgan Hamon**[2], Sean Porazinski[2], Maria Kavallaris[3], Kristopher A. Kilian[1], Justin Gooding[1]

[1]School of Chemistry, UNSW, Sydney, Australia,[2]Inventia Life Science, Alexandria, Australia,[3]Children's Cancer Institute, Lowy Cancer Research Centre, Sydney, Australia

Antibody-drug conjugates (ADCs) are a rapidly evolving class of biotherapeutics designed to deliver potent cytotoxic agents directly to cancer cells while minimizing systemic toxicity. ADCs offer this highly targeted approach by combining the selectivity of antibodies with the lethality of small-molecule drugs. However, their preclinical development still faces substantial challenges, including species-specific differences in antigen expression and antibody binding that complicate translational studies, often leading to discrepancies between preclinical efficacy and clinical outcomes. As a result, there is growing interest in developing more predictive preclinical models, including those that incorporate extracellular matrix (ECM) components into three-dimensional (3D) culture models which can help dissect how microenvironmental factors influence ADC target engagement. Such models provide a more physiologically relevant environment to assess ADC diffusion and payload delivery.

Using Inventia Life Science's RASTRUM^{TM} Allegro platform, we developed and validated the utility of high-throughput 3D bioprinted patient-derived colorectal cancer (CRC) models for the testing of a CEACAM5-targeted ADC in two CRC subtypes. These engineered hydrogel-based tumoroid models, using the Gibco^{TM} OncoPro^{TM} CRC Tumoroid Cell Lines (ThermoFisher Scientific), were tuned to mimic the stiffness and ECM composition of CRC tumors and maintained subtype-specific molecular and phenotypic features. This allowed comparisons of ADC efficacy versus standard-of-care chemotherapies and here we show clinically-relevant differential drug responses between subtypes, with the ADC demonstrating enhanced cytotoxicity over chemotherapy alone.

We also provide evidence for the ease of assessing target expression in situ by immunofluorescence imaging of models. Furthermore, the ability to test on-target cytotoxicity dependence was demonstrated by blocking target binding with anti-CEACAM5, which reduced ADC cytotoxicity in the sensitive tumoroid models.

This scalable and reproducible workflow is applicable across many cancer types, and bridges the gap between oversimplified in vitro assays and complex in vivo systems, offering more predictive insights into ADC performance by using models that incorporate physical and biochemical features relevant in patient tumors.

#4399 ANT045: A novel format, antibody fragment drug-conjugate (FDC) product for challenging cMET-expressing solid tumors.

Mahendra Deonarain, Bryan Edwards, Gokhan Yahioglu, Isabel Perez-Castro, Sam Ness, Anja Pomowski, Laura Bouche, Soraya Diez-Posada, Lowri Davies, Howard Desmond

Antikor Biopharma Ltd, Stevenage, United Kingdom

Antibody Fragment Drug Conjugates (FDCs), a new product class tailored for solid tumors promise many advantages over conventional ADCs including rapid tumor penetration and faster and safer systemic clearance. However, these formats have been technologically-challenging to apply in oncology. Our novel approach enables high-Drug:Antibody Ratios (DARs) whilst retaining effective binding and other favourable biophysical properties. To achieve this, single-chain Fvs and other recombinant antibody formats must be considered in context with complex linker-payload chemical moieties. In some cases, antibody surface charge needs to be manipulated to achieve high DARs. This platform technology has led to our lead product, ANT-045 is a cMET-targeted FDC addressing a wide range of solid tumors. ANT-045 demonstrates superior tumor cure efficacy in cMET high, moderate and low CDX and PDX gastric cancer xenograft models and better tolerability compared to the leading competitor ADCs, notably telisotuzumab vedotin. In a non-GLP, non-human primate study, ANT-045 was well tolerated with a predicted half-life in humans of around 12-14 hours supporting a viable clinical dosing strategy with a wide therapeutic window. Insights into how FDCs behave *in vivo* through quantitative uptake studies and toxicological parameters will be shared and how these have informed our follow-up products.

#4400 Degrader antibody conjugates (DACs) as a next-generation therapeutic approach for selective and potent targeted protein degradation in EGFR-positive cancers.

Jihye Lee[1], Soohyun Lee[1], Jiyoung Kim[1], Han Wool Kim[1], So Hyuk Kim[1], Onnuri Bae[2], Jeonghwa Han[2], Je Ho Ryu[2], **Song Hee Lee**[1]

[1]Ubix Therapeutics Co., Ltd., Seoul, Korea, Republic of,[2]Ubix Therapeutics Co., Ltd., Incheon, Korea, Republic of

Antibody Drug Conjugates (ADCs) have become an established therapeutic modality in oncology; however, challenges such as payload-associated systemic toxicity and the emergence of resistance to conventional cytotoxic payloads underscore the need for next-generation payload. Degrader Antibody Conjugates (DACs) have recently attracted attention as an alternative strategy that leverages targeted protein degradation rather than traditional toxin-mediated cytotoxicity. In this study, we synthesized a panel of DACs by generating diverse linker-payload (LP) designs engineered for targeted degradation and conjugating them to cetuximab. These DACs were evaluated across multiple cell lines for their degradation potency and anti-proliferative activity. In several EGFR-positive models, specific DAC constructs demonstrated significantly enhanced degradation efficiency relative to the corresponding free payloads, accompanied by improved inhibition of cellular proliferation. *In vivo* pharmacodynamic studies confirmed selective degradation of the target protein in EGFR-positive tissues, whereas no degradation was detected in EGFR-negative tissues, demonstrating the high specificity of the DAC mechanism. Overall, our findings show that our DAC platform exhibits potent on-target antitumor activity in relevant indications while minimizing off-target toxicity in non-expressing tissues. These results establish a proof-of-concept for DACs as a safer and mechanistically differentiated therapeutic approach warranting further development.

#4401 A novel antibody-drug conjugate targeting alkaline phosphatases ALPP and ALPPL2 in solid tumors.

Yujun Huang, Xiao Liang, Yajuan Xue

Hepius Therapeutics, Suzhou, China

Alkaline phosphatase placental (ALPP) and ALP-like 2 (ALPPL2) are highly expressed in a wide set of solid tumors, including ovarian, endometrial, gastric and non-small cell lung cancers. Their expression is highly restricted in normal tissues. ALPP/ALPPL2 are attractive targets for antibody-drug conjugate (ADC) and CAR-T therapies. HP-004 is a novel ADC targeting both ALPP and ALPPL2, with high selectivity and enhanced internalization efficiency. HP-004 specifically binds ALPP/ALPPL2 but not the related isozymes ALPI or ALPL, minimizing potential on-target off-tumor liability. In cellular internalization assays using ALPP/ALPPL2 high- and low-expressing tumor cells, HP-004 demonstrated higher uptake and an improved capacity to deliver cytotoxic payload intracellularly across a range of target expression levels. HP-004 is site-specifically conjugated with monomethyl auristatin E (MMAE) with an average DAR about 4. In vitro, HP-004 induced potent target-dependent cytotoxicity in ALPP/ALPPL2-overexpressing tumor cell lines, with an IC_{50} of approximately 248 pM. In the ALPP/ALPPL2-positive NCI-H1651 xenograft lung cancer model, HP-004 administration achieved near-complete tumor regression at 3 mg/kg (Q2W X4), with complete tumor regression in 6 of 8 mice, demonstrating a robust antitumor activity. HP-004 is further being evaluated in cell line- and patient-derived xenograft models with different expression levels of ALPP and ALPPL2. In parallel, bispecific ADC formats incorporating HP-004 are being explored to further enhance therapeutic index and extend activity to heterogeneous or low-antigen tumors. Collectively, our data support HP-004 as a highly selective ADC candidate with superior internalization, strong preclinical efficacy, and promising potential for translation in solid tumors expressing ALPP/ALPPL2.

#4402 EGFR and LGR5 dual-targeting antibody-drug conjugate-based therapeutic strategies for the improved treatment of colorectal cancer.

Peyton C. High, Zhengdong Liang, Maya Cappellino, Tiffani Blackburn, Cara Guernsey-Biddle, Shraddha Subramanian, Yueh-Ming Shyu, Adela Aldana, Yukimatsu Toh, Kendra S. Carmon

Institute of Molecular Medicine, UT Health Houston, Houston, TX

Colorectal cancer (CRC) remains the second-leading cause of cancer-associated death in the United States, indicating an urgent need for improved therapies. Antibody-drug conjugates (ADCs) are a promising class of therapeutics that function as “biological missiles,” employing the specificity of monoclonal antibodies to direct highly potent drug payloads to cancer cells while sparing normal tissues. We have developed ADCs targeting leucine-rich repeat-containing G-protein coupled receptor 5 (LGR5), a marker of normal adult intestinal stem cells and CRC stem-like cells with roles in CRC tumorigenesis, tumor progression, metastasis, and drug resistance. While LGR5-targeting ADCs incorporating microtubule inhibitors promoted tumor regression in select xenograft models and were well-tolerated, tumors eventually relapse following treatment cessation due to LGR5 downregulation and suboptimal ADC payload selection (Gong et al. 2016, *Molecular Cancer Therapeutics*). Thus, this work aims to investigate multi-targeting therapeutic strategies with improved LGR5-targeting ADCs to improve CRC care and prevent relapse. Our work showed that therapies targeting the epidermal growth factor receptor (EGFR), including cetuximab (CTX) which is approved for $KRAS^{WT}$metastatic CRC, increased LGR5 protein levels in CRC cell lines, tumor organoids, and mouse models independent of *KRAS* mutational status. To evaluate EGFR and LGR5 dual-targeting approaches, we generated a novel LGR5-targeting ADC incorporating a topoisomerase I inhibitor payload via site-specific conjugation that was well-tolerated in immunocompetent mice. Importantly, combination of CTX with LGR5-targeting ADCs significantly enhanced anti-tumor efficacy and extends survival as compared to ADC and CTX monotherapies in RAS^{MUT} CRC patient-derived xenografts (High et al. 2025, *Cell Reports Medicine*). Still, tumors eventually relapsed following combination treatment, warranting investigation into alternative dosing regimens and dual-targeting modalities. We have therefore generated two EGFR:LGR5 bispecific antibodies (bsAbs) that promote lysosome-mediated EGFR degradation. EGFR:LGR5 bsAbs demonstrated minimal cytotoxicity in CRC cells, necessitating drug conjugation to generate highly potent EGFR:LGR5 bispecific ADCs (bsADCs). Importantly, EGFR:LGR5 bsADCs exert 100- to 1000-fold enhanced potency over LGR5 ADCs with identical linker-payloads in LGR5/EGFR-expressing CRC cell lines of varying genetic backgrounds. These promising findings warrant further investigation into the anti-tumor efficacy of EGFR:LGR5 bsADC monotherapy versus combination therapy of CTX and LGR5 ADCs in CRC xenograft models. Taken together, this work strongly rationalizes dual-targeting of EGFR and LGR5 as an effective therapeutic option for CRC and other EGFR- and LGR5-expressing cancers.

#4403 A fast and robust development process providing new highly internalized anti-hHER2 antibody-drug conjugates.

Eric Chabrol, Marie-Claire Phelipot, Cecile Lemoigne, Julie Lichiere, Nadjiba Mares, Alice Aymard, Alexandre Bagnolini, Sophie Mesnard, Caroline Huber, Matthieu Tassa, Ester Morgado, **Jacques Fieschi**

Mimabs, Marseille, France

Purpose: The aim of this study was to establish an accelerated and de-risked workflow for the generation of potent anti-hHER2 antibody-drug conjugates (ADCs), addressing key bottlenecks that currently limit the efficiency, predictability, and overall success rate of ADC discovery.
Methods: We implemented a fully integrated four-step strategy. (1) A multisite immunization protocol was developed to rapidly induce robust anti-hHER2 responses, enabling the isolation of high-titer antibodies in less than two weeks; antibodies generated with this accelerated protocol were benchmarked against a classical schedule. (2) Antibody-secreting plasma cells were isolated and ranked on the Bruker Beacon single-cell platform based on antigen binding and relative affinity prior to sequencing and recombinant expression. (3) A microscale, robotics-assisted production workflow was established to express and purify dozens of antibodies in parallel. Binding affinity was measured by bio-layer interferometry BLI, and internalization kinetics were quantified using a new lanthanide-based pH-sensitive probe. (4) A two-stage ADC synthesis pipeline was created using enzymatic conjugation and click chemistry. A first library of ADCs was generated by coupling 24 antibodies to MMAF at DAR4, followed by cytotoxicity assessment on patient-derived xenograft-derived cells (PDX-DC). The most promising hits were then reformatted into a second ADC library conjugated to multiple linker-payload combinations at diverse DARs with the same conjugation strategy.
Results: The rapid immunization protocol consistently produced highly internalized anti-hHER2 antibodies, some surpassing those from classical schedule and trastuzumab. Beacon-based screening enabled efficient prioritization of clones with superior affinity. In the first ADC library, multiple candidates showed strong cytotoxic activity on PDX-DC models. Subsequent optimization through linker-payload engineering further enhanced potency for selected candidates.
Conclusions: This integrated and optimized workflow accelerates ADC generation from immunization to functional readout while reducing technical risk at each stage. It enabled the rapid identification of novel anti-hHER2 antibodies with enhanced internalization and highly potent ADC derivatives. This approach is broadly applicable to future ADC discovery programs targeting diverse antigens.

#4404 Diverse VHH antibodies targeting multiple LGR5 epitopes for cancer therapy.

Chenrui Xu[1], Yifan Li[1], Trang Nguyen[2], Roger Shek[2], Longfei Chong[1], Tek H. Lee[2], Yuxiang Lang[1], Li Yi[2], **Per Greisen**[2]

[1]BioMap Research, BioMap Inc, Beijing, China,[2]BioMap Research, BioMap Inc, Palo Alto, CA

Background: LGR5 is a validated therapeutic target highly expressed in cancer stem cells and solid tumors. Petosemtamab, an EGFR/LGR5 bispecific antibody, confirms its druggability. Single-domain antibodies (VHHs) provide advantages over conventional antibodies through small size, high tissue penetration, and scalable manufacturing. We aimed to create a panel of VHH binders against LGR5 with broad epitope diversity and favorable biophysical traits for therapeutic use.
Methods: VHHs were designed using AI-based structure and sequence-guided modeling targeting recombinant human LGR5 extracellular domain. Chain-of-thought optimization was applied to improve multiple parameters simultaneously, including affinity, thermal stability (Tm), expression yield, and hydrophobic interaction chromatography (HIC) behavior. Top candidates were evaluated for kinetics via surface plasmon resonance, epitope mapping by cryo-EM using N-glycan knockout variants, thermal stability by differential scanning fluorimetry, and expression in mammalian systems. Specificity was tested against related receptors LGR4 and LGR6.
Results: Multiple VHH clones showed high-affinity binding to LGR5, with KD values in the nanomolar range. Cryo-EM mapping revealed distinct, non-overlapping epitopes across the LGR5 extracellular domain, providing full structural coverage of potential binding sites. The panel included both LGR5-selective and pan-LGR binders, offering flexibility in therapeutic design. R-spondin competition assays identified ligand-blocking and non-competing VHHs targeting alternate epitopes. All lead molecules displayed strong stability (Tm >65°C) and robust expression, supporting high manufacturability. These characteristics enable both pathway inhibition and targeted payload delivery approaches to eliminate LGR5+ cancer stem cells.
Conclusions: AI-driven protein engineering produced a diverse, high-quality panel of LGR5-targeted VHHs with multi-epitope coverage, broad affinity range, and strong manufacturability. Chain-of-thought optimization improved multiple parameters in parallel, accelerating VHH development. This library enables rational design of bispecific and multispecific therapeutics for enhanced tumor targeting and represents a foundation for next-generation LGR5-directed ADCs, bispecifics, and CAR-T therapies.

#4405 Real-time, label-free assessment of HER2-targeted antibody-drug conjugate therapies.

Danny Flanigan, BEN STREETER, STACIE CHVATAL, DANIEL MILLARD

Axion BioSystems, Atlanta, GA

Antibody-drug conjugates (ADCs) are made of monoclonal antibodies covalently linked to small molecule drugs that, together, can improve both components' anti-tumor effects. Several ADCs are targeted towards human epidermal growth factor receptor 2 (HER2), a cell surface receptor that is overexpressed in many cancers. Its increased expression in tumor cells makes HER2 an attractive target for cytotoxic therapies, allowing for the specific killing of cancer cells while minimizing off-target effects. Here, we developed an in vitro assay to measure the cytotoxic capacity of ADCs that use the HER2-targeted monoclonal antibody trastuzumab. This assay was performed in a real-time, label-free manner using the Maestro Z platform. The Maestro Z measures electrical impedance via electrodes embedded in the surface of the well to monitor cell growth and proliferation. To assess the cytotoxic effects of one HER2-targeted ADC, trastuzumab-deruxtecan (DS-8201a, branded as ENHERTU®), 5,000 HER2-positive SKOV3 cells were plated in CytoView Z plates and monitored for 24 hours before being dosed with increasing amounts of DS-8201a. SKOV3 cells were killed in a dose-dependent manner, and higher doses of DS-8201a led to larger decreases in SKOV3 impedance, indicative of greater SKOV3 death. SKOV3 cytolysis at the highest dose reached 90.9% at ~ 5 days post dose, and the EC50 value was calculated to be 30.7 µg/mL. We also tested the effects of DS-8201a against other cell types with varying degrees of HER2 expression, including A549 (low HER2 expression) and MDA-MB-231 (no HER2 expression) cells. As expected, impedance data showed that DS-8201a had enhanced cytotoxic effects on the high HER2-expressing SKOV3 cells compared to the other two cell types with lower HER2 expression. Finally, we compared the cytotoxic effects of DS-8201a to another trastuzumab-based ADC, trastuzumab-emtasine (T-DM1, branded as Kadcyla®) on the Maestro Z. Taken together, these results show that the cytotoxic capacity of ADC therapies toward HER2 positive cell types can be screened using the Maestro Z. The assay presented here can be used to further develop ADC therapies aimed at HER2-positive cancers as well as ADCs toward other cancer-specific targets.

#4406 Mouse analog of micvotabart pelidotin, an antibody-drug conjugate targeting extradomain-B of fibronectin, demonstrates anti-tumor efficacy in an immunotherapy-refractory syngeneic head and neck squamous cell carcinoma model.

Anthony B. Rodriguez, Amanda Facklam, Justin Trickett, Sara Lewandowski, Matthew Iovino, Chuan Shen, Frank Wang, Nicolas Severe, Marsha Crochiere

Pyxis Oncology, Boston, MA

Head and neck squamous cell carcinoma (HNSCC) is a difficult-to-treat indication, with current standard of care providing limited long-term survival, underscoring the need for more effective treatment options. Micvotabart pelidotin (MICVO) is a first-in-concept antibody-drug conjugate targeting extradomain-B of fibronectin (EDB+FN), a non-cellular component of the tumor extracellular matrix that is abundantly expressed in the stroma of many malignancies, including HNSCC, but minimally in normal adult tissues, making it an attractive drug-delivery target. In preclinical studies, a murine analog of MICVO (maMICVO) demonstrated pronounced anti-tumor activity, enhanced T cell tumor infiltration, and synergy with anti-PD1, resulting in greater efficacy in syngeneic triple-negative breast cancer models, including one refractory to immunotherapy. MICVO also showed broad anti-tumor activity across multiple patient-derived xenograft models, with particularly strong responses in HNSCC. Consistent with these findings, preliminary results from a Phase 1 Part 1 trial (NCT05720117) showed favorable anti-tumor activity with MICVO monotherapy across several solid tumor types, including HNSCC. This clinical observation is further supported by the present study, in which strong maMICVO activity was observed in the poorly immunogenic, immunotherapy-refractory mouse oral carcinoma 2 (MOC2) syngeneic HNSCC model. *In vitro*, MOC2 cells exhibited minimal EDB+FN expression at baseline. However, tumors established in immunocompetent mice with these cells displayed markedly elevated EDB+FN expression within the extracellular space, suggesting that signals arising during tumor growth drive EDB+FN induction. To evaluate efficacy, mice bearing subcutaneous MOC2 tumors were treated with up to 6 mg/kg maMICVO, with tumor growth and body weight monitored. Treatment was well tolerated at all doses, and a dose-dependent anti-tumor effect was observed, with 6 mg/kg producing the greatest tumor growth inhibition. Notably, image analysis of MOC2 tumors after maMICVO treatment revealed trends of increased CD8 T cell infiltration, reduced regulatory T cell frequencies, and elevated PD-L1 expression, suggesting modulation of the tumor-immune landscape that may enhance susceptibility to anti-PD1 therapy in this model. Ongoing studies aim to determine whether maMICVO synergizes with anti-PD1 to enhance efficacy in this immunotherapy-refractory MOC2 model and to further define the immune changes driving this response at the cellular, molecular, and spatial levels. Collectively, these findings support the continued clinical evaluation of MICVO both as a monotherapy (NCT05720117) and in combination with pembrolizumab (NCT06795412) in difficult-to-treat HNSCC.

#4407 Integrative design of PSM101 Lock-antibody for EGFR-positive tumors through clinical protease profiling and structure-based computer simulation.

Yi-An Cheng[1], Yun-Chi Lu[2], Yu-Chi Lee[1], Chen-Yung Hung[1]

[1]Reseach and development center, PrecisemAb Biotech Co., Ltd., Taipei, Taiwan,[2]President, PrecisemAb Biotech Co., Ltd., Taipei, Taiwan

Objective: On-target toxicity remains a major limitation of anti-EGFR antibodies, as exemplified by a 9.8% discontinuation rate in cetuximab-treated patients due to skin toxicity. Protease-activated pro-antibodies can improve tumor selectivity; however, their performance is limited by heterogenous clinical protease activity and antibody-specific CDR structural constraints. We aimed to develop an optimized EGFR Lock-antibody (PSM101) with improved blocking efficiency, high tumor-specific cleavability, and minimal normal-tissue binding.
Methods: PSM101 was engineered by fusing the Antibody Lock™ masking domain, tumor-associated protease substrates, and optimized linkers to an anti-EGFR antibody. Clinical tumor tissues were profiled to identify highly active protease substrates across multiple cancer types. An automated structure-based simulation platform (MSCS 2.0) was established to predict cover rate and protease cleavability for variant designs. Lead PSM101 molecules were evaluated for (1) binding to human normal cells (flow cytometry), (2) protease activation in clinical tumor tissues (IHZ assay), and (3) antitumor efficacy in EGFR-positive CDX and PDX mouse models.
Results: Clinical protease profiling from head and neck, lung, colon, and gastric tumors identified substrates with high and consistent tumor-associated cleavage activity. MSCS 2.0 successfully predicted variants with optimal masking coverage and cleavability, enabling rational selection of the final PSM101 design. PSM101 demonstrated a 100-200-fold reduction in binding to human normal cells compared with cetuximab, and showed robust activation in head and neck tumor tissues. In vivo, PSM101 achieved significant antitumor activity in both CDX and PDX models.
Conclusion: We developed a protease-activated EGFR Lock-antibody, PSM101, with markedly improved tumor selectivity and strong therapeutic efficacy. MSCS 2.0 provides a predictive framework for early-stage optimization of pro-antibodies, which may accelerate next-generation antibody drug development and reduce clinical toxicity. Ongoing studies include safety evaluation of PSM101 in cynomolgus monkeys.

#4409 Comparing potential bispecific formats comprising of trastuzumab and a humanized OKT3.

Sabrina Mateos, Catherine Bladen, Abbie Hardisty, Emily Blackwood, Holly Guz, Stacey Walker, Stephen Anderson, Michael Fiebig

Vector Laboratories, Inc., Newark, CA

Purpose: This abstract showcases how Absolute Antibody (a Vector Laboratories company) generate bi-specific antibodies based on existing monoclonal antibody therapeutics molecules, compare the constructs and feasibility in order to produce “well-behaved multi-specifics”.
Experimental Procedures: Our recombinant platform converts any antibody into customizable multispecific formats with defined Fc mutations, enabling precise control of effector function. Using trastuzumab and a humanized OKT3 variant as binding arms, we generated and expressed a panel of bispecific constructs, purified them to high quality, and compared their expression profiles, monomer content, and binding. These variants now serve as a reference set for ongoing functional and biophysical characterization studies.
Conclusions: Recent reports list 79 multi-specific antibodies in the clinic, while Absolute Antibody (a Vector Laboratories company) has produced more than 180 engineered formats. In this study, we built and analyzed 17 bispecific designs, revealing that Fc-containing architectures, scFv placement, and interface engineering strongly affect expression and stability. This reference panel highlights how design choices shape bispecific performance and is available for collaborative research.

#4410 The discovery and development of a bispecific T cell engager prodrug targeting ENPP3.

Li Chen[1], Lindi Wang[1], Yingyu Li[1], Xin Wang[1], Yang Xin[1], Mingzhu Shao[1], Jiangtao Ning[1], Ziyu Chen[1], Cheng Luo[1], Jingjing Nie[1], Yue Wu[1], Tingting Yang[1], Hai Huang[1], Miaomiao Song[1], **Yu Liang**[2]

[1]Probio, Inc, Nanjing, China,[2]Probio, Inc, Pennington, NJ

T cell engager (TCE) antibodies have been proven to be effective for a variety of hematological malignancies, with at least 10 marketed drugs to date; however, their efficacy in many solid tumors is still very limited due to a number of challenges. One of the leading challenges is the lack of tumor-specific targets, leading to an increased risk of on-target, off-tumor toxicity. An approach to address this challenge is to build a “prodrug” TCE that is conditionally activated in the tumor microenvironment (TME), taking advantages of various masking technology platforms that block the release of active TCE drug outside of the TME. To develop such a novel TCE molecule with improved tumor selectivity, potency, and safety profile, we first discovered a masking peptide specific to a CD3 VHH antibody that we previously developed, and demonstrated that the masked CD3 VHH can effectively reduce T cell activation several hundred-fold. Next, we fused this masking peptide to the CD3 VHH arm via a proteolytically-labile linker containing sequence motifs sensitive to proteases enriched in the TME, and showed that upon cleavage by proteases, the T cell-activating potency of such a masked CD3 VHH can be effectively recovered. Finally, with such a CD3 VHH armed with cleavable linker and masking peptide, we built a series of prodrug TCE molecules targeting ENPP3 (ectonucleotide pyrophosphatase/phosphodiesterase family member 3), a tumor associated antigen with good tumor selectivity for renal cell carcinoma. Our *in vitro* validation studies demonstrated that the potency of these TCE prodrugs in killing ENPP3+ tumor cells can be restored to a similar level as the unmasked, active TCE molecule upon proteolytic cleavage. Our *in vivo* studies using an ENPP3+ CDX model with transplanted human PBMCs demonstrated two important points: (i) the prodrug/masked ENPP3-targeted TCE can potently inhibit tumor growth to a comparable level as the unmasked version and clinical benchmarks, and (ii) the prodrug TCE can be dosed at least 100-fold higher than the active drugs without any observed toxicity, suggesting a greatly improved safety profile. Further preclinical development of these ENPP3-targeted prodrug TCE molecules, including pharmacokinetics and toxicity studies in non-human primates, is ongoing.

#4411 Discovery of mutation-independent cKit degrading bispecific antibodies that suppress tumor growth in preclinical models of GIST.

Kenneth Ng, Shruti Yadav, Brianna McIntosh, Andy Goodrich, Hai Tran, Josef Gramespacher, Kimberly Hoi, Sara Yan, Brian Hiller, Adison McLaggan, Zhong Huang, Noah Solomon, John Coan, Jon Sitrin, Shyra Gardai, **Ken Flanagan**

Epibiologics, San Mateo, CA

Extracellular targeted protein degradation (eTPD) has emerged as a promising drug modality focused on the selective elimination of extracellular and transmembrane proteins. Unlike intracellular protein degraders, such as proteolysis targeting chimeras (PROTACs) and molecular glues, which rely on ubiquitin-proteasome pathways, extracellular degraders can harness a variety of internalizing receptors that can be tailored to specific targets and tumor types. EpiTACs are a novel type of extracellular targeted protein degrader (eTPD) defined as bispecific antibodies designed to bind a protein of interest (POI) with one arm and a degrading cell-surface receptor with the other. When the receptor is engaged, it carries the POI target into the cell, leading to selective degradation of the POI on receptor-expressing cells. EpiTACs combine favorable pharmacological and manufacturing properties of antibodies with the ability to engineer tissue specificity aiming to enhance efficacy while reducing off-target toxicity. To demonstrate the potential of this platform, we developed EpiTACs to the canonical receptor tyrosine kinase c-KIT. c-KIT is a critical driver of gastrointestinal stromal tumor (GIST) pathogenesis, with activating mutations representing the primary oncogenic event. Current kinase inhibitors are limited by the inevitable emergence of secondary resistance mutations. EpiTACs offer a compelling alternative by eliminating c-KIT itself, rather than merely inhibiting its activity, thereby overcoming mutation-dependent resistance and providing a potentially more durable therapeutic strategy. Importantly, c-KIT is also expressed on healthy cells, including hematopoietic stem cells (HSCs), highlighting the need for approaches that selectively target tumor cells while sparing normal tissue. We generated over 50 c-KIT-targeting EpiTACs spanning 10 degrading receptors expressed on GIST cells but absent from HSCs. These constructs were screened in tumor cell-based assays for c-KIT internalization and degradation. One such construct preserved degrading receptor expression, allowing for sustained catalytic degradation of the POI, which resulted in markedly reduced c-KIT levels and strong efficacy in vitro and in CDX and PDX mouse models. This EpiTAC demonstrates limited toxicity to HSCs, and could be used as a complementary approach as well as a front line combination opportunity with standard of care. In conclusion, eTPD of c-KIT using EpiTACs represents a promising new therapeutic modality and expands the toolbox of extracellular targeted degraders that can be applied in a target-, tissue-, and disease-specific manner.

#4412 Discovery and characterization of GI-128: A PD-L1 x LILRB1/2/4 bispecific antibody as a macrophage engager.

Seong Hun Kim, Eunji Ahn, Min Sang Yoon, Ji Cheol Kim, Hye Jun Park, Wonjae Lee, Hyuckjun Mok, Eun Jin Lee, Jisoo Kim, Young Min Oh, Kook Hwan Kim, Myoung Ho Jang

GI Innovation Inc., Seoul, Korea, Republic of

Immunosuppressive activity of myeloid cells within the tumor microenvironment (TME) contributes significantly to tumor immune evasion. Leukocyte immunoglobulin-like receptor subfamily B (LILRB) members are inhibitory receptors primarily expressed on myeloid cells. LILRB1, LILRB2 and LILRB4 are upregulated on tumor-infiltrating myeloid cells across many cancers. LILRB1 and LILRB2 suppress cytotoxic T cell and NK cell activity through interactions with their ligands such as HLA-G and HLA-G/β2m. LILRB4 interacts with extracellular matrix proteins and subsequently promotes myeloid-mediated immunosuppression, leading to impairment of anti-tumor immunity. Although immune checkpoint inhibitors (ICIs) show broad clinical benefit, many patients are refractory or develop acquired resistance. ICI-resistant tumors often exhibit increased polarization of immunostimulatory M1 to immunosuppressive M2 tumor-associated macrophages. As macrophages are abundant in the TME across many cancer types, reprogramming of tumoricidal macrophages and their engagement with tumor cells could be a promising approach to elicit effective anti-tumor responses. Since high LILRBs expression correlate with poor prognosis and ICI non-responsiveness, and PD-L1 is highly expressed in multiple cancer types or positively correlates with LILRBs expression, we designed GI-128, a macrophage-engaging bispecific antibody composed of an anti-PD-L1 sdAb (single domain antibody) and an anti-LILRBs sdAb. Here, we showed that GI-128 candidates exhibited high affinity for both PD-L1 and LILRB1/2/4 and effectively suppressed their receptor-ligand interactions against each target in cell-based blockade assay or cell-based reporter assay. In functional assays using immune cells, GI-128 candidates enhanced macrophage-mediated phagocytosis of tumor cells. Furthermore, they promoted pro-inflammatory cytokine production in LPS-stimulated PBMC-derived monocytes and induced M1 polarization during macrophage differentiation. In addition, a trans-binding assay showed that GI-128 candidates bound simultaneously to PD-L1-expressing cells and to LILRB1-, LILRB2- or LILRB4-expressing cells, implying their functionality as macrophage-engaging molecules. These findings suggest that GI-128, a bispecific macrophage engager, has a promising potential to reinvigorate tumoricidal macrophage function in immunosuppressed PD-L1-positive tumors. *In vivo* anti-tumor efficacy of GI-128 is being investigated.

#4413 KRAS amplification creates a targetable pMHC antigen for T cell engager therapy to overcome KRAS inhibitor resistance.

Lorenzo Maso, Diamond N. Mensah, Angelina Pizzo, Sergio A. Rodriguez-Aponte, Samantha Sze, Weifeng Liu, Sean T. Toenjes, Paul Da Silva Jardine, Christoph Rader, Lauren E. Stopfer

Aethon Therapeutics, New York, NY

KRAS amplification has emerged as a shared mechanism of resistance to KRAS-targeted therapies, including $KRAS^{G12C}$ and KRAS-multi small molecule inhibitors. Wild-type KRAS allele amplification also defines a subset of aggressive gastroesophageal cancers with poor outcomes. To exploit this alteration, we sought a mutation-agnostic, HLA-A*02:01-restricted KRAS pMHC antigen selectively presented in KRAS-amplified tumors. Using peptide prediction & targeted immunopeptidomics, we identified the amplified antigen “kAMP.A2,” enabling a strategy to selectively target KRAS-amplified tumors with a bispecific pMHC×CD3 T cell engager (TCE). Quantitative immunopeptidomics across multiple models estimated kAMP.A2 at ~10^2-10^3 copies-per-cell (CPC) in KRAS-amplified cell lines (MKN1*, 119 CPC; COR-L23*, 555; HSKTC*, 1432) and undetectable or <10 CPC in non-amplified cell lines (A375, NCI-H661, ND; NCI-H520*, 9). A*02:01-negative lines (*) were A*02:01-engineered. KRAS pathway inhibition further increased antigen levels: treatment of 10 nM RMC-7977 in COR-L23 cells (G12V; KRAS CN=16), produced a 2.5× rise in surface HLA and an 8-fold increase in kAMP.A2, reaching ~4,000 CPC at 48 h. KRAS amplification thereby establishes an exploitable pMHC therapeutic window—analogous to gp100 or PRAME—that is further broadened by KRAS inhibition. Importantly, NRAS & HRAS paralogs of kAMP.A2 were not detected in any model. Consistent with this, stability profiling showed kAMP.A2 to be markedly more stable at 37 °C ($t_{½}$ ≈ 45 min) than NRAS/HRAS peptides ($t_{½}$ < 4 min), supporting kAMP.A2 as a selective TCE target with minimal paralog cross-reactivity. Screening our ultra-large human naïve antibody library with phage/yeast display and stringent counter-selection yielded the TCR-mimicking antibody PK313, exhibiting high affinity (K_D = 5.3 nM) and strict specificity confirmed by SPR as well as by X-scan and healthy-tissue pMHC libraries (>10^2 & ~10^4 peptides) with no high-affinity off-targets. A 2.8-Å cryo-EM structure revealed extensive kAMP.A2-specific contacts. Reformatted as a TCE, PK313 induced potent cytotoxicity in KRAS-amplified models (MKN1*, EC_{50} = 1.1 nM; COR-L23*, 150 pM; HSKTC*, 160 pM) and showed enhanced activity with KRAS inhibitors. Structure-guided maturation is underway to advance PK313 toward development candidate nomination. Our data demonstrate that KRAS amplification—whether intrinsic or emerging under therapeutic pressure—creates a robust, tumor-amplified pMHC antigen with exceptional potential for therapeutic exploitation. PK313 enables selective targeting of KRAS-amplified tumors as a monotherapy or in combination with KRAS small molecule inhibitors to enhance treatment durability and provides a therapeutic strategy for A*02:01 patients (~42% in US population), who are currently excluded from A*03/A*11 KRAS-mutant neoantigen TCR-T/CAR-T/TCE programs.

#4414 A bispecific antibody-drug conjugate targeting protein tyrosine kinase 7 and fibroblast activation protein alpha simultaneously acts on tumor cells and the tumor microenvironment.

Yifan Zhan, Shi Chen, Jingen Xu, Xiaofang Chen, Changping Zheng, Xianfei Pan, Shaojie Wang, Simin Xia, Haijia Yu, Yujie Feng, Guoyuan Peng, Huifeng Jia, Xiaopei Cui, Xiangyang Zhu

Shanghai Huaota Biopharmaceutical, Shanghai, China

Bispecific antibody-drug conjugates (Bs-ADCs) represent a significant advancement over traditional ADCs by addressing key limitations, including tumor selectivity, on-target/off-tumor toxicity, tumor heterogeneity, antigen escape, inefficient internalization, and low payload delivery efficiency. By simultaneously targeting tumor cells and cancer-associated fibroblasts (CAFs), Bs-ADCs not only enrich drug concentration at the tumor site but also disrupt the tumor's supportive stroma, thereby improving drug penetration. We have developed a Bs-ADC, HB0085, which targets tumor cells through protein tyrosine kinase 7 (PTK7) and CAFs through fibroblast activation protein (FAP), delivering a topoisomerase I inhibitor (TOP1i) payload to tumor. HB0085 has demonstrated potent antitumor activities both in vitro and in vivo. In multiple patient-derived xenograft (PDX) experiments, HB0085 achieved a tumor growth inhibition (TGI) rate greater than 70% in 42.9% (3/7) of lung cancer models and 83.3% (5/6) of pancreatic cancer models. Notably, HB0085 exhibited superior efficacy compared to combination therapy with individual monospecific ADCs targeting PTK7 and FAP in PDX models. Furthermore, when combined with the bispecific antibody HB0025 (targeting PD-L1/VEGF), the antitumor activity of HB0085 was significantly enhanced. These results position HB0085 as a promising therapeutic candidate for a range of solid tumors.

#4415 AI-powered analysis of millions of IHC images identifies 19 spatially highly co-expressed protein pairs to enable bispecific antibody development.

Sukjun Kim[1], Hosik Kim[1], Biagio Brattoli[1], Sergio Pereira[1], Siraj Mahamed Ali[2]

[1]Lunit Inc., Seoul, Korea, Republic of,[2]Lunit USA Inc., Cambridge, MA

Background: Developing effective bispecific antibodies requires identifying target protein pairs that are co-expressed within the same spatial context of a given tumor. However, discovering such co-expressed targets is challenging due to the vast combinatorial search space across the human proteome. AI-powered analysis of IHC images enables systematic identification of spatially co-expressed protein pairs, facilitating rational bispecific antibody design.
Methods: We analyzed 6.8M IHC-stained TMA core images from the Human Protein Atlas, where 21144 different antibodies were used to stain 15303 human proteins. Serial section pairs were identified using a feature-matching-based image similarity algorithm. For each pair, positive and negative cells were detected from the IHC images using the Lunit SCOPE uIHC model. The spatial similarity of expression between two proteins was quantified using the intersection over union (IoU) of their positive cell regions.
Result: From all possible image pairs generated by combining every two images from 1.5M positively stained TMA cores, 26730 pairs were identified as serial sections based on image similarity analysis. By selecting pairs in which the positive cell regions overlapped (IoU ≥ 70) and only consisted of plasma membrane proteins, we identified 19 pairs across 10 tumor types with the most pairs in bladder cancer. B7-H3 was co-expressed with NT5E or JAG1 in bladder cancer, and with NT5E in cervical cancer. In thyroid cancer, CLDN3 was co-expressed with ROBO1.
Conclusion: We developed an AI-powered pipeline for spatial analysis of IHC images and applied it to a large publicly available data source, enabling systematic identification of co-expressed protein pairs. This approach can guide the design of tumor type specific bispecific antibodies as demonstrated by the possibility of targeting B7-H3 and simultaneously either the ectonucleotidase NT5E or the Notch ligand JAG1.

List of identified co-expressed target pairs by tumor types.

Tumor type	**Number of pairs**	**List of pairs (A x B)**
Bladder	7	B7-H3 x NT5E, B7-H3 x JAG1, PIEZO2 x GPR142, DDR1 x IL6ST, ITGA3 x BTN3A3, CSF1R x BTN3A3, LSR x SORT1
Cervix	2	B7-H3 x NT5E, DDR1 x ICOSLG
Pancreas	2	SLC4A4 x PKD2L1, DCHS1 x GFRAL
Brain	1	TRPV2 x CSPG4
Head and Neck	1	DCHS1 x GFRAL
Liver	1	CDH8 x KCNE3
Lung	1	SLC4A4 x PKD2L1
Testis	1	PIEZO2 x GPR142
Thyroid	1	CLDN3 x ROBO1
Uterine	1	FZD1 x IGF1R

#4416 Overcoming the limited monospecific target landscape in cancer via discovery of tumor selective AND and OR gate bispecifics.

Daniel Holdbrook, **Katherine Vousden**, Michael Hunter, Roy Pettipher, Mark Edwards

Promatix Biosciences Ltd., London, United Kingdom

The pool of membrane proteins suitable for monospecific antibody-drug conjugates (ADCs) is inherently limited, restricting tumor selectivity and leaving many cancers without actionable antigens. Bispecific ADCs unlock a much larger combinatorial target universe by pairing antigens, enabling AND-gate designs that enforce dual expression for engagement and OR-gate designs that extend coverage where individual markers are insufficient. However, rational construction of such bispecifics depends on identifying antigen pairs that are co-expressed in tumors but absent - or expressed only individually - in normal tissues. To meet this need, we developed a discovery framework that combines quantitative proteomic profiling across more than 14 tumor types, matched normal tissues, and cell lines with computational modeling of cancer-normal specificity. This approach systematically evaluates both AND- and OR-logic potential across all bispecific ADC pairings currently under clinical or preclinical investigation, while also uncovering previously unexplored combinations with favorable selectivity profiles. Our analysis confirms that the universe of high-selectivity monospecific targets is extremely small, whereas the application of AND-logic markedly expands the number of viable tumor-restricted pairings by exploiting cancer-specific co-expression signatures. OR-logic designs provide complementary value by maintaining or improving selectivity while accommodating tumor expression heterogeneity. Among existing clinical bispecific ADC programs, only a limited subset demonstrates true AND-gate behavior, with the EGFR/MET pairing showing the most robust tumor-restricted co-expression profile. Beyond the current landscape, the platform identifies novel AND-gate opportunities with predicted improvements in therapeutic index. Functional evaluation of one such candidate validated the model's prediction of avidity-driven dual engagement and tumor-selective cytotoxicity. Collectively, these findings demonstrate that a proteomics-driven AND/OR bispecific discovery platform can substantially expand the therapeutic target space beyond what is achievable with monospecific ADCs, enabling the development of safer and more selective next-generation cancer therapeutics.

#4417 GS24-B025, a novel CDH17- and CEA-directed bispecific antibody-drug conjugate, for the treatment of colorectal cancer.

Zeng Qi, **Fu Li**, Liping Shao, Yuting Lu, Chong Ding, Nan Li, Huan Wang, Weiming He, Qiangqiang Deng, Peng Qi, Wenqiang Zhai, Yihui Lin, Xiaozhen Wang, Fanglong Yang, Siqin Wang, Lei Jin, John L. Xu

Changchun GeneScience Pharmaceutical Co., Ltd., Shanghai, China

Background: Colorectal cancer (CRC) is the third most common cancer worldwide and the second leading cause of cancer deaths. Often diagnosed at advanced stages with limited treatment options, substantial unmet need remains in the metastatic setting of CRC (mCRC). Both CDH17 and CEA are highly expressed tumor-associated antigens (TAAs) in CRC, representing promising therapeutic targets. GS24-B025, a dual CDH17- and CEA-targeting ADC comprising topoisomerase 1 inhibitor payloads site-specifically conjugated to a CDH17 x CEA bsAb by a proprietary peptide-based cleavable linker with a drug-to-antibody ratio (DAR) of 8, is currently in development as a potential therapy for mCRC.
Methods: Membrane expression of CDH17 and CEA was assessed in CRC tissue microarrays (TMAs) by immunohistochemistry (IHC). Binding affinity and activity of GS24-B025 to CDH17 and CEA were determined by Biacore and flow cytometry, respectively. *In vitro* cytotoxicity and bystander killing effect of GS24-B025 were examined in a Cell Titer-Glo assay in CRC cell lines. *In vivo* anti-tumor efficacy of GS24-B025 was investigated in the CRC xenograft models in mice. Pharmacokinetics was studied in cynomolgus monkeys.
Results: CDH17 and CEA were found to be highly co-expressed in CRC tissues (N=209), and thus, dual targeting of CDH17 and CEA may enable broader patient coverage across and provide benefit to the entire CRC population. GS24-B025 showed single-digit nanomolar affinity to both CDH17 and CEA and potent binding to $CDH17^+$ and CEA^+ tumor cells, resulting in efficient internalization, and displayed robust cytotoxicity and bystander killing activity against CRC cell lines *in vitro* (with an EC50 in the sub-nanomolar range). Furthermore, GS24-B025 effectively induced tumor regression across different levels of CDH17 and/or CEA expression and demonstrated superior *in vivo* efficacy *versus* benchmark ADCs, including in-house generated M9140 and TORL-3-600. Furthermore, GS24-B025 featured a favorable pharmacokinetic profile in cynomolgus monkeys.
Conclusion: These data suggest the potential of GS24-B025 as an effective treatment option for CRC patients and support its further evaluation in IND-enabling studies.

#4418 Preclinical characterization of a potential best-in-class camptothecin-based antibody-drug conjugate targeting ADAM metallopeptidase domain 9.

Rui Liu, Lan Ding, Yushi Chi, Ge Song, Kuichao Qu, Wan-jen Yang, Kun Yan, Jinbo Liu, Huixin Yan, Xiaoling Yuan, Ying Chen, Zhenjian Li, Chen Hu, Jijun Yuan

Shanghai Henlius Biotech, Inc., Shanghai, China

Introduction: ADAM metallopeptidase domain 9 (ADAM9), a member of the disintegrin and metalloproteinase, mediates proteolytic shedding of cytokines and growth factors. ADAM9 dysregulation promotes tumor progression, metastasis, and pathological angiogenesis. ADAM9 is overexpressed in various solid tumors, including pancreatic, lung, gastric, and breast cancers, with low expression in normal adult tissues. Previously, the clinical development of ADAM9-targeted ADC IMGC-936 was terminated due to maytansinoid-related ocular toxicities. Herein, we developed a next-generation ADAM9 ADC using a camptothecin-based linker-payload, which is anticipated to avoid ocular toxicity and possess expanded therapeutic index.

Methods: ADC cytotoxicity was evaluated using the CellTiter-Glo (CTG) assay in Jurkat (ADAM9-negative), Calu-3 (intermediate ADAM9 expression), and NCI-H1693 (high ADAM9 expression) cell lines. Bystander activity was assessed in Jurkat cells co-cultured with CHOK1-hADAM9 cells, with Jurkat viability determined by CTG. ADC stability in human and rat plasma was monitored over 14 days, with payload release quantified by LC-MS. Accelerated stability was examined by incubating ADCs at 25 °C for 7 days, followed by drug antibody ratio (DAR) and size exclusion chromatography monomer fraction analysis. *In vivo* efficacy was investigated in Calu-3 (non-squamous NSCLC, *EGFR* wildtype) and DLD-1 (CRC, MSI-H, *KRAS* G13D) cell line-derived xenograft (CDX) mouse models. A PK study was conducted in Sprague-Dawley rats administered intravenously with ADAM9 ADC 5 mg/kg.

Results: The parental antibody exhibited nanomolar affinity for human and cynomolgus ADAM9, with no cross-reactivity to rodent orthologs or other ADAM family members. Antibody internalization in MKN-45, MiaPaCa-2, and Calu-3 cells were time-dependent and highly efficient (>50% at 4 h), while the ADC showed comparable or enhanced internalization. The ADAM9-ADC demonstrated potent cytotoxicity and bystander killing effects. In Calu-3 CDX models, a single 3 mg/kg dose elicited 109.3% tumor growth inhibition (benchmark ADC, 91.1%). In DLD-1 CDX models, TGIs reached 90.2% and 66.8% at 3 and 8 mg/kg, respectively, significantly outperforming the benchmark (39.2%) at 3mg/kg. The ADC also displayed excellent plasma stability, with minimal DAR reduction and aggregation in accelerated and freeze-thaw stability assays. The ADAM9 ADC also exhibited a favorable pharmacokinetic profile in rats, characterized by minimal free toxin release and antibody-like half-life.

Conclusion: Preclinical studies reveal that the ADAM9-ADC exhibits potent *in vitro* cytotoxicity and superior in vivo antitumor efficacy relative to benchmarks. Pilot toxicology studies in cynomolgus monkeys are ongoing. Further clinical development is warranted.

#4419 Development of a first-in-class camptothecin-based antibody-drug conjugate targeting ALPP/ALPPL2 with potent antitumor activity and excellent tolerability.

Rui Liu, Lingli Zhang, Fan Yang, Junjie Zhang, Wan-Jen Yang, Xiaoling Yuan, Jichen Sha, Yushi Chi, Ge Song, Weiguang Qu, Zhiliang Lv, Qian Zou, Huixin Yan, Chen Hu, Jijun Yuan

Shanghai Henlius Biotech, Inc., Shanghai, China

Introduction: ALPP (alkaline phosphatase, placental) and ALPPL2 (alkaline phosphatase, placental-like 2) emerge as promising targets due to their expression across multiple solid tumors, including ovarian (60%), endometrial (50%), pancreatic (30%), and gastric cancer (15%) along with minimal expression in normal adult tissues. We developed a novel ALPP/ALPPL2-directed antibody-drug conjugate (ADC) incorporated a proprietary camptothecin-derived payload linked through a protease-cleavable linker to a high-affinity monoclonal antibody. Preclinical studies demonstrate robust antitumor activity with favorable safety, supporting its potential to benefit patients with refractory advanced solid tumors.

Methods: Parental antibody binding to ALPP/ALPPL2-positive cells was evaluated by flow cytometry. Selectivity against related phosphatases (hALPL and hALPI) was confirmed via enzyme-linked immunosorbent assay. ALPP/ALPPL2-ADC cytotoxicity was assessed using CellTiter-Glo (CTG) in ALPPL2-positive cells (HEP2, NCI-H1651). Bystander killing was quantified in co-cultures of ALPPL2-positive HEP2 cells and Jurkat controls by measuring Jurkat viability with CTG assay. *In vivo* efficacy was examined in Capan-1 pancreatic adenocarcinoma cell line-derived xenograft (CDX) model and LD1-0017-200702 gastric patient-derived xenograft (PDX) models. Pharmacokinetics and toxicology were characterized in cynomolgus monkeys at 20 and 40 mg/kg, administered every three weeks for three cycles.

Results: The parental ALPP/ALPPL2 antibody demonstrated high specificity for human and cynomolgus ALPP/ALPPL2, with no cross-reactivity to related phosphatases (hALPL and hALPI). The ALPP/ALPPL2-ADC (drug antibody ratio of 8), incorporating a proprietary camptothecin-based linker-payload, exhibited target mediated cytotoxicity in HEP2 (ALPP/ALPPL2^{high}) and NCI-H1651 (ALPP/ALPPL2^{medium}) cells *in vitro*. The ADC also showed a 50-fold greater bystander killing effect compared with a deruxtecan-based ADC. *In vivo*, a single 1 mg/kg dose induced profound tumor regression in the Capan-1 CDX model, while in the gastric adenocarcinoma PDX model refractory to an ADC with an MMAE payload, a single 8 mg/kg dose achieved deep tumor remission. In non-human primates, the ALPP/ALPPL2 showed linear pharmacokinetics and excellent tolerability (highest non severely toxic dose ≥40 mg/kg).

Conclusion: ALPP/ALPPL2-ADC is a promising therapeutic candidate for solid tumors, particularly gynecologic cancers. As a first-in-class camptothecin-based ADC targeting ALPP/ALPPL2, it combines high antibody specificity with robust antitumor efficacy and favorable tolerability, supporting advancement into clinical development.

: Antibody-Drug Conjugates and Linker Engineering 3
Poster Session

#4423 Advancing ADC therapeutics with next-generation site-specific glycan conjugation and dual-payload flexibility.

Wei-Chien Tang, Yu-Hung Chen, Chih-Kang Chang, Ting-Wei Liu, Hung-Yi Lin, Wei-Jhen Huang, Chi-Huan Lu, Ren-Yu Hsu, Nan-Hsuan Wang, Ya-Chi Chen, Teng-Yi Huang

OBI Pharma, Inc, Taipei, Taiwan

The unique technology by enabling site-specific glycan-based conjugation via a proprietary dual-function enzyme offers an innovative approach for developing antibody-drug conjugates (ADCs). This advanced technology facilitates the production of homogeneous ADCs at a specific drug-to-antibody ratio (DAR) from DAR2 to DAR16, while maintaining the integrity and function of the native antibody. A key feature of the technology is its proprietary linker, specifically designed to enhance payload stability and enable selective release within the tumor, thereby potentially broadening the therapeutic index.
Expanding upon its core capabilities, the new technologies serve as a dual-payload platform, enabling the development of site-specific ADCs carrying two distinct payloads. This technology allows for flexible DAR construction, including both equal and asymmetric payload ratios, providing versatility to tailor ADCs for optimized therapeutic outcomes. Moreover, the ability to specify distinct conjugation sites further enhances its flexibility for diverse payload combinations, including cytotoxic agents, immunomodulators, anti-tumor inhibitors, and degraders. The platform also accommodates both mono- and multi-specific antibodies, broadening its applicability across therapeutic modalities.
Here we used microtubule inhibitor and Topoisomerase I inhibitor to demonstrate the site-specific dual-payload platform. In preclinical studies, the site-specific dual-payload ADCs exhibited superior cytotoxicity and promising antitumor activity in various tumor models, compared to approved and benchmark single payload ADCs, underscoring their potential for enhanced antitumor efficacy. Importantly, these ADCs maintained structural integrity and
avoided antibody aggregation. These features provide a strong foundation for the future clinical development of biomolecules derived from this site-specific dual-payload technology.
Through the integration of glycan engineering, dual-function enzymatic control, proprietary linker chemistry, and flexible payload conjugation, the site-specific dual-payload technology suite provides a robust and adaptable solution to overcome key limitations in current ADC design. Continued innovation and clinical translation of the site-specific dual-payload platform may unlock new therapeutic possibilities to overcome drug resistance and is applicable across oncology and beyond.

#4424 Preclinical efficacy of a first-in-class anti-Integrin α/β ADC in hard-to-treat solid tumors.

Qinhong Ma, Daizong Li, Kewei Zhao, Mary Q. Xu, **Mason Lu**

MedAbome, Inc., Fremont, CA

Integrin (ITG) α/β is a heterodimeric type I transmembrane glycoprotein composed of one α and one β integrin subunit. It mediates cell-cell and cell-extracellular matrix (ECM) interactions and elicits subsequent signaling cascades that regulate cell adhesion, motility, proliferation, survival, and gene expression. The aberrant overexpression of ITGα/β has been observed across a variety of solid tumors, and it supports cancer progression and metastasis, suggesting that it may serve as a potential therapeutic target. Using our proprietary live-cell immunization (LC-I) and high-throughput screening (LC-HTS) platforms, we generated and developed MAb51-31, an anti-ITGα/β monoclonal antibody (mAb), which selectively recognizes a tumor-restricted conformational epitope of ITGα/β. MAb51-31 exhibited no cross-reactivity with normal cells or tissues. Both the chimeric and humanized versions of MAb51-31 displayed high binding affinity to recombinant ITGα/β ($K_D \approx 1.4$ nM). MAb51-31-cAb, engineered with two point-mutations in each Fc region, was conjugated to MMAE via an MC-Vc-PAB linker to generate MAb51-31-ADC (DAR4). MAb51-31-ADC demonstrated potent antiproliferative effects *in vitro*, with cytotoxicity correlating with its internalization efficiency across various solid tumor cell lines. In cell line-derived xenograft (CDX) models of triple-negative breast cancer (TNBC), non-small cell lung cancer (NSCLC), gastric cancer (GC), and other solid tumors, a single intraperitoneal (*i.p.*) dose of MAb51-31-ADC at 4, 7, or 10 mg/kg effectively inhibited tumor growth, resulting in complete tumor regression within 24~30 days post-treatment. Initial toxicology assessments indicated that MAb51-31-ADC was well tolerated, with no notable safety concerns observed. MAb51-31-ADC is a promising therapeutic candidate for treating solid tumors, with selective recognition of a tumor-specific ITGα/β epitope potentially enabling strong antitumor efficacy and reduced off-target effects. Ongoing studies include evaluation of MAb51-31-ADC in patient-derived xenograft (PDX) models of gastrointestinal (GI) cancers, as well as retrospective analyses of target expression in tumor samples, to further support its clinical development.

#4426 Novel tumor microenvironment (TME)-activated, pan-RASi and Topo1i dual-payload linker enables safe broad RAS inhibition and overcomes Topo1i resistance.

Zhengsong Gu, Cheng Liu, **Yuan Liu**

Affinity Biopharmaceutical Co., Ltd., Shanghai, China

Pan-RAS inhibitors target RAS mutations in tumor cells but also affect wild-type RAS in normal tissues. Consequently, pan-RASi-related skin toxicities such as rash and acneiform dermatitis commonly occur, narrowing their therapeutic window. QHL-P1711 is a potent pan-RAS inhibitor which effectively suppresses the proliferation of wild type NRAS and HRAS tumor cells and tumor cells with $KRAS^{G12C}$, $KRAS^{G12D}$ and $KRAS^{G12V}$ mutations. In cytotoxicity assays, QHL-P1711 demonstrated synergistic effects with DXd (a Topo1 inhibitor) in MIA PaCA-2^{G12C}, AGS^{G12D} and Capan-1^{G12V} tumor cells.

TMEAlinker is a clinically validated, selectively activated linker in the tumor microenvironment (TME) by legumain, an active protease highly overexpressed in the TME while exhibiting negligible expression in skin endothelial cells. By using the dual-payload TMEAlinker, both pan-RASi (QHL-P1711) and DXd can be conjugated to an EGFR-TROP2 bispecific antibody to construct a dual-payload ADC EGFR-TROP2-TMEAlinker-RASi-DXd (IMD2146). The highly hydrophilic dual-payload TMEAlinker effectively addressed CMC challenges and enabled homogeneous formation of dual-payload ADCs with a drug-to-antibody ratio (DAR) of 8+8.

IMD2146 exhibited superior efficacy than single-payload ADCs and pan-RAS inhibitor treatment at equivalent pan-RASi molar doses in the NCL-H1975 tumor model. Notably, IMD2146 retained antitumor activity in the PA-1 Topo1i-resistant tumor model, whereas the single-payload ADC (EGFR-TROP2-TMEAlinker-DXd) showed no efficacy. In human plasma at 37 °C, <1% of free pan-RASi was released after 7 days of incubation of IMD2146, indicating excellent plasma stability. In preclinical toxicology studies in cynomolgus monkeys, IMD2146 was well tolerated after repeated dosing at 50 mg/kg. Pharmacokinetic analysis in cynomolgus monkeys revealed high plasma concentrations of IMD2146 with minimal levels of free pan-RASi and free DXd, further confirming its stability in circulation.

In summary, these results demonstrate that the dual-payload TMEAlinker design provides a novel strategy to achieve systemic safety with broad RAS inhibition while effectively overcoming Topo1i resistance. This approach integrates precise TME activation with dual-mechanism targeting, offering a promising therapeutic platform for RAS-driven tumors while minimizing systemic toxicity.

#4427 Development of CLIO-8221: A HER2-targeted multi-payload ADC to address ADC resistance.

Alyson Smith[1], Ben Ayers[2], Shalini Paliwal[2], Bhushan Dharmadhikari[2], Jerome Boyd-Kirkup[1]

[1]Callio Therapeutics, Seattle, WA,[2]Hummingbird Bio, Singapore, Singapore

Antibody drug conjugates (ADCs) are transforming the treatment landscape for patients across tumor types, particularly HER2 expressing cancers, however they continue to be limited by narrow therapeutic indexes and rapidly emerging resistance. Studies have confirmed that most ADC patients retain target expression post progression, suggesting that treatment resistance emerges in part because of payload insensitivity. Patient samples have highlighted DNA damage response activity as one important cause of reduced efficacy and resistance to Topoisomerase 1 inhibitor (TOP1i) payloads, therefore, blockade of DNA damage repair pathways in conjunction with TOP1i may drive better and more durable efficacy. Dual payload ADCs are a novel modality with the potential for efficient delivery of combination therapies to the same tumor cell at the same time, balancing PK and exposure profiles. We have developed CLIO-8221, a novel anti-HER2 dual payload ADC conjugated to both TOP1i and a potent DNA damage response inhibitor (ATRi), designed for optimal efficacy and tolerability. CLIO-8221 is an Fc-engineered anti-HER2 antibody conjugated site-specifically via MTGase to a hydrophilic branched linker carrying both a Topo1 inhibitor and an ATR inhibitor, with a DAR of 4 for each payload. ELISA, SPR, flow cytometry and live cell imaging were used for ADC characterization. The pharmacologic activity of CLIO-8221 was assessed using proliferation assays, cell line-derived xenograft studies and non-human primate tolerability studies (NHP). CLIO-8221 is rapidly internalized into lysosomes in HER2 expressing tumor cells to release TOP1i and ATRi payloads with strong bystander effect. CLIO-8221 shows *in vitro* cell killing activity across cell lines with a range of HER2 expression levels and Trastuzumab-DXd (T-Dxd) sensitivities, and drives tumor regressions after a single dose in T-DXd-resistant and refractory xenograft models, with strong durable activity seen at 3 mg/kg. The optimized Fc and linker engineering reduces off-target uptake via abrogated FcγR binding and decreased macropinocytosis. Toxicokinetic studies in NHPs demonstrate high tolerability with minimal systemic free payload exposure and no significant CLIO-8221 changes in safety endpoints up to 70mg/kg. CLIO-8221 has dose dependent exposure with comparable PK profiles between the total antibody (mAb) and conjugated mAb and a half-life of 8-12 days. CLIO-8221 is a first-in-class anti-HER2 dual payload ADC that allows targeted delivery of TOP1i and ATRi payloads to HER2 expressing tumors to maximize anti-tumor efficacy, overcome TOP1i resistance, and reduce systemic toxicity. Our findings strongly support the development of CLIO-8221 as a potential therapeutic option for HER2-positive cancers and a phase 1/2 study of CLIO-8221 in patients with advanced solid tumors has been initiated.

#4430 WuXiTecan2: A hydrophilic exatecan linker-payload for dual-payload ADC discovery.

Hu Chen, Qirui Fan, Zili Xu, Xiaomei Li, Ding Wei, Lin Zhang, Chenghu Hu, Cindy Cheng, Marie Zhu

Discovery and development, WuXi XDC, Shanghai, China

Background: Exatecan, a camptothecin-derived topoisomerase inhibitor, demonstrates high potency along with robust bystander activity. Several exatecan-based ADCs against diverse targets have now entered into late-stage clinical trials. In parallel, the need to overcome resistance mechanisms have intensified interest in dual-payload ADC strategies, with exatecan emerging as a compelling payload option in these combination formats. However, its hydrophobic physicochemical properties can lead to ADC aggregation, non-specific uptake, reduced plasma stability, particularly at DAR8, or in dual-payload settings. Therefore, the introduction of hydrophilic moieties via linker design is essential to improve ADC hydrophilicity and physicochemical behavior. Here, we developed a super-hydrophilic linker payload, named WuXiTecan2, that overcomes exatecan's hydrophobicity and shows strong efficacy and good tolerability in vitro and in-vivo, both as DAR8 ADC and in dual-payload ADC formats.

Methods: WuXiTecan2 was conjugated to Trastuzumab at DAR8 or formulated as a trastuzumab-dual payload ADC paired with an MMAE payload using WuXiDARX Technology. The resulting ADCs were fully characterized by HIC-HPLC, SEC-HPLC, and LC-MS. The in-vitro activity was assessed across breast and gastric cancer cell lines with varied HER2 expressions. Plasma stability was evaluated in the mouse, and human plasma. In-vivo efficacy was determined in Her2 expressing CDX models, and the tolerability of trastuzumab-WuXiTecan2 ADC(DAR8) was evaluated in mice and preliminary cynomolgus monkey studies.

Results: WuXitecan2 was conjugated to trastuzumab at DAR8 and incorporated into a dual-payload ADC pairing with MMAE payload. Both formats were successfully generated and demonstrated highly uniform conjugation profiles. Notably, the introduction of WuXiTecan2 showed excellent ADC hydrophilicity, which is very close to naked antibody. In-vitro, both ADC formats displayed sub-nanomolar IC50 across a panel of breast and gastric cancer cell lines spanning HER2 expression levels. Both DAR8 and dual-payload ADCs showed improved plasma stability in mouse and human plasma, consistent with the enhanced hydrophilicity of the linker and its stabilizing effect on the exatecan payload. In Her2-expressing CDX models, the dual-payload ADC achieved superior tumor growth inhibition relative to the single-payload DAR8 ADC at comparable doses. Treatment was well tolerated; the trastuzumab-WuXiTecan2 DAR8 ADC demonstrated acceptable tolerability in mouse studies at a single dose up to 250mg/kg,and tolerated well in preliminary cynomolgus monkey studies at 45mg/kg, Q3Wx3.

Conclusions: WuXitecan2, enabled by the hydrophilic linker moiety design, demonstrated strong efficacy, stability and tolerability, supporting its use as a promising dual-payload ADC component.

#4431 ZW427, a Ly6E-targeting antibody drug conjugate bearing a novel pan-RAS inhibitor payload for the treatment of RAS mutated cancers.

Dunja Urosev[1], Vidhi Khanna[1], Ambroise Wu[1], Jodi Wong[1], Saki Konomura[2], Elizabeth Porter[1], Matthew Bonderud[1], Victoria Harman-McKenna[1], Taixiang Wang[1], Linglan Fu[1], Diego Alonzo[1], Devika Sim[1], Adele Chan[1], Allysha Bissessur[1], Spencer Boisjoli[1], Michael Lee[1], Germanna Righetto[1], Jesse Leblanc[1], Raffaele Colombo[1], Graham Garnett[1], Jamie Rich[1], Stuart Barnscher[1]

[1]Zymeworks Inc., Vancouver, BC, Canada,[2]None, None, BC, Canada

Aberrant RAS signaling is implicated as an oncogenic driver in up to 30% of cancers. Mutant selective RAS inhibitors (RASi) have been clinically approved in select indications, but their durable efficacy is hampered by acquired alterations that render tumors refractory to drug. Pan-RASi are showing broad clinical promise, but their full potential has been limited by toxicities likely arising from on-target inhibition of wild-type RAS in normal tissues, as well as by the emergence of resistance. These challenges may be improved upon by optimizing delivery of a RASi via an antibody drug conjugate mechanism. Lymphocyte antigen 6 family member E (Ly6E) is a GPI anchored cell surface protein with minimal presence in normal tissues that is prevalently overexpressed in many solid tumors including those which commonly feature oncogenic RAS mutations, such as NSCLC, PDAC, and CRC. We sought to leverage the ability of an ADC to increase the delivery of a novel pan-RASi payload to tumors for improved response, and to provide a differentiated safety profile that mitigates the toxicity limitations of current small molecule pan-RASi.

ZW427 comprises a novel Ly6E-targeted humanized IgG1 antibody conjugated to a novel pan-RAS inhibitor via a cleavable linker. The anti-Ly6E antibody was discovered and optimized for ADC application, with a focus on binding, specificity, internalization and payload delivery to tumor cell lines. To study the therapeutic potential of ZW427, *in vitro* ADC cytotoxicity was assessed in spheroids derived from a panel of RAS mutated cancer cell lines. Internalization and spheroid penetration were evaluated, and tumor cell co-culture assays were performed to assess bystander-mediated cell killing potential. Anti-tumor activity of ZW427 was investigated in multiple RAS mutated mouse xenograft models with a range of Ly6E-expression. Pharmacodynamic aspects of RAS inhibition were also assessed.

ZW427 exhibited target specific binding to cancer cells, highly effective internalization and bystander-mediated killing. Importantly, the ADC demonstrated potent and target-specific cytotoxicity in multiple Ly6E-expressing cancer cell spheroids. A single administration of ZW427 resulted in anti-tumor activity across a range of xenograft models. The pan-RASi ADC platform that has been developed shows encouraging tolerability in mice and an imminent toxicology study of ZW427 in non-human primates will further define its safety profile. Overall, the data supports the potential of ZW427 as a novel, highly differentiated therapeutic agent against Ly6E-expressing RAS mutant cancer indications.

#4432 LNF2105, a next-generation nectin-4-targeted ADC with a specially designed linker and a DXD analogue.

Zhongsong Zhu, Shili Wang, Jinhua Xu, Fanliang Cheng, Yuqiang Zhu, Peibiao Zhang, Guimin Zhang, Lili Zhao, **Zhenyu Li**

Lunan Pharmaceutical Group Co., Ltd., Linyi, China

Background: Nectin-4 is an attractive tumor-associated antigen, with over-expression in various solid tumors including UC, TNBC, CC, NSCLC, and HNSCC, while minimal expression in normal tissues. High Nectin-4 expression is closely associated with tumor development and poor prognosis, acting as a crucial biomarker for cancer recurrence and metastasis. Currently, only one Nectin-4 ADC with MMAE as the payload, Enfortumab Vedotin (EV), has been approved for marketing. However,EV has the issue of non-uniform DAR values, which can result in drug heterogeneity. Moreover, there is a black box warning in its instruction for severe and fatal skin adverse reactions. Therefore, we developed a novel Nectin-4-targeted ADC drug with a new mechanism, LNF2105 whose homogenous drug-antibody ratio and novel linker chemistry increase the stability of the conjugate in the systemic circulation, enabling highly efficient drug delivery and avoiding off-target toxicity.

Methods: To measure the bystander killing effect, CHO-GFP and MCF-7 cell lines were used. To assess serum stability, LNF2105 and DS8201 were incubated at 37℃ for up to 25 days in human plasma; free DXD was quantified by LC/MS-MS. For *in vitro* studies, assays for competitive ability and specificity, binding affinity, internalization, ADCC activity, and killing activity were performed. The *in vivo* antitumor efficacy of LNF2105 was evaluated in MDA-MB-468, xPC3, NCI-H322, and SW780 in subcutaneous xenograft models.PK properties were studied in cynomolgus monkeys, and safety studies of the payload and ADC were conducted in rats and cynomolgus monkeys, respectively. In general toxicology studies, cynomolgus monkeys and ICR mice were used.

Results: LNF2105 appeared as a homogeneous ADC composed of a Nectin-4-targeting monoclonal antibody conjugated to a Topo I inhibitor using interchain-disulfide-based site-specific conjugation technology, with DAR 8. A significant bystander killing effect were observed. Compared to DS8201, the payload dropout rate of LNF2105 was much slower and its plasma stability was higher. In various solid tumor xenograft models, LNF2105 demonstrated dose-dependent tumor suppression, with efficacy comparable to or superior to that of EV, which may be attributed to the site-specific conjugation. In addition, LNF2105 demonstrated a favorable safety profile, and the only side effect on the skin of monkeys was reversible. Ocular, pulmonary, and hematologic toxic side effects—common in Nectin-4-targeted therapy—were not observed. The HNSTD in monkey was 6 mg/kg, with milder adverse events compared with those of EV.

Conclusions: Overall, LNF2105 is a Nectin-4-directed ADC drug with a specially designed linker and a DXD analogue payload. Next generation site-specific conjugation technologies endow the drug with excellent homogeneity, remarkable preclinical antitumor activity, and a favorable safety profile.

#4433 Preclinical evaluation of LM-364^{TME}: A next-generation anti-Nectin4 ADC with promising efficacy and reduced toxicity.

Lei Shi, Yun Zhang, Rongrong Huang, Xia Qin, Da Fei, Yuan Li, **Wei Cao**

LaNova Medicines, Shanghai, China

Background: Antibody-drug conjugates (ADCs) has shown significant efficacy across multiple tumor types. Nectin-4, an adhesion molecule with limited expression in normal tissues (restricted to skin and secretory glands), is overexpressed in bladder, triple-negative breast, and other epithelial cancers. The clinical success of enfortumab vedotin valudated Nectin-4 as a therapeutic target; however, dose-limiting skin rash and neuropathy arise from on target, off-tumor toxicity due to low Nectin-4 epxression in nomal tissues. Extracelluar adenine nucleotides (ANP:ATP/ADP/AMP) accumulate to micromolar concentrations within the tumor microenvironment (TME), while remaining at nanomolar levels in heathy tissues. LM-364^{TME} is a novel anti-Nectin-4 ADC designed to exploit this metabolic difference. It comprises a humanized antibody endineered for ANP-dependent binding to Nectin-4, conjugated via a cleavable linker to topoisomerase I inhibitor payload, with a drug-to-antibody ration of 8.

Methods: Binding activity, specificity, and cross-species reactivity of LM-364^{TME} were evaluated by flow cytometry. Internalization was evaluated using a pH-sensitive fluorescent probe. Cytotoxicity was measured via CellTiter-Glo luminescent cell viability assay. *In vivo* anti-tumor activity of LM-364^{TME} was evaluated in Nectin 4-positive cell line-derived xenografts (CDX) and patient-derived xenografts (PDX) models. Repeated-dose toxicity studies were performed in Sprague-Dawley rats and rhesus monkeys.

Results: LM-364^{TME} exhibited strong ANP-dependent binding to Nectin 4, with an EC_{50} of 0.02 nM to huNectin4 protein and 0.187 -1.837 nM in Nectin-4 positive tumor cells under high ANP conditions, butnegligible binding in the absence of ANP, resulting a large selectivity window. LM-364^{TME} also exhibited cross-reactivity with Nectin-4 in rodent and non-human primate models. LM-364^{TME} showed robust ANP-dependent internalization and cytotoxicity in in MDA-MB-468 and huNectin 4 CHOK1 cells. *In vivo*, LM-364^{TME} treatment (3-6 mg/kg) significantly induced tumor growth and regression in multiple models, including MDA-MB-468 (TGI 119.1%), urothelial carcinoma PDX (TGI 107.46%) , esophageal cancer PDX (TGI 86.73%), and cervical cancer PDX (TGI 168.79%). In repeat-dose studies, LM-364^{TME} was well tolerated in both rats and rhesus monkeys.

Conclusion: LM-364^{TME} is an ANP-dependent, conditionally active anti-Nectin-4-ADC that demonstrates potent and selective antitumor activity with favorable safety profile in preclinical models. These data support LM-364^{TME} as a promising next-generation Nectin-4-targeted therapy with the potential to improve the therapeutic index of this class.

Keywords: Nectin-4, antibody-drug conjugate, LM-364^{TME}, solid tumors

Disclosure: The study was funded by LaNova Medicines Limited, China.

#4434 *In vitro* and *in vivo* study of C^2LP-ADC & CLP^2-ADC targeting human breast and gastric cancer.

Xingquan Ma[1], Greg Liang[1], Weihua Shi[1], Bing Li[2], Shuwei Lu[1], **Xinxin Yang**[1], Qikuan Chen[1], Guilan Wang[1], Yao Ma[2]

[1]Shanghai ChemPartner Co., Ltd., Shanghai, China,[2]ChemPartner Co., Ltd., Boston, MA

Antibody-Drug Conjugates are a class of targeted cancer therapeutics that combine the specificity of monoclonal antibodies with the potency of cytotoxic agents. This design enables selective delivery of the agents to cancer cells, while avoiding healthy tissue. Some of the challenges that remain with the development of these treatments is the narrowness of the therapeutic window and significant off target toxicity due to non-specific release of the payload. One of the other major challenges is tumor resistance. Leveraging our experience in linker synthesis, we set out to design next-generation linkers that address the persistent challenges of ADC development. Our strategy centered on creating a cleavage cascade system incorporating two distinct cleavage events, enhancing linker robustness and reducing the risk of non-specific payload release (C^2LP-ADC). As a potential solution to drug resistance, we engineered linkers with the ability to tailor the Drug-to-Antibody Ratio (DAR), enabling incorporation of multiple payloads (CLP^2-ADC). We synthesized and conjugated analogues of known ADCs for Anti-HER cancers using both C^2LP and CLP^2 linkers. The C^2LP was compared *in vitro* and *in vivo* to a reference ADC, demonstrating improved therapeutic index and decreased off-target toxicity, with the test subjects maintaining body mass for longer than those treated with the reference-ADC. In addition, the linker-payload complex was demonstrated to be stable in plasma for much longer than the reference-ADC. *In vitro* treatment of resistant cell lines with CLP^2-ADC demonstrated enhanced therapeutic efficacy with respect to the reference-ADC.These findings highlight the critical role of linker technology in optimizing ADC performance. Incorporation of C^2LP and CLP^2 linkers can substantially improve safety, stability, and therapeutic efficacy in ADCs targeting HER-positive breast and gastric cancers, offering a promising strategy for overcoming resistance and minimizing systemic toxicity.

#4435 Transforming ADC development with novel linker architectures and payload optimization.

Gengcheng Jack Yang, Xudong Wei

Payload-linker Department, WuXi XDC, Cranbury, NJ

Antibody-drug conjugates (ADCs) are an expanding class of targeted cancer therapies, and innovations in linker and payload chemistry are critical to improving therapeutic index and clinical outcomes. We present four complementary strategies designed to enhance ADC performance and manufacturability. First, a novel linker adapter, N-(ortho-hydroxyphenyl)-N-methylcarbamate, enables controlled side-chain modification and rapid payload release, resulting in pronounced tumor regression in colonic cancer xenograft models. Second, a Val-Ala-based double self-immolative linker-payload platform was developed to optimize hydroxyl group-containing payload integration. A trastuzumab-DXd ADC constructed using this platform demonstrated improved stability, cathepsin B sensitivity, potent bystander effect, and a broad therapeutic index in HER2-positive and -negative xenografts, with favorable safety profiles in preclinical toxicology studies. Additionally, we introduce a streamlined two-step synthesis of a disaccharide linker for glycosite-specific conjugation, reducing the traditional >15-step process and enabling cost-effective production of homogeneous ADCs with enhanced quality and consistency. Finally, we report the first ADC incorporating homocamptothecin as a payload, achieving antitumor activity comparable to Enhertu at 3 mg/kg while demonstrating improved tolerability in NCI-N87 xenograft models. Collectively, these innovations establish a versatile platform for next-generation ADCs, combining precision targeting, improved pharmacological properties, and scalable manufacturing to advance clinical oncology.

#4436 Sutro's site-specific dual-payload ADCs combining TOPO1i and DNA damage response inhibitors to enhance efficacy, overcome resistance, and improve safety.

Krishna Bajjuri, Robert Yuan, Daniel Calarese, Rhoneil Pena, Ravi Singh, Young Park, Cuong Tran, Abigail Yu, Xiaofan Li, Guifen Xu, Yihong Zhou, Brian Vuillemenot, Werner Rubas, Genevive Hernandez, Alice Yam, Gang Yin, Hans-Peter Gerber

Sutro Biopharma Inc, South San Francisco, CA

Antibody-drug conjugates (ADCs) have demonstrated transformative potential in oncology, but enhancing efficacy of ADC against low-antigen and heterogeneous tumors while overcoming resistance and maintaining safety remain a major challenge. Resistance to single-payload ADCs, particularly TOPO1i based ADCs, is often driven by payload-specific mechanisms such as enhanced DNA repair or upregulation of drug efflux pumps, limiting sustained clinical responses. Sequential administration of TOPO1i ADCs frequently fails to restore efficacy, underscoring the need for novel, multi mechanistic strategies. Topoisomerase I inhibitors (TOPO1i) induce DNA breaks that collapse replication forks, but their efficacy is constrained by rapid repair via PARP and ATR dependent pathways. DNA damage response inhibitors (DDRi), such as PARPi and ATRi, block these repairs, restoring TOPO1i sensitivity in resistant, SLFN11-deficient, or repair-proficient tumors. This combination enforces checkpoint failure and prevents fork repair, providing a strong rationale for synergistic antitumor activity while limiting the development and progression of acquired resistance. Although combining TOPO1 inhibition with DDRi has a strong mechanistic rationale, clinical application is constrained by overlapping and non-overlapping toxicities. To overcome these challenges, we developed site-specific dual-payload ADCs (dpADCs) to co-deliver TOPO1i and proprietary DDR inhibitors, including PARPi or ATRi that are not substrates for drug efflux pumps. This strategy leverages synthetic lethality by pairing TOPO1i-induced DNA damage with DDR blockade, selectively enhancing cytotoxicity in target-antigen expressing tumor cells. Key challenges in developing TOPO1i × DDRi dpADCs include optimizing DDRi properties suitable for ADC delivery, selecting payload ratios, maintaining conjugate homogeneity, ensuring linker stability, and mitigating systemic toxicity. By leveraging Sutro's cell-free expression platform, precise dual-conjugation technology, and hydrophilic tumor-selective β-glucuronidase cleavable linkers, we engineered homogeneous, site-specific dpADCs with tunable drug-to-antibody ratios (DARs). These design features enhance solubility, stability, and pharmacokinetics while preserving payload synergy. We demonstrate that Sutro's site-specific TOPO1i × DDRi dual-payload ADCs (dpADCs) exhibit superior anti-tumor activity compared to single-payload ADCs, including in models resistant to TOPO1i ADCs. The targeted co-delivery of TOPO1i and DDRi has the potential to minimize off-target toxicity typically associated with systemic DDR inhibition, thereby broadening the therapeutic window and streamlining preclinical and clinical development compared to separate combination regimens.

#4437 Preclinical development of XNW28012, an antibody drug conjugate targeting tissue factor for treatment of solid tumors.

Yonghan Hu[1], Zhe Zhang[2], Yuanbao Li[2], Liang Kong[2], Shihua Wang[2], Zhenwei Wu[2], Xiaocheng Hu[2], Ka Ruan[2], Wengui Wang[2], Guorong Li[1], Qifeng Shi[2], Haiyang Wei[2], Xiaojun Liu[2], Meijie Le[1], Jing Qiang[1]

[1]Evopoint, Shanghai, China,[2]Evopoint, Suzhou, China

Tissue factor (TF) is a transmembrane protein that serves as the primary initiator of physiological hemostasis. TF binds coagulation factor VII (FVII), promotes its activation, and enhances the proteolytic activity of FVIIa to initiate the extrinsic pathway of blood coagulation. To prevent any improper coagulation cascade activation, TF is normally not expressed by cells exposed to flowing blood such as endothelial cells. Elevated TF expression has been reported in multiple solid cancers, such as cervical cancer, esophageal cancer, and pancreatic cancer. TF is well-internalized into lysosomes and given these various features, represents a favorable target for an antibody-drug conjugate (ADC) modality.XNW28012 is a TF-targeting ADC comprised of a humanized IgG1 antibody conjugated with a potent DNA topoisomerase I inhibitor *via* a protease-cleavable linker with a drug-antibody ratio (DAR) of 8. The tripeptide linker is highly stable in blood and cleavable in the tumor microenvironment and in tumor cell lysosomes. In preclinical studies, XNW28012 can bind to TF on cell surface, enter the cell through internalization effect, and then exhibits similar efficacy with toxin, such as inhibition of cell proliferation, cell cycle arrest, DNA damage response and apoptosis. XNW28012 also exhibits significant antitumor efficacy in multiple tumor xenograft models, including cervical cancer (CaSki), ovarian cancer (OVCAR8), pancreatic cancer (HPAF-II), etc. *In vivo* efficacy is dose-dependent and test dosages are well-tolerated, with minimum effective dose at 1 mg/kg/dose weekly. At the well-tolerated 3 or 10 mg/kg dosage, XNW28012 achieves partial tumor regression (PR) and complete tumor regression (CR) in most xenograft models. XNW28012 combined with SOC showed synergistic effect in multiple xenograft models. The antibody has minimal effect on blood coagulation through antibody screening and therefore no bleeding adverse effect (AE) is observed in toxicity studies.In pharmacokinetic studies, the ADME characteristics of XNW28012 confirmed the designed attributes of the ADC that directs toward the target antigen expressed on the cancer cell surface, and has excellent stability in the bloodstream and the exposure of payload was very low, leading to reduced toxicity. In toxicity studies, XNW28012 displays good tolerability with wide therapeutic windows in Cynomolgus monkeys. It is particularly important to note that XNW28012 has no toxic effect on the lungs and eyes, and no bleeding risk was observed in monkeys.Taken together, preclinical data suggest that XNW28012 could be a promising new antitumor agent for further investigation in clinical trials. Clinical activity of XNW28012 is currently under evaluation in a Phase I/II clinical trial (CTR20233056) and a Phase III clinical trial (CTR20252545).

#4438 A novel synergistic dual-payload TROP2 ADC (CTPH-03) delivering enhanced safety by increased MTD.

Myeong Joo Kim, Soyeon Lim, Dahyun Kim, Han ah Kim, Jaebeom Park, Eunseok Choi, Da wo Jeong, Ji Eun Choi, Young Sang Kim, Seung Chan Kim, Hyo Jin Kang, **Chang-Sun Lee**

Celltrion Pharm, Inc., Incheon, Korea, Republic of

Dual-payload antibody drug conjugates (ADCs) have gained increasing attention due to their potential to overcome limitations of single-payload ADCs. Depending on the combination strategy, dual-payload formats have been reported in order to mitigate tumor heterogeneity or to address resistance that may develop with single payload ADCs. Our dual-payload approach is differentiated from these approaches by aiming to identify two distinct payloads that could provide synergistic anti-tumor activities while minimizing overlapping unwanted side effects. Through extensive combination screening campaigns, we have discovered payload pairs that synergize each other by ZIP score experiments. TROP2 is a perfect target antigen to validate our dual-payload ADC format since it is a clinically validated. Although there are two FDA-approved ADCs, Trodelvy and Datroway, anti-tumor efficacy from these TROP2 ADCs have been subpar due to dose-limiting toxicities. We have developed a novel TROP2-targeting dual-payload ADC (AD^2C) by using MMAE-based dual-payload combination to address this unmet need. The presentation highlights advantages of the synergistic dual-payload TROP2 ADC over known single-payload ADCs or other dual-payload ADC formats by demonstrating, (1) *in vitro* cytotoxicity for cancer cells having different TROP2 expression levels (2) *in vivo* efficacy in various CDX(cancer-cell derived xenograft) models (3) *in vivo* ADC stability in rats and monkeys by PK(pharmacokinetics) studies, and (4) preliminary toxicity studies conducted in mice and monkeys.In due course, we are currently in preparation of PDX efficacy studies for further confirming its *in vivo* efficacy over various patient-derived tumor cells, and IND-enabling toxicology studies in order to quickly move forward the dual-payload TROP2 ADC(AD^2C) into clinical study.

#4439 Preclinical assessment of HWK-007, a next-generation, PTK7-targeting ADC with novel bioconjugation and linker-payload technology.

Kathy S. Keegan[1], Shihe Hou[1], Ashwini B. Pai[1], Enrico Bellomo[1], Erik Kratzer[1], Victor Peykov[1], Bryan Ball[1], Xia Wang[2], Qingling Lu[2], Lei Wu[2], Jijie Gu[2], David J. Lennon[1], David Dornan[1]

[1]Whitehawk Therapeutics, Morristown, NJ,[2]WuXi Biologics, Shanghai, China

Protein tyrosine kinase-7 (PTK7) is a catalytically-inactive receptor tyrosine kinase that promotes tumor progression through the Wnt/planar cell polarity (PCP), phosphatidylinositol 3-kinase/protein kinase B (PI3K/AKT), mitogen-activated protein kinase (MAPK), and vascular endothelial growth factor (VEGF) pathways. Overexpression of PTK7 contributes to metastasis, chemoresistance, and poor clinical outcomes in multiple tumor types. PTK7 is overexpressed in up to 70% of solid tumors, including—but not limited to—lung, ovarian, and endometrial cancers, and has low expression in normal cells, making it an attractive target for an antibody-drug conjugate (ADC). Results from early clinical trials of cofetuzumab pelidotin, a PTK7-targeted, auristatin-based ADC, showed promising signs of clinical activity. HWK-007 is a next-generation, PTK7-targeting ADC that comprises an Fc effector-attenuated IgG1 antibody conjugated to the DNA topoisomerase I inhibitor CPT116, with a drug-to-antibody ratio of 6. HWK-007 incorporates novel bioconjugation (carbon bridge cysteine re-pairing) and advanced linker-payload technologies, designed to maximize intracellular delivery while minimizing systemic exposure of free payload. The mechanism of action of HWK-007 was investigated in preclinical models of cancer. Results showed that HWK-007 bound specifically to cells expressing PTK7, was internalized through receptor-mediated endocytosis into lysosomes, and induced DNA damage resulting in loss of cell viability. Potent antitumor activity was demonstrated in multiple xenograft tumor models, with durable tumor regression observed with as low a dosage as 1 mg/kg single dose; this antitumor activity was superior to that of cofetuzumab pelidotin at equivalent doses. HWK-007 showed a notable bystander killing effect *in vitro*, suggesting the ability to elicit activity against heterogeneous tumors. HWK-007 demonstrated a favorable pharmacokinetic profile in non-human primates (NHP), with an extended half-life and very low levels of free payload observed (0.0067% of the AUC). Repeat-dose toxicology studies in NHP determined a highest non-severely toxic dose (HNSTD) of 60 mg/kg. Combined with preclinical efficacy results, these data suggest a therapeutic index that is suitable for testing in humans. In summary, HWK-007 is a highly potent and selective, next-generation, PTK7-targeted ADC. A phase I dose-escalation study is planned to evaluate HWK-007 in patients with advanced solid tumors.

#4440 Preclinical assessment of HWK-206, a next-generation, biparatopic, SEZ6-targeting ADC with novel bioconjugation and linker-payload technology.

Kathy S. Keegan[1], Shihe Hou[1], Ashwini B. Pai[1], Enrico Bellomo[1], Erik Kratzer[1], Victor Peykov[1], Bryan Ball[1], Lei Wu[2], Mengmeng Sun[2], Lu Jiang[2], Jijie Gu[2], David J. Lennon[1], David Dornan[1]

[1]Whitehawk Therapeutics, Morristown, NJ,[2]WuXi Biologics, Shanghai, China

Seizure-related 6 homolog (SEZ6) is a cell-surface transmembrane protein that plays a role in neuronal development. SEZ6 expression is highly elevated in neuroendocrine (NE) tumors, including, but not limited to, small cell lung cancer (SCLC), brain or central nervous system cancers, and NE tumors of prostate and bladder origin, and has limited expression in normal tissues. In SCLC, SEZ6 expression is correlated with worse survival outcomes. Single-epitope, SEZ6-directed antibody-drug conjugates (ADCs), such as ABBV-706, have shown initial promise in SCLC and NE neoplasms, but with some potential challenges attributed to side effects associated with these agents. HWK-206 is a next-generation ADC that utilizes a biparatopic antibody (bpAb) approach to target SEZ6, with an Fc effector-attenuated IgG1 antibody conjugated to the novel DNA topoisomerase I inhibitor, CPT116. HWK-206 was designed using novel bioconjugation (carbon bridge cysteine re-pairing) and advanced linker-payload technologies to maximize intracellular delivery while minimizing systemic exposure of free payload. The mechanism of action of the HWK-206 bpAb was investigated in preclinical SCLC models. Results showed that the HWK-206 bpAb bound to SEZ6 with higher affinity than the parental antibodies or that reported previously for ABBV-706. HWK-206 induced DNA damage and loss of SCLC tumor cell viability. Furthermore, the HWK-206 bpAb demonstrated superior binding, receptor-mediated internalization, and reduction in viability of SCLC tumor cells expressing varying levels of SEZ6, compared with the parental antibodies and historical benchmarks. Potent antitumor activity was observed in various SCLC xenograft tumor models, with tumor regression observed at single doses as low as 2 mg/kg. HWK-206 demonstrated a bystander killing effect *in vitro*, suggesting the ability to elicit activity against heterogeneous tumors. The pharmacokinetic (PK) and safety profiles of HWK-206 were evaluated in nonclinical toxicology studies. HWK-206 demonstrated a favorable PK profile and was well tolerated. In summary, HWK-206 is a highly potent and selective next-generation, biparatopic, SEZ6-targeted ADC that warrants further investigation. A planned phase I dose-escalation study will investigate HWK-206 in patients with advanced solid tumors.

#4441 Preclinical characterization of novel LIV1 antibody drug conjugates.

Fei Teng, Huanhuan Guo, Xinlai Yao, Lizhi Qin, Lei Shi, Xu Lin, **Yi Gu**, Xueming Qian

Transcenta Therapeutics Co., Limited, Suzhou, China

Background: LIV1 is a member of the zinc transporter family. With limited normal tissue expression, LIV1 was found to be overexpressed with high prevalence in breast (93%), prostate (72%) and lung (10%) cancers, and considered as an attractive cell surface target for developing ADC therapeutics. We have generated 48D6, a proprietary novel humanized anti-LIV1 mAb with high affinity, specificity, internalization ability, unique epitope and improved pharmacokinetics (PK) profile in mice. Then we developed 48D6 based ADCs using glycotransferase mediated site-specific conjugation with Topo I inhibitor (ADC-2) or MMAE (ADC-3), and characterized their anti-tumor activities in preclinical PDX/CDX models and exploratory toxicity in mice.
Methods: PK properties were studied with single dose (i.v.) of 3 or 10 mg/kg of both naked antibodies and ADCs in Balb/c mice. To evaluate anti-tumor activities, nude mice were subcutaneously implanted with LIV1-expressing PDX tumor blocks. When tumors reached ~200mm3, mice were treated (i.v.) with isotype control-ADC or LIV1 ADCs. To explore the combination efficacy of LIV1 ADCs and PD-1 antibody, we established LIV1/PDL1 co-expressing NCI-H460-LIV1 CDX model in human PBMC reconstituted mice. For exploratory tox study, mice were i.v. injected with LIV1 ADC or 48D6 at 10, 30, 60 mg/kg every week for 3 times, then recovered for 5 weeks.
Results: The T1/2 of of 48D6 antibody is 13.8~15.6 days relative to 1.7~3.3 days for Ladiratuzumab analog in mice. After conjugation into ADCs, the T1/2 of 48D6 ADC-2 ranged 10.4~11.6 days while that of SGN-LIV1A analog in mice is 3.7~3.9 days. Topo I inhibitor payload based ADC-2 displayed strong anti-tumor activities in LIV1 expressing NSCLC and breast PDX models. However, for LIV1 expressing prostate PDX models, two doses of ADC-2 did not inhibit tumor growth significantly. Thus MMAE-based ADC-3 replaced ADC-2 from the 3rd dose. Interestingly ADC-3 inhibited the growth of the prostate tumor significantly. In a LIV1 high expressing prostate PDX, the tumor growth was suppressed by ADC-3 for over 70 days after the dosing was stopped on Day 28. In the LIV1/PDL1 co-expressing NCI-H460-LIV1 CDX model, combination group inhibited tumor growth significantly better than single agent group. In exploratory tox study, ADC-2 were well tolerated following repeated administrations in mice at all doses tested. Slight lesions were observed in 60 mg/kg group during the treatment period and fully recovered at the end of the recovery period. Based on these results, the maximum tolerated dose (MTD) of ADC-2 in mice was determined at 60 mg/kg.
Conclusions: LIV1 targeting ADC-2 and ADC-3 exhibited strong anti-tumor activities as monotherapy in PDX models and the anti-tumor activity is further enhanced by checkpoint inhibitor. ADC-2 displayed excellent tolerability profile in mice. These results support further investigation of our LIV1 ADCs in LIV1 positive solid tumors.

#4442 Targeting ITGB4 with a topoisomerase I ADC: Preclinical antitumor activity in colorectal and head and neck cancers.

Mi Young Cha, **Hyunuk Kim**, Hyunkyung Yu, Youngeun Ha, Kitae Park, Seungmin Byun, Bu-Nam Jeon, Mira Kim, Gyeongyeon Kim, Sangmoo Park, Wuhwui An, Suah Choi, Yura Kang, Hansoo Park

Genome & Company, Suwon-si, Korea, Republic of

Integrin beta 4 (ITGB4) was identified as a promising tumor-specific antigen through the GNOCLE™ platform, a drug discovery engine that leverages real-world clinical data. ITGB4 is highly expressed in various solid tumors, including head & neck, colorectal, and esophageal cancers, but shows minimal expression in matched normal tissues, as confirmed through immunohistochemistry analysis, supporting a favorable therapeutic window. In cancer progression, ITGB4 promotes epithelial detachment, migration, and invasion. Its high expression is linked to resistance to chemo and targeted therapies and correlates with poor prognosis and aggressive tumor behavior. Based on its tumor-specific profile and functional relevance, ITGB4 was selected as an attractive target for antibody-drug conjugate (ADC) development. Here, we report the preclinical activity and safety of GENA-120, an ITGB4-targeting ADC composed of a humanized anti-ITGB4 antibody (GENA-120B17), a cleavable hydrophilic linker (LinkerE) designed to minimize retro-Michael elimination, and the topoisomerase I inhibitor payload exatecan. GENA-120B17 demonstrated high binding affinity to ITGB4, as well as efficient internalization into ITGB4-expressing cancer cells. Because ITGB4 exclusively dimerizes with integrin α6 to form α6β4 and interacts with its extracellular ligand, the binding and functional role of GENA-120B17 were further investigated in the context of α6β4-ligand interactions. Off-target screening confirmed high specificity to the primary target, with no detectable binding to irrelevant targets. GENA-120 was readily internalized into ITGB4-positive cancer cell lines and showed efficient lysosomal trafficking. In cellular assays, GENA-120 exhibited potent, target-dependent cytotoxic activity against multiple cancer cell lines. GENA-120 also demonstrated strong bystander activity in co-culture systems of ITGB4-positive and negative cancer cells. In addition, treatment with GENA-120 significantly increased ATP and HMGB1 release from ITGB4-positive cancer cells, indicating the induction of immunogenic cell death. In in vivo studies, GENA-120 demonstrated potent antitumor activity in ITGB4-positive cell-derived colorectal and head & neck cancer xenograft models (COLO205, LS174T, and FaDu). GENA-120 exhibited high stability in mouse, cynomolgus monkey, and human serum, as well as a favorable pharmacokinetic profile in mice. It was well tolerated in mice at single doses up to 140 mg/kg, with no maximum tolerated dose reached and no dose-limiting toxicities observed. These robust preclinical data, demonstrating strong efficacy, favorable pharmacokinetics, excellent cross-species serum stability, and a promising safety profile, support the continued development of GENA-120 as a therapeutic candidate for ITGB4-expressing solid tumors, including colorectal and head & neck cancers.

#4443 Preclinical development of GENA-104 ADC, an exatecan-based novel antibody-drug conjugate targeting CNTN4, for solid tumors.

Mi Young Cha, Hyunkyung Yu, Hyunuk Kim, Kitae Park, Youngeun Ha, Seungmin Byun, Jiyeong Lee, Mira Kim, Bu-Nam Jeon, Soojung Moon, Gyeongyeon Kim, Gyeong-Jin Cheon, Hansoo Park

Genome & Company, Suwon-si, Korea, Republic of

Contactin 4 (CNTN4) has emerged as a novel immune checkpoint molecule, previously shown to suppress T cell activity through interaction with amyloid precursor protein on T cells. Immunohistochemical (IHC) analysis revealed elevated CNTN4 expression across multiple tumor types, most notably in melanoma, liver, and endometrial cancers, while its expression remains low in normal tissues, including immune cells. Leveraging this tumor-specific expression profile, we developed an antibody-drug conjugate (ADC) targeting CNTN4, designated GENA-104A16B.LinkerE.Ex (hereafter referred to as GENA-104 ADC). This ADC consists of GENA-104A16.hIgG1, an anti-CNTN4 antibody engineered with reduced effector function, conjugated via cysteine to a hydrophilic, cleavable linker (Linker E) designed to minimize retro-Michael elimination. Linker E is an improved version of Linker D and demonstrated robust serum stability across species. The payload is exatecan, a potent topoisomerase I inhibitor, incorporated at a high drug-to-antibody ratio. GENA-104 ADC demonstrates potent cytotoxicity in CNTN4-positive cancer cells while maintaining low Fcγ receptor-mediated cytotoxicity, an advantageous safety feature for ADCs. Mechanistically, it induces tumor cell death through multiple pathways: direct cytotoxicity via internalization, lysosomal trafficking, and payload release; a bystander effect; and immunogenic cell death. Additionally, it enhances T cell-mediated cytotoxicity through immune checkpoint blockade. *In vivo*, GENA-104 ADC showed robust anti-tumor efficacy in fibrosarcoma (HT1080) and hepatocellular carcinoma (HEPG2) xenograft models. Using IHC analysis, CNTN4 expression was evaluated in 23 patient-derived xenograft (PDX) tissues, including gastric, hepatic, NSCLC, pancreatic, and prostate cancers, as well as sarcoma. High CNTN4 expression (H-score >250) was observed in 11 tissues, notably in 4 of 5 sarcoma models. Moreover, CNTN4 gene expression generally showed a positive correlation with H-scores. Ex vivo and in vivo evaluations of the GENA-104 ADC using PDX models are currently in progress, and updated results will be presented. Non-GLP toxicology in Sprague-Dawley rats and cynomolgus monkeys is in progress, with safety updates to follow. Taken together, these findings support the therapeutic potential of GENA-104 ADC as a targeted treatment strategy for CNTN4-expressing solid tumors. This research represents a meaningful step toward the development of precision oncology therapeutics that may offer improved outcomes for patients with limited treatment options.

#4444 Integrin alpha-2 (ITGA2) is a novel and well-suited antibody-drug conjugate (ADC) target.

Sophie Colombo[1], Vincent Martin[1], Aurelie Courtin[1], Sylvain Roqueviere[1], Lou-Amelia Revellin[1], Benjamin Beaufils[1], Catherine C. L. Wong[2], Pei Han[2], Wei Li[2], Yu Song[2], Qing Zhou[3], Feng He[3], Chuanying Xu[3], Weihong Nian[3], Mary Jane Hinrichs[4], Elisabetta Leo[5]

[1]Ipsen, Paris, France,[2]Foreseen Bio, Shangai, China,[3]Escugen Bio, Shangai, China,[4]Ipsen, Boston, MA,[5]Ipsen, London, United Kingdom

Background: IPN60300 is a novel, potential first-in-class ADC targeting ITGA2, a subunit of the heterodimeric transmembrane receptor integrin α2/β1 involved in cell adhesion and signal transduction. The ADC is designed to deliver exatecan, a potent topoisomerase I inhibitor, to ITGA2-expressing cancer cells. Here, we present a summary of newly generated and publicly available data indicating that the expression pattern of ITGA2 is well-suited for an ADC target. ITGA2 shows low expression in normal tissue and marked overexpression in various solid tumors, in particular gastrointestinal malignancies, where ITGA2 is known to contribute to tumor progression via extracellular matrix signaling and epithelial-mesenchymal transition. Furthermore, we confirm that IPN60300 activity in preclinical models is dependent on ITGA2 expression.
Methods: ITGA2 RNA and protein expression data were extracted from public databases (GEPIA 2, cProSite) and published literature. Additional expression data were generated through immunohistochemical analysis on human tissue microarrays (TMAs). Target-dependent anti-cancer activity was assessed in preclinical models with differential ITGA2 expression.
Results: ITGA2 is expressed ubiquitously at low levels in normal tissue, but is restricted to few cell types, in particular epithelial cells. In contrast, ITGA2 is overexpressed in several cancers, in particular in gastrointestinal tract tumors. Both transcriptomics and proteomics data demonstrate a strong differential expression of ITGA2 between tumor and normal tissue, with high overexpression in cholangiocarcinoma, pancreatic, colorectal, esophageal and stomach cancers, among other indications. Published literature further supports that in many cancer patient samples, ITGA2 is highly expressed in tumor cells. In addition, we confirm this expression pattern on TMAs, and show that overall, >90% of gastrointestinal tumor samples present ITGA2 expression, with a majority displaying medium-to-high expression levels. In preclinical studies, IPN60300 showed potent in vitro ITGA2-dependent cytotoxicity in cells overexpressing ITGA2 compared to the parental cell line. Consistently, in vivo, IPN60300 demonstrated strong anti-tumor activity in mice bearing ITGA2-expressing tumors, whereas no efficacy was observed in mice with ITGA2 knockout tumors.
Conclusion: The ITGA2 expression pattern makes it a well-suited ADC target, and IPN60300 efficacy in preclinical models is dependent on ITGA2 expression. These findings support IPN60300 as a promising first-in-class ADC for individuals harboring ITGA2-expressing tumors. IPN60300 is advancing to a First-in-Human clinical trial (NCT07213817).

#4445 Diverse ADC novel payloads, comprehensive screening and evaluation platform.

Ying Meng, Qian Wang, Min Kang, Xuan Qiao, Chanrui Wang, Yixiao Zhao, Jiangtao Lin, Jiamei Zhao, Li Li, **Tiejun Bing**

ICE Bioscience, Beijing, China

By combining the potency of payload with the specificity of antibody, Antibody-drug conjugate (ADC) is an innovative and promising drug modality for cancer therapy, possessing the advantages of both chemotherapy and immunotherapy. As ADC technology development continues to advance, more novel types of payloads are being actively explored.
ICE Bioscience employed different screening approaches including biochemical, biophysical, cell-based, and LC/MS-based assays for payload screening and evaluation. To be specific, the methods for cytotoxic drug evaluations include microtubule polymerization assay, NMT1/2 FI assay, different biochemical assays for DNA-damage response (DDR) targets, and DNA topoisomerase inhibition assay; For degrader payloads, spectral shifts or HTRF can be applied for measuring binary/ternary complex formation, HiBiT system and WB assay for quantifying target degradation; For STING agonist/antagonist payload, ICE has ready-to-use assays for detecting STING binding, STING activation and cytokine release. Cell panels of different types of cancer cell lines, ADC-related drug-resistant cell lines, immunogenic cell death (ICD) evaluation, in vitro hematotoxicity prediction, as well as ADME evaluation especially permeability and lysosome stability assays are valuable for all different types of payloads.
Based on 15 years of experience in early drug discovery, from target validation to pre-clinical candidate identification, our well-established ADC integrated platform can support comprehensive payload screening and evaluation early-stage drug discovery projects of traditional ADCs and emerging new ADC formats, including different cytotoxic payloads, novel degrader payloads and immune-related payloads, which can greatly accelerate ADC early-stage research.

#4447 Next generation molecular tools for evaluating antibody drug conjugates in 3D systems.

Jayanth Surya Narayanan Shankara Narayanan, Ryan Holly

Thermo Fisher Scientific, Eugene, OR

The development of effective anti-cancer drugs relies on accurately evaluating therapeutic antibodies. Three-dimensional (3D) tumoroids, which closely mimic the tumor microenvironment, help provide a promising platform for these evaluations. Our research focuses on validating therapeutics using antibody degradation trackers and antibody drug conjugates within 3D tumoroids. LysoLight tagged antibodies are fluorogenic in lysosomes, allowing visualization of antibody behavior within tumoroids, enabling insights into antibody degradation. Our studies showed higher Cetuximab uptake and localization to lysosomes in EGFR-overexpressing lung adenocarcinoma tumoroids, while non-specific antibodies or EGFR-null tumoroids showed minimal LysoLight activity. Additionally, we generated MMAE conjugated therapeutic antibodies using the new SiteClick rapid antibody conjugation technique, that allowed rapid screening of candidates from selected monoclonal antibodies to identify candidates with favorable therapeutic potential. High-throughput assays within 3D tumoroids enabled us to evaluate binding affinity, internalization rates, and cytotoxic effects. Our findings indicated that a MMAE conjugated EGFR targeted antibody-drug conjugate, facilitated a targeted cell penetration of drugs in colon cancer tumoroids and induced cell death. Integrating antibody degradation trackers and high-throughput Ab screenings within 3D tumoroids offers a robust platform for evaluating therapeutic efficacy, by providing a more accurate representation of their behavior in vivo.

#4448 3D-tumor organoid, over 2D-cell, is more predictive of *in vivo* anti-cancer pharmacology in assessing ADC candidates.

Tao Yang[1], Jun Zhou[2], Hang Ke[3], Jessie Jingjing Wang[4], Jiawen Gao[5], Qing Li[5], Jinxi Wang[5], Feiyu Peng[3], Cen Chen[1], Lei Zhang[3], Faming Zhang[3], **Henry Li**[1]

[1]Hanx Bio, Wuhan, China,[2]Crown Bioscience, Inc., San Diego, CA,[3]Hanx Biopharmaceuticals, Ltd, Wuhan, China,[4]Crown Bioscience, Inc., Taicang, China,[5]CrownBio, Taicang, China

ADC is a promising anti-cancer modality lately for widened therapeutic window (TW) due to tumor-specific targeting by direct binding to tumor cell-associated antigen (TAA), internalization and payload releasing/cytotoxicity induction. The conventional evaluation of lead ADC candidates usually involves the following steps: 1) ELISA-based binding to recombinant TAA protein; 2) TAA^+-2D-cell culture for assessing binding, internalization and cytotoxicity; 3) anti-tumor pharmacology using TAA^+ xenograft tumor models. This process is largely based on the assumption that 2D cancer cell line culture is predictive of *in vivo* tumor models. However, 2D-assay is frequently not reflective of tumor pharmaology assay from time to time due to distinct architectures of tumor (cell), rendering the process unproductive. Considering 3D tumor organoid being more reflective of tumor than 2D cell culture, we hypothesized that addition of 3D-tumor organoid culture as a new tier of assessment, right before *in vivo* tumor pharmacology, could make the process more productive. In this report, we set out to test this hypothesis by using three antibodies (Ab1, 2 and 3) against three different epitopes of PD-L1 and their corresponding ADCs (ADC1, 2, 3) with the same payload/DAR-value for binding/ internalizations/cytotoxicity in several $PD\text{-}L1^+$ cancer cell lines. Despite similar high-affinity to PD-L1 recombinant protein or $PD\text{-}L1^+$ cells, ADC-1 exhibited the strongest internalization/cytotoxicity in $PD\text{-}L1^+$ tumor cell lines, whereas ADC2 and 3 showed significantly lower activity (up to 1000x folds in differences). In another word, only ADC1 looks promising as an ADC candidate for further development. However, when all three ADCs were tested *in vitro* using 3D-tumor organoids, all ADCs demonstrated potent and comparable activities, sharp contrasting to those seen in 2D-cultures. We then tested them in the same 2D-cell-derived xenograft tumor models (CDXs), the results of which are consistent with those from 3D-tumor organoid cultures, but not those from 2D-cell cultures. These confirmed better transnationality of 3D-organoids over 2D-cells. Together, these findings support a practical workflow in which 2D assays serve as early benchmarks, while 3-D organoids provide a more predictive *in vitro* readout of ADC pharmacology prior to *in vivo* confirmation. We believe that the process of 2-D (benchmark) → 3-D organoids (translational) → in vivo (validate) can more efficiently streamline preclinical ADC triage. Furthermore, if the hypothesis that 2D (monolayer) culture is more representative of normal tissues, while 3D-tumor organoid is more representative of tumor architecture, is true, we could further suggest that 3D tumor and 2D cell culture differentiation assay could help to identify more tumor-specific ADC candidates with widen TW, *e.g.* ADC2 and ADC3 described in this report.

#4449 Functional organoid screening uncovers target dependency and bystander killing in TROP2 ADCs.

Jialei Sun, Marten Hornsveld, Lenno Krenning, Dorrith Verstegen, Peng Han, Zhongman Sun, Caitlyn Hulsebosch, Dione Blok, Peter van Schaik, Mali He, Huike Ju, Yi Sun, Mariusz Madej, Hester Bange, Jun Zhou, Peng Wang, Ludovic Bourre, Marrit Putker

Organoid, Crown Bioscience, Inc., San Diego, CA

Introduction: TROP2-targeted antibody-drug conjugates (ADCs) represent a promising therapeutic class for multiple tumor types with elevated TROP2 expression. Membrane-permeable payloads can induce bystander killing, making functional, physiologically relevant testing crucial. We developed an advanced organoid-based ADC evaluation workflow combining large-scale patient-derived (xenograft) organoid (PD(X)O) screening, CRISPR-engineered isogenic models, and 3D high-content imaging (HCI) to assess potency, target dependency, and bystander effects.
Methods: Two TROP2 ADCs - an experimental exatecan-based ADC linked via a hydrophilic, cleavable linker, and datopotamab-deruxtecan (Dato-Dxd; DS-1062) - were evaluated in the organoid screening platform, where models were selected irrespective of TROP2 expression. The exatecan-based ADC was tested in 109 PD(X)Os (101 tumor, 8 normal) across ten cancer types using nine-point dose-response. Dato-Dxd was screened using six-point dose-response assays in 142 PD(X)Os (132 tumor; 10 normal) spanning nine tumor types. Drug incubation ran over five days, and efficacy was determined by ATP-based cell viability assay. Free payloads exatecan and Dxd (both naked and linker-conjugated) served as controls. CRISPR/Cas9-generated TROP2 knockout (KO) organoid pairs were labeled with fluorescent/luminescent reporters for target HCI-based dependency and bystander effect assays.
Results: The exatecan-based ADC demonstrated high overall efficacy (68.6% showed >50% inhibition at the highest dose of 1 μM), with pancreatic models even showing 100% sensitivity, and 32.4% of organoids achieving IC_{50} < 0.1 μM. Payloads alone were strongly cytotoxic in most models (93.3% of models sensitive with IC_{50} < 0.03 μM) with similar potency for exatecan and Dxd, whereas linker-conjugated Dxd was significantly less cytotoxic (average IC_{50} > 0.1μM). Dato-Dxd responses varied across the PD(X)O panel (54% showed >50% inhibition at 0.1μM, 37% IC_{50} < 0.1μM). For both TROP2 ADCs, a correlation between efficacy and TROP2 mRNA abundance was observed. In isogenic KO organoid models, loss of TROP2 abrogated Dato-Dxd responses, confirming target dependency. Mixed-culture assays quantified Dato-Dxd bystander killing, validating membrane-permeable payload action in neighboring cells.
Conclusion: The combined organoid screening and HCI workflow provides a robust, translationally relevant platform for ADC evaluation, integrating efficacy profiling, mechanistic validation, and functional bystander effect modeling. CRISPR-generated isogenic organoids enable precise dissection of target dependency and resistance, supporting the preclinical optimization of TROP2-targeted ADCs.

: Drug Combinations, Repurposing, and Differentiation
Poster Session

#4453 Ataxia telangiectasia and Rad3 related kinase inhibitors and gemcitabine induce synergistic killing of uterine leiomyosarcoma cells.

Megan Doherty, Minnie Malik, Montanna Macias-Young, Adora Jacobs, Yuka Otsuka, William H. Catherino

Uniformed Services University, Bethesda, MD

Introduction: Uterine leiomyosarcoma (uLMS) is a rare, lethal gynecological cancer. Therapeutic response to standard-of-care chemotherapy for uLMS is hindered because cancer cells can activate DNA damage response (DDR) pathways. For example, gemcitabine stalls replication forks and halts DNA synthesis. This activates Ataxia telangiectasia and Rad3 related kinase (ATR), which aids DDR by repairing stalled replication forks and delaying cell cycle progression. Therefore, we investigated the potential for ATR inhibitors to enhance the potency and efficacy of chemotherapy for uLMS *in vitro*.

Methods: CellTitre Glo, Bliss Independence analysis, and Multidimensional Synergy of Combinations (MuSyC) assessed synergy between three ATRi (elimusertib, ceralasertib, berzosertib) and SOC chemotherapy (gemcitabine, doxorubicin, docetaxel) in three commercially available (SK-LMS-1, SK-UT-1B, SK-UT-1) and two patient-derived uLMS cell lines (ACI-44A, ACI-44B). Following treatment of gemcitabine alone, elimusertib alone, or gemcitabine + elimusertib, flow cytometry was performed to analyze cell cycle phase distribution using propidium iodine-stained cells, as well as to assess apoptosis and necrosis using annexin V and sytox blue-stained cells. Western blotting investigated protein expression of ATR pathway proteins, DNA damage markers, and apoptosis markers.

Results: ATR inhibitors synergized most strongly with gemcitabine, with elimusertib + gemcitabine emerging as the most synergistic combination across all five cell lines. In contrast, combinations of ATRi with doxorubicin or docetaxel showed minimal to no synergy. ATRi enhanced gemcitabine potency in all cell lines by significantly reducing its EC50. Elimusertib also increased gemcitabine's cytoxicity. In SK-UT-1B cells, the combination increased apoptotic cells by 51.4% (14.7% vs 9.7%, $p < 0.05$) and necrotic cells by 120.2% (24.7% vs 11.2%, $p < 0.001$) compared to gemcitabine alone. Elimusertib did not prevent gemcitabine-induced S phase arrest but increased the sub-G1 population, consistent with enhanced cell death. Western blot analysis confirmed that elimusertib inhibited downstream ATR signaling, including CHK1 S345 phosphorylation blockage, and that the combination produced greater DNA damage and apoptosis - evidenced by increased p-H2AX (S139) and cleaved caspase-3 expression - than either agent alone.

Conclusions: Elimusertib strongly synergizes with gemcitabine *in vitro* across uLMS cell lines by potentiating DNA damage and apoptosis. The lack of synergy with docetaxel or doxorubicin underscores gemcitabine as the most effective combination with ATR inhibitors. These finds support further preclinical and clinical evaluation of elimusertib + gemcitabine as a promising novel therapy for uterine leiomyosarcoma.

#4454 AI-driven discovery of an IRP2-EGFR dual-targeting strategy reveals synergistic antitumor efficacy in colorectal cancer.

Soseul Won[1], Jieon Hwang[2], Sejeong Park[3], Sunkyu Kim[3], Sanghoon Lee[3], Areum Park[4], Hyuk Lee[4], Joong-Bae Ahn[2], Jaewoo Kang[3], Sang Joon Shin[2]

[1]Department of Clinical Drug Discovery and Development, Yonsei University College of Medicine, Seoul, Korea, Republic of,[2]Division of Medical Oncology, Department of Internal Medicine, Yonsei Cancer Center, Seoul, Korea, Republic of,[3]AIGEN Sciences, Seoul, Korea, Republic of,[4]Infectious Diseases Therapeutic Research Center, Korea Research Institute of Chemical Technology, Daejeon, Korea, Republic of

Background: IRP2 is a key regulator of intracellular iron homeostasis and is known to be overexpressed in colorectal cancer (CRC). As a relatively novel therapeutic target, IRP2 has been implicated in tumor progression, and our previous study demonstrated the antitumor effects of IRP2 inhibitors. To broaden the therapeutic potential of IRP2 inhibition and establish effective combination strategies, we applied a multifaceted AI-based predictive approach to identify compounds capable of synergizing with the IRP2 inhibitor.
Methods: We predicted compounds capable of producing a synergistic effect with IRP2 inhibition using an AI-based model on the AIGEN InSight platform. Cell viability was assessed using CCK-8, and synergy scores were calculated using the SynergyFinder 3.0. To investigate the mechanism underlying the combination effect at the RNA level, we performed RNA sequencing (RNA-seq) and identified differentially expressed genes (DEGs) using the DESeq2 R package. Pathway enrichment analysis was conducted, and key findings were validated in CRC cell lines using qRT-PCR and western blotting.
Results: Based on the AI-driven prediction model, Osimertinib was identified as a top-ranked candidate, achieving an AI-score of 0.73, which places it within the top 0.03% of all evaluated compounds. IRP2 inhibitor was subsequently optimized to generate KS-20260 with improved potency. The combination of KS-20260 and Osimertinib exhibited differential synergy scores across seven colorectal cancer cell lines. Notably, LoVo and DLD-1 cells showed the highest synergy scores of 10.845 and 7.843, respectively, and the combination treatment markedly reduced the protein levels of IRP2 and phosphorylated EGFR compared with single-agent treatments. Using RNA-seq data from LoVo cells treated with KS-20260, Osimertinib, or their combination, we analyzed pathways that were more affected by the combination treatment than the additive effect, defined as the average response of individual treatments. The Gene Set Enrichment Analysis (GSEA) revealed a significant downregulation of cell-cycle-related gene sets (e.g., CELL_CYCLE and CELL_CYCLE_PHASE_TRANSITION). Supporting these transcriptomic findings, the mRNA expression of key cell-cycle regulators, including CDK1, AURKB, CENPF, and E2F8, was decreased in the combination-treated cells. Furthermore, in the preliminary in vivo experiment, the combination-treated group (TGI 57.01%) exhibited a greater reduction in both tumor volume and tumor weight compared with the single-agent treatment groups (KS-20260, 38.37%; Osimertinib, 20.57%).
Conclusion: This study demonstrates that KS-20260 and Osimertinib combination therapy disrupts cell-cycle progression and enhances antitumor efficacy in colorectal cancer, supporting dual IRP2-EGFR targeting as a promising therapeutic strategy.

#4455 Efficacy of Tumor Treating Fields (TTFields) together with standard chemotherapy and PD-L1 blockage in preclinical models of small cell lung carcinoma.

Rotem Engelman[1], Lina Somri-Gannam[1], Talya Borkum[1], Roni Blatt[1], Daria Gerasimova[1], Shay Cahal[1], Catherine Tempel Brami[1], Mai Shai[1], **Yiftah Barsheshet**[1], Eyal Dor-On[1], Itai Tzchori[1], Adi Haber[1], Moshe Giladi[1], Uri Weinberg[2], Yoram Palti[1]

[1]Novocure Ltd, Haifa, Israel,[2]Novocure GmbH, Baar, Switzerland

Introduction: SCLC is a highly aggressive cancer treated with platinum-etoposide chemotherapy, immunotherapy, and radiotherapy. Tumor Treating Fields (TTFields), an FDA-approved therapy for several solid tumors, has been shown to enhance chemotherapy and immunotherapy treatment efficacy. Here, we assessed the potential of TTFields to augment the effects of chemotherapy and PD-1 inhibition in preclinical SCLC models.

Methods: Human SCLC cell lines (H196, DMS-53) were exposed to 150 kHz TTFields (1.62 V/cm RMS, 120 h; 1 V/cm RMS, 72 h), alone or with the chemotherapy combination cisplatin and etoposide (0.15 µM and 0.3 µM; 0.25 µM and 0.5 µM). Treatment efficacy was assessed by cell count and colony formation, combined to determine overall response. Protein expression in the Fanconi anemia-BRCA DNA repair pathway was analyzed by western blot, and DNA damage was quantified via γH2AX fluorescence microscopy. Immunogenic cell death (ICD) was evaluated by flow cytometry for ATP depletion (quinacrine staining) and surface calreticulin, and by Homogeneous Time Resolved Fluorescence (HTRF) assay for HMGB1 release. In vivo, mice orthotopically implanted with murine KP3 SCLC cells received TTFields (150 kHz) or sham-heat for 10 days starting seven days post-implantation, with or without cisplatin (2 mg/kg), etoposide (8 mg/kg), and anti-PD-L1 (10 mg/kg) administered intraperitoneally. Tumor burden was monitored by MRI at treatment initiation and completion, and tumor weight measured at endpoint. DNA damage was examined by γH2AX immunohistochemistry and by flow cytometry of tumor single-cell suspensions.

Results: TTFields and the chemotherapy combination each reduced cell counts and increased overall treatment efficacy compared with control, with greater effects observed when applied simultaneously. While TTFields or chemotherapy alone induced minimal DNA damage and ICD, concurrent application markedly enhanced both endpoints relative to control and single treatments. TTFields exposure suppressed expression of Fanconi anemia-BRCA pathway proteins essential for homologous recombination repair. In mice, TTFields reduced tumor growth, with further suppression observed when delivered together with cisplatin, etoposide, and anti-PD-1 therapy. Enhanced DNA damage was likewise detected under concurrent TTFields and immunochemotherapy exposure.

Conclusions: In preclinical SCLC models, TTFields showed antitumor activity and augmented the effects of standard chemoimmunotherapy. By interfering with DNA repair, TTFields intensify the cytotoxic impact of DNA-damaging chemotherapeutics, while their ability to trigger immunogenic cell death may potentiate immune checkpoint blockade. These complementary mechanisms highlight TTFields as a promising modality to reinforce the efficacy of existing therapeutic approaches in SCLC.

#4456 Tumor Treating Fields (TTFields) potentiate antitumor and immune responses to standard immunochemotherapy in non-small cell lung cancer models.

Boris Brant[1], **Yiftah Barsheshet**[1], Tali Voloshin[1], Tal Kan[1], Tharwat Haj Khalil[1], Simona Zisman-Rozen[1], Lilach Koren[1], Avital Vorontsov[1], Bella Koltun[1], Cfir David[1], Anat Klein-Goldberg[1], Efrat Zemer-Tov[1], Adi Haber[1], Moshe Giladi[1], Uri Weinberg[2], Yoram Palti[1]

[1]Novocure Ltd, Haifa, Israel,[2]Novocure GmbH, Baar, Switzerland

Introduction: Tumor Treating Fields (TTFields) are low-intensity alternating electric fields that disrupt mitotic processes in cancer cells, promoting downstream immunogenic cell death (ICD), and leading to activation of antitumor immunity. TTFields are approved for treatment of metastatic non-small cell lung cancer (NSCLC) following progression on platinum-based chemotherapy, together with immune checkpoint inhibitors (ICIs) or docetaxel. The ongoing LUNAR-2 trial (NCT06216301) is evaluating first-line TTFields with the anti-PD-1 pembrolizumab and platinum-based chemotherapy in metastatic NSCLC. The present study assessed the therapeutic efficacy and immunological effects of TTFields administered alongside anti-PD-1, cisplatin, and pemetrexed (PCP) in preclinical NSCLC models.

Methods: Human A549 NSCLC cells were exposed to TTFields (150 kHz, 1.7 V/cm RMS, 72 h) with or without cisplatin and pemetrexed (CP; 1.5 and 6.3 μM, respectively). Cell count, apoptosis (assessed by annexin V/7-AAD staining), and ICD markers surface calreticulin exposure and ATP depletion (quinacrine staining) were evaluated by flow cytometry In vivo, C57Bl/6 mice were orthotopically implanted with LL/2 lung carcinoma cells and allowed seven days for tumor establishment. The mice were then randomized into four groups: control, TTFields, anti-PD-1/cisplatin/pemetrexed (PCP), or TTFields + PCP. Treatment included continuous TTFields (150 kHz) or sham (heat) for 10 days and intraperitoneal injections of anti-PD-1 (10 mg/kg), cisplatin (1 mg/kg), and pemetrexed (6 mg/kg) or vehicle every 72 hours (three doses). Tumor localization was confirmed by MRI at study initiation, and at study end tumors were measured (MRI and weight) and processed to single cell suspensions for flow cytometric analysis of tumor-infiltrating lymphocytes. IFN-γ and granzyme B expression in $CD8^+$ T cells were assessed following PMA/ionomycin stimulation.

Results: Chemotherapy at the tested doses exerted minimal cytotoxic or pro-apoptotic effects on A549 cells and negligibly induced ICD. TTFields exposure reduced cell counts, increased apoptosis, and enhanced ICD markers, including calreticulin exposure and ATP depletion; however to a higher extent in the presence of CP chemotherapy. In vivo, TTFields or PCP each limited tumor growth compared with controls, while the concomitant regimen resulted in the smallest tumor volumes. Both PCP and TTFields + PCP increased tumor infiltration of $CD3^+$ T cells, particularly $CD8^+$. The TTFields + PCP group showed the highest proportion of IFN-γ- and granzyme B-producing $CD8^+$ T cells, indicating an elevated cytotoxic immune response.

Conclusions: TTFields enhanced the antitumor and immunostimulatory effects of standard immunochemotherapy in NSCLC preclinical models, supporting its therapeutic potential as an immune-modulating modality.

#4457 A novel CerS2 activator, DH20931, synergizes with doxorubicin to overcome therapeutic resistance in breast cancer.

Hissah Alatawi[1], Haritha H. Nair[1], Lingbao Ai[2], Abhisheak Sharma[3], Christopher Vulpe[4], Arun K. Sharma[5], Coy D. Heldermon[2], **Satya Narayan**[1]

[1]Physiology and Aging, University of Florida, Gainesville, FL,[2]Medicine, University of Florida, Gainesville, FL,[3]Pharmaceutics, University of Florida, Gainesville, FL,[4]Physiological Sciences, University of Florida, Gainesville, FL,[5]Molecular and Precision Medicine, Penn State Cancer Institute, Hershey, PA

Background: Doxorubicin (DOXO) efficacy in triple-negative breast cancer (TNBC) is severely limited by acquired resistance and dose-limiting cardiotoxicity. We identified ceramide synthase 2 (CerS2), producer of tumor-suppressive very long-chain ceramides (VLCCs), as a prognostic marker and therapeutic target in breast cancer (BC). We previously developed DH20931, a CerS2 activator that inhibits growth across BC subtypes by inducing lipotoxic endoplasmic reticulum (ER) stress. We hypothesized that DH20931 could sensitize BC cells to DOXO and reverse resistance.
Methods: The synergistic efficacy of DH20931 and DOXO was evaluated in parental and DOXO-resistant BC cell lines, e.g., MDA-MB-231, 4T1. Synergy was quantified using the Chou-Talalay method (Combination Index, CI). Mechanisms were assessed via confocal microscopy (DOXO uptake), immunoblotting (ER stress, apoptosis markers) and *in vivo* efficacy.
Results: The DH20931 combination significantly reduced the required IC_{50} of DOXO by 3-8-fold. DH20931 demonstrated strong synergy with DOXO (CI <1) across all tested BC cell lines, including DOXO-resistant models. The synergy was eliminated in CerS2-knockout cells indicating CerS2 target engagement. Mechanistically, the combination therapy resulted in hyper-activation of the UPR, maximized ATF4/CHOP/PUMA expression, and a marked increase in cleaved caspase-3 compared to either agent alone. *In vivo*, the DH20931+DOXO combination significantly inhibited tumor growth compared to DH20931 and DOXO monotherapy.
Conclusion: DH20931 effectively sensitizes BC cells to Doxorubicin and reverses DOXO-resistance, likely by enhancing CerS2-mediated lipotoxic ER-stress. This synergistic approach offers a promising clinical strategy to improve DOXO efficacy, reduce its cardiotoxicity by allowing dose reduction, and improve outcomes for patients with TNBC and other BC subtypes.

#4458 Enhancing the antitumor efficacy using a combination of FGFR4 inhibitor(H3B-6527) and oxaliplatin in gastric cancer.

Nadeem Bhat, Mohammed Soutto, Ahmed Gomaa, Shoumin Zhu, Selma Maacha, Marwah Al-Mathkour, Melanie Genoula, Oliver McDonald, Wael El-Rifai

University of Miami, Miami, FL

Background: Chemotherapy resistance continues to be a major obstacle in treating gastric cancer. This study investigates whether combining the FGFR4 inhibitor (H3B-6527) with Oxaliplatin can enhance treatment effectiveness in preclinical models, with emphasis on their combined impact on tumor growth inhibition and cell-death pathways.
Material and Methods: To assess the effectiveness of the H3B-6527 and oxaliplatin combination, we utilized IC50 assays, colony formation tests, patient-derived xenograft (PDX) models, immunofluorescence, immunohistochemistry, western blotting and caspase-3/7 luminescence assays. These methods allowed us to evaluate how the combined treatment influences tumor cell proliferation, DNA damage, and apoptosis in gastric cancer cell lines (MKN28 and HGC27) as well as in tumor tissues.
Results: IC50 analyses showed that both MKN28 and HGC27 cells were markedly more sensitive to the combination treatment than to either drug alone. Colony formation assays further demonstrated a substantial reduction in colony numbers with the combined therapy, underscoring its stronger anti-proliferative effect. In PDX mouse models, the combination produced significant tumor growth suppression and extended overall survival compared to controls. IF and IHC analyses revealed increased DNA damage, indicated by elevated γH2AX, decreased proliferation (Ki67), and higher apoptosis (cleaved caspase-3). Caspase-3/7 luminescence assays confirmed enhanced apoptotic activity in treated cells. Western blotting also showed increased cleaved PARP and γH2AX levels in both gastric cancer cell lines and PDX samples, supporting the heightened DNA damage and apoptosis triggered by the combined treatment.
Conclusions: This study highlights the strong synergistic effect of H3B-6527 and oxaliplatin in inducing apoptosis, increasing DNA damage, and suppressing tumor growth in gastric cancer models. The results offer strong support for the potential clinical use of this combination as an effective treatment approach, particularly for gastric cancer patients who exhibit chemoresistance.

#4459 Repurposed FDA-approved agents for hepatic artery infusion in colorectal liver metastases.

Manasa Ravi[1], Colin M. Court[2], April Risinger[1]

[1]UT Health Science Center at San Antonio, San Antonio, TX,[2]Division of Surgical Oncology and Endocrine Surgery, UT Health Science Center at San Antonio, San Antonio, TX

Colorectal cancer (CRC) remains a leading cause of cancer-related death, with liver metastases (CRLM) representing the most common cause of mortality. Despite advances in systemic therapy, outcomes for patients with CRLM remain poor, underscoring a critical need for improved, liver-directed treatment strategies. Hepatic artery infusion (HAI) pumps are an effective method to deliver high local concentrations of chemotherapy directly to the liver while limiting systemic toxicity. The currently-standard of care compounds for HAI have limited efficacy and elevated hepatotoxicity, emphasizing the demand for treatment regimens that have better patient outcomes. In this project, we explored a drug repurposing strategy by evaluating FDA-approved chemotherapeutic agents with pharmacokinetic properties compatible with HAI delivery. Drugs were selected using established pharmacokinetic databases and then tested in vitro using CRC cell models and a normal epithelial liver cell line to assess cytotoxicity and dose-response. In addition, we investigated the therapeutic potential of combining a microtubule destabilizer with an FDA-approved fatty acid synthase (FASN) inhibitor. Synergy experiments demonstrated enhanced cytotoxic effects when chemotherapeutics were combined with the FASN inhibitor, suggesting that there is potential for a novel treatment regimen for patients presenting with this disease. These preliminary findings support drug repurposing within the context of HAI delivery as a clinically translatable approach. By utilizing existing FDA-approved compounds of both chemotherapeutic agents and metabolic inhibitors, this strategy may lay the groundwork for novel therapies for patients with CRLM. Further preclinical and translational studies will be necessary to define optimal drug combinations and dosing regimens, with the ultimate goal of expanding therapeutic options and improving outcomes for this high-risk patient population.

#4460 Drug repurposing in Nectin-4-positive epithelial ovarian cancer.

Xiaoyan Zhong[1], Runying Long[2], Ruiqian Zhang[1], Ling Shan Hung[1], Can Cui[1], Chen Bao[1], Kui Liu[1], Cho Wing Li[1], Haonan Lu[1], Kar Loen Chan[1]

[1]Department of Obstetrics and Gynaecology, The University of Hong Kong, Hong Kong SAR, Hong Kong,[2]Materials Innovation Institute for Life Sciences and Energy (MILES), HKU-SIRI, Shenzhen, China

Objectives: Antibody-drug conjugates (ADCs) are promising therapeutic biologics for cancer treatment, and Mirvetuximab soravtansine (MIRV) is currently the only FDA-approved ADC for treating folate receptor alpha (FRα) positive platinum-resistant epithelial ovarian cancer (PROC). Results from the Phase 3 EV-302/KEYNOTE-A39 trial indicate that the combination of Nectin-4-directed ADC Enfortumab Vedotin-ejfv (anti-Nectin-4 ADC) and pembrolizumab yields better treatment outcomes than platinum-based chemotherapy in patients with metastatic urothelial carcinoma. The study aims to investigate the potential of repurposing anti-Nectin-4 ADC as a therapeutic strategy for epithelial ovarian cancer (EOC), and to explore effective combination therapies targeting Nectin-4-positive EOC tumors.
Methodology: Nectin-4 expression in EOC was validated through multiplex immunohistochemistry (MIHC) in our institutional tissue cohort and corroborated in independent public datasets. In vitro efficacy of anti-Nectin-4 ADC was evaluated using cytotoxicity, apoptosis, and clonogenic assays in EOC cell lines. Anti-tumor activity was investigated in patient-derived organoid models and xenograft models.
Result: Nectin-4 expression in EOC is heterogeneous but generally elevated compared to matched normal tissues. The Nectin-4-targeted ADC demonstrated significant cytotoxicity in Nectin-4-positive EOC cell lines. Both in silico and in vitro analyses revealed that Nectin-4-positive tumors are sensitive to two FDA-approved compounds, potentially due to dysregulated fatty acid metabolism. In vivo studies confirmed that anti-Nectin-4 ADC monotherapy effectively suppressed tumor growth, and combination treatments further enhanced survival outcomes.
Conclusion: This study demonstrates the therapeutic potential of Nectin-4-targeted agents in preclinical models of Nectin-4-positive EOC, supporting their advancement toward clinical translation. Additionally, the findings suggest that repurposing Nectin-4-guided combination therapy could expand and enhance treatment options for EOC.

#4461 Nebivolol exhibits cell growth inhibition in drug-resistant HR+/HER2- breast cancer and anti-tumoral synergism with abemaciclib *in vitro*.

Chia-Ling Wu, Meghana Trivedi, Shivaani Suresh Kanna

University of Houston, College of Pharmacy, Houston, TX

Background: We are investigating nebivolol, a third-generation beta-blocker, as a drug-repurposing candidate for breast cancer (BC). While prior studies have focused on triple-negative BC, we evaluated its efficacy and potency in hormone receptor-positive, HER2-negative (HR+/HER2-) BC, which is the most prevalent subtype. Since HR+/HER2- BC is typically treated with endocrine therapy (ET) alone or in combination with CDK4/6 inhibitors (CDK4/6i), we also assessed the effects of nebivolol in ET- and CDK4/6i-resistant models, as well as in combination with ET and CDK4/6i.
Methods: The efficacy and potency (IC50) of nebivolol were evaluated using MCF7 and T47D parental cells and their estrogen deprivation-resistant (EDR), palbociclib-resistant (PalboR), and EDR/PalboR derivatives. Cells were treated with vehicle or nebivolol (0.01 to 30 μM). Efficacy (% inhibition at 30 μM) and IC50 of nebivolol were determined using a three-parameter non-linear regression model using GraphPad Prism v.10. For evaluating drug combinations, concentration ranges of the drugs (nebivolol with palbociclib or abemaciclib) were selected based on their estimated IC50 values in the concentration-response matrices. Growth inhibition was quantified using the EnSight™ Multimode Plate Reader, and drug interaction was analyzed using CompuSyn (combination index, CI) and SynergyFinder (Loewe synergy score). A parallel analysis was performed to determine the statistical significance between combination and single-agent groups using One-way ANOVA, followed by Tukey multiple comparison test.
Results: Nebivolol inhibited growth in parental and ET- and CDK4/6i-resistant MCF7 and T47D cells in a concentration-dependent manner. Efficacy (%) and potency (μM) of nebivolol were as follows: MCF7-P [84.1 and 7.9]; EDR [79.1 and 12.3]; PalboR [73.5 and 13]; EDR/PalboR [68.4 and 20.4]; T47D-P [96.1 and 5.8]; EDR [94.6 and 5.4]; PalboR [86.7 and 5.7]; EDR/PalboR [91.6 and 5.2]. Additionally, nebivolol demonstrated synergism with abemaciclib in Chou-Talalay and Loewe analysis. Effective combinations included 1 or 10 μM and 0.3-10 μM of nebivolol with 30-300 nM of abemaciclib (CI < 1 in Chou-Talalay method) in MCF7P and T47DP, respectively, suggesting synergy. Significant % inhibition in combination compared to single agent alone was observed at 3 μM of nebivolol with 100 or 300 μM abemaciclib in MCF7P and 0.3-3 μM of nebivolol with 30 nM of abemaciclib in T47DP cells. Loewe analysis also revealed nebivolol-abemaciclib synergism, with the most synergistic area score of >10 (12.51 in MCF7P and 41.14 in T47DP).
Conclusion: Nebivolol inhibited the growth of HR+/HER2- BC cell lines sensitive or resistant to ET and/or CDK4/6i and synergized with abemaciclib. Ongoing studies are evaluating nebivolol and abemaciclib in other cell-based assays and combination with ET for enhanced therapeutic potential.

#4462 Nebivolol inhibits cell growth, inhibits autophagic flux, and enhances growth inhibition in combination with bicalutamide in prostate cancer cells.

Swarnil Mandal[1], Chia-Ling Wu[2], Shivaani S. Kanna[1], **Wangjia Cao**[2], Meghana V. Trivedi[3]

[1]Department of Pharmacy Practice and Translational Research, University of Houston, Houston, TX,[2]Department of Pharmacological and Pharmaceutical Sciences, University of Houston, Houston, TX,[3]University of Houston, Houston, TX

Introduction: Nebivolol, a β1-adrenergic receptor blocker, is being explored as a repurposed therapeutic for breast cancer, showing inhibition of cell growth and autophagic flux. This study evaluated nebivolol's anti-tumor effects in prostate cancer (PCa) cells and determined whether it enhances the effect of the androgen receptor antagonist bicalutamide.

Methods: PCa cell lines, LNCap and 22Rv1, were treated with vehicle or nebivolol (0.01-30μM) for 7 days to assess cell growth using the EnSight™ Multimode Plate Reader. Clonogenic growth was measured after 14-15 days of vehicle or nebivolol (0.1-10μM). Autophagy and lysosome formation were evaluated after 24-hour treatment with vehicle, nebivolol (1 or 10μM), or chloroquine (50μM) using Hoechst 33342, Cyto-ID® Green, and Lyso-ID® Red staining followed by confocal imaging. Combination studies with nebivolol and bicalutamide (0-30μM) were performed over 7-day using concentration-response curves to access growth inhibition and interaction effects. IC_{50} values were calculated by non-linear regression curve analysis. LC3B protein expression was measured in 22Rv1 cells by immunoblotting following vehicle or nebivolol (10μM) treatment for 24, 48, and 72 hours. Statistical significance was determined using paired student's t-test or one-way ANOVA followed by Dunnett's multiple comparison test, as appropriate, using GraphPad Prism v.10. Drug synergism of nebivolol and bicalutamide was tested by CompuSyn software using the Chou-Talalay method.

Results: Nebivolol inhibited cell growth (IC_{50}: 37.1μM in LNCap; 9.8μM in 22Rv1) and suppressed clonogenic potential (IC_{50}: 1.1μM in LNCap; 2.5μM in 22Rv1) in a concentration-dependent manner. Nebivolol (10μM) significantly increased autophagosome and lysosome accumulation compared with vehicle ($p<0.05$). Nebivolol significantly upregulated LC3B protein expression in 22Rv1 cells in a time-dependent manner ($p<0.05$), suggesting inhibition of autophagic flux. Chou-Talalay analysis indicated a potential synergism at 1 to 30μM bicalutamide in combination with nebivolol 10 to 30μM, with combination index<1.

Conclusion: Nebivolol inhibited PCa cell growth and clonogenic potential, and inhibited autophagic flux with increased LC3B expression. Furthermore, nebivolol enhanced growth inhibition when combined with bicalutamide. These findings support further investigation of nebivolol, with/without bicalutamide, in PCa.

#4463 Repurposing the anti-dementia drug memantine, (a dualα7-nAChR NMDAR antagonist) as an anti-cancer agent in human squamous cell lung cancer.

Javan Christian[1], Sarah L. Miles[2], Kritsa L. Denning[3], Kushal J. Modi[4], Reagan S. Light[4], Piyali Dasgupta[4], Yi Charlie Chen[5]

[1]Marshall University, Huntington, WV,[2]Biological Sciences, Marshall University, Huntington, WV,[3]Pathology, Marshall University, Huntington, WV,[4]Biomedical Sciences, Marshall University, Huntington, WV,[5]Bluefield State University, Bluefield, WV

Purpose of the study: Memantine is a drug used in clinical practice to combat dementia associated with mild-to-moderate Alzheimer's disease. Traditionally, memantine is an NMDAR receptor antagonist, but published reports show that it has multiple molecular targets apart from NMDAR. Nicotinic acetylcholine receptors (nAChRs) are a class of ion-channel receptors which mediate the bioactivity of nicotine. Published reports reveal that memantine functions as an antagonist to a particular kind of nAChR, namely the alpha-7-nicotinic receptor (α7-nAChR). The binding affinity of memantine for α7-nAChRs is stronger than its affinity for the NMDAR receptor. Squamous cell lung carcinoma (LUSC) is a type of non-small cell lung cancer (NSCLC) that typically develops in one of the air passages (bronchi) of the lungs. The primary objective of our research project was to repurpose the drug memantine as a growth-inhibitory agent in LUSCs.
Experimental procedures. Data from the TCGA atlas show that the α7-nAChR is overexpressed on patient-isolated LUSC tumors relative to matched normal tissue. Our research has shown that the α7-nAChR is upregulated in LUSC tissues and LUSC cell lines relative to normal lung epithelial cells. It is well known that almost 30% of LUSC patients continue to smoke after diagnosis, and many LUSC patients are exposed to nicotine via smoking-cessation devices like patches and gums. Therefore, we decided to evaluate the antiproliferative activity of memantine on nicotine-induced LUSC cells. Proliferating Cell Nuclear Antigen (PCNA) ELISA assays revealed that memantine robustly inhibited nicotine-induced proliferation of LUSCs. The growth-inhibitory activity of memantine was further confirmed in chicken chorioallantoic membrane (CAM) model systems of LUSC. Additionally, the anti-tumor activity of memantine was measured in two independent mice models, namely the cell derived xenograft (CDX) mouse model and the patient derived xenograft (PDX) mouse model. Finally, siRNA methodology was used to delineate the signaling pathways underlying the anti-proliferative activity of memantine in LUSC.
Results: Memantine potently inhibited nicotine-induced proliferation across a panel of human LUSC cell lines. The presence of memantine induced cell cycle arrest (at G1/S phase) in nicotine-treated LUSC cells and the anti-proliferative activity of memantine was also observed in chicken CAM models of LUSC. Finally, the administration of memantine via dietary methods decreased nicotine-induced growth of LUSC tumors in both CDX and PDX tumors in immunodeficient mice models. Depletion of the α7-nAChR expression by siRNA methodology abrogated the anti-proliferative activity of memantine in human LUSC cells.
Conclusions: The drug memantine could be repurposed as a potent anti-cancer drug for the treatment of LUSC.

#4464 Repurposing nebivolol with CPI-613 for triple-negative breast cancer: Linking *in-vitro* synergy to *in-vivo* exposure.

Mikayla Skillman[1], Airong Li[1], Junhyoung Park[2], Amir Mohammad-Gholizadeh[1], Fatima Dagher[1], Meghana Trivedi[3], Benny Kaiparettu[2], Diana S-L Chow[1]

[1]University of Houston, Houston, TX,[2]Baylor College of Medicine, Houston, TX,[3]Department of Pharmacy Practice and Translational Research, University of Houston, Houston, TX

Triple-negative breast cancer (TNBC) is an aggressive subtype lacking ER, PR, and HER2 expressions, making chemotherapy the default standard of care with high relapse and late-onset toxicities. Drug repurposing offers a rapid, cost-effective path to safer, mechanism-based therapies using agents with known safety. Nebivolol (NEB), an FDA-approved third-generation β_1-blocker, shows anti-cancer activity in preclinical models and is believed to act in part by inhibiting oxidative phosphorylation and angiogenesis, although its precise mechanism remains incompletely defined, while CPI-613 (CPI), a lipoate analog that targets pyruvate and α-ketoglutarate dehydrogenases, disrupts mitochondrial metabolism. We hypothesized that dual metabolic targeting would suppress TNBC growth. Murine 4T1 cells were treated with NEB (0.5-16 μM) and CPI (5-250 μM) in fixed ratios. MTT assays (72 h) and Chou-Talalay analysis identified 4-8 μM NEB + 5-50 μM CPI as the optimal synergistic ratio (>90% inhibition, CI < 0.2). *In vivo*, orthotopic 4T1-Luc tumors were established by mammary fat-pad injection in BALB/c mice and treated with vehicle (N=5), NEB (10 mg/kg QD) (N=5), CPI (25 mg/kg BID) (N=5), or NEB + CPI (NC) (N=6), 5 days/week for 3 weeks. All treatments significantly reduced tumor growth versus vehicle on day 28 ($p < 0.01$-0.001). Mean tumor volumes (mm^3 ± SD) were: Vehicle 1484.9 ± 492.4; NEB 595.8 ± 134.6; CPI 634.7 ± 116.9; NEB + CPI 702.5 ± 352.0. Tumor weights showed the same pattern ($p < 0.0001$), with all treated groups significantly lower than vehicle but no difference among NEB, CPI, and combination. LC-MS/MS confirmed intratumoral concentrations of NEB and CPI (NEB 42.2 ± 20.4 ng/g; CPI 22.7 ± 6.6 ng/g; combo NEB 39.3 ± 39.8, CPI 16.8 ± 8.5 ng/g). Systemic PK was similar across groups, though CPI in NC showed reduced volume of distribution vs single CPI ($p = 0.0368$). Tumors collected 23 h post-dose were used to calculate molar concentrations (μM = [ng/g × ρ_tumor (g/mL)] / MW), where density (ρ = weight/volume) was derived from caliper volume. Tumor concentrations in μM were NEB 0.093 ± 0.051, CPI 0.043 ± 0.011; combo NEB 0.067 ± 0.080, CPI 0.031 ± 0.022—below the *in-vitro* synergistic range and not reaching the optimal ratio, which may explain the lack of combination benefit over single agents. PK/PD analyses showed moderate, non-significant trends ($r = 0.26$-0.70). NEB and CPI inhibited TNBC growth, but the combination did not outperform single agents. Sub-synergistic, ratio-mismatched tumor exposure may underlie this outcome; upcoming tumor PK studies will determine whether the synergistic ratio is reached within the dosing interval to guide dose optimization.

#4465 Miconazole induces cell cycle arrest and apoptosis in prostate cancer cells via a p53-mediated pathway: A Drug repurposing strategy.

Eswara Naga Hanuma Kumar Ghali[1], Lindsey Shim[1], Rahul Tiwari[1], Rajasekhar Baru[1], Anupam Dhasmana[1], Chang Ryan Jisoo[2], Sung Yun Jung[2], Vivek Kumar Kashyap[1], Neeraj Chauhan[1], Subhash C. Chauhan[1], Murali M. Yallapu[1]

[1]Medicine and Oncology, University of Texas Rio Grande Valley, McAllen, TX,[2]Baylor College of Medicine, Houston, TX

Purpose of the study: This study explores the repurposing of FDA-approved antifungal drugs as potential therapeutics for prostate cancer.
Background: Prostate cancer remains the second leading cause of cancer-related deaths among men in the United States. The American Cancer Society estimated about 313,780 new cases and 35,770 deaths projected from prostate cancer in 2025. Current treatments, including radiation, chemotherapy, hormone therapy, and other emerging modalities, are often associated with long-term adverse effects, underscoring the need for novel therapeutic strategies.
Procedures: We screened antifungal drugs using CCK-8, colony formation, invasion, and migration assays to identify the most effective compound against prostate cancer cells. The lead hit molecule, miconazole, was further evaluated for its pro-apoptotic and cell cycle regulatory effects using confocal and scanning electron microscopy, flow cytometry, and Western blotting. Proteomic profiling and pathway enrichment analyses were performed to identify key molecular targets. The binding affinities of miconazole were evaluated via molecular docking.
Results: Miconazole significantly inhibited prostate cancer cell proliferation, clonogenic capacity, invasion, and migration properties compared to other antifungal agents. Mechanistic studies revealed G0/G1 cell cycle arrest through downregulation of cyclin D3, CDK2, CDK4, and PCNA, and induction of apoptosis via upregulation of p53, p21, p27, cl-PARP, cl-caspase-3, alongside suppression of PARP-1 and caspase-3. Further, proteomic analysis revealed that miconazole significantly regulated many proteins that are responsible for cell cycle arrest and apoptosis. Molecular docking demonstrated that miconazole exhibited strong binding affinities with PARP1 (-8.97 kcal/mol) and cyclin D3 (-8.50 kcal/mol), moderate binding affinities with CDK4 (-7.19 kcal/mol) and CDK2 (-6.15 kcal/mol), and lower binding affinities with PCNA (-5.14 kcal/mol), TP53 (-4.89 kcal/mol), and CDKN1B (-3.50 kcal/mol). No significant binding was found with caspase-3 (+65.04 kcal/mol).
Conclusions: These findings highlight miconazole as a promising candidate for drug repurposing in prostate cancer therapy, offering a potential foundation for future combination strategies.
Keywords: Prostate cancer; Repurposing; Antifungal drugs; Miconazole; Apoptosis; Proteomics

#4466 Clinical-grade CK2 inhibitor CX-4945 synergistically enhances venetoclax-mediated antileukemic activity in preclinical acute myeloid leukemia models.

Upendarrao Golla, Muhammad Danial, Rajesh Rajaiah, Marudhu Pandiyan Shanmugam, Koby Duke, Katherine Mercer, Yi Qiu, Sinisa Dovat, Yasin Uzun, Hong Zheng, Suming Huang, Chandrika G. Behura

Penn State College of Medicine, Hershey, PA

Introduction: Dysregulated apoptotic machinery and signaling contribute to acquire resistance to regimens containing venetoclax (VEN), a BCL2 (B-cell lymphoma-2) inhibitor, in acute myeloid leukemia (AML) and pose a clinical challenge. Casein kinase 2 (CK2) is a serine/threonine kinase with 300+ substrates and regulate cell cycle, survival, differentiation, and apoptosis. Its aberrant activity promotes disease progression, poor prognosis, and drug resistance. CX-4945 (CX), a selective CK2 inhibitor, shows potent anticancer activity in leukemia and other solid tumors. Here, we tested combined CK2 and BCL2 targeting with CX and VEN in pre-clinical AML models.

Methods: Cytotoxic and pro-apoptotic effects of the CX+VEN combo were tested in AML cell lines and primary samples by WST and annexin V assays. The ZIP synergy score was determined by SynergyFinder tool. Flow cytometry and immunoblotting assessed cell surface markers, various apoptosis regulators along with CK2 target levels after drug treatment. Dynamic BH3 profiling assessed priming of VEN-resistant (VR) cells to apoptosis after CX treatment. Transcriptome of VR-AML cells with and without drug treatment was analyzed by RNA sequencing. *In vivo* efficacy of CX+VEN combo was tested in cell line and patient-derived xenograft (PDX) mouse models.

Results: CK2α (*CSNK2A1*) expression exhibited negative correlation similar to that of *BCL2* levels with VEN activity in BeatAML cohort and VR-AML cells showed higher CK2 activity. CX+VEN combo showed synergistic cytotoxicity and augmented apoptosis in VEN-sensitive (MOLM13, HL60, THP1), VR-AML (U937, MOLM13/VR, HL60/VR) cell lines, and PDX cells *in vitro*. CX treatment enhanced VR-AML cells priming to BH3 peptides and increased cytochrome c release. Also, CX+VEN combo effectively induced apoptosis and decreased leukemia stem cells (CD34+CD38-) and chemo-resistant (CD47+CD123+) subpopulations in VR-AML cells. AML cells showed downregulation of CK2 activity and other pro-survival BCL2 member family proteins with increased PARP activity after CX+VEN combo treatment. Functional enrichment analysis of transcriptome after CX+VEN combo treatment showed upregulation of cell cycle arrest, TP53 and apoptotic signature genes that were repressed in VR-AML cells. Lastly, CX+VEN combo effectively decreased leukemia burden and prolonged overall median survival of xenograft (CDX/PDX) mice *in vivo*.

Conclusions: CX+VEN combo showed a superior antileukemic activity in different pre-clinical AML models and CK2 inhibition overcome VEN resistance. CX-4945 (Silmitasertib) has favorable pharmacokinetics with good tolerability in human studies and is being evaluated in early phases of clinical trial. Our findings provide a rationale for CK2 and BCL2 co-targeting as an effective approach for AML treatment and to overcome VEN resistance.

#4467 Synergistic antileukemic activity of JAK inhibition combined with cytarabine in acute megakaryoblastic leukemia.

Akira Shimada[1], Shiho Aoki[1], Hiroko Hayakawa[2], Erico Jimbo[3], Narumi Omika[3], Kaito Furuya[3], Hideya Asai[3], Hiroki Yoshinari[3], Hitomi Niijima[3], Yuta Kawahara[3], Kentaro Ushijima[4], Masakazu Mimaki[5], Mitsuteru Hiwatari[5]

[1]Jichi Medical University, Tochigi, Japan,[2]Research Equipment Center, Jichi Medical University, Tochigi, Japan,[3]Pediatrics, Jichi Medical University, Tochigi, Japan,[4]Faculty of Pharmaceutical Sciences, Yamaguchi University of Science, Yamaguchi, Japan,[5]Pediatrics, Teikyo University, Tokyo, Japan

Background: Acute megakaryoblastic leukemia (AMKL) remains a therapeutic challenge, with limited responsiveness to standard cytarabine-based regimens and frequent microenvironment-mediated resistance. Aberrant activation of the JAK-STAT signaling pathway has been implicated in AMKL pathogenesis but has not been fully exploited therapeutically in combination with cytarabine.
Methods: We evaluated the antileukemic efficacy of combining a JAK inhibitor with cytarabine across multiple preclinical models: (i) AMKL cell lines (including CMK, CMY, MKPL1, UT7, MOLM16, Mo7e) assessing viability, apoptosis, and combination index; (ii) three-dimensional (3D) co-culture with mesenchymal cells (MSCs) modelling bone-marrow niche-mediated protection; and (iii) murine xenograft models of AMKL assessing leukemic burden and survival.
Results: In cell-line experiments, the JAK inhibitor plus cytarabine demonstrated marked synergy (combination index < 0.7) with significantly increased apoptosis (Annexin V+) and reduced proliferation compared to either agent alone. In the 3D MSC co-culture model, the microenvironment protected AMKL cells from cytarabine-induced death, but this protective effect was abrogated by JAK inhibition, restoring cytarabine sensitivity especially in MOLM16 and MKPL1 cells. In vivo, combination therapy significantly reduced leukemic burden ($p < 0.05$) and significantly prolonged median survival compared to cytarabine alone. Mechanistically, ruxolitinib suppressed phosphorylation of STAT3 and STAT5 and exerted a synergistic effect in combination with cytarabine; however, this inhibitory effect on phosphorylation was attenuated under the 3D co-culture condition.
Conclusions: Our results provide robust preclinical evidence that combining JAK inhibition with cytarabine yields synergistic antileukemic effects in AMKL, including in a niche-protected context, and significantly improves in vivo outcomes. This data strongly supports the rationale for clinical evaluation of this combination in AMKL patients, especially those with JAK-STAT pathway activation.

#4468 WNK1 inhibition induces AML differentiation via ERK-CEBPβ signaling.

Jordan D. Cress, Emily Katoni, Parameswaran Ramakrishnan

Case Western Reserve University, Cleveland, OH

Impaired differentiation is a key pathological feature of Acute Myeloid Leukemia (AML). AML differentiation-inducing agents such as all-trans retinoic acid (ATRA) have shown great promise to treat AML patients as seen by improved overall survival and relapse rates. However, this success has been limited to a subset of AML patients, namely those with Acute Promyelocytic Leukemia (APL). This highlights the need to identify more differentiation therapy options that could be effective for other AML subtypes. In this study, we identified With-no-Lysine(K) kinase 1 (WNK1) as a novel regulator of AML differentiation arrest. We show evidence of WNK1 dysregulation in AML patients demonstrated by its increased expression and activity compared to healthy controls. Targeting WNK1 through genetic or pharmacologic inhibition induced granulocytic differentiation of AML cell lines in vitro. WNK1 inhibition also caused cell cycle arrest and apoptosis. Furthermore, oral administration of WNK1 inhibitor reduced leukemic burden in AML xenograft models. We observed that knocking down expression of WNK1 substrates SPAK and OSR1 mirrored the effects of WNK1 inhibition suggesting their involvement in mediating pro-leukemic functions of WNK1. Mechanistically, we show that WNK1 inhibition induces differentiation by promoting MEK-ERK activity and increasing C/EBPβ activity and expression, resulting in increased transcription of myeloid differentiation genes. Finally, we illustrate that combining WNK1 inhibition with ATRA further boosts ATRA's efficacy, synergistically increasing differentiation, apoptosis, and cell cycle arrest. C/EBPβ expression was also enhanced by this combination treatment, suggesting a role for C/EBPβ in mediating these anti-leukemic effects. Taken together, our findings suggest that WNK1 negatively regulates ERK phosphorylation and activity, likely through SPAK/OSR1. Inhibiting WNK1 releases ERK suppression, increasing C/EBPβ activity and expression which leads to myeloid differentiation. Overall, our findings reveal a novel role for WNK1 in promoting differentiation arrest and highlight its potential as a new therapeutic target for AML treatment.

#4469 FACT Complex — A gatekeeper of differentiation in AML.

Soumya Sharma[1], Sagarajit Mohanty[2], Stefan R. Sweha[2], Kazuya Fukasawa[2], Jieun Jeong[2], Katerina V. Gurova[3], Hans-Guido Wendel[2]

[1]Department of Physiology and Biophysics, Weill Cornell Medicine, New York, NY;, Cancer Biology and Genetics Program, Memorial Sloan Kettering Cancer Center, New York, NY,[2]Cancer Biology and Genetics Program, Memorial Sloan Kettering Cancer Center, New York, NY,[3]Department of Cell Stress Biology, Roswell Park Cancer Institute, Buffalo, NY

Acute Myeloid Leukemia (AML) is an aggressive hematological malignancy with a dismal 5-year survival rate of ~32%. Given that the treatment of AML remains an unmet clinical need, it is critical to identify novel, therapeutic targets in AML. Differentiation blockade is the key problem in AML. Hallmarks of AML include myeloid progenitors proliferating constantly and failing to terminally differentiate into their mature, functional counterparts such as macrophages. Presently, there are only a few differentiation therapies for AML traversing the regulatory drug development pipeline. Available differentiation therapies are limited to specific subtypes of AML, for example, All-Trans Retinoic Acid (ATRA) for Promyelocytic Leukemia (PML) and Enasidenib for IDH2-mutated AML.To identify genes encoding druggable proteins essential in maintaining the undifferentiated state of AML, we designed a creative CRISPR screen. The screen revealed that FACT (FAcilitates Chromatin Transcription) complex is required for AML to maintain this undifferentiated state. The FACT complex is a key histone chaperone that stabilizes nucleosomes during transcription, DNA replication, and DNA repair. The FACT complex is overexpressed in AML patient samples, and its expression is significantly associated with poor patient prognosis. Little is known about its function in AML. In the present study, our goal is to explore the mechanistic role of FACT complex in AML differentiation. We also intend to exploit the dependency of the FACT complex in AML to develop therapeutic approaches to target AML.

#4470 Combination of NAMPT inhibitors plus pyrimidine analog antimetabolites floxuridine and 5-FU impair rhabdomyosarcoma proliferation and survival.

Jamie Gudyka[1], Choh Yeung[1], Senna Munnikhuysen[1], Christina M. Robinson[2], Amy James[2], Xiaohu Zhang[3], David Holland[3], Michele Ceribelli[3], Simone Difilippantonio[2], Craig J. Thomas[3], Christine M. Heske[1]

[1]Pediatric Oncology Branch, National Cancer Institute, Bethesda, MD,[2]Laboratory Animal Sciences Program, Frederick National Laboratory for Cancer Research, Fredrick, MD,[3]Division of Preclinical Innovation, National Center for Advancing Translational Sciences, Rockville, MD

Pediatric rhabdomyosarcoma (RMS) is a soft tissue sarcoma of high unmet need that requires novel treatment approaches. Nicotinamide phosphoribosyltransferase (NAMPT) catalyzes the rate limiting step of the nicotinamide adenine dinucleotide (NAD^+) salvage pathway. Previously, we showed that RMS is highly sensitive to NAMPT inhibition, with *in vivo* RMS models undergoing tumor regression upon treatment with the NAMPT inhibitor OT-82. However, we observed recurrence after cessation of treatment, suggesting single agent therapy is not durable. The aim of this project is to identify and evaluate drug combinations that synergize with NAMPT inhibitors in RMS in an effort to improve treatments for patients with RMS. To identify synergistic drug combinations, we used a matrix drug screen of 2 RMS cell lines (Rh30 (fusion-positive (FP)) and Rh36 (fusion-negative (FN)) testing 2 NAMPT inhibitors (daporinad and GNE-618) in combination with 62 other anticancer agents. We identified that floxuridine, a pyrimidine analog antimetabolite, was the most highly synergistic agent with both NAMPT inhibitors. Validation of the screen results using longitudinal proliferation assays confirmed synergy between floxuridine and an additional NAMPT inhibitor, OT-82, across additional FP and FN RMS cell lines. Doses of each drug that had minimal effect on proliferation as single agents resulted in durable cell death when combined. Notably, when this combination was tested in proliferating non-cancer cell lines, there was a minimal effect on proliferation, suggesting a therapeutic window exists. Rescue experiments using nicotinamide mononucleotide (NMN), the product of NAMPT, reversed the antiproliferative effect of the combination, indicating that the synergy is NAD^+ dependent. Protein analysis revealed that floxuridine-related ternary complex formation of thymidylate synthase is blocked by NAD^+ loss mediated by NAMPT inhibition. To evaluate this combination for potential translation into the clinic, we extended our testing to include clinical agents, including RPT1G (Remedy Plan Therapeutics), a NAMPT inhibitor currently under early phase evaluation, and 5-FU, a prodrug of floxuridine. Validation studies of these agents using longitudinal proliferation assays again demonstrated that single agent doses had minimal effect on proliferation but when combined, resulted in persistent cell death. Preliminary toxicity testing in Rh30 tumor-bearing NSG mice demonstrated tolerability of OT-82 plus 5-FU up to the highest doses tested (15 mg/kg and 25 mg/kg respectively) and reduced tumor volume. Efficacy experiments are ongoing and will be reported. These findings demonstrate that combining NAMPT inhibitors with floxuridine or 5-FU results in significant synergy and preliminarily suggest that this is a promising and feasible combination regimen for patients with RMS.

#4471 Synergistic metabolic inhibition with 2-DG and metformin loaded electrospun scaffolds disrupts glioblastoma redox balance and glycolytic output.
Bryce William Jewett

Northern Arizona University, Flagstaff, AZ

Glioblastoma (GBM) displays exceptional metabolic plasticity. Beyond the canonical Warburg Effect, which demonstrates preferential reliance on aerobic glycolysis despite sufficient oxygen, GBM can upregulate oxidative phosphorylation to maintain proliferation and redox balance under glycolytic stress. Targeting both pathways simultaneously represents a promising strategy to overcome this resilience. This study evaluates the synergistic effects of 2-deoxy-D-glucose (2-DG), a glycolytic inhibitor, and metformin, a mitochondrial complex I modulator, delivered through electrospun polycaprolactone scaffolds engineered for localized release at the tumor resection margin.Concentration range-finding was conducted by quantifying total metabolic activity via PrestoBlue and normalizing to total DNA content via CyQUANT. Mechanistic assays included mitochondrial membrane potential (ΔΨm) via JC-1 and reactive oxygen species via CellROX. Viability was assessed using Trypan Blue. Scaffolds were electrospun de novo, drug-loaded, and evaluated for structural integrity to determine feasibility for sustained local delivery. Parallel studies are extending this work to primary human astrocytes to assess differential sensitivity in noncancerous glial tissue.Dual treatment produced a synergistic reduction in metabolic index and viability that surpassed monotherapy and exceeded the response to temozolomide. Mechanistically, combined inhibition induced a hyperpolarized ΔΨm consistent with stress-driven proton-gradient accumulation under impaired ATP synthesis rather than improved mitochondrial function. Reactive oxygen species measurements indicated redox imbalance characteristic of mitochondrial stress. Trypan Blue analysis confirmed near-complete loss of viable GBM cells by day five. Electrospun scaffolds incorporated both agents effectively and retained fiber morphology compatible with controlled release.These findings indicate that simultaneous inhibition of glycolysis and mitochondrial respiration precipitates bioenergetic failure in glioblastoma cells through coordinated disruption of ATP production, ΔΨm homeostasis, and redox stability. Integrating this strategy into drug-releasing electrospun scaffolds offers a platform for localized metabolic therapy at resection margins while minimizing systemic exposure. Ongoing studies include astrocyte toxicity profiling, scaffold release kinetics, and application to three-dimensional tumorsphere models.

#4472 Combination of medroxyprogesterone acetate (MPA) and a WEE1 or ATR inhibitor enhances anti-tumor activity of estrogen receptor-positive endometrial cancer cells.

Yuki Takemoto, Yasuto Kinose, Li Han, Mai Koizumi, Yan Wang, Kanako Kasuya, Aasa Shimizu, Erika Nakatsuka, Mahiru Kawano, Kenjiro Sawada, Michiko Kodama

Department of Obstetrics and Gynecology, Graduate School of Medicine, the University of Osaka, Suita-city, Japan

Objectives: Hormonal therapy is an important treatment option for patients with early-stage, low-grade endometrial cancer who desire fertility preservation, as well as for those with advanced or recurrent disease resistant to chemotherapy and immune checkpoint inhibitors. Based on evidence that estrogen signaling regulates cell cycle progression via cyclin D1 transcription, the combination of endocrine therapy with cyclin-dependent kinase 4/6 inhibitors has become a pivotal strategy in the management of estrogen receptor-positive (ER+) recurrent breast cancer in recent years. However, clinical trials investigating similar approaches in ER+ recurrent endometrial cancer have shown only limited responses so far. The aim of this study is to develop a novel therapeutic strategy combining hormonal therapy with targeted therapy for ER+ endometrial cancer.

Methods: The anti-tumor effects of combining hormonal therapies were assessed, using ER+ endometrial cancer cells, ARK1 and MFE280. Tamoxifen, letrozole, fulvestrant, and medroxyprogesterone acetate (MPA, 25 μM for MFE280; 30 μM for ARK1) were used as hormone therapies. As drugs for targeted therapies, either the ATR inhibitor (ATRi) AZD6738 (2.5 μM) or the WEE1 inhibitor (WEE1i) MK1775 (0.1 μM) was employed. The anti-tumor effect of *ESR1* knockdown via siRNA was also examined. The synergistic effects of MPA and ATRi/WEE1i were evaluated by coefficient of drug interaction (CDI) methods.

Results: Among these hormone therapies, only MPA showed a distinct dose-dependent anti-tumor effect, and thus it was selected for combination with molecular-targeted agents. MPA and ATRi synergistically decreased cell viability compared with control in both cell lines, reducing viability to 0.48-, 0.40-, and 0.16-fold in ARK1 and to 0.83-, 0.85-, and 0.56-fold in MFE280 by MPA monotherapy, ATRi monotherapy, and MPA-ATRi combination therapy, respectively. The CDI values of the MPA-ATRi combination were less than 1 (ARK1 = 0.81; MFE280 = 0.79). When *ESR1* was knocked down, the cell viability under MPA-ATRi combination treatment was 0.37-fold in ARK1 and 0.74-fold in MFE280 relative to the control, suggesting that *ESR1* knockdown attenuated the anti-tumor effects of the combination therapy. In contrast, MPA and WEE1i exhibited only additive effects in ARK1 cells, reducing viability to 0.39-, 0.71-, and 0.30-fold following MPA monotherapy, WEE1i monotherapy, and MPA-WEE1i combination therapy, respectively. The CDI value for the combination was approximately 1, consistent with an additive interaction.

Conclusion: We found that the combination of MPA and ATRi markedly enhances anti-tumor activity in ER+ endometrial cancer, in an ERα expression-dependent manner. Future studies are needed to elucidate the mechanism of these synergistic effects.

#4473 Advancing new rational drug combinations to treat mutant KRAS-driven pancreatic adenocarcinoma.

Brajendra K. Tripathi[1], Sophia M. Shahin[1], Elise Van Meter[1], Marian E. Durkin[1], Xiaolan Qian[1], Ross Lake[2], James H. Doroshow[3], Dunrui Wang[1], Douglas R. Lowy[1]

[1]Laboratory of Cellular Oncology, National Cancer Institute, Bethesda, MD,[2]Laboratory of Genitourinary Cancer Pathogenesis, National Cancer Institute, Bethesda, MD,[3]Developmental Therapeutics Branch, National Cancer Institute, Bethesda, MD

Pancreatic ductal adenocarcinoma (PDAC) is a highly aggressive malignancy with a poor prognosis, largely due to late diagnosis and limited response to currently available therapies. Identifying effective drug combinations that harness PDAC-specific vulnerabilities remains a major challenge for molecularly targeted therapy. Oncogenic mutations in the *KRAS* gene, which are found in over 90% of PDAC patients, play a critical role in PDAC. Although KRAS inhibitors may be found to be clinically useful for treating PDAC, it is likely that resistance will develop in most patients when given as single agent treatment. To overcome this anticipated limitation, effective drug combinations that include KRAS inhibitors will be necessary. We have determined in preclinical human and mouse lung cancer models that RAS facilitates the export of nuclear proteins into the cytoplasm via a mechanism independent of canonical RAS signaling (Tripathi et al., 2024, *Nature Cancer*). This observation suggests that new drug combinations that cooperate with the inhibition of the RAS nuclear export function might be suitable for targeted cancer therapy. Our preclinical PDAC studies suggest that the newly identified RAS-dependent nuclear export mechanism is also relevant to PDAC and may have implications for developing new drug combinations for PDAC treatment. In human PDAC models, we have found that the DLC1 tumor suppressor protein is a critical downstream target of KRAS-dependent nuclear protein export. Perinuclear binding of KRAS-GTP to RanGAP1 promotes the hydrolysis of RAN-GTP to RAN-GDP and the consequent release of nuclear protein cargo into the cytoplasm. In human PDAC models, export of the nuclear EZH2 methyltransferase into the cytoplasm leads to methylation of the cytoplasmic DLC1 protein, making it susceptible to ubiquitin-dependent proteasomal degradation. Conversely, KRAS inhibition prevents the nuclear export of EZH2, leading to an increase in DLC1 protein levels. Consistent with these findings, analysis of the Clinical Proteomic Tumor Analysis Consortium (CPTAC) database indicates DLC1 protein levels in PDAC are lower than would be expected from the relatively high *DLC1* mRNA expression in these tumors. Remarkably, the low levels of DLC1 protein in PDAC are inversely correlated with the high levels of the FBXW5 E3 ubiquitin ligase. Our preclinical PDAC studies show that a three-drug combination, comprising a KRAS inhibitor plus AKT and SRC inhibitors, exhibits significantly greater antitumor activity than the KRAS inhibitor alone. The cooperative effect of the three-drug combination arises as the KRAS inhibitor increases DLC1 protein levels, while AKT and SRC kinase inhibitors block phosphorylations that attenuate DLC1 tumor suppressor activity. Mechanistically, this three-drug combination enhances antitumor effects in mutant *KRAS* PDAC by stabilizing and reactivating the DLC1 tumor suppressor protein.

#4474 Cannabidiol enhances etoposide efficacy in non-small cell lung cancer by engaging a p53-mTOR-TFEB lysosomal death program.

Youngsic Jeon[1], Hyukjoon Kwon[1], Young Nyun Park[2], Taejung Kim[1], **Young-Joo Kim**[1]

[1]Korea Institute of Science and Technology (KIST), Gangneung, Korea, Republic of,[2]Yonsei University College of Medicine, Seoul, Korea, Republic of

The search for more effective and safer cancer therapies has intensified interest in combination regimens that repurpose well-established agents. Here, we investigated whether cannabidiol (CBD), a cannabis-derived compound clinically used for pediatric epilepsy, can potentiate the anticancer activity of etoposide in non-small cell lung cancer (NSCLC). Among multiple chemotherapeutics tested, etoposide displayed the most pronounced reduction in NSCLC cell viability when combined with CBD, indicating a robust synergistic interaction. To elucidate the underlying mechanisms, we performed comprehensive transcriptomic and proteomic profiling, revealing that the CBD-etoposide combination up-regulated gene programs associated with autophagic cell death while concomitantly downregulating key oncogenic drivers linked to tumor progression. Mechanistically, this autophagic cell death was associated with PI3K-AKT-mTOR pathway inactivation and required functional p53. Importantly, downstream of mTOR suppression, the combination was associated with reduced TFEB phosphorylation, enhanced TFEB nuclear translocation, and increased transcriptional activation of lysosome-related gene networks, consistent with amplification of lysosomal stress programs that can contribute to lysosome-associated cell death. Notably, the therapeutic synergy was independent of classical cannabinoid receptors and transient receptor potential channels, supporting a noncanonical mode of CBD action. We also performed pharmacological blockade experiments using antagonists of PPARγ and GPR55 to test whether these pathways contribute to the CBD-etoposide response. Collectively, our findings suggest that CBD combined with etoposide represents a promising strategy to enhance treatment efficacy in NSCLC—particularly in tumors retaining p53 function—by concurrently engaging autophagic/lysosomal cell death programs and suppressing oncogenic signaling beyond canonical cannabinoid pathways.

#4475 Neuroendocrine-like dedifferentiation mediates resistance to EGFR inhibitors via the NRG1/HER3 axis.

Alessandra Morselli[1], Chiara Miroglio[1], William Kothalawala[2], Donatella Romaniello, Idan Lahat[3], Paola Cecchi[1], Davide Zilio[1], Michelangelo Fiorentino[4], Andrea Ardizzoni[1], Yosef Yarden[5], Yaara Oren[3], Balazs Gyorffy[6], **Mattia Lauriola**[1]

[1]University of Bologna, Bologna, Italy,[2]Budapest, Hungary, Semmelweis University, Hungary,[3]Tel Aviv University, Tel AViv, Israel,[4]Pathologist, Istituto Oncologico Addarii, University of Bologna, Bologna, Italy,[5]Weizmann Institute of Science, Rehovot, Israel,[6]Semmelweis University, Budapest, Hungary

Non-small cell lung cancer (NSCLC) patients with activating EGFR mutations, such as exon 19 deletions (del746-750) and the L858R point mutation in exon 21, respond well to third-generation tyrosine kinase inhibitors (TKIs) like osimertinib. However, resistance inevitably emerges, limiting the long-term efficacy of these therapies. In this study, we investigated non-genomic mechanisms that enable drug tolerant persister cells to survive and cycle under EGFR inhibition, likely by exploiting alternative signaling routes. One such mechanism involves the upregulation of HER3. However, the precise molecular and cellular basis for HER3 dependency in NSCLC patients who progress on TKI therapy remains poorly understood. We employed a combination of immortalized and patient-derived cell lines, alongside advanced single-cell sequencing technologies, to elucidate the underlying biology. Our findings reveal that EGFR/HER3 axis upregulation dependency represents an early mechanism of response to TKI treatment, specifically enriched in pulmonary alveolar type I and II cancer cells. This dependency is driven and maintained by paracrine signaling involving secreted factors, with neuregulin-1 (NRG1) playing a central role. NRG1 is primarily secreted by the tumor stroma and by cancer cells undergoing neuroendocrine (NE)-like dedifferentiation, contributing to the resistance mechanisms, leading to invasiveness and metastatic progression. Notably, animal studies demonstrated that the combination of an NRG1-neutralizing antibody with a dual EGFR blockade, achieved through a TKI and an anti-EGFR antibody, eradicated tumors *in vivo*. These results highlight the critical role of HER3 signaling and its interplay with EGFR and the tumor microenvironment in mediating TKI resistance, and suggest a compelling therapeutic strategy for overcoming resistance in NSCLC.

#4476 Repurposing PARP inhibitors in molecularly defined subgroups of peritoneal metastatic colorectal cancer (pmCRC): Preclinical analysis of patient-derived xenograft (PDX) models.

Mathias Dahlmann[1], Beate Rau[2], Safak Gul-Klein[2], Bernadette Brzezicha[1], Marlen Keil[1], **Antje Wengner**[1], Jens Hoffmann[1], Sebastian Stintzing[3], Ulrike S. Stein[4], Wolfgang Walther[1], Loredana Vecchione[3]

[1]Experimental Pharmacology & Oncology Berlin-Buch GmbH, Berlin, Germany,[2]Department of Surgery, Charite - University Medicine Berlin, Berlin, Germany,[3]Department of Hematology, Oncology, and Cancer Immunology, (CCM), Charité - University Medicine Berlin, Berlin, Germany,[4]Translational Oncology of Solid Tumors, Experimental and Clinical Research Center, Charite - University Medicine Berlin, and Max-Delbruck-Center for Molecular Medicine in the Helmholtz Association, Berlin, Germany

Peritoneal metastatic colorectal cancer (pmCRC) has the worst outcome compared to metastatic CRC patients with metastases in other organs, such as liver or lung. More importantly, despite of the improvement of both systemic and peritoneal specific treatment, 50% to 90% of patients experience relapse and progression of the disease, leading to premature death. Precision oncology has successfully improved the overall survival of several solid and non-solid malignancies. For CRC, large volumes of information have been acquired regarding the molecular aberrations, characterizing both lung and liver metastases from CRC, thus leading to a more personalized treatment approach. On the contrary, this has not yet been done for pmCRC. In a comprehensive effort to close this gap and to identify new predictive signatures to drug responses in pmCRC, we previously established a novel platform of matched preclinical pmCRC models, including 14 patient-derived xenografts (PDX) of peritoneal metastases from a total of 10 pmCRC patients and showed that tumors intrinsically resistant to 5-Fluorouracil (5-FU) were enriched in alterations of the DNA damage response and repair (DDR) machinery. We therefore hypothesize, that those tumors are responsive to DDR inhibitors such as olaparib. In order to prove our hypothesis, we generated a new cohort of 48 pmCRC PDX, characterized by RNA sequencing. Based on both transcriptomic and mutational profiles, we classified 14 PDX as homologous recombination deficient (HRD) and 34 PDX as proficient. The most common alteration identified in the HRD positive group were loss-of-function frameshift insertions/deletions in BRCA1/2, in addition to other homologous recombination repair genes (HRRmut). Clinical data, in particular treatment response data, were combined with the genomic profiles of the respective PDX models, supporting the prediction of 5-FU resistance. Subsequently, a total of 12 pmCRC models predicted to be resistant to 5-FU-based treatment regimens, but sensitive to PARP due to HRD, were treated with 5-FU or olaparib alone, as well as in combination. Response data will be presented. Our study highlights the importance of molecular profiling for better personalized treatment.

#4477 Resistance interception: Development of novel immune checkpoint inhibitor as dynamic combination with Anti-PD-1 to overcome resistance.

Lynda Chin, Ronan O'Hagan, Magali Pederzoli-Ribeil

Apricity Health, Inc., Houston, TX

Background: Durable benefit from anti-PD1 therapy is limited by adaptive resistance that evolves under therapeutic pressure which is often missed by static pretreatment tumor profiling. We developed Dynamic Precision™ to mine longitudinal plasma proteomic profiling before and on-treatment to identify adaptive immune resistance drivers. With dynamic blood-based biomarkers to detect emerging resistance as early on-treatment, we establish a window before clinical progression to intercept resistance with precision drug and extend anti-PD-1 therapeutic benefit.
Methods: We analyzed serial plasma proteomics from melanoma patients on standard-of-care anti-PD1 therapy to define dynamic non-responder signatures and identify actionable immune targets driving resistance, including AH004, a novel B-cell checkpoint. Mining of public multi-omic datasets defined tumor contexts associated with AH004 biology.
Results: In this study, we conducted Dynamic Precision™ analysis of 2.7 million plasma proteomic data points from 300+ melanoma patients before and on anti-PD1 standard-of-care treatment. AH004 was found to be differentially regulated in ~17% of anti-PD1 non-responders after one treatment cycle. Mechanistically, as a checkpoint on B-cells, AH004 inhibits T and NK effector cell function and promotes an immunosuppressive tumor milieu. Analysis of public multi-omic datasets showed that AH004+ tumors exhibit an inflamed-but-ineffective (“pseudohot”) phenotype and have poor ICI response.
Utilizing Alloy Therapeutics’ antibody discovery platform, we have generated and characterized 24 antibody clones with high affinity binding to cell-surface human AH004 and inhibition of ligand binding. Functional characterization is ongoing.
Conclusions: Resistance Interception represents a paradigm shift from reactive to proactive combination therapy, using blood-based biomarker surveillance to detect emerging immune-mediated resistance and guide targeted intervention before clinical progression.
AH004 is a tractable B-cell checkpoint associated with anti-PD1 resistance and pseudo-hot tumor phenotypes. A biomarker-guided “resistance interception” strategy—adding AH004 blockade as the signal emerges—may extend anti-PD1 efficacy and increase durable response rate.

#4478 Synergistic antitumor activity of tumor-treating fields and multiselect-RAS (ON) inhibitor RMC-6236 in pancreatic ductal adenocarcinoma.

Ishita Saha, Santanu Bhattacharya, Debabrata Mukhopadhyay, Hani M. Babiker

Mayo Clinic Florida, Jacksonville, FL

RMC-6236 (daraxonrasib) is a novel multiselect RAS(ON) inhibitor under investigation for pancreatic ductal adenocarcinoma (PDAC) and other RAS-mutant cancers. This compound shares structural similarities with RMC-7977 and exhibits a conserved binding site and interaction pattern within the tri-complex formed between active RAS (RAS(ON)) proteins and cyclophilin A (CypA). Tumor Treating Fields (TTFields) are low-intensity, alternating electric fields that disrupt mitosis and have shown clinical benefit in solid tumors. The PANOVA-3 trial demonstrated that TTFields combined with gemcitabine plus nab-paclitaxel improved survival, pain control, and quality of life in locally advanced PDAC. Our previous work demonstrated that TTFields abrogate oncogenic KRAS pathway. We thus hypothesize a potential for increase in effectievness with the combination. In this study, the metastatic PDAC cell line AsPC-1 was treated with TTFields (150 kHz, 1.8 V/cm), RMC-6236 (15 nM; sub-IC_{50}), or combination. A sub-IC_{50} concentration (15 nM) of RMC-6236 was selected based on MTS assay results, and subsequent experiments were performed at this dose. The MTS assay revealed that both TTFields and RMC-6236 independently reduced AsPC-1 cell viability, with a more pronounced reduction observed at 72 hours compared to 48 hours. RMC-6236 alone produced minimal effects at either 48 hours (85.82 ± 13.9%) or 72 hours (90.48 ± 15.4%) compared with control (100.0 ± 8.4%, 48 h; 100.0 ± 8.2%, 72 h). TTFields treatment significantly reduced viability to 74.42 ± 21.4% at 48 hours and 50.17 ± 26.5% at 72 hours. The combination treatment (TTFields + RMC-6236) further decreased viability to 63.8 ± 25.2% at 48 hours and 40.93 ± 18.1% at 72 hours, demonstrating synergistic cytotoxicity relative to monotherapy. Clonogenic assays were performed to evaluate cell survival fractions following treatment with RMC-6236, TTFields, and their combination. Cell migration was assessed using scratch assays, revealing that untreated cells exhibited a migration rate of 91.49 ± 0.85%, RMC-6236-treated cells showed 89.48 ± 1.3%, TTFields alone reduced migration to 61.33 ± 16.3%, and combination treatment markedly suppressed migration to 24.6 ± 22.13% . For every case we were compared with 72h cell migration rate with 0 h migration rate. These findings indicate that TTFields alone significantly impair cellular motility, while their combination with RMC-6236 results in a profound anti-migratory effect, substantially inhibiting wound closure. Additionally, western blot analysis was performed to assess changes in KRAS protein expression, a key PDAC biomarker. Overall, our results demonstrate that the combination of TTFields and RMC-6236 significantly inhibits PDAC cell growth, migration, and survival at sub-IC_{50} concentrations, suggesting a promising alternative therapeutic approach for PDAC management.

: Epigenetic Modulators 1
Poster Session

#4482 Catalytic inhibition of NSD2 demonstrates *in vitro* antitumor activity in head and neck squamous cell carcinoma.

Amr Ismail[1], Iuliia Topchu[2], Tingting Zhang[3], Ahmed Ismail[4], Peter Makhov[5], Jia Xu[6], Kang Le[7], Michael Soth[7], Yanis Boumber[1]

[1]Medicine - Hematology and Oncology, University of Alabama at Birmingham, Birmingham, AL,[2]Institute of Fundamental Medicine and Biology, Kazan Federal University, Kazan, Russian Federation,[3]Department of Oncology, Shengli Oilfield Central Hospital, Dongying, China,[4]Medicine, Eastern Virginia Medical School at Old Dominion University, Norfolk, VA,[5]Fox Chase Cancer Center, Philadelphia, PA,[6]Genetics, University of Alabama at Birmingham, Birmingham, AL,[7]Institute for Applied Cancer Science, MD Anderson Cancer Center, Houston, TX

NSD2 is a histone methyltransferase that catalyzes H3K36 dimethylation and is frequently altered or overexpressed in diverse cancers. Recent work has demonstrated that selective NSD2 catalytic inhibitors suppress tumor growth in preclinical models of pancreatic and lung cancer by reprogramming chromatin and transcriptional states. However, the effect of NSD2 catalytic inhibition in other solid and hematologic malignancies remains undefined. Prior studies from our lab and others demonstrated that NSD2 depletion suppresses HNSCC cell growth. We therefore evaluated the activity of a highly selective NSD2 inhibitor (IACS-17817) and its enantiomer (IACS-17818) as a negative control in head and neck squamous cell carcinoma (HNSCC) JHU-11 and FaDu cell lines, as well as in the RPMI-8402 acute lymphoblastic leukemia (ALL) cell line, which carries an NSD2-activating mutation. Cells were treated with escalating concentrations of the inhibitor for 72 hours, and cells were treated with a fixed concentration of the compounds at serial time points. Then, global H3K36me2 levels were tested via western blotting. IACS-17817 decreased H3K36me2 levels in a time and concentration-dependent manner, with a significant drop at treatment concentrations as low as 10 nM of the active compound after 72 hours in all cell lines tested. IACS-17817 showed an onset of action as early as 24 hours in HNSCC and 48 hours in ALL cells. NSD2 inhibition suppressed the proliferation of HNSCC cells as measured by clonogenic assays in a time- and concentration-dependent manner. ALL RPMI-8402 methylcellulose cell survival is also being evaluated, and results are pending. Combination treatment with IACS-17817 and the PARP inhibitor olaparib demonstrated additive cytotoxicity compared to single agents in HNSCC cells, as shown in clonogenic assays. These findings broaden the known therapeutic scope of NSD2 catalytic inhibition from pancreatic and lung cancers to head and neck squamous cell carcinoma (HNSCC), highlighting NSD2 as a convergent oncogenic driver and supporting further preclinical development of NSD2-targeting agents for clinical translation.

#4483 The KAT6/7 inhibitor IDE574 disrupts tumor lineage identity and drug tolerance to deliver robust antitumor activity in biomarker selected indications.

Manav Gupta, Scott R. Tyler, Nour Ghaddar, Carl Schultz, Pranav Gupta, Steven L. Spivak, Katelyn N. Lukas, Zabrisky Roland, Anjali Bisaria, Mona Khalaj, Mason Appel, Oscar Aubi, Kelly S. Trego, Parker Y. Jameson, Jacob Burch-Konda, Angelica Gonzalez-Sanchez, Brittany Cruzan, Rushika Pandya, Jay Prakash Jain, Michael E. Dalziel, Julie Deichert, Sunjay Sethi, Ivan G. Shabalin, Jonathon S. Ryan, Daniel M. Walden, Muzaffar Alam, Daniel Severance, Amber C. Donahue, Edward Chan, Rebeca Choy, Diana M. Munoz, Richard Zang, Xin Linghu, Peter Teriete, Christian R. Frey, Yuchen Bai, Claire L. Neilan, Josh Taygerly, Paul A. Barsanti, Michael A. White, Brian T. Jones

Ideaya Biosciences, South San Francisco, CA

Intra-tumoral heterogeneity often limits therapy benefit due to intrinsic and adaptive phenotypic diversification via interactions between somatic variation and epigenetic regulation. Important opportunities to overcome this challenge may lie in new therapies that target obligatory lineage-specific gene regulatory programs and constrain emergence of drug tolerant cell states. Lysine acetyltransferases (KATs) are a promising epigenetic target class due to their roles in the establishment and maintenance of permissive chromatin architecture that supports both tumor lineage identity and adaptive plasticity. In particular, KAT6A, KAT6B and KAT7 collaboratively promote oncogenic transcription programs via acetylation of histone H3 at K9, K14, and K23. Preclinical modeling of dual KAT6/KAT7 inhibition has demonstrated pathway modulation and antitumor activity that is superior to selective inhibition of KAT6, highlighting the essential role of KAT7 in sustaining tumorigenic transcription factor activity. Furthermore, the clinical KAT6 inhibitor monotherapy experience in ER+ mBC indicates an opportunity to augment therapeutic benefit by maximizing pathway modulation and preventing acquired resistance. Here we describe IDE574, a potent dual KAT6/KAT7 inhibitor with high selectivity over related KAT5/KAT8 enzymes. IDE574 demonstrated robust suppression of both H3K23ac and H3K14ac in multiple cancer models. This was concomitant with selective chromatin condensation at locations typically occupied by lineage survival transcription factors including FOXA1 in NSCLC and GATA3/ESR1 in ER+ mBC. RNA-seq analysis of drug response and an unbiased evaluation of affected biological systems with a custom RAG AI method, indicated perturbation of lineage identity and epigenetic remodeling. scRNA-seq and protein profiling of PDX-derived ER+ mBC cells revealed that dual KAT6/7 blockade likely overcomes acquired resistance by inhibiting emergence of drug-tolerant persister cells and renewal of cancer stem-like cells. In contrast to selective inhibition of KAT6, IDE574 reduced ALDH+, CD133+, and CD44+/CD24- cell populations, and inhibited clonogenic capacity. Consistent with this biology, IDE574 delivered deeper and durable antitumor activity in aggressive ER+ mBC PDX models including ESR1 mutant backgrounds reported to be resistant to the clinical KAT6 inhibitor even when combined with palbociclib and fulvestrant. Pan-cancer cell viability assessments and xenograft studies with IDE574 revealed indication opportunities in addition to mBC, including predictive biomarker-associated subsets of NSCLC and bowel cancer. These preclinical findings combined with favorable drug-like properties and non-clinical safety profile support evaluation of IDE574 in the clinic as a treatment option for patients with biomarker positive disease.

#4484 Characterization and pre-clinical development of LG-CBP/p300 inhibitor, a potent and selective bromodomain inhibitor of CBP/p300.

Sinae Lee, Yuna Chang, Ik Sun Kim, Sung Woong Jang, Rira Kim, Gyungah Pak, Bitna Oh, Byung Gyu Kim, Sugyeong Woo

Life Sciences R&D, LG Chem, Ltd., Seoul, Korea, Republic of

[Background] Acute Myeloid Leukemia (AML) is a heterogeneous hematologic malignancy characterized by uncontrolled proliferation and impaired differentiation of myeloid progenitors. Despite advances in targeted and combination therapies, relapse and resistance remain major clinical challenges, underscoring the need for novel therapeutic approaches. Epigenetic dysregulation is a hallmark of AML, with transcriptional co-activators CBP (CREBBP) and p300 (EP300) emerging as key regulators of leukemogenesis. These histone acetyltransferases (HATs) catalyze acetylation of histone H3 lysine 27 (H3K27), promoting open chromatin and transcriptional activation of genes involved in cell proliferation and differentiation. Aberrant CBP/p300 activity sustains oncogenic transcriptional programs driven by factors such as MYC and MYB. Preclinical studies have demonstrated that pharmacologic inhibition of CBP/p300 suppresses leukemic cell growth and reduces leukemia-initiating potential, supporting CBP/p300 as a promising therapeutic target in AML. In this study, we evaluated the antileukemic efficacy and molecular mechanism of a selective CBP/p300 inhibitor in AML models to assess its translational potential.
[Method] The antileukemic activity of the LG-CBP/p300 inhibitor was assessed in AML cell lines and in vivo mouse models. Cell viability was measured using CellTiter-Glo®. H3K27ac levels were analyzed by flow cytometry. The expression of MYC and MYB were quantified by reverse transcription quantitative PCR (RT-qPCR) and western blot. Pharmacodynamic and efficacy studies were conducted in both subcutaneous and disseminated xenograft AML mouse models.
[Result] The LG-CBP/p300 inhibitor exhibited potent anti-proliferative activity in AML cell lines, with IC_{50} values in the nanomolar range. The compound was effective across AML cell lines regardless of the presence or absence of common AML-associated mutations. Target engagement was confirmed by concentration-dependent reductions in H3K27ac levels and downregulation of MYC and MYB mRNA expression. In in vivo studies using AML cell lines resistant to venetoclax, this inhibitor significantly suppressed tumor growth in a dose-dependent manner in a subcutaneous xenograft model. Moreover, in a systemic AML mouse model, it reduced leukemia burden and prolonged survival.
[Conclusions] Selective inhibition of CBP/p300 exerts potent antileukemic effects by regulating multiple oncogenes. The LG-CBP/p300 inhibitor represents a promising epigenetic therapeutic strategy for AML with strong translational potential.

#4485 ASTU-045, a novel METTL3 inhibitor with anti-tumor activity in the MC38 syngeneic mouse model.

Laurence Mevellec[1], Nicolas George[2], Ludovic Waeckel[3], Remi Longuespee[4], Nathalie Weidner[4], Hugues Prevet[1], Celine Ronin[4], Jean-Michel Linget[3], Anna Bonhoure[4], Roland Blanque[3], Sabine Gratzer[4]

[1]NOVALIX, Val de Reuil, France,[2]AQEMIA, Paris, France,[3]NOVALIX, Romainville, France,[4]NOVALIX, Strasbourg, France

N^6-methyladenosine (m^6A) is the most prevalent modification of eukaryotic mRNA and plays a crucial role in gene regulation. Methyltransferase-like 3 (METTL3), the key catalytic component of the m^6A methyltransferase complex, is primarily responsible for depositing m^6A on target RNA. METTL3 is highly expressed in various cancers and is closely associated with tumor development. Previous studies have also shown that METTL3 inhibition activates anti-tumor immunity and reshapes the tumor microenvironment. Using structure-based drug design owing to the generation of multiple high resolution crystal structures of ligands bound to the METTL3-METTL14 complex, we developed novel METTL3 inhibitors. This effort led to the identification of ASTU-045, a selective METTL3 inhibitor that demonstrated cellular target engagement (m^6A inhibition) and, in an *in vitro* co-culture system, showed strong, concentration dependent enhancement of PBMC-mediated killing of cancer cells. In the MC38 colorectal syngeneic model, oral administration of ASTU-045 to immune-competent, tumor-bearing mice resulted in tumor stasis. Combination treatment with ASTU-045 and an anti-PD1 antibody produced significant tumor regression. Strong target engagement was also observed in the spleen under both treatment conditions. In summary, we identified ASTU-045 as a novel, selective METTL3 inhibitor with high efficacy in the MC38 syngeneic model.

#4486 The MTA-cooperative PRMT5 inhibitor CTS3497 alone and in synergy with mechanism-based combination targeted therapies for the treatment of *MTAP*-deleted cancers.

Yilin Liu[1], Xinyue Duan[1], Hui Shi[1], Qiugeng Ouyang[1], Jiaxin Huang[1], Meng Wang[1], Xingnian Fu[1], Yiqin Wang[2], Guoliang Xu[2], Haiping Wu[1]

[1]CytosinLab Therapeutics Co., Ltd., Hangzhou, China,[2]Center for Excellence in Molecular Cell Science, Chinese Academy of Science, Shanghai, China

Homozygous deletion of chr9p21/*CDKN2A*/*MTAP* occurs in approximately 15% of human cancers and represents a high unmet medical need. Protein arginine methyltransferase 5 (PRMT5), a key member of the type-II PRMT family, has emerged as a synthetic-lethal target for $MTAP^{null}$ cancers. The MTA-cooperative PRMT5 inhibitor CTS3497, currently in Phase I/II trials (NCT06971523), exhibited potent cell growth inhibition with a low single-digit nM IC50 and 171-fold high selectivity for $MTAP^{null}$ over isogenic $MTAP^{wt}$ cells. *In vivo*, CTS3497 led to tumor inhibition or deep regression in $MTAP^{null}$ xenograft models of various lineages, notably $MTAP^{null}$ orthotopic glioma. The brain penetration property of CTS3497 underscores its therapeutic potential for both primary brain tumors and brain metastases. Mechanism-based therapeutic combinations were explored to improve response and defeat emergent resistance of standard of care (SOC) targeted agents. Co-targeting type I and type II PRMTs with CTS2190 (currently in Phase II trial, NCT06224387) and CTS3497 demonstrated strong synergy against $MTAP^{null}$ tumors *in vitro* and *in vivo*, especially in intractable pancreatic cancer. Moreover, the synergy of CTS2190 and CTS3497 was also significant in $MTAP^{null}$ cells that were established acquired resistance to PRMT5 inhibitors, suggesting the potential combinational use of the dual PRMT inhibitors post PRMT5 targeted therapy. In addition, combination of CTS3497 and osimertinib (EGFR-TKI) enhanced anti-tumor efficacy and suppressed acquired resistance to osimertinib in $MTAP^{null}EGFR^{mut}$ lung cancer xenografts. Furthermore, CTS3497 effectively reversed resistance to adagrasib ($KRAS^{G12C}$) in an adagrasib-resistant $MTAP^{null}$ model, resulting in profound tumor regression without regrowth even after discontinuation of treatment. CTS3497 also synergized with Bcl-2/xL inhibitors by promoting apoptosis, more prominently in $MTAP^{null}$ $BCL2L1^{amp}$ tumor cells. In summary, CTS3497 exhibits strong antitumor activity alone and in combination with clinically feasible targeted agents including but not limited to type I PRMT, EGFR, KRAS and Bcl-2/xL inhibitors. CTS3497 represents a promising synthetic-lethal precision medicine for patients with MTAP-deficient cancers either as a single agent or in combination with rational combination partners. Particularly, combination of CTS3497 with CTS2190, a type I PRMT inhibitor, may provide a potential solution for patients post PRMT5 targeted therapy.

#4487 CTS2190, a first-in-class PRMT1 inhibitor in phase I/II clinical development, demonstrates robust and broad monotherapy efficacy and provides a rationale for novel combinations based on translational findings.

Hui Shi[1], Qiugeng Ouyang[1], Jiaxin Huang[1], Xingnian Fu[1], Guoliang Xu[2], Haiping Wu[1]

[1]CytosinLab Therapeutics Co., Ltd., Hangzhou, China,[2]Center for Excellence in Molecular Cell Science, Chinese Academy of Sciences, Shanghai, China

Background: Protein arginine methyltransferase 1 (PRMT1) is a master epigenetic regulator implicated in oncogenesis through diverse mechanisms, including signal transduction, DNA damage repair, and immune evasion. CTS2190 was designed as a first-in-class, oral PRMT1 inhibitor to achieve high selectivity and minimize off-target toxicity. This agent is currently being evaluated in a phase I/II clinical trial (NCT06224387) and has shown encouraging efficacy and a favorable safety profile, with no thrombotic events observed, in heavily pretreated patients with advanced solid tumors.

Methods: The potency and selectivity of CTS2190 were characterized through biochemical and cellular assays. Its monotherapy efficacy was evaluated in multiple cell-derived xenograft (CDX) and patient-derived xenograft (PDX) models. Furthermore, the combinatorial potential of CTS2190 was investigated with targeted therapies (Enzalutamide, Osimertinib, Gilteritinib), a radioligand therapy (Lu177-PSMA), and an anti-PD-1 antibody across relevant *in vivo* models. Tumor growth and immune profiling were assessed.

Results: CTS2190 exhibited high selectivity for PRMT1 and potent dose-dependent antitumor activity as a single agent in various CDX and PDX models, leading to significant tumor growth inhibition. This robust monotherapy efficacy provided a strong foundation for exploring combinations. CTS2190 demonstrated robust synergistic antitumor activity with all combination partners. It enhanced the efficacy of targeted agents, sensitized tumors to radiation, and remodeled the tumor immune microenvironment.

Conclusion: The compelling single-agent activity of CTS2190 in preclinical models corroborates its ongoing clinical investigation. The broad and potent synergy observed with targeted, radioligand, and immunotherapeutic agents provides a strong mechanistic rationale for the imminent clinical development of novel CTS2190-based combination regimens, positioning it as a versatile therapeutic strategy for multiple cancers.

#4488 Targeting non-canonical PRC2 functions via small-molecule degradation: A novel therapeutic strategy for prostate cancer and other solid tumors.

Hui Shi[1], Xinyue Duan[1], Jiaxin Huang[1], Qiugeng Ouyang[1], Xingnian Fu[1], Guoliang Xu[2], Haiping Wu[1]

[1]CytosinLab Therapeutics Co., Ltd., Hangzhou, China,[2]Center for Excellence in Molecular Cell Science, Chinese Academy of Sciences, Shanghai, China

Background: The Polycomb Repressive Complex 2 (PRC2) is a key epigenetic regulator responsible for histone H3 lysine 27 methylation (H3K27me3) and is implicated in essential cellular processes. However, its core components, EZH2 and EED, also exert extensive non-conventional functions through protein-protein interactions (PPIs) with other proteins, independent of its methyltransferase activity. Aberrant activation or overexpression of PRC2 components, particularly EZH2, drives oncogenesis and tumor progression in a variety of cancers. While several enzymatic inhibitors targeting PRC2 components (EZH2, EED, and EZH1/2) have been developed, their therapeutic efficacy remains limited, particularly in solid tumors, where clinical responses are often modest and transient. Notably, emerging evidence from KO/KD models, as well as PROTACs underscores the non-canonical, non-enzymatic functions in tumor maintenance, positioning PRC2 as a more effective therapeutic target. PROTAC-based degraders targeting these functions show promise but are hampered by poor permeability and stability. We developed novel small-molecule PRC2 degraders to overcome these limitations.

Methods: Small molecular lead candidates CTS3353 and CTS3952 were evaluated for their -PRC2 degradation efficacy, and *in vitro* antiproliferative effects across multiple cancer cell lines (e.g., mCRPC cell 22Rv1, DLBCL Karpas422). Pharmacokinetic and *in vivo* efficacy were performed in cell-derived xenograft (CDX) models of prostate cancer (especially in mCRPC) and DLBCL.

Results: CTS3353 and CTS3952 achieved potent PRC2 downregulation through complex disruption in 22Rv1 and Karpass422 cells. They exhibited superior cell permeability and metabolic stability compared to conventional PROTAC-based degraders. Both compounds induced sustained suppression of PRC2 components, leading to potent anti-proliferative effects. In mCRPC CDX models, CTS3353 and CTS3952 achieved robust antitumor activity, reducing tumor burden and improving survival without observable systemic toxicity. These effects were attributed to the disruption of PRC2's non-canonical functions rather than its histone methyltransferase activity.

Conclusions: Our findings highlight the therapeutic potential of targeting the non-enzymatic functions of PRC2 through small-molecule degradation. CTS3353 and CTS3952 represent a new class of potent and bioavailable PRC2 degraders with promising preclinical efficacy in solid tumor models such as mCRPC and TNBC. This strategy provides a foundation for next-generation PRC2-directed cancer therapies beyond enzymatic inhibition.

#4489 CAAP1 loss uncovers vulnerability of MTAP-deficient NSCLC to PRMT5 inhibition with AZD3470.

Jelena Urosevic[1], Angelos Papadopoulos[2], Shaun Moore[1], Ted Hong[3], Valentina Quarantotti[2], Harriet Southgate[1], Maximilian Wechsung[2], Lukasz Magiera[1], Daniel Barrell[2], Grainne Gernon[2], Elissavet Kentepozidou[2], Laura Rosenberg[2], Anisha Solanki[1], James T. Lynch[1], Stephen Fawell[4], Ho Man Chan[4], Susan Critchlow[1], Emma Dean[1]

[1]Oncology Targeted Discovery, Oncology R&D, AstraZeneca, Cambridge, United Kingdom,[2]Discovery Sciences, Biopharmaceuticals R&D, AstraZeneca, Cambridge, United Kingdom,[3]Data Science, Oncology R&D, AstraZeneca, Waltham, MA,[4]Oncology Targeted Discovery, Oncology R&D, AstraZeneca, Waltham, MA

Introduction: This study aimed to identify genes that sensitize NSCLC cells to AZD3470, an MTA-cooperative PRMT5 inhibitor that targets MTAP-deficient tumors while sparing normal tissues. Early clinical data for this class of drugs as monotherapy has shown objective response rates (ORRs) of approximately 20% across multiple tumor indications. Encouragingly, the duration of response and disease control rates are substantial, suggesting that PRMT5 inhibitors may play a significant role in disease stabilization. While these findings are promising, they also highlight the need to further improve clinical efficacy. Therefore, we aimed to identify genetic alterations—beyond MTAP deficiency—that contribute to sensitivity to PRMT5 inhibition.
Experimental procedures: To identify genes associated with sensitivity to AZD3470 we performed a genome-wide CRISPR screen across six NSCLC cell lines. Hit validation was conducted using two NSCLC CRISPR/Cas9 generated isogenic pairs. RNAseq, cell cycle analysis, apoptosis assay and γH2AX staining were used to provide mechanistic insight for AZD3470 sensitization. Finally, findings were validated in 29 NSCLC PDX models.
Results: The genome-wide CRISPR screen identified CAAP1 loss as one of the top sensitizers to AZD3470 treatment. The CAAP1 (Caspase activity and apoptosis inhibitor 1) gene is located on chromosome 9p21, in close proximity to MTAP, and was found to be co-deleted with MTAP in approximately 20% of tumors. CRISPR screen results were further validated using HCC15 and NCI-H838 CAAP1 KO/WT isogenic pairs in long term proliferation assays, where CAAP1 null cells showed increased sensitivity to AZD3470 compared to CAAP1 WT cells. In addition, cell cycle analysis of the NCI-H838 and HCC15 CAAP1 KO cells after 96h of treatment with 1μM AZD3470 showed a higher percentage of cells in G2/M phase compared to CAAP1 WT cells. Moreover, CAAP1 deficiency potentiated both DNA damage and apoptosis induced by AZD3470. RNAseq analysis of HCC15 CAAP1 KO/WT isogenic cell line pairs revealed significant number of differentially spliced events in CAAP1 KO versus CAAP1 WT cells that increased with AZD3470 dose. Notably, the most abundant changes were detected in the transcripts with skipped exons that were enriched for pathways such as DNA repair or cell cycle consistent with the increased DNA damage and cell cycle alterations detected in CAAP1 null cells treated with AZD3470. Finally, our findings were confirmed using PDX models, where 71% of NSCLC PDXs in which AZD3470 induced regression were CAAP1 null.
Conclusions: In summary, CAAP1 deletion in MTAP-null tumors increases sensitivity to AZD3470, both in vivo and in vitro, by potentiating AZD3470 induced cell cycle alterations and DNA damage, potentially through the regulation of alternative splicing.

#4490 PRMT5 inhibition alters cellular chromatin landscape and drives vulnerability to BH3 mimetics in mantle cell lymphoma.

Christoph Weigel[1], Claire Hinterschied[1], Shirsha Koirala[1], Mackenzie Long[1], Shelby Sloan[1], Jessica Weist[1], Lynda Villagomez[2], Allesandro La Ferlita[1], Coinne Gao[1], Ian Hout[1], Sydney Leon[1], Fiona Brown-Burke[1], Betsy Pray[1], Maggie Harper[1], Neha Bhagwat[3], Kris Vaddi[3], Peggy A. Scherle[3], Cem Meydan[4], Selina Chen-Kiang[5], Maurizio DiLiberto[5], Olivier Elemento[4], Christopher E. Mason[4], Jihye Paik[5], Lapo Alinari[1], Rosa Lapalombella[1], Lalit Sehgal[1], Robert Baiocchi[1]

[1]The Ohio State University Comprehensive Cancer Center, Columbus, OH,[2]Department of Pediatrics, The Ohio State University and Nationwide Children's Hospital, Columbus, OH,[3]Prelude Therapeutics, Wilmington, DE,[4]Department of Physiology and Biophysics, Institute for Computational Biomedicine, Weill Cornell Medicine, New York, NY,[5]Department of Pathology and Laboratory Medicine, Weill Cornell Medicine, New York, NY

Background: Mantle cell lymphoma (MCL) is a rare and incurable blood cancer, comprising 10% of Non-Hodgkin lymphomas. Especially in relapse settings, there remains a crucial need for novel treatments. The enzyme protein arginine methyltransferase 5 (PRMT5) is an oncogenic driver in MCL which targets both histones and non-histone proteins for posttranslational symmetric arginine dimethylation (me2s). BCL2 family proteins govern apoptosis and their dysregulation is a hallmark of MCL, but treatment with pharmacological inhibitors (BH3 mimetics) has had limited success. We hypothesized that transcriptional and epigenomic perturbations via PRMT5 inhibitors (PRMT5i) will sensitize MCL cells to BH3 mimetics for synergistic drug action.
Methods: Plate- and flow-cytometry-based BH3 profiling was used to read out the apoptotic priming state of n=5 MCL cell lines and n=2 primary patient samples. Effects of the small molecule PRMT5i PRT382 were assessed via BH3 profiling, transcriptomics (RNA sequencing) and genome-wide histone modification profiling (CUT&RUN sequencing for H3K4me3, H3K27me3, H3K27ac and two me2s marks H3R8me2s and H4R3me2s). Drug combination effects of PRT382 and BH3-mimetics (navitoclax, A852/A-1331852, PRT1419) were tested in MCL cell lines (n=5). Efficacy of navitoclax and PRT808, a related PRMT5i, was assessed alone or in combination in a murine patient-derived xenograft (PDX) model of aggressive, relapsed MCL.
Results: Global analysis of histone modifications and RNA expression revealed strong association around transcription start sites (adjusted $p<0.0001$), including for PRMT5-mediated H4R3me2s (adjusted $p<0.0001$), but revealed no pronounced global loss of histone arginine methylation under PRT382. Epigenomic responses to PRT382 were highly distinct in MCL models Z-138 and CCMCL1, with the latter revealing lowered global H3K4me3 ($p<0.0001$) at loci specifically enriched for cell cycle pathways (adjusted $p<0.0001$). BH3 profiling revealed vulnerabilities to mitochondrial insults in cell lines, PDX cells, and patient samples, which was correlated with pro-survival BCL2 family RNA- and protein expression ($p<0.01$). Pronounced sensitization to depolarization with PRT382 in Z-138, but not CCMCL1, was reflective of transcriptomic differences in these models. We observed strong synergistic reduction in cell viability with n=16 distinct PRMT5i/BH3 mimetic combinations ($p<0.01$). In our PDX model, the PRT808/navitoclax combination outperformed single treatment cohorts in survival (median 93 vs. 65/75 days for PRT808/navitoclax alone, $p<0.01$) and circulating disease ($p<0.01$).
Conclusions: Our study showed the broad synergistic potential of combining PRMT5i and BH3 mimetics both in vitro and in vivo. PRMT5i lead to epigenome-wide modulation of chromatin states with potential to create vulnerabilities to targeted agents.

#4491 HDAC inhibitors induce NOX5 expression in human uveal melanoma cells in a Brd4-Sp1/Sp3-dependent manner.

Smitha Antony, Ballachanda N. Devaiah, Mariam M. Konate, Yongzhong Wu, Guojian Jiang, Jennifer L. Meitzler, Jiamo Lu, Becky A. Diebold, David J. Mallick, Krishnendu K. Roy, Dinah S. Singer, James H. Doroshow

National Cancer Institute, NIH/DHHS, Bethesda, MD

Epigenetic reprogramming, particularly histone deacetylation (HDAC), and reactive oxygen species (ROS) play key roles in melanoma progression and the development of drug resistance. While various histone deacetylase inhibitors (HDACi) are already in clinical use for hematological cancers, recent studies indicate their potential effectiveness in melanoma models as well. Given the increasing interest in enhancing the therapeutic efficacy of HDACi, we investigated the molecular mechanisms underlying their association with ROS formation in melanomas. Uveal melanoma (UM), a rare and aggressive eye cancer, has been identified in the TCGA dataset as expressing the highest levels of the superoxide-producing enzyme NADPH oxidase 5 (NOX5) among all human cancers. Our study demonstrates that HDACi treatment increases NOX5 expression in UM cell lines. This upregulation is accompanied by elevated extracellular ROS, which is suppressed when NOX5 is silenced. The use of actinomycin D and cycloheximide significantly reduced HDACi-induced NOX5 expression, suggesting regulation at both transcriptional and translational levels. HDACi treatment also led to accumulation of acetylated histones H3 and H4. Since histone acetylation (particularly H4K5/8/12Ac) recruits BRD4 to facilitate transcription, we evaluated the effect of BRD4 knockdown or exposure to BRD4 inhibitors on NOX5 levels in UM cells. Both approaches reduced NOX5 expression induced by HDACi. Furthermore, dual silencing of the transcription factors Sp1 and Sp3 markedly attenuated both basal and HDACi-induced expression of NOX5. ChIP assays revealed that HDACi treatment increases chromatin-associated acetylated histone H3, phosphorylated RNA polymerase II (p-Ser2), BRD4, Sp1, and Sp3 at the NOX5 promoter region. Collectively, these findings suggest that HDACi-mediated upregulation of NOX5 in UM cells occurs, at least in part, via transcriptional activation of the NOX5 promoter. This process is driven by HDACi-induced histone hyperacetylation, which enhances the recruitment of BRD4, Sp1, and Sp3 to the promoter region, thereby facilitating RNA polymerase II-dependent transcription. Given that HDAC inhibition elevates both NOX5 expression and ROS production, co-targeting HDACs and NOX5 may offer a novel and effective therapeutic strategy in the treatment of UM.

#4492 Linking VHL and SETD2 in a common oncogenic pathway that converges on the mitotic spindle.

Manga Motrapu[1], Pratim Chowdhury[2], Sung Yun Jung[2], Xiaoli Wang[2], Ashley Boice[2], Ruhee Dere[2]

[1]Center for Precision Environmental Health, Baylor College of Medicine, Houston, TX,[2]

Background: Loss of chromosome 3p is a landmark event in clear cell renal cell carcinoma (ccRCC) that results in mono-allelic loss of *VHL* (*von Hippel-Lindau*) and *SETD2* (*Set-domain containing 2*) (and other tumor suppressors co-located on 3p). Second hits in *VHL* inactivate this key tumor suppressor, initiating tumor progression. SETD2, a histone methyltransferase, has been previously shown to have a dual function in methylating both histones and microtubules, thereby contributing to the histone and tubulin codes. Methylation by SETD2 on microtubules occurs at the mitotic spindle and is essential for normal mitosis and cytokinesis; the loss of SETD2 acts as a strong driver of apoptosis. This raises a conundrum of how cancer cells survive the early mono-allelic loss of *SETD2*, escaping cell death.

Methods: Using biochemical kinase assays and mass spectrometry, we have identified SETD2 as a substrate for AURKA. Additionally, we have employed immunoblotting and immunofluorescence assays to investigate the phosphorylation of SETD2 and its effects on both chromatin and cytoskeleton targets.

Results: We have identified the mitotic kinase, Aurora kinase A (AURKA), as a regulator of SETD2. Our data uncover SETD2 as a unique substrate for phosphorylation by AURKA, with mass spectrometry identifying serine 2080 (S2080) as the site of phosphorylation on SETD2. We found that phosphorylation of SETD2 by AURKA at S2080 contributes to its methyltransferase (i.e., enzymatic) activity on microtubules but does not impact chromatin methylation at H3K36, which remains unchanged. We demonstrate that VHL regulates SETD2 through AURKA, and the loss of phosphorylation on SETD2 leads to mitotic defects and genomic instability. Importantly, we demonstrate that inhibition of AURKA is synthetic lethal in the setting of *VHL* and *SETD2* deficiency.

Conclusions: AURKA expression levels are high in *VHL*-null cells, resulting from an inability of VHL to target AURKA for degradation, and our data now highlight a direct link between VHL and SETD2, two tumor suppressors believed to drive RCC pathogenesis independently. In summary, our data reveal a tumor-specific vulnerability linked to mitotic fragility that can be precisely targeted to drive mitotic catastrophe ultimately.

*Presenting and primary author.

#4493 Comprehensive assay approaches for PRMT5 targeted drug discovery.

Jianghong Wu, Charles Schmidt, Jamin Steffen, Joseph J. Ferry, Li Liang, Shawn McGinley, Joshua Rettew, Yong Wan, Haiching Ma

Reaction Biology, Malvern, PA

Protein arginine methyltransferase 5 (PRMT5) is a type II methyltransferase that symmetrically dimethylates arginine residues on histone and non-histone proteins, an essential epigenetic modification that shapes chromatin structure and regulates gene expression. Through these activities, PRMT5 controls key cellular processes, including transcription, RNA splicing, DNA repair, and signal transduction. PRMT5 operates in complex with MEP50, which is required for efficient catalytic activity. Dysregulated PRMT5 is strongly associated with diseases, particularly cancer. PRMT5 is frequently overexpressed in breast, lung, prostate, and hematologic malignancies, where it promotes tumor growth, metastasis, and therapy resistance. Small-molecule PRMT5 inhibitors have emerged as promising agents that block methyltransferase activity, reverse aberrant epigenetic marks, and disrupt oncogenic pathways. Here, we established comprehensive assay platforms for PRMT5-targeted drug discovery and validated them using five known inhibitors (LLY-283, JNJ-64619178, GSK591, EPZ015666, and GSK33326595). Our biochemical FlashPlate assay demonstrated potent inhibition of PRMT5/MEP50 activity, with IC_{50} values in the low nanomolar range (0.6-17 nM). Surface Plasmon Resonance (SPR) revealed distinct binding profiles: substrate-competitive inhibitors (EPZ015666, GSK33326595, GSK591) showed weak affinity for apo PRMT5, enhanced by cofactors (MTA, SAH, SAM), whereas cofactor-competitive LLY-283 bound tightly to apo PRMT5 but exhibited >50-fold reduced affinity with cofactors. JNJ-64619178 displayed reduced signal upon cofactor binding, driven by a slow off-rate consistent with pseudo-irreversible inhibition. NanoBRET target engagement intracellular assay results indicated that the PRMT5 inhibitors engaged with the PRMT5/MEP50 complex within one hour of incubation in live HEK293 cells, and Western blot confirmed inhibition of histone H4R3me2s methylation, a key substrate of PRMT5, in MV4-11, Jeko-1, 22RV1, and PC3 cancer cell lines. Collectively, these platforms enable identification, optimization, and mechanistic characterization of PRMT5 inhibitors, accelerating development of selective and potent therapeutic candidates.

#4494 A highly selective KAT6/7 dual inhibitor with best-in-class potential and favorable pharmacokinetic profile.

Yang Yang, Xin Nie, Zhen Mi, **Yin Guo**, Yinyin Zhang, Yong Peng, Lei Zhang

Beijing Konruns Pharmaceutical Co., Ltd., Beijing, China

A growing body of published studies suggested the important role for epigenetic regulation in promoting tumor heterogeneity. Targeting these epigenetic proteins becomes an exciting and attainable approach for several cancer types with unmet clinical needs.

MYST-family acetyltransferases, KAT6A/B and KAT7 (HBO1), maintain promoter-proximal H3 acetylation (e.g., H3K23ac, H3K14ac) that sustains lineage transcription in multiple cancers. First-generation KAT6-selective agents have shown early clinical activity in $ER^+/HER2^-$ breast cancer but can produce predominantly cytostatic responses. We here report an orally bioavailable dual KAT6/7 inhibitor, KC1086, designed to produce deeper promoter closure, broaden lineage program suppression, and translate into tumor regressions with superior efficacy and a favorable safety window.

KC1086 showed sub-10 nM potency on KAT6A/B and potent KAT7 inhibition (IC_{50} around 16 nM) with wide selectivity over KAT5/8. In addition, KC1086 retained activity under elevated Acetyl-CoA (AcCoA), indicating reduced co-factor competition liability. Unlike PF-07248144, KC1086 did not drive significant Malonyl-CoA accumulation, while maintaining on-target AcCoA modulation, suggesting potentially much less hepatotoxicity. In ER^+ breast cancer cells, KC1086 durably suppressed H3K23ac/H3K14ac, which outperformed PF-07248144 on biomarker depth and duration.

KC1086 monotherapy exhibited strong tumor growth inhibition in various xenograft models. Combinations of KC1086 further demonstrated enhanced efficacy: (i) with Palbociclib (CDK4/6 inhibitor) (TGI 101%) in ZR-75-1 ER^+ breast cancer xenograft model; (ii) with Fulvestrant (Estrogen Receptor Antagonist) (TGI 83%) in xxT47D breast cancer models yielding tumor regressions and survival benefit. Furthermore, KC1086 demonstrated favorable PK profile and significant safety window: linear PK, high oral bioavailability, minimum drug accumulation and clean safety pharmacology (eg. CV, CNS and respiratory).

In conclusion, we demonstrated equipotent dual inhibition of KAT6/7 delivering potentially deeper chromatin closure than KAT6-selective blockade, which translated into robust monotherapy activity and combination synergy across ER^+ breast cancer, ovarian cancer as well as other tumor models, with favorable preclinical safety. These data supported clinical development of KC1086 as a dual KAT6/7 inhibitor with best-in-class potential.

#4495 TACC3 inhibition with KC1101 drives mitotic catastrophe and broad antitumor activity.

Lei Zhang, Xin Nie, Zhen Mi, **Yin Guo**, Xiaona Yang, Yinyin Zhang, Huaying Wang, Bingqian Li, Yong Peng, Yang Yang

Beijing Konruns Pharmaceutical Co., Ltd., Beijing, China

TACC3, an oncogenic member of the transforming acidic coiled-coil domain-containing protein (TACC) family, is a core component of multi-protein complexes regulating microtubule and centrosome-related processes. Aberrant overexpression of TACC3 is found across multiple cancers with centrosome instability and worse prognosis. Emerging evidence further highlights TACC3 as a therapeutic vulnerability, particularly in highly aggressive cancers characterized with centrosome amplification.

We have profiled our selective TACC3 inhibitor -- KC1101 via cell proliferation assays across diverse cancer cell lines. KC1101 demonstrated potent anti-proliferative effects, approximately 2-fold more potent than AO-252, an oral TACC3 inhibitor currently in Phase I. Meanwhile, no cytotoxicity was observed in primary hepatocytes or PBMCs. Further studies indicated KC1101 triggered robust cell-cycle arrest at G2/M phase and markedly increased multipolar spindle formation, consistent with on-target disruption of TACC3-dependent spindle regulation. With once-daily oral dosing, KC1101 demonstrated superior antitumor activity in vivo across TNBC (MDA-MB-231, CAL-51) and colon (HCT116) xenograft models. At 20 mpk, KC1101 achieved 94.4% TGI in CAL-51 and 61.1% TGI in HCT-116, outperforming AO-252 (24.7% and 54.2%, respectively). Encouragingly, KC1101 also produced significant tumor suppression in an intracranial TNBC (MDA-MB-231-Luc) and AML (MOLM-13-Luc) model. All the data highlighted high therapeutic potential of KC1101. A wide safety margin in exploratory toxicology, coupled with low interspecies PK variability in mouse, rat, and dog, supports future clinical investigation.

In conclusion, KC1101 delivers best-in-class potential for TACC3-addicted tumors by coupling strong mitotic-catastrophe biology with consistent, QD oral efficacy—including intracranial and hematologic settings—while avoiding primary-cell cytotoxicity. Collectively with the clinical precedent for TACC3 inhibition (AO-252), these data nominate KC1101 for IND in 2026.

#4496 Imofinostat, a histone deacetylase inhibitor, enhances anti-tumoral activity on colorectal cancer with an immune checkpoint inhibitor.

Chung-Yen Li[1], Chin-Wen Wei[1], Ka-Po Tse[1], Shih-Han Huang[1], Tzu-Hsien Yang[1], Meng-Chieh Lin[2], Chien-Ting Lin[3], Sue-Ming Chang[1], Mark Shiuh-Sheng Horng[1], John Tsu-An Hsu[1], Kien Thiam Tan[1]

[1]AnBogen Therapeutics, Inc., Taipei, Taiwan,[2]Yang Ming Regenerative Therapeutics Co., Taipei, Taiwan,[3]National Taiwan University Cancer Center, Taipei, Taiwan

Background: Histone deacetylase (HDAC) inhibitors have been shown to exert immunomodulatory effects and enhance immune responses elicited by immune checkpoint inhibitors (ICIs). Imofinostat (ABT-301) is an HDAC inhibitor with potent activity against class I HDACs and moderate activity against class IIb HDACs. In this study, we investigated the therapeutic efficacy and underlying immunomodulatory mechanisms of imofinostat combined with ICI-based regimens in colorectal cancer (CRC).

Methods: Imofinostat was evaluated in combination with ICIs (anti-mPD-1 or anti-PD-L1) in both murine syngeneic (CT26) and human microsatellite stable (MSS) CRC cell line-derived xenograft (CDX) models (HT29) with or without antiangiogenic agent aflibercept. Transcriptomic profiling was performed using the NanoString IO360 panel, while immune cell alterations and functional markers were analyzed by flow cytometry and immunohistochemistry (IHC).

Results: In the CT26 syngeneic mouse model, the combination of imofinostat with avelumab (anti-PD-L1) induced complete tumor regression in 7 of 8 animals. Notably, of those achieving complete remission, 6 of 7 remained tumor-free following tumor re-challenge, indicating the establishment of durable anti-tumor immunity. This combination demonstrated superior efficacy compared to the pan-HDAC inhibitor vorinostat and the class I-selective HDAC inhibitor tucidinostat in parallel CT26 models. In the HT29 CRC model co-engrafted with patient-derived PBMCs, an additive anti-tumor effect was observed with the combination of imofinostat and nivolumab (anti-PD-1), which was further enhanced by the addition of aflibercept. Gene Set Enrichment Analysis (GSEA) revealed that imofinostat, alone and in combination, significantly enriched gene signatures associated with central memory T-cells. The combination treatment also increased infiltrated cytotoxic $CD4^+$ and $CD8^+$ T cells ($IFN\text{-}\gamma^+$ or $GzmB^+$) and reduced monocytic-myeloid-derived suppressor cells (M-MDSCs) in PBMCs.

Conclusion: Imofinostat synergizes with ICI by targeting mechanisms of immune suppression, including the reduction of M-MDSCs in PBMCs, while concurrently promoting the development of robust cytotoxic and memory T-cell responses. This provides a strong rationale for the clinical investigation of imofinostat in combination with ICIs for CRC.

#4497 Imofinostat enhances chemotherapy response by targeting HDAC3-NRF2 pathway in KRAS-mutant pancreatic cancer.

Yi-Chen Lin, Ka-Po Tse, Chung-Yen Li, Tzu-Hsien Yang, Shih-Han Huang, Sue-Ming Chang, Mark Shiuh-Sheng Horng, John Tsu-An Hsu, Kien Thiam Tan

Anbogen Therapeutics, Inc., Taipei, Taiwan

Background: Aberrant HDAC3 activation in solid tumors contributes to therapeutic resistance and poor prognosis. Inhibition of HDAC3 has therefore emerged as a potential strategy to overcome resistance to chemo-, radio-, and immunotherapies. Imofinostat (also known as ABT-301), a hydroxamic acid-based HDAC inhibitor, exhibits potent HDAC class I selectivity with preferential inhibition of HDAC3 (IC_{50} = 7 nM). This study evaluated the antitumor efficacy of imofinostat, alone or in combination with standard therapies, in cancers exhibiting high HDAC3 dependency.

Methods: HDAC3 dependency was assessed across cancer types using the DepMap database. The *in vitro* anti-proliferation effects of imofinostat, alone or in combination with gemcitabine, were measured via standard cell viability assays across multiple cancer cell lines. RNA sequencing and Western blot analyses were conducted to examine transcriptomic and protein expression changes following imofinostat treatment. *In vivo* efficacy of imofinostat, alone or in combination with chemotherapies, was evaluated in KRAS-mutant pancreatic ductal adenocarcinoma (PDAC) xenograft models.

Results: DepMap analysis revealed PDAC, bladder cancer, brain tumors, and leukemia as malignancies with pronounced HDAC3 dependency. *In vitro*, imofinostat inhibited cell proliferation in PDAC cell lines (GI_{50} 0.3 - 4.8 μM) and bladder cancer cell lines (GI_{50} 0.2 - 0.5 μM), demonstrating synergistic effects with gemcitabine and pemetrexed, respectively. Mechanistically, transcriptomic profiling in PDAC revealed imofinostat downregulated antioxidant genes (*NQO1*, *GPX4*, *GSS*, *COQ2*) and upregulated ferroptosis-associated genes (*STEAP3*, *FTL*, *SLC39A14*, *CP*). Consistently, Western blot analysis of KRAS-mutant PDAC xenografts confirmed target engagement (increased histone H3 acetylation) and reduced expression of NRF2 and its targets (NQO1, SLC7A11). Together, these findings indicate that imofinostat suppresses NRF2-driven antioxidant programs, enhances ferroptotic susceptibility and exposes metabolic vulnerabilities linked to oncogenic KRAS. *In vivo,* imofinostat alone or in combination with gemcitabine significantly inhibited tumor growth in NRF2-high, KRAS-mutant xenograft models.

Conclusion: Imofinostat exerts potent anti-tumor activity via HDAC3 inhibition, exploiting the HDAC3-NRF2 vulnerability in KRAS-mutant PDAC models. Its combination with gemcitabine further enhanced efficacy, supporting the clinical potential of imofinostat with DNA-damaging or metabolic agents in NRF2-activated cancers.

#4498 Discovery of novel SMARCA2 small molecule inhibitors with best-in-class potency and selectivity for the treatment of SMARCA4-mutant cancers.

Lijs Beke[1], Sandrine Grosse[1], Shaun Martin[2], Godelieve Lammens[1], Pieter Peeters[1], Bart Stoops[1], Sandrine Vendeville[1], Stephane De Cesco[1], Kenneth Goossens[2], Sara Musch[2], David Moreno Delgado[2], Line Oste[2], Pierre Raboisson[1], Francois Gonzalvez[1]

[1]Onco3R Therapeutics, Leuven, Belgium,[2]Former Galapagos employee, Mechelen, Belgium

Patients with homozygous loss-of-function (LOF) mutations in SMARCA4 constitute a molecularly distinct subgroup of non-small-cell lung cancer (NSCLC), encompassing approximately 5% of all patients. This subset is defined by its mutual exclusivity with other oncogenic drivers and demonstrates resistance to standard treatments, including radiotherapy, chemotherapy, and PD-L1 inhibitors. Notably, SMARCA4 LOF can co-occur with KRAS-G12C mutations, leading to resistance against KRAS-targeted therapies.

Mechanistically, the loss of SMARCA4 function creates a synthetic lethal dependency on SMARCA2, a vulnerability that has been validated through both genetic and pharmacological approaches. However, the development of selective SMARCA2 inhibitors remains challenging due to the high sequence homology between SMARCA2 and SMARCA4—yet achieving selectivity is critical for clinical success. Previous clinical trials with a dual SMARCA4/2 inhibitor were discontinued due to safety concerns, highlighting the urgent need for potent and selective SMARCA2 inhibitors. Addressing this therapeutic gap could unlock the full potential of targeting SMARCA2 in SMARCA4-deficient cancers.

At Onco3R Therapeutics, our patient-centric strategy—combining deep translational science with rational, structure-based and AI-augmented drug design—has led to the discovery of a novel series of SMARCA2-selective small molecule inhibitors with a best-in-class potency and selectivity profile. Lead compounds exhibited single digit to sub-nanomolar activity and over 30-fold selectivity for SMARCA2 versus SMARCA4, as demonstrated in a KRT80 qRT-PCR assay using SMARCA2/4 isogenic knockout cell lines.

Notably, these lead compounds combined potent anti-proliferative effects in SMARCA4-deficient cells with favourable in vitro ADME characteristics, a supportive safety profile and pharmacokinetic properties suitable for in vivo evaluation. Following oral administration, the compounds achieved sustained target engagement and elicited pronounced anti-tumor activity in a SMARCA4-deficient RERF-LC-A1 CDX mouse model without evidence of SMARCA4-related body weight loss.

These unique SMARCA2-selective lead compounds are currently further profiled as potential clinical candidate with the ultimate goal of delivering transformative efficacy and enhanced safety for patients with SMARCA4-deficient cancers.

#4499 KAT6i prifetrastat combines with PI3K pathway inhibitors to drive superior efficacy in preclinical models of PIK3CA mutated ER+ BC.

Kamakoti Prakash Bhat, Joan Q. Cao, Christopher Beldon Proffitt, Jelena Petrovic, Xinmeng Jasmine Mu, Kyle Spinler, Colin Ashton Flaveny, Thomas A. Paul, Joal Garrido Mayor, Heather Neumann, Shikhar Sharma

Tumor Biology, Pfizer, Inc. Medical Oncology, San Diego, CA

KAT6A, and its paralog KAT6B, are histone lysine acetyltransferases (HATs) that acetylate histone H3K23 and regulate lineage-specific transcriptional programs. KAT6A/B activity is dysregulated in cancer, resulting in an oncogenic function for KAT6A/B in several tumor types, including in breast cancer. Prifetrastat is a first in class catalytic inhibitor of KAT6A and KAT6B with selectivity over other HAT enzymes. KAT6A/B inhibition results in downregulation of key pathways including estrogen signaling, cell cycle and MYC, resulting in anti-tumor activity in ER+ breast cancer. Here, we evaluate the activity of prifetrastat across a panel of breast cancer cell lines comprising different subtypes. Prifetrastat response was enriched in ER+, luminal subset of breast cancer cell lines with activity observed in both PIK3CA mutant and WT cells. Transcriptomic and chromatin accessibility analyses demonstrate that KAT6i treatment inhibits similar pathways in both PIK3CA WT and mutant cell lines. In vivo PDX studies also confirm the efficacy of prifetrastat in PIK3CA mutated models. Given the potential interplay between the mechanisms of action of KAT6i and PI3Kα inhibition in ER+ BC, we explored the potential of combining prifetrastat with PI3Kα inhibitors. In vitro drug combination studies demonstrate synergy between prifetrastat and several PI3Kα inhibitors including alpelisib and inavolisib as well as mutant selective PI3Kα inhibitors such as tersolisib across cell lines harboring PIK3CA helical or kinase domain mutations. Mechanistically, the combination of prifetrastat with PI3Kα inhibitors leads to further suppression of ER pathway genes and cell cycle pathways as compared to monotherapy activity. Finally, the triple combination of prifetrastat + Fulvesterant with PI3Kα inhibitors drives deeper tumor growth inhibition in PIK3CA mutant ER+ PDX models in vivo. Overall, we find that KAT6A/B inhibitors can effectively be combined with PI3Kα inhibitors and endocrine therapy to further drive efficacy in PIK3CA-mutant ER+BC indicating that the triplet combination could present a promising therapeutic option for this population.

#4500 Embryonic ectoderm development (EED) inhibitor APG-5918 synergizes with topoisomerase I inhibitors in preclinical small-cell lung cancer (SCLC) models through epigenetic priming of chemosensitivity.

Yan Yin[1], Zhiyan Liang[2], Baisong Li[1], Zhou Yu[1], Daojie Liu[1], Dajun Yang[1], Yifan Zhai[2]

[1]Ascentage Pharma (Suzhou) Co., Ltd., Suzhou, China,[2]Ascentage Pharma Group Inc., Rockville, MD

SCLC initially responds to platinum-based chemotherapy but rapidly acquires resistance, resulting in poor prognosis. PRC2-mediated epigenetic silencing represses Schlafen 11 (SLFN11)—a biomarker of sensitivity to DNA-damaging therapies—contributing to resistance. EZH2, the PRC2 catalytic subunit, promotes chemoresistance via SLFN11 repression. EED, another core PRC2 subunit, stabilizes the complex and maintains its methyltransferase activity, making it an attractive target. Topoisomerase I inhibitors, such as topotecan and irinotecan, are used in relapsed SCLC, but efficacy is limited when SLFN11 is epigenetically suppressed. APG-5918, a selective and investigational EED inhibitor, disrupts PRC2 function. This study evaluated antitumor activity of APG-5918 combined with topoisomerase I inhibitors in preclinical SCLC models.

In vitro antiproliferation was assessed using human SCLC cell lines (NCI-H446, NCI-H69, NCI-H889, DMS-114); cell viability via CellTiter-Glo® luminescent assays; apoptosis with Annexin V/PI flow cytometry; molecular mechanisms via western blot; and in vivo antitumor efficacy using a subcutaneous NCI-H446 cell-derived xenograft (CDX) model.

APG-5918 synergized with topoisomerase I inhibitors (topotecan or SN-38, the active metabolite of irinotecan) to suppress proliferation and induce apoptosis in SCLC cell lines. In NCI-H446 CDX, single-agent APG-5918 (100 mg/kg) or irinotecan (5 mg/kg) at 27 days showed limited efficacy (T/C: 115.79% and 61.58%, respectively). The combination significantly enhanced antitumor activity, achieving a T/C value of 38.92% ($p < 0.05$ vs. vehicle) and a synergistic index of 1.83. No significant body-weight changes indicated favorable safety. Mechanistically, APG-5918 reduced H3K27me3 confirming on-target epigenetic modulation, and upregulated SLFN11 and p21 (CDKN1A). This EED inhibition reverses epigenetic silencing of chemosensitivity genes and sensitizes tumor cells to topoisomerase I inhibitors. Notably, topotecan or SN-38 alone increased H3K27me3, indicating that compensatory epigenetic repression was countered by APG-5918. The combination further downregulated PRC2 components (EED, EZH1, EZH2, SUZ12), suppressed cell-cycle regulators (pRb, CDK4, CDK6), and induced DNA damage (γH2A.X) and apoptotic markers (cleaved PARP-1, cleaved caspase-3, BIM, Noxa), supporting a synergistic proapoptotic mechanism.

APG-5918 synergistically enhances antitumor activity of topoisomerase I inhibitors in preclinical SCLC models by reversing PRC2-mediated epigenetic silencing of SLFN11 and amplifying DNA damage, cell-cycle arrest, and apoptosis. These findings support clinical investigation of APG-5918 combined with DNA-damaging agents as a promising strategy for SCLC.

#4501 Targeting the epigenetic adaptor protein menin in multiple myeloma.

Emily Gruber[1], Sree Kumar[1], Rheana Franich[1], Tiffany Khong[2], Daniel Neville[1], Andrew Spencer[2], Omer Gilan[2], Lev Kats[1]

[1]Peter MacCallum Cancer Centre, Melbourne, Australia,[2]Australian Centre for Blood Diseases, Monash University, Melbourne, Australia

The interaction between the epigenetic proteins Menin and MLL1 is critical for sustaining the expression of self-renewal genes in specific subsets of acute leukemias. Disrupting the Menin-MLL1 interaction with Menin inhibitors (iMenin) is showing promising overall response rates in leukemia clinical trials, however, iMenin are not known to be active in other cancers. We analysed DepMap and discovered that many multiple myeloma (MM) cell lines are highly dependent on Menin/MLL1 for proliferation. MM is a common plasma cell malignancy that remains largely incurable, despite the plethora of treatments available. The objectives of our study are to understand the role of the Menin/MLL1 complex in MM, determine the efficacy of iMenin in MM pre-clinical models and identify biomarkers of response to enable the rapid and successful translation of iMenin into the myeloma setting.

To assess the efficacy of iMenin in MM, we performed growth assays across 13 commercially available cell lines and 9 early passage patient-derived MM cells (physiologically relevant model). We found that ~30% were highly sensitive to iMenin with a substantial impact on viability and proliferation, with an additional ~40% showing a significant anti-proliferative response. Sensitivity was significantly correlated with the absence of the MYC t(8;14) translocation. Importantly, iMenin showed *in vivo* efficacy in a xenograft and in the syngeneic Vk*MYC-32052 model of MM.

RNA-, ChIP- and chromatin conformation sequencing found that iMenin sensitivity was characterized by the deposition of Menin/MLL1 at the super-enhancer of IRF4, with iMenin evicting Menin/MLL1 from chromatin and suppressing IRF4 and its target genes. Genome-wide CRISPR screening was performed to identify the molecular determinants of iMenin response in MM. This identified the EP300/CREBBP/NCOR1 axis as a key modulator of iMenin sensitivity. To further advance the translational potential of iMenin, we tested several combination strategies. Among the most effective was the combination of Menin and EP300/CREBBP inhibitors, which demonstrated synergistic activity even in models which were unresponsive to the single-agents, including JJN3 cells *in vitro* and the syngeneic *in vivo* Vk*MYC-14551 model. Molecular analyses uncovered deep suppression of IRF4, via disruption of the canonical IRF4 super-enhancer, as the mechanism underpinning the synergy between Menin and EP300/CREBBP inhibitors.

Taken together, Menin regulates the pan-myeloma essential transcription factor IRF4 and is a promising and clinically actionable target in MM.

#4502 Expanding the PRISM platform: Addition of new hematologic models and a 10-day assay improve drug sensitivity mapping for epigenetic targets.

Colleen T. Harrington, Antonella Masciotti, Ursula Widocki, Laura Doherty, Tenzin Sangpo, Li Wang, Mustafa Kocak, Anthony Fazio, Aydin Golabi, Rachael Barry, Emily Reeves, John Davis, Melissa Ronan, Matthew G. Rees, Jennifer A. Roth

Cancer Program, Broad Institute, Cambridge, MA

Despite major advances in targeted therapies, cancer remains a leading cause of death among pediatric, adolescent, and adult populations, emphasizing the need for continued therapeutic innovation. The PRISM assay enables large-scale evaluation of oncology agents by barcoding and pooling over 900 cancer cell lines with extensive genomic and functional characterization. This platform enables systematic analysis of drug potency, selectivity, and rapid identification of genomic correlates of sensitivity. To broaden the coverage of pediatric, hematologic, and rare tumor types in the PRISM assay and enhance our ability to investigate novel therapeutics for these disease areas, we expanded the PRISM cell line panel in collaboration with the Pediatric Cancer Dependencies Accelerator to include 109 additional lines, including 21 pediatric, 60 hematopoietic, and 14 previously unrepresented subtypes. We re-profiled compounds with predicted activity in new cell models and found that many compounds targeting heme-centric proteins such as BCL6, FLT3, IKZF3, EP300, EZH2, EED had stronger correlations with target dependency. Targeting of epigenetic drivers is an attractive therapeutic strategy for hematopoietic tumors, so we sought to compare clinically relevant epigenetic targeting compounds in PRISM. For example, mevrometostat more selectively targets EZH2-dependent cell lines compared to other EZH2 inhibitors profiled after 5 days of treatment. However, the observed potency of many epigenetic targeting compounds is somewhat limited in a 5-day assay, as the mechanistic nature of these compounds often requires a longer incubation period to enact their cytotoxic effects. We developed a 10-day PRISM assay for our hematopoietic cell collection and re-screened mevrometostat as part of an assay validation screen. We observed greater potency, selectivity, and stronger correlations with EZH2 dependency for mevrometostat in the 10-day assay compared to the 5-day assay. Future assay development will enable higher throughput screening of slow-acting compounds against our hematopoietic cell lines. Taken all together, these advances position PRISM to accelerate hematologic and pediatric cancer research by expanding disease-relevant models and enabling long-duration single-agent screening at scale. All data will be made publicly available on depmap.org, providing a resource for the cancer research community to explore novel therapeutic opportunities.

#4503 RCZY-843: A potential best-in-class, second-generation menin-MLL inhibitor engineered to overcome clinically observed menin-mutation-mediated resistance, with superior preclinical efficacy and safety in acute leukemia models.

Xiaojing (Celia) Chen[1], Zhengyong Wan[1], Xiaohong Liu[1], Qiaoni You[1], Shenjun Li[2], Ling Wang[2], Shanshan Bi[2], Jing Jiang[2], Jianming Bao[1]

[1]Rongchang Pharmaceuticals, Ltd., Yantai, China,[2]RemeGen Co., Ltd., Yantai, China

Menin, encoded by the MEN1 gene, is a ubiquitously expressed scaffold protein that regulates gene transcriptions and key signaling pathways. The menin-MLL1 (KMT2A) complex drives aberrant HOX/MEIS1 expression, promoting leukemogenesis in KMT2A-rearranged or NPM1-mutant acute leukemias. Disrupting this interaction is a validated therapeutic strategy, as evidenced by FDA approvals of Syndax's revumenib (initially for R/R KMT2A-rearranged acute leukemia in November 2024, expanded to R/R NPM1-mutant AML in October 2025) and Kura's ziftomenib (for R/R NPM1-mutant AML in November 2025). However, first-generation menin inhibitors rapidly develop clinical acquired resistance driven by MEN1 somatic mutations—especially loss-of-function alterations eliminating menin dependency—urgently requiring next-generation, mutation-resilient menin inhibitors. Herein, we report RCZY-843, a novel, highly potent, orally bioavailable second-generation menin-MLL inhibitor with superior preclinical efficacy against acute leukemias. Surface plasmon resonance assays show its picomolar binding affinity to wild-type menin—4-fold and 5-fold stronger than SNDX-5613 and KO-539, respectively. Fluorescence polarization assays further confirm its potent disruption of the menin-MLL interaction in the presence of clinically observed resistance mutations (M327I/V, G331R, T349M) with substantially lower IC_{50} values than approved or clinical-stage menin inhibitors (SNDX-5613, KO-539, JNJ-75276617). RCZY-843 exerts potent growth inhibition in KMT2A-rearranged/NPM1-mutant cell lines, with >476-fold selectivity over wild-type MLL HL-60 cells and demonstrates favorable drug-like properties, including robust in vitro ADME characteristics, a clean safety profile (hERG IC_{50} >30 μM), and excellent pharmacokinetics across preclinical species. Notably, it exhibits a longer half-life ($T_{1/2}$) and ~3-fold higher oral bioavailability than SNDX-5613 in rat. In AML xenograft models (MV-4-11, OCI-AML-3), orally administered RCZY-843 achieves tumor growth inhibition comparable to SNDX-5613 at only one-third to one-tenth of the dose, accompanied by higher plasma exposure and preferential tumor distribution. Compared to SNDX-5613, RCZY-843 further demonstrates favorable PK/PD characteristics—including stronger and more durable MEIS1 mRNA suppression—along with good in vivo tolerability, and a wide therapeutic window, as supported by a 14-day rat DRF toxicity study. In conclusion, RCZY-843 is a potential best-in-class, second-generation menin-MLL inhibitor capable of overcoming MEN1 mutation-mediated acquired resistance, with robust preclinical efficacy and a favorable safety profile for the treatment of KMT2A-rearranged/NPM1-mutant acute leukemias.

#4504 Synergistic antitumor activity of the MTA-cooperative PRMT5 inhibitor ABSK131 in combination with multiple therapeutic agents in diverse cancer models.

Bin Shen, Qianqian Chen, Xiao Chen, Jie Wang, Jie Zhang, Manqi Liu, Hongping Yu, **Nannan Zhang**

Abbisko Therapeutics Co., Ltd., Shanghai, China

Background: Homozygous deletion of *MTAP* occurs in ~10-15% of solid tumors and frequently coexists with major oncogenic drivers such as *EGFR* and *KRAS*, providing a strong rationale for combining their inhibitors with MTA-cooperative PRMT5 inhibitor. Moreover, low *MTAP* expression is linked to poorer survival in NSCLC treated with chemoimmunotherapy, underscoring the need for novel, effective therapeutic strategies in *MTAP*-deleted tumors. ABSK131, a highly potent and selective MTA-cooperative PRMT5 inhibitor discovered by Abbisko, is under clinical evaluation. Here, we investigated the potential of ABSK131 combined with multiple therapeutic agents to enhance antitumor efficacy across diverse cancer models preclinically.

Methods: Synergistic activity of ABSK131 with various agents was evaluated using *in vitro* antiproliferative assays across various cancer cell lines, primarily from NSCLC and PDAC origins. Combination partners included chemotherapy agents and the inhibitors targeting KRAS, EGFR, MAT2A, etc. Synergy was quantified by combination index analysis. Prioritized combinations were further tested in xenograft models reflecting clinically relevant biomarker-defined contexts, including in combination with KRAS, EGFR inhibitors, and standard chemotherapy.

Results: ABSK131 demonstrated strong *in vitro* synergy with multiple KRAS inhibitors in anti-proliferation assays. In *KRAS*-mutant and *MTAP*-deleted models, ABSK131 led to robust tumor growth inhibition when combined with KRAS G12C inhibitor AMG510 or KRAS G12D inhibitor ABSK141. In *EGFR*-mutant and *MTAP*-deleted NSCLC, ABSK131 combined with osimertinib produced enhanced anti-proliferative and *in vivo* antitumor efficacy. ABSK131 plus MAT2A inhibitor IDE397 induced consistent synergy across diverse cell types, indicating a broadly applicable mechanistic interaction. Additionally, synergy was observed with carboplatin in multiple NSCLC models *in vitro* and *in vivo*.

Conclusion: ABSK131 synergizes with multiple therapeutic classes across *MTAP*-deleted models, providing compelling preclinical support for developing ABSK131-based combination strategies in genetically defined patient populations in clinic.

#4505 IDE892 is a highly potent and selective PRMT5 inhibitor, with MTA-positive and SAM-negative cooperativity, optimized for development in MTAPdel cancers in combination with the allosteric MAT2A inhibitor IDE397.

Arjun A. Rao, Marcus M. Fischer, Rebeca M. Choy, Angelica M. Gonzalez-Sanchez, Natalie Bresnahan, Zhipeng Fang, Mason J. Appel, Atul Rathore, Oscar Aubi, Shannon Faris, Parker Y. Jameson, Zabrisky Roland, David Trinh, Kelly Trego, John Vivian, Michael E. Dalziel, Christian R. Frey, Yuchen Bai, Jasgit Sachdev, Claire L. Neilan, Jay Prakash Jain, Michael A. White, Paul A. Barsanti, Peter Teriete, Melissa Fleury

Computational Biology, Ideaya Biosciences, South San Francisco, CA

Homozygous deletion of MTAP frequently co-occurs with the adjacent CDKN2A tumor suppressor on chromosome 9p21.3 in human cancers. Loss of MTAP activity creates an acute dependency on MAT2A, the rate-limiting enzyme for SAM synthesis, to produce sufficient SAM to overcome MTA suppression of PRMT5 and to support the folate cycle via 1-carbon metabolism. Proof-of-concept therapeutic targeting of this vulnerability has been achieved by allosteric inhibition of MAT2A or by MTA-cooperative inhibition of PRMT5. However, variability of response highlights the opportunity to continue to improve outcomes with combination therapy strategies. Preclinical profiling has indicated the extent of MTA accumulation in tumor cells and intrinsic or acquired resistance mechanisms are key determinants of antitumor activity. Notably, co-administration of appropriately designed MAT2A and PRMT5 inhibitors can deliver durable tumor regressions and complete responses in multiple MTAPdel PDX models recalcitrant to either monotherapy. Here we describe the biochemical, cell biological, and in vivo efficacy profiles of IDE892, an MTA-cooperative PRMT5 inhibitor purposely designed to exploit the therapeutic opportunity associated with combined inhibition of PRMT5 and MAT2A. Extensive biophysical and biochemical characterization of the IDE397 mode-of-inhibition of MAT2A yielded a mechanistic model that accounts for MTAPdel tumor-specific activity of IDE397 due to allostery-dependent preservation of basal MAT2A activity, maintaining SAM levels above the threshold required to sustain function in normal tissues. In addition, extensive evaluation of the kinetic and equilibrium binding parameters of metabolite and inhibitor exchange on PRMT5 revealed key relationships that specify MTA-cooperativity as well as slow on-rate binding kinetics to the SAM-bound state (negative cooperativity) relative to the apo state. These findings informed the design of IDE892 that optimized efficacy and tolerability in combination with allosteric inhibition of MAT2A. IDE892 demonstrated at least 1,400-fold selective binding to MTA-PRMT5 versus SAM-PRMT5 complexes (by SPR) and robust MTAPdel-specific PRMT5 pathway inhibition in vitro and in vivo. Whole transcriptome, proteome, and mRNA/tRNA methylome analyses indicated both shared and distinct contributions of IDE397 and IDE892 to perturbation of MTAPdel cellular systems which translated to robust combination benefit in MTAPdel CDX and PDX models. These preclinical studies indicate that the combination of IDE892/IDE397 has the potential to deliver durable therapeutic activity for patients harboring MTAPdel tumors; an opportunity that is currently under evaluation in phase 1 clinical trials.

#4506 H11 is a first-in-class bifunctional HDAC and autophagy inhibitor with potent antileukemic activity.

Natalie L. Hakim[1], Claudia M. Espitia[1], Sruthi Sureshkumar[1], Madison Gamble[1], Bi Fangchao[2], Wei Wang[2], Kevin Kelly[3], Jennifer S. Carew[1], Steffan T. Nawrocki[1]

[1]Cancer Center, University of Arizona, Tucson, AZ,[2]Pharmacology Toxicology, University of Arizona, Tucson, AZ,[3]Hematology, University of Southern California, Los Angeles, CA

Acute myeloid leukemia (AML) is a highly aggressive hematologic malignancy characterized by the accumulation of immature myeloid blasts that disrupt hematopoiesis. Although initial remissions can be achieved with standard chemotherapy, relapse is frequent and durable responses remain uncommon. This underscores the need for new therapeutic strategies that can overcome established resistance mechanisms. Disruption of epigenetic homeostasis is a common feature of AML pathogenesis and offers an opportunity for targeted therapy. Histone deacetylase (HDAC) inhibitors are one class of agents that induce epigenetic reprogramming and have previously demonstrated antileukemic activity. However, their efficacy is blunted by the activation of cytoprotective autophagy. Simultaneous blockade of HDAC activity and autophagic flux therefore represents a rational approach to enhance therapeutic benefit. To address this, we developed H11, a first-in-class bifunctional small molecule engineered to concurrently inhibit HDACs and suppress autophagy. H11 potently reduced viability and triggered apoptosis across genetically diverse AML models and primary AML specimens from patients including those with adverse features such as *FLT3-ITD* and loss of p53 function. H11 retained potent activity in models resistant to frontline therapies, indicating its potential to overcome both epigenetic and lysosomal-mediated resistance mechanisms. Importantly, H11 demonstrated strong therapeutic selectivity with very limited effects against normal CD34+ bone marrow progenitors. Mechanistic studies demonstrated robust HDAC inhibition, evidenced by increased global histone acetylation, coupled with impaired autophagic degradation, reflected by p62 accumulation, lysosomal deacidification, and blocked autophagic flux. H11 treatment also decreased the expression of the oncogenic transcription factor c-Myc and increased CDKN1A (p21), consistent with epigenetic reprogramming and disruption of AML survival circuitry. Because epigenetic dysregulation is a hallmark of AML, we next evaluated H11 in combination with the FDA-approved hypomethylating agent azacitidine (AZA). The H11-AZA combination produced strong synergy, markedly enhancing cytotoxicity across multiple AML cell lines and significantly extending overall survival in an orthotopic FLT3-ITD+ mouse xenograft model of AML. Together, these findings establish H11 as a first-in-class dual HDAC-autophagy inhibitor that integrates epigenetic modulation with autophagy suppression to promote apoptosis and disrupt adaptive AML survival pathways. This coordinated mechanism of action highlights H11 as a promising next-generation therapeutic with strong potential to improve clinical outcomes in patients with AML.

: Hematologic Malignancies and Novel Therapeutic Modalities
Poster Session

#4510 Comprehensive surfaceome proteomics uncovers CD70 as a novel immunotherapeutic target in natural killer/T cell lymphoma (NKTL).

Ern Sen Chew[1], Nurulhuda Mustafa[2], Wai Khang Yong[1], Vartika Khanchandani[1], Rui Xue Lee[1], Anand Jeyasekharan[1], Dennis Kappei[1], Siok Bian Ng[3], Wee Joo Chng[1]

[1]Cancer Science Institute of Singapore, National University of Singapore, Singapore, Singapore,[2]Pharmacology, National University of Singapore, Singapore, Singapore,[3]Department of Pathology, Yong Loo Lin School of Medicine, National University of Singapore, Singapore, Singapore

Natural killer/ T cell lymphoma (NKTL), a subtype of non-Hodgkin lymphoma, is an Epstein-Barr virus (EBV) associated lympho-proliferative disease prevalent in Asia and South America. Current treatments options are inadequate with treatments such as conventional radiotherapy or chemotherapy having limited efficacy. Moreover, efficacy of newer therapies such as targeted therapies or immunotherapies has been less than ideal in clinical trials likely due to heterogeneous nature of disease. Novel treatments which are more efficacious, such as immunotherapy with higher specificity and less cytotoxicity, will have to be formulated. Hence, this project aims to identify new targets and develop novel antibody-based therapies against NKTL. First step in antibody-based therapy development involves identification of suitable targets. Here, we combined aminooxy-biotin labeling followed by streptavidin enrichment with label-free quantitative mass spectrometry analysis to systematically profile the plasma membrane landscape of NKTL. Considering a lack of proper pipeline for plasma membrane annotation, we designed a unique membrane annotation pipeline based off publicly available databases, including UniProt, Gene Ontology and in silico surfaceome database, SURFY. Strategy for prioritization of targets with highest immunotherapeutic potential was employed by looking at target specificity and accessibility. Plasma membrane profiling via this method of analysis was successful with GO terms enrichment of the significant proteins in different cell lines pre-membrane protein annotation revealing molecular functions and biological processes associated with surface membrane proteins such as signalling receptor activity and adhesion. Our method of immunotherapeutic potential analysis revealed CD70, ITGA4 and CD48 as top targets with CD70 having highest potential. CD70 is a tightly regulated immune co-stimulatory ligand which is aberrantly expressed in different malignancies. Expression of CD70 was validated on multiple NKTL cell lines while PBMCs and primary NK cells from healthy donors were CD70 negative. Substantial internalization of CD70 was validated via FACS, immunofluorescence and Fab-ZAP assays, revealing potential as an antibody-drug conjugate (ADC) target for NKTL. Cusatuzumab, anti-CD70 monoclonal antibody currently in clinical trials for other malignancies, elicited strong antibody effector functions such as complement dependent cytotoxicity (CDC) and antibody dependent cellular cytotoxicity (ADCC) in NKTL. Lastly, in-house generated ADC through conjugation of Cusatuzumab with MMAE via VC-PAB linker showed efficacious response in NKTL. As such, our work characterized plasma membrane landscape of NKTL and shed light on targets with potential to become novel treatments for this dreadful disease.

#4511 Dual targeting of IKKβ and NR4A1 for AML therapy.

Chandra Kumar Maharjan[1], Yi Liu[1], Yufeng Xiao[1], Bristy Podder[1], Tyler Montgomery[1], Lei Wang[2], Myung-Chul Kim[3], Zeng Jin[4], Seyedehalaleh Anvar[1], Alexandra Stevens[5], Ryan Kolb[1], Chen Zhao[6], Zhijian Qian[7], Jatinder K. Lamba[1], Guangrong Zheng[1], Weizhou Zhang[1]

[1]University of Florida, Gainesville, FL,[2]Genentech, South San Francisco, CA,[3]Kyungpook National University, Gainesville, Korea, Republic of,[4]University of Florida College of Medicine, Gainesville, FL,[5]Texas Children's Hospital, Houston, TX,[6]Case Western Reserve University, Cleveland, OH,[7]City of Hope Comprehensive Cancer Center, Monrovia, CA

Acute myeloid leukemia (AML) is a common aggressive blood cancer with a lethality rate among the highest of all leukemia subtypes. Cure rates of available therapeutic options are very low, underscoring an urgent need to develop more effective drugs. Here we identify IKKβ and NR4A1 as two closely related, clinically meaningful drivers of AML progression, and develop a proteolysis targeting chimera (PROTAC) drug that degrades both the proteins. IKKβ and the downstream NF-κB signaling are aberrantly activated in around 40% AML patients. However, IKKβ inhibitors exhibit serious side effects such as neutrophilia, limiting their therapeutic development. As opposed to the previously reported AML-suppressive role, we found that NR4A1 can also promote AML pathogenesis in different contexts. Moreover, IKKβ and NR4A1 were found to be highly expressed in AMLs associated with poor clinical outcomes, positively regulate each other's expression, and synergize to maintain AML cell viability. We designed, synthesized, and validated an array of celastrol-based PROTACs as celastrol binds to both IKKβ and NR4A1, and identified one lead PROTAC, A9, that effectively kills several AML cell lines and primary human AML cells. Mechanistically, A9-induced AML cell killing was found to be dependent on CRBN E3 ligase-mediated dual degradation of IKKβ and NR4A1. *In vivo*, A9 attenuated AML disease progression in a clinically relevant KMT2A::MLLT3 mouse model and didn't induce neutrophilia. Our results reveal a potentially novel strategy to treat intractable and aggressive AMLs in the clinic.

#4512 WASP activation by BM011 triggers mitochondrial collapse and aldolase-dependent glycolytic vulnerability in lymphoma.

Filippo Spriano[1], Luciano Cascione[1], Stephen Croke[2], Digvijay Gahtory[2], Maurits van den Nieuwboer[2], Francesco Bertoni[1]

[1]Institute of Oncology Research, Universita della Svizzera italiana, Bellinzona, Switzerland,[2]BIMINI Biotech B.V., Leiden, Netherlands

Background. BM011 is the first-in-class WASP (Wiskott-Aldrich Syndrome Protein) activator (Spriano et al, 2024). WASP regulates cytoskeletal remodeling, immune synapse formation, vesicle trafficking, and mechano-metabolic coupling. Aberrant actin dynamics and rewiring of the WASP pathway contribute to proliferation, metabolic flexibility, and stress resistance in lymphomas and other cancers. Here, we investigated the mechanism of action of BM011 by combining transcriptomics, proteomics, and a genome-wide CRISPR-Cas9 knockout screen in lymphoma cells treated with the compound.

Methods. JEKO1 mantle cell lymphoma cells were treated with BM011 for 8h and analyzed by RNA-Seq and mass spectrometry (MS). A genome-wide CRISPR-Cas9 knockout screen was conducted following 14-day exposure to BM011.

Results. Proteomics revealed a strong downregulation of mitochondrial import and respiratory chain proteins in BM011-treated cells, while many RNAs coding for the same molecules were upregulated, consistent with an attempt to compensate for mitochondrial stress. Similarly, ribosomal proteins decreased, while ribosomal transcripts increased, suggesting a proteotoxic stress response and a translational offset. Stress-response genes (e.g., HSPA family), cytoskeleton, and apoptotic pathways were strongly induced, indicating proteotoxic pressure, cytoskeleton remodeling, and apoptosis induction following cytoskeletal forcing. At the genetic screen, the loss of many mitochondrial respiratory chain genes sensitized cells to BM011, confirming their importance in mitigating BM011-induced mitochondrial collapse. In contrast, the knockout of FUNDC2 and TIMM23, not part of the mitochondrial respiratory chain, conferred resistance, likely due to the interruption of mitochondrial quality control and decreased apoptosis upon BM011 treatment. The genetic screen also revealed a divergent vulnerability to glycolysis. Knockout of genes coding for enzymes of the upper glycolytic process (HK2, PFKM, PFKL, GPI, PFKFB3) conferred resistance, while knockout of genes coding for proteins in the lower part of glycolysis (PGK1, ENO1, PKM, PFKFB4) increased sensitivity. This pointed to aldolase and the fructose-1,6-bisphosphate node as a critical metabolic point. Aldolase can indeed bind to F-actin and WASP, inhibiting actin polymerization. Additionally, an excess of fructose-1,6-bisphosphate (F16bP) inhibits aldolase binding to F-actin. We proved that F16bP supplementation or aldolase inhibition increased the sensitivity of BM011 in otherwise resistant lymphoma cells.

Conclusion. BM011-driven activation of WASP induces cytoskeletal stress, mitochondrial import failure, and a proteotoxic response, with upper-glycolysis and aldolase acting as a metabolic safety valve. These reveal druggable metabolic-cytoskeletal vulnerabilities in lymphoma.

#4513 Structural surface protein targets for AML.

James Dowell, Daniel Benjamin, Patric Sadecki, Jonathan Schmitz, Anjali Nelliat, Anna Ritter, **Neal C. Goodwin**

Immuto Scientific, Inc., Madison, WI

Background: Nearly all current antibody- or CAR-T-directed therapies in AML (e.g., CD33) target antigens that are also expressed (often at lower levels) on healthy hematopoietic stem/progenitor cells (HSPCs), causing dose-limiting myeloablation or prolonged cytopenias. Driven by this critical need for tumor-specific targets, we developed a deep learning approach that combines structural proteomics with multi-modal biological network integration and high-throughput protein complex structure prediction to predict potential targets based on predicted surface localization, changes in protein-protein interactions (PPIs), degree of conformational change, and estimated potential therapeutic relevance.
Methods: Protein tagging reagents were used to quantify changes in amino acid surface accessibility and solvent accessibility (SASA) via quantitative LC-MS/MS. Using this innovative approach, changes in the global structural surfaceome of NOMO-1 AML cells treated with all-trans retinoic acid (atRA) were compared with those of vehicle-treated cells. Peptides with significant SASA changes (FDR: $q < 0.05$; $\log_2$ fold-change > +/-1) were filtered using a surfaceome localization score, and conformational ensembles generated for this protein list were scored by a custom GNN-based structure encoder fine-tuned on surface proteomics data. Further, to identify PPIs with interface SASA changes, an all-by-all list of protein pairs was first fed to a graph attention-based module integrating multiple data modalities to retain high-confidence interactions, which were subsequently passed to AlphaFold-Multimer for complex structure prediction, and final target PPIs were predicted by a scoring function based on interface SASA.
Results: The global structural analysis identified 20,933 modified peptides from 3,540 proteins, of which 2,627 peptides from 1,089 proteins exhibited significant changes in SASA. These proteins and the corresponding 1089×1089 candidate PPIs were analyzed by our AI/ML pipeline to generate a final ranked list of potential structural targets, with the top candidates demonstrating high predicted affinity and specificity against AML. The data set achieved in the current study has successfully identified new surface targets in response to atRA treatment that are independent of atRA-RARA differentiation.
Conclusion: Our structural proteomics platform significantly broadens the potential druggable space in AML by identifying novel structural surface targets. The data set achieved in the current study has successfully identified new surface targets in response to multiple atRA-induced mechanisms. The top-ranked structural targets from this study are being evaluated as potential antibody-drug conjugates (ADCs)-based therapies for AML.

#4514 Development and validation of a CyTOF assay for measuring phosphoproteins in AML blast cell populations in whole blood from AML patients.

Steven R. Pirie-Shepherd[1], Crystal Tarrago[2], Wenxin Zheng[3], **Sen Zhang**[3], Hamish Wright[2]

[1]Schrodinger, San Diego, CA,[2]Schrodinger, New York City, NY,[3]Schrodinger, Cambridge, MA

CDC7 (Cell Division Cycle 7-related protein kinase), also known as DBF4-dependent kinase (DDK), is a critical serine/threonine cell cycle protein kinase indispensable for maintaining DNA replication fork progression and stability, particularly under conditions of replication stress. CDC7 activates fork protection and restart mechanisms, including the phosphorylation and activation of MCM2 (Minichromosome Maintenance protein 2) at Ser40. Inhibition of CDC7 disrupts the capacity of cancer cells to ameliorate replication stress and repair DNA damage, leading to the accumulation of DNA damage, incomplete DNA replication, apoptosis, and cellular demise. Consequently, CDC7 represents a promising therapeutic target in cancer, especially for hematologic malignancies such as acute myeloid leukemia (AML).

Given that pMCM2 (phosphorylated MCM2) serves as a biomarker of CDC7 inhibition, the development of a CyTOF assay to quantify pMCM2 and gH2AX (a downstream marker of dsDNA damage) in cells holds significant utility in clinical trials evaluating CDC7 inhibitors. Precise measurement of these phosphoproteins in whole blood AML blast cells for example is expected to provide insights into a drug's mechanism of action and its efficacy in AML patients.

We present the development and validation of a cytometry by time-of-flight (CyTOF) assay designed to measure pMCM2 and gH2AX in blast cell populations prevalent in AML patients and comparing a one step fixation process and a two-step fixation process. Initial investigations demonstrated the feasibility of characterizing the phenotype of AML blast cells using cell surface markers such as CD34, HLADR, CD33, and CD123, as well as assessing the cellular state with respect to the presence or absence of pMCM2 and gH2AX, and quantifying changes in Median Channel Value (MCV) in response to proliferation stimulators or inhibitors. We further detail the development and validation of the assay, along with an assessment of the comparability between a one-step PROT-1 fixation process versus two-step SLST (Stable Lyse Stable Store) fixation process. The finalized assay utilizing the SLST fixation process could facilitate the monitoring of treatment response and the identification of potential biomarkers in clinical trials, which could have utility in investigating disruptions to the DNA damage response (DDR) in blood cancers.

(AI was used to refine the text of this abstract)

#4515 Clinically relevant AML modeling with *in vitro* bone marrow niche and *in vivo* PDX approaches.

Talita Stessuk, Hanna Vermeer, Afsaneh Golestani, Jolie Flach, Jessie Wang, Qingzhi Liu, Jinping Liu, Gera Goverse, Marrit Putker, Ludovic Bourre

Crown Bioscience, Inc., San Diego, CA

Introduction Acute Myeloid Leukemia (AML) remains therapeutically challenging due to various genetic alterations, drug resistance, and relapse at the clinical stage. Preclinical evaluation is therefore critical to identify effective novel therapeutic strategies. Optimal ex vivo growth and in vivo engraftment of primary AML cells are challenging, and current preclinical screening of oncology drugs is often compromised by the lack of advanced models that mimic therapeutical response in the native human bone marrow niche (BMN). To address this challenge, we present the integration of our 3D BMN in vitro platform composed of hematopoietic cells cultured on the perivascular site to capture response and resistance patterns with in vivo AML Patient Derived Xenograft (PDX) models, giving translational preclinical insights for therapy development. Methods Three AML PDX models were systemically engrafted in immunodeficient mice and exposed to standard of care (SoC) drug panels containing FLT3 and IDH inhibitors, as well as classical chemotherapy. Endpoint readouts included survival, clinical signs, and peripheral leukemic burden by flow cytometry (blood, bone marrow, spleen). In parallel, human CD45+ cells from the same AML PDX models were integrated in 3D mesenchymal-endothelial networks (BMN platform) and exposed to SoC and targeted drug panels for 10 days. Quantitative assessment of the in vitro drug effects was performed using a proprietary automated high content imaging (HCI) analysis platform. Immunofluorescence (IF) staining, NSG, cytogenetics, and flow cytometry were used for in-depth characterization of AML PDX. Results Engraftment of AML PDX (AM9626, AM9627, and AM9628) cells into mice was validated upon evaluation of leukemia signs, immunophenotypic profiling, and histopathology. Tumor burden growth (% of hCD45+) assessment across AML PDX models harboring FLT3 and IDH1 mutations revealed sensitivity and resistance patterns to targeted inhibitors and SoC agents. HCI analysis showed decreased AML PDX cell counts at the highest doses of FLT3 and IDH1 inhibitors in comparison to the control in the BMN platform, identifying different drug sensitivities across the PDX models upon support and protection provided by human mesenchymal and endothelial cells. Conclusion Here, we present a combination of advanced, patient-relevant preclinical platforms that offer valuable information on how a drug performs under divergent conditions. The in vivo AML PDX system recapitulates disease progression and enables systemic pharmacokinetic and pharmacodynamic assessment. In parallel, the in vitro BMN platform provides a quantitative measurement of treatment response in leukemia cells attached to the perivascular site. These findings underscore the utility of integrating in vitro and in vivo preclinical models to support AML therapeutic development and prioritize compounds for clinical translation.

#4517 Triamterene inhibits NRF2^{Mut} as a molecular glue.

Yahui Li[1], Zachary Ladd[2], Haining Wang[3], Candice Bui-Linh[4], Boopathi Subramaniyan[1], Chorlada Paiboonrungruang[4], Huan Li[1], Yan Ma[1], Kiera Chang[1], Katherine Gao[1], Maiya Ang[1], Francis Spitz[1], Zhaohui Xiong[4], Xiaoxin Luke Chen[1]

[1]Cooper University Health Care, Camden, NJ,[2]Cooper Medical School of Rowan University, Camden, NJ,[3]Insilico Medicine Canada Inc, Montreal, QC, Canada,[4]Coriell Institute for Medical Research, Camden, NJ

Background: NFE2-like bZIP transcription factor 2 (NRF2, encoded by *NFE2L2*) is a master regulator of the oxidative stress response. Under normal conditions, NRF2 is ubiquitinated and degraded via the proteasome following its interaction with Kelch-like ECH-associated protein 1 (KEAP1). Persistent activation of NRF2, commonly caused by gain-of-function *NFE2L2* or loss-of-function *KEAP1* mutations, is frequently observed in human esophageal squamous cell carcinoma (ESCC) and contributes to tumor progression and therapeutic resistance, underscoring the urgent need for effective therapeutic strategies against NRF2-addicted ESCC. Despite its importance, targeting NRF2 pharmacologically has proven challenging, as it is considered an 'undruggable' target due to its function as a transcription factor lacking classical enzymatic pockets or well-defined ligand-binding sites. In a previous high-throughput NRF2 reporter screen, we identified triamterene (TRM), an FDA-approved potassium-sparing diuretic, as a potential NRF2 inhibitor. The effects of TRM on NRF2 expression were validated by Western blot in two NRF2^{Mut} ESCC cell lines (KYSE70 and TE14). This study is aimed at understanding its efficacy *in vivo* and its mechanisms of action.

Methods: *In vivo* efficacy of TRM was evaluated using both a genetically engineered mouse model (GEMM) and a cell line-derived xenograft (CDX) model. Mechanistic studies including biochemical assays (ubiquitination and proximity ligation assay [PLA]) and biophysical analyses (isothermal titration calorimetry [ITC], surface plasmon resonance [SPR], hydrogen-deuterium exchange mass spectrometry [HDX-MS], and molecular docking), were conducted to elucidate the mechanism of action of TRM.

Results: TRM significantly suppressed tumor growth and NRF2 signaling in the NRF2^{W24C} ESCC CDX and the NRF2^{D29H} GEMM model. Mechanistically, TRM shortened the half-life of NRF2^{W24C} by promoting KEAP1-dependent ubiquitination and degradation. PLA confirmed enhanced KEAP1-NRF2^{W24C} interaction both *in vitro* and *in vivo* following TRM treatment. ITC demonstrated high-affinity binding between TRM and human recombinant KEAP1 (Kd = 0.975 μM). SPR analysis revealed that TRM enhanced the interaction between the DLG^{W24C} peptide and the Kelch domain, but not between DLG^{WT} and Kelch. HDX-MS identified two TRM-binding sites on KEAP1, including residues 397-417, consistent with molecular docking predictions implicating Arg^{415} as a critical residue for TRM binding.

Conclusion: TRM selectively inhibits NRF2^{Mut} ESCC by restoring KEAP1-mediated NRF2 degradation through direct binding to the Kelch domain of KEAP1. These findings support TRM as a promising therapeutic candidate for NRF2-addicted cancers. Ongoing studies aim to further define the structural basis of TRM-KEAP1 interaction and its role in modulating NRF2 stability and signaling.

#4518 Preclinical assessment of BT5528 anti-tumor activity in patient-derived xenograft (PDX) models of pancreatic ductal adenocarcinoma (PDAC).

Lukas Stanczuk[1], Assunta De Rienzo[2], Gavin Bennett[1]

[1]BicycleTx Ltd, Cambridge, United Kingdom,[2]BicycleTx Ltd, Cambridge, MA

Background: Erythropoietin-producing hepatocellular receptor A2 (EphA2) is a receptor tyrosine kinase critical for cell development; it is highly expressed in a range of solid tumors, and its expression correlates with higher grade, later stage disease, and poor prognosis. There is high unmet need for patients with EphA2-expressing tumors, including pancreatic cancer, which has one of the highest EphA2 expression levels across solid tumors. BT5528 is a Bicycle® Drug Conjugate (BDC®), comprising a highly selective EphA2-targeting bicyclic peptide conjugated to the cytotoxin MMAE via a stable valine-citrulline cleavable linker. BT5528 has low molecular weight (4.4 kDa), enabling rapid and efficient delivery of the BDC® to the tumor and subsequent payload release, with minimal systemic exposure to the conjugate. Here we evaluate EphA2 expression and antitumor activity of BT5528 in murine PDX models of PDAC.
Methods: Cohorts of female NOD SCID gamma (NSG) mice were used to generate 16 PDAC PDX models by subcutaneous implantation of patient-derived PDAC tumors into the left abdominal flank. Flash frozen paraffin embedded tumor samples from vehicle treated mice were used to assess EphA2 expression by immunohistochemistry (IHC); Tumor Proportion Score (TPS) was calculated as the number of membrane EphA2+ cells/total number of viable tumor cells x 100. Tumor-bearing mice were treated once weekly for 4 weeks with either vehicle control or BT5528 (3 mg/kg IV). Tumor growth was monitored by caliper measurements and tumor volume was calculated as $[(\text{width})^2 \times \text{length}]/2$. Tumor growth inhibition (TGI) was estimated for each treatment group per model using the average response across replicates after 4 weeks.Results: Of 16 PDAC PDX models tested, all 16 displayed some degree of EphA2 membrane staining, with 16/16 considered positive (TPS ≥1%), including models JH029 (20%), Panc163 (30%), and Panc421 (90%). Fourteen of 16 PDAC PDX models were assessed for antitumor activity. Six of 14 models showed high sensitivity to BT5528 (TGI ≥100%), including JH029 (157%), Panc163 (114%), and Panc421 (110%), with most models showing some level of sensitivity to BT5528 (only 3/14 had TGI <50%). Anti-tumor activity of BT5528 was not affected by the extent of desmoplasia, with TGI scores roughly equivalent across mature, intermediate, and immature tumor models. No increase in response was seen with increasing membrane EphA2 TPS.
Conclusions: Expression of EphA2 was found in all PDAC PDX models. Most models were sensitive to BT5528 treatment, which was not affected by the degree of desmoplasia or membrane EphA2 TPS. These results may reflect a lack of truly EphA2-negative models in this analysis. These data support the potential for BT5528 to offer a novel option for the treatment of PDAC.

#4519 FS-207: A potential best-in-class WRN helicase inhibitor for treating MSI-H cancers.

Bin Li, Cai Wu, Yaqian Liu, Linsen Li, Yan Ma, Dongbo Li

Foresight Therapeutics Co., Ltd., Hefei, China

Microsatellite instability-high (MSI-H) cancers, characterized by impaired DNA mismatch repair (MMR), are vulnerable to synthetic lethal targeting of Werner Syndrome RecQ helicase (WRN). Although PD-1 inhibitors are the standard treatment for MSI-H tumors, their response rate is around 40%-60%, with many patients eventually developing resistance and relapse. WRN inhibition offers a promising alternative therapeutic strategy, potentially overcoming resistance to PD-1 inhibitors. We discovered FS-207, a potent and selective small-molecule inhibitor of WRN helicase, using Foresight Therapeutics' multimodal drug discovery platform. FS-207 demonstrates low nanomolar potency in inhibiting WRN helicase/ATPase activity and exhibits over 1000-fold selectivity against other RecQ helicases. Inhibition of WRN by FS-207 induces chromosomal structure aberrances, leading to selective killing of MSI-H cancer cells via the DNA damage response pathway. FS-207 is well tolerated, with excellent pharmacokinetic properties. Its potent inhibition of WRN helicase, combined with favorable oral bioavailability, translates into robust and durable efficacy in MSI-H cancer cell line derived (CDX) and patient-derived (PDX) xenograft models. Notably, tumor regression was observed in mice dosed at 5 mg/kg or higher in these models. Study results, including efficacy and pharmacodynamic responses, will be presented. Our findings position FS-207 as a promising, potentially best-in-class WRN helicase inhibitor for the treatment of MSI-H cancers, owing to its superior efficacy, durability, and selectivity. FS-207 is poised to enter clinical trials in 2026.

#4520 Development of terfenadine-derived small-molecule inhibitors of TFE3-O dimerization for translocation renal cell carcinoma.

Christian Migliarese[1], Mohd Abdullaha[1], Ilaria Delle Fontane[2], David E. Heppner[3], Roberto Pili[4]

[1]University at Buffalo SUNY, Buffalo, NY,[2]University of Lausanne, Lausanne, Switzerland,[3]University at Buffalo, Department of Chemistry, Buffalo, NY,[4]University at Buffalo, Buffalo, NY

Translocation renal cell carcinoma (tRCC) is an aggressive kidney cancer subtype with poor clinical outcome and no effective standard therapies. It is characterized by gene fusions involving members of the MiT transcription factor family, most commonly TFE3 fused to various partner genes. Work from our laboratory has previously identified the antihistamine terfenadine as a promising compound capable of inhibiting TFE3 dimerization, highlighting dimerization as a targetable mechanism in tRCC. These findings suggest that disrupting TFE3 fusion protein dimerization may enhance therapeutic response and could be leveraged in combination with existing treatment options, including tyrosine kinase inhibitors (TKIs).

The purpose of this study was to optimize terfenadine-derived tool compounds and identify novel small molecules that enhance its antiproliferative activity while reducing terfenadine well-known long QT associated cardiotoxicity. We aimed to determine whether these derivatives selectively inhibit dimerization of TFE3 fusion proteins and improve activity against tRCC diminishing hERG interaction and cardiotoxicity. Two series of terfenadine analogs based on chemical structure modifications were synthesized to evaluate groups specific functional contribution. All compounds were purified and structurally verified by NMR, LTQ mass spectrometry, and HPLC. Their antiproliferative activity was assessed in tRCC cell lines harboring distinct TFE3 fusions (R07: SPFQ-TFE3; UOK-109: NONO-TFE3; UOK-146: PRCC-TFE3). FRET-based assays are being established to measure inhibition of TFE3/TFE3-O dimerization, and hERG activity monitored.

Several newly synthesized compounds, in particular two leading candidates exhibited improved antiproliferative effects (IC_{50}s ~2 µM) as compared to terfenadine (IC_{50}s ~7 µM). These results provide a foundation for further structural refinement and assessment of pharmacological properties with modifications also aiming to reduce its cardiotoxic effect. Combination studies with TKIs demonstrated that co-treatment with terfenadine significantly reduced IC50 values relative to monotherapy, as confirmed by Combination Index analysis. This supports the hypothesis that inhibiting TFE3 fusion protein dimerization enhances drug response to TKIs, potentially by reducing drug sequestration in the lysosome.

In conclusion, this work identifies terfenadine derivatives with improved antiproliferative potential and reduced predicted cardiotoxicity, and highlights TFE3 dimerization as a therapeutically targetable mechanism that may help overcome drug resistance in tRCC.

#4521 Use of a p120 RasGAP glue to inhibit KRas in NF1-null cells.

Anastasiia Gerasimova[1], Sven Miller[1], Jonathan Chernoff[2]

[1]Fox Chase Cancer Center, Philadelphia, PA,[2]Fox Chase Cancer Center, Jenkintown, PA

Neurofibromatosis type 1 (NF1) is an autosomal dominant genetic disorder that is associated with a spectrum of pathologies including glioma, autism spectrum disorder, Lisch nodules of the iris and neurofibroma. The *NF1* gene encodes neurofibromin, a Ras GTPase-activating protein. Deletion or disabling mutations in *NF1* gene result in an absence of neurofibromin and sustained Ras activation, driving uncontrolled cell proliferation and tumorigenesis. Targeting the Ras protein directly has until recently proved challenging due to the lack of binding cavities on molecular surface and due to its high affinity for GTP/GDP.

Purpose: Our study aims to evaluate the efficacy of novel molecular glues designed to modulate Ras activity by increasing its binding to p120RasGAP, a ubiquitously expressed negative regulator of Ras that, like NF1, augments the GTPase activity of Ras, assisting its conversion from active Ras-GTP to inactive, Ras-GDP. The goal is to use these compounds to enable p120RasGAP to functionally replace neurofibromin in *NF1*-deficient cells, restoring normal Ras signaling.

Methods: We used an artificial intelligence/machine learning (AI/ML) protocol to identify potential molecular glues that should stabilize the p120RasGAP/Ras complex. To assess the impact of these compounds, we used NF1-deficient cell line and employed Western Blot analysis to measure changes in phosphorylated ERK (p-ERK) levels as a downstream marker of Ras activity. In addition, we used shRNA-mediated knockdown of the RASA1 gene, which encodes p120RasGAP protein, to verify whether the observed effects are dependent on the proposed Ras/RasGAP interaction mechanism. To assess direct interaction, purified recombinant KRAS and p120RasGAP were used in AlphaScreen binding assay. Compound binding was further validated by surface plasmon resonance (SPR).

Results: Preliminary data indicate a reduction in p-ERK levels upon treatment with novel compounds, suggesting partial suppression of Ras signaling. Furthermore, in p120RasGAP knockdown cells, the molecular glues had a less potent effect in reducing p-ERK levels, suggesting that our compounds act through the proposed mechanism rather than producing off-target effects. Of the three most perspective candidates, one promoted significant binding of KRAS to p120RasGAP in an AlphaScreen assay. This result was also confirmed by SPR.

Conclusion: AL/ML methods can be used to design molecular glues that stabilize the interaction of p120RasGAP to Ras, providing a promising avenue for targeted NF1 therapies. Such compounds might be useful in reducing Ras activity in NF1-mutant cells. We aim to further characterize this interaction using STD NMR and initiate crystallization trials to determine the structural basis of binding.

#4522 Advancing protein engineering through AcroAIxTM: AI-driven strategies for enhanced structure and function optimization.

Spencer Chiang[1], Jane Liu[1], **Lisa Chou**[2], An Ouyang[2], Lili Qin[1]

[1]ACROBiosystems Co., Ltd., Beijing, China,[2]ACROBiosystems Inc., Newark, DE

Recombinant proteins are indispensable tools in biomanufacturing, underpinning drug development and manufacturing processes ranging from biologics to cell therapies. Cellular pathways are driven by the modulation of varying signaling pathways comprising of numerous proteins and membrane receptors. However, reproducing certain proteins ex vivo poses a significant challenge, especially when the tertiary and quaternary structure are complex. This results in a protein that suffers from limited stability, short half-life, and inconsistent bioactivity which further restricts reproducibility, production costs, and poses a significant barrier to scalable manufacturing. In many cases, traditional protein engineering strategies, while valuable, are constrained by experimental throughput and limited predictive accuracy. To overcome this challenge, AcroAIxTM is an artificial intelligence-driven protein design platform that integrates structural modeling, machine learning, and sequence-function prediction to systematically generate high-performing protein variants. By optimizing key biophysical parameters, AcroAIxTM enables the rational enhancement of recombinant proteins for improved conformational stability, functional half-life, and binding efficiency. These advances are particularly impactful in cell culture applications, where growth factors such as interleukin-21 (IL-21) and fibroblast growth factor 2 (FGF-basic) are essential. Heat-stable forms of IL-21 and FGF-basic were developed to maintain their bioactivity and half-life in 37ºC media for 3 days. The resulting cytokine remains active for a longer period and improves cell counts significantly under a reduced-feeding protocol compared to wild types. As such, engineering variants with enhanced stability and bioactivity can directly improves culture robustness, reduce factor replenishment requirements, and increase the efficiency of cell-based manufacturing workflows. By bridging computational design with experimental validation, the AcroAIxTM platform establishes a transformative framework for recombinant protein innovation, advancing both general biomanufacturing practices and cell culture-driven therapeutic production.

#4524 LDHA-positive neutrophils drive Treg-mediated immune tolerance to promote resistance to pan-RAS inhibitors in pancreatic cancer.

Xiangyan Jiang[1], Xiaoe He[1], Wen Wei[1], Qichen He[1], Lei Shi[2], **Zuoyi Jiao**[1]

[1]Lanzhou University, Lanzhou, China,[2]Cancer Research UK Manchester Institute, Manchester

KRAS is the most common and critical oncogenic mutation in pancreatic cancer, with a mutation rate exceeding 90%. The pan-RAS inhibitor RMC-6236 (Daraxonrasib) has shown promising progress in clinical trials and has been designated as a breakthrough therapy by the FDA. However, resistance to RAS-targeted drugs is inevitable. Here, we collected tumor tissues from KPC mice treated with the pan-RAS inhibitor RMC-6236, both at the time of tumor shrinkage and after the development of acquired resistance, and performed single-cell sequencing. We found that regulatory T cells (Tregs) decreased after treatment but increased after resistance. Similarly, myeloid immune cells exhibited similar subpopulation changes in both treated and acquired resistant states, with LDHA-positive tumor-associated neutrophils (TANs) significantly reduced after RMC-6236 treatment, but replenished after the development of acquired resistance. Mechanistically, LDHA-positive neutrophils upregulate PD-L1 expression via STAT3 signaling and NETs, and promote the immune suppressive effect of Tregs through PD-L1/PD-1 interactions. Additionally, the ablation of LDHA in neutrophils combined with RMC-6236 significantly inhibited tumor growth in KPC mice and restored pancreatic cancer sensitivity to RMC-6236. In conclusion, this study reveals the tumor microenvironment regulatory mechanisms underlying resistance to pan-RAS inhibitor RMC-6236 and proposes a promising strategy for overcoming RAS inhibitor resistance.

#4525 Potential of Rac and Cdc42 inhibitors as pancreatic cancer therapeutics.

Anamaris Torres-Sanchez, Ailed Cruz-Collazo, Nilmary Grafals, Stephanie Dorta-Estremera, Suranganie Dharmawardhane Flanagan

Biochemistry, University of Puerto Rico Medical Sciences Campus, San Juan, PR

Pancreatic ductal adenocarcinoma (PDAC) remains one of the deadliest forms of cancer, with a distinct extracellular matrix and immunosuppressive tumor microenvironment. Existing chemotherapies are hampered by toxicity and demonstrate poor clinical response. Therapies targeting the KRAS G12D mutation, prevalent in pancreatic cancer, have yet to receive FDA approval. Therefore, there is a critical need for novel targeted therapies for PDAC. These therapies should simultaneously target metastatic cancer cells and immunosuppressive cells such as tumor-associated macrophages (TAMS), since they promote pancreatic cancer progression. Ras-activated related GTPases Rac and Cdc42 are ideal targets for pancreatic cancer therapy because they regulate migration, invasion, polarity, viability, and survival in cancer cells and immune cells. Therefore, we developed Rac and Cdc42 inhibitors for metastatic diseases such as PDAC to target cancer and its immunosuppressive environment. The hypothesis tested in this study is that Rac/Cdc42 inhibitors will simultaneously target the migration and activity of cancer cells and macrophage-like cells in the TME. We assessed the potential of the dual Rac and Cdc42 inhibitors MBQ-167 and MBQ-168, which block guanine nucleotide association with Rac and Cdc42. The effects of vehicle, MBQ-167 or MBQ-168 were tested in human and mouse PDAC cells or macrophages by performing pulldown assays for Rac and Cdc42 activation, MTT assays for cell viability, wound-healing assays for cell migration, phagocytosis, as well as co-culture assays with PDAC cells and macrophages. Results demonstrated that Rac and Cdc42 inhibitors significantly reduced active Rac and Cdc42 in pancreatic and macrophage cells. Both MBQ-167 and MBQ-168 reduced pancreatic cancer cell viability, without affecting macrophage viability, and inhibited cell morphology and migration. In co-culture using Transwells, MBQ-167 and MBQ-168 decreased pancreatic cancer cell migration from the top wells, with macrophages in the bottom wells, and reduced inflammatory mediators such as IL-6, CHI3L1 and S100A8 and S100A9 levels in conditioned media. A preliminary study was also conducted in C57BL6 mice bearing orthotopic KPC (KRas G12D, p53 null, Cre) tumors to test the effect of vehicle or 10mg MBQ-167 administered by IP 5X a week for 21 days. MBQ-167 treatment decreased tumor growth and increased survival compared to vehicle treatments. In conclusion, MBQ-167 and MBQ-168 pose as potential therapeutics for PDAC due to their ability to target both pancreatic and macrophage-like cells.

#4526 Activation of the RXR nuclear receptor improves survival and the therapeutic window of immunotherapy in murine breast cancer.

Ana S. Leal

Division of Hematology and Oncology, Indiana University School of Medicine, Indianapolis, IN

The retinoid X receptor (RXR) is a member of the nuclear receptor superfamily of ligand-dependent transcription factors. Bexarotene, the only approved RXR agonist, is used in refractory cutaneous T cell lymphoma but lacks effect on solid tumors. Based on structure-activity-relationships (SAR) we selected MSU42011, as a more potent and specific RXR agonist.Treatment with the RXR agonist MSU42011 (300 mg/Kg diet) reduced tumor burden and increased survival in a MMTV-Neu murine model of HER2+ breast cancer (p=0.01, 55 days vs 62 days median survival, respectively). HER2 breast cancer patients have not benefited from the approval of immunotherapy. However, HER2 positive stomach cancer patients see benefit when treated with anti-PD1, which is now approved for clinical use. We previously shown that MSU42011 can be combined with immunotherapy in a lung cancer murine model, therefore we tested the combination of MSU42011 with anti-PD1 in MMTV-Neu mice. The combination of MSU42011+anti-PD1 significantly (median survival 69 days) increases survival when compared with mice that receive either only control (p=0.008) or anti-PD1 (p= 0.05, median survival 53 days). No obvious side effects were observed in either anti-PD1 alone or in combination with MSU42011 groups. MMTV-Neu mice were treated as above and euthanized at 40 days after treatment initiation for tumor immunophenotyping. Mice receiving MSU42011 or MSU42011+anti-PD1 showed a significant reduction in the expression of CD206 and PDL-1, two immunosuppressive molecules, in inflammatory (p=0.03) and resident (p=0.05, p=0.005) monocytes. CD11c (p=0.04) and CD11b (p=0.03) tumor associated macrophages (TAMs) had a significant reduction in PDL-1 expression in both MSU42011 and MSU42011+anti-PD1 groups. The reduction in the immunosuppressive CD206 and PDL-1 expression in the myeloid lineage, was associated with a significant increase in the infiltration of CD8 T cells (p=0.01), as well as in the activation markers of CD8 T cells (CD44, p=0.05; CD69, p=0.007).In the highly aggressive MMTV-PyMT murine model of triple negative breast cancer (TNBC), MSU42011 treatment significantly (p= 0.001) prolonged survival (median 39 vs 49 days). Flow cytometry of tumors at 28 days of treatment showed a decreased number of TAMs (36.6% vs 20.2%) and an increased number of CD8 T cells (3.4% vs 5.9%). Moreover at this time point only 1 of 10 mice had visible lung metastasis in the MSU42011 group compared with control where 4 of 10 mice had lung metastasis, additionally, one mouse that had a bone metastasis. In conclusion, MSU42011 increased recruitment and activation of CD8 T cells and a decrease of tumor promoting myeloid cells in both HER2+ and TNBC murine mammary tumors. These data, in combination with our previous work shows that the RXR agonist MSU42011 reduces tumor growth by modulating the tumor microenvironment and can safely be combined with anti-PD1.

#4528 The basal cell-derived matricellular protein SPON2 suppresses luminal cell oxidative phosphorylation and cancer progression by blocking the SLC38A1/mTOR metabolic axis.
Pengfei (Paul) Lu

University of South China, Hengyang, Hunan, China

Tumor resistance, largely driven by cellular heterogeneity and complex interactions within the tumor microenvironment (TME), remains a central challenge in oncology. In breast cancer, the crosstalk between basal-like cancer stem cells (bCSCs) and luminal niche cells is hypothesized to be a critical driver of therapy resistance, yet the underlying molecular mechanisms are poorly defined. Here, we identify and characterize SPON2, a matricellular protein secreted by basal cells, as a master regulator of luminal cell metabolism and function. Mechanistically, SPON2 directly binds to the amino acid transporter SLC38A1 on luminal cells, thereby blocking the glutamine-leucine exchange and consequently suppressing PI3K-AKT-mTOR signaling. This inhibition leads to a profound reduction in oxidative phosphorylation (OXPHOS) and energy metabolism in luminal cells. Phenotypically, *Spon2*-knockout mice exhibit aberrantly increased and accelerated mammary ductal branching. Conversely, SPON2 overexpression in vitro potently inhibits organoid formation, branching morphogenesis, and epithelial proliferation. Crucially, SPON2 exerts potent tumor-suppressive effects across multiple breast cancer subtypes, including Luminal A and triple-negative breast cancer (TNBC). Our findings establish SPON2 as a basal-derived paracrine signal that is essential for maintaining metabolic homeostasis in the mammary gland and the TME. This work unveils the SPON2-SLC38A1-mTOR axis as a fundamental pathway of metabolic communication between cell populations, providing a novel conceptual framework for understanding breast cancer heterogeneity and a promising therapeutic target for overcoming drug resistance.

#4529 Antibody-drug conjugates for the treatment of hematologic malignancies.

Priya Hays

Hays Documentation Specialists LLC, San Mateo, CA

Belantamab mafodotin is composed of a monoclonal antibody targeting BCMA and is conjugated to the cytotoxic payload monomethyl auristatin F (MMAF), a microtubule disrupting agent, and is approved for multiple myeloma. Its efficacy was evaluated in DREAMM-7, an open-label, randomized trial in adults with R/R multiple myeloma with at least one prior therapy. The mPFS was 31.3 months (95% CI: 23.5, NR) in the BVd arm and 10.4 months (95% CI: 7, 13.4) in the DVd arm (HR 0.31, 95% CI: 0.21, 0.47). The mOS was NR and 35.7 months (95% CI: 21.1, NR) in respective arms (HR 0.49, 95% CI: 0.32, 0.76). Gemtuzumab oxogamicin targets the CD33 receptor on myeloid cells and is approved for AML. Its approval in combination with CT for adults was based on ALFA-0701, a multicenter, randomized, open-label phase 3 study of 271 patients with newly-diagnosed, de novo AML. The second trial, MyloFrance-1, a phase 2, single-arm, open-label study, included 57 patients with CD33-positive AML in first relapse. Fifteen (26%; 95% CI: 16% - 40%) patients achieved CR following a single course of gemtuzumab ozogamicin. Inotuzumab ozogamicin targets the CD22 receptor on B-cell precursor leukemic cells and is approved for ALL in pediatric patients with R/R CD22-positive B-cell precursor ALL. Efficacy was evaluated in a multicenter, single-arm, open-label study and the main efficacy outcome measures were complete remission (CR), duration of CR, and the proportion of patients with MRD negative CR. CR was defined as < 5% blasts in the bone marrow and the absence of peripheral blood leukemia blasts, full recovery of peripheral blood counts and resolution of any extramedullary disease. MRD was defined by leukemic cells comprising < 1 × 10-4 (<0.01%) of bone marrow nucleated cells. 22/53 (42%, 95% CI: 28.1, 55.9%) achieved CR and the median duration of CR was 8.2 months (95% CI: 2.6, NE). The MRD negativity rate in patients with CR was 21/22 [95.5% (95% CI: 77.2, 99.9)] based on flow cytometry, and 19/22 [86.4% (95% CI: 65.1, 97.1] based on RQ-PCR. Brentuximab vedotin is composed of a monoclonal antibody targeting the CD20 antigen and conjugated to microtubule disrupting agent monomethyl auristatin, which serves as the payload, for chronic Hodgkin's lymphoma. Approval was based on ECHELON-3, a randomized, double-blind, placebo-controlled trial enrolling 230 adult patients with R/R LBCL who were ineligible to receive an auto-HSCT or CAR T-cell therapy. The major efficacy outcome measure was OS. Additional efficacy outcome measures included PFS and ORR. The trial demonstrated a statistically significant improvement in OS, PFS and ORR. mOS of 13.8 months (95% CI: 10.3, 18.8) in the BV+R2 arm and 8.5 months (95% CI: 5.4, 11.7) in the Pbo+R2 arm (HR 0.63, 95% CI: 0.45, 0.89) were shown. mPFS was 4.2 months (95% CI: 2.9, 7.1) with BV+R2 and 2.6 months (95% CI: 1.4, 3.1) with Pbo+R2 (HR 0.53, 95% CI: 0.38, 0.73). The ORR was 64.3% (95% CI: 54.7, 73.1) and 41.5% (95% CI: 32.5, 51.0), respectively.

#4530 Synergistic targeting of Mediator complex and BCL-2 reveals a novel therapeutic strategy for acute myeloid leukemia.

Camille Aitchedji[1], Celine Moison[1], Deanne Gracias[1], Rodrigo Mendoza-Sanchez[2], Simon Fortier[1], Jean-Francois Spinella[1], Tara Macrae[1], Nadine Mayotte[1], Melanie Frechette[1], Valerie Blouin-Chagnon[1], Koryne Leveille[1], Rejean Ruel[2], Anne Marinier[2], Guy Sauvageau[1], Josee Hebert[3]

[1]Molecular Genetics of Stem Cells Research Unit, Institute for Research in Immunology and Cancer (IRIC), Montreal, QC, Canada,[2]Drug Discovery Unit, Institute for Research in Immunology and Cancer (IRIC), Montreal, QC, Canada,[3]Division of Hematology-Oncology and Leukemia Cell Bank of Quebec, Hopital Maisonneuve-Rosemont, Montreal, QC, Canada

Background: Acute myeloid leukemia (AML) is a heterogeneous and aggressive hematologic malignancy characterized by the uncontrolled proliferation of myeloid stem and progenitor cells. Despite therapeutic advances, the 5-year survival rate remains low, underscoring the urgent need for novel therapeutic strategies.
Methods: To meet this need and identify new anti-leukemic agents, we conducted a high-throughput cell viability screen of 10,000 small molecules using 56 different primary AML specimens of diverse genetic anomalies. Molecules showing highly correlated inhibition profiles were grouped into 21 compound correlation clusters (CCCs). The overall hypothesis was that compounds sharing highly correlated inhibition profiles most likely act on the same biological pathway / molecular target. Among the various CCC identified, CCC163, which include compound AML874, emerged as a potent and selective anti-leukemic hit.
Results: Integrated pharmacological and CRISPR-Cas9 screening revealed the Mediator complex as the molecular target of AML874. Mechanistic studies confirmed that AML874 inhibits Mediator complex function through CDK8/CDK19 kinase inhibition, leading to transcriptional dysregulation and loss of Mediator structural integrity. Kinase-dead CDK8 rescue assays confirmed that AML874 activity depends on CDK8 kinase function. Notably, FLT3-mutated AML primary specimens exhibited increased sensitivity to AML874, indicating a potential subtype-specific therapeutic opportunity. Structure-activity relationship profiling of AML874 analogs further supported the dependency on Mediator complex disruption for anti-leukemic activity. Finally, combination studies demonstrated strong synergy between AML874 and the BCL2 inhibitor venetoclax both in vitro and in vivo, resulting in markedly improved anti-leukemic activity in xenograft models.
Conclusions: This work identifies the Mediator complex as a novel vulnerability in AML and positions CDK8/CDK19 inhibition, alone or in combination with Venetoclax, as a promising strategy for the development of next-generation targeted therapies for this disease.

: Next-Generation Targeted Therapies Directed Against Tumor Surface Antigens
Poster Session

#4533 Discovery and characterization of CARs against novel, highly selective solid tumor targets identified using the Oncolinkage platform.

McKensie Collins, Benjamin Hallisey, Andrew Astley, Murray O. Robinson

Rubik Therapeutics, Cambridge, MA

CAR T cell therapy has demonstrated remarkable efficacy in treating hematologic malignancies. However, these therapies have been largely unsuccessful in solid tumors, which account for approximately 90% of cancer diagnoses. A critical obstacle to developing CAR T cell therapies for solid tumors is the lack of surface-expressed targets that are selectively present on tumors and not healthy tissues. Identification of tumor-restricted targets is essential to avoid on-target, off-tumor toxicity, which has proven therapeutically limiting for several CAR T therapies, including anti-PSMA and MSLN CARs. To address this challenge, we developed Oncolinkage, a computational platform to discover novel, selectively expressed surface targets whose upregulation is linked to an inciting oncogenic event through the non-specific nature of genomic mutation. As these events drive tumor formation, oncolinked targets are under positive selection, resulting in uniform expression and resistance to loss, making them ideal CAR targets. We first selected a set of ten surface targets that exhibited oncolinked properties--restricted expression in normal tissues, but dysregulated expression in tumors-and identified antibodies that bound cells for 9/10 targets examined. Binding was confirmed by CRISPR/Cas9 knockout of the gene of interest and assessed by flow cytometry. Next, 4-1BB/CD3z CARs were generated for each target using the VH/VL regions of the identified antibodies for scFv generation. After lentiviral transduction of CAR constructs into Jurkat E6.1 cells, active CARs were identified for multiple targets by assessing antigen-dependent CD69 upregulation in overnight co-culture experiments with target-expressing cell lines. The most advanced CAR binds a surface protein whose cancer-specific amplification is observed in subsets of multiple solid tumors, including lung and prostate cancers. This CAR was advanced into primary donor T cells for functional validation. Cytotoxicity was assessed against cell lines exhibiting varying antigen densities of the target protein to demonstrate anti-tumor efficacy at expression levels comparable to primary human tumors. Together, this study highlights the potential of the Oncolinkage platform to efficiently identify and validate multiple novel CAR targets and demonstrates pre-clinical efficacy of solid tumor-directed CARs based on this platform.

#4534 FGF19/ FGFR4 Axis: A key driver in tumorigenesis and treatment resistance in colorectal cancer.

Anh Nguyen, **Bruce M. Boman**

Helen F. Graham Cancer Center & Research Institute, Newark, DE

Colorectal cancer (CRC) remains one of the most treatment-resistant malignancies, yet the mechanisms underlying this resistance are not fully understood. Our GOAL is to define these mechanisms and identify new therapeutic targets to improve treatment outcomes. We investigate the role of the Fibroblast Growth Factor (FGF) signaling, particularly the FGF19/FGF Receptor (FGFR) 4 axis, in CRC tumor growth and therapeutic response. This axis is compelling because our preliminary data show that: *(i)* FGF19 and FGFR4 are co-overexpressed in human CRC, based on publicly available single-cell RNA-seq and bulk RNA-seq of our paired patient specimens; *(ii)* FGF19 overexpression correlates with worse relapse-free survival (RFS) in the TCGA-COAD cohort; and *(iii)* both FGF19 and FGFR4 expression correlate with poor overall survival (OS). Importantly, FGF19/FGFR4 signaling is an upstream regulator of the MAPK and WNT/β-catenin pathways, key drivers of tumorigenesis and treatment resistance in CRC. We HYPOTHESIZE that autoactivation of the FGF19/FGFR4 axis promotes tumor growth, survival, and treatment resistance in CRC. To dissect this axis's functional contributions, CRC cell lines underwent selective FGFR4 inhibition or induced FGF19 overexpression. Effects on viability, proliferation, clonogenic growth, invasion, and drug sensitivity were assessed using established in vitro assays, while mechanistic changes were examined by qRT-PCR and Western blotting. Functionally, targeting FGFR4 with the selective inhibitor BLU9931 impacted all critical cancer hallmarks: increased apoptosis, reduced proliferation, suppressed clonogenic capacity, and diminished invasion. Pre-treatment with BLU9931 sensitized cells to 5-fluorouracil (5-FU), a standard chemotherapeutic agent, enhancing cytotoxicity synergistically. Conversely, FGF19 overexpression activated ERK1/2 and β-catenin signaling to promote proliferation, induced resistance to 5-FU by maintaining cells in the G1-protective phase, and facilitated rapid post-chemotherapy recovery. Our findings support the hypothesis that the FGF19-FGFR4 axis is a key driver of CRC progression and therapy resistance, underscoring the rationale for developing targeted therapies against this tumor-specific signaling axis.

#4535 Targeting LPAR1 as a potential therapeutic strategy for glioblastoma.

Satoshi Takagi, Sumie Koike, Ryohei Katayama

Japanese Foundation for Cancer Research, Tokyo, Japan

Glioblastoma (GBM) is the most aggressive primary brain tumor, with a poor prognosis and a 5-year survival rate of 10%, despite multimodal treatment combining surgery, radiotherapy, and chemotherapy. Due to its high invasiveness, complete surgical resection is challenging, making postoperative radiotherapy and chemotherapy indispensable. Temozolomide (TMZ), a DNA alkylating agent, remains the only FDA-approved therapeutic agent for GBM, novel therapeutic agents for GBM are warranted. In this study, to identify potential therapeutic targets in GBM, we conducted an siRNA-based screening of G protein-coupled receptors (GPCRs) and identified lysophosphatidic acid receptor 1 (LPAR1) as a key molecule whose knockdown significantly reduced the GBM cell viability. LPA, a bioactive lipid mediator, signals through six receptors (LPAR1-6), with LPAR1 particularly implicated in cytoskeletal remodeling, migration, proliferation, and differentiation. Analysis of TCGA data revealed that LPAR1 is highly expressed in brain tumors compared to other cancer types. *In vitro*, LPAR1 knockdown significantly suppressed cell proliferation and induced PARP cleavage, a hallmark of apoptosis, in several GBM cell lines expressing LPAR1. LPA treatment enhanced proliferation of LPAR1-positive GBM cell lines in a concentration-dependent manner and this effect was cancelled by both genetic and pharmacological inhibition of LPAR1. These results indicate that the LPA-LPAR1 axis plays a critical role in promoting GBM cell proliferation and survival. Further analysis using phospho-Kinase arrays and pathway-specific inhibitors revealed that the PI3K/Akt signaling pathway downstream of LPAR1 is involved in these pro-survival effects. In an orthotopic GBM xenograft model, oral administration of the LPAR1 antagonist BMS-986020 significantly suppressed tumor growth in brain. Additionally, combinatorial treatment with BMS-986020 and TMZ lowered the IC_{50} value of TMZ *in vitro*, suggesting a potential synergistic cytotoxic effect. We have previously reported the potential of LPAR1 antagonists as therapeutic agents for osteosarcoma (Takagi S *et al. Oncogene* 2021); our current findings suggest that LPAR1 antagonists would be promising therapeutic option for GBM treatment.

#4536 GFS784, a next-generation ADC with a novel panRAS(ON) inhibitor payload.

Feng Yan, Jichen Zhao, Jingyang Zhang, Li Wang, Yumei Li, Siyuan Le, Fusheng Zhou, Jiong Lan, Qiang Lu

Genfleet Therapeutics, Shanghai, China

Background: Antibody drug conjugate (ADC) has proven an effective drug modality and keeps evolving with innovations explored on each of its components. However, the potential coordination between the antibody and the payload of an ADC is usually overlooked efficacy-wise. Here we introduce the development of a novel panRAS (ON) inhibitor payload and more importantly, the Functional Antibody and Synergistic conjugate(FAScon^{TM}), a novel ADC design which employes the antibody-payload synergy to further enhance the therapeutic activity of an ADC beyond precision delivery. The preclinical profile of an exemplified FAScon GFS784, an EGFR-panRASi ADC is presented for concept demonstration.
Methods: GFS784 was established by conjugating Cetuximab with a panRAS(ON) inhibitor GF005095 via a proprietary, cleavable linker at DAR of 8. The anti-growth activity of GFS784 was tested in cell lines with different RAS genotypes. The bystander effect of GFS784 was investigated by comparing its effect on the growth of an EGFR negative cell line when mono-cultured or co-cultured with an EGFR-positive cell line. The plasma stability of GFS784 was studied via incubation in vitro or injection into mice. CDX tumor mouse models were used to explore the in vivo efficacy of GFS784.
Results: The pan-RAS(ON) inhibitor payload GF005095 employes cyclophilin A to target K/H/N-RAS mutants or wild type proteins and demonstrated higher anti-growth activity than DXd in vitro. GFS784 bound to and was internalized into tumor cells in an EGFR-dependent manner. GFS784 showed broad and potent anti-proliferation activity in EGFR-expressed tumor cell lines addicted to mutant or wild type RAS genes with a sub-nanomolar median IC_{50}, which is significantly lower than that of an EGFR-DXd ADC. GFS784 demonstrated significant bystander effect in vitro. GFS784 showed good plasma stability when tested in vitro and in animals. GFS784 at dose levels of 1-5 mg/kg via i.v., q3W showed robust therapeutic efficacy in RAS-mutant CDX models which were either sensitive or resistant to the DXd counterpart. Compared with combination therapy using Cetuximab and RMC-6236 at clinical equivalent doses, GFS784 demonstrated comparable efficacy but better tolerability in CDX mice. GFS784 also induced deep tumor regression in both Osimertinib-sensitive and resistant EGFR-mutant NSCLC CDX models.
Conclusions: GFS784 has a satisfactory preclinical profile as an ADC candidate. GFS784 is effective in CDX models resistant to DXd ADC or Osimertinib, suggesting the potential as a next-generation ADC and an alternative solution for TKI resistance. Therefore, GFS784 provides a promising solution for treating RAS mutant or EGFR-altered tumors and a further clinical investigation is warranted.

#4537 Modified acetate salt form of GHRH-antagonist retains anti-leukemic activity against acute myelogenous leukemia.

Joel Costoya[1], Elizabeth Costoya[2], Medhi Wangpaichitr[3], Wei Sha[4], Joaquin J. Jimenez[5]

[1]Department of Biochemistry and Molecular Biology, University of Miami Miller School of Medicine, Miami, FL,[2]College of Arts, Sciences & Education, Florida International University, Miami, FL,[3]DeWitt Daughtry Family Department of Surgery, Division of Cardiothoracic Surgery, University of Miami Miller School of Medicine, Miami, FL,[4]Bruce W. Carter Veterans Affairs Medical Center, Miami, FL,[5]Phillip Frost Department of Dermatology and Cutaneous Surgery, University of Miami Miller School of Medicine, Miami, FL

Acute myeloid leukemia (AML) is a heterogenous hematological malignancy characterized by an accumulation of immature myelocytic cells resulting from aberrancies to programs underlying the survival, proliferation, and maturation of myeloid progenitor cells during hematopoiesis. Despite continuous improvement in AML therapies, five-year survival rates remain at 31.7%, and standard induction therapy relies on the use of intense chemotherapeutic regimes, followed by HSCT if applicable. This underscores the need for novel therapies, ideally without introducing adverse events as side effects to treatment. GHRH antagonists, represent a new therapeutic modality and pre-clinically have shown robust activity against various cancer types with minimal peripheral toxicity. Previously we demonstrated MIA-602, a GHRH antagonist, to have significant anti-leukemic activity both *in-vitro* and *in-vivo* against APL and an all-trans retinoic acid/arsenic trioxide (RAA) resistant clone, as well as AML and a doxorubicin resistant (DR) clone. When MIA-602 was combined with standard therapy in non-resistant models, the anti-leukemic effect produced was made even more potent. Whilst in resistant models, MIA-602 monotherapy retained its significant anti-leukemic activity, implying a distinct mechanism of action independent from that of traditional therapeutic modalities. Here we tested a more clinically acceptable acetate salt form of MIA-602, MIA-602 Ac, and showed that it retained significant anti-leukemic activity against both APL and AML *in-vitro* as well as versus their RAA and DR analogs, respectively. In order to assess retention of MIA-602Ac's anti-leukemic efficacy, NB4 and NB4-RAA cells, were cultured with increasing doses of MIA-602Ac ranging from 0.05 to 5 µmol/L. K562 and K562-DR cells, were cultured with MIA-602Ac alone or combined with doxorubicin at varying concentrations ranging from 0.05 to 5 µmol/L and 0.005 to 0.05 µg/ml respectively, using doxorubicin as the standard-of-care comparator. Cell viability was measured 24h and 48h post-treatment. Our results show that MIA-602Ac maintained a significant dose- and time-dependent anti-leukemic effect as seen previously with MIA-602. Synergism of GHRH antagonism with standard of care therapies was preserved. MIA-602Ac as a monotherapy could still produce significant anti-leukemic effects in resistant cell lines. In conclusion, further clinical investigation of MIA-602Ac as a monotherapy, or adjuvant therapy for the treatment of acute myeloid leukemia is warranted, given its continued preclinical success and improvements made to toxicity.

#4539 A MUC1-C-targeting ADC exhibits potent antitumor activity against neuroendocrine prostate cancer in both intact and testosterone-depleted preclinical models.

Surender Kharbanda[1], Rehan Ahmad[1], Deepak Raina[1], Changchuin Mao[1], Sourav Choudhary[2], Brian Lawney[3], Nandita Sreenivasalu[1], Govind Panchamoorthy[1], Neeraj Agarwal[4], Ravi Jasuja[1]

[1]R&D, Xyone Therapeutics Inc., Canton, MA,[2]Birla Institute of Technology and Science, Hyderabad, India,[3]Dana Farber Cancer Institute, Boston, MA,[4]Asst. Professor, Div. of Med. Onc., University of Utah Huntsman Cancer Institute, Salt Lake City, UT

Background: Prostate cancer (PC) is one of the most frequently diagnosed malignancies in men and remains the second leading cause of cancer-related mortality. The castration-resistant and neuroendocrine variants (CRPC/NEPC) are especially challenging to treat, as these tumors often lose dependence on androgen receptor signaling and become refractory to androgen-targeted therapies. Although prostate-specific membrane antigen (PSMA) is a valuable surface target in many forms of PC, its absence in PSMA-negative tumors necessitates alternative therapeutic markers. One such marker is MUC1, whose expression becomes markedly upregulated in PSMA-negative disease. Notably, aberrant MUC1 expression is a hallmark of CRPC/NEPC and is strongly associated with aggressive tumor behavior and poor clinical outcomes.
Methods: In-vitro cytotoxic activity of MUC1-C targeting ADC (XYA02-8) was evaluated in a series of prostate cancer cell lines. Preclinical antitumor activity was evaluated in-vivo in both intact and castrated nude mice to model androgen replete and depleted states in PC patients.
Results: We find that the MUC1-C mAb 7B8* binds to ~90% cells compared to isotype control in CRPC/NEPC in-vitro. To develop multiple ADC formulations and to optimize the candidate, Quality by Design (QbD, FDA) approach was utilized, leveraging the Design of Experiments (DOE) statistical framework. XYA02-8-ADC exhibits efficient internalization at 3 hours at 37^{o}C in multiple CRPC/NEPC cell lines and displayed potent cytotoxicity in in-vitro. Both intact and castrated nude mice with established tumor xenografts were treated with 7.5 mg/kg QW x 3 i.v. and monitored for over two-month post treatment. Significant (~70%) tumor growth inhibition was observed with XYA02-8-ADC without an accompanying weight loss and/or tissue toxicity. Interestingly, the antitumor activity persists in both intact and castrated nude mice xenografts demonstrating that targeting MUC1-C present a unique opportunity for tumor abrogation downstream of androgen signaling.
Conclusions: XYA02-8-ADC demonstrates strong antitumor activity with a favorable safety profile in CRPC/NEPC models. Notably, its ability to retain efficacy even under testosterone-replete conditions highlights an important therapeutic opportunity: targeting MUC1-C with XYA02-8-ADC without relying on androgen-deprivation strategies. These findings open a promising avenue for developing effective treatments that avoid the systemic adverse effects associated with hormonal deprivation.* https://patents.google.com/patent/US20230265208A1/en

#4540 BC602: An IND-enabling stage LGR5x EGFR bispecific antibody with superior anti-tumor efficacy in mouse CDX and PDX models.

Zhe Shao, Tao Wang, Wen Chao Jia, Keng Hoe Lok, **Zhong Zong Pan**

Dragon Boat Biopharmaceutical, Shanghai, China

Epidermal growth factor receptor (EGFR) is a key driver oncogene in the tumorigenesis of many cancer types. EGFR targeting antibodies are approved mainly in EGFR overexpression cancers including colorectal cancer (CRC), head and neck squamous carcinoma (HNSCC), and squamous non-small cell lung cancer (NSCLC). These antibodies exert their function by binding to the extracellular domain(s) to block ligand binding and to induce receptor internalization and degradation. To further enhance EGFR internalization and degradation, we developed an asymmetric LGR5*EGFR bispecific antibody (BsAb) BC602, with one arm as VHH targeting leucine-rich repeat-containing G-protein coupled receptor 5 (LGR5), and the other arm as Fab targeting EGFR. To further increase the anti-tumor activity, BC602 Fc is engineered for enhanced FcγRIII binding and ADCC activity. In ELISA and BLI assays, BC602 binds to the LGR5 protein and EGFR protein with high affinity, respectively. In LGR5 and EGFR expressing cell lines,BC602 showed high binding affinity to cell surface receptors at single digit nM, while isotype control antibody showed no binding. In the pH-rodo internalization assay, BC602 induced significantly higher internalization magnitude than EGFR antibody or LGR5 antibody alone in both cell lines. In growth inhibition assay using the patient-derived organoids (PDO), BC602 showed potent inhibitory activity, much stronger than EGFR antibody. The antitumor efficacy of BC602 was studied in several mouse CDX and PDX models. BC602 demonstrated dose-dependent anti-tumor efficacy, with the antitumor efficacy stronger than EGFR antibody, superior or comparable to its competitor in clinical development stage. In AGS mouse xenograft tumor model, BC602 at 5 mg/kg showed a TGI of 72% while EGFR antibody had a TGI of 50%. In A431-LGR5 mouse xenograft tumor model, BC602 at 1/3/10 mg/kg showed TGI of 42%, 67%, and 83% respectively. BC602 showed no effect on mouse body weight or showed any other safety concerns in these mouse models. BC602 demonstrated good physicochemical properties for CMC, with a high production yield. Non-clinical GLP PK and toxicity studies of BC602 and 200L scale clinical batch production are ongoing. IND filing is expected in 2026 Q3, and the planned indications include cancer types that overexpress both EGFR and LGR5 including HNSCC and CRC.

#4541 DR319-DP: A Nectin-4/Trop-2 bispecific ADC with an avidity-driven VHH design and dual-MOA payloads.

Xiaofang Wen[1], Wenwen Duan[1], Gaofeng Yao[1], Shaoqi Liu[1], Yonglu Chen[1], Teng Li[1], Xiaoyu Qian[1], Zhenxing Zhou[1], Jingjin Fang[1], Jie Zhao[1], Ke Chen[1], Yi Yang[2], Yanshan Huang[1]

[1]Zhejiang Doer Biologics Co., Ltd, Hangzhou, China,[2]Glyco-therapy Biotechnology Co. Ltd., Hangzhou, China

Trop-2 and Nectin-4 have emerged as attractive targets for the development of next-generation antibody-drug conjugates (ADCs). However, the emergence of drug resistance remains a critical challenge in ADC therapy. Combination strategies represent a promising approach to enhance therapeutic efficacy and mitigate resistance. Notably, Trop-2 and Nectin-4 exhibit high and frequent co-expression across multiple solid tumors, while showing limited or moderate expression in normal tissues. In clinical attempts, the combination of sacituzumab govitecan (SG) and enfortumab vedotin (EV) has demonstrated substantially improved efficacy in early-phase trials for metastatic urothelial carcinoma. However, toxicities arising from both “off-target, off-tumor” and “on-target, off-tumor” effects remain a major concern. To maximize antitumor efficacy while minimizing systemic toxicity, we developed an avidity-driven bispecific antibody, DR319, featuring a “1+1” bispecific format that incorporates a low-affinity but high-avidity anti-Trop-2 VHH arm. We demonstrated that DR319 enables potent, high-avidity binding to Nectin-4/Trop-2 dual-positive tumor cells in our diverse cell line panel, while minimizing binding to Trop-2 single-positive cells, thereby mechanistically reducing on-target toxicities. We then conjugated DR319 to a novel Topoisomerase I inhibitor (TopoI) linker-payload (CPD3) featuring improved plasma stability, generating DR319-CPD3 (DAR 6). Our results showed that DR319-CPD3 exhibited superior antitumor efficacy in CDX models compared with benchmark mono-targeting ADCs with TopoI payloads, even those using the same CPD3. Furthermore, we generated a dual-payloads ADC, DR319-DP, with a DAR of 4 TopoI + 2 microtubule inhibitor (MTI), through a one-step glyco-conjugation strategy. This construct is designed to deliver synergistic, orthogonal mechanisms of action (MOA) to address tumor heterogeneity and therapeutic resistance. In our studies, DR319-DP demonstrated excellent target and bystander killing and achieved more potent and durable tumor suppression than mono-targeting ADCs (with either TopoI or MTI payloads) and DR319-CPD3, across multiple CDX and PDX models. Additionally, our characterization confirmed that DR319-DP displayed excellent thermal and plasma stability, along with a favorable pharmacokinetic (PK) profile in mice and cynomolgus monkeys. DR319 is precision-engineered with an avidity-driven backbone to minimize the on-target toxicities that limit current Nectin-4 and Trop-2 therapies. The incorporation of synergistic dual-MOA payloads (DP) into DR319 provides a comprehensive strategy to maximize efficacy and overcome resistance. These preclinical data strongly support the clinical development of DR319 ADCs as a potential best-in-class therapeutic for solid tumors.

#4542 Zanidatamab modulates multiple pathways involved in tumor growth and survival and is efficacious post T-DXd.

Ankur Karmokar[1], Emanuele Loro[2], Al Hassan Kyakulaga[3], Desmond Lau[4], Nina Weisser[4], Genevieve Desjardins[4], Prajwal Raghunatha[4], Edwin Clark[1], Robin Humphreys[1], **Kedar S. Vaidya[1]**

[1]Oncology Research, Jazz Pharmaceuticals, Palo Alto, CA,[2]Bioinformatics, Jazz Pharmaceuticals, Palo Alto, CA,[3]DMPK, Jazz Pharmaceuticals, Palo Alto, CA,[4]Zymeworks, Vancouver, BC, Canada

Zanidatamab (Ziihera), a biparatopic antibody against the human epidermal growth factor receptor-2 (HER2), is currently approved in previously treated advanced HER2+ biliary tract cancer. To understand the specificity of binding, affinity of zanidatamab and the one-armed antibodies (OAAs) that comprise the Fab and scFv of zanidatamab, to WT HER2 extracellular domain (ECD) and mutein HER2 ECD domains were determined by surface plasmon resonance. The anti-HER2 Fab bound HER2 ECD II, and the anti-HER2 scFv bound HER2 ECD IV generated a Kd of 0.25 and 0.48 nM, respectively. Zanidatamab bound HER2 ECD with a lower Kd (0.047 nM) when compared to HER2 ECD II (0.31 nM) or HER2 ECD IV muteins (0.26 nM), demonstrating the avidity of Fab and scFv paratopes. To further understand MoA of zanidatamab, a multi-omics analysis including whole transcriptomics, proteomics and phospho-proteomics was performed on BT-474 HER2-amplified breast cancer xenograft tumors exposed to zanidatamab. A combination of unbiased analyses showed that zanidatamab significantly altered key pathways associated with DNA damage/repair, cell cycle, and MAPK signaling in a dose- and time-dependent manner. Expanded analysis of in vivo response demonstrated that zanidatamab is efficacious post T-DXd (trastuzumab deruxtecan) therapy. Mice bearing BT-474 HER2-amplified tumors were treated with T-DXd to regression and regrowth to baseline followed by treatment with zanidatamab. Zanidatamab was efficacious on these progressed tumors with 100% regressions following the first dose. These data demonstrate HER2 domain specific binding affinity, zanidatamab impacting key cellular pathways in driving *in vivo* efficacy, and potential utility in a post-T-DXd population.

#4543 A novel CDH17-targeted radioligand therapy overcomes resistance to microtubule and topoisomerase I inhibitor ADCs and achieves potent efficacy in GI-tract tumors.

Abdul Mondal[1], Garima Kaushik[1], Marina Bell[1], Maxwell Hilbert[1], Arnab Mukharjee[1], Dennis Beckford[2], Paul Heverly[2], Michael Ritchie[1], Kakajan Komurov[1]

[1]Corellia AI, Rockville, MD,[2]Champions Oncology, Rockville, MD

CDH17 (Cadherin 17) is a single-pass transmembrane protein that is highly and widely expressed in adenocarcinomas of the colon, stomach, and pancreas, as well as in subsets of ovarian and lung cancers. Here, we describe the development of a CDH17-targeted antibody-drug and a radioligand conjugate, their in vivo efficacy across a large panel of GI-tract PDX tumors, and the pharmacokinetic and safety profiles in non-human primates. A fully human monoclonal antibody against CDH17 was generated and conjugated to Deruxtecan at a DAR of 8 (CO-ADC-010). CO-ADC-010 demonstrated rapid internalization and potent CDH17-dependent cytotoxicity, along with favorable plasma stability, pharmacokinetics, and manufacturability. In a large-scale in vivo efficacy study, CO-ADC-010 achieved >90% tumor growth inhibition (TGI) in 80% of tested PDX models. This performance significantly surpassed a comparator ADC carrying MMAE at DAR 4, which showed a similar TGI in only 33% of models, suggesting better suitability of topoisomerase-based payloads for CDH17-directed delivery. In non-human primates, a single-dose exploratory toxicology study of CO-ADC-010 at 10, 30, and 45 mg/kg revealed no target-related toxicities at any dose, with all clinical and pathological findings deemed mild and reversible.Despite strong initial responses to CO-ADC-010, many tumors relapsed over prolonged treatment due to acquired resistance to the payload, while CDH17 expression was not altered. To overcome the limitations of the *de novo* and acquired resistance to the ADC treatments, we also developed a CDH17-targeted radioligand therapy (RLT) using the same antibody scaffold. We demonstrate that CDH17-targeted RLT shows broad and durable responses across the PDX panel, including full activity in models refractory to Deruxtecan-based ADCs, demonstrating the superiority of RLT in these indications in overcoming drug resistance and achieving durable responses. These data collectively support CDH17-targeted RLT as a promising therapeutic approach for CDH17-positive gastrointestinal malignancies.

#4544 Predictive biomarkers and combination strategies to overcome resistance to HER2- and TROP2-directed antibody drug conjugates with topoisomerase I inhibitor payloads in SCLC.

Kavya Ramkumar, C. Allison Stewart, Shui-Ping So, Runsheng Wang, Azusa Tanimoto, Alberto Duarte Jr., Jenna H. Gray, Li Shen, Lixia Diao, Yuanxin Xi, Qi Wang, Alejandra G. Serrano, Luisa M. Solis Soto, Jing Wang, Bingnan Zhang, Carl M. Gay, Lauren A. Byers

UT MD Anderson Cancer Center, Houston, TX

Treatment-naïve small cell lung cancer (SCLC) is highly sensitive to frontline chemotherapy; however relapsed SCLC acquires broad chemoresistance that renders conventional second line agents like topotecan, a topoisomerase inhibitor (TOP1i), largely ineffective. Recent clinical trials with surface targeting strategies such as antibody drug conjugates (ADCs) with TOP1i-based payloads have demonstrated strong responses in relapsed small SCLC. Identifying biomarkers of response and resistance to these agents will be important to optimize the effectiveness of this new therapeutic class. We previously showed that non-neuroendocrine SCLC tumors express low levels of *DLL3* and *SEZ6*, but high levels of *TACSTD2* (TROP2) and *ERBB2* (HER2). In this study, we examined the activities of different HER2- and TROP2-directed ADCs with TOP1i- and non-TOP1i-based payloads in SCLC cell lines. While target expression did not correlate with ADC sensitivity, SCLC cell lines with high SLFN11 levels showed greater sensitivity to TOP1i-based HER2- and TROP2-ADCs and their payloads. SLFN11 knockdown confirmed that SLFN11 loss reduces ADC sensitivity. Notably, combination with an ATR inhibitor sensitized resistant SLFN11-low SCLC cell lines to TOP1i-based ADCs. In contrast, sensitivity to a non-TOP1i-based HER2 ADC was not associated with SLFN11 expression. High cMYC and *ABCB1* (P-glycoprotein) levels were also associated with resistance to TOP1i-based ADC, but not to non-TOP1i ADCs. Mechanistically, TOP1i-based HER2- and TROP2-ADCs induced significant DNA damage and apoptosis. Increases in PDL-1 expression, STING-chemokine *CCL5,* along with extracellular ATP were also detected, indicating induction of immunogenic responses and supporting combinations with immunotherapy. Overall, these results identify SLFN11 as a clinical biomarker for patient selection and provide preclinical support for combinations with ATR inhibitor or using alternate non-TOP1i-based ADCs to overcome resistance to TOP1i-based HER2- and TROP2-ADCs.

#4545 Targeting heparan sulfate proteoglycans in pancreatic cancer with *Salmonella* expressing bacterial heparinase III.

Nancy Danielle Ebelt, Suvithanandhini Loganathan, Lara C. Avsharian, Edwin R. Manuel

Immuno-oncology, Beckman Research Institute of The City of Hope, Duarte, CA

Heparan sulfate proteoglycans (HSPG) regulate processes that drive tumor progression and promote treatment resistance in pancreatic ductal adenocarcinoma (PDAC), including increased fatty acid metabolism, sustained survival signaling, high fibrosis, and increased macropinocytosis. HSPG are regulated in a pro-tumor manner by site-specific cleavage of their heparan sulfate chains by mammalian heparanase; however, alternative cleavage by bacterial heparinase III (HepIII) has been shown to deactivate these proteins and prevent downstream pro-tumor signaling. To broadly target HSPG on tumor cells surfaces, we have expressed a highly active bacterial HepIII from *Bacteroides* on a clinically evaluated, attenuated strain of *Salmonella typhimurium*, YS1646 (YS-HepIII). This tumor-targeting YS both continuously expresses active HepIII enzyme and limits its expression to tumor tissue using an inducible system to circumvent toxicities that might arise from systemic HepIII treatment. Analysis of human PDAC cell lines treated with YS-HepIII *in vitro* as well as of human PDAC xenograft tumors treated *in vivo* shows evidence of decreased macropinocytosis, reduced survival signaling, lipid storage depletion, and decreased expression of translation machinery. These vulnerabilities sensitize tumors to FDA approved cancer therapies. This translatable therapeutic has the potential to improve PDAC patient survival, an unmet medical need.

#4546 HER2- and TROP2-antibody-drug conjugates in small cell lung cancer cell lines and 3D culture: Efficacy and role of target expression.

Jenna Gray, Kavya Ramkumar, C. Allison Stewart, Runsheng Wang, Alberto Duarte, Azusa Tanimoto, Robert J. Cardnell, Lauren Averett Byers, Carl M. Gay

UT MD Anderson Cancer Center, Houston, TX

Small cell lung cancer (SCLC) is an aggressive neuroendocrine cancer characterized by robust responsiveness to frontline chemotherapy and immunotherapy followed by rapid resistance and poor survival. Recently, cell-surface targeting drugs, such as T-cell engagers (tarlatamab) and antibody-drug conjugates (ADCs), have demonstrated significant responses in relapsed SCLC patients. Paradoxically, the efficacy of TROP2-ADCs and HER2-ADCs both have failed to correlate with the level of target expression in both SCLC and breast cancer patients, yielding difficulty in predicting the patient population which would receive benefit from these treatments. Treatment efficacy across a range of expression may be due to tumor heterogeneity and the delivery of the payload to a cell presenting the target resulting in a bystander effect on cells with low or no expression. SCLC cell lines and dissociated PDX tumors were evaluated for development of spheroids, which better mimic a solid tumor than 2D cell culture. The growth of these spheroids and PDX organoids were evaluated following treatment with HER2-ADC (trastuzumab deruxtecan), TROP2-ADC (sacituzumab govitecan), tarlatamab, activated T-cells, and combinations of these. Effect of complete siRNA knockdown of the surface target on the efficacy of targeted ADCs was also determined. HER2- and TROP2-ADCs slowed growth of the spheroids as compared to the control. Additionally, the combination of TROP2-ADC, tarlatamab, and T-cells caused contraction of the spheroids. Notably, the tarlatamab and T-cells arm demonstrated what is likely a pseudo-progression sometimes seen in patients as T-cells infiltrate and begin to kill tumor cells. Knockdown of ERBB2 and TACSTD2 demonstrated no demonstrable difference in ADC sensitivity. In conclusion, HER2- and TROP2-ADCs demonstrated efficacy in these models and may be used in combinatorial approaches in the future. Additionally, co-cultured cell line spheroids could provide a better model of tumor heterogeneity. Lastly, HER2- and TROP2- levels are not predictive biomarkers for ADC sensitivity, suggesting that other biomarkers should be explored to identify responsive patient populations.

#4547 TRO-02, a conditionally activated EGFR-targeting ADC incorporating TROCAD^{TM} and TROSIG^{TM} platforms, shows enhanced tumor selectivity and potent efficacy.

Young Hun Lee, Do Hyeon Kim, Eun Young Shim, Eunhyun Choi, Jong Un Cho, Myoungki Baek, Sung Ho Woo

TriOar Inc., Daejeon, Korea, Republic of

Epidermal growth factor receptor (EGFR) represents a validated therapeutic target across multiple solid tumor indications, including non-small cell lung cancer, head and neck squamous cell carcinoma, and colorectal cancer. However, EGFR expression in normal epithelial tissues, particularly skin, has limited the therapeutic window of EGFR-targeted therapies, often causing dose-limiting toxicities that impair clinical efficacy. To overcome this challenge, we developed TRO-02, a novel conditionally activated EGFR-targeting antibody-drug conjugate (ADC) that selectively activates in the tumor microenvironment while remaining masked in healthy tissues. TRO-02 is a DAR8-type ADC generated by conjugating a potent topoisomerase I inhibitor to panitumumab via a cleavable, stable, and hydrophilic TROSIG^{TM} linker. Furthermore, it incorporates our proprietary TROCAD^{TM} platform, which provides dual functions: (1) masking the panitumumab to prevent EGFR binding until proteolytic cleavage by tumor-associated proteases, and (2) guiding the ADC to the tumors by targeting annexin A1, which is highly expressed on tumor vasculature and facilitates transcytosis. This dual mechanism allows TRO-02 achieve both specific activation within the tumor microenvironment and selective tumor delivery. In vitro, the masked TRO-02 exhibited approximately 100-fold weaker binding to EGFR than the activated ADC, confirming effective suppression of target engagement. The unmasked TRO-02 displayed sub-nanomolar cytotoxicity against EGFR-expressing tumor cells, whereas the masked form showed markedly reduced cytotoxicity, with 30- to 100-fold lower potency depending on the cell type compared with the unmasked form. In MDA-MB-231 xenograft model, a single dose of 0.3 and 1 mg/kg achieved 65% and 98 % tumor growth inhibition, respectively. Rat plasma stability studies showed high stability, with >85% of intact ADC remaining after 7 days of incubation. Furthermore, pharmacokinetic analysis in rats demonstrated favorable PK properties ($t_{1/2}$ = 4.47 days, AUC = 163.52 day·μg/mL, CL = 25.05 mL/day/kg, Vd = 0.08 L/kg at 4 mg/kg), indicating high in vivo stability and low clearance. Collectively, these findings demonstrate that TRO-02 is a conditionally activated EGFR-targeting ADC with improved therapeutic index, achieving potent antitumor efficacy while minimizing on-target/off-tumor toxicity.

#4548 Therapeutically targeting B7-H6 with antibody-drug conjugates for diffuse large B-cell lymphoma.

Qiaoling Ye, Ye Lu, Chulin Sha, Peng Guo

Hangzhou Institute of Medicine, Chinese Academy of Sciences, Hangzhou, China

Background: Diffuse large B-cell lymphoma (DLBCL) remains fatal in ~40% of patients who relapse after first-line R-CHOP chemoimmunotherapy. Although CD19- and CD79b-targeted ADCs offer additional therapeutic options, their benefit is limited by on-target depletion of normal B cells, restricting the therapeutic window. To identify tumor-selective antigens with minimal normal-tissue expression, we performed multi-omics analyses across lymphoma datasets and identified B7-H6 (NCR3LG1) as a cancer-enriched surface protein. B7-H6 is undetectable in healthy tissues, consistently elevated in DLBCL, and further inducible by cellular stress, suggesting a therapeutically exploitable vulnerability.
Methods: Monoclonal antibodies against B7-H6 were conjugated to monomethyl auristatin E (MMAE) or DXd to generate B7-H6-targeted ADCs. Antigen-dependent cytotoxicity and selectivity were evaluated across B7-H6-high DLBCL cell lines and normal epithelial or hematopoietic cells. Tumor targeting and biodistribution were assessed by IVIS imaging using fluorescently labeled antibodies. Antitumor efficacy was evaluated in subcutaneous DLBCL xenograft models by tumor growth inhibition and treatment durability. Mechanistic studies assessed NKp30 engagement, immune-evasion pathways, and Fc-dependent effector activity.
Results: B7-H6 ADCs induced strong antigen-dependent cytotoxicity, eliminating B7-H6-high DLBCL cells while sparing normal cells. IVIS imaging demonstrated highly selective tumor accumulation with minimal off-tumor uptake in major organs, indicating a favorable biodistribution profile. In multiple DLBCL xenograft models, both MMAE- and DXd-based B7-H6 ADCs produced significant and sustained tumor regression, outperforming the unconjugated antibody and standard chemotherapy. Mechanistically, B7-H6 acted as an immune-modulatory ligand that engaged NKp30, enabling DLBCL cells to diminish NK-cell activity. B7-H6 ADCs counteracted this immune-evasion mechanism by directly delivering cytotoxic payloads to antigen-expressing cells. The intact Fc domain further promoted Fcγ-receptor-mediated NK- and macrophage-dependent effector functions, complementing payload-mediated killing.
Conclusions: B7-H6 is a tumor-selective, immune-regulatory, and mechanistically validated target for next-generation ADC development in DLBCL. B7-H6 ADCs demonstrate potent tumor-selective activity, favorable biodistribution, and dual mechanisms of antitumor action, providing a promising strategy to overcome the limitations of existing DLBCL therapies.

#4549 Discovery of HMPL-A580, a first-in-class antibody-targeted therapy conjugate (ATTC) of a novel PI3K/PIKK inhibitor payload linked to an anti-EGFR antibody.

Yu Cai, Xiangling Chen, Shishuang Chen, Na Yang, Yan Xu, Huijing Yu, Shiming Fan, Haibin Yang, Min Cheng, Nelson Ng, Jianlin He, Shaohui Shen, Weigang He, wei shao, xiaoming dai, Yajing Bai, Yizhen Yang, linfang wang, Jian Wang, Weihan Zhang, Yongxin Ren, Guangxiu Dai, Michael Shi, Weiguo Su

HUTCHMED Ltd., Shanghai, China

Background: EGFR is highly expressed in multiple types of solid tumors and well recognized as a driving force in tumorigenesis and disease progression. Modulation of the PI3K/AKT/mTOR (PAM) pathway is required for EGFR-mediated tumorigenesis or conferred resistance to EGFR-targeted therapy. Importantly, PAM pathway inhibition synergizes anti-EGFR therapy to enhance anti-tumor activity. Consequently, an Antibody-Targeted Therapy Conjugate ("ATTC") with a PI3K/PIKK small molecule inhibitor conjugated to an EGFR antibody is developed and expected to enhance anti-tumor efficacy of anti-EGFR therapy while reducing off-tumor toxicities of PAM inhibitors. HMPL-A580 is a first-in-class ATTC comprising of a highly selective and potent PI3K/PIKK inhibitor payload linked to an anti-EGFR IgG1 antibody, via a cleavable linker.
Methods: EGFR binding and internalization were evaluated by FACS. Confocal microscopic imaging was used to monitor endocytosis. Cell viability was measured by CCK-8 or luminescence in 3D cell viability assays. Multiple human xenograft tumors were applied in immune-deficient mice to investigate the anti-tumor activity of HMPL-A580.
Results: The payload of HMPL-A580 potently inhibited PI3K and PIKK family kinases, with IC_{50} ranging around 1 to 10 nM. Eurofins profiling across 418 kinases revealed the payload has excellent selectivity. By conjugating this potent payload with an anti-EGFR antibody via a cleavable linker, the ATTC compound HMPL-A580 demonstrated robust anti-tumor effect. Upon binding to EGFR-expression cancer cell line, HMPL-A580 underwent rapid internalization, lysosomal trafficking, payload release, and PAM and PIKK signaling inhibition to induce tumor cell apoptosis. In a 38-human solid tumor cell line panel, HMPL-A580 potently inhibited EGFR-expression tumor cell proliferation. The tumor cells harboring EGFR high expression, EGFR mut or PAM alterations were more sensitive to HMPL-A580. HMPL-A580 showed a strong bystander effect when EGFR-negative cells co-cultured with EGFR-expression cells. In human tumor xenograft models in mice, HMPL-A580, administered intravenously at 1~10 mg/kg once weekly for two weeks, demonstrated a dose / exposure-dependent anti-tumor activity in multiple EGFR-expression models, which is associated with much stronger target inhibition and suppression of downstream functions than antibody and payload alone treatment. The preliminary results demonstrated that HMPL-A580 was stable in human, monkey, rat and mouse plasma, and showed favorable PK property in cynomolgus monkeys.
Conclusion: HMPL-A580 demonstrates strong anti-tumor activity in preclinical models and good PK characteristics, supporting further clinical evaluation.

#4550 Tumor cell surface targeting of high-grade neuroendocrine carcinomas.

C. Allison Stewart, Kavya Ramkumar, Azusa Tanimoto, Runsheng Wang, Alberto Duarte, Angelo Chen, Alejandra Serrano, Yuanxin Xi, Lixia Diao, Qi Wang, Li Shen, Alexa Halliday, Shui Ping So, Luisa Solis Soto, Jing Wang, Bingnan Zhang, Lauren A. Byers, Carl M. Gay

UT MD Anderson Cancer Center, Houston, TX

High-grade neuroendocrine carcinomas (hgNECs) are aggressive malignancies that arise, most commonly, from the aerodigestive tracts, though, more rarely from other sites. Frustratingly, hgNECs are, initially, exquisitely sensitive to chemotherapy and/or radiation, but these responses are short-lived and inevitable relapses occur. Recent therapeutic developments have focused on hgNEC-associated cell surface antigens which, when targeted with an antibody, can serve as beacons for delivery of cytotoxic or immunologic payloads. T-cell engagers (TCEs) and/or antibody-drug conjugates (ADCs) against hgNEC antigens, including DLL3 and SEZ6, have demonstrated unprecedented responses in relapsed hgNECs. In some cases, such as small cell lung cancer (SCLC), the expression of these antigens is nearly ubiquitous and sensitivity to surface-targeting therapies is contingent primarily on payload. However, in other hgNECs, neuroendocrine (NE) features, including DLL3 and SEZ6 expression, are bimodal, which necessitates strategies for patient selection and alternative antigens for NE-low hgNECs. DLL3 levels have been evaluated by CLIA-validated immunohistochemistry in >340 patients at MDACC, including those diagnosed with rare extrapulmonary hgNECs (i.e., Merkel cell carcinoma, small cell of the breast, thyroid, etc.) for off-label use of tarlatamab (DLL3-targeting TCE). We utilized expression data from public hgNEC cohorts, as well as our own patient and preclinical model cohorts to characterize the relationship between known cell surface target expression (i.e., DLL3, etc.), various established biomarkers, including NE status and SLFN11, and sensitivity to surface targeting therapies. NE status defined two major subsets of hgNECs. NE-high specimens expressed high DLL3 and SEZ6 and were responsive to therapies targeting these antigens. In contrast, the NE-low subsets expressed high TROP2 and HER2. Surprisingly, target expression was not the dominant predictive biomarker for ADCs targeting these antigens as, instead, biomarkers of payload sensitivity (e.g. SLFN11 for topoisomerase I inhibitor payloads, P=0.01) offered superior insight into efficacy. Surface-targeting therapies represent a new paradigm for hgNEC therapeutics and while DLL3- and SEZ6-targeting therapies are showing promise across all hgNECs, their impact will be limited outside SCLC without patient selection. Utilizing biomarkers, including those for target expression, inflammatory potential, and payload sensitivity, will be critical to optimize drug selection for patients with these malignancies.

#4551 Nano-protomers targeted at tumor metastasis.

Rebecca Benhaghnazar[1], Dutsin Sirvinas[1], Joseph Aceves[1], Ryan Cho[1], Felix Alonso-Valenteen[2], Nelyda Gonzalez[2], Ravinder Abrol[3], Robin Shaw[4], Lali Medina-Kauwe[1]

[1]Biomedical Sciences, Cedars Sinai Medical Center, Los Angeles, CA,[2]Cedars Sinai Medical Center, Los Angeles, CA,[3]cal state university Northridge, Northridge, CA,[4]University of Utah, Salt Lake City, UT

Therapeutic failure in many highly aggressive cancers is often driven by early metastatic spread and poor delivery of effective treatments. Protein-based therapeutics represent an attractive alternative to small-molecule drugs due to their strong biological activity, target selectivity, and generally limited off-target effects. In this work, we investigated whether a HER3-directed fusion construct, HPK, can function as a carrier to transport three different protein payloads—GFP, Gelonin, and GJA1-20k—into HER3-positive tumor cells. By incorporating a simple tagging motif onto each cargo, we assessed HPK's capacity to load the proteins, recognize HER3 on the tumor cell surface, and promote internal uptake. Our findings show that HPK engages HER3 with high specificity, mediates efficient entry into cancer cells, and delivers intact, functional protein therapeutics. In vivo studies using melanoma and triple-negative breast cancer (TNBC) models further demonstrate that HPK enables payload activity within tumors. Collectively, these results identify HPK as a promising vehicle for successful protein delivery and highlight its potential utility in treating HER3-expressing cancers.

#4552 BSI-730, a first-in-class HER2xPD-L1 bi-specific ADC, demonstrates potent anti-tumor activity in HER2-low models via selective tumor cell killing and immune modulation.

Hui-Han Hu[1], Xiaoyao Hao[1], Yue Gao[1], Hongyan Li[1], Jinyu Liu[1], Jinge Zhao[1], Yi Lu[1], Liezhou Ji[1], Zhigang Ma[1], Mingjiu Chen[1], Kedan Lin[2]

[1]Biosion Inc., Nanjing, China,[2]Biosion USA Inc., Delaware, DE

Background: HER2-targeting ADCs approved worldwide benefit patients with HER2-positive/overexpression, yet the efficacy in HER2-low/null setting is limited. HER2-positive cancers often display adaptive resistance to HER2-targeted therapies, driven in part by PD-L1-mediated immunosuppression. Current clinical readouts on HER2-targeting ADCs combined with immune checkpoint modulators and PD-L1-targeting ADCs support the dual targeting design. Engaging HER2 and PD-L1 simultaneously enables enhanced internalization, selective tumor cell killing, and promoted anti-tumor immune response via payload-induced immunogenic cell death, subsequently improving efficacy in HER2-low/null patients.

Methods: The HER2xPD-L1 bi-specific antibody was composed of trastuzumab and the humanized anti-PD-L1 antibody identified from A/J mice immunized with PD-L1-ECD-Fc. The *in vitro* characterization of the bi-specific construct, including simultaneous dual target binding, internalization, and PD-1/PD-L1 signal blocking, has been reported previously. The bi-specific antibody was conjugated to exatecan via a glyco-site-specific conjugation technology in a DAR of 4. The *in vitro* cytotoxicity of BSI-730 was evaluated across cancer cell lines with various expression levels of HER2 and PD-L1. The anti-tumor activity of BSI-730 was investigated in animal models with low/null HER2 expression. The CMC developability as well as the stability of BSI-730 in mouse and human plasma were also assessed.

Results: BSI-730 simultaneously bound to HER2 and PD-L1 with high affinity and showed strong PD-1/PD-L1 signal blocking activity as well as efficient internalization regardless target expression. BSI-730 exhibited potent *in vitro* cytotoxic activity across cell lines with various expression levels of HER2 and PD-L1. The potency of BSI-730 was higher than and comparable to T-Dxd in HER2-low and high expressing cell lines, respectively. In a HER2-null breast cancer CDX model (MDA-MB-231), a single administration of BSI-730 resulted in a significant anti-tumor activity, which was higher than T-Dxd at the same dose level. BSI-730 possesses favorable CMC developability profile.

Conclusion: BSI-730 is a first-in-class HER2xPD-L1 bi-specific ADC tailored for HER2-low/null patients leveraging dual function of selective cell killing and immune modulation. The current pre-clinical data highlight the potential of BSI-730 in HER2-low setting and further pharmacokinetics, toxicity, and IND-enabling studies are underway.

#4553 BSI-128 (AK2024) enhances trastuzumab function and potentiates trastuzumab-deruxtecan activity across HER2-positive preclinical models.

Hui-Han Hu[1], Yinghui Dou[2], Hongyan Li[1], Liansheng Cheng[2], Jinyu Liu[1], Li Wei[2], Wenwen Dai[1], Daoqin Liu[2], Hui Wang[1], Ting Xu[2], Xiaoyao Hao[1], Yue Gao[1], Jinge Zhao[1], Yi Lu[1], Mingjiu Chen[1], Kedan Lin[3]

[1]Biosion Inc., Nanjing, China,[2]Anhui Anke Biotechnology (Group) Co., Ltd., Hefei, China,[3]Biosion USA Inc., Delaware, DE

Background: HER2-targeted therapy continues to evolve with the development of synergistic antibody combinations and novel payload-coupled modalities. Pertuzumab, the first approved trastuzumab-efficacy booster, demonstrates clinical benefit when combined with trastuzumab or trastuzumab-deruxtecan (T-Dxd) in HER2-positive breast cancer. BSI-128 (AK2024), a HER2-targeting monoclonal antibody identified through trastuzumab-synergy-based functional screening, has been characterized as a differentiated trastuzumab efficacy enhancer. Here, we further evaluate the synergistic cytotoxicity and anti-tumor activity of BSI-128 in combination with T-Dxd across HER2-positive *in vitro* and *in vivo* models.

Methods: The binding epitope of BSI-128 was compared with trastuzumab, pertuzumab, and a competing antibody of similar epitope class HLX22 analog (synthetic antibody generated from published Henlius sequence). Trastuzumab-mediated cell binding, HER2 internalization, and antibody-dependent cell-mediated cytotoxicity (ADCC) in the presence of BSI-128 were assessed by flow cytometry, pH-sensitive internalization probes, and ADCC reporter assay. *In vitro* cytotoxicity assays for BSI-128 ± T-Dxd were performed using a 1:1 antibody ratio. *In vivo* synergy studies evaluated BSI-128 with sub-efficacious doses of T-Dxd in HER2-positive xenograft models. The efficacy comparisons were performed against pertuzumab and HLX22 analog.

Results: BSI-128 engaged a HER2 epitope distinct from trastuzumab and pertuzumab and partially overlapping with the HLX22 analog. Despite epitope proximity, BSI-128 did not block trastuzumab binding, unlike the HLX22 analog. When combined at equal molar ratios, BSI-128 plus trastuzumab induced an approximate 2-fold increase in HER2 internalization compared with trastuzumab alone, and this enhancement exceeded that observed with pertuzumab or HLX22 analog combinations. Trastuzumab-mediated ADCC activity was maintained despite a 50% reduction in trastuzumab concentration when BSI-128 was added. Superior synergy of BSI-128 with trastuzumab relative to pertuzumab and HLX22 analog was confirmed in multiple HER2-positive *in vitro* and *in vivo* models. The presence of BSI-128 enhanced T-Dxd *in vitro* cytotoxicity by 2-fold in HER2-positive cells, whereas pertuzumab did not augment T-Dxd activity. BSI-128 also significantly potentiated the anti-tumor activity of T-Dxd in HER2-positive animal models.

Conclusion: These data robustly support BSI-128 as a differentiated trastuzumab-synergy antibody with improved performance relative to pertuzumab and the competing synergy antibody when combined with T-Dxd. These findings support the clinical development of BSI-128 plus T-Dxd for HER2-positive gastric cancer and other T-Dxd-approved indications. BSI-128 is currently being evaluated in a Phase 1 clinical trial.

#4554 Correlation of GI cancer antigens expression or association with patient survival outcomes using TCGA data.

Catherine Wu[1], Salique Hassan Shaham[2], Manish Tripathi[2]

[1]School of Medicine, University of Texas Rio Grande Valley, Edinburg, TX,[2]Oncology and Medicine ISU, South Texas Center of Excellence in Cancer Research, School of Medicine, The University of Texas Rio Grande Valley, McAllen, TX

Background: Cancers of the GI system, including the esophagus, stomach, colon, rectum, pancreas, liver, and biliary tract, comprise a significant portion of the global cancer burden. Recently, tumor-associated antigens (TAAs) have been shown to be useful in targeted cancer therapies and as markers. Although many GI cancer-related TAAs have been identified, treatments could be improved if they could target multiple antigen profiles simultaneously. This study first examines the expression of eight well-known GI cancer-specific TAAs: MMP7, TACSTD2, FOLR1, EPCAM, AADAT, MSLN, CLDN18, and CEACAM5; then it investigates their relationships with each other and with patient survival.

Methods: The Cancer Genome Atlas (TCGA) database; UALCAN was used to analyze the expression profile of TAA in normal and tumor samples, along with their significance. The effects of each TAA on survivability (Kaplan-Meier) and their significance were also analyzed. Survival plots and significance were calculated using log-rank tests. Lastly, Pearson correlations between the eight antigens across all seven cancers were obtained from the Gene Expression Profiling Interactive Analysis (GEPIA) portal.

Results: Across GI cancers show that TAA expression varies from that in normal tissue. MMP7 and MSLN are the most commonly upregulated. Most cancers exhibit three or more antigens that are increased, except for LIHC, where MMP7, EPCAM, and AADAT are downregulated. Only five of eight TAAs correlate with survival: EPCAM and MMP7 in STAD, FOLR1 and CLDN18 in LIHC, EPCAM in ESCA, and MSLN in PAAD. Correlations are mostly weak to moderate, except TACSTD2, which is negatively correlated with all ESCA antigens.

Conclusion: Since MMP7 and MSLN are broadly upregulated in GI cancers, these TAAs could be studied further as potential targets for pan-GI therapies. Cancers with multiple high-impact upregulations associated with survival may be suitable for treatment with multi-antigen antibody or CAR-T therapies, such as EPCAM and MMP7 for STAD. Additionally, the weak correlations among the TAAs suggest that somewhat independent mechanisms might regulate their expression. Therefore, this implies that therapies targeting a single antigen may not be fully effective.

: Novel Antitumor Agents 2
Poster Session

#4558 First disclosure of a highly potent and selective oral KRAS G12V inhibitor PSTA-6208.

Wenxi Li, Lihong Hu, zhenzhen Zhu, Yingchun Liu, Tao Yu, Qianwei Jiang, **Chi-Chung Chan**, Jian Li, Shuhui Chen

Prospect Therapeutics, Nanjing, China

Introduction:
The KRAS G12V mutation is a major oncogenic driver in numerous cancers, promoting tumorigenesis and metastasis via constitutive activation of the MAPK pathway. Although the advent of KRAS-targeted therapy has yielded approved G12C inhibitors and clinical candidates for G12D and pan-KRAS inhibition, a significant unmet need remains for KRAS G12V-driven cancers. Here, we present PSTA-6208, a novel, orally bioavailable KRAS G12V inhibitor with sub-nanomolar cellular potency, marked efficacy in preclinical models, and high selectivity over wild-type KRAS, positioning it as a promising therapeutic candidate for KRAS G12V-positive tumors.
Methods and Results:
PSTA-6208 demonstrated potent and selective anti-proliferative activity in a panel of KRAS G12V-mutant cell lines, with IC_{50} values around 0.1 nM in most cells. In head-to-head comparisons, PSTA-6208 was 17-fold more potent than RMC-5127. This activity was mechanistically linked to MAPK pathway suppression, as evidenced by inhibition of phospho-ERK in KRAS G12V-mutant CAPAN-1 cells (IC_{50} = 1 nM). PSTA-6208 showed >500 folds selectivity over wild-type KRAS cells.
PSTA-6208 exhibited favorable oral pharmacokinetics across multiple species, with low systemic clearance, a prolonged half-life (~10 hours), and high plasma exposure. These properties supported once-daily dosing, which achieved tumor regression in mice at doses as low as 3 mg/kg.
PSTA-6208 induced profound, dose-dependent tumor growth inhibition and regression in multiple KRAS G12V xenograft models. In the NCI-H727 model, daily oral administration of PSTA-6208 at 1, 3, and 10 mg/kg for 21 days resulted in tumor growth inhibition (TGI) of 82%, 108%, and 112%, respectively. Notably, treatment with PSTA-6208 at 10 mg/kg led to near-complete tumor regression (complete response) by Day 21. All treatment groups were well-tolerated, with no significant adverse effects reported.
Conclusions:
PSTA-6208 is a potent, highly selective, and orally bioavailable KRAS G12V inhibitor. Its compelling preclinical profile—including sub-nanomolar cellular potency, exceptional selectivity, favorable pharmacokinetics, and robust *in vivo* efficacy culminating in tumor regression at low doses—strongly supports its further development as a clinical candidate for KRAS G12V-driven cancers.

#4559 PLM-103: A dual-mechanism YES1/YAP pathway inhibitor exhibiting broad antitumor efficacy and immuno-oncology synergy.

Soo Jin Kim[1], Kyoung Mee Kim[1], Jaehyeon Kim[1], Soo Yeon Jang[1], **Yong-Chul Kim**[2]

[1]PeLeMed, Co. Ltd., Seoul, Korea, Republic of,[2]Gwangju Institute of Science & Technology, Gwangju, Korea, Republic of

The Hippo-YAP pathway is a key regulator of tumor progression, metastasis, and immune evasion. Aberrant activation of YAP promotes epithelial-mesenchymal transition (EMT), suppresses immune cell infiltration, and contributes to poor immune responsiveness in various cancers. YES1, a Src family kinase, functions as a critical upstream activator of YAP nuclear signaling, and its oncogenic amplification has been reported in multiple YAP-driven malignancies. Therefore, pharmacologic inhibition of YES1 represents a promising approach to suppress YAP (Yes-Associated Protein) activity and identify new therapeutic strategies targeting YAP-dependent tumors. PLM-103 is a novel small-molecule inhibitor that potently inhibits YES1 kinase and concurrently suppresses TEAD-mediated transcription, leading to robust inactivation of YAP signaling. Through this dual mechanism, PLM-103 achieves TEAD inhibition comparable to classical TEAD inhibitors but exhibits superior suppression of cell proliferation and downstream oncogenic signaling, translating into potent in vivo antitumor efficacy. Unlike conventional TEAD inhibitors whose activity is largely restricted to mesothelioma, PLM-103 demonstrates broad spectrum antitumor activity across YAP-driven cancers including esophageal squamous cell carcinoma (ESCC), renal cell carcinoma (RCC), pancreatic ductal adenocarcinoma (PDAC), and mesothelioma. In the KYSE70 ESCC xenograft model, PLM-103 monotherapy exhibited a remarkable antitumor effect, achieving complete tumor regression (CR) in 4 out of 7 mice. In this in vivo model, PLM-103 treatment significantly reduced the expression of CYR61 and CTGF, YAP target genes, confirming effective suppression of YAP transcriptional activity in tumors. Mouse PK study demonstrated that PLM-103 is orally available and provides sufficient systemic exposure to exert its pharmacologic effects. Additional ADME and safety profiling, including metabolic stability, plasma protein binding, and hERG assay, confirmed that PLM-103 possesses favorable drug-like properties suitable for further development. When combined with the immune checkpoint inhibitor anti-PD-1 antibody, PLM-103 exhibited remarkable synergistic efficacy characterized by enhanced infiltration of $CD8^+$ effector T cells and reduced regulatory T (Treg) cells within the tumor microenvironment. The combination of PLM-103 with anti-PD-1 therapy resulted in durable complete responses, underscoring the potent immunomodulatory and immune-potentiating capacity of PLM-103. Collectively, these findings establish PLM-103 as a highly promising next-generation anticancer agent that integrates targeted YES1/YAP pathway inhibition with robust immunomodulatory activity, providing dual and complementary mechanisms capable of addressing a broad range of YAP-driven malignancies.

#4560 CTPS1 as a metabolic vulnerability and novel therapeutic target in breast and ovarian cancer.

Xiyin Wang[1], Michael Emch[1], Lauren Voll[1], Rebecca Epp[2], Esther Rodman[3], Noa Odell[1], Hannah Smith[1], Nicole Pearson[1], Xiaonan Hou[4], Matthew Goetz[4], Scott Kaufmann[4], S. John Weroha[4], Phillip Beer[5], John Hawse[1]

[1]Department of Biochemistry and Molecular Biology, Mayo Clinic, Rochester, MN,[2]Case Western Reserve University, Cleveland, OH,[3]Vincent Center for Reproductive Biology, Mass General Brigham, Boston, MA,[4]Department of Oncology, Mayo Clinic, Rochester, MN,[5]Step Pharma, Saint-Genis-Pouilly, France

Breast and ovarian cancers are major causes of cancer mortality in women with frequent relapse after curative intent treatment, underscoring the need for novel therapeutics. To this end, we identified CTPS1 as an essential gene in multiple breast and ovarian cancer models, including those resistant to chemotherapy and PARP inhibitors.

CTPS1 and CTPS2 are responsible for *de novo* synthesis of cytidine triphosphate (CTP) which is required for DNA/RNA polymerization, phospholipid synthesis and protein glycosylation. We found CTPS1 to be the predominant isoform expressed in cancer cells, with significantly higher levels in advanced and resistant disease models compared to normal tissue, benign lesions and treatment naïve cancers. Using CTPS1 siRNAs and CTPS1-dTAG (degradation tag) cell lines, we discovered that depletion of CTPS1 induces S-phase cell cycle arrest followed by apoptosis.

Leveraging a first-in-class, highly selective, and orally bioavailable CTPS1 inhibitor (STP938) developed by Step Pharma, we identified nanomolar IC50 values across a panel of cell lines, both in 2D and 3D culture systems, and potent anti-neoplastic activity *ex vivo* and *in vivo* using patient-derived xenograft (PDX) models. STP938 also synergized with standard-of-care chemotherapy agents and PARP inhibitors, including in therapy-resistant models.

Given the essentiality of CTP for biosynthetic processes, we performed bulk and single cell RNA-seq, total and phospho-proteomics, metabolomics, and lipidomic strategies to examine changes induced by acute and chronic STP938 exposure. This revealed that cancer cells are able to overcome pharmacologic CTPS1 inhibition by rewiring of pyrimidine and purine synthesis pathways, upregulation of the pentose phosphate pathway, and extensive remodeling of lipid synthesis pathways including shifts in PC/PE content, increased lysophospholipid production, and altered mitochondrial lipid composition (decreased cardiolipin and increased PG).

To identify genetic drivers of STP938 resistance and synthetic lethal vulnerabilities, we performed a genome-wide CRISPR knockout screen together with a PRISM drug sensitivity screen. Genes regulating dNTP biosynthesis, S-phase progression, and RNA processing were identified as primary escape mechanisms, while DHODH inhibitors, purine and nucleoside analogs, and mitosis modifiers were implicated as synthetic lethal opportunities.

Notably, we discovered that 25% of ovarian tumors lack CTPS2 protein expression, suggesting near complete reliance on CTPS1 for survival. Thus, a Phase 1a/b clinical trial of STP938 (NCT06297525) has been initiated, including an expansion cohort for patients with CTPS2-null ovarian tumors. These laboratory discoveries and ongoing clinical efforts aim to enable broader uptake of this novel therapeutic approach to improve long-term outcomes in patients with CTPS1-dependent disease.

#4561 Cbl-b inhibition with ISM3830 restores innate and adaptive immunity and demonstrates antitumor activity against solid tumors *in vitro* and *in vivo*.

Zhongying Cao[1], Fanye Meng[1], Jinxin Liu[1], Zhilin Ning[1], Jiaojiao Yu[1], David Gennert[2], **Suguna Rachakonda**[2], Man Zhang[1], Xin Cai[1], Xiao Ding[1], Alex Zhavoronkov[2]

[1]Insilico Medicine, Shanghai, China,[2]Insilico Medicine, Cambridge, MA

Therapeutic inhibition of immune checkpoints, such as CTLA-4 and PD-1/PD-L1, has dramatically improved outcomes for cancer patients, yet there remains a critical need for the majority of patients who relapse or insufficiently respond to current checkpoint inhibitor treatments. Cbl-b is an intracellular immune checkpoint downstream of both CD28 and CTLA-4 signaling that negatively regulates activation of T cells, NK cells, dendritic cells, and mast cells, representing a promising, distinct target for cancer immunotherapy. Here, we describe a novel Cbl-b inhibitor, ISM3830, which demonstrated strong Cbl-b inhibition *in vitro* and *in vivo*, leading to enhanced activation of primary human T cells and NK cells.

Comprehensive metabolic and pharmacokinetic profiling showed that ISM3830 has low drug-drug interaction potential, minimal off-target risk, and low in vitro clearance across multiple species. ISM3830 treatment led to increased IL-2 and IFN-γ release in primary human T and NK cells upon anti-CD3 stimulation, with minimal cytotoxicity up to 10 μM. ISM3830 treatment also restored T cell function in the immunosuppressive tumor microenvironment in the presence of PGE2 or adenosine and significantly recovered the function of exhausted T cells. Oral administration of ISM3830 suppressed tumor growth in CT26 and MC38 syngeneic mouse models, with a significant synergistic effect when combined at a dose of 10 mpk with anti-PD-1, achieving a 96% tumor growth inhibition (TGI) rate and complete tumor regression (CR) in 6 out of 8 animals. Notably, ISM3830 also conferred protection against CT26 tumor rechallenge in cured mice by increasing effector memory T cells and NK cells, indicating ISM3830 induced long-term tumor immunity. In vivo pharmacokinetic studies also demonstrated low clearance (CL < 30% Qh) and an average oral bioavailability of 71% across preclinical species, including mice, rats, dogs, and monkeys. Toxicology studies in mice and dogs indicated a favorable safety profile compared to other small-molecule Cbl-b inhibitors. Human dose projection suggested lower effective doses with sustained target coverage. These data together demonstrate ISM3830 potently activates the innate and adaptive immune responses, sustains antitumor efficacy in animal models, and synergizes with other immune checkpoint inhibitors while maintaining favorable pharmacokinetic and safety profile suitable for clinical development. This work supports the further development of ISM3830 as an immune checkpoint inhibitor to treat various solid tumors.

#4562 ISM6210, a potent and selective CDK4 inhibitor for the treatment of HR+/HER2- breast cancer.

Yilin Yang[1], Zhongying Cao[1], Zhisen Zhang[1], Fanye Meng[1], Jinxin Liu[1], Jiamin Zheng[1], Zuoxiao Shi[1], Ling Wang[1], David Gennert[2], **Suguna Rachakonda**[2], Xiao Ding[1], Xin Cai[1], Man Zhang[1], Feng Ren[1], Alex Zhavoronkov[2]

[1]Insilico Medicine, Shanghai, China,[2]Insilico Medicine, Cambridge, MA

CDK4/6 kinases drive the G1-S cell cycle transition, and overactive cyclin-CDK4/6 complexes are common across cancer types. While clinically approved CDK4/6 inhibitors have benefited patients with HR+/HER2- breast cancer, their efficacy is constrained by dose-limiting hematological toxicities, particularly CDK6-driven myelosuppression. Hematopoietic stem cell activation relies primarily on CDK6, but breast cancer cells are more dependent on CDK4, suggesting a potential therapeutic window for a CDK4-selective inhibitor. Here, we report the development and preclinical characterization of ISM6210, an orally bioavailable CDK4 inhibitor with high selectivity over CDK6.

ISM6210 demonstrated potent inhibition of the CDK4/Cyclin D1 complex in enzymatic assays with nanomolar IC50 values and good selectivity over CDK6 and other CDKs. Kinome profiling revealed minimal off-target activity, confirming its high selectivity. In cellular assays, ISM6210 selectively targeted CDK4-dependent breast cancer cells over CDK6-dependent cells. Notably, in human hematopoietic stem cell assays, ISM6210 exhibited an IC50 value about 30-fold higher than the dual CDK4/6 inhibitor Palbociclib against human hematopoietic stem cells, suggesting reduced myelosuppressive potential. Mechanistically, ISM6210 effectively blocked Rb phosphorylation and the G1/S cell cycle transition, resulting in growth arrest in HR+ breast cancer cell lines. In vivo, ISM6210 achieved robust anti-tumor activity at 30 mg/kg BID across multiple HR+ breast cancer xenograft models with notable tumor enrichment.

In addition to its robust biological potency and high selectivity, ISM6210 exhibited favorable drug-like properties, including desirable in vitro ADMET profiles, excellent in vivo exposure and clearance, and good oral bioavailability across multiple preclinical species. Collectively, these findings establish ISM6210 as a potent and selective CDK4 inhibitor that delivers strong efficacy and a promising hematologic safety margin for HR+/HER2- breast cancer treatment.

#4563 Small molecules inhibited dysregulated STAT3-proinflammatory axis and induced antitumor responses in pancreatic and breast cancer.

Rasaq Akinsola[1], Monday Ogaba Ogese[1], Lihong Huo[2], Yue Chen[1], Francisco Lopez-Tapia[1], Richard T. Waldron[3], Aurelia Lugea[3], Stephen J. Pandol[4], James Turkson[1]

[1]Department of Medicine, Division of Medical Oncology and Cancer Biology Program, Cedars-Sinai Medical Center, Los Angeles, CA,[2]Department of Medicine, Division of Gastroenterology, Cedars-Sinai Medical Center, Los Angeles, CA,[3]Department of Medicine, Division of Gastroenterology and Cancer Biology Program, Cedars-Sinai Medical Center, Los Angeles, CA,[4]Department of Medicine, Division of Gastroenterology, and Cancer Therapeutics Program, Cedars-Sinai Medical Center, Los Angeles, CA

Signal transducer and activator of transcription 3 (STAT3) is a promising anti-cancer therapeutic target that promotes tumor development and progression. To study the STAT3-specific mechanisms underpinning tumor formation and that underlie the responses to its targeting, we used the validated mutant *Kras*^{G12D} (KC) mice that under high-fat diet (HFD) has a high pancreatic adenocarcinoma (PDAC) incidence and progression, human cancer-associated fibroblasts (CAFs), PDAC and triple-negative breast cancer (TNBC) cells and xenograft models and interrogated STAT3 activity with two small molecule inhibitors, H182 and H279. Human CAFs, PDAC and TNBC cells harboring aberrantly-active STAT3 responded to growth factor and cytokine stimulation by further enhancing phospho-tyrosine-STAT3 (pYSTAT3) levels. Likewise, upon feeding KC mice the HFD, pYSTAT3 was strongly increased in cells that tracked along a path of altered phenotype, including acinar-ductal-metaplasia (ADM) elements, neoplastic ducts, stromal and immune cells, but was not present in normal acinar cells, in parallel with the development of pancreatic intraepithelial neoplasia (PanIN) lesions. To define the contexts of the pYSTAT3 and the phenotype changes, we probed the cells and mouse models with the inhibitors. The pYSTAT3 levels in the cells were suppressed early by H182 and H279 treatment. In PDAC cells, prolonged treatments with H182 severely shifted the secretome, including decreased IL-6-stimulated production of IL-8, SERPINE1, CXCL1, CXCL12, CCL2 and MIF, repressed the expression of genes involved in immune evasion, angiogenesis, cell proliferation, migration, oxidative stress and tumor progression, and upregulated tumor suppressor genes. In PDAC or TNBC cells, similar prolonged treatments with H182 or H279 also suppressed the expression of anti-apoptotic Mcl-1, Bcl-xL and c-Myc, pro-invasive matrix metalloproteinase 9, and the epithelial-mesenchymal transition proteins, SNAIL, Twist, Snug and ZEB, while inducing E-cadherin and pro-apoptotic Bax, Bad, PUMA and BIM. Treatments of PDAC and TNBC cells with the inhibitors also led to DNA damage, γH2AX, ATM and Chk2 induction, mitochondrial oxygen consumption rate impairment, cell cycle arrest at the G2/M phase, decreased viability, migration and invasiveness *in vitro*, and apoptosis. H182 treatment prevented acinar cell de-differentiation into ADM/PanINs, in parallel with decreased pro-fibroinflammatory gene expression in the pancreas, such as CXCL12, CCL2, and CCL5 in HFD-fed KC mice, and inhibited growth of PDAC subcutaneous xenografts in mice. Together, the findings support a hyperactivated STAT3-pro-fibroinflammatory cytokines and chemokines axis in diverse cell types within tumors that is critical in tumor initiation and progression. Inhibiting STAT3 functions may be a preventative and therapeutic approach against cancer.

#4564 Dual mechanisms of PARP7 inhibition driving potent antitumor activity.

Iksoo Jang, Dajeong Kim, Daehyeon Seong, Jeong Yoon Shin, Kyu Hwan Kim, SeungHyun Song, Joon Yonug Hwang, Hong Sik Han, Kyung Seok Lee, Jongho Cho, Ki Moon Ryu, Mi-Kyung Kim

Dong-A ST, Yongin-si, Korea, Republic of

PARP7 is a mono-ADP-ribosyltransferase that transfers a single ADP-ribose moiety to its substrates, thereby modulating protein function and contributing to the regulation of type I interferon (IFN) signaling and cellular homeostasis. In cancer models, PARP7 inhibition exhibits strong antitumor activity through a dual mechanism involving activation of the type I IFN pathway and direct tumor-intrinsic effects within cancer cells. We have developed a couple of series of novel PARP7 inhibitors, and in this study, we focused on characterizing the molecular features associated with responsiveness to PARP7 inhibitors in parallel with mechanistic studies using the clinical-stage benchmark, RBN-2397. First, in the context of antitumor immune activation, we hypothesized that interferon-stimulated gene (ISG) induction upon PARP7 inhibition is positively correlated with antitumor activity. In mouse syngeneic models, cancer cells showing strong ISG induction upon PARP7 inhibition exhibited greater antitumor responses. Combination with chemotherapeutic agents that increase cytosolic double-stranded DNA (dsDNA) further enhanced ISG induction and antitumor activity. To define ISG induction responsiveness, we screened more than 40 human cancer cell lines and categorized them as ISG responders or non-responders. Responders exhibited gene expression patterns characterized by elevated innate immune signaling and reduced genome stability. In addition to its immuno-oncological activity, PARP7 inhibition exerts an intrinsic, cell-autonomous antitumor effect, suggesting a dual mechanism of action for PARP7-targeted therapy. This intrinsic cytotoxic effect acts independently of the catalytic inhibition responsible for immune activation. While multiple mechanisms have been proposed, our data support that a PARP7 inhibitor-induced chromatin-associated trapping process represents a critical event leading to nuclear accumulation of PARP7 and subsequent DNA damage. Additionally, we confirmed that intracellular PARP7 expression is essential for PARP7 inhibitor-induced cytotoxicity. Furthermore, using the CRISPR-Cas9 system, we validated an additional key factor involved in this intrinsic cytotoxicity. Collectively, our findings demonstrate that PARP7 inhibition elicits a dual mechanism involving ISG induction and intrinsic cytotoxicity, resulting in robust antitumor activity. The key regulatory factors underlying this dual mechanism may serve as potential biomarkers for patient selection in future clinical trials and help identify individuals most likely to benefit from PARP7-targeted therapy.

#4565 Preclinical evaluation of GFH276 monotherapy and combination therapy for RAS-mutant tumors.

Feng Yan, Jichen Zhao, Jingyang Zhang, Siyuan Le, Fusheng Zhou, Jiong Lan, Qiang Lu

Genfleet Therapeutics, Shanghai, China

Background: RAS mutations are found in 90% PDAC, 50% CRC, 30% NSCLC, 27% cholangiocarcinomas, 20% uterine corpus endometrial carcinomas and some other types of tumors. KRAS G12C was the first RAS mutant clinically conquered, yet targeting other isoforms remains unresolved. GFH276, an investigational molecular-glue panRAS(ON) inhibitor currently being evaluated in a Phase 1 trial (NCT07198321), has previously shown potent activity across RAS-mutant models and demonstrated MOA-derived superiority to SIIP-based KRAS inhibitors and dose-level advantage over the competitor compound. Here we present a further pre-clinical assessment of GFH276 monotherapy and its rational combination with distinct therapeutic agents.
Methods: BULB/c nude mice bearing CDX tumors harboring different KRAS mutations were used to determine the anti-tumor efficacy of GFH276 monotherapy or its combination with Cetuximab. BULB/c mice bearing CT-26 tumors engineered to harbor KRAS G12C mutation were used to compare GFH276 monotherapy with its combination with an anti-mouse PD-1 mAb.
Results: Across a serial of NSCLC, CRC and PDAC CDX models, daily oral administration of 3 mg/kg of GFH276 drove significant anti-tumor efficacy. In a cholangiocarcinoma and an endometrial tumor models, GFH276 also inhibited tumor growth in a dose-dependent manner. Considering the validated synergism between KRAS G12C inhibitors and EGFR mAbs in clinic, combination therapy of GFH276 plus Cetuximab was also investigated and the result showed that co-administration with Cetuximab enhanced the efficacy of GFH276 significantly. Coordination between GFH276 and immunotherapy was also explored in the syngeneic CT26-KRAS^{G12C} mouse model. In this model, 21-day treatment with 0.3-3 mg/kg of GFH276 elicited significant anti-tumor effect and all animals from the 3 mg/kg group were tumor free. Co-treatment with an anti-mouse PD-1 antibody not only synergized with GFH276 dosing , but also helped maintain the tumor free status after GFH276 dosing was stopped for another 79 days.
Conclusions: GFH276 monotherapy was effective in mouse models harboring tumors originating from most common RAS-mutant cancers. GFH276 also showed synergistic effects with anti-EGFR mAb and immunotherapy. These results depict the promising therapeutic potential of GFH276 in broad indications via different application strategies.

#4566 Discovery and characterization of CKD-9001, a novel PARP1-selective inhibitor and DNA trapper with enhanced efficacy and an improved toxicity profile in HRD cancers.

Yuji Kim, Moosung Ko, Gun-Woo Park, Yoo-Kyung Song, Hye-Jin Hong, Keesoo Nam, Junho Cho, Younghue Han, Jaeyoung Lee, Dahae Lee, Jiyeon Back, Seong-Ho Hong, Ju Young Song, Jinsol Park, Hyunmo Yang, Nina Ha, Se-Mi Kim, In-Chang Hwang, Changsik Lee, Sung Jun Kang

CKD Pharmaceutical Corp., Seoul, Korea, Republic of

Poly(ADP-ribose) polymerase (PARP) inhibitors have been established as therapeutic agents for patients with homologous recombination repair (HRR) deficiencies, such as BRCA1/2 mutations, in ovarian, breast, prostate, and pancreatic cancers. Currently, pan-PARP inhibitors that have received approval target both PARP1 and PARP2, demonstrating potent antitumor activity. However, PARP2 inhibition has been identified as a major contributor to hematologic toxicity, resulting in dose limitations and treatment discontinuation. Given PARP1's role as the primary enzyme in sensing single-strand breaks and regulating DNA repair processes, the development of PARP1-selective inhibitors has emerged as a promising strategy to achieve potent antitumor efficacy while minimizing toxicity compared with conventional pan-PARP inhibitors. In this study, we present the preclinical development of CKD-9001, a novel PARP1-selective inhibitor and potent DNA trapper.We developed CKD-9001, a next-generation PARP1-selective inhibitor, and evaluated its preclinical efficacy and toxicity profile against the leading agents, olaparib and saruparib. Our findings demonstrated excellent selectivity for PARP1, as evidenced by its high levels of enzymatic inhibition and DNA-trapping potency.*In vitro* studies demonstrated that CKD-9001 exhibited potent antiproliferative effects, with IC_{50} values ≤10 nM in HRR-deficient and BRCA2-knockout cancer cell lines. *In vivo* studies showed remarkable antitumor efficacy of CKD-9001, even at low doses, in HRR-deficient animal models. Furthermore, pharmacokinetic and safety analyses confirmed that CKD-9001 markedly reduced hematologic toxicity and significantly improved the safety margin compared with conventional pan-PARP inhibitors. In addition, we found that CKD-9001 was capable of penetrating the blood-brain barrier (BBB).In conclusion, CKD-9001 is a next-generation PARP1-selective inhibitor that successfully combines enhanced efficacy with remarkably low toxicity, demonstrating outstanding therapeutic potential in HRD cancers.

#4567 A novel PARP7 inhibitor exhibits dual antitumor activity through immune activation and tumor-intrinsic growth inhibition.

Dajeong Kim, Iksoo Jang, Daehyeon Seong, Jeongyoon Shin, Kyu Hwan Kim, SeungHyun Song, Joon Yonug Hwang, Hong Sik Han, Kyung Seok Lee, Boram Lee, Soo-Jung Choi, Song-Yi Lee, Dae Young Lee, Jinhoon Jeong, Hojeong Hong, Haneol Kim, Jongho Cho, Ki Moon Ryu, Mi-Kyung Kim

Dong-A ST, Yongin-si, Korea, Republic of

PARP7 (TIPARP, TCDD-induced poly[ADP-ribose] polymerase) is a stress-inducible mono-ADP-ribosyltransferase frequently overexpressed across multiple cancer types. Elevated PARP7 expression has been implicated in tumor progression, immune evasion, and the establishment of an immunosuppressive tumor microenvironment (TME). Mechanistically, in cancer cells, PARP7 negatively regulates type I interferon (IFN) signaling by mono-ADP-ribosylating TBK1, thereby suppressing nucleic acid sensing and dampening antitumor immune activation within the TME. Pharmacological inhibition of PARP7 restores IFN signaling and potentiates immune-mediated antitumor responses. In addition to immune activation, PARP7 inhibition exerts tumor-intrinsic antitumor effects through multiple cellular mechanisms, culminating in direct tumor cell growth inhibition. Collectively, these findings suggest that targeting PARP7 may offer superior therapeutic potential compared with current immuno-oncology (IO) approaches by coupling immune activation with tumor-intrinsic control. In this study, we identified a novel small-molecule PARP7 inhibitor, referred to as compound 1, which exerts dual anticancer mechanisms. Compound 1 demonstrated potent inhibition of PARP7 enzymatic activity in biochemical assays and markedly reduced global mono-ADP-ribosylation (MARylation) in PARP7-inducible SK-MES-1 cells, thereby confirming its activity at the cellular level. From an IO perspective, compound 1 robustly induced interferon-stimulated gene (ISG) expression in RAW-Lucia ISG cells and various cancer cell lines. It also enhanced the activation of multiple immune cell subsets, showing pronounced effects particularly under TME-mimicking conditions. Compound 1 exhibited strong monotherapy activity in syngeneic tumor models and achieved complete responses (CR) when combined with anti-PD-1 or standard chemotherapies. Beyond immune modulation, PARP7 inhibition also mediates tumor-intrinsic growth inhibition. We identified a chromatin-associated trapping mechanism as a primary driver of these intrinsic effects. Correspondingly, compound 1 produced potent growth inhibition across multiple cancer cell lines, including NCI-H1373, and significantly suppressed tumor growth in xenograft models. Notably, across both mechanisms, compound 1 demonstrated comparable or superior activity to RBN2397, a PARP7 inhibitor under clinical evaluation. In summary, our findings highlight PARP7 inhibition as a promising therapeutic strategy that integrates immune activation with tumor-intrinsic growth inhibition. The novel PARP7 inhibitor, compound 1, consistently demonstrated this dual mechanism across diverse preclinical models, supporting its potential as a next-generation therapeutic candidate with both immune-mediated and tumor-intrinsic antitumor activity.

#4568 Inhibition of nicotinamide phosphoribosyltransferase (NAMPT) impairs cellular viability, affects energy metabolism, induces DNA damage, and drives tumor regression in preclinical models of neuroblastoma.

Amy Yu[1], Sophia Varriano[1], Victor J. Collins[1], Ariana E. Nelson[1], Abantika Chakraborty[1], Unsun Lee[1], Amy James[2], Kristine Isanogle[2], Nimit Patel[3], Joong Kim[3], Ming Sun[1], Ye Yang[4], Ying Wu[5], Krithika Bhuvaneshwar[5], Bhushan L. Thakur[6], Arnulfo Mendoza[1], Sameer H. Issaq[7], Mirit I. Aladjem[6], John F. Shern[1], Parthav Jailwala[5], Joseph D. Kalen[3], Simone Difilippantonio[2], Craig J. Thomas[8], Daniel R. Crooks[4], Rosa Nguyen[1], Carol J. Thiele[1], Christine M. Heske[1]

[1]Pediatric Oncology Branch, National Cancer Institute, Bethesda, MD,[2]Animal Research Technical Support, Laboratory Animal Sciences Program, Frederick National Laboratory for Cancer Research, Frederick, MD,[3]Small Animal Imaging Program, Laboratory Animal Sciences Program, Frederick National Laboratory for Cancer Research, Frederick, MD, [4]Clinical Cancer Metabolism Facility, Urologic Oncology Branch, National Cancer Institute, Bethesda, MD,[5]Advanced Biomedical Computational Science, Frederick National Laboratory for Cancer Research, Frederick, MD,[6]Developmental Therapeutics Branch, National Cancer Institute, Bethesda, MD,[7]Urologic Oncology Branch, National Cancer Institute, Bethesda, MD,[8]Division of Preclinical Innovation, National Center for Advancing Translational Sciences, Rockville, MD

Cancer cell metabolism is altered to meet increased metabolic demands of proliferating cancer cells. Reprogrammed metabolic pathways represent cell type and context specific therapeutic opportunities. Targeting NAD^+ production via inhibition of the NAD^+ salvage pathway presents one potential opportunity, as NAD^+ is essential for energy metabolism and other downstream processes. Presently, NAMPT is the only clinically targetable enzyme in this pathway. We conducted a high-throughput cancer cell line screen and identified that neuroblastoma (NB) cells are significantly more sensitive to NAMPT inhibitors (NAMPTis) than most other solid tumors, with IC50 values >20-fold less than the cell line panel average. NB is the most common extracranial solid tumor in children, accounting for 15% of pediatric cancer deaths. We used 2 clinical NAMPTis under early phase study (OT-82 and KPT-9274) to validate our drug screen results in 10 molecularly diverse NB cell lines including 2 NB PDX-derived cell lines. We investigated the mechanistic effects of NAMPT inhibition on NAD^+-dependent pathways and analyzed the *in vivo* effects of OT-82 in 3 orthotopic NB models. Treatment of NB cell lines with NAMPTis results in failure of cells to proliferate following replacement with drug-free media at 48h, suggesting irreversible cell death. Furthermore, NAMPTi treatment results in neither apoptotic nor necroptotic cell death but induces autophagy. NAMPTis reduce intracellular NAD^+ levels and co-treatment with NMN, the product of NAMPT, fully rescues cell viability, verifying NAD^+-dependence and on-target activity of each NAMPTi. Moreover, we observed reductions in ATP of 50% and >90% after 24h and 72h of treatment, respectively. Examination of drug effects on glucose metabolism using extracellular flux and metabolomics analyses demonstrated cell line-specific effects, including reduction in oxidative phosphorylation and/or glycolysis with depletion of metabolites produced via NAD^+-consuming enzymes. Investigation of the effects of NAMPTis on other key NAD^+ consuming enzymes including sirtuin 1 (SIRT1) and poly (ADP-ribose) polymerase (PARP), demonstrated significant loss of activity of both enzymes in a time-dependent manner. As loss of PARP and SIRT1 activity can compromise DNA repair, comet assays were used to assess the extent of DNA damage, revealing increased DNA damage upon NAMPTi treatment in all models. *In vivo* studies of OT-82 in orthotopic xenografts demonstrated significant tumor shrinkage. Across models, 23/26 mouse tumors had average volume reductions of 67% (range 10%-99%). Together, these data demonstrate that in NB, multiple critical pathways are impacted by the loss of NAD^+ mediated by NAMPT inhibition and suggest NAMPTis may have translational potential as a novel agent against NB.

#4569 D3S-003, an orally bioavailable potent and selective dual-state inhibitor targeting both GDP- and GTP-bound KRAS G12D.

Jing Zhang[1], Tienan Wang[1], Robert A. Mook Jr.[2], Haibo Xie[1], Shaonan Wang[1], Zhiqiang Zheng[1], Xin Xiong[1], Hui Wang[1], Zhi Jian Chen[1]

[1]D3 Bio, Inc., Shanghai, China,[2]Department of Medicine, Duke University Medical Center, Durham, NC

KRAS G12D is the most prevalent KRAS mutation in human cancers and represents a highly attractive yet challenging oncogenic target. Compared with KRAS G12C, the intrinsic hydrolysis rate of KRAS G12D is significantly slower, resulting in a more persistent active (GTP-bound) state that limits the efficacy of GDP-state inhibitors. To address this challenge, we identified D3S-003, a potent and selective small-molecule inhibitor that targets both the GDP-bound (OFF) and GTP-bound (ON) forms of KRAS G12D through intensive optimization guided by molecular dynamics and co-crystal-based SAR interrogation. In SPR binding assays, D3S-003 sub-nanomolar affinity for both GDP-bound and GTP-bound KRAS G12D, with a target residence half-life exceeding 13 hours on the GDP-bound form, a key feature enabling a covalent-like inhibition. In biochemical assays, D3S-003 inhibited GDP-bound KRAS G12D nucleotide exchange and disrupted GTP-bound KRAS G12D-cRAF interaction with single-digit nanomolar IC_{50} values, validating its dual-state molecular mechanism of action. In cellular assays, D3S-003 demonstrated nanomolar IC_{50} inhibition in both p-ERK inhibition and proliferation across a panel of KRAS G12D-mutant cell lines, while maintaining high selectivity over KRAS non-G12D lines. Notably, D3S-003 showed improved potency and selectivity compared with RMC-9805, an investigational KRAS G12D (ON) inhibitor currently in clinical trials. D3S-003 exhibits desirable drug-like properties, oral bioavailability across multiple preclinical species, and a robust GLP safety profile. In i*n vivo* studies, it demonstrated robust antitumor activity in KRAS G12D-driven HPAC pancreatic cancer xenografts, requiring only 17.5 nM·h and 56 nM·h free drug AUC to achieve 30% tumor regression (PR) and 100% complete remission (CR), respectively. Across a broad panel of PDX and CDX models of NSCLC and pancreatic cancer with KRAS G12D mutations and diverse genetic backgrounds, D3S-003 achieved a 70% overall response rate (ORR), indicating broad efficacy across these tumor types. Together, these findings highlight D3S-003 as a potent and selective KRAS G12D dual-state inhibitor with strong translational potential. A Phase 1 first-in-human (FIH) study is currently being planned.

#4570 HEC228032, an orally bioavailable molecular glue pan-RAS (ON) inhibitor with highly potent anti-tumor efficacy.

Haiwang Liu, Lingling Chen, Yangyang Meng, Hong Huang, Ming Li, Ning Kang, Yahui Feng, Ziting Liu, Jing Li, Kai Lin, Yingjun Zhang

HEC Pharma Co. Ltd, Shenzhen, China

Background: The RAS oncogene, one of the most frequently mutated drivers in human cancer, is pathogenic in approximately 25% of malignancies, with particularly high prevalence in pancreatic ductal adenocarcinoma, colorectal carcinoma, and non-small cell lung cancer. Approved RAS inhibitors are predominantly limited to the KRAS G12C mutation, leaving a substantial patient population with other KRAS mutations (e.g., G12D, G12V, G13D, Q61R, etc.) or NRAS/HRAS mutations underserved. The emergence of resistance to these agents further underscores the critical need for broad-spectrum pan-RAS inhibitors.

Methods: The affinity of HEC228032 for Cyclophilin A (CypA) and KRAS mutants (G12C/D/V, etc.), as well as its disruption of RAS-RAF interactions, was evaluated using HTRF binding assays. Its anti-proliferative activity was assessed via CTG assays in tumor cell lines. Pharmacodynamic and anti-tumor efficacy were investigated in multiple KRAS-dependent xenograft models *in vivo*.

Results: HEC228032 exhibited high binding affinity for CypA and KRAS mutants (G12C, G12V, G12D, etc) and potently disrupted KRAS-RAF interactions. It demonstrated superior *in vitro* potency compared to RMC-6236, inhibiting proliferation across multiple RAS-mutant cell lines with sub-nanomolar IC50 values. In KRAS-mutant xenograft models (including PK59 (G12D), HPAC (G12D), and LU99 (G12C)), HEC228032 administered orally once daily at 3-10 mg/kg induced dose-dependent tumor regression, with good tolerability over 21 days. Furthermore, HEC228032 achieved higher oral exposure than RMC-6236 in mice, rats, and beagle dogs.

Conclusions: HEC228032 is a promising pan-RAS(ON) inhibitor, characterized by potent antitumor activity against diverse RAS mutants, favorable pharmacokinetic properties, and an excellent tolerability profile, supporting its strong potential for clinical development.

#4571 Discovery and characterization of RGT-490, a mutant selective PI3Kα inhibitor.

Jing Han[1], Kailiang Wang[1], Feng Zhao[1], Xinjuan Wang[1], Xiaoming Ren[1], Xiuliang Huang[1], Xiumei Chen[1], Teng Feng[1], Xin Hua[1], Zhuanzhuan Zhang[1], Lili Yao[1], Jing Lin[1], Wenge Zhong[2], Julie Xie[2]

[1]Qilu Regor Therapeutics Inc., Shanghai, China,[2]Regor Pharmaceuticals Inc., Boston, MA

PI3Kα is frequently mutated and overactivated in a variety of human cancers including breast, gynecological, head and neck, and colorectal cancers. Clinical use and efficacy of the approved PI3Kα inhibitors alpelisib and inavolisib are limited by the side effects associated with wild-type (WT) PI3Kα inhibition, prominently hyperglycemia, rash, stomatitis and GI toxicities. RGT-490 is a potent and mutant selective PI3Kα inhibitor discovered by deploying Computer Accelerated Rational Design (CARD) technology platform. It demonstrated potent anti-proliferation activity in PIK3CA mutated cancer cells. In ER+ breast cancer T47D xenograft model, RGT-490 robustly suppressed Akt phosphorylation and induced significant apoptosis without increasing insulin or glucose levels. In addition, RGT-490 caused near-complete tumor regressions in T47D models without any apparent toxicity. As an allosteric PI3Kα inhibitor, RGT-490 overcame the resistance to orthosteric inhibitors alpelisib and inavolisib resulted from the secondary mutations in the ATP binding pocket. In HER2+ breast cancer HCC1954 cells, RGT-490 suppressed the resistance to HER2 inhibition caused by PI3Kα mutation. With potent activity and excellent selectivity, RGT-490 provides opportunity to reduce WT PI3Kα-associated toxicities, enable deeper target coverage and achieve further improved clinical efficacy in PI3Kα mutant patients. RGT-490 phase 1 study is planned 1H2026.

#4572 Discovery of SY-14556, a highly potent and selective small molecule reactivator of p53 Y220C mutant with differentiated preclinical profile.

Hongjuan Li, Zhenbang Lou, Xiaopeng Li, Chang Lu, Shikang Cheng, Bo Li, Xianxing Shang, Xiaofeng Zhai, Yan Zhu, Hong Luo, **Yinghui Sun**

Shouyao Holding (Beijing) Co., Ltd., Beijing, China

As a key tumor suppressor, p53 binds to DNA and transcriptionally activates target genes to regulate cell-cycle arrest, DNA damage repair, apoptosis, and multiple other antiproliferative processes. *TP53* is the most frequently mutated gene in human cancer, and Y220C is one hot-spot mutation occurring in approximately 1% of solid tumors. Pharmacologic stabilization and reactivation of the Y220C mutant to a wild-type-like conformation is a validated therapeutic strategy, as demonstrated by the clinical activity of PC14586 (rezatapopt). Here, we characterize SY-14556 as a highly potent and selective p53 Y220C reactivator. In biochemical assay, SY-14556 induced p53 Y220C DNA binding with an EC_{50} < 5 nM. In luciferase reporter assay, SY-14556 activated wild-type p53 transcriptional activity with an EC_{50} < 50 nM. Across a panel of p53 Y220C-mutant cancer cell lines, SY-14556 inhibited proliferation (IC_{50} 20-100 nM) with >100-fold selectivity over p53-WT cells. Consistent with high-fidelity p53 pathway reactivation, SY-14556 also dose-dependently activated p53 target genes expression including p21 and MDM2, inducing cell cycle arrest and apoptosis. *In vivo,* SY-14556 demonstrated robust anti-tumor activity in several p53 Y220C-mutant cell line-derived xenograft (CDX) models. Furthermore, SY-14556 displayed favorable PK properties and tolerability in preclinical studies. In conclusion, SY-14556 is a best-in class p53-Y220C reactivator with robust preclinical efficacy and safety. These data support its advancement into clinical trials for p53 Y220C-mutant solid tumors.

#4573 JMKX007129 is a next generation of androgen receptor inhibitor targeting N-terminal domain for the treatment of metastatic castration-resistant prostate cancers.

Shengjian Huang, Gang Deng, Liyan Yue, Xiaodong Zhang, Aishen Gong, Xiumei Li, Nan Liu, Shurong Yang, Amin Wang, Jiayu Zhao, Jianbiao Peng

Shanghai Jeyou Pharmaceutical Co., Ltd., Shanghai, China

Background: Androgen receptor ligand binding domain (AR LBD) mutations are one of the key factors leading to resistance to AR inhibitors or degraders in castration-resistant prostate cancer (CRPC). As a result, inhibitors targeting other domains of AR, such as the NTD, have become a major focus in current drug development efforts to overcome this resistance. However, the clinical development of Anitens-based AR-NTD inhibitors has encountered setbacks due to insufficient activity and selectivity. Therefore, there is an urgent need to develop AR-NTD inhibitors with higher potency, improved selectivity, and enhanced safety profiles.

Methods: Based on the core structure of Anitens, we conducted rational design and obtained the lead compound JMKX007129. A comprehensive suite of in vitro and in vivo characterizations was subsequently performed. These evaluations included assessments of its target binding affinity, mechanism of action, in vitro and in vivo efficacy, pharmacokinetic and toxicological profiles, as well as its combination effects with existing AR inhibitors and degraders.

Results: Compound JMKX007129 demonstrated excellent in vitro and in vivo activity and selectivity. Cellular Thermal Shift Assay (CETSA) confirmed that JMKX007129 simultaneously engages both full-length AR (in LnCap cells) and the splice variant AR-V7 (in 22RV1 cells). Reporter gene and qPCR assays demonstrated that JMKX007129 effectively (EC50≈20 nM) modulates the transcription of downstream genes of both AR and AR-V7. It potently inhibited the proliferation of AR-positive prostate cancer cells, exhibiting a selectivity window of approximately 20-fold over AR-negative cells. JMKX007129 displayed favorable pharmacokinetic properties in mice, rats, and dogs, which translated into robust in vivo antitumor efficacy. Significant activity was observed in models sensitive to AR inhibitors (LnCap) as well as in those with acquired resistance (VCap, 22RV1), accompanied by a favorable tolerability profile. Finally, JMKX007129 exhibited a synergistic anti-proliferative effect in combination with AR inhibitors or degraders in 22RV1 cells.

Conclusions: In summary, we have successfully developed JMKX007129, a novel small-molecule compound targeting the AR-NTD. Preclinical studies demonstrate that JMKX007129, both as a monotherapy and in combination with AR inhibitors or degraders, exhibits promising in vitro and in vivo efficacy and a favorable safety profile, indicating its potential to overcome resistance mediated by AR LBD mutations. IND-enabling studies for JMKX007129 are currently underway.

#4574 Highly potent inhibitors of RAD51, with first-in-class potential, targeting HR-proficient cancers.

Alessandro Galbiati, Daniela Asa, Pietro Picconi, Annamaria Marra, Claudia Stellato, Patrizia Banfi, Liviana Cozzi, Fabio Gasparri, Frank Narjes, Claudia Perrera, **Alessia Montagnoli**

Nerviano Medical Sciences, Nerviano, Italy

BACKGROUND: Targeting DNA repair pathways to selectively eliminate cancer cells has seen a huge success with multiple PARP1 inhibitors (PARPi) approved in different solid tumor indications. RAD51 is a key DNA repair gene with an important role in maintaining genomic stability by mediating homologous recombination repair (HRR) and promoting replication fork protection. Impairment of HRR reduces cell fitness in genetic backgrounds with high replication stress and sensitizes cancer cells to DNA-damaging agents and DNA Damage Response (DDR) inhibitors.
METHODS: A drug discovery campaign was conducted to identify novel small-molecule inhibitors of BRCA2-RAD51 protein-protein interaction (PPI). Structure-based drug design was employed to develop multiple compound series. Biochemical potency was assessed using a Fluorescence Polarization (FP) assay and an ATPase assay to measure the DNA-induced activity of RAD51, which is reliant on RAD51 self-oligomerization. A cellular reporter assay to measure HRR proficiency and a high content imaging assay to measure RAD51 foci formation were developed to assess compounds target engagement.
RESULTS: We have identified proprietary RAD51 PPI inhibitors, orally bioavailable, demonstrating single-digit nanomolar biochemical potency on RAD51 and anti-proliferative activity in a subset of cancer cell lines. These include cell lines resistant to cisplatin or PARP1 inhibitors with a sensitivity profile distinct from RAD51 genetic depletion (based on the analysis of DepMap dataset). The anti-proliferative potency correlates with biochemical potency, cellular target engagement and activation of DNA damage response, confirming the expected on-target mechanism of action.
CONCLUSIONS: The novel mechanism of action, with potential for combination with DNA damaging agents and DDR inhibitors, positions Nerviano Medical Sciences' RAD51 inhibitors as promising first-in-class candidates for further development across multiple cancer types resistant to standard of care.

#4575 Non-clinical characterization of Mocertatug Rezetecan (GSK5733584), a novel B7-H4-directed antibody-drug conjugate.

Jeremy Waight[1], Yuanfeng Zhou[2], Danni Sun[2], Lu Zhang[3], Jon Chung[4], Michael Adam[1], Wenjin Zhou[3], Pengchao Qiu[3], Jifa Fan[3], Anna Strobl[5], Jaegil Kim[4], Aishwarya Bhaskar[1], Srujana Neelam[1], Geeta Sharma[4], Shannon McKearnan[1], Huifeng Niu[2], Takahiro Sato[1], Derek Poore[1], Alexander Cocks[5], Prajna Behera[4], Chris Hopson[1], Ken Hance[1], Richard Davidson[5]

[1]GSK, Collegeville, PA,[2]Hansoh Pharmaceutical Group Co., Ltd, Shanghai, China,[3]Hansoh Pharmaceutical Group Co., Ltd., Shanghai, China,[4]GSK, Waltham, MA,[5]GSK, London, United Kingdom

B7-H4 (B7 homolog 4 protein), also known as B7S1 (B7 superfamily member 1) or VTCN1 (V-set domain-containing T cell activation inhibitor 1), is an important immunoregulatory ligand in the B7-CD28 family. B7-H4 is overexpressed in various tumor tissues such as breast, ovarian, uterine, and lung cancers. B7-H4 has been described to both attenuate T cell function (e.g., proliferation, cytokine secretion and cell cycle) as well as promote tumor cell proliferation, invasion, and metastasis. Consistent with its described immunoregulatory and tumor promoting role, B7-H4 is associated with poor prognosis and negative clinicopathological features in patients with advanced tumors. Due to its overexpression in tumors and tumor-promoting functions, B7-H4 represents an attractive target for tumor-selective therapies like antibody-drug conjugates (ADCs). Mocertatug Rezetecan (Mo-Rez) is a novel ADC that combines a humanized anti-B7-H4 immunoglobulin G1 monoclonal antibody with an exatecan-derived topoisomerase I (TOPO1) inhibitor (SHR-9265, GSK5757810A, average DAR of 6).

Here we describe various non-clinical characteristics of Mo-Rez, including biophysical, functional, and mechanistic attributes of the ADC. In vitro, Mo-Rez demonstrated concentration-dependent binding to B7-H4-expressing tumor cells, which resulted in time-dependent B7-H4 internalization and subsequent cellular cytotoxicity. Consistent with its TOPO1i payload characteristics, Mo-Rez also exhibited cell cycle arrest (S-phase) and bystander killing capability. In vivo, Mo-Rez exhibited significant and dose-dependent tumor growth inhibition (TGI) towards MX-1 (breast) and RL95-2 (endometrial) CDX models. Similar anti-tumor activity was observed across human PDX models of breast cancer, cholangiocarcinoma, cervical cancer, and ovarian cancer. Notably, Mo-Rez antitumor responses were observed in both homologous recombination deficient and proficient (HRD and HRP, respectively) ovarian cancer PDX models.

Importantly, the strong antitumor activity in ovarian models align with recent clinical data for Mo-Rez in heavily pretreated platinum-resistant ovarian cancer (PROC, 48.5% ORR). Collectively, these findings support Mo-Rez as a promising cancer therapy and its rapidly progressing global clinical development (BEHOLD trials).

#4576 2X-121/ stenoparib - a novel, dual inhibitor of PARP and tankyrase in phase 2 clinical trials in advanced ovarian cancer- blocks the WNT signaling pathway and inhibits growth of human colorectal cancer cell lines at clinically relevant drug concentrations.

Louis F. Stancato[1], Sydney Leohr[1], Mustapha Moussaif[1], Mogens Winkel Madsen[2], Steen Knudsen[2], Annette Nielsen[2], Mette Jacobsen[2], Peter Gimsing[2], Thomas Jensen[2], **Jeremy R. Graff**[2]

[1]Indiana Biosciences Research Institute, Indianapolis, IN,[2]Allarity Therapeutics, Inc., Tarpon Springs, FL

2X-121 (stenoparib/ E7499) is a novel inhibitor of PARP1/2 (1nM ~IC50) and Tankyrase 1/2 (IC50 ~50nm). As such, 2X-121 impairs DNA repair while simultaneously inhibiting the WNT/ß-catenin oncogenic signaling pathway. 2X-121 has shown durable clinical benefit in a phase 2 study in patients with advanced, platinum resistant and refractory ovarian cancer as a single agent dosed twice daily, regardless of BRCA status. A new protocol is currently enrolling platinum resistant or ineligible ovarian cancer patients to further deepen the clinical understanding of 2X-121 mediated clinical benefit.

The clinical experience in ovarian cancer patients has shown benefit in $BRCA^{wt}$ patients- patients who typically do not show durable clinical benefit from first generation PARP inhibitors. These data may suggest that, in addition to PARP 1/2 inhibition, the added activity of 2X-121 inhibiting tankyrase and the WNT pathway may contribute to the therapeutic mechanism of action for 2X-121. Accordingly, 2X-121 may be therapeutically useful as an inhibitor of the WNT pathway for cancers not typically sensitive to PARP 1/2 inhibition. Colorectal cancers are not typically sensitive to PARP1/2 inhibition. However, approximately 80% of colorectal cancers (CRCs) do show mutational activation of the canonical WNT pathway, which may impart resistance to standard chemotherapy. Moreover, WNT pathway activation may also enable a cancer initiating cell/ cancer stem cell-like phenotype enabling the cellular plasticity that often characterizes advanced malignancies.

We therefore sought to explore the therapeutic activity of 2X-121 in a panel of CRC cell lines chosen for a spectrum of WNT pathway activating mutations. We show that 2X-121 inhibits growth of multiple colorectal cancer cell lines in monolayer and 3D culture conditions. 2X-121 also inhibits the WNT pathway, stabilizing Axin, reducing activated beta-catenin, and generally blocking WNT pathway activation in CRC cell lines harboring TCF-LEF reporters. The reduction in cell number following 2X-121 treatment may reflect both cytostasis and direct cell killing. Importantly, these effects are evident at clinically relevant drug concentrations for 2X-121. Collectively, these data provide the foundation to explore the clinical potential of 2X-121 in colorectal cancers as well as other cancers where WNT pathway activation is prevalent.

#4577 Targeting midkine-driven oncogenic signaling with HBS-101: A novel therapeutic strategy for lung cancer.

Roberto Borea[1], Francesco Drago[1], Malaak Sammour[2], Nigita Giovanni[2], Serena Li Zhao[3], Blake R. Peterson[4], Hareesh B. Nair[5], Christian Rolfo[2], Eswar Shankar[2]

[1]Department of Internal Medicine, Division of Medical Oncology, The Ohio State University Comprehensive Cancer Center, College of Medicine, Columbus, OH,[2]Division of Medical Oncology, Department of Internal Medicine, The Ohio State University Comprehensive Cancer Center, College of Medicine, Columbus, OH,[3]The Ohio State University College of Pharmacy, Columbus, OH,[4]Division of Medicinal Chemistry & Pharmacognosy, The Ohio State University, Columbus, OH,[5]Department of Molecular and Translational Medicine, Texas Tech University Health Science Center El Paso, El Paso, TX

Midkine (MDK), a heparin-binding growth factor, is aberrantly overexpressed in non-small cell lung cancer (NSCLC) and small cell lung cancer (SCLC), where it drives tumor progression, angiogenesis, EMT, and therapy resistance via PI3K/Akt, MAPK/ERK, and Notch pathways. Despite progress with low-dose computed tomography (LDCT) screening for lung cancer, high false-positive rates, cumulative radiation exposure, and suboptimal sensitivity are still major concerns. These limitations underscore the need for novel, noninvasive biomarkers to enhance early detection and guide the development of targeted therapies. Circulating MDK in serum and urine is a promising biomarker, and HBS-101, a first-in-class small-molecule inhibitor, selectively blocks MDK-receptor interactions and downstream oncogenic signaling, offering a biomarker-guided therapy.MDK expression was analyzed across tumor and normal tissues using The Cancer Genome Atlas Program (TCGA) and the Genotype-Tissue Expression (GTEx) data. Anti-tumor efficacy of HBS-101 was evaluated in vivo using an SW1573 NSCLC xenograft model treated intraperitoneally with HBS-101 (5 or 10 mg/kg) for 56 days and in vitro using a 3D SCLC organoid model (SB-17-54) across 0-200 µM to determine IC_{50} values. Tumor growth, body weight, systemic toxicity, and gene expression were monitored.RNA analyses revealed broad MDK overexpression in both NSCLC and SCLC, with significantly elevated levels in lung adenocarcinoma and squamous cell carcinoma compared to matched normal tissues. HBS-101 treatment led to a statistically significant dose-dependent tumor growth inhibition in NSCLC xenografts, reducing tumor volume by 55-60% compared to control ($p<0.01$) without systemic toxicity. In SCLC organoids, HBS-101 demonstrated potent growth inhibition with an IC_{50} of 5.09 µM.Ongoing works include synthesizing fluorescent MDK derivatives and HBS-101 analogues to elucidate receptor interactions and enable high-throughput screening, and profiling MDK in *EGFR*-mutated NSCLC cell lines (PC-9, H1975) and their Osimertinib-resistant derivatives aim to define the MDK axis and its role in therapeutic resistance. Taken together, our findings validate MDK as both a circulating biomarker and a druggable target, and position HBS-101 as a promising candidate for precision lung cancer therapy. If validated, MDK inhibition could overcome EGFR-TKI resistance and enable MDK-based patient stratification, guiding next-generation inhibitors and early detection strategies.

#4578 Discovery of a Best-in-Class small molecule p53 Y220C reactivator: Breaking through the potency ceiling.

Ruben Boon[1], Jo Alen[1], Nihed Draoui[2], Koen Vandyck[2], Elke Behaeghel[1], Godelieve Lammens[1], Sandrine Vendeville[1], Lijs Beke[1], Pieter Peeters[1], Stephane De Cesco[1], Bart Stoops[1], Pierre Raboisson[1], **Francois Gonzalvez**[1], Carla De Legher[3]

[1]Onco3R Therapeutics, Leuven, Belgium,[2]Former Galapagos employee, Mechelen, Belgium,[3]Onco3R Therapeutics, Heverlee, Belgium

The tumor suppressor p53 is inactivated in approximately 50% of human cancers. In about 1% of solid tumors, a specific Y220C point mutation induces p53 misfolding, leading to its inactivation. This mutation also creates a unique, druggable pocket on the protein's surface, making it a promising target for cancer therapy. The first-generation small molecule reactivator (PC14586, Rezatapopt), designed to bind to this pocket, to refold p53 and to restore its tumor-suppressive functions, has shown clinical efficacy in patients harboring the Y220C mutations.
However, this first-generation compound is limited by modest potency, necessitating high dosing in patients. This high-dose requirement increases the risk of adverse events and narrows the therapeutic window, as monotherapy and even more so in combination regimens. As a result, this compound fails to deliver the drug pressure needed to reach full reactivation of this critical tumor suppressor. Thus, there is a clear need to discover and develop a highly potent p53 small molecule reactivator to fully unlock the therapeutic potential of this promising target.
At Onco3R Therapeutics, our patient centric approach, integrating deep translational science with rational, structure-based and AI-augmented drug design, has led to the identification of best-in-class series of p53 Y220C reactivators. Our lead series exhibits more than 200-fold superior potency compared to the clinical compound PC14586 (Rezatapopt) across diverse preclinical assays, including biochemical p53 refolding, cellular p53 refolding, and cellular p21 induction.
Importantly, our lead series, characterized by strong potency and long residence times in vitro, significantly sustains target engagement and P53 reactivation in cells. This profile enables robust activation of the pro-apoptotic protein PUMA and induces potent, selective cytotoxicity in p53 Y220C mutant cells and in an isogenic cell model. In line with their superior cellular activity and in combination with optimized key ADME, safety parameters, and favorable in vivo PK profiles across species, our leads reach similar efficacy in vivo as PC145586 at much lower exposure.
In conclusion, we have identified unique p53 Y220C small molecule reactivators with clear best-in-class cellular potency and favorable drug-like properties. We are currently further profiling these leads as potential drug candidates to achieve superior efficacy at substantially lower doses, maximizing the safety window to ultimately deliver better outcomes to cancer patients with p53 Y220C mutations.

#4579 Preclinical evaluation of a novel hyperbolic NAMPT inhibitor in combination with pan-RAS targeted therapies in pancreatic ductal adenocarcinoma.

Husain Yar Khan[1], Mohammed Najeeb Al Hallak[1], Sahar F. Bannoura[1], Md. Hafiz Uddin[1], Bin Bao[1], Mohamad Walid Sukkari[1], Adeeb Aboukameel[1], Khalil Choucair[1], Hugo Jimenez[1], Grayson Barker[1], Callum McGrath[1], Ganji Purnachandra Nagaraju[2], Rafic Beydoun[1], Yang Shi[1], Philip A. Philip[3], Azeddine Atfi[1], Bassel El-Rayes[2], Ramzi M. Mohammad[1], Min Wu[4], Michael Schelle[4], Boris C. Pasche[1], Asfar S. Azmi[1]

[1]Wayne State University School of Medicine, Karmanos Cancer Institute, Detroit, MI,[2]University of Alabama at Birmingham, O'Neill Comprehensive Cancer Center, Birmingham, AL,[3]Henry Ford Cancer Institute - Henry Ford Health System, Detroit, MI,[4]Remedy Plan Therapeutics, Gaithersburg, MD

Background: Pancreatic ductal adenocarcinoma (PDAC) remains highly lethal, driven by near-universal KRAS mutations and profound metabolic dependence on nicotinamide adenine dinucleotide (NAD). NAMPT, the rate-limiting enzyme of the NAD salvage pathway, is frequently upregulated in KRAS-driven tumors, suggesting metabolic co-dependence. We evaluated whether simultaneous blockade of NAMPT and KRAS signaling enhances antitumor efficacy in PDAC.
Methods: KRAS-NAMPT expression correlations were analyzed in TCGA PDAC samples (n=179). Multiple KRAS-mutant PDAC cellular models, including KRASG12C inhibitor, KRASG12D inhibitor, and pan-RAS inhibitor (RMC6236)-resistant lines were treated with the hyperbolic NAMPT inhibitor RPT-E-037, RMC6236, or both. Antitumor activity was assessed in 2D viability assays, 3D spheroid cultures, and patient-derived 2D/3D co-culture systems. Drug interactions were calculated using combination index (CI) analysis.
Results: TCGA analysis revealed a fairly strong positive correlation between KRAS and NAMPT expression (Spearman ρ=0.59). RMC6236-resistant PDAC cells displayed increased NAMPT expression and heightened sensitivity to RPT-E-037 compared to parental cells. Similar NAMPT upregulation and enhanced NAMPT inhibitor sensitivity were observed in KRASG12C and KRASG12D inhibitor-resistant models. Across KRAS-mutant PDAC lines, RPT-E-037 combined with RMC6236 produced robust synergy (CI<1) in both 2D and 3D cultures. In patient-derived PDAC co-culture systems, the combination significantly reduced tumor mass, dismantled compact spheroid architecture, and disrupted tumor-stroma interactions more effectively than either agent alone. KRASG12D-mutant metastatic patient rapid autopsy tissue-derived and KPC mice tumor-derived subcutaneous and orthotopic xenograft studies with the combination are ongoing.
Conclusion: Dual inhibition of NAMPT-mediated NAD biosynthesis and KRAS signaling yields synergistic antitumor activity in PDAC, including models resistant to KRAS-targeted therapies. These findings support NAMPT-KRAS co-dependency as a therapeutically actionable vulnerability and justify further translational and in vivo studies to guide clinical development and biomarker-based patient selection."Generative AI was used for improving the language of the abstract".

#4580 Novel PCNA inhibitor AOH1996 synergizes with KRAS-targeted therapies in pancreatic ductal adenocarcinoma.

Sahar F. Bannoura[1], **Husain Y. Khan**[1], Md Hafiz Uddin[1], Amro Aboukameel[1], Yin Wan[1], Bin Bao[1], Adeeb Aboukameel[1], Rafic Beydoun[2], Pouya Haratipour[3], Long Gu[3], Muhammad Wasif Saif[1], Robert J. Hickey[3], Linda H. Malkas[3], Yang Shi[1], Mohammed Najeeb Al Hallak[1], Ramzi M. Mohammad[1], Boris C. Pasche[1], Asfar S. Azmi[1]

[1]Barbara Ann Karmanos Cancer Institute, Wayne State University School of Medicine, Detroit, MI,[2]Department of Pathology, Barbara Ann Karmanos Cancer Institute, Wayne State University School of Medicine, Detroit, MI,[3]Beckman Research Institute of The City of Hope, Duarte, CA

Background: Pancreatic ductal adenocarcinoma (PDAC) is a highly lethal malignancy driven predominantly by oncogenic KRAS mutations. Proliferating cell nuclear antigen (PCNA) is a ring-shaped clamp protein that encircles DNA and regulates replication, repair, and resolution of transcription-replication conflicts; processes hyperactivated in PDAC. AOH1996 is a first-in-class, selective PCNA inhibitor currently in Phase I clinical trials. PCNA has predicted synthetic lethal interactions with KRAS, suggesting combination potential with emerging KRAS inhibitors. This study evaluated AOH1996 alone and in combination with KRAS-targeted agents in PDAC models.

Methods: In this study, we investigated the use of AOH1996 in preclinical models of KRAS-mutant PDAC. We determined cell viability and growth inhibition by MTT, colony formation and spheroid assays. Apoptosis and the cell cycle were analyzed by flow cytometry. RNA-seq, RT-qPCR and western blot were performed for mechanistic evaluations. Drug combination synergy modeling was performed using SynergyFinder. In vivo efficacy was assessed in PDAC xenograft models treated with AOH1996, KRAS inhibitors (MRTX1133, sotorasib, and RMC-6236), or combinations. Residual tumors were analyzed for pERK and pAKT signaling changes.

Results: AOH1996 showed potent, dose-dependent cytotoxicity in multiple PDAC cell lines and 3D spheroids (IC_{50}: 0.5-1.5 μM). RNA-seq revealed broad transcriptional alterations, with enrichment of MAPK, PI3K-Akt and Hippo signaling pathways. Across KRAS G12C and G12D models, AOH1996 exhibited strong synergy with KRAS inhibitors, including MRTX1133, sotorasib, adagrasib, and RMC-6236. Combination therapy caused marked G1 and G2/M phase arrest, increased Annexin V-positive apoptosis, and dual suppression of pERK and pAKT. In patient-derived tumoroids, AOH1996 plus RMC-6236 significantly reduced viability compared to single agents. In vivo, AOH1996 combined with MRTX1133 or with sotorasib produced robust tumor regressions with no significant weight loss, supporting tolerability.

Conclusions: AOH1996 is a promising therapeutic candidate for PDAC, demonstrating potent single-agent activity and strong synergy with clinically relevant KRAS inhibitors across in vitro, ex vivo, and in vivo models. The combination induces profound apoptotic and cell-cycle effects and disrupts key KRAS effector pathways. These results support further translational development of AOH1996-based combination regimens for patients with KRAS-mutant PDAC.

#4581 Small molecule restoring mutant p53R273H DNA binding and activity.

Anne Kingsland[1], Kyle P. Kisor[1], Emil Alexov[2], **Diane L. Barber**[1]

[1]University of California San Francisco, San Francisco, CA,[2]Clemson University, Clemson, SC

Although mutations in TP53 are the most frequent genetic alteration in human cancers, approaches that target mutant p53 to restore p53-wild type (WT) tumor suppressor functions have had limited success and there are currently no FDA-approved therapeutics targeting mutant p53. We report a membrane-permeant small molecule, Compound K, that selectively increases tumor suppressor functions of p53-R273H, one of the two most common p53 mutants in cancers. Key to understanding the loss of tumor suppressor functions of p53-R273H is deprotonation of His273 at the higher intracellular pH (pHi) of cancer cells, which attenuates binding to the negatively charged phosphate backbone of DNA. We identified Compound K in a computational screen of 3.5 million small molecules for targeting deprotonated His273 and imparting a positive charge to restore electrostatic binding to DNA, like positively charged WT p53-Arg273. We find that Compound K selectively increases DNA binding by p53-R273H at the higher pH of cancer cells with no effect on DNA binding by p53-R273H at the lower pH of untransformed cells, or by p53-WT, p53-R175H, and other pH-regulated transcription factors at lower and higher pH values. Compound K also restores p53-WT functions in human PANC-1 pancreatic cancer cells that are homozygous for p53-R273H, with limited effects in human HPDE untransformed pancreatic epithelial cells, including >4200 DEGs in PANC-1 and <200 DEGs in HPDE, as determined by RNA-seq. In PANC-1 cells Compound K increases expression of loss-of-function, anti-tumorigenic genes, including GADD45A, KLF6, and IFIT2, and decreases expression of gain-of-function pro-tumorigenic genes, including CDC20, PLK1, AURKA, and for TGF-β signaling, as determined by RNA-seq and immunoblotting cell lysates. Compound K also selectively decreases viability of PANC-1 cells with no effect on HPDE cells, and tumorigenicity, determined by 80% reduced colony formation in soft agar. Our findings are an important step toward the unmet need of developing therapeutics targeting mutant p53 to limit cancer progression. Additionally, beyond p53-R273H, Arg>His mutations are enriched in many cancers, most notably medulloblastoma, acute myeloid leukemia, and pancreatic and prostate cancers, which makes our approach of targeting an Arg>His substitution to restore a positive charge have broad cancer therapeutic promise.

#4582 Targeting MEIS2 in platinum resistant ovarian cancer.

Yinu Wang[1], Natalia Obrochta[2], Jennifer Heo[1], Junzui Li[1], Natalia Maria Masnica[3], Daniela E. Matei[1]

[1]OB/GYN, Northwestern University, Chicago, IL,[2]Department of Neurobiology, Northwestern University, Evanston, IL,[3]Weinberg School of Arts and Sciences, Northwestern University, Evanston, IL

Background: Recurrent ovarian cancer (OC) develops chemoresistance, which is fatal. Cancer stem cells (CSCs) have been hypothesized to be responsible for driving chemoresistance and tumor relapse. Myeloid Ecotropic Insertion Site 2 (MEIS) is a homeobox transcription factor (TF) that is deregulated in various cancers, playing critical roles in regulating stem cell identity and cell fate decisions. Here, I examined the role of MEIS2 in regulating stemness features that promote chemoresistance of OC, and the impact of a MEIS2 blockade on OC initiation and progression.
Methods: Paired isogenic OC cell lines (platinum sensitive (Pt-S) and resistant (Pt-R)) were used. MEIS2 expression level in these cells was assessed by q-RT-PCR and Western Blotting. The effects of MEIS2 inhibition (by using a pharmacological inhibitor MEISi and biological knockdown (KD)) and overexpression (OE) on OC cell survival and chemosensitivity were assessed using colony formation and cell viability assay, and on stemness features by flow cytometry for analysis of ALDH+ CSC population and measurement of stemness-related gene expression. MEIS2 direct binding targets in OC cells were examined using ChIP-seq and validated using q-PCR. The anti-tumor effects of MEIS2 inhibition on Pt-R OC cells and tumor initiation were tested in vivo.
Results: MEIS2 expression levels were increased in Pt-R vs. Pt-S OC cells at mRNA and protein levels. Treatment with MEIS2i (500nM-1μM) reduced the number of colonies in OC cells by at least 2-fold and resensitized Pt-R OC cells to cisplatin ($p<0.05$). Treatment with MEIS2i (250nM-1uM, 48 hours) decreased ALDH+ CSCs population by at least ~2-fold ($p<0.05$) and inhibited the expression of stemness-associated genes ALDH1 isoforms and Sox2 ($p<0.05$), compared to vehicle control. MEIS2 KD decreased the CSC population by two-fold ($p<0.05$) and inhibited stemness gene expression ($p<0.05$). By integrating ChIP-seq and RNA-seq, we identified that stemness-associated gene ALDH1A2 is a direct binding target of MEIS2 in OC cells, contributing to the maintenance of stemness and chemoresistant features. We further validated the MEIS2 binding region on the enhancer region of the ALDH1A2 genes using ChIP-qPCR, which is highly conserved across multiple species. In vivo, OC xenografts derived from MEIS2 KD OVCAR5 cells were more responsive to carboplatin ($p<0.05$) compared with control xenografts, and MEIS2 KD inhibited tumor-initiating capacity. Importantly, MEISi treatment alone (25μM/100μL, 5 days, 2 weeks) or in combination with carboplatin (25mg/kg, once/week, 2 weeks) suppressed OVCAR5 Pt-R xenograft tumor growth and inhibited ALDH+ CSC population in the tumor residuals.
Conclusions: Altogether, blocking MEIS2 in OC cells inhibits stemness traits that contribute to chemoresistance and tumor relapse, suggesting that MEIS2 is a potential new treatment target in OC therapy.

#4583 Multitarget kinase inhibitor olverembatinib (HQP1351) is efficacious and synergizes with chemotherapy in preclinical models of endometrial carcinoma (EC).

Yan Xiong[1], Zhiyan Liang[2], Huidan Yu[1], Bingxing Wu[1], Guoqin Zhai[1], Zhou Yu[1], Dajun Yang[1], Yifan Zhai[2]

[1]Ascentage Pharma (Suzhou) Co., Ltd., Suzhou, China,[2]Ascentage Pharma Group Inc., Rockville, MD

Background: EC is the most common uterine cancer. Treatments for certain subtypes or advanced disease are limited. Olverembatinib is an investigational multikinase inhibitor targeting factors such as VEGFR1-3, FGFRs, SRC, PDGFRs, and RET. Drug sensitivity screening of 883 human cancer cell lines showed that EC is the second-most sensitive tumor type to olverembatinib, prompting us to explore antitumor effects of olverembatinib alone or combined with standard-of-care chemotherapy in preclinical EC models.

Methods: PRISM (Profiling Relative Inhibition Simultaneously in Mixtures) was used to screen olverembatinib activity in multiple cancer cell lines. Cell viability was assessed using CellTiter-Glo® assays, and apoptosis was measured by flow cytometry. Western blotting was used to illustrate mechanisms of action. Subcutaneous MFE296 and AN3CA cell line-derived xenograft (CDX) models were established to evaluate antitumor effects *in vivo*.

Results: Olverembatinib inhibited proliferation of 31 EC cell lines across different histological types, with IC_{50} values ranging from subnanomolar to ~4 μM. Olverembatinib was significantly more potent (IC_{50} up to 100-fold lower) than lenvatinib in cell growth inhibition in AN3CA, HEC-1B, RL95-2, and Ishikawa cells. Combinations of olverembatinib and paclitaxel or carboplatin were evaluated in AN3CA, HEC-1B, MFE296, and Ishikawa cells. All were resistant to carboplatin. Olverembatinib synergized with paclitaxel to inhibit cell proliferation and promote apoptosis. In the MFE296 CDX model, olverembatinib showed dose-dependent antitumor activity at day 29 with respective T/C values of 61.72% and 39.04% at 5 and 10 mg/kg. Combining paclitaxel (10 mg/kg) and carboplatin (50 mg/kg) with olverembatinib (10 mg/kg) significantly enhanced the latter's antitumor activity, with a T/C value of 9.08% and synergistic index of 1.37. Antitumor effects of olverembatinib and synergy with chemotherapy were recapitulated in AN3CA CDX models. No significant body weight loss was observed. Mechanistically, olverembatinib suppressed phosphorylation of oncogenic FGFR2, SRC, and PI3K-AKT (the most frequently altered pathway in EC) and downstream factors STAT3 and ERK. When olverembatinib was combined with chemotherapy, synergistic downregulation of the above pathways, cell cycle proteins (pRB, CDK4, and CDK6), and augmentation of apoptotic markers (cleaved caspase3 and PARP) and DNA damage marker (γH2AX) were observed, as well as modulation of epithelial-mesenchymal transition (tumor metastasis) markers.

Conclusions: In a broad range of preclinical *in vitro* and *in vivo* EC models, olverembatinib is efficacious and synergizes with chemotherapy to promote antitumor effects. The findings support future clinical evaluation of olverembatinib and its combination with other approved treatment options in EC.

#4584 Effects of ergosterol peroxide on proteostasis disruption in triple negative breast cancer cells.

Michelle Martinez-Montemayor[1], Aliyah Bocachica-Adorno[2], Adriana Aponte-Ramos[3], Taotao Ling[4], Fatima Rivas[4]

[1]Universidad Central del Caribe, Bayamon, PR,[2]University of Puerto Rico, Bayamon, PR,[3]Universidad Interamericana, Bayamon, PR,[4]Louisiana State University, Baton Rouge, LA

Triple-negative breast cancer (TNBC) is a highly aggressive and heterogeneous subtype of breast cancer characterized by the absence of estrogen receptor, progesterone receptor, and HER2 expression, known for its high malignancy, invasiveness, and propensity for metastasis. Due to the lack of targeted therapies, TNBC patients typically undergo multimodality chemotherapy with cytotoxic agents like taxanes, anthracyclines, and cyclophosphamide. Therefore, there is an urgent need for selective therapies for TNBC. Natural products have gained significant attention for their potential in cancer therapy, as around 60% of clinically approved anticancer drugs were inspired by secondary metabolites found in nature. In our laboratory, we work with Ergosterol Peroxide (EP), a bioactive compound extracted from the *Ganoderma lucidum* mushroom. We discovered that the natural product EP exhibits selective cytotoxicity against TNBC models, demonstrating activity in the low micromolar range while sparing normal cells. Our studies indicate that EP exerts its anticancer effects by disrupting critical cellular processes including proteostasis, protein synthesis, and protein degradation pathways. We hypothesize that EP compromises TNBC cell viability by disrupting proteostatic balance. Mechanistically, we propose that EP inhibits protein synthesis and induces mitochondrial dysfunction, which collectively impair the ability of TNBC cells to restore protein homeostasis, ultimately resulting in cell death**.** To validate our hypothesis, we performed protein synthesis assays in two TNBC cell models, SUM149 and MDA-MB-231. Veh (0.2% DMSO), EP (20μM), or cyclophosphamide (1μM, positive control) were administered for 6 or 24h. EP effects on protein aggregation, under Veh, EP, or MG132 (positive control) in SUM149 or MDA-MB-231 TNBC cells and MCF10A non-cancerous cells, we used an aggresome assay. Finally, to assess protein degradation we performed western blots probing for ubiquitin. We previously established that EP increases ROS levels in TNBC cells. EP affects protein synthesis, compared to negative vehicle control treated cells, and in reduced capacity when compared to cyclophosphamide. Moreover, EP significantly increases protein aggregation, although the signal detected for MG132 was greater. Finally, EP decreases cancer cell degradation, as seen by decreased levels of ubiquitin when treated after 24h. In summary, EP demonstrates the capacity to modulate proteostasis in TNBC cells. Further investigation is warranted to comprehensively characterize the intricate mechanistic pathways by which EP exerts its anticancer effects in this malignancy.

#4585 A novel thioxanthenone activates p47phox to exploit redox vulnerabilities in acute myeloid leukemia.

Madison Gamble[1], Claudia M. Espitia[1], Sruthi Sureshkumar[1], Natalie Hakim[1], Kevin R. Kelly[2], Wei Wang[3], Steffan T. Nawrocki[1], Jennifer S. Carew[1]

[1]Cancer Center, University of Arizona, Tucson, AZ,[2]Hematology, University of Southern California, Los Angeles, CA,[3]Pharmacology and Toxicology, University of Arizona, Tucson, AZ

Acute myeloid leukemia (AML) is an aggressive hematologic malignancy with poor outcomes, particularly among older adults and patients harboring adverse-risk features such as FLT3-ITD and p53 mutations. Relapsed or refractory (R/R) AML remains largely incurable, underscoring the urgent need for new therapies that selectively target leukemia-specific survival pathways while sparing normal hematopoiesis. Through a focused medicinal chemistry campaign, we optimized an understudied thioxanthenone chemotype and identified 06-30 as a potent lead compound with broad anti-AML activity. 06-30 induces robust and selective cytotoxicity across genetically diverse AML cell lines including models resistant to standard of care agents (cytarabine, azacitidine), and demonstrates strong activity in primary AML blasts with adverse molecular profiles. Unbiased integrative proteomic and transcriptomic analyses revealed p47phox (NCF1), a cytosolic organizer subunit of the NADPH oxidase complex, as the top common drug-induced target following 06-30 treatment with >9-fold increases in protein abundance and >50-fold increases in mRNA levels. Although p47phox is well established in host defense and inflammatory reactive oxygen species (ROS) generation, its role in AML pathogenesis and therapeutic sensitivity remains undefined. We hypothesize that p47phox functions as a pharmacodynamically regulated effector of 06-30 that drives ROS-mediated DNA damage and apoptosis in AML by exploiting leukemia-specific redox dysregulation. Supporting this hypothesis, shRNA-mediated silencing of p47phox significantly diminished 06-30-induced ROS generation and apoptosis and antioxidant co-treatment similarly blunted cell death. Importantly, 06-30 demonstrated selective toxicity toward AML cells while sparing normal CD34+ bone marrow progenitors, consistent with the enhanced antioxidant capacity of normal hematopoietic cells and establishing a clear therapeutic window. *In vivo*, 06-30 significantly extended overall survival and was very well tolerated. *Ex vivo* analyses demonstrated that its antileukemic efficacy was associated with increased p47phox expression and oxidative DNA damage as quantified by 8-oxoguanine levels. To our knowledge, no anticancer pharmacologic activators of p47phox have been previously described. Thus, thioxanthenone 06-30 represents both a first-in-class mechanistic probe and a promising therapeutic lead for redox-based targeting in AML. Together, these findings provide strong rationale for the further preclinical development and eventually clinical investigation of 06-30 as a strategy to exploit redox vulnerabilities in leukemia and improve outcomes for patients with limited therapeutic options.

#4586 p97/VCP inhibition with CB-5339 induces REDD1-dependent antitumor activity in renal cell carcinoma.

Sruthi Sureshkumar[1], Claudia M. Espitia[1], Maria Janina Carrera Espinoza[1], Madison Gamble[1], Natalie Hakim[1], Kevin Kelly[2], Jennifer S. Carew[1], Steffan T. Nawrocki[1]

[1]Cancer Center, University of Arizona, Tucson, AZ,[2]Hematology, University of Southern California, Los Angeles, CA

Renal cell carcinoma (RCC) is the tenth most common cancer in the United States and disproportionately affects Hispanic and Native American populations, who experience higher incidence and mortality. Although current therapies targeting tyrosine kinases and immune checkpoints have extended survival, most patients ultimately develop resistance. This emphasizes the need for novel treatment strategies that disrupt essential survival pathways. The AAA+ ATPase p97/valosin-containing protein (VCP) is a central regulator of protein quality control that extracts misfolded or unfolded proteins from the endoplasmic reticulum (ER) for degradation, thereby preventing proteotoxic stress. We demonstrated that genetic knockdown of p97 significantly reduced RCC cell viability, supporting p97 as an essential survival factor and a promising therapeutic target. Consistent with this, the orally bioavailable, clinically relevant p97 inhibitor CB-5339 potently induced ER stress and apoptosis across human RCC cell lines and in Hispanic and Native American patient-derived xenograft (PDX) models. Transcriptomic profiling identified REDD1 as the most strongly upregulated gene following CB-5339 treatment. CRISPR-mediated knockout studies showed that REDD1 was required for maximal induction of ER stress and apoptosis, indicating that CB-5339 triggers a REDD1-dependent stress response. Because REDD1 is a negative regulator of mTORC1, we further assessed downstream effects on nutrient-sensing pathways. CB-5339 treatment inhibited mTORC1 activity and activated autophagy, as confirmed by autophagic flux assays using the lysosomal inhibitor bafilomycin-A1. Therefore, we hypothesized that combining p97 inhibition with autophagy blockade would enhance cytotoxicity by preventing the compensatory autophagic response. Consistent with this, co-treatment with CB-5339 and the lysosomal autophagy inhibitor ROC-325 produced strong synergy, significantly increasing apoptosis and reducing viability compared with either agent alone. In RCC xenograft models, the combination achieved marked tumor suppression, robust induction of apoptotic signaling, and excellent tolerability. Together, these results identify p97 as a novel therapeutic vulnerability in RCC and demonstrate that CB-5339's anticancer effects are driven by REDD1-mediated ER stress and cell death. The synergistic efficacy of CB-5339 and ROC-325 highlights the therapeutic potential of combining proteostasis disruption with autophagy inhibition. Moreover, the use of multiple RCC PDX models enhances the translational relevance of this approach and provides a strong rationale for clinical investigation of p97 inhibition alone and in combination with autophagy-targeting agents in RCC.

#4587 USP10 inhibition with GL-320 enhances chemo-immunotherapy efficacy and overcomes resistance in NSCLC.

Sadaf Dorandish[1], Komal Bhayekar[1], Prahlad Parajuli[1], Amirreza Samarbakhsh[1], Babita Kushwaha[2], Yubin Ge[3], Navnath Gavande[1]

[1]Pharmaceutical Sciences, Wayne State University-Eugene Applebaum College of Pharmacy and Health Sciences, Detroit, MI,[2]Pharmaceutical Sciences, Wayne State University, Detroit, MI,[3]Pharmaceutical Sciences, Wayne State University-School of Medicine, Detroit, MI

Platinum-based chemotherapy combined with immunotherapy remains the frontline regimen for advanced non-small cell lung cancer (NSCLC), yet most patients ultimately relapse due to acquired resistance. A major contributor to this resistance is hyperactivation of the DNA damage response (DDR), which enables tumor cells to repair chemotherapy-induced lesions, evade cytotoxicity, and suppress immunogenic signaling. The deubiquitinating enzyme USP10 stabilizes multiple DDR and pro-survival proteins, making it an attractive target for re-sensitizing resistant tumors. Inhibiting USP10 may attenuate DNA repair, disrupt oncogenic pathways, and enhance anti-tumor immune activation. GL-320, a potent and selective small-molecule USP10 inhibitor developed in our laboratory, was evaluated across NSCLC models using integrated biochemical, cellular, and molecular assays. MTT and colony formation studies demonstrated robust, dose-dependent suppression of proliferation and clonogenic survival, while CellTiter-Glo and combination colony assays showed that GL-320 effectively re-sensitized cisplatin-resistant cells. CETSA confirmed direct intracellular USP10 engagement. Comet assays and immunofluorescence imaging revealed increased DNA fragmentation and elevated γH2AX, PARP1, and 53BP1 foci, indicating impaired DNA repair capacity. Flow cytometry demonstrated early G_0/G_1 arrest accompanied by ATM/ATR activation and increased pChk1 and γH2AX. Co-treatment with ATM and pan-caspase inhibitors confirmed the involvement of DDR signaling and caspase-dependent apoptosis. Broader mechanistic profiling showed modulation of DDR and checkpoint proteins (MSH2, p21, MDM2, p53), destabilization of survival factors (HDAC6, CD36), and induction of autophagy (p62, Beclin-1, LC3-II). Importantly, GL-320 induced strong immunogenic stress, marked by increased GRP78/BiP, caspase-8 activation, calreticulin exposure, and reduced CD47 expression, hallmarks of endoplasmic reticulum stress and immunogenic cell death. Collectively, GL-320 mediated USP10 inhibition disrupts DDR signaling, activates autophagy and caspase-dependent apoptosis, and triggers immunogenic cell death, thereby restoring cisplatin sensitivity and potentially enhancing response to immunotherapy. These multifaceted effects position USP10 as a promising therapeutic target for overcoming treatment resistance and stimulating anti-tumor immunity in NSCLC.

: Proximity-Induced Drug Discovery 1
Poster Session

#4591 SC3613 (IN-207387), a mutant-selective EGFR degrader, exhibits potent anti-tumor activity and improved safety profile in EGFR TKI-resistant NSCLC.

Jun Gyu Kim[1], Jihoon Choi[1], Ok Young Lee[1], Young Jun Park[1], Young Min Jeong[1], Choongsil Lee[1], Seo Yoon Jeong[1], Hye Yeon Lee[1], Yu Jin Lee[1], Hyesun Lee[1], Dae Young Lee[1], Ah Yeon Park[1], Hyoeun Jo[1], Sun Ho Choi[1], Sun Ho Jeon[1], Ji-Young An[2], Jong Hyun Lee[2], Yang Hun Tae[2], Mirae An[2], Keunho Lee[2], Jong Ryoul Choi[2], Bong Tae Kim[2], Mi-Kyung Kim[1]

[1]Dong-A ST, Youngin-si, Korea, Republic of,[2]Innovative Drug Discovery R&D Institute, HK inno.N Corp., Gyeonggi-do, Korea, Republic of

Non-small cell lung cancer (NSCLC) accounts for approximately 85% of all lung cancers, with activating mutations in the epidermal growth factor receptor (EGFR) strongly associated with tumor progression and poor clinical outcomes. Among these mutations, the L858R mutation in *exon 21* serves as a major oncogenic driver that confers initial sensitivity to EGFR tyrosine kinase inhibitors (TKIs). However, patients with L858R-driven tumors exhibit a poorer prognosis and shorter progression-free survival even with third-generation EGFR TKIs, such as osimertinib, compared with those harboring *exon 19* deletions, underscoring a substantial unmet clinical need in this molecular subgroup. In addition, the emergence of secondary resistance mutations, including C797S, further limits the long-term efficacy of current TKIs. To address these challenges, targeted protein degradation has emerged as a promising strategy to eliminate both activating and resistance-associated mutant EGFR. We developed SC3613 (IN-207387), a novel heterobifunctional degrader designed to selectively bind an allosteric pocket of mutant EGFR while sparing the wild-type receptor, thereby minimizing off-target toxicities. SC3613 efficiently induced ubiquitin-proteasome-mediated degradation across L858R-containing EGFR variants, including L858R/C797S, and exhibited potent anti-proliferative activity in patient-derived cells harboring resistant EGFR mutations. A potent antitumor effect was also observed in NCI-H1975 (L858R/T790M) cells. Consistent with effective target engagement, SC3613 treatment resulted in marked suppression of downstream EGFR signaling pathways. Importantly, SC3613 demonstrated a superior safety profile. In BALB/c nude mice, SC3613 produced substantially lower levels of skin keratosis on the face, neck, and abdomen compared with osimertinib, indicating a reduced incidence of cutaneous adverse effects and a broader therapeutic window. Furthermore, orally administrated SC3613 induced potent, dose-dependent anti-tumor activity in multiple EGFR TKI-resistant xenograft model. Treatment led to a high incidence of durable complete tumor regressions without associated body-weight loss, highlighting its favorable tolerability. Collectively, these findings identify SC3613 as a potent, highly mutant-selective, and orally active EGFR degrader with robust anti-tumor efficacy and improved safety. SC3613 represents a promising next-generation therapeutic candidate for NSCLC patients harboring activating and resistance mutations such as L858R, T790M, and C797S.

#4592 The highly selective and potent reversible-covalent FGFR4 inhibitor, BB102, induces targeted-protein degradation through lysosomal autophagy.

Min Li, Qi Wang, Gongping Duan, Xiaoyi Ma, Junheng Wang, Lijie Wei, **Xingmin Zhang**

BroadenBio Co., Ltd., Beijing, China

Introduction: Fibroblast growth factor 19 (FGF19) overexpression contributes to the tumorigenesis of certain forms of hepatocellular carcinoma (HCC) and fibroblast growth factor receptor 4 (FGFR4) mutations have been found in rhabdomyosarcoma, breast, colorectal, and gastric cancer. Thus, FGFR4 is considered as a novel target to treat cancer with hyperactivated FGF19/FGFR4 signaling. We previously reported BB102 was a highly selective and potent reversible-covalent FGFR4 inhibitor. Here we demonstrated for the first time that BB102 not only inhibited FGFR4 kinase activity but also induced FGFR4 degradation through lysosomal autophagy.

Methods: BB102 was developed through structure-based drug design, and optimized by SAR analysis and medicinal chemistry iteration. Biochemical and cell-based assays were applied in evaluation of BB102 inhibitory activity. Parallel artificial membrane permeability assay (PAMPA) and permeability in MDCK-MDR1 cell line were conducted. The degradation of FGFR4 protein induced by BB102 was demonstrated in both tumor cell lines and tumors from xenograft models in mice.

Results: BB102 inhibited FGFR4 kinase activity with IC_{50} of 2.5 nM and displayed >400-fold selectivity against the other 206 kinases tested. BB102 blocked the phosphorylation of the downstream protein ERK with IC_{50} of 2.4 nM. BB102 exhibited strong inhibitory effects on the cell proliferation with the high expression of both FGF19 and FGFR4, or FGFR4-mutated tumor cells and suppressed tumor growth in mouse models. PAMPA and permeability in MDCK-MDR1 cell line had shown BB102 was permeable to blood-brain barrier (BBB) and BB102 was found in the rat brain tissues. BB102 clearly induced FGFR4 protein degradation in FGFR4 over-expressed HuH-7, Hep3B, and SJCRH30 cancer cell lines, which was blocked by Bafilomycin A1, an inhibitor of lysosomal autophagy. BB102 induced degradation of FGFR4 only in the tumors but not in the normal lungs and livers from xenograft mouse models.

Conclusion: BB102 is a degrader of FGFR4 with highly selective and potent reversible-covalent FGFR4 kinase inhibition. BB102 has remarkable antitumor activity in mice bearing HCC tumor xenografts. It is permeable to BBB. It has shown safe profiles in the phase Ia study and preliminary promising efficacy in the phase Ib study.

#4593 PBI-381, a development candidate PROTAC for KRasG12D solid tumors.

Bing Zhang[1], Yuxin Liu[1], Yufeng Chen[1], Danqiu Lin[1], Jinhua Chai[1], Yang Meng[1], Mixue Tong[1], Ganng Yang[1], Michael Xiang[2], Liping Zhao[1], Rui Yang[1], **Lan Xu**[2], He Zhou[1], Jason Xiang[1]

[1]Polymed Biopharmaceuticals, Hangzhou, China,[2]Polymed Biopharmaceuticals, Cambridge, MA

Kras gain-of-function mutations are prominent cancer drivers in pancreatic, colorectal, lung and other solid tumors. While several small molecule inhibitors against KRasG12C have been approved to treat non-small cell lung and colorectal cancers, either as single agent or in combination, there is still a great unmet need for other more prevalent Kras mutations such as KrasG12D. Furthermore, given the complexity of KRasG12D molecular mode of action and its downstream signaling branches, whether complete elimination of the KRasG12D protein or functional inhibition of its signaling activity has a bigger impact on cancer cells remains an open question. Therefore, Proteolysis Targeting Chimera (PROTAC)-based Kras degraders may bring differentiated clinical benefits to patients with Kras-mutant solid tumors. At present, ASP3082 (Astellas Pharma) and PT0253 (PAQ Therapeutics) are the only two KRasG12D PROTAC degraders that have entered clinical trials.Polymed Biopharmaceuticals has generated a series of potent and selective PROTAC molecules targeting the KRasG12D mutant protein. *In vitro*, these PROTAC molecules exhibited DC_{50} (degradation IC_{50}) < 1 nM and D_{max} (maximal % of degradation) > 98% against KRasG12D in cancer cell lines harboring this mutation. Moreover, as measured by cancer cell growth inhibition, the Polymed PROTAC molecules are highly selective against cells with the KRasG12D mutation while sparing cells harboring KRasG12V, KRasG12C or cells with amplified wild type KRas. More importantly, in KRasG12D pancreatic cancer xenograft model PK59, treatment with the lead molecule PBI-381 resulted in robust tumor regression without impact on body weight and any other noticeable adverse effects on the mice after 4 weeks of treatment. A good PK/PD/efficacy relationship was also observed with PBI-381. Preliminary ADME, *in vitro* safety and drug-drug interaction assessments further supported PBI-381 as a development candidate for advancing into the clinic.Compared to the most clinically advanced KRasG12D PROTAC ASP3082, PBI-381 has superior potency and more favorable tissue distribution for a drug designed to treat solid tumors. In head-to-head comparison studies using xenograft models, PBI-381 also exhibited significantly higher anti-tumor activity than ASP3082. IND-enabling activities on PBI-381 are underway to progress the compound further towards the clinic.

#4594 LY4584180, a novel BCL6 molecular glue, demonstrates antitumor efficacy in preclinical models of B Cell NHL.

Candace Langan[1], Nicholas E. Brown[1], Bryan G. Perria[1], Petia Gatzeva-Topalova[1], Bonita D. Jones[1], Lisa J. Kindler[1], Wayne D. Blosser[1], Rebecca J. Metivier[2], Eric S. Fischer[2], Xueqian Gong[1], Nathan A. Brooks[1]

[1]Eli Lilly and Company, Indianapolis, IN,[2]Department of Cancer Biology, Dana-Farber Cancer Institute, MA, and Department of Biological Chemistry and Molecular Pharmacology, Harvard Medical School, Boston, MA

B-cell lymphoma 6 (BCL6) is a protooncogene and key molecular driver of DLBCL, FL, and other B-cell malignancies. BCL6 gene alterations such as chromosomal translocations or somatic mutations, lead to deregulation of BCL6 expression, contributing to poorly prognostic double- and triple-hit lymphomas.[1] Given its role in repressing genes involved in DNA damage response, cell cycle checkpoints, and differentiation,[2] BCL6 is a promising drug target for the treatment of non-Hodgkin Lymphomas (NHL). Small molecule inhibitors have been ineffective in disrupting BCL6-mediated oncogenic activity; emerging evidence suggests that degradation of BCL6 is essential for antitumor activity.[3] Here, we describe the characterization of LY4584180, an oral, highly selective, small molecule BCL6 molecular glue. LY4584180 induces BCL6 homodimerization at the BTB/POZ domain, resulting in BCL6 polymers sequestered into cellular aggregates, leading to polyubiquitination of the BCL6 aggregates by E3 ligases, and subsequent degradation by the proteasome. The unique non-cereblon dependent degradation mechanism allows combination with IMiDs and may also reduce a key mechanism for on-target drug resistance, in comparison to other ligand directed cereblon degraders. LY4584180 has demonstrated rapid, potent, and concentration-dependent degradation of BCL6 protein in both transcriptionally defined DLBCL subtypes, activated B-cell (ABC; OCI-Ly10) and germinal center B-cell (GCB; Farage and SU-DHL-4). DC_{50} (concentration of LY4584180 resulting in 50% degradation of BCL6) values ranged from 1 to 22 nM at 24 hrs with maximal degradation (~96-97%) observed within 2 hrs, as quantified by Mesoscale Diagnostics ELISA. Furthermore, LY4584180 demonstrated anti-proliferative activity across a panel of human NHL cell lines with mid- to high-BCL6 expression, including ABC and GCB DLBCL subtypes. Additionally, in a mass spectrometry-based proteomics study using SU-DHL-4 cells, the compound selectively reduced BCL6 relative to its effects on the global proteome. In DLBCL cell line-derived xenograft models, LY4584180 demonstrated robust dose-dependent BCL6 degradation and antitumor activity ($p<0.001$), including tumor regression at multiple dose levels, with no significant body weight loss. These results demonstrate the ability of LY4584180 to selectively degrade BCL6, exert antiproliferative effects across a panel of malignant human B-cell lines, and exhibit antitumor activity *in vivo*. These findings suggest that LY4584180 has the potential to be effective in patients with hematologic malignancies. NOVA-BCL6-1, a phase 1 clinical trial evaluating LY4584180 in patients with NHL is currently enrolling (NCT07226843). [1]Xu J, et al. *Cancer Res* 2024, 84: Abstract 6062 [2]Liongue C, et al. *Int J Mol Sci* 2024, 25:10968 [3]Groocock L, et al. *Blood* 2024; 144 (Supplement 1): 957

#4595 A first-in-class potent EZH2 degrader, AXT-1003, exhibits robust anti-tumor activity across multiple lymphomas and solid tumors.

Yong Yang, Huiya Huang, Enxing Zhou, Yan Lin, Qian Gao, Alex Xu

Axter Therapeutics, Beijing, China

Enhancer of Zeste Homolog 2 (EZH2) acts as the core enzymatic component of the Polycomb Repressive Complex 2 (PRC2), which mediates trimethylation of histone H3 lysine 27 (H3K27Me3) to maintain the epigenetic repression of target genes. Mutated and/or dysregulated EZH2 expression is a hallmark of various cancers and is frequently correlated with poor patient prognosis. Several S-adenosylmethionine (SAM)-competitive EZH2 inhibitors, which suppress methyltransferase activity of EZH2, have clinically shown promising results in treating sarcoma and lymphoma, including the FDA-approved tazemetostat (EPZ-6438). However, monotherapy with these EZH2 inhibitors has limited efficacy in most solid tumors, even though they effectively reduce the H3K27Me3. Growing evidence suggests that EZH2 commonly functions noncanonically, in a methyltransferase-independent manner, as a transcriptional coactivator through associating with oncogenic transcription factors in solid tumors. Therefore, targeting EZH2 with degradation can be advantageous for the treatment of EZH2-dependent cancers. Herein, we reported the development of a first-in-class, oral, and potent EZH2 degrader, AXT-1003. Across multiple *in vitro* and *in vivo* tumor models, this degrader promoted a dose- and time-dependent reduction of EZH2 protein, which led to significant inhibition of H3K27Me3. Meanwhile, AXT-1003 had no significant effect on EZH2 at transcriptional levels, and its protein expression was restored by MG-132 (proteasome inhibitor). Our ubiquitinomics and proteomics studies demonstrated that AXT-1003 simultaneously triggered ubiquitination and degradation of EZH2 protein, suggesting AXT-1003 serves as an EZH2-targeting degrader via the ubiquitin-proteasome pathway. Additionally, AXT-1003 effectively inhibited enzymatic activity of wild-type EZH2 and its mutants at nanomolar concentrations in a non-SAM-competitive manner and exhibited greater selectivity for EZH2 inhibition than EPZ-6438. AXT-1003 exhibited broader and stronger anti-proliferative activities against various lymphoma cell lines with wild-type or mutated EZH2 as well as solid tumor cell lines. Notably, in the patient-derived organoid (PDO) models from ovarian clear cell carcinoma (OCCC) samples, AXT-1003 displayed superior efficacy compared with cisplatin or mevrometostat (PF-06821497), regardless of ARID1A status. AXT-1003 suppressed tumor growth more effectively than EPZ-6438 in several cancer cell-derived xenograft (CDX) mice models. Furthermore, the *in vivo* combination treatment of AXT-1003 with enzalutamide showed synergistic efficacy in a prostate cancer (LNCaP) CDX mice model. In conclusion, our preclinical data highlight the therapeutic potential of AXT-1003 and support its ongoing clinical evaluation in patients with EZH2-driven cancers.

#4596 The combination of the AR PROTAC AZD9750 and AKT inhibitor capivasertib delivers improved efficacy over monotherapy in prostate cancer.

Antonio Ramos-Montoya[1], Chrysiis Michaloglou[1], Nuria Galeano-Dalmau[1], Ana Quiroga[1], Michael Niedbala[2], Claire Crafter[1]

[1]Oncology R&D, AstraZeneca, Cambridge, United Kingdom,[2]Oncology R&D, AstraZeneca, Waltham, MA

The PI3K-AKT pathway is frequently activated in prostate cancer through *PTEN* genetic alterations—primarily homozygous deletion in tumor cells—and is associated with poor clinical outcomes. Capivasertib, a potent, oral, selective inhibitor of AKT1/2/3, inhibits proliferation in prostate cancer cell lines with PTEN alterations. Preclinical evidence demonstrates reciprocal feedback between AR and PI3K-AKT signaling, providing a strong rationale for combined pathway blockade. Consistent with this, in the Phase III CAPItello-281 trial (NCT04493853), capivasertib plus abiraterone and ADT achieved a statistically significant improvement in radiographic progression-free survival versus abiraterone and ADT in patients with *PTEN*-deficient *de novo* metastatic hormone-sensitive prostate cancer (mHSPC). Abiraterone, an androgen receptor pathway inhibitor (ARPI), is a key standard-of-care treatment in mHSPC, yet resistance inevitably emerges via mechanisms such as AR amplification and ligand-binding domain mutations. AZD9750 is a novel AR-directed proteolysis targeting chimera (AR-PROTAC) that co-engages AR and the E3 ligase CRBN to promote AR ubiquitination and degradation, achieving deeper suppression of AR signaling and activity against both wild-type and mutant AR, with the potential to overcome resistance to current standards of care. Given the robust preclinical and clinical evidence supporting combinations of AKT inhibitors with AR pathway suppression, we evaluated whether AZD9750 could combine effectively with capivasertib in preclinical prostate cancer models. *In vitro*, combining AZD9750 and capivasertib in LNCaP (PTEN null) and VCaP (PTEN wt) cell lines enhanced antiproliferative activity and induced apoptosis, accompanied by inhibition of AKT pathway signaling (reduced pS6 and pPRAS40) and AR signaling (decreased PSA expression). In PTEN-null patient-derived xenograft prostate tumor models (both HSPC and CRPC), the combination consistently delivered significantly greater efficacy than either monotherapy, including 73% tumor growth inhibition (TGI) in TM00298 (vs AZD9750 52% TGI and capivasertib 14% TGI) and >100% TGI with 25% regression in MR041 (vs AZD9750 90% TGI and capivasertib 61% TGI), with similar benefits observed in other models. These findings indicate that in PTEN-null prostate cancer AZD9750 mediated AR degradation synergizes with AKT inhibition by capivasertib to enhance antitumor efficacy and support clinical evaluation of the AR-PROTAC-AKT inhibitor combination in PTEN-deficient prostate cancer.

#4598 An orally bioavailable, specific PLK1 bifunctional degrader for the treatment of small cell lung cancer and other cancers.

Keum Young Kang[1], Im Suk Min[1], Seong Hye Ahn[1], Gi Bbeum Lee[1], Sol Hee Noh[1], Yeon Jung Song[1], Hyun Lim[1], Boas Nam[1], Hanbit Lee[1], Su Gwon Lee[1], Woojeung Song[2], Kyungsik Ha[1], Junyang Jung[2], Jihoon Ryu[1], Soo Hee Ryu[1], Na Young Lee[1], Seong Hoon Kim[1], **Hwajin Lee**[2]

[1]UPPThera, inc., Incheon, Korea, Republic of,[2]College of Medicine, Kyung Hee University, Seoul, Korea, Republic of

Polo-like kinase 1 (PLK1) is a G2/M phase checkpoint protein that regulates signaling pathways critical for cell cycle progression, making it a key contributor to cancer cell proliferation and tumorigenesis. Due to its essential role across diverse cell types, PLK1 has emerged as an attractive therapeutic target for various cancers. Although several PLK1 inhibitors have reached clinical evaluation, most have failed to demonstrate efficacy at doses that show tolerable toxicity, highlighting the need for novel therapeutic approaches to effectively target PLK1. UP1002 is an orally administered, selective bifunctional PLK1 degrader which has been designed to potentially overcome such limitations. UP1002 promotes the proximity between PLK1 and cereblon (CRBN), leading to selective PLK1 degradation through a proteasome-dependent mechanism. Unlike traditional PLK1 inhibitors, UP1002 prevents PLK1 accumulation during G2/M arrest and induces robust cell cycle arrest and apoptosis. In preclinical models, UP1002 monotherapy demonstrated significant antitumor efficacy in multiple cancer types, which achieved near-complete tumor regression in a subset of dosing groups while reducing toxicity compared to canonical PLK1 inhibitors. Moreover, combinations of UP1002 with multiple approved therapies showed synergistic or additive antitumor activity, highlighting its potential to enhance current treatment regimens. Together, these findings suggest that UP1002 has therapeutic potential in small-cell lung cancer and may extend its efficacy to additional cancer types.

#4599 Rationally designed allosteric EGFR degrader SC3499 (IN-207375) selectively eliminates mutant EGFR and overcomes osimertinib resistance in non-small cell lung cancer.

Jihoon Choi[1], Jun Gyu Kim[1], Yu Jin Lee[1], Young Jun Park[1], Ok Young Lee[1], Young Min Jeong[1], Choongsil Lee[1], Seo Yoon Jeong [1], Hye Yeon Lee[1], Hye Sun Lee[1], Moon Jung Goo[1], Hyun Woo Park[1], Ah Yeon Park[1], Hyoeun Jo[1], Sun Ho Choi[1], Soo jung Choi[1], Dae Young Lee[1], Sun Ho Jeon[1], Jong Ryoul Choi[2], Jong Hyun Lee[2], Mirae An[2], Keunho Lee[2], Yanghun Tae[2], Ji-Young An[2], Bong Tae Kim[2], Mi-Kyung Kim[1]

[1]Dong-A ST Co. Ltd, Seoul, Korea, Republic of,[2]HK inno.N Corp, Seongnam, Korea, Republic of

Epidermal growth factor receptor (EGFR) tyrosine kinase inhibitors (TKIs) have demonstrated remarkable therapeutic efficacy in patients with non-small cell lung cancer (NSCLC) harboring activating EGFR mutations. However, acquired resistance often driven by secondary EGFR mutations remains a major clinical challenge. Although the third-generation covalent inhibitor osimertinib effectively overcomes T790M-mediated resistance and is widely used as first-line therapy. Nevertheless, resistance to osimertinib eventually develops, and patients with the EGFR L858R mutation often experience less durable responses than those with *exon 19* deletions. Therapeutic options for patients who progress after osimertinib remain limited. Targeted protein degraders act through a catalytic, event-driven mechanism that can reduce on-target resistance relative to occupancy-driven inhibitors. SC3499 is an orally active, allosteric bifunctional degrader rationally designed to selectively target mutant EGFR containing the oncogenic L858R mutation. In preclinical studies, SC3499 demonstrated potent and durable antitumor activity in both in vitro and in vivo L858R-driven NSCLC models. Importantly, SC3499 maintained full activity against multiple resistance mutations, including L858R/C797S, L858R/T790M, and L858R/T790M/C797S, which confer resistance to approved EGFR TKIs such as osimertinib. In in vivo studies, SC3499 exhibited favorable pharmacokinetic properties, excellent oral bioavailability, and induced marked tumor regression with once-daily oral dosing. Broad kinase profiling showed exceptional kinase selectivity, and global proteomic analysis confirmed selective degradation of mutant EGFR without affecting unrelated proteins or other cereblon (CRBN) substrates. These results support SC3499 as a promising, orally active, allosteric EGFR degrader capable of overcoming resistance to current EGFR-targeted therapies, including osimertinib, and providing durable antitumor responses in EGFR-mutant NSCLC.

#4600 Discovery of PLX-66140, a first-in-class, potent and selective CDK2 molecular glue degrader for CCNE1-amplified tumors.

Leenus Martin, Jean-Francois Brazeau, Nasrin Rastgoo, Quinn Spalding, Gabrielle Blanco, Kyohei Hayashi, Susan Song, Jianguo Ma, Shu You, Campos Alex, Jay Chung, Farhana Barmare, Kevin Freeman-Cook, Peggy A. Thompson

Plexium, San Diego, CA

Introduction: Dysregulation of the cell cycle is a hallmark of many cancers. The Cyclin-Dependent Kinases (CDKs) with their cyclin binding partners are associated with cell cycle progression and transcriptional regulation. Targeting CDK2 is a key therapeutic strategy in oncology, especially in Cyclin E1 (CCNE1) amplified/overexpressed and ER+ breast cancers. CCNE1 amplification/overexpression and activation of its canonical binding partner CDK2 is a major resistance mechanism in CDK4/6i breast cancer therapy. In addition, elevated CCNE1 expression and complexation with CDK2 promotes aberrant cell cycling which is associated with poor prognosis in ovarian, breast and uterine cancers. Targeting CDK2 using small molecule active site inhibitor-based approaches have advanced into the clinic; however, maintaining selective CDK2 inhibition at efficacious exposures is challenging due to the high sequence homology across other CDKs. Molecular glue degraders have the potential to selectively target CDK2 and provide improved clinical benefit while minimizing off-target toxicities.

Results: Here we report the discovery of our development candidate, PLX-66140, a novel, potent and selective cereblon (CRBN) based CDK2 molecular glue degrader for the treatment of CCNE1 amplified cancers. Plexium's ultra-high throughput screening platform and medicinal chemistry optimization efforts identified our lead molecular glue degrader that induces CRBN-CDK2 ternary complex formation and demonstrates proteasomal dependent, CRBN-mediated degradation of CDK2 in cell-based assays. Global proteomics confirms that PLX-66140 degrades CDK2 selectively without modulating known cereblon neosubstrates and exhibits dose dependent modulation of E2F target genes. Potent, deep and selective degradation of CDK2 with PLX-66140 treatment, results in robust inhibition of RB phosphorylation, cell cycle arrest and antiproliferative activity in a panel of CCNE1 amplified cancer cell lines. In contrast to ATP-competitive small molecule inhibitors, PLX-66140 demonstrates selective inhibition of cell cycle arrest and proliferation in CCNE1 amplified cells, and minimal activity in non-CCNE1 amplified cells, highlighting the selectivity and potential superior safety profile over inhibitors. Oral administration of PLX-66140 in tumor bearing mice demonstrates robust target degradation and enhanced anti-tumor activity over ATP-competitive inhibitors in multiple CCNE1 amplified xenograft models at well tolerated doses.

Conclusion: Our development candidate, PLX-66140 provides compelling preclinical evidence and scientific rationale for clinical development in CDK4/6 inhibitor-naïve and -resistant $HR^+/HER2^-$ breast cancer along with CCNE1 amplified solid tumors.

#4601 Rational design of potent androgen receptor degraders via AI-assisted molecular modeling and validation of anti-tumor efficacy in prostate cancer.

Chih-Chang Chou, You-Sheng Lin, Cheng-Li Chou, Kuan-Hung Chen, Shu-Jen Chen, Chu-Chiang Lin

AnHorn Medicines Co., Ltd., Taipei, Taiwan

The androgen receptor (AR) plays a central role in the progression of prostate cancer, and its sustained signaling remains a major challenge in castration-resistant prostate cancer (CRPC). Targeted protein degradation of the AR offers a promising therapeutic strategy to overcome therapeutic resistance that limits the efficacy of current AR antagonists. To rationally design novel AR degraders, we employed AnHorn's proprietary AIMCADD (Artificial Intelligence-bio-Informatic-MedChem-Computer-Aided Drug Design) platform to predict the three-dimensional binding conformations between the AR ligand-binding domain (AR-LBD) and CRBN E3 ligase. Molecular dynamics (MD) simulations were used to calculate binding free energies and identify the most stable AR-CRBN ternary complex. Based on this complex, the binding conformations of AR-LBD and CRBN warheads were obtained via molecular docking, followed by AI-assisted linker generation using AIMLinker, a deep neural network-based algorithm, to construct a virtual library of degrader candidates. Molecular docking and dynamic simulations were further applied to evaluate ternary complex stability and binding affinity, from which a subset of top-ranked candidates were selected for experimental validation. Lead candidates effectively induced AR degradation in LNCaP, 22Rv1, and VCaP cells. Notably, these degraders also retained activity against clinically relevant AR mutants frequently observed in CRPC patients, including L702H, T878A, H875Y, W742C, and F877L. The degradation was abolished by co-treatment with the proteasome inhibitor MG132, confirming a ubiquitin-proteasome-dependent mechanism. Direct binding of the lead compound to AR was further verified by drug affinity responsive target stability (DARTS) assay. Quantitative RT-PCR analysis revealed a marked downregulation of AR downstream targets, *KLK3* (PSA), suggesting the loss of AR transcriptional activity. In cell viability assays, the most potent compound selectively suppressed proliferation of AR-positive prostate cancer cells, with minimal cytotoxicity in normal cells. In xenograft animal models, once daily administration significantly reduced tumor volume and prostate specific antigen (PSA) level in plasma without observable systemic toxicity. In summary, through AI-assisted molecular design and computational screening, we developed a potent AR degrader that efficiently induces proteasome-dependent AR degradation, suppresses AR transcriptional activity, and exhibits robust anti-tumor efficacy *in vivo*. These results highlight a promising therapeutic approach for advanced prostate cancer through targeted AR degradation.

#4602 Dual HDAC3/8 PROTAC degraders exert anti-tumor and immunomodulating effects in diffuse large B-cell lymphoma.

Michael Y. He[1], Yufeng Xiao[2], Mehran Bakhtiari[1], Ting Liu[1], Wenxi Xu[1], David G. Brooks[1], Housheng Hansen He[1], Guangrong Zheng[2], Robert Kridel[1]

[1]UHN Princess Margaret Cancer Centre, Toronto, ON, Canada,[2]University of Florida, Gainesville, FL

Critical challenges remain in the clinical management of diffuse large B-cell lymphoma (DLBCL), as up to 40% of patients experience disease relapse or refractoriness. Despite the use of novel therapies, relapsed/refractory DLBCL results in a high risk of mortality, especially in the activated B-cell-like (ABC) subtype. Developing new therapeutic options for those patients becomes a pressing and clinically unmet need. Here, we explore the combined targeting of histone deacetylase (HDAC) 3 and 8 by targeted protein degradation to combat epigenetic deregulation in DLBCL. Through a comprehensive screen using single or dual HDAC3/8-targeting compounds in 12 DLBCL cell lines, we discovered that a highly selective, potent, first-in-class dual HDAC3/8 proteolysis-targeting chimera (PROTAC) degrader YX968 potently suppressed cell survival and proliferation. This effect was particularly more prominent and significantly stronger than single HDAC3 or 8 PROTACs in the ABC-DLBCL cell lines. Further functional evaluations revealed that YX968 specifically induced caspase-3-mediated apoptosis and caused cell cycle arrest. Mechanistically, YX968 profoundly upregulated H3K27 acetylation (H3K27ac), a key epigenetic mark for enhancer regulation, and generated a unique transcriptomic profile with downregulated genes associated with cell cycle regulation and upregulated genes implicated in immune activation. Moreover, we validated the gene expression results using flow cytometry for upregulated surface protein expression of the antigen presentation markers MHC-I and II, and detected enhanced $CD8^+$ T-cell-induced cytotoxicity by YX968 in an in vitro T-cell co-culture assay, indicating its immunomodulating activities to potentiate anti-tumor immunity. Although YX968 showed in vitro efficacy, we found that it had poor metabolic stability, which precluded its potential in vivo application. To enhance the translation value of our approach, we developed a second-generation dual HDAC3/8 PROTAC (YX226) with improved metabolic stability while maintaining potent degradation, cell-killing, and immunomodulating activities. Using global proteomics, we confirmed the on-target activity of YX226 to selectively degrade HDAC3 and 8 but not the other HDAC isoforms. Importantly, we observed significant in vivo HDAC3/8 protein degradation and tumor growth inhibition by YX226 in a xenograft lymphoma model without adverse reduction of body weight, providing proof-of-principle evidence for in vivo efficacy and safety of a dual HDAC3/8 PROTAC. In conclusion, our findings demonstrate that dual HDAC3/8 PROTAC degraders induce significant anti-tumor and immunomodulating effects in our preclinical DLBCL models, supporting further development and evaluation of our second-generation bioavailable compound YX226 as a novel treatment option for DLBCL.

#4603 Favorable DMPK properties enable development of a novel arylsulfonamide RBM39 molecular glue degrader, PPI-101, for the treatment of neuroblastoma.

Jian Wu, Lei Zhou, Yongzhi Gao, Shanshan Wang, Qi Zhang, Jingping Mei, Fang Bai, Song Feng, **James X. Rong**

Peak Perform Innova, Shanghai, China

Background: E7820 and related arylsulfonamides have recently been recognized as molecular glues that recruit the splicing factor RBM39 to the CRL4-DCAF15 E3 ligase complex, triggering RBM39 ubiquitination and degradation. Despite clinical evaluation, these degraders have shown limited efficacy and dose-limiting hematotoxicity. The underlying in vivo pharmacology of RBM39 degraders remains poorly defined, hindering optimization.
Methods: We characterized the pharmacokinetic (PK), pharmacodynamic (PD), and efficacy relationships of E7820 and analogs (PPI-101, R134, R111, R011) in an IMR32 neuroblastoma xenograft model. Compounds were administered orally once daily for 28 days. Tumor growth inhibition (TGI), plasma/tumor exposures, and RBM39 protein levels were quantified to establish PK/PD relationships and identify next-generation RBM39 degraders with improved therapeutic index (TI).
Results: E7820, PPI-101, R134, and R011 achieved complete tumor growth inhibition at 30 mg/kg. TGI correlated with unbound exposure normalized by cellular DC50 values, exhibiting a sigmoidal relationship between efficacy and exposure multiples. Following 3-day dosing, tumor RBM39 remained ≥75% depleted for up to 30 hours after the last dose, even when unbound plasma and tumor concentrations had fallen >300-fold below DC50, indicating slow RBM39 recovery kinetics and sustained pharmacodynamic effect. PPI-101 showed the most favorable DMPK profile, with the lowest human plasma protein binding, the highest volume of distribution (Vss = 0.77 L/kg)—an indicator of drug distribution between plasma and peripheral tissues—and superior tumor penetration (tumor/plasma ratio = 1.0, ~50% higher than E7820). Consequently, lower plasma exposure was required for equivalent tumor coverage, reducing systemic exposure and the risk of hematologic toxicity. Preliminary toxicology studies revealed a markedly improved TI (14 for PPI-101 vs <2.7 for E7820), consistent with reduced reticulocyte and lymphocyte suppression.
Conclusions: This study defines, for the first time, the in vivo PK/PD relationships governing RBM39 degradation and demonstrates that favorable distribution properties can markedly enhance therapeutic index. PPI-101 emerges as a potent and safer RBM39 degrader candidate for neuroblastoma therapy, warranting GLP toxicology and IND-enabling development.

#4604 Preclinical efficacy of a PROTAC pan-KRAS degrader in a KRAS G12D syngeneic mouse model and concurrent immune tumor microenvironment changes.

Jason M. Berk, Andrea Lopez-Arroyo, Dana M. Klug, John P. Caldwell, Peter Hegan, Samantha Andella, Jessica Kraus, Amanda Chapman, Jennifer Pizzano, Mark Bookbinder, Gregory Cadelina, Debbie Gordon, Kim Davenport, Wendy Wu, Madeline A. Dorso, Morena Scopel, Rebecca Conrad, William Corwin, Goutham Pattabiraman, Keith R. Hornberger, Angela Cacace, Ignacio J. Juncadella, Kathryn D. Smith

Arvinas Operations, Inc., New Haven, CT

Missense mutations in *KRAS* occur in ~20% of cancers. Although 2 KRAS inhibitors have been approved for patients with *KRAS* G12C-mutated disease, resistance quickly develops; moreover, no approved agents target other KRAS mutants. We developed a tool PROteolysis TArgeting Chimera (PROTAC) pan-KRAS degrader that induces the ubiquitination and subsequent proteasomal degradation of KRAS; it potently and selectively degrades active and inactive KRAS forms. Selective KRAS degradation that spares HRAS and NRAS may yield a higher therapeutic index than current investigational RAS inhibitors targeting all RAS isoforms. Additionally, the iterative activity of the PROTAC pan-KRAS degrader may overcome resistance driven by *KRAS* upregulation, a common RAS inhibitor resistance mechanism. Mutant KRAS is an established intrinsic driver of an immunosuppressive tumor microenvironment (TME), which can be alleviated by KRAS inhibition, suggesting potential synergy with immune checkpoint blockade (ICB). We compared the antitumor activity of PROTAC-driven KRAS degradation vs RAS inhibition (± ICB with an anti-programmed death-1 antibody) and the effects on TME in a KRAS G12D murine colorectal cancer model, CT-26. Our PROTAC potently degraded mutant KRAS and exhibited antiproliferative effects in spheroids that were comparable to a clinical RAS(ON) inhibitor. Oral administration of the PROTAC pan-KRAS degrader as a single agent in the CT-26 model led to substantial KRAS degradation (>85%), robust and durable suppression of mitogen-activated protein kinase pathway activity, and substantial tumor growth inhibition, including complete responses (CRs). The PROTAC pan-KRAS degrader combined with ICB led to deeper and more rapid tumor regressions, resulting in a higher rate of CRs and longer post-treatment survival, compared with the RAS(ON) inhibitor plus ICB. To characterize TME changes, tumors treated with the PROTAC pan-KRAS degrader or RAS(ON) inhibitor (± ICB) were compared by bulk RNA sequencing (RNAseq) and tumor-infiltration leukocyte (TIL) analysis. RNAseq revealed strong RAS pathway suppression by both agents, leading to altered gene expression in tumor-intrinsic and extrinsic molecular pathways. KRAS degradation demonstrated a differential positive enrichment for key immune-related pathways associated with antitumor immunity and immune activation, suggesting PROTAC-specific immune TME changes may contribute to its antitumor effects. TIL analysis demonstrated statistically significant changes in immune populations, including cytotoxic T cells and myeloid cells, after PROTAC treatment. The observed rapid tumor regressions, paired with deeper immune response and longer survival, suggest that the PROTAC pan-KRAS degrader is more efficacious and permissive to ICB combination than a RAS(ON) inhibitor in an immunocompetent tumor model system.

#4605 Brigatinib based degraders as a therapeutic strategy for triple negative breast cancer.

Manu Khosla[1], Suresh Alahari[1], Guangdi Wang[2]

[1]Biochemistry and Molecular Biology, Louisiana State University Health Sciences Center, New Orleans, LA,[2]Xavier University of Louisiana, New Orleans, LA

Background: Treatment of patients with triple-negative breast cancer (TNBC) has been challenging due to the absence of well-defined molecular targets and high invasive and proliferative capabilities of these cells. Therefore, new therapeutic strategies for treatment of TNBC are urgently needed. Protease-targeted chimeras (PROTACs) are a class of emerging therapeutic inhibitors that recruit the ubiquitin E3 ligase to selectively degrade proteins. PROTAC degrader technology has shown robust results in inhibiting TNBC progression.
Methods: RNA sequencing and analysis were done. Samples were submitted to PamGene for kinome profiling and analysis. Western blotting was performed to visualize protein expression. MTT assays were carried out to evaluate cell viability. Colony formation assays assessed changes in clonogenicity. Data were analyzed using Graph Pad Prism Software 8 using one-way ANOVA and the unpaired two-tailed Students t-test. All data were evaluated in triplicate against control cells.
Results: Analysis of RNA sequencing in LM2-4175 TNBC cells treated with our target degrader showed increased genes associated with apoptosis and a decrease in genes associated with cell cycle checkpoint, DNA replication, and regulation of P53 signal transduction pathways. Kinase activity profiling of MDAMB231-LM2-4175 TNBC cells treated with our degrader showed a significant reduction in serine/threonine kinases (STKs) associated with Mitogen-activated protein kinase (MAPK) and cyclin-dependent kinase (CDK) families. In addition, we noticed a significant decrease in protein tyrosine kinases (PTK) associated with ephrin receptor proteins. Western blot analysis confirmed targeted degradation of Focal Adhesion Kinase in multiple TNBC cell lines (MDAMB-231-LM2-4175, MDAMB-468, and 4QXTB). MTT analysis of cell proliferation showed our degrader selectively targeted
MDAMB231, MDAMB231-LM2-4175, MDAMB-468, and 4QXTB (Primary)TNBC cells over our non-neoplastic cell line, MCF10A, in a nanomolar range. Colony formation assays also showed our degrader was able to reduce clonogenicity in TNBC cell lines MDAMB231-LM2-4175, MDAMB-468, and 4QXTB.
Conclusions:Breast cancer is a diverse and intricate disease which is known to have unique inter- and intra-tumoral characteristics. We have identified a candidate PROTAC which can selectively target TNBC cells while minimally affecting normal bystander cells at nanomolar ranges in vitro. The further development of this degrader can serve as the fundamental basis for a novel therapeutic treatment in TNBC.

#4606 Rational development of novel DCAF16-mediated SMARCA2 selective Targeted Glues™ for the treatment of SMARCA4 deficient tumors.

James T. Lynch, Martin Ambler, Nicole Zordan, Claudia De Fusco, Laura Casares Perez, Kathryn Bosson, Alexander Fawcett, Paula MacGregor, Tarun Narwani, Colin T. R. Davies, Mahad Gatti Lou, Edward Hooper-Greenhill, Liliana Greger, Giles A. Brown, Martin Pass, Louise K. Modis

Amphista Therapeutics, Cambridge, United Kingdom

SMARCA2 and SMARCA4 are mutually exclusive catalytic subunits of the SWI/SNF chromatin remodelling complex. In non-small cell lung cancer (NSCLC), SMARCA4 mutations are observed in >5% patients and are associated with poor prognosis and advanced disease. Selective degradation of SMARCA2 exploits paralogue dependency in SMARCA4-deficient tumors to impact disease burden with minimal toxicity in normal tissues.

Here, we report the rational design and optimisation of a novel class of SMARCA2 degraders that exploit a Targeted Glue™ mechanism to induce DCAF16-dependent proteasomal degradation. Amphista's degraders potently drive >95% SMARCA2 degradation within 4 hours, resulting in deep suppression of biomarkers KRT80 and PLAU *in vitro*. Further, we observe exceptional degradation specificity for SMARCA2, as revealed by global proteomics and, critical for a best-in-class molecule, achieve near complete selectivity over SMARCA4 in a SMARCA4 WT model.

Comprehensive mode of action studies, including E3-ligase knock-out and cysteine mutant rescue experiments demonstrate that our SMARCA2 Targeted Glues™ induce degradation via selective recruitment of DCAF16 and covalent interaction with a single DCAF16 cysteine residue. Structural studies, including generation of multiple high resolution (sub-3Å) cryo EM ternary complex structures have enabled informed structure-activity relationship optimisations of degradation potency, kinetics and selectivity. Consequently, optimised compounds can deliver fast, deep degradation of SMARCA2 as demonstrated *in-vivo* in a disease-relevant SMARCA4 mutant model.

We have achieved compound profiles that uniquely position Amphista to deliver class-leading SMARCA2 degraders for the treatment of SMARCA4-mutant NSCLC.

#4607 Preclinical evaluation of a cardiosafe first-in-class MCL-1 degrader for the treatment of hematological malignancies.

Tomasz Tomczyk, Anna Maria Serwotka-Suszczak, Robert Dyjas, Jose Arencibia, Monika Milewicz, Klaudia Poniatowska, Jolanta Skalska, Andrzej Tracz, Diana Trębicka, Karolina Wojcik, Sylvain Cottens, Piotr Kowalczyk, Paweł Dobrzański, Michał Biśta, Katarzyna Brach, Toshimitsu Takagi, Martyna Pastok, Justyna Adamczyk, Iwona Mames, Michał Walczak

Captor Therapeutics S.A., Wrocław, Poland

MCL-1, a member of the Bcl-2 family of apoptosis regulators, is a critical pro-survival factor implicated in tumor maintenance and therapeutic resistance across a wide range of cancers. Although several MCL-1 inhibitors have entered clinical development, many were discontinued due to dose-limiting cardiac toxicity. Targeted protein degradation offers an alternative strategy with potential advantages, including improved selectivity, prolonged pharmacodynamic effects, and reduced risk of adverse cardiac events.

Here, we describe the discovery and preclinical characterization of a novel bifunctional compound designed to selectively degrade MCL-1 for the treatment of hematological malignancies. Biophysical assays confirmed ternary complex formation between the degrader, MCL-1, and an E3 ligase. The compound induces proteasome-dependent degradation of MCL-1, leading to apoptosis and cell death in a broad panel of human cancer cell lines, with low nanomolar potency (pIC_{50} ~9 for MV4-11, OPM-2, and DMS114). Cytotoxic effects were observed across leukemia, lung cancer, and multiple myeloma models, while sparing normal and primary cells. In human iPSC-derived cardiomyocytes, the degrader caused only transient reduction of MCL-1 levels, in contrast to MCL-1 inhibitors that induced 6-15-fold MCL-1 upregulation persisting after washout, a mechanism linked to elevated cardiac troponin in clinical trials.

In vivo, the compound demonstrated strong antitumor activity in AML xenograft models, inducing MCL-1 degradation and tumor growth inhibition. Combination with low-dose venetoclax (7.5 mpk) promoted tumor regression at 5 mpk using an intermittent dosing regimen (2 days on/5 days off). In non-human primates, the compound exhibited a favorable pharmacokinetic/pharmacodynamic profile with effective MCL-1 degradation and no evidence of cardiac toxicity at exposures exceeding predicted human efficacious levels.

In conclusion, we have developed a highly potent and selective bifunctional MCL-1 degrader that shows robust activity *in vitro* and *in vivo*, complete target coverage, and a favorable safety margin compared with MCL-1 inhibitors. These findings support MCL-1 degradation as a promising therapeutic approach for hematologic malignancies. The compound is advancing through IND/CTA-enabling studies, with a first-in-human Phase 1 trial planned for 2026.

#4608 GSK5471713: A novel, selective oral androgen receptor degrader with best-in-class potential for the treatment of prostate cancer.

Christine Thompson[1], Yang Lee[2], Melissa C. Musso[1], Kwok-Ho Chan[3], Kamelia Behnia[1], Edward Hooper-Greenhill[3], Christian S. Sherk[1], Nanhua Deng[2], Nadeesha Rajapaksha[1], Mansi Babbar[1], Sarah Gerhart[1], Julie Bullock[1], Kenneth W. Hance[1], Benjamin Schwartz[2], Laure Rittie[1], Christopher P. Tinworth[3], **Anastasia Wyce**[1]

[1]GSK, Collegeville, PA,[2]GSK, Cambridge, MA,[3]GSK, Stevenage, United Kingdom

The androgen receptor (AR) is a ligand-dependent transcription factor that controls expression of genes involved in normal prostate development and is a critical driver of prostate cancer growth and survival. Patients with locally advanced or metastatic disease are frequently treated with AR pathway inhibitors (ARPIs) targeting AR (e.g., enzalutamide) and/or androgen synthesis (e.g., abiraterone), and while these therapies offer survival benefit, patients frequently develop resistance via reactivation of AR signaling. AR pathway re-activation is often mediated by direct alterations to AR, including gene amplification, structural rearrangements, point mutations in the ligand binding domain (LBD), and co-expression of constitutively active splice variants. In total, AR alterations are observed in >60% of metastatic castration resistant prostate cancer (mCRPC) patients and are associated with resistance to ARPIs.

Heterobifunctional degraders recruit proteins of interest to the ubiquitin-proteasome system for targeted degradation. As these molecules degrade their target protein, they offer an opportunity to overcome or avoid resistance mechanisms impacting inhibitors of functional activity. We disclose herein GSK5471713 as a potent and selective oral AR degrader, comprised of an AR LBD ligand linked to a binder of the E3 ubiquitin ligase CRBN. GSK5471713 potently degrades all clinically relevant forms of full-length AR, including wild type, LBD mutants, and in amplified settings. Similar to other AR degraders currently in clinical development, it functions as a dual AR degrader and antagonist. GSK5471713 potently degrades full-length AR in prostate cancer cell lines *in vitro*, resulting in transcriptional down-regulation of AR-dependent genes and gene signatures and inhibition of cell growth. Increased potency is observed for GSK5471713 in prostate cancer cell lines *in vitro* compared to both enzalutamide and other AR degraders. *In vivo*, GSK5471713 induces time- and dose-dependent AR degradation in prostate cancer xenografts. Daily oral administration induces dose-dependent tumor growth inhibition and tumor regressions, with commensurate decreases in plasma PSA levels. Comparison of the *in vivo* activity of GSK5471713 to enzalutamide and other AR degraders dosed at clinical exposure equivalents suggest an opportunity for differentiated efficacy. In total, these data demonstrate GSK5471713 as a potential best-in-class AR degrader offering benefit to patients with prostate cancer. GSK5471713 is expected to advance into Phase 1 clinical studies in early 2026.

#4609 Discovery and development of PRMT5/MEP50 degraders for the selective targeting of MTAP-null cancers.

Yue Zhong, Qian Chao, Yan Xiong, Husnu Kaniskan, Jian Jin

Departments of Pharmacological Sciences and Oncological Sciences, Icahn School of Medicine at Mount Sinai, New York, NY

Protein arginine methyltransferase 5 (PRMT5) is an important regulator of various biological processes through the mono- and symmetric dimethylation of protein substrates. PRMT5 is overexpressed in multiple human cancers, and its overexpression is often associated with poor prognosis. We recently reported MS115, a best-in-class PRMT5 degrader that potently and selectively degraded PRMT5 and its coactivator, MEP50, in concentration-, time-, and ubiquitin-proteasome system-dependent manners. MS115 displayed markedly improved PRMT5/MEP50 degradation potency over published PRMT5 degraders, which translated to superior antiproliferative effect in both breast and prostate cancer cells. More importantly, MS115 exhibited safer cytotoxicity profile compared to existing PRMT5 degraders and inhibitors in normal cells. Nonetheless, residual antiproliferative activity in MTAP-proficient cells highlights the need for improved therapeutic selectivity. To address this limitation, we tackled the synthetic lethality between PRMT5 and MTAP loss. MTAP homozygous deletions, present in approximately 15% of human cancers, lead to accumulation of methylthioadenosine (MTA), an endogenous PRMT5 inhibitor. By leveraging MTA-cooperative PRMT5 inhibitors, we generated a series of PRMT5/MEP50 degraders that selectively degraded PRMT5 and MEP50 and suppressed proliferation in MTAP-null cancer cells, while sparing MTAP-wild-type counterparts across breast cancer and cholangiocarcinoma models. This targeted selectivity enables the study of both catalytic and non-catalytic functions of PRMT5 with substantially improved tolerability. Collectively, we have discovered MS115 and multiple MTA-cooperative PRMT5/MEP50 degraders with enhanced potency and safety, providing valuable chemical probes and promising candidates for the treatment of cancers driven by PRMT5 dysregulation.

#4610 The B-hCRBN mice model facilitates PROTACs studies based on CRBN ligands.

Jay Zhang, Yue Zhang, Chonghui Liu, Ying Zhao, Xiao Liu, Jiansu Zhang

Biocytogen, Waltham, MA

In recent years, CRBN ligands have gradually become popular E3 ligase ligands. They can be used to design and synthesize PROTACs and molecular glue degraders, playing an important role in these fields. CRBN, together with DDB1 (damaged DNA binding protein 1), Cul4A (Cullin 4A), and ROC1, forms the E3 ubiquitin ligase complex (CRL4). As a substrate receptor, CRBN binds certain proteins, promoting their ubiquitination and proteasome-dependent degradation. Through its E3 ligase function, CRBN regulates the degradation of various proteins, which is crucial for cell growth, differentiation, and apoptosis. CRBN is expressed not only in tumor cells but also in normal cells. In the treatment of multiple myeloma (MM), immunomodulatory drugs targeting CRBN (such as thalidomide and lenalidomide) show significant efficacy. These drugs alter the substrate specificity of CRBN, inducing degradation of tumor-associated proteins and thereby inhibiting cancer cell growth. Additionally, CRBN-based PROTACs (Proteolysis Targeting Chimeras) are currently being developed as a novel cancer treatment strategy. CRBN-based PROTACs recruit the CRBN complex to the target protein, leading to its polyubiquitination and subsequent proteasome degradation.Biocytogen has developed the B-hCRBN mouse model. The CDS of the human CRBN gene that encodes the full-length protein was inserted into the mouse *Crbn* exons 2-3. The B-hCRBN mice will express the human CRBN protein, while mouse *Crbn* will no longer be expressed. Heart, liver, spleen, lung, kidney, stomach, small intestine, colon, and cortex were collected from homozygous B-hCRBN mice. Human *CRBN* mRNA was only detectable in homozygous B-hCRBN mice. The cortex, liver, lung, kidney, and spleen were collected from homozygous B-hCRBN mice, and then analyzed by western blot with anti-CRBN antibody. CRBN was detectable in homozygous B-hCRBN mice. Naïve CD4+ T cells from B-hCRBN mice have increased production of IL-2 when treated with Lenalidomide. CC-885 exhibits marked toxicity exclusively in B-hCRBN mice, with no detectable toxicity observed in wild-type mice. The body weight, complete blood count, and blood biochemistry of male and female B-hCRBN mice were analyzed. The main organs were dissected, weighed, and analyzed by H&E staining. No obvious abnormalities were found in all the organs detected (brain, heart, lung, liver, spleen, stomach, small intestine, colon, kidney, uterus, ovary, and testis). In summary, the development of the B-hCRBN mouse model has been successful, as it successfully expresses the human CRBN protein and can be used functionally. Tumor cell lines inoculated in B-hCRBN mice can be used to study the *in vivo* efficacy and safety evaluation of CRBN small molecule drugs, molecular glue drugs based on CRBN, or PROTAC drugs based on CRBN.

#4611 Small-molecule stabilization of non-native c-Myc multimer drives degradation using an IDP-targeting discovery platform.

Markus K. Muellner[1], Christian Kuehne[2], Michael Ahrweiler[2], Antony Crisp[1], Florian Kellner[1], Katharina Strasser[1], Paulina Pacak[1], Bechir Zitouni[1], Joonsun Lee[1], Milanka Gavrilovic[1], Lisa Wurm[1], Bernadette Winter[1], Manuela Richter[1], Fiona Liebig[1], Noel Riedl[1], Christoph Berger[1], Stefan Seidl[1], David Fischer[1], Christine Triska[1]

[1]RDP Pharma AG, Romanshorn, Switzerland,[2]RDP Pharma AG

Intrinsically disordered proteins (IDPs) such as c-Myc remain largely undrugged despite their central role in cancer. We developed Prompt Degrader™, a computational platform that predicts transient ordered conformations in IDPs and identifies drug-like, orally bioavailable, non-covalent small molecules that stabilize degradation-prone states. Using in silico modeling of a c-Myc homodimer pocket, we identified compounds predicted to stabilize dimerization and to promote targeted protein degradation of c-Myc via a mechanism distinct from conventional PROTACs or molecular glues. Our hit RDP-02004 induced rapid, dose-dependent loss of c-Myc protein (DC_{50} ~5-10 µM) and apoptosis across diverse MYC-dependent cancer cell lines, including multiple myeloma, lung and triple-negative breast cancer, with selectivity over non-transformed cells. RDP-02004 showed high microsomal stability and broad in vivo activity, suppressing tumor growth in three xenograft models after oral dosing. Minimal weight loss and only mild hepatic and renal findings were observed. Mechanistic studies indicated engagement of multiple protein quality-control pathways, consistent with clearance of misfolded c-Myc species. The proteasome inhibitor MG-132, the ubiquitin-activating enzyme inhibitor TAK-243, and the autophagy inhibitor Autophinib each rescued c-Myc levels after compound treatment, implicating both ubiquitin-proteasome and aggrephagy-like mechanisms. Based on these findings, we screened scaffold-divergent analogues and identified RDP-09024, which likewise showed potent c-Myc degradation and cytotoxicity with an improved off-target profile. Direct target engagement of recombinant c-Myc protein was confirmed by ligand-observed STD and WaterLOGSY NMR experiments, in which RDP-09024 showed no binding to a negative-control protein. We confirmed the predicted binding mode and pocket of RDP-09024 via hydrogen-deuterium exchange mass spectrometry (HDX-MS) with or without compound, revealing a flexible loop on c-Myc directly involved in RDP-09024 binding. Prompt Degrader™ compounds were active ex vivo in $CD138^+$ multiple myeloma patient cells as well as in xenograft models and showed a significantly improved selectivity profile versus non-cancer cells. Structure-activity and pharmacophore analyses, together with structure-based design, yielded additional series with improved properties and activity (DC_{50} < 1 µM). These data provide proof of concept that exploiting IDP conformational ensembles to stabilize degradable c-Myc assemblies can generate small-molecule c-Myc degraders and support further optimization of this platform toward safer, more selective anti-MYC therapeutics.

#4612 Application of mechanistic preclinical PK/PD/efficacy modeling to support combination strategy for AZD9750, a novel oral androgen receptor degrader (PROTAC).

Ana Quiroga[1], Pablo Morentin Gutierrez[1], Antonio Ramos-Montoya[1], Chrysiis Michaloglou[1], Nuria Galeano-Dalmau[1], Claire Crafter[1], Aaron Smith[1], Jamie Scott[1], Michael Niedbala[2]

[1]AstraZeneca, Cambridge, United Kingdom,[2]AstraZeneca, Waltham, MA

The androgen receptor (AR) is highly expressed in prostate cancers and is a clinically validated target in oncology. AZD9750 is a novel potent oral selective AR Proteolysis-targeting chimera (PROTAC) with a suitable pharmacological profile to be used in combination with a variety of other therapeutics such as capivasertib, a potent pan-AKT kinase inhibitor with anti-tumor activity in tumors with PIK3CA and PTEN mutations, and saruparib, a PARP1-selective inhibitor especially effective against tumors with mutations in genes like BRCA1 and BRCA2. We present here the preclinical PK/PD/Efficacy modeling work used to understand the anti-tumor mechanism of AZD9750 in combination with AKT and PARP inhibitors. We developed a novel mechanistic mathematical model applied to in vivo preclinical hormone sensitive, ARwt prostate PDX models C901 and MR041. C901 has homologous deletion of BRCA2 and MR041 is PTEN null, making them appropriate candidates for combination with PARP and AKT inhibitors, respectively. The PK module of the model describes the compound exposure in monotherapy and combination. The PD module describes the AR, AKT, GSK3β and S6 total and phosphorylated levels measured by Western Blotting and PARylation levels measured by ELISA. In the efficacy module, the levels of AR, pS6 and PARylation were linked to tumor growth inhibition while pGSK3β and PARylation levels were linked to induction of apoptosis; subsequently, these parameters determine the tumor size. All model parameters were derived from internal studies; some were estimated using Non-Linear Mixed Effect modeling of individual longitudinal PK, PD biomarkers and tumor size data taken from several studies. The model describes well the relationship between plasma concentration of the different compounds and PD biomarkers modulation both in monotherapy and in combination. Furthermore, the mathematical model is capable of explaining the enhanced anti-tumor efficacy in combination as a function of the different biomarkers' modulation. This study provides quantitative mechanistic insights into the AZD9750 combination with AKT and PARP inhibitors. The study enriches our understanding of biomarkers relevant to AR-PROTACs, PARP inhibitors, and AKT inhibitors, informing the selection of biomarkers for monitoring in clinical trials. Additionally, it quantifies the extent of biomarker modulation required to achieve maximal antitumor activity and supports rational combination strategies, as well as dose and schedule optimization for clinical development.

#4613 ZMS-4426, an oral degrader of SMARCA2 shows potent anti-tumor activity, but variant selectivity against SMARCA4 across species.

Lu Liu, Fanxun Zeng, Ruonan Chen, Mengnan Hu, Yao Guo, Wenjing Li, Mei Lan, Liting Xue, Zhengtao Li, Renheng Tang

State Key Laboratory of Neurology and Oncology Drug Development, Simcere Zaiming Pharmaceutical Co., Ltd., Shanghai, China

Mammalian SWI/SNF complexes always contain one of two mutually exclusive and structurally highly related ATPases: SMARCA2/BRM or SMARCA4/BRG1, as its catalytic subunit. It is reported that SMARCA4 is absent in a serial of cancers, and these SMARCA4 deficient cancer cells are highly dependent on its paralog SMARCA2 for survival. Therefore, it holds great therapeutic promise to treat SMARCA4 deficient cancers with selective SMARCA2 degraders. Here, we reported ZMS-4426, a highly selective SMARCA2 degrader. In HiBiT knock-in HeLa cells, it potently degraded SMARCA2 with a >10,000-fold selectivity over SMARCA4. The global proteome data also indicated that ZMS-4426 was highly specific in degrading the expected target proteins SMARCA2. Furthermore, ZMS-4426 demonstrated high degradation selectivity of SMARCA2 over SMARCA4 in a variety of human cancer cell lines and PBMCs of multiple species. However, in dog PBMCs, the degradation selectivity between SMARCA2 and SMARCA4 varies among individuals.Due to the high selectivity over SMARCA4, ZMS-4426 effectively inhibited the proliferation of SMARCA4 deficient cells, and inhibited the proliferation of neither SMARCA2/4-WT cells nor SMARCA2/4-DEL cells. Furthermore, the *in vitro* synergistic effects were observed when SMARCA4-loss NSCLC cells were treated with ZMS-4426 in combination with docetaxel.ZMS-4426 exhibited good oral availability in mice, rats, and dog. In the NSCLC NCI-H838 CDX model, ZMS-4426 effectively inhibited tumor growth, and the tumor growth inhibition (TGI) correlated well with SMARCA2 degradation in tumors. Further, the combination treatment of ZMS-4426 and nab-paclitaxel effectively suppressed tumor growth to a greater extent than either agent alone.

However, ZMS-4426 was not tolerated in dog for 7-day treatment at 2 mpk. Strong degradation of SMARCA4 in lung was detected, suggesting poor *in vivo* degradation selectivity in dog. Further, in monkey, the treatment of ZMS-4426 for 7-day at 1.5 mpk resulted in body weight loss and deep degradation of SMARCA4 in PBMCs, indicating that *in vitro* degradation selectivity in monkey PBMCs did not maintained *in vivo*.Similar findings were also observed in rats. In a head-to-head comparison with compound A (a reference molecule from WO2025194405, Prelude Therapeutics), treatment of ZMS-4426 and compound A for 4-day at 5 mpk intravenous injection in rats both induced complete degradation of SMARCA4 at 24 hours post-dose, indicating that neither compound preserved its selectivity profile *in vivo*.In conclusion, our potent and selective SMARCA2 degrader, ZMS-4426 induces strong synthetic lethality in SMARCA4 deficient cells both *in vitro* and *in vivo*. However, more studies are needed to elucidate discrepancy in degradation selectivity between *in vitro* and *in vivo* results.

#4614 Evaluation of targeted protein degraders using high-throughput ubiquitination assays for mechanistic and SAR analysis.

Yuzhou Xu, Jichuan Zhang, Yanfei Hu, Ye Tian, Min Lyu, Yinfei Yin

Shanghai ChemPartner Co., Ltd., Shanghai, China

Targeted Protein Degraders (TPDs) represent a paradigm shift from traditional occupancy-driven inhibition to event-driven pharmacology by harnessing the ubiquitin-proteasome system for selective protein elimination. Despite their therapeutic potential, the rational design of effective degraders, particularly Molecular Glues, remains a significant challenge due to the complex interplay between binding cooperativity, ubiquitination efficiency, and degradation kinetics. To better understand these mechanisms, we established a suite of preclinical assays to systematically evaluate TPD activity across key mechanistic steps, including ternary complex formation, ubiquitination induction, cellular uptake, and target protein degradation in cellular and *in vivo* models. During the early screening of degrader libraries, medicinal chemists require efficient methods to assess structure-activity relationships (SARs). Comparative studies revealed that the ubiquitination assay provides a more predictive measure of cellular degradation efficiency than ternary complex formation assays. While ternary complex assays characterize binding affinity, cooperativity, and complex stability among the target, degrader, and E3 ligase, they fail to capture conformational changes necessary for productive ubiquitination. Our data demonstrate that ubiquitination assays offer deeper mechanistic insights with high throughput and scalability, enabling rapid generation of robust datasets for data-driven SAR development. This approach effectively bridges the gap between structural optimization and functional outcomes, accelerating the rational design of next-generation degraders with improved potency and selectivity for therapeutic applications.

#4615 Preclinical characterization and evaluation of JSB462 (Luxdegalutamide), a novel AR degrader, and its combinations in prostate cancer.

Stephane Ferretti[1], Daniel A. Guthy[1], Marco Taddio[1], Marc Hattenberger[1], Marion Dourdoigne[1], Ramona Stump[1], Sabina Ciaghi[1], Mylene Lanter[1], Alessandra Amadori[1], Laurent Laborde[1], Asif Khan[2], Rafael Caparica[1], James Warburton[3], **Marta Cortes Cros**[1]

[1]Novartis Pharma AG, Basel, Switzerland,[2]Novartis Pharmaceuticals UK, London, United Kingdom,[3]Novartis Pharmaceuticals Corporation, East Hanover, NJ

The androgen receptor (AR) is a key therapeutic target in prostate cancer, being an important tumor driver in patients with metastatic hormone-sensitive prostate cancer (mHSPC), and AR alterations are a key mechanism of acquired resistance to androgen deprivation therapy (ADT) and androgen receptor pathway inhibitors (ARPIs) in those with metastatic castration resistant prostate cancer (mCRPC). JSB462 (Luxdegalutamide, formerly ARV-766) is an orally bioavailable proteolysis targeting chimera (PROTAC®) that induces a protein-protein interaction between AR and the Cereblon (CRBN) E3 substrate receptor, resulting in the ubiquitination of AR and its subsequent degradation via the proteasome. JSB462 is efficacious against wild type AR as well as clinically relevant AR ligand binding domain (LBD) mutants that confer resistance to ADT and ARPIs, including AR L702H, H875Y, and T878A mutations. AR degradation overcomes limitations of conventional AR antagonists that only inhibit AR activity and cannot compensate for the feedback loop leading to AR upregulation. JSB462 demonstrates potent AR degradation at sub-nanomolar concentrations *in vitro* and dose-dependent tumor growth inhibition in mouse xenograft models, including those resistant to enzalutamide and with high levels of AR. In addition to degrading the androgen receptor, JSB462 also exhibits direct antagonistic activity against AR signaling, inhibiting AR-driven transcriptional programs independent of receptor abundance. Beyond single agent activity, we have also explored biology-guided combination opportunities to maximize JSB462 efficacy. Abiraterone inhibits AR activity by targeting CYP17A1 and reducing synthesis of androgen receptor ligands, and combination with JSB462 leads to sustained AR pathway inhibition and improved *in vivo* efficacy. JSB462 treatment leads to sustained upregulation of PSMA in multiple prostate cancer cell lines, and pre-treatment of prostate tumor xenografts with JSB462 in combination with a sub-efficacious single dose of the PSMA-targeting radioligand therapy (RLT) Lutetium (^{177}Lu) Vipivotide Tetraxetan (Pluvicto®) led to sustained tumor growth inhibition. In a phase I/II trial, JSB462 was well tolerated and showed encouraging antitumor activity in pretreated patients with mCRPC. Here, we show preclinical combination data of JSB462 with abiraterone and Pluvicto® that support further investigation of these regimens. Towards that end, two phase 2 trials of JSB462 in combination with abiraterone in patients with high-volume mHSPC (NCT06991556) as well as in combination with Pluvicto® in patients with mCRPC (NCT07047118) are ongoing.

#4616 Integrated organoid screening approaches enable preclinical assessment of protein degrader efficacy and target engagement.

Marten Hornsveld[1], Dennis van der Grinten[1], Dorrith Verstegen[1], Shannon Kouters[1], Esther Kingma[1], Tomas Veenendaal[1], Mariusz Madej[1], Aaron Hua[2], Jinxi Wang[2], Lenno Krenning[1], Jessie Wang[2], **Marrit Putker**[1], Ludovic Bourre[3]

[1]Crown Bioscience Netherlands B.V., Leiden, Netherlands,[2]Crown Bioscience Taicang, Taicang, China,[3]Crown Bioscience, Inc., San Diego, CA

Introduction Proteolysis-targeting chimeras (PROTACs) and molecular glues are novel therapeutics designed for selective protein degradation, offering new avenues for targeted cancer treatment. Two cereblon (CRBN)-mediated protein degrader candidates, CC-885 (GSPT1 degrader; molecular glue) and ARV-471 (estrogen receptor (ER) degrader; PROTAC), were evaluated using patient-derived organoids to address the unmet need for physiologically relevant platforms in preclinical protein degrader development.

Methods: CC-885 was screened using the OrganoidXplore™ CellTiterGlo assay at 6 doses across 98 NGS characterized organoids derived from six tissue types (colorectal, cervical, gastric, head and neck, lung, and pancreatic cancer), including non-diseased models. ARV-471 efficacy was assessed in ten organoid models of ER-sensitive indications (breast, ovarian) in high content imaging (HCI) assays. CC-885 sensitivity was validated in HCI assay for a selection of models, and GSPT1 and ER degradation were assessed in immuno-fluorescent (IF) assays. CC-885-sensitive models were selected to generate CRISPR/Cas9-mediated CRBN knockout organoid models. (Patient-matched) PDX models were subcutaneously engrafted in immunodeficient mice, and in vivo efficacy was evaluated by tumor growth inhibition (TGI) measurement.

Results: Large panel organoid screening of CC-885 revealed heterogeneous tumor responses (IC50s ranging from ~0.1nM to 50nM) that did not correlate to GSPT1 or CRBN mRNA expression levels. In isogenic KO organoid models, loss of CRBN abrogated CC-885 responses, confirming E3-ligase dependency. HCI studies validated CC-885 responses and quantified target engagement and degradation through IF staining. ARV-471 efficacy testing in ER positive organoids by HCI demonstrated both robust activity and ER degradation. The integration of efficacy and target engagement through HCI provided a mechanistic link between observed responses and molecular mode-of-action. Lastly, findings from organoid screens were compared to responses in matched patient-derived xenograft (PDX) models.

Conclusion: Organoids offer genomically stable, patient-derived models that capture patient diversity and tumor heterogeneity, enabling clinically translatable insights for precision medicine. Our results establish organoid-based screening platforms (OrganoidXploreTM), combining CTG and HCI modalities, as robust tools for preclinical protein degrader evaluation. These platforms uniquely enable identification of tumor subtypes likely to respond to targeted degradation and will potentially facilitate translational biomarker discovery through simultaneous efficacy and mechanistic readouts. PDXO to PDX follow-up opportunities further underscore the utility of these platforms for guiding early therapeutic development and target selection in oncology.

#4617 NRX-0305, an orally bioavailable, CNS penetrant pan-mutant BRAF degrader demonstrates robust efficacy in intracranial models of melanoma brain metastasis and primary glioma.

Alexandra Borodovsky, Ya-Wen Lu, Ge Peng, Karthik Arumugam, Paul L. Auger, Delia Bradford, Lilly G. Carlson, Scott K. Kimura, Daniel Medina-Cleghorn, Mariah J. Mesner, Davorka Messmer, Madeleine P. Nemchek, Ryan B. Rountree, Rusha M. Sardhara, Sangita Sridharan, Jennifer M. Stokes, Leslie Tong, Alexandra M. S. Trotier, Jennifer S. Tung, Ge Wei, Jeffrey Wu, Jordan Ye, Gwenn M. Hansen

Nurix Therapeutics, Inc., Brisbane, CA

Mutations in *BRAF*, a key component of the MAPK pathway, drive constitutive pathway activation and oncogenic transformation across multiple tumor types. *BRAF* V600 mutations occur in approximately 40–50% of cutaneous melanomas, of which 30–50% develop brain metastases during disease. CNS progression is common following acquired resistance to BRAF inhibitor and MEK inhibitor combination therapy, with 40–60% of patients experiencing intracranial relapse despite initial systemic response. *BRAF* mutations are also detected in ~5–8% of primary gliomas, predominantly in pediatric and epithelioid subtypes. Although approved BRAF inhibitors provide meaningful benefit to patients with Class 1 mutations, there is a high unmet need for patients with brain involvement due to limited CNS activity of existing therapies.We developed NRX-0305, a CNS-penetrant, pan-mutant BRAF degrader designed to selectively degrade mutant BRAF across Class 1/2/3 mutant tumors while sparing wildtype BRAF. Pharmacokinetic and pharmacodynamic studies following oral dosing confirmed brain exposure, robust BRAF degradation, and pathway inhibition. Daily oral administration of NRX-0305 demonstrated potent single-agent efficacy in multiple intracranial models of BRAF-mutant melanoma and glioma. In a BRAF inhibitor-resistant melanoma brain metastasis PDX model, NRX-0305 achieved dose-dependent efficacy and significantly improved survival relative to vehicle and dabrafenib treatment, demonstrating superiority to clinically approved BRAF inhibitors.These findings establish pan-mutant BRAF degradation as a promising therapeutic strategy for BRAF-mutant CNS malignancies and highlight NRX-0305's potential to overcome the limited CNS activity and treatment-emergent resistance associated with BRAF targeted therapies.

#4618 TRI-611, a development stage molecular glue degrader of ALK for the treatment of ALK-positive NSCLC including central nervous system metastases.

Andrew R. Conery, Daniel S. La, Artyom A. Alekseyenko, David Marcoux, Aaron G. Bart, Matt L. Harlow, Patrick R. Arsenault, Nico R. Cantone, Rebecca L. Casaubon, Hari B. Kamadurai, Aravind Prasad Medikonda, Duncan E. Nunes, Tim J. Wigle, Maolin Yu, Aleksandra Zagulyaeva, Christine Zarate, Kathleen I. Seyb, Patrick Trojer, Vito J. Palombella

Triana Biomedicines, Lexington, MA

Therapeutic inhibition of Anaplastic Lymphoma Kinase (ALK) has transformed the treatment of ALK fusion-positive non-small cell lung carcinoma (NSCLC), but ALK tyrosine kinase inhibitors (TKIs) suffer from liabilities common to all orthosteric inhibitors, such as off-target kinase inhibition and resistance alleles in and around the TKI binding site. Molecular glue degraders (MGDs) that engage the $CRL4^{CRBN}$ E3 ligase to promote neosubstrate degradation offer an alternative therapeutic approach. Here we describe TRI-611, a potent, brain-penetrant MGD that promotes the proximity of ALK and CRBN via a unique, non-G loop degron interface that is distal from the kinase active site. TRI-611 functions by engaging CRBN to create a neosurface that interacts with the C-lobe of the ALK kinase domain. This ALK:TRI-611:CRBN ternary complex promotes ALK polyubiquitination and CRBN-dependent degradation of ALK proteins, including ALK fusions such as EML4-ALK, and oncogenic, transmembrane ALK. Cellular degradation of EML4-ALK is rapid (occurring within 1-2 hours), robust (>90% maximum degradation), and durable (recovery half-life of more than 15 hours after compound withdrawal). Cellular proteomics profiling demonstrates the profound selectivity of TRI-611 across CRBN neosubstrates and the kinome (including key off-target kinase families such as NTRK), consistent with the unique degron interface located in a less conserved region of ALK. TRI-611 treatment leads to inhibition of downstream signaling and subsequent selective anti-proliferation of ALK-positive cell lines. TRI-611 is orally bioavailable and brain penetrant, with daily oral dosing leading to deep and durable degradation of endogenous EML4-ALK and tumor regression in both subcutaneous and intracranial xenograft models of ALK-positive NSCLC. TRI-611 represents the first example of a development stage degrader targeting an oncogenic gene fusion and has the potential to expand the arsenal of meaningful therapeutic options for ALK-positive NSCLC patients. The discovery of TRI-611 additionally broadens the reach of CRBN-modulating MGDs by exploiting a previously undescribed degron.

#4619 Disabling oncogenic signaling with Apertor Interceptors - Proximity inducing bisteric molecules.

Andrew Robertson, Shinji Kasahara, Jennifer Schmidt, Bo Pang, Nage Yarravarapu, Diego Garrido Ruiz, Rose Citron, Arash Samadi, Denisse Martinez, Nefeli Chanoutsi, Colleen Mulvihill, Arushi Singhai, Vinh Thai, Raissa Estrela Curado, Ericka Mendez, Edmund Graziani, **Lawrence Lum**

Apertor Pharmaceuticals, South San Francisco, CA

All proteins including those encoded by corrupted DNA in diseased tissues, convey cellular instructions in partnership with other physically interacting proteins. Disrupting these protein-protein interactions (PPIs) to achieve therapeutic goals face a number of daunting chemistry challenges, including the shallow chemical-target interfaces to achieve selective PPI disruption typically found in cell membrane penetrant small molecules. Here we introduce bisteric molecules (AP Interceptors) that are able to traverse the cell membrane and recruit abundantly expressed members of the intracellular FKBP protein family to achieve selective disruption of PPIs essential to the function of several oncogenic driver proteins. We demonstrate the durable effects of AP Interceptors in blocking the growth of cancerous cells harboring alterations in KRAS and present a mechanistic account of their anti-cancer activity.

#4620 RCZY-698: An orally bioavailable, highly potent, and selective reversible KRAS^{G12V} (ON)-state inhibitor with robust antitumor activity in preclinical models of KRAS^{G12V}-driven solid tumors.

Xiaojing (Celia) Chen, Lin Wang, Xiaohong Liu, Zhengyong Wan, Qiaoni You, Jianming Bao

Rongchang Pharmaceuticals, Ltd., Yantai, China

The KRAS^{G12V} mutation is the second most common oncogenic RAS alteration, particularly as a driver mutation in pancreatic (~34%), colorectal (~21%), and non-small cell lung cancers (~5%). It is associated with poor prognosis in affected cancer patients. Due to its very low GTPase activity, which impairs hydrolysis of RAS-bound GTP to RAS-bound GDP, the mutant protein spends most of its time in the active (GTP-bound) state with limited cycling. As a result, an off-state KRAS^{G12V} inhibitor targeting the conformation of GDP-bound (inactive) state would theoretically be ineffective at blocking downstream signaling pathways such as MAPK and PI3K-AKT, as the mutant protein rarely accesses its GDP-bound state. The lack of a nucleophilic side chain at position 12 (valine) of KRAS^{G12V} precludes development of covalent inhibitors targeting the mutation site directly. Currently, no direct inhibitors targeting KRAS^{G12V} have been approved, representing a significant unmet medical need. RCZY-698, developed by Rongchang Pharmaceuticals, is a novel, highly potent, orally bioavailable, and mutant-selective non-covalent tri-complex inhibitor that specifically targets the GTP-bound (ON) conformation of KRAS^{G12V}. It potently disrupts the interaction between KRAS^{G12V} and downstream effector proteins, thereby robustly suppressing key signaling cascades, including the MAPK pathway mechanistically, RCZY-698 engages cyclophilin A (CypA) specifically to form a stable ternary complex with KRAS^{G12V}, conferring exceptional selectivity over wild-type KRAS. In a panel of KRAS^{G12V}-mutant tumor cell lines, RCZY-698 elicits potent antiproliferative effects, demonstrating superior in vitro growth inhibition compared with RMC-5127. This compound exhibits favorable in vitro absorption, distribution, metabolism, and excretion (ADME) characteristics, alongside distinctive oral pharmacokinetic profiles across multiple species. In human KRAS^{G12V}-mutant xenograft models, RCZY-698 induces dose-dependent tumor regression at well-tolerated doses, achieving comparable tumor growth inhibition (TGI) to RMC-5127 at substantially lower exposures. Collectively, these data delineate the discovery and preclinical profiling of RCZY-698 as a novel oral non-covalent KRAS^{G12V}(ON)-selective tri-complex inhibitor with compelling in vitro potency and in vivo efficacy. Further efforts and characterization work are being implemented to complete the preclinical candidate (PCC) data package for RCZY-698.

: Strategies to Enhance the Therapeutic Index of Radiotherapy
Poster Session

#3329 Targeting DNA Damage Response Dependencies for Radiosensitization in Li-Fraumeni Syndrome.

Madeleine Driscoll[1], Paula R. Quaglietta[1], David Malkin[2]

[1]Genetics and Genome Biology, The Hospital for Sick Children, Toronto, ON, Canada,[2]The Hospital for Sick Children, Toronto, ON, Canada

Li-Fraumeni Syndrome (LFS) is a hereditary cancer predisposition syndrome associated with germline *TP53* mutations, leading to a significantly increased lifetime cancer risk. Individuals with LFS display striking clinical heterogeneity, including variation in tumour onset, aggressiveness, and metastasis, highlighting the need to better understand genetic modifiers and their influence on cancer susceptibility.

Recent work from our lab suggests that variation in Wnt signalling may be contributing to this clinical diversity. The Wnt pathway regulates many cellular processes, including proliferation, differentiation, and stemness. When hyperactivated, it can promote oncogenesis by stabilizing β-catenin levels, activating transcriptional programs that support tumour initiation and progression. Whole-genome sequencing on a large, multi-institutional cohort of LFS patients has identified Wnt-pathway variants that appear to decrease cancer risk and are associated with improved survival. These variants are predicted to dampen β-catenin signalling, pointing toward a novel mechanism that may act to counterbalance TP53-driven oncogenesis.

To further investigate the differences contributing to heterogeneity in LFS, we are developing a proteomic atlas of patient-derived dermal fibroblasts, representing a range of clinical presentations: wild-type (n=5), clinically unaffected LFS carriers (n=7), and LFS individuals with known malignancies (n=6). Baseline protein expression was quantified using mass spectrometry, and Wnt-related proteins were identified for further testing. To explore the functional mechanisms of these variants, siRNA-mediated knockdowns will be used to examine how short-term reductions in Wnt expression affect cancer-associated cell phenotypes.

Preliminary analyses have identified that LFS fibroblasts demonstrate increased expression of Wnt receptors compared to wild-type, suggesting a baseline priming towards Wnt activation. Gene set enrichment analysis demonstrated an enrichment of β-catenin, Lef1, and Myc transcriptional programs in LFS cells, consistent with a strongly activated Wnt signalling state. Together, these findings support hyperactive Wnt signalling as a defining feature of the LFS cellular environment and a contributing factor to TP53-driven oncogenesis.

By integrating proteomic profiling with functional variant validation, this work examines how Wnt-modifying variants contribute to the tumorigenic environment in LFS. The results of this study will help us to better understand the biological heterogeneity seen among LFS patients and lay the groundwork for future research into Wnt modifiers as therapeutic interventions. Beyond the scope of this project, the LFS fibroblast proteomic atlas may act as a novel resource for the LFS and *TP53* research communities, providing unbiased quantification of proteins across different clinical outcomes.

#4624 Investigation of the efficacy of reduced coenzyme Q10 (CoQ10) for alleviating acute intestinal toxicity associated with pelvic radiotherapy: A randomized, placebo-controlled, double-blind comparative study.

Satoshi Seno[1], Akifumi Kajiwara[1], Yasuyuki Shimizu[1], Kazuma Iwashita[1], Kana Kobayashi[1], Qin Qin[2], Qu Zhang[3], Hatamei Takabayashi[1], Kanako Suda[1], Hiroki Kawaguchi[1], Takeaki Ishihara[1], Daisuke Miyawaki[1], Sae Murakami[4], Yoshito Terai[5], Ryohei Sasaki[1]

[1]Radiation Oncology, Kobe University Graduate School of Medicine, Kobe, Japan,[2]Radiation Oncology, Nanjing Medical University First Affiliated Hospital, Jiangsu Province Hospital, Nanjing, China,[3]Radiation Oncology, Tongji Medical College, Hubei Cancer Hospital, Huazhong University of Science and Technology, Wuhan, China,[4]Clinical & Translational Research Center, Kobe University Graduate School of Medicine, Kobe, Japan,[5]Obstetrics and Gynecology, Kobe University Graduate School of Medicine, Kobe, Japan

Background: Diarrhea is one of the major acute adverse effects in patients undergoing pelvic radiotherapy, often impairing treatment continuity and quality of life. Despite its clinical importance, the pathogenesis of radiation-induced diarrhea (RID) remains inadequately understood, and effective prophylactic strategies have yet to be established. Reduced coenzyme Q10 (rCoQ10) possesses antioxidant properties capable of neutralizing activated reactive oxygen species generated during irradiation. This study aimed to evaluate whether oral administration of rCoQ10 could mitigate intestinal mucosal damage and reduce the severity of diarrhea in patients receiving curative pelvic radiotherapy.

Materials and Methods: This randomized, placebo-controlled clinical study included patients with cervical, endometrial, or vaginal cancer (FIGO 2018 Stage IB-IVA) treated with radiotherapy at Kobe University Hospital between June 2021 and November 2023. Eligible patients were ≥20 years old, had ECOG Performance Status 0-2, and provided written informed consent. A total of 47 patients were randomized into rCoQ10 and placebo groups. Participants received three 200 mg soft capsules of rCoQ10 or placebo orally once daily starting 5-7 days before radiotherapy. From the first day of radiotherapy, capsules were taken once daily approximately one hour before each irradiation session. Thirty patients (63.8%) underwent IMRT, and 33 patients (70.2%) received concurrent chemotherapy with weekly cisplatin (40 mg/m²). Adverse events, including diarrhea, were graded according to CTCAE version 5.0. The primary endpoint was the maximum increase in the number of daily bowel movements during the radiotherapy period. Analyses were adjusted for chemotherapy use and radiotherapy modality.

Results: Among the 47 enrolled patients, 44 were evaluable for analysis (two withdrew consent and one discontinued due to cognitive decline). The median maximum increase in bowel movements was 5.3 in the rCoQ10 group and 5.8 in the placebo group, showing no significant difference ($p = 0.937$). While the overall incidence and severity distribution of diarrhea did not significantly differ, a trend toward reduced occurrence of Grade 2 diarrhea was observed in the rCoQ10 group. The 2-year progression-free survival was 80.4% in the rCoQ10 group and 84.0% in the placebo group ($p = 0.491$), indicating no negative influence on oncologic treatment efficacy. No serious adverse events related to rCoQ10 were reported.

Conclusions: Although the primary endpoint was not met, rCoQ10 showed a potential benefit in reducing moderate diarrhea in patients undergoing pelvic radiotherapy, without compromising cancer treatment outcomes. Further large-scale studies are warranted to clarify its clinical utility as a supportive therapy.

#4625 Mechanistic insights into the radioprotective action of GM-0111 via CCL5 inhibition and endothelial-immune modulation.

Kholod A. Elhasany[1], Shukran Alizada[2], Sushanto Kumar Saha[3], Thomas A. Zangle[2], Abigail Pulsipher[1], Hamid Ghandehari[1]

[1]Molecular Pharmaceutics, College of Pharmacy, University of Utah, Salt Lake City, UT,[2]Department of Chemical Engineering, University of Utah, Salt Lake City, UT,[3]Department of Biomedical Engineering, University of Utah, Salt Lake City, UT

Radiation-induced proctitis (RIP) is a painful inflammatory condition of the rectum affecting up to 20% of cancer patients undergoing pelvic radiation. RIP manifests as a broad spectrum of side effects, which may lead to discontinuation of cancer treatment, and surgical intervention. Current therapeutics are merely symptomatic, highlighting the need for new effective prophylactics. We have demonstrated that synthetic glycosaminoglycan, GM-0111, has promising activity in mitigating the tissue-damaging effects of ionizing radiation when administered prophylactically in a murine model of RIP. We found that immune cell infiltration, and rectal tissue expression of CCL5, a potent chemotactic agent for mast cells and other immune cells, and its associated signaling pathways were significantly reduced with GM-0111 compared to irradiated controls. The mechanisms by which GM-0111 interacts with CCL5 and exerts its prophylactic effects against RIP have yet to be elucidated. We therefore performed a series of *in vitro* studies using immune and endothelial cells implicated in different stages of RIP. As mast cells hyperplasia and activation have been implicated in RIP development, we hypothesized that GM-0111 inhibits mast cell chemotaxis and degranulation, thereby reducing the immunological response resulting from radiation, including immune cell chemotaxis, activation, and viability and reactive oxygen species (ROS) generation. To test our hypothesis, the effect of GM-0111 treatment on CCL5 secretion and mediated responses was assessed in endothelial cells (HUVECs) and mast cells (P-815 and RBL-2H3). Due to the significant crosstalk between mast cells and macrophages, we also evaluated mast cell degranulation, ROS production, and cell viability using a colorimetric assay, flow cytometry, and quantitative phase imaging. We found that GM-0111 inhibited CCL5-induced chemotaxis with the IC_{50} of 82 nM. GM-0111 showed strong binding to CCL5 with K_d 3.34 ± 1.21 nM which may play a significant role in inhibiting its chemotactic effect. We also investigated the effect of GM-0111 on CCL5 released from TNF-α- and IFN-ɣ-activated HUVECs, whereby 10 µM GM-0111 caused an 8-fold reduction in CCL5 secretion, suggesting that GM-0111 also interferes with CCL5 production. GM-0111 (10 µM) was found to exert cytoprotective effects on RAW 264.7 cells irradiated with 2.5 Gy and 5 Gy, which may be attributed to decreased ROS production. Collectively, these data demonstrate that GM-0111 exerts coordinated radioprotective effects by attenuating oxidative stress, inhibiting endothelial CCL5 production, and blocking mast cell recruitment. This integrated mechanism positions GM-0111 as a promising prophylactic candidate against radiation-induced injury for supportive cancer care. We would like to acknowledge NIH (5R01CA227225-05) (HG) and NIH (R01CA276653) (TAZ) for funding this project.

#4626 Radioprotective fullerene derivative as a potential systemic therapeutic to alleviate radiation-induced cardiovascular disease.

Khadijeh Koushki[1], Prapannajeet Biswal[1], Joseph B K Kim[2], Ngoc Tuyet Tra[1], Prudhvi C. Mallepaddi[1], Naren Gundapaneni[1], Sai Kumar Samala[1], Lydia WT Cheung[1], Geraldine Vijay[1], Sivareddy Kotla[3], Yuri Mackeyev[1], Sunil Krishnan[1]

[1]Neurosurgery, UT Health Houston, Houston, TX,[2]Department of Radiation Oncology, MD Anderson Cancer Center, Houston, TX,[3]Department of Cardiology, MD Anderson Cancer Center, Houston, TX

Despite advances in radiation therapy (RT), radiation-induced cardiovascular disease remains a major cause of long-term morbidity and mortality in cancer survivors, increasing cardiovascular risk by 10-30% within 5-10 years after treatment. Excess reactive oxygen species (ROS) are major drivers of RT-induced endothelial injury and cardiovascular dysfunction, causing direct oxidative damage to DNA, lipids, and proteins and activating inflammatory pathways that sustain endothelial dysfunction. Targeting ROS-mediated injury, therefore, represents a promising strategy to mitigate the cardiovascular toxicity of radiation therapy. Fullerenes (C60) and their derivatives are potent antioxidants and are referred to as "free radical scavengers" because of their ability to readily interact with and neutralize free radicals. Despite promising reports of the antioxidant and anti-inflammatory activity of C60 fullerenes in recent years, translating C60 into clinic application is challenging due to their inherent lipophilicity and insolubility in aqueous media. To address this challenge, we have developed a novel chemistry for the custom synthesis of C60 derivatized with serinol (C60-ser). This derivative is neutral, amphiphilic and exquisitely soluble in water. Our data demonstrated that C60-ser is non-toxic and can protect non-malignant normal endothelial cells, but not cancer cells, from RT-mediated damage. Mechanistically, C60-ser radioprotection is exerted by both neutralizing RT-induced free radicals and inducing antioxidant response pathway and activity of antioxidant enzymes to neutralize RT-induced free radicals. The resultant radioprotective effects include preservation of mitochondrial respiratory capacity and reduction in DNA damage, senescence, and inflammatory responses of endothelial cells, which together enhance the long-term cell survival after RT. Remarkably, C60-ser treatment upregulates the expression of the transcription factor Nrf2 and promotes its nuclear translocation, thereby activating the Nrf2-antioxidant response element (ARE) signaling axis for the expression of downstream antioxidant enzymes (catalase, SOD2, HO-1, NQO1, and TRX1) in normal cells but not in cancer cells. Collectively, these results highlight a critical role of the Nrf2-ARE pathway in mediating the effects of C60-ser against oxidative stress. This study advances the realization of the clinical translation of C60-ser for reducing RT-induced toxicity in cardiovascular tissues of cancer patients.

#4627 Receptor-targeted gold nanospheres strengthen radiation efficacy and reprogram tumor immunity.

Bhoomika Muruvekere Lakshmisha[1], Prudhvi Chand Mallepaddi[1], Prapannajeet Biswal[1], Ngoc Tuyet Tra[1], Aria Sabbagh[1], Ayobami Fidelix[2], Sai Kumar Samala[1], Gabrielle Krouse[1], P M Quan Mai[1], Khadijeh Koushki[1], Lydia WT Cheung[1], Geraldine V Vijay[1], Yuri Mackeyev[1], Sunil Krishnan[1]

[1]Vivian L. Smith Department of Neurosurgery, University of Texas Health Science Center at Houston, Houston, TX,[2]Baylor College of Medicine, Houston, TX

Radiation therapy is an essential component of colorectal cancer management. However, it is limited by anatomical constraints, toxicity, and modest immune activation. When tumors are laden with high atomic number (Z) elements and exposed to ionizing radiation, a higher radiation dose is deposited within the tumor. This radiosensitization, achieved here using gold nanospheres (GNS), is boosted by a greater degree of free radical formation resulting in greater DNA damage with GNS + radiation. Recent evidence shows that unrepaired DNA damage can lead to chromosome missegregation and the formation of immature nuclei called micronuclei. The poorly formed nuclear envelope around these micronuclei exposes DNA to cytoplasmic sensors, triggering a type I interferon response and innate immune activation. Based on this, we hypothesized that GNS amplifies X-ray therapy and elicits unique immune responses. To improve receptor-mediated internalization into colorectal cancer cells overexpressing epidermal growth factor receptor (EGFR), we employed our prototype, cetuximab-conjugated gold nanospheres (cGNS). Cetuximab (monoclonal antibody targeting EGFR) was attached to 30 nm gold nanospheres using thiol polyethylene glycol (PEG) for improved biocompatibility. Two murine colorectal cancer cell lines engineered to overexpress human EGFR, CT26-EGFR and MC38-EGFR, were used to test cGNS and a pegylated control (pGNS). Cellular uptake of the GNSs was shown by Inductively Coupled Plasma Mass Spectrometry and dark-field microscopy. Clonogenic survival assays assessed radiosensitization, while immune activation was examined using flow cytometry, immunoblotting, cytokine arrays, and macrophage polarization assays. Following radiosensitization, we observed upregulation of the cGAS-STING pathway and pro-inflammatory cytokines. Conditioned media applied to RAW 264.7 macrophages increased the M1/M2 macrophage ratio, indicating enhanced innate immune activation. We next used the CT26 syngeneic mouse model to assess GNS biodistribution, the extent of radiosensitization, immune cell infiltration, and potential abscopal effects. Efficacy studies demonstrated that cGNS outperformed pGNS in combination with radiation. Immune studies incorporating immune checkpoint inhibitors are currently underway. By integrating nanotechnology with radiation oncology and immunotherapy, this project lays the groundwork for advancing nanomaterial-based radio-immunotherapy toward clinical translation.

#4628 Mitochondrial serine/threonine phosphatase, phosphoglycerate mutase 5 (PGAM5) is a novel target to promote abdominal radiotherapy.

Shujah Hamid Rehman, Rishi Man Chugh, Payel Bhanja, Stacey Krepel, Subhrajit Saha

University of Kansas Medical Center, Kansas City, KS

Pancreatic cancer patients frequently undergo radiotherapy, which carries a significant risk of toxicity to the small bowel and gastrointestinal tissues. Therapeutic outcomes in pancreatic cancer often depend on delivering higher radiation doses, and thus strategies that minimize gastrointestinal toxicity without compromising tumor radiosensitivity would be profoundly beneficial to patients. Radiation induced oxidative stress plays a significant role in radiation induced toxicity in intestinal epithelial cells. However, mitigation of gastrointestinal toxicity requires reduction of oxidative stress and stimulation of epithelial regeneration through activation of WNT/β-catenin signaling. Mitochondrial serine/threonine phosphatase, phosphoglycerate mutase 5 (PGAM5), is involved in activation of oxidative stress along with inhibition of WNT/β-catenin signaling. PGAM5, located in the mitochondrial membrane, inhibits nuclear translocation of NRF2 and thereby represses NRF2-dependent antioxidant gene expression. Moreover, PGAM5 induces β-catenin degradation by dephosphorylating DVL2, a β-catenin destruction complex**.** We have observed PGAM5 expression significantly increased in intestinal epithelium in response to irradiation. Pharmacological inhibition of PGAM5 using a novel small molecule-based modulator LFHP-1c (3 mg/kg BW, subcutaneous) at 24 hours post irradiation mitigates gastrointestinal toxicity. Mice exposed to partial body irradiation (PBI) with 2.5% bone marrow shielding (LD100/15) followed by LFHP-1c treatment demonstrated significant improvement of mice survival (90% mice survived beyond 30 day) ($p< 0.00002$) compared to irradiated control where all the mice died within 14 days. Histopathological analyses demonstrated preservation of crypt-villus structures in the jejunum sections of LFHP-1c-treated mice compared to untreated irradiated mice. LFHP-1c treatment significantly ($p<0.005$) induced stabilization and nuclear translocation of NRF2, along with increased nuclear localization of β-catenin, indicating activation of the WNT/β-catenin signaling pathway in the irradiated intestinal epithelium. LFHP-1c treatment in irradiated organoids from Lgr5/eGFP-IRES-Cre-ERT2; R26-ACTB-tdTomato-EGFP mice intestine demonstrated mitigation of radiation induced toxicity and significant improvement in Lgr5+ve intestinal stem cell survival. In mice model of Pancreatic tumors, LFHP-1c treatment did not compromise the radiosensitivity of Kras positive KPC cells. In conclusion, our studies using mice model of radiation induced genotoxic stress and ex vivo organoid model demonstrated that PGAM5 can be a potential target to promote therapeutic ratio for abdominal radiotherapy.

#4629 Modeling pharmacokinetics and efficacy of the ATM inhibitor WSD0628 in GBM and melanoma metastasis PDX models.

Ann Catherine Mladek[1], Juhee Oh[2], Sneha Rathi[2], Lily Liu[3], Danielle M. Burgenske[1], Brett L. Carlson[1], Katrina K. Bakken[1], Lauren L. Ott[1], Zeng Hu[1], Wei Zhong[3], William F. Elmquist[2], Jann N. Sarkaria[1]

[1]Radiation Oncology, Mayo Clinic, Rochester, MN,[2]Department of Pharmaceutics- College of Pharmacy, University of Minnesota, Minneapolis, MN,[3]Wayshine Biopharm, Corona, CA

Radiation is a cornerstone of glioblastoma (GBM) treatment, however, the majority of tumors progress within the radiation field due to inherent radiotherapy (RT) resistance. The integration of highly potent radiosensitizers, such as the ATM inhibitors AZD1390 or WSD0628, could reverse resistance and significantly improve local control of these tumors. However, the achievable brain tumor exposure of these inhibitors may be limited by drug exposure in skin and mucosa, leading to enhanced radiation toxicity. To support the clinical development of WSD0628, we developed pharmacokinetic (PK)-efficacy models to help interpret ongoing PK analyses. A model based on in vitro cell studies was based on the in vitro observations that 30 nM WSD0628 provided maximum ATM inhibition and the extent of radiosensitization was directly related to the duration of drug incubation after irradiation, up to a maximum of 24 hours. The unbound WSD0628 concentration, measured by rapid equilibrium dialysis, was 66% of the total concentration in cell culture media, and was used to define an optimal radiosensitizing target of 20 nM free WSD0628 for 4 to 24 hours. Previous PK analyses showed that the free, unbound fraction (fu) of WSD0628 in plasma and brain tumor tissue are 0.02 and 0.054, respectively, and the brain tumor-to-plasma ratio is 0.32 in GBM43 patient-derived xenografts (PDXs). From these data, a total drug level of 1160 nM in plasma is predicted to achieve unbound drug levels above the 20 nM WSD0628 target unbound concentration. To validate this prediction, parallel in vivo dose-ranging studies were performed in orthotopic PDXs. Mice with orthotopic GBM43 were randomized to treatment with RT (8 Gy x1) alone or in combination with a range of WSD0628 doses. RT combined with 0.25 mg/kg and 1 mg/kg WSD0628 had no impact on survival, compared to RT alone, while median survival increased by 1.3-fold for RT combined with 2.5 mg/kg, 1.7-fold with 5 mg/kg, and 3.2-fold with 10 mg/kg WSD0628. A similar dose-response was observed in an M12 melanoma brain metastasis PDX. Based on PK modeling of these drug doses, 2.5 mg/kg dosing will maintain total WSD0628 plasma levels above 1160 nM for 11.9 hours, 5 mg/kg for 23.6 hours, and 10 mg/kg for 40 hours. Taken together, we have developed a model to predict efficacious dosing of a brain tumor based on the free drug hypothesis, which allows integration of multiple aspects of in vitro modeling with measured drug levels in animal models to predict total plasma levels associated with robust sensitizing effects. Assuming similar tissue to plasma partitioning in human GBM, this model could be directly applied to interpret the ongoing Phase 1 PK analysis of WSD0628 in recurrent GBM.

#4630 CD46-targeted dual-modality alpha-particle and cytotoxic payload-loaded antibody for enhanced treatment of metastatic castration-resistant prostate cancer.

Anil Bidkar[1], Scott Bidlingmaier[2], Anju Wadhwa[3], Kondapa Naidu Bobba[3], Shubhankar Naik[4], Cheng Xue[3], Athira Raveendran[3], Megha Basak[3], Jonathan Chou[3], Rahul Aggarwal[3], Henry VanBrocklin[3], Youngho Seo[3], Bin Liu[3], Robert Flavell[3]

[1]Radiology and Biomedical Imaging, University of California San Francisco, San Francisco, CA,[2]Department of Anesthesia, University of California San Francisco, San Francisco, CA,[3]University of California San Francisco, San Francisco, CA,[4]University of California Berkeley, Berkeley, CA

Background: CD46 is a validated therapeutic target broadly expressed in prostate cancer, including metastatic castration-resistant and PSMA-low or neuroendocrine subtypes. The CD46-targeting YS5 antibody supports two complementary therapeutic platforms: a CD46-directed antibody-drug conjugate (YS5-MMAE) and a radioimmunoconjugate delivering the alpha-emitter actinium-225 (^{225}Ac-YS5). Each monotherapy induces tumor regression, yet dose escalation increases systemic toxicity, underscoring the need for a combined approach.

Methods: Two combination strategies were evaluated: (1) co-administration of YS5-MMAE with ^{225}Ac-Macropa-PEG4-YS5, and (2) a dual-labeled construct, ^{225}Ac-Macropa-PEG4-YS5-MMAE, integrating both payloads on a single scaffold. The dual construct was synthesized by conjugating MMAE to YS5, attaching the Macropa-PEG4 chelator, and radiolabeling with ^{225}Ac. Radiochemical purity, antigen binding, and in vitro stability were confirmed. In vitro cytotoxicity was assessed in 22Rv1 prostate cancer cells, and in vivo efficacy was tested in 22Rv1 tumor-bearing mice (n = 9 per group) receiving saline, YS5-MMAE (1.8 mg/kg), ^{225}Ac-YS5 (0.125 μCi), their combination, or the dual-labeled construct.

Results: In vitro, combination therapy induced greater cytotoxicity than either monotherapy, indicating synergistic interaction. In vivo, median survival was 24 days for saline, 30 for YS5-MMAE, and 66 for ^{225}Ac-YS5. Co-administration of YS5-MMAE and ^{225}Ac-Macropa-PEG4-YS5 extended survival beyond 80 days, with delayed tumor progression. In contrast, the dual-labeled construct achieved survival exceeding 90 days, accompanied by durable tumor regression and minimal renal or hematologic toxicity. Both combination and dual-modality therapies exhibited enhanced therapeutic efficacy compared to single-agent treatments.

Conclusion: Simultaneous alpha-particle and cytotoxic targeting of CD46 produces synergistic effects, improving tumor control while reducing dose-limiting toxicity. The dual-labeled construct represents a next-generation radiotheranostic platform combining targeted alpha therapy and cytotoxic payload delivery, offering enhanced potency, safety, and translational potential for advanced prostate cancer therapy.

#4631 Utilizing a dual action agent for targeted neuroendocrine tumor therapy.

Tyler M. Bateman[1], Sukhen C. Ghosh[2], Solmaz AghaAmiri[2], Majid Momeny[2], Servando Hernandez Vargas[1], Jack T. Adams[1], Vahid Khalaj[2], Ali Azhdarinia[2]

[1]Experimental Therapeutics, UT Health Houston, Houston, TX,[2]Experimental Therapeutics, Institute of Molecular Medicine, Houston, TX

Neuroendocrine tumors (NETs) are rare, heterogeneous neoplasms with an incidence of 8 per 100,000 individuals, a rate that has increased significantly over the past four decades. These tumors frequently overexpress somatostatin receptor subtype 2 (SSTR2), enabling a form of NET-targeted radiotherapy called peptide-receptor radionuclide therapy (PRRT). Although PRRT improves progression-free survival (PFS), over half of patients in the NETTER-2 trial did not respond, and recurrence often occurs after the four FDA-approved therapy cycles. Strategies to improve outcomes for patients on PRRT have been explored, such as combining PRRT with the DNA alkylating agent temozolomide (TMZ). This combination has improved objective response rates but has not significantly extended overall or progression-free survival.

To overcome these limitations, our lab developed tumor-targeted TMZ (ttTMZ), a drug conjugate that selectively delivers its chemotherapeutic payload directly to SSTR2-positive tumors and can chelate radioisotopes for imaging and therapy. Chelation of gallium-67 (^{67}Ga) by ttTMZ yields ^{67}Ga-ttTMZ, a dual-action agent that combines radiotherapy and chemotherapy in a single targeted construct. The Auger emitter ^{67}Ga has high linear energy transfer (4–4500 keV/μm) and a small radius of emission (2.4 μm), properties that lead to increased damage from emissions and decreased off-target effects, respectively.

Radiolabeling ttTMZ with ^{67}Ga yields ^{67}Ga-ttTMZ with >95% efficiency. We evaluated ^{67}Ga-ttTMZ in IMR-32 cells using Western blotting for cleaved PARP and γ-H2AX to assess apoptosis and DNA damage, respectively. Optimal dosing was identified as 0.5 MBq/mL ^{67}Ga and 100 μM ttTMZ. γ-H2AX immunofluorescence confirmed a dose-dependent increase in DNA damage. *In vivo* PET imaging with ^{68}Ga-ttTMZ demonstrated selective localization to SSTR2-positive tumors and rapid clearance in dual-implant mouse models 1 h post-injection.

These findings demonstrate that ^{67}Ga-ttTMZ induces significant DNA damage and apoptosis. Western blotting and γ-H2AX immunofluorescence microscopy results both indicate that DNA damage is a primary mechanism of action for ^{67}Ga-ttTMZ. The selective tumor targeting and dual-action mechanism of ^{67}Ga-ttTMZ highlight its potential as a next-generation combination therapeutic for NETs, addressing key limitations of current PRRT and TMZ combination therapy.

#4632 LSD1 inhibition enhances radiotherapy efficacy in OSCC by attenuating SUMOylation and activating NK cells.

Chumki Choudhury[1], Amit Kumar Chakraborty[1], Rajnikant Raut[1], Marilia Takada[2], Bikash Sahay[2], Minh-Tam Truong[3], Daniel L. Gustafson[4], Jenna Burton[4], Manish V. Bais[1]

[1]BU School of Medicine, Boston, MA,[2]College of Veterinary Medicine, University of Florida, Gainesville, FL,[3]Boston Medical College, Boston, MA,[4]Associate Professor, Clinical Sciences, Colorado State University, Fort Collins, CO

Background: Oral squamous cell carcinoma (OSCC) is a prevalent and deadly cancer, with limited treatment success using radiation therapy (RT) alone. This study investigated the role of lysine-specific demethylase 1 (LSD1) in promoting oncogenic signaling, resistance to RT, and immunosuppression in OSCC. We hypothesized that targeting LSD1-specific mechanisms, in combination with RT, could inhibit OSCC growth and immune evasion.

Methods: We employed a 4NQO-treated progressive mouse OSCC model to identify the molecular and cellular changes during radiotherapy and LSD1 inhibition (with SP2509) in combination with radiation. To identify these changes, we used RNA-seq for pathway-related changes, flow cytometry for immune regulation, and *in vitro* cell culture techniques for ChIP, qRT-PCR, and pathway validation. Finally, we treated feline spontaneous OSCC with a combination of SP2509 and radiation to test its efficacy.

Results: RT combined with the LSD1 inhibitor SP2509 promoted the infiltration of natural killer (NK) cells and dendritic cell (DC)-mediated antitumor immunity in mouse OSCC preneoplasia. Feline OSCC treated with an LSD1 inhibitor and RT showed reduced tumor growth. In vitro studies have demonstrated that combination therapy induces the activation of IFNγ+ CD8+ T cells and NK cells. RNA sequencing showed that the combination therapy attenuated the cell cycle and CDK-related pathways. Clinical OSCC samples treated with RT exhibited inhibition of CD8+ T cells, while the combination of an LSD1 inhibitor and RT recovered CD8+ T cell proliferation with a significant increase in NK cell population in mouse OSCC and peripheral blood mononuclear cells co-cultured with human OSCC cells (HSC3). It was also observed that LSD1 inhibition in OSCC, both in vivo and *in vitro,* attenuated SUMOylation pathways and downregulated the SUMO1 gene while upregulating NKG2DL-related genes such as MICB in humans and their mouse analog RAEγ. Using ChIP-qPCR, we observed that LSD1 inhibition increased H3K9me2 methylation at the SUMO1 gene locus and decreased H3K4me2 methylation. LSD1 inhibition in combination with radiotherapy in feline OSCC attenuates cancer growth.

Conclusion: SP2509 treatment enhances the efficacy of radiation therapy by inhibiting SUMOylation pathways, which increases NK cells by NKG2DL-NKG2D axis activation, thereby inducing anti-tumor immunity.

#4633 Theranostic evaluation of ^{68}Ga-PMSA, ^{177}Lu PSMA therapy, and biomarker guided immunotherapy and DDR inhibitor combinations in LNCaP prostate cancer xenografts.

Juliana Maynard, Anita Liu, Benedetta Arno, Tracy Hall, William Drewe, Kerry Shea, Andrzej Rutkowski, Grace Haydon, Tiffany-Jane Allen, Fiona Yau, Liviu Lucaciu, Mikaela Griffiths, Gayle Marshall

Medicines Discovery Catapult, Ltd., Alderley Park, United Kingdom

Background and Rationale. PSMA-targeted radioligand therapy with ^{177}Lu-PMSA is a promising treatment for metastatic castration-resistant prostate cancer. To optimise its clinical translation, preclinical models are required to link to diagnostic imaging with dosimetry, assess biomarkers or response, and evaluate sensitising combination. We conducted an in vivo study using LNCaP xenograft model comparing ^{177}Lu-PSMA monotherapy with immunotherapy, DDR inhibition and combinations, integrating multimodal imaging, pharmacokinetics, toxicity, and ex vivo biomarker analyses.

Methods. Male immunodeficient mice bearing LNCaP tumours (100-150mm^3) underwent baseline ^{18}F-PSMA PET/CT to confirm uptake and lesion dosimetry, then were randomised into 6 cohorts (n 8-10). 1. Vehicle; 2. ^{177}Lu-PSMA monotherapy (minimal effective dose); 3. anti-PD-1; 4. ^{177}Lu plus anti-PD-1; 5. ^{177}Lu plus PARP inhibitor, 6. Triple combination. Longitudinal ^{18}F-PSMA at 7, 14, and 28 days monitored early metabolic response, alongside tumour volume and body weight. Blood samples post ^{177}Lu (1-96 h) informed PK and clearance, with concurrent CBC and serum chemistry to assess systemic toxicity. At endpoint, tumours were harvested for immunostaining and molecular analysis for markers of proliferation, immune response and DDR inhibition. In addition, exploratory γH2AX in PBMCs and ctDNA profiling were assessed as translational biomarkers.

Results. ^{18}F-PSMA-PET early uptake and diagnostic assessment correlated with ^{177}Lu efficacy. Minimal dose ^{177}Lu maintained significant anti-tumour activity and reduced haematologic toxicity. Combination with anti-PD-1 enhanced efficacy via radio sensitisation. Triple therapy produced maximal tumour suppression with manageable toxicity. Ex vivo biomarkers provided mechanistic insight and predictive correlates across cohorts.

Conclusions. This integrated preclinical study demonstrates that ^{177}Lu-PSMA efficiency is enhanced by immunotherapy and DDR inhibition. Multimodal imaging, PK, toxicity, and biomarker analyses inform rational dosing, combination design, and translational strategies for future clinical trials in prostate cancer.

#4634 Pretreatment with pan-integrin inhibitor GLPG-0187 sensitizes GBM cells to radiation.

Maryam Ghandali[1], Ianlan Zhou[2], Wafik S. El-Deiry[3]

[1]Brown university, Providence, RI,[2]Brown University, Providence, RI,[3]Legorreta Cancer Center at Brown University, Providence, RI

Glioblastoma multiforme (GBM) is the most common primary CNS tumor in adults. Treatment of GBM involves a combination of radiation, chemotherapy, and surgery. Despite significant advancements in radiotherapy, treatment response in GBM remains limited due to challenges such as radioresistance and tumor recurrence. Multiple biological factors contribute to this resistance, including hypoxia, tumor microenvironment interactions, and DNA damage response and repair mechanisms. Previous studies have highlighted the role of integrins in promoting tumor radio resistance under both normoxic and hypoxic conditions. Based on this, we hypothesized that pretreatment of GBM cells with a pan-integrin inhibitor could enhance radiation sensitivity by blocking integrin-mediated pro-survival signaling before radiation-induced stress. In our study, U251 and SNB19 GBM cell lines were treated with GLPG-0187 24 hours before irradiation under both normoxic and hypoxic conditions. CellTiter-Glo (CTG) assays were performed 48 hours post-irradiation, and the combination effects were analyzed using Combenefit software. Under normoxic conditions, pretreatment with GLPG-0187 increased radiation sensitivity in both cell lines. Under hypoxic conditions, pretreatment still enhanced sensitivity, although the effect was attenuated compared to normoxic conditions. Our ongoing studies are expanding these findings to include additional GBM and diffuse intrinsic pontine glioma (DIPG) cell lines and are exploring the molecular pathways affected by this combination treatment. Overall, our results indicate that pan-integrin inhibition prior to radiotherapy could be a promising strategy to improve treatment outcomes in GBM patients.

#4635 Mapping PSMA-617 sensitivity in prostate cancer PDX models to enable combination therapy and resistance studies.

Rocio Matesanz Sanchez[1], Karg Margarete[1], Nikoline Nielsen[1], Marina Simon Martin[1], Kira Ropke Jorgensen[1], Mette Munk Wessek[1], Rasmussen Patricia[1], Anne Hessellund Langhave[1], Louise Juul Nielsen[1], Jacobsen Helle Jane[1], Neal D. Shore[2], Sebastian Gnosa[1], Michael Wick[3], **Carsten Haagen Nielsen**[1]

[1]Minerva Imaging ApS, Olstykke, Denmark,[2]The START Center for Cancer Research - Carolinas, Myrtle Beach, SC,[3]The START Center for Cancer Research-XenoSTART, San Antonio, TX

Prostate cancer represents the second most frequently diagnosed malignancy and ranks fifth in cancer-related mortality worldwide among men. Therapeutic strategies include the FDA-approved radioligand therapy (RLT) [^{177}Lu]Lu-vipivotide tetraxetan ([^{177}Lu]Lu-PSMA-617, Pluvicto), indicated for PSMA-positive metastatic castration-resistant prostate cancer (mCRPC) following progression on hormone therapy and/or chemotherapy. Given the favourable toxicity profile of [^{177}Lu]Lu-PSMA-617, clinical investigations are exploring its application earlier in the therapeutic sequence. Nevertheless, a substantial proportion of patients exhibit only transient responses or fail to respond due to intrinsic or acquired resistance mechanisms, underscoring the need for combination regimens incorporating chemotherapeutics, radiosensitizers, targeted agents, and/or immunotherapies. Robust preclinical models are essential for evaluating such combination strategies, as they enable controlled assessment of treatment efficacy within biologically relevant systems. Patient-derived xenografts (PDXs) retain the genomic, histopathologic, and pharmacologic characteristics of the original tumors, providing reliable predictive power for clinical outcomes. Consequently, well-validated PDX models are critical for elucidating synergistic interactions and guiding translational application of novel combinatorial approaches. We utilized a panel of prostate cancer PDX models selected based on PSMA expression, quantified by immunohistochemistry and AI-driven image analysis (Visiopharm). PSMA-expressing tumors validated by IHC before the treatment were treated with ~1 mCi (30-37 MBq) of [^{177}Lu]Lu-PSMA-617 and tumor uptake of was evaluated using SPECT/CT. Tumor growth was monitored longitudinally, and therapeutic efficacy was assessed using tumor growth inhibition (TGI) and time to progression (TTP). To model acquired resistance, a [^{177}Lu]Lu-PSMA-617-resistant PDX (ST1273/RTR; XenoSTART) was derived from an initially sensitive tumor (ST1273; XenoSTART). This model tolerated up to 30 MBq of [^{177}Lu]Lu-PSMA-617, while PSMA expression and radioligand uptake remained comparable between parental and resistant tumors. As proof-of-concept, PARP inhibition with olaparib was evaluated as a radiosensitizer in ST1273/RTR. Tumor relapse occurred 29 days post-[^{177}Lu]Lu-PSMA-617 monotherapy, whereas combination treatment extended relapse to 49 days, demonstrating enhanced antitumor efficacy. Collectively, these fully characterized prostate PDX models-validated for PSMA expression and [^{177}Lu]Lu-PSMA-617 responsiveness-integrated with comprehensive clinical data, establish a robust, translationally relevant platform for preclinical evaluation of innovative combinatorial strategies in RLT.

#4636 Deciphering radiation sensitivity identifies MDM2 as a targetable driver of synergistic radiosensitization in TP53 wild-type lung adenocarcinoma.

Chan Hoon Maeng[1], Jieon Hwang[2], Joong Bae Ahn[2], Sang Joon Shin[2]

[1]Department of Medicine, Yonsei University College of Medicine, Seoul, Korea, Republic of,[2]Division of Medical Oncology, Department of Internal Medicine, Yonsei Cancer Center, Seoul, Korea, Republic of

Background: Resistance to ionizing radiation (IR) remains a major obstacle to effective radiotherapy. Beyond its classical role as a negative regulator of p53, MDM2's broader contribution to radioresistance remains insufficiently understood. Given that lung adenocarcinoma (LUAD) exhibits heterogeneous responses to radiotherapy, defining molecular determinants of radiation sensitivity may reveal actionable targets. In this context, we sought to identify such determinants and to determine whether MDM2 represents a critical and therapeutically targetable regulator capable of enhancing radiotherapy efficacy in LUAD.

Methods: LUAD cell lines (A549, NCI-H460, NCI-H650, NCI-H1573) were stratified into IR-sensitive and IR-insensitive groups using clonogenic survival following irradiation. Transcriptomic profiles and DepMap CRISPR dependency datasets were integrated to uncover potential molecular determinants of radiation sensitivity. Pharmacologic MDM2 inhibition (idasanutlin) was tested alone or in combination with IR across LUAD cell lines with distinct TP53 backgrounds. Clonogenic assays, 3D spheroid cultures, and xenografts were used to assess treatment responses in 2D, 3D, and *in vivo* settings.

Results: Clonogenic survival analysis revealed distinct IR-sensitive and IR-insensitive subsets among LUAD cell lines. Integrated analyses demonstrated that MDM2 dependency was markedly higher in TP53 wild-type IR-insensitive cells, suggesting a p53-proficient context for MDM2-driven radioresistance. In line with this prediction, MDM2 inhibition alone (idasanutlin monotherapy) induced more pronounced growth inhibition in p53 wild-type compared with p53-mutant cells. The IR-idasanutlin combination produced robust synergistic cytotoxicity, profoundly reducing clonogenic survival and causing spheroid shrinkage accompanied by markedly elevated EthD-1 fluorescence intensity, indicating increased cell death. In an NCI-H460 xenograft model, idasanutlin (15 mpk, p.o. daily) combined with IR (4 Gy) yielded the highest tumor growth inhibition (TGI = 77.1%, $p < 0.001$) without body-weight loss, demonstrating strong *in vivo* synergistic efficacy and tolerability. These findings underscore the translational potential of MDM2 blockade as a radiosensitizing strategy in p53-proficient tumors.

Conclusions: Our findings demonstrate that MDM2 dependency, revealed through integrative omics analyses, represents a therapeutic vulnerability underlying IR-resistance in p53-proficient LUAD. Combining idasanutlin with radiotherapy effectively overcomes this resistance, highlighting MDM2 as a robust and actionable target for enhancing radiation response in cancers driven by high MDM2 activity.

#4637 Alpha-particle radiotherapy combined with anti-CTLA-4 synergistically overcomes radioresistance and induces local and systemic antitumor immunity in PDAC.

Marco Reis[1], Poliana C. Marinello[2], Walison Augusto da Silva Brito[2], Scott Bright[2], Mark Wasley[2], Alexandre Rubinstein[2], Ronen Sega[3], Vered Bachar[3], Gabriel O. Sawakuchi[2]

[1]Radiation Physics & BioSciences, UT MD Anderson Cancer Center & Rice University, Houston, TX,[2]Radiation Physics, UT MD Anderson Cancer Center, Houston, TX,[3]Alpha Tau Medical Ltd, Jerusalem, Israel

Pancreatic ductal adenocarcinoma (PDAC) is the third leading cause of cancer death in the U.S., with over 90% of patients presenting mutant KRAS (mtKRAS). Increased radioresistance and elevated CTLA-4 expression are hallmarks driven by mtKRAS. Radiation has only shown meaningful efficacy in PDAC at very high doses that are not achievable with conventional radiotherapy due to toxicity to adjacent organs. Additionally, although CTLA-4 upregulation suggests a therapeutic target, PDAC shows limited response to immune checkpoint blockade because of its highly immunosuppressive tumor microenvironment. We propose to sensitize a cold mtKRAS murine PDAC model (KPC) to anti-CTLA-4 (aCTLA-4) by overcoming radioresistance using Diffusing Alpha-emitters Radiation Therapy (Alpha DaRT), an intratumoral source of alpha particles with >1,000-fold greater ionization density than photons. This enables delivery of very high doses directly to the tumor while sparing healthy tissue. To further enhance this effect, an ATR inhibitor will impair DNA repair, increasing susceptibility to treatment. To assess local tumor response, mice received 5×10^5 cells in the left leg, and after 7 days (day 0) one DaRT source (inert or active) was implanted. ATRi (75 mg/kg) or DMSO was administered orally on days 0, 1, 2, 7, 8, and 9, and aCTLA-4 or IgG was injected intraperitoneally every 3 days starting on day 3 (4 doses). Animals with complete regression (>100 days tumor-free) were rechallenged on day 130. To assess systemic immunity, mice received 5×10^5 KPC cells in the left leg and 1×10^5 in the right leg, and after 10 days (day 0) one DaRT source was implanted in the left leg. The drug schedule was identical, except mice received six doses of aCTLA-4. The triple therapy (Alpha DaRT + ATRi + aCTLA-4) induced significantly ($p<0.05$) greater tumor growth delay compared to control, monotherapies, and duotherapies, excluding Alpha DaRT + aCTLA-4, from day 25 onward. By day 41, all control and monotherapy mice reached euthanasia criteria, whereas 60% and 70% of the Alpha DaRT + aCTLA-4 and triple therapy groups remained alive. Complete tumor regression >100 days was sustained in 40% and 50% of mice, respectively. Upon rechallenge, no tumors regrew in the Alpha DaRT + aCTLA-4 group, and only 1 of 5 in the triple therapy group showed regrowth. A significant ($p<0.0001$) synergistic effect was observed between Alpha DaRT and aCTLA-4. For systemic immunity, Alpha DaRT + aCTLA-4 and the triple therapy induced greater tumor growth delay in both the irradiated and unirradiated tumors compared to all other treatments. In conclusion, Alpha DaRT combined with aCTLA-4 generates durable local and systemic antitumor responses in mtKRAS PDAC, offering a strategy to overcome KRAS-mediated radioresistance and immune evasion.

#4638 Oncolytic herpes simplex virus, M002, increases the antitumor radiation response by decreasing the G2/M arrest in murine rhabdomyosarcoma orthotopic allograft cells.

Maryam G. Shaikh[1], Nazia Nazam[1], Morgan L. Brown[1], Pranava Nande[1], Ali M. Eakes[1], Shamza Manzoor[2], Joel C. Opara[1], James M. Markert[3], Jamie M. Aye[4], Elizabeth A. Beierle[1]

[1]Surgery, University of Alabama at Birmingham, Birmingham, AL,[2]Department of Neurosurgery, University of Alabama at Birmingham, Birmingham, AL,[3]Neurosurgery, University of Alabama at Birmingham (UAB), Birmingham, AL,[4]Pediatrics, University of Alabama at Birmingham (UAB), Birmingham, AL

Introduction: Rhabdomyosarcoma (RMS) represents the predominant soft tissue sarcoma in children. For most RMS patients, multimodality therapy is employed to achieve optimal outcomes, incorporating chemotherapy, radiotherapy (RT) and surgery. RT, although an integral component of local control, often results in significant long-term sequelae. Further, children with RMS who relapse after RT continue to experience the poorest outcomes. These issues underscore the need to develop strategies to minimize late toxicities and improve therapeutic index. Investigations have indicated that RT-induced antigen release amplifies the immune response triggered by oncolytic viruses (OVs), and viral infection of tumor cells impedes the repair of RT-induced DNA damage, both enhancing RT efficacy. We previously showed that treatment of murine orthotopic allograft (OA)-RMS cells with an oncolytic Herpes Simplex Virus (oHSV), M002, enhanced the response to RT. These findings led us to investigate the mechanism by which M002 enhances the antitumor response to RT in OA-RMS cells.
Methods: Murine OA-RMS cells were treated with M002 (0 or 5 plaque forming units (PFU)/cell) for 24 hours and whole cell RNA sequencing was performed. RT doses were delivered as X-rays at 275 kV and 10.0 mA. Viability was measured using almarBlue. Cell cycle distribution was assessed by flow cytometry.
Summary of results: OA-RMS cells demonstrated resistance to RT as measured by no significant change in viability between control cells and RT treated cells on post-treatment day 6. RNA sequence data and pathway analysis of M002 (5 PFU/cell) treated OA-RMS cells showed significant downregulation of genes involved in the G2/M pathway. Combined treatment with 2 Gy RT and M002 abrogated G2/M phase arrest caused by RT alone. The percentage of OA-RMS cells arrested at the G2/M phase increased after 2 Gy RT to 24.4% compared to 8.3% in the control cells. Combined treatment with M002 and RT decreased the percentage of OA-RMS cells arrested at G2/M phase to 2.5%. Combining M002 with RT significantly increased the sub-G1 population compared to the control group, indicating dying and apoptotic cells.
Conclusion: We demonstrate that the oHSV, M002, significantly suppresses the genes regulating the G2/M phase of the cell cycle in OA-RMS cells. Combining RT with M002 reduced the G2/M phase arrest caused by RT. The loss of G2/M arrest was accompanied by an increase in cell death. These results indicate that M002 is a promising strategy to disrupt the G2/M checkpoint, a mechanism through which RT-resistant RMS tumors function.

#4639 Redox modulation by gold nanorods enhances radiosensitivity in MOLT 4 cells.

Paras Jawaid[1], Mati Ur Rehman[2], Azhar Hussain Rajabali[3], Ather Enam[4]

[1]Biological and Biomedical Sciences, Centre of oncological research in surgery, Aga Khan University Hospital - Karachi, Pakistan, Karachi, Pakistan,[2]Biological and Biomedical Sciences, Aga Khan University hospital, Karachi, Pakistan,[3]Biological and Biomedical Sciences, Aga Khan University Hospital - Karachi, Pakistan, Karachi, Pakistan,[4]Neurosurgery, Centre for regenerative medicine and stem cell research, Aga Khan University Hospital - Karachi, Pakistan, Karachi, Pakistan

Gold nanoparticles have gained increasing interest because of their unique optical properties. Among different shapes of nanoparticles, gold nanoparticles (Au-NPs) with non-spherical shape, such as gold nanorods (Au-NR), are gaining particular attention for various applications because of their facile synthesis and modification. They can be conjugated with different molecules for biomedical applications, such as tumor imaging and therapy. Previously, we have shown that small sized Au-NPs possess distinct effects depending on the treatment modality; they protect against x-ray induced apoptosis while enhancing apoptosis induced by ultrasound and helium based cold atmospheric plasma. Therefore, this study is intended to investigate the effects of Au-NR, on x-ray (2.5 Gy) induced apoptosis as well as mediating molecular pathways in MOLT 4 cells *in-vitro*. The effect of Au-NR on x-ray induced apoptosis was determined by observing the changes in intracellular reactive oxygen species (ROS) formation and apoptotic signalling pathways. The results indicate that cells pre-treated with 10 nm size of Au-NR at a dose of 0.1 and 0.5 µg significantly enhanced apoptosis. Typical morphological changes were observed by using Giemsa staining which shows the enhanced apoptotic cell death in combination treatment. Loss of mitochondrial membrane potential, glutathione and intracellular calcium ion level was significantly enhanced; observed by using flow cytometry. Furthermore, western blot analysis was employed to determine the expression of caspase-3, and Bcl-2 family proteins. In this study we have shown for the first time that in combination treatment, Au-NR significantly enhanced the low dose of x-ray-induced apoptotic cell death. Our finding indicates that the combination treatment of cancer will be emerged as a critical approach to achieve remarkable anticancer effects.

#4640 Benefit of combining DLL3 targeted alpha therapy with standard of care in preclinical small cell lung cancer models.

Hanan Babeker[1], Emma Cummins[1], Alex Mandel[1], Lily Li[1], Etienne Melese[1], Rachael Brake[2], Iva Kulić[1]

[1]Abdera Therapeutics Inc., Vancouver, BC, Canada,[2]Abdera Therapeutics Inc., San Francisco, CA

ABD147 is a human delta-like ligand 3 (DLL3) engineered antibody designed with optimized pharmacokinetics and biodistribution to preferentially deliver actinium-225 (^{225}Ac) to DLL3 expressing tumor cells resulting in potent antitumor activity in preclinical models. ^{225}Ac-ABD147 is built using Abdera's Radio Optimized Vector Engineering (ROVEr™) platform and is currently in phase I clinical trials for small cell lung cancer (SCLC) and large cell neuroendocrine carcinoma (LCNEC). SCLC is an aggressive neuroendocrine malignancy characterized by rapid progression and high relapse rates despite initial response to standard-of-care (SOC) treatment, including platinum-based chemotherapy and immune checkpoint inhibitors, underscoring the unmet need for therapies that improve tumor control and prolong survival. SCLCs are intrinsically radiosensitive and along with other neuroendocrine cancers commonly express DLL3 on the cell surface. Targeted alpha therapy induces difficult to repair DNA double-strand breaks and can promote immunogenic cell death enhancing SOC tumor-directed cytotoxicity by overwhelming DNA repair pathways and overcoming resistance. A single administration of ^{225}Ac-ABD147 or a murine DLL3 ROVEr™ was assessed in combination with SOC in DLL3-expressing chemo-resistant SCLC cell line derived xenograft models or a syngeneic model. The combination treatment was tolerated and outperformed SOC alone for anti-tumor efficacy, sustained tumor responses and prolonged survival across models. In conclusion, DLL3-targeted alpha therapy demonstrates potent anti-tumor activity in combination with SOC across multiple SCLC models. These findings suggest ^{225}Ac-ABD147 has a combinatorial benefit that could support an add-on to a SOC therapeutic approach in the clinic.

#4641 Highly soluble prodrug boronophenylalanine (L-BPA) dipeptide, exhibits notable tumor suppression whilst inducing cancer vaccine effect post neutron irradiation treatment.

Samkeliso Dlamini[1], Michael Torgov[1], Arthur Raitano[1], Jason Quintana[1], Tioga Martin[1], Chunying Zhang[1], Maria Christina Malinao[1], Maki Ikeura[1], Linnette Capo[1], Karen Morrison[1], Robert Dorn[1], Kotaro Matsumoto[2], Aoi Komatsu[2], Yuya Higashi[2], Takushi Takata[3], Yoshinori Sakurai[4], Minoru Suzuki[4], Fuyuhiko Tamanoi[2], Kendall Morrison[1]

[1]Medicinal Chemistry, TAE Life Sciences, Santa Monica, CA,[2]Institute for Advanced Study, Institute for Integrated Cell-Material Science, Kyoto University, Japan,[3]Institute for Advanced Study, Institute for Integrated Radiation and Nuclear Science, Kyoto University, Japan,[4]Institute for Integrated Radiation and Nuclear Science, Kyoto University, Japan

Boron Neutron Capture Therapy (BNCT) is an emerging cancer treatment modality that has seen a resurgence due to its efficacy and the advent of compact neutron beam devices. BNCT is a binary cancer treatment that combines selective boron delivery with epithermal neutron irradiation. When ^{10}B-enriched compounds accumulate in tumor cells and capture low-energy neutrons, the reaction generates high-linear energy transfer (LET) α-particles and ^{7}Li nuclei that deposit their energy within a few microns, producing irreparable DNA double-strand breaks and tumor cell death while sparing normal tissues. The clinical success of BNCT critically depends on the selective delivery of sufficient boron to tumors. Currently, 4- l-boronophenylalanine (l-BPA) is the leading BNCT agent, as it exploits LAT-1 (SLC7A5), a transporter highly expressed in many solid tumors. However, l-BPA suffers from poor solubility, severely limiting the maximum intravenous dose that can be administered and thereby constraining therapeutic efficacy. Here we report the synthesis and evaluation of highly soluble ^{10}B-enriched l-BPA-based dipeptides as next-generation boron delivery agents. These dipeptides, incorporating hydrophilic peptide linkages, enabled substantially higher intravenous bolus doses in mice compared to l-BPA while maintaining favorable biodistribution. In vivo, the dipeptides were rapidly cleaved by endogenous proteases, releasing l-BPA de novo within tumors. Neutron irradiation of syngeneic CT26 tumors in dipeptide-treated mice produced complete and durable tumor regressions, accompanied by immunological effects including a vaccine response and abscopal tumor suppression. By contrast, l-BPA administered at its solubility-limited maximal dose and using the same irradiation produced only transient growth delay without durable regression or immune activation. These findings establish dipeptides as a promising strategy to overcome the solubility limitations of l-BPA, enabling higher boron delivery, improved tumor control, and immune-mediated benefits. This approach could significantly expand the therapeutic potential of BNCT.

#4642 Defining radiosensitivity indicators to predict prognosis using patient-derived organoids in oral cancer.

Sumin Kang[1], Mi Rim Lee[1], Jonghyun Lee[1], Dongkwan Shin[1], Jong-Ho Lee[1], Ikjae Kwon[2], Jiyoung Lee[1], Yu-Sun Lee[1], Sun-il Choi[1], Hye Won Shon[1], Gyeongmin Kang[1], Sung Woen Choi[3], Yun-Hee Kim[1]

[1]National Cancer Center, Goyang-si, Korea, Republic of,[2]School of Dentistry, Seoul National University, Seoul, Korea, Republic of,[3]National Cancer Center, Goyaing-si, Korea, Republic of

Over 60% of patients with oral cancer are diagnosed at advanced stages, and the standard treatment was surgery followed by adjuvant radiotherapy. Nevertheless, 30-50% of patients experience recurrence within two years, whereas patients with radiosensitive tumors may be exposed to unnecessarily high radiation doses. Therefore, predicting radiotherapy response and stratifying patients is essential for personalized treatment approaches and improving clinical outcomes. Patient-derived organoids (PDOs) are robust preclinical models that recapitulate the characteristics of patients' tumors. In this study, we defined radiation sensitivity indicators using an oral cancer PDO library comprising 102 patient-derived organoids. Dose-dependent radiation responses were evaluated for 68 PDOs and correlated with clinical data. When organoids were classified based on the mean survival fraction at 2 Gy (SF2), patients in the high-SF2 group exhibited a significantly shorter recurrence-free survival. It suggests that PDO-based assessment of radiation response may serve as a useful predictor of clinical outcomes. In addition, a radiation sensitivity-related pathway score was generated from differentially expressed genes (DEGs) identified in radiosensitive PDOs and applied to The Cancer Genome Atlas (TCGA) oral cancer cohort. Patients were classified into low- and high-score groups according to the sensitivity score. The high-score group had a significantly more favorable survival prognosis. Furthermore, to identify a tissue-detectable radiation sensitivity marker (RSM), we selected the gene associated with the most enriched pathway in the low-SF2 organoid group, resulting in the identification of a candidate marker, RSM-1. Subsequent immunohistochemical (IHC) analysis demonstrated that RSM-1 was expressed at higher levels in tumors from patients without recurrence. Overall, this study utilized patient-derived organoids to evaluate radiation responses, derive a radiosensitivity score, and identify a clinically relevant biomarker. By integrating molecular and phenotypic tumor characteristics, this approach provides reliable prognostic indicators, enabling prediction of patients' radiation responses and supporting personalized therapeutic strategies to improve prognosis in oral cancer.

#4643 Microsatellite instability as a determinant of chemoradiotherapy sensitivity in colorectal cancer: Integrated clinical, radiomic, and 3D organoid-based analyses.

Hyowon Hong[1], Shin Kim[2], Sang Jun Byun[3], Seong Kyu Baek[3], hyewon lee[2], sung wook bae[3]

[1]Research Affairs, Keimyung University Dongsan Medical Center, Daegu, Korea, Republic of,[2]Keimyung University School of Medicine, Daegu, Korea, Republic of,[3]Keimyung University Dongsan Medical Center, Daegu, Korea, Republic of

Background: Microsatellite instability (MSI) is an established biomarker affecting immunotherapy outcomes and may influence DNA damage responses following chemoradiotherapy (CRT). While clinical studies have reported favorable CRT outcomes in MSI-high (MSI-H) colorectal tumors, the biological basis for differential radiosensitivity remains incompletely understood. To address this gap, we integrated clinical-radiomic analyses with functional assays using 3D organoid models derived from MSI-H and microsatellite-stable (MSS) colorectal cancer (CRC) cell lines.
Methods: Clinical data from 87 rectal cancer patients receiving neoadjuvant CRT were analyzed. MSI status was determined by PCR and immunohistochemistry for MLH1, MSH2, MSH6, and PMS2. Radiomic features were extracted from pre-CRT CT images, and a machine learning model was trained to classify MSI status. For biological validation, 4 MSI-H (HCT116, HCT15, RKO, DLD-1) and 5 MSS cell lines (HT29, CACO2, SW480, COLO205, COLO320DM) were subjected to graded irradiation. Cells were embedded in 70% Matrigel or BME to generate 3D organoids. Radiation responses were evaluated using Calcein-AM-based viability area analysis, ATP-based 3D CellTiter-Glo assays, and area-under-curve (AUC) quantification across 0-8 Gy.
Results: MSI tumors were exclusively found in the responder group (18.52%) and absent in non-responders ($P<0.05$). Pathological downstaging (T0-T2) was significantly higher in responders (88.89% vs. 38.33%, $P<0.001$), with increased nodal clearance (N0; 92.59% vs. 61.67%, $P=0.003$). In 3D organoid models, MSI-H cell lines displayed markedly greater radiosensitivity than MSS lines. MSI-H organoids showed stronger growth inhibition and lower viability in both Calcein-AM and ATP 3D assays, resulting in reduced radiation-response AUC values. In contrast, MSS organoids maintained higher viability and metabolic activity after irradiation, indicating relative radioresistance.
Conclusion: MSI-H colorectal cancer demonstrated consistently higher chemoradiotherapy sensitivity across clinical outcomes, radiomic signatures, and 3D organoid-based functional assays. The enhanced radiosensitivity observed in MSI-H organoids suggests that deficiencies in DNA mismatch repair may contribute to increased susceptibility to radiation-induced damage, although the precise molecular pathways have not yet been fully defined. These integrated findings support the potential value of combining MSI testing with organoid-based functional profiling to refine patient stratification and guide personalized CRT approaches in colorectal cancer. Validation in larger and ethnically diverse cohorts will be necessary to confirm generalizability.

#4644 Protein kinase D1 modulates LET- and dose-dependent radiosensitivity in prostate cancer cells.

Joseph McGrath[1], Sanjeev Shukla[1], Mohammad Saki[2], Hardev Grewal[2], Jiyeon Park[2], Mark Artz[2], K.C. Balaji[1]

[1]Urology, University of Florida Health, Jacksonville, FL,[2]University of Florida Health Proton Therapy Institute, Jacksonville, FL

Protein kinase D1 (PrKD1) participates in DNA damage response signaling, but its role in modulating dose- and linear energy transfer (LET)-dependent radiosensitivity in prostate cancer remains poorly defined. We evaluated the effect of PrKD1 loss on clonogenic survival following photon and proton irradiation to determine whether PrKD1 influences radiosensitivity across clinically relevant dose ranges. LNCaP and their PrKD1-knockdown derivative (shPrKD1) prostate cancer cells were exposed to 0-4 Gy X-rays or proton irradiation delivered at increasing dose-averaged LET (PL2-PL4 = 2-4 keV/µm). Clonogenic survival was normalized to unirradiated controls, and linear-quadratic modeling was used to derive D10, D37, and relative biological effectiveness (RBE) values. Both cell lines showed a dose-dependent decline in survival, but their response profiles diverged with dose and LET. LNCaP cells were more radioresistant at 1 Gy and demonstrated a steep loss of viability from 2-4 Gy with LET-associated sensitization that was most evident at PL4 and at higher doses. In contrast, shPrKD1 cells exhibited greater sensitivity at low-to-intermediate doses (≤2 Gy), a more linear survival curve, and reduced LET dependence. The survival curves crossed at higher doses, with shPrKD1 more sensitive at clinically relevant doses yet relatively more resistant at high, near-ablative doses. D10 values ranged from 5.2-5.7 Gy in shPrKD1 versus 4.2-5.1 Gy in LNCaP, with both cell lines showing greatest sensitization at PL4. RBE values remained modest (~1.0-1.2) but increased slightly with LET in shPrKD1, indicating enhanced sensitivity at intermediate doses. These findings demonstrate that PrKD1 loss enhances radiosensitivity in the fractionated dose range and attenuates LET-dependent effects, identifying protein kinase D1 as a modulator of radiation response and a potential biomarker for optimizing proton and photon therapy strategies in prostate cancer.

#4645 Integrative transcriptomic and CRISPRi screening identifies determinants of intrinsic radiosensitivity in breast cancer.

Breanna Nicole McBean[1], Priyanka S. Rana[2], Reine Abou Zeidane[3], Alexander Davis[2], Vesna Mercer[2], Benjamin Hauk[3], Anna Michmerhuizen[1], Samuel Lichtman-Mikol[3], Camila Diedrich[2], Kari Wilder-Romans[1], Mingfang Tao[3], Alan P. Boyle[1], Corey Speers[2]

[1]University of Michigan, Ann Arbor, MI,[2]University of Alabama Birmingham, Birmingham, AL,[3]Case Western Reserve University School of Medicine, Cleveland, OH

Background: Breast cancer (BC) remains a leading cause of cancer-related mortality among women, and radiation therapy (RT) is a cornerstone of its management. Despite its efficacy, more than 15% of patients experience locoregional recurrence following RT, highlighting a critical need to define the molecular determinants of RT response and resistance. We hypothesized that transcriptomic changes that occur after ionizing radiation in intrinsically radiosensitive and radioresistant BC models would offer mechanistic insight into mediators of this differential response. To investigate this, we performed *in vitro* RNA-sequencing across a panel of BC cell lines spanning a spectrum of intrinsic radiosensitivity to characterize radiation-induced transcriptional programs. Recognizing that key mediators of radioresistance may not exhibit differential expression, we complemented this approach with a genome-wide CRISPR interference (CRISPRi) screen to identify additional functional targets that modulate radiosensitivity. Together, these studies aim to elucidate novel molecular pathways underlying RT resistance and inform future therapeutic strategies
Methods: Eight BC cell lines were treated with 4 Gy RT and RNA was collected 24 hours after treatment for RNA-seq. Differential gene expression analysis with DESeq2 was performed, followed by pathway analysis with Advaita Bioinformatics' iPathwayGuide. For the CRISPRi experiments, dCas9-KRAB-expressing BT-549 cells were transfected with the Dolcetto library and treated with 3 fractions of 3 Gy RT. DNA was isolated for sequencing to determine sgRNA abundance 7 days after the last dose of radiation and analyzed with MAGeCK.
Results: Radiation induced significant transcriptional changes across both radiosensitive and radioresistant models, with highly enriched pathways including cell cycle regulation, DNA replication, and the Fanconi anemia pathway. The CRISPRi screen identified canonical regulators of the DNA damage response as modulators of radiosensitivity, as well as less-characterized candidates such as the potassium channel modifier *KCNG3* and the spliceosome component *U2AF1*, with mechanistic studies now underway.
Conclusions: Ionizing radiation activates transcriptomic programs predominantly involving expression changes in DNA damage response-replated pathways, consistent with top hits identified in the CRISPRi functional screen. Importantly, the screen also reveals previously underexplored mechanisms of radiosensitization, including perturbations in alternative splicing and potassium channel signaling. Together, these findings highlight biologic vulnerabilities that may underlie intrinsic radioresistance and nominate potential targets for therapeutic intervention in women at high risk of local BC recurrence.

#4646 Validation of a panel of fibroblast activation protein expressing cell line derived xenograft models as a platform for the development of targeted radioligand therapeutics.

Michael Batey, James Suchy, Taylor Hotz, Michael Milhollen, Kayla Duval, Jackson Chan, Karen Gelinas, Michael Bruce, Michelle Petrozzi, William Maccuaig, Neil Rollins, Jennifer Tavares, Erin Snay, Kyeara Mack-Henry, Soumya Ullas

Perceptive Discovery, Needham, MA

Targeted radioligand therapy (RLT) has emerged as a promising strategy for precision oncology, enabling selective tumor targeting while reducing collateral damage to healthy tissue. A major challenge in advancing novel RLT agents, however, is the limited availability of well-validated preclinical models for assessing target-specific efficacy. Fibroblast Activation Protein (FAP), a membrane-bound protein with minimal expression in normal tissues but high prevalence in cancer-associated fibroblasts and glioblastoma (GBM) cells, represents an attractive therapeutic target. FAP-2286, a FAP-binding peptide radiolabeled with lutetium-177 (^{177}Lu), offers potential as both an imaging and therapeutic agent. In this study, we evaluate target expression and compare the anti-tumor efficacy of ^{177}Lu-FAP-2286 across multiple immunocompromised mouse models bearing subcutaneous, cell line-derived tumors. Our findings underscore the critical role of model selection in preclinical development and highlight its importance for rational decision-making in RLT programs.

#4647 Development and validation of a panel of cell line derived xenograft models representing multiple tumor indications for the evaluation of targeted radioligand therapeutics.

Michael Batey, James Suchy, Taylor Hotz, Michael Bruce, Jennifer Tavares, Erin Snay, Neil Rollins, Jackson Chan, Karen Gelinas, Kayla Duval, William Maccuaig, Michael Milhollen, Michelle Petrozzi, Kyeara Mack-Henry, Soumya Ullas

Perceptive Discovery, Boston, MA

Targeted radioligand therapy (RLT) represents a significant advancement in precision oncology, enabling selective tumor targeting while minimizing damage to healthy tissue. However, the development of innovative RLT agents is often hindered by the limited availability of robust, well-validated preclinical models needed to evaluate target-specific efficacy. Here, we demonstrate the development and validation of a comprehensive panel of in vitro screening assays and in vivo cell line-derived xenografts, including models such as Colo205, MiaPaca2, SHP-77, HT29, A549, LNCaP, and 22Rv1, which express key targets relevant to radioligand therapy. These models provide an ideal pathway for evaluating novel agents in this rapidly growing field, covering targets such as TROP2, CAIX, DLL3, FAP, and PSMA across a range of indications including glioblastoma, colorectal, lung, pancreatic, and prostate cancers. We also discuss the use of *in vivo* and *ex vivo* imaging techniques such as single photon emission computed tomography (SPECT) and cryo fluorescence tomography (CFT) . These studies highlight the utility of these platforms for the preclinical development of a wide range of target-based therapies, with potential applications spanning multiple therapeutic modalities including RLT, antibody-drug conjugates (ADCs), and small molecules.

#4648 Targeting alternative end-joining overcomes *miR-21-5p*-mediated radioresistance in oral squamous cell carcinoma.

Lin Ma[1], Nilupaier Tayier[2], Weitao Hu[3], Junyang Chen[2], Yanhe Li[2], Lu Wen[2], Yonghui Luo[2], Xinghan Li[3], **Qi Liu**[4]

[1]Department of Stomatology, Shenzhen University General Hospital, Institute of Stomatological Research, Shenzhen University, Shenzhen, China,[2]Shenzhen University, Shenzhen, China,[3]Department of Stomatology, Shenzhen University General Hospital, Institute of Stomatological Research, Shenzhen University, Shenzhen, China,[4]International Cancer Center, Shenzhen University, Shenzhen, China

Radiation resistance remains a major barrier to effective radiotherapy in oral squamous cell carcinoma (OSCC), yet its molecular basis is incompletely defined. Here, we uncover activation of the alternative end-joining (alt-EJ) DNA repair pathway as a key driver of miR-21-5p-mediated radioresistance in OSCC. Comprehensive miRNA profiling of radioresistant OSCC clones revealed distinct expression signatures marked by robust upregulation of miR-21-5p and miR-486-5p, coupled with reduced miR-320b and miR-1248. Functional assays, including clonogenic survival and syngeneic mouse tumor models, demonstrated that enforced expression of miR-21-5p markedly enhanced radioresistance, accompanied by sustained DNA damage response signaling and improved double-strand break (DSB) repair capacity. Transcriptomic and genomic analyses of the TCGA-HNSC cohort revealed that high miR-21-5p expression correlates with suppression of canonical DNA repair targets, poor radiotherapy outcomes, elevated tumor mutational burden (TMB), and an increased frequency of microhomology-mediated insertions/deletions, consistent with heightened alt-EJ activity. Cross-validation in independent OSCC datasets and local tumor panels confirmed that miR-21-5p-overexpressing tumors exhibit strong activation of alt-EJ gene programs, including upregulation of PARP1, POLQ, and associated accessory factors. Analysis of diverse cancer cell line databases further established that miR-21-5p activity positively correlates with alt-EJ gene expression independent of microenvironmental influence. Mechanistically, miR-21-5p overexpression shifted DSB repair dependence from homologous recombination and classical non-homologous end-joining toward alt-EJ. Pharmacologic or genetic suppression of alt-EJ components (PARP1 or POLQ) disrupted DSB resolution and effectively restored radiosensitivity in miR-21-5p-high OSCC cells. Notably, radiosensitization by PARP inhibition was abrogated in POLQ-deficient cells, confirming a POLQ-dependent mechanism. In vivo, miR-21-5p-driven OSCC tumors exhibited enhanced expression of alt-EJ signatures, increased radioresistance, and high TMB. Combination treatment with irradiation and PARP blockade suppressed tumor growth, diminished alt-EJ gene expression, and prolonged survival in a syngeneic mouse model. Collectively, these findings establish a novel miR-21-5p/alt-EJ signaling axis as a central determinant of radioresistance in OSCC. Targeting alt-EJ represents a promising therapeutic strategy to overcome miR-21-5p-mediated treatment failure and improve radiotherapy efficacy in head and neck cancers.

: Cell Death Regulation and Therapeutic Resistance in Cancer
Poster Session

#4652 Deciphering neutrophil heterogeneity to enhance therapeutic efficacy of TRAIL (Tumor necrosis factor-related apoptosis-inducing ligand) in triple negative breast cancers.

Manjari Kundu Sil[1], Wenqi Wu[2], Lichun Ma[2], Stan Lipkowitz[1]

[1]Women's Malignancies Branch, National Institute of Health, CCR, NCI, Bethesda, MD,[2]Cancer Data Science Laboratory, National Institute of Health, CCR, NCI, Bethesda, MD

TRAIL induces apoptosis in many preclinical cancer models including breast cancer models and has been extensively studied as a potential cancer therapeutic target. However, the clinical efficacy of TRAIL agonists is limited, suggesting that there are unknown modulatory mechanisms responsible for the lack of activity in patients. Our prior work demonstrated that TRAIL induces various cytokines (CXCL1, CXCL2, CXCL3, CXCL8, CXCL11, IL6) via NFKB2-dependent pathway in triple negative breast cancers (TNBC), promoting the recruitment of immunosuppressive neutrophils, suggesting that neutrophil-mediated regulation of the tumor immune microenvironment modulates TRAIL activity in TNBC. Thus, this study aims 1) to characterize the neutrophil heterogeneity induced by TRAIL as well as derived factors from TRAIL treated TNBC, and 2) to identify targetable pathways that could reprogram neutrophils towards an anti-tumor phenotype, thus enhancing TRAIL efficacy. To address this, neutrophils isolated from a healthy donor were incubated with 4 different conditions: serum-free media (SFM), SFM supplemented with TRAIL (SFM-T), conditioned media from TNBC (CM), or conditioned media from TRAIL-treated TNBC (T-CM). Single cell RNA sequencing (scRNA-seq) of neutrophils (43,420 cells) across the 4 conditions indicated that there are 10 transcriptionally distinct clusters. These findings were further validated with scRNA-seq of pooled neutrophils from 5 different healthy individuals (35,500 cells). *t*-SNE analysis identified similar transcriptionally distinct states encompassing inflammation, antigen presentation, and ribosome biogenesis programs, demonstrating remarkable neutrophil heterogeneity. Based on literature and functional relevance, we focused on 2 key clusters that were increased upon treatment of the neutrophils with T-CM identified in both experiments. One is enriched for antigen-presentation genes and immunosuppressive markers such as *CCL4*, *CD274*, *IL1A*, and *IL1B*, and a second enriched for ribosome biogenesis-related genes including *DDX21*, *UTP18*, *LAGE3*, and *NPM1*. These clusters also exhibited low expression of IFN-gamma/alpha-responsive genes, further suggesting the immunosuppressive role of T-CM. In contrast, SFM-T treatment resulted in a population with markers regulating neutrophil-specific function (e.g. NETosis, degranulation). The Sc-RNA-seq findings are currently being confirmed by gene expression analysis and surface staining methods. Collectively, our study delineates a potential mechanistic role of supernatants from TRAIL treated TNBC cells and neutrophil plasticity. These findings imply that targeting the innate immune system may modulate the effects of TRAIL on TNBC tumors enhancing the therapeutic outcomes.

#4653 TC-PTP-mediated regulation of p38 MAPK signaling induces epidermal apoptosis in response to UVB irradiation.

Rodrigo Vidales, Lindsey Shim, Subhash Chauhan, Dae Joon Kim

University of Texas Rio Grande Valley, McAllen, TX

T-cell protein tyrosine phosphatase (TC-PTP) is a non-receptor PTP that has been shown to have various roles in signaling pathways. Our previous studies have demonstrated that the TC-PTP deficiency in the epidermis can exacerbate hyperplastic response by inducing epidermal cell proliferation in response to tumor promoter TPA or UVB exposure. This implies that TC-PTP plays a tumor-suppressive role in the epidermis and provides protection against UVB radiation, which is well known to contribute to skin cancer development. In the present study, we aim to elucidate the molecular mechanisms by which TC-PTP influences the p38 MAPK pathway and its subsequent effects on cellular responses to UVB exposure. We utilized transgenic mice that specifically overexpress TC-PTP in the epidermis (*K5HA.Ptpn2*) and immortalized primary keratinocytes (IPKs) derived from both FVB mice (TC-PTP/WT) and *K5HA.Ptpn2* mice (TC-PTP/OVER). Upon UVB irradiation, the overexpression of TC-PTP in keratinocytes leads to an increase in apoptosis, which plays a protective role by removing damaged cells. Consistent with *in vitro* results, epidermal thickness induced by UVB was significantly decreased in *K5HA.Ptpn2* mice. The phosphorylation of p38 MAPK was increased progressively over time, reaching its peak expression at 12 hours post-UVB exposure in both TC-PTP/OVER IPKs and *K5HA.Ptpn2* mice. This effect was not observed in similarly treated control IPKs and FVB mice. Western blot analysis revealed a significant increase in the levels of cleaved Caspase-3 and PARP in TC-PTP/OVER IPKs following UVB treatment. FACS analysis confirmed that higher levels of apoptotic cells were observed in TC-PTP/OVER IPKs compared to TC-PTP/WT IPKs following UVB treatment. Similarly, annexin V staining was particularly more pronounced in TC-PTP overexpressing keratinocytes compared to control keratinocytes. Pretreatment with SB203580, p38 MAPK inhibitor, before UVB exposure led to an increase in cell viability in TC-PTP/OVER IPKs with decreased apoptotic response, suggesting that UVB-induced apoptotic response is mediated via the TC-PTP/p38 MAPK axis. Our findings reveal insights into the protective role of TC-PTP against UVB-induced skin damage via the regulation of p38 MAPK signaling pathway. Understanding the interaction between TC-PTP and the p38 MAPK signaling pathway is essential, as these underlying molecular mechanisms could be a potential therapeutic target for skin cancer prevention and treatment.

#4654 *Leptospermum petersonii* methanol and ethyl acetate crude extracts as antimetastatic and apoptotic effects against pancreatic and prostate cancer cells.

Lesetja Motadi[1], Maria Matlou[2]

[1]University of Johannesburg, Johannesburg, South Africa,[2]Biochemistry, University of Johannesburg, Johannesburg, South Africa

Cancer remains number one health care challenge worldwide with an estimation of 1 in 9 people developing cancer in their lifetime. As cancer becomes increasingly prevalent, research focuses on finding palliative care and natural treatments that could transform cancer therapeutics. The aim of the project was to investigate the anti-cancer and anti-metastatic effects of medicinal plant *Leptospermum petersonii*'s active compounds against pancreatic and prostate cancer cells. The following techniques were employed: TLC, Column and NMR chromatography, alamarblue assay, ATP assay, wound healing assay, Hoechst Staining, caspase assay, Agarose gel (DNA fragmentation analysis) and RT-PCR. Through cell viability assay and IC_{50} of approximately 100 µg/mL for the methanolic crude extract was identified with greater cytotoxic effect on MIA PaCa-2 than PC3 cells. The EtOAc extract showed cytotoxicity indices IC_{50} > 100 µg/mL signifying 60% of the cells were viable even at a dose of 100 µg/mL and thus led to the termination of additional testing because of its ineffective potency. Caspase 3/7 assay and DNA fragmentation had shown some positive result in support of apoptosis. Wound healing demonstrated untreated cells healed the gap in 24 hours, whereas treated cells took longer to do so. Gene expression showed upregulation of RB1 and checkpoint 1 which are necessary for DNA damage and apoptosis induction. In conclusion, the results suggest that there might be compounds within *L. petersonii* extracts that can be exploited for anticancer agent.

#4655 Carnosic acid inhibits proliferation and induces apoptosis of breast cancer cells.

Amanda L. Kornel, Evangelia Tsiani

Brock University, St. Catharines, ON, Canada

Breast cancer remains a major cause of cancer-related mortality among women worldwide, contributing to an estimated 670,000 deaths in 2022. Although advances in early detection and systemic therapy have improved outcomes, incidence rates continue to rise, and therapeutic resistance—particularly in aggressive subtypes such as triple-negative breast cancer (TNBC)—remains a critical challenge. Plant-derived chemicals have historically served as a source of anticancer agents, exemplified by the clinical success of paclitaxel, highlighting the continued potential of plant-derived compounds.In this study, we examined the anticancer effects of carnosic acid (CA), a polyphenolic diterpene abundant in rosemary, sage, and oregano, across multiple breast cancer subtypes. CA significantly suppressed proliferation of TNBC cell lines (MDA-MB-231, HCC70, HCC1143) and Luminal A cell lines (MCF7, T47D) in a dose-dependent manner with IC_{50} values in the range of 30 to 78 μM, (MDA-MB-231: 77.92 μM; HCC70: 63.51μM; HCC1143: 38.56 μM; T47D: 30.29μM).CA induced apoptotic cell death, confirmed by increased Annexin V/PI staining and elevated levels of cleaved PARP in MDA-MB-231, MCF7, and T47D cells. Additionally, CA promoted autophagy, demonstrated by enhanced LC3A/B-II accumulation and increased Beclin-1 expression.These anti-proliferative and pro-apoptotic effects of CA were associated with robust activation of AMP-activated protein kinase (AMPK) signaling, as evidenced by increased phosphorylation of AMPK and its downstream target, acetyl-CoA carboxylase (ACC).Collectively, these data indicate that carnosic acid suppresses breast cancer cell proliferation, induces apoptosis and autophagy with a concomitant AMPK activation. These findings support CA as a promising plant-derived therapeutic candidate and justify further evaluation in in vivo breast cancer models.

#4656 A Novel FOLR1 and TRAIL-R2 targeting bispecific antibody to treat ovarian cancer.

Shiva Bhowmik[1], William Brady[2]

[1]Purdue University, West Lafayette, IN,[2]University of Washington, Seattle, WA

We report a first-in-class tumor antigen dependent apoptotic inducing bispecific antibody, TRAILBody™, that co-targets FOLR1 and TRAIL-R2, selectively inducing TRAIL-R2 mediated apoptotic cell death with superior selectivity and efficacy. In a head-to-head comparison with the recently approved ADC drug, Elahere, FOLR1 TRAILBody showed superior activity. Extensive in vitro and in vivo analyses across ovarian cancer cell lines, patient-derived xenografts (PDX), and murine models demonstrate that FOLR1 TRAILBody drive high-level tumor-specific apoptosis independent of ADCC, significantly overcoming limitations of FcγR-mediated TRAIL-R2 clustering. Mechanistically, FOLR1 functions as a clustering anchor for TRAIL-R2, yielding enhanced receptor oligomerization, rapid caspase-3 activation, and robust cell death in FOLR1+ ovarian cancer models. Preclinical models confirm optimal stability, avidity, and selective tumor localization with minimized off-target toxicity. Notably, FOLR1 TRAILBody show superior regression of cisplatin-resistant PDX tumors and improved safety profile compared to clinically tested monospecific TRAIL-R2 antibody agonists, including minimized liver accumulation and hepatotoxicity with reduced levels of AST/ALT in blood. This study reveals a previously unappreciated mechanism in antibody therapeutics: the use of a tumor-enriched anchor (FOLR1) to optimize death receptor clustering and activation, enabling a quantum leap in apoptotic signaling and therapeutic index for ovarian cancer. The TRAILBody platform thus offers a foundation for next-generation immuno-oncology agents and revives hope for the clinical translation of death receptor agonism, particularly in solid tumors marked by immune exclusion and therapeutic resistance.

#4657 Antigenic cancer persister cells survive direct T cell attack.

Brandon E. Mauch[1], Michael Wang[2], August (Gus) Finley Williams[2], Tania Barazande-Pour[1], Filipe Araujo-Hoffman[3], Sophie Harris[4], Cooper Lathrop[1], Matthew Hangauer[5]

[1]UCSD Moores Cancer Center, La Jolla, CA,[2]University of California San Diego - UCSD, La Jolla, CA,[3]Stanford University, Stanford, CA,[4]The University of Miami Miller School of Medicine, Miami, FL,[5]UC San Diego Health, San Diego, CA

Cancer persister cells survive cytotoxic drug stress through nongenetic mechanisms, but it is unclear whether cancer cells enter a similar survival state during immunotherapy. Using a long-term coculture model of human melanoma cells with antigen-specific CTLs, we found that antigenic cancer cells can enter a persister state in response to CTL attack and survive despite delivery of granzyme B, mitochondrial outer membrane permeabilization, and apoptotic caspase activation. Although both CTL- and drug-tolerant persister cells undergo sublethal apoptosis, they differ markedly in their transcriptomes, pro- and anti-apoptotic factors, and vulnerabilities, including opposite ferroptosis sensitivities. CTL-tolerant persister cells occupy a caspase-inhibited state partially dependent on inhibitor of apoptosis proteins, yet exhibit multiple stress-dependent features including DNA damage and mutagenesis, and are growth-arrested as a result of IFNγ-IDO1-mediated tryptophan starvation. Apoptotic caspase activity protects CTL-tolerant persister cells from potent caspase-independent death and suppresses type I IFN production. Persister cell features are enriched in inflamed tumors that regressed during immunotherapy in vivo and in surgically resected human melanoma ex vivo. These findings reveal a sublethal apoptotic persister state that allows cancer cells to survive CTL attack and identify a targetable barrier to durable immunotherapy responses.

#4658 Novel Bcl-2/Bcl-xL inhibitor, LP-118, enhances apoptosis induction by the CDK2/9 inhibitor, fadraciclib, in BRAF(V600E) human colorectal cancer cells.

Md Mohiuddin[1], Vanda Povoa[2], Beatriz Sebo[2], Rita Fior[2], Frank A. Sinicrope[1]

[1]Department of Medicine, Gastrointestinal Research Unit, Mayo Clinic Alix School of Medicine, Rochester, MN,[2]Champalimaud Centre for the Unknown, Champalimaud Research, Champalimaud Foundation, Lisbon, Portugal

Background: The *BRAF(V600E)* mutation in colorectal cancer (CRC) is associated with treatment resistance and a poor prognosis. CDK2/9 is frequently activated in human cancers, and we have previously shown that $BRAF^{V600E}$ can upregulate MCL-1, which can be suppressed by the selective CDK2/9 inhibitor fadraciclib. Herein, we determined whether targeting CDK2/9 by fadraciclib can be enhanced by concurrent Bcl-2/Bcl-xL inhibition using LP-118, which minimizes platelet toxicity in patients, compared to the Bcl-2 inhibitor venetoclax. Effects of the drugs on apoptosis, colony formation and tumor growth were studied in a zebrafish model.

Methods: We utilized isogenic human RKO ($BRAF^{V600E/V600E/WT}$) and T29 ($BRAF^{WT/-/-}$) CRC cell lines in addition to HCT-116 ($BRAF^{WT}$) and *Bax* knockout (HCT-$116^{Bax-/-}$) CRC cells. Cells were treated for 24h with fadraciclib (500nM) plus encorafenib (500nM) in the presence or absence of LP-118 (1μM) or venetoclax (1μM). Apoptosis and cell growth inhibition were assessed using annexin V/PI staining and colony formation assays, respectively. Expression of MCL-1, Bcl-xL, Bcl-2, PARP, and cleaved caspase-3 (Asp175) proteins was analyzed. In a zebrafish tumor xenograft model, the effects of the drugs on caspase-3 cleavage and tumor growth were then evaluated.

Results: Fadraciclib suppressed MCL-1 expression, induced apoptosis and significantly inhibited colony formation in all CRC cell lines. However, this effect was enhanced by encorafenib only in RKO ($BRAF^{V600E/V600E/WT}$) cells. The addition of LP-118 to fadraciclib plus encorafenib potently enhanced apoptosis induction, shown by annexin V and cleavage of PARP, caspase-3, in RKO and HCT-116 cell lines, which was synergistic and *Bax* dependent. Treatment with LP-118 combined with fadraciclib and encorafenib suppressed both Bcl-xL and MCL-1 expression in RKO cells. The addition of LP-118 to fadraciclib plus encorafenib enhanced apoptosis (annexin V) to a greater extent than did venetoclax. In a zebrafish tumor xenograft model, the addition of LP-118 to fadraciclib plus encorafenib significantly enhanced caspase-3 activation and reduced the tumor xenograft size.

Conclusion: LP-118 synergistically enhanced the antitumor activity of fadraciclib plus encorafenib in $BRAF^{V600E}$ human CRC cells, and to a greater extent than did venetoclax. Mechanistically, targeting Bcl-2/Bcl-xL concurrent with inhibition of MCL-1 and CDK2/9 by fadraciclib potently induced apoptosis and suppressed tumor cell growth. These findings suggest a novel and effective therapeutic strategy for $BRAF^{V600E}$ human CRCs.

#4660 Mcl-1 inhibitors and antidepressants as enhancers of chemotherapy response in pleural mesothelioma.

Francisco A. Molina-Pelayo[1], Cristian G. Medina[1], Jaylon C. Aggison[1], Naren Li[1], Siqi Wu[1], Hainin Yang[2], Michele Carbone[2], Yuan Xu[1], Robert T. Ripley[1]

[1]Surgery, Baylor College of Medicine, Houston, TX,[2]University of Hawaii Cancer Center, Honolulu, HI

Background: Pleural mesothelioma (PM) remains a highly lethal malignancy with limited therapeutic options. Chemotherapy with cisplatin (CDDP) and pemetrexed provides modest benefit which is limited by primary resistance mechanisms involving dysregulated apoptotic signaling. Myeloid Cell Leukemia (MCL)-1 is a Bcl-2 family member that blocks apoptosis by targeting the mitochondria which works synergistically with activation of autophagy to promote chemoresistance. Targeting MCL-1 lowers the apoptotic threshold and may suppress autophagy to enhance chemosensitivity and improve therapeutic response. This study aimed to determine whether combining MCL-1 inhibition with the antidepressant, desmethyl-clomipramine (DCMI), will enhance chemosensitivity via autophagy in PM cells.

Methods: IC_{50} calculations of CDDP, the MCL-1 inhibitor (AZD-5991), DCMI and the combinations were performed in PM cell lines H28 and H2452. Synergistic interactions were quantified using the Highest Single Agent (HSA) model. To explore autophagy, cells were treated with the autophagy inhibitor, chloroquine (CQ, 10 μM), as a positive control and analyzed for known markers, LC3 and p62, by Western blot. In addition, MCL-1 expression after DCMI combination treatments was evaluated. Cell death and apoptosis were evaluated by flow cytometry (Anexin V and PI) following treatment. Mitochondrial and glycolytic metabolic parameters were quantified by Seahorse XF.

Results: CDDP + AZD-5991 exhibited robust synergy (HSA = 10.51, $p < 0.0001$ in H2452; HSA = 9.06, $p < 0.0001$ in H28). In contrast, CDDP and DCMI produced limited interaction in H2452 cells (HSA = 2.48, $p = 0.0015$) and a near-additive effect in H28 cells (HSA = 0.76, $p = 0.175$). However, the combination of CDDP, AZD-5991, and DCMI revealed synergistic activity at lower AZD-5991 concentrations, suggesting enhanced potency. DCMI promoted accumulation of p62 and delayed LC3-II processing, consistent with inhibition of autophagy. Furthermore, DCMI + AZD-5991 increased apoptotic cells relative to CDDP alone. These findings suggest enhancement of apoptotic signaling via combined inhibition of autophagy and MCL-1 activity. Seahorse analysis revealed that DCMI decreased basal respiration in H2452, with no effect on H28 bioenergetics. MCL-1 decreases under CDDP + DCMI versus CDDP alone, indicating that DCMI enhances apoptotic priming via MCL-1 suppression and mitochondrial dysfunction.

Conclusion: These findings support that complementary mechanisms of DCMI blocking autophagy and MCL-1 promoted apoptosis will enhance the response to cisplatin. This cooperative mechanism reveals metabolic and anti-apoptotic vulnerabilities that could be exploited to overcome chemoresistance in mesothelioma. Further investigation is warranted to assess whether blocking autophagy will increase patient's response to chemotherapy.

#4661 Expression of the ferroptosis suppressor FSP1 but not GPX4 shows significant adverse prognostic effect in diffuse large B-cell lymphoma with wild-type *TP53*.

Beibei Lyu[1], Zijun Xu-Monette[1], Xiaoxian X. Zhao[2], Eric D. Hsi[3], Ming Chen[4], Carlo Visco[5], Alexandar Tzankov[6], Karen Dybkaer[7], Mu-En Wang[4], Chang Wang[1], Qingyan Au[8], Harry Nunns[8], Zenggang Pan[9], Benjamin Parsons[10], Santiago Montes-Moreno[11], Fenghuang Zhan[12], Michael B. Moller[13], Leon Bernal-Mizrachi[2], Youli Zu[14], Shanxiang Zhang[15], Weina Chen[16], Govind Bhagat[17], Yong Li[18], KEN H. YOUNG[1]

[1]Department of Pathology, Duke University Medical Center, Durham, NC,[2]Wake Forest University School of Medicine, Winston-Salem, NC,[3]Mayo Clinic, Rochester, MN,[4]Duke University School of Medicine, Durham, NC,[5]University of Verona, Verona, Italy,[6]University Hospital Basel, Basel, Switzerland,[7]Aalborg University Hospital, Aalborg, Denmark,[8]NeoGenomics Laboratories, Aliso Viejo, CA,[9]University of Colorado School of Medicine, Aurora, CO,[10]Gundersen Lutheran Health System, La Crosse, WI,[11]Hospital Universitario Marques de Valdecilla/IDIVAL, Santander, Spain,[12]University of Arkansas, Little Rock, AR,[13]Odense University Hospital, Odense, Denmark,[14]Assoc. Professor of Pathology, The Methodist Hospital-Cornell University, Houston, TX,[15]Duke University Medical Center, Omaha, NE,[16]University of Texas Southwestern Medical Center, Durham, NC,[17]Columbia University Irving Medical Center, New York, NY,[18]Baylor College of Medicine, Houston, TX

Introduction: Diffuse large B-cell lymphoma (DLBCL) is the most common type of malignant lymphoma. Previous studies have shown that DLBCL cells are susceptible to GPX4 (Glutathione peroxidase 4)-regulated ferroptosis, an iron-dependent type of programmed cell death characterized by increased reactive oxygen species and excessive lipid peroxidation. In addition to GPX4, FSP1 (Ferroptosis suppressor protein 1, previously known as AIFM2) is a glutathione-independent repressor of ferroptosis that has shown prognostic significance in solid tumors. In this study, we aimed to reveal the significance of GPX4 and FSP1 in DLBCL.

Patients and Methods: We performed immunohistochemistry (IHC) for GPX4 and FSP1 in a large cohorts of patients with de novo DLBCL, and evaluated their cytoplasmic and nuclear expression. Prognostic analysis was performed for FSP1 and GPX4 expression in patients treated with rituximab (R)-CHOP or CHOP chemotherapy, respective of TP53 mutation status, as p53 regulates ferroptosis and TP53 mutation is associated with poorer prognosis in DLBCL.

Results: FSP1 expression with a ≥10% cutoff was positive in 42.3% of DLBCL cases. Patients with TP53 mutations had a non-significant trend of higher mean FSP1 expression than those with wild-type (Wt) TP53 (P=0.11). Prognostic analysis revealed that cytoplasmic FSP1$^+$ expression was associated with significantly poorer overall survival and progression-free survival in Wt-TP53 DLBCLs treated with R-CHOP (P=0.016 and P=0.003, respectively), and only showed non-significant unfavorable trends in TP53 mutated DLBCLs and patients treated with CHOP. In contrast, GPX4 expression did not show a significant unfavorable prognostic effect in DLBCL, and in fact, was associated with a non-significant trend of better survival. Previously we have quantified immune cell abundance and PD-1/PD-L1 expression in the tumor microenvironment of the study cohort using multiplex fluorescent IHC. Correlative analysis found that FSP1$^+$ patients had significantly higher mean and median abundance of CD68$^+$ cells (both M1 and M2 macrophages) and CD11c$^+$ cells than FSP1- patients. Further analysis in Wt-TP53 and mutated TP53 subcohorts found that only in the TP53 mutated DLBCL subcohort, FSP1 expression was associated with significantly higher mean and median CD163$^-$CD68$^+$ (M1) and overall CD68$^+$ macrophages, whereas in the Wt-TP53 DLBCL subcohort, FSP1 expression was associated with significantly higher median (but not mean) CD163$^+$CD68$^+$ (M2) macrophages and CD11c$^+$ cells.

Summary: Cytoplasmic FSP1 expression but not GPX4 had significantly adverse prognostic effect in patients with Wt-TP53 DLBCL treated with standard immunochemotherapy. Our results also suggest that in addition to ferroptosis regulation, macrophage abundance was relevant for the prognostic effects of FSP1 expression.

#4662 The mitochondrial antioxidant mitoquinone alters cancer cell death outcomes in response to therapy.

Christopher W. Clark[1], Xingping Qin[1], Cameron Fraser[2], Jessalyn Ubellacker[2], Kristopher A. Sarosiek[1]

[1]Environmental Health, Harvard T.H. Chan School of Public Health, Boston, MA,[2]Molecular Metabolism, Harvard T.H. Chan School of Public Health, Boston, MA

Background: Cell death resistant cancer cells are challenging to treat with existing therapies and are major drivers of recurrence, morbidity, and mortality. Novel cell death-modulating drugs show promise for enhancing the therapeutic efficacy of first-line chemotherapeutic agents and may potentially improve patient outcomes. Both apoptosis and ferroptosis sensitivities are known to be modulated by changes in the redox environment from excessive oxidative stress, however, the mechanisms that determine cell commitment to each form of cell death are unclear. Therefore, to investigate how cell death outcomes might be adapted by changes to the cellular redox environment we used the mitochondrial antioxidant Mitoquinone (MitoQ) as a tool compound to dissect differences between apoptosis and ferroptosis outcomes in response to chemotherapeutic agents.

Methods: Wild-type and $BAX^{-/-}BAK^{-/-}$ HeLa (human cervical cancer) cells, as well as B16-F10 (metastatic murine melanoma) wild-type cells were treated with MitoQ (0.1-1 μM) alone or in combination with either an apoptosis-inducing cocktail of BH3 mimetics (1 μM ABT-263 + 1 μM S63845) or a ferroptosis-inducing cocktail (1 μM RSL3 + 1 μM Erastin2). Inhibitors of apoptosis (Q-VD-OPh) and ferroptosis (Ferrostatin-1) were used as controls to confirm the cell death modality. After 48 hours, cell viability and stage of cell death were assessed by flow cytometry using TMRE staining, CellEvent Green Caspase 3/7 Reporter, Annexin V, and DAPI to detect mitochondrial outer membrane permeabilization, caspase activation, phosphatidylserine externalization and plasma membrane permeabilization, respectively.

Results: In wild-type cancer cell lines, increasing MitoQ concentrations (doses up to 0.3 μM) enhanced the induction of apoptosis in response to BH3 mimetics but suppressed ferroptosis induction in response to GPX4/System xc^- inhibition. Across all three cell lines, treatment with high doses of single-agent MitoQ (1 μM and above) induced a significant increase in cell death, even in BAX/BAK-deficient cells.

Conclusion: These findings suggest that modulation of mitochondrial oxidative stress via MitoQ modulates cancer cell death outcomes, promoting apoptosis while suppressing ferroptosis at low doses. Further work is needed to elucidate the molecular mechanisms underlying these effects and their implications for modulating cancer cell death modalities to improve cancer therapy outcomes.

#4663 BGB-21447, a next-generation Bcl-2 inhibitor, demonstrates superior potency and overcomes Venetoclax resistance in preclinical models of hematologic malignancies.

Shuran Li[1], Shasha Yang[1], Xiaolong Yang[1], Yanwen Ma[1], Shining Nie[1], Longbo Yin[1], Qin Wang[1], Haimei Xing[1], Zhu Mei[1], Ali Wang[1], Xiaolin Liu[1], Ying Guo[1], Haitao Wang[1], Weiwei Song[1], Lin Li[1], Lu Lyu[1], Yiwen Wang[1], Jin Wei[1], Chuanxiu Wang[1], Ye Liu[1], Xi Yuan[1], Yunhang Guo[1], Yu Shen[2], Lai Wang[2], Xiaomin Song[1]

[1]BeOne Medicines (Beijing) I GmbH, Beijing, China,[2]BeOne Medicines (Shanghai) Research & Development I GmbH, Beijing, China

Bcl-2 is a key anti-apoptotic gatekeeper that controls intrinsic apoptosis pathway. Its overexpression or aberrant activation is frequently observed in hematologic malignancies, where it promotes tumorigenesis and confers resistance to chemotherapy. Venetoclax (VEN), the first-in-class Bcl-2 inhibitor approved for R/R CLL and AML, shows modest efficacy in non-Hodgkin lymphoma and is compromised by acquired BCL2 mutations (e.g., G101V, D103Y).

Herein, we report the preclinical characterization of BGB-21447, a highly potent and selective next-generation Bcl-2 inhibitor that demonstrates remarkably better potency than VEN across multiple hematologic cancer cell lines and effectively targets a broad spectrum of VEN-resistant Bcl-2 mutations. BGB-21447 displays ≥121-fold higher selectivity for Bcl-2 over Bcl-xL, Bcl-W, Mcl-1 and Bcl2A1. Across a panel of 9 hematologic lines, it consistently achieved lower IC_{50} values than VEN (0.18-6.6 nM vs 4.8-238 nM for Ven). In RS4;11 cells overexpressing Bcl2 mutants, BGB-21447 achieved IC_{50} values of 11-44 nM IC_{50}s, including G101V (15 nM vs 3854 nM for VEN) and D103Y (44 nM vs 4731 nM for VEN). Its anti-proliferative effects were accompanied by hallmark features of intrinsic apoptosis, including caspase-3/7 activation, phosphatidylserine externalization (Annexin V positivity), and sub-G0/G1 DNA accumulation.

In PK/PD studies, oral administration of BGB-21447 demonstrated a clear exposure-response relationship in both RS4;11 wild-type and Bcl-2-G101V knock-in xenograft models, with cleaved caspase-3 levels correlating with intratumoral drug concentration. At 1.5 mg/kg, BGB-21447 showed superior antitumor efficacy compared to VEN at 15 mg/kg and ABBV-453 (AbbVie's selective Bcl-2 inhibitor) at 1.5 mg/mL. in the RS4;11 WT model. Notably, BGB-21447 showed robust antitumor effects in VEN-insensitive models, including the Toledo (DLBCL), RS4;11 Bcl2-G101V, and RS4;11 Bcl2-D103Y xenografts. No significant weight loss or laboratory toxicities were observed.

In conclusion, BGB-21447 surpasses VEN in potency and mutant coverage, and durably inhibits VEN-resistant tumors at well-tolerated doses in preclinical models. These findings support the ongoing Phase 1 clinical trials (NCT05828589, NCT06756932) evaluating BGB-21447 in B-cell malignancies and metastatic breast cancer.

#4664 Impacts of endothelial cell autophagy inhibition on tumorigenesis.

Nancy Esmeralda Leon-Rivera, Brayden Chin, Teresa Monkkonen

Biology, San Diego State University, San Diego, CA

Metastasis is the leading cause of cancer related mortality, and this burden is particularly severe in breast cancers lacking hormone receptor expression. These patients have limited treatment options and poorer outcomes. Endothelial cells are important regulators of metastasis, as they control vascular integrity and migration of circulating tumor cells into other tissues. Inhibition of autophagy, a conserved degradative process which promotes metabolic adaptation in tumor cells, is being tested as a targeted therapy for breast and other cancers. However, the impact of autophagy inhibition on the tumor vasculature and metastasis is poorly understood. To determine how endothelial autophagy influences breast tumor progression, we generated endothelial cell specific *Atg12* and *Atg5* knockout (ECKO) mice driven by the Cdh5CreER vascular endothelial cadherin promoter. In orthotopic transplantation of *MMTV-PyMT* tumor organoids and genetic crosses to *PyMT* mice, *Atg12* ECKO mice displayed delayed primary tumor growth compared to controls. Mid- stage *Atg12* ECKO tumors exhibited increased apoptosis, whereas proliferation and necrosis were unchanged at endpoint, indicating that endothelial cell autophagy promotes efficient tumor cell survival during mid-stage cancer progression. Despite increased $CD31^+$ vascular density, *Atg12* ECKO tumors demonstrated elevated HIF1-α, consistent with impaired vascular function and hypoxia. Following surgical resection of primary tumors, *Atg12* ECKO mice demonstrated higher rates of tumor recurrence and lung metastasis, and tail vein injection of *PyMT* cells into tumor naïve mice confirmed enhanced metastatic outgrowth. To test whether these effects were tumor type specific, we used the Rat insulin promoter-SV40 Large T antigen (RIP-Tag) model of pancreatic neuroendocrine tumors, which are highly vascular and sensitive to anti-angiogenic therapy. Neither early nor late endothelial deletion of *Atg12* altered primary tumor burden or survival, in contrast to the *PyMT* findings. However, *Atg12* ECKO mice displayed increased liver micrometastasis, indicating that the effects of endothelial autophagy loss are highly context specific. These results highlight the context dependent roles of endothelial autophagy in shaping tumor growth and metastasis, underscoring the need to consider strategies to limit changes to metastasis with autophagy inhibition strategies in cancer therapy.

#4665 Programmable multivalent siRNA nanostructure rewires apoptosis by co-silencing MCL-1 and BCL-XL in glioblastoma.

Qianhui Feng, Henry Lin, Yichen Yan, Rong Zheng, Yang Xu, Hao Yan

Arizona State University, Tempe, AZ

Background: Glioblastoma is one of the most aggressive and treatment-resistant brain cancers. Many standard treatments fail because glioblastoma cells rely on powerful survival proteins, especially MCL-1 and BCL-XL, to block cell death, which stabilizes mitochondrial integrity, suppresses caspase activation, and maintains the survival of glioblastoma. Pharmacologic inhibitors of these proteins face dose-limiting toxicities and incomplete target suppression. To overcome these barriers, we engineered a multivalent siRNA nanostructure that enhances functional activation of RNAi modules within tumor cells.

Methods:A branched multivalent siRNA nanostructure was first engineered using GFP-targeting siRNAs to validate multivalent RNAi performance in U251-GFP glioblastoma cells. This model enabled assessment of cooperative gene silencing, spatial organization-dependent activity, and prolonged knockdown efficiency. Upon confirming the effectiveness of multivalent RNAi silencing, the nanostructure was redesigned to present siRNAs targeting MCL-1 and BCL-XL, thereby overcoming anti-apoptotic signaling and engaging the intrinsic apoptosis pathways. Functional testing, including qPCR, confocal microscopy, western blotting, mitochondria-dependent apoptosis assays, and long-term knockdown stability, was conducted to evaluate dual-gene silencing and apoptotic activation in U251 glioblastoma cells.

Results: The GFP-targeting multivalent siRNA nanostructure exhibited strong cooperative silencing in U251-GFP cells, achieving a sustained reduction in GFP fluorescence of over 90% for up to 7 days, demonstrating enhanced potency, improved intracellular stability, and superior durability compared to a single siRNA. The therapeutic multivalent siRNA nanostructure targets MCL-1 and BCL-XL, achieving robust dual-gene suppression at both mRNA and protein levels. Co-silencing of these anti-apoptotic nodes triggered mitochondrial activation of caspase-9/3 signaling, confirming reactivation of the apoptotic pathway. Cells exhibited a pronounced loss of viability and reduced colony-forming capacity.

Conclusions: This study established a programmable multivalent siRNA nanostructure capable of both validating multivalent RNAi using GFP and achieving therapeutic co-targeting of MCL-1 and BCL-XL to overcome apoptotic resistance in glioblastoma. The observed strong apoptotic activation supports the potential of this modular RNAi nanotechnology for treating refractory and malignancies. This approach offers a clinically translatable, programmable strategy for next-generation multi-target RNA interference therapies.

#4666 CAPZB suppresses disulfidptosis through SQOR interaction to drive intrahepatic cholangiocarcinoma progression and therapeutic vulnerability.

Jiangqiao Yao[1], Tong Chen[1], Ziyan Chen[1], Gang Chen[2], **Chongming Zheng**[3], Yi Wang[1]

[1]Department of Epidemiology and Biostatistics, Wenzhou Medical University, Wenzhou, China,[2]The First Affiliated Hospital of Wenzhou Medical University, Wenzhou Medical University, Wenzhou, China,[3]The First Affiliated Hospital of Wenzhou Medical University, Wenzhou, China

Background: Intrahepatic cholangiocarcinoma (ICC) is an aggressive malignancy with limited therapeutic options. Disulfidptosis, a novel cell death modality triggered by disulfide stress, represents a promising therapeutic target. While CAPZB has been implicated in disulfidptosis, its role in ICC remains undefined. This study investigates whether CAPZB regulates disulfidptosis via SQOR to promote ICC progression.

Methods: Transcriptomic analysis of three ICC cohorts (n=98) and single-cell RNA-seq (n=4) evaluated CAPZB expression and prognostic significance. CAPZB was genetically modulated in ICC cell lines using shRNA/overexpression constructs. Disulfidptosis was induced by glucose deprivation and assessed via cell viability, F-actin staining, and NADP+/NADPH/GSH/GSSG ratios. Protein interactions were identified by IP-MS and validated by co-immunoprecipitation. AKT/NICD mouse models evaluated in vivo tumor progression. Patient-derived organoids were treated with GLUT1 inhibitor BAY-876.

Results: CAPZB was significantly overexpressed in ICC tissues and correlated with poor overall survival ($p<0.01$). Single-cell analysis revealed elevated CAPZB in malignant cholangiocytes. CAPZB knockdown suppressed proliferation, migration, and invasion, while overexpression enhanced malignant phenotypes. IP-MS identified SQOR as a CAPZB-interacting protein, with strong expression correlation ($p<0.001$). CAPZB knockdown promoted disulfidptosis under glucose deprivation, increasing cell death ($p<0.001$), F-actin contraction, and NADP+/NADPH ratio. SQOR overexpression partially rescued these effects. In vivo, CAPZB knockdown reduced tumor burden ($p<0.01$). Patient-derived organoids showed BAY-876 sensitivity (IC_{50}=0.315 μM). Combination therapy with CAPZB knockdown and BAY-876 demonstrated synergistic anti-tumor efficacy ($p<0.001$). Conclusions: CAPZB is a disulfidptosis-related oncogene that drives ICC progression by interacting with SQOR to maintain redox homeostasis and suppress disulfidptosis. Targeting CAPZB alone or with GLUT1 inhibitors induces synthetic lethality via disulfidptosis, offering a promising therapeutic strategy.

Clinical Significance: This study identifies the CAPZB-SQOR axis as a novel disulfidptosis regulator in ICC and demonstrates synergistic anti-tumor effects of dual targeting CAPZB and glucose metabolism, providing a translational framework for disulfidptosis-based therapies.

#4667 Targeting ULK1 overcomes autophagy-mediated chemoresistance in cancer cell.

Eun-Jung Kim, Youngjun Park

Jeju National University, Jeju-si, Korea, Republic of

Autophagy is a tightly regulated, lysosomedependent recycling process that preserves energy balance and proteostasis during stress, thereby promoting cell survival. Although chemotherapy aims to eliminate malignant cells, many tumors acquire resistance by engaging prosurvival autophagy. To disable this escape, we targeted Unc51like kinase 1 (ULK1), the initiator of autophagosome biogenesis. We generated a library by modifying reported ULK1 inhibitor scaffolds and screened for blockade of autophagic flux using an LC3GFPmCherry tandem reporter. Western blotting verified ontarget suppression, including phosphorylated ATG13 reduction and p62 accumulation, which nominated a novel lead compound. By treating this compound with standard chemotherapeutics in multiple cancer cell lines, cell death was increased concomitant with the blunted autophagic flux. These data support ULK1 as a tractable node to overcome autophagymediated chemoresistance and rationalize ULK1 inhibition as a combination strategy to deepen chemotherapy responses. Future study will evaluate antitumor efficacy and tolerability in vivo to advance a novel ULK1 inhibitor toward preclinical development.

#4668 Targeting the histone acetyltransferase GCN5 sensitizes cancer cells to ferroptosis.

Ling-Chu Chang[1], Shih-Kai Chiang[2], Shuen-Ei Chen[2]

[1]China Medical University Hospital, Taichung, Taiwan,[2]National Chung Hsing University, Taichung, Taiwan

Ferroptosis is an iron-dependent form of regulated cell death with emerging significance in cancer. However, its full regulatory network, particularly epigenetic regulation, remains poorly understood. Here, we identify the histone acetyltransferase GCN5 as a critical novel mediator of ferroptosis. We demonstrate that the ferroptosis inducers Erastin and RSL3 trigger reactive oxygen species (ROS) production, lipid peroxidation, and labile iron accumulation in a GCN5-dependent manner. Genetic knockdown or pharmacological inhibition of GCN5 ameliorated Erastin/RSL3-induced mitochondrial dysfunction (including ROS, lipid peroxidation, and impaired dynamics), restored endoplasmic reticulum (ER) homeostasis, and normalized autophagic flux. Furthermore, Erastin/RSL3 upregulated several transcription factors in a GCN5-dependent manner. Notably, HDAC inhibitor-induced cell death was synergistically enhanced by Erastin or RSL3, suggesting a compelling combination therapy strategy.In conclusion, our work establishes GCN5 as a central regulator of ferroptosis, governing its execution through mitochondrial, autophagic, and nuclear pathways. These findings nominate GCN5 as a therapeutic target to sensitize cancers to ferroptosis.

#4669 Label free identification of cancer cell death pathways via holotomography and deep learning as an early pharmacodynamic biomarker.

Minwook Kim[1], Park Weisun[1], Geon Kim[1], Sanggeun Oh[2], **Juyeon Park**[1], Jihwan Yu[1], Hyun-Suk Min[2], Sumin Lee[3], Won Do Heo[1], YongKeun Park[1]

[1]KAIST, Daejeon, Korea, Republic of,[2]Tomocube, Inc., Daejeon Metropolitan, Korea, Republic of,[3]Sumin Lee (Individual)

Accurate measurement of regulated cell death (RCD)—including apoptosis, necroptosis, and necrosis—is critical for oncology drug development and mechanism-of-action studies. Conventional fluorescence assays introduce phototoxicity, labeling bias, and incompatibility with long-term or high-frequency pharmacodynamic monitoring. We developed a fully label-free platform that integrates 3D holotomography (HT) and deep learning to classify RCD phenotypes directly from intrinsic refractive-index (RI) signatures, enabling non-perturbative, mechanism-aware drug-response biomarkers.HeLa cells were induced into apoptosis, necroptosis, or necrosis using canonical biochemical triggers, with fluorescence markers (Annexin V, PI, Hoechst) used solely for ground truth. 3D RI tomograms acquired by HT-X1 Plus were converted to 2D maximum-intensity-projection (MIP) patches to train an ImageNet-pretrained CNN to classify five states (live-control, live-treated, apoptosis, necroptosis, necrosis) using a sliding-window/majority-vote strategy. Temporal concordance was evaluated through synchronized HT–fluorescence time-lapse imaging and flow cytometry. For subtle drug-induced phenotypes (doxorubicin, cisplatin), performance of full 3D volumetric models was compared with 2-D projections to assess the necessity of depth information. Cross-cell-line robustness was tested on A549 cells with minimal fine-tuning.The five-state classifier achieved 99.3% accuracy on held-out HeLa datasets, with misclassifications limited to the apoptosis–necroptosis boundary. HT-based predictions identified early necroptotic transitions 2–4 hours before Annexin V/PI fluorescence, and population-level dynamics closely matched flow cytometry, establishing an earlier, dye-free pharmacodynamic window. In drug-response experiments, 3D volumetric models outperformed all 2D approaches, capturing spatially heterogeneous, mechanism-rich morphological signatures (76–88% accuracy in 3D vs. 50–55% in 2D MIP and 0% in SUM projections). The HeLa-trained model generalized poorly to A549 cells initially (50.4% accuracy), but small-data fine-tuning restored near-perfect performance, demonstrating practical assay portability across cancer cell types.Holotomography-based AI provides a fully label-free, segmentation-free, real-time biomarker for distinguishing RCD pathways and quantifying early drug responses with high accuracy. The platform detects necroptosis hours earlier than biochemical assays, resolves subtle drug-induced morphologies, and adapts rapidly to new cell types. These capabilities position HT-AI as a scalable pharmacodynamic tool for mechanism-of-action profiling, cytotoxicity testing, and high-content oncology drug discovery, enabling longitudinal, non-destructive phenotyping beyond fluorescence-based methods.

#4670 Multimodal mechanistic control of autophagy by the CtBP1/KAISO/TRIM28 Complex in breast cancer cells.

Young-Ho Lee[1], Kevin L. Gardner[2]

[1]Columbia university, New York, NY,[2]Vagelos College of Physicians & Surgeons, New York, NY

Autophagy plays a context-dependent role in breast cancer progression, alternately promoting or suppressing tumor survival. However, the transcriptional and metabolic mechanisms for autophagy remain poorly understood. Here, we identify a CtBP1/Kaiso/Trim28 transcriptional regulatory complex as a key metabolic sensor that coordinates both transcriptional control of autophagy genes in the nucleus and structural regulation of autophagic machinery in the cytoplasm. We demonstrate that this CtBP1/Kaiso/Trim28 complex mediates multimodal control of autophagy in response to glucose availability. Genome-wide chromatin occupancy (CNR-seq) and transcriptomic profiling (RNA-seq) across luminal (MCF7) and triple-negative (MDA-MB-231) breast cancer cells reveal that CtBP1 directs complex assembly at promoters of key autophagy-related genes, including *ULK1*, *MTOR*, *VPS34*, and *TFEB*. Loss of CtBP1 or Kaiso leads to de-regulation of these targets, underscoring their cooperative role in maintaining autophagic balance. Proximity ligation assays detect CtBP1/Kaiso/Trim28 complexes in both nucleus and cytoplasm, highlighting their “moonlighting” function together with autophagic components such as LC3 in regulating autophagosome formation and stability. Several of these complexes display glucose-dependent dynamics, directly linking metabolic flux to autophagic regulation. Together, these findings uncover a previously unrecognized CtBP1-linked multimodal mechanism that integrates metabolic signals with both transcriptional and structural control of autophagy. The defined coordination between CtBP1, Kaiso, and Trim28 establishes a critical metabolic-autophagy axis in breast cancer and suggests new therapeutic strategies targeting CtBP1-mediated metabolic adaptation in therapy-resistant tumors.

#4671 Autophagy alterations in KRAS-mutant colorectal cancer following PRMT5 inhibition.

Komalpreet Kaur[1], Danbee Chae[1], Daniel Aguaiza[1], Netanel Louloueian[1], Shloimie Lowy[1], SANJAY GOEL[2], Radhashree Maitra[1]

[1]Biology, Yeshiva University, New York, NY,[2]Oncology, Rutgers Cancer Institute, New Brunswick, NJ

Introduction: The KRAS mutation is found in 45% of Colorectal Cancer (CRC) patients. Evidence indicates upregulation of Protein Arginine Methyltransferase 5 (PRMT5) expression in 75% of KRAS-mutated CRC patient tumor samples and suggesting PRMT5 as a surrogate therapeutic target for KRAS Mutant CRC treatment. The exact mechanism of crosstalk between PRMT5 and mutant KRAS is poorly understood. This study evaluates the mechanism of autophagy induction under PRMT5 inhibition and the possible apoptotic transition.
Methodology: Four CRC cell lines, HCT116, SW640 (KRAS mutant), HKE3, and LIM2405 (KRAS wild type), were treated with three inhibitors, EPZ015666 (EPZ), GSK3326595 (GSK), and AMG-193 (AMG), each at 0.5 μM, 1 μM, and 10 μM, and assessed at 24 h and 48 h. Western blot analysis was conducted for ATG5, BECLIN1, BRG1, LC3B, ULK1, and ACTIN (housekeeping) to quantify autophagy regulation. Fold-change values and p-values were used to determine significance, and comparisons were made across drug, dose, time point, and KRAS mutation status.
Results: All three PRMT5 inhibitors elicited the autophagy pathway, with varying temporal and dose-dependent effects. EPZ showed autophagy induction at most doses at 24 h, yet regulation fluctuated over further timepoints, suggesting induction without any clear shift toward either sustained flux or apoptosis. GSK demonstrated mild early induction at 24 h, which was followed by marked reductions. Notably, at 0.5 μM concentration, ULK1 ($p=0.002$) and BECLIN1 ($p=0.023$) were significantly downregulated at 48 h, suggesting that an initial trigger of the pathway is followed by autophagy collapse. AMG caused the highest activation with strong induction (Fold Change>2.5, $p=0.045$), observed at 48 h at concentrations of 1 and 10 μM; however, the absence of significant increases to LC3B suggests impaired flux and a transition toward apoptosis. EPZ and GSK both also demonstrated BECLIN1-independent initiation of autophagy across early doses and timepoints.
Conclusion: Across four CRC lines, PRMT5 inhibition enhanced autophagy signaling, significantly in KRAS-mutant backgrounds. AMG consistently caused the strongest activation across early and late autophagy markers, indicating potent disruption of PRMT5-regulated stress-response circuits. We are currently investigating the onset of apoptosis under these treatment conditions by western blotting and gene expression by transcriptomics. This work aims to identify therapeutic targets within the autophagy-apoptosis axis to improve PRMT5 inhibitor-mediated cancer cell killing.

#4672 Neuropeptide Y Y1 receptor inhibition induces autophagy to limit colorectal cancer progression.

Sooraj Kakkat, Prabhat Suman, Aris Richter, Steven B McClellan, Debanjan Chakroborty, Chandrani Sarkar

University of South Alabama, Mobile, AL

Introduction: Deregulation of autophagy in colorectal cancer (CRC) increases cell proliferation, disrupts intestinal epithelial cell homeostasis, and contributes to therapeutic resistance. Therefore, determining the mechanisms by which CRC cells evade autophagy is important for developing new therapeutic strategies. The present study aimed to investigate the role of neuropeptide Y (NPY), a neurohormone that is overexpressed in CRC, and its receptors in regulating CRC cell growth and survival.
Methods: The status of NPY and Y1 receptor (Y1R) expressions in CT26 (ATCC) and MC38 (Kerafast) mouse CRC cells was determined by western blot analysis. NPY and Y1R expressions in human colon adenocarcinomas and mouse colon cancer tissues were determined by immunohistochemistry. In vitro cell proliferation assays and flow cytometry were performed to determine the effects of blocking Y1R by antagonist (BIBO3304 trifluoroacetate) or by siRNA-mediated silencing of Y1R in CT26 and MC38 cells. Western blot and qRT-PCR were also performed to determine the changes related to autophagy upon blocking/silencing Y1R. To elucidate the underlying mechanism of Y1R inhibition-induced autophagy, the signaling pathway was analyzed. The impact of the Y1R inhibition on tumor growth and progression was assessed in vivo.
Results and Conclusion: Our analysis revealed a significant increase in NPY and Y1R expressions in human colon adenocarcinoma and mouse orthotopic CRC tissues. NPY is primarily secreted by CRC cells that express Y1R on their surfaces. Suppression of Y1R with both an antagonist and siRNA resulted in significant inhibition of proliferation and increased autophagy in CRC cells. Also, the levels of autophagy markers (ATG3, ATG12, ATG16L, LC3A, ATG5, LC3B and BECN1) were significantly enhanced with the inhibition of Y1R. Further analysis revealed that autophagy was induced in CRC cells via AMPK activation, leading to mTOR inhibition. Our results, therefore, indicate that targeting Y1R with clinically safe antagonists may represent a promising therapeutic strategy to suppress tumor growth and restore autophagy-mediated tumor suppression in CRC. These findings suggest a decisive role for the NPY/Y1R axis in regulating CRC cell behavior and indicate the potential of targeting Y1R with clinically safe Y1R inhibitors to improve therapeutic outcomes in CRC.

#4673 Targeting BCL2 pathway to enhance immunogenicity in *ALK+* NSCLC.

Batkhishig Munkhjargal[1], Sudha Mudumana Sadasivan[2], Shirish M. Gadgeel[3], Amanda Pilling[4]

[1]Henry Ford Health System, Detroit, MI,[2]Henry Ford Health System, Troy, MI,[3]Henry Ford Hospital, Detroit, MI,[4]Hematology/Oncology, Henry Ford Health System, Detroit, MI

Background: Translocations of the Anaplastic Lymphoma Kinase (ALK) gene occur in 3-5% of Non-Small Cell Lung Cancer (NSCLC) patients and are treated with ALK tyrosine kinase inhibitors (TKIs). However, resistance to ALK TKIs develop through on-target mutations and bypass signaling. Treatment response to ALK TKIs also relies on apoptosis, a complex mechanism regulated by BCL2 family proteins. Therefore, dysregulation of this pathway promotes tumor progression and therapy resistance. It has been reported that cancer cells depend on anti-apoptotic proteins of BCL-2 family (e.g. BCL-2, MCL-1, BCL-xL) for their survival. This has led to the development of BH3 mimetics, which are inhibitors of anti-apoptotic proteins. ALK+ NSCLC is considered an immune “cold” tumor with low immunogenicity, demonstrated by fewer neoantigens and lack of cytotoxic tumor-infiltrating lymphocytes (TILs), leading to limited efficacy of immune checkpoint-targeting therapies in these patients. Some TKIs have been reported to elicit durable antitumor immunity by inducing immunogenic cell death (ICD) through the release of damage-associated molecular patterns (DAMPs). However, this has not been studied in the context of ALK+ NSCLC.We hypothesized that ALK-directed therapy in combination with BH3 mimetics would initiate ICD through the release of DAMPs and increase sensitivity to ALK TKIs.

Methods: We evaluated the efficacy of ALK TKIs (Lorlatinib, Alectinib) alone and in combination with the BH3 mimetics navitoclax (BCL-2/BCL-xL inhibitor), venetoclax (BCL-2 inhibitor) and s63845 (MCL-1 inhibitor) to induce damage-associated molecular patterns (DAMPs) in ALK+ NSCLC cell lines.

Results: ALK+ cancer cell lines exhibited high expression of MCL-1 and BCL-xL proteins, indicating their dependency on BCL-2 family proteins for survival. The addition of BH3 mimetics enhanced apoptosis induction, as evidenced by increased PARP cleavage, and further reduced colony formation efficiency compared to ALK TKI single-agent treatment. Both ALK TKI single agent and combination treatment with BH3 mimetics induced key DAMPs essential for ICD, including: (1) increased type I interferon signaling via IFN-β (3-7-fold) and CXCL10 (2-3-fold); (2) peak release of extracellular ATP at 7 hours of treatment; and (3) enhanced phosphorylation of eIF2α compared to the control.

Conclusions: ALK-directed therapy has the potential to induce immunogenic cell death (ICD) and elicit antitumor immune responses. Combining BH3 mimetics with ALK TKIs can be a promising therapeutic strategy to enhance anti-tumor immunity and overcome ALK TKI resistance in ALK+ NSCLC

#4674 Activation of a STAT3/LATS1 signaling axis by folate receptor alpha enables breast cancer cells to resist ferroptosis.

Prajakta Prasad Ambegaokar[1], Hira Goel[2], Arthur M. Mercurio[3]

[1]Molecular, Cell and Cancer Biology, UMass Chan Medical School, Worcester, MA,[2]Research Assistant Professor, Cancer Bio. Dept., Univ. of Massachusetts Medical School, Worcester, MA,[3]Interim Chair & Professor, Dept. of Cancer Bio., University of Massachusetts Medical School, Worcester, MA

Dynamic changes occurring in the tumor microenvironment that carcinoma cells encounter during their progression can trigger ferroptosis, a form of cell death characterized by the iron-dependent lipid peroxidation of cell membranes. This phenomenon is exacerbated during metastasis as tumor cells in circulation are exposed to conditions of matrix-detachment, oxidative stress and high iron concentration. Many tumor cells withstand these conditions to survive, which suggests they have acquired mechanisms to resist ferroptotic stimuli. Our goal in this study was to identify specific cell surface proteins expressed on breast cancer cells that promote ferroptosis resistance since such proteins can serve as therapeutic targets. To achieve this goal, we used an unbiased approach that involved analysis of single-cell RNA sequencing data (scRNA-seq) that we obtained from an organoid derived from a breast cancer patient that was exposed to a ferroptosis-inducing drug, imidazole ketone erastin (IKE). Differential gene expression analysis of this scRNA seq revealed that folate receptor α (FRα) is significantly expressed in ferroptosis non-responder populations. Subsequently, we demonstrated a causal role for FRα in promoting resistance to ferroptosis induced by both IKE and matrix detachment in breast cancer cell lines (CAL51 and T47D). We verified the ability of FRα to activate STAT3 and observed that STAT3 drives ferroptosis resistance in our model. To understand how STAT3 promotes ferroptosis resistance, we identified LATS1, a key regulator of Hippo signaling that phosphorylates and inactivates YAP and TAZ. Using chromatin immunoprecipitation, we observed that STAT3 binds to the LATS1 promoter region and that inhibition of STAT3 reduces LATS1 gene and protein expression. We also found that STAT3-mediated regulation of LATS1 inhibits YAP, which is known to promote ferroptosis sensitivity. To investigate a mechanism for how inhibition of YAP by STAT3/LATS1 contributes to ferroptosis resistance, we focused on the ability of YAP to regulate Acyl-CoA synthetase long-chain family member 4 (ACSL4), an enzyme that triggers ferroptosis by remodeling lipid membranes in cells. Our data revealed that STAT3 and LATS1 have a causal role in inhibiting YAP-mediated induction of ASCL4 expression. Together, these data highlight a novel role for FRα in promoting ferroptosis resistance by a mechanism that is dependent on LATS1. Ongoing studies are aimed at investigating the ability of FRα and LATS1 to enhance metastasis by promoting ferroptosis resistance. This work also suggests that FRα could be an effective therapeutic target for mitigating metastatic breast cancer.

#4675 Integrated real-time impedance and fluorescence imaging to characterize NETosis.

Tian Wang[1], **Xiaoyu Zhang**[2], Grace Yang[1], Peifang Ye[1], Nancy Li[2]

[1]Agilent Technologies, Hangzhou, China,[2]Agilent Technologies, La Jolla, CA

NETosis is a specialized form of neutrophil cell death characterized by the release of web-like DNA structures and associated proteins, known as neutrophil extracellular traps (NETs). Two main pathways mediate NETosis[1,2]: (1) classical “suicidal” NETosis, which involves cell lysis following NET release, typically occurs within 3-4 hours and depends on reactive oxygen species (ROS) generation via NADPH oxidase; and (2) “vital” NETosis, where NETs are extruded through vesicles within 1-2 hours while the cell remains intact. NETosis plays a dual role in host defense and disease, contributing to antimicrobial immunity as well as pathological inflammation, thrombosis, and autoimmunity[3]. In this study, differentiated neutrophil-like HL-60 (dHL-60) and primary human neutrophils were treated with a small set of compounds: PMA, which triggers suicidal NETosis; A23187, a pharmacological agent that induces rapid, vital NETosis; and camptothecin, an apoptotic compound. To visualize NET formation, the cells were cultured in media containing eTox Green, a membrane-impermeable DNA-binding dye. The morphological and physiological changes were continuously monitored via both impedance readout, reported as Cell Index, and live-cell imaging simultaneously on an xCELLigence RTCA eSight system. Our results show that: (1) the extent of DNA-binding dye staining distinguished apoptosis from NETosis, with NETosis inducers PMA and A23187 producing larger green fluorescence areas than the apoptotic agent camptothecin, reflecting that extruded NETs are substantially larger than nuclei; (2) suicidal NETosis induced by PMA was differentiated from vital NETosis triggered by A23187 based on ROS dependency—NET release was completely inhibited by DPI, an NADPH oxidase blocker, after PMA treatment but not after A23187 exposure. Additional distinctions included earlier onset of NET extrusion with A23187 and neutrophil death following PMA stimulation but not A23187 treatment; and (3) PMA-induced NETosis was associated with a transition from suspension to adherent states, which was monitored and quantified by impedance measurements. In conclusion, this real-time, noninvasive impedance-imaging approach enables visualization of NETosis, quantification of NET release kinetics via fluorescence imaging, and monitoring of neutrophil transitions between suspension and adherent states through impedance measurements. This integrated method provides a robust and versatile platform for mechanistic NETosis studies, drug-screening applications, and broader investigations into neutrophil-driven pathologies.

#4676 Therapeutic exploitation of AUTAC in hematologic malignancies with cardiac protection.

Ahmed M. Elshazly, Nayyerehalsadat Hosseini, Senthil K. Radhakrishnan

Virginia Commonwealth University, Richmond, VA

Background: Myeloid cell leukemia-1 (Mcl1) is a critical member of the Bcl_2 family that plays an essential role in regulating apoptosis and maintaining mitochondrial integrity, particularly within cardiac tissue. While Mcl1 overexpression is a major driver of resistance to multiple anticancer therapies, its pharmacologic inhibition has been hampered by dose-limiting cardiotoxicity, representing a significant and unresolved challenge in cardio-oncology. The development of safer therapeutic strategies that selectively target Mcl1 in cancer cells while sparing cardiac cells remains a high-priority goal. In this study, our group investigated a novel autophagy-targeting chimera (AUTAC) designed to selectively degrade Mcl1 via the autophagy-lysosomal pathway. We aimed to determine whether AUTAC could induce selective cytotoxicity in multiple myeloma cells while preserving cardiac cell viability and mitochondrial function.
Methods: Multiple myeloma cell lines (U266B1, RPMI-8226) and cardiac cell lines (AC16, H9c2) were used as tumor and cardiac models, respectively. Cell viability was assessed using the CellTiter-Glo assay and IncuCyte live-cell imaging. Mitochondrial membrane potential was measured by TMRE fluorescence. Effects of AUTAC on Mcl1 and autophagy dynamics were evaluated by Western blotting, confocal microscopy, and inhibition studies with 3-methyladenine (3-MA) and chloroquine (CQ). To confirm autophagy dependence, ATG5 was knocked down using shRNA.
Results: Treatment with AUTAC selectively induced lysosomal degradation of Mcl1, without detectable effects on other anti-apoptotic Bcl_2 family members, including Bcl_2 and Bcl_{xL}. Pharmacological inhibition of autophagy with 3-MA (early-stage inhibitor) or CQ (late-stage inhibitor) effectively blocked AUTAC-mediated Mcl1 degradation, confirming that the process required an intact autophagy-lysosomal pathway. Furthermore, knockdown of ATG5 abolished Mcl1 reduction, reinforcing the autophagy dependence of this degradation mechanism. Functionally, AUTAC treatment led to a greater than 50% reduction in cell viability in U266B1 and RPMI-8226 multiple myeloma cells, accompanied by increased apoptotic signaling. In contrast, AUTAC caused minimal cytotoxicity in AC16 and H9c2 cells, maintaining mitochondrial function and morphology. Compared with conventional Mcl1 inhibitors, AUTAC exhibited substantially reduced cardiotoxicity, underscoring its favorable safety profile.
Conclusions: Targeted lysosomal degradation of Mcl1 via AUTAC represents a promising therapeutic strategy that repurposes autophagy for selective oncogenic protein removal. AUTAC effectively degraded Mcl1 in malignant cells while sparing cardiac cells from apoptosis and mitochondrial injury, highlighting its potential as a next-generation, cardio-safe alternative to conventional Mcl1 inhibitors.

#4677 Estrogen induces cell death in non- reproductive cancer cells through disrupting mitotic spindle assembly.

Pu Liang[1], Song Zeng[2], Wei Chen[3], Dong Li[3], Wei Feng[4], Xiaopeng Hu[2], Wensheng Wei[5], Xin Liang[3], Xi Wang[1]

[1]Beijing Ditan Hospital, Capital Medical University, Beijing, China,[2]Beijing Chaoyang Hospital, Capital Medical University, Beijing, China,[3]School of Life Sciences, Tsinghua University, Beijing, China,[4]Institute of Biophysics, Chinese Academy of Sciences, Beijing, China,[5]School of Life Sciences, Peking University, Beijing, China

Cancer epidemiology shows consistent sex dimorphism across many non reproductive cancers: males typically have earlier onset, higher incidence, and worse outcomes. While these differences have been partly attributed to differential exposure to risk factors, they persist after adjustment, implicating intrinsic biological contributors. Changes in cancer behavior around the menopausal transition further implicate estrogenic environments in modulating core processes such as cell division and tumor survival. Here, we examine effects of high concentrations of estrogen on proliferation in multiple non reproductive cancer types, including bladder cancer. We find that estrogen induces tumor cell death through a mechanism independent of classical estrogen receptors (ERα, ERβ, and GPER). To identify mediators of this cytotoxicity, we conducted an unbiased whole genome CRISPR knockout screen. Notably, the ten most significant genes—KIFC1, TPX2, LIN37, KIF4A, KIF18B, KIF2C, WDR62, CLASP1, CLIP1, and VPS37C—are all required for spindle assembly and function. These results implicate spindle assembly as a key determinant of cellular sensitivity to estrogen. Kinetic studies showed that estrogen inhibits both microtubule polymerization and depolymerization. Biochemical analysis identifies estrogen binds αβ-tubulin dimers and acts as a negative catalyst of microtubule dynamics, impairing spindle assembly, disrupting mitosis, and triggering cell cycle-associated death pathways. Consistent with this model, overexpression of the microtubule polymerase Ch-TOG attenuates estrogen's effects. Together, these data suggest that elevated estrogen levels can compromise spindle assembly and promote tumor cell death, providing a potential mechanism by which reproductive age females may be relatively protected from many non reproductive cancers and offering insight into the sex disparities observed in epidemiological studies.

: Insights into Genomic Instability
Poster Session

#4681 Probing the RecQL4 homolog Hrq1: A genetic suppressor screen identifies critical functional features.

Robert H. Simmons, Matthew Bochman

Molecular and Cellular Biochemistry, Indiana University, Bloomington, IN

The DNA repair helicase RECQL4 is a potent oncogene whose dysregulation is a hallmark of multiple cancers and diseases of genomic instability. Overexpression of RECQL4 is observed in human breast, ovarian, and liver cancers, where its expression is a biomarker for poor prognosis. Conversely, germline loss-of-function perturbations in the ATPase domain of the protein are linked to genetic diseases like Rothmund-Thomson syndrome that are characterized by high risk of developing osteosarcoma and lymphoma. This bifurcated role highlights that RECQL4 dosage and activity must be precisely tuned. Additionally, RECQL4 has a highly conserved function in the repair of DNA interstrand crosslink (ICL) damaging agents such as platinum-based chemotherapeutics, making this an important protein to understand for overcoming chemoresistance. However, mechanistic studies of RECQL4 are difficult to study *in vivo* as well as overexpress and purify because its N terminus contains an essential replication-initiation domain equivalent to *Saccharomyces cerevisiae's* Sld2. Therefore, we study the *S. cerevisiae* homologue of RECQL4, Hrq1. We use this model to discover more details about this protein's functions that can then be linked back to the human system. The ATPase-dead mutant of Hrq1 (*hrq1-K318A*) is profoundly hypersensitive to the ICL agent diepoxy butane (DEB), exhibiting a lethality far greater than the complete deletion strain (*hrq1Δ*). This defines a dominant-negative "protein-trapping" or "roadblock" phenotype. To identify how this toxic protein-DNA complex is resolved, we generated spontaneous suppressor colonies by plating *hrq1-K318A* strains on DEB. Whole-genome sequencing revealed that over 90% of screened colonies in the *hrq1-K318A* strain had a secondary mutation within the *hrq1* gene itself. Crucially, spot dilution assays confirmed that these intragenic suppressors rescue the K318A hypersensitivity back to the level of the *hrq1Δ* deletion. This provides powerful genetic evidence for the "roadblock" hypothesis, demonstrating the suppressors function by "defusing" the toxic K318A protein, reverting its phenotype to a simple loss-of-function. Further analysis of those results has revealed that many of the mutations are at highly conserved residues amongst RECQL4 and its homologues, suggesting important functional properties at those sites. Finally, we compared these genetic suppressors to a rationally-designed, DNA-binding-deficient mutant (*hrq1-R739A*). While *in vitro* assays confirmed reduced DNA binding, this mutation *in vivo* provided only a slight rescue of the K318A toxicity. This finding suggests the dominant-negative "trap" is a complex intermediate stabilized by more than DNA-binding alone—likely including key protein-protein interactions—and reveals critical mechanistic nuances for the design of future RECQL4-targeting therapeutics.

#4682 Metabolic enzymes as protective modulator of BRCA2 haploinsufficiency and genome instability.

Xiao Zi Huang[1], Tuan Zea Tan[2], C. Pawan K. Patro[2], Li Ren Kong[3], Ashok R. Venkitaraman[2]

[1]NUS Centre for Cancer Research, Yong Loo Lin School of Medicine, National University of Singapore (NUS), Singapore, Singapore,[2]Cancer Science Institute of Singapore, Singapore, Singapore,[3]Lee Kong Chian School of Medicine, Nanyang Technological University, Singapore, Singapore

Germline mutations in the BRCA2 tumor suppressor gene predispose individuals to various cancers. Our lab previously discovered that endogenous reactive metabolites selectively degrade BRCA2 below the protective threshold and transiently induced BRCA2 haploinsufficiency. This functional insufficiency promotes genome instability and drives cancer evolution, establishing a direct mechanistic link between metabolic stress and carcinogenesis. My project aims to uncover the cellular mechanisms that counteract metabolic stress and prevent BRCA2 depletion. I hypothesise that specific metabolic enzymes act as protective buffers by detoxifying reactive metabolites and maintaining BRCA2 stability. To investigate this, I employed isogenic cells modeling two distinct classes of BRCA2 mutations - truncating (+/3036del4) and missense (+/D2723H) mutations. These mutations differ in protein expression, subcellular localisation and some of the biochemical properties, making them ideal to examine how different subtypes of BRCA2 mutations influence cellular metabolic requirements.Using a dual-readout targeted metabolic CRISPR-Cas9 knockout screening, I identified metabolic genes essential for cell survival and maintenance of genome stability. The primary screen revealed subtype-specific dependencies, with truncating mutants showing heightened sensitivity to perturbations in energy metabolism, whereas missense mutants relied on DNA damage response-linked metabolic pathways. Focused analysis of the top hits identified distinct metabolic responses associated with energy balance, reactive oxygen species accumulation and ER homeostasis. Ongoing work focuses on mechanistic validation of high-priority candidate genes to elucidate how specific metabolic pathways safeguard BRCA2 function under stress. These findings reveal mutation-specific metabolic vulnerabilities and provide a foundation for identifying potential metabolic interventions to preserved genome stability in BRCA2 mutation carriers.

#4683 Loss of nuclear integrity at persistent DNA bridges ties PARP inhibitors to cGAS/STING signaling.

Ece Kocak[1], Kerry A. Larkin[1], Nicholas R. Ader[2], Yiduo Hu[3], Kevin Li[1], C. Patrick Lusk[1], Anna Dominika Staniszewska[4], Mark R. Albertella[4], Megan C. King[1]

[1]Cell Biology, Yale School of Medicine, New Haven, CT,[2]Biology, UNC Greensboro, Greensboro, NC,[3]Medical Oncology, University of Kansas Medical Center, Westwood, KS,[4]Oncology Targeted Discovery, AstraZeneca, Cambridge, United Kingdom

BRCA mutant tumors, deficient in homologous recombination DNA repair (HRR), exhibit some of the highest levels of tumor cell-intrinsic interferon (IFN)-stimulated gene (ISG) expression among The Cancer Genome Atlas primary tumors, consistent with preclinical studies tying DNA repair deficiency to increased ISG expression through an as yet poorly understood mechanism. The goal of our ongoing studies is to examine the contribution of mitotic errors to IFN signaling in BRCA-deficient cancer. We find that DNA bridges that persist beyond the abscission checkpoint into the following interphase occur more frequently with *BRCA1* deficiency. Treatment with PARP inhibitors (PARPi) including olaparib, saruparib, and AZD9574, which cause targeted tumor cell death of BRCA-deficient cells, further increases the frequency of persistent bridges. Similarly, PARPi induce an elevated number of persistent bridges in BRCA2-deficient prostate tumor xenografts but not in those that are competent for HRR. Our findings show that the majority of persistent bridges recruit the cytosolic DNA sensor cGAS *in vitro*, suggesting a loss of nuclear integrity that exposes the bridging DNA to the cytoplasm. Indeed, performing the first correlative light and electron microscopy (CLEM) of persistent DNA bridges, we find nuclear envelope (NE) ruptures at PARPi-induced bridges. cGAS is maximally activated by non-nucleosomal DNA, and we find the bridging DNA to be highly accessible as assessed by Tn5 transposition (ATAC-see). Surprisingly, our CLEM data reveals efficient NE repair at persistent bridges, which we tie to the robust recruitment of the NE repair factors BAF, LEM2 and CHMP7. This NE repair network may influence cGAS activation by the bridging DNA thereby influencing ISG expression. Consistent with this, knockdown of the most upstream NE repair factor, BAF, increases ISG expression and synergizes with PARPi. Taken together, our results demonstrate that PARPi treatment increases the frequency of persistent DNA bridges that are over-stretched, non-nucleosomal, and defective in nuclear integrity, leading to activation of cGAS-dependent IFN signaling. We are additionally investigating the prevalence of persistent bridges in patient samples and xenograft models to explore their potential use as a biomarker for PARPi sensitivity. Further elucidating the mechanisms contributing to ISG expression in BRCA-deficient cancers will provide novel insights into strategies for maximizing the therapeutic potential of PARPi treatment.

#4684 A RHNO1-ATR/Chk1 positive feedback loop sustains the cellular DNA replication stress response.

Niphat Jirapongwattana, Carley M. Conover, Catalina Trujillo Jaramillo, Adam R. Karpf

Eppley Institute, University of Nebraska Medical Center, Omaha, NE

Cancer cells are continually challenged by both intrinsic and extrinsic stresses that interfere with DNA replication, causing DNA replication stress (DRS). DRS can fuel cancer progression by increasing genomic instability, but if left unregulated, it can also cause widespread DNA damage and cell death. Consequently, cancer cells are highly dependent on the ATR/Chk1 signaling pathway to regulate DRS and ensure survival. Rad9-Hus1-Rad1 interacting nuclear orphan 1 (RHNO1) is a novel component of the ATR/Chk1 pathway and is often overexpressed in cancer cells with high DRS, where it contributes to chemotherapy resistance. However, the precise function of RHNO1 in the DRS response is still largely unknown. Here, we investigated the roles of RHNO1 in cancer progression and DRS response using an ovarian cancer cell (OVC) model in both in vitro and in vivo systems. Furthermore, we generated an endogenously HiBiT-tagged and degron-tagged RHNO1 cell line to precisely track RHNO1 levels and temporally deplete RHNO1 during different phases of the DRS response in HEK293T cells. Depletion of RHNO1 significantly reduces OVC proliferation rate, clonogenicity, and in vivo tumor growth, while extending host mouse survival. RHNO1 knockdown sensitized cells to hydroxyurea (HU), increasing cell death and micronuclei formation. Mechanistically, RHNO1 was upregulated and stabilized following DRS. Notably, we show that RHNO1 stabilization is mediated by ATR/Chk1 phosphorylation, which is also required for RHNO1 translocation to stressed replication forks. Interestingly, chromatin recruitment of RHNO1 appears to be independent of 9-1-1, a DNA clamp complex previously known to bind RHNO1. Furthermore, cells with stable RHNO1 knockdown demonstrated normal initial ATR/Chk1 signaling activation in response to HU treatment, however, at later time points, the absence of RHNO1 caused premature termination of ATR/Chk1 signaling despite the persistence of DRS. These findings are consistent with a dispensable role of RHNO1 in the initial activation of the ATR/Chk1 pathway but a key role in sustaining the ATR/Chk1 response. In summary, we demonstrated the RHNO1 promote critical OVC phenotypes and uncovered a novel positive feedback loop between RHNO1 and ATR/Chk1 signaling. This work identifies RHNO1 as a key component in maintaining the DRS response, highlighting its potential as a therapeutic target for cancers reliant on ATR/Chk1 signaling.

#4685 Intestinal inflammation triggers *POLE*^{P286R}-driven ultramutated colorectal cancer.

Md Kawsar Mustofa, He Zhang, Diego H. Castrillon, Hasan Zaki

UT Southwestern Medical Center, Dallas, TX

Pathogenic variants of DNA polymerase ε (POLE), such as P286R, result in high tumor mutational burden (TMB), particularly in endometrium and colorectal cancer (CRC). Here, we investigated the role of *POLE* mutations in CRC using a conditional mouse model expressing the *Pole*^{P286R} mutation in intestinal epithelial cells. We generated *LSL-Pole*^{P286R} knock-in mice and crossed them with *Vilin-Cre* mice to obtain intestinal epithelial cell-specific *Pole*^{P286R} mutant mice (PVC). Spontaneous tumor development in the small intestine and colon of PVC mice was monitored. *Additionally, effect of inflammation on POLE-driven colorectal tumorigenesis was monitored following induction of colitis with 2.5% dextran sulfate sodium (DSS).* PVC developed invasive adenocarcinoma in the small intestine (SI) with partial penetrance but did not develop any tumor in colon spontaneously. Surprisingly, induction of chronic colitis with DSS resulted in colorectal tumor development with 100% penetrance in PVC mice but not control wild-type mice. Tumors of PVC mice were pathologically diverse, with low-grade and high-grade dysplasia and invasive adenocarcinoma. Whole genome sequencing demonstrated that colorectal tumors of PVC mice bear high TMB, including recurring mutations in *Apc* and *Ctnnb1*. Consistently, there was increased expression of proliferative genes, including *cMyc, Ccnd1, Ki67,* and *Lgr5* and higher activation of Wnt/β-catenin, NF-κB, and ERK pathways. Notably, mice expressing intestinal *Pole*^{P286R} recovered faster from acute DSS-induced mucosal injury, prior to the development of tumors. In vitro organoid culture further confirmed that *Pole*^{P286R} mutant intestinal organoids grow faster and larger than those from control mice. These findings demonstrate that POLE plays a crucial role in the maintenance of intestinal genomic stability, and inflammation plays an essential role in driving ultra-mutated CRC in the presence of pathogenic *POLE* variants.

#4686 Lymphatic niches shield stem cells from malignant fate.

Ananya Goyal, Madison Conte, Shiri Gur-Cohen

UC San Diego, La Jolla, CA

Oncogenic mutations arise frequently in young tissues, yet most remain clinically silent, suggesting that non-genetic variables may act as major drivers of cancer initiation. With age, this landscape of tolerance gradually diminishes, allowing mutated cells to bypass restraint and initiate tumorigenesis. Although cancer has long been considered as a hallmark disease of aging, recent evidence shows its incidence is now rising sharply in younger individuals, particularly of squamous cell carcinomas (SCCs). Understanding how mutated cells tolerate oncogenic stress in youth, and why this tolerance collapses over time, may provide opportunities for preventive intervention. These considerations are particularly important in the context of stem cells (SCs) which serve as the cells of origin for many cancers and whose fate and fitness are tightly orchestrated by their microenvironment, or “niches.” Yet, the niche-derived signals that precede and direct tumor formation remain poorly understood. The lymphatic vasculature, recently identified as a SC niche, is consistently remodeled in tumors and associated with heightened risk of metastasis and death among cancer patients. To investigate the impact of the lymphatic niches on early-stage tumorigenesis, we used skin SCC as a model, and examined SC tolerance to oncogenic stress under lymphatic loss-of-function conditions. Deep volumetric imaging revealed that lymphatic dysfunction predisposes stem cells to genomic instability, marked by accumulation of DNA damage indicators such as γH2AX in non-dividing cells, even in the absence of carcinogen exposure. These findings suggest that intact lymphatic niches protect SCs from genomic instability and preserve tissue homeostasis. Using a novel stem cell-lymphatic organotypic model, we found that SCs co-cultured with lymphatic vessels exhibited reduced DNA damage compared to those cultured with stromal cells following exposure to suboptimal carcinogenic insults. To directly test whether lymphatic dysfunction accelerates tumorigenesis, we induced *Kras* activation and *p53* loss in *Sox9+* hair follicle SCs. Pharmacological perturbation of lymphatics in this model led expansion of mutant clones in the epidermis within three weeks post-induction and significantly earlier tumor onset. Together, these findings uncover a previously unrecognized role for the lymphatic vasculature in reprogramming stem cell vulnerability to oncogenic stress. By linking lymphatic integrity to genomic stability, this work highlights lymphatic-driven regulation as a potential target for early detection and prevention of SC-derived cancers, including age related metastatic disease.

#4687 The BRCT domain is a modular platform for signal transduction in the DNA damage response.

Nicholas Woods[1], **Thales Nepomuceno**[2], Rebekah Baskin[3], Rafael Mesquita[4], Volha Golubeva[5], Xueli Li[2], Nicholas Palermo[6], John M. Koomen[2], Alvaro N. Monteiro[2]

[1]UNMC Eppley Institute, F&P Buffett Cancer Center, Omaha, NE,[2]Moffitt Cancer Center, Tampa, FL,[3]Graduate Student, St. Jude Children's Research Hospital, Memphis, TN,[4]Federal University of Rio de Janeiro, Rio de Janeiro, Brazil,[5]Ohio State University, Columbus, OH,[6]University of Nebraska, Omaha, NE

Protein modular domains are critical for the cellular response to intra- and extracellular signaling, facilitating the assembly of dynamic multi-protein complexes in response to specific stimuli. The BRCA1 C-Terminal (BRCT) domain is present in 23 proteins in the human proteome, containing 46 individual BRCT modules organized as 14 singletons, 16 tandems, and one quartet of BRCT functional units. The BRCT singleton consists of a central core of four parallel beta sheets flanked by two alpha helices on one side and one alpha helix on the opposite side. The BRCT domain is a versatile protein-modular domain that has emerged as an integrator of signals in maintaining genomic integrity. We previously charted the protein-protein interaction network of seven tandem BRCT domains (tBRCT), revealing previously unknown components in DNA damage signaling. Here, we present a comprehensive BRCT-centered human protein-protein interaction network (PPN) comprising 46 BRCT domains organized into various domain architectures, building on our previous work. This network was determined by integrating data from literature curation, yeast two-hybrid (Y2H) screens, and tandem affinity purification coupled to mass spectrometry (TAP-MS) and comprises 3,162 highly curated BRCT-dependent interactions and 1,672 unique human proteins. The BRCT-containing protein PAXIP1 (also known as PTIP) is critical for DNA double-strand break repair by non-homologous end joining. PAXIP1 has a distinctive structural organization, containing three tBRCT domains, which present a unique set of PPN. Interestingly, the last four BRCT domains form a unique quartet (qBRCT) in the human proteome, binding to a set of proteins not observed in either of the tBRCTs alone. These data indicate that distinct interacting partners may be recruited by different combinations of higher-order BRCT domain organization to assemble inter- or intramolecular complexes, accommodating combinatorial interactions in response to genotoxic stimuli. Moreover, we mapped 62 unique phosphorylation sites at 19 BRCT domains. We identified that PAXIP1 qBRCT phosphorylation alters its binding to gH2AX, providing an additional layer of regulation by modulating BRCT-mediated ligand recognition. The BRCT PPN resource charted here provides a comprehensive analysis of these modular protein domains in the human proteome, contributing to an understanding of cancer and its response to genotoxic clinical therapies.

#4688 The nuclease EXO1 promotes genomic instability by degrading nascent DNA in BRCA-proficient cells.

Alexandra Nusawardhana, Claudia M. Nicolae, George-Lucian Moldovan

Molecular and Precision Medicine, Penn State College of Medicine, Hershey, PA

Genomic instability promotes carcinogenesis. DNA repair genes are generally considered tumor suppressors, as their inactivation is observed in tumors and is associated with carcinogenesis. Mutations in BRCA1 and BRCA2 genes are observed in breast, ovarian, and other cancers. BRCA pathway inactivation results in defective homologous recombination DNA repair, as well as in degradation of nascent DNA during replication stress. This degradation is catalyzed by nucleases including MRE11 and EXO1, and occurs at two types of DNA structures which are formed upon replication stress, namely single stranded DNA (ssDNA) gaps and reversed replication forks, eventually causing double strand DNA break (DSB) formation. However, most tumors are BRCA pathway-proficient. Here, we show that EXO1 is overexpressed in a significant proportion of tumors. EXO1 overexpression causes the degradation of nascent DNA at both ssDNA gaps and reversed forks, through its exonuclease catalytic activity. Importantly, EXO1-mediated nascent strand degradation occurs efficiently in BRCA-proficient cells, through its cooperation with MRE11. This results in increased DSB formation and hypersensitivity to genotoxic agents. We thus identify increased EXO1 activity as a mechanism of genomic instability similar to BRCA pathway inactivation, but occurring more frequently in tumors compared to BRCA inactivation.

#4689 Dynamic and defective repair of extrachromosomal DNA drives genome instability in cancer.

Shu Zhang[1], Yanbo Wang[2], Thomas B. K. Watkins[1], Xiaowei Yan[3], Aditi Gnanasekar[3], Jun Tang[3], Ivy T. Wong[3], Howard Y. Chang[4], Paul S. Mischel[2]

[1]Pathology, Stanford University, Stanford, CA,[2]Stanford University School of Medicine, Stanford, CA,[3]Stanford University, Stanford, CA,[4]Amgen, Stanford, CA

Extrachromosomal DNA (ecDNA) is megabase-sized circular DNA amplified exclusively in tumor cells, driving poor outcomes and therapeutic resistance. EcDNA represents a distinct form of genome instability associated with heightened replication stress and DNA damage. However, how ecDNA manages these elevated damage levels remains unclear. Here, we used long-read sequencing and live-cell imaging to investigate DNA damage repair dynamics and genomic patterns in isogenic cell lines harboring either ecDNA or homogeneously staining region (HSR). We found that damaged ecDNAs are preferentially sequestered into micronuclei following induction of double-strand breaks. This process triggers additional DNA damage beyond the initial lesions and impairs homologous recombination (HR) during knock-in by CRISPR-Cas9. Structural variant analyses further revealed that although ecDNA damage initiates HR repair, the process is frequently incomplete or aberrant. Analysis of whole-genome sequencing data from 14,778 tumors across 39 cancer types in the Genomics England cohort confirmed that ecDNA-positive cancers exhibit enriched HR deficiency (HRD) mutational signatures, even after excluding cases with canonical HRD driver mutations. Together, these findings delineate the dynamic and error-prone repair of ecDNA, linking it to HRD-associated genomic alterations. Our study exposes vulnerabilities of ecDNA-positive cancers that may be therapeutically exploited through synthetic lethality related to HRD.

#4691 Assessing prognostic and therapeutic associations across EMAST, MSI, and MSS among African Americans colorectal cancer subtypes.

Hassan Brim[1], Mudasir Rashid[1], Ahmed Imran[1], Somtochukwu Abazu[1], yumna siddiqui[1], Shweta Dixit[1], Anas Brim[1], Wardah Bajwa[1], Mrinalini Deverapal[1], Rumaisa Rashid[1], Aurmin Amirmokri[1], Chibuzor Nwachukwu[1], Neda Dezfuli,[1], Rabia Zafar[1], Gholamreza Oskrochi[2], Zaki Sherif[1], Adeyinka O Laiyemo[1], John Carethers[3], Babak Shokrani[1], **Hassan Ashktorab**[1]

[1]Howard University, DC, DC,[2]American University of the Middle East, Egaila, Kuwait,[3]UC San Diego, San Diego, CA

Background: Elevated Microsatellite Alterations at Selected Tetranucleotide Repeats (EMAST), microsatellite instability-high (MSI), and microsatellite stability (MSS) represent distinct forms of genomic instability and characterize colorectal cancer (CRC) genotypes related to DNA mismatch repair (MMR) deficiency and proficiency. EMAST is reported with a higher prevalence among African American (AA) vs White rectal cancers. The full clinical significance and phenotype of EMAST and its relationship with tumor characteristics, treatment factors, and patient outcomes remain unclear.

Aim: We compared clinical characteristics, treatment patterns, and survival outcomes across EMAST, MSI, and MSS genotypes among AA CRC patients, and evaluated whether these genotypes have distinct prognostic or therapeutic associations.

Methods: We retrospectively analyzed 304 CRC patients at Howard University, the majority being from AAs. Patients' CRCs were assessed for EMAST, MSI, and MSS via fragment analysis. Clinical variables, including demographics, survival, tumor location, and treatment history, were compared across groups. Remission and recurrence outcomes were assessed. Statistical significance was determined using p-values provided in the dataset.

Results: Patients with EMAST CRCs demonstrated higher overall[JC1] mortality when compared with patients with MSI and MSS CRCs (32% vs 18% vs 14%, respectively). The higher mortality between patients with MSI versus MSS CRCs may reflect a greater proportion of stage III tumors in the MSI vs MSS subgroup (n=14, 48.3% vs n=91, 39%) as advanced stage is strongly associated with poor survival. Patients with MSI CRCs demonstrated more right-sided tumors (46%) than patients with MSS (13%) or EMAST (15%) CRCs. Symptom-wise, gastrointestinal bleeding was the most frequent occurring in 25%, 19% and 12% of patients with MSS, EMAST, and MSI CRCs, respectively. Treatment-wise, chemotherapy was administered to 57%, 63% and 57% of patients with EMAST, MSI, and MSS CRCs, and 84%, 100%, 76%, respectively, were treated with radiotherapy. However, patient benefit was not equal based on the higher mortality of patients with EMAST CRCs. Demographic and clinical variables showed no significant differences ($p>0.05$) between patients with EMAST, MSS, and MSI CRCs. Similarly, we identified no differences among the 3 groups in overall survival or remission and recurrence rates ($p>0.05$).

Conclusions: Patients with EMAST CRCs have the highest mortality despite similar treatment exposures and comparable demographic and clinical characteristics amongst our three groups. As expected, patients with MSI CRCs demonstrate a predominance of right-sided cancers. Overall, the EMAST genotype aligns with being a biological modifier that associates with poorer patient outcomes.

#4692 Environmental toxin-induced m6A RNA modification promotes R-loop accumulation and chromosomal instability.

Rebekah Gridley[1], Palakshi Bandapalli[1], Sharmila Govindaraj[1], Siddhant Meshram[2], Suvo Chatterjee[2], Gurdeep Singh[1], **Arunkumar Ganesan**[1]

[1]Cell Biology & Physiology, University of New Mexico Health Sciences Center, Albuquerque, NM,[2]Department of Epidemiology and Biostatistics, Indiana University, Bloomington, IN

Chromosome instability (CIN) is a defining feature of cancer and a driver of tumor evolution. While genetic and epigenetic mechanisms underlying CIN are well characterized, the role of environmental carcinogens remains underexplored. Hexavalent chromium [Cr(VI)], a widespread groundwater contaminant in the United States, particularly in New Mexico, has been epidemiologically linked to increased cancer risk. Our study investigates the molecular consequences of Cr(VI) exposure in normal human colon epithelial cells, revealing a novel RNA-mediated pathway contributing to CIN. We demonstrate that Cr(VI) exposure induces epigenetic reprogramming, including the loss of repressive histone marks and disruption of heterochromatin. Notably, Cr(VI) downregulates METTL3, a key RNA N6-methyladenosine (m6A) methyltransferase, leading to reduced m6A modification and accumulation of genome-wide R-loops. Since m6A methylation is critical for R-loop resolution, its loss impairs RNA processing and genome stability. These findings suggest that Cr(VI)-induced m6A deficiency promotes R-loop persistence, thereby compromising genome integrity and facilitating CIN. Our investigation reveals a novel mechanism by which an environmental toxin induces genomic instability through RNA epigenetic dysregulation. It highlights the role of RNA modifications in genome stability and underscores the need to consider environmental exposures in cancer risk.

#4693 The cancer testis antigen, HORMAD1, promotes genomic stability in lung adenocarcinoma.

Ronnesha Johnson[1], Angelique Whitehurst[2], Anthony J. Davis[1], Luis Reza Herrera[1]

[1]UTSW, Dallas, TX,[2]Asst. Prof., Dept. of Pharmacology, UT Southwestern Simmons Comp. Cancer Ctr., Dallas, TX

Cancer-testis antigens (CTAs) are proteins whose expressions are typically restricted to the testes but are aberrantly expressed in cancer. There are over 200 known CTAs, most of which have no known function in cancer. In the testis, HORMA Domain Containing Protein 1 (HORMAD1) is expressed in meiotic cells, and recruits proteins to sister chromosomes for the exchange of genetic information during crossing over. HORMAD1 is necessary for crossing over, and mice lacking HORMAD1 are healthy, yet infertile. HORMAD1 is aberrantly expressed in approximately 50% of lung adenocarcinoma patient samples. Patient tumor expression data reveal that high HORMAD1 expression correlates with poor overall patient survival and increased mutational burden. HORMAD1-positive tumors are enriched for genes essential for the DNA replication stress response and DNA repair, including MRE11 and RAD51. HORMAD1 promotes the formation of RAD51 filaments, which accumulate in response to replication stress. Cancer cells undergo chronic replication stress and are able to proliferate while evading catastrophic DNA damage. To determine if HORMAD1 is directly associated with proteins involved in DNA metabolism, we conducted immunoprecipitation mass spectrometry and found that endogenous HORMAD1 associates with a subset of proteins involved in the replication stress response. We found that cells lacking HORMAD1 undergo nascent DNA strand degradation, which is mediated by the MRE11-DNA2-BLM pathway. Moreover, we found that HORMAD1 protects stalled replication forks that are remolded by F-Box DNA Helicase 1 (FBH1) to maintain fork stability. FBH1 negatively regulates the activity of RAD51 via displacement from DNA and/or through ubiquitination for degradation. We found that loss of HORMAD1 leads to single strand DNA gaps during replication. Moreover, we found that HORMAD1 protects FBH1-mediated gaps during replication, but the mechanism as to how HORMAD1 protects these gaps is unknown. We hypothesize that HORMAD1 recruits RAD51 to FBH1-mediated single strand gaps during replication to protect these gaps from degradation and promote genomic stability. Our data suggest that aberrant HORMAD1 expression reduces replication stress-induced DNA damage accumulation to prevent genomic instability. This research gives insight into the mechanism by which HORMAD1 promotes genomic stability and how this process can be targeted for lung adenocarcinoma treatment.

#4694 Oxidative base damage to telomeres sensitizes cancer cells to ATR inhibition.

Alex Garbouchian[1], Natalia Cestari Moreno[1], Aninda Dey[1], Patricia Lynn Opresko[2], **Ryan Barnes**[1]

[1]University of Kansas Medical Center, Kansas City, KS,[2]University of Pittsburgh, Pittsburgh, PA

Targeted inhibition of DNA damage response proteins has received significant clinical attention owing to the success of PARP inhibitors. Due to the loss of G1/S checkpoint proteins like p16 and p53, cancer cells are reliant on the G2/M checkpoint to cope with elevated DNA replication stress, making them vulnerable to ATR and Chk1 inhibition. Cancer cells also experience elevated levels of oxidative stress, and targeting this is another therapeutic strategy, especially in photodynamic therapy. Our group has developed a chemoptogenetic tool (FAP-TRF1) which allows for targeted induction of singlet oxygen mediated 8-oxo-guianine (8oxoG) at telomeres. We previously demonstrated a single induction of 8oxoG at telomeres in cancer cells was sufficient to induce replication stress but was well tolerated at the cellular level. This led us to hypothesize that oxidative base damage to telomeres may sensitize cancer cells to low dose ATR inhibition. In this study we found inhibition of ATR, Chk1, or Wee1 after induction of telomeric 8oxoG significantly induced genome instability and reduced viability of cancer cells. This occurred at doses markedly less than those required to increase instability in non-cancer cells, and at levels in the cancer cells which the drug alone had no effect. We found p53 was critically protective of the non-cancerous cells in our model. We determined genome instability after 8oxoG induction and ATR inhibition was enhanced when cells were damaged in S-phase and when Mre11 was inhibited, while CDC7 inhibition restored stability. This phenotype resulted in an increased amount of time required to complete mitosis suggesting cells entered mitosis with unresolved replication intermediates. Indeed, pharmacologic prevention of mitotic entry during ATR inhibition rescued the genome instability caused by telomere oxidation. Together our findings indicate that manipulating the levels of reactive oxygen species in cancer cells may be an effective therapeutic alongside ATR inhibitors, allowing for tumor destruction while mitigating off-target effects to non-diseased tissue.

#4695 Distinct genomic remodeling in Li Fraumeni Syndrome breast cancer.

Nabamita Boruah[1], Renyta Moses[1], Ryan Hausler[1], Heena Desai[1], Maliha Tayab[2], Ahn Le[1], Gregory Kelly[1], Anupama Nayak[1], Kara Maxwell[1]

[1]University of Pennsylvania, Philadelphia, PA,[2]Jefferson University, Philadelphia, PA

Background: Pathogenic germline variants (PGVs) in *TP53* cause Li-Fraumeni Syndrome (LFS), a hereditary multicancer predisposition syndrome. Among females with LFS, breast cancer (BC) is the most prevalent malignancy, affecting 80-90% of carriers, typically at a much earlier age than sporadic cases and frequently exhibiting HER2 positivity. Interestingly, LFS-BC displays a high burden of short- amplified segments of aneuploidy (SAAS), suggesting that germline *TP53* loss may drive tumorigenesis through distinct genomic mechanisms that remain poorly understood.
Methods: To elucidate genotype-phenotype correlations underlying these unique genomic features, we performed whole-genome sequencing (WGS) and targeted sequencing on invasive ductal carcinoma (IDC), ductal carcinoma in situ (DCIS), and matched adjacent and contralateral normal breast tissues from individuals with LFS. Data were compared to early-onset nonLFS-BC and to The Cancer Genome Atlas (TCGA) tumors harboring either wild-type or somatic *TP53* mutations.
Results: Across hormone receptor (HR) subtypes, expected increases in genomic instability were observed in triple-negative versus ER+ nonLFS-BC. However, overall instability measures were similar or lower in LFS-BC. Specifically, in ER+ tumors, microsatellite instability (MSI) and aneuploidy scores were significantly lower in LFS-BC compared to nonLFS-BC. In contrast, LFS-BC exhibited a notable increase in segmental allelic imbalance (AI) with high-level amplifications-particularly within HER2+ subtypes. These amplified regions were significantly shorter than those in nonLFS-BC and often encompassed oncogenes such as *ERBB2*, defining a distinct SAAS phenotype. Unlike sporadic *TP53*-mutant breast cancers in TCGA, which showed globally elevated aneuploidy and HRD, LFS-BC uniquely accumulated focal, short amplifications. WGS of LFS DCIS and invasive tumors revealed predominant chromosomal instability (CN9) and chromothripsis (CN5) copy number signatures, with minimal whole-genome doubling. Amplicon Architect analysis identified ecDNA structures in 14 of 19 tumors, including *ERBB2*-containing ecDNA in 3/6 DCIS and 5/9 HER2+ IDCs with 4 and 8 number of ecDNA structure in each category respevtively. Our work is consistent with prior reports of ecDNA in ~23% of breast cancers and up to 46% of HER2+ cases.
Conclusion: LFS-associated breast cancers are defined by a unique genomic remodeling pattern characterized by focal, high-level amplifications within short aneuploid amplified segments (SAAS) and frequent ecDNA formation. These features distinguish LFS-BC from sporadic *TP53*-mutant tumors and highlight a germline *TP53*-driven mechanism of oncogene amplification and structural genome evolution.

#4696 Oncogenic transcriptional rewiring in micronuclei.

Duaa Hassan Al-Rawi[1], Danguole Norkunaite[1], Kaden Southard[1], Mercedes Duran[1], Xuelan Chen[1], Andrew William McPherson[1], Scott W. Lowe[1], Sohrab Shah[1], Samuel F. Bakhoum[2]

[1]Memorial Sloan Kettering Cancer Center, New York, NY,[2]Memorial Sloan Kettering Cancer Center, Rye, NY

Chromosomal instability (CIN) is a well-known feature of aggressive tumors, yet the distinct oncogenic mechanisms associated with CIN remain an area of active discovery. We previously demonstrated that in addition to driving karyotypic heterogeneity, chromosomal localization into micronuclei (MN)—the extranuclear bodies formed from missegregated chromosomes— causes epigenetic dysregulation. Moreover, we and others had previously demonstrated that micronuclei were largely silenced. Here we took a multimodal approach to examine the transcriptional behavior of micronuclei, using imaging-based approaches as well as purification of nascent RNA from micronuclei. We show that despite global dampening, micronuclei are transcriptionally active. Across epithelial and cancer cell models, micronuclei display robust nascent RNA synthesis. GSEA of differentially expressed micronuclear genes reveals an enrichment of MYC programs as well as preferential transcription of short genes with fewer introns. This is consistent with constrained RNA processing within the micronuclear environment. Overexpression of a panel of transcription factors reveals that MYC upregulates micronuclear transcription. A chromosome-specific missegregation system confirms that these transcriptional effects occur on the missegregated chromosome itself, linking mitotic errors to locus-directed transcriptional change. Analyses of TCGA and SPECTRUM ovarian cancer datasets connect regions of copy number alteration with micronuclear transcriptional signatures, underscoring clinical relevance. Together, these findings establish a direct and novel relationship between chromosomal missegregation and oncogenic transcription. Chromosomal localization to micronuclei endows cancer cells with locus-specific transcriptional programs and reveals new oncogenic mechanisms in CIN-high disease.

#4698 Quantifying ongoing chromosomal instability using single-cell whole-genome sequencing.

Barbara Hernando[1], Blas Chaves-Urbano[1], Maria Escobar-Rey[1], Alice Cadiz[1], Angel Fernandez-Sanroman[1], Marina Torres[1], Sara Barrambana[1], Carmen G. Lechuga[1], Carmen Guerra[1], Mariano Barbacid[1], Maria Garcia-Perez[2], Patricia G. Santamaria[1], **Geoff Macintyre**[1]

[1]Spanish National Cancer Research Ctr. (CNIO), Madrid, Spain,[2]Institute for Biomedical Research Sols-Morreale (IIBM), Spanish National Research Council-Universidad Autonoma de Madrid (CSIC-UAM), Madrid, Spain

Chromosomal instability (CIN) describes the set of processes that generate numerical and structural DNA changes that typically operate during tumourigenesis. High-resolution readouts of DNA changes can be achieved using whole-genome sequencing (WGS) and the distinct patterns of copy number aberrations seen in these data can then be used to infer which type of CIN operated on the genome[1-3]. However, this static readout only provides evidence of historical or past CIN, as bulk WGS lacks the resolution needed to identify ongoing CIN that is actively shaping genome evolution.

To address this limitation, we have developed a computational framework that leverages single-cell whole-genome sequencing (scWGS) to identify and quantify ongoing CIN by detecting cell-unique copy number alterations and probabilistically mapping them to known CIN signatures[2]. We assessed performance by generating in vitro models with 4 types of induced CIN via CRISPR knockout of DNA repair genes or drug perturbation, and correctly identifying the induced-CIN type in each case.

Applied to near-diploid *BRCA1/2*-deficient hTERT-RPE1 models, we show that only single-cell, and not bulk, WGS can reveal ongoing homologous recombination deficiency (HRD) scars, enabling accurate identification of sensitivity to PARP inhibitors. In 4 pancreatic cancer organoids treated with platinum-based chemotherapy, ongoing HRD scars correctly identified the most sensitive organoid, which was misclassified as resistant using bulk WGS. Analysis of scWGS from 8 triple-negative breast cancers further reveal that impaired non-homologous end joining (NHEJ) is associated with subclonal diversification. Consistent with this observation, activity levels of CX10 (a CIN signature linked to NHEJ impairment[1]) was significantly higher in 119 metastatic TNBCs compared with 60 primary tumours (p-value=0.0085, Wilcoxon test), suggesting a link between defective NHEJ, subclonal evolution and increased metastatic potential.

Together, these results show that our framework reveals treatment-relevant, recent CIN processes undetected by bulk sequencing, and it offers a robust tool for dissecting tumour evolution. Our study supports expanding biomarker-guided therapies by targeting active CIN rather than historical genomic scars.

References: [1]Macintyre et al. Nat Genetics, 2018; [2]Drews et al. Nature, 2022; [3]Thompson et al. Nat Genetics, 2025

#4699 CK2α is a novel phosphoinositide effector of PIPKIIα and PIPKIIβ in DNA damage repair.

Gavril Limet Ibaan, Suyong Choi

University of Nebraska Medical Center, Omaha, NE

Phosphoinositides (PIs) are a class of lipid second messengers that coordinate signaling events at the membrane interface. This canonical role belies the presence of rich PI metabolism within the nucleus, where emerging functions reveal pivotal contributions to oncogenesis. Despite this, effectors that transduce this lipid network are largely obscure. In particular, dysregulation of nuclear phosphatidylinositol 4,5-bisphosphate ($PI4,5P_2$) and its generative kinases PIPKIIα and PIPKIIβ are salient in breast cancer progression and prognosis, yet the mechanistic basis for how they drive oncogenesis remains enigmatic. Identification of the underlying pathways, therefore, remains a critical question that could inform novel therapeutic strategies. To investigate their nuclear function, we examined $PI4,5P_2$ dynamics by immunofluorescence (IF) and observed accumulation at γH2A.X-positive DNA lesions. Consistent with this, DNA damage response (DDR) assays quantifying caspase activation, growth and genomic integrity revealed that PIPKIIα/β double-knockout breast cancer cells exhibited genotoxic hypersensitivity and exacerbated genomic fragmentation. These observations implicated PIPKIIα/β in DDR signaling. Through mass spectrometric profiling of nuclear extracts, we identified CK2α as an interactor of PIPKIIα and PIPKIIβ. This interaction was validated by endogenous co-immunoprecipitation and further supported by *in vitro* binding assays between purified recombinant proteins and proximity ligation immunofluorescence, which together revealed direct and nuclear-restricted engagement. Cells lacking PIPKIIα/β selectively compromised CK2α activity elicited in response to DNA damage, but not mitogenic stimulation. Interrogation of CK2α-dependent DDR substrates further demonstrated impaired downstream signaling, substantiating PIPKIIα/β control over CK2α in the DDR. To probe lipid signaling transduction, we performed structural, biochemical, and *in silico* assays that uncovered a PI-binding polybasic motif (PBM) in CK2α (residues 71-80) adjacent to the binding interface of its regulatory subunit CK2β; further mutation of this PBM diminished $PI4,5P_2$ binding. This motivated the hypothesis that $PI4,5P_2$ supplants CK2β, releasing monomeric CK2α, thereby redirecting its substrate specificity. Accordingly, PIPKIIα/β depletion enhanced endogenous CK2α-CK2β association while concurrently diminishing its interaction with the DDR-substrate XRCC1. Our findings support a model in which PIPKIIα/PIPKIIβ synthesizes $PI4,5P_2$ following DNA damage to liberate nuclear CK2α from CK2β and potentiate the DDR. Late-stage breast cancers may upregulate this pathway to mitigate otherwise lethal genetic insults and promote survival against their intrinsic genomic instability, defining a previously unrecognized nuclear $PI4,5P_2$ signaling axis that promotes tumor progression.

: Metabolic Alterations in Colorectal and Gastrointestinal Cancers
Poster Session

#4703 Sex-specific metabolic features in pre-cancerous polyps identified in Puerto Rican stool samples: A pilot study.

Melissa Gabriela Soto-Santiago[1], Gabriel Borges Velez[1], Leslie A. Casiano Agosto[1], Luis R. Llanos[1], Ibis R. Vera-Urbina[2], Josue Perez-Santiago[1], Maria Gonzalez-Pons[1]

[1]University of Puerto Rico Comprehensive Cancer Center, San Juan, PR,[2]University of Puerto Rico, San Juan, PR

Background: Colorectal cancer (CRC) is the leading cause of cancer deaths in Puerto Rico when combining men and women, with notable differences in presentation according to sex. Men have a higher incidence of CRC, with a higher overall mortality, while women are more often diagnosed with proximal tumors that respond less effectively to conventional therapies. This pattern suggests the existence of underlying sex-specific pathways that influence CRC development. Metabolite abundance analysis offers a comprehensive approach to identifying biochemical alterations associated with disease mechanisms and progression. This study aimed to characterize metabolite differences in stool between pre-cancerous polyps and healthy samples, and to explore sex-specific metabolic differences in a Hispanic cohort.
Methods: A case-control design was used to analyze stool samples from ninety-seven Puerto Rican participants (68 females, 29 males) with and without colorectal adenomas. Gas chromatography-mass spectrometry was used for metabolite identification; afterwards spectral peak data was normalized and analyzed using MetaboAnalyst 6.0 and RStudio. Significance was assessed using paired t-test for pairwise comparisons and 2-way ANOVA for multivariate analysis.
Results: Fifty-nine metabolites were detected across samples, with significant abundance differences between polyps and controls observed in females: β-alanine (adjusted $p=0.0014$) and N-acetyl-L-aspartic acid (adjusted $p=0.0017$). We observed different top metabolites in males: Thapsic acid (nominal $p= 0.019$) and cholesterol (nominal $p = 0.035$). In a multivariate analysis, seven metabolites were identified in polyps vs controls, adjusting for sex (nominal $p<0.05$): Nicotinic acid, β-alanine, 3,4-Dihydroxyhydrocinnamic acid, Isoleucine, Callitrisic acid, Palmitoleic acid, and Thapsic acid.
Conclusion: The different metabolite profiles observed in males versus females provide evidence supporting different carcinogenic mechanisms according to sex, which may contribute to the CRC differences in presentation and outcomes reported. The metabolites detected could be potential biomarker candidates and we will be examining microbiome integration analyses with additional samples and even matching across groups. Together, these efforts will enable a more precise delineation of sex-dependent metabolic pathways that can ultimately inform tailored CRC risk stratification and prevention strategies.

#4704 Disruption in cholesterol homeostasis by free fatty acid promote colon cancer by modulating CCL20.

Janani Muralidharan[1], Ankit Bhatt[1], Jaliya M. Mims[2], Gene Hughes[3], Paige Marcelline[1], Sejong Bae[4], Shailesh Singh[1], **Hina Mir**[1]

[1]Morehouse School of Medicine, Atlanta, GA,[2]Spelman College, Atlanta, GA,[3]Morehouse College, Atlanta, GA,[4]Auguta University School of Public Health, Augusta, GA

Background: Colorectal cancer (CRC) displays metabolically flexible but dysregulated lipid homeostasis, involving increased lipid synthesis, altered fatty acid uptake, enhanced storage, and remodeling of membranes and cholesterol pools. These processes interact with inflammatory signaling networks and may support cancer progression. CCL20, a chemokine elevated in lipid-rich and inflammatory CRC microenvironments, has been implicated in tumor progression, but its relationship with lipid metabolic regulation remains unclear. This study examines possible interactions between lipid metabolism and CCL20 signaling, and specifically its effects on lipid accumulation, membrane biophysics, and cholesterol metabolic programs in CRC models.
Methods: CRC cell lines (Caco2, DLD1, HCT116) were exposed to free fatty acids (FFAs) differing in chain length (C12, C16) and saturation (C16:0, C18:1(9)). CCL20 production was quantified by ELISA. FFA uptake was assessed using Lauric acid (C12) and palmitic acid (C16). Lipid accumulation was assessed by BODIPY mean fluorescence intensity normalized to cell size. Membrane fluidity was measured using Laurdan generalized polarization (GP) and fluorescence imaging. Total, cellular and secreted cholesterol, as well as ratio of esterified and free cholesterol ratios were measured alongside expression of cholesterol-associated enzymes, including HMGCR, SOAT2, and SREBP2. CCL20-overexpressing HCT116 cells were included to validate effects of CCL20.
Results: Data indicate that FFAs of differing lengths may variably modulate CCL20 expression. Distinct patterns of FFA internalization and accumulation, and membrane fluidity shifts were observed in CRC cell line with differential CCL20 signaling. Levels of cholesterol and expression of key metabolic enzymes were found to be associated with CCL20 modulation.
Conclusions: These findings establish a clear link between lipid metabolism and CCL20 expression and function in CRC cells. Ongoing studies aim to validate these observations and develop a unified model of CCL20-driven metabolic regulation in colorectal cancer.

#4705 A clearer picture of cachexia: Leveraging body composition imaging in C26 tumored mice.

Cheryl Davis[1], Liz Bailey[2], Mollie McArthur[3], Melissa Tran[3], Ben Hoerner[4], Victoria Caruso[4], Helen Ketteringham[3], Corrine Silvio[4], Shannan Paul[4], Delaney McCormick[5], Jocelyn Saurbaugh[5], Chris Holding[6], Aliccia Koznecki[6], Dawn Lusk[4], Shorena Nadaraia-Hoke[4], Kathleen Hutchinson[4]

[1]Reaction Biology Europe GmbH, Freiburg im Breisgau, Germany,[2]Reaction Biology Corp, Boston, MA,[3]Reaction Biology Corp, Malvern, PA,[4]Reaction Biology Corp, Hummelstown, PA,[5]Reaction Biology Corp, Lancaster, PA,[6]Reaction Biology Corp, Hershey, PA

Cancer cachexia remains a major unmet need in oncology, characterized by progressive loss of skeletal muscle and adipose tissue that negatively impacts treatment tolerance and survival. Anamorelin (AML), a ghrelin receptor agonist, is currently the only approved therapeutic for cancer cachexia; however, its clinical benefits remain modest, highlighting the need for improved preclinical models and more informative physiological endpoints. Here, we established and characterized a C26 colorectal carcinoma cachexia model using both traditional metrics and non-invasive body composition imaging performed on a Bruker MiniSpec. This platform enabled longitudinal quantification of lean and fat mass changes with high sensitivity, providing a refined assessment of cachexia progression and therapeutic response.In vitro and in vivo studies confirmed the robust cachexia-inducing phenotype of the C26 model. Consistent with published literature, AML treatment increased food intake in tumor-bearing mice but did not reduce circulating pro-inflammatory cytokines. Combination therapy, evaluated based on the mechanistic rationale that AML-mediated appetite stimulation may complement the anti-inflammatory activity of CYA, demonstrated enhanced preservation of body mass and adipose tissue compared with either monotherapy. Our findings support the utility of integrating body composition imaging with standard physiological and biochemical measures to generate a comprehensive efficacy profile. These results highlight the value of this refined platform for evaluating emerging cachexia therapeutics and suggest that multi-modal combinations such as CYA+AML may provide superior benefit over current single-agent approaches.

#4706 Mechanoplasmonics: Integrating nanoplasmonic materials and stiffness tunable hydrogels for real-time, label-free cellular analysis.

Cason M. Hancock[1], Harlie Rios[2], Alexander McGhee[3], Swarna Ganesh[3]

[1]UA Comprehensive Cancer Center, University of Arizona, Tucson, AZ,[2]Biomedical Engineering, University of Arizona Cancer Center, Tucson, AZ,[3]UA Comprehensive Cancer Center, Biomedical Engineering, University of Arizona, Tucson, AZ

Understanding how cellular biochemical states respond to mechanical stimuli requires analytical approaches capable of probing molecular signatures. We present a multifunctionalplatform that integrates Surface-Enhanced Raman spectroscopy (SERS),silver nanoparticles,and stiffness-tunable hydrogels to investigate mechanochemical interactions at single-cell and, insome instances, single-molecule resolutions. Silver nanoparticles were synthesized via controlled reduction process to optimize size morphology for strong localized surface plasmon resonance.Characterization confirmed the monodisperse nanoparticles with pronounced optical resonances in the visible range, enabling substantial electromagnetic field enhancement and highly sensitive detection of biomolecular vibrations.Hydrogels with tunable stiffness were fabricated by modulating cross linking density while keeping chemical composition and surface functionalization constant. This design provided a controlled range of elastic moduli to emulate diverse physiological and pathological tissue conditions. Healthy and cancerous colorectal cells were cultured on hydrogels with dispersed SERS nanoparticles, creating a mechanically defined and optically accessible interface for molecular imaging and analysis.Raman spectra acquired from cells on soft versus stiff hydrogels revealed reproducible differences in vibrational modes corresponding to lipids, proteins, and nucleic acids. The high enhancement factors produced by the silver nanoparticles enabled these spectral changes to be detected with exceptional sensitivity, offering insight into how extracellular stiffness modulates intracellular chemical composition. These results suggest that mechanical cues lead to measurable biochemical remodeling at the molecular level, detectable through the enhancedRaman scattering signatures of key cellular components. Combining nanoplasmonics and tunable mechanical substrates, our mechanoplasmonic platform captures real-time, label-free molecular responses of living cells to their physical environment. The ability to detect single-molecule spectral features within biologically relevant contexts demonstrates the analytical strength and versatility of this hybrid system. More broadly, the approach bridges the disciplines of mechanobiology, materials science, and nanophotonics, providing a foundation for future studies on stiffness-mediated cell signaling and potential diagnostic tools that exploit mechanical-biochemical coupling for early detection of disease progression or therapeutic response.

#4707 Repurposing statins activates compensatory glutathione metabolism as synergistic vulnerability in colorectal cancer.

Jieqing FENG[1], Jianming LI[2], Hong YAN[2], Zongwei CAI[1]

[1]Department of Chemistry, Hong Kong Baptist University, Kowloon, Hong Kong,[2]Department of Biology, Hong Kong Baptist University, Kowloon, Hong Kong

Metabolic adaptations upon intrinsic and environmental stressors enable cancer cells to resist treatment and sustain proliferation. Understanding of adaptive rewiring and compensatory mechanisms is a pivotal strategy to develop effective treatment options. Statins are receiving increasing attention in the prevention of colorectal cancer (CRC), but the biological mechanism is elusive. Here, we demonstrate that six statins show effective tumor repression capacity in a dose-dependent manner. We next observe that administration of statin alone is not sufficient to induce programmed cell death because inhibitors of ferroptosis, apoptosis, necroptosis, and autophagy fail to rescue the cell viability. To further understand the therapeutic vulnerability, untargeted metabolic analysis is employed to detect the reprogramming metabolites. Pathway analysis shows glutathione metabolism is significantly perturbed. Meanwhile, dramatic increases of cysteine and gamma-glutamylcysteine are widely observed while the reduced glutathione (GSH) and oxidized glutathione (GSSG) levels are decreased, linked to redox imbalance and ferroptosis. Western blotting shows statins have similar effects as RSL3 on increasing the expression of glutamate-cysteine ligase catalytic subunit (GCLC), which catalyzes the rate-limiting step of GSH synthesis, and its inhibition is associated with ferroptosis induction. In contrast, CRC cells show increasing reliance on glutathione peroxidase 4 (GPX4) upon statins treatment when compare to RSL3. Collectively, compensatory upregulation of GCLC indicates combinations of statins and GCLC inhibitors may enhance antiproliferative efficacy of targeting GSH metabolism.

#4708 Metabolomics signatures with multidrug-resistant colorectal cancer cells.

Christopher Farrell

Clemson University, Clemson, SC

Colorectal cancer is one of the deadliest cancers with almost 50,000 deaths each year in the US. Many of the deaths are due to a serious issue of multidrug resistance (MDR) where the cancer cells are unaffected by chemotherapy resistance. The use of metabolic profiling in MDR cancer cells may be useful for identifying weaknesses in the cells. This study analyzes the metabolomic profiles of colorectal cancer cell lines that were treated for a long-term with chemotherapy medication and a non-chemotherapy drug. We treated the colorectal cancer cell lines with medications for approximately 3-4 months and monitored drug resistant markers through expression analysis using qPCR. Once the markers were confirmed using RNASeq and western blots, the cells analyzed for Biolog Phenotype Mammalian Microarray 1 (PM-M1) to assess the metabolic profile of the drug-resistant colon cancer cells. The PM-M1 assay allowed us to evaluate the production of NADH in the presence of different carbon-based energy sources, providing functional information on the major energy pathways of the cells. Other PM-M assays helped to identify and validate possible trends pathways such as glycolysis and major energy sources. Exposing the cells to atorvastatin (10 and 40 μM), the chemotherapeutic drug doxorubicin (positive control), or untreated/DMSO (negative control) resulted in the overexpression of *ABCB1* by the 5th month of the study with bi-weekly treatments of the medication. The protein analysis with western blots and RNASeq analysis confirmed the expression of the transporter. Comparison of the NADH levels from the cells exposed to DMSO (negative control) to the ones from the cells exposed to doxorubicin (positive controls), we noted 21 compounds showing differences. The cells exposed to atorvastatin showed dose-dependent trends: the NADH levels observed with the 10 μM dose showed very few differences when compared to both DMSO- and doxorubicin-treated cells, while the ones with the 40 μM dose were significantly decreased, with lower NADH levels than both DMSO- and doxorubicin-treated cells in about one third of the PM-M1 wells. Overall, our experiments confirmed that the MDR cancer cells in the doxorubicin and 10 μM atorvastatin, showed very little difference from the negative control in metabolic profiling, while the 40 μM atorvastatin-treated cells caused a drastic reduction of energy production, with deleterious effects on compounds encompassing various metabolic pathways. In conclusion, this study provides a promising approach, both alone and in combination with molecular tools by exploring potential biomarkers and molecular targets for treatment development. These results provide insight into how selective pressures through medication can cause the cells to still be able to slowly develop back to the original metabolic levels once they are resistant to the drug.

#4709 Metabolic reprogramming through SREBP2-driven cholesterol synthesis in CAFs of CMS4 colorectal cancer.

Iguru Omori[1], hiroaki kasashima[1], Yukina Kusunoki[2], Nobuhiro Naito[1], Zizhou Wang[1], Yuki Seki[1], Kenji Kuroda[1], Yuichiro Miki[1], Mami Yoshii[1], Tatsuro Tamura[1], Masatsune Shibutani[1], Takahiro Toyokawa[1], Masakazu Yashiro[3], Yu Muta[4], Yuki Nakanishi[4], Kiyoshi Maeda[1]

[1]Department of Gastroenterological Surgery, Osaka Metropolitan University Graduate School of Med., Osaka, Japan,[2]Pathophysiology, Osaka Metropolitan University Graduate School of Medicine, Osaka, Japan,[3]Molecular Oncology and Therapeutics, Osaka Metropolitan University Graduate School of Medicine, Osaka, Japan,[4]Gastroenterology and Hepatology, Kyoto University, Kyoto, Japan

Colorectal cancer has been stratified based on gene expression profiles into consensus molecular subtypes (CMS). Among these, the mesenchymal subtype (CMS4), which accounts for approximately 23% of cases, is associated with a particularly poor prognosis compared with the other subtypes. It has been increasingly recognized that the high malignancy of CMS4 colorectal cancer is driven by activation of the tumor stroma, predominantly composed of CAFs, and by its interactions with cancer cells within the tumor microenvironment (TME). However, the mechanisms remain to be unclear. Cholesterol is essential for cancer, particularly through its roles in membrane integrity and intracellular signaling. Dysregulation of cholesterol homeostasis has been implicated in cancer progression. Recent studies have shown that activation of SREBP2, a key transcription factor for cholesterol biosynthesis, contributes to the development of aggressive serrated colorectal tumors characterized by desmoplasia. However, the metabolic state of cancer-associated fibroblasts (CAFs), particularly regarding cholesterol metabolism, remains unclear. We analyzed bulk RNA sequencing data from 10 colorectal cancer samples. Gene set enrichment analysis (GSEA) was performed to compare CAFs from CMS4 tumors with those from other CMS subtypes. Subsequently, we established CAF lines derived from CMS4 and the other subtype tumors and examined the impact of CAF cholesterol metabolism on tumor progression. We revealed that CMS4-CAFs exhibited significant enrichment of gene sets related to cholesterol homeostasis. In particular expression levels of SREBP2 and its downstream genes were markedly upregulated in CMS4-CAFs. Furthermore our *in vitro* results showed that inhibition of cholesterol biosynthesis or SREBF2 knocking down reduced the proliferative capacity of CMS4-CAFs and suppressed tumor migration. These findings highlight a potential metabolic feature of CAFs in CMS4 colorectal cancer that may contribute to tumor aggressiveness.

#4710 Comprehensive metabolomic profiling of FFPE human tissues reveals key metabolic reprogramming in colorectal cancer and associated pathways.

Tom Cohen[1], Ashima Mehta[1], Adam Richardson[1], Monil Gandhi[1], Douglas Guzior[1], Kevin Cho[2], Ethan Stancliffe[1], Gary Patti[2]

[1]Panome Bio, St. Louis, MO,[2]Washington University in St. Louis, St. Louis, MO

Introduction: Formalin-fixed paraffin-embedded (FFPE) tissues are invaluable for retrospective clinical studies due to superior morphological preservation and easy storage, but their use in metabolomics is limited by a lack of established sample preparation protocols and concerns over metabolite stability. Here we optimized a novel FFPE metabolomic workflow and validated findings with matched fresh-frozen (FF) samples to identify metabolic signatures altered in human colorectal cancer (CRC).

Methods: We analyzed 12 FFPE human tissue samples, comprising 6 paired tumor and Nearby Adjacent Tissue (NAT) specimens from adenocarcinoma patients, alongside matched FF samples for validation. Global metabolomics assays were performed on both polar and lipid fractions using a next-generation mass spectrometry platform.

Results: Metabolic profiling detected 2,564 unique metabolites across 200+ classes from FFPE tissues with low technical variation (median CV < 5%). Unsupervised analyses showed clear tumor-NAT distinctions. Statistical analysis identified 200 differential metabolites ($|\log2(fc)| > 1$, $p < 0.05$). Pathway analysis revealed 39 altered pathways ($p<0.05$), with upregulated diacylglycerophosphoinositols and downregulated triacylglycerols in tumors being the most significant findings. Consistent upregulation of central carbon metabolites and amino acids indicated metabolic reprogramming for biosynthesis and oxidative stress buffering. FF sample validation showed concordance across the most significant hits and pathways identified, confirming the robustness and biological relevance of FFPE-derived signatures.

Conclusion: Our study confirms FFPE metabolomic profiling reliably identifies significant metabolic perturbations in human cancer, consistent with FF findings. The identified shifts in lipid, central carbon, and amino acid metabolism highlight extensive metabolic reprogramming in CRC. FFPE archives are a valuable resource for large-scale retrospective clinical metabolomics studies, offering a powerful avenue for discovery research in human genetics and disease, and for identifying novel biomarkers.

#4711 Investigating synergistic impact of diet-induced hyperinsulinemia and mutant *Kras* on colorectal cancer metastasis.

Anindita Mahanty[1], Cara Wallingford[2], Alexa Magstadt[3], Revan Hammontree[2], Jennifer Davis[4]

[1]Cancer Biology, University of Kansas Medical Center, Kansas City, KS,[2]Cancer Biology, Kansas University Medical Center, Kansas City, KS,[3]Kansas University Lawrence, Lawrence, KS,[4]University of Kansas Cancer Center, Kansas City, KS

Purpose: This study examines how chronic high-fat-sugar (HFS) diet-induced metabolic dysfunction affects cancer metastasis in an in vivo, genetically engineered iKAP model (inducible Kras, Apc, and p53) (Boutin et al., Genes & Development, *2017, 31:370).*

Methods: 8-10 weeks old mice are randomized to either a 10% low-fat-sugar/LFS (healthy diet) or a 45% high-fat-sugar/HFS (western-style diet) to induce hyperinsulinemia and metabolic dysfunction before tumor initiation. The development of metabolic dysfunction is monitored using Echo-MRI for alterations in body composition, a glucose tolerance test (GTT), and endpoint steatosis. Upon tumor induction, tumor growth rates are measured to compare tumor burden in relation to diet and Kras mutation status. Micro- and macro-metastases are being recorded and compared using micro-CT imaging and endpoint tissue histopathology. In parallel, a complementary *in vitro* study using a panel of isogenic colorectal cancer cell lines is underway to evaluate the effect of insulin-mediated cell migration and invasion through scratch and trans-well assays, as well as downstream signaling analyses by Western blot.

Result: Our preliminary *in vivo* findings demonstrate signals of metabolic dysfunctions, including higher body fat percentage, lower glucose tolerance, and the development of hepatic steatosis in HFS-fed iKAP mice. Mice on the 45% high-fat diet showed higher liver disease scores compared to those on the 10% fat diet. Inclusions of hepatocyte ballooning and inflammation were noticeably increased in the high-fat group. Current findings indicate a diet-dependent increase in liver steatosis in 45% HFS mice relative to the 10% control group.

Conclusion: Based on preliminary findings, an HFS diet effectively induces metabolic dysfunction in the iKAP *in vivo* model. This context may support investigating hyperinsulinemia-oncogenic *Kras* crosstalk in CRC progression and metastasis. Additional mice and sex-based analyses will further validate and strengthen these findings. Moving forward, chronic hyperinsulinemia reprograms metabolism and intracellular signaling in the presence of mutant *Kras* to expand tumor metastatic spread, is an open question.

#4712 Targeting NRF2-regulated polyamine and glutathione metabolism enhances chemotherapy efficacy in colorectal cancer based on KRAS status.

Jiamin Li[1], Jieqing Feng[1], Fuyue Wang[1], Yingjie Zhang[2], Hong Yan[1], Zongwei Cai[3]

[1]Hong Kong Baptist University, Hong Kong, China,[2]The University of Hong Kong, Hong Kong, China,[3]Eastern Institute of Technology, Zhejiang, China

Metabolic reprogramming is a hallmark of colorectal cancer and is strongly influenced by oncogenic KRAS mutations, which contributes to reduced drug responsiveness and poor clinical outcomes. Inducing ferroptosis—a form of iron-dependent, lipid peroxidation-driven cell death—has emerged as a promising strategy to augment chemotherapy response by disrupting this adaptive metabolic state. However, the interplay between KRAS-specific metabolism and ferroptosis-induced drug sensitivity remains incompletely understood and could enable precision therapeutic interventions. In our study, we integrated public datasets and in vitro experiments to investigate the drug combination effect and how the metabolism will be altered. We first utilized drug sensitivity data from CRC cell lines, and we found that drug response varied by KRAS status and engaged distinct ferroptotic dependencies: KRAS-mutant cells showed increased reliance on iron-handling genes (*FTH1, FTL, SLC11A2*), whereas KRAS wild-type cells were more vulnerable to disruption of GPX4-mediated antioxidant defense. Given that NRF2 coordinates ferroptosis through both iron homeostasis and antioxidant responses, pharmacologic inhibition of NRF2 using Brusatol across four CRC cell lines (representing wild type, KRAS G12D, and KRAS G13D) markedly enhanced chemotherapy efficacy, with the strongest effect observed in KRAS G12D lines, followed by wild-type cells. Regarding non-targeted metabolomics analysis, co-treatment with Brusatol and Oxaliplatin or 5-Fluorouracil rendered dysregulated pathways that fuel cancer growth and progression, including methionine cycle, nucleotide synthesis as well as energy metabolism only in wild-type cells and $KRAS^{G12D}$ mutant which accounted for improved inhibitory effect. Moreover, distinctive alterations depending on KRAS mutation were observed under this combination therapy, manifesting KRAS mutants (comprising $KRAS^{G12D}$ and $KRAS^{G13D}$) demonstrated an blockage of polyamine catabolism with extremely decreased acetylspermine, whereas wild-type cells suffered elevated oxidative stress with severe GSH exhaustion and GSH/GSSG ratio reduction. In light of clinical unavailability of Brusatol, we successfully repositioned several clinically viable antineoplastic drugs and a panel of therapeutic agents under preclinical status for emerging tumor combat utilizing a transcriptional-based silico drug repurposing approach. Our findings highlighted NRF2 deprivation-mediated polyamine metabolism as a potential target for chemosensitivity and provided a clinically-approved therapeutic option in $KRAS^{G12D}$ CRC, brightening the path for targeted therapy and translation medicine.

#4713 Targeting glycogen metabolism in cancer-associated fibroblasts alleviates immunosuppression and inhibits colorectal cancer malignancy.

Xudong Zhu, Yuning Zhou, Haoxiang Zhang, Yinping Jiang, Jinpeng Liu, Chi Wang, **B. Mark Evers**, Qingding Wang

UK Markey Cancer Center, Lexington, KY

Background: Cancer-associated fibroblasts (CAFs) are the major sources of secreted cytokines and chemokines contributing to the shaping of immunosuppressive tumor microenvironment (TME). Dysregulation of glycogen metabolism is integral to cancer cell proliferation and metastasis. The purpose of this study was to identify whether targeting glycogen metabolism in CAFs could alleviate immunosuppression and inhibit colorectal cancer (CRC) growth.

Methods: Human CAFs (hCAFs) were isolated from CRC patient samples. $APC^{f/f}$; CDX2-Cre/ERT2 mice were injected with tamoxifen to induce adenoma formation. Mouse CAFs (mCAFs) were isolated and cultured. The expression of glycogen phosphorylase liver form (PYGL), phospho-PYGL, hexokinase 2 (HK2), GLUT1, IL6, CLCF1, LIF, and CXCL6 was determined by either real time (RT)-PCR or western blot. Glycogen levels were determined using a Glycogen Analysis Kit. Cell proliferation was determined using WST-1. Extracellular acidification rate (ECAR) was determined utilizing an Agilent Seahorse XFe96 extracellular flux analyzer. To determine whether targeting PYGL would inhibit tumor growth, $APC^{f/f}$; CDX2-Cre/ERT2 and MC38 mouse tumor models were used.

Results: (**i**) Elevated glucose metabolism in CAFs was found compared to normal fibroblasts. (**ii**) Treatment of hCAFs with either conditioned medium (CM) derived from HCT116 CRC cells or TGFβ resulted in activated glycogen metabolism as noted by increased expression of p-PYGL/PYGL and the reduced level of glycogen in hCAFs. Moreover, CM increased the expression of IL6 family cytokines such as IL6, CLCF1, LIF and CXCL6 in hCAFs. (**iii**) Inhibition of glycogen metabolism by knockdown of PYGL or treatment with the PYG inhibitor, CP-91149, significantly repressed hCAFs proliferation and reduced the expression of these cytokines in hCAFs. Knockdown of PYGL decreased glycolytic activity as noted by decreased ECAR. (**iv**) Treatment with CP-91149 significantly inhibited tumor growth. In addition, mCAF cells co-implanted with MC38 cells increased MC38 tumor growth; this increase was attenuated by knockdown of PYGL in mCAFs.

Conclusion: Our results demonstrate that glycogen metabolism is crucial for promoting CAF immunosuppressive functions. Importantly, our findings suggest that targeting glycogen metabolism in CAFs alleviates immunosuppression and inhibits CRC malignancy.

#4714 Tumor-associated macrophage creatine metabolic reprogramming enhances hnRNPA1 phase separation and promotes colorectal cancer stemness and recurrence.

Zhengran Zhou, Xuanhui Liu, Yifan Zheng, Zhengyu Wei, Zerong Cai, Yufeng Chen, Peishan Hu, Xiaojian Wu

The Sixth Affiliated Hospital of Sun Yat-sen University, Guangzhou, China

BACKGROUND: Creatine, a common nutritional supplement, has gained increasing attention in tumorigenesis and development. Our previous study found that creatine is a key metabolic biomarker for colorectal cancer (CRC) recurrence. Further studies are urgently needed to reveal the mechanism by which creatine metabolic reprogramming induces CRC relapse.
METHODS: Targeted metabolomics analysis of creatine was dynamically performed on plasma samples of 160 CRC patients including 30 relapse cases. Creatine metabolism-related genes were investigated in TCGA, ICGC-ARGO database (a large multi-omics study of CRC in China), and CRC single-cell transcriptome datasets. Single-cell RNA sequencing and spatial transcriptomics sequencing were carried out on locally recurrent CRC tissues. Creatine metabolic reprogramming and its effect on CRC stemness were investigated in tumor-associated macrophages (TAMs) and CRC cell lines, patient-derived organoids, and murine models. Limited proteolysis-mass spectrometry (LiP-MS) and RNA-sequencing were performed to illustrate creatine-protein interaction and the regulation of relative signal pathways.
RESULTS: In recurrent CRC cases, creatine level gradually increased over time after the first radical surgery until recurrence. GATM, the key enzyme for creatine synthesis, was found to be enriched in TAMs, while creatine transporter SLC6A8 was highly expressed by malignant cells. Their expression levels were found significantly higher in patients who were going to relapse and they were positively correlated with that of LDHA, the acidic micronment marker. Creatine synthesis in TAMs was found upregulated, especially in acidic condition or after the addition of lactate, and the lactylation level of H3 histone was found elevated. Isotope tracking assays indicated that creatine can be taken up by CRC cells through SLC6A8. The addition of creatine significantly enhanced the self-renewal ability of CRC cells and activated tumor stemness pathways, which could be reversed by SLC6A8 inhibitors. LiP-MS and CETSA assay revealed that creatine directly interacted with hnRNPA1 and enhancement of hnRNPA1 phase separation was observed after the addition of creatine. Function of creatine-hnRNPA1-stemness axis was verified in vivo and in vitro subsequently.
CONCLUSIONS: Creatine has been identified as a biomarker for the dynamic monitoring of post-surgery CRC recurrence. Macrophages in the tumor microenvironment have undergone metabolic reprogramming of creatine, and TAMs-derived creatine contributed to CRC recurrence. Creatine promotes tumor stemness and malignancy via directly interacting with hnRNPA1 and enhancing its phase separation. Therapeutic strategies targeting creatine metabolism and hnRNPA1 have the potential to reduce CRC recurrence.

#4715 Detection of mitochondria-targeting anticancer agents in tumor organoids.

Yoonseok Kam, Lisa Winer, Natalia Romero

Agilent Technologies, Inc., Lexington, MA

Mitochondrial reprogramming is a hallmark of cancer, enabling tumor cells to adapt to hostile microenvironments and resist therapy. While some cancers suppress oxidative phosphorylation, others remain highly dependent on mitochondrial respiration, making mitochondria an attractive therapeutic target. This study presents a robust workflow for evaluating mitochondrial function and drug-induced mitochondrial toxicity in cancer organoids using the Agilent Seahorse XF Flex Analyzer and XF Flex Organoid Microplate. Colon cancer cell line-derived organoids embedded in Matrigel were used to evaluate the mitochondrial inhibitory effects of metformin, a well-characterized metabolic modulator. The Seahorse XF 3D Mito Stress Test and XF Mito Tox Assay enabled real-time measurement of oxygen consumption rate (OCR) and quantification of mitochondrial toxicity via the Mito Tox Index (MTI) - a unitless metric that differentiates between inhibition and uncoupling. The workflow incorporates optimized organoid seeding, image-based normalization, and reproducible metabolic profiling using the XF Flex Organoid Microplate. Results demonstrated dose-dependent mitochondrial inhibition by metformin and revealed differential susceptibility between 2D monolayer and 3D organoid cultures. These findings validate the compatibility of XF technology for organoid-based metabolic profiling in preclinical cancer research and underscore the utility of the MTI for cross-model potency comparisons of mitochondrial-targeting agents. This approach supports the development of new approach methodologies (NAMs) aligned with FDA initiatives to reduce animal testing and improve clinical translatability. The workflow is readily adaptable to patient-derived organoid (PDO) models, offering a scalable platform for screening mitochondrial-targeting therapies in oncology.

#4716 Disruption of mitochondrial dynamics alters DNA repair capacity in colon cancer.

Marion D. Creech[1], Erin M. Wolf Horrell[2], Tianyan Gao[3]

[1]Molecular and Cellular Biochemistry, Univ. of Kentucky College of Medicine, Lexington, KY,[2]Department of Surgery, Univ. of Kentucky College of Medicine, Lexington, KY,[3]Markey Cancer Center, Univ. of Kentucky College of Medicine, Lexington, KY

Mitochondrial dynamics refers to a collection of mitochondrial movements, including fission, fusion, and transport. Cancer cells are known to adjust mitochondrial dynamics to provide the metabolic plasticity needed for cell growth, proliferation and migration. We have shown previously that Drp1, a key regulator of mitochondrial fission, plays an important role in mediating fatty acid-induced activation of Wnt/β-catenin signaling in colon cancer. In this study, we determined the functional interaction between mitochondrial dynamics and DNA damage response in colon cancer cells. To disrupt mitochondrial fission, inducible Drp1 knockdown colon cancer cell lines were generated using lentivirus-mediated RNAi. Control and Drp1 knockdown cells were treated with radiation or chemotherapy drug irinotecan to induce DNA damage response. The extent of DNA damage as well as the activation of DNA repair signaling were analyzed by western blot and RT-qPCR. We found that Drp1 was activated upon irinotecan or radiation treatment as shown by increased phosphorylation at S616 site. Interestingly, the expression of γH2AX, a DNA damage marker, induced by irinotecan or radiation treatment was increased in Drp1 knockdown cells, whereas the expression and activation of DNA damage sensing proteins (e.g., ATM and ATR) remained unchanged. To determine if increased fatty acid uptake alters DNA damage, we showed that the presence of exogenous fatty acids attenuated γH2AX expression induced by radiation in control cells whereas knockdown of Drp1 blunted this response. Functionally, the addition of fatty acids increased, while silencing Drp1 decreased, cell survival post radiation as measured by colony formation assays. However, the pro-survival effect of fatty acids was largely abolished in Drp1 knockdown cells. Taken together, our results suggest that fatty acid uptake may enhance DNA repair via a mitochondrial fission-dependent mechanism. This study establishes a functional link between fatty acid metabolism, mitochondrial dynamics, and DNA damage response in colon cancer cells.

#4717 TBK1/IKKβ-mediated CAD phosphorylation links pyrimidine synthesis blockade and chemosensitization to innate immune activation.

Taolin Xie, Chi Liang, Hansong Xia, Anjie Lu, Chao Qin, Xinchi Xie, Wayne Yeh, Pinghui Feng

Herman Ostrow School of Dentistry, University of Southern California, Los Angeles, CA

Metabolic reprogramming is a hallmark of cancer. Aberrantly-activated metabolic enzymes fuel tumor progression through multiple mechanisms, including tumor cell proliferation, metastasis and drug resistance. Elucidating the regulatory mechanism of metabolic enzymes in cancer is thus of vital importance, which will pave a way to novel anti-tumor therapies. The first three steps of *de novo* pyrimidine synthesis are mediated by a multi-functional enzyme known as carbamoyl-phosphate synthetase 2, aspartate transcarbamylase, and dihydroorotase (CAD). Our lab have identified CAD as a protein deamidase that deamidates the NF-κB transcriptional factor RelA, shunting RelA from mediating the transcription of inflammatory cytokines to glycolytic enzymes. CAD thereby acts as a cellular metabolic node that fuels cancer cell proliferation by mediating pyrimidine synthesis and aerobic glycolysis. Indeed, CAD has been characterized as a critical oncogenic factor in a variety of malignancies. However, whether and how CAD is regulated by innate immune response remain unexplored. In this study, we report that innate immune activation dramatically impairs CAD enzymatic activity in colon cancer cells. Mechanistically, CAD is phosphorylated at multiple residues by two key innate immune protein kinases, TANK-binding kinase-1 (TBK1) and inhibitor of NF-κB kinase-β (IKKβ). TBK1 / IKKβ-mediated phosphorylation significantly attenuates both pyrimidine synthetase and protein deamidase activity of CAD, subsequently suppressing colon cancer cell metabolic reprogramming and proliferation. Furthermore, TBK1 / IKKβ-mediated CAD phoshorylation results in pyrimidine depletion and an imbalance in cellular nucleotide pool, which sensitizes colon cancer cells to DNA damage agents. Pharmacological activation of innate immune signaling by stimulator of interferon gene (STING) agonist can thereby inhibit intratumoral CAD activity and boost chemotherapy agents-induced DNA damage, highlighting a novel combination therapy. Besides, in a panel of cancer cell lines in which TBK1 acts as an oncogene, TBK1 is switched to activate CAD via growth factor signaling pathway, implicating context-dependent roles of TBK1 in regulating CAD. In summary, our study reveals an unprecedented crosstalk that places pyrimidine synthesis as a downstream ramification of innate immune activation. These findings provide fresh insights into how innate immune signaling reshapes tumor metabolic landscape, and offer a mechanistic rationale for combining STING agonists with chemotherapy as a highly potent approach to improve cancer treatment.

#4718 Redox reprogramming protects colon cancer cells from disulfidptosis under glucose deprivation.

Elimelech Nesher, Subha Ranjan Das, Igor Koman

Ariel University, Ariel, Israel

Cancer cells thrive in the tumor microenvironment by reprogramming their metabolism and adapting to severe nutritional stress. Although some cancer cells can withstand prolonged glucose deprivation, the molecular mechanisms underlying this resilience remain poorly understood. In this study, we investigated how glucose deprivation-resistant (GDR) colon cancer cells survive sustained glucose starvation, focusing on their ability to counteract oxidative stress and disulfidptosis, a recently described form of cell death driven by disulfide stress.We established long-term glucose-deprived cultures of colon cancer cells and compared quiescent populations with GDR cells that had resumed proliferation. Metabolic rewiring was assessed using Seahorse XF metabolic flux analysis and LC-MS-based metabolomics to map energy production pathways and metabolite changes. RNA sequencing was performed to identify transcriptional alterations, including those associated with disulfidptosis. Cytoskeletal integrity was evaluated by phalloidin staining, and cell viability was measured using the resazurin assay. To test whether redox support could restore survival, we conducted rescue experiments with antioxidants such as N-acetylcysteine and S-adenosylmethionine, as well as thiol-reducing agents including 2-mercaptoethanol and dithiothreitol, under both glucose-deprived and docetaxel-induced stress conditions.We found that upon glucose depletion, a subpopulation of colon cancer cells enters a dormant state characterized by elevated ROS, loss of mitochondrial membrane potential, extensive DNA damage, and cytoskeletal collapse. In contrast, the surviving GDR cells adapt by shifting from glycolysis to oxidative phosphorylation (OXPHOS). Metabolomic profiling revealed increased levels of TCA cycle intermediates and a pronounced enrichment of redox-active metabolites, including cystine, glutamate, glutamine, γ-glutamylcysteine, reduced GSH, and oxidized GSSG. Transcriptomic analyses further supported this metabolic transition, showing marked upregulation of disulfidptosis-associated genes. Functionally, these adaptations enhanced redox buffering capacity and reduced sensitivity to disulfide-induced cytotoxicity. Notably, supplementation with antioxidants and thiol-reducing agents preserved cytoskeletal integrity and improved overall cell viability, indicating that strengthening redox homeostasis is sufficient to counteract disulfidptosis, even under the combined stresses of chemotherapy and glucose deprivation.In conclusion, GDR colon cancer cells evade disulfidptosis by reprogramming metabolism toward OXPHOS and enhancing redox defense mechanisms that maintain cytoskeletal integrity. Targeting these adaptive redox pathways may provide a promising strategy to eliminate cells that survive glucose deprivation through metabolic plasticity.

#4719 Dissecting metabolism-driven transcriptional reprogramming in human colon and liver cancer cells.

Subhamoy Datta[1], Emilia Kotinurmi[1], Konsta Karttunen[1], Biswajyoti Sahu[2], **Paivi Pihlajamaa**[1]

[1]Applied Tumor Genomics Research Program, Faculty of Medicine, University of Helsinki, Helsinki, Finland,[2]Norwegian Centre for Molecular Biomedicine and Medicine and Applied Tumor Genomics Research Program, University of Helsinki, Finland; University of Oslo, Oslo, Norway

Cellular metabolism is a dynamic process that supports tissue homeostasis, growth, and environmental adaptation. Cancer cells exploit this by rewiring metabolic pathways in response to oncogenic cues and microenvironmental pressures. While oncogene-driven metabolic reprogramming is an established cancer hallmark, the extent to which specific metabolic enzymes shape the chromatin and transcriptional landscape of cancer cells remains incompletely understood. Here, we systematically interrogate how loss of individual metabolic enzymes rewires gene expression programs through chromatin-based mechanisms. We performed a CROP-seq screen targeting key metabolic enzymes across major pathways, including the tricarboxylic acid cycle, glycolysis, nucleotide synthesis, amino acid metabolism, fatty acid biosynthesis, and glutaminolysis, combined with single-cell RNA-seq in HCT116 colon cancer cells. Differential expression analysis relative to non-targeting controls revealed substantial transcriptional changes upon loss of several enzymes, indicating strong metabolic control over gene regulatory states. Interestingly, silencing of ACSS2 (acyl-CoA synthetase short-chain family member 2; acetate-to-acetyl-CoA pathway) elicited one of the most pronounced transcriptional effects, and similarly a broad gene expression shift was observed upon shRNA-mediated ACSS2 silencing followed by bulk RNA-seq in HepG2 liver cancer cells. ACSS2 converts acetate into acetyl-CoA in both the cytosol and nucleus, positioning it as a direct metabolic regulator of histone acetylation and chromatin accessibility. Notably, loss of metabolic enzymes upstream of acetyl-CoA production, including fumarate hydratase (FH; tricarboxylic acid cycle) and pyruvate dehydrogenase beta subunit (PDHB; pyruvate-to-acetyl-CoA conversion), induced compensatory upregulation of ACSS2, suggesting a feedback mechanism that maintains nuclear acetyl-CoA availability. Ongoing work couples these transcriptional profiles with ChIP-seq profiling of histone acetylation and other chromatin marks, enabling direct linkage between metabolic perturbation, chromatin remodeling, and transcriptional outcomes. Together, this study reveals how metabolic dependencies converge on chromatin-mediated transcriptional control and contributes to a broader understanding of how metabolic state influences gene regulation in cancer. Full results and mechanistic insights will be presented at the meeting.

#4720 Glutamine transporter ASCT2 as a therapeutic target in HPV positive organoid models of HNSCC.

Shu-Yun Cheng, Ella Jackert, Liyang Tang, Daniel Kwon, Niels Kokot, Uttam Sinha, Yang Chai, Albert Y. Han

University of Southern California, Los Angeles, CA

Background: Head and neck squamous cell carcinoma (HNSCC) is the sixth most common cancer worldwide, with Human Papillomavirus (HPV) - 16 infections being a cause. Previous studies have shown that glutamine is a crucial amino acid that provides carbon and nitrogen for proliferating cells. In particular, some cancer cells increase the uptake of glutamine through metabolic reprogramming. However, our understanding of glutamine metabolism and transport remains limited in HNSCC. In this study, we will be investigating glutamine transport, specifically ASCT2, in patient-derived normal tonsil organoid and HPV16-positive tonsil organoids.

Methods: Tonsil tissue is obtained from tonsillectomy and process for organoid generation. Through mechanical and enzymatic dissociation, tonsil tissue is dissociated into single cell suspension and plated in extracellular matrices. HPV16 lentivirus is used to infect tonsil organoids and used as premalignant HPV16-positive HNSCC model. RNA of the normal tonsil and HPV+ organoids were extracted for qPCR analysis. V-9302, an ASCT2 competitive antagonist, was treated to the organoids for IC_{50}.

Results: In this study, the glutamine transporter, ASCT2, was investigated in patient-derived normal tonsil organoid and HPV16-positive tonsil organoids. Both organoid models exhibit ASCT2 through qPCR analysis, with HPV16-positive tonsil organoids exhibiting less ASCT2 (FC 0.64 $p<0.00$) than normal tonsil organoids. To see if ASCT2 can be a therapeutic target, V-9302 was treated to normal tonsil organoids and HPV16-positive tonsil organoids. V-9302 IC_{50} of the organoids were obtained, with HPV16-positive organoids being more sensitive (IC_{50}: 15.37 μM) than normal tonsil organoids (IC_{50}: 20.50 μM).

Conclusion: Glutamine is an essential amino acid for cell growth and proliferation, especially in fast growing tumors. With V-9302 being more sensitive to HPV16-positive organoids, V-9302 shows the potential to be used as a therapeutic drug for HNSCC treatment. Future studies will focus on V-9302 sensitivity in patient-derived HNSCC tumor organoids.

#4721 Cross-species multi-omics mapping of APC/KRAS-driven metabolic networks.

Mahima Bharti[1], Swagata Maity[1], Marcos Calderon[1], Peng Zhang[1], Augustine Takyi[2], Marco Marchetti[3], Paul Stewart[2], Bruce A. Edgar[1]

[1]Department of Oncological Sciences, Huntsman Cancer Institute, University of Utah, Salt Lake City, UT,[2]Department of Nutrition & Integrative Physiology, Huntsman Cancer Institute, University of Utah, Salt Lake City, UT,[3]Eccles Institute of Human Genetics, University of Utah, Salt Lake City, UT

Colorectal cancer (CRC) is the third most diagnosed malignancy and the second leading cause of cancer-related deaths worldwide. Over 70% of CRCs harbor activating mutations in the EGFR/KRAS and WNT/APC pathway genes, which regulate intestinal stem cells (ISCs) proliferation and differentiation. While these oncogenic pathways are well depicted for their transcriptional effects, their metabolic interactions and cooperative roles in tumor progression remain unclear. Our preliminary data reveal that EGFR signaling promotes ISC self-renewal through an anabolic program that redirects carbohydrates to biosynthetic pathways while using fatty acid oxidation (FAO) to sustain ATP production. Published evidence also suggests that WNT/APC signaling induces similar metabolic changes. Here we show that co-activation of WNT/APC and EGFR/KRAS signaling reprograms cellular metabolism, generating cancer-specific vulnerabilities distinct from those induced by either mutation alone. To test this, we employ an integrated multimodal and multi-omics strategy that combines transcriptomics, metabolomics, lipidomics, and proteomics across *Drosophila* models and patient-derived organoids (PDOs). This approach maps metabolic changes under normal and oncogenic conditions involving EGFR/RAS and WNT/APC pathways. In *Drosophila*, ISC-derived cell clones carrying Apc^{Δ}, Ras^{G12V}, or dual $Apc^{\Delta}; Ras^{G12V}$ mutations reveal that dual-hit clones show enhanced proliferation, altered morphology, and cancer-like phenotypes, unlike single hits. Transcriptomic and metabolomic analyses identified distinct differentially expressed genes (DEGs) and metabolic profiles in the dual-hit state, particularly in mitochondrial, lipid, and nucleotide biosynthetic pathways. Integrated multi-omic analyses further identified unique metabolic modules reflecting synergistic reprogramming. Parallel studies in patient-derived cancerous (CRC) organoids show similar patterns: compared to normal control gut organoids, CRC organoids displayed altered morphology, transcription, and metabolism, including reprogrammed lipid and amino acid metabolism and enhanced glycolytic and mitochondrial activity. Following prioritization by evolutionary conservation and multi-omic integration, ~40 candidate genes (e.g., *r, mt:ND4L, eloF, Ak1*) will be functionally tested via RNAi or inhibitors in Apc^{Δ} Ras^{G12V} *Drosophila* ISC clones and *APC/KRAS* colon organoids to assess tumor-suppressive effects. Validated effectors will be evaluated in mouse and xenograft models to identify targetable metabolic dependencies. Together, these findings demonstrate that concurrent APC and KRAS mutations establish a unique synergistic metabolic program driving aggressive CRC. By integrating multi-omics and cross-species models, this study is finding conserved, cancer-specific metabolic effectors as promising therapeutic targets in colorectal cancer.

#4722 Genetic background shapes mitochondrial metabolic adaptations underlying thyroid cancer progression.

Vincenzo Davide Pantina[1], Chiara Modica[1], Francesco Verona[2], Giulia Bozzari[1], Roberta Drago[1], Caterina D'accardo[1], Gaetana Porcelli[2], Sebastiano Di Bella[1], Rosario Brancato[2], Pierre Sonveaux[3], Matilde Todaro[2], Giorgio Stassi[1]

[1]Department of Precision Medicine in the Medical, Surgical and Critical Care Areas, University of Pa, University of Palermo, Palermo, Italy,[2]Department of Health Promotion, Mother and Child Care, Internal Medicine and Medical Specialties (P, University of Palermo, Palermo, Italy,[3]Catholic University of Louvain School of Medicine, Brussels, Belgium

Introduction: Anaplastic Thyroid Cancer (ATC) is characterized by rapid progression and unclear dissemination mechanisms. Tumor evolution is not solely defined by the selective pressure acting on pre-existing subclones, but is intricately intertwined with the rapid, environmentally mediated acquisition of adaptive phenotypes. Metabolic plasticity is a critical process that lies at the intersection of these complementary evolutionary paradigms, actively fueling malignant progression and conferring metastatic competence. Elucidating how metabolic rewiring contributes to the emergence and expansion of highly invasive ATC clones is critical to counteract TC progression

Experimental procedures: We established a TC tumorigenesis model by leveraging human embryonic stem cells and CRISPR/Cas9 genome engineering to generate distinct TC progenitor cells, harbouring specific mutations. We developed highly invasive in vitro TC cells to identify the metabolic signatures linked to cellular aggressiveness. The data were corroborated in orthotopic TC mouse models, which recapitulated the disease progression. The metabolic profile was characterized by measuring oxygen consumption rate (OCR), extracellular acidification rate (ECAR). RNA-seq data were analyzed to obtain transcriptomic and metabolism-related signatures associated with specific genetic background. Cells were treated with MitoQ, Treatment effects were assessed on primary tumor growth and metastatic dissemination.

New, unpublished data: We observed that BRAF V600E single/double-mutated cells cluster based on their metabolic profile and undergo a similar metabolic shift during the selection of super-invasive subpopulations. BRAFV600E-mutated ATC-derived aggressive clones experience a reprogramming toward oxidative phosphorylation (OXPHOS). ATC superoxide clones exhibit heightened mitochondrial respiration, increased mitochondrial membrane potential, and accumulation of mitochondrial reactive oxygen species, in line with their enhanced invasive capacity. Leveraging this metabolic dependency uncovered a therapeutic opportunity: treatment with the mitochondria-targeted antioxidant MitoQ significantly reduced cellular invasiveness in vitro and suppressed lung metastasis formation in vivo in mouse models. This defined metabolic vulnerability provides a distinct signature that may aid in stratifying relevant thyroid cancer patient subsets.

Conclusions: Our study demonstrates that mitochondrial metabolic rewiring is not a universal feature of ATC but is instead tightly dictated by the tumor's genetic background. These findings underscore the critical interplay between genetic context and metabolic adaptation, providing a refined framework for developing targeted therapeutic strategies aimed at pharmacologically restraining the metastatic progression of BRAFV600E-mutated ATC

#4723 Dysregulated lipid metabolism accompanies chromosomal instability in obesity-associated oesophageal adenocarcinoma.

Yun Suen Kho[1], Aiswarya Nair[2], Daryl Kai Ann Chia[3], Supriya Srivastava[4], Jimmy Bok Yan So[3], Asim Shabbir[3], Li Ren Kong[5], Ashok R. Venkitaraman[2]

[1]School of Medicine, NUS Centre for Cancer Research, Cancer Science Institute of Singapore, National University of Singapore, Singapore, Singapore,[2]Cancer Science Institute of Singapore, Singapore, Singapore,[3]Department of Surgery, National University Hospital, National University Health System, Singapore, Singapore,[4]Department of Medicine, National University of Singapore, Singapore, Singapore,[5]Lee Kong Chian School of Medicine, Nanyang Technological University, Singapore, Singapore

Background - The global rise in obesity has been paralleled with increasing incidence of obesity-associated cancers, including OAC. While epidemiological studies have shown a strong link between obesity and increased risk of OAC, the underlying mechanism remains poorly understood. We hypothesized that toxic metabolites associated with obesity can induce chromosomal instability, thereby provoking carcinogenesis in OAC.

Method - To investigate obesity-associated metabolic and genomic alterations in OAC, we performed metabolomics, immunohistochemistry (IHC) and whole-genome sequencing on paired malignant and non-malignant gastroesophageal junction (GEJ) tissues from individuals with varying body mass index (BMI). To model early events during obesity-associated tumorigenesis, we have developed long-term organoid cultures from normal simple columnar epithelial biopsies obtained during bariatric surgeries, to test the effects of long-term growth in a high lipid environment.

Results - Our preliminary results suggested an association between obesity and dysregulated lipid metabolism in both non-malignant and OAC tissues. Obese non-malignant tissues showed an elevation in toxic lipid metabolite, 4-hydroxy-2-nonenal (4-HNE) and higher oxidative stress with elevated oxidative DNA damage markers. Obese tumour tissues exhibited a higher tumour mutational burden and genomic instability score, suggesting that obesity may result in a distinct, genomically unstable OAC subtype. To recapitulate these obesity-associated alterations, organoids were grown in a high lipid environment. Prolonged culture induced morphological changes, with reduced differentiation markers and increased stemness. Notably, lipid withdrawal restored the organoid morphology, demonstrating that lipid-rich conditions can transiently alter epithelial cell states and may contribute to tumour initiation.

Conclusion - Our preliminary results suggest the existence of an obesity-associated OAC subtype driven by lipid-mediated metabolic and genomic dysregulation. The organoid model serves as an *in vitro* platform for dissecting early events in obesity-associated tumorigenesis and highlights the potential role of toxic lipid metabolites in cancer initiation.

#4724 Elevated plasma trimethylamine-N-oxide (TMAO) levels correlate with better clinical and molecular responses in immunotherapy-treated resectable gastroesophageal cancer and pleural mesothelioma.

Rachel J. Keogh[1], Paul K. Lee[1], N.V. Rajeshkumar[1], Blair V. Landon[1], Joshua E. Reuss[2], Jaime Wehr[1], Gavin Pereira[1], Amna Jamali[1], Noushin Niknafs[1], Ronan J. Kelly[3], Ali H. Zaidi[4], Josephine L. Feliciano[1], Julie R. Brahmer[1], Vincent K. Lam[1], Patrick M. Forde[1], Chi V. Dang[1], Valsamo Anagnostou[1]

[1]Johns Hopkins University School of Medicine, Baltimore, MD,[2]Georgetown Univ. School of Medicine, Washington, WA,[3]Charles A. Sammons Cancer Center Baylor University Medical Center, Dallas, TX,[4]Allegheny Health Network Cancer Institute, Pittsburgh, PA

Background: Microbiome-derived metabolites have demonstrated significant impact on immunotherapy response, particularly in the context of immune checkpoint blockade (ICB). Trimethylamine-N-oxide (TMAO), an amine oxide generated when gut bacteria metabolize dietary choline, has been identified in preclinical studies to enhance anti-tumor immune responses. Here, we evaluated circulating choline metabolites with respect to clinical outcomes and circulating tumor DNA (ctDNA) residual disease in patients with resectable cancers receiving neoadjuvant ICB.
Methods: Pre-treatment choline, trimethylamine (TMA) and TMAO plasma concentrations from 51 patients with stage I-III diffuse pleural mesothelioma (DPM; n = 25 patients; NCT03918252) or stage II/III esophageal/gastro-esophageal junction cancer (E/GEJ; n = 26 patients; NCT03044613) on neoadjuvant ICB, were quantified via liquid chromatography-mass spectrometry (SCIEX Triple Quad 6500+). Clinical outcomes were compared across metabolite thresholds, as were ctDNA residual disease through tumor-informed cell-free DNA (cfDNA) whole-genome sequencing (WGS). ctDNA residual disease in the DPM cohort was measured by intersecting tumor (n = 28), white blood cell (n = 28), and plasma (n = 97) WGS.
Results: In the DPM cohort, median baseline choline, TMA and TMAO concentrations were 3970, 2840 and 256 ng/mL, respectively. Higher baseline TMAO levels were associated with lower ctDNA residual disease at C2D1 (Fisher's exact, p = 0.028), C3D1 (Fisher's exact, p = 0.057) and pre-surgery (Fisher's exact, p = 0.01). Further, patients with higher TMAO had either undetectable ctDNA throughout the neoadjuvant window or ≥95% reduction in cfDNA tumor fraction from baseline to pre-surgery (Fisher's exact, p = 0.028). In this cohort, ctDNA residual disease strongly correlated with progression-free and overall survival (log-rank, p < 0.05). In the E/GEJ cohort, median baseline choline, TMA and TMAO concentrations were 279, 2945 and 4175 ng/mL, respectively. Patients who attained a major pathologic response had numerically higher TMAO levels (Fisher's exact, p = 0.078). In line with the findings in the DPM cohort, patients in the E/GEJ cohort with lower TMAO (lowest quintile; <197 ng/mL) had shorter overall survival (log-rank, p = 0.034) compared to those with higher TMAO concentration (≥197 ng/mL), an association that remained significant after adjusting for clinicopathological variables (Cox multivariable, p = 0.04).
Conclusion: Our findings indicate that higher plasma TMAO levels may be linked to molecular ctDNA response and better clinical outcomes with neoadjuvant ICB, further supporting a potential immunomodulatory role of choline metabolites in enhancing immunotherapy response.

: Metabolic Features of Thoracic and Urologic Cancers
Poster Session

#4728 Loss of LKB1 promotes lactate utiliaztion in *KRAS*-mutant lung adenocarcinoma.

Yu Qian[1], David Molkentine[1], Yifan Kong[1], Amirali Karimi[1], Qian Huang[1], Chendong Yang[2], Ralph J. DeBerardinis[2], John V. Heymach[1]

[1]UT MD Anderson Cancer Center, Houston, TX,[2]Children's Medical Center Research Institute, University of Texas Southwestern Medical Center, Dallas, TX

Loss of function of the tumor suppressor LKB1, which is encoded by the gene *STK11*, represents about 20% in non-small cell lung cancer (NSCLC). LKB1 is frequently co-mutated with *KRAS*, and LKB1-deficiency is associated with resistance to anti-PD1 therapy but remain partial response to anti-PD1/CTLA4 dual checkpoint blockade. We previously found that LKB1 loss led to increased lactate levels in the tumor microenvironment and suppressed anti-tumor immunity. However, whether LKB1-deficient tumor cells directly benefit from the lactate rich environment remains unclear. We hypothesized that LKB1 deficiency enhances lactate utilization and promotes a malignant phenotype. We performed metabolic profiling on Kras mutant LKB1-proficient (K) and -deficient (KL) cells treated with lactate. Seahorse assay was performed in K and KL cells to measure lactate utilization in vitro, and isotope tracing was conducted in vitro and in vivo. Single-cell RNAseq (scRNAseq) data from murine syngeneic tumors and clinical samples were used to assess the lactate metabolism score in KRAS mutant tumors with or without LKB1/*STK11* alterations. We treated K and KL cells with lactate as the carbon source and performed metabolic profiling. The data showed that altered metabolites were enriched in several pathways including TCA cycle. We observed that KL cells showed increased oxidative phosphorylation (OXPHOS) and GSH and NADPH levels when cultured with lactate, suggesting that LKB1-deficient cells had an enhanced ability to utilize OXPHOS and maintain redox homeostasis when using lactate as an energy source. Moreover, [U-13C]lactate tracing revealed that isotopologues were significantly enriched in pyruvate and TCA components such as citrate, glutamate and malate in KL cells, indicating the enhanced lactate incorporation into the TCA cycle, which was consistent with the observed elevated OXPHOS. Next, we injected K and KL murine cells into mice to establish syngeneic tumor models. Animals were infused with [U-13C]lactate to detect the isotopologues distribution in vivo. KL tumors showed significantly enhanced lactate incorporation as compared to K tumors. Genetically engineered mouse models of K and KL lung cancer similarly showed that increased amounts of lactate transformed into citrate, succinate and malate. Finally, we analyzed data from clinical samples infused with [U-13C]lactate, although the sample size was limited, patients with *KRAS*/*STK11* co-mutation showed a trend towards increased labeling of TCA cycle metabolites as compared to patients with *KRAS* or *KRAS*/*TP53* co-mutation. Additionally, scRNAseq data from murine tumors and clinical samples showed significantly elevated lactate metabolic score in KL tumors. Collectively, our data indicates that LKB1-deficient tumors increase lactate incorporation and utilization, suggesting that targeting lactate metabolism as a novel therapeutic approach for this recalcitrant subgroup.

#4729 LINE-1 retrotransposition drives lipid metabolic reprogramming and immune suppression in lung squamous cell carcinoma via cPLA2/5-LOX axis.

Rui Zhang, Wenjing Tian, Pengpeng Liu, Jinpu Yu

Tianjin Medical Univ. Cancer Inst. & Hospital, Tianjin, China

Background: Long interspersed nuclear element-1 (LINE-1; L1) retrotransposition is frequent in lung squamous cell carcinoma (LUSC), yet its functional impact remains largely unelucidated. We previously identified recurrent L1-ATP8B1 (L1 insertion in ATP8B1) associated with poor prognosis. Given ATP8B1's role in lipid homeostasis, we hypothesize L1-ATP8B1 drives lipid metabolic reprogramming to promote LUSC progression.
Methods: We integrated transcriptomic analyses of The Cancer Genome Atlas (TCGA) and validation cohorts with targeted metabolomics, functional assays, and tumor-immune cell co-culture systems. Mechanistic studies were conducted via genetic perturbation, pharmacologic inhibition, and rescue experiments in both in vitro and in vivo models.
Results: Gene Ontology and KEGG enrichment analysis revealed L1-ATP8B1 correlated with deregulated lipid metabolism, particularly arachidonic acid (AA) metabolism. Metabolomic profiling results confirmed elevated AA-derived 5-HETE and 5-oxo-ETE (the oxidation metabolite of 5-HETE) in L1-ATP8B1-over-expressing cells. Mechanistically, L1-ATP8B1 up-regulated the transcriptional levels of PLA2G4 and ALOX5 to enhance AA release and 5-HETE generation. Pharmacologic inhibition of the activity of their metabolic enzymes cytosolic phospholipase A_2 ($cPLA_2$) and 5-lipoxygenase (5-LOX) abrogated tumor progression, whereas exogenous 5-oxo-ETE rescued the effects. Further, we found L1-ATP8B1 induced immune suppression by recruiting myeloid-derived suppressor cells (MDSCs). Co-culture experiments demonstrated 5-oxo-ETE enhanced the immunosuppressive function of MDSCs by activating non-canonical NF-κB signaling, thereby inhibiting T cell proliferation and IFN-γ production-an effect reversed by 5-LOX inhibition.
Conclusions: Our findings uncover a previously unrecognized L1/cPLA2/5-LOX/NF-κB axis linking lipid metabolic reprogramming to LUSC immune evasion. L1-ATP8B1 drives tumor aggressiveness and immune suppression via lipid mediators. Targeting this pathway is a promising therapeutic strategy to overcome immune resistance in LUSC.

#4730 Construction of a prognostic model for small-cell lung cancer based on lipid metabolism related proteins.

Haohua Zhu[1], **Aijuan Yu**[2], Huiyang Shi[3], Jingyu Lu[3], Kai Zhu[3], Miaohan Wang[3], Yi Liu[2], Naizhong Zheng[2], Xingsheng Hu[3]

[1]Cancer Center, Aerospace Center Hospital, Beijing, China,[2]DeepKinase Biotechnologies Ltd., Beijing, China,[3]Department of Medical Oncology, National Cancer Center/National Clinical Research Center for Cancer/Cancer Hospital, Chinese Academy of Medical Sciences & Peking Union Medical College, Beijing, China

Small cell lung cancer (SCLC) is a highly invasive tumor with poor prognosis. There is an urgent need to develop novel biomarkers to identify patients with high-risk SCLC and optimize individual treatment strategies. We conducted a comprehensive, mass spectrometry-based proteomic analysis of 120 tumors (90 primary, 15 lymph node, 15 brain) from 105 SCLC patients. Metabolic transformation has become a hallmark of cancer. Additionally, we have found a correlation between lipid metabolism and the recurrence and metastasis of SCLC in our previous study, based on this deep, unbiased proteomic profiling. This analysis aimed to construct a prognostic risk score for SCLC using lipid metabolism related proteins and explore the underlying molecular biological mechanisms. We first identified 940 proteins related to lipid metabolism, of which 51 were associated with the prognosis of patients. The unsupervised consensus clustering results showed two different lipid metabolism patterns for SCLC, which was associated with patient prognosis and immune cell infiltration. Eight survival related lipid metabolism proteins were further identified through LASSO regression to construct a prognostic risk score, which is an independent prognostic factor for SCLC patients and validated in an independent cohort. The correlation of risk score with neuronal characteristics and anti-tumor immune response was revealed through pathway enrichment analysis of differentially expressed proteins between low-risk and high-risk groups. Finally, low-risk group showed significantly higher sensitivity to almost all chemotherapy and targeted therapy drugs compared to the high-risk group.

#4731 Cysteine oxidation is required for brain metastasis in lung cancer.

Maolin Ge

Mass General Cancer Center, Boston, MA

Most cysteine residues are believed to require a reduced state for activity and their oxidation by reactive oxygen species (ROS) is traditionally viewed as damaging to proteins. However, it stands that some cysteines that must be oxidized for protein function, yet their identity remains largely unknown. To answer this question, we lowered ROS levels in 55 lung cancer cell lines and analyzed the cellular consequences using cysteine-focused chemical proteomics paired with functional CRISPR screens. This integrated approach revealed hundreds of impacted cysteines required for proliferation. We focused on NDUFA10•C253 in mitochondrial complex I, which we find exists in a more oxidized state in some human brain metastases. This cysteine is dynamically regulated by antioxidant pathways and its oxidation is required for complex I stability and supports metastasis to the brain. Collectively, we demarcate oxidized cysteines essential for cell fitness and disease states including metastasis.

#4732 Anaplastic lymphoma kinase harnesses the SLC4A7 bicarbonate transporter to intensify de novo nucleotide synthesis in neuroblastoma and lung cancer..

Ruth Palmer[1], Wei-Yun Lai[1], Tzu-Po Chuang[1], Joel Johansson[1], Emre Can Tuysuz[1], Dan E. Lind[1], Alexander Schmidt[2], Michael N. Hall[3], Bengt Hallberg[1]

[1]Institute of Biomedicine, University of Gothenburg, Gothenburg, Sweden,[2]Biozentrum, University of Basel, Basel, Switzerland,[3]University of Basel, Basel, Switzerland

There is growing recognition of how metabolic dependencies influence sensitivity or resistance to neuroblastoma (NB) therapies. In this regard, the impact of Anaplastic Lymphoma Kinase (ALK), a receptor tyrosine kinase which is mutated in approximately 10% of primary NB cases, and a clinical target in NB on cellular metabolism is unclear. In this study, we combined phosphoproteomics and BioID-mediated proximity interaction screening in neuroblastoma cell lines, identifying the sodium bicarbonate transporter SLC4A7, a member of the Solute Carrier (SLC) family, and the multifunctional protein Carbamoyl Phosphate Synthetase 2-Aspartate Transcarbamylase-Dihydroorotase (CAD) downstream of ALK signaling in NB cells. SLC4A7 and CAD are both important molecular components in the metabolism of pyrimidine nucleotides. ALK activation leads to phosphorylation of both SLC4A7 and CAD, resulting in increased sodium bicarbonate transport and pyrimidine biosynthesis that is blocked by the addition of ALK tyrosine kinase inhibitors (TKIs). Combined targeting of both ALK signaling and nucleotide synthesis leads to a more effective inhibition of NB tumor growth in both cell and genetically modified mouse NB models. Finally, we show that SLC4A7 and CAD are also targets in ALK-driven non-small cell lung cancer (NSCLC), revealing a novel therapeutic strategy that leverages metabolomic dependencies to target ALK-driven malignancies such as NB and NSCLC.

#4734 Metabolomic profiling among non-small cell lung cancer and non-cancer populations: A case-control study.

Yoo-Min Koh[1], Jae Jeong Yang[2], Mi-Jeong Yoo[3], Qiuyin Cai[4], Feifei Xiao[2], Hiren Mehta[2], Lizi Wu[2], Hyung-Suk Yoon[2]

[1]Yale University, New Haven, CT,[2]University of Florida, Gainesville, FL,[3]Clarkson University, Potsdam, NY,[4]Vanderbilt University Medical Center, Nashville, TN

Lung cancer is the second most common cancer in the United States, with an estimated 124,730 deaths projected in 2025. Non-small cell lung cancer (NSCLC) accounts for 80-85% of all lung cancer cases, making it the predominant form of the disease. 27.4-28.1% of NSCLC cases are diagnosed at early stages, indicating the need for biomarker testing, which enhances detection accuracy beyond imaging-based approaches alone. Metabolomics enables the comprehensive identification of NSCLC-specific metabolites, revealing distinct biochemical alterations that inform the discovery of novel diagnostic biomarkers and could be utilized to further investigate outcomes and therapeutic targets. Therefore, we conducted a pilot metabolomics study using a case-control design to identify differentially abundant metabolites between NSCLC patients and non-cancer controls, with the goal of discovering potential metabolomic biomarkers associated with NSCLC. A total of 80 NSCLC patients (45.6% male; mean age=65.4) and 40 non-cancer control individuals (24.3% male; mean age=40.2) were included in this study. Global metabolomic profiling from serum samples of the study population utilizing the Orbitrap Fusion and the TSQ Altis QqQ mass spectrometry interfaced with the Vanquish Horizon UHPLC system at the UF ICBR Proteomics & Mass Spectrometry. Differentially abundant metabolites were determined using Mann-Whitney U-tests with Benjamini-Hochberg FDR correction and fold-change threshold. Global metabolomic profiling identified 5,307 metabolites, of which 626 (11.8%) were differentially abundant between NSCLC patients and non-cancer controls using stringent criteria (FDR<0.01, FC≥4). 455 metabolites were less abundant, and 171 were more abundant in NSCLC. The results from PCA demonstrated a separation between NSCLC patients and non-cancer controls, with PC1 and PC2 accounting for 25% of the total variance. OPLS-DA confirmed the discrimination of metabolic profiles between NSCLC patients and non-cancer controls. Network analysis revealed dysregulation in metabolic pathways, including the urea cycle, TCA cycle, amino acid metabolism, and polyamine biosynthesis. Key metabolites, including hypoxanthine, adipic acid, and betaine, were significantly less abundant in NSCLC. Pathway enrichment analysis identified enrichment in purine and pyrimidine metabolism, suggesting altered nucleotide metabolism associated with NSCLC. Larger prospective studies are warranted to validate these metabolomic biomarkers for clinical application in NSCLC. Future investigations will evaluate their utility in predicting prognosis, treatment response, and survival. The implementation of these NSCLC-specific metabolomic signatures in clinical practice could enhance prognostic accuracy and inform personalized treatment strategies, ultimately improving outcomes and survival.

#4735 Designing a novel 3D co-culture model incorporating patient T-cells to study lipid metabolism as a metabolic vulnerability in KRAS driven non-small cell lung cancer.

Saoirse Flanagan[1], Robyn Stanley[2], Sze Ying Tan[2], Beatrice Malacrida[3], Noemie Petit[4], David O'Reilly[5], Jarushka Naidoo[5], Shane Browne[4], Paul Murray[1], Catriona M. Dowling[2]

[1]School of Medicine, University of Limerick, Limerick, Ireland,[2]Department of Medicine, Royal College of Surgeons in Ireland, Dublin, Ireland,[3]Centre for Tumour Microenvironment, Barts Cancer Institute, Queen Mary University of London, London, United Kingdom,[4]Tissue Engineering Research Group, Department of Anatomy & Regenerative Medicine, Royal College of Surgeons in Ireland, Dublin, Ireland,[5]Beaumont Hospital, Dublin, Ireland

Non-small cell lung cancer (NSCLC) accounts for 80-85% of all lung cancers worldwide, with KRAS-driven NSCLC representing 30% of these cases. Although immunotherapy has improved outcomes in lung cancer, only 27-46% of patients respond initially to immune checkpoint inhibitors (ICIs). One cohort of patients that do not respond to such treatment include those with KRAS-driven NSCLC harbouring a co-mutation in the LKB1 gene (KL), who have significantly poorer responses to immunotherapy compared to those with a KRAS and TP53 co-mutation (KP). However, the reason for this difference in response to immunotherapy is largely unknown. Recent studies demonstrate that metabolic vulnerabilities in KL genotypes can influence therapeutic response. We aim to identify and target these vulnerabilities in KL NSCLC, with the aim to enhance response to immunotherapy. Using the cBioPortal mRNA database and publicly available patient protein data, we completed a bioinformatic analysis of key genes, proteins, and metabolites involved in major metabolic pathways. Lipid metabolism displayed significant differences between KP and KL genotypes, specifically β-oxidation and fatty acid synthesis. Following this, we conducted a drug screen using inhibitors targeting lipid metabolism. Fatty acid synthase (FASN) inhibitor, TVB-2640, showed the greatest efficacy in KL cells. Moreover, functional assays demonstrated reduced colony formation and migration following FASN inhibition in KL cells. Separately, we have successfully established novel 3D co-culture models of NSCLC cell lines and T-cells. This was achieved by embedding A549 NSCLC cells in a collagen gel matrix, with peripheral blood mononuclear cells (PBMCs) from patients with NSCLC enrolled on PLAN clinical trial (Trial ID: NCT05542485) added to the surrounding media. PBMCs were isolated, activated and expanded for 7 days using CD3, CD28 and IL-2. Following expansion, the T-cells were added to the A549 co-culture model for a further 4 days. These co-cultures were then paraffin embedded and stained using immunohistochemistry (IHC). Results demonstrated positive Ki67 staining and low cleaved caspase-3, indicating cell proliferation and minimal cell death. Moreover, IHC and flow cytometry analysis revealed 12% and 19% CD3 positive staining respectively, confirming successful T-cell infiltration in our co-culture model. In conclusion, we have identified fatty acid synthesis as a metabolic vulnerability in KL NSCLC. Targeting this pathway could be a potential therapeutic option for patients with this genotype of NSCLC. Moreover, we have developed a novel 3D co-culture model using NSCLC cells and patient T-cells. Further analysis, supported by our 3D co-culture model, aims to analyse the consequences of targeting fatty acid synthesis in combination with immunotherapy in the KL genotype of NSCLC.

#4736 Trace metal signatures in non-small cell lung cancer: A pilot study of patients attended at Mount Sinai Hospital in New York City.

Diddier Prada[1], Manish Arora[1], Julio landero[1], Jamshid Abdul Ghafar[1], Rachel Brody[2], Oscar Arrieta[3], Fred R. Hirsch[2]

[1]Icahn School of Medicine at Mount Sinai, New York, NY,[2]Mt. Sinai Medical Center Tisch Cancer Institute, New York, NY,[3]Instituto Nacional de Cancerologia (INCan), Mexico City, Mexico

Abstract Background: Non-small cell lung cancer (NSCLC) is increasing worldwide, yet the environmental and mechanistic contributors driving tumor development and aggressiveness remain poorly defined. Metals and trace elements—ubiquitously present in air pollution—can induce oxidative stress, potentially generating DNA damage that remodels tumor metabolism and promotes malignancy. We evaluated the feasibility of integrating metal profiling in malignant and normal NSCLC tissues and identified preliminary correlations between trace elements and malignancy status.
Methods: Ten OCT-embedded lung adenocarcinoma cases from an urban cohort of patients attended and biobanked at the Mount Sinai Biorepository underwent laser-capture microdissection to isolate paired tumor and adjacent normal tissue. Twenty-three metals and trace elements were quantified using Inductively Coupled Plasma Mass Spectrometry (ICP-MS) following nitric acid digestion. Logistic regression models (unadjusted due to sample size) were used to evaluate associations with tumor status. Linear regressions were used for tumor size.
Results: Tumor tissue demonstrated distinct metal signatures. Magnesium (Mg) and selenium (Se) were significantly enriched in tumors (Mg: Odds ratio [OR]=4.79, 95% Confidence Interval [95% CI]: 1.10-20.82; Se: OR=18.93, 95% CI: 1.48-242.44), while nickel (Ni) and zinc (Zn) showed positive trends toward tumor accumulation. Iron (Fe) was markedly higher in normal tissue. Additional analyses revealed inverse associations between tumor size and chromium (Cr; β = -1.34, 95%CI: -2.41, -0.27, p = 0.02*), manganese (Mn; β = -1.06, 95%CI: -2.32, 0.199, p = 0.09*), and cesium (Cs; β = -1.10, 95%CI: -2.16, -0.04, p = 0.04*).
Conclusions: Preliminary data demonstrate the feasibility of multiple metal and trace element quantification in NSCLC tissues, revealing potential specific perturbations associated with tumor presence and aggressiveness. The observed enrichment of Mg, Se, and Ni in tumors supports a potential mechanistic link between metal exposure, trace element imbalance, and malignant phenotypes, which may contribute to NSCLC tumorigenesis in urban populations. Ongoing analyses will integrate mitochondrial mtDNA heteroplasmy variants from these NSCLC samples to elucidate metal-mitochondrial interactions driving tumor biology.
Keywords: "NSCLC," "Trace Metals," "Environmental Carcinogenesis," "Tumor Microenvironment."

#4737 Utilizing patient-derived organoid tumor models to combat chemo-immunotherapy resistance in NSCLC.

Manojavan Nagarajan[1], Chunjing Wu[2], Dao M. Nguyen[3], Estelamari Rodriguez[1], Emily Kim[4], Diane Lim[5], George Theodore[2], Irving Vidaurre[2], Wei Sha[2], Adeline Murphy[2], Jose Gomez[2], Durga Prasad Gannamedi Hinder[1], David Lombard[1], Lynn G. Feun[6], Niramol Savaraj[5], Medhi Wangpaichitr[5]

[1]Univ. of Miami/Sylvester Comprehensive Cancer Center, Miami, FL,[2]VA Medical Ctr., Miami, FL,[3]Associate Professor & Chief, Thoracic Onc., University of Miami, Miami, FL,[4]Wistar Institute, Miami, FL,[5]Univ. of Miami/VA Medical Ctr., Miami, FL,[6]Univ. of Miami Sylvester Comprehensive Cancer Ctr., Miami, FL

Immune checkpoint inhibitors (ICIs) have transformed the treatment landscape for non-small cell lung cancer (NSCLC), yet only a subset of patients achieves durable benefit due to primary and acquired resistance. We previously reported elevated kynurenine (KYN) in cisplatin-resistant NSCLC. KYN, produced by indoleamine 2,3-dioxygenase 1 (IDO1) and tryptophan 2,3-dioxygenase (TDO2), promotes immune evasion by diminishing $CD8^+$ T-cell responses and expanding regulatory T cells (Tregs). Clinical failure of selective IDO1 inhibition in cancer suggests compensatory TDO2 upregulation as one of the resistance mechanisms. To target redundant KYN production, we evaluated the efficacy of a dual IDO1/TDO2 inhibitor (AT-0174; Antido Therapeutics) in preclinical models of cisplatin-resistant NSCLC. Efficacy and mechanism were assessed in vivo via a syngeneic orthotopic mouse model. Dual inhibition significantly reduced tumor volume ($n=10$, $p<0.01$) and prolonged survival in the mouse model. These effects correlated with increased activity of $CD8^+$ T cells and natural killer (NK) cells, as well as reduced frequencies of immunosuppressive Tregs and myeloid-derived suppressor cells (MDSCs). Combining AT-0174 with anti-PD-1 therapy produced a synergistic effect, further suppressing tumor growth and significantly improving survival in mice (log-rank, $p=0.0001$). We then developed a patient-derived organoid tumor (PDOT) platform that closely recapitulates the molecular and metabolic features of each patient's NSCLC. Single-cell RNA sequencing demonstrated ~70% transcriptional similarity to original tumors, and metabolomic profiling confirmed comparable pathway activity. IDO1 protein was detected in all PDOTs. Co-culture with patient-matched PBMCs revealed that PDOTs with high baseline PD-L1 and kynurenine (KYN) expression were highly sensitive to dual IDO/TDO inhibition combined with pembrolizumab, resulting in increased immune cell infiltration ($n = 10$, $p < 0.005$). This microfluidic PDOT system enables functional, patient-specific assessment of KYN pathway reliance, supporting timely stratification of NSCLC patients and rational design of combination regimens integrating metabolic targeting with immune checkpoint inhibitors. These findings provide a strong rationale for clinical evaluation of dual IDO/TDO inhibitors alongside checkpoint blockade.

#4738 Pharmacological activation of PI3Kα triggers cancer cell death under metabolic stress.

Benoit Bilanges[1], Ralitsa Madsen[2], Daniele Morelli[1], Thomas Jones[3], Wayne Pearce[1], Etienne Leveille[4], Mustafa Kocak[5], Eden Bramson[6], Mark Bekala[1], Roger Williams[7], Nicholas McGranahan[3], Markus Muschen[8], William R. Sellers[5], Henning Walczak[1], Bart Vanhaesebroeck[9]

[1]University College London (UCL) Cancer Institute, London, United Kingdom,[2]MRC-Protein Phosphorylation and Ubiquitylation Unit, School of Life Sciences, University of Dundee, Dundee, United Kingdom,[3]Cancer Research UK Lung Cancer Centre of Excellence, UCL Cancer Institute, London, United Kingdom,[4]Yale School of Medicine, New Haven, CT,[5]Broad Institute of Harvard and MIT, Cambridge MA, Dana-Farber Cancer Institute and Harvard Medical School,, Boston, MA,[6]Center of Molecular and Cellular Oncology, Yale University, New Haven, Connecticut, USA, New Haven, CT,[7]MRC Laboratory of Molecular Biology, Cambridge, United Kingdom,[8]Center of Molecular and Cellular Oncology, Yale University, New Haven, CT,[9]Centre Lead, Centre for Cell Signalling, University College London Cancer Institute, London

Cancer cells maintain oncogenic signalling within a survival “fitness zone”. While conventional targetœed therapies suppress this signalling below a critical threshold, excessive activation of the same pathways can also be lethal to cell, an observation currently being explored as a novel therapeutic approach in cancer. In this study, we report that hyperactivation of PI3Kα, one of the most frequently oncogenically activated PI3K isoforms, using the small-molecule PI3Kα activator UCL-TRO-1938 (further referred to as 1938) induces cytotoxicity in cancer cell lines while sparing non-transformed cells. This PI3K activation-induced cell death (PI3K-AICD) depends on AKT/mTORC1 activity, only occurs under serum starvation and is enhanced by low O_2 levels. This hyperactivation lethality is mechanistically linked to an irreconcilable metabolic conflict by simultaneously activating anabolic PI3K/mTORC1 signalling in a catabolic (hypoxic) state, resulting in an unresolvable energy crisis and ultimately cell death. In serum-deprived lung cancer cell lines, 1938 induces a magnified endoplasmic reticulum stress response which, along with PI3K-AICD, can be mitigated by supplementation with unsaturated fatty acids, suggesting a critical metabolic dependency on lipid metabolism for driving this cell death response. Consequently, co-treatment with 1938 and inhibitors of stearoyl-CoA desaturase-1 (SCD1), an O_2-dependent enzyme essential for fatty acid desaturation, amplifies the PI3K-AICD response. In summary, these findings demonstrate that enhancing an oncogenic pathway central to metabolic control can selectively kill cancer cells.

#4739 Targeting PGK1 enhances enzalutamide efficacy in resistant prostate cancer.

Min Zhang, Ruixin Wang, Xiaoqi Liu

Toxicology and Cancer Biology, Univ. of Kentucky College of Medicine, Lexington, KY

Enzalutamide is a standard AR-targeting therapy for advanced prostate cancer (PCa), yet intrinsic and acquired resistance remain major barriers to durable response. To identify regulators of enzalutamide sensitivity, we performed a kinome-wide CRISPR-Cas9 knockout screen in the intrinsically resistant 22Rv1 cell line. Phosphoglycerate kinase 1 (PGK1), a key glycolytic enzyme, emerged as a top negatively selected gene, indicating that its loss increases enzalutamide susceptibility. PGK1 inhibition or genetic deletion reduced viability, colony formation, migration, and invasion in 22Rv1 cells, validating its role in maintaining the aggressive phenotype of resistant PCa. Bulk RNA-seq analysis of PGK1 knockdown cells revealed increased AR signaling pathway activity, suggesting compensatory AR reactivation following metabolic disruption. Combination MTT assays showed synergistic efficacy between PGK1 inhibition and enzalutamide, supporting a metabolic-hormonal interaction that enhances AR-directed therapy response. Mechanistically, Seahorse analysis demonstrated that PGK1 inhibition decreases glycolytic rate in resistant PCa cells, indicating impaired metabolic compensation as a potential mechanism of sensitization. Future work includes xenograft studies using 22Rv1 and LNCaP PDX models, ATP flux assays, mitochondrial stress test, lipid metabolism, and pathway-level analysis. These findings identify PGK1 as a metabolic vulnerability and highlight its therapeutic potential to overcome enzalutamide resistance in advanced prostate cancer.

#4740 Exploiting ketone body metabolism as a therapeutic vulnerability in prostate cancer.

Pablo Sanchis[1], Agustina Ayelen Sabater[2], Jiabin Dong[3], Peter Shepherd[3], Nicolas Anselmino[4], Paul G. Corn[3], Elba Vazquez[5], Christopher J. Logothetis[6], Daniel Frigo[3], Geraldine Gueron[5], Estefania Labanca[7]

[1]UT MD Anderson Cancer Center, Houston, TX, USA; CONICET-Universidad de Buenos Aires, Instituto de Quimica Biologica (IQUIBICEN), Argentina; Universidad Argentina de la Empresa (UADE), Instituto de Tecnologia (INTEC), Buenos Aires, Argentina,[2]UT MD Anderson Cancer Center; CONICET-Universidad de Buenos Aires, Instituto de Quimica Biologica (IQUIBICEN), Argentina; Universidad Argentina de la Empresa (UADE), Instituto de Tecnologia (INTEC), Buenos Aires, Argentina, Houston, TX,[3]UT MD Anderson Cancer Center, Houston, TX,[4]University of Buenos Aires, CABA, Argentina,[5]University of Buenos Aires, Buenos Aires, Argentina,[6]Chairman/Professor, Gu Med. Onc., UT MD Anderson Cancer Center, Houston, TX,[7]UT MD Anderson Cancer Ctr., Houston, TX

Prostate cancer (PCa) progression remains a major clinical challenge with limited therapeutic options, and the complexity of metabolic pathways fueling advanced PCa rests poorly understood. We have identified a shift from glycolysis to ketone body (KB) metabolism in castration-resistant PCa (CRPC), with an upregulation of ketolytic/ketogenic enzymes. From these, ACAT1 is a potential therapeutic candidate, as its expression is elevated in aggressive PCa and associates with unfavorable clinical outcomes. Here, we investigated the contribution of the bone niche -the dominant PCa metastatic site- to KB metabolism during PCa progression and evaluated ACAT1 inhibition as a treatment strategy for advanced disease. Co-culture experiments between PCa cells and bone progenitors (MC3T3, Raw264.7) were used to evaluate bone-driven metabolic adaptations. To validate *in vivo* the effect of the bone niche, we implanted MDA PCa patient-derived xenograft (PDX) 183 either intrafemorally (*i.f.*) or subcutaneously (*s.c.*) in sham or castrated CB17 SCID mice. We assessed cell viability in PCa cells lines and in PDX-derived organoids (PDX.DO), treated with increasing concentrations of ACAT1 inhibitor, arecoline hydrobromide (AH). ACAT1 and phospho-ACAT1 levels were measured by Western blot and immunofluorescence. Intracellular KB and ATP content were quantified by luciferase-based assays. Lipid uptake and accumulation were quantified by flow cytometry using Bodipy probes. *In vivo*, mice bearing MDA PCa PDXs 183, 203 and 173 were treated with AH (50 mg/kg/day i.p., 21 days). Tumor volume, KB content, and ACAT1 modulation were evaluated. We observed transcriptional activation of lipid and KB metabolism in PC3 cells from PCa-bone co-cultures, and consistently, in *i.f.* PDXs compared to matched *s.c.* tumors, alongside a significant increase in ACAT1 expression levels. Castration dynamically modulated ACAT1 levels in MDA PCa 183 tumors growing *i.f.*, with initial downregulation followed by restoration over time, underscoring KB metabolism as a mechanism of resistance within the bone niche. Functional studies showed that AH treatment reduced cell viability in PC3, C42B, and 22Rv1 cells, as well as PDX.DO, decreased ACAT1 and phospho-ACAT1 expression, lowered KB levels, and altered lipid dynamics by increasing lipid accumulation, uptake, and decreasing ATP content ($P<0.05$). *In vivo*, AH treatment in MDA PCa 183 tumors led to a significant reduction in tumor volume and intratumoral KB content ($P<0.05$). Moreover, in the CRPC model MDA PCa 203 -derived from a longitudinal sample of the same patient as 183-, and in the aggressive hormone-naïve model MDA PCa 173, AH treatment significantly reduced both tumor volume and KB content ($P<0.05$). In conclusion, our findings reveal KB metabolism as a critical vulnerability in PCa progression, with ACAT1 emerging as a druggable target whose inhibition disrupts tumor growth and metabolic fitness.

#4741 Loss of SIRT3 promotes metabolic and epigenetic dysregulation in aggressive prostate cancer.

Xiaochen Yu[1], Alphonse Nicholas Dimeck[1], Eriko Katsuta[1], Spencer Rosario[2], Mark Long[3], Song Liu[3], Kent Nastiuk[4], Hai Wang[5], Subhamoy Dasgupta[1]

[1]Department of Cell Stress Biology, Roswell Park Comprehensive Cancer Center, Buffalo, NY,[2]Department of Medicine, Roswell Park Comprehensive Cancer Center, Buffalo, NY,[3]Department of Biostatistics and Bioinformatics, Roswell Park Comprehensive Cancer Center, Buffalo, NY,[4]Department of Cancer Genetics & Genomics, Roswell Park Comprehensive Cancer Center, Buffalo, NY,[5]Department of Molecular & Cellular Biology, Roswell Park Comprehensive Cancer Center, Buffalo, NY

Prostate cancer is one of the leading causes of cancer-related deaths among men worldwide. Localized prostate tumors in certain patients relapse after surgery, radiation therapy or androgen deprivation therapy (ADT), leading to an aggressive metastatic recurrent disease. We recently found that in prostate cancer patients, SIRT3 (sirtuin 3) expression is significantly decreased in advanced metastatic disease compared to localized tumors. SIRT3 is a mitochondrial deacetylase that modulates the biochemical functions of its substrates by regulating their acetylation status. Restoration of SIRT3 levels in human and mouse prostate tumors reduced prostate cancer progression in both immune-deficient and immune competent animals. Transcriptomic profiling and targeted metabolomics analysis of bulk tumors revealed that SIRT3 regulates one-carbon metabolism pathway by controlling the levels of s-adenosyl methionine (SAM) pools. Mechanistic studies indicated that SIRT3 interacts with the rate limiting enzymes MAT1A and MAT2A that catalyze the conversion of methionine to SAM. Biochemical experiments indicated that SIRT3 deacetylates MAT1A/MAT2A which may contribute towards increased SAM synthesis. Additionally, we found that restoration of SIRT3 levels in prostate tumors increased macrophage reprogramming in the tumor microenvironment of the syngeneic mouse models. These findings provide rationale for our working hypothesis that SIRT3 may modulate prostate tumor-immune microenvironment by regulating one-carbon metabolism, and its loss accelerates lethal prostate cancer progression. Supported by NCI grants: R01CA285707 and R01CA252092 to S.D.

#4742 Investigating the crosstalk between metabolic reprogramming and epigenetic modifications in bone metastatic prostate cancer.

Madison Aust, Abbas Jawadwala, Ephraim Jeremiah Gardner, Surendra Gulla, Tej K. Sharma, Remi M. Adelaiye-Ogala

University at Buffalo, State University of New York, Buffalo, NY

Prostate cancer (PCa) is the second leading cause of cancer-related deaths in the United States. PCa is heavily influenced by the androgen receptor (AR). Throughout disease progression, AR overrides treatment efforts to promote proliferation and survival, often leading to metastatic disease, at which point the management of the disease becomes challenging. Approximately 80% of metastatic disease occurs in the bone, which is the most common site of PCa metastasis. Studies have shown that metabolic activity in the bone microenvironment is crucial, and metabolic reprogramming is required to support the functional requirements of cancer cells, such as continued proliferation. In PCa, increased lipid metabolism plasticity, dysregulation of glycolysis, and OXPHOS dysfunction are linked to worse prognosis. We have also learnt that reprogramming can influence, and be influenced by, epigenetic modification. We performed global proteomic and transcriptomic analyses across five patient-derived xenograft models established from patients with metastatic disease, revealing significant concordance in metabolic processes. Validation studies using Western blot confirmed our results from the mass spectrometry proteomic data. FASN and LDHA protein expression were consistent with gene expression. Next, we determined the implications of FASN inhibition on cell proliferation (live-cell imaging, Incucyte) and metabolism (Cell Titre Glo, which measures cell metabolism by quantifying adenosine triphosphate (ATP) present in all metabolically active cells) in the bone metastatic C4-2B cell line. We observed decreased proliferation. At the molecular level, we observed decreased expression of AR, ZEB1, LDHA, and EZH2. These observations were not observed in the LNCaP (non-bone metastatic model) cell line. Ongoing studies will provide more insight into the cross-talk between AR signaling, EZH2, and metabolic reprogramming in bone metastasis of prostate cancer.

#4743 Dual inhibition of PIKfyve and FASN reveals therapeutic potential in neuroendocrine prostate cancer.

Yang Zheng[1], Caleb Cheng[1], Yizhi Cao[1], Gabriel Cruz[1], Yuping Zhang[1], Radha Paturu[1], Somnath Mahapatra[1], Jing Hu[1], Rahul Mannan[1], Huseyin Karaburk[1], Rupam Bhattacharyya[1], Yitong Yin[1], Xuhong Cao[1], Hui Xue[2], Chungen Li[3], Zhen Wang[3], Stephanie Miner[1], Ulka N. Vaishampayan[1], Vaibhav Sahai[1], Lois S. Weisman[1], Ke Ding[3], Costas Andreas Lyssiotis[1], Yuzhuo Wang[2], Yuanyuan Qiao[1], Arul M. Chinnaiyan[1]

[1]University of Michigan, Ann Arbor, MI,[2]The University of British Columbia, Vancouver, BC, Canada,[3]Shanghai Institute of Organic Chemistry, Chinese Academy of Sciences, Shanghai, China

Background: Neuroendocrine prostate cancer (NEPC) is emerging rapidly as a resistance phenotype to androgen receptor pathway inhibitors in castration-resistant prostate cancer. NEPC persists in a profoundly hypoxic microenvironment, yet the mechanisms enabling tumor adaptation to this hostile niche remain largely undefined. We hypothesized that NEPC depends on stress-adaptive lysosomal programs mediated by the lipid kinase PIKfyve that can be targeted therapeutically.
Methods: PIKfyve expression was assessed by immunohistochemistry and RNA-ISH in clinical NEPC specimens. Functional studies used newly derived NEPC cell lines and established cell line (NCI-H660), and multiple NEPC PDX/CDX models. Pharmacologic and genetic perturbations of PIKfyve were evaluated *in vitro* and *in vivo*. Global transcriptomic, proteomic and lysosome-focused profiling were used to assess downstream responses. Combination studies explored the therapeutic impact of concurrently inhibiting PIKfyve and the lipogenic enzyme FASN. Cell death and pharmacodynamic endpoints included apoptotic markers and TUNEL staining.
Results: PIKfyve was consistently elevated in primary and metastatic NEPC and was required for tumor cell survival. Pharmacologic inhibition of PIKfyve led to robust antitumor activity across multiple NEPC models, producing marked apoptosis and sustained tumor regressions. Multi-omic analyses indicated that PIKfyve inhibition activated compensatory lipid metabolic programs, including increased reliance on FASN. Notably, concurrent inhibition of PIKfyve and FASN resulted in enhanced tumor cell death and superior antitumor efficacy *in vivo* compared with single agents.
Conclusions: NEPC exhibits a stress-associated metabolic dependency involving PIKfyve and adaptive lipogenic pathways. Co-targeting PIKfyve and FASN induces a potent therapeutic response in preclinical models, supporting further investigation of this combinatorial strategy as a promising approach for treating NEPC.

#4744 Metabolomic profiling of fresh and formalin-fixed paraffin-embedded samples reveals metabolome alterations in penile cancer.

Andres Enrique Hernandez-Gonzalez[1], Maria Sanchez-Vazquez[2], Luis Torres-Pena[3], Keren Valentin-Lopez[4], Carlos A. Rivera-Lopez[5], Brandon Torres-Rivera[6], Maria Marcos-Martinez[6], Antonio Puras-Baez[5], Nataliya Chorna[4], Magaly Martinez-Ferrer[2]

[1]Department of Pharmaceutical Sciences, University of Puerto Rico, Medical Sciences Campus, School of Pharmacy, San Juan, PR,[2]Division of Cancer Clinical & Translational Research, University of Puerto Rico, Comprehensive Cancer Center, San Juan, PR,[3]Department of Biology, University of Puerto Rico, Rio Piedras Campus, San Juan, PR,[4]Department of Biochemistry, University of Puerto Rico, Medical Sciences Campus, School of Medicine, San Juan, PR,[5]Department of Surgery, Urology Section, University of Puerto Rico, Medical Sciences Campus, School of Medicine, San Juan, Puerto Rico,[6]Department of Pathology, University of Puerto Rico, Medical Sciences Campus, School of Medicine, San Juan, PR

Penile squamous cell carcinoma represents a significant source of morbidity and mortality in Puerto Rico, with HPV-associated cases comprising 56% of cases. The link between clinical variables and metabolomic alterations has not been studied in penile cancer. This study aimed to characterize the non-targeted metabolomic profiles of fresh and formalin-fixed paraffin-embedded (FFPE) penile cancer samples to identify correlations with patient clinical variables: HPV infection status, tumor stage and tumor grade. In this study, 14 fresh and 37 FFPE penile cancer samples were processed for metabolomic analysis. HPV infection status was determined using INNO-Lipa HPV Genotyping and RHA kit HPV SPF10-LiPA25 kits. Sample aliquots were analyzed using GCMS/MS-TQ8050 equipment. Clinical variables were provided by the Departments of Pathology and Surgery. Filtering of raw data was conducted using AMDIS 32 and the NIST MS Spectrum database. Statistical analysis (T-test and Mann-Whitney test) of metabolomic profiles was done using MetaboAnalyst 6.0. Our study identified 52 metabolites in the fresh penile cancer sample cohort and 18 metabolites in the FFPE penile cancer sample cohort. The fresh sample cohort yielded eight metabolite classes: amino acids, sugar alcohols, fatty acids, carboxylic acids, nucleic acids, sterols, cofactor and vitamins, and others. The FFPE cohort yielded five metabolite classes: amino acids, sugar alcohols, fatty acids, carboxylic acids, and others. Statistical findings suggest that HPV infection status and tumor stage are significantly correlated with alterations in expression of several metabolites in both sample cohorts: isoleucine (p value = 0.011), homoserine (p-value = 0.0001), cysteine (p-value = 0.0385), glycolic acid (p-value = 0.0215), methylmalonic acid (p-value = 0.0475), malic acid (p-value = 0.0483) and heptanoic acid (p-value = 0.0461). Statistical findings found no significant correlation between tumor grade and metabolomic alterations. Our findings suggest that HPV infection status and tumor stage are associated with altered metabolomic pathways in penile cancer. Further understanding is needed to establish the clinical relevance of these altered metabolites and their potential role as novel metabolomic biomarkers or therapeutic targets to improve treatment outcomes for this disease.

#4745 Tumor-intrinsic Warburg effect as the driver and therapeutic target for cancer-associated cachexia in mouse models.

Shaozi Fu, **Vincent Pham**, Victoria Sanchez, Yaxing Nie, Kasie Liu, Chenhui He, Yu Luan, Lingtao Jin, Gang Huang

UT Health San Antonio, San Antonio, TX

Cancer-associated cachexia (CAC) is a multifactorial metabolic syndrome affecting 50-80% of patients with advanced malignancies and still lacks FDA-approved interventions. It manifests as progressive loss of body weight, depletion of adipose and skeletal muscle tissues, metabolic inflexibility, and anemia, collectively worsening prognosis and compromising responses to systemic therapy. Accumulating evidence indicates that tumor-intrinsic metabolic reprogramming can sustain aggressive tumor growth and drive systemic energy imbalance, yet the specific molecular events linking oncogenic programs to host peripheral wasting remain incompletely defined. To dissect this tumor-intrinsic axis, we established subcutaneous tumor models in C57BL/6 mice using isogenic KP lung cancer cells ($Kras^{G12D/+}$; $p53^{-/-}$), KPL cells carrying additional Lkb1 loss ($Kras^{G12D/+}$; $p53^{-/-}$; $Lkb1^{-/-}$), and B16F10 melanoma. KPL and B16F10 tumors induced a more severe cachectic phenotype than KP tumors, characterized by greater body weight decline, pronounced loss of adipose tissue and skeletal muscle, and more severe anemia. Thus, this KP/KPL isogenic tumor models provide us an opportunity to dissect the underlying mechanisms for CAC. First, we found that KPL tumors grew faster and relied more heavily on glycolytic metabolism than KP controls. Integrated proteomic and metabolomic profiling confirmed a shift toward aerobic glycolysis in KPL tumors, consistent with a strengthened Warburg effect. Follow-up experiments indicated that this metabolic shift was linked to LKB1 loss and heightened HIF activity. To test therapeutic relevance, we treated KPL- and B16F10-bearing mice with an FDA-approved HIF-2α inhibitor Belzutifan. Belzutifan reduced adipose and muscle loss, suggesting that dampening HIF signaling can lessen cancer-associated wasting, although anemia did not improve under this treatment, likely because systemic HIF-2α blockade reduces erythropoietin (EPO) production in these CAC mouse models. Collectively, our data identifies HIF-driven tumor-intrinsic Warburg effect as a central contributor to CAC in mouse models. Targeting HIF signaling can attenuate tumor-induced wasting and provides mechanistic proof-of-concept for metabolic reprogramming-directed CAC therapy although anemia issues remain. Moreover, our data indicated that rational combination regimens, such as co-administration of EPO, will be required to deliver full muscular, adipose, and hematologic rescue in CAC. These preclinical data warrant further investigation in patient-derived model systems, and eventually in clinical trials.

#4746 Downregulation of PDLIM2 promotes tumor growth through regulation of oncometabolites and HIF-1α pathway.

Tsung-Hsien Chuang[1], Jing-Xing Yang[2], Yu-Chen Chuang[2], Jen-Chih Tseng[2], Yi-Ling Liu[2], Chao-Yang Lai[3]

[1]Buddhist Tzu Chi Medical Foundation, Hualien Tzu Chi Hospital, Hualien, Taiwan,[2]National Health Research Institutes, Miaoli, Taiwan,[3]Asia University, Taichung, Taiwan

Cancer is increasingly recognized as a disease driven by dysregulated cellular metabolism, and elucidating the molecular mechanisms behind these metabolic alterations is essential for developing effective targeted therapies. In present study, we investigated the pro-tumorigenic role of PDLIM2 (PDZ and LIM domain 2) downregulation in lung cancer progression, with a particular focus on its impact on mitochondrial metabolism and hypoxia-inducible factor-1α (HIF-1α) signaling. Our analysis revealed that PDLIM2 expression is significantly downregulated in lung cancer tissues, and this reduction correlates with unfavorable patient prognosis. Transcriptomic profiling indicated that PDLIM2 regulates a network of genes associated with mitochondrial function. Mechanistically, PDLIM2 downregulation impaired the expression of tricarboxylic acid (TCA) cycle genes, notably those encoding succinate dehydrogenase (SDH) subunits. This disruption led to mitochondrial dysfunction, accumulation of succinate and other oncometabolites. These metabolic disturbances contributed to the stabilization and activation of HIF-1α, a transcription factor known to drive tumor progression under hypoxic conditions. Further studies indicated that HIF-1α expression is elevated across all stages of lung cancer, and its levels are inversely correlated with PDLIM2 expression in patient samples. To further validate this axis, we performed an in vivo study with cancer animal model using PX-478, an orally bioavailable HIF-1α inhibitor. Treatment with PX-478 significantly attenuated the tumor growth promoted by PDLIM2 knockdown, supporting the functional relevance of HIF-1α activation in mediating the oncogenic consequences of PDLIM2 loss. Collectively, these findings highlight a novel regulatory link between PDLIM2, mitochondrial metabolism, and HIF-1α signaling in lung cancer. They emphasize the tumor-promoting effects of PDLIM2 downregulation and suggest that therapeutic inhibition of HIF-1α may represent a promising precision strategy for patients with PDLIM2-deficient tumors.

#4747 Chronic E-cigarette aerosol exposure induces metabolic, translational, and immune reprogramming in mice: A serum proteomics analysis.

Rizwana Begum, Ganesan Muthusamy, Shreya Pokharel, Biplov Sapkota, Poorna Sai Vaddi, Shang SU, Abhishek Pandit, Naveen Chintala Ramulu, Joseph Francis

Louisiana State University, Baton Rouge, LA

Background: E-cigarette aerosol exposure has been associated with inflammation and oxidative stress; however, its systemic metabolic effects remain poorly understood. Because circulating serum proteins capture early physiological perturbations, we examined how chronic e-cigarette exposure alters metabolic, translational, and immune pathways using a controlled mouse model.
Methods: We subjected C57BL/6 mice to chronic exposure to e-cigarette aerosols for 10 weeks, with filtered-air controls. Serum samples were collected and analyzed through untargeted LC-MS/MS proteomics. Gene Set Enrichment Analysis (GSEA) was performed using GO, KEGG, Hallmark, and MSigDB immune signatures to identify pathway-level alterations in metabolism, redox biology, translational control, and immune signaling.
Results: Our findings reveal that chronic exposure to e-cigarette aerosols triggers metabolic reprogramming, marked by significant enrichment of pathways related to oxidative phosphorylation, fatty acid metabolism, pyruvate metabolism, vesicle trafficking, and detoxification of reactive oxygen species (ROS). We observed increased levels of redox-adaptive and glycolytic proteins (PKM, IDH1/2, NQO1, GSTM1/2, GSS), indicating a shift toward NADPH-driven antioxidant metabolism and mitochondrial remodeling, consistent with systemic metabolic stress. This metabolic shift was accompanied by strong translational reprogramming, including enrichment of ribonucleoprotein complex assembly and mRNA processing pathways. Increased expression of translation-associated factors, such as eIF4A2, further supported activation of an stress-responsive translational program. Immune analyses revealed selective enrichment of natural killer (NK) cell-associated pathways, indicating altered NK cell functional signatures following chronic e-cigarette exposure. This targeted shift in innate immunity is consistent with the observed metabolic and translational remodeling, as NK cell activity relies heavily on glycolytic and stress-adaptive translational programs.
Conclusion: Chronic e-cigarette exposure leads to interconnected changes in metabolic, translational, and immune processes in mice. The resultant shifts towards antioxidant and glycolytic pathways, stress-responsive translation, and altered immune signaling suggest that metabolic-immune crosstalk serves as an early systemic mechanism of vaping toxicity, warranting targeted validation through metabolic, translational, and immune profiling.

: Oncogenic Transcription Factors and Cancer Programs
Poster Session

#4751 SOX4 upregulation contributes to ovarian cancer initiation through a stress-adaptation program.

Jayaprakash Mandal[1], Brielle Hayward Piatkovskyi[1], Md Masud Rana[2], Tu-Yung Chang[1], Tian-Li Wang[2], Ie-Ming Shih[1]

[1]Gynecology and Obstetrics, Johns Hopkins University School of Medicine, Baltimore, MD,[2]Pathology, Johns Hopkins University School of Medicine, Baltimore, MD

High-grade serous carcinoma (HGSC) is a clinically aggressive subtype of ovarian epithelial cancer, mainly because of late diagnosis and the development of therapy resistance. Our Ovarian Precancer Atlas study provides a molecular map of HGSC development, and one of our most exciting findings is the identification of a transcription factor, SOX4. SOX4 is a developmentally regulated transcription factor belonging to the SRY-related HMG-box family. It regulates cell fate, lineage determination, and differentiation. Our spatial transcriptomic and immunohistochemical analyses show an upregulation of SOX4 in HGSC and its precancerous lesion, STIC. However, the biological significance of this finding remains unclear. Spatial transcriptomics and Immunohistochemical analyses confirmed progressive SOX4 upregulation in STIC and HGSC tissues. siRNA-mediated SOX4 knockdown in fallopian tube epithelial (FT241, FT2821) and HGSC (UWB1.289 ± BRCA1) models reduced proliferation and colony formation, indicating that endogenous SOX4 is required for cell growth and survival. Conversely, acute SOX4 induction in doxycycline-inducible OVCAR8 models decreased proliferation, clonogenicity, and wound healing, while elevating ROS and ProteoStat-measured proteotoxic stress—indicating a SOX4-induced cellular stress environment. RNAseq analyses also revealed expression of genes involved in reprogramming and redox homeostasis. When the inducible cells were cultured continuously under doxycycline for approximately two months, they underwent stable phenotypic remodeling and regained proliferative fitness, paralleling the enhanced tumorigenicity observed in vivo. This suggests that chronic SOX4 activation drives a transition from an initial stress-induced to a stress-adapted proliferative state that enables malignant progression. Before this adaptive remodeling is complete, SOX4-high cells exhibited heightened vulnerability to ER stress and proteasome inhibition—revealing a stress-sensitized therapeutic window selectively targetable in SOX4-high tumors. SOX4-induced cells showed synergistic reduction in cell proliferation and apoptosis when combined with MG132 or Tunicamycin. This study reveals a new mechanism by which transformed cells exploit SOX4-induced proteomic stress and turn it to their advantage in tumor progression after overcoming a selection pressure. SOX4 induces an oxidative/proteotoxic stress state that temporarily hinders growth in vitro but promotes tumorigenicity in vivo through adaptive remodeling. This process highlights a time-limited, stress-sensitive therapeutic window—before full adaptation, during which ER and proteasome challenges are especially effective. These findings position SOX4 as both a mechanistic driver of stress adaptation in HGSC carcinogenesis and a biomarker to select HGSC patients for targeted stress-modulating therapies.

#4752 HMGA1: An epigenetic driver of colon carcinogenesis by inducing FGF19 signals which can be targeted with FGFR4 receptor blockade.

Yuze Du[1], Li Luo[2], Jung-Hyun Kim[3], Bailey West[4], Tatianna Larman[5], Leslie Cope[6], Eric R. Fearon[7], Cynthia Sears[8], Linda Resar[9]

[1]Molecular Microbiology and Immunology, Johns Hopkins Bloomberg School of Public Health, Baltimore, MD,[2]Johns Hopkins University School of Medicine, Baltimore, MD,[3]Research Institute, National Cancer Center, Goyang-si, Gyeonggido, Korea, Republic of,[4]Pathobiology Graduate Program, Johns Hopkins University School of Medicine, Baltimore, MD,[5]Pat Gastrointestinal Liver Pathology, Johns Hopkins University School of Medicine, Baltimore, MD,[6]Onc Bioinformatics, Johns Hopkins University School of Medicine, Baltimore, MD,[7]Oncology, University of Michigan, Ann Arbor, MI,[8]DOM Infectious Disease, Johns Hopkins University School of Medicine, Baltimore, MD,[9]Hematology, Johns Hopkins University School of Medicine, Baltimore, MD

Advanced colorectal cancer (CRC) continues to be a significant healthcare burden with increasing incidence in younger patients, necessitating the development of novel targeted therapies. The gene encoding the High Mobility Group A1 (HMGA1) chromatin regulator is enriched in adult stem cells, including colon stem cells, and diverse tumors where high levels portend adverse clinical outcomes. Indeed, *HMGA1* is among the genes most highly overexpressed in CRC compared to nonmalignant colon epithelium. To define targetable mechanisms underlying HMGA1 in colon carcinogenesis, we performed gene expression studies (bulk, single cell RNA sequencing) and chromatin accessibility assays (ATACseq) in preclinical models and human tumors which unveiled the FGF19 growth factor as a downstream effector of HMGA1 in CRC. We had previously discovered that disrupting FGF19 signaling with the clinical inhibitor to the FGFR4 receptor (BLU9931) in KPC mouse models of pancreatic cancer and human orthotopic xenografts decreases pancreatic tumor and stroma formation while prolonging survival. In mice with intestinal epithelial cells harboring *Adenomatous polyposis coli* (Apc^{Min}) inactivation, we found that *Hmga1* is induced following inoculation with enterotoxigenic *Bacteroides fragilis* (ETBF), a common oncogenic bacterium in humans with CRC. In this model, ETBF inoculation results in robust distal colon tumorigenesis and HMGA1-dependent amplification of Wnt signaling. HMGA1 also activates murine *FGF19* (*Fgf15*) expression. Strikingly, in human CRC tumors, *HMGA1* and *FGF19* are also up-regulated and positively correlated (r=0.71, $P<0.00001$; TCGA). Further, silencing *HMGA1* in human CRC cell lines (SW620) represses *FGF19* expression. By ATACseq in mouse colon crypt cells with *Apc* inactivation, HMGA1 enhances chromatin accessibility at the murine *Fgf15* locus ($P<0.001$), suggesting that HMGA1 opens chromatin to activate *Fgf15* expression. We therefore tested whether FGFR4 inhibition has anti-tumor efficacy in CRC by treating human CRC cells (SW620) with BLU9931. FGFR4 blockade disrupts clonogenicity in a dose-dependent fashion, recapitulating effects of *HMGA1* silencing. Together, these data illuminate the HMGA1-FGF19 axis as a novel epigenetic pathway driving colon carcinogenesis and a promising therapeutic target.

#4753 The SOX2-RUNX2/TEAD4 signaling axis drives ESCC progression and exposes therapeutic vulnerabilities via Hippo/MAPK pathways.

Shangwei Sun[1], Yixiao Li[1], Yating Xu[1], **Jin Zhou**[1], Adam Bass[2], ZHONG WU[1]

[1]West China Hospital of Sichuan University, Chengdu City, China,[2]Gastrointestinal Oncology Service, Department of Medicine, Memorial Sloan Kettering Cancer Center, New York, NY

SOX2 has been identified as a frequent genomic amplification and potent oncogenic driver in esophageal squamous cell carcinoma (ESCC). We previously generated an ESCC organoid model based on *Trp53*/*Cdkn2a* knockout and *Sox2* overexpression, and subsequently demonstrated the critical epigenetic and transcriptional functions of SOX2 during ESCC development. However, effectively targeting *SOX2*-driven ESCC remains challenging. To define the transcriptional and epigenomic mechanisms downstream of SOX2 and identify targetable vulnerabilities, we profiled our ESCC organoid model and human ESCC cell lines with SOX2 overexpression via RNA-seq, ATAC-seq, SOX2 ChIP-seq, and H3K27ac ChIP-seq. Our findings show that SOX2 upregulates RUNX2 by forming super-enhancers at its cis-regulatory elements. This RUNX2 protein then functions as a cofactor, binding directly to SOX2. By integrating RUNX2 ChIP-seq data with the above multi-omic profiles, we revealed that SOX2 and RUNX2 co-regulate a broad spectrum of oncogenic pathways, among which the Hippo pathway was prominently enriched. Multi-omic analyses revealed that SOX2 and RUNX2 are significantly enriched at the cis-regulatory elements of key Hippo pathway genes—such as *YAP1*, *TEAD4*, *CTGF*, and *CYR61*—and cooperatively regulate their expression. We found that TEAD4, a key Hippo pathway transcription factor, also interacts directly with SOX2. It notably co-occupied SOX2-established super-enhancers, leading to the upregulation of the downstream MAPK pathway. Furthermore, in human ESCC cell lines, SOX2 knockdown downregulated RUNX2, TEAD4, and their downstream targets. Consistently, silencing RUNX2 or TEAD4 suppressed the corresponding Hippo and MAPK signaling pathways. Collectively, these findings uncover a critical role for the SOX2-RUNX2/TEAD4-Hippo/MAPK signaling axis in SOX2-driven ESCC development. Therefore, we evaluated the therapeutic efficacy of the MEK inhibitor trametinib, the TEAD4 inhibitor IAG933, and the BRD4 inhibitor JQ1 using both organoid and cell line models. These agents significantly suppressed ESCC proliferation in vitro and in vivo. Notably, combinatorial treatment strategies demonstrated synergistic effects, resulting in enhanced cytotoxicity. In conclusion, our study uncovers a novel epigenetic mechanism driving *SOX2*-amplified ESCC and identifies the SOX2-RUNX2/TEAD4 axis as a promising therapeutic target. These findings provide a strong preclinical rationale for evaluating therapeutic strategies targeting this axis in clinical trials for patients with this aggressive malignancy.

#4754 ADT-induced stress elevates CDKN2AIP to promote neuroendocrine prostate cancer.

Benjamin Chen[1], Pranabananda Dutta[2], Jerry Salinas[3], Ali Andalibi[4], Kamrul Hasan[5]

[1]Cornell University, Ithaca, NY,[2]Charles R. Drew University of Medicine & Science, Los Angeles, CA,[3]California State University, Dominguez Hills, Dominguez Hills, CA,[4]Office of the Provost, Charles R. Drew University of Medicine & Science, Los Angeles, CA,[5]Internal Medicine, Charles R. Drew University of Medicine & Science, Los Angeles, CA

Approximately 80-90% of prostate cancers (PC) initially depend on androgen signaling for growth, making androgen deprivation therapy (ADT) the standard first-line treatment. However, chronic ADT imposes metabolic and oxidative stress that drives therapeutic resistance and progression to castration-resistant prostate cancer (CRPC). A subset of CRPC tumors further acquires a neuroendocrine (NE) phenotype, leading to the development of neuroendocrine prostate cancer (NEPC), an aggressive, therapy-refractory disease with no effective treatment options. Understanding the molecular mechanisms and identifying key drivers of this phenotypic transition are therefore critical. Analysis of NEPC patient datasets revealed elevated expression of CARF (CDKN2AIP), a stress-responsive RNA regulatory factor whose role in lineage plasticity is unknown. Using an ADT-conditioned LNCaP model, we observed upregulation of CARF together with NEPC-associated regulators SIRT1, CHGA, SYP, and c-MYC, as shown by immunostaining, immunoblotting, and RT-qPCR. Silencing CARF via shRNA significantly reduced the expression of these NE markers, indicating that CARF is required to sustain their induction under ADT. Mechanistically, exposure to H_2O_2-induced oxidative stress increased CARF and SIRT1 expression, suggesting that ADT-associated oxidative stress upregulates CARF and contributes to NEPC development. We further found that ADT increased the expression of the splicing regulator SRSF3, while CARF knockdown suppressed SRSF3, implicating CARF in an alternative splicing pathway that facilitates NE lineage reprogramming.Overall, these findings identify a CARF-SRSF3 signaling axis that integrates oxidative stress and RNA regulation to promote neuroendocrine differentiation in prostate cancer. This pathway represents a potential therapeutic target for preventing or reversing NE transdifferentiation and treatment resistance in advanced disease.

#4755 Novel SOX2-targeting bioPROTACs as multi-faceted anti-tumor agents overcoming resistance to standard therapies in lung cancers.

Yeryoung Yong, Saeyi Lim, Hyerin Song, Yuna Jeon, Kiyoung Choi, Seunghyun Lee, **Jaehyun Choi**

Genexine, Inc., Seoul, Korea, Republic of

SOX2 is one of the pluripotency transcription factors and has been well-known for its crucial role in tumor development through promoting cancer cell survival, metastasis, stemness, and drug resistance. Numerous studies have reported the overexpression of SOX2 in various tumor tissues, such as ovarian, esophageal, and head and neck cancers, and demonstrated an associated poor prognosis. Thus, SOX2 has emerged as a therapeutic target for anti-tumor agents, but directly targeting SOX2 has been proven to be difficult since SOX2 is an “undruggable” transcription factor. Here, we show the versatile anti-tumor efficacy of our SOX2 bioPROTACs as first-in-class SOX2 degraders. Our SOX2 bioPROTACs are composed of a nanobody against SOX2 with high affinity and modified E3 ligases with deletion of natural substrate binding domain, which in turn achieve highly selective degradation of SOX2 protein. First, we validated the potent SOX2 protein degradation and therapeutic efficacy of SOX2 bioPROTACs in lung squamous cell carcinoma (LUSC) cells, which present difficulties for targeted therapy due to the lack of common oncogenic driver mutations. Given that SOX2 is amplified in about 40% of LUSC patients, our SOX2 bioPROTACs offer a promising alternative for patients currently lacking effective therapeutic options. In addition, we confirmed SOX2 overexpression in several chemo-resistant cell lines, and subsequently demonstrated that SOX2 bioPROTACs exhibit synergistic efficacy in combination with chemotherapy via SOX2 degradation. We also verified remarkable tumor growth inhibition in chemo-resistant patient-derived xenograft models upon co-treatment with SOX2 bioPROTACs and chemotherapy, thereby firmly establishing their potential to bypass existing drug resistance. Notably, diverse EGFR-TKIs induced elevated SOX2 levels in EGFR-mutant lung cancer cells and we found that the combination of SOX2 bioPROTACs and EGFR-TKIs resulted in a significant improvement in therapeutic efficacy compared to EGFR-TKI alone. Furthermore, the induction level of SOX2 by EGFR-TKIs was much higher than that of ADC targets, such as TROP2, HER2, or MET, which are actively being developed for combination therapy to overcome EGFR-TKI resistance. This suggests the potential superiority of our SOX2 bioPROTACs as a combination partner for EGFR-TKIs. Finally, we developed the clinically applicable drug product by utilizing a lung-targeted lipid nanoparticle (LNP), and confirmed its potent anti-tumor efficacy upon intravenous injection into an orthotopic lung cancer model. Taken together, our novel SOX2 bioPROTACs exert superior anti-tumor efficacy through multi-faceted mechanisms, positioning them as optimal therapeutic candidates for patients who face challenges in treatment due to the limitations of existing therapies.

#4756 Evaluation of strategies to target the Myc oncogene.

Maria Ahn, Aimee Blair, Juan Bueren-Calabuig, Barbara Farkas, Charlotte Hodson, John Lyons, Stanislava Panova, **Mark Wade**, George Ward, Alison Woolford

Astex Pharmaceuticals, Cambridge, United Kingdom

Aim: Myc overexpression or dysregulation is a hallmark of most malignancies, yet targeting of Myc-driven cancers remains a clinically unmet need[1]. Both indirect and direct modalities of Myc inhibition have been evaluated. Indirect Myc targeting via inhibition of its binding to partner proteins is challenging due to issues around redundancy and patient selection. Furthermore, antisense and other epigenetic approaches have so far failed. While direct targeting is challenging due to the intrinsically disordered nature of Myc[2], peptides/miniproteins, such as OmoMYC[3] (which essentially prevent the interaction of Myc with its obligate heterodimeric binding partner, Max) are being tested in the clinic. It is currently unclear whether a small molecule approach for Myc inhibition will be feasible. Here, we used biophysical, biochemical and functional assays to test published tool compounds that are reported to target Myc. Based on publicly available data, we also present strategies for selection of patients with Myc-driven cancer.
Methods: Commercially available Myc targeting compounds were tested in direct Myc:Max binding assays using NMR. OmoMYC was synthesized and purified by Peak Proteins. An HTRF DNA binding assay was developed to investigate functional binding of recombinant Myc:Max complexes to DNA using consensus E-Box or control oligonucleotides. Myc and Max have been overexpressed in HEK293T cell lines to generate cell lysates for biochemical testing.
Results: Compounds reported to directly inhibit Myc did not bind to the MYC/MAX heterodimer in our assays. We confirmed the ability of OmoMYC to displace Myc binding to the canonical E-box sequence in biochemical assays and in cell lysates. We also identified biomarkers that are predictive of increased sensitivity to genetic inhibition of Myc, which may facilitate patient selection strategies.
Conclusion: Early data from clinical trials with OmoMYC suggest that direct targeting of Myc is feasible. Small molecule inhibition of Myc would offer distinct pharmacological advantages and is, therefore, a first-in-class opportunity. A significant improvement in the affinity of Myc-targeting small molecules will be required to fully validate its potential as an oncology target.
References:1) Whitfield J.R. and Soucek L., MYC in cancer: from undruggable target to clinical trials, Nat. Rev. Drug Disc. (2025)2) Madden S.K. et al., Taking the Myc out of cancer: toward therapeutic strategies to directly inhibit c-Myc, Mol. Can. (2021)3) Demma M.J. et al., Omomyc reveals new mechanisms to inhibit the MYC Oncogene, MCB (2019)

#4757 *CREBBP* drives tumorigenicity via aberrant IL-1α signaling in *EP300* altered bladder cancer.

James August Rodrigues[1], Hikmat A. Al-Ahmadie[1], Sizhi P. Gao[1], Jiaqian Luo[1], Jacob Tallman[1], Fengshen Kuo[1], Merve Basar[1], Cansu Yol[1], Jordan Eichholz[1], Alejandra Lopez Rojas[1], Ecenur Turkay[1], Jonathan E. Rosenberg[1], Gopa Iyer[2], Eugene J. Pietzak[1], Dan Li[1], Dana Schoeps[1], Shipra Shukla[1], Zoe Jacobs[1], Chen Khuan Wong[1], Woo Hyun Cho[1], Ping Chi[1], David B. Solit[1], Yu Chen[1]

[1]Memorial Sloan Kettering Cancer Center, New York, NY,[2]Clinical Instructor, Medical Oncology, Memorial Sloan Kettering Cancer Center, New York, NY

EP300 and *CREBBP* encode p300 and CBP respectively, which are H3K27 acetylases. Both *EP300* and *CREBBP* mutated in a subset of urothelial cancers (~15% for *EP300* or *CREBBP*). The *EP300* and *CREBBP* genes have ~60% sequence similarity and thus have been presumed to have largely overlapping functional roles in cell homeostasis and cancer pathogenesis. To characterize the role of *EP300* mutations in urothelial cancer pathogenesis and to identify non-redundant roles of these paralogues, we generated *EP300* and *CREBBP* isogenic knockout urothelial cancer cell lines and characterized low passage mutant and wild type for *EP300* and *CREBBP* urothelial cancer-derived patient derived organoids. *EP300* KO and loss-of-function mutation was associated with enhanced cell growth in soft agar, increased invasive potential *in vitro* and altered cellular metabolism. These gain-of-function phenotypes were mediated by enhanced JAK-STAT3 activation resulting from IL-6 trans-signaling, the proximal driver of which was increased transcription and production of IL-1á. Notably, isogenic BLCA cells with *CREBBP* knockout did not confer IL-1á hypersecretion or hyperactivation of the IL-6/JAK1/STAT3 signaling axis indicating that this is a phenomenon was specific to *EP300* loss-of-function. Transcriptomic analysis of Parental, EP300 KO, and CREBBP KO RT112 clones revealed that *CREBBP* KO significantly depressed *IL1A* transcript levels which *EP300* KO significantly elevated. Additionally, *CREBBP* inactivated BLCA lines could not upregulate *IL1A* expression following genotoxic stress in contrast to parental and *EP300* null cell lines. Using an inducible short hairpin RNA construct targeting *CREBBP*, we also find that *CREBBP* knockdown rescued *IL1A* upregulation in *EP300* ko clones that coincided with a significant growth defect. Pharmacologic inhibition via the p300/CBP specific inhibitor A485 also abolished *IL1A* upregulation and caused significant growth defect in *EP300* KO cells. *EP300* null clones were also significantly more sensitive to A485 treatment than either *CREBBP* null urothelial cell or parental cell lines. In sum, our results identify regulation of IL-1á-JAK-STAT3 signaling as a novel non-redundancy between *EP300* and *CREBBP* that could be exploited therapeutically in patient with *EP300* loss-of-function mutations.

#4758 MYC-BCL6 state transition drives metabolomic cycling and leukemia-initiating capacity in B-ALL.

Zhangliang Cheng[1], Ruoyi Shi[1], Kohei Kume[1], Mark Robinson[1], Richard Kim[1], Kadriye Nehir Cosgun[1], Yujin Bao[2], Siyi Chen[3], Mina Xu[4], Joerg Bewersdorf[5], Markus Muschen[1]

[1]Center of Molecular and Cellular Oncology and Department of Immunobiology, Yale School of Medicine, New Haven, CT,[2]Department of Physics and Department of Cell Biology, Yale School of Medicine, New Haven, CT,[3]Department of Immunobiology, Yale School of Medicine, New Haven, CT,[4]Department of Pathology, Yale School of Medicine, New Haven, CT,[5]Department of Cell Biology, Yale School of Medicine, New Haven, CT

Background and significance: Stemness in AML is defined by a rare leukemia-initiating cell (LIC) population, but analogous LICs in B-ALL have remained elusive (Kelly 2007, Le Viseur 2008, Rehe 2013). Given that LICs in AML are drug-resistant and initiate relapses, identifying an LIC population in B-ALL would be consequential.
Results: Time-lapse studies of patient-derived B-ALL cells revealed that most B-ALL cells were continuously proliferating, while subpopulations underwent periodic transitions between quiescent and proliferative states. Gene expression studies identified MYC as the top-ranking gene in 'proliferative' and BCL6 in 'quiescent' B-ALL cells. To dissect MYC-BCL6 dynamics, we knocked in dual reporters with mNeonGreen fused to MYC and mScarlet fused to BCL6 in patient-derived B-ALL (PDX). Time-lapse imaging revealed proliferative cells expressed MYC with no detectable BCL6, whereas PDX also included 'alternating' cells that underwent repeated transitions between MYC+ BCL6– and MYC– BCL6+ states. Approximately 30% of BCR-ABL1 B-ALL and >50% of RAS-pathway B-ALL consisted of 'alternating' cells. Transitions occurred independently of the ~36-hour cell-division cycle, with ~3-hour MYC phases and ~6-hour BCL6 phases. Integrated ChIP-seq, RNA-seq, and metabolomics showed that MYC-high cells are much larger and activate glycolysis and protein-synthesis programs, whereas BCL6-high cells are small and enriched for phosphatidylethanolamine (PtdEtn) synthesis, essential for autophagosome formation. To directly link MYC-BCL6 dynamics with growth, we combined quantitative phase microscopy and time-lapse fluorescence to measure single-cell dry mass. MYC-high cells accumulated biomass at twice the rate of BCL6-high cells (0.018 vs 0.009 pg/min), producing stepwise trajectories aligned with each MYC/BCL6 state transition. To experimentally induce transitions, we engineered PDX with MYC-dTAG knock-in alleles and employed the BCL6 PROTAC ARV-393. Acute MYC degradation caused rapid shrinkage and reduced dry mass, whereas BCL6 degradation decreased autophagy and increased biomass, confirming opposing MYC-driven anabolic and BCL6-driven catabolic programs. To functionally study 'steady' (MYC-only) and 'alternating' (MYC/BCL6) B-ALL populations, we developed a cell-sorting strategy that enriched each of the two populations to a purity of 85% as confirmed by subsequent time-lapse imaging. Extreme limiting dilution and series transplantation experiments revealed MYC-BCL6 alternating B-ALL cells significantly enriched for LIC (1 in 124) compared to MYC-only population (1 in 574) and initiated fatal leukemia after short latency.
Conclusion: These findings reveal a MYC-BCL6 state-transition program in B-ALL that coordinates quiescence-proliferation cycling, anabolic-catabolic metabolism, and leukemia-initiating potential.

#4759 NELFE and SMARCB1 cooperate to regulate chromatin accessibility and allow MYC-driven gene activation in hepatocellular carcinoma.

Alvaro Lucci, Anna E. Barry, Laura M. Reynolds, Brittany N. Ruiz, Trish Nguyen, Pongsakorn Choochuen, Kai Zhang, Hien T. Dang

Department of Surgery, Thomas Jefferson University, Philadelphia, PA

Liver cancer is a serious and growing problem in the United States, with cases having more than tripled since 1980. Although there have been some advances in diagnosis and treatment, the five-year survival rate remains below 20%. Hepatocellular carcinoma (HCC), the most common type of liver cancer, often involves aberrant activation of the MYC gene, which helps cancer cells grow and survive. Unfortunately, MYC is very difficult to target directly with drugs. As such, researchers are interested in understanding proteins that control or support MYC's activity. One such protein is NELFE, which regulates gene expression by regulating how genes are turned on and off. We believe NELFE is important because it helps MYC access and activate its target genes, promoting cancer growth. To study this, we used CRISPR/Cas9 to remove NELFE from liver cancer cells and performed ATAC-seq and ChIP-seq experiments to see how this affected MYC and the structure of DNA. We found that without NELFE, the DNA became less accessible, and MYC was less able to bind near important genes. However, NELFE does not directly bind to these MYC sites, suggesting it works together with another protein. Mass spectrometry of NELFE identified SMARCB1, a component of the SWI/SNF chromatin remodeling complex, as a major interacting partner that links NELFE to MYC. Although SMARCB1 is widely known as a tumor suppressor in many cancers, in our liver cancer system, it appears to act as an oncogene, promoting cancer growth. We also showed that NELFE and SMARCB1 form special phase-separated structures in cells that help organize DNA, influencing both paused and non-paused genes. These structures keep the chromatin open, allowing MYC to be more active and interact with its target genes. Moreover, when NELFE is missing, SMARCB1 and MYC cannot interact properly, leading to reduced gene activation by MYC. In summary, NELFE helps MYC promote liver cancer by working with SMARCB1 to change how DNA is organized. Understanding this relationship could lead to new treatments for liver cancers that depend on MYC.

#4760 Uncovering a highly transforming, Myc-stabilizing isoform of dipeptidase-1 in colorectal cancer.

Elizabeth Grace Fisher[1], Sarah E. Glass[2], Chelsie K. Sievers[2], Zheng Cao[2], Matthew E. Bechard[3], Samuel T. Ellis[3], Radhika Aramnadla[3], Ping Zhao[2], Ryan T. Smith[2], Yu Wang[4], James N. Higginbotham[3], Frank Revetta[5], M. Kay Washington[5], Martha J. Shrubsole[6], Qi Liu[7], Ken S. Lau[8], Bruce Aronow[9], Robert J. Coffey[2]

[1]Cancer Biology Program, Vanderbilt University School of Medicine, Nashville, TN,[2]Department of Medicine, Vanderbilt University Medical Center, Nashville, TN,[3]Epithelial Biology Center, Vanderbilt University Medical Center, Nashville, TN,[4]Department of Biostatistics, Vanderbilt University Medical Center, Nashville, TN,[5]Department of Pathology, Microbiology, and Immunology, Vanderbilt University Medical Center, Nashville, TN,[6]Division of Epidemiology, Vanderbilt Epidemiology Center, Nashville, TN,[7]Center for Quantitative Sciences, Vanderbilt University Medical Center, Nashville, TN,[8]Center for Computational Systems Biology, Vanderbilt University, Nashville, TN,[9]Department of Biomedical Informatics, University of Cincinnati, Cincinnati, OH

Protein isoforms play significant roles in cancer progression as they can impact localization, binding partners, and functions, especially when it comes to pro-tumorigenic properties. One protein in particular, dipeptidase-1 (DPEP1), was identified 25 years ago as a cell-surface protein upregulated in adenomas and colorectal cancers (CRCs) in comparison to normal colonic tissue. We have found that a diffuse staining pattern of DPEP1, not a cell-surface localization, leads to worse overall and progression-free survival for CRC patients. Spurred by the inconsistency of an intracellular DPEP1 staining pattern for a cell surface protein, we discovered two isoforms of DPEP1 that differ in their C-terminal sequence. This difference reflects an absence of a glycosylphosphatidylinositol anchorage signal sequence in a novel, undescribed isoform of DPEP1, that we have termed DPEP1 Isoform B. We found expression of DPEP1 Isoform B in CRC patient tissue samples which, upon immunohistochemical staining, revealed an intracellular localization of DPEP1 in cells. DPEP1 Isoform B expression transforms a non-tumorigenic cell line to form large, invasive tumors in nude mice and upregulates pro-tumorigenic gene programs including Myc targets, epithelial-to-mesenchymal transition, and angiogenesis as identified by RNA-seq. Surprisingly, in a CRC cell line, we find that DPEP1 Isoform B binds to Myc, increasing its half-life 2-fold. Utilizing TCGA data sets, we deployed a strategy to examine long transcripts and found that DPEP1 Isoform B was present in 91% of CRC patients, with 28% of patients having high expression of DPEP1 Isoform B. To contrast, DPEP1 Isoform A was present in 68% of CRC patients, having high expression in 26% of patients. Overall, our work demonstrates the discovery of a novel isoform of DPEP1, which given its high incidence in CRC, warrants further investigation as a predicative biomarker as well as a novel therapeutic target.

#4761 Investigation of the role of N-MYC in lung neuroendocrine carcinoma.

Hiroki Yamamoto[1], Takashi Sato[1], Yuri Yagami[1], Ryosuke Inoue[1], Hiromi Matsuo[1], Hideo Watanabe[2], Naoki Katsuhiko[1]

[1]Kitasato University School of Medicine, Sagamihara, Japan,[2]Division of Pulmonary, Critical Care and Sleep Medicine, Department of Medicine, Icahn School of Medicine at Mount Sinai, New York, NY

Small cell lung cancer and large cell neuroendocrine carcinoma are classified as high-grade neuroendocrine tumors of the lung, representing extremely aggressive, life-threatening cancers with limited treatment options among various lung cancers. In these cancers, amplification of MYC family transcription factors: c-MYC, L-MYC and N-MYC is found to be mutually exclusive and overall account for ~20%. In addition, recent studies have reported that L-MYC and c-MYC control lineage plasticity across molecular subtypes of small cell lung cancer defined by lineage-specific transcription factors such as ASCL-1 and NEUROD-1. Compared with L-MYC and c-MYC, the role of N-MYC, a lineage factor highly expressed in several tumors derived from neural cell lineages and a subset of neuroendocrine lung cancers, have not been described clearly. In this study, we aimed to investigate the role of N-MYC as a lineage-specific factors in neuroendocrine lung cancers. First, we investigated N-MYC binding profiles in N-MYC-high neuroendocrine lung cancer cell lines and found that genes related to neural cell differentiation were enriched in genes near N-MYC bound regions. Next, examination of genome-wide Myc-accessible regions in neuroendocrine lung cancer cell lines revealed that a fraction of peaks that overlapped between N-MYC- and c-MYC-classified cells, suggesting common functional binding of N-MYC and c-MYC. When we overexpressed N-MYC in L-MYC- or c-MYC-classified cells, expression profiles of the neuroendocrine lineage factors did not change, which was different from the previous findings on the relationships between L-MYC and c-MYC. Our findings suggest that N-MYC regulates distinct transcriptional program among the MYC family members although N-MYC and c-MYC share common binding profile.

#4762 KIF11 regulates EWS-FLI1 and EWS-ATF1 target gene expression in Ewing and clear cell sarcomas.

Hannah Louise Walker-Mimms, Nicole Londono, Neelkamal Chaudhary, David Bean, Yi Liao, Lancia N.F. Darville, Jose Serrano-Velez, Yalin Liao, Jiqiang Yao, Andrew Smith, Fumi Kinose, Xueli Li, Joseph O. Johnson, Smitha R. Pillai, Eric B. Haura, Mingxiang Teng, Uwe Rix, Derek R. Duckett

Moffitt Cancer Center, Tampa, FL

Clear Cell Sarcoma (CCS) and Ewing Sarcoma (ES) have a poor 5-year survival rate and lack targeted therapies. The cancers are driven by aberrant fusion proteins generated through chromosomal translocations, EWS-FLI1 (ES) and EWS-ATF1 (CCS). These fusion proteins activate and repress target genes by targeting enhancers located on the distal intergenic sites, thereby driving the survival and proliferation of ES and CCS. Direct pharmacological targeting of these fusion proteins has been difficult due to their highly disordered structure. Therefore, we sought to identify alternative targets essential to EWS-FLI1 and EWS-ATF1 driven tumor cells. Using a small molecule library screen, we identified that KIF11 inhibitors selectively reduce the viability of ES and CCS cells. Investigating the underlying mechanism of action revealed that the KIF11 inhibitor, filanesib, induces G2/M arrest in ES and CCS cells. This result was translatable in CCS *in vivo* and in relapse-resistant metastatic ES PDXs *in vivo*. Interestingly, we observed that KIF11 interacted with the fusion proteins specifically during mitosis in both ES and CCS. Furthermore, knockdown of KIF11 results in the loss of the EWS-ATF1 fusion protein globally and visually during mitosis. KIF11 knockdown leads to a significant reduction in chromatin accessibility at many of the fusion proteins' target distal intergenic sites as measured with ATAC-Seq. While the relationship between KIF11 and the fusion proteins remains to be fully explored, our data suggest that KIF11 is essential in maintaining the fusion proteins' ability to target their downstream genes during mitosis. We aim to further elucidate why the fusion proteins in ES and CCS remain bound to target genes during mitosis. Furthermore, based on these findings, we are focused on developing KIF11 degraders to further improve the efficacy of targeting KIF11 in ES and CCS. This work has been supported in part by the Flow Cytometry, Analytical Microscopy, Biostatistics and Bioinformatics, Proteomics and Metabolomics, and Molecular Genomics Cores as well as the Nikon Center for Excellence at the H. Lee Moffitt Cancer Center & Research Institute, a comprehensive cancer center designated by the National Cancer Institute and funded in part by Moffitt's Cancer Center Support Grant (P30-CA076292)

#4763 Alternative splicing of ABI1 by enzalutamide treatment drives tumor plasticity in prostate cancer.

Kevin M. Lin[1], Anna Seidl[1], Tanner Waldman[1], Xiang Li[1], Eva Corey[2], Adam G. Sowalsky[3], Leszek Kotula[1]

[1]Urology; Biochemistry and Molecular Biology, SUNY Upstate Medical University, Syracuse, NY,[2]University of Washington, Seattle, WA,[3]National Cancer Institute, Bethesda, MD

Prostate cancer affects nearly 1.4 million new patients each year and is the second leading cause of cancer-related deaths. While initial stages of disease are driven by androgen receptor (AR) signaling and treatable with androgen-depravation therapies (ADT) and androgen receptor pathway inhibitors (ARPIs), tumors frequently recur with resistance to these therapies. The development of resistance is driven by tumor plasticity in which mutations, epigenetic changes, and alternative splicing generate phenotypic alterations that allow for adaptations to circumvent AR inhibition.Recent studies have shown that treatment with second generation ARPIs such as enzalutamide may be the very driver of the plasticity leading to its resistance. Enzalutamide treatment has been shown to induce global splicing changes, and promote a high-grade, treatment-resistant, neuroendocrine phenotype. One potential link between the changes in RNA-splicing and the development of a neuroendocrine phenotype is Abelson Interactor 1 (ABI1), a multi-isoform scaffolding protein known to be a regulator of prostate cancer progression. In this study, we aimed to identify how ARPI treatment induces isoform-specific changes in ABI1, and how these changes drive prostate cancer progression. Using a combination of cell line, patient-derived and animal models of prostate cancer, we were able to determine that ARPI treatment deregulates inclusion of ABI1-exon 4, which is critical to ABI1's DNA-binding ability. This dysregulation in turn alters the expression of many genes involved in pathways of transcriptional regulation and stress response during enzalutamide treatment. Taken together, these findings shed new light on the mechanisms behind the development of enzalutamide resistance and provide a novel target in treatment-resistant prostate cancer.

#4764 Exploring the anti-proliferative impact of PBX1 perturbation in enzalutamide-resistant CRPC.

Ephraim J. Gardner[1], Surendra Gulla[1], Sasikumar Ponnusamy[1], Abbas Jawadwala[1], Madison Aust[1], Remi M. Adelaiye-Ogala[2]

[1]University at Buffalo, State University of New York, Buffalo, NY,[2]University at Buffalo, Buffalo, NY

Advanced prostate cancer (PCa) is often driven by upregulated activity of the androgen receptor (AR) and is clinically targeted by second-generation AR-antagonists such as Enzalutamide. Though patients initially respond to treatment, many develop resistance, leading to disease advancement and poor prognosis. We have focused on a mechanism involving an AR cistrome switch from a canonical to a noncanonical cistrome as PCa becomes Enzalutamide-resistant. As collaborating protein partners drive transcriptional activity, we employed core regulatory circuitry analysis in Enzalutamide-resistant PCa cell line models to identify novel TF candidates that may mediate non-canonical AR cistrome reprogramming, including Pre-B-cell leukemia homeobox 1 (PBX1), a TALE homeodomain TF. We previously showed that PBX1 is highly expressed in castrate-resistant and Enzalutamide-resistant (EnzaR-CRPC) cell line models compared with sensitive models. We have also demonstrated that PBX1 inhibition has an anti-proliferative effect in a high-PBX1-expressing EnzaR-CRPC cell line, with synergism observed with continuous Enzalutamide treatment. In the current study, we perturbed PBX1 expression in an EnzaR-CRPC cell line by shRNA (PBX1 KD) and CRISPR-Cas9 (PBX1 KO). Western blotting, RT-qPCR, and genomic DNA analysis validated a significant reduction in PBX1 protein and gene levels. Similar to previous observations with PBX1 inhibitors, PBX1 KD and PBX1 KO cells showed an initial, prominent decrease in proliferation compared to their respective controls. Interestingly, PBX1 KO clones after several passages regained increased proliferation. On the contrary, the PBX1 KD cells continue to demonstrate anti-proliferation. Ongoing transcriptomic and genome-wide DNA analysis will provide a clear understanding of the biological pathways affected by PBX1 perturbation and, most importantly, of changes in the AR and PBX1 cistrome, promoter, and enhancer landscape at low levels of PBX1 (PBX1 KD) vs. complete elimination of PBX1 (PBX1 KO). This would provide a better insight into (i) AR-PBX1 transcriptional axis and PBX1's role in promoting treatment-resistant, advanced PCa, (ii) the long-term implications for PBX1 suppression, and (iii) the best treatment strategy for targeting both PBX1 and AR for a durable positive outcome in advanced treatment-resistant CRPC.

#4765 Induction of epidermal like differentiation irreversibly limits the invasive and metastatic potential of basal like breast cancer cells.

Justin Hui[1], Andrea E. Doak[1], Nicole Rhoads[1], Ruijin Yang[1], Jimin Park[1], Cory L. Simpson[2], Manu Setty[1], Kevin J. Cheung[1]

[1]Fred Hutchinson Cancer Center, Seattle, WA,[2]University of Washington, Seattle, WA

Triple-negative breast cancer (TNBC) exhibits the worst overall survival compared to other breast cancer subtypes and has the most limited treatment options. Molecularly, most TNBCs are classified as basal-like and are associated with aggressive metastasis and drug resistance.A major hurdle in the development of effective therapeutics is tumor cell state and phenotypic plasticity that confer fitness advantages for growth, therapeutic resistance, and invasion. In this study, we sought to identify transcription factors that regulate basal-like plasticity for collective invasion. Using mouse mammary tumor organoids and time course single-cell RNA sequencing, we show that transcription factor KLF4 is a potent suppressor of basal-like invasion plasticity.Unexpectedly, we observed that KLF4 overexpression potently induced a molecular program recapitulating the classical differentiation of basal epidermal cells processively toward a biologically dead cornified outer skin layer. Overexpression of KLF4 induced hallmark markers of epidermal differentiation such as keratin 10, desmosomal cadherins, loricrin, and multicellular features of maturing epidermis, including cell piling, keratinization, and increased desmosomes, all putative anti-invasive features. Induction of epidermal differentiation, specifically in basal but not mesenchymal or luminal breast tumor cells, resulted in terminal differentiation in vitro and irreversible loss of colony-forming potential, indicative of tumor subtype-specific vulnerability. In vivo, KLF4 potently suppressed metastatic outgrowth of human basal TNBC in an intracardiac metastasis assay. In human breast tumors, we observed 50% of tumors expressed KLF4 RNA yet lacked KLF4 protein. Mechanistically, we show that basal-like TNBCs actively degrade KLF4protein to limit epidermal differentiation, which was overcome by proteasome inhibitors. In sum, these data uncover epidermal differentiation as a latent plasticity switch of highly metastatic basal-like breast cancer cells, making them irreversibly more cohesive, and point to KLF4protein stabilization as a therapeutic strategy.

#4767 Targeted antagonism of the activator protein 1 transcription factor complex results in potent anti-tumor activity in HNSCC models.

Karen Mendelson, Zachary F. Mattes, Siok Leong, Ricardo Ramirez, Mark Koester, Claudio Scuoppo, Julia Diehl, Erin Gallagher, Binh Lee, Franco Abbate, Lila Ghamsari, Gene Merutka, Barry J. Kappel, Abi Vainstein-Haras, Jim A. Rotolo

Sapience Therapeutics, Tarrytown, NY

The AP-1 transcription factor complex, comprised of Fos and Jun family heterodimers, plays a pivotal role in tumor progression and metastasis of head and neck squamous cell carcinoma (HNSCC), where expression of AP-1 component Fra1 positively correlates with poor prognosis. As dimerization is required for AP-1 complex DNA binding and transcriptional activity, we designed Fra1 antagonizing peptide (FraAP) to disrupt complex formation and prevent associated activity. Low nanomolar FraAP binding affinity to Fra1 and Jun and selectivity towards AP-1 family members was demonstrated by bio-layer interferometry (BLI), fluorescence polarization, and DNA ELISA assays. Immunofluorescence imaging reveals rapid FraAP cell entry into both the cytoplasmic and nuclear compartments of HNSCC cells, while proximity ligation assays (PLA) and co-immunoprecipitation experiments demonstrate FraAP antagonism of cJun and Fra1 protein-protein interactions and reporter assays confirm inhibition of AP-1 transcriptional activity in vitro. To investigate the impact of FraAP on tumor cell transcriptomics, RNAseq and pathway enrichment analysis identified a significant impact of FraAP on AP-1-regulated pathways including tumor cell apoptosis, invasion and proliferation. Corresponding functional in vitro assays support transcriptomic observations, as FraAP induces dose-dependent Annexin V+ apoptosis by flow cytometry; promotes a phenotypic mesenchymal to epithelial transition characterized by decreased mesenchymal marker N-cadherin and increased epithelial marker E-cadherin, leading to an inhibitory effect on invasion in Boyden chamber assays; and induces G1 arrest characterized by upregulation of CDKN1A, reduction of CDK4, CDK6, and CCND1 expression, and hypophosphorylation of Rb. The impact of FraAP on CDK4 and CDK6 expression prompted investigation of the combination activity of FraAP with the CDK4/6 inhibitor abemaciclib. Data identifies synergistic anti-tumor activity in vitro in assays of cytotoxicity, clonogenic formation, orosphere formation, and cell signaling. Further, while FraAP results in significant anti-tumor activity as a monotherapy in HNSCC subcutaneous xenograft models, combination of subpharmacologic FraAP and abemaciclib results in enhanced tumor growth inhibition. In summary, these data support FraAP as a potent peptide antagonist of the AP-1 transcription factor family that warrants further development as a novel therapeutic option for AP-1 driven tumors such as HNSCC.

#4768 From peptide screens to biological insights, FOXO4 and the PBAF complex.

Dieu An Hoang Nguyen[1], Andrea Cochran[2], Shalini Gupta[1], E Megan Flynn[1]

[1]Genentech, Inc., South San Francisco, CA,[2]Early Discovery Biochemistry, Genentech, Inc., South San Francisco, CA

Bromodomains are ubiquitous among chromatin regulators, and while they are potentially exciting therapeutic targets for cancer, the specific functions of many of them remain unknown. In a high-throughput peptide screen for potential bromodomain binding partners, acetylated peptides of transcription factors FOXO1/3/4 emerged as significant binders to the polybromo protein PBRM1, a subunit of the SWI/SNF chromatin remodeler PBAF. FOXOs are of particular interest because they are well-conserved mediators of stress adaptation in cells and are regulated by several PTMs. Under oxidative stress, FOXOs are acetylated and translocate to the nucleus, where PBRM1, within PBAF, resides. We sought to characterize the interaction between acetylated FOXOs and PBRM1 and their potential cooperation in stress responses. (1) We validated the interaction by Isothermal titration calorimetry (ITC) and found acetylated FOXO peptides bind to PBRM1 bromodomains with affinities comparable to peptides including the preferred histone modification, H3K14ac. (2) Using purified, site-specifically acetylated FOXO4 proteins as bait, we purified interactors for mass spec analysis, finding that FOXO4 acetylated at K189 interacts with PBAF components. (3) We employed genomic profiling assays ATAC-seq, CUT&RUN-seq, and Bru-Seq to dissect the role of FOXO4 under endogenous conditions versus oxidative stress, with select studies also performed in FOXO4 CRISPR knockout cells. We identified peaks where FOXO4 and PBRM1 co-localize and exhibit changes in peak intensity under acute stress. We also established a transcriptional profile of cellular response to oxidative stress and compared affected genes to the genes bound by FOXO4 and PBRM1. While our findings suggest that the FOXO4-PBRM1 interaction may not be the key driver of transcription in the oxidative stress response, this framework allows us to systematically assess other potential functions of the interaction. Together, by combining biophysical, biochemical, cell growth assays, and functional genomics assays, we have defined a likely aspect of the biology of the tumor suppressor PBRM1, namely regulation of FOXO transcription factor genomic localization.

#4769 Unravelling the transcriptome in mantle cell lymphoma.

Chioniso Patience Masamha[1], Mahesh Gupta[1], Demiah Lockett[1], Caiden Lukan[1], Lael Pasipamire[1], Jie Li[2]

[1]Pharmaceutical Sciences, Butler University, Indianapolis, IN,[2]UC Davis, Davis, CA

Many studies in the incurable B-cell hematological malignancy, mantle cell lymphoma (MCL), have focused on identifying mutations in oncogenes and tumor suppressor genes. Next-generation sequencing technologies have opened the potential to discover other global changes that contribute to the malignancy. In particular, sequencing the RNA can help us uncover transcriptome diversity resulting from alternative splicing, alternative polyadenylation (resulting in different 3'UTRs), generation of fusion transcripts as well as non-coding RNAs. The goal of this study was to characterize the transcriptome of MCL. We performed long-read Iso Sequencing and short-read RNA Sequencing on RNA samples from three MCL cell lines. The data was analyzed to identify novel transcripts as well as alternative splicing and alternative polyadenylation patterns. Select transcripts were validated using different types of PCR, Sanger Sequencing and other molecular biology techniques. Our heatmap showed that while there was always overlap between highly upregulated and downregulated transcripts in two cell lines, each cell line had its own unique gene signature. We were able to identify different variants arising from alternative splicing and alternative promoter usage in several genes including glutaminase (GLS1) by overlaying our long-read sequencing and short-read sequencing data. Our qRT-PCR and Western blot results confirmed the presence of the two most prevalent GLS1 alternatively spliced variants GAC and KGA. At the protein level, all the MCL cell lines expressed higher levels of the GAC isoform than B-cells. The GAC isoform is the form most commonly associated with cancer since the mRNA lacks a target site for miR-23 and an AU rich element (ARE) which are both potent modulators of the KGA isoform. When we looked at alternative polyadenylation, we found that the ATM gene, which is a major contributor to MCL pathogenesis, undergoes shortening of the 3'UTR in MCL cell lines. Using SQANTI3 on our long-read sequencing data, we found that transcripts were in 9 different structural categories and only ~30% of our transcripts mapped to annotated genes. We also identified fusion transcripts from our long-read sequencing data. As a proof of concept, we validated the ubiquitous fusion transcript, CTBS::GNG5, in our MCL cell lines using PCR and Sanger Sequencing. We also detected it in MCL patient samples using PCR. So far, we have identified heterogeneity as well as overlaps in levels of the differentially expressed genes in MCL. Use of both short-read and long-read sequencing technology has uncovered transcripts in MCL cell lines arising from alternative splicing, alternative polyadenylation as well as fusion transcripts. This comprehensive analysis of the MCL transcriptome can provide potential biomarkers and therapeutic targets. Our analysis is currently ongoing.

#4770 Molecular features of patient-derived triple-negative breast cancer models based on super-enhancer-associated transcriptional regulators and biomarkers.

Kuniko Horie[1], Kazuhiro Ikeda[1], Satoshi Inoue[2]

[1]Saitama Medical University, Saitama, Japan,[2]Professor, Dept. of Anti-Aging Med., TMIG - Tokyo Metropolitan Institute of Gerontology, Tokyo, Japan

Super-enhancers (SEs) have been defined as particular genomic regions with clusters of consecutive enhancers, which provide cell- or stage-specific context. SEs are often determined by high-level enrichment for genomic binding of transcriptional coactivators and active chromatin marks such as histone H3 with acetylated K27. In this study, we aim to characterize similarity and specificity of SE-associated gene profiles of patient-derived models of triple-negative breast cancer (TNBC) obtained from distinct advanced cases. We identified SE-associated genes for these models based on the integrated study of RNA-sequencing and chromatin immunoprecipitation (ChIP) sequencing for H3K27ac binding. Since these patient-derived cancer models were generated through a spheroid culture technique, stemness markers such as *CD44* and *MYC* were identified as predominant SE-associated genes in the majority of cases. We further identified MYBL1 as a critical SE-associated transcription factor among basal-like cancer cases. Silencing of MYBL1 in TNBC patient-derived and cell line models showed that this transcription factor contributes to cell proliferation and the regulation of mitosis-associated gene expression. Immunohistochemical study for MYBL1 in our TNBC cohort showed that MYBL1 immunoreactivity is a potential poor prognostic factor for TNBC patients. The present findings suggest that the characterization of SE-associated transcriptional regulators and biomarkers will facilitate the understanding of molecular features of TNBC subtypes and the development of alternative potential therapeutic targets for the advanced disease.

#4771 DEL data-driven discovery of Brachyury (TBXT) ligands toward chordoma therapeutics.

Zhen Chen[1], Rebecca Swett[1], Miklos Feher[2], AJ Baghaie[1], Jeffrey Santandrea[2], Philippe McGee[2], Massaba Keita[2], Jenny Liu[1], **Ying Zhang**[1], Jithender Vakiti[2], Natalia Sannikova[2], Julien Pomarole[2], Timothy Morgan[2], Jean-Christophe Grenier-Petel[2], Aurelien Coelho[2], Ryan Walsh[1], Dylan Hale[2], Faraz Hussain[2], Arnaud Clerc[2]

[1]X-Chem Pharmaceuticals, Waltham, MA,[2]X-Chem Pharmaceuticals, Montreal, QC, Canada

Aberrant expression of the transcription factor Brachyury (also known as TBXT) drives the growth of chordoma, a rare bone cancer with limited treatment options. While transcription factors are traditionally considered undruggable by small molecules, advances in DNA-encoded library (DEL) screening and data-driven drug discovery technologies are challenging this conventional wisdom. To discover noncovalent small molecule ligands for Brachyury, we screened X-Chem's DEL deck comprising >150 billion diverse compounds against the Brachyury DNA-binding domain. The screen produced a rich dataset where ~73k compounds, representing >500 distinct chemical families, showed positive enrichment signal. Using X-Chem's Chemomics platform, we translated this dataset into actionable chemical matter from three avenues: (1) off-DNA resynthesis of exact DEL-encoded structures (library compounds) that are prioritized by our DEL-to-pharmacophore (Del2Ph4) analysis workflow, (2) compounds in commercial catalogs that score highly in Machine Learning (ML) models built from the DEL data and Del2Ph4 analysis, and (3) rapid parallel synthesis of analogs of enriched library compounds using multicomponent reactions. SPR assays using full-length Brachyury protein, independently run by the Chordoma Foundation, have confirmed target-binding activity for several chemically distinct compounds. These results highlight the power of X-Chem's drug discovery platform and offer a path forward for Brachyury-targeted chordoma therapeutics.

#4772 snoRNA-guided ribosome heterogeneity in a model of NSCLC collective invasion.

Sarah F. Webster[1], Yi-Ru Li[1], Virginie Marchand[2], Tala O. Khatib[3], Ryan M. Nottingham[4], Lutfur Rahman[1], Janna K. Mouw[3], Alan M. Lambowitz[4], Blerta Xhemalce[1], Yuri Motorin[5], Adam I. Marcus[3], Homa Ghalei[1]

[1]Biochemistry, Emory University, Atlanta, GA,[2]UMS2008 IBSLor, Universite de Lorraine, Vandoeuvre-les-Nancy, France,[3]Hematology and Medical Oncology, Emory University, Atlanta, GA,[4]Molecular Biosciences and Oncology, University of Texas at Austin, Austin, TX,[5]UMR7365 IMoPA, Universite de Lorraine, Vandoeuvre-les-Nancy, France

The processing, folding, and chemical modification of ribosomal RNAs (rRNAs) are critical for proper ribosome assembly and function and are tightly coordinated by a complex network of proteins and non-coding RNAs (ncRNAs). Among these, an abundant group of ncRNAs, small nucleolar RNAs (snoRNAs), guide the folding and site-specific modification of over 200 nucleotides in human rRNAs. Emerging evidence has linked changes in rRNA modification pattern to distinct tumor stages, but how rRNA modification heterogeneity manifests and contributes to cancer progression remains unknown. One mechanism driving cancer progression to metastasis is collective invasion, which is defined by the presence of cooperative subpopulations within a tumor. Previous work by the Marcus lab isolated two cell subpopulations, leaders and followers, from the H1299 cell line based on their distinct phenotypes. To assess the role of snoRNA-guided modification heterogeneity in invasion, we applied an unbiased genome-wide sequencing approach to leader and follower subpopulations to map rRNA modifications and snoRNAs. We identified 418 snoRNAs in leaders and followers. Of the differentially expressed snoRNAs, 60% are predicted to be ribosome targeting. Analysis of the snoRNA-guided rRNA modifications, revealed differential modification status at specific sites on the rRNA between leaders and followers. The majority of the top differentially modified sites are among the known dynamically modified sites across different cancers and tissues. While the sites of modification heterogeneity are not localized to a distinct site on the ribosome, they fall within key functional regions near the decoding center, subunit bridges, within the L1 stalk, and near the binding site of key ribosomal proteins. Overall, a weakly positive Spearman correlation of <0.3 between snoRNA abundance and rRNA modification status suggests snoRNA abundance alone does not inform the global rRNA modification pattern. To uncouple the roles of snoRNA expression and rRNA modification, we apply a set of biochemical tools and demonstrate that leaders and followers have differential growth and translation capacities that can be changed by altering snoRNA expression. Collectively, our data reveal novel modulators of growth and translation in NSCLC and shed light on the molecular principles underlying ribosomal modification heterogeneity in invasive cancer cells.

#4773 MYC associated transcriptional heterogeneity at the single cell level.

Saravana Gowtham Baskaran[1], Min-Zhi Jiang[2], Ada Tam[1], Hongkai Ji[2], Chi Van Dang[1]

[1]Johns Hopkins University School of Medicine, Baltimore, MD,[2]Johns Hopkins University Bloomberg School of Public Health, Baltimore, MD

Background: Tumor heterogeneity allows cancer cells to adapt to microenvironmental stress and resist therapies. MYC is commonly amplified in human cancers and its expression can be heterogeneous due to variations in extrachromosomal DNA (ecDNA) and the pulsatile nature of MYC expression. However, the heterogeneity of the MYC responsive transcriptome among single cells is unknown. Here, we evaluate the heterogeneity of MYC transcriptional response in vitro in an inducible MYC cancer cell line.
Methods: We used the P493-6 human B cell line model of Epstein-Barr Virus associated Burkitt's lymphoma (BL) with tetracycline-repressible (Tet-OFF) ectopic MYC expression. We modulated MYC expression by addition of tetracycline and performed paired bulk and single-cell RNA-sequencing (scRNA-seq). To further characterize the transcriptional response of these cells with different MYC levels, we turned off MYC in these cells and then turned it back on to capture cells with increasing levels of MYC over time and performed paired bulk and single-cell RNA sequencing.
Results: We observed heterogeneous expression of MYC and strikingly diverse expression of MYC responsive genes at the single cell level. After MYC induction with the removal of tetracycline, we observe a time-dependent decrease in STAT1 and other immune-related gene expression and movement of single cell transcriptomic clusters in high dimensional space visualized with tSNE plotting. Intriguingly, we observed a small cluster of CD58+ cells whose position in the tSNE space is unaltered by MYC status. We surmise that this cluster behaves like 'stem' cells capable of repopulating the entire population of P493 cells. Interestingly, we also see this small cluster of cells in some patient-derived BL cell lines.
Conclusions: Overall, we provide detailed evidence of MYC driven transcriptional heterogeneity at the single cell level. Our preliminary evidence of this unique 'stem-cell' like population of cells in BL warrants further study.

#4774 Targeting Beta-catenin in colorectal cancer: Novel molecular glue drug candidates by Coltac's BOND+ platform.

Yaron Sfadyah[1], Orli Even-Or[1], Michael Mullokandov[1], Hana Boocholez-Vardi[1], Valeria Arkadash[1], Alexandra Brodezki[1], Daniel Feder[1], **Liraz Harel**[1], Elon Yariv[2], Gali Prag[2]

[1]Coltac Therapeutics, Yavne, Israel,[2]School of Biochemistry Neurobiology Biophysics, Tel Aviv University, Tel Aviv, Israel

β-Catenin is a central oncogenic driver through its regulation of the Wnt signaling pathway, controlling cell proliferation, metastasis, drug resistance, across multiple cancer types. Its critical role is well-established in colorectal cancer (CRC), hepatocellular carcinoma, endometrial cancer, desmoid tumors, and subsets of ovarian cancer. In over 90% of colorectal cancers, Wnt/β-catenin pathway mutations elevate β-catenin levels, promoting tumorigenesis and poor prognosis. Restoring control of aberrant Wnt signaling in β-catenin–driven cancers hold significant potential to suppress tumor growth and improve clinical outcomes. Targeted protein degradation (TPD) by molecular glues offers a promising therapeutic strategy for modulating oncogenic drivers such as β-catenin proteins, historically considered challenging for conventional small-molecule inhibition. Discovery of selective glues remains limited by low throughput screening methods, weak detection sensitivity, and the complexity of E3-substrate biology. Coltac Therapeutics developed BOND+ a proprietary bacterial ubiquitin-dependent positive-selection screening system designed to identify molecular glues that enhance E3 ligase-target engagement. This synthetic platform converts functional ubiquitination events into bacterial growth, by leveraging the bacterial environment, which lacks deubiquitinases, proteasomal and lysosomal degradation systems, redundant E3 ligases, and any ubiquitylation-dependent degradation machinery, thus enabling direct, low-signal to noise readouts of functional target engagement. Identified hits are further validated in mammalian cell assays, followed by mechanistic studies and continuous optimization through medicinal chemistry and in silico refinement. Using BOND+ platform we identified selective molecular glue candidates that promote proteasome-dependent degradation of β-catenin and modulate downstream associated signaling. Lead compounds demonstrated up to 100-fold inhibition potency relative to initial hits, with preferential anti-tumor activity effects in various CRC Wnt-dependent cancer cell models. Early mechanistic studies confirmed target selectivity and E3-ligase dependence. Structure activity relationship (SAR) optimization and in vivo pharmacology studies refined potency and translational potential. Despite β-catenin central role in CRC there are no approved therapies directly target β-catenin, highlighting a significant unmet need. Coltac's BOND+ platform enabled rapid discovery and validation supporting therapeutic drugs for β-catenin. We demonstrated potent antitumor activity highlighting Coltac's molecular glue as a new drug candidate in β-catenin-driven cancers.

#4775 Reflux-induced NEK2 activates cap-dependent mRNA translation program in esophageal adenocarcinoma.

Lei Chen[1], Chloe Xiao[1], Tianling Hu[1], Oliver Gene McDonald[2], Steven Xi Chen[3], Heng Lu[1], Zheng Chen[1], Alexander Zaika[1], Wael El-Rifai[1], Dunfa Peng[1]

[1]Surgery, University of Miami Miller School of Medicine, Miami, FL,[2]Pathology, University of Miami Miller School of Medicine, Miami, FL,[3]Public Health Sciences, University of Miami Miller School of Medicine, Miami, FL

Background: The incidence of esophageal adenocarcinoma (EAC) has increased more than sevenfold in the United States and Western countries over the past four decades; however, patient prognosis remains poor, with a five-year survival rate of less than 20%. Dysregulation of mRNA translation, especially the cap-dependent mechanism mediated by eIF4F complex, was found in many human cancers. Aberrant expression and phosphorylation of eIF4E, the rate-limiting component of eIF4F complex, has been evidenced to promote oncogenic translation programs in human cancers. Constitutive overexpression of NEK2, a serine/threonine kinase of the NEK protein kinase family, has been reported to mediate tumor progression and drug resistance in cancer cells. Our study aims to investigate the role of NEK2 in regulating cap-dependent mRNA translation and translational significance of NEK2/eIF4E signaling in EAC.
Methods and Results: We first confirmed activation of the cap-dependent translation using a luciferase reporter assay and increased protein levels of its key factors, such as p-eIF4E, eIF4E, p-4EBP1, and 4EBP1, by western blotting, in the scenarios with either transient or repeated ABS exposure. However, the levels of p-mTOR, mTOR, eIF4A, and eIF4G remained unchanged. Meanwhile, intrinsic overexpression of NEK2 protein was observed in EAC patients, esophageal cell lines of dysplasia/EAC, and ABS-exposure-induced cell models. Overexpression and silence of NEK2 underlined its role in mediating activation of cap-dependent translation under reflux conditions. The co-overexpression of NEK2 and eIF4E was identified by immunofluorescent staining in EAC cells and immunohistochemistry staining in human TMA, indicating their potential interaction. Mechanically, we discovered that NEK2 contributes to cap-dependent translation by stabilizing eIF4E protein and regulated its phosphorylation in an MNK-dependent manner. Exotic overexpression of NEK2 significantly promoted colony formation capacities of tumor cells, while NEK2 silencing greatly suppressed tumor growth and expansion in cells/3D tumor spheres. Moreover, activation of NEK2/eIF4E signaling was proved to facilitate tumor cell survival in the presence of oxaliplatin. NEK2 silencing re-sensitized resistant EAC cells to chemotherapeutic drugs by magnifying apoptosis. Remarkably, the combination therapy of oxaliplatin and pharmacological inhibitor of NEK2, T-1101, synergized in inducing cell death, with minimized interruption on non-neoplastic cells. This finding was further confirmed in EAC-cell-line-derived xenograft models.
Conclusion: Our data elucidates novel functions of NEK2/eIF4E signaling axis in promoting cancer progression and drug resistance. Combination therapy of chemotherapeutic drugs with NEK2 inhibitor provides a promising strategy for treatment of EAC patients.

#4776 Lurbinectedin alters EWS::FLI1 binding to chromatin to poison transcription.

Zachary P. Tolstyka[1], Raphael D. Lopez[2], Sridhar M. Veluvolu[2], Emma Hiscock[1], Andrew Fuller[1], Mia Lollo[1], Emily Seiden[1], Rachael Hinshaw[1], Lauren Gaetano[2], Elizabeth Wilson[2], Gretchen Lam[1], Rebecca Kaufman[2], Elissa Boguslawski[1], Michelle Paulsen[1], Ishwarya Narayanan[1], Jenna Gedminas[2], Mats Ljungman[1], Patrick J. Grohar[1]

[1]University of Michigan Medical School, Ann Arbor, MI,[2]Children's Hospital of Philadelphia, Philadelphia, PA

Relapsed Ewing sarcoma has dismal outcomes and has had minimal treatment advancements in the last 30 years - there is a critical need for the development of new treatments. The tumor is uniquely dependent on the oncogenic EWS::FLI1 fusion transcription factor to develop and maintain malignancy. Lurbinectedin is a small molecule analog of the natural product trabectedin that has shown efficacy in multiple cancers including Ewing sarcoma. The mechanism of toxicity of lurbinectedin in Ewing sarcoma is under investigation.

Lurbinectedin exposure alters EWS::FLI1 trafficking into the nucleolus as measured by confocal microscopy. The subsequent impact of drug exposure on EWS::FLI1 binding to chromatin was determined by CUT&Tag and confirmed by chromatin fractionation. Transcription was assessed by qPCR and RNAseq, and BRUseq was utilized to determine the impact on nascent transcription. Further mechanistic clarification was determined by proximity ligation mass spectrometry. Ultimately, the integration of CUT&Tag of EWS::FLI1 with Bru-seq (CUT, Tag, and Bru) following treatment with lurbinectedin elucidated the effects of the drug on EWS::FLI1 binding and alteration of downstream transcription.

Exposure of Ewing sarcoma cells to lurbinectedin alters EWS::FLI1 distribution in the nucleus to the nucleolus. The relocalized EWS::FLI1 can be trapped in the nucleolus by use of potentiators that inhibit HSP70. The relocalization is driven by altered MAPK signaling and can be rescued by siRNA silencing of MAPK pathway members. The effect is rooted in wild-type function of the FET family of proteins and is associated with altered EWS::FLI1 binding at response elements leading to alteration of the transcriptome. Both transcription initiation and elongation are altered. Importantly, these effects on EWS::FLI1 are both dose and time dependent and can be further amplified with MAPK perturbants.

Treatment with lurbinectedin induces relocalization of the oncogenic transcription factor EWS::FLI1 to the nucleolus leading to transcriptional suppression of EWS::FLI1 target genes and a striking decrease in cell viability. This modulation of EWS::FLI1 binding to chromatin occurs in both a concentration and time dependent manner. Intriguingly, the impact appears to be dependent on gene length: there is greater transcription alteration in longer genes compared to shorter genes.

#4777 Core tension and control: Fxr1 mediates mechanoregulation via ahnak in head and neck cancer.

Anitha Vijayakumar[1], Samuel John[1], Tae-Hyung Kim[2], Breege V. Howley[3], Viswanathan Palanisamy[1]

[1]Department of Internal Medicine, UNM Comprehensive Cancer Center, University of New Mexico, Albuquerque, NM,[2]Department of Pathology, UNM Comprehensive Cancer Center, University of New Mexico, Albuquerque, NM,[3]Department of Biochemistry and Molecular Biology, Medical University of South Carolina, South Carolina, SC

Background: Head and neck squamous cell carcinoma (HNSCC) is the sixth most prevalent cancer globally and is marked by aggressive invasion, high metastatic potential, and a persistently low 5-year survival rate (~50%). Emerging evidence highlights the roles of cytoskeletal remodeling and altered cellular biomechanics, including stiffness, viscoelasticity, and deformability, in promoting cancer cell migration and invasion. However, the molecular regulators of these biomechanical properties in HNSCC remain poorly defined.
Methods: We investigated the role of Fragile X-Related Protein 1 (FXR1), an RNA-binding protein, in modulating tumor biomechanics and invasion in cancer cells. FXR1 knockdown (KD) was performed in HNSCC cell lines, followed by transcriptomic, cytoskeletal, and biomechanical analyses. Functional assays, including cell motility, stiffness, and tumor growth in vitro and in syngeneic mouse models, were performed to define the tumorigenic role of FXR1 in oral cancer.
Results: FXR1 silencing significantly upregulated AHNAK, a large scaffolding protein implicated in cytoskeletal organization. This upregulation was associated with reduced F-actin polymerization, impaired lamellipodia formation, decreased cellular stiffness, and diminished invasive and migratory properties of oral cancer cells. Dual knockdown of FXR1 and AHNAK partially restored F-actin architecture, lamellipodia formation, and cell stiffness, suggesting a functional interplay between the FXR1-associated protein network. Mechanistically, further evidence demonstrated that FXR1 KD activated the Hippo signaling pathway via LATS2, leading to the cytosolic accumulation of phosphorylated YAP (P-YAP), implicating FXR1's role in mechanotransduction. In vivo, WT and FXR1 KD-derived xenografts exhibited significantly reduced tumor volume in syngeneic mouse models with immune cell activation.
Conclusions: FXR1 promotes HNSCC progression by repressing AHNAK and enhancing F-actin dynamics, thereby increasing cellular stiffness, invasion, and migration. Our findings reveal a novel FXR1-AHNAK-F-actin axis that regulates tumor biomechanics and invasiveness of oral tumors, offering new mechanistic insights and identifying FXR1 as a promising therapeutic target in HNSCC.

#4778 FOXR2 reverses MDM2-mediated but not MDM4-mediated p53 repression.

Wei-Hsiung Yang[1], Anmol P. Patel[2], William H. Yang[3]

[1]Biomedical SCiences, Mercer University School of Medicine, Savannah, GA,[2]Mercer University School of Medicine, Savannah, GA,[3]Medical College of Georgia at Augusta University, Augusta, GA

Despite advances in therapy, cancer remains a major health challenge in the 21st century, with mortality rate ranging from approximately 11% to 25%. The tumor suppressor p53, a protein critical for cancer development and prevention, is regulated by numerous interacting partners. In our previous unpublished findings, we identified that FOXR2 (an epigenetically regulated pan-cancer oncogene) is able to module p53 activity. Consequently, in the present investigation, we broaden our exploration to examine how FOXR2 regulates p53 transactivation. We first found that FOXR2 enhances p53 transactivation in a dose-dependent manner in H1299 (p53 NULL) cells. Given that MDM2 and MDM4 (MDMX) are major p53 negative regulators, we then tested whether FOXR2 could counteract MDM2- and MDM4-mediated p53 repression. We found that FOXR2 dose-dependently reverses MDM2-mediated p53 transactivation. However, FOXR2 has minimal or no effect on MDM4-mediated p53 repression. Moreover, our data suggests that FOXR2 is capable of binding to p53. Finally, we found that FOXR2 increases wild-type (WT) p53, but not G245S (hotspot mutation) p53, transactivation. Taken together, our preliminary results demonstrate that FOXR2 is a novel protein to regulate p53 activity likely involving MDM2 competition due to possible p53-FOXR2 interaction. This data is presented to substantiate the concept that p53's activity is governed by a complex and still-expanding network of interactions.

#4779 IL-6/STAT3 signaling mediates MYB dysregulation in prostate cancer: Implications for aggressive disease progression and racial disparities.

Vinayaraj Ellu Valappil[1], Shashi Anand[1], Kunwar Somesh Vikramdeo[1], Ranjana Mitra[2], Seema Singh[1], Ajay P. Singh[1]

[1]Department of Cell and Molecular Biology, Cancer Center and Research Institute, University of Mississippi Medical Center, Jackson, MS,[2]College of Medicine, Roseman University of Health Sciences, Las Vegas, NV

We have previously reported a role for MYB in the progression, aggressiveness, and therapy resistance of prostate cancer. Notably, we also observed racially disparate MYB expression, with higher levels being present in prostate cancer from Black patients, correlating with advanced tumor grade and shorter time to biochemical recurrence. In this study, we investigated the molecular mechanisms underlying MYB dysregulation in prostate cancer that could potentially be linked to its higher levels in Black patients. We found that serum levels of IL-6 were significantly elevated in Black patients with prostate cancer, and treatment of prostate cancer cell lines with IL-6 resulted in a dose- and time-dependent upregulation of MYB expression. IL-6-induced MYB upregulation was abolished when cells were pre-treated with either an IL-6 neutralizing antibody (Tocilizumab) or a STAT3 inhibitor (Stattic). Notably, AR-negative cell lines exhibited high basal MYB expression, which was slightly reduced by Tocilizumab treatment but drastically reduced upon STAT3 inhibition, suggesting that it is a significant regulator of MYB overexpression in prostate cancer. Chromatin immunoprecipitation (ChIP) analysis revealed increased STAT3 binding to the MYB in the first intronic region, following IL-6 treatment, which was reduced upon pre-treatment with Tocilizumab or Stattic. Additionally, in this region, we observed enhanced recruitment of CDK9, a key component of the P-TEFb complex, which is shown to facilitate the release of the MYB transcriptional pause through Ser2 phosphorylation in the c-terminal domain of RNA polymerase II. Pre-treatment of prostate cancer cells with a CDK9 inhibitor also attenuated IL-6-induced MYB expression. Finally, silencing MYB or treating cells with a CDK9 inhibitor significantly impaired IL-6-mediated proliferation, migration, and invasion of prostate cancer cells. These findings establish IL-6/STAT3 signaling as a critical regulator of MYB expression in prostate cancer, highlighting its potential role in prostate cancer pathogenesis and racial disparities.

: Angiogenesis
Poster Session

#4783 An mRNA vaccine targeting angiogenesis elicits a robust immune response and inhibits tumor growth and angiogenesis in two mouse melanoma models.

Srdan Tadic, Laura Ochoa-Callejero, Judit Narro Iniguez, Josune Garcia-Sanmartin, Alfredo Martinez

Angiogenesis Study Group, Center for Biomedical Research of La Rioja (CIBIR), Logrono, Spain

Background: Angiogenesis is essential for tumor growth, metastasis, and the establishment of an immunosuppressive microenvironment. By supporting nutrient delivery and modulating immune cell infiltration, tumor-driven angiogenesis promotes both malignant progression and immune evasion. Among its key regulators, adrenomedullin (AM) is a potent pro-angiogenic factor frequently overexpressed in solid tumors. To explore its therapeutic potential, we developed an mRNA vaccine encoding a fusion antigen composed of a small keyhole limpet hemocyanin (KLH) peptide, as a hapten, linked to mouse AM.
Methods: The in vitro transcribed mRNA was encapsulated in lipid nanoparticles (LNPs) and administered to C57BL/6 mice, with empty LNPs serving as controls. The vaccine was evaluated in two distinct melanoma models: an experimental lung metastasis model induced by intravenous injection of B16-F10 melanoma cells, and a subcutaneous melanoma model. After four immunizations, melanoma cells were injected, followed by a fifth immunization. Mice were sacrificed once tumors reached humane endpoints and blood and organs were analyzed.
Results: Vaccinated mice exhibited significant increases in anti-AM IgG titers ($p= 0.040$) and CD8+ T cell numbers ($p=0.033$) compared to controls. In the lung metastasis model, immunization resulted in a significant reduction in both the number ($p=0.028$) and size of lung metastases ($p=0.020$) as well as a decrease in the number of tumor-associated blood vessels ($p=0.046$), without disrupting normal vasculature as assessed in SMAA-GFP transgenic mice. In the subcutaneous model, vaccination delayed tumor initiation ($p=0.005$) and reduced tumor volume ($p=0.004$), accompanied by decreased tumor angiogenesis ($p=0.045$). Importantly, no systemic toxicity or significant changes in weight were observed.
Conclusion: By targeting angiogenesis, the KLH-AM mRNA vaccine effectively impaired tumor growth in melanoma models. These results highlight AM as an important pro-angiogenic factor driving tumor vascularization and support further development of AM-directed mRNA therapeutic vaccination as a strategy to disrupt angiogenesis-dependent tumor progression.This study was funded by Agencia Estatal de Investigacion (AEI, Spain)'s project PID2022-136735OB-I00.

#4784 Galectin-1 as a central regulator of angiogenesis and metabolic reprogramming in glioblastoma.

Luisina B. Ripari[1], Joaquin P. Merlo[2], Mariana B. Vera[3], Olivia Morris-Hanon[3], Monica B. Mezmezian[4], Marcos Hermida[5], Gustavo E. Sevlever[3], Diego O. Croci[6], Guillermo A. Videla-Richardson*[1], Gabriel A. Rabinovich*[7]

[1]Laboratorio de Investigacion Aplicada a las Neurociencias (LIAN-INEU-Fleni), Fundacion para la Lucha de las Enfermedades Neurologicas de la Infancia (Fleni); Laboratorio de Glicomedicina, Instituto de Biologia y Medicina Experimental (IBYME-CONICET), Buenos Aires, Argentina,[2]Laboratorio de Glicomedicina, Instituto de Biologia y Medicina Experimental (IBYME-CONICET); UADE - INTEC, Buenos Aires, Argentina,[3]Laboratorio de Investigacion Aplicada a las Neurociencias (LIAN-INEU-Fleni), Fundacion para la Lucha de las Enfermedades Neurologicas de la Infancia (Fleni), Buenos Aires, Argentina,[4]Laboratorio de Neuropatologia y Biologia Molecular, Fundacion para la Lucha de las Enfermedades Neurologicas de la Infancia (Fleni), Buenos Aires, Argentina,[5]Departamento perinatal, Hospital Nacional Prof. Alejandro Posadas, Buenos Aires, Argentina,[6]Instituto de Histologia y Embriologia de Mendoza (IHEM-CONICET), Buenos Aires, Argentina,[7]Laboratorio de Glicomedicina, Instituto de Biologia y Medicina Experimental (IBYME-CONICET), Buenos Aires, Argentina

Glioblastoma (GB) is the most aggressive tumor of the central nervous system characterized by rapid growth and remarkable resistance to current therapies. Its biology is shaped by profound inter- and intra-tumoral heterogeneity, a highly immunosuppressive microenvironment, and a strong dependence on metabolic and vascular adaptations that allow tumor cells to thrive under hypoxic and nutrient-poor conditions. A subpopulation enriched in glioma stem-like cells (GSCs) plays a central role in these adaptations, sustaining tumor expansion through flexible metabolic and angiogenic programs. Galectin-1 (GAL1), a glycan-binding lectin with multiple roles in the tumor microenvironment, is considerably elevated in gliomas. This led us to investigate whether GAL1 could act as a common regulator of both metabolism and angiogenesis in GB. We established patient-derived GSC lines (G02, G03, G08, G09), a model that preserves the clinical heterogeneity typical of this disease. RNA-seq and functional assays revealed clear differences among cell lines. G02 showed an endothelial-like signature and promoted endothelial cell migration, while G03 was enriched in angiogenesis-related pathways and formed robust tube-like structures in vitro, in line with higher VEGF secretion ($p<0.01$). Biopsies from the corresponding patients (G02 and G03) recapitulated this biology, displaying broad areas of microvascular proliferation. Inhibition of GAL1 with antibodies or siRNA reduced tube formation mainly in G03, suggesting that not all angiogenic profiles are likely dependent on GAL1. Metabolic analysis further supported this idea. Seahorse analysis showed that G02 and G03 respond to GAL1 depletion by shifting toward opposite metabolic programs, and complementary assays (TMRE, MitoSOX) revealed high mitochondrial activity in G02 (FC=2), while G09 displayed impaired OXPHOS (FC=0.5). Together, our data indicate that both secreted and intracellular GAL1 contribute to the metabolic and angiogenic adaptations that sustain GB growth. These results emphasize that GSCs rely on distinct yet coordinated strategies to obtain resources, and position GAL1 as a central regulator of these processes. Defining the cellular and functional profiles that determine sensitivity to GAL1 inhibition may help guide the development of more precise anti-angiogenic or metabolic therapies for glioblastoma.

#4785 Thermal regulation of dysbiotic tumor vasculature.

Amie A. Brint, Hailey Kristian, Samir Jenkins, Robert Griffin, **Ruud Petrus Dings**

University of Arkansas for Medical Sciences, Little Rock, AR

Antibiotic use has substantially increased over the years. Although oral antibiotics treat infections, they also drastically change the gut microbiota, disturbing commensal bacteria that are essential for maintaining a number of homeostatic processes. Our recent published and unpublished work have shown that GI-tract dysbiosis causes drastic changes to the stroma of distal tumors, resulting in accelerated cancer progression of various solid tumors. We discovered that dysbiosis induces a significant suppression of adhesion molecules on tumor endothelial cells. Conversely, localized hyperthermia has been increasingly recognized to elicit various cellular responses, yet the effects of hyperthermia on the tumor vasculature during ABX-induced dysbiosis are unknown. We found that hyperthermia (60 min of either 41.5 °C or 43 °C, as compared to 37 °C) influenced various adhesion molecules to different degrees. Especially hyperthermic exposure of 43 °C for 1 hr was able to overcome the adhesion-molecule suppression found on the tumor vasculature during dysbiosis. Functional studies with splenocytes and T cells demonstrated that the induced increase in vasculature adhesion molecules caused increased tethering of leukocytes. Although further studies are warranted, these results demonstrate that hyperthermia exerts immune modulating effects and is capable of overcoming the dysbiosis-induced phenotype. Since current systemic anti-cancer treatments are often limited by their toxicities, localized hyperthermia may become a viable alternative in the future.

#4786 AI-powered deep phenotyping: Vision transformers quantify vessel normalization and immune efficacy in a 3D vascularized tumor-on-a-chip.

Delaney K. Donnelly, Byungjun Lee, Junfeng Wang, Sabrina Figueroa Buezo, Hyeon-geun Park, Bushra Rajput, Yeongmin Choi, Jiho Kim, Jihye Baek, Eunjeong Kim, Joseph Harris, Kyusuk Baek, Branka Mitrovic, Tsung-Li Liu, Aneesh Sathe, Sanghee Yoo

Qureator, Inc., San Diego, CA

Introduction: Dysfunctional, chaotic tumor vasculature creates a hostile physical barrier to immune infiltration, severely limiting the efficacy of immunotherapies. Conventional models fail to replicate this structural complexity or the dynamic interplay between vessels and immune cells. To address this, we validated a high-throughput, AI-driven vascularized tumor microenvironment (TME) platform designed not only to model this barrier but to rigorously quantify tumor-induced angiogenesis, vessel normalization, and downstream immune cell behaviors.
Methods: Using the Qureator's microphysiological system (MPS), we generated a patient-derived gastric cancer model with perfusable vasculature. To validate predictive utility, models were treated with FDA-approved anti-angiogenic agents (e.g., Ramucirumab, a second-line therapy for gastric cancer) and a panel of vessel normalization reagents. We developed a customized, machine learning-powered Vision Transformer (ViT) pipeline to analyze immunofluorescence images. Unlike traditional morphological tools, our ViT approach utilizes self-attention mechanisms to capture global dependencies, allowing for the rigorous quantification of high-dimensional deep phenotyping features.
Results: The platform established a clinically relevant TME where Ramucirumab treatment significantly reduced peritumoral vessel density, accurately recapitulating clinical anti-angiogenic effects. Beyond simple density metrics, our ViT-based deep phenotyping identified distinct phenotypic clusters among different normalization reagents based on complex, non-linear features such as vessel tortuosity, branch density, and pericyte coverage. Crucially, this high-dimensional AI analysis revealed a direct functional correlation: reagents that induced a specific "normalized" vascular signature were strongly associated with a measurable increase in T cell-mediated killing efficiency, linking restored vascular morphology to improved therapeutic outcomes.
Conclusion: This AI-enabled TME platform represents a powerful New Approach Methodologies (NAMs), integrating deep learning with complex biology to perform "deep phenotyping" of the tumor microenvironment. By precisely linking vascular morphology to functional immune outcomes, it accelerates the discovery of therapies that restore the TME to a treatment-responsive state.

#4787 Glutaminolysis promotes cancer-associated angiogenesis via the GLS1-TNC signaling pathway.

Jianqiang Yang, Zhenzhen Fu, Soumya Vijaya Kuma, Fanghui Chen, **Yong Teng**

Emory University, Atlanta, GA

Glutaminolysis, a metabolic pathway in which glutamine is converted into glutamate and subsequently into α-ketoglutarate, supports cancer progression by supplying energy and biosynthetic precursors that sustain tumor cell growth, survival, and metabolic flexibility. While its metabolic functions have been extensively studied, its contribution to tumor angiogenesis is not well defined. In this study, we demonstrate that knockdown of glutaminase 1 (GLS1), a key regulator of glutaminolysis, in head and neck cancer (HNC) xenografts markedly reduced intratumoral CD31⁺ endothelial cells, consistent with impaired angiogenesis. In vitro, HUVECs exposed to exosomes from GLS1-deficient HNC cells exhibited diminished migratory capacity and reduced tube formation compared with those treated with control-derived exosomes. Proteomic analysis by LC-MS revealed that exosomes lacking GLS1 were deficient in tenascin-C (TNC), a matricellular protein with established pro-angiogenic activity. Mechanistic studies showed that GLS1 loss triggered USP1-dependent proteasomal degradation of caveolin-1 (CAV1), a critical regulator of exosome biogenesis. Because CAV1 promotes the incorporation of TNC into exosomes, GLS1 deficiency disrupted the CAV1-TNC signaling axis, resulting in exosomes lacking pro-angiogenic cargo. Consequently, these defective exosomes failed to activate extracellular matrix remodeling and adhesion pathways in HUVECs, thereby limiting endothelial migration and angiogenic capacity. Together, these findings uncover a previously unrecognized role for GLS1 in promoting tumor angiogenesis and further suggest that targeting GLS1 could not only suppress tumor metabolism but also inhibit angiogenesis in HNC.

#4788 PSMA-expressing tumor vasculature in renal cell carcinoma: spatial, functional, and therapeutic implications.

Ryuta Watanabe[1], Keito Kagimoto[1], Mami Chosei[2], Tomohisa Sakaue[3], Mie Kurata[4], Noriyoshi Miura[1], Riko Kitazawa[5], Tadahiko Kikugawa[1], Shigeki Higashiyama[6], Takashi Saika[1]

[1]Department of Urology, Ehime University Graduate School of Medicine, Toon, Japan,[2]Department of Biochemistry and Molecular Genetics, Ehime University Graduate School of Medicine, Toon, Japan,[3]Department of Cardiovascular and Thoracic Surgery, Ehime University Graduate School of Medicine, Toon, Japan,[4]Department of Analytical Pathology, Ehime University Graduate School of Medicine, Toon, Japan,[5]Division of Diagnostic Pathology, Ehime University Hospital, Toon, Japan,[6]Department of Oncogenesis and Growth Regulation, Osaka International Cancer Institute, Osaka, Japan

Background

Prostate-specific membrane antigen (PSMA) is an established diagnostic and therapeutic target in prostate cancer, widely utilized in PSMA-PET imaging and PSMA-directed radioligand therapy. Beyond prostate cancer, PSMA has also been reported in the tumor-associated vasculature of several solid tumors, suggesting its potential as a vascular marker and therapeutic target. In renal cell carcinoma (RCC), PSMA-positive vessels have been described, yet their spatial distribution, mechanisms of induction, contribution to angiogenesis, and therapeutic relevance remain insufficiently defined.

Methods

Spatial transcriptomic analysis (10x Genomics Visium) was performed to characterize the spatial localization of FOLH1 (PSMA) expression and associated transcriptional changes within RCC tissues. Immunohistochemistry for PSMA and CD31 was conducted on 45 RCC cases to evaluate associations with recurrence and venous invasion. Endothelial cells were exposed to RCC-derived conditioned medium and differential centrifugation fractions to assess PSMA induction, angiogenic activity, and transcriptional alterations. A Caki1 xenograft model was used to investigate the therapeutic effect of the PSMA inhibitor 2-PMPA.

Results

Spatial analysis showed that FOLH1 expression was concentrated within peritumoral vascular regions and overlapped with areas exhibiting increased expression of angiogenesis-related genes. Immunohistochemistry confirmed that PSMA expression was restricted to tumor-associated vessels, and strong PSMA expression was significantly associated with recurrence and venous invasion. Among RCC-derived fractions, only the 10,000 g pellet robustly induced endothelial PSMA expression, enhanced tube formation, and activated angiogenesis-related transcriptional programs. In vivo, treatment with 2-PMPA significantly reduced tumor growth and microvessel density.

Conclusions

PSMA-positive vasculature in RCC represents an endothelial phenotype induced by tumor-derived vesicles and functionally contributes to angiogenesis. The association between strong PSMA expression and aggressive clinicopathologic features, together with the anti-angiogenic effect of PSMA inhibition, highlights PSMA-positive vessels as a promising therapeutic target in RCC. These findings provide a molecular basis for extending PSMA-targeted imaging and therapeutic strategies—well established in prostate cancer—to PSMA-positive RCC.

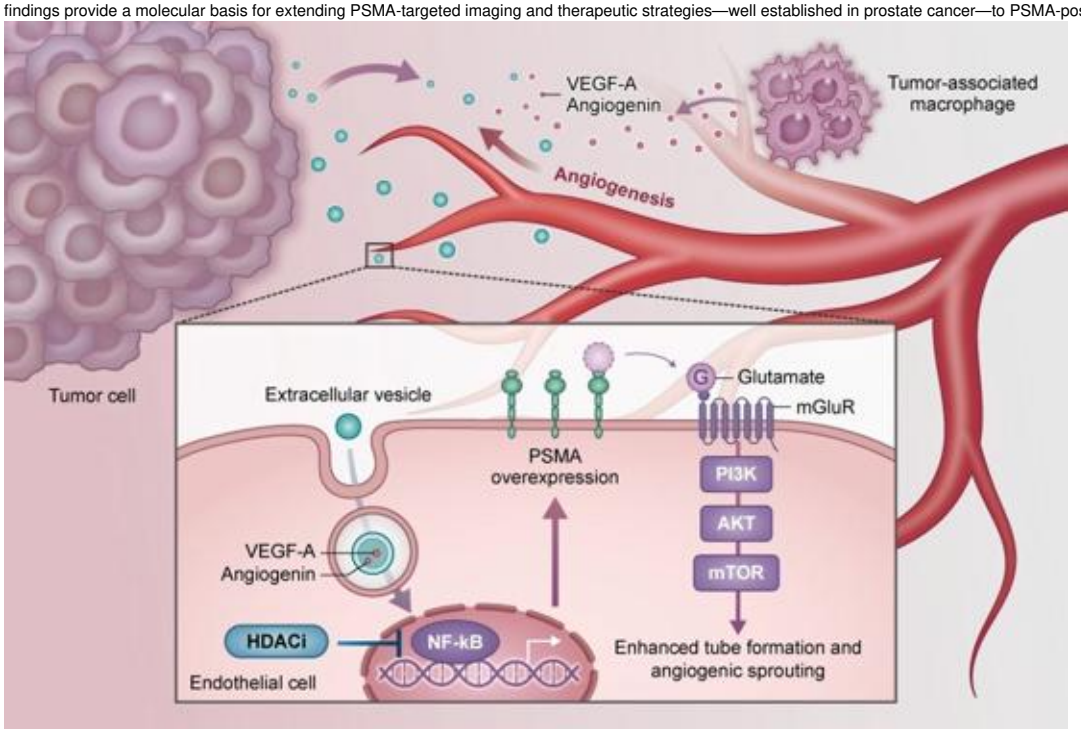

#4789 Apelin is a candidate driver for neuromuscular junction recovery from cancer cachexia.

Alice Wang, Tobias Janowitz

Cold Spring Harbor Laboratory, Cold Spring Harbor, NY

Cancer cachexia is a systemic wasting condition that affects multiple organs and failure to recover from the condition ultimately leads to death. It is estimated to affect as many as 80% of patients with cancer and accounts for up to 20% of cancer deaths. Cancer cachexia is characterized by negative energy balance leading to weight loss and organ atrophy. Cancer cachexia results in decreased physical ability, reduced therapy efficacy, and increased mortality and morbidity. There is emerging evidence that hormone signaling drives inter-organ changes in cancer cachexia development, including changes in the brain, liver and muscle. I have developed a cancer cachexia mouse model in which both cancer cachexia development and recovery can be studied in the same animal. Using this model, I observed decreased muscle mass during cancer cachexia development and increased muscle mass during cancer cachexia recovery. By performing unbiased analyses on quadriceps RNA sequencing data from cachectic and recovering mouse, I identified a cluster of genes indicating alterations in the neuromuscular junctions. This suggests that neuromuscular junctions (NMJ) may play a role in muscle atrophy and regeneration in cancer cachexia. By focusing my analyses on circulating hormones, I identified apelin as the most upregulated hormone in the skeletal muscle during cancer cachexia recovery. Apelin has been associated with age-related muscle atrophy, muscle function and the neuromuscular junction. I have modulated apelin level systemically and demonstrated that systemic apelin administration decreased intramuscular E3 ligase (protein degradation) and increased Pax7 (regeneration) marker in the lower leg muscle. These findings have been corroborated by detailed histopathology analyses. My work establishes a novel mouse model that enables studying cachexia development and recovery in the same mice. This model may lead to the discovery of new treatment options that can prevent or treat cancer cachexia. In addition, my work suggests that there may be potential targetable mechanisms for accelerating muscle recovery from cancer cachexia.

#4790 Cancer reprograms the remote vascular microenvironment to promote atherosclerosis.

Lingfeng Luo[1], Changhao Fu[1], Kai-Uwe Jarr[2], Richard Baylis[3], Virginia Sun[3], Julius Heemelaar[3], Moritz von Scheidt[4], Daniela Ramirez[4], Johannes Krefting[4], Nadja Sachs[5], Justus Wettich[5], Hanna Winter[5], Hua Gao[1], Fudi Wang[1], Allen M. Haas[6], Kevin T. Nead[7], Lars Magdefessel[5], Heribert Schunkert[4], Tomas Neilan[3], Nicholas J. Leeper[1]

[1]Surgery, Stanford University, Stanford, CA,[2]Cardiology, Angiology, and Pneumology, Heidelberg University Hospital, Stanford, Germany,[3]Medicine, Massachusetts General Hospital, Boston, MA,[4]Surgery, Technische Universitat Munchen, Munich, Germany,[5]Vascular and Endovascular Surgery, Technical University Munich, Munich, Germany,[6]University of Texas MD Anderson Cancer Center, Houston, TX,[7]Radiation Oncology, University of Texas MD Anderson Cancer Center, Houston, TX

Cancer releases a broad repertoire of circulating cytokines and angiogenic factors that remodel distant tissues. However, the remote vascular consequences of tumor-derived inflammatory signaling remain incompletely understood. Our preliminary data suggest that cancer activates a TNF-driven, LRG1-dependent endothelial pro-angiogenic pathway implicated in remote vascular remodeling. We profiled vascular responses to colorectal tumors using bulk and single-cell RNA sequencing of aortic tissues from tumor-bearing versus control mice across diverse backgrounds, endothelial assays stimulated with tumor-conditioned media, O-link proteomics to define tumor-induced circulating mediators, and in vivo perturbation of the TNF-LRG1 axis using a TNF-neutralizing antibody or endothelial-targeted AAV-LRG1 knockdown. Across independent human datasets, we further observed that large cohort studies from both Europe and the United States demonstrate an increased risk of atherosclerotic CVD in cancer survivors, tumor resection is associated with a reduced risk of atherosclerotic events, and biobank tissues from cancer patients display elevated vascular TNF-LRG1 signaling, supporting clinical relevance. In conclusion, cancer upregulates TNF to activate an LRG1-dependent endothelial pathway, driving angiogenesis and vascular remodeling. These findings uncover a previously unrecognized tumor-CVD interaction and identify the TNF-LRG1 axis as a potential therapeutic target to mitigate cancer-induced vascular dysfunction.

#4791 The role of endothelial cell remodeling in driving immunotherapy resistance of hepatocellular carcinoma.

Baoyi YIN[1], Shufen CHEN[1], Zhewen XIONG[1], Patrick WONG[1], Zhuo Yu[2], Stephan CHAN[1], Alfred Sze Lok CHENG[1]

[1]The Chinese University of Hong Kong, Hong Kong, Hong Kong,[2]Shuguang Hospital Affiliated to Shanghai University of Traditional Chinese Medicine, Shanghai, China

Background: Hepatocellular carcinoma (HCC) has shown limited durable responses to immune checkpoint blockade (ICB) therapies due to tumor microenvironment (TME)heterogeneity. Combining anti-vascular endothelial growth factor (VEGF) with ICB has enhanced therapeutic efficacy, but the limited benefits suggest that understanding endothelial cell (EC) remodeling beyond angiogenesis is essential for enhancing ICB effectiveness. Integrated analyses identified a novel transcription factor(TF) transcriptional program, coupled with elevated bromodomain and extra terminal domain (BET) protein BRD4 expression, that was associated with EC remodeling in ICB-resistant HCC. Emerging studies have shown that this TF functions depend on BRD4 through its recruitment to a specific enhancer region, and inhibiting BRD4 with BET inhibitors can reduce its expression. Hence, we aim to delineate the microenvironmental cue that direct EC remodeling for tumor immunosuppression and their role in promoting ICB resistance.
Methods: Single-cell transcriptomic profiling was performed on samples from a Phase II clinical trial of pembrolizumab in HCC patients (NCT03419481). An ICB-resistant HCC mouse model generated via iterative selection was utilized for validation. BET inhibitor AZD5153, administered in nanoparticle formulations, was used to suppress BRD4 and TF expression selectively in ECs. Quantitative immunofluorescence and flow cytometry was employed for EC assessment and intratumoral immune microenvironment.
Results: scRNA-seq analysis revealed that tumor vessels in ICB non-responders were enriched with disorganized macrovascular-like endothelial cells (MaVEC), which likely originate from liver sinusoidal endothelial cells (LEC). Suggesting a dynamic trans-differentiation process from LEC to MaVEC during the development of ICB resistance. Notably, we identified a novel TF as the top regulon in MaVEC, exhibiting increased transcription factor activity along the LEC-to-MaVEC trajectory, and closely associated with BRD4 in MaVEC. Treatment with the EC-targeted nanoparticle-delivered AZD5153 can suppress this TF expression, caused remarkable intratumoral MaVEC-to-LEC reversion and reshaped the intratumoral immune microenvironment, leading to an augmented anti-PD-L1 efficacy.
Conclusions: Our study reveals that the dynamic trans-differentiation from LEC to MaVEC is related with ICB resistance in HCC. Blocking this EC transformation shifts the TME from immunosuppressive to stimulatory, re-sensitizing tumors to anti-PD-L1 therapy. This project may yield new strategies to counter adaptive immune resistance in HCC.
Keywords: Hepatocellular carcinoma, Immune-checkpoint blockade, Endothelial cells remodeling.
Acknowledgement: The work is funded by General Research Fund (14118424) & AstraZeneca Pre-clinical Oncology Research Programme & Li Ka Shing Foundation.

#4792 Krüppel-like factor 8 promotes triple negative breast cancer angiogenesis and metastasis through matrix metalloproteinases.

Ebaa Y. Ababneh, Heng Lu, Chunjiang He, Chao Shen, Lin Yu, Satadru K. Lahiri, Debarati Mukherjee, Xianhui Wang, Jihe Zhao

Burnett School of Biomedical Sciences, College of Medicine, University of Central Florida, Orlando, FL

Krüppel-like factor 8 (KLF8) is a transcription factor known to promote breast cancer. KLF8 upregulates matrix metalloproteinases (MMPs) that degrade the extracellular matrix (ECM) and are associated with enhanced angiogenesis. However, KLF8's role in BC angiogenesis through MMPs has not been elucidated. We hypothesize that KLF8's upregulation of MMPs promotes an angiogenic switch in triple-negative breast cancer (TNBC), the most aggressive breast cancer subtype, by degrading the ECM to create physical space and increase the bioavailability of pro-angiogenic factors. Inducible KLF8 overexpression (MCF10A-Ras) and knockdown (MDA-MB-231) cell models were used to study the function of KLF8 *in vitro*. We employed the broad-spectrum matrix metalloproteinase (MMP) inhibitor GM6001 to confirm dependency, endothelial tube formation and HUVEC recruitment assays to evaluate angiogenesis potential, Quantitative real-time PCR (qRT-PCR) and Vascular Endothelial Growth Factor (VEGF)-A ELISA to measure growth factor expression and active factor release. Findings were then validated using the *in vivo* xenograft tumor growth and tail vein lung metastasis assays, angiogenesis in excised tumors was quantitatively evaluated using microvessel density staining (cluster of differentiation 31 (CD31)), with MMP rescue experiments used to establish molecular pathway. Our results show that KLF8 overexpression promotes endothelial cell migration and tube formation in an MMP-dependent manner. The KLF8-MMP-VEGF axis is established using VEGFA ELISA that shows KLF8-dependent accumulation of active VEGF in conditioned medium. This effect was eliminated by MMP inhibition, Notably, KLF8 does affect VEGF mRNA expression. *In vivo* experiments validate these results showing that KLF8 overexpression markedly increases angiogenesis, xenograft tumor growth, and lung metastasis. On the other hand, MMP-9 or MMP-14 rescue in the knockdown cells restores the effects of KLF8 knockdown. Poor distant metastasis-free survival and elevated angiogenic markers are associated with high KLF8 expression in human breast cancer cohorts. In conclusion, our work demonstrates KLF8's role in promoting TNBC metastasis by activating MMP9 and MMP14, which in turn enhances the angiogenic microenvironment through the release of soluble VEGF. This work advances our understanding of KLF8's carcinogenic function and suggests that KLF8-MMP signaling could be a promising antiangiogenic therapeutic target for TNBC.

#4793 Tumor-intrinsic CD80 mediates cancer stemness and vascular mimicry in aggressive oral squamous cell carcinoma.

Yu-Lin Chen[1], Shih Sheng Jiang[1], Shih-Han Huang[1], Ssu-Han Wang[1], Fang-Yu Tsai[1], Yen-Chung Chiu[1], Kai-Ping Chang[2], Daw-Yang Hwang[3], Ko-Jiunn Liu[3], Yu-Wen Su[1], Ya-Wen Chen[1]

[1]National Health Research Institute, Miaoli County, Taiwan,[2]Chang Gung University, Taoyuan, Taiwan,[3]National Health Research Institute, Tainan, Taiwan

Background Intratumoral heterogeneity drives oral squamous cell carcinoma (OSCC) progression by fostering tumor cell plasticity. This plasticity poses a major therapeutic challenge. We identified the immune molecule CD80 as a potential driver of this process and dissected its non-canonical, tumor-intrinsic functions.

Methods Syngeneic OSCC sublines were established through *in vivo* selection. Gene profiling and single-cell RNA sequencing (scRNA-seq) of mouse tumors, integrated with human datasets, identified candidate drivers. CD80 function was interrogated using shRNA knockdown, cell sorting, and assays of tumorigenesis, cancer stemness, and vascular mimicry (VM) in mouse models and human OSCC cells. SOX2 rescue experiments assessed mechanistic dependency.

Results Gene expression profiling and scRNA-seq identified the co-stimulatory molecule CD80 as highly expressed in the aggressive sublines, and its expression correlated with poor patient prognosis in OSCC. Crucially, CD80 knockdown reduced tumor burden in immunocompetent and immunodeficient mice, demonstrating a tumor cell-intrinsic oncogenic role independent of its canonical function in adaptive immunity. Mechanistically, CD80 enhanced cancer stemness, as evidenced by increased sphere formation and SOX2 expression. *In vivo* scRNA-seq data indicated that $CD80^+$ tumor cells were associated with EMT-active, metabolic, and angiogenesis pathways. Moreover, CD80 knockdown impaired vessel-like formation *in vitro*, while CD80-high tumors displayed prominent VM *in vivo*. Ectopic SOX2 expression rescued both sphere and vessel-like formation in CD80 knockdown cells, suggesting that CD80-mediated oncogenic effects are partly SOX2-dependent.

Conclusions Our findings reveal a novel, non-immunological role for CD80 in driving OSCC progression. By promoting cancer stemness and VM via a CD80-SOX2 axis positions CD80 as a promising therapeutic target.

#4794 Prognostic relevance of angiogenesis-associated genes in gliomas: Influence of idh/1p19q status and opportunities for antiangiogenic immunotherapy strategies.

Pijush Das[1], Kevin A. Camphausen[2], Uma Shankavaram[2]

[1]National Cancer Institute, National Institutes of Health (NIH), Bethesda, MD,[2]National Cancer Institute, Bethesda, MD

Background: Angiogenesis, the formation of new blood vessels, is central to glioma progression and supports tumor growth and invasion. Early identification of aggressive biology in lower-grade gliomas (LGG) is essential for guiding treatment decisions. We developed an immune-oriented angiogenesis gene signature that characterizes aggressive tumor phenotypes in LGG and glioblastoma (GBM). The study also evaluates its association with key glioma biomarkers, including IDH mutations and 1p/19q co-deletions, and assesses its prognostic relevance across both tumor types.
Objective: To develop and validate an immune-oriented angiogenesis gene signature that identifies aggressive glioma biology, predicts patient prognosis in LGG and GBM, and evaluates its relationship with IDH mutation and 1p/19q co-deletion status.
Methods: We analyzed LGG and GBM samples from The Cancer Genome Atlas (TCGA). Immune infiltration levels were estimated using EPIC, and samples were classified into high and low infiltration groups. Differentially expressed genes between these groups were identified, followed by Weighted Gene Co-expression Network Analysis (WGCNA) to cluster co-expressed genes into modules. Fisher's exact test was used to assess enrichment of WGCNA module genes within the Hallmark Angiogenesis gene set, prioritizing overlapping genes. Associations with IDH status, 1p/19q co-deletion, and patient survival were evaluated using Cox regression, Kaplan-Meier analysis, and time-dependent ROC curves. Validation was performed in the Chinese Glioma Genome Atlas (CGGA) and two single-cell datasets (pLGG: GSE222850; GBM: GSE138794).
Results: The derived immune-oriented angiogenesis signature was significantly associated with IDH mutation and 1p/19q subtypes (Adj. $p \leq 0.05$) and strongly predicted patient outcomes. Higher signature expression correlated with poorer survival and remained independently prognostic in multivariate analyses (e.g., TCGA LGG $p = 3.28\times10^{-7}$; CGGA LGG $p = 1.08\times10^{-8}$). The signature showed strong predictive accuracy in time-dependent ROC analyses (TCGA LGG AUCs: 1-year 0.959, 3-year 0.873, 5-year 0.812). Gene expression patterns observed in LGG showed a progressive trend consistent with certain GBM subgroups. In single-cell datasets, most genes showed significant differential expression between high and low immune infiltration groups (Adj. $p \leq 0.05$).
Conclusion: We identified and validated an immune-oriented angiogenesis gene signature that integrates genetic, molecular, and clinical features across gliomas. The signature demonstrates strong prognostic value in both LGG and GBM and reflects increasing angiogenic activity along glioma progression. This gene set may serve as a practical tool for patient risk stratification and offers potential targets for future therapeutic strategies.

#4796 CXCL17 Drives angiogenesis to promote progression in cutaneous squamous cell carcinoma.

Alok R. Khandelwal, Cherie-Ann O. Nathan, Keerthan Jaganmohan

Otolaryngology, Head and Neck Surgery, LSU Health Shreveport, Shreveport, LA

Cutaneous squamous cell carcinoma (cSCC) represents a growing public health challenge, with 200,000 Americans diagnosed annually and limited therapeutic interventions. Despite widespread awareness of ultraviolet B (UVB) radiation as a primary etiologic factor, current prevention strategies remain inadequate, underscoring the urgent need for mechanism-based approaches to interrupt cSCC development and progression. Our investigation unveils a critical molecular mechanism by which CXCL17 drives pro-angiogenic signaling in human microvascular endothelial cells. Comprehensive molecular analysis revealed a profound activation of key oncogenic and angiogenic pathways upon CXCL17 treatment, with significant phosphorylation of endothelial nitric oxide synthase (eNOS), protein kinase B (pAKT), nuclear factor kappa B (NFκB), and hypoxia-inducible factor-1α (HIF-1α). The coordinated activation of these signaling molecules suggests a robust angiogenic reprogramming mechanism. Notably, eNOS phosphorylation indicates enhanced nitric oxide production, a critical mediator of endothelial proliferation and vessel formation. Concurrent AKT activation promotes endothelial cell survival, while NFκB and HIF-1α upregulation demonstrates metabolic and inflammatory adaptations that support aggressive vascular remodeling. Syngeneic Tumor-Cell Xenograft model corroborated these molecular findings, demonstrating significantly reduced CD31 staining in CXCL17-knockout tumors, directly linking CXCL17 to tumor angiogenesis. Clinical correlation studies further substantiated CXCL17's role in metastatic potential, with elevated expression associated with increased perineural invasion and tumor aggressiveness. Our comprehensive analysis establishes CXCL17 as a pivotal molecular orchestrator of angiogenic processes in cutaneous squamous cell carcinoma, offering novel insights into tumor progression mechanisms.

#4797 Antagonistic SMAD2/3 control of TIMP-1, VEGF-A, and hypoxia signaling in myofibroblasts shapes histotype-specific angiogenesis in lung cancer.

Jordi Alcaraz[1], Natalia Isabel Diaz Valdivia[1], Paula Duch[1], Marselina Arshakyan[1], Amelia Parker[2], Alejandro Bernardo Suarez[1], Danielle Park[3], Erik Sahai[3], Noemi Reguart[4], Derek C. Radisky[5], Oriol Casanovas[6]

[1]Universitat de Barcelona, Barcelona, Spain,[2]Garvan Institute of Medical Research, Darlinghurst, Australia,[3]The Francis Crick Institute, London, United Kingdom,[4]Medical Oncology Department, Hospital Clinic i Provincial de Barcelona, Barcelona, Spain,[5]Mayo Clinic Florida, Jacksonville, FL,[6]Catalan Institute of Oncology, Barcelona, Spain

Non-small cell lung cancer (NSCLC) exhibits strikingly different responses to antiangiogenic therapies between its two major histologic subtypes, lung adenocarcinoma (LUAD) and squamous cell carcinoma (LUSC), suggesting an histotype-specific regulation of angiogenesis. Cancer-associated fibroblasts (CAFs) commonly exhibit an activated/myofibroblast-like phenotype in NSCLC, and are emerging as key modulators of tumor progression; however, their contribution to angiogenic control remains undefined. Here, we investigated angiogenesis and hypoxia signatures in NSCLC and integrated bulk RNA-seq, scRNA-seq, CAF secretome profiling, genetic perturbations, and functional in vitro and in vivo assays to dissect the histotype-dependent production of pro-angiogenic factors by CAFs. We observed greater angiogenesis and reduced necrosis/hypoxia in LUAD compared to LUSC across multiple patient cohorts. The LUAD-CAF secretome was primed for angiogenesis through SMAD3-dependent overproduction of key regulators, most notably TIMP-1 and VEGF-A. We also uncovered a previously unrecognized role for TIMP-1 in promoting endothelial hyper-branching. In contrast, LUSC-CAFs displayed attenuated angiogenic activity despite robust HIF-1α upregulation and an hypoxia-associated transcriptional program, due to their epigenetic repression of SMAD3 and compensatory increase in SMAD2. Collectively, these results reveal that CAFs critically shape the distinct angiogenic landscapes of LUAD and LUSC through opposing SMAD2/3 regulation of TIMP-1, VEGF-A, and hypoxia signaling. These results further highlight the therapeutic potential of targeting stromal SMAD3/TIMP-1 in LUAD or microenvironmental stressors such as hypoxia and acidosis in LUSC. In addition, these findings provide a biological framework for understanding histotype-specific patterns of dissemination, immune evasion, and response to antiangiogenic therapies in NSCLC.

#4798 Comparison of three vascular endothelial markers in the evaluation of microvessel density in cutaneous melanoma.

Nolwabo Moyakhe[1], Benny Mosoane[1], Tebogo Marutha[2], Rahaba Marima[2], **Zodwa Dlamini**[2], Meshack Bida[1]

[1]Department of Anatomical Pathology, University of Pretoria, Pretoria, South Africa,[2]Pan African Cancer Research Institute (PACRI), University of Pretoria, Pretoria, South Africa

Background

Angiogenesis underpins tumor growth, survival, and metastasis in many solid cancers, including malignant melanoma. One way to quantify tumor angiogenesis is to assess microvessel density (MVD) using endothelial immunohistochemical markers. In routine practice, anti-factor VIII-related antigen, anti-CD31, and anti-CD34 are all used for this purpose, but how they stack up against each other in cutaneous melanoma is still not very clear. We compared these three markers to determine which is the most useful for MVD evaluation in this specific context.

Methods

We conducted an analytical comparative study using archival cutaneous melanoma samples collected between 2015 and 2021 at the University of Pretoria. Immunohistochemistry with anti-factor VIII, anti-CD31, and anti-CD34 antibodies was performed on 102 tissue sections from 34 cases. Three pathologists independently counted the microvessels in 10 high-power fields (200× magnification) for each marker. Data were analyzed using repeated-measures ANOVA with post-hoc testing ($p<0.05$).

Results

The mean MVDs were 77.33 (±29.57) for anti-CD34, 61.67 (±34.85) for anti-CD31, and 58.67 (±23.51) for anti-factor VIII. Anti-CD34 highlighted significantly more microvessels than anti-CD31 or anti-factor VIII ($p=0.003$). Post-hoc analysis confirmed significant differences between CD31 and CD34, and between CD34 and factor VIII ($p=0.001$). In contrast, anti-CD31 and anti-factor VIII did not show a meaningful difference in sensitivity or specificity for microvessel detection.

Conclusion

In this series, anti-CD34 performed better than anti-CD31 and anti-factor VIII in highlighting MVD in cutaneous melanoma. This is in line with reports from other solid tumors, suggesting that CD34 tends to pick up more vessels. While our sample size is modest and drawn from a single center, the data support the use of anti-CD34 as the preferred marker for intratumoral MVD assessment in surgical pathology, ideally alongside clinicopathological correlation and, where needed, complementary markers.

#4799 Lymphangiogenesis in the uterine horns: Implication of the Netrin-1 and UNC5B signaling pathway in physiology and cancer.

Lia Barcons, Nicolas Rama, Patrick Mehlen

Cancer Research Center of Lyon (CRCL), Lyon, France

The lymphatic system consists of an open, unidirectional network of lymphatic vessels maintaining tissue homeostasis, intestinal absorption, immunosurveillance and immunomodulation. These vessels are lined by lymphatic endothelial cells (LECs). Lymphangiogenesis, defined as sprouting of new lymphatic vessels from pre-existing vessels or embryonic veins, is the main mechanism driving the formation and expansion of lymphatic networks during embryogenesis and in adults under physiological conditions.
This process involves numerous molecules, most notably VEGF-C, but also axon-guidance cues such as Netrins (Hu et al., 2024). Lymphangiogenesis shares many features with angiogenesis, which depends mainly on VEGF-A, but also Netrin-1. Netrin-1, acting through its receptor UNC5B, regulates vascular endothelial migration and branching, thereby stabilizing the vascular network (Lu et al., 2004).
In our laboratory, scRNAseq analysis of murine uterine horns revealed that Netrin-1 and UNC5B are specifically expressed by LECs. The lymphatic network of uterine horns has never been investigated, nor has the role of the Netrin-1 and UNC5B in lymphangiogenesis in general. We hypothesize that Netrin-1 and UNC5B contributes to lymphatic network development by regulating LEC migration and tubulogenesis. Our preliminary in vivo data describe the expression patterns of Netrin-1 and UNC5B during lymphatic development in murine uterine horns. UNC5B and Netrin-1 knockout models are being generated to define their functional roles. In vitro studies on human dermal LECs are assessing Netrin-1 effects on migration and tubulogenesis.
The lymphatic system is a key route for metastatic dissemination, notably in endometrial cancer (Donoghue et al., 2007). Uterine horns are continuously lined by the endometrium, suggesting that lymphatic vessels within uterine horns may provide a pathway for endometrial cancer cell dissemination. Although Netrin-1 is normally absent in adult tissues, it is re-expressed in tumors, where it promotes tumor progression. If Netrin-1 contributes to lymphangiogenesis in uterine horns, it may similarly modulate lymphatic vessel formation and thereby facilitate metastasis in endometrial cancer.
Consistent with this, preliminary results showed that the neutralizing antibody anti-Netrin-1 in mice grafted with endometrial cancer cells significantly reduces lung metastases. The knockout models will help define how Netrin-1 and UNC5B could regulate lymphatic-dependent metastatic spread.
This project aims to characterize lymphangiogenesis in uterine horns and to define the roles of Netrin-1 and UNC5B in physiological and tumor contexts. Ultimately, this work may support new therapeutic applications for the anti-Netrin-1 antibody developed in our laboratory, currently in phase II clinical trial.

#4800 Targeting CD160 as an immunotherapy approach to modulate tumor angiogenesis and improve outcomes in triple-negative breast cancer.

Abdel-Ilah Aziz[1], Maxence Mocquery-Corre[2], Chloe Jean[2], Jessica Thevenard-Devy[2], Alexandre Berquand[2], Sabrina Haddou[2], Cathy Hachet[2], Andre F. Martins[3], Rachid El fatimy[1], Laurent Duca[2], Armand Bensussan[1], Sanae Ben Mkaddem*[1], Jerome Devy*[2]

[1]Faculty of Medical Sciences, UM6P Hospitals, Mohammed VI Polytechnic University, Ben Guerir, Morocco,[2]Universite de Reims-Champagne-Ardennes, UMR CNRS/URCA 7369, MEDyC, Reims, France,[3]Werner Siemens Imaging Center, Department of Preclinical Imaging and Radiopharmacy, Eberhard Karls University,, Tubingen, Germany, Germany

Triple-negative breast cancer (TNBC) is an aggressive subtype with limited treatment options and poor clinical outcomes. While immune checkpoint inhibitors (ICIs) have shown promise in TNBC, many patients remain unresponsive, highlighting the urgent need for new immunotherapeutic targets and mechanisms. CD160, a GPI-anchored receptor expressed on cytotoxic immune and endothelial cells, we have recently been proposed CD160 as a novel immune checkpoint inhibitor in solid tumors (Scheffges, Devy, *et al.* 2024). In this study, we investigated CD160 as a dual therapeutic target in TNBC, combining immunoregulatory and anti-angiogenic potential. Using a novel high-affinity monoclonal antibody against CD160, we demonstrate that targeting this receptor significantly inhibits pathological angiogenesis and promotes vascular normalization *in vitro* and *ex vivo*, without inducing cytotoxicity. These effects may contribute to enhanced immune infiltration and improved tumor perfusion, ultimately improving patient survival. To better understand CD160's mechanism of action, we explored its molecular interactions in human endothelial cells. Super-resolution microscopy and functional assays revealed that CD160 physically associates with LRP1, identifying it as a potential co-receptor involved in its vascular effects. These findings support the development of CD160-targeted immunotherapy as a promising strategy for TNBC, acting both as an immune checkpoint inhibitor and a modulator of the tumor vasculature.

References : Scheffges C, Devy J, Giustiniani J, Francois S, Cartier L, Merrouche Y, Foussat A, Potteaux S, Bensussan A, Marie-Cardine A. Identification of CD160-TM as a tumor target on triple negative breast cancers: possible therapeutic applications. Breast Cancer Res. 2024 Feb 15;26(1):28. doi: 10.1186/s13058-024-01785-x. PMID: 38360636; PMCID: PMC10870674.

#4801 DDR2 positive endothelial cells promote angiogenesis and metastasis in breast tumors.

Alessandra DiMauro[1], Audrey Brenot[1], Julien Lesage[1], Jade Weber[1], Vasilios Morikis[1], Jason D. Weber[2], Gregory D. Longmore[3]

[1]Washington University in St. Louis, St. Louis, MO,[2]Assoc. Professor, Dept. of Internal Medicine, Washington University, Saint Louis, MO,[3]Washington University School of Medicine, St. Louis, MO

The collagen receptor DDR2, a receptor tyrosine kinase, contributes to breast cancer progression through actions in both invasive tumor cells and tumor stromal cells. In the tumor stroma, DDR2 is predominantly expressed by cancer associated fibroblasts (CAFs) and therein contributes to the formation of a tumor permissive ECM which facilitates metastasis. Through an analysis of human breast tumor scRNAseq data and multiplex immunohistochemistry, we noted that DDR2 is also expressed by a subset of tumor $CD31^+$ endothelial and $LYVE1^+/CD31^+$ lymphatic cells. To determine whether this endothelial cell $DDR2^+$ population contributes to breast cancer progression, and if so how, we genetically depleted $Ddr2^{fl/fl}$ from endothelial cells using inducible $Cdh5\text{-}Cre^{ERT2}$ in the context of MMTV-PyMT mouse breast tumor model. In endothelial $Ddr2^{-/-}$ breast tumors there was no significant difference in primary tumor burden or total number of $CD31^+$ endothelial cells within the tumor; however, there was a significant reduction in lung metastases. Closer analyses revealed a decrease in $CD31^+$ vessel length and area in primary tumors from these mice and an associated increase in hypoxia. When VEGF-containing Matrigel plugs were implanted subcutaneously in ubiquitous DDR2 null mice, $CD31^+$ vessel growth into the plug was reduced. Vessel outgrowth from aortic rings from global DDR2 null mice was decreased. These data suggested some migratory defect in $Ddr2^{-/-}$ endothelial cells. To test this possibility directly, we developed, characterized, and utilized a microfluidic device wherein ECs are subjected to mechanical fluid flow within a 3D fibrin matrix. Genetic depletion of *Ddr2* and antibody inhibition of DDR2 both resulted in reduced EC migration. In summary, we find that DDR2 is present in a subset of ECs, possibly tip cells, and impacts tumoral and non-tumoral angiogenesis *in vivo* and *in vitro.*

#4802 Evaluation of the circulating angiome in cancer: Translational assessment of a 44-plex angiogenesis biomarker panel.

Hans Layman[1], Mai Abdel-Ghani[1], Grace Galen[1], Rony Garcia-Vivas[1], Jenna Slezak[1], Anu Mathew[1], Mingyue Wang[1], Catherine Demos[1], Pankaj Oberoi[1], Andrew B. Nixon[2], Jacob N. Wohlstadter[1]

[1]Meso Scale Diagnostics, LLC, Gaithersburg, MD,[2]Duke Univ. Medical Ctr., Durham, NC

Angiogenesis, the formation of new blood vessels from existing vasculature, is a hallmark of tumor progression, enabling malignant growth, invasion, and metastasis. Tumor-associated angiogenesis leads to the formation of leaky, poorly perfused vessels and localized hypoxia, fostering metabolic stress, immune evasion, and resistance to therapies. Vascular normalization through targeting of VEGF, Ang-2, and PDGF pathways can restore perfusion, enhance immune infiltration, and improve response. Although anti-angiogenic agents are widely used, no predictive biomarker identifies individuals that are likely to benefit. Previously, biomarker development for anti-angiogenic therapies focused on few vascular factors and did not capture the complexity of angiogenic signaling. To address this, we developed a 44-marker angiogenesis panel enabling high-throughput profiling of pro- and anti-angiogenic mediators relevant to oncology and vascular biology. Forty-four biomarkers encompassing established pro- and anti-angiogenic mediators (e.g., VEGF-A, Ang-2, Tie-2, IL-6) were literature-curated. Antibody pairs for each assay were optimized for the electrochemiluminescence detection-based MESO SCALE DISCOVERY (MSD) U-PLEX® platform. Double-spun platelet-poor EDTA plasma samples from Duke University was tested to identify a common diluent. Analytical characterization included LLOD/LLOQ, precision, spike recovery, and dilution linearity/parallelism determinations. The interclass correlation coefficient (ICC) and biological variance were evaluated using longitudinally collected plasma from 28 participants (27-79 y.o.), incorporating diurnal (morning and afternoon) draws over two months. Pharmacodynamic biomarker modulation was explored using retrospective plasma samples from two NCI studies —Cabozantinib + Panitumumab (NCT02008383) and Bevacizumab (NCT00416637). All assays met the predefined criteria, with >90% of assays achieving intra-/inter-assay precision of <15% CV. A single diluent supported multiplex compatibility. Dynamic ranges spanned 3-5 orders of magnitude, with analytical sensitivity for low and high abundance markers ranging from 0.06 pg/mL (IL-6) to 67.4 pg/mL (vWF), demonstrating sub-pg/mL detection. ICC analyses revealed good to excellent variable marker stability across the panel over two months. Retrospective analysis of both sets of NCI study samples demonstrated an association between (a) baseline markers and outcomes (OS, PFS) and (b) pharmacodynamic responses and expected treatment-induced changes, highlighting the value of the biomarker panel. This 44-plex panel demonstrates robust analytical performance, sensitivity, and reproducibility on the MSD® U-PLEX platform. The assay supports harmonized angiogenesis profiling, enabling standardized angiogenesis biomarker assessment in oncology research.

#4803 Ascites protects against ferroptosis and enables the peritoneal spread of ovarian cancer.

Yasaman Setayeshpour[1], Ssu-Yu Chen[1], Divya L. Dayanidhi[1], Yunji Lee[1], Shao-Chin Wu[1], Juan J. Aristizabal-Henao[2], Jianli Wu[1], Chao Chieh (Jerry) Lin[1], Nazanin Setayeshpour[1], Chiara Federico[1], Alexander A. Mestre[1], Michael A. Kiebish[2], Andrew Berchuck[1], David S. Hsu[1], Zhiqing Huang[1], Susan K. Murphy[1], Jen-Tsan Ashley Chi[1]

[1]Duke University, Durham, NC,[2]BPGbio, Waltham, MA

One of the most common sites of metastasis in ovarian cancer (OVCA) is the peritoneum. Often, this spread is accompanied by the accumulation of a fluid called ascites in the peritoneal cavity. Despite its common occurrence in metastatic OVCA patients, ascites and its influence on the peritoneal spread of OVCA are poorly understood. Interestingly, OVCA cells are vulnerable to ferroptosis, a type of cell death caused by lipid hydroperoxides. Hence, how these ferroptosis-sensitive OVCA cells persist in their spread to the peritoneum remains unknown. Here, we show that ascites robustly protects OVCA cell lines, patient-derived tumor cells and organoids against ferroptosis and enhances the peritoneal spread of OVCA cells in mice. Mechanistically, ascites downregulates the mitochondrial enzyme, 3-hydroxy-3-methylglutaryl-CoA synthase 2 (*HMGCS2*), which contributes to an increase in lipid droplets. Additionally, upon ferroptosis induction, ascites represses the upregulation of the transferrin receptor, *TFRC*, thereby decreasing cellular labile iron levels. Furthermore, we show that lipid-lowering fibrates reverse cellular changes induced by ascites, and they attenuate the peritoneal spread of OVCA cells in mice. Our findings implicate the importance of ascites in ferroptosis protection and the peritoneal spread of OVCA, and they suggest that targeting the ferroptosis protection by ascites may present a novel therapeutic approach to limit OVCA metastasis.

#4804 Synchronously implanted cold tumor abrogates anti-PD-1 response of hot tumor in a syngeneic mouse model.

Hao Sun, Ying Zheng, Luke Tsai, Xia Ding, Cassandra Rosemond

HD Biosciences, Inc. A WuXi AppTec company, San Diego, CA

Background and Objective: Synchronous cancer describes a new or second primary cancer that develops at the same time as the first primary cancer, either in the same organ or in a different organ with the same molecular basis. Synchronous cancer is not considered metastatic relapse. The prevalence of synchronous cancer varies depending on the cancer type, but overall, it is a rare event occurring in 4.5% to 11.7% of patients with multiple primary malignancies. The impact of a second primary tumor on the progression and treatment response of the first tumor remains poorly understood. This study investigates the interaction between two distinct primary tumors- MC38 colorectal cancer and LL/2 lung cancer- in a synchronous syngeneic mouse model. Specifically, we evaluated how the presence of LL/2 tumor influences the efficacy of anti-PD-1 immunotherapy against MC38 tumor. Changes in immune cell population and cytokine profiles in circulation and within the MC38 tumor microenvironment were also examined. These findings shed light on how inter-tumoral communication affects therapeutic efficacy in the presence of synchronous malignancies.

Method and Result: C57BL/6 mice were inoculated subcutaneously with 5 x 10^5 MC38 cells on the right flank. Mice in group 1 and 3 received an additional MC38 inoculation on the left flank, while group 2 and 4 received 5 x 10^5 LL/2 cells at the left flank. When MC38 tumor reached approximately 100 mm^3, mice were treated with 10 mg/kg of anti-PD-1 antibody intraperitoneally every 4 days. Tumor growth, body weights, immune cell populations, and cytokine levels in blood and tumor tissues were assessed after 10 days of treatment. The body weights of the mice remained no significant differences between groups. Interestingly, although the tumor volumes in group 2 were only slightly higher than in group 2, the tumor volumes in group 4 were significantly higher than in group 3, indicating the presence of LL/2 tumor greatly impaired the efficacy of anti-PD-1 immunotherapy against MC38 tumor. FACS analysis and cytokine analysis confirmed the changes of immune profiling that led to the insensitive of MC38 tumor to the immunotherapy.

Conclusion: The presence of a second primary cancer can profoundly affect the immune checkpoint inhibitor therapeutic response of the first primary tumor through inter-tumoral immune modulation. These findings emphasize the importance of evaluating tumor-tumor communication when designing treatment strategies for patients with synchronous cancer. WuXi AppTec Biology-IVPU offers bilateral tumors models and comprehensive in vivo capability for preclinical oncology drug efficacy studies.

#4805 Investigating the interaction between GBM and perivascular niche using an engineered brain microenvironment model.

Sheridan Ke-Wing Fok[1], Hanrong Ye[2], Ahmad Khalil[2], Brendan Harley[1]

[1]University of Illinois at Urbana-Champaign, Urbana, IL,[2]Biomedical Engineering, Boston University, Boston, MA

Introduction: Glioblastoma (GBM) is the largest histological group among brain tumors, accounting for 47.8% of malignant brain tumors in the adult population; its high infiltrative nature and incidence of tumor recurrence make GBM lethal and untreatable. Vessel co-option occurs when GBM invades the vasculature; tumor cells hijack pre-existing vessels and utilize it to move inside the brain. To understand GBM mechanisms and facilitate therapeutic developments against tumor recurrence, a tumor microenvironment model for vessel co-option is required. Our lab has previously developed a gelatin hydrogel platform using a photopolymerizable methacrylamide-functionalized gelatin (GelMA). This platform was coupled with the synthetic zinc finger gene regulator (SynZiFTR) to overexpress pro- and anti- angiogenic factors to control vascular formation. We aim to use this model to study the interaction between GBM and the perivascular niche.
Materials: Sequences of human PDGFR-β and ANG-2 were obtained from the NCBI database, which were later inserted into the vector backbone using a Gibson assembly cloning kit. The gelatin hydrogel model is generated by encapsulating a mixture of brain microvascular endothelial cells, normal human astrocyte, and pericytes (3:1: 1, 3 x 10^6 BMVECs/mL); PVN cells were resuspended with GBM spheroid in the GelMA-LAP solution and then polymerized by exposure to UV light.
Results: SynZiFTR containing human PDGFR-β was transduced into human brain vascular pericytes (HBVPs). Immunostaining showed a significant increase in PDGFR-β expression and vessel formation when encapsulated in the GelMA hydrogel with NHAs and BMVECs. Conditioned media collected from this pro-angiogenic microenvironment significantly increased tumor cell migration. We further validated the effect of this vessel network on GBM behavior by encapsulating GBM spheroid into the hydrogel model. We observed a similar increase in cellular outgrowth, and a reduced effect of TMZ on GBM spheroids. Ongoing efforts are expanding the study to consider maturation processes, where we observe overexpression of ANG-2 reduces the overall density of vessel formation, yet conditioned media from more mature vessel networks promotes GBM invasion into the surrounding hydrogel environment.
Conclusion: Our data demonstrate that the cytokines and growth factors released from pro- and anti-angiogenic brain microenvironments significantly affect tumor behaviors. Ongoing efforts seek to co-encapsulate GBM spheroids in engineered vascular hydrogels (overexpressed ANG-2) to more deeply investigate reciprocal interactions between GBM and perivascular cell compartments that shape vessel co-option and GBM invasion. We believe this model would greatly facilitate the development of new therapeutics against GBM recurrence and understanding of vessel co-option.

: Contextual Determinants of Cancer Stemness and Tumor Aggressiveness
Poster Session

#4809 The role of estradiol and estrogen receptors in lung cancer: A focus on sex differences.

Omar A. Borges-Sosa, Maksat Babayev, Carolyn D. Ekpruke, Dustin Rousselle, Patricia Silveyra

Environmental and Occupational Health, Indiana University, Bloomington, IN

Background: Lung cancer (LC) is the first and second most diagnosed cancer in males and females, respectively. Despite advancements, LC remains the leading cause of cancer-related mortality worldwide. Recent discoveries have reopened the discussion about the potential influence of hormonal factors on sex differences in LC outcomes. Among these factors, the role of 17β-estradiol (E2) in LC tumor progression is still unclear. This study aims to understand the influence of E2 and its possible role in cell proliferation and tumor growth in LC.
Methods: To study the contribution of E2 to metabolic activity in vitro, we exposed male and female human bronchial epithelial (HBE) cell lines (BEAS-2B, 16HBEC14o-, and HBEC3-KT), and human and murine LC cell lines (NCI-H441, NCI-1650, NCI-1975, A549, LL/2-Luc2) to seven different concentrations of E2 (from 1pM to 1uM), or vehicle (control) in E2-free medium. MTT assay was conducted after 24, 48, and 72hrs of exposure. We then studied specific E2 pathway mechanisms of cell proliferation in selected conditions. To study sex differences in tumor growth in vivo, we orthotopically injected LL/2-Luc2 murine cells into the left lung of 6-9-week-old C57BL/6J male and female mice. The mice were euthanized at 21 days post-injection or before if they reached humane endpoint.
Results: HBE cell lines did not show increased metabolic activity in response to physiological E2 concentrations; however, some cell lines showed a significant increase at the highest concentration (1uM) compared with the control. On the other hand, NCI-H441, NCI-1650, and LL/2-Luc2 showed a significant increase at earlier time points and at lower concentrations of E2. A549 and NCI-1975 did not show increased activity at any E2 concentration compared with control. Additionally, we found that LC cell lines with increased metabolic activity showed a significant increase in expression of genes related to angiogenesis (VEGFA), estrogen metabolism (CYP1B1), and ER pathway co-activation (GREB1) compared with their vehicle-treated cells. In contrast, HBE cell lines did not exhibit these changes, even at the highest E2 concentration, although some showed increased metabolic activity. In vivo, our preliminary results have shown an increased survival in female mice compared with male mice at 21 days post-orthotopic injection with LL/2-Luc2.
Conclusion: The preliminary data suggests that estrogen signaling stimulates metabolic activity and gene pathways associated with tumor progression in some LC cell lines. These effects may be related to the individual cell lines' ER expression or mutations. Unveiling these and other mechanisms by which E2 increases cell metabolic activity and induces gene expression highlights the translational potential of targeting the ER pathway or its downstream effectors in LC. Our preliminary in vivo mouse model results with LL/2-Luc2 show increased survival in male C57BL6/J mice compared to females.

#4810 Cisplatin-oral microbiota synergistic role in HNSCC aggressiveness and its clinical relevance.

Partha Jyoti Saikia[1], Lekhika Pathak[1], Bidisha Pal[2], Upasha Sarmah[1], Tulika Sarma[3], Chayanika Das[3], Debduti Datta[1], Rupam Das[4], Bikul Das[5]

[1]Department of Cancer and stem cell biology, KaviKrishna Laboratory, Guwahati, India,[2]Department of Experimental Therapeutics, Thoreau Laboratory for Global Health, M2D2, University of Massachusetts, Lowell, Massachusetts, Massachusetts, MA,[3]KaviKrishna Telemedicine Care, Sualkuchi, Assam, India,[4]KaviKrishna Laboratory, Guwahati, India,[5]Department of Cancer and Stem Cell Biology, KaviKrishna Laboratory, Guwahati, India

Background: Cisplatin-based chemotherapy remains a cornerstone for treating Head and NeckSquamous Cell Carcinoma (HNSCC). However, its therapeutic success is often limited inpatients with advanced-stage disease (Stage III-IIIb). Emerging evidence indicates thatchemotherapy itself may induce or select for aggressive, therapy-resistant tumor phenotypes.Meanwhile, dysbiosis of the oral microbiota—particularly involving Fusobacterium nucleatumand Porphyromonas gingivalis—has been implicated in HNSCC progression and immuneevasion. Yet, the synergistic interplay between cisplatin treatment and oral microbial ecologyremains poorly understood. Here, we investigate whether oral microbiota enhance cisplatin-induced aggressiveness via reprogramming of cancer stem cell (CSC) phenotypes, particularlythe Tumor Stemness Defense (TSD) state, which represents an adaptive altruistic response totherapy-induced stress.
Methods: Saliva samples were prospectively collected from 15 HNSCC patients prior toinitiation of cisplatin-based chemotherapy. The microbiome composition was analyzed using16S rRNA gene sequencing and targeted qPCR for F. nucleatum and P. gingivalis. In vitro,these isolates were co-cultured with SAS HNSCC cells (MOI 50:1) and treated with cisplatin(1-5 μM) for three days. Post-treatment recovery was monitored up to 14 days, withassessments of colony formation, migration, and expression of TSD-associated stemnessmarkers (EpCAM, ABCG2, HIF-2α, Myc, SOX2, OCT4, NANOG). Clinically, post-therapysalivary microbiota was correlated with patient outcomes and tumor hypoxia profiles.
Results: Co-exposure of SAS cells to cisplatin and F. nucleatum or P. gingivalis led to theemergence of a TSD-like phenotype, characterized by elevated expression of HIF-2α, ABCG2,and Myc, increased clonogenic survival, and enhanced migration capacity. Thisreprogramming effect was attenuated by TLR4 inhibition. Patient saliva analysis revealed thatelevated microbial LPS load and enrichment of F. nucleatum correlated with poorchemotherapy response and higher CTC count during treatment.
Conclusion: Our findings reveal that the oral microbiota synergizes with cisplatin to promotetherapy-induced adaptive stemness in HNSCC. This mechanism, involving microbialLPS/TLR4 signaling and HIF-2α activation, suggests that oral microbial dysbiosis may act asa co-driver of tumor evolution under chemotherapeutic stress. Targeting microbiota-chemotherapy interactions may offer a new avenue to reduce post-therapy relapse.
References: 1. doi: 10.3389/fimmu.2024.1336882 **2.** doi: 10.3389/fimmu.2023.1198269 **3**. doi:10.1620/tjem.253.249. PMID: 33840648.

#4811 Surgical resection versus non-surgical treatment for hepatocellular carcinoma with portal vein tumor thrombosis: A comprehensive systematic review and meta-analysis.

Seok-Hwan Kim[1], Sang Hoon Kim[2]

[1]Surgery, Chungnam National University Hospital, Daejeon, Korea, Republic of,[2]Surgery, Asan Medical Center, Seoul, Korea, Republic of

Background: The role of surgical resection (SR) as a primary treatment for hepatocellular carcinoma (HCC) with portal vein tumor thrombosis (PVTT) remains uncertain.
Methods: A comprehensive search of electronic databases from January 2000 to April 2024 identified studies comparing SR with transarterial chemoembolization (TACE), combined TACE and radiation therapy (TACE-RT), or sorafenib. Meta-analyses were conducted for comparison groups with at least three eligible studies. Hazard ratios (HRs) with 95 percent confidence intervals (CIs) for overall survival (OS) were extracted or reconstructed from Kaplan-Meier curves.
Results: Twelve retrospective cohort studies involving 4,498 patients were included. SR demonstrated superior long-term OS compared with TACE in Vp1-2 (5-year OS: HR 0.53, 95% CI 0.35-0.79) and Vp3 (5-year OS: HR 0.68, 95% CI 0.61-0.75), with comparable outcomes in Vp4. SR and TACE-RT showed similar 1- and 3-year OS, although SR demonstrated a clear 5-year OS advantage in Vp1-3 PVTT (HR 0.48, 95% CI 0.31-0.74). Compared with sorafenib, SR provided superior OS in Vp1-2 (3-year OS: HR 0.26, 95% CI 0.18-0.38) and comparable OS in Vp3. Sensitivity analyses supported the robustness of these findings, and no substantial publication bias was detected.
Conclusion: Based on current evidence, SR is not inferior to non-surgical treatments including TACE, TACE-RT, and sorafenib in patients with HCC and PVTT and provides meaningful long-term survival benefits, particularly in those with segmental PVTT (Vp1-Vp2). Further comparative studies incorporating immunotherapy are needed in future research.
Key words: Hepatocellular carcinoma; tumor thrombosis; resection; transarterial chemoembolization; meta-analysis.

#4812 Ontario Tumour Bank: Accelerating commercial oncology research and development with quality samples and data.

Riley Cox[1], Katarina Maksimovic[1], Larry Phouthavongsy[1], Anumta Amir[1], Ilinca Lungu[1], Terry Hawrysh[2], Dianne Chadwick[1], Lincoln Stein[1]

[1]Ontario Tumour Bank, Ontario Institute for Cancer Research, Toronto, ON, Canada,[2]Patient and Family Advisory Council, Ontario Institute for Cancer Research, Toronto, ON, Canada

The Ontario Tumour Bank (OTB) is a core research resource at the Ontario Institute for Cancer Research, a collaborative research institute that conducts and enables research to find cancer earlier and treat it more effectively. With 20+ years of expertise in biobanking, OTB has collected 150,000+ samples and 15,000+ whole slide images (WSIs) from 22,500+ participants across 30+ solid tumor sites. Each oncology case is comprehensively annotated with diagnostic, treatment and health data for up to 5 years. OTB has a strong record of supporting research, with acknowledgements in 200+ publications and 70,000+ citations. Recently, OTB has experienced an increased demand from commercial research clients. OTB's samples and data can be used for many commercial applications, including fresh tumor tissue for rapid drug screening; frozen tumor and normal adjacent tissue for metabolomics; formalin-fixed paraffin-embedded tumor tissue for diagnostic assay development; plasma for predictive blood tests for cancer detection and monitoring; and WSIs combined with longitudinal health record data for prognostic AI model development. Academic biobanks such as OTB have several challenges when working with commercial research clients. These include ensuring its resources are visible and accessible to the commercial research community, as well as obtaining appropriate participant consent, ethics and contractual approvals. OTB has mitigated these challenges by asking participants to agree to a broad informed consent that includes use of their samples and data in commercial research and creating a researcher-focused website (ontariotumourbank.ca) that allows clients to submit inquiries and start the sample and data request process online. Each request is received by OTB's dedicated senior client coordinator, who is the central point-of-contact for each client and facilitates each project from start to finish. To meet evolving research needs, commercial clients are provided access is to OTB's deep "research ready" inventory as well as custom fresh tumor and blood collections shipped overnight immediately after collection. The number and proportion of projects, samples and data provided to commercial clients - including venture capital-supported biotechnology startups in Canada, the US and globally - has steadily increased over the past 5 years and now represents 1/3 of OTB's business. By streamlining the request process for commercial clients, OTB has demonstrated its ability to meet the unmet demands of this sector, including emerging predictive AI model development in research and medicine. Supporting commercial research projects ensures that access to OTB's deep inventory of quality samples and data is consistent with the wishes of our generous patient participants to support diverse academic and industry research, all while contributing to OTB's long-term financial sustainability.

#4813 Diabetes mellitus related fibroblast activation as a premetastatic niche enhances lung metastasis.

Lingfeng Fu, Takatsugu Ishimoto

The Cancer Institute JFCR, Tokyo, Japan

Distant metastasis is a major determinant of poor prognosis in cancer. Epidemiological data indicate that diabetes markedly increases lung metastasis (LM) in patients with gastric cancer (GC); however, the underlying mechanisms remain unclear. Here, we report that high glucose stimulates GC cells to secrete extracellular vesicles (EVs) that activate FAP+ fibroblasts in the lung to establish a premetastatic niche and enhance metastasis. Transcriptomic and proteomic analyses revealed that high glucose activates FOXM1, promoting CEP55 transcription and its incorporation into EVs. Circulating CEP55-EVs trigger CEP55-pFAK-FAP signaling in lung fibroblasts, driving their activation. This results in extracellular matrix remodeling by tenascin-C secretion and scaffold formation to facilitate GC cell colonization. Finally, we demonstrate that the antidiabetic drug glimepiride suppresses fibroblast activation and significantly reduces LM. These findings reveal a diabetes-driven mechanism of LM mediated by CEP55-EVs and suggest a potent therapeutic strategy to inhibit LM using conventional antidiabetic drugs

#4815 Temporal control of EMT via the miR-200c/Zeb1 regulatory circuit to uncover the drivers of stemness in pancreatic cancer.

Andrew Karam, Divya Murthy, Petra den Hollander, Joseph Zhu, Sendurai A. Mani

Legorreta Cancer Center, Brown University, Providence, RI

Pancreatic cancer is poised to become the second leading cause of cancer-related deaths by 2030, with most fatalities resulting from metastasis. During metastatic progression, tumor cells undergo epithelial-to-mesenchymal transition (EMT), a developmental program that enhances motility, stemness, and resistance to stressors such as chemotherapy. Targeting EMT-induced cancer cells is therefore an urgent therapeutic priority. To investigate the EMT spectrum, we developed a doxycycline-inducible system that enables controlled induction of epithelial or mesenchymal states through the miR-200c/Zeb1 axis. Induction of miR-200c suppresses Zeb1 and promotes epithelial identity, whereas Zeb1 induction drives mesenchymal features. Although this regulatory circuit is well studied in other cancers, its role in pancreatic cancer remains poorly understood. Across human and mouse pancreatic cancer cell lines (PANC-1, CFPAC, FC1242, FC1199), miR-200c induction upregulates E-cadherin, while Zeb1 induction decreases E-cadherin and increases vimentin. In stemness assays, Zeb1 induction exerts minimal or even negative effects on sphere formation, whereas carcinoma cells expressing mesenchymal markers consistently display high stem-like capacity. Overexpression of miR-200c markedly suppresses the cancer stem cell phenotype, highlighting its role as a potent regulator of epithelial identity. Overall, our findings establish miR-200c as a central driver of the epithelial, less invasive state in pancreatic cancer and suggest that developing therapeutic strategies that upregulate miR-200c hold strong potential to prevent metastasis and improve overall survival for pancreatic cancer patients.

#4816 Single-cell transcriptomic analysis reveals KRT17 as a prognostic tumor-initiating cell marker in ovarian cancer.

Jie Wu, Tat San Lau, Kit Ying Loucia Chan, Chi Chiu Wang

Department of Obstetrics and Gynaecology, The Chinese University of Hong Kong, Hong Kong, China

Background: Ovarian cancer (OV) is characterized by high rates of recurrence and chemoresistance, which are largely attributed to a subpopulation of cancer cells known as tumor-initiating cells (TICs). The identification of specific biomarkers for TICs is crucial for developing novel prognostic tools and targeted therapies. This study aimed to identify and validate potential TIC markers in OV using a comprehensive bioinformatics approach at the single-cell level.
Methods: We performed an integrated analysis of publicly available single-cell RNA sequencing datasets from ovarian cancer patients. Malignant epithelial cells were first identified by inferring copy number variations (CNVs). To characterize the heterogeneity within these malignant cells, we quantified cellular stemness using CytoTRACE, reconstructed the differentiation trajectory with Monocle3, and analyzed the cell cycle to assess proliferative states. By integrating these multi-dimensional analyses, we identified a distinct cell subpopulation exhibiting high stemness, an undifferentiated state, and a unique gene expression signature, which we designated as the TIC-like cluster. Candidate markers were defined as the genes specifically upregulated within this functionally characterized cluster. The prognostic significance of the top candidate was then evaluated using bulk RNA-seq and clinical data from an independent cohort from our institution.
Results: Our analysis successfully identified a distinct subcluster of malignant cells exhibiting significant TIC properties. Differential gene expression analysis of this subcluster pinpointed Keratin 17 (KRT17) as a top-ranking, specifically expressed gene. Crucially, survival analysis demonstrated that high expression of KRT17 was significantly associated with worse overall survival and progression-free survival.
Conclusion: Through a multi-faceted bioinformatic pipeline, our study identifies KRT17 as a robust candidate marker for TICs in ovarian cancer. The strong correlation between high KRT17 expression and poor patient prognosis underscores its potential as a valuable prognostic biomarker. These findings provide a strong rationale for future experimental studies to validate the functional role of KRT17 in OV tumorigenesis and its utility as a therapeutic target.

#4817 The role of cancer cell-derived TWEAK in promoting a cancer stem-like phenotype in ovarian cancer cells.

Steffy Mathew, Luisjesus S. Cruz, Mikella Robinson, Sofia Howe, Greg J. Jordan, Dishant Vandra, Harshada Sapre, Carrie Danielle House

San Diego State University, San Diego, CA

Ovarian cancer is the most lethal gynecological cancer in the United States, with over 80% of patients relapsing after chemotherapy. Recurrent ovarian cancer may be due to cancer stem-like cells (CSCs) that are drug resistant and capable of long-term self-renewal and reestablishment of tumors. Previous studies in our lab suggest that TWEAK, a cytokine enriched in ovarian tumors, enhances CSC development and survival. Additionally, inhibiting TWEAK in combination with chemotherapy was shown to significantly prolong survival and remission in mouse models. The source of TWEAK in ovarian cancer remains unidentified, but in normal tissues it is primarily produced by myeloid cells. A recent pancreatic cancer study identified cancer cells as a novel source of TWEAK and preliminary data from our lab suggests that TWEAK protein expression in ovarian cancer cells is significantly increased (2-fold) following chemotherapy treatment. Therefore, we hypothesize that cancer cell-derived TWEAK is a unique driver of CSC phenotypes in ovarian cancer cells. To explore this hypothesis, we generated and validated shRNA knockdown of TWEAK in OVCAR8 and CAOV4 ovarian cancer cell lines at the gene and protein level. To assess TWEAK-mediated tumor formation, we sorted for CSCs and non-CSCs in shNeg and shTWEAK cells and intraperitoneally injected cells into a xenograft mouse model. We found significantly decreased tumor formation in non-CSC shTWEAK tumors compared to non-CSC shNeg tumors ($p<0.05$). Moreover, the calculated stem cell frequency was significantly reduced in the shTWEAK non-CSCs compared to the shNeg non-CSCs and shTWEAK CSCs ($p=0.0144$ and $p=0.0086$, respectively). This data suggests that stem cell frequency is dependent on TWEAK expression. Experiments are underway to assess spheroid formation ability, chemoresistance, and expression of stemness genes in the CSC and non-CSC shNeg and shTWEAK cells. By targeting factors like TWEAK that promote a CSC phenotype, we hope to identify alternative therapeutic strategies to inhibit CSC development and prevent relapse in ovarian cancer.

#4818 Establishing novel, representative prostate cancer cell lines from fresh prostatectomy tissues via an optimized protocol.

Tuong Vi V. Nguyen[1], Steven C. Smith[2], Lance J. Hampton[3], Victoria J. Findlay[4], David P. Turner[4]

[1]VCU Massey Comprehensive Cancer Center, Richmond, VA,[2]Pathology, VCU Massey Comprehensive Cancer Center, Richmond, VA,[3]Urology, VCU Massey Comprehensive Cancer Center, Richmond, VA,[4]Surgery, VCU Massey Comprehensive Cancer Center, Richmond, VA

Background: The existing panel of prostate cancer (PCa) cell lines, often established from metastatic sites or after extensive passaging, frequently fails to fully recapitulate the genetic heterogeneity and tumor microenvironment dependence of primary prostate tumors. Additionally, there is a crucial need for diverse, population-specific cell lines to investigate the biological factors underlying disparities in patient outcomes and therapeutic response. To address this critical resource gap, we optimized and validated a highly efficient protocol for the de novo establishment of patient-derived, primary PCa cell lines from fresh surgical specimens.
Methods: Patients were consented in accordance with VCU IRB protocol #20210623, and their self-reported race was recorded as either White (W) or African American (AA). Fresh tissues were obtained as punched biopsies from 36 radical prostatectomy specimens. Each specimen yielded 1-3 biopsy samples. H&E slides were graded by a licensed pathologist. Optimized from Maitland et al. 2016 protocol, tissue samples digested enzymatically were separated into distinct populations through differential centrifugation, and propagated in optimal media for epithelial and fibroblastic cell lines. The cellular origin of patient-matched lines were confirmed using cytochemistry and further characterized through proliferation assays, Western blot, and short tandem repeat (STR) profiling.
Results: The optimized protocol, carried out in the latter quarter of the trial, demonstrated high efficacy with an 86% success rate (13 out of 15 samples), bringing the total to 30 novel, matched PCa epithelial and fibroblast cell lines successfully established from 18 patients. Among the 30 samples, 18 were benign (11 W and 7 AA) and 10 were cancerous (6 W and 4 AA). Additionally, 3 patient prostatic specimens yielded matched cell lines from both the tumor and the contralateral non-malignant tissue. Critically, these cell lines retained the expression of androgen receptor (AR) and prostate-specific antigen (PSA). Furthermore, the lines exhibited heterogeneous growth patterns reflecting the diversity of the source tumors.
Conclusion: We have established a robust, highly effective protocol for generating patient-derived, primary PCa cell lines directly from prostatectomy tissues. These novel, characterized models significantly enrich the translational research toolkit, providing invaluable resources for several critical applications, including biomarker identification, understanding tumor initiation and progression, resistance mechanism studies, drug discovery and validation, and, most importantly, for studying population-specific differences to guide the development of truly equitable and personalized treatment strategies.

#4819 Gene knockout or selective inhibition of AKT-3, but not AKT-1 or AKT-2 isoform, enhances apoptosis in CD133+ melanoma cancer stem cells treated with the MEK inhibitor trametinib.

Cynthia M. Simbulan-Rosenthal, **Nusrat Islam**, Dhyana Yan, Ingrid Mandala Kol, Noah Smith, Dean S. Rosenthal

Biochemistry and Molecular & Cellular Biology, Georgetown University School of Medicine, Washington, DC

CD133-expressing melanoma-initiating stem cells are associated with tumorigenesis, metastasis, and drug resistance in malignant human melanoma. CD133 knockout (KO) or doxycycline (Dox)-inducible expression shows that CD133 activates an alternate survival pathway, PI3K/AKT, bypassing the MAPK pathway, resulting in apoptosis inhibition, increased melanoma cell survival, and resistance to the MEK-inhibitor trametinib. Combinational inhibition of the MAPK and PI3K/AKT pathways with trametinib and the pan-AKT inhibitor capivasertib synergistically induces melanoma cell apoptosis *in vitro* and inhibits tumor growth *in vivo*. To determine the relative contributions of each of three AKT isoforms, AKT-1, -2, and -3, to apoptosis inhibition, we used CRISPR-Cas9 KO or pharmacological inhibitors of each isoform, in combination with trametinib in a Dox-inducible NRAS-mutant melanoma cell line BAKP. Immunoblot analysis with anti-AKT-1, -2, or -3 and DNA sequence analysis confirmed gene knockout. BAKP control cells and cells with single or triple KO of each or all of the AKT isoforms were then exposed to trametinib, alone or in combination with capivasertib, and subjected to Annexin V apoptosis assays and immunoblot analysis with antibodies to apoptosis markers. Single KO of AKT-2 or -3, but not AKT-1, sensitized BAKP cells exposed to trametinib alone, partially obviating the requirement for inhibition of AKT by capivasertib. Triple KO of all three isoforms further sensitized cells to trametinib alone. We next investigated apoptosis induction by selective inhibitors of each of the AKT isoforms; afuresertib for AKT-1, CCT128930 for AKT-2, or uprosertib for AKT-3, as a monotherapy or in combination with trametinib. The combination of uprosertib and trametinib proved to be the most effective in synergistically inducing apoptosis in melanoma cells, even targeting the CD133-expressing melanoma stem cells. Together, this indicates that AKT-3 plays an essential role in apoptosis inhibition, consistent with reports that implicate AKT-3 in drug resistance in melanoma and glioblastoma. Cells treated with trametinib, alone or combined with capivasertib or uprosertib, exhibited loss of mitochondrial membrane potential, suggesting a mitochondrial pathway of apoptosis. Future studies will focus on optimizing the effect of selective inhibitors of AKT-3 in dose response experiments, and test its effects in *in vivo* mouse xenograft studies. Simultaneously targeting the AKT and MAPK survival pathways with trametinib and uprosertib underscores the importance of combination therapies to eliminate recalcitrant melanoma stem cells.

#4820 TIM-3 as a prospective target to eliminate pancreatic cancer stem cells.

Prapannajeet Biswal, Prudhvi Chand Mallepaddi, Bhoomika Murvekere Lakshmisha, Tuyet Ngoc Tra, Sai Kumar Samala, Khadijeh Koushki, P.M. Quan Mai, Arjun Vasan, Gabrielle Krouse, Yuri Mackeyev, Lydia WT Cheung, Sunil Krishnan, Geraldine Vidhya Vijay

Neurosurgery, UT Health Houston, Houston, TX

Background : Pancreatic cancer (PDAC) is nonresponsive to conventional therapies and poor survival is the norm. A small percentage of malignant cells undergo epithelial-mesenchymal transition to evolve into pancreatic cancer cells stem cells (PCSCs) that evade therapy and subsequently give rise to residual/recurrent tumors and also drive therapy resistance. While radiotherapy (RT), is a cornerstone of PDAC management, it promotes EMT via activation of TGF-β, NF-kB and Akt/GSK-3β pathways. TIM-3 (HAVCR-2) a cell surface marker traditionally designates exhausted T-cells. However TIM-3 overexpression is being increasingly reported in solid tumors. We report RT induced TIM-3 overexpression in PDAC and propose that RT triggered TIM-3, on pancreatic cancer cells could serve as a novel target in selectively eliminating PCSCs.

Methods : GEO datasets were analyzed with the Seurat package in R to evaluate TIM-3 expression across tissue types (benign pancreatic tissue, non metastatic primary PDAC/Pm0, primary of metastatic PDAC/Pm1 and matched liver metastases/Lm). TIM-3 expression between treatment naive and chemo-RT treated tumors was also compared. In vitro, murine (Panc02-ova, KPC) and human (PANC-1, MIA PaCa-2) pancreatic cancer cells were treated with increasing doses of RT alone or in combination with NRF-2 / ATM inhibitor to either simulate a high oxidative stress environment or inhibit DNA repair pathways. Following treatments, TIM-3 expression in these samples were evaluated using RT-qPCR, western blotting, flow cytometry and immunofluorescence. In vivo, Panc-02 xenografts in C57BL/6 mice were irradiated (10Gy RT at 320Kv & 13.2 mA). Tumors were collected, 24 hrs post RT, and dissociated. Single cells thus obtained were assessed for the expression of TIM-3, using flow cytometry.

Results : Advanced stages of cancer (Pm1 and Lm tumors) demonstrated greater TIM-3 expression compared to Pm0 tumors. Further, increased TIM-3 expression was noted in chemo-RT treated tumors compared to untreated tumors. In vitro, RT dose dependent increase in TIM-3 mRNA and protein levels was recorded and cells subjected to 10Gy RT showcase maximal TIM-3 expression (Control < 3Gy < 6Gy < 10Gy). Addition of NRF2 inhibitor or ATM inhibitor before exposing cells to RT further increased TIM-3 levels.The TIM-3+ cells exhibited higher CD24+ and CD44+ positivity, indicating its association with PCSC phenotype.

Conclusion : Our results indicate that TIM-3 can be employed as a specific marker to designate PCSCs in addition to the classical stem cell phenotype (ESA+ CD24+ CD44+). Increased mRNA, total protein and TIM-3 levels post RT are possibly driven by elevated oxidative stress in addition to RT induced ds-DNA breaks. The novel role of TIM-3 as a PCSC marker, establishes it as an ideal candidate for targeting both immune-suppressive T cells and therapy resistant PCSCs.

#4821 Investigating FOXC2-dependent mechanisms regulating stem cell Identity in breast cancer.

Joanna Joyce Maddela[1], Petra den Hollander[1], Nick Allen Kuburich[2], Maria Castaneda[3], Mika Pietila[3], Mercy Adewumi[4], Sendurai A. Mani[2]

[1]Department of Pathology and Medicine, Legorreta Cancer Center at Brown University, Providence, RI,[2]Legorreta Cancer Center at Brown University, Providence, RI,[3]MD Anderson Cancer Center, Houston, TX,[4]Department of Pathology and Laboratory Medicine, Legorreta Cancer Center at Brown University, Providence, RI

Stem cells maintain tissue homeostasis by balancing self-renewal and differentiation, a process shaped by how fate determinants are stabilized and partitioned during mitosis. Disruption of these mechanisms can either generate cancer stem cells (CSCs) that drive tumor progression or deplete CSCs that lead to the elimination of the tumor. In triple-negative breast cancer (TNBC), the embryonic transcription factor FOXC2 is aberrantly reactivated, leading to induction of EMT, the gain of CSC properties, and poor patient outcomes. Although our lab has shown that FOXC2 levels fluctuate across the cell cycle, the cues governing this regulation remain unclear. Since PLK1 is a key mitotic kinase and a targetable vulnerability in aggressive TNBC, we investigated whether FOXC2 is regulated by PLK1-mediated phosphorylation. Pharmacologic PLK1 inhibition (Volasertib) reduces FOXC2 protein levels, and this loss is reversed by the proteasome inhibitor MG132, suggesting that PLK1-dependent phosphorylation stabilizes FOXC2. Using SUM159 cells expressing phospho-ablated (S125A, T465A) and phospho-mimetic (S125E, T465E) FOXC2 mutants, we evaluated its CSC-related function, including mammosphere assays, and found that phosphorylation influences FOXC2's role in maintaining CSC traits. Biochemical pulldown, immunoblotting, and imaging assays support a potential interaction and role for FOXC2 and PLK1. Promoter analysis of the PLK1 promoter identified FOXC2 binding sites near the transcription start site, suggesting possible reciprocal control. Live-cell imaging further indicates that FOXC2 is spatially regulated during mitosis and that phosphorylation may affect its chromatin association and inheritance. Collectively, our findings suggest PLK1-dependent phosphorylation of FOXC2 may stabilize the FOXC2 protein and influence its function during mitosis and regulate stem cell identity in daughter cells during cell division.

#4822 Investigating the role of miR-27a-3p in the WNT signaling pathway in colorectal cancer stem cells.

Molly A. Lausten, Victoria A. Stark, Caroline O. B. Facey, Lynn M. Opdenaker, **Bruce M. Boman**

Helen F. Graham Cancer Center & Research Institute, Newark, DE

Cancer stem cell (CSC) overpopulation drives colorectal cancer (CRC) development and growth, but molecular mechanisms are unclear. CSCs functional phenotypic characteristics include signaling pathway dysregulation. CRC CSCs, in particular, are defined by their high WNT signaling activity, particularly those defined by the stem cell maker leucine-rich-repeat containing G protein-coupled receptor 5 (LGR5). A growing body of scientific evidence indicates that miRNAs, involved in post-transcriptional gene expression, play an important role in maintaining the CSC phenotype. However, the exact mechanism is still unknown. Our goal is to investigate how miRNAs contribute to the SC origin of CRC. My preliminary experiments used HT-29 CRC cells and NanoString profiling to identify miRNAs enriched in FACS-isolated CSCs. I discovered that miR-27a-3p is differentially upregulated in LGR5+ CSCs versus LGR5- cells. Analysis of available deep sequencing data also shows that the canonical miR-27a-3p is the highest expressed isoform in human CRC and is significantly upregulated during the colonic adenoma-carcinoma progression. *miR-27a-3p* has been shown to: i) be enriched in human CSCs in CRC utilizing other CSCs markers and methods; ii) activate or repress WNT signaling activity in various cancers; iii) increase chemoresistance in various cancers. The exact mechanism by which *miR-27a-3p* functions in CRC to regulate WNT signaling has not been elucidated. *Hypothesis*: miR-27a-3p is enriched in CRC and the LGR5+ SC subpopulation; miR-27a-3p promotes WNT signaling expression through repression of WNT antagonist targets. A significant increase in cellular proliferation was seen in the HT-29 stable lentiviral overexpressing cell line, and an increase in the WNT target genes mRNA of LGR, cMYC, cyclin D1, MET, and CD44. Decreases in LGR5, cMYC, cyclin D1, and MET were seen in the HCT116 stable lentiviral knockdown CRC cell line. My findings show that miR-27a-3p modulates WNT signaling in CRC cell lines by targeting WNT antagonistic targets that affect the stability and expression of β-catenin.

#4823 Development of a multi-institutional integrated resource platform linking primary and secondary biospecimens in gynecologic cancers.

Yoon Joo Kim, Jue Young Kim, Ha-Yeon Shin, Yookyung Lee, Jae-Hoon Kim

Department of Obstetrics and Gynecology, Gangnam Severance Hospital, Yonsei University College of Medicine, Seoul, Korea, Republic of

Background:
Gynecologic cancers exhibit substantial molecular and histopathologic heterogeneity, highlighting the need for infrastructures that integrate high-quality biospecimens with multi-omics and functional resources. To address this need, we established a seven-center framework that collects standardized primary biospecimens and generates secondary resources for gynecologic cancers, supported by integrated clinical and pathological datasets.
Methods:
Primary biospecimens—including serum, plasma, buffy coat, urine, ascites, frozen tumor tissues, and formalin-fixed paraffin-embedded (FFPE) blocks—were collected under Standard Operating Procedures (SOPs), with pre-analytical variables recorded using the Standard PRE analytical Code (SPREC). Frozen tissues supported high-depth whole-genome sequencing (WGS) and the development of patient-derived xenograft (PDX) and organoid models. FFPE blocks were used to construct tissue microarrays (TMAs). Human ovarian surface epithelial (HOSE) cells were subjected to standard immortalization procedures to establish stable cell lines.
Results:
As of November 5, 2025, 372 patients (161 endometrial, 101 ovarian, 104 cervical cancers, and 6 rare tumors) had been enrolled, yielding more than 6,000 primary biospecimens. WGS was performed using tumor-normal paired samples when available, generating 403 datasets: 215 tumor genomes (60×/90×) and 188 normal genomes (30×), representing 191 endometrial, 35 ovarian, and 177 cervical cancer cases. TMAs were constructed with 373 endometrial, 260 cervical, 490 ovarian cores. In addition, 17 PDX models were established (7 endometrial, 8 cervical, 2 ovarian), along with two organoid models and five IHOSE cell lines. Importantly, the primary biospecimens, WGS datasets, and PDX models were all generated from the same patients, creating a patient-matched resource that enables direct integration of genomic, pathologic, and functional data at the individual-patient level.
Conclusions:
This multi-institutional platform integrates standardized primary biospecimens with a broad set of secondary resources, providing a rare patient-linked structure in gynecologic cancers. The combined availability of WGS datasets, TMAs, PDX and organoid models, and IHOSE cell lines supports genomic-pathologic correlation, biomarker development, and functional studies of therapeutic response. Its scalable design offers a durable infrastructure for advancing gynecologic cancer research.

: Epithelial-to-Mesenchymal Transition
Poster Session

#4827 Lymphatic vasculature as a non-genetic driver of tumorigenesis.

Celeste K. Kanne, Jeremy Horrell, Hodaya Knafo, Savannah Martin, Aditya Verma, Ananya Goyal, Madison Conte, Shiri Gur-Cohen

University of California San Diego, La Jolla, CA

Harboring genetic mutations with oncogenic potential is common, yet not everyone develops cancer. This suggests that non-genetic factors contribute to tumor initiation and progression. In epithelial cancers such as squamous cell carcinoma (SCC), stem cells exhibit plasticity, transforming from an epithelial to a mesenchymal identity through the epithelial-to-mesenchymal transition, a process linked to metastasis. The lymphatic vasculature, known for fluid balance and immune trafficking, also supports the stem cell niche. Given this dynamic, we hypothesized that lymphatic vessels may represent a non-genetic element that drives cancer progression by altering stem cell behavior. To characterize lymphatic arrangement in benign versus advanced tumors, we performed high resolution 3D whole-mount immunofluorescence imaging on optically cleared benign papillomas and progressed skin SCCs. Compared to papillomas, advanced SCCs exhibited greater lymphatic association and integration. Spatial transcriptomics showed that regions enriched for lymphatic signals aligned with domains expressing hybrid epithelial-mesenchymal states in SCCs, suggesting that lymphatic positioning helps define the spatial architecture of these transitional tumor states. To test whether lymphatic vessels are required for tumor progression, we used both chemical and genetic (SOX9-CreER; $Kras^{mut}$; $p53^{fl/fl}$; $YFP^{fl/fl}$) mouse models of skin SCC. Tumors subjected to local lymphatic dysfunction stabilized or regressed in size, while matched controls continued to progress. Immunofluorescence revealed increased epithelial identity and reduced mesenchymal identity in regressing tumors, consistent with a shift toward a more epithelial and therapeutically responsive state. These findings suggest that lymphatic cues shape the regulatory programs governing tumor cell evolution. To define these programs, we profiled papillomas and SCCs using single cell RNA sequencing. The analyses resolved distinct epithelial, hybrid, and mesenchymal states. The hybrid state emerged as a key transition point, marked by selective induction of a secreted factor with a pro-lymphatic signature, suggesting a potential role in linking lymphatic cues to tumor cell evolution and malignant progression. Using a fluorescent lentiviral reporter, we confirmed that the secreted cue becomes highly expressed in advanced tumors *in vivo*. Functionally, silencing the pro-lymphatic cue in tumors derived from tumor-initiating cells slowed progression, demonstrating its active role in driving tumorigenesis. Together, these findings reveal that lymphatic interactions with tumor-initiating cells form a central regulatory axis in SCC, positioning the lymphatic vasculature as a promising therapeutic entry point to restrain malignant progression.

#4828 Dynamic androgen signaling orchestrates epithelial-mesenchymal transitions and epigenetic memory in prostate cancer.

Zhongchi Li[1], John Blenis[2]

[1]Pharmacology, Weill Cornell Medicine, New York, NY,[2]Professor of Pharmacology, Weill Cornell Medical College, New York, NY

Prostate cancer is one of the most aging-associated malignancies, with incidence rising sharply in older men. Although hyperactivation of the androgen receptor (AR) promotes tumor growth and provides the rationale for androgen deprivation therapy (ADT), circulating androgen levels paradoxically decline with age. This contradiction underscores the need to interpret AR function in a context-dependent manner. Epithelial-mesenchymal transition (EMT) is a central driver of metastasis and a common stress-adaptation program. AR-targeted therapies, including ADT and enzalutamide, can induce partial EMT and promote aggressive tumor states, yet how prostate tumor cells dynamically modulate AR signaling during this process remains unclear. Here, we exposed androgen dependent prostate tumor cells to androgen withdrawal, enzalutamide, or TGFβ stimulation and profiled AR activity, EMT markers, and metastatic behaviors across distinct stages of stress adaptation. Both AR inhibition and TGFβ signaling triggered EMT, marked by early suppression of AR activity. This initial AR downregulation was required for tumor cells to acquire mesenchymal features and enhanced motility. After TGFβ is removed, steroidogenesis was recovered, gradually restoring AR signaling. Late-phase AR reactivation promoted mesenchymal-epithelial transition (MET), re-establishing epithelial identity and stabilizing cell state. Steroidogenesis was essential for this EMT-MET rebalancing, as its inhibition induce redox oxidative imbalance and disrupted the completion of the adaptive cycle. Cells completing this EMT-MET transition became more resistant to androgen deprivation, proliferated more rapidly in spheroid culture, and exhibited globally elevated histone propionylation, indicating the establishment of an epigenetic “memory” that reinforces tumor plasticity. Together, these findings define a dynamic AR-EMT-steroidogenesis circuit that governs prostate cancer plasticity and therapeutic adaptation. This model provides a potential explanation for the paradox of increased prostate cancer incidence despite declining androgen levels with age. It also suggests that restoring AR activity may suppress EMT and metastasis, and that targeting histone propionylation could prevent therapy-induced aggressiveness and synergize with AR-directed therapies.

#4829 The defining features of hybrid epithelial-mesenchymal state in head and neck cancer.

Po-Han Lin[1], Yu-Shuen Tsai[1], Hsing-Hsiang Wang[2], Jie-Hong Song[2], Chih-Hung Chung[1], Muh-Hwa Yang[2]

[1]Cancer and Immunology Research Center, National Yang Ming Chiao Tung University, Taipei, Taiwan,[2]Institute of Clinical Medicine, National Yang Ming Chiao Tung University, Taipei, Taiwan

Epithelial-mesenchymal plasticity represents a major axis of tumor cell adaptation, enabling cancer cells to dynamically and reversibly transition between epithelial and mesenchymal states through epithelial-mesenchymal transition (EMT) and its reverse process, mesenchymal-epithelial transition (MET). EMT is an evolutionarily conserved cellular plasticity program that allows cancer cells to adopt multiple intermediate phenotypes along an epithelial-mesenchymal spectrum. Notably, complete EMT is relatively rare in human tumors, as most cancer cells do not fully activate terminal mesenchymal markers. Instead, they adopt an intermediate or hybrid epithelial/mesenchymal (hybrid E/M) state, also referred to as partial EMT, in which epithelial traits are retained while mesenchymal features are gradually acquired. In this study, we focus on elucidating the clinical significance of the hybrid E/M state in head and neck squamous cell carcinoma (HNSCC) and investigate whether this transitional phenotype is governed by specific molecular regulators. By integrating multi-omics clinical datasets and spatial transcriptomic analyses of patient tumor tissues, we found that the tumor invasive front exhibits marked cellular heterogeneity, which strongly correlates with the hybrid epithelial/mesenchymal cell phenotype. Digital Spatial Profiling analysis revealed that epithelial markers were evenly distributed between the primary and metastatic lymph node tumor regions. In contrast, mesenchymal markers were highly expressed in outer invasive regions and metastatic tumor sites. By analyzing both TCGA datasets and our own RNA-seq cohort, we found that the hybrid E/M phenotype is significantly associated with advanced tumor stage in HNSCC patients. Through single-cell transcriptomic profiling of clinical HNSCC samples, we found that hybrid E/M cells represent a unique cell state defined by their enriched expression of adhesion-related markers. We further developed an in vitro platform to model hybrid epithelial-mesenchymal transition and performed ATAC-seq profiling. Our analysis revealed that members of the GATA transcription factor family, particularly GATA3, play a crucial role in maintaining this intermediate state. Surprisingly, depletion of GATA3 led to a disruption of the hybrid epithelial/mesenchymal phenotype. Taken together, our findings provide compelling evidence that the hybrid epithelial/mesenchymal state is not only clinically relevant in HNSCC but is also shaped by distinct molecular mechanisms. Hybrid E/M cells display a unique adhesion-related gene expression profile, suggestive of a specialized function in promoting collective invasion during tumor progression. These findings enhance our understanding of EMT plasticity and highlight hybrid E/M cells and their control mechanisms as promising targets for slowing tumor evolution and metastasis.

#4830 Mic60-low breast cancer cells activate epithelial-mesenchymal transition and support aggressive tumor growth.

Camilla Esposito[1], Michela Perego[2], Elisabetta Panza[1], Giuseppe Cirino[1], Dario Altieri[2]

[1]Department of Pharmacy, University of Naples "Federico II", Naples, Italy,[2]The Wistar Institute, Philadelphia, PA

Background & Objectives: Breast cancer (BC) is the most frequent malignancy in women and a leading cause of cancer-related mortality worldwide. Despite advances in early detection and therapy, BC heterogeneity remains a major clinical challenge. Recent evidence highlights the role of mitochondria in sustaining BC aggressiveness and metabolic reprogramming. An shRNA screen identified Mic60 (also known as Mitofilin) as a mitochondrial gene whose reduced expression is associated with enhanced tumor cell invasion and altered proliferation. Mic60, part of the MICOS multiprotein complex, ensures cristae architecture, respiratory complex organization, and outer membrane biogenesis. Notably, Mic60 loss reduces mitochondrial fitness, contributing to aggressive disease. We investigated how Mic60 influences BC phenotype with regard to epithelial-mesenchymal transition (EMT) modulation in vitro and tumorigenic potential in vivo.
Materials & Methods: Mic60 silencing was achieved using small interfering RNA (siRNA) and short hairpin RNA (shRNA) in human and murine BC cell lines. Gene expression was analyzed by RT-qPCR, protein levels by Western blotting and flow cytometry. Migration and invasion were assessed in vitro using transwell assays with and without Matrigel, quantified by microscopy. In vivo tumorigenic capacity was evaluated in immunocompetent mice injected with syngeneic AT3 cells stably silenced for Mic60.
Results: Mic60 silencing induced EMT master regulators (Twist, Snail, Lbx1, Zeb2) in both human and murine BC cell lines. This transcriptional increase was accompanied by elevated N-cadherin and reduced E-cadherin and EpCAM expression. Moreover, Mic60 silencing upregulated NF-κB signaling, a key transcription factor linking inflammation, EMT, and cancer. Functionally, silenced cells exhibited enhanced migration and invasion in vitro. When injected into immunocompetent mice, AT3 Mic60-silenced cells displayed accelerated tumor growth in vivo.
Conclusions: Mic60 downmodulation activates EMT in BC cells, promoting migratory and invasive behavior. This phenotype is accompanied by NF-κB pathway activation, linking Mic60 loss to pro-tumorigenic signaling. In vivo, Mic60 depletion drives increased tumor growth, confirming the relevance of EMT activation in cancer progression. These findings extend previous observations on Mic60 in breast cancer, directly supporting its role in tumor progression and disease aggressiveness.

#4831 Inducible models of EMT reveal dynamic changes in the tumor-immune microenvironment.

Breanna Demestichas[1], Tanvi Visal[2], Petra den Hollander[1], Nick Kuburich[1], Sendurai A. Mani[1]

[1]Brown University, Providence, RI,[2]The University of Texas MD Anderson Cancer Center, Hosuton, TX

Epithelial-to-mesenchymal transition (EMT) drives tumor cell plasticity, stemness, and metastasis, yet the dynamic consequences of EMT activation on the tumor microenvironment remain poorly defined. Doxycycline-regulated EMT-inducible systems offer a powerful strategy to study reversible EMT programs with precise temporal control in both in vitro and in vivo settings. In this study, we developed doxycycline-inducible miR-200 and ZEB1 models in the D2A1 and EMT6 breast cancer cell lines to interrogate EMT regulation across diverse contexts. Doxycycline treatment produced robust EMT inhibition in miR-200 models and EMT activation in ZEB1 models, accompanied by expected morphological changes. In vivo, doxycycline-induced miR-200 expression suppressed EMT marker expression and reshaped the tumor immune microenvironment. Specifically, miR-200 induction increased intratumoral $CD8^+$ T cells, reduced $Arg1^+$ macrophages, and decreased platelet accumulation, as confirmed by immunohistochemistry. Cytokine profiling revealed shifts in inflammatory and immune-recruiting signals, and single-cell RNA sequencing showed enhanced MHC-I antigen presentation pathways and altered immune activation states upon EMT inhibition. Together, these results demonstrate that doxycycline-inducible EMT models faithfully recapitulate epithelial-mesenchymal plasticity and uncover key EMT-dependent changes in stemness and immune composition. Ongoing studies aim to define the mechanisms through which miR-200-mediated EMT suppression drives these immune shifts. These inducible systems provide a powerful framework for dissecting how EMT dynamics shape tumor-immune interactions and may offer insight into therapy responsiveness.

#4832 Developing advanced tumoroid models driven by epithelial-to-mesenchymal transition with a novelxeno-free andbiofunctionalhydrogel system.

Alejandra I. Ferrer Diaz, John Huang

TheWell Bioscience, Inc, Monmouth Junction, NJ

Epithelial-to-mesenchymal transition (EMT) is a key biological process that facilitates cancer metastasis to distant organs. Most preclinical studies investigating EMT are conducted using traditional two-dimensional (2D) culture models, which fail to recapitulate the in vivo tumor microenvironment, limiting the translational relevance of their findings to clinical settings. Consequently, three-dimensional (3D) culture systems have emerged as a superior approach for modeling metastatic processes and evaluating therapeutic candidates. However, these models typically rely on animal-derived extracellular matrices like Matrigel, which are poorly defined, exhibit batch-to-batch variability, and lack mechanical and biochemical stability, thereby compromising experimental reproducibility and clinical translation. In this study, we developed tumoroids from two cancer types known to undergo EMT such as glioblastoma multiforme (GBM) and breast cancer using VitroGel® hydrogel, a fully synthetic and biocompatible hydrogel system. The VitroGel® hydrogel is tunable in both mechanical and biofunctional properties, making it a powerful tool for generating advanced tumoroid models that might require distinct microenvironments. The tumoroids were generated from a single spheroid formed in ultra-low attachment, u-shaped, 96-well plates, which were then embedded in VitroGel® hydrogel diluted in our xeno-free supplement. Within the first three days after adding the hydrogel, the cells began migrating from the spheroid into the matrix, developing a tube-like structure with rapidly proliferating cells. By day seven, the tumoroids exhibited an outer layer enriched with EMT marker-positive cells expressing vimentin and N-cadherin, while the spheroid core and tube-like structure were mostly composed of cells expressing the cancer stem cell–associated markers Oct4 and Sox2**.** The tumoroids were susceptible to standard chemotherapies, including temozolomide and 5-fluororacil, indicating that these structures developed in the xeno-free hydrogel are a suitable system for drug screening studies.Additionally, to enhance the physiological relevance of the tumoroid model, we aimed to mimic tumor-vasculature interactions by performing co-cultures of tumoroids with endothelial cells. The endothelial cells penetrated the matrix and migrated towards the tumoroids, enhancing their long-term survival. Altogether, these findings demonstrate that the xeno-free hydrogel system supports the development of robust 3D cancer models, providing a platform for the evaluation of therapeutic drug candidates.

#4833 Identification of protein kinase signaling networks activating partial EMT as therapeutic targets in non-small cell lung cancer.

Mohaddase Hamidi[1], Kenneth Omolo[1], Amir Yarmahmoodi[2], Margret B. Einarson[3], Yan Zhou[3], Adam Karami[4], Korrey W. Hart[1], Adrian Dizon[1], Shrey Sitaram[1], Kathy Q. Cai[3], Pedro Torres-Ayuso[2]

[1]Cancer and Cellular Biology, Temple University Lewis Katz School of Medicine, Philadelphia, PA,[2]Temple University Lewis Katz School of Medicine, Philadelphia, PA,[3]Fox Chase Cancer Center, Philadelphia, PA,[4]Fels Cancer Institute for Personalized Medicine, Lewis Katz School of Medicine, Temple University, Philadelphia, PA

Non-small cell lung cancer (NSCLC), of which one-third are lung squamous cell carcinomas (LUSC), is the leading cause of cancer-related death in the US. LUSC treatments primarily involve platinum-based chemotherapy and immune checkpoint blockade. However, only 20% of patients benefit long-term, underscoring a critical need for strategies that improve treatment efficacy. We have identified partial epithelial-to-mesenchymal transition (pEMT) as a key mechanism hindering treatment efficacy in LSCC. pEMT is a cell state in which cancer cells display epithelial and mesenchymal characteristics, and is associated with heightened cell migration/invasion, survival, and treatment resistance. Therefore, we sought to identify phosphorylation networks that could reverse pEMT and, thereby, sensitize LSCC to treatment. We have identified a STE20-family kinase network as a central signaling node sustaining pEMT in LSCC cells. RNAseq analysis of STE20-inhibited LSCC cells revealed transcriptional reprogramming of LSCC indicative of reversion to an epithelial-like phenotype. Consistently, we observed increased expression of epithelial markers (E-cadherin, EpCAM), and reduced levels of mesenchymal markers (vimentin, CD44). Furthermore, STE20 depletion or inhibition suppressed key pEMT functions, including migration, invasion, and clonogenic potential. Our current studies are aimed at identifying the underlying mechanisms of the observed phenotypes. Our initial analysis indicates that STE20 is required for the activation of the YAP/TAZ and MYC transcriptional programs. Last, to lay the groundwork for combination treatments, we conducted a high-throughput screen using a library of clinically relevant compounds in combination with STE20 inhibitors. This screen showed potential synergism with platinum-based chemotherapy, which we are investigating *in vitro* and *in vivo*. In conclusion, we have uncovered a STE20 phosphorylation module that sustains pEMT in NSCLC cells and represents an actionable vulnerability that can be targeted to sensitize NSCLCs to first-line treatments.

#4834 Keratin 17 correlates with epithelial-to-mesenchymal transition in pancreatic ductal adenocarcinoma.

Shayan Sarkar, Lyanne Delgado Coka, Robert S. Powers, Natalia Marchenko, Kenneth Shroyer

Pathology, Stony Brook University, Renaissance School of Medicine, Stony Brook, NY

Background: Pancreatic ductal adenocarcinoma (PDAC) accounts for more than 90% of all pancreatic malignancies and has a 5-year survival rate of 13%. Approximately, 80% of the patients are diagnosed at later stages with metastatic disease characterized by widespread invasion. One of the key biological pathways that lead to this metastatic spread is Epithelial to Mesenchymal Transition (EMT) - a highly plastic process that allows cancer cells to gain invasive properties by switching from an epithelial to a mesenchymal phenotype. Keratin 17 (K17), a component of the basal-like PDAC signature associated with poor prognosis, has been shown to promote pancreatic cancer metastases and induce EMT in bladder, esophageal, and lung cancers. In this study, we test the hypothesis that K17 is associated with EMT in PDAC, contributing to the poor prognosis of the disease.
Methods: We performed integrative single-cell transcriptomic analyses (scRNA-seq) of publicly available datasets comprising of 42 treatment-naïve PDACs to identify cancer-related pathways associated with K17 expression. Differential gene expression and pathway enrichment analyses were conducted in RStudio using the Hallmark gene sets from MSigDB and Gene Ontology (GO) terms. To validate the scRNA-seq results, we performed cyclic multiplex immunofluorescence imaging using the MACSima platform on FFPE tissue microarrays, along with immunohistochemistry (IHC) on whole-slide FFPE sections of human PDAC samples. These analyses were conducted to assess the spatial distribution of K17 and its correlation with the expression of top EMT-associated markers identified through scRNA-seq.
Results: scRNA-seq analysis revealed that K17-positive PDAC cells exhibited transcriptional enrichment of the EMT pathway, with ANXA1, S100A4, GPC1, LAMC2, WWTR1, and LAMA3 identified as top associated markers. Multiplex immunofluorescence image analysis confirmed that K17-positive tumor regions displayed reduced epithelial differentiation as indicated by low GATA-6 and E-cadherin score. Among the markers identified by scRNA-seq, LAMC2, an established biomarker of EMT, demonstrated the most significant positive correlation with K17 and was confirmed using IHC.
Conclusions: K17 marks a transcriptionally distinct and highly invasive PDAC subpopulation characterized by robust EMT activation. LAMC2 emerges as the EMT marker most closely associated with K17 at both transcriptomic and protein levels, suggesting a K17-LAMC2 axis that maybe a major driver of EMT in PDAC.

#4835 Morphological effects of cytokeratin 8/18 and vimentin coexpression in vulvar cancer cells.

Jani E. Lewis, Avinash Gopal, Sara M. Mongelli, Abby R. Stevenson

Biology, State University of New York at Geneseo, Geneseo, NY

Vulvar squamous cell carcinoma (VSCC) is a rare but aggressive malignancy that primarily affects women over the age of 60, with the earliest stages often obscured by vulvar lichen sclerosus (VLS). VLS is commonly treated with ultrapotent corticosteroids such as clobetasol. Our previous studies demonstrated that clobetasol treatment of A431 vulvar cancer cells results in the loss of the cell-cell junction proteins E- and P-cadherin and the subsequent gain of the intermediate filament protein vimentin. The resulting cells (referred to as A431D) do not form adherens junctions nor desmosomes. Loss of E- and P-cadherin and gain of vimentin expression is consistent with an epithelial-to-mesenchymal transition (EMT), a process associated with cancer progression and acquisition of a more aggressive phenotype. Despite these changes, A431D cells retain expression of the epithelial intermediate filaments cytokeratins 8/18. Our analyses revealed colocalization of cytokeratin 8/18 and vimentin within A431D cells. In the absence of cadherin-mediated junctions, the organization of both filament systems, and the overall morphology of the cells, resembles that of fibroblasts. It is only upon exogenous expression of an E-cadherin-plakoglobin construct, that desmosome and adherens junctions form. In the studies presented we tested the hypothesis that vimentin is driving the morphology of the A431D cells in spite of continued cytokeratin 8/18 expression even when E- and P-cadherin or E-plakoglobin were exogenously expressed in these cells. A431D cells were transfected with plasmids containing E-, P-, or a construct of E-plakoglobin and the resulting cells were examined for localization of vimentin and cytokeratin 8/18 by confocal microscopy.

#4836 High dietary cholesterol promotes epithelial-to-mesenchymal transition and invasion in colorectal cancer via the Wnt/Snai2 axis of transcriptional regulation.

Blake M. Arciga[1], Zaynab Shakkour[2], Vikas Satyananda[1], Van Nguyen[3], Jussuf T. Kaifi[1], Satyanarayana Rachagani[4]

[1]Surgery, Univ. of Missouri School of Medicine, Columbia, MO,[2]Univ. of Missouri School of Medicine, Columbia, MO,[3]Pathology and Anatomical Sciences, Univ. of Missouri School of Medicine, Columbia, MO,[4]Veterinary Medicine and Surgery, Univ. of Missouri, Columbia, MO

Introduction: Colorectal cancer (CRC) progression is frequently influenced by diet and lifestyle factors, and these variables can affect clinical outcomes. We have previously reported that modulation of cholesterol levels can facilitate epithelial-to-mesenchymal transition (EMT) and invasion in CRC. However, the exact signaling mechanisms driving this process have not yet been identified. In this study, we sought to further characterize the invasive phenotype associated with high cholesterol *in vivo*, and to investigate transcriptome-level changes that occur in response to a high cholesterol diet, in search of mechanistic insights.

Methods: We generated a variable-diet $APC^{fl/fl}CDX\text{-}Cre^{ER}$ CRC mouse model, in which the mice were fed either a high cholesterol diet (2% cholesterol), a low cholesterol diet (1% cholesterol), or a chow diet (0% cholesterol) for 6-8 weeks. Tumor growth was induced by intraperitoneal tamoxifen injection. Four weeks after injection, colon tissue samples were collected. Formalin-fixed sections were stained with hematoxylin and eosin (H+E), and examined for histological indicators of invasion by a clinical pathologist in a blinded manner. The epithelial markers claudin-1, Zo-1, and E-cadherin were stained by multiplex immunofluorescence. Frozen colon samples from chow diet-fed and high cholesterol-fed mice were submitted for bulk RNA sequencing. KEGG pathway enrichment analysis of differentially expressed genes was performed using the limma package in R.

Results: H+E-stained colon tumor sections from mice fed the high cholesterol diet showed markedly more extensive desmoplastic reactions and increased cancer invasiveness compared to the chow diet-fed mice, with low cholesterol-fed mice displaying an intermediate phenotype. Immunofluorescence revealed that expression and junctional co-localization of claudin-1, Zo-1, and E-cadherin were consistently downregulated in the tumor cells of high cholesterol-fed mice compared to mice fed either the low cholesterol or chow diet. Expression of genes involved in the Wnt signaling pathway was found to be significantly upregulated in high cholesterol-fed mice relative to chow diet-fed mice, as was expression of the EMT transcription factor Snai2 (Slug).

Conclusions: High dietary cholesterol promotes an EMT-like phenotype in CRC, which involves a loss of epithelial gene expression and activation of Wnt signaling. Notably, high cholesterol increases expression of the transcription factor Snai2 (Slug), which is known to be induced by Wnt signaling and to suppress expression of Cldn1, Zo1, and E-cadherin. These findings indicate that high cholesterol promotes EMT in CRC via a Wnt-dependent mechanism of transcriptional regulation, which could potentially increase the risk of invasion and metastasis in CRC patients affected by high cholesterol.

#4837 Mechanistic studies on the role of GABA type A ($GABA_A$) ion channel receptor in tumor invasion and metastasis in triple negative breast cancer.

Yasmeen Ahmed[1], Mark Garewal[2], Kenneth Myers[2], Isabelle Mercier[1], Asha Suryanarayanan[3]

[1]Department of Pharmaceutical Sciences, Saint Joseph's University, Philadelphia, PA,[2]Department of Biology, Saint Joseph's University, Philadelphia, PA,[3]Department of Physician Assistant Studies, Saint Joseph's University, Philadelphia, PA

Triple-negative breast cancer (TNBC) represents 15-20 percent of breast cancer cases and is associated with aggressive progression, metastasis, and limited treatment options. TNBC treatment relies on surgery, radiation, and chemotherapy, but these approaches are non-selective and highly toxic, emphasizing the need for novel molecular targets. Traditionally known for mediating inhibitory neurotransmission through chloride ion conductance, recent evidence implicates γ-aminobutyric acid type A ion channel-coupled receptors ($GABA_A$ R) in cancer cell proliferation, migration, and metastasis. Our previous studies demonstrated that β3 and α1 $GABA_A$ R subunits are overexpressed in TNBC cells, promoting chloride influx and cell survival. We also showed that pharmacological inhibition or shRNA-mediated $GABA_A$ R β3 subunit knockdown reduces proliferation and induces cell cycle arrest of TNBC cell lines. Epithelial-mesenchymal transition (EMT) drives cancer metastasis by enabling cells to lose adhesion, reorganize the cytoskeleton, degrade the extracellular matrix, and gain migratory properties. The steroid receptor coactivator and focal adhesion kinase (Src-FAK) axis plays a central role in these processes by regulating cell remodeling, promoting cell proliferation, and migration. Src-FAK activation also stimulates the PI3K/AKT pathway, enhancing cell survival and resistance to apoptosis. In addition, FAK activates Rho-GTPases, which regulate actin cytoskeleton reorganization and cell motility. In this study, we investigated whether $GABA_A$ R β3 subunit knockdown and pharmacological inhibition alter the invasive potential and EMT in TNBC. Our results showed that inhibiting $GABA_A$ R genetically and pharmacologically significantly reduced the invasive potential and reversed the EMT, as evidenced by decreased expression of mesenchymal markers (vimentin and N-cadherin) and increased expression of the epithelial marker E-cadherin as determined by Western blot analysis. Furthermore, β3 subunit knockdown decreased the expression of total Src and reduced the phosphorylation of both Src and FAK. Morphological assessment further demonstrated that β3 subunit knockdown reduced cell size, disrupted actin stress fibers, and altered actin distribution, consistent with impaired migratory capacity. To further define the molecular mechanisms downstream of $GABA_A$ R signaling, we will perform RNA sequencing on control and β3 knockdown TNBC cells to identify transcriptional pathways involved in invasion and metastasis. Collectively, these findings reveal that $GABA_A$ R β3 promotes TNBC cell proliferation, EMT, and invasion through Src-FAK signaling, highlighting GABAergic signaling as a promising therapeutic target in metastatic breast cancer.

#4838 An EMT-driven Exoc7 splicing switch controls the PRPF19-GATA3 axis to destabilize the hybrid E/M state.

Hsing-Hsiang Wang[1], Po-Han Lin[2], Yu-Shuen Tsai[2], Tsan-Jan Chen[3], Wen-Ching Wang[3], Muh-Hwa Yang[1]

[1]Institute of Clinical Medicine, National Yang Ming Chiao Tung University, Taipei, Taiwan,[2]Cancer and Immunology Research Center, National Yang Ming Chiao Tung University, Taipei, Taiwan,[3]Institute of Molecular and Cellular Biology, College of Life Sciences and Medicine, National Tsing Hua University, Hsinchu, Taiwan

The epithelial-mesenchymal transition (EMT) is a dynamic process that cancer cells exploit to gain metastatic competence, with the hybrid E/M state—co-expressing both epithelial and mesenchymal markers—being particularly critical due to its heightened plasticity and association with aggressive disease. However, the molecular mechanisms that stabilize this hybrid phenotype and govern its reversible transition to a full mesenchymal state remain a central unanswered question. Our research identified the transcription factor GATA3 as a key stabilizer of the hybrid E/M state in head and neck squamous cell carcinoma (HNSCC). Surprisingly, we found that induction of core EMT transcription factors leads to a reduction in GATA3 protein levels but does not alter its mRNA levels. This led us to explore the possibility that a post-translational mechanism drives this regulation. We analyzed the GATA3-interactome and identified PRPF19, a dual splicing factor and E3 ubiquitin ligase, as the enzyme responsible for GATA3 ubiquitination. Notably, while PRPF19 expression remains constant during EMT, its ligase activity is precisely regulated by alternative splicing. The EMT-driven loss of epithelial spliceosome switches the Exoc7 gene product from the epithelial isoform 5 (Exoc7-iso5) to the mesenchymal isoform 2 (Exoc7-iso2). Mechanistically, PRPF19 preferentially binds to Exoc7-iso5, and this interaction acts as a molecular brake by inhibiting the full cofactor assembly essential for the E3 ligase activity of PRPF19. Consequently, the EMT-associated loss of Exoc7-iso5 unleashes PRPF19, leading to unrestrained GATA3 ubiquitination and degradation. Crucially, restoring Exoc7-iso5 expression successfully rescued GATA3 protein levels and epithelial markers, formally confirming a splicing-dependent regulatory mechanism. Collectively, we propose an integrated model in which EMT-driven alternative splicing of Exoc7 serves as a functional switch to control PRPF19 E3 ligase activity, thereby targeting GATA3 for degradation to dismantle the hybrid E/M state and drive mesenchymal commitment in HNSCC, revealing this axis as a possible regulatory mechanism that controls the stability and reversibility of the hybrid E/M state.

#4839 PTPRE receptor tyrosine phosphatase in matrix-stiffness-driven EMT and breast cancer metastasis.

Calista A. Horta, Laurent Fattet, Zhimin Hu, Khoa Doan, Aida Mestre-Farrera, Qingrong Li, Dong Wang, Jing Yang

University of California, San Diego, San Diego, CA

Mechanical cues from the extracellular matrix (ECM) regulate various cellular processes in cell proliferation, migration and differentiation via distinct mechanotransduction pathways. In breast cancer patients, increase in tumor tissue stiffness is correlated with distant metastasis and poor outcome. Previous studies show that, cell invasion and metastasis. Using 3D reconstituted extracellular matrixes that recapitulate the range of physiological stiffness from normal mammary glands to breast tumors, we previously reported that increased ECM stiffness promotes Epithelial-Mesenchymal Transition (EMT) and identified the TWIST1 transcription factor as a key player driving EMT and invasion in response to increasing ECM stiffness. High ECM stiffness activates the LYN tyrosine kinase, which phosphorylates TWIST1 and promotes TWIST1 to enter the nucleus, thus triggering EMT and invasion. To understand how LYN is activated at high ECM stiffness, we performed an unbiased screen for tyrosine phosphatases that is required for high stiffness-induced EMT and invasion in basal-subtype mammary cells. This screen identified a novel role of protein tyrosine phosphatase epsilon (PTPRE) in TWIST1/LYN mechanotransduction. We show that genetic deletion of PTPRE blocked high ECM stiffness-induced EMT and invasion in human and mouse TNBC cell-derived acini as well as in patient-derived triple-negative breast cancer (TNBC) organoids, demonstrating a conserved role of PTPRE in stiffness-induced invasion. Mechanistically, knockdown or pharmacological inhibition of PTPRE blocks LYN activation, TWIST1 nuclear translocation and EMT at high stiffness. Biochemical analyses and AlphaFold modeling suggest that PTPRE bind to LYN and dephosphorylates Tyr507 to activate the LYN kinase. Functionally, treatment of mice carrying TNBC PDX tumors with a PTPRE inhibitor decreased local invasion and lung metastasis. This study identifies a novel role for PTPRE in matrix-stiffness induced EMT and metastasis in TNBC and broadens the repertoire of actionable targets implicated in breast cancer metastasis. The importance of mechanical force and tissue stiffness in regulating breast cancer invasion and metastasis has only recently been appreciated. This study raises the promise to target novel mechanotransduction pathways and mechanoregulators to combat breast tumor invasion and metastasis.

#4840 KPNA2 drives cancer stemness, which enhances drug resistance and facilitates cancer progression in lung adenocarcinoma.

Seongran Cho[1], Inyoung Cheon[1], Seoree Kim[2], Yoon Ho Ko[3], Young-Ho Ahn[4]

[1]Ewha Womans University, Seoul, Korea, Republic of,[2]Seoul St. Mary's Hospital, Seoul, Korea, Republic of,[3]Catholic University of Korea, Seoul, Korea, Republic of,[4]Molecular Medicine, Ewha Womans University School of Medicine, Seoul, Korea, Republic of

KPNA2 (Importin α1) is a nuclear transport protein that shuttles nuclear proteins into the nucleus. While its role in cancer-associated fibroblasts and the tumor microenvironment is known, its direct function in lung cancer cells remains to be fully elucidated. In this study, we found that high KPNA2 expression is associated with poor prognosis in patients with lung adenocarcinoma. KPNA2 knockdown significantly impaired cell migration and invasion and sensitized cells to anticancer drugs in vitro. In vivo, KPNA2 depletion decreased primary tumor growth and metastasis in an orthotopic model. Mechanistically, RNA sequencing revealed that KPNA2 regulates the epithelial-mesenchymal transition (EMT) pathway. Functional studies demonstrated that KPNA2 specifically increases the responsiveness of lung cancer cells to EMT-inducing factors like TGFβ, evidenced by enhanced plasticity in 3D Matrigel cultures. These findings establish KPNA2 as a critical regulator of lung cancer stemness and chemoresistance, representing a potential therapeutic target to suppress metastasis.

#4841 ZEB1 drives pro-metastatic membrane trafficking through upregulation of REEP2 in lung adenocarcinoma.

Kevin Fulp, Oluwafunminiyi Emmanuel Obaleye, Guan-Yu Xiao

University of Kentucky, Lexington, KY

Membrane trafficking governs the transport of proteins to intracellular and extracellular locations to maintain cell homeostasis. Although this process is frequently disrupted during cancer progression, the underlying mechanisms remain largely unknown. As a result, there are currently no effective drugs that target membrane trafficking. Recent evidence has demonstrated that epithelial-to-mesenchymal transition (EMT) in lung adenocarcinoma (LUAD) employs a membrane trafficking program to coordinate cancer cell invasion and immunosuppression in the tumor microenvironment (TME). To further dissect the pro-tumorigenic membrane trafficking program, we initiated an in vivo CRISPRi screen to assess more than 2,000 membrane trafficking-related genes in a syngeneic mouse LUAD model. This screen identified REEP2, an endoplasmic reticulum (ER) shaping protein, as a novel regulator of EMT-dependent membrane trafficking. High REEP2 expression is associated with poor prognosis in LUAD patients, and REEP2 depletion decreases LUAD proliferation, migration, and invasion both in vitro and in vivo. REEP2 expression is positively correlated with expression of the EMT-driver, ZEB1, which is known to regulate gene expression via miRNA regulation. Our findings show that ZEB1 upregulates REEP2 expression by silencing miR-183 and miR-193a. Pro-metastatic secretion relies on the transport of cargo from the ER to the Golgi, and then to the plasma membrane. We discovered that REEP2 is necessary for colocalization of the ER exit site (ERES) protein SEC24D with the Golgi to facilitate cargo trafficking and ultimately drive secretion of pro-tumorigenic factors. This REEP2-driven secretome promotes cancer progression by increasing LUAD proliferation, migration, and immunosuppressive tumor microenvironment. Altogether, these findings establish REEP2 as a novel mediator of the EMT-driven pro-metastatic membrane trafficking program, revealing a specific vulnerability in mesenchymal LUAD.

#4842 SNAIL2 drives the hybrid epithelial-mesenchymal transcriptional network that reveals selective, druggable anti-invasion vulnerabilities in HNSCC.

Ananya Pal[1], Fudong Wang[1], Michael Moore[2], Yi-Hsuan Chang[1], Marina Nogueira[1], Rachel Paolini[3], Robi D. Mitra[4], Sidharth V. Puram[2]

[1]Otolaryngology, Washington University School of Medicine in St. Louis, St. Louis, MO,[2]Genetics and Otolaryngology, Washington University School of Medicine in St. Louis, St. Louis, MO,[3]Medicine and Oncology, Washington University School of Medicine in St. Louis, St. Louis, MO,[4]The Edison Family Center for Genome Sciences & Systems Biology and McDonnell Genome Institute, Washington University School of Medicine in St. Louis, St. Louis, MO

In nearly all solid tumors, metastatic progression remains the major barrier to long-term disease control and is the most common reason for death. Current anticancer agents largely target proliferation, causing toxicity in normal proliferating cells and limiting their use as long-term adjuvant therapy to suppress metastatic dissemination. Notably, no FDA-approved therapy selectively inhibits invasion without impairing normal cell viability, underscoring a major gap in metastasis-directed treatment. In head and neck squamous cell carcinoma (HNSCC), invasion and metastasis are driven by hybrid epithelial-mesenchymal (E/M) states, yet the upstream regulatory circuitry governing these states remains poorly defined and therapeutically unaddressed. Here, through comprehensive correlative and loss-of-function analyses of the six canonical EMT transcription factors (TFs), we identify SNAI2 (encoding Snail2) as the dominant EMT-TF regulating hybrid-E/M states in HNSCC. Functional assays across multiple models demonstrate that SNAI2 is both necessary and sufficient to drive invasion and metastasis. We mapped genome-wide binding sites of Snail2 (via Calling Cards) and integrated this with RNA-seq to uncover the first genome scale direct Snail2 regulon in hybrid-E/M cells. To determine which genes controlled by Snail2 act as effectors for its metastatic phenotypes, we performed a large-scale functional screen to identify invasion-specific vulnerabilities and nominate druggable nodes. Remarkably, of the 48 direct SNAI2 targets we analyzed, 21 (43 percent) function as bona fide invasion drivers in multiple lines establishing the first systematic delineation of the upstream transcriptional architecture governing the hybrid-E/M invasive phenotype in HNSCC. Importantly, we identify two key downstream effectors, NID1 (basement membrane glycoprotein) and BNC2 (zinc-finger transcription factor) as actionable therapeutic targets. Pharmacologic inhibition of NID1 and BNC2 markedly reduces invasion in vitro and suppresses metastasis in vivo at doses ~10-fold lower than those associated with toxicity. Notably, BNC2 activates SNAI2 expression, forming a reinforcing SNAI2-BNC2 positive feedback transcriptional circuit that sustains the hybrid-E/M invasive program. Together, these findings position SNAI2 at the apex of the hybrid-E/M transcriptional network in HNSCC and expose selective, drug-vulnerable anti-metastatic nodes with high translational potential. This work establishes a blueprint for developing the first generation of long-term low-toxicity anti-metastatic therapies deployable in the adjuvant setting to prevent metastatic progression.

#4843 Smarca1 maintains PAX3-FOXO1 fusion oncogene and coordinates EMT networks through chromatin remodeling.

Ashwaq K. Aljabri[1], Matt Geisler[2], Marielle E. Yohe[3], Judith K. Davie[4]

[1]Independent Researcher, Columbia, MD,[2]Plant Biology, School of Biological Sciences, Southern Illinois University, Carbondale, IL,[3]Laboratory of Cell and Developmental Signaling, National Cancer Institute (NCI), Center for Cancer Research (CCR), Frederick, MD,[4]Biochemistry and Molecular Biology, Southern Illinois University School of Medicine, Carbondale, IL

Aggressive fusion positive rhabdomyosarcoma driven by the PAX3-FOXO1 oncogene remains therapeutically challenging with poor outcomes. High SMARCA1 expression marked poorer survival outcomes, indicating prognostic significance. The chromatin remodeling factor SMARCA1 shows preferential expression in fusion positive tumors, yet its functional role in sustaining oncogenic programs has not been defined. SMARCA1 function was investigated using CRISPR Cas9 knockout combined with multi-omics profiling. All detected PAX3-FOXO1 transcripts became undetectable, showing that SMARCA1 is required for fusion expression. Fusion transcript abundance showed nearly perfect quantitative correlation with downstream key oncogenic targets including FGFR4, SNAI2, MYOD1, MYCN, ALK, ID2, IGF2, and CXCR4. Fusion levels determine the magnitude of its transcriptional output. My prior findings established, SMARCA1 acts as a master coordinator of epithelial mesenchymal transition (EMT) networks. Knockout caused simultaneous suppression of all four core EMT transcription factors SNAI1, SNAI2, ZEB1, and ZEB2 which represent both direct and indirect targets of the fusion oncogene. Their upstream regulatory pathways collapsed concurrently, including complete loss of canonical SMAD dependent TGF-β signaling and multiple non canonical branches involving PI3K, AKT, RAS, MAPK, mTOR, and NF-κB pathways. WNT/β-catenin signaling was likewise dismantled. Despite the elimination of detectable PAX3-FOXO1 mRNA, suppression of EMT transcription factors, and collapse of their upstream signaling networks, EMT gene signatures paradoxically showed strong enrichment with elevated mesenchymal markers. However, this fusion independent EMT transcriptional state failed to produce functional cellular plasticity. Migration was abolished and invasion markedly impaired, indicating that transcriptional activation alone is insufficient without proper chromatin architecture. Building on our earlier observation that SMARCA1 regulates EMT pathways, our profiling indicates that YAP-TAZ-TEAD remains active as a fusion-independent EMT module despite the collapse of the canonical fusion-driven EMT network. These findings establish that SMARCA1 maintains PAX3-FOXO1 expression and governs the organization of EMT transcription factor networks together with their upstream signaling dependencies. Together, these findings show that SMARCA1 is required to maintain PAX3-FOXO1 expression, organize EMT transcription factor networks and their upstream signaling pathways, and demonstrate that chromatin architecture is essential for converting transcriptional programs into functional behavior, and reveal chromatin dependency as a targetable vulnerability in fusion driven cancers, effectively transforming the historically undruggable PAX3-FOXO1 fusion into a druggable chromatin dependent weakness.<!--EndFragment-->

#4844 Gli2 regulation of EMT in TNBC invasion.

Emily A. Jaremba[1], Erik Beadle[2], Julie Rhoades[2]

[1]Program in Cancer Biology, Vanderbilt University, Nashville, TN,[2]Division of Hematology and Oncology, Vanderbilt University Medical Center, Nashville, TN

Despite improvements in survival for patients with primary disease only, breast cancer remains a leading cause of cancer-related death for women in part due to the propensity of breast cancer to metastasize and develop therapy resistance. Triple negative breast cancer (TNBC) has high metastatic potential, and an estimated 30-50% of patients develop tumors that are resistant to chemotherapies. To metastasize, tumors undergo epithelial-to-mesenchymal transition (EMT), in which transcriptional alterations allow tumor cells to become more invasive through reduced adhesion and increased motility. In addition to facilitating the early stages of metastasis and allowing tumors to invade, EMT has been associated with a more plastic, stem-like phenotype that may lead to therapy resistance. Thus, preventing the acquisition of an EMT phenotype may offer a dual role in inhibiting metastatic potential as well as resensitizing therapy-resistant tumors in patients with TNBC. While the Hedgehog (HH) signaling pathway is primarily active during embryonic development, its aberrant activation has been observed to promote tumor growth, invasion, metastasis, and chemoresistance. Previous data have shown that components of the HH pathway are upregulated in clinical samples of breast cancer in patients with greater mesenchymal gene signatures and those with metastatic disease. Additionally, Gli2 (Glioma-associated oncogene 2), a downstream transcriptional regulator of HH signaling, correlates with poorer patient outcomes. Thus, we hypothesize that Gli2 transcriptionally regulates EMT-associated genes, therefore promoting invasive potential in TNBC. We examined the pharmacological inhibition of Gli2 and found a reduction in EMT marker expression in TNBC cell lines. Specifically, we have identified genes such as *Cldn1* (FC = 0.382, p = 0.0003), *Zeb2* (FC = 0.426, p = 0.0005), and *Spp1* (FC = 0.163, p = 0.0009) as potential targets of Gli2-mediated EMT. We will use Cleavage Under Targets & Release Using Nuclease (CUT&RUN) sequencing to identify regions of DNA bound by Gli2, followed by comparison to genes that have differentially expressed RNA transcripts upon inhibition of Gli2. Following confirmation of Gli2-regulation of EMT-associated genes, we will genetically knockdown these target genes in Gli2-overexpressing TNBC cell lines and overexpress these genes in Gli2-knockdown TNBC cell lines. We will then perform transwell migration and invasion assays as well as *ex vivo* invasion assays on decellularized extracellular matrix (dECM) scaffolds from mouse mammary fat pads using the above cell models to assess the rescue or depletion of EMT phenotypes. The proposed studies will provide insight into the mechanisms by which Gli2 regulates EMT and invasion in TNBC. Elucidating direct transcriptional regulation of Gli2 on the EMT program may provide insight into potential therapeutic targets to reduce metastatic burden and combat chemoresistance in TNBC patients.

#4846 Stromal MTA1 silencing reprograms mesenchymal stem cells to suppress EMT and distant metastasis in triple-negative breast cancer.

Adel Zaid I Mutahar[1], Bharathi P Salimath[2]

[1]Department of Surgery, Stanford University School of Medicine, Stanford Cancer Institute,, Palo Alto, CA,[2]Department of Studies in Biotechnology, University of Mysore, Mysore, India

Background: Metastasis-associated protein-1 (MTA1) is a chromatin regulator that drives epithelial-to-mesenchymal transition (EMT), invasion, and metastatic competence in aggressive cancers including triple-negative breast cancer (TNBC). While tumor-cell MTA1 roles are well documented, its stromal contribution within mesenchymal stem cells (MSCs)—key regulators of the tumor microenvironment—remains largely unexplored. We investigated whether genetic silencing of MTA1 in human MSCs reprograms the tumor microenvironment to restrain TNBC progression and distant metastasis.

Methods: Human MSCs were stably transfected with MTA1-shRNA or scrambled control. Knockdown was confirmed by qPCR and immunoblotting. Functional assays included MMP-2 activity, osteogenic differentiation markers (RUNX2, DMP1), endothelial tube formation, and TNBC (MDA-MB-231) 3D spheroid migration, invasion, and EMT profiling. Orthotopic MSC-TNBC spheroid co-implants were established in NSG mice (n=5-8/group) to assess tumor growth, lung and brain metastases, and histologic EMT and proliferation markers. Metastasis was quantified using macrometastatic scoring, H&E staining, IHC, and micro-CT of the lungs and whole body.

Results: MTA1 knockdown reduced MSC-MTA1 expression by >80% and suppressed MMP-2 activity by 66%. Osteogenic differentiation was markedly reduced (RUNX2 and DMP1 each ↓>60%), and angiogenic tube formation decreased by 61%. In 3D co-culture, MTA1-KD MSCs reduced TNBC migration (↓54%) and invasion (↓57%) and induced EMT reversal with increased E-cadherin and decreased Vimentin and Snail. In vivo, MTA1-KD MSCs significantly inhibited tumor growth (~48% reduction at day 56). Lung and brain metastases were profoundly reduced, with a 93% decrease in lung micrometastatic foci validated by macrometastasis scoring, H&E, IHC, and micro-CT imaging. Tumors and metastatic lesions showed reduced Ki-67, N-cadherin, and Vimentin, confirming impaired proliferation and EMT signaling.

Conclusion: Our data reveal that MTA1 acts as a master stromal determinant of metastatic competence and that its suppression in MSCs yields marked inhibition of tumor-stroma crosstalk driving EMT, invasion, and organotropic colonization. The profound reduction of lung and brain metastases—validated across macroscopic, histologic, immunophenotypic, and imaging platforms—highlights the therapeutic leverage gained by targeting stromal epigenetic programs rather than tumor cells alone. These findings nominate stromal MTA1 inhibition as a powerful, mechanistically grounded strategy to remodel the metastatic niche and provide a strong translational strategy for engineering MSC-based interventions for high-risk TNBC.

#4847 Characterisation of C6ORF15 as a marker for epithelial-mesenchymal transition and lymph node metastasis in colorectal cancer.

Dedrick Kok Hong Chan

National University of Singapore (NUS), Singapore, Singapore

Introduction Lymph node metastasis in colorectal cancer (CRC) correlates with poor prognosis, yet its molecular drivers remain unknown. This study aimed to identify novel targets associated with lymph node metastasis.

Methods Colon cancers were classified into "expanding" and "metastatic" phenotypes using TCGA data. Transcriptomic profiles were analyzed by RNA-seq and GSEA. *C6ORF15* knockout (KO) and overexpression (OE) in HCT116 and SW480 cells were achieved via CRISPR-Cas9 and lentiviral transduction, validated by Sanger sequencing and Western blot. Functional effects were assessed through proliferation, migration, and invasion assays, and Western blot for EMT markers. Immunoprecipitation-mass spectrometry (IP-MS) was performed in *C6ORF15*-OE HCT116 cells to identify potential interactors.

Results TCGA analysis identified a median CRC tumor size of 5.375 cm, enabling classification into ‘expanding’ (>5 cm, no lymph node involvement) and ‘metastatic’ (≤5 cm, early lymph node involvement) phenotypes. Kaplan-Meier analysis showed significantly poorer survival in the ‘metastatic’ group (p = 0.0145). GSEA identified epithelial-mesenchymal transition (EMT) as the top enriched Hallmark in ‘metastatic’ tumors (NES = 1.81, FDR q = 0), with *C6ORF15* highly upregulated (LogFC = 2.37, p = 2.06E-07), confirmed by immunohistochemistry in patient-derived tissue specimens.

In isogenic cell lines, *C6ORF15* KO downregulated the EMT gene set (NES = -1.44, FDR q = 0.1), reducing SNAI1/2 while preserving CDH1/2, shifting cells toward a non-metastatic epithelial phenotype with reduced proliferation, migration, and invasion. Conversely, OE cells exhibited aggravated partial EMT characteristics, marked by downregulation of CDH1 and upregulation of selected mesenchymal markers (CDH2, SLUG, and SNAI1) in a cell line-dependent manner, shifting cells toward a more aggressive metastatic phenotype with enhanced proliferation, migration, and invasion.

IP-MS identified FAT1 as one of two potential C6ORF15 interactors.

FAT1 OE is known to upregulate EMT and is associated with CRC. In isogenic cell lines, *C6ORF15* OE rescued EMT activity in *FAT1* KO cells, while *C6ORF15* KO downregulated EMT in *FAT1* OE cells, suggesting that *C6ORF15* effects on EMT may persist independent of *FAT1* expression.

Conclusion *C6ORF15* may promote EMT and early CRC metastasis involving lymph nodes, showing potential as a target for future therapies.

#4848 Multi-transcriptomics reveal the potential involvement of RAB27A in promoting epithelial-mesenchymal transition in pancreatic cancer.

Zhanghao Li, Wing Ho Chan, Huiyi Guan, Sifan Yu, Aiping Lyu, Jin Liu*

Hong Kong Baptist University, Hong Kong, China

Background: Pancreatic adenocarcinoma (PAAD) is a lethal malignancy with early metastasis, a process driven by epithelial-mesenchymal transition (EMT). Although RAB27A is implicated in cancer progression, its specific role in regulating EMT in PAAD remains unclear.
Objective: This study aims to investigate the role of RAB27A in PAAD-associated EMT and to characterize its functional impact on malignant phenotypes.Methods: RAB27A expression and its correlation with patient survival were analyzed in the TCGA-PAAD cohort. Spatial transcriptomics was used to assess its enrichment in tumor regions. Gene Set Enrichment Analysis (GSEA) was performed to link RAB27A expression to the EMT program. For functional characterization, RAB27A was knocked down via siRNA in human (PANC-1) and murine (Panc-02) PAAD cell lines. Cellular proliferation, migration, and invasion were quantified by colony formation, wound healing, and transwell assays respectively. Protein levels of key EMT markers were assessed by Western blot.
Results: Bioinformatic analysis revealed that high RAB27A expression was significantly associated with poor patient survival in PAAD. Spatial transcriptomics demonstrated a strong positive spatial correlation between RAB27A expression and tumor-annotated regions. GSEA linked high RAB27A expression to an activated EMT gene signature. Functionally, RAB27A knockdown markedly inhibited proliferation, migration, and invasion in PAAD cells. This functional suppression was accompanied by a molecular shift consistent with an attenuation of EMT, including increased E-cadherin and decreased N-cadherin levels.Conclusion: Our findings implicate the potential involvement of RAB27A in promoting EMT in pancreatic cancer.
Future Directions: Future studies will focus on elucidating the precise molecular mechanisms by which RAB27A regulates EMT and evaluate the therapeutic potential of targeting RAB27A in pancreatic cancer.

: In Vitro Models 2: 2D, 3D, Organoids, and Spheroids
Poster Session

#4852 Unraveling the molecular events driving *BRCA1*-associated transformation in novel models of early müllerian cancer.

Carly A. Tompkins[1], Victoria R. Cerda[2], Marcela Haro[1], Quentin Chartreux[1], Andrew J. Li[2], Simon A. Gayther[3], B.J. Rimel[4], Fabiola Medeiros[5], Kate Lawrenson[1]

[1]Center for Inherited Oncogenesis, Department of Obstetrics and Gynecology, University of Texas Health Science Center at San Antonio, San Antonio, TX, [2]Division of Gynecologic Oncology, Department of Obstetrics and Gynecology, Cedars-Sinai Medical Center, Los Angeles, CA,[3]Center for Inherited Oncogenesis, Department of Medicine, University of Texas Health Science Center at San Antonio, San Antonio, TX,[4]Department of Gynecologic Oncology, Fred Hutchinson Cancer Center, University of Washington, Seattle, WA,[5]Department of Pathology and Laboratory Medicine, Department of Computational Biomedicine, Cedars-Sinai Medical Center, Los Angeles, CA

Clinical and translational research studies over the last two decades have revealed that high-grade serous carcinomas (HGSCs) primarily originate from fallopian tube secretory epithelial cells (FTSECs). Germline mutations in *BRCA1/2* are the strongest risk factors associated with HGSC development, but the earliest stages of neoplastic transformation, and the precise role in increasing cancer risk in FTSECs, remains poorly understood. To address this need, novel FTSEC models were generated by harvesting epithelial cells from fallopian tube fimbria by exfoliative cytology, a protocol that allowed for the use of tissue for both clinical and research applications. The study included 4 patients with high-risk germline *BRCA1* mutations undergoing risk-reducing prophylactic salpingo-oophorectomy surgery, and 4 average risk patients undergoing salpingectomy for reasons unrelated to ovarian cancer risk. Immortalization and features of neoplastic transformation were induced by transducing cells with a cDNA encoding *TERT*, dominant negative *p53*, mutant $CDK4^{R24C}$, and *CMYC*. Transduced cells bypassed replicative senescence and maintained expression of gynecologic epithelial keratins and FTSEC lineage marker PAX8. To explore if FTSECs with high-risk *BRCA1* mutations were more prone to neoplastic transformation and DNA damage, colony formation assay, and camptothecin treatment with immunofluorescent analysis of γH2A.X, 53BP1, and Rad51, were assessed. We found that high-risk FTSECs displayed increased *MYC*-induced colony formation and DNA damage compared to average-risk FTSECs. Single cell RNA-sequencing of high-risk tubal brushings identified upregulated expression of genes encoding the electron transport chain, suggesting a metabolic alteration may characterize the precancer niche in *BRCA1*-mutant fallopian tubes. Using Agilent's Seahorse assay, we found that oxidative phosphorylation is significantly decreased in high-risk FTSECs compared to FTSECs from average risk patients. Additionally, high-risk FTSECs exhibit decreased mitochondria fission. Decreased mitochondria fission coupled with a decrease in oxidative phosphorylation, suggests metabolic defects may be occurring due to the lack of mitochondria turnover and persistence of dysfunctional mitochondria. These observations uncover a new aspect of *BRCA1* biology and give new insight into metabolic perturbations occurring in high-risk fallopian tube epithelia. This work provides new models to study early tumorigenesis in the fallopian tube of high-risk mutation carriers, and demonstrates the utility of these models to investigate mechanisms underlying elevated cancer susceptibility in high-risk mutation carriers. More importantly, they have the potential to serve as models for biomarker discovery to identify early-stage markers to aid in Stage I diagnoses in the general population.

#4853 A comprehensive endometrial cancer organoid biobank reveals subtype-specific transcriptional programs and therapeutic targets.

Mali Barbi[1], Shalini Gupta[2], Santhilal Subhash[2], Divya Gowthaman[3], Arielle Katcher[3], Megan Gorman[3], Brian Yueh[4], Erdogan Akyildiz[4], Uma Mahesh[2], Devin Gee[5], Nyasha Chambwe[5], Charlie Chung[4], Marina Frimer[3], Gary L. Goldberg[3], Semir Beyaz[4]

[1]Hematology and Medical Oncology, Northwell Health Cancer Institute, New Hyde Park, NY,[2]Department of Biosciences and Bioengineering, Indian Institute of Technology Jammu, Jammu, India,[3]Department of Obstetrics and Gynecology, Division of Gynecologic Oncology, Northwell Health, New Hyde Park, NY,[4]Cold Spring Harbor Laboratory, Cold Spring Harbor, NY,[5]The Feinstein Institute for Medical Research, Manhasset, NY

Background: Endometrial cancer (EC) is a clinically and biologically heterogeneous disease with unequal outcomes, particularly among high-grade tumors that disproportionately affect racially diverse populations. Existing preclinical models incompletely capture this heterogeneity. We established a large, racially diverse EC patient-derived organoid (PDO) biobank with matched normal to define subtype-specific molecular programs and actionable vulnerabilities.

Methods: Tumors and matched normal endometrium were prospectively collected (n=380). Morphologic fidelity was assessed by histology and immunophenotyping. Multi-omic profiling evaluated driver retention and defined subtype-specific transcriptional states. High-throughput drug screening identified candidate vulnerabilities.

Results: A total of 319 samples were included, with a ~93% PDO establishment rate, and matched tumor-normal PDOs generated across major EC histologies. PDOs recapitulated the key architectural and protein-expression features of their parental tumors, including TP53-abnormal serous phenotypes and mixed epithelial-mesenchymal organization in carcinosarcoma (CS). PDOs also preserved the key genomic characteristics, including TP53, PTEN, and PIK3CA alterations. Transcriptomic profiling revealed distinct subtype programs. Endometrioid PDOs showed Wnt-associated epithelial renewal with reduced apoptosis, p53, mTORC1, and inflammatory signaling. Serous PDOs displayed TP53-abnormal, MYC-and cell-cycle-enriched programs with uniformly suppressed interferon signaling. CS exhibited hybrid epithelial-mesenchymal features with activation of Hedgehog and myogenic pathways and broad suppression of NF-kB and interferon signaling. Stratification by p53 stability and MSI status defined opposing hyperproliferative versus immune-active axes. High-throughput drug screening identified class I HDAC inhibitor (romidepsin, RD) as a consistent activity signal. RD-perturbation RNA-seq in CS showed extensive remodeling at 10 nM, with downregulation of core G2-M/E2F mitotic regulators and suppression of CS-associated secreted factors, accompanied by restoration of antigen-presentation and interferon-responsive genes. Pathway analysis demonstrated coordinated suppression of mitotic modules and reactivation of cytokine and immune signaling. RD inhibited the TPX2-CDK1-KIF11 mitotic module, indicating a druggable spindle-dependency circuit in CS.

Conclusions: This large, racially diverse EC PDO biobank provides a robust preclinical platform that captures EC heterogeneity and enables controlled, subtype-resolved analyses. Integrated multi-omics and functional perturbation identify a spindle-dependency axis in CS, supporting subtype-specific and ancestry-aware therapy development.

#4854 Mutational profiling of patient tumor organoids for clinical variable association and markers of therapeutic response in mucinous appendiceal cancers.

Daniel J. Gironda[1], Cecilia R. Schaaf[1], Steven D. Forsythe[2], R. Andrew Erali[3], Tiefu Liu[1], Ming Leung[1], Ashok K. Pullikuth[1], Helen R. Bernardirathgeb[3], Eleftherios Makris[3], Shay Soker[1], Edward A. Levine[3], Konstantinos I. Votanopoulos[3], Lance D. Miller[1]

[1]Cancer Biology, Wake Forest University School of Medicine, Winston Salem, NC,[2]Surgical Oncology, The University of Alabama at Birmingham, Birmingham, AL,[3]Surgical Oncology, Wake Forest University School of Medicine, Winston Salem, NC

Background: Mucinous Appendiceal Cancer (mAC) is a rare and poorly characterized malignancy with no known molecular targets and is treated using colorectal cancer protocols. In this study, we employed whole-exome sequencing (WES) on 3D cultures to investigate how mAC-specific oncogenic programming associates with patient clinical variables and therapeutic responses.
Methods: Patient-derived tumor organoids (PTOs) were generated from multiple mAC lesions from patients undergoing cytoreductive surgery and hyperthermic intraperitoneal chemotherapy under IRB approval. PTOs were treated with FOLFOX or FOLFIRI for 72 hours with response measured by Cell TiterGlo to determine a response phenotype. A subset of PTOs from 10 patients and 31 tumor deposits were treated with DMSO vehicle, FOLFOX, or FOLFIRI, after which genomic DNA was isolated and sequenced on an Illumina NextSeq 6000. GATK and DRAGEN pipelines were used for mutation calling, and alterations associated with drug response were analyzed by Ingenuity Pathway Analysis (IPA), with stratification informed by relevant patient clinical variables.
Results: Across the 10 mAC cases profiled, WES identified a total of 28,245 mutations, including therapeutically actionable KRAS G12D variants in 40% of cases. No targetable alterations were detected in BRAF, EGFR, or ALK. When pooling all pre-treated PTOs and averaging the variant allele frequency (VAF) across all 31 lesions, with a focus on mutations with an average VAF >=10% and present in at least 2/10 patients, individual gene mutations that were undetectable (i.e. VAF=0%) after FOLFIRI treatment included TAX1BP1, PDXK, ZFPM2, and H1FX-AS1. The lone genetic mutation undetectable after FOLFOX treatment was LINC01197, with mutations in SORD and ZBTB24 associated with a complete clonal loss after either FOLFIRI or FOLFOX treatment. Of note, SORD overexpression is implicated in the migration of CRC via upregulation of the mevalonate pathway. IPA canonical pathway analysis of patients progressing within 2 years revealed alterations in D-Myo-Inositol regulation associated pathways, whereas progression-free patients displayed alterations in pathways related to insulin-like growth factor uptake and iron regulation. Further pathway analysis was performed to discover mutations that differentiate pathways by sex, race, tumor grade, TNM scores, obesity status, among other clinical variables.
Conclusions: Comprehensive mutational profiling of mAC using paired PTO models via WES is feasible and clinically informative, enabling the detection of actionable oncogenic drivers and chemotherapy-sensitive clonal populations. These data provide the first integrated framework linking mAC-specific genomic alterations to patient outcomes and therapeutic responses and offers new biological insight into the molecular underpinnings of mAC.

#4855 Cystathionine beta-synthase drives transcoelomic metastasis in ovarian cancer.

Pallab Shaw[1], ARPAN DEY BHOWMIK[2], Akrit Pran Jaswal[1], Resham Bhattacharya[2], Priyabrata Mukherjee[1], Shailendra Kumar Dhar Dwivedi[2], Geeta Rao[1]

[1]Pathology, OU Health Stephenson Cancer Center, Oklahoma City, OK,[2]Obstetrics and Gynecology, OU Health Stephenson Cancer Center, Oklahoma City, OK

Ovarian cancer (OvCa) disseminates predominantly by transcoelomic metastasis, where exfoliated tumor cells survive as multicellular spheroids, adhere to the omentum, and establish peritoneal invasion. This process is largely dependent on spheroid viability (anoikis resistance) and efficient omental adhesion. We investigated whether the cystathionine β-synthase (CBS), which has been previously associated with other aspects of OvCa progression, can also functionally drive intraperitoneal metastasis. We integrated (i) publicly available multi-cohort patient data with survival analyses, (ii) an in-house HGSOC tissue microarray (TMA; n=109) scored for CBS with clinicopathologic correlation to peritoneal/omental metastasis, and (iii) mechanistic assays involving OvCa 2D monolayer and 3D spheroid models, including proteomics, to identify key players of CBS-mediated metastasis. High CBS expression was found to be positively correlated with worse patient survival and with clinically observed peritoneal/omental metastasis in the TMA cohort. Functionally, CBS maintained spheroid viability and compact architecture by stabilizing SP1 and sustaining ITGB1, a key mediator of mesothelial adherence on omentum via its interaction with fibronectin engagement. CBS silencing deteriorated spheroid structure, reduced $CD24^+$ subpopulations, downregulated EMT/stemness programs, and attenuated omental homing in vivo. Further, H_2S supplementation restored SP1 along with ITGB1, causing promulgated fibronectin adhesion, and spheroid survival, supporting a causal CBS→H_2S→SP1→ITGB1 pathway as the underlying mechanism of CBS-mediated OvCa transcoelomic metastasis. Therefore, the CBS-SP1-ITGB1 axis mechanistically facilitates the survival and omental adhesion of metastatic spheroids, underscoring CBS's candidacy as a target for anti-metastatic therapy.

#4856 Quantifying the dual effect of anti-tumor and pro-tumor human neutrophils on natural killer cell behaviors in a microphysiological system.

Shuai Shao, Caroline N. Jones

Biomedical Engineering, UT Southwestern Medical Center and UT Dallas, Dallas, TX

Neutrophils can promote tumor progression by inhibiting the antitumor activity of natural killer (NK) cells known as the first line of defense against cancer. Studies in mice show that neutrophils can be polarized toward either an anti-tumor “N1” or a pro-tumor “N2” state. However, it is unknown how N1 and N2 neutrophil subtypes influence NK cell behaviors differently in human cancer. It is also challenging to monitor neutrophil-NK cell interactions in the human tumor tissue. Here, we engineered a human cell-based microphysiological system to measure the distinct effect of N1 and N2 neutrophil subtypes on NK cell migration, motility, tumor cytotoxicity, and tumor infiltration. We fabricated a three-channel microfluidic chip using standard lithography. To model the preferential migration of NK cells toward different neutrophil subtypes (scenario 1), the two side channels of the microfluidic chip were seeded with LPS, IFN-γ, and IFN-β-polarized N1 and TGF-β-polarized N2 HL-60 neutrophils respectively and the central channel was seeded with NK-92MI cells. To model NK cell cytotoxicity against tumor (scenario 2), the side channels were seeded with a mixture of NK-92MI cells, PANC-1 pancreatic tumor spheroids, and N1 or N2 neutrophils. All cells were embedded in 3D collagen hydrogel to mimic the extracellular matrix of the pancreatic tumor tissue. Time-lapse imaging and end-point confocal imaging were performed to capture NK cell migration and motility in scenario 1 and tumor spheroid apoptosis and NK cell-tumor infiltration in scenario 2. NK-92MI cells showed both a higher percentage of migration (12.07 vs. 5.11% at t=24 h, $p<0.001$) and a higher maximum rate of migration (1.31 vs. 0.73%/h, $p<0.01$) to N1 neutrophils than to N2 neutrophils over 24 h. NK-92MI cells showed a higher motility after migration to N2 neutrophils than N1 neutrophils in speed (1.07 vs. 0.80 μm/min at t=12 h), displacement (9.89 vs. 6.89 μm at t=12 h), and directionality (0.43 vs. 0.36 at t=24 h) ($p< 0.0001$). Hence, NK-92MI cells showed preferential migration to N1 over N2 neutrophils, although they slowed down after migration to N1 compared to N2 neutrophils. Moreover, N1 neutrophils restored NK cell cytotoxicity against tumor spheroids (0.97 vs. 1.01, $p>0.99$) while N2 neutrophils suppressed it (0.97 vs. 0.54, $p<0.0001$), although both N1 and N2 neutrophils inhibited NK cell infiltration in tumor spheroids (control vs. N1 vs. N2: 8.04 vs. 5.87 vs. 5.49%, $p<0.01$). We also found that N1 neutrophils secreted a higher level of NK cell chemokine IP-10 and induced higher expressions of activation markers CD107a and IFN-γ by NK-92MI cells than N2 neutrophils. This study reveals the dual role of human neutrophils in modulating NK cell behaviors and the complex neutrophil-NK cell crosstalk, suggesting reprogramming neutrophils to reverse the immunosuppression on NK cells as a potential therapeutic strategy for cancer.

#4857 A panel of patient-derived organoid models from rare cancers for high-throughput preclinical pharmacology studies.

Nathan P. Coussens[1], Thomas S. Dexheimer[1], Zahra Davoudi[1], Thomas Silvers[1], Eric M. Jones[1], Bryce M. N. Butler[1], John R. Britt[1], Luke Stockwin[1], Dianne Newton[1], Carmen Allegra[2], James H. Doroshow[2], Beverly A. Teicher[2]

[1]Applied and Developmental Research Directorate, Frederick National Laboratory for Cancer Research, Frederick, MD,[2]Division of Cancer Treatment and Diagnosis, National Cancer Institute, Bethesda, MD

Twenty-five patient-derived organoid models from rare cancer types were selected from the NCI's Patient-Derived Models Repository (https://pdmr.cancer.gov) to serve in a high-throughput screening panel for preclinical pharmacology studies. The models were derived from primary (16; 64%) or metastatic (9; 36%) tumors of patients (56% female, 44% male) with varied ancestries, ranging in age from 32-87 yrs, that were either previously treated (13; 52%) or treatment naïve (12; 48%). The panel included a range of cancer types, including one breast, seven digestive/gastrointestinal, one neuroendocrine, four gynecologic, seven head and neck, and five musculoskeletal. Variations were determined in microsatellite stability and genetics, including clinically relevant oncogenic variants of RAS, BRAF, and PIK3CA. A high-throughput pilot screen was conducted with a library of 166 FDA-approved oncology drugs tested at five concentrations with a 1-log dilution series ranging from 0.01 µM to 100 µM. After a seven-day drug exposure period, cell viability was determined by the CellTiter-Glo 3D endpoint assay. The overall assay performance was excellent with average Z'-factor values from nine microplates per organoid model ranging between 0.54 (0.49 - 0.63) to 0.89 (0.86 - 0.91), with an overall average of 0.67 (0.44 - 0.91). Under assay conditions, the organoid models exhibited diverse morphologies and varied growth kinetics with doubling times ranging from 48 - 363 h with an average of 129 h. Among the patients that received prior chemotherapy, four had a partial response as the best outcome, two of which were sarcoma patients treated with regimens including doxorubicin, vincristine, and etoposide. Interestingly, the organoids derived from the two patients demonstrated ≥1 log of cytotoxicity following exposure to these drugs and others at concentrations below the clinical Cmax. A patient with lip/oral cavity squamous cell carcinoma partially responded to a regimen including temozolomide and the corresponding organoid demonstrated ≥1 log of cytotoxicity following exposure to temozolomide and other drugs below the clinical Cmax. A patient with stomach adenocarcinoma partially responded to a regimen with 5-fluorouracil and cisplatin, but the organoid was minimally sensitive to these drugs. However, genomic characterizations of the tumor tissue indicated an amplification of ERBB2 and the organoid demonstrated sensitivity to the ERBB2 inhibitors neratinib, dacomitinib, and lapatinib below their respective clinical Cmax value. Altogether, these data underscore the potential utility of organoids for assessing tumor responses and exploring novel treatment modalities for underserved malignancies. Funded by NCI Contract No. 75N91019D00024 & 75N91020F00032.

#4858 Combined pan and precision targeting in extrachromosomal DNA-positive gastric cancer.

Gengyi Zou[1], Melissa Pizzi[1], Aryanasingh Bhati[1], Bansi Vanparia[1], Wei-Chieh Yu[2], Ailing Scott[1], Yibo Fan[1], Calena Brown-Abel[1], Liyong Zeng[1], Johnson Amoah[1], Tanaya Alexander Washington[1], Yuan-Hung Lo[2], Vineet Bafna[3], Shilpa Dhar[1], Jaffer Ajani[1]

[1]GI Med Oncology, UT MD Anderson Cancer Center, Houston, TX,[2]Molecular & Cellular Oncology, UT MD Anderson Cancer Center, Houston, TX,[3]University of California, San Diego, CA

Gastric adenocarcinoma (GAC) remains a major health challenge with high mortality due to late diagnosis, therapy resistance, and limited targeted options. Extrachromosomal DNA (ecDNA)—circular DNA elements carrying amplified oncogenes such as MYC, ERBB2, and EGFR—enhances transcriptional output, therapy resistance, and genomic instability. However, its role in GAC is poorly understood, and current models fail to recapitulate patient tumor complexity. Patient-derived organoids (PDOs) preserve tumor-specific features, including ecDNA, providing an ideal platform for mechanistic and therapeutic exploration.We hypothesize that ecDNA drives unique oncogenic programs in GAC that create exploitable vulnerabilities. Analysis of 221 TCGA-STAD samples with AmpliconArchitect identified ecDNA in 33.3% of primary tumors, absent in matched normal blood. ecDNA+ tumors showed distinct amplification patterns, with proteomic profiling revealing CHEK1 and TFRC enrichment, suggesting co-targetable vulnerabilities. To model these tumors, we established a PDO biobank comprising 5 primary and 9 ascites-derived PDOs. ecDNA was detected in 5/9 (55.6%) ascites-derived and 1/5 (20%) primary PDOs, consistent with ecDNA enrichment in metastatic settings. Amplified oncogenes included PTP4A3, for which inhibitors are available.RNA-seq comparison of ecDNA+ PDO 385 with ecDNA- PDOs (4666, 4601) revealed distinct transcriptional programs, with enriched expression on chromosomes 8 and 20. Transcription factor analysis identified MYC, also amplified as ecDNA. Immunofluorescence confirmed higher TFRC, CHEK1, MYC, and PRL3 (PTP4A3) expression and increased Ki67 in ecDNA+ PDO 385, supporting oncogene overexpression and aggressive growth. Drug screening predicted compounds reversing the ecDNA+ signature. Functional assays showed the TFRC inhibitor (TfR-1-IN-1) reduced proliferation of ecDNA+ PDO 385, while CHK1 inhibition had modest effects. Combined TFRC and CHK1 inhibition synergistically suppressed ecDNA+ PDO growth, with minimal effects on ecDNA- controls. These results highlight the selective vulnerability of ecDNA-driven tumors to co-targeting strategies. Using a PDO biobank, we aim to uncover and exploit vulnerabilities in ecDNA-positive GAC.

#4859 A novel sarcoma tumoroid platform preserving the tumor microenvironment to guide personalized immunotherapy.

Tony Ezzat[1], Nathaniel Ruppert[2], Elizabeth Nowak[3], Danny G. Cho[3], Masahiro Hitomi[4], Tyler E. Miller[5], Gary K. Schwartz[5], Jacob G. Scott[5], Zachary D. Burke[6]

[1]The Cleveland Clinic Lerner College of Medicine, Cleveland, OH,[2]Case Western Reserve University School of Medicine, Cleveland, OH,[3]The Cleveland Clinic, Cleveland, OH,[4]Project Staff, Dept. of Stem Cell Biology and Regenerative Medicine, The Cleveland Clinic, Cleveland, OH,[5]Case Comprehensive Cancer Center, Cleveland, OH,[6]Orthopedic Surgery, The Cleveland Clinic, Cleveland, OH

Sarcomas are rare, aggressive mesenchymal cancers with over 80 subtypes. Although they represent a small fraction of adult cancers, sarcomas comprise over 20% of pediatric solid tumors and carry poor outcomes for patients with advanced disease. Preclinical modeling remains challenging: traditional 2D cultures fail to preserve the tumor microenvironment (TME), while conventional 3D organoid platforms rely on enzymatic dissociation, which disrupts cellular interactions essential for TME integrity. Patient-derived xenografts, though more representative, are costly and low-throughput. To address these limitations, this study aims to develop reproducible 3D sarcoma tumoroids as a translational platform for functional studies and therapeutic testing that preserves the TME.

Freshly resected sarcoma specimens were mechanically cut into small fragments without enzymatic dissociation, preserving the TME in each fragment, and cultured in suspension or matrix-embedded conditions. Media formulations and growth factor combinations were evaluated across sarcoma subtypes to optimize culture performance. Tumoroid formation and growth were monitored for 14 days using brightfield microscopy, quantitative area analysis, and alamarBlue viability assay. Structural integrity and TME preservation were assessed by hematoxylin and eosin (H&E) staining and immunohistochemistry (IHC). Cytotoxic response assays were performed using standard chemotherapeutic agents, including doxorubicin and methotrexate, to evaluate drug sensitivity in 3D culture over a 5-day treatment period.

Established tumoroids maintained consistent 3D morphology and viability over 14 days, with Mammocult medium plus growth factors supporting the strongest proliferation. Quantitative growth analysis showed a progressive increase in tumoroid area and metabolic activity, indicating stable expansion under optimized conditions. H&E staining confirmed retention of tumor cells, stroma, and histologic architecture across osteosarcoma, dedifferentiated liposarcoma, and chondrosarcoma for over 10 days. IHC staining for CD45 confirmed the presence of immune and stromal cell populations within the cultures, indicating preservation of the native TME. Chemotherapeutic testing using methotrexate and doxorubicin revealed cytotoxic effects through H&E and Live/Dead staining, validating the model's responsiveness and functional relevance.

These findings demonstrate that mechanically dissociated sarcoma tissues can generate viable, subtype-representative tumoroids while maintaining key TME features. Future efforts will focus on expanding therapeutic testing, integrating immune co-culture systems to better recapitulate the sarcoma TME, and applying spatial transcriptomics and single-cell RNA sequencing to uncover cellular heterogeneity and guide precision oncology for sarcoma patients.

#4860 Predicting therapy efficacy and revealing tumor heterogeneity using patient-derived 3D bioprinted ovarian cancer models.

Jiangang Zhang[1], Huiyu Yang[2], Ying Shan[3], Zihan Zhong[4], Ziren Kong[5], Yuning Sun[1], Huayu Yang[6], Lingya Pan[3], Yilei Mao[6], Ying Jin[3]

[1]Department of Head and Neck Surgery, National Cancer Center/National Clinical Research Center for Cancer/Cancer Hospital, Chinese Academy of Medical Sciences and Peking Union Medical College, Beijing, China,[2]Department of Neurosurgery, Xuanwu Hospital, Capital Medical University, Beijing, China,[3]Department of Obstetrics and Gynecology, Peking Union Medical College Hospital, Beijing, China,[4]National Cancer Center/National Clinical Research Center for Cancer/Cancer Hospital, Chinese Academy of Medical Sciences and Peking Union Medical College, Beijing, China,[5]Cancer Hospital Chinese Academy of Medical Sciences, Beijing, China,[6]Department of Liver Surgery, Peking Union Medical College Hospital, Beijing, China

Ovarian cancer is the most lethal gynecologic malignancy, characterized by tumor heterogeneity and a high recurrence rate. Patient-derived *in vitro* tumor models offer a promising strategy for individualized drug screening to overcome limitations of systemic therapy. Among existing modeling methodologies, 3D bioprinting exhibits advantages including high-throughput, high fidelity, and a drug screening timeline of 8 days. Here, we present experimental data of a cohort of novel 3D bioprinted patient-derived ovarian cancer (3DP-OC) models. We established 3DP-OC models by mixing primary ovarian cancer cells with Gelatin Methacryloyl (GelMA) and photoinitiator, and bioprinting in a layer-by-layer manner. In total, 3DP-OC from 79 patients were successfully established, including 61 high-grade serous ovarian cancer patients, 9 ovarian clear cell carcinoma patients, 4 ovarian sarcoma patients, 4 ovarian endometrioid carcinoma patients, and 1 ovarian neuroendocrine cancer patient. 113 3DP-OC models were constructed from different tissue origins (primary lesion and metastatic sites) with high cell viability maintained throughout bioprinting and prolonged *in vitro* culture. Bulk RNA sequencing and immunohistochemistry confirmed that key molecular markers and Ki-67 levels in 3DP-OC models closely resembled those of their paired tumor tissues, demonstrating that 3DP-OC can serve as a patient avatar for drug sensitivity testing. On days *in vitro* 5, 3DP-OC models were exposed to gradient concentrations of 15 frequently used chemotherapeutic and targeted drugs in ovarian cancer including paclitaxel, carboplatin, olaparib, *etc.* Cell viability was quantified to calculate IC_{50} values of different anti-tumor drugs. Drug sensitivity testing revealed substantial interpatient heterogeneity in therapeutic responses. To further investigate whether this response heterogeneity has clinical relevance, we conducted a prospective observational cohort study that enrolled 41 stage III/IV newly diagnosed ovarian cancer patients. Patients were divided into “3DP-OC identified sensitive group” or “3DP-OC identified resistant group” according to 3DP-OC IC_{50} values of anti-tumor drugs they received. The median follow-up time for all patients was 580.5 days. The 3DP-OC identified sensitive group exhibited significantly prolonged progression-free survival compared to the 3DP-OC identified resistant group ($P < 0.05$), with disease progression observed in 16.7% (4/24) and 52.9% (9/17) of patients, respectively. In this study, we established a 3D bioprinted patient-derived cancer model with high success rate of establishment, low intra-batch heterogeneity, and high biological fidelity. 3DP-OC model holds promise for predictive utility in precision oncology as well as the potential to serve as an innovative platform that bridges fundamental cancer research and clinical practice.

#4861 Modeling IDH-mutant low-grade astrocytoma using human embryonic stem cells.

Greta Henriette Ghita, Yanhong Yang, Viviane Tabar

Memorial Sloan Kettering Cancer Center, New York, NY

Introduction: Few existing models accurately recapitulate and sustain the phenotype of IDH-mutant low-grade gliomas (LGGs). Maintaining a stable IDH-mutant glioma line remains a major challenge, as patient-derived cultures rapidly lose mutant IDH expression due to selective pressure favoring more aggressive, IDH wild-type cells. To address this limitation, we developed an inducible human embryonic stem cell (hESC)-derived model for longitudinal studies of IDH-mutant Low-Grade Astrocytoma (LGA) pathogenesis, progression, and therapeutic response.
Methods: We engineered hESCs to carry a doxycycline-inducible IDH1-R132H mutation, with or without CRISPR/Cas9-mediated knockouts of TP53 and ATRX. These combinations generated three isogenic lines: IDH-mutant alone, IDH-mutant/TP53-null, and IDH-mutant/TP53-ATRX-null. This allows for the dissection of how common co-mutations influence glioma initiation and evolution. Cells underwent neural induction to the progenitor stage to model early gliomagenesis, with induction of mutant IDH expression being verified via Western blot. Tumorigenic potential and progression are currently being assessed both in vitro and in vivo.
Results: Upon differentiation to the neural progenitor stage, IDH1-R132H induction produced hallmark features of LGG biology, including elevated γH2AX, a marker of DNA damage response associated with IDH-mutant gliomas. Induced cells exhibited slower proliferation and limited invasiveness compared to non-induced controls, mirroring the slower growth of patient-derived LGGs. In vivo, IDH-mutant xenografts demonstrated delayed tumor expansion relative to IDH-wild-type counterparts. Ongoing studies are comparing therapeutic responses between our hESC-derived model and patient-derived lines to evaluate its translational utility for preclinical drug testing and longitudinal progression studies.
Conclusions: We established an inducible hESC-based model with the capability to recapitulate the behavior and characteristics of IDH-mutant LGA. This platform could overcome the instability of patient-derived lines, enabling controlled, long-term studies of glioma evolution and treatment response. Our model provides a powerful system to dissect how IDH and cooperating mutations drive gliomagenesis and to test targeted therapies across disease stages.

#4862 Development of a high-throughput multimodal patient-derived platform integrating autologous fibroblasts and tumor-infiltrating lymphocytes for colorectal cancer drug discovery.

Lewis Campbell, Agapitos Patakas, Athanasios Koulis, Hannah Findlay, Daria Paruzina, Cameron Fyfe, Ellen Main

RoukenBio, Motherwell, United Kingdom

Background:
Colorectal cancer (CRC) remains one of the leading causes of cancer-related mortality, driven by extensive molecular heterogeneity and the emergence of therapy-resistant subclones. Conventional *in vitro* models fail to reproduce the complexity of the tumor microenvironment (TME). To address this, we developed a high-throughput, multimodal patient-derived tumoroid (PDTO) platform incorporating autologous tumor-infiltrating lymphocytes (TILs) and / or cancer-associated fibroblasts (CAFs), enabling integrated pharmacologic, genomic, and immunologic analyses for translational drug discovery.
Methods:
Matched tumor and adjacent normal tissues were collected from CRC patients under the NHSGGC biorepository ethics approval (REC 22/WS/0020). PDTOs, CAFs, and TILs were isolated, expanded, and cryopreserved under optimised protocols that maintain molecular signature of the parental tumor. Each patient derived model was subjected to multi-omic characterisation, including whole-exome sequencing, and bulk RNA sequencing. Derived models were treated with standard-of-care drugs (SOC) to assess sensitivity/resistance, tumoroid survival and viability post treatment, which was analysed by high throughput fluorescent imaging, flow cytometry and multiplex cytokine profiling.
Results:
To date, five PDTO, CAF, TIL models, including mono-, dual-, and tri-culture formats have been successfully established from both primary and metastatic CRC samples encompassing diverse mutational backgrounds. Integrated mutational burden analysis together with transcriptional and clinical data revealed discrete transcriptional clusters associated with microsatellite status, immune infiltration, and drug response patterns. SOC regimens demonstrated expected cytotoxic profiles, confirming physiological relevance of the models. Initial experiments indicated that inclusion of immune and stromal component confirm that incorporating CAFs and TILs modifies pharmacologic response profiles.
Conclusions:
This multimodal CRC tumoroid platform recapitulates the epithelial, stromal, and immune components of the native TME. Its integration of clinical, genomic, and gene expression datasets enables high-content functional screening and predictive biomarker discovery. The platform supports translational drug development while reducing the need for large-scale expansion across heterogeneous patient cohorts by capturing most dominant CRC molecular subtypes and intratumoral complexity within each culture system.

#4863 Innovative xeno free synthetic hydrogel supports iPSC derived intestinal organoids and colorectal cancer (CRC) organoid growth, An advanced organoid platform for therapeutic screening.

Kalhara R. Menikdiwela, JOHN HUANG

Research and Development, TheWell Bioscience Inc., Monmouth Junction, NJ

Colorectal cancer (CRC) is the fourth most commonly diagnosed cancer and the second leading cause of cancer death in the United States of America. Organoids, specifically CRC organoids have emerged as a powerful preclinical model as they closely recapitulate patient-specific tumor features, including tumor morphology, genetics and treatment response. However, most organoid culture systems heavily rely on animal-based hydrogel systems, which are tumor-derived and consist of a large number of undefined components, introducing batch variability, thus limiting their translational relevance. To overcome these limitations, we developed and engineered an innovative xeno-free synthetic hydrogel system (VitroGel) to provide mechanical support and a tunable extracellular environment for advanced CRC organoid research. Human iPSCs were first cultured in synthetic hydrogel VitroGel STEM, to generate uniform spheroids. Using stepwise differentiation with endoderm-inducing and mid-gut patterning media, spheroids were guided toward intestinal lineage commitment. Immature intestinal organoids were subsequently transferred into VitroGel ORGANOID with intestine-specific medium to generate mature intestinal organoids with stable expansion. Similarly, patient-derived CRC organoids were cultured in synthetic hydrogel system, resulting in reproducible growth and structural integrity. To further evaluate the utility of the VitroGel system for modeling tumor-epithelium interactions, we established an advanced co-culture model by integrating iPSC-derived intestinal organoids with Wnt3a-overexpressing, RFP-labeled Caco-2 cells within VitroGel. Activation of the Wnt pathway induced tumor-like phenotypes within the organoid structures, enabling the development of intestinal organoids with enhanced tumor characteristics. Overall, the synthetic hydrogel VitroGel ORGANOID provides a next-generation matrix that enhances the reproducibility, scalability, and translational relevance of intestinal and CRC organoid models, including advanced tumor-epithelium co-culture. By eliminating the limitations of animal-derived extracellular matrices, VitroGel represents a significant advancement for precision oncology and drug discovery.

#4864 A leiomyosarcoma cell model based on smooth muscle-committed *TP53*-knockout iPSCs identifies novel actionable pathways..

Annalisa Astolfi[1], Livia Gozzellino[2], Alice Costa[3], Ilenia Motta[2], Margherita Nannini[1], Maria Concetta Nigro[1], Martina Lops[2], Maria Giulia Pirini[3], Antonio De Leo[1], Gianandrea Pasquinelli[1], Maria A. Pantaleo[1]

[1]University of Bologna, IRCCS Azienda Ospedaliero-Universitaria di Bologna, Bologna, Italy,[2]University of Bologna, Bologna, Italy,[3]IRCCS Azienda Ospedaliero-Universitaria di Bologna, Bologna, Italy

Leiomyosarcoma (LMS) is a mesenchymal tumor of smooth muscle origin, representing one of the most common types of soft tissue sarcoma. The genetic landscape of LMS is driven by *TP53* mutation that recurs in more than 60% of patients. Leiomyosarcoma prognosis is still disappointing, since up to now no drug combination has shown relevant clinical activity in the advanced or metastatic setting and the role of adjuvant therapy remains controversial. The aim of this project was to dissect the vulnerability of the most recurrent genetic lesion in a LMS model to identify novel actionable pathways. To this end we developed a cell model system recapitulating LMS molecular and lineage phenotypes by engineering donor-derived induced pluripotent stem cells (iPSC) at the *TP53* locus using Crispr/Cas9 system. The model was then differentiated towards smooth muscle and characterized by gene expression profiling, protein and transcript biomarker expression, *in vitro* 2D and 3D cell growth and drug response testing. *TP53*-edited cell pool was subcloned to select lines carrying either homozygous or compound heterozygous frameshift mutations (*TP53* Knockout, KO). Mesoderm lineage commitment upregulated specific mesoderm markers (T, Mixl1, CD56) in both parental (iPSC WT) and *TP53* KO lines, while only *TP53* KO cells significantly downregulated p53-target genes. Differentiation towards smooth muscle showed upregulation of terminal smooth muscle markers at the transcript (ACTA2, ACTG2, TAGLN) and protein level (alpha-SMA, Cnn1) in iPSC WT and *TP53* KO clones. At the phenotypic level *TP53* loss promoted cell growth at early and late stages of smooth muscle differentiation (2 - 2.5-fold induction, $p<0.001$), and significantly induced 3D spheroid cell growth with respect to the wild type counterpart (3.6-fold, $p<0.001$). Gene expression profiling during smooth muscle differentiation uncovered the malignant phenotype driven by *TP53* knockout, shown by the upregulation of the CINSARC signature that is associated to tumor aggressiveness in sarcomas. Moreover, it identified *FBXW7* as the most significantly silenced gene immediately after *TP53* ($p<0.001$). Analysis of the TCGA Firehose Legacy dataset confirmed that *FBXW7* was significantly downregulated in *TP53*-mutant or deleted sarcomas with respect to WT tumors. Since it is known that *FBXW7*-deficient cells are more sensitive to Tigecycline, a drug that targets mitochondrial translation, we tested the drug in *TP53* KO LMS model, showing that smooth muscle-committed *TP53* KO cells are three times more sensitive to this compound than wild type cells. This study shows that *TP53* KO LMS iPSC model is an effective tool for target discovery, and that *FBXW7* pathway could be an amenable target in *TP53*-mutant LMS. The research leading to these results has received funding from AIRC under IG 2024 - ID. 30644 project - P.I. Astolfi Annalisa.

#4865 Functional assessment of patient drug sensitivity using AI-powered image analysis on patient-derived organoids and micoorganoid spheres.

Abraham Lin[1], Maxim Le Compte[2], Divya L. Dayanidhi[3], Edgar Cardenas De La Hoz[4], Rebecca Stone[5], Tyler Gilcrest[5], Geert Roeyen[6], Filip Lardon[1], Christophe Deben[1]

[1]Center for Oncological Research, University of Antwerp, Wilrijk, Belgium,[2]University of Antwerp, Wilrijk, Belgium,[3]Medical Center, Duke University, Durham, NC,[4]Industrial Vision Lab, University of Antwerp, Antwerp, Belgium,[5]Orbits Oncology, Palo Alto, CA,[6]University Hospital Antwerp, Edegem, Belgium

Lately, there has been a push for new laboratory models that more accurately represent human biology than traditional models. These include miniature tumor models such as, patient-derived organoids (PDOs) and MicorOrganoidSpheres (MOS), which act as functional avatars of patient tumors and treatment response[1,2]. While recent studies provided first evidence that patient responses to standard-of-care therapies could be recapitulated, these studies were only able to predict clinical responses in a subset of patients[3]. This limitation largely stems from the analytical methods used, namely CellTiter-Glo 3D[4], which rely on a bulk, endpoint analysis and only extracts a fraction of clinically relevant insights that PDOs provide[5]. Therefore, we hypothesized that using kinetic, higher-dimensional analysis methods, further improves the predictive performance of PDOs. We combined live-imaging techniques with AI-driven analysis to capture dynamic drug responses. Using a fully characterized a PDO panel (n=8) from patients with pancreatic ductal adenocarcinoma (PDAC) and a fully characterized MOS panel (n=43) from patients with colorectal cancer, we matched our multiparametric analysis with retrospective clinical patient response to standard of care therapies (e.g. gemcitabine-paclitaxel, FOLFIRINOX, oxaliplatin). Our PDO analysis quantified resistant and sensitive PDO clones within the patient, and identified patient-specific sensitives to therapy that were in-line with progression-free survival of matched patients ($R=0.97$)[6]. This was a significant improvement to the relative viability readouts from CellTiter-Glo3D ($R^2=0.26$). Our MOS analysis correlated with patient sensitivity and resistance to oxaliplatin. Taken together, our work highlights the importance of using sophisticated analysis methods to measure the complexity new laboratory models, such as MOS and PDOs. Our ongoing work include developing more robust predictive models, using the multiparametric readouts of our analysis platform.

1. Hadj Bachir, E., et al. *Biol Cell* 114 (2021) 2. Ding, S., et al. *Cell Stem Cell* 29 (2022) 3. Driehuis, E., et al. *Proc Natl Acad Sci* 116 (2019) 4. Sachs, N., et al. *Cell* 172 (2018) 5. Phan, N., et al. *Commun Biol* 2 (2019) 6. Le Compte, M., et al. *npj Precis Oncol* (2023)

#4866 Interactions between colorectal cancer cells and cancer-associated fibroblasts across desmoplastic reaction subtypes.

Wataru Kosaka[1], Keigo Murakami[2], Yota Akamori[1], Hideaki Karasawa[1], Yuki Yasuda[1], Ichiro Ise[1], Tomoyuki Ono[1], Megumi Murakami[1], Yoshihiro Sato[1], Gumpei Yoshimatsu[1], Hideyuki Suzuki[1], Takashi Kamei[1], Shinobu Ohnuma[1], Toru Furukawa[2], Michiaki Unno[1]

[1]Department of Surgery, Tohoku University Graduate School of Medicine, Sendai, Japan,[2]Department of Investigative Pathology, Tohoku University Graduate School of Medicine, Sendai, Japan

The desmoplastic reaction (DR) at the invasive front of colorectal cancer (CRC) has recently gained increasing attention as an important prognostic indicator and as a histological hallmark that reflects tumor-stroma interactions. DR is classified into mature, intermediate, and immature patterns based on stromal morphology, each representing distinct biological states of the surrounding microenvironment. Previous clinicopathological studies have demonstrated that immature and intermediate DR are associated with unfavorable outcomes; however, the biological mechanisms underlying these prognostic differences remain insufficiently understood. Because cancer-associated fibroblasts (CAFs) constitute the predominant stromal component of DR and critically influence stromal architecture, we aimed to clarify CRC-CAF interactions by combining analyses from a well-characterized clinical cohort and a three-dimensional co-culture system incorporating patient-derived CRC organoids and CAFs.We retrospectively identified 269 consecutive patients who underwent surgical resection for CRC (pT3 or higher) between 2013 and 2018 at our institution. Clinicopathological and prognostic variables were examined in detail, with a focused analysis of 191 stage II/III patients who did not receive preoperative therapy to reduce treatment-related confounding. Primary CRC organoids and CAFs were established from resected tumors under standardized culture conditions, and the DR subtype corresponding to each CAF line was determined histologically. To further explore stromal biology, proteomic profiling was performed to characterize DR subtype-specific protein expression signatures and to investigate molecular features associated with stromal phenotypes.Immature DR demonstrated significant associations with aggressive clinicopathological characteristics, including higher T (T3 66.0%, T4 34.0% P-value : 0.0011) and N (pN1-3 62.3% P-value : < 0,001) categories, vascular invasion (positive 98.1% P-value : < 0,001), and other indicators of tumor invasiveness, whereas mature DR was linked to more favorable clinical outcomes. In three-dimensional co-culture assays, CRC organoids exhibited the greatest proliferative expansion when paired with immature CAFs, emphasizing the functional relevance of stromal immaturity in promoting tumor growth (P-value : < 0.05). Proteomic analysis revealed clear segregation among DR subtypes, reflecting distinct protein expression profiles characteristic of each subtype. Notably, in immature DR, pathways related to cell adhesion centered on integrins, actin-regulation pathways, and fatty acid metabolism were among the top enriched pathways.These findings support DR classification as a clinically meaningful prognostic factor in CRC and indicate that immature CAFs play a key role in promoting CRC cell growth.

#4867 The radiosensitivity index (RSI): A patient-derived organoid platform for predicting radioresistance in cervical cancer.

Young Joo Lee[1], Ju Hee Oh[2], Eun Hye Choi[2], Kyung Jin Eoh[3], Sang Wun Kim[2], Yoo-Na Kim[2], Ji Hyun Lee[2], Eun Ji Nam[2]

[1]Department of Obstetrics and Gynecology, Kyung Hee University Hospital at Gangdong, Kyung Hee University College of Medicine, Seoul, Korea, Republic of,[2]Department of Obstetrics and Gynecology, Women's Cancer Center, Yonsei Cancer Center, Institute of Women's Life Medical Science, Yonsei University College of Medicine, Seoul, Korea, Republic of,[3]Department of Obstetrics and Gynecology, Yongin Severance Hospital, Yonsei University College of Medicine, Yongin, Korea, Republic of

Purpose Radiotherapy is one of the major treatment modalities for cervical cancer; however, treatment responses vary among patients, and no reliable method currently exists to predict individual radiosensitivity. We aim to establish a radiosensitivity index (RSI) model using cervical cancer patient-derived organoids (PDOs) and to evaluate its clinical performance in relation to actual patient outcomes.

Patients and Methods Fresh cervical cancer tissues were obtained from 14 patients at diagnosis, and clinical information including stage, radiation history, histology, recurrence, and progression-free survival was retrieved from their medical records. Organoids were established from patient-derived cervical cancer tissues, and their histopathological and genomic features were compared with the original tumors to confirm reproducibility and model fidelity. Each organoid underwent irradiation assays to evaluate radiosensitivity. Radiation-response metrics including area under the survival curve (AUC-survival), growth rate-adjusted slope (GR-slope), and ΔG2/M% as well as clinical stage were standardized using z-score normalization and integrated into a composite RSI. Predictive performance of the RSI was assessed using receiver operating characteristic (ROC) curve analysis, and AUC, sensitivity, specificity, PPV, and NPV were calculated based on Youden's index. Kaplan-Meier analysis was performed to evaluate differences in survival outcomes according to RSI-predicted radiosensitivity.

Results All 14 PDOs successfully underwent irradiation assays, and multiparametric integration of AUC-survival, GR-slope, ΔG2/M%, and clinical stage yielded an individualized RSI value. The RSI effectively predicted recurrence after radiotherapy (AUC = 0.844, p = 0.039; sensitivity 80.0%, specificity 88.9%). In addition, the predicted recurrence probability was significantly higher in recurrent patients compared with non-recurrent patients. Survival analysis demonstrated a trend toward improved progression-free survival in the RSI-predicted radiosensitive group compared with the radioresistant group (median 42.3 vs. 15.5 months, p=0.257), suggesting concordance between RSI-based predictions and actual clinical outcomes.

Conclusions We successfully developed a personalized preclinical platform based on a cervical cancer PDO-derived RSI model. This is the first PDO-based approach that predicts individual radiosensitivity and validates these predictions against actual clinical outcomes. The RSI model may serve as a preclinical decision-support tool to personalize treatment decisions and guide radiotherapy optimization for cervical cancer patients.

#4868 Modelling glioblastoma sensitivity to irradiation with a patient derived xenograft-derived 3D platform.

Fu-Ju Chou[1], Annamaria Rapisarda[1], Marianna Zipeto[1], Michael Ritchie[1], Markus Hippich[1], Daniel Ciznadija[2], BanuPriya Sridharan[3], Veena Jagannathan[1], Gilad Silberberg[1], **Stefano Cairo**[1]

[1]Champions Oncology (Rockville, MD), Rockville, MD,[2]Champions Oncology, Hackensack, NJ,[3]Champions Oncology, Inc. (Hackensack, NJ), Hackensack, NJ

Glioblastoma (GBM) remains one of the most aggressive and treatment-refractory brain tumors, characterized by profound cellular heterogeneity, infiltrative growth, and intrinsic resistance to conventional therapies, including radiotherapy. To better understand differential tumor responses to irradiation, a series of short & long-term viability assays were conducted using glioblastoma patient-derived xenograft organoids (PDXO) to evaluate sensitivity to X-ray exposure. Multiple GBM models were included in the analysis, in a 4-day irradiation assay, & an expanded panel of ten models in a 14-day extended assay. Organoids were established in ultra-low attachment 96-well plates at defined seeding and cultured in triplicate. Following initial organoid formation, PDXOs were exposed to X-ray irradiation at doses of 2 Gray (Gy) for the short-term & 4 Gy for the extended assay. Endpoints included morphological assessment of three-dimensional structure formation, bright-field imaging, & quantitative viability measurements using the CellTiter-Glo® luminescent assay. Organoid size & integrity were monitored over time, focusing on structures measuring ≥50 µm in diameter. The 4-day assay revealed a general lack of sensitivity to irradiation across all tested models, suggesting that short-term exposure is inadequate for capturing delayed or cumulative cytotoxic effects typical of radiation-induced damage. In contrast, the 14-day assay, which incorporated both higher radiation dose & extended culture duration, successfully discriminated between irradiation-sensitive & resistant models. Several organoids displayed marked viability loss, reaching up to 92% reduction relative to control, while others displayed high viability, illustrating the broad heterogeneity of GBM responses to radiation. Analysis of molecular correlates revealed no consistent relationship between irradiation response and patient demographic variables, indicating that intrinsic tumor biology, rather than clinical factors, drives sensitivity. Notably, models harboring epidermal growth factor receptor (EGFR) amplification tended to exhibit enhanced susceptibility to irradiation, aligning with prior evidence implicating EGFR signaling in radiation response modulation. Conversely, models demonstrating resistance displayed transcriptional enrichment of mitochondrial integrity and oxidative stress-related pathways, implicating metabolic and redox homeostasis in radiotolerance. These data suggest that oxidative damage repair mechanisms and mitochondrial stress tolerance may serve as critical determinants of radiation resistance in GBM. Overall, this work underscores the importance of physiologically relevant, longitudinal preclinical models in guiding precision radiotherapy approaches for glioblastoma and in identifying novel targets to overcome therapeutic resistance.

#4870 Isolation, characterization and establishment of male breast cancer cells from male breast cancer patient-derived tumor (PDT).

Samikshya Kandel[1], Kathy Robinson[2], Ricardo Cosyleon[2], Daotai Nie[3], Krishna A. Rao[4]

[1]Medical Microbiology, Immunology and Cell Biology, Southern Illinois University School of Medicine, Springfield, IL,[2]SIU School of Medicine, Simmons Cancer Institute/Center for Clinical Research, Springfield, IL,[3]Southern Illinois University School of Medicine, Springfield, IL,[4]Professor, Internal Medicine, Medical Microbiology, Immunology and Cell Biology, Southern Illinois University School of Medicine, Springfield, IL

Breast cancer is one of the most common cancers worldwide, but it is more fatal and rarer among men. There are no male patient derived breast cancer cell lines commercially available, limiting research on breast cancers in the male patients. Consequently, most research and therapeutic approaches are largely based on female research subjects because of limited information on male mammary carcinoma. Thus, development of male breast cancer cell lines would provide an excellent biological and preclinical model to study male specific mammary carcinoma. This study aims to establish novel male breast cancer cell lines using tumors derived from male mammary carcinoma patients. Mammary tumors were obtained from three consented male breast cancer patients undergoing mastectomy at the Simmons Cancer Institute. The breast tumor tissues were minced, enzymatically digested overnight at 370c, strained using sterile strainer, and centrifuged to pellet the cells on the following day. The pellets were suspended in HUMEC Ready Mix media and cultured for several weeks until adherent epithelial cells started to grow. The epithelial cell populations were purified by positive flow sorting using EpCAM antibody (epithelial marker) and considered immortal upon reaching passage 20. Out of three tumor samples, two unique male breast cancer cell lines from two different tumor samples have been successfully cultured and named as male breast cancer cell-1(MBCC-1) and male breast cancer cell-2 (MBCC-2). During the flow sorting, MBCC-1, which is currently in passage-50, was noted to be 70% epithelial (EpCAM positive) while MBCC-2 cells, which are currently at passage-19, were 20% EpCAM positive. The average circularity and diameter of the MBCC-1 ranges between 0.6-0.8uM and 12-19 microns while the average population doubling time is forty-two hours. Further, MBCC-1 is capable of anchorage independent growth by soft agar colony formation assay and shows positive expression for Cytokeratin, CD24, CD44, ALDH1, cKIT, ki-67 but is negative for Collagen-IV and fibroblast activation protein (FAP) protein. Studies are ongoing to further characterize both the male breast cancer cell lines, including biomarkers, gene expression profiling, karyotyping, cell proliferation rate, soft agar colony formation assay, nutrient dependency tests, and tumorigenicity assays. In summary, two novel male breast cancer cell lines have been established for studying the biology of male breast cancers.

#4872 3D bioprinting of fresh NSCLC: The Lung3Dprint proof of concept study.

Aurelie Cadiou[1], Clarisse Thiollier-Schmitt[1], Gabrielle Devret[2], Raphaele Guelminger[3], Tanguy Fenouil[4], Corinne Perrin[5], Camille Leonce[1], Samantha Ballesta[6], Gaetan Pochon[6], Nicolas Alcala[7], Lars Petter Jordheim[1], Charles Dumontet[1], Michael Duruisseaux[1]

[1]Cancer Research Center of Lyon (CRCL), Lyon, France,[2]Service de chirurgie thoracique, Hopital Louis Pradel, Hospices Civils de Lyon, Lyon, France,[3]Hospices Civils de Lyon, Lyon, France,[4]Groupement Hospitalier Est, Institut de Pathologie Multisite - Site Est, Hospices Civils de Lyon, Bron, France,[5]Groupement Hospitalier Est, Tissu-Tumorotheque Est, CRB HCL, Hospices Civils de Lyon, Bron, France,[6]3D-ONCO platform, Cancer Research Center of Lyon (CRCL), Lyon, France,[7]International Agency for Research on Cancer, Lyon, France

3D bioprinted models are emerging to bridge the gap between 2D systems and animal models, advancing the efficiency and accuracy of preclinical workflows. This work aimed to (i) develop an innovative methodology to generate patient-derived bioprinted lung cancer (PDBLC) models that aim to reflect the heterogeneity of the parent tumor, and (ii) evaluate these models as a relevant ex vivo drug screening tool. Fresh Non-Small Cell Lung Cancer (NSCLC) samples were obtained from March to October 2025 at Hospices Civils de Lyon, dissociated and embedded into a fibrinogen-alginate-gelatin bioink (0.5 to 5x10^6 cells/mL of bioink). PDBLC models were obtained by extrusion-based bioprinting using a Cellink BIO X^{TM}, with post-conditioning polymerization using thrombin, transglutaminase, and calcium. PDBLC models were then placed in a dedicated lung cancer cell culture medium and analyzed at different time points, using a non-disruptive method (PrestoBlue^{TM} assay) and disruptive methods (flow cytometry and immunohistochemistry). Flow cytometry markers include EpCAM and CK-7/-8 to identify tumor cells, CD31 for endothelial cells, CD45, CD3, and CD19 for leukocyte infiltrate, and FAP, α-SMA and PDGFR-β for analysis of cancer-associated fibroblasts. Tumor and non-tumor cell contents were quantified as number of cells per object and their percentage of total live cells present. Nine samples have presently been bioprinted and analyzed. PrestoBlue^{TM} assay enabled non-specific monitoring of the model's metabolic activity over time. The median percentage of tumor cells in the bioink was estimated at 40% (range: 11 - 85). The percentage of viable tumor cells on days 7 and 14 were dependent on the initial concentration of cells in the bioink, ranging from 5 to 84%. The absolute number of tumor cells per PDBLC model tended to stabilize with time. The absolute percentage of viable tumor cells tended to increase between day 0 and day 14, with a median fold-change of 1.7-fold (range: -0.76 - 7.2). This was notably due to the decrease in the leukocyte infiltration as well as the endothelial subpopulation. Leukocyte subpopulation remaining 14 days after bioprinting was found to be T lymphocytes (CD45+ CD3+). Exposure of PDBLC models to conventional and targeted therapies used in NSCLC patients is ongoing and results will be presented. 3D bioprinting offers a relatively inexpensive and rapid means to evaluate fresh tumor samples. Our preliminary data show that our model not only supports fresh NSCLC cell survival for up to 22 days, but also maintains the primary tumor's heterogeneity over this period. The use of these 3D models as a drug-screening platform is being evaluated and would be relevant for translational research and clinical practice.

#4873 Reconstructing drug-tolerant persister (DTP) niches in iPSC-derived alveolar lung cancer organoids for spatio-temporal dissection of cell-cell interactions and ligand-receptor targets.

Toshio Suzuki[1], Harry Choi[2], Erik Johansson[2], Tetsuharu Nagamoto[2], Ayako Suzuki[3], Takuji Suzuki[1], Katsuya Tsuchihara[4], Yutaka Suzuki[3], Yuki Yamamoto[2]

[1]Department of Respirology, Chiba University, Chiba, Japan,[2]HiLung Inc., Kyoto, Japan,[3]Department of Computational Biology and Medical Sciences, Graduate School of Frontier Sciences, The University of Tokyo, Kashiwa, Japan,[4]Exploratory Oncology Research and Clinical Trial Center, National Cancer Center, Kashiwa, Japan

Purpose: TKIs and ADCs have transformed NSCLC therapy, yet most patients relapse without detectable resistant mutations due to drug-tolerant persister (DTP) cells. Although immune evasion and CAF-mediated remodeling are well recognized, the contribution of lung-specific epithelial and ECM components to protective niche formation remains unclear. Systems that recapitulate alveolar architecture are needed to reveal targetable mechanisms.
Methods: We developed a three-dimensional system, termed MicroEnvironment-Embedded Tumor in Fibroblast-integrated Organoid Alveolar MicroStructure (MEET-FOAms), by integrating human iPSC-derived alveolar organoids with NSCLC lines harboring *EGFR* exon19 deletion or *ERBB2* exon20 insertion. Organoids were exposed to osimertinib, erlotinib, or trastuzumab-deruxtecan. Longitudinal single-cell RNA-seq and Xenium 5K spatial transcriptomics mapped lineage trajectories, ligand-receptor networks, and ECM remodeling.
Results: Analysis of cancer cell clusters revealed that, even before drug exposure, a distinct subset persisted within the alveolar organoid background. These clusters lacked resistance mutations and were transcriptionally aligned with persister-like states, suggesting that the alveolar niche may inherently sustain DTP populations independently of drug pressure. Following TKI treatment, a stress-adaptive DTP subpopulation remained stable, relying on stromal-epithelial communication and ECM-receptor engagement. Under ADC exposure, an epithelium-associated DTP program was maintained via adhesion networks originating from alveolar epithelial cells, enabling protection from cytotoxic payload delivery. Spatial multi-omics profiling delineated organized multicellular interactions underpinning these responses. Intervention studies showed: (1) ADCs with bystander effect eliminated DTPs along with surrounding niche cells; (2) neutralizing CAF-derived factors suppressed DTP expansion; and (3) blocking ECM-related adhesion pathways disrupted persister maintenance.
Conclusions: With MEET-FOAms, we experimentally reconstructed lung cancer tissue architecture by introducing oncogene-driven NSCLC cells into a human iPSC-derived alveolar background, elucidating that persister-like clusters exist prior to therapy and are sustained by lung-specific niche interactions. Unlike prior models emphasizing CAFs or immune escape alone, this organoid platform highlights the underexplored role of alveolar epithelial cells and ECM in priming and maintaining DTP states. These findings suggest that such persister niches may act as reservoirs from which genetically resistant clones eventually emerge, supporting a paradigm expansion into therapeutic strategies that target multicellular remodeling in drug-tolerant NSCLC.

#4874 Preclinical assessment of HER2 CAR-T cells using tumor and GI organoid models to define therapeutic window.

Julia B. Schueler[1], Ina Rohleff[1], Tania Martianez Canales[2], Kanstantsin Lashuk[1], Youri von Elsswilk[2], Namrata Jayanth[2], Ludovico Buti[2]

[1]Charles River Laboratories, Freiburg, Germany,[2]Charles River Laboratories, Leiden, Netherlands

Anti-HER2 therapies have significantly improved outcomes for metastatic breast cancer patients with HER2+ tumors. Beyond antibody-based approaches such as trastuzumab, HER2-targeted CAR-T cells are emerging as promising options for solid tumors. However, the clinical translation of cancer therapies is often hindered by off-target toxicities, particularly in the gastrointestinal (GI) tract. CAR-T cells, can cause epithelial damage, leading to adverse events such as diarrhea and mucosal inflammation. To address this, we employed 3D iPSC-derived intestinal organoids (HIOs) as a human physiologically relevant model to assess GI toxicity. Using viability assays, cleaved caspase 3 and 7, we evaluated both direct cytotoxic and immune-mediated epithelial injury in HIOs co-cultured with PBMCs. In parallel, we investigated the efficacy of HER2-targeting CAR-T cells versus trastuzumab as positive control in HER2+ and HER2– human cancer cell lines (SK-OV3, JIMT-1, Hs578T) in 2D and 3D in vitro models. Tumor growth and invasion of the CAR-T cells was measured via fluorescence-based live cell imaging. On the last experiment day, a metabolic read-out (CellTiter-Glo, CTG assay) was performed. CAR-T cells demonstrated potent, dose-dependent cytotoxicity against HER2+ spheroids, including trastuzumab-resistant JIMT-1, while sparing HER2– Hs578T cells. Trastuzumab was effective only in SK-OV3. The un-transduced T cells proved to be ineffective. In parallel, the CAR T cells induced epithelial injury in the HIOs indicating possible safety concerns in later drug development stages. Also, in this assay the untransduced T cells from the same donor did not induce any cytotoxicity. In summary, the integration of intestinal organoid-based toxicity screening with tumor efficacy assays enabled a more precise definition of the therapeutic window for HER2 CAR-T cells. This dual-platform approach enhances preclinical evaluation by simultaneously capturing efficacy and GI safety, supporting the development of cell therapies with improved translational potential.

#4875 Modeling GBM-vasculature interaction on chip.

Promise Emeh[1], Alan Fetah[1], Jade Admiraal[1], Marleen Bokkers[1], Kevin Jimenez-Cowell[2], **Will Allen**[1], Nienke Wevers[1], Martine Lamfers[3], Clemens M. Dirven[2], Todd Burton[1], Karla Queiroz[1]

[1]MIMETAS B.V, Oegstgeest, Netherlands,[2]Department of NeuroSurgery, Erasmus MC-University Medical Center Rotterdam, Rotterdam, Netherlands,[3]Erasmus Medical Ctr., Rotterdam, Netherlands

Background: The tumor microenvironment (TME) of glioblastoma (GBM) is highly complex and dynamic, playing a pivotal role in tumor progression and therapeutic resistance. Comprising diverse components including blood vessels, immune cells, and the blood-brain barrier, the heterogeneous TME forms distinct niches that critically shape tumor behavior. Recent TME-based classification has delineated three subtypes TMELow, TMEMed, and TMEHigh distinguished by varying vascular and immune cell compositions.
Methods: This study focuses on elucidating the vascular interactions within the GBM-TME interface. To achieve this, we developed a brain-specific 3D vascular network by integrating primary human brain-derived endothelial and stromal cells within an extracellular matrix (ECM) on a microfluidic platform. Following the establishment of the brain vascular network model, GBM cell lines were incorporated to examine tumor-vasculature interactions in a 3D context. GBM integration was performed via two distinct strategies: co-seeding with vascular-forming cells within the ECM at the start of culture, or grafting tumor cells onto a pre-established vascular bed culture to facilitate invasion assays.
Results: The resulting perfusable model recapitulates key features of the brain vasculature, including the expression of adherens junction markers CD31 and VE-cadherin, tight junction marker Claudin-5, and the strategic alignment of stromal cells along vascular structures. Preliminary results from the integration of GBM in the vascular network model indicate that, irrespective of the seeding method, GBM cells preferentially localize along vascular structures, suggesting an intrinsic tropism toward the vasculature. Notably, co-cultures of GBM with vascular networks exhibited significantly higher proliferative and invasive capacity compared to GBM monocultures, highlighting the pro-tumorigenic influence of the vascular microenvironment.
Conclusion: The brain vascular network model demonstrates physiological relevance, robustness, and scalability making it suitable for medium- to high-throughput applications. This multifaceted platform offers a unique opportunity to functionally model and stratify GBM TME subtypes in vitro, with the potential to uncover novel therapeutic targets within the vascular and immune niches of the tumor ecosystem.

#4876 Cytokine supplementation for improved tumoroid-immune cell co-culture.

Shyanne Salen, **Colin D. Paul**, Sydney Hawkins, Matthew R. Dallas, David Kuninger

Thermo Fisher Scientific, Frederick, MD

Immunotherapies for solid cancers rely on robust engagement between immune and epithelial tumor cells within the tumor microenvironment. However, culture conditions that simultaneously sustain epithelial and tumor-infiltrating immune cell viability during short-term ex vivo culture remain poorly defined. Patient-derived tumoroids, multicellular organoid systems that recapitulate cancer cells in vitro but lack the immune cell component of tumors, enable interrogation of tumor-immune interactions in vitro via addback of immune cells. To explore an alternative approach, namely short-term co-culture of tumor and immune cells, we optimized OncoPro™ Tumoroid Culture Medium to promote immune cell survival and composition stability during culture of patient-derived dissociated tumor cell (DTC) digests. Initial studies showed that healthy donor PBMCs cultured in OncoPro medium alone lost approximately 80% of viable cells after 5 days. A design of experiments (DOE) screen of 13 cytokines and growth factors identified combinations that enhanced PBMC survival while maintaining balanced immune subpopulations. Among these, IL-2, GM-CSF, IL-15, IL-4, and BAFF emerged as candidates that increased PBMC cell counts relative to non-supplemented medium across multiple donors and helped preserve lymphocyte, monocyte, NK, helper T, and cytotoxic T cell proportions within 10% of baseline. Using this list of cytokine cocktails, we next assessed culture conditions supporting both immune ($CD45^+$) and epithelial ($EpCAM^+$) cell populations in colorectal cancer DTCs. Three donors were evaluated in a blocked DOE framework to control for donor variability. We evaluated both embedded culture where cells were encapsulated in Geltrex™ Flex matrix before media overlay, as well as suspension culture where cells were plated in OncoPro medium supplemented with Y-27632, 2% (v/v) Geltrex Flex matrix, and cytokines, and analyzed after 5 days by flow cytometry. Tube-based dissociation yielded ~25% higher recovery than in-plate dissociation, and bead-based enumeration cytometry using CountBright™ absolute counting beads agreed within ~25% of Trypan Blue-based counts made prior to staining samples for flow cytometry. Suspension culture favored immune cell viability, whereas embedding in Geltrex Flex matrix modestly improved tumoroid recovery but reduced $CD45^+$ cell survival. Across donors, cultures supplemented with IL-2, IL-15, GM-CSF, and BAFF achieved the highest total viable cell recovery and the lowest change in immune composition. Together, these results establish a cytokine-optimized medium that enhances immune cell viability and stability during short-term tumoroid co-culture, enabling improved modeling of the microenvironment and facilitating downstream studies of tumor-immune interactions and therapeutic response.

#4877 A high-throughput 3D tumor-immune co-culture platform for evaluating immune checkpoint inhibitors.

Laure-Anne Ligeon, Tabea Gamma, Zuzanna Kotkowska, Charlotte Veser, Irina Agarkova, Sue Grepper, Madhu Nag-LAL

Insphero, Schlieren, Switzerland

The development of immune checkpoint inhibitors (ICIs) requires preclinical models that accurately reflect interactions between human tumor and immune cells. Conventional 2D systems lack architectural and immunological relevance, and animal models often fail to capture human checkpoint regulation. There is therefore a strong need for physiologically relevant and scalable *in vitro* platforms to improve the predictive power of early-stage ICI evaluation.To address this need, we developed a high-throughput 3D tumor-immune co-culture platform to model checkpoint activity and quantify immune-mediated tumor responses. Tumor microtissues were generated in the Akura™384 format and treated to induce inhibitory ligand expression, while human immune cells were stimulated through defined co-stimulatory pathways to induce checkpoint receptor expression. After establishing the co-cultures, we applied reference ICIs or control antibodies and assessed responses using multiple assays. Apoptotic tumor cell death was quantified using Caspase-3/7 Glo®, and tumor integrity was monitored through fluorescence-based viability assays. Immune activation was evaluated using multiplex cytokine and cytolytic mediator profiling. High-content imaging was used to visualize immune-tumor interactions, spheroid structural changes, and immune infiltration depth, supported by automated segmentation workflows. Flow cytometry analysis provided phenotypic information on immune activation and checkpoint receptor modulation. To extend the platform beyond lymphoid checkpoints, we established a myeloid module in which pH-sensitive dye-labeled tumor spheroids were co-cultured with fluorescent macrophages to quantify phagocytic uptake.Checkpoint blockade enhanced immune effector function across these readouts. We observed increased caspase-3/7 activation and reduced viability of tumor spheroids. Cytokine profiling revealed elevated inflammatory and cytolytic mediator release, and imaging demonstrated deep immune penetration into the 3D architecture. Flow cytometry confirmed activation-associated immune phenotypes, while the myeloid module showed increased macrophage-tumor engagement and phagocytosis.In summary, this 3D co-culture platform provides a physiologically relevant, robust, and scalable system for characterizing human tumor-immune interactions and evaluating ICI activity. Its integration of microtissue engineering with multiparametric functional and phenotypic assays offered a translational approach for more predictive preclinical assessment and accelerated development of next-generation ICIs and biosimilars.

#4878 Modeling tumor microenvironment-mediated resistance in NSCLC using a high-throughput spheroid microarray platform.

Alireza Rahnama[1], Maddalena Arrighi[1], Ines Pulido Endrino[2], Takeshi Shimamura[2], Ian Papautsky[2]

[1]Biomedical Engineering, University of Illinois at Chicago, Chicago, IL,[2]University of Illinois at Chicago, Chicago, IL

Therapeutic resistance in EGFR- and KRAS-mutant non-small cell lung cancer (NSCLC) remains a major clinical challenge, often driven by dynamic interactions within the tumor microenvironment (TME). While third-generation EGFR inhibitors have improved outcomes, compensatory stromal signaling can undermine efficacy. Conventional models fail to capture paracrine-mediated resistance mechanisms. To investigate paracrine-mediated resistance mechanisms, a high-throughput spheroid microarray platform was developed to investigate how fibroblast- and endothelial-derived factors influence drug sensitivity across NSCLC genotypes. The platform was used to generate uniform 3D spheroids of NSCLC cell lines (H358, H1975, HCC827) harboring KRAS G12C or EGFR mutations. Agarose microwells were molded within standard 24-well plates using PDMS stamps fabricated by soft lithography. Spheroids were cultured in media conditioned by WI-38 fibroblasts, HUVEC endothelial cells, or both to simulate stromal signaling. Following a 72-hour treatment with osimertinib or adagrasib, spheroid viability was assessed using Calcein AM, Propidium Iodide, and Hoechst staining, followed by fluorescent imaging and quantitative analysis. Drug response was compared across conditions to evaluate TME-mediated resistance, with H1975 spheroids showing approximately 25% higher viability in HUVEC-conditioned media compared to control. Similarly, H358 spheroids exposed to WI-38-conditioned media showed attenuated response to adagrasib, consistent with prior findings. Combined fibroblast and endothelial conditioning further diminished drug efficacy, suggesting additive or synergistic effects. Spheroid viability remained high (>83%) across conditions, and uniformity was maintained (<22% coefficient of variance), supporting the platform's robustness for mechanistic studies. These findings highlight the role of soluble stromal factors in modulating therapeutic response and underscore the potential of this platform. Future integration with patient-derived organoids and multiplexed signaling analyses may uncover actionable targets to overcome resistance and guide combination strategies in EGFR- and KRAS-mutant NSCLC.

#4879 Bladder cancer organoids as a translational models to model disease biology and assess new therapies.

Emilie Decaup[1], Celine Rouget[1], Amandine Prioux-Quartier[1], Claire Beraud[1], Nadege Bidan[1], Xavier Game[2], Philippe Lluel[1]

[1]Urosphere, Toulouse, France,[2]CHU Toulouse, Toulouse, France

Background : Inter-patient heterogeneity in bladder cancer (BC) remains a major driver of treatment failure, highlighting the need for more personalized therapeutic approaches. Org anoids represent valuable preclinical models capturing this diversity. We established a BC organoid biobank comprising 20 models that have been extensively characterized at phenotypic, pharmacological and molecular levels. The aim of this study was to demonstrate the relevance of our biobank in terms of specifications and disease representation. In addition, we illustrated the utility of these models for evaluating targeted therapies, using Enfortumab-vedotin (EV) as a proof of concept.

Methods : Urothelial progenitors were isolated from tumor samples, seeded in Matrigel® and culture medium was added. Molecular characterization was performed by whole exome and transcriptome sequencing. Morphology of organoids was determined by optical microscopy. To evaluate targeted-therapy, organoids were treated with EV (from 0.3 to 10 µg/mL) for 5 days. Cell viability was measured with CellTiter-Glo3D® assay.

Results : All organoid models were developed following a strict quality framework: cultures were expanded beyond passage 6, cryopreserved, and demonstrated a 100% post-thaw recovery rate. The biobank captured the full pathological spectrum, from non-invasive pTa to metastatic pT4 stages. It reflected the anatomical diversity of urothelial carcinoma, with models derived from both bladder and ureteral tumors. Omics analyses revealed the presence of key molecular alterations commonly observed in BC patients, including FGFR3 and TP53 mutations. Organoid morphology, categorized as solid, hollow, or mixed, correlated with tumor stage and metastatic models exhibited features of epithelial-mesenchymal transition. For EV evaluation, we assessed Nectin-4 expression across the biobank and observed heterogeneous expression levels. Interestingly, organoid responses to EV were not strictly correlated with Nectin-4 expression with low response for models with high Nectin-4 expression.

Conclusion : Overall, our BC organoid biobank constitutes a high-quality collection of clinically annotated and comprehensively characterizes models ensuring robustness, stability, and reproducibility across experiments. It faithfully captured the pathological diversity and inter-patient heterogeneity observed in BC. These organoid models represent powerful tools for assessing novel targeted therapies, and the availability of a broad biobank enables the extrapolation of patient-specific responses, paving the way toward personalized medicine.

#4880 An in-vitro vascularized micro-tumor model of cervical cancer.

Daniela Gaebler, Christopher C. W. Hughes, Stephanie J. Hachey

University of California Irvine, Irvine, CA

Cervical cancer is a significant global health burden, ranking as the fourth most common cancer in women worldwide, with approximately 660,000 new cases each year, the majority of which occur in low- and middle-income countries. Despite the availability of preventive screening and HPV vaccination, cervical cancer remains a leading cause of cancer-related deaths, particularly in cases of advanced or recurrent disease. Current standard of care treatment approaches rely on a combination of cisplatin-based chemotherapy and radiotherapy. However, treatment resistance and disease recurrence continue to pose major challenges, underscoring the critical need for improved therapeutic strategies and more predictive preclinical models.
Currently, up to 95% of drugs that show promise in preclinical trials fail to receive FDA approval due to poor efficacy and tumor resistance. These high failure rates can be attributed to unphysiological testing conditions neglecting the tumor microenvironment, as well as poor model systems failing to predict drug-induced pharmacological responses in the human body. To address these shortcomings in cervical cancer research and reliably predict the efficacy of drugs intended for human use, we have invented a novel organ-on-a-chip platform called the vascularized micro-tumor (VMT). The VMT microfluidic device allows for the de novo formation of micro-vessels, which are cocultured with cancer cells and associated stroma. Critically, the micro-vessels enable the physiological delivery of nutrients, drugs and immune cells into the complex 3D tumor microenvironment and hence constitute a powerful tool for physiological disease modeling and drug screening approaches. Here, we present the establishment of a cervical cancer VMT model based on well-characterized, commercially available tumor cell lines and demonstrate treatment responses to standard of care cisplatin-based chemotherapy and radiotherapy.

#4881 Fabrication and characterization of echogenic microbubbles for in vitro modeling of blood-brain barrier (BBB) disruption via focused ultrasound.

Nathan Han[1], Nabhan Fakrudin[2], Frederic Zenhausern[2], Jian Gu[2]

[1]Duke University, Durham, NC,[2]University of Arizona, Phoenix, AZ

The blood-brain barrier (BBB) presents a major obstacle to the delivery of many promising pharmacological agents to the central nervous system. The BBB is composed of tightly connected endothelial cells that regulate molecular exchange to maintain brain homeostasis. While this is beneficial for protecting the brain, over 98% of small-molecule and almost 100% of large-molecule drugs are blocked by the BBB, limiting treatment options for neurological diseases. Recently, bubble-assisted focused ultrasound (BaFUS) has emerged as a non-invasive strategy to transiently disrupt the BBB and facilitate targeted drug delivery by injected gas bubbles in the bloodstream. We previously developed a custom ultrasound-transparent organ-on-chip (UST-OoC) platform for modeling BaFUS-mediated BBB disruption *in vitro*. In this study, we report on the optimization and characterization of a microbubble formulation for use in BaFUS. Microbubbles were synthesized using a phospholipid-based protocol and characterized by dynamic light scattering (DLS) and zeta potential measurements. The formulation produced ~1 µm microbubbles with a neutral zeta potential and a concentration of 2.4×10^{10} bubbles/mL. Acoustic testing showed strong, sustained bubble cavitation across flow rates of 150-300 µL/min. An acoustic dose-response sweep revealed non-linear stable cavitation and inertial cavitation thresholds to be 0.08 and 0.32 MPa. These lab-fabricated microbubbles have the advantages of low cost and easy adjustment of size and concentration. The UST-OoC platform enables human-based *in vitro* modeling for real-time visualization of barrier disruption, quantitative permeability assessment, and systematic optimization of acoustic parameters, including pressure, frequency, and duty cycle under controlled flow conditions. This integrated system provides a scalable, reproducible preclinical tool for evaluating microbubble performance and BaFUS protocols prior to *in vivo* translation. By establishing human-based BBB models, standardized methods for microbubble fabrication, acoustic characterization, and barrier disruption modeling, this platform addresses key translational gaps in developing BaFUS-enhanced drug delivery for brain disorders.

: Microbiome-Tumor-Immune Crosstalk
Poster Session

#4885 Association of an ectopic upper gastrointestinal microbiome with multiple primary lung cancers: A multi-site cross-sectional study.

Guotian Pei[1], Yaqiong Guo[2], Na Lyu[3], Yuqing Huang[1]

[1]Department of Thoracic Surgery, Beijing Haidian Hospital (Haidian Section of Peking University Third Hospital), Beijing, China,[2]Institute of Biotechnology and Health, Beijing Academy of Science and Technology, Beijing, China,[3]CAS Key Laboratory of Pathogenic Microbiology and Immunology, Chinese Academy of Sciences, Beijing, China

Background: The etiology of multiple primary lung cancers (MPLC), defined by their independent multifocal origins, remains largely unknown, particularly the contribution of the microbiome. Gastroesophageal reflux disease (GERD) is an established risk factor for lung cancer, but its specific association with MPLC and the potential for GERD-mediated translocation of upper gastrointestinal (UGI) microbiota into pulmonary nodules (PNs) has not been investigated. We hypothesized that GERD facilitates UGI-to-lung microbial translocation, contributing to a pro-carcinogenic microenvironment in MPLC.
Materials and Methods: In this prospective case-control study (NCT06973499), GERD symptom burden was assessed in 149 MPLC, 41 solitary primary lung cancer (SPLC), and 119 healthy controls using the validated GERD-Q questionnaire. For a subset of 21 MPLC patients, we performed comprehensive multi-site microbiome profiling using PacBio full-length 16S rRNA gene sequencing on samples from seven anatomical compartments, including the UGI tract and multiple resected PNs. Rigorous contamination controls were employed. Microbial source tracking (SourceTracker2) was used to quantify UGI bacterial translocation, with strain-level identity confirmed via phylogenetic analysis.
Results: MPLC patients exhibited a significantly higher prevalence of high-risk GERD symptoms (GERD-Q score >8) compared to healthy controls (26.2% vs. 16.0%; OR = 1.87, 95% CI 1.01-3.44, P=0.048); this association was not observed in SPLC patients (P=0.87). Crucially, microbial source tracking identified a significant, ectopic UGI-derived bacterial signature in 22.9% of PNs (8 of 35 nodules) from MPLC patients. Linking the symptom to the microbe, a post-hoc analysis revealed a strong trend where MPLC patients with a high GERD burden showed a greater proportional contribution of UGI microbiota to their PNs compared to those with a low GERD burden (P = 0.0692). Finally, high-resolution phylogenetic analysis confirmed shared, identical strains of *Prevotella melaninogenica* and *Gemella haemolysans* across UGI and pulmonary sites within the same individuals, providing definitive evidence of active translocation.
Conclusion: This study provides the first direct, multi-site evidence linking GERD symptom burden to the active translocation of UGI microbiota into pulmonary nodules in MPLC patients. We introduce the 'GERD-microbial translocation-multifocal carcinogenesis' axis as a novel pathogenic pathway that may contribute to the etiology and heterogeneity of MPLC. Our findings identify the UGI-lung axis as a potential target for novel diagnostic and therapeutic strategies, suggesting that managing GERD or targeting the translocated pathobiome could represent a new paradigm for MPLC prevention or interception.

#4886 Integrative analysis reveals bacterial load as a determinant of molecular and immune phenotypes in colorectal cancer.

Subha Singh[1], Travis D. Kerr[1], Melissa Lumish[2], Ying Ni[1], Natalie Silver[1], Daniel McGrail[1]

[1]Cancer Sciences, Cleveland Clinic Research, Cleveland, OH,[2]Department of Hematology and Oncology, University Hospitals Seidman Cancer Center, Cleveland, OH

Colorectal cancer (CRC) ranks as the third most frequently diagnosed cancer and the second leading cause of cancer deaths globally. The incidence and mortality rates vary widely across regions, being highest in developed countries but it is increasing rapidly in low- and middle-income nations due to aging population, urbanization and adoption of Western lifestyles. Phenotypically, CRC can broadly be divided into tumors with microsatellite instability (MSI) and those that are microsatellite stable (MSS). MSI tumors typically arise in the right colon and are driven by hypermutation from loss of function in DNA mismatch repair (MMR) genes, such as *MLH1* or *MSH2*. We recently found that the overall bacterial load in a tumor, rather than relative abundance of any specific taxa, is the primary driver of microbial-based immunosuppression in head and neck squamous cell carcinoma. However, how bacterial load is associated with clinicopathological features and molecular phenotypes of CRC remains unknown. To address this, we performed a comprehensive analysis of bacterial load in CRC tumors. We found that bacterial load was independently enriched in both MSI tumors and tumors with lymphatic invasion. After controlling for MSI status, tumors with high bacteria were more likely to be *TP53* and *APC* wildtype and exhibited elevated inflammatory signaling at both the gene and protein level. Further analysis of systems-level metabolic rewiring indicated elevated levels of glycoprotein metabolism in high bacterial tumors, which have previously been associated with bacteria adhesion to tumor cells. Together, these findings offer the first landscape of how the bacterial load is associated with clinicopathological and molecular alterations, which may have implications for patient prognosis and treatment strategies.

#4887 Mapping the cellular landscape of intratumoral bacteria in colorectal cancer using single-cell transcriptomics.

Ian Wesley Folkert[1], Abderrahman Day[2], Ashish Damania[2], Matthew C. Wong[2], Taylor Neilson[3], Ryan Morgan[3], Scott Kopetz[4], Joshua Smith[5], Jennifer A. Wargo[4], Nadim J. Ajami[2], John P. Shen[6], Michael Geoffrey White[4]

[1]Department of Surgery, Penn Medicine, Philadelphia, PA,[2]Department of Genomic Medicine, The University of Texas MD Anderson Cancer Center, Houston, TX,[3]Department of Surgical Oncology, The University of Texas MD Anderson Cancer Center, Houston, TX,[4]UT MD Anderson Cancer Center, Houston, TX,[5]Department of Colon & Rectal Surgery, The University of Texas MD Anderson Cancer Center, Houston, TX,[6]Department of Gastrointestinal Medical Oncology, The University of Texas MD Anderson Cancer Center, Houston, TX

Tumor-associated microbes are increasingly investigated across cancer types. In CRC, intratumoral microbes are associated with detrimental treatment responses and clinical outcomes. However, critical gaps remain in understanding how individual cells within the TME respond to microbial presence. Defining these cellular responses could provide mechanistic insights into microbe-host interactions in cancer and reveal novel therapeutic targets.

To map the cellular landscape of intratumoral bacteria in CRC, we developed a custom analytical pipeline integrating single-cell transcriptomics with metagenomic profiling. We performed scRNA-seq on 150 samples from 146 CRC patients across 85 primary tumors, 60 liver metastases, and 5 peritoneal metastases. Unsupervised clustering was performed using Seurat 5.1.0, with cells annotated using PanglaoDB and canonical markers. Single-cell reads were aggregated and mapped against NCBI and SILVA databases.

Starting with $1.09x10^9$ reads from 650,485 cells, we applied stringent quality filters including trimming, human genome filtering (removing 98.7% of reads), and a custom k-mer diversity filter to exclude likely contaminants. This final filter eliminated 96% of remaining reads and 92% of initially identified taxonomies, addressing the challenge of ambient contamination in scRNA-seq data. Our pipeline ultimately retained 18,115 high-confidence bacterial reads (<0.001% of total) from 4,888 cells (0.8%), representing 1,237 unique taxa. After contaminant exclusion, we identified 89 species across 48 genera, including Bacteroides fragilis, Parvimonas micra, Gemella morbillorum, and Fusobacterium nucleatum. Bacterial reads were mapped to cells using barcodes. Clustering identified 16 cell populations with bacterial signals across all major cell types and tumor sites. In this exploratory single-cell analysis, cells from primary colon tumors exhibited increased bacterial diversity compared to cells from liver metastases ($p<0.01$). Within primary colon tumors, cells from MSI-H tumors (n=15) demonstrated significantly higher bacterial reads than cells from MSS tumors (n=67, 95% CI [2.425, 12.691], $p = 0.006$). Furthermore, the presence of bacteria-positive cells in primary colon tumors was associated with significantly worse patient survival compared to tumors without detectable intracellular bacteria (HR 4.90, 95% CI [1.08, 22.2], $p = 0.039$).

Our findings demonstrate that bacterial reads, although present at extremely low abundance, can be retrieved from scRNA-seq data when stringent contamination controls are applied. The taxonomic resolution achieved provides proof-of-concept for investigating microbe-host interactions at single-cell resolution. This study establishes a methodological foundation for leveraging single-cell technologies to probe the complex interplay between tumors and their microbiome.

#4888 Association of intratumoral *Fusobacterium nucleatum* with stromal remodeling and immune exclusion in esophageal squamous cell carcinoma.

Takashi Ofuchi[1], Qingjiang Hu[2], Kosuke Kanemitsu[1], Koshi Mimori[2], Masaaki Iwatsuki[1]

[1]Kumamoto University Hospital, Kumamoto, Japan,[2]Kyushu University Beppu Hospital, Beppu, Japan

Background: *Fusobacterium nucleatum* (*F. nucleatum*), an oral anaerobe, has been linked to tumor progression and immune suppression in esophageal squamous cell carcinoma (ESCC). However, its relationship with stromal remodeling and immune exclusion within the tumor microenvironment (TME) remains unclear.

Methods: We performed integrated analyses combining metagenomic profiling, transcriptomic deconvolution, and histopathologic validation in 93 TCGA-ESCC cases and 126 resected tumors. *F. nucleatum* status was determined using Centrifuge and quantitative PCR. Immune and stromal cell fractions were estimated by CIBERSORT and EPIC. Immunohistochemistry (IHC) for α-smooth muscle actin (α-SMA) and NF-κB p65 (RelA) assessed cancer-associated fibroblast (CAF) activation and inflammatory signaling, and fluorescence in situ hybridization (FISH) visualized *F. nucleatum* within tumors. Clinicopathologic variables, including ECOG performance status, were compared between *F. nucleatum*-positive and -negative cases.

Results: Twenty-three of 93 TCGA-ESCC tumors (25%) were *F. nucleatum*-positive (≥0.02% relative abundance). Gene set enrichment analysis revealed activation of TNFα/NF-κB and epithelial-mesenchymal transition pathways in *F. nucleatum*-positive tumors. CIBERSORT showed reduced $CD8^+$ T-cell infiltration, while EPIC demonstrated a higher CAF fraction (0.72 vs. 0.45, $P < 0.01$). In the validation cohort, IHC confirmed increased α-SMA expression in *F. nucleatum*-positive tumors, consistent with transcriptomic results. FISH identified *F. nucleatum* signals within tumor cells adjacent to α-SMA-positive fibroblasts, suggesting spatial proximity between infection and stromal activation. Nuclear RelA localization was significantly more frequent in *F. nucleatum*-positive tumors, indicating NF-κB activation. Cases with both strong α-SMA expression and nuclear RelA were markedly enriched in the *F. nucleatum*-positive group ($P < 0.01$). These findings support a model in which *F. nucleatum* activates NF-κB-mediated cytokine signaling that promotes fibroblast recruitment and stromal expansion, contributing to immune exclusion. Clinically, *F. nucleatum* positivity was associated with poorer performance status despite similar tumor stages, suggesting colonization may reflect systemic vulnerability or impaired oral hygiene.

Conclusions: Intratumoral *F. nucleatum* is associated with an NF-κB-activated, fibroblast-rich, and $CD8^+$ T-cell-poor TME in ESCC. By promoting stromal remodeling and immune exclusion, *F. nucleatum* may enhance tumor aggressiveness. These findings highlight the interplay between microbial colonization, stromal activation, and host condition, offering insight into potential microbiome-stroma-immune interactions in ESCC.

#4889 Distinct tumor microbiome profiles in triple negative breast cancer compared to other breast cancer subtypes: A pilot study.

Yangbo Sun, Chi-Yang Chiu, Jay H. Fowke, Karen Johnson

University of Tennessee Health Science Center, Memphis, TN

Background: Emerging evidence suggests that the tumor microbiome may influence breast cancer biology and therapeutic responses. However, few studies have characterized microbial differences across breast cancer subtypes, particularly triple-negative breast cancer (TNBC), which tends to have poor prognosis and limited targeted therapies, compared with other subtypes. We conducted a pilot study to compare the microbiome in TNBC versus other subtypes.

Methods: DNA was extracted from 25 formalin-fixed paraffin-embedded (FFPE) tumor tissues, including 4 TNBC cases and 21 non-TNBC cases. 16S rRNA gene sequencing was performed to characterize bacterial composition. Relative abundance was analyzed at multiple taxonomic levels. Differential abundance between TNBC and other subtypes was evaluated using linear regression.

Results: Distinct microbial signatures were observed between TNBC and other subtypes. At the phylum level, TNBC tissues were enriched in *Fusobacteriota* compared with non-TNBC tissues (*p* value=0.03). At the family level, TNBC tissues showed higher relative abundance of *Dermacoccaceae*, *Fusobacteriaceae*, and *Rikenellaceae*, and lower abundance of *Oscillospiraceae (p* values<0.05*)*. At the genus level, TNBC tumors were enriched in *Dermacoccus*, *Rothia*, and *Alistipes*, while *UCG-002* was reduced compared to other subtypes (*p* values <0.05).

Conclusions: This pilot study reveals distinct microbial composition in TNBC tissues compared with other breast cancer subtypes, characterized by enrichment of *Fusobacteriota* and specific genera such as *Dermacoccus* and *Rothia*. These findings suggest potential microbiome-mediated mechanisms contributing to TNBC biology and warrant validation in larger, well-annotated cohorts.

#4890 Patients with high body mass index share tumor microbial profiles with CpG island methylator phenotype-high or early-onset colorectal cancers.

KuoHsing Chen[1], Jyh-Shiuan Hsu[2], Yu-Li Su[3], Shih-Chiang Lin[4], Been-Ren Lin[5], Kai-Lung Tsai[6], Li-Ming Tseng[7], Yi-Hsin Liang[8], Jia-Huei Tsai[9], Chien-Chen Tsai[10], Ting-Ting Liu[11], Mong-Hsun Tsai[12], Kun-Huei Yeh[13]

[1]Medical Oncology, National Taiwan University Cancer Center (NTUCC), Taipei City, Taiwan,[2]Institute of Biotechnology, National Taiwan University, Taipei, Taiwan., Taipei City, Taiwan,[3]Division of Hematology Oncology, Department of Internal Medicine, Kaohsiung Chang Gung Memorial Hospital, Kaohsiung, Taiwan,[4]Oncology and Hematology, Far Eastern Memorial Hospital, New Taipei City, Taiwan,[5]Surgery, National Taiwan University Cancer Center, Taipei, Taiwan,[6]Division of Colon & Rectal Surgery, Kaohsiung Chang Gung Memorial Hospital,, Kaohsiung, Taiwan,[7]Division of Colorectal Surgery, Far Eastern Memorial Hospital, New Taipei City, Taiwan,[8]National Taiwan University College of Medicine, Taipei, Taiwan,[9]Department of Pathology, National Taiwan University Hospital, Taipei, Taiwan,[10]Department of Anatomical pathology, Far Eastern Memorial Hospital, New Taipei City, Taiwan,[11]Department of Anatomic Pathology, Kaohsiung Chang Gung Memorial Hospital, Kaohsiung, Taiwan,[12]Institute of Biotechnology, National Taiwan University, Taipei, Taiwan,[13]Dept. of Oncology, National Taiwan University Hospital, Taipei, Taiwan

BackgroundTumor microbiota plays a significant role in colorectal cancer (CRC) by influencing tumor development and progression. Our previous study demonstrated a significant association between high body mass index (high BMI, BMI ≥ 27.5 kg/m^2) and CpG island methylator phenotype-high (CIMP-high) in early-onset CRC (EOCRC, age < 50y). The present study investigates whether tumor microbiota may mediate this association in CRC.

Materials and methods We enrolled 140 patients with CRC and 30 patients with polyps from the biobank of National Taiwan University Hospital, respectively. The tumor and adjacent normal part in each tumor or polyp were collected. V3-V4 regions of bacterial 16S ribosomal RNA gene were amplified and then amplicons were sequenced on the MiSeq system. Patients' clinicopathological characteristics were also recorded. CIMP status was defined by using a 5-gene panel (*p16, MINT1, MINT2, MINT31 and MLH1*) and MethyLight assay. Analysis of diversity and LefSe (Linear discriminant analysis Effect Size) of tumor microbiota were performed and the results were compared between each subgroup.

ResultsIn total, 121 CRC tumors (CRC-T), 115 adjacent normal (CRC-N) and 26 polyps (polyp-T and polyp-N) passed the quality control (sequencing depth > 5000 reads). Microbiota α diversity is significantly lower in CRC compared to that in polyps (p = 1.3 x 10^{-11}). Microbiota α diversity is also reduced in CRC patients with high BMI compared to those with low BMI (p = 0.042). LefSe analyses revealed specific microbiota enriched in each subgroup, including EOCRC, high BMI, and CIMP-high. The Venn diagram revealed multiple overlapping bacteria taxa between the high BMI and the CIMP-high or EOCRC subgroups.

ConclusionWe found the diversity of microbiota in CRC with high BMI is significantly lower than that in CRC with low BMI and identified specific bacteria taxa shared between high BMI and CIMP-high or EOCRC tumors. The clinical applications of these bacterial taxa warrant further exploration.

#4891 Paired metagenomic profiling reveals site-specific microbial composition and conserved diversity in the oral cavity of head and neck cancer patients.

Jada Tschetter[1], Rachel Elsey[2], McKenna Perrin[2], David Starks[2], Benjamin Solomon[2], William Spanos[2], Sarah Viet[3], Cody Silvernail[3], Jason L. Petersen[3], Erik A. Ehli[3], Tobias Meissner[2], Casey T. Finnicum[3]

[1]Sanford School of Medecine, University of South Dakota, Vermillion, SD,[2]Avera Cancer Institute, Sioux Falls, SD,[3]Genetics, Avera McKennan, Sioux Falls, SD

Background: The extent to which microbial diversity and composition vary across oral subsites within an individual remains poorly defined, limiting the reproducibility of microbiome-based biomarkers and the standardization of sampling strategies. We investigated compositional and diversity differences between paired tonsil and saliva samples to characterize microbial ecology across oral compartments in HNC patients.

Methods: Paired tonsil and saliva samples were collected from 25 patients diagnosed with head and neck squamous cell carcinoma (NCT05142033) (median age = 63 years [IQR 53-73]; 76% male, 96% White). The cohort included 68% oral cavity, 20% oropharyngeal, 8% laryngeal, and 4% cutaneous primaries. Shotgun metagenomic sequencing was performed on all samples. Beta diversity was assessed using paired permutational multivariate analysis of variance (PERMANOVA) on Bray-Curtis dissimilarity matrices with restricted permutations to account for individual variation. Species-level differential abundance was tested using paired Wilcoxon signed-rank tests with false discovery rate (FDR) correction. Additionally, alpha diversity metrics were compared between sites.

Results: Microbial composition differed significantly between tonsil and saliva samples (PERMANOVA: $F=1.00$, $R^2=2.0\%$, $p=0.001$). Twenty species showed significant abundance differences after FDR correction ($q<0.05$). Fifteen species were increased in saliva versus tonsils, including *Rothia aeria* (FDR=0.004), *Actinomyces naeslundii* (FDR=0.008), and *Streptococcus sanguinis* (FDR=0.009). Five species decreased in saliva, including *Prevotella scopos*, *Prevotella jejuni*, and *Campylobacter concisus*. Despite compositional differences, alpha diversity metrics were equivalent between sites (Shannon index: tonsil 3.73±0.59 vs saliva 3.71±0.70, $p=0.565$; observed species: 3135±1567 vs 3251±1228, $p=0.708$). Individual-level differences in evenness significantly correlated with compositional dissimilarity (Spearman rho=0.450, $p=0.024$), indicating that diversity and composition co-vary within individuals.

Conclusions: Tonsil and saliva harbor distinct microbial communities yet maintain equivalent species diversity levels. This pattern demonstrates niche conservatism in the oral cavity. The paired study design was essential for detecting these differences, as massive individual variation dominated over site-specific effects. These findings have implications for understanding oral microbiome ecology in head and neck cancer and suggest that sampling site selection is critical for microbiome-based biomarker discovery.

#4892 Janus villus chip identifies an anaerobic probiotic that suppresses tumor growth in mice.

Saeyeon Shin[1], **Jaeyoung SHIN**[2], Gwan Myeong Seo[3], Hyungji Jo[4], Sejong Oh[1], Sungsu Park[3]

[1]Animal Science, Chonnam National University, Gwangju, Korea, Republic of,[2]OrganoPlus, Suwon, Korea, Republic of,[3]Mechanical Engineering, Sungkyunkwan University, Suwon, Korea, Republic of,[4]Metabiohealth, Sungkyunkwan University, Suwon, Korea, Republic of

Chronic intestinal inflammation disrupts epithelial integrity and reshapes the tumor immune microenvironment (TIME), accelerating colorectal cancer progression. We investigated how the strict anaerobic mucin-binding probiotic *Bifidobacterium adolescentis* OP820 modulates inflammation-driven epithelial and immune dysfunction using a Janus oxygen-gradient villus chip and in vivo models. Because *Bifidobacterium* requires strict anaerobic conditions for viability and physiological activity, the villus chip—engineered with an anaerobic apex and oxygenated base to reproduce the native villus oxygen gradient—was essential for accurately modeling OP820-epithelium interactions. Under these conditions, epithelial cells upregulated *MUC13* and *MUC17*, generating a mucin-rich glycocalyx to which OP820 adhered strongly, reflecting its natural niche preference. Transcriptomic profiling revealed that OP820 modulates inflammatory signaling by elevating CCL8, TGFA, and MMP12—genes linked to epithelial repair and immunoregulatory remodeling—while suppressing TSLP, FLT3LG, and IL18, which are typically associated with heightened inflammatory stress. These coordinated shifts indicate that OP820 promotes a resolution-oriented immune state rather than amplifying inflammation. The effects were consistent across monolayer, spheroid, and villus-chip models, underscoring the robustness of OP820's immunomodulatory activity under strict anaerobic conditions that reflect its physiological habitat. In vivo, OP820 demonstrated dual therapeutic activity. In the DSS-induced colitis model, it attenuated mucosal injury and preserved epithelial structure, supporting its inflammation-resolving function. In the colorectal cancer xenograft model, intravenous OP820 administration significantly reduced tumor burden, and OP820 cells were detected within the tumor microenvironment, suggesting that intratumoral localization may underlie its immune-modulating and tumor-suppressive activity. The presence of a strict anaerobe within tumors implies the existence of permissive micro-niches and points to direct modulation of local cytokine or stromal networks. Collectively, these findings identify OP820 as a microbiome-derived therapeutic capable of reinforcing epithelial barrier recovery and reprogramming inflammation-driven tumor microenvironments. By integrating villus-chip modeling with in vivo validation, this study highlights OP820's potential as a mechanism-based intervention for inflammation-associated colorectal cancer.

#4893 Profiling the ovarian cancer-specific intratumoral microbiome.

Ryosuke Sonobe, Miho Suzuki, Keiko Shinjo, Yutaka Kondo

Division of Cancer Biology, Graduate School of Medicine, Nagoya University, Nagoya, Japan

Interactions between tumors and their associated microbiota have recently emerged as a novel dimension of cancer biology. These microbes can influence tumor initiation, immune evasion, and therapeutic response. Although several cancers, such as colorectal and esophageal cancer, harbor distinct microbial communities that shape their tumor microenvironment, the presence and functional relevance of intratumoral bacteria in ovarian cancer, the most lethal gynecologic malignancy, remain largely unexplored. Using pan-bacterial 16S rRNA fluorescence in situ hybridization (FISH), we detected bacterial signals in approximately 60% of ovarian cancer specimens, whereas benign ovarian tissues were nearly negative. The signals were predominantly localized (>80%) within the tumor stroma. To further characterize the bacterial composition, 16S rRNA sequencing identified a unique intratumoral microbiota dominated by *Phyllobacterium, Rhodococcus* and *Fusobacterium*. To assess the biological impact of these bacteria, we established an in vivo mouse model by introducing the ovarian cancer-resident bacteria via intraperitoneal injection, followed by transplantation of mouse ovarian cancer cells. Tumor growth was approximately 3-fold higher in bacteria-exposed mice than in controls. These findings demonstrate that bacterial exposure can enhance tumor progression, potentially through remodeling of the tumor microenvironment. Collectively, our results reveal that ovarian cancer harbors a distinct, stromal-localized intratumoral microbiota that contributes to tumor progression. We propose that bacterial colonization of the tumor stroma may act as a chronic inflammatory niche, promoting fibroblast activation, angiogenesis, and immune modulation.

#4894 *Pseudomonas*-derived LPS promotes metastatic behavior in papillary thyroid cancer metastasis is attenuated by Hashimoto's thyroiditis.

Yue Che, Wei Kou, Haoran Feng, Qiwu Zhao, Zhuoran Liu, Jie Kuang, Weihua Qiu

Department of General Surgery, Ruijin Hospital, Shanghai Jiao Tong University School of Medicine, Shanghai, China

Background: Intratumoral microbiota can influence cancer progression through immune and metabolic interactions. Papillary thyroid cancer (PTC) frequently coexists with Hashimoto's thyroiditis (HT), an autoimmune condition that remodels the tumor immune microenvironment. However, how microbe-derived molecules contribute to PTC metastasis, and how autoimmune cytokines modulate these effects, remains poorly understood.

Methods: Tumor and matched adjacent tissues from 75 PTC patients were analyzed using 16S rRNA sequencing, and microbial functional pathways were inferred with PICRUSt2. The pro-metastatic activity of *Pseudomonas*-derived lipopolysaccharide (LPS) was evaluated using wound-healing and Transwell assays, with polymyxin B to confirm LPS specificity. NF-κB activation and EMT markers were analyzed by Western blotting. To model the autoimmune cytokine milieu of HT, PTC cells were treated with recombinant IFN-γ. For *in vivo* validation, LPS-stimulated PTC cells were injected intravenously into NCG mice to establish a spontaneous lung metastasis model.

Results: Patients with lymph node metastasis (LNM) exhibited increased *Pseudomonas* abundance and enhanced predicted LPS biosynthetic activity. In contrast, HT^+ tumors showed reduced *Pseudomonas* levels and diminished LPS pathway activity compared with HT^- tumors. After adjusting for age and TNM stage, *Pseudomonas* abundance remained positively associated with LNM within the HT subgroup. Propensity score-matched mediation analysis further indicated that HT conferred a protective effect against LNM, whereas the pro-metastatic effect of *Pseudomonas* partially counteracted this protection. *In vitro*, *Pseudomonas*-derived LPS promoted PTC cell migration and invasion in a dose- and time-dependent manner through TLR4-NF-κB activation, accompanied by increased phosphorylated NF-κB and N-cadherin; these effects were substantially diminished by polymyxin B. Under an HT-like cytokine environment, IFN-γ markedly attenuated both LPS-induced NF-κB activation and invasive behavior. *In vivo*, mice receiving LPS-pretreated PTC cells developed significantly more pulmonary metastatic foci.

Conclusions: *Pseudomonas* functions as a potential pro-metastatic bacterium in PTC with its LPS promoting PTC cell invasiveness through TLR4-NF-κB-EMT pathway. HT is associated with reduced *Pseudomonas* abundance, weakening this pro-metastatic signaling and contributing to the lower LNM risk observed in HT patients. These findings highlight the importance of microbial-immune interactions in PTC metastasis and suggest potential therapeutic targets for PTC prevention and treatment.

#4895 *Helicobacter pylori*-driven T cell stress in tumors as a mediator of resistance to immune checkpoint blockade in gastric cancer.

Donghyeok Seol[1], Jieun Lee[1], Junwoo Jo[2], Chanmi Bang[1], Hyeon Jeong Oh[1], Sejoon Lee[1], Mira Yoo[1], Duyeong Hwang[1], So Hyun Kang[1], Young Suk Park[1], Sang-Hoon Ahn[1], Masami Yamamoto[3], Tetsuya Tsukamoto[4], Sachiyo Nomura[5], Qi Su[6], Seong-Ho Kong[7], Do Joong Park[7], Hyuk-Joon Lee[7], Hyung-Ho Kim[1], Charles Lee[8], Han-Kwang Yang[7], Sunjae Lee[9], Yun-Suhk Suh[1]

[1]Seoul National University Bundang Hospital, Seongnam, Korea, Republic of,[2]Gwangju Institute of Science and Technology, Gwangju, Korea, Republic of,[3]Nippon Veterinary and Life Science University, Tokyo, Japan,[4]Fujita Health University, Toyoake, Aichi, Japan,[5]Hoshi University, Tokyo, Japan,[6]The Chinese University of Hong Kong, Hong Kong SAR, China,[7]Seoul National University College of Medicine, Seoul, Korea, Republic of,[8]The Jackson Laboratory for Genomic Medicine, Farmington, CT,[9]Korea Advanced Institute of Science and Technology (KAIST), Daejeon, Korea, Republic of

The influence of microbiota residing within tumors on patient response to immunotherapies for gastric cancer (GC) is not yet fully understood. We aim to define the characteristics and functional role of tumor-resident microbiota in the context of immune checkpoint inhibitor (ICI) efficacy in GC. A comprehensive multi-omics analysis was performed on samples from 137 GC patients, all of whom were treatment-naïve regarding chemo- or antibiotics. This extensive dataset included both metagenomes and host transcriptomes, with single-cell RNA sequencing data. To achieve accurate quantification, we developed a novel tumor-resident microbial index (TM index) that compared taxon-level load between tumor tissue and matched normal tissue. Treatment responses were subsequently validated using syngeneic mouse models with a cancer-bacteria co-culture platform. Abundance analyses consistently highlighted *Helicobacter pylori* as the only species significantly decreased in tumor tissue compared to paired normal tissue. Metagenome-assembled genomes showed patient-specific *H. pylori* strains, maintaining over 99% genomic identity across the paired samples. The TM_{HP} index indicated that high levels of *H. pylori* were predominantly found in the genomically stable (GS) subtype, characterized by a partially preserved normal physiology. Single-cell RNA sequencing data showed that *H. pylori*-infected cells exhibit a signature of elevated T cell stress, correlating with the overexpression of *HSPA1A*. Critically, *H. pylori* significantly compromised the therapeutic effectiveness of anti-PD-L1 by reducing the infiltration of T cells in mouse models. However, a negative effect was not observed with standard 5-fluorouracil or oxaliplatin treatments. Our findings implicate *H. pylori* as a mediator of immunotherapy resistance and a therapeutically actionable target for overcoming ICI resistance in GC.

#4896 *Sphingomonas*-driven sphingosine signalling enhances neoadjuvant therapy responses in digestive system cancers.

Bin Wang, Xiuchao Wang, Jihui Hao

Tianjin Medical Univ. Cancer Inst. & Hospital, Tianjin, China

Neoadjuvant therapy (NAT) is becoming an essential component in the management of digestive system malignancies, yet whether the microbiome modulates NAT efficacy remains unclear. Here, we profile the intratumoral microbiome of patients with digestive system cancers following NAT and identify *Sphingomonas* as markedly enriched in pancreatic ductal adenocarcinoma (PDAC) tumors from responders. *Sphingomonas* was likewise detected in gastric and colorectal cancers with favourable NAT responses. Using mouse models, we show that *Sphingomonas* stably colonizes pancreatic, gastric, and colorectal tumors and augments NAT efficacy through secretion of sphingosine. Mechanistically, *Sphingomonas*-derived sphingosine binds lipid raft structures on the plasma membrane and is preferentially internalized by immune cells, where it selectively activates the ceramide-sphingomyelin synthetic pathway rather than the Sphingosine-1-Phosphate (S1P) pathway. This process amplifies lipid raft organization, promotes immune synapse formation, and enhances immune-mediated tumor cell killing. We further develop a lipid-raft-targeted sphingosine delivery system that boosts immune activation and sensitizes tumors to NAT. Together, these findings uncover a previously unrecognized microbial determinant of NAT responsiveness in digestive system cancers and provide a conceptual and translational framework for microbiome-based patient stratification and therapeutic sensitization.

#4897 Characterization of the intratumoral microbiota in non endemic EBV associated nasopharyngeal carcinoma.

Deborah Lenoci[1], Federico Rossignoli[1], Armando Giuseppe Licata[1], Marta Lucchetta[1], Ilenia Rolli[1], Marica Ficorilli[1], Antonello Manocchio[2], Noemi Crippa[2], Walter Ferrari Bravo[2], Federica Manoni[2], Monica Zucchini[3], Francesca Taverna[3], Stefano Cavalieri[2], Lisa Licitra[2], Loris De Cecco[1], Salvatore Alfieri[2]

[1]Integrated Biology of Rare Tumors, Department of Experimental Oncology, Fondazione IRCCS Istituto Nazionale dei Tumori, Milan, Italy,[2]Head and Neck Medical Oncology Department, Fondazione IRCCS Istituto Nazionale dei Tumori, Milan, Italy,[3]Department of Immunohematology and Transfusion Medicine Service, Fondazione IRCCS Istituto Nazionale dei Tumori, Milan, Italy

Epstein-Barr virus (EBV) related nasopharyngeal carcinoma (NPC) is an epithelial malignancy arising from the nasopharyngeal mucosal lining. A high incidence of EBV related NPC is recorded in endemic areas (EA), East and Southeast Asia. Microbiota resides the upper respiratory tract including nasopharynx. Thus, intratumoral microbiota (ITM) in EA EBV related NPC has been characterized with Corynebacterium and Staphylococcus being the most predominant taxa. Currently, ITM profile in NPC remain unexplored in non endemic area (NEA). We hypothesized that the ITM in NEA NPC is associated to tumor biology. In our previously NEA EBV related NPC study, we stratified patients into three transcriptional clusters (Cl1: immune active; Cl2: defense response; Cl3: proliferative), with Cl3 displaying the poorest prognosis. Hence, the present work investigates the ITM composition according to our clusters' model. Formalin-fixed paraffin embedded (FFPE) samples from 94 NEA NPC EBV related cases were collected. Total RNA was extracted using miRneasy kit (Qiagen) and libraries were generated using QuantSeq 3' mRNA (Lexogen) and sequenced on the NextSeq500 (Illumina). The ITM composition and immune cell deconvolution (xCell) were inferred from RNAseq data. Differential abundance analyses (LEfSe) among clusters and correlation analyses between immune cells populations and differentially abundant taxa were conducted. To validate the RNAseq findings and assess spatial colocalization patterns, spatial and metatranscriptomics (SMT) (Stereoseq OMNI for FFPE, STOmics) was performed on one representative case per cluster. 297 bacterial taxa were detected in our NEA cohort. LEfSe comparisons showed that Bacteroidota and Pseudomonadota were enriched in Cl1 vs Cl2, while Bacillaceae dominated in Cl2. Actinomycetota was more prevalent in Cl1 vs Cl3. Correlation analyses showed that most differentially abundant taxa, found in clusters' comparison, were positively associated with fibroblast and stroma score and inversely correlated with CD8+ and CD4+ T cell populations. SMT profiling confirmed intratumoral bacteria expression: Cl1 and Cl2 exhibited higher bacterial proportion in respect to EBV (the latter expressed in 14.6% and 23.6%, respectively), while Cl3 displayed both bacterial and EBV signals, with a predominant EBV expression (52.5%). SMT analyses is ongoing to disclose co expression patterns between immune cells, intratumoral bacteria and EBV. This study provides the first characterization of the ITM in NEA EBV related NPC. Higher EBV expression was detected in Cl3, the subgroup associated with the poorest prognosis, suggesting a possible synergistic interplay between EBV and specific bacterial taxa in the NPC pathogenesis. These findings highlight the impact of the microbiome on the tumor microenvironment and support its potential as biomarker in NEA EBV related NPC.

#4898 Gut virus shapes distal tumor immunity: fecal phage transfer from long-term pancreatic cancer survivors delays tumor progression.

Xiaoqing Wang, Jiakun Wang, Hongji Dai, Bin Wang

Tianjin Medical University Cancer Institute and Hospital, Tianjin, China

Gut bacteria and fungi have been implicated in promoting tumor progression in patients with pancreatic ductal adenocarcinoma (PDAC). However, the role of the gut virus in PDAC pathogenesis remains poorly defined. Here, we systematically compared the fecal virus of long-term survivors (LTS) and short-term survivors (STS) of PDAC, and identified striking compositional differences between the two groups. Through fecal virus transplantation into murine orthotopic PDAC models, we demonstrated that the LTS-derived virus significantly delayed tumor progression. Mechanistically, LTS samples were characterized by a reduced abundance of Akkermansia muciniphila-targeting phages (Akkermannviridae), leading to significantly increased intestinal *Akkermansia* following transplantation compared to STS. *Akkermansia*-derived metabolite 2-PMPA exerted tumor-suppressive effects by promoting migration of intestinal group 3 innate lymphoid cells (ILC3s) into the tumor, where they modulated IL-17 signaling and enhanced $CD8^+$ T cell infiltration, thereby orchestrating an anti-tumor immune response. Our study provides the first causal evidence that the gut virus can regulate the progression of pancreatic cancers through a bacteriophage-microbiota-metabolite-innate/adaptive immunity axis, offering new insights into microbiome-targeted interventions and immunotherapeutic strategies for distal tumors.

#4899 A dysbiotic polymicrobial signature characterized by oral pathogens links the oral-gastric axis to gastric carcinogenesis in a high-risk Chilean cohort.

Javier Figueroa[1], Marcelo Garrido[2], Arnoldo Riquelme[3], Matias Munoz Medel[4], Franz Villaroel-Espindola[2], Fernan Gomez-Valenzuela[2], **Ignacio Retamal**[2]

[1]Universidad Adofo Ibanez, Santiago, Chile,[2]Universidad Mayor, Santiago, Chile,[3]Pontificia Universidad Catolica de Chile, Santiago, Chile,[4]Celerity Clinical Research, Santiago, Chile

Objectives:Gastric cancer (GC) remains a formidable global health challenge, particularly in high-risk regions like Chile. The traditional etiological model centered on *Helicobacter pylori* is insufficient to explain the full spectrum of disease. This study aimed to identify a robust, polymicrobial signature in GC tissue and test the hypothesis that the Oral-Gastric Axis drives the carcinogenic process via chronic colonization by translocated oral pathogens.
Methods: We employed high-throughput 16S rRNA amplicon sequencing to profile the gastric microbiome in tissue samples from a Chilean cohort (15 GC patients [CAN], 15 healthy controls [NOC]). Microbial composition, alpha diversity (richness, evenness), and differential abundance were assessed using non-parametric tests (Mann-Whitney U) and statistically validated through supervised machine learning approaches, including Random Forest and penalized regression models (Lasso/Ridge), to ensure robust biomarker selection.
ResultsThe GC microbiome showed a profound dysbiotic shift, characterized by a significant increase in species richness (Observed ASVs, ACE, Chao1; $p<0.001$) but marked ecological unevenness. A core four-genus signature consistently differentiated CAN from NOC tissue: *Fusobacterium* (MWU $p=0.024$), *Lactobacillus* (MWU $p=0.038$), *Neisseria* (MWU $p=0.005$), and *Prevotella* (MWU $p=0.023$). The oral pathogens *Neisseria* (Random Forest Rank 1) and Fusobacterium (enriched in CAN) were identified as the top predictive features. Mechanistic insights suggest Fusobacterium contributes to immune evasion by promoting the recruitment of PD-L1-expressing tumor-associated neutrophils, linking this signature directly to immunotherapy targets.
Conclusions: Gastric cancer is associated with a distinct, pathologically unstable polymicrobial signature dominated by known oral pathogens. This robust signature provides compelling quantitative evidence supporting the Oral-Gastric Axis Hypothesis. The identified microbial community offers promising candidates for novel non-invasive diagnostic biomarkers and suggests new therapeutic strategies, such as targeted depletion of pro-tumorigenic oral microbes to sensitize tumors to immune checkpoint blockade therapy in gastric cancer.

#4900 Microbiome derived lactate promotes immunosuppression and radiation resistance.

Christy Charles, David Lo, Jennifer L. Anderson, Ratna Veeramachaneni, Francisco Saenz, Anastasios Maniakas, MIchael T. Spiotto, Andrew G. Sikora, Lauren Elizabeth Colbert

UT MD Anderson Cancer Center, Houston, TX

The cervical microbiome plays a pivotal role in shaping vaginal health and influencing tumor prognosis. Tumor associated microbes secrete bioactive metabolites that modulate both tumor behavior and its surrounding microenvironment. Our lab previously identified a species of L-Lactate producing *Lactobacillus* (LAB), *Lactobacillus iners* (*L. iners*), to be associated with poor chemoradiation response. In vitro experiments revealed that conditioned media from *L. iners* enhances radiation resistance in cervical cancer cells—a phenomenon replicated by direct lactate supplementation. This study aims to characterize the impact of microbiome-derived lactate on the tumor microenvironment.

Hypothesis: We propose that L-lactate produced by cancer-derived LAB supports tumor progression by fostering an immunosuppressive niche.

Methods: LAB strains were isolated via targeted culture from cervical, vaginal, vulvar, and oral cavity cancers. These isolates were used in co-culture systems and to generate cell-free bacterial conditioned media (CFS) to assess their capacity to interact with cancer cells and promote tumor-supportive conditions. For initial studies, we focused on cervical cancer isolates. To evaluate LAB-derived lactate's role in radiation resistance, we performed cell viability assays (CyQUANT) on HeLa, SiHa, and CaSki cervical cancer lines exposed to CFS from patient-derived LAB and radiation. Lactate production was quantified using the Diazyme D-/L-Lactate rapid test kit, enabling precise source attribution between bacterial and tumor origins. We developed a syngeneic lactate exposure model using mEER (mouse oral line) xenografts in C57BL/6 mice, administering weekly intratumoral lactate injections. The tumors were radiated after the tumors reached ~75mm^3. To evaluate the immune landscape, multiplex immunofluorescence using the Lunaphore COMET microfluidic platform was performed on mEER tumors.

Results: Cervical cancer cells exhibited increased radiation resistance when co-cultured with L-lactate-producing LAB, the isoform preferentially metabolized by human cells. LAB emerged as the dominant source of lactate in co-culture, confirming its role in driving lactate accumulation within the tumor microenvironment. In vivo, lactate-treated tumors grew significantly larger post-radiation (mean volume 48 mm³ vs. 74 mm³, $p < 0.0001$). Immune profiling revealed elevated T-cell infiltration, with a skew toward regulatory T cells and reduced CD8$^+$ populations. The lactate-rich microenvironment showed marked upregulation of immune checkpoint proteins CTLA4 and PD-L1, suggesting functional exhaustion of infiltrating immune cells.

#4901 Biodiversity and biogeography of the multi-kingdom cancer microbiome.

Anders B. Dohlman[1], Robin Mjelle[2], Henry M. Wood[3], Alaina Shumate[1], Iris T.-h. Lee[1], Gianmarco Piccinno[4], Phil Quirke[3], Curtis Huttenhower[5], Nicola Segata[6], Matthew L. Meyerson[1]

[1]Dana-Farber Cancer Institute, Boston, MA,[2]Norwegian University of Science and Technology, Trondheim, Norway,[3]Leeds Institute of Molecular Medicine, Leeds, United Kingdom,[4]University of Trento, Trento, Italy,[5]Harvard T.H. Chan School of Public Health, Boston, MA,[6]Computational Metagenomics Lab, University of Trento, Trento, Italy

There is growing evidence that microorganisms represent an important component of the tumor microenvironment. However, conflicting reports regarding the cancer microbiome have left the extent of microbial presence across cancer types unclear, highlighting the need for more robust methods for identifying tumor-associated microorganisms. Leveraging the completed human reference genome, we built a host-subtraction and microbial classification pipeline to accurately identify tumor-associated microorganisms in whole-genome sequencing data, which we validated and benchmarked on *in silico* and *in vitro* mixtures of human and microbial DNA. We used this pipeline to perform the largest pan-cancer microbiome analysis to date, spanning 16,369 high-depth tumor whole genomes from the UK 100,000 Genomes Project. After decontamination, microbial signatures were indistinguishable from background in most cancer types. However, in oral, esophageal, gastric, and colorectal cancers, we detected multi-kingdom polymicrobial communities, including bacteria, fungi, viruses, and archaea. In some oral and colorectal cancers, we also detected the parasite *Trichomonas vaginalis*. These microbial communities varied by tumor site and subtype, with increased microbial colonization of microsatellite-instable and POLE/POLD1-mutated tumors. This pattern was driven by a correlation between microbial load and tumor mutation burden across cancer types that was independent of genomic subtype. Additionally, we observed an over tenfold depletion of *Akkermansia muciniphila* in early-onset colorectal cancer. Together, our analysis helps resolve the microbial landscape of cancer and provides a new tumor microbiome atlas for future studies.

#4902 Gut bacteria as hidden architects of stemness maintenance in the progression of pancreatic cancer.

Kirtana Arikath, Seoung Ryoung Choi, Annant Bir Kaur, Nivedeta Krishna Kumar, Venkatesh Varadharaj, Zahraa Wajih Alsafwani, Neelanjana Gayen, Poompozhil Mathivanan, Wyatt Petersen, Prabagaran Narayanasamy, Surinder K. Batra, Moorthy P. Ponnusamy

University of Nebraska Medical Center, Omaha, NE

Background: Pancreatic ductal adenocarcinoma (PDAC) is one of the deadliest cancers, defined by an aggressive tumor microenvironment (TME) and a small pool of cancer stem cells (CSCs) that fuel recurrence and therapy resistance. Evidence suggests that bacteria migrating from the gut to the pancreas reshape the TME to sustain these CSCs. Although microbial imbalance is linked to other cancers, its role in PDAC stemness remains unclear. This study investigates how gut-derived microbes and their metabolites reprogram the tumor niche to enrich CSCs and accelerate PDAC progression.

Methodology: Clinical profiling of PDAC patient samples was performed to identify diverse microbial species that contribute to dysbiosis. We performed tissue validation using 16S rRNA FISH (fluorescent *In-situ* hybridization) and lipopolysaccharide (LPS) staining to localize these bacteria in human and murine PDAC tissues. To define microbial effects, we exposed PDAC and normal pancreatic cell lines to bacterial supernatants, live bacteria, or purified LPS, followed by functional validation through tumor sphere, serial dilution, and colony assays with CSC markers assessed by immunofluorescence, western blotting, and qPCR. We next applied Omics Integration using LC-MS of bacterial supernatants and RNA sequencing of Antibiotics (Abx) treated mice to identify microbial metabolites and signaling pathways linked to CSC enrichment. In our *In-Vivo* studies using $Kras^{LSL\text{-}G12D/+}$;Pdx1-Cre (KC), $Kras^{LSL\text{-}G12D/+}$;$Trp53^{R172H/+}$;Pdx1-Cre (KPC), and C57BL/6J (C57) mice treated with Abx, we evaluated how microbiome depletion reshapes CSC dynamics and PDAC progression.

Results: Clinical Profiling of 62 resected PDAC samples showed that the basal-like subtype is enriched with *Pseudomonas aeruginosa, Acinetobacter baumannii*, and *Sphingopyxis macrogoltabida*, linking microbial dysbiosis to tumor aggressiveness. *In-situ* hybridization and LPS staining revealed stage-dependent bacterial accumulation in human PDAC and in KC and KPC tumors. LPS or bacterial supernatants elevated CSC and proliferation markers including SOX2, SOX9, NANOG, Cyclin A, and p-ERK, while normal pancreatic cells remained unchanged. Co-culture with *P.aeruginosa* and *S.macrogoltabida* produced the strongest stemness induction with LPS-CD44 co-localization. Functional assays and KPC organoids confirmed enhanced self-renewal and growth, most pronounced with *S.macrogoltabida* supernatant. Abx treatment in xenograft tumors altered tumor growth, and KC and KPC mice showed reduced PanIN lesions with decreased CD44 and Ki67 expression, consistent with loss of CSC maintenance.

Conclusion:A dysbiotic microbiome within the PDAC microenvironment sustains CSC-driven aggressiveness through metabolite-mediated signaling. Targeting this microbiome-stemness axis may offer a therapeutic approach to limit PDAC progression and improve patient outcomes.

#4903 Explore the effects of *Fusobacterium nucleatum* on chemotherapy response in colorectal cancer at spatial and single-cell resolution.

Yuting Shan[1], Lilin Wang[1], Matthew Jeon[1], R. Stephanie Huang[2]

[1]University of Minnesota, College of Pharmacy, Minneapolis, MN,[2]Asst. Professor, Dept. of Medicine, University of Minnesota, Minneapolis, MN

Introduction: Emerging evidence implicates intratumoral microbiota such as Fusobacterium nucleatum (Fn) in modulating therapeutic response and clinical outcomes in colorectal cancer (CRC). Here, we leveraged tumor transcriptomic data to predict the efficacy of hundreds of chemotherapies at single-cell resolution in the presence or absence of Fn, aiming to identify drugs with differential efficacy under each condition.

Methods: Two CRC cell lines (HT29 and HCT116) were co-cultured with or without Fn and sequenced using the 10x Genomics platform. In parallel, a CRC patient tumor was profiled using 10x Genomics Visium spatial transcriptomics. Raw sequencing data from both the cell lines and the patient sample were obtained from published sources and aligned to references to generate single-cell RNA and Fn count matrices. Drug sensitivity for each cell was predicted using scIDUC, a previously validated single-cell level transcriptome-based drug response prediction model. This enables prediction of >350 drugs for their likelihood of response in each cell derived from either cell line or patient sample. We then compared the predicted drug sensitivity between Fn-positive and Fn-negative cells for each drug. Differential expression and gene set enrichment analyses were conducted to identify Fn-associated molecular pathways.

Results: After quality control, 11,624 cells from the CRC cell lines and 3,105 spatial spots from the patient sample were retained, each with >20,000 genes quantified. Among standard-of-care agents used to treat CRC, oxaliplatin was consistently predicted to have reduced efficacy in Fn-positive cells ($P < 2.2 \times 10^{-16}$ for HT29 and HCT116; $P < 0.01$ for the CRC sample). In contrast, 5-fluorouracil was predicted to be less effective in Fn-positive cells in the patient sample but more effective in cell lines. Notably, dasatinib, a BCR-ABL inhibitor, was consistently predicted to exhibit enhanced efficacy in Fn-positive cells. Transcriptomic analyses revealed upregulation of tumor growth and drug-resistance genes, including JUN, DDIT4, and BIRC3, in Fn-enriched CRC cells.

Discussion: This study provides one of the first spatial and single-cell perspectives on how intratumoral microbiota shape chemotherapy response in CRC. Our findings suggest that F. nucleatum status may serve as a predictive biomarker for chemotherapy efficacy and a potential guide for drug repurposing and treatment stratification in colorectal cancer.

#4904 Reprogramming of the non-pathogenic *E. coli* surface architecture to create next-generation immune engagers for potent cancer therapies.

Shaobo Yang[1], Anna Clara Bader[1], Stephanie Sendker[1], Ashley Hu[1], Alice Chen[1], Daniel Chen[1], Hetal Nath[1], Eden Bobilev[1], Michal Sheffer[1], Veronica W. Hui[1], Tereza Kochs[1], Andreia Maia[1], Fuguo Liu[1], Xingyu Deng[1], Maily Nguyen[1], Mila Stanojevic[1], Mubin Tarannum[2], Alaa Ali[1], Roman Shapiro[1], Young Rock Chung[1], Erin M. Parry[1], Julissa G. Tello[1], Stephanie K. Dougan[3], Marco Campisi[1], David A. Barbie[1], John Koreth[3], Robert J. Soiffer[1], Catherine J. Wu[4], Jerome Ritz[5], Rizwan Romee[3]

[1]Medical Oncology, Dana-Farber Cancer Institute, Boston, MA,[2]DFCI/Harvard Medical School, Boston, MA,[3]Dana-Farber Cancer Institute, Boston, MA,[4]Dana-Farber Cancer Institute, Brookline, MA,[5]Professor of Medicine, Dana-Farber Cancer Institute, Boston, MA

Background: Multi-specific immune engagers show therapeutic promise but are limited by systemic toxicities (e.g., cytokine release syndrome, CRS), short half-lives, and poor infiltration into the immunosuppressive tumor microenvironment (TME). Tumor-homing bacteria offer a targeted delivery strategy capable of overcoming restricted infiltration and TME-mediated suppression. Building on our *E. coli* K-12 surface display platform for localized cytokine delivery (Yang et al., *Nat Biotechnol*, 2024), we developed *Live Immune Modulating Engagers* (LIME), engineered *E. coli* co-displaying scFvs against tumor-associated antigens and effector-cell receptors (T or NK). We hypothesize that dual-display LIME enhances anti-tumor immunity by enabling localized effector-cell activation and precise tumor-immune cell bridging.

Methods: *E. coli* was engineered to display scFvs targeting TAAs (CD19, Mesothelin, DLL3, etc.) and immune receptors (CD3, NKG2D, etc.) using optimized outer-membrane scaffolds, confirmed by flow cytometry. In vitro co-cultures with primary human T or NK cells assessed binding, activation (CD25/CD69), and cytotoxicity (7-AAD/Annexin V). In syngeneic A20 and KPC tumor models, mice received intravenous LIME ± anti-PD-1 (i.p.) or RMC-7977 (oral). In DLL3$^+$ H69 xenografts, NSG mice were infused with human CD3$^+$ T cells followed by LIME, benchmarked against the FDA-approved engager Tarlatamab. Tumor growth was monitored and analyzed by flow cytometry, multiplex ELISA, and CFU quantification.

Results: In vitro, LIME activated T or NK cells and enhanced killing across a broad panel of tumor cell lines, including Small cell lung cancer, Glioblastoma, Pancreatic ductal adenocarcinoma, etc. In vivo, CD19 LIME cured ~34% of A20-bearing mice and achieved ~80% cures when combined with anti-PD-1, generating durable immune memory. Mesothelin LIME significantly inhibited KPC tumor progression, with extended survival upon RMC-7977 co-treatment. DLL3 LIME provided superior tumor control compared with Tarlatamab in H69 xenografts. Mechanistically, LIME reprogrammed the TME by activating T and NK cells, driving macrophage repolarization toward an M1 state, and enhancing DC activation in draining lymph nodes. Bacteria remained enriched in tumors, and no evidence of CRS was observed in plasma.

Conclusions: LIME represents a versatile platform that enables localized, immune engagement, overcomes major barriers in solid tumors, and outperforms existing immune engagers while maintaining a favorable safety profile.

#4905 Microbiome-wide association study identifies crosstalk between tumor-associated microbes and the human tumor microenvironment.

Nathan O. Siemers, Naouel El Asri, Corinne Danan, Karen L. Abbott

Theralytica, Inc., Mountain View, CA

Summary: Using recently refined measures of microbiome abundance in TCGA samples, we use quantitative models, in combination with human RNA-seq and RNA signatures, to identify microbial strains associated with functional modulation of the tumor microenvironment (TME), with implications for prognosis and therapy.

Methods: Determining the influence of intra- and peri-tumoral microbes on cancer outcomes is an active area of investigation. Progress has been limited in part by technical challenges to accurate quantitation of microbial species across large clinical cohorts, such as The Cancer Genome Atlas (TCGA). Recent advances in this area have produced refined tumor microbiome estimates across thousands of TCGA samples (Ge et al. 2025). We exploited the refined microbiome information to perform associative modeling between strain abundances and TME signals in human TCGA RNA-seq and -signature data. We reasoned that identifying direct associations between microbe abundances and tumor transcription might add support to a given microbe's importance. Linear models were constructed based on these data and selected technical and clinical covariates across 25 distinct human tumor types. Human RNA abundances and RNA signatures were selected based on potential to identify mechanistic and regulatory elements associated with microbial presence, as well as to infer differences in abundance of human TME cell types.

Results: We observed associations between microbe abundances and human transcription, confirming previously reported findings and identifying novel associations. In some cases, these associations were both specific to limited microbial strains and tumor type. For example, the relationships between an alpha-interferon-based RNA signature and microbial strains in serous ovarian carcinoma revealed only a small number of microbes in association, most of which were specific to ovarian cancer.

Conclusion: By exploiting advances in microbiome quantitation, a large clinical cancer cohort, and an associative study framework, we identified a subset of microbial species in association with human tumor transcriptional profiles. Although limited by the associative nature of the study, these species are candidates for future efforts that evaluate their mechanistic roles in the TME. The analysis adds to the body of evidence from preclinical models and early clinical observations that microbial elements in patient tumors can modulate tumor and TME function, influencing prognosis and response to therapy.

#4907 Obligate anaerobes in the gut drive pancreatic cancer metastasis.

Adriana Zingone[1], Senthil K. Muthuswamy[2], **Norihiro Yamaguchi**[1]

[1]National Cancer Institute, Bethesda, MD,[2]National Cancer Institute Center for Cancer Research, Bethesda, MD

Introduction: Tumoral microbiota is a strong predictor of gastrointestinal cancer outcome. However, our efforts to identify bacterial molecular drivers of cancer progression are hindered by 1) the lack of an efficient anaerobic bacterial culturing system and 2) the fact that >90% of the human gut microbiota are anaerobes. This predicament limits our capability to conduct mechanistic studies in tumor microbiota research. To fill this gap, we sought to establish a novel experimental system to propagate metastasis-associated tumoral microbiota by leveraging a curated, culturable human gut microbiota library. **Methods:** We established a gnotobiotic system by sequentially administering the curated human gut microbiota library via oral gavage in germ-free C57BL/6 mice. Subsequently, the mice underwent intrapancreatic injections of syngeneic KPC pancreatic cancer cells. Liver metastatic foci, primary pancreatic cancer, and the duodenum with their associated bacteria were subject to 16s sequencing and direct culture-based propagation. **Results:** To validate the feasibility of our experimental platform in identifying bacterial species despite the expected low biomass, we conducted proof-of-concept experiments by intrapancreatically injecting KPC cancer cell lines in wild-type C57BL/6 mice. Liver metastatic foci, primary pancreas tumors, and the duodenum were subject to 16S sequencing and direct culture. A Bray-Curtis dissimilarity matrix-based PCoA plot revealed apparent dissimilarity between tumor-bearing mouse samples and corresponding mock-surgery non-tumor-bearing samples, in a sample-site-agnostic manner, suggesting a systemic impact of the tumor-bearing state. Clostridium species were particularly enriched in primary pancreatic tumors and liver metastatic samples, suggesting biological pressure in hypoxic tumors and the hypoxic liver microenvironment that favors obligate anaerobes. Co-injections of KPC cancer cells and Clostridium species promoted liver metastasis more than 10-fold. Moreover, Clostridium-conditioned media also enhanced liver metastasis, suggesting a critical role for bacteria-derived soluble factors in regulating metastasis. **Conclusion:** The observed symbiosis between metastasizing pancreatic cancer cells and obligate anaerobes warrants further searches of similar co-opted bacteria-cancer interactions in other cancers. Our discovery of pro-metastatic bacteria-derived soluble factors paves the way for developing bacteria-derived, yet live microorganism-free, scalable therapeutics by blocking their interactions with host cells. In summary, we identified novel bacteria-derived soluble factors that strongly drive cancer metastasis.

#4908 Functional interrogation of pancreatic cancer resident microbes reveals their role in host modulation.

Vidhi Chandra[1], Le Li[1], Seyda Baydogan[1], Fuduan Peng[1], Thais Bartelli[1], Haoyue Liu[1], Fernando Jimenez-Arancon[1], David Romanin[1], Javier A. Gomez[1], Steven Maron[2], Erick M. Riquelme[3], Mark Hurd[1], Anirban Maitra[1], Luis A. Diaz[2], Ismet Sahin[4], Adriana Paulucci-Holthauzen[1], Jared K. Burks[1], Huamin Wang[1], Jay Kolls[5], James R. White[6], Linghua Wang[1], Michael P. Kim[1], Florencia McAllister[1]

[1]UT MD Anderson Cancer Center, Houston, TX,[2]Memorial Sloan Kettering Cancer Center, New York, NY,[3]Pontificia Universidad Catolica de Chile, Santiago, Chile,[4]Texas Southern University, Houston, TX,[5]Tulane University, New Orleans, LA,[6]Resphera Biosciences, Baltimore, MD

Tumor resident microbes are a well-recognized component of the tumor microenvironment. Microbial subcellular location across tumors along with their functionality remains to be determined. Bulk microbial profiling techniques lack subcellular and spatial resolution and ultimately cannot distinguish between microbial signals or live microbial presence. To address these limitations, we performed orthogonal methods for functional microbial-host characterization. We first developed advanced quantitative fluorescent imaging methodologies that allows visualization of microbial cellular compartmentalization across three different tumor types (total n=30). Using this methodology, we performed spatial microbial transcriptomics at the regional and single cell levels to determine microbial distribution and to interrogate microbial regulation of tumor cell signaling in human pancreatic tumors (n=55). To confirm presence of viable microbes, we performed multiplexed culturomics of patient tumors and normal adjacent tissue specimens (n=80), followed by Whole Genomic Sequencing (WGS) analysis. We tested the effect of the isolated clinical strains on tumor cell signaling pathways with *in vitro* co-culture assays, and upon genetic fluorescent labelling we defined their role on *in vivo* tumor growth in murine models. These experiments confirmed their role in promoting tumors, driving resistance to therapeutics and modulation of host signaling mechanisms. Overall, our results identified several pathways under microbial regulation within cancer cells that can drive immune evasion through impaired antigen presentation. In summary, using multiple complimentary novel methodologies we characterize the microbial niche of tumors (MiNT) that uncover microbial regulation of host cell signaling and patient outcomes. Microbial modulatory approaches may be needed to reverse resistance to therapies in pancreatic cancer.

#4909 Microbial stimuli differentially regulate astrocyte and glioblastoma cell phenotypes.

Ariana N. De Jesus-Carrasquillo[1], Claudia M. Ramos-Lugo[1], Aliaha Serpa-Figueroa[1], Alondra Soto-Nieves[2], Alexander Y. Morla-Sevilla[2], Yaraliz Corchado-Vargas[1], Joseph M. Torres-Cruz[3], Yisel M. Cantres-Rosario[4]

[1]University of Puerto Rico - Comprehensive Cancer Center, San Juan, PR,[2]University of Puerto Rico - Rio Piedras Campus, San Juan, PR,[3]University of Puerto Rico - Medical Sciences Campus, San Juan, PR,[4]Microbiology and Medical Zoology, University of Puerto Rico - Medical Sciences Campus, San Juan, PR

Glioblastoma multiforme (GBM), an astrocytoma, is the most prevalent and aggressive primary brain tumor. These tumors present with an intricate molecular profile and resistance to treatment, thus resulting in poor prognosis. Astrocytes, the most abundant cells in the brain, maintain the blood-brain barrier (BBB) and support metabolic homeostasis. Studies have shown that, when exposed to inflammation, they can acquire a reactive phenotype, possibly contributing brain carcinogenesis. However, the mechanisms behind their role in tumor development remain unclear, highlighting the need to further understand the phenotype of astrocytes in GBM. Lipopolysaccharides (LPS) from periodontal disease-causing pathogen *Porphyromonas gingivalis* (Pg) are known endotoxins capable of crossing the BBB, inducing strong inflammatory responses. Thus, understanding the role of common microbial products in the brain microenvironment, and their influence on GBM pathogenesis is key. To assess this response, astrocytes and U87-GBM cells were cultured and exposed directly to Pg-LPS, *Staphylococcus aureus* lipoteichoic acids (Sa-LTA) and *Escherichia coli* lipopolysaccharides (Ec-LPS). Indirect treatments were also performed using astrocyte-conditioned media (ACM) primed with Pg-LPS, Sa-LTA and Ec-LPC. After 24- and 48-hour exposures, cytokine and protein expression were measured by ELLA assays and immunofluorescence (IF) respectively. Viability was assessed via MTT Assay. At 24 hours, exposure to Pg-LPS significantly increased astrocyte metabolic activity when compared to other treatments ($p = 0.042$), though this effect was not observed at 48 hours. IF staining of proliferation marker Ki67 in astrocytes revealed a significant increase when treated with Pg-LPS ($p = 0.033$) for 24H. In contrast, Pg-LPS-primed ACM for 48H, decreased proliferation in GBM cells compared to untreated ($p = 0.007$), directly treated U87-GBM cells with Pg-LPS ($p = 0.003$), and not-primed astrocyte-conditioned media ($p = 0.024$). GBM cells expressed consistently higher levels of Ki67 than all astrocyte treatments and viability remained unchanged across treatments. Moreover, Pg-LPS-primed ACM presented detectable levels of IL-10, IFN-a2, IL-4 and TGF-beta. Our results suggest that Pg-LPS promotes a shift toward an anti-inflammatory phenotype and may reduce proliferation in GBM cells. Further studies are needed to elucidate how Pg-LPS-conditioned astrocytes modulate GBM progression.

: Novel Experimental Platforms and Causal Inference
Poster Session

#4913 Single-cell intercellular CRISPR screen reveals stromal regulators of colorectal cancer plasticity.

Corinne Molyneux, Rhianna O'Sullivan, Alistair Wilkinson, Nick Li, Shauna Crampsie, Petra Vlckova, Aurelie Dobric, Chris Tape

Cancer Institute, University College London, London, United Kingdom

Colorectal cancer (CRC) displays high levels of non-genetic phenotypic plasticity, enabling cancer cells to dynamically shift between distinct functional states, resulting in therapy evasion and disease progression. This plasticity is driven by both intrinsic transcriptional programmes within epithelial cancer cells and extrinsic cues from the tumour microenvironment.
To explore the molecular mechanisms underlying this process, we performed single-cell transcriptomic profiling of ten CRC patient-derived organoid (PDO) models co-cultured with or without cancer-associated fibroblasts (CAFs). Across all CRC PDOs, we observed varying admixtures of proliferative colonic stem cells (proCSC) and slow-cycling, onco-foetal, revival colonic stem cells (revCSC). In response to stromal cues some PDOs underwent pronounced transcriptional reprogramming towards the chemoresistant revCSC state. However, this CAF-induced epithelial plasticity was highly patient-specific with some PDOs maintaining an intrinsic stem cell equilibrium. We identified the transcriptional regulator DACH1 as a defining marker of CRC cells with high stromal responsiveness and this factor was consistently downregulated upon CAF interaction.
To functionally identify the stromal signals mediating this stem cell reprogramming, we developed an arrayed CRISPR screening platform to systematically perturb the CAF secretome during direct PDO-CAF co-culture. Perturbed co-cultures were assessed via multiplexed mass cytometry to capture the PDO response to the genetically-edited CAF population at single cell resolution. This approach revealed the key regulators of proCSC-to-revCSC transdetermination with prostaglandin E2 (PGE_2) emerging as the primary effector of stromal-induced CRC plasticity changes.
These findings demonstrate that CRC phenotypic plasticity is regulated by cell-intrinsic transcriptional states and stromal-derived signals, provide new mechanistic insight into therapy failure and describe a potential therapeutic intervention strategy to overcome plasticity driven chemoresistance.

#4914 Defining the immunoregulatory molecular drivers of dendritic cells using CRISPR screens in ex-vivo modelsvivo models.

Mukta Asnani, Jiekun Yang

Rutgers University - New Brunswick, New Brunswick, NJ

Conventional dendritic cell type 1 (cDC1) plays a central and indispensable role in coordinating antitumor T-cell responses by producing cytokines such as IL-12 and expressing key regulatory molecules including PD-L1. Despite their importance in shaping antitumor immunity and influencing responses to modern immunotherapies, the molecular mechanisms controlling cDC1 activation and maturation remain poorly defined. This gap in knowledge is compounded by the extremely low abundance of cDC1 within the tumor microenvironment (TME), which limits the ability to experimentally interrogate their biology and apply genetic perturbation tools at scale. To address these challenges, we developed, optimized, and compared robust ex vivo differentiation systems capable of generating physiologically relevant cDC1-like cells from both murine and human hematopoietic stem cells (HSCs).Using a carefully designed two-stage culture platform incorporating Fms-like tyrosine kinase 3 ligand (Flt3L), DLL1-mediated Notch signaling, and granulocyte-macrophage colony-stimulating factor (GM-CSF), we efficiently produced $CD103^+$ cDC1-like populations from mouse bone marrow progenitors and $Clec9a^+CD141^+$ cDC1-like cells from G-CSF-mobilized human peripheral blood $CD34^+$ HSCs. These ex-vivo derived cells closely mirrored their in-vivo counterparts, exhibiting the expected surface immunophenotypes, high IL-12 secretion upon stimulation measured by ELISA, and strong functional responsiveness to TLR agonists and cell-associated antigens. Upon activation, cells consistently upregulated classical maturation markers including PD-L1, MHCII, and CD40, demonstrating their ability to undergo appropriate immune stimulation-driven maturation.To support downstream genetic studies, we optimized viral transduction strategies for primary HSCs, a major technical barrier in the field. An ecotropic retroviral system combined with retronectin substantially improved gene delivery efficiency in murine cells, while an amphotropic pseudotyped retroviral approach enhanced transduction of human $CD34^+$ HSCs. These advances enable reliable introduction of CRISPR-based perturbations into precursor cells prior to differentiation.Together, this scalable, high-yield differentiation and gene-delivery platform provides a powerful foundation for conducting CRISPR-based genetic screens aimed at identifying the molecular regulators orchestrating cDC1 activation and maturation. These insights have the potential to inform the development of next-generation immunotherapies that harness or enhance dendritic cell-driven antitumor immunity.Defining the immunoregulatory molecular drivers of dendritic cells using CRISPR screens in ex-vivo models

#4915 Using functional CRISPR screening to investigate metabolic genes in lung squamous cell carcinoma adoptive T cell therapy.

Verra Ngwa, Jin Chen

Vanderbilt University Medical Center, Nashville, TN

Lung squamous cell carcinoma (LUSC) represents 30% of non-small cell lung cancer (NSCLC) cases and has a high mortality rate with limited targeted therapies. Unlike lung adenocarcinoma (LUAD), which has seen advancements in targeted therapies, LUSC has not benefited from similar breakthroughs despite having similar genetic abnormalities. While immune checkpoint inhibitor therapies have shown promise in some LUSC patients, a significant portion does not respond effectively, leaving limited treatment options. The metabolic landscape of tumors plays a crucial role in shaping the efficacy of immunotherapies, especially adoptive T cell therapies. However, identifying actionable metabolic vulnerabilities involved in T cell therapy is poorly understood. Here, we performed a high-throughput CRISPR-Cas9 screen targeting metabolic genes in an orthotopic LUSC mouse model to identify key metabolic enzymes that would sensitize the tumors to adoptive $CD8^+$ T cell therapy. By comparing sgRNA enrichment and depletion between tumors treated with adoptive T cells and those receiving PBS, we identified genes that are involved in the fatty acid biosynthesis pathway as potential suppressors of T cell-mediated killing in this tumor model. Moreover, pilot experiments indicate that loss of these genes promote invitro cytotoxic killing when tumor cells were co-cultured with T cells. Additionally, in vivo studies showed a decrease in tumor growth. Experiments are underway to evaluate the effect of adoptive T cell therapy in vivo.

#4916 StromaBlast™: A novel CRISPR-based functional genomics platform to identify therapeutic targets within the tumor microenvironment.

Abdullah Al Emran[1], Lu Gong[1], Nick Patsoukis[1], Yi Yang[1], Ruth Fekade[1], Fen Ma[1], Jahnavi Tatineni[1], Renhong Tang[2], Amin Al-Shami[1], Pankaj Seth[1], Tamas Oravecz[1]

[1]Simcere Zaiming, Cambridge, MA,[2]Simcere Zaiming, Shanghai, China

Background: The solid tumor microenvironment (TME) plays a critical role in regulating tumor progression, metastasis, and therapeutic resistance. It is a complex network of cancer-associated fibroblasts (CAFs), immune cells, endothelial cells, extracellular matrix (ECM), and soluble mediators. Recent advances in oncology have shifted the therapeutic paradigm from a cancer cell-centric to a TME-centric model, underscoring the importance of stromal components in shaping tumor behavior. Among these, CAFs represent the functionally dominant stromal population, driving resistance through multifaceted mechanisms including ECM remodeling, paracrine signaling, and metabolic reprogramming. These processes collectively create a protective niche that fosters drug tolerance and immune evasion.

Methods: To overcome the limitations of traditional discovery screens that rely solely on monoculture cancer models, we developed StromaBlast™, a next-generation CRISPR screening platform which incorporates co-cultures of cancer cells, CAFs, and immune cells. Using both Cas9-mediated knockout and dCas9-based activation approaches, we performed a comprehensive CRISPR surfaceome screen in lung cancer cells under conditions that simulate therapeutic antibody exposure and T-cell mediated killing in fibrotic tumors. Our screen was optimized to identify essential interaction networks and novel therapeutic targets involved in CAF-cancer-immune cell crosstalk.

Results: The StromaBlast™ screen uncovered several novel and known targets that are essential for cancer cell survival and communication within a CAF-rich microenvironment. Comparative analyses distinguished targets exhibiting CAF dependency from those functioning independently of stromal interactions. Functional validation confirmed the critical role of select targets in sustaining cancer cell viability in the presence of CAFs. These findings nominate actionable targets amenable to development as biologics, including T-cell engagers and antibody-drug conjugates, designed to disrupt CAF-cancer cell interactions and restore anti-tumor immune activity.

Conclusion: Fibrotic, CAF-enriched tumors are notoriously resistant to immunotherapy and antibody-based treatments due to CAF-ECM-mediated physical barriers and immune suppression. StromaBlast™ represents a transformative platform for discovering therapeutic targets that can overcome this resistance. Targeting CAF-dependent vulnerabilities identified through this approach holds the potential to convert immune-cold, fibrotic tumors into immune-active, therapy-sensitive states - advancing precision oncology and improving patient outcomes.

#4917 Establishment of patient-derived lung epithelial progenitor lines as a foundation for autologous immune and tumor modeling.

Sanaz Keshavarz Shahbaz[1], Florentina Marches[1], Te-Chia Wu[1], Mohammed Toufiq[1], Andrew Salner[2], Peter Yu[2], Adolfo Garcia-Sastre[3], Karolina Palucka[1]

[1]The Jackson Laboratory for Genomic Medicine, Farmington, CT,[2]Hartford HealthCare Cancer Institute, Hartford, CT,[3]Department of Microbiology, Icahn School of Medicine at Mount Sinai, New York, NY

Lung cancer is the leading cause of cancer-related mortality worldwide. Resistance to immunotherapy significantly limits durable clinical benefit. Elucidating the interactions between epithelial and immune compartments within the lung tumor microenvironment is critical for the development of effective interventions. However, most preclinical systems do not preserve patient-specific epithelial programs or support autologous immune modeling.The purpose of this study was to generate and characterize patient-derived lung epithelial progenitor lines from uninvolved tissues of lung cancer patients as a foundation for future immune and tumor co-culture platforms. Epithelial progenitor organoids were established from uninvolved lung tissues of adenocarcinoma and squamous cell carcinoma patients and maintained to passage 5 (P5) under defined, growth factor–optimized conditions. Identity and quality were verified by pan-cytokeratin immunostaining and fibronectin. Progenitor lines were expanded and cryopreserved to create a biobank supporting downstream air–liquid interface (ALI) and immune co-culture assays. Parallel spatial imaging of matched tumor and uninvolved tissues, along with RNA sequencing of progenitor cell lines, will be performed to analyze the immune and stromal architecture, providing integrative context for model development.Sixteen stable progenitor lines were generated (7 female, 9 males; 9 adenocarcinoma, 7 squamous cell carcinoma) with consistent morphology and long-term viability. Cryopreserved stocks and associated patient-matched materials (tumor blocks, uninvolved tissues, PBMCs, and serum) are now being integrated into functional ALI and immune co-culture assays.In conclusion, this work establishes a comprehensive biobank of lung epithelial progenitor lines derived from cancer-adjacent tissues, enabling next-generation autologous models to explore immune regulation, aging, and therapeutic resistance in lung cancer.

#4918 Bioprinted multicellular microenvironments to accelerate immunotherapy discovery in pancreatic cancer.

Aji Istadi[1], **Ali McCorkindale**[2], Silvia Lombardi[1], Inna Navarro[1], Diego Chacon Fajardo[1], Henry Barraclough-Franks[1], David Hermann[1], Sean Porazinski[2], Marco J. Herold[3], Paul Timpson[1], Greg Neely[4], Marina Pajic[1]

[1]Garvan Institute of Medical Research, Darlinghurst, Australia,[2]Inventia Life Science, Alexandria, Australia,[3]Olivia Newton-John Cancer Research Institute, Victoria, Australia,[4]Charles Perkins Centre, The University of Sydney, Camperdown, Australia

90% of pancreatic cancer (PC) patients succumb to the disease [1], necessitating development of more effective treatments. PC tumors are characterized by dense fibrotic stromal regions that contain complex, highly remodelled extracellular matrices. These fibrotic regions create protective niches promoting growth and shielding cancer cells from therapies [2]. These regions, along with other immunosuppressive elements within the tumor, prevent robust immune responses against the cancer cells, limiting immunotherapy efficacy.

Accurately modeling fibrotic microenvironments in preclinical settings remains challenging. Two-dimensional models can incorporate multiple cell types and extracellular matrices, but fail to replicate nutrient and drug gradients that exist in tumors. These architectural features are particularly important when studying immune interactions, as T cells are often spatially excluded from tumor niches in patients [3]. Furthermore, in vivo models can lack sufficient immune components, make dissecting causal effects of therapies difficult and are limited by throughput costs.

We present development and characterization of 3D in vitro co-culture models incorporating cancer, stroma, immune and microenvironment components using the RASTRUM^{TM} Allegro bioprinter from Inventia Life Science. We investigate the role of CAFs in supporting immune evasion and analyze cancer-T cell dynamics in various contexts. Using single-cell RNA sequencing we show this physiologically-relevant system better mimics native PC tumors while maintaining scalability for drug screening. The modular design facilitates combinatorial drug testing and mechanistic dissection of therapy effects across distinct cell populations. This model will be utilised to identify combination therapies that are more effective in vivo, streamlining preclinical testing, particularly for immunotherapies and immunomodulators.

References

1. Stoffel EM, Brand RE, Goggins M. Pancreatic Cancer: Changing Epidemiology and New Approaches to Risk Assessment, Early Detection, and Prevention. Gastroenterology. 2023 Apr;164(5):752-765.
2. Neesse A, Bauer CA, Öhlund D et al. Stromal biology and therapy in pancreatic cancer: ready for clinical translation? Gut. 2019 Jan;68(1):159-171.
3. Carstens JL, Correa de Sampaio P, Yang D et al. Spatial computation of intratumoral T cells correlates with survival of patients with pancreatic cancer. Nat Comm. 2017 Apr 27;8:15095.

#4919 Decoding the tumor microenvironment of NF1 tumors using spatial and cell-type specific analyses of patient-derived organoids.

Alberto Mendoza-Valderrey[1], Michael J. Lippincott[2], Huyen Thi Lam Nguyen[1], Jenna Tomkinson[2], Cameron Mattson[2], Dave Bunten[2], Summer Norris[1], Jeremy Jacobson[3], Jackson Chin[3], Paul Piehowski[3], Le Day[3], Chelsea Hutchinson Bunch[3], Christopher Anderton[3], Brittney Gorman[3], Sara Gosline[3], Gregory P. Way[2], Alice Soragni[1]

[1]Department of Orthopaedic Surgery, David Geffen School of Medicine, University of California Los Angeles, Los Angeles, CA,[2]Department of Biomedical Informatics, University of Colorado School of Medicine, Aurora, CO,[3]Earth and Biological Sciences Directorate, Pacific Northwest National Laboratory, Richland, WA

Neurofibromatosis Type I (NF1) is a tumor-predisposing genetic syndrome driven by germline variants in the tumor suppressor gene *NF1*. Patients with NF1 frequently develop benign peripheral nerve sheath tumors, including cutaneous and plexiform neurofibromas (cNFs, pNFs), which are associated with significant comorbidities. Notably, a proportion of pNFs can progress to malignant peripheral nerve sheath tumors (MPNSTs), aggressive soft tissue sarcomas, in approximately 15% of patients. Current therapies for NF1 associated tumors are extremely limited, being the MEK 1/2 inhibitors selumetinib and mirdametinib the only FDA-approved drugs for patients with symptomatic inoperable pNFs. However, both treatments are not curative and require continuous administration, with associated toxicities that highlight the need for alternative therapies. NF1 tumors present a complex microenvironment comprising different cell types including Schwann cells, fibroblasts, and mast cells embedded in a dense extracellular matrix (ECM). Efforts to identify effective non-surgical treatments are constrained by the rarity of these tumors, their marked cellular heterogeneity, their abundant ECM deposition, and the lack of patient-derived models that accurately recapitulate these complex features. We have developed patient-derived organoids of both neurofibromas (*Nguyen et al, Cell Reports Methods* 2024) and MPNSTs (*Al Shihabi et al, Cell Stem Cell* 2024) that preserve the cellular and molecular characteristics of parental tumors, providing robust tractable models for drug discovery studies. Here, we are developing a single-cell typing, image-based assay, integrating multiplex immunofluorescence with computational techniques, to evaluate the impact of drugs on individual cell subpopulations within NF1 organoids. This methodology will be coupled with our high throughput mini-ring organoid screening platform (*Phan et al, Communications Biology 2019; Al Shihabi et al, Science Advances 2022*), to rapidly screen FDA-approved drugs, along with a modified 3D-compatible Cell Painting assay for providing unbiased phenotypic readouts of the impact of therapeutic agents on each cell type as well as proteomics approaches. By integrating these methods, we aim to address the challenges posed by the cellular heterogeneity of NF1-associated tumors and to identify precision therapeutic strategies for NF1 patients.

#4920 Decoding phenotypic and functional states of *in vivo*-mimetic 3D human pancreatic CAF/ECM units through sequential high-plex IF.

Mariia Dmitrieva, Edna Cukierman, Janusz Franco-Barraza

Dr. Edna Cukierman's laboratory, Fox Chase Cancer Center, Philadelphia, PA

Background: Pancreatic ductal adenocarcinoma (PDAC) is characterized by extensive desmoplasia, with cancer-associated fibroblasts (CAFs) dominating the tumor microenvironment (TME) and driving collagen-rich extracellular matrix (ECM) deposition. While resident pancreatic fibroblasts exert natural tumor-restrictive functions, CAF/ECM units adopt both tumor-promoting and tumor-suppressive phenotypes, critically shaping tumor progression, therapeutic response, and patient outcomes. Defining inter-patient heterogeneity in CAF/ECM phenotypic traits and understanding their functional shifts in response to therapy is essential for predicting clinical outcomes, predicting therapy responses, and identifying new TME-targeting strategies.
Methods: We developed a human PDAC TME-within-a-chip integrating fresh tissue-derived 3D CAF/ECM units cultured in customized microfluidic chambers on glass slides. High-plex sequential immunofluorescence (seqIF™) on the COMET™ platform standardized ~20 mesenchymal biomarkers to distinguish tumor-supportive from tumor-restrictive CAF phenotypes. Automated image analysis (HORIZON™ software) quantified single-cell, subcellular, and extracellular marker expression patterns.
Results: CAF activation-state interventions revealed marked alterations in canonical TGFβ signaling, reduced Ki67-positive cell proliferation, and changes in ECM architecture and composition, reflecting shifts in stromal functional states. This integrated platform effectively resolved CAF/ECM unit heterogeneity and tracked TME adaptations in response to therapeutic perturbation.
Conclusions: This technological advancement provides a robust, medium-throughput framework for dissecting CAF heterogeneity and exploring stromal biology in PDAC (and other cancers). The platform enables comprehensive profiling from minimal starting material while substantially reducing antibody consumption and processing time compared to conventional methods, establishing a scalable foundation for functional screening and evaluating therapeutic interventions in complex TMEs.

#4921 An advanced 3D vascularized tumor immune microenvironment on a chip for predictive efficacy and toxicity testing of IO therapeutics.

Junfeng Wang, Byungjun Lee, Delaney Donnelly, Sabrina Figueroa Buezo, Bushra Rajput, Jihye Baek, Hyeon-geun Park, Eunjeong Kim, Joseph Harris, Aneesh Sathe, Tsung-Li Liu, Branka Mitrovic, Kyusuk Baek, Sanghee Yoo

Qureator, Inc., San Diego, CA

Introduction: Conventional pre-clinical models for immuno-oncology (IO) therapeutics, such as animal models, suffer from irrelevant biology and ecosystems, while simple 2D/3D *in vitro* assays lack the complexity of the human tumor microenvironment. These gaps lead to poor prediction of clinical outcomes, including immune-related toxicities. To address this translational gap, we developed and validated an advanced, patient-relevant 3D vascularized tumor immune microenvironment (vTIME) on-a-chip model for the predictive assessment of IO drug efficacy and toxicity—a platform now proven to generate data packages supporting Investigational New Drug (IND) approval.

Methods: Within proprietary microfluidic CurioChips, we established the vTIME model by co-culturing patient-derived organoids in hydrogel with stromal cells and endothelial cells (HUVECs). In this co-culture, endothelial cells are self-assembled into a perfusable vascular network. We subsequently introduced human monocytes, which migrated into the tumor bed and differentiated to build an immunosuppressive microenvironment. The transformation of immune microenvironment was characterized by multiple cytokine changes. We then validated the model's predictive utility using a clinical stage T-cell engager (TCE) for dual efficacy and toxicity evaluation. The tumor killing and T cell activations are measured by immunofluorescent images, immune cell profiling and secretome analysis.

Results: The model successfully recapitulated a clinically relevant, immunosuppressive TME: monocytes differentiated into tumor-promoting macrophages, fibroblasts converted to CAF-like cells, and metastatic organoids demonstrated vascular invasion. For efficacy testing, TCE-mediated cancer-killing was observed in a dose-dependent manner; however, this efficacy was significantly diminished in the presence of immunosuppressive macrophages, demonstrating the model's ability to avoid the overestimation of efficacy seen in simpler systems. For toxicity assessment, the complete vTIME model captured the key cascade of cytokine release syndrome (CRS). TCE treatment induced a characteristic kinetic, with an initial IFNγ peak followed by a substantial IL-6 elevation. Critically, we also captured significant, CRS-linked vessel toxicity post-TCE treatment, a key initiating event of organ failure in patients.

Conclusion: These findings demonstrate that our advanced 3D vTIME-on-a-chip platform represents one of the powerful New Approach Methodologies (NAMs), which is reliable and predictive for the dual assessment of novel IO therapeutics. It is capable of capturing complex immune-mediated responses, identifying the therapeutic "sweet spot" balancing efficacy and toxicity, and modeling CRS-driven vascular damage not seen in conventional systems.

#4922 Development of vascularized 3D tumoroid models using microphysiological systems.

Geetika Sahni[1], Hooi Linn Loo[1], **Colin D. Paul**[2], Matthew R. Dallas[2], Sei Hien Lim[1], Kuan Chee Mun[1]

[1]AIM Biotech Pte Ltd, Singapore, Singapore,[2]Thermo Fisher Scientific, Frederick, MD

The adoption of New Approach Methodologies (NAMs) in drug discovery and toxicology is accelerating as the field seeks human-relevant predictive models to replace animal testing. Microphysiological systems (MPS) are leading this transition by enabling physiologically relevant, reproducible in vitro models. Here, we demonstrate construction of vascularized tumoroid models using AIM Biotech's VasQ Kit and organiX™ platform and Thermo Fisher Scientific patient-derived OncoPro™ Tumoroid Cell Lines. These models combine a microfluidic system optimized for complex three-dimensional (3D) co-cultures with physiologically-relevant tumoroid (cancer organoid) lines. Endothelial cells and fibroblasts, which came pre-validated in the VasQ Kit, were co-cultured with OncoPro tumoroid models in hydrogel matrices to generate perfusable vascular networks. Tumoroids derived from colorectal (HuCo1044-GFP) and lung (HuLu051421) cancers were integrated into organiX devices to assess tumor-vasculature interactions. Fluorescent and confocal imaging with Texas Red-dextran, anti-CD31, and CellEvent™ Caspase-3/7 reagents were used to visualize perfusion, vascular architecture, and apoptosis within tumoroids.

Perfusable vascular networks reproducibly formed around patient-derived tumoroids, recapitulating critical features of the tumor microenvironment (TME). Confocal imaging revealed active vasculature-tumoroid interfaces, with endothelial networks penetrating hydrogel matrices and surrounding tumor masses. Quantification of apoptotic markers and spatial analysis of immune or stromal cell compartments demonstrated the model's capability for assessing drug response and cellular infiltration.

This method establishes a standardized and human-relevant MPS model for vascularized tumoroids, enabling mechanistic studies of tumor biology, immune cell trafficking, and therapeutic efficacy. This integrated approach supports the broader transition toward NAMs and offers a translationally relevant platform for immuno-oncology and precision medicine research.

#4923 A micro-vascularized pancreatic ductal adenocarcinoma-on-chip model recapitulates immune exclusion and altered T cell polarization.

Thomas Sommermann[1], Amelie Paillereau[1], Alina Deipenbrock[2], Nicole Teusch[2], Martin Raasch[1], Knut Rennert[1]

[1]Dynamic42, Jena, Germany,[2]Institute of Pharmaceutical Biology and Biotechnology, Heinrich-Heine-University Dusseldorf, Dusseldorf, Germany

Pancreatic ductal adenocarcinoma (PDAC) demonstrates strong immune evasion by reshaping the tumor microenvironment (TME) into an anti-inflammatory, immunosuppressive niche. This process involves creating chemokine gradients and physical barriers that hinder the recruitment and infiltration of immune effector cells.To study these interactions under physiologically relevant conditions, we developed a PDAC-on-chip model using a microfluidic three-channel biochip. The system was based on PDAC co-spheroids composed of primary cancer-associated fibroblasts (CAFs) and Panc1 tumor cells embedded in an extracellular matrix within a dedicated chip channel. Over 10 days, fibroblasts generated a fibrotic barrier exceeding 100 µm around the tumor core. Concurrently, endothelial cells integrated into the matrix formed a perfusable microvascular network directly interfacing with the TME. Various immune cell populations were introduced into the vascular channel, and their transmigration across a porous membrane through the microvasculature into the complex TME was tracked over time using live-cell imaging and flow cytometry.Our findings show that PDAC-on-chip models effectively restrict T cell infiltration, reinforcing the concept of active immune exclusion by the tumor. Moreover, activated CD8 T cells recovered from the chip exhibited an altered activation phenotype characterized by HLA-DR downregulation and 4.1BB upregulation. This microvascularized PDAC-on-chip platform faithfully reproduces key features of PDAC immune evasion observed in vivo and provides a promising tool for evaluating immunotherapeutic strategies in a controlled microphysiological setting.

#4924 Decellularized lung biomatrix models to investigate microenvironmental regulation of organ-selective tropism in metastatic breast cancer.

Kasra Goodarzi[1], Yi Yin[1], Maureen Aliru[2], Andrew Z. Wang[1]

[1]University of Texas Southwestern Medical Center, Dallas, TX,[2]Harold C. Simmons Comprehensive Cancer Center, Dallas, TX

Background: Breast cancer is the most frequently diagnosed malignancy and a leading cause of cancer-related death in women. Metastatic disease is the main cause of breast cancer mortality, with lung as a key metastatic organ. Although a variety of tumor models, ranging from conventional two-dimensional (2D) systems to in vivo models, have been used to study breast cancer lung metastasis, they do not fully recapitulate lung specific microenvironment.
Methods: To study the role and impact of organ microenvironment on the tropism of breast cancer cells, we used parental and lung-metastatic variants of MDA-MB-231cells by seeding the various cell densities (25 k, 15 k, 5 k, 2.5 k, 1 k, and 0.5 k cell/cm²) on decellularized lung matrices. The decellularized lung biomatrix scaffolds were harvested from rats using perfusion protocol. To assess cell activity, ATP-based luminescence assays were performed for all conditions and normalized to the corresponding control condition (cells cultured in the absence of lung biomatrix).
Results: Normalized ATP measurements showed that decellularized lung biomatrix differentially modulated the metabolic activity of parental and lung-metastatic MDA-MB-231 cells. Across almost all seeding densities and biomatrix concentrations, the lung-metastatic variant generally exhibited higher growth velocity than the parental line, suggesting that the lung-derived matrix provides a more favorable microenvironment for the metastatic cells through enhanced cell-matrix interactions that activate proliferative signaling pathways. This difference was most evident at higher cell seeding densities and higher protein concentrations of decellularized lung biomatrix. At 25 k, 15 k, and 5 k cells/cm², the lung-metastatic cells displayed a clear increase in normalized metabolic activity relative to the parental cells at 200 and 300 µg/cm². In contrast, at cell densities of 2.5 k, 1 k, and 0.5 k cells/cm², normalized ATP values for parental and metastatic cells were comparable across all matrix protein densities within 5 days culture period. Ongoing work aims to further characterize cellular activities and cell-matrix signaling pathways in the lung-mimetic scaffolds.
Conclusion: Our ex vivo model based on decellularized lung biomatrix scaffolds demonstrates that lung specific microenvironmental cues selectively enhance the metabolic activity of lung-metastatic breast cancer cells relative to parental cells, supporting microenvironmental regulation of organ specific metastatic preference.

#4925 Unlocking the extracellular matrix as a source of novel targets: A matrisome-based platform to characterize the tumor microenvironment.

Edward Long, Cecilia Pennica, Lisa Sassi, Seyed Mahfouzi, Filippo Prestinoni, Luca Frenguelli, Gareth Muirhead, Kovilen Sawmynaden, Athiva Shankar, Tu Vinh, Matthew J. Edwards, Chris Stevenson, Emma Huang, **Sam Cooper**, Giuseppe Mazza

Engitix Therapeutics, London, United Kingdom

Background:
The extracellular matrix (ECM) is a bioactive environment key to tumorigenesis and disease progression. Yet despite evidence that multiple ultra-selective ECM targets exist, efforts to leverage the ECM for therapeutic targeting have remained centered on fibronectin isoforms.
Methods:
We leveraged a decellularization protocol focused on preserving stable ECM targets to characterize the matrisome in three cancer indications, including moderately to poorly differentiated pancreatic ductal adenocarcinoma (PDAC) tumors (n = 5; stage IA-IIB), moderately differentiated primary colorectal cancer (CRC) tumors (n = 5; stages I-IIIB), and CRC liver metastases (CRC-LM; n = 5; stage IV). For each indication, we decellularized tumor and background whole-tissue samples using mechanical and chemical approaches. This method enables the removal of cells while preserving 3D ECM structure and composition. Decellularized ECM was then analyzed histologically and with proteomics via TMT DDA mass spectrometry (MS).
Results:
Analysis of CRC and CRC-LM tumor and adjacent non-tumor tissue samples identified 1,080 commonly expressed proteins, 79 of which were core matrix proteins and 67 matrix-associated. Tumor-specific matrisome signatures clearly differentiated tumor from non-tumor adjacent tissue samples for both indications—83 and 96 ECM proteins were differentially expressed in CRC and CRC-LM, respectively (FDR < 0.05). Analysis of PDAC tumors and adjacent non-tumor tissue samples detected 854 proteins, including 103 core matrisome and 77 matrisome-associated proteins. In addition, we identified a PDAC signature of 109 ECM proteins differentially regulated between tumor and background. Critically, comparison of highly enriched targets identified by this study with both bulk and single-cell RNA data indicated that a number of these targets are ultra-selective and could thus serve as valuable ECM-stable candidates for therapeutic targeting.
Conclusions:
TMT-MS analysis of decellularized tumors and adjacent non-tumor tissues defined a novel, tumor-specific matrisome signature enriched for stably bound proteins. Integration of this dataset with transcriptomic data identified specific ECM pathways and targets that may be valuable for therapeutic targeting.

#4926 Modeling the metaplastic triple negative breast cancer matrix.

Elizabeth Martin[1], Katherine Hebert[2], Mackenzie Hawes[2], Thomas Cheng[2], Delia Carlino[3], Matthew E. Burow[4], Bridgette M. Collins-Burow[2], Jorge Belgodere[2]

[1]Tulane Univ. Health Sciences Ctr., New Orleans, LA,[2]Tulane University School of Medicine, New Orleans, LA,[3]Tulane Cancer Center, New Orleans, LA,[4]Associate Professor of Medicine & Surgery, Tulane University School of Medicine, New Orleans, LA

Metaplastic breast cancer accounts for >1% of all breast cancers and is marked by an aggressive phenotype with poor patient survival. Individuals diagnosed with metaplastic breast cancer have higher rates of recurrence, metastasis, and limited therapeutics options. Further the five-year survival rate of metaplastic breast cancer is 55%. Metaplastic breast cancer is characterized by unique histological features and recent evidence suggests that metaplastic breast tumors have extensive extracellular matrix (ECM) remodeling, including altered protein expression and increased ECM stiffness. Due to the scarcity of this tumor type, accurate modeling of the metaplastic ECM would provide enhanced *in vitro* testing and ultimately guide the discovery of novel targeted treatments for this rare disease. Here we demonstrate changes in the metaplastic TNBC tumor microenvironment and preliminary modeling of the metaplastic matrix *in vitro*. Specifically, SEM imaging revealed enhanced pore size and stiffness in the metaplastic tumor compared to matched distal breast adipose tissue. Further, metaplastic TNBC had significant enrichment for ECM proteins, notably glycoproteins (MFAP2, POSTN, FN1), compared to distal adipose. The enhanced expression of the glycoprotein MFAP2 in primary metaplastic and non-metaplastic TNBC breast cancer cell lines demonstrated enrichment of genes associated with the biological process: epithelial-to-mesenchymal transition. In depth analysis of genes elevated with MFAP2 expression in metaplastic TNBC demonstrated elevated expression of genes associated with a cancer stem like phenotype and ECM remodeling. Overall, our results establish an extracellular signature and onco-architecture for the metaplastic triple-negative tumor type.

#4927 Expression profiles of TCF-4 variants across digestive system cancers quantified by a novel PNA-directed qPCR assay.

Hironori Koga, Yasuko Imamura, Tomoya Sudo

Kurume University Research Center for Innovative Cancer Therapy, Kurume-shi, Japan

Background: TCF-4, a key transcription factor in the Wnt/β-catenin pathway, produces multiple splice variants with distinct functions. Although our group previously identified 14 variants in liver cancer cells, quantitative assessment across digestive system cancers has been limited by the low resolution of conventional assays. To address this unmet need, we developed a peptide nucleic acid (PNA)-directed PCR clamping-based quantitative RT-PCR system enabling precise discrimination of individual TCF-4 splice variants.
Purpose: To establish a robust quantitative framework for variant-level TCF-4 expression analysis and delineate organ-specific expression patterns across digestive cancer cell lines and colorectal cancer (CRC) tissues, with emphasis on the functionally distinct variants TCF-4J (SxxSS–) and TCF-4K (SxxSS+). Methods: A PNA-qPCR platform was constructed for sensitive discrimination of closely related TCF-4 splice variants. Sixteen cell lines representing liver, stomach, colorectum, pancreas, and pancreatic neuroendocrine tumors were analyzed. TCF-4J and TCF-4K expression levels were further quantified in 39 paired CRC tissues and adjacent mucosa (IRB-approved). An exploratory subgroup analysis was performed using quartile-based stratification of tumor TCF-4J expression.
Results: The PNA-qPCR system enabled specific quantification of 14 TCF-4 variants. Distinct organ-dependent expression signatures were observed: liver cancer cell lines showed a predominantly TCF-4B-dominant pattern, whereas gastric, colorectal, and pancreatic cancer lines exhibited TCF-4J-dominant profiles, indicating lineage-specific variant usage rather than differentiation-dependent changes. In CRC tissues, TCF-4J was significantly upregulated relative to noncancerous mucosa, whereas TCF-4K expression remained low. Exploratory quartile analysis revealed that patients in the lowest 25% of tumor TCF-4J expression had no distant metastasis, and this subgroup showed a trend toward longer overall survival compared with higher-expression cases (51 vs. 23 months).
Conclusions: This study establishes a sensitive quantitative platform for TCF-4 variant profiling and reveals striking organ-specific differences in variant usage across digestive system malignancies. The inverse relationship between low TCF-4J expression and metastatic progression in CRC suggests potential biological relevance. Integration of this bulk RNA-based framework with single-cell and spatial transcriptomic approaches will be essential to elucidate variant-specific regulation and intratumoral heterogeneity.

#4928 Immune signaling reporter cell lines enable quantitative monitoring of crosstalk among cancer, innate, and adaptive immune cells in tumor microenvironment model.

Hyeyoun Chang, John G. Foulke, Luping Chen, Meghan Sikes, Catherine McManus, Fang Tian

ATCC, Manassas, VA

Background: T cell-targeted immunotherapies have led to major clinical gains, yet many patients fail to respond or develop resistance due to the immunosuppressive tumor microenvironment (TME). Increasing evidence shows that B cells and myeloid cells also influence antitumor immunity, but accessible models capable of capturing interactions among cancer cells and multiple immune cell types remain limited. To address this gap, we developed immune signaling reporter cell lines that allow real-time, quantitative monitoring of NFAT- and NF-κB-driven activation pathways. These models enable capturing dynamic interactions among multiple immune cell lineages and cancer cells relevant to immunotherapy response.

Methods: Six luciferase-based reporter lines derived from T cells, B cells, or myeloid cells were engineered with NFAT or NF-κB response elements driving luciferase expression. The models retain high endogenous expression of checkpoint receptors, including PD-1, TIGIT, and GITR in T cell reporters and SIRPα, Siglec-10, LILRB1, and B7-1 in myeloid reporters. Reporter activation was assessed following pathway-specific stimulation: PMA and ionomycin for NFAT and TNF-α or T cell-conditioned media for NF-κB. The B cell NF-κB reporter with elevated basal activity was further tested with an NF-κB inhibitor. In addition, all reporters were evaluated in co-culture with primary immune and cancer cells.

Results: Stimuli activating NFAT or NF-κB signaling produced strong, dose-dependent increases in luciferase activity, while pathway inhibition reduced signal as expected. Co-culture with primary immune and cancer cells generated diverse activation patterns, reflecting context-dependent signaling shaped by interactions within the TME.

Conclusions: These reporter cell lines provide a scalable platform for monitoring NFAT- and NF-κB-driven immune activation across T, B, and myeloid lineages. They support sensitive, reproducible evaluation of immune responses, enable mechanistic studies of dynamic immune crosstalk, and evaluation of combinatorial immunotherapy strategies within the TME.

#4929 CAR-Tmigration andcytotoxicity in atumor-vasculature-on-chipmodel.

Luuk de Haan, Aleksandra Olczyk, Thomas Olivier, Joris Wesselius, **Will Allen**, Johnny Suiker, Todd Burton, Lenie van den Broek, Karla Queiroz

MIMETAS B.V, Oegstgeest, Netherlands

CAR-T cell therapies have shown remarkable success in hematologic malignancies; however, their efficacy in solid tumors remains limited. This is primarily due to the complex tumor microenvironment (TME), which creates immunosuppressive conditions and physical barriers that hinder CAR-T infiltration and function. Current in vitro models fail to replicate these critical parameters, limiting the ability to predict clinical performance. To address this gap, we developed a tumor-vasculature-on-chip model using the OrganoPlate platform, enabling perfusion of CAR-T cells through a functional endothelial vessel adjacent to a tumor compartment. This setup allows assessment of key processes such as extravasation, migration, and killing kinetics in a physiologically relevant context. EpCAM-positive HT-29 colorectal cancer cells and EpCAM-negative A375 melanoma cells were co-cultured with an endothelial tubule to evaluate EpCAM-targeting CAR-T cells. CAR-T cells selectively killed EpCAM-positive HT-29 cells while sparing EpCAM-negative A375 cells, demonstrating antigen-specific activity. Killing was dose-dependent, and endothelial integrity was maintained at most CAR-T concentrations but disrupted at the highest doses, revealing a therapeutic window. We further compared CAR-T constructs with different co-stimulatory domains (CD28 vs. 4-1BB) and observed reduced potency with 4-1BB. Addition of IL-2 enhanced CAR-T cytotoxicity. Cytokine profiling showed increased IFN-γ, TNF-α, and IL-6 over time, and morphometric analysis confirmed endothelial disruption at high effector-to-target ratios. The platform was also used to study combination strategies, including immune checkpoint inhibitors and temozolomide. This modular, scalable organ-on-chip system enables phenotypic and functional characterization of CAR-T cells under relevant conditions.

#4930 Cell Avidity: The Next-Gen cell binding assay to understand therapeutic mechanism of action through quantifying cell-cell and cell-protein interaction strength.

Keith Bailey[1], Riley Pihl[1], Michael SAVAGE[2], Trey Simpson[3]

[1]LUMICKS, Amsterdam, Netherlands,[2]LUMICKS, New York, NY,[3]LUMICKS, Boston, MA

While conventional assays such as affinity, cytokine secretion, and cytotoxicity provide valuable data at a molecular level, this information is insufficient to fully characterize and select the best cellular therapies. There is still a lack of understanding about the biophysical cell-cell interactions that drive functional processes.

Methods: Cell avidity, the integrated strength of multivalent interactions between an effector cell and its target, can help elucidate the mechanism of action for therapeutic candidates. Our Cell Avidity platform challenges these interacting pairs using contactless force and quantifies the strength of binding between effector and target cells to distinguish productive from unproductive cell binding in a physiological context. This biophysical metric provides a unique view into cell binding characteristics to interrogate binding potency, selectivity, sensitivity, and kinetics.

Results: Here, we review recent publications highlighting how researchers have used Cell Avidity to: • Fine-tune the affinity/cell avidity of CAR-T cells to mitigate on-target off-tumor toxicity in renal cell carcinoma. • Assess the impact of Venetoclax treatment on NK cells, finding improvements to cytoskeleton remodeling and lytic granule polarization, which contributed to a more efficient IS, enhancing NK cell-mediated killing of AML cells. • Format-tune bispecific T cell engagers to enhance efficacy against renal cell carcinoma • Validate binding mechanism of tandem CAR-T cells to overcome tumor heterogeneity • Engineer CAR-T cells secreting a T-cell engaging molecule to overcome a challenging tumor microenvironment in pancreatic adenocarcinoma. • Elucidate mechanism of action of tandem CAR-T targeting heterogenous solid tumors • Phenotype the tumor-primed NK cells for cell binding and function.

Conclusions: We developed a Cell Avidity platform that enables the characterization and screening of molecular binders and cellular products, including antibodies, small molecules, and cell therapies. Cell Avidity provides comprehensive information on potency, selectivity, sensitivity, and kinetics, offering key insights into the mechanism of action for cell therapies.

#4931 Development of a CyTOF panel for macrophage polarization and functional assessment under treatment conditions.

Poornima Gourabathini[1], Rachel Weil[2], **Kimberly Q. McKinney**[3], Jeffrey S. Huo[1], Kenzie Wells[4], Kaitlyn Smith[5], David M. Loeb[2], Javier Oesterheld[4]

[1]Atrium Health Wake Forest Baptist Comprehensive Cancer Center, Charlotte, NC,[2]Albert Einstein College of Medicine, Bronx, NY,[3]Pediatric Oncology Research Laboratory, Atrium Health Wake Forest Baptist Comprehensive Cancer Center, Charlotte, NC,[4]Atrium Health Levine, Charlotte, NC,[5]Wake Forest Baptist Health, Winston Salem, NC

Purpose: Tumor associated macrophages (TAMs) are prevalent in the sarcoma tumor microenvironment, and often contribute to immune suppression, angiogenesis, and tumor progression. TAMs exhibit a spectrum of polarization states, ranging from anti-tumor (M1) to tumor-supportive (M2) functions. Mass cytometry (CyTOF) enables high-dimensional single-cell profiling, making it ideal for dissecting the presence and abundance of various macrophage phenotypes within a tumor. This study aimed to design and validate a CyTOF panel targeting macrophages and associated immune markers, to characterize macrophage polarization states and evaluate treatment induced changes in macrophage subtypes.

Methods: A mouse macrophage-focused CyTOF panel was developed comprised of 40 markers, including lineage markers, activation markers, and cytokine-associated proteins relevant to M1/M2 phenotypes and other immune cell populations. For optimization of antibody titration and staining conditions, macrophage polarization was performed *in vitro* using the commercially available mouse-derived macrophage cell line RAW 264.7. Macrophage polarization states were induced under standard conditions: M1: LPS + IFN-γ and M2a: IL-4 + IL-13, M2b- OVA, Anti-OVA IgG, M2c- IL-10, and M2d-NECA stimuli. Following validation, the panel was applied to a mouse model of orthotopically implanted osteosarcoma cells treated with a novel compound to quantify the TAM polarization and associated immune networks. Tumor tissue samples were dissociated into single cell suspensions, stained using the CyTOF panel, and analyzed using dimensionality reduction (UMAP) and clustering algorithms.

Results: The 40-marker CyTOF panel was successfully used to identify and characterize macrophage subtype populations in vitro as well as in mouse xenograft tumors. In vitro polarization of mouse RAW264.7 cells showed distinct phenotypic clusters corresponding to M1 and M2 subtypes. These results also enabled effective antibody titration. Treatment of orthotopically implanted osteosarcoma tumors with the novel compound resulted in increased expression of M1 markers and a reduction in M2-associated markers compared to vehicle control, indicating a shift in macrophage polarization induced by this compound.

Conclusion: The developed CyTOF panel provides a robust platform for high-resolution analysis of macrophage polarization and treatment-induced phenotypic changes, offering more detailed investigation of immune modulation strategies. This panel could be applied as a tool for future investigations focused on macrophage subpopulations and their functional roles and will allow for further dissection of the tumor immune microenvironment, advancing the understanding of immunological variability in response to treatment.

#4932 Establishment and characterisation of PDTOs and CAFs for the development of a co-culture system in pancreatic periampullary adenocarcinoma.

Panagiotis Sarametidis[1], Jojanneke Stoof[1], Laura Ivers[2], Jean Murphy[3], Niall Swan[3], Luca Benigno[3], Fiona Hand[3], Kevin C. Conlon[3], Paul B. Mullan[4], Maeve Lowery[5], Naomi P. Walsh[1]

[1]Dublin City University, Dublin, Ireland,[2]Life Sciences Institute, Dublin City University, Dublin, Ireland,[3]St. Vincent's University Hospital, Dublin, Ireland,[4]Postdoctoral Fellow, Dept. of Oncology, Queen's University Belfast, Belfast,[5]Trinity St James Cancer Institute, Dublin, Ireland

Periampullary adenocarcinoma (PAC) constitutes a diverse group of malignancies originating from the pancreatic head (60%), the ampulla of Vater (20%), the distal common bile duct (10%), and the duodenum (10%). The pancreatic tumour microenvironment (TME) is a major driver of tumour progression and therapeutic resistance, with cancer-associated fibroblasts (CAFs) emerging as central contributors. Representing a heterogeneous population within the TME, CAFs actively mediate stromal remodelling through complex interactions with tumour cells as well as with immune and stromal components. Detailed characterisation of CAF phenotypes is essential to define their impact to PAC pathobiology and to facilitate the design of novel therapeutic strategies against this highly aggressive malignancy.Patient-derived tumour organoids (PDTOs) and CAFs were isolated from freshly obtained primary PAC specimens. CAFs subtypes were characterised by immunofluorescence staining for key CAF proteins and transcriptomic sequencing. PDTOs were characterised by genomic sequencing. Drug screening of PDTOs with talazoparib and olaparib was conducted to examine the correlation between an HRD mutation and sensitivity to PARP inhibitors.4 PDTOs and 4 CAFs were successfully derived and cultured from PAC specimens. CAF cell lines showed positive expression of fibroblast markers α-SMA and vimentin, and showed heterogeneous intensity and expression of CAF markers such as PDGFR and FAP. They were categorised into antigen-presenting (apCAFs), inflammatory (iCAFs) and myofibroblastic (myCAFs) subgroups based on the RNA expression of key genes. MyCAFs were grouped based on the expression levels of CTGF, COL1A1, POSTN and ACTA2 genes. CD74 and HLA genes were chosen for the characterisation of apCAFs, while iCAFs were characterised based on the expression of IL-1/6/11, FAP and CXCL1/2 genes. Mutational profiling of the PDTOs identified a missense ATM variant c.5558A>T (p.Asp1853Val) in an intestinal-type adenocarcinoma, which was sensitive to olaparib (1.66 μM) and talazoparib (0.45 μM).PDTOs and CAFs serve as a useful model for studying the cellular architecture and heterogeneity of PAC in vitro. Building on this, defined CAF heterogeneity will be assessed for its association with immunosuppressive versus immunostimulatory profiles, and T cells, along with immunotherapeutic agents, will be incorporated into the co-cultures. These models will provide valuable insights into PAC tumour-stroma-immune biology and form the basis for advanced co-cultures to test strategies targeting the TME.

#4934 Identifying molecular regulators of ovarian tumor cell attachment to peritoneal mesothelial cells under shear stress using an *ex-vivo* microfluidic model.

Jillian A. Martin[1], Breanna Baker[2], Vasilios Morikis[1], Alessandra DiMauro[1], Gregory D. Longmore[1], Whitney R. Grither[3]

[1]Medical Oncology, Washington University School of Medicine, St. Louis, MO,[2]Hematology, Washington University School of Medicine, St. Louis, MO,[3]Obstetrics and Gynecology, Washington University School of Medicine in St. Louis, St. Louis, MO

Ovarian cancer metastasis is unique in that the primary tumor and the initial metastatic site, the peritoneal mesothelial layer, share the same cavity. Early spread of ovarian cancer involves tumor cell shedding from primary ovarian tumors, which then circulate throughout the abdominal cavity to attach and invade mesothelium covering the abdominal organs. During peritoneal migration, ovarian tumor cells are also exposed to ascitic fluid, and the influence of this fluid flow on tumor cell attachment to mesothelium is poorly understood. To address this problem, we developed and characterized a robust microfluidic device incorporating ovarian tumor cell attachment to mesothelial cells in the presence of fluid flow. Mesothelial cells are cultured within the microfluidic device for 48 hours, and ovarian cancer cells are introduced at fixed flow rates for 7 minutes. Using live cell video imaging and analysis, we can quantify the extent of tumor cell adhesion. We find that factor(s) secreted by ovarian tumor cells significantly increase tumor cell adhesion to mesothelium. To identify candidate molecules modulating this cell-cell communication, we performed bulk mRNA sequencing of mesothelial cells treated with ovarian tumor cell culture supernatant and proteomics of the ovarian tumor cell secreted media. From these analyses, we have identified numerous potential candidate molecules. One of these molecules, cadherin-12, is downregulated in mesothelial cells in response to tumor cell culture supernatant exposure both in vitro and in vivo. Genetic depletion of cadherin-12 in mouse peritoneal mesothelial cells results in altered mesothelial barrier function, fibroblastic differentiation, and increased tumor cell adhesion to mesothelium. Our results suggest that cadherin-12 plays a role in maintaining peritoneal mesothelial integrity and is manipulated by some factor(s) secreted by ovarian tumor cells during early ovarian cancer metastasis.

#4935 Cell cycle regulation by PAX3-FOXO1 via WEE1 kinase in fusion-positive rhabdomyosarcoma.

Chandra Kaladhar Vemula, JinSeok Park

Hematology and oncology, Children's Hospital Los Angeles, Los Angeles, CA

IntroductionFusion-positive rhabdomyosarcoma (FPRMS) is a highly aggressive form of the most common childhood muscle cancer, rhabdomyosarcoma. A distinct genetic signature, the PAX3-FOXO1 (P3F) fusion gene, characterizes a subtype of the most common pediatric soft tissue sarcoma. We aim to understand the collective cell invasion by determining how leader-follower cellular cooperation, P3F signaling, and the cell-cycle checkpoint kinase WEE1 drive tumor growth and invasion, and whether inhibiting WEE1 can blunt these behaviors.
Brief Experimental Procedures To understand the collective cell invasion of FPRMS, we utilize a 3D "mini-tumor" (spheroid) model that recapitulates leader cells at the invasive front and rapidly proliferating follower cells behind them. We paired this with live-cell reporters of cell-cycle checkpoint activity and proliferation. We analyzed the transcriptome of FPRMS cells with P3F knockdown (PFKD) to confirm whether P3F regulates cell cycle checkpoints and DNA replication. Additionally, we employ ChIP-seq to identify the P3F-regulated genes and pharmacological WEE1 inhibition.
ResultsOur preliminary data show that follower cells exhibit higher P3F expression, increased proliferation, and elevated WEE1 activity relative to other regions, consistent with a fast-cycling compartment that mechanically supports leader-directed invasion. These findings suggest that P3F upregulates WEE1-dependent programs, which fuel follower growth and cooperative invasion. Additionally, we use P3F knockdown to demonstrate, via RNA-seq, the Negative enrichment of gene sets associated with the G1/S transition and DNA replication in PFKD FPRMS cells. PAX3-FOXO1 regulates cell cycle progression by S-phase arrest. Furthermore, P3F regulates cell cycle progression by reducing the expression of pCDK2 and the double-strand break regulatory gene γH2A.X.
ConclusionsTogether, the data support a model in which P3F-driven WEE1 signaling sustains the follower population that powers collective invasion in FPRMS. Targeting WEE1 slows growth and invasion in our 3D model, suggesting that WEE1 inhibition is a therapeutic strategy worthy of further evaluation in patient-derived specimens and preclinical studies.

#4936 Dissecting tumor microenvironment and cellular adaptation in ovarian cancer models using Bio-Rad ddSEQ Single-Cell 3' RNA-Seq technology.

Errile Pusod[1], Madison Uyemura[2], Patricia Schnepp[1], Aqila Ahmed[1], Angelica P. Olcott[3], Adnan Chowdhury[3], Michelle Racey[3], Elizabeth Dreskin[3], Zhen Ni Zhou[4], Analisa DiFeo[2]

[1]Bio-Rad Laboratories, Ann Arbor, MI,[2]Department of Pathology, University of Michigan, Ann Arbor, MI,[3]Bio-Rad Laboratories, Hercules, CA,[4]Department of Obstetrics and Gynecology, University of Michigan, Ann Arbor, MI

Ovarian cancer remains one of the most lethal gynecologic malignancies due to its complex biology and the challenges associated with early detection and effective treatment. Advances in single-cell RNA sequencing technologies have enabled researchers to dissect cellular heterogeneity within tumors and gain deeper insight into the dynamic interactions between cancer cells and their microenvironment. By leveraging innovative single-cell analysis tools, analysis of gene expression profiles at single-cell resolution can be performed across various cancer models, providing valuable information on tumor evolution, therapeutic response, and mechanisms driving tumorigenesis.Single-cell and single-nucleus RNA sequencing were performed using the Bio-Rad ddSEQ 3’ Single-Cell RNA-Seq Kit on multiple cancer models—including a primary high-grade serous ovarian tumor, a patient-derived cancer cell line (PDCC), and a patient-derived xenograft (PDX)—all originating from the same patient. The objective of this study is to investigate the role of the tumor microenvironment in modulating gene expression patterns that support the persistence and adaptation of cancer cells in various patient-derived models. By comparing single-cell transcriptomic profiles across these models, we aim to identify key regulatory pathways and microenvironmental signals that influence cellular behavior. These insights may advance our understanding of tumor cell adaptation mechanisms and facilitate the development of more physiologically relevant models for cancer research. Integration of single-cell data from various cancer models showed concordance of distinct clusters suggesting changes in gene expression specific to the cancer model utilized. We identified cancer cells as well as fibroblasts, endothelial cells, T and B cells, and myeloid cells in the primary tumor sample. Additionally, enrichment of cancer cells expressing increased levels of *PHGDH* and *PSAT1*, genes associated in serine metabolism pathway that is crucial in tumorigenesis was observed in PDCC samples - data which were previously confirmed with bulk RNA-Seq. The Bio-Rad ddSEQ 3’ RNA-Seq kit enables robust analysis of various *in vitro* and *in vivo* cancer models due to the capability of running many samples simultaneously, generating high-quality single-cell data. The observed concordance of distinct expression profiles—particularly the upregulation of serine metabolism genes in enriched cancer cell populations—highlights the power of single-cell approaches to uncover both cellular diversity and model-specific molecular features. These findings underscore the value of high-throughput single-cell technologies for advancing our understanding of ovarian cancer biology, with implications for improving cancer models and identifying potential therapeutic targets.

#4937 Enabling transcriptome-wide single cell RNA sequencing from FFPE tissues with Evercode WT combinatorial barcoding.

Aisling Sinclair, Ajay Sapre, Alec Salvino, Guillermo Gallareta-Olivares, Vuong Tran, Joey Pangallo, Gokhan Demirkan, Sam You, Charles Roco, Alexander Rosenberg

Parse Biosciences, Inc., Seattle, WA

Formalin-fixed, paraffin-embedded (FFPE) tissues represent a vast and underutilized resource of patient data for retrospective and translational research. While FFPE enables long-term preservation of valuable clinical specimens, RNA degradation and fragmentation have historically hindered its compatibility with single cell RNA sequencing (scRNA seq). Currently, researchers have relied on probe-based FFPE profiling approaches and are limited to predefined target sets, restricting transcriptome coverage and discovery potential.

Here, we introduce a novel split-pool combinatorial barcoding method for FFPE tissue that captures the full transcriptome through dual priming with both poly dT and random hexamer reverse transcription primers. This workflow extends the scalability of Parse's single-cell technology to FFPE tissues, enabling unbiased transcriptome-wide analysis of millions of cells and hundreds of samples within a single experiment. By capturing a broad range of RNA biotypes, this approach delivers deeper insights into cellular function and disease mechanisms.

As a proof of concept, FFPE tissues from multiple organs, including kidney, brain, lymph node, liver, and breast tumor, were processed using our novel Evercode Whole Transcriptome (WT) for FFPE assay. The resulting single cell datasets demonstrated high-resolution identification of cell types across diverse tissue types. Comparative analyses between FFPE and matched fresh frozen samples revealed concordance in gene expression patterns and cell type proportions, validating the approach's complete capture of sample biology. In cancer samples, complex cellular biology was captured from the detection of tumor infiltrating lymphocytes to cancer associated fibroblasts.

By enabling transcriptome wide scRNA-seq from thousands to millions of cells from FFPE-preserved tissues across hundreds of samples simultaneously, this method greatly expands access to single cell analyses of archival specimens, offering a powerful platform for translational oncology, biomarker discovery, and precision medicine research.

#4938 Elucidation and pharmacologic targeting of master regulator proteins representing mechanistic determinants of macrophage state and immunoevasive potential.

Gaetano Viscido[1], Mikko Turunen[1], Zhouzerui Liu[2], Justyn Chang[2], Meghna S. Raman[2], Leo B. Dupire[1], Hanrui Zhang[3], Tim Olsen[2], Jeremy Worley[4], Aleksandar Obradovic[5], Andrea Califano[6]

[1]Systems Biology Department, Columbia University, New York, NY,[2]Chan Zuckerberg Biohub, New York, NY,[3]Cardiovascular Genomics Program, Department of Medicine, Columbia University Irving Medical Center, New York, NY,[4]Columbia University and Chan Zuckerberg Biohub, New York, NY,[5]Columbia University, New York, NY,[6]Dept. of Systems Biology and Dept. of Medicine and Dept. of Biomedical Informatics and Dept. of Biochemistry & Molecular Biophysics, and HICCC, Columbia University Irving Medical Center; Chan Zuckerberg Biohub, New York, NY

PURPOSE: Macrophages (mΦ) exhibit extensive transcriptional plasticity within the tumor microenvironment (TME). While M1 mΦ promote anti-tumor immunity, regulatory M2 mΦ drive tumor progression and resistance to immune checkpoint therapy. In a recent study, Obradovic et al. (Cell 2021) used VIPER, a network-based algorithm that infers protein activity from transcriptomic data, to identify a highly immunosuppressive TAM subset in clear cell renal carcinoma (ccRCC) characterized by TREM2$^+$/C1Q$^+$/APOE$^+$ (TCA$^+$) expression. TCA$^+$ mΦ were associated with poor prognosis, metastasis, and immune evasion. We aim to identify Master Regulator (MR) proteins that mechanistically control the TCA$^+$ program and may serve as actionable targets for selective depletion or reprogramming of these cells toward neutral, antitumor or pro-inflammatory states.

METHODS: We performed pooled single-cell CRISPR interference (CRISPRi) via Perturb-seq targeting 50 candidate MRs identified by VIPER from genes differentially expressed in TCA$^+$ versus M0/M1 mΦs, followed by time-resolved scRNA-seq. THP-1 monocytes were differentiated and polarized to the M2 state using IL-4 and IL-13 for 48 hours, then profiled across seven time points spanning M2 polarization (0, 6, 12, 24, 48, 96, 192 hr). Approximately 100,000 cells per time point were analyzed, along with ~10,000 unperturbed THP-1-derived M0, M1, and M2 mΦs as references. We aim to generate perturbational RNA-seq profiles of TCA$^+$ mΦs with >350 drugs using PLATE-seq to identify compounds that either target individual MRs (OncoTarget) or invert the global MR-activity signature (OncoTreat), thus phenocopying validated genetic perturbations.

UNPUBLISHED DATA: We generated a comprehensive dataset comprising ~700,000 time-resolved (~100,000 cells per time point), genetically perturbed mΦs, enabling high-resolution characterization of MR-specific transcriptional responses across the full course of M2/TCA$^+$ polarization. The dataset captures early, intermediate, and late transcriptional changes induced by targeted repression of candidate MRs, providing a dynamic view of the regulatory architecture underlying the acquisition and maintenance of the TCA$^+$ state. We will integrate with >350 drug-perturbation profiles to establish a matched pharmacologic resource for downstream identification of compounds capable of modulating MR activity or globally shifting the TCA$^+$ transcriptional program.

CONCLUSION: This study provides a large-scale, time-resolved map of regulatory programs in immunosuppressive TCA$^+$ mΦs, with the aim of identifying and targeting Master Regulators to invert their immunosuppressive phenotype. This framework offers a path to neutralize mΦ-mediated immunosuppression and improve responses to immune checkpoint therapy.

#4939 Quantifying tumor immune escape through immunogenic tension mapping.

June-Young Koh[1], Ludmil B. Alexandrov[2]

[1]UCSD, San Diego, CA,[2]UC San Diego Health, San Diego, CA

Predicting response to immunotherapy remains challenging because biomarkers such as TMB, PD-L1 expression, and bulk immune infiltration offer only static snapshots of tumor biology and fail to capture the cumulative influence of immune pressure over time. Immune pressure leaves discernible footprints on tumor evolution, and characterizing these signatures may help distinguish tumors shaped by immune editing from those that have escaped immune surveillance. Comparing observed tumor genomes with patient-specific neutral expectations provides a direct framework for revealing such evolutionary deviations. Using TCGA colorectal cancers, we generated mutational-signature-matched neutral simulations and quantified how far each tumor diverged across multiple evolutionary metrics. Observed coding mutations showed substantially greater dispersion than neutral simulations. Although the cohort appeared near-neutral overall, tumors showing strong deviation in one metric consistently deviated across others, revealing a coherent subset under stronger selective pressure. These strongly deviated tumors aligned with well-established hypermutated categories—including POLE-mutated hypermutated tumors and MSI-H/indel-rich tumors—and displayed steep TMB gradients (44.8 vs 5.3 mut/Mb across quartiles). They also exhibited stronger immune-associated features, including significant higher CD8-related infiltration and elevated CD103 ratios in extreme cases, suggesting that immune activity contributes to the observed evolutionary divergence. To evaluate whether broader mutation patterns capture deeper evolutionary structure, we embedded observed and simulated mutation catalogs into a genomic foundation model. The resulting latent space clearly distinguished strongly deviated tumors from near-neutral cases, and also separated molecular subtypes and each sample's mutational-signature composition. These findings suggest that zero-shot sequence representations capture contextual patterns linked to immune-driven tumor evolution. Because these embeddings encode mutation context at a finer resolution than classical summaries, they can recover evolutionary trajectories and underlying mechanisms that remain obscured in low-dimensional metrics. Together, these results show that immune-linked evolutionary divergence is detectable even when cohort-level averages appear neutral. Tumors that diverge most strongly from neutral expectation correspond to hypermutated biology and increased CD8-driven immune activity. Evolution-based approaches—especially when combined with foundation-model embeddings—offer a scalable framework for quantifying historical immune pressure and refining immunologic stratification beyond conventional biomarkers.

#4940 A hybrid mathematical model: Emergent CAF structures and their impact on cancer progression.

Junho Lee, Eunjung Kim

Center for Natural Product Systems Biology, Korea Institute of Science and Technology, Gangneung, Korea, Republic of

Cancer-associated fibroblasts (CAFs) are key regulators of the tumor microenvironment (TME), exhibiting diverse phenotypes that exert both anti- and pro-tumorigenic effects. To investigate how this heterogeneity shapes cancer progression and therapy response, we first developed an ordinary differential equation (ODE) model, which assumes a well-mixed, homogeneous, and non-spatial TME. This mean-field framework captures cancer-immune-CAF interactions and predicts that CAF composition strongly influences treatment outcomes sometimes making single-agent therapies as effective as multi-drug combinations, or conversely rendering even triple-combination therapies ineffective. These results highlight CAF composition as a potential biomarker for guiding less invasive, CAF-informed therapeutic strategies.

To overcome the limitations of non-spatial ODE models, we developed a hybrid Agent-Based Model-Partial Differential Equation-Ordinary Differential Equation (ABM-PDE-ODE) framework. In this spatial model, cancer cells, T cells, and CAFs are represented as individual agents that migrate, proliferate, or die based on local environmental cues. Diffusible factors including oxygen, CXCL, IFN-gamma, and TGF-beta are modeled by PDEs to generate spatial gradients, while each T cell independently solves an ODE-based PD-1/PD-L1 binding equation to determine its activation or exhaustion state. This multiscale model resolves spatial heterogeneity, local immunosuppressive niches, and CAF-driven barriers to immune infiltration phenomena that cannot be captured in the well-mixed ODE system.

Together, these complementary modeling approaches provide a unified multiscale framework to evaluate how CAF phenotypic diversity shapes cancer dynamics and treatment response, and they offer new opportunities for CAF-informed, spatially guided personalized therapy design.

: Spatial Niches and Functional Boundaries within the Tumor Microenvironment 1
Poster Session

#4944 Chromogenic triplex characterization of breast and gastrointestinal cancers for biomarker discovery and spatial image analysis.

Andrew Fuller[1], Stacey Margerrison[1], **Scott J. Anderson**[1], Anne Hellebust[2]

[1]Leica Biosystems, Buffalo Grove, IL,[2]Indica Labs, Albuquerque, NM

Background: HER2 and PD-L1 expression serve as key biomarkers in breast and gastrointestinal (GI) cancer research. The tumor immune microenvironment, particularly the presence of tumor-infiltrating lymphocytes (TILs), also plays a critical role in these cancers, with mounting evidence of the importance of the signaling between the tumor and its environment. In this study, we evaluated two multiplex chromogenic immunohistochemistry (IHC) assays, HER2/PD-L1/CD3 and HER2/PD-L1/CD8, to assess the relationships among their expressions and related signaling pathways.
Methods: Formalin-fixed, paraffin-embedded (FFPE)tissue sections from HER2-expressing and/orPD-L1-positive breast and GI cancers were stained using CD3/HER2/PD-L1 andCD8/HER2/PD-L1 chromogenic multiplex IHC assays on the BOND RX RUO automated stainer from Leica Biosystems. The assays employed the Chromoplex III Triple Detection RUO system from LeicaBiosystems. Whole-slide imaging was performed on the Aperio GT 450 DX scanner, and HALO® digital image analysis from Indica Labs was used to quantify biomarker expression with the Multiplex IHC module leveraging HALO AI nuclear and membrane segmentation. Relationships between identified tumor cells and immune infiltrates were further interrogated with the Spatial Analysis module
Results: In HER2-positive breast cancer, expression of PD-L1and TIL markers (CD3, CD8) varied, with a subset of cases showing high CD8+ T-cell infiltration, potentially indicative of a more immunogenic phenotype.HALO AI analysis provides insights into proximity ofCD3, CD8 and PDL1 positive infiltrating cells to HER2positive carcinoma cells within breast and stomach carcinoma cases providing valuable spatial analysis using chromogenic multiplexing.Visualization of 3 markers simultaneously using ChromoPlex III Triple Detection RUO allows automated spatial analysis of tumor samples.In HER2 positive breast cancer and stomach cancer cases higher density of CD3+ cells and CD8+ cells shown to be in closer proximity to HER2 positive cells with the highest number of CD3 or CD8+ cells seen within 10uM of a HER2+ cell.
Conclusions: ChromoPlex III Triple Detection RUO can be used as a tool to identify 3 simultaneous markers in FFPE tissue using automated staining (BOND RX). As an example -multiplex chromogenic IHC staining of HER2, PD-L1,and CD3/CD8 provides valuable insights into the interplay between the tumor and the immune cell microenvironment in breast and GI cancers. The use of whole-slide digital pathology (Aperio GT 450 DX) and HALO AI Image Analysis, enables high-throughput assessment of multiplex chromogenic stained slides. HALO AI Image Analysis is a powerful tool for automated quantification of marker expression and proximity analysis.

#4945 Distinct colorectal cancer tumor cell subtypes revealed by single-cell and spatial transcriptomics.

Ji Hye Choi[1], Yeong Hak Bang[2], Kyung Yeon Han[3], Woong-Yang Park[4]

[1]Sungkyunkwan University, Seoul, Korea, Republic of,[2]University of Ulsan College of Medicine, Seoul,[3]Translational Genomics Center, Seoul, Korea, Republic of,[4]GENINUS, Seoul, Korea, Republic of

Background: Colorectal cancer is highly heterogeneous, exhibiting diverse tumor characteristics. However, studies focusing on the epithelial cell compartment remain limited. Here, we aimed to comprehensively profile CRC epithelial cells, define tumor-specific subtypes, and explore their spatial distributions and prognostic implications.
Method: We performed single-cell RNA sequencing of 65 primary CRC samples, along with 13 liver metastasis, 33 colon normal, and 8 liver normal controls. Epithelial cell clusters were classified using non-negative matrix factorization. After characterizing their transcriptional and developmental features, we mapped the subtypes to spatial transcriptomic data to assess spatial localization patterns within the tumor.
Results: We analyzed a total of 273,711 cells including 64,911 epithelial cells. Among these epithelial cells, 14 tumor-associated epithelial clusters were identified after excluding low-quality and normal-like clusters. Of these, seven clusters consistently abundant across multiple samples were selected for further analyses: C1 (inflamed), C2 (ribosomal), C3 (epithelial-mesenchymal transition; EMT), C4 (goblet-like), C5 (MHC II), C6 (oxidative phosphorylation), and C8 (proliferating). C1 and C3 were enriched in advanced-stage tumors and associated with poor prognosis in TCGA data. Trajectory inference suggested a developmental continuum from C8 toward C1 and C3, indicating potential tumor cell evolution toward EMT and inflamed states. Spatial transcriptomic analysis using both Visium and Xenium datasets revealed distinct localization patterns: C2, C6 and C8 were concentrated in the tumor core, whereas C1 and C3 were predominantly enriched at the tumor margin. Interestingly, tumor budding regions were predominantly composed of these C3 clusters, consistent with the EMT-like characteristics of tumor buds. Notably, co-localization analysis revealed subtype-specific epithelial-immune-stromal niches, in which myofibroblastic cancer-associated fibroblasts and *SPP1*$^{+}$ macrophages were spatially associated with C3 clusters, suggesting potential crosstalk that may promote tumor invasion and immune modulation.
Conclusions: We profiled colorectal cancer epithelial cells and identified distinct tumor cell subtypes with unique transcriptional and spatial characteristics. These subtypes exhibited dynamic interactions with the surrounding tumor microenvironment, suggesting that epithelial plasticity and spatial crosstalk may collectively drive tumor progression and immune evasion.

#4946 Osteopontin spatially rewires tumor-immune niches to promote colon cancer liver metastasis.

Patrick Czabala[1], Yang Zhao[1], John Klement[1], Dafeng Yang[1], Dakota Poschel[1], Kendra Fick[1], Zainab Tiamiyu[1], Martina Zoccheddu[1], Kristen Carver[1], Priscilla Redd[1], Patricia Schoenlein[1], Jennifer Waller[2], Huidong Shi[1], Kebin Liu[1]

[1]Biochemistry and Molecular Biology, Augusta University, Augusta, GA,[2]Biostatistics, Data Science, and Epidemiology, School of Public Health, Augusta University, Augusta, GA

Osteopontin (OPN) is a secreted extracellular matrix protein that regulates T cells, myeloid cells, and tumor cells. Although OPN is a known biomarker of colorectal cancer (CRC) progression and liver metastasis, the cellular circuitry linking OPN-producing and OPN-responsive cells in the metastatic liver microenvironment remains poorly defined. Here, we investigated how tumor-derived and host-derived OPN remodel this microenvironment to promote disease progression. Using orthotopic mouse models, we found that deleting OPN in either tumor cells or host cells was sufficient to increase T cell infiltration and suppress liver metastasis, whereas dual deletion produced an even greater reduction in metastatic burden. To define niche-specific programs, we applied COSMX spatial transcriptomics to mouse liver metastasis tissues, profiling 1,000 signature genes across 1,179,351 cells. We determined that tumor-derived OPN reprograms immune-inactive niches enriched for highly proliferative cancer cells, and that host-derived OPN rewires niches characterized by low monocyte and T cell abundance and enriched stem-like cancer cells. Mechanistically, tumor-derived OPN activates the MEK/ERK pathway to promote tumor cell proliferation. To translate these findings, we tested OPN blockade immunotherapy in mouse models. OPN blockade immunotherapy significantly suppressed tumor growth and increased immune cell infiltration in both syngeneic models and humanized mouse models of CRC liver metastasis. Together, these data identify tumor- and host-derived OPN as nonredundant, pro-metastatic drivers of proliferation, immune suppression, and niche remodeling, and support OPN inhibition as a promising immunomodulatory strategy for CRC liver metastasis.

#4947 Spatially organized transcriptional programs and tumor-stroma interfaces shape immunotherapy response in microsatellite instability-high gastrointestinal cancers.

Xueshuai Han[1], Kohei Yamashita[1], Melissa Pool Pizzi[2], Kyung Serk Cho[1], Enyu Dai[1], Kai Yu[1], Yunhe Liu[1], Yibo Dai[1], Tian Chu[1], Matheus Sewastjanow-Silva[1], Hiro Yoshimura[1], Yibo Fan[1], Rebecca Waters[1], Qiong Gan[1], Feng Yin[1], Shilpa S. Dhar[1], Isadora Martins[1], Jason Willis[1], Mariela B. Murphy[1], Jenny Li[1], Brian D. Badgwell[1], Van K. Morris[1], Michael J. Overman[1], Linghua Wang[1], Jaffer A. Ajani[1]

[1]UT MD Anderson Cancer Center, Houston, TX,[2]Gastrointestinal Medical Oncology, UT MD Anderson Cancer Center, Houston, TX

Background: Immune checkpoint blockade (ICB) has significantly improved outcomes in microsatellite instability-high (MSI-H) gastrointestinal cancers, yet more than half of patients do not achieve durable remission despite initial tumor regression. Clinical decisions guided solely by MSI status and radiographic response provide limited ability to anticipate long-term benefit or inform choices regarding surgery and treatment modification. The development of spatially informed molecular predictors of sustained response would therefore address a critical unmet need in the management of MSI-H tumors.

Methods: Spatial transcriptomic profiling was performed on 18 tumor specimens from 13 patients with gastric, colorectal, or esophageal cancers, including 11 MSI-H and 2 MSS tumors, collected before and after ICB therapy. All tissues were assayed using the 10x Genomics Visium platform. Pathology-guided spot annotation was combined with transcriptional Meta-program analysis, spatial deconvolution, niche interaction mapping, and ligand-receptor modeling to characterize tumor-immune-stromal organization across sustained complete responders (CR) and non-sustained responders (NR).

Results: We found that tumor cell meta-programs (MPs) exhibited distinct spatial gradients across different response groups. The epithelial-mesenchymal transition MPs was enriched at the invasive margin of pre-treatment NR (pre-NR) tumor tissue and diminished toward the core, while the Cycling-high-Interferon MPs peaked at the periphery of pre-CR tumor tissue. These findings indicate that transcriptional programs are spatially compartmentalized within the tumor. Next, we investigated how the spatial organization of the tumor microenvironment (TME) differed between response groups. In pre-CR tumors, malignant cells colocalized with B cells and T follicular helper cells within tertiary lymphoid structures (TLSs), whereas in pre-NR tumors, they were associated with macrophages and cancer-associated fibroblasts. Notably, TLSs from CR tumors exhibited stronger immune activation signatures irrespective of their maturation state. Cell-cell communication analysis further revealed immune activation at the tumor-stroma interface in sustained-CR tumors, contrasting with immunosuppressive signaling in NR tumors.

Conclusions: Our study reveals distinct spatial and transcriptional programs underlying differential responses to ICB in MSI-H gastrointestinal cancers, highlighting the pivotal role of tumor-immune-stromal organization in shaping therapeutic outcomes and guiding future strategies to enhance immunotherapy efficacy.

#4948 Spatial architectures of colorectal cancer microenvironment underlying immune checkpoint inhibitor response.

Chuyan Liu[1], Hang Yin[2], Joon Sang Lee[3], Julien Tessier[4], Junbum Kim[2], Donald Jackson[3], Angela Hadjipanayis[4], Olivier Elemento[5]

[1]Graduate School of Medical Sciences, Weill Cornell Medicine, New York, NY,[2]Department of Systems and Computational Biomedicine, Weill Cornell Medicine, New York, NY,[3]Precision Oncology, Sanofi, Cambridge, MA,[4]Precision Medicine and Computational Biology, Sanofi, Cambridge, MA,[5]Caryl and Israel Englander Institute for Precision Medicine, Weill Cornell Medicine, New York, NY

Colorectal cancer (CRC) remains a leading cause of cancer mortality. Immune checkpoint inhibitors (ICI) are among the most effective systemic therapies, yet they benefit only a subset of MSI-H/MMRd patients. To investigate how spatial tumor-immune-stromal organization contributes to heterogeneous treatment responses, we profiled FFPE CRC tissues from PD-1 inhibitor pembrolizumab-treated (n=10) and treatment-naïve (n=14) patients using the CosMx Spatial Molecular Imager (SMI) with a 1,000-gene single-cell panel. After image processing and cell segmentation, cell states were annotated through unsupervised Leiden clustering, gene-module scoring, and supervised InsituType prediction using a public CRC single-cell atlas, followed by spatial analyses including niche identification, neighborhood enrichment, distance-based metrics, and ligand-receptor inference. Across 24 patients (balanced sex distribution; stages I-IV; median age 66.5), ICI-treated tumors exhibited markedly higher frequencies of all $CD8^+$ T cell subsets, $CXCL8^+$ cancer-associated fibroblasts (CAFs), myofibroblasts, and diverse macrophage and neutrophil populations compared with treatment-naïve tumors, alongside higher proportions of CMS1-like malignant cells. *De novo* nonnegative matrix factorization (NMF) revealed eight tumor-intrinsic programs, with Inflammatory/MHC-II, Type I IFN/Antigen Presentation, and Innate Inflammatory programs enriched in ICI-exposed tumors, whereas Invasion/Angiogenesis, Proliferation/Stress, and CEA-high programs characterized untreated tumors. Spatial mapping uncovered two recurrent architectures: immune-infiltrated tumors enriched for tertiary lymphoid structures (TLSs) marked by T-B lymphocyte aggregates and focal LTB and CXCL13 expression, as well as fibroblast-dominated tumors demonstrating stromal encapsulation, limited immune intermixing, and preliminary enrichment of CAF-immune suppressive ligand-receptor circuits. Together, these findings delineate inflamed versus fibrotic CRC microenvironments with distinct tumor-immune communication states. Integration of spatial features with clinical response will support refined stratification for ICI-based therapy and nominate TLS density, CAF patterning, and specific ligand-receptor modules as candidate spatial biomarkers for predicting or modulating treatment responsiveness.

#4949 High resolution spatial transcriptomics reveals dynamic remodeling of the tumor microenvironment during prostate cancer progression.

Jiayi Zhou, Gabriel Cruz, Somnath Mahapatra, Radha Paturu, Hanbyul Cho, Xuhong Cao, Fengyun Su, Rui Wang, Dan Robinson, Yi-Mi Wu, Rohit Mehra, Kayla Muschong, Christine Caldwell Smith, Chelsea Decker, Chandan Kumar-Sinha, Saravana Mohan Dhanasekaran, Rahul Mannan, Yuping Zhang, Arul Chinnaiyan

University of Michigan, Ann Arbor, MI

Prostate cancer exhibits diverse cellular composition, and the interaction between the tumor epithelial and tumor microenvironment (TME) cell types plays a crucial role in disease progression. However, due to technical limitations, systematic characterization of microenvironmental influences on prostate cancer progression remains insufficient. This study combined an assembled single-cell transcriptomic data (163 prostate samples; 756,000 high-quality cells) with the spatial data we obtained from 20 primary prostate tumors using the Visium HD platform to create high-resolution spatial profiles of the TME in prostate cancer. Our approach enabled detailed investigation of the dynamic remodeling of TME during prostate cancer progression from benign to low- and high-grade lesions. Our spatial transcriptomics data cohort includes 13 high-grade (grade group>=2) and 7 low-grade cases (grade group 1). We used the single cell clustering results as a reference and applied robust cell type decomposition (RCTD) to annotate the Visium HD data. In total, we identified 15 major cell types within the microenvironment and observed significant differences in the distribution of TME cell types and their frequency across benign, low-grade, and high-grade prostate cancers areas. Inflammatory fibroblasts and their gene signature were more prevalent in benign and low-grade microenvironments, whereas they decreased in high-grade TME. Conversely, myofibroblasts and their gene signature were enriched in high-grade TMEs. Within the smooth muscle populations, the more proliferative and migratory synthetic type (THY1-high) is increased in high-grade TMEs, while the contractile type (RERGL-high) was enriched in benign and low-grade microenvironments. Among endothelial cells, the abundant pro-angiogenesis subpopulation (EDNRB-high) was noted in high-grade TMEs, in contrast to the preferential enrichment of anti-angiogenesis subpopulation (RGS16-high), in localized to benign and low-grade microenvironments. Our findings uncover variations in the TME across tumor stages and implicate several important cell types that may influence prostate cancer progression, offering clues for future therapeutic exploration.

#4950 Spatially resolved multiomic profiling of cancer tissue with DISS enables variant mapping across tissue landscape.

Vivian Tran Dien, Tyler Lopez, Connor Thompson, Ben Krajacich, Adeline Mah, Andrew Altomare, Mariam Dawood, Neam Dawood, Keerthana Elango, Daniel Honigfort, Ryan Kelley, Michael Kim, Jean Kwon, Seana Lymer, Kyle Metcalfe, Jacob Moreno, Duuluu Naranbat, Evan O'Brien, Tristin Rammel, Carlos Ruiz Perez, Ramreddy Tippana, David White, Kelly Wiseman, Jennifer Wong, Jane Yao, Grace Yeo, Matthew Kellinger, Sinan Arslan, Michael Previte

Element Biosciences, Inc., San Diego, CA

Clonal evolution within the tumor microenvironment is central to understanding disease initiation, progression, and therapeutic response and resistance. Resolving these dynamics requires high accuracy spatial transcriptomics that can map driver mutations and cellular phenotypes directly in intact tissue. Direct in Sample Sequencing (DISS) on AVITI24™ enables the measurement of transcriptome and targeted gene expression directly in intact tissues sections without library preparation, linking genotype and phenotype at high resolution to resolve the complex clonal architecture in the tumor microenvironment. AVITI24™ utilizes two complementary approaches for spatial profiling with DISS: a 3' transcriptome method using poly-T probes to capture polyadenylated mRNA, and a targeted strategy employing custom probes designed against expressed variants or a panel of hundreds of RNA markers. The AVITI24™ system automatically performs probe hybridization, cDNA extension, probe circularization, and rolling-circle amplification onboard. DISS chemistry is designed for flexibility, using single-ended probes and supporting up to 100 sequencing cycles with >80% Q30, enabling sensitive detection of a broad range of expressed variants including SNPs, indels, and fusions through long, high quality reads of the transcriptome, not currently capable with dual-sided probe or padlock-based detection methods. To demonstrate variant detection in cancer with DISS, we profiled somatic driver mutations expressed in fresh frozen and FFPE colorectal cancer sections, including multiple hot-spot SNVs in KRAS and TP53, TGFBR2 and APC indels, and ALK gene fusions. Targeted DISS achieved sensitive detection of mutations with variant allele frequency (VAF) down to 5% for genes of diverse expression levels. Utilizing unbi2ased transcriptomic profiling, we accurately resolved major cell types within the tumor microenvironment, with results from sequential tissue sections demonstrating high concordance with RNA seq ($R^2 = 0.7$). Spatial mapping of these alterations onto tissue morphology uncovered regional clonal architecture and mutational heterogeneity within intact tumor microenvironments. Using DISS chemistry in tissue, transcriptomics from the same tissue section across a panel of custom genomic targets enabled a highly personalized and sensitive approach to identify both cell types and their associated oncogenic mutations with spatial precision.

#4951 Unraveling the role of APOE/APOC1/SPP1/TREM2-positive lipid-Associated macrophages in destructive venous invasion and metastasis of colorectal cancer.

Sanha Hwang

Seoul National University, Seoul, Korea, Republic of

Background/Objective
Venous invasion (VI) is strongly linked to recurrence and poor outcomes in colorectal cancer, especially when the vessel wall is breached (destructive VI). The cellular programs that distinguish destructive VI from intraluminal VI remain unclear. We hypothesized that lipid-associated macrophages (LAMs) co-expressing APOE, APOC1, SPP1 and TREM2 remodel the VI niche via lipid metabolic reprogramming, immune suppression and matrix/vascular remodelling, thereby driving metastatic spread.
Methods
We analysed 103 metastatic colorectal cancer patients across three platforms. Using GeoMx Digital Spatial Profiler on 67 samples we compared regions of destructive VI tumours, VI-negative tumours and control vessels. We re-analysed published single-cell RNA-seq data from 60 matched primary-liver-metastasis pairs for myeloid re-clustering, differential expression and pathway analysis. We applied Xenium in situ sequencing (5k panel) on 36 tissues to spatially map macrophage states around VI boundaries. Standard normalization, batch correction, multiple-testing control and ring-based spatial enrichment around destructive VI edges were applied, with primary contrasts of destructive VI versus VI-negative/control regions.
Results
Across platforms we found a convergent myeloid program. In GeoMx data, tumour microenvironments adjacent to destructive VI exhibited consistent up-regulation of APOE, APOC1 and SPP1, along with cathepsins (eg CTSB/CTSL), and enrichment of protein secretion, glycolysis and complement/coagulation pathways compared to VI-negative tumours and control vessels. The single-cell dataset revealed a distinct TREM2$^+$ TAM cluster co-expressing APOE/APOC1/SPP1 with lipid-oxidative signatures, matching LAM-like macrophages. In Xenium spatial data these macrophages preferentially accumulated at destructive VI boundaries, aligning exactly with suppressed T-cell activity at sites of vascular breach and tumour escape. Our data confirm a functional interaction between APOE and LRP1, supporting a Jun-APOE-LRP1 axis in colorectal cancer invasion and metastasis.
Conclusions
Our multi-platform study nominates APOE/APOC1/SPP1/TREM2$^+$ LAMs as central players in the destructive VI niche in colorectal cancer, integrating lipid-metabolic rewiring with matrix/vascular remodelling and immune suppression at vascular breach sites. The confirmed involvement of the Jun-APOE-LRP1 axis points to this pathway as a therapeutic target. These findings support translational efforts to target TREM2 and the APOE-LRP1 axis to intercept metastatic seeding via venous invasion. Functional validation is underway.

#4952 Spatial Transcriptomics reveals core resistance niches distinguishing non-MPR from MPR in NSCLC after neoadjuvant chemoimmunotherapy.

Seo Hye Park[1], Jeongbin Park[1], Hongyoon Choi[1], Jaemoon Koh[2], Taeyoung Yun[3], Jihyeon Park[3], Bubse Na[3], Samina Park[3], In Kyu Park[3], Chang Hyun Kang[3], Young Tae Kim[3], Kwon Joong Na[1]

[1]Portrai, Inc., Seoul, Korea, Republic of,[2]Department of Pathology, Seoul National University Hospital, Seoul, Korea, Republic of,[3]Department of Thoracic and Cardiovascular Surgery, Seoul National University Hospital, Seoul, Korea, Republic of

Background

Neoadjuvant chemoimmunotherapy (nCIT) is increasingly used in NSCLC. Major pathologic response (MPR) is a robust prognostic marker, yet bulk or single-cell assessments of residual tumor do not capture how spatially heterogeneous TMEs yield non-MPR. Using FFPE Visium CytAssist spatial transcriptomics, we defined tissue-scale core resistance niches distinguishing MPR from non-MPR after nCIT and asked whether these niches delineate spatially targetable compartments.

Methods

FFPE resections from 10 nCIT-treated patients were profiled; MPR status followed IASLC criteria. Blocks were selected by residual tumor burden (MPR 5-10%; non-MPR 70-90%). We compared global programs (DEG, GSEA/Reactome, cell-cycle), inferred cell composition (cell2location), analyzed context-specific ligand-receptor and metabolic states, and spatially mapped resistance axes (DDR, NRF2/ferroptosis, MDR/ABC) and TACSTD2 (TROP2).

Results

Non-MPR activated cell-cycle/transcription/DNA-repair programs and showed a proliferative landscape, whereas MPR was ECM/immune-enriched and quiescent. Deconvolution mapped deep T-cell/myeloid infiltration into MPR cores/borders, while non-MPR cores remained epithelial-dense. Ligand-receptor mapping showed immune-recruiting ECM-integrin/syndecan and CX3CL1-ITGAV at MPR boundaries but LGALS9-HAVCR2, MIF-CD74, and TIMP1-CD63 within non-MPR cores, extending into peritumor tissue. Non-MPR exhibited hyper-metabolic, antioxidant-buffered states (glycolysis, OXPHOS/TCA, glutathione), with differences attenuating in cancer-only analyses, implicating TME contribution; resistance axes were higher in non-MPR and formed contiguous core hotspots. TROP2 was core-enriched in a subset and often overlapped NRF2/MDR-high niches with low signal in adjacent non-tumor, although TROP2-independent resistant cores were also observed.

Conclusion

Spatial transcriptomics defined non-MPR by a core-centered, resistance-rich TME that is proliferative, immune-suppressive, and metabolically flexible, contrasting with the immune-permissive, quiescent landscape of MPR. Dismantling core resistance niches, restoring immune access, and tempering metabolic buffering emerge as organizing principles for overcoming residual disease. TROP2-aligned cores represent a compartment-selective subset, whereas TROP2-independent cores argue for complementary strategies.

#4953 Spatial tissue architecture as a unifying principle of tumor and microenvironmental states in adult gliomas.

Anna Mathioudaki[1], Zaira Seferbekova[1], Samuel P. Rutz[1], Michael Ritter[1], Domenico Calafato[1], Gleb Rukhovich[1], Felix Hinz[2], Philipp Mahlknecht[2], Franziska M. Ippen[2], Ekaterina Popova[3], Sophia Schinkewitsch[4], Nela Runa Koeberer[4], Nina Wilhelm[1], Pooja Sant[5], Jan-Philipp Malm[5], Sascha Dietrich[3], Christel Herold-Mende[6], Nima Etminan[7], Antje Wick[8], Sandro Krieg[9], Michael Platten[10], Andreas von Deimling[2], Felix Sahm[2], Abigail Suwala[2], Moritz Gerstung[1]

[1]AI in Oncology, German Cancer Research Center (DKFZ), Heidelberg, Germany,[2]Department of Neuropathology, Institute of Pathology, Heidelberg University Hospital, Heidelberg, Germany,[3]Department of Hematology, Oncology and Clinical Immunology, Medical Faculty and University Hospital Dusseldorf, Dusseldorf, Germany,[4]Department of Neuropathology, Institute of Pathology, University Hospital Heidelberg, Heidelberg, Germany,[5]Single Cell Open Lab, German Cancer Research Center (DKFZ), Heidelberg, Germany,[6]Division of Experimental Neurosurgery, Department of Neurosurgery, Heidelberg University Hospital, Heidelberg, Germany,[7]Department of Neurosurgery, University Hospital Mannheim, Medical Faculty Mannheim (UMM), University of Heidelberg, Mannheim, Germany,[8]Department of Neurology, University Hospital Heidelberg, Heidelberg, Germany,[9]Department of Neurosurgery, Heidelberg University Hospital, Heidelberg, Germany,[10]Clinical Cooperation Unit Neuroimmunology and Brain Tumor Immunology, German Consortium for Translat, German Cancer Research Center (DKFZ), Heidelberg, Germany

Adult gliomas exhibit substantial molecular and pathological variation. Prior single-cell studies have characterized intratumoral heterogeneity; in glioblastoma, tumor cells adopt lineage-associated programs—such as oligodendrocyte- and neuro- progenitor (OPC, NPC), astrocyte (AC) and mesenchymal (MES) like states. However, how these states recur across other gliomas remains unclear. Given their shared environment, defining conserved versus entity-specific tumor characteristics is essential for understanding glioma heterogeneity.

Here, we analyzed 310 tumor cores from 284 patients spanning oligodendroglioma, astrocytoma, glioblastoma, and ependymoma, using single-cell spatial transcriptomics with a 344-gene panel (10x Xenium). This approach yielded a dataset of 2.8 million cells, including 18 tumor microenvironment (TME) cell types. To further probe local interactions, we profiled a validation cohort of astrocytomas using a 5,096-genes panel and multiplexed immunofluorescence (57 proteins).

Our data revealed 9 recurrent tumor states across gliomas, organized into neighborhoods shaped by local cellular interactions. These formed structured layers, with OPC-/NPC-like tumors near cortical interfaces and AC-like regions forming a continuum with MES1-gliosis. Neighborhoods were largely subtype-specific suggesting that tissue organization and not cell composition alone, underlies glioma heterogeneity. Consistently, methylation classification—central to subtype definition in gliomas—stratified the cohort into 13 classes with distinct neighborhood profiles, including characteristic architectures in RTK1, RTK2, and MES glioblastomas.

Neighborhoods also showed distinct TME variation: $P2RY12^{+}$ microglia were enriched in AC-like and MES1-gliosis regions, while $CD163^{+}$ myeloid cells concentrated in MES1-gliosis and MES2-hypoxia niches. These immune patterns corresponded to neighborhood-specific inflammatory programs and at the entity level to myeloid-dominated inflammation in ependymoma and low inflammation in oligodendroglioma.

Beyond neighborhood definition, we evaluated their diagnostic potential. In astrocytoma, AC-like enrichment marked favorable prognosis, whereas MES1-like prevalence defined high-risk patients. Given this, we asked whether neighborhoods show histopathological correlates in routine H&E. Morphology embeddings extracted with histopathology foundation models recovered clusters mirroring niche composition, indicating that neighborhoods can be inferred from H&E morphology and incorporated into diagnostic workflows.

Collectively, these findings link glioma microanatomy heterogeneity by connecting tumor states to their TME. By capturing spatially dependent programs, our work provides a framework for integrating spatial architecture into biological understanding, diagnosis, and risk stratification.

#4954 Integrated scRNAseq andspatial RNAseq analysis of aggressive prostatic adenocarcinoma identifies *TIGIT-NECTIN 2/3* and *TIGIT/PVR*immunosuppressive interactions.

Jerry A. Ombor[1], Anurendra Kumar[2], Jatin Gandhi[1], Rakesh Shiradkar[3], Tilak Pathak[1], Cynthia L. Winham[1], Ismaheel O. Lawal[1], Olayinka A. Abiodun-Ojo[1], Lara Harik[1], Saurabh Sinha[2], Martin G. Sanda[1], David M. Schuster[1], Adeboye O. Osunkoya[1], **Carlos S. Moreno**[1]

[1]Emory University, Atlanta, GA,[2]Georgia Institute of Technology, Atlanta, GA,[3]Indiana University, Indianapolis, IN

Background: Our understanding of the mechanisms of tumor immunosuppression in the tumor microenvironment (TME) of aggressive prostatic adenocarcinoma (PCa) at the single-cell level is limited. Integrated Visium-HD Spatial RNAseq analysis and 10X Flex sequencing of formalin-fixed paraffin-embedded (FFPE) tissue can provide unique insights into the mechanisms of immunosuppression in the 'immune cold' TME of PCa.

Design: Visium-HD Spatial RNAseq analysis was performed on FFPE blocks from radical prostatectomy specimens of 12 patients of which six had lymph node metastases (LNM) and six did not. All specimens were also analyzed by 10X Flex sequencing, and data from each scRNAseq dataset were integrated with spatial RNAseq data. VisiumHD bins were processed with H&E images to generate cell-level expression data using the bin2cell package, and cell types were annotated. Ligand-receptor interactions were identified using the CellWhisper algorithm.

Results: Mean patient age was 63 years (range: 50-77 years). Gleason scores ranged from 7-10 (Grade group 3-5). Patients with LNM had more significant enrichment for gene signatures associated with inflammation and immune responses and high numbers of naïve regulatory T cells (Naïve Treg) near the invasive front of the aggressive tumor foci. The inflamed stroma adjacent to PCa in patients with LNM was enriched in expression of antigen-presenting genes, but also in immunosuppressive gene signatures. In addition, there was significant enrichment for spatial co-expression of the immunosuppressive receptor *TIGIT* and the *NECTIN2, NECTIN3,* and *PVR* ligands. *TIGIT* was expressed in CD4 and CD8 expressing cells and CD14+ monocytes, while *NECTIN2, NECTIN3,* and *PVR* were expressed in tumor cells, suggesting that this is one of the mechanisms of immunosuppression in aggressive PCa.

Conclusions: High-definition spatial RNAseq analysis with integrated 10X Flex scRNAseq enabled identification of mechanisms of immunosuppression in the TME of PCa. Targeting *TIGIT-NECTIN2/3* and/or *TIGIT/PVR* interactions may be a potential immunotherapeutic strategy for the management of patients with aggressive PCa.

#4955 Basescope™ duplex assay enables same-slide detection of short RNA targets including isoforms.

Sonali A. Deshpande, **Alvin J. Y. Ling**, Julia Yu, Anushka Dikhshit, Li-Chong Wang

Bio-Techne, Newark, CA

Background Genetic changes in mammalian genes including exon skipping and point mutations play a crucial role in oncogenesis and predicting patient survival and disease prognosis. Studies have shown that cancer cell lines can be distinguished from non-cancer cell line based on gene transcript isoform. As example, MET (receptor tyrosine kinase) exon 14 skipping mutation and EGFR exon 19, 21 deletion or exon 20 insertion mutation have emerged as a biomarker in various cancer types. Additionally, alternative-splicing plays a crucial role in disease progression and therapeutic response. Spatial visualization of gene isoform holds the potential of providing better understanding of tumor microenvironment.

Methods We developed a next-generation, manual and fully automated fluorescent assays on the Leica platform that enables specific and simultaneous detection of highly similar RNA targets - isoform-specific exon-exon junctions. The assay utilizes specificity and sensitivity of RNAscope™ technology to visualize single RNA molecule on formalin fixed paraffin embedded (FFPE) tissue and cell pellets. To validate the new workflow, endogenous control genes were detected using 1zz probes on HeLa cell pellets and Mouse multi tissue array. Signal and background were quantitatively compared to original BaseScope 1zz probes. To visualize MET exon 14 skipping (METΔ14), MET WT exon and exon 14-15 junction specific probes were detected on the WT and variant positive cell pellets. Further, exon 13-15 or exon 14-15 junction probe and exon 15 probes were duplexed and co-detected in MET WT and Δ14 cell pellets, respectively using BaseScope duplex assay that utilizes streamlined RNAscope chemistry to potentially co-detect mRNAs, proteins and protein-protein interactions.

Results Signal (as determined by dot counts/cell) from control gene using new BaseScope technology was comparable to signal generated using original BaseScope assay. Next, we visualized specific signal from METΔ14 exon junction probe on MET mutant pellet and WT MET probe on WT cell pellet, using dual fluorophores to identify both isoforms on the same slide. No signal was observed from mutant probe in WT pellet indicating specificity of the assay. Similarly, MET exon 14-15 junction probe and exon 15 probes were duplexed in the assay and visualized using two distinct fluorophores on wild-type cell pellet. Exon 13-15 junction probe and exon 15 probe were duplexed and co-detected using two fluorophores on mutant cell pellet. These results demonstrate the assay's efficacy in same-slide detection of cells expressing two short targets.

Conclusions This BaseScope Duplex assay provides spatial resolution of isoform and point mutation-specific gene expression, offering a powerful tool for exploring cell-specific transcript variants within the tumor microenvironment and potentially advancing precision oncology research.

#4956 Spatial and vascular microenvironmental features predict tumor-infiltrating lymphocyte expansion in glioblastoma.

Jodie Jepson[1], Kenan Zhang[2], Anna Corcoran[2], Elizabeth Owens[1], Kelly M. Hotchkiss[2], Beth H. Shaz[2], Kyra Van Batavia[2], Jose R. Conejo-Garcia[1], John Hickey[2], Mustafa Khasraw[3]

[1]Duke University School of Medicine, Durham, NC,[2]Duke University, Durham, NC,[3]Duke Cancer Institute, Durham, NC

Introduction/Rationale: Adoptive transfer of tumor-infiltrating lymphocytes (TILs) has demonstrated meaningful clinical activity in several solid tumors, yet its application in glioblastoma is challenged by profound immune dysfunction, sparse T-cell infiltration, and spatially restricted immune niches that constrain the outgrowth of tumor-reactive lymphocytes ex vivo. A deeper understanding of the spatial, cellular, and vascular features that distinguish tumors capable of yielding TIL cultures from those that fail may identify microenvironmental determinants of successful expansion and guide patient selection or microenvironment-modifying strategies for future TIL-based therapies.

Methods: TIL expansion was attempted in 40 tumors, 24 (60%) yielded successful yield in an optimized rapid expansion protocol (REP). Expanded products were characterized by spectral flow cytometry and TCRseq. A subset of TIL-positive (TIL^+; n = 5) and TIL-negative (TIL^-; n = 6) tumors underwent bulk RNA and TCRseq, single-cell RNAseq, CODEX multiplex spatial proteomics, and Xenium in situ spatial transcriptomics to define immune cell states, spatially organized niches, receptor-ligand communication networks, and vascular architecture.

Results: Expanded TILs proliferated 100-1000-fold from pre-REP to REP and were enriched for $CD4^+$ cells, with both $CD4^+$ and $CD8^+$ compartments dominated by effector-memory phenotypes and containing minimal naïve or regulatory subsets. Although overall T-cell infiltration in tumors was low (<3% of all cells), TIL^+ tumors contained more stem-like $TCF7^+$ $CD8^+$ T cells and exhibited lower expression of HAVCR2 and TOX, consistent with reduced terminal exhaustion. Spatial analysis demonstrated 2.3-fold higher $CD31^+$ endothelial density and significantly shorter T cell-endothelium distances in TIL^+ tumors ($p < 0.05$), indicating more accessible vascular niches. In contrast, TIL^- tumors exhibited 1.6-fold stronger inhibitory TAM-microglia signaling, whereas TIL^+ regions were enriched for T cell-endothelial and TAM-macrophage interactions, reflecting a more permissive immune architecture.

Conclusion: Our data highlight vascular accessibility, immune spatial organization, and reduced inhibitory myeloid signaling as key determinants of successful TIL expansion in glioblastoma. The integration of spatial transcriptomics, multiplex proteomics, and single-cell sequencing identifies microenvironmental hallmarks associated with TIL outgrowth and suggests that modulating vascular or myeloid niches may enhance the feasibility and effectiveness of TIL-based therapies in glioblastoma. These insights support microenvironment-guided patient selection and inform the development of combination approaches aimed at reconditioning the glioblastoma tumor microenvironment to improve responsiveness to cell-based immunotherapy.

#4957 Spatially resolved profiling of the tumor microenvironment and therapeutic response in SMARCB1-deficient epithelioid sarcoma.

Jiayi Fan, Jeffrey Quinn, Wesley Tansey

Computational Oncology, Memorial Sloan Kettering Cancer Center, New York, NY

Epithelioid sarcoma (ES) is a rare, aggressive soft-tissue sarcoma driven by biallelic loss of SMARCB1. It primarily affects adolescents and young adults and has poor clinical outcomes. The EZH2 inhibitor tazemetostat is the only FDA-approved targeted therapy for ES, yet most tumors show primary resistance or relapse after treatment. How the ES tumor microenvironment (TME) is spatially organized, and how it is reshaped by therapy, remains poorly understood. Here, we profiled 64 tumor tissue microassay (TMA) samples from 19 patients using the 10X Xenium 5k platform. An analysis pipeline integrating automated cell-type annotation, spatial neighborhood characterization, and ligand-receptor interaction (LRI) inference, and therapy response was established. Spatial niche analysis identified tumor associated M2 like macrophages that limit effector T cell development in the early lymphoid aggregates. Further, LRI analysis identified a detailed communication network involving immune suppression, tumor proliferation and angiogenesis in the TME. Comparative analyses using paired pre and post tazemetostat samples further revealed consistent treatment associated transcriptional shifts. Most post treatment tumors showed up regulation of inflammatory and mesenchymal transition pathways. Notably, patients who responded clinically displayed the opposite features. Together, the genes and pathways that become activated after tazemetostat exposure may highlight potential targets that could be explored in combination with EZH2 inhibition. Moreover, cancer-associated fibroblasts (CAFs) were highly abundant in ES. Distal and proximal tumors exhibited divergent CAF subgroups, with distal tumors showing a higher prevalence of CAF programs associated with matrix remodeling and migratory signaling that may facilitate tumor dissemination. These findings provide one of the first large-scale spatially resolved maps of ES.

#4958 Spatial transcriptomic profiling reveals heterogeneity in desmoplastic small round cell tumor.

Elana Sverdlik[1], Jeffrey Quinn[2], Jiayi Fan[2], Christopher Tosh[2], Tamar Feinberg[2], Melania Franchini[3], Jovana Pavisic[2], Shanita Li[2], Andoyo Ndengu[2], Glorymar Ibanez Sanchez[2], Emily Stockfisch[2], Filemon Dela Cruz[2], Andrew L. Kung[4], Joshua Honeyman[2], Emily Slotkin[2], Wesley Tansey[2]

[1]Gerstner Sloan Kettering - Graduate School of Biomedical Sciences, New York, NY,[2]Memorial Sloan Kettering Cancer Center, New York, NY,[3]Herbert Irving Comprehensive Cancer Ctr., New York, NY,[4]Chief, Division of Pediatric Hematology/, Memorial Sloan Kettering Cancer Center, New York, NY

Desmoplastic small round cell tumor (DSRCT) is a rare, aggressive soft tissue sarcoma driven by the chimeric fusion protein EWSR1-WT1 that modulates oncogenic gene expression programs in DSRCT tumor cells. Despite this defined molecular driver, treatment response and survival outcomes vary substantially between DSRCT patients (5-year survival ~ 15%). We hypothesize that treatment outcome variability reflects heterogeneity in tumor cell phenotypic states, microenvironmental architecture, and signaling networks. Here we profiled seven peritoneal and lymph node metastatic tumor sites across four DSRCT patients using Xenium 5K spatial transcriptomics on tissue microarrays (1,383,406 cells). We integrated snRNA-seq data from 15 DSRCT samples (251,087 cells) for cell type annotation, identifying patient-specific tumor subtypes through per-patient Leiden clustering (resolution=0.2) and CAF subtypes through marker gene scoring. This revealed 14 patient-specific tumor subtypes (3-4 per patient), three CAF subtypes (apCAFs, myCAFs, iCAFs), macrophages, T cells, and endothelial cells.

#4959 Trekker enables high-sensitivity, single-cell spatial profiling of the FFPE lung SCC tumor microenvironment without segmentation or deconvolution.

Cedric R. Uytingco, Alec Barret, Julie Wilhelmy, Bryant Ngo, Chenglong Xia, Jonathan Sakkos, Diksha Kool, Wanxin Wang, Christina Chang, Christina Fan, Andrew Farmer

Spatial Genomics R&D, Takara Bio USA, San Jose, CA

Squamous cell carcinoma (SCC) is a highly heterogeneous malignancy characterized by complex cellular architecture, variable patterns of immune infiltration, and diverse stromal interactions that influence progression, metastatic potential, and therapeutic response. A detailed understanding of the SCC tumor microenvironment (TME) is therefore essential for identifying biomarkers, resolving resistant niches, and guiding precision oncology strategies. Although single-cell sequencing captures cellular diversity, it lacks spatial context, while most spatial transcriptomics platforms depend on complex protocols, proprietary reagents, and computationally intensive segmentation, deconvolution, or binning steps that limit true single-cell resolution—especially in FFPE clinical samples. To address these challenges, we present Trekker, a flexible, next-generation single-cell spatial transcriptomics platform that delivers spatial context with the simplicity of standard snRNA-seq. Using a Slide-tag-inspired spatial tagging approach (Russel et al., 2023), Trekker™ indexes nuclei directly within intact tissue sections and is compatible with same-section H&E staining for direct histopathological correlation. The workflow requires no specialized instrumentation and integrates seamlessly with a fixed snRNA-seq protocol, enabling high-sensitivity, single-nucleus expression and spatial data without modifying established laboratory practices. By applying Trekker to FFPE human lung squamous cell carcinoma specimens, we generated high-resolution spatial maps of malignant cells, stromal elements, and diverse immune populations. Because each nucleus carries its own spatial barcode, downstream analysis bypasses cell segmentation, unmixing, and binning, allowing users to analyze the data using familiar single-cell bioinformatics pipelines. This streamlined approach supports robust characterization of SCC architecture, tumor-immune interaction zones, and spatially informed differential gene expression. By combining ease of implementation, FFPE flexibility, reduced computational complexity, and high-sensitivity single-cell spatial resolution, Trekker provides an accessible and powerful platform for cancer researchers. This technology enables deeper, more intuitive exploration of SCC tumor ecosystems and has the potential to accelerate biomarker discovery and therapeutic development.

#4960 Cross-platform comparison of spatial transcriptomics technologies in an FFPE lung squamous cell carcinoma sample.

Bryan Bell, Cedric Uytingco, Alec Barrett, Bryant Ngo, Jonathan Sakkos, Diksha Kool, Wanxin Wang, Melissa del Rosario, Christina Chang, Christina Fan, Andrew Farmer

Takara Bio USA, San Jose, CA

Spatial transcriptomics technologies vary widely in methodology, spatial resolution, sensitivity, and compatibility with FFPE tissues, yet comparative data generated from the same clinical specimen remain limited. We conducted a benchmarking study using a single FFPE lung squamous cell carcinoma block to evaluate Takara Trekker™ alongside Visium, Visium HD, and Xenium. Sections from the same block were processed with each platform following standard workflows. Trekker employs a unique spatial-tagging strategy that preserves the positional identity of intact nuclei and integrates seamlessly with the 10x Flex assay, enabling true single-cell–resolution spatial profiling. Visium HD and Visium provide array-based mRNA capture and Xenium enabled targeted in situ detection. Data were processed with platform-specific pipelines.Within the same tumor region, Trekker delivered higher gene recovery and captured malignant, immune, and stromal populations with spatial patterns broadly aligned with histopathology. Comparisons with Visium HD showed overall spatial concordance in major tumor and stromal features. Trekker's increased sensitivity relative to Visium HD and Visium resulted in deeper transcriptome coverage and clearer separation of transcriptionally distinct tumor states. The nuclei-based workflow also supported reliable detection of lower expressing genes. Xenium offered high-resolution, targeted measurements that aligned with Trekker's major spatial features, though its panel limited unbiased transcriptome-wide discovery.Across platforms, integrated analysis showed that Trekker provided strong concordance with both high-resolution imaging-based signals and array-level structure while preserving the advantages of whole-transcriptome profiling from FFPE. These findings demonstrate that Trekker enables high-resolution, scalable, and unbiased spatial characterization of archival lung cancer tissue and complements existing spatial technologies by combining flexible FFPE compatibility with comprehensive molecular detection.

#4961 Cell type-specific adipokine signaling networks in the breast tumor microenvironment uncovered by high-plex spatial imaging.

Samarth Singhal[1], Amber Rockson[2], Hanina Hibshoosh[3], Parin Shah[3], Fatemeh Derakhshan[3], Diane Chen[3], Alireza Salem[3], Benjamin Izar[3], Kevin L. Gardner[4], Coral O. Omene[5], Daniel Fernandez[6], Adrienne L. Castillo[6], Emma Armstrong[6], Ijeamaka Anyene Fumagalli[6], Elizabeth M. Cespedes Feliciano[7], Sandeep K. Singhal[8], **Adana A. M. Llanos**[2]

[1]University of North Dakota,[2]Epidemiology, Columbia University Mailman School of Public Health, New York, NY,[3]Columbia University Irving Medical Center, New York, NY,[4]Vagelos College of Physicians & Surgeons, New York, NY,[5]Clinical Instructor, Dept. of Medicine, Rutgers Cancer Institute of New Jersey, New Brunswick, NJ,[6]Kaiser Permanente Northern California, Oakland, CA,[7]Kaiser Permanente, Oakland, CA,[8]University of North Dakota, Grand Forks, ND

Background Adiposity is linked to adverse breast cancer outcomes, but mechanisms connecting adipose signaling to tumor progression remain unclear. Adipokines like leptin and adiponectin, and their receptors, may influence tumor behavior via paracrine and autocrine interactions across tumor, stromal, and immune cells in the breast tumor microenvironment (TME). Using high-plex spatial molecular imaging, we mapped adipokine expression and cell type-specific signaling networks to reveal adiposity-related differences in tumor biology.
Methods Single-cell spatial transcriptomics was performed using the CosMx Spatial Molecular Imager (Human 6K Panel) on breast tumors and matched adjacent tissues. Cells were segmented and classified into tumor epithelium, stroma, and immune compartments via an AI framework. LEP, LEPR, ADIPOQ, ADIPOR1, and ADIPOR2 were quantified to derive compartment-specific positivity rates, mean/very high expression, potential 5-gene co-expression, and composite adipokine signature scores and expression was compared with non-tumor cells and cells from adjacent tissues, and correlated with select clinical variables.
Results In 259 women with stage II-III breast cancer (49% postmenopausal, 47% Black, 53% Hispanic, 62% ER-positive, 17% HER2-positive), adipokine and receptor expression was consistently higher in tumor cells than stromal or immune cells. All five adiposity genes showed elevated expression in tumor cells versus stroma and immune cells. In the tumor epithelial compartment, ADIPOR1, ADIPOR2, and LEPR exhibited markedly high-end expression versus adjacent epithelium ($P < 10^{-16}$), defining a tumor-intrinsic adipokine receptor program. Tumor epithelial 5-gene signature scores and co-expression of ≥2 adipokine genes were enriched in a subset of tumors and modestly inversely associated with tumor size. In stroma, ADIPOR1, ADIPOR2, and LEPR formed a tightly coordinated module; stromal ADIPOR1 positivity and higher stromal adipokine signature scores were enriched in higher-grade and ER-negative tumors, indicating a grade- and subtype-linked stromal adipokine phenotype. In the immune compartment, ADIPOR1 and ADIPOR2 were broadly detectable at lower intensity, correlated with LEPR and immune-specific adipokine scores, consistent with a distinct immune-focused axis. Across compartments, 5-gene signatures captured coherent TME-wide adipokine programs remodeled in tumor versus adjacent tissue and showing compartment-specific associations with BMI, grade, ER status, and tumor size.
Conclusion Single-cell spatial profiling reveals a compartmentalized adipokine architecture in the breast TME, including a heightened tumor epithelial receptor program, a grade-linked stromal module, and an immune-associated axis that together form integrated adipokine signatures strongly connected to clinicopathologic features.

#4962 Spatial transcriptomics reveals distinct ASCL1 and ASCL2 gene expression patterns in advanced prostate cancer.

Fan Wei[1], Joy C. Yang[1], Kenneth Iczkowski[2], Marc A. Dall'Era[1], Chengfei Liu[1]

[1]Department of Urologic Surgery, University of California Davis, Sacramento, CA,[2]Department of Pathology and Laboratory Medicine, University of California Davis, Sacramento, CA

Background: ASCL1 and ASCL2 are bHLH transcription factors aberrantly reactivated in advanced prostate cancer. ASCL1 drives neuroendocrine differentiation by activating neuronal genes to promote androgen receptor (AR) independence. ASCL2, regulated by Wnt/β-catenin signaling, maintains stem-like programs and facilitates epithelial to neuroendocrine transition under androgen deprivation. Both factors promote lineage plasticity leading to castration-resistant and neuroendocrine prostate cancer (NEPC). This study examines their distinct gene expression patterns to elucidate how ASCL1 and ASCL2 contribute to lineage transitions and identify potential targets to block transdifferentiation.
Methods: Spatial transcriptomic profiling was performed on a Gleason 10 prostate cancer specimen using the 10x Genomics Visium platform. Regions with ASCL1-high, ASCL2-high, or ASCL1/ASCL2-low expression were analyzed for differential gene expression using Loupe Browser, heatmaps, volcano and violin plots, and pathway enrichment via Gene Set Enrichment Assay (GSEA). A patient derived (PDX) model derived from the same patient was subjected to castration, and intact (n=4) and relapsed (n=6) tumors underwent RNA-seq and GSEA. A spontaneously immortalized prostate cancer cell line, UCDCaP, was derived from the same patient, and its castration-resistant derivative, UCDCaP-CR, was established through serial castration-relapse cycles in mouse passages. Key genes were validated by qRT-PCR and Western blotting.
Results: ASCL1 and ASCL2 were expressed in a mutually exclusive manner in prostate cancer patient tissues. Compared with ASCL2-high regions, ASCL1-high areas showed higher expression of WNT5A, FOLH1 (PSMA), KRT15, and PROX1, but lower levels of AR, AKR1C3, MAOA, and MET. GSEA indicated enrichment of E2F, Myc, DNA repair, translation, and neural lineage pathways in ASCL1-high regions, while interferon signaling, androgen response, extracellular matrix, and epithelial-mesenchymal transition (EMT) pathways were enriched in ASCL2-high regions. Castration-relapsed PDX tumors exhibited increased AR, AKR1C3, ASCL1, and ASCL2, with reduced FOXA1, FOXJ1, DUSP1, and ALDH1A3. Parallel analyses in UCDCaP-CR cells showed upregulated ASCL2 and neuroendocrine markers, and downregulated ASCL1, PTEN, AR response, and P53 pathways.
Conclusions: ASCL1 and ASCL2 define distinct molecular states in prostate cancer. ASCL1 is linked to neural lineage and proliferative pathways, whereas ASCL2 is associated with androgen response and EMT programs. Their mutual exclusivity suggests divergent mechanisms of lineage plasticity. The transition toward ASCL2 dominance in castration-relapsed models, accompanied by neuroendocrine marker upregulation and loss of AR and P53 signaling, highlights their dynamic interplay in driving therapy resistance and neuroendocrine differentiation.

#4963 Cross platform validation of spatial domain identification reveals concordant tumor microenvironment architecture in NSCLC using integrated spatial transcriptomics and multiplex immunofluorescence.

Zeinab Mokhtari[1], Mint Htun[2], Debayan Mukherjee[2], Nima Vakili[1], Deon Hildebrand[2], Crysthiane Ishiy[2], Anna Pasto[2], Sue Griffin[2], **Paul Barber**[2], Tony NG[2]

[1]GSK, Heidelberg, Germany,[2]GSK, Stevenage, United Kingdom

Background: Spatial organization of the tumor microenvironment (TME) in non-small cell lung cancer (NSCLC) influences therapeutic response, yet the reproducibility of spatial domain identification across platforms remains unclear. We performed spatial transcriptomics (STx) and multiplex immunofluorescence (mIF) on surgically resected NSCLC specimens to validate spatial domain identification and characterize TME architecture between lung adenocarcinoma (LUAD) and squamous cell carcinoma (LUSC).
Methods: Formalin-fixed paraffin-embedded NSCLC tissue was analyzed using spatial profiling platforms. STx was performed using Xenium platform with cell type annotation via TACCO optimal transport-based label transfer from public NSCLC single-cell RNA sequencing data. mIF was performed using Leica Cell Dive platform. Spatial domain identification was achieved independently on both platforms: foundational deep learning models identified tissue domains in STx data, while Cell Charter method with transfer variational autoencoder (trVAE) determined cellular architecture in mIF images. Cross-platform validation assessed concordance of spatial domain boundaries and composition between STx and mIF based modalities.
Results: Spatial domain identification revealed strong concordance between STx and mIF platforms across multiple tissue compartments. Tumor epithelial domains identified transcriptomically overlapped with EpCAM-defined regions in mIF. Cancer-associated fibroblast (CAF)-enriched stromal and tertiary lymphoid structure (TLS) domains showed consistent boundaries and composition across modalities. Computationally-defined spatial domains accurately reflected histological features without manual annotation. LUSC samples exhibited expanded CAF-enriched stromal domains with reduced T-cell infiltration compared to LUAD, indicating distinct immune-stromal organization between subtypes.
Conclusions: We demonstrate robust cross-platform validation of spatial domain identification in NSCLC tissue, with computational methods accurately recapitulating biological compartments across transcriptomic and proteomic modalities. The strong concordance between STx and mIF spatial domains establishes confidence in automated tissue segmentation approaches for TME characterization. Spatial domain analyses reveal distinct microenvironmental architectures between LUAD and LUSC, with differential organization of stromal and immune compartments. This validated spatial domain framework provides a reproducible approach for high-resolution TME mapping and may enable identification of spatially-defined biomarkers for precision therapy selection in NSCLC.

#4964 Spatial interaction between Gli1 high tumor cells and M2 macrophages predicts survival and recurrence in gastric cancer.

Dae Yeong Kim[1], Dae-Hee Lee[2], Sang Cheul Oh[3]

[1]Institute of Convergence New Drug Development, Korea University College of Medicine, Seoul, Korea, Republic of,[2]Gangneung-Wonju National University, Gangneung, Korea, Republic of,[3]Dept. of Oncology, Korea University, UT MD Anderson Cancer Center, Seoul, Korea, Republic of

Purpose: This study investigated the prognostic significance of GLI1 expression in gastric cancer by analyzing its association with the infiltration and spatial proximity of tumor-associated M2 macrophages identified by CD163 and CD206. We evaluated how the combined GLI1-M2 macrophage spatial phenotype influences clinical outcomes, including survival and recurrence patterns.
Methods: GLI1 expression and M2 macrophage infiltration were assessed using immunohistochemistry and spatial biology approaches, including multiplex immunofluorescence and machine-learning-based digital pathology. CD163 and CD206 defined M2 macrophage populations. Spatial metrics included GLI1 expression intensity, M2 macrophage density, and the intercellular distance between GLI1-positive tumor cells and CD163/CD206-positive macrophages. Associations with clinical outcomes were analyzed using Kaplan-Meier survival curves and multivariate Cox regression.
Results: High GLI1 expression demonstrated a strong correlation with increased infiltration of CD163/CD206-positive M2 macrophages ($p=0.001$) and reduced spatial distance between tumor cells and M2 macrophages ($p=0.01$). The GLI1-high and M2-close phenotype was associated with markedly reduced overall survival, higher recurrence rates including early relapse, and a microenvironment enriched with immunosuppressive and tumor-promoting signals. In contrast, tumors with lower GLI1 expression and greater separation from M2 macrophages showed improved survival outcomes and reduced recurrence.
Conclusions: GLI1 expression and the spatial proximity of CD163/CD206-positive M2 macrophages serve as strong prognostic indicators in gastric cancer. The GLI1-high and M2-close phenotype identifies a clinically vulnerable subgroup with significantly poorer outcomes. These findings highlight the biological relevance of the GLI1-M2 macrophage axis and suggest that targeting GLI1 signaling or reprogramming M2 macrophages may provide therapeutic benefit and reduce recurrence risk in gastric cancer.

#4965 Sarcomatoid transformation rewires the immune spatial landscape and checkpoint regulation in chromophobe renal cell carcinoma.

Wafaa Bzeih[1], Yan Tang[1], Tiegang Han[1], Andrew J. Sedgewick[2], Nathan D. Maulding[2], Carmen Priolo[1], Katrina Collins[3], Hadi Mansour[1], Joelle Chami[1], Michelle M. Stein[2], Justin Guinney[2], Michel Alchoueiry[1], Jessica F. Williams[4], Michelle S. Hirsch[4], Pavlos Msaouel[5], Elizabeth P. Henske[1]

[1]Department of Medicine, Harvard Medical School/Brigham and Women's Hospital, Boston, MA,[2]Tempus AI, Inc., Chigaco, IL,[3]Indiana University School of Medicine, Indianapolis, IN,[4]Department of Pathology, Harvard Medical School / Brigham and Women's Hospital, Boston, MA,[5]Genitourinary Medical Oncology, The University of Texas MD Anderson Cancer Center, Houston, TX

Background: Chromophobe renal cell carcinoma (ChRCC) is the second most common non-clear cell RCC. Patients with metastatic ChRCC have a poor prognosis with a median overall survival of ~2 years. Sarcomatoid transformation occurs in ~5% of ChRCC and is associated with increased metastatic risk and reduced survival. In clear cell RCC, the sarcomatoid phenotype is associated with an immune-inflamed state and enhanced responsiveness to immunotherapy. The immune landscape of sarcomatoid ChRCC and how it differs from classic ChRCC remain poorly defined. To address this, we performed a spatial comparison of the immune microenvironment in classic versus sarcomatoid ChRCC.

Results: The 10x Genomics Xenium Prime Assay with 5k-plex target panels was performed on 10 ChRCC tumors (5 classic and 5 sarcomatoid). Hallmark pathway enrichment and differential expression analysis of pseudo-bulk data showed that sarcomatoid transformation is associated with activation of epithelial-mesenchymal transition, proliferation, and inflammatory response pathways ($p < 0.05$). Examining the spatial distribution of single cells, classic tumors showed an immune-excluded microenvironment, with T cells and macrophages localized to the tumor periphery. In contrast, sarcomatoid tumors exhibited an immune-infiltrated microenvironment, with T cells and macrophages present within the tumor bed. Sarcomatoid tumors showed an upregulation of CTLA4 across multiple T cell subsets, including cytotoxic $CD8^+$ T cells, naïve T cells, and regulatory T cells, compared to classic tumors. Additionally, in sarcomatoid tumors, cytotoxic $CD8^+$ T cells exhibited increased expression of LAG3 compared to classic tumors. Using metastasis as a proxy for sarcomatoid transformation, we compared 113 primary ChRCC tumors and 27 metastatic ChRCC tumors using bulk RNA-seq (Tempus xR). Expression profiles and immune deconvolution showed a shift from the immune-excluded, indolent primary state to an immune-modulated metastatic state marked by increased gamma delta T-cell abundance, higher LAG3 expression and decreased T cell exhaustion score (FDR < 0.05).

Conclusion: By generating the first spatially resolved immune map of ChRCC, we showed that sarcomatoid ChRCC exhibits an immune-infiltrated microenvironment with intra-tumoral T cells and macrophages, accompanied by increased expression of immune checkpoint genes including, but not limited to CTLA4 and LAG3. This higher CTLA4 is of interest given the SUNNIFORECAST trial result, where combined CTLA4 and PD1 blockade achieved a 27% objective response rate in ChRCC. We also show that metastatic progression is associated with a shift toward a gamma delta T cell-enriched immune state. Together, these findings reveal potential therapeutic vulnerabilities and support further evaluation of immune checkpoint blockade in ChRCC.

#4966 A single-cell spatial proteomic analysis of the TNBC microenvironment defines genotype-specific features.

Dana Pueschl[1], Danielle Bragen[1], Jia-Ren Lin[2], Anupma Nayak[1], Derek A. Oldridge[3], Kate Bennett[1], Victoria Fang[1], kConFab Investigators, Kenneth Offit[4], Andrew K. Godwin[5], Paul A. James[6], Phuong L. Mai[7], Soo Hwang Teo[8], Antonis Antoniou[9], Georgia Chenevix-Trench[10], E. John Wherry[1], Susan M. Domchek[1], Katherine L. Nathanson[1]

[1]University of Pennsylvania, Philadelphia, PA,[2]Harvard Medical School, Boston, MA,[3]The Children's Hospital of Philadelphia, Philadelphia, PA,[4]Memorial Sloan Kettering Cancer Center, New York, NY,[5]University of Kansas Cancer Center, Kansas City, KS,[6]Peter MacCallum Cancer Center, Melbourne, Australia,[7]University of Pittsburgh, Pittsburgh, PA,[8]Cancer Research Malaysia, Subang Jaya, Malaysia,[9]University of Cambridge, Cambridge, United Kingdom,[10]QIMR Berghofer Medical Research Institute, Brisbane, Australia

Breast cancer in women with germline BRCA1/2 pathogenic variants (g*BRCA1/2*) are generally treated with platinum-based therapies and PARP inhibitors (PARPi) with resistance commonly emerging. As the tumor microenvironment (TME) in *gBRCA1* triple-negative breast cancer (TNBC) is enriched with tumor-infiltrating lymphocytes (TILs) and CD8 T cells, treatment trials have been done combining PARPi and immune checkpoint inhibitors (ICIs) in *BRCA1* TNBC. This combination has not been shown to be more effective than PARPi alone. Evaluating the TME in *gBRCA1/2* TNBC may help identify tumors most likely to benefit from PARPi/ICI therapy. We performed a detailed spatial proteomic analysis to characterize tumor-immune cell interactions in patients with *gBRCA1/2* and wild-type (WT) TNBC with spatial tissue multiplexing (PhenoCycler) in 101 g*BRCA1*, 24 g*BRCA2*, and 30 WT TNBCs with matched RNAseq for 34 g*BRCA1*, 8 g*BRCA2*, and 16 WT TNBCs. A 43-plex antibody panel was developed featuring markers of DNA damage and repair, immune subtypes and exhaustion. We detected single tumor cells (PANCK+) in S/G2 phase (Geminin+) with double-stranded DNA breaks (γH2AX+) and DNA repair capacity (RAD51+) across all three cohorts. g*BRCA1/2* TNBC patients exhibited a significantly lower proportion of tumor cells with homologous recombination proficiency (HRP) (g*BRCA1* p = 0.006; g*BRCA2* p = 0.007) compared to WT TNBC. CD4 & CD8 T cells, and CD20 B cells had intact DNA repair in WT and g*BRCA1/2* TNBC. The frequency of CD8+ T (p=0.016) and CD20 B (p=0.003) cells was significantly higher in g *BRCA1* compared to WT TNBC; BRCA2 and WT TNBC showed no differences. A detailed characterization of CD8 T cells revealed significantly increased numbers of potentially dysfunctional CD8 T cells in BRCA1 (TOX, p<0.0001; LAG-3, p=0.028; PD-1, p=0.033) and BRCA2 (LAG-3, p=0.033) compared to WT TNBC. We observed two types of TMEs in g*BRCA1* TNBC: 1) CD8 low (mean<9.38%) with 1.4-fold increased immune checkpoint (PD-1) expression (mean: 15.4%) and high DNA damage in tumor cells; and 2) CD8 high (>9.38%) with reduced PD-1 and low DNA damage in tumor cells. Our findings suggest that although g*BRCA1/2* variants lead to DNA damage and impaired repair in tumor cells, T cells (CD4, CD8) and B cells (CD20) retain intact DNA repair mechanisms. We also found that g*BRCA1/2* TNBCs exhibit higher levels of immune checkpoint proteins LAG-3 and PD-1 on CD8 T cells compared to WT TNBC. This finding suggests the potential utility of additional ICI (LAG-3, PD-1) beyond PD-L1 blockade. Importantly, patients with g*BRCA1*-associated TNBC exhibit two different TMEs, suggesting that the response to ICI- and DNA-damaging-based therapies may differ between tumors, and anticipated prior to treatment. Defining treatment-naïve TME is crucial for designing personalized, targeted ICI strategies for individuals with *BRCA*-mutated TNBC.

#4967 Spatial divergence across glioblastoma multi-regional biopsies and corresponding neurosphere cultures.

Roberto Salatino[1], Jacob Geisberg[2], Arantxa Romero Toledo[1], Benjamin Oakes[1], Dobeen Hwang[1], Cristina Vincentelli[3], Oszkar Szentirmai[4], Thomas O. McDonald[2], Franziska Michor[2], **Michalina Janiszewska**[1]

[1]The Wertheim UF Scripps Institute, Jupiter, FL,[2]Dana-Farber Cancer Institute, Boston, MA,[3]Mount Sinai Medical Center, Miami Beach, FL,[4]Cleveland Clininc Martin Health, Port St. Lucie, FL

Glioblastoma (GBM), the most aggressive brain tumor, remains an unmet medical need, as only 6.8% of patients survive 5 years post diagnosis. Lack of effective treatment for GBM is largely driven by high level of intratumor heterogeneity, which is poorly captured by the current models of the disease used for drug discovery. Several recent studies demonstrated that spatial organization of the GBM tumor tissue is another highly heterogeneous aspect of this disease. Despite these observations, and availability of imaging-guided surgical navigation that allows for tumor-wide sampling to account for variation between distant regions of the tumor, typical drug screening is performed on cell lines derived from a single biopsy and does not account for GBM heterogeneity.

Here, we profiled matching MRI-guided multi-region primary tumor biopsies from 6 GBM cases (n=40 biopsies) and corresponding neurosphere cultures (n=30) derived from these spatially distinct tumor samples. The tumors represented all three GBM subtypes, with some biopsies classifying as a different subtype than the rest. Whole exome sequencing-based clonal analysis of the tumor samples confirmed their heterogenous nature, with 3-5 clones found in each biopsy.

Interestingly, the neurosphere cultures derived from different areas of the same tumor retained their diversity with respect to metabolism of 5-ALA, used in fluorescence-guided tumor resection, varying proliferative capacity and distinct transcriptional programs. Tumor periphery, which is thought to harbor cells driving local recurrence after surgery, gave rise to neurospheres with higher expression of cell cycle and DNA repair genes. The lines representing tumor periphery and not accumulating 5-ALA had high levels of MYC activity.

Since these cells are thought to drive local recurrence, targeting these tumor subpopulations could have a significant clinical benefit. To inhibit these pathways, we selected a panel of 7 drugs based on their recent evaluation in clinical trials for GBM patients, and tested their ability to affect proliferation of our neurosphere lines. We found that the responses to these drugs were variable between the neurospheres derived from distinct regions of the same tumor. Unexpectedly, we found that the cellular composition of the original tumor sample, predicted based on bulk transcriptomic data, can be linked to drug response outcomes derived from respective neurosphere line.

Our study demonstrates that the tumor-wide diversity of phenotypes of GBM can be propagated *in vitro*. Our results suggest that, at least in part, the transcriptional programs retained by GBM cells in vitro reflect their history of selection in distinct microenvironments in the tumor.

#4968 Comprehensive multi-omic profiling of the tumor-immune microenvironment using Xenium transcriptomics and Hyperion XTi Imaging Mass Cytometry.

Wendell Smith[1], Elim Cheung[2], JingHao Tian[2], Qanber Raza[1], Toby Astill[1], Daniel Zangrando[1], Nina Lane[1], Tommy Tran[2], Rikita Gakhar[2], Vidyodhaya Sundaram[2]

[1]Standard BioTools Inc., South San Francisco, CA,[2]BioChain Institute Inc., Newark, CA

Spatial multi-omics has become a powerful strategy for resolving cellular heterogeneity and precisely characterizing the tissue microenvironment, surpassing the biological resolution achievable with RNA-only or protein-only spatial assays. To address the limitations of single-modality profiling, we established an integrated workflow that combines Xenium in situ transcriptomics with Standard BioTools' Hyperion XTi Imaging Mass Cytometry (IMC) system. This approach is designed to enable coordinated, high-parameter analysis of transcriptomic and proteomic features within the same tissue regions, supporting deeper investigation of microenvironmental structure and function. Using a human primary FFPE multi-tissue panel comprising stomach large cell carcinoma, colon adenocarcinoma, invasive ductal carcinoma, and lung squamous cell carcinoma, BioChain generated spatially resolved Xenium transcriptomic data and mapped cell populations using lineage-defining markers. Major epithelial, stromal, endothelial, lymphoid, and myeloid compartments were identified, and architectural features—including tumor nests, stromal boundaries, tertiary lymphoid structures, and mixed immune aggregates—were delineated. For each region of interest, transcriptomic readouts were distilled into concise microenvironmental summaries reflecting immune infiltration intensity, lymphoid organization, cytotoxic activity, stromal composition, and checkpoint-associated transcriptional programs. These region-level profiles enabled cross-tissue comparison of microenvironmental classes across heterogeneous tumor types. Hyperion XTi IMC profiling of the same tissue regions provided a complementary proteomic view with high spatial and phenotypic resolution. The expanded protein panel resolved functional states associated with immune activation, suppression, proliferation, and tissue remodeling. Overlapping immune and stromal markers supported alignment of proteomic signals with the Xenium transcriptomic map, allowing corresponding cellular neighborhoods to be referenced across modalities. Together, these datasets established a multi-omic spatial framework that links cellular identity to protein-level functional dynamics within shared tissue coordinates. Overall, this combined transcriptomic-proteomic strategy establishes a scalable and practical template for comprehensive spatial profiling using limited FFPE material. The workflow is compatible with existing analysis tools, readily adaptable to new panels or tissue types, and well positioned for future development of spatially informed biomarkers and mechanistic insights into complex tissue ecosystems.

#4969 Automated multiomics assay with over 100 biomarkers for in-depth spatial profiling of the tumor microenvironment in multiple cancer types.

Marion Bonnet[1], Cansaran Saygili-Demir[1], Kim Handel[1], Pedro Machado[1], **Alix Failletaz**[1], Debia Wakhloo[2], Anushka Dikshit[2], Maria Giuseppina Procopio[1], Saska Brajkovic[1]

[1]Lunaphore, a Bio-Techne brand, Tolochenaz, Switzerland,[2]Advanced Cell Diagnostics, a Bio-Techne brand, Newark, CA

Background

The tumor microenvironment (TME) plays a pivotal role in cancer progression, immune evasion, and therapeutic response. Understanding the spatial organization and functional states of cells within the TME is essential for advancing immuno-oncology and precision medicine [PMID: 40102282]. However, simultaneous visualization of secreted molecules and cellular phenotypes in situ remains a major challenge in the spatial biology field [PMID: 39930476]. Here, we employed an automated hyperplex multiomics assay to simultaneously detect RNA and protein expressions to spatially map cell phenotypes and their functional states in the TME of multiple cancer types.

Methods

We examined a formalin-fixed paraffin-embedded tissue microarray (TMA) comprising various human cancer types: prostate, lung, breast, colorectal, melanoma, and lymphoma. A TMA section was stained and imaged on the COMET™ platform, integrating RNAscope™ HiPlex Pro for transcript detection and sequential immunofluorescence (seqIF™) for proteomic analysis [PMID: 22166544; 37813886; 41065276]. Image was analyzed using HORIZON™ software to extract single-cell and spatial features.

Results

The automated multiomics approach enabled the concomitant in situ detection of over 100 biomolecular targets, including 12 transcripts and more than 90 proteins on the same section. High-resolution spatial profiling of the TME allowed accurate mapping of cancer, stromal, vascular and diverse immune cell subsets. It further revealed key molecular features associated with tumor-suppressor or proto-oncogene activity, including markers of proliferation, apoptosis, and immune checkpoint regulation. Concurrent detection of cytokine and chemokine transcripts highlighted localized immune signaling and cell-cell communication within tumor and stromal compartments.

Conclusions

This multiomics workflow offers a powerful tool for in-depth characterization of the TME across multiple cancer types, while significantly reducing sample consumption. Spatial profiling provides new opportunities to dissect the tissue architecture and immune dynamics to identify functional cell states and interactions to be exploited in immunotherapy and personalized medicine.

#4970 Transcriptomic analysis reveals myoepithelial cell reprogramming in invasive breast cancer.

Mohamed M. Haq[1], Curtis Benson[2], Meik Kunz[2], Elim Cheung[3]

[1]HCA Houston Healthcare Southeast, Pasadena, TX,[2]The Bioinformatics CRO, Sanford, FL,[3]BioChain Institute Inc., Newark, CA

INTRODUCTION: Myoepithelial cells (MECs) in ductal carcinoma in situ (DCIS), although morphologically similar to normal MECs, exhibit distinct functional properties that promote progression to invasive breast cancer. To investigate MEC alterations in invasive disease (IDC), we performed a transcriptomic comparison of MECs within IDC and adjacent normal breast tissues from the same patient specimens.

METHODS: Breast cancer tissue specimens were obtained from HCA Houston Healthcare Southeast (Pasadena, TX). MEC presence within invasive ductal carcinoma (IDC) was validated by α-smooth muscle actin (αSMA) staining and confirmed by a pathologist. Seven untreated, loco-regional invasive breast carcinoma FFPE blocks were sent to BioChain Institute for spatial transcriptomic profiling using the GeoMx Digital Spatial Profiler (DSP, NanoString). H&E staining was used to identify suitable regions, and a 3 mm core tissue microarray (TMA) was constructed using both tumor and adjacent normal tissues. MEC transcriptomes were profiled on 5 µm TMA sections, with ROIs selected based on αSMA, PanCK, and Syto13 staining to distinguish MECs from stroma, and indexing oligonucleotides were collected for sequencing. Libraries were prepared and sequenced on an Illumina NextSeq2000 platform. Bioinformatics analyses were conducted in R by The Bioinformatics CRO using EdgeR, fgsea, and clusterProfiler, with normalization, differential expression, gene set enrichment analysis and functional pathway analysis revealing molecular distinctions between tumor-associated and adjacent normal MECs.

RESULTS: Our analysis revealed profound molecular reprogramming across three principal domains: extracellular matrix interactions, epithelial-mesenchymal transition, and cellular signaling. Key molecular alterations included (1) widespread upregulation of 17 distinct collagen isoform genes, indicating active stromal remodeling; (2) increased expression of matrix metalloproteinases (*MMP2*, *MMP9*, *MMP11*, and *MMP14*), suggesting compromised basement membrane integrity; and (3) significant dysregulation of epithelial markers (*KRT5*, *KRT7*, and *KRT14*), characteristic of a transitional phenotype resembling cancer-associated fibroblasts. Additional findings included elevated expression of pro-tumorigenic genes (*SPARC*, *POSTN*) and integrin subunits, alongside alterations in growth factor signaling pathways. These findings, although limited by the sample size and the transcriptomic approach, align with previously reported molecular alterations associated with myoepithelial reprogramming in DCIS-associated MECs.

CONCLUSION: This comprehensive transcriptomic analysis demonstrates significant molecular plasticity of myoepithelial cells within the IDC microenvironment, consistent with a phenotypic transition from tumor-suppressive to tumor-promoting function.

#4972 KIT exon 9 versus exon 11 mutations imprint distinct spatial and phenotypic immune microenvironments in gastrointestinal stromal tumors.

Jean-Philippe Guegan[1], Jean-Michel Coindre[2], Carine Ngo[3], Antoine Bougouin[4], Christophe Rey[5], Catherine SAUTES-FRIDMAN[6], Wolf Herve Fridman[6], Armelle Dufresne[7], Alban Bessede[5], **Antoine Italiano**[8]

[1]Immunospot, Cleveland, OH,[2]Institute Bergonie, Bordeaux, France,[3]Carine Ngo (Individual),[4]Sorbonne University, Paris, France,[5]ImmuSmol, Pessac, France,[6]INSERM U1138 (Centre de Recherche des Cordeliers), Paris, France,[7]Leon Berard Center, Lyon, France,[8]Institute Bergonie, Bordeaux cedex, France

Background:
The tumor microenvironment (TME) is a key determinant of progression and treatment response in gastrointestinal stromal tumors (GIST). Oncogenic KIT mutations in different exons (exon 9 vs exon 11) are clinically relevant, but their impact on immune and stromal architecture in situ remains insufficiently understood. We hypothesized that KIT exon 9 and exon 11 mutations drive distinct spatial transcriptional programs and immune cell compositions.

Methods:
FFPE samples from KIT-mutated GIST (exon 9 and exon 11) were profiled using the NanoString GeoMx® Whole Transcriptome Atlas (18,695 protein-coding genes). Eleven areas of illumination per case were selected in tumor and peritumoral regions and segmented into $CD45^+$ (immune-enriched) and $CD45^-$ (tumor/stromal) compartments. Cell-type abundances in $CD45^+$ segments were estimated with SpatialDecon. In parallel, three multiplex immunofluorescence (mIF) panels (DOG1/CD11c/CD11b/CD68/CD45/HLA-DR; DOG1/CD45RO/CD56/CD4/CD8/CD20; DOG1/CD45/CD16/CD56) were applied to independent retrospective GIST cohorts (n=170), and cell densities were quantified in tumor and stromal compartments using QuPath-based segmentation and FACS-like phenotyping.

Results:
GeoMx analysis identified 2315 differentially expressed genes in $CD45^+$ tumor regions between exon 9 and exon 11 tumors, indicating exon-specific immune transcriptional programs. SpatialDecon deconvolution revealed that exon 11-mutant tumors exhibited higher NK-cell scores (adjusted $p \approx 6\times10^{-6}$), whereas exon 9-mutant tumors showed higher fibroblast (adjusted $p \approx 6\times10^{-6}$) and $CD8^+$ memory T-cell signals (adjusted $p \approx 1.9\times10^{-4}$). In the large mIF cohorts, unsupervised analyses of DOG1-gated tumor regions confirmed robust technical performance of all three panels and demonstrated genotype-segregated TME patterns KIT-mutant cases, and within them exon 9 vs exon 11 tumors, occupied distinct regions in PCA space, with exon 11 tumors showing higher $CD56^+$ (NK/NKT) and myeloid ($CD11b^+$/$CD68^+$/HLA-DR^+) densities, whereas $CD8^+CD45RO^+$ memory T cells were more abundant in exon 9 tumors, independently of PDGFRA-mutant GIST. Across panels, these phenotypic differences aligned with the GeoMx-derived enrichment of NK cells in exon 11 tumors and of and $CD8^+$ memory T cells in exon 9 tumors.

Conclusions:
Integrated spatial transcriptomics and multiplex IF demonstrate that KIT exon 9 and exon 11 mutations are associated with distinct immune and stromal microenvironments in GIST, characterized by an NK-cell-enriched, myeloid cells , less fibroblast- and $CD8^+$ memory T-cell-dense niche in exon 11 tumors and the converse pattern in exon 9 tumors. These data support the concept that the precise KIT exon mutated imprints the TME and should be considered when designing genotype-adapted combinations of kinase inhibition and immunotherapy.

TUMOR BIOLOGY: Tumor-Immune Crosstalk
Poster Session

#4976 Upregulation of a B7 family protein drives immune escape in therapy-induced senescent cancer cells.

Donghee Kang[1], Min-Ji Kim[1], Hyung Jung Hwang[1], Jeong Minwoo[2], Jong-Ho Cha[2], Jae-Seon Lee[2]

[1]Research Center for Controlling Intercellular Communication, Inha University, Incheon, Korea, Republic of,[2]Program in Biomedical Science and Engineering, Inha University, Incheon, Korea, Republic of

Background: Conventional cancer therapies, including ionizing radiation (IR) and chemotherapy, often drive tumor cells into a cellular senescence state. Accumulating evidence suggests that senescent tumor cells contribute to the establishment of an immunosuppressive tumor microenvironment (TME) and promote tumor recurrence. A B7 family protein, an immune checkpoint protein, is frequently overexpressed across various tumor types and is known to suppress T-cell activity, thereby facilitating immune evasion and resistance to immunotherapy. However, the molecular mechanisms underlying the role of this B7 family protein in therapy-induced senescent (TIS) cancer cells remain poorly understood.
Methods: To elucidate the molecular mechanisms and immunoregulatory roles of the B7 family protein in TIS, we analyzed The Cancer Genome Atlas (TCGA) database to assess its expression across multiple cancer types. We further examined changes in its expression following IR or doxorubicin treatment in several human cancer cell lines, including A549 (lung), HCT116 wild-type (colon), HepG2 (liver), MIA PaCa-2 (pancreas), DU145 (prostate), and U2OS (bone). The role of the B7 family protein in cellular senescence was evaluated through gene knockdown experiments, and its impact on immune function was investigated using T cell-mediated cytotoxicity assays.
Results: TCGA analysis revealed that the B7 family protein is highly expressed across diverse cancer types. Following IR or doxorubicin treatment, its expression was significantly upregulated in senescent cancer cells across multiple cell lines. Depletion of the B7 family protein did not alter the senescence phenotype, indicating that it is not directly involved in regulating cellular senescence. Mechanistically, its upregulation in IR-induced senescent cancer cells occurred predominantly at the transcriptional level rather than through post-transcriptional or post-translational mechanisms. Notably, depletion of the B7 family protein markedly enhanced T-cell infiltration and cytotoxic activity against senescent cancer cells, demonstrating that its upregulation impairs antitumor immunity in TIS.
Conclusions: Our findings reveal the B7 family protein acts as a key regulator of immune suppression during therapy-induced senescence. This upregulation enables senescent cancer cells to evade T-cell mediated immune attack. Thus, inhibiting B7 family protein may offer a strategy to restore anti-improve immunity and improve therapeutic outcomes.

#4977 Programmed cell death ligand 1 (PD-L1) expression across molecular subtypes of human high-grade ductal carcinoma in situ (DCIS) of the breast.

Hossein Schandiz[1], Lorant Farkas[2], Berit Gravdehaug[3], Elin Edda Seland Agustsdottir[3], Torill Sauer[4], Jurgen Geisler[1]

[1]Department of Oncology, Akershus University Hospital, Lorenskog, Norway,[2]Department of Pathology, Oslo University Hospital, Oslo, Norway,[3]Department of Breast and Endocrine Surgery, Akershus University Hospital, Lorenskog, Norway,[4]Institute of Clinical Medicine, Faculty of Medicine, University of Oslo, Oslo, Norway

Background: The expression of PD-L1 in tumor-infiltrating lymphocytes (TILs) in tumor microenvironment (TME) of high-grade breast DCIS is currently unknown.
Methods: Formalin-fixed paraffin-embedded specimens from 494 female patients diagnosed with DCIS between 1996-2018 were available to routine diagnostic immunohistochemical (IHC) staining. ER and PR IHC positivity was defined as ≥1% positive tumor cells, and HER2 IHC was scored based on the updated guidelines of the American Society of Clinical Oncology and the College of American Pathologists, as in routine diagnostic procedures. HER2 silver in situ hybridization was performed when the IHC score was 2+. We calculated the Ki67 ratio by counting 200 intraductal epithelial cells in two separate hotspot foci. DCIS cases were classified as Luminal A (LumA), LumB HER2$^-$, LumB HER2$^+$, HER2-enriched, or triple-negative (TPN) subtypes according to the 2013 St. Gallen guidelines, which is used for molecular subtyping of invasive breast carcinoma. Each subtype was sorted into “Pure”: without an invasive component and “W/invasive”: with an invasive component. We calculated the PD-L1 IHC ratio by counting (up to) 1000 immune cells divided by positive PD-L1 cells. PD-L1 expression was dichotomized at a threshold of 1%. We assessed the associations between PD-L1 status, subtype, and other variables, including age, Ki67, DCIS extension, and invasiveness.
Results: We identified a significant proportion of TILs in 149/484 (31%) cases. 100% of these cases were high-grade DCIS. We successfully stained 118/149 cases with PD-L1 IHC, and 73/118 (63%) expressed PD-L1 ≥1%. In 92/149 (62%) cases with TILs, strong membrane-positive HER2 overexpression was observed (25% LumB HER2$^+$ and 37% HER2-enriched subtype, $p < 0.0001$). A significant number (31/60; 52%) of the “W/invasive” cases contained TILs, compared to “Pure” (118/362; 32%) ($p < 0.0055$). PD-L1 ≥1% was most prevalent in HER2-enriched (48.6%) and LumB HER2$^+$ (25%) subtypes, with lower representation in LumA (12.5%), LumB HER2$^-$ (9.7%), and TPN (4.2%) subtypes. However, comparison of the PD-L1 ≥1% status across subtypes yielded a non-significant chi-square result ($p = 0.2734$). PD-L1 expression was not significantly associated with “W/invasive” cases ($p = 0.0765$). Significant differences were observed across subtypes among cases expressing PD-L1 ≥1% for Ki67 ($p = 0.0325$) and DCIS extension ($p = 0.0323$), but not for age ($p = 0.4329$) or invasive status ($p = 0.6722$).
Conclusions: PD-L1 ≥1% was more common in HER2-driven subtypes, but its distribution was not subtype-dependent. PD-L1 expression also lacked a significant association with invasiveness. These findings demonstrated strong PD-L1 expression in high-grade DCIS, although the utility of PD-L1 as a standalone biomarker for subtype stratification or prediction of invasive potential in DCIS patients could be limited.

#4978 MHC class 1 expression and distribution of multiple immune cells in chemotherapy-naïve triple-negative breast cancers: lack of antigen-presentation can bring high TILs and good prognosis, possibly via decreased regulatory T-cell composition.

Makiko Yamashita[1], Akira I. Hida[2], Naomi Gondo[3], Yasuyo Ohi[4], Shigehisa Kitano[1]

[1]Department of Advanced Medical Development, Cancer Institute Hospital, Tokyo, Japan,[2]Department of Pathology, Matsuyama Shimin Hospital, Ehime, Japan,[3]Department of Breast Surgery, Sagara Hospital, Kagoshima, Japan,[4]Department of Pathology, Sagara Hospital, Kagoshima, Japan

Triple-negative breast cancers (TNBCs) have not been candidates for targeted therapies because they are negative for ER, PgR, and HER2. In addition, the aggressive nature of TNBCs makes their treatment challenging. However, recent advances include immune checkpoint inhibitors (ICIs), which are effective against some TNBCs. The abundance of tumor-infiltrating lymphocytes (TILs) in the cancer microenvironment correlates with better prognosis, and improved efficacy of chemotherapy and ICIs. We don't know yet in detail what makes the difference, high or low TIL, and wanted to investigate cancer immunity cycles.

We retrospectively recruited 153 consecutive TNBC patients from a single institution, all of whom had primary curative surgery and standard adjuvant chemotherapy. Representative surgical samples were immunohistochemically stained for MHC class 1 and evaluated by a pathologist in a score of 3 (diffusely positive) to 0 (almost negative). Heterogeneous staining was scored as 2 (positive area>50%) or 1 (positive area<50%). TILs were estimated after hematoxylin & eosin staining, and relapse-free survival was recorded. Thirty cases with different levels of MHC expression were stained for CD3, CD4, CD8, CD20, CD56, CD204, FoxP3, and pan-cytokeratin using a multi-fluorescence technique. Six-hundred small areas of interest were selected and assigned to one of four categories according to tumoral MHC (positive/negative) and stromal TILs (high/low). Staining signals were calculated on the images, and clustered to determine the distribution of cells in areas of tumor or stroma.

TIL abundance was an independent prognostic factor (HR: 2.52, p=0.013). MHC class 1 expression was diffusely positive in many cases (score 3 in 88 of 153 cases), and four cases were negative (score 0). MHC positivity correlated with higher TILs; nevertheless, the four cases with an MHC score of 0 had high TILs (42.5% on average) and showed no recurrence or death during the mean follow-up period of 14.5 years. Detailed composition of immune cells in areas of high TIL showed infiltration by many CD3+ and CD20+ cells, while CD204+ cells were numerous in areas of low TIL. MHC class 1-negative areas had fewer FoxP3+ cells than positive areas, even in areas of high TIL. There was no significant difference in CD56+ cell number between MHC-positive and -negative areas. Cluster analysis of immune cells revealed CD204 to be a major divider of the population.

MHC class 1-negative TNBCs contained relatively high TILs, the main components of which were CD3+ and CD20+ cells. The presence of FoxP3+ cells seems to require HMC class 1, and the lack of negative regulation by FoxP3 might have resulted in high TIL and better prognosis. Our findings indicate a missing link between antigen presentation and T-cell recruitment.

#4979 CD155- binding peptide enhances antitumor activity of T cells and cytotoxic activity of a lytic peptide in colon tumor.

Gunassekaran Gowri Rangaswamy[1], Poongkavithai Vadevoo Sri Murugan[2], Byungheon Lee[2]

[1]Biochemistry, Kyungpook National University, Daegu, Korea, Republic of,[2]Kyungpook National University, Daegu, Korea, Republic of

CD155 is an immunoglobulin-like protein overexpressed in most tumor cells and promotes the proliferation, adhesion, and migration/invasion of tumor cells. CD155 has multiple immune checkpoint receptors, including CD226, TIGIT, CD96, CD112R (PVRIG) and KIR2DL5. These ligands bind with different affinities to PVR-like protein receptors, thus exerting immune-activating or immunosuppressive functions.CD155 binds to TIGIT with far higher affinity than binds to CD96 or CD226. Moreover, the CD155 immunosuppressive target TIGIT, CD96 competes with the immune activation target CD226 to inhibit immune system activation. As a result, TIGIT exerts an immunosuppressive impact on immune cells by preventing CD226-mediated co-stimulation. Upregulation of CD155 in colon tumor is associated with poor patient outcomes, which highlights its potential as therapeutic target. Using a phage-displayed peptide library, we identified a peptide that binds CD155 with a high affinity (CD155pep). Treatment of CT26 colon tumor cells with CD155pep during co-cultures with CD8+ T cells down-regulated CD155 expression of the tumor cells and enhanced antitumor activity of T cells, including the release of granzyme B, interferon-γ, and tumor necrosis factor-α, and the increase of tumor cells lysis. In addition, treatment of tumor-associated macrophages with CD155pep during co-cultures with CD8+ T cells decreased anti-inflammatory IL-10 production while increasing pro-inflammatory IL-12 secretion of macrophages. Furthermore, CD155pep-linked lytic peptide showed a selective toxicity in tumor cells over normal cells and inhibited tumor growth in mice. These results highlight the therapeutic potential of CD155pep and CD155pep-linked lytic peptide for targeted therapy of CD155-high tumors.

#4980 Clinical and prognostic significance of spatial distribution of CD163-positive tumor-associated macrophages in pleural mesothelioma.

Ryota Sumitomo[1], Tetsuya Fukui[1], Masashi Kobayashi[2], Hiroaki Sakai[3], Toshi Menju[1]

[1]Kyoto University Hospital, Kyoto, Japan,[2]Department of Thoracic Surgery, SHOWA Medical University, Tokyo, Japan,[3]Hyogo Prefectural Amagasaki General Medical Center, Hyogo, Japan

Objectives: Pleural mesothelioma (PM) remains a fatal malignancy despite multimodal therapy. Macrophages activated by asbestos and tumor-derived factors may develop into tumor-associated macrophages (TAMs) with tumor-promoting properties. However, the spatial distribution and clinical impact of these TAMs in PM remain poorly defined.

Methods: We retrospectively analyzed 101 consecutive patients with PM treated at Kyoto University Hospital and Hyogo Prefectural Amagasaki General Medical Center between 1998 and 2010. CD163 immunohistochemistry was performed to quantify pro-tumoral TAMs in intratumoral and peritumoral regions, while Ki-67 staining assessed tumor proliferation. The intratumoral region was defined as an area within the tumor or, if not feasible, as a field containing ≥70% tumor tissue. The peritumoral region was defined as an adjacent stromal area containing >70% stroma. Optimal cutoffs for TAM densities were determined using the minimum p-value method with pretreatment C-reactive protein (CRP). Overall survival (OS) was estimated using the Kaplan-Meier method, and the Cox regression model was employed for univariable and multivariable analyses to examine factors influencing survival.

Results: Intratumoral and peritumoral CD163-positive TAM densities were 660.8 ± 565.9 and 223.1 ± 195.6 cells/mm², respectively, and were moderately correlated ($r = 0.505$, $p < 0.001$). Both intratumoral and peritumoral TAM densities correlated with CRP ($r = 0.283$ and 0.255, $p < 0.05$) and Ki-67 ($r = 0.498$ and 0.435, $p < 0.001$). Intratumoral TAMs were more abundant in sarcomatoid histology ($p < 0.001$) and in advanced stage ($p = 0.043$), whereas peritumoral TAMs showed no significant associations with clinicopathologic factors. High CD163-positive TAM density predicted poorer OS in both regions: intratumoral high versus low groups showed 5-year OS rates of 13.3% and 23.2% ($p = 0.044$), and peritumoral high versus low groups showed 5-year OS rates of 13.2% and 24.1% ($p = 0.046$). In multivariable analysis, peritumoral CD163-positive TAM-high status (HR = 1.700, 95% CI 1.034-2.796, $p = 0.037$) remained an independent prognostic factor along with stage and histology.

Conclusions: In PM, high densities of CD163-positive TAMs were associated with systemic inflammation and tumor proliferation. The spatial distribution of these TAMs may indicate a prognostically relevant tumor immune microenvironment, and peritumoral TAMs in particular showed independent prognostic significance. These findings suggest that TAM spatial profiling may serve as a practical biomarker for risk stratification.

#4981 New thought and strategy of liver cancer immunotherapy.

Gen-Sheng Feng

UC San Diego School of Medicine, La Jolla, CA

This study is to explore new strategy of liver cancer immunotherapy. Despite the great success of immunotherapy in a broad range of cancers, the vast majority of cancer patients showed poor response. Approximately 17% liver cancer patients responded to monotherapy of pembrolizumab and 20% responded to nivolumab. A combination of nivolumab and ipilimumab increased the response rate to 30% in HCC. Simultaneous blockade of PD-L1 and VEGF signaling using atezolizumab and bevacizumab achieved better overall and progression-free survival than sorafenib in HCC.

Our previous data showed that monotherapy with anti-PD-L1 antibody exhibited no inhibitory effect in primary liver cancer driven by classical oncogenes in mice. Given a robust induction of PD-L1 expression by polyIC in the liver, we reasoned that the synthetic dsRNA could sensitize hepatic response to αPD-L1 treatment. Indeed, combined treatment of polyIC and anti-PD-L1 showed markedly improved efficacy in mouse HCC models.

A combinatorial therapy of polyIC and anti-PD-L1 exhibited an intriguing synergistic effect in liver tumors. We interrogated the compositions and changes of immune cell subtypes infiltrated into the tumors grown subcutaneously or in the liver, as well as the whole liver of tumor-bearing mice. The data suggest that it is the tumor microenvironment, rather than the tumor cells, that determine the response to immunotherapy.

We have also found that the polyIC+antiPD-L1 combination exhibited more potent anti-tumor effect than antiPD-L1+antiVEGFA. Further, we demonstrate that a monotherapy of liver-targeting lipid nanoparticles that encapsulate polyIC (polyIC-LNP) is sufficient to suppress both primary and metastasized liver tumor progression in mouse models.

Current working address: Institute of Cancer Research, Shenzhen Bay Laboratory

#4982 Targeting collagen receptor CD49b enhances PD-L1 blockade by promoting CD8⁺ T-cell immunity in breast cancer.

Ibrahim R. Eissa[1], Kenneth K. Tanabe[2]

[1]Massachusetts General Hospital, Boston, MA,[2]Massachusettes General Hospital, Boston, MA

Background: Immune checkpoints blockade (ICB) have improved cancer outcomes, but its efficacy in breast cancer remain limited by an immunosuppressive tumor microenvironment and dense extracellular matrix (ECM). Collagen, the main ECM component, supports tumor progression and immune evasion via integrin-mediated signaling and DDRs receptors. The collagen receptor CD49b (integrin α2) promotes tumor adhesion. This study evaluated whether CD49b targeting enhances PD-L1 blockade to overcome ECM-driven resistance.
Methods: Expression of CD49b, CD29, and DDR1 were profiled in breast cancer cell lines by flow cytometry, along with MHC-I and PD-L1. Collagen adhesion assays followed CD49b inhibition using Vatelizumab (anti-human CD49b), HMα2 (anti-mouse CD49b), or CRISPR/Cas9 knockout in 4T1 cells. Transcriptomic datasets (CCLE, scRNA-seq, spatial transcriptomics) were analyzed to define collagen receptor localization in breast cancer TME. In vivo, 4T1-bearing mice were treated with anti-PD-L1, anti-CD49b, or the combination, followed by analysis of tumor growth and tumor immune infiltration.
Results: CD49b and CD29 were highly expressed in MCF7, T47D, and 4T1 cells, while MDA-MB-231 cells showed low levels and weak collagen adhesion. CD49b blockade or knockout impaired adhesion and delayed tumor growth in vivo without affecting proliferation. Transcriptomic analysis confirmed CD49b enrichment in malignant cells. Dual CD49b and PD-L1 inhibition showed a synergistic antitumor activity, significantly reducing tumor burden and increasing $CD8^+$ T-cell infiltration and IFN-γ expression, consistent with enhanced cytotoxic immunity.
Conclusions: CD49b mediates tumor-ECM interaction in breast cancer. Combined CD49b and PD-L1 blockade remodels the TME, enhances $CD8^+$ T-cell-driven responses, and represents a promising therapeutic strategy to overcome ICB resistance in collagen enriched tumors.

#4984 Dissociative, spatial, and functional single-cell profiling reveals antigen-driven exhaustion and chemotactic failure of tumor-reactive T cells in HPV-negative HNSCC.

Joseph Zenga[1], Musaddiq Awan[1], Fumou Sun[1], Stuart J. Wong[1], Abdullah Memon[1], Tyce Kearl[1], Ean Norenberg[1], Margaret L. Hoang[2], Joseph M. Beechem[3], Eric Hobbs[4], Ashley Heck[2], Rachel Liu[2], Daniel McGuire[2], Erin Piazza[2], Peiman Hematti[1], Heather Himburg[1]

[1]Medical College of Wisconsin, Milwaukee, WI,[2]Bruker Spatial Biology, Seattle, WA,[3]Bruker Spatial Biology, Piedmont, CA,[4]Bruker Cellular Analysis, Emeryville, CA

Introduction: HPV-negative head and neck squamous cell carcinoma (HNSCC) remains highly lethal, and even the recent KEYNOTE-689 trial showed limited response to PD-1 blockade. To clarify mechanisms of immunoresistance, we performed multi-omic single-cell profiling of HPV-negative HNSCC to define the states, clonotypes, and spatial niches of tumor-reactive T cells.
Methods: Two patients with untreated HPV-negative HNSCC underwent surgical tumor sampling. Biopsies were allocated for dissociative single-cell RNA and TCR sequencing, for single-cell spatial whole transcriptome imaging with TCR add-in on the Bruker CosMx platform, and for functional co-culture of autologous tumor cells and tumor-infiltrating lymphocytes (TILs) on the Bruker Beacon system with robotic retrieval of reactive clones followed by single-cell TCR sequencing.
Results: Dissociative and spatial datasets were high quality, and dissociative clustering guided spatial annotation. Two tumor-reactive TIL populations emerged: a transcriptionally reactive population marked by terminal exhaustion and clonal hyper-expansion, and a functionally reactive population identified on the Beacon platform through tumor-killing and IFNγ secretion. Neither appeared in adjacent normal mucosa. Spatial projection showed functionally reactive clonotypes progressing along a pseudotime continuum from minimally exhausted stromal states toward a deeply exhausted yet proliferative state within malignant epithelial islands. Transcriptionally reactive TILs shared this exhausted-proliferative phenotype and primarily localized within tumor islands. Conversely, Tregs and immunosuppressive macrophages were confined to stromal regions and showed minimal spatial overlap with tumor-reactive T cells. Malignant epithelium strongly enriched CXCL14 (> ten-fold over stroma), yet tumor-reactive TILs remained rare, with a tumor-to-reactive T cell ratio greater than 20 to 1.
Conclusions: This is the first study to integrate dissociative, spatial, and functional single-cell analytics to define tumor-reactive TIL biology in solid tumors. We find that tumor-reactive T cells can infiltrate malignant epithelial islands, and that their deepest infiltration corresponds to the most exhausted states, indicating that chronic antigen stimulation is the primary driver of dysfunction. The confinement of suppressive cells to stromal niches suggests that their influence is exerted through maintenance of a restrictive barrier stroma rather than through proximity-based inhibition. Together, these findings highlight insufficient chemotactic recruitment of tumor-reactive T cells as a central barrier to effective antitumor immunity. The strong epithelial enrichment of CXCL14 positions it as a promising candidate for enhancing tumor-directed T cell migration.

#4985 The role of CD5L in regulating liver immune cells.

Diala S. Alhousari[1], Handan Hong[2], Taojian Tu[2], Bangyan L. Stiles[3]

[1]USC School of Pharmacy, Los Angeles, CA,[2]USC - University of Southern California, Los Angeles, CA,[3]Assistant Professor, USC School of Pharmacy, Los Angeles, CA

CD5-like molecule (CD5L) is a soluble glycoprotein primarily produced and secreted by macrophages. As a member of the scavenger receptor cysteine-rich (SRCR) superfamily, CD5L regulates many biological processes such as apoptosis, pathogen recognition, immune responses, autophagy, cell polarization, and lipid metabolism, highlighting its crucial role in tissue homeostasis and its involvement in inflammation and cancer. In liver cancer, elevated serum CD5L levels have been observed in patients with steatohepatitis and hepatocellular carcinoma (HCC), supporting its potential as a diagnostic biomarker. Steatosis and steatohepatitis are key comorbidities that promote HCC development and are linked to poor therapeutic outcomes, particularly resistance to immune checkpoint inhibitors. Given that liver inflammation and lipid metabolism are involved in the progression of liver cancer, both of which are closely correlated with CD5L activity, this suggests that CD5L could play a pivotal role in shaping the tumor microenvironment of HCC. In this study, we found that CD5L is predominantly produced by liver macrophages and that its expression is significantly upregulated in multiple models of liver injury. Additionally, we observed that elevated serum CD5L levels were observed to correlated with the severity of liver damage. Clinically, we found that patients with hepatocellular carcinoma (HCC) displayed higher serum CD5L levels compared to controls, and increased CD5L levels were associated with poorer responses to immune checkpoint therapies. Functionally, we demonstrated that CD5L enhances lipid uptake in hepatocytes and hepatic stellate cells and promotes macrophage survival under palmitic acid-induced stress, findings consistent with its previously reported biological roles. Although CD5L's role in supporting macrophage survival is well established, its precise role in immune regulation remains less clearly defined. Our data indicate that CD5L produced by liver macrophages can modulate the chemotaxis of hepatic immune cells, particularly T cells and NKT cells. In macrophages and adipocytes, CD36, a scavenger receptor, mediates CD5L's effects on lipid metabolism. Notably, CD8+ T cells and regulatory T cells also express CD36, suggesting that CD5L may influence their function through CD36-dependent pathways. However, our findings show that while CD5L acts on T cells via CD36, it impacts NKT cells through a CD36-independent mechanism. Our study further investigates the impact of CD5L on liver immune cells' functional properties. Overall, CD5L is an upregulated secreted protein that plays an important role in regulating liver immune cells during liver diseases.

#4986 Identification of tumor microenvironment for high infiltration of lymphocytes in triple negative breast cancer.

Sowon Choi[1], Hee Jin Lee[2], Byung-Kwan Jeong[2], Hyun Je Kim[1]

[1]Seoul National University, Seoul, Korea, Republic of,[2]Asan Medical Center, Seoul, Korea, Republic of

Elucidating the roles of intra-tumoral macrophage subtypes that promote a high-TIL microenvironment in triple-negative breast cancer. High levels of tumor-infiltrating lymphocytes (TILs) within the stromal compartment are associated with favorable prognosis and improved response to immune checkpoint blockade in triple-negative breast cancer (TNBC). To elucidate the mechanisms underlying the divergence between TIL-high and TIL-low tumor microenvironments (TMEs), we analyzed treatment-naïve, early-stage TNBC samples. We profiled the TME of 21 patients using single-cell-resolution spatial transcriptomics on FFPE tissue microarray blocks. Patients were classified into high TIL group with over 60% ratio of TIL in stroma. sTILs (0-100%) were evaluated on H&E-stained slides, and tumors with sTIL ≥ 60% and ≤ 10% were classified as high and low TIL, respectively. These thresholds are stricter than the commonly used sTIL ≥ 50% and < 30% cutoffs associated with distant RFS. Using this classification, 11 patients were assigned to the TIL-high group and 10 to the TIL-low group. We clustered 40 cell types for TNBC samples using Xenium 5K platform and identified 12 spatial domains by uncovering recurrent cellular neighborhoods (RCNs) that share similar spatial patterns using SCIMAP(v2.2.11). Among those 12 spatial domains, domain 9 and domain 0 represented tumor center and tumor edge, respectively. We identified 10 myeloid cell subtypes and discovered macrophage subtype MC2 expressing LDHA and PLAUR are enriched specifically in tumor domains consisting of domain 9 and 0. Interestingly, the MC2(LDHA_PLAUR) subtype present low PLAUR expression in TIL-high group compared to TIL-low group in tumor domains. Although the proportion of infiltrating MC2 (LDHA_PLAUR) macrophages within tumor domains was higher in the TIL-high group compared with the TIL-low group, the expression level of PLAUR within MC2 cells was paradoxically lower in the TIL-high group. Additionally, the MC2(LDHA_PLAUR) expressed more IFN-stimulated genes such as CXCL9, GBP5, and IRF1 in TIL-high group compared to TIL-low group. PLAUR has been known for inducing HIF1A highly in tumor microenvironment. As HIF1A hinders IFNG-signaling important to establish TIL-high environments, high expression of PLAUR promotes inhibition of IFNG-signaling in macrophages. So, low expression of PLAUR for MC2 in TIL-high group helps normal IFNG-signaling pathways in macrophages. Taken together, these findings indicate MC2 macrophages located in both the cancer center and edge regions showed reduced PLAUR expression, rendering them less susceptible to HIF1A-driven suppression and allowing sustained IFNG-signaling in high-TIL tumors. This suggests that these MC2 cells help establish an intra-tumoral environment conducive to TIL infiltration by continuously supplying CXCL9, CXCL10, and CXCL11.

#4987 Dual roles of JNK1 and JNK2 in TNBC progression and tumor microenvironment immune modulation reveal a novel therapeutic vulnerability.

Bharat Singh Kuntal[1], Xuemei Xie[1], Xanthe stern[1], Kendall Nakaoka[2], Marilisa Fujimoto[2], Marisa William[2], Madixx Muramoto[2], Naoto T. Ueno[3]

[1]Cancer Biology, University of Hawai'i Cancer Center, Honolulu, HI,[2]University of Hawai'i at Manoa, Honolulu, HI,[3]Translational and Clinical Research, University of Hawai'i Cancer Center, Honolulu, HI

Background: Triple-negative breast cancer (TNBC), one of the most lethal breast cancer subtypes, is driven by hyperactive oncogenic pathways that promote tumor growth and suppress antitumor immunity. Aberrantly high c-Jun N-terminal kinase (JNK) signaling is emerging as a key driver of tumor progression and immune evasion; however, the distinct roles of JNK1 and JNK2 in TNBC are largely undefined. This knowledge gap constrains efforts to exploit JNK biology for therapeutic advancement. Here, we investigated how each isoform drives tumor-intrinsic behavior and remodels the tumor microenvironment (TME). We hypothesized that both JNK1 and JNK2 drive TNBC growth and promote an immunosuppressive TME, and that loss of either isoform reprograms the TME toward a more immune-permissive, antitumor state. **Methods:** The impact of JNK signaling inhibition on PyMT-N TNBC cell growth was evaluated pharmacologically, using the pan-JNK inhibitor JNK-IN-8, and genetically, by knocking out JNK using the CRISPR-Cas9 system. Cell growth was evaluated using CellTiter-Blue viability and clonogenic assays. Immunocompetent syngeneic C57BL/6 mice bearing JNK1-, JNK2-, or dual-knockout (KO) tumors were used to assess tumor-intrinsic roles of each isoform; in parallel, *jnk1*$^{-/-}$ and *jnk2*$^{-/-}$ C57BL/6 mice bearing JNK-KO tumors were used to distinguish host-dependent effects. Immune cell tumor infiltration was quantified by flow cytometry. Cytokines were profiled by cytokine arrays and validated by ELISA and qPCR.**Results:** JNK-IN-8 (5 μm) suppressed PyMT-N cell growth by 85.1%, while KO of JNK1, JNK2, or both reduced colony formation by 55.3%, 67.7%, and 42.0%, respectively. Intratumoral JNK1 or JNK2 KO reduced tumor growth by 44.2% and 53.4%, respectively, and dual KO produced the most profound effect. These results highlight the strong tumor-intrinsic dependence of TNBC on both isoforms. Compared with Cas9 controls, JNK1-KO and JNK2-KO tumors exhibited increases in activated $CD8^+$ T cells (83.4% and 53.3%, respectively) and reductions in Tregs (37.9% and 24.9%, respectively), indicating a shift toward an immunoactive TME. Furthermore, JNK1-KO and JNK2-KO tumors showed reduced TSLP expression and increased IGF-1 expression, suggesting JNK's regulation of these cytokines. In host-dependent studies using *jnk1*$^{-/-}$ and *jnk2*$^{-/-}$ C57BL/6 mice, loss of either isoform reduced tumor growth, though to a lesser degree than intratumoral KO. Host JNK1 deficiency increased M1 macrophages and NK cells, while JNK2 deficiency increased $CD8^+$ T cells and NK cells; both showed reduced Tregs, indicating the induction of an immunoactive TME.**Conclusion**: Both intratumoral JNK1 and JNK2 are critical drivers of TNBC growth and TME immunosuppression, and their loss reprograms the TME toward robust antitumor immunity, positioning JNK signaling as a compelling therapeutic target in TNBC.

#4988 Comprehensive tumor microenvironment analysis identifies a suppressive immune landscape in stemness-high hepatocellular carcinoma.

Woo Young Kwon[1], Sungho Ko[2], Sungwoo Cho[2], Song-A Park[2], Sihun Cho[2], Sung Hwan Lee[1]

[1]Omics & Real-world Data-driven AI for Precision Medicine Lab, Seongnam, Korea, Republic of,[2]Humanase Co., Ltd., Seongnam, Korea, Republic of

Introduction: Hepatocellular carcinoma (HCC) remains a leading cause of cancer mortality, driven by late detection and limited therapeutic efficacy. A prior molecular classification defined five transcriptomic subtypes, among which the stemness-high (STM) subtype exhibits the poorest survival and pronounced stemness programs. Given the scarcity of effective treatments for this high-risk population, it is critical to characterize their tumor immune landscape and evaluate potential sensitivity to immune checkpoint inhibitors (ICIs). Here, we systematically profiled the immunologic features of STM tumors to assess their immunogenicity and likelihood of benefiting from ICIs.

Methods: Four resectable HCC transcriptomic cohorts (Korea, Samsung, Zhongshan, and Modena) were analyzed. STM subtype assignment was performed using the Bayesian Compound Covariate Predictor (BCCP) with previously defined STM signatures. Immune deconvolution was conducted using TIMER 3.0 (CIBERSORT, MCP-counter, EPIC), and immune cell states were assessed by EcoTyper. Immune dysfunction and exclusion were quantified using TIDE. Survival outcomes were evaluated by Kaplan-Meier analysis.

Results: Across all cohorts, STM tumors demonstrated significantly worse overall survival and recurrence-free survival. Clinically, STM tumors were enriched for adverse pathological features, including higher T stage, poor differentiation, and increased vascular invasion.Immune profiling revealed a profoundly suppressive tumor microenvironment, characterized by elevated M0 macrophages, regulatory T cells, myeloid-derived suppressor-like signatures, and abundant cancer-associated fibroblasts (CAFs). EcoTyper identified enrichment of pro-migratory fibroblasts, exhausted and Treg-like $CD4^+$ T cell states, and tumor-associated endothelial and epithelial programs.TIDE analysis demonstrated high exclusion and dysfunction scores, along with increased CD274 (PD-L1) and Merck18 expression, collectively indicating an immune-excluded, poorly immunogenic, and ICI-resistant profile.

Conclusions: The STM subtype of HCC is defined by a markedly immunosuppressive and immune-excluded tumor microenvironment with dysfunctional T cell states, CAF/MDSC infiltration, and angiogenic activity. These features are strongly associated with resistance to ICIs, suggesting that immune checkpoint blockade alone is unlikely to be effective. Alternative or combination therapeutic strategies will be required to improve outcomes in this high-risk molecular subtype.

#4989 SIPA1 deficiency reprograms mesenchymal stromal cells differentiaion and enhance the T cell immunity in the tumor microenvironment.

Yan Xu, Kentaro Sumida, Ryuhei Kawakami, Masakazu Hattori, Nagahiro Minato

Kyoto University, Kyoto, Japan

Background: Sipa1 (Signal-induced proliferation-associated gene 1) is a Rap1 GTPase-activating protein implicated in cellular adhesion and immune regulation. However, its functions within the tumor microenvironment (TME) remain unclear. Sipa1$^{-/-}$ mice resistant to Bcr-Abl^{+} leukemia by coordinated interplay between MSCs and immune T cells.

Methods: In this research, we clearly demonstrated that Sipa1$^{-/-}$ mice also showed increased resistance to different epithelial cancer cells such as MC38 intestinal and IPmN pancreatic cancers accompanied with increased stromal reaction and T cells infiltration. To clarify the stromal response in the anti-tumor mechanism, tumor resident mesenchymal stromal cells (MSCs) were sorted and subjected to Single cell RNA sequencing (scRNA-seq).

Results: Three major MSCs subsets which have distinct gene expression profiles were identified: αSMA+ myofibroblast CAFs(myCAF), inflammatory CAFs(iCAF), and antigen-presenting CAFs(apCAFs). In Sipa1$^{-/-}$ tumor, iCAFs were significantly enriched, whereas the proportion of myCAFs decreased relative to WT tumors. Sipa1 expression levels across MSCs subsets followed the hierarchy myCAF > apCAFs > iCAF, suggesting a role for Sipa1 in MSCs lineage determination. These findings indicate that Sipa1 is required for MSCs differentiation into myCAF, and that Sipa1 deficient MSCs transdifferentiate from myCAF to iCAF. Functionally, MSCs from Sipa1$^{-/-}$ tumors exhibited significant upregulation of CXCL9 and immunohistochemical analyses demonstrated enhanced IFNγ-STAT1signaling in Sipa1$^{-/-}$ MSCs. In vitro experiments using MC38 cells and other stromal cells revealed that Sipa1 interacted directly with STAT1/pSTAT1 and suppresses its activation, suggesting that Sipa1 negatively regulates the IFNγ-STAT1 axis.

Conclusion: All of the results demonstrate that Sipa1 is a critical regulator of MSCs-to-CAF differentiation and CAF functional programming in the TME. Sipa1 deficiency drives MSCs toward an iCAF-like, CXCL9 producing, immunostimulatory phenotype, which promoting enhanced T cell recruitment and anti-tumor immunity. These findings identify Sipa1 as a previously unrecognized stromal checkpoint controlling T cell responses against tumors and highlight Sipa1 as a potential therapeutic target to improve cancer immunotherapy.

#4990 Single-cell mass cytometry reveals T-cell exhaustion in sentinel nodes of ER+ breast cancer without histological detectable metastases.

Inga Hansine Rye[1], Marit Otterlei FJortoft[1], Karin Teien Lande[1], Margit Riis[1], Ole Christian lingjarde[2], Oystein Garred[3], Colin LaMont[4], June Myklebust[4], Kanutte Huse[4], Hege Russnes[1]

[1]Cancer Genetics, Oslo University Hospital, Institute for Cancer Research, Oslo, Norway,[2]University of Oslo, Institute for informatics, Oslo, Norway,[3]Pathology, Oslo University Hospital, Oslo, Norway,[4]Cancer Immunology, Oslo University Hospital, institute for Cancer Research, Oslo, Norway

Introduction: Tumor cell infiltration in regional lymph nodes is a strong prognostic marker and guides treatment decisions in breast cancer. While the immune landscape of primary tumors has been widely studied, the composition of immune cells in sentinel (SN) and axillary lymph nodes (ALN) remains less understood. Clarifying how tumor cells shape the nodal immune microenvironment may provide insights into metastasis, cancer progression, and potential therapeutic strategies.

Materials and methods: We analysed tumor draininglymph nodes from a prospective cohort of 458 treatment-naïve patients with primary operable breast cancer, representing all breast cancer subtypes. Lymph node status included negative nodes (n=357), sentinel node-positive (SN+, n=88), and axillary lymph node-positive (ALN+, n=13). Comprehensive immunophenotyping was performed by mass cytometry (CyTOF) using a 48-antibody panel. The panel included lineage markers, cell type-defining markers, and markers of activation and exhaustion.Data were processed using semi-automated FlowSOM clustering with manual clean-up to remove dead cells, doublets, and technical noise. This enabled identification of immune, tumor, apoptotic, and unclassified cell populations.After quality control, 468 lymph nodes comprising more than 45 million single cells were included in the final analysis.

Results: Patients with ALN+ disease had shorter time to distant metastasis than those with SN+ or SN- nodes. Compared with SN- samples, ALN+ samples showed enrichment of exhausted T cells as well as germinal center B (GC B) cells and plasma cells, both in the full cohort and within the estrogen receptor-positive (ER+) subgroup. No immune composition differences were observed across breast cancer subtypes in SN- samples. SN+ samples from triple-negative breast cancer (TNBC) demonstrated a trend toward increased GC B and plasma cells, resembling the immune profile of ALN+ nodes, suggesting that even small SN metastases can trigger early immune activation. In SN- samples from half of the ER+ patients, a subset displayed pronounced T-cell exhaustion. These nodes were enriched for cases that appeared negative by routine pathology but contained tumor cells detectable by CyTOF.

Conclusion: SN and ALN immune profiles in breast cancer are highly heterogeneous and show limited correlation with subtype, clinical variables, or outcome. Metastatic tumor cells promote T-cell exhaustion and immunosuppression, detectable in nearly half of ER+ cases. Importantly, T-cell exhaustion coincided with CyTOF-detected tumor cells that were missed by conventional pathology, indicating that even small tumor deposits can reshape the immune landscape. These findings highlight the potential of immune profiling to uncover occult tumor involvement in lymph nodes.

#4991 Stromal MAOB promotes prostate cancer growth by suppressing antitumor immunity.

Jing Wei, Hsiang Ching Huang, Kaisheng Yuan, Alivia O'Brien, Boyang Wu

Washington State University, Spokane, WA

Background: Stromal fibroblasts are a key component and regulator of the tumor microenvironment (TME), influencing tumor growth and shaping immune responses. Although stromal-epithelial interactions are known to drive prostate tumor development and progression, the specific stromal factors that modulate the tumor immune milieu in prostate cancer, a notoriously immune-cold malignancy, remain poorly understood. In this study, we investigate the role, mechanism, and therapeutic potential of monoamine oxidase B (MAOB), a mitochondrial enzyme that catalyzes the oxidative deamination of monoamines, in regulating prostate tumor immunity and growth.
Methods: The prostatic stromal fibroblasts from Maob knockout (KO) or wild-type (WT) male mice were isolated and co-inoculated with RM-1 mouse prostate cancer cells as subcutaneous implants in immunocompetent C57BL/6 or immunodeficient NSG male mice. Orthotopic RM-1 tumors were also established in the prostates of Maob-KO or WT mice. Tumor growth was monitored, and tumor-infiltrating immune cell profiles were analyzed using flow cytometry. Cytokine and chemokine secretion by Maob-KO and WT stromal fibroblasts was measured with antibody arrays.
Results: Stromal Maob deficiency markedly suppressed the growth of co-inoculated RM1 tumors in immunocompetent C57BL/6 mice, while it had only a marginal effect on RM1 tumor growth in immunodeficient NSG mice, indicating a tumor immune response triggered by stromal Maob. RM1 tumors grown in the prostates of Maob-KO mice also appeared notably smaller compared to those in WT mice. Both subcutaneous and orthotopic tumors with Maob-KO stroma exhibited increased infiltration of total and $CD8^+$ T cells, along with fewer myeloid-derived suppressor cells, M2 macrophages, and T regulatory cells. In orthotopic tumors, T-cell activity was further elevated in stromal Maob-ablated tumors, as evidenced by higher numbers of Ifnγ and Gzmb-expressing cells. Mechanistically, Maob-KO stromal fibroblasts secrete lower levels of Il-6, Ccl5, Ccl11, and Cxcl12 compared to WT counterparts, which are known to create an immunosuppressive TME.
Conclusion: Our findings identify MAOB as a potential stromal mediator of immune evasion in prostate cancer and a stromal-focused therapeutic target to enhance prostate cancer immunotherapies.
Funding Acknowledgements: This work was supported by NIH/NCI grants R01CA258634, R37CA233658, and R01CA279528 to BJW.

#4992 Activin A promotes PDAC progression via immunosuppression and non-canonical signaling.

Mark B. Wiley, Jessica Bauer, Yuchen Wang, Barbara Jung

UC San Diego School of Medicine, La Jolla, CA

The five-year survival rate for pancreatic cancer patients remains at 13%. More than 90% of these patients are diagnosed with pancreatic ductal adenocarcinoma (PDAC). Acute pancreatitis and chronic pancreatitis are risk factors for developing PDAC suggesting a strong inflammatory role for disease initiation. Recently, we found that activin a (activin), a TGFβ superfamily member, drives inflammation in acute pancreatitis via recruitment of macrophages and activation of neutrophils. In keeping with this, we recently showed that PDAC patients with high activin expression in the stroma have a worse prognosis and that inhibition of activin in mice decreased metastasis suggesting PDAC patients might benefit from activin inhibition. Here, we expand our studies in PDAC in the setting of inflammation and activin signaling. Digital Spatial Profiling (DSP) was performed on a tissue microarray of PDAC patients which permitted visualization and separation of images based on PanCK and activin localization. Tumor and stroma compartments were separated via PanCK expression and the quantification of 56 proteins was performed in activin (+) and (-) areas within each compartment. Western blots were employed to quantify the phosphorylation of p38 and SMAD2/3 in MIA PaCa-2, and AsPC-1 pancreatic cancer cell lines treated with/out activin. DSP data revealed activin (+) areas in the tumoral compartment had reduced total immune, total T cell, T helper, and memory T cell infiltrations when compared to activin (-) areas. This effect was coupled to increased markers of the MAPK and PI3K pathways in activin (+) areas. *In vitro*, activin stimulated phosphorylation of p-38, p-90, and SMAD2/3 in primary pancreatic cancer cells, but not in metastatic pancreatic cancer cells suggesting that activin may mediate stage-specific outcomes. Taken together, these data suggest that activin is a targetable molecule promoting a cancer supportive microenvironment in PDAC.

#4993 Tumor-associated macrophages promote oral squamous cell carcinoma development.

Manlin Shao[1], Carlos Caulin[2]

[1]Cancer Biology, Univ of Arizona College of Med - Tucson, Tucson, AZ,[2]Assistant Professor, H&N Surgery Research, University of Arizona, Tucson, AZ

Oral squamous cell carcinoma (OSCC), the most common oral malignancy, is characterized by poor prognosis, risk factors of tobacco and alcohol, and epithelial-specific mutations. Within the tumor microenvironment (TME) of OSCC, tumor-associated macrophages (TAMs) are key immune cells recruited to the tumor site and can be polarized into different phenotypes with either pro-inflammatory or anti-inflammatory functions. Therefore, there is a significant need to understand the role of TAMs in the OSCC microenvironment and the interaction between TAMs and cancer cells that may impact OSCC's aggressiveness and therapy resistance. Our lab has established cell lines from mouse oral tumors generated by activation of epithelial-specific mutations in mouse oral epithelium using both genetic and carcinogenic systems. Using these models, we employed an orthotopic and immunocompetent approach to study the specific functions of TAMs on the OSCC TME with surrounding lymphoid organs and highly dense vascularity. After orthotopic implantation, these cell lines developed oral tumors with high levels of TAM infiltration. To determine the role of TAMs in oral tumor development we depleted macrophages systemically with an anti-mouse Colony Stimulating Factor-1 Receptor (CSF1R). Results showed a significantly decreased tumor growth in mice injected with anti-CSF1R compared to untreated mice. Immunohistochemistry confirmed the loss of TAMs from the tumors treated with anti-CSF1R. Ongoing studies focus on investigating how macrophages remodel the tumor immune microenvironment of OSCC and modulate the malignant properties of oral cancer cells. We envision that these studies will help develop prevention and therapeutic approaches by targeting the pro-tumorigenic activities of TAMs in OSCC.

#4994 Exosome-targeted xmot-shRNA as a modular platform to dissect signaling pathways driving tolerogenic dendritic cells in the tumor microenvironment.

Mahere Rezazade Bazaz[1], Michael P. Plebanek[1], Y-Van Nguyen[1], Xueying Wang[2], Balamayooran Theivanthiran[1], Brent A. Hanks[1]

[1]UNC Lineberger Comprehensive Cancer Center, Chapel Hill, NC,[2]Department of Pharmacology and Cancer Biology, Department of Pharmacology and Cancer Biology, Duke University, Durham, NC

Dendritic cells (DCs) orchestrate tumor-targeted immunity and are essential for immune checkpoint inhibitor (ICI) efficacy, but ICI responses often fail when tumors drive DCs into a pro-tolerogenic state exhibiting an impaired capacity to stimulate $CD8^+$ T cell activation and an enhanced ability to drive $CD4^+FoxP3^+$ regulatory T cell (Treg) differentiation. Despite the potent impact of DC tolerization on the generation of anti-tumor immunity, the pathways involved in their development *in vivo* are poorly understood. We have previously demonstrated that tolerogenic DCs in the tumor microenvironment maintain increased fatty acid oxidation (FAO) and this metabolic program fuels indoleamine-2,3-dioxygenase 1 (IDO1) activation and downstream Treg development. A pivotal check point in this pathway is the rate limiting enzyme, carnitine palmitoyltransferase 1a (CPT1a). Tumor-derived extracellular vesicles (EVs) are abundantly released in response to stress and can transfer regulatory RNAs to infiltrating immune cells. DCs are highly proficient at engulfing these EVs within tumors. A defined 3′ exosome-enriched motif (xmot) sequence can selectively load oligonucleotides into these vesicles, providing an opportunity to exploit tumor EV biogenesis for shRNA delivery. Here, we aimed to utilize the xmot-shRNA platform to selectively silence *Cpt1a* in DCs to suppress FAO and prevent Treg development.*Cpt1a*-targeted shRNA is fused to a 3′ exosome-enrichment trafficking motif and utilized to generate a xmot-shCpt1a-expressing $BRAF^{V600E}$-$PTEN^{-/-}$ melanoma cell line. The tumor EVs were confirmed to harbor *Cpt1a*-shRNA by qrt-PCR and found to suppress both DC *Cpt1a* expression and DC oxidative phosphorylation *in vitro*. In order to track selective DC targeting *in vivo*, the platform was equipped with an EV-enriched CD81-mEmerald marker protein. Using this approach, $mEmerald^+$ DCs infiltrating xmot-shCpt1a-expressing $BRAF^{V600E}$-$PTEN^{-/-}$ melanomas were isolated by fluorescence-activated cell sorting and found to exhibit suppressed *Cpt1a* expression levels. By comparing with control $BRAF^{V600E}$-$PTEN^{-/-}$ melanomas, this work demonstrated xmot-shCpt1a-expression to inhibit intra-tumoral $CD4^+FoxP3^+$ Treg accumulation, enhance tumor $CD8^+$ T cell infiltration and activation, and suppress $BRAF^{V600E}$-$PTEN^{-/-}$ melanoma progression. Collectively, this study serves as a proof-of-principle for the xmot-shRNA/CD81-mEmerald platform as a modular delivery system for dissecting signaling pathways contributing to the development of tolerized DCs within the tumor microenvironment. This approach is now being utilized to probe additional regulatory circuits contributing to DC tolerization *in vivo*.

#4995 LAMP3+ migratory dendritic cells establish immune-accessible tumor microenvironment in non-Hodgkin lymphoma.

Yulong Wei[1], David Alexander Braun[2], Ya-Chi Ho[1]

[1]Microbial Pathogenesis, Yale School of Medicine, New Haven, CT,[2]Medical Oncology and Hematology, Yale School of Medicine, New Haven, CT

Effective anti-tumor immunity requires functional tumor infiltrating lymphocytes (TILs) to migrate into the tumor nest, recognize tumor antigens, and exert effector function despite suppressive tumor microenvironment (TME). Compared to immune-accessible “hot” tumors, immune-inaccessible “cold” tumors lack immune cell infiltration and resist immunotherapy. Concomitant viral infections in the tumor further shape TME heterogeneity, promoting an immunoregulatory state that limits anti-tumor immunity. We aim to dissect spatial heterogeneity in the TME to identify immune determinants of T cell infiltration and effector function that underlie hot versus cold tumors in non-Hodgkin lymphoma (NHL). Using pre-treatment snap-frozen tumors with and without viral infections (EBV and HIV) from 12 NHL patients (6 HIV+ and 6 HIV–, including 3 ABC-DLBCL, 7 GCB-DLBCL, and 2 EBV+ Burkitt lymphoma) and lymph nodes from 17 donor without NHL (9 HIV+ and 8 HIV–), we performed single-cell multi-omics (paired ATAC-seq and RNA-seq in the same nucleus) and profiled 415,548 cells, including 127,455 cancer cells and 40,730 TILs. From matched tissues, we performed spatial transcriptomics (10x Xenium immuno-oncology panel with 100 custom probes, including HIV- and EBV-specific probes) in 69 tissue sections. Across HIV+ and HIV– NHL tumor sections, we found spatially discrete tumor regions with high type I Interferon stimulated gene (ISG) expression that did not correlate with local EBV or HIV expression, excluding viral-induced type I IFN responses as the primary drivers of ISG gradients. Joint single-cell multi-omics and spatial transcriptomics profiling revealed that LAMP3+ migratory dendritic cells (LAMP3+ mDCs) established discrete ISG-high niches characterized by CXCL9 and CXCL10 expression from fibroblastic reticular cells, increased infiltration of CXCR3+ cytotoxic CD8 T cells, and ISG-high cancer cells that upregulated MHC class I and II with reduced proliferation. In contrast, in tumor nests without LAMP3+ mDCs, TIL infiltration was minimal, and cancer cells did not express ISG, had decreased MHC I and MHC II expression, and maintained proliferation capacity. Ligand-receptor analysis with NicheNet (single-cell) and CellNEST (spatial transcriptomics) revealed that LAMP3+ mDCs supported both TIL cytotoxicity via IL-15 trans-presentation and TIL exhaustion through PD-L1-PD-1 engagement. In addition to TIL exhaustion, gene-regulatory networks revealed that HIV-induced suppressive TME was shaped by MAF, which drove CD4+ T cells towards a type I regulatory (Tr1) phenotype (*MAF*, *IKZF2*, *TIGIT*, *CTLA4*, *IL2RB*, and *IL12RB2*). Overall, we identified LAMP3+ mDC-defined niches that drives type I IFN gradients and coordinates immune effector recruitment and function. Our study nominates LAMP3+ mDCs as immunotherapy targets to promote TIL migration into cold tumors and enhance anti-tumor immunity.

#4996 Biomarker discovery and the targeting of tumor immune suppression in Renal Cell Carcinoma.

Giuliana P. Mognol[1], Erpei Wang[1], William Harris[2], Tami Von Schalscha[1], Birkley S. Lim[2], Rayan Jouny[2], Ahmed Abdelhak[3], Rana R. McKay[4], Judith Varner[1]

[1]Pathology, University of California, San Diego, San Diego, CA,[2]Moores Cancer Center, University of California, San Diego, San Diego, CA,[3]Neurology, University of California, San Francisco, San Francisco, CA,[4]Medicine, University of California, San Diego, San Diego, CA

Metastatic renal cell carcinoma (RCC) remains highly lethal despite advances in immunotherapy, highlighting the need for improved diagnostic biomarkers and therapeutic strategies that overcome immune suppression and identify patients most likely to benefit from specific treatments. RCC tumors contain high levels of pro-angiogenic, immune-suppressive macrophages that contribute to therapeutic resistance and correlate with poor survival. To address the hypothesis that circulating and tumor-derived biomarkers can inform personalized therapeutic strategies, we prospectively collected 26 fresh surgical RCC tumors with matched peripheral blood, along with peripheral blood from 20 healthy donors. We isolated serum and peripheral blood mononuclear cells (PBMCs) from normal and RCC patients for comprehensive profiling. Serum was analyzed by Olink and Illumina high-throughput proteomics to detect more than 5,000 and 9,000 serum proteins, respectively. PBMCs were analyzed by 25-color flow-based immunophenotyping and by single-cell RNA sequencing. Tumor specimens also analyzed by single-cell RNA sequencing and immunocytochemistry. To identify novel strategies to treat RCC, we established ex vivo tumor slice cultures of early stage RCC specimens and tested the impact of novel innate immune therapeutics on myeloid and T cell content and state, as well as on tumor and immune cell survival. Combined, these approaches enabled the identification of biomarkers of disease progression and immune response in RCC patients. By integrating serum proteomics, single-cell profiling and functional ex vivo tumor modeling as well as the impact of new therapeutic strategies, these results may inform biomarker-guided therapeutic strategies and may identify novel therapeutic strategies that can enhance durable responses and improve clinical outcomes for patients with RCC.

#4997 TME profiling in Colombian men with suspected prostate cancer.

Dayanne M. Rodriguez Hernandez[1], Jovanny Zabaleta[2], Luis D Valle[3], Rafael Parra-Medina[1], Carmen L. Roa[1], Alvaro Gutierrez[4], Mateo Barros Barraza[1], Alba Lucia Combita[1]

[1]Instituto Nacional de Cancerologia, Bogota, Colombia,[2]Interdisciplinary Oncology, LSU Health New Orleans, New Orleans, LA,[3]Pathology, LSU Health New Orleans, New Orleans, LA,[4]Urobosque, Bogota, Colombia

Prostate cancer (PCa) features a heterogeneous tumor microenvironment (TME) that shapes evolution and therapeutic response. Although immune and stromal composition have emerged as source of prognostic biomarkers, these components remain poorly characterized in Latin American populations. No previous study has integrated computational immune deconvolution with in situ validation in this context. We aimed to define TME remodeling across malignant, adjacent, and benign prostate tissue in a Colombian cohort.RNA-seq data from 75 patients with suspected PCa were TMM-normalized and analyzed using differential expression models adjusted for PSA, age, and Gleason grade. Immune composition and stromal enrichment were inferred using CIBERSORT and xCell. For validation, six TMAs were constructed from 20 prostatectomy patients: five TMAs included three PCa-positive cases each (Gleason grades 3+3, 3+4, 4+3, 4+4, 4+5) sampling tumor and adjacent tissue, and one TMA contained benign tissue from five PCa-negative cases. IHC quantified $CD8^+$ T-cell and $CD11b^+$ myeloid infiltration.Deconvolution revealed distinct immune shifts between malignant and benign tissue. PCa-positive samples showed significant enrichment of M1 macrophages ($p=0.02$), plasmacytoid dendritic cells ($p<0.001$), and Th1 cells ($p=0.0075$), alongside elevated stromal scores ($p=0.0014$), indicating a predominantly inflammatory TME. In contrast, PCa-negative samples displayed higher mast cells, hematopoietic stem cells, common myeloid progenitors (all $p<0.0001$), NK cells ($p=0.0009$), $CD8^+$ effector memory T cells ($p=0.0006$), and $CD4^+$ naïve T cells ($p=0.0047$), consistent with an immunologically quiescent state. IHC validation confirmed increased $CD8^+$ T-cell infiltration in tumor versus adjacent ($p<0.001$) and benign tissue ($p=0.016$), and higher $CD11b^+$ myeloid infiltration versus adjacent ($p=0.002$) and benign tissue ($p=0.040$). Critically, $CD11b^+$ infiltration correlated with Gleason grade, while $CD8^+$ infiltration remained elevated across all grades.This study provides the first multimodal TME profiling in a Colombian PCa cohort. Integration of RNA-seq deconvolution with TMA-based IHC reveals immune remodeling characterized by enrichment of cytotoxic T cells and myeloid populations in malignant tissue. The grade-dependent $CD11b^+$ infiltration suggests potential as a stratification biomarker for immunotherapy and supports therapeutic targeting of myeloid cells in underrepresented populations.

#4998 ImmunoPET imaging of human tumor associated macrophages.

Ayla Vaughn Embs[1], Borna Roohani[1], Robin Kumar[1], Dajah Nash[1], Chloe La Prairie[2], Mann Dangarwala[1], Harriet M. Kluger[3], Ping Zhang[2], Benjamin Larimer[1], Bernadette V. Marquez-Nostra[1]

[1]Radiology, University of Alabama at Birmingham, Birmingham, AL,[2]Pediatric Dentistry, University of Alabama at Birmingham, Birmingham, AL,[3]Yale University, New Haven, CT

Introduction: Macrophages are valuable imaging targets for inflammatory diseases, as they may reflect prognosis and response to therapy. Current noninvasive imaging agents that target different markers of macrophages are either nonspecific or preferentially identify the immunosuppressive macrophage subset. Here, we report the development of the first positron emission tomography (PET) tracer that targets human CD68 (huCD68), the clinically established pan-macrophage marker and its evaluation in the tumor microenvironment (TME).

Methods: Fab8, previously identified through phage display, was conjugated with p-SCN-Bn-DFO chelator and radiolabeled with ^{89}Zr to obtain [^{89}Zr]Zr-DFO-Fab8. Binding specificity of the tracer was evaluated in vitro using THP-1 macrophages, and THP-1 undifferentiated cells was used as a control. NSG mice (n = 3) were inoculated with MDA-MB-231 cells, a triple negative breast cancer cell line that does not express huCD68, subcutaneously to both shoulders. After tumor growth, the mice were then intratumorally injected with THP-1 macrophages on the right tumor to establish a new model of human macrophages in the TME. As a control, undifferentiated THP-1 cells were injected into the left tumors at 1 h before tracer injection. These mice were then injected with 100 µL of 930 kBq (6.3 µg mass dose) of [^{89}Zr]Zr-DFO-Fab8 and PET imaging was performed at 1 and 6 h post-injection (p.i.). The specific uptake of [^{89}Zr]Zr-DFO-Fab8 was determined by calculating tumor-to-heart Standardized Uptake Value Ratios (SUVR). The presence of CD68 in the tumors were biologically validated by immunofluorescence (IF) staining.

Results: [^{89}Zr]Zr-DFO-Fab8 was produced with radiochemical yield >95%. [^{89}Zr]Zr-DFO-Fab8 had significantly higher binding in THP-1 macrophages (10 ± 1.5 %) than in THP-1 undifferentiated cells (3.4 ± 0.11 % ; p = 0.016). The SUVR of [^{89}Zr]Zr-DFO-Fab8 in THP-1 macrophages was determined to be 0.34 ± 0.05 and 0.48 ± 0.07 and in undifferentiated THP-1 was 0.18 ± 0.03 and 0.29 ± 0.03, at 1 and 6 h p.i. respectively. Tracer uptake in the THP-1 macrophage tumors was significantly higher than that in the undifferentiated THP-1 tumors at 1 and 6 h p.i. (p = 0.0120 and p = 0.0041, respectively). IF results showed more huCD68 staining in the THP-1 macrophage tumors vs the THP-1 undifferentiated tumors, further validating our immunoPET results.

Conclusion: We have developed the first immunoPET tracer targeting human CD68. [^{89}Zr]Zr-DFO-Fab8 binds specifically to huCD68 in both an in vitro and in vivo model, making it a promising tracer for noninvasive imaging of macrophage burden in various diseases for future clinical studies.

#4999 GFRAL is not required for PDAC tumor development and TME immune cell suppression.

Emma Crockett Funk[1], Abasi-ama Udeme[1], Cynthia F. Wright[2], Jenna Schwesig[1], Michael C. Ostrowski[3], Teresa A. Zimmers[4], Leonidas G. Koniaris[5], David Wang[3], Denis C. Guttridge[3]

[1]Pediatrics, Medical University of South Carolina, Charleston, SC,[2]Associate Professor, Path. & Lab. Med., Medical University of South Carolina, Charleston, SC,[3]Medical University of South Carolina, Charleston, SC,[4]OHSU Knight Cancer Institute, Portland, OR,[5]Surgery, Oregon Health Sciences University, Portland, OR

Growth Differentiation Factor 15 (GDF15) is a stress-induced cytokine upregulated in several cancers, including pancreatic cancer. Its most well-known role is signaling through GFRAL in the brain to induce an anorexia/cachexia syndrome. Outside the brain, GDF15 acts as an immunosuppressor. In cancer, GDF15 is thought to leverage this function to protect tumors from immune surveillance. Recently, much attention has been drawn to the relationship between GDF15 and T cell activity, as blocking GDF15 has been shown to enhance responses to anti-PD-1 therapies. Interestingly, the only known receptor for GDF15 is GFRAL, whose expression is restricted to a subpopulation of neurons located in the brainstem. As GDF15 emerges as a target for enhancing immune cell activity, the role of GFRAL in this relationship remains underexplored in animal models of cancer. The purpose of this study is to evaluate the necessity of GFRAL in mediating the immunosuppressive activity of GDF15 with relevance to pancreatic ductal adenocarcinoma (PDAC), the most aggressive form of pancreatic cancer. To test this, T cells were isolated from the whole spleen of immunocompetent mice and activated in the presence of conditioned media (CM) from murine KPC PDAC cells (*Pdx^{Cre}; $Kras^{+/G12D}$; $Trp53^{fl/fl}$).* In culture, we find that CM containing GDF15 suppressed the proliferation of CD4 and CD8 T cells. qRT-PCR confirmed that T cells lack GFRAL expression, suggesting that GDF15-mediated suppression of T cell activity does not require its canonical receptor. Additionally, KPC CM equally inhibited the proliferation of T cells isolated from *$GFRAL^{+/+}$* and *$GFRAL^{-/-}$* mice. We previously showed that GDF15 is required for early-stage development of pancreatic cancer in mice. To determine if this function of GDF15 is mediated through GFRAL, KPC cells were orthotopically injected into the pancreas of immunocompetent *$GFRAL^{+/+}$* and *$GFRAL^{-/-}$* mice. No significant differences in tumor burden or overall survival were observed between *$GFRAL^{+/+}$* and *$GFRAL^{-/-}$* mice at the experimental endpoint. In addition, both *$GFRAL^{+/+}$* and *$GFRAL^{-/-}$* mice exhibited similar myeloid and lymphoid immune responses to tumor implantation compared to non-tumor controls. Moreover, expression of the T cell exhaustion marker PD-1 remained consistent between groups. These results suggest that GDF15 modulates the tumor microenvironment independently of its sole known receptor, GFRAL. Further, disruption of the GDF15-GFRAL signaling axis does not alter the immune cell landscape or enhance T cell expansion. These findings provide valuable insights into the immunomodulatory function of GDF15 in PDAC and the possible distinct roles that the GDF15-GFRAL signaling axis has in regulating anorexia/cachexia vs tumorigenesis.

#5000 Activin receptor subtype-2A regulates innate immune cell activation and non-canonical signaling in pancreatic cancer cells.

Yuchen Wang[1], Mark B. Wiley[2], Jessica Bauer[1], Xinru Wang[3], Jordi Guillem-Marti[4], David Lee[5], David Baker[5], Barbara Jung[1]

[1]Medicine, UC San Diego School of Medicine, La Jolla, CA,[2]UC San Diego School of Medicine, La Jolla, CA,[3]Biochemistry, University of Washington, Seattle, WA,[4]Universitat Politecnica de Catalunya, BarcelonaTech, Barcelona, Spain,[5]University of Washington, Seattle, WA

More than 50% of all pancreatic cancer patients present with distant metastasis at the time of diagnosis highlighting the need for early biomarkers of pancreatic cancer progression. Inflammatory disorders of the pancreas increases the risk for developing pancreatic cancer suggesting an inflammatory component to disease initiation. Our research team has previously shown that activin A (activin), a critical inflammatory cytokine, contributes to pancreatitis development through activation of innate immune cells. Furthermore, activin co-localizes with pancreatic intraepithelial neoplasm (PanIN) lesions in a mouse model of inflammation assisted pancreatic ductal adenocarcinoma (PDAC). Here, we will test the hypothesis that activin is an early, targetable biomarker of PDAC. Western blots were performed to quantify pSMAD2/3, pERK, and PI3K on pancreatic cancer cells stimulated with activin in the presence/absence of anti-activin neutralizing antibody or a highly specific activin receptor subtype-2A (ACVR2A) inhibitor. qPCR was performed to quantify chemokine receptor expression in RAW264.7 macrophages and neutrophil-like HL-60 cells exposed to the same conditions. Transwell migration assays were performed on RAW264.6 macrophages exposed to conditioned media from pancreatic stellate cells treated with activin in the presence/absence of anti-activin neutralizing antibody or the ACVR2A inhibitor. Preliminary data suggests ACVR2A regulates SMAD2/3 phosphorylation in pancreatic cancer cells. We also observed ACVR2A dependent increases in the migratory capacity of macrophages that was regulated via activin. Taken together, these data suggest activin mediates PDAC initiation and progression via activin-mediated ACVR2A signaling.

#5001 Dynamics of HER2-driven MHC I immune evasion utilizing PWK x NeuT mice.

Ryann Ray[1], Hui-En Chou[2], WEI-ZEN WEI[3], **Jennifer Jacob**[1]

[1]Michigan State University, East Lansing, MI,[2]Biochemistry and Molecular Biology, Michigan State University, East Lansing, MI,[3]Oncology, Wayne State University Karmaos Cancer Institute, Detroit, MI

Loss of Major Histocompatibility Complex I (MHC I) is a critical immune evasion mechanism in breast cancer, often associated with aggressive disease and reduced response to immunotherapy. Given the known inverse correlation between HER2/neu expression and MHC I levels, we sought to develop a model to study the kinetics of this immune-editing process. We crossed the spontaneous HER2/neu-expressing BALB NeuT model onto a Diversity Outbred (DO) background and identified that the PWK background strain significantly accelerates tumor onset. PWKxNeuT mice developed tumors at an average of 11.5 weeks of age, substantially earlier than the parental BALB NeuT (17 weeks, $p = 0.0001$). Paradoxically, single cell RNA sequencing (scRNA-Seq) revealed that PWKxNeuT tumors harbored an increased immune infiltrate (8% CD3+ T cells) compared to BALB NeuT (2% CD3+ T cells). FFPE tumor tissue from NeuT and PWKxNeuT was analyzed using proteomics in collaboration with the iDEA Proteomics Core (Little Rock, Arkansas) using the label-free DIA approach. tumor tissue showed significant down-regulation of proteins essential for antigen processing and presentation, including tapasin, TAP1, and TAP2 ($p = 0.0003$), indicative of a systemic reduction in functional MHC I and II levels and resolving the paradox. Furthermore, we confirmed that the increased immune infiltrate in PWKxNeuT mice was functional. PWKxNeuT and BALB NeuT mice were vaccinated with DNA encoding HER2/neu together with pGM-CSF (im, ep) three times beginning at 8 weeks of age. Sera was collected to assess antibody production and peripheral blood was collected to determine T cell response by ELISPOT. Mice receiving control DNA developed tumors at an average of 11 weeks of age, compared with an average of 17 weeks for vaccinated mice, with some mice protected to 23.5 weeks of age ($p = 0.007$). Neu-specific T cells were identified in PWK background mice as were significantly increased neu antibodies compared with BALB NeuT mice. Thus, the PWKxNeuT model simultaneously displays accelerated HER2-driven tumorigenesis and a profound defect in the MHC presentation pathway, making it an ideal, genetically defined system to kinetically dissect how HER2 signaling drives the loss of MHC I during breast cancer progression. Current work is identifying changes in MHC levels and infiltrates over time in BALB NeuT and PWKxNeuT mice.

#5002 Notch4 blockade reprograms tumor-associated macrophages and enhances anti-tumor inflammatory signature in breast cancer.

Katherine A. Alexander[1], Jason Eng[2], Yu Kato[3], Bhairavi Swaminathan[2], Debdutta Mandal[2], Yajath Narra[2], L. A. Naiche[2], Yasuhiro Funahashi[4], Junji Matsui[5], Jan Kitajewski[6]

[1]Department of Pharmaceutical Sciences, University of Illinois at Chicago, Chicago, IL,[2]Department of Physiology and Biophysics, University of Illinois at Chicago, Chicago, IL,[3]Eisai Co., Ltd., Tsukuba-Shi, Japan,[4]Eisai Inc., Tokyo, Japan,[5]Eisai Co., Ltd., Woodcliff Lake, NJ,[6]University of Illinois Cancer Center, Chicago, IL

Macrophages play a crucial role in the tumor microenvironment (TME) and significantly influence pro- or anti-tumor immunity in breast cancer. Though macrophages often participate in pro-inflammatory tumor surveillance and elimination during early phases of tumor development, during later stages, they may become immunosuppressive, pro-angiogenic, pro-metastatic, and/or facilitative of a pro-tumor TME. The Notch pathway is essential for the differentiation of tumor-associated macrophages (TAMs) through the core canonical transcription factor, RBPJκ. However, individual Notch receptors (Notch1-4) have been shown to have varying effects on TAM polarization, with Notch1 and Notch2 displaying both pro- and anti-inflammatory activity. In peritoneal macrophages, Notch4 responds to inflammatory cues by limiting pro-inflammatory cytokine production and is upregulated during M2 induction. Notch4 promotes breast tumor initiation and maintains breast cancer stem cells. We have previously demonstrated that Notch4 inhibition with a novel, first-in-class neutralizing antibody, E7011, caused reduced tumor growth in mouse models of multiple tumor types, including mammary carcinoma. However, it is currently unclear whether the efficacy of anti-Notch4 treatment is mediated by Notch4 regulation of TAM function in breast cancer. We have demonstrated longitudinal increases in total macrophage populations following Notch4 blockade, accompanied by a decrease in myeloid-derived suppressor cells (MDSCs), which contribute to an immunosuppressive TME. Single-cell RNA sequencing of Py8119 mammary tumors treated with a murine analog of E7011 (6-3-A6) revealed a significant increase in the number of macrophages, and particularly Stab1+ TAMs, a subpopulation of TAMs that exhibits strong immunosuppressive activity and supports tumor growth by dysregulating antigen presentation and inducing resistance to checkpoint inhibitors. Analysis of the Stab1+ TAM transcriptome from tumors treated with 6-3-A6 showed decreased expression of markers associated with anti-inflammatory and “pro-tumor” macrophage activity, and an increase in pro-inflammatory mediators, notably the Dectin-2 pathway. This suggests that Notch4 blockade via 6-3-A6 functionally alters the traditionally pro-tumor Stab1+ TAM cluster towards a tumor-destructive, phagocytic macrophage phenotype. Taken together, these new insights into the functional reprogramming of pro-tumor Stab1+ TAMs towards a pro-inflammatory phenotype and decrease in immunosuppressive MDSCs following Notch4 blockade underscore a role for Notch4 in shaping a pro-tumor microenvironment. Ongoing genetic studies aim to elucidate the mechanism of Notch4-induced TAM immunosuppression and identify opportunities to enhance the efficacy of current immunotherapies by targeting Notch4 blockade in breast cancer.

#5003 Treg-specific inhibition of hedgehog signaling alters their function and impedes the growth of murine triple-negative breast cancer.

Ian Miranda, Courtney Swain, Brandon J. Metge, Lalita Shevde

Department of Pathology, Heersink School of Medicine, University of Alabama at Birmingham, Birmingham, AL

The central purpose of this study is to uncover and mechanistically describe the role of Hedgehog (Hh) signaling in CD4+ regulatory T cells (Tregs) in the context of murine triple negative breast cancer (TNBC). We employ a novel genetically engineered mouse model, murine TNBC models, flow cytometry, and targeted molecular assays to provide compelling evidence that inhibiting Hh activity in Tregs mitigates their suppressive function and subsequently slows tumor growth. TNBC is an aggressive form of breast cancer with limited treatment options. Any therapeutic benefits can be stifled by an immunosuppressive tumor microenvironment (TME) often found in TNBC due to an abundance of Tregs. Tregs are under transcriptional control of Foxp3, suppress other tumor-infiltrating lymphocytes and innate immune cells, and are associated with worse patient outcomes.Hh signaling normally plays a key role in embryonic development, tissue regeneration, and stem-cell renewal. Importantly, Hh signaling is aberrantly upregulated in a quarter of all cancers, and in TNBC, it has been implicated in drug resistance, tumor growth, migration, and invasion. Recent work from our lab has demonstrated that systemic pharmacological inhibition of Hh signaling led to a decrease in Treg abundance and function in the TME of TNBC.In this study, we report that inducible ablation of the Hh transcription factor, *Gli2*, in a Foxp3-dependent manner, impedes mammary tumor growth. The resultant TME is characterized by decreased abundance of Tregs and an increase in inflammatory Th17s. To uncover the mechanism behind these changes, we utilized RNA-seq and chromatin immunoprecipitation qPCR (ChIP-qPCR). Our data demonstrate that *Gli2* ablation alters the transcriptional controls in Tregs leading them to pivot towards inflammatory Th17 cells. These changes in Tregs functionally reduce the immunosuppressive nature of the TME of TNBC and permit an inflammatory TME, thereby reducing tumor growth. Cumulatively, these findings introduce a novel strategy for immunotherapy to target and impair Tregs in the TME of TNBC.

: Signaling Pathways, Metabolism, and Emerging Therapeutic Targets
Poster Session

#5007 ELAVL3 post-transcriptionally regulation of the NOTCH2 signaling pathway shapes the plasticity of small cell lung cancer.

Shuangsi Liao[1], Zichong Peng[1], Kai Kang[1], Shanghai Liu[1], Hui Wang[1], Yufeng Zhang[1], Ren Luo[1], Linglu Yi[1], Feifei Na[2], Guo Lin[1], Yue Zheng[1], Jianxin Xue[1], You Lu[1], Zhuoran Yao[1]

[1]West China Hospital of Sichuan University, Chengdu City, China,[2]Sichuan University, Chengdu, China

Background: Small cell lung cancer (SCLC) is a highly aggressive and heterogeneous malignancy, typically classified into four phenotypic subtypes by different transcription factors, referred to as ANYP. Recent studies have highlighted the plasticity between these subtypes, especially neuroendocrine (NE)/ non-NE states, which closely linked to treatment resistance. Emerging evidence suggests that stabilizing the SCLC phenotype could be advantageous for improving clinical outcomes. In this study, we identified a novel RNA-binding protein, ELAVL3, as a key player in the plasticity of SCLC. We discovered that ELAVL3 promotes a more NE-like progression of SCLC by post-transcriptionally disrupting the NOTCH2 signaling pathway. This finding offers new insights into the molecular mechanisms driving SCLC plasticity and proposes potential targets for therapeutic intervention.
Methods and Result: Through analysis of single-cell RNA sequencing data from 20 of our SCLC patients and some public databases, ELAVL3 expression is found to be positively correlated with NE signatures in both SCLC cell lines and patient tumors. Transcriptomic analysis and Western blotting results in SCLC cell lines showed that pharmacological inhibition of ELAVL3 with xxx activates NOTCH signaling pathways and induces the loss of NE features, while *ELAVL3* overexpression reduces NOTCH2 mRNA levels and helps to maintain the NE characteristics. Some molecular experiments, including RNA immunoprecipitation (RIP)-qPCR, RIP-sequencing and RNA pulldown, further discovered that ELAVL3 extensively binds to and interferes with the RNA stability of NOTCH2 signaling pathway members, thereby enhancing the NE program.Our previous studies have found that immunotherapy (IO) combined with radiotherapy (RT) can be effective for chemotherapy resistant subcutaneous SCLC, which is non-NE type, for a certain period of time. By single-cell RNA sequencing of tumor at multiple time points after IO+RT, we identified a close association among highly expressed *ELAVL3*, inactivated NOTCH signaling, restored NE characteristics and acquired therapy resistance. After testing various combination therapies in SCLC cell lines, patient-derived organoids, patient-derived tumor xenograft model, and murine SCLC model, we revealed that the inhibition of ELAVL3 hold their differentiation into non-NE types, which better corresponded to the immuno-combination therapies for SCLC after chemotherapy resistance.
Conclusions: This study nominates ELAVL3 as a key regulator of the NE state plasticity and defines a novel therapeutic strategy for SCLC.

#5008 Combination therapy with AKT and MEK inhibitors is effective in patient-derived models of adrenocortical carcinoma.

Suresh Kumar[1], Yoo Sun Kim[1], Nai-Yun Sun[1], George Karadimov[1], Yasuhiro Arakawa[1], Briana N. Cortez[1], Diana Varghese[1], Arnulfo Mendoza[1], Katja Kiseljak-Vassiliades[2], Margaret E. Wierman[2], Jonathan M. Hernandez[1], Chuong D. Hoang[1], Noemi Kedei[1], Xiaoling Luo[1], Stephen Hewitt[1], Yves Pommier[1], Craig Thomas[1], Jaydira Del Rivero[1], **Nitin Roper**[1]

[1]Center for Cancer Research, Bethesda, MD,[2]Colorado University, Aurora, CO

Adrenocortical carcinoma (ACC) is a rare malignancy with frequent metastases and poor survival due to chemoresistance and the lack of targetable oncogenic drivers. ~80% of ACC tumors overexpress IGF2, yet targeting the IGF2-IGFR1 axis in ACC has not been successful in the clinic. Here, we hypothesized that targeting additional survival pathways in combination with IGFR1 inhibition would be more effective in ACC than IGFR1 inhibition alone. Using a high-throughput screening platform (n=2803 compounds), we identified inhibitors of the MAPK pathway, to be highly synergistic with IGFR1 inhibition. MEK inhibitors were chosen for further evaluation given the safety, tolerability, and broad clinical activity. IGFR1 and MEK inhibitors were strongly synergistic in cytotoxicity across ACC cell lines (n=2) and short-term ACC organoids (PDOs) (n=8) derived from surgical tissue resections. Genetic depletion of IGF2 significantly inhibited growth with MEK inhibition and genetic depletion of MEK1 inhibited growth with IGFR1 inhibition in ACC cell lines. We then sought to identify signaling pathways downstream of IGFR1 that may be more amenable to clinical translation as IGF1R inhibitors are not FDA approved in cancer. Surprisingly, we found that linsitinib completely downregulated phospho-AKT suggesting AKT is a key downstream pathway of IGF2-IGFR1 in ACC. Accordingly, we observed strong synergy in cytotoxicity with combined AKT and MEK inhibition among ACC cell lines and short-term ACC PDOs. In vivo, the 2-drug AKT and MEK inhibitor combination demonstrated greater anti-tumor activity than either agent alone in an ACC cell-line xenograft and two chemoresistant ACC patient-derived xenograft models. Our results demonstrate a novel, active drug combination in refractory ACC that warrants clinical investigation.

#5009 A tumor-derived PTHrP-calcium axis drives cardiac dysfunction to connect cancer cachexia with mortality.

Tuba Mansoor Thakir, Sam Oscar Kleeman, Miriam Ferrer Gonzalez, Tobias Janowitz

Cold Spring Harbor Laboratory, Cold Spring Harbor, NY

Cancer cachexia (CC) contributes significantly to cancer-associated mortality, yet the mechanisms leading to death in CC remain poorly defined. We investigated whether cardiac dysfunction is a driver of CC-associated mortality. Using continuous ECG telemetry and echocardiography during disease progression in the C26 model of CC, we comprehensively assessed the effect of cachexia on electrical and mechanical components of cardiac function. The development of cachexia was associated with significantly reduced mean stroke volume (baseline 30 µL vs. cachectic 13 µL, $p = 0.001$) and cardiac output (baseline 18 mL/min vs. cachectic 8 mL/min, $p = 0.02$), with significantly increased cardiac muscle atrophy at endpoint (baseline 145 mg vs. cachectic 110 mg, $p < 0.0001$). Mortality was preceded by progressive conduction abnormalities, including first- and second-degree atrioventricular block, bradyarrhythmias, and atrial fibrillation. The onset of cachexia was associated with significantly reduced mean QTc duration (baseline 55 ms vs. cachectic 40 ms, $p = 0.002$), which correlated with marked hypercalcemia (baseline 8 mg/dL vs. cachectic 15 mg/dL, $p < 0.0001$) and hypophosphatemia (baseline 6.5 mg/dL vs. cachectic 4.5 mg/dL, $p = 0.0044$). As an explanation for perturbed calcium homeostasis, we identified RNA and protein expression of parathyroid hormone-related protein (PTHrP) in C26 cancer cells. To investigate whether hypercalcemia was a driver of cachexia-associated cardiac dysfunction, we pharmacologically suppressed calcium levels with continuously infused zoledronic acid (ZA). ZA infusion significantly lowered mean plasma calcium ($p = 0.05$), delayed the onset of cachexia ($p = 0.03$), and partially preserved stroke volume and cardiac output. We hypothesized that if hypercalcemia is PTHrP-dependent, then isogenic PTHrP knockout in the C26 cell line would obviate cachexia. Mice bearing PTHrP-KO tumors remained non-cachectic with preserved electrical function (mean QTc: scramble 40 ms vs. KO 55 ms, $p = 0.01$) and preserved mechanical function (mean cardiac output: scramble 8 mL/min vs. KO 16 mL/min, $p = 0.03$) despite comparable tumor size to scramble controls. Taken together, these preclinical data demonstrate that tumor-derived PTHrP plays a major role in driving cachexia and associated cardiac dysfunction in the C26 model, and that cardiac dysfunction may be a final common pathway of mortality in CC. Our findings raise the possibility that PTHrP-driven cachexia may be a biologically distinct and therapeutically relevant subgroup of cancer cachexia.

#5010 Loss of SHP phosphorylation reprograms lipid metabolism to promote colorectal tumorigenesis.

Ting Fu

University of Wisconsin-Madison, Madison, WI

Background: Small Heterodimer Partner (SHP/NR0B2) is a central metabolic regulator that integrates bile acid and lipid signaling with intestinal homeostasis. SHP activity is enhanced by phosphorylation at a conserved threonine residue (Thr-58 in mouse; Thr-55 in human), mediated by PKCζ downstream of FGF19 and bile acid receptor activation. While this modification is known to regulate bile acid and lipid metabolism, its role in colorectal cancer (CRC) is unknown.

Methods & Results: To determine how impaired SHP phosphorylation influences colorectal tumorigenesis, we analyzed knock-in mice expressing a phosphorylation-defective SHP mutant (SHP-T58A) in multiple CRC models. To determine how loss of SHP phosphorylation influences cell proliferation, we compared organoids generated from SHP-WT and SHP-T58A mice on both wild-type and *Apc*Min/+ backgrounds. Across both genotypes, SHP-T58A organoids displayed markedly increased budding, growth rate, and stem-cell-associated gene expression, indicating enhanced intestinal stem cell proliferation. Consistent with this, SHP-T58A mice subjected to AOM/DSS exhibited significantly greater colonic tumor multiplicity and tumor area, accompanied by increased SREBP1 activation, elevated FASN and SCD1 expression, and enhanced lipogenic lipid accumulation within tumors. Even in the acute DSS injury model, SHP-T58A colons showed exaggerated epithelial proliferation and dysregulated metabolic gene expression, suggesting that defective SHP phosphorylation alters epithelial regenerative responses and primes the tissue toward tumor-promoting metabolic states. In human HCT116 cells, CRISPR sgSHP knockout lines reconstituted with SHP-WT or SHP-T58A demonstrated that SHP-T58A drives higher proliferation, colony formation, and migration. Gene expression analyses showed activation of oncogenic and stemness-related programs (LGR5, SOX9, CD44, MYC,MET) together with induction of lipogenic genes (SREBF1, FASN, SCD1). In HCT116 mediated xenografted mice, SHP-T58A group formed significantly larger tumors in NSG mice than their SHP-WT counterparts, accompanied by increased SREBP1 signaling and lipid accumulation. Importantly, in parallel human genomic analyses, we identified SHP mutations located near the Thr-55 regulatory region in individuals with early-onset obesity and early-onset colorectal cancer, suggesting that disruption of this phosphorylation-dependent regulatory module may have broader clinical relevance.

Conclusion: Loss of SHP phosphorylation is a key metabolic switch that enhances stemness, activates lipogenesis, and promotes colorectal tumorigenesis in both mouse and human models. SHP phosphorylation status may represent a previously unrecognized metabolic vulnerability in CRC.

#5011 Targeting DUSP1 overcomes resistance to ^{177}Lu-DOTATATE in neuroendocrine tumors.

Majid Momeny, Solmaz AghaAmiri, Servando Hernandez Vargas, Sukhen C. Ghosh, Tyler M. Bateman, Jack T. Adams, Nafiseh Ghazanfari, Vahid Khalaj, Ali Azhdarinia

UT Health Houston, Houston, TX

Background: Neuroendocrine tumors (NETs) often present as metastatic or unresectable disease, and while ^{177}Lu-DOTATATE PRRT benefits SSTR2-positive patients, its modest response rate highlights the need for improved combinations. DUSP1, a MAPK phosphatase regulating JNK/p38, is elevated in multiple cancers, yet its role in NETs is unknown. Given the contribution of MAPK signaling to therapy resistance, we hypothesized that DUSP1 inhibition enhances NET sensitivity to ^{177}Lu-DOTATATE.

Materials and Methods: We compared DUSP1 mRNA levels in primary versus metastatic NETs using public transcriptomic datasets and assessed DUSP1 protein across NET cell lines and two PDX models by Western blot. Functional studies with the DUSP1 inhibitor BCI measured viability, clonogenic survival, apoptosis, mitochondrial depolarization, ROS and MAPK activation, with RNA-seq defining transcriptional changes. Rescue experiments used CC90001, ISRIB, NAC, DUSP1 overexpression, and the JNK1-K55R mutant. Synergy with PRRT was evaluated by combining BCI with sub-lethal ^{177}Lu-DOTATATE.

Results: Transcriptomic profiling showed elevated DUSP1 in lymph-node metastases versus primary NETs, and DUSP1 protein was highly expressed across NET cell lines and PDX models. BCI (1-2.5 μM) markedly reduced viability and clonogenic survival (~80% at 1 μM) and induced apoptosis (cleaved PARP ~6-fold, caspase-3/7 ~4-fold, ΔΨm loss ~2-fold). RNA-seq and Western blotting confirmed strong activation of pro-apoptotic JNK1/2 and p38. JNK inhibition, the JNK1-K55R mutant, and DUSP1 overexpression each rescued cells, whereas DUSP1 knockdown induced apoptosis—establishing DUSP1 as a key NET survival factor. RNA-seq also revealed ER-stress activation (XBP1s, ATF4, CHOP). ISRIB blocked ER stress and rescued cells, while NAC suppressed ROS, prevented MAPK/ER-stress activation, and fully rescued cells, indicating that DUSP1 inhibition triggers a ROS-dependent cascade converging on JNK and ER-stress pathways. Combining BCI with ^{177}Lu-DOTATATE produced strong synergy (CI < 0.5) with enhanced apoptosis. JNK inhibition and ISRIB each rescued combination-induced apoptosis (~60% and ~40%), showing that both pathways are required for PRRT sensitization.

Conclusion: DUSP1 is an actionable therapeutic vulnerability in NETs. Its inhibition induces ROS-driven activation of pro-apoptotic MAPK and ER-stress pathways, potentiating ^{177}Lu-DOTATATE. These findings provide preclinical support for DUSP1-targeted combination strategies, with ongoing *in vivo* studies needed to advance this approach toward clinical translation.

#5012 Multiomic profiling reveals ligand and cell specific regulatory programs of LXR selective modulation in myeloid immune cells.

Yifan Fei[1], Rajendra K C[2], Mark Flory[3], Natalia Julianna Krawczynska[4], Yu Wang[5], Kevin T. VanBortle[4], Hisham Mohammed[3], Erik R. Nelson[5]

[1]Molecular and intergrative physiology, Urbana, IL,[2]University of Illinois Urbana-Champaign, Champaign, IL,[3]Oregon Health & Science University, Portland, OR,[4]University of Illinois Urbana-Champaign, champaign, IL,[5]University of Illinois at Urbana-Champaign, Urbana, IL

Selective modulation of steroid nuclear receptors such as estrogen (ER), glucocorticoid (GR), and androgen receptors (AR) has advanced cancer therapy by enabling precise control of receptor signaling. However, selective modulation of other nuclear receptors remains underexplored. Liver X receptors (LXRs) are key regulators of cholesterol homeostasis, inflammation, and immune responses. LXR ligands have shown antiproliferative and immunomodulatory effects across multiple cancers, including prostate, breast, and colorectal cancers, as well as hematologic tumors. Certain LXR ligands also attenuate immunosuppressive cell populations in the tumor microenvironment, making LXR a promising therapeutic target.
However, many synthetic LXR agonists have shown adverse metabolic and neurologic effects and their impact on tumor progression is often inconsistent, suggesting potential ligand- and cell-specific modulation. Understanding the mechanisms underlying such selective LXR modulation, inspired by established selective modulation strategies for ER and AR related cancers, may enable the development of safer and more effective LXR-directed cancer therapies.To elucidate the mechanism of selective LXR modulation in myeloid cells, we performed multi-omics profiling (RNA-seq, ATAC-seq, and RIME proteomics) on murine bone marrow derived macrophages and dendritic cells treated with seven LXR ligands. We observed both shared and ligand- or cell-specific transcriptional and chromatin accessibility patterns. Notably, 27-hydroxycholesterol (27HC) suppressed interferon/STAT1 programs in macrophages and induced a MYC/E2F associated immunosuppressive state, whereas dendritic cells exhibited suppression of interferon stimulated genes and MYC/E2F program.T cell proliferation can be suppressed by 27HC treated macrophages. Preliminary functional assays suggested that this effect could be reversed by inhibiting E2F pathway (CDK4/6 blockade) or by targeting NF-κB, STAT3, or HDAC2 signaling in macrophages. These findings delineate cell-specific mechanisms of LXR selective modulation and suggest that targeting LXR may fine-tune E2F, NF-κB, STAT3, and HDAC2 dependent signaling that impacting macrophage-T cell crosstalk and thereby enhance T cell antitumor function.

#5013 Comprehensive characterization of DICER1 mutations and two hit tumorigenesis mechanisms in follicular thyroid carcinoma using multi-omics analysis.

Dakyung Lee[1], Young Ah Lee[1], Yeonju Kyoung[2], Seong-Keun Yoo[3], Sun-Wha Im[1], Jaeyong Choi[1], Yoo Hyung Kim[1], Dohyun Han[4], Young Joo Park[1], Jong-Il Kim[1]

[1]Seoul National University College of Medicine, Seoul, Korea, Republic of,[2]Seoul National University, Seoul, Korea, Republic of,[3]Samsung Medical Center, Seoul, Korea, Republic of,[4]Seoul National University Hospital, Seoul, Korea, Republic of

Background: DICER1 is an essential RNase III enzyme for microRNA (miRNA) processing. Germline loss-of-function (LoF) variants cause DICER1 syndrome and predispose younger individuals to tumors including follicular thyroid carcinoma (FTC). Somatic RNase IIIb hotspot mutations are characteristic, but how germline LoF, somatic hits, and tissue-specific regulatory networks drive FTC is not fully understood.
Methods: We analyzed DICER1-mutant FTC (n=20) using whole-exome sequencing, miRNA-seq, RNA-seq, and proteomics, and compared them with wild-type tumors (wt-T, n=61). Tumors were classified as syndrome-associated (syn-T, n=7) or sporadic (spo-T, n=13). Integrative analyses included allelic imbalance, pathway enrichment, and network modeling (WGCNA).
Results: Clinically, spo-T patients were significantly younger than wt-T, indicating an age-specific window for DICER1-driven FTC. Most tumors showed biallelic disruption through RNase IIIb hotspot mutations with secondary LoF events, and allelic imbalance confirmed two-hit inactivation even when only one mutation was detected.In syndrome-normal tissues, substantial mRNA dysregulation occurred without miRNA changes, suggesting DICER1 haploinsufficiency acts independently of global miRNA loss.In DICER1-mutant tumors, cell-cycle, mTOR, and Wnt pathways were strongly upregulated, whereas immune programs were broadly suppressed. The thyroid stem-cell marker REXO1 was specifically elevated, indicating a stem-like phenotype. Network analysis highlighted CTNNB1 and let-7i as key regulators of the DICER1 transcriptional program. Although DICER1- and RAS-mutant FTCs shared some downstream signaling modules, DICER1-mutant tumors retained a distinct expression identity. WGCNA identified a DICER1-specific cell-cycle module and a partially shared DICER1-RAS Wnt/MAPK module.
Conclusion: DICER1 functions as a distinct oncogenic driver in FTC, following a biallelic inactivation model and producing unique proliferative, immune-suppressed, and stem-like transcriptional states. These findings refine the mechanism of DICER1-associated thyroid tumorigenesis and suggest potential lineage-specific therapeutic targets.

#5014 *CDC73* loss does not augment cyclin D1-driven parathyroid tumorigenesis in transgenic mice.

Jen-Yuan C. Kao[1], Callie Burke[2], Justin Bellizzi[2], Andrew Arnold[1], Jessica Costa-Guda[2]

[1]Univ. of Connecticut School of Medicine, Farmington, CT,[2]UConn Health, Farmington, CT

Loss-of-function mutations in the *CDC73* tumor suppressor gene, encoding parafibromin, are the most common genetic alteration in parathyroid carcinoma. Germline *CDC73* mutation causes Hyperparathyroidism-Jaw Tumor Syndrome (HPT-JT), a rare tumor predisposition syndrome including parathyroid carcinoma, and both germline and somatic *CDC73* mutations are seen in patients with sporadically presenting parathyroid cancer. Oncogenic amplification of *CCND1*, which encodes cyclin D1, is another frequent finding in parathyroid carcinoma. Parathyroid-targeted overexpression, via a PTH-cyclin D1 (PCD) transgene, leads to parathyroid tumorigenesis, but not parathyroid malignancy, in transgenic mice. The absence of appropriate preclinical models has hindered the development of preventative strategies for patients with germline *CDC73* mutation and of non-surgical treatments for parathyroid cancer in general. Thus, we sought to develop a model system that could mimic the clinical course of *CDC73*/parafibromin-deficient parathyroid carcinoma, including robust parathyroid hormone (PTH)-dependent hypercalcemia and invasion/metastasis. To this end, we crossed parathyroid-targeted *CDC73* null mice with PCD transgenic mice, producing offspring with both *CDC73* deficiency and cyclin D1 overexpression in parathyroid cells. Double mutant mice were compared to PCD mice and wildtype littermate controls. Mice were monitored for the progression of parathyroid tumorigenesis by monthly blood collection and evaluation of serum calcium and PTH. Mice were euthanized at 18 months of age. The parathyroid glands and surrounding tissue were dissected *en bloc* and evaluated histologically for general morphology, local invasion, and parathyroid cell proliferation via Ki-67 immunostaining. While PCD-positive mice developed hypercalcemia, a hallmark of parathyroid tumorigenesis, as expected, no significant differences in calcium levels were observed between mice with both *CDC73* deficiency and cyclin D1 overexpression as compared to mice with cyclin D1 overexpression alone. Similarly, general parathyroid gland morphology and parathyroid cell proliferation were comparable between the two groups; local tumor invasion was not observed in either group. While the combined disruption of *Cdc73* and the overexpression of cyclin D1 did not result in the development of parathyroid carcinoma in our mouse model, this model system may provide valuable insight into genetic modifiers of parathyroid tumorigenesis. Background strain is known to affect the phenotype of many genetically modified mouse models, including parathyroid-targeted *Cdc73* deletion; however, the responsible genetic modifiers remain unknown. Our model system could serve as a key reagent in identifying genetic modifiers with relevance to parathyroid tumor development.

#5015 Targeting insulin to improve endometrial cancer.

Alexander Emmanuelli[1], Ezequiel Dantas[2], Marcus DaSilva Goncalves[2]

[1]Medicine, NYU Langone Medical Center, New York, NY,[2]NYU Langone Health, New York, NY

Insulin and insulin-like growth factor stimulate the growth of the endometrial mucosa by binding cell surface receptors that activate the phosphatidylinositol-3 kinase (PI3K) signaling pathway. PI3K hyperactivity is sufficient to initiate carcinoma in the uterine epithelia, where this signaling pathway promotes proliferation by activating several intracellular targets, including AKT and mTOR. Enhancement of the PI3K signaling pathway dominates the genetics of human endometrial cancer. Mutations in *PIK3CA*, encoding the p110a subunit of PI3K, and loss of function mutations in *PTEN*, a molecular off switch for the PI3K activity, are among the most frequently mutated genes in endometrial cancer. Although this high mutational burden suggests druggable targets, pharmacological inhibition of the PI3K pathway has had limited clinical outcomes. Our group has previously demonstrated that hyperinsulinemia, a clinical biomarker of endometrial cancer, limits the efficacy of PI3K inhibitors in mice and that systemic insulin can be reduced by feeding mice a very low carbohydrate (ketogenic) diet (VLCD). The combination of VLCD and PI3K inhibition can abolish tumor growth in mouse models of cancer, but the relationship between PI3K inhibition and the dysregulation of systemic glucose homeostasis has yet to be resolved in endometrial cancer. To evaluate the effects of systemic insulin on endometrial cancer growth and the efficacy of PI3K inhibition we established clinically relevant endometrial cancer xenografts via patient-derived organoids. In this study, we demonstrate that hyperinsulinemia is a modifiable factor that limits the efficacy of PI3K inhibition in endometrial cancer. By employing diazoxide and canagliflozin, pharmacological agents that counteract hyperinsulinemia, we can decrease insulin levels in the tumor while enhancing the apoptotic response to the PI3K inhibitors copanlisib and alpelisib. Additionally, we show that ketogenic diet reduces systemic insulin and improves efficacy of PI3K inhibition in xenograft models of endometrial cancer. These findings have significant implications for ongoing clinical trials of PI3K pathway inhibitors and suggest a method for increased treatment efficacy in cancer patients.

#5016 Oncogenic PIK3CA mutation enhances cyclin D1-driven parathyroid tumorigenesis in transgenic mice.

Maia Jakubowski, Callie Burke, Justin Bellizzi, Andrew Arnold, Jessica Costa-Guda

UConn Health, Farmington, CT

Parathyroid carcinoma is a rare but life-threatening malignancy. Limited treatment options are available for the more than 50% of parathyroid carcinoma patients who develop recurrent disease following surgery with curative intent. Many such patients will become refractory to medical management, eventually succumbing to the sustained, progressive hypercalcemia caused by parathyroid hormone-secreting tumors. Identification of genetic/molecular aberrations that might serve as “actionable targets” for pharmacologic intervention in parathyroid carcinoma have uncovered frequent inactivation of the CDC73 tumor suppressor gene, amplification of the cyclin D1 oncogene and activating mutations of the PI3K/MTOR pathway. We sought to combine these frequent tumor driving mutations to develop a novel preclinical model that could mimic the clinical course of recurrent/metastatic parathyroid carcinoma, for study of disease progression and to eventually develop/test novel preventative/therapeutic interventions. To this end, we crossed existing mouse models with genetic alterations known to occur in human parathyroid carcinomas, namely PTH-cyclinD1 transgenic mice (PCD), oncogenic Pik3ca mutant mice (Pik3caH1047R) and parathyroid-specific Cdc73 knockout mice. PCD mice develop biochemical hyperparathyroidism and parathyroid tumors with known kinetics. Mice harboring double and triple genetic modifications were evaluated independently and compared to PCD and wild type littermate controls. Assessment of progression of biochemical hyperparathyroidism was evaluated by monthly blood collection followed by measurement of serum calcium and parathyroid hormone (PTH). We observed that activation of Pik3ca in the absence of cyclin D1 overexpression was insufficient to drive parathyroid tumorigenesis and that loss of Cdc73 did not appear to enhance parathyroid tumorigenesis beyond the contribution of cyclin D1 overexpression. However, crossed mice harboring activating mutations of both cyclin D1 and Pik3ca developed more severe biochemical primary hyperparathyroidism than those with activated cyclin D1 alone. Some PCDxPik3caH1047R mice developed atypical histologic features consistent with aggressive parathyroid tumors. Thus, the combination of activated Pik3ca and cyclin D1 overexpression appears to yield a more aggressive parathyroid tumor phenotype. Our findings carry important potential therapeutic implications: the combination of cdk4/6 inhibitors with PI3K/MTOR inhibitors is under active investigation in other tumor types and the efficacy of such combination therapy merits investigation in parathyroid carcinomas which may harbor both cyclin D1 amplifications and activating mutations in PI3K/MTOR.

#5017 Targeting human melanoma growth with non-calcemic vitamin d3 hydroxyderivative: A synergistic approach with vemurafenib.

Senthilkumar Ravichandran[1], Ewa Podgorska[1], Zorica Janjetovic[1], Tae-Kang Kim[1], Gitali Ganguli Indra[2], Arup K. Indra[2], Andrzej T. Slominski[1]

[1]Department of Dermatology, School of Medicine, The University of Alabama at Birmingham, Birmingham, AL,[2]Department of Pharmaceutical Sciences, Oregon State University College of Pharmacy, Corvallis, OR

Background: Melanoma remains a major clinical challenge due to its resistance to current targeted therapies, emphasizing the need for new preventive and therapeutic strategies. The vitamin D receptor (VDR) and its ligands are promising, low-toxicity targets. Our team has discovered an alternative, noncanonical vitamin D-metabolic pathway initiated by CYP11A1, generating hydroxyderivatives such as 20(OH)D_3 with antioxidative, photoprotective, and anticancer activities through VDR and other nuclear receptors (LXR, AhR, ROR). We hypothesize that 20(OH)D_3, alone or combined with vemurafenib (VEM), can inhibit melanoma tumorigenic behavior through VDR-dependent and independent mechanisms.

Methods: *In vitro* studies used migration, CFU, and PrestoBlue viability assays on melanoma lines (WM3960, WM1366, WM3942, WBM550). Spheroid assays utilized 3D culture and TUNEL staining to assess apoptosis. *In vivo* efficacy was evaluated in nude mice implanted with either wild-type (WT) or VDR-knockout ($VDR^{-/-}$) WM164 ($BRAF^{V600E}$) melanoma cells. Mice received vehicle, 20(OH)D_3 VEM, or combination therapy three times weekly. Tumor growth and necrosis were monitored, and protein expression was analyzed by Western blotting.

Results: Cell migration assays demonstrated that the treatment with novel vitamin D_3 derivatives markedly inhibited the migratory capacity of WM3960 PDX melanoma cells. CFUs further confirmed a significant reduction in melanoma cell growth across several melanoma cell lines. Viability assay revealed decreased fluorescence intensity in treated cells relative to controls, indicating reduced metabolic activity, viability, and proliferation. No apoptosis was detected using the TUNEL System, suggesting that the observed effects were primarily cytostatic rather than apoptotic. *In vivo*, WT WM164 xenografts treated with the combination of 20(OH)D_3 and VEM exhibited the strongest tumor suppression, followed by VEM monotherapy, whereas 20(OH)D_3 alone had minimal impact. In $VDR^{-/-}$ tumors, both VEM and combination treatments achieved comparable inhibition, indicating both VDR-dependent and independent mechanisms of action. Western blot confirmed synergistic downregulation of phospho AKT, ERK1/2, and NF-κB signaling pathways in combination-treated tumors, consistent with enhanced suppression of oncogenic signaling. Notably, male mice displayed greater sensitivity to the combination therapy compared with females.

Conclusion: The non-calcemic vitamin D_3 derivative 20(OH)D_3, especially when combined with vemurafenib, inhibits human melanoma growth by blocking oncogenic signaling pathways, independent of apoptosis. Due to its natural origin, safety profile, and pathway selectivity, 20(OH)D_3 has strong potential as a preventive and therapeutic agent against melanoma progression and metastasis.

#5019 Preclinical mechanistic PK/PD/Efficacy modeling for AZD4241, a novel oral estrogen receptor (ER) degrader (PROTAC), to support dose selection during early clinical development.

Ana Quiroga, Pablo Morentin Gutierrez, Lynet Nyoni, Natalie Cureton, Mandy Lawson, Aaron Smith, Thomas Hayhow, Neil Gibson

AstraZeneca, Cambridge, United Kingdom

The high prevalence of ER-positive breast cancer and the emergence of resistance to current endocrine therapies highlight the need for more effective ER degraders. AZD4241 is a novel, potent, orally bioavailable, and selective ER proteolysis-targeting chimera (PROTAC) scheduled to enter clinical evaluation in 2026. We describe preclinical pharmacokinetic/pharmacodynamic (PK/PD) and efficacy modeling that quantifies the relationships among drug exposure, ERα degradation, and antitumor activity, thereby defining the extent of compound plasma exposure and target modulation required to achieve efficacy. These translational analyses are intended to inform dose selection and guide early clinical development of AZD4241.We developed a mechanistic mathematical model to quantify the exposure-target-response profile of AZD4241 in in-vivo patient-derived xenograft (PDX) models harboring either wild-type or mutated ESR1. The PK module characterized plasma concentrations across a range of doses. An indirect-response PK/PD module incorporated AZD4241 mechanism of action, whereby the compound accelerates ERα degradation yielding reductions in total ER protein measured by Western blot. The integrated PK/PD/Efficacy model linked plasma exposure, ERα levels, and tumor growth kinetics in the PDX models. Model parameters were estimated via nonlinear mixed-effects (NLME) modeling using individual longitudinal PK, PD biomarker, and tumor volume data aggregated across multiple studies. The mathematical model captured the dose-dependent reduction of ERα and the associated inhibition of tumor growth observed in the PDX models. The level of ER degradation required to induce tumor regressions on the PDX models was also quantified and will be presented. This work provides quantitative, mechanistic insight into how exposure drives biomarker modulation and antitumor responses, delineating the level of ERα degradation required for robust efficacy in endocrine-sensitive PDX models. The framework supports interpretation of compound-induced PD effects in patients under defined dosing regimens and supplies translational evidence to enable dose selection in early clinical development.

#5020 Oxysterol sulfotransferase in prostate cancer inhibition: Cell-intrinsic and -extrinsic roles.

Bobae Park[1], Zhao Zhang[1], Chiou-Miin Wang[1], Mohin Patel[1], Yaguang Liu[2], Chia-Nung Hung[1], Bandana Chatterjee[1]

[1]Molecular Medicine, The University of Texas at San Antonio-UT Health, San Antonio, TX,[2]Pathology & Laboratory Medicine, The University of Texas at San Antonio-UT Health, San Antonio, TX

Oxysterol sulfotransferase (SULT2B) mediates enzymatic sulfation of oxysterols. SULT2B can modulate lipid metabolism by interfering with oxysterol-induced activation of the LXR nuclear receptor, since sulfated oxysterols are LXR inert. Poor survival is linked to reduced SULT2B in primary prostate cancer, and the enzyme is undetectable in clinical metastases of castration resistant prostate cancer (CRPC). SULT2B-null CRPC xenografts show escalated growth while SULT2B-high tumors are growth suppressed, show reduced tumor-emitted bioluminescence and sustain apoptosis. SULT2B silenced cells are more aggressive - evident from EMT-like induction; activated ERK survival signal; and enhanced invasion. To gain mechanistic insight, we probed PC3 CRPC cells for cell-intrinsic and -extrinsic changes due to ectopic SULT2B expression.

Results: Single-cell RNA sequences of SULT2B-high PC3 (SA) & control PC3 (VA) cells revealed transition of neuroendocrine-like PC3 from mesenchymal to epithelial traits afforded by SULT2B. UMAP showed a cluster of SA cells (cluster 7) spatially well-resolved from all other clusters. Bioinformatic probing of cluster 7 cells showed them enriched in epithelial markers and deficient in mesenchymal markers. Down genes in cluster 7 include FOXA2, SOX4, MMP16, Fibronectin 1 - all drivers of lethal CRPC. Notably, CD59 - a sialic acid containing cell surface glycoprotein - is a down gene in cluster 7 and in all SA clusters combined. CD59 is a ligand for Siglec-9 - a lectin that binds sialic acid and resides on macrophages (MΦ) & other myeloids. CD59 binding to Siglec-9 may aid immune evasion since blocking Siglec-9 interaction with sialylated glycoproteins prevented immune cells infiltration to prostate tumor and inhibited PC xenograft (PMID 39436703). Inflammatory genes - such as for NFκB1 & CXCL1, CXCL8 chemokines - are induced in cluster 7 cells and in all SA cell clusters together. RT-qPCR confirmed the changes. AKR1C3 - a key androgen biosynthesis driving enzyme - was elevated in SULT2B-silenced C4-2B CRPC cells *in vitro*. Multiplex immunofluorescence showed colocalization of $CD86^+$ M1MΦ (pro-inflammatory, immune-boosting) with SULT2B+ cells of SA xenograft, and $CD163^+/CD206^+$ M2MΦ (anti-inflammatory, immune-suppressive) infiltration to $AKR1C3^+$ tumor cells of VA xenograft. AKR1C3 is expressed copiously in VA xenograft, colocalizing with M2MΦ, while it is markedly reduced in M1MΦ-enriched SA xenograft. Reciprocal AKR1C3 and SULT2B expression is consistent with our finding that AKR1C3 is upregulated by oxysterol-LXR signaling.

Conclusion: Results highlight dual impacts of SULT2B on CRPC - regulating cancer cell metabolism and also shaping cancer-immune cells interplay by altering MΦ dynamics at tumor microenvironment. In depth molecular insights into cell-intrinsic and -extrinsic roles of SULT2B may uncover new avenue(s) for limiting lethal progression of prostate cancer

#5021 Role of *ZFX* variants in parathyroid tumorigenesis.

Sara Halili, Lucas Iommazzo, Callie Burke, Justin Bellizzi, Jessica Costa-Guda, Andrew Arnold

Center for Molecular Oncology, University of Connecticut School of Medicine, Farmington, CT

Somatic alterations in *ZFX*, a conserved zinc-finger transcription factor involved in stem cell maintenance and proliferation, have been reported across various malignancies including endometrioid carcinoma, melanoma, acute lymphoblastic leukemia, and diffuse large B cell lymphoma. Emerging evidence also links *ZFX* variants in zinc finger domains 12 and 13 to parathyroid tumorigenesis. Parathyroid gland tumors cause dysregulated calcium homeostasis and increased risk for bone fractures and kidney stones. While most people with parathyroid tumors have only one single gland affected (~85%), the remaining 15% have multigland disease (MGD). This condition, previously known as parathyroid hyperplasia, has distinct clinical implications including higher rates of recurrence and association with genetic syndromes, such as multiple endocrine neoplasia type 1, that may entail risk for family members. A few studies have reported germline variants in *ZFX* associated with MGD; however, the contribution of *ZFX* variants in MGD remains poorly understood.To assess the contribution of *ZFX* variants in MGD, we screened parathyroid tumor DNA from 26 patients with MGD for variants in zinc finger domains 12 and 13. We identified the variant p.Arg764Trp in one sample and confirmed it to be germline. This variant has been previously reported as both germline and somatic in parathyroid adenomas and as a somatic variant in other malignancies, but has not been reported in MGD. We subsequently screened germline DNA from an additional cohort of 47 patients with MGD and found no variants in the coding sequence of zinc finger domains 12 and 13. The finding of the p.Arg764Trp variant in this cohort further supports the contribution of *ZFX* variants to MGD. The mechanisms by which such variants predispose affected patients for MGD as opposed to solitary parathyroid tumors merit further investigation. Additionally, while we were unable to access family history in the patient with the p.Arg764Trp variant, a previously reported three-generation family with a different *ZFX* variant (p.Tyr774Cys) included four females diagnosed with hyperparathyroidism, with one proband having MGD. This familial pattern raises important considerations for genetic testing and counseling of family members of patients with *ZFX* variants.

#5022 Hormonal alterations distinguishing high-risk women from breast cancer patients across the menopause transition.

Jiaqing Hao[1], Reilly T. Enos[2], Sam Rosin[3], Jinyu Wang[1], Shanshan Liu[1], Melissa A. Curry[4], Sonia L. Sugg[4], Marinella Temprosa[3], E. Angela Murphy[2], Bing Li[1]

[1]Department of Pathology, University of Iowa, Iowa City, IA,[2]Department of Pathology, Microbiology, and Immunology, University of South Carolina, Columbia, SC,[3]Department of Biostatistics and Bioinformatics, The George Washington University, Rockville, MD,[4]Department of Surgery, University of Iowa, Iowa City, IA

Hormonal level changes during the menopause transition have been proposed to influence breast cancer risk. Epidemiologic studies indicate that postmenopausal women with higher circulating estrogen levels are at an increased risk of developing breast cancer, suggesting that alterations in hormone profiles may reflect disease progression. However, few studies have investigated hormonal differences between high-risk women and those with active cancer. In this study, we measured 11 common hormones in plasma samples from 206 women, including 80 diagnosed with breast cancer and 126 high-risk but cancer-free women. We found that plasma levels of estrone (E1), estradiol (E2), deoxycorticosterone (DOC), and progesterone (PROG) were significantly lower in premenopausal breast cancer patients compared to high-risk women. Correlation analyses revealed that E1 levels were positively associated with body mass index (BMI) in postmenopausal high-risk individuals, while E2 levels showed a similar positive correlation in postmenopausal cancer patients. In contrast, BMI was negatively correlated with cortisol, testosterone, and 17α-deoxypregnenolone in postmenopausal high-risk women. These findings suggest that hormonal alterations, specificially reduced levels of E1, E2, DOC, and PROG, distinguish premenopausal high-risk women from those with active breast cancer. The menopause-dependent changes in hormone-BMI associations indicate that metabolic-hormonal interactions may drive the transition from cancer susceptibility to malignancy.

#5024 USP8, a survival gatekeeper turned oncogenic trigger via hyperactivation of the integrated stress response.

Debjani Mandal[1], Santosh Kumar[1], Dhruval Bhatt[1], Yan Li[2], Kory Johnson[3], Maric Dragan[4], Prashant Chittiboina[1]

[1]Neurosurgery Unit for Pituitary and Inheritable Diseases, NIH-National Institute of Neurological Disorders and Stroke, Bethesda, MD, [2]Protein/peptide sequencing facility. National Institute of Neurological Disorders and Stroke, NIH-National Institute of Neurological Disorders and Stroke, National Institutes of Health, Bethesda, MD,[3]DIR Bioinformatics Section, NIH-National Institute of Neurological Disorders and Stroke, National Institutes of Health, Bethesda, MD,[4]Flow and Imaging Cytometry Core Facility, NIH-National Institute of Neurological Disorders and Stroke, National Institutes of Health, Bethesda, MD

Eukaryotic deubiquitinase enzymes (DUBs) play a vital role in maintaining cellular homeostasis by deubiquitinating substrates marked for degradation. Of the ~100 DUBs discovered in humans, USP8 is unique for its association with human tumors including Cushing's disease (activating mutation), and solid cancers (genomic overexpression). The mechanisms underlying USP8 in tumorigenesis remain unknown. We first found that USP8 is essential for cell survival using CRISPR-Cas9-mediated homozygous excision and RNA interference. To circumvent obligate lethality, identify the substrates of USP8, and determine pathways dysregulated in human tumors with elevated USP8 activity, we engineered a GFP-auxin inducible degron (AID) at the endogenous USP8 locus in DLD1 cells. Additionally, we assayed both transient and long-term interactors using a promiscuous biotinylator BirA fused to a USP8 lentiviral construct. We performed cell survival, apoptosis assays, immunocytochemistry, western blot, RNAseq, and TMT labeled LC/MS, TUBE and IP-LC/MS study. We found that with auxin activation, DLD1USP8-GFP-AID had >80% reduction in USP8 within 30 minutes. At 6 hours, LC/MS revealed a profound alteration of the proteome and phosphoproteome with suppression of eukaryotic elongational initiation factor-2 (EIF2) signaling. We found that USP8 triggers the Integrated Stress Response (ISR), as measured by an ATF4 reporter assay. Consistently, USP8 overexpression led to a concordant elevation of EIF2 signaling and enrichment of EIF2 signaling peptides in cells expressing the USP8-BirA construct. Moreover, USP8 overexpression in PERK and GCN2 knockout lines suggests that USP8 activates ISR via both the amino acid deprivation (GCN2) and unfolded protein response (PERK) pathways. Taken together, our findings indicate that USP8 activation induces the Integrated Stress Response (ISR) through EIF2α phosphorylation and subsequent activation of the transcription factor ATF4. We propose that tumor cells hijack ISR signaling to promote pro-survival pathways, an effect that can be reversed by pharmacological inhibition of ISR using ISRIB. ISR pathway inhibition or decrease of USP8 activity shows a significant reduction of tumor volume in a syngeneic mouse model. These results reveal targetable downstream pathways of USP8 activation, offering potential therapeutic strategies to improve outcomes in patients with Chusing's disease and solid tumors.

: Diet, Alcohol, and Tobacco, and Other Lifestyle Factors
Poster Session

#5028 Joint association of body mass index and waist circumference with head and neck cancer mortality risk in Asian population.

Sangjun Lee, Sue K. Park

Department of Preventive Medicine, Seoul National University College of Medicine, Seoul, Korea, Republic of

Background: Low body mass index (BMI) has been linked to higher head and neck cancer (HNC) mortality, but the roles of general and central obesity in Asian populations are unclear. Most epidemiologic studies have evaluated BMI or waist circumference (WC) separately. We investigated the joint associations of BMI and WC with HNC mortality in Asian prospective cohorts.

Methods: We conducted a pooled analysis of population-based cohorts in the Asia Cohort Consortium with follow up for cause specific HNC mortality. BMI (kg/m^2) was categorized using Asia-Pacific cut offs (<18.5, 18.5-22.9, 23.0-24.9, 25.0-27.4, 27.5-29.9, ≥30), and WC into sex specific quintiles and WHO obesity thresholds (≥90 cm in men, ≥80 cm in women). We also constructed joint BMI-WC and BMI-smoking categories. Multivariable Cox models estimated hazard ratios (HRs) and 95% confidence intervals (CIs), adjusting for age, sex, smoking status, alcohol intake, cohort, diabetes, and hypertension, with additional adjustment for height in WC models; analyses were stratified by smoking.

Results: Compared with normal BMI (18.5-22.9 kg/m^2), underweight participants (<18.5) had more than a two fold higher risk of HNC mortality (HR 2.19, 95% CI 1.75-2.74), whereas those with BMI 27.5-29.9 had lower risk (HR 0.53, 95% CI 0.37-0.77), and intermediate categories showed similar inverse associations. WC showed a parallel inverse pattern; compared with the lowest quintile, higher quintiles had lower HNC mortality (e.g. Q4 HR 0.49, 95% CI 0.33-0.72; p trend<0.01). In smoking stratified analyses, underweight remained strongly associated with HNC mortality in both never smokers (HR 2.56, 95% CI 1.92-3.40) and smokers (HR 1.73, 95% CI 1.19-2.52). Joint BMI-smoking models using never smokers with normal BMI as the reference showed markedly elevated risk among underweight smokers (HR 3.76, 95% CI 2.53-5.60) and excess risk among normal BMI smokers (HR 2.19, 95% CI 1.70-2.83). In joint BMI-WC categories, underweight individuals with normal WC had higher HNC mortality (HR 2.29, 95% CI 1.47-3.56), whereas those with BMI ≥30.0 and normal WC had lower risk (HR 0.67, 95% CI 0.47-0.96); adding WC did not materially change BMI-HNC associations.

Conclusion: In these Asian cohorts, smaller body size-low BMI and small WC-was consistently associated with higher HNC mortality, whereas overweight and moderate obesity were associated with lower mortality. BMI was a stronger predictor than WC, suggesting that overall body mass may be more relevant than central adiposity for HNC mortality. These findings highlight the importance of incorporating baseline nutritional status and smoking history into risk stratification and survivorship care.

#5029 Employment status and adherence to physical activity guidelines among U.S. cancer survivors: An analysis of the National Health Interview Survey.

Alexis Clouser[1], Benjamin C. Amick III[1], Christopher Walter[2], Jaimi Allen[1]

[1]Epidemiology, University of Arkansas for Medical Sciences, Little Rock, AR,[2]College of Health Professions, University of Arkansas for Medical Sciences, Little Rock, AR

Background: Physical activity (PA) is a critical, modifiable lifestyle factor that improves cancer survivorship outcomes, including reduced recurrence and lower mortality. However, many cancer survivors fail to meet recommended PA guidelines (150 min of aerobic PA and 2 days of strength training per week). Socioeconomic and structural factors such as employment status are key determinants of health behaviors. As many survivors return to work, the influence of employment on their ability to engage in PA is an understudied area. This study examined the relationship between employment and PA among U.S. adults including those with cancer.
Methods: This cross-sectional study used pooled data from the 2020 and 2022 National Health Interview Survey (n=57,101), including cancer survivors. The independent variable was employment. The dependent variable, physical activity (PA) status, was categorized into four levels based on HHS guidelines (meeting both aerobic and strength, aerobic-only, strength-only, or neither). Multinomial logistic regression was used to calculate relative risk ratios for employment status across physical activity categories, adjusted for covariates.
Results: Preliminary results using adjusted multinomial logistic regression showed that, relative to meeting neither criteria, employment was significantly associated with a 9% higher relative risk of meeting both aerobic and strength physical activity criteria (RRR = 1.09; 95% CI, 1.02-1.16). Employment status was not significantly associated with meeting strength-only (RRR = 1.05; 95% CI, 0.96-1.16) or aerobic-only criteria (RRR = 1.00; 95% CI, 0.95-1.06). For the distinct populations of U.S. citizens with cancer, employment was not significant for any of the physical activity categories.
Conclusion: Preliminary findings suggest that while employment is associated with higher aerobic and muscle strengthening physical activity in the general population, this association does not hold true for cancer survivors. This suggests that returning to work may not offer the same PA benefit for survivors, potentially due to factors like persistent fatigue or other cancer-related symptoms. These results emphasize the need for targeted, low-cost physical activity interventions for non-working individuals and accessible workplace wellness programs designed specifically to mitigate PA barriers for working cancer survivors and improve long-term outcomes.

#5030 An evaluation of c-reactive protein and sleep in women with breast cancer using the All of Us dataset.

Layja J. Grant[1], Lauren K. Evans[2], Ivan T. Jubilee[3], Nelson R. Lemieux[4], **KiTani Parker Lemieux**[5]

[1]Public Health, Xavier University of Louisiana, New Orleans, LA,[2]Basic Pharmaceutical Sciences, Xavier University of Louisiana College of Pharmacy, New Orleans, LA,[3]Division of Basic Pharmaceutical Sciences, Xavier University of Louisiana- College of Pharmacy, New Orleans, LA,[4]Seven Star Academy, Inc, Harvey, LA,[5]Xavier University of Louisiana - College of Pharmacy, New Orleans, LA

Background: Women who have breast cancer are likely to encounter sleep disturbances for various reasons. Wellness is associated with the quality of sleep one receives, and the quality of sleep is also associated with healing. Continuous sleep disturbances could lead to a poorer quality of life. Therefore, we used the SDoH survey in the All of Us dataset to evaluate noise in the neighborhoods of participants with breast cancer as a measure of sleep disturbances. Women with breast cancer and poor sleep quality may experience disease progression which could be correlated by inflammation biomarkers, such as c-reactive protein.

Methods: According to the SDoH survey from the All of Us version 8 dataset, participants were divided into two cohorts, noisy and non-noisy living environments. We used multiple statistical tests to compare the groups' data. The Welch's t-test was used to compare the two cohorts and their awake, light, deep, and REM sleep level in minutes. We also used the Mann Whitney U test to compare the four levels of sleep. The correlation between sleep length and c-reactive protein was tested by Pearson's correlation coefficient. Each test was completed via Jupyter notebook using Python coding.

Results: Upon update of the All of Us dataset version 8 update, about two-hundred and ninety-nine breast malignancy-diagnosed women met the inclusion criteria of the cohort to compare noise levels of their neighborhood, quality of sleep level, and the measurement of their C-reactive protein via FitBit data and surveys. There was no statistically significant difference between noise levels and minutes of sleep or sleep level and c-reactive protein measurements.

Conclusion: It is well-established that quality sleep is essential for overall wellness. The data we collected did not establish correlation between sleep level and C-reactive protein measurements. While our outcomes are not as we predicted, it is important to know that the data were skewed, as the two cohorts were not evenly distributed. Furthermore, despite the addition of participants in the version 8 dataset, we observed that the representation of medically underserved and understudied communities was still deficient. To provide more population representative data, there needs to be more diversity amongst the participants providing pertinent data.

#5031 Integrating real-world wearable data into breast cancer risk assessment: Evidence from the *All of Us* Research Program.

Yoav Weber[1], Arshia Ilaty[2], Xuanxi Kuang[3], Emily Lan Nguyen[3], Abel Plaza-Florido[1], Shlomit Radom-Aizik[1], Argyrios Ziogas[1], Amir M. Rahmani[4], Hannah Lui Park[1]

[1]UCI School of Medicine, Irvine, CA,[2]UCI Donald Bren School of Information and Computer Sciences, Irvine, CA,[3]UC Irvine, Irvine, CA,[4]UCI School of Nursing, Irvine, CA

Lifestyle and genetic factors are known contributors to breast cancer risk, yet their integration with clinical data into breast cancer risk assessment remains limited. Traditional, self-reported lifestyle measures are subject to recall bias, whereas wearable devices provide objective, continuous measurements of physical activity and sleep behaviors. Using data from the National Institutes of Health *All of Us* Research Program (n=633,540 participants), we conducted a retrospective matched case-control study to evaluate the association between objectively captured wearable data and breast cancer risk, and to establish a scalable analytical framework for causal and machine learning modeling. Females diagnosed with breast cancer at age ≥50 years with at least five valid weeks of Fitbit data (two or more days per week) within the five years preceding diagnosis (n=154) were each matched to up to 20 cancer-free controls by date of birth (±1 year) and availability of wearable data within the same time temporal window. Numerical variables were analyzed using Wilcoxon signed-rank tests, and categorical variables via chi-square analysis. Cases exhibited lower average daily steps (6766 ± 3040) compared to controls (7248 ± 3266; p=0.011), as well as fewer daily light active and very active minutes (179.8 ± 69.0 and 13.6 ± 13.7 vs. 190.2 ± 69.3 and 16.0 ± 16.9; p = 0.043 and p < 0.001, respectively). Sleep metrics were not significantly different between groups, while family history of breast cancer was more common among cases (p < 0.001). Building on these findings, we propose a multimodal integrative framework that merges wearable, survey, and electronic health record data, with future incorporation of genomic features and causal inference techniques (e.g., propensity score matching and causal forests) to refine individualized risk estimation. Explainable machine learning approaches, including ensemble and time-series models, will enable interpretable and dynamically updated risk predictions. This study demonstrates the feasibility of using real-world wearable data within the *All of Us* infrastructure and underscores the translational potential of multimodal, causal, and interpretable modeling for precision breast cancer screening and prevention at a population scale.

#5032 Physical activity and overall and cancer-specific mortality in postmenopausal women with breast cancer: A competing risks analysis with 19-year follow-up.

Jaime I. Castillo Silva[1], Lina S. Palacio Mejia[1], Juan E. Hernandez Avila[1], Salvador Zamora Munoz[2], Rocio Rodriguez Valentin[1], Angelica Angeles Llerenas[1], Amado Jimenez Avila[3], Gabriela Torres Mejia[1]

[1]Instituto Nacional de Salud Publica, Cuernavaca, Mexico,[2]Universidad Nacional Autonoma de Mexico, Mexico City, Mexico,[3]Hospital Regional Alta Especialidad de Ixtapaluca, Ixtapaluca, Mexico

Background: As breast cancer survivors live longer, non-cancer mortality competes with cancer mortality. However, many studies evaluating physical activity have not accounted for competing risks or adequately tested effect modification by menopausal status. Therefore, we aimed to assess the association between physical activity and mortality in women with breast cancer, accounting for menopausal status and competing risks.
Methods: We analyzed 1000 breast cancer cases from the multicenter CAMA study in Mexico with 19-year follow-up. Usual hours of leisure-time moderate-to-vigorous physical activity before breast cancer diagnosis or symptoms were dichotomized at 2.5 h/week. Primary outcomes were overall, cancer, and non-cancer mortality. We used a two-stage analysis: (1) Cox model for overall mortality testing menopausal status as an effect modifier, and (2) Fine-Gray competing risks models in strata with significant effects. Models were adjusted for DAG-derived clinical, lifestyle, and socioeconomic confounders. Missing data were handled using Multiple Imputation by Chained Equations with Random Forest.
Results: Menopausal status significantly modified the association between physical activity and overall mortality (p=0.035). In postmenopausal women (n=584), physical activity was associated with reduced mortality (Table), with no significant association in premenopausal women.
Conclusions: In postmenopausal women with breast cancer, physical activity before diagnosis or symptoms was associated with lower overall mortality at long-term follow-up. This benefit reflects significantly lower cancer-specific mortality when accounting for competing non-cancer mortality. These findings underscore the importance of physical activity after menopause and highlight the need for methodological approaches that jointly consider menopausal status and competing risks in survivorship research.

Association of physical activity and mortality outcomes in postmenopausal women with breast cancer

Outcome	**HR/sHR (95% CI)**	**p-value**
Overall mortality	0.59 (0.41-0.84)	0.004
Cancer mortality	0.63 (0.40-0.98)	0.042
Non-cancer mortality	0.63 (0.35-1.14)	0.125
Models adjusted for age, clinical stage, comorbidities, Diet Inflammatory Index, alcohol, smoking, education, residence, and healthcare access. HR = hazard ratio (Cox model); sHR = subdistribution hazard ratio (Fine-Gray models).		

#5033 Association between ultra-processed foods and PI3K/AKT/MTOR signaling pathway protein expression in breast tumor tissue of Black women.

Tengteng Wang[1], Bo Qin[1], Fred K. Tabung[2], Steven Zheng[1], Nur Zeinomar[1], Chi-Chen Hong[3], Christine B. Ambrosone[3], Elisa V. Bandera[1], Ting-Yuan David Cheng[4]

[1]Rutgers Cancer Institute, New Brunswick, NJ,[2]The Ohio State University College of Medicine, Columbus, OH,[3]Roswell Park Comprehensive Cancer Center, Buffalo, NY,[4]The Ohio State University, Columbus, OH

Background: Ultra-processed food (UPF) consumption has been linked to increased breast cancer risk and poorer outcomes, potentially through metabolic/insulin resistance pathways. The PI3K/AKT/MTOR signaling pathways are frequently dysregulated in breast tumors. However, little is known about how UPF intake influences this pathway in breast tissue, particularly among Black women, who experience highest breast cancer mortality. Examining these associations may clarify diet-related molecular mechanisms underlying breast cancer disparities.
Methods: We investigated tumor FFPE samples from 439 breast cancer cases who self-identified as Black/African American and participated in the well-established population-based study, the Women's Circle of Health Study. Tumor expressions for MTOR, phosphorylated (p)-MTOR, p-AKT, and p-P70S6K were analyzed by immunohistochemistry (IHC) and digitally scored (H-score 1%-300%). Foods and drinks consumed over 12 months before breast cancer diagnosis were assessed during home interviews by validated food-frequency questionnaires. UPFs were classified according to their degree of processing using the NOVA classification system. Multivariable logistic regression models estimated odds ratios (ORs) and 95% confidence intervals (CIs) for associations between UPF intake (per 1-SD increase) and protein expression (positive [H-score>0] vs. negative [H-score=0]), adjusting for age of breast cancer diagnosis, socioeconomic status, total energy intake, and body mass index at diagnosis.
Results: Our participants consumed an average of 5.5 UPF servings/day before breast cancer diagnosis. More than 90% of tumors expressed MTOR and p-MTOR markers, whereas p-AKT and p-P70S6K were detected in 38% and 42% of cases, respectively. Higher UPF consumption was significantly associated with increased odds of nuclear p-AKT-positive tumors (OR = 1.23; 95% CI: 1.00-1.51) and cytoplasmic p-P70S6K-positive tumors (OR = 1.20; 95% CI: 1.00-1.47). Associations remained robust after restricting analyses to women with estrogen receptor (ER)-positive tumors or those without type 2 diabetes. However, heterogeneity by ER status was observed for MTOR expression: higher UPF intake was significantly associated with a threefold greater odds of cytoplasmic MTOR-positive tumors among ER-negative subtype (OR = 3.27; 95% CI: 1.19-16.46) but not among those with ER-positive cancer (OR = 0.91; 95% CI: 0.68-1.22; P-interaction=0.02).
Conclusion: Our findings suggest that higher UPF intake was associated with activation of downstream PI3K/AKT/MTOR pathway in breast tumor tissue, highlighting a potential biological mechanism linking UPFs to breast cancer development. A deeper understanding of how UPF consumption influences tumor signaling may inform the development of tailored dietary recommendations and interventions for Black women.

#5034 Ultra-processed food intake and inflammatory markers in breast cancer survivors.

Minsu Cho[1], Sihan Song[2], Zisun Kim[3], Hyun Jo Youn[4], Jihyoung Cho[5], Jun Won Min[6], Yoo Seok Kim[7], Jihyoun Lee[8], Seho Park[9], Joon Jeong[10], Jung Eun Lee[1]

[1]Department of Food and Nutrition, Seoul National University, Seoul, Korea, Republic of,[2]Division of Public Health Sciences, Department of Surgery, Washington University School of Medicine, St. Louis, MO,[3]Department of Surgery, Soonchunhyang University Bucheon Hospital, Bucheon, Korea, Republic of,[4]Department of Surgery, Jeonbuk National University Medical School, Jeonju, Korea, Republic of,[5]Division of Breast and Thyroid Surgery, Department of Surgery, Koo Hospital, Daegu, Korea, Republic of,[6]Department of Surgery, College of Medicine, Dankook University, Cheonan, Korea, Republic of,[7]Department of Surgery, College of Medicine, Chosun University, Gwangju, Korea, Republic of,[8]Department of Surgery, Soonchunhyang University Seoul Hospital, Seoul, Korea, Republic of,[9]Division of Breast Surgery, Department of Surgery, Yonsei University College of Medicine, Seoul, Korea, Republic of,[10]Department of Surgery, Gangnam Severance Hospital, Yonsei University College of Medicine, Seoul, Korea, Republic of

Objectives: This study aimed to examine the associations between ultra-processed food intake and inflammatory markers among Korean breast cancer survivors.
Methods: A total of 641 breast cancer survivors were included. Ultra-processed food intake was assessed using 3-day dietary records or a validated food frequency questionnaire. Plasma levels of high-sensitivity C-reactive protein (hs-CRP), interleukin-6, interleukin-8, tumor necrosis factor-α, and adiponectin were measured. A composite inflammatory z-score was calculated from these five biomarkers. Multivariate logistic regression and general linear models were used to estimate odds ratios (ORs) and least-squares (LS) means for inflammatory markers.
Results: Total ultra-processed food intake was not associated with inflammatory markers overall. However, the associations varied by menopausal status at diagnosis, estrogen/progesterone receptor (ER/PR) subtype, and age. Comparing extreme quartiles of ultra-processed food intake, ORs (95% confidence intervals, CIs) for an increased composite inflammatory z-score were 0.57 (0.28, 1.19) and 3.10 (1.20, 8.00) among participants who were premenopausal and postmenopausal at diagnosis, respectively (p for interaction < 0.01). LS means (95% CIs) for hs-CRP (mg/L) in the lowest and highest quartiles of ultra-processed food intake were 0.28 (0.16, 0.51) and 0.59 (0.33, 1.06) among those with ER/PR-negative tumors (p for trend = 0.03), whereas the corresponding values were 0.41 (0.31, 0.53) and 0.48 (0.37, 0.61) among those with other subtypes (p for trend = 0.67); the interaction did not reach statistical significance (p for interaction = 0.26). For reduced adiponectin, ORs (95% CIs) comparing extreme quartiles of ultra-processed food intake were 0.57 (0.26, 1.26) in those aged < 50 years and 2.65 (1.20, 5.88) in those aged ≥ 50 years (p for interaction = 0.03). When we examined the associations of ultra-processed food subgroups, higher intake of packaged and instant noodles was associated with increased hs-CRP.
Conclusions: Higher ultra-processed food intake was associated with unfavorable inflammatory profiles among Korean breast cancer survivors who were postmenopausal at diagnosis, ER/PR-negative, or aged 50 years and older. Among ultra-processed food subgroups, greater intake of packaged and instant noodles was associated with higher hs-CRP.
Acknowledgements: This research was supported by the National Research Foundation of Korea grants, funded by the Ministry of Science and ICT (2014R1A2A2A01007794, 2019R1F1A1061017, 2021R1F1A1062476, and RS-2025-00560416).

#5035 The impact of genetic and lifestyle factors on the risk of invasive postmenopausal breast cancer in the multiethnic cohort study.

Chenya Zhao[1], Gertraud Maskarinec[2], David Conti[3], Christopher A. Haiman[3], Loic Le Marchand[2], Lynne R. Wilkens[2], Fei Chen[3], Eunjung Lee[1]

[1]University of Southern California, Los Angeles, CA,[2]University of Hawai'i Cancer Center, Honolulu, HI,[3]Center for Genetic Epidemiology, University of Southern California, Los Angeles, CA

Background: Adherence to a healthy lifestyle has been consistently associated with reduced breast cancer risk, but whether this benefit varies by genetic susceptibility remains unclear, particularly among racially and ethnically diverse populations. This study evaluated whether the association between a Healthy Lifestyle Index Score (HLIS) and breast cancer risk differs by a 313-variant polygenic risk score (PRS) among postmenopausal women in the Multiethnic Cohort (MEC).
Methods: HLIS (range: 0-7) was constructed based on the 2018 World Cancer Research Fund/American Institute for Cancer Research Cancer Prevention Recommendations and included nine dietary and lifestyle components: fruit and vegetable intake, total fiber intake, red meat intake, alcohol consumption, physical activity, body mass index (BMI), waist circumference (WC), smoking status, and sugar-sweetened drink intake. HLIS was categorized into tertiles (low, intermediate, high) according to its distribution among non-cases. Hazard ratios (HRs) and 95% confidence intervals (CIs) were estimated using multivariable Cox proportional hazards models with age as the time metric. The parsimonious model was adjusted for family history of breast cancer, educational attainment, type of menopause, parity, daily energy intake, PRS, and the top 10 principal components (PCs), while the extended model was additionally adjusted for history of diabetes, age at menopause, age of menarche, and hormone use. Analyses were further stratified by PRS (above vs. below the median), and interaction was tested using a likelihood ratio test.
Results: Among the 22,725 postmenopausal women (non-Hispanic White [22.2%], African American [12.9%], Native Hawaiian [8.1%], Japanese American [37.5%], and Latino [19.2%]), 1,174 developed breast cancer during an average follow-up of 12.2 years. Higher HLIS was associated with a significantly lower risk of breast cancer. Compared to women in the low HLIS tertile, breast cancer risk was 12% lower (HR = 0.88; 95% CI: 0.77-1.00; P = 0.05) in the intermediate tertile and 34% lower (HR = 0.66; 95% CI: 0.56-0.77; P < 0.001) in the high tertile, with similar results in the extended model. This inverse association appeared to be driven by BMI (obese vs. normal: HR=1.36, 95% CI: 1.13-1.64, P=0.001) and WC (≥88 cm vs. <80 cm: HR=1.43, 95% CI = 1.19-1.72, P < 0.001). PRS was significantly associated with breast cancer risk (per-SD HR = 1.37; 95% CI: 1.29-1.45; P < 0.001). The inverse association between HLIS and breast cancer risk was similar across PRS strata, with no significant interaction (P-int = 0.48).
Conclusion: In this multiethnic cohort of postmenopausal women, adherence to a healthy lifestyle was associated with a reduced risk of breast cancer, regardless of low or high PRS, supporting the importance of lifestyle modification as a key preventive strategy for breast cancer across diverse populations.

#5036 Ultra-processed foods and disease-free survival after colorectal cancer diagnosis: Findings from the Colocare Study.

Patricia A. Erickson[1], Rachel Hoobler[1], Victoria Maria Bandera[1], Victoria Damerell[2], Ildiko Strehli[1], Megan Mclaws[1], Lyen Huang[1], Jessica N. Cohan[1], Erin Siegel[3], Doratha Armenthus Byrd[4], Adetunji T. Toriola[5], David Shibata[6], Christopher I. Li[7], Jane C. Figueiredo[8], Biljana Gigic[9], Mary Playdon[1], Sheetal Hardikar[1], Cornelia M. Ulrich[1]

[1]University of Utah Huntsman Cancer Institute, Salt Lake City, UT,[2]Department of General, Visceral and Transplantation Surgery, Heidelberg University Hospital, Heidelberg, Germany,[3]Colorectal Cancer Alliance, Washington, DC,[4]Moffitt Cancer Center, Tampa, FL,[5]Department of Surgery, Washington University School of Medicine, St. Louis, MO,[6]Assoc. Professor of Surgical Onc., Div. of Interdiscipl. Onc., University of Tennessee Health Science Center - Memphis, Memphis, TN,[7]Fred Hutch Cancer Center, Seattle, WA,[8]Samuel Oschin Comprehensive Cancer Institute, Los Angeles, CA,[9]Heidelberg University Hospital (UKHD), Heidelberg, Germany

Introduction: Ultra-processed foods (UPFs), industrially formulated products high in fat, sugar, and additives, account for ~60% of daily calories in the United States. UPF intake has been linked to obesity, diabetes, and risk of some cancers, yet its impact on colorectal cancer (CRC) survivorship remains unclear. CRC survivors often face treatment-related dietary challenges and may rely on UPFs for convenience or to meet energy needs.
Methods: We analyzed 418 stage I-III CRC patients in the ColoCare Study across four U.S. sites. Baseline demographic, lifestyle, and clinical data were collected. Dietary intake was assessed 6 months post-diagnosis using a food frequency questionnaire (FFQ) reflecting the prior six months. Foods were classified into one of four NOVA groups: unprocessed, minimally processed, processed, and ultra-processed foods (UPFs). We focused on UPF intake (NOVA Group 4), categorized into quartiles (Quartile 1 = lowest; Quartile 4 = highest) using two metrics: absolute intake (grams/day) and relative intake (percent of total grams/day). Cox proportional models estimated hazard ratios (HRs) and 95% confidence intervals (CIs) for disease-free-survival (DFS), adjusting for study site, age, sex, tumor site adjuvant treatment, BMI, and total caloric intake (kcal). Sensitivity analyses without BMI/kcal adjustment were also done.
Results: Participants had a mean age of 58 years (standard deviation [SD]=13y) and a mean BMI of 29 kg/m² (SD=6.8). 50% of participants were female, 49% were diagnosed with stage III CRC, and 59% with colon cancer. The median follow-up was 4 years (SD=2y). UPFs comprised ~16% of the total daily food intake by weight. The mean Healthy Eating Index (HEI) score was 63 (SD=10), but scores decreased across quartiles of UPF consumption ($p < 0.001$). When evaluated by g/day, BMI differed by UPF quartiles (p=0.04), and a similar pattern was observed when quartiles of % g/day were used (p=0.12). UPF consumption, whether in g/day or percent of total intake, was not significantly associated with DFS. For g/day quartiles, HRs (95% CI) for quartiles 2-4 vs 1 were 0.92 (0.52-1.65), 0.88 (0.47-1.62), and 0.88 (0.45-1.74). For percentage-based quartiles, HRs were 1.12 (0.61- 2.09), 1.02 (0.54-1.93), and 1.27 (0.70-2.30). Results were consistent in both unadjusted models and those without BMI/kcal adjustment.
Discussion: In this large, multi-center cohort, UPF intake was common among CRC survivors and associated with lower diet quality. However, UPF consumption was not associated with DFS, regardless of whether intake was measured in g/day or percentage of total intake. Modest differences in HR direction likely reflect how absolute versus relative intake captures dietary patterns. These findings offer important insights into post-diagnosis diet and cancer outcomes.

#5037 Liquid and solid fructose intake and colorectal cancer mortality by physical activity in U.S. prospective cohorts.

Hanseul Kim[1], Jihye Yun[1], Carrie R. Daniel-MacDougall[1], Long H. Nguyen[2], Edward L. Giovannucci[3]

[1]The University of Texas MD Anderson Cancer Center, Houston, TX,[2]Massachusetts General Hospital, Boston, MA,[3]Harvard TH Chan School of Public Health, Boston, MA

Background: We recently found that liquid fructose promotes colorectal cancer (CRC) metastasis in preclinical models, including human cancer cell lines and mice (Feng et al., 2025). In humans, fructose is consumed in both liquid and solid forms (Li et al., 2023), but whether these sources relate differently to CRC mortality is unknown. Additionally, physical activity may modify the metabolic effects of fructose (Tappy & Rosset, 2019).

Methods: We assessed pre- and post-diagnostic liquid and solid fructose intakes using quadrennial food frequency questionnaires in the Nurses' Health Study (1984-2018) and Health Professionals Follow-Up Study (1990-2018). Nutrient intakes were energy-adjusted using the residual method. Post-diagnostic fructose intake was assessed at least six months but no more than four years after diagnosis. Liquid fructose was derived from sugar-sweetened beverages and juice, and solid fructose was calculated as total minus liquid fructose. Cox proportional hazards models were used to estimate hazard ratios (HRs) for fructose intake and CRC-specific mortality, stratified by pre-diagnostic physical activity (<11.5 vs. ≥11.5 metabolic equivalent of task [MET]-hrs/wk) and adjusted for demographics, tumor characteristics, lifestyle factors, and diet.

Results: Among 724 CRC patients with low pre-diagnostic physical activity (<11.5 MET-hrs/wk), we observed 96 CRC-specific deaths over 7,412 person-years. Higher post-diagnostic, but not pre-diagnostic, liquid and solid fructose intakes were associated with higher CRC-specific mortality. Post-diagnostic liquid fructose showed the strongest association with CRC mortality (Multivariable [MV]-adjusted HR per 5 g/day, 1.18; 95% CI, 1.04-1.34; P-value, 0.011), whereas post-diagnostic solid fructose showed a more modest association (MV-adjusted HR per 20 g/day, 1.04; 95% CI, 1.01-1.06; P-value, 0.002). Among 705 patients (6,611 person-years; 95 CRC-specific deaths) with high pre-diagnostic physical activity (≥11.5 MET-hrs/wk), neither liquid nor solid fructose intake, pre- or post-diagnostic, was associated with CRC-specific mortality. These findings showed that the positive associations between fructose intake and CRC mortality were observed for individuals with low physical activity, confined to post-diagnostic fructose intake, and stronger for liquid than for solid fructose.

Conclusions: Higher post-diagnostic fructose intake, especially from liquid sources, was associated with increased CRC-specific mortality among patients with low physical activity. These findings suggest a potential interaction between physical activity and fructose intake in the context of CRC mortality and highlight the importance of food choices in CRC survivorship.

#5038 Associations of WCRF/AICR recommendations with survival and chemotherapy outcomes in colon cancer: CALGB/SWOG 80702 (Alliance).

En Cheng[1], Chao Ma[2], Qian Shi[3], Anthony F. Shields[4], Peter T. Campbell[1], Ardaman P. Shergill[5], Katherine A. Guthrie[6], Felix Couture[7], Philip Kuebler[8], Pankaj Kumar[9], Benjamin Tan[10], Smitha S. Krishnamurthi[11], Kimmie Ng[2], Eileen M. O'Reilly[12], Justin C. Brown[13], Philip A. Philip[4], Jeffrey A. Meyerhardt[2]

[1]Department of Epidemiology and Population Health, Albert Einstein College of Medicine, Bronx, NY,[2]Department of Medical Oncology, Dana-Farber Cancer Institute, Boston, MA,[3]Alliance Statistics and Data Management Center, Mayo Clinic, Rochester, MN,[4]Department of Oncology, Karmanos Cancer Institute, Wayne State University, Detroit, MI,[5]Department of Medicine, University of Chicago Pritzker School of Medicine, Chicago, IL,[6]SWOG Statistics and Data Management Center, Fred Hutchinson Cancer Center, Seattle, WA,[7]Hotel-Dieu de Quebec, Quebec, QC, Canada,[8]Columbus NCI Community Oncology Research Program, Columbus, OH,[9]Illinois CancerCare PC, Peoria, IL,[10]Siteman Cancer Center, Washington University School of Medicine, St Louis, MO,[11]Department of Hematology and Medical Oncology, Cleveland Clinic, Cleveland, OH,[12]Memorial Sloan Kettering Cancer Center, Weill Cornell Medical Center, New York, NY,[13]Exercise & Cancer Biology Research Program, AdventHealth, Orlando, FL

Background: Adhering to 2018 World Cancer Research Fund (WCRF)/American Institute for Cancer Research (AICR) Cancer Prevention Recommendations is reportedly associated with better survival among long-term colon cancer survivors (likely affected by immortal time bias). Thus, it is important to validate survival benefits by assessing adherence shortly after diagnosis, and further investigation is needed to examine its association with chemotherapy outcomes.

Methods: Using an NCI-sponsored adjuvant chemotherapy trial conducted in patients with stage III colon cancer (CALGB/SWOG 80702; NCT01150045), we included 1,666 patients who returned valid Willett food frequency questionnaires (FFQ) at chemotherapy initiation and derived WCRF/AICR scores accordingly (higher score suggesting higher adherence). The primary outcome was disease-free survival (time from FFQ completion to recurrence or death), and secondary outcomes were reduced relative dose intensity (RDI; <85% suggesting worse completion) and severe toxicities (grade ≥3 for any chemotherapy-related toxicity). To estimate the associations of WCRF/AICR scores (quartiles) with survival and chemotherapy outcomes, we conducted multivariable Cox proportional hazards regression for disease-free survival and multivariable logistic regression for reduced RDI and severe toxicities.

Results: Compared to those in the lowest quartile of the WCRF/AICR score, patients in the highest quartile had significantly better disease-free survival (hazard ratio: 0.75 [0.58, 0.98], P_{trend} = 0.02) and lower risk of reduced RDI (odds ratio [OR]: 0.74 [0.54, 1.00], P_{trend} = 0.03), but not for severe toxicities (OR: 1.24 [0.93, 1.67], P_{trend} = 0.11).

Conclusions: In patients with stage III colon cancer, higher adherence to WCRF/AICR recommendations was associated with better survival and chemotherapy completion, but not for severe toxicities.

Funding: https://acknowledgments.alliancefound.org

Table. Adjusted Associations of WCRF/AICR Recommendations with Survival and Chemotherapy Outcomes

Survival and Chemotherapy Outcomes	Q1	Q2	Q3	Q4	P_{trend}
Disease-free survival					
Number of events/at risk	133/393	134/492	74/323	114/458	
Hazard ratio	1.00	0.83 (0.65, 1.05)	0.68 (0.51, 0.91)	0.75 (0.58, 0.98)	0.02
Reduced RDI					
Number of events/at risk	156/393	191/492	131/323	208/458	
Odds ratio	1.00	0.97 (0.72, 1.30)	0.95 (0.69, 1.32)	0.74 (0.54, 1.00)	0.003
Severe toxicities					
Number of events/at risk	174/393	230/492	172/323	227/458	
Odds ratio	1.00	1.10 (0.83, 1.46)	1.41 (1.03, 1.93)	1.24 (0.93, 1.67)	0.11

#5039 Dietary patterns in young lung cancer: mutation-specific environmental associations.

Sarah D. Gorbatov[1], Marisa A. Bittoni[2], Anna H. Wu[3], Allison Harper[4], Kotait Virginia[4], Narjust Florez[5], Barbara J. Gitlitz[3], Jorge J. Nieva[3]

[1]California Northstate College of Medicine, Elk Grove, CA,[2]The Ohio State University, Columbus, OH,[3]Keck School of Medicine, University of Southern California, Los Angeles, CA,[4]Addario Lung Cancer Medical Institute, San Carlos, CA,[5]Dana-Farber Cancer Institute, Boston, MA

Following peak tobacco incidence in the mid-1980's there has been a large reduction in lung cancer incidence among men that has not been seen among women. Lung cancer at a young age is now more common among women than men, reversing a decades long pattern. We sought to characterize environmental exposures among young lung cancer patients to understand potential drivers of this change in the epidemiologic profile of young lung cancer patients. We analyzed 187 patients (157 females, 84%) from the Epidemiology of Young Lung Cancer (YLC) study (ClinicalTrials.gov identifier: NCT04640259) using mutation-based grouping by shared biological mechanisms: EGFR Pathway (EGFR+ERBB2), Fusion Positive (ALK+ROS1+RET+NTRK), and Other/Mixed Mutations (including MET exon 14 skipping, TP53, KRAS, BRAF, and additional alterations). Of these, 166 patients (138 females, 83.1%) completed validated food frequency questionnaires. Dietary quality was assessed using the Healthy Eating Index-2015 (HEI-2015) and compared to U.S. reference values from NHANES. Dietary categories with elevated contaminant residue potential were identified using published literature. Statistical comparisons employed one-sample t-tests against reference means and chi-square tests for categorical variables. The EGFR groups and ALK groups had tobacco use history in 32.8% and 13.4% of patients respectively. All groups had similarly high levels of oral contraceptive exposure among women (75-100%). Dietary analysis revealed that EGFR Pathway, Fusion Positive, and Other/Mixed Mutations patients demonstrated HEI-2015 scores (out of 100) of 64.9 ± 10.7, 65.5 ± 9.8, and 63.5 ± 9.5 respectively, compared with the US reference of 58. YLC women demonstrated higher dietary quality scores than men (65.6 ± 9.7 vs. 61.8 ± 11.3), both exceeded U.S. reference values of 60 for females and 56 for males. These YLC patients also consumed more foods from dietary categories associated with elevated contaminant exposure potential, as reflected by higher HEI-2015 component scores (out of 5) for total vegetables (4.2 vs. 3.5), fruits (3.3 vs. 2.5), and whole grains (3.9 vs. 2.6). YLC patients have a diet pattern of higher diet quality, with higher exposure to whole fruits, vegetables and whole grains. While these food groups are presumed to have good health benefits, there is an emerging, under-appreciated literature that produce based whole foods often contain high pesticide/herbicide contaminants. Further investigation of the role of pesticide contaminated fruits/vegetables/whole grains is timely to assess its role, if any, in the changing lung cancer prevalence over the last 4 decades.

#5040 Dietary advanced glycation end-products and risks of lung cancer and chronic respiratory diseases.

Ailing Qin[1], Fubin Liu[1], Yu Peng[1], Peng Wang[1], Changyu Si[1], Xixuan Wang[1], Jianxiao Gong[1], Huijun Zhou[1], Jiale Gu[1], Ming Zhang[2], **Fangfang Song**[1]

[1]Tianjin Medical Univ. Cancer Inst. & Hospital, Tianjin, China,[2]Shenzhen Prevention and Treatment Center for Occupational Diseases, Shenzhen, China

Background: Advanced glycation end-products (AGEs) can promote inflammation and oxidative stress, and are involved in the onset of various chronic diseases. Diet has been identified as a major source of exogenous AGEs. However, epidemiological evidence regarding the role of dietary AGEs in respiratory-related diseases remains scarce.
Methods: We included 153,897 participants from the UK Biobank, for whom food consumption information was collected via 24-hour dietary questionnaires. We estimated the daily intakes of total AGEs comprising N^{ε}-(carboxymethyl)-lysine (CML), N^{ε}-(1-carboxyethyl)-lysine (CEL), and N^{δ}-(5-hydro-5-methyl-4-imidazolon-2-yl)-ornithine (MG-H1), and categorized them into 17 food groups. Multivariable Cox proportional hazards models were used to estimate the hazards ratios (HRs) and 95% confidence intervals (CIs) of total and different food-derived AGEs with lung cancer and chronic respiratory diseases.
Results: After a median follow-up of 10.57 and 10.81 years, 1,073 cases of lung cancer and 19,584 cases of chronic respiratory disease were ascertained, respectively. Higher intakes of total AGEs, CML, CEL, and MG-H1 were associated with lower risks of lung cancer (mainly lung adenocarcinoma, $HRs_{Q5\ vs.\ Q1}$: 0.60-0.72) and chronic respiratory diseases (asthma, COPD, IPF, and pneumonia, $HRs_{Q5\ vs.\ Q1}$: 0.67-0.91). Additionally, meats-derived AGEs were related to an increased lung cancer risk ($HR_{Q5\ vs.\ Q1}$ =1.26, 95% CI: 1.04-1.53), whereas a reduced risk of lung cancer was associated with AGEs from nuts ($HR_{Q5\ vs.\ Q1}$=0.69, 95% CI: 0.59-0.81). Beverages-, meats-, potatoes-, and sweets-derived AGEs increased the risk of chronic respiratory diseases by 4%~10% (P_{trend} <0.05), while increased intakes of AGEs from cereals, vegetables and fruits, nuts and most other foods presented a protective trend against chronic respiratory diseases (P_{trend} <0.05).
Conclusions: There existed an inverse association of dietary AGEs exposure with lung cancer and chronic respiratory diseases. The different role of AGEs by diverse food sources needs to be emphasized when assessing their impacts on health outcomes.

#5041 Recruiting men who smoke for lung cancer risk research: Lessons learned using the electronic health record and community recruitment strategies.

Trista A. Beard, Diana L. Morales, Kelsie Campbell, Alexandra L. Lindgren, Chanita Hughes Halbert

Population and Public Health Sciences, Keck School of Medicine of USC, Los Angeles, CA

Introduction: Electronic Health Records (EHRs) are broadly used for research recruitment; however, reported social histories such as smoking status are inconsistently reported, incomplete, or inaccurate. The goal of this review is to analyze lessons learned in recruiting men for a stress reactivity study and compare various recruitment yields across EHR versus community strategies.
Methods: In a large Los Angeles tertiary health system, we conducted two EHR driven outreach waves from January 2024-June 2025 targeting African American/Black and non-Hispanic White men aged 21-75. The first wave utilized a natural language processing (NLP) query of a combination of notes, smoking-related terms, and smoking-related health history. The second wave manually queried discrete social history fields that recorded tobacco use. Recruitment from the first two waves was standardized, with potential participants contacted via multiple text, phone calls, and email attempts. Parallel community recruitment used targeted social media advertisements linked to a REDCap survey screener, plus recontact of a prior smoking cohort who consented to future studies. Primary measured outcomes were the consent rate, contact rate, and proportion misclassified as smokers (those who were identified via EHR as smokers but reported being “never-users”).
Results: In EHR wave 1 (NLP wave), 579 participants were approached, with 171 (29%) reached and 16 consented (2.8%). Among those who declined, 77 (49.6%) reported having a never-smoking history. EHR wave 2 (discrete fields) had more participants (1,374 patients): 141 (10.2%) were reached, and 16 (1.2%) consented to join the study. Community ads screened 1,488 potential participants, 404 were eligible (27.2%) and 110 consented to participate in study activities (27.2%).
Conclusions: EHR recruitment alone, particularly when NLP driven, was demonstrated to misclassify presumed smokers and yielded low consent rates. Wave 2 (discrete field of social history) yielded improvement in specificity but not engagement. Social media targeted outreach generated the most positive recruitment activity; however, this requires phone verification to ensure individual authenticity. Multimodal recruitment, coupled with standardized, longitudinal EHR capture of smoking intensity (in pack-years) and history is essential for representative and accurate enrollment and improving lung cancer screening referral uptake.

#5042 Attributable cancer in Asia: A heterogeneous picture.

Monireh Sadat Seyyedsalehi[1], **Paolo Boffetta**[2]

[1]University of Bologna, Bologna, Italy,[2]Stony Brook University, Stony Brook, NY

Published estimates of cancer burden attributable to modifiable factors in Asia are not comparable due to heterogeneous methodologies. A comprehensive analysis is needed to characterize regional variations and inform prevention strategies. We estimated population attributable fractions (PAFs) for major avoidable cancer risk factors across Asian countries grouped into West Asia, South Asia, South-East Asia, Central Asia, and selected East Asian countries (China, Mongolia and North Korea; Japan and South Korea). Data sources included region-specific exposure estimates and established relative risks from international evaluations. Risk factors analyzed included tobacco use, alcohol consumption, infections, dietary factors, occupational factors, and excess body weight. PAFs were computed separately for individual risk factors and cancer types. Substantial heterogeneity was observed across Asia in the contribution of modifiable risk factors to cancer burden (table 1). Tobacco, infections, and alcohol were consistently among the leading contributors, although their ranking varied by region. Diet and excess body weight contributed substantially to several countries, with marked regional differences. Overall, PAFs for many risk factors were higher than those reported in Europe and the Americas. The distribution of cancer types with the highest attributable fractions differed across regions, reflecting variations in exposure patterns and baseline incidence. The burden of cancer attributable to modifiable factors in Asia is substantial yet highly heterogeneous across regions. Improving the availability and quality of exposure data is needed for more accurate assessments. Expansion of comparable, methodologically harmonized PAF estimation across additional Asian countries will strengthen regional cancer prevention strategies. Future work should incorporate temporal exposure trends and broaden the range of risk factors evaluated.

Table 1. PAFs expressed as percentages, for major modifiable cancer risk factors referring to all cancers combined in Asia.

Risk Factor	Gender	West	Center	South	Southeast	China+ North Korea+ Mongolia	Japan+ South Korea
All factors in the analysis	Both	30.82	40.54	36.85	38.29	42.44	40.55
All factors in the analysis	Male	35.95	48.15	43.25	47.09	55.89	45.87
All factors in the analysis	Female	24.45	36.07	34.34	31.78	30.85	28.98
Diet *	Both	8.55	12.07	6.14	9.78	11.12	7.93
Diet *	Male	9.75	15.35	6.51	11.17	12.47	8.47
Diet *	Female	6.54	8.99	5.6	8.08	9.34	6.45
Infection **	Both	8.66	18.43	14.11	16.32	15.13	14.11
Infection **	Male	8.14	15.24	7.19	13.72	15.71	13.74
Infection **	Female	8.01	19.91	20.24	17.53	13.77	11.43
BMI > 25	Both	6.2	6.29	2.63	2.46	3.38	5.5
BMI > 25	Male	3.73	4.05	1.48	1.64	3.71	5.35
BMI > 25	Female	8.01	7.72	3.5	2.8	3.01	4.75
Alcohol drinking	Both	0.9	3.66	2.6	2.54	4.11	6.05
Alcohol drinking	Male	1.54	7.16	5.59	5.04	7.54	8.63
Alcohol drinking	Female	0.44	2.11	1.16	1.09	1.95	3.22
Tobacco smoking	Both	11.03	7.42	11.21	12.83	17.25	15.77
Tobacco smoking	Male	19.89	21.02	26.13	27.51	33.59	23.97
Tobacco smoking	Female	4.04	1.91	3.76	5.03	6.61	7.2

*Including Low fruit and vegetable intake, high red and processed meat intake, dairy intake, fish intake

**Including Helicobacter pylori, Hepatitis B virus, Hepatitis C virus, Human Papillomavirus virus

#5043 AI-generated pictorial alcohol warnings strongly increase motivation to reduce drinking through enhanced attention, learning, and emotional processing: A mediation analysis.

Taghrid Asfar[1], Frank J. Penedo[2], Olusanya Joshua Oluwole[1], Eric Brown[1], Erin N. Kobetz[3], Carmen Calfa[4]

[1]University of Miami Miller School of Medicine, Miami, FL,[2]University of Miami, Miami, FL,[3]Assistant Professor, Dept. of Epidem. & Pub. Health, University of Miami, Miller School of Medicine, Miami, FL,[4]Univ. of Miami Sylvester Comprehensive Cancer Ctr., Plantation, FL

Background: Alcohol is the 3rd leading cause of cancer in the US, linked to seven types, but only 30% of Americans are aware. Health warning messages can effectively communicate this risk, though the mechanism remains unclear.
Objective: This study examined if AI-generated pictorial messages (graphic, neutral) surpass text messages and explored mediators affecting motivation to reduce alcohol use.
Methods: In March 2025, a national online crossover experiment with 596 U.S. adult alcohol users (49.3% female; aged 21 +) evaluated 8 alcohol-cancer risk messages (4 general, 4 cancer-specific), each at 3 intensities: text, neutral pictorial, and graphic pictorial (n = 24). Each participant viewed two randomly assigned messages out of the 8, each at 3 intensities (n = 6), in a counterbalanced order. The primary outcome was motivation to reduce alcohol in the next 30 days. Mediators were attention, perceived learning, believability, fear, and avoidance. We used multilevel structural equation modeling to estimate parallel and serial mediation pathways, comparing graphic vs. text, neutral vs. text, and graphic vs. neutral, while adjusting for age, sex, alcohol level consumption (moderate, heavy), alcohol social norms, and message order and specificity (general vs. cancer-specific).
Results: Graphic and neutral pictorials drew more attention, perceived learning, believability, and fear than text messages ($p<0.01$ for all). Graphic pictorials also increased avoidance relative to both neutral and text messages. In parallel mediation models, graphic pictorials had a significant total effect on motivation ($\beta = 0.91$, SE = 0.12), with 93.6% of the effect mediated through indirect paths, primarily through attention (47.2%) and fear (24.3%). Neutral pictorials also increased motivation compared to text messages ($\beta= 0.47$, SE= 0.10), with 99.3% of the effect mediated, mainly by attention (56.8%) and believability (16.7%). Graphic pictorials outperformed neutral ones ($\beta= 0.439$, SE = 0.092, $p < 0.001$ for all), with 87.6% of the effect mediated mainly through attention and fear. Serial mediation analyses confirmed attention as the primary upstream driver. For graphic vs. text comparisons, sequential paths through attention and believability (31.8%), attention and fear (22.9%), and attention and learning (17.6%) significantly predicted motivation. Similar patterns were observed in comparing neutral vs. text and graphic vs. neutral. Across all models, the direct effects of message intensity on motivation were not significant.
Conclusions: AI-generated pictorial alcohol warnings, particularly graphics, substantially increase motivation to reduce alcohol consumption by enhancing attention, fear, perceived learning, and believability. These findings highlight AI's role in improving alcohol-cancer risk communication.

#5044 Changes in providers' delivery of cigarette smoking interventions for cancer prevention after the implementation of a tobacco-free workplace program in healthcare centers serving rural and medically underserved areas in Texas.

Ammar D. Siddiqi[1], Nikhil K. Patel[2], Maggie Britton[3], Tzuan A. Chen[4], Isabel Martinez Leal[3], Teresa Williams[5], Kathleen Casey[5], Lorraine R. Reitzel[3]

[1]University of California, San Francisco, San Francisco, CA,[2]Vanderbilt University, Nashville, TN,[3]UT MD Anderson Cancer Center, Houston, TX,[4]University of Houston, Houston, TX,[5]Integral Care, Austin, TX

Cigarette smoking is elevated in rural and medically underserved areas of the US, contributing to greater tobacco-related cancer morbidity and mortality among residents relative to their urban counterparts. Consequently, there is an opportunity for cancer prevention via use of evidence-based interventions for cigarette smoking in settings where rural and medically underserved adults receive care. The implementation of tobacco-free workplace programs in urban healthcare centers has improved providers' intervention delivery for cigarette use; however, evidence regarding their effectiveness in centers serving rural and medically underserved populations is limited and cannot be assumed, given potentially unique barriers to program adoption. This work seeks to redress this gap by examining changes in providers' delivery of the 5As, an evidence-based intervention for cigarette use, from pre- to post-implementation of a tobacco-free workplace program in centers serving these areas. Healthcare centers (N=9 centers with 17 clinics), together serving 79,266 unique patients annually across 81 rural/partially rural counties and 63 counties with medically underserved areas in Texas, implemented a multi-component tobacco-free workplace program between 2021 and 2025. The program included provider training on evidence-based strategies to address patients' cigarette use with an emphasis on the 5As: Ask about patients' cigarette use, Advise them to quit, Assess their interest in quitting, Assist them to quit, and Arrange a follow-up meeting to support the quit attempt. Providers completed an anonymous e-survey before (N=184) and after (N=126) program implementation, reporting their use of the 5As in the past month. Linear mixed models were used to assess differences between pre- and post-implementation, accounting for nesting of healthcare providers within center. Providers demonstrated clinically meaningful improvements in cigarette intervention provision. From pre- to post-implementation, providers Asked a greater proportion of patients about their cigarette use (57.96% to 72.17%; p=0.08). For patients who smoked, they were significantly more likely to Advise them to quit (45.40% to 68.64%; p=0.01), Assess their interest in quitting (38.86% to 63.44%; p=0.01), Assist in a quit attempt (22.97% to 50.60%; p<0.01), and Arrange a follow-up (17.76% to 39.84%; p<0.01). Results support the promise of tobacco-free workplace programs to address tobacco-related cancer disparities in rural and medically underserved areas by improving providers' use of evidence-based cigarette screening and intervention practices. Future work should examine implementation strategies that support the long-term sustainability of such interventions in this setting.

#5045 Patterns of tobacco use, cessation interventions, and lung cancer screening in rural vs. urban areas over time; a 10-year retrospective cohort study.

Brianna Tranby[1], Paul A. Decker[1], Jiang Ruoxiang[1], David Midthun[1], Lori C. Sakoda[2], Melinda C. Aldrich[3], Debra Friedman[3], Adoma Manful[3], Oindrila Bhattacharyya[4], Christi Patten[1], Chyke A. Doubeni[4]

[1]Mayo Clinic, Rochester, MN,[2]Kaiser Permanente, Oakland, CA,[3]Vanderbilt University Medical Center, Nashville, TN,[4]The Ohio State University Wexner Medical Center, Columbus, OH

Introduction: Lung cancer rates differ across rural and urban areas, but few studies have evaluated rural-urban differences across the risk-screening continuum. We examined smoking, cessation interventions, and lung cancer screening patterns across the rural-urban continuum in a geographically defined area over 10 years.
Materials and Methods: A retrospective cohort study (2014-2023) was conducted using clinical data from the Rochester Epidemiology Project, derived from healthcare encounters in a 27-county region of the midwestern United States. Patients ages 40-80 were included. We used Rural-Urban Commuting Area codes to assign residence as urban, rural, or highly rural. We examined yearly smoking prevalence, cessation intervention (pharmacotherapy, counseling), and low-dose computed tomography (LDCT) lung cancer screening.
Results: Over the 10-year study period, the sample size ranged from 305,530 to 340,411 people annually with 36-38% urban, 56-57% rural, and 6-7% highly rural. Current smoking prevalence declined from 14 to 12% over the 10-year period (range=12-16%; p=0.06) and was consistently lower in urban areas (range=10-14%) than rural (range=12-17.0%) and highly rural areas (range=12-18%; p=<0.001). Among individuals who currently smoked with no history of lung cancer, yearly smoking cessation intervention ranged from 16% to 23%, increasing over the 10-year period (p=<0.001). Cessation medication (varenicline, bupropion, or nicotine replacement) prescription consistently increased overall over time but remained higher in urban than rural and highly rural areas (p=<0.001). Cessation counseling rates also increased overall over time and were similar between urban and rural areas and lower in highly rural areas (p=<0.001). Among people who had ever-smoked aged 50-80 years with no diagnosis of lung cancer, LDCT screening increased from 0.0% to 3.1% over the study period. Increases were higher in urban areas (0.0-3.6%) and similar in rural and highly rural areas (0.0-2.8% and 0.0-2.9%, respectively; p=<0.001). Among people who currently smoked, LDCT screening also increased over the study period (0.0-6.4%), with higher increases in urban (0.1-8.0%) than rural (0.0-5.7%) or highly rural (0.1-6.1%) areas (p=<0.001). After the new screening guidelines in 2021, rates in all areas increased year-on-year.
Conclusion: In this cohort, we found that smoking prevalence, cessation interventions, and lung cancer screening improved from 2014-2023 across the rural-urban continuum. Unfortunately, smoking prevalence remained higher and cessation interventions and screening rates lower in rural compared to urban areas. The persistent patterns underscore the need for strategies to overcome barriers for rural residents and improve lung cancer prevention and early detection in all areas.

#5046 Integrating omics data unravels potential mechanisms linking diet-related inflammation and colorectal cancer risk.

Emmanouil Bouras[1], Jun Li[2], Franzel J. B. Van Duijnhoven[3], Ulrike Peters[4], Edward L. Giovannucci[2], Konstantinos K. Tsilidis[1], Marc J. Gunter[1]

[1]Department of Epidemiology and Biostatistics, School of Public Health, Imperial College London, London, United Kingdom,[2]Department of Epidemiology, Harvard T.H. Chan School of Public Health, Boston, MA,[3]Division of Human Nutrition and Health, Wageningen University & Research, Wageningen, Netherlands,[4]Fred Hutchinson Cancer Center, Seattle, WA

Although diet-related inflammation has been linked to colorectal cancer (CRC) risk, the biological mechanisms underlying this association remain unclear. We conducted integrative analyses of diet, clinical, and multi-omics data in a prospective cohort to investigate potential molecular pathways linking diet-related inflammation to CRC risk. We used the Energy-adjusted Dietary Inflammatory Index (EDII) to proxy diet-related inflammation in 203,770 UK Biobank participants with at least one 24-hour dietary recall. The index has been extensively validated in previous studies, and we further examined its associations with inflammatory proteins interleukin-6 (IL6), interleukin-18 (IL18), TNF receptor superfamily member 1B (TNFRSF1B), and adiponectin in our study, adjusting for age, sex, BMI, smoking, and non-steroidal anti-inflammatory drug use. We derived metabolic (mEDII) and proteomic (pEDII) signatures of the EDII using stability selection and cross-validated elastic net modelling, and examined their associations with CRC risk using regression models, adjusting for the aforementioned confounders. Genetic determinants of the signatures were identified through multi-trait GWAS analyses, and signals were prioritized via Ensembl's Variant Effect Predictor. We explored potentially shared variants using colocalization analyses, integrating GWAS data for mEDII and pEDII, gene expression in colon and visceral fat tissue (GTEx v8), and CRC risk (185,616 participants, including 78,473 CRC cases). The EDII showed positive associations with plasma IL-6 (beta per SD increase = 0.039; 95%CI: 0.025, 0.052), IL-18 (0.060; 0.046, 0.075), and TNFRSF1B (0.057; 0.043, 0.072), and an inverse association with adiponectin (-0.025; -0.037, -0.013). The mEDII comprised 26 metabolites and the pEDII comprised 21 proteins, each explaining approximately 11.5% of EDII variance. Over a median follow-up of 9.8 years, 1,427 CRC cases occurred (42.9% in women), of which 934 (65.4%) in the colon. There was a suggestive positive association between EDII and colon cancer risk in men (OR per SD increase = 1.11; 95%CI: 1.01, 1.22). The mEDII was positively associated with colon cancer risk across both sexes, independently of EDII (OR per SD increase = 1.14; 95%CI: 1.01, 1.29). GWAS identified 19 loci for mEDII and pEDII, with potential functional consequences for 102 genes. We found evidence for a shared genetic basis across both signatures, CRC risk, and gene expression in colon tissue [in the Fatty Acid Desaturase 1 (*FADS1*), Ras Interacting Protein 1 (*RASIP1*), and MEF2 Activating Motif and SAP Domain Containing Transcriptional Regulator (*MAMSTR*) regions], and in visceral fat [in the *FADS1* and Transmembrane Protein 258 (*TMEM258*) regions]. Diet-related inflammation may contribute to CRC risk through mechanisms involving lipid metabolism, endothelial function, and intestinal inflammation.

#5047 Associations of self-reported sleep duration and sleep quality with cancer risk: A pooled analysis of 6 prospective cohorts.

Charlie Zhong[1], Pedro Saint-Maurice[2], Rashmi Sinha[3], Laura Beane Freeman[3], Wei Zheng[4], Xiao-Ou Shu[4], Garnet L. Anderson[5], Trang VoPham[5], Charles E. Matthews[3], Alpa V. Patel[1], Erika Rees-Punia[1], Steven C. Moore[3]

[1]American Cancer Society, Atlanta, GA,[2]Champalimaud Foundation, Lisbon, Portugal,[3]Division of Cancer Epidemiology & Genetics, National Cancer Institute, Bethesda, MD,[4]Vanderbilt University Medical Center, Nashville, TN,[5]Fred Hutchinson Cancer Center, Seattle, WA

A third of adults report poor sleep health which may be from short sleep (<7 hours/day), long sleep (>9 hours/day), or poor quality of sleep. Sleep health involves getting the right amount of restful sleep each day and poor sleep health is associated with increased morbidity and mortality, including certain types of cancer. There is evidence linking more common cancers, such as breast, colon, and lung, to both short and long sleep duration, but less is known about sleep quality and other cancer types. We sought to evaluate the association between sleep duration and quality with risk from 29 types of cancer. We conducted a pooled random-effects meta-analysis of 6 prospective United States and Asian cohorts in the National Cancer Institute Cohort Consortium with self-reported sleep duration and quality. Cox regression was used to calculate hazard ratios (HR) and 95% confidence intervals (95% CI) for associations with incidence of overall cancer as well as 29 types of cancer; adjusted for age, sex, race/ethnicity, education, body mass index, alcohol consumption, and smoking status. Sleep duration (hours) was modeled as a 5:2 weekday:weekend weighted average and quality was based on reported trouble sleeping or restless sleep (<1 night/week or rarely/never vs 1+ nights/week). A total of 643,860 participants (median [range] age, 62 [34-99] years, 58% female) were included in the analysis. Over a median of 12 years of follow-up, there were 138,606 cancer diagnoses. Compared to National Sleep Foundation's recommended sleep duration of 7-9 hours/day in adults, short sleep duration was associated with reduced risk of overall cancers (HR 0.98; 95% CI 0.97, 0.99), as well as breast (n = 24,386; HR 0.95; 95% CI 0.92, 0.97) and prostate cancer (n = 24,593; HR 0.97; 95% CI 0.94, 1.00); and increased risk of small intestine (n = 510; HR 1.26; 95% CI 1.05, 1.52) and head and neck cancers (n = 3,433; HR 1.09; 95% CI 1.02, 1.18). Long sleep duration was associated with increased risk of head and neck cancers (HR 1.19; 95% CI 1.03, 1.39). Restless sleep was associated with decreased risk of breast cancer (n = 12,515; HR 0.95; 95% CI 0.90, 0.99) and increased risk of hepatocellular carcinoma (n = 352; HR 1.31; 95% CI 1.03, 1.67). We did not observe any associations with trouble sleeping. Short sleep duration appeared to be protective against overall cancer risk, potentially due to the association with lower risks of breast and prostate cancer. However, short sleep was associated with higher risks of small intestine and head and neck cancers. Long sleep duration was also associated with increased risk of head and neck cancers. While we observed associations between restless sleep and breast cancer and hepatocellular carcinoma, only 2 cohorts asked about restless sleep. These results highlight the complex relationship between sleep and cancer risk and the importance of assessing individual cancer types.

#5048 The association of sleep duration and quality with obesity-related cancers: Results from the health examinees study.

Sinyoung Cho[1], Sukhong Min[2], Hyobin Lee[2], So-Yoon Lee[2], Daehee Kang[2]

[1]Seoul National University Hospital, Seoul, Korea, Republic of,[2]Seoul National University College of Medicine, Seoul, Korea, Republic of

This study aims to investigate the associations of self-reported sleep duration and quality with obesity-related cancer risk in a large-scale Korean population. This prospective cohort study utilized data from the Health Examinees-Gem (HEXA-G) cohort, comprising adults aged ≥40 years. A total of 126,866 participants who provided information on both sleep duration and quality were included in the present study. Sleep duration was self-reported at baseline and categorized into <6 hours, 6-<8 hours, and ≥8 hours. Sleep quality was assessed using four independent questions, including nonrestorative sleep, daytime fatigue, difficulty in initiating sleep, and nighttime anxiety. Cancer cases were identified through national cancer registration data from the Korea Central Cancer Registry of the Korea National Cancer Center. This study adopted obesity-related cancers, defined by the International Agency for Research on Cancer. Cox proportional hazards models were used to estimate hazard ratios (HRs) and 95% confidence intervals (CIs), with follow-up beginning two years after the age at enrollment and continuing until the first cancer diagnosis, loss to follow-up, or the end of the study (December 31, 2018). During the median follow-up period of 7.3 years (range, years), 7,284 incident all-site cancer cases, including 4,113 obesity-related cancer cases, were documented. Long sleep duration (≥8 h) was significantly associated with obesity-related cancer (1.08; 1.01-1.16), marginally associated with all-site cancer (1.05; 1.00-1.11), and not associated with non-obesity-related cancer. Compared with participants reporting each sleep quality component “not at all,” those reporting nonrestorative sleep “sometimes” (1.08; 1.01-1.16) or “most of the time” (1.11; 1.01-1.22) showed higher obesity-related cancer risk; those reporting initiation difficulty “sometimes” was associated with obesity-related cancer risk (1.08; 1.01-1.16), whereas daytime fatigue and nighttime anxiety showed no significant associations. Reporting sleep ≥8 h with nonrestorative sleep (“sometimes”) increased all-site cancer (1.10; 1.01-1.20) and obesity-related cancer risk (1.24; 1.11-1.39). Reporting sleep ≥8 h with daytime fatigue increased all-site cancer (1.18; 1.06-1.31) and obesity-related cancer risk (1.19; 1.04-1.37). Reporting sleep ≥8 h with initiation difficulty increased all-site cancer (1.16; 1.04-1.30) and obesity-related cancer risk (1.26; 1.13-1.41). Long sleep duration was significantly associated with obesity-related cancer risk. Long sleep duration combined with nonrestorative sleep, daytime fatigue, initiation difficulties, or nighttime anxiety had positive associations with all-site and obesity-related cancer risks, but not with non-obesity-related cancers.

#5049 Prospective evaluation of dietary intake of essential metals and pancreatic cancer risk: The Multiethnic Cohort Study.

Yi-Chuan Yu[1], Sihao Han[2], Adelynn Paik[2], Song-Yi Park[3], Shannon Sullivan[4], Eric Kawaguchi[5], Loic Le Marchand[6], Lynne R. Wilkens[3], Christopher A. Haiman[7], Veronica Wendy Setiawan[2], Brian Huang[2]

[1]Keck School of Medicine of USC, Los Angeles, CA,[2]USC Norris Comprehensive Cancer Center, Los Angeles, CA,[3]Population Sciences in the Pacific Program, University of Hawai'i Cancer Center, Honolulu, HI,[4]Department of Laboratory Medicine and Pathology, University of Minnesota Medical School, Minneapolis, MN,[5]Department of Population and Public Health Sciences, University of Southern California, Los Angeles, CA,[6]University of Hawai'i Cancer Center, Honolulu, HI,[7]Co-Director, USC Genomics Ctr., USC Norris Comprehensive Cancer Center, Los Angeles, CA

Background: Evidence suggests that dietary intake levels of essential metals are linked to the development of or protection against pancreatic adenocarcinoma (PDAC). However, results from existing epidemiological studies remain inconsistent, often limited by retrospective designs and recall bias. We aim to prospectively investigate the relationship between dietary intake of essential metals and the risk of PDAC in a large, racially and ethnically diverse U.S. population.

Methods: Data were from the Multiethnic Cohort Study, a large population-based prospective cohort study established between 1993 and 1996 in Los Angeles and Hawaii, comprised of participants from five main racial and ethnic groups (African American, Japanese American, Latino, Native Hawaiian, and White). Incident PDAC cases were identified through linkage with the state SEER cancer registries. Dietary intake densities (intake per 1,000 kcal per day) of seven essential metals (copper, selenium, zinc, manganese, iron, calcium, and magnesium) were estimated from a baseline quantitative food frequency questionnaire and modeled as quartiles. Participants were excluded if they were of other racial/ethnic groups, had implausible dietary data, a prior diagnosis of PDAC, or inconsistent/incomplete follow-up time. Cox proportional hazards regression models (with age since cohort entry as time metric) were used to estimate hazard ratios (HRs) and 95% confidence intervals (CIs) for PDAC risk associated with intake of each essential metal , adjusting for age, sex, race/ethnicity, body mass index, history of diabetes, alcohol use, smoking status, education, family history of PDAC, and total daily energy intake.

Results: After an average follow-up of 20.2 years, 2,119 of 195,061 at-risk participants developed PDAC. Compared with the lowest quartile (5.7 - 44.9 mcg/1,000 kcal/day), participants in the highest quartile (58.0 - 131.9 mcg/1,000 kcal/day) of selenium intake had a 17% higher risk of developing PDAC (HR=1.17, 95% CI: 1.03-1.34, P-trend=0.048). No evidence of heterogeneity across sex and race/ethnicity was observed (all P's-heterogeneity>0.05); however associations appeared stronger for White (HR=1.27, 95% CI: 0.95-1.70), African American (HR=1.29, 95% CI: 0.96-1.73) and Latino (HR=1.32, 95% CI: 0.96-1.80) participants. No significant associations were observed for dietary intakes of copper, zinc, manganese, iron, calcium, and magnesium.

Conclusion: Elevated selenium dietary intake is associated with an increased risk of PDAC in this large, racially and ethnically diverse U.S. population. Further large-scale prospective studies are warranted to confirm this association and elucidate the underlying biological mechanisms .

#5050 Healthier pre-diagnosis lifestyle and long-term survival in patients after diagnosis of colorectal cancer: Evidence from the Singapore Chinese Health Study.

Peh Joo Ho[1], Aizhen Jin[2], Jian-Min Yuan[3], Woon-Puay Koh[2], Adeline L. H. Seow[2]

[1]Saw Swee Hock School of Public Health, National University of Singapore (NUS), Singapore, Singapore,[2]National University of Singapore (NUS), Singapore, Singapore,[3]University of Pittsburgh, Pittsburgh, PA

Purpose To quantify survival differences between colorectal cancer (CRC) patients with healthier and those with less healthy pre-diagnosis lifestyles using restricted mean survival time (RMST) at 5 and 10 years, and to assess which lifestyle components contribute to these differences.

Methods Incident CRC cases (n = 2124) were identified from the Singapore Chinese Health Study, a prospective cohort of 63 257 adults enrolled in 1993-1998. Cancer status and cause of death were obtained via linkage with the National Disease Registry through 31 December 2015. A pre-diagnosis lifestyle score (0-7) incorporated BMI and smoking, sleep duration, diet, and weekly physical activity at baseline. RMST differences comparing less healthy (scores 0-3) versus healthier (4-7) lifestyles were estimated at 5- and 10-years post-diagnosis, adjusted for CRC stage (early, late) and age at diagnosis, sex, education attainment, and the interval between lifestyle assessment and diagnosis.

Results Over a median follow-up of 4.8 years (IQR 1.2-11.8) from CRC diagnosis, 1557 deaths occurred, including 1103 CRC-specific deaths. Late-stage diagnosis was associated with shorter survival than early stage by 1.53 years (95% CI 1.35 to 1.72) at 5 years and 3.33 years (2.93 to 3.72) at 10 years. The median interval between lifestyle assessment and diagnosis was 12.2 years (IQR 6.9 to 16.7). RMST for all-cause deaths was significantly improved by a healthier lifestyle but results for CRC-specific deaths were mixed. For all-cause mortality, adjusted RMST differences (less healthy - healthier) were −0.15 (95% CI −0.32 to 0.01) at 5 years and −0.37 (−0.71 to −0.02) at 10 years. CRC-specific mortality: At 5 years, the adjusted RMST difference (less healthy – healthier) was −0.15 years (−0.32 to 0.02), and at 10 years it was −0.34 years (−0.71 to 0.03). Among patients diagnosed at age ≤70 years, healthier pre-diagnosis lifestyles were associated with modestly longer survival, with a 10-year CRC-specific RMST gain of 0.58 years (0.03 to 1.13), while other estimates were borderline or not significant. Lifestyle components associated with improved CRC-specific survival included diet (lower vs higher AHEI category: 5-year RMST difference −0.20 (−0.38 to −0.02); 10-year −0.46 (−0.84 to −0.08)) and weekly physical activity (no vs yes: 5-year −0.19 (−0.37 to −0.02); 10-year −0.42 (−0.78 to −0.06)). Similar results were obtained for all-cause death. Smoking and sleep duration were not significantly associated with survival.

Conclusions A healthier pre-diagnosis lifestyle was associated with improved long-term survival in CRC patients. Short-term differences were modest after accounting for CRC stage at diagnosis, underscoring the importance of early detection. Having maintained healthy behaviors before diagnosis may favorably influence long-term outcomes among CRC patients.

#5051 A multi-center hospital-based case-control study of lymphoid and myeloid neoplasms (AsiaLymph): Study design and initial findings for education, body mass index, and family history.

Qing Lan[1], Lauren M. Hurwitz[1], John K. Chan[2], Tai Hing Lam[3], Kexin Chen[4], Yok Lam Kwong[5], Xu Caigang[6], Brian CH Chiu[7], Raymond Liang[8], Ip Dennis[3], Wei Hu[1], Bryan Bassig[9], Mark Purdue[1], Jun Xu[3], Sarah Locke[1], Sophia S. Wang[10], James R. Cerhan[11], Sonja Berndt[1], Jonathan N. Hofmann[1], Jianxin Shi[1], Kai Yu[1], Shahinaz Gadalla[1], Lisa J. McReynolds[1], Rena Jones[1], Hongji Dai[4], Zhangyan Lyu[4], Lugui Qiu[12], Wei Liu[12], Huilai Zhang[13], Xianhuo Wang[13], Lindsay M. Morton[1], Stephen Chanock[1], Martha Linet[1], Melissa C. Friesen[1], Roel Vermeulen[14], Nathaniel Rothman[1]

[1]NCI Div. of Cancer Epidemiology & Genetics, Bethesda, MD,[2]Queen Elizabeth Hospital, Hong Kong, Hong Kong,[3]School of Public Health, Li Ka Shing (LKS) Faculty of Medicine, University of Hong Kong, Hong Kong, Hong Kong,[4]Tianjin Medical University Cancer Institute and Hospital, Tianjin Medical University, Tianjin, China,[5]Queen Mary Hospital, Hong Kong, Hong Kong,[6]Department of Hematology, Hematology Research Laboratory, West China Hospital, Sichuan University, Chengdu, China,[7]Associate Professor, Dept. of Health Studies, University of Chicago, Chicago, IL,[8]Hong Kong Sanatorium & Hospital, Hong Kong, Hong Kong,[9]Saville Cancer Screening and Prevention Center, Inova Schar Cancer Institute, Inova Health System, Fairfax, VA,[10]City of Hope National Medical Center, Duarte, CA,[11]Mayo Clinic College of Medicine and Science, Rochester, MN,[12]Institute of Hematology & Blood Diseases Hospital, Chinese Academy of Medical Sciences & Peking Union Medical College, Tianjin, China,[13]Tianjin Medical University Cancer Institute and Hospital, Tianjin, China,[14]Utrecht University, Utrecht, Netherlands

Background: Epidemiologic and other studies have identified environmental, occupational, and genetic risk factors for lymphoid and myeloid malignancies, but most studies have been conducted in Western populations. Investigations in populations with differing exposure patterns, distributions of disease subtypes, and genetic architecture are needed to fully understand hematopoietic tumor etiology. **Methods:** We conducted a large, multicenter, hospital-based case-control study of lymphoid and myeloid neoplasms in East Asia (AsiaLymph), including 5,671 lymphoid cases, 1,879 myeloid cases, and 3,858 controls. Participants completed a computer-assisted personal interview and provided biospecimens. Cases underwent central pathology review and were coded into the WHO Classification. Herein, we describe the study methods in detail and report association results for education, body mass index, and family history.**Results:** Greater BMI at age 20 but not at age 40 was associated with odds of total lymphoid neoplasm (per 5 kg/m^2 increase: OR [95% CI]: 1.18 [1.09-1.27]), total myeloid neoplasm (OR [95% CI]: 1.17 [1.05-1.29]), and several subtypes. Greater educational attainment was associated with increased odds of total lymphoid neoplasm (for college vs. less than primary education: OR [95% CI]: 1.41 [1.21-1.65]) but not myeloid neoplasm (OR [95% CI]: 1.17 [0.95-1.45]; p-heterogeneity=0.02). There were also positive associations between family history of hematologic cancer in first degree relatives and odds of lymphoid neoplasm (OR [95% CI]: 1.53 [1.15-2.03]) and myeloid neoplasm (OR [95% CI]: 1.65 [1.11-2.44]) and specific subtypes. None of the evaluated risk factors were associated with NK/T-cell lymphoma, which supports a distinct etiology for this subtype. **Conclusion:** The AsiaLymph Study is one of the largest molecular epidemiology studies of both lymphoid and myeloid neoplasms with standardized World Health Organization classification of histopathologic subtypes and will serve as a valuable resource for etiologic investigations into risk factors for these malignancies.

#5052 A network approach using Gaussian graphical models to evaluate dietary patterns and colorectal cancer risk in the UK Biobank.

Jiyoung Hwang, Sooyoung Cho, Aesun Shin

Seoul National University, Seoul, Korea, Republic of

Background: Current research on the link between dietary patterns and colorectal cancer (CRC) has relied on methods that summarize intake without accounting for the structural dependencies among food groups. Gaussian graphical models (GGMs) derive dietary patterns by capturing how foods are consumed in relation to one another, offering a network-based view of overall eating behavior.
Objectives: We aimed to identify dietary patterns using GGMs and to examine their associations with incident CRC in the UK Biobank.
Methods: This prospective cohort study included 105,676 UK Biobank participants with 24-hour recall dietary data. Dietary patterns were identified using GGMs constructed from 43 food groups, and participants were classified into tertiles of each pattern score. Cox proportional hazards models were applied to estimate hazard ratios (HRs) and 95% confidence intervals (CIs), adjusting for demographic, lifestyle, and clinical factors.
Results: Over a median follow-up of 10.1 years, 1,026 cases of CRC were newly diagnosed. The network identified four dietary patterns consisting of different food groups. In sex-stratified analyses, the processed food and dessert pattern was associated with higher CRC risk in male, with the highest tertile showing increased risk (HR = 1.23; 95% CI: 1.00-1.50; *P*-trend = 0.048). In female, the balanced pattern was inversely associated with CRC, with the highest tertile showing lower risk (HR = 0.82; 95% CI: 0.60-0.93; *P*-trend = 0.041). No significant associations were observed for the other dietary patterns, including the protein-based and beverage patterns, in the total or sex-stratified analyses.
Conclusions: Network-based dietary patterns identified through GGMs showed different sex-specific associations with CRC risk. By addressing pairwise correlations between food variables while controlling for indirect effects from other foods, this approach captures dietary structures with greater specificity than traditional pattern methods. These results contribute to a clearer understanding of how sex-specific dietary patterns relate to CRC risk within existing epidemiologic evidence.

#5053 Comparison of machine learning-based dimensionality reduction methods for dietary patterns and their predictability of cancer risk in a large cohort study.

Hyobin Lee[1], Dongseok Heo[2], Sukhong Min[1], Sinyoung Cho[1], So-Yoon Lee[1], Ji-Yeob Choi[3], Bongwon Suh[4], Daehee Kang[1]

[1]Department of Preventive Medicine, Seoul National University College of Medicine, Seoul, Korea, Republic of,[2]Integrated Major in Innovative Medical Science, Seoul National University Graduate School, Seoul, Korea, Republic of,[3]Department of Biomedical Sciences, Seoul National University Graduate School, Seoul, Korea, Republic of,[4]Department of Intelligence and Information, Seoul National University, Seoul, Korea, Republic of

Background & Aims Dietary pattern analysis is essential in nutritional epidemiology, yet traditional clustering approaches may be limited by their inability to capture latent dietary structures. This study compared three dimensionality reduction techniques—Principal Component Analysis (PCA), Uniform Manifold Approximation and Projection (UMAP), and Autoencoders (AE)—for dietary pattern development, and further examined associations of AE-derived dietary patterns with cancer incidence in a large prospective cohort study.
Methods Data were obtained from 130,472 participants enrolled in the Health Examinees-Gem (HEXA-G) study (2004-2013), who completed a validated food frequency questionnaire. PCA, UMAP, and AE were each applied prior to k-means clustering. Cluster quality was assessed using silhouette coefficients, and variable contributions were evaluated using SHAP values. External validation was conducted by applying the HEXA-trained encoder to the Korean National Health and Nutrition Examination Survey (KNHANES). Cancer incidence was ascertained through linkage with the Korea Central Cancer Registry up to December 31, 2018. Multivariable Cox proportional hazards models estimated hazard ratios (HRs) and 95% confidence intervals (CIs) for total and site-specific cancers, focusing on the seven most common cancers in Korea.
Results Without dimensionality reduction, the silhouette coefficient was 0.05; PCA rarely exceeded 0.2, UMAP reached ~0.4, and AE achieved >0.35, providing competitive cluster quality with the most balanced variable contributions. Ten dietary patterns were identified: Balanced, Selective, Rice, Bread, Vegetables, Dairy, Meat, Processed meat, Noodles, and Salty. External validation using KNHANES produced similar silhouette values (~0.36) and preserved centroid positions, confirming transferability. Over a median follow-up of 9.4 years, 7,390 cancer cases occurred. No significant associations were observed for total cancer; however, site-specific analyses revealed that the Processed meat pattern in men was associated with higher colorectal cancer risk (HR = 1.98, 95% CI: 1.12-3.49), and the Selective pattern with higher gastric cancer risk (HR = 1.32, 95% CI: 1.03-1.70) compared to the Balanced pattern. In women, the Bread pattern was associated with lower gastric cancer risk (HR = 0.53, 95% CI: 0.32-0.89).
Conclusion Among the dimensionality reduction techniques, AE achieved the most favorable balance of cluster quality and variable contribution balance, supporting its utility for developing dietary patterns. These findings demonstrate that machine learning-based dimensionality reduction methods, particularly AEs, can strengthen dietary pattern development and capture meaningful associations with cancer risk.

#5054 E-cigarette use among cancer survivors who are ineligible for lung cancer screening.

Priyanka N. Srinivasan[1], Eric Liu[1], Amrita Mukunda[1], Melinda Hsu[2], Hui Xie[3], Qian Wang[4]

[1]Case Western Reserve University School of Medicine, Cleveland, OH,[2]University Hospitals, Cleveland, OH,[3]University of Wisconsin-Milwaukee Zilber College of Public Health, Milwaukee, WI,[4]Seidman Cancer Center University Hospitals, Cleveland, OH

Significance: Cancer survivors are at higher risk of developing lung cancer than the general population due to shared risk factors (e.g. cigarette smoking), treatment (e.g. prior chest irritation) and genetic susceptibilities. Though it has been widely promoted as a smoking cessation tool, preclinical studies have suggested that e-cigarettes contain carcinogens similar to those found in combustible cigarettes. Approximately 15% of cancer survivors reported life-time e-cigarette use. As current lung cancer screening (LCS) criteria primarily focuses on age and combustible smoking history, individuals who are never- or light-smokers but who use e-cigarettes may be excluded from screening. We aim to assess prevalence of e-cigarette use among LCS-ineligible cancer survivors and compare it to their non-cancer survivor peers.

Methods: Data were extracted from Behavioral Risk Factor Surveillance System from 2022 to 2024. Individuals ineligible for LCS according to USPSTF 2021 guidelines (i.e. aged 50-80 years, smoked at least 20 pack years and quitted within past 15 years for former smokers) were included. Cancer survivors with history of lung cancer were excluded. Chi-square tests and multivariate logistic regressions were used to compare current e-cigarette use prevalence between cancer survivors and non-cancer survivors. All analyses were weighted. A p-value of <0.05 was considered statistically significant.

Results: 694,576 patients (342,841,347 weighted) were included, of which 10.9% were cancer survivors. The average age was 68 (61-74) and 60 (50-69) for cancer survivors and non-cancer survivors, respectively. Overall, 2.6% and 3.6% of cancer survivors and non-cancer survivors reported currently using e-cigarettes, respectively (p<0.001). After adjusting for age, sex, race/ethnicity, education, income, marital status and combustible smoking status, cancer survivors were more likely to be current e-cigarette users (aOR=1.10, 95%CI: 0.99-1.23) than non-cancer survivors. Among individuals aged 40-49 years, cancer survivors were 21% more likely to report currently using e-cigarettes than non-cancer survivors (9.3% vs 7.2%, p<0.001; aOR=1.21; 95%CI: 1.02-1.44). In addition, male cancer survivors (aOR=1.22; 95%CI: 1.01-1.46), and cancer survivors who never smoked combustible cigarettes (aOR=1.52; 95%CI: 1.13-2.05) were more likely to report currently using e-cigarettes.

Conclusion: Our results showed that among adults ineligible for LCS, cancer survivors were more likely to report currently using e-cigarettes, with the highest prevalence observed in younger individuals, men, and never-smokers. The findings are concerning as e-cigarette use may add to their pre-existing elevated risk profile. Future studies are needed to assess long-term risks of e-cigarette use in this population and to inform potential refinements to risk assessment and screening eligibility among cancer survivors.

#5055 The association of allostatic load (AL) with diagnosis of monoclonal gammopathy of undetermined significance (MGUS) and progression to multiple myeloma (MM).

Mark Aaron Fiala, Qingyuan Tan, Mei Wang, Su-Hsin Chang

Washington Univeristy School of Medicine, St. Louis, MO

Introduction: AL is a measure of the physiological burden of chronic stress. There is no direct measurement; rather, indices are created based on available biomarkers for endocrine dysfunction. This study aimed to determine whether increased AL was associated with a higher odds of having MGUS and if AL was associated with an increased risk of progression from MGUS to MM in the nationwide Veterans Health Administration (VHA).

Methods: Diagnosis of MGUS from 2003-2024 and subsequent progression to MM were confirmed by a published natural language processing algorithm (doi 10.1200/CCI.23.00081). AL was calculated using six biomarkers: body mass index (BMI), alkaline phosphatase (ALP), albumin (ALB), creatinine (CR), creatinine clearance (CRCL), and white blood count (WBC). For each, patients who were in the "worst" quartile were awarded 1 point, with the exception of BMI, where all with a BMI $\geq$25 was awarded 1 point. For Aim 1, patients were indexed at first BMI measurement following their 50th birthday. MGUS cases we matched (1:1) to controls of the same age and index date (within 6 months). MGUS diagnosis was treated as a time-to-event analysis with death being a competing risk. For Aim 2, patients were indexed at time of MGUS diagnosis. Progression to MM was treated as a time-to-event analysis with death being a competing risk. Patients who progressed, died, or lost-to-follow-up within 6 months of diagnosis were excluded.

Results: In Aim 1, 4855 cases of MGUS were matched to 4855 controls. The median age was 62 years, 94% were Male, and 60% were non-Hispanic White (NHW), 24% were non-Hispanic Black (NHB), and 16% were another race/ethnicity or were unclassified. The median AL score was 2. For each 1-unit increase in AL score, the risk of being diagnosed with MGUS increased by 14% (aHR 1.14; 95% CI 1.11-1.18); $p < 0.001$). In Aim 2, 42683 cases of MGUS were identified. The median age was 73 years, 96% were Male, and 61% were non-Hispanic White (NHW), 26% were non-Hispanic Black (NHB), and 13% were another race/ethnicity or were unclassified. The median AL score was 2. In total, 3194 (7%) of cases progressed to MM and 21104 (49%) died without progression after a median follow-up of 46 months. For each 1-unit increase in AL score, the risk progression to MM decreased by 10% (aHR 0.91; 95% CI 0.89-0.94); $p < 0.001$). In post-hoc analyses, we determined that four components of the AL score, ALP, CR, CRCL, and WBC were associated with lower risk (all $p < 0.001$), while BMI and ALB were associated with higher risk. Patients with a BMI $\geq$25 had a 21% increased risk in progression (HR 1.21; 95% CI 1.14-1.32; $p < 0.001$) and patients in the lowest quartile of albumin ($\leq$3.5g/dL) had a 17% increased risk in progression (HR 1.17; 95% CI 1.05-1.30; $p = 0.003$).

Conclusions: AL score is a potential biomarker to determine who is at higher risk for MGUS, but its association with risk of progression to MM is unclear.

#5056 Metabolic disease and risk for thyroid cancer in a predominantly Black and low-income cohort.

Jessica Rampy, Xijing Han, Xiangzhu Zhu, Xiao-Ou Shu, Vivian L. Weiss, Martha J. Shrubsole

Vanderbilt University Medical Center, Nashville, TN

Background: Thyroid cancer incidence and mortality are rising in the U.S., as is metabolic disease. Some studies have shown in predominantly Non-Hispanic White populations that obesity and diabetes are positively associated with thyroid cancer risk while physical activity is inversely associated. However, comparatively little is known about metabolic diseases as risk factors for thyroid cancer among Black Americans and low-income Americans, despite a high prevalence of these factors within these populations.
Methods: The Southern Community Cohort Study is a prospective cohort study of >84,000 participants enrolled between 2002 to 2009 designed to evaluate the etiology of cancer and other health conditions in the southeastern U.S. states including for Black individuals (~2/3) and individuals with low income (~1/2). Self-reported body mass index (BMI), diabetes diagnosis, and physical activity levels were collected at baseline. Thyroid cancer incidence was ascertained through state cancer registry linkages. BMI was categorized as normal/underweight: <25 kg/m^2, overweight: 25–<30 kg/m^2, and obese: ≥30 kg/m^2. Participants with missing data were excluded, leaving 68,532 participants and 135 incident cases. We used Cox proportional hazards models adjusted for potential confounders to evaluate risk factors for thyroid cancer overall and stratified by sex, self-reported race, and income.
Results: The mean enrollment age was 51.8 years, with a median follow-up of 12.6 years. In comparison to normal/underweight, being overweight (HR: 2.39; 95% CI: 1.30-4.40) or having obesity (HR: 2.56; 95% CI: 1.44-4.58) were both associated with increased thyroid cancer risk (P_{trend}: <0.01). These associations were also observed for female participants (HR: 2.55; 95% CI: 1.26-5.20 and HR: 2.55; 95% CI: 1.30-5.00, respectively; P_{trend}: 0.02). Obesity was also associated with increased risk for Non-Hispanic Black participants (HR: 2.81; 95% CI: 1.19-6.63; P_{trend}: 0.02) and for those with household income <$15,000 (HR: 5.42; 95% CI: 1.92-15.3; P_{trend}: <0.01). No statistically significant association was observed for obesity among those with higher income although being overweight was associated with a two-fold increased risk in comparison to normal/underweight. Neither overweight nor obesity was associated with risk for male or Non-Hispanic White participants, possibly due to a smaller sample size. History of diabetes and physical activity were not independently associated with thyroid cancer risk.
Conclusions: Thyroid cancer risk is associated with obesity in a predominantly Black and low-income population, in line with previous findings in other populations. However, neither diabetes nor physical activity were associated. These findings suggest that obesity prevention and treatment should be evaluated as potential prevention strategies for thyroid cancer risk.

#5057 Clinical and lifestyle determinants of all-cause mortality among high-risk prostate cancer patients: Findings from a multicenter longitudinal cohort, 1990-2024.

Cynthia R. Robbins[1], Jiji Jiang[1], Sally Elsamanoudi[1], Paul Campbell[2], Sean P. Stroup[3], Jennifer Cullen[4], Gregory Chesnut[1], Jongeun Rhee[1]

[1]Center for Prostate Disease Research (CDPR), Murtha Cancer Center Research Program, Uniformed Services University of the Health Sciences, Bethesda, MD,[2]U.S. Naval Research Laboratory, Washington, DC,[3]Department of Surgery, Uniformed Services University of the Health Sciences, Bethesda, MD,[4]Houston Methodist Cancer Center, Houston, TX

Patients with high-risk prostate cancer (PCa) have substantially elevated risks of disease progression and mortality, yet outcomes remain highly variable. Emerging evidence suggests that comorbidities, obesity, and smoking contribute to PCa progression and overall survival through metabolic and inflammatory pathways. However, few studies have evaluated how these factors interact to influence mortality in high-risk PCa patients. We examined individual and combined effects of clinical and lifestyle factors on all-cause mortality in a large, longitudinal cohort of high-risk patients treated within military treatment facilities.

Male patients with newly diagnosed National Comprehensive Cancer Network-defined high-risk PCa who underwent radical prostatectomy (RP), external beam radiation therapy (EBRT), and androgen deprivation therapy (ADT) were included from the Center for Prostate Disease Research Multicenter National Database (1990-2024; n=2,713). Multivariable Cox regression analyses were conducted to evaluate associations between lifestyle factors (obesity, smoking) and self-reported comorbidity conditions at enrollment and all-cause mortality across treatment groups.

Median age at diagnosis was 68 years; 66% self-identified as White and 26% as African American. Overall, 44% underwent EBRT, 34% RP, and 14% ADT. During follow-up, 45% of patients died. Chronic obstructive pulmonary disease (COPD) was a strong predictor of increased all-cause mortality across all treatment groups [RP, Hazard Ratio (HR)=1.98 (1.13, 3.50); EBRT, HR=1.52 (1.09, 2.16); ADT, HR=1.65 (0.98, 2.75)]. The association was more apparent among ever smokers in RP group [HR=2.58 vs. never, HR=0.58] and among non-obese patients in RP [HR=2.21 vs. obese, HR=1.27] and EBRT [HR=1.80 vs. 1.01] groups. Hypertension and diabetes were also marginally associated with higher mortality across treatment groups, with stronger associations among ever smokers in RP [hypertension, HR=1.58 vs. 0.77; diabetes HR=1.6 vs. 0.49]. Coronary artery disease was a significant predictor of mortality among EBRT patients [HR=1.34 (1.03, 1.74)] but not in other groups. Renal insufficiency was associated with increased mortality in EBRT [HR=1.84 (1.16, 2.93)] and ADT [HR=1.38 (0.70, 2.73)], with a stronger association never smokers [EBRT, HR=8.45 vs. ever, HR=1.29].

COPD, hypertension, and diabethes were consistently associated with increased all-cause mortality in high-risk PCa patients, with modest effect modification by smoking and obesity status. These findings highlight the importance of integrated management of comorbidities and lifestyle risk factors to improve survivorship in this high-risk patients.

: Etiology and Molecular Epidemiology Approaches to Decipher Cancer Disparities
Poster Session

#5061 Allele frequency variation in people of European and admixed African ancestry in the United States do not fully explain incidence differences in adult-type diffuse glioma.
Christine Ann Pittman Ballard[1], Carol Kruchko[2], Mackenzie Price[2], Quinn T. Ostrom[3]

[1]Epidemiology, University of North Carolina at Chapel Hill, Chapel Hill, NC,[2]Central Brain Tumor Registry of the United States, Pewaukee, WI,[3]Duke University School of Medicine, Durham, NC

BackgroundGlioma is a heterogeneous group of tumors that make up the most common type of primary malignant brain tumor. Incidence varies globally, with highest rates in Europe and North America and lowest in Asia and Africa. Within the United States, these tumors are most common in individuals who are non-Hispanic White. Previously, genome-wide association studies (GWAS) have identified 25 single nucleotide polymorphisms (SNPs) which affect risk for glioma (European only), most of which have subtype-specific differences. SNP allele frequencies (AF) vary between continental populations. We estimated population-level incidence for adult-type diffuse glioma subtypes and calculated the difference between observed variation and variation attributable to AF differences.

MethodsRace/ethnicity-stratified age-adjusted incidence rates for glioma subtypes (Astrocytoma with *IDH1/2* mutation [IDHmut], Astrocytoma with wildtype *IDH1/2* [IDHwt], and Oligodendroglioma with *IDH1/2* mutation and 1p/19q codeletion [IDHmut-codel]) from diagnosis years 2018-2022 were calculated using the Central Brain Tumor Registry of the United States, an aggregation of CDC's National Program of Cancer Registries and NCI's SEER. Incidence rate ratios (IRR_O) were estimated as compared to non-Hispanic White. Effect estimates for known glioma risk SNPs were extracted from a prior subtype-specific glioma GWAS (Labreche, 2018) for SNPs with $p<4x10^{-4}$. AF were extracted from the Allele Frequency Aggregator for the European and African American populations. We calculated the normalized IRR (IRR_N) for each SNP based on population AF and summed these to estimate the incidence variation attributable to AF. IRR_N was calculated by multiplying the beta by the corresponding AF.

ResultsAs compared to individuals who are non-Hispanic White, incidence was decreased in non-Hispanic Black individuals for all subtypes [IDHmut IRR_O=0.40, IDHwt IRR_O=0.49, IDHmut-codel IRR_O=0.29]. IRR_N were attenuated as compared to observed rates [IDH-mut IRR_N=0.78, IDH-wt IRR_N=0.75, IDHmut-codel IRR_N=0.64]. The IRR_N is higher compared to the IRR_O, with the greatest differences being observed in the non-Hispanic Black population.

ConclusionIRR_N fail to fully explain population differences in incidence of glioma. This may be a result of limited ancestral diversity in GWAS, which have not assessed SNPs in individuals who are African American. Sample sizes for subtype-specific GWAS have been small and underpowered. These SNPs do not capture all genetic risk for glioma (all identified SNPs explain 30% of heritable risk), and there is significant 'missing heritability.' These results emphasize the need for inclusion of more diverse populations in glioma genetic epidemiology to ensure accurate genetic risk estimation.

#5062 Genetic ancestry-associated features of the colorectal cancer T-cell landscape.

Ya-Yu Tsai[1], Marco Matejcic[1], Daniel Sobieski[1], Eric M. Cockman[1], Esther Jean-Baptiste[2], Nathalie T. Nguyen[3], Edna Gordian[4], Jose Oliveras Torres[5], Hannah J. Hoehn[2], Kritika Shankar[1], Diana B. Diaz[2], Rusche Wilson[1], Karina Brito[1], Allyson Koepfler[1], Nicole Catalina Lorona[3], Domenico Coppola[6], Ozlen Saglam[7], Clifton Fulmer[8], Kun Jiang[6], Seth Felder[9], Julian Sanchez[9], Mariana C. Stern[10], Douglas Cress[4], Erin M. Siegel[11], Jamie K. Teer[12], Jane C. Figueiredo[3], Stephanie L. Schmit[1]

[1]Genomic Sciences & System Biology, Cleveland Clinic Research, Cleveland, OH,[2]Non-Therapeutic Research Office, H. Lee Moffitt Cancer Center & Research Institute, Tampa, FL,[3]Department of Medicine, Samuel Oschin Comprehensive Cancer Institute, Cedars Sinai Medical Center, Los Angeles, CA,[4]Department of Molecular Oncology, H. Lee Moffitt Cancer Center & Research Institute, Tampa, FL,[5]Department of Microbiology, Ponce Health Sciences University, Ponce, PR,[6]Department of Anatomic Pathology, H. Lee Moffitt Cancer Center & Research Institute, Tampa, FL,[7]California University Science and Medicine, Colton, CA,[8]Diagnostics Institute, Robert J. Tomsich Department of Pathology and Laboratory Medicine, Cleveland Clinic, Cleveland, OH,[9]Department of Gastrointestinal Oncology, H. Lee Moffitt Cancer Center & Research Institute, Tampa, FL,[10]Department of Population and Public Health Sciences, USC Norris Comprehensive Cancer Center, Los Angeles, CA,[11]Department of Cancer Epidemiology, H. Lee Moffitt Cancer Center & Research Institute, Tampa, FL,[12]Department of Biostatistics and Bioinformatics, H. Lee Moffitt Cancer Center & Research Institute, Tampa, FL

Introduction: Tumor-infiltrating lymphocytes (TILs) are positive prognostic indicators in colorectal cancer (CRC), yet factors driving their variability beyond microsatellite instability (MSI) are poorly defined. Prior studies suggest that genetic ancestry may influence systemic and tumor-associated immune responses. We tested the hypothesis that global genetic ancestry is independently associated with distinct T-cell features in the CRC tumor immune microenvironment.

Methods: In 230 patients with CRC from the Latino Colorectal Cancer Consortium, we quantified tumor-associated T-cell repertoires using immunoSEQ TCRβ assays for T-cell receptor (TCR) abundance and clonality (log-transformed), pathologist-scored TILs per high-powered field (dichotomized ≥2 vs <2; N=180), and whole-exome sequencing (WES)-inferred TCRα (TCRA) fractions (dichotomized ≥0.03 vs <0.03; N=192). Genetic ancestry proportions (European [EUR], African [AFR], East Asian [EAS], Indigenous American [NAT], South Asian [SAS]) were estimated from germline/normal genotypes from WES via supervised ADMIXTURE (using 1kGP/HGDP references). Correlations between TCR features were evaluated using Spearman coefficients. Logistic/linear regression examined the associations between immune features (TCR abundance, TCR clonality, TILs, and TCRA fractions) and individual ancestry proportions, adjusting for age, sex, tumor location, and MSI status. To account for the constrained sum of ancestral components, we applied an additive log-ratio transformation (ALR), expressing AFR, EAS, SAS, and NAT ancestries as log ratios relative to EUR. These ALRs were fitted into a multivariable logistic/linear regression model, and the overall contribution of genetic ancestry to each immune feature was tested using a 4-df likelihood-ratio test (4-df LRT).

Results: Various T-cell quantification metrics were positively correlated, with pathologist-reviewed TILs showing significant correlations with TCR abundance, clonality, and TCRA fractions (ρ=0.29, 0.29, and 0.22, respectively). CRC patients with higher TCRA fractions were more likely to have higher EUR ancestry (Odds Ratio [OR]: 12.85; 95% Confidence Interval [CI]: 1.09-151.70, p=0.043) and lower NAT ancestry (OR: 0.06, 95% CI: 0.005-0.70, p=0.025). Higher TCR clonality showed a suggestive association with lower EUR proportions (p=0.076) and higher NAT proportions (p=0.084). We found no association with overall genetic ancestry and any T-cell feature in the compositional analysis (4-df LRT>0.05).

Conclusion: Our findings suggest that specific genetic ancestry components may be associated with T-cell landscapes in CRC. These results indicate that genetic background may influence the host anti-tumor immune response in CRC, highlighting the importance of integrating genetic ancestry into personalized risk stratification and precision medicine approaches.

#5063 Ancestry-linked, stage-specific delay to tertiary care is associated with survival differences in colorectal cancer.

Sharafudeen Dahiru Abubakar, Henry Walch, Christina Lee, David Gomez Sanchez, Chin-Tung Chen, Stefanie Gerstberger, Kanika Arora, Farheen Shah, Tejiri E. Agbamu, Michele Waters, Christopher J. Fong, Justin Jee, Michael F. Berger, Karuna Ganesh, Debyani Chakravarty, Walid Khaled Chatila, Nikolaus Schultz, Rona Yaeger, Julio Garcia-Aguilar, Francisco Sanchez-Vega

Memorial Sloan Kettering Cancer Center, New York, NY

Background: African-ancestry (AFR) patients with colorectal cancer (CRC) have worse overall survival (OS) than non-AFR patients. While biological and socioeconomic (SES) factors are known to play a role, delayed access to specialized care remains a critical, underexplored driver of this inequity. This study investigates how the time from diagnosis (Dx) to arrival at a tertiary cancer center interacts with ancestry, disease stage, SES, and genomics to affect OS.
Methods: We analyzed data from 4,328 CRC patients (259 AFR, 4,069 non-AFR) treated at Memorial Sloan Kettering Cancer Center (MSK) since 2014. Tumors were sequenced with MSK-IMPACT, a targeted DNA sequencing assay that profiles genomic changes in 341-505 genes. Genetic ancestry was inferred from sequencing data with >80% African ancestry fraction grouped as AFR. OncoKB identified clinically actionable genomic alterations. Covariates included tumor location, stage at Dx, time from Dx to MSK arrival (Early ≤90 days vs Late >90 days), insurance type and metastatic burden. OS from Dx was compared using Kaplan-Meier curves and log-rank test, with left-truncation for genomic sequencing date.
Results: AFR patients had worse OS from Dx than Non-AFR patients (median 39.3 vs 62.7 months, p<0.001). This difference remained when stratified by stage at Dx (Stage I-III: 65.3 vs 96 months, p<0.001; Stage IV: 31.6 vs 36.7 months, p=0.03). AFR patients also had significantly longer delays from Dx to arrival (median: 22 [IQR: 10, 173] vs 14 [IQR: 6, 38] days; p<0.001) and a higher proportion of late arrivals (28.7 vs 17.1%, p<0.001). This difference was more evident in Stage I-III (49.6 vs 25.9%, p<0.001) than in Stage IV (6.3 vs 5.6%, p=0.69). There was no significant difference in OS between AFR and Non-AFR for Stage I-III early (median: Not Reached (NR) vs NR, p=0.98), Stage I-III late (median: 36 vs 43.5 months, p=0.24), and Stage IV late (median:43.7 vs 33.9 months, p=0.48) arrival, but was significant in Stage IV early arrival (median: 31.6 vs 36.9 months, p=0.034). Patients diagnosed with Stage I-III disease who arrived late at MSK were often Stage IV at their time of arrival (AFR: 68.9%, Non-AFR 65.8%) but this was much less frequent among early arrivals (AFR: 6.1%, Non-AFR: 2.6%); and was linked to higher Medicaid use in both AFR (10.8% vs 1.5%; p=0.03) and Non-AFR (4.4% vs 2.4%; p=0.015) patients. AFR had higher KRAS mutation frequency compared to Non-AFR across all stages and arrival groups (Stage I-III Early: 51.5 vs 38.8%, p=0.04; Stage I-III Late: 58.2 vs 47.2%, p=0.10; Stage IV Early: 58.5 vs 44.5%, p=0.004; Stage IV Late: 75 vs 50.5%, p=0.28).
Conclusion: Delayed specialized care appears to be linked to CRC survival gaps in AFR patients, especially in the non-metastatic setting where timely multidisciplinary care is crucial. Expediting referral of AFR patients to tertiary care centers could help to achieve CRC outcome equity.

#5064 Ancestry-associated epigenetic differences in chronic lymphocytic leukemia.

Zhiquan Wang[1], Huihuang Yan[1], Mingma Sherpa[1], Daniel Bihnam[2], Cristine Allmer[1], Chantal McCabe[1], Daniel O'Brien[1], Dennis P. Robinson[1], James R. Cerhan[3], Neil E. Kay[1], Sameer A. Parikh[1], Esteban Braggio[4], Susan Slager[1]

[1]Mayo Clinic, Rochester, MN,[2]Mayo Clinic, Phoenix, AZ,[3]Mayo Clinic College of Medicine and Science, Rochester, MN,[4]Mayo Clinic Arizona, Scottsdale, AZ

Background: CLL incidence differs by ancestry, with higher rates in individuals of European ancestry (EA) than African ancestry (AA). The contribution of epigenetic variation to these disparities remains unclear. We investigated chromatin accessibility, histone modifications, and gene expression in CLL patients of EA and AA to identify ancestry-associated epigenetic signatures.
Methods: ATAC-seq was performed on blood clonal B cells from 15 AA and 51 EA patients; CUT&Tag profiling of six histone marks (H3K4me1, H3K4me3, H3K27ac, H3K9me3, H3K27me3, H3K36me3) was done in 8 AA and 12 EA cases; RNA-seq was generated for all samples. Ancestry was genetically confirmed. Differential regions were linked to genes using ENCODE and Hi-C datasets.
Results: ATAC-seq revealed 4,955 regions with increased and 3,000 with decreased accessibility in AA vs EA (fold change >2, FDR ≤0.05). Regions with increased accessibility mapped to 2,313 genes; 599 were upregulated and enriched in TNF-α/NF-κB (p=1.40E-53) and apoptosis pathways (p=6.90E-11). Regions with decreased accessibility linked to 1,953 genes; 317 were downregulated, enriched in interferon-γ response (p=1.04E-03) and IL-6/JAK/STAT3 signaling (p=6.41E-03). Histone profiling showed ancestry-specific changes across all marks. For H3K27ac (active enhancer), 68 genes with a decreased signal in AA were downregulated and enriched in interferon-γ (p=1.55E-06) and IL-6/JAK/STAT3 (p=9.62E-05) pathways. Increased H3K27me3 (repressive histone modification) in AA affected 399 genes enriched in IL-6/JAK/STAT3 (p=8.13E-09) and interferon-γ (p=2.48E-05) pathways. These findings suggest coordinated regulation by active and repressive chromatin states.
Conclusions: Despite limited sample size, this study suggests differences between AA and EA ancestries may exist in epigenetic signatures in CLL, implicating chromatin accessibility and histone modifications in pathways relevant to tumor biology. These signatures may also contribute to the differences in CLL incidence by ancestry. Future studies with more patients and functional validation experiments are needed to clarify the role of these epigenetic differences in CLL pathogenesis.

#5065 Ancestry-related differences in genomic mutations between African American and European American prostate cancer patients.

Nicholas S. Korvink[1], Arash Rezazadeh[2], Omid Yazdanpanah[3], Michael McClelland[3], Farahnaz Rahmatpanah[1]

[1]Pathology, University of California, Irvine, Irvine, CA,[2]Hematology/Oncology, University of California, Irvine, Irvine, CA,[3]University of California, Irvine, Irvine, CA

Background. Somatic mutations accumulate with age in prostate cancer (PCa) tumorigenesis, affecting key driver genes including FOXA1 and SPOP. Significant ancestry-related differences exist in PCa's mutational landscape: CDK12 mutations occur twice as frequently in African Americans (AA) versus European Americans (EA), while TMPRSS2-ERG fusion is more common in EA (~50%) than AA (~25%). Despite these differences, comprehensive genome-wide mutational comparisons remain limited. This study elucidates genome-wide mutational differences between ancestries to identify ancestry-specific molecular signatures for improved risk stratification and personalized treatment.

Methods. We analyzed whole-genome DNA sequencing from 19 patients across three cohorts: Africans (AF, n=5) from the European Nucleotide Archive (PRJNA412953), AA (n=11), and EA (n=3) from TCGA. Sequencing files aligned to hg38 were processed using R codes and Strand NGS software for recalibration, realignment, and SNP detection. After removing statistical outliers, we compared mutational burden categories including substitutions, insertions, deletions, complex mutations, zygosity patterns, transition/transversion mutations, Ti/Tv ratios, and dbSNP variants. Statistical analysis employed Mann-Whitney U test for groups ≥5 samples or 10,000-iteration permutation test for smaller groups.

Results. Whole-genome SNP analysis revealed distinct patterns across AF, AA, and EA. AA versus EA showed significant differences ($p<0.05$) in most categories: all basic variant types (substitutions: $p=0.0149$; insertions: $p=0.0181$; deletions: $p=0.0181$), zygosity patterns (homozygous: $p=0.0174$; heterozygous: $p=0.0236$), transition/transversion mutations (both $p=0.0149$), Ti/Tv ratios ($p=0.0174$), and known dbSNP variants ($p=0.0149$). Complex variants ($p=0.1708$) and novel variants ($p=0.2766$) showed no significant differences. AF versus AA revealed significant differences ($p<0.05$) in nearly all categories: substitutions ($p=0.0176$), insertions ($p=0.005$), deletions ($p=0.0169$), complex variants ($p=0.0169$), heterozygous variants ($p=0.0211$), transitions ($p=0.0176$), transversions ($p=0.0052$), Ti/Tv ratios ($p=0.0047$), and both known ($p=0.0046$) and novel ($p=0.0186$) variants, except homozygous variants ($p=0.7155$). These findings indicate AA have developed distinct genetic profiles compared to continental AF, likely from admixture and environmental factors.

Conclusion. This genome-wide analysis demonstrates significant ancestry-specific mutational differences in PCa, with AA exhibiting distinct profiles from both AF and EA due to admixture and environmental factors. These findings underscore the need for diverse genomic databases, personalized precision oncology, and validation in larger cohorts.

#5066 Association between genetic ancestry and somatic mutational profiles in colorectal cancer.

Marco Matejcic[1], Jamie Teer[2], Daniel Sobieski[3], Eric M. Cockman[3], Esther Jean-Baptiste[4], Nathalie Nguyen[5], Diana B. Diaz[6], Ya-Yu Tsai[1], Hannah J. Hoehn[4], Kritika Shankar[3], Rusche Wilson[3], Karina Brito[3], Allyson Koepfler[3], Seth Felder[7], Julian Sanchez[7], Nicole Catalina Lorona[5], W. Douglas Cress[8], Teresita Munoz-Antonia[9], Idhaliz Flores[9], Edna Gordian[8], Jose Oliveras Torres[10], Ozlen Saglam[11], Kun Jiang[12], Clifton Fulmer[13], Domenico Coppola[12], Erin M. Siegel[14], Mariana C. Stern[15], Jane C. Figueiredo[5], Stephanie L. Schmit[16]

[1]Genomic Sciences and System Biology, Cleveland Clinic Lerner College of Medicine, Cleveland, OH,[2]Department of Biostatistics and Bioinformatics, Moffitt Cancer Center, Tampa, FL,[3]Genomic Sciences and System Biology, Cleveland Clinic, Cleveland, OH,[4]Non-Therapeutic Research Office, Moffitt Cancer Center, Tampa, FL,[5]Department of Medicine, Samuel Oschin Comprehensive Cancer Institute, Los Angeles, CA,[6]Moffitt Cancer Center, Tampa, FL,[7]Department of Gastrointestinal Oncology, Moffitt Cancer Center, Tampa, FL,[8]Department of Molecular Oncology, Moffitt Cancer Center, Tampa, FL,[9]Puerto Rico Biobank, Ponce Health Sciences University, Ponce, Puerto Rico,[10]Department of Microbiology, Ponce Health Sciences University, Ponce, PR,[11]California University Science and Medicine, Colton, CA,[12]Department of Anatomic Pathology, Moffitt Cancer Center, Tampa, FL,[13]Diagnostics Institute, Robert J. Tomsich Department of Pathology and Laboratory Medicine, Cleveland Clinic, Cleveland, OH,[14]Department of Cancer Epidemiology, Moffitt Cancer Center, Tampa, FL,[15]Department of Population and Public Health Sciences, USC Norris Comprehensive Cancer Center, Los Angeles, CA,[16]Genomic Sciences and System Biology, Cleveland Clinic, Cleveland Clinic, OH

Colorectal cancer (CRC) mortality rates differ across populations and differences are not fully accounted for by sociodemographic factors and access to care. Opportunities exist to better understand biological determinants of disparities by expanding cancer genomic datasets to include profiles of tumors from patients from varied communities. Using whole-exome sequencing data from the Latino Colorectal Cancer Consortium (LC3) and additional datasets, we characterized somatic mutational profiles by ethnicity and genetically-inferred ancestry. We hypothesized that ancestral haplotypes that vary across populations contribute to differential somatic mutational profiles. Somatic mutations were called from paired tumor and germline/normal samples using an analysis pipeline including Burrows-Wheeler MEM Aligner, the Genome Analysis Toolkit (GATK), MuTect, Strelka, MuSE, SomaticSniper, freebayes, and Lancet. Inherited variants were identified using GATK. Global proportions of African, East Asian, European, Native American, and South Asian ancestries were estimated using ADMIXTURE based on the 1000 Genomes Project and the Human Genome Diversity Project. Among the 1,243 primary CRC cases included, 391 (31.5%) were Latino, 488 (39.3%) were non-Latino. Associations between global ancestry and somatic mutational features were examined using logistic regression. Among commonly mutated genes in CRC, tumors from Latino participants exhibited lower frequencies of mutations in *BRAF* (OR=0.59, 95%CI=0.34-0.99, p=0.048), *CTNBB1* (OR=0.54, 95%CI=0.30-0.96, p=0.037), *FBXW7* (OR=0.61, 95%CI=0.38-0.99, p=0.045), *KRAS* (OR=0.71, 95%CI=0.52-0.95, p=0.023), but higher frequency of mutations in *CDC27* (OR=11.74, 95%CI=1.39-99.09, p=0.024) and *SMAD2* (OR=2.30, 95%CI=1.08-4.89, p=0.03) compared to non-Latino patients. In addition, African ancestry was significantly associated with higher odds of mutations in *APC* (OR=1.10, 95%CI=1.02-1.18, p=0.013) and *PIK3CA* (OR=1.08, 95%CI=1.00-1.15, p=0.037), while Native American ancestry was associated with lower odds of mutations in *BRAF* (OR=0.83, 95%CI=0.70-0.97, p=0.02) and *FBXW7* (OR=0.85, 95%CI=0.75-0.97, p=0.012). Genome-wide analyses revealed that global genetic ancestry was associated with mutation status in *CFAP54*, *LMBRD2*, *MUC12*, and *TTC6* (FDR-adjusted 4-df LRT p<0.05). Native American ancestry was associated with reduced odds of mutations in *LMBRD2* (OR= 0.47, 95%CI=0.24-0.95, p=0.034), but with higher odds of mutations in *CFAP54* (OR=1.32, 95%CI=1.17-1.49, p=7.55x10^{-06}), *MUC12* (OR=1.29, 95%CI=1.08-1.55, p=0.0049), and *TTC6* (OR=1.31, 95%CI=1.11-1.53, p=0.0011). Tumor mutation burden was significantly reduced in Latino patients compared to non-Latino patients (OR= 0.78, 95%CI=0.64-0.94, p=0.012). These findings advance precision medicine efforts by improving our understanding of ancestry-associated molecular heterogeneity.

#5067 Prospective epigenome-wide association study of pancreatic cancer risk in a multiethnic population.

Xinman Zhang[1], Sihao Han[1], Brandon Quon[2], Adelynn Paik[1], Veronica Wendy Setiawan[1], David V. Conti[1], Kimberly D. Siegmund[1], Heinz Josef Lenz[3], Lenora W. M. Loo[4], Loic Le Marchand[2], Lynne R. Wilkens[2], Christopher A. Haimen[1], Alexandra M. Binder[2], Sung-Shim Lani Park[2], Brian Huang[1]

[1]Department of Population and Public Health Sciences, Keck School of Medicine, University of Southern California, Los Angeles, CA,[2]Population Sciences of the Pacific Program-Epidemiology, University of Hawaii Cancer Center, Honolulu, HI,[3]Department of Medicine, Keck School of Medicine, University of Southern California, Los Angeles, CA,[4]Cancer Biology Program, University of Hawaii Cancer Center, Honolulu, HI

Background: Pancreatic ductal adenocarcinoma (PDAC) is a highly lethal cancer, with known differences in incidence across populations in the US. Epigenome-wide association studies (EWAS) have identified DNA methylation markers of PDAC risk, but have been mostly performed in European ancestry populations with small sample sizes and post-diagnostic samples. Prospective EWAS in diverse populations may reveal novel biomarkers and provide insights into racial/ethnic differences in PDAC biology.

Methods: Using a nested case-control design, we conducted an EWAS of PDAC risk in the Multiethnic Cohort, a large prospective cohort of African American, Japanese American, Latino, Native Hawaiian, and White residents of Los Angeles and Hawaii. Incident PDAC cases (N=689) were matched to controls (N=806) on age, sex, race/ethnicity, year of blood draw, and study site. DNA methylation was measured in pre-diagnostic blood using the Illumina EPICv2 array (>930,000 CpG sites). Associations between DNA methylation at each CpG site and PDAC risk was assessed using conditional logistic regression, adjusting for matching factors, diabetes, family history of PDAC, smoking, BMI, and DNA methylation-predicted lymphocyte cell type proportions. Differentially methylated region (DMR) and pathway analyses were further conducted. The most significant results were examined in a prior EWAS of PDAC in the Nurses' Health Study, Physicians' Health Study and Health Professionals Follow-up Study (N=393 cases/431 controls).

Results: We identified 105 CpG sites significantly associated with PDAC risk ($p<9\times10^{-8}$). The top CpG sites were annotated to genes related to tumor suppression, metabolism, and inflammation (e.g., *TRAK1*, *INPP5A*, *ACOX3*, *WBP1L*, *RASSF8-AS1).* Most of the top CpG sites exhibited a positive association between DNA methylation levels and PDAC risk (odds ratios [OR] per 0.01 increase in methylation beta value 1.03-2.33). Heterogeneity across race/ethnicity was observed for one site in *ZNF713*, which was associated with PDAC in Native Hawaiians only (OR 1.65, 95% CI 1.52-1.80; p-heterogeneity$<6.6\text{x}10^{-25}$). DMR analysis revealed 738 regions associated with PDAC (FDR-adjusted $p<0.05$), with the top regions annotated to genes related to genetic regulation and cancer progression (e.g. *PRMT7*, *NDUFC1*, *NAA15*, *TFDP1).* KEGG and GO pathway analyses identified 18 and 388 significantly enriched pathways, respectively ($p < 0.05$); the top pathways were DNA replication and catalytic complex. In the validation analyses, none of the 105 sites reached significance ($p<0.01$), but 26 showed the consistent direction of association.

Conclusions: In this multiethnic population, differential methylation in genes related to cancer, inflammation, and metabolism were associated with PDAC risk. Further studies integrating larger discovery and validation data are warranted to elucidate underlying mechanisms across populations.

#5069 Ethnic differences in the immune landscape and gene signature in prostate cancer.

Shiv S. Verma[1], Pingfu Fu[2], Gregory T. MacLennan[3], Lee E. Ponsky[4], Sanjay Gupta[1]

[1]Case Western Reserve University School of Medicine, Cleveland, OH,[2]Population and Quantitative Health Sciences, Case Western Reserve University, Cleveland, OH,[3]Pathology, Case Western Reserve University, Cleveland, OH,[4]Urology, University Hospitals Cleveland Medical Center, Cleveland, OH

Prostate cancer is a biologically and clinically heterogeneous disease, with incidence and mortality rates that vary substantially across racial and ethnic groups. Among Black American (BA) men, the incidence of prostate cancer is approximately 60% higher, and the mortality rate is two to three times greater than that observed in White American (WA) men. These disparities are multifactorial, involving both biological and social determinants such as genetic predisposition, comorbidities, socioeconomic status, environmental exposures, and cultural influences. While these factors obviously contribute to disease outcomes, growing evidence highlights the crucial role of the tumor immune microenvironment and its associated gene signatures in shaping prostate cancer biology and progression. To investigate ethnic variations in tumor immune gene signatures, we analyzed transcriptomic data from 35 radical prostatectomy specimens from treatment-naïve patients, including 20 BA and 15 WA men. Gene expression profiles from tumor and adjacent normal tissues were examined using EPIC, xCell, and Ingenuity Pathway Analysis. Differential gene expression was determined by rank testing, and prognostic associations were assessed via univariate Cox regression. WA tumors are enriched for pathways associated with neuroinflammation and oxidative phosphorylation including IL-8 signaling, neuroinflammation, dendritic cell maturation, oxidative phosphorylation, PKCθ signaling in T cells, and NFAT-mediated immune regulation, while PPAR and PD-1/PD-L1 pathways were less active. In contrast, BA tumors are characterized by increased activation of pro-inflammatory and immune-regulatory pathways; display elevated CREB signaling, Th1/Th2 activation, dendritic cell maturation, IL-17 and TREM1 signaling, and IL-17A/F-mediated cytokine production, with reduced activity in PD-1/PD-L1, ILK, IL-3, VEGF, and B-cell receptor pathways. Thirteen immune cell types showed race-specific gene expression patterns including ARG1, FA2H, FBXO39, IGLL3P, KLKB1, MERTK, SEMA3G, and TRPV5 markedly expressed in WA tumors, whereas ARSL, BAALC, CCL23, EPHA2, IGFL2, KRT5, NTM, and NDP upregulated in BA tumors. These results reveal distinct immune-oncological landscapes between BA and WA prostate tumors, highlighting pro-inflammatory pathway enrichment in BA men and underscoring opportunities for ethnicity-specific, genomically informed therapies.

#5070 How stress gets under the skin: Everyday discrimination, inflammation and cancer risk in older adults.

Cameron Brown, Lauren Brown

USC-Leonard Davis School of Gerontology, Los Angeles, CA

Cancer is a devastating disease predominately affecting older adults, with adults 65+ accounting for 70% of cancer-related deaths and over 60% of new diagnoses. Preliminary studies show that Black and Hispanic/Latine older adults are at an increased risk of diagnosis of advanced staged cancers and experience higher mortality rates from cancer than older adults of other racial/ethnic groups. Inflammation is one such risk factors in these sub-groups, specifically through chronic stressors like everyday discrimination (EDD). One way to measure this stress pathway is via inflammatory biomarkers like C-Reactive Protein (CRP) and Soluble Tumor Necrosis Factor-1 (sTNFR-1). Improving our understanding of the intersection between EDD and inflammatory biomarkers in disaggregated populations will help us identify high-risk groups to improve timeliness and diagnosis. We examined whether EDD is associated with elevated CRP and sTRNFR-1 levels, ultimately increasing cancer risk for minoritized populations. This study included White (n=3,187), Black (n=443), and Hispanic/Latine (n=375) older adults in the U.S. who were 65-95 years old in the 2016 *Health and Retirement Venus Blood Biomarker Subsample*. Results show that Black older adults experience more EDD and have higher average CRP [(4.93 mg/L (0.41)] and sTNFR-1 [(1840.88 pg/mL (85.3)] levels than White [CRP= 3.95 mg/L (0.16) ; sTNFR-1= 1807.21 pg/mL (20.7)] and Hispanic/Latine [CRP=4.50 mg/L (0.41); sTNFR-1=1806.75 pg/mL (67.43)] older adults. OLS regression models show reporting more experiences of EDD is associated with higher CRP levels (β;= 0.23; p=0.03), specifically in Black older adults, but is not associated with higher levels of sTNFR-1. Logistic regression models show sTNFR-1 (OR=1.00; p=0.04) significantly increases the odds of being diagnosed with cancer in the full sample. Findings suggest that experiences of EDD may increase cancer risk, via inflammatory pathways like CRP.

#5071 Stress and breast cancer risk among Asian American females: The CRANE Study.

Scarlett L. Gomez[1], Katherine Lin[2], V. Wendy Setiawan[3]

[1]Epidemiology & Biostatistics, University of California, San Francisco, San Francisco, CA,[2]University of California, San Francisco, San Francisco, CA,[3]University of Southern California, Los Angelens, CA

Background: Breast cancer incidence rates among Asian American (AA) women have risen rapidly, 2.3% annually since 2012, far outpacing the overall US trend. The increase is particularly stark for early-onset cases (<50 years), at 2.9% per year since 2016. Significant increases were observed across nearly all AA groups, stages and subtypes, with especially sharp rises in late-stage and triple-negative breast cancer. Foreign-born AA now face higher risk relative to US-born AA, even after accounting for established risk factors. These evolving patterns point to emerging, unrecognized risk factors. The CRANE Study (Breast Cancer Risk among Asian Americans) investigates multilevel determinants, from environmental to biological, that drive the contemporary elevated risk in this population. This abstract describes preliminary social stressor results.

Methods: The CRANE Study, initiated in 2022, is a population-based case-control study of breast cancer in AA in California. The study integrates epidemiologic data on established and emerging risk factors with geospatial data (including residential histories), cancer registry data, and biospecimens (saliva and hair), alongside access to medical records and tumor specimens. AA women with recently-diagnosed breast cancer are identified through the Greater Bay Area and Los Angeles County cancer registries. Controls, matched to cases by ethnicity, age, and region, are recruited using multiple modalities to represent the population at risk.

Results: To date, 317 cases and 368 controls have been enrolled (39% Chinese, 18% Filipina, 9% Japanese, and 8% each Korean, South Asian, and Southeast Asian). Among cases, 48% were younger than age 50 at diagnosis, ranging from 16% among Japanese to 71% among Koreans. Most were diagnosed at stage I disease (70%). Tumor subtypes included 68% HR+/HER2-, 20% HER2+ (14% among Koreans to 29% among South Asians), and 8.5% triple-negative cancer. Compared to controls, cases were more likely to be foreign-born (72% vs. 54%) and less acculturated (65% vs. 81% English proficient), and have higher BMI (20% vs. 14% BMI≥27.5) and later menarche (50% vs. 45% at ≥13 years). However, cases reported lower levels of stress (20% vs 24% in the highest quartile of immigrant stress) and racism (15% vs. 22% in the highest quartile of anti-Asian racism) compared to controls. Despite reporting fewer stressors, more cases than controls expended higher levels of effortful coping on the John Henryism scale (29% vs. 24% in the highest quartile).

Conclusions: The CRANE Study provides a unique and timely platform to investigate how environmental, social, and biological factors interact to shape breast cancer risk in this population. By focusing on AA, who are experiencing notable increases in early-onset and triple-negative breast cancers, CRANE aims to identify novel risk factors and pathways that may help explain emerging breast cancer trends in both AA and the broader US population.

#5072 Discriminatory capacity of allostatic load score in colorectal cancer: A pilot case-control study.

Hilmaris Centeno-Girona[1], Maria Gonzalez-Pons[2], Elba V. Caraballo-Rivera[1]

[1]Shared Resources and Scientific Operations, University of Puerto Rico Comprehensive Cancer Center, San Juan, Puerto Rico,[2]Clinical and Translational Cancer Research, University of Puerto Rico Comprehensive Cancer Center, San Juan, Puerto Rico

Colorectal cancer (CRC) represents the leading cause of cancer-related deaths in Puerto Rico. Allostatic load (AL) reflects a cumulative dysregulation across inflammatory, neuroendocrine, and metabolic systems. It may serve as a composite index for distinguishing CRC cases from controls. Unlike individual markers, AL captures multi-system physiological dysregulation observed in CRC patients. This study aimed to assess the discriminatory capacity of a composite AL score derived from inflammatory, neuroendocrine, and metabolic biomarkers for distinguishing CRC patients from healthy controls in a sample of Hispanics individuals living in Puerto Rico (HPR).This case-control study used plasma samples from the Puerto Rico Familial Colorectal Cancer Registry (PURIFICAR) including 18 CRC cases and 18 healthy controls. AL score was constructed using control derived percentile scoring (75th percentile cutoffs, 25th for IGF-1) across 8 markers: IL-1β, TNF-α, IL-8, MCP-1, CRP (inflammatory), cortisol (neuroendocrine), and IGF-1 and BMI (metabolic). Logistic regression models evaluated discriminatory capacity with progressive adjustment for demographic and sociodemographic factors. Area under the curve (AUC) comparisons were performed using DeLong's test. Analyses were performed in Stata 18. Participants had a median age of 48 years (range: 34-65) and 44% were male. CRC cases had significantly lower BMI (median 23.8 vs 28.2, p=0.016), higher educational attainment (50% vs 33%, p=0.31), and lower private insurance coverage (33% vs 56%, p=0.18) than controls. The AL score showed higher median values in cases versus controls. Higher AL scores were associated with increased odds of CRC in unadjusted analysis (OR=1.26, p=0.295), which strengthened slightly after adjusting for age and sex (OR=1.30, p=0.247). When including education and insurance type for the full model, the association remained similar (OR=1.25, p=0.362). Private insurance demonstrated a marginally significant protective association (OR=0.20, p=0.075). Discriminatory capacity was modest for AL alone (AUC=0.619) and remained similar after demographic adjustment (AUC=0.590) but improved with full adjustment (AUC=0.713). DeLong's test indicated non-significant differences between models (Model 1 vs 2: p=0.626; Model 1 vs 3: p=0.329; Model 2 vs 3: p=0.171). This pilot study demonstrated non-significant associations between AL score and CRC, though discriminatory capacity improved with sociodemographic adjustment. The marginally significant protective effect of private insurance suggests healthcare access may influence CRC risk independent of physiological stress burden. These findings support the feasibility of AL measurement in HPR populations and highlight the importance of considering structural determinants of health in CRC risk assessment. Validation in larger samples is warranted.

#5073 Disparities in timeliness of cancer diagnosis across a multi-site academic health system.

Vivian Hoang Tran[1], Suraj M. Rajan[1], Matthew P. Banegas[1], Winta Mehtsun[2], Brent Rose[1], James Murphy[1], Melody Schiaffino[1], Joshua Demb[1], Noe C. Crespo[3], Humberto Parada[1], Corinne McDaniels-Davidson[3], Elena Martinez[1]

[1]Center for Health Equity Education & Research, UC San Diego Moores Cancer Center, La Jolla, CA,[2]UC San Diego School of Medicine, La Jolla, CA,[3]San Diego State University School of Public Health, San Diego, CA

Background: Early cancer diagnosis is crucial for improving survival and quality of life. Understanding which patient populations are at higher risk for late-stage diagnosis within a healthcare system is a crucial step toward achieving health equity. This study examines demographic, clinical, and socioeconomic factors associated with late-stage diagnosis, defined as stage III/IV diagnoses using the American Joint Committee on Cancer (AJCC) criteria.
Methods: A retrospective cohort study of 12,721 patients diagnosed with breast, colorectal, or lung cancer within the University of California health system database. Multivariable logistic regression was used to identify various factors associated with late-stage diagnosis.
Results: 14.1% of patients were diagnosed at a late-stage (stage III/IV). In adjusted analyses, patients with colorectal (OR: 4.76; 95% CI: 4.12-5.50) and lung cancer (OR: 12.82; 95% CI: 11.01-14.92) had significantly higher odds of late-stage diagnosis compared to breast cancer (reference group). A higher Area Deprivation Index (ADI) was significantly associated with increased odds of late-stage diagnosis (OR: 1.03 per 1-unit increase; 95% CI: 1.01-1.05). Neither race nor ethnicity was an independent predictor of late-stage diagnosis in the final adjusted model.
Conclusion: Cancer type is the strongest predictor of a late-stage diagnosis. Additionally, greater neighborhood-level socioeconomic disadvantage (measured by ADI) is a significant, independent risk factor. These findings highlight the need for targeted screening and diagnostic interventions that incorporate geospatial analyses, particularly for lung and colorectal cancer patients in socioeconomically disadvantaged communities.

#5074 Transcriptomic and SNP profiling reveals early-onset and ethnicity-associated signatures in colorectal cancer.

Soumya Nair[1], Betty Huang[2], Umme Tania[1], Brian Grajeda[1], Md Zahirul Islam Khan[1], Michael Schatz[2], Rajiv McCoy[2], Sourav Roy[1]

[1]The University of Texas at El Paso, El Paso, TX,[2]John Hopkins University, Baltimore, MD

Colorectal cancer (CRC) is the second deadliest cancer in the United States, with early-onset (age < 50) cases rising significantly over the past decade. Although early-stage (I/II) CRC is treatable with a higher survival rate, these tumors often present with poor outcomes, particularly among minority groups like Hispanics. Hispanics experience higher rates of late-stage (III/IV) diagnosis than Non-Hispanic Whites (NHW), suggesting that both genetic and non-genetic factors may contribute to this disparity. To identify potential biological contributors to early-onset and ethnicity-associated disparities, we investigated transcriptomic and genotypic biomarkers that may improve screening and prognosis. We performed RNA sequencing on CRC tissues and normal tissues adjacent to the tumor (NATs) from Hispanic and NHW patients. Gene level quantification was obtained using two independent pipelines - Rsubread and Salmon. DESeq2 analysis, identified 996 differentially expressed genes (DEGs, log2 foldchange ≥ 2.0 and ≤ -2.0 and a false discovery rate of 0.05) common to both the tools between CRC and NAT samples. When analyzed within each ethnic cohort 1251 DEGs were identified in Hispanics and 899 in NHWs. Notably, within the Hispanic group, 311 DEGs were common between early-onset and late-stage Hispanic CRC samples compared to NHWs. Pathway enrichment analyses using Ingenuity Pathway Analysis and Gene Set Enrichment Analysis revealed significant dysregulation of the cell cycle regulatory pathways including the Mitotic G2-G2/M phases, Mitotic G1 phase and G1/S transition, as well as Cell cycle checkpoints, pathways critical for apoptosis, and tumor progression. Interaction analysis further revealed 138 DEGs (log2 foldchange ≥ 1.0 and ≤ -1.0 and p- value ≤ 0.05) display a significant association with CRC occurrence in the Hispanic cohort. Additionally, variant discovery and annotation using the Genome Analysis Toolkit (GATK) and Snpeff workflows, identified 383 variants either unique to or abundant in Hispanic CRC samples and predicted to have high or moderate functional impact. Among these, analysis of SNP-associated genes revealed that the downregulation of NCF1, carrying the rs10614 variant, was significantly correlated with tumor status in the Hispanic CRC cohort. Reduced NCF1 expression is associated with ROS deficiency induced colitis-mediated tumorigenesis. Overall, our findings reveal Hispanic-specific transcriptomic and genotypic signatures that may underlie CRC disparities and identify potential biomarkers for improved screening. Further functional studies in Hispanic patient tissues and patient-derived organoid models will help elucidate the biological roles of these genes and variants, ultimately promoting the development of early-screening strategies and targeted therapies for high-risk populations.

#5075 Integrated clinicopathologic, genomic and transcriptomic characterization of gastric cancer by race/ethnicity in a national multi-institutional cohort.

Kyle D. Klingbeil[1], Sinead Cullina[2], Natalie N. Martinez[1], Mariah B. Blegen[1], Kyla E. Wright[1], R. Vanessa Mora Molina[1], Ami Hayashi[1], Adam J. Dugan[2], Unnati Jariwala[2], Stamatina Fragkogianni[2], Jonathan Boiarsky[3], Lee S. Rosen[3], Mark D. Girgis[1], Brian E. Kadera[1]

[1]Department of Surgery, Division of Surgical Oncology, UCLA Health, Los Angeles, CA,[2]Tempus AI, Inc., Chicago, IL,[3]Department of Medicine, Division of Hematology-Oncology, UCLA Health, Los Angeles, CA

Background: Although gastric cancer outcomes vary by race/ethnicity, a molecular basis for these differences has not been fully elucidated. To address this gap, we used the Tempus Lens Platform (Tempus AI, Inc., Chicago, IL) to query the multimodal de-identified database in order to establish and subsequently analyze a cohort of patients with gastric adenocarcinoma who underwent germline and tumor testing using xT (DNA) and xR (RNA).

Methods: Patients were categorized by R/E. RNA-seq data were normalized as transcripts per million (TPM) and reported as log2(TPM+1). Single-sample Gene Set Enrichment Analysis (ssGSEA) using Hallmark gene sets was used to compare cell signaling pathway activity. Real-world overall survival (rwOS) was defined as the time from biopsy to death or last known follow-up. rwOS survival curves were estimated using the Kaplan Meier (KM) approach and differences tested using log-rank tests. Hazard ratios (HR) were calculated using Cox proportional hazard models.

Results: Among 1,842 patients with reported race/ethnicity data, 1,186 (64%) identified as White, 327 (17.7%) as Hispanic/Latino (HL), 217 (11.8%) as Black or African American (AA) and 112 (6.1%) as Asian. In the multivariable Cox model, compared to White patients, rwOS was longer for HL (HR 0.65, 95% CI 0.48-0.88, p=0.005) and Asian (HR 0.64, 95% CI 0.41-0.98, p=0.042) patients. Asian patients had longer median rwOS compared to White patients (19 vs 10.9 months, log-rank p<0.001). Compared to White patients, HL patients were younger at diagnosis (median 57 vs 67 years, p<0.001) and a greater proportion were female (45% vs 28%, p<0.001). Tumor grade, microsatellite instability, tumor mutational burden, and *CLDN18.2* expression differed significantly across groups (all p<0.01), whereas HER2 and PD-L1 status did not. At the genomic level, the frequency of somatic alterations in *TP53* (57% HL vs 75% White), *CDKN2A* (11% Asian vs 21% White), *CDH1* (6.9% AA vs 16% HL) differed between groups (all p,q<0.001). Pathogenic germline variants were identified in 10.1% of AA, 10.7% of Asian, 10.7% of HL, and 15.8% of White patients, most commonly involving *HDAC2*, *ATR*, *ATM*, and *MUTYH*, respectively. Transcriptomic profiling via ssGSEA revealed an inflammatory pathway activation among HL and Asian patients, with a significant increase in IL6/JAK/STAT3 and IFN-γ signaling vs White patients (all q<0.001). HL patients also demonstrated greater enrichment of the IL2/STAT5, TNFα and complement response pathways vs White patients (q<0.001).

Conclusion: This study represents the largest and most diverse clinico-genomic analysis of gastric cancer. Collectively, these findings highlight distinct clinical presentations, molecular alterations and survival outcomes by race/ethnicity, promoting the critical need for broad molecular testing to inform precision cancer care.

#5076 Disparities across demographic, behavioral, and socioeconomic factors in lung cancer stage at diagnosis: An EPIC EHR study from the University of Maryland Medical System.

Leila Abar[1], Sally N. Adebamowo[2], Clement Adebamowo[1]

[1]University of Maryland, Baltimore, Baltimore, MD,[2]University of Maryland School of Medicine, Baltimore, MD

Background: Lung cancer is the leading cause of cancer mortality in Maryland and the US with sex, socioeconomic factors, and insurance status disparities in stage at diagnosis. There is a rising burden among younger adults, never-smokers, women and racial/ethnic minorities, who often present with advanced disease and may not qualify for screening using current USPSTF guidelines. In this study, we evaluate the associations between age, smoking status, race, sex, and insurance status, and the stage at diagnosis using large real-world EHR datasets.
Methods: We conducted a retrospective cross-sectional study of 6,446 adults diagnosed with lung cancer (ICD-10: C34) using EPIC electronic medical records from the University of Maryland Medical System between January 2016 and December 2024. We extracted age, sex, race, ethnicity, smoking status, insurance type, and stage at diagnosis classified as early (I-II) or advanced (III-IV) from the records. We used t tests for continuous variables and χ^2 tests for categorical variables.
Results: Overall, 38% of patients were diagnosed with early-stage lung cancer and 62% with advanced disease. Advanced stage disease was commoner among younger patients, (mean age 68 vs 70 years, $p<0.001$), and those younger than 50 years (77%, $p<0.001$). Though there were more women (52%) in the study population, men were more likely to present with advanced disease (64% vs 59%, $p<0.001$). The study population was predominantly white (73%) but there was no association between race and stage ($p=0.06$). Current smokers were most likely to present with advanced disease (66%, $p<0.001$). Patients on Medicaid (78%) and uninsured individuals (65%) had a higher likelihood of advanced-stage diagnosis compared with those covered by Medicare (58%) or private insurance (66%).
Conclusions: Younger adults, males, current smokers, and patients on Medicaid or having no insurance were more likely to present with advanced lung cancer. These findings highlight disparities in lung cancer diagnosis and underscore the need for further research.

#5077 Investigating IL-6-driven inflammation and gene-environment interactions in colorectal cancer disparities among Puerto Rican Hispanics.

Luis Daniel Borrero-Garcia, Melissa Chavez, Olga Diaz-Miranda, Leslie Casiano, Maria Gonzalez-Pons

Clinical and Translational Cancer Research, University of Puerto Rico Comprehensive Cancer Center, San Juan, PR

Early-onset colorectal cancer (EOCRC) is rising in Puerto Rico despite an overall decline in colorectal cancer (CRC) incidence. Interleukin-6 (IL-6), a pro-inflammatory cytokine, has been implicated in CRC progression through inflammatory signaling, immune disruption, and DNA damage. This study explores the association between circulating IL-6 levels and IL-6-related single nucleotide polymorphisms (SNPs) in EOCRC patients to examine if IL-6 contributes to cancer disparities. A case-control design was used with CRC patients (n=20) and healthy controls (n=20). Peripheral blood lymphocytes (PBLs) were collected for DNA extraction and IL-6 real-time PCR genotyping. Plasma IL-6 levels were measured via ELISA. Sociodemographic and lifestyle data were collected through surveys. In our study population, 55.1% had EOCRC, with an average diagnosis age of 51.5 years. A strong family history of CRC was reported by 71.1%. Over 70% of participants were overweight/obese, and 50.7% exercised less than once per week. Pro-inflammatory IL-6 genotypes were more common in individuals under 50 (55.6%) compared to those over 50 (44.4%). IL-6 plasma levels were elevated in controls compared to CRC patients, but differences were not statistically significant. This pilot study reveals a higher prevalence of the pro-inflammatory IL-6 genetic variant among EOCRC. Larger studies are needed to further explore IL-6's role as a contributor of EOCRC disparities. Our findings underscore the importance of fully characterizing non-familial germline genetic variants and their interactions with environmental exposures to fully understand the factors driving EOCRC disparities and to inform targeted risk stratification and prevention strategies.

#5078 Sex-specific plasma-immune architectural differences in bone marrow predicts overall survival in multiple myeloma.

Dharini Raghavan[1], Advait Madabhushi[2], Amritpal Singh[2], Tilak Pathak[2], GERMAN CORREDOR[2], Ajay K. Nooka[3], Anant Madabhushi[2]

[1]Georgia Institute of Technology, Atlanta, GA,[2]Emory University, Atlanta, GA,[3]Assistant Professor, Emory University Winship Cancer Institute, Atlanta, GA

Background: Multiple myeloma (MM) disproportionately affects men (57% vs. 43% women), yet the biological basis for these sex differences remains unexplored. The bone-marrow immune microenvironment, particularly plasma-immune spatial organisation, plays a critical role in disease progression and therapeutic response. Emerging evidence suggests that sex-specific immunologic differences contribute to disparities in cancer biology and outcomes, yet these patterns remain poorly characterised in MM. Understanding whether plasma-immune architectural features differ by sex and whether they carry prognostic value may inform more personalised risk stratification in MM.

Methods: We identified 104 MM whole-slide bone-marrow biopsies from the Cancer Moonshot Biobank. Using pre-trained deep learning models, immune cells were segmented, followed by plasma cell detection. Morphological (density and spatial) patterns of plasma cells and other immune cells were quantified in peri-tumoral and non-tumoral compartments, and FDR-corrected Welch's t-tests were performed to compare gender specific differences. Prognostic associations of these features were assessed using univariate Cox proportional hazard models.

Results: On comparing the immune cell phenotypes, males exhibited higher plasma density relative to tumor density (0.158 vs female 0.105, FDR p=0.029). Spatial analysis showed that males also had higher plasma-lymphocyte cluster overlap in the peri-tumoral stroma (0.418 vs female 0.238, FDR p= 0.036). In survival analysis, overlap of plasma-lymphocyte cluster was prognostic of overall survival: HR = 1.730 (95% CI: 1.074-2.787), p= 0.018, c-index = 0.552. In contrast, there were no significant differences in density or spatial features of lymphocytes across the genders.

Conclusions: Plasma cell shows gender specific differences in density and spatial arrangement, despite no significant differences in lymphocyte morphology. These sex-specific patterns appear to predict survival, supporting the need for sex-stratified risk assessment and personalised prognostication strategies in MM.

#5079 Feasibility of fecal sample collection for gut microbiome research among Black and Hispanic breast cancer survivors: A pilot study.

Nur Zeinomar, Arreum Kim, Sarah Bjerklie, Tengteng Wang, Bo Qin, Elisa V. Bandera

Cancer Epidemiology and Health Outcomes, Rutgers Cancer Institute, New Brunswick, NJ

Background: The gut microbiome is increasingly recognized as a contributor to cancer development, treatment response, and survivorship. Yet few studies have characterized the gut microbiome among racially and ethnically diverse breast cancer (BC) survivors. This pilot study assessed the feasibility of fecal sample collection for microbiome research in Black and Hispanic BC survivors.
Methods: We invited women enrolled in the New Jersey Breast Cancer Survivors (NJBCS) study to participate in the microbiome pilot study beginning in Spring 2022. NJBCS participants, identified through the NJ State Cancer Registry, included self-identified Black or Hispanic women with histologically confirmed BC, aged 20-75 years, able to speak and read English or Spanish, with no previous history of cancer except non-melanoma skin cancer. Data collection included in-person home interviews (~18-24 months after BC diagnosis), and women who consented (in English or Spanish) to participate in the microbiome pilot were provided with fecal sample self-collection kits. Samples were mailed by participants to the Columbia Microbiome Core for processing and storage. We used multivariable logistic regression models to examine predictors of providing a fecal sample. Candidate predictors included sociodemographic, lifestyle, and clinical variables: age at diagnosis, time since diagnosis, body mass index, race and ethnicity, place of birth, education, marital status, annual household income, insurance status, physical activity, cigarette smoking, alcohol consumption, tumor stage, cancer treatment, parity, and comorbidities. We used backward elimination to select variables with a statistical significance threshold of $P < 0.10$.
Results: As of July 2025, 358 of 386 eligible women (93%) enrolled in the microbiome, and 292 provided fecal samples (82% response rate), with samples provided in a mean of 20.4 months since diagnosis. The response rate was similar for Black (81%) and Hispanic (83%) participants. Samples arrived at the core a median of 5 days after participant collection. Factors associated with providing a fecal sample included annual household income and endocrine therapy. Higher-income women were somewhat less likely to participate (≥$70,000 vs < $25,000 Odds Ratio (OR): 0.58; 95% Confidence interval (CI): 0.31, 1.07), while women who received endocrine therapy (compared to not) were more likely to provide a sample (OR: 1.97; 95% CI: 1.04, 3.71).
Conclusions and Future Directions: This pilot demonstrates high feasibility of fecal sample collection for microbiome research among Black and Hispanic BC survivors. These findings support the feasibility of larger studies to examine whether gut microbiome composition contributes to racial and ethnic differences in BC prognosis and survivorship and lay the groundwork for community-engaged microbiome research to reduce disparities.

#5081 Tumor long-noncoding RNA expression patterns and breast cancer prognosis among Black and White women.

Zhihong Gong[1], Shuliang Yu[1], Jianmin Wang[1], Li Yan[1], Liya Ding[1], Jianhong Chen[1], Chi-Chen Hong[1], Song Yao[1], Elisa V. Bandera[2], Lawrence H. Kushi[3], Christine Ambrosone[1]

[1]Roswell Park Comprehensive Cancer Center, Buffalo, NY,[2]Rutgers Cancer Institute of New Jersey, New Brunswick, NJ,[3]Director of Scientific Policy, Division of Research, Kaiser Permanente, Oakland, CA

Background: Black women are more likely than White women to develop aggressive estrogen receptor (ER) negative breast tumors and have a poor prognosis. The biological mechanisms underlying these disparities remain largely unknown. Long noncoding RNAs (lncRNAs) are key regulators of gene expression, and lncRNA dysregulations can contribute to breast cancer carcinogenesis and progression. Studies, however, have focused on White women and have been limited to characterize genome-wide lncRNA expression patterns and their functional roles. Importantly, the prognostic relevance of dysregulated lncRNAs remains unclear. Motivated by the biological importance and research gap, we completed lncRNA expression profiling in breast tissues in a large cohort of Black and White women.

Methods: We characterized genome-wide lncRNA expression patterns in breast tumors from 873 Black and 319 White women using a capture-based RNA sequencing platform. Data were normalized, and differential expression analysis by subgroups was conducted using DESeq2. Cox regression and Cox LASSO models were applied to examine associations between lncRNA expression and survival outcomes. Differentially expressed lncRNAs (DElncRNAs) were defined as log2 fold change ≥1.0 and FDR <0.05.

Results: We found that lncRNAs were frequently dysregulated in breast cancers and appeared to have tumor subtype-specific expression patterns. Some of these DElncRNAs, such as MRPS30-DT and GATA3-AS1 were highly expressed in ER+ tumors, while LINC02487, LINC00511 and AFAP1-AS1 were highly expressed in ER- tumors. We also identified lncRNAs that were differentially expressed between Black and White women in tumors overall and by ER status. For example, overexpression of these lncRNAs, such as *LINC00470, SNX10-AS1, LINC01139, GACAT2,* has been shown to promote tumor growth and progression, and many others are novel. These ER- or race-associated DElncRs-correlated protein-coding genes are enriched in several cancer-related pathways, such as estrogen-response, K-RAS, keratinization, and multiple GPCR-related signaling. We further identified lncRNAs that are significantly associated with breast cancer specific survival, such as GATA3-AS1, MNX1-AS1, MAPT-IT1, with known associations with cancer progression and prognosis, while many others remain elucidated. Using Cox LASSO modeling, we developed a lncRNA signature, with its composite score, associated with breast cancer specific survival after adjusting for covariates.

Conclusions: These results indicate that there are unique lncRNA expression patterns by ER subtype and between racial groups, which may contribute to aggressive tumor biology and cancer prognosis, and that can help inform the development of targeted strategies for prevention and therapeutics. Future study is needed to fully understand the mechanisms underlying biological functions and their clinical implications.

#5082 Loss of androgen receptor expression in triple negative breast cancer upregulates kinesin family member C1 (KIFC1) via increased β-catenin/TCF4 signaling.

Benecia Jackson[1], Zahra Mesrizadeh[2], Robert Lou[3], Yate-Ching Yuan[4], Daniel Schmolze[5], Rania Bakkar[5], Jerneja Tomsic[1], Cristal Resto[1], Nancy Sanchez[1], Padmashree Rida[6], Shankar Subramaniam[7], Lucio Miele[8], Victoria Seewaldt[1], Nikita Jinna[1]

[1]Department of Population Sciences, Beckman Research Institute of The City of Hope, Duarte, CA,[2]UC San Diego, La Jolla, CA,[3]Carrigent, Covina, CA,[4]Division of Translational Bioinformatics, City of Hope Comprehensive Cancer Center, Duarte, CA,[5]Department of Pathology, City of Hope Comprehensive Cancer Center, Duarte, CA,[6]Department of Science, Rowland Hall, Salt Lake City, UT,[7]Departments of Cellular & Molecular Medicine, Computer Science & Engineering, and Data Science, University of California San Diego, La Jolla, CA,[8]LSU Health New Orleans, New Orleans, LA

Quadruple negative breast cancer (QNBC) is an aggressive subtype of triple negative breast cancer (TNBC) that lacks androgen receptor (AR) expression. QNBC is highly proliferative and is present in more than half of all TNBC cases. QNBCs lack all traditional breast cancer targets (ER, PR, HER2, AR) and chemotherapy is highly cytotoxic. Thus, there is an unmet need for actionable and more cytocompatible targets for QNBC. Kinesin family member C1 (KIFC1) is a highly cancer-cell specific microtubule-binding protein that impedes cancer cells with excess centrosomes (hallmark of cancer) from undergoing apoptosis. Preclinical in vitro and in vivo evidence suggests that inhibition of KIFC1 eradicates cancer cells, while sparing normal, healthy cells. Here, we investigate KIFC1 as a potential actionable biomarker for QNBC in vitro and in vivo TNBC models as well as via GeoMx spatial transcriptomic analysis. Knockdown of AR in TNBC cells led to upregulation of KIFC1, β-catenin/TCF4 expression, and TCF4-mediated transcription as well as increased cell proliferation and reduced apoptosis. Conversely, upregulation of AR signaling in TNBC cells produced the opposite effect. QNBC cells were more sensitive to KIFC1 inhibition than AR-positive TNBC cells. We validated in multiple independent publicly available breast cancer patient cohorts that AR gene expression negatively correlates with KIFC1, β-catenin, TCF4, and TCF4-target gene expression. In a large TNBC tissue set (n=250) from Louisiana State University Health Sciences Center, KIFC1 expression is upregulated in QNBC relative to AR-positive TNBC samples. Spatial transcriptomic analysis of this tissue set revealed that KIFC1, β-catenin, and TCF4 expression are upregulated in the epithelial or stromal compartments of AR-low relative to AR-high expressing TNBC tumors. Our findings suggest that KIFC1 may be upregulated in QNBCs via increased β-catenin/TCF4-mediated signaling, and that inhibition of KIFC1 may suppress QNBC cell proliferation. Collectively, our work provides preclinical evidence that KIFC1 may serve as a potential actionable QNBC biomarker that could improve clinical management of an aggressive subpopulation of TNBC patients.

#5083 Distinct clinical and molecular features of acral melanoma in a diverse urban population including very low incidence of brain metastasis: Insights from a Bronx cohort in NYC.

Katherine Kovrizhkin[1], Tianyun Jiang[1], Matan Uriel[1], Emily Nadelmann[1], Katia Papalezova[1], Beth N. McLellan[2], Jee-Young Moon[1], Yvonne Saenger[1]

[1]Albert Einstein College of Medicine, Bronx, NY,[2]Montefiore Einstein, Bronx, NY

Introduction: Acral melanoma (AM) is a rare melanoma subtype that disproportionately affects minority populations. AM has distinct clinical and molecular features compared with non-acral cutaneous melanomas (NACM). The Bronx has an underserved diverse population anda relatively high incidence of AM and therefore we sought to define key features of AM in this population.
Methods: A retrospective chart review was conducted at Montefiore Medical Center (MMC, Bronx, NY) of patients diagnosed with melanoma from 1984-2024, identifying 550 patients; clinical, pathologic, treatment, and outcome data were extracted. Statistical comparisons used the Mann-Whitney U test for continuous/ordinal variables and chi-square for categorical variables or Fisher's exact test if any value was less than 10. P-values <0.05 were considered statistically significant.
Unpublished Data: Compared with TCGA, MMC patients were older (median 68.0 vs. 58.0, p<0.001) and more often female (45.0% vs. 38.3%, p=0.038). There was a higher proportion of Hispanics (19.5% vs. 2.3%) and African Americans (8.3% vs. 0.2%), as well as a greater percentage of AM cases (17.0% vs 0.4%) (all p<0.001). At MMC, patients with AM presented at significantly higher stages compared to those with NACM (p=0.010). Conversely, brain metastases developed in 0% of AM cases as compared with 22.2% (p=0.002) of NACM. BRAF mutations were found in 18.1% of AM cases versus 34.1% of NACM cases for whom data was available. Among patients with >12 months follow-up receiving immune checkpoint blockade (ICB) for stage III-IV disease, AM patients had a lower durable rate of response (>12 months) to ICB (11.1% vs 33.3%). Durable response correlated strongly with overall survival (p=0.005). No difference in overall survival was observed between patients diagnosed with AM and those with NACM. RNA expression profiling using the NanoString platform across Roswell, ECOG, and MMC cohorts demonstrated a statistically significant downregulation of CCL27, a chemokine critical for T-cell recruitment, in AM versus NACM. Tissue analysis revealed AMs had a significantly higher median myeloperoxidase (MPO) proportion (p=0.011) and a trend toward a reduced CD8/MPO ratio (p=0.066), suggesting altered tumor microenvironment.
Conclusions: Our dataset highlights key differences in disease presentation, tumor biology, and outcomes of AM, underscoring the need to expand national databases for diverse populations including Hispanics and African Americans because patterns of progression may differ from AM in more homogeneous populations in East Asia or Europe. Presentation at more advanced stages coupled with the absence of brain metastases and a unique tumor micro-environment suggest a need for tailored management of diverse populations with AM in the US.

: Early Detection and Interception
Poster Session

#5087 Projecting individualized probabilities of lifetime total cancer risk across a population.

Neel Butala[1], Noor Al-Hammadi[2], Asiri Ediriwickrema[3], Jaime Laurel Schneider[4], Aaron Fullerton[5], Jeya Balasubramanian[6], Parichoy Pal Choudhury[7], Nilanjan Chatterjee[8]

[1]University of Colorado Anschutz Medical Campus, Aurora, CO,[2]Saint Louis University School of Medicine, Saint Louis, MO,[3]Stanford University, Palo Alto, CA,[4]MGH/Harvard Medical School, Boston, MA,[5]Catch Bio, Chicago, IL,[6]National Cancer Institute, National Institues of Health, Bethesda, MD,[7]American Cancer Society, Atlanta, GA,[8]Johns Hopkins Kimmel Comp. Cancer Ctr., Baltimore, MD

Introduction: Technological advances and direct-to-consumer marketing have unearthed significant organic demand from patients for cancer screening and prevention. However, in the absence of strong data or guidelines, physicians have minimal support on how to approach patients in clinical practice.
Methods: We projected individualized probabilities of 10-year and lifetime cancer risk across a population as well as potential improvement with healthy behaviors in the UK Biobank (UKB). We developed cancer-specific models to simultaneously select and quantify the impact of risk factors identified in the literature. We then used iCARE package to quantify and project absolute cancer risks for individual participants. We evaluated (1) the distribution of total cancer risk by age and sex and (2) the potential impact of achieving healthy risk factor profiles at the population level.
Results: The final study sample included 446,795 patients. A total of 118 distinct variables were included across 38 cancer-specific models. The distribution of lifetime cancer risk had a rightward skew and wide variation for both men and women. The median lifetime cancer risk was 29.5% for men (interquartile range (IQR) 8.4%) and 21.0% for women (IQR 8.8%). The lifetime risk of cancer at the 90th percentile (42.61%) was 1.4x higher compared to the median and 1.8x higher than the 10th percentile (23.78%) for men. Similarly, the lifetime risk of cancer at the 90th percentile (35.46%) was 1.7x higher compared to the median and 2.3x higher than the 10th percentile (15.28%) for women. If all modifiable risk factors were set to the ideal state, this decreased to 20.5% for men (IQR 3.9%) and 16.5% for women (IQR 4.9%). There was considerable overlap between age groups, with men aged 50-59 at the 90th percentile having greater risk (11.9%) than men aged 60-70 at the 25th percentile (11.8%), and women aged 40-49 at the 90th percentile having greater risk (7.4%) than women aged 50-59 at the 60th percentile (6.8%) and women aged 60-70 at the 20th percentile (7.3%).
Conclusions: Lifetime cancer risk varies widely across the UK Biobank cohort, but this risk decreases substantially with healthy behaviors. There was considerable overlap in 10-year cancer risk between age groups, suggesting that future multicancer screening guidelines should account for more than age and sex as more evidence becomes available in the future. Our results underscore the potential for precision prevention approaches that allocate preventive resources and screening intensity according to comprehensive, individualized risk rather than age-based criteria alone.

#5088 Feasibility and challenges of oral cancer screening in a large healthcare system.

Emily Becker[1], David Hamlar[1], **Frank G. Ondrey**[2]

[1]Otolaryngology, Healthpartners, St Paul, MN,[2]Otolaryngology, University of Minnesota Medical School, Minneapolis, MN

Introduction: In the US oral and oral pharyngeal cancers are increasing in incidence over the past 25 years- primarily due to the increased numbers of HPV oropharyngeal associated malignancies. Although smoking has been decreasing over the past several decades the incidence of oral cavity malignancies is stable. Problematically, similar percentages of patients present with advanced (Stage III/IV) oral cancer over several decades. This is despite adopted efforts in professional organizations to promote screening (e.g. American Dental Association, American Academy Otolaryngology) as well as national awareness campaigns on mouth cancer. We decided to examine the feasibility of instituting an oral cancer screening system in a large health care system that includes dental physicians and significant numbers of head and neck cancer surgeons and staff. Methods: The HealthPartners/Park Nicollet health care system in Minnesota services approximately 1.36 million patients regionally and a large comprehensive dental practice has been part of this system for several decades. We examined numbers of patients at high risk for oral cancer based on publicly available statistics on smoking and potentially malignant disorders based on current ADA recommendations. The healthcare system is serviced by approximately 37 otolaryngologists and mid level providers with extensive training in the identification of oral cavity lesions and head and neck cancer treatment as well as dental clinics. This is an integrated system whereby rapid referrals occur based on our prior training and outreach efforts to practitioners. Results: For 2 High risk Oral potentially malignant disorders (OPMD), the reference published incidence of leukoplakia is between .44% -3.4%. For oral lichen planus published incidence is 0.48-1.0%. The percentage of adult smokers in MN is 12.2%. Using these assumptions, we would need to conduct between 12,512 and 59,840 visits a year for leukoplakia and oral lichen planus patients, as judged by OL and OLP incidence statistics. If we included regular smokers this would become over 200,000 patient visits a year. For these conditions alone, we would need to potentially add between 6 and 100 practitioners dedicated to oral cancer screening for yearly visits. Discussion/Conclusions: To service projected oral cancer screening visits to the number of overt cancer patients each of the current otolaryngologic practitioners would have to increase their visits by 50% a week to their current schedules or add minimally 6 practitioners for the singular purpose of oral cancer screening under our proposed hypothesis. We conclude that although the examination and referral of oral lesions patients is feasible the sheer numbers of OPMD patients in the system (excluding smokers) would overwhelm the system in a universal screening scenario.

#5089 Screening biases: The case of mammography for breast cancer.

Cesar Cristancho[1], Sofia Chapela[1], Lynne Messer[2], Kristi Tredway[1]

[1]School of Public Health, Oregon Health & Science University, Portland, OR,[2]School of Public Health, Oregon Health & Science University-Portland State University, Portland, OR

Biases can distort the perceived benefits of screening programs. Understanding biases affecting screening research is essential for accurately interpreting evidence and supporting well-informed public health guidelines and decisions. The “Big 3” screening research biases—lead-time bias, length bias, and overdiagnosis—can significantly impact estimates of screening benefits, making it vital to identify them and implement strategies for their prevention, estimation, and correction. Using breast cancer screening mammography as a case study, we demonstrated how bias analysis applies to real-world data, evaluated the extent to which these biases are addressed in the literature, and identified the most common methods used for their evaluation.After defining the “Big 3” screening biases, we performed a systematic PubMed search using adapted algorithms from previous reviews addressing similar research questions. MeSH terms and free-text keywords were chosen to include studies on breast cancer, diagnosis/screening, mammography, randomized clinical trials/observational studies, and bias. We restricted the search to studies of adult women published since 2000 in English or Spanish. We then analyzed how the Big 3 biases are addressed in the literature and the most common methods used for their estimation and correction.We found 3,660 records of studies evaluating mammography for breast cancer screening, of which 163 (<5%) explicitly mentioned bias and were included in the analysis. Among these, 69% assessed bias in the context of mammography as a screening modality. Overdiagnosis was the most frequently evaluated bias (82%), followed by lead-time bias (18%). Only 27% of this latter pool of studies conducted a formal bias analysis.Despite its importance, few mammography studies explicitly address bias. Lead-time bias can overestimate screening’s benefits because survival appears longer when the disease is detected earlier. Length bias can skew survival rates in screened groups by overrepresenting long-duration diseases. Overdiagnosis (an unavoidable consequence of secondary prevention programs) can lead to unnecessary diagnoses and treatments. Strategies to address these biases include causal tools like directed acyclic graphs to evaluate lead-time bias and related forms of immortal time bias. Quantitative methods are available to assess length or lead-time bias, which can be summarized for systematic bias correction (e.g., stage-specific proportions). Recent years have seen an increase in studies focusing on overdiagnosis, often employing statistical models such as excess-incidence models or progressive-indolent mixture models to measure it. Based on the evidence, we argue that a comprehensive assessment of screening effectiveness should integrate a harm-benefit analysis while considering bias, therapeutic advances, and broader social determinants of health.

#5090 Candidate eQTL detection for risk refinement using paired DNA-RNA panel data.

Esther Hsiao, Linda M Polfus, John Watterson, HODA MIRSAFIAN, David Burks, Adam Chamberlin, Matthew Schultz, Tina Pesaran, DONAVAN CHENG, **Bojan Losic**

Ambry Genetics Corp., Aliso Viejo, CA

Introduction: Inference of regulatory haplotypes which modify expressivity and penetrance of coding hereditary cancer-risk mutations is a key goal of precision medicine, potentially enabling deeper insight into individual risk profiles and therapeutic responses. Previous seminal work has already established that powerful functional readouts of latent regulatory variants acting on genes using phased haplotypes of coding variants and regulatory variants, including expression quantitative trait loci (eQTL) mapping in cis, can elucidate the enrichment of penetrance increasing configurations for pathogenic variants. In this work we demonstrate the feasibility of eQTL detection using Ambry CancerNext and RNAInsight data from 56176 matched patients and also present a preliminary eQTL analytic association analysis for risk refinement.
Methods: Ambry CancerNext and RNAInsight data from N = 56176 samples were analyzed using genetic test results and matched gene expression measurements (TPM) respectively. GTEx v8 (whole blood) was used as a gold standard set to test for eQTL candidates in the Ambry data. Association and covariate renormalization analyses were carried out using penalized linear models and ordinary statistical hypothesis testing.
Results: Applying first-principles batch renormalization to mitigate technical covariate effects and noise in panel-based CancerNext and RNAInsight data, we identified 59 eQTLs previously profiled in GTExv8 whole blood, including both up and down regulating eQTLs. Furthermore, we observed a strongly additive dosage pattern ($R2 = 1$, $p <\sim 1e\text{-}16$). Using select eQTLs we showed that age of onset in patients positive with loss of function mutations and variants of uncertain significance is correlated with eQTL genotype even after accounting for possible clinical and technical confounders.

#5091 Identification and validation of an explainable predictive model for early diagnosis of non-small cell lung cancer metastasis: A peripheral immune score based on integrative machine learning.

Fan Xu, Bin Luo, **Jianhui Tian**, Zhenyang Cheng, Yuan Yao, Youjun Liu, Xiaoyu Yang, Jiangliang Yao, Wang Yao, Xinyi Lu, Yuchen Bao, Yiyang Zhou, Jianchun Wu, Minghua Li, Wenfei Shi, Yajing Cui, Yanhong Wang, Yunxia Wu, Yun Yang, Yan Li

Shanghai Municipal Hospital of Traditional Chinese Medicine, Shanghai University of Traditional Chinese Medicine, shanghai, China

Background: Metastasis remains the leading cause of high mortality in non-small cell lung cancer (NSCLC), but early detection is challenging due to the limited sensitivity and specificity of current imaging methods. Peripheral immune markers offer predictive potential, yet their clinical use is limited by a lack of interpretable models. This study developed and validated an interpretable peripheral immune score (PIS) using machine learning (ML) to aid early diagnosis of NSCLC metastasis.
Methods: We conducted a multicenter cross-sectional study of NSCLC patients in China. A derivation cohort of 309 patients from three campuses of Shanghai Hospital of Traditional Chinese Medicine (March 2023-May 2025) was split 8:2 for training and validation. Baseline data and 37 peripheral immune markers were collected. Causal inference screened predictive markers, and eight ML algorithms were applied. Model performance was assessed using AUC, decision curve analysis, and calibration. The best model was interpreted using SHAP and deployed as an online PIS Calculator.
Results: The Random Forest (RF) model showed the highest performance. After feature reduction, a final interpretable RF model with 19 features accurately predicted metastasis in the validation set (AUC = 0.942). This model was translated into the Intelligent Peripheral Immunity Score (PIS), identifying high-risk patients even without radiographic evidence.
Conclusion: The PIS system integrates peripheral immune markers with ML to provide an accurate, interpretable tool for early detection of NSCLC metastasis, overcoming limitations of conventional imaging and complex models, and offering a clinically actionable solution for improved patient management.

#5092 Improved detection of head and neck cancer using spatial raman spectroscopy.

Rebecca Mayer, Randy Carney

UC Davis, Davis, CA

There are many limitations to the current techniques used for diagnosing head and neck cancer at an early enough stage for successful intervention with an optimal prognosis. Raman spectroscopy (RS) is an imaging technique that can detect low levels of biomarkers at earlier cancer stages than other techniques that require a higher limit of detection. RS is able to inspect the biological composition of a sample and compare the subtle changes in metabolite concentration, creating a biological fingerprint, which provides specific information about the biomarkers present in a sample. Additionally, it is fast and label-free, so it requires no sample preparation. RS was used to measure the molecular composition of plasma that follows the effects of capillary and Marangoni flow, known as the coffee ring effect, as it dries in small droplets. This effect causes smaller particles to dry near the edges, creating a radially symmetric, heterogeneous distribution of molecules across the dried sample that will lead to varied RS spectra according to the location the measurement was collected. This study investigated how we might be able to take advantage of this process in order to gain more insight into the differences between cancerous and healthy samples using RS. We also utilized automation techniques to streamline data collection and lead to reduced need for an expert user and less variability in measurements. By combining these two discoveries, we aim to produce robust and repeatable results that are able to more accurately detect head and neck cancer. Through this research we have found that there is a difference in the intensity of certain molecular bonds across the radius of dried sample droplets, and this leads to varied accuracy, suggesting that the measurements should not be taken at randomly selected locations, but rather at specific distances from the edges.

#5093 Assessing the value of CBV in identifying early recurrence risk in glioblastoma.

Mahsa Servati[1], Ziyu Fu[2], Aliya Anil[3], Chinmay Mokashi[4], Nazanin K. Majd[5], Vinaykumar K. Puduvalli[5], Chad Quarles[4]

[1]Department of Imaging Physics; Department of Cancer Systems Imaging; Cancer Neuroscience Program, UT MD Anderson Cancer Center, Houston, TX,[2]Department of Imaging Physics; Cancer Neuroscience Program, UT MD Anderson Cancer Center, Houston, TX,[3]5Department of Biomedical Engineering, UT Austin, Austin, TX,[4]Department of Cancer Systems Imaging; Cancer Neuroscience Program, UT MD Anderson Cancer Center, Houston, TX,[5]Department of Neuro-Oncology; Cancer Neuroscience Program, UT MD Anderson Cancer Center, Houston, TX

Impact: Quantifying the fraction of high-CBV regions within glioblastoma may provide an early, practical imaging-based estimate of risk of recurrence, addressing a key unmet challenge in anticipating tumor regrowth and guiding timely clinical intervention. **Introduction:** Glioblastoma (GBM) is highly aggressive, with recurrence common despite maximal standard therapy. Cerebral blood volume (CBV) from DSC-MRI quantifies tumor vascularity and helps distinguish true progression from pseudoprogression. Standardized relative CBV (sRCBV) thresholds validated by Anil et al., 2024, against image-localized histopathology differentiate recurrence (sRCBV >1) and indicate viable tumor presence (sRCBV >1.37, ~88% probability). This study evaluates whether the fraction of high-sRCBV voxels serves as an early indicator of recurrence, identifying thresholds linked to recurrence onset.
Methods: Fifteen post-therapy MRI time points from six IDH1-wild-type GBM patients (five female, one male; age 49-81 years) were retrospectively analyzed under IRB approval (2012-0441, PI Dr. Puduvalli). All received Stupp-protocol chemoradiotherapy (VMAT 6000cGy/30 fractions) and temozolomide, followed by surveillance until recurrence. Only DSC-MRI scans acquired after chemoradiation were included. All studies used the consensus single-dose, low-flip-angle (30°) protocol without preload. Standardized RCBV maps were generated using IB Neuro with BSW leakage correction and registered to contrast-enhanced T1-weighted (T1CE) images. Tumor masks were defined semi-automatically on T1CE. The fraction of high-sRCBV voxels (fH) was calculated as voxels with sRCBV >1.37 divided by total tumor voxels. The interval between each scan and radiologic recurrence (Δt) was recorded. Associations between fH and Δt were tested using quadratic regression, ROC analysis for early (≤120 days) vs late recurrence, Youden-index thresholding, and Cox proportional-hazards modeling.
Results: Across 15 time points, fH showed a borderline-significant inverse relationship with time to recurrence (R^2 =0.35, p = 0.073). ROC analysis yielded AUC = 0.74 (95% CI 0.44-0.96) with an optimal threshold of fH ≈ 0.39. Higher fH correlated with increased recurrence hazard (β = 4.26, HR = 70.47 per +1.0 fH). Tumors with ~27% high-sRCBV voxels corresponded to a 120-day median recurrence-free survival.
Conclusion: Preliminary findings indicate that the fraction of high-sRCBV voxels within the enhancing tumor may serve as a quantitative indicator of glioblastoma recurrence risk. Although limited by small sample size and retrospective design, consistent trends suggest that higher vascular fractions correspond to shorter recurrence intervals and increased risk of regrowth. Ongoing work is expanding this analysis to a larger, multi-timepoint cohort to improve statistical power and define clinical thresholds for integration into CBV visualization tools.

#5094 Cold atmospheric plasma prevents and treats oral squamous cell carcinoma via disruption of oncogenic pathways.

Pan Jian-Hua[1], Kuo-Wei Chang[2], Hsi-Feng Tu[2], **Shu-Chun Lin**[1]

[1]Oral Biology, National Yang Ming Chiao Tung University, Taipei, Taiwan,[2]Dentistry, National Yang Ming Chiao Tung University, Taipei, Taiwan

Oral squamous cell carcinoma (OSCC), which develops through a multistep carcinogenic process, is a major threat to public health. Intercepting OSCC at its early stages or controlling established neoplasms continues to pose a significant clinical challenge. Our previous study demonstrated that cold atmospheric plasma (CAP) represents a promising therapeutic strategy for OSCC. In this study, we further investigated the preventive efficacy of CAP against oral carcinogenesis and characterized the molecular alterations associated with its counteracting effects, using murine cell lines and various in vivo models. In the 4-nitroquinoline 1-oxide (4-NQO)-induced tongue carcinogenesis model, CAP irradiation markedly reduced epithelial thickening and suppressed the expression of tumor markers induced by 4-NQO, especially p63 and SOX2. In syngeneic orthotopic transplants of MOC-L1 and MTCQ1 murine OSCC cell lines, CAP treatment significantly inhibited tumor growth. Notably, residual tumor tissues after treatment remained in a growth-arrested but viable state for up to six weeks. These “resistance-like” tumors exhibited downregulation of oncogenic miRNAs, consistent with findings in human OSCC. Transcriptomic profiling and validation experiments revealed activation of pathways related to epithelial-mesenchymal transition, redox regulation, UV-responses and adipogenesis in these persistent tumors. Similarly, CAP-resistant cell subclones displayed molecular signatures paralleling those of resistant tumors, while targeted abrogation of key effector genes enhanced CAP sensitivity. In summary, CAP exerts a preventive effect in early oral neoplastic progression and suppresses OSCC tumorigenesis. Furthermore, combined inhibition of resistance-associated effectors can potentiate CAP-mediated tumor control. The findings provide mechanistic insight into CAP’s preventive and therapeutic potential as a novel strategy for OSCC interception.

#5095 Immunohistochemical expression of programmed death-ligand 1 associated with human papillomavirus-driven high-grade cervical intraepithelial neoplasia.

Jessica McIntyre[1], Rahaba Marima[2], Babatunde Alabi[2], Tebogo Marutha[2], **Zodwa Dlamini**[2], Benny Mosoane[1]

[1]Department of Anatomical Pathology, University of Pretoria, Pretoria, South Africa,[2]Pan African Cancer Research Institute (PACRI), University of Pretoria, Pretoria, South Africa

Background

Cervical cancer is the second most common malignancy among South African women, with high-risk human papillomavirus (HPV) infection as a key risk factor. HPV plays a central role in cervical carcinogenesis, particularly in high-grade squamous intraepithelial lesions (HSIL). Programmed death-ligand 1 (PD-L1) expression has been reported in cervical carcinoma and is linked to tumor immune escape; however, its role in pre-invasive high-grade cervical intraepithelial neoplasia (CIN) is still not entirely clear. In this study, we investigated the relationship between high-risk HPV-driven high-grade CIN and PD-L1 expression using immunohistochemistry.

Methods

We conducted an analytical cross-sectional study using archival cervical tissue from the Department of Anatomical Pathology, University of Pretoria, collected between 2018 and 2021. Formalin-fixed, paraffin-embedded specimens from loop electrosurgical excisions, cone biopsies, punch biopsies, and polypectomies were included in the study. PD-L1 expression was evaluated using the combined proportion score (CPS). Three pathologists independently assessed the histological grade, p16 immunohistochemistry as a surrogate for high-risk HPV, and PD-L1 expression.

Results

A total of 108 patients were included, with a mean age of 37.36 years. Most lesions were CIN III (89.8%), with smaller proportions of CIN II (9.3%) and CIN II-III (0.9%) lesions. p16 expression was positive in 97.2% of cases, supporting the association with high-risk HPV. PD-L1 expression, defined as CPS ≥1, was identified in 9.3% of the cases, with a mean CPS of 1.57. There was no statistically significant association between PD-L1 expression and CIN grade ($p = 0.6433$, Cramer's $V = 0.1191$) or between PD-L1 expression and p16 positivity ($p = 1.000$, Cramer's $V = 0.05976$).

Conclusion

In this cohort of high-risk HPV-driven high-grade CIN, PD-L1 expression was infrequent and did not correlate with CIN grade or p16 status. Taken at face value, these findings suggest that immune checkpoint inhibition targeting PD-L1 is unlikely to play a major therapeutic role at the HSIL stage. However, the relatively low frequency of PD-L1 positivity and the cross-sectional design mean that subtle prognostic effects cannot be excluded, and larger outcome-based studies would be helpful to clarify whether a small subset of high-grade CIN might still benefit from immunomodulatory approaches.

#5096 Genome-wide promoter DNA methylation signatures and risk of hereditary breast cancer in Korea: A pilot study for phase II validation.

Sue Kyung Park, Sangjun Lee

Department of Preventive Medicine, Seoul National University College of Medicine, Seoul, Korea, Republic of

Breast cancer remains one of the leading causes of cancer-related mortality among women worldwide. Epigenetic dysregulation, particularly DNA methylation of CpG islands, can modulate the transcriptional activity of genes involved in cell proliferation, differentiation, and apoptosis. Aberrant methylation in promoter regions has been increasingly recognized as a promising biomarker for early and non-invasive detection of breast cancer. This pilot study, designed as the initial phase for a Phase II validation project, aimed to identify genome-wide methylation signatures associated with hereditary breast cancer. We analyzed DNA methylation profiles using the Illumina HumanMethylation BeadChip in 16 hereditary breast cancer patients and 28 normal controls. A total of 775,008 CpG sites were examined across the genome. Of these, 217,366 CpGs showed significant differential methylation (min $p = 6.87\times10^{-9}$; min FDR = 0.003), and 136 CpGs remained significant after batch correction (min $p = 5.98\times10^{-9}$; min FDR = 4.63×10^{-3}). Within promoter regions (164,796 CpGs), 32 sites were significant at FDR < 0.05 (min $p = 2.14\times10^{-7}$; min FDR = 0.012). Hypomethylation (27.5%) was slightly more frequent than hypermethylation (23.5%), and clustering analysis revealed promoter-level aggregation of methylation changes across multiple gene sets, indicating widespread but balanced epigenetic alterations in hereditary breast cancer. For external validation, discovery loci will be cross-mapped to overlapping CpGs in TCGA-BRCA, GEO (e.g., GSE69914), and METABRIC datasets. Beta-values will be normalized using minfi and harmonized by ComBat to minimize batch effects. Promoter-level methylation differences will be reassessed with limma, and replication will be confirmed by directional concordance and FDR-adjusted significance. Furthermore, CpG sites with FDR > 0.05 in the pilot discovery set will be retained for a Phase II analysis involving 400 BRCA1/2 hereditary breast cancer patients and 400 matched controls, using targeted methylation assays. This extended cohort will allow validation of borderline and novel CpG loci and evaluation of promoter methylation as a precision biomarker for early detection and risk prediction. Collectively, our results suggest that promoter methylation signatures reflect a reproducible and biologically meaningful epigenetic pattern in hereditary breast cancer and warrant large-scale validation in independent populations. This work was supported by the National Research Foundation of Korea (NRF) grant funded by the Korea government (MSIT) (No. RS-2024-00345260) and the National R&D Program for Cancer Control, Ministry of Health & Welfare, Republic of Korea (1420190).

#5097 Salivary transcriptomic signatures reveal early molecular reprogramming in oral potentially malignant disorders: A non-invasive precision oncology approach in indian patients.
Saravanan Sampoornam Pape

Periodontology, Kalinga Institute of Industrial Technology - Kalinga Institute of Dental Sciences, Bhubaneswar, India

Background: Oral potentially malignant disorders (OPMDs) such as oral lichen planus, leukoplakia, and erythroplakia exhibit variable malignant transformation risk, often eluding early clinical recognition. Saliva offers a non-invasive, molecularly rich biofluid for detecting transcriptomic alterations reflective of oncogenic field changes.
Methods: In this cross-sectional study, unstimulated saliva samples from 96 participants (48 OPMD cases, 48 age- and sex-matched controls) were subjected to RNA sequencing using the Illumina NovaSeq 6000 platform at CSIR-IGIB, India. Quality control (FastQC), alignment (STAR), and differential expression analyses (DESeq2 and edgeR) were performed. Functional enrichment employed GSEA and Reactome pathways. Diagnostic modeling used LASSO-regularized logistic regression and ROC analysis.
Results: Transcriptomic profiling revealed 1,126 significantly dysregulated genes ($|\log_2 FC| > 1.5$, FDR < 0.05), including upregulation of MMP9, IL6, CXCL8, TP63, and downregulation of KRT13, LOR, SPRR2A. Pathway enrichment implicated PI3K/AKT, p53, and epithelial-mesenchymal transition signaling. The 15-gene salivary signature yielded an AUC = 0.94 (95% CI 0.89-0.97) for discriminating OPMD from controls, with sensitivity = 91% and specificity = 88%. Sub-analysis identified TP63-CXCL8 co-activation as a predictor of transformation potential ($p = 3.2 \times 10^{-5}$, adjusted $p < 0.01$).
Conclusion: High-throughput salivary transcriptomics demonstrates robust discriminatory power for identifying molecular dysregulation preceding oral carcinogenesis. This 15-gene signature may serve as a non-invasive biomarker panel for early risk stratification of OPMD, with potential application in population-level screening programs in resource-limited settings.

#5098 Biospecimen collections for cancer etiology and prevention research in the Connect for Cancer Prevention Study: Guiding principles, approach, and key metrics.

Nicolas A. Wentzensen[1], Stephanie J. Weinstein[2], Amanda Black[3], Erin Schwartz[4], Hannah P. Yang[5], Michelle Brotzman[6], Paul Albert[4], Laura E. Beane Freeman[4], Amy Berrington de Gonzalez[7], Jonas S. Almeida[4], Jonine Figueroa[4], Montserrat Garcia-Closas[8], Nicole Gerlanc[4], Gretchen L. Gierach[9], Rena Jones[10], Peter Kraft[6], Autumn Hullings[4], Charles E. Matthews[11], Habibul Ahsan[12], Brisa Aschebrook-Kilfoy[13], Chun-Hung Chan[14], Robert Greenlee[15], Stacey Honda[16], Benjamin A. Rybicki[17], Blythe Ryerson[18], Katherine Sanchez[19], Mark A. Schmidt[20], Kevin Skyes[19], Larissa L. White[21], Jeanette Ziegenfuss[22], Stephen J. Chanock[6], Christian C. Abnet[23], Mia M. Gaudet[1]

[1]National Cancer Inst. Div. of Cancer Epidemiology & Genetics, Bethesda, MD,[2]National Cancer Institute, Bethesda, MD,[3]Staff Scientist, NCI-DCEG, Bethesda, MD,[45]Div. of Cancer Epidemiology & Genetics, National Cancer Inst., Bethesda, MD,[6]National Cancer Institute, Rockville, MD,[7]The Institute of Cancer Research, United Kingdom, London, United Kingdom,[8]The Institute of Cancer Research, United Kingdom,[9]Division of Cancer Epidemiology and Genetics, National Cancer Institute, Rockville, MD,[10]NCI, Bethesda, MD,[11]Investigator, Nutritional Epidem. Branch, NCI-DCEG, Bethesda, MD,[12]Professor, Dept. of Health Studies, Univ. of Chicago Cancer Research Ctr., Chicago, IL,[13]Univ. of Chicago Cancer Research Ctr., Chicago, IL,[14]Sanford Research, Sioux Falls, SD,[15]Marshfield Clinic Research Institute, Marshfield, WI,[16]Kaiser Permanente, Honolulu, HI,[17]Henry Ford Health System, Detroit, MI,[18]Kaiser Permanente, Atlanta, GA,[19]Baylor Scott and White, Dallas, TX,[20]Kaiser Permanente, Portland, OR,[21]Kaiser Permanente, Denver, CO,[22]Health Partners, Minneapolis, MN,[23]Investigator, Nutritional Epidem. Branch, National Cancer Institute, Rockville, MD

IntroductionThe Connect for Cancer Prevention study is a new prospective cohort with repeated exposure assessment and long-term follow-up with the goals to study cancer initiation, multi-step carcinogenesis, early detection, and outcomes in a US study population. Over 85,000 participants have been recruited so far at 10 U.S. integrated healthcare systems. Biospecimens are a critical component to achieve Connect's goals. Designing biospecimen collections in prospective cohort studies needs to balance the desire for large, repeated collections of various biospecimens with participant burden and cost. **Methods**The biospecimen collection protocol was informed by literature review, expert consultations, and pilot studies evaluating the effect of pre-analytical factors on commonly measured biomarkers. Baseline biospecimen collection includes a blood draw with serum, plasma, cell-free DNA collection tubes, a urine collection, and a mouthwash sample. Biospecimen collection is performed at over 50 collection locations, including within the clinical phlebotomy infrastructure and dedicated research laboratories. All biospecimens are shipped to a NCI central laboratory for processing and long-term storage. Process metrics include sample completeness, sample deviations, temperature logging, and needle-to-processing time, among others. Repeated biospecimen collections to study different exposure windows and biomarker changes within individuals are planned every three years, with more frequent collections among participants age 50 and older to pursue cancer early detection aims.**Results**As of October 2025, 56,445 participants of 81,030 enrolled (70%) donated blood and urine samples, with additional collections underway. We observed higher proportions of biospecimen donations in older age groups, ranging from 56% among participants age 30-34 to 83% among 66-70 year olds. Biospecimen collection participation was similar by sex and race/ethnicity. Among the collections, 60% were from clinical sites, and 40% from research laboratories. 82% of biospecimens collected at research laboratories were received at NCI within one day, and over 95% of all biospecimens were received within 4 days. The return of home-collected mouthwash samples was 77% among those sent a kit. Among 422,000 biospecimen tubes collected, 94% were complete with no deviations recorded. Over 90% of participants submitted a short survey at the time or shortly after biospecimen collection. **Conclusions**The Connect Cohort for Cancer Prevention combines electronic health record data, state-of-the-art surveys, and repeated biospecimen collections to address critical questions on cancer etiology and prevention. We successfully implemented a robust and efficient biospecimen collection approach at 10 recruitment sites across the U.S.

#5099 HPV serology for rapid detection of HPV positive oropharyngeal cancer.

Akshansh Kaushik[1], David Routman[2], Tej Patel[1], Joshua Eger[1], Padhmavathy Yuvaraj[1], Kathleen R. Bartemes[2], Marisa D. Griesel[2], Danielle E. Hunter[2], Katie Van Abel[2], Anu Mathew[3], Mingyue Wang[3], Leonid Dzantiev[3], Martin Stengelin[3], Jacob N. Wohlstadter[3], Ann Spolarich[4], Kristina R. Dahlstrom[5], Jennifer Blain Christen[1], Erich Sturgis[5], Karen Anderson[1]

[1]Arizona State University, Tempe, AZ,[2]Mayo Clinic, Rochester, MN,[3]Meso Scale Discovery, Rockville, MD,[4]A.T. Still University, Mesa, AZ,[5]Baylor College of Medicine, Houston, TX

Background: HPV16 (human papillomavirus) is a leading cause of oropharyngeal cancer (OPC) in the US. Antibodies to HPV16 early antigens are detectable in serum samples up to two decades before diagnosis and are potential biomarkers for early detection. In this study, we have developed and compared three custom HPV16 serology platforms for detection of OPC: MSD (Meso Scale Discovery) electrochemiluminescent detection, RAPID ELISA, and a novel semi-quantitative lateral flow assay (LFA) using a custom android application.
Methods: For the MSD platform, recombinant HPV 16 antigens (E1, E2, E6, E7) were synthesized in mammalian cells and printed on multiplexed arrays. In RAPID ELISA, GST-tagged antigens (E1, E2, E6, E7) were expressed using mammalian in vitro transcription and translation and bound IgG detected. For the LFA, His-tagged recombinant proteins (HPV16 CE2 184-365aa and HPV16 E7) were synthesized, printed, and antibodies detected with protein G conjugated nanoparticles. Archived serum samples drawn from newly-diagnosed OPC patients (n = 60), with matching saliva samples (n=54, MSD assay only) were obtained from Mayo Clinic. Unmatched controls (n = 46) were obtained from AT Still. For the lateral flow assay, colorimetric image analysis was done using a titration curve of known concentration of monoclonal antibody. We optimized the biomarker panel (E2, E6, and E7 for MSD and ELISA, and for LFA E2, and E7) by using multiparametric analysis and plotting the receiver operating curves to the test performance, and assays were compared using the Cohen's kappa statistic.
Results: At 98% specificity, the MSD HPV16 serologic assay achieved 88% sensitivity, similar to RAPID ELISA, and the LFA assay at 85% sensitivity. The signal intensities for saliva samples were weaker at 24% sensitivity. The Cohen's kappa value ranged from 0.74 to 0.78 for the comparison between all three assays. There was only one sample among all the cases that was negative by all three serology tests.
Conclusion: All three assays have strong concordance for the detection of HPV16 early antigen serology. All the tests can facilitate large scale HPV serology research.

#5100 A next-generation extracellular vesicle and particle-based liquid biopsy for early lung cancer detection.

Toumy Guettouche[1], Caroline Schissel[2], Daniel P. Salem[1], Troy B. Hawkins[1], Aaron Chevalier[1], Ibukunoluwapo O. Zabrowski[1], Brittany Grimes[1], Timothy Santos-Heiman[1], Nina Insixiengmay[1], Gabrielle N. Barcaskey[1], Katherine S. Yang[1], MacKenzie S. King[1], Mahmoud M. Bassam[1], Michael J. Smith[1], Anish Panda[2], Travis B. Sullivan[2], Prasanth Reddy[1], Dawn R. Mattoon[1], Kimberly M. Rieger-Christ[2]

[1]Mercy BioAnalytics, Waltham, MA,[2]Translational Research, Lahey Hospital & Medical Center, Burlington, MA

Background: Early detection of lung cancer (LC) remains a critical unmet need, as most patients are diagnosed at advanced stages when treatment is less effective. The current standard of care for detection, computed tomography lung screening (CTLS), is constrained by limited uptake, emphasizing the need for a more universally accessible approach. Circulating extracellular vesicles and particles (EVPs) offer a minimally invasive source of tumor-derived biomarkers reflective of underlying tumor biology. We developed an EVP-based liquid biopsy assay for LC detection that aims to achieve high sensitivity through detection of vesicles and particles released abundantly by tumor cells and high specificity by assessing multiple cancer-associated biomarkers colocalized on the same EVP surface.

Methods: The LC Test, consisting of a predefined biomarker panel and classifier was locked following a training study. A blinded case-control study was conducted using plasma samples from individuals enrolled in a routine LC screening program and from those enrolled in a lung cancer study in those who never smoked. The study included two arms: 1) High-risk participants with a history of tobacco use without evidence of lung cancer (n = 75; 37 Lung-RADS 1, 38 Lung-RADS 2) and participants with lung adenocarcinoma (LUAD) (n = 20; median tumor diameter 1.8 cm), and small-cell carcinoma (SCLC; n=5), and 2) participants who never smoked without evidence of lung cancer (n = 74) and with LUAD (n = 26; median tumor diameter 2.3 cm), and squamous cell carcinoma (LUSC; n= 1). The design enabled evaluation of assay performance for the detection of LCs arising in high and average risk individuals, with strong representation of early-stage disease (71% Stage I/II).

Results: Using a pre-specified locked classifier with specificity set to 90%, the LC Test achieved an overall sensitivity of 47.8% for LUAD and 35.3% for Stage I/II disease in high-risk participants. For SCLC, overall sensitivity was 60%. Among those who never smoked, the assay demonstrated 50% overall sensitivity and 31.3% sensitivity for Stage I/II LUAD. The biomarker panel test score correlated with predicted tumor size at blood draw (R = 0.60; p = 0.0048). The smallest detected tumor measured 0.8 cm in diameter.

Conclusions: The LC Test enables sensitive and specific detection of early-stage LC in both high-risk individuals undergoing screening and those who never smoked, with incidentally or clinically detected disease. Assay performance approaches that of CTLS, supporting its potential as a minimally invasive complement or, in select settings, as an alternative for imaging-based screening. These findings warrant further evaluation of the LC Test in larger clinical studies.

#5101 Advancing access and equity in colorectal cancer screening: Key insights from Cycles of Impact Philadelphia Initiative.

Kimberly McNeil[1], David Barreto[2], Eveline Phillips[3], Mallorie Jones[4], Carmen E. Guerra[5], Paige Edmonds[1], Corrine Rhodes[4], Shivan J. Mehta[6], Keyirah Williams[4]

[1]Colorectal Cancer Alliance, Washington, DC,[2]Johns Hopkins Medicine, Baltimore, MD,[3]University of Pennsylvania Health System, Philadelphia, PA,[4]University of Pennsylvania, Philadelphia, PA,[5]Perelman School of Med. Univ. of Pennsylvania, Philadelphia, PA,[6]Medicine, University of Pennsylvania, Philadelphia, PA

Background: Colorectal cancer (CRC) is the second leading cause of cancer death in the U.S., disproportionately affecting Black Americans due to systematic barriers and medical mistrust. The Cycles of Impact (COI) Philadelphia Initiative was a collaboration between the Colorectal Cancer Alliance, Independence Blue Cross, and University of Pennsylvania Medicine designed to reduce disparities through an integrated multi-level strategy of centralized outreach, behavioral health engagement, and community activation.
Methods: Between 2022-2025, COI distributed over 2,400 fecal immunochemical test (FIT) kits and executed three key interventions: (1) centralized outreach to 1,888 unscreened Black patients through proactive phone, text messaging, and navigation support; (2) integration of CRC screening within a 28-day residential substance use treatment facility utilizing on-site education and an incentive program; and (3) broad community engagement through faith-based events, digital media campaigns, and healthcare partnerships.
Results: Out of 1,888 patients reached through centralized outreach, 97 completed FIT, with 7 positive), and 82 underwent colonoscopy, detecting adenomas in (35) 43% and adenocarcinoma in 1%. In the behavioral health facility, 125 of 155 eligible residents (81%) completed FITs, with 13.5% positive results and successful linkage to colonoscopy. Across all COI activities, 2,736 participants were engaged, 430 screenings completed, and 126 adenomas, 8 advanced neoplasms, and 1 instance of stage IV cancer detected. Follow-up completion after positive FIT averaged 27.8%.
Conclusion: Equity-driven, multi-level interventions including centralized navigation, behavioral health integration, and community partnerships led to colorectal cancer screening and detection among Black Philadelphians who may otherwise have not been screened. Deploying navigators in trusted community settings and establishing payer-academic collaborations created a scalable, sustainable model to address racial disparities in colorectal cancer outcomes.

#5103 AI-empowered cancer risk assessment model based on routine laboratory tests for enriching individuals at high risk of cancer.

Mao Mao[1], Yi Luan[2], Yong Shen[3], Shiyong Li[1], Shibin Long[1], Wei Wu[1]

[1]SeekIn, Shenzhen, Guangdong, China,[2]Sun Yat-sen Memorial Hospital, Sun Yatsen University, Guangzhou, Guangdong, China,[3]The Affiliated Cancer Hospital of Zhengzhou University and Henan Cancer Hospital, Zhengzhou, Henan, China

Background: Early cancer detection improves survival, yet population-wide screening remains costly and logistically challenging. Traditional cancer risk models, such as lifestyle-based assessments and polygenic risk scores, offer limited sensitivity. In contrast, routine laboratory tests (complete blood count, urinalysis, and biochemical panels) are already widely performed in primary care and may harbor latent cancer signals. We developed an AI-based cancer risk assessment (CRA) model using these existing data to enrich cancer cases and improve the cost-effectiveness of downstream multi-cancer early detection (MCED) tests.

Methods: Routine laboratory data from 5,376 individuals (1,399 cancer; 3,977 non-cancer) across two hospitals were retrospectively collected and split into training and validation cohorts. A total of 43 features were selected to calculate CRA scores using a gradient boosting framework. All participants also underwent OncoSeek testing, a validated MCED assay combining multiple protein tumor markers with clinical data, applied to CRA-positive individuals.

Results: The CRA model achieved AUCs of 0.738 and 0.802, with sensitivities of 87.5% and 90.0% at specificities of 50.0% and 47.2% in the training and validation cohorts. Among individuals predicted positive (CRA > 0.4, n = 3241), cancer prevalence increased from 26.0% to 38.2% (1.5-fold enrichment). In this enriched group, OncoSeek achieved 37.0% sensitivity at 97.3% specificity, and 56.6% sensitivity when restricted to its covered 14 cancer types. Furthermore, within the high-risk subgroup (CRA > 0.88, n = 231), 65.4% were cancer patients, with a higher proportion of advanced disease (Stage IV: 42.2%) than the overall cohort (25.0%), indicating potential to flag patients needing prompt diagnostic evaluation.A population-level simulation in 1 million adults ≥50 years (incidence = 0.9%) showed that adding CRA before OncoSeek increased cancer incidence to 1.5% (1.7-fold), reduced false positives by 33.3%, and halved total screening cost ($80.0 M → $40.5 M), lowering cost per detected case by 44.1%, demonstrating improved efficiency and cost-effectiveness.

Conclusion: The AI-based CRA model, leveraging routine primary care data, provides substantially higher sensitivity and broader applicability than polygenic risk scores. Beyond enriching cancer incidence for screening, CRA can also flag individuals with strong cancer signals who may require prompt diagnostic evaluation in EMR system. When integrated as a front-end enrichment step before MCED testing, this approach effectively filters out low-risk individuals, reduces unnecessary downstream testing, and halves screening costs with only a modest (~9%) sensitivity reduction. The combined CRA + MCED framework offers a scalable and economically sustainable pathway for precision population-level cancer early detection.

#5104 Cost-effectiveness analysis of integrating multi-cancer early detection into current cancer screenings in the United States.

Mao Mao[1], Shuaipeng Geng[2], Shiyong Li[1], Yinyin Chang[2], Shujia Hao[1]

[1]SeekIn, Shenzhen, Guangdong, China,[2]Shenyou Bio, Zhengzhou, Henan, China

Background: Cancer remains a major global health challenge. While standard-of-care (SoC) screenings (e.g., colonoscopy, mammography) improve early detection and survival, limitations persist: many cancer types lack screening guidelines, existing methods are single-cancer early detection (SCED) tests, and invasive protocols with low adherence lead to inefficiencies. Multi-cancer early detection (MCED) tests using liquid biopsy technologies provide a potential solution by screening for multiple cancers, including those not targeted by current SoC, within a single test. From a health economic perspective, supplementing SoC with MCED could enhance cost-effectiveness by broadening detection and reducing missed diagnoses.

Methods: This modeling study evaluated two strategies: 1) integrating MCED testing into SoC screenings, and 2) optimizing colorectal cancer screening with a two-step process (FIT followed by colonoscopy), further enhanced by MCED. U.S. SoC screening data from 2021 for five common cancers (breast, cervical, colorectal, lung, prostate), U.S. Census 2020 statistics, and real-world screening cohort parameters informed screening population overlap, cancer incidence, and detection rates for both SoC screenings and MCED.

Results: Among 75.6 million individuals screened in 2021, SoC alone detected 193,554 cancer cases at a total cost of $43.2 billion ($223,034 per detected case). Integrating SeekIn's two-step MCED test (OnceSeek followed by SeekInCare, $190 per person) raised total cost to $57.5 billion but increased detected cases to 539,909, nearly three times SoC alone, while halving the cost per case to $106,556. In contrast, using GRAIL's Galleri MCED ($949 per person) increased detected cases further, with an additional 297,141 cases, but escalated total costs to $114.9 billion. Notably, optimizing the colorectal screening protocol (FIT followed by colonoscopy) reduced SoC spending by $22.1 billion, covering all participants' TwoStep MCED costs and achieving a surplus of $7.7 billion. This strategy yielded 531,556 detected cases (2.7x SoC) and reduced per-case cost to $66,637 (29.9% of SoC).

Conclusion: Integrating cost-effective MCED tests, such as TwoStep test, into current SoC screenings can substantially improve cancer detection, lower per-case identification costs, and keep overall expenditures manageable. Targeted optimization, exemplified by a FIT-first colorectal approach, maximizes cost savings and amplifies the benefits of adding MCED tests to established national screening programs, all without requiring an increase in the overall budget. Collectively, these findings highlight a unique opportunity: with thoughtful integration, MCED can reshape population health by delivering timely, accessible, and affordable screening that saves more lives.

#5105 *CervicalMethDx*: Precision risk stratification of high-risk HPV samples to reduce unnecessary colposcopy referrals and improve the quality of value-based care.

Yanira Gonzalez Rodriguez[1], Ashley Ramos-Lopez[1], Laura Palmieri[2], Amanda Garcia-Negron[1], Paola Quinonez-Mendez[1], Guie Beeu Guerrero Hunt[2], Alvaro Gutierrez Colima[3], Carolina Teran[4], Adhi Guerrero Thillet[1], Mariana Brait[2], Priscilla Brebi Mieville[3], Carmen Ili[5], Teresa Diaz-Montes[6], Josefina Romaguera[7], Bruce Trock[8], David Sidransky[9], Carolina Larronde[3], Rafael E. Guerrero-Preston[1]

[1]LifeGene-Biomarks, Inc, San Juan, PR,[2]Oncology, Johns Hopkins Medical Insts., Baltimore, MD,[3]Center of Excellence in Translational Medicine (CEMT-BIOREN), Universidad de la Frontera, Temuco, Chile,[4]Facultad de Medicina, Universidad San Francisco Xavier of Chuquisaca,, Sucre, Bolivia, Plurinational State of,[5]Center of Excellence in Translational Medicine (CEMT-BIOREN), Universidad de La Frontera, Temuco, Chile,[6]Gynecologic Oncology Center, Mercy Medical Center, Baltimore, MD,[7]Obstetrics and Gynecology, University of Puerto Rico School of Medicine, San Juan, PR,[8]Brady Urological Institute,, Johns Hopkins Medical Insts., Baltimore, MD,[9]Lab Director, Otolaryngology, Johns Hopkins Medical Insts., Baltimore, MD

Oncogenic human papillomavirus (hrHPV) screening identifies many transient infections, but few clinically significant precancers, generating high rates of unnecessary colposcopy referrals. In the United States, 70-80% of women referred for hrHPV-positive colposcopy lack actionable precancerous diagnoses. Given that >90% of hrHPV infections clear naturally within 12-24 months, there is an urgent need for objective molecular triage tools to optimize colposcopy-driven biopsy selection and enhance value-based cervical cancer care.

The *CervicalMethDx* precision methylation platform was evaluated using 1,618 samples from IRB-approved studies across Puerto Rico, Latin America, and the United States. Independent datasets and specimen types were tested, including Digene and PreservCyt media, as well as self-collected vaginal swabs. Diagnostic performance metrics (sensitivity, specificity, AUC) were compared across *CervicalMethDx* assay versions (1.0 singleplex, 1.5 six-gene panel, 2.0 duplex). Cross-assay reproducibility and anatomic-site concordance were assessed using correlation and generalized estimating equation (GEE) models.

CervicalMethDx 1.0 detected cervical intraepithelial neoplasia grade 2 or higher (CIN2+) lesions with 96% sensitivity, 84% specificity, and an area under the ROC curve (AUC) of 0.99 in hrHPV-positive Digene samples (n = 108, University of Puerto Rico). In the ESTAMPA Latin American trial (n = 759), CIN3+ detection reached 67% sensitivity, 59% specificity, and an AUC of 0.65. The *CervicalMethDx* 1.5 six-gene panel identified squamous intraepithelial lesion (SIL) cytology with 94% sensitivity, 57% specificity, and an AUC of 0.85 in CLIA-certified PreservCyt samples (n = 377). No significant methylation differences ($p > 0.05$) were observed between paired cervical and self-collected vaginal swabs (n = 100 each), demonstrating strong intra-individual concordance. *ZNF516* methylation correlated across singleplex and duplex assays ($r = 0.51$, $p = 0.01$). GEE modeling showed a negative within-Pearson correlation ($\rho = -0.64$) between paired cervical and vaginal sites, confirming consistent site-dependent variation and reproducibility.

CervicalMethDx provides a robust precision-methylation approach for risk stratification of hrHPV-positive samples with the potential to reduce unnecessary colposcopy referrals and biopsies. The assay's reproducibility across self-collected and clinician-collected specimens supports its potential integration into at-home hrHPV testing workflows, advancing equitable and value-based cervical cancer screening worldwide

#5106 Endurance of HPV self-collection to detect disease: Histopathological follow up up to 16 months.

Sangini Sheth[1], Megan Fitzpatrick[2], Karl Hibler[3], Catherine Behrens[4]

[1]Obstetrics, Gynecology & Reproductive Sciences, Gynecology, Yale University, New Haven, CT,[2]Clinical, Teal Health, Inc., San Francisco, CA,[3]Independent Statistician, Bradenton, FL,[4]Women's Healthcare and Biotechnology Consultant, San Francisco, CA

Background: HPV self-collection (SC) expands access to cervical cancer screening (CCS) and is equivalent to clinician-collected (CC) sampling. Longer-term histopathological data after SC is essential to ensure durable sensitivity.

Methods: 599 enrolled in the SELF-CERV study evaluating the Teal Wand SC device and underwent SC and CC primary HPV testing at baseline (reported previously [1]), with SoC colposcopy and biopsy/excisions per guidelines. Pathology results were collected after baseline to 490 days for secondary analysis to fill the evidence gap. Diagnostic performance metrics (Sen, Sp, negative predictive value-NPV) and cumulative incidence rate (CIR) were calculated for SC versus CC HPV testing among those with high grade squamous intraepithelial lesions (HSIL) or worse (CIN2+).

Results: Of 599 paired SC and CC HPV results, 280 (46.7%) had pathology results within 490 days of the study visit and 57 (9.5%) were diagnosed with CIN2+. SC HPV testing showed high Sen for CIN2+, equivalent to CC testing (TABLE), ratio of Sen 1.00, similar to that observed at baseline, ratio 1.00). The NPV amongst those with pathology was 96.7% (59/61). The CIR per genotype group was not statistically significantly different for SC and CC: HPV16 had the highest ratio both at the study visit (SC: 31%, CC: 33%) and at 16 months later (SC: 47%, CC: 49%), followed by 12 Other HPV (SC: 17%, CC: 18% at study visit; SC: 24%, CC: 25% at 16 mo), and HPV18 (SC &CC: 5% at study visit, SC & CC: 21% at 16 mo).

Conclusions: SC HPV testing maintained high Sen for detection of CIN2+ in the 16 mo following study enrollment and high NPV of a SC HPV negative, both equivalent to CC.

Impact: To our knowledge, this is the first prospective study to evaluate pathology outcomes up to 16 mo following HPV SC, which strengthens confidence in SC as an effective CCS option that expands access, ensures appropriate clinical triage following SC, and warrants further inclusion in CCS guidelines. [1] https://pubmed.ncbi.nlm.nih.gov/40388167/

Diagnostic performance of HPV testing for detection of HSIL+

	SC (n/N; 95% CI)	**SC (n/N; 95% CI)**
Sen CIN2+	96.5% (55/57; 88.1-99.0)	96.5% (55/57; 88.1-99.0)
Sen CIN3+	97.1% (34/35; 85.5-99.5)	100% (35/35; 90.1-100)

#5107 Feasibility and interim results from the prospective international LS-URO study: Urine tumor DNA-based screening for urothelial cancer in Lynch syndrome carriers.

Jussi Nikkola[1], **Lauri Ryyppo**[1], Juuso Vuorinen[1], Jack V. Bacon[2], John Pham[2], Sara Singh[3], Lauren Deneault[2], Chuyi Zheng[3], Hanna Selin[1], Paivi Martikainen[1], Cecily Q. Bernales[2], Melissa Koudjanian[2], Kirsi Pylvanainen[4], Matti Nykter[1], Thea Veitonmaki[5], Jukka-Pekka Mecklin[4], Alexander Wyatt[2], Kasmintan Schrader[3], Toni Seppala[1], Peter C. Black[2], Gillian Vandekerkhove[2], Matti Annala[1]

[1]Tampere University, Tampere, Finland,[2]Vancouver Prostate Centre, Vancouver, BC, Canada,[3]Hereditary Cancer Program, BC Cancer Agency, Vancouver, BC, Canada,[4]The Wellbeing Services County of Central Finland, Jyvaskyla, Finland,[5]Tampere University Hospital, Tampere, Finland

Introduction: Lynch syndrome (LS) is a hereditary cancer syndrome caused by germline variants in DNA mismatch repair (MMR) genes (*MSH2*, *MLH1*, *MSH6* and *PMS2*), with up to 25% lifetime risk for urothelial cancer (UC). LS-UCs are commonly located in the upper urothelial tract, where tumors are difficult to detect early. No evidence-based screening strategy exists. We and others have shown that UC can be sensitively detected using urine tumor DNA (utDNA) mutation analysis.
Methods: LS-URO is an international, prospective, multicenter study enrolling LS carriers aged 50-75 years from the Finnish LS Registry and the BC Cancer Hereditary Cancer Program. Participants receive an at-home 100-mL urine collection kit (with preservative) for mail return. Urine cell pellet DNA is analyzed using the UroScout 25-gene deep targeted sequencing assay, which includes common UC drivers (e.g., *FGFR3*, *ARID1A*, *KMT2D*) and MMR genes. Samples with ≥2 somatic mutations are reviewed by a molecular tumor board, with utDNA-positive cases examined by cystoscopy, urine cytology and imaging, as well as repeat urine sequencing.
Results: Between May 2023 and October 2025, 213 participants were recruited, and 160 returned urine samples. Mean participant satisfaction with the urine collection procedure was 4.46/5. utDNA analysis is complete for 135 participants (76 Finland, 59 Canada). Nine (6.7%) participants were utDNA-positive with a median cancer fraction of 9% (range 4-17%) and median of four somatic mutations detected per sample (range 3-18). In 8/9 (89%) utDNA-positive participants, a somatic *MMR* second hit beyond the germline defect was detected. A total of 28 follow-up urine samples from five initially utDNA-positive participants revealed consistent detection of original mutations, with new mutations emerging in four. Eight out of nine (89%) positive participants harbored an *FGFR3* hotspot mutation (of which 88% *R248C*), whereas only one out of nine (11%) carried a *TERT* promoter mutation, consistent with our published observation that such mutations are rare in LS-UC. Two asymptomatic UC cases have been confirmed (one at initial examination, one 28 months after the first utDNA-positive screening sample during protocol-scheduled follow-up CT imaging). Four positive cases are pending initial urologic investigation, and the remainder are under continued surveillance through additional sampling and clinical follow-up.
Conclusions: utDNA-based screening in LS is feasible, well accepted, and enables early, non-invasive cancer detection. Interim results demonstrate high compliance and promising diagnostic yield, pending long-term clinical follow-up. These findings support large-scale implementation of urine biopsy-based screening, to be further evaluated in the randomized PREDI-LYNCH trial.

#5108 Screening colonoscopy yields among adults aged 40 to 49 years after new screening guidelines.

Xiangyuan Qi[1], Xiaomei Wu[2], Bo Zhu[3]

[1]Cancer Hospital of China Medical University/Liaoning Cancer Hospital & Institute, Shenyang, Liaoning Province, China,[2]The First Hospital of China Medical University, Shenyang, Liaoning Province, China,[3]Liaoning Cancer Hospital & Institute, Shenyang, Liaoning Province, China

Objective: To analyze screening colonoscopy yields among adults aged 40 to 49 years since China Guideline for the Screening, Early Detection and Early Treatment of colorectal cancer (2020, Beijing) expanded the screening initiation age to 40, thus providing evidence to support lowering the screening initiation age to 40.
Method: This population-based cross-sectional study was part of the framework of the Cancer Screening Program initiated by the Chinese government. We included residents aged 40-59 who underwent their first screening colonoscopy in 2020-2024. The study outcomes included: colorectal cancer (colon or rectal adenocarcinoma); advanced lesions (at least one adenoma ≥10mm or at least one adenoma with villous components or high-grade dysplasia); and other benign lesions. Robust Poisson regression was used to estimate the adjusted risk ratios (aRRs) for outcomes between age groups, with 50- to 59-year-olds serving as the reference group. Regression models were adjusted for region, sex, comorbidities, body mass index (BMI), and tobacco smoking history.
Result: A total of 5040 eligible patients underwent a screening colonoscopy in 2020-2024, including 1529 aged 40-49 and 3511 aged 50-59. Females comprised 60.5% of the overall cohort, 53.7% had comorbidity, 23.7% had a history of tobacco smoking, and 39.7% had body mass index>=24 (calculated as weight in kilograms divided by height in meters squared). Screening colonoscopy outcomes were generally slightly less frequent among the younger group compared with the older group, only the aRR for other benign lesions (12.0% vs. 19.4%; aRR, 0.67; 95% CI, 0.54-0.82) and negative (85.8% vs 77.3%; aRR, 1.06; 95% CI, 1.04-1.09) were statistically significant. All other colonoscopy findings did not differ significantly between the 2 age groups, including for advanced lesions (1.7% vs. 2.6%; aRR, 0.69; 95% CI, 0.39-1.22) and colorectal cancer (0.3% vs. 0.5%; aRR, 0.55; 95% CI, 0.19-1.57). In addition, there were no significant differences between age groups for all lesion types among women. Other than for other benign lesions and negative, there were no significant differences in the types of lesions among men.
Conclusion: The current study findings extend the observation of similar screening colonoscopy detection rates for advanced lesions and colorectal cancer in those aged 40 to 49 years vs 50 to 59 years and support the suggestion that there is likely no need to reduce advanced lesions and colorectal cancer detection rate benchmarks because of the infusion of younger patients into the screening pool. The similar rates of advanced lesions and colorectal cancer detection between age groups also provide support for lowering the start of screening initiation to age 40 years.

Keywords: Colorectal cancer; Screening Colonoscopy; advanced lesions

#5109 Stage at diagnosis and tumor characteristics among screen-detected breast cancer cases in Cartagena, Colombia.

Laura C. Pinzon-Martinez, Ines Benedetti, Luis F. Viana

School of Medicine, Histopathology Research Group, Universidad de Cartagena, Cartagena, Colombia

INTRODUCTION: The implementation of breast cancer screening programs aims for an early diagnosis and timely management. In Colombia, national regulations recommend biennial mammography for women aged 50 - 69 years. Patients with mammographic findings suggestive of malignancy are referred for biopsy. Limited data exists on screening performance and stage distribution in Cartagena.
OBJECTIVE: To characterize the stage at diagnosis and clinical and pathological features of women participating in a breast cancer screening program in Cartagena, Colombia.
METHODS: A retrospective study which included women screened for breast cancer between January 2019 and February 2023 with BIRADS 4A, 4B, 4C, and 5 mammographic results. Data were collected from mammography and biopsy reports and medical records. Associations between clinical and pathological variables were evaluated, including age, BI-RADS category, histological type and grade, ER, PR, and HER2 status, Ki-67 index, tumor size, multifocality, axillary lymph node involvement, metastatic disease, and TNM stage. A p-value < 0.05 was considered statistically significant.
RESULTS: 211 women were included (mean age=58.9, SD=11.3). 39,8% (n=84) mammograms were reported as BI-RADS-5, 97.5% had a histopathological diagnosis of cancer, compared to 81.8%, 47% and 40% of patients classified as BI-RADS 4C, 4B and 4A, respectively. Women with malignant diagnoses were significantly older than those with benign findings (p = 0.021, t test). At the time of diagnosis, tumor size was predominantly between 2 and 5 cm (T2), most tumors were unicentric, 42.9% had lymph node involvement and 8.2% had metastases. Most patients (50%) were diagnosed at intermediate stages (IIA-IIB), a significant proportion (20%) at stage III, and 7% at stage IV. Invasive ductal carcinoma represented 76.2% of cases, followed by invasive lobular carcinoma. The predominant subtype was HR+/HER2- (62%), and a high proportion of triple-negative breast cancer (HR-/HER2-) was observed (23%). The Ki67 index greater than 20% was observed in 51.7% of the cases and there was a significant association between histological type and Ki67 index (p=0.014, Fisher test).CONCLUSION: Stage at diagnosis of screen-detected breast cancers in this program cannot be considered neither very early nor very late. This suggests that while the screening program has improved, opportunities remain to strengthen early detection and screening efforts. The higher-than-expected malignancy rate in the BI-RADS 4A category may indicate a population with more aggressive disease biology. Although the predominant histological subtype is associated with better prognosis and effective therapies, the relatively high incidence of triple-negative breast cancer may be related to population-specific risk factors and carries therapeutic and prognostic implications that should be further investigated.

#5110 Early life exposure to antibiotics and early onset colorectal cancer.

Qiuyi Mao[1], Niti Jani[2], Varsha Gowda[1], Thrisha Mote[1], Anna Bassler[1], Shyam Ganesh Babu[1], Victoria Zottoli[1], Hannah Villanueva[1], Mariko Maja[1], Maredith Richardson[1], Maria Marjorette Ociones Pena[3]

[1]Biological Sciences, University of South Carolina, Columbia, SC,[2]University of South Carolina, Columbia, SC,[3]Research Associate Professor, University of South Carolina School of Medicine, Columbia, SC

Colorectal cancer (CRC) is the second leading cause of cancer related deaths in the United States and worldwide. Recently, the overall incidence of CRC has been decreasing presumably due to early screening and healthy lifestyles. However, CRC in individuals under 50 years old, known as early-onset colorectal cancer (EOCRC)**,** has been increasing at an alarming rate in the since the 1980s. It is a growing global epidemic with cases rising from 11% to 20 % between 1995 to 2019 and is expected to increase by 140% by 2030. The underlying causes and mechanisms as to why otherwise healthy young adults are susceptible is poorly understood. Based on our current knowledge of the disease, we hypothesized that EOCRC is caused exposure to exposomes that have been increasing globally in parallel with increases in EOCRC with each birth cohort; that impact the gut microbiome causing dysbiosis and inflammation in the distal colon and rectum, the anatomical site of EOCRC; and those that can affect humans at different development stages from conception to adulthood. Among the potential factors is the use of antibiotics, particularly in the early stages of life.In this study, we hypothesize that there are development windows of susceptibility wherein exposure to commonly prescribed pediatric antibiotics (β-lactams or macrolides) can increase the risk of developing EOCRC. Using a mouse model of EOCRC, we defined corresponding developmental windows of susceptibility over an individual's lifetime. Here, we test if exposure to a single round of antibiotics at the perinatal and juvenile windows can impact risk of developing EOCRC. A/J mice at the perinatal stage were treated by gavage-feeding lactating dams who then passed the antibiotics to their offspring. After weaning, the offspring were treated with azoxymethane (AOM), a carcinogen, and tumor burden was determined after tumor outgrowth. Four-week-old mice were gavage-fed the antibiotics, exposed to AOM and tumor burden assessed as above. Our findings suggest that the impact of antibiotics on EOCRC risk was affected by exposure at specific developmental windows of susceptibility. Maternal antibiotic administration altered the gut microbiota in offspring which persisted over the long term. This effect was associated with changes in gut microbial structure and abundance, and an increase in pro-inflammatory bacterial strains, which correlated with elevated inflammation and tumor burden in offspring.

#5111 The global inequality in cervical cancer screening: An evidence synthesis.

Ruijun Xin[1], Xiaomei Wu[2], Bo Zhu[1]

[1]Liaoning Cancer Hospital & Institute, Shenyang, Liaoning Province, China,[2]The First Hospital of China Medical University, Shenyang, Liaoning Province, China

Background: The rising global burden of cervical cancer and persistent inequalities in screening access underscore the need to strengthen implementation. Therefore, we compiled the cervical cancer screening guidelines from different countries/regions and evaluated their implementation status and coverage situation.
Methods: In this study, we conducted comprehensive search of the PubMed, Embase and Web of Science databases (from their establishment to February 1, 2025), websites and the World Health Organization (WHO) database. Studies included in our analysis provide detailed information on the official cervical cancer screening recommendations for each country. All indicators were stratified based on factors such as human development index (HDI), income level, geographical location, WHO regions, disease risk, and age. The systematic review was prospectively registered at Prospero (registration number: CRD420251087263).
Results: Our study incorporated data from 77 countries/regions, only 62.3% (48/77) of them provided the year of published/updated protocol. Cytology was the primary screening test in 62 (80.5%) of 77 countries. Visual inspection with acetic acid (VIA) was the most recommended test in low HDI countries. The number of countries using Human papillomavirus (HPV) is relatively small. Screening coverage was associated with HDI/income (low HDI: 12.43% vs very high HDI: 49.74%; high-income: 51.68% vs low income and middle-income countries [LMICs]:34.45%), with high-risk regions (29.88%) significantly lower than other areas (46.76%). Age-stratified analysis showed minimal coverage in the 20-29 and 70-79 groups, while coverage peaked in the 30-39 group. Our results also showed substantial heterogeneity in screening quality indicators (positive rate, further assessment rate, detection rate, and positive predictive value [PPV]).
Conclusions: This study highlights global inequities in cervical cancer screening guidelines, particularly in the transition of screening methods among different countries/regions. Global cervical cancer coverage remains significantly below the target of 70%. Accelerate screening strategies, improve screening-diagnosis-treatment accessibility, establish monitoring systems, and strengthen global cooperation. Key words: Cervical cancer; Global health; Health policy;Screening, Coverage, Systematic review

#5112 Assessing hematologic pattern variation in AI-based blood cell analysis for ovarian cancer risk detection.

Eun Ji Song[1], Se Ik Kim[2], Hanbyoul Cho[3], Yookyung Lee[4], Heeyeon Jung[1], Hyejin Lee[1], Yoon Joo Kim[4], TaeJin Ahn[1], Yong Sang Song[5], **Eunyong Ahn**[1], Jae-Hoon Kim[4]

[1]ForetellMyHealth, Inc., Gyeongsangbuk-do, Pohang-si, Korea, Republic of,[2]Seoul National University Hospital, Seoul, Korea, Republic of,[3]Department of Obstetrics and Gynecology, Yonsei University Health System, Seoul, Korea, Republic of,[4]Yonsei University Health System, Seoul, Korea, Republic of,[5]Myongji Hospital, Goyang-si, Gyeonggi-do, Korea, Republic of

Ovarian cancer(OC) lacks reliable early detection methods, and blood cell-derived inflammatory signatures have emerged as potential non-invasive indicators. However, these hematologic patterns may vary across individuals and sample-processing conditions. This study applies an AI-driven blood cell analysis model to a new cohort and evaluates feature-level variability relevant to OC risk detection.

Peripheral blood was collected to evaluate hematologic patterns associated with OC detection from asymptomatic controls, patients with benign ovarian or uterine tumors, and patients with newly diagnosed OC. Samples were transported under refrigerated conditions and processed within 28 hours for complete blood count analysis. Composite hematologic indices were calculated from measured parameters and input into our previously developed AI-driven blood cell analysis model to evaluate OC risk signals. Residual samples were additionally used to obtain platelet images for exploratory morphological assessment.

Among 135 samples analyzed, including 16 OC cases, the AI-driven blood cell analysis model produced 6 true positives, 10 false negatives, 17 false positives, and 102 true negatives, yielding a sensitivity of 37.5%, specificity of 85.7%, PPV 26.1%, and NPV 91.9%. True-positive cases showed pronounced inflammatory activation with markedly elevated SII, NLR, and PLR and the lowest lymphocyte counts. False positives demonstrated similarly high inflammatory indices but disproportionately elevated platelet counts. False-negative OCs exhibited near-normal inflammatory markers yet had the highest RDW-CV, MPV, and PDW, indicating a morphology-dominant rather than inflammation-dominant hematologic phenotype.

Although overall performance was lower than in our previous dataset using the same AI-driven blood cell analysis model, the consistency of feature importance suggests that the inflammatory signal remains stable. Reduced sensitivity is likely related to pre-analytical differences, as samples were refrigerated and processed after transport. False-negative cases showed a morphology-dominant profile not captured by inflammation-based indices, indicating that some OCs lack strong systemic inflammatory signatures. To address this limitation, we are acquiring platelet-level image data to develop a complementary morphology-focused diagnostic approach.

The reproducibility of key hematologic patterns across datasets supports the biological relevance of AI-driven blood cell analysis for OC signal detection. However, reduced performance under altered processing conditions and the presence of morphology-dominant tumors highlight the limitations of inflammation-focused models. Incorporating platelet-image features may enhance detection of under-represented phenotypes and improve diagnostic coverage across OC subtypes.

#5113 Multiple myeloma screening education.

Karie Feldman[1], Diana Basali[1], Kimberly Bell[1], Pamela Combs[2], Beth Faiman[1], Anwer Faiz[1], Raymond D. Jackson[1], Jack Khouri[3], Stacy Mathews[1], Sandra Mazzoni[1], Kayona Moore[4], Natasha Patel[1], Shahzad Raza[1], Mark D. Ribbins[1], Christy Samaras[1], Louis Williams[1], Jason Valent[1], **Heather McKee Hurwitz**[1]

[1]The Cleveland Clinic, Cancer Institute, Cleveland, OH,[2]Office of Nursing Education and Professional Development, The Cleveland Clinic, Cleveland, OH,[3]Hematology and Medical Oncology, Cleveland Clinic, Cleveland, OH,[4]University of Cincinnati College of Medicine, Cincinnati, OH

Background: The lack of federal screening guidelines and limited knowledge of multiple myeloma (MM) among the public and primary care providers contributes to late-stage detection of MM when the disease is harder to treat. Black Americans over 50 are at higher risk for MM but are often diagnosed later than other groups. Given similar or improved outcomes with early detection, this study aims to implement a multi-level community-based intervention. Improved health literacy about cancer risk can lead to better decision making in MM care.
Methods: To encourage MM screening in Black Americans, our study engaged providers in continuing medical education seminars (CME), provided brochures with basic MM education at health fairs, and engaged high-risk individuals in on-site MM screening and a knowledge retention pre-test and post-test. A multidisciplinary team created the CME, which included information about the MM disease process, the benefits and methods of early detection and how to address abnormal results. Community events were designed for screening and included participation from outreach staff, navigators, clinicians, and phlebotomists. Participant education relied on an original community brochure that included information such as defining MM, its symptoms and its prominence among Black Americans. Knowledge retention questions were designed by the clinical team to highlight information covered in the brochure.
Results: Participants were recruited via convenience sampling from June 2023 through December 2024. The robust educational program included training 46 health care providers in three CME seminars, conducting 22 screening events, and providing education and monoclonal protein screening to identify MM and its precursors for 199 Black individuals over age 50. Overall scores on MM knowledge measures were consistent with a mean score of 2.8 on a five-point scale immediately after exposure to educational materials to 2.9 after at least one week had passed and screening results had been provided. The lack of decline in the score suggests that participants retained the knowledge about MM that they gained during their participation in screening. Screening results identified 21 participants (11%) with Monoclonal Gammopathy of Undetermined Significance (MGUS), a precursor condition to MM, all of whom received follow-up care.
Conclusions: Our community-based screening program combined educational opportunities for providers and patients alongside on-site screening to identify individuals with MM precursor conditions in high-risk populations. Further research should aim to expand the reach of interventions and to recruit randomized samples to allow for measurement of baseline knowledge and to generalize findings. Screening programs that meet high-risk populations in their community, intervene at multiple levels, and educate people about their risk can be effective ways to identify the individuals most likely to benefit from MM screening.

#5114 Analysis of variation in global breast cancer screening indicators: A systematic analysis.

Jiaqi Guo[1], Ruijun Xin[1], Xiaomei Wu[2], Bo Zhu[1]

[1]Department of Cancer Prevention and Treatment, Cancer Hospital of China Medical University/Liaoning Cancer Hospital & Institute, Shenyang, Liaoning Province, China,[2]Department of Clinical Epidemiology and Centre of Evidence-Based Medicine, The First Hospital of China Medical University, Shenyang, Liaoning Province, China

Background: The coverage rate of breast cancer screening is a key indicator for measuring the effectiveness of screening. Comprehensive studies on the global coverage rate of breast cancer screening are still insufficient at present, and existing evidence suggests that screening rates remain suboptimal in many regions. Therefore, this study aims to systematically assess the current status of global breast cancer screening programs and focus on analyzing their coverage. Based on existing data, we have systematically sorted out and presented the implementation of breast cancer screening at the global, regional and national levels.

Methods: We systematically searched the PubMed, Web of Science, and Embase databases (from their inception to August 12, 2025), and supplemented the search with relevant official websites and the World Health Organization database. A total of 75 countries and regions' breast cancer screening policies and coverage data were included. The following key information was incorporated: screening methods, screening intervals, and specific circumstances of providing free services, etc. On this basis, we further analyzed the specific contents of breast cancer screening guidelines in various countries and systematically evaluated the global differences in screening coverage. To deeply explore the influencing factors behind the differences, detailed subgroup analyses were conducted based on the Human Development Index (HDI) level, continent distribution, World Health Organization (WHO) regions, and different age groups. The systematic review was prospectively registered in PROSPERO (registration number: CRD420251233260).

Results: Among the 75 countries and regions included, 35 (46.7%) countries have established official breast cancer screening guidelines. Regarding screening methods, mammography/digital breast tomosynthesis (DBT) is the most commonly adopted approach, used in 49 (65.3%) countries. In resource-limited countries and regions, clinical breast examination (CBE) is the most frequently recommended screening method. The average coverage rate of breast cancer screening is 50.2% (95% CI: 36.6%-58.8%). Stratified analysis by age shows that the screening coverage rate in the 50-69 age group is significantly higher than that in the 40-49 and 70-79 age groups.

Conclusions: At present, the coverage rate of breast cancer screening in most countries around the world remains at a relatively low level. To bridge this gap, it is necessary to systematically identify influencing factors, formulate targeted strategies, and actively promote their implementation to effectively enhance the coverage level of breast cancer screening.

Key words: Breast cancer; Breast cancer screening; Coverage rate; Systematic review

#5115 A multi-omic liquid biopsy for the earlier detection of colorectal cancer.

James M. Cameron, Holly J. Butler, David S. Palmer, Rose G. McHardy, Alexandra Sala, Matthew J. Baker

Dxcover Ltd., Glasgow, United Kingdom

Background: Timely diagnosis and intervention in colorectal cancer (CRC) are critical to improving patient outcomes and limiting disease progression. Screening of average-risk individuals is essential for detecting tumors at an earlier, more treatable stage. However, adherence to current screening programs remains suboptimal. Liquid biopsies represent a promising alternative to stool-based tests and may play a key role in optimizing CRC detection and diagnostic pathways.
Methods: In this study, 957 patients were recruited across various clinical sites in the USA: 48 CRC, 157 advanced precancerous lesions (APL), 331 non-advanced lesions (NAL) and 421 with a negative colonoscopy diagnosis. Blood was obtained from patients either prior to scheduled colonoscopy or before surgical resection and any anti-cancer therapies. Streck plasma samples were analyzed by the Dxcover® Liquid Biopsy Platform and classified with machine learning algorithms.
Results: When CRC was classified against all other groups, the receiver operating characteristic curve generated an area under the curve value of 0.95, and test sensitivity and specificity were 90% and 89%, respectively. The diagnostic model accurately predicted 75% of stage I (3/4), 100% of stage II (15/15), 93% of stage III (14/15) and 100% of stage IV (6/6) CRCs. For the advanced colorectal neoplasia model, 29% of APL were detected.
Conclusion: A simple blood test with high sensitivity for early-stage colorectal cancer could significantly enhance patient outcomes. With continued development, this liquid biopsy has the potential to make a substantial impact on the early detection of CRC.

#5116 Assessing blood- and stool-based tests for colorectal cancer detection.

James M. Cameron[1], Holly Butler[1], David Palmer[1], Rose McHardy[1], Amanda Alty[2], Peter Mitchell[2], Edward Parkin[2], Matthew Baker[1]

[1]Dxcover Ltd., Glasgow, United Kingdom,[2]Lancashire Teaching Hospitals NHS Foundation Trust, Preston, United Kingdom

Background: Colorectal cancer (CRC) is one of the most common and deadliest cancers worldwide, and incidence rates are rising. However, early detection and intervention can improve the survival rates and quality of life of affected patients. The Dxcover Liquid Biopsy Platform is a rapid multi-omic liquid biopsy that interrogates a blood sample with infrared radiation and produces a distinctive signature that represents the whole biomolecular profile of the sample. The liquid biopsy has been reported previously as a standalone test, but also has potential to be employed in combination with other information sources, such as biomarker data, and clinical risk factors.
Methods: In this study, samples from 1377 patients were collected across sites in the USA (n=989) and UK (n=388). Blood was obtained from patients either prior to scheduled colonoscopy or before surgical resection and any anti-cancer therapies. Streck plasma samples were analyzed by the Dxcover Liquid Biopsy Platform. Carcinoembryonic Antigen (CEA) values were determined for all samples. Fecal hemoglobin levels from fecal immunochemical testing (FIT) were also obtained for the UK samples. Machine learning algorithms were developed to compare test performance and assess combinations.
Results: Initially, machine learning models were developed for the spectral dataset alone. The area under the curve (AUC) was 0.95 and the model reported consistent detection rates across CRC stages. There was limited diagnostic utility reported for CEA alone (37% sensitivity with 80% specificity). There was no improvement to the spectral model with the inclusion of CEA. For the UK cohort with FIT results, the FIT only model (AUC=0.83) was enhanced by the addition of spectral data, with the combined model (spectra+FIT) reporting an AUC of 0.90.
Conclusions: There is potential for combining this liquid biopsy with orthogonal tests, such as FIT testing or other blood-based biomarkers. A rapid liquid biopsy that is sensitive to early-stage CRC could substantially improve patient outcomes. Current screening programs have addressable limitations and the emergence of new alternative technologies is vital to support earlier CRC detection.

: New Ligands and Inhibitors
Poster Session

#5118 *In silico* discovery of potent small molecule inhibitors targeting the AR N-terminal domain for treating castration-resistant prostate cancer.

Patrick Kunz[1], Thomas Alanine[2], Babette Schade[3], Ben Cossins[2], Sandro Bottaro[1], Daniele Peterle[1], Flavia Giamogante[3], Elia Gamba[3], Sasha Soldati[3], Nathalie Wyss[3], Lixin Yang[3], Michele Invernizzi[3], Michael Habeck[3], Rudy Rubini[3], Melissa Kachura[3], Dmitry Dmitry Ryzhenkov[3], Matteo Cerrina[3], Fabio Airoldi[3], Valentina Ceserani[3], Alice Santopolo[3], Heidi Derks[3], Stefano Ruschetta[3], Andrew Allen[2], David Lowe[2], Carlo Fisicaro[3], Ken Carson[2], Patrik Foerch[2], Kevin Sprott[2], Kamil Tamiola[2]

[1]Experimental Biophysics, Peptone Switzerland AG, Bellinzona, Switzerland,[2]Peptone Ltd., London, United Kingdom,[3]Peptone Switzerland AG, Bellinzona, Switzerland

Castration-resistant prostate cancer (CRPC) remains an unsolved clinical challenge due to resistance mechanisms that occur upon treatment with androgen receptor pathway inhibitors (ARPI). Since the hallmarks of resistance are (i) AR amplification, (ii) the occurrence of splice variants like AR-V7 and (iii) mutations in the ligand binding domain (LBD), the novel concept of targeting the disordered N-terminal domain (NTD) of the androgen receptor is a compelling way of inhibiting AR in the context of castration-resistance. Here, we describe the discovery of small-molecule AR-NTD inhibitors by leveraging Peptone's HDX-MS and in silico platform. A virtual screen against a highly dynamic segment of the NTD yielded binders that were further developed into a series with potent in vivo activity. Binding was confirmed by multiple biophysical approaches, including a proprietary ultra-fast mixing hydrogen-deuterium exchange mass spectrometry (HDX-MS), NMR spectroscopy, spectral shift analysis, and cellular NanoBit assays, all of which validated direct interaction with the NTD. Our lead compounds exhibit potent cellular activity across a range of in vitro models. In AR full-length (FL-AR) and AR-V7 luciferase reporter assays, as well as LNCaP proliferation assays, potencies between 10-100 nM were obtained. Activity in the VCaP CRPC cell model was similarly strong, clearly outperforming standard-of-care compounds like Enzalutamide and Darolutamide and reaching equal potency to PROTACs. Mode of action (MoA) studies demonstrated that the lead compounds suppress the formation of FL-AR and AR-V7 homodimers (NanoBit assay), inhibit nuclear translocation of AR, and can efficiently downregulate AR-target genes in a dose-dependent manner in qPCR assays. The lead series displays drug-like physicochemical, ADME, and pharmacokinetic profiles, conducive to rapid preclinical and clinical development, while providing distinct differentiation over novel modalities such as PROTACs and RIPTACs. Our findings highlight the therapeutic promise of targeting the AR-NTD in CRPC via a unique, structure-driven approach, with small molecules that combine a novel mechanism with potent anti-tumor activity.

#5119 P015, a highly selective PARP7&12 dual inhibitor.

Jinwen Huang, Hao Huang, **Steve Shen**

Convalife Pharmaceuticals, Shanghai, China

Background: The poly(ADP-ribose) polymerase (PARP) family plays critical roles in DNA damage repair, cellular stress responses, and tumor immune modulation. Among them, PARP7 and PARP12 have been implicated in innate immunity and tumor microenvironment remodeling. Selective inhibition of PARP7&12 holds promise for cancer therapy by modulating immune responses and cell survival pathways. However, potent and selective small-molecule inhibitors targeting PARP7&12 remain scarce, creating an urgent need for the development of candidate compounds with superior enzymatic inhibitory activity.

Methods and Materials: Based on structure-activity relationship (SAR) studies and accelerated by the Convalife "AIDRUG.WORK" molecular design platform, we designed and optimized small-molecule inhibitors targeting PARP7&12, leading to the identification of the candidate compound P015. In vitro enzymatic assays were performed to evaluate the inhibitory activity of P015 against human PARP7 and PARP12. IC_{50} values were calculated by fitting concentration-response curves. The current work primarily focuses on characterizing enzymatic-level activity to validate the feasibility of P015 as a PARP7&12 inhibitor.

Results: Enzymatic assay results demonstrated that P015 exhibited potent inhibitory activity against both PARP7 and PARP12, with IC_{50} values below 10 nM for both enzymes. These findings indicate that P015 possesses exceptionally strong affinity and inhibitory potency for PARP7&12 at the enzymatic level, establishing a foundation for further investigation of P015 as a highly active PARP7&12 inhibitor.

Conclusions: We have identified and preliminarily characterized P015, a small-molecule inhibitor with sub-10 nM IC_{50} values against PARP7&12 at the enzymatic level. Although current experimental data are primarily derived from in vitro enzyme activity assays, the results suggest that P015 has significant potential for further cellular and in vivo pharmacological and mechanistic studies, and may be developed as a novel anti-cancer candidate drug targeting the PARP7&12 pathway.

#5120 Design and discovery of BH-501242, a novel pan-KRAS on/off inhibitor targeting KRAS switch II pocket.

Eugene Rui, Nancy Ling, Wei Deng, Ping Jiang, Zhenping Wang, Yue Hu, Joshua Choi, Danan Li, Evan Rogers, Anindya Sarkar, Levan Darjania, Geoffrey Oxnard, Jean Cui

BlossomHill Therapeutics, Inc., San Diego, CA

KRAS mutations are involved in approximately 25% of all tumors and are frequent oncogenic drivers in lung (32%), colorectal (40%), and pancreatic cancers (85-90%). The most common *KRAS* driver mutations are on codon 12 and 13, including G12C, G12D, G12V, G12R, G13A, G13D, etc. The G12C mutation has been effectively targeted using a covalent strategy that exploits the unique reactivity of the cysteine residue. Other mutations, however, require inhibitors with high intrinsic binding affinity with KRAS to be effective in clinic. MRTX1133 was the first to demonstrate low single-digit nM cell potency for G12D mutation; however, the inhibitor lacked the ADME properties required for a successful oral drug. Since then, multiple KRAS inhibitors targeting G12D, G12V, or pan-KRAS mutations have advanced into clinical trials. Leveraging our structure-based drug design expertise, we designed a novel chemical scaffold targeting KRAS switch II pocket and identified the pan-KRAS inhibitor, BH-501242 after lead optimization on potency, ADME/PK, and safety properties. BH-501242 demonstrated excellent potency and target engagement across a broad spectrum of *KRAS* mutations and achieved sub-nM to low single-digit nM IC_{50} values in cellular anti-proliferation assays and anti-phosphorylation assays against downstream kinase ERK. In a panel of 15 cell lines with *KRAS* G12D mutation, 10 cell lines with G12V, and 11 cell lines with G12C, BH-501242 showed superior anti-cell proliferation activity with median IC_{50}s of 1.31 nM (0.40 nM for GP2D - 9.96 nM for SUIT-2), 3.55 nM (1.84 nM for SW620 - 19.7 nM for SW900), and 2.13 nM (0.68 nM for SW1463 - 5.79 nM for SW756) against *KRAS* G12D, G12V, and G12C mutant cells, respectively. BH-501242 also demonstrated outstanding cell potency against other *KRAS* mutations including G12S, G12F, G12A, G13D and K117N. Mechanistically, BH-501242 tightly binds with both active (GTP-bound or “on”) and inactive (GDP-bound or “off”) forms of mutant KRAS, effectively blocking its interaction with downstream effector c-RAF, and inhibiting the phosphorylation of ERK. Synergistic effects were observed in combination with EGFR antibody cetuximab in colony formation assays with *KRAS* mutant cells. PK profiling revealed oral bioavailability of BH-501242 in multiple species and dose dependent plasma exposures in mouse xenograft tumor models. BH-501242 demonstrated excellent anti-tumor activity in multiple CDX mouse models with various KRAS mutations, including GP2D and HPAC models with G12D mutation, H441 with G12V, and MiaPaca-2 with G12C, etc. In conclusion, the strong preclinical profile provides a strong rationale for the advancement of BH-501242 into further development.

#5121 Targeting peripheral α_{2A}-adrenoceptors as a dual-benefit approach for integrated cancer therapy and supportive care.

Zhiqiang Cheng[1], Yang Xu[1], Larry Zhu[2]

[1]Aglaeapharma INC., Camden, DE,[2]Alpherabio LLC, Boston, MA

Background: Emerging evidence highlights sympathetic innervation is a key component of the tumor microenvironment, and that denervation effectively suppresses tumor growth, revealing new therapeutic opportunities (Vera Thiel, Nature 2025). α_{2A}-adrenoceptor (α_{2A}AR) agonists like clonidine are potent regulators of sympathetic activity, and have demonstrated antitumor efficacy (Jingjing Zhu, Nature 2023), yet their application in oncology can be severely limited by the central nervous system (CNS)-mediated adverse effects, including sedation and hypothermia. To overcome this challenge, we developed CC10230, a novel peripherally restricted α_{2A}AR agonist designed to provide sustained antitumor therapy without dose-limiting CNS toxicity.

Method: A focused compound library was generated through rational design and screened based on *in vitro* α_{2A}AR potency, P-gp efflux ratio, and oral bioavailability. Peripheral restriction of the lead compound was confirmed using *in vivo* distribution pharmacokinetic. Anti-tumor activity was assessed in the MC38 subcutaneous tumor model in mice, and anti-allodynic efficacy was evaluated in the NCTC-2572 cell-induced bone cancer pain model in mice. All clinical observations, including behavior and safety monitoring, were conducted in accordance with CRO's standard operating procedure (SOP).

Result: CC10230 was selected as a lead compound based on its high α_{2A}AR activity (EC_{50}= 7.5 nM, Ki = 58.1 nM), strong P-gp substrate properties (efflux ratio = 51.0), and a favorable oral bioavailability (44.6%). Pharmacokinetic studies confirmed minimal CNS penetration (Kp,uu,brain < 0.03), markedly lower than that of clonidine, supporting strong peripheral restriction. In the MC38 model, CC10230 (5 mg/kg, b.i.d., p.o.) significantly suppressed tumor growth, achieving a TGI of 62.3% at Day 17. Clonidine (5 mg/kg, b.i.d., p.o.) as a positive control also achieved significant TGI but was poorly tolerated, causing pronounced somnolence, hypothermia, and 18.1% body weight loss. In contrast, CC10230 showed no tolerability issues. Additionally, CC10230 exhibited robust efficacy in cancer pain model, confirming its dual therapeutic benefits.

Conclusion: These findings establish peripheral α_{2A}AR activation as a promising two-pronged translational strategy for integrated oncology care, simultaneously inhibiting tumor progression and alleviating cancer-related pain while circumventing CNS-mediated side effects. The favorable safety profile of CC10230 supports its potential for sustained antitumor therapy without the tolerability limitations of conventional α_{2A}AR agonists.

#5122 Regulating m6A-RNA modification as new therapies for cancer.

Tariq Rana

UC San Diego, La Jolla, CA

The role of post-transcriptional modifications of mRNA in regulation of gene expression, stem-cell maintenance, and differentiation has gained significant interest. Transcriptome-wide mapping has revealed that the most abundant internal mRNA modification is the N^6-methyladenosine (m6A), which is present in > 25% of all mRNAs. The N^6-methylation of adenosine is a reversible modification controlled by a multiprotein complex comprised primarily of METTL3 and METTL14, which is responsible for the methylation step, and by two Fe(II)-α-ketoglutarate-dependent dioxygenases, ALKBH5 and FTO, which drive the reverse, demethylation step. In addition, FTO, but not ALKBH5, is responsible for the demethylation of N^6, 2'-*O*-dimethyladenosine (m6Am), a prevalent modification frequently found at the 5′ cap-adjacent adenosine of mRNA where it plays a critical role in controlling mRNA stability and translation. In GBM, reduced levels of m6A and m6Am are involved in cell proliferation, survival, and differentiation. As such pathways are known to be directly linked to acquisition of stem-like cell properties in GBM and other solid and hematological tumors, m6A dysregulation is believed to play a role in the generation of stem-like tumor initiating cells and tumorigenesis where such properties are known to be important for tumor progression, recurrence, and resistance. In GSCs, knockdown of the m6A demethylases FTO and its homolog ALKBH5 suppresses GSC-induced tumorigenesis. Moreover, FTO inhibition prolongs lifespan in tumor bearing mice. Recently, we identified novel inhibitors of FTO that impaired sphere formation of GSCs in 3D organoid models in a manner comparable to FTO silencing. Further medicinal chemistry efforts in this area led to the discovery of a novel series of drug-like small molecules, exemplified by the oxetane derivative FTO-43N that selectively inhibit FTO over ALKBH5. These molecules act as competitive inhibitors of FTO and demonstrate potent antiproliferative effects in glioblastoma. These promising results indicate that selective inhibition of FTO could be an effective strategy to target the resistant stem-cell populations in GBM. Furthermore, assessment of *in vitro* safety pharmacology (CEREP SafetyScan) and brain/plasma PK suggest that FTO-43N and related compounds are an attractive selective FTO inhibitors as drug candidates for the treatment of GBM. Accordingly, using structure-based design strategies combined with advanced *in vitro* and *in vivo* modeling systems, lead-optimization studies to identify candidate FTO inhibitors with pharmacokinetic (PK), *in vivo* efficacy, and safety/tolerability profiles suitable for further drug development.

#5123 C018, a potent and selective CDK4&9 dual inhibitor.

Jinwen Huang, Zhongyuan Li, Steve Shen

Convalife Pharmaceuticals, Shanghai, China

Background: CDK4&6 inhibitors have been approved for the treatment of metastatic ER+&HER2- breast cancer, either as monotherapy or in combination with endocrine therapy. However, many patients develop resistance to CDK4&6 inhibition through multiple mechanisms, including loss of the tumor suppressor Rb, hyperactivation of CDK4&6, and&or upregulation of CDK2&Cyclin E1 expression and activity, resulting in a significant unmet clinical need. CDK9 plays a critical role in RNA transcription as a catalytic subunit of positive transcription elongation factor b (P-TEFb), which phosphorylates the negative elongation factor (NELF), DRB sensitivity-inducing factor (DSIF), and the Ser2 residue within the C-terminal domain (CTD) of RNA polymerase II (Pol II), ultimately triggering transcriptional elongation. Accumulating evidence suggests that CDK9 activity may contribute to palbociclib resistance mechanisms, and targeting CDK9 represents a promising strategy to overcome resistance in breast cancer.
Methods and Materials:Based on structure-activity relationship (SAR) studies and accelerated by the Convalife "AIDRUG.WORK" molecular design platform, we completed the early-stage screening of CDK4&9 inhibitors. The lead compound demonstrated >30-fold selectivity for CDK4 over CDK6 and >80-fold selectivity for CDK9 over CDK6. To explore the therapeutic potential of CDK4&9 dual inhibitors against palbociclib-resistant tumors, we evaluated the effects of CDK4&9 inhibition on cell viability using both palbociclib-sensitive and palbociclib-resistant MCF-7 cell lines.
Results:The CDK4&9 inhibitor significantly impaired the viability of both palbociclib-sensitive and palbociclib-resistant MCF-7 cell lines through concurrent inhibition of CDK4 and CDK9 activity.
Conclusions:Our findings demonstrate that simultaneous inhibition of CDK4 and CDK9 may exert synergistic effects in overcoming palbociclib resistance. CDK4&9 dual inhibition represents a promising therapeutic strategy to overcome both endocrine therapy and CDK4&6 inhibitor resistance in ER+ breast cancer, warranting further clinical development as a novel approach for treating resistant breast cancer.

#5124 Identification and structural characterization of a novel PCNA-interacting small molecule scaffold.

Jennifer Jossart[1], Ning Ma[2], Pouya Haratipour[2], Caroline Li[3], Long Gu[3], Terrence O'Brien[4], Nagarajan Vaidehi[5], Linda H. Malkas[3], Robert Hickey[1], Jeff J. Perry[6]

[1]Cancer Biology and Molecular Medicine, Beckman Research Institute of The City of Hope, Duarte, CA,[2]Beckman Research Institute of the City of Hope, Duarte, CA,[3]Beckman Research Institute of The City of Hope, Duarte, CA,[4]Atomwise, San Francisco, CA,[5]City of Hope National Medical Center, Duarte, CA,[6]Beckman Research Institute at the City of Hope, Duarte, CA

Proliferating cell nuclear antigen (PCNA) plays essential roles in DNA replication, repair, transcription, and cell-cycle regulation, making it an attractive yet historically difficult target in cancer therapy. Building on our development of AOH1996, a first-in-class small molecule currently in Phase I clinical evaluation for solid and liquid tumors, we sought to identify additional PCNA-interacting chemotypes that could expand therapeutic opportunities and inform next-generation inhibitor design. Using an artificial intelligence-guided computer-aided drug discovery workflow, we screened more than ten million drug-like compounds and prioritized candidates through differential scanning fluorimetry. This approach led to the identification of COH005, a previously unreported small-molecule scaffold that binds PCNA. X-ray crystallography demonstrated that COH005 engages the major PCNA-interacting-protein (PIP)-box binding pocket, a critical interface for PCNA-mediated protein-protein interactions. Cellular thermal shift assays (CETSA) validated direct COH005-PCNA engagement in cells similar to clinical IND, AOH1996. To assess selectivity, we performed protein-structure frustration analysis comparing COH005 interactions with PCNA against an unrelated anti-target, revealing energetically favorable binding unique to PCNA. Together, these studies establish COH005 as a novel PCNA-interacting scaffold with strong potential for therapeutic development. This work provides a structural and mechanistic foundation for designing next-generation PCNA-targeted agents with improved specificity and pharmacological properties.

#5125 Discovery of a novel, selective brain penetrant CDK4 inhibitor for targeted cancer therapy.

Boris Rogovoy[1], Dmitrii Shkil[2], Ruben Karapetian[2], Elena Bulanova[2], Alexei Rjakhovskiy[2], Sergey Shevyakov[2], Tudor Oprea[3], Amy Burd[1], Iain Dukes[1], Nikolay Savchuk[1]

[1]Eilean Therapeutics, Dover, DE,[2]ChemDiv Inc, San Diego, CA,[3]Expert Systems, Inc., San Diego, CA

In breast and other malignancies, CDK4 overactivation commonly occurs as a result of sustained endocrine and mitogenic inputs, dysregulated cyclin D1 expression, or the genetic loss or functional impairment of INK4 family inhibitors, or loss of endogenous inhibitors such as p16. Approved CDK4/6 inhibitors (palbociclib, ribociclib, and abemaciclib) are associated with hematologic toxicity, including neutropenia, linked to CDK6 rather than CDK4 inhibition. Since these drugs block CDK6, drug dosing is restricted by bone marrow suppression rather than anti-tumor efficacy. HR+ breast cancer cells are more dependent on CDK4 than CDK6 for proliferation, whereas normal hematopoiesis relies predominantly on CDK6. Loss of CDK4 alone does not impair blood cell development in mice, while CDK6 and its partner cyclin D3 play a key role in stem cell activation, erythroid and myeloid differentiation, and neutrophil maintenance. This divergence establishes a therapeutic window: Selective blockade of CDK4 could suppress tumor growth while sparing bone marrow function. Clinical benefits in patients with brain metastases have been documented. However, dose-limiting toxicity may prevent the gain in overall outcome. CDK4-selective inhibition represents a strategic evolution in targeting cell-cycle dysregulation. By sparing CDK6, agents aim to overcome the main toxicity barrier of dual CDK4/6 inhibitors, enabling more potent and sustained CDK4 blockade. Here, we describe AL-0433, a novel, selective brain penetrant CDK4 inhibitor with excellent *in vitro* and *in vivo* activity.

Methods: AL-0433 was developed using resistance-aware, structure-based design, via AI-enabled virtual screening and medicinal chemistry at Expert Systems. Potency was evaluated against CDK1, 2, 4, 6, 9, and GSK3b in biochemical assays, and cytotoxicity was assessed in breast, ovarian, and glioblastoma cell lines. Pharmacokinetic (PK) properties were characterized in murines and dogs. Anti-tumor efficacy was tested in MCF-7 xenograft models as a single agent and in combination with other anti-tumor agents.

Results: AL-0433 exhibited low-nanomolar CDK4 inhibition (2.7 nM) with 30-fold selectivity over CDK6, and 1000-fold selectivity over CDK1, CDK2, and CDK9. AL-0433 showed potent cytotoxicity in breast, ovarian, and glioblastoma cells (20-950 nM). Mechanism of action studies in MCF-7 cells demonstrated inhibition of pRB phosphorylation. AL-0433 demonstrated excellent oral bioavailability with high blood-brain barrier (BBB) permeability, making it particularly advantageous for treating both primary and metastatic tumors, as well as brain tumors such as glioblastoma.

Conclusion: AL-0433 is a promising, AI-designed, selective CDK4 inhibitor with broad activity across breast, ovarian, and glioblastoma cell lines. Its favorable PK profile, preclinical efficacy, and rational design strategy support further clinical development

#5127 Structure-guided discovery of potent and selective DGKα inhibitors for targeted cancer therapy.

Farag E. S. Mosa, Khaled Barakat

Faculty of Pharmacy and Pharmaceutical Sciences, University of Alberta, Edmonton, AB, Canada

Introduction: Cancer remains a major cause of morbidity and mortality in North America. Diacylglycerol kinases (DGKs) are key regulators of lipid-mediated signaling, converting diacylglycerol (DAG) to phosphatidic acid (PA), two bioactive second messengers that orchestrate diverse cellular pathways. The DGK families comprise ten isoforms classified into five subtypes. Among these, DGKα—a type I isoform—plays critical roles in immune regulation, neuronal signaling, and membrane remodeling. In the context of cancer, DGKα enhances tumor cell proliferation and survival while suppressing cytotoxic T-cell and natural killer (NK) cell activity, thereby facilitating immune evasion. DGKα also promotes PD-L1 expression, further reinforcing tumor immune escape. Dysregulated DGKα signaling similarly contributes to immune dysfunction. To address these pathological roles, we aim to develop highly selective DGKα inhibitors by exploiting a distinct allosteric pocket to achieve precise and isoform-specific modulation of the enzyme.
Methods: We generated high-confidence structural models of DGK isoforms including (α, β) using state-of-the-art AI prediction platforms, complemented by molecular dynamics (MD) simulations and binding free-energy methodologies. Structural models of DGKα and DGKβ were constructed in the presence of biologically relevant cofactors (ATP, Ca^{2+}, Zn^{2+}, Mg^{2+}) to capture catalytically competent conformations. Each model underwent extensive validation through long-timescale MD simulations, and dominant conformational ensembles were extracted via clustering analyses. A generative-design pipeline was subsequently deployed to create and prioritize novel small-molecule inhibitors based on predicted potency, isoform selectivity, and physicochemical suitability. Top-ranked candidates were further interrogated through molecular docking, MD refinement, and free-energy calculations to characterize their binding poses.
Results: The DGKα structural models demonstrated strong concordance with available in vitro data, supporting their suitability for downstream computational analyses. Molecular docking identified a previously uncharacterized allosteric pocket capable of accommodating the generative-AI-derived compounds. MM-PBSA analyses of MD trajectories provided binding free-energy estimates and revealed key residues that mediate ligand engagement and stabilize the inhibitor-protein complexes.
Conclusion: S532, L556, H606, Y558, and F559 mediate ligand recognition, enabling elucidation of the mechanistic basis that underlies the interactions of two lead chemotypes. Several designed molecules exhibit marked isoform selectivity, displaying substantially stronger predicted affinity for DGKα than for DGKβ. Together, these insights provide a structural framework for the rational development of selective DGKα inhibitors.

#5128 Accelerated discovery of novel RORγT modulators using an AI-driven platform integrating generative chemistry and mechanistic PK simulation.

Jeremy Jones[1], Rafal Bachorz[1], Michael Lawless[1], Joanna Pastwinska[2], Anna Salkowska[2], Marcin Ratajewski[2]

[1]Simulations Plus, Inc., Lancaster, CA,[2]Polish Academy of Sciences, Lodz, Poland

The application of artificial intelligence (AI) in oncology drug discovery offers the potential to significantly accelerate and de-risk the identification of novel therapeutic agents. In this study, we present the successful application of an AI-driven drug design (AIDD) platform to discover new classes of RORγT ligands, both agonists and inverse agonists. RORγT, a nuclear receptor central to Th17 cell differentiation and IL-17 signaling, has emerged as a promising target for auto-immune diseases as well as cancer immunology, and both classes of ligands have therapeutic potential.

Our AIDD platform integrates quantitative structure-activity relationship (QSAR) modeling, ADMET property predictions, high-throughput mechanistic PK simulations, 3D volumetric/pharmacophore similarity scoring, and synthetic accessibility assessments at the point of initial compound design. Importantly, compound prioritization is guided by a multi-criteria decision analysis multi-parameter optimization (MPO) algorithm, which incorporates these features to balance potency, ADMET/PK, and chemical tractability to optimize candidate selection. This approach enables systematic decision-making across multiple parameters, reducing reliance on trial-and-error screening.

In our initial Design/Make/Test cycle, 27 novel compounds were synthesized and tested. Remarkably, 70% demonstrated >25% inhibition of RORγT activity in cell-based assays. The top candidate had an IC_{50} of 1.51 uM and favorable in vitro ADME, with high concordance between predicted and measured values. Based on these results, a second set of inverse agonists was designed. 14/19 (74%) were active, with 4 having improved potency. In vitro and in vivo ADMET and PK testing is ongoing. In parallel work, we identified a novel class of RORγT agonists, which could find application in cancer immunotherapy; further development of this class is ongoing as well.

This work demonstrates how a platform integrating generative chemistry with mechanistic PK simulations and MPO can be used to accelerate the development of viable drug candidates, in this case, against an important clinical target, RORγT

#5129 Discovery and development of a novel PI3K-CDK4/6 dual inhibitor PC-13 for the treatment of breast cancer.

Xinyun Zhang[1], Jiaqi Hu[1], Xiaoxue Li[1], Qian Wang[2], Yanan Zhao[2], Qiang Xia[2], Jinhua Wang[1], Heng Xu[1], **Tj (Tiejun) Bing**[2]

[1]Institute of Materia Medica, Chinese Academy of Medical Sciences and Peking Union Medical College, Beijing, China,[2]ICE Bioscience, Beijing, China

Breast cancer continues to be a major cause of cancer-associated mortality globally, underscoring the urgent need for innovative therapeutic strategies. In this study, we report the discovery and preclinical characterization of PC-13, a potential first-in-class dual inhibitor targeting both PI3K and CDK4/6. PC-13 demonstrates nanomolar-level potency against PI3K and CDK4/6 kinases, high selectivity across a broad panel of kinases, and potent antiproliferative effects in multiple breast cancer cell lines. Furthermore, PC-13 exhibits reasonable pharmacokinetic properties and achieves significant tumor growth suppression in a T47D xenograft model, with efficacy comparable to the Palbociclib-Buparlisib combination regimen, while maintaining a promising safety profile. Our findings highlight the potential of concurrent PI3K and CDK4/6 inhibition as a novel and effective therapeutic approach for breast cancer, supporting further development of PC-13 as a clinical candidate.

#5130 Identification and characterization of pan-mutant selective PI3Kα inhibitors with the capability of PI3Kα H1047R protein degradation.

Chengshan Niu*,#, Shengli Dong*,#, Shaoqing Chen*, Kaige Ji, Zhengfei Guo, Maolin Zheng, Mingtao Chen, Yuanjie Li, Meihua Li, Hongqiang Li, Yu Yu, Xinlong Yang, Zhiyong He, Apeng Liang, Zhou Yin, Wei Wu, Jun Li*, Yusheng Wu

TYK Medicines, Inc., Changxing, Zhejiang, China

Introduction: PIK3CA, a PI3K isoform, is one of the most frequently mutated genes in human cancers. PIK3CA mutations are highly enriched at “hotspot” sites in the helical (E542K, E545K) and kinase (H1047R/L) domains. Orthosteric inhibitors of PI3Kα, such as alpelisib and inavolisib, have been approved for the treatment of patients with advanced HR+/HER2– breast cancer. Selective targeting of mutant PI3Kα is anticipated to enhance antitumor efficacy and mitigate the toxicity associated with wild-type PI3Kα inhibition in normal tissue. Allosteric and mutant-selective PI3Kα inhibitors, including RLY-2608 (NCT06982521) and LY4064809 (STX-478, NCT07174336), have been successfully developed in the clinical phase III stage.

Results: Several allosteric and potent pan-mutant PI3Kα inhibitors developed by TYK Medicines exhibited high selectivity over wild-type (WT) PI3Kα. Our observations revealed that the compounds inhibited AKT phosphorylation in the T47D (PI3Kα H1047R) cell line with an IC_{50} in the single-digit nanomolar range, demonstrating nearly 200 times more selectivity compared to SK-BR-3 (PI3Kα WT) cells at same time. In *in vitro* antiproliferative assays, the compounds displayed superior antiproliferative activity against various PI3Kα mutant cells, including T47D, HCC1954 (PI3Kα H1047R), and MCF7 (PI3Kα E545K), compared to STX-478 and RLY-2608. For instance, TY-3659 was four and thirteen times more selective in T47D and MCF7 cells, respectively, than RLY-2608, aligning with the PI3Kα kinase inhibition assays. In addition, TY-3659 effectively degraded PI3Kα mutant protein in HCC1954 and MDA MB 453 (PI3Kα H1047R) cells. In the mouse HCC1954 and Cal33 (PI3Kα H1047R) CDX models, the compounds exhibited potent tumor-inhibitory activity, excellent tolerance, good DMPK properties, and desirable drug-like characteristics. No effects on fasting plasma glucose levels were observed after four days of treatment in the insulin tolerance test.

In conclusion, we identified potent allosteric and pan-mutant selective PI3Kα inhibitors capable of degrading PI3Kα mutant protein. Our findings suggest that TYK compounds can significantly enhance the therapeutic index of PI3Kα-mutant cancers without causing PI3Kα WT-related toxicity.

# Chengshan Niu and Shengli Dong contributed equally to this work.

*Correspondence authors

#5131 HDM2021, a potent and selective CBL-B inhibitor exhibits robust immunomodulatory efficacy for anti-tumor therapy.

Shulun Chen, Mengting Zhao, Zhimin Zhang, Jingwen E, Xi Yang, Xinyu Dai, Zhenna Xia, Xin Xu, **Dongzhou Liu**

Global R&D Center, Huadong Medicine, Hangzhou, China

Introduction: The E3 ligase Casitas B-lineage lymphoma proto-oncogene B (CBL-B) is a critical negative regulator of immune activation. It controls T-cell and NK cell activation by lowering the threshold for effector cell activation, driving effector cell proliferation and inflammation, and reducing susceptibility to suppression by Tregs, MDSCs, and macrophages. Tumors exploit this pathway as a mechanism of immune evasion. To address this resistance, we are developing a potent CBL-B inhibitor designed to enhance intrinsic immune cell function, rescue anti-tumor immunity, and achieve clinical efficacy in immunotherapy-resistant patients.

Methods: A series of CBL-B inhibitors with novel scaffolds have been synthesized and screened for activity and drug-like properties. Compound binding to the CBL-B protein was evaluated using TR-FRET and surface plasmon resonance (SPR) assays. Immunomodulatory activity was assessed *in vitro* in T cells or NK cells by measuring cytokine release via ELISA. Pharmacokinetic studies were conducted in mice and dogs, with serial blood samples analyzed by LC-MS/MS. The toxicology assessment was conducted using an *in vitro* safety panel and *in vivo* 14-day dose range finding (DRF) study in mice. Proof-of-concept *in vivo* efficacy was demonstrated in subcutaneous xenograft mouse models.

Results: Through systematic molecular design and rigorous drug-likeness screening, we have identified HDM2021 as a promising drug candidate. This compound demonstrated high-affinity binding to CBL-B (K_d < 1 nM) and a prolonged target dissociation half-life. Functionally, it activated both T cells and NK cells and exhibited potent tumor-killing activity in T cell-tumor cell co-culture assays. Furthermore, HDM2021 exhibited excellent target selectivity in safety panel assays (44 targets) and minimal hERG channel inhibition (IC50 > 20 μM). In particular, HDM2021 was well tolerated in mice at a dose of 80 mg/kg in a DRF study, indicating an optimal safety profile. It also displayed moderate pharmacokinetic properties in both mice and dogs. Notably, in multiple xenograft models, HDM2021 demonstrated robust antitumor efficacy in combination with PD-1 antibody, and sustained tumor regression was maintained after treatment withdrawal.

Conclusion: HDM2021 has demonstrated potent CBL-B inhibition and robust efficacy in both *in vitro* and *in vivo* models. It also exhibits improved pharmacokinetic properties, high target selectivity, and a favorable safety profile. These findings support its further development as a novel immunomodulatory drug candidate for anti-tumor therapy. IND-enabling studies have been initiated for clinical studies.

#5132 Discovery and preclinical evaluation of a potent, orally bioavailable, highly selective, small molecule non-covalent KRAS[G12D] inhibitor.

Alexei Pushechnikov[1], Volodymyr Kysil[2], Ruben Karapetian[3], Stepan Mochalov[4], Aleksei Riakhovskii[4], Elena Bulanova[4], Nikolay Savchuk[5], Iain Dukes[5]

[1]Expert Systems, Inc., San Diego, CA,[2]ChemDiv, Inc., San Diego, CA,[3]Expert Systems, Inc, Dover, DE,[4]Navegador Biosciences, Cantanhede, Portugal,[5]Eilean Therapeutics LLC, Philadelphia, PA

KRAS[G12D] oncogenic mutation is present in ~35% of pancreatic, 13% of colorectal, and 4% of non-small cell lung cancers. The mutation also occurs in other cancer types, albeit less frequently. Here we would like to present compelling evidences that ZE98-0277 has potent and selective activity in KRAS[G12D] mutant cell lines and in vivo models.
ZE98-0277 drug candidate demonstrates strong in vitro activity (IC50 KRAS[G12D] 6.3 nM) and oral PK, bioavailability ~20-40% in mice and monkeys, broad therapeutic window (>100x in cellular models), good safety and tolerability, favorable ADME properties (solubility, stability, permeability, low hERG inhibition, minimal off-target effects), effective tumor suppression in multiple mouse xenograft models.
These preclinical results demonstrate that ZE98-0277 is a potent, selective, and orally bioavailable KRAS[G12D] inhibitor, strongly efficacious against KRAS[G12D] mutant tumors slated for further development.

#5133 Design, synthesis and pharmacological evaluation of ACC1 selective inhibitors for cancer treatment.

Ryo Mizojiri, Moriteru Asano, Daisuke Tomita, Hiroshi Banno, Noriyuki Nii, Masako Sasaki, Hiroyuki Sumi, Yoshihiko Satoh, Yukiko Yamamoto, Takeo Moriya, Yoshinori Satomi, Hironobu Maezaki

Takeda Pharmaceutical Company Ltd. (Japan), Kanagawa, Japan

Acetyl-CoA carboxylase (ACC) is an enzyme that regulates the rate-limiting step in lipid synthesis, converts acetyl-CoA to malonyl-CoA, and is attracting attention as a drug discovery target in a wide range of areas, including metabolic diseases, oncology, and immunology. There are two subtypes of ACC, and among them, ACC1 has been reported to be highly expressed in human cancer cells, and is therefore expected to be a candidate for the development of new cancer therapeutics. Aiming to develop novel and selective ACC1 inhibitors, we initiated synthetic development from pyrrolopyridine derivative and benzoxazole derivative as lead compounds. In terms of pyrrolopyridine derivative, modification of substituents dramatically improved ACC1 inhibitory activity and PK profiles to identify in vivo tool compound which showed potent PD activity. On the other hand, in benzoxazole derivative, linkers and terminal parts were developed for improving enzymatic activity. As a result, we found 2-phenylbenzoxazole compound, which exhibits very strong selective ACC1 inhibitory activity. Furthermore, we continued to investigate reducing lipophilicity to improve solubility toward the generation of in vivo tool compounds, and found ureido compound with good selective ACC1 inhibitory activity and PK profiles. This compound showed significant anti-tumor efficacy in 786-O xenograft mice at an oral dose of 30 mg/kg, bid (T/C = 0.5%) along with potent and prolonged PD activity. Further investigation toward ACC1 specific inhibitor discovered monocyclic derivatives. Among them, oxazole compound exhibited more potent in vivo efficacy than ureido compound in several xenograft mice models. This finding was the first example to show anti-tumor efficacy by the treatment with ACC1 specific inhibitor as a single agent.

#5135 Targeting EGFR cysteine 775 in EGFR mutant lung cancer.

Jie Jiang[1], Zhengnian Li[2], Yaning Wang[2], Stephen J. Collins[1], Felix H. Gottlieb[1], Prafulla C. Gokhale[3], Michael J. Eck[3], Pasi A. Janne[3], Jianwei Che[1], Nathanael S. Gray[2], Tinghu Zhang[2]

[1]Dana-Farber Cancer Insistitute, Boston, MA,[2]Stanford University, Stanford, CA,[3]Dana-Farber Cancer Institute, Boston, MA

Covalent targeting of EGFR cysteine 797 by osimertinib is one of the most successful breakthroughs in targeted therapy, fundamentally transforming the treatment landscape for non-small cell lung cancer (NSCLC) patients. However, resistance driven by mutation of C797 remains a major clinical challenge. Developing novel covalent strategies beyond C797 targeting presents a compelling opportunity for next-generation EGFR inhibitors. We first demonstrated that cysteine 775, located deep within the ATP-binding pocket, is accessible by a rationally designed covalent molecule ZNL-3, which exhibited strong efficacy in osimertinib-resistant mouse models. To further enhance resilience to resistance-causing mutations, we developed a dual-warhead, bident compound—YNW-1—which covalently targets both cysteine 775 and 797 simultaneously. YNW-1 is the first molecule to exhibit balanced reactive efficiency on both cysteines, rendering single-site mutations ineffective to confer resistance. The discovery of ZNL-3 and YNW-1 represents significant advancements in EGFR-targeted drug development, and further optimization toward clinical translation is a worthwhile strategy.

#5136 Multi-targeted MNK inhibitors as anticancer agents for AML.

Sophie Derusha[1], Erika Lisabeth[2], **Sonali Kurup**[3]

[1]Ferris State University, Big Rapids, MI,[2]Assay Development and Drug Repurposing Core, Michigan State University, East Lansing, MI,[3]Pharmaceutical Sciences, Ferris State University, Big Rapids, MI

Mutant FMS-like tyrosine kinase 3 (FLT3) is implicated as an oncogenic driver in over 30% of acute myeloid leukemia (AML) cases. While several FLT3-targeted drugs have been approved, resistance develops rapidly through varied mechanisms, including RAS mutations. The mitogen-activated protein kinase-interacting kinases (MNK1 and MNK2) are the only kinases that phosphorylate the eukaryotic translation initiation factor 4E (eIF4E). Dysregulation of the MNK-eIF4E axis has been seen in acute myeloid leukemia (AML) and MNK inhibitors have shown antiproliferative effects in AML. The kinases, MNK1 and MNK2 are activated by p38 mitogen-activated protein (MAP) kinase and extracellular signal-regulated kinase (ERK), downstream of FLT3 and RAS in the RAS/RAF/ERK signaling cascade. The aurora kinases (AURKA and AURKB) are also overexpressed in AML. Synergistic anticancer effects have been observed in AML for AURK inhibitors in combination with FLT3 targeted drugs. Multitargeted inhibition of varied oncogenic drivers could be anticipated to demonstrate improved anticancer effects in AML, particularly resistant AML. We have identified novel compounds as multi-targeted MNK inhibitors that bind with nanomolar potencies to MNK1, MNK2, FLT3 and AURKB. The compounds show single-digit micromolar inhibition of AML cells expressing mutant FLT3 (MV-411) and are equipotent to tomivosertib, a clinically investigated MNK inhibitor that was included as a standard for comparison. The design, synthesis, and anticancer effects of multi-targeted MNK inhibitors will be described.

#5137 KBD880 is a potent and selective GPC3 peptide binder for treatment of HCC.

Hongzhu Chu, Yang Chen, Yonggang Wei, Fei Ye, Jing Zhang, Zhiyong Li, **Xiaoke Liu**, Jiannan Cui

Kangbaida (Sichuan) Biopharmaceutical Technology Co., Ltd, Chengdu, China

Background: The membrane-associated glycoprotein Glypican-3 (GPC3) is highly overexpressed in hepatocellular carcinoma (HCC) while exhibiting minimal to no expression in normal tissues. This tumor-specific expression profile makes GPC3 an ideal target for developing radiopharmaceutical therapies to treat HCC, a leading cause of cancer-related deaths worldwide.
Methods: DOTA-KBD-GPC3 (KBD880) is a radiopharmaceutical conjugate composed of a novel GPC3-binding macrocyclic peptide, a linker, and a DOTA chelator for complexation with therapeutic radioisotopes. The binding affinity of the ^{175}Lu-labeled conjugate was characterized by surface plasmon resonance and competitive flow cytometry. Subsequently, Target-mediated cellular internalization kinetics were quantified via radiometric assays. In vivo, the biodistribution and therapeutic efficacy of the ^{177}Lu-labeled conjugate were evaluated in HepG2 HCC xenograft model.
Results: ^{175}Lu-KBD880 exhibited high-affinity binding to both human and murine GPC3, with equilibrium dissociation constants (KD) of 2.20 nM and 2.02 nM, respectively, as determined by surface plasmon resonance. In addition, ^{175}Lu-KBD880 showed potent binding to GPC3-expressing HepG2 cells (IC_{50}= 9.3 nM). A high proportion of non-canonical amino acids and fragments with favorable drug-like properties were used to achieve a balance of potency, permeability, and physicochemical properties. ^{175}Lu-KBD880 exhibited excellent permeability, an optimal half-life and substantial systemic exposure in mice. The therapeutic conjugate, ^{177}Lu-KBD880, exhibited rapid and efficient internalization, achieving cellular uptake ratios of 50-60%. ^{177}Lu-KBD880 displayed an excellent in vivo profile, characterized by high tumor retention, rapid renal clearance, and minimal off-target uptake. This favorable biodistribution translated into significant and sustained tumor growth inhibition following monotherapy in GPC3-positive HCC xenografts.
Conclusions: KBD880 is a potent and selective, peptide-based radiopharmaceutical agent developed for targeting GPC3-expressing tumors. Its favorable preclinical characteristics—including an optimal pharmacokinetic profile, targeted biodistribution, and durable monotherapy efficacy—strongly support its development as a theranostic agent for patients with GPC3-positive malignancies.

#5138 Chemical optimization of an orally bioavailable macrocyclic peptide KRAS inhibitors that achieve KRAS selectivity by recognizing a single amino acid difference.

Mirai Kage, Hatsuo Kawada, Koji Takano, Atsushi Matsuo, Yoshihisa Murata, Satoshi Hashimoto, Minoru Tamiya, Tomoya Kotake, Shino Kuramoto, Takashi Yamano, Machiko Irie, Kazuhiro Ohara, Yuuji Sakurai, Kenichi Nomura, Yuya Morita, Ryuji Hayashi, Yuma Wakamiya, Kana Takei, Hiroshi Tanaka, Yoshikazu Nishimura, Hitoshi Iikura, Takuya Shiraishi, Mikimasa Tanada

Chugai Pharmaceutical Co., Ltd., Yokohama, Kanagawa, Japan

Macrocyclic peptides represent a promising modality for targeting intracellular proteins that are traditionally considered "undruggable" by small molecules or antibodies. Their tunable physicochemical properties allow for engineering of membrane permeability and metabolic stability, enabling oral bioavailability and intracellular engagement. A classic example is cyclosporine A, which exhibits both oral absorption and intracellular activity. To expand the drug-like potential of this class, we developed an mRNA display platform optimized for the selection of bioactive cyclic peptides with favorable pharmacokinetic profiles. This platform enables the identification of peptides capable of passive cell membrane permeation and oral absorption without the need for permeation enhancers. Using this technology, we previously reported LUNA18 (Paluratide), a mid-sized cyclic peptide that binds reversibly to GDP-bound RAS isoforms (KRAS, NRAS, HRAS), inhibiting their signaling (J. Am. Chem. Soc. 2023, 145, 16610). In this presentation, we report the structural optimization research that led to the development of AUBE00, a next-generation pan-KRAS inhibitor derived from the LUNA18 scaffold. AUBE00 was engineered to achieve KRAS isoform selectivity by targeting His95, a residue uniquely present in KRAS but absent in NRAS and HRAS. KRAS selectivity was achieved through a targeted interaction with His95, a KRAS-specific amino acid residue. A key challenge in this process was the inherent flexibility of the cyclic peptide scaffold. To address this, we introduced a partial fixation by bridging the peptide backbone near His95, enabling a precise interaction with the residue. As a result, we achieved approximately 14-fold selectivity over NRAS and 10-fold selectivity over HRAS. Importantly, this structural optimization was accomplished while maintaining the favorable pharmacokinetic profile of the parent compound, LUNA18. AUBE00 is an 11-residue hydrophobic cyclic peptide lacking dissociable side chains. It exhibits high membrane permeability (Caco-2 P_{app} = 2.2 × 10^{-6} cm/s) and strong binding affinity to KRAS (K_D = 92 pM). Notably, AUBE00 demonstrates moderate oral bioavailability (F = 24-65%) across three animal species without specialized formulation. In mouse xenograft models, oral administration of AUBE00 resulted in robust antitumor efficacy. A Phase 1 clinical trial in patients with advanced solid tumors is currently ongoing.

#5139 A novel toll-like receptor antagonist lead for glioblastoma and pancreatic and breast cancer.

Milan Makale, Wolfgang Wrasidlo

UC San Diego School of Medicine, La Jolla, CA

EMS-312 a dual toll-like receptor (TLR2/9) antagonist is the product of a structure activity testing campaign that involved 400+ synthesized analogs. This compound represents a *first-in-class* approach to suppressing the inflammatory network that fuels aggressive cancers. EMS-312 selectively blocks the intracellular TLR2/9-MyD88 signaling complex. As shown in Table 1, EMS-312 is orally available and crosses the blood-brain barrier. By targeting a shared innate-immune pathway, EMS312 can address multiple indications—from glioblastoma, triple negative breast cancer, and pancreatic cancer while also qualifying for orphan and fast-track designations. Comprehensive composition-of-matter patents have been issued and are active through 2039. EMS312 shows a clean safety and ADME package, with compelling early proof of tumor-cell and microglial suppression. EMS-312 sits at the locus of oncology where big pharma currently appears to have a pipeline gap, giving this drug lead candidate significant partnering and acquisition potential.

EMS-312: Physicochemical and pharmacological properties

Parameter	Desired value	EMS-312
Plasma Stability	>80% 1hr	99%
P-gp	No	No
Alb Lig	1E6 cm/sec	1.7E6 cm/sec
Micros stability	>80% 1 min	94%
hERG block	IC50/ICmax	Yes
P450 inhib	<50%@ 10 u/m	<17%
CYPP2D6 substr	No	No
CYPP3A4 induc	No	No
Genotoxic	No	No
circ t1/2	>1 hr	4.79 hrs
vol dist	<10L/Kg	3.8
Clearance	<30 ml/mg/kg	13.6
oral bioavail	>30%	89%
brain/Plasma ratio	>0.3	1.5

#5140 Development of hydrophilic and metabolically stable heterocyclic AOH1996 analogues for pediatric AML oral liquid formulations.

Pouya Haratipour[1], Melissa Valerio[2], Michaela R. Jacobs[1], Maryam Zangi[1], Long Gu[3], Caroline Li[3], Robert Lingeman[3], Jennifer Jossart[1], Jefferson J. Perry[1], Le Xuan Truong Nguyen[2], Linda H. Malkas[3], Robert J. Hickey[1]

[1]Cancer Biology and Molecular Medicine, Beckman Research Institute of The City of Hope, Duarte, CA,[2]Department of Hematologic Malignancies Translational Science, Beckman Research Institute of The City of Hope, Duarte, CA,[3]Department of Molecular Diagnostics & Experimental Therapeutics, Beckman Research Institute of The City of Hope, Duarte, CA

Proliferating cell nuclear antigen (PCNA) is a key regulator of at least 11 essential cellular processes, including DNA replication and repair, transcription, cell cycle progression, apoptosis induction, transcription-replication conflict resolution, energy metabolism, chromosome maintenance, mitosis, and immune surveillance. In tumor cells, PCNA exists as a cancer-associated acidic isoform (caPCNA), while non-malignant cells express only a basic isoform (nmPCNA). The absence of caPCNA in normal cells makes it an attractive target for selective cancer therapy. We previously developed AOH1996, a first-in-class small molecule that selectively inhibits caPCNA, inducing apoptosis in cancer cells without detectable toxicity in non-malignant cells. AOH1996 binds to caPCNA, stabilizes its trimeric structure, decreases chromatin association, and suppresses tumor cell proliferation. AOH1996 is orally bioavailable and is currently being evaluated in two first-in-human Phase I clinical trials: one for treatment refractory solid tumors (NCT05227326) and the other for acute myeloid leukemia (NCT06763341). No dose-limiting toxicities have been observed to date, with ongoing dose escalation currently reaching 1110 mg PO BID. In this study, we aimed to enhance the aqueous solubility and pharmacokinetic properties of AOH1996 through strategic single-point heteroatom substitutions. By replacing selected aromatic carbons with nitrogen atoms, we generated a series of quinoline, isoquinoline, and pyridine analogues optimized for liquid oral formulations that will be ultimately compatible with pediatric administration for AML. Structure-activity relationship (SAR) analyses across these three heterocyclic scaffolds identified several analogues with improved solubility, potency, selectivity, and metabolic stability when compared to the clinical lead. For example, introducing two nitrogen atoms into the aromatic regions of one analogue reduced the CLogP to 3.35 (vs. 4.46 for AOH1996) while maintaining IC_{50} values comparable to the parent compound. This reduction in lipophilicity corresponds to an estimated ~13-fold increase in aqueous solubility, making this analogue more amenable to liquid formulation for oral administration. Over 30 novel AOH analogues were synthesized and evaluated for antiproliferative activity across eight tumor cell lines (including Molm-13, THP-1, HTB-0225, SK-N-AS, HCT116, U251, and MDA-MB-468), as well as in AML mouse models. Synthetic routes, biological data, and preliminary *in vivo* results will be presented. Together, these findings lay the groundwork for the next generation of AOH-based therapeutics with improved physicochemical and pharmacological properties suitable for pediatric oncology applications.

#5141 ZMS-4084, a potent and selective WRN inhibitor induces significant tumor regression and sustained complete responses in MSI-H tumor models.

Weikun Wang, Guimei Yang, Liting Xue, Yao Guo, Wenjing Li, Renhong Tang, **Zhengtao Li**

State Key Laboratory of Neurology and Oncology Drug Development, Simcere Zaiming Pharmaceutical Co, Ltd., Shanghai, China

Microsatellite instability-high status (MSI-H) is typically prevalent in endometrial, gastrointestinal, ovarian and colorectal cancers. The RecQ helicase WRN has been identified as a synthetic lethal target in MSI-H cancers and represents a promising therapeutic candidate in this context. The two clinical-stage WRN inhibitors, HRO761 and RO7589831, have demonstrated the clinical efficacy in phase I trials. Here we report the discovery of a novel and potent WRN inhibitor, ZMS-4084. Surface plasmon resonance analysis revealed that ZMS-4084 binds specifically to the WRN helicase domain with high affinity (KD=1.08E-08 M). ZMS-4084 selectively inhibited WRN ATPase activity with an IC_{50} of 0.05 μM, and exhibited over 2,000-fold selectivity over other RecQ family helicases. Intracellular mechanistic study demonstrated that ZMS-4084 induces apoptosis and inhibits proliferation of HCT116 (MSI-H) cells with an EC_{50} of 0.024 μM, accompanied by WRN degradation and accumulation of DNA damage signified by p21 expression and other markers. In a panel of 124 tumor cell lines, ZMD-4084 selectively inhibited the viability of MSI-H cell lines without significant effects on microsatellite stable (MSS) cell lines, indicating high selectivity and a potentially favorable safety profile. Notably, ZMD-4084 effectively suppressed the growth of MSI-H patient-derived organoids, including those previously exposed to standard-of- care therapies such as chemotherapy, anti-EGFR agents, and/or immunotherapy. *In vitro* ADME and *in vivo* pharmacokinetics studies demonstrated favorable physicochemical properties and dose-proportional oral bioavailability across preclinical species, supporting its potential for oral administration in humans. Daily administration of ZMS-4084 resulted dose-dependent antitumor efficacy in xenograft models derived from MSI-H human tumors. In the Ishikawa xenograft model, daily dosing at 2.5 mg/kg induced 100% tumor regression, and complete responses (CRs) were achieved in five out of six aminals at 15 mg/kg. Even in the less sensitive RKO xenograft model, 100% tumor regression and several CRs were observed at a dose of 20 mg/kg. No treatment-related abnormalities were observed across all dose regimens in non-GLP preclinical safety studies. In conclusion, we have developed a novel WRN inhibitor, ZMS-4084, which demonstrates robust antitumor activity in both xenograft models and patient-derived organoids representing diverse MSI-H tumor types. Given the synthetic lethality between WRN inhibition and MSI-H status, along with its broad antitumor activity across multiple tumor lineages, ZMS-4084 holds strong potential as a tissue-agnostic therapeutic agent for patients with MSI-H tumors.

#5142 PRMT5 inhibitor SCR-6920 downregulates HIF-1α and exhibits synergistic antitumor activity with Bevacizumab.

Guimei Yang, Huixia Dou, Liting Xue, Yao Guo, Wenjing Li, Zhen Li, **Zhengtao Li**, Renheng Tang

State Key Laboratory of Neurology and Oncology Drug Development, Simcere Zaiming Pharmaceutical Co, Ltd., Shanghai, China

PRMT5 has emerged as a promising epigenetic target for cancer therapy, yet its potential in rational combination strategies remains inadequately explored. This study aims to characterize the novel, oral PRMT5 inhibitor SCR-6920, with a particular focus on its ability to synergize with anti-angiogenic therapy by modulating the hypoxia-inducible factor-1α (HIF-1α)/vascular endothelial growth factor (VEGF) axis. SCR-6920 is a potent and highly selective PRMT5 inhibitor that has undergone extensive preclinical evaluation and is currently in phase 1 clinical trials (NCT05528055). It demonstrated broad antitumor efficacy across a panel of cancer cell lines *in vitro* and in xenograft models *in vivo*. A key finding from RNA-seq analysis was that PRMT5 inhibition by SCR-6920 led to the downregulation of angiogenesis pathways, particularly those involving VEGF. Subsequent mechanistic studies revealed that SCR-6920 significantly reduced hypoxia-induced HIF-1α protein levels without altering its mRNA expression. This effect was mediated by promoting the ubiquitination and subsequent proteasomal degradation of the HIF-1α protein. Consequently, SCR-6920 treatment resulted in the decreased expression and secretion of VEGF, a major downstream target of HIF-1α. Based on this mechanism targeting the HIF-1α/VEGF axis, we investigated and demonstrated a robust synergistic antitumor effect between SCR-6920 and the anti-VEGF antibody bevacizumab in an ovarian cancer xenograft model. This combination resulted in significantly enhanced tumor growth suppression without an increase in toxicity, providing a strong mechanistic rationale for this combination strategy. Furthermore, SCR-6920 exhibited synergistic or additive effects when combined with several standard-of-care chemotherapies and targeted agents for solid tumors, including paclitaxel, docetaxel, doxorubicin, and olaparib. In summary, our work identifies SCR-6920 as a promising clinical-stage PRMT5 inhibitor with a unique ability to destabilize HIF-1α and suppress VEGF signaling. The unveiled mechanism, whereby PRMT5 inhibition promotes HIF-1α degradation, provides the foundation for the observed synergistic activity with bevacizumab. These findings position SCR-6920 as a compelling clinical candidate for solid tumors, particularly in rational combinations aimed at overcoming resistance to anti-angiogenic therapy.

#5145 A novel highly potent multiple-RAS inhibitor ZMS-2195 efficiently blocks MAPK pathway activation and induces robust anti-tumor growth effects in preclinical models.

Zhengtao Li, Guimei Yang, Huixia Dou, Wei Zhu, Xiang Chen, Yao Guo, Wenjing Li, Liting Xue, Renhong Tang

State Key Laboratory of Neurology and Oncology Drug Development, Simcere Zaiming Pharmaceutical Co, Ltd., Shanghai, China

Variants in the RAS family (HRAS, NRAS and KRAS) represent among the most prevalent oncogenic mutations identified in cancer. Approximately 19% of cancer patients harbor RAS mutations, which are typically associated with poor clinical outcomes. Multi-RAS inhibitor may overcome resistance by hitting a broader range of targets than single-mutant inhibitors. As such, multi-RAS inhibitors are anticipated to offer therapeutic potential across a wide range of RAS-driven malignancies. Here we report ZMS-2195, a novel and highly potent Multi-RAS inhibitor. Biochemical assays assessing disruption of the RAS-RAF complex demonstrated that ZMS-2195 effectively inhibited the interaction between multiple RAS variants—including KRAS, NRAS, and HRAS mutants and wild-type forms—and the RAF-RBD domain, with digital nanomolar IC_{50} values. The cellular MAPK pathway inhibition was confirmed through robust suppression of phosphorylated ERK in representative cancer cell lines harboring diverse *RAS* mutant alleles. Consistent with the biochemical activity observed against multiple RAS variants and cellular pERK inhibition potency in RAS mutant cell lines, ZMS-2195 caused potent growth inhibition of KRAS mutant cancer cell lines, exemplified by Miapaca-2 ($KRAS^{G12C/G12C}$, PDAC), AsPC-1($KRAS^{G12D/G12D}$, PDAC) and SW403 ($KRAS^{G12V/WT}$, CRC) with IC_{50} values of 0.8, 1.3 and 0.3 nmol/L, respectively. Wild-type *RAS* (RAS^{WT}) cancer cells with GTP-activated RAS from upstream mutations were equally sensitive to ZMS-2195, exemplified by H1975($EGFR^{mut}$, NSCLC) with an IC_{50} of 6.7 nmol/L. Conversely, RAS^{WT} cancer cells harboring downstream *BRAF* mutations or RAS-independent normal cells were essentially insensitive to ZMS-2195. Favorable oral bioavailability and pharmacokinetic profiles were exhibited in pre-clinical species. Oral administration of ZMS-2195 resulted in dose-dependent and sustained suppression of RAS pathway signaling, as evidenced by reduced human DUSP6 mRNA expression levels in tumor lysates. Daily dosing of ZMS-2195 produced dose-dependent antitumor activity in xenograft models derived from RAS-driven human tumor xenograft model *in vivo*. At a dose of 0.8 mg/kg, ZMS-2195 induced tumor regression in PK59 ($KRAS^{G12D/WT}$, PDAC) xenograft model. In summary, ZMS-2159 is a potent Multi-RAS inhibitor with robust activity against RAS-driven tumor cells, supporting its further development as a target therapy for cancers driven by diverse RAS aberrations.

#5146 Discovery of a novel ALK inhibitor ZM-8195 that targets ALK compound mutations with superior TRK selectivity.

Zhen Li, Yajing Liu, Mengying Li, Jing Dai, Xuefeng Wang, Yuan Cheng, Xue An, Jing Chen, Jianan Wang, Yuandong Zheng, Wenjing Li, Liting Xue, **Zhengtao Li**, Renghong Tang

State Key Laboratory of Neurology and Oncology Drug Development, Simcere Zaiming Pharmaceutical Co., Ltd., Shanghai, China

ALK fusions are common oncogenic drivers. Approximately 5% of NSCLC patients are ALK-positive, with 30% to 40% developing brain metastases. ALK inhibitors are primarily used to treat ALK-positive patients. However, sequential therapy with second- and third-generation inhibitors is susceptible to resistance mutations, compromising clinical efficacy. Concurrently, inhibition of TRK-family kinases (TRKA, TRKB, and TRKC) elicits broad central nervous system (CNS) adverse effects, further limiting their utility. Therefore, there is an urgent need to develop a new generation of ALK inhibitors to cover a broader population of drug-resistant mutations with brain penetrance and superior TRK selectivity. Here, we identified ZM-8195, a potent and selective ALK inhibitor. In *in vitro* evaluation, ZM-8195 showed low nano-molar activities against EML-ALK fusion and G1202R/L1196M mutation in biochemical and cell proliferation assay. ZM-8195 exhibited minimal activity against TRK-family kinases, with selectivity indices for TRKB over ALK wild-type or mutant exceeding 100-fold. ZM-8195 also showed potent anti-proliferation activity in different ALK compound mutant cell lines with IC_{50} from 0.5-24 nM. ZM-8195 effectively inhibited H3122(EML4-ALK V1) and BaF3(EML4-ALK V1(G1202R/L1196M)) tumor growth with complete tumor regression. In a BaF3 G1202R/L1196M orthotopic brain model, ZM-8195 also demonstrated robust anti-tumor efficacy. ZM-8195 was well tolerated in rodents and non-rodents. Based on its favorable activity, selectivity, pharmacokinetic profiles and safety, ZM-8195 is currently in IND enabling stage.

#5147 A novel investigation of the cyclin A/B inhibitor ZMS-7506 demonstrates robust anti-tumor efficacy both *in vitro* and *in vivo*.

Guimei Yang, Ruina Wang, Weikun Wang, Liting Xue, Xiaokang Qin, Renhong Tang, **Zhengtao Li**

State Key Laboratory of Neurology and Oncology Drug Development, Simcere Zaiming Pharmaceutical Co, Ltd., shanghai, China

Cyclins A and B are critical regulators of the transition from the S phase to the G2/M phase of the cell cycle. Abnormal expression and activity of these cyclins are hallmarks of cancer. Disruption of the interaction between E2F and the cyclin A2-CDK2 complex results in hyperactivation of E2F, leading to apoptosis and synthetic lethality in E2F-driven tumors. Small cell lung cancer (SCLC) cell lines commonly exhibit dysregulated E2F activity due to near-universal loss-of-function mutations in RB1 and TP53. We have developed ZMS-7506, a potent oral Cyclin A/B inhibitor, which demonstrated a median IC_{50} of approximately 40 nM in anti-proliferation assays using a panel of SCLC cell lines. Moreover, ZMS-7506 selectively inhibited the proliferation of ovarian cancer OVCAR3 cells, with a GI_{50} value below 20 nM. In the meanwhile, ZMS-7506 exhibited a GI_{50} greater than 10 μM in normal human embryonic lung fibroblasts (WI38), indicating a favorable therapeutic window. Mechanistically, ZMS-7506 induced G2/M cell cycle arrest and upregulated markers associated with apoptosis and mitotic arrest, including p-KNL1, p-HH3, p-PARP, and p-γ-H2AX. These findings suggest that ZMS-7506 activates the spindle assembly checkpoint (SAC), thereby inducing mitotic arrest and apoptosis. ZMS-7506 also exhibited moderate oral bioavailability in pre-clinical species such as dogs, which supported the oral administration in human. Moreover, ZMS-7506 exhibited robust antitumor efficacy as a monotherapy in the SCLC NCI-H69 xenograft mouse model. In summary, ZMS-7506 is a highly selective oral Cyclin A/B inhibitor with promising therapeutic potential as a monotherapy for cancers characterized by elevated E2F activity.

: Targeted Protein Degradation and Induced Proximity
Poster Session

#5151 Design and synthesis of highly efficacious CRBN-based pan-KRAS degraders targeting cancers with KRAS G12D, G12V and G12C mutations.

Changwei Wang[1], Prithwish Ghosh[1], Shicheng Jin[1], Longchuan Bai[2], Donna McEachern[1], Angelo Aguilar[2], Qiuxia Li[3], Bo Wen[3], DUXIN SUN[2], Shaomeng Wang[1]

[1]Departments of Internal Medicine, University of Michigan, Ann Arbor, MI,[2]University of Michigan, Ann Arbor, MI,[3]Department of Pharmaceutical Sciences, University of Michigan, Ann Arbor, MI

Oncogenic mutation of KRAS is one of the most promising targets for cancer. Treatment with inhibitors inevitably lead to rapid onset of resistance, and loss of therapeutic effect after months. KRAS PROTACs may offer superior efficacy by eliminating mutated protein, disrupting scaffolding function and activating immune response, thus overcoming the rapid development of resistance. Using new E3 ligands developed in house, our compounds achieved less than 1 nM DC_{50} and IC_{50} in *in vitro* assays with G12D, G12V and G12C mutated cell lines. They exhibited excellent pharmacokinetic and pharmacodynamic properties in mice, and outstanding pharmacokinetic in rats, dogs, and monkeys. At 10 mg/kg, qW, the compounds achieved a remarkable TGI of over 92% in SW620 xenograft, a robust and challenging model of $KRAS^{G12V}$ mutation. Additionally in an efficacy study with mice bearing SW1990 xenograft, at 10 mg/kg, qW, the compounds regressed the tumors by over 90%.

#5152 Targeted degradation of KRAS using the AUTOTAC platform.

Su Ran Mun[1], Su Jin Lee[1], Hyeong-Reh C. Kim[2], Yong Tae Kwon[1]

[1]Seoul National University, Seoul, Korea, Republic of,[2]Department of Pathology, Barbara Ann Karmanos Institute, Wayne State University School of Medicine, Detroit, MI

RAS is one of the most frequently mutated oncogenes in human cancers, with KRAS mutations being particularly prevalent: accounting for approximately 95% of pancreatic cancers, 45% of colorectal cancers, and 20% of lung cancers. Due to its lack of deep pockets for ligand binding, RAS has long been considered an “undruggable target,” despite more than three decades of intensive drug discovery efforts. Although small-molecule inhibitors targeting KRAS G12C have recently been developed, their therapeutic effect is limited to this specific mutation, underscoring the need for strategies capable of targeting a broader range of KRAS variants.AUTOphagy TArgeting Chimera (AUTOTAC) is a recently developed targeted protein degradation platform that harnesses the autophagy pathway to eliminate pathological proteins. In this study, we applied AUTOTAC technology to RAS, generating RAS-AUTOTAC, a bifunctional small molecule composed of a Target-Binding Ligand (TBL) linked to an Autophagy-Targeting Ligand (ATL). Upon binding to RAS via the TBL, the ATL component recruits the ZZ domain of p62, inducing p62 oligomerization and initiating autophagic degradation. During this process, RAS becomes biologically inactivated and sequestered into autophagosomes. RAS-AUTOTAC suppresses downstream oncogenic signaling through p62 oligomerization and subsequent autophagic degradation. Importantly, RAS-AUTOTAC selectively recognizes the GTP-bound active form of RAS and effectively suppresses RAS signaling across multiple KRAS variants. Moreover, RAS-AUTOTAC demonstrated tumor growth inhibition in animal models, supporting its functional activity *in vivo*.Collectively, our results provide a mechanistic basis for applying AUTOTAC to RAS-driven cancers.

#5153 Characterization of second-generation AUTOTACs targeting the androgen receptor for castrate-resistant prostate cancer treatment.

Tri Pham[1], Su Jin Lee[2], Y. Mindy Huang[3], Matthew Han[4], Tae-Hyun Bae[2], Brianna Temby[5], Isabella Schena[6], Abdo J. Najy[1], Harmant Grewal[7], Jenna Poole[1], Young Tae Kwon[8], Hyeong-Reh C. Kim[9]

[1]Pathology, Karmanos Cancer Institute, Wayne State University School of Medicine, Detroit, MI,[2]Department of Biomedical Sciences, College of Medicine, Seoul National University College of Medicine, Seoul, Korea, Republic of,[3]Physics and Astronomy, Wayne State University, Detroit, MI,[4]International School, Bellevue, WA,[5]Oncology, Karmanos Cancer Institute, Wayne State University School of Medicine, Detroit, MI,[6]Department of Pathology, Karmanos Cancer Institute, Wayne State University School of Medicine, Detroit, MI,[7]Michigan State University College of Osteopathic Medicine, East Lansing, MI,[8]Department of Biomedical Sciences, Seoul National University College of Medicine, Seoul, Korea, Republic of,[9]Pathology, Oncology, Karmanos Cancer Institute, Wayne State University School of Medicine, Detroit, MI

Background: The androgen receptor (AR) drives the progression of prostate cancer (PCa), including castrate-resistant PCa (CRPC). Therapeutic resistance is often mediated by AR mutations and splice variants like AR-v7, which circumvent conventional AR-targeting therapies. AUTOTACs (Autophagy-Targeting Chimeras) is a novel platform for targeted protein degradation via the autophagy-lysosomal pathway. We previously reported the characterization of ATC-324, the first-generation AR-targeting AUTOTAC utilizing enzalutamide (ENZ) as a target-binding ligand (TBL) and YT 6-2 as an autophagy targeting ligand (ATL). The current study evaluates two second-generation AR AUTOTACs, ATB-238 and ATB-239, designed to improve the efficacy and stability in degrading AR and its variants.

Methods: AR-null PCa model: PC3. Androgen-sensitive PCa models: LNCaP, LAPC4. CRPC models: CWR-R1, 22Rv1. Immunoblotting measured relative protein levels. p62 siRNA and bafilomycin A1 were used to study autophagy-dependent drug mechanism. An AR activity reporter assay quantified AR transcriptional activity. Cytotoxicity was evaluated using the WST1 assay. Molecular docking, mutagenesis assays, and proximity ligation assay (PLA) were used to assess ATB-238- and ATB-239-induced AR:p62 complex formation. Bone-in-culture array (BICA) was used to assess the therapeutic potential of ATB-238- and ATB-239 in 22Rv1 in the bone microenvironment. Docetaxel, a first-line chemotherapy for PCa, was used to study synergy with AR AUTOTACs.

Results: ATB-238 and ATB-239 demonstrated improved degradation of AR isoforms and significantly reduced AR transcriptional activity, including AR-v7-driven activity. ATB-238 demonstrated cytotoxicity against AR-positive cells (LAPC4, CWR-R1, 22Rv1), but not AR-null cells (PC3). Molecular docking predicts that ATB-238 and ATB-239 bind to R139, K141, L166, and F168 within the zz domain of p62. Mutation of these residues into Alanine abolished AR:p62 interaction and p62 oligomerization induced by ATB-239. ATB-238 and ATB-239 exhibited high potency against 22Rv1 micrometastases in BICA, while ATB-238 synergizes with docetaxel in killing LNCaP and CWR-R1 cells.

Conclusion: ATB-238 and ATB-239 represent significant advances in AR-targeted therapeutics, capable of degrading AR variants and overcoming therapy resistance. The ongoing intra-iliac-artery xenograft studies will assess their potential to inhibit PCa bone metastasis, an incurable stage of the disease. These findings highlight the therapeutic promise of AUTOTAC technology in addressing critical challenges in CRPC treatment.

#5154 Proteolysis and gene silencing targeting chimera (PROGENTAC).

Abhay Prasad, Rong Zheng, Deeksha Satyabola, Yang Xu, Yichen Yan, Hao Yan

Biodesign Center for Molecular Design and Biomimetics, Arizona State University, Tempe, AZ

Introduction: In biological systems, nucleic acids mirror computational networks, integrating digital genetic codes with analog molecular interactions to achieve precise, context-dependent control of life processes. Harnessing this property provides an opportunity to design programmable therapeutics with exceptional specificity and minimal toxicity. Building on this inspiration, we devised a method for the conditional activation of a dual-functional nucleic acid construct comprising gene-silencing antisense oligonucleotide (ASO) and protein degrader, a DNA-based proteolysis-targeting chimera. We have coined the term “Proteolysis Gene Silencing Targeting Chimera” (PROGENTAC) to describe this technology. This dual functionality of conditional PROGENTAC offers several advantages, such as enhanced specificity and combating multidrug-resistant in complex diseases[1]. The molecular design of PROGENTAC consists of three elements: 1) DNA-templated, spatially controlled protein-degrading chimera (DTAC) platform[2]; 2) ASO for targeted gene modulation; and 3) rationally proposed conditional nucleic acid-based molecular framework that regulate PROGENTAC activity[3] in response to disease-specific intracellular cues or chemical trigger.

Experimental Procedures: In house solid phase oligo synthesis was utilized to construct both DTAC and modified ASO constructs. In house organic synthesis was utilized to modify small molecule-based inhibitors. Electrophoretic mobility shift assay (EMSA) was utilized to visualize conditional activation of PROGENTAC in cell-free based media. Fluorescence resonance energy transfer (FRET) assay was utilized to evaluate kinetics of PROGENTAC activation. Additional experiments were conducted including, Cell treatments, Western blots, Confocal imaging, Flow Cytometry, Proteomics, and Cytotoxicity assays.

Results and Summary: Three cancer cell lines U251, A549 and AU565 showed excellent activity of DTAC that targets Cyclin D1-CDK4/6 complex protein with efficacy of DC_{50} of 20-100 nM range. For a proof of concept, we successfully constructed GFP protein silencing ASO construct with various nucleic acid modifications such as 2’-OMe, locked nucleic acid (LNA), and phosphorothioate (PS backbone). The optimal chemically modified potent ASO construct was successfully integrated with DTAC in PROGENTAC molecular framework. PROGENTAC construct was evaluated for structural stability and conditional activation to release both protein degrading DTAC and gene silencing ASO modalities. In the conference we will further talk about extended cellular results and therapeutic properties of PROGENTAC.

Citation: 1) Dagogo-Jack, I. & Shaw, A. T. Nat Rev Clin Oncol 15, 81-94 (2018); 2) Zheng, L. et al. J. Am. Chem. Soc. 2025, 147, 33, 29742-29755; 3) Yan, H., Zhang, X., Shen, Z. et al. Nature 415, 62-65 (2002).

#5156 Development of FBXW7 binders for targeted protein degradation.

Shenghao Guo[1], Becky Leifer[2], Yichen Xiang[1], Angela N. Koehler[2]

[1]Massachusetts Institute of Technology (MIT), Cambridge, MA,[2]Koch Inst. for Integrative Cancer Research at MIT, Cambridge, MA

Protein-protein interactions (PPIs) play essential roles in almost all the physiological processes in human cells. Inducing or enhancing the proximity of specific PPIs for targeted protein degradation (TPD) has received much attention. TPD caused by induced protein proximity is usually achieved by two categories of small molecules: molecular glues and proteolysis targeting chimeras (PROTACs). Both categories utilize the ubiquitin-mediated proteolysis system for degradation, in which E3 ligases play vital roles in substrate recognition. Despite the fact that there are over 600 E3 ligases in the human system, only less than 10% are investigated for TPD. Here we report the discovery of a set of potential binders for FBXW7, an E3 ligase and key tumor suppressor for which no previous binders have been found. Our project aims to discover potent small-molecule binders to FBXW7, which can be used as new warheads for PROTAC design for TPD and eventually suppression of various cancers. Taking advantage of our high-throughput screening technology, Small Molecule Microarrays (SMMs), we successfully identified 3 groups of compounds (44 total) that potentially bind to FBXW7 after screening our 65,000 'drug-like' small molecule library. This is done by printing these small molecules directly onto glass chips and incubating with in-house purified His-tag FBXW7, and then recognizing with fluorescence-conjugated antibody. We then performed secondary assays using nanoDSF, in which multiple small molecules from one of the groups induced over 0.3 ℃ change in the melting point of FBXW7, indicating binding activity. Interestingly, these small molecules share very similar chemical structures, which differ from others by merely one functional group on one of the 6-membered rings. Following thermo shift assay indicates that these small molecule candidates stabilize FBXW7 in a dose-dependent manner shown by western blot. So far, our leading compound is shown to have a binding affinity of 0.3μM to FBXW7 using ITC. Attempts to synthesize and test these binders for a set of proof-of-concept PROTACs are in progress. In summary, our findings identify a new set of potential binders to FBXW7, which expands the toolbox for PROTAC design. We also prove the strength of SMM as a viable methodology for the exploration of more E3 ligase binders, which will greatly benefit the development of tools in TPD for cancer therapeutics.

#5157 Discovery and characterization of XNW34017, a first-in-class, orally bioavailable, and brain-penetrant AURKA-MYC degrader.

Liqun Chen[1], Haoran Li[1], Xiuchun Zhang[1], Chong Peng[1], Zhe Zhang[1], Shihua Wang[1], Liang Kong[1], Jiajing Xu[1], Xiaocheng Hu[1], Zhenwei Wu[1], Yanfei Wang[1], Wengui Wang[1], Haiyang Wei[1], **Yonghan Hu**[2], Xiaojun Liu[1], Meijie Le[2], Jing Qiang[2]

[1]Evopoint, Suzhou, China,[2]Evopoint, Shanghai, China

Aurora-A is a serine/threonine kinase essential for mitotic progression and is overexpressed in a broad range of solid tumors and hematological malignancies. Inhibiting AURKA's kinase activity can suppress tumor progression. Several AURKA inhibitors have been developed and tested in clinical trials. Although AURKA inhibitors have shown strong preclinical efficacy, their clinical development was not successful. Beyond its catalytic role, AURKA can stabilize MYC family proteins to protect them from proteasomal degradation. Consequently, unlike the AURKA inhibitors, degraders of AURKA can eliminate the entire AURKA protein, simultaneously abolishing its kinase activity and scaffolding function. Compared with inhibitors, this dual mechanism may offer enhanced antitumor efficacy and expanded therapeutic window, making degradation of AURKA and subsequent MYC a more effective therapeutic strategy. Based on this rationale, we developed the first-in-class bifunctional AURKA degraders, which have shown efficient degradation of AURKA and MYC family proteins (c-Myc, L-Myc, and N-Myc) in MYC-driven cell lines. MoA studies with early lead compounds confirmed that AURKA degradation is on-target, E3- and UPS-dependent. qPCR experiment further demonstrated that neither AURKA nor MYC protein level change is associated with transcriptional changes, validating our therapeutic strategy of degrading AURKA to induce MYC degradation. After extensive optimization, XNW34017 was selected as the development candidate. XNW34017 exhibits favorable PK properties, including >50% oral bioavailability across species (mouse, rat, and dog), and evidence of brain penetration. The compound selectively and potently degrades AURKA, leading to subsequent degradation of MYC family proteins. In the NCI-H209 SCLC model with L-MYC overexpression, oral QD dosing of XNW34017 induced rapid AURKA degradation at day 1 and efficient L-MYC degradation at day 3, which then led to complete tumor regression. PD studies revealed a strong correlation between L-MYC degradation and enhanced tumor response. In tumor models with c-MYC and N-MYC overexpression, XNW34017 also demonstrated superior tumor growth inhibition (TGI) while AURKA inhibitor showed limited efficacy. Notably, in the NCI-H1975 NSCLC brain metastasis model with c-MYC overexpression, oral QD dosing of XNW34017 achieved 98% TGI at day 21, demonstrating its efficacy against MYC-driven CNS disease. DRF and GLP toxicity studies of XNW34017 in rats and dogs demonstrated good tolerability with a reasonable safety margin, suggesting that the clinical risks are manageable. Observed toxicities were consistent with on-target degradation of AURKA, with no unexpected safety risk observed. Together, our MOA and preclinical studies support the advancement of XNW34017 into clinical development for MYC-driven malignancies.

#5158 Preclinical characterization of HY809382, a highly potent and orally bioavailable PRC2 PROTAC, for the treatment of lymphoma and solid tumors.

Huangtao Jin[1], Juan Du[1], Ruwei Wang[1], Zengrong Li[1], Ting Zhang[1], Xing Yu[1], Ming Weng[1], Xiaoxiao Wang[1], Xiaohong Hou[1], Feifei Yang[1], Xin Li[1], Weixing Zhu[1], Liming Zhang[1], Lei Chen[1], Sai Yang[1], Feng Xu[1], Qian Ma[1], **Ruowen Zhang**[2], Xiaotian Huang[1]

[1]Yangtze River Pharmaceutical (Group) Co., Ltd., Taizhou, China,[2]Medicilon USA Corp, Lexington, MA

The Polycomb repressive complex 2 (PRC2) is a key epigenetic regulator that mediates gene silencing through the catalysis of histone H3 lysine 27 trimethylation (H3K27me3). This activity facilitates repression of tumor suppressor genes as well as immune-related transcripts. The core subunits of PRC2 comprise EED, SUZ12, and the catalytic component EZH1 or EZH2. Aberrations of PRC2 components, including mutation and overexpression, have been identified across a range of cancers, highlighting PRC2 as a promising therapeutic target. Although targeting EZH2 has been the primary approach in PRC2 inhibitor development, leading to the FDA approval of Tazemetostat as the first-in-class agent, no PRC2 degraders have yet progressed to clinical trials. The PRC2 degraders provide several potential advantages, such as overcoming acquired resistance to approved EZH2 inhibitors, disrupting the stability of the PRC2 complex, and enhancing efficacy against lymphoma and solid tumors. Herein we disclose HY809382, an orally bioavailable PRC2-targeting PROTAC molecule, as a candidate therapeutic for lymphoma and solid tumors. HY809382 demonstrated degradation of the target protein EED at nanomolar (nM) concentrations, without altering protein levels of known CRBN neo-substrates such as IKZF1/3, GSPT1 and CK1α. Proteomic analysis confirmed that HY809382 selectively degraded the target protein EED and its co-complex partner EZH2, demonstrating excellent degradation specificity. The antiproliferative activity of HY809382 surpassed that of approved or clinically investigated small molecule inhibitors targeting PRC2 components. HY809382 exhibited favourable oral pharmacokinetics in preclinical species, with bioavailability (F)≥ 40%. Once-daily oral administration of HY809382 demonstrated significant, dose-dependent tumor growth inhibition in Karpas-422 (DLBCL), G401 (rhabdoid tumor) and 22Rv-1 (prostate cancer) cell-derived xenograft models, outperforming approved or clinically investigated PRC2-related inhibitors. IHC analysis confirmed HY809382-mediated downregulation of key on-target pharmacodynamic markers (e.g., H3K27me3, EED and EZH2) in tumor tissues. A 44-target safety screen indicated a clean off-target profile, and the compound showed low risks of cardiotoxicity and genotoxicity, as supported by hERG inhibition and the mini-Ames tests, respectively. Preliminary non-GLP repeated-dose toxicity studies in mice and cynomolgus monkeys indicated that HY809382 was well tolerated, with estimated therapeutic windows of >95 and >25, respectively. These findings support the potential of HY809382 as a best-in-class PRC2 degrader and warrant its further evaluation in IND-enabling studies.

#5159 Rational development of novel FBXO22-mediated TEAD Targeted Glues™ for mesothelioma and NSCLC treatment.

Marta Carrara, Martin Fisher, Alice Fletcher, Callum Hamby, Jack Miles, Colin T. Davies, Sara Bisetto, Paula MacGregor, Edward Hooper-Greenhill, Aleksandra Azevedo, Martin O'Rourke, Dominic CG Owens, Liliana Greger, Ivan Del Barco Barrantes, Giles Brown, Martin Pass, Louise K. Modis

Amphista Therapeutics, Cambridge, United Kingdom

TEAD transcription factors are critical effectors of the Hippo signalling pathway and represent promising therapeutic targets in cancers with pathway dysregulation. We report the rational discovery and optimization of a novel class of TEAD degraders that exploit a Targeted Glue™ mechanism to achieve FBXO22-dependent proteasomal degradation. Our novel degraders with differentiated chemical matter demonstrate exceptional degradation profiles (sub-nM DC50, >90% Dmax), coupled with outstanding on-pathway selectivity as measured by global proteomics vs >7000 other proteins measured. Through comprehensive mechanistic studies, we elucidated that our warheads engage FBXO22 via covalent modification of C326. This structural understanding, enabled by high-resolution ternary complex cryo-EM data, facilitated systematic structure-activity relationship optimization of both degradation potency and kinetic parameters. In vitro, our lead compounds exhibited deep (>150% GImax) and potent (nM GI50) anti-proliferative activity in mesothelioma, with synergistic efficacy observed in combination with EGFR inhibitors in EGFR-mutant NSCLC models. Critically, our optimized compounds achieved oral bioavailability and demonstrated robust in vivo activity, representing the first demonstration of FBXO22-mediated degradation in vivo. In mesothelioma xenograft models, we observed rapid (2h, first time point measured), deep (>95%) and sustained (≥72h) TEAD degradation leading to prolonged biomarker inhibition. Our work provides critical design principles for this degrader class and validates FBXO22-TEAD degradation as a therapeutically relevant approach for Hippo pathway-driven cancers, with promise in mesothelioma and combination strategies for EGFR-mutant NSCLC.

#5161 HJ-004, a potent and selective pan-EGFR mutation targeted protein degrader (TPD) that effectively overcomes osimertinib resistance in EGFR-mutant NSCLC.

Li Zeng, Yao Liu, Ya Geng, Yue Zhu

Jing Medicine Technology (Shanghai) Ltd., Shanghai, China

Background: Although three generations of EGFR tyrosine kinase inhibitors (TKIs) have achieved remarkable clinical success, resistance driven by secondary EGFR mutations remains a major therapeutic challenge in non-small cell lung cancer (NSCLC). To address this unmet need, we developed HJ-004, a potent, selective, and orally bioavailable pan-EGFR mutation degrader that targets classical, rare, and exon 20 insertion mutations.

Methods and Results: HJ-004 induces potent and selective degradation of mutant EGFR proteins, but not wild-type EGFR, in Ba/F3 and human cell lines harboring diverse EGFR alterations, with DC_{50} values below 5 nM, and exhibits strong antiproliferative activity. Mechanistic studies confirmed E3 ligase-mediated ubiquitination and proteasomal degradation. *In vivo*, HJ-004 produces dose-dependent tumor regression in both murine and human-derived cell-derived xenograft (CDX) and patient-derived xenograft (PDX) models carrying various resistant EGFR genotypes. Pharmacokinetic evaluation demonstrated favorable PK properties, including 30-40% oral bioavailability across multiple species and sustained exposure supporting once-daily dosing. Importantly, HJ-004 exhibits an approximately 10-fold therapeutic window in both mice and monkeys, without any notable skin rashes or diarrhea, indicating excellent selectivity and safety margin.

Conclusions: HJ-004 represents a first-in-class pan-EGFR mutation targeted protein degrader that effectively overcomes osimertinib resistance across classical, rare, and exon 20 insertion variants. Its potent degradation activity, broad antitumor efficacy, and favorable pharmacokinetic and safety profiles support advancement into clinical development as a next-generation therapy for EGFR-mutated NSCLC. HJ-004 was independently developed by Jing Medicine Technology (Shanghai) Ltd., and has received IND clearance from both the U.S. FDA and China NMPA.

#5163 Leveraging selective degradation of CBP and EP300 for potent anti-cancer activity.

Karolina Mizeracka, Elizabeth Wittenborn, Darshan Sappal, Laura La Bonte, Danette L. Daniels

Foghorn Therapeutics, Watertown, MA

Numerous cancers have shown dependency on one of two paralog histone acetyltransferases, CREB binding protein (CBP) or E1A binding protein (EP300). Genomic screens have identified a bidirectional synthetic lethal relationship for these two proteins, such that, for example, EP300-mutant gastric and colorectal malignancies strongly depend on CBP function for growth and survival. Additionally, the divergent biology of these targets can underly selective lineage dependencies. For example, hematological cancers are exquisitely sensitive to loss of EP300, even in the presence of functionally intact CBP. Previously developed inhibitors that disrupt activity of both enzymes have resulted in hematopoietic toxicity, and selectively drugging these targets to improve the therapeutic window has been a significant challenge. Here we describe our platform to develop fast, potent, and selective CBP and EP300 degraders that remove only one of the targets, while sparing the activity of its paralog. We elucidate the mechanisms underlying selective degradation through cellular, structural, and biophysical assays of ternary complex formation and ubiquitination between the target proteins and the E3 ligase VHL. We find that our selective degraders likely drive differential target ubiquitination and degradation through differences in ternary complex stability and the induction of divergent orientations between the bromodomains of the respective target relative to VHL. Additionally, we demonstrate that CBP and EP300 selective degraders show strong anti-proliferative effects across numerous oncology indications that are dependent on either target. Importantly, treatment with our selective degraders at efficacious doses is not associated with hematopoietic toxicity, providing evidence that specific targeting of one of the paralogs provides a wider therapeutic window than dual inhibition.

#5164 Exploration of novel E3 ligase to support targeted protein degradation drug discovery.

Zuyuan Shen, Yunyun He, Rui Wang, Nengwei Xu, **Peichuan Zhang**, Lingbing Sun

In Vitro Biology Unit, WuXi AppTec, Shanghai, China

Targeted protein degradation is a new drug discovery strategy that harnesses mainly the power of the ubiquitin-proteasome system (UPS) to degrade selectively disease-causing proteins. A key mechanism of UPS degrader molecules, including molecular glues and proteolysis-targeting chimeras (PROTACs), relies on their ability to bring target proteins into proximity with E3 ligases or complexes for ubiquitination and subsequent degradation at the proteasome. The human genome encodes at least 600 E3 ligases, of which two complexes (i.e., $CUL4^{CRBN}$ and $CUL2^{VHL}$) are predominantly employed in the TPD field. This has raised concerns about issues like target diversity and specificity and drug resistance, and thus, prompts a strong need to look for novel, ligandable E3 ligases that can be exploited to support TPD drug discovery.

To this date, we have surveyed a small panel of E3 ligase components, by utilizing the DNA-encoded library (DEL) screening technology, and identified GID4 (homolog of the yeast glucose-induced degradation deficient complex 4), substrate receptor of the CTLH E3 complex, as a top candidate that showed promising ligandability to small molecules. The GID4-binding hit molecules were validated, structure-optimized, and conjugated with a linker and BRD4-binding moiety to generate a number of PROTACs for targeting BRD4, a transcription regulator that plays an important role in promoting tumorigenesis.

We demonstrated that these GID4-BRD4 PROTACs can mediate biochemical ternary binding (with EC_{50} < 1 nM) and induce BRD4 degradation in cancer cell lines (with DC_{50} < 1 uM). We also solved the crystallography structure of the ternary complex to look into potential working mechanism for one PROTAC. Using the direct-to-biology (D2B) high-throughput approach, we also have optimized the PROTACs and identified structures that can enhance degradation efficacy.

Taken together, we have shown that, as a proof-of-concept, affinity-based DEL selection may help explore ligandability of proteins of interest and lead to the discovery of novel ligands and PROTACs for novel E3 ligases. Of note, our work has been corroborated by another independent study, which reported that GID4 E3 ligase can be leveraged for protein degradation (Li et al., *Nat. Struct. Mol. Biol.* 2025).

#5166 NRX-4972, a selective, oral, Aurora kinase A degrader, demonstrates increased efficacy in an SCLC tumor model, and greater *in vitro* synergy than an AURKA inhibitor.

Hua Tian[1], **Ryan B. Rountree**[1], Jeffrey T. Mihalic[1], Eric R. Wegrzyniak[1], Ge Wei[1], Karthik Arumugam[1], Paul L. Auger[1], Graham J. Carlson[2], Robert T. Cass[1], Tarra Knotts[1], Filippo Marchioni[1], Daniel Medina-Cleghorn[1], Michael G. Mormino[1], Madeleine P. Nemchek[1], Rusha M. Sardhara[1], Sangita Sridharan[1], Austin Tenn-McClellan[1], Simon Vezina-Dawod[2], Gwenn M. Hansen[1]

[1]Nurix Therapeutics, Inc., Brisbane, CA,[2]Nurix Therapeutics, Inc., The Woodlands, TX

Aurora kinase A (AURKA) is frequently overexpressed in adult solid tumors, hematologic malignancies, and pediatric cancers. AURKA is a critical regulator of mitosis. Cancer cell lines particularly sensitive to AURKA loss include those derived from *MYCN*-amplified tumors (e.g., neuroblastoma) and from tumors with *RB1* loss, such as neuroendocrine small cell cancers and CDK4/6-resistant breast cancers (Mou et al., 2021). Several AURKA inhibitors are effective in preclinical tumor models but have failed to translate into clinical efficacy. Recent studies have found that AURKA has kinase-independent scaffolding functions that are not effectively blocked through enzymatic inhibition (Otto, et al, Cancer Cell, 2009; Buchel, et al., Cell Reports, 2017).

To address the limitations of inhibitors, we developed NRX-4972, a CNS-penetrant, orally bioavailable and highly selective degrader of AURKA designed to remove both enzymatic and scaffolding functions. NRX-4972 has a superior PK/PD profile compared with an AURKA inhibitor and more effectively induces DNA damage, apoptosis, and G2/M arrest. Previously, we demonstrated that once-daily oral administration of NRX-4972 provides robust efficacy in the H82 mouse tumor model of SCLC, while an AURKA inhibitor is ineffective (Tian et al.; AACR; Cancer Res 2025;85(8_Suppl_1): Abstract 6379). Here, we demonstrate that NRX-4972 achieves superior efficacy in the same tumor model when administered twice-daily (BID). After over two months of treatment with NRX-4972, 60% of mice survived to the end of the study. In contrast, none of the mice treated BID with the AURKA inhibitors alisertib or LY3295668 survived to the end of the study.

To evaluate the benefit of AURKA degradation over inhibition in the combination setting, we performed an in vitro synergy screen across SCLC, NSCLC, and TNBC cancer cell lines. NRX-4972 and LY3295668 were compared in combination with a range of chemotherapeutics and targeted agents, and cell viability was evaluated for synergy using the Bliss independence model. The highest synergy scores were found in combination with NRX-4972, and more combinations with NRX-4972 resulted in synergy than with LY3295668. These data suggest that eliminating the kinase and scaffolding functions through degradation of AURKA increases the vulnerability of cancer cells to combination therapy.

Collectively, NRX-4972's superior preclinical profile highlights the potential of AURKA degraders to overcome the limitations of AURKA inhibitors and achieve meaningful therapeutic benefit.

#5167 Design and applications of novel hydrophobic CRBN binders.

Hailong Yang, Qingbo Xu, Yongqiang Wang, Zhenyu Wu, **Hongbo Zhang**

HitChem, Wilmington, DE

Cereblon (CRBN) molecular glue degraders engage target proteins through a shallow binding pocket, representing a promising strategy to expand the druggable proteome. However, a key challenge in the structure-based discovery of CRBN molecular glues lies in the conformational diversity induced at the CRBN-substrate interface. Different CRBN binders can modulate this interface in distinct ways, ultimately determining which substrate proteins are recruited and defining compound selectivity.In this study, we designed and identified several novel CRBN binders exhibiting excellent or acceptable binary binding affinities. Compared with previously reported CRBN ligands, our compounds possess unique structural features and enhanced hydrophobic properties. Derivatives based on these scaffolds enabled the construction of a CRBN molecular glue library that extends into previously unexplored, CRBN-biased chemical space. This library provides a high-quality toolbox to accelerate the discovery of new targets using the CRBN molecular glue degrader approach.

#5168 Expanding the landscape of targeted protein degradation: E3-agnostic discovery and proprietary ligand identification.

Kanae Gamo, Shinya Yokosaka, Michiko Watanabe, Tomoaki Hayashi, Shigeyuki Mori, Naomi Asahara, Noriyasu Sano, Shigeru Furukubo, Kazuteru Aoki

FIMECS, Inc., Fujisawa, Japan

Targeted protein degradation (TPD) is a promising therapeutic modality, but its broader application is constrained by the lack of established strategies to select optimal E3 ligases for specific targets. Although many E3 ligases exist, only a few have been leveraged in degraders currently undergoing clinical trials, leaving much of the ligase space unexplored. To address this challenge, a proprietary TPD discovery platform enables rational E3 ligase selection in a high-throughput manner through a workflow that integrates fragment-based diversity-oriented synthesis (DOS) with phenotypic screening in relevant cell models. This workflow, supported by in-house capabilities for high-throughput compound synthesis, generates diverse chemical scaffolds and identifies degrader candidates with desired activity profiles. Phenotypic screening ensures functional relevance and facilitates the discovery of compounds that engage E3 ligases not previously applied in TPD, thereby expanding the scope of ligase-targeted degradation strategies. Lead compounds are refined through optimization and E3 ligase deconvolution to confirm ligase engagement and improve molecular properties such as potency, selectivity, and drug-likeness. Once novel E3 ligase binders are identified through this process, they open up new application opportunities. One path is to incorporate the binder into our internal E3 ligase toolbox and apply it to other targets as part of bifunctional degrader design. Another is to evaluate whether the binder can function as a molecular glue, enabling degradation through neo-substrate recruitment. Importantly, our phenotypic screening approach has led to the identification of proprietary E3 ligases with low expression in bone marrow and hematopoietic tissues. Degraders based on these E3 ligase binders demonstrate the potential to avoid bone marrow toxicity—a major concern for cancer targets—while maintaining robust activity. This strategy not only enables the development of orally bioavailable molecules with improved pharmacokinetics and broad target applicability, but also provides a path to safer TPD therapeutics. By expanding the usable E3 ligase toolbox, this proprietary platform unlocks new degrader modalities and supports the development of therapeutics with improved physicochemical properties, including orally bioavailable candidates. This presentation will highlight case studies demonstrating how this platform contributes to the advancement of novel E3 ligase-based TPD, offering a scalable, versatile, and forward-looking solution to a key bottleneck in the field.

#5169 Identification and optimization of pyridylbenzylamine analog 1 as potent and selective Helios degrader.

Ashok Purandare[1], Godwin Kumi[1], Guo Li[1], Aaron Balog[1], Emily Cherney[1], Michael Barnes[2], Satheesh Nair[3], Sirish K. Lakharaju[1], Xin Li[4], Robin Moore[4], Petia Shipkova[4], Silvi Chacko[4], Cullen Cavallaro[1], Ling Li[1], Kimberly Foster[4], Keith DiPetrillo[4], Gerry Everlof[4], Kevin Stefanski[4], Steven Levine[5], Lihong Shi[6], Jinqi Liu[5], Helen Pham[7], Ari Salinger[7], Ashok Dongre[7], Shailesh Dudhgaonkar[3], Debarati Mazumder[8], Anuradha Gupta[3], Vetrichelvan Muthalagu[3], Madhusudhan Ravindran[8], Yan Chen, Weifang Shan, Suresh Babu Viswa Krishna Penmetsa, Carolyn Weigelt, Robert Borzilleri, Louis Lombardo, Gregory Vite, John Hunt

[1]Discovery Chemistry, Bristol Myers Squibb Company, Princeton, NJ,[2]Discovery Biology, Bristol Myers Squibb Company, Seattle, WA,[3]Discovery Chemistry, Bristol Myers Squibb Company, Bangalore, India,[4]PCO, Bristol Myers Squibb Company, Princeton, NJ,[5]LDO, Bristol Myers Squibb Company, Princeton, NJ,[6]LDO, Bristol Myers Squibb Company, San Diego, CA,[7]LDO, Bristol Myers Squibb Company, Cambridge, MA,[8]LDO, Bristol Myers Squibb Company, Bangalore, India

Small molecule approaches that enhance antitumor immunity have the potential to broaden the benefit of cancer immunotherapy as monotherapies or in combination with immune checkpoint inhibitors (ICIs). Indeed, despite the success of ICIs, resistance and limited response in some patients highlight the need for alternative strategies. FOXP3+ regulatory T (Treg) cells within the tumor microenvironment (TME) suppress antitumor immunity and limit the efficacy of ICIs in some tumor types. Transcriptional reprogramming of Treg cells represents a novel and promising therapeutic approach to treat such patients. IKZF2 (Helios), a zinc finger transcription factor selectively expressed in Treg cells, contributes to the transcriptional immunosuppressive phenotype of these cells, including silencing of IL-2 expression. Genetic deletion of IKZF2 in FOXP3+ cells enhances antitumor responses in preclinical models, establishing it as a nonredundant regulator of Treg cell function. Although transcription factors have traditionally been considered “undruggable,” the discovery of cereblon (CRBN)-mediated degradation of zinc finger proteins by immunomodulatory imide drugs (IMiDs™) has enabled targeted protein degradation (TPD) of factors such as IKZF1 (Ikaros) and IKZF3 (Aiolos). We recently disclosed the discovery of a potent and selective IKZF2 degrader, BMS-986449, derived from lenalidomide/pomalidomide scaffolds. Herein, we report SAR optimization studies leading to the identification of a pyridylbenzylamine appended lenalidomide analog (compound 1) with excellent Helios degradation activity and improved selectivity over related neosubstrates (e.g. IKZF1, IKZF3, and CK1α). In addition, 1 also exhibited favorable ADME properties and robust in vivo pharmacodynamic effects in a mouse syngeneic model.

#5170 Design and optimization of small-molecule PROTACs targeting KRAS.

Fidelix Ayobami[1], Sai Kumar Samala[2], **Ngoc Tuyet Tra**[2], Geraldine V. Raja[2], Yuri Mackeyev[2], Sunil Krishnan[2]

[1]Baylor College of Medicine, Houston, TX,[2]Vivian L. Smith Department of Neurosurgery, The University of Texas Health Science Center at Houston, Houston, TX

KRAS is one of the most frequently mutated oncogenes in cancer and is strongly associated with poor outcomes. For decades, it has been considered ‘undruggable’ because its surface lacks the deep binding pockets that small-molecule drugs can typically target and the very strong affinity to GTP/GDP makes it difficult for drugs to outcompete GTP. Recently, advances in structural biology led to the discovery of a regulatory allosteric pocket in the KRAS(G12D) mutant, which has opened the door to new therapeutic approaches for pancreatic cancer; unfortunately, single-agent allosteric inhibitors have shown little anti-cancer activity in patients. PROTACs (proteolysis-targeting chimeras) offer advantages over traditional inhibitors by degrading entire proteins independent of active sites or deep, hydrophobic binding pockets, making them attractive for hard-to-target proteins like KRAS.

In our lab, we carried out an *in silico* screen and identified Pixantrone as the top hit for a possible KRAS-binding warhead. Based on this, we synthesized a library of PROTACs with various lengths of alkyl linkers tethering Pixantrone, the warhead targeting KRAS, to Pomalidomide, a well-known E3 ligase recruiter. We then assessed our PROTACs’ effectiveness in degrading KRAS and the corresponding effects in pancreatic cancer cell lines. In addition, we evaluated the MAPK signaling cascade, one of the KRAS downstream pathways. Evaluation of the Pixantrone-based PROTACs showed limited KRAS degradation and no significant effects on MAPK signaling or cell death, as assessed by cell viability and immunoblotting assays. These findings suggest that Pixantrone is not a suitable warhead for KRAS targeting. Moving forward, we are shifting our efforts toward validating other candidates from the screen, since PROTAC efficacy may be independent of kinase inhibition efficacy of the warhead alone. If successful, an improved PROTAC design may overcome the clinical ineffectiveness of the current generation of allosteric inhibitors.

#5171 The EGFR-PROTAC molecule TY-2719 attenuates acquired resistance to 3rd-generation EGFR TKIs and augments the efficacy of KRAS mutant inhibitors in solid tumors.

Apeng Liang*,#, Shengli Dong*,#, Shaoqing Chen*, Hongqiang Li, Zhiyong He, Zhengfei Guo, Meihua Li, Shunxun Han, Guangbin Liu, Xi Wang, Yanyan Liu, Ling Fang, Yi Long, Xiang Zhang, Wei Wu, Chengshan Niu, Jun Li, Yusheng Wu

TYK Medicines, Inc., Changxing, Zhejiang, China

Introduction: Acquired resistance to EGFR-TKIs poses a significant challenge in the clinical management of non-small-cell lung cancer (NSCLC). TY-2719, an effective oral, broad-spectrum EGFR-PROTAC developed by TYK Medicines, was designed to overcome the resistance associated with third-generation EGFR-TKIs. TY-2719 not only demonstrated an excellent safety profile but also enhanced the efficacy of KRAS mutant inhibitors in NSCLC and pancreatic ductal adenocarcinoma (PDAC) models.

Results: TY-2719 effectively degraded EGFR with the L858R mutation in NSCLC H3255 cells and the L858R/T790M/C797S and 19del/C797S mutations in BaF3 cells. However, it did not degrade EGFR in cells expressing wild-type EGFR, such as A549 and H358 cells. It demonstrated excellent antiproliferative activity against EGFR mutants but did not inhibit the growth of normal cells, including NHEK, MCF-10A, IOSE-80, and FHC cells. TY-2719 overcame osimertinib resistance in BaF3 L858R/C797S and BaF3 del19/C797S CDX mouse models and enhanced the efficacy of Divarasib (GDC-6036) and pan-KRASi Daroxonrasib (RMC-6236) in NSCLC H1972 and H2122 cells, as well as Daroxonrasib in MiaPaca 2 (PDAC, KRAS G12D), AsPC-1, SU.86.86, PANC-1 (PDAC, KRAS G12D), and Capan-1 (PDAC KRAS G12V). Common side effects of EGFR-TKIs, including osimertinib, are skin reactions and diarrhea due to wild-type EGFR inhibition in normal tissues. The DMPK characteristics of TY-2719 were excellent, with superior toxicity profiles in Sprague-Dawley rat experiments. The body weights of male and female rats showed no difference between the 100 mg/kg (mpk) TY-2719 treated group and the vehicle group after three weeks of treatment. No diarrhea was observed in rats treated with 100 mg/kg TY-2719, either. In the BN Norway female rat rash experiment, after 28 days, all rats in the 37.5 mpk gefitinib control group showed obvious rash symptoms, whereas in the TY-2719 100 mpk group, all rats' skin appeared normal. Meanwhile, treatment with 100 mpk TY-2719 had no significant effect on the body weight of Norway rats compared to that of the vehicle group.Taken together, we have identified a potent and safe EGFR-PROTAC molecule which may grant new therapeutic opportunities to overcome drug resistance of 3rd -generation EGFR TKIs in NSCLC patients and enhance the efficacy of KRAS mutant inhibitors in NSCLC and PDAC.

#Shengli Dong and Apeng Liang contributed equally to this work.

* Correspondence authors.

#5172 Mechanistic insights into PLK1 target inhibition in ovarian cancer: Functional suppression and PROTAC-based therapeutic agents.

jaesung Ryu, Baek MooJun, HyoWook Gil, Eunjung Yang, Kwangseock Kim, Taewan Kim, Kong Hyejeong, Beamjun Park, Jeong Kyu Bang, **Seob Jeon**

Soonchunhyang University Cheonan Hospital, Cheonan, Korea, Republic of

OBJECTIVE
This study aimed to identify the oncogenic role of PLK1(Polo-like kinase 1) in ovarian cancer and evaluate its potential as a PROTAC therapeutic target candidate. We also investigated the change in the functional properties of cancer by PLK1 inhibition and whether it is possible to improve cell viability rate through PROTAC-based PLK1 protein degradation.
METHODS
Functional studies were conducted using PLK1 siRNA in SKOV3 cell lines. Changes in cell proliferation, migration, invasion, and wound-healing ability were evaluated following PLK1 silencing. Quantitative RT-PCR was used to measure PLK1 expression in cell lines and in benign, malignant ovarian tumor tissue samples.In addition, we evaluated the effect on sensitivity in ovarian cancer cell lines and paclitaxel-resistant ovarian cancer cell lines using PLK1 target PROTAC.
RESULTS
Expression of PLK1 at the RNA level is significantly overexpressed in ovarian cancer cells compared to normal cells. Also, PLK1 expression was significantly overexpressed in malignant ovarian tumor compared to benign ovarian neoplasm. PLK1 silencing significantly reduced cell proliferation and decreased migration and invasion by 50-60%. Cell viability assays performed in both parental and paclitaxel-resistant ovarian cancer cell lines demonstrated that treatment with the PLK1-targeting PROTAC resulted in a significantly higher level of cell death compared to paclitaxel.
CONCLUSION
Our results demonstrate that PLK1 inhibition at both the RNA and protein levels suppresses the metastatic characteristics of ovarian cancer and highlights its potential as a therapeutic target. Targeting PLK1 in ovarian cancer may contribute to the inhibition of metastatic aibilty and the overcoming of chemoresistance.

#5173 Identification of a small molecule degrader targeting SALL4 oncogene.

Kim Anh L. Vu[1], **Shiva Moein**[2], Kalpana Kumari[1], Bee Hui Liu[1], Miao Liu[2], Chong Gao[2], Li Feng[1], Mahmoud Bassal[2], Douglas Auld[3], Dominik Casalena[3], Qiling Zhou[1], Daniel G. Tenen[4], Li Chai[5]

[1]Cancer Science Institute of Singapore, Singapore, Singapore,[2]Harvard Medical School/Brigham and Women's Hospital, Boston, MA,[3]Novartis Institute for BioMedical Research, Cambridge, MA,[4]Harvard Stem Cell Institute, Boston, MA,[5]Harvard Medical School/ Brigham and Women's Hospital, Boston, MA

Recent studies have shown that immunomodulatory imide drugs (IMiDs) could degrade SALL4 through a proteasome-dependent mechanism. Intriguingly, we found that IMiDs do not affect SALL4-positive cancer cell survival. Further studies revealed IMiDs could only degrade SALL4A, one of the SALL4 isoforms. This suggests that SALL4B, the isoform not affected by IMiDs, might be essential or compensating SALL4A in supporting cancer cell survival. Indeed, knocking downSALL4B increased apoptosis and inhibited cancer cell growth, similar to knocking down bothSALL4A and B. Moreover, SALL4B gain-of-function alone led to liver tumor formation in mice. Through high-throughput screening, we discovered a new non-IMiD degrader that targetsSALL4A and SALL4B via proteasomal degradation, showing potent anti-cancer activity by inhibiting cancer cell proliferation in culture and *in vivo* tumor growth by 70%. Gene expression profiling via RNA-sequencing identified a shared drug and SALL4B knock down gene signature in hepatocellular carcinoma (HCC) cells, including pathways involved in DNA damage response and DNA replication. Our findings highlight the importance of understanding drug action and oncogenesis at the isoform level to develop more effective cancer therapeutics.

#5174 High-throughput capillary immunoassays enable precise quantitation of protein degrader potency and kinetics in oncology discovery.

Charles Haitjema[1], Francisco Ramirez[1], Bhamini Purandare[1], Pallavi Joshi[1], Chris Heger[2]

[1]Bio-Techne, San Jose, CA,[2]Bio-Techne, Minneapolis, MN

Protein degraders such as PROteolysis TArgeting Chimeras (PROTAC degraders) have transformed oncology drug discovery by enabling catalytic removal of disease-relevant proteins rather than occupancy-based inhibition. To effectively rank and optimize degrader candidates, discovery teams need quantitative, reproducible assays that resolve both potency (e.g., DC_{50}, *D*max) and degradation kinetics across large panels of compounds, concentrations, and time points. Conventional Western blotting lacks the throughput and consistency required for this role early in the screening funnel.

Here, we demonstrate how Simple Western capillary immunoassays with the Leo system enables precise, quantitative degrader assessment with 96-sample throughput for upstream primary and secondary screening. Using androgen receptor (AR) degraders in AR-expressing MDA-MB-453 breast cancer cells as a model system, this method delivered robust, dose- and time-dependent AR degradation profiles with single-digit coefficients of variation and highly consistent DC_{50}, *D*max, and degradation rate (kdeg) estimates between biological and technical replicates.

The open antibody platform flexibility of Leo provides endogenous protein expression measurements for orthogonal validation of model systems such as anti-HiBiT antibodies. By resolving proteins by size, Leo can distinguish true target degradation from artifacts in plate-based assays (e.g., luminescent or fluorescence reporter loss), thereby validating plate-based screening hits and revealing false readouts that lack corresponding size-resolved changes in the target or reporter.

These results establish high-throughput Simple Western assays on Leo as a fit-for-purpose solution for precise degrader quantitation at scale. The combination of open, antibody-agnostic detection chemistry, size-resolved readouts, and 96-sample throughput enables richer pharmacologic insight earlier in oncology screening funnels and supports data-driven prioritization and orthogonal validation of protein degrader candidates before advancing into more complex, resource-intensive models.

#5175 Discovery and characterization of once in a month intravenous and orally bioavailable SMARCA2 degraders for treating SMARCA4 mutant cancers.

Bilash Kuila, Kiran B. Aithal, Sandeep Vitthal Dukare, Charamanna KB, Khaji Abdul Rawoof, Prasath Kothandaraman, Amit A. Dhudashiya, Nandish C, Payel Das, Anuradha Gadeval, Madhu K L, Bhagwan Mahadeo Dhaytadak, Gopinath CH, T Jagadeesh Kumar, Suraj Tgore, Mohamad Fairus Bin Abdul Kadir, Leena Khare, Ranadeep Bokalial, Samiulla DS, Subhendu Mukherjee, Saravanan Thiyagarajan, Kavitha Nellore, Rajesh Eswarappa, Girish Daginakatte, Chandrasekhar Abbineni, Sanjeev Giri, Murali Ramachandra, **Susanta Samajdar**

Aurigene Oncology Limited, Bangalore, India

The BAF (SWI/SNF) chromatin remodelling complex is a multi-subunit assembly that regulates chromatin accessibility via ATP-dependent nucleosome repositioning, thereby modulating transcription, DNA recombination & repair, and mitotic chromosome segregation. Its catalytic activity is mediated by two mutually exclusive ATPases, SMARCA2 (BRM) and SMARCA4 (BRG1). In SMARCA4-deficient tumors, oncogenic dependency shifts to the residual SMARCA2-containing SWI/SNF complex, establishing a synthetic lethal vulnerability. This dependency has been validated through genetic silencing studies, positioning SMARCA2 as a compelling therapeutic target in SMARCA4-mutant cancers. We report the identification and preclinical development of highly potent and selective SMARCA2 degraders based on rational design by optimizing assemblies of SMARCA2/4 bromodomain binders, degron-linking moieties, and ligands for specific E3 ligases. Design prioritization was guided by our proprietary ternary complex modelling algorithm, ALMOND (ALgorithm for MOdeling Neosubstrate Degraders). Selected compounds were synthesized and evaluated across multiple cellular assays to assess mechanistic and functional outcomes. Several compounds demonstrated potent and selective SMARCA2 degradation, eliciting distinct phenotypic responses in a panel of SMARCA4-mutant cell lines. The lead IV compound demonstrated robust anti-tumor efficacy in multiple SMARCA4 mutant xenograft models with confirmed target degradation, at well tolerated doses. IND application was accepted by USFDA for this compound. Formulation efforts helped in identification of long-acting IV formulation which demonstrated significant efficacy following once in 4 weeks administration. Subsequent ADME optimization yielded compounds with favourable oral bioavailability across tested species. Furthermore, the lead degrader exhibited robust antitumor efficacy in multiple SMARCA4-deficient CDX models at well-tolerated doses. Repeat-dose tolerability studies in non-rodent species are ongoing to support candidate nomination by Q4 2025.

#5176 Selective degradation of SMARCA4 as a therapeutic strategy in SMARCA4 driven cancers.

Bilash Kuila, Sandeep Dukare, Kiran Aithal B, Charamanna KB, Khaji Abdul Rawoof, Amit A. Dhudashiya, Nandish C, karthik S, Payel Das, Gopinath CH, Suraj Tgore, Gauri Rahul Petkar, Mohamad Fairus Bin Abdul Kadir, Leena Khare, Ranadeep Bokalial, Samiulla DS, Subhendu Mukherjee, Saravanan Thiyagarajan, Kavitha Nellore, Rajesh Eswarappa, Girish Daginakatte, Chandrasekhar Abbineni, Sanjeev Giri, Murali Ramachandra, **Susanta Samajdar**

Aurigene Oncology Limited, Bangalore, India

The BAF (SWI/SNF) chromatin remodelling complex regulates nucleosome positioning and DNA accessibility, influencing transcription, recombination, repair, and mitotic chromosome decatenation. It contains two mutually exclusive ATPases, SMARCA2 (BRM) and SMARCA4 (BRG1). SMARCA4 is frequently overexpressed in several cancers and is associated with aggressive phenotypes and poor prognosis. Genetic knockdown of SMARCA4 reduces proliferation and sensitizes tumors to chemotherapeutics, validating SMARCA4 as a therapeutic target. Synthetic lethality between SMARCA4 and PTEN further supports its clinical relevance. Here, we developed a first-in-class SMARCA4-selective degrader using hetero-bifunctional molecules that combine SMARCA2/4 bromodomain inhibitors with E3 ligase ligands. Design prioritization was guided by our proprietary ternary complex modelling algorithm, ALMOND (ALgorithm for MOdeling Neosubstrate Degraders). Multiple linker chemistries and exit vectors were explored based on rational designs which resulted in selective SMARCA4 degraders with good anti-proliferative activity in multiple cancer cell lines. Lead compound exhibited potent anti-proliferative effects in hematological and prostate cancer models, while SMARCA4-mutant cell lines showed minimal sensitivity, confirming target dependency. Preliminary tolerability and efficacy studies support the therapeutic potential of SMARCA4 degradation. These findings establish proof-of-concept for targeting SMARCA4 via targeted protein degradation as a novel strategy for treating SMARCA4-driven cancers with improved safety margin. Advanced in-vivo studies are in progress to complete candidate nomination by Q1 2026

#5177 Exceptionally selective and orally bioavailable p300 degraders for the treatment of CBP-mutant and p300-dependent cancers.

Iram Khan Iqbal, Krishna Chaitanya T, Kishore Narayanan, Naveen Kumar R, Aravind A. B, Avinash Kumar, Dabbeeru Madhu Babu, Pathur Obanna, Ankita Manna, Rabin Madhaiyan, Damodhran B, Shraddha B Shirsat, Shilpa S Nayak, Suraj T Gore, Mohamad Fairus, Girish Daginakatte, Rajesh Eswarappa, Chandrasekhar Abbineni, Saravanan Thiyagarajan, Murali Ramachandra, **Susanta Samajdar**

Aurigene Oncology Limited, Bangalore, India

EP300 (or p300) acts as histone acetyltransferase (HAT) and transcriptional adapter or co-activator regulating transcription via chromatin remodelling. Both histone and non-histone proteins are acetylated by p300. p300 functions by scaffolding or as a co-activator and enhancer of different transcription factors like HIF1a, BRCA-1, p53, NFκB, c-Myc, estrogen receptor (ER) and androgen receptor (AR) as well as other proteins such as PD-L1 and FOXP3. Selective targeting of p300 is expected to lead to therapeutic efficacy in CBP-mutant and p300-dependent malignancies with high degree of tolerability as a result of sparing the other paralog CBP in normal cells. CBP mutant cancers comprise of several solid and haematological malignancies such as bladder, lung, colorectal, melanoma, DLBCL, MM etc. and p300-dependent malignancies include prostate cancer, in which p300 plays a major role for androgen-dependent and independent transactivation of the AR, MYCN-amplified neuroblastoma and ER+ breast cancers. Conventional CBP/p300 BD inhibitors lack paralog selectivity due to high sequence homology, leading to adverse effects like severe thrombocytopenia in clinical settings. We have adopted a degrader approach to solve this selectivity challenge by means of a differentiated ternary complex. Herein, we report first-in-class highly potent and paralog selective p300 degraders with excellent selectivity over CBP along with other bromodomain containing proteins such as BRD4 and CRBN neosubstrates such as GSPT1. These degraders induce synthetic lethality in CBP loss-of-function mutant cell lines by selectively degrading p300 and demonstrate strong antiproliferative effects across CBP-mutant and p300-dependent models, including AR-positive prostate cancer. Identified p300 selective degraders exhibited good oral bioavailability and were well tolerated in rodents without showing thrombocytopenia. Demonstration of efficacy in CBP mutant and AR-positive CDX models is underway and will be presented subsequently. In summary, we have identified highly selective degraders of p300 with desirable profile. Efforts are in progress towards nominating a development candidate by Q1 2026.

#5178 Discovery and characterization of a selective p300 degrader reveals deep anti-tumor activity in CBP mutant cancers.

Harshil Dhruv, Andrew Fedoriw, Xuqing Zhang, Michael Russell, Jeremy Roach, Nathan Kendsersky, Nelisa Bechtel, Kelsey Annen, Brian Vidal, Timothy Dougherty, Clemente Aguilar-Bonavides, Elham Behshad, Sudeep Banjade, Corey Strickland, Wenxue Wu, Larry Jolivette, Helai Mohammad, Ryan Kruger

SK Lifescience Labs, KOP, PA

Paralogous protein pairs harboring loss-of-function mutations in one member have emerged as a promising opportunity in precision oncology, owing to their well-defined mechanistic complementarity. Among these, CBP and p300 are acetyltransferase paralogs whose functional redundancy has been exploited in genomic screens revealing synthetic lethality in CBP-deficient cancers when p300 is targeted. However, efforts to develop p300-specific inhibitors have been hampered by high sequence homology within functional domains, while dual p300/CBP inhibitors have faced on-target hematologic toxicities from simultaneous inhibition of both paralogs. Here, the discovery of potent, selective p300 degraders that exhibit robust efficacy across multiple CBP loss-of-function (LoF) cancer models is reported.Efforts at SKLSL led to the discovery of an optimized heterobifunctional degrader that induces rapid and selective p300 degradation (DC_{90} < 10 nM, Dmax >90%) within 2 hours, with no detectable CBP degradation up to 48 h (DC_{50} > 10 µM). Mechanistic studies confirmed an on-target mode of action, with complete loss of H3K27 acetylation observed in CBP knockout (KO) H1299 cells (IC_{50} < 0.5 nM, Max Inh > 97%), while p300 KO and wild-type cells remained unaffected (IC_{50} > 10 µM). Correspondingly, growth inhibition was restricted to CBP KO cells (gIC_{50} < 5 nM), confirming p300 dependence.To support these findings, computational analysis was performed to identify endogenous cell lines with putative CBP loss-of-function (LoF) mutations across a range of cancer types, including bladder cancer, SCLC, DLBCL, and CRC. CBP LoF cell lines exhibited strong sensitivity to p300 degradation, with a median gIC_{50} ≤ 1 nM (n = 19), while CBP wild-type and non-LoF mutant lines remained largely unresponsive (median gIC_{50} > 10 µM, n = 15). Importantly, the observed growth inhibition in CBP LoF lines closely correlated with robust suppression of H3K27 acetylation and downregulation of c-Myc, reinforcing the on-target mechanism of action. These in vitro results translated into striking in vivo efficacy: once-daily oral dosing of the p300 degrader (30 mpk) led to near-complete p300 degradation in tumors and marked tumor regression (TR) across xenograft models, including SW780 (TR = 82%, bladder cancer), NCI-H1876 (TR = 100%, SCLC), PFIEFFER (TR = 98%, DLBCL), and KARPAS422 (TR = 20%, DLBCL).Furthermore, bone marrow colony-forming assays demonstrated a markedly improved safety profile, with the p300-selective degrader showing minimal hematologic toxicity (IC_{50} >10 µM) compared to a clinical stage dual p300/CBP inhibitor (IC_{50} = 121 nM) or dual degrader (IC_{50} = 16 nM).Collectively, these results establish selective p300 degradation as a powerful therapeutic strategy for CBP loss-of-function cancers, offering robust anti-tumor activity and a significantly enhanced therapeutic index relative to dual inhibition.

#5179 Discovery and characterization of a selective p300 degrader reveals broad anti-tumor activity in p300-dependent cancers.

Harshil Dhruv, Andrew Fedoriw, Xuqing Zhang, Michael Russell, Jeremy Roach, Nathan Kendsersky, Nelisa Bechtel, Kelsey Annen, Brian Vidal, Timothy Dougherty, Clemente Aguilar-Bonavides, Elham Behshad, Sudeep Banjade, Corey Strickland, Wenxue Wu, Larry Jolivette, Helai Mohammad, Ryan Kruger

SK Lifescience labs, KOP, PA

p300 and CBP are paralogous lysine acetyltransferases with both shared and distinct roles in cancer. p300 acts as a key transcriptional co-activator in tumors driven by lineage- or tumor-specific gene programs, such as AR^+ prostate and hematologic cancers. While efforts to develop p300-specific inhibitors have been hindered by high sequence homology with CBP, dual p300/CBP inhibitors have shown limited clinical progress due to on-target hematologic toxicity resulting directly from simultaneous inhibition of both paralogs. Here, the discovery of a selective p300 degrader with potent activity in castration-resistant prostate cancer and multiple myeloma, where p300 is essential for oncogenic signaling, reported.[LJ1] Efforts at SKLSL led to the discovery of [SK2] an optimized heterobifunctional degrader that exhibits rapid and selective p300 degradation (DC_{90} < 10 nM, Dmax > 90%) within 2 hours and no CBP degradation up to 48 h (DC_{50} > 10 µM). Mechanistic studies confirm an on-target effect, with complete loss of H3K27 acetylation in CBP knockout (KO) H1299 cells (IC_{50} < 0.5 nM, Max Inh > 97%), while p300 KO and wild-type cells remain unaffected (IC_{50} > 10 µM). Across a panel of prostate cancer lines, p300 degradation caused robust growth suppression in AR^+ cells and downregulation of c-Myc and AR, key transcriptional drivers of tumorigenesis. In a panel of multiple myeloma cell lines, p300 degraders displayed superior potency compared with dual p300/CBP inhibitors and pomalidomide. Importantly, these *in vitro* findings translated into efficacy *in vivo*. Once-daily oral administration at 30 mpk in xenograft models led to near-complete tumor p300 degradation and strong anti-tumor efficacy, with tumor growth inhibition (TGI) of 100% (VCaP, AR^+ CRPC), 77% (LNCaP, AR^+ CRPC), and 86% (OPM2, multiple myeloma).Furthermore, bone marrow colony-forming assays revealed a significantly improved safety margin (IC_{50} > 10 µM) relative to a dual p300/CBP inhibitor (IC_{50} = 121 nM) and a dual degrader (IC_{50} = 16 nM), supporting an enhanced therapeutic index.Collectively, these findings establish that selective p300 degradation delivers potent anti-tumor efficacy while minimizing hematologic toxicity, offering a promising therapeutic approach for p300-dependent cancers driven by either lineage-specific or tumor-intrinsic p300 essentiality.

#5180 Engaged but not degraded: Proteome-wide CETSA in degrader research.

Tomas Friman, Soren Bruhn, Merve Kacal, Alexey Chernobrovkin, Daniel Martinez Molina

Pelago Bioscience AB, Solna, Sweden

Targeted protein degradation has emerged as a promising strategy to address protein targets considered undruggable by small-molecule inhibitors. Moreover, proteins vulnerable to inhibition can still possess scaffolding functions that can sustain biological effects, making degradation a compelling alternative. Degraders, however, inherit the selectivity of their pharmacologically active components; for bifunctional degraders/PROTACs, two ligands contribute to this composite selectivity. Unbiased quantitative proteomics is commonly used to monitor degrader selectivity. Still, not all proteins that bind a degrader are subsequently degraded, and traditional protein-ligand interactions may persist at relevant concentrations. The Cellular Thermal Shift Assay (CETSA®) measures target engagement by detecting interactions between compounds and their cognate proteins in lysates or intact cells, without modifying compounds, proteins, or the cellular environment. Coupled to mass spectrometry (MS), CETSA enables unbiased, proteome-wide monitoring of compound-protein interactions. An MS readout can also report protein degradation when the protein of interest (POI) has a suitable half-life. Here, we demonstrate how CETSA coupled to MS can deconvolute protein binding of PROTACs targeting BRD4, CDK4/6, and CDK9, and compare the selectivity profiles of full PROTACs with their individual warheads. All investigated PROTACs and warheads showed target engagement and/or degradation of their intended targets. In intact cells, downstream biological effects were also observed; for example, effects on the CDK4/6 substrate RB1 were seen with the CDK4/6-targeting PROTAC BSJ-03-204 and its kinase-binding warhead palbociclib. In contrast, the CDK9-targeting PROTAC THAL-SNS-032 did not affect RB1, whereas its kinase-binding warhead SNS-032 did. As expected, THAL-SNS-032 induced degradation of the annotated target CDK9 and its associated cyclin T1. We also observed target engagement without degradation for additional proteins, including other kinases. GSK3A and GSK3B, as well as their downstream substrate FOXK1, were thermally shifted but not degraded by the PROTAC (consistent with the profile of SNS-032). Overall, a CETSA-MS workflow can concurrently reveal degradation, target engagement, and downstream biological effects, including liabilities arising from engagement without degradation. This integrated perspective improves selectivity assessment and supports the design and interpretation of degrader campaigns.

: Adoptive Cell Therapy 2
Poster Session

#5183 High-throughput *ex vivo* TCR-T cells screening identifies aggrephagy-driven, therapy-resistant clones in KRAS-mutant PDAC.

Masoumeh Eshaghi[1], Fei Miao[1], Ali Abdollahzadeh[2], Sixing Chen[3], Jacopo Chiaro[4], Elahe Kamali G[1], Joshua Glover[5], Vineeth Koneru[1], Michael C. Milone[6], Miren L Baroja[1], Gerald P. Linette[7], Beatriz M. Carreno[7], Emma E. Furth[8], Vincenzo Cerullo[4], Joseph Fraietta[9], Carl H. June[10], Friederike Herbst-Nowrouzi[1]

[1]Center for Cellular Immunotherapies, Perelman School of Medicine, University of Pennsylvania, Philadelphia, PA,[2]A.I. Virtanen Institute for Molecular Sciences, University of Eastern Finland, Philadelphia, Finland,[3]Department of Genetics, Perelman School of Medicine, University of Pennsylvania, Philadelphia, PA,[4]Helsinki Institute of Life Science (HiLIFE), University of Helsinki, Helsinki, Finland,[5]The Stem Cell & Xenograft Core (SCXC), Perelman School of Medicine, University of Pennsylvania, Philadelphia, PA,[6]Department of Pathology and Laboratory Medicine, Perelman School of Medicine, University of Pennsylvania, Philadelphia, PA,[7]University of Pennsylvania, Philadelphia, PA,[8]Hospital of the University of Pennsylvania, Philadelphia, PA,[9]Department of Microbiology, Perelman School of Medicine, University of Pennsylvania, Philadelphia, PA,[10]Program Director of Translational Research, Abramson Family Cancer Research Inst, University of Pennsylvania, Philadelphia, PA

Background: Pancreatic ductal adenocarcinoma (PDAC) is characterized by frequent KRAS-G12 oncogenic mutations, low immune cell infiltration, and early metastatic spread, leading to poor outcomes. Selective pressure from systemic therapies promotes the emergence of resistant clones and relapse. Patient-derived models that capture tumor heterogeneity are needed to optimize T cell receptor-engineered T cell (TCR-T) strategies and anticipate mechanisms of resistance.

Methods: We developed a high-throughput *ex vivo* screening platform to test cell-based immunotherapies in patient-derived PDAC spheroids. KRAS-G12V-specific $CD8^+$ TCR-T cells were co-cultured with KRAS-mutant 3D tumor spheroids under graded levels of cytotoxic pressure and monitored using automated image cytometry. Microcavity plates enabled parallel tracking of thousands of spheroids across two sequential TCR-T challenges. Surviving cells were profiled by single-cell RNA sequencing (scRNA-seq), followed by 2D regrowth assays and orthotopic transplantation into NSG mice to assess tumor-initiating capacity.

Results: High-throughput resistance screening of over 33,000 microcavities revealed that 6.6% of 3D-PDAC spheroids remained viable after repeated TCR-T cell challenge, enriching for rare resistant subclones. After the first challenge, most cells exhibited an antiviral-like inflammatory response, characterized by increased levels of MX1, MX2, RIG-I, and interferon-stimulated gene expression. scRNA-seq after re-challenge revealed proliferating cells with upregulation of MHC II molecules and TUBA1B-associated aggrephagy pathways, implicating aggrephagy in immune escape. Resistant cells retained tumor-initiating potential and generated distant metastases in orthotopic NSG models ($n = 10$). *In vitro*, paclitaxel, a microtubule disassembly inhibitor, reduced colony formation by TCR-T-escaped clones, supporting a rationale for combination therapy.

Conclusions: High-throughput *ex vivo* cytotoxicity screening of patient-derived PDAC models reveals aggrephagy-enriched, therapy-resistant clones and nominates rational combination partners such as paclitaxel. This platform may help anticipate patient-specific resistance to KRAS-targeted TCR-T therapy and guide the design of preventative combination strategies.

#5184 From tLNP selection to *in vitro/vivo* efficiency evaluation: *In vivo* CAR-T therapy.

Shunchuan Zhang, Qi Xin, Gang Liu, Jingxian Liu, **Jun Liu**, Pei Wu, Jingwei Huang, Mengwen Huang, Zhongyao Ma, Letian Kuai, Wenji Su

WuXi AppTec, Shanghai, China

Targeted lipid nanoparticle (tLNP)-mediated in vivo CAR-T technology delivers mRNA encoding CAR directly to T cells in the body. This enables in situ engineering of T cells and provides an innovative solution to overcome the bottlenecks of traditional CAR-T therapies, such as complex processes, long cycle times, and high production costs. In this study, we first constructed the linear and circular mRNA structures of CD19 CAR and verified their expression and cytotoxicity through in vitro experiments. The results showed that, compared to linear CAR, circular CAR had a higher transfection positivity rate and expression level, as well as a stronger sustained expression ability. Additionally, the cytotoxicity results indicated that T cells transfected with circular CAR exhibited a more potent killing effect on $CD19^+$ Raji cells than those transfected with linear CAR. Furthermore, by optimizing the LNP formulation and process, we obtained an unfunctionalized LNP formulation capable of efficiently transfecting activated T cells, providing a powerful tool for the validation and optimization of CAR mRNA expression. Meanwhile, CD3 or CD8 antibodies were conjugated to the lipid nanoparticle surface to construct targeted vectors such as CD3-tLNP and CD8-tLNP. By utilizing specific ionizable lipids or combining antibody conjugation with spleen-targeting formulations, tLNP can selectively target T cells while maintaining low levels of liver expression, resulting in reduced side effects. In the NALM-6 systemic model with PBMC engrafted, CD19 in vivo CAR-T can significantly inhibit tumor growth and markedly extend the survival of mice without causing weight loss. Additionally, we monitored the distribution and levels of CAR-T cells in various tissues, organs, and peripheral blood at multiple time points. Additionally, we administered in vivo CART to immunocompetent mice, humanized with CD3/CD8/CD19, and monitored the changes in B cell levels in peripheral blood and spleen after administration. During the treatment period, the amount of B cell in mice were continuously suppressed, demonstrating that in vivo CAR-T can thoroughly eliminate B cells. In summary, our study demonstrates that the integration of CAR mRNA preparation, tLNP selection and optimization, along with in vitro evaluation and in vivo tumor and autoimmune disease models, could be instrumental for the design and development of in vivo CAR-T therapies.

#5185 Flow cytometry-based monitoring of CAR-T cell persistence and immune phenotypes pre- and post-infusion: Challenges in Phase 1/2 hematologic malignancy trials.

Jackie Benko, Bhagyaraj Ella, Samantha Splitt, **Angelina Bisconte**, Rachel Owen, Deborah J. Phippard

Precision for Medicine, Frederick, MD

Chimeric antigen receptor T-cell (CAR-T) therapies that support hematological malignancies have recently had their treatment efficacy determined by both clinical outcomes and specific assessments of the CAR-T cells themselves. Assay validation typically uses control CAR-T cells spiked into healthy PBMCs, which do not fully replicate the phenotypic and scatter characteristics of patient-derived CAR-T cells after infusion. This discrepancy introduces challenges in gating accuracy and data interpretation.

Precision for Medicine (PfM) developed and validated a multiparameter flow cytometry assay to quantify CAR-T persistence and characterize immune phenotypes, including CD4, CD8 subsets, memory, effector differentiation, and activation/exhaustion markers. In the development and validation control CAR-T cells were used to establish the gating strategy.

Post-infusion CAR-positive cells exhibited altered scatter profiles and marker expression compared to validation controls. Inter-assay controls ensured baseline reproducibility, but adaptive gating strategies were required for accurate identification of CAR-T populations in patient samples. These adjustments enabled robust persistence tracking and immune profiling. Clinical sample analysis was performed on peripheral blood mononuclear cells (PBMCs) pre- and post-infusion. Differences between validation controls and post-infusion CAR-T cells underscore the need for dynamic and flexible gating strategies. Addressing these challenges is critical for reliable immune monitoring in oncology trials and for correlating CAR-T persistence with clinical outcomes.

#5186 Pro-inflammatory cytokine primed Wharton's jelly mesenchymal stem cells: A potent immunomodulatory strategy to combat pancreatic cancer.

Sangeeta Choudhury, Poonam Yadav, Mohd Saad, Vikrant Singh, Rohini Tamang

Sir Ganga Ram Hospital, New Delhi, India

Background & Aim: Mesenchymal stem cells (MSCs) from umbilical cord (UC) have the potential therapeutic applications in context of injured, immune related & inflammatory diseases due to high proliferation rate, multilineage differentiation potential and immune tolerance properties. While clinical trials have clearly demonstrated strong safety records, efficacy of MSCs is still modest and inconsistent. Hypothesizing that priming MSCs prior to administration can improve their therapeutic efficacy, present study investigates the modulation of MSC behaviour through cytokine priming and assesses their effectiveness in ameliorating tumor apoptosis. Proteomic analysis shows compositional changes post cytokine priming.

Method: Wharton's jelly derived MSCs (hWJMSCs) were primed with tumor necrosis factor-alpha (TNF-α; 25ng/ml) and interferon-gamma (IFN-γ; 25ng/ml), incubated for 24 hrs at 37°C/5%CO2, their morphological alterations, multi-lineage differentiation potentials (osteocytes/chondrocytes/adipocytes), immunophenotypying (CD90+73+105+44+34-45-19- HLADR-), Adhesion molecules (ICAM, VCAM, NCAM) migration capabilities were examined.Label-free quantitative LCMS (nLC/MS/MS coupled to Orbitrap fusion Tribrid mass-spectrometer) analysis was performed on more than 2400 proteins identified. Further, immunogenic potentials are being tested using PBMNCs from healthy human donors.

Result: hWJMSCs primed with TNF-α (hWJMSC-T)/IFN-γ (HWJMSC-I) showed >90% expression of $CD90^{+}73^{+}105^{+}44^{+}$. Microscopically morphological distinction stained with phyalloidin/DAPI observed showed hWJMSC-T as elongated and flattened cells and Complement & coagulation cascade and Pro-angiogenic proteome signature in abundance, suggesting their role in innate immunity homeostasis. On the other hand, IFN-γ induction showed immune-modulating protein signature of infection/inflammation especially, Guanylate-binding proteins. Differentially expressed protein signature points towards modulation of NOD-like receptor signaling and cell adhesion molecule pathways.

Conclusion: Data herein provides the evidences that stem cell properties of regenerative capability remains conserved and do not compromise under inflammatory conditions. Additionally, primed hWJMSCs can modulate or prevent infection most likely via cross-talk between cascades of defense systems. Thus, suggesting a potential role as alternate strategy to regulate inflammation and/or reshape inflammatory microenvironment.

Keywords: Mesenchymal stem cells, pro-inflammatory cytokines, inflammation, immunomodulation

#5187 IL-21-Enhanced NK cells: A mitochondrial fitness enhancement for targeting glioblastoma stem cells.

Mayra Shanley[1], Sufang Li[1], Mandira Manandhar[1], Giacomo Sferruzza[1], Rafet Basar[1], May Daher[1], Jinzhuang Dou[1], Joy Gumin[1], Ana Karen Nunez Cortes[1], Sunil Acharya[1], Donghai Xiong[1], Hila Shaim[2], Frederick F. Lang[1], Navin Varadarajan[3], Ken Chen[4], Katayoun Rezvani[1]

[1]UT MD Anderson Cancer Center, Houston, TX,[2]Stem Cell Transplantation and Cellular Therapy, MD Anderson Cancer Center, Pearland, TX,[3]University of Houston, Houston, TX,[4]Asst. Professor, Dept. of Bioinformatics & Computational Bio., UT MD Anderson Cancer Center, Houston, TX

Glioblastoma (GBM), an aggressive brain cancer, recurs due to the resistance of glioblastoma stem cells (GSCs) to conventional therapies. We recently showed that cord blood-derived NK cells (CBNK) armed with cytokines like IL-21 exhibit enhanced anti-tumor activity against GSCs, showing superior killing capacity after multiple re-challenges. IL-21 transduction enhances NK cell diversity, polyfunctionality, and mitochondrial fitness, improving tumor control and survival in an in vivo glioblastoma model without toxicity. A deeper dive into the cellular mechanisms revealed that IL-21 transduction triggers significant changes in the metabolic and mitochondrial profiles of NK cells. RNA sequencing revealed that IL-21 transduction upregulates genes involved in metabolic reprogramming, mitophagy, and mitochondrial health, including *KLF2*, *GZMH*, *CLIC3*, and *CEBPD*. Further investigations into mitochondrial function confirmed improved mitochondrial respiration (OCR) and reduced glycolytic activity (ECAR) in IL-21 CBNK cells, indicating enhanced mitochondrial fitness. Confocal microscopy revealed that IL-21 CBNK cells had smaller mitochondria, a hallmark of mitophagy, which was significantly different from other cytokine-transduced or non-transduced CBNK cells. Furthermore, mitochondrial-related proteins, including Mitofusin-2 and DRP1, were upregulated in IL-21 NK cells, confirming improved mitochondrial dynamics. Inhibition of mitophagy reversed the enhanced killing ability of IL-21 transduced CBNK cells. Seahorse Mito Fuel tests identified glucose and fatty acids as the primary fuel sources for IL-21 CBNK mitochondria. Blocking these fuels impaired their anti-tumor activity, further supporting the role of mitochondrial metabolism in IL-21-driven NK cell fitness. Additionally, CEBPD, a key transcription factor involved in mitophagy and mitochondrial metabolism, was upregulated in IL-21 transduced CBNK cells, further enhancing their mitochondrial function and anti-tumor efficacy. These results suggest that IL-21 enhances NK cell anti-tumor potency through metabolic reprogramming, mitochondrial fitness, and CEBPD-driven mitophagy, offering a promising therapeutic strategy for glioblastoma.

#5189 Generating EZH2-inhibitor resistant CAR-T cells to sustain function for combination therapy.

Katherine Bronson[1], Daniel Fil[2], Megan R. Reed[2], Billie Heflin[2], Sydnye Shuttlewoth[2], Brian S. Koss[3], Alan Tackett[4]

[1]UAMS Winthrop P. Rockefeller Cancer Institute, Little Rock, AR,[2]University of Arkansas for Medical Sciences, Little Rock, AR, Little Rock, AR,[3]University of Arkansas for Medical Sciences, Little Rock, AR,[4]UAMS Winthrop P. Rockefeller Cancer Institute, Little Rock, AR, Little Rock, AR

Background: EZH2, a histone methyltransferase and core component of the PRC2 complex, is often overexpressed in tumors and contributes to immune evasion. EZH2 inhibition has been shown to reprogram cancer cells toward a more immunogenic state and enhance lymphocyte infiltration into tumors in preclinical models. These findings have led to growing interest in combining EZH2 inhibitors with adoptive cell therapies. EPZ-6438 (Tazemetostat), a potent EZH2 inhibitor (EZH2i), is FDA-approved for epithelioid sarcoma and follicular lymphoma and is under investigation in multiple solid and liquid tumors. However, EZH2 is also critical for preserving T cell epigenetic stability and function. Here, we investigate this therapeutic tradeoff and show that while EZH2i may enhance tumor immunogenicity it impairs long-term CAR-T cell persistence.

Methods: Human $CD8^+/CD3^+$ T cells were activated with CD3/CD28/CD2 and transduced on day 0 with a CD19-specific CAR lentiviral vector. On day 3, CAR-T cells were edited with CRISPR/Cas9 to introduce EZH2i-resistant mutations into the endogenous *EZH2* gene. On day 9, CAR-T cells were co-cultured with nuclear RFP-labeled $CD19^+$ target cells with or without 0, 0.5, 1, 2 μM EZH2i. Tumor cell count was measured every 4 hours using automated imaging, and fresh tumor cells and drug were added every 48 hours until loss of T cell tumor control. This was repeated in the OT1 T cell murine system with RFP-labeled $SIINFEKL^+$ B16F10 melanoma cells. In parallel, $CD8^+/CD3^+$ T cells cultured with or without chronic exposure to 1 μM EZH2i were used for phenotype and functional analysis. Histone H3K27me3 levels and PD-1, CTLA-4, and LAG-3 expression were measured by immunoblot. Polyfunctionality ($IL\text{-}2^+/IFN\text{-}\gamma^+/GZMB^+$) was measured via flow cytometry.

Results: EZH2i treatment did not impair initial CAR-T cytotoxicity against tumor cells. However, prolonged co-culture revealed a significant decline in tumor control past the fourth round of co-culturing. EZH2i-treated WT CAR-T cells sustained tumor clearance for an average of 5.7 killing rounds compared to 14.0 rounds in untreated controls ($p=0.0002$, $n=3$). Immunoblots confirmed loss of the repressive histone mark H3K27me3 following chronic EZH2i exposure ($p<0.0001$, $n=8$), alongside elevated expression of exhaustion markers: PD-1 (1.6-fold, $p=0.0502$, $n=8$), CTLA-4 (7.4-fold, $p<0.0001$, $n=6$), and LAG-3 (53.3-fold, $p=0.0198$, $n=6$). Flow cytometry further revealed a reduced frequency of polyfunctional ($IL\text{-}2^+/IFN\text{-}\gamma^+/GZMB^+$) $CD8^+$ T cells and a shift toward an exhausted phenotype.

Conclusions: We demonstrate that while EZH2i does not impair the short-term function of CAR-T cells, prolonged exposure significantly reduces persistence and anti-tumor efficacy. To overcome this limitation, we are developing strategies to engineer CAR-T cells resistant to EZH2i, enabling future combination therapies that harness both EZH2 inhibition and adoptive T-cell therapy.

#5190 Advancing FCRL5 directed immunotherapy for improved treatment of B cell lymphoma.

Chakrapani Tripathi, John Nguyen, Fang-chi Hsu, Frank Luh, Yun Yen

Sino-American Cancer Foundation, Covina, CA

Despite significant advances in B-cell lymphoma therapies including monoclonal antibodies, bispecific T-cell engagers (BiTEs), and CD19/CD20-directed chimeric antigen receptor (CAR) T-cell therapies disease relapse and treatment resistance remain major clinical challenges. The principal driver of therapeutic failure is antigen escape, characterized by the downregulation or loss of CD19 and/or CD20 on malignant B cells[1], rendering current immunotherapies ineffective. These limitations underscore the urgent need for alternative target antigens and next-generation immunotherapeutic strategies capable of circumventing antigen loss. Fc receptor-like 5 (FcRL5), a transmembrane immunoglobulin superfamily protein selectively expressed on malignant B cells and plasma cells with minimal expression in normal tissues[2], represents a compelling tumor-associated antigen. We generated and functionally characterized FcRL5-targeted CAR T cells using nanobody-based single-domain antibodies (VHHs) derived from an immunized llama library. Anti-FcRL5 VHHs were incorporated into second-generation CAR constructs incorporating 4-1BB-CD3ζ signaling domains. CAR candidates were first screened in Jurkat NFAT-GFP reporter cells for surface expression, antigen-specific activation, and basal tonic signaling to identify top performers. Selected CAR constructs were further evaluated in primary human CD3+ T cells for FcRL5-dependent activation, cytotoxicity, cytokine secretion, and memory differentiation following co-culture with FcRL5+ diffuse large B-cell lymphoma (DLBCL) cell lines (Su-DHL-6, Toledo) and FcRL5$^-$ controls. These analyses demonstrated robust and selective activation, potent effector function, and strong cytotoxicity against FcRL5-expressing lymphoma cells, highlighting their therapeutic potential. Collectively, these findings establish FcRL5-targeted nanobody-based CAR T cells as a promising next-generation immunotherapy capable of overcoming antigen escape in B-cell lymphomas. Evaluated alone or in combination with FDA-approved targets, FcRL5 CAR T cells hold strong potential for translation into first-in-human clinical trials for patients with relapsed or refractory disease. **Funding:** Supported by the SACF Drug Discovery Research Fund **References:** 1.Spiegel JY, et al. *Nat Med* 2021;27:1419-31.2.Capone M, et al. *J Clin Cell Immunol* 2016;7:427.

#5191 Multiscale engineering of PTPRZ1 CAR T cells through affinity-tuned binders and modular architecture optimization.

Aditya A. Mohan[1], Barbara Lipes[1], Rushil Yerrabelli[1], Kisha Kamini Patel[2], Charla Gentry[1], Ariel Gonzalez[1], John Sampson[3], Peter E. Fecci[4], Michael Gunn[1], Anoop Patel[1]

[1]Duke University, Durham, NC,[2]University of Pennsylvania, Philadelphia, PA,[3]University of Colorado, Aurora, CO,[4]Duke University Medical Center, Durham, NC

Glioblastoma remains universally lethal, with rapid recurrence and a median survival of less than two years. Current CAR T approaches in glioblastoma have been limited by a lack of uniformly expressed and therapeutically actionable antigens. Using integrated single-cell and single-nucleus atlases, we identify PTPRZ1 as a consistently and highly expressed surface antigen across malignant glioblastoma states with minimal expression in non-neoplastic neural lineages. To translate this target, we developed a binder engineering pipeline combining mouse immunization, phage display with counter-selection against PTPRG, and yeast based directed evolution to generate a panel of scFv and nanobody binders with a spectrum of affinities that recognize the same PTPRZ1 epitope. This panel enables systematic tuning of CAR antigen sensitivity and functional thresholds and allows direct comparison of how binder format and affinity shape CAR activity against endogenous antigen. We incorporated these affinity-graded binders into a modular CAR backbone and constructed a combinatorial CAR library that varies hinge domains, transmembrane regions, and costimulatory modules. Primary human T cells transduced with pooled CAR libraries were screened against patient-derived glioma stem cells to quantify how each architectural module influences CAR function as an isolated component and how combinations of modules synergize to enhance activation, cytotoxicity, proliferation, resistance to exhaustion, and durability under chronic stimulation. This screening strategy also enabled the identification of recurrent architectural features that support persistence and metabolic fitness in solid tumor settings. Individual validation studies confirmed that both scFv and nanobody CARs targeting the identical epitope exhibit distinct activation and persistence profiles, and that optimal performance arises from specific pairings of hinge, transmembrane, and costimulatory domains. Safety studies using human epilepsy-derived cortical slice cultures reveal minimal off-tumor cytotoxicity and preserved neural architecture following exposure to PTPRZ1-targeting CAR T cells. Collectively, these data nominate affinity-tuned PTPRZ1 binders and optimized CAR architectures as strong candidates for translation and provide generalizable design principles for improving CAR T therapy in solid tumors.

#5192 Single-cell profiling reveals immune circuit disruption preceding CAR-T relapse in B-ALL.

Zhouting Zhu[1], Na Li[2], Zhaoyang Jia[2], Yufei Deng[2], Lujing Wu[2], Hui Hui[2], Victor Wong[3], Tariq M. Rana[2]

[1]Graduate School of Biomedical Sciences, Sanford Burnham Prebys Institute, La Jolla, CA,[2]Department of Cellular and Molecular Medicine, University of California San Diego, La Jolla, CA,[3]Rady Children's Hospital, San Diego, CA

Chimeric antigen receptor T (CAR-T) cell therapy has transformed treatment outcomes for B-cell acute lymphoblastic leukemia (B-ALL), yet disease relapse remains a major clinical challenge. To elucidate mechanisms underlying relapse, we analyzed longitudinal single-cell RNA-seq profiles from peripheral blood mononuclear cells (PBMCs) of five B-ALL patients treated with CAR-T cells. Within total T cells, MHCII$^+$ CD8$^+$T cells were markedly reduced at relapse, whereas naive-like CD8$^+$ T cells were enriched. Trajectory reconstruction revealed that antigen-processing and antigen-presentation pathways are critical for the transition from naive-like to MHCII$^+$ CD8$^+$ T cells. In relapsed patients, MHCII$^+$ CD8$^+$ T cells exhibited impaired progression along this trajectory and remained transcriptionally similar to the naive-like state. Within the monocyte lineage, antigen-presenting monocytes in relapsed patients skewed toward a non-classical phenotype, characterized by enhanced chemotaxis, taxis, and oxidative phosphorylation, whereas a patient who maintained remission to day 360 displayed antigen-processing, antigen-presentation, and type I interferon activation signatures. Analysis of B-ALL cells revealed that relapsed leukemic cells exhibit increased stemness, “don’t-eat-me” signaling, and immaturity scores, along with reduced mature B-cell differentiation signatures. Together, our multi-patient single-cell analysis reveals a coordinated dysregulation of monocytes, CD8$^+$ T-cell antigen presentation, and intrinsic leukemic cell states during CAR-T relapse, highlighting a potential B-ALL-monocyte-T-cell axis that may drive immune evasion and inform strategies to prevent or treat CAR-T failure.

#5193 Novel SynKIR-310 outperforms CD3-based second-generation CD28 or 41BB co-stimulated CAR T in B-cell non-Hodgkin lymphoma xenograft mice and shows early clinical signal.

Megan C. Blair[1], Jun Xu[1], Nora Yucel[1], Tony Truong[1], William Stanley[1], Michael Tees[2], Olivia Dermody[1], Susan K. Howard[1], Andrea Campanile[1], Michael Milone[3], Don L. Siegel[3], Laura A. Johnson[1]

[1]Verismo Therapeutics, Philadelphia, PA,[2]Colorado Blood Cancer Institute, Denver, CO,[3]Department of Pathology and Laboratory Medicine and Center for Cellular Immunotherapies, University of Pennsylvania, Philadelphia, PA

Over half of B-NHL patients (pts) receiving FDA-approved CD19-targeting chimeric antigen receptor (CAR) T experience progressive disease within 1 year[1], demonstrating need for more durable therapies. Unlike CD3-based single-chain CAR, killer immunoglobulin-like receptor (KIR)-based CAR have a multi-chain design derived from natural killer (NK) cells[2] with separated antigen binding and activation signals, and reduced tonic signaling and off-target activity[3]. SynKIR-310 is an autologous T cell therapy targeting CD19 with canine-derived single chain variable fragment (scFv), DS191. We previously compared SynKIR-310 to single-chain FMC63-41BBζ (tisagenlecleucel analog) for anti-tumor functionality in NALM6 B-cell leukemia-engrafted NOD-SCID-IL2Rγc$^{-/-}$ (NSG) mice. SynKIR-310 showed faster tumor regression and increased tumor control with reduced systemic cytokines and comparable T cell persistence[4]. Here we evaluated SynKIR-310 in B-NHL Raji cell Burkitt lymphoma xenograft NSG mice compared with FMC63-41BBζ and single-chain FMC63-CD28ζ (axicabtagene ciloleucel analog). Mice were IV injected with Raji tumors and then IV injected with T cells. Tumor progression was monitored by bioluminescent imaging. In this Raji model, SynKIR-310 and FMC63-41BBζ showed comparable anti-tumor efficacy and increased overall survival, while FMC63-CD28ζ had no impact over negative control animals despite similar T cell persistence across groups. SynKIR-310 and FMC63-41BBζ produced similar levels of cytokines *in vivo*, while FMC63-CD28ζ produced significantly more cytokines at both early and late timepoints, despite worse tumor control. At the early timepoint, FMC63-CD28ζ produced 11-fold more IL-2 than SynKIR-310 and FMC63-41BBζ, while IFNγ and TNFα were comparable across groups. At the late timepoint, FMC63-CD28ζ produced 11-fold more IFNγ and 9-fold more TNFα, compared to SynKIR-310 and FMC63-41BBζ. SynKIR-310 achieves significantly improved tumor control compared to FMC63-CD28ζ in a Raji B-NHL mouse model, with reduced cytokine production. We have previously shown SynKIR-310 has superior anti-tumor efficacy over FMC63-41BBζ in a leukemia NALM6 model, here FMC63-41BBζ and SynKIR-310 had comparable anti-tumor efficacy against B-NHL Raji, though SynKIR-310 was the only group with 100% survival. These data support a potentially increased benefit-risk profile of SynKIR-310 compared with conventional CD3-based CAR T and merits further investigation in patients with B-NHL. We are enrolling pts in a Phase 1 first-in human multi-site U.S.-based clinical trial for relapsed/refractory B-NHL, including pts with or without prior exposure to CAR T (NCT06544265). Early clinical pt data will be presented.

1 Cappell KM *Nat Rev Clin Oncol* 2023 2 Wang E *Cancer Immunol Res* 2015 3 Yucel N *JITC* Nov 2025 Abst 298 4 Blair M *Blood* Dec 2025 Abst 4103

#5194 Oncolytic virus infected tumors drive AP-1 and IRF signaling in NK cells to sustain anti tumor activity.

Hila Shaim[1], Cheryl Jiang[1], Mayra Shanley[1], Hind Rafei[1], Jiajinlong Kang[1], Yu-Sung Hsu[1], Huihui Fan[1], Patrick Zhang[1], Rafet Basar[1], May Daher[1], Qingnan Liang[1], Donghai Xiong[1], Joy Gumin[1], Viswakalyan Kotapali[1], Corry Jones[1], April Gilbert[1], Luis Muniz-Feliciano[1], Gary M. Deyter[1], Pinaki Banerjee[1], Madison Moore[1], Ye Ethan Li[1], Dexing Fang[1], Sunil Acharya[1], Inci Biederstadt[1], Hong Jiang[1], Nadima Uprety[1], Rejeena Shrestha[1], Byron Jia[1], Alexander Biederstadt[1], Paul Daniel[1], Maliha Munir[1], Mecit Kaplan[1], Mayela Mendt[1], Oluwatosin Banjo[1], Vakul Mohanty[1], Jinzhuang Dou[1], Xianli Jiang[1], Elizabeth Shpall[1], Ken Chen[2], Abhinav Jain[3], Frederick F. Lang[1], Candelaria Gomez-Manzano[1], Juan Fueyo[1], Katayoun Rezvani[1]

[1]UT MD Anderson Cancer Center, Houston, TX,[2]Asst. Professor, Dept. of Bioinformatics & Computational Bio., UT MD Anderson Cancer Center, Houston, TX,[3]Dept. of Biochem. & Molec. Biology, UT MD Anderson Cancer Center, Houston, TX

Background: Natural killer (NK) cells play a crucial role in cancer immunosurveillance. They infiltrate the tumor microenvironment and kill tumor cells by integrating activating signals from stress-induced ligands on cancer cells and inhibitory signals, mediated by the major histocompatibility immune complex (HLA), that preserve self-tolerance. However, their effectiveness against solid tumors is limited by tumor-driven immune-suppression. Oncolytic viruses (OV) can potentially overcome this barrier by selectively infecting tumor cells and stimulating antitumor immunity. We thus combined the oncolytic adenovirus Delta24-RGD with NK cells to target aggressive solid tumors, aiming to define the mechanisms underlying virus-induced NK cell hyperactivation and supporting clinical translation of this approach.
Methods: We conducted in vitro and in vivo studies to evaluate the cytotoxicity of ex vivo-expanded cord blood-derived NK cells against Delta24-RGD-infected pancreatic ductal adenocarcinoma and glioblastoma cells. In vitro, OV-infected tumor cells were co-cultured with NK cells, followed by CyTOF phenotyping and cytotoxicity evaluation using xCelligence and Incucyte. Long-term cytotoxic capacity was assessed by first co-culturing NK cells with OV-infected or non-infected tumor cells, isolating NK cells and then testing their serial killing against fresh tumor targets. In vivo efficacy was tested using patient-derived xenograft glioblastoma mouse models. Mechanistic workup included ATAC-seq, bulk RNA-seq, CUT&RUN, and CRISPR-Cas9 knockout of JUNB and FOS.
Results: NK cells exhibited synergistic cytotoxicity against OV-infected PDAC and glioblastoma cells and acquired an enhanced activation phenotype with increased expression of DNAM-1, NKG2D, CD94, NKp30, CD25, CD69, ICOS, T-bet, TRAIL, and CD107a. OV-infected tumor cells upregulated stress ligands including B7-H6, MICA/B, and ULBP1 and downregulated HLA-I. In vivo, the combination therapy significantly reduced tumor growth and extended survival in glioblastoma models. NK hyperactivation required direct contact with OV-infected tumor cells, likely driven by virus-mediated modulation of NK-ligand expression on tumor cells. Robustly activated NK cells maintained enhanced cytotoxicity through repeated tumor rechallenges, indicating durable functional reprogramming. Mechanistic studies revealed AP-1 activation followed by type I interferon signaling. Disruption of JUNB and FOS, as well as chemical AP-1 inhibition reduced this effect. CUT&RUN confirmed AP-1 dependent transcriptional programs supporting cytotoxicity.
Conclusion: Oncolytic viruses synergistically enhance sustained NK cell antitumor activity by reprogramming AP-1 driven transcriptional responses. This combination strategy provides a mechanistic foundation for advancing NK cell-based therapies against solid tumors.

#5195 Next-generation CAR-T cells that target only tumor stroma and matrix: Collagen-binding IL-12-expressing FAP-CAR-T show strong anti-tumor efficacy but are safe.

Jun Ishihara[1], Chiu Po Chaun[1], Koichi Sasaki[2]

[1]Imperial College London, London, United Kingdom,[2]Imperial College London, London

Fibrotic tumor subtypes have been identified across multiple solid malignancies, including pancreatic, breast, lung, and colorectal cancers. These fibrotic tumors are generally difficult-to-treat and are characterized by extensive desmoplastic stroma and pronounced heterogeneity. The fibrotic tumor microenvironment (TME) not only serves as a physical barrier that impedes therapeutic penetration and immune cell infiltration but also contributes to therapeutic resistance, rendering these cancers particularly challenging to treat. Cancer-associated fibroblasts (CAFs), which are abundant in the TME, have emerged as a promising therapeutic target. In this study, we developed a novel chimeric antigen receptor T cell (CAR-T) therapy specifically targeting fibroblast activation protein (FAP) expressed on CAFs. After binding to FAP, NFAT signalling enables the subsequent local secretion of collagen-binding domain-fused interleukin-12 (CBD-IL-12) from CAR-T cells. This CAR-T cells only remove CAF but also concentrate collagen-binding IL-12 in the tumor to enhance host immune activation within the tumor microenvironment. The CBD-IL-12 expressing FAP CAR-T cells exhibited effective cytotoxicity against fibroblast cell lines in vitro. In vivo, CBD-IL-12 expressing FAP CAR-T cells significantly suppressed tumor progression of murine breast cancer and pancreatic cancers, which were better than 2nd generation FAP CAR-T or wt IL-12-expressing CAR-T. Importantly, CBD-fusion to IL-12 in the CAR-T design improved accumulation of IL-12 within tumor tissues >10 times, whereas minimizing systemic IL-12 exposure and reducing associated toxicities. Immunophenotyping revealed increased infiltration of $CD8^+$ cytotoxic T lymphocytes and reduced regulatory T cells (Tregs) in the TME of mice treated with CBD-IL-12-expressing FAP CAR-T, compared to those treated with FAP CAR-T alone or with wt IL-12 secretion. This dual-function CAR-T approach serves to first deplete CAFs, thereby disrupting the physical barrier impeding immune cell infiltration, and second, to activate anti-tumor immunity through localized IL-12 delivery. We have created a new therapeutic concept, which utilizes CAR-T cells for non-tumor antigen target, but still activates immune cells locally in the tumors, which could be a universal purpose CAR-T cells for multiple cancer types, especially for fibrotic or post-x-ray tumors.

#5197 Metabolically supercharged NK cells engineered with adenoviral E4ORF-1.

Maliha Munir[1], Madison Moore[1], Silvia Tiberti[1], Rafet Basar[1], Byron Jia[1], Leen Kheirbek[1], Nadima Uprety[1], Francia Reyes Silva[1], Rejeena Shrestha[1], Ana K. Nunez Cortes[1], Mayra Shanley[1], Sunil Acharya[2], Jeong-Min Park[1], Bin Liu[1], Pinaki Banerjee[1], Paul Lin[1], Donghai Xiong[1], Enli Liu[1], Alia Ghrayeb[1], Eyal Gottlieb[1], Elizabeth Joan Shpall[3], Katayoun Rezvani[1], **May Daher**[1]

[1]UT MD Anderson Cancer Center, Houston, TX,[2]Molecular and Cellular Oncology, UT MD Anderson Cancer Center, Houston, TX,[3]Professor of Medicine, Dept. of Stem Cell Transplant & Cell Therapy, UT MD Anderson Cancer Center, Houston, TX

Background: Chimeric antigen receptor (CAR) T and natural killer (NK) cells have achieved success in hematologic malignancies but show limited efficacy in solid tumors. A major barrier is the metabolically hostile solid tumor microenvironment (TME), where hypoxia, acidosis, and nutrient deprivation impair immune cell fitness, cytotoxicity, and persistence. Current metabolic engineering strategies that enhance single nutrient uptake or target one metabolic pathway provide only partial benefit and remain vulnerable to tumor metabolic plasticity. A critical unmet need is the development of immune cells with metabolic flexibility rather than single-pathway dependence. To address this, we explored a strategy inspired by viral metabolic rewiring. During adenoviral infection, the viral protein E4ORF-1 activates PI3K-AKT signaling, stabilizes MYC, augments nutrient uptake, and enhances glycolysis, oxidative phosphorylation (OXPHOS), and fatty acid oxidation (FAO). We hypothesized that engineering E4ORF-1 into NK cells would generate a viral-like metabolic state capable of withstanding nutrient restriction in solid tumors.
Methods: Metabolic characterization included mitochondrial mass and membrane potential, Seahorse assays, and SCENITH. CAR-NK cells were cocultured with solid tumor cell lines, and cytotoxicity was quantified using xCelligence and IncuCyte platforms. In vivo efficacy was tested in xenograft models of hematologic (MOLM14) and solid tumors (SKOV3). Mechanistic studies incorporated bulk RNAseq, CyTOF profiling, and CRISPR-Cas9 knockout of AMPK.
Results: E4ORF-1 expression significantly enhanced NK cell antitumor function across tumor models and sustained cytotoxicity and metabolic fitness under glucose-, glutamine-, or lipid-limited conditions. Western blotting confirmed coordinated upregulation of nutrient transporters and metabolic enzymes across glycolysis, OXPHOS, and FAO. E4ORF-1 NK cells also maintained a cytotoxic advantage under targeted metabolic inhibition; despite blockade of glycolysis, OXPHOS, FAO, or glutamine metabolism, they consistently demonstrated superior tumor killing, underscoring enhanced metabolic adaptability. Transcriptomic profiling showed preserved cytokine signaling and metabolic signatures even under nutrient restriction or after tumor challenge. Mechanistic studies identified AMPK as a central metabolic integrator required for the E4ORF-1 phenotype, as CRISPR deletion of AMPK abrogated metabolic and functional advantages. Incorporation of E4ORF-1 into CAR-NK cells improved tumor control and survival in vivo.
Conclusion: E4ORF-1 enhances NK cell metabolic flexibility, enabling sustained antitumor activity and improving therapeutic potential for solid tumors. These findings establish viral gene-mediated metabolic rewiring as a promising platform to strengthen CAR-NK cell fitness and overcome nutrient competition in the TME.

#5198 A non-viral mRNA engineering platform for rapid, same-day immune-cell therapies.

Chen Wu[1], Christoph Schaefers[2], Malvika Gupta[2], Kevin Regan[2], Zuoyi Shao[2], Andre De Menezes Silva Corraes,[2], Virginia Van Keulen[2], Jacob Hirdler[2], Tobias Peikert[3], Timothy D. Wiltshire[4], Haidong Dong[5], Yi Lin[2]

[1]Biochemistry and Molecular Biology, Mayo Clinic College of Medicine and Science, Rochester, MN,[2]Mayo Clinic, Rochester, MN,[3]Pulmonary and Critical Care Medicine, Mayo Clinic College of Medicine and Science, Rochester, MN,[4]Senior Research Fellow, Mayo Clinic, Rochester, MN,[5]Mayo Clinic College of Medicine and Science, Rochester, MN

Background: Cellular immunotherapy has transformed cancer treatment, but success in solid tumors remains limited by long manufacturing times, high costs, and the need for viral vectors that permanently modify DNA. To address this, we examined electroporation (EP) and mechanoporation (MP) approach to transfect T cells with mRNA to enable the development of a bedside immune cell editing platform. NKG7, natural killer cell granule-7, was previously demonstrated to play key function in activating T-cell cytotoxicity function. mRNA transfection of T cells with NKG-7 can increase these cells' anti-tumor cell killing. We examine EP and MP methods for NKG7 transfection in primary peripheral blood mononuclear cells (PBMCs) from healthy donors.
Method: Synthetic Clean Cap mRNAs encoding NKG7 or NKG7 with membrane-bound cRNA IL-2 were introduced into PBMCs by electroporation (MaxCyte) or mechanoporation (Portal Bio). T cell expression of NKG7 and IL-2 were analyzed by CytoFlex flow and Kaluza.
Result: The yield at EP and MP were comparable at 0.615+/-0.09% and 0.597+/-0.16%, respectively. Viability were high at above 80% for 3 days after EP and MP. NKG7 and NKG7+cIL-2 mRNA transfection led to different NKG7 expression kinetics in T-cells and between EP and MP. With EP, CD4 T-cells showed an increase in NKG7 expressions with the highest MFI ratio (NKG7 MFI/ IgG MFI) compared to mock EP at Day 1 for the NKG7 -only EP (1.25 ± 0.38) and at Day 2 for NKG7+cIL-2 EP (1.20 ± 0.27). $CD8^+$ T cells displayed a similar trend, with peak NKG7 expression at Day 1 for NKG7 EP (1.22 ± 0.76) and Day 2 for NKG7+cIL-2 EP (1.21 ± 0.90). However, MP did not enhance NKG7 expression in $CD4^+$ T cells. NKG7 expression peaked at Day 1 for both NKG7 (1.28 ± 0.42) and NKG7 + cIL-2 (1.24 ± 0.20). IL2 expression peaked at Day 1 for both EP and MP: EP, $CD4^+$ T (91.5% ± 4.4), $CD8^+$ T (92.7% ± 12.8); MP, $CD4^+$ T (88.9% ± 31.7), $CD8^+$ T (84.7% ± 9.6). Functional assays for anti-tumor cell killing of these transfected cells are currently ongoing.
Conclusions: We report that EP of PBMC can transfect all cell populations. MP may yield comparable yield, viability and NKG7 expression in CD8 T cells compared to EP, but without the need to isolate CD8 T cells from PBMC. EP and MP method can be used for bedside immune cell transfection depending on the target and cell populations of interest.

#5199 uPAR-targeting CAR-NK cells enhance cytotoxicity against acute myeloid leukemia.

Xingliang Guo[1], Nadima Uprety[2], Rejeena Shrestha[2], Francia Reyes Silva[1], Sunil Acharya[2], Bijender Kumar[3], Bin Liu[2], Dexing Fang[2], Bingqian Hu[2], Sha Wang[2], May Daher[1], Ana K. Nunez Cortes[2], Corry Jones[2], LaTretta Harris[2], Vernikka Woods[2], Jerrell E. Scott[2], April Gilbert[2], Cornelio Santibanez[2], Katayoun Rezvani[2], Rafet Basar[1]

[1]Department of Stem Cell Transplantation and Cellular Therapy, The University of Texas MD Anderson Cancer Center, Houston, TX,[2]Institute for Cell Therapy Discovery and Innovation, The University of Texas MD Anderson Cancer Center, Houston, TX,[3]Division of Hematology Oncology, VCU Massey Comprehensive Cancer Center, Richmond, VA

Background: Relapsed/refractory acute myeloid leukemia (AML) remains difficult to treat, highlighting the need for new therapies. NK cell-based immunotherapy offers potent antitumor activity with low risk of GVHD or severe CRS. The urokinase plasminogen activator receptor (uPAR), encoded by *PLAUR*, is highly expressed on malignant and senescent cells while largely absent from healthy HSCs and most normal vital organs. We found *PLAUR* significantly upregulated in AML and confirmed strong uPAR surface expression on primary blasts. Based on this favorable profile, we developed an off-the-shelf uPAR-targeted CAR-NK platform with a CD28 costimulatory domain and secreted IL-15 to enhance persistence.
Methods: Cord blood-derived NK cells were preactivated with IL-12/15/18 and transduced to express (i) uPAR-CAR, (ii) IL-15, or (iii) uPAR-CAR/IL-15. CAR expression, cytokine production, and phenotype were assessed by flow cytometry, ELISA, and CyTOF, respectively. Antileukemic activity against AML cell lines (MV4-11, THP-1, OCI-AML3) and primary blasts was tested by IncuCyte real-time killing and Annexin V staining. Long-term activity was assessed by sequential tumor rechallenge. In vivo efficacy was evaluated in NSG mice engrafted with luciferase-labeled OCI-AML3 and treated with a single NK infusion.
Results: uPAR was highly expressed on AML blasts but minimal on healthy HSCs/HSPCs, confirming its suitability as a CAR-NK target. uPAR-CAR/IL-15 NK cells were efficiently generated, secreted IL-15, and expanded robustly. In vitro, they showed markedly enhanced and antigen-specific killing of all uPAR+ AML lines and primary blasts compared with CAR-only, IL-15-only, or non-transduced NK cells ($p < 0.0001$), while *PLAUR*-knockout cells resisted killing. uPAR-CAR/IL-15 NK cells produced more IFN-γ and TNF-α and maintained superior function during repeated tumor exposure, with CyTOF revealing an activation/cytotoxicity-enriched metacluster. In vivo, a single uPAR-CAR/IL-15 NK infusion significantly reduced leukemia burden, delayed progression, and improved NK persistence in bone marrow. Compared with non-transduced NKs, tumor burden in peripheral blood ($p < 0.05$), bone marrow ($p = 0.001$), and spleen ($p < 0.01$) was substantially reduced, with no observed toxicity or weight loss. Taken together, uPAR is a safe, selective AML target. uPAR-CAR NK cells, particularly when armored with IL-15, display potent, antigen-specific, and durable antileukemic activity, supporting advancement of this platform for AML therapy.

#5200 Preclinical evaluation of armored DLL3 biepitope compound nanobody CAR T cells.

Byeong-Hyeok Choi[1], Ga-Ram Hwang[1], Morgan Flaherty[1], Vincent M. DeStefano[1], Masayuki Wada[1], Kevin Pinz[1], Jennifer E. Chow[1], Nabil Hagag[1], Yu Ma[2], Luo Jing[2], Yupo Ma[1]

[1]iCell Gene Therapeutics, Stony Brook, NY,[2]iCAR Bio Therapeutics Ltd, Zhongshan, China

Introduction

Delta-like ligand 3 (DLL3) is markedly and selectively expressed in small cell lung cancer (SCLC) and other high-grade neuroendocrine tumors with minimal expression in normal tissues, making it an attractive target for cellular immunotherapy. DLL3-directed CAR approaches in solid tumors have shown limited durability, underscoring the need for improved potency. To address these challenges, we developed DLL3 bi-epitope compound nanobody CAR T cells. We incorporate IL-18 armoring to enhance effector cell survival and function. Herein we report the feasibility of an armored DLL3 bi-epitope cCAR T construct.

Experimental Procedures

Alpacas were immunized with recombinant human DLL3 extracellular domain protein. Peripheral blood mononuclear cell (PBMC) mRNA was extracted and converted into a VHH (nanobody) to generate a library. The library was panned against DLL3 antigen to enrich for high-affinity binders, which were identified through ELISA screening and cellular binding analysis by flow cytometry. VHH clone sequencing were used to generate our cCAR. The DLL3 bi-epitope cCAR T is comprised of two unique and independently functioning CAR units targeting different DLL3 epitopes reducing risk of tumor evasion due to antigenic variation. A DLL3-targeting nanobody pair was used to generate DLL3 bi-epitope cCAR. Human T cells were activated and transduced to produce CAR T cells. CAR expression was assessed by flow cytometry. Cytotoxicity was evaluated using SHP-77 (endogenous DLL3$^+$) and REH-DLL3xp (overexpressing DLL3) targets. NSG mice received CAR T cells to assess antitumor activity.

Results

The bi-epitope DLL3 cCAR T construct demonstrates potent cytotoxicity lysing target cells in vitro and in vivo. At various effector-to-target ratios, the cCAR was observed to have strong killing activity and specificity against the primary tumor cell line and artificially DLL3-
expressing cell line. The cCAR also demonstrated strong potency in SHP-77 xenograft mouse models.

Conclusions

Our bi-epitope armored DLL3 cCAR T therapy demonstrated exceptional efficacy in vitro and in vivo. These results support future investigation of our cCAR in patients with SCLC and/or DLL3 expressing neuroendocrine tumors.

#5201 Tuning gated CAR-T cells for enhanced activity against acute myeloid leukemia.

Shawn Barman[1], Molly Shields[1], Tatiana Fourfouris[1], Ki Jun Lee[1], Naiomi Desai[1], Devon Bell[1], Ethan BenDavid[1], Justin Pfahler[1], Ayesha Khan[1], Sanjana Tottempudi[1], Armita Shadfar[1], Yong-Mi Kim[2], BABAK MOGHIMI[1]

[1]USC/CHLA, Los Angeles, CA,[2]Children's Hospital Los Angeles, Los Angeles, CA

Background: Conventional Chimeric Antigen Receptor (CAR) T-cell therapies for Acute Myeloid Leukemia (AML) face persistent challenges, including limited T-cell fitness, resistance emergence, and on-target, off-tumor toxicity. To overcome these limitations, we previously developed logically gated CAR-T cells using Synthetic Notch (SynNotch) circuits targeting two AML antigens, CD33 and CD123. In this system, CD33 engagement triggers expression of a gated CD123 CAR, leading to greater precision, improved metabolic fitness, reduced exhaustion, and longer in vivo persistence. Despite these benefits, gated CAR-T cells exhibit modestly reduced potency compared with conventional CAR-T cells. We hypothesize that incorporating modified intensity signaling elements into the gated architecture will enhance cytotoxicity while preserving the favorable metabolic and immunological profiles of gated CAR-T cells.
Methods: To enhance downstream activation, we engineered a panel of CAR signaling constructs, including CD3ζ ITAM-modified and ZAP70-based signaling modules. These designs were assessed using an NFAT reporter assay, allowing quantification of inducible signaling strength across constructs.
Results: Gated CAR-T cells expressing these enhanced signaling modules demonstrated accelerated and more robust activation, with a clear dose-dependent increase in NFAT reporter activity. Furthermore, we successfully incorporated the optimized signaling elements into a single open-reading-frame CAR design, enabling efficient expression and positioning these constructs for forthcoming translational testing.
Conclusion: Augmenting T-cell receptor-proximal signaling within the gated CAR framework increases activation and improves functional potency. We anticipate that these high-intensity gated CAR-T cells will maintain the metabolic advantages characteristic of SynNotch-gated systems. Ongoing studies are evaluating their efficacy, fitness, and safety in relevant AML models.

#5202 Predictive models for hematologic toxicity after CAR-T therapy: A systematic review of current risk scores and unmet AI needs.

Mansha Gupta[1], Abhijith Vemulapalli[2], Swathi Cherukuri[3], Rithish Nimmagadda[4], Akhil Jain[5]

[1]Midwestern University - Glendale Campus, Glendale, AZ,[2]Guntur Medical College, Guntur, India,[3]Mayo Clinic, Jacksonville, FL,[4]One Brooklyn Health - Interfaith Medical Center, New York, NY,[5]University of Iowa Hospitals and Clinics, Iowa City, IA

Background: Hematologic toxicity, including early and prolonged neutropenia, anemia, and thrombocytopenia, is among the most common and clinically significant complications after CD19, CD20, CD22 and BCMA-directed CAR-T therapy. Several clinical scoresmost notably CAR-HEMATOTOX (CAR-HT) and the refined ALL-HThave been developed to predict post-infusion cytopenias, but their comparative performance across diseases has not been systematically evaluated. No prior review has summarized existing models or assessed the need for AI-based predictive approaches.
Methods: We conducted a systematic review of studies that developed or validated predictive models or risk scores for hematologic toxicity after CAR-T therapy in hematologic malignancies. Eligible studies included clinical, cytokine-based, or composite predictors and reported discrimination metrics such as area under the curve (AUC). Extracted variables included CAR-T product, target antigen, disease type, predictors used, model type, validation strategy, and performance statistics. Results were synthesized qualitatively due to heterogeneity in model structure and outcome definitions.
Results: Studies on the CAR-HT score in B-cell lymphomas and multiple myelomas reported AUC values of 0.89 and 0.82, respectively, for predicting severe or long-term neutropenia after CD19 and BCMA-directed CAR-T therapy. Studies on the ALL-HT score (a modified/refined version of CAR-HT replacing ferritin with bone-marrow burden to improve discrimination in B-ALL) reported AUC 0.84-0.90 for predicting prolonged neutropenia and worse overall survivability (OS) after CD19/CD22 CAR-T. A multicenter study including aggressive/indolent NHL, MM/PCL, and ALL patients treated with CD19, CD20, or BCMA CAR-T reported AUC 0.87 (eIPM-Pre) and 0.88 (eIPM-Post) for predicting ICA-HT. A CD19 CAR-T study in B-ALL and LBCL reported AUC 0.85 for an early hematotoxicity nomogram using TNF- and CRP.
Conclusion: Existing prediction tools for hematologic toxicity after CAR-T therapy demonstrate strong but disease-specific performance. Yet inconsistent endpoints and heterogeneous predictors limit clinical generalizability. No current model incorporates contemporary AI or machine-learning methods, underscoring a significant unmet need. Advanced predictive frameworks may allow earlier identification of patients at risk for severe or prolonged cytopenias and guide more individualized supportive care, with the potential to reduce downstream complications.

#5203 Phosphorylated IRF7 enhances antitumor activity of GPC3-targeted CAR T cells in solid tumors.

Inci Cevher Zeytin[1], Che-Hsing Li[1], David de la Cerda[1], Leidy Diana Caraballo Galva[2], Andras Attila Heczey[1]

[1]Ben Towne Center for Childhood Cancer and Blood Disorders Research, Seattle Children's Research Institute, Seattle, WA, [2]Pediatrics - Oncology, Baylor College of Medicine, Houston, TX

Glypican-3 (GPC3) is highly expressed in hepatocellular carcinoma (HCC) and hepatoblastoma (HBL), but not in healthy mature tissues; thus, represents a promising immunotherapeutic target. In a recent study, GPC3-CAR or IL15 co-expressing GPC3-CAR T cells (15.CAR) were safe in patients, IL15 co-expression significantly enhanced CAR T cell expansion and resulted in a disease control rate of 66% and antitumor response rate of 33%. To elucidate molecular programs associated with therapeutic response, single cell RNA sequencing of tumor infiltrating CAR T cells was performed and unique transcriptomic profile differences were identified associated with antitumor responses including downregulation of SWI/SNF and upregulation of FOS/JUN and Type I Interferon family members. Transcription factor motif enrichment analyses identified Interferon regulatory factor 7 (IRF7) as the dominant transcriptional driver of genes upregulated in responders. We hypothesized that IRF7 will boost the antitumor activity and this study examined the role of wild type and constitutively active IRF7 expression in GPC3-CAR T cells (IRF7.CAR and pIRF7.CAR, respectively).Compared with 15.CAR T cells, IRF7.CAR and pIRF7.CAR T cells showed significantly higher naïve (CD45RA+ CCR7+ CD62L+; CD4 p=0.0348; in CD8 p=0.0163;), Central memory (CM, CD45RO+ CCR7+ CD62L+; CD4 p= 0.0382), LAG3+ (CD4 p=0.0236, CD8 p=0.0030) and significantly lower effector memory (TEM, CD45RA- CCR7- CD62L-; CD4 p= 0.0221) cell population at baseline, post-manufacturing based on flow cytometry. IRF7.CAR and pIRF7.CAR T cells had higher expansion and significantly improved killing efficacy ($p<0.001$) in repeated tumor-challenge assays using the IncuCyte system. Finally, In vivo, pIRF7GPC3+ cells showed more rapid tumor clearance under both high (5x10^6)- and low-dose (3x10^6) conditions in NSG-MHC I/II double knockout mice bearing HCC and HBL xenografts. These findings demonstrate that pIRF7 enhances CAR T-cell function. Incorporation of pIRF7 into GPC3-targeted CARs represents a novel strategy to improve efficacy against solid tumors.

#5204 CD5-directed CAR5/IL-15 NK cells as a therapeutic platform for T-cell malignancies.

Rafet Basar, **Sunil Acharya**, Nadima Uprety, May Daher, Francia Reyes Silva, Rejeena Shrestha, Bin Liu, Mayra Shanley, Merve Dede, Pinaki Banerjee, Ping Li, Paul Lin, Enli Liu, Donghai Xiong, Ken Chen, David Marin, Elizabeth Joan Shpall, Katayoun Rezvani

UT MD Anderson Cancer Center, Houston, TX

Background: Engineered NK cells have increasingly emerged as a powerful allogeneic cell therapy platform, with multiple trials demonstrating meaningful anti-tumor responses, durable clinical activity, and an excellent safety profile without GVHD and low cytokine-release toxicity. Their suitability for large-scale manufacturing makes CAR-NK cells particularly attractive for broad clinical use. T-cell lymphomas and leukemias remain difficult to treat, and although CD5 is a widely expressed and clinically actionable target, CAR-T cell development has been limited by fratricide and manufacturing barriers. A CD5-directed NK cell that avoids these limitations is therefore attractive in this setting.
Methods: We developed iC9/CAR5/IL-15 NK cells, an off-the-shelf engineered NK-cell therapy targeting $CD5^+$ tumors without fratricide or GVHD. The construct incorporates IL-15 to enhance persistence and the inducible caspase 9 (iC9) safety switch for controlled elimination if needed. A panel of CD5-targeting CAR constructs incorporating different intracellular signaling was generated and screened to identify constructs that optimized NK-cell activation, cytotoxicity, cytokine production, metabolic fitness, and functional persistence. These were tested against multiple $CD5^+$ T-ALL and T-cell lymphoma models, followed by in vivo evaluation in xenograft systems and safety testing against normal human tissues and long-term culture.
Results: Several signaling domains mediated strong anti-tumor activity, each with distinct advantages. CD28- and DAP10-based designs demonstrated the most consistent performance, supporting potent cytotoxicity and enhanced NK-cell activation. After comparing functional reproducibility, including cytotoxicity, cytokine production, proliferation, and serial killing, and considering manufacturing feasibility together with our prior clinical experience using CD28- signaling in CAR-NK products, the CD28-based iC9/CAR5/IL-15 NK construct was selected as the lead therapeutic candidate. In vivo, CD28-based iC9/CAR5/IL-15 NK cells resulted in rapid tumor regression and a significant survival benefit in $CD5^+$ T-ALL xenograft models. Safety studies confirmed the absence of off-target cytotoxicity, and prolonged culture showed no autonomous expansion or phenotypic instability.
Conclusion: iC9/CAR5/IL-15 NK cells overcome the barriers that have hindered CD5-directed CAR-T cell approaches, offering a scalable off-the-shelf therapy for aggressive T-cell malignancies. A Phase I/II clinical trial evaluating this therapy in relapsed/refractory $CD5^+$ T-cell cancers is now open and accruing at our center.

#5205 Assessing donor heterogeneity in CAR-T cells with massively parallel mixed lymphocyte reactions.

Lujing Wu[1], Lina Mohamad[1], Michelle Mantilla[1], Johnathan Lu[1], Ansuman T. Satpathy[2], Theodore Roth[3]

[1]Pathology, Stanford University, Stanford, CA,[2]Stanford University,[3]Stanford University, San Francisco, CA

Donor heterogeneity is a major source of variation in CAR-T cell functions which leads to inconsistencies in both clinical efficacy and pre-clinical studies to enhance CAR-T cell functions. However, assessing T cell donor heterogeneity with a large sample size is costly and time-consuming. Here, we developed a Massively Parallel - Mixed Lymphocytes Reaction (MP-MLR) assay that allows pooling and simultaneously testing of CAR-T cells from multiple human donors. Combining with pooled genetic perturbation technologies, we conducted pooled screening in more than 50 T cell donors for enhanced CAR-T cell proliferation under repetitive tumor stimulations, with a library of candidate genetic perturbations proposed to enhance CAR-T or T cell functions. While we identified genetic perturbations with consistent effect on CAR-T cells across donors, the majority of perturbations showed various levels of donor dependencies, and this observation was confirmed with arrayed validation of selected perturbations on specific donors. Furthermore, we performed multi-parameters pooled screening in-vitro and in-vivo for systematic discovery of generalizable and donor specific genetic perturbations enhancing CAR-T cell pre-clinical therapeutic efficacies. Overall, we presented an efficient and cost-effective strategy for assessing donor variabilities in CAR-T cells, predicting patient specific effects of genetic perturbations on CAR-T cells efficacies, and potentially identifying of personalized optimal genetic perturbation for enhancing CAR-T cell functions.

#5206 Mitochondrial remodeling sustains CAR-NK stemness for superior tumor control.

Silvia Tiberti[1], Madison Moore[2], Maliha Munir[1], Merve Dede[1], Byron Jia[1], Leen Kheirbek[1], Rejeena Shrestha[1], Nadima Uprety[1], Jeong-Min Park[1], Vernikka Woods[1], Corry Jones[1], Patrick Zhang[1], Dexing Fang[1], Huihui Fan[1], Maria Laura Centomo[1], Francia Reyes Silva[1], Mayra Shanley[1], Sunil Acharya[1], Ye Ethan Li[1], Bin Liu[1], Pinaki Banerjee[3], Rafet Basar[1], Katayoun Rezvani[1], May Daher[1]

[1]UT MD Anderson Cancer Center, Houston, TX,[2]UT MD Anderson Cancer Center, Houston, TX, Houston, TX,[3]UT MD Anderson Cancer Center, houston, TX

Background: NK cell-based therapies are a promising off-the-shelf strategy for cancer treatment. Their inherent safety and lack of graft-versus-host disease make NK cells an attractive platform for CAR engineering, combining innate cytotoxicity with receptor specificity. However, clinical efficacy in solid tumors is limited by poor persistence and rapid metabolic exhaustion in the tumor microenvironment (TME). Strategies that enhance metabolic fitness and delay differentiation are essential. Inspired by stem-cell culture systems, we tested whether Albumin Polyvinylalcohol Essential Lipids (APEL), a defined medium used to support iPSC differentiation into embryoid bodies and NK cells, could preserve CAR-NK stemness and improve metabolic fitness and function.
Methods: CAR-NK cells expanded with APEL (CAR-NK_{stem}) were compared with CAR-NK cells expanded in conventional NK cell media (CAR-NK_{conv}). Metabolic profiling included mitochondrial mass and potential profiling, Seahorse assays to measure glycolysis and oxidative phosphorylation, nutrient competition assays to assess metabolic flexibility. CAR-NK cells were cultured with various hematologic and solid tumor cell lines, followed by cytotoxicity evaluation using 2D xCelligence and 3D Incucyte including rechallenge assays to assess serial killing capacity. In vivo efficacy was tested using various xenograft mouse models of hematologic cancers (MOLM14, MM1s) and solid tumors (786-0 ongoing). Mechanistic studies included multiomics profiling by bulk RNA-seq and ATAC-seq, CyTOF, and mitochondrial-transfer assays.
Results: Our data show that early metabolic reprogramming of CAR-NK_{stem} during expansion drove the development of enlarged and highly active mitochondria, increased spare respiratory capacity (SRC), and superior metabolic flexibility. This metabolic state stabilized stem-like features and limited terminal differentiation via chromatin remodeling toward persistence and memory-associated programs. Functionally, CAR-NK_{stem} cells showed improved proliferation, sustained serial killing, superior nutrient competition, and enhanced tumor control in vitro and in vivo. Mechanistically, mitochondrial transfer from CAR-NK_{stem} cells enhanced cytotoxicity and persistence in recipient NK cells, highlighting mitochondrial remodeling as a key driver of functional fitness.
Conclusion: These findings demonstrate that targeted metabolic reprogramming during manufacturing can generate stem-like, highly persistent CAR-NK cells and offer a broadly applicable, immediately translatable strategy for cancer immunotherapy.

: Biological and Clinical Consequences of Cancer Therapy
Poster Session

#5211 Lung adenocarcinoma and urothelial carcinoma: Analysis of double cancer in Chang-Gung Medical Foundation.

Feng-Che Kuan[1], Meng-Hung Lin[2], Chung-Sheng Shi[3]

[1]Oncology, Chang Gung Memorial Hosp. - Chiayi Branch, Putzu City, Taiwan,[2]Chang-Gung Memorial Hospital, Chia-Yi Branch, Puzi, Taiwan,[3]Chang Gung University, Taoyuan County, Taiwan

Background: Aristolochic acids (AA) form carcinogenic DNA adducts, which can be detected in human urinary tract (kidney, ureter, and urinary bladder), liver, and non-target tissues such as pancreas, breast, and lung. AA is blamed for urothelial carcinoma (UC) but its carcinogenic role on lung cancer is still under debate. This study plans to investigate the characteristics of double cancers with urothelial carcinoma and lung adenocarcinoma (LA). Methods: We conducted this multi-institutional cohort study in Taiwan. Two independent cohorts were retrieved from Chang-Gung Research Database (CGRD). The first cohort (UCLA) included patients with double cancers with urothelial carcinoma (UC) and lung adenocarcinoma (LA) from 1994 to 2023 and the second cohort (CGMH-EGFRm) with EGFR-mutated LA from 2011 to 2020. UCLA was further divided into groups according to the sequence of cancer development (group 1: index diagnosis date of UC before LA; group 2: simultaneous LA and UC; group 3:LA before UC), and CGMH-EGFRm was divided into activating EGFR-mutations (group 4) and other mutations (group 5). The last follow-up time was Dec 30, 2023. Descriptive statistics are provided with Chi-Squared and Fisher's Exact Test. $P<0.05$ was set to be statistic significance.Results: From 1994 to 2023, cohort 1 comprised of 196 patients of which 126 in group 1, 30 in group 2, and 40 in group 3 and from 2011 to 2020 cohort 2 comprised of 3,427 patients. The last follow-up time was Dec 30, 2023, and the mean age of group 1, 2, and 3 was 73, 73, and 67, respectively. The male gender in group 1, 2, and 3 was 65.9%, 66.7%, and 67.5%, and smoking habit was 30.2%, 26.7%, and 42.5%, respectively. The baseline characteristics such as age, gender, smoking habits were different from group 1 to 5, while in UCLA cohort, gender and smoking habits were similar. The median interval of diagnosis between double cancer was 2381.5 (range: 131 to 10556), 8.5 (0 to 84) and 755.5 (98 to 4390) days, respectively. After 2000s (based on year of diagnosis with UC), there was an increasing trend in group 2 and 3. The anatomical locations of LA was similar between groups 1 to 3 ($p=0.660$), and a trend of increasing renal pelvis and ureter UC in group 3 ($p=0.104$). Conclusion: 1.1% of UC can develop LA in CGRD. Further genomic analysis between groups was warranted to elucidate the carcinogenic role of AA in double cancers.

#5213 T-cell transcriptome affected by therapy-related clonal hematopoiesis in long-term survivors of pediatric cancers.

Nadezhda V. Terekhanova, Sivaraman Natarajan, Bensheng Ju, Kohei Hagiwara, Li Dong, Zhaoming Wang, Leslie L. Robison, John Easton, Jinghui Zhang

St. Jude Children's Research Hospital, Memphis, TN

Our previously published work on the St. Jude Lifetime Cohort Study (SJLIFE), a retrospectively constructed cohort with prospective follow-up of long-term survivors of pediatric cancer, unveiled the phenomenon of accelerated clonal hematopoiesis (CH) associated with prior exposure to radiotherapy and chemotherapy. *STAT3* Y640F, a hotspot mutation specifically linked to prior exposure to procarbazine in Hodgkin Lymphoma (HL) survivors, was most frequent in the SJLIFE cohort. Based on joint profiling of DNA amplicons and cell-surface proteins at single cell resolution using the MissionBio platform, we found *STAT3* Y640F mutation in blood leukocytes from 6 out of 10 HL survivors. Importantly, *STAT3* Y640F was enriched in cells clustered within CD8 T-cells, indicating that mutation-positive cells have reprogramed the transcriptome that gave selective growth advantage to a subset of those cells. To investigate this, we performed PacBio scKinnex assay to generate full-length transcriptomes at single cell level, enabling integration of CH mutations with gene expression profiles. An initial analysis using blood samples of HL survivors yielded limited information as few mutant cells were detected due to the low mutation frequency (≤1%) and *STAT3* expression. To enrich for the mutant cells, we performed sorting for CD8+ T-cells followed by scKinnex for three samples which yielded sufficient number of mutant cells (14 to 26 cells per sample) for gene expression analysis. For each sorted sample 4,396 to 5,416 cells were profiled, and clustering by gene expression revealed 11-14 subpopulations per sample. Guided by the expression status of marker genes, we performed cell annotation and identified multiple CD8 T-cell subsets, including naive, central memory, effector memory, and terminally differentiated effector memory cells. *STAT3* mutant cells were present only in a few of these subpopulations: 3 out of 13 (23%), 1 out of 14 (7%), and 2 out of 11 (18%) in these three samples with an average frequency of 40% in each subpopulation. Nearly all mutant-positive clusters showed increased expression of *STAT3* gene; four out of the five (80%) such clusters exhibited high expression of cytotoxic markers, including *GZMB*, *GZMH*, *FGFBP2* and *NKG7*, while the remaining one showed high expression of stress response markers from FOS/JUN pathway (*JUN*, *JUNB*, and *FOS*). To our best knowledge, this is the first study that shows CH mutation can confer selective advantage to specific functional cell subsets of CD8 T-cells and analysis of gene-regulatory network changes related to *STAT3* Y640F mutation in those cell subpopulations is currently ongoing. Our study also demonstrates that cell sorting followed by scKinnex can be an effective strategy for studying the functional impact of rare CH mutations at the single cell resolution in relevant cell types.

#5214 The mutational landscape underlying the late effects of anthracyclines on tumor, blood, and heart genomes.

Mathepan Jeya Mahendralingam[1], Mehdi Layeghifard[1], Timmy Wen[1], Burcak Otlu[2], Seema Mital[1], Filio Billia[3], Adam Shlien[4]

[1]The Hospital for Sick Children, Toronto, ON, Canada,[2]Middle East Technical University, Ankara, Turkey,[3]Toronto General Hospital Research Institute, Toronto, ON, Canada,[4]Graduate Student, Dept. of Genetics & Genome Bio., The Hospital for Sick Children, Toronto, ON, Canada

Motivation: Anthracyclines, an essential chemotherapy, disproportionately contributes to several late effects burdening survivors of cancer, including cancer relapse, therapy-related blood cancers, and fatal cardiotoxicity. Despite decades of clinical use, the mechanisms underlying these late effects - particularly how anthracyclines damage the genome of neoplastic and non-neoplastic tissues (blood and heart) - remain poorly understood. A deeper understanding of the tissue-specific mutational outcomes of anthracyclines could yield promising biomarkers to improve survivorship care for survivors of cancer.

Methods: We assembled a cohort of untreated or anthracycline-treated tumor, blood, and heart samples. Tumors and blood were leveraged from childhood cancer patients enrolled in the SickKids Cancer Sequencing Program. Heart samples were obtained from cancer survivors who received anthracyclines and later developed severe cardiotoxicity that required a heart transplant. We sequenced the DNA of each tissue type to identify anthracycline-induced somatic mutations.

Results: Our initial results revealed minimal genome-wide mutational differences between anthracycline-treated versus untreated samples across all tissue types. We hypothesized that anthracyclines may cause localized mutagenesis in unique genomic topographies. Indeed, we found that anthracycline-treated tissues had a strong enrichment of somatic mutations in open chromatin of their respective cell of origin but differed based on the mutation type. Anthracycline-treated tumors had an enrichment of single nucleotide variants in promoters and introns, but depletion of deletions in exonic regions. However, leveraging matched blood samples from these cancer patients demonstrated that anthracycline-treated blood samples had an enrichment for deletions in open chromatin of various blood cell types. Despite the heart's non-proliferative capacity, anthracycline-treated hearts had a significant enrichment of insertion-deletions in fetal cardiomyocyte open chromatin and non-B DNA regions. Lastly, comparative analysis of the somatic mutational profiles of anthracycline-exposed hearts, tumors, and blood samples, we uncovered previously underappreciated tissue-specific mutational signatures.

Significance: This study is the first to characterize the tissue-specific genomic consequences of anthracyclines on tumors, blood, and heart. The early identification of high-risk patients will transform survivorship care, ensuring children with cancer do not merely survive their diagnosis - they thrive beyond it.

#5215 Metabolic and lipidomic changes in early asparaginase hepatotoxicity in mice.

Veronica Ruiz-Torres[1], Jennifer J. Chia[2], Michael D. Cohen[3], Jia Tan[3], Kevin J. Williams[4], Nedas Matulionis[4], Abby Krall[4], Heather R. Christofk[5], Etan Orgel[6], **Steven D. Mittelman**[7]

[1]UCLA Mattel Children's Hospital and Instituto de Investigacion, Desarrollo e Innovacion en Biotecnologia Sanitaria de Elche (IDiBE), Universitas Miguel Hernandez (UMH), Los Angeles, CA,[2]Department of Pathology and Laboratory Medicine, UCLA and Jonsson Comprehensive Cancer Center, University of California, Los Angeles, CA, Los Angeles, CA,[3]UCLA - University of California Los Angeles, Los Angeles, CA,[4]UCLA, Los Angeles, CA,[5]UCLA David Geffen School of Medicine, Los Angeles, CA,[6]Pediatric Hematology/Oncology, Children's Hospital Los Angeles, Los Angeles, CA,[7]UCLA Mattel Childrens Hospital, Los Angeles, CA

Asparaginase (ASNase) is an effective treatment for pediatric acute lymphoblastic leukemia but is limited by hepatotoxicity, particularly in obese patients. While ASNase has been shown to induce adipocyte lipolysis and hepatocyte integrated stress response, the mechanisms by which ASNase causes hepatosteatosis and hepatotoxicity remain unclear. We previously examined the effects of PEG-ASNase on livers in mice seven days after injection. However, by this timepoint, livers were severely steatotic. Therefore, to uncover early effects of ASNase, we treated obese and control 18-week-old male C57Bl6 mice with one IP dose of 3,000 IU/kg pegylated-ASNase and analyzed livers three days later. ASNase caused significant hepatosteatosis already 3 days after injection (n=6; Table). ASNase increased liver unsaturated triglycerides and decreased phosphatidylcholine and lysophosphatidylcholine. Metabolomics identified decreases in s-adenylmethionine (SAM), 5-Aminoimidazole-4-carboxamide ribonucleoside (AICAR), and glutathione to glutathione disulfide ratio (GSH:GSSG, Table), indicating oxidative stress. These lipidomic and metabolomic changes were more pronounced in obese mice. RNAseq identified lower expression of palatin-like phospholipase domain containing protein 3 (PNPLA3) after ASNase (-4.8 to -5.1 $\log_2$fold change, $p<0.001$). qPCR showed low PNPLA3 expression in obese compared to control vehicle livers ($p<0.001$) and confirmed substantial suppression after ASNase in both groups (Table). Our results show that within three days, ASNase induces hepatic steatosis, oxidative stress lower phosphatidylcholine levels and suppression of PNPLA3 expression. These effects appear to be magnified in obesity. Since phosphatidylcholine and PNPLA3 are known to be related to metabolic dysfunction associated steatotic liver disease (MASLD), these effects are likely contributory to ASNase hepatotoxicity. Further work is needed to fully understand the mechanisms of these changes.

Liver changes with ASNase treatment

	Lean VEH	Lean PEG	p value	Obese VEH	Obese PEG	p value
Steatosis Score	0±0	2.833±0.477	0.002	2.667±0.333	3.833±0.401	0.050
GSH:GSSG (normalized)	1.000±0.071	0.546±0.049	0.001	0.404±0.060	0.662±0.038	0.006
PNPLA3 (RQ)	1.234±0.771	0.016±0.007	0.011	0.026±0.009	0.005±0.002	0.072

#5216 Novel transdermal curcumin attenuates cisplatin induced neuropathy in a mouse model of breast cancer.

Yugal Goel[1], Carolina Mireles[1], Dahlia Ordaz[2], Kendall O'Daniel[1], Kristen A. Peterson[1], Naomi Lomeli[2], Reina Lomeli[1], Daniela A. Bota[2], Joel Friedman[3], Kalpna Gupta[1]

[1]Hematology/Oncology, Department of Medicine, University of California, Irvine, CA,[2]Department of Neurology, Department of Medicine, University of California, Irvine, CA,[3]Department of Microbiology and Immunology, Albert Einstein College of Medicine, Bronx, NY

Cisplatin-induced neuropathy remains a major challenge to treat. Cisplatin disrupts mitochondrial homeostasis and increases reactive oxygen species (ROS) contributing to neuronal injury. We examined the ability of curcumin to prevent CIPN because it has antioxidant and neuroprotective properties. However, a major challenge is the reduced absorption and bioavailability of oral and systemically administered curcumin. To address this challenge, we used a novel transdermal curcumin (TDC) preparation which is bioavailable in the blood and central nervous system after topical application to the abdomen of mice. We used a transgenic mouse model of breast cancer (C3TAg) which shows the evolutionary spectrum of human breast cancer and its isotype control FVB/N mice. At ~4 months of age female C3TAg mice develop palpable tumors and demonstrate mechanical, thermal and musculoskeletal hyperalgesia ($P<0.0001$ vs FVB/N). Mice were treated with vehicle or cisplatin (2.3 mg/kg/day i.p.) for two cycles of 5-days and 5 days of rest in the presence or absence of TDC/VAS-101 (0.1 mL) applied daily by rubbing on the abdomen of mice through the endpoint. Similar to cisplatin, TDC alone significantly reduced tumor weight ($P<0.05$ vs vehicle), and didn't decrease the anti-tumor efficacy of cisplatin. By day 5, cisplatin induced significant mechanical and cold hyperalgesia in both strains ($p<0.001$ vs vehicle and BL), and musculoskeletal hyperalgesia at day 16 in C3TAg mice ($P<0.001$ vs BL; $P<0.0001$ vs vehicle). TDC co-treatment significantly attenuated cisplatin induced hyperalgesia (mechanical and cold, $P<0.0001$ vs cisplatin) and prevented musculoskeletal hyperalgesia ($P<0.001$ vs cisplatin). Notably, in C3TAg mice, TDC alone significantly decreased constitutive mechanical ($P<0.001$ vs vehicle; $P<0.01$ vs BL) and cold hyperalgesia ($P<0.01$ vs vehicle). These changes in hyperalgesia were accompanied by a significant reduction in phospho-p38 mitogen-activated protein kinase (MAPK) in dorsal root ganglion (DRG) neurons in C3TAg mice co-treated with TDC and cisplatin compared to cisplatin treatment ($P<0.001$) suggesting the activation of pain signaling. Furthermore, in primary DRG neurons and HT22 hippocampal neuronal cell line in culture, cisplatin elevated ROS and caused mitochondrial depolarization ($P<0.0001$; $P<0.001$ vs vehicle), which was prevented by TDC ($P<0.0001$). In HT22 neurons, cisplatin increased calcium release and lowered subsequent metabolic activity and viability ($P<0.001$ vs. vehicle), which were significantly inhibited by TDC ($P<0.001$), indicating that TDC targets the pain generating Ca^{2+} release from neuronal cells. In conclusion, TDC alleviates cancer- and chemotherapy-related hyperalgesia via inhibition of p38 MAPK and oxidative stress, while restoring mitochondrial function and limiting tumor growth. Thus, the novel TDC has a translational potential for preventing CIPN.

#5217 Mast cell activation leads to cisplatin-induced peripheral neuropathy.

Carolina Mireles[1], Donovan A. Argueta[1], Raghda Fouda[1], Sonal Joshi[2], Daniela A. Bota[3], Kalpna Gupta[1]

[1]Medicine, University of California, Irvine, Irvine, CA,[2]Medicine, University of Minnesota, Minneapolis, MN,[3]Neurology, University of California, Irvine, Irvine, CA

Chemotherapy-induced peripheral neuropathy (CIPN) is a painful side effect of treating cancer with cisplatin. Cisplatin is a platinum-based chemotherapeutic that induces mast cell activation. Mast cells reside in close proximity of the epidermal layer, vasculature and nerve fibers in the skin. Tryptase and other noxious substances released by mast cells activate nociceptors via protease activated receptor -2 (PAR2) leading to pain. We hypothesized that cisplatin-induced mast cell activation leads to nerve injury and neuropathic pain. We used C57BL/6, wild-type (WT) and mast cell knockout (MC-KO) mice with a spontaneous c-kit "sash" mutation (Kit*W-sh*) on a C57BL/6 background. Male and female mice were treated with cisplatin (i.p., 2.3 mg/kg/day), for 5 days of treatment followed by 5 days of saline (i.p.) for 2 cycles; or pre-treated with 100 mg/kg/day imatinib, an inhibitor of c-Kit and mast cell activation. Mechanical, cold, and thermal hyperalgesia were assessed at regular intervals. At day 18, cisplatin-treated mice showed a significant increase in mechanical hyperalgesia ($p<0.001$), cold hyperalgesia ($p<0.05$), and heat hyperalgesia ($p<0.0001$) compared to vehicle-treated mice. There were no changes in WT mice treated with imatinib or imatinib with cisplatin or in MC-KO mice treated with cisplatin for mechanical or thermal hyperalgesia, suggesting the involvement of mast cells in CIPN. Dorsal skin sections were co-stained with histone H3 (mast cell traps), FcεR1 (mast cell marker), and NF200 (nerve bundles). Cisplatin-treated mice showed activated mast cells surrounding nerve bundles, causing the expulsion of dense traps of citrullinated histones and podia extending into nerve fibers, causing nerve damage. The vehicle-treated mice showed intact, undisturbed thick nerve bundles without mast cell activation. Compared to vehicle, cisplatin-treated WT mice showed a significant increase in the number of non-degranulating and degranulating mast cells in dorsal ($p<0.05$) and toe skin ($p<0.001$, $p<0.0001$, respectively). We found a significant increase in cutaneous chymase ($p<0.01$), and tryptase ($p<0.01$), and plasma chymase ($p<0.5$), and tryptase ($p<0.01$) levels in cisplatin-treated compared to vehicle-treated WT mice. Human mast cells, HMC1.2, were incubated with 2, 5, and 10 µg/ml cisplatin or vehicle for 10 and 70 min, followed by analysis of chymase and tryptase in the conditioned medium. At the lowest dose of 2 µg/ml, cisplatin significantly stimulated the time-dependent release of chymase and tryptase compared to vehicle ($p<0.01$ for both). Together, our data show the novel phenomenon of mast cell traps upon cisplatin treatment leading to nerve injury, while tryptase released from mast cells may activate PAR-2 leading to the painful symptoms of CIPN. We speculate that the cotreatment of cisplatin with imatinib or other mast cell stabilizers such as cromolyn may ameliorate the painful symptoms of CIPN.

#5218 Leveraging a PARP inhibitor as neuroprotection against chemotherapy induced cognitive impairments.

Dahlia A. Ordaz, Shashi Jain, Daniela A. Bota

Neurology, University of California Irvine, Irvine, CA

Platinum-based (Pt) chemotherapies are lifesaving for many cancers, yet they induce persistent DNA damage and neuroinflammation that can profoundly alter cognitive function, collectively known as chemotherapy-induced cognitive impairments (CICI). The molecular drivers of these long-lasting effects remain mostly unknown, but symptoms include impaired concentration, memory deficits, and declines in speech and motor function this suggesting significant hippocampal vulnerability. Cisplatin, a widely used Pt agent causes extensive DNA crosslinking and robust proinflammatory signaling. Emerging evidence implicates poly (ADP-ribose) polymerase 1 (PARP1) in this process; when persistently activated by cisplatin-induced DNA damage- PARP1 drives metabolic dysfunction, inflammatory amplification, and impaired neuronal repair. PARP1 inhibitors have shown neuroprotective effects in other neurodegenerative disorders, reducing neuroinflammation and delaying functional decline. We hypothesized that excessive PARP1 activation contributes significantly to cisplatin-induced hippocampal dysfunction, and that targeted PARP inhibition could mitigate these neurotoxic cascades and preserve neuronal health. To determine whether the PARP inhibitor niraparib acts as a neuroprotective or rescue agent, we evaluated multiple treatment windows in vitro using mouse neural stem cells (MNSCs) from C57BL/6 mice. Cells were exposed to cisplatin (IC_{50}: 0.4 µM) with niraparib (1 µM) administered pre-, post-, or concurrently. Niraparib significantly improved viability across all time points compared to cisplatin alone ($p<0.0001$). In primary hippocampal neurons (cisplatin IC_{50}: 0.6 µM), combination treatment markedly increased PSD95 puncta and dendritic branching ($p<0.0001$), indicating preserved synaptic structure. To ensure that niraparib's neuroprotection did not dimmish cisplatin's anticancer efficacy, we tested the same low-dose combination in ID8/MOSEC and SKOV3.ip1 (IC_{50}: 34.11 µM and IC_{50}: 13.5 µM) ovarian cancer cell lines. No increase in viability was observed relative to cisplatin alone, confirming that niraparib did not interfere with cisplatin cytotoxicity. Together, these findings suggest that niraparib mitigates cisplatin-induced neurotoxicity while maintaining anti-cancer activity. Our next phase will evaluate niraparib alongside clinically relevant cisplatin dosing in C57BL/6 mice to assess cognitive outcomes in vivo. This works aims to clarify the mechanisms underlying CICI and identify strategies to improve quality of life and survivorship patients undergoing treatment.

#5219 Systemic therapy and cardiovascular disease in adolescent and young adult breast cancer survivors.

Theresa H. M. Keegan[1], Candice A. M. Sauder[1], Ann M. Brunson[1], Renata Abrahao[1], Anne C. Kirchhoff[2], Eric Haupt[3], Mallory Casperson[4], Ted Wun[1], Chun R. Chao[3], Andrew B. Smitherman[5], Hazel B. Nichols[6], Jessica Chubak[7], Erin E. Hahn[3], Lawrence H. Kushi[8], Kathryn J. Ruddy[9]

[1]UC Davis Comprehensive Cancer Center, Sacramento, CA,[2]University of Utah, Salt Lake City, UT,[3]Kaiser Permanente Southern California, Pasadena, CA,[4]Cactus Cancer Society, Oakland, CA,[5]University of North Carolina Chapel Hill, Chapel Hill, NC,[6]University of North Carolina at Chapel Hill, Chapel Hill, NC,[7]Kaiser Permanente Washington Health Research Institute, Seattle, WA,[8]Kaiser Permanente Northern California, Oakland, CA,[9]Mayo Clinic Cancer Center, Rochester, MN

Breast cancer (BC) is the most common cancer among female adolescents and young adults (AYAs; 15-39 years). While advances in treatment have improved survival, cardiovascular disease (CVD) can result from systemic therapies, and CVD is a leading cause of death in AYA cancer survivors. AYAs with BC face nearly a four-fold increased risk of CVD compared to their peers without cancer. However, data on the effects of systemic treatment on CVD in this population remains limited. We estimated risk of CVD in AYAs diagnosed with invasive BC (2006-2020), who survived ≥2 years, and were diagnosed and treated in the Kaiser Permanente (KP) Northern and Southern California. Patients were categorized by receipt of anthracycline-, alkylating-, HER2-, platinum-, and taxane-based therapies within 2 years of diagnosis. We examined the cumulative incidence of CVD starting 2 years post-diagnosis and used Cox proportional hazards regression to determine factors associated with CVD. Among 3,071 AYAs, 35.1% were non-Hispanic (NH) White, 31.6% were Hispanic, 18.3% were NH Asian, and 8.2% were NH Black. Most received systemic therapy (90.6%), including anthracycline- and alkylator without HER2-targeted therapy (41.9%) and HER2-targeted therapy without anthracycline (20.9%). Fewer AYAs received a taxane and alkylator (13.0%) or anthracycline with alkylator and taxane along with a HER2-targeting agent (6.4%). Mean follow-up after cancer diagnosis was 7.2 years (range: 2.0-17.5). The 10-year cumulative incidence of CVD was highest among AYAs who received anthracycline/alkylator/taxane/HER2-targeting therapy (19.6%), intermediate for those with anthracycline/alkylator without HER2-targeting therapy (13.0%) and those who received HER2-targeted therapy without anthracycline (14.6%), and lowest for those who received taxane/alkylator (7.3%). In the multivariable model adjusted for demographic factors and radiation, compared to taxane/alkylator, anthracycline/alkylator/taxane/HER2-targeting therapy (hazard ratio (HR)=2.63, 95% confidence interval (CI) 1.56-4.43); anthracycline/alkylator without HER2-targeting therapy (HR=1.75, CI 1.13-2.71); and HER2-targeting therapy without anthracycline (HR=2.13, CI 1.11-4.09) were associated with an increased risk of CVD. CVD risk was similar for taxane/alkylator and no systemic therapy. Other factors associated with higher risk of CVD included NH Black race/ethnicity (HR=1.90, CI 1.32-2.73 vs. NH White) and public health insurance (HR=1.67, CI 1.00-2.78 vs private). This study identifies AYA BC survivors at higher risk of CVD based on treatment regimens received, with highest risks found for those receiving anthracycline/alkylator/taxane/HER2 treatment combinations. In addition, AYAs of Black race/ethnicity and those with public health insurance experienced more CVD, underscoring the need for targeted interventions to mitigate these disparities.

#5220 Association between metabolic syndrome and risk of second primary malignancy among patients with a history of cancer.

Pragati Advani[1], Nicolas F. Schlecht[2], Christina Crabtree-Ide[3], Sarah Mullin[4], Oday Karadsheh[5], Tessa Faye Flores[6], Han Yu[4], Kayla Catalfamo[4], Mary E. Reid[7], Sai Yendamuri[1]

[1]Department of Thoracic Surgery, Roswell Park Comprehensive Cancer Center, Buffalo, NY,[2]Cancer Prevention and Control, Roswell Park Comprehensive Cancer Center, Buffalo, NY,[3]Cancer Screening Outreach and Survivorship, Roswell Park Comprehensive Cancer Center, Buffalo, NY,[4]Biostatistics and Bioinformatics, Roswell Park Comprehensive Cancer Center, Buffalo, NY,[5]Division of Endocrinology, Roswell Park Comprehensive Cancer Center, Buffalo, NY,[6]Department of Medicine, Roswell Park Comprehensive Cancer Center, Buffalo, NY,[7]Cancer Screening, Survivorship and Mentorship, Roswell Park Comprehensive Cancer Center, Buffalo, NY

Background: Prior studies have reported associations between modifiable comorbid conditions such as obesity, insulin resistance, hypertension, and hyperlipidemia (collectively known as Metabolic Syndrome [MetS]) and the risk of first primary cancer (FPC). However, the role of MetS on the risk of a second primary malignancy (SPM), a histologically and clonally distinct tumor that develops in a cancer survivor, is a heavily understudied area. Given that ~1 in 5 cancer survivors get diagnosed with a SPM in their lifetime, the purpose of this investigation was to understand the complex interplay between MetS, its individual components, other patient-related risk factors and risk of SPM.

Methods: The study cohort included 11,617 cancer patients who survived at least 12 months after their FPC diagnosis without a disease event (death, SPM or recurrence) and seen at the Roswell Park Comprehensive Cancer Center's dedicated survivorship clinic. Data on specific biomarkers to capture individual components of MetS was abstracted from electronic medical records. Patients were identified as having MetS if they had at least three of four MetS conditions (obesity, insulin resistance, hypertension, and hyperlipidemia). The association between MetS and risk of SPM was evaluated using Fine-Gray sub distribution hazard models adjusting for age, sex, smoking status, and TNM stage at FPC diagnosis.

Results: A total of 10,462 patients (90%) had data on ≥3 MetS conditions. Of those, 8,910 had fewer than three MetS conditions, while 1,552 had three or more. Overall, 4,963 patients developed SPMs ≥12 months after FPC diagnosis. In our multivariable analyses, we found that presence of MetS was independently associated with a significantly increased risk of SPM (Hazard Ratio [HR]=1.20; 95% Confidence Interval=1.01-1.40; P=0.043). Additionally, the risk of SPM increased significantly with number of MetS conditions (P<0.001). A majority of patients were obese (Body Mass Index ≥30 kg/m) (70%), and obesity was one of the primary conditions driving the increased SPM risk associated with MetS (HR=1.54; P=0.013). Among the other patient-related risk factors adjusted for, older age was associated with increased SPM risk (HR=1.02, P<0.001), whereas being a non-/former-smoker was associated with a decreased SPM risk compared to current smokers (HR=0.72, P<0.001, HR=0.83, P=0.019, respectively) as was having a higher stage of FPC (TNM III-IV vs. I-II) (HR=0.33, P<0.001).

Conclusion: MetS is significantly associated with the risk of developing SPMs among cancer survivors, with the risk of SPM increasing with number of MetS conditions, of which obesity was the strongest predictor. SPMs have emerged as an important concern for cancer survivors as treatment options for FPC have improved. Further research into the interrelationship between MetS conditions in cancer survivors and risk of SPM is therefore warranted.

#5221 Racial/ethnic disparities in risk of second primary malignancy among women in the Pathways Study of breast cancer survivors.

Pragati Gole Advani[1], Lia D'Addario[2], Cecile A. Laurent[2], Janise M. Roh[2], Marilyn L. Kwan[3], Theresa H. Keegan[4], Isaac J. Ergas[2], Scarlett L. Gomez[5], Han Yu[6], Christine B. Ambrosone[7], Lawrence H. Kushi[8]

[1]Department of Thoracic Surgery, Roswell Park Comprehensive Cancer Center, Buffalo, NY,[2]Division of Research, Kaiser Permanente Northern California, Pleasanton, CA,[3]Research Scientist, Div. of Research, Kaiser Permanente Northern California, Oakland, CA,[4]Hematology and Oncology, University of California Davis Comprehensive Cancer Center, Sacramento, CA,[5]Department of Epidemiology and Biostatistics, University of California, San Francisco, CA,[6]Biostatistics and Bioinformatics, Roswell Park Comprehensive Cancer Center, Buffalo, NY,[7]Department of Cancer Prevention and Control, Roswell Park Cancer Institute, Buffalo, NY,[8]Director of Scientific Policy, Division of Research, Kaiser Permanente, Oakland, CA

Background: Breast cancer (BC) survivors face a significantly increased risk of developing a second primary malignancy (SPM). While late-effects of cancer treatments contribute to SPM risk, shared behavioral and genetic factors that lead to the initial BC may also affect development of SPM. Previous studies have reported significant racial/ethnic disparities in BC incidence and mortality; however, few have examined disparities on the risk of SPM after BC. The aim of this study was to evaluate SPM risk across racial and ethnic groups of women with BC.

Methods: We examined risk of SPM in the Pathways Study, a prospective cohort study of 4,504 women with newly diagnosed, invasive BC between the years 2006 and 2013, at Kaiser Permanente Northern California (KPNC). Associations between self-identified race/ethnicity (categorized as non-Hispanic White [White], non-Hispanic Black [Black], non-Hispanic Asian American/Pacific Islander [AAPI] and Hispanic/Latino [H/L]) and SPM was evaluated using a univariate Fine-Gray sub distribution hazard model. Models were adjusted for age, stage, grade, hormone receptor status and treatment type. Due to small numbers, 92 American Indian/Alaska Native participants were excluded. Follow-up was from date of BC diagnosis to SPM, disenrollment from the KPNC health plan, death, or December 31, 2022, whichever came first.

Results: Of the 4,412 BC patients included in the study, 2,950 (66.9%) were White, 351 (8.0%) Black, 599 (13.6%) AAPI and 512 (11.6%) were H/L. Overall, 612 (13.6%) developed a SPM (median follow-up time=14.2 years; range=9.8-17.3). Among 521 patients with known SPM sites, breast (197, 37.8%), reproductive organs (74, 14.2%) and lung (48, 9.2%) were most common sites. In multivariable analyses, we found that compared with White women, H/L had a significantly decreased risk of developing a SPM (Hazard Ratio [HR]=0.64; 95% Confidence Interval [95%CI]=0.43-0.95). Although we also observed lower risk of SPM in AAPI and Black women (HRs of 0.71, 95%CI=0.49-1.02; and 0.79, 95%CI=0.51-1.22, respectively), these associations did not reach statistical significance. Besides race/ethnicity, age at BC diagnosis was also a significant predictor of SPM risk. Older age at diagnosis (60-69 and 70+ years) was associated with significantly increased SPM risk (HR_{60-69}=1.66, 95% CI=1.17-2.34 and HR_{70+}=2.37, 95% CI=1.64-3.41) compared with women diagnosed at <50 years.

Conclusion: We observed substantial disparities in SPM risk by race/ethnicity in the KPNC BC survivor's cohort, with H/L patients experiencing lower risk than Whites, whereas those in the older age group (60+ years) experienced higher risks. Further research to understand drivers of these racial, ethnic and age-related heterogeneity is warranted. Tailored surveillance strategies accounting for these characteristics may help reduce disparities among BC survivors.

#5222 Multifactorial risks for multiple primary cancers.

Johnathan Amsalem, Ying Liu, Aliya Khurram, Yelena Kemel, Andrew Marderstein, Mitul Waghmare, Semanti Mukherjee, Michael Conry, Vignesh Ravichandran, Saibaba Magunta, Ritika Kundra, Matthew Buas, Christopher Fong, Justin Jee, Michael Berger, Jian Carrot-Zhang, Zsofia Stadler, Venkatraman Seshan, Nikolaus Schultz, Kenneth Offit, Vijai Joseph

Memorial Sloan Kettering Cancer Center, New York, NY

Background: Advances in cancer treatment and surveillance have increased survivorship, consequently elevating the risk of multiple primary cancers (MPC). However, distinguishing single primaries (SP) and MPC from recurrences or metastases remains a key barrier to studying gene and environmental drivers of second malignancies at scale.
Methods: We developed an automated algorithm to classify tumors as distinct primaries versus recurrences/metastases using IARC criteria, curated exceptions, and clinical and molecular data from Memorial Sloan Kettering's Cancer Data Science Initiative in 91,906 cancer patients. The classifier was validated against an expert-adjudicated dataset. Standardized incidence ratios (SIRs) were computed using age and sex-adjusted SEER-21 reference rates. To assess therapy-related risk, MPCs were stratified by exposure and analyzed for latency and survival. Inherited etiology based on rare germline pathogenic variants (PV) and cancer-specific polygenic risk scores (PRS) was assessed.
Results: The classifier achieved 93% concordance in distinguishing MPC from SP tumors. Applied to 91,906 patients in the MSK-IMPACT cohort, the algorithm identified 16,990 (18.5%) with MPC. Among metachronous cases, the median latency to a second primary was 8.2 years. Twenty-one cancer pairs showed elevated SIRs, including four matching known hereditary syndromes. Excess risk persisted in non-carriers of PV, suggesting polygenic or exposure-related causes. Treatment-related pairs included ovary-leukemia (SIR=5.7), breast-leukemia (SIR=4.0), breast-lung (SIR=2.9), breast-uterus (SIR=2.7), and male bladder-lung (SIR=3.3). Therapy exposure significantly modified risk and latency. Tamoxifen exposure conferred a 3.5-fold higher uterine cancer hazard with earlier onset yet improved survival. Among radiotherapy-exposed breast cancer survivors (n=3,482), higher chest irradiation correlated with a 4-fold secondary lung cancer hazard. Platinum exposure for ovarian cancer (n=2,811) increased Acute Myeloid leukemia (AML) hazard by 4.4-fold while alkylating agents for breast cancer (n=9,497) conferred a 2.9-fold AML risk, with shorter latency supporting treatment-related mechanisms. In male bladder cancer survivors, smokers had 9.1-fold increased hazard of subsequent lung cancer (n=1,316). Among smokers, older age at bladder cancer diagnosis predicted shorter latency to lung cancer. Increased SIR persisted in several cancer pairs, even after accounting for rare PV and PRS, suggesting undiscovered genetic and environmental factors and interactions.
Conclusions: Automated classification of MPC reveals genetic and exposure-related patterns in secondary cancer risk, timing, and survival. Ongoing work is integrating tumor genomics as well as polygenic risk scores to identify inherited and therapy-related drivers of cancer development and aggressiveness. (Supported by MSK Niehaus Center and BCRF).

#5223 Risk factors for early locoregional recurrence among young-onset breast cancer patients: Findings from a single institutional prospective dataset.

Kristen D. Brantley[1], Tonia Parker[2], Julie Vincuilla[3], Alyssa R. Martin[1], Elizabeth A. Mittendorf[3], Catherine Stever[1], Craig Snow[1], Rebecca A. Ottesen[1], Sara M. Tolaney[1], Tari A. King[4], Nancy U. Lin[1], Ann H. Partridge[1]

[1]Department of Medical Oncology, Dana-Farber Cancer Institute, Boston, MA,[2]Breast Oncology Program, Dana-Farber Cancer Institute, Boston, MA,[3]Division of Breast Surgery, Brigham and Women's Hospital, Boston, MA,[4]Division of Breast Surgery, Emory University School of Medicine, Atlanta, GA

Introduction: While women diagnosed with breast cancer at young ages remain at risk of locoregional recurrence in long-term survivorship, predictors of risk remain unclear.
Methods: Women ≤40 years of age diagnosed with breast cancer for which they underwent surgery between January 2016 and April 2023 (N=1,088) were identified from a prospectively maintained database with detailed clinicopathologic and treatment information collected. The primary outcome was locoregional recurrence (≥6 months after primary BC diagnosis) without concurrent distant metastasis. Univariable associations between patient characteristics, primary tumor and treatment variables, and outcome were assessed via Fine and Gray subdistribution models, considering distant metastasis and death as competing risks. Backward selection of variables by AIC was performed using crr step in R to build a multivariable model predicting risk of locoregional recurrence. A sensitivity analysis was completed among individuals who did not have a mastectomy.
Results: A total of 1,053 women ≤40 years of age who did not experience a competing risk within the first 6 months were included. Mean age at first BC diagnosis was 35.3 (SD=4.2) years. Most patients were diagnosed with Stage 1 or 2 disease (77%) and had (HR)+/HER2- tumors (51%) [HR+/HER2+ (18%), HR-/HER2- (16%), HR-/HER2+ (10%), unknown HER2 (5%)]. Over a median of 3.6 (IQR=3.3-3.8) years of follow up, 34 women had a local or regional recurrence without concurrent metastasis. In univariable models, higher hazard of locoregional recurrence was associated with *in situ* disease (vs. invasive, p=0.05), smaller tumor size (p=0.005), lumpectomy (vs. mastectomy, p<0.001), non-receipt of endocrine therapy (ET) if HR+ (vs. HR+ w/ ET, p=0.009), and non-receipt of adjuvant chemotherapy (p=0.004). The multivariable model was tested among individuals with non-missing grade and stage (N=1037, events=34). Variables selected included stage (stage 3 vs. stage 1: aSHR=3.41, p=0.04), HR and ET combined (HR+ w/o ET vs. HR+ w/ET: aSHR=3.60, p=0.007), and surgery and RT combined (mastectomy only vs. lumpectomy+RT: aSHR=0.22, p=0.003; mastectomy+RT vs. lumpectomy+RT: aSHR=0.08, p<0.001). Other variables (age, race, BMI, known germline mutations, tumor grade, HER2 status, and adjuvant chemotherapy) were not selected. When restricted to individuals without mastectomy (N=405, events=26), receipt of ET emerged as the key predictor of locoregional recurrence (HR+ w/o ET vs. HR+ w/ET: aSHR=3.09, p=0.02).
Conclusion: In a modern cohort of young BC patients, receipt of ET for HR+ disease emerged as the most important factor in predicting hazard of early locoregional recurrences. This highlights the importance of recommending ET for young BC patients with HR+ disease, while finding ways to increase tolerability of ET for young BC patients to encourage adherence.

#5224 Shifting the gut microbiome to alleviate anti-cancer treatment-induced cardiovascular toxicity.

Zipporah Cornelius, Adam Wilson, Valerie Payne, Eleanor Cyrus, Kenysha YJ. Clear, David R. Soto-Pantoja, Katherine L. Cook

Cancer Biology, Wake Forest School of Medicine, Winston-Salem, NC

Introduction: Postmenopausal women with metastatic hormone receptor-positive (HR+) breast cancer are treated with either aromatase inhibitors (AIs), or Faslodex (fulvestrant, ICI), in combination with cyclin-dependent kinase 4/6 inhibitors (CDK4/6i). Despite the improvement in breast cancer outcomes, follow-up studies demonstrate the combination treatment is associated with cardiovascular toxicities. Previous studies have shown *Lactobacillus* probiotics supplementation shifts the gut microbiome, reduces breast tumorigenesis, and improved menopause-induced cardiometabolic syndrome. However, limited studies have investigated *Lactobacillus* probiotics on improving cardio-oncological outcomes.

Materials/Methods: Eight-week-old female BALB/c mice (n = 60) were placed on a Western diet. At ten weeks of age, syngeneic 4T1.2ER+ breast cancer cells (1×10^6 cells) were transplanted into the left inguinal mammary fat pad. Tumors were allowed to reach 100 mm^3 before initiating treatment, which was administered for 21 days. Mice were randomized by tumor volume into treatment groups: untreated control, probiotics (Probx; 2×10^8 CFU *Lactobacillus* spp.), Letrozole (AI)+Ribociclib (CDK4/6i), Faslodex (ICI)+CDK4/6i, Probx+AI+ CDK4/6i, or Probx+ICI + CDK4/6i. Tumor volume and weight were measured three times weekly using calipers. Vevo cardiac ultrasound was performed at the end of the study.

Results: In the 4T1.2ER+ breast cancer animal model, the addition of probiotics with the combinational therapeutics (AIs or ICI with CDK4/6i) significantly reduced tumor volume validating the potential of the probiotic to increase the anti-tumor efficacy of the therapeutics. Furthermore, our cardiac data displayed both ICI+CDK4/6i and AI+CDK4/6i-treated groups significantly increased diastolic dysfunction parameters (E'E and IVRT) that were reduced in groups supplemented with *Lactobacillus* probiotics. We show addition of *Lactobacillus* probiotics reduced cardiac fibrosis induced by endocrine-targeting therapies+CDK4/6i treatment. Additionally, we assessed the expression of pro-fibrotic TGF-β/Smad-dependent pathway. We also determined the impact of therapies on oxidative stress markers in cardiac tissue. Lastly, we performed untargeted metabolomics on plasma and proteomics on cardiac tissue to determine potential molecular mechanisms mediated by Lactobacillus probiotic interventions.

Conclusion: Our findings highlight CDK4/6i and endocrine-targeting therapies promote cardiac fibrotic deposition and result in diastolic dysfunction. However, *Lactobacillus* probiotic supplementation significantly improved treatment efficacy, ameliorated drug-induced cardiac dysfunction, and may regulate pro-fibrotic activity. Our data provides a feasible and accessible approach to address drug toxicity in the cardio-oncology setting.

#5225 Is endothelial dysfunction induced by aromatase inhibitors reversible after treatment?.

Mohamed Dabour[1], Adnan Shaaban[2], Jack Wolf[3], Daniel Duprez[4], Douglas Yee[5], Beshay Zordoky[1], Anne Blaes[6]

[1]University of Minnesota, College of Pharmacy, Minneapolis, MN,[2]Division of Cardiology, AdventHealth, Orlando, FL,[3]University of Minnesota, Minneapolis, MN,[4]Cardiovascular Division, University of Minnesota, Minneapolis, MN,[5]Division of Hematology, Oncology, and Transplantation, University of Minnesota, Minneapolis, MN,[6]Division of Hematology and Oncology, University of Minnesota, Minneapolis, MN

Introduction: Breast cancer accounts for about one-third of all new female cancer diagnoses and remains the second leading cause of cancer-related mortality among women. Aromatase inhibitors (AIs) are a standard therapy for postmenopausal women with hormone receptor-positive breast cancer, improving disease-free survival compared to tamoxifen. However, prolonged AI use is linked to increased cardiovascular (CV) risk, including hypertension, dyslipidemia, and endothelial dysfunction, likely due to estrogen depletion. We previously demonstrated early impairment in endothelial function during AI therapy. This study assessed whether AI-induced endothelial dysfunction is reversible after AI discontinuation.

Methods: Patients were recruited before or within one month of AI initiation (Pre/Early AI), at multiple time points during AI therapy, and after AI discontinuation (Post-AI) from two prospective studies: Aromatase Inhibitors and Vascular Health (AIVH) and Vascular Assessment in Breast Cancer Survivors Taking Aromatase Inhibitors (VABC). Patients with hypertension, hyperlipidemia, diabetes, or tobacco use were excluded. Vascular assessments, including the EndoPAT ratio for endothelial function and large and small artery elasticity indices for arterial stiffness, were conducted using the non-invasive EndoPAT 2000 and the HDI/PulseWave CR-2000 CV Profiling System. Lower EndoPAT ratios predict increased risk for future CV events and adverse outcomes. Plasma levels of estradiol, lipid profiles, interleukin-6 (IL-6), and tumor necrosis factor-alpha (TNF-α) were also measured. To evaluate the longitudinal changes in endothelial function during AI therapy, a model was fit using generalized estimating equations to assess how the EndoPAT ratio changed over time on AI.

Results: EndoPAT ratio, was significantly impaired during AI therapy compared to the Pre/Early AI (Pre/Early AI mean: 1.92; AI mean: 1.03; $p< 0.0001$). The EndoPAT ratio declined as early as 6 months on AI (model-based mean at 6 months: 1.19, p-value = 0.0097) and showed a progressive decline with increasing duration of AI use (e.g., model-based mean at 5 years on AI: 0.92; $p = 0.0003$). Importantly, after AI discontinuation, the EndoPAT ratio was only partially and not significantly restored (mean: 1.12) despite the full restoration of estradiol levels and the long post-treatment follow-up period (mean: 3.93 years; range: 1.53-5.34). No significant differences were observed in large and small artery elasticity, blood pressure, or lipid profiles between groups. Circulating IL-6 and TNF-α significantly decreased following AI discontinuation compared to during AI ($p < 0.05$).

Conclusion: AI therapy is associated with significant and progressive endothelial dysfunction, which does not fully recover after treatment cessation, highlighting the importance of CV monitoring in breast cancer patients receiving long-term AI therapy.

#5226 The role of pancreatic adenocarcinoma cancer-stromal interactions on cardiac structure and function.

Anna E. Gibson[1], Praveen Bhoopathi[1], Adolfo Mauro[1], Eleonora Mezzaroma[2], Vignesh Vudatha[2], Arunima Punjala[2], Vashti L. Bandy[1], Fadi Salloum[1], Jose G. Trevino[3]

[1]VCU Health, Richmond, VA,[2]Virginia Commonwealth University, Richmond, VA,[3]Div. of Surgical Oncology, VCU Massey Cancer Center, Richmond, VA

Pancreatic ductal adenocarcinoma (PDAC) has a dismal 5-year survival of <13% despite advances in therapy. Patients with PDAC also experience significantly lower cardiac-specific median survival compared to those with other GI cancers. While cancer cachexia impacts survival through skeletal muscle loss, the contribution of cardiac function to outcomes in PDAC is unknown. We aim to evaluate cardiac tissue structure and function in the most representative human preclinical model. This will provide insight into cardiac remodeling associated with PDAC and its clinical implication for possible interventions to improve overall survival. We implanted a PDAC patient-derived xenograft (PDX) into five NSG mice heterotopically and five NSG mice orthotopically, with five NSG mice receiving sham surgeries as controls. Tumor volumes were monitored weekly and once reaching 1.5cm, echocardiography and Millar catheterization were performed to assess cardiac structure and function between the three groups. Cardiac muscle, gastrocnemius muscle and tumors were collected for histologic and molecular analysis, including staining for structural assessment RNA sequencing to assess for changes associated with tumor burden, which is ongoing. An ANOVA and simple unpaired t-test were used with a significance value set at $p < 0.05$.Global longitudinal strain (GLS) measured by echocardiogram was within the normal values (-18 to -25%) across the groups, with no significant difference between the means of the sham (–20.3%), heterotopic (–21.2%), and orthotopic (–19.9%) groups. However, there is a slight trend showing a decline in GLS in the orthotopic group compared to the control group. The PV Loop data show a decline in left ventricular compliance (EDPVR) means in the heterotopic group (0.86) and orthotopic group (1.06) compared to the control group (0.22). The orthotopic group EDPVR mean is statistically different from the control group mean, with a simple unpaired t-test p-value of 0.02. The slight reduction in GLS observed in the orthotopic group relative to controls may indicate the presence of early systolic impairment in PDAC-bearing mice. Additionally, the results suggest that tumor burden is associated with impaired EDPVR, with the orthotopic group showing more stiffening as evidenced by a significantly elevated EDPVR when compared to the control group. This may indicate early diastolic dysfunction in the context of tumor related cardiac remodeling. We also anticipate that PDAC bearing mice will exhibit cardiac tissue remodeling, characterized by histological changes and transcriptional alterations linking cardiac decline and cancer progression. Recognizing early cardiac changes in patients with PDAC will help identify interventions that may ultimately improve treatment tolerance and clinical outcomes.

#5227 Clone wars: Evidence of clonal stability in a longitudinal prospective cohort of cancer survivors with serial NGS analysis.

Anmol Goyal, Akriti Jain, Salendra Singh, Ying Ni, Emmett Samsa, Kristen Sykes, Sujata Patil, Abhay Singh

Cleveland Clinic, Cleveland, OH

Introduction: Hematopoietic stem and progenitor cells with preleukemic mutations (mut^{n}s), collectively termed clonal hematopoiesis (CHIP) serve as the cellular origin of myeloid neoplasms (MN). While risk of MN development varies, its natural history and transformation potential remain poorly defined. We present findings from our ongoing 10-year CHIP protocol using serial NGS to monitor clonal evolution and MN in cancer survivors.

Methods: Retrospective analysis of 210 prospective pts from March 2020 to June 2024. Mut^{n}s were classified CHIP+ if they had a variant allele frequency (VAF) ≥2% (or ≥1% for *IDH1, IDH2,* and *JAK2*). Clonal evolution was evaluated by annual VAF changes adjusted for age-related increases (e.g. *DNMT3A* increases by ~2%/yr based on published data). Mut^{n}s were classified as slow (≤5%/yr: *DNMT3A, TET2, ASXL1*), intermediate (5-10%/yr: *TP53, PPM1D, IDH1/2, KRAS, NRAS, SF3B1*), or fast-growing (>10%/yr: *JAK2, SRSF2*). BPearson's Chi-squared, Fisher's exact, and Wilcoxon rank-sum tests were used.

Results: Of 210 pts, 42 (20%) had at least one CHIP+ mut^n. Median age was higher in CHIP+ vs. CHIP- pts (66 vs. 59 years, p<0.001). CHIP+ was not significantly associated with sex, race, family history, smoking, alcohol use, prior cancer types (e.g., breast, head and neck) or treatment (chemo, radiation, surgery). Of 487 samples, 56 had detectable somatic mut^{n}s. The most frequent mut^n were *DNMT3A* (n=27), *PPM1D* (n=10), and *TET2* (n=9). By expected growth kinetics, 37 (66%) mut^n were slow-growing, 12 (21.4%) intermediate, 2 (3.5%) fast-growing, and 4 (7.14%) of unknown kinetic category.

Beyond VAF-kinetics-based progression, 12 pts developed new mut^n in subsequent years - *DNMT3A (n=8), PPM1D (n=2).* Some later became undetectable, suggesting transient clones. In total, 12 pts (1 by VAF kinetics, 11 by new mut^n acquisition) clonally progressed over 5 years of this study (5.7%).

6 pts regressed by year 2, with gene mut^n VAFs becoming undetectable. These included mut^n in *PPM1D* (n=2), *CBL* (n=2), *TP53* (n=1), and *DNMT3A* (n=1). Three more pts regressed in year 3, and 1 in year 4. In all, 10 pts showed regression over 5 years (17.8%). Notably, 5 of 10 had received interventions for cardiac comorbidities. Overall, ~94% pts had clonal stability/regression. Slow-growing mut^{n}s - *DNMT3A* and *TET2* had median rates of 0.83% and 2.11%, (historical rates ≤5%). Intermediate mut^{n}s like *TP53* and *PPM1D* had median rates of 1.64% and -0.625%, below the expected 5-10% annual rise. *JAK2,* a fast-growing mut^n, also showed a lower rate of 0.19%.

Conclusion: Despite being a high-risk population due to prior solid malignancy and exposure to chemo/radiation, most pts in our five-year longitudinal study showed clonal stability. Even among those who progressed, VAF kinetics remained stable post-detection. CHIP's inflammatory link to cardiovascular disease suggests preventive cardiology may impact clonal behavior.

#5229 Hair loss in cancer patients receiving small molecule inhibitors: Evidence from clinical trials.

Isabella Kamholtz[1], Simonetta I. Gaumond[2], Joaquin Jimenez[3]

[1]Dr Phillip Frost Department of Dermatology and Cutaneous Surgery, University of Miami Miller School of Medicine, Miami, FL,[2]Department of Biochemistry and Molecular Biology, University of Miami Miller School of Medicine, Miami, FL,[3]University of Miami Miller School of Medicine, Miami, FL

Alopecia remains one of the most common and distressing side effects of cancer therapy. While traditionally associated with cytotoxic chemotherapy, increasing evidence shows that small molecule inhibitors, targeting pathways such as FGFR, BRAF, and Src/ABL, can also induce clinically significant hair loss. However, incidence and severity patterns remain poorly characterized across small molecule inhibitor monotherapy. A scoping review of PubMed and Embase was conducted to identify clinical trials reporting alopecia in cancer patients treated with small molecule therapies. Eligible agents included kinase inhibitors (e.g., BRAF, KIT, FGFR, multikinase, Hedgehog pathway) and hormonal agents. Studies were excluded if they comprised preclinical studies, case reports, case series, reviews, or biologic therapies. Data on alopecia incidence, severity, and clinical presentation were extracted and synthesized qualitatively across small molecule drug classes. Eighteen clinical trials were included in this review, with alopecia incidence ranging from 9% to 63%. Hedgehog pathway inhibitors induced the highest overall rates, ranging from 20-30% with saridegib and glasdegib, and up to 63% with vismodegib. FGFR inhibitors (pemigatinib, infigratinib) and other kinase inhibitors (ripretinib, vemurafenib, sorafenib, AZD0424) demonstrated moderate rates (22-48%). Lower alopecia incidence was reported with aromatase inhibitors (anastrozole, lenostrozole) and the aurora B kinase inhibitor BI 811283, ranging from 9 to 21%. Across these monotherapies, alopecia was predominantly grade 1-2, with grade 3 alopecia or above occurring in less than 1% of patients. Although alopecia events were low-grade, their psychosocial impact remains significant. The higher incidences seen with Hedgehog inhibitors, compared with aromatase inhibitors, highlight how pathway-specific disruption of follicular signaling contributes to hair loss. Further research into the molecular mechanisms of these agents may help clinicians better anticipate and manage this side effect.

#5230 Alopecia in cancer immunotherapy: Incidence and patterns with monoclonal antibodies and antibody-drug conjugates.

Isabella Kamholtz[1], Simonetta I. Gaumond[2], Joaquin Jimenez[3]

[1]Dr Phillip Frost Department of Dermatology and Cutaneous Surgery, University of Miami Miller School of Medicine, Miami, FL,[2]Department of Biochemistry and Molecular Biology, University of Miami Miller School of Medicine, Miami, FL,[3]University of Miami Miller School of Medicine, Miami, FL

The treatment landscape in oncology is evolving, with a shift toward more targeted approaches, including biologic immunomodulators. These agents are designed to minimize systemic toxicity and offer greater precision than traditional chemotherapy, yet they are not without adverse effects. Emerging data suggests that biologic therapies, such as antibody-drug conjugates, immune checkpoint inhibitors, and interferons, may induce alopecia in cancer patients. A scoping review was conducted using PubMed and Embase to identify clinical studies reporting alopecia in cancer patients treated with biologic therapies. Eligible agents included monoclonal antibodies such as antibody-drug conjugates (e.g., trastuzumab deruxtecan), immune checkpoint inhibitors (e.g., anti-PD-1, anti-PD-L1, anti-CTLA-4) and cytokine-targeting biologics (e.g., interferons, anti-IL therapies). Case reports, preclinical studies, and reviews were excluded. Data on alopecia incidence, severity, and clinical presentation were qualitatively synthesized across antibody classes. Nine clinical trials met inclusion criteria, encompassing 1,924 patients. Antibody-drug conjugates (ADCs), including datopotamab deruxtecan, trastuzumab deruxtecan, tisotumab vedotin, enfortumab vedotin, and disitamab vedotin, showed the highest rates of alopecia, ranging from 37% to 56% (predominantly grade 1-2). These ADCs, which delivered topoisomerase I or microtubule inhibitors, were used in patients with breast, cervical, urothelial, non-small cell lung cancer, and other solid tumors. In contrast, immune checkpoint inhibitors such as cemiplimab (anti-PD-1) and trastuzumab (anti-HER2) were rarely associated with alopecia (1-2.2% incidence, grade 1-2) in lung and breast cancer patients, respectively. Interferon alfa-2b, a type I interferon receptor agonist, demonstrated a time-dependent effect, with alopecia (grade 1-3) reported in 9% of melanoma patients receiving one month therapy versus 28% in those on one year regimens. The higher incidence of alopecia observed with ADCs likely reflects the effects of the chemotherapeutic payloads they deliver, rather than the antibody itself. In contrast, antibody-only and interferon therapies demonstrated substantially lower rates (1-28%). Recognizing these trends across biologic classes can help clinicians set patient expectations, guide counseling, and implement supportive measures for those experiencing hair loss throughout treatment.

#5231 GAS6 signaling links smoke-filled environments to increased invasion and communication in gastric and lung cancer models.

Emilee N. Humphreys, Derek Clarke, Kristen Noyes, Madeline Boyer, Juan Arroyo, Amber Gonda

Cell Biology and Physiology, Brigham Young University, Provo, UT

A key determinant of cancer severity is its invasion potential—the ability of malignant cells to spread from their primary site across a border and establish secondary tumors in distant tissues. One major environmental factor commonly seen in society today is the use of stimulants, such as nicotine and other nicotine-containing substances. Nicotine has been found to influence the pathogenesis of many different cancer types including lung cancer, gastric cancer, and many other types. In addition to the neurological effects, scientists have identified a gene that encodes for a gamma-carboxyglutamic acid-containing protein (known as GAS6) that has been found to play a role in cell proliferation. Additionally, GAS6 is found to have a role in the inflammation and immune effects that contribute to the invasion potential of cancer. To determine that GAS6 affects the cell invasion potential and increase cell proliferation, we altered the environment of gastric adenocarcinoma cells (AGS) and human alveolar basal epithelial adenocarcinoma cells (A549) by infusing smoke from both cigarettes and electronic cigarettes, found to increase GAS6 levels , as well as GAS6 specifically into the cell culture media. We then isolated exosomes, nano-sized extracellular vesicles containing proteins, lipids, and more derived from their parent cells. Exosomes have emerged as critical mediators in cancer progression due to their essential roles in tumor growth, immune modulation, and the metastatic process, making them a significant focus of current cancer research. In doing so, we found that GAS6 increased cell proliferation, exosome production, and invasion potential in gastric and cancer cell lines, suggesting the potential of GAS6 as a biomarker for invasive potential in cancer cell types.

: Biomarkers Predictive of Therapeutic Benefit 5
Poster Session

#5235 Real world prediction and biological characterization of sotorasib sensitivity using multimodal AI and liquid biopsy genomic inputs.

Maayan Baron, Felicia Kuperwaser, Sepideh Foroutan, Sunil Kumar, Dillon Tracy, Kevin Freisen, Brandon Funkhouser, Zong Miao, Nathaniel Tann, Fahad Khan, Sean Klei, Jordan Wolinsky, Taylor Wood, Jean Michel Rouly, Nick Lee, Ripple Khera, Anshu Jain, Jeff Sherman, **Emily A. Vucic**

Zephyr AI, McLean, VA

Background: KRAS G12C inhibitors such as sotorasib have expanded options for NSCLC, but clinical benefit is variable and no validated biomarkers beyond the KRAS G12C mutation exist. Reported resistance mechanisms include MAPK reactivation, co-occurring alterations, lineage plasticity, and TME programs. Liquid biopsy is widely used for treatment selection— including Guardant360 CDx, the FDA-approved test for sotorasib—motivating computational approaches that operate on standard clinical assays. AIM-Bx is a multimodal, biologically interpretable AI model that predicts small-molecule response from routine inputs and outputs drug-response predictions, Vulnerability Networks (predicted CRISPR perturbation sensitivities), and reconstructed expression profiles. We evaluated whether AIM-Bx could predict real-world sotorasib benefit using commercial liquid biopsy data.
Methods: NSCLC patients with KRAS G12C mutations treated with sotorasib (n = 39) were identified using Guardant360 CDx liquid biopsy linked to outcomes (rwOS, rwPFS) from Optum® Market Clarity. ctDNA profiling within 24 months prior to treatment was required. AIM-Bx inputs included mutation and copy-number alterations from the 74-gene panel, limited clinical features, and drug-specific structural embeddings. For each patient, AIM-Bx generated a sensitivity prediction, a Vulnerability Network, and a reconstructed expression profile. Performance was assessed using Kaplan-Meier analysis and Cox regression; available clinical covariates were evaluated as confounders.
Results: AIM-Bx significantly stratified patients by benefit. Predicted-sensitive patients showed longer rw-PFS (median 14 vs. 4 months; $p < 0.05$) and rw-OS (14 vs. 7 months; $p < 0.05$). In Cox analyses, KRAS mutation category, histology, sex, and age > 65 were not significantly associated with outcomes. Biological interpretation revealed distinct features: predicted-sensitive tumors showed enriched KRAS/RAS-effector signaling, GEFs, CCND1-linked cell-cycle programs, and metabolic pathways including OXPHOS, HIF, and YAP/TAZ. Predicted non-responders displayed more heterogeneous dependencies and were enriched for downregulation of RAS-pathway programs and upregulation of EMT- and NOTCH-associated signatures.
Conclusions: This retrospective study demonstrates the feasibility of predicting sotorasib benefit directly from liquid biopsy NGS using a multimodal AI model. AIM-Bx identifies biological programs beyond KRAS mutation status that may influence therapeutic sensitivity, suggesting hypotheses for vulnerability-based patient selection and potential combination strategies. Because AIM-Bx operates on routinely available inputs—including the FDA-approved CDx assay used for sotorasib eligibility—it may support future prospective evaluation without new assays.

#5236 Updated exploratory biomarker analysis of cadonilimab plus regorafenib as second-line or later therapy in advanced hepatocellular carcinoma: Identification of Bola3 as a potential predictive biomarker.

Yang Liu[1], Jin Zhang[1], Qi Qi[2], Dandan Wu[1], **Linze Xu**[1], Yueguo Li[3], Huikai Li[2]

[1]Department of Hepatobiliary Cancer, Liver Cancer Center, Tianjin Medical University Cancer Institute & Hospital, National Clinical Research Center for Cancer, Key Laboratory of Cancer Prevention and Therapy, Tianjin's Clinical Research Center for Cancer, Tianjin, China,[2]Department of Hepatobiliary and Pancreatic Oncology, Tianjin Cancer Hospital Airport Hospital, Tianjin, China,[3]Department of Laboratory, Tianjin Medical University Cancer Institute and Hospital, National Clinical Research Center for Cancer, Tianjin Key Laboratory of Digestive Cancer, Key Laboratory of Cancer Prevention and Therapy, Tianjin's Clinical Research Cent, Tianjin, China

Background: Cadonilimab, a first-in-class bispecific antibody targeting PD-1 and CTLA-4, in combination with regorafenib, a multikinase inhibitor approved for second-line treatment of hepatocellular carcinoma (HCC), has demonstrated promising antitumor activity and manageable safety in heavily pretreated patients with advanced HCC (aHCC). We previously reported the updated clinical outcomes at the 2025 AACR Annual Meeting (Abstract #CT172, NCT05644379). Here, we present updated findings from an exploratory biomarker analysis focusing on the potential predictive role of BOLA3 in treatment response.

Methods: Paired plasma samples were collected before and during treatment for cell-free RNA sequencing (cfRNA-seq) to evaluate transcriptional dynamics. Differential expression analysis was performed using DESeq2 (FDR ≤ 0.10), and Hallmark GSEA was applied to assess mitochondrial and immune-related pathway changes. ELISA quantified soluble PD-1 and CTLA-4 at baseline and early on-treatment, calculating individual values. In a prespecified patient subset, baseline tumor tissues underwent semi-quantitative BOLA3 immunohistochemistry (IHC). Multiplex immunofluorescence (mIF) was performed for BOLA3, TOMM20, PD-L1, CD8α, and DAPI, enabling cell-level quantification and comparison of tumor versus peritumoral spatial distribution.

Results: ELISA detected stable levels of soluble PD-1 and CTLA-4 pre- and on-treatment, with early individual dynamics observed; however, these levels did not correlate with treatment response. cfRNA-seq revealed decreased BOLA3 in the PR patient and increased BOLA3 in the PD patient after treatment. Pathway analysis indicated PD-associated enrichment of mitochondrial signaling and weaker inflammatory response, whereas PR showed the opposite trend. Baseline BOLA3 IHC aligned with transcriptomic findings: higher BOLA3 expression was observed in patients with disease progression versus disease control, maintaining directional association when analyzed as a continuous variable. Preliminary mIF suggested that responders exhibited lower BOLA3/TOMM20 and higher PD-L1/CD8, while progressors showed the reverse phenotype.

Conclusions: Integrated exploratory analyses nominate BOLA3 as a candidate outcome-associated biomarker and support a model in which responders exhibit a mitochondria-low, inflamed-high phenotype. These findings provide early, complementary evidence that BOLA3-related features may inform patient stratification, with further validation underway. Research Sponsor: The Joint Funds of the Natural Science Foundation of Tianjin (No.25JCLZJC00120).

#5237 The significant co-expression of claudin-3(CLDN3) and B7-H3(CD276) as a potential biomarker for targeted therapy in neuroendocrine carcinomas.

Ji-Hye Nam[1], Ju-Yeon Kim[1], Jae Choi[2], Minjung Sung[3], Jae Hwan Kang[4], Hobin Yang[5], Yoon-la Choi[6], Young Kee Shin[7]

[1]Logone Bio-Convergence Research Foundation, Seoul, Korea, Republic of,[2]R&D Center, ABION Inc., Seoul, Korea, Republic of,[3]Laboratory of Molecular and Digital Pathology for Theranostics, Samsung Medical Center, Sungkyunkwan University School of Medicine, Seoul, Korea, Republic of,[4]Department of Health Sciences and Technology, SAIHST, Sungkyunkwan University School of Medicine, Seoul, Korea, Republic of,[5]College of Pharmacy, Kyungsung University, Busan, Korea, Republic of,[6]Department of Pathology and Translational Genomics, Samsung Medical Center, Sungkyunkwan University School of Medicine, Seoul, Korea, Republic of,[7]Department of Molecular Medicine and Biopharmaceutical Sciences, Graduate School of Convergence Scie, Seoul National University, Seoul, Korea, Republic of

Despite the elevated mortality rate associated with neuroendocrine carcinomas (SCLC and LCNEC; large cell neuroendocrine carcinomas), the development of novel therapeutic targets has been limited by the predominance of non-targetable driver mutations. Consequently, the identification of viable therapeutic targets has become increasingly important, with proteins such as Claudin-3 (CLDN3) and B7-H3 emerging as promising candidates for targeted therapy. CLDN3, a key component of tight junctions in epithelial and endothelial cells, is frequently dysregulated in various cancers. Although CLDN3 is also present in normal tissues, its enhanced surface accessibility in tumor cells highlights its potential as a therapeutic target. Recent studies have demonstrated that CLDN3 is highly expressed in most neuroendocrine neoplasms, and its positivity has been linked to poor prognosis in clear cell renal cell carcinoma. Similarly, B7-H3 has gained attention as a promising target in neuroendocrine tumors, particularly SCLC. The high expression of B7-H3 is consistent across molecular subtypes in SCLC, supporting its relevance for protein-level characterization and the development of novel therapeutic strategies. In this context, the purpose of the present study was to evaluate CLDN3 and B7-H3 as therapeutic target biomarkers using a validated multiplex immunohistochemistry (IHC) platform. A total of 94 cases of formalin-fixed, paraffin-embedded tissues obtained from surgical resection or biopsy were retrospectively collected. All cases were diagnosed as neuroendocrine carcinoma, including SCLC, LCNEC, or combined neuroendocrine carcinoma. A tyramide signal amplification-based 7-plex IHC assay panel has been developed for the evaluation of therapeutic target biomarkers. The expression levels of CLDN3 were elicited by two different methods: single IHC and multiplex IHC assay. These were analysed with a high sensitivity of 93.3% and an area under the curve (AUC) of 0.964 under the receiver operating characteristic (ROC) curve. Among the four targeted biomarkers analyzed using a validated 7-plex IHC method, CLDN3 and B7-H3 were identified as potential therapeutic target biomarkers for neuroendocrine carcinomas. This validated multiplex IHC panel serves as a useful platform for supporting therapeutic development in neuroendocrine carcinomas.

#5238 Retrospective study for clinical biomarkers to guide post-EGFR-TKI treatment strategies in EGFR-mutant NSCLC.

Tadaaki Yamada[1], Kenji Morimoto[1], Naoki Furuya[2], Hisashi Tanaka[3], Akihiro Yoshimura[4], Tomohiro Oba[5], Makoto Hibino[6], Takahito Fukuda[7], Yasuhiro Goto[8], Akira Nakao[9], Shinsuke Ogusu[10], Yuta Okazaki[11], Taishi Harada[12], Takayo Ota[13], Ken Masubuchi[14], Tae Hata[15], Koji Mikami[16], Shoki Matsumoto[17], Ryoichi Honda[18], Koji Date[19], Yusuke Chihara[20], Koichi Takayama[1]

[1]Kyoto Prefectural University of Medicine, Kyoto, Japan,[2]St. Marianna University School of Medicine, Kanagawa, Japan,[3]Hirosaki University Graduate School of Medicine, Hirosaki, Japan,[4]Japanese Red Cross Kyoto Daini Hospital, Kyoto, Japan,[5]Saitama Red Cross Hospital, Saitama, Japan,[6]Shonan Fujisawa Tokushukai Hospital, Fujisawa, Japan,[7]Nagasaki University Graduate School of Biomedical Sciences, Nagasaki, Nagasaki, Japan,[8]Fujita Health University School of Medicine, Toyoake, Japan,[9]Fukuoka University Hospital, Fukuoka, Japan,[10]Saga University, Saga, Japan,[11]Kansai Medical University, Osaka, Japan,[12]Fukuchiyama City Hospital, Fukuchiyama, Japan,[13]Izumi City General Hospital, Izumi, Japan,[14]Gunma Prefectural Cancer Center, Ota, Japan,[15]Rakuwakai Otowa Hospital, Kyoto, Japan,[16]Hyogo Medical University, School of Medicine, Nishinomiya, Japan,[17]Japanese Red Cross Kyoto Daiichi Hospital, Kyoto, Japan,[18]Kokuho Asahi Chuo Hospital, Asahi, Japan,[19]Kyoto Chubu Medical Center, Nantan, Japan,[20]Uji-Tokushukai Medical Center, Uji, Japan

Background: In patients with non-small cell lung cancer (NSCLC) harboring epidermal growth factor receptor (EGFR) mutations, the combination of atezolizumab, bevacizumab, carboplatin, and paclitaxel (ABCP) has demonstrated encouraging efficacy following prior treatment with EGFR tyrosine kinase inhibitors (EGFR-TKIs). However, real-world evidence comparing ABCP with standard platinum-based chemotherapy remains unclear.
Methods: We conducted a multicenter retrospective study including 408 patients with advanced or recurrent EGFR-mutant NSCLC who received either platinum-based chemotherapy (with or without bevacizumab) or ABCP after EGFR-TKI treatment at 20 institutions in Japan. Clinical outcomes were evaluated using propensity score matching to adjust for baseline characteristics.
Results: After propensity score matching, there were no significant differences in progression-free survival (PFS) or overall survival (OS) between the Chemo/Chemo + BEV and ABCP groups (median PFS, $p = 0.44$; median OS, $p = 0.84$). In the subgroup of patients with programmed death-ligand 1 (PD-L1) expression ≥50%, the ABCP group exhibited significantly longer PFS compared with the Chemo/Chemo + BEV group ($p = 0.02$).
Conclusions: Among patients with EGFR-mutant NSCLC previously treated with EGFR-TKIs, those with high PD-L1 expression may derive greater benefit from ABCP therapy compared with platinum-based chemotherapy, suggesting that ABCP could represent a more promising treatment option in this subgroup.

#5239 Biomarker dynamics in the completed phase I study of DT-9081: An analysis of *ex vivo* cytokine stimulation, urinary PGEM, and tumoral biomarkers in advanced solid tumors.

Thomas Maurin[1], Lola Lecru[1], Antoine Mousson[1], Orphee Blanchard[1], Malaury Schappler[1], Christophe Le Tourneau[2], Zahra Castel-Ajgal[3], Jean-Pascal Machiels[4], Rachel Galot[4], Nuria Kotecki[5], Christiane Jungels[5], Jean-Pierre Delord[6], Iphigenie Korakis[6], Camille Dietsch[1], Luc Baron[1], Maria Jesus Garcia Leon[1], Edith Steinberg[1], Katia Saulnier[1], Samira El-Farouk[1], Calire Jouffroy-Zeller[1], Anne Quesnel[1], Carolina Duarte[1], Abdelkrim Taamma[1], Anne-Laure Blayo[1], Thibaut Brugat[1], Nathalie Lenne[1], Jean-Marie Cuillerot[1], **Stephan Schann**[1]

[1]Domain Therapeutics, Illkirch, France,[2]Institut Gustave Roussy, Villejuif, France,[3]Institut Curie, Paris, France,[4]Cliniques Universitaires Saint-Luc, Louvain, Belgium,[5]Institut Jules Bordet, Bruxelles, Belgium,[6]Institut Universiatire du Cancer de Toulouse, Toulouse, France

Background: DT-9081, a novel EP4R-antagonist, recently completed its Phase I study in patients with advanced solid tumors (NCT05582850). In addition to establishing safety, tolerability, and pharmacodynamic signals, integrated biomarker analyses were conducted to gain insights into its mechanism of action and therapeutic potential.

Objectives: This abstract presents a comprehensive evaluation of multiple biomarkers from the completed Phase I study of DT-9081. The analyses include:Ex vivo cytokine stimulation examining IL-10, IL-5, MIP-1α, and TNFα concentrationUrinary prostaglandin E metabolite (tetranor-PGEM) levels, measured by LC-MS/MS Tumor tissue expression of mPGES and COX2 enzymes, as well as PD-L1, assessed pre- and post-treatmentPlasma cytokine levels

Methods: Peripheral blood mononuclear cells from subjects were isolated and subjected to *ex vivo* cytokine stimulation, with subsequent quantification of IL-10, IL-5, MIP-1α, and TNFα using validated immunoassays. Urine samples were analyzed for PGEM levels by LC-MS/MS. Tumor biopsies, collected at baseline and after treatment, were examined by multiplex immunofluorescence to determine the expression levels of mPGES, COX2, and PD-L1. Additionally, plasma samples were collected at serial timepoints, and cytokine concentrations were measured.

Results:Biomarker assessments revealed that DT-9081 treatment modulated immune responses as evidenced by restauration of *ex vivo* cytokine release profiles (IL-10, IL-5, MIP-1α, and TNFα). Increase in urinary PGEM levels was consistent with modulation of the prostaglandin pathway. Tumor tissue analyses demonstrated alterations in the expression of mPGES and COX2 enzymes following treatment, and changes in PD-L1 expression were observed, suggesting potential implications for combination with immune checkpoint inhibitors. Plasma cytokine data provided additional evidence of

systemic immunomodulation. Integrated analysis suggest that DT-9081 favors a Th1, antitumoral immune response.

Conclusions: The integrated biomarker evaluation from the completed Phase I study of DT-9081 offers valuable insights into its immunomodulatory effects in advanced solid tumors. The combined analysis of *ex vivo* cytokine stimulation, urinary PGEM levels, and tumor biomarker expression (mPGES, COX2, and PD-L1) supports the engagement of multiple pathways involved in the anti-tumoral response after treatement with DT-9081. These results lay the groundwork for further clinical development and potential combination strategies in immuno-oncology.

Keywords: DT-9081, EP4R antagonist, small molecule, solid tumors, immuno-oncology, phase I/ trial, biomarker, NCT05582850.

#5240 A CXCL10/11 and CCL19 duplex chromogenic assay complements PD-L1 immunohistochemistry in non-small cell lung cancer.

Alexander L. Tang[1], Liad Elmelech[1], William L. Tang[1], Maxwell Spurrell[2], Maria Ganci[3], Yiwen He[4], Catherine B. Meador[3], Christopher S. Nabel[3], Jessica J. Lin[3], Mari Mino-Kenudson[3], Nir Hacohen[5], Justin F. Gainor[3], Jonathan H. Chen[6]

[1]Broad Institute, Cambridge, MA,[2]Yale University, New Haven, CT,[3]Massachusetts General Hospital, Boston, MA,[4]Northwestern University, Chicago, IL,[5]Massachusetts General Hospital/Broad Institute, Boston, MA,[6]Northwestern University/Broad Institute, Chicago, IL

Purpose: PD-1 blockade is a standard first-line treatment for advanced non-small cell lung cancer (NSCLC). PD-L1 tumor proportion score (TPS) by immunohistochemistry (IHC), a key predictor of response to PD-1 blockade, is imperfect, underscoring the need for additional predictive biomarkers. Immunity hubs and stem-immunity hubs have been shown to correlate with response, but these have been mainly characterized through spatial transcriptomics, and multiplexed immunofluorescence, which are not readily scalable to clinical workflows. We developed a clinically compatible chromogenic duplex assay that quantifies these multicellular immune networks using the chemokines CXCL10/11 and CCL19 to predict response.
Experimental Design: We stained tissue from 65 metastatic NSCLC tumors for CXCL10/11 and CCL19 using chromogenic in situ hybridization (cISH). We created three separate scoring approaches, 1. percentage of CXCL10/11+ cells, 2. percentage of CXCL10/11+ tiles (immunity hubs), and 3. percentage of CXCL10/11+ and CCL19+ tiles (stem-immunity hubs), in order to stratify patients and determine whether respective scoring approaches were predictive of response. Objective response rates were assessed using RECIST v1.1.
Results: 57 patients with NSCLC treated with single-agent PD-(L)1 inhibitors were identified and samples were procured before treatment. The majority of patients (56%) had a PD-L1 TPS of 50% or above. Across the cohort, the overall response rate was 37% and the median progression free survival of 119 days. The PD-L1 TPS (>50%) had 71.4% sensitivity, 56.3% specificity, 50% positive predictive value, and 75% negative predictive value (Fisher's exact test: p=0.089). The stem-immunity hub scoring approach with cISH combined with PD-L1 TPS had 100% sensitivity, 53% specificity, 58% positive predictive value, and 100% negative predictive value (Fisher's exact test: p<0.0001). Notably, the stem-immunity cISH scoring approach identified all responders who were not previously classified as PD-L1 TPS high.
Conclusions: cISH detection of stem-immunity hubs using CXCL10/11 and CCL19 complements PD-L1 IHC. Integration of this spatial biomarker with PD-L1 testing may refine immunotherapy treatment strategies in NSCLC.

#5241 Personalized fusion measurable residual disease detection in acute myeloid leukemia using droplet digital PCR.

Asra Noor[1], Xiaojuan Cao[2], Maggie J. Cox[2], Francesca Ferraro[2], David H. Spencer[2], Stephen T. Oh[2], Grant A. Challen[2], Andrew L. Young[2]

[1]Washington University In St. Louis, Saint Louis, MO,[2]Washington University in St. Louis, Saint Louis, MO

Acute myeloid leukemia (AML) is an aggressive cancer, of which 30-40% are driven by gene fusions. Effective therapy selection often requires accurate assessment of disease burden—termed measurable residual disease (MRD) detection. MRD is typically assessed with multiparameter flow cytometry (MPFC) or RT-qPCR, which are limited by accuracy, cost, turnaround time or applicability. MPFC has a reported limit of detection of 1:1,000 to 1:10,000, but 20% of MRD negative patients by MPFC relapse within weeks to months. MPFC requires an invasive bone marrow biopsy, so testing is infrequent and critical treatment decisions are often based on a single measurement (e.g. end of induction). In fusion driven AML, the fusion itself is a robust biomarker of disease. Unfortunately, only the most common gene fusions (e.g. BCR-ABL and PML-RARA) have RT-qPCR-based MRD assays. But there are hundreds of gene fusions that drive AML that do not have a molecular MRD assay. To address this limitation, we have developed personalized gene fusion MRD detection using droplet digital PCR (ddPCR). We utilize diagnostic sequencing to define a patient's unique fusion, design their personalized MRD assay and validate the assay to a limit of detection of 1 in 100,000. We applied this approach in a cohort of 20 AML and acute lymphoblastic leukemia (ALL) patients harboring diverse gene fusions including *KMT2A* (with partners including *AF9, AF10*, *AF4, ELL, ENL*, *AF6*, *AF1q*), *RUNX::RUNX1T1*, *PAX5::MLLT3, EP300::KMT2A* and *BCR::ABL*. We focused on *KMT2A* fusions due to their heterogeneity and clinical need for molecular MRD given the development of Menin inhibitors. Using personalized ddPCR assays, we analyzed 155 patient specimens (median 4.5, range 1-24 per participant) collected at diagnosis, throughout treatment, and during surveillance from bone marrow aspirates (n=31) and peripheral blood samples (n=124). We identified disease recurrence in eight patients by ddPCR 38-103 days before standard of care MPFC-based testing or clinical relapse. In our study, every patient with increasing fusion burden relapsed and every patient who remained in long-term remission cleared their fusion. Fusion transcript abundance was similar in peripheral blood and bone marrow specimens obtained concurrently, demonstrating non-invasive peripheral blood sampling may be able to replace bone marrow biopsy for fusion-based MRD detection. In conclusion, personalized gene fusion MRD testing by ddPCR is highly sensitive and specific for disease recurrence. This approach is ideal for real-time clinical decision-making given the low limit of detection, non-invasive testing from the peripheral blood, and rapid turnaround time (1-2 days). Future work is focused on building trials to assess clinical utility. Long-term this has the potential to improve treatment selection and drive better patient outcomes.

#5242 Down regulation of HPV 16 and NF-KB and upregulation of gigaxonin and immune markers in APG-157 treated head and neck cancer: A phase 2A clinical investigation.

Saroj K. Basak[1], Bhavani Shankara Gowda[2], Manasvini Kala[2], Jin Zhong[3], Trent Su[4], Daniel Sanghoon Shin[5], Marilene B. Wang[6], **Eri S. Srivatsan**[2]

[1]Surgery, VAGLAHS, Los Angeles, CA,[2]Surgery, VAGLAHS/David Geffen School of Medicine at UCLA, Los Angeles, CA,[3]Pathology, VAGLAHS/David Geffen School of Medicine at UCLA, Los Angeles, CA,[4]Pathology, David Geffen School of Medicine at UCLA, Los Angeles, CA,[5]Medicine, Michael E Debakey VA Medical Center, Houston, TX,[6]Head and Neck Surgery, VAGLAHS/David Geffen School of Medicine at UCLA, Los Angeles, CA

Background: Persistent HPV 16 expression and NF-κB activation drive inflammation and immune suppression in head and neck squamous cell carcinoma (HNSCC). APG-157 is a proprietary oral botanical immunomodulator with anti-inflammatory and tumor-microenvironment (TME) reprogramming activity. This Phase 2A clinical study evaluated its molecular and immunologic effects in patients with HNSCC.

Methods: Fourteen patients received APG-157 (200 mg TID for 4 weeks) under IRB approval at VAGLAHS. Paired pre- and post-treatment saliva and tumor biopsies (n=24) were analyzed for HPV 16 E7 integration and expression by qPCR/RT-qPCR, and for expression of p16, NF-κB, gigaxonin, E-cadherin, and Snail by molecular and immunohistochemical assays. Paired PBMCs from 5 patients underwent single-cell RNA sequencing (scRNA-seq) to characterize systemic immune modulation.

Results: PCR identified presence of HPV 16 E7 sequences in 2/7 OC and 4/7 OPC (total of 6/14) pre-APG-157 samples. Expression of p16 by IHC showed p16 positivity in 4/7 OC and 7/7 OPC samples. APG-157 treatment reduced HPV 16 E7 integration and expression levels in 4 of 6 HPV 16 E7 pre-APG-157 positive samples in the saliva and tumor, confirming a direct antiviral effect. NF-κB expression decreased concordantly, whereas gigaxonin (a cytoskeletal regulator linked to NF-κB degradation) increased, suggesting restoration of proteasomal regulation and suppression of inflammatory signaling. Expression of epithelial integrity markers (E-cadherin↑, Snail↓) improved, indicating a shift towards a less invasive phenotype. Notably, salivary HPV 16 detection correlated with tumor expression, validating saliva as a non-invasive biomarker for HPV-driven diseases. scRNA-seq of PBMCs revealed post-treatment expansion of activated B cells and effector T-cell clusters consistent with systemic immune activation. These findings indicate that APG-157 exerts coordinated local and systemic immunomodulatory effects by simultaneously suppressing oncogenic viral and inflammatory pathways and enhancing lymphocyte function.

Conclusions: APG-157 demonstrates dual antiviral and immunoregulatory activity in HNSCC, suppressing HPV 16 and NF-κB while promoting immune activation and epithelial restoration. APG-157 uniquely enhances gigaxonin-mediated NF-κB regulation and downregulates HPV 16 E7 expression, defining a new therapeutic axis for oral immunomodulation. These data support the continued development of APG-157 as an oral immunotherapy for HPV-driven and immunologically “cold” head and neck cancers, both as a monotherapy and as a combinatorial agent with chemo-radiation or immune checkpoint inhibitors.

#5243 Profiling of peripheral LAG-3+CD8+ T cells: An immune cell population associated with immunotherapy resistance.

Ariel Kogan Zajdman[1], Cory A. Brennick[1], Kayla J. Foster[1], Sydney A. Riddick[1], Tatiana Shcheglova[1], Matthew Adamow[2], Jasme Lee[3], Ronglai Shen[3], Katherine S. Panageas[3], Xiyu Peng[4], Margaret K. Callahan[1]

[1]Department of Immunology and Neag Comprehensive Cancer Center, University of Connecticut School of Medicine, Farmington, CT,[2]Immune Monitoring Facility, Memorial Sloan Kettering Cancer Center, New York City, NY,[3]Department of Epidemiology and Biostatistics, Memorial Sloan Kettering Cancer Center, New York City, NY,[4]Department of Statistics, Texas A&M University, College Station, TX

Despite the success of immune checkpoint blockade (ICB), many patients fail to respond, highlighting a need for predictive biomarkers. We previously identified pre-treatment differences in peripheral blood mononuclear cells (PBMCs) from patients treated with ICB using an 11-color flow cytometry panel. These differences grouped patients into 3 distinct immune phenotypes, or immunotypes (Shen et al Sci Trans Med, 2021). Immunotype 1 (IT-1) was characterized by higher numbers of LAG-3^{+}CD8^{+} T cells and associated with poor response and overall survival (OS) after anti-PD-1 therapy. IT-2 was characterized by lower LAG-3^{+}CD8^{+} and better outcomes; IT-3, by the presence of additional cell populations not present in IT-1 or IT-2. Here, we aim to establish a deeper understanding of LAG-3^{+}CD8^{+} T cells, the defining cell population of the IT-1 phenotype.

We analyzed banked pre-treatment PBMC samples from patients with melanoma (n=30) and urothelial carcinoma (UC, n=48) previously assessed to have IT-1, IT-2, or IT-3, using a 28-color spectral flow cytometry assay, with single-cell RNA sequencing of a representative IT-1 sample.

Compared with LAG-3^{-}CD8^{+} cells, LAG-3^{+}CD8^{+} T cells displayed higher expression of cytotoxic, terminal differentiation markers (GzmB, CD57, T-bet, Eomes) and lower expression of homing (CCR4, CXCR5, CCR7) and costimulatory molecules (ICOS, CD27, CD28, CD127). Consistent with our flow cytometry data, transcriptomic profiling revealed upregulation of GZMB, B3GAT1, TBX21, and EOMES, as well as downregulation of CCR4, CCR7, ICOS, CD27, CD28, and IL7R. These findings were further validated in an independent melanoma scRNA-seq dataset (Huuhtanen et al J. Clin. Invest, 2023). Finally, we evaluated samples from patients with the IT-2/3 phenotypes, confirming this pattern to be unique to IT-1.

Our results reveal a distinct phenotypic signature defining LAG-3^{+}CD8^{+} T cells, the hallmark of IT-1. These findings refine the definition of IT-1, highlight immune-phenotype differences between the IT-1 and IT-2/3, and suggest mechanisms, such as altered costimulation and trafficking, that underlie ICB resistance.

#5244 Genomic HLA class I allelic imbalance undermines enduring immunotherapy response in advanced non small cell lung cancer.

Yiting Dong#[1], Shun Wang#[2], Wenbin Li*[2], Zhijie Wang*[1], Jie Wang*[1]

[1]Department of Medical Oncology, National Cancer Center/National Clinical Research Center for Cancer/Cancer Hospital, Chinese Academy of Medical Sciences and Peking Union Medical College, Beijing, China,[2]Department of Pathology, National Cancer Center/National Clinical Research Center for Cancer/Cancer Hospital, Chinese Academy of Medical Sciences and Peking Union Medical College, Beijing, China

Human leukocyte antigen class I (HLA-I) molecules are essential for neoantigen presentation and T cell recognition, yet the clinical significance of allelic imbalance within HLA-I genes (HLA-AI) in immune checkpoint inhibitor (ICI) therapy remains undefined. Here, we established haplotype-specific, coverage-based (cHLA-AI) and plasma-derived (bHLA-AI) models compatible with routine clinical sequencing, based on 292 fully heterozygous patients with paired tumor and blood samples from the phase III CHOICE-01 trial. Tumor mutational burden (TMB)-low tumors with HLA-AI derived no benefit from first-line immunochemotherapy, whereas all other patients achieved significant survival gains (mOS 16.53 vs. 29.57 months, HR = 2.29, 95% CI 1.59-3.30, p < 0.001,interaction P = 0.019; mPFS 5.59 vs. 9.92 months, HR = 2.02, 95% CI 1.43-2.90, p < 0.001, interaction P = 0.016). These findings were validated in the RATIONALE-304 and RATIONALE-307 trials and independent real-world cohorts, and extended to cfDNA (bHLA-AI), where integrated tissue-plasma assessment delineated four therapeutic trajectories. Incorporating cHLA-AI with pathology, PD-L1 and TMB significantly improved 2-year OS prediction (DeLong's P = 0.003). Multi-omic profiling linked cHLA-AI to active DNA damage response signaling, high TMB, elevated intratumor heterogeneity (ITH-high), pronounced chromosomal instability (CIN-high), immune-cold microenvironments, and failure of on-treatment TCR expansion, while longitudinal sampling revealed its late, branching emergence under immune pressure. Pan-cancer profiling (N = 5,989) demonstrated consistent associations with TMB and proliferative activity (Ki-67 index). Collectively, these results establish cHLA-AI as a pivotal biomarker bridging genomic instability, immune evasion, and therapeutic outcome, providing a framework for stratified immunotherapy in non-small cell lung cancer and beyond.

#5246 Immune profiling and targetable biomarkers in NSCLC: Toward rational design of CKI-based combinations.

Rania Gaspo[1], Alexandra Jean[2], Renaud Burrer[2], Jerome Sallette[3], Amanda Finan-Marchi[2], Marie Gerus-Durand[2]

[1]Cerba Research, Laval, QC, Canada,[2]Cerba Research, Montpellier, France,[3]Cerba Research, Paris, France

Background: Actionable mutations guide first-line targeted therapies in non-small cell lung cancer (NSCLC), yet resistance frequently develops. Immune checkpoint inhibitors (CKIs) improve outcomes, and recent evidence suggests potential synergy with targeted agents for rare NSCLC biomarkers. This study explored correlations between actionable targets and immune contexture to inform combination strategies.

Methods: Twenty-five NSCLC FFPE resected specimens were analyzed by immunohistochemistry for PD-L1 (clone 22C3), ALK, ROS1, HER2, EGFR, pan-TRK, BRAF, c-Met, and MEK1. Two in-house multiplex panels (PD-1/PD-L1/CD3/CD8 and CD3/CD8/FoxP3) assessed PD-1, PD-L1, and T-cell subsets. Chromogenic simplex IHC stains were scored by a thoracic oncology pathologist per clinical standards or literature; immune populations were quantified in tumor and non-tumor regions using Halo image analysis.

Results: Targetable protein expression largely reflected published prevalence. PD-L1 correlated positively with c-Met, MEK1, and EGFR, but not HER2. HER2 expressions were associated with increased helper and cytotoxic T cells, supporting limited benefit of PD-1/PD-L1 blockade in HER2-positive NSCLC while suggesting alternative immunomodulators. MEK1+ tumor cells showed strong correlation with infiltrating immune cells and PD-1 expression, reinforcing MEK1 inhibition as a promising approach to counter immune evasion. No correlation was observed between PD-L1 and PD-1+ cytotoxic T cells, highlighting the need to assess both PD-1 and PD-L1 for optimal CKI efficacy.

Conclusions: Immune profiling within the tumor microenvironment may complement actionable target testing and guide rational design of CKI-based combination therapies in NSCLC.

This text has been revised with the assistance of Microsoft Copilot to comply with the specified character limit.

#5247 Integrating immunohistochemistry for biomarker detection in NSCLC: A step toward precision therapy.

Rania Gaspo[1], Renaud Burrer[2], Jerome Sallette[3], Amanda Finan-Marchi[2], Marie Gerus-Durand[4]

[1]Cerba Research, Laval, QC, Canada,[2]Cerba Research, Montpellier, France,[3]Cerba Research, Paris, France,[4]Cerba Research Histalim, Montpellier, France

Background: Advances in NSCLC treatment increasingly rely on biomarker-driven strategies, with targeted therapies outperforming cytotoxic agents. However, rapid progress in precision medicine poses challenges for translating biomarker recommendations into clinical practice. Accurate characterization is essential to ensure timely and appropriate therapy selection.
Methods: We analyzed 30 adult primary NSCLC FFPE tumors (n=25 unknown biomarker status; n=5 known biomarker controls) using immunohistochemistry (IHC) for actionable and exploratory targets: ALK, ROS1, BRAF, EGFR, c-Met, pan-TRK, HER2, and MEK1. Biomarker frequency, intensity, and specificity were assessed, and correlations between expression patterns were investigated. All slides were scored by a thoracic oncology pathologist per clinical standards or literature.
Results: Among five known controls, concordance was observed for HER2, c-Met, and EGFR, while discrepancies occurred for ALK (focal staining requiring reflex FISH/next-generation sequencing (NGS) confirmation) and BRAF. Controls were originally identified by NGS, which is generally more sensitive than IHC. Negative staining for BRAF was consistent with a non-V600E mutation in the control specimen. Correlation trends were noted between c-Met and MEK1, and between EGFR and HER2. Frequencies of ALK, c-Met, and HER2 aligned with literature, while EGFR and MEK1 appeared higher, suggesting IHC may serve as an initial screen before reflex NGS testing. No positivity was observed for BRAF, ROS1, or pan-TRK, consistent with their rarity in NSCLC.
Conclusions: IHC remains a valuable screening tool for detecting most actionable biomarkers, particularly in settings lacking NGS capabilities. Its integration into routine pathology may optimize patient selection for targeted therapies and clinical trials.
This text has been revised with the assistance of Microsoft Copilot to comply with the specified character limit.

#5248 Single-cell multi-omics reveals co-mutation of *TP53* and epigenetic gene driving myeloid transformation in B-ALL following CAR-T therapy.

Shuang Zhao[1], Yanjing Tang[2], Meng Su[2], Bowen Cui[1], Rongrong Fan[1], Han Wang[1], Liu Yang[2], Lixia Ding[2], Ronghua Wang[1], Huiying Sun[1], Ying Zhong[1], Qiaoqiao Shi[1], Yuxuan Guo[1], Lili Song[2], Xinyu Wan[2], Tianyi Wang[2], Jing Yang[2], Benshang Li[2], Yu Liu[1]

[1]Pediatric Translational Medicine Institute, Shanghai Children's Medical Center, School of Medicine, Shanghai Jiao Tong University, shanghai, China,[2]National Health Committee Key Laboratory of Pediatric Hematology & Oncology, Shanghai Children's Medical Center, School of Medicine, Shanghai Jiao Tong University, shanghai, China

Lineage switch is a rare phenomenon, occurring in less than 1% of leukemia cases. However, with the advent of CD19-targeted immunotherapies such as CAR-T and blinatumomab, it has emerged as a significant complication. Identifying patients at high risk for lineage switch prior to immunotherapy is critical, yet predictive biomarkers remain unclear. In a cohort of 65 B-ALL patients who relapsed after CAR-T therapy, we identified one case of myeloid lineage switch with unknown mechanism. Transcriptomic sequencing across three timepoints: pre-CAR-T, first CAR-T relapse, and second CAR-T relapse (myeloid switch) confirmed a consistent driver gene profile (*ETV6*::*RUNX1* fusion, *NF1*, *WNK1* and *CIC* mutations), ruling out a secondary malignancy. To elucidate the mechanism, we performed single-cell DNA-protein sequencing (Mission Bio Tapestri platform) and single-cell RNA sequencing (10x Genomics platform). At first CAR-T relapse, we identified five distinct clones. After CAR-T therapy, three clones were undetectable, whereas two clones persisted and underwent rapid expansion, concomitant with myeloid lineage switch. Notably, both of these clones harboring mutations in *TP53* and epigenetic regulator *STAG2*. We further discovered a distinct population of lineage-infidelity cells (CD117+CD71+ CD34+CD38+CD56+CD19dim) that co-express myeloid and B-lineage markers, representing a heightened plasticity that may facilitate CAR-T evasion. Projection of our scRNA-seq data onto a normal developmental atlas showed pre-CAR-T sample from the lineage-switch case encompassed a broad spectrum, whereas control case of CD19-negative relapse due to *CD19* mutation were confined to the pro-B/pre-B stages. Based on these findings, we hypothesized that co-mutation of *TP53* and epigenetic regulators predisposes cells to lineage switch. To validate this finding, we performed a longitudinal flow cytometry analysis. Patients were stratified into two groups: a co-mutation group (n=4) harboring *TP53* and epigenetic gene mutations, and a control group (n=2) lacking these mutations. The co-mutation group exhibited significant downregulation of the B-lineage marker CD19 and concurrent upregulation of the myeloid marker following CAR-T treatment. In contrast, the control group showed no notable changes. In conclusion, our data suggests that co-mutations in *TP53* and epigenetic genes enhance plasticity in B-ALL. Under the selective pressure of CD19 CAR-T therapy, subclones harboring these mutations are preferentially expanded, leading to lineage switch. We propose monitoring myeloid marker expressing subclones in B-ALL patients carrying co-mutations in *TP53* and epigenetic genes during immunotherapy is important to improve their prognosis.

#5249 Longitudinal liquid biopsy identifies an early predictive biomarker of immune checkpoint blockade response in head and neck squamous cell carcinoma.

Robert Saddawi-Konefka[1], Binbin Wang[2], Lauren M. Clubb[3], Cynthia Tang[4], Di Wu[5], Sumit Mukherjee[6], Sahil Sahni[7], Saugato Rahman Dhruba[6], Sumeet Patiyal[6], Chi-Ping Day[8], Parth Anil Desai[9], Clint Tanner Allen[10], Kun Wang[11], J. Silvio Gutkind[12], Eytan Ruppin[13]

[1]UT MD Anderson Cancer Center, Houston, TX,[2]NIH-NCI, Bethesda, MD,[3]Pharmacology, UC San Diego, San Diego, CA,[4]Stanford, Palo Alto, CA,[5]University of Illinois at Urbana-Champaign, Champaign, IL,[6]National Cancer Institute - Cancer Data Science Laboratory (CDSL), Bethesda, MD,[7]MSKCC, New York, NY,[8]NCI, Bethesda, MD,[9]Fox Chase Cancer Center, Philadelphia, PA,[10]National Insts. of Health, Bethesda, MD,[11]University of Illinois Urbana-Champaign, Urbana, IL,[12]UC San Diego, San Diego, CA,[13]National Cancer Institute, Rockville, MD

Immune checkpoint inhibition (ICI) has emerged as a pivotal therapy for head and neck squamous cell carcinoma (HNSCC), yet the development of predictive biomarkers to guide its clinical application has significantly lagged. Current biomarkers such as tumor mutational burden and PD-L1 fail to capture systemic immune dynamics that may better reflect host immune fitness and the coordinated immune response driving durable tumor control. We hypothesized that early treatment-induced changes in circulating immune repertoires could provide a dynamic, non-invasive readout of ICI responsiveness. Using a time-resolved, multi-omic approach in a murine HNSCC model, we characterized peripheral immune responses to anti-PD-1 across defined pre- and on-treatment timepoints. Single-cell transcriptomics and paired T/B cell receptor analyses revealed an early and robust, but transient, expansion of effector memory T and B cell repertoires in responders, preceding tumor regression. Temporal changes in effector T and B cell abundance, clonality, and gene expression strongly predicted immunotherapy response, with early on-treatment timepoints emerging as the optimal window for assessing treatment response. These dynamic immune features informed a composite transcriptional signature, Liquid Biomarker for Immuno-Oncology (LiBIO), derived from effector T and B cell programs that accurately predicts ICI response in independent human HNSCC cohorts and outperforms contemporary biomarkers such as PD-L1 combined positive score and tumor mutational burden. LiBIO further generalizes to melanoma, non-small cell lung cancer, and breast cancer without retraining, suggesting that early peripheral immune dynamics capture conserved features of effective antitumor immunity across cancer types. Collectively, these findings support the premise that antitumor immune responses initiated regionally in tumor-draining lymphatics give rise to transient, stereotyped peripheral immune responses that precede successful primary tumor control, and that peripheral immune events can serve as a foundation for liquid biomarker discovery. This innovative approach represents a paradigm shift from static, tumor-centric biomarkers to dynamic monitoring of host immunity, enabling real-time treatment adaptation during the critical early window of immune activation.

#5250 Method development and workflow optimization of a CTC-based biomarker assay to predict response to CDK4/6 inhibitors in HR+/HER2- breast cancer.

Mantasha Tabassum[1], Shivaani Suresh Kanna[1], Wangjia Cao[1], Suneel Kumar[2], Mothaffar F. Rimawi[2], George Miles[2], Meghana Trivedi[1]

[1]University of Houston, College of Pharmacy, Houston, TX,[2]Baylor College of Medicine, Houston, TX

Introduction: CDK4/6 inhibitors (CDK4/6i) are the standard of care for hormone receptor-positive/HER2-negative breast cancer (HR+/HER2- BC). Yet resistance is common and often characterized by loss or dysfunction of the Retinoblastoma (Rb) protein or inadequate suppression of its phosphorylation. Circulating tumor cells (CTCs) offer minimally invasive means to monitor tumor biology. Here, we describe the analytical performance of a multiplex immunofluorescence (mIF) assay integrated with an image-analysis pipeline to quantify Rb and phospho-Rb (pRb) expression on CTCs and evaluation of cell recovery efficiency by CTCeptor, a microfluidic CTC isolation platform.

Methods: The mIF assay utilized antibodies against Rb (AF595), pRb (AF488), cytokeratin (CK, AF647), and CD45 (AF555), with DAPI for nuclear staining. Antibody specificity and minimal non-specific binding were verified using single-marker staining and isotype controls. Assay performance (sensitivity, specificity, signal-to-noise ratio (SNR), and dynamic range) was evaluated using positive (MCF7, T47D) and negative (T47D-PalboR, MDA-MB-468, or leukocytes) control cell lines. Healthy donor leukocytes were spiked with control cell lines to simulate patient-derived matrices. Various blocking buffers, wash buffers, and cell attachment methods were compared. Cell recovery was evaluated after processing blood spiked with MCF7 cells using CTCeptor followed by staining with anti-CK-AF647, anti-CD45-AF555, and DAPI in HyPICC chamber. Imaging was performed on Leica STED SP8 or Nikon N-STORM microscopes. Quantitative analysis of mean fluorescence intensity (MFI) was conducted using FIJI, and statistical analysis was performed using GraphPad Prism v10.

Results: The optimized mIF with integrated image analysis pipeline demonstrated high analytical sensitivity (Rb: 84%, pRb: 83%) and specificity (Rb: 96%, pRb: 100%). SNRs were 5 for Rb and 50 for pRb, with dynamic range exceeding two log units for both markers. Single-marker staining and isotype controls confirmed antibody specificity and minimal non-specific binding. Based on comparative analyses, 1% BSA + 0.5% goat serum was selected as the blocking buffer, and Triton-based buffer as the wash buffer. RareCyte® cell attachment method yielded superior cell retention (79%). Recovery rate after processing the spiked blood with MCF7 cells using CTCeptor followed by staining in HyPICC chamber ranged from 40-60%.

Conclusion: We have developed and optimized a quantitative mIF assay and image analysis workflow to detect Rb and pRb expression on CTCs. Future studies will assess the predictive biomarker utility of the assay by measuring Rb and pRb dynamics on CTCs in metastatic HR+/HER2- BC patients before and after CDK4/6i therapy.

Acknowledgement: This research was funded by CPRIT (RP210148) and NCATS CTSA pilot grant (1UM1TR004539-01A1).

#5251 Precise description of metabolomic states using NGS uncover new potential biomarkers of response to TKIs in ccRCC.

Alina Tarasova, Stanislav Kurpe, Andrey Kravets, **Nikita Kotlov**

BostonGene Corporation, Waltham, MA

Renal cell carcinomas (RCC) undergo extensive metabolic reprogramming, which support tumor progression and therapy resistance. Understanding these changes is essential for identifying resistance mechanisms and therapeutic targets. While RNA sequencing enables estimation of metabolic changes, current gene expression-based metabolomic signatures often lack specificity and include unrelated or conflicting genes. Here, we combine transcriptomic and metabolomic data to create refined metabolic signatures for glycolysis (Glyc), the kynurenine pathway of tryptophan catabolism (Trp), and the urea cycle (UC), which may inform prediction of tyrosine kinase inhibitors (TKIs) response in patients with clear cell RCC (ccRCC).

To develop metabolic signatures, an initial gene pool was assembled by merging unique genes from existing metabolomic signatures in MSigDB (v2024.1) database. This gene list was refined using part of BostonGene ccRCC metacohort (701 samples), by filtering them based on technical and biological criteria: (i) median expression ≥ 2 TPM; (ii) positive Spearman cross-correlation among genes in the signature; and (iii) confirmed biological relevance through correlation with paired metabolomic and NGS data, retaining only genes with $r > 0.2$ to target metabolites (like L-lactic acid, kynurenine, or urea). Clinical significance of signatures, focusing on associations with TKI response, was assessed using data from the metacohort with available therapy response (853 samples). Overall, TME and survival analysis was assessed on the whole metacohort (n = 4,583).

All metabolic signatures demonstrated statistically significant differences between tumor and normal samples ($P < 0.001$), with higher scores for Glyc and Trp signatures in tumors and lower scores for the UC signature, consistent with previously reported findings. Notably, our signatures showed the strongest differentiation between tumor and normal samples compared to publicly available signatures. The metabolic signatures were also significantly associated with tumor microenvironment (TME) subtypes ($P < 0.001$) (Bagaev et al., 2021, *Cancer Cell*). Higher Trp signature scores were observed in immune-enriched subtype, whereas lower Trp and higher UC signature scores were found in the immune-depleted subtype. Survival analysis revealed that low UC scores correlated with worse overall survival ($P < 0.001$, MW U-test). In TKI-treated patients, complete responders exhibited higher Trp scores, while those with progressive disease had lower UC scores, which were associated with significantly poorer overall survival.

We developed metabolism-based gene signatures and demonstrated that the Trp and UC signatures strongly correlate with TKI response and patient survival. The UC and Trp pathways represent novel candidate biomarkers for future patient stratification aimed at overcoming TKI resistance in RCC.

#5252 Computational modeling of comprehensive genomic profiling to predict chemo-immunotherapy benefit in early stage NSCLC.

Prashant Nair[1], Kishor Promod[1], Ansu Kumar[1], Swati Khandelwal[1], Ambreen Ambreen[1], Susheel George[1], Mamatha Patil[1], Deepak Lala[1], Ashokraja Bala[1], Veena Balakrishnan[1], Shweta Kapoor[1], Drew Watson[1], **James Wingrove**[1], Tejas Patil[2]

[1]Cellworks Group, Inc., South San Francisco, CA,[2]University of Colorado Anschutz Medical Campus, Aurora, CO

Background: Immune checkpoint inhibition (ICI), alone and in combination with chemotherapy (ICI+C), has transformed the treatment landscape for non-small cell lung cancer (NSCLC). We have previously reported results from the myCare-040 study[1], where we validated an algorithm capable of distinguishing advanced NSCLC patients with favorable ICI+C benefit from those with no benefit. To understand whether the underlying molecular mechanisms used by the algorithm are conserved across disease stages, we have evaluated the algorithm in a cohort of patients with early stage NSCLC receiving adjuvant ICI or ICI + C.

Design: The ΔTRI algorithm uses Cellworks' computational model of a patient's tumor genomics to predict biomarker changes related to disease progression and potential benefit from ICI+C therapy. The previously validated ΔTRI and clinical threshold (16) were evaluated in 51 non-squamous, early stage NSCLC patients (Stage I=20, Stage II=12, Stage IIIA=19) receiving adjuvant ICI or ICI+C ,with complete clinical and genomic information (Foundation One CDx) derived from the nationwide (US-based) de-identified ConcertAI Genomics360 database.

Results: Patients in the ΔTRI High Benefit Group (ΔTRI ≥ 16, n = 11), had an incremental benefit in median OS of 19.4 months with the addition of chemotherapy to ICI (logrank $p = 0.057$, median OS ICI = 7 months vs ICI+C = 26.6 months). In contrast, patients in the ΔTRI No Benefit Group (ΔTRI < 16, n = 40) showed no improvement in OS when receiving ICI+C (logrank $p = 0.84$, median OS ICI = 13 months vs ICI+C = 9 months). A likelihood ratio test of interaction between the linear ΔTRI and treatment (ICI versus ICI+C) was significant (LR $p = 0.038$). Cut-point optimization for the early stage population (ΔTRI= 9) improved the logrank statistics in the High Benefit Group (ΔTRI ≥ 9; logrank $p = 0.003$).

Conclusions: Although developed and validated in patients with advanced NSCLC, the ΔTRI also predicted incremental chemotherapy benefit in an real-world cohort of patients with early stage NSCLC receiving adjuvant ICI or ICI+C. Further work is needed to understand how these observations could be translated into clinical use.

1 Aggarawal et al, WCLC 2025

#5253 Molecular correlates of progression-free survival in recurrent gliomas treated with pembrolizumab.

Shameel Shafqat[1], Muhammad Asad Maqbool[1], Hussam Al Kateb[2], Terry C. Burns[3], Jian L. Campian[4], Shannon P. Fortin Ensign[5], Evanthia Galanis[4], Julie E. Hammack[6], Cristaine M. Ida[2], Mitch L. Klebig[2], Timothy J. Kaufmann[7], Autumn C. Moon[2], Maciej M. Mrugala[8], Bryan J. Neth[9], Alyx B. Porter[8], Michael W. Ruff[9], Ugur T. Sener[9], Wendy J. Sherman[6], Joon H. Uhm[9], Rachael A. Vaubel[2], Sani H. Kizilbash[4]

[1]Comprehensive Cancer Center, Mayo Clinic, Rochester, MN,[2]Department of Laboratory and Pathology Medicine, Mayo Clinic, Rochester, MN,[3]Department of Neurological Surgery, Mayo Clinic, Rochester, MN,[4]Department of Oncology, Mayo Clinic, Rochester, MN,[5]Department of Oncology, Mayo Clinic, Phoenix, AZ,[6]Department of Neurology, Mayo Clinic, Jacksonville, FL,[7]Department of Radiology, Mayo Clinic, Rochester, MN,[8]Department of Neurology, Mayo Clinic, Phoenix, AZ,[9]Department of Neurology, Mayo Clinic, Rochester, MN

Background: Pembrolizumab has been increasingly used off label for recurrent gliomas, yet biomarkers predicting response are poorly defined. Gliomas exhibit substantial molecular heterogeneity across Glioblastoma, IDH-wildtype (GBM), Astrocytoma, IDH-Mutant (A-IDHm), and Oligodendroglioma, 1p/19q co-deleted (OLIGO), which may influence immunotherapy efficacy. This study aimed to identify molecular predictors of progression-free survival (PFS) in recurrent glioma patients treated with pembrolizumab.
Methods: Adults ≥18 years with recurrent glioma receiving ≥2 cycles of pembrolizumab between 2014 - 2024 were retrospectively identified across Mayo Clinic. Next-generation sequencing (NGS) reports were reviewed and archival tumor tissue resected prior to pembrolizumab initiation was analyzed when available. Comprehensive molecular profiling was performed using the Mayo Clinic Solid Tumor Panel which employs the Illumina Tru-Sight Oncology 500 High-Throughput NGS assay. Progression was assessed using RANO 2.0 criteria. Genomic alterations (clinically relevant sequences and/or copy-number variants) were evaluated using the Kaplan-Meier method, with differences in PFS compared using the log-rank test.
Results: Thirty-three patients were included [median (range) age: 44.0 (21-76) years; 63.6% male]. The interval between tumor tissue sampling and pembrolizumab initiation was 9.9 (0.9-176.1) months, and median treatment duration was 2.8 (1.4-10.4) months. Median PFS for the overall cohort was 2.4 (0.8-15.2) months, and median overall survival from pembrolizumab initiation was 6.9 (0.9-48.2) months. Patients with OLIGO (n=8) had a longer PFS [4.6 (1.9-15.2) months] than either A-IDHm [n=11; PFS 2.1 (1.1-4.4) months] or GBM [n=14; PFS 2.3 (0.8-9.2) months]. Within OLIGO, CDKN2A/B heterozygous deletion (n=3) predicted a shorter PFS (3.9 vs 10.9 months; p=0.0462), while in A-IDHm, FANC mutation (n=2) was associated with a longer PFS (4.17 vs 1.61 months; p=0.0224). No significant associations with PFS were observed for other altered genes or pathways evaluated, including but not limited to Tumor Mutational Burden, EGFR, RB1, TP53, FUBP1, NF 1 or 2, PTEN, PDGFRA, PIK3CA, PIK3R1, CDK4, KRAS, MLH1, MLH2, MSH6 genomic alterations or CDKN2A/B homozygous deletion (all p>0.05).
Conclusions: Pembrolizumab shows limited overall efficacy in recurrent gliomas, however, exploratory analyses identified several subtype-specific genomic alterations that may correlate with PFS. These hypothesis-generating findings highlight the potential influence of underlying tumor biology on immunotherapy response and warrant further validation in larger, prospective cohorts.

#5254 Copy number amplification of PSG is associated with poor survival in female lung adenocarcinoma patients.

Jung Hun Oh, Yingjie Zhu, Himangi Srivastava, Leyla Ebrahimpour, Rena Elkin, Larry Norton, Nadeem Riaz, Joseph O. Deasy

Memorial Sloan Kettering Cancer Center, New York, NY

Pregnancy-specific glycoproteins (PSGs) play a pivotal role in establishing and maintaining maternal immune tolerance during pregnancy, preventing fetal rejection through targeted modulation of innate and adaptive immune responses. In our previous work, we found that elevated tumor mRNA expression of PSG genes was associated with worse overall survival in lung cancer, with a significantly stronger effect observed in female patients. Based on this finding, we hypothesized that PSG copy number alterations (CNAs) show a similar sex-dependent effect on survival in lung cancer. We assessed the sex-specific impact of PSG CNAs using two lung adenocarcinoma (LUAD) cohorts: The Cancer Genome Atlas (TCGA) LUAD cohort (269 females, 234 males) and the Memorial Sloan Kettering Cancer Center (MSK)-IMPACT LUAD cohort (2,450 females, 1,413 males). CNAs in the TCGA LUAD dataset were retrieved from cBioPortal and CNAs in the MSK-IMPACT dataset were determined using the FACETS algorithm. Differences in overall survival between patients with PSG copy number gain and those without were assessed using Kaplan-Meier analysis with log-rank test. Tumor mutational burden (TMB) was also compared between the two groups using a two-sample t-test. In the TCGA cohort, female patients with PSG copy number gain (n=48) showed significantly worse overall survival compared to those without copy number gain (n=221; log-rank p=0.0039). In contrast, no significant survival difference was observed in males with PSG copy number gain (n=60) vs. those without (n=174; log-rank p=0.1902). In the MSK-IMPACT cohort, female patients with PSG copy number gain (n=426) showed significantly worse overall survival compared to those without copy number gain (n=2,024; log-rank $p=7.5\times10^{-6}$; hazard ratio [HR]=1.46, 95% CI: 1.24-1.73). In males, PSG copy number gain was associated with a significantly weaker trend toward poorer survival (n=276 with PSG copy number gain vs. n=1,137 without; log-rank p=0.0089; HR=1.29, 95% CI: 1.07-1.56). Notably, TMB was significantly higher in patients with PSG copy number gain compared to those without, in both females and males ($p<0.0001$ for both). Among patients receiving immunotherapy in the MSK-IMPACT cohort, no significant survival difference was observed between those with and without PSG copy number gain in both female (n=344) and male (n=248) groups. In this study, we demonstrated that copy number gains of PSG are associated with significantly worse overall survival in female LUAD patients compared to male LUAD patients, and this sex-dependent association is unlikely to be relevant to tumor immunity. These results highlight PSG copy number status as a novel sex-specific prognostic biomarker in lung cancer. These findings warrant further investigation into the underlying biological mechanisms and support future exploration of PSG-targeted therapeutic strategies tailored to female lung cancer patients.

#5255 KRAS subtype may modify the poor immunotherapy response in pancreatic cancer: Evidence from early phase trials.

Dilsa Mizrak Kaya[1], Yangruijue Ma[2], Tarik Demir[3], Aparna Kalyan[1], Sheetal Kircher[4], Mary Mulcahy[4], Al B. Benson III[4], Ruohui Chen[2], Devalingam Mahalingam[1]

[1]Department of Developmental Therapeutics, Northwestern University Feinberg School of Medicine, Chicago, IL,[2]Department of Preventive Medicine-Biostatistics and Informatics, Northwestern University Feinberg School of Medicine, Chicago, IL,[3]Division of Medical Oncology, The Ohio State University, Columbus, OH,[4]Department of Medical Oncology, Northwestern University Feinberg School of Medicine, Chicago, IL

Background: PDAC is characterized by a near universal presence of KRAS mutations and limited responsiveness to immunotherapy. Biologic heterogeneity among KRAS subtypes may shape tumor immunobiology and treatment resistance.
Methods: We evaluated 109 patients with advanced PDAC treated on early phase trials (08/2014 to 08/2023). PFS and OS were estimated, cox regression models assessed clinical and molecular predictors of survival.
Results: Of 109 patients, 64% had KRAS mutations, 18% were KRAS wild, and 17% had unknown KRAS status. Median age was 65 and 83% had liver metastases. KRAS subtype distribution was G12D (46%), G12V (31%), G12R (13%), and other variants (10%). Immunomodulatory agents were administered in 39% of patients, most commonly in the 1L (49%). mOS and PFS for the entire cohort were 5.65 and 2.73 months, respectively. The restricted mean OS (7.54 vs. 8.65, p=0.53) and PFS (3.82 vs. 4.24, p=0.7) did not differ between KRAS-mutant and KRAS wild. Among KRAS-mutant patients, those receiving immunomodulator therapy had shorter OS compared with those who did not, with the strongest association observed in KRAS G12D (Table 1). This pattern was not seen in the KRAS wild-type. On univariate analysis, immunotherapy exposure, number of prior treatment lines, and liver metastasis were each associated with inferior OS. On multivariate analysis, immunotherapy exposure demonstrated a non-significant trend toward inferior OS (HR 1.61, 95% CI 0.98-2.66; p=0.06), while others remained independently associated with worse OS, suggesting confounding in the unadjusted association between immunotherapy and survival.
Conclusion: Our findings suggest that among KRAS mutant PDAC - particularly G12D - receipt of immunotherapy in early phase trials was associated with shorter OS. This may reflect underlying biology or confounding by treatment line and disease burden and warrant validation by KRAS subtype-informed studies.
Table 1: mOS by KRAS and immunotherapy exposure

KRAS		Immunotherapy (n)		mOS (months)	p
wild		yes (n=7)		4.47	0.08
	no (n=13)		7.43		
mutant		yes (n=27)		2.63	***0.03***
	no (n=43)		7.52		
G12D		yes (n=13)		2.07	***0.04***
	no (n=19)		7.79		
G12V		yes (n=7)		4.04	0.48
	no (n=15)		10.22		
others		yes (n=7)		2.33	0.20
	no (n=9)		5.75		

#5256 Association of NME1, CXCL12, VDR, DNMT1, CAV1, IL27, and IL33 polymorphisms with breast cancer susceptibility in Bangladeshi women: A case-control and *in silico* study.
Mohammad Safiqul Islam, Md Abdul Barek

Department of Pharmacy, Noakhali Science and Technology University, Noakhali, Bangladesh

Purpose: Breast cancer (BC) remains one of the most common cancers and a leading cause of death among women worldwide. Despite therapeutic advances, identifying genetic factors that influence susceptibility is crucial for populations at high risk. This study aimed to investigate whether polymorphisms in *NME1* (rs16949649), *CXCL12* (rs2839693, rs1801157), *VDR* (rs7975232, rs731236, rs2228570), *DNMT1* (rs16999593), *CAV1* (rs3807987), *IL27* (rs181206), and *IL33* (rs7044343) are linked to BC in Bangladeshi women, combining case-control data with in-silico analysis.
Methods: We analyzed 250 histologically confirmed BC cases and 250 age-matched healthy controls. Genotyping was carried out by PCR-RFLP. Odds ratios (ORs) with 95% confidence intervals (CIs) were calculated, and $p<0.05$ was considered significant. To complement these findings, in-silico predictions of variant impact were performed using GEPIA, UALCAN, SIFT, PolyPhen-2, CADD, PredictSNP, Mutation Assessor, MuPro, and I-Mutant.
Results: *NME1* rs16949649 showed a significant association with BC (dominant model: OR=2.24, p=0.040; allele model: OR=2.44, p=0.045). *CXCL12* rs2839693 also increased risk (dominant model: OR=1.69, p=0.017; allele model: OR=1.67, p=0.008). Among *VDR* variants, rs7975232 and rs731236 were positively associated with BC, whereas rs2228570 was protective (additive model 2: OR=0.36, p=0.009). No meaningful associations were observed for *DNMT1* rs16999593, *CAV1* rs3807987, *IL27* rs181206, *IL33* rs7044343, or *CXCL12* rs1801157 in the case-control analysis. Interestingly, in-silico modeling suggested that *DNMT1* rs16999593 (H97R) could reduce protein stability, with some predictors indicating possible disease relevance. For *IL33* rs7044343 (C>T), the T allele was predicted to increase BC susceptibility, reflecting IL-33's context-dependent roles in tumor biology.
Conclusions: This study highlights *NME1* rs16949649, *CXCL12* rs2839693, and *VDR* variants (rs7975232, rs731236, rs2228570) as important genetic markers of BC risk in Bangladeshi women. While case-control analysis did not confirm significant effects for *DNMT1* and *IL33*, computational predictions suggest they may influence protein function and deserve further exploration. Integrating genetic association with in-silico analysis can provide deeper insights into breast cancer susceptibility in underrepresented populations.

#5257 Armored TIL GT201 induces potent tumor-specific TCR expansion and durable antitumor responses in advanced solid tumor.

Pin Wang[1], Rong Zhou[2], Yong Han[2], Zhengxiang Han[3], Weijia Fang[4], Kai Chen[5], Youguo Chen[5], Liqing Ma[6], Lili Lu[6], Derun Shen[6], Jiahui Jin[6], Yiyang Tan[6], Ke Liu[6], Zhenjiang Liu[6], Jingman Wang[6], Zhao Xu[6], Jingwei Sun[6], Jun Cui[6], Jing Yu[6], Yue He[2], Yarong Liu[6]

[1]University of Southern California, Los Angeles, CA,[2]Department of Oral Maxillofacial & Head and Neck Oncology, Shanghai Ninth People's Hospital, Shanghai, China,[3]Oncology Department, the Affiliated Hospital of Xuzhou Medical University, Xuzhou, China,[4]Department of Medical Oncology, the First Affiliated Hospital, Zhejiang University, Hangzhou, China,[5]The First Affiliated Hospital of Soochow University, Suzhou, China,[6]Grit Biotechnology, Shanghai, China

Background: Tumor-infiltrating lymphocyte (TIL) therapy has demonstrated activity in solid tumors but remains constrained by T-cell exhaustion and an immunosuppressive tumor microenvironment. GT201 is an engineered, cytokine-armored TIL product expressing membrane-bound IL-15 (mbIL-15) designed to enhance TIL persistence and antitumor function. A multi-center, open-label, single-arm exploratory clinical study was initiated to evaluate the safety, tolerability, and preliminary efficacy of GT201 in patients with advanced solid tumor.

Method: The primary endpoint was to evaluate the tolerance and safety profile according to CTCAE v5.0. Secondary endpoints included preliminary efficacy measures such as overall response rate (ORR), disease control rate (DCR), assessed per RECIST v1.1, as well as pharmacokinetics of GT201. Exploratory endpoint included longitudinal tumor biopsies and peripheral blood sampling, analyzed by single-cell RNA/TCR sequencing and bulk TCR sequencing to track clonal dynamics and identify tumor-specific TCRs.

Result: As of November 4, 2025, twelve patients were enrolled (median age 52.5 years; median of two prior lines of therapy). GT201 demonstrated a favorable safety profile: most AEs were Grade 1-2, while Grade ≥3 events were attributable to lymphodepleting chemotherapy or IL-2 support and resolved within 14 days. Preliminary efficacy signals were encouraging, with an ORR of 58.3% (7/12) and a DCR of 83.3% (10/12), including two complete responses (16.7%) and five partial responses (41.7%). Correlative multi-omics profiling revealed that mbIL-15-expressing cells were enriched in post-infusion tumor samples, and their corresponding TCRs underwent marked clonal expansion. A putative tumor-specific T-cell subset (4-1BB$^+$CD8$^+$ with high effector/exhaustion and low stemness signatures in tumor samples pre- and post-infusion) was preferentially expanded during manufacturing and showed a pronounced expansion peak in peripheral blood between Days 7-28 in responders. This subset was scarce at baseline and exhibited minimal expansion in non-responders. In contrast, “TIL-only” TCRs, which were clonotypes present in the infused product but absent pre-infusion, did not expand in peripheral blood in any patient.

Conclusion: GT201 exhibited a manageable safety profile and encouraging early efficacy in patients with advanced solid tumor, with ongoing enrollment to further inform clinical outcomes. Integrated multi-omics analyses indicate that expansion of tumor-specific TCRs, during both manufacturing and post-infusion in responding patients, correlates more strongly with clinical benefit than expansion of TIL-only TCRs. Continued longitudinal sampling and functional validation of putative tumor-specific clonotypes will be essential to establish their utility as biomarkers of response in GT201 therapy.

#5258 Monitoring of molecular response during immunotherapy by circulating tumor DNA in non-small cell lung cancer.

Johanna Svensson[1], Maria Yhr[1], Per Torstensson[2], Levent Akyurek[3], Andreas Hallqvist[4], Sukanya Raghavan[5], **Anna Rohlin**[1]

[1]Department of Clinical Genetics and Genomics, Sahlgrenska University Hospital, Goteborg, Sweden,[2]Department of Pulmonary Medicine, Skaraborg Hospital, Goteborg, Sweden,[3]Department of Clinical Pathology, Institute of Biomedicine, Sahlgrenska University Hospital, Goteborg, Sweden,[4]Department of Oncology, Sahlgrenska University Hospital, Goteborg, Sweden,[5]Department of Microbiology and Immunology, Institute for Biomedicine, Sahlgrenska Academy, University of Gothenburg, Goteborg, Sweden

Background: Patients with non-small cell lung cancer (NSCLC) may benefit from immune checkpoint blockade (ICB) targeting PD-1/PD-L1. However, only 20-40% of patients respond to ICB. Circulating tumor DNA (ctDNA) analysis in plasma offers a non-invasive biomarker for treatment monitoring. Previous studies have shown that ctDNA detection can predict clinical response earlier than standard radiological evaluation.
Objective: This study aimed to evaluate the detection and dynamics of somatic tumor-specific DNA variants in ctDNA during early treatment cycles, with the goal of identifying molecular response patterns.
Methods: Thirty-three stage III-IV NSCLC patients treated with ICB were prospectively included. ctDNA levels were analyzed longitudinally at baseline and up to five timepoints during treatment. Based on initial tumor sequencing, four to fifteen patient-specific somatic variants were selected according to pathogenicity classification and variant allele frequency. These variants were monitored at each timepoint using ultrasensitive sequencing assays (Simsen Diagnostics). A model for ctDNA-based response assessment was developed and compared with clinical outcomes defined by RECIST criteria from CT scans performed every third month after ICB initiation. Results Overall, 78.8% (26/33) of patients showed ctDNA results concordant with CT imaging when applying the molecular response model. Thirteen patients with non-detectable ctDNA at baseline had significantly longer overall survival compared with baseline ctDNA-positive patients, independent of radiological response at 3 months. Six patients experienced early progression, which was detected by ctDNA up to six weeks before clinical evaluation by CT scan. Longitudinal ctDNA patterns varied depending on metastatic site and sampling timepoint. The genomic landscape of non-responders was further explored using complementary methodologies.
Conclusion: ctDNA monitoring, based on the selection of informative tumor-specific DNA variants, provides a sensitive tool for evaluating treatment response in NSCLC. ctDNA dynamics correlated well with clinical outcomes and enabled earlier detection of progression or response compared with radiological imaging. Longitudinal ctDNA analysis underscores the importance of frequent sampling and highlights its potential to improve patient management in routine clinical practice.

#5260 *DNMT3A*-mutated tumor-infiltrating clonal hematopoiesis predicts immune checkpoint inhibitor response in advanced non-small cell lung cancer.

Geun-Ho Park, Cheolyong Joe, Hyemin Kim, Eunjoo Oh, Naeun Lee, Subin Kim, Junsu Choe, Jinyong Kim, Sehhoon Park, Hyun-Ae Jung, Jong-Mu Sun, Jin Seok Ahn, Myung-Ju Ahn, Joo Kyung Park, Se-Hoon Lee

Department of Medicine, Sungkyunkwan University School of Medicine, Samsung Medical Center, Seoul, Korea, Republic of

Introduction: Clonal hematopoiesis (CH) arises from the clonal expansion of hematopoietic stem cells and has been associated with an increased risk of hematologic malignancies, as well as adverse clinical outcomes across various solid tumors. Recent studies have shown that CH-mutated immune cells can infiltrate solid tumors, with notable enrichment in non-small cell lung cancer (NSCLC), where they may influence the local tumor microenvironment. However, the relevance of TI-CH in the context of immune checkpoint inhibitor (ICI) therapy remains poorly understood. Here, we investigated the immunologic characteristics of TI-CH and its association with ICI efficacy in patients with advanced NSCLC.

Methods: We analyzed whole-exome sequencing (WES) data from 600 ICI-treated patients with advanced NSCLC. Variant assessment was restricted to the most recurrent CH driver genes *DNMT3A*, *TET2*, and *ASXL1* (DTA), using a variant allele frequency (VAF) cutoff of ≥ 2%. Analysis of high-depth panel sequencing with paired peripheral-blood samples confirmed that tumor-detected DTA mutations were of hematopoietic origin, leading to their classification as putative TI-CH.

Results: The median depth of tumor WES data was 275.2× (range 145.9-469.5×). Putative TI-CH was identified in 12.5% of patients, with prevalence increasing with age (R^2 = 0.83, *P*=0.011). TI-CH mutations occurred at low VAF (median VAF 0.052, range 0.021-0.320) and were predominantly single-mutation events. No significant difference in sequencing depth was observed between TI-CH positive and negative groups (*P*=0.397).TI-CH-positive group showed a trend toward longer progression-free survival (PFS) (hazard ratio [HR] 0.77; 95% confidence interval [CI] 0.59-1.01; *P*=0.056) and had significantly better overall survival (OS) (HR 0.73; 95% CI 0.56-0.96; *P*=0.024). Especially, the *DNMT3A*-mutated TI-CH group exhibited significantly improved median PFS and OS compared with those without *DNMT3A* mutations (HR 0.57; 95% CI 0.40-0.83; *P* < 0.01; HR 0.51; 95% CI 0.35-0.75; *P*< 0.001). The *DNMT3A*-mutated group also demonstrated a higher response rate (45.0% vs 24.7%; *P* < 0.01). In contrast, *TET2*- and *ASXL1*-mutated TI-CH groups showed no significant difference in survival outcomes.In multivariable analysis adjusting for relevant clinical factors, DNMT3A-mutated TI-CH remained independently associated with prolonged PFS (adjusted HR 0.65; 95% CI 0.44-0.95; *P*=0.027) and OS (adjusted HR 0.64; 95% CI 0.43-0.95; *P*=0.028).

Conclusions: In this study, we characterized the landscape of TI-CH in advanced NSCLC, revealing that favorable efficacy of ICI is linked specifically to *DNMT3A* mutations. Collectively, these findings highlight *DNMT3A*-mutated TI-CH as a distinct predictive biomarker for ICI efficacy in advanced NSCLC.

#5261 Serial plasma tumor-informed next generation sequencing as a new efficacy metric to guide immunotherapy treatment discontinuation.

Meghan J. Mooradian[1], Aleigha Lawless[2], Julianne Czapla[2], Amaya Gasco[3], Patrick Boyle[3], Merrida Childress[3], Ryan J. Sullivan[4]

[1]Mass General Brigham Cancer Institute, Boston, MA,[2]Mass General Brigham, Boston, MA,[3]Foundation Medicine, Cambridge, MA,[4]Harvard Medical School/Massachusetts General Hospital, Boston, MA

Background: Immune checkpoint inhibition (ICI) is a front-line standard-of-care treatment for patients with metastatic melanoma (MM). However, there are critical questions pertaining to optimal ICI management, particularly the ideal duration of therapy, for which biomarker guidance is lacking. Identifying patients who are safely able to receive a shorter course of ICI (<2 years), thereby limiting physical and financial toxicity, is an unmet need. In this non-randomized, prospective interventional trial (NCT06146920) we evaluated the use of the FDA-approved companion diagnostic test, FoundationOne®CDx (F1CDx), and the laboratory developed test FoundationOne®Tracker, a tissue-informed personalized ctDNA monitoring assay, as an efficacy metric to guide treatment discontinuation.

Methods: Eligible patients had radiographic evidence of disease control (stable disease or response) on ICI (>12 months but ≤18 months) without the development of dose-limiting immune-related adverse event/s (irAEs). After successful sequencing with F1CDx, the FoundationOne Tracker assay was generated. Patients ctDNA positive were excluded. The ctDNA negative (neg) patients stopped ICI and continued with active surveillance, including standard of care imaging as well as serial ctDNA via FoundationOne Tracker at 1month, 2month, 3month and subsequently every 3months up to 1 year. Patients were followed for an additional year to monitor for recurrence. The primary endpoint was PFS 12-month post-ICI cessation.

Results: From March 2024 through September 2024, 12 patients with MM were screened with two becoming ineligible due to development of an irAE prior to ICI cessation and one due to inadequate tissue for F1CDx. Of enrolled patients (n=9), six had cutaneous MM, one mucosal MM and two with MM from an unknown primary. ICI regimens included nivolumab-relatlimab (n=5), ipilimumab-nivolumab (n=2) and pembrolizumab (n=3) with a median duration on therapy of 13.9 mths. The best radiographic response prior to ICI cessation was Partial Response in 6, Complete Response in 3; in those who underwent PET imaging (n=6), 3 had a complete metabolic response (CMR), and 3 had a near-CMR. All patients remained ctDNA neg at 12months post-ICI cessation and after a median of 14.9 months (13.4-19.2) following enrollment, all patients remain ctDNA neg with no clinical or radiographic evidence of progression.

Conclusion: ctDNA guided therapy decisions for advanced cancers is an active area under clinical investigation. To our knowledge, this is the first interventional study utilizing ctDNA to discontinue immunotherapy in patients with MM. Although this study was halted early due to programmatic decisions by the sponsor, the data from this small cohort highlights the potential benefit of ctDNA in guiding treatment discontinuation; further prospective study is needed.

: Effects of Ionizing Radiation on Normal Tissues and FLASH Radiation Research
Poster Session

#5264 An *in vivo*-validated dual-mechanism model explains and guides FLASH radiotherapy for normal-tissue sparing.

Lixiang Guo[1], Anthony Davis[1], Albert van der Kogel[2], **Ken KangHsin Wang**[1]

[1]Radiation Oncology, UT Southwestern Medical Center, Dallas, TX,[2]University of Wisconsin, Madison, WI

The clinical effectiveness of radiotherapy (RT) is often limited by normal tissue toxicity. FLASH-RT, delivered at ultra-high dose rate (UHDR, >40 Gy/s), can markedly reduce normal tissue injury without compromising tumor control—a phenomenon known as the FLASH effect. Despite considerable interest in FLASH clinical translation, a critical challenge remains, the mechanisms underlying the FLASH effect are not understood. Published studies are often confounded by differences in organ type, endpoints, and beam parameters. This uncertainty impacts the selection of dose rate and dose required to optimize FLASH effect. Normal tissue sparing under FLASH-RT is widely attributed to rapid physicochemical reactions. Two leading hypotheses have emerged: radiolytic oxygen depletion (ROD), in which transient O_2 depletion reduces the oxygen enhancement ratio (OER) and DNA damage; and radical-radical recombination (RRR), in which elevated radical concentrations promote recombination of lipid peroxyl radicals, suppressing lipid peroxidation (LP) and apoptotic signaling. However, neither mechanism alone fully explains experimental observations. We propose that the FLASH sparing effect could arise from the synergistic contributions of ROD and RRR, as both affect cellular damage through distinct pathways. Given the complexity of physicochemical reactions induced by irradiation, computational modeling is essential in elucidating FLASH mechanisms. We developed a physicochemical model that integrates both mechanisms. The OER-weighted dose serves as a surrogate for DNA double strand break (D_{DSB}), while the dose resulting in LOOH formation quantifies LP-related toxicity (D_{LP}). The overall tissue toxicity is represented by the Damage Equivalent Dose (DED) as sum of D_{DSB} and D_{LP}. Our results show that DED generates a consistent normal tissue complication probability (NTCP) curve that accurately captures published data on FLASH sparing of acute GI toxicity and late brain toxicity, across a wide range of UHDR and conventional dose rate (CONV) conditions, whereas dose alone fails to do so. Furthermore, the brain toxicity correlates with D_{LP}, supporting an RRR-dominated mechanism, whereas GI toxicity correlates with both D_{DSB} and D_{LP}, indicating synergistic contributions of ROD and RRR. We further present iso-FLASH tissue sparing maps that delineate dose and dose-rate ranges where FLASH sparing is expected, stratified by organ type and endpoint. Finally, we apply this model to investigate the effects of average dose rate and dose per pulse reported in abdominal irradiation studies, providing insights into parameters governing FLASH-mediated tissue sparing. In sum, this physicochemical model provides an unified and important mechanistic framework that advances our understanding of FLASH-RT sparing effects and guides the optimization of dosimetric parameters for clinical translation.

#5265 FLASH radiotherapy improves survival in mouse glioblastoma and spares circulating antigen reactive CD8$^+$T-cells.

Yanxia Ma[1], Nhat Nguyen[1], Xuehong Gui[2], Edgardo Aguilar[3], Luke Connell[3], Denae Neill[3], Emil Schuler[3], Chibawanye I. Ene[1]

[1]Department of Neurosurgery, The University of Texas MD Anderson Cancer Center, Houston, TX,[2]Department of Leukemia, The University of Texas MD Anderson Cancer Center, Houston, TX,[3]Department of Radiation Physics, Division of Radiation Oncology, The University of Texas MD Anderson Cancer Center, Houston, TX

Introduction: Glioblastoma is a lethal brain tumor with poor response to current therapies, which include surgery, chemotherapy, and conventional radiation therapy (CONV-RT). Although, CONV-RT (0.01Gy/second) to brain tumors stimulate tumor antigen release, it also recruits immunosuppressive myeloid-derived suppressor cells and is associated with neurotoxicity. Ultrahigh-dose-rate or FLASH-RT, which delivers CONV-RT doses over a significantly shorter period (more than 40Gy/second) maintains tumor control, reduces normal tissue injury and is less immunosuppressive compared to CONV-RT across multiple cancer types. In our study, we compared the effects of FLASH-RT to CONV RT in syngeneic mouse GL261 glioblastoma-bearing mice. We hypothesized that FLASH-RT would be equally or more effective than CONV-RT for tumor control and result in less immunosuppression within the tumor and systemically.

Methods: We stereotactically implanted 2×10^5 mouse GL261 cells into the right forebrain of C57BL/6 mice. Five days after tumor initiation, tumor bearing mice were treated with Sham-RT (control), CONV-RT (mean dose rate > 0.373 Gy/s), or FLASH-RT (mean dose rate >$3.6x10^6$ Gy/s). Brain tumor tissue and peripheral blood were collected on days 5 and 12 after treatment. To assess for changes in the tumor microenvironment after CONV-RT or FLASH-RT, we performed 10x Xenium spatial transcriptomics analysis (stRNA-seq; brain tumor, n = 6 mice per group), Lunaphore COMET multiplexed immunofluorescence assay (brain tumor, n = 6 mice per group), and flow cytometry (peripheral mononuclear cells, n = 6 mice per group). We also evaluated survival outcomes following treatment (n = 8 mice per group).

Results: FLASH-RT significantly improved overall survival rate of GL261 bearing mice compared to CONV-RT ($P < 0.05$) and Sham-RT ($P < 0.001$). FLASH-RT treatment markedly increased intratumoral CD8+ T-cell infiltration compared with CONV-RT ($P < 0.01$) and Sham-RT ($P < 0.01$). We also found that compared to FLASH-RT, CONV-RT caused a significant decrease in circulating PD-1$^+$CD8$^+$ T-cells ($P < 0.01$), a potent antigen reactive cytotoxic T-cell population previously identified in human patients with glioblastoma.

Conclusion: FLASH-RT is associated with better tumor control in mouse GL261 glioblastoma, increased intratumoral CD8+ T-cell infiltration, and preserves circulating antigen reactive PD1$^+$CD8$^+$ T-cells. These results indicate that FLASH-RT may synergize better with immune checkpoint inhibitors to re-invigorate anti-tumor T-cell responses against glioblastoma.

#5266 FLASH radiotherapy maintains tumor control and enables safe re-irradiation while preserving normal tissue in breast cancer PDX models.

Adel Zaid I Mutahar[1], Banita Verma[2], Stavros Melemenidis[3], Suparna Dutt[4], Kerriann M. Casey[5], Zhen Qi[2], Angera Hsiao-Chi Kuo[6], Kathleen C. Horst[7], Edward Elliot Graves[2], Michael F. Clarke[8], Billy W. Loo[9], Frederick M. Dirbas[10]

[1]Department of Surgery, School of Medicine, Stanford Cancer Institute, Stanford University School of Medicine, Stanford, CA,[2]Stanford University, Stanford, CA,[3]Department of Radiology, Stanford University, Palo Alto, CA,[4]Medicine, Stanford University School of Medicine, Stanford, CA,[5]Department of Comparative Medicine, Stanford University, Palo Alto, CA,[6]Stanford Univ., Foster City, CA,[7]Department of Radiation Oncology, Stanford University, Palo Alto, CA,[8]Associate Director, Stanford University School of Medicine, Stanford, CA,[9]Stanford University School of Medicine, Stanford, CA,[10]Stanford Cancer Institute, Stanford, CA

Background: Radiotherapy is central to breast cancer treatment but is limited by acute and cumulative skin toxicity, especially in large-field treatments and re-irradiation. Ultra-high-dose-rate FLASH radiotherapy (FLASH-RT, ≥ 40 Gy/s) may widen the therapeutic window by reducing normal-tissue injury without compromising tumor control. However, breast-directed and patient-derived models remain underexplored, including the effects of FLASH under repeated-irradiation conditions.
Methods: We integrated an orthotopic triple-negative breast cancer (TNBC) patient-derived xenograft (PDX) model and hemithoracic normal-tissue models to compare FLASH-RT (180 Gy/s) with CONV-RT (0.03 Gy/s). TNBC-bearing NRG mice received single-fraction of 30Gy electron irradiation via a custom stereotactic jig enabling mammary-targeted or hemithoracic fields. A separate cohort of non-tumor-bearing NRG mice underwent left-chest re-irradiation to assess cumulative tolerance. Endpoints included tumor regression, recurrence, survival, and graded skin toxicity; ongoing analyses incorporate histopathology and single-cell/spatial transcriptomics to elucidate FLASH-mediated tissue responses and mechanisms of normal-tissue sparing.
Results: FLASH-RT achieved equivalent tumor control to CONV-RT in TNBC-PDX models, with both modalities inducing complete regression by day 16 and maintaining clearance for two weeks before recurrence at day 32 post-RT. In contrast, normal-tissue responses diverged markedly: FLASH-RT significantly reduced acute skin toxicity (median score 0 vs. 5; $p<0.0001$), eliminated ulceration, and extended survival (120 vs. 90 days post-implantation) in tumor bearing mice. In non-tumor-bearing NRG mice, FLASH-RT also improved tolerance to cumulative thoracic irradiation; mice receiving a second 25Gy left-chest FLASH irradiation dose showed no clinical decline, whereas CONV-RT animals developed progressive toxicity requiring euthanasia within three months of re-irradiation. Multi-omics analyses are underway to define mechanisms of early tissue sparing and improved re-irradiation response.
Conclusions: FLASH-RT maintains tumor-control efficacy equivalent to CONV-RT while significantly reducing skin toxicity in TNBC-PDX models and improving normal-tissue tolerance to re-irradiation in non-tumor-bearing NRG mice. These findings support FLASH-RT as a clinically promising strategy that may expand safe re-treatment options and broaden curative radiotherapy opportunities in breast cancer. Mechanistic studies are ongoing to elucidate the biological basis of early tissue sparing and guide translation into breast-conserving and post-mastectomy treatment settings.

#5267 Reprogramming of pyruvate metabolism overcomes sex-specific differences in intestinal stem cell radiosensitivity and improves the therapeutic ratio for abdominal irradiation.
Stacey Krepel, Payel Bhanja, Rishi Man Chugh, Shujah Hamid Rehman, Subhrajit Saha

University of Kansas Medical Center, Kansas City, KS

Our study was done to elucidate the mechanism of sex-dependent differences in radiotherapy (RT) response in males versus females, and then utilize this mechanism to help prevent intestinal radiation toxicity. More than 50% of patients with gastrointestinal (GI) cancers undergo abdominal radiotherapy. However, intestinal epithelial radiosensitivity is a major limiting factor to delivering a tumoricidal dose. Personalized differences, including sex-specific differences in radiosensitivity, is one of the key determining factors in radiotherapy outcome. Using a mouse model of abdominal irradiation and a human intestinal organoid model, we previously demonstrated that healthy male intestinal stem cells are more radiosensitive than females due to higher rates of oxidative phosphorylation (OXPHOS) and production of reactive oxidative species (ROS). In the present study, we demonstrate that these higher rates of OXPHOS in males are due to increased expression of the Mitochondrial Pyruvate Carrier (MPC), which transports pyruvate into the mitochondria for flux through the TCA cycle, and, ultimately, the OXPHOS pathway. Genetic deletion of the MPC in Lgr5-EGFP-positive ISCs increases ISC survival following the reduction in radiation-induced mitochondrial pyruvate oxidation in both male and female organoids. In both human intestinal organoids and a mouse model of radiation-induced gastrointestinal syndrome, treatment with MPC inhibitor, UK5099, normalized these differences in radiation responses between males and females. Moreover, our study in a mouse model of pancreatic adenocarcinoma also establishes UK5099 as a radio-modulator for pancreatic cancer, as combination of RT+ UK5099 treatment significantly reduces tumor growth and alters the immunosuppressive tumor immune microenvironment compared to irradiated control. These findings clearly suggest that pyruvate metabolism and MPC can be a potential target to promote therapeutic ratio of abdominal radiotherapy.

#5268 Genetic inhibition of FTO does not exacerbate the severity of radiation-induced oral mucositis in C57BL/6 mice.

Margaret Pan[1], Leighton Pu[2], Stavros Melemenidis[2], Edward Elliot Graves[3], Kerriann M. Casey[2], Erinn Rankin[3]

[1]Stanford University School of Medicine, Stanford, CA,[2]Stanford University School of Medicine, stanford, CA,[3]Stanford University, Stanford, CA

Oral mucositis is a severe side effect of cancer treatment in patients with head and neck cancer. These ulcerative lesions often interfere with eating and swallowing, making recovery more difficult and potentially delaying treatment. In this study, we evaluated the impact of genetic inhibition of fat-mass and obesity-associated gene (FTO), an m6A RNA demethylase, on the severity of radiation-induced oral mucositis in C57BL6/J mice. Tongues were collected 10 days following administration of 18 Gy irradiation to the head and neck region. Histopathology demonstrated equivalent damage between FTO-knockout (KO) and wild-type (WT) mice following radiation. Thus, FTO inhibition does not exacerbate normal tissue damage following radiation and supports further investigation of FTO as a potential therapeutic target in head and neck squamous cell carcinoma (HNSCC).

#5269 Low-dose radiation therapy for peripheral joint osteoarthritis: Early U.S. community experience with pain, function, and medication outcomes.

Emily Schwartz[1], Michael Anderson[2], Russell Nevins[3], Kelsey Moakler[2], Andrew Cohen[4], Michael Sinopoli[4], Samuel Francis[4], Bradley Newby[2], Matthew Schwartz[5]

[1]University of Miami, Coral Gables, FL,[2]Comprehensive Cancer Centers of Nevada, Henderson, NV,[3]Desert Orthopaedic Center, Las Vegas, NV,[4]Comprehensive Cancer Centers of Nevada, Las Vegas, NV,[5]University of Nevada, Las Vegas (UNLV), Las Vegas, NV

Background / Significance: Osteoarthritis (OA) causes chronic pain and functional decline in older adults, yet treatment options are limited for patients who cannot tolerate long-term NSAIDs or opioids. Low-dose radiation therapy (LDRT) has shown efficacy in European studies, but U.S. data are sparse. This student-led study reports early outcomes from a community oncology practice implementing LDRT for OA, focusing on pain, function, and analgesic trends.
Methods: Thirty patients (55 joints) with OA were treated with LDRT (3 Gy in 5-6 fractions, 0.5 Gy/fraction). Pain was assessed using the Numeric Rating Scale (NRS, 0-10) and patient-assessed global improvement using the von Pannewitz Score (VPS, 0-4) at baseline, end of treatment (EOT), and ~1-month follow-up. Analgesic use was recorded at both time points. Paired t-tests and one-way ANOVA by joint site were used to assess changes.
Results: Mean baseline NRS = 8.0 (±1.2); follow-up = 3.3 (±2.1), a mean reduction of 4.7 points ($p < 0.001$). Eighty-three percent (25/30) achieved ≥2-point improvement; 70% (21/30) ≥3 points; 40% (12/30) ≥5 points. VPS at follow-up indicated moderate improvement in 39%, excellent in 25%, and complete response in 9%. Analgesic use decreased in 23% (7/30), and no patients required escalation or new medications. No ≥ Grade 2 toxicities occurred.
Conclusions: LDRT was safe, feasible, and provided substantial pain relief and improved function with parallel reductions in analgesic use. The absence of medication escalation underscores its potential as a non-pharmacologic, opioid-sparing therapy for OA pain. These real-world U.S. data support further prospective evaluation of LDRT in geriatric pain management.
Disclosure: No external funding or conflicts of interest. Study conducted under student investigator leadership with faculty supervision.

#5270 Cell-free RNA changes precede symptomatic radiation pneumonitis in cancer patients receiving thoracic radiotherapy.

Isabel Jabara, Noah Kastelowitz, Monica Nesselbush, Nick Phillips, Michael S. Binkley, Rene F. Bonilla, Kevin Liu, Alice Jiang, Nataliya Kovalchuk, Ash A. Alizadeh, Maximilian Diehn

Stanford University, Stanford, CA

Cancer therapies are limited by normal tissue toxicity. Radiation pneumonitis (RP) is a dose-limiting toxicity that commonly occurs in cancer patients who receive thoracic radiation therapy. RP is caused by inflammation and increased vascular permeability in the lungs and can lead to severe pulmonary symptoms and sometimes death. Currently, the strongest predictors of RP are radiation dose metrics, such as the volume of normal lung receiving ≥20 Gy (V20) or mean lung dose (Dmean); however, these have only modest predictive accuracy. Therefore, it is currently not possible to accurately identify patients who might benefit from RP-directed therapy prior to developing symptoms and there remains an unmet need for sensitive, non-invasive biomarkers to identify patients at risk for RP before symptoms develop. Plasma cell-free RNA (cfRNA) is a promising analyte that enables non-invasive profiling of gene expression in diverse tissues. Our group recently developed an ultrasensitive method called RARE-Seq to detect low abundance transcriptional signatures in cfRNA (Nesselbush et al. *Nature* 2025). In this study, we applied RARE-Seq to analyze cfRNA from 160 plasma samples from 56 lung cancer patients, 34 of whom developed RP, collected before, during, and after radiation therapy. We observed enrichment of lung- and airway-specific gene transcripts in cfRNA from patients with symptomatic RP compared to those who received radiation but did not develop RP. Additionally, pre-symptomatic samples from patients who later developed RP were enriched for cfRNA signatures of lung pneumocytes, suggesting early molecular changes preceding clinical symptoms. Lastly, we identified cfRNA signatures that distinguished symptomatic RP from non-RP samples with an AUC of 0.85 and pre-symptomatic RP from non-RP samples with an AUC of 0.77, significantly outperforming the classic dosimetric predictors lung V20 and Dmean (V20 P = 4.9e-5, Dmean P = 7.4e-5, paired DeLong test). Collectively, these findings demonstrate proof of concept that cfRNA profiling can predict radiation-induced toxicities before onset of symptoms, establishing it as a potentially transformative biomarker for improving monitoring and personalized management of patients treated with radiation therapy.

#5271 Pain signaling in dogs undergoing radiotherapy for head and neck cancer.

Faihaa A. Ahmed, Thitsana Ingkasri, Sophi Schofield, Effie Palyvou, Santosh K. Mishra, B. Duncan x Lascelles, Michael M. Nolan

Clinical Sciences, North Carolina State University, Raleigh, NC

A frequent side effect of radiotherapy (RT) for head and neck cancer is intense pain. While the biological basis of acute orofacial radiation-associated pain (RAP) remains unclear, it may involve pathways related to cold sensation and signaling. One important cold-sensing receptor is TRPM8 (Transient Receptor Potential Melastatin 8), which may be activated by the neurotrophic factor artemin (ARTN) through its main receptor, GFRα3. To investigate whether radiation induces the release of ARTN, resulting in TRPM8 signaling pathway modulation and subsequent RAP, a prospective clinical trial enrolled 24 pet dogs undergoing RT (32 or 36 Gy total, given in four-weekly fractions) for either oral melanoma or intranasal carcinoma. Radiotoxicity was scored at each visit, per Veterinary Radiation Therapy Oncology Group criteria. Pain was assessed using a previously validated composite oral and maxillofacial pain scale. Oral mucosal biopsies were collected from the RT field immediately before the first fraction, after the fourth/final fraction, and two weeks post-RT, to assess gene expression using bulk RNA-sequencing and protein expression of ARTN and GFRα3 via immunohistochemistry and immunofluorescence. Blood was collected at these time points and before the second fraction to quantify ARTN in serum using ELISA. Data were analyzed using two-way ANOVA. At the end of RT, 79% of all dogs had grade 1-2 oral mucositis; by the two-week recheck, only 58% had persistent mucositis. Pain severity scores were variable. In oral mucosa collected at the end of RT, there were 1,406 significantly differentially expressed genes at 32 Gy and 1,898 at 36 Gy. At the end of RT, ARTN increased 1.11-fold ($P < 0.01$) in 32 Gy-treated dogs and 1.35-fold in those received 36 Gy ($P < 0.01$). GFRα3 expression decreased by 1.02-fold ($P = 0.02$) in 36 Gy-treated dogs at the end of RT and by 1.23-fold after RT ($P = 0.01$). There were no significant changes in TRPM8 gene expression. Protein expression of ARTN and GFRα3 was unchanged in oral mucosa and neither mucositis nor pain severity correlated with ARTN or GFRα3 levels. However, there was a significant increase in serum concentrations of ARTN levels ($P= 0.01$) in dogs whose pain worsened after RT. Elevated circulating ARTN mirrors prior observations in dogs with mild radiodermatitis. Increased ARTN mRNA expression in the oral mucosa after irradiation suggests that the irradiated tissue itself is a key source of the circulating ligand. Interestingly, this occurred alongside downregulation of GFRα3 mRNA and without a clear relationship between local protein expression and the severity of radiation-associated pathology. The unexpected ligand-receptor imbalance suggests that after irradiation, increased ARTN reflects nerve regeneration and tissue repair, while reduced GFRα3 may result from nerve damage or silencing. Thus, the apparent inverse correlation may reflect tissue reorganization and adaptive signaling.

#5272 Development of a novel radiation-induced vaginal tissue injury model.

Julie Hakim[1], Dan Kennedy[1], Melissa Grunlan[2], Manuel Rausch[3], Ashley Hicks[3], Elizabeth Cosgriff-Hernandez[3]

[1]Baylor College of Medicine, Houston, TX,[2]Texas A&M Engineering Experiment Station, College Station, TX,[3]University of Texas at Austin, Austin, TX

Introduction: Vaginal stenosis (VS), characterized by thickening and shortening of the vaginal wall tissue, occurs in up to 80% of women receiving pelvic radiotherapy (PRT), the most common treatment for gynecologic cancers. Yet, a critical barrier to developing more effective therapies is a lack of clinically relevant models to dissect underlying mechanisms. Using the Food and Drug Administration gold-standard for vaginal irritation testing, we have developed a rabbit model of radiation-induced vaginal injury.
Methods: Female New Zealand white rabbits were either left untreated or radiated at low dose (LD) (6 Gy) or high dose (HD) (20 Gy) by external beam radiation. After the final radiation fraction, vaginoscopies were conducted once per week for six weeks. Changes to vaginal tissue were scored using five clinical morphological parameters for VS: mucosal pallor, telangiectasia, fragility of the vaginal wall, ulceration, and adhesions/occlusion. Gross vaginal tissue was measured to determine changes in length and diameter. Histopathologic changes to vaginal tissue were determined under H&E and Masson's trichrome.
Results: Vaginoscopy of HD rabbits revealed a consistently higher degree of changes to the vaginal tissue. Compared to untreated rabbits, high-dose radiation induced vaginal wall thinning, smooth muscle tissue loss, replacement fibrosis, and increased interstitial fibrosis. HD-treated rabbits also demonstrated higher VS scores. While the inner perimeter of vaginas from high-dose rabbits decreased compared to untreated control rabbits, the difference was not statistically significant.
Conclusion: Here, we present a radiation-induced vaginal injury model of VS. Given the current gaps in available animal models for basic and translational research in vaginal health, the proposed model addresses key anatomical and physiological parameters that parallel the human vagina. This innovative model will strengthen the translational-to-clinical pipeline by enhancing the rigor of therapeutic testing after radiotherapy.

#5273 Signaling pathway insights into spaceflight cancer risks.

Anu R I[1], Josef Borg[1], JangKeun Kim[2], Tricia Larose[3], Ryan T. Scott[4], Joseph Borg[1], Christopher E. Mason[2], Afshin Beheshti[5], Kurt van der Speeten[6]

[1]University of Malta, Msida, Malta,[2]Weill Cornell Medicine, New York, NY,[3]University of Oslo, Oslo, Norway,[4]NASA Ames Research Center, Moffett Field, CA,[5]University of Pittsburgh, Pittsburgh, KS,[6]Hasselt University, Genk, Belgium

Spaceflight is a stochastic risk factor for development of cancer in astronauts and experimental data beyond low earth orbit is scarce[1]. Our understanding of role of tumorigenic pathways in the context of space biology is limited. We compared differentially expressed genes (DEGs), signaling pathways, and cancer hallmarks between human tumor tissue with Spaceflight data from civilian astronauts on private missions and rodents on Space missions[2].Astronaut RNA Seq data from the Inspiration4 (I4) mission and NASA Twin study were used conjointly with data from space-flown rodents and compared to transcriptome from organ-matched human tumor counterparts from NCI Genomic Data Commons. The peripheral blood transcriptome of the I4 crew revealed a temporal trend of oncogenic gene dysregulation from pre-flight to 82 days after return to Earth (R+82). Early post-flight window showed activation of pro-tumorigenic and immune-mediated genes namely *KRAS, MTOR, STAT3, RARA,* and *PIK3CA* on R+1 (immediate post-spaceflight), of which sustained activation of key genes were observed on R+45 (45 days post return to Earth) and on R+82. DNA damage repair genes such as *MRE11, ATR, ABL1, RAD51B, RAD51D, FANCA*, and *CREBBP* were activated in parallel. Over time, most regulatory genes recovered, but therapeutic targets namely *ALK, ROS1, NTRK3, POLE, RAD51D, MTAP, ESR1, FGFR3, TSC1, STK11, ABL1, CREBBP, RAF1, NRG1, BCL6,* and *KMT2D* were found to be upregulated post-flight after readjusting to Earth, irrespective of inter-individual variability. Sustained upregulation of stemness factors *STAT3* and *FOXP1* indicate adaptivity or immune system tuning post-stress but warrants attention for long term studies for potential oncogenic risks.In parallel, multi-organ sorted patient and rodent data offered staggering insights into tumorigenic roles of major signaling cascades in cancer. Significant overlaps in DEGs were observed between primary human tumors and spaceflown models notably in Breast (p 4.84E-57, OR 7.7), Colon (p 9.24E-46, OR 25), Kidney (p 9.21E-62, OR 9.3), Lung (p 1.38E-51, OR 28), and Skin (p1.23E-85, OR 119). GSEA analysis revealed pro-tumorigenic pathway enrichment. For example, in breast, we observed activation in pathways of MYC targets (NES 2.17, FDRq 0.003), mTORC (NES 2.42, FDRq 0.000), PI3K pathway (NES 1.31, FDRq 0.123), DNA damage repair (NES 1.76, FDRq 0.002), Oxidative Phosphorylation (NES 3.28, FDRq 0.000), and ROS cascades (NES 2.10, FDRq 0.000).The distinction between signaling pathway dysregulations in healthy tissue, benign tumors, stress-induced tissue, and florid malignancy remains a question. Sustained activation of pathways post-spaceflight in astronauts is a crucial finding that mirrors a cellular environment observed in human pre-malignant tissues. Simultaneously, the significant similarity in cellular pathways between tumors and spaceflight petitions cognizance of the bivalent nature of pathways in cancer[3].

#5274 Impact of ultra-high dose rate (FLASH) versus conventional radiotherapy on tumor control in wild-type and cGAS-knockout mice.

Banita Verma[1], Adel Mutahar[1], Stavros Melemenidis[2], Rohit Verma[3], Lucy Whitemore[1], Suparna Dutt[2], Kathleen C. Horst[2], Edward Elliot Graves[2], Michael F. Clarke[4], Lingyin Li[5], Billy W. Loo[2], Frederick M. Dirbas[1]

[1]General Surgery, Stanford University School of Medicine, Stanford, CA,[2]Radiation Oncology, Stanford University School of Medicine, Stanford, CA,[3]Neurosurgery, Stanford University School of Medicine, Stanford, CA,[4]Med/Stem Cell, Stanford University School of Medicine, Stanford, CA,[5]Stanford Biochemistry, Sarafan ChEM-H and Arc Institute, Stanford University School of Medicine, Stanford, CA

Background: Radiotherapy (RT) is central to breast cancer (BC) management but limited by normal tissue toxicity. Conventional RT (CONV; ≤0.03 Gy/s) controls tumors but often causes skin inflammation, compromises treatment intensity and quality of life. Ultra-high dose-rate FLASH RT (>40 Gy/s) achieves comparable tumor control with markedly reduced tissue injury ("FLASH effect"), yet its mechanism of tumor control and sparing of normal tissue remains unclear. Ionizing radiation activates the cGAS-STING pathway through DNA damage, triggering proinflammatory cytokine production and tissue injury, yet has also been implicated with improvement in the antitumor immune response. Emerging data suggest that FLASH may attenuate or abrogate cGAS-STING signaling leading to reduced inflammation and tissue injury. This study investigated the role of cGAS signaling in mediating the differential effects of FLASH and CONV RT on normal tissue toxicity and tumor control using wild-type (WT) C57BL/6 and cGAS double knockout (cGAS -/- KO) mice.

Methods: PYMT117 BC cells were orthotopically implanted into the third mammary fat pad of 6-8-week-old female WT and cGAS-/- mice. Once tumors reached ~50 mm^3, mice received a single 30 Gy dose of either FLASH or CONV RT targeted to the tumor site. Tumor growth and skin toxicity (graded 0-5) were measured every other day. Euthanasia was performed upon excessive tumor burden or skin injury. Data were analyzed by two-way ANOVA followed by Tukey's post hoc test ($p < 0.05$).

Results: Both FLASH and CONV RT significantly reduced tumor volume ($p < 0.001$), with complete regression by day 14. Tumor recurrence occurred around day 25 in all groups. In WT mice, both modalities produced comparable tumor control, with CONV showing a slight but non-significant trend toward smaller recurrent tumors and few complete responses but caused severe skin toxicity (score 5) requiring euthanasia by day 50-60. In contrast, FLASH treated mice showed equivalent tumor suppression markedly reducing skin toxicity (score ≤ 3 in 2/10 mice). Notably, the cGAS-/- mice exhibited minimal or no visible toxicity with either modality, except one CONV-treated mouse (score 2).

Conclusion: FLASH RT significantly reduces normal tissue toxicity compared to CONV RT while maintaining equivalent tumor control: improved tumor control might be achievable through higher FLASH doses because of the improved therapeutic index over CONV RT. The minimal toxicity observed following FLASH RT, together with the absence of toxicity in cGAS-/- mice, also supports the possibility that FLASH may limit early inflammatory responses and tissue injury by suppression or abrogation of cGAS-STING activation. These findings support FLASH RT as a promising, less-toxic radiotherapeutic approach and highlights the potential of suppression of the cGAS-STING pathway to improve treatment outcomes in BC.

#5275 Mechanistic insights into the anti-tumor activity of ^{212}Pb-PSMA radioligand therapy.

Feifei Liu, Melissa Monterosso, Didier Boucher, Anna Amiss, Stelle Shakti, Kwong Ching Li, Chanwoo Kim, Aimee Horsfall, Kevin Kuan, William Tieu, Stephen Rose, Simon Puttick, Joana Brilhante, Gary Li, Anna Karmann, Thomas Kryza

AdvanCell Pty Ltd, Sydney, Australia

Introduction: Prostate-specific membrane antigen (PSMA)-targeted radioligand therapy (RLT) with lutetium-177 (^{177}Lu) has demonstrated clinical benefit in prostate cancer (PC). Although alpha-emitters offer superior cytotoxic efficacy, the complex toxicity profile of actinium-225 (^{225}Ac)-PSMA limits its therapeutic application. Lead-212 (^{212}Pb) possesses favorable physical properties, including high linear energy transfer, a 10.6-hour half-life, and a simple decay scheme with a single alpha-emitting daughter nuclide, enabling precise, potent radiation delivery at the cellular level. In this study, we combine *in vitro* and *in vivo* models with multiomics and functional assays to elucidate the mechanisms underlying the anti-tumor efficacy of PSMA-targeted RLT.

Materials and Methods: ^{212}Pb-ADVC001, a novel ^{212}Pb-based PSMA-targeting RLT in Phase I/II clinical development (NCT05720130) for the treatment of metastatic PC, was used as the ^{212}Pb-PSMA-RLT agent. ^{177}Lu-PSMA-I&T was used as the ^{177}Lu-PSMA-RLT agent. The kinetic mechanisms associated with ^{212}Pb-ADVC001 mediated cell-death were investigated *in vitro* and *ex vivo* using transcriptomics and proteomics analyses. To validate the omics findings, functional assays were conducted to assess the effects of ^{212}Pb-PSMA on PC's cell cycle progression, reactive oxygen species (ROS) generation, and lipid peroxidation in PC cells.

Results: ^{212}Pb-ADVC001 displayed potent cytotoxic activity with a mean EC_{50} of 2.7, 7.2 and 3.3 kBq/mL in PC cell lines PC-3-PIP (PSMA^{high}), C4-2 (PSMA^{int}) and LNCaP (PSMA^{int}), respectively. Transcriptomic and proteomic analysis of *in vitro* treated PC cells and *in vivo* tumors harvested longitudinally revealed multiple mechanisms of action involving DNA damage, cell cycle arrest and cell death, and immune response modulation. *In vitro* functional assays confirmed the involvement of ROS production, lipid peroxidation, and cell cycle arrest upon treatment with ^{212}Pb-ADVC001. Particularly, ^{212}Pb-ADVC001 caused significant DNA damage, and reduced DNA content in the S-phase of the cell cycle with a concomitant increase in the G1- and G2/M-phase arrest compared to ^{177}Lu-PSMA-I&T ($p < 0.05$).

Conclusion: Multiomics analyses highlighted the involvement of multiple mechanisms of action in the efficacy of ^{212}Pb-ADVC001 which collectively resulted in effective cancer cell death. Mechanistic studies furthered the understanding of PC radiobiology and cellular responses to beta- and alpha-based RLT with the identification of a cell cycle arrest in PC specifically induced by ^{212}Pb-PSMA.

#5276 [^{123}I]CC1, a radiopharmaceutical for Targeted radionuclide therapy (TRT), exploits PARP binding and trapping to amplify DNA damage and cytotoxicity in human cancer cell lines..

Luis Hernandez Cano[1], Nerea Delgado Mayenco[1], Hilleen Kramer[1], Elmar Diekstra[1], Francesca Amoroso[1], Sreelakshmi Unnikrishnan[1], George Alachouzos[2], Wiktor Szymanski[2], Frank A. Kruyt[3], Bart Cornelissen[1]

[1]Nuclear Medicine and Molecular Imaging, University Medical Center Groningen, Groningen, Netherlands,[2]Nanomedicine and Drug Targeting, University of Groningen, Groningen, Netherlands,[3]Medical Oncology, University Medical Center Groningen, Groningen, Netherlands

We investigated whether the antitumor effects of [^{123}I]CC1, a PARP-binding radiopharmaceutical emitting very short-range ionising Auger electrons with potential use in Targeted Radionuclide Therapy (TRT), are driven by PARP trapping. Trapping will prolong its residence time on DNA and triggers more DNA damage. We tested this in PSN1 and U87 human cancer cell lines exposed to [^{123}I]CC1, by assessing PARP levels in the chromatin fraction via western blot and quantifying ^{123}I counts in nuclear and cytoplasmic fractions using a gamma counter. Downstream effects were evaluated using γH2AX immunofluorescence as a marker of DNA damage and DNA fiber assays to measure replication speed. Furthermore, we modulated PARP association with DNA by using methyl methanesulfonate (MMS) to increase and the PARG inhibitor JA2131 to decrease trapped PARP, using western blot and gamma counter to analyze how [^{123}I]CC1 tracks PARP movements from chromatin to nuclear soluble fraction. Finally, γH2AX immunofluorescence was used to assess whether combinatory treatments with MMS or PARGi affect the ability of [^{123}I]CC1 in producing DNA damage. [^{123}I]CC1 elevated trapped PARP levels on DNA in PSN1 and U87 cells, followed by a rapid increase in γH2AX foci. Interestingly, DNA fiber assays showed that replication was markedly hindered in PSN1 at 30 min and 24 h, indicating substantial DNA damage. Pretreatment with 0.01% MMS before [^{123}I]CC1 addition further elevated PARP levels compared to [^{123}I]CC1 alone, resulting in greater chromatin ^{123}I accumulation. In contrast, PARG inhibitor treatment reduced PARP residence time on DNA, and in combination with [^{123}I]CC1 decreased DNA ^{123}I delivery. Finally, assessment of γH2AX at 30 min and 24 hours showed that MMS pretreatment enhanced DNA damage induced by [^{123}I]CC1 greater damage than MMS alone, demonstrating an additive effect, whereas PARGI pretreatment had no significant effect.The results indicate that the cytotoxic effect of [^{123}I]CC1 is mediated by PARP trapping, which underlies its potent antitumoral activity previously observed by our group. Furthermore, modulation of the PARylation cycle alters delivery of radioactivity to DNA and the extent of DNA damage, suggesting a strategy to enhance the therapeutic benefit of [^{123}I]CC1 and its potential for clinical translation.

#5277 Alpha- and beta-emitter radiopharmaceutical therapy combined with dual immune checkpoint inhibitors yields distinct control of primary and metastatic tumors.

Yujuan Wang[1], Alexander Wertheim Verona[2], Bhoomika Raj Pillai[2], Tracy Berg[1], Caroline Kerr[1], Jamey P. Weichert[3], Reinier Hernandez[4], Bryan P. Bednarz[4], Zachary S. Morris[1]

[1]Department of Human Oncology, University of Wisconsin School of Medicine and Public Health, Madison, WI,[2]College of Agricultural and Life Sciences, University of Wisconsin-Madison, Madison, WI,[3]Department of Radiology, University of Wisconsin School of Medicine and Public Health, Madison, WI,[4]Department of Medical Physics, University of Wisconsin School of Medicine and Public Health, Madison, WI

Background: The therapeutic challenge of advanced and metastatic solid tumors may be addressed by immune checkpoint inhibitors (ICIs) for some patients, but most exhibit primary or acquired resistance. Combination with radiopharmaceutical therapy (RPT) provides promise in overcoming ICI resistance by delivering radiation to all lesions. Selecting radionuclides of differing physical properties, such as linear energy transfer (LET) and path length, are an optimizable feature of RPT. For instance, α-emitters such as ^{225}Ac deliver high LET radiation over short ranges suitable for targeting microscopic disease, whereas β-emitters such as ^{90}Y release lower LET radiation over longer distances suitable for macroscopic primary tumors. The optimal radionuclide type and dose to control coexisting macro- and micro-disease in advanced tumors remain undefined. To define rational strategies for metastatic disease, we evaluate differential therapeutic efficacy of α- and β-emitting RPTs when combined with dual ICIs in controlling concurrent macroscopic and microscopic tumors.

Methods: Dosimetry was estimated using the Monte Carlo-based RAPID platform informed by serial PET/CT or SPECT/CT imaging and/or ex vivo biodistribution. Female C57BL/6 mice (6-8 weeks) were implanted subcutaneously with 2×10^6 MOC2 cells in the flank on day -5 resulting in a macroscopic (~70 mm^3) tumor at the time of RPT. To model micro-metastatic disease, we injected 1×10^6 MOC2 cells intravenously on the morning prior to RPT. Mice received either ^{90}Y-NM600 (2, 12, or 20 Gy) or ^{225}Ac-NM600 (0.5, 2, or 6 Gy) on day 1, or were assigned to a no-radiation control group. Dual ICIs (anti-CTLA-4 + anti-PD-L1; 100 µg each) were administered
intraperitoneally on days −1, 2, and 5 relative to RPT. Lymphopenia was monitored weekly using an HM5 analyzer up to expected isotope decay. Mice were euthanized when macroscopic tumors exceeded 20 mm in any dimension or on independent health-monitoring criteria for moribundity.

Results: We identified an optimal dose of either ^{225}Ac- or ^{90}Y-NM600 that inhibited primary tumor growth and increased survival in a mixed tumor model. However, proportions of mice that were euthanized at the 20 mm primary tumor cut-off versus those that were euthanized prior to that endpoint because of moribundity differed between ^{225}Ac- and ^{90}Y-NM600. 50% of ^{225}Ac-NM600 mice were euthanized for reaching the 20 mm primary tumor endpoint, while no mice in the ^{90}Y-NM600 group were euthanized for primary tumor size and were instead euthanized for moribundity.

Conclusions: Further testing is required to identify the cause of differing moribundity amongst the ^{225}Ac-NM600 versus ^{90}Y-NM600 treatment groups; however, these findings suggest differing effects on disease progression in a mixed tumor model when treated with radionuclides of differing properties.

: Epigenetics, Cytogenetics, and Clinical Molecular Genetics
Poster Session

#5281 A novel viral-derived epigenetic gene therapy delivered via mRNA-lipid nanoparticles to inhibit HPV-associated malignancies.

Fan Yang[1], Yan-Ning Yu[1], Liliana Echavarria[1], Leo Holguin[1], Sarah Schroeder[1], Shasha Li[1], Michelle Afkhami[2], Diana Bell[3], Krupal Patel[4], **Tristan A. Scott**[1]

[1]City of Hope Comprehensive Cancer Ctr., Duarte, CA,[2]Comprehensive Cancer Ctr., Duarte, CA, United States, City of Hope, CA,[3]University of Pittsburgh Medical Center, Pittsburgh, PA,[4]Department of Surgery, City of Hope Comprehensive Cancer Ctr., Duarte, CA

Human Papillomavirus (HPV) is associated with a range of malignancies, including oropharyngeal, cervical, and anal carcinomas. Approximately 47,000 carcinoma cases annually in USA are attributed to HPV causing significant morbidity and mortality. Integration of the episomal HPV genome into the host's DNA is a critical event in oncogenesis. HPV's long control region (LCR) promoter overexpresses the viral E6 and E7 proteins, which inhibit the tumor suppressors p53 and Rb1 respectively, driving the oncogenic transformation. E6 and E7 are also critical for tumor maintenance by creating a state of 'oncogene addiction', making them ideal targets for therapeutic intervention. They are considered undruggable, but they present ideal targets for gene therapy interventions. However, gene therapies face significant challenges such as targeting multiple HPV oncogenes within sequence-diverse high-risk HPV subtypes. To this end, we have exploited a viral self-regulatory genetic circuit to develop a compact, single component epigenetic repressor (BE2K). BE2K targets highly conserved sites in the LCR which can silence multiple oncogenes simultaneously in virtually all HPV subtypes. BE2K inhibited the proliferation of high-risk HPV16 and HPV18-associated oropharyngeal, cervical, and anal cancer cell lines. BE2K had no effect on non-HPV associated cell lines. BE2K suppressed E6 and E7 expression resulting in reactivation of the p53 tumor suppressor and caspase-mediated apoptosis. Global mRNA profiling confirmed E6 and E7 reduction, an increase in p53 signaling and apoptosis pathways, as well as a reduction in the E2F transcription factor targets, downstream of Rb1. Of note, an upregulation in interferon pathways and inflammatory response was observed, which may additionally contribute to the anti-proliferative effects in HPV-associated cancers in an immune-competent context. To deliver BE2K intratumorally, it was formulated as mRNA in MC3 lipid nanoparticles (LNPs). An HPV-associated head and neck SCC154 xenograft model in NSG mice was used and LNP-mRNA BE2K reduced tumor volume and improved clinical scores in the mice compared to controls. Immunohistochemistry showed an elevated p53 with a reduction in the Ki-67. Safety profiling showed no effect on serum ALT/AST levels, or liver and spleen histology. To validate our findings, a patient-derived xenograft (PDX) model was established from a primary tonsil HPV-associated head and neck squamous cell cancer. Preliminary experiments in the PDX showed that BE2K treatment resulted in a correlation between tumor growth inhibition and p53 and caspase-3 activation. Overall, BE2K, as a scalable LNP-mRNA formulation, represents a promising new epigenetic mRNA treatment towards a more generalizable gene therapy for HPV-associated malignancies.

#5282 Splicing disruption using a CLK inhibitor shows activity in malignant rhabdoid tumor pre-clinical models.

Clemence Basse[1], Pawel Sobczuk[1], Andrea Gazzo[1], Tom Zhang[1], Marissa Mattar[1], Inna Khodos[2], Elisa De Stanchina[3], Romel Somwar[1], Neerav N. Shukla[4], Marc Ladanyi[1]

[1]LADANYI Lab, Memorial Sloan Kettering Cancer Center, New York, NY,[2]Anti-tumor Core Facility, Pharmacology Program, Memorial Sloan Kettering Cancer Center, NEW YORK, NY,[3]Anti-tumor Core Facility, Pharmacology Program, Memorial Sloan Kettering Cancer Center, New York, NY,[4]Department of Pediatrics, Memorial Sloan Kettering Cancer Center,, New York, NY

BACKGROUND. Malignant Rhabdoid Tumors (MRT) are rare lethal tumors affecting young children and characterized by genetic loss of *SMARCB1*. SMARCB1 is a core subunit of the canonical BAF (cBAF) chromatin-remodeling complex and its loss disrupts canonical BAF assembly leading to dependence on alternative BAF complexes (not containing SMARCB1), notably the non-canonical BAF (ncBAF) complex, which contains BRD9 instead. MRT cells activate Wnt/beta-catenin signaling based on impaired repression of Wnt/beta-catenin target genes by TCF/LEF in the absence of a functional cBAF complex, representing a specific therapeutic vulnerability, as well as an overall dependence on the ncBAF complex which makes BRD9 another specific vulnerability. CLK inhibition via its effects on phosphorylation of splicing factors is known to inhibit Wnt/beta-catenin signaling by disrupting canonical splicing of TCF/LEF, and BRD9 has been reported to be downregulated in the context of splicing factor alterations. We hypothesized that the CLK/DYRK inhibitor SM09419, an analogue of the clinical stage CLK/DYRK inhibitor cirtuvivint/SM08502 (both developed by Biosplice Therapeutics, Inc./TenaRx, Inc.) could be active in MRT cells.

METHODS. Established MRT cell lines and patient-derived xenograft (PDX) models were used for *in vitro* and *in vivo* experiments. Proliferation and growth were examined using Alamar Blue viability dye or colony forming assays. Cell cycle analysis was assessed by flow cytometry. mRNA expression and splice forms were evaluated by RNAseq, qPCR, RT-PCR, and long read sequencing. *In vivo* efficacy studies were conducted in NSG mice harboring MRT PDXs.

RESULTS. SM09419 inhibited growth *in vitro* of six (A204, G401, JMRTK2, KYM-1, TM87-16, TTC549) MRT cell lines with IC_{50} <200 nM for all cell lines. Cell cycle profiling showed increased arrest at G0/G1. SM09419 treatment resulted in upregulation of the cell cycle inhibitors p21 and p27, elevation of the pro-apoptotic markers cleaved PARP, BIM and PUMA and increased caspase 3/7 activity. RNAseq of MRT cell lines A204 and TTC549 treated with SM09419 showed downregulation of *WNT*/beta-catenin transcriptional targets and qPCR confirmed aberrant splicing of WNT pathway repressors LEF/TCF. Additionally, SM09419 significantly reduced BRD9 canonical transcripts in both cell lines and qPCR confirmed aberrant splicing of BRD9. In three MRT PDX models, SM09419 treatment (12.5 mg/kg and 25 mg/kg) for at least 40 days after implantation suppressed growth in a dose-dependent manner.

CONCLUSION. The splicing inhibitor SM09419 exerts promising anti-tumoral effects in MRT models. Mechanistically, CLK inhibition as monotherapy may be hitting at least two known key vulnerabilities in MRT, namely Wnt/β-catenin signaling and ncBAF function (via BRD9 misplicing). These findings provide a rationale for further early phase clinical trials of CLK inhibitors in MRT.

#5283 Cloud-based computational framework for individualized genomic analysis in pediatric acute lymphoblastic leukemia: A nationwide multi-center real-world clinical study.

Han Wang[1], Jiaoyang Cai[1], Jie Yu[2], Shaoyan Hu[3], Yongjun Fang[4], Ju Gao[5], Jian Li[6], Hua Jiang[7], Xiuli Ju[8], Sixi Liu[9], Wenyong Kuang[10], Runming Jin[11], Liangchun Yang[12], Xuedong Wu[13], Xiaowen Zhai[14], Qun Hu[15], Hui Jiang[16], Ningling Wang[17], Chi Kong Li[18], Lirong Sun[19], Jiao Jin[20], Chun Li[21], Changda Liang[22], Yan Dai[23], Kaili Pan[24], Hao Xiong[25], Ching-Hon Pui[26], Shuhong Shen[27], Yu Liu[1]

[1]Shanghai Children's Medical Center, School of Medicine, Shanghai Jiao Tong University, Shanghai, China,[2]Chongqing Medical University Affiliated Children's Hospital, Chongqing, China,[3]Children's Hospital of Soochow Universit, Suzhou, China,[4]Nanjing Children's Hospital Affiliated to Nanjing Medical University, Nanjing, China,[5]West China Second University Hospital, Sichuan University, Chengdu, China,[6]Fujian Medical University Union Hospital, Fuzhou, China,[7]Guangzhou Women and Children's Medical Center, Guangzhou, China,[8]Qilu Hospital of Shandong University, Jinan, China,[9]Shenzhen Children's Hospital, Shenzhen, China,[10]Hunan Children's Hospital, Changsha, China,[11]Union Hospital of Tongji Medical College, Huazhong University of Science and Technology, Wuhan, China,[12]Xiangya Hospital Central South University, Changsha, China,[13]Nanfang Hospital, Southern Medical University, Guangzhou, China,[14]Children's hospital of Fudan university, Shanghai, China,[15]Tongji Hospital of Tongji Medical College, Huazhong University of Science and Technology, Wuhan, China,[16]Shanghai Children's Hospital, School of Medicine, Shanghai Jiao Tong University, Shanghai, China,[17]Anhui Medical University Second Affiliated Hospital, Hefei, China,[18]Hong Kong Children's Hospital, Hong Kong, Hong Kong,[19]Affiliated Hospital of Qingdao University, Qingdao, China,[20]The Affiliated Hospital of Guizhou University, Guiyang, China,[21]Anhui Provincial Hosptical, Anhui, China,[22]Jiangxi Provincial Children's Hospital, Nanchang, China,[23]The People's Hospital of Guangxi Zhuang Autonomous Region, Nanning, China,[24]Xi 'an Northwest Women and Children Hospital, Xi 'an, China,[25]Wuhan Children's Hospital, Wuhan, China,[26]Chair, Dept. of Oncology, St. Jude Children's Research Hospital, Memphis, TN,[27]Department of Hematology & Oncology, Shanghai Children's Medical Center, School of Medicine, Shanghai Jiao Tong University, Shanghai, China

Acute lymphoblastic leukemia (ALL) is the most common childhood cancer. While genomic studies have identified key molecular subtypes and aberrations in ALL, it requires integrating multi-omics data to complete complex and time-consuming analyses in large retrospective cohorts. It is challenging to perform individualized clinical genomic analysis in real-world.

We present a nationwide precision genomic study as part of the Chinese Children Cancer Group ALL 2020 clinical trial. Between 2020 and 2023, 6486 pediatric ALL patients were enrolled from 25 medical centers across 15 provinces in China. RNA-seq was performed for 5103 patients during diagnosis. We developed the National Children's Medical Center ALL Bio-Cloud (NCMC-ABC), an automated, cloud-based framework for real-time RNA-seq data process. NCMC-ABC is designed to analyze multiple clinically relevant genomic aberrations from single RNA-seq data, including molecular subtypes, coding and noncoding driver mutations, fusions and CNVs. The median turnaround time from sample collection to clinical reporting was 14 days across all hospitals, aligning with clinical treatment timelines.

We established a molecular subtype classification framework for pediatric ALL, and successfully classified 94.94% of B-ALLs into 20 subtypes and 86.38% of T-ALLs into 11 subtypes. This framework significantly improved the traditional MICM approach, which classified only 48.58% of B-ALLs and did not account for T-ALL subtypes. The enhanced classification is due to the improved detection of key fusions (*DUX4*, *PAX5*, *ZNF384*, *MEF2D* rearrangements) and mutations (*PAX5* P80R and *IKZF1* N159Y). Meanwhile, we achieved more precise subtyping of HYPO, HYPER and KMT2A BALLs. The refined subtypes unveiled a distinct profile of Chinese B-ALL patients, with higher frequencies of HYPER, ETV6, DUX4 and PH subtypes, and lower frequencies of Ph-like, iAMP21 and HYPO, compared to Western cohorts. Importantly, the refined framework directly improved the risk stratification of patients.

We identified a median of 2.44 pathogenic SNPs/indels and 1.28 fusions per patient. The driver mutations were detected in 259 genes in B-ALL and 156 in T-ALL. We observed different driver mutation profiles in our cohort compared to the Western cohort. Mutations in RAS pathway (*NRAS*, *KRAS* and *PTPN11*) were more frequent in Chinese patients, whereas the JAK-STAT (*JAK2*, *IL7R*, *SH2B3* and *CRLF2*) pathway was more frequently mutated in Western cohort. We observed direct clinical relevance of these aberrations. For example, patients with *TP53* and *NR3C1* mutations showed inferior treatment response.

The implementation of NCMC-ABC in a nationwide multicenter pediatric ALL clinical trial demonstrated its effectiveness and feasibility in real-world, improving risk stratification and therapeutic decision making in clinic.

#5284 Epigenetic clusters identified in Hispanic/LatinX colorectal cancers reveal novel molecular subtypes.

Seeta Rajpara[1], Vicky Yamamoto[2], Carmen Chavez[1], John D. Carpten[3], David W. Craig[4], Heinz-Josef Lenz[5], Bodour Salhia[5]

[1]Keck School of Medicine of USC, Los Angeles, CA,[2]Keck School of Medicine, Los Angeles, CA,[3]Department of Integrative Translational Sciences, City of Hope Comprehensive Cancer Center, Duarte, CA,[4]City of Hope Comprehensive Cancer Center, Duarte, CA,[5]USC Norris Comprehensive Cancer Center, Los Angeles, CA

Introduction: Colorectal cancer (CRC) incidence and mortality are rising among Hispanic/LatinX (HL) individuals, yet they remain underrepresented in genomic studies. As a result, it is unknown whether HL CRCs harbor distinct epigenetic or biological features. We addressed this gap by profiling HL CRC tumors using genome-wide DNA methylation and integrating these data with matched transcriptomic and genomic datasets.

Methods: We generated DNA methylation profiles for 104 HL CRC tumors using the Illumina EPIC v2 array. RNA-seq (n=92) and whole-exome sequencing (WES; n=89) were available for integrative analyses. TCGA non-Hispanic White (NHW) CRCs served as a reference cohort. CIMP status was assigned using promoter methylation values for eight canonical CIMP markers (MLH1, IGF2, CACNA1G, NEUROG1, RUNX3, SOCS1, CRABP1, CDKN2A). Unsupervised clustering of the top most variable CpGs was used to define methylation subtypes. Pathway interpretation was performed by summarizing CpGs into gene-context scores across cancer related pathways. Matched RNA-seq and WES data were used to characterize transcriptional and mutational features of each subtype and validate DNA methylation pathway interpretation. CMS classifications, MSI status were assigned for comparison.

Results: CIMP patterns in HL CRCs differed markedly from NHW tumors in TCGA. Only 1% of HL MSI tumors were CIMP-H (vs. 7.1% in NHW MSI CRCs), and 11% were CIMP-0 (vs. 3.4% in NHW), indicating a decoupling of MSI and CIMP-H status. Unsupervised clustering identified six novel methylation-defined subtypes (HL-C1 to HL-C6) with distinct immune, stromal, metabolic, and epigenetic features. These subtypes also differed by mean age at diagnosis and global methylation: HL-C1 (58.7y, β=0.493), HL-C2 (51.2y, β=0.358), HL-C3 (60.1y, β=0.428), HL-C4 (51.9y, β=0.222), HL-C5 (52.8y, β=0.460), and HL-C6 (44.5y, β=0.608). Integration with RNA-seq confirmed concordant pathway activation across overlapping samples. Somatic mutations further distinguished subtypes: TP53 mutations were reduced in HL-C6 (37.5% vs. ~66% in other clusters), while MLH1 mutations were enriched (12.5%). CMS assignments did not recapitulate these six HL-specific subtypes.

Conclusion: HL CRCs display molecular features not captured by existing CIMP or CMS frameworks. The distinct methylation subtypes identified here offer new insight into HL CRC biology and provide a foundation for refining future molecular studies in this population.

#5285 Toward a functional characterization of polygenic modifiers of *BRCA2* associated prostate cancer risk.

Kenneth Offit, Sanchari Bhattacharyya, Matthew Buas, Brett Carver, Jonathan Fainberg, Yelena Kemel, Catherine Fanjoy, Viaji Joseph, Kathryn Graz, Xu Zhang, Shiv Prakash Verma, Ninghui Mao, Kyrie Pappas, Mitul Waghmare

Memorial Sloan Kettering Cancer Center, New York, NY

Introduction: Male carriers of *BRCA2* pathogenic variants are at elevated risk of prostate cancer (PC), with wide variation in disease frequency observed (88% vs. 34%) for men in the top versus bottom 5th percentile of a 147-SNP prostate cancer polygenic risk score (PRS) (PMID: 34320204). Causal variants and genes at most of these PRS loci remain uncharacterized, limiting our understanding of the molecular mediators and biological mechanisms underlying putative modifiers of *BRCA2* risk.
Methods: We adopted our published informatics pipeline to prioritize candidate functional variants at PC risk loci using Functional Potential Scores (FPS), assembled from disease-relevant annotations of chromatin accessibility, histone marks, and transcriptional factor (TF) binding. We identified 74 loci with a high-scoring lead SNP or strongly correlated variant ($r2>0.80$), typically mapping to a predicted enhancer region, and selected several such loci for experimental interrogation: 10q25, 11q13, 12q14, 19p13. Genomic fragments spanning prioritized SNPs were cloned in forward and reverse orientations upstream of a minimal promoter driving Nanoluc luciferase (pNL3.1), and luciferase reporter assays were conducted to evaluate allele-specific enhancer activity in normal prostate (RWPE-1) and PC cell lines (LnCAP, VCAP and 22PC). CRISPR genome editing studies are underway to assess the impact of enhancers and risk alleles on regional gene expression profiles.
Results: Three of the four candidate enhancer fragments tested exhibited enhancer activity in at least two cell lines -- 10q25/SNP5, 11q13/SNP10, 19p13/SNP17. Among these, the enhancer at 10q25 exhibited allele-specific activity, with up to ~two-fold stronger signal observed for allele C versus T in both normal and cancer cell lines. Initial studies also suggested allelic specificity for enhancers at 11q13 (SNP10 G>T) and 19p13 (SNP17 G>A). At 10q25, the functional variant identified maps to the third intron of *TCF7L2*, a critical gene in the Wnt signaling pathway, in a region bound by several key TFs in prostate including androgen receptor and FOXA1. Functional studies of validated target genes are being conducted with and without genotoxic stressors using human organoid cultures we have established from prostate biopsies of men with *BRCA2* mutations.
Conclusions: Our findings support the utility of the FPS informatics framework for prioritizing likely functional/causal variants at inherited cancer susceptibility loci and provide a foundation for downstream functional assays using physiologic model systems to investigate causal mechanisms of genetic modifiers of *BRCA2*-associated prostate cancer risk. (Supported by the Breast Cancer Research Foundation, CureBRCA, the MSK Niehaus Center and the Sabin Foundation)

#5286 Molecular and immune landscape of HER2-amplified colorectal cancer.

Sunyoung Lee[1], Michelle Weitz[2], Adam Dugan[2], Saif Nirzhor[2], Kayla Layng[2], Scott Kopetz[1], James Yu[1], Asif Rashid[3], Funda Meric-Bernstam[1], Mohamed Nuh[4], Monica Hsiang[4], Kanwal Pratap Singh Raghav[1]

[1]UT MD Anderson Cancer Center, Houston, TX,[2]Tempus AI, Inc, Chicago, IL,[3]Div. of Path. & Lab. Med., UT MD Anderson Cancer Center, Houston, TX,[4]Department of Medicine, Baylor College of Medicine, Houston, TX

Background: HER2 amplification defines a biologically distinct subset of colorectal cancer (CRC), yet its transcriptomic and immune correlates remain incompletely characterized. We profiled HER2-amplified CRCs to delineate clinicogenomic, immune, and transcriptomic features associated with ERBB2-driven oncogenesis.
Methods: We used Tempus Lens (Tempus AI, Inc., Chicago, IL) to query the Tempus multimodal de-identified database and identify patients with stage III/IV CRC who underwent Tempus xT (DNA) and xR (RNA) testing with tumor purity ≥30%. HER2 amplification was defined as *ERBB2* copy number (CN) ≥6. Demographic and clinical characteristics, somatic and germline alterations, quanTIseq-based immune cell infiltration estimates, and biomarkers (TMB, PD-L1, MSI) were compared. RNA-seq data were normalized to $\log_2$(TPM+1), and differential expression and pathway enrichment analyses on the hallmark gene set using fgsea compared HER2-amplified and non-amplified tumors.
Results: Among 16,394 patients with diagnoses of colon or rectal adenocarcinoma, 445 (2.7%) were HER2-amplified. These tumors occurred at a younger median age (58 vs. 60 years, p=0.001) and were more often left-sided (70% vs. 57%, p=0.011). Where data were available, *ERBB2* amplification showed 88% (36/41) concordance with external HER2 IHC/ISH and a correlation between *ERBB2* copy number and mRNA expression (ρ=0.38, p<0.001), demonstrating concordance across DNA, RNA, and protein levels. *ERBB2*-activating mutations, most frequently V777L (3.15%), followed by G776V, S310F, and H878Y, co-occurred in 9.2% of amplified tumors, suggesting dual genomic and structural activation. HER2-amplified CRCs had fewer *KRAS* mutations (14% vs. 48%, p<0.001; *G12D* most common), lower mean TMB (5 vs. 8 mut/Mb, p<0.001), and were universally MSS (MSI-H 0%). Germline mutation frequencies were similar between groups, with *CHEK2* and *MUTYH* most frequent. HER2-amplified tumors demonstrated reduced infiltration of M1 macrophages, NK cells, and Tregs (all p<0.01) and lacked significant enrichment of antigen-presentation, Th1, checkpoint, or co-stimulatory signatures (q=0.06-0.08), indicating a relatively immune-inactive microenvironment compared to non-amplified CRCs. Gene set enrichment analysis revealed a trend toward positive enrichment of cell-cycle and DNA replication programs (*E2F, MCM, PLK1, AURKB, TOP2A*) and suppression of *KRAS* signaling in HER2-amplified patients.
Conclusions: HER2-amplified CRCs exhibit a coordinated *ERBB2* activation axis linking DNA amplification, mRNA overexpression, and protein upregulation. These tumors are characterized by a hyperproliferative yet immune-depleted transcriptional profile. The biological interplay between HER2 signaling, proliferation, and immune modulation warrants further study, and future work should include clinical outcome correlations.

#5287 Parent-of-Origin-Aware genomic analysis in hereditary cancer: identifying the side of the family at risk using only the proband's blood sample.

Lilian Cordova[1], Vahid Akbari[1], Tiffany Leung[2], Kieran O'Neill[3], Katherine Dixon[3], Alexandra Roston[4], Eugene Cheung[5], Chuyi Zheng[5], Millicent Sharman[6], Alshanee Sharma[5], Steve Bilobram[3], Yaoqing Shen[3], Janine Senz[7], Yanni Wang[2], Daniel Chan[2], Alexandra Fok[5], Jennifer Nuk[5], Quang Hong[6], Robin Coope[3], Eric Chuah[7], Simon Chan[3], Hyun-Wu Lee[3], Yongjun Zhao[3], Miruna Bala[3], Karen Mungall[3], Andrew Mungall[3], Richard Moore[3], Nur Diana Binte Ishak[8], Siao Ting Chong[8], Ee Ling Chew[8], Ashley McDonald[9], Anna Martinez[9], Gregory Kelly[10], Rosella Delgado[10], Caitlin Orr[10], Joanne Yuen Yie Ngeow[8], Kara N. Maxwell[11], Stephen B. Gruber[12], Dean Regier[13], Alice Virani[6], Louis Lefebvre[6], Fabio Feldman[5], Marco Marra[6], Sophie Sun[14], Stephen Yip[15], Peter Lansdorp[1], Steven John Jones[3], Kasmintan Schrader[5]

[1]Medical Genetics, University of British Columbia, Vancouver, BC, Canada,[2]Terry Fox Laboratory, BC Cancer, Vancouver, BC, Canada,[3]Canada's Michael Smith Genome Sciences Centre, BC Cancer, Vancouver, BC, Canada,[4]University of British Columbia Faculty of Medicine, Vancouver, BC, Canada,[5]Hereditary Cancer Program, BC Cancer, Vancouver, BC, Canada,[6]University of British Columbia, Vancouver, BC, Canada,[7]BC Cancer, Vancouver, BC, Canada,[8]Cancer Genetics Service, National Cancer Centre Singapore, Singapore, Singapore,[9]City of Hope National Medical Center, Duarte, CA,[10]University of Pennsylvania, Philadelphia, PA,[11]Perelman School of Med. Univ. of Pennsylvania, Philadelphia, PA,[12]City of Hope National Medical Center, Los Angeles, CA,[13]School of Population and Public Health, University of British Columbia, Vancouver, BC, Canada,[14]Medical Oncology, BC Cancer, Vancouver, BC, Canada,[15]BC Cancer

Background: Determining the parent of origin (PofO) of a variant in hereditary cancer guides counseling, risk management, recurrence risk assessment, and variant classification. In conditions involving genes with PofO effects, such as *SDHD*, *SDHAF2* and *MAX*, this information can determine whether disease will manifest. Current approaches rely on family-based testing, yet uptake among eligible first-degree relatives remains low, with fewer than 30% undergoing testing, creating a major barrier in hereditary cancer.To address this gap, we developed Parent-of-Origin-Aware Genomic Analysis (POAga), a method that integrates chromosome-scale haplotyping with DNA methylation at differentially imprinted regions to assign PofO without parental data. To validate POAga, we applied it to individuals with hereditary cancer and known segregation of their pathogenic variants, and compared the predicted PofO with the established segregation to assess concordance and limitations.**Methods:** Blood samples are being collected from individuals with pathogenic variants in hereditary cancer genes, representing broad ranges of ages, ancestries, and cancer histories. Parental segregation was previously known or established through confirmatory testing. Predicted PofO is compared with true segregation to assess concordance. All samples undergo Strand-seq and long-read sequencing under an REB-approved protocol.**Results:** To date, 285 samples with 290 pathogenic variants have been analyzed across the following genes: *BRCA2* (n=46), *BRCA1* (n=42), *MSH2* (n=34), *SDHD* (n=29), *MLH1* (n=27), *MSH6* (n=26), *PMS2* (n=20), *PALB2* (n=15), *TP53* (n=14), *ATM* (n=14), *CDH1* (n=9), *CHEK2* (n=3), *EPCAM* (n=2), *SDHAF2* (n=2), *MUTYH* (n=2), *CDKN2A* (n=1), *POT1* (n=1), *RAD51D* (n=1), and *SDHC* (n=1). PofO was assigned for 250 variants, with 98.4% concordance (246/250). PofO could not be determined for 40 variants (13.8%, 40/290), mainly due to insufficient allele-specific methylation at imprinted regions or extended homozygosity that impeded phasing. Misassignments were rare and mainly due to stochastic phasing errors, unresolved inversions, or random allelic methylation at imprinted regions.**Conclusion:** POAga achieves clinical-grade accuracy in assigning PofO from a single blood sample in hereditary cancer. This directly addresses a major barrier in clinical genetics, particularly when parental samples are unavailable. For genes with PofO effects, this information can determine whether disease will manifest. By enabling reliable segregation without parental testing, POAga helps direct clinical efforts toward those truly at risk and improves the clinical interpretation of variants. Ongoing analyses will refine its performance and support its adoption as a transformative tool in hereditary cancer genomics.

#5288 HMA-induced oncogene reactivation as a driver of disease progression in MDS.

Junsu Kwon[1], Yanjing Liu[2], Mahmoud A. Bassal[3], Julie A.I. Thoms[4], Emiliano Fabiani[5], John Pimanda[4], Maria T. Voso[6], Daniel G. Tenen[3], Li Chai[1]

[1]Brigham and Women's Hospital, Harvard Medical School, Boston, MA,[2]Broad Institute, Boston, MA,[3]Harvard Stem Cell Institute, Harvard Medical School, Boston, MA,[4]University of New South Wales, Sydney, Australia,[5]UniCamillus-Saint Camillus International University of Health Sciences, Rome, Italy,[6]University of Rome Tor Vergata, Rome, Italy

Hypomethylating agents (HMAs), including azacitidine and decitabine, are widely used for high-risk myelodysplastic syndromes (MDS) and selected AML, yet most patients eventually relapse, and survival after HMA failure remains dismal. HMAs were long assumed to function primarily by reactivating tumor suppressor genes through DNA demethylation. However, our recent work demonstrated that HMAs paradoxically upregulate the oncofetal gene SALL4, and that this induction strongly correlates with inferior overall survival, challenging existing paradigms. Emerging data suggest that additional cancer-germline antigen genes (CGAGs) may be similarly reactivated, generating oncogenic programs that facilitate resistance and leukemic progression. To investigate this, we profiled paired pre- and post-HMA patient marrow samples using RNA-seq and methylation analysis. We observed consistent post-treatment upregulation and promoter hypomethylation of SALL4 and multiple CGAGs, including PIWIL2, HORMAD1, and DDX43. Induction was more pronounced in patients with progression or treatment failure. Functional studies in MDS cell models revealed that forced expression of SALL4 or selected CGAGs enhanced proliferation, impaired myeloid differentiation, and reduced sensitivity to HMAs. Conversely, shRNA-mediated depletion mitigated these phenotypes. CRISPR-DiR-driven locus-specific demethylation of SALL4 recapitulated HMA-associated activation and conferred a proliferative advantage, confirming a causal role for promoter demethylation in SALL4 reactivation. We next evaluated therapeutic vulnerabilities associated with this pathway. Treatment with a newly developed small-molecule SALL4 degrader (SH6) reduced viability in SALL4-high models and reversed HMA-induced resistance phenotypes. Combination treatment with HMA + SH6 demonstrated enhanced cytotoxicity compared to either agent alone. Ongoing studies are expanding this approach to additional CGAG targets and mapping resistant subpopulations using single-cell transcriptomic and epigenetic profiling. Together, these findings reveal that HMA therapy can trigger unintended activation of oncogenic CGAG programs that drive MDS progression. They support a new mechanistic framework in which treatment-induced epigenetic reawakening promotes malignant fitness, and they identify SALL4 and CGAGs as high-value biomarkers and therapeutic targets. This work motivates development of companion diagnostic strategies and combination regimens pairing HMAs with targeted degraders to prevent therapy-induced disease acceleration and improve patient outcomes.

#5289 Native domain-interaction rewiring collapses the AR neo-enhanceosome in prostate cancer.

Jie Luo[1], Jianzhang Yang[2], Yuanyuan Qiao[3], Jean Ching-Yi Tien[1], Eleanor Young[2], sumit Das[1], Jocelyn Cai[1], Kenneth Gu[4], Shaomeng Wang[2], Arul M. Chinnaiyan[1]

[1]University of Michigan, Ann Arbor, MI,[2]University of Michigan, ANN ARBOR, MI,[3]University of Michigan Medical School, Ann Arbor, MI,[4]Rogel Cancer Center, Ann Arbor, MI

The androgen receptor (AR) signaling axis remains active in metastatic castration-resistant prostate cancer (mCRPC) through adaptive mechanisms that sustain oncogenic transcriptional programs despite androgen deprivation. AR cooperates with the histone acetyltransferase p300 and other cofactors to assemble cancer-specific “neo-enhanceosomes” via highly organized domain–domain interactions that drive oncogenic gene expression. Here, we introduce a new class of chemical-induced proximity compounds, termed Domain-ALTeration Chimeras (DALTACs), which represent a distinct modality designed to rewire endogenous protein complexes by altering native domain interactions rather than degrading or inhibiting individual proteins. Our first-in-class compound, AR–p300 DALTAC-1, enforces proximity between the AR ligand-binding domain and the p300 bromodomain, thereby miswiring their native architecture and locking the complex in a non-productive configuration. This domain reconfiguration elicits a “super-inhibitory” effect that suppresses AR target gene transcription and cell proliferation more potently than concurrent inhibition of AR and p300. Mechanistically, DALTAC-1 reprograms the substrate spectrum of p300, diminishing histone H2B N-terminal acetylation (H2BNTac) and triggering the collapse of the oncogenic enhancer network. Strikingly, DALTAC-1 displays remarkable lineage selectivity, exerting potent activity in AR-driven prostate cancer cells and organoids while sparing AR-negative or non-prostate lineage tissues. In multiple prostate cancer models, DALTAC-1 exhibits robust antitumor efficacy and tumor regression with favorable tolerability. Collectively, this study establishes the DALTAC modality as a new therapeutic concept that manipulates protein complex topology to reprogram cellular function, offering a versatile and generalizable strategy to rewire diverse transcriptional, epigenetic, and signaling complexes across different cancer types. Importantly, the exquisite lineage selectivity of DALTAC-1 minimizes effects on normal tissues, underscoring its strong clinical translational potential with a low likelihood of safety concerns.

#5290 Investigating the intrinsic epigenetic dependencies of estrogen receptor positive and ESR1 mutant breast cancer.

Andrej Coleski, Eleanor Young, Sumit Das, Xuhong Cao, Shannon VanAken, Fengyun Su, Yizhi Cao, Rui Wang, James M. Rae, Abhijit Parolia, Yuanyuan Qiao, Lanbo Xiao, Arul M. Chinnaiyan

University of Michigan, Ann Arbor, MI

Background: Estrogen receptor alpha (ERα) is a nuclear steroid hormone receptor that regulates transcription through DNA binding. ER is a lineage defining transcription factor (TF) that drives approximately 70% of breast cancer (BC) cases expressing the receptor. Aromatase inhibitor or selective estrogen receptor modulator treatment are first-line endocrine therapies for the treatment of ER$^+$ BC, and they function by disrupting ligand availability or antagonizing ER, respectively. Activating mutations in *ESR1*, the gene encoding ERα, are enriched in approximately 25% of metastatic cases. *ESR1* mutations lock ER in an active conformation, conferring ligand-independent signaling, endocrine therapy resistance, and increased proliferative capacity. Both wild-type and mutant ER primarily act through enhancer elements rather than promoters, relying on a network of transcriptional co-factors and chromatin remodeling complexes to facilitate enhancer accessibility. Targeting these epigenetic dependencies represents a promising therapeutic strategy. The mammalian SWI/SNF (mSWI/SNF) chromatin remodeling complex interacts with ER-associated transcription factors, including FOXA1, and supports enhancer activity and ER recruitment. Thus, disrupting mSWI/SNF function may impair ER-driven transcriptional programs in ER$^+$ BC.

Methods: mSWI/SNF activity was perturbed using either a dual PROTAC degrader of SMARCA2/4 or a selective SMARCA2/4 ATPase inhibitor. Pharmacological effect was assessed in a variety of preclinical models of ER$^+$ and *ESR1* mutant BC including cell lines and patient-derived xenografts (PDX). Mechanisms of action of ER signaling disruption and mSWI/SNF dependence were investigated using multi-omics techniques such as RNA-seq, ATAC-seq, ChIP-seq, and RIME.

Results: We showed that ER$^+$ BC cell lines are preferentially sensitive to mSWI/SNF complex inactivation at nanomolar concentrations of both compounds. We also demonstrated significant anti-tumor activity in both ER wild type and mutant PDX models. This anti-proliferative phenotype is shown to be driven by ER signaling axis disruption, with key downstream targets like c-Myc and CCND1 being downregulated. Mechanistically, we demonstrate these effects are mediated by reduced chromatin accessibility at enhancer regions, changes in the FOXA1 and ER cistromes, and a disruption of the ER interactome.

Conclusions: We establish the mSWI/SNF complex as a critical epigenetic dependency that sustains ER transcriptional activity in ER+ BC. Therapeutic targeting of SMARCA2/4 effectively disrupts enhancer function, impairs ER signaling, and suppresses tumor growth. mSWI/SNF-directed therapies therefore represent a promising strategy for advanced and endocrine-resistant ER+ breast cancers.

#5291 EZH2-AR non-canonical axis activation in TKI-resistant RCC: Differential effects of lenvatinib and cabozantinib.

Christian Migliarese[1], Abbas Jawadwala[1], Sabrina A. Orsi[1], Stephanie Metcalf[2], Saranya Rajendran[3], Peter C. Hollenhorst[3], Roberto Pili[1]

[1]University at Buffalo, SUNY, Buffalo, NY,[2]Indiana University School of Medicine, Bloomington, IN,[3]Indiana University, Bloomington, IN

Tyrosine kinase inhibitors (TKIs) are critical to the treatment of renal cell carcinoma (RCC). However, recurrent and metastatic RCC frequently develop resistance to TKIs, limiting therapeutic options. Understanding the molecular mechanisms underlying this resistance is crucial for improving patient outcomes. Our previous studies have identified EZH2 and the androgen receptor (AR) as key regulators of acquired resistance to the TKI . Inhibiting EZH2 or AR restores sunitinib sensitivity in vitro and in vivo, highlighting these molecules as therapeutic targets potentially shared across TKIs .To investigate the interplay between EZH2 and AR, we compared sunitinib-resistant 786-0 cells (786-0^{RS}) with drug-naive 786-0 cells overexpressing AR (786-0^{AR}). Chromatin immunoprecipitation sequencing revealed that AR and EZH2 co-occupy genomic loci exclusively in resistant cells. Sunitinib treatment induced nuclear translocation of AR in 786-0^{AR}, with AR binding at EZH2-occupied sites. Mass spectrometry further showed high phosphorylation of AR at S81 and S213, markers of ligand-independent activation, in 786-0^{RS}, which was absent in 786-0^{AR}.786-0^{RS} cells undergo EZH2-dependent reprogramming of the tyrosine kinome via a likely non-canonical mechanism. Co-expression of a phosphomimetic EZH2 mutant (S21D) with AR promoted sunitinib resistance, whereas wild-type or phosphonull (S21A) EZH2 did not. Expanded phosphoproteomic analyses revealed extensive rewiring of serine/threonine signaling networks in sunitinib resistant cells, including enrichment of EGFR-driven MAPK and AKT pathways. Interestingly, preliminary data indicate that cabozantinib does not induce AR and EZH2 upregulation like other TKIs such as lenvatinib. Moreover, cabozantinib appears to prevent compensatory pathway activation triggered by lenvantinib, suggesting a distinct resistance profile. Consistently, AR expression is observed in RCC lines resistant to sunitinib, dovitinib, and lenvatinib, but not with cabozantinib treatment. Ongoing phosphoproteomic analysis will dissect the difference across the TKIsdrugs. Overall, our findings suggest that EZH2-dependent kinase reprogramming drives AR phosphorylation and activation, contributing to drug resistance to selective TKIs. Cabozantinibunique ability to bypass AR/EZH2 upregulation underscores the need to explore alternative resistance pathways.

#5292 Epigenetic modulators romidepsin and mithramycin A reactivate tumor-suppressive programs and suppress c-MYC under hyperthermic conditions in colorectal peritoneal metastasis.

Yazid Ghanem[1], Gena Topper[1], Sahil Jethi[2], Jessica Collier[1], Marlena Buonasorte[1], Yong Ki Hong[1], **Weam Othman Elbezanti**[1]

[1]Surgery, Cooper University Health Care, Camden, NJ,[2]Cooper Medical School of Rowan University (CMSRU), Camden, NJ

Colorectal peritoneal metastasis remains difficult to treat despite advances in cytoreductive surgery and hyperthermic intraperitoneal chemotherapy (HIPEC). Emerging evidence indicates that epigenetic dysregulation contributes to therapeutic resistance by repressing tumor suppressor pathways and sustaining oncogenic transcriptional programs. To evaluate whether epigenetically active agents improve antitumor responses relevant to HIPEC, we compared the histone deacetylase inhibitor romidepsin (Ro) and the Sp1 transcription factor inhibitor mithramycin A (MA) with the standard HIPEC agent mitomycin C (MMC) in HCT116 and HT29 colorectal cancer cells exposed to normothermic (37°C) or hyperthermic (42°C) conditions for 90 minutes. Both Ro and MA induced greater cytotoxicity, reduced clonogenic survival, and more strongly inhibited migration relative to MMC. Mechanistically, these agents robustly increased p21 and cleaved caspase-3 expression, consistent with reactivation of tumor-suppressive and apoptotic programs, while markedly suppressing c-MYC. Transcriptomic analysis further revealed that Ro and MA restored the expression of multiple epigenetically silenced tumor suppressor genes, including *SPRY2*, *HIC1*, *TIMP3*, and *DKK1*, indicating broad reversal of transcriptional repression. Hyperthermia variably augmented drug responses in a pathway-dependent manner, suggesting synergistic interactions between heat stress and chromatin remodeling. Ongoing studies using a murine HIPEC model with HCT116 peritoneal xenografts will define the molecular correlates and therapeutic potential of integrating epigenetic modulators into HIPEC-based regimens for colorectal peritoneal metastasis.

#5293 Targeting the oncogenic RNA m6A reader YTHDF2 inhibits oral squamous cell carcinoma by preventing p53 degradation.

Anitha Pandi[1], Vijayashree Priyadharsini Jayaseelan[1], Paramasivam Arumugam[2]

[1]Clinical genetics lab, Saveetha Dental College and Hospitals, Chennai, India,[2]Molecular biology lab, Saveetha Dental College and Hospitals, Chennai, India

Background: The N6-methyladenosine (m6A) RNA modification machinery has emerged as a critical modulator in cancer biology, however, the function of m6A “reader” proteins in oral squamous cell carcinoma (OSCC) is not fully understand. YTH domain family protein 2 (YTHDF2) is a prominent m6A-binding protein (m6A “reader”) that facilitates the degradation of methylated mRNAs and has been associated with tumorigenesis by targeting destabilization on clusters of tumor suppressor mRNAs. Nevertheless, the exact mechanism how YTHDF2 promotes OSCC proliferation and regulates p53 activity is in dire lack of elucidation. This study investigated the oncogenic role of YTHDF2 in OSCC and evaluated its potential as both a diagnostic biomarker and a therapeutic target.
Methods: The mRNA and protein levels of YTHDF2 were examined in OSCC tissues, matched adjacent non-cancerous specimens as well as OSCC cell lines by quantitative real-time PCR (qRT-PCR) and Western blot. Furthermore, the TCGA-OSCC dataset were employed to evaluate YTHDF2 expression, its clinicopathological characteristics and prognostic value. Functional assays including proliferation, colony formation and wound-healing assays were performed to evaluate the oncogenic phenotypes in YTHDF2-depleted OSCC cell lines. The antitumor effects were examined in vitro via OSCC cell lines and patient-derived organoids (PDOs) derived from OSCC patients who received a selective YTHDF2 inhibitor.
Results: YTHDF2 was remarkably up-regulated in OSCC tissues and cell lines compared with non-tumor tissues and normal cells, $P < 0.001$. Overexpression of YTHDF2 is correlated with OSCC development, progression and poor prognosis. YTHDF2 knockdown dramatically impaired OSCC cell proliferation, migration and tumorsphere formation. Functionally, YTHDF2 physically interacted with m6A-modified p53 transcripts and promoted their degradation. Inhibition of YTHDF2 significantly promoted the stability and protein expression of p53. YTHDF2 inhibitor impeded growth, migration, colony formation, tumorsphere and organoid development of cancer cells.
Conclusions: Our results recognize YTHDF2 as an oncogenic m6A reader promoting the OSCC progression by increasing p53 mRNA degradation. Our findings indicate that YTHDF2 can be exploited therapeutically and tumor suppressively as a candidate antitumor approach in OSCC.

#5294 Epigenetic modulation by DNMT-1 inhibitor induces cell death in SK-N-AS neuroblastoma cells.

Shyam Sundar Jaganathan, Umamaheswari Natarajan, Appu Rathinavelu

Rumbaugh Goodwin Institute for Cancer Research, Barry and Judy Silverman College of Pharmacy, Nova Southeastern University, Fort Lauderdale, FL

Neuroblastoma (NB) is one of the most common extra-cranial solid tumors that is typically found in newborns and infants. Unfortunately, most children are present with advanced diseases and have poor prognosis at the time of diagnosis. Although the treatment of neuroblastoma has significantly improved with recent therapeutic strategies, many patients still do not benefit from them. As a result, new treatment approaches that can control aggressive and resistant tumors are urgently needed. Epigenetic regulation through DNA methylation and histone modifications have been shown to play a critical role in neuroblastoma progression, similar to the phenomenon seen in many other types of cancers. In this regard, DNMT's are commonly upregulated in aggressive neuroblastoma cells, contributing to transcriptional repression of tumor suppressor pathways. Therefore, in this study, we investigated the effect of the DNMT/G9a inhibitor CM-272 on cell survival in SK-N-AS neuroblastoma cells. Treatment of neuroblastoma cells with CM-272 at a concentration of 2 μM resulted in significant cell death, due to activation of the programmed cell death (PCD) cascade caused by elevated levels of apoptotic markers. In addition, CM-272 markedly suppressed DNMT-1 expression, confirming its ability to disrupt DNA methylation dependent gene silencing. In multiple cancer types, apoptosis induction was validated by enhanced cleavage of PARP accompanied by elevation of BAX and Caspases. Furthermore, CM-272 treatment elevated BAX expression, with downregulated BCL-2 levels, Intrinsic Pathway activation. In addition to the above analyses, miRNA expression profiling was performed using the NanoString Human miRNA panel. To fully explore post-transcriptional regulatory mechanisms that may be associated with CM-272 treatment. Together, these results demonstrate that CM-272 can induces apoptosis in SK-N-AS neuroblastoma cells by targeting epigenetic regulators and activating cell death pathways. Our findings suggest that CM-272 has strong therapeutic potential, as an epigenetic modifier drug, particularly in neuroblastoma tumors that are resistant to conventional treatments. Acknowledgements: This project was supported by the National Pediatric Cancer Foundation (NPCF). This research was also partially funded by the Bankhead Coley Infrastructure Development Grant from the Florida Department of Health that was awarded to A.R. through the Department of Pharmacology of the University of Miami (Coral Gables, Florida USA). The authors would like to thank Royal Dames of Cancer Research Inc. (Ft. Lauderdale, Florida) for their financial support in conducting this research

#5295 Integrative identification and functional interrogation of DNA methylation-mediated epigenetic gene alterations in pancreatic cancer.

Sanghee Nam, **Galam Leem**, Seungmin Bang

Division of Gastroenterology, Department of Internal Medicine, Yonsei University College of Medicine, Seoul, Korea, Republic of

Background: Pancreatic ductal adenocarcinoma (PDAC) remains a highly lethal malignancy with limited treatment options and a lack of effective molecular targets. Recent studies have highlighted the critical role of epigenetic modifications in the pathogenesis of various cancers.
Methods: To identify targetable epigenetic modifications in PDAC, we analyzed publicly available genomic datasets from pancreatic cancer patients and conducted genomic analysis of pancreatic cancer cell lines and patient-derived cell lines. The functional significance of the identified epigenetic modification was assessed by modulating its expression through DNA demethylation and overexpression experiments.
Results: We found that neurofilament (NEFL) was consistently and significantly downregulated in both pancreatic cancer patients and cell lines. We restored the expression of NEFL by DNA demethylation and overexpression in pancreatic cancer cell lines and found that NEFL overexpression reduced cancer cell proliferation, colony formation, invasion, and migration. Finally, we performed RNA sequencing to analyze the changes in gene expression profiles following NEFL overexpression.
Discussion: Our findings indicate that the epigenetic silencing of NEFL plays a crucial role in pancreatic caner progression. This study highlights the potential of targeted modification of DNA methylation as a promising novel therapeutic strategy for PDAC.
Key words: Pancreatic cancer; Neurofilament; DNA hypermethylation; epigenetic modification.

#5296 Epigenetic and transcriptional drivers of mucinous breast carcinoma.

Lorenzo Ferrando[1], Higinio Dopeso[2], Laxmi Gusain[2], Edaise M da Silva[2], Thais Basili de Oliveira[2], Lounes Djerroudi[3], Hannah Y. Wen[2], Hong Zhang[2], Edi Brogi[2], Richard P. Koche[4], Pierre-Jacques Hamard[4], Larry Norton[5], Jorge S. Reis-Filho[2], Britta Weigelt[2], Fresia Pareja[2]

[1]Department of Internal Medicine, University of Genoa, Genoa, Italy,[2]Department of Pathology and Laboratory Medicine, Memorial Sloan Kettering Cancer Center, New York, NY,[3]Deparment of Pathology, Curie Institute, Paris, France,[4]Center for Epigenetics Research, Memorial Sloan Kettering Cancer Center, New York, NY,[5]Department of Medicine, Breast Service, Memorial Sloan Kettering Cancer Center, New York, NY

Background: Mucinous breast cancer (MucBC) is an uncommon histologic subtype of estrogen receptor (ER)-positive/HER2-negative breast cancer (BC) characterized by tumor cells floating in pools of mucin. In contrast to ER-positive/HER2-negative invasive ductal carcinoma of no special type (IDC-NST), MucBCs harbor fewer *PIK3CA* mutations and typically lack concurrent 1q gains/16q losses. Yet, no pathognomonic genetic alterations have been identified to explain their mucinous phenotype. Here, we sought to determine whether MucBCs might be driven by distinctive epigenetic alterations.

Methods: We analyzed 40 pure MucBCs using genome-wide DNA methylation profiling (n=40) and/or RNA-sequencing (n=27). We evaluated DNA methylation age, epigenetic mitotic score, and integrated methylation-transcriptomic profiles, comparing MucBCs with IDC-NSTs from The Cancer Genome Atlas (TCGA) lacking *PIK3CA* mutations and concurrent 1q gains/16q losses to minimize genetic confounding factors. IDC-NSTs were matched at a 1:1 ratio by menopausal status, ER/HER2 status and histologic grade. The ER-positive/HER2-negative CAMA1, ZR-75-1 and MCF7 breast cancer cell lines were used to interrogate candidate pathways and transcriptomic changes.

Results: Compared to matched IDC-NSTs, MucBCs exhibited accelerated DNA methylation age relative to patient chronological age ($p=0.015$), indicative of epigenetic dysregulation, lower epigenetic mitotic scores ($p=0.0071$), and pronounced global enhancer hypomethylation ($p< 0.001$). Integrated methylation-transcriptome analyses identified *ZBTB20* and *ZNF133* as key transcriptional regulators in MucBCs (FDR < 0.05), as well as significant dysregulation of the TGF-β and estrogen-response pathways (FDR<0.05). In CAMA1 and ZR-75-1 BC cells, pharmacologic inhibition of the TGF-β pathway led to increased expression of mucin-encoding genes (*MUC2*, *MUC20*, *MUCL1*, *MUC5B*), while silencing of *ZBTB20* or *ZNF133* resulted in reduced mucin gene expression. In MCF7 cells, overexpression of ZBTB20 or ZNF133 similarly resulted in upregulation of mucin encoding genes and induced transcriptional changes in the TGF-β pathway, including downregulation of *TGFBR1, TGFB1, SMAD3* and *TRIM33* (*TIF1γ*) and upregulation of ID1, mirroring patterns observed in MucBCs.

Conclusions: MucBC display accelerated DNA methylation age and widespread enhancer hypomethylation, underscoring profound epigenomic dysregulation. Key transcription factors, including *ZBTB20* and *ZNF133*, appear to orchestrate mucin gene expression as well as TGF-β pathway reprogramming, contributing to the mucinous phenotype of MucBC.

#5297 Distinct genomic and pathway-level alterations in early-onset colorectal cancer: A large-scale Korean cohort analysis.

Ah Reum Lim[1], Boyeon Kim[2], Minsoo Kim[3], Soohyeon Lee[4]

[1]Korea University Ansan Hospital, Ansan, Korea, Republic of,[2]Korea University, Seoul,[3]Korea University Anam Hospital, Anam, Korea, Republic of,[4]Korea Univ. Medical Center, Seoul, Korea, Republic of

Background: Early-onset colorectal cancer (EOC) is rising in incidence globally, yet its genomic landscape in Asian populations remains inadequately characterized. Understanding molecular differences between EOC and traditional-onset colorectal cancer (TOC) is essential for clarifying age-related tumor biology.

Patients and methods: Genomic profiles from 1,675 nationwide colorectal cancer patients (2017-2021) were analyzed using targeted next-generation sequencing. EOC was defined as diagnosis at ≤50 years and TOC as >50 years. Mutational frequencies, spectra, pathway enrichment, and co-occurrence patterns were compared between EOC and TOC using R-based pipelines, including Fisher's exact test with FDR adjustment and maftools. Functional and protein-protein interaction analyses (DAVID, Metascape/MCODE) were performed to identify enriched pathways, and HRD-associated genes were additionally assessed for nonsense and frameshift loss-of-function variants.

Results: Among 1,675 patients (428 EOC; 1,247 TOC), EOC showed higher rates of TMB-high tumors (18% vs. 12%, p = 0.009) and MSI-high tumors (5.1% vs. 2.2%, p = 0.003), indicating a greater prevalence of hypermutated phenotypes in younger individuals. EOC also demonstrated higher mutation rates in *SMAD4, FAT3, and KMT2D*, each increased by approximately 3-4% compared with TOC. In contrast, classical colorectal cancer drivers such as *APC, KRAS, TP53*, and *WNT*-related genes were more frequently altered in TOC. In mutational spectrum analysis, EOC exhibited a modestly higher transition-to-transversion ratio, consistent with greater intrinsic genomic instability. Pathway analysis demonstrated enrichment of NOTCH, PI3K, Hippo, TGF-β, cell-cycle, and MYC pathways in EOC, while RTK-RAS and WNT pathways predominated in TOC. Ninety-one genes showed significantly higher mutation frequencies in EOC (FDR < 0.05). Loss-of-function mutations in HRD-related genes (*BRCA1/2, PALB2, RAD51C/D, ATM, CHEK2*) were also more frequent in EOC (11.4% vs. 8%), supporting the greater contribution of homologous recombination defects in early-onset disease. Co-occurrence network analyses revealed EOC-specific clusters involving chromatin remodeling and DNA repair modules, including a dominant DNA repair supercluster ($\log_{10}(P) = -16.5$ to -18.6), alongside enriched epigenetic and transcriptional regulation modules.

Conclusions: EOC exhibits distinct genomic and pathway-level characteristics, including higher genomic instability and enrichment of chromatin remodeling and DNA repair. These findings indicate that EOC represents a biologically unique subtype of colorectal cancer that may benefit from age-specific or HRD-targeted therapeutic strategies. Future work integrating germline sequencing with somatic profiles will help more comprehensively clarify the age-related molecular features of EOC.

#5298 Impact of genomic and clinical factors on therapeutic response to arly-phase epigenetic therapies: An international cohort from two major phase I units.

Manuel Pedregal[1], Harold Nathan Tan[2], Mercedes Avedillo[1], Ignacio Mahillo[3], Ester Garcia[4], Bernard Gaston Doger de Speville[4], Miriam Dorta[4], Jordi Rodon Ahnert[5], Victor Moreno Garcia[4]

[1]START - Madrid - FJD, Madrid, Spain,[2]The University of Texas MD Anderson Cancer Center, Conroe, TX,[3]MADRID - FJD - Unidad de estadistica y epidemiologia., Madrid, Spain,[4]START - Madrid - FJD, MADRID, Spain,[5]UT MD Anderson Cancer Center, Conroe, TX

Introduction: Epigenetic agents—including inhibitors of BET bromodomains, PRMT5, EZH2, and other chromatin regulators—have emerged as promising therapeutic strategies across solid tumors. However, clinical activity remains variable, and robust predictive biomarkers are lacking. We conducted a retrospective two-center analysis to characterize outcomes of patients treated with these compounds in early-phase trials and to evaluate the contribution of next-generation sequencing (NGS) profiles to interpatient variability.

Methods: A total of 262 patients treated within phase I trials of epigenetic agents at two academic early-phase drug development units were included. Clinical data (demographics, tumor type, ECOG status, prior therapies) and NGS results (pathogenic variants, VUS, short variants) were harmonized across centers into a unified dataset. Associations with overall survival (OS) were assessed using two-sided univariable Cox proportional hazards models. Hazard ratios (HR), 95% confidence intervals (CI), proportional hazards assumptions, Akaike Information Criteria (AIC), and C-statistics were reported.

Results: Median age was 59.9 years (IQR 51-69), and 55% were female. Most patients had metastatic disease (88.2%), ECOG 1 (59.2%), prior chemotherapy (78.5%), and prior immunotherapy (70.9%), with a median of 3 prior systemic lines (IQR 1-4). The median number of metastatic sites was 2 (IQR 1-3). Patients received diverse epigenetic compounds, most commonly BET inhibitors (46.6%), PRMT5 inhibitors (22.5%), HDAC inhibitors (14.1%), and EZH2 inhibitors (8.4%), across tumor types including gastrointestinal (21.4%), thoracic (19.8%), CNS (12.6%), and sarcoma/GIST (12.6%). Best overall response included 10% CR/PR (n=21), 39.7% SD (n=104), and 44.6% PD (n=117), reflecting modest clinical activity.In the clinical Cox model, worse OS was associated with higher metastatic burden (HR 1.19; 95% CI, 1.08-1.32; p<0.001), prior chemotherapy (HR 1.64; 95% CI, 1.17-2.31; p=0.004), and increasing prior lines (HR 1.05; 95% CI, 1.00-1.11; p=0.044). Age was also statistically significant (HR 0.99; 95% CI, 0.98-1.00; p=0.029). In the genomic Cox model, short EGFR variants were significantly associated with worse OS (HR 2.74; 95% CI, 1.36-5.52; p=0.005). Other alterations, including pathogenic EGFR mutations (HR 1.83; p=0.065), ATM (HR 3.00; p=0.066), and ASPM (HR 0.29; p=0.087) variants showed non-significant trends.

Conclusions: Epigenetic therapies showed modest activity in this heterogeneous early-phase cohort. Clinical factors—but not individual genomic alterations—were modestly prognostic for survival. These findings underscore the need for integrated
biomarker approaches beyond single-gene predictors to optimize patient selection in epigenetic drug development.

#5299 Epigenetic modulation by MDM2 and DNMT inhibitor promotes cell cycle arrest and programmed cell death in neuroblastoma cells.

Sruthika Talanki[1], Helen Le[2], Aashi Chhabra[3], Rhea Hede[4], Jose Nazario[5], Pragya Srivastava[2], Greeshma Davu[2], Shyam Jaganathan[5], Umamaheswari Natarajan[6], Appu Rathinavelu[5]

[1]Rumbaugh Goodwin Institute for Cancer Research, College of Psychology, Nova Southeastern University, Fort Lauderdale, FL,[2]Rumbaugh Goodwin Institute for Cancer Research, Halmos College of Arts and Sciences, Nova Southeastern University, Fort Lauderdale, FL,[3]Rumbaugh Goodwin Institute for Cancer Research, Kiran C. Patel College of Osteopathic Medicine, Nova Southeastern University, Fort Lauderdale, FL,[4]Rumbaugh Goodwin Institute for Cancer Research, Kiran C. Patel College of Osteopathic Medicine, Hochberg-Miniaci Razor's Edge Research Scholars Program, Nova Southeastern University, Fort Lauderdale, FL,[5]Rumbaugh Goodwin Institute for Cancer Research, Barry and Judy Silverman College of Pharmacy, Nova Southeastern University, Fort Lauderdale, FL,[6]Rumbaugh Goodwin Institute for Cancer Research, Halmos College of Arts and Sciences, Barry and Judy Silverman College of Pharmacy, Nova Southeastern University, Fort Lauderdale, FL

Neuroblastoma isa pediatricmalignancythat affects childrenmostly under the age of 5 yearsold. Thismalignancyoriginatesfrom neural crest cells (called neuroblasts) that can be found inthe adrenal glands, neck, chest, or pelvicareas. Although varioustreatments are availablefortreatingneuroblastoma, experimentaland literatureevidencesuggest that epigeneticmodificationscan triggercell cycle arrest and induceprogrammed cell death (PCD), such asapoptosis,providinga potentialtherapeuticavenue for achievinggreater success duringneuroblastoma treatments. Our study investigatedwhether the MDM2 and DNMT inhibitorscould block DNMTs, and concurrently upregulate TET and p21, to inducecell cycle arrest andapoptoticcell death inIMR-32 and SK-N-AS cells. To assess the effects of RG-7388, CM-272,and SGI-1027, the neuroblastoma cells were treated for 24 hrs, then qRT-PCR analyses wereconducted to evaluate the gene expressionlevels of DNMT-1, DNMT-3A, DNMT-3B, G9a,EZH2, TET-2, TET-3, MDM2, p53, p21, and PARP. In addition,the proteinexpressionlevels ofthe previouslylistedgenes were evaluated through western blot methods to quantifythe changesinepigenetic,cell cycle, and apoptosis-relatedbiomarkers.Interestingly, the qRT-PCR analysisshowed a downregulationof DNMT-1, DNMT-3A, DNMT-3B, G9a, and EZH2 levels intheCM-272 and SGI-1027 treated SK-N-AS cells compared to the control. In both IMR-32 andSK-N-AS cells, the western blot analysisrevealed DNMT-1 downregulation,cleavage of PARP,and upregulationof BAX followingthe drug treatments. So far, our findingsindicatethatRG-7388, CM-272, and SGI-1027 treatments effectivelydownregulate the expressionof DNMTs, whileupregulatingp21 levels inIMR-32 cells, leadingto cell cycle arrest andapoptosis.The abilityof these experimentalcompounds to inducecell cycle arrest and cell deathsuggests that further evaluationof these compounds could lead to the identificationof apromisingtherapeuticagent for treatingaggressiveneuroblastoma.(Thisprojectwas supported by the NationalPediatricCancer Foundation(NPCF) and The RoyalDames of Cancer Research Inc., Ft. Lauderdale, Florida)

#5300 Clinical utility of whole genome sequencing for upfront risk stratification in AML and MDS patients.

Kerry D. Fitzgerald[1], Dennis D. Krutkin[1], Jenny Brouckaert[2], Traci Pawlowski[2], Pratheesh Sathyan[2], James Han[2], Tong Liu[1], Yuanyu Cao[1], Xiaojun Guan[1], Jake Humphrey[3], Grant Hogg[1], John Howitt[3], Amanda Williamson[3], Shakti Ramkissoon[3], Marcia Eisenberg[3], Brian Caveney[3], Eric A. Severson[3], Eyad Almasri[1], Jonathan Williams[1], Taylor J. Jensen[3]

[1]Labcorp, Inc., San Diego, CA,[2]Illumina, Inc., San Diego, CA,[3]Labcorp, Inc., Durham, NC

Acute Myeloid Leukemia (AML) and Myelodysplastic Syndromes (MDS) are hematologic malignancies that require a quick and accurate risk stratification for guiding treatment decisions. In this study, we retrospectively assessed the accuracy and utility of Whole Genome Sequencing (WGS) using clinical samples previously tested at Labcorp with FISH, Chromosomal banding, microarray, single gene molecular technologies, and/or NGS. Samples were selected based on presence of structural variants (SVs), Copy Number Variants (CNVs), or clinically significant mutations e.g. FLT3-ITD, and included controls and healthy donors. 90 total samples were included with 74 suspected of having AML/MDS. To determine WGS performance, all available clinical testing results were leveraged; samples were also assayed on Labcorp's 141 gene pan-heme NGS assay that reports somatic small variants when VAF >3%, as well as 16 CNVs. Sensitivity and specificity were calculated for single nucleotide variants (SNVs), indels, and CNVs overlapping the pan-heme NGS panel, as well as SVs and CNVs from other clinical testing results. Libraries prepared using Illumina's PCR-free Tagmentation kit were sequenced on a NovaSeq X Plus and analyzed using Illumina's DRAGEN Heme WGS pipeline in Illumina Connected Analytics; variants were scored and interpreted using Illumina Connected Insights. Estimated TAT: 67 hours per batch of 15 samples before director review and sign out. Mean genomic coverage for the cohort was 160X. Excluding events with FISH probe positivity <10%, WGS detected 116/121 SVs and 122/127 CNVs identified by cytogenetic/FISH analysis (sensitivity 0.96 and 0.98, respectively). The comparator targeted NGS assay averages 400X read depth. WGS detected 426/427 (.998) variants >10% VAF and 441/447 (.989) variants >5% VAF. Additional clinically relevant findings were identified with WGS in regions not covered by the comparator assays. Calculating performance for reportable SNVs >10% we observed a positive predictive value (PPV) of 100% with no known false positives (FPs). SV and CNV false negatives (FNs) were driven by variants below the Limit of Detection (LOD) expected for WGS. SNV FPs and FNs were from minor fluctuation between the two methods near the performance threshold. Using the Platinum Genome Cell line NA12878 and healthy donors, specificity was 100% with no FPs detected across 11 replicates and 9 individuals evaluating SNVs/indels within the pan-Heme ROI. Utilizing a WGS approach we observed increased sensitivity compared to similar previously reported studies, likely resulting from improved technology and increased sequencing depth. Compared to current laboratory assays WGS has comparable accuracy, sensitivity, and specificity, with additional benefits in clinical utility, cost reduction, improved workflow, TAT, and robustness.

#5301 Evaluating the molecular landscape of genetic mutations among Black patients with acute myeloid leukemia.

Eno-obong B. Udoh[1], Xiaoying (Nicole) Chen[2], Sarah J. Philip[3], Yazeed Sawalha[4], Yazan F. Madanat[5], Ameera Rose[6], Teodora Kuzmanovic[6], John C. Molina[7], Moaath K. Mustafa Ali[7], Akriti G. Jain[7], Abhay Singh[7], Sophia Balderman[7], Babal Kant Jha[8], Ronald Sobecks[7], Betty K. Hamilton[7], Sudipto Mukherjee[7], Aaron Gerds[7], Hetty Carraway[7], Jaroslaw P. Maciejewski[8], Mikkael Sekeres[9], Anjali Advani[7]

[1]Cleveland Clinic Lerner College of Medicine, Cleveland, OH,[2]Department of Quantitative Health Sciences, Cleveland Clinic Lerner Research Institute, Cleveland, OH,[3]Division of Medical Oncology & Malignant Hematology, Houston Methodist Hospital, Houston, TX,[4]Division of Hematology, The Ohio State University, Columbus, OH,[5]Harold C. Simmons Comprehensive Cancer Center, UT Southwestern Medical Center, Dallas, TX,[6]Cleveland Clinic Foundation, Cleveland, OH,[7]Department of Hematology and Medical Oncology, Cleveland Clinic Taussig Cancer Institute, Cleveland, OH,[8]Department of Translational Hematology and Oncology Research, Cleveland Clinic Lerner Research Institute, Cleveland, OH,[9]Sylvester Comprehensive Cancer Center, University of Miami Miller School of Medicine, Miami, FL

Introduction: Acute myeloid leukemia (AML) is an aggressive blood cancer driven by genetic changes that disrupt hematopoiesis. It is characterized by poor survival, with two-thirds of patients dying within 5 years. Non-Hispanic Black patients with AML have higher mortality rates compared to White patients despite favorable disease factors like low-risk cytogenetics and younger age. Risk stratification in AML has been greatly improved by the inclusion of tools such as next generation sequencing (NGS) in the prognostication of AML. However, little is known about the molecular landscape and prognostic relevance of mutations in Black patients with AML. This study characterizes the genetic profiles of Black patients with AML at the Cleveland Clinic.

Method: This retrospective, single-center, cohort study included patients diagnosed with AML between 2002 and 2022. Clinical data were obtained from electronic medical records and stored securely. Molecular data were obtained from NGS platforms of genes frequently mutated in AML. Overall survival (OS) was limited to patients receiving intensive induction chemotherapy and estimated using Kaplan-Meier method.

Results: Overall, there were 118 (9.34%) Black patients among our cohort of 1,264 AML patients. 55% of these patients were male and the median age at diagnosis was 62 years. Karyotype analysis revealed that majority (68%) of Black patients had an abnormal karyotype driven by trisomy 8 (23.0%), -7 or del (7q) (17.6%), or -5 or del (5q) (16.2%) abnormalities, of which the latter two represent adverse risk disease. Most of these patients (65%) were treated with intensive induction chemotherapy and of these 30% (n=23) underwent a bone marrow transplant. NGS was available for 49.1% (n = 58) of Black patients and revealed a predominance of mutations in genes involved in DNA methylation: *DNMT3A* (24%, n=14) and *TET2* (21%, n=12). Median OS was 24 months (95% CI: 14-46months) with a 5-year OS rate of 27% (95% CI:18-40%), lower than the national average of 32.9%. Older age (>60), poor risk cytogenetics, non-intensive chemotherapy, *TET2*, and *ASXL1* were associated with worse survival in univariable analysis ($p<0.05$). Upon adjusting for prognostic variables, only poor risk cytogenetics remained significant ($p=0.02$).

Conclusion: *DNMT3A* and *TET2* mutations were most observed in Black patients with AML in this cohort at similar frequencies compared to population studies. These genes are observed in clonal hematopoiesis indicating early events in leukemogenesis. Their prognostic significance remains undefined but may inform future studies addressing outcome disparities through better risk stratification and the development of targeted therapies. Study limitations include small sample size, NGS availability and self-reported race/ethnicity. Comparative analysis with White patients and prospective studies with genetic ancestry testing are needed.

#5302 Defining the landscape of TP53 mutations in acute myeloid leukemia.

Joseph Stenberg[1], Jordan Redemann[1], Jessica Lewis-Gonzalez[2], Rama Gullapalli[1], Charles Foucar[2]

[1]Department of Pathology, University of New Mexico, Albuquerque, NM,[2]Department of Hematology and Oncology, University of New Mexico, Albuquerque, NM

Background and Objective: The *TP53* gene is one of the most frequently mutated genes in human cancers. *TP53* mutations can be classified as functional, partially functional, or nonfunctional. In gynecologic cancers, this information has been used to identify patients who are sensitive to bevacizumab and has led to the exploration across multiple cancer types of "p53 reactivators" to restore normal p53 activity. In myeloid neoplasms, the 10 most commonly mutated amino acid residues account for 30% of all *TP53* mutations, all located within the DNA-binding domain. However, protein functionality has not been sufficiently described in the context of acute myeloid leukemia (AML). The main goal of this study is to analyze the functional classification of *TP53* mutations in AML.
Methods: *TP53*-mutated AML cases were identified by searching for "TP53" in next-generation sequencing reports within TriCore Reference Laboratories' laboratory information system. Cases were individually reviewed to include those with an AML diagnosis (n=76) and those treated at the University of New Mexico (UNM) (n=12). Molecular, cytogenetic, histologic findings, laboratory values, and clinical data were collected and recorded in REDCap, a secure translational research database. The National Cancer Institute's TP53 Database was used to classify *TP53* mutations and assign functional classifications.
Results: Of the 76 patients, 43 had a single *TP53* mutation and 21 had two or more *TP53* mutations. A total of 89 *TP53* mutations were identified, including 68 non-functional mutations, five partially functional mutations, one functional mutation, and 15 unclassified mutations. Twelve patients (12/76) received treatment at UNM and had additional cytogenetic and prognostic data. Seven patients (7/12) had a complex karyotype, and six patients (6/12) had chromosome 17 alterations at diagnosis. 11 patients (11/12) had non-functional or unclassified *TP53* mutations. These patients had a median overall survival of 6.4 months. A single patient (1/12) was found to have a functional *TP53* mutation and is currently alive 17.6 months after diagnosis.
Conclusion: Our findings indicate that a majority of patients diagnosed with *TP53*-mutated AML have non-functional mutations. However, a single patient with a functional *TP53* mutation showed a significantly better clinical course. Further subclassification of *TP53* mutation functionality may be necessary for accurate prognosis predictions and for novel therapeutic approaches.

: Liquid Biopsies: Circulating Nucleic Acids 4
Poster Session

#5306 Transcriptomic analysis of small extracellular vesicles in metastatic breast cancer.

Emmanuel Acheampong[1], Tumisang Ntereke[1], Katie Dixon[1], Karen Page[1], Shradha Bhagani[1], Naila Abid[1], Marc Wadsley[1], Rebecca Allsopp[1], Charles Coombes[2], Jacqui Shaw[1]

[1]University of Leicester, Leicester, United Kingdom,[2]Imperial College, London, United Kingdom

Introduction: Small extracellular vesicles (sEVs) are emerging as a valuable liquid biopsy tool for cancer, complementing cell-free DNA and circulating tumour cells. These nanoscale, membrane-bound particles, secreted by all cell types, carry DNA, RNA, proteins, and lipid cargo that reflect their cellular origin. sEV-RNAs are implicated in cancer progression, metastasis, and therapeutic resistance. We demonstrate a workflow for isolating sEV-RNAs from plasma for RNA sequencing.
Methods: We used sensitive MCF7 and fulvestrant-resistant MCF7 (FULVR-MCF7) breast cancer cell lines to optimise a workflow that combines ExoGAG technology for EV isolation with the Ion AmpliSeq™ Transcriptome gene expression kit (AmpliSeq™) for profiling sEVs on the Ion Torrent S5XL system. AmpliSeq™ detects 20,802 mRNA targets from low RNA inputs, making it suitable for analysing the limited RNA from sEVs. The ExoGAG-AmpliSeq™ workflow was validated using sEV-RNA samples from the plasma of 5 patients with metastatic breast cancer (mBCa) and 3 healthy female controls.
Results: Evaluation of different cell line RNA concentrations (500pg - 10ng) demonstrated that a 1ng RNA input yielded robust sequencing output, with high mapped reads and accurate measurement of AmpliSeq target regions and gene detection comparable to the standard 10ng input. We then applied the workflow to compare ExoGAG-isolated sEV-RNA from exosome-depleted FBS cell culture medium of MCF7 and FULVR-MCF7 cell lines using 1ng RNA input. All samples met library quality control metrics, and sequencing yielded an average of 12 million reads per sample. Technical replicates of MCF7 and FULVR sEVs RNA samples showed minimal variation in raw gene read counts (Pearson's $r \geq 0.95$). Differential gene expression analysis using DESeq2 identified 1331 significantly differentially expressed genes (FDR < 0.05), with 680 upregulated and 651 downregulated. Gene Ontology analysis indicated downregulation of sensory perception and metabolite transport pathways, and upregulation of antiviral and immune signalling pathways, including type I interferon and lymphocyte activation. These findings highlight altered intercellular communication associated with drug resistance. In the mBCa patient samples, 248 genes showed significant expression changes, with 83 upregulated and 165 downregulated relative to healthy controls. HLA-B and ENPP1, both associated with EV and exosome biology, and AGAP2, linked to endosomal trafficking for vesicle formation, ranked among the top 10 significant genes. Pathway analysis showed these genes were significantly enriched in biological pathways involved in system development, intracellular signal transduction, and regulation of cellular processes.
Conclusions: The ExoGAG-AmpliSeq™ workflow is feasible for recovering and analysing plasma-derived sEV-RNA and developing gene signatures as breast cancer biomarkers.

#5307 Analytical performance of an ultrasensitive whole genome sequencing assay for molecular residual disease detection.

Andrew Georgiadis[1], Christopher Greco[1], Cynthia Maddox[1], Paul McGregor[1], Cesar Nalvarte[1], Kaitlin Victor[1], Amanda Harvey[1], Shelby Bain[1], Robert Summersgill[1], Ana Perez-Lebron[1], Liam Cox[1], Stephen Higgings[1], David Riley[1], Samuel Angiuoli[1], Marcia Eisenberg[2], Brian Caveney[2], Eric Severson[2], Taylor J. Jenson[2], Shakti Ramkissoon[2], Mark Sausen[1]

[1]Laboratory Corporation of America, Baltimore, MD,[2]Laboratory Corporation of America, Durham, NC

In non-metastatic cancers after curative intent intervention, a significant subset of patients retain tumor cells which can lead to disease recurrence. These residual tumor cells can be detected through ultra-sensitive circulating tumor DNA (ctDNA) assays and reported as molecular residual disease (MRD). The most common approaches generally utilize patient-specific, bespoke panels, which have extended turnaround times for initial testing and relatively high cell-free DNA (cfDNA) input requirements. Here we present a non-bespoke approach based on whole genome sequencing (WGS), which leverages native duplex error correction using the Ultima Genomics (UG) sequencing platform for rapid turnaround times for initial testing with low cfDNA input. Specifically, patient tumor, white blood cell, and plasma derived DNA were sequenced to approximately 80x, 30x, and 80x depth, respectively, through a PCR-free WGS workflow on the UG 100 platform. These data were demultiplexed and aligned on-instrument to the hg38 human reference genome. Paired variant calling for matched tumor and white blood cell samples was performed with the UG-adapted DeepVariant algorithm, and subsequently filtered to retain only tumor-specific single nucleotide variants (SNVs). Plasma variant analyses at those tumor-specific SNV positions were performed to leverage the paired plus-minus sequencing (ppmSeq) approach and allowed for ≥Q60 base quality, equating to a theoretical $1x10^{-6}$ error rate. ctDNA status and abundance was then assessed based on the level of the sample-specific machine learning model weighted and normalized signal compared to a reference population of noncancerous donor plasma samples (n=85). We assessed analytical specificity for 120 noncancerous donor plasma samples evaluated against clinical whole-genome somatic mutation profiles and demonstrated a specificity > 99.5%. Analytical sensitivity for ctDNA detection was assessed using five commercially available cell lines across ten levels between 1 - 500 parts per million (ppm) and demonstrated a 95% limit of detection < 5 ppm. Additionally, analytical concordance was evaluated in pre-surgical, treatment naïve plasma samples across a cohort of patients with bladder, breast, colon, and colorectal cancers. Taken together, these data support the significant potential for tumor-informed, non-bespoke MRD approaches for ctDNA detection across a broad range of solid tumor types and curative-intent clinical settings.

#5308 Monitoring treatment response in metastatic breast cancer patients using an mDETECT assay.

Keira Frosst[1], Brooke E. Wilson[2], Katarzyna J. Jerzak[3], Christopher R. Mueller[1]

[1]Queen's University, Cancer Research Institute, Kingston, ON, Canada,[2]Kingston Health Sciences Centre, Kingston, ON, Canada,[3]Sunnybrook Health Sciences Centre, Toronto, ON, Canada

Metastatic breast cancer treatment response is currently monitored with CT-scans every 3-6 months leaving many patients on ineffective therapy while their disease progresses. We have developed the methylation DETEction of Circulating Tumour DNA (mDETECT) assay, a targeted DNA methylation-based Next Generation Sequencing liquid biopsy designed to detect cancer specific DNA methylation patterns. The breast cancer assay targets 60 hypermethylated regions (>400 CpGs), detects all subtypes of breast cancer, is quantitative for molecules of methylated DNA, and shows 93% sensitivity at 100% specificity for TNBC with a limit of detection of 0.025%. It is both tumour and treatment agnostic as well as being compact (2 million sequencing reads per sample) making it ideal for frequent disease monitoring.

We are conducting a prospective multi-centre observational cohort study to monitor metastatic breast cancer patients using the mDETECT liquid biopsy as they undergo treatment. Metastatic breast cancer patients are eligible regardless of subtype or treatment and are followed through treatment changes. 20mL of blood is collected at each standard of care blood draw for up to 3 years. Patients are assessed for response to treatment and monitored for disease progression.

Over 120 participants have been enrolled to date with recruitment ongoing, generating over 500 timepoints (0-22 timepoints/patient). Initial patients with completed longitudinal timepoints have been assessed using the mDETECT assay. Although complete clinical and radiological outcome data are not yet available, early molecular results show decreasing mDETECT levels during treatment and increasing levels prior to treatment change or disease progression.

These preliminary findings demonstrate the potential of methylation-based monitoring for metastatic breast cancer patients, a key clinical need as there are many therapy options available and complex treatment sequence decisions to be made. We will evaluate whether specific mDETECT trajectories predict disease progression and durable treatment response. Ongoing follow-up and integration of radiology data will further assess the predictive value of mDETECT in monitoring metastatic breast cancer.

The mDETECT assay may allow for more timely treatment decision-making in metastatic breast cancer, improving outcomes and reducing prolonged exposure to ineffective therapy.

#5309 Baseline ctDNA profiling identifies molecular predictors of resistance to second-generation ALK inhibitors in EML4-ALK-positive NSCLC.

Emma Roger Sonderbek[1], Maiken Parm Ulhoi[2], Peter Meldgaard[2], Boe Sandahl Sorensen[2]

[1]Aarhus University, Aarhus, Denmark,[2]Aarhus University Hospital, Aarhus, Denmark

Introduction: Lung cancer remains the leading cause of cancer-related death worldwide. Although tyrosine kinase inhibitors (TKIs) have improved outcomes for EML4-ALK-positive non-small cell lung cancer (NSCLC), most patients experience disease progression. Understanding the clinical and molecular factors that drive resistance is essential for guiding more effective treatment strategies.
Aim: To identify molecular features associated with treatment resistance and survival in patients receiving first-line alectinib or brigatinib.
Patients and Methods: Seventy-two patients with EML4-ALK-positive NSCLC treated with first-line alectinib or brigatinib were included. Plasma samples were obtained at baseline, during treatment, and at disease progression. Circulating tumor DNA (ctDNA) was analyzed using cancer personalized profiling by deep sequencing (CAPP-seq) and the R/Bioconductor package, *DNAfusion*, recently developed in our lab. ctDNA features at progression and at baseline were correlated to time to progression (TTP) and overall survival (OS).
Results: During a median follow-up of 27 months, 54% (39/72) of patients developed disease progression. *ALK* on-target resistance mutations at progression were observed exclusively in short EML4-ALK variants (40% vs 0% in long variants, $p<0.05$). Patients with short variants also had numerically shorter TTP (14 vs 35 months, $p=0.12$) and OS (38 months vs NE, $p=0.16$). Baseline ctDNA profiles were analyzed to assess associations with clinical outcomes. Patients with a high plasma mutation load (>1 mutation) had significantly shorter TTP (13 vs 51 months, $p<0.05$) and OS (36 months vs NE, $p<0.05$) compared with those with a low load (0-1 mutation). In addition, *TP53* mutations were strongly associated with poor outcomes (TTP: 10 vs 45 months, $p<0.05$; OS: 12 months vs NE, $p<0.05$).
Conclusion: Development of *ALK* on-target resistance mutations at progression demonstrates a significant association with short EML4-ALK variants. A high mutation load and *TP53* mutations at baseline identify patients at risk of early progression and poor survival under second-generation ALK TKI treatment. These findings suggest that ctDNA-based molecular profiling may help guide personalized treatment strategies and improve survival outcomes for EML4-ALK-positive NSCLC.

#5310 Dynamic changes in ctDNA methylation predict early response to immunotherapy in advanced esophageal cancer.

Hui Zhang#[1], Yu Lang#[1], Yaping Dong#[2], Wei Li#[3], Jialin Lin[4], Lu Yang[5], Jiapeng Kang[6], Wenqiang Yu*[7], Changshun Yang*[8], Jingxun Wu*[1], Qiyuan Li*[9], Feng Ye*[1], Weiwei Tang*[1]

[1]Department of Medical Oncology, The First Affiliated Hospital of Xiamen University, School of Medicine, Xiamen University, The School of Clinical Medicine of Fujian, Medical University, Xiamen, China,[2]Department of research and development，Shanghai Epiprobe Biotechnology Co.,Ltd, Shanghai, China,[3]Fudan University Shanghai Cancer Center, Department of Radiotherapy, Shanghai Medical College, Fudan University, Shanghai, China,[4]Department of Medical Oncology, National Cancer Center/National Clinical Research Center for Cancer/Cancer Hospital, Chinese Academy of Medical Sciences and Peking Union Medical College, Beijing, China,[5]Department of Medical Oncology,Weifang people's Hospital, Weifang Medical University, Weifang, China,[6]Department of Medical Oncology, Zhangzhou Municipal Hospital, Zhangzhou Municipal Hospital Affiliated of Fujian Medical University, Zhangzhou, China,[7]Shanghai Public Health Clinical Center and Department of General Surgery, Huashan Hospital, Institutes of Biomedical Sciences, Shanghai Medical College, Fudan University, Shanghai, China,[8]Department of Surgical Oncology, Fujian Provincial Hospital, Fuzhou, China,[9]Department of Hematology, The First Affiliated Hospital of Xiamen University and Institute of Hematology, School of Medicine, Xiamen University, Xiamen, China

Background: Immune checkpoint inhibitors (ICIs) improve the prognosis of advanced esophageal cancer (ESCA), yet accurate response prediction remains challenging. Traditional biomarkers and imaging often lack timely reflection of disease progression. Circulating tumor DNA (ctDNA) methylation offers novel, non-invasive, real-time monitoring. In this study, we evaluated the early dynamic ctDNA methylation changes in advanced ESCA and predicted ICI response and survival.

Methods: This observational exploratory study enrolled advanced ESCA patients on ICI treatment.Peripheral blood samples were collected at baseline and regularly throughout treatment.Plasma ctDNA was subjected to methylation sequencing. Patients were stratified into "decreased" (methylation score reduction from baseline) and "non-decreased" (stable or increased scores) groups based on dynamic changes. Kaplan-Meier and log-rank tests assessed methylation score dynamics' association with progression-free survival (PFS) and overall survival (OS). Consistency between ctDNA dynamics and imaging efficacy (RECIST 1.1) was also evaluated.

Results: Baseline ctDNA methylation levels did not significantly correlate with outcomes (p=0.1); however,dynamic changes were strongly prognostic. The "decreased" group demonstrated significantly longer PFS (26.0 vs. 15.85 months; p<0.05) and median OS (35.0 vs. 27.0 months; p=0.01) compared to the "non-decreased" group. CtDNA-defined response occurred significantly earlier than radiological response (1.55 vs. 4.0 months, p<0.05). Median time to ctDNA-defined progression (2.52 vs. 4.0 months) also preceded imaging progression, without statistical significance (p=0.15).

Conclusion: Dynamic ctDNA methylation monitoring presents a promising non-invasive approach for assessing ICI efficacy in advanced ESCA. A reduction in post-treatment ctDNA methylation levels significantly correlated with prolonged survival. ctDNA dynamics enabled earlier prediction of treatment response and progression than radiological assessment, highlighting its potential for timely detection. These findings underscore the value of dynamic ctDNA methylation analysis as a novel early efficacy marker.

#These authors contributed equally: Hui Zhang, Yu Lang,Yaping Dong,Wei Li

*Correspondence to:Dr. Weiwei Tang, weiweitang008@xmu.edu.cn;Dr. Feng Ye, yefengdoctor@xmu.edu.cn;Dr. Qiyuan Li, qiyuan.li@xmu.edu.cn; Dr.Jingxun Wu,wujingxun@xmu.edu.cn;Dr. Changshun Yang, 282483331@qq.com;Dr. Wenqiang Yu .wenqiangyu@fudan.edu.cn

FUNDING: This study was supported by the National Natural Science Foundation of China (Grant No. 81702414), Natural Science Foundation of Fujian Province of China (Grant No. 2020J05306) and Xiamen Medical and Health Guidance Project (Grant No. 3502Z20244ZD1023).

#5311 Tracking prostate cancer progression by deep whole genome sequencing of primary tumors and longitudinal circulating tumor DNAs.

Samira Rahimirad[1], Eleonora Scarlata[1], Lucie Hamel[1], Seta Derderian[1], Ginette McKercher[1], Fadi Brimo[2], Fred Saad[3], Armen Aprikian[4], Simone Chevalier[1]

[1]Urologic Oncology Research Group, Cancer Research Program, Research Institute of the McGill University Health Center (RI-MUHC), Montreal, QC, Canada, [2]Pathology, McGill University, Montreal, QC, Canada,[3]Surgery, Centre Hospitalier Universitaire de Montreal, Montreal, QC, Canada,[4]Surgery, McGill University, Montreal, QC, Canada

Background: Although prostate cancer (PCa) generally has a high survival rate, some patients develop aggressive disease. Identifying reliable markers of progression and therapeutic response is essential for improving management. Cell-free DNA (cfDNA) in blood provides a minimally invasive means to monitor tumor evolution through liquid biopsy. In this study, we compared primary tumors from severe PCa patients versus long-term disease-free individuals to identify genomic alterations linked to aggressiveness. We also tracked tumor-shared alterations in circulating tumor DNA (ctDNA) and discovered exclusive modifications emerging during progression. Methods: Banked fresh frozen prostate tissues from radical prostatectomy cases (lethal PCa=80, disease-free=35) were processed to identify tumor foci and macro-dissect cores of high cellularity (>75%) for DNA extraction. Serial plasma collections from six lethal cases were used to isolate cfDNA. Sequencing of tumors, matched germline blood DNAs, and cfDNAs was performed to identify copy number variations (CNVs) and mutations. Results: Already established and novel CNVs were found in tumors of both lethal and disease-free cases. Comparing their CNVs showed shared alterations associated with PCa development and disease recurrence, also pinpointing genomic signatures specifically associated with PCa severity. Clinical analysis of lethal cases revealed genomic deletions associated with rapid recurrence, metastases, castration-resistance, and short overall survival. Longitudinal cfDNA analysis unveiled rising ctDNA fractions when patients reached the metastatic and late stages. Although genomic amplifications were rare in primary tumors, they were common during progression. Tumor-shared alterations were found in the ctDNA during progression, along with newly discovered ctDNA-exclusive modifications. Furthermore, clonal ctDNA alterations became sub-clonal during treatment and re-emerged in the blood two years later in relation to treatment resistance. Evidence of tumor-shared and unique clonal evolutions was identified in the advanced disease stages, speaking for intra-tumoral and metastatic cellular heterogeneity. Conclusion: The identification of novel genomic changes in tumor DNA and ctDNAs in advanced disease is enhancing our knowledge of PCa severity. Findings on ctDNA underscore the significance of longitudinal liquid biopsy for monitoring disease progression. They could contribute to the development of novel diagnostic tests that enable earlier, more effective treatment and ultimately reduce PCa lethality.

#5312 Digital PCR-based plasma DNA methylationassayfor noninvasive molecular subtyping of small cell lung cancer: A prospective feasibility study.

Jin-Soo Kim[1], Mi Young Kim[1], Jeemin Yim[2], Yun Young Lee[3], Joon An[3], Jinil Han[3], Ji Eun Kim[2], Youngho Moon[3]

[1]Internal Medicine, Seoul Metropolitan Government Seoul National University Boramae Medical Center, Seoul, Korea, Republic of,[2]Pathology, Seoul Metropolitan Government Seoul National University Boramae Medical Center, Seoul, Korea, Republic of,[3]Gencurix, Inc., Seoul, Korea, Republic of

Background: Small cell lung cancer (SCLC) is an aggressive neuroendocrine tumor with limited treatment options and poor survival outcomes. Although recent studies highlight the clinical relevance of molecular subtypes for therapeutic stratification, tissue-based subtyping is often infeasible because most patients receive chemotherapy rather than surgical resection. This study aimed to develop and clinically evaluate a digital PCR assay for subtype-specific methylation profiling using plasma samples.
Methods: Twenty patients with pathologically confirmed SCLC were prospectively enrolled at Seoul National University Boramae Medical Center from April 2023 to September 2025. Plasma samples were collected prior to systemic therapy, and molecular subtypes were classified as NEUROD1-type (N-type; n = 1), ASCL1-type (A-type; n = 16), POU2F3-type (P-type; n = 3), or SCLC-I type (I-type; n = 0). Plasma-derived molecular subtypes determined by the digital PCR-based methylation assay were compared with these clinical classifications.
Results: Subtype-associated methylation markers were identified through integrative analysis of publicly available methylation array and expression datasets from the National Cancer Institute Small Cell Lung Cancer Screening Project. These candidate loci were integrated into a 4-plex digital PCR assay, which demonstrated clear subtype-enriched methylation patterns across representative SCLC cell lines. In 20 prospectively collected plasma samples, all targets were successfully quantified with sufficient clinical performance. Plasma-derived molecular subtypes showed overall concordance of 85.0% (17/20) with clinical classifications, with detection sensitivities of 100.0% (1/1) for N-type, 87.5% (14/16) for A-type, and 66.7% (2/3) for P-type cases. These findings support the feasibility of plasma-based methylation profiling for noninvasive SCLC molecular subtyping.
Conclusion: This study demonstrates the feasibility of using a digital PCR-based methylation assay to classify SCLC molecular subtypes from plasma. Larger validation cohorts are warranted to refine cutoffs and confirm clinical utility.

#5313 Fragmentomic analysis of cfDNA WGS at regulatory regions generates gene-level expression-like traits for subtype analysis in breast cancer.

Jonathan H. Shepherd[1], Jeff Burdine[1], Yoichiro Shibata[1], Gregory M. Mayhew[1], Gabe Milburn[1], Michael V. Milburn[1], Matthew LaBella[2], Shalee Killpack[2], Kirk L. Pappan[1], **James M. Davison**[1], Kirk Beebe[1]

[1]GeneCentric Therapeutics, Inc., Durham, NC,[2]Myriad Genetics, Salt Lake City, UT

Introduction: Analysis of cell-free DNA (cfDNA) from liquid biopsy provides a rapid, repeatable, and non-invasive means to study tumor biology. In breast cancer, invasive tissue biopsies and immunohistochemistry (IHC) remain the standard for determining molecular subtype and treatment selection. However, fragmentomic analysis of cfDNA whole genome sequencing (WGS) can yield biologically meaningful surrogates of tumor transcriptional states through its relationship with nucleosome positioning. Here, we describe a WGS-based fragmentomic pipeline that recapitulates gene-level, expression-like traits from cfDNA. These traits enable the development of fragmentomic classifiers reflective of tissue expression markers such as hormone receptor and HER2.

Experimental Procedures: Matched FFPE tumor blocks and plasma samples from 25 consenting patients with breast cancer were analyzed. Plasma cfDNA underwent WGS to 30-40× depth, and matched FFPE RNA was profiled by RNA sequencing. cfDNA reads were processed through a fragmentomic pipeline quantifying fragment size and coverage properties across predefined regulatory regions assigned to nearby genes. Gene-level expression from RNA-seq was analyzed and established breast cancer molecular subtype classifiers were applied. Fragmentomic signals were correlated with RNA expression for the same genes. Samples were split into training (n = 17) and test (n = 8) sets, and features with Pearson correlation > 0.4 were used in an elastic net model to predict *ESR1* expression from cfDNA fragmentomic data.

Results: The elastic net model's predicted *ESR1* score showed a Spearman correlation of 0.99 ($p = 0.003$) in the training set and 0.64 ($p = 0.10$) in the test set. Heatmaps of fragmentomic signal at model-selected regions mirrored corresponding RNA-seq expression patterns. Genes identified by the model included *DLG5* and *MTUS1* (both upregulated in samples with high *ESR1* expression), and *SMC4* (downregulated in samples with high *ESR1* expression), consistent with known ER-associated biology.

Summary and Conclusions: These findings demonstrate that cfDNA fragmentomic patterns derived from high-depth WGS can recapitulate gene-level, expression-like traits reflective of tumor biology in breast cancer. Integrating regulatory-region fragmentomics with expression-informed modeling enables non-invasive inference of molecular phenotypes such as estrogen receptor status directly from plasma. The deep WGS data, supported by RNA-seq, could also be leveraged to define target regions to enable gene-level expression fragmentomics in targeted hybrid capture panels. This approach highlights the potential of cfDNA fragmentomics as a surrogate for tissue-based transcriptomic and IHC profiling, supporting development of liquid biopsy-based classifiers for breast cancer subtyping and therapeutic stratification.

#5314 Combining gene expression and mutation profiling in a single cfDNA assay through the addition of a custom hybrid capture panel targeting gene regulatory regions to a commercial CGP panel.

Gregory M. Mayhew[1], Jonathan H. Shepherd[1], Yoichiro Shibata[1], Jeff Burdine[1], Gabriel V. Milburn[1], Kirk L. Pappan[1], Nripesh Prasad[2], Michael V. Milburn[1], **James M. Davison**[1], Kirk Beebe[1]

[1]GeneCentric Therapeutics, Inc., Durham, NC,[2]Discovery Life Sciences, Madison, AL

Introduction: Analysis of cell-free DNA (cfDNA) provides a rapid, repeatable, and non-invasive window into tumor biology, yet tissue biopsies are still often needed for accurate phenotyping and treatment guidance. A liquid biopsy approach that captures both genomic alterations and expression-like features could strengthen patient monitoring and lessen biopsy reliance. Here, we integrate a custom hybrid-capture panel targeting gene regulatory regions with a comprehensive genomic profiling (CGP) panel into a single cfDNA sequencing assay. Our bioinformatic pipeline calculates variant allele frequencies (VAF) and extracts fragmentomic features that reproducibly correlate with gene expression, enabling non-invasive tumor phenotyping.Top of FormBottom of Form

Experimental Procedures: Matched FFPE tumor and plasma samples from 31 breast cancer patients were collected and analyzed, along with 11 additional unmatched plasma samples; all patients provided consent. Plasma cfDNA underwent sequencing in a single assay that integrated custom hybrid-capture baits for regulatory regions of 2,704 genes (2.44 Mb) with a CGP panel covering 562 genes (2.4 Mb). Matched FFPE RNA was profiled by RNA sequencing. cfDNA reads were processed through a multi-omic pipeline for quantifying fragmentomic properties across predefined regions assigned to nearby genes and a gene alteration analysis for VAF. Fragmentomic signals were correlated with RNA expression for the same genes. Association of fragmentomic signal, gene expression, and associated tumor biology was assessed.

Results: Fragmentomic features with high Pearson correlation to matched tissue RNA-seq were observed and were used to train a breast cancer model comprised of 34 features. Model-selected features showed a more distinctly matched correlation structure to breast tumor tissue RNA-seq than did randomly sampled features. Mapping model-selected genes to 31 breast tumor gene expression ontologies showed an enrichment for genes, such as *EZH1*, previously associated with breast cancer. Additional associations with ER status, Ki67%, and HER2 status demonstrated the potential utility of this assay for measuring these markers in blood.

Summary and Conclusions: Our findings show that cfDNA fragmentomic patterns captured using both CGP and custom panels, together with AI modeling, can recapitulate gene-level expression traits and enable tissue-free, plasma-based inference of tumor molecular phenotypes. By integrating fragmentomic signals with standard DNA-alteration profiling, hybrid-capture cfDNA sequencing provides two complementary molecular data layers from the same assay. Combining these capabilities can enhance biomarker discovery and may ultimately support clinical decision-making in precision oncology.

#5315 Analytical precision and cross-platform replicability of cfDNA-based genome-wide multi-feature classifiers for early cancer detection.

Vishruth Girish[1], Alice C. Eastman[1], Adrianna L. Bartolomucci[1], Akshaya V. Annapragada[1], Hope Orjuela[1], Carter Norton[1], Daniel H. Du[1], Sarah Short[1], Christopher M. Cherry[1], James R. White[1], Shashikant Koul[1], Vilmos Adleff[1], Zachariah H. Foda[2], Jillian Phallen[1], Victor E. Velculescu[1], Robert B. Scharpf[3]

[1]The Sidney Kimmel Comprehensive Cancer Center, Johns Hopkins University School of Medicine, Baltimore, MD,[2]Department of Medicine, Johns Hopkins University School of Medicine, Baltimore, MD,[3]Department of Biostatistics, Johns Hopkins University Bloomberg School of Public Health, Baltimore, MD

Introduction: Genome-wide liquid biopsies offer a non-invasive approach to cancer detection, management, and monitoring, and are increasingly being adopted across the cancer care continuum. These approaches interrogate a multitude of genomic features of the cell-free DNA (cfDNA) fragmentome, providing potential performance advantages over traditional imaging and other blood-based biomarkers. As cfDNA-based fragmentome methods move towards clinical deployment, validating their analytical precision and replicability across sequencing platforms is essential to realize their full clinical potential.

Methods: We developed an automation-compatible two-step plate protocol that combines end repair and A-tailing to process 48 samples in parallel. To systematically assess the analytical precision of this protocol, we designed a precision study using large volume (~20 mL) plasma from 12 individuals without cancer and individuals with lung (n=10) or liver (n=2) cancer. Three unique pre-specified plate layouts ensured that there was a minimum of 12 genomic library replicates per donor, with distinct row and column assignments within and between plates. In parallel, cfDNA was processed using our previously published three-step tube protocol, with a minimum of 6 genomic library replicates across three unique tube layouts. Each operator processed two unique plate and two unique tube layouts, with 3 ng input cfDNA for all libraries.

Results: Library yields were higher with the tube-based three-step protocol compared to the plate-based two-step protocol (6.51 nM vs 5.25 nM). Presequencing analyses revealed measurable operator effects in library QC metrics across matched replicates. All libraries were sequenced genome-wide to a mean depth of 1-2x on both the NovaSeq 6000 and NovaSeq X. Post-sequencing, locked computational pipelines for alignment and feature summarization were applied uniformly, generating genome-wide fragmentation in non-overlapping 5 Mb bins via short (100-150 bp) to long (151-220 bp) fragment ratios (S/L ratios), chromosome arm-level measures of aneuploidy, and lung and liver cancer classifier scores. The intra- and inter-batch precision of these features and classifier scores was assessed by implementing a Bayesian hierarchical model using the Stan software.

Conclusions: This study aims to provide a detailed assessment of assay- and platform-driven variability in cfDNA-based features and classifiers. Initial findings support the feasibility of scalable, automation-compatible plate-based protocols, and emphasize the need for robust workflows in clinical implementation. Ongoing analyses will determine the stability of classifier performance across protocol and sequencing platform transitions, informing best practices for evolving liquid biopsy technologies.

#5316 Analytical validation of SPIRAL: An integrated genomic and epigenomic liquid biopsy assay.

Lei Wang, Peiru Liu, Chaoran Zheng, Shanshan Yu, Yalan Jin, Fujun Qiu, Bo Yang, Yuan Sun, Xiaotian Wang, Shuailai Wu, **Zhihong Zhang**

Burning Rock Dx, Guangzhou, China

Introduction: Genomic and epigenomic alterations serve as key biomarkers for tumor detection, yet conventional approaches require separate workflows and DNA inputs for each signal type, which is impractical when sample quantity is limited. Because tumor initiation and progression arise from coordinated genomic and epigenomic dysregulation, simultaneous assessment of both layers is critical for accurate tumor classification, mechanistic insight, and clinical decision-making. Genomic profiling captures oncogenic drivers such as mutations, copy number alterations, and fusions, whereas epigenomic features—particularly DNA methylation—provide complementary information on histological subtype, gene regulation, prognosis, and tumor burden. To address the limitations of segregated assays, we developed SPIRAL (Single Portion Input Resourceful Assay of Liquid biopsy), an integrated multi-omics method that generates genomic and methylation libraries from the same DNA aliquot. Here, we present a preliminary evaluation of SPIRAL in a liquid biopsy setting, demonstrating its ability to concurrently profile genomic and epigenomic signals from a single blood-derived DNA sample.

Results: Analytical validation of SPIRAL was conducted using both cell line-derived and clinical samples. For genomic detection, the observed LoD95 was 0.8% for SNVs/indels (0.3% for hotspot variants), 0.3% for fusions, 20% tumor fraction for CNAs at six copies, 30% tumor fraction for homozygous deletions, and 1% tumor fraction for MSI. For epigenomic analysis, the LoD95 for global methylation was 5×10^{-5} in cell lines and 1×10^{-4} in clinical samples, with a limit of quantitation of 0.05% and a specificity of 98% in clinical samples. The LoD for promoter methylation was 1%.

Conclusion: SPIRAL is a liquid biopsy technology capable of simultaneously profiling genomic and epigenomic alterations from the same portion of cfDNA. In addition to comprehensive genomic profiling, it enables tissue-free MRD detection, therapy-response monitoring through tumor-fraction quantification, tumor subtyping, and broader phenotypic characterization. This integrated approach provides a robust platform for biomarker discovery and has the potential to substantially advance precision cancer management.

#5317 Evaluation of circulating tumor DNA as a biomarker for early relapse detection and molecular profiling in patients with high-risk neuroblastoma.

Natalia Wojciechowska[1], David Farbo[1], **Tiffany Duque**[2], Angela Brentlinger[1], Chelsee Greer[1], Anish Ray[1]

[1]Cook Children's Medical Center, Fort Worth, TX,[2]University of North Texas Health Science Center, Fort Worth, TX

Neuroblastoma (NBL) is the most common extracranial solid tumor of childhood, and nearly half of patients are diagnosed with high-risk disease. Patients with high-risk NBL often present with metastasis and frequently develop drug resistance; the 5-year survival rate is about 50%. Standard diagnostic and surveillance modalities not only involve radiation exposure and possible procedural sedation in pediatric patients, but also lack the ability to effectively monitor genetic evolution and heterogeneity. Circulating tumor DNA (ctDNA) has emerged as a minimally invasive biomarker capable of detecting microscopic disease, offering potential advantages for earlier relapse identification, reduced radiation exposure, and improved accessibility. We conducted a retrospective chart review of 13 patients with high-risk NBL, capturing salient clinical, molecular, diagnostic, and therapeutic information for each patient. Using this data, clinical evaluations of treatment response were recorded according to the revised International Neuroblastoma Response Criteria (INRC). Plasma samples taken in tandem with these evaluations were sequenced, and the ctDNA results were used to examine recurrence-associated ctDNA positivity and explore shared genomic alterations across patients. Additionally, variant information collected from tumor sequencing - performed as part of routine clinical care - was compared to the variants found in ctDNA sequencing. We found that 11 relapse-associated time points had preceding ctDNA measurements; among these, 72% were ctDNA-positive prior to radiographic relapse. Samples positive for ctDNA, with higher variant allele frequency (VAF), and with higher tumor fraction (TF) were significantly associated with stable or progressive disease, whereas complete response correlated strongly with samples negative for ctDNA. Progressive disease was associated with increasing VAF and TF, while partial response was associated with decreasing VAF. Six patients had concordant sequencing results; however, ctDNA failed to detect certain key alterations, including HRAS K117N and HGF amplification. Conversely, ctDNA detected several variants not observed in tumor sequencing, including alterations in tumor suppressor genes such as TP53 and CHEK2, as well as a rare germline SMARCA4 Variant of Uncertain Significance (VUS). ctDNA demonstrates promising utility as a non-invasive tool for monitoring treatment response and predicting relapse in high-risk NBL while also showing potential to reveal clinically relevant genetic alterations. Although our interpretation is limited by small sample size, heterogeneous sampling, and analytical bias, these findings support further prospective evaluation of ctDNA as a complementary biomarker to current imaging-based surveillance strategies.

#5318 A low-cost, ultra-fast, low-input amplicon NGS workflow for rapid cancer profiling.

Fang Liu, Kemin Zhou, Pan Du, Binggang Xiang

Predicine, Inc., Hayward, CA

Background: Liquid biopsy-based analysis of cell-free DNA (cfDNA) from plasma and urine has emerged as a powerful, non-invasive strategy for identifying clinically actionable oncogenic mutations. However, rapid and accurate detection of low-frequency variants remains technically challenging, particularly when working with limited input DNA. Predicine has developed an amplicon-based NGS platform to overcome these barriers through high analytical sensitivity, superior error suppression, and an accelerated workflow to support precision oncology applications.

Methods: A streamlined amplicon-based NGS workflow was established for sensitive detection of clinically relevant alterations in *FGFR (16 variants)*, *PIK3CA (62 variants)*, *ESR1 (25 variants)*, *KRAS* (21 variants), EGFR (62 variants) as well as additional variants commonly implicated in breast, prostate, bladder, lung and GIST cancers. The assay leverages Predicine's proprietary error-correction technology to suppress sequencing artifacts and enhance variant-calling accuracy. Sequencing-ready libraries were generated within three hours using a protocol optimized for low-input cfDNA. Analytical performance, including sensitivity and specificity, was systematically evaluated.

Results: This study demonstrated high analytical performance for detecting mutations in FGFR, PIK3CA, ESR1, KRAS, EGFR, and other clinically actionable targets across plasma and urine cfDNA. The streamlined workflow delivered ≥98% uniform coverage and >95% on-target rates across all target regions. Low-frequency variants were consistently detected at allele frequencies as low as ≤0.25% using 30 ng of cfDNA. The assay features a rapid library preparation process with a short hands-on time, enabling sequencing-ready samples to be generated within three hours, further supporting fast turnaround for liquid biopsy analysis. Specificity exceeded 98% in healthy donor cfDNA samples, indicating minimal background noise and low false-positive rates. While the evaluation focused on liquid biopsy specimens, the same rapid and efficient workflow is also compatible with FFPE-derived DNA, extending its applicability to tissue-based mutation profiling.

Conclusions: We report a low-cost, rapid, and high-throughput NGS solution for cfDNA analysis from plasma, urine and FFPE tissue DNA, offering a unified approach for mutation profiling across both liquid biopsy and tissue samples. This flexibility, combined with exceptional sensitivity, minimized error rates, low DNA input requirements, and fast turnaround time, positions this amplicon-based NGS assay as a powerful tool for clinical research, cancer diagnostics, and longitudinal disease monitoring.

#5319 Circulating tumor DNA (ctDNA)-based profiling of acquired resistance to the fibroblast growth factor receptor (FGFR)2/3 inhibitor lavengratinib(ABSK061) in patient(pt)s with advanced solid tumors.

Yue Wang[1], Chunyu Zhou[1], Liyun Zhao[1], Chaoze Cheng[1], Zhixuan Zhu[1], Zishuo Wang[1], Peng Zhang[1], Jing Zhang[1], Hua Zou[1], Jing Ji[1], Hongping Yu[1], Ji Zhu[2], Yan Zhao[3], Dewei Li[4], Yongsheng Li[4], Wei Li[5], Yanru Qin[6], Shujun Yang[7], **Nannan Zhang**[1]

[1]Abbisko Therapeutics, Shanghai, China,[2]Zhejiang Cancer Hospital, Hangzhou, China,[3]Liaoning Cancer Hospital & Institute, Shenyang, China,[4]Chongqing university Cancer Hospital, Chongqing, China,[5]The First Hospital of Jilin University, Changchun, China,[6]The First Affiliated Hospital of Zhengzhou University, Zhengzhou, China,[7]Henan Cancer Hospital, Zhengzhou, China

Background: Aberrant activation of FGFR signaling is implicated in tumorigenesis across multiple cancer types. Lavengratinib, the first-in-class selective FGFR2/3 inhibitor, showed encouraging efficacy and a favorable safety profile as monotherapy in pts with *FGFR2/3* alterations in a phase 1 study (NCT05244551). We used next-generation sequencing (NGS) of ctDNA to define the molecular mechanism of acquired resistance to lavengratinib.

Method: Pts with *FGFR2/3* activating alterations who had progressed on or declined standard therapy, and who had no prior FGFR inhibitor treatment, were treated with lavengratinib. Pts with both baseline and post-progression ctDNA samples were included in the study. Sequential ctDNA profiling (Onco Sonar, Genetron) was performed to compare genomic alterations at baseline and at disease progression.

Result: Seventeen pts with paired baseline and post-progression ctDNA samples were analyzed in this study, containing individuals with cholangiocarcinoma (CCA), gastric cancer (GC), non-small-cell lung cancer (NSCLC), cervical cancer and urothelial carcinoma. All the pts initially achieved an objective response or stable disease before developing progression. Seven pts acquired one or more secondary mutations in the kinase domain of FGFR2 or FGFR3. In *FGFR2*-altered pts, 15 residues in FGFR2 kinase domain were found mutated at the time of resistance to lavengratinib. The molecular brake residue N549 was the most frequently affected site. Additional recurrent mutations involved L617, the molecular brake residue E565 and the gatekeeper residue V564, particularly in *FGFR2*-amplified GC and CCA with *FGFR2* fusion. These putative cases of *FGFR2* acquired resistance in GC were consistently polyclonal, a pattern also commonly observed in CCA. In one cervical cancer pt with *FGFR3* S249C, an emergent *FGFR3* M528I was detected at progression. In contrast, *FGFR2*-altered NSCLC was prone to develop acquired alterations in genes involved in RTK/RAS pathways other than *FGFR2*, suggesting the resistance mainly driven by bypass mechanisms in this indication. Moreover, *ATM*, a key gene in the DNA damage response (DDR) network, exhibited the highest incidence of off-target emergent mutations across tumor types.

Conclusion: This study revealed diverse genomic mechanisms imparting acquired resistance to the selective FGFR2/3 Inhibitor lavengratinib, including secondary FGFR2/3 kinase domain mutations as well as off-target alterations in RTK/RAS and DDR pathways. In GC and CCA, polyclonal FGFR2 acquired mutations represent a convergent, on-target resistance mechanism to FGFR inhibition. These findings provide molecular insights into resistance mechanisms and guide the combination and sequential therapy strategies to overcome resistance in FGFR2/3 driven advanced solid tumors.

#5320 Leveraging enhanced conversion efficiency of the KAPA EvoPrep Boost workflow for urine ctDNA detection.

Angela Apessos[1], Maria Shin[1], Yanpeng Xi[2], Stephanie J. Yaung[3], Indira Wu[1]

[1]Roche Molecular Systems, Pleasanton, CA,[2]Roche Sequencing Solutions, Pleasanton, CA,[3]Roche Sequencing Solutions, Santa Clara, CA

Bladder cancer is the 9th most common cancer type globally, and early detection is often associated with a better prognosis. While tissue biopsy is the gold standard, its invasiveness limits disease detection and monitoring. Liquid biopsy is a less-invasive alternative, typically using plasma to monitor for circulating tumor DNA (ctDNA). In recent years, urine has emerged as a potentially superior source of ctDNA in bladder cancer studies, as it comes in direct contact with the tumor tissue[1]. However, high concentrations of DNAases in urine result in shorter cell free DNA (cfDNA) fragments and a lower concentration of cfDNA in the sample. Accurate analysis therefore relies on a sensitive and efficient sample preparation workflow. The KAPA EvoPrep Boost workflow employs an engineered ligase and an optimized amplification system, which improve library conversion efficiency and uniformity. The enhanced library preparation performance makes it a promising tool for analyzing poor quality and low input cfDNA obtained from urine. Urine cfDNA (ucfDNA) was isolated from healthy donors and archived bladder cancer samples and characterized. UcfDNA was converted using KAPA EvoPrep Boost and another commercially available library preparation kit for comparison, followed by target enrichment using the KAPA HyperCap Oncology Panel, which is a 214 Kb (capture) target enrichment panel covering the coding region of 13 genes involved in somatic oncology in addition to hotspot variants across 69 genes. The libraries were sequenced on an Illumina NovaSeq 6000 System and analyzed with a Roche KAPA Somatic DNA RUO Pipeline. Population databases of known single nucleotide polymorphisms were used to filter out putative germline mutations given matched normals were not available for the bladder cancer samples.Using Seraseq ctDNA Complete Reference Material, assay sensitivity in detecting variants from common oncogenic regions was established at 1ng cfDNA input. Compared to the alternative library preparation kit, KAPA EvoPrep Boost achieved higher coverage uniformity and lower error rates when tested with low input ucfDNA samples from healthy donors. Furthermore, using the KAPA EvoPrep Boost workflow coupled with the KAPA HyperCap Oncology Panel, variants in genes that are often mutated in bladder cancer development were detected in the cell-free DNA shed into the urine by the tumor. In summary, we describe a complete workflow for the analysis of low input and potentially poorer quality cfDNA isolated from urine. The improved conversion efficiency and genome equivalent recovery rates achieved by using the KAPA EvoPrep Boost Kit will be a useful research tool for bladder cancer and potentially other urinary tract cancers.KAPA products are For Research Use Only. Not for use in diagnostic procedures. 1.Ou Z, *et al.* Detection of bladder cancer using urinary cell-free DNA and cellular DNA. Clin Transl Med. 2020; 9(1):4.

#5321 Comprehensive profiling of urine microRNAs in prostate cancer patients.

Matias A. Bustos[1], Yoko Koh[2], Jaime Moon[2], Dai Takamatsu[2], SooMin Kim[2], Gianna Jimenez[3], David L. Krasne[4], Timothy G. Wilson[3], Dave S. B. Hoon[2]

[1]Translational and Precision Medicine, Providence Saint John's Health Center, Santa Monica, CA,[2]Translational and Molecular Medicine, Providence Saint John's Health Center, Santa Monica, CA,[3]Urology and Urologic Oncology, Providence Saint John's Health Center, Santa Monica, CA,[4]Division of Surgical Pathology, Providence Saint John's Health Center, Santa Monica, CA

The diagnosis of early-stage and locally advanced prostate cancer (PCa) continues to present significant clinical challenges. While prostate-specific antigen (PSA) remains the only serum biomarker currently used for PCa detection, its specificity is low, limiting its effectiveness. Although multiparametric magnetic resonance imaging serves as a valuable diagnostic resource, there are many inherent risks, including missing the target lesion during evaluation. This study was designed to identify urine cell-free microRNAs (cfmiRs) as diagnostic markers for patients with PCa of different stages (pT1a-pT3b). Briefly, urine samples were collected from 100 patients diagnosed with PCa and 22 individuals without PCa. Total RNA was isolated from 1 mL of urine using JBS Cell-free RNA & microRNA Isolation Kit and the automated JpurX-S200 isolation system according to manufacturer's protocol. Purified miRNAs were analyzed using an NGS-based approach to quantify 2,083 distinct microRNAs (miRs). Differential expression analysis using DESeq2 revealed 664 differentially expressed miRs in the urine of PCa patients, among which 95 cfmiRs were upregulated. Machine learning analysis considering both upregulated and downregulated cfmiRs led to the development of 10-cfmiR signature based on importance-scores. The 10-cfmiR signature showed strong performance on receiving operating characteristic (ROC) curve analysis [area under the curve (AUC) = 0.88, specificity = 0.91, sensitivity = 0.72, $p < 8.31e-09$]. When considering only upregulated cfmiRs, we found a 16-cfmiR and a 54-cfmiR signatures, which demonstrated good diagnostic performance for PCa [AUC = 0.77, specificity = 0.64, sensitivity = 0.84, $p < 1.84e-06$; AUC = 0.82, specificity = 0.82, sensitivity = 0.73, $p<1.90e-06$]. The diagnostic accuracy observed for the cfmiR signature was further conserved when focusing specifically on let-7a-5p [AUC = 0.79, specificity = 0.73, sensitivity = 0.76, $p < 0.001$] and let-7b-5p [AUC = 0.80, specificity = 0.73, sensitivity = 0.69, $p < 0.001$]. Specific cfmiR signatures were associated with higher grade groups and elevated PSA levels. The cfmiR signatures identified in this study were also compared with the cfmiRs identified in a previous study analyzing a cohort of early-stage pT2 PCa patients. Notably, 109 cfmiRs were detected consistently in both groups, with 93.75% (15 out of 16) of the cfmiRs in the 16-cfmiR signature being upregulated and present in both comparisons. In summary, this study successfully quantified and identified potential cfmiR signatures in urine samples from PCa patients at all stages. Specific urine cfmiRs may offer an advantage to distinguish patients with more aggressive disease. The findings suggest that urine is a robust source of cfmiRs with promising potential for the diagnosis of individuals with PCa.

#5322 Non-invasive tracking of clonal evolution and treatment response through liquid biopsies.

Farhia Kabeer[1], Matteo Lepur[2], Branden Lynch[3], Emilia Hurtado[3], Janine Senz[3], Ding Ma[3], Vinci Au[3], Caroline Baril[3], Gavin Ha[4], Samuel Aparicio[3], Jessica N. McAlpine[5], Alexandre Bouchard-Cote[2], David G. Huntsman[1], Yvette Drew[6], Andrew Roth[7]

[1]Department of Pathology and Laboratory Medicine, Faculty of Medicine, University of British Columbia, Vancouver, BC, Canada,[2]Department of Statistics, University of British Columbia, Vancouver, BC, Canada,[3]Molecular Oncology, BC Cancer Research Institute, Vancouver, BC, Canada,[4]Fred Hutchinson Cancer Center, Seattle, WA,[5]Department of Obstetrics & Gynaecology, University of British Columbia, Vancouver, BC, Canada,[6]Department of Gynaecology and Obstetrics, Division of Medical Oncology, Faculty of Medicine, University of British Columbia, Vancouver, BC, Canada,[7]Department of Pathology and Laboratory Medicine, Department of Computer Science, University of British Columbia, Vancouver, BC, Canada

Background: High-grade serous ovarian cancer shows high genomic instability and heterogeneous tumorsubpopulations that drive variable therapy responses and treatment failure. Tracking tumor cellpopulation changes during treatment is crucial for understanding cancer response, resistance, andmetastasis. Clonal dynamics reflects selective sweeps, fitness-enhancing genomic alterations,and spatially restricted subpopulation outgrowth. To capture these dynamics, we developed atumor-informed framework that resolves haplotype-specific copy number (HSCN) states fromsingle cell whole genome sequencing (scWGS). These high-resolution clonal profiles areintegrated into a Bayesian circulating tumor DNA (ctDNA) deconvolution method, cfClone,enabling sensitive, biologically interpretable quantification of clonal shifts from liquid biopsies.

Methods: Plasma ctDNA was collected from 20 high-grade serous ovarian cancer (HGSOC) patients,along with tumor samples from multiple sites. Single-cell whole-genome sequencing (scWGS)was performed and analyzed with HapClone, a Bayesian model reconstructing the geneticstructure and dynamics of tumor clones. HapClone generated haplotype-specific copy-number(HSCN) profiles reflecting allele-specific amplifications, deletions, and structural changes. Theseprofiles were then used to deconvolute clonal contributions in plasma with cfClone, and residualanalyses revealed hidden tumor subpopulations.

Results: In HGSOC cases, integrating scWGS-derived clonal states with cfDNA enabled reconstructionof tumor dynamics, quantification of clonal growth across metastatic sites, and identification ofthe dominant clone driving recurrence, indicating that metastasis is driven by the recurrent clonerather than new clones. cfClone longitudinal tracking in one case revealed tumor-fractionchanges over multiple time points, highlighting resistant subclones emerging during therapy.Including tumor content allowed detection of clones and quantitative assessment of responsedynamics, such as rapid clonal responses in another case. Differences between refractory andsensitive clones were identified, showing how longitudinal data reveal resistance mechanisms.The HSCN framework detected greater clonal diversity than state of the art structural-variant-based methods.

Conclusions: scWGS-informed HSCN analysis combined with ctDNA deconvolution provides a sensitive,biologically grounded approach to track tumor evolution, identify resistant clones, and measurectDNA. This framework enables real-time monitoring of tumor changes and has strong potentialto guide precision cancer treatment by enabling non-invasive monitoring of clonal dynamics inresponse to therapeutic decisions by linking clonal dynamics to therapy decisions in a non-invasive way.

#5323 Circulating tumor DNA dynamics predict the response to neoadjuvant chemotherapy but not long-term outcomes in *PIK3CA*-mutated breast cancer.

Ayaka Sato[1], Takayuki Ueno[2], Shunji Takahashi[3], Yoshinori Murakami[4], Masahiko Tanabe[1]

[1]Department of Breast and Endocrine Surgery, The Graduate School of Medicine, The University of Tokyo, Tokyo, Japan,[2]Japanese Foundation for Cancer Research, Tokyo, Japan,[3]The Cancer Institute Hospital of JFCR, Tokyo, Japan,[4]Senior Professor, Department of Molecular Biology, Nippon Medical School, Tokyo, Japan

Background: The clinical significance of circulating tumor DNA (ctDNA) dynamics in *PIK3CA*-mutated breast cancer treated with neoadjuvant chemotherapy (NAC) remains unclear. We evaluated whether ctDNA patterns defined between baseline and pre-surgery are associated with pathological complete response (pCR) and long-term distant outcomes.

Methods: A total of 122 patients with stage I-III breast cancer who were scheduled to receive NAC between May 2016 and September 2017 were prospectively enrolled in this study. Tumor DNA extracted from pretreatment formalin-fixed, paraffin-embedded (FFPE) biopsy specimens was analyzed for *PIK3CA* hotspot mutations (E542K, E545K, and H1047R) using droplet digital PCR (ddPCR). Blood samples were collected at baseline (pre-NAC), pre-surgery, and post-surgery. Tumor-matched *PIK3CA*-mutated ctDNA was quantified by ddPCR. ctDNA dynamics between baseline and pre-surgery were categorized into four patterns: persistent-negative (-/-), cleared (+/-), persistent-positive (+/+), and post-NAC-emergent (-/+). pCR was defined as the complete disappearance of invasive carcinoma in both the breast and lymph nodes. Distant metastasis was assessed after a median follow-up of 96 months (range, 9-108).

Results: Tumor DNA was extracted from 113 primary tumors in 122 patients. *PIK3CA* mutations were detected in 36 (32%) of the 113 tumors. Plasma samples were available from 34 (94%) of 36 patients with *PIK3CA*-mutated tumors. Among these 34 patients, the ctDNA patterns were as follows: 17 were persistent-negative, 14 were cleared, two were persistent-positive, and one was post-NAC-emergent. Post-surgical ctDNA was negative in all patients. pCR occurred in nine patients (26%), including five of 17 persistent-negative patients and four of 14 cleared patients, whereas none of the persistent-positive or post-NAC-emergent patients achieved pCR. Follow-up for distant recurrence was available for 33 patients. Distant metastasis developed in five patients: Three in the persistent-negative group, one in the cleared group, and one in the persistent-positive group. Although persistent-positive patients showed a numerically higher metastatic rate (one of two), most late distant relapses arose from preoperative ctDNA-negative patterns.

Conclusions: In *PIK3CA*-mutated breast cancer treated with NAC, pre-surgical ctDNA positivity indicated residual disease but did not reliably predict long-term outcomes. A two-point ctDNA assessment may be insufficient for prognostic stratification. Further long-term follow-up and large-scale studies are needed to validate these findings.

#5324 Circulating tumor DNA detects minimal residual disease and predicts outcomes in esophageal cancer after esophagectomy.

Qingjiang Hu[1], Eiji Oki[2], Yasue Kimura[3], Hajime Otsu[1], Yusuke Yonemura[1], Koshi Mimori[1]

[1]Department of Surgery, Kyushu University Beppu Hospital, Beppu, Japan,[2]Kyushu University Hospital, Fukuoka, Japan,[3]Department of Gastrointestinal surgery, Kyushu Cancer Center, Fukuoka, Japan

BackgroundCirculating tumor DNA (ctDNA) monitoring shows promise for detecting minimal residual disease (MRD) and predicting prognosis in various cancers. This study evaluated ctDNA for detecting MRD and predicting outcomes in patients with esophageal cancer (EC) after esophagectomy.**Methods**We conducted a two-step observational study with a retrospective cohort (cohort 1) and a prospective cohort (cohort 2) of 40 EC patients who underwent upfront surgery or neoadjuvant chemotherapy (NAC) followed by esophagectomy. Plasma samples were collected at six time points: pre-therapy, post-NAC, and 1, 3, 6, and 12 months post-surgery. ctDNA was assessed using a 250-gene panel and its association with clinical outcomes was analyzed.**Results**Tumor-informed ctDNA levels were significantly correlated with tumor stage (*P*=0.01). Changes in ctDNA levels predicted tumor progression, with an area under the curve of 0.77. Postsurgical ctDNA positivity correlated with reduced recurrence-free survival (RFS) in cohort 1 (n=6, Log-rank *P*=0.034) and progression-free survival (PFS) in cohort 2 (n=34, Log-rank *P*=0.025) compared to ctDNA-negative patients. Combined analysis showed that postsurgical ctDNA positivity was associated with shorter PFS (hazard ratio [HR]=12.6, 95% confidence interval [CI]: 1.6-99.0; *P*=0.002) across all patients (n=40) and shorter RFS (HR=11.1, 95% CI: 1.4-89.0; *P*=0.006) in those who underwent R0 resection (n=37). ctDNA positivity predicted recurrence at a median of 90 days before radiographic evidence.**Conclusions**This study showed a strong correlation between ctDNA status and postsurgical prognosis in EC patients. ctDNA assessments can effectively detect MRD and guide postoperative management strategies.

#5325 Cell-free DNA fragmentomes for treatment response monitoring in patients with metastatic colorectal cancer: The Dolphin study.

Denise E. van Steijn[1], Lorenzo Rinaldi[2], Adria Closa[1], Erica Peters[2], Alissa Konicki[2], Mariska Bierkens[1], Haoyue Wang[3], Marjolein Greuter[3], Birgit Lissenberg-Witte[4], Veerle Coupe[3], Amoolya Singh[2], Timothy McDaniel[2], Meike de Wit[1], Anna Houben[5], Daan van den Broek[6], Miriam Koopman[5], Gerrit Meijer[1], Max Lahaye[7], Manon Braat[8], Victor Velculescu[9], Jeanine Roodhart[8], Nicholas Dracopoli[2], Frederieke van der Baan[6], Geraldine Vink[6], Niels Kok[10], Remond Fijneman[1]

[1]Department of Pathology, Netherlands Cancer Institute, Amsterdam, Netherlands,[2]DELFI Diagnostics, Baltimore, MD,[3]Department of Epidemiology and Data Science, Amsterdam University Medical Centers, Amsterdam, Netherlands,[4]Department of Data Science and Biostatistics, Julius Center for Health Sciences and Primary Care/University Medical Center Utrecht, Utrecht, Netherlands,[5]Department of Medical Oncology, University Medical Center Utrecht, Utrecht University, Utrecht, Netherlands,[6]Department of Laboratory Medicine, Netherlands Cancer Institute, Amsterdam, Netherlands,[7]Department of Radiology, Netherlands Cancer Institute, Amsterdam, Netherlands,[8]Department of Radiology, University Medical Center Utrecht, Utrecht University, Utrecht, Netherlands,[9]Sidney Kimmel Comprehensive Cancer Center, Johns Hopkins University School of Medicine, Baltimore, MD,[10]Department of Surgical Oncology, Netherlands Cancer Institute, Amsterdam, Netherlands

Introduction: Accurate monitoring of tumor response in patients with metastatic colorectal cancer (mCRC) undergoing systemic therapy is essential to enable timely and informed treatment decisions. Although CT imaging is currently the standard-modality, it has limitations including limited accuracy for detecting small lesions, as well as inter-reader variability. A reliable blood-based biomarker may enable a more precise and dynamic assessment of treatment response. Circulating tumor DNA (ctDNA) is indicative of cancer cell burden and may complement CT imaging for evaluating treatment responses. DELFI tumor fraction (DELFI-TF) is a mutation- and tumor-independent ctDNA assay which has demonstrated potential for longitudinal monitoring of treatment response. The DOLPHIN study aims to evaluate the clinical added value of DELFI-TF to conventional imaging-based response monitoring in patients with mCRC.

Method: DOLPHIN is a prospective, observational substudy of the Prospective Dutch Colorectal Cancer Cohort, in which blood samples are collected longitudinally in conjunction with routine CT imaging in mCRC patients. ctDNA levels are longitudinally assessed using the DELFI-TF ctDNA assay, a locked and validated machine learning model that quantifies tumor burden using cell-free DNA (cfDNA) fragmentomic data derived from low-coverage whole genome sequencing. Simultaneously, ddPCR analysis is performed on samples from patients with a tumor tissue-confirmed RAS or BRAF mutation. The primary endpoint of this study is the association between changes in ctDNA levels and clinically determined treatment response. Secondary endpoints include the correlation between ctDNA dynamics and clinical, biochemical, and radiological responses at multiple timepoints during systemic treatment (I), lead time of ctDNA testing compared with CT imaging for identifying progressive disease (II), prognostic value of longitudinal ctDNA testing (III) and the cost-effectiveness of various monitoring approaches (IV).

Results: Between March 16 2023 and October 16 2025, 504 patients were enrolled before starting the second line of treatment. Nine patients were excluded due to incorrect entry criteria. A comprehensive overview of patient demographics and clinical characteristics will be presented at the conference. In total 2214 blood samples and 2468 CT scans have been collected, with collection planned to continue until March 2026. To date, 2186 samples (86.8%) have been successfully matched to a corresponding CT scan, and 1881 (86.0%) of these were obtained within 14 days of imaging.

Conclusion: In the ongoing DOLPHIN study, we successfully aligned a majority of blood samples with corresponding CT scans. This study will determine whether DELFI-TF can complement treatment response monitoring in mCRC patients and potentially enable parts of follow-up to be shifted to the home setting.

#5326 High throughput genomic profiling of tissue and liquid biopsy samples reveals targetable mutations in NSCLC patients from the Indian population.

Amit Kumar[1], Puja Sinha[2], Rama Chandran[2], Shobit Gupta[2], **Giulliana Tessarin**[3]

[1]Genes2Me, Gurugram, India,[2]Genes2me Pvt Ltd,, Gurugram, India,[3]Genes2me Pvt Ltd, Gurugram, India

Background: Non-Small Cell Lung Cancer (NSCLC), accounts for approximately 85% of lung cancer cases and ranking as the foremost cause of cancer related deaths globally, is both highly aggressive and uniquely characterized by the broadest spectrum of approved targeted treatments. Comprehensive genomic profiling (CGP) using next-generation sequencing (NGS) has become integral to clinical practice, with tissue and plasma-based analysis of cell free circulating tumor DNA (ctDNA) representing the most established and widely adopted modality in NSCLC. Addressing the scarcity of molecular data in Indian NSCLC patients, this study aims to delineate the mutational spectrum through NGS based profiling of FFPE and plasma ctDNA samples, driving advances in targeted therapy and precision medicine.

Methods: The study included 45 FFPE tissue and plasma specimens from NSCLC patients, enabling a robust comparison of solid and liquid biopsy approaches. Comprehensive genomic profiling was performed on a total of 45 samples using the G2M PanCan CGP assay, which targets 681 clinically relevant genes with approximately 1.7 Mb of genomic regions and was sequenced on the Illumina platform. Bioinformatics analysis was conducted using the GATK v4.1.2 somatic variant calling pipeline, and downstream visualization of mutational landscapes and hotspot regions was achieved using MAF tools.

Results: Consistent mutations were detected in both FFPE tissue and plasma ctDNA samples, with prominent alterations in TP53 showing the highest frequency and clinical relevance, accompanied by alterations in EGFR, ASXL1 and ARID1A. With variant allele frequencies of 6-39% in FFPE and 0.9-3.0% in liquid biopsy samples, the assay proved effective across sample types, producing a highly concordant mutational profile. TP53 was the most frequently mutated gene, exhibiting hotspot variants such as G325, P152L, H179D, and L194R, underscoring its critical role in NSCLC pathogenesis.

Conclusions: By mapping mutations in key NSCLC associated genes, the investigation confirms that NGS-based comprehensive genomic profiling delivers reliable and concordant detection across FFPE tissue and plasma ctDNA samples. This finding highlights the assay's utility for integrating tissue and liquid biopsy into routine clinical practice, empowering clinicians with accurate genomic insights to guide targeted mutation driven therapy decisions.

#5327 Utilization of urinary cell-free DNA as an informative biomaterial for comprehensive genomic profiling.

Robert Summersgill[1], Jesse Fox[1], Patrick Horn[1], LaRonda White[1], Vito Caropreso[1], Amy Meltzer[1], Ana Perez-Lebron[1], Kenneth Valkenburg[1], Eric Severson[2], Taylor J. Jenson[2], Shakti Ramkissoon[2], Brian Caveney[2], Marcia Eisenberg[2]

[1]Labcorp, Baltimore, MD,[2]Labcorp, Durham, NC

Background: Urinary cell-free DNA (UcfDNA) could soon prove to be a valuable non-invasive sampling analyte for next-generation sequencing (NGS) assays, particularly in urological cancers. Additionally, enabling at-home collection for cancer testing could lead to higher rates of adherence to testing schedules. In this proof-of-concept study, we intended to establish a baseline for how to effectively extract UcfDNA from urine with the potential of applying it as a sample type in assays such as Labcorp Plasma Complete™.

Methods: Extraction efficiency was compared across 4 different on-market cfDNA extraction methods, 3 manual kits (1 bead-based, 1 column-based, and 1 column/bead-based hybrid) and 1 automated bead-based kit. This comparison used 5 mL urine samples (n=10) that were stored at room temperature for 8-25 months. All samples were collected from patients with known solid tumor cancers. Extracted UcfDNA was characterized using both a fluorometer and a cfDNA bioanalyzer with a pre-determined cfDNA base pair range (50-700 bp). Next, larger volume (15 mL) extractions were conducted using 2 of the 4 previously tested extraction kits (the column/bead-based hybrid kit and automated bead-based kit) utilizing samples (n=6) collected with a urine stabilizing additive and stored at -80°C for 9-20 months. These extractions produced sufficient UcfDNA and were assessed for comprehensive genomic profiling in duplicate using Labcorp Plasma Complete. Post sequencing quality metrics were analyzed to determine the performance and reliability of the data. Lastly, mutation profiles were assessed for reproducibility between replicates and across extraction methods.

Results: The results show that multiple urine extraction methods produce viable yields with significant variability (2 - 900 ng) and these were influenced by cancer type and pre-analytical factors such as sample handling and storage. Regarding post-sequencing quality metrics, the extraction kits had little impact. However, the quality of material extracted from each kit was variable, indicated by differences in sequencing ratios. Comprehensive genomic profiling results indicate robust performance, with a > 90% call rate when identifying variants > 0.8% variant allele frequency (VAF) across replicates. The assay also identified multiple variants with 100% call rate across sample replicates and extraction methods, including clinically significant variants such as a TERT promotor mutation and an ALK translocation.

Conclusions: The findings show that UcfDNA is an extractable biomaterial when properly handled, and it also has great potential to be used for comprehensive genomic profiling in urological cancer samples with Labcorp NGS assays such as Labcorp Plasma Complete.

#5328 Analytical performance of magnetic bead-based cfDNA extraction with a low input targeted DNA enrichment.

Mayer Saidian[1], Yingmin Wang[2], Heng Wang[2], Yun Bao[3], Jason Saenz[1], Carlos Hernandez[1], Cameron Van Dieren[1], Daniel Cedeno[1], Nafiseh Jafari[1]

[1]nRichDX, Irvine, CA,[2]Agilent Technologies, Inc., Santa Clara, CA,[3]Agilent Technologies, Inc., Snata Clara, CA

Introduction: Analytical alignment between cfDNA extraction chemistry and downstream targeted-DNA assays is essential for reliable molecular counting, especially at low plasma input. This study evaluated whether two magnetic bead-based cfDNA extraction methods generate equivalent or distinguishable performance within a low-input targeted DNA enrichment workflow.
Methods: Experiment I (Human plasma, n = 8): Sixteen 3-mL plasma aliquots per donor were extracted in parallel using two bead-based kits—the Revolution cfDNA Max 20 Kit and MagMAX—producing paired eluates from identical input samples. QC included electrophoretic cfDNA quantification (50-700 bp), nucleosomal-profile assessment, and detection of high-molecular-weight (HMW) carryover. Experiment II (Contrived spike-in): Plasma matrices containing a 0.2% allele-frequency cfDNA spike-in were extracted in duplicate from 1-mL inputs using the same extraction kits.The primary endpoints were the library-eligible cfDNA concentration and molecule recovery following Agilent's Avida low-input targeted DNA enrichment workflow. Secondary endpoints included VAF concordance, on-target fraction, background noise, and library complexity.
Results: Across both experiments, cfDNA from the two bead-based extractions met the minimal QC thresholds; however, the Revolution cfDNA Max 20 Kit consistently demonstrated superior analytical performance, including: higher recovery of library-eligible cfDNA concentration (50-700 bp), more defined mono-/di-nucleosomal peak structure, less frequent HMW carryover, and stronger QC suitability for low-frequency (0.2%) variant interrogation.Spike-in experiments showed that eluates generated by this method more reliably met the requirements for low-input targeted DNA enrichment, supporting higher confidence in downstream molecular counting. Sequencing of paired eluates is ongoing and will quantify differences in molecule recovery, VAF precision, and background suppression.
Conclusions: Both magnetic bead-based methods generated cfDNA suitable for low-input targeted sequencing; however, the Revolution cfDNA Max 20 Kit delivered superior cfDNA yield, fragment-quality metrics, and overall pre-analytical performance. Pending sequencing results will further define the magnitude of analytical advantage and support optimized recommendations for pre-analytical workflows in low-input liquid biopsy assays.
AI Disclosure: Portions of this abstract were generated using an AI-assisted tool and subsequently reviewed and edited by the authors.

#5329 Unlocking transrenal DNA: New methods for stabilizing and isolating small cfDNA in urine.

Daniela Mancarella-Langer[1], Franziska Kaiser[1], Daniel Groelz[1], Moritz Rath[1], Nguyen Van Nhi Le[2], Eric Provencher[1], Michelle Walther[1]

[1]PreAnalytiX GmbH, Hombrechtikon, Switzerland,[2]QIAGEN GmbH, Hilden, Germany

Introduction: Urine liquid biopsy is emerging as a non-invasive approach for disease monitoring and early detection. Transrenal DNA, cell-free DNA that passes from plasma through the kidney into urine, contains promising biomarkers that may expand the applications of urine liquid biopsy beyond urological malignancies. Due to the size restriction of the renal barrier, transrenal DNA is shorter than urological cfDNA (<50 bp). However, the analysis of urine cfDNA is challenging as it is prone to rapid degradation. Furthermore, isolating short DNA fragments from the complex urine matrix demands optimized extraction protocols. The presented study addressed key technical challenges in urine liquid biopsy, presenting optimized workflows for stabilization, isolation, and analysis of urine cfDNA to realize the full potential of transrenal DNA research.
Methods: Urine was collected from apparently healthy, consented individuals and either stabilized or left unstabilized. Urine samples were spiked with a DNA ladder with defined size fragments ranging from 10 to 300 bp. DNA was either isolated from urine on the day of collection, stabilization and spike-in, or after urine storage. DNA spike-in was also performed in phosphate-buffered saline. DNA was isolated either manually or automated with several commercially available cfDNA isolation technologies. The isolated cfDNA was analyzed by capillary gel electrophoresis.
Results: All isolation kits tested were suitable for isolation of cfDNA down to 50 bp. Smaller DNA fragments down to 35 bp could be isolated with the miRNA protocol of the manual QIAamp® Circulating Nucleic Acid Kit as well as with automated isolation using the QIAsymphony® DSP Circulating DNA Kit and the EZ1&2® ccfDNA Kit. With the integration of new nucleic acid binding beads into the automated isolation with the QIAsymphony DSP Circulating DNA Kit, isolation of cfDNA down to 20 bp was possible. To test the need for urine stabilization for efficient isolation of small cfDNA from urine, the spike-in DNA was isolated from unstabilized urine as well as urine stabilized with the PAXgene® Urine Liquid Biopsy Set. For unstabilized samples, the ladder fragments could not be detected even when isolated within hours of urine collection, indicating rapid degradation of the ladder DNA. For stabilized urine samples, the DNA ladder spike-in could be detected even after days of storage.
Conclusion: This study emphasizes the critical role for urine stabilization for efficient isolation of a wide range of cfDNA sizes. The isolation technology defines the cfDNA size range available for analysis and should be chosen based on the cfDNA population of interest. The PAXgene Urine Liquid Biopsy Set, combined with manual or automated isolation technologies, enables recovery of small cfDNA fragments and hence, transrenal DNA research.

: Precision Oncology and Real World Data
Poster Session

#5333 Profiling membrane antigen expression of select antibody-drug conjugate (ADC) targets in *EGFR*-altered non-small cell lung cancer treated with osimertinib.

Kevin Lu[1], Tali Azenkot[2], Ellen B. Jaeger[3], Unnati Jariwala[3], Stamatina Fragkogianni[3], Jacob Mercer[3], Jyoti D. Patel[3], Sandip P. Patel[2]

[1]UC San Diego School of Medicine, La Jolla, CA,[2]UC San Diego Moores Cancer Center, La Jolla, CA,[3]Tempus AI Inc, Chicago, IL

Background: Resistance to EGFR-Tyrosine Kinase Inhibitors (TKIs) in patients with NSCLC represents an unmet clinical need. Bypass pathway upregulation is a key mechanism of resistance and represents a potential target for therapeutic agents such as Antibody-Drug Conjugates (ADCs). This study evaluates the RNA expression of select ADC targets in NSCLC patients treated with osimertinib (osi).

Methods: The Tempus Lens Platform was used to identify a cohort (n=583 patients) of classical *EGFR*-altered NSCLC with DNA (xT) and RNA (xR) testing treated with first-line osi monotherapy (mono) or osi with chemotherapy (combo). RNA-seq data of select ADC membrane targets, including *ERBB2*, *ERBB3*, *MET*, *NECTIN4*, and *TACSTD2* (TROP2) were quantified as transcripts per million (TPM), reported as log2(TPM + 1) and compared using Wilcoxon rank-sum test. Median RNA expression in each gene was defined relative to the pre-treatment *EGFR*-altered cohort. We examined real world overall survival (rwOS) and hazard ratio (HR) from Cox proportional hazards model.

Results: Among 583 patients, median (range) age at diagnosis was 66 (27-88) years old while 68% were female. In all samples, the highest median gene expression was identified in *ERBB2*, *MET*, and *TACSTD2* (TROP2) (7.46, 7.38, 7.57). When comparing first-line pre- and post-treatment samples, there was a significant increase in median gene expression of *MET* (7.23 vs 7.85; p<0.001) however decreases in median expression of *NECTIN4* (5.22 vs 4.90; p=0.005) and *ERBB2* (7.48 vs 7.38; p=0.021). In pre-osi mono patients (n=378), median rwOS was 29.8 months. Of the five genes assessed, only *MET* expression was associated with worse rwOS (HR 1.25; p=0.001). In the mono group, those with above-median *MET* expression at pre-treatment had a worse rwOS than those with below-median expression (26.1 vs. 31.5 months; p=0.007). Above-median *MET* expression was associated with worse rwOS compared to below median (HR 1.52; p=0.008).

Conclusion: In patients with *EGFR*-altered NSCLC, we identified high expression of *ERBB2*, *MET*, and *TACSTD2* (TROP2) in both pre- and post-treated samples. This may provide rationale for use of these ADC targets in second-line therapy, such as seen in recent approvals for trastuzumab deruxtecan in *ERBB2*-mutated, telisotuzumab vedotin in *c-MET* over-expressing, and datopotamab deruxtecan in *EGFR*-altered NSCLC. Notably, high *MET* pre-treatment expression was associated with poor survival outcome and appeared to be associated with post-osimertinib resistance. Further investigation is required to evaluate *MET* expression as a predictive biomarker for *MET*-targeting agents to overcome innate and acquired EGFR-TKI resistance.

#5334 Genomic profiling of lung cancer in Guizhou province and comparative performance of DNA-NGS versus DNA+RNA-NGS for fusion detection.

Weiwei Ouyang, Yichao Geng, Chuang Tian

The Affiliated Hospital of Guizhou Medical University, Department of Oncology, China

Background: Targeted therapy plays a crucial role in non-small cell lung cancer (NSCLC), making accurate genomic profiling essential for treatment selection. RNA-based fusion detection has been increasingly recommended by major guidelines due to its superior analytical performance, yet real-world evidence remains limited. This study characterized the genomic landscape of NSCLC in Guizhou Province and compared DNA-based next-generation sequencing (DNA-NGS) with combined DNA+RNA sequencing (D+R-NGS), particularly for fusion detection.
Methods: From 2017 to 2024, 880 tumor samples from 571 NSCLC patients underwent NGS testing, including 750 samples analyzed by DNA-NGS and 130 by D+R-NGS. Somatic SNVs/indels, copy-number variations (CNVs), and gene fusions were comprehensively assessed and compared across platforms.
Results: Across all samples, 2,051 SNVs/indels, 198 CNVs, and 73 gene fusions were identified. *EGFR* (53%) and *TP53* (45%) were the most common mutations, consistent with previously reported Chinese NSCLC data. Except for one large-cell neuroendocrine carcinoma, all fusion-positive cases were adenocarcinomas, with female patients representing a higher proportion (60.2%).Fusion detection rates differed substantially between platforms. The D+R-NGS group showed a significantly higher fusion detection rate than DNA-NGS (15.4% vs. 7.1%, $p = 0.003$). And the D+R-NGS also had a numerically higher detection rate (13.5% VS 8.1%, p=0.095), even when significant differences were lost after filtering multiple samples from the same patient. Fusion subtype analysis indicated similar overall patterns, with ALK rearrangements most common in both groups (45% in D+R-NGS; 64% in DNA-NGS). Notably, the detection of *MET* exon 14 skipping was substantially higher in the D+R-NGS cohort (20%) compared with DNA-NGS (2.4%).This difference may be related to the fact that the MET exon 14 skipping on DNA is usually caused by the variant drive of intron 13 or 14, regions that are challenging to assess using DNA-based assays, whereas RNA sequencing provides inherent structural advantages for detecting such events.Importantly, the improvement in fusion detection with D+R-NGS did not reduce sensitivity for other mutation types. Instead, actionable alterations such as *EGFR* (64.7% vs. 46.1%) and *KRAS* (12.9% vs. 6.53%) were identified at higher rates in the D+R-NGS group, suggesting broader analytical benefits.
Conclusions: The genomic profile of NSCLC in Guizhou Province aligns with broader Chinese cohorts. Combined DNA+RNA sequencing significantly enhances fusion detection while maintaining strong performance for SNVs/indels and CNVs. These findings support integrating RNA into routine NGS workflows to improve diagnostic accuracy and guide targeted therapy more effectively in NSCLC.

#5335 Integrated machine learning and large language models reveal molecular determinants of survival and treatment response in KRAS-mutant lung cancer.

Qingtian Li[1], Albert Lee[2], Wei Wu[3], Trever G. Bivona[3]

[1]Department of Medicine, UCSF - University of California San Francisco, San Francisco, CA,[2]IT Academic Research Services, UCSF - University of California San Francisco, San Francisco, CA,[3]UCSF - University of California San Francisco, San Francisco, CA

Background: KRAS activating mutations are the most prevalent oncogenic drivers in non-small cell lung cancer (NSCLC), with KRAS G12C as the dominant subtype. FDA-approved small-molecule inhibitors (sotorasib and adagrasib) have improved outcomes in KRAS G12C positive patients, though responses remain heterogeneous. To dissect clinical and molecular determinants of treatment response and overall survival, we analyzed large KRAS-mutant NSCLC cohorts with multimodal clinical annotation and targeted sequencing, integrating computational and machine learning (ML) approaches.

Methods: 679 KRAS-mutant NSCLC patients including 43 patients treated with KRAS inhibitors were retrieved from UCSF Information Commons (data released in March 2025). Clinical, pathological, targeted tumor exome sequencing, survival, and treatment-response data were extracted from clinical notes using SQL-based algorithms and large language models. Structured datasets were generated for ML models including random forest (RF), multilayer perceptron (MLP), and XGBoost (XGB). An independent MSK-IMPACT cohort (n=2,152) was used for validation. All computational analyses were performed on the UCSF Wynton HPC cluster.

Results: Comparing co-occurring mutations between UCSF KRAS G12C (n=185) and non-G12C KRAS (n=494) treatment naïve tumors, we identified 14 significant differential mutations (Fisher's exact test, BH-corrected $p<0.05$). LRP1B, KEAP1, RUNX1T1, ATP6AP1, ZFTA, TRAF7, and NF2 gene mutations were enriched in the KRAS G12C cohort. Clinical genetic data predicted KRAS inhibitor treatment outcomes (TO) (stable vs progressive disease) and overall survival (OS) with modest accuracies by models of RF (TO:0.67, OS:0.64), MLP (TO:0.83, OS:0.73), and XGB (TO: 0.67, OS:0.73). Intriguingly, the models identified co-mutations of NAV3, COL2A1, MLH3, PTPRD, and SOS2 associated with stable tumor disease, co-mutations of IGFBP3, SPEN and PTPRB correlated with progressive tumor disease, whereas co-mutations of DUSP4, WHSC1, EBF1 and MAP2K4 are potential covariates for poor OS. ML prediction of OS using MSK-IMPACT cohort with clinico-genetic test data achieved AUROC values of 0.80 (RF), 0.72 (MLP), and 0.81 (XGB), respectively. Feature-importance analyses highlighted metastasis, tumor mutation burden (TMB), and mutations in ERCC5, BCOR, and SPEN as major predictors of poor OS.

Conclusion: Analysis of real-world multimodal clinical data revealed distinct biological and genomic features between KRAS G12C and non-G12C NSCLC, as well as key determinants of survival and treatment response. This study demonstrates the value of LLM-generated structured clinical data for AI/ML-driven oncology research with hypotheses generation and highlights its potential to improve personalized treatment decision-making.

#5336 Distinct *KRAS* mutation codons differentially associate with microsatellite instability in colorectal carcinoma.

Mark Evans[1], Vishal Chandan[2], Kenna Shaw[3], Scott Kopetz[4], Anirban Maitra[5], **Julian Bryan**[6]

[1]Caris Life Sciences, Irving, TX,[2]UC Irvine School of Medicine, Irvine, CA,[3]Sheikh Khalifa Bin Zayed Al Nahyan Institute for Personalized Cancer Therapy, UT MD Anderson Cancer Ctr., Houston, TX,[4]UT MD Anderson Cancer Center, Houston, TX,[5]NYU Langone Health, New York, NY,[6]MD Anderson Cancer Center, Houston, TX

Background: MSI/MMR and *KRAS* are key biomarkers in colorectal carcinomas (CRC) for PD1 inhibitors, EGFR mAbs, and KRAS G12C inhibitors. MSI High is reported to be less common in *KRAS* mutant CRC. However, because *KRAS* mutation location influences protein function and CRC pathophysiology, we hypothesized that MSI also differs by *KRAS* mutation site.
Methods: MSI High prevalence was assessed by *KRAS* mutation location in CRCs using logistic regression in 2 databases: MSK-CHORD, and Caris CODEai. *BRAF* V600E CRCs were excluded.
Results: In MSK-CHORD's 4,805 CRCs (non*BRAF* V600E, *NRAS* wt, and no prior EGFRmab), 8.7% were MSI-H. However, MSI-H prevalence differed markedly by *KRAS* mutation site: 8.8% of *KRAS* wt and 13.5-15.9% of codon 13/61/146 CRCs; but only 5.1% of codon 12 mutant CRCs were MSI-H (all p≤0.001). Notably, MSI-H also varied within *KRAS* codons: only 2.0% of G12C and 2.8% of G12V (both C>A) were MSI-H, vs 7.8% of G12D, 4.8% of G12A, and 3.8% of G12S. For confirmation of institutional findings, we analyzed data from a large reference laboratory. In Caris CODEai's 83,532 non*BRAF* V600E CRCs, 5.4% were MSI-H. Again, MSI-H prevalence varied by *KRAS* mutation site: 6.4% of *KRAS* wt, 5.6-6.9% of codon 13/61/117/146, and 19.2-26.9% of codon 14/59 mutant CRCs were MSI-H; compared to only 1.9% of codon 12 mut CRCs (all p<0.001). We then tested this finding in other cancer types in Caris CODEai. A similar result was observed in pancreatic cancer: among 40,497 only 0.7% were MSI-H, from 0.7% of *KRAS* wt to 0.4-0.5% of codon 12/61, but 7.8% of codon 13 (p<0.001).
Conclusions: MSI-H prevalence varied by *KRAS* mutation location in CRC, with codon 12 muts—especially C>A—associated with low MSI-H rates, whereas codon 13/59/61/146 muts were enriched among MSI-H CRCs. Our data suggest that MSI/MMR mutational processes are associated with distinct codon-resolved *KRAS* biology and may give rise to specific *KRAS* muts, which warrants further investigation and could refine predictive biomarker interpretation.

MSI-High prevalence by KRAS status in MSK-CHORD CRC

***KRAS*_status**		**Total_n**	**MSI-H_n**	**MSI-H_%**
wt		2510	222	8.8
codon_12		1517	78	5.1
codon_13		436	49	13.5
codon_59		10	5	50.0
codon_61		94	13	13.8
codon_117		26	8	30.8
codon_146		164	26	15.9
in_codon_12	G12A_(C>G)	104	5	4.8
	G12C_(C>A)	153	3	2.0
	G12D_(C>T)	658	51	7.8
	G12R_(C>G)	24	2	8.3
	G12S_(C>T)	105	4	3.8
	G12V_(C>A)	469	13	2.8
in_codon_13	G13C_(C>A)	19	2	10.5
	G13D_(C>T)	412	55	13.4
in_codon_61	Q61H_(T>G,T>A)	50	5	10.0
	Q61K_ (GA>TT, G>T, GA>TG)	21	8	38.1
	Q61L_(T>A)	7	0	0
	Q61R_(T>C, TT>GC)	15	0	0
in_codon_146	A146P_(C>G)	9	2	22.2
	A146T_(C>T)	128	23	18.0
	A146V_(G>A)	26	1	3.9
in_codon_59	A59T_(C>T)	10	5	50.0
in_codon_117	K117N_(T>A,T>G)	24	8	33.3

#5337 MSI colon adenocarcinoma transcriptomic subtypes are biomarkers of response to immunotherapy.

Matthew B. Maxwell[1], Akul Singhania[1], Michelle Stein[1], Radia Johnson[1], Van K. Morris[2], Andrew J. Sedgewick[1], Scott Kopetz[2], Justin Guinney[1]

[1]Tempus AI, Inc., Chicago, IL,[2]UT MD Anderson Cancer Center, Houston, TX

Background: Microsatellite instability-high (MSI) is a predictive biomarker for response to immune checkpoint inhibitors (ICI) in metastatic colon adenocarcinoma (COAD), but not all patients respond to ICI. Thus, there is a clinical need to develop novel biomarkers to more accurately predict ICI response in metastatic MSI-COAD.
Methods: The transcriptomic subtyping cohort consisted of 793 primary tumor MSI-COAD samples with DNA & RNA-seq (Tempus xT/xR) from Tempus' real-world database. The ICI cohort consisted of 59 metastatic MSI-COAD patients who had a primary tumor sample profiled via Tempus xT/xR. We performed transcriptomic subtyping via non-negative matrix factorization (NMF). Survival analyses were performed via risk set adjusted Kaplan-Meier and CoxPH models with right censor cutoff of 48 months post ICI. Consensus molecular subtype (CMS) calls were made using Tempus CMS classifier, immune deconvolution was performed using xCell, and GSEA using fgsea. A FDR < .05 was considered significant.
Results: Clustering of primary MSI-COAD tumor transcriptomes revealed two subtypes that we named "Immune/Stromal" (C1, n=390) and "Goblet/Enterocyte" (C2, n=403). C1 tumors displayed significantly higher proportion of CD8+ T cells, cytolytic scores, and enrichment of EMT, TNFα, and IFNα/γ response gene sets. C2 tumors displayed significantly higher expression of goblet cell and enterocyte marker genes and enrichment of metabolic gene sets. LOF mutations in epigenetic regulators ARID1A, ARID1B, and EP300 were enriched in C1 tumors. In the ICI cohort of metastatic MSI-COAD patients, C2 was associated with significantly shorter PFS (HR = 6.6, 95% CI: 2.2-19.6, p < 0.0001) and OS (HR = 4.4, 95% CI: 1.4-13.3, p < 0.001). In C2 patients, the median PFS and OS following ICI were 8 and 34 months, respectively; in C1, neither median was reached. C2's association with shorter PFS but not OS following ICI was independent of ICI regimen, line of therapy, collection procedure type, age, sex, and TMB in a CoxPH model (HR = 7.0, 95% CI: 1.8-26.6, p = 0.005). In the subset of our ICI cohort treated with Nivolumab + Ipilimumab (n=10), we observed that 4/4 C2 patients progressed within 6 months of treatment while 0/6 C1 patients progressed (p = 0.049, HR = Inf). Finally, we demonstrate that NMF subtypes presented here have a stronger association with PFS in CoxPH models following ICI compared to CMS subtypes (CMS3 vs CMS1 HR=3.5, 95% CI: 1.1-11.1, p = 0.04, CMS4 vs CMS1 HR = 4.2, 95% CI: 0.7-24.6, p = 0.11).
Conclusions: We identified novel MSI-COAD transcriptomic subtypes that stratify patient response to ICI, including Nivolumab + Ipilimumab. In addition to personalizing patient care, these subtypes could inform clinical trial design and target discovery by identifying patients with an unmet clinical need.
Acknowledgements: We acknowledge FightCRC for funding this study and colleagues at Tempus AI and FightCRC for helpful discussion.

#5338 Clinicogenomic predictors of first-line immune checkpoint inhibitor outcomes in non-small cell lung cancer: A nationwide C-CAT cohort from Japan.

Mika Iwasaki[1], Takahiro Ando[1], Koki Fujii[1], Kousuke Watanabe[1], Katsutoshi Oda[2], Hidenori Kage[1]

[1]Department of Respiratory Medicine, The University of Tokyo, Tokyo, Japan,[2]Division of Integrative Genomics, The University of Tokyo, Tokyo, Japan

Background: The efficacy of immune checkpoint inhibitors (ICIs) in non-small cell lung cancer (NSCLC) varies, underscoring the need for predictive biomarkers. Programmed death-ligand 1 (PD-L1) and tumor mutational burden (TMB) are widely used but have limited sensitivity and specificity. Increasing evidence suggests that genomic alterations shape immune responses and influence ICI outcomes. However, data from large-scale real-world cohorts, particularly in East Asian patients, remain limited.

Methods: We retrospectively analyzed the Center for Cancer Genomics and Advanced Therapeutics (C-CAT) database, integrating comprehensive genomic profiling (CGP) results with clinical information from cancer patients across Japan, encompassing 99.7% of all CGP tests under the national insurance program. A total of 1,629 patients with stage IV NSCLC received first-line ICI-based therapy between 2019 and 2025. The primary endpoint was time to treatment failure (TTF); the secondary endpoint was overall survival (OS). We used age-stratified Cox models adjusted for covariates. Genomic covariates included *KRAS, KEAP1*, and *STK11*, with additional genes from an exploratory screening. To clarify interaction effects, we further expressed results as wild-type-referenced hazard ratios for *KRAS*-only, *KEAP1*-only, *STK11*-only, and their co-mutations (*KRAS-KEAP1* and *KRAS-STK11*). Sensitivity analyses included a formalin-fixed paraffin-embedded (FFPE)-only subset with TMB available (n = 1,095, categorized as <10 vs ≥10 mut/Mb), and models also adjusting for ECOG performance status (0, 1, ≥ 2).

Results: *BRAF* mutation was independently associated with longer TTF (HR 0.77, 95% CI 0.59-1.00; $p = 0.049$), whereas *KRAS*, *KEAP1*, and *STK11* alone showed no significant associations (HRs 1.21, 1.08, and 1.09; all $p > 0.21$). A significant *KRAS-KEAP1* interaction was associated with shorter TTF (HR 1.89, 95% CI 1.06-3.36; p = 0.032). Compared with PD-L1 ≥ 50%, PD-L1 < 1% was associated with shorter TTF (HR 1.17; $p = 0.041$). In a four-level comparison versus wild-type, *KRAS*-only and *KEAP1*-only were not significant (HRs 1.09 and 1.21), whereas the *KRAS-KEAP1* co-mutation was associated with higher risk of treatment failure (HR 2.48, 95% CI 1.50-4.10; $p < 0.001$). Results were consistent in FFPE-only subsets with TMB data. *KEAP1* ($p < 0.001$) and *STK11* ($p = 0.001$) were associated with worse OS, while *BRAF* showed no significant difference ($p = 0.840$).

Conclusions: In first-line ICI-treated stage IV NSCLC, *KRAS-KEAP1* co-mutation, not *KRAS* or *KEAP1* alone, identifies patients at high risk of early failure, whereas *BRAF* was associated with longer TTF. These findings highlight the importance of co-mutation profiling in guiding treatment selection and warrant prospective validation with integrative models incorporating PD-L1 and TMB.

#5339 Prevalence and distinct biological programs of small cell lung cancer molecular subtypes revealed by real-world clinico-genomics database.

Yige Luo[1], Lujia Wang[2], Nadine Jahchan[3], Peter Ansell[4], Xi Zhao[1], Weilong Zhao[1]

[1]Quantitative Medicine & Genomics, AbbVie Bay Area, South San Francisco, CA,[2]Data & Statistical Science, AbbVie Bay Area, South San Francisco, CA,[3]Precision Medicine, AbbVie Bay Area, South San Francisco, CA,[4]Precision Medicine, AbbVie Inc., North Chicago, IL

Background: Molecular subtypes of Small Cell Lung Cancer (SCLC) highlight patient heterogeneity and continue to carry potential as predictive biomarkers. Resistance to Immune Checkpoint inhibitor (ICI) and impact of RW treatments remain outstanding. We aim to enhance understanding of SCLC subtype biology and therapeutic implications by leveraging the multi-modal RWD with curated outcome and treatment pattern.

Methods: We analyzed a US-based SCLC cohort (381 samples; 376 patients) from Caris-ConcertAI linked clinico-genomic database. We performed Non-negative Matrix Factorization (NMF) on transcriptomic data from patients with treatment-naïve samples (n=230), and applied to treatment-experienced samples (n=66). Subsequent treatments included ICI+chemo (n=179) and chemo only (n=49). PD-L1 IHC results are based on the 22c3 assay using tumor percent cutoff of 1%. Gene signatures are obtained from MSigDB.

Findings: Consistent with previous literature, expression of lineage-defining transcription factors varied across four NMF subtypes. Two groups (NMF1-SCLC-A/N, 33.5% treatment-naïve vs. 33.3% experienced; NMF2-SCLC-A-like, 15.2% vs. 19.7%) were neuroendocrine (NE)-enriched; two (NMF3-SCLC-I, 28.7% vs. 21.2%; NMF4-SCLC-P-like, 22.6% vs. 13.6%) displayed immune features, with prevalence remained in post-treated samples. NMF1 showed activated transcriptional programs of ASCL1/NEUROD1, high proliferation signatures, and low immune infiltration—consistent with classical NE subtypes. NMF2 exhibited ASCL1-associated activity, while its elevated metabolic pathways differ from canonical SCLC-A. NMF3 resembled the inflamed SCLC-I subtype, with broad immune signatures, confirmed by higher prevalence of PD-L1 IHC positivity. Yet the promise of an efficacious ICI therapy could be dampened by concurrently heightened immunosuppressive TGF-β/fibrosis pathways. REST/NOTCH activation and low NE features in NMF3 indicated YAP1-driven NE dedifferentiation, accompanied by hypoxia-related programs (angiogenesis, KRAS signaling) that may inform targeted therapy. NMF4 matched canonical SCLC-P with POU2F3 activation and MYC overexpression. Though atypical, the concurrent expression between POU2F3 and NEUROD1 may point to MYC-driven subtype mixing. Preliminary analysis revealed NMF3-SCLC-I subtype with the best prognosis. Survival outcomes vary by treatment received within NMF subtypes, warranting further validations on their predictive values.

Conclusion: SCLC molecular subtypes from this US RW cohort align and extend those from global clinical trial cohorts, revealing distinct clusters enriched with metabolic pathway and subtype mixing. Current SoC regimen has limited impact on the subtype prevalence. The analysis of RW outcome associated with subtypes' unique pathway activation will inform novel treatment strategies.

#5340 Landscape of ALK fusion breakpoints and subtypes: A comparative analysis of DNA-NGS versus RNA-NGSs.

Yanwei Li, Yanli Chen, Yameng Cui

Tianjin Medical University Cancer institute and Hospital, Tianjin, China

Background: ALK fusions are important therapeutic biomarkers across solid tumors, and accumulating evidence shows that fusion breakpoints, isoforms, and fusion orientations influence response to ALK tyrosine kinase inhibitors (TKIs). Non-canonical or reciprocal fusions and rare breakpoints may yield nonfunctional transcripts and lead to inferior outcomes. Understanding the differences in ALK fusion profiles detected by DNA-based and RNA-based next-generation sequencing (NGS) is therefore critical for optimizing molecular testing and guiding targeted therapy.
Methods: A total of 34,085 solid tumor patients were analyzed, including 15,957 tested by DNA-NGS and 18,128 by RNA-NGS. ALK fusion positivity, fusion orientations, and characteristics of subtypes were compared between DNA- and RNA-based sequencing approaches.
Results: DNA-NGS identified 358 ALK-positive patients carrying 547 fusions, while RNA-NGS identified 469 patients with 482 fusions. RNA-NGS showed a significantly higher positivity rate than DNA-NGS (2.6% vs. 2.2%, $p = 0.043$). The two approaches differed markedly in fusion multiplicity: 57.5% of DNA-positive patients harbored multiple fusions, including one patient with eight partners, whereas only 2.5% of RNA-positive patients showed multiple events. Additionally, 27 DNA-NGS cases carried exclusively non-canonical reciprocal or non-reciprocal fusions, suggesting potential nonfunctional variants that complicate therapeutic interpretation.Fusion orientation and partner diversity also varied substantially. All RNA-detected fusions were canonical 5′→3′ events, involving 11 partner genes; EML4 accounted for 97%, followed by KLC1, DCTN1, and KIF5B (each <1%). Conversely, the DNA-NGS cohort included 3.8% 3'→3' fusions, 5.6% 5'→5' fusions, and among the 5'→3' events, only 70% represented canonical forward fusions. In total, 38 partner genes were identified in the DNA group, with EML4 remaining most prevalent (85.5%), followed by KIF5B (2.0%) and STRN (1.2%). Only five fusion partners overlapped between the two detection modalities.Breakpoint diversity was greater in DNA-NGS (21 breakpoint types vs. 17 in RNA-NGS). Although EML4-ALK isoform distributions were similar ($p = 0.55$), DNA-NGS identified more atypical short-variant breakpoints (3.1% vs. 2.1%), which are associated with lower protein expression and poorer TKI response.
Conclusions: RNA-NGS achieved a higher detection rate and a cleaner, more biologically meaningful ALK fusion profile, with fewer multi-partner or non-canonical events and predominately functional fusion isoforms. DNA-NGS frequently identified complex or potentially nonfunctional structures that may mislead therapeutic decisions. These findings suggest that RNA-NGS provides a more accurate representation of transcriptionally active ALK drivers and may be better suited to guide ALK-targeted therapy.

#5341 Real-world landscape of BRAF fusions in chinese patients with lung and colorectal cancers: Insights from 26,248 DNA-NGS and RNA-NGS tests.

Li Wang, Wanpu Wang, Xinyan Pan, Ming Tang, Juanjuan Zhang

Department of Pathology, The First People's Hospital of Yunnan Province, Kunming, China

Background: Although rare, *BRAF* fusions are highly actionable alterations with strong responses to targeted therapy, particularly in lung and colorectal cancers. Their significant clinical relevance makes accurate detection essential, despite challenges posed by their low frequency and heterogeneous structures across sequencing technology. This study provides a large real-world analysis of *BRAF* fusion characteristics in Chinese lung and colorectal cancer patients, focusing on fusion partners, co-mutations, and differences between DNA-based and RNA-based next-generation sequencing (NGS).

Methods: A total of 26,248 patients underwent NGS testing, including 11,337 analyzed by DNA-NGS and 14,911 by RNA-NGS. *BRAF* fusions, partner genes, breakpoint patterns, and co-occurring driver alterations were systematically evaluated. Detection performance and fusion configuration differences were compared between DNA-NGS and RNA-NGS.

Results: Among all patients, 55 individuals (0.43%) carried 65 distinct *BRAF* fusions, with a higher proportion of female patients (58.5%). IMMP2L was the most common fusion partner (11.1%), followed by *TRIM24* (7.9%), *CD74* (6.3%), and *MKRN1* (6.3%). Co-mutations were identified in 30 fusion-positive patients, 90% of whom had lung cancer, consistent with reports suggesting *BRAF* fusions often emerge as secondary events after targeted therapy.Overall *BRAF* fusion prevalence did not differ significantly between DNA-NGS and RNA-NGS (0.24% vs. 0.19%, $p = 0.45$). However, the two platforms showed marked differences in fusion structure. All RNA-NGS-detected fusions were canonical 5′-3′ events, with *BRAF* exon 10 and exon 2 as the most frequent breakpoints (28.6%). In contrast, only 55.6% of DNA-NGS-detected cases showed canonical 5′-3′ fusions. Six of these also carried reciprocal or non-reciprocal rearrangements, while 12 cases harbored only non-canonical reciprocal configurations, suggesting that several DNA-NGS-identified events may not be transcriptionally functional or may represent structural variants lacking RNA expression.Importantly, the most frequent subtype, *IMMP2L-BRAF*, was detected exclusively in the RNA-NGS cohort, suggesting potential technical limitations in resolving *IMMP2L*-related breakpoints at the DNA level and underscoring the methodological advantages of RNA profiling.

Conclusions: This large real-world cohort outlines the *BRAF* fusion landscape in Chinese lung and colorectal cancers and reveals substantial discordance between DNA-NGS and RNA-NGS. The distinct partner spectrum and structural differences observed reinforce the value of RNA-based sequencing for accurate detection of clinically actionable *BRAF* fusions, supporting the integration of RNA analysis to optimize molecular testing and guide targeted therapeutic decisions.

#5342 Analysis of RNA expression of 47 cell surface proteins in real-world small cell lung cancer patients.

Sana Parveen[1], Emma T. Corcoran[2], Sebastia Franch-Exposito[2], Prerna Jain[2], Jacob Mercer[2], Abdul R. Naqash[3], Christine M. Lovly[4], Paul Fields[2], Hui-Zi Chen[5]

[1]Medical College of Wisconsin, Wauwatosa, WI,[2]Tempus AI, Chicago, IL,[3]Department of Medicine, University of Oklahoma, Oklahoma City, OK,[4]Department of Medical Oncology & Therapeutics Research, City of Hope Comprehensive Cancer Ctr., Duarte, CA,[5]Division of Hematology & Oncology, Department of Medicine, Medical College of Wisconsin, Wauwatosa, WI

Small cell lung cancer (SCLC) is an aggressive, smoking-induced bronchogenic lung cancer with few effective treatment options and an abysmal prognosis. Almost all patients relapse after initial induction chemotherapy and immunotherapy, and clinical benefit from subsequent therapies including tarlatamab-dlle (a DLL3 bispecific T cell engager) are limited. Herein, we performed an exploratory analysis of RNA expression of 47 cell surface proteins (CSPs) and 11 selected associated ligands in SCLC patients sequenced with Tempus xT (DNA-seq) and xR (RNA-seq). The CSPs include targets of immune checkpoint inhibitors (ICIs) and antibody-drug conjugates (ADCs) that are either FDA approved or currently evaluated in clinical trials. CSPs with important roles in modulating the tumor microenvironment (both tumor and stromal cell markers) were also evaluated. Leveraging Tempus dataset's clinical and molecular annotations, we stratified SCLC patients by subtypes (ASCL1, NEUROD1, POU2F3, Inflamed), treatment status (naïve vs. treated), and disease stage (limited vs. extensive). Non-parametric statistical tests (Wilcoxon Rank-Sum Test, Kolmogorov-Smirnov (KS) Test and Anderson-Darling (AD) Test) were applied to uncover robust differential expression patterns across these strata. We interrogated N=1,353 patients for CSP gene expression by subtype. We demonstrate that expression of certain CSPs are enriched in multiple (>2) SCLC subtypes including *DLL3*, *SEZ6*, *CEACAM5*, *CD276* and *MUC1*. We further identified subtype-specific CSP expression including *SSTR2* in NEUROD1 as well as *NECTIN4* and *ERBB3* in POU2F3. ICI targets including *CTLA4*, *PDCD1*, and *CD274* as well as the ADC target *TACSTD2* were increased in Inflamed and to a lesser extent the POU2F3 subtypes. With respect to disease stage, ICI and ADC targets such as *CTLA4*, *CD274*, *PDCD1*, *TIGIT*, *ICOS*, *TACSTD2*, and *MUC1* were significantly ($p<0.05$) more highly expressed in LS-SCLC (N=210) than in ES-SCLC (N=1,137). With respect to treatment status, we detected significantly ($p<0.05$) higher expression of *CTLA4*, *PDCD1*, *TIGIT*, *TACSTD2*, and *ITGB6* in treatment-naïve (N=744) than in SCLC patients who had received at least one line of systemic treatment (N=384). Although protein-level validation will be important and should be done when feasible, our exploratory analysis demonstrates that RNA expression of clinically relevant CSPs in SCLC patients may be influenced by subtype classification, cancer stage, and treatment status.

#5344 Variant allele frequency machine learning model identifies unique TP53-mutant phenotypes with worse post-operative survival in pancreatic cancer.

Imaad Said[1], Eugene Chen[2], Megan Zeller[2], Mohammed Aldakkak[1], Matthew Sochor[2], Bhabishya Neupane[2], Kshitij Gaur[2], Mandana Kamgar[3], Alexandria Phan[2], Janice Zhao[2], Samih Thalji[1], Beth Erickson[1], Christina Small-Tom[2], Callisia Clarke[2], Kathleen K. Christians[1], Nikki K. Lytle[1], Thomas McFall[2], William A. Hall[1], Anai N. Kothari[1], Douglas B. Evans[4], **Yongwoo David Seo**[2]

[1]Medical College of Wisconsin, Wawautosa, WI,[2]Medical College of Wisconsin, Wauwatosa, WI,[3]Medical College of Wisconsin, Milwaukee, WI,[4]Dept. of Surgery, Medical College of Wisconsin, Milwaukee, WI

Introduction: Even after neoadjuvant therapy (NAT) and resection for localized pancreatic ductal adenocarcinoma (PDAC), overall survival (OS) varies greatly. Clinical factors such as positive lymph nodes (LNs) can stratify risk, but greater precision is needed; comprehensive genomic profiling (CGP) can bridge this gap. We present a novel method of combining machine learning (ML) with variant allelic frequency (VAF) to identify drivers of OS.

Methods: We identified all localized PDAC patients who completed NAT, resection, and had CGP data. Stratifying OS from surgery by median, an XGBoost ML framework was utilized to extract features of importance using clinicopathologic variables, as well as VAFs for any present pathogenic mutations (with VAF=0% for wildtype [wt]). Model performance was evaluated using area under the curve (AUC) and Shapley additive explanation plots (SHAP), with Kaplan-Meier curves for clinical validation. In patients with available whole transcriptome data, DESeq2 was utilized for differential expression profiling.

Results: Among 110 patients with CGP data, 89 (81%) were KRAS mutated (G12D 33%, G12V 23%, and G12R 18%), and 67 (61%) had pathogenic TP53 mutation (mut). Initial models using known pathogenic mut VAFs identified TP53 as the highest impact feature. Addition of TP53 VAF, when combined with time-of-surgery clinical variables (age, comorbidity index, pathologic LN and T stage, lymphovascular or perineural invasion), improved prediction of OS (AUC = 0.81), vs. clinical variables alone (AUC = 0.73). SHAP analysis showed high TP53 VAF and LN+ status as the two highest contributing features for poor OS. When categorized by TP53 and LN status, TP53 mut/LN+ patients had significantly worse OS than all other groups (median 11.0 mo [95%CI 7.4-15.3] vs. 23.0 mo [20.4-32.1], p<0.0001); there was no difference in OS between TP53 wt/LN+, TP53 mut/LN-, and TP53 wt/LN-. When stratified into high vs. low VAF by median (6.5%), only high VAF patients had worse OS (10.7 mo [6.7-22.0]) compared to wt(25.9 mo [16.5-38.7], p=0.05.)78 of the 110 patients had bulk transcriptomic data available on the same specimens. TP53 mut tumors had significantly higher expression of LYPD2 (one of the human lymphocyte antigen-6 proteins associated with worse outcomes; log10 fold 4.4, p<1e-9), as well as keratin genes KRT13 (log10 fold 2.3, p <0.0001) and KRT15 (log10 fold 1.3, p <0.0001) - associated with basal subtypes and worse outcomes.

Conclusion: VAF analysis from CGP can uncover novel predictive targets for post-surgical outcomes. TP53 mut tumors express higher levels of genes associated with worse prognosis (e.g. LYPD2, KRT genes). When present with LN+, TP53 mut confers worst OS and may be a clonally dependent process (based on VAF). Post surgical TP53 mut/LN+ cohorts should be stratified as high risk and be considered for adjuvant treatment and clinical trials.

#5345 Large-scale genomic analysis of pancreatic cancer in a real-world patient population.

Avinash Ramu[1], Vasily Aushev[1], J. Bryce Ortiz[1], Alyssa Antonopoulos[1], Maria Diab[2], Philip A. Philip[3], David Kwon[3], Soma Subramaniam[1], Adham Jurdi[1], Gregory P. Botta[4]

[1]Natera, Inc., Austin, TX,[2]Division of Hematology and Medical Oncology, Department of Internal Medicine, Henry Ford Health and Michigan State University, Detroit, MI,[3]Henry Ford Pancreatic Cancer Center, and Department of Surgery, Henry Ford Health, Detroit, MI,[4]Division of Hematology and Oncology, Department of Medicine, University of California San Diego Moores Cancer Center, La Jolla, CA

Pancreatic cancer (PC) remains one of the deadliest malignancies, with minimal improvement in survival over recent decades. Fundamental questions persist regarding how genomic alterations influence PC biology and therapeutic response. Using a large multi-modal real-world genomic database, we sought to characterize the mutational and transcriptional landscape of PC and identify patterns that may inform future precision medicine approaches. Whole-exome sequencing (WES) data from tumor tissue samples were analyzed for patients with PC included in Natera's proprietary Real-World Database. Sequencing was performed as part of the tumor-informed, personalized Signatera™ circulating tumor DNA assay designed between May 2019-Nov 2024. After excluding cases of low tumor mutational burden and variant allele frequency, a total of 3,664 patients were included in the analysis. Variant calling was performed using Mutect2 and VarScan2. For prevalence analysis, only non-synonymous somatic SNVs and INDELs were included. Germline variant analysis was performed for 128 cancer predisposition genes in both tumor and normal samples; ClinVar pathogenic/likely pathogenic (P/LP) germline variants were retained. RNA sequencing data, from Altera™ tumor genomic profiling test (Natera, Inc.), were available for 658 patients, of whom 391 had matched WES data. Among the 3,664 patients with PC, the male/female ratio was [50%/50%], and the stage distribution was: I (14.6%%), II (24.4%), III (24.8%), IV (28.2%), and unknown (7.9%). Genetic ancestry composition included European (74.5%), African (10.9%), Latino/Admixed American (7.9%), East Asian (5.0%), and South Asian (1.5%) populations. The most frequently somatically mutated genes were *KRAS* (78%), *TP53* (62%), *CDKN2A* (18%), *SMAD4* (18%), and *ARID1A* (8%). The most common individual somatic variants were $KRAS^{G12D}$ (32%), $KRAS^{G12V}$ (25%), $KRAS^{G12R}$ (13%), $TP53^{R175H}$ (5%), and $KRAS^{Q61H}$ (4%). No statistically significant ancestry-based differences were observed in either gene or variant-level frequencies. P/LP germline variants were detected in 210 patients, comprising 149 unique variants across 34 genes, most commonly *ATM*, *BRCA2*, *MUTYH*, *BRCA1*, and *PALB2*. Among RNA-Seq profiled tumors, expression analysis identified patients with basal and classical molecular subtypes associated with distinct genomic features and clinical outcomes.

This real-world study represents one of the most extensive characterizations of PC to date, integrating WES, germline, and RNA-Seq data from over 3,500 patients. The findings confirm the predominance of canonical driver alterations (*KRAS*, *TP53*, *CDKN2A*, *SMAD4*) and highlight germline and transcriptomic diversity across the disease spectrum. Ongoing analyses are assessing transcriptional variation across *KRAS* and other genomic features and will link these profiles with survival outcomes to determine clinical relevance.

#5346 Prognostic impact and clinical characteristics of *KRAS* mutations and *CDKN2A* loss in *IDH1*-mutant intrahepatic cholangiocarcinoma.

Eiichiro So[1], Chigusa Morizane[1], Kouya Shiraishi[2], Nobuyoshi Hiraoka[3], Miyuki Sone[4], Takafumi Koyama[5], Rui Kitadai[6], Yusuke Okuma[7], Takashi Kohno[2], Tetsuro Shiraishi[2], Yuno Goto[1], Shiho Hakui[1], Kiyoaki Ochi[1], Keita Fujisaki[1], Kazunori Onuma[1], Yasuhiro Komori[1], Daiki Yamashige[1], Mao Okada[1], Shota Harai[1], Yuta Maruki[1], Yasuyuki Kawamoto[1], Yoshikuni Nagashio[1], Susumu Hijioka[1], Hideki Ueno[1], Kenro Hirata[8], Takanori Kanai[8], Takuji Okusaka[1]

[1]Department of Hepatobiliary and Pancreatic Oncology, National Cancer Center Hospital, Tokyo, Japan,[2]Division of Genome Biology, National Cancer Center Research Institute, Tokyo, Japan,[3]Division of Pathology and Clinical Laboratories, National Cancer Center Hospital, Tokyo, Japan,[4]Department of Diagnostic Radiology, National Cancer Center Hospital, Tokyo, Japan,[5]Department of Experimental Therapeutics, National Cancer Center Hospital, Tokyo, Japan,[6]Department of Medical Oncology, National Cancer Center Hospital, Tokyo, Japan,[7]Department of Thoracic Oncology, National Cancer Center Hospital, Tokyo, Japan,[8]Division of Gastroenterology and Hepatology, Department of Internal Medicine, Keio University School of Medicine, Tokyo, Japan

Background: In the ClarIDHy trial, ivosidenib significantly improved progression-free survival (PFS) compared with placebo in patients with previously treated *IDH1*-mutant cholangiocarcinoma (CCA) and is currently awaiting insurance approval in Japan. However, approximately 40% of patients in both arms experience disease progression within 2 months, suggesting underlying biological heterogeneity within *IDH1*-mutant CCA. We hypothesized that genomic co-alterations may serve as potential determinants of this heterogeneity.
Methods: We analyzed patients with intrahepatic cholangiocarcinoma (iCCA) in the Center for Cancer Genomics and Advanced Therapeutics (C-CAT) database between June 2019 and June 2025. Point mutations were annotated using OncoKB, and copy number variants and rearrangements were evaluated using C-CAT (approval number CDU2021-001N). Additionally, we reviewed institutional patients with *IDH1*-mutant iCCA diagnosed between October 2001 and October 2025, with detailed pathological and radiological assessments (approval number 2018-149).
Results: Among 2484 patients with iCCA, 353 had *IDH1* mutations (14.2%). *IDH1*-mutant iCCA tended to show longer overall survival (OS) and time to treatment failure (TTF) for first-line therapy than *IDH1*-wild type (median OS, 22.4 vs. 20.1 months; HR, 0.83; *P*=0.054; median TTF, 7.8 vs. 6.4 months; HR, 0.87; *P*=0.068). In *IDH1*-mutant iCCA, *KRAS* mutations and *CDKN2A* loss were less frequent than *IDH1*-wild type (*KRAS* mutations, 11.6% vs. 27.6%, *P*<0.001; *CDKN2A* loss, 17.8% vs. 27.5%, *P*<0.001). Among *IDH1*-mutant iCCA, *KRAS* mutations showed a trend toward shorter OS (median, 17.0 vs. 23.2; HR, 1.60; *P*=0.069) and were associated with shorter TTF (median, 5.7 vs. 8.5 months; HR, 1.86; *P*=0.0039). *CDKN2A* loss was correlated with shorter OS (median, 17.6 vs. 23.7 months; HR, 1.58; *P*=0.037). *IDH1*-mutant iCCA without *KRAS* mutations or *CDKN2A* loss demonstrated significantly longer OS (median, 24.9 vs. 17.6 months; HR, 0.61, *P*=0.010) and TTF (median, 8.4 vs. 6.1 months; HR, 0.70, *P*=0.020) than the other subsets. In multivariate analysis, *KRAS* mutations predicted shorter OS (HR, 1.75; *P*=0.046) and TTF (HR, 1.77; *P*=0.012). In an institutional cohort of 37 patients, only one case was pathologically classified as large-duct type and harbored *KRAS* mutation, with all other cases classified as small-duct type. Radiologically, *IDH1*-mutant iCCA without *KRAS* mutations and *CDKN2A* loss tended to present in a peripheral location (60.0% vs. 33.3%) and intratumoral transversing vessels (84.0% vs. 55.6%).
Conclusions: *IDH1* mutations less frequently co-occur with *KRAS* mutations and *CDKN2A* loss. *IDH1*-mutant iCCA without these co-alterations exhibited favorable clinical outcomes and distinct radiopathological characteristics, highlighting the biological heterogeneity associated with genomic co-alterations in *IDH1*-mutant iCCA.

#5347 Real-world clinicogenomic comparison of early- and average- onset gastric cancer.

Hannah McDonald, Lilia Turcios, Neelima Hosamani, Abu Saleh Mosa Faisal, Chi Wang, Joseph Kim, **Mautin Barry-Hundeyin**

University of Kentucky, Lexington, KY

In recent decades, there has been an unprecedented rise in gastric cancer among younger individuals, contrasting with a decline among older individuals. However, the biological underpinnings of gastric cancer in younger individuals remain poorly understood. We described the clinicopathologic and genomic characteristics of early-onset gastric cancer (EOGC) compared to average-onset gastric cancer (AOGC). We analyzed 311 patients using the multi-institutional prospective Oncology Research Information Exchange Network (ORIEN) database to compare demographic, clinicopathologic, genomic, and survival outcomes between EOGC (<50 years; N=72) vs AOGC (>50 years N=239). Genomic, germline, and RNA sequencing data were analyzed and compared between the cohorts. Mutational and immune signatures were also processed. EOGC patients exhibited significantly higher rates of pain at diagnosis (53% vs 30% *p=0.001*), but not anemia or reflux. EOGC patients were more likely to present with stage III/IV disease (70% vs 45% *p=0.006*) and diffuse/signet ring histology (47% vs 16% *p=0.002*). Consequently, OS was decreased in the younger cohort (HR 1.52; p=0.03). Somatic mutational load was decreased in young patients. Significantly mutated genes in the entire cohort included *CDH1*, *ARID1A*, *TP53*, *PIK3CA,* but *CDH1* was more frequently mutated in the EOGC cohort (40% vs 18% *p=0.09*). Significant differences in RNA expression were observed, with upregulated epithelial mesenchymal transition (EMT), myogenesis, and apical junction. Immune deconvolution revealed a predominance of M2 macrophages, mast cells, and $CD4^+$ T cell subsets, but no differences between cohorts. Early-onset gastric cancer has unique clinical and genomic features. Pathway dysregulation in EOGC may contribute to tumorigenesis and therapy resistance. This study underscores the necessity for further research into novel therapies, biomarker discovery, and early detection methodologies in younger individuals.

#5348 Tumor remodeling pathways are enriched in the tumor microenvironment of obesity-associated colorectal cancer.

Yu Fujiwara[1], Sarbajit Mukherjee[2], Yali Zhang[1], Jianmin Wang[1], Emily Baiyee Toegel[3], Tiago Biachi De Castria[4], Bodour Salhia[5], Anne M. Noonan[6], Michael J. Cavnar[7], Dae Won Kim[4], Muneeb Rehman[8], Patrick B. Boland[9], Melissa L. Fishel[10], Carlos H.F. Chan[11], Michele M. Gage[12], Hassan Hatoum[13], Julia White[14], Robert J. Rounbehler[15], Michelle Churchman[15], Deepak Vadehra[1]

[1]Roswell Park Comprehensive Cancer Center, Buffalo, NY,[2]Miami Cancer Institute, Baptist Health South Florida, Miami, FL,[3]University of Colorado Cancer Center, Aurora, CO,[4]Moffitt Cancer Center, Tampa, FL,[5]USC Norris Comprehensive Cancer Center, Los Angeles, CA,[6]Ohio State University, Columbus, OH,[7]Markey Cancer Center, Lexington, KY,[8]University of Virginia, Charlottesville, VA,[9]Rutgers Cancer Institute, New Brunswick, NJ,[10]IU Simon Comprehensive Cancer Center, Indianapolis, IN,[11]Carver College of Medicine, University of Iowa, Iowa City, IA,[12]Murtha Cancer Center, Bethesda, MD,[13]Oklahoma University Stephenson Cancer Center, Oklahoma City, OK,[14]University of Kansas Cancer Center, Kansas City, KS,[15]Aster Insights, Tampa, FL

Background: Obesity is a known risk factor for colorectal cancer (CRC) that promotes systemic inflammation and T-cell dysfunction, yet the characteristics of the tumor immune microenvironment (TIME) in obesity-associated CRC are not well-defined. Therefore, we performed a comprehensive analysis to characterize the unique immunological and genomic features of obesity-associated CRC.

Methods: We performed genomic and transcriptomic analyses of patients with CRC stratified by body mass index (BMI) - obese (BMI ≥30), overweight (25≤ BMI <30), normal (18≤ BMI <25), and underweight (BMI<18). Data were obtained from the Oncology Research Information Exchange Network (ORIEN). Differential gene expression (DGE) and gene set enrichment analyses (GSEA) were performed to identify differentially expressed immune-related genes and altered biological pathways; immune deconvolution was performed to explore tumor immune microenvironment composition using CIBERSORT. Concurrently, genomic data were explored to compare the alteration frequency of selected genes (*APC, KRAS, TP53, SMAD4, PIK3CA, BRAF, NRAS, TGFBR2, MLH1, MSH2, MSH6, PMS2, CTNNB1,* and *PTEN*) using a Fisher's exact test. Statistical models were adjusted for covariates such as age, gender, and disease stage to isolate the effects of obesity.

Results: Overall, 939 patients (obese: n=355; overweight: n=326; normal: n=242; underweight: n=16) were included. Male sex was more common as weight increases ($p<0.0001$) but disease stage was well balanced across BMI groups ($p=0.581$). GSEA revealed that obesity was significantly associated with pathways related to tissue remodeling, including epithelial-mesenchymal transition, coagulation, and angiogenesis. Conversely, normal weight status was characterized by the upregulation of metabolic processes such as oxidative phosphorylation and fatty acid metabolism, alongside pathways governing cell cycle progression and DNA repair (normalized enrichment score ≥ 2.0, adjusted p value <0.05). Although immune cell compositions via immune deconvolution did not differ between obese and normal weight groups, DGE analysis revealed higher expression of several immune checkpoint related genes such as CD276 (B7H3) and SIRPα (CD47 ligand) in the obesity group and CD73 (NT5E) and apoptosis-inducing gene, TNFSF10 (TRAIL) in the normal weight. The alteration frequency of selected genes was not significantly different between obese and normal groups.

Conclusions: CRC with obesity is characterized by tumor remodeling whereas CRC without obesity had more upregulated metabolic processes in the TME. Differential expression status of key immune checkpoints between cases with and without obesity could indicate a tailored therapeutic target in this disease entity.

#5349 Refining tumor mutational burden as a predictive biomarker for pembrolizumab: A real-world analysis of 1,899 Japanese patients.

Tomoyo Yasuda[1], Mio Yumura[1], Azusa Hamasaki[1], Tongyi Fei[1], Takashi Kubo[2], Hitoshi Ichikawa[3], Takashi Kohno[3], Kuniko Sunami[2]

[1]Sysmex Corporation, Hyogo, Japan,[2]National Cancer Center Hospital, Tokyo, Japan,[3]National Cancer Center Research Institute, Tokyo, Japan

Tumor mutational burden (TMB) is a key biomarker for predicting the response to immune checkpoint inhibitors (ICIs). However, its predictive accuracy in real-world clinical practice, particularly in Asian populations, remains inadequately evaluated. We addressed this issue by analyzing real-world data from 63,952 patients registered in the Center for Cancer Genomics and Advanced Therapeutics (C-CAT) database, which integrates genomic and clinical information from Japanese patients with various advanced solid tumors. We assessed the therapeutic efficacy of pembrolizumab in 1,899 patients who underwent one of three comprehensive genomic profiling tests: FoundationOne CDx, the OncoGuide NCC Oncopanel System, or the GenMine TOP Cancer Genome Profiling System. Based on the reported TMB values, patients were classified as TMB-high (≥10 mutations per megabase) or TMB-low (<10 mutations per megabase). The objective response rate (ORR) among 946 TMB-high patients exceeded 30% and was significantly higher than that observed in 953 TMB-low patients (16.8%, $P < 0.001$). Notably, patients with borderline TMB values (10 to less than 13 mutations per megabase) exhibited relatively modest responses (20.8%). The ORR improved when hotspot mutations were excluded from the TMB calculation, suggesting that this adjustment enhances the predictive accuracy of TMB. These findings support the clinical utility of TMB as a biomarker for predicting ICI response in routine oncology practice. In particular, excluding hotspot mutations from TMB calculations may improve response prediction in patients whose TMB values are near the threshold.

#5350 Evaluating prognostic biomarkers in advanced epithelial ovarian carcinoma using machine learning on real-world data.

Carlos Ronchi, **Coryandar Coulomb**, Frances Peterson, Danielle Bloch, Kathleen Burke

Tempus AI, Inc., Chicago, IL

Introduction: Real-world data (RWD) offers a valuable tool for identifying novel prognostic factors in heterogeneous diseases. We leveraged the Tempus multimodal RWD database to analyze outcomes for patients with advanced epithelial ovarian carcinoma (EOC) and primary peritoneal carcinoma (PPC). Our primary objective was to apply machine learning (ML) models to identify and evaluate clinical prognostic biomarkers for real world progression-free survival (rwPFS). A secondary objective was to build a well-characterized, real-world cohort of patients receiving standard-of-care (SoC) treatment to serve as a foundation for this analysis.

Methods: Using the Tempus database we constructed a retrospective real-world clinical biomarker cohort of 3016 patients with Stage III/IV EOC or PPC who received first-line (1L) carboplatin and paclitaxel and had a reductive surgery prior to or within 30 days of 1L treatment start. We included relevant clinical variables, such as CA125, race, ECOG, obesity status, histology, and lymphocyte counts. rwPFS was analyzed using Kaplan-Meier and Cox proportional hazard models. Using this cohort, we trained Random Survival Forest (RSF), Cox Regression, and Regularized Cox Regression models to predict rwPFS risk. Model interpretability and feature importance were assessed using SHAP (SHapley Additive exPlanations) values.

Results: The median rwPFS (mPFS) for this cohort was 18.5 months (95% CI: 17.5-19.6), establishing a baseline for this advanced SoC-treated population. The RSF model, trained on the clinical biomarker cohort (N=2769, 80% training, 10% validation, 10% test), demonstrated prognostic performance for rwPFS (AUC = 0.7 at 18 months). SHAP analysis of the RSF model confirmed CA125 as the most significant prognostic feature, consistent with clinical practice. Obesity (BMI threshold > 30) was identified as an important prognostic feature, with obese patients having higher SHAP values compared to non-obese. A stratified analysis showed that CA125 levels were prognostic in non-obese patients (mPFS, Low vs. High: 20.2 [95% CI: 16.1-24.2] vs. 14.7 months [95% CI: 13.0-16.3]), whereas for obese patients mPFS estimates were similar across the two CA125 groups (mPFS, Low vs. High: 14.7 [95% CI: 12.5-20.9] vs. 14.3 months [95% CI: [11.2-17.5]).

Conclusions: Our study demonstrates the utility of applying ML models to large-scale, multimodal RWD to identify and validate prognostic factors in advanced EOC and PPC. Our models confirmed the primary prognostic power of CA125 and identified obesity as an independent prognostic factor. The observed differential prognostic impact of CA125 between obese groups highlights a potential health disparity and underscores the need for further investigation into population-specific biomarkers to ensure the development of equitable prognostic models.

#5351 Epidemiology of folate receptor alpha expression in ovarian cancer by age, race/ethnicity, and histotype in a real-world, US-based clinicogenomic database.

Rebecca C. Arend[1], Kent F. Hoskins[2], Jenny S. Guadamuz[3], Gregory S. Calip[4], Megan A. Clarke[4], Yookyung Christy Choi[4], Qu Zhang[4], Ricardo R. Lastra[5], Amanda L. Strickland[6], Sarah K. Lynam[7]

[1]University of Alabama at Birmingham, Birmingham, AL,[2]University of Illinois Chicago, Chicago, IL,[3]University of California Berkeley, Berkeley, CA,[4]AbbVie, Inc., North Chicago, IL,[5]The University of Chicago, Chicago, IL,[6]University of North Carolina at Chapel Hill, Chapel Hill, NC,[7]University Hospitals Seidman Cancer Center, Cleveland, OH

Ovarian cancer (OC) is molecularly heterogeneous, requiring biomarkers to guide personalized therapy. Folate receptor alpha (FRα) is an actionable biomarker with therapeutic implications. We evaluated FRα expression in OC by age, race/ethnicity, and histotype using real-world US clinicogenomic data.

We conducted a cross-sectional analysis of patients diagnosed with ovarian, fallopian tube, or primary peritoneal cancer from 2019 to 2025 using the ConcertAI RWD360™ database linked to Caris Life Sciences genomic data. FRα testing was done using the VENTANA FOLR1 (FOLR1-2.1) RxDx Assay (Roche Diagnostics); FRα-high was defined as ≥75% of tumor cells with ≥2+ membrane staining. Stratified prevalence rates and multivariable prevalence rate ratios (RRs) with 95% CIs were estimated using modified Poisson regression. Sensitivity and exploratory analyses evaluated associations with FRα expression in the full, unselected OC clinicogenomic database, applying a validated machine learning classifier trained on whole transcriptome RNAseq to predict FRα-high expression (N=3045).

Among 1155 patients with OC who received FRα testing, median age was 66 years (y) (IQR, 58-73); 71% were non-Hispanic White and 61% had high-grade serous histology. FRα-high expression was observed in 33%, with higher prevalence in high-grade serous (43%) compared to less common histotypes (low-grade serous, 24%; endometrioid, 6%; clear cell, 2%; carcinosarcoma, 9%) (*P*<0.001). There were no significant associations between FRα-high prevalence and age after adjusting for histotype (<50, Reference; 50-64, aRR 0.95, 95% CI 0.69-1.31; 65-74, aRR 1.15, 95% CI 0.84-1.57; ≥75 y, aRR 1.18, 95% CI 0.85-1.63). FRα-high prevalence did not differ by race/ethnicity (*P*=0.933) including after adjustment for age and histotype: non-Hispanic Black, 34% (aRR 1.03 [95% CI, 0.78-1.35]); non-Hispanic Asian, 29% (aRR 0.97, 95% CI 0.57-1.65); Hispanic, 30% (aRR 0.95, 95% CI 0.64-1.40); non-Hispanic White (32%, Reference). In sensitivity analyses restricted to high-grade serous histology, consistent associations with age and race/ethnicity were observed. In exploratory analyses, similar associations were observed in the broader database.

FRα-high expression does not significantly differ by age or racial/ethnic group and is most prevalent in high-grade serous OC. These findings further support FRα as an OC biomarker with broad clinical applicability across demographics and demonstrate the importance of accounting for potential confounding by histotype in studies of FRα-high prevalence. Further adoption of FRα testing in the work-up for advanced OC provides important information to ensure patients have access to all eligible treatment options and biomarker-directed clinical trials, particularly for underrepresented groups and those facing disparities in access to healthcare.

#5352 Genomic and ancestry-associated determinants of survival in gynecologic cancers.

Laura Chambers[1], Avinash Ramu[2], Vasily N. Aushev[2], Susan Rojahn[2], Alyssa Antonopoulos[2], Carly B. Scalise[2], Faraz Salmasi[2], Minetta C. Liu[2], Adam C. ElNaggar[2], Rebecca C. Arend[3]

[1]The Ohio State University, Columbus, OH,[2]Natera, Inc., Austin, TX,[3]Obstetrics and Gynecology, University of Alabama at Birmingham, Birmingham, AL

Survival outcomes for gynecologic cancers vary across populations; however, the genomic and other factors that contribute to these differences are poorly defined. We leveraged a large, real-world dataset to examine how genetic ancestry, tumor genomics, and histology are associated with overall survival (OS) in endometrial (EC), ovarian (OC), and cervical cancer (CC). This retrospective analysis used integrated data from whole-exome sequencing (WES), medical claims, mortality records, and electronic health records in Natera's proprietary de-identified Real-World Database. Tumor and germline WES data were obtained as part of the workflow for a personalized, tumor-informed mPCR-NGS circulating-tumor DNA assay (Signatera™, Natera Inc.). Variants, microsatellite instability (MSI), and genetic ancestry were analyzed. Ancestry was inferred by EthSeq and classified into predefined groups: African (AFR), American, East Asian (EAS), European (EUR), and South Asian. Cancer histologies were extracted from clinical records using natural language processing. OS associations were evaluated using Cox proportional hazards models. A total of 2,574 EC, 2,425 OC, and 773 CC patients were included. In EC, AFR ancestry was associated with worse OS compared to EUR ancestry (HR 1.56, p=0.013), especially in stage I/II patients (HR 2.1, p=0.03). The most frequent variants in EC were in *PTEN* (46.5% of patients), *PIK3CA* (40.6%), *TP53* (38.0%), and *ARID1A* (37.8%). Variants in *TP53* (stage I/II: HR 2.1, p<0.001; stage III/IV: HR 2.1, p<0.0001) and *KMT2B* (stage III/IV: HR 1.48, p=0.04) were linked with worse OS, while variants in *PTEN* (stage I/II: HR 0.5, p=0.002; stage III/IV: HR 0.44, p<0.0001) and *ARID1A* (stage I/II: HR 0.6, p=0.02; stage III/IV: HR 0.5, p<0.0001) were associated with better OS. Microsatellite stable (MSS) EC tumors had a worse OS than MSI-High (MSS vs MSI-H: HR 2.0, p<0.001). In OC, stage I AFR patients had worse OS compared to EUR patients (HR 7.5, p=0.04). OC tumor variants were most common in *TP53* (59.7%), *PIK3CA* (11.4%), *and ARID1A* (10.5%), consistent with established OC biology. No associations with OS and variants, MSI, or histology were identified. In CC, AFR ancestry was associated with worse OS vs EUR (HR 2.0, p=0.04). *PIK3CA* variants were common (29.5% of patients) and associated with worse OS in stage II/III/IV patients (HR 1.9, p=0.015). No OS differences by histology were observed. Across cancers, AFR and EAS ancestry showed distinct histologic distributions compared with EUR. In conclusion, genetic ancestry was independently associated with OS across gynecologic cancers, particularly among AFR-ancestry patients with EC and CC. Specific genomic features (e.g., MSI status and *TP53, PTEN, ARID1A, PIK3CA,* and *KMT2B* variants) further define risk. Further study of ancestry-informed genomic and pathologic data into clinical research may reduce survival disparities in gynecologic malignancies.

#5354 Extrachromosomal DNA shapes aggressive transcriptional states in multiple myeloma.

Hi Eun Jung[1], Saeam Shin[2], Yu Ri Kim[3], Ja Min Byun[4], Youngil Koh[4], Junshik Hong[4], Dong-Yeop Shin[4], Inho Kim[4], Hoon Kim[5], Hyunsoo Cho[4]

[1]Biomedical Research Institute, Seoul National University Hospital, Seoul, Korea, Republic of,[2]Department of Laboratory Medicine, Yonsei University College of Medicine, Seoul, Korea, Republic of,[3]Department of Internal Medicine, Yonsei University College of Medicine, Seoul, Korea, Republic of,[4]Department of Internal Medicine, Seoul National University Hospital, Seoul, Korea, Republic of,[5]Department of Biopharmaceutical Convergence, School of Pharmacy, Sungkyunkwan University, Suwon-si, Korea, Republic of

Background:
Extrachromosomal DNA (ecDNA) is increasingly recognized as a key driver of oncogene amplification, intratumoral heterogeneity, and poor clinical outcomes across solid tumors. However, its significance in multiple myeloma remains largely unexplored. Multiple myeloma is characterized by marked genomic instability including hyperdiploidy or IgH translocations, and widespread structural rearrangements that underlie biological heterogeneity and therapy resistance. Defining whether ecDNA contributes an additional layer of genomic complexity in this disease therefore represents an important unmet need.
Methods:
Whole-genome sequencing (WGS) BAM files of patient tumor samples from the Multiple Myeloma Research Foundation (MMRF) CoMMpass study were analyzed using the AmpliconSuite pipeline to identify circularized DNA amplicons indicative of ecDNA. Matched transcriptome (RNA-seq) data and clinical metadata from the same cohort were integrated to evaluate the prognostic impact of gene expression associated with ecDNA-harboring loci. Gene Set Enrichment Analysis (GSEA) was performed using the *clusterProfiler* R package to assess pathway-level biological signatures linked to ecDNA-positive tumors.
Results:
We identified ecDNA in 28 of 904 patients (3.1%) from the MMRF CoMMpass dataset. Despite the low prevalence, ecDNA-positive myeloma patients exhibited significantly inferior survival compared with patients without ecDNA. Frequently amplified ecDNA loci contained oncogenes such as *MYC, TNFRSF17 (BCMA),* and *SNX29,* as well as pro-tumoral lncRNAs including *CASC11* and *PVT1.* GSEA revealed strong enrichment of MYC and E2F targets, oxidative phosphorylation, and PI3K-AKT-mTOR and mTORC1 signaling in ecDNA-positive tumors, highlighting transcriptional addiction and metabolic activation. These pathways align with known mechanisms of proliferation, metabolic rewiring, and treatment resistance in multiple myeloma.
Conclusions:
ecDNA-positive myeloma represents a biologically aggressive subset characterized by oncogene-enriched circular amplicons and hyperactivated proliferative and metabolic programs. Myeloma patients with ecDNA showed significantly worse survival, supporting ecDNA as a previously underrecognized high-risk feature. These findings highlight ecDNA as potential therapeutic vulnerabilities in myeloma and warrant further investigation.

#5356 Leveraging a real-world clinicogenomic database for post-sequencing quality assessment in solid tumor comprehensive genomic profiling (CGP).

Erin N. Newburn[1], Rebecca A. Previs[1], Michelle F. Green[1], Kyle C. Strickland[1], Heidi Ko[1], Taylor Jensen[2], Eric Severson[1], Hardik Parikh[3], Maria-Fernanda Senosain[3], Jie An[1], Erik Van Roey[3], Daniel Metzger[1], R.J. Seager[3], Mark Sausen[4], Jennifer Jackson[4], Kenneth Valkenburg[4], Brian Caveney[5], Marcia Eisenberg[5], Shakti Ramkissoon[1]

[1]Labcorp, Durham, NC,[2]Labcorp, Fuquay-Varina, NC,[3]OmniSeq, LLC, Buffalo, NY,[4]PGDx, Baltimore, MD,[5]Labcorp, Burlington, NC

The quantity and integrity of DNA and RNA extracted from formalin-fixed paraffin-embedded (FFPE) tumor specimens can vary significantly due to factors such as block age, fixation conditions, protein crosslinking, and the presence of chemical inhibitors. Over a decade of research has demonstrated that, with optimized pre- and post-analytical workflows, FFPE samples can serve as reliable input material for both clinical and research-based next-generation sequencing (NGS) applications. Certain tumor types present additional challenges for nucleic acid extraction due to their biological characteristics, such as high metabolic activity and elevated nuclease levels. To evaluate sequencing quality across diverse tumor tissue types, we analyzed post-sequencing metrics from clinical tests performed over a 12-month period using the OmniSeq INSIGHT test for CGP. The cohort included 8,645 solid tumor samples representing 19 distinct cancer types. The most frequently profiled tumors were lung (N=3,984), colorectal (N=1,211), breast (N=578), pancreatic (N=398), prostate (N=331), uterine (N=252), esophageal (N=232), and head and neck (N=221). Key post-sequencing quality metrics that assess sequencing coverage and on target mapping were evaluated. Across all indications, high-quality data metrics were consistently achieved for both DNA and RNA, underscoring the robustness of the workflow regardless of tumor type. These findings support the scalability and reliability of CGP using FFPE tissue across a broad spectrum of solid tumors, reinforcing its utility in clinical oncology and research applications for high-quality genomic reporting.

#5357 Molecular tumor registries - A learning system for real world data (RWD).

Erik Larsen[1], Chenbo Sun[2], Michele Cosi[3], Rudy Salcido[3], Sarah Roberts[3], Nirav Merchant[3], Justin Starren[4], **Ritu Pandey**[5]

[1]University of Arizona Cancer Center, Tucson, AZ,[2]Cellular and Molecular Medicine, Tucson, AZ,[3]University of Arizona, Tucson, AZ,[4]Center for Bioinformatics and Biostatistics, Tucson, AZ,[5]University of Arizona Cancer Center, Center for Biomedical Informatics and Biostatistics, Cellular and Molecular Medicine, Tucson, AZ

Background: Genomic data is a key component for drug discovery and precision medicine, an innovative approach for tailoring treatment and prevention that is useful for clinicians and researchers. Patient care now often involves comprehensive genomic profiling through certified clinical lab vendors. The clinical interpretation of molecular alterations is at the heart of providing the value of precision medicine and yet this Real-World Data is not always seamlessly integrated along with Real World Evidence (RWE) in electronic health records (EHR). We present the challenges and lessons learned in developing an end-to-end secure platform, along with the opportunities that a molecular registry opens for RWE in clinical care and research.
Design: The molecular tumor registry IMPACT (Individual Molecular Registry of Patients for Accelerated Clinical and Translational Medicine) is built within a secure data enclave, “Soteria”, a HIPAA compliant high-performance compute (HPC) cluster. The software tools include an R package of JSON parsers to extract NGS and other results and store them within a DuckDB. An interactive RShiny web application is deployed on a secure VM within the secure enclave. This provides a real-time, de-identified genomics data feed of test metadata including tumor site, test types, genes, variants, and several associated elements for every case. Optimized data pipelines have been constructed for bulk NGS files, for comprehensive analysis. AI tools have been deployed for connecting the National Clinical Trial registry and associated FDA-approved targeted drugs.
Results: The data is accelerating in size as more tests are being ordered by clinicians and new tests are developed by the vendors. Common challenges are a) time devoted to advance the process due to legal hurdles and inflexible contracts, b) lack of common nomenclature and data formats to compare and interpret results across vendors, c) constant change of technology and tests and d) Integration with the EHR. The registry opens up opportunities - 1) to normalize and harmonize results across vendors, 2) enable genomically informed clinical trials and patient recruitment, 3) facilitate a molecular tumor board, 4) enable cohort discovery and integrative analysis with RWE data from EHR, 5) support biomedical trainee education 6) provide opportunity to deploy LLM (Large Language Models)-powered tools for data investigation and deep learning models for research.
Conclusions: The learning system, IMPACT, enables bringing molecular sequencing and clinical data together in a secure enclave to learn from RWD from patients utilizing power discovery approaches. Real-world insights from visualizing the pan-cancer results from both a high and granular level is an invaluable resource for accelerating research and treatment strategies across cancers, the epitome of translational research.

#5358 Disparities between genomic alterations and clinical trial representation in precision oncology.

Jingyao Zhang[1], Raoul Santiago[2], Kamila Bakirhan[3], Tenzin Tamdin[1]

[1]Danbury Hospital, Danbury, CT,[2]CHU Laval Research Ctr., Quebec, QC, Canada,[3]Praxair Cancer Center, Danbury Hospital, Danbury, CT

Background: Precision oncology has shifted from histology-based treatment toward molecularly driven frameworks, but it remains unclear whether clinical trial priorities align with the real-world genomic landscape. This study evaluated biomarker-driven solid tumor trials from 2010 to 2025 and compared trial representation with genomic prevalence in TCGA.
Methods: Interventional solid tumor trials (2010-2025) were extracted from the AACT ClinicalTrials.gov database and processed in Python. Adult solid tumor studies were identified via structured filters, and 30 predefined biomarkers were detected through text-mining of titles, eligibility criteria, and interventions. Manual review removed false positives, and biomarker names were harmonized across AACT and TCGA. TMB-high was defined as ≥10 mutations per megabase, and MSI-high was defined as MSIsensor score ≥10. Trials were categorized by phase, sponsor type, and tissue specificity. Representation ratios (trial frequency ÷ TCGA genomic prevalence) were calculated, with ratios >1.5 classified as over-represented, 0.5-1.5 as balanced, and <0.5 as under-represented. TCGA overall survival (OS) analyses were performed for each biomarker.
Results: Among 7,259 biomarker-driven solid tumor trials, 19.4% were tissue-agnostic, 54.5% were industry-sponsored, and 79.6% were early-phase (I/II). Of the 30 biomarkers analyzed, 6 (20%) were over-represented, 16 (53%) were balanced, and 8 (27%) were under-represented relative to their TCGA genomic prevalence. Over-represented biomarkers included EGFR (28.4% vs 8%), VEGFA (12.5% vs 2%), FGFR3 (6.0% vs 3%), and HER2 (12.4% vs 6%), reflecting prioritization of highly druggable oncogenic drivers. In contrast, under-represented biomarkers included TP53 (2.0% vs 37%), STK11 (0.5% vs 8%), KEAP1 (0.2% vs 4%), TMB-high (2.9% vs 12%), and CDKN2A (7.3% vs 17%), most of which were tumor suppressors without approved targeted therapies and have recognized immune relevance. Alterations in TP53, CDKN2A, and KEAP1 were associated with significantly shorter OS in TCGA (all $p < 0.001$), underscoring their prognostic significance despite limited clinical trial representation.
Conclusions: Current oncology trials disproportionately focus on established, targetable oncogenes, while high-prevalence tumor suppressor alterations and immune-related biomarkers remain underrepresented. This mismatch highlights a translational gap between genomic prevalence and clinical trial design and underscores opportunities to broaden biomarker inclusion, expand tissue-agnostic frameworks, and integrate real-world genomic data to advance equitable precision oncology.

#5359 Precision oncology in practice: Comprehensive genomic profiling identifies actionable alterations and guides therapeutic selection in 756 clinical solid tumors.

Sarabjot Pabla[1], Sushant Khadgi[2], Anjana N. Bhattacharya[2], Asia Chang[3], Mark Gardner[2]

[1]Quest Diagnostics, Baltimore, MD,[2]Quest Diagnostics, Secaucus, NJ,[3]Quest Diagnostics, San Franscisco, CA

Background: Comprehensive genomic profiling (CGP) of solid tumors is increasingly used to inform targeted and immune-directed therapies; real-world performance data are needed to guide further adoption. This study reports multi-laboratory experience running the TSO500 (TruSight Oncology 500) solid tumor assay on 756 clinical FFPE samples across different tumor types and evaluates, variant tier and biomarker distribution that impacts treatment decisions.

Methods: TSO500 was performed on 756 routine clinical specimens, where DNA/RNA were isolated from FFPE specimens. Sequencing was performed at two sites using NovaSeq600. Post sequencing, NGS data was analyzed using Illumina TSO500 analysis pipeline. SNVs, INDELs, Copy Number Alterations were estimated from DNA whereas gene fusions were estimated and reported using tumor RNA. Variants were classified as per AMP/ASCO/CAP tiers. Other biomarkers including tumor mutational burden (TMB) and microsatellite instability (MSI) were reported. Clinical decision impact was assessed by variant Tier classification.

Results: Of the 756 clinically reported samples, major disease types included lung cancer (63.3%), colorectal cancer (11.51%), solid neoplasm (9.26%), pancreatic cancer (5.16%), melanoma (1.72%) and breast cancer (1.19%). of the 12,461 reported variants across all samples, 19.3% (2407/12461) were classified by AMP variant classification. 50% (1216/2407) of these variants were actionable variants (AMP Tier I/II). Tier III variants of unknown significance comprised 29.3% (705/2407) and Tier IV/benign 20.2% (486/2407). Clinically relevant biomarkers detected included high TMB (≥10 mut/Mb) in 32.8% and MSI-high in 3.3% of cases; gene fusions were detected in 9.8% (74/756). CGP results informed treatment selection (Variants with strong clinical significance (e.g., those with FDA-approved therapies or included in professional guidelines) in 30% of cases and Variants with potential clinical significance (e.g., supported by preclinical data, case reports, or ongoing clinical trials in 58% of overall specimens tested. Additionally, Tier 3 variants of unknown significance were reported in 60% of cases.

Conclusions: In this large real-world study, our CGP assay delivered identified actionable genomic alterations in nearly half of cases across diverse solid tumors. These results demonstrate the high-throughput CGP assay, provide scalable detection of molecular alterations to support precision oncology, enabling reporting and therapy selection of hundreds of samples per week.

: Prognostic Biomarkers 3
Poster Session

#5363 Validation of microenvironment gene signatures from FFPE to predict nasopharyngeal cancer prognosis.

Yi Ren[1], Wei Keat Teo[1], Bingcheng Wu[2], Joseph W. Foley[1], Chee Yit Lim[1], Serene Chor Hiang Siow[1], Han Lee Goh[1], Eugenia Li Ling Yeo[3], Enya Hui Wen Ong[3], Melvin Lee Kiang Chua[3], Jianjun Liu[4], Kwok Seng Loh[1], Raymond Tsang[1], Joshua K. Tay[1]

[1]Department of Otolaryngology, National University of Singapore (NUS), Singapore, Singapore,[2]Department of Pathology, National University Hospital, Singapore, Singapore,[3]Division of Medical Sciences, National Cancer Centre Singapore, Singapore, Singapore,[4]Human Genetics, Genome Institute of Singapore, , Agency for Science, Technology and Research (A*STAR), Singapore, Singapore

Background: Nasopharyngeal carcinoma (NPC) is endemic to Southern China and Southeast Asia. Gene expression profiling and biomarker identification in NPC with conventional bulk RNAseq has been challenging due to substantial heterogeneity in cellular composition and limited tissue availability. While we have previously described the microdissected gene expression landscape of NPC and its tumor microenvironment (TME) subtypes, prognostic gene signatures for treatment response remain poorly defined.

Methods: We obtained formalin-fixed paraffin-embedded (FFPE) biopsies from 64 NPC patients matched for stage but with different clinical outcomes, i.e., the treatment failure group (recurrent/metastatic disease) and the survivor group (remained disease-free). Laser-capture microdissection was performed to isolate the tumor epithelial (TUM) and TME regions based on H&E staining and pathologist annotation. Gene expression libraries were prepared using a specialized RNAseq protocol optimized for FFPE tissues. Following next generation sequencing, bioinformatic analyses were performed to develop gene signatures predictive of clinical outcomes.

Results: After quality control, 277 gene expression libraries were analyzed, consisting of 154 TUM and 123 TME libraries. Unsupervised consensus clustering of TME libraries identified three conserved clusters (average Silhouette width = 0.89). These TME clusters were characterized as immune (C1), epithelial-infiltrative (C2), and stromal (C3) gene signatures based on gene set enrichment analysis (GSEA) and in-silico deconvolution. Notably, 63.2% and 72.7% of TME libraries in C1 and C3 were from survivors, while 61.5% in C2 were from treatment failures (chi-square test, $p = 0.0397$). Gene signatures for TME clusters were derived from upregulated genes in each cluster, and single-sample GSEA (ssGSEA) was used to calculate signature scores in two independent NPC cohorts (PMID:28851814 and PMID:40412382). Consistently, Kaplan-Meier analyses showed that patients with high C1 or low C2 scores had better progression-free survival (log-rank p-values 0.005 to 0.031). Interestingly, these TME cluster gene signatures outperformed the gene signature derived directly from the treatment failure versus survivor comparison in TME, suggesting that biologically meaningful TME-based gene signatures capture prognostic signal more robustly and generalize better across cohorts.

Conclusions: In this study, we identified three distinct TME clusters in NPC and derived gene signatures that consistently predict progression-free survival across cohorts. These results highlight the value of TME-based biomarkers for risk stratification and precision medicine. Importantly, our FFPE LCM RNAseq workflow enabled high-quality, cell type-specific profiling from archival biopsies, supporting its utility for uncovering clinically relevant biomarkers.

#5364 Neutrophilic skin infiltrates in patients with acute myeloid leukemia (AML) are clonal and associate with poor overall survival.

Gabby Tesfaye[1], Yazan Abu-Shihab[1], Deedra Nicolet[2], Jill Buss[2], Andrea Laganson[2], Catherine Chung[2], SANAM LOGHAVI[2], Benjamin Kaffenberger[3], **Ann-Kathrin Eisfeld**[4]

[1]The Ohio State University Comprehensive Cancer Center, Columbus, OH,[23]The Ohio State University Wexner Medical Center, Columbus, OH,[4]Postdoctoral Fellow, Dept. of Human Cancer Genetics, Ohio State University College of Medicine, Columbus, OH

Background: Acute myeloid leukemia (AML) is an aggressive hematologic malignancy. While blast infiltration (leukemia cutis, LC) is a known extramedullary disease, reactive neutrophilic dermatoses (like Sweet's syndrome) are common, but their etiology remains unclear. We aimed to determine if these lesions represent an atypical leukemic process.
Methods: We analyzed the clinical and molecular characteristics, including survival outcomes, in 1,019 consecutive AML patients for histopathologically evaluated skin lesions (10 days prior and up to 60 days post-diagnosis). Patients with reactive neutrophilic dermatoses underwent confirmation for absence of leukemic blasts. We then performed paired tumor/normal whole-exome sequencing on bone marrow (BM) and FFPE-derived skin biopsy tissues for 8 such patients.
Results: Dermatology consultation was required in 31% of patients. While reactive inflammation generally showed high complete remission (CR) rates (91%), patients with reactive neutrophilic dermatoses had the shortest disease-free survival (DFS) of all patient groups, with a median DFS of only 13 months. Clinically, these patients frequently harbored NPM1 (27%), IDH1/2 (41%), and FLT3-ITD (23%) mutations. Next, we sequenced paired samples from 4 patients whose skin lesions were confirmed as blast-free. Remarkably, sequencing of the skin lesions revealed AML gene mutations identical to those found in the BM blasts, with near-identical variant allele fractions (VAFs) in both tissues. Three of four patients also harbored mutations in genes encoding keratin-associated proteins.
Conclusions: Morphologically normal, mutationally clonal, neutrophilic infiltrates represent a distinct extramedullary manifestation of leukemia that differs from classical leukemia cutis but has significant clinical and biological relevance (poor survival). A similar phenomenon is known for chronic myelomonocytic leukemia (CMML). If validated, this may identify an underappreciated type of leukemic involvement and possible escape mechanism.

#5365 Clinicopathological and prognostic analyses of colorectal cancer with neuroendocrine differentiation.

Yuki Yasuda[1], Keigo Murakami[2], Hideaki Karasawa[1], Wataru Kosaka[1], Yota Akamori[1], Ichiro Ise[1], Tomoyuki Ono[1], Megumi Murakami[1], Yoshihiro Sato[1], Gumpei Yoshimatsu[1], Hideyuki Suzuki[1], Takashi Kamei[1], Shinobu Ohnuma[1], Toru Furukawa[2], Michiaki Unno[1]

[1]Department of Surgery, Tohoku University Graduate School of Medicine, Sendai, Japan,[2]Department of Investigative Pathology, Tohoku University Graduate School of Medicine, Sendai, Japan

Background: A subset of colorectal cancers (CRCs) exhibits neuroendocrine differentiation (NED), characterized by the expression of neuroendocrine markers such as synaptophysin and chromogranin A. Although NED has been reported to be associated with aggressive behavior and poor prognosis in other cancer types, the clinicopathological and prognostic significance of NED in CRC remains unclear due to limited and inconsistent evidence. A better understanding of CRC with NED may provide insights into its molecular characteristics and potential therapeutic strategies.
Methods: Patients with pathological stage II-IV CRC who underwent surgical resection at our institution between 2013 and 2017 were retrospectively analyzed. Immunohistochemical staining for synaptophysin was performed on formalin-fixed, paraffin-embedded tissue sections. NED was defined as positive when the H-score for synaptophysin was ≥4. Clinicopathological features—including lymphovascular and perineural invasion, desmoplastic reaction pattern, tumor budding grade, and poorly differentiated cluster (PDC) grade—were compared between NED-positive and NED-negative groups. Overall survival (OS) and relapse-free survival (RFS) were analyzed using Kaplan-Meier method.
Results: Among 261 evaluable CRC cases, 21 (8.0%) were classified as NED-positive based on synaptophysin expression. The NED-positive group included 9 males and 12 females, with a median age of 68 years old (range, 17-91 years old). The TNM classification (8th edition) was as follows: pathological stage II (n=4, 4.1%), stage III (n=10, 9.3%), and stage IV (n=7, 12.5%) of the total cases in each stage. Compared with NED-negative CRCs, the NED-positive group more frequently exhibited the following features: perineural invasion (61.9% vs. 31.3%), high-grade tumor budding (G2/G3: 61.9% vs. 33.8%) and PDC (G2/G3: 47.6% vs. 21.3%). The median OS and RFS for the NED-positive group were 78 months and 28 months, respectively. The 5-year OS and RFS rates were 71.9% and 35.3% in the NED-positive group, compared with 75.1% and 67.1% in the NED-negative group, respectively. RFS was significantly shorter in CRCs with NED than in those without (log-rank test, p=0.0073).
Conclusions: The presence of NED tended to be associated with perineural invasion and high-grade PDC, suggesting a trend toward more aggressive histopathological features. RFS was significantly shorter in CRCs with NED than in those without, indicating a possible association between NED and early recurrence.

#5366 Prognostic value of tumor-informed circulating tumor DNA in non-small cell lung cancer after curative treatment: real-world cohort with long-term follow-up.

Soyun Lim[1], Jisoo Lee[1], Julianne Jin[1], Anthony Wong[1], Youjin Oh[1], Sung Mi Yoon[1], Jeeyeon Lee[2], Joo Hee Park[1], Soowon Lee[1], Timothy Hong[1], Bella Kim[1], Sanghwa Kim[1], Liam Il-Young Chung[1], Young Kwang Chae[3]

[1]Northwestern University Feinberg School of Medicine, Chicago, IL,[2]Kyungpook National University Hospital, Daegu, Korea, Republic of,[3]Robert H. Lurie Comprehensive Cancer Center of Northwestern University, Northwestern University Feinberg School of Medicine, Chicago, IL

Background: Circulating tumor DNA (ctDNA) is a biomarker for detecting molecular residual disease (MRD) and predicting recurrence in cancer patients. Our group previously reported the first real-world data of ctDNA-based MRD detection. We now investigate its long-term prognostic value with extended follow-up in the real-world cohort of non-small cell lung cancer (NSCLC) patients treated with curative-intent.

Methods: Longitudinal ctDNA monitoring was performed using a commercially available personalized, tumor-informed assay (Signatera) in 116 patients with NSCLC. Plasma samples were collected post-treatment, and ctDNA status was evaluated within the 6-month MRD window, and longitudinally thereafter. Recurrence-free survival (RFS) and overall survival (OS) were assessed according to ctDNA status. For ctDNA(+) patients, plasma-based next-generation sequencing (NGS; Guardant360) at MRD timepoint was performed when available and compared with baseline tissue NGS results (PGDx or Tempus xT).

Results: A total of 116 patients across stages I-IV (stage I: 41.4%, stage II: 30.2%, stage III: 21.6%, and stage IV: 6.9%) were identified (90 adenocarcinoma, 23 squamous cell carcinoma, 2 adenosquamous and 1 other). Median age at diagnosis was 66 years (range: 23-86 years) and median follow-up was 33 months (range: 4-120 months). MRD results were available for 99 patients within 6 months of curative-intent treatment. Within the 6-month MRD window, ctDNA(+) was associated with inferior RFS (aHR: 24.3; 95% CI: 3.2-186.8; $p < 0.001$), with a median RFS of 8.5 months. ctDNA(+) during longitudinal surveillance beyond MRD window was associated with inferior RFS (HR: 8.0, 95% CI: 3.4-18.9; $p < 0.001$) and OS (HR: 11.6, 95% CI: 3.4-39.8; $p < 0.001$), with median RFS of 10.8 months. Among patients with both tissue NGS (tNGS) and blood NGS (bNGS) profiling results, 8 patients were ctDNA(+). Among them, 5 patients had at least one overlapping gene mutation at the variant level between tNGS and bNGS. All 5 of these patients recurred, while the other 3 patients (who did not have an overlapping gene mutation at the variant level) did not recur. The matched group consisted mostly of stage III cases (4 of 5), with one stage II, whereas the unmatched group included one each of stage I, II and IV cases.

Conclusion: This first real-world report with extended follow-up provides real-world evidence that tumor-informed, personalized ctDNA monitoring is a clinically valuable tool for predicting long-term outcomes in patients with NSCLC after curative-intent treatment. Although interpretation is limited by the small sample size, blood NGS at ctDNA(+) may reflect potential subclonal evolution and molecular heterogeneity. These findings support the prognostic value of ctDNA and its potential integration into personalized cancer management.

#5367 Clinical and molecular features of CD276 (B7H3) in liver metastases of pancreatic cancer.

Go Igarashi[1], Shuichi Mitsunaga[1], Nobuaki Okumura[2], Kanae Inoue[1], Tomonao Taira[1], Taro Shibuki[1], Tomoyuki Satake[1], Masataka Amisaki[1], Mitsuhito Sasaki[1], Hideaki Takahashi[1], Hiroshi Imaoka[1], Masafumi Ikeda[1]

[1]Hepatobiliary and Pancreatic Oncology, National Cancer Center Hospital East, Kashiwa-shi, Japan,[2]Institute for Protein Research, Osaka University, Suita-shi, Japan

Introduction: CD276 (B7-H3), a modulator of tumor-microenvironment as affecting cadherin expression, has a prognostic impact in the different types of cancers including pancreatic ductal adenocarcinoma (PDAC). In metastatic PDAC, these roles in CD276 have not been fully understood. Using liver metastasis (LM)-derived transcriptome and reversed-phased protein array (RPPA) data, we evaluated CD276 expressions of LMs on clinical outcomes and molecular features in metastatic PDAC.

Methods: Needle-biopsied specimens from treatment-naïve LMs of PDAC were collected for protein and RNA extraction. A 435-protein expression was measured on RPPA. The impact of each protein level stratified with median value was tested using univariate Cox regression hazard model. The top 3 prognostic proteins and clinical prognostic factors such as Eastern Cooperative Oncology Group Performance Status (ECOG-PS) and serum level of C-reactive protein (CRP) were evaluated in multivariate Cox regression hazard model. To investigate clinical relevance of CD276, our study population was stratified based on the median value of CD276 mRNA expression level detected on cDNA microarray, followed by differential gene expression analysis and subsequent Gene Ontology (GO) analysis between the two groups surveying for CD276 high-related genes/ pathways.

Results: RPPA data was obtained from LMs of 42 patients (Male: 64.2%; median age: 66 years). The tumor proteome data showed that overall survival times were prolonged in the patients with intratumoral high expression of Aurora-A, PGDFR-beta, and CD276 as compared to those without. Independent prognostic impacts were found in CD276 high (hazard ratio: 0.148 [95% confidence interval: 0.005 to 0.434]), ECOG-PS 1 or more (4.651 [1.713 to 12.63]), and CRP high (6.440 [2.498 to 16.60]) in multivariate analysis. Transcriptome data were evaluated in 40 of 42 LMs. The 116 genes were identified as CD276 high-related genes. GO terms associated with CD276 high were cadherin binding (GO:0045296), cell adhesion molecule binding (GO:0050839), and protein binding (GO:0005515). LMs with high CD276 protein expression showed high protein expression in E-cadherin ($P<0.001$) and tended to be low in protein expression of N-cadherin ($P=0.097$) as compared to those with low CD276 protein expression.

Conclusion: High expression of CD276 protein in liver metastasis of PDAC was an independent favorable prognostic factor and related to increasing E-cadherin expression in tumor. Further study is needed to explore the roles of CD276 in metastatic PDAC.

#5368 The prognostic role of pretreatment neutrophil-to-lymphocyte ratio in a multiethnic cohort of breast cancer patients.

Armaan Jamal[1], Lendy Chu[2], Jincong Q. Freeman[1], Rita Nanda[3], Olufunmilayo I. Olopade[3], Wenji Guo[3], Dezheng Huo[1]

[1]Department of Public Health Sciences, University of Chicago, Chicago, IL,[2]Internal Medicine Residency Program, University of Chicago, Chicago, IL,[3]Department of Medicine, University of Chicago, Chicago, IL

Introduction: The neutrophil-to-lymphocyte ratio (NLR) is a marker of systemic inflammation linked to poor outcomes in several solid tumor malignancies, including breast cancer. Prior studies have shown that its prognostic significance in breast cancer differs by molecular subtype; however, these studies have rarely accounted for racial variation in baseline NLR values, which may affect the interpretation of threshold-based analyses. This study evaluates the prognostic value of pretreatment NLR in breast cancer and whether associations between NLR and survival outcomes differ by race and tumor subtype.

Methods: We conducted a retrospective analysis of 754 patients from the Chicago Multiethnic Epidemiologic Breast Cancer Cohort. Eligible patients had an NLR measurement ≤1 year prior to treatment initiation. NLR was analyzed as both continuous and binary variables, using a cohort-wide median cutoff (2.07) and race-specific cutoffs (3.11 for White and 2.56 for Black patients). Outcomes included recurrence-free survival (RFS), overall survival (OS), breast cancer-specific survival (BCSS), and other-cause (OC) mortality. Cox and competing risk regression models were used to estimate the associations between NLR and survival outcomes, adjusting for demographic and clinical covariates.

Results: Among 754 patients (mean age at diagnosis 55.9 years), 383 were Black, 308 were White, and 63 were categorized as Other. The median pretreatment NLR was lower in Black patients (1.78, IQR 1.30-2.61) compared to White (2.38, IQR 1.69-3.11) and Other racial patients (2.06, IQR 1.41-2.89). In adjusted analyses, each doubling of NLR was associated with worse RFS (adjusted hazard ratio [aHR] 1.24, 95% CI 1.02-1.52), OS (aHR 1.20, 95% CI 0.98-1.48), and OC mortality (aSHR 1.42, 95% CI 1.07-1.89). When modeled as a binary variable, high NLR (≥2.07) was associated only with higher OC mortality (adjusted sub-distribution hazard ratio [aSHR] 2.11, 95% CI 1.11-4.02). Stratified analyses showed that the association between NLR and survival outcomes was most pronounced in HER2-negative and hormone receptor-positive tumors, whereas no significant associations were observed in hormone receptor-negative tumors. When using race-specific thresholds, high NLR (≥2.56) was significantly associated with worse RFS (aHR 2.02, 95% CI 1.27-3.21), OS (aHR 1.93, 95% CI 1.15-3.21), and BCSS (aSHR 2.31, 95% CI 1.12-4.78) in Black patients, but not in White patients.

Conclusion: Our study demonstrates that pretreatment NLR may be used as a prognostic marker for breast cancer outcomes, but its predictive value varies by race and tumor subtype. Baseline racial differences in NLR underscore the need for race-specific thresholds. Larger, diverse studies are needed to validate these findings and clarify underlying biological mechanisms.

#5369 CCR8+ regulatory T cells represent a promising prognostic marker for non-small cell lung cancer (NSCLC).

Santosh K. Singh[1], Manoj K. Mishra[2], Eric Flenaugh[3], Gabriella M. Oprea-Ilies[4], Brian M. Rivers[1], James W. Lillard[1], Shailesh Singh[1], Rajesh Singh[1]

[1]Morehouse School of Medicine, Atlanta, GA,[2]Alabama State University, Montgomery, AL,[3]Pulmonary and Critical Care & Interventional Pulmonary Medicine, Atlanta, GA,[4]Winship Cancer Institute of Emory, Atlanta, GA

Non-small cell lung cancer (NSCLC) contains a highly diverse immune landscape, making it challenging to identify markers that truly reflect how the tumor interacts with the immune system. Recent research has identified CCR8 as a key marker for a particularly suppressive group of regulatory T cells (Tregs) that accumulate within tumors. In this study, we aimed to investigate the impact of CCR8$^+$ Tregs on disease outcomes in NSCLC and to deepen our understanding of their role in facilitating tumor evasion of the immune response. We employed various techniques, including multiparametric flow cytometry, RNA sequencing, and spatial immunohistochemistry, using NSCLC cell lines (H1299 and H1573) and patient-derived tumor samples to assess their effects. We observed that CCR8$^+$ Tregs were significantly enriched within tumor tissue compared to adjacent normal lung tissue. These CCR8$^+$ Tregs expressed higher levels of potent immunosuppressive molecules, including CTLA-4, TIGIT, and IL-10, as well as genes associated with TGF-β signaling, distinguishing them from CCR8$^-$ Tregs. Tumors with a high density of CCR8$^+$ Tregs had fewer CD8$^+$ T cells, reduced effector cytokine production, and lower levels of granzyme B, indicating weakened antitumor immunity. Additionally, patients with elevated CCR8$^+$ Treg infiltration tended to have more advanced diseases and shorter progression-free and overall survival, even after adjusting for standard clinical factors. Statistical modeling confirmed that CCR8$^+$ Treg levels independently predict patient outcomes. Further analysis and *in vitro* assays using NSCLC cell lines revealed that CCL1-CCR8 interactions likely drive the recruitment and retention of these cells within tumors. Overall, our findings show that CCR8$^+$ Tregs represent a uniquely suppressive immune population and a strong prognostic marker in NSCLC, supporting the development of therapies that specifically target CCR8 to enhance antitumor immunity.

#5370 Prognostic and metastasis-associated roles of IL-6 and IL-8 in patients with stage IV gastric cancer.

Jinsoo Jang[1], Chan Hee Park[1], Woo Sun Kwon[1], Tae Soo Kim[1], Sun Young Rha[2]

[1]Song-dang Institute for Cancer Research, Yonsei University College of Medicine, Seoul, Korea, Republic of,[2]Yonsei University College of Medicine, Seoul, Korea, Republic of

Background: Cytokine-driven inflammation is increasingly recognized as a key determinant of tumor progression and metastatic behavior in gastric cancer. Interleukin-6 (IL-6) and interleukin-8 (IL-8) are central mediators of immune suppression, angiogenesis, and systemic inflammatory activation, yet their clinical significance in advanced gastric cancer remains insufficiently defined.
Methods: Pre-treatment blood samples from 186 patients with HER2-negative stage IV gastric cancer treated at Severance Hospital between May 2019 and March 2025 were analyzed. Serum IL-6 and IL-8 levels were quantified by ELISA in patients with stage IV gastric cancer prior to systemic therapy. Patients were stratified into high- and low-expression groups using predefined cutoffs. PD-L1 expression was assessed by immunohistochemistry using the PD-L1 IHC 22C3 pharmDx assay and quantified by combined positive score (CPS). Associations with metastatic patterns and overall survival (OS) were assessed using nonparametric tests and Kaplan-Meier analysis.
Results: High cytokine expression was strongly associated with inferior clinical outcomes. Patients with high IL-6 levels (≥4.6862 pg/mL) showed significantly reduced OS compared with the IL-6-low group (HR 1.96, 95% CI 1.31-2.94; P=0.0008). A similar but more pronounced effect was observed for IL-8, where high expression (≥7.5801 pg/mL) was associated with markedly worse survival (HR 2.79, 95% CI 1.89-4.10; P < 0.0001). No correlation was observed between IL-6 and PD-L1 expression or between IL-8 and PD-L1 expression at any CPS cutoff. Cytokine levels also demonstrated metastatic pattern specificity: IL-6 was significantly elevated in patients with bone metastasis (P = 0.018) including IL-8 (P = 0.039), whereas IL-8 was markedly increased in those with liver metastasis (P = 0.002). These findings suggest that systemic cytokine elevation reflects both tumor aggressiveness and distinct metastatic phenotypes.
Conclusion: IL-6 and IL-8 are strong, accessible biomarkers associated with poor survival and characteristic metastatic patterns in advanced gastric cancer. Their integration into clinical risk assessment may improve biological stratification and inform future therapeutic strategies.

#5371 Annexin A3 expression is prevalent but highly variable in human cancer: A tissue microarray study involving 5,914 cancers from 105 tumor entities.

Clara von Bargen[1], Nayira Hakimi[1], Fiete Gehrisch[1], Anne Menz[1], Florian Lutz[1], Viktoria Chirico[1], Florian Viehweger[1], David Dum[1], Ria Schlichter[1], Andrea Hinsch[1], Christoph Fraune[1], Christian Bernreuther[1], Seyma Buyucek[1], Martina Kluth[1], Claudia Hube-Magg[1], Georgia Makrypidi-Fraune[1], Nina Schraps[1], Katharina Moller[1], Andreas M. Luebke[1], Patrick Lebok[1], Guido Sauter[1], Maximilian Lennartz[1], Till S. Clauditz[1], Andreas H. Marx[2], Ronald Simon[1], Eike Burandt[1], Natalia Gorbokon[1], Maria C. Tsourlakis[1], Sarah Minner[1], Till Krech[1], Morton Freytag[1], Viktor Reiswich[1], **Stefan Steurer**[1]

[1]Institute of Pathology, University Medical Center Hamburg-Eppendorf, Hamburg, Germany,[2]Department of Pathology, Academic Hospital Fuerth, Fuerth, Germany

Annexin A3 (ANXA3) is a member of the annexin family of calcium-dependent phospholipid-binding proteins which plays a major role in various membrane-related processes, including membrane organization, repair, vesicle trafficking, and regulation of ion channels. Its diverse functions extend across various cellular processes such as apoptosis, cell growth, inflammation, and differentiation. Altered ANXA3 expression has been found in several cancer types. To better comprehend the role of ANXA3 in cancer, ANXA3 expression was analyzed by immunohistochemistry (IHC) on tissue microarrays (TMAs) containing 5,914 samples from 105 different tumor types. ANXA3 staining was seen in 3,490 (72.3%) of the 4,824 analyzable tumors, and was considered weak in 18.2%, moderate in 10.2%, and strong in 44.0% of cases. Of 105 tumor categories, 87 (82.9%) showed ANXA3 expression in at least one case, 69 (65.7%) showed ANXA3 staining in at least 50% of cases, and 78 (74.3%) included at least one case with strong ANXA3 positivity. Among tumors with at least 10 evaluable samples, the highest rates of tumors with strong ANXA3 positivity were observed in ampullary (100.0%) and ductal adenocarcinoma of the pancreas (90.9%), adenocarcinoma of the cervix uteri (95.7%),gastrointestinal stromal tumor (GIST; 90.4%), colorectal adenocarcinoma (90.0%), gastric adenocarcinoma of the intestinal (88.7%) and diffuse (81.6%), basal cell carcinoma of the skin (88.2%), gallbladder adenocarcinoma (88.2%),esophageal adenocarcinoma (87.8%), prostatic adenocarcinoma (83.8%), endometroid (82.5%), serous (78.9%) and mucinous (72.7%) carcinoma of the ovary, papillary renal cell carcinoma (63.2%), cholangiocarcinoma (77.8%), endometroid (76.3%) and serous (50.0%) endometrial carcinoma, squamous cell carcinomas from different organs of origin (up to 61.9%), testicular seminoma (53.8%), carcinosarcoma of the ovary (53.3%), lobular (52.3%), mucinous (40.0%) and tubular (38.9%) carcinoma of the breast, clear cell carcinoma of the ovary (42.1%), muscle-invasive urothelial carcinoma (41.4%), carcinosarcoma of the uterus (40.0%), Brenner tumor (39.3%), invasive breast carcinoma of no special type (NST; 36.1%), urothelial carcinoma of the kidney pelvis (29.8%) and yolk sac tumors of the testis (27.3%). In breast cancer NST, low ANXA3 expression was linked to aggressive tumor phenotype. Strong ANXA3 staining was seen in 100.0% of Gleason 3+3, 87.3% of Gleason 4+4, and in 65.8% of Gleason 5+5 carcinomas of the prostate ($p<0.0001$). In breast cancer NST, low ANXA3 expression was linked to high grade of malignancy ($p<0.0001$). In summary, the data from this study provide a catalogue of ANXA3 expression in human cancer, demonstrate that ANXA3 levels are highly variable in most tumor entities, and show that ANXA3 immunostaining is associated with prognostic tumor features in at least some tumor types.

#5372 Fragmentomics analysis of targeted hybrid capture NGS cfDNA gene panel data yields an orthogonal genomic dimension for developing a robust prognostic model for metastatic breast cancer patients.

Gregory M. Mayhew, Jonathan H. Shepherd, Jeff Burdine, Yoichiro Shibata, Gabriel V. Milburn, Michael V. Milburn, Kirk L. Pappan, **James M. Davison**, Kirk Beebe

GeneCentric Therapeutics, Inc., Durham, NC, NC

Introduction: Analysis of cfDNA fragment distributions, or fragmentomics, yields information about the transcriptional activity of genes but mostly has been applied to WGS and WES datasets. The widespread use of targeted hybrid capture NGS cfDNA gene panels provide a rich data source for mining orthogonal fragmentomic features for developing novel algorithmic signatures for prognosis and predicting response. Here, we applied an uniquely developed fragmentomic computational method for hybrid capture panel data to a prospective study of HER2 negative, metastatic breast cancer patients, who were all treated with paclitaxel and bevacizumab.

Experimental Procedures*:* Fastq files from baseline (n=182) and associated clinical data were downloaded from NCBI (PRJNA745047). Raw sequencing (avg. depth ~2600x) data from a custom panel targeting 48 breast cancer associated genes and 8 cancer gene promoters were processed through a proprietary pipeline to get a fragmentomics matrix comprised of 2936 features. Samples were split into a train-test set (2/3-1/3) balanced on overall survival and key clinical variables. Overall survival (OS) and triple negative (TN) signatures using fragmentomics matrix features in training samples with the glmnet package in R. Association between the OS signature and OS was evaluated using the log-rank test and multivariable cox models. Association between the TN signature and TN status was evaluated using the Wilcoxon test and AUC.

Results: An OS signature developed in the training set used 56 fragmentomics features. The association between the signature and OS was directionally uniform in low and high tumor content strata (tumor content defined using the available VAF data) in both training and test data sets (and each nominal log-rank test p-value < 0.05). In the test set, the addition of the fragmentomics signature to a multivariable OS model that already included parameters for TN status, tumor grade, and metastatic site significantly improved the model fit (LRT p-value = 0.009), with a signature hazard ratio of 2.50 (95% CI 1.25-4.99). The TN status signature developed in the training set used 56 fragmentomics features of which 6 overlapped with the OS signature. In the test set, the signature was markedly correlated with TN status (Wilcoxon p-value = 0.0052) with an AUC of 0.75.

Summary and Conclusions: This work demonstrates the utility of cfDNA hybrid capture fragmentomic data for developing robust predictors even in low tumor fraction samples of overall survival and TN status. Although additional validation is warranted, these signatures could represent potential biomarkers that could assist in clinical decision making. This work also supports the possibility of retrospectively using any cfDNA panel sequencing dataset for fragmentomics analysis to identify predictive biomarkers.

#5373 Prognostic impacts of skeletal muscle gene expression and cachexia in advanced colorectal cancer.

Vashti L. Bandy[1], Arunima Punjala[2], Praveen Bhoopathi[1], Vignesh Vudatha[1], KATARZYNA TYC[1], Mikhail G. Dozmorov[1], Leopoldo Fernandez[1], Andrew R. Judge[3], Sarah M. Judge[4], Anna Gibson[5]

[1]Virginia Commonwealth University, Richmond, VA,[2]Virginia Commonwealth University - VCU, Richmond, VA,[3]University of Florida, Gainesville, FL,[4]University of Flordia, Gainesville, FL,[5]VCU Health, Richmond, VA

Background: Cancer cachexia is a complex metabolic syndrome characterized by severe muscle loss, reduced physical function, and diminished therapeutic response. Despite its clinical impacts, the transcriptional landscape of cachexia in patients with advanced peritoneal carcinomatosis from metastatic colorectal cancer (pmCRC) remains poorly defined. Our study aims to characterize alterations in skeletal muscle with associated cachexia in pmCRC patients.
Methods: Muscle biopsies were obtained from 17 pmCRC patients consented for IRB tissue collection and undergoing cytoreductive surgery with hyperthermic intraperitoneal chemotherapy (CRS/HIPEC), classified as myopenic (n=7) or non-myopenic (n=11) based on skeletal muscle index (SMI cm2/m2). Biopsies were sent for RNA sequencing and differential expression analysis was performed utilizing statistical algorithms within edgeR software. We compared the two cohorts and selected differentially expressed genes (DEGs) with significantly increased or decreased expression (>2-fold change and p-value <0.05). Enrichment analysis identified gene sets and pathways relevant to cachexia pathophysiology. Last, survival analysis was performed to assess the prognostic value of identified DEGs in predicting patient outcomes.
Results: Our analysis revealed 231 genes DEGs, including 75 upregulated and 156 downregulated genes in the myopenic group. Enrichment analysis exhibited several pathways involved in immune cell signaling. Overall survival analysis revealed associations with survival outcomes for seven DEGs-six of which have associated prognostic value in colorectal cancer or other cancer variants including pancreatic adenocarcinoma, hepatocellular carcinoma, renal cell carcinoma and oral squamous cell carcinoma. High expression of one DEG and low expression of the remaining prognostic genes were linked with poor survival in our patient cohort.
Conclusions: Our study highlights molecular features of cancer-induced cachexia in pmCRC and several potential diagnostic and prognostic biomarkers.

#5374 Immune checkpoint protein expression of PD-1 shows prognostic significance in large B-cell lymphomas of the central nervous system.

Sara Francesca Santagostino[1], Derek M. Devine[2], John DeWitt[3], Alissa A. Thomas[4], Ashley K. Volaric[3]

[1]Larner College of Medicine at The University of Vermont, Burlington, VT,[2]Biomedical Statistics Research Core, Larner College of Medicine at The University of Vermont, Burlington, VT,[3]Department of Pathology and Laboratory Medicine, Larner College of Medicine at The University of Vermont, Burlington, VT,[4]Department of Neurological Sciences, University of Vermont Medical Center, Burlington, VT

Large B-cell lymphomas of the central nervous system are rare but aggressive neoplasms that uniquely involve immune privileged sites. Targeted immune-based therapies are limited, but immune checkpoint inhibition involving programmed cell death protein 1 (PD-1) and its ligand (PD-L1) are being investigated for relapse/refractory disease. However, the prognostic significance of PD-1 and PD-L1 expression across primary and secondary presentations (PCNSL and SCNSL, respectively) is unknown. We evaluated the prognostic indicators of PD-1 and PD-L1 immunohistochemical expression in a rural-based clinical cohort of both PCNSL and SCNSL. We performed immunohistochemical studies (IHC) for PD-1 (NAT 105, Cell Marque) and PD-L1 (SP263, Ventana) on a curated cohort of CNS lymphomas (n=36) from a rural patient population with PCNSL (n=27) or SCNSL (n=9). Positivity was defined as ≥5% cellular staining. Clinical groups were stratified by patient age, therapy response (durable response- DR or relapse/refractory- RR), and PD-1/PD-L1 IHC expression. All survival analyses were conducted on 33 evaluable patients, none of whom received immune checkpoint inhibitors. Prognostic indicators of overall survival (OS), progression-free survival (PFS), time to progression (TTP), and time to response (TTR) were evaluated and associated with PD-1/PD-L1 expression using Kaplan-Meier methods, log-rank tests, and unadjusted Cox proportional hazards models. Our analysis revealed robust expression rates for PD-1 (67%) and PD-L1 (75%) across all tumors. Importantly, in PCNSL, PD-1 positivity was significantly associated with shorter OS. In the PD-1-positive subgroup, PCNSL exhibited significantly longer PFS/TTP than SCNSL. In addition, there was stratification of OS and PFS by DR and RR clinical status across all tumors, with DR exhibiting longer OS and PFS than RR tumors. Interestingly, PD-1 positivity was associated with faster TTR, particularly for PCNSL, indicating earlier treatment response than SCNSL. PD-L1 expression was not significantly associated with survival outcomes or treatment response. While age was not associated with PFS overall, SCNSL patients older than 65 showed a trend toward shorter PFS. PFS and TTP were identical in this dataset. In conclusion, PD-1 positivity in large B-cell lymphomas of the CNS, particularly for primary presentations, is predictive of earlier treatment response without translating to improved OS or PFS/TTP. These findings highlight the importance of clinical context (disease presentation and extent) and suggest that early-response kinetics like TTR offer complementary biological insight distinct from long-term survival outcomes. Larger studies are needed to further define the prognostic influence of immune checkpoint proteins in large B-cell lymphomas of immune-privileged sites.

#5375 Development of reference standards for clonal evolution and measurable residual disease in acute myeloid leukemia.

Colt W. Nash, Matthew G. Butler, Ojaswee Dahal, Jayanthi Ramprakash, Andrew T. Anfora, Yves Konigshofer

LGC Clinical Diagnostics, Gaithersburg, MD

Here, we describe novel reference standards for measurable residual disease (MRD) and clonal evolution in acute myeloid leukemia (AML). About a third of patients with AML harbor somatic mutations in NPM1 and FLT3, and it is not uncommon for AML to start with a mutation in NPM1 or an internal tandem duplication (ITD) in FLT3, respond to a therapy with remission, and have the other mutation appear during relapse as a result of clonal evolution. To support the development and validation of molecular diagnostic assays that assess MRD and clonal evolution, we created reference standards where several clonal AML cell lines with added mutations are combined with peripheral blood mononuclear cells (PBMCs). These clones represent different combinations of an NPM1 mutation, a short FLT3-ITD, and a long FLT3-ITD to support single-cell assays that can evaluate the mutations in a given cell. Additional PBMCs are provided to dilute these clones to MRD levels and for assays that are designed to use the DNA and/or RNA input from around 2 million cells (i.e., 10 micrograms). On a commercial single-cell assay, it was possible to identify and separate the individual clones. Additionally, it was possible to dilute the cells to MRD levels and detect the mutations by NGS. In conclusion, we have generated cell-based reference standards with combinations of an NPM1 mutation and FLT3-ITDs, which are designed for the development and validation of molecular biology-based AML assays. Using the same methodology, it should also be possible to generate clones with mutations in other genes to reflect clonal evolution in AML.

#5376 EGFR/RAS/SIAH pathway-centered biomarker-based prediction of tumor relapse/chemo-resistance/patient survival in TNBC.

Amy H. Tang[1], Mary L. Guye[2], Billur Samli[3], Janet S. Winston[3], Richard A. Hoefer[4]

[1]Biomedical and Translational Sciences, Old Dominion University, Norfolk, VA,[2]Surgical Oncology, Sentara Surgery Specialists, Newport News, VA,[3]Pathology Sciences Medical Group, Sentara Norfolk General Hospital, Norfolk, VA,[4]Sentara Health Research Center, Sentara Cancer Network, Norfolk, VA

Introduction: Triple-negative breast cancer (TNBC) is an aggressive breast cancer subtype that disproportionately affects BRCA1 mutation carriers and young Black/white women. Pembrolizumab and neoadjuvant chemotherapy (NACT) has become the new standard of care (SOC) for high-risk early-stage TNBC. Pathologic complete response (pCR) predicts good outcome, whereas pathologic incomplete response (pIR) with high-risk residual cancer burden (RCB) is correlated with early tumor relapse, chemo-IO-resistance, and poor survival. Many similarly treated patients with identical TNM and RCB classifications experience clear treatment disparity, distinct relapse rates, and disparate survival. Current methods fall short in predicting relapse/resistance/survival with high precision in the clinic.

Methods: We have conducted IHC staining of EGFR, Ki67, and SIAH expression in a large cohort of TNBC patients (577), of which 48% patients are Black/AA and 48% patients are white patients, from the Sentara Cancer Network. The Sentara Comprehensive Breast Centers have served our military veterans (Naval Norfolk Station) as well as many socio-economically disadvantaged, medically underserved, and underinsured low-income patients from Hampton Roads Virginia, with a racially diverse population of 1.8 million.

Results: We reported that high SIAH expression in residual tumors post-NACT reflects persistent EGFR/K-RAS/SIAH pathway activation (ON), predicts ineffective SOC therapy, continuous tumor growth post-NACT, which predicts early relapse, chemo-resistance, and poor survival. Conversely, no or super-low SIAH expression in residual tumors post-NACT reflects effective SOC therapy, EGFR/K-RAS/SIAH pathway inactivation (OFF), which predicts tumor remission and prolonged survival. We found that our Black/AA TNBC patients suffer a significantly higher mortality and reduced survival when compared to their white counterparts in this study, similar to the SEER/CDC databases.

Conclusions: We found that persistent EGFR/RAS/SIAH pathway activation is a major driving force in TNBC malignancy. As an evolutionarily conserved RING-domain E3 ligase, SIAH is a new prognostic biomarker for patient risk stratification, tumor relapse prediction, and racial disparity detection in TNBC. SIAH is a major tumor vulnerability in TNBC malignancy. We aim to demonstrate the prognostic power of SIAH and develop a SIAH-centered biomarker panel for patient risk stratification and relapse/resistance/survival prediction in high-risk TNBC.

#5377 Prediction of relapse risk in favorable outcome AML from DNA methylation data.

Jamie Endicott[1], Ruslan Strogantsev[2], CRISTINA TOGNON[2], Hisham Mohammed[2], Elie A. Traer[3]

[1]CEDAR, OHSU Knight Cancer Institute, Portland, OR,[2]OHSU Knight Cancer Institute, Portland, OR,[3]Instructor, Ctr. for Hematologic Malignancies, Oregon Health & Science University, Portland, OR

In patients diagnosed with acute myeloid leukemia (AML), several genetic profiles are designated as ‘favorable outcome’ such as presence of NPM1 mutation or certain translocations. Despite sharing these genetic commonalities, many patients still relapse.

Due in part to the high frequency of AML driver mutations occurring in genes involved in epigenetic regulation, we profiled genome wide DNA methylation for blood and bone marrow specimens from favorable risk AML patients at diagnosis, follow-up, remission, and relapse.

We identified differentially methylated regions (DMRs) present at diagnosis and remission which separated patients on relapse outcome. These DMRs were enriched in biologically meaningful chromatin regions (e.g. association with certain modifications) and some overlap genes with previously demonstrated significance for patient outcome.

Interestingly, many of the remission time point DMRs had effect sizes much greater than we would expect from minimal residual disease present in the bulk sample, suggesting a shift in normal cell populations or stem cell compartment between outcome groups. We further profiled DNA methylation in single cells to investigate cell state composition and heterogeneity across the course of disease.

Further, we created a DNA methylation-based predictor of relapse risk that again separates patients at diagnosis and remission. Our findings have the potential for utility both in treatment strategy approaches and in better understanding the biology of relapse in AML.

#5378 GDF-15 reflects host physiological stress rather than tumor progression in colorectal cancer patients.

Tasuku Kaise[1], Hideaki Karasawa[1], Keigo Murakami[2], Ichiro Ise[1], Tomoyuki Ono[1], Megumi Murakami[1], Yoshihiro Sato[1], Gumpei Yoshimatsu[1], Hideyuki Suzuki[1], Takaaki Abe[3], Takashi Kamei[1], Shinobu Ohnuma[1], Toru Furukawa[2], Michiaki Unno[1]

[1]Department of Surgery, Tohoku University Graduate School of Medicine, Sendai, Japan,[2]Department of investigative Pathology, Tohoku Graduate School of Medicine, Sendai, Japan,[3]Department of Clinical Biology and Hormonal Regulation, Tohoku University Graduate School of Medicine, Sendai, Japan

GDF-15 (growth differentiation factor 15) is a stress-responsive cytokine within the TGF-β (transforming growth factor-β) superfamily that is secreted in response to tissue injury and cellular stress. It increases under various pathological conditions, including cardiovascular, renal, and malignant diseases. In colorectal cancer (CRC), plasma GDF-15 levels are elevated compared with healthy individuals, and higher concentrations have been associated with worse prognosis. However, whether GDF-15 reflects tumor characteristics or host physiology remains unclear. This study aimed to clarify the clinical significance of GDF-15 in CRC by integrating analyses of plasma levels, tumor tissue expression, and gut microbiota composition. Seventy patients with CRC who underwent surgery between November 2021 and September 2023 were enrolled. Plasma GDF-15 levels were examined in relation to age, serum albumin (Alb), tumor stage, and other comprehensive nutritional and clinical parameters. GDF-15 expression in tumor tissue was evaluated by immunohistochemistry, and a semiquantitative histoscore (H-score) was calculated using the digital pathology software QuPath. Preoperative fecal samples were analyzed by 16S rRNA sequencing. For microbiota analysis, patients were classified into high and low plasma GDF-15 groups based on the median value, and microbial diversity and composition were compared between the groups. Plasma GDF-15 correlated positively with age ($r = 0.58$, $p < 0.001$) and negatively with Alb ($r = -0.54$, $p < 0.0001$). Levels were higher in advanced T categories (T3+4 vs. T1+2, $p < 0.05$) and higher stages (II-IV vs. I, $p < 0.05$); however, these associations disappeared after adjustment for age and Alb (T category, $p = 0.72$; stage, $p = 0.86$). These findings indicate that plasma GDF-15 reflects host physiological stress rather than tumor progression.
GDF-15 expression in tumor tissue, assessed by H-score, showed no correlation with plasma GDF-15 ($r = 0.06$, $p = 0.62$), age ($r = 0.09$, $p = 0.47$), or Alb ($r = -0.09$, $p = 0.48$), and did not vary by tumor depth ($p = 0.97$) or stage ($p = 0.75$). Gut microbiota analysis revealed no difference in α-diversity. In contrast, β-diversity differed significantly in both weighted and unweighted UniFrac analyses ($p < 0.05$), indicating compositional shifts associated with elevated plasma GDF-15. In conclusion, GDF-15 functions as a host-derived marker that reflects systemic physiological stress associated with aging and malnutrition rather than tumor burden. Furthermore, concurrent microbial alterations in patients with elevated GDF-15 suggest a potential role for GDF-15 as an integrative biomarker linking host physiological stress to intestinal environmental changes in colorectal cancer.

#5379 Prognostic significance of STING expression in patients with resected lung adenocarcinoma.

Jung-Jyh Hung[1], Ying-Shiun Kao[2]

[1]National Yang Ming Chiao Tung University and Taipei Veterans General Hospital, Taipei, Taiwan,[2]Taipei Veterans General Hospital, Taipei, Taiwan

Background: Lung cancer is the leading cause of cancer death worldwide. Tumor recurrence is the most common cause of treatment failure after surgical resection. STING (Stimulator of Interferon [IFN] Genes) is a protein responsible for controlling anticancer immune responses to leaked self- or non-self DNA. Recent studies have shown in animal models that knocking out STING and cGAS expression results in a nonresponse to PD-L1 checkpoint therapy. STING and cGAS are thus thought to be essential for the antitumor response of PD-1/PD-L1 checkpoint inhibition. Several studies have reported that STING expression was decreased in tumor in hepatocellular, gastric and colorectal cancer, and in melanoma. STING is frequently lost during tumor progression, and loss of STING/cGAS correlates with poor survival. The prognostic value of STING expression in patients with resected lung adenocarcinoma has not been well demonstrated.
Methods: A total of 68 patients with resected lung adenocarcinoma were included in the study. STING expression was determined by immunohistochemistry in tumor specimens. The prognostic value of STING expression and its relationship with clinicopathological variables were investigated. We have screened the expression of STING in several lung cancer cell lines. STING knockdown or transfection will be performed in suitable lung cancer cell lines. Western blotting analysis will be performed to demonstrated STING, E-cadherin and vimentin expression.
Results: High STING expression was shown in 45 (66.2%) of the 68 lung tumor samples. Predominant pattern group (lepidic/acinar/papillary vs. micropapillary/solid) ($P = 0.662$) was not significantly associated with STING expression. Univariate analysis indicated that high STING expression (HR, 0.158; 95% CI, 0.032 to 0.787; $P = 0.024$) was a significant prognostic factor for better disease-free survival (DFS). In multivariate analysis, predominant pattern group (lepidic/acinar/papillary vs. micropapillary/solid) (HR, 5.764; 95% CI, 1.054 to 31.537; $P = 0.043$) was a significant prognostic factor for DFS. High STING expression (HR, 0.073; 95% CI, 0.009 to 0.617; $P = 0.016$) was also a significant prognostic factor for better DFS.
Conclusions: High STING expression was a significant prognostic factor for better DFS in patients with surgical resected lung adenocarcinoma. This information is useful to stratify high-risk patients of recurrence after resection of lung adenocarcinoma.

#5380 Prognostic utility of minimal residual disease detection using circulating tumor DNA in early-stage breast cancer: A systematic review and meta-analysis.

Panuch Eiamprapaporn[1], Thiti Susiriwatananont[1], Yaohua Ma[1], Hataiwan Ratanabunjerdkul[2], Panchanin Patanayindee[2], Lucksika Wanichtanom[3], E. Aubrey Thompson[4], Saranya Chumsri[1]

[1]Mayo Clinic, Jacksonville, FL,[2]Internal Medicine, Thammasat University, Bangkok, Thailand,[3]Internal Medicine, Lucksika Wanichtanom, Bangkok, Thailand,[4]Comprehensive Cancer Center, Mayo Clinic, Jacksonville, FL

Circulating tumor DNA (ctDNA)-based minimal residual disease (MRD) detection is a paradigm shift for risk stratification in early-stage breast cancer (eBC) surveillance. While the prognostic signal is clear, comprehensive synthesis across molecular subtypes remains limited, hindering the translation of prognostic findings into actionable, intervention-guided trials. We conducted a systematic review and meta-analysis following PROSPERO registration (CRD420251122005). Databases including PubMed/MEDLINE, Embase, and Cochrane CENTRAL were searched through September 2025. Studies involving eBC (stage I-III) patients with ctDNA-based MRD detection using validated assays, survival outcomes, and ≥12 months follow-up were included. Random-effects meta-analysis assessed the pooled hazard ratio (HR) for disease recurrence. Subgroup analyses explicitly evaluated molecular subtypes (TNBC, HER2+, HR+/HER2-) based on detection performance and gene mutation profiles. From 1,246 records, 59 studies were included, encompassing 12,847 eBC patients. Meta-analysis demonstrated an extreme prognostic value of disease-free survival from 26 studies with a pooled HR of 9.95 (95% CI: 6.50-15.25, p<0.0001). High heterogeneity was observed (I2=67.2%), largely driven by differences in tumor biology and assay technology. Subtype-specific analysis highlighted distinct shedding rates: TNBC showed the highest baseline detection (80–83.8%) and sensitivity (85–90%). HR+/HER2-showed the lowest baseline detection (14.6–30%). Gene mutation analysis revealed actionability: TP53 predominated in TNBC, while PIK3CA, ESR1, and AKT1 mutations were more frequent in HR+/HER2- disease. Crucially, the time from ctDNA detection to clinical recurrence provided a consistent median lead time of 10.2 months (range 7.5–16months), with cases detected up to 68 months prior. Specificity exceeded 95% across all subtypes. This meta-analysis establishes ctDNA-based MRD detection as a clinically valid biomarker with a nearly 10-fold increased recurrence riskin ctDNA-positive patients. The high heterogeneity underscores the necessity of tailored, subtype-specific surveillance protocols and selection of ultra-sensitive assays. The consistent ~10-month lead time defines a critical intervention window, providing a clear rationale for ongoing and future randomized clinical trials evaluating ctDNA-guided therapeutic intensification against the distinct molecular profiles observed in each breast cancer subtype.

#5381 Integrated analysis for identification of risk stratification biomarkers for colon cancer.

Andrea J. O'Hara[1], Priya Roy[2], Dhwani Mulani[2], Ethan Stancliffe[3], Tom Cohen[3], Hemant Roy[2], Haythem Latif[1]

[1]GENEWIZ, LLC, South Plainfield, NJ,[2]Baylor College of Medicine, Houston, TX,[3]Panome Bio, St Louis, MO

Introduction: Colorectal cancer (CRC) remains the second leading cause of cancer-related deaths worldwide, underscoring the critical need for improved early detection and risk stratification methods. While polyps are detected in up to 40% of colonoscopies, most are negative for significant lesions, with only about 10% showing advanced adenomas or carcinomas. Although colonoscopy remains the gold standard for CRC screening, it has major limitations in predicting progression from benign neoplasia to advanced adenomas or carcinomas. Precision approaches that integrate molecular insights are necessary to identify biomarkers for risk stratification and better understand which individuals with colon neoplasia are at increased risk to develop advanced adenomas or carcinomas.

Methods: This study leverages a multi-modal, integrated analysis of spatial transcriptomics, bulk RNA-sequencing, and metabolomics—an approach that has not been comprehensively applied to risk stratification in CRC. A set of 10 colorectal samples, five from cases that have progressed to CRC and five that have not, were selected for deep multiomics analysis. Starting with spatial transcriptomics from FFPE, single cell analysis across a slice was explored for each sample across the specimen, with a focus on variability between groups across the colonic crypts, tube-like glands in the colon and rectum that produce mucus and renew the intestinal lining. An additional slice of tissue was analyzed for bulk RNA-sequencing. Finally, adjacent tissue from the same individual was analyzed for bulk metabolomics, to identify and quantify the small molecules present within each sample.

Results: Integrated bioinformatics analyses were used to compare and combine bulk results, along with clinical and demographic data associated with these samples, for downstream pathway and processes analysis. In addition, these results were further analyzed to cross-compare and validate single cell spatial findings.

Conclusion: With this integrated multiomics approach, spatial transcriptomics provides high-resolution insights into gene expression within the structural context of the colonic crypts, while bulk metabolomics captures a systemic overview of metabolic alterations linked to neoplastic progression. By identifying key biomarkers and pathways associated with CRC progression, this study aims to pave the way for personalized screening strategies and targeted interventions to reduce the burden of advanced colorectal cancer.

#5382 The Yin and Yang of sphingosine kinase 2 (SPHK2): Opposing regulation by nuclear and cytoplasmic localization in lung cancer progression.

Tsung-Ching Lai[1], Wei-Jiunn Lee[1], Jer-Hwa Chang[1], Ming-Hsien Chien[2]

[1]Wanfang Hospital, Taipei, Taiwan,[2]Asst. Professor, Taipei Medical Univ., Taipei, Taiwan

Sphingosine-1-phosphate (S1P) is a pleiotropic lipid mediator, generated primarily by SPHK1 and SPHK2, regulating cell survival, migration, and angiogenesis. While SPHK1 and SPHK2 have been reported as oncogenes, our prognostic analysis of TCGA-LUAD (Lung Adenocarcinoma) revealed opposite roles for the two enzymes, suggesting a dual function for SPHK2. We investigated the hypothesized tumor suppressor function of SPHK2. Unlike SPHK1, SPHK2 is capable of nuclear localization. Our data showed that high levels of nuclear-localized SPHK2 in tissue correlate with a better prognosis for lung cancer patients. Overexpression of SPHK2 within the nucleus significantly reduced cell proliferation and migration capacity. Furthermore, general SPHK2 overexpression enhanced sensitivity to the drug FTY720, but this sensitivity was reduced when SPHK2 was overexpressed specifically in the nucleus. This suggests that the localization of SPHK2 in the cytoplasm versus the nucleus results in opposing functions. The TCGA-LUAD expression profile likely reflects SPHK2's dominant tumor-suppressor role due to a higher proportion of its expression being nuclear.

#5383 Construction and assessment of the stemness-telomere survival risk framework (STSRF) for precision breast cancer therapy: Insights from multi-omic approaches.

Zhiyuan Bo[1], Jingpei Long[1], Fang Wan[1], Fangfang Chen[1], Jiajun Li[2], Zhengxiao Zhao[3]

[1]Department of Surgery, Women's Hospital School of Medicine Zhejiang University, Hangzhou, China,[2]The Second Affiliated Hospital and Yuying Children's Hospital of Wenzhou Medical University, Wenzhou, China,[3]Department of Oncology, the First Affiliated Hospital of Zhejiang Chinese Medical University, Hangzhou, China

Background and Aims: Breast cancer (BRCA) remains a major clinical challenge due to its molecular heterogeneity and therapy resistance. Stemness and telomere-related genes are key contributors to tumor progression, but their interplay is poorly defined. This study aims to construct a Stemness-Telomere Survival Risk Framework (STSRF) to improve risk stratification and guide precision treatment.

Methods: We integrated single-cell and bulk RNA sequencing data (n = 1684 BRCA patients) with WGCNA and 101 machine learning model combinations within a LOOCV framework to build the STSRF. Immune infiltration was assessed using seven algorithms and deep learning on histopathological images. Biological functions were explored via multi-omic enrichment analyses. Drug sensitivity data from DepMap, GDSC, CMap, CTRP, and PRISM supported therapeutic predictions. Causal relationships were validated using Mendelian randomization (MR), and expression patterns were confirmed by RT-qPCR and immunohistochemistry (IHC).

Results: STSRF showed strong prognostic power (highest 1-, 3-, 5-year AUCs: 0.930, 0.807, 0.766). High- and low-risk groups were effectively stratified, correlating with immune infiltration and clinical traits. High-risk patients were linked to immune-cold phenotypes and may benefit from chemotherapy combined with HDAC inhibitors, while low-risk patients, associated with immune-hot phenotypes and lower IC50 values for chemotherapy agents, may respond better to immunotherapy or chemotherapy. Single-cell and MR analyses confirmed the biological relevance of STSRF genes to BRCA risk. Experimental validation supported key gene expression patterns.

Conclusions: STSRF is a robust framework integrating stemness and telomere biology to predict prognosis and inform personalized therapies in BRCA.

: Redefining Targeted Therapy: Bispecific T-Cell Engagers and Antibody-Drug Conjugates 2
Poster Session

#5388 Dual targeting of CEACAM6 and EGFR with a bispecific antibody induces EGFR degradation and overcomes anti-EGFR resistance.

Ming-Heng Wu, Chee Voon Yap, Yao-Tsung Tsai

Taipei Medical University, Taipei, Taiwan

Epidermal growth factor receptor (EGFR) protein stability is an important determinant of tumor progression and therapeutic response. Here, we identified carcinoembryonic antigen-related cell adhesion molecule 6 (CEACAM6) as a previously unrecognized post-translational stabilizer of EGFR. CEACAM6 expression positively correlated with EGFR protein, but not mRNA, in clinical specimens. Mechanistically, CEACAM6 sequesters EGFR into CEACAM6-enriched lipid rafts, which delays the raft-associated endocytosis and lysosomal degradation of EGFR. This retention maintains EGFR clustering and sustains downstream ERK, AKT, and SRC signaling, promoting migration, invasion, and anoikis resistance, ultimately contributing to resistance against anti-EGFR therapeutics.
To therapeutically exploit this vulnerability, we developed an anti-CEACAM6/EGFR bispecific antibody (BsAb) that simultaneously engages both antigens on the tumor cell surface. The BsAb induces potent antigen crosslinking that triggers efficient EGFR internalization and redirects it toward lysosomal degradation, thereby bypassing the CEACAM6-dependent blockade of EGFR turnover. In addition, the BsAb efficiently suppressed the progression and metastasis of colorectal and lung cancer in xenograft models. These findings identify CEACAM6 as a critical regulator of EGFR stability and demonstrate that dual targeting with the bispecific antibody can induce EGFR degradation, thereby overcoming EGFR-driven malignancy.

#5389 CC312, a novel CD19/CD3/CD28 tri-specific T cell engager, leads to rapid and deep B-cell depletion and has broad potential for development in autoimmune diseases.

Mingyuan Sun[1], Yingfeng Huang[2], Ruixia Zhang[2], Zhen Jing[2], **Xiaofang Zhang**[2], Yuchao Wei[2], Junyuan Qi[1]

[1]Institute of Hematology & Blood Diseases Hospital, Tianjin, China,[2]CytoCares (Shanghai) Inc., Shanghai, China

Background: CD19-targeted T cell engagers (TCEs) have the potential to induce B-cell depletion with potential better safety than CAR-T therapy and off-the-shelf convenience. However, T cell dysfunction and exhaustion contribute to treatment failure following anti-CD19 bispecific TCE. In this study, we developed CC312, a novel tri-specific TCE that integrates CD28 co-stimulation with CD3 and CD19 targeting. CD28 signaling in CC312 has been proved obviously with non-exhausted T cell phenotype.
Objective: The potential of CC312 in treating relapsed/refractory autoimmune diseases will be explored in the clinical setting (NCT06888960).
Methods: This 3 + 3 design, dose-escalation study determined adverse events and the maximum tolerated dose (MTD) of CC312 in patients with autoimmune diseases. CC312 was administered intravenously twice per week at 5 different dose levels (5 to 40 μg). Safety, pharmacokinetic/pharmacodynamic profiles, and primary efficacy parameters—including B-lymphocyte counts of peripheral blood and bone marrow, autoantibodies and biomarkers—will be evaluated for 48 weeks. Primary efficacy endpoint is the SLE Responder Index 4 (SRI-4) criteria.
Results: To date, 10 patients with refractory SLE received 1 to 3 cycles of CC312 treatment. The safety profile remained favorable, with no observed dose-limiting toxicities (DLTs), immune effector cell-associated neurotoxicity syndrome (ICANS), or cytokine release syndrome (CRS) of grade ≥2. A consistent pattern of low-level release for CRS-associated cytokines (IL-6, TNF-α, and IL-10) was observed. CC312 consistently and dose-dependently depleted peripheral B cells in most patients. Among those patients who were followed up ≥24 weeks, B cell reconstitution was observed at week 24 without recurrence of clinical symptoms, suggesting immune reconstitution. $CD19^+$ B cells subsets of bone marrow were completely diminished in the 20~30 μg cohorts at week 8 or week 12. 75% of patients (3/4) achieved an SRI-4 response at week 36, with decreased SLEDAI-2K scores and improvement in clinical symptoms, 100% responders have maintained SRI-4 response. In patient 3, the SLEDAI-2K score fell to zero after treatment and remained stable through week 36. C3 levels and anti-dsDNA antibody levels remained stable for most patients.
Conclusion: In this study, the highest dose currently administered was 30 μg, and CC312 still exhibited favorable safety profiles, with no ICANS or grade ≥2 CRS. Rapid, near-complete depletion of peripheral $CD19^+$ B lymphocytes was achieved at all cohorts. Furthermore, deep and complete depletion of $CD19^+$ B cells in bone marrow was also achieved for 20 μg and 30 ug cohort. Long-term (up to 6~9 months) SRI-4 response was observed across the cohorts and improvement in clinical symptoms.

#5390 Mechanistic drivers of FAP-targeted ADC performance.

Atanasio Pandiella[1], Monica Redondo-Puente[1], Maria del Carmen Gomez-Garcia[1], Patricia Gonzalez[2], Isabel Egana[2], Roland Kontermann[3], Oliver Seifert[3], Jorge Galino[4], Sonia Montero-Molina[4], Jose Luis Hernandez[4], Juan Daniel Sanjuan[4], Guillermo Quintas[4], Ignacio Garcia[2], Manuel Hidalgo[5], Laureano Simon[2], Myriam Fabre[2]

[1]Agencia Estatal Consejo Superior De Investigaciones Cientificas, MADRID, Spain,[2]Oncomatryx Biopharma S.L., Derio, Spain,[3]University of Stuttgart, Stuttgart, Germany,[4]Health and Biomedicine Department, Leitat Technological Center, Terrassa, Spain,[5]NYU Langone Health Perlmutter Cancer Ctr., New York, NY

Cancer-associated fibroblasts (CAFs), the main stromal cell population within the tumor microenvironment (TME), play a pivotal role in cancer progression, metastasis, and immune evasion. To target this compartment, two antibody-drug conjugates (ADCs), OMTX705 and OMTX105, were developed against fibroblast activation protein (FAP) expressed on CAFs. Both share the same human IgG1 antibody backbone (OMTX005) but differ in linker-payload chemistry: OMTX705 carries the cytolysin A1B1, whereas OMTX105 includes monomethyl auristatin E (MMAE). Despite similar drug-antibody ratios (DAR ≈ 4), their distinct vc-PABA-derived linkers confer differential stability and intracellular processing characteristics.We performed a comprehensive characterization of their mechanisms of action, including internalization, intracellular trafficking, and bystander cytotoxicity, in vitro and in vivo, as well as plasma stability and maximum tolerated dose (MTD) analyses to assess their pharmacological and safety profiles. Both ADCs displayed potent antitumor effects but differed markedly in their intracellular fate and pharmacodynamic properties. OMTX105 demonstrated faster processing and stronger bystander killing, leading to higher antitumor activity in murine xenografts; however, its effective dose was close to the MTD in rat, limiting its therapeutic window. In contrast, OMTX705 exhibited slower intracellular processing, resulting in a sustained and controlled payload release. This translated into a longer-lasting effect in vivo, with CAFs acting as a drug reservoir prolonging cytotoxic activity in neighboring tumor cells, while maintaining a superior safety profile.Remarkably, both ADCs exhibited in humanized xenograft mice a shared immunomodulatory activity, promoting infiltration of $CD4^+$ and $CD8^+$ T lymphocytes within the TME—particularly $CD8^+$ cells in treated tumors—suggesting that FAP-targeted ADCs facilitate immune cell recruitment compared to control. This was confirmed in clinical samples from patients treated with OMTX705, currently under clinical development. In these patients, CAF disruption, much lower FAP expression and higher $CD8^+$ and $CD4^+$ cell infiltration was detected in tumor areas co-localizing with the OMTX705 payload signal, providing evidence that OMTX705 enhances local immune activation and supports an antitumor immune response.Overall, these findings reveal both cytotoxic and immunomodulatory functions for FAP-targeted ADCs within the TME and provide molecular mechanistic insights into their bystander effect, emphasizing how differences in linker-payload chemistry critically determine efficacy, durability of response, immune engagement, and tolerability. This study highlights OMTX705 potential as a safer FAP-targeted ADC with long-lasting effect and underlines the importance of biology-driven linker-payload engineering for next-generation stroma-directed ADC anticancer therapies.

#5391 A versatile KY-HC-mouse™nanobody platform enabling tumor-anchored, conditionally active 4-1BB bispecific antibodies.

Xiaoting Liang, Siyu Li, Jie Xu, Hao Peng, **Feng Hao**, Jinying Ning

Kyinno Biotechnology Co., LTD, Beijing, China

4-1BB (CD137) is an attractive co-stimulatory receptor for boosting anti-tumor T-cell responses, but first-generation systemic 4-1BB agonist antibodies have been limited by dose-limiting toxicity, highlighting the need for tumor-anchored, conditionally active agonists with an improved benefit-risk profile. We established a proprietary heavy-chain-only mouse (KY-HC-mouse™) platform to generate relatively low-affinity anti-4-1BB nanobodies that block 4-1BB/4-1BBL binding and require cross-linking for strong signaling, thereby conferring built-in conditional agonism. These nanobodies were formatted into Fc-silenced IgG (LALA mutation) bispecifics targeting PSMA (PSMA×4-1BB, KA-2722), CD19 (CD19×4-1BB, KA-6859) and CDH17 (CDH17×4-1BB, KA-A3438), as well as a trispecific antibody targeting CDH17×CLDN18.2×4-1BB (KA-A3601). CDH17×CLDN18.2×4-1BB (KA-A3601) was designed based on the frequent co-expression of CDH17 and CLDN18.2 in gastrointestinal tumors, enabling dual-antigen anchoring of 4-1BB co-stimulation. All molecules show relatively reduced 4-1BB binding compared with benchmark agonists but retain strong, high-avidity binding to their respective tumor antigens and drive potent, antigen-dependent activation of 4-1BB reporter cells. CD19×4-1BB (KA-6859) further demonstrates robust *in vivo* efficacy in hu-PBMC lymphoma models when combined with a CD20×CD3 T-cell engager Glofitamab, with clear tumor growth inhibition at 3 mg/kg KA-6859 plus 0.15mg/kg CD20×CD3 (QW*3), and exhibits favorable pharmacokinetics with sustained serum exposure in mice. CDH17×4-1BB (KA-A3438) and CDH17×CLDN18.2×4-1BB (KA-A3601) show strong tumor growth inhibition in MC38-CDH17 and MC38-CDH17-CLDN18.2 tumors established in B-h4-1BB C57BL/6 humanized 4-1BB (h4-1BB) mice, respectively, without ALT/AST elevation, indicating absence of detectable hepatotoxicity. CD19×4-1BB (KA-6859) exhibits a transient ExpiCHO-S expression yield of ~393 mg/L and a favorable pharmacokinetic profile in C57BL/6 mice, with terminal half-lives of approximately 16-21 days after i.v. dosing and ~10 days after s.c. dosing, and an s.c. bioavailability of ~82%. KA-6859 also displays high thermal stability and good overall stability, indicating favorable developability.Together, these data position the KY-HC-mouse™ 4-1BB nanobody platform as a versatile foundation for next-generation, tumor-anchored 4-1BB bispecifics and multispecifics, and for future combinations with checkpoint inhibitors in solid and hematologic malignancies.

#5392 Targeting solid tumors with pH-dependent dual-specific TCEs: First-in-human development of CT-202.

Stanley Roberts[1], Kelly Byrnes-Blake[2], Heather Ansorge[3], Eric Butz[4], **Daniel Olson**[5]

[1]SAR Safety Assessment, Northbrook, IL,[2]Northwest PK Solutions, LLC, Cordova, AK,[3]Context Therapeutics Inc, Philadelpha, PA,[4]Context Therapeutics Inc, Philadelphia, PA,[5]University of Chicago, Chicago, IL

Introduction: Nectin-4 has emerged as a clinically validated antigen for the treatment of urothelial, colorectal, lung, breast, and other solid malignancies. However, Nectin-4's physiological expression in epidermal keratinocytes restricts the utility of potent immunotherapeutic strategies such as bispecific T cell engagers (TCEs) and chimeric antigen receptor T cells (CAR-Ts), due to on-target, off-tumor toxicity. CT-202 is a fully humanized, dual pH-dependent Nectin-4 x CD3 bispecific TCE engineered to widen the therapeutic window by selectively targeting Nectin-4 and CD3 within the acidic tumor microenvironment (TME).

Methods: CT-202 was characterized for pH-dependent binding to both Nectin-4 and CD3, employing *in vitro* affinity assays across pH gradients mimicking physiological (pH 7.4) and tumoral (pH ~6.5) conditions. *In vivo* pharmacology and safety assessments were performed in non-human primates comparing CT-202 and non-pH-dependent bispecific controls. *In vitro* functional assays, including cytotoxicity and cytokine release, were used to determine dose-response relationships to inform initial human dosing strategies.

Results: CT-202 demonstrated high affinity and specificity for Nectin-4 and CD3 exclusively at the lower pH characteristic of the TME; at neutral pH, binding was markedly attenuated. This conditional dual engagement was essential for effective T cell-mediated cytotoxicity against tumor targets *in vitro*. In non-human primate toxicology studies, CT-202 exhibited a >30-fold improvement in the Highest Not Severely Toxic Dosage (HNSTD) relative to traditional bispecifics lacking pH modulation, delineating a superior safety profile. Integrated analysis of *in vitro* potency and *in vivo* toxicology data supported a rational selection of starting dose for forthcoming clinical investigation.

Conclusion: CT-202 represents a novel dual pH-selective bispecific TCE targeting Nectin-4 x CD3, designed to optimize tumor selectivity and minimize off-tumor toxicity. Preclinical data validate the differentiated pharmacological and safety attributes of this modality, justifying its advancement to first-in-human Phase 1 trials. This approach highlights the potential of dual pH-dependent bispecific antibodies as a next-generation platform for the selective immunotherapy of Nectin-4-expressing solid tumors.

#5393 Preclinical efficacy and safety profile of NPX125, a novel ADC targeting B7-H7.

Silvia Ferrati, Emilien Loeuillard, Susannah L. Hewitt, Matthew Peter Rausch, Bijan Etemad-Gilbertson, Jamie Strand, Riale Gilligan, Katalin Kis-Toth, Yasmin Hashambhoy-Ramsay, Emma Wang, Leena Gandhi, Tatiana Novobrantseva

NextPoint Therapeutics, Cambridge, MA

Introduction: B7-H7 is a member of the B7 family, with strong expression in multiple cancer indications in addition to its known role as an immune regulator. B7-H7 upregulation is correlated with poor patient outcomes while its normal tissue expression is limited, making it very attractive for targeting tumors. Here, we report the development of NPX125, a novel B7-H7-targeting antibody-drug conjugate with a potent DNA topoisomerase I inhibitor and a novel linker. NPX125 has potent *in vitro* activity, stable pharmacokinetic profile, favorable safety profile, and *in vivo* antitumor responses in nonclinical studies.

Methods: The target specificity and species cross-reactivity of NPX125 were assessed by flow cytometry on endogenous B7-H7+ and overexpressing B7-H7 cell lines. Internalization was tracked with Fabfluor-pH reporter conjugated-NPX125 using Incucyte® imaging. Its pharmacologic activities were evaluated in several human cancer cell lines *in vitro* by luminescence-based cell viability assays and in xenograft mouse models *in vivo*. The safety profile was evaluated in a dose escalation toxicokinetic study in cynomolgus monkeys. Animals were evaluated for 4 weeks after a single intravenous dose of NPX125. Clinical observations, hematology, chemistry, cytokine, and immunophenotyping samples were collected. At completion, pathology evaluation of selected tissues was performed. NPX125 pharmacokinetics was assessed in rats and monkeys by measurement of both total and drug-conjugated antibodies.

Results: NPX125 showed cross reactivity to human and monkey B7-H7 with on-cell binding. Incucyte® imaging analyses in a HER2 positive cell line showed faster internalization compared to Trastuzumab-Dxd. NPX125 demonstrated cytotoxic activity in tumor cell lines (EC50 ~ 0.19 nM to 2.95 nM) with a wide range of B7-H7 expression levels and significant bystander effect on B7-H7 negative cell lines. NPX125 was tested in several *in vivo* tumor models expressing a wide range of B7-H7 protein levels, demonstrating anti-tumor activity. Furthermore, NPX125 was stable in circulation with minimal free payload release in rats and monkeys (T1/2 = 352 and 135 hr, respectively and ~0.07% of the total injected payload released at Cmax in NHP). NPX125 was well tolerated in monkeys with a NOAEL of at least 10 mg/kg and no NPX125-related changes in clinical signs, body weight, food appetence, hematology, clinical chemistry, urinalysis, immunophenotyping, and organ weights. Increases in IL-1RA and IL-8 concentrations were noted with possible dose proportionality. Possible NPX125-related findings were present in the gastrointestinal tract.

Conclusions: NPX125 exerted potent antitumor activity against B7-H7-expressing tumors in *in vitro* and *in vivo* models and showed favorable pharmacokinetic and safety profiles in nonclinical species. The data presented here supports clinical development of NPX125 as a promising treatment strategy.

#5394 Novel multispecific T cell engagers exploit avidity for highly selective targeting of B-myeloid mixed-phenotype acute leukemia.

Sophie Jamet[1], Huiyuan Zhang[1], Ray Ruff[1], Irene Chen[1], Sally Ditzler[1], Kiersten Tucker[1], Hailey Hentschel[1], Jessica Chantel Ramadhin[2], James M. Olson[1], Jason Price[1], Mignon L. Loh[1]

[1]Seattle Children's Research Institute, Seattle, WA,[2]Taconic Biosciences, Inc., Los Angeles, CA

Introduction. B-myeloid mixed-phenotype acute leukemia (B-MPAL) is a high-risk leukemia subtype co-expressing lymphoid and myeloid surface antigens. Cure rates remain low, especially in adults (OS 20% to 50%). Current therapies are heterogeneous, borrowing from either ALL or AML regimens. MPAL cells uniquely co-express both lymphoid markers (e.g. CD19) and myeloid markers (e.g. CD33), a dual expression profile not shared by normal hematopoietic cells. We hypothesize that a Multispecific T cell Engager (MTE) engineered to preferentially bind cells expressing CD19 AND CD33 will achieve high selectivity compared to single-antigen targeting. We thus designed MTEs that bind both CD19 and CD33 on MPAL cells and CD3 on T cells. We fine-tuned the affinity of the CD19 and CD33 binders to leverage avidity; this ensures poor binding to single-positive (SP) normal cells but high-avidity binding to double-positive (DP) leukemia cells. This strategy aims to induce deep remissions and improve safety over single-target agents like Blinatumomab.

Methods. We successfully designed and produced 30 tri-specific CD19/CD33/CD3 MTEs, utilizing components derived from de-risked or FDA-approved therapeutics. Our MTE framework is an asymmetric "knob into hole" human IgG1 scaffold incorporating effector silencing mutations. *In vitro* assays tested binding and T cell cytotoxicity against DP, SP, or negative cell lines. Top candidates were tested *in vivo* using a luciferase-labeled JIH-5 xenograft (CD19+ CD33+) model in NSG-SGM3 mice. Engrafted mice received repeated weekly doses of MTEs and human T cells, with disease progression tracked via IVIS imaging.

Results. *In vitro* data confirm successful dual-antigen targeting and dramatic specificity improvements using lower-affinity binders. For multiple candidates, we observed much lower cytotoxicity for SP cells, with up to a 7-log difference in IC50 between DP and SP cells, demonstrating an AND logic-gated treatment within a single molecule. Initial preclinical *in vivo* data show successful control of disease progression in xenografted mice at well-tolerated doses. Crucially, we conducted safety studies in huNOG-EXL humanized mice (engrafted with CD34+ cells) to test toxicity on normal human hematopoietic cells. Dose titration confirmed the selective sparing of normal human B cells and CD33+ myeloid cells, a major advancement over single-targeting therapies.

Conclusions. By taking advantage of the unique DP features of B-MPAL cells, we developed a novel immunotherapy that offers improved half-life, potency, selectivity, and safety. This work establishes proof of concept that the combinatorial use of binders with optimized affinity generates highly specific immunotherapies with minimal normal cell cytotoxicity via an avidity-driven mechanism, paving the way for safer and more effective treatments.

#5397 A novel anti-CD3×CD28×STEAP1 tri-specific T-cell engager with enhanced and durable antitumor responses in prostate cancer.

Ge Song, Aiying Xiong, Seng Zhu, Xuemei Tian, Xiaoling Yuan, Wanli Zhang, Wan-Jen Yang, Xiansong Xiong, Ling Ding, Haixiang Yu, Xiaoli Hou, Pingao Yan, Qingyu Wang, Xiao Zou, Chen Hu, Jijun Yuan

Shanghai Henlius Biotech, Inc., Shanghai, China

Introduction: Limited efficacy has been achieved with immunotherapy for prostate cancer, largely due to an immunosuppressive or “immune desert” tumor microenvironment, poor T-cell infiltration, or lack of robust tumor-specific targets. To overcome these barriers, we have developed an anti-CD3×CD28×STEAP1 tri-specific T-cell engager (TCE) that redirects T cells to prostate tumors with high levels of STEAP1 and improves T cells through co-delivering CD3 and CD28 signals.

Methods: T cell-dependent cellular cytotoxicity was assessed using a luciferase assay or flow cytometry. Concurrently, cytokine secretion in cell culture supernatants was analyzed using a multiplex bead-based flow cytometric assay. To evaluate T-cell proliferation and memory formation, peripheral blood mononuclear cells (PBMCs) were co-cultured with C4-2B cells and subsequently analyzed by flow cytometry. The sustained cytotoxic potency of T cells was further examined in a repeated antigen challenge model, and cytotoxicity was measured after each cycle using a luciferase assay. *In vivo*, antitumor efficacy was investigated in humanized PBMC/C4-2, LNCaP and patient-derived xenograft (PDX) xenograft models. Additionally, a pilot toxicology was studied in cynomolgus monkeys.

Results: Anti-CD3×CD28×STEAP1 TCE exhibited a target-dependent T-cell activation and cytotoxicity, especially under conditions with a low T effector to tumor cell ratio (1:5-1:10). HLX3902 demonstrated enhanced T cell function and sustained *in vitro* cytotoxicity compared with bispecific TCEs and their combinations, showing superior T-cell proliferation and enhanced expansion of memory T cells. Furthermore, Anti-CD3×CD28×STEAP1 TCE demonstrated superior and sustained antitumor activity in both humanized PBMC/cell line-derived xenograft and PDX models at a single 0.01 mg/kg dose, with increased T-cell infiltration, activation, and persistent intratumoral CD8+ T cells resulting from CD28 co-stimulation compared to AMG509. Anti-CD3×CD28×STEAP1 TCE was well tolerated in cynomolgus monkeys after weekly intravenous administration at a dose of 45 μg/kg/QW

Conclusion: We developed a novel tri-specific TCE with optimized CD3 and CD28 signaling, effectively co-engages T cells and STEAP1-expressing tumor cells. It elicits potent, target-dependent T-cell activation and cytotoxicity, The incorporation of CD28 signaling significantly improved T-cell persistence and sustained functional activity against repeated antigen challenges *in vitro* and *in vivo*. It was well tolerated in cynomolgus monkeys, supporting its potential for clinical development, and positions as a best-in-class molecule with Investigational New Drug submission anticipated in Q1 2026. This tri-specific co-stimulatory platform may be extended to treat immunosuppressive or “immune desert” solid tumors.

#5399 QLS2309, a trifunctional NKp46/CD16a-NK cell engager targeting CD70 enhances efficacy against acute myeloid leukemia via mitigating the refraction to therapeutic antibody-dependent cytotoxicity.

Liuqing Yang[1], Ruimei Li[1], Xiaoran Wu[2], Shuyong Zhao[2], Hua Ying[1], Weikang Tao[1]

[1]Shanghai Qilu Pharmaceutical Research and Development Center LTD., Shanghai, China,[2]Qilu Pharmaceutical Co., Ltd., Jinan, China

Acute myeloid leukemia (AML), the most prevalent acute leukemia in adults, is characterized by clonal expansion of myeloid precursors in the bone marrow (BM) and peripheral blood. Despite advancements in treatment, unmet medical needs persist in AML, with up to 50% of patients relapsing after initial chemotherapy and older patients facing a poor prognosis. CD70, a member of the tumor necrosis factor family, is expressed in over 80% of AML blasts and exhibits high specificity for leukemia stem cells (LSCs), while normal hematopoietic stem cells (HSCs) and immune cells show minimal or no expression. This makes CD70 an attractive therapeutic target for AML. However, approximately one-third of AML patients express the high-affinity Fc receptor CD64, which may impair the tumor-killing efficacy caused by Fc-mediated ADCC of therapeutical monoclonal antibodies. To address this challenge, we generated a trifunctional natural killer cell engager (NKCE), QLS2309, which targets AML blasts via binding to CD70 and engages NK cells via binding to NKp46/CD16a on NK cells. QLS2309 is a human IgG1 bispecific antibody featuring an anti-NKp46 nanobody (VHH) and an anti-CD70 antigen-binding fragment (Fab). Unlike anti-CD70 monoclonal antibodies, QLS2309 retained potent antitumor activity against primary AML blasts regardless of CD64 expression. Additionally, it selectively induced NK cell activation and cytokine secretion only in the presence of AML cells. *In vivo* studies demonstrated dose-dependent tumor growth inhibition with QLS2309, showing superior efficacy compared to cusatuzumab (an ADCC-enhanced monoclonal antibody). Single-dose pharmacokinetics in non-human primates (NHPs) revealed linear exposure, while multiple-dose toxicokinetics showed no significant accumulation. A GLP toxicity study in cynomolgus monkeys (QW × 4) confirmed favorable safety, with QLS2309 well-tolerated up to 100 mg/kg and minimal cytokine release. In conclusion, QLS2309 combines excellent efficacy, favorable pharmacokinetics, and a strong safety profile, outperforming cusatuzumab. These data support QLS2309 as a promising novel therapy for AML. A Phase 1 dose-escalation study in CD70+ relapsed/refractory hematologic malignancies is currently ongoing (NCT07173595).

#5400 QLS2313, a CD79b/CD20 tri-specific T cell engager with dual-targeting strategy developed as a new therapeutics for the treatment of DLBCL.

Ting Lu[1], **Liuqing Yang**[1], Fujia Yao[1], Dongdong Wu[1], Shuyong Zhao[2], Hua Ying[1], Weikang Tao[1]

[1]Shanghai Qilu Pharmaceutical Research and Development Center, Shanghai, China,[2]Qilu Pharmaceutical Co., Ltd., Jinan, China

Diffuse large B-cell lymphoma (DLBCL) is the most prevalent subtype of non-Hodgkin lymphoma (NHL), with approximately 40% of patients developing refractory disease or relapsing after initial therapy response. While CD20-targeted T cell engagers (TCEs) have demonstrated clinical efficacy and gained FDA approval for DLBCL, studies indicate that CD20 expression loss occurs in 8-64% of patients following CD20-directed therapies. This loss is often associated with transformation to high-grade lymphoma and poor overall survival. To address this challenge, Dual targeting another DLBCL surface antigen as well as CD20 may enhance therapeutic effects. CD79b is a well-validated therapeutic target expressed in 90% of DLBCL cases anditis critical for the viability of DLBCL cells. Unlike CD20, CD79b-targeted agents are less prone to resistance caused by antigen loss, making it an attractive TCE target. Therefore, a TCE dual targeting of CD79b and CD20 may overcome resistance and improve efficacy compared to a single-antigen targeting TCE. QLS2313 is a human IgG1 tri-specific antibody featuring an anti-CD3 single-chain variable fragment (scFv), an anti-CD20 Fab, an anti-CD79b Fab, and an effector-silent Fc region. *In vitro*, QLS2313 exhibited higher affinity for DLBCL cell lines than JNJ-80948543 (a clinical-stage CD79b/CD20 TCE from Janssen) while demonstrating significantly lower affinity for primary human T cells and Jurkat cells compared to JNJ-80948543 and FDA-approved CD20/CD3 bi-specifics (mosunetuzumab and glofitamab). QLS2313 effectively depleted both dual- and single-target-expressing cells, showing superior cytotoxicity to JNJ-80948543 and lower IL-6 release than glofitamab. *In vivo*, QLS2313 demonstrated linear pharmacokinetics in triple transgenic (human CD3/CD20/CD79b) mice, with a half-life of ~5 days. It inhibited tumor growth in a dose-dependent manner and exhibited greater antitumor efficacy than JNJ-80948543, particularly in CD20-low expression models. QLS2313 was well tolerated in a transgenic mice (QW × 4) GLP toxicity study, with the highest non-severely toxic dose (HNSTD) at 30 mg/kg for both intravenous and subcutaneous administration. In conclusion, QLS2313 show superior efficacy, favorable pharmacokinetics and safety profile, which support the clinical development of this novel therapy for DLBCL treatment.

#5401 A novel bispecific ADC targeting Nectin-4 and HER2 demonstrates superior and broad antitumor efficacy in preclinical models.

Jinxiu Hou, Tingting Gu, Chuan Chen, Chenpeng Su, Xiaoqian Chen, Dandan Liu, Jiyuan Tian, Zhihang Liu, Yongxin Shang, Rongmei Yan, Kezhen Ye, Liang Tian, Jian Peng, Zhenping Zhu

Earendil Labs, Wilmington, DE

Recently Nectin-4 has emerged as a prominent oncological target due to its high expression across various solid tumors (e.g., urothelial carcinoma, breast cancer, lung cancer, and pancreatic cancer) with restricted expression in normal adult tissues. The clinical significance of Nectin-4 is underscored by the FDA's approval of enfortumab vedotin (EV) for the treatment of urothelial carcinoma. Several novel therapeutic modalities targeting Nectin-4 are under active investigation for cancer therapies. Herein, we describe the design and development of a panel of bispecific antibodies (bsAbs) targeting both Nectin-4 and HER2. Each individual binding arms of the bsAb were engineered and fine-tuned to moderate affinity in order to instill an avidity-driven binding to cells co-expressing both target antigens. The formats of bsAbs were further optimized for favorable developability. The lead BsAb was subsequently conjugated with varieties of cytotoxic payloads to generate bispecific ADC candidates. Several assays were established to exam cell-binding, internalization, and biological activities of the bispecific ADC in cancer cells that express either one or both of the tumor antigens. Internalization assays demonstrated that the BsAbs were endocytosed in tumor cells co-expressing Nectin-4 and HER2 more efficiently than monoclonal antibodies against Nectin-4 or HER2. The antitumor activity of the bispecific ADCs in multiple CDX mouse models were assessed. The lead bsADC demonstrated potent efficacy in CDX models with varying target expression levels, indicating its potential for a broad anti-tumor spectrum for UC and other solid tumors with dual HER2/Nectin-4 antigen expression.

#5402 Engineering and development of a novel bispecific ADC targeting EGFR and FGFR2b.

Liang Zhu, Chuan Chen, Chenpeng Su, Mei Tian, Xiaoqian Chen, Dandan Liu, Jiyuan Tian, Yang He, Yongxin Shang, Rongmei Yan, Kezhen Ye, Liang Tian, Jian Peng, Zhenping Zhu

Earendil Labs., Wilmington, DE

EGFR is a clinically validated oncogenic driver frequently overexpressed in gastric cancer. Fibroblast growth factor receptor 2b (FGFR2b), a transmembrane receptor tyrosine kinase,is likewise overexpressed in approximately 30% of gastric and gastroesophageal junction (GEJ) cancers, and is associated with poor prognosis. Notably, subsets of gastric tumors co-express EGFR and FGFR2b, indicating potential cooperative signaling that contributes to tumor progression and therapeutic resistance. Bemarituzumab, an afucosylated FGFR2b monoclonal antibody has shown efficacy in the clinical study for the treatment in patients with FGFR2b-positive GC and GEJ cancer. However, the clinical application of bemarituzumab is accompanied by safety concerns. The corneal adverse events were frequently observed. Co-expression of EGFR and FGFR2b presents an attractive opportunity for a dual targeting strategy and supports the bispecific design that could potentially address the safety issues. In this study, we developed several bispecific antibodies (bsAb) targeting EGFR and FGFR2b. These bsAb demonstrated enhanced binding avidity and superior internalization efficiency compared with bemarituzumab and BG-C137 mAb analogs in $EGFR^+/FGFR2b^+$ dual expressing cancer cell lines. Our EGFR×FGFR2b bsAb function as a partial FGFR2b ligand blocker, and only weakly inhibiting FGF7 while sparing FGF10-mediated signaling, thus with the potential to reduce on-target toxicity associated with FGF7/FGF10 blockade. Several bsAb ADC were generated with various cytotoxic payloads and are being tested in vitro and in vivo studies.

#5404 Tumor cell targeted granzyme B demonstrates direct cytotoxic action and indirect immunogenic cell death mediated through numerous defined proteins.

Khalid A. Mohamedali[1], Madhuri Wadehra[2], Lawrence H. Cheung[1], Michael G. Rosenblum[1]

[1]Translational Medical Sciences, Texas A&M University Health Science Center, Houston, TX,[2]UCLA David Geffen School of Medicine, Los Angeles, CA

The primary effect of antibody-directed therapeutics is the delivery of cytotoxic payloads directly to antigen-expressing tumor cells resulting in activating cell death mechanisms in the target cells while sparing nonmalignant cells and reducing systemic toxicity. Cytotoxic payloads with the additional capacity to initiate immune activation mechanisms directed against tumor cells as a secondary effect of targeted therapy have the added benefit of initiating “immunogenic cell death” (ICD), which allows further control over residual tumor cells which may be antigen-negative or resistant to the initial cytotoxic effect. Our previous studies in two syngeneic breast cancer mouse models showed that an EMP2-targeted granzyme B fusion significantly enhanced the tumor levels of CD45+ immune cells and tumor-inhibitory M1 macrophages, as well as decreased tumor-supporting M2 macrophages. Tumor cells undergoing ICD express and secrete immunogenic factors such as damage-associated molecular patterns (DAMPs) that are critical in immune cell recruitment and the initiation of immunogenic apoptosis. Accordingly, we investigated whether targeted granzyme B delivery into human tumor cells resulted in the release or expression of DAMP proteins. We tested three human cell lines with varying levels of antigen expression for FOLRa, Fn14, EMP2 and HER2 with scFv-based constructs targeting each of these antigens and delivering the cytotoxic payload granzyme B. In vitro cytotoxicity against each cell line for all four constructs was found to be in the low nanomolar range. Treatment with all four constructs over 72 hours against log-phase tumor cells resulted in the detection of HMGB1 in the conditioned media while detection of released Annexin A1 was restricted to HEY A8 cells targeted via FOLRa. We characterized HMGB1 and Annexin A1 release into the media in a dose dependent (0-100 nM) and time-dependent (4-72h) manner and correlated these events with real-time release of ATP into the conditioned media. Furthermore, we characterized the expression of Calreticulin on the cell surface of each of these cell lines by flow cytometry and investigated the onset of caspase activation by fluorescence imaging. Further studies are ongoing to identify other DAMP-related proteins which may mediate the secondary immunogenic bystander effect against tumor cells. These data support a proposed “dual mechanism” for GrB-based therapeutics which include a direct, antigen-mediated cytotoxic effect and a secondary, immune-mediated effect which can target both antigen-positive and antigen-negative tumors. Research conducted, in whole or in part, by the Clayton Foundation for Research and generously supported by the NCI R21 CA163971.

#5405 STX002: A GPC3-targeted antibody-drug conjugate with potent and durable antitumor activity in preclinical models of hepatocellular carcinoma.

Deepak Rohila, Sameena Wani, Atul Tandon, Jianhua Zhao, Anindya Bagchi, **Ashutosh Tiwari**

Styx Biotechnologies Inc, San Diego, CA

Hepatocellular carcinoma (HCC) remains a leading cause of cancer mortality with limited therapeutic options, highlighting the need for novel targeted therapies. Glypican-3 (GPC3) is highly expressed in HCC and minimally present in normal adult tissues, making it an attractive antigen for antibody-drug conjugate (ADC) development. STX002 is a next-generation ADC composed of a humanized anti-GPC3 antibody site-specifically conjugated to a potent topoisomerase I inhibitor payload via a cleavable linker. Topoisomerase I inhibitor-based ADCs have shown broad clinical benefit across solid tumors, and STX002 aims to leverage this class against a genetically and molecularly defined HCC target. STX002 demonstrated high-affinity, selective binding to GPC3 and robust internalization in GPC3-positive cells, resulting in potent target-dependent cytotoxicity with sub-nanomolar IC_{50} values and a measurable bystander effect. In vivo, STX002 induced deep and durable tumor regressions across a panel of GPC3-expressing HCC CDX and PDX models, including models refractory to standard-of-care tyrosine kinase inhibitors. Pharmacokinetic and tolerability studies revealed favorable systemic exposure, linker stability, and a wide therapeutic index with minimal off-target toxicity. Collectively, these data support STX002 as a differentiated GPC3-targeted topo-I ADC with strong preclinical efficacy and translational potential. STX002 represents a promising therapeutic candidate for addressing the substantial unmet need in HCC and warrants advancement toward IND-enabling studies and clinical development.

#5406 A novel AI-engineered biparatopic DLL3/CD3 T cell engager demonstrates potent preclinical efficacy and a promising safety profile.

Chuan Chen, Yue Wu, Chenpeng Su, Dandan Liu, Jiyuan Tian, Yujuan Li, Yongxin Shang, Xiaoqian Chen, Rongmei Yan, Liang Tian, Jian Peng, Zhenping Zhu

Earendil Labs, Wilmington, DE

Purpose: This study aimed to develop and characterize a novel biparatopic T-cell engager (TCE) targeting DLL3 for the treatment of small cell lung cancer (SCLC) and other neuroendocrine carcinomas (NECs).
Methods: Using an AI-engineered multispecific antibody platform, we engineered a biparatopic DLL3/CD3 TCE to bind two distinct epitopes on DLL3 while engaging CD3 on T cells. Binding affinities were systematically optimized to enhance tumor targeting and minimize off-T cell activation. The molecule was evaluated *in vitro* activity for T cell-dependent cytotoxicity, T cell activation, and cytokine release and in vivo efficacy using human SCLC cell lines-derived xenograft models. Safety was assessed in transgenic mice and cynomolgus monkeys.
Results: The biparatopic DLL3/CD3 TCE demonstrated potent and specific cytotoxicity against DLL3-expressing cell lines, while limiting T cell activation and cytokine release. In murine models, it achieved significant tumor growth inhibition at lower doses than a benchmark TCE (tarlatamab analog). The molecule exhibited good tolerability at doses up to 30 mpk in transgenic mice and 10 mpk (administered via step-dosing) in monkeys, without significant adverse effects.
Conclusion: The biparatopic DLL3/CD3 TCE exhibits robust preclinical efficacy and a favorable safety profile, supporting its further development as a targeted immunotherapy for DLL3-positive SCLC and NECs.

#5407 Mechanism of CAPRIN-1 membrane localization in cancer and development of TRK-950, a humanized anti-CAPRIN-1 antibody.

Yoshitaka Minamida, Shoichi Ohno, Kazushi Tachibana, Ukei Wasai, Takayuki Fujita, Takashi Morimoto, Fumiyoshi Okano

New Frontiers Research Laboratories, Toray Industries, Inc., Kamakura, Japan

CAPRIN-1, initially reported as a cytoplasmic protein, has emerged as a novel cancer-specific therapeutic target. CAPRIN-1 is highly expressed on the cell membrane surface of a broad range of solid tumors, but not on normal cells (Okano, F et al., Cancer Res Commun 2023). However, the molecular mechanism underlying this cancer-specific membrane localization of CAPRIN-1 remains unclear. In this study, we aimed to elucidate the mechanism responsible for CAPRIN-1 membrane expression in cancer. We identified “Protein X” as a CAPRIN-1-binding partner under certain stress conditions. Our data indicate that “Protein X” is required for stress-induced membrane localization of CAPRIN-1 in cancer cells. Based on the promising expression profile of CAPRIN-1, we developed a humanized anti-CAPRIN-1 antibody, TRK-950, currently under clinical development. TRK-950 demonstrated safety and tolerability in a Phase-1 study (NCT02990481), and Phase-2 trials are ongoing in patients with gastric cancer (NCT06038578) and melanoma (NCT05423262). In parallel with clinical studies, we conducted non-clinical investigations to clarify TRK-950’s anti-tumor mechanism. Our findings show that macrophage-mediated ADCP via Fcg receptors is critical for the TRK-950 efficacy as demonstrated using FcgR knockout and macrophage-depleted mouse models. Furthermore, TRK-950 combined with several approved anticancer drugs exhibited enhanced anti-tumor activity both *in vitro* and *in vivo*. In addition to the naked antibody, we are developing CAPRIN-1-targeted modalities such as ADCs and will present these encouraging results at this meeting. Collectively, these data support CAPRIN-1 as a promising target for antibody-based therapies.

: Retrospective Observational Studies
Poster Session

#5411 Primary osteosarcoma of the short bones: A Surveillance, Epidemiology, and End Results Program (SEER) retrospective study.

Jarrell Imamura[1], Elizabeth Nowak[2], Arda Durmaz[2], Jacob G. Scott[2], Zachary Burke[2]

[1]Genomic Medicine and Systems Biology, Cleveland Clinic Research, Cleveland, OH,[2]Cleveland Clinic, Cleveland, OH

Introduction:
Osteosarcoma (OS) is the most common primary solid malignancy of bone and accounts for 2% of all childhood cancers. OS is most often found in the long bones of the extremities, in particular the femur, tibia, and humerus. However, it is rarely found in the short bones of the upper and lower extremity. This study seeks to address the existing gap in the literature on the incidence, treatment, and outcomes of OS of the short bones of the upper and lower extremity.
Methods:
Cases of primary short bone OS were identified using the National Cancer Institute Surveillance, Epidemiology, and End Results (SEER) Program database, containing 8,216,169 cancer cases from 2000 to 2020. Demographic, clinical, and treatment characteristics were collected, and univariate and multivariate regression analysis was conducted to determine the relationship between disease-specific survival and tumor spread, tumor size, tumor grade, surgery type, and primary site.
Results:
Cases of primary short bone OS made up 2.2% of all OS cases in the database. The majority of cases were male, and the most common age group ranged from ages 15 to 39. Within the 201-patient cohort, 58.2% were treated with chemotherapy and 4.5% received radiation therapy. Surgery information was available for 170 patients—50.6% of that group underwent limb-sparing surgery, 31.8% of patients underwent amputation, and 17.6% did not have surgery. Univariate analysis revealed grade and disease spread to be statistically significant predictors of survival; however, upon multivariate analysis, only localized disease was correlated with better disease-specific survival. Interestingly, there was no survival difference between patients treated with amputation versus patients who underwent limb salvage surgery.
Conclusions:
The results of this study confirm that OS of this location is a rare entity that generally follows the demographic distribution of the more common long bone variant. The results also signal that limb salvage is a reasonable treatment option for this group, given the lack of survival difference between limb salvage surgery and amputation.

#5412 Eyelid malignancies on the rise? A population-based analysis of merkel cell carcinoma, melanoma, and sebaceous carcinoma from the SEER database.

Said Yaseen[1], Bashar I. Almaraziq[2], Shaimaa A. Abdelmoneim[3], Ahmed S. Al Sakini[4], Mohamed Ahmed Ali[5], Joud K. Alhousani[1], Leen Abu Rabi[1], **Ahmad Farouk Alzein**[6], Issam Khourshid[7], Shahd Alsharif[1], Hamza Khoursheed[1], Mohammad Almajali[1], Hashem Abu Serhan[8]

[1]Jordan University of Science and Technology, Irbid, Jordan,[2]Hashemite University, Zarqa, Jordan,[3]Egyptian Ministry of Health and Population, Alexandria, Egypt,[4]University of Baghdad, Baghdad, Iraq,[5]South Valley University, Qena, Egypt,[6]University of Illinois Chicago, Chicago, IL,[7]Victoria Hospital, Scotland, Kirkcaldy, United Kingdom,[8]Hamad Medical Coorporation, Doha, Qatar

Purpose:
This study sought to analyze temporal incidence trends for malignant melanoma (MM), Merkel cell carcinoma (MCC), and sebaceous gland carcinoma (SGC) of the eyelid and to predict future patterns using population-based data.
Methods:
A retrospective analysis was conducted using the Surveillance, Epidemiology,and End Results (SEER) database from 2000-2021. Time-series models, including Autoregressive Integrated Moving Average (ARIMA) and Neural Network Autoregression (NNAR), were applied to estimate incidence rates (IRs) per 100,000, stratified by tumor type, sex, age, and race. Model selection was based on minimizing Root Mean Square Error (RMSE). Poisson regression was used to assess the impact of age and sex on IRs.
Results:
The overall IR for these malignancies showed an increase from 2000 to 2015,followed by a slight decline and a subsequent rise in 2021; a 10-year forecast projects a continued modest increase. Subtype analysis revealed variable trends: MM incidence is projected to rise, while MCC and SGC incidence rates are forecasted to remain relatively stable. Poisson regression identified age >60 years as a highly significant risk factor, dramatically increasing the incidence rate ratio (IRR) for both MM (IRR 17.1) and SGC (IRR 25.4). Gender was not a significant factor. Racial disparities were evident; White individuals had the highest incidence of MM, whereas Asian or Pacific Islander individuals had the highest incidence of SGC.
Conclusion:
Malignant eyelid tumors exhibit distinct patterns. MCC has the highest metastatic risk, sebaceous adenocarcinoma varies by race, and surgery remains key

#5413 Real-world (RW) outcomes by race in patients (pts) receiving first-line (1L) treatment (tx) for advanced/metastatic (a/m) gastric, gastroesophageal junction, or esophageal adenocarcinoma (GC/GEJC/EAC).

Jin Gu[1], Ravindra Gupta[1], Daniel O. Koralek[1], Aliki Taylor[1], Jaffer A. Ajani[2]

[1]Gilead Sciences, Foster City, CA,[2]Department of Gastrointestinal Medical Oncology, The University of Texas MD Anderson Cancer Center, Houston, TX

Prior studies show racial disparities in tx access and mortality in GC/GEJC/EAC, yet the effect of race on 1L tx outcomes is unclear. We evaluated tx patterns and outcomes by race in pts who received 1L tx for GC/GEJC/EAC in the US. This retrospective, observational study used the Flatiron Health Research Database. Adults starting 1L tx between May 1, 2021, and Nov 30, 2024 for HER2-negative/unknown GC/GEJC/EAC were included. End of follow-up was May 31, 2025 to allow for ≥6 months of follow-up. Flatiron categorized self-reported race as White, Black/African American (Black), Asian, or other (multiple categories/not listed). RW overall survival (OS), time to next tx/death (TTNTD), and time to tx discontinuation (TTD) were estimated via the Kaplan-Meier method and compared between race categories. Of 2128 eligible pts, 61% were White, 8% Black, 3% Asian, 8% other, and 20% unknown race. Most were treated in community-based oncology practices (77%-79%). Median age was similar across racial groups (69 years); 25% (White), 76% (Black), and 77% (Asian) of pts had GC. Median OS (12.0 vs 13.0 months) and TTNTD (7.6 vs 6.7 months) were similar in Black vs White pts; median TTD was numerically longer in Black vs White pts (4.3 vs 2.3 months). However, the differences in clinical outcomes between Black and White pts were not statistically significant (hazard ratio [95% confidence interval]: OS, 0.97 [0.78-1.20]; TTNTD, 0.93 [0.77-1.13]; TTD, 0.92 [0.76-1.10]) after adjusting for key baseline confounders (Table). These findings underscore the potential impact of equitable 1L tx access in minimizing racial disparities in pts with HER2-negative/unknown a/m GC/GEJC/EAC. Larger studies are needed to assess the influence of disease prognosis and other variables, but this study highlights the value of RW data in advancing health equity and guiding future clinical interventions.

Table. Clinical outcomes by race[a]

Median (HR vs White; 95% CI), mo	**White (n = 1290)**	**Black/African American (n = 174)**	**Asian (n = 68)**	**Other (n = 170)**
rwOS	13.0 (Referent)	12.0 (0.97; 0.78-1.20)	16.6 (0.88; 0.60-1.27)	13.0 (0.90; 0.72-1.12)
rwTTNTD	6.7 (Referent)	7.6 (0.93; 0.77-1.13)	8.6 (0.87; 0.63-1.20)	7.4 (0.95; 0.78-1.16)
rwTTD	2.3 (Referent)	4.3 (0.92; 0.76-1.10)	5.0 (0.79; 0.59-1.07)	4.5 (0.81; 0.67-0.98)

HR, hazard ratio; mo, months; rwOS, real-world overall survival; rwTTD, real-world time to treatment discontinuation; rwTTNTD, real-world time to next treatment or death.

[a]Analysis excluded pts with unknown race.

#5414 Clinical outcomes and treatment outcomes of stage IV large cell lung cancer based on two national database analysis.

Wongi Woo[1], Seoin Kim[2], Jongwoo Kim[2], Vincent Lopez[1], Kirun Chohan[1], David Thota[1], Yeena Lee[1], Christian Wong[1], Amrut Savadkar[1], Yoonjin Cha[3], Duk Hwan Moon[4], Sungsoo Lee[4], Young Kwang Chae[5]

[1]St. Joseph's Medical Center Stockton, Stockton, CA,[2]Metrowest Medical Center, Framingham, MA,[3]Yonsei University College of Medicine, Seoul, Korea, Republic of,[4]Gangnam Severance Hospital, Seoul, Korea, Republic of,[5]Northwestern Univ. Feinberg School of Medicine, Chicago, IL

Background: Large cell lung cancer (LCLC) is an uncommon neuroendocrine subtype of non-small cell lung cancer with limited therapeutic options and poor prognosis. Evidence regarding survival patterns in stage IV LCLC, particularly across different treatment modalities, remains scarce. This study aimed to evaluate clinical characteristics, treatment patterns, and survival outcomes using two national cohorts.

Methods: Patients with stage IV LCLC diagnosed between 2000 and 2021 were identified from the Surveillance, Epidemiology, and End Results Program (SEER) 17 registries. Eligible cases were stage IV LCLC according to the 7th or 8th TNM classification; demographic, clinicopathologic, socioeconomic, and available molecular data were collected. Kaplan-Meier analyses compared overall survival (OS) and cancer-specific survival (CSS) across treatment groups: no treatment, chemotherapy, and combined surgery plus chemotherapy. Cox proportional hazards models were used to identify independent predictors of CSS. In addition, publicly available data from the Korean National Health Insurance System (KNHIS) were analyzed to assess the impact of epidermal growth factor receptor (EGFR) mutation on survival.

Results: A total of 3,478 patients were included. In the SEER cohort, 3-year OS differed substantially by treatment modality: 2.2% with no treatment, 7.1% with chemotherapy, and 13.3% with surgery plus chemotherapy. Similar trends were observed for CSS. In multivariable analysis, age >65 years (hazard ratio (HR) 1.16 [95% confidence interval (CI) 1.08-1.25], p<0.0001), male sex (HR 1.17[95% CI 1.09-1.26], p<0.0001), and low household income (HR 1.18[95% CI 1.08-1.30], p<0.0001) were independently associated with higher cancer-related mortality. Compared with chemotherapy alone, surgery combined with chemotherapy reduced mortality (HR 0.78[95% CI 0.70-0.87], p<0.0001). Among the KNHIS cohort, EGFR mutations were detected in 303 of 666 patients (45.5%); however, the presence of EGFR mutation did not confer a significant survival benefit among patients who received chemotherapy (HR 0.821 [95% CI 0.63-1.07], p=0.146).

Conclusions: Despite the overall poor prognosis, treatment significantly influences outcomes in stage IV LCLC. Chemotherapy provides a clear survival benefit, and multimodal therapy that includes surgery offers the greatest improvement, potentially reflecting increased access to molecular testing and targeted therapy. Further investigation— including the potential benefits of tyrosine-kinase inhibitors in EGFR-mutated disease, systematic evaluation of other actionable mutations, and ongoing studies of immunotherapy after platinum-based regimens— is needed to define optimal management strategies for this rare subtype.

#5415 Association between time-dependent postoperative vitamin D levels and survival in early-onset colorectal cancer patients undergoing curative surgery: A real-world database analysis .

Yimiao Zeng[1], Bingya Ma[1], Matthew C. Coleman[2], John Y. Ha[3], Jason Zell[4], Yunxia Lu[1]

[1]Department of Population Health & Disease Prevention, Joe C. Wen School of Population &Public Health, UC-Irvine, Irvine, CA,[2]Joe C. Wen School of Population & Public Health, UC-Irvine, Irvine, CA,[3]School of Medicine, Case Western Reserve University, Cleveland, OH,[4]School of Medicine, UC-Irvine, Irvine, CA

Background: Previous studies have found high vitamin D levels are associated with improved colorectal cancer (CRC) survival. However, no reports have focused on early-onset CRC (EOCRC, CRC diagnosed before age 50), whose incidence has increased dramatically in the United States and many other countries. Moreover, previous studies rarely considered the timing of vitamin D measurements, the dynamic change in vitamin D levels, and patients' comorbidity conditions, which may confound the association.
Methods: Using the University of California Health Data Warehouse (UCHDW), an electronic health record (EHR) database encompassing data from six UC medical centers from 2012 through 2025, we initiated an EOCRC patient cohort. EOCRC patients who had no prior history of malignancy, underwent curative surgery, and had at least one vitamin D measurement after surgery were included in the study. Vitamin D level was treated as both continuous variable and categorical variable (Vitamin D deficiency: 25(OH)D < 20ng/mL; Vitamin D insufficiency: 20ng/mL ≤ 25(OH)D <30ng/mL; Vitamin D sufficiency: 25(OH)D ≥ 30ng/mL). To account for dynamic changes in vitamin D levels, postoperative vitamin D levels were treated as time-dependent variables. A time-dependent Cox regression model was performed and hazard ratio (HR) and 95% confidence intervals (CI) were estimated to measure the association between Vitamin D and EOCRC survival.
Results: We identified 424 eligible EOCRC patients, with an average follow-up time of 5.42 years. Each patient had an average of 2.68 postoperative vitamin D measurements, and 83 patients died during the follow-up period. Data was organized as person-time structure for the time-dependent cox regression model and were adjusted for age, gender, race, tumor locations, body mass index (BMI), socioeconomic status, comorbidity index, and seasons of vitamin D measurement. Patients with vitamin D sufficiency (HR 0.36, 95%CI 0.21-0.65) and insufficiency (HR 0.34, 95%CI 0.18-0.64) were associated with a better survival compared with patients with Vitamin D deficiency. When vitamin D level was treated as a continuous variable in the model, higher vitamin D levels were still associated with better overall survival (HR 0.96, 95%CI 0.94-0.99).
Conclusion: This is the first study to investigate the association between vitamin D levels and EOCRC survival using a time-dependent Cox regression model. Our results show that postoperative vitamin D non-deficiency status is associated with better survival compared to vitamin D deficiency. Our findings may provide evidence for clinical management of vitamin D levels in EOCRC patients.

#5416 Preoperative albumin is associated with unplanned readmission following soft tissue sarcoma resection.

Erin J. Kim[1], Christopher M. Liu[2], Pearce B. Haldeman[2], Michael Gedestad[3], Conner Trimm[2], James H. Flint[2], Frank Chiarappa[2]

[1]University of California, San Diego School of Medicine, La Jolla, CA,[2]Department of Orthopaedic Surgery, University of California, San Diego, La Jolla, CA,[3]Department of Plastic Surgery, University of California, San Diego, La Jolla, CA

Introduction: Treatment of soft tissue sarcomas (STS) revolves around surgical resection. Post-operative readmission is common and is associated with patient morbidity and increased healthcare costs. This study sought to identify risk factors for unplanned readmission and quantify the cost of such events.
Experimental Procedures: Extremity STS patients who underwent resection from 2018 to 2022 at a tertiary referral center were included. Demographics, comorbidities, tumor characteristics, treatment, and surgical findings were collected. Postoperative complications, readmissions, local recurrence, reoperations, and disease-specific survival were also obtained. Risk factors for readmission were evaluated via Pearson correlation testing. Binomial logistic regression modeling was subsequently utilized for variables with p-values < 0.2.
Results: Among 131 patients (mean follow-up 21 ± 10 months), overall postoperative complication rate was 36%, local recurrence rate was 9%, reoperation rate was 20%, and disease-specific survival rate was 96%. Unplanned readmission occurred in 32% of patients at a mean of 19 days after discharge (Range: 6-121). ASA class, preoperative hemoglobin, preoperative albumin, and complications during the index hospitalization were significantly associated with readmission. After multivariate analysis, preoperative serum albumin remained independently associated with unplanned readmission (OR = 0.077; 95% CI = 0.005, 0.15). Mean readmission cost was $76,605.39 (Standard Deviation: $101,981.78).
Conclusions: Unplanned readmission after STS resection is common and is associated with substantial financial burden. Low preoperative serum albumin is associated with increased readmission risk, underscoring the potential value of preoperative nutritional optimization and intervention. Studies with larger patient cohorts and additional nutritional markers are needed.

Patient Characteristics and their Associations with Unplanned Readmission

Demographics and Comorbidities		**P-value**
Age (years), Mean (SD)	61 (16)	0.92
Male, n (%)	61 (54)	0.21
BMI (kg/m^2), Mean (SD)	28 (6.4)	0.19
Diabetes Mellitus, n (%)	21 (19)	0.10
COPD, n (%)	10 (9.2)	0.14
Osteoporosis, n (%)	10 (9.2)	0.26
ASA Class, Mean (SD)	2.6 (0.6)	**0.0009**
Preoperative Serum and Tumor Metrics		**P-value**
Hemoglobin (g/dL), Mean (SD)	12.7 (1.79)	**0.03**
Albumin (g/dL), Mean (SD)	4.02 (0.681)	**0.001**
Tumor Location - Proximal Lower Extremity, n (%)	73 (64)	0.16
FNCLCC Grade (1/2/3), n (%)	15 (13)/34 (30)/63 (57)	0.25
Tumor Size (cm), Mean (SD)	10.0 (1.5-40)	**0.01**
Treatment and Surgical Metrics		**P-value**
Preoperative Radiation, n (%)	61 (54)	0.14
OR Time (minutes), Mean (SD)	468 (306)	**0.05**
Estimated Blood Loss (mL), Mean (SD)	172 (516)	**0.05**
Hospital LOS (days), Mean (SD)	4.3 (5.6)	**0.05**
Complications During Operative Hospitalization, n (%)	17 (15)	**0.03**
Independent Risk Factors of Unplanned Readmission Following Multivariate Analysis	**OR (95% CI)**	**P-value**
Preoperative Serum Albumin	0.077 (0.005, 0.15)	**0.03**
Diabetes Mellitus	1.4 (0.70, 2.1)	0.12
Preoperative Radiation	9 (0.98, 17.02)	0.07

#5417 Recurrence-free survival in patients with early-stage HPV-associated adenocarcinoma of the cervix stratified by Silva patterns.

Ana Lucia Rosario Santos[1], Hisham Bahmad[2], Jovanka Ravix[3], Andre Pinto[2], Navya Nair[1]

[1]Obstetrics, Gynecology, and Reproductive Sciences, University of Miami Miller School of Medicine, Miami, FL,[2]Pathology and Laboratory Medicine, University of Miami Miller School of Medicine, Miami, FL,[3]Medical Scientist Training Program, University of Miami Miller School of Medicine, Miami, FL

Background: HPV-associated adenocarcinoma of the cervix presents challenges in adjuvant treatment compared to squamous cell carcinoma of the cervix. Silva Pattern-based classification has emerged as a histomorphologic predictor supplementing the traditional Sedlis Criteria established in GOG 92. While not part of FIGO staging, it is considered in clinical guidelines, as the Silva Pattern C confers a higher risk of nodal metastasis and disease recurrence; however, its prognostic role in early-stage disease and in patients who do not meet Sedlis criteria remains less defined. We aimed to determine whether Recurrence-free survival (RFS) in patients with early-stage HPV-associated adenocarcinoma of the cervix differs between patients with Silva Pattern C and those with A/B. We hypothesize that Silva Pattern C can guide adjuvant management in patients with negative Sedlis Criteria.

Methods: We conducted a retrospective study of patients with surgically treated FIGO Stage IA-IB2 HPV-associated adenocarcinoma of the cervix. Cases were identified through our institutional pathology database under an IRB-approved protocol (2015 to 2025). Pathology specimens from cone biopsies and hysterectomies were reviewed by gynecologic pathologists. Silva patterns were assigned accordingly. Clinical data were obtained from electronic medical records. The study outcome was to determine the RFS, measured from diagnosis to recurrence or to the last follow-up. A Kaplan-Meier analysis was used to compare Silva patterns A/B vs. pattern C.

Results: Our sample consisted of 13 patients with HPV-associated adenocarcinoma of the cervix. We identified 6 patients with Silva Patterns A/B and 7 with Silva Pattern C. Three recurrences occurred exclusively in the Silva Pattern C group. RFS was 42.9% in Silva C and 100% in Silva A/B (log-rank *p*-value: 0.4142). Median follow-up was 29 months (6-108 months) for Silva Pattern C and 15 months (0-46 months) for Silva Pattern A/B. All recurrences occurred in patients with FIGO stage IA2-IB1 disease who did not meet Sedlis Criteria for adjuvant radiation. Times to recurrence were 10, 24, and 90 months.

Conclusions: Patients with Silva Pattern C experienced worse RFS. None of the patients with Silva Pattern C who recurred met Sedlis criteria for adjuvant radiation. Sedlis criteria mainly guide squamous cell carcinoma management; only 12% of GOG 92 patients had adenocarcinoma, limiting its use for this group. Our findings suggest that the Silva pattern C may provide clinically actionable prognostic information and can help guide multidisciplinary discussions regarding adjuvant management. Prospective validation of clinical algorithms incorporating Silva pattern-based classification in larger cohorts is warranted.

#5418 COVID-19 infection and impact on cancer recurrence: Comprehensive results from over 32,000 patients with breast cancer.

Shiliang Zhang[1], Eric Yang[2], Marla Lipsyc-Sharf[1], Alexis LeVee[1], Carlos Cordon-Cardo[3], Aditya Bardia[1]

[1]Department of Medicine, Division of Hematology and Oncology, UCLA Health, Los Angeles, CA,[2]UCLA College of Letters and Sciences, Los Angeles, CA,[3]Department of Pathology, Icahn School of Medicine at Mount Sinai, New York, NY

Background: The impact of COVID-19 infection on breast cancer recurrence remains poorly understood. SARS-CoV-2 infection is associated with systemic immune dysregulation, including lymphopenia, chronic inflammation, and altered interferon signaling, which may compromise tumor immune surveillance. We aimed to evaluate the association between COVID-19 infection and recurrence outcomes in patients with breast cancer.

Methods: We identified patients diagnosed with localized breast cancer between 1/1/2011 and 12/31/2024 using ICD-10 codes, excluding those with metastatic disease codes prior to or at initial diagnosis, at an academic center. COVID-19 infection was identified through diagnostic codes. Recurrence was defined by ICD codes for metastatic disease occurring after initial diagnosis, and time to recurrence was measured from first breast cancer diagnosis to first metastatic code. Sites of recurrence were determined using specific ICD-10 codes. Hazard ratios were estimated using Cox proportional hazards models. Kaplan-Meier curves were generated for time-to-event analyses, and log-rank tests were used for group comparisons.

Results: Of 32,871 eligible patients, 18,297 had tumors that were ER positive (ER+), 3,563 were ER negative (ER-), and 11,011 had unknown ER status. Median age at diagnosis was 63. Median follow-up time was 47 months. Of the entire cohort, 3325 (10.12%) developed distant or lymph node metastasis. Among 2,449 patients with COVID-19 after breast cancer diagnosis, 11.15% experienced distant recurrence and 15.35% experienced any recurrence, compared with 7.65% and 9.69%, respectively, in patients without post-diagnosis COVID-19. COVID-19 infection was associated with higher risk of any recurrence (HR 1.21; 95% CI 1.08-1.34; p<0.001). Subtype analyses showed higher risk of any recurrence associated with COVID-19 in ER+ patients (HR 1.42; p<0.001) and a trend towards higher risk in ER- patients (HR 1.18; p=0.169). Five-year invasive disease-free survival was lower in patients who had COVID-19 (85.7% vs. 88.6%; p<0.001). Bulk RNA sequencing from rapid autopsy studies demonstrated downregulation of HLA and p53 creating an immunosuppressive and pro-tumorigenic microenvironment, facilitating cancer growth and disease recurrence.

Conclusions: COVID-19 infection following breast cancer diagnosis was associated with increased risk of recurrence, particularly in patients with ER+ disease, mediated in part by downregulation of tumor suppressor and immunosurveillance-related genes. These findings underscore the need for continued clinical surveillance and mechanistic studies exploring immune recovery and tumor progression in breast cancer survivors affected by COVID-19.

#5419 Persistent opioid use during long-term lung cancer survivorship: When did it start?.

Ziwei Zhu[1], Yiye Zhang[1], Hao Zhang[2], Rulla Tamimi[1], Yuhua Bao[1]

[1]Weill Cornell Medicine, New York, NY,[2]University of Alabama at Birmingham, Birmingham, AL

Introduction: Lung cancer survivors had a high rate of long-term opioid use. Prolonged opioid use was associated with reduced survival and increased recurrence. It is unknown to what extent opioids initiated during cancer treatment accounted for long-term use. This study aims to characterize the patterns of opioid use in the first year of lung cancer long-term survivorship (LTS) and the history of opioid prescriptions (Rxs) by such patterns.

Method: We used the 2010-19 SEER-Medicare linked data to identify a sample of lung cancer survivors enrolled in traditional Medicare Parts A&B and Part D for ≥84 months - 12 months before and 72 months after (including) the month of lung cancer diagnosis, who had ≥1 opioid Rx during the first year of LTS (months 61-72 post diagnosis). We constructed a sequence of daily opioid possession status (0/1) for each patient over the first year of LTS. We applied agglomerative hierarchical clustering to identify groups with distinct patterns. For each patient over the 84 months, we identified the earliest opioid Rx observed, earliest opioid episode that was ≥30 days, and earliest episode that was ≥90 days, if any. Episodes were defined based on filling date and days of supply of consecutive opioid Rxs; a gap of ≥30 days ends the episode.

Results: 1,176 survivors were identified with ≥1 opioid Rxs in the first year of LTS. Clustering identified three groups: “persistent use” (N=301, 26%), “intermittent use” (N=176, 15%), and “sporadic use” (N=699, 60%), with median days of opioid possession of 343, 168, and 10, respectively. More than 90% of the persistent-use group had their first opioid Rx before lung cancer diagnosis. There was a sharp gradient across the 3 groups in percentage with first 30- or 90- day episode before cancer diagnosis (Table).

Conclusions: An overwhelming proportion of survivors with persistent or intermittent opioid Rxs during first year of LTS started opioid therapies and, to a less extent, long-term opioid therapies, prior to lung cancer diagnosis.

Earliest opioid prescription and long-term episodes observed across three groups of survivors

	Persistent Use (N = 301)	**Intermittent Use (N = 176)**	**Sporadic Use (N = 699)**
Earliest Opioid Prescription Observed			
12 months before diagnosis	276 (92%)	144 (82%)	463 (66%)
Months 1 - 12 after diagnosis	20 (6.5%)	28 (16%)	188 (27%)
Months 13-60 after diagnosis	5 (1.7%)	4 (2.3%)	32 (4.6%)
Months 61-72 after diagnosis	0 (0%)	0 (0%)	16 (2.3%)
Never	N/A	N/A	N/A
Earliest 30-Day Opioid Episode Observed			
12 months before diagnosis	250 (83%)	114 (65%)	220 (31%)
Months 1 - 12 after diagnosis	36 (12%)	37 (21%)	163 (23%)
Months 13-60 after diagnosis	14 (4.7%)	19 (11%)	85 (12%)
Months 61-72 after diagnosis	1 (0.33%)	6 (3.4%)	58 (8.3%)
Never	0 (0%)	0 (0%)	173 (25%)
Earliest 90-Day Opioid Episode Observed			
12 months before diagnosis	226 (75%)	79 (45%)	104 (15%)
Months 1 - 12 after diagnosis	34 (11%)	28 (16%)	49 (7.0%)
Months 13-60 after diagnosis	38 (13%)	43 (24%)	58 (8.3%)
Months 61-72 after diagnosis	3 (1.0%)	15 (8.5%)	33 (4.8%)
Never	0 (0%)	11 (6.3%)	455 (65%)

#5420 Identifying dynamic subtypes of cancer cachexia using longitudinal clinical lab values.

Jamie Wang[1], Ed Reznik[2], Wesley Tansey[2]

[1]Physiology, Biophysics & Systems Biology, Weill Cornell Medicine, New York, NY,[2]Computational Oncology, Memorial Sloan Kettering Cancer Center, New York, NY

Cancer cachexia is a wasting syndrome estimated to affect roughly 50% of all cancer patients and is most commonly identified using a simple weight loss criterion. The heterogeneity in plausible cachexia weight loss mechanisms, along with their potential to evolve over time, suggests the existence of distinct, dynamic subtypes of cachexia. Clinical lab values are frequently measured and, although they do not grant direct mechanistic insight, they provide rich temporal information about patient latent states. In a cohort of lung adenocarcinoma patients from Memorial Sloan Kettering Cancer Center, we clustered 1,630 cachectic episodes using 28 longitudinally measured clinical lab values and body mass index. Clustering was performed using K-means with Dynamic Time Warping Barycenter Averaging to handle trajectories with varying lengths. We identified 4 major clusters with differentiating patterns including a group with relatively higher red cell distribution width and relatively lower mean corpuscular volume and mean corpuscular hemoglobin. Another cluster had lab values that are more consistent with normal ranges, indicating a possible non-cachectic group of weight loss patients. This study demonstrates the potential of longitudinal clinical lab values for stratifying cachexia patients and identifying intervention points in patient care that can improve outcomes.

#5421 Determining the benefit of comprehensive molecular testing in advanced cancers: BostonGene and Exigent Genomic INsight (BEGIN) study.

Sibel Blau[1], Katherine Sanchez[2], Eric Schaefer[3], Julio A. Peguero[4], Paul Zito[5], Dheeraj Kodali[6], Artem Tarasov[7], Rheanna Carter[7], Kayla Hendricks[7], Anna Love[7], Lile Kontselidze[7], Polina Turova[7], Viktor Smirnov[7], Anna Ogloblina[7], Konstantin Rumyantsev[7], Neeharika Makani[7], Alexander Bagaev[7], Nathan Fowler[7]

[1]Northwest Medical Specialties, Seattle, WA,[2]New Mexico Cancer Center, Albuquerque, NM,[3]Highland Oncology Group, Rogers, AR,[4]Oncology Consultants, Houston, TX,[5]Oklahoma Cancer Specialists and Research Institute, Tulsa, OK,[6]Stockton Hematology Oncology Medical Group, Stockton, CA,[7]BostonGene Corporation, Waltham, MA

Introduction: Growing evidence suggests that comprehensive genomic and molecular testing has the potential to enable more precise, effective, and individualized cancer care. However, outside of trials, testing is inconsistent, and adoption into practice is limited. The BostonGene and Exigent Genomic INsight Study (BEGIN; NCT06272864) is an ongoing, prospective, multi-site study evaluating the clinical utility and actionability of integrated DNA/RNA comprehensive genomic profiling (CGP) in community settings. Using the multimodal Tumor Portrait test, CLIA-certified whole-exome sequencing (WES), whole-transcriptome RNA-seq, and tumor microenvironment (TME) subtyping were performed in pts. with advanced tumors.

Methods: We consented and prospectively enrolled adult pts. with advanced breast cancer, non-small cell lung cancer (NSCLC), melanoma, or sarcoma at six community practice sites within the Exigent Research Network. All pts. underwent WES, RNA-seq, and TME profiling using the Tumor Portrait test. Actionable findings were defined by links to FDA-approved or NCCN®-recommended therapies or eligibility for biomarker-matched clinical trials. RNA-seq expression of targetable molecules (e.g., *ERBB2* [HER2], *CD274* [PD-L1]) was also classified as actionable. Absence of driver mutations were not reported. Demographics, prior therapy, treatment decisions, and clinical outcomes were collected at 6 and 12 mos.

Results: We analyzed 156 pts. (breast, n = 87; NSCLC, n = 41; melanoma, n = 21; sarcoma, n = 7) with ≥6 mos. of follow-up after report delivery. The median turn around time for comprehensive testing was 8 business days. Out of 221 screened pts., the sample failure rate was 14.4% (32/221). Actionable findings were identified in 93% of pts. (145/156), with ~10% (15/145) attributable to RNA-seq and missed by DNA-only testing. Actionable finding rates by tumor type were: breast, 95.4%; NSCLC, 87.8%; melanoma, 95.2%; and sarcoma, 71.4%. At least one NCCN®/FDA-linked CGP biomarker was identified in 71 of 156 pts. (45.5%). Post-testing follow-up was available for 138 pts.; median follow-up was 6 mos., with 68/156 (43.5%) at ≥12 mos. RNA or DNA findings directly informed or altered the clinical course through the initiation of genomically matched systemic therapy and/or referral to biomarker-selected trials in 10% of pts.

Conclusions: Integrated DNA/RNA CGP identified actionable findings in 93% of pts., with 10% of actionable findings being identified by RNA expression that were missed by DNA testing. This study demonstrates the clinical utility of combined exome-transcriptome profiling for precision oncology in community practice, which directly impacts patients' therapeutic options. Continued follow-up with BEGIN will assess the impact on patient-related outcomes, including progression-free and overall survival, as well as clinical trial accrual.

#5422 Turnaround time between NSCLC diagnosis to genomic testing using reflexive next generation sequencing.

Sahar Forootan Sedigh[1], Sydney F. Denney[1], Katharine Thomas, MD[2]

[1]University of Nevada School of Medicine, Reno, NV,[2]Renown Regional Medical Center, Reno, NV

Background: Lung cancer is the leading cause of cancer mortality in both men and women in the United States, accounting for 1 in 5 of all cancer deaths. Identifying driver mutations in lung cancer allows clinicians to choose targeted therapies, offering higher response rates and fewer adverse effects. Timeliness to treatment of non-small cell lung cancer (NSCLC), which contributes approximately 87% of lung cancer cases, is expected to improve outcomes by facilitating biomarker-directed treatment in the first-line setting. In this study, we evaluated and compared the turnaround time (TAT) between NSCLC diagnosis and genomic result reporting before and after the initiation of reflexive next generation sequence (NGS) testing.
Methods: A single institution retrospective study was conducted using time zero as the specimen collection date from biopsy/surgical resection to NGS report release date before (N=23) and after (N=26) the implementation of reflexive NGS testing. Reflexive NGS testing was defined as an institutional policy in which a pathologist automatically ordered NGS testing during diagnostic biopsy reporting. Prior to this policy, the NGS testing was ordered at the discretion of the treating oncologist. We used FoundationOne companion diagnostic (CDx), an NGS diagnostic test, to identify tumor mutation profiles to detect biomarkers with FDA-approved targeted therapies. TAT in pre- and post-reflexive cohorts was compared using a two-sample t-test.
Results: A total of 49 patients were included, 23 patients before and 26 patients after reflexive testing. The mean TAT from specimen collection to NGS report release date decreased from 31.8 days pre-reflexive to 18.9 days (40.6% reduction, $p = 0.001$) after implementation of reflexive testing. Median TAT decreased from 31 to 17 days. The range narrowed from 49 to 27 days and standard deviation of TAT decreased from 15 to 6.5 days, indicating a more consistent TAT post-reflexive testing. Evaluating TAT from specimen collection date to order date, the mean TAT decreased from 18.3 days pre-reflexive to 5.53 days (69.8% reduction, $p = 0.0001$) post-reflexive testing with median TAT decreasing from 15 to 4 days and the range decreasing from 48 to 23 days. The standard deviation of TAT also decreased from 13 to 5 days, showing a more consistent TAT after implementation of reflexive NGS testing.
Conclusion: Reflexive NGS testing significantly reduced both ordering time by 69.8% and reporting time by 40.6%. These findings highlight the substantial improvement in diagnostic efficiency and workflow. The reduction in TAT will allow for an earlier initiation of targeted therapies in patients with NSCLC. Future studies will investigate the clinical benefit of reflexive NGS testing in reducing hospitalizations, time to treatment initiation, and improved patient outcomes.

#5423 A Bayesian framework for evaluating somatic copy number variants into comparative genomic analysis of multifocal non-small cell lung cancer.

Claire Teigen, Ying-Chun Lo, Sounak Gupta, Stephanie Smoley, Beth Pitel, Hussam Al Kateb, Gopi Sivasankaran, Benjamin Kipp, Ande Rumilla, Gang Zheng, Kevin Halling, Katherine Geiersbach

Mayo Clinic, Rochester, MN

Introduction: Clinical staging of multifocal non-small cell lung cancer (NSCLC) is facilitated by comparative genomic analysis of separate tumor nodules, but the role of genome-wide copy number profiling for this purpose is uncertain.
Methods: We analyzed single nucleotide variants (SNVs), gene fusions, small copy number variants (gene amplifications and homozygous deletions) (sCNVs), and large-scale copy number variants (lCNVs) in a retrospective cohort of 34 patients with >1 lung cancer nodule tested on a previously validated tumor-only 515-gene next generation sequencing (NGS) panel (MayoComplete Solid Tumor Panel). For patients with <2 shared SNVs, a Bayesian approach was formulated to calculate the probability of shared versus independent events occurring in different tumor nodules in the same patient. The prevalence of specific lCNVs in NSCLC was derived from an independent dataset of 100 NSCLC peers tested by the same panel, and the prevalence of SNVs, fusions, and sCNVs in NSCLC was derived from publicly available data. Alterations unique to different tumor nodules and suspected germline alterations were excluded from the Bayesian analysis.
Results: There were 54 total comparisons for 34 patients. Eleven of the patients (32.4%) had >=2 shared SNVs along with one or more shared lCNVs also identified in each patient. Eight patients (23.5%) had no shared SNVs, gene fusions, sCNVs, or lCNVs. Using the Bayesian approach for the remaining fifteen (44.1%) patients with at least one shared alteration (SNVs, sCNVs, and lCNVs), the probability of clonal relatedness ranged from 73% for a shared whole arm or whole chromosome lCNV to >99% for tumors with two or more shared alterations including multiple or complex lCNVs and SNVs. Whole chromosome or whole arm lCNVs were sometimes shared between tumor nodules with different driver SNVs.
Conclusions: Incorporating lCNVs into comparative genomic analysis provides additional evidence of clonal relatedness in a subset of multifocal NSCLCs. However, differences in bioinformatics pipelines for calling lCNVs, concerns over the imprecision of genome-wide copy number profiling, and uncertainty regarding the temporal relationship between lCNVs and carcinogenesis (including somatic events possibly related to “field cancerization”) create challenges for integrating lCNVs into comparative genomic analysis with standard clinical workflows for tumor-only NGS on paraffin embedded tissue sections. Our simplified approach mitigates some of the uncertainty introduced by incorporating lCNVs into clonality determination.

#5424 Detection of rare oncogenic fusions through concurrent DNA and RNA next-generation sequencing in a pan-cancer clinical setting.

Lisa Gai[1], Molly Murnane[1], Malvika Pillai[1], Matthew Campbell[1], Bradley Bowles[1], Kyle A. Beauchamp[1], Rotem Ben-Shachar[2], Gregory Omerza[1], Razelle Kurzrock[3], Nathan David Seligson[4], Halla S. Nimeiri[1], Justin Guinney[1]

[1]Tempus AI, Inc, Chicago, IL,[2]GeneDX, Stamford, CT,[3]Medical College of Wisconsin, Milwaukee, WI,[4]Department of Pharmacotherapy and Translational Research, University of Florida, Jacksonville, FL

Background: Concurrent DNA and RNA testing is the gold standard for detection of oncogenic gene fusions with an associated targeted therapy. However, rare fusions without such therapies can also impact patient care by informing diagnosis, prognosis, or potential resistance to therapy. Targeted panel DNA assays are typically optimized for a small number of fusion genes, making use of RNA testing particularly salient for rare fusions. Here we quantify the benefit of concurrent DNA and RNA testing over DNA alone for such fusions, in a large real-world dataset of 74,182 patients with advanced cancer.

Methods: We retrospectively analyzed deidentified records from the Tempus multimodal database of metastatic solid tumor samples from non-pediatric patients who underwent testing with both targeted panel DNA-next generation sequencing (NGS) and whole-exome RNA-NGS assays (Tempus xT and xR, respectively). Fusions both on and off the xT panel without an associated targeted therapy were considered for the study. Fusions were identified through the Tempus bioinformatic workflow, which runs RNA-NGS and DNA-NGS pipelines concurrently, followed by pathologist review.

Results: Of the 74,182 patients in the cohort, 4,776 (6.4%) had at least one oncogenic fusion without an FDA-approved targeted therapy, with a total of 4,845 such fusions in the dataset. Of these fusions, 85.0% (4,119/4,845) involved genes present on the xT panel, with 56.6% (2,744) involving genes optimized for detecting rearrangements on the xT panel. Across all fusions in the study, 2,561 (52.9%) were detected by RNA-NGS only. For rare fusions involving genes on the xT panel and those with optimized detection in xT, 44.7% (1,841/4,119) and 23.9% (656/3,744) were detected in RNA only, respectively.

The most common fusions in this dataset were TMPRSS2-ERG (n=2,247) with 23.4% detected only in RNA. RNA-only detection rates were particularly high for ESR1-CCDC170 (211/213, 99.1%) and PTPRK-RSPO3 (280/280, 100%). TMPRSS2 is optimized for fusion detection by xT, ESR1 is on xT but not targeted for rearrangements, and PTPRK- RSPO3 does not appear on xT.

Conclusions: We show that RNA testing greatly enhances detection of rare fusions without an associated FDA-approved targeted therapy in a real-world setting. This benefit of RNA testing is most apparent for fusions not on a DNA-NGS targeted panel, but fusions targeted on the xT panel also showed increased detection with concurrent RNA testing. Among the fusions with high rates of RNA-only detection, ESR1-CCDC170 is associated with more aggressive ER+ breast cancers, and PTPRK-RSPO3 may modulate WNT signaling in colorectal cancer. Other clinically relevant fusions also showed enhanced detection from RNA-NGS. Overall, these findings suggest RNA testing could enhance detection of rare oncogenic fusions to better inform patient care.

#5425 Clinical and genomic characterization of biliary tract tumors (BTT) with ARID1A mutations: A case-control study.

Giulia Massaro[1], Manuel Pedegral[2], Diana Rosero[1], Brezo Martinez Amores[3], Ester Garcia[4], Eva Ruiz Hispan[1], Miriam Dorta[4], Diego Casado[5], Carlos Garzon[6], Bernard Gaston Doger de Speville[4], Raquel Fuentes[1], Victor Moreno Garcia[7], **Angela Lamarca**[8]

[1]Fundacion Jimenez Diaz University Hospital, Madrid, Spain,[2]START-Madrid; Fundacion Jimenez Diaz University Hopsital, Madrid, Spain,[3]Rey Juan Carlos University Hospital, Madrid, Spain,[4]START-Madrid; Fundacion Jimenez Diaz University Hospital, Madrid, Spain,[5]General de Villalba University Hospital, Madrid, Spain,[6]Infanta Elena University Hospital, Madrid, Spain,[7]START Madrid; Fundacion Jimenez Diaz University Hospital; Health Research Institute-Fundacion Jimenez Diaz University Hospital (IIS-FJD), Madrid, Spain,[8]Fundacion Jimenez Diaz University Hospital; Health Research Institute-Fundacion Jimenez Diaz University Hospital (IIS-FJD), Madrid, Spain

Introduction: ARID1A is a tumor suppressor gene involved in chromatin remodeling and is commonly mutated across several cancer types. In biliary tract cancer (BTC), the clinical and genomic landscape of ARID1A mutations remains poorly defined. This study aims to characterize the demographic, clinical, and molecular features of patients (pts) with ARID1A-mutated (ARID1A-mut) BTC compared with a control cohort harboring wild-type (ARID1A-wt) ARID1A.

Methods: From a consecutive retrospective cohort of 146 pts with molecularly profiled BTC, 14 (9.6%) exhibited pathogenic ARID1A mutations. Of these, 13 (8.9%) with available clinical data were compared to a randomly selected group of 13 ARID1A-wt controls. The study was approved by the local ethics committeee.

Resuls Out of 146 patients screened, total of 27 were found eligible: 14 ARID1A-mut and 13 ARID1A-wt. ARID1A-mut pts (vs ARID1A-wt) were predominantly female (77% vs 46%; p=0.23). Median age was 64 years. Primary tumor distribution was intrahepatic (76.9%), hilar (15.4%), and gallbladder (7.7%) (p=1). Disease stage at diagnosis, performance status, and first-line (1L) treatment regimens were comparable across both cohorts. ARID1A-mut pts showed a trend toward higher partial response (PR) rates to 1L therapy (53.9% vs 30.1%; p=0.43). Median progression-free survival (PFS) on 1L treatment was similar (11.4 vs 9.3 months; HR 0.67, 95% CI 0.29-1.57; p=0.36), as was overall survival (OS) (21.4 vs 22.5 months; HR 1.47, 95% CI 0.51-4.28; p=0.48). Genomic profiling revealed a distinct co-alteration pattern: BAP1 (28.6% vs 0%; p=0.09), IDH1 (21.4% vs 0%; p=0.22), and PBRM1 (28.6% vs 7.7%; p=0.33) were more frequent in ARID1A-mut pts, whereas TP53 (38.5% vs 28.6%; p=0.69), KRAS (30.8% vs 16.7%; p=0.38), and DNMT3A (23.1% vs 0%; p=0.09) predominated in the ARID1A-WT cohort.

Conclusion: BTC with ARID1A mutations represents a distinct molecular subgroup characterized by a trend toward improved partial response and enrichment in epigenetic co-alterations. Prospective validation is warranted to assess the prognostic and therapeutic implications. Targeted therapeutic strategies against ARID1A in BTC should be further explored in early-phase (I/II) clinical trials.

#5426 Anatomic origins of primary skeletal tumors effect metastatic and prognostic behaviors.

Matthew Duazo, Aayush Bhatawadekar, Dillon Pekoff, Maria Plummer, Brian Beatty

NYIT College Of Osteopathic Med (NYITCOM), Old Westbury, NY

Introduction:
This study investigates the histology of nonmetastatic primary skeletal tumors related to their anatomic origin and its influence on 5-year survival outcomes.
Methodology:
Deidentified patient data were obtained from the National Cancer Institute's Surveillance, Epidemiology, and End Results (SEER) database. Inclusion criteria included: (1) diagnosis of a primary bone cancer with anatomical location of origin, classified using ICD-O-3 anatomic site codes; (2) documented absence of metastasis to the brain, lung, liver, or bone; (3) cause-specific death and survival duration; and (4) available histology codes. Patients were stratified by primary tumor location and histologic sub-type. Kaplan-Meier survival curves were used to estimate survival, and group differences were assessed with pairwise log-rank tests. A p-value <0.05 was considered statistically significant.
Results:
The top five most common nonmetastatic skeletal tumors by histology are Chondrosarcoma, Osteosarcoma, Chondroma, Ewing Sarcoma, and Diffuse Large B-Cell Lymphoma (DLBCL). The tumor location distribution and 5-year survival for each histological subclass are outlined in Table 1.
Conclusion:
The differences in anatomic origin of primary bone tumors when controlled for histologic category influences patient mortality. There are distinct differences in overall survival compared among origin sites, signifying a location-based influence on disease severity and survival. The knowledge of anatomic origin differences of survival of various histologic categories of bone cancer can improve clinical decision making and create more accurate, locational based planning when looking at prognosis and disease progression.

#5427 Weekend radiotherapy for oncologic emergencies: A single-institution analysis of indications and practice patterns.

Ahmed Allibhai, Asiyah Allibhai

Holy Trinity School, Richmond Hill, ON, Canada

Purpose: Oncologic complications can arise that require emergency radiotherapy (RT) outside of standard working hours. This study documents the incidence, indications, RT dose/fractionation and outcomes for patients receiving RT on weekends/scheduled holidays at a single institution.
Methods: Patients receiving RT on weekends (Saturday, Sunday, or long weekend holidays) from January 2022 through December 2024 were identified retrospectively. Patient demographics, primary cancer diagnosis, clinical indication, treatment site, dose/fractionation, inpatient status, treatment completion, and survival were collected and analyzed.
Results: Over three years, 122 patients received emergency weekend RT. Median age was 67 years (39-98); 63.1% male, 66.4% inpatients. Patients most commonly presented with lung (25.4%), gastrointestinal (23.8%), and hematologic (18.0%) malignancies. The top three indications for emergency weekend RT included spinal cord compression (38.9%), GI bleeding (20.7%), or obstructive airway/lung disease (7.6%). The most common RT regimen was 20 Gy in 5 fractions (80.3%), with most patients receiving two days of treatment (54.1%). Six patients (4.9%) did not complete their course of treatment owing to clinical deterioration. One-month mortality was 13.1% and three-month mortality was 36.9%.
Conclusions: Weekend RT is predominantly used to manage well-identified oncologic emergencies such as spinal cord compression and tumor-related bleeding. The high inpatient proportion and substantial short-term mortality reflect advanced disease burden requiring urgent intervention. These findings demonstrate the importance and incidence of weekend radiotherapy services and provide evidence to help inform staffing & resource allocation as well as institutional policies.

#5428 Impact of double primary cancer on survival in patients with non-small cell lung cancer: Large-scale cohort.

Hyun Ae Jung[1], Sang Ah Chi[1], Allison Park[2], Sehhoon Park[1], Jong-Mu Sun[1], Se-Hoon Lee[1], Jin Seok Ahn[1], Myung-Ju Ahn[1], Kyunga Kim[1]

[1]Samsung Medical Center, Seoul, Korea, Republic of,[2]Cornell University, Boston, MA

Background: Although survival outcomes for non-small cell lung cancer (NSCLC) have improved with advances in treatment, the increasing number of long-term survivors has brought greater attention to double primary cancers (DPCs). This study aimed to evaluate the frequency and distribution of double primary cancers (DPC) in patients with NSCLC and to assess their impact on survival outcomes.

Methods: This study evaluated clinical variables of patients diagnosed with NSCLC between 2008 and 2024. The types of DPCs were identified, and the impact of DPC occurrence and timing on the survival outcomes of NSCLC was analyzed. To minimize the influence of lead-time bias, this study applied Cox regression models incorporating time-varying covariates. Multivariable analyses were then performed to evaluate the prognostic impact of DPC timing on survival, adjusting for age, smoking status, stage, histology, DPC duration, multiple primary cancer status, and the presence of EGFR mutations or ALK rearrangements.

Results: Among a total of 34,593 patients diagnosed with NSCLC, 4,339 (12.5%) were identified as having DPC, and 455 (1.3%) had multiple primary cancers (MPCs) involving three or more malignancies. Among the total 34,593 patients with NSCLC, DPC was identified before NSCLC in 2,345 patients (6.8%), concurrently in 1,039 (3.0%), and after NSCLC diagnosis in 1,155 (3.3%). The incidence of DPC was slightly higher in males (12.9%) than in females (12.0%) and showed an inverse association with NSCLC stage—occurring in 17.8%, 13.0%, 9.4%, and 6.4% of patients with stage I, II, III, and IV disease, respectively. In males, the most frequent DPCs were gastric cancer (2.7%), colorectal cancer (2.1%), prostate cancer (2.1%), and liver cancer (1.0%). Among 32,170 patients after excluding those with post-NSCLC DPC, pre-existing DPC was associated with worse survival compared with no DPC (adjusted HR = 1.146, $P = 0.0018$). However, DPC diagnosed more than 5 years before NSCLC showed no significant effect on survival (adjusted HR = 1.094, $P = 0.1965$), whereas DPC within 5 years conferred poorer outcomes (adjusted HR = 1.180, $P = 0.0018$).

In a time-varying Cox model including 31,827 patients with concurrent or post-NSCLC DPC, the development of DPC after NSCLC remained independently associated with worse survival (adjusted HR = 1.377, $P < 0.0001$).

Conclusions: DPC diagnosed more than 5 years before NSCLC had no impact on survival, whereas DPC occurring within 5 years before or after NSCLC was independently associated with worse outcomes. These findings underscore the importance of increased vigilance and individualized management strategies for NSCLC patients with recent or subsequent DPCs, particularly in an era of improving long-term survival.

#5429 REAL-AML: Real-world predictors of early mortality and treatment inequities in acute myeloid leukemia across a multi-institutional U.S. cohort.

Randa Elzein[1], Safa Elzein[2]

[1]Medicine, SUNY Upstate Medical University, Syracuse, NY,[2]Hematology Oncology, SUNY Upstate Medical University, Syracuse, NY

Despite therapeutic advances, early mortality (<60 days) in newly diagnosed acute myeloid leukemia (AML) remains 15-25% in routine care, particularly among older and socioeconomically vulnerable patients. Randomized trials under-represent these groups, limiting generalizability. We conducted a multi-institutional, equity-focused analysis to identify modifiable determinants of early mortality and propose operational benchmarks for quality improvement.Adults (≥18 y) with newly diagnosed AML between 2016-2024 were identified from a federated, de-identified electronic-health-record network encompassing >35 U.S. health systems. Primary endpoint: 60-day mortality from diagnosis. Predictors included demographics, comorbidities, insurance type, urban/rural residence, facility type, cytogenetic risk, and receipt/timing of induction chemotherapy or hypomethylating-agent (HMA) regimens. Multilevel logistic regression with site random effects estimated adjusted odds ratios (aORs). Fairness analysis evaluated subgroup calibration by race, sex, and payer. Interrupted time-series modeling assessed 2020-2024 adoption of targeted agents (FLT3, IDH1/2 inhibitors). Only aggregate outputs were analyzed.Among 7,842 patients (median age 66; 47% female; 22% Black or Hispanic; 28% Medicaid/uninsured), overall 60-day mortality was 19.4% (95% CI 18.5-20.3). Independent predictors: age >70 y (aOR 2.43, 2.10-2.82), Medicaid/uninsured (aOR 1.54, 1.30-1.83), diagnosis at non-academic centers (aOR 1.39, 1.21-1.59), ECOG ≥2 (aOR 1.71, 1.50-1.95), and treatment initiation >5 days after diagnosis (aOR 1.46, 1.28-1.67). Adoption of targeted agents increased from 6% (2018) to 29% (2024), corresponding with a 5.1-point mortality reduction (p=0.003). Fairness analysis showed minimal calibration drift (ΔBrier <0.005) across demographic subgroups. Scenario modeling suggested that reducing treatment delays to ≤3 days could lower early mortality by ≈2.7% absolute (14% relative) nationwide.REAL-AML defines pragmatic, measurable drivers of early mortality in AML and identifies actionable levers-timely induction, equitable access to targeted agents, and improved insurance continuity-that could yield substantial survival benefit. This is the largest multi-system, equity-audited AML outcomes study to date and provides a template for real-world precision-implementation trials in hematologic malignancies.

#5430 Allostatic load connects tumor genomics, disease trajectory, and pre-diagnosis wearable activity.

Christopher J. Fong[1], Kaicheng U[1], Cheryl Phua[1], Xuechun Bai[1], Karl Pichotta[1], Kathryn Tsai[2], Anzhi Chen[1], Meixuan Zhang[1], Jie Yu[1], Whitney Underwood[1], Chenlian Fu[1], Michele Waters[1], Sanna Goyert[3], Adam Schoenfeld[1], Nikolaus Schultz[1], Justin Jee[1], Jessica Scott[1], Luke Pike[1], Jian Carrot-Zhang[1]

[1]Memorial Sloan Kettering Cancer Center, New York, NY,[2]University of Illinois, Champaign, IL,[3]CUNY School of Medicine City College of New York, New York, NY

Background: Allostatic load (AL), a composite index of physiological stress from routine labs and vitals, reflects multisystem strain and predicts survival in cancer. Building on prior validation of cancer-modulated AL (cmAL), we examined how cmAL varies across disease states, relates to tumor genomics, and aligns with wearable-measured activity before diagnosis.
Methods: We analyzed 12,689 adults treated at MSK with pre-treatment labs and vitals across NSCLC, colorectal, prostate, ovarian, breast, pancreatic, endometrial, and bladder cancers. cmAL was computed from ten cardiovascular, metabolic, renal, and immune biomarkers and compared across disease phases using rank-sum tests with multiple-testing correction. Per-cancer-type genomic models used multivariable logistic regression relating cmAL to recurrent oncogenic alterations while adjusting for clinical covariates and comorbidity burden. Wearable activity was evaluated in 77 MSK patients (Apple HealthKit) and 1,867 All of Us participants (Fitbit) using median daily step counts across cmAL levels, Spearman correlation, and continuous trend tests. Pre-diagnosis steps were summarized using a 90-day window before first cancer diagnosis.
Results: cmAL decreased during remission (median change -0.42, $p<0.001$) and increased with progression (median change +0.61, $p<0.001$), with the highest values observed within six months of death ($p<1\times10^{-40}$). Higher cmAL correlated with cardiometabolic comorbidity (diabetes OR=0.74; renal OR=0.54). In NSCLC, higher cmAL was less common in patients with EGFR mutations and more common in those with KRAS mutations. Across both wearable datasets, higher cmAL was linked to lower pre-diagnosis activity. In the MSK cohort, median daily steps declined from 4,914 at (cmAL=1) to 1,092 at (cmAL=5) (Spearman $\rho=-0.388$, $p=0.0005$). In All of Us, median steps declined from 6,276 (cmAL=1) to 4,091 (cmAL=5) ($\rho=-0.248$, $p<0.0001$), demonstrating reproducibility in a population cohort.
Conclusions: cmAL increases with disease progression and quantifies cumulative physiologic strain across body systems. Elevated cmAL is associated with specific genomic patterns in NSCLC, greater comorbidity burden, and lower pre-diagnosis step counts in both institutional and population cohorts. These findings support cmAL as a scalable and potentially modifiable biomarker integrating molecular, physiologic, and behavioral domains in real-world cancer survivorship.

: Application of Bioinformatics to Cancer Biology 5
Poster Session

#5434 Immune cell infiltration analysis of lung cancer based on proteomics.

Ruoxian Zhang[1], Liangcheng Lyu[2]

[1]Fudan University, Shanghai, China,[2]Peking University, beijing, China

Lung cancer remains a leading cause of cancer-related mortality, accounting for nearly one-quarter of all cancer deaths. Its initiation, progression, and metastasis are tightly influenced by the tumor microenvironment, within which diverse immune cell populations play critical roles. Quantifying tumor-infiltrating immune cells is therefore essential for understanding lung cancer biology and improving therapeutic strategies. While numerous computational methods have been developed for immune infiltration analysis based on transcriptomic data, algorithms optimized for proteomics data are largely unavailable, and the applicability of existing transcriptome-based tools to proteomic datasets remains unclear.In this study, we developed a deconvolution-based algorithm tailored for proteomics data to quantify tumor-infiltrating immune cells in lung cancer. Using a support vector regression model constructed from an immune signature matrix, we decomposed tumor tissue proteomics profiles into proportions of distinct immune cell types. Application of this algorithm to lung cancer proteomics datasets revealed that MO non-classical cells, NK cells, and T4-EMRA cells exhibited the highest infiltration levels. Integrating proteomics and clinical data, we further performed NMF-based subtyping and identified two immune-associated subtypes. Cluster 1, characterized by poorer prognosis, showed significant enrichment in complement cascade signaling, IGF transport and uptake regulation, and post-translational protein phosphorylation pathways. Additionally, NK cells and several $CD4^+$ T-cell subsets were more abundant in Cluster 1 than in Cluster 2, indicating stronger immune infiltration and elevated immune activity, potentially contributing to adverse clinical outcomes.These findings provide a proteomics-based framework for immune infiltration analysis and offer new insights into lung cancer molecular subtyping and precision oncology.

#5436 Spatial identification of hypoxic and normoxic dormancy hotspots predicting in her2-positive and metastatic breast cancer.

Tzu-Hung Hsiao[1], Fan Jhen Liu[2], Yu-Ting Kang[1], Kuo Yen Huang[2], Yidong Chen[3]

[1]Department of Medical Research, Taichung Veterans General Hospital, Taichung City, Taiwan,[2]Graduate School of Advanced Technology, National Taiwan University, Taipei City, Taiwan,[3]Greehey Children's Cancer Research Institute, UT Health San Antonio, San Antonio, TX

One of the major clinical challenges in breast cancer is overcoming therapeutic resistance and metastatic relapse. Such relapses are often driven by residual tumor cells that resist therapy by entering a dormant, non-proliferative state and later reawaken after variable latent periods. In this study, we applied spatial transcriptomics-Visium HD platform to a HER2-positive breast tumor sample from a patient who developed brain metastasis one year after treatment. By integrating dormancy-associated transcriptional programs with spatial colocalization, we aimed to predict cells with dormancy potential. We curated eight dormancy-related genes to construct a DormancyScore and intersected it with G0/G1 cell-cycle arrest signatures to identify dormancy-like cells. Kernel density estimation (KDE) and Ripley's K were used to quantify spatial aggregation and define dormancy hotspots. Using Intersection-over-Union (IoU) to evaluate the overlap between dormancy hotspots and HALLMARK pathway hotspots, we observed substantial colocalization with hypoxia. To further dissect the role of oxygenation in maintaining dormancy, hotspots were stratified into hypoxic dormancy hotspots (HDH) and normoxic dormancy hotspots (NDH). HDH exhibited enriched response to stress, defense, and inflammatory programs, accompanied by surrounding stromal accumulation of ECM-remodeling CAFs and TAMs. In contrast, NDH were enriched for oxidative phosphorylation, ATP synthesis, and biosynthetic processes, reflecting a distinct functional state under normoxia. This study lays the foundation for expanded cohort analyses to determine whether dormancy cells arising from different oxygenation states are associated with varying risks or timing of breast cancer metastasis, and to further evaluate the robustness of density-based and colocalization-based approaches for detecting dormant tumor cells.

#5437 Sensitive detection of rare cfDNA variants utilizing molecular technologies and a novel informatics platform: A combined genomic and proteomic MRD application.

Emma Kaitlyn Longshore[1], Ethan Barnett[2], Ingrid T. Erazo[2], Leisa Jackson[1], Helen Halpin[1], Reis Pestano[1], Patricia Schnepp[3], Adam Corner[3], Howard I. Scher[2], Gary A. Pestano[1]

[1]Biodesix, Inc., Louisville, CO,[2]Memorial Sloan Kettering Cancer Center, New York, NY,[3]Bio-Rad, Hercules, CA

Advances in next-generation sequencing (NGS) are producing massive amounts of data at rapidly declining costs. Effective processing of millions of high-depth sequencing reads while maintaining sensitivity and specificity is a growing challenge in the design of new molecular tests. One critical application is detection and subsequent monitoring of rare variants in plasma for molecular residual disease (MRD). Our MRD testing strategy utilizes a preliminary proteomic risk of recurrence mass spectrometry assay to stratify high-risk baseline samples as likely to need further monitoring, followed by design of bespoke ddPCR assays to mark recurrence in the follow-up plasma of the high-risk population. To qualify assays for genomic monitoring, we developed a novel informatics pipeline utilizing approximately 24 million reads and 1 million structural variant calls to profile a cohort of 14 metastatic castration resistant prostate cancer patients (mCRPCa). Tissue-derived NGS data were systematically analyzed to identify a MRD fingerprint for monitoring molecular recurrence in post-treatment plasma specimens. We achieved sequencing depths of 64-367x across the cohort. Data filtering strategies included quality score (≥20), identical homology (≤5), structural variant size, and intersection of multiple gold-standard bioinformatics tools, Delly and Manta. Analytical turnaround time was 16.5 - 72 hours from raw NGS data to designed primers. Bespoke primers were successfully designed or available off-the-shelf for all evaluated patients. Initial studies identified tissue-informed variants derived from four mCRPCa patients with matched baseline plasma. 6/6 of the tested variants were found in the matched patient plasma specimens. Significantly, longitudinal ctDNA analyses identified clearance of AR p.L702H from circulation in a patient with evidence of radiographic and biochemical response to docetaxel after progression on multiple lines of AR signaling inhibitors (ARSI). AR p.L702H is an acquired resistance mechanism to ARSIs, and the elimination of sub-clonal cell populations harboring the alteration could indicate restored sensitivity to these agents. Additionally, declines in ctDNA coincided with declines in serum PSA. This report showcases the design of a novel MRD test combining proteomics for early and impactful risk of recurrence stratification with cost-effective and rapid genomic PCR monitoring in the follow-up plasma of patients at a high-risk of recurrence, for utility in real-world clinical diagnostics laboratories

#5438 Transcript isoform diversity in esophageal squamous cell carcinoma: Insights into tumor heterogeneity and therapeutic targets in Africa.

Sikhumbuzo Z. Mbatha[1], Mohammed Alaouna[2], Botle Precious Damane[1], Tebogo Marutha[2], Rodney Hulll[2], Jonathan Featherston[3], Aristotelis Chatziioannou[4], **Zodwa Dlamini**[2]

[1]Department of Surgery, Steve Biko Academic Hospital, University of Pretoria, Pretoria, South Africa,[2]Pan African Cancer Research Institute (PACRI), University of Pretoria, Pretoria, South Africa,[3]Division of National Health Laboratory Service, The National Institute For Communicable Diseases Of South Africa, Sandringham, South Africa,[4]Center of Systems Biology, Biomedical Research Foundation of the Academy of Athens, Kallithea, Greece

Background: Esophageal squamous cell carcinoma (ESCC) is a major cause of cancer mortality in sub-Saharan Africa, particularly African ESCC corridor. The region's complex etiology, including viral infections, may influence RNA processing such as alternative splicing (AS), a critical but understudied mechanism in ESCC biology. This study characterized the transcriptome wide AS landscape in African ESCC and assessed whether HPV and HIV infections contribute to splicing dysregulation and structural protein alterations.
Methods: A cross-sectional study was conducted between February to December 2024 involving 29 patients with histologically confirmed ESCC and verified HIV status. Paired tumor/ adjacent normal endoscopic biopsies were collected and subjected to histological evaluation, HPV genotyping, and RNA sequencing. Alternative splicing profiles were investigated, with a focus on their association with viral status. Computational structural modeling and molecular docking was used to predict the functional impact of tumor-specific splice variant.
Results and Discussion: Skipped exons were the predominant AS event, followed by alternative 5′ and 3′ splice sites. Substantial patient-specific heterogeneity emerged, with the protocadherin gene family most affected, implicating disrupted cellular adhesion and invasion. Dysregulated non-coding RNAs (DGCR5, LINC00641) further reflected loss of tumor-suppressive control. A tumor-enriched 3′ splice-site variant in CXADR was predicted to alter junctional signaling. Stratification by viral status (HIV+/HPV+, HIV+/HPV-, HIV-/HPV+, HIV-/HPV-) revealed no significant effect on overall splicing burden.
Conclusion: African ESCC exhibits a distinct, skipped-exon-dominated AS signature that drives molecular diversity independent of HIV/HPV status, highlighting AS as a promising diagnostic and therapeutic axis for precision oncology in Africa.

#5439 Shared and divergent transcriptional signatures of ductal cells in distal human cholangiocarcinoma at a single cell resolution.

Meng Ting Chen[1], Jon M. Harrison[1], David R. Ruddy[2], Michelle Piquette[2], Jon Chang[2], Viviana Cremasco[2], Andrew L. Warshaw[1], Carlos Fernandez-Del Castillo[1], Andrew S. Liss[1], Divyansh Agarwal[1]

[1]Department of Surgery, Massachusetts General Hospital and Harvard Medical School, Boston, MA,[2]Novartis Institutes for BioMedical Research, Cambridge, MA

Background: While chronic pancreatitis (CP) has long been recognized as a risk factor for pancreatic ductal adenocarcinoma, recent work has shown an elevated risk of biliary tract malignancies in patients with pancreatitis. However, the underlying mechanisms and the genomic similarities that might explicate this association remain elusive. Inflammation is thought to be a precipitating risk factor for cholangiocarcinoma; however, whether the inflammatory milieu of chronic pancreatitis also contributes to this risk is unclear. To address this gap, we characterized the shared and unique genomic signatures between patients with chronic pancreatitis and those with distal cholangiocarcinoma (dCCA), compared to normal healthy individuals.
Methods: We performed single cell RNA sequencing (scRNA-seq) from pancreata or tumor specimens obtained from 3 healthy human subjects, 3 patients with CP, and 2 individuals with dCCA. After ascribing cell-type identities and delineation of ductal cell clusters, we performed inference of copy number variations as well as functional perturbations at the gene and pathway level in ductal cell from the three patient cohorts - normal, CP and dCCA.
Results: scRNA-seq revealed 35 different cell clusters across ~120,000 cells from the three patient cohorts. Based on semi-supervised learning, we identified 13 cell types in our data; additional analysis revealed that the Ductal cell cluster could be further sub-classified into two cell populations with disparate genomic signature. We further identified amplification/duplication of chromosomes 1, 7, 11, 12 and 18 in the Ductal A cluster from the dCCA cohort through two orthogonal approaches. Pseudobulking analysis suggested an upregulation of laminins in Ductal A subcluster, and Ligand-receptor analysis further revealed LAMC2 as a key target gene in the Ductal cell cluster, with putative fibroinflammation mediated by *TGFB1* and *FGF2* receptors. While laminin upregulation was unique to dCCA and not observed in CP, *TGFB1* and *FGF2* receptor-driven signaling was a shared feature in ductal cells across both CP and dCCA.
Conclusions: We discovered a novel ductal cell population in dCCA that exhibits upregulation of laminins compared to normal pancreas and CP. Further still, the expression of ligand, receptor, and target genes in the dCCA extracellular matrix highlights how the TGFB1-FGF2-LAMC2 axis might be contributing to the desmoplastic process observed in dCCA tumors.

#5441 Structural and kinetic effects of R361H SMAD4 mutation on TGF-ß signaling in colorectal cancer.

Evan Boczko[1], Isaac Silverman[1], Yisrael Wiener[1], Sanjay Goel[2], Radhashree Maitra[1]

[1]Biology, Yeshiva University, New York, NY,[2]Rutgers Cancer Institute of New Jersey, New Brunswick, NJ

Introduction: SMAD4 mutations disrupt TGF-ß signaling in colorectal cancer. We focus on the recurrent MH2-domain R361H mutation, whose structural and interaction effects remain unclear. Using structural modeling, docking, and molecular dynamics, we assess how R361H alters SMAD4 stability and binding to SMAD1/2/3/5.
Methodology: AlphaFold models of SMAD1-5 were obtained from RCSB, and the R361H mutation was introduced to SMAD4 with PyMOL. Wildtype and mutant SMAD4 were docked separately to each R-SMAD with ClusPro. The resulting complexes were subsequently repaired, solvated, and parameterized in GROMACS. Molecular dynamics simulations were run for 100 ns per complex. Global and domain-specific RMSD/RMSF were computed with GROMACS. MMPBSA.py was used to calculate binding energies and per-residue contributions.
Results: R361H mutation altered SMAD4-R-SMAD complex stability in a partner-specific way. At the complex level, SMAD4-SMAD1 and SMAD4-SMAD3 showed only small changes in overall RMSD (Δcomplex ≈ −0.05 nm for SMAD1 and +0.07 nm for SMAD3, MUT - WT). In contrast, SMAD4-SMAD2 and SMAD4-SMAD5 were clearly destabilized, with much larger RMSD shifts (Δcomplex ≈ +0.34 and +0.50 nm, respectively).Across all four complexes, R-SMAD linkers became more flexible in the mutant (+0.10-0.34 nm) while SMAD4 MH2 mobility increased in the SMAD1, SMAD3, and SMAD5 complexes.RMSF analysis localized these changes to SMAD4 residues ~470-490 and 540-550 and to partner-specific regions in each R-SMAD.Energy decomposition revealed distinct mechanisms for each partner. In the SMAD1-SMAD4 complex, strongly interacting residues in wildtype and mutant showed minimal overlap; PyMOL alignment (RMSD ≈ 36 Å) and docking scores indicate that R361H drives an alternative, remodeled binding mode rather than simply weakening the wildtype interface. In the SMAD2-SMAD4 complex, a hydrophobic to polar patch interaction (SMAD4 274-281, SMAD2 181-187) becomes less favorable in the mutant, consistent with increased SMAD4 RMSF and higher complex RMSD. In the SMAD3-SMAD4 complex, a key R420SMAD3-E417SMAD4 salt bridge is weakened by ~3 kcal/mol in the mutant. RMSF data indicate that in the wildtype, a flexible C-terminal tail frequently adopts the orientation needed for this interaction, whereas the mutant tail is more rigid in a less favorable orientation. In the SMAD5-SMAD4 complex, the mutant gains favorable contacts between SMAD5 residues 185-188 and a polar SMAD4 patch (263-268), with increased SMAD4 MH2 mobility (~0.2 nm).
Conclusion: This framework suggests that R361H remodels SMAD4-R-SMAD interfaces in a partner-specific manner, inducing marked reorganization with SMAD1 and more nuanced shifts in SMAD2/3/5. These partner-specific interfaces may represent druggable surfaces for restoring tumor-suppressive TGF-ß responses or selectively constraining pro-metastatic signaling in R361H-mutant colorectal cancer.

#5442 Identifying cell-cell interactions across spatial scales in spatial transcriptomics.

Alex C. Soupir[1], Mitchell T. Hayes[1], Brandon J. Manley[1], Lauren Cole Peres[1], Julia Wrobel[2], BROOKE FRIDLEY[3]

[1]Moffitt Cancer Center, Tampa, FL,[2]Emory University, Atlanta, GA,[3]Childrens Mercy Hospital, Kansas City, MO

Introduction: Single-cell spatial transcriptomics provides rich data for the gene expression profiles at cellular resolutions. This level of data offers the ability to estimate interactions between cells and associate those interactions with clinical information such as survival or response to immunotherapy. Previously, we had shown that *COL4A1* and *ITGAV* are significantly more spatially enriched in primary clear cell renal cell carcinoma (ccRCC) tumors after exposure to immunotherapy (IO), specifically showing high expression in malignant cells and fibroblasts/myofibroblasts. We assessed this interaction by using K=3, but spatial proximity is also an important consideration to explore.

Methods: To address true spatial context, we developed a functional data analysis approach to profile cell-cell interactions at varying spatial scales. We used 14 stromal compartment FOVs (8x IO naïve, 6x IO exposed) from Soupir et. al. (2024). Bivariate Moran's I was calculated for COL4A1 and ITGAV using row standardized weights from Gaussian transformed distances. The bandwidth of the kernel was varied from 0 to 250 to calculate Moran's I as a function of bandwidth, I(h), using 100 permutations to determine complete spatial randomness (CSR). CSR was subtracted from I(h) (Degree of I(h)) to make values comparable across samples. We used functional principal component (FPC) analysis to analyze the full Degree of I(h) curves. FPC scores were used to compare the IO naïve and IO exposed tumors. Results from our approach were compared to SpatialDM, another approach based on Moran's I, with h=75.

Results: FOVs from tumors exposed to IO showed a distinct, positive Degree of I(h) curve with a peak at a bandwidth between 25-50 while FOVs from IO naïve tumors were each unique in either shape or sign of Degree of I(h). Calculating (FPCs) from all Degree of I(h) curves showed that FPC1 describes the overall strength of the spatial relationship (positive scores indicate overall elevated and negative scores indicate overall decreased interaction) while FPC2 describes whether the interaction occurs at a near/far scale. Plotting FPC2 vs FPC1, FPC1 perfectly separates IO naïve from IO exposed FOVs (Wilcox Test p=0.00067, where IO exposed FOVs have a positive FPC1 score and FPC2 scores around 0 (no change in near/far). SpatialDM's global I didn't show significant differences between IO exposures (Wilcox Test p=0.1079)

Conclusion: The application of our approach to ccRCC indicates that COL4A1 and ITGAV in these stroma FOVs from IO exposed primary ccRCC tumors are more strongly spatially related across spatial scales than stroma FOVs from IO naïve primary ccRCC tumors. Our approach also showed a significantly stronger spatial association than SpatialDM. Further research is needed to better understand the underlying cause of this shift, which may lead to new drug targets.

#5443 Copy number loss and somatic loss of heterozygosity calling in liquid- and tissue-based genomic profiling.

Hao Wang[1], Andrew Gross[1], **Adrian Bubie**[1], Lauren Lawrence[1], Reagan Barnett[1], Bernard Herman[1], Matthew Ellis[1], Tingting Jiang[2]

[1]Guardant Health, Redwood City, CA,[2]Guardant Health, San Diego, CA

Introduction: Copy number loss (CNL) alterations are common oncogenic driver events important for therapy selection and clinical trial matching in several cancer types. We developed a CNL detection approach that pairs a purpose-built panel with a ploidy-aware, multi-signal model to sensitively detect loss of heterozygosity (LoH) and homozygous deletion (homdel) events from ~1MB to chromosome scale in both plasma- and FFPE-derived samples.

Method: We employed hybrid-capture assays (Guardant360 Liquid and Guardant360 Tissue, Guardant Health, Palo Alto, CA) that target more than 700 cancer-associated genes and incorporate a dense tiling of common single-nucleotide polymorphisms (SNPs) to optimize segmentation resolution. Read depth and SNP minor allele fraction (MAF) are integrated within a ploidy-aware likelihood framework that jointly estimates tumor fraction (TF), ploidy, and allele-specific copy number (CN). Highly polymorphic loci (e.g. HLA) are handled with a unique target design that mitigates polymorphism and artifacts while preserving true deletions. A single caller operates across specimen types, with material-specific adjustments for ctDNA and FFPE tissue. Validation of the caller performance established deletion limit of detection (LoD), sensitivity, specificity and limit of blank (LoB) using a combination of clinical and contrived cell-free DNA (cfDNA) and genomic DNA (gDNA) samples.

Result: Joint tumor fraction (TF)/CNL inference reduces miscalls and improves allele-specific state assignment in polyploid genomes at low TF. The CNL reportable range extends to >500 genes including coverage of the HLA locus, homologous recombination (HRR) and DNA mismatch repair (MMR) pathways. LoD was established at 20% TF in cfDNA and 30% in tissue-derived gDNA, and LoB was demonstrated with a per-sample false positive rate of <5%. Both analytes demonstrated ≥90% sensitivity across the reportable range, and clinical precision established at ≥90% PPA for samples above LoD. HLA deletion calling, while known to be technically challenging, demonstrated similar overall performance to other genes. Among 117k plasma and 43k tissue samples from patients with advanced cancer, this method yielded reportable deletion 10.8% (plasma) and 18.6% (tissue) cases, substantially improving diagnostic yield.

Conclusion: We demonstrate that ploidy- and TF-aware deletion caller approach sensitively and accurately detects CNLs irrespective of gene identity, including in traditionally difficult-to-map regions like the HLA locus, in both cfDNA and gDNA inputs. This ability is a critical component of modern comprehensive genomic profiling, which must include robust detection of clinically relevant copy number alterations to better inform cancer treatment decisions.

#5444 Analytical validation of HLA class I allele typing in a liquid biopsy platform.

Adrian Bubie[1], Sante Gnerre[2], Marisa Juntilla[1], Reagan Barnett[1], Matthew Ellis[1], Tingting Jiang[2]

[1]Bioinformatics, Guardant Health Inc, Redwood City, CA,[2]Guardant Health, San Diego, CA

Background: Human Leukocyte Antigen (HLA) genotyping is an emerging biomarker for immunotherapy efficacy in several solid tumor types but can be particularly challenging to genotype with standard NGS due to the locus' inherent variability. Accurate HLA typing from cell-free DNA (cfDNA) enables non-invasive biomarker assessment for therapy selection and clinical trial matching and can be provided as incidental to standard liquid biopsy without the additive cost of white blood cell sequencing. Using a novel algorithm to enable HLA genotyping as part of Guardant360 Liquid (Guardant Health, Palo Alto, CA), we present analytical validation of HLA class-I allele typing (HLA-A, -B, -C) and demonstrate concordance with paired tissue assay results.
Methods: The cfDNA genotyping algorithm leverages perfect read-pair alignments against a database of more than 16000 known HLA alleles, identifying the most supported allele pairs (germline configuration) based on the read coverage from amongst reference alleles. Analytical validation assessed accuracy using 32 samples with orthogonal HLA data from a validated commercial assay. Limit of detection (LoD) was established through *in silico* downsampling at 5 coverage levels ranging from high to challenging inputs near the test minimum using 4 samples with 5 replicates per level. Precision was evaluated using 6 clinical samples at 5ng input tested across 5 operator, reagent lot, and instrument combinations. Concordance with HLA genotyping in tissue was assessed by comparing 80 paired patient samples run on both Guardant360 Liquid and Guardant360 Tissue.
Results: Guardant360 Liquid demonstrated high accuracy with 97.3% positive percent agreement (PPA) [95% CI: 93.8-99.1%] for HLA class-I alleles. Among evaluable results, 100% concordance was achieved for homozygous alleles (16/16) and 97.0% for heterozygous alleles (163/168). LoD was established at the lowest input level allowed for the assay with 100% detection rate across all tested levels. Precision at 1-5X LoD demonstrated 100% PPA across multiple testing conditions. Paired tissue-liquid concordance analysis showed 97.5% overall PPA (231/237 alleles) across HLA-A (80/80, 100%), HLA-B (77/80, 96.3%), and HLA-C (74/77, 96.1%), with discordances primarily attributed to tumor-specific loss of heterozygosity or minor SNP differences between closely related alleles.
Conclusions: Guardant360 Liquid HLA typing demonstrates robust analytical performance with high accuracy, sensitivity, and precision in cfDNA with accelerated turnaround times compared to standard genotyping assays. Strong concordance between paired tissue and liquid samples validate the algorithm's performance in cfDNA. This non-invasive HLA typing capability enables comprehensive biomarker profiling for immunotherapy selection and clinical trial eligibility assessment in patients with advanced solid cancers.

#5445 Macrophage metabolic rewiring underpins the distinct immunological architecture of invasive mucinous adenocarcinoma revealed through layered molecular profiling.

ShinYoung Park[1], KyungA Kim[2], Chung Lee[2], Byungjin Hwang[3], Hyo Sup Shim[2]

[1]Department of Biomedical Sciences, Graduate School of Medical Science, Brain Korea 21 Project, Yonsei University College of Medicine, Seoul, Korea, Republic of,[2]Department of Pathology, Yonsei University College of Medicine, Seoul, Korea, Republic of,[3]Department of Biomedical Sciences, Yonsei University College of Medicine, Seoul, Korea, Republic of

Invasive mucinous adenocarcinoma (IMA) is a rare variant of lung adenocarcinoma whose biological underpinnings remain poorly resolved, and the factors governing its distinct clinical behavior are not fully understood. To elucidate the cellular architecture of IMA, we generated a high-resolution single-cell transcriptomic atlas from ten IMA tumors and performed comparative analyses against datasets from invasive non-mucinous adenocarcinoma (INMA). Our data revealed that the IMA tumor microenvironment is shaped by a pronounced reshaping of the myeloid compartment, characterized by the expansion of select macrophage populations displaying transcriptional signatures associated with regulatory and metabolically activated states. These macrophages constituted a dominant cellular component in IMA and were positioned at the center of immunomodulatory pathways within the tumor ecosystem. Concomitantly, IMA exhibited a sharp reduction of multiple T cell subsets, accompanied by transcriptional indicators of functional attenuation, and a shift in the B cell compartment toward quiescent phenotypes consistent with disrupted lymphoid organization. Together, these features point to a coordinated landscape of adaptive immune dysfunction. Cell-cell communication analyses further supported this immunological configuration, uncovering immunoregulatory signals specifically strengthened in IMA that involved macrophage-to-lymphocyte and macrophage-to-epithelial interactions absent in INMA. On the epithelial axis, IMA tumors displayed a prominent enrichment of a mucin-producing epithelial population with transcriptional programs associated with mucin secretion and structural remodeling. Pseudotemporal modeling identified a differentiation trajectory linking alveolar epithelial cells to mucin-producing cells, bifurcating between IMA and INMA and suggesting that IMA harbors a lineage evolution distinct from the non-mucinous counterpart. Taken together, these results define IMA as a tumor ecosystem in which a remodeled macrophage compartment intersects with epithelial specialization to reinforce an immunosuppressive microenvironment. By outlining the interplay between myeloid activation, adaptive immune impairment, and mucin-associated epithelial differentiation, this work provides a cellular framework for understanding the unique biology of IMA and highlights potential therapeutic avenues that may benefit its clinical management.

#5446 BRCA1, RNA-binding proteins, and miR-18a, a molecular tri(umph) in breast carcinoma.

Raiyan Satti, Anjana Saxena, Shaneen M. Singh

Brooklyn College, Brooklyn, NY

Breast cancer frequently involves widespread dysregulation of miRNAs, and changes in their processing can influence tumor behavior. RNA binding proteins (RBPs) are key post-transcriptional regulators that predominantly control gene expression through RNA metabolism. Dysregulation of RBPs is implicated in therapy resistance of breast cancer and targeting key RBPs can be a promising therapeutic approach to reverse this resistance. Earlier we identified a group of RBPs as common interactors of BRCA1 and RBP-nucleolin (NCL), namely heterogeneous nuclear ribonucleoprotein A1 (HNRNPA1), heterogeneous nuclear ribonucleoprotein D (HNRNPD), polyadenylate binding protein cytoplasmic 1(PABPC1), and TAR DNA-binding protein 43 (TDP-43). We published computational models of these RBPs, including NCL for their competitive versus synergistic binding with miR-21, based on predicted docking scenarios. NCL and the biogenesis of the six-miRs that it regulates are frequently overexpressed in breast cancer and are directly implicated in tumor growth and progression. Similarly, the miR-17-92 cluster which includes miR-18a is often upregulated in malignancies, including breast tumors. In estrogen receptor-positive breast cancer, it has been shown that miR-18a directly targets the 3'UTR of ER-α, increasing resistance to hormonal therapy. Although it is known that HNRNPA1 binds the terminal loop of pri-miR-18a and enhances its processing by the microprocessor complex, how NCL interacts with miR-18a is completely unknown. Interestingly, targeting NCL either by silencing or using NCL-specific aptamers directly impacts its control of various miRs, and hence inhibition of tumor growth. In this study, we have focused on the two RBPs, NCL and HNRNPA1 and their interaction with miR-18a in the context of breast cancer. We have modeled the full primary miR-18a and show its predicted interaction with the RNA-binding domains (RBDs) of NCL and HNRNPA1. We compare and contrast the molecular interactions and highlight the key residues involved in the interaction interface for the RBPs and miR-18a with an end goal to suggest potential targetable sites for therapeutics.

#5447 *In silico* analysis of GSK3α to identify novel potential ligands for cancer therapy.

Neha Sylvia Walter, Sanchit Dora, **Jasmeet Kaur**

Postgraduate Institute of Medical Education and Research (PGIMER), Chandigarh, India

Cancer prevails as the leading mortality cause worldwide. Constraints like drug resistance and adverse immune events urge the need to find novel treatment targets in cancer patients. Glycogen synthase kinase 3 (GSK3) is a multifunctional kinase that has context-dependent dual role in cancer. Out of the two highly homologous mammalian isoforms of GSK3 (i.e. GSK3α and GSK3β), we explored the predictive and prognostic role, and novel potential ligands for GSK3α. *GSK3A* gene expression was compared in normal and tumor tissues using TNM plot (https://tnmplot.com/analysis/). Kaplan-Meier plotter (https://kmplot.com/analysis/) was used to correlate *GSK3A* mRNA expression with survival in cancer patients receiving immunotherapy, for a 240 months follow-up threshold and using median expression. ROC plotter (https://www.rocplot.com) was used to analyze the predictive role of *GSK3A* gene in cancer patients receiving immunotherapy. The data from KM- and ROC-Plotter was analyzed using Graphpad PRISM 8. Logrank P, 95% confidence intervals and Hazard ratio (HR) were calculated and P value of < 0.05 was considered to be statistically significant. Five ligand libraries from Selleckchem chemical database were docked with GSK3α protein using PyRx Vina Wizard for virtual screening. Ligands with favorable binding energies were validated for drug-likeliness using ProTox 3.0 (https://tox-new.charite.de/protox_II/). *GSK3A* gene expression was significantly higher in twelve tumors than normal tissue and two normal than tumor tissue. Higher *GSK3A* mRNA expression was significantly correlated with better OS and not PFS in patients receiving immunotherapy. ROC analysis showed that *GSK3A* gene expression was significantly associated with combined response to anti-PD-L1 and anti-CTLA-4 therapy, and not to anti-PD-1 therapy. Molecular docking predicted several ligands with strong binding affinity to GSK3α. Shortlisted drugs based on their docking scores were analyzed for their drug-likeliness. MOLI001171, MOLI001205 and Formylmethanofuran were found to be potent GSK3α ligands with potential for cancer therapy.

#5448 A serotonin transcriptional axis shapes immune phenotypes and clinical outcomes in lung cancer.

Ecem Kalemoglu[1], Salih Akgun[2], Ayse Caner[3]

[1]Internal Medicine, Rutgers University - Jersey City Medical Center, Jersey City, NJ,[2]Internal Medicine, JFK University Medical Center, Edison, NJ,[3]Department of Basic Oncology, Institute of Health Sciences, Ege University, Izmir, Turkey

Background
Neuromodulator-metabolite pathways are emerging regulators of tumor-immune interactions. A recent study showed that neurotransmitter signaling remodels immune infiltration. Building on this framework, we developed a serotonin transcriptional axis incorporating TPH/HTR synthesis, MAOA/IDO1 degradation, and SLC6A4 transport to characterize immune states in lung adenocarcinoma (LUAD) and lung squamous carcinoma (LUSC).
Methods
TCGA RNA-seq data were processed via Xena. Row-z-scaled serotonin genes generated Up, Down, and composite Axis scores. k-means defined serotonin phenotypes. Immune checkpoints, cytotoxic programs, chemokines, and immune-cell surrogates (CD8A, FOXP3, NCAM1, IRF5, CD163, MS4A1, ITGAX) were assessed using Wilcoxon testing, correlation matrices, limma DEGs, Hallmark GSEA, and KM/Cox survival.
AI tools (ChatGPT) were used for editing, grammar, and text condensation.
Results
In LUAD, three phenotypes emerged: C1 (MAOA/IDO1-high, immune-cold), C2 (serotonin-depleted), and C3 (TPH/HTR-high, immune-hot).
C3 demonstrated strong activation of CD8A, IFNG, GZMB, PRF1, CXCL9/10/13 and checkpoints including PDCD1, CD274, CTLA4, LAG3, TIGIT ($p<0.001$).
Serotonin Axis Score correlated positively with CD8 T cells, NK cells, dendritic cells, B cells, and M1 markers, and negatively with CD163, indicating an inflamed, antigen-presenting TME.
GSEA showed C3 enrichment for interferon and inflammatory programs; C1 favored metabolic/MYC pathways.
Survival differed significantly across clusters ($p=0.0014$), with C3 best and C1 worst; high serotonin axis trended toward improved OS ($p=0.055$).In LUSC, the same phenotypes recurred, confirming cross-histology reproducibility. C3 again showed the strongest immune activation with elevated cytotoxic and checkpoint expression.
Serotonin activation associated with CD8A, NK signatures, MS4A1, ITGAX, and M1 markers, whereas serotonin suppression correlated with CD163-high M2 states.
GSEA showed C3 enrichment for IFN-α/γ and inflammatory pathways; C1 enriched for OXPHOS/MYC programs.
Cluster OS was not significant ($p=0.63$), but continuous Serotonin Axis Score predicted improved OS ($p=0.039$).
Conclusions
Serotonin pathway states reproducibly shape immune landscapes and survival across LUAD and LUSC. Serotonin activation aligns with cytotoxic infiltration, chemokine-rich inflammation, dendritic/B-cell signatures, M1 polarization, checkpoint expression, inflamed GSEA programs, and improved survival. These findings extend neuromodulator-TME concepts from recent study and identify the serotonin axis as a cross-histology biomarker and potential immunomodulatory target.

#5449 The effects of survivorship patterns and survival parameters on cancer risk across vertebrates.

Olivia K. Corrao[1], Walker Mellon[1], Zachary Taylor Compton[2], Harley Richker[1], Gissel Marquez Alcaraz[1], Stefania Kapsetaki[3], Joel Brown[4], Orsolya Vincze[5], Mathieu Giraudeau[6], Michael Lynch[1], Carlo C. Maley[7]

[1]Biodesign Institute, Arizona State University, Tempe, AZ,[2]University of Arizona, Tucson, AZ,[3]Institute of Molecular Biology and Biotechnology of the Foundation for Research and Technology-Hellas, Heraklion, Greece,[4]Moffitt Cancer Center, Tampa, FL,[5]French National Center for Scientific Research, Bordeaux, France,[6]University of La Rochelle, La Rochelle, France,[7]Arizona State Univ. Biodesign Institute, Tempe, AZ

Cancer is a disease that affects all multicellular organisms. However, evolutionary pressures resulted in a diverse range of life history traits, including survivorship patterns, across all species that may significantly impact susceptibility to cancer. This study aims to identify the effects of survivorship patterns and survival parameters in vertebrate species on neoplasia and cancer prevalence. The data used contains necropsy records of 29,702 individual organisms, spanning 100 different species in 4 clades: Mammalia, Reptilia, Amphibia, and Aves. The Rage software in R was used to generate survivorship models and calculate survivorship patterns for each species. Five survival parameters were estimated for each species using the Siler model and the fmsb software in R. We found that species that exhibit a Type I or Type III survivorship pattern have a higher prevalence of both neoplasia and cancer, whereas Type II species develop significantly less neoplasia and cancer. Similarly, we found that species with a low extrinsic mortality rate in the senescent stage have an increased risk of both neoplasia and cancer. This comparative study highlights the effects of life history strategies on cancer and allows for further research on mechanisms of cancer suppression in species with low cancer risk and potential applications to cancer treatment plans in humans.

#5450 Decoding ADC payload dynamics with a spatial transcriptomics-integrated tumor microenvironment PK model.

Sungwoo Bae, Jeongbin Park, Jin Yeong Choi, Daeseung Lee, Hyung-Jun Im, Hongyoon Choi

Portrai, Inc., Seoul, Korea, Republic of

Background: The inherent heterogeneity of the tumor microenvironment (TME) complicates the prediction of antibody-drug conjugate (ADC) payload delivery and the mechanism of resistance. The advent of spatial transcriptomics (ST) enables high-resolution molecular profiling, allowing in silico pharmacokinetics (PK) modeling within the TME as a proxy for payload delivery. This study aimed to develop a TME-PK platform, validate it preclinically, and integrate human TME data to inform how ADC payload delivery can be optimized in clinically relevant settings.
Method: We developed an in silico TME-PK model parameterized using target expression and endothelial density derived from ST (Visium/Visium HD) grids. It enables quantification of payload distribution in a time-dependent manner by solving kinetic equations mapped onto ST data, incorporating vessel distribution, linker-cleavage enzymatic activity, and target expression patterns. To validate these findings, we used a FaDu xenograft mouse model that received either fluorescently labeled cetuximab or panitumumab. Tumors were collected at two and 40 hours for distribution imaging and ST. We then used the model to simulate payload delivery in 52 stomach adenocarcinoma (STAD) patients across a wide K_D range (pM to 10 μM) to find optimal targets and range of ADC characteristics. The peak concentration of the intratumoral payload was then calculated for each ST of the patient tumor.
Results: The 2 and 40-hour antibody distribution predicted by the TME-PK model correlated significantly with observed fluorescence intensity from experimental data (Spearman's rho > 0.65, $p < 0.05$). The model was then evaluated for the relationship between intratumoral target expression levels and the sensitivity of payload delivery to K_D, revealing a strong positive correlation (Spearman's rho: 0.94, $p < 0.05$). For highly expressed targets (e.g., CEACAM5), payload concentration rapidly saturated even at modest binding affinities (higher K_D). However, very high affinity (low K_D) induced a potent binding-site barrier, causing ADC accumulation in perivascular regions and preventing tumor core penetration. Conversely, for low-expression targets (e.g., NECTIN-4), a very high affinity (low K_D) was essential to achieve adequate payload concentration and enhanced tumor core delivery.
Conclusion: We established a spatially-resolved TME-PK framework, which was validated preclinically using experimental xenograft data. Its application to STAD patient data confirmed known pharmacological phenomena, such as the binding-site barrier effect. This demonstrates the TME-PK model as a crucial tool for optimizing ADC payload delivery, showing that the optimal kinetic properties of antibody must be balanced against the spatial patterns of target expression and relationship with tumor microenvironment to ensure both binding and tissue penetration.

#5451 Omicology: A comprehensive AI/LLM/NLP-based web resource for the ontology, phylogeny, and practical navigation of omics literature.

James M. Melott, **John N. Weinstein**

UT MD Anderson Cancer Center, Houston, TX

Introduction: We present here a public website, omicology.com, which includes extensive information on omic research domains and features a specialized omics search engine. Omics started as a simple suffix for research based on molecular profiling of genes, proteins, and other (biological) molecules in aggregate. The etymology, from ancient Greek or possibly Sanskrit, is debated. Application of the suffix to dozens of research fields starting in the 1990s (Weinstein 1998) was often derided as jargon. “Where’s the hypothesis?” was a common critique - and reason for rejecting manuscripts or proposals. But given the draft human genome in 2001, synergy between omic and hypothesis-driven research gradually gained acceptance. In 2000, 2010, 2020, and 2025, there were 6, 61, 267, and >700 omics terms, respectively. More recently, high-throughput single-cell, spatially-resolved, and temporally-resolved omic technologies have provided new dimensions to our pursuit of precision medicine for cancer.

Methods: Our starting point for development of the search engine database was 6,980,243 full-text Open Access PubMed Central articles plus various metadata. It included 5,699 omics terms. Our NLP, use of LLM resources, and careful manual curation have produced 702 omics terms. Refinement of such lists is complicated by eccentricities of language, misspellings, alternative spellings, suffixes like ‘nomics’ (e.g., in economics), not ‘omics,’ and ambiguous terms like ‘chromosomics.’

AI tools (Elicit, Cursor, Google, and ChatGPT) have provided useful design and content ideas for a static html prototype website. An agentic AI coding tool has assisted our development of a dynamic full-stack, human-curated version (currently 34,124 lines of code and content) based on the prototype (for publicly roll-out before AACR 2026).

Representative Results: The most frequent omic terms are Genomics (257,617 articles), Proteomics (123,697), Metabolomics, (80,023), and Transcriptomics (78,279). Metagenomics, radiomics, lipidomics, epigenomics, pharmacogenomics, and phosphoproteomics complete the top 10.

Our data on the top 702 terms currently include usage numbers for each document section, publication date, curation status, a brief LLM-generated description, and more.

Conclusions: The open-source, updatable Omicology.com website will provide an expanding repertoire of information and perspectives on omics plus specialized omics search capabilities. Biomedical perspective will be aided by the senior author’s long-term experience in omic research beginning with his initiation and leadership of the first omic/multi-omic NCI project, molecular profiling of the NCI-60 (e.g., Weinstein, et al., Science, 1997). Methods used here for omics can provide a template for research on other hard-to-analyze fields, complementing the capabilities of such resources as PubMed Central.

#5452 Deep learning enables matched-normal free estimation of tumor mutational burden from whole exome reads in colorectal cancer.

Amrita Chattopadhyay[1], Liang-Yu Lin[2], Ching-Tai Chen[3], Eric Y. Chuang[4]

[1]Institute of Epidemiology and Preventive Medicine, College of Public Health, National Taiwan University, Taipei, Taiwan,[2]Graduate Institute of Biomedical Electronics and Bioinformatics, National Taiwan University., Institute of Epidemiology and Preventive Medicine, College of Public Health, National Taiwan University, Taipei, Taiwan,[3]Department of Computer Science, University of Taipei, Taipei, Taiwan,[4]Graduate Institute of Biomedical Electronics and Bioinformatics, National Taiwan University, Taipei, Taiwan

Tumor mutational burden (TMB) is a key biomarker for immune checkpoint inhibitor (ICI) therapy. However, its clinical implementation in colorectal cancer (CRC) remains limited by the cost of matched normal sequencing and by inconsistent TMB estimates across pipelines. We developed a tumor only, deep learning pipeline using raw whole exome sequencing (WES) reads. First, tumor purity was predicted using genomic language model (gLM) sequence features, read depth, and clinical data, the purity embedding from which were integrated with genomic and coverage features to estimate log transformed TMB. The model was trained with five fold cross validation on 121 CRC tumor samples; 29 matched-normal samples were gradually added to evaluate generalization. Across ten random experiments, the best purity model achieved an average mean-squared error (MSE) of 0.026 and concordance index (C index) of 0.93. Incorporating purity embedding improved TMB prediction accuracy, achieving MSE of 0.096 and CI of 0.62, nearly halving the error compared with a more complex baseline using reduced input reads. This framework enables rapid, TMB estimation directly from tumor only WES data, removing the need for matched normal or ad hoc filtering. By improving accessibility and consistency of TMB measurement, the method may enhance identification of CRC patients most likely to benefit from ICI therapy, particularly in resource-limited clinical settings.

#5453 Machine learning accelerates discovery of synergistic- PI3K-mTOR combinations for robust tumor growth inhibition in KRAS G12 mutant patient-derived xenografts.

Emily Eastwood, Yuan-Hung Chien, Jose Lopez-Ramos, Paris Offor, Warren Andrews, Long Hoang Do, **Raffaella Pippa**

Certis Oncology Solutions, San Diego, CA

Identifying effective drug combinations remains a major challenge in oncology, primarily due to inherent resistance and the limited clinical fidelity of conventional in vitro screening data. To address this translational barrier, we established a robust platform utilizing Certis Oncology's proprietary patient-derived xenograft (PDX) models, which offer high correlation with clinical responses, to predict and validate synergistic therapeutic regimens.

Our approach leveraged CertisAI^{TM}, an ensemble of proprietary machine learning (ML) models trained on high-throughput combination experiments. CertisAI^{TM} successfully prioritized combinations targeting the PI3K and mTOR pathways as lead candidates for treating aggressive KRAS G12 mutant tumors, spanning non-small cell lung, gastric, pancreatic, and colorectal cancers. We experimentally evaluated a comprehensive matrix of six PI3K inhibitors and four mTOR inhibitors across distinct KRAS G12 mutant PDX models. These ex-vivo studies rigorously demonstrated that the dual inhibition of the PI3K-mTOR axis resulted in potent, synergistic anti-tumor activity, consistently yielding efficient and sustained tumor cell reduction across all tested models. Notably, a key synergistic combination—involving Everolimus or Tacrolimus (mTORi) paired with Inavolisib (PI3Ki)—translated directly to significant therapeutic benefit in the PDX setting.

These findings validate our PDX-informed strategy for rapidly identifying clinically relevant, synergistic combinations. The demonstrated efficacy of the Everolimus/Tacrolimus + Inavolisib combination provides compelling preclinical evidence, establishing this dual-agent approach as a strong therapeutic candidate for clinical evaluation in KRAS G12 mutant solid tumors.

#5454 Identification of microRNA clusters as predictors of chemotherapy response in acute myeloid leukemia.

Ziang Chen[1], Jennifer Rangel Ambriz[1], Yu-Hsuan Fu[1], David Eugene Frankhouser[1], Denis O'Meally[1], Lianjun Zhang[1], Ying-Chieh Chen[1], Sergio Branciamore[1], Jihyun Irizarry[1], Bin Zhang[1], Guido Marcucci[2], Russell Rockne[1], Ya-Huei Kuo[1]

[1]Beckman Research Institute of The City of Hope, Duarte, CA,[2]City of Hope National Medical Center, Duarte, CA

Acute myeloid leukemia (AML) is a cancer of the myeloid cell lineage characterized by acquired gene mutations and chromosomal abnormalities. We have previously shown that AML initiation and progression can be predicted by applying a state-transition theory to the analysis of time-series messenger RNA (mRNA) and microRNA (miRNA) sequencing data from peripheral blood mononuclear cells (PBMCs) collected during disease development. We showed that AML initiation and progression in mouse models can be tracked via blood mononuclear cell transcriptomes and modeled as particle undergoing Brownian motion in a double-well potential with critical points for health, transition, and leukemia. Building on this framework, our current study evaluates chemotherapy response using time-series sequencing data from an AML mouse model. We plotted mRNA and miRNA transcriptome trajectories over time and found that chemotherapy initially shifted both trajectories away from the leukemic state toward the healthy state, followed by relapse back toward leukemic state. Notably, miRNA responses showed a delay of 2 weeks behind mRNA. To investigate the cause of delayed miRNA transcriptomic response to chemotherapy, we performed Weighted Gene Co-expression Network Analysis (WGCNA) on miRNA expression profiles to identify co-expressed clusters. By projecting each miRNA cluster onto the leukemia state-space[YK1] , we identified a cluster that exhibit strong contribution to the AML state transition. This is a cluster of 30 miRNAs with coordinated expression patterns, significantly upregulated and associated with delayed transcriptomic response post-chemotherapy.Notably, 80% of these miRNAs are located within the DLK1-DIO3 imprinted region (chromosome 14q32 in humans, 12qF1 in mice), a locus previously implicated in stress response, acute promyelocytic leukemia (APL), solid tumors, and type 2 diabetes. However, their involvement in standard-of-care chemotherapy responses in AML has not been previously reported.Further mechanistic analysis revealed a regulatory mechanism in which high expression of these miRNAs suppresses the PI3K/mTOR signaling pathway. Inhibiting the PI3K/mTOR pathway lowers reactive oxygen species (ROS) production, which creates an environment for leukemia stem cells (LSC) to survive. Since chemotherapy primarily eliminates leukemic blast cells, the persistence of LSCs may significantly contribute to relapse.Our findings highlight the power of state-space modeling to uncover dynamic regulatory mechanisms and identify miRNA-driven factors that may lead to AML relapse after chemotherapy.

#5455 RNA-seq profiling identifies FOX genes as potential CRC biomarkers.

Yakshi Nicole Ortiz-Maldonado, **Hilmaris Centeno-Girona**, Camille Zenon-Melendez, Sheila Natalie Lopez-Acevedo, Elba V. Caraballo

Division of Shared Resources and Scientific Operations, University of Puerto Rico Comprehensive Cancer Center, San Juan, Puerto Rico

Colorectal cancer (CRC) remains a leading cause of cancer-related deaths worldwide, including Puerto Rico, highlighting the urgent need for reliable biomarkers to enable earlier and more accurate detection. The FOX family of transcription factors regulates key cellular processes, including cell proliferation, apoptosis, metabolism, and immune regulation. However, their expression patterns and diagnostic utility in Hispanics individuals living in Puerto Rico (HPR) have not been characterized. The aim of this study is to characterize FOX gene expression profiles across healthy and CRC individuals and evaluate their prognostic and diagnostic performance in HPR.

Tissue samples from 28 participants in the Puerto Rico Familial Colorectal Cancer Registry (PURIFICAR) cohort (13 controls-healthy normal mucosa, 7 early-stage, and 8 advanced-stage CRC tumors) were used for RNA extraction and bulk RNA sequencing. Differential gene expression was performed using DESeq2 (|log2 fold change|>2, adjusted $p<0.05$). Four FOX signature scores were constructed from significant non-collinear FOX genes (VIF<10) using Gene Set Variation Analysis. Kaplan Meier survival analysis was performed for each differentially expressed FOX gene using publicly available colon cancer data. Gene associations with CRC status were evaluated using binomial generalized linear models (GLM), unadjusted and adjusted for age and BMI. Diagnostic performance was assessed using sensitivity, specificity, and AUC-ROC. Significance was set at 0.05. Statistical analyses were performed using R, version 4.3.3.Expression profiles of 35 FOX genes separated samples into distinct clusters by early- and advanced-stages of CRC and controls. Of 12 differentially expressed genes, 5 genes were upregulated (FOXC1, FOXC2-AS1, FOXH1, FOXN2, FOXQ1), while 7 were downregulated (FOXA1, FOXA3 FOXD2, FOXD3-AS1, FOXE3, FOXF2, FOXO1) in CRC relative to controls. Kaplan-Meier analysis showed that higher expression of 4 genes (FOXA3, FOXC1, FOXF2, FOXQ1) was associated with reduced survival probabilities in CRC patients, whereas higher expression of FOXA1 and FOXN2 was associated with improved survival ($p<0.05$). In unadjusted analysis, FOXQ1 expression and a 6-gene FOX signature, including FOXC1 and FOXQ1, significantly increased CRC odds ($p<0.05$), while 7 genes significantly decreased CRC odds. After adjusting for age and BMI, protective associations were observed for FOXE3 (OR:0.19), and FOXD2 (OR:0.42), while FOXQ1 (OR:1.45) and FOXC1 (OR:2.83) showed the largest increased odds of CRC.

Multiple FOX genes were differentially expressed in CRC, with FOXC1 and FOXQ1 showing significant associations with both survival of CRC patients and disease risk. A FOX gene signature further improved diagnostic performance. These findings support the potential of FOX transcription factors as clinically relevant biomarkers for HPR.

#5456 Multiplatform bioinformatic profiling identifies TTK and NEK2 as survival-associated drivers in triple-negative breast cancer.

Alexandra N. Aquino-Acevedo[1], **Esther M. Irizarry-Quintana**[2], Angel D. Colon-Burgos[1], Marileana Rodriguez-Ruiz[3], Joel A. Orengo-Orengo[1], Elliott Rodriguez-Lopez[1], Melanie E. Cruz-Robles[1], Harold I. Saavedra[1]

[1]Basic Sciences, Ponce Health Sciences University, Ponce, PR,[2]U54 REC InterAmerican Undergraduate Program, Ponce Health Sciences University, Ponce, PR,[3]Moffitt U54 Summer Research Program, Ponce Health Sciences University, Ponce, PR

Introduction: Triple-negative breast cancer (TNBC) is an aggressive subtype characterized by the absence of ER, PR, and HER2 receptors, limiting targeted therapeutic options and contributing to poorer outcomes among women. Prior evidence from our group indicates that mitotic kinases TTK and NEK2 are frequently overexpressed in TNBC, promoting centrosome amplification and invasive behaviour. Therefore, we aim to further explore how these mitotic kinases impact biological processes and the overall survival of TNBC patients.
Hypothesis: Mitotic kinases, such as TTK and NEK2, play a pivotal role in EMT and metastatic processes in TNBC, while their overexpression leads to a lower overall survival of TNBC patients.
Method: To functionally assess this hypothesis, we performed a series of bioinformatic analyses using the TCGA and STRING databases to evaluate the molecular processes associated with TTK and NEK2 expression. We also collected information from the Kaplan Meier (KM) Plotter database to evaluate the correlation between TTK and NEK2 expression on BC patients' overall survival.
Results: mRNA expression profiles from TCGA demonstrated significantly elevated TTK and NEK2 levels across TNBC groups. Moreover, high expression of both mitotic kinases correlated with reduced overall survival in KM analyses. STRING network analysis revealed enrichment for β-catenin binding, cell-to-cell junction regulation, and mesenchymal differentiation, supporting a role for these kinases in EMT-associated processes.
Conclusion: Collectively, these data provide complementary bioinformatic evidence that the mitotic kinases TTK and NEK2 contribute to EMT activation and invasive potential in TNBC. Their overexpression in patient tumors correlates with poor survival outcomes. Thus, these results highlight TTK and NEK2 as promising molecular targets for limiting TNBC progression and metastasis.

#5457 From tumor to model: Transcriptomic and therapeutic insights from patient-derived colorectal cancer organoids.

Matthew Graziano, Ajeet Singh, Stephen Friend, Ruby E. Thamert, Utsav Sharma, Abhay Andar, Jonathan Jacobs, **Carolina Lucchesi**

Microphysiological Systems, American Type Culture Collection (ATCC), Manassas, VA

Background: Colorectal cancer (CRC) is the world's second leading cause of cancer deaths, often diagnosed late due to its silent onset. To drive breakthroughs in drug discovery, scientists use both traditional cell lines and patient-derived models. The Human Cancer Models Initiative (HCMI)—a collaboration among the National Cancer Institute, Cancer Research UK, Wellcome Sanger Institute, Hubrecht Organoid Technology, and ATCC—has built a collection of clinically annotated CRC organoids that capture tumor biology and genetic diversity. Understanding differences in gene expression between organoids and conventional cell lines is key to improving disease models and developing better therapies.
Methods: Six CRC organoid models from unique donors and ten CRC cell lines were expanded and analyzed via RNA sequencing. The models were derived from primary tissues across ten anatomical sites. Transcriptomic profiles were compared among models and against tumor data from The Cancer Genome Atlas (TCGA). A subset of models was screened for drug sensitivity using a panel of six compounds targeting molecular pathways identified by RNA-seq. Dose-response curves were generated, and IC50 values were calculated. Post-treatment cultures were evaluated using a luminescent ATP viability assay to assess drug response.
Results: Patient-derived CRC organoids showed high genomic concordance with matched tumors, including shared single-nucleotide variants and ~30-40% overlap in extrachromosomal DNA features. KRAS mutation discrepancies (e.g., G12D/G12V vs. G12R) indicated clonal evolution. Key driver mutations (APC, TP53, KRAS, PIK3CA, SMAD4) were consistently detected, corresponding with Oncomine targets. Histopathology confirmed retention of tumor-specific markers. Drug screening revealed variable responses across organoids, with fluorescence-based viability assays confirming model-specific sensitivities. Transcriptomic analysis highlighted molecular heterogeneity and distinct subtype-specific expression patterns. Several genes were consistently expressed across models, suggesting shared oncogenic pathways.
Conclusion: CRC organoids from HCMI faithfully recapitulate key transcriptomic and mutational features of patient tumors while revealing diverse drug responses. These models offer valuable platforms for precision oncology, enabling the identification of variant-specific vulnerabilities and supporting personalized treatment strategies.

#5458 Single-cell metabolic flux analysis defines distinct metabolic programs across tumor-infiltrating immune cells.

Yue Fang[1], Changlin Wan[1], Haiqi Zhu[2], Zheng An[1], Pengtao Dang[1], Chi Zhang[1], Sha Cao[1]

[1]Biomedical engineering, Oregon Health & Science University, Portland, OR,[2]Computer Science, Indiana University, Bloomington, IN

Metabolism strongly influences how immune cells become activated, differentiate, and lose function in the tumor microenvironment. Understanding the metabolic programs that define different tumor-infiltrating immune cell subtypes is important for identifying pathways that could be targeted to improve immune responses in cancer, yet the distinct metabolic features of major immune cell types—including T cells, myeloid cells, NK cells, and B cells—are still not well defined. To address this, we collected multiple tumor-derived scRNA-seq datasets (>500,000 cells across ~30 immune cell subtypes). Using these datasets, we conducted metabolic flux inference to identify immune cell-specific metabolic states in the tumor microenvironment. scRNA-seq datasets of tumor-infiltrating immune cells were first analyzed using Seurat, where cell type and subtype identities were assigned based on canonical marker genes and confirmed with additional annotation tools. Pseudobulk and meta-cell representations were created to reduce sparsity, and metabolic flux was estimated using our in-house tool MPOCtrL, which infers reaction-level activity from gene expression using curated metabolic gene lists. Dimensionality reduction and clustering were applied to compare metabolic patterns across immune cell types and subtypes. In particular, for T cells, we have discovered distinct metabolic phenotypes for different T cell subtypes. Exhausted T cells showed high serine and glutamate metabolism, low glucose uptake, and reduced β-oxidation, while T follicular helper cells showed opposite trends with low serine and glutamate metabolism but high glucose uptake and elevated glycolysis. Glycolysis was also high in Th1-like cells but reduced in CD4 cytotoxic effector and Tn-like cells. Lactate-associated flux was enriched in Treg and Trm cells, while Tcm and Tn-like cells showed low lactate production. Ketone body metabolism was high in Th17-biased CD4 T cells and low in Trm cells. Fatty acid pathways varied across subsets, with Tn-like cells showing low fatty acid synthesis and Th1-like cells showing high β-oxidation. Pentose phosphate pathway activity remained uniformly low across T-cell subsets. This analysis reveals clear metabolic patterns across immune cell types and subtypes in the tumor microenvironment. By defining these metabolic programs, our work provides a basis for identifying metabolic pathways that could be targeted to change immune cell behavior and improve anti-tumor immunity.

#5460 Elucidation of breakage-fusion-bridge (BFB)-mediated *EGFR* amplification in lenvatinib-resistant hepatocellular carcinoma.

JungHyun (Jenny) Kim[1], Ji Young Kim[1], Hyeonu Yang[1], Sang Yun Ha[2], Han-Na Kim[1], Hoon Kim[3], Yeup Yoon[4], Wonseok Kang[5]

[1]Samsung Medical Center, Samsung Advanced Institute for Health Sciences and Technology (SAIHST), Seoul, Korea, Republic of,[2]Pathology, Samsung Medical Center, Seoul, Korea, Republic of,[3]School of Pharmacy, Sungkyunkwan University, Suwon, Korea, Republic of,[4]Samsung Medical Center, Sungkyunkwan University School of Medicine, Seoul, Korea, Republic of,[5]Gastroenterology and Hepatology, Samsung Medical Center, Sungkyunkwan University School of Medicine, Seoul, Korea, Republic of

Lenvatinib, a multi-targeted tyrosine kinase inhibitor, is widely used as a first-line therapy for patients with immunotherapy-ineligible hepatocellular carcinoma (HCC). However, its clinical benefit is often compromised by the development of resistance. Understanding the genomic alterations driving resistance is critical to improving therapeutic outcomes in HCC. In this study, a lenvatinib-resistant HCC cell line, Huh7, was established by exposing parental sensitive cells to increasing concentrations of lenvatinib. To elucidate the mechanisms underlying drug resistance, short- and long-read whole genome sequencing (WGS), whole transcriptome sequencing (WTS), and western blot were performed. Comparative analysis of genomic alterations between parental and resistant cells revealed marked differences in copy number (CN) profiles. In resistant cells, *EGFR* showed the most prominent CN gain, increasing from 6 to 21 copies. Detailed breakpoint analysis utilizing LUMPY identified fold-back inversions that directly corresponded with genomic locations exhibiting significant CN alterations, indicative of the hallmark features of breakage-fusion-bridge (BFB) cycles. These findings were confirmed by Sniffles-based long-read SV calling. Transcriptomic and protein-level analyses using WTS and Western blotting, respectively, showed increased EGFR expression. Gene set enrichment analysis showed significant enrichment of ERBB and MAPK pathways. Mechanistically, activation of the EGFR-PAK2-ERK5 axis was observed, suggesting that lenvatinib-induced blockade of VEGFR/FGFR promotes a bypass survival signal through EGFR downstream pathways. Combined treatment with lenvatinib and erlotinib, an EGFR inhibitor, reduced viability and restored sensitivity. Clinically, lenvatinib-treated HCC patients with high EGFR immunohistochemistry scores exhibited shorter progression-free survival, and public HCC cell line datasets consistently showed poor responses in *EGFR*-amplified cells. In conclusion, our findings suggest BFB-driven *EGFR* amplification as a key structural and functional driver of lenvatinib resistance in HCC. Lenvatinib combined with an EGFR inhibitor may offer a treatment option for patients with HCC exhibiting elevated EGFR expression.

#5461 Molecular genetic profiling of a *de novo* neuroendocrine prostate cancer in a patient-derived xenograft (PDX) and organoid model from an African ancestry patient.

Tej Sharma, Surendra Gulla, Sasikumar Ponnusamy, Abbas Jawadwala, Ephraim Gardner, Roberto Pili, Maddie Aust, John Bodkin, John Tomaszewski, Remi-adelaya Ogala

Jacobs School of Medicine and Biomedical Sciences, Buffalo, NY

Patient-derived xenograft (PDX) and organoid (PDO) models are powerful tools to study how prostate cancer (PCa) develops and responds to treatment, especially in populations that are often underrepresented. In this study, we report the first de novo neuroendocrine prostate cancer (NEPC) case from an African American male who had localized disease with no prior treatment before surgery. The tumor was classified as pT2N0, Gleason score 7 (4+3), and had a PSA level of 3.6. A portion of the patient's tumor tissue was used to generate PDX and PDO models, and another portion was used for downstream molecular analyses. To identify genetic changes driving aggressive tumor behavior, we performed whole-exome sequencing on DNA from the primary tumor and the first passage of the associated PDX model generated (p0) using the Illumina Exome Kit and the Twist Biosciences Exome Panel 2.0. Bioinformatic analysis was performed using Nextflow pipelines (nf-core/sarek) to detect somatic single-nucleotide variants (SNVs), mutations, structural variants, and copy number variations (using CNVkit). Our results reveal variant annotation links of genetic changes associated with PCa progression. Western blot analysis and immunohistochemistry (IHC) demonstrated increased expression of neuroendocrine markers, SYP. Furthermore, we observed similar mutations and copy number changes in genes previously reported in NEPCs. Moreover, novel markers provide deeper insight into molecular drivers of prostate cancer and could guide the development of targeted treatments for aggressive, high-risk localized PCa.

: Deep Learning in Cancer
Poster Session

#5465 Improving early cancer detection by training scalable deep neural networks to extract tumor signal from cell-free DNA.

Jackson A. Killian[1], Kade Pettie[1], Kyle Gowen[1], Shiva Farashahi[1], Esther Brown[2], Feras Hantash[2], Jocelyn Charlton[1], Franziska Michor[3], Kieran I. Chacko[1], Dorna Kashef[1]

[1]Machine Learning and Computational Biology, Harbinger Health, Cambridge, MA,[2]Clinical Laboratory, Harbinger Health, Cambridge, MA,[3]Data Science, Dana-Farber Cancer Institute, Boston, MA

Introduction: Blood-based liquid biopsies offer potential for non-invasive cancer screening. However, detecting early-stage disease is complicated by low levels of circulating tumor biomarkers and background noise from normal cells. To address this, we developed a novel deep-learning framework to detect cancer signal at the resolution of single DNA reads. Applied to bisulfite-converted cell-free DNA (cfDNA) samples, our method significantly improves early-stage cancer sensitivity.
Methods: We designed a massively parallel 2-D convolutional neural network architecture that differentiates cancer and non-cancer signal in cfDNA by learning local methylation patterns at thousands of genomic regions. The model takes next generation sequencing (NGS) data as input, encodes aligned sequences within genomic windows as images, and outputs informative feature vectors for classification. However, training is complicated by two real-world data limitations: (1) disease samples contain a mix of unlabeled fragments from normal and diseased cells, and (2) acquiring sufficient early-stage disease data is costly, burdensome, and time-intensive. To address these, we designed a novel data generation technique that (1) assigns positive labels for groups of reads via in silico spike-in of tumor biopsy reads and (2) generates large, diverse datasets via fine-tuned in silico mixing of non-cancer cfDNA reads. Our model's architecture has key advantages: compact input encoding, interpretable saliency maps, and scalable parallel architecture: we trained on 720TB of data across 10 million genomic bases in a single day, highlighting our framework's efficiency.
Results: We validated our method with targeted bisulfite sequencing data from the CORE-HH clinical study (NCT05435066, N=1229 non-cancers, N=1118 cancers, including N=599 Stage I/II). We pretrained the model on 1.3 billion training examples generated using a held-out set of non-cancer plasma (N=174) and tumor tissue biopsies (N=505). Predictions on data from clinical samples yielded feature vectors, with saliency maps confirming the model highlights biopsy-learned patterns. In a 10x5 cross-validation, classifiers trained on these feature vectors improved overall sensitivity by 9.9 points (Stage I: +6.5 pts, II: +17.6 pts, III: +14.3 pts, IV: +9.5 pts) at 98.5% specificity, compared to classifiers trained on region-wide average methylation values. These performance improvements, coupled with the scalability of the framework, underscore its potential as a transformative tool in the early diagnosis of cancer and establish a foundation for training models on NGS data in other liquid biopsy assays. Future work will investigate the potential to incorporate per-read embeddings from DNA-based large language models, without sacrificing scalability.

#5467 Integrating intra- and inter-cell gene-gene interactions into deep omics data analysis for enhanced single-cell cancer biology.

Qingyue Wei[1], Sheng Liu[1], Chuanbao Zhang[2], Zixia Zhou[1], Wei Emma Wu[1], Md Tauhidul Islam[1], Lei Xing[1]

[1]Stanford University, Stanford, CA,[2]Beijing Tiantan Hospital, Capital Medical University, Beijing, China

Single-cell RNA sequencing (scRNA-seq) is widely used in cancer research to dissect tumor heterogeneity, characterize malignant and immune cell states, and identify dysregulated regulatory programs. However, accurately accounting the gene-gene interactions in cellular samples remains challenging due to the high dimensionality and nonstructured sequences of single-cell data. Existing Transformer-based approaches often rely on oversimplified gene-embedding strategies—such as ordering, coarse value binning, or direct value projection—that reduce biological resolution and overlook key regulatory dependencies. Moreover, most current methods emphasize intra-cell interactions while neglecting population-level patterns that are essential for understanding tumor microenvironmental regulation. To address these limitations, we propose a novel dual-branch Transformer framework that explicitly integrates intra-cell and inter-cell gene-gene interactions. The method comprises two complementary branches: (1) an intra-cell interaction branch that uses a Transformer augmented with interaction-aware embeddings to capture fine-grained regulatory relationships within individual cells based on graph-derived gene representations; and (2) an inter-cell interaction branch that applies a Vision Transformer (ViT) to image-based representations of single-cell profiles, spatially organized to reflect global gene-gene interaction structures across cell populations. A cross-attention module links the two branches, enabling coordinated learning between intracellular and intercellular regulatory signals. Extensive evaluation across diverse downstream tasks—such as cell-type classification, including cancer cell recognition and characterization; gene regulatory network inference; and protein abundance prediction—demonstrates that this interaction-aware architecture consistently outperforms state-of-the-art approaches. Notably, the framework achieves approximately a 30% average improvement in protein abundance prediction, a 4% improvement in cell-type classification accuracy, and a 4% improvement in gene regulatory network inference performance. By jointly capturing cell-intrinsic regulatory signals and population-level interaction patterns, the proposed framework offers a powerful computational strategy for dissecting tumor heterogeneity and characterizing regulatory interactions between malignant and microenvironmental cell populations.

#5468 Deep learning-based analysis reveals patient-level proton radiation therapy trajectories using single-cell PBMC chromatin images.

Hannah M. Schluter[1], Trinadha Rao Sornapudi[2], Dominic Leiser[3], Sandra Koller[2], Zeynep Karavelioglu[2], Caroline Uhler[1], Damien Weber[3], G. V. Shivashankar[4]

[1]Laboratory for Information and Decision Systems, Massachusetts Institute of Technology, Cambridge, MA,[2]Division of Biology and Chemistry, Paul-Scherrer Institute, Villingen, Switzerland,[3]Center for Proton Therapy, Paul-Scherrer Institute, Villingen, Switzerland,[4]Department of Health Sciences and Technology, ETH Zurich, Zurich, Switzerland

Introduction: The development of non-invasive, simple, and accurate methods to predict patient response to cancer therapy remains an open challenge. Proton radiation therapy (PRT) is increasingly used for hard-to-reach tumors or those in sensitive areas. However, it remains more expensive than other radiation therapies and while considered safer than conventional radiation therapy, its short- and long-term side effects are still not well explored. Therefore, developing an early measure for patient response is a critical research direction. Here we sought to test whether chromatin images of peripheral blood mononuclear cells (PBMCs) contain sufficient information to track patients' trajectories during and after PRT.
Methods: We collected blood samples at five timepoints (before, during, at the end of, and twice after PRT) from 150 patients across various cancers including Central Nervous System and Head & Neck cancers, and 50 healthy volunteers. PBMCs were isolated, stained with DAPI to label the DNA, and imaged with a confocal microscope. We applied machine learning methods to single-cell crops of the PBMCs to: 1) classify healthy vs. cancer patients, 2) derive patient-level similarity-to-healthy scores, and 3) predict patient trajectories. To account for the possibility that variation in PBMC proportions might be a key difference between healthy and cancer patients, we adopted a multiple-instance learning (MIL) approach. MIL is a form of weakly-supervised learning that automatically discovers which features and which cells are important within a collection of cells.
Results: By comparing chromatin images of PBMCs from cancer patients and healthy volunteers using our MIL framework, we identified cancer-specific alterations in PBMC chromatin architecture induced by tumor-derived signals in the bloodstream. Longitudinal tracking across five time points revealed three distinct patient subgroups. Patients whose PBMC profiles shifted toward greater similarity to healthy volunteers after therapy were less likely to experience disease recurrence. Furthermore, our MIL framework enabled prediction of patients' likelihood of returning to a healthy state after therapy, based solely on pre-treatment PBMC chromatin images, within the largest cancer type population in our study, Head & Neck cancer.
Conclusion: In summary, we demonstrated that simple chromatin images derived from liquid biopsies can serve as a non-invasive, easily obtained, and inexpensive biomarker for monitoring patient trajectories during PRT. This motivates further investigation of the use of PBMC chromatin images in the context of cancer screening and treatment monitoring, and more broadly in other disease contexts where PBMCs have been previously studied as potential biomarkers.

#5469 Data-efficient morphological deep learning for fine-grained Gleason grading based on AI-triaged 3D pathology.

Renao Yan[1], Gan Gao[1], Andrew Song[2], Huai-Ching Hsieh[3], Yujie Zhao[1], Cristina Almagro-Perez[4], Lawrence D. True[5], Faisal Mahmood[2], Priti Lal[6], Anant Madabhushi[7], Jonathan TC Liu[3]

[1]University of Washington, Seattle, WA,[2]Harvard Medical School, Boston, MA,[3]Stanford University, Palo Alto, CA,[4]Harvard-MIT Division of Health Sciences and Technology, Massachusetts Institute of Technology, Cambridge, MA,[5]Professor, Dept. of Pathology, University of Washington, Seattle, WA,[6]Pathology and Laboratory Medicine, University of Pennsylvania, Philadelphia, PA,[7]Emory University, Atlanta, GA

Prostate cancer risk assessment relies on 2D histology, which samples only a small portion of tissue and lacks 3D architectural context, often leading to ambiguities. Slide-free 3D pathology using open-top light-sheet microscopy provides volumetric views of intact biopsies, offering richer morphological information without destructive sectioning. Yet the massive scale of 3D datasets makes manual review impractical. Prior work has shown that AI-triage models can identify high-risk 2D sections within 3D pathology datasets for time-efficient pathologist review, but these models are trained on limited labeled datasets, and thus prone to overfitting, especially for fine-grained multiclass tasks (e.g., Gleason grading). To address this, we investigate whether data-efficient, segmentation-guided prototype learning can better capture morphological patterns for improved Gleason grading. To enable fine-grained Gleason grading under limited supervision, we developed SCOPE, a Segmentation-guided CrOss-slice PrototypE learning framework for 3D pathology. Prototype learning helps mitigate overfitting by mapping large numbers of patch features into compact prototype features, each of which represents a distinct tissue morphology. To adapt this paradigm to 3D pathology, we first pretrain on unlabeled 3D volumes to initialize prototypes that capture the broad morphological diversity of the cohort. We then use 3D segmentation masks as structural priors to guide prototype refinement. In addition to the prototype learning, we adopt a 2.5D multiple-instance learning (MIL) strategy that incorporates context from neighboring slices to improve the feature quality for each slice of interest. Aggregated prototype features from each slice are used to train classifiers for grading. To evaluate our approach, we applied SCOPE to a cohort of 59 prostate cancer patients with slice-level annotations (Gleason grades) established by consensus among three pathologists. Using a leave-one-out cross-validation protocol, our framework achieved an AUC of 0.819 for the fine-grained Gleason grading task (i.e., GG1, GG2, GG3, or GG > 3). In comparison, the baseline prototype learning model achieved an AUC of 0.699. We further quantified the contribution of each component in SCOPE, finding that segmentation-guided features contribute the most, followed by the 2.5D MIL formulation and clustering-based pretraining. In summary, SCOPE confirms that data-efficient, segmentation-guided prototype learning can capture fine-grained 3D morphological patterns that improve prostate cancer Gleason grading. By integrating clustering-based pretraining with segmentation-derived structural priors and a 2.5D MIL formulation, SCOPE delivers a high-performance, interpretable, and clinically actionable AI-triage tool for 3D pathology when labeled data is limited.

#5470 Low-magnification deep learning model for rapid HER2 status prediction from H&E whole-slide images.

Ziyu Su[1], Abdul Rehman Akbar[1], Usama Sajjad[1], Sansar Babu Tiwari[1], Elshad Hasanov[2], Arya Mariam Roy[3], Zaibo Li[1], Daniel G. Stover[4], Muhammad Khalid Khan Niazi[1]

[1]Department of Pathology, The Ohio State University Wexner Medical Center, Columbus, OH,[2]Internal Medicine, The Ohio State University Comprehensive Cancer Center, Columbus, OH,[3]Division of Medical Oncology, The Ohio State University Comprehensive Cancer Center, Columbus, OH,[4]Department of Medical Oncology, The Ohio State University Wexner Medical Center, Columbus, OH

Background: HER2 (human epidermal growth factor receptor 2) overexpression is a pivotal biomarker for breast cancer prognosis and targeted therapy selection. Conventional assessment requires immunohistochemistry (IHC) and/or in situ hybridization (ISH), which are costly, time-consuming, and constrained by limited tissue and resource availability. In contrast, hematoxylin-and-eosin (H&E) slides are routinely acquired for diagnosis. Leveraging deep learning to infer HER2 status directly from H&E whole-slide images (WSIs) could substantially streamline the diagnostic workflow and reduce cost. However, existing deep learning models typically operate at high magnifications, resulting in slow slide-level processing and high computational costs, which hinder scalability and limit their integration into real-time clinical workflows.
Methods: To predict HER2 overexpression directly from routine H&E whole-slide images (WSIs), we developed a streamlined deep-learning model tailored for low-magnification pathology images. The approach extracts meaningful histologic features from each slide and integrates them at the whole-slide level to generate a binary prediction of HER2 status (positive vs negative). Model development and validation were performed using the TCGA-BRCA dataset, applying a five-fold cross-validation strategy to ensure robustness and generalizability. In each fold, 467 WSIs were used for training and 145 for testing. HER2 status in TCGA was determined primarily by IHC, supplemented with ISH results.
Results: Our model achieved an AUC of 0.7280.029 and an F1-score of 0.6530.054. In comparison, the state-of-the-art deep learning model UNI2 achieved an AUC of 0.7150.010 and F1-score of 0.6270.036. Despite comparable accuracy, our model demonstrated markedly higher efficiency, processing 8.8 whole-slide images per minute—approximately 30 faster than UNI2—while requiring significantly less computational and storage resources.
Conclusions: This study highlights the potential of our deep learning model to predict HER2 status from low-magnification H&E WSIs. Our model's efficiency and scalability highlight its potential for integration into digital pathology workflows, enabling near real-time molecular screening without the need for additional staining or cloud-based computation. This level of efficiency further strengthens its suitability for real-world deployment, particularly in settings with high volume or limited computational resources. These findings support the feasibility of deep learning-driven virtual biomarker prediction as a practical step toward accessible, AI-assisted precision oncology.

#5471 Genie-ADLA: A deep learning algorithm for methylation-based multiple cancer early detection (MCED).

Kezhong Chen[1], Ziyu Li[2], Xiaojian Wu[3], Jian Huang[4], Guoyue Lv[5], Weiping Wen[6], Dahong Zhang[7], Xiangyu Zhao[8], Danbo Wang[9], Zhihua Liu[10], Lixin Sun[11], Shu Wang[12], Xiangnan Li[13], Zhigang Li[14], Jiandong Tai[15], Jiayin Yang[16], Zhentong Wei[17], Ming Cai[18], Qiang Zhang[9], Songbing He[19], Shuhua Yi[20], Shenhong Qu[21], Wenhui Zhao[22], Xianjun Yu[23], Ruixia Guo[13], Jianhong Lian[11], Desong Yang[24], Huaiwu Lu[25], Xi Guo[26], Yan Zhang[27], Zhuowei Liu[28], Yingjiang Ye[29], Chang Lin[30], Jie Gao[31], Xuanhui Liu[32], Yushu Guo[33], Suying Ding[13], **Guoqiang Zhao**[34], Yanzhan Yang[34], Jiangyu Li[34], Shiqing Chen[34], Hui Yu[34], Fang Liu[34], Yang Wang[34], Min Li[34], Baoliang Zhu[34], Yonghui Li[34], Xiaohui Wu[34], Fan Yang[1], Jun Wang[1]

[1]Thoracic Oncology Institute and Department of Thoracic Surgery, Peking University People's Hospital, Beijing, China,[2]Peking University Cancer Hospital and Institute, Beijing, China,[3]Department of General Surgery (Colorectal Surgery), The Sixth Affiliated Hospital, Sun Yat-sen University, Guangzhou, China,[4]The Department of Breast Surgery, Second Affiliated Hospital, Zhejiang University School of Medicine, Hangzhou, China,[5]Department of Hepatobiliary and Pancreatic Surgery, General Surgery Center, First Hospital of Jilin University, Changchun, China,[6]Department of Otolaryngology, The First Affiliated Hospital, Sun Yat-sen University, Guangzhou, China,[7]Urology & Nephrology Center, Department of Urology, Zhejiang Provincial People's Hospital (Affiliated People's Hospital), Hangzhou Medical College, Hangzhou, China,[8]Peking University People's Hospital, Peking Universtiy Institute of Hematology, Beijing, China,[9]Liaoning Provincial Cancer Hospital, Shenyang, China,[10]Cancer Hospital, Chinese Academy of Medical Sciences, Beijing, China,[11]Department of General Surgery, Shanxi Cancer Hospital, Taiyuan, China,[12]Breast Disease Center, Peking University People's Hospital, Beijing, China,[13]The First Affiliated Hospital of Zhengzhou University, Zhengzhou, China,[14]Department of Thoracic Surgery, Shanghai Chest Hospital, Shanghai Jiao Tong University School of medicine, Shanghai, China,[15]Department of Colorectal&anal Surgery, General Surgery Center, First Hospital of Jilin University, Changchun, China,[16]The Department of Liver Surgery of West China Hospital, Sichuan University, Chengdu, China,[17]Department of Obstetrics and Gynecology, The First Hospital of Jilin University, Changchun, China,[18]Department of Urology, The Second Affiliated Hospital, School of Medicine, Zhejiang University, Hangzhou, China,[19]The First Affiliated Hospital of Soochow University Department of General Surgery, Suzhou, China,[20]National Clinical Research Center for Blood Diseases, Institute of Hematology & Blood Diseases Hospital, Chinese Academy of Medical Sciences & Peking Union Medical College, Tianjin, China,[21]Department of Otolaryngology-Head and Neck Surgery, Guangxi Zhuang Autonomous Region People's Hospital, Nanning, China,[22]Harbin Medical University Cancer Hospital, Harbin, China,[23]Department of Pancreatic Surgery, Fudan University Shanghai Cancer Center, Shanghai, China,[24]Hunan Cancer Hospital & The Affiliated Cancer Hospital of Xiangya School of Medicine, Central South University, Changsha, China,[25]Department of Gynecologic Oncology, Sun Yat-Sen Memorial Hospital, Sun Yat-Sen University, Guangzhou, China,[26]Department of Urology, Hunan Provincial People's Hospital, the First Affiliated Hospital of Hunan Normal University, Changsha, China,[27]Department of Oncology, Shijiazhuang People's Hospital, Shijiazhuang, China,[28]Sun Yat-sen University Cancer Center, Guangzhou, China,[29]Department of Gastrointestinal Surgery, Peking University People's Hospital, Beijing, China,[30]Otorhinolaryngology Department of the First Affiliated Hospital of Fujian Medical University, Fuzhou, China,[31]Department of Hepatobiliary Surgery, Peking University Organ Transplantation Institute, Peking University People's Hospital, Beijing, China,[32]The Sixth Affiliated Hospital, Sun Yat-sen University, Guangzhou, China,[33]Health Management Center, Peking University People's Hospital, Beijing, China,[34]Shanghai Xiaohe Medical Laboratory Co. Ltd., Shanghai, China

Background: Methylation-based analysis of cell-free DNA (cfDNA) has emerged as a key technology for MCED. However, existing approaches rely on traditional machine learning algorithms, which inherently limit detection performance. With the rapid advancement of artificial intelligence (AI), we have developed Genie-ADLA, a deep learning algorithm designed specifically for MCED. By integrating state-of-the-art deep neural network architectures with the intrinsic patterns inherent in methylation data, Genie-ADLA significantly enhanced MCED performance.
Methods: Genie-ADLA was trained and evaluated on a dataset of 4,781 participants aged 40-75 years, including 2,702 pathologically confirmed cancer cases across 16 cancer types and 2,079 non-cancer controls (NCT06217900). The training set comprised 3,217 samples (1,756 cancer cases and 1,461 non-cancer controls), and the model's performance was evaluated on an independent test set of 1,564 samples (618 non-cancer controls and 946 cancer cases). To address challenges inherent to methylation data—high dimensionality, sparsity, and noise—we applied feature dimensionality reduction and embedding strategies, reducing computational burden, mitigating overfitting, and improving learning efficiency. An ensemble learning approach further strengthened robustness and generalization.
Results: Across all stages of 16 cancer types, Genie-ADLA achieved an overall sensitivity of 63.43% (600/946, 95% CI: [60.26%, 66.50%]) at 99.3% (612/618, 95% CI: [97.90%, 99.64%]) specificity in the test cohort. Compared with the XGBoost model trained on the same dataset, Genie-ADLA demonstrated improved overall sensitivity in 11 of the 16 cancer types, with an average increase of 4.86%.For stage I-III cancer patients, the sensitivities at 99.3% specificity showed notable gains over XGBoost: colorectal cancer achieved 76.98% (97/126, 95% CI: [68.65%, 84.01%]), an improvement of 9.52% from 67.46%; esophageal cancer reached 80.95% (51/63, 95% CI: [69.09%, 89.75%]), up 6.35% from 74.60%; breast cancer reached 37.14% (26/70, 95% CI: [25.89%, 49.52%]), improving by 5.71% from 31.43%. Lung cancer was subdivided into adenocarcinoma and non-adenocarcinoma, with stage I-III sensitivities of 40.90% (27/66, 95% CI: [28.95%, 53.71%]) in adenocarcinoma, an increase of 10.6%, and 84.44% (38/45, 95% CI: [70.54%, 93.51%]) in non-adenocarcinoma, improving by 2.22%.
Conclusions: Genie-ADLA, leveraging advanced deep neural network architectures and data processing strategies, substantially elevates the performance ceiling of methylation-based early cancer detection, offering a new paradigm for AI-driven cancer screening.

#5472 Deep learning reveals hidden pan-cancer drug signatures across the brain-gut axis through latent space modeling of 6.6 million single-cell perturbations.

Noha Samir Ismail[1], Kourosh Salehi-Ashtiani[2]

[1]New York University-Abu Dhabi / New York University-New York, Abu-Dhabi, NY,[2]New York University-Abu Dhabi, Abu Dhabi, United Arab Emirates

The brain-gut axis represents a bidirectional communication network increasingly recognized in cancer pathogenesis, yet shared therapeutic vulnerabilities between brain and gastric cancers remain unexplored. We applied deep learning on massive single-cell data to discover the drugperturbation signatures that elicit concordant responses across both tumor types.

We trained a Compositional Perturbation Autoencoder (CPA) on 6.6 million single-cell RNA-sequencing profiles from four cancer cell lines: two brain glioblastomas (A-172, H4) and two gastric carcinomas (KATO III, SNU-1), treated with 332 drugs from the Tahoe-100M dataset. The model compressed high-dimensional transcriptional responses into 128-dimensional latentrepresentations, capturing the complex drug-specific transcriptional perturbation signatures while removing confounders through adversarial training. We computed cross-tissue similarity scores between brain and gastric cancer responses in a learned latent space, capturing complex nonlinear patterns. Additionally, non-Negative Matrix Factorization (NMF) was applied todiscover data-driven pathway modules, and Gene Set Enrichment Analysis (GSEA) validated biological convergence using MSigDB pathway databases.

The model achieved a validation R^2 of 0.74 for gene expression prediction, with effective disentanglement of biological and technical confounders. We identified 49 pan-cancer drug candidates exhibiting high cross-tissue concordance (similarity > 0.7), including FDA-approved agents and investigational compounds. Top candidates included Erythromycin (similarity 0.752), Lonafarnib (0.747), and Capmatinib (0.742), exhibiting pathway module similarity of (0.78- 0.79). Furthermore, NMF revealed 15 latent pathway modules, with modules 7 and 15 significantly enriched in pan-cancer candidates (Spearman $\rho = 0.118$, $p < 0.05$). GSEAconfirmed convergence on inflammatory (NF-κB/IL-6), proliferation (RAS/MAPK), and survival (MET/mTOR) pathways (FDR < 0.05).

This work establishes a framework for discovering shared therapeutic vulnerabilities across anatomically distinct cancers in the brain-gut axis. The identified pan-cancer signatures provide mechanistically validated candidates for repurposing and rational combination therapy development in both brain and gastric malignancies. Deep learning enabled critical capabilities impossible with traditional bioinformatics:(1) automatic confounder removal via adversarial training, (2) discovery of functional drug similarity in compressed latent space capturing nonlinear response patterns, (3) unsupervised pathway module identification from learned representations. This enables mechanism-agnostic discovery of clinically validated pan-cancer therapeutics. AI tools were used in data analysis and editing this abstract.

#5473 A deep learning framework for extracting comprehensive single-cell biophysical profiles from brightfield images.

Nicholas Calistri, Selim Olcum, **Robert Kimmerling**, Steven Wasserman, Rachel LaBella, Madeleine Vacha, Katelin Katsis, Reginald Aikins, Maria Ssozi

Travera, Medford, MA

Single-cell biophysical measurements including mass, volume, density, and morphology provide a highly integrative readout of cellular state. We have previously demonstrated that these measurements enable rapid assessment of tumor cell drug response and immune cell functional fitness. As part of a CLIA-certified workflow with a two-day reporting turnaround, this approach enables clinically actionable decision support across diverse solid tumor malignancies and prediction of immune checkpoint blockade response. However, the complex instrumentation and expert operation required for these multiparametric measurements confine their use to CLIA laboratories as LDTs, limiting accessibility in community hospitals and deployment to large diagnostic networks. Here we describe a deep learning approach that estimates single-cell biophysical properties from brightfield imaging data alone. Specifically, we trained a Vector Quantized Variational Autoencoder (VQ-VAE) based model using more than 20 million paired multiparametric measurements as ground truth. This training data linked measurements of single-cell mass, volume, density, and morphological features extracted from inline brightfield images for each individual cell. The model was trained to minimize prediction error for biophysical measurements from images alone, creating a framework where simple imaging can serve as a proxy for comprehensive biophysical profiling. The biophysical inference model accurately predicted single-cell mass (RMSE < 2pg) and volume (RMSE < 15fL) from brightfield images with an R^2 >0.95, exceeding the performance of existing gold-standard instrumentation.

When deployed alongside our multiparametric platform, biophysical inference increased single-cell throughput more than 50-fold while maintaining measurement concordance. Notably, image-only predictions of immune cell activation readout, previously shown to predict neoadjuvant ICB response, achieved 95% accuracy, functionally equivalent to direct biophysical measurements in our CLIA-validated workflow.

This work establishes a paradigm for inferring quantitative biophysical properties from brightfield microscopy, bridging high-content single-cell biophysics with scalable imaging workflows. Unlike existing approaches relying on large patient cohorts to correlate high-dimensional features with outcomes, our framework uses experimentally measured biophysical parameters as interpretable intermediates linking images to patient response. Millions of single-cell measurements acquired rapidly and inexpensively provide an efficient training foundation. Furthermore, the framework enables tiered deployment: core laboratories use the full multiparametric platform for measurements and model training, while peripheral sites deploy low-cost imaging for routine applications.

#5474 Dyna-Q Reinforcement Learning for breast tumor malignancy classification using phantom-trained models applied to human data.

Chang-hee Won[1], Arpita Das[1], Dina Caroline[2]

[1]Electrical and Computer Engineering, Temple University, Philadelphia, PA,[2]Radiology, Temple University Hospital, Philadelphia, PA

Background: Obtaining large, well-annotated human datasets remains one of the major barriers to progress in biomedical AI. Ethical restrictions, patient burden, and institutional review processes limit access to clinical samples, making it difficult to train generalizable machine learning models. This issue is particularly acute in histopathology and tumor classification studies. Building on the concept of phantom-to-human transfer learning demonstrated by Das et al. (IEEE Sensors 2024), we propose a new Dyna-Q reinforcement learning framework that leverages tactile sensing to assess tumor malignancy. The model is trained exclusively on phantom data and applies a zero-shot knowledge transfer strategy to unseen human datasets, using interpretable mechanical features as the bridge between synthetic and biological domains.
Methods: In this study, we utilized a Tactile Sensing System to generate images correlated with the mechanical properties (size, depth, and elasticity) of breast tumors. Tactile data were first collected from breast phantoms. Using these data, we developed a deep Dyna-Q learning model for tumor classification. A deep neural network served as the decision-making agent and was trained in a self-supervised manner to classify tumor malignancy. The training process relied exclusively on phantom-derived tactile features of breast tumors, using a total of 9,000 balanced phantom data samples. Subsequently, we collected tactile data from 40 human patients. The trained deep Dyna-Q reinforcement learning model was then tested directly on the unseen human data to classify breast tumor malignancy, with pathology results serving as the ground truth.
Results: Despite the inherent domain gap between phantom models and human tissue, our approach achieved promising performance: an overall accuracy of 76.5%, sensitivity of 62.9%, and specificity of 73.5%. These findings indicate that clinically meaningful signals can be transferred across domains using tactile features, even without direct human training samples. By eliminating the need for retraining human data, this method substantially reduces reliance on scarce clinical datasets and offers a scalable solution for early-stage diagnostic modeling.
Conclusions: This study highlights the feasibility of a tactile, reinforcement learning-based AI system for tumor classification in data-limited biomedical settings. By exploiting phantom data as a training substrate, the approach minimizes dependence on scarce clinical samples and provides an ethical, scalable framework for early diagnostic modeling. Beyond breast cancer, this paradigm could be extended to other organ systems where tissue-mimicking phantoms are available, offering a practical path toward cost-effective and generalizable AI-driven diagnostics.

#5476 GLEAM: Democratizing high-quality machine learning for cancer research.

Paulo Cilas Morais Lyra Junior[1], Junhao Qiu[1], Khai Dang[1], Alyssa Pybus[1], Maansi Singh[1], Qiang Gu[2], Luke Sargent[2], Allison L. Creason[2], Jeremy Goecks[1]

[1]Moffitt Cancer Center, Tampa, FL,[2]Knight Cancer Institute, Oregon Health & Science University, Portland, OR

Machine learning (ML) has revolutionized biomedical research, enabling accurate prediction from large and often high-dimensional datasets through statistical modeling and pattern recognition. Examples of ML applications include predicting patient responses to cancer therapies and classifying cancer lesions. However, the lack of accessible, well-structured guidance on how to develop, validate, and communicate ML models continues to limit their routine and effective use in research. To address this gap, we introduce the second-generation ML toolkit for the Galaxy platform, a widely used bioinformatics workbench. Named Galaxy Learning and Modeling (GLEAM), it is built around four core principles that target critical barriers in cancer research: no-code accessibility through a web interface; adherence to best practices via standardized setups and reports; reproducibility by recording parameters, data versions, environments, and workflows; and scalability through native Galaxy integration. Our goal is to provide end-to-end ML tools that enable researchers to configure, run, evaluate, and share publication-ready analyses. GLEAM integrates three learner tools: (1) Tabular Learner for structured data, (2) Image Learner for pixel-based inputs, and (3) Multimodal Learner for heterogeneous data. The AutoML backends are PyCaret, Ludwig, and AutoGluon, respectively. Users supply datasets, labels, and optional metadata, and GLEAM automates preprocessing, feature extraction, algorithm selection, hyperparameter tuning, and cross-validation. As a proof of concept, we reproduced results from published studies using GLEAM tools by running their publicly available datasets and comparing model metrics to benchmark tool quality. On the HAM10000 dermoscopy dataset, the Image Learner, using a deep-learning model, achieved accuracy 0.86 (vs. 0.86 in published models), precision 0.85 (vs. 0.88), recall 0.85 (vs. 0.85), and F1 score 0.85 (vs. 0.86), matching state-of-the-art outcomes for skin lesion classification on this dataset. On the LORIS immunotherapy-response dataset, the Tabular Learner achieved accuracy 0.80 (vs. 0.70), AUC 0.76 (vs. 0.75), and PR-AUC 0.55 (vs. 0.56), demonstrating robust prediction of treatment response. Using the HANCOCK dataset to predict survival in head and neck cancer, the Multimodal Learner achieved an ROC AUC of 0.74 (vs. 0.79). This modest decrease reflects a different modeling strategy, in which two engineered structured modalities were replaced with raw image and plain-text inputs, substantially reducing preprocessing complexity while maintaining competitive predictive performance. By embedding the GLEAM toolkit within Galaxy, we shift the focus from tool development to knowledge extraction. As a result, the framework produces high-quality, transparent, and shareable models that accelerate data-driven discovery and support cancer research.

#5477 AI-driven *de novo* design of miniproteins targeting mutant p53 peptide-MHC-I complex for cancer immunotherapy.

Fengze Jin, Puja Singh, Hanyong Chen, Christopher Warlick, **Yibin Deng**

Department of Urology, University of Minnesota Medical School, Minneapolis, MN

Genetic alterations in the tumor suppressor p53 occur in nearly every type of human cancer, with mutation rates ranging from 10% to nearly 100%, averaging about 50% in cancer patients. Over 80% of these mutations are missense mutations in the p53 DNA-binding domain (DBD), with the p53-R175H mutation being the most common "hot spot," occurring in approximately 5% of p53-mutated cases. Clinically, p53-R175H mutation in cancer patients are significantly associated with decreased overall survival compared to cancer patients with wild-type p53. Biologically, missense mutations in the p53 gene, particularly "hot-spot" mutations, including p53-R175H, result in the high expression of mutant p53 protein in cancer cells. These features suggest that expression of mutant p53-R175H protein could serve as an attractive therapeutic target. However, targeting the intracellular oncoprotein mutant p53-R175H has proven extremely challenging and remains a major unmet need in cancer therapy. Interestingly, the mutant p53-R175H protein can be processed by the proteasome into a 9-mer peptide, presented on the cancer cell surface by human leukocyte antigen (HLA)-A*02:01, a common major histocompatibility complex (MHC) class I allele in the U.S. population (40%), providing a “unique” target for immunotherapy by harnessing immune cells—such as T cells—to eliminate cancer cells carrying mutant p53R-175H. Traditional efforts to develop T cell receptors (TCRs) or monoclonal antibodies (mAbs) against the peptide-MHC-I complex have largely failed due to low affinity, limited specificity, and multi-year development timelines. Recent advances demonstrate that artificial intelligence (AI)-designed miniproteins (less than 150 amino acids) targeting peptide-MHC class I complexes can be engineered into chimeric antigen receptor (CAR)-T cells, enabling robust T-cell activation and potent recognition and elimination of tumor cells. To accelerate the discovery of miniprotein-mediated therapeutics, we have developed and integrated multiple AI-driven platforms for *de novo* design of p53-R175H peptide-MHC-I-complex binding miniproteins, including diverse backbone generation, protein sequence optimization, and enhanced high-throughput computational screening of peptide-MHC-I-miniprotein complexes. Top candidates have undergone, or are currently undergoing, experimental validation as engineered T/NK cell engagers and CAR-T/NK cells to kill cancer cells. In summary, our integrated AI-driven framework enables rapid and personalized cancer immunotherapy by transforming previously “undruggable” intracellular oncoproteins—including, but not limited to, mutant p53—into actionable immunotherapeutic targets.

#5478 Benchmarking gene expression foundation models on bulk RNA-Seq data.

Jong Hyun Kim[1], Sunwoo Yu[1], Soonyoung Lee[1], Tae Hyun Hwang[2], Jongseong Jang[1], Janghyeon Lee[1]

[1]Bio Intelligence Lab, LG AI Research, Seoul, Korea, Republic of,[2]Department of Surgery, Vanderbilt University Medical Center, Saint Johns, FL

Introduction: Recent advances in single-cell RNA (scRNA) foundation models have enabled large-scale learning of gene-gene relationships across cell types. Although these models are pre-trained on single-cell data, many studies have begun applying them to bulk RNA-seq datasets, assuming cellular level representations can generalize to tissue data. However, no systematic benchmark has evaluated whether scRNA-based foundation models truly generalize to bulk RNA-seq data or how their performance compares with models trained on bulk data. Here, we systematically evaluate gene expression foundation models for transferability and distributional bias between single-cell and bulk RNA-seq data using TCGA.

Methods: We compared publicly available models with released weights, including six single-cell models (CellFM, GeneFormer, scBERT, scFoundation, scGPT, and scLong) and BulkFormer, a model trained on bulk RNA-seq data. Embeddings were extracted following each model's published procedures. When not specified, average pooling over valid gene tokens was applied. Gene expression inputs were normalized according to each model's original preprocessing. Hyperparameter were tuned, and the best configuration was used for final evaluation. Performance was assessed via linear probing on fixed embeddings for two downstream tasks: gene mutation classification and survival prediction. Classification and survival tasks were evaluated using AUROC and C-index, respectively. Results were averaged across ten random data splits.

Results: In pan-cancer mutation prediction tasks involving six biomarker genes, CellFM achieved the highest performance (0.870 ± 0.053), followed by scFoundation (0.858 ± 0.056) and BulkFormer (0.827 ± 0.058). GeneFormer (0.822 ± 0.060) and scGPT (0.673 ± 0.077) showed moderate generalization (0.81-0.82), while scBERT (0.614 ± 0.054) and scLong (0.597 ± 0.053) exhibited limited transferability. A consistent trend was observed in subtype-specific mutation tasks across BRCA, COAD, LUAD, and RCC, where CellFM and scFoundation maintained the top performance, followed by BulkFormer. In survival prediction across 14 cancer types, scFoundation (0.672 ± 0.081) and CellFM (0.665 ± 0.078) achieved the best overall performance, comparable to BulkFormer (0.839 ± 0.086). While scBERT (0.599 ± 0.054) and scLong (0.589 ± 0.052) showed limited generalization.

Conclusion: In conclusion, models that effectively learn gene-gene interactions during pretraining can generalize across bulk RNA-seq data despite distributional differences. This suggests that the key to cross-domain performance lies not in model size or data scale, but in how well biological relationships are captured within learned representations. These results highlight the importance of biologically grounded pretraining for achieving robust generalization across transcriptomic domains.

#5479 Optical spectral fingerprinting for anthracycline detection in synthetic clinical biofluids.

Atara R. Israel[1], Yunjung Kim[2], Adnan Arnaout[1], Myesha Thahsin[1], Yumna Ahmed[1], Zachary Cohen[1], Amelia Ryan[1], Syeda Rahman[1], Mijin Kim[3], Ryan Williams[4]

[1]Biomedical Engineering, City College of New York, New York, NY,[2]Chemistry, Hanyang University, Seoul, Korea, Republic of,[3]Chemistry and Biochemistry, Georgia Institute of Technology, Atlanta, GA,[4]Stony Brook University, Stony Brook, NY

Anthracyclines, commonly used as chemotherapies, are highly effective at inducing apoptosis in cancer cells but also affect healthy cells; cardiotoxicity being a major side effect of chemotherapy administration as anthracyclines accumulate in cardiac tissue. The inability to monitor their accumulation in vivo in a noninvasive, rapid, and continuous manner presents a challenge in early diagnosis of cardiotoxicity and therapeutic drug monitoring of anthracyclines. While there are established guidelines for dosing this class of drugs, the high interpatient variability coupled with variable pharmacology make it difficult to gauge when cardiotoxicity may begin developing. To reduce this risk and more effectively understand these drugs' pharmacology, we developed fluorescent nanosensors using single walled carbon nanotubes (SWCNT) that can rapidly and continuously monitor anthracycline accumulation in a concentration-dependent manner. SWCNT have the innate ability to fluoresce stably in the near infrared region, which is tissue-transparent. Several species of fluorescent SWCNT exist due to structural chirality which have independent excitation/emission wavelengths. SWCNT are dispersed with ssDNA for individual dispersion, which imparts hydrophilicity and fluorescence, and promotes interaction with anthracyclines. To create chemical library diversity, multi-species SWCNT were dispersed with 12 unique ssDNAs and challenged with four anthracyclines: daunorubicin, doxorubicin, epirubicin, and idarubicin, at concentrations ranging from 0.1-100 μM. Using spectral fingerprinting, spectral changes and ssDNA-SWCNT pairings were analyzed using principal component (PCA) analysis to determine which factors most contributed to anthracycline detection. PCA differentiated sensor responses above 5 μM and provided insight into which ssDNA-SWCNT species combinations were best suited for detecting each anthracycline. Further analysis using binary classification was done using machine learning models k-nearest neighbor (k-NN) and support vector machine (SVM) to determine the accuracy of classifying each anthracycline's concentration-based spectral changes in buffer and synthetic biofluids. We found that the models were strongly predictive for detection of daunorubicin and idarubicin, exhibiting 100% cross validation, test accuracy, and validation in synthetic biofluids. Multi-class classification distinguished anthracycline type by spectral fingerprint, with 100% accuracy using Decision Tree and eXtreme Gradient Boosting. Future work will use these ssDNA-SWCNT species combinations to develop a noninvasive therapeutic drug monitoring tool to monitor accumulation at the tumor and in the heart during chemotherapy. We anticipate this work leading to a tool to improve tolerance for anthracycline chemotherapy by establishing personalized pharmacological treatment windows.

#5480 Artificial intelligence-designed peptide PROTACs suppress TNBC by regulating PD-L1 palmitoylation.

Miao Liu

Harvard Medical School/MIT, Boston, MA

Background: Triple-negative breast cancer (TNBC) responds poorly to immune checkpoint blockade (ICB), partly due to sustained PD-L1 expression on tumor cells. PD-L1 palmitoylation enhances its membrane stability and limits internalization, contributing to immune evasion. Modulating PD-L1 palmitoylation therefore represents an attractive strategy to overcome ICB resistance. Here, we developed an Artificial Intelligence-designed peptide PROTAC platform to regulate PD-L1 palmitoylation and restore anti-tumor immunity in TNBC.
Methods: Using an Artificial Intelligence-guided structural peptide-design workflow, we generated membrane-permeable peptide PROTACs composed of: (1) a high-affinity DHHC3-binding peptide, (2) a cell-penetrating peptide module, and (3) a small-molecule E3 ligase ligand. TNBC models (MDA-MB-231 and 4T1) were used to evaluate the effects of these degraders on DHHC3 levels, PD-L1 palmitoylation, PD-L1 expression, T-cell activation, apoptosis, and in vivo antitumor efficacy.
Results: The lead Artificial Intelligence-designed degrader efficiently reduced DHHC3, leading to substantial suppression of PD-L1 palmitoylation and marked downregulation of PD-L1 protein at nanomolar concentrations. In vitro, the degrader significantly enhanced T-cell-mediated cytotoxicity and increased IFN-γ and TNF-α secretion. In ICB-resistant 4T1 TNBC models, systemic administration of the peptide PROTAC resulted in strong tumor growth inhibition, outperforming PD-L1 monoclonal antibodies and small-molecule PD-L1 inhibitors. Tumor tissues showed increased apoptosis, reduced Ki67, robust loss of PD-L1, and no detectable systemic toxicity.
Conclusions: Artificial Intelligence-designed peptide PROTACs effectively suppress TNBC by regulating PD-L1 palmitoylation. This strategy expands the therapeutic potential of targeted protein degradation and provides a promising approach for highly aggressive and treatment-refractory TNBC.

#5481 Learning the mechanisms of chemotherapy response using a pathway-informed transformer.

Zach Wallace[1], Ingoo Lee[2], Nicole M. Mattson[2], Sungjoon Park[3], Akshat Singhal[4], Xiaoyu Zhao[2], Trey Ideker[2]

[1]UC San Diego, La Jolla, CA,[2]University of California San Diego - UCSD, La Jolla, CA,[3]UC San Diego School of Medicine, La Jolla, CA,[4]UCSD Medical Ctr., San Diego, CA

Predicting how a cancer patient will respond to chemotherapy remains challenging, as the molecular determinants of drug sensitivity and resistance are incompletely understood. Advances in interpretable AI and transformer-based modeling offer an opportunity to improve prediction while revealing deeper mechanistic insight. Here, we introduce the *Drug Response Pathway-Informed Transformer (DRPT)*, a hierarchical graph transformer that accurately predicts and explains response to 12 replication-stress-inducing chemotherapies. DRPT learns signals beyond broad genomic burdens such as copy-number alteration load and tumor mutation burden, identifying 37 systems and 206 genetic alterations that govern drug response. Prominent drivers include transcriptional regulation (ASXL1, DNMT3B, TOP1, ZNF217), cell-cycle control (AURKA, CDKN2B, CDK6), and DNA-damage response (CDKN2A, PMS2, TP53), alongside unexpected contributors in extracellular matrix organization (FGF10, DMD), particularly for topoisomerase inhibitors such as doxorubicin, etoposide, and camptothecin. Using patient cohorts from TCGA and MSK-CHORD, we validate DRPT's predictive power, demonstrating significant stratification of survival outcomes across pan-cancer and subtype-specific settings. Overall, this work shows that pathway-informed graph transformers can both reliably predict chemotherapy response and reveal mechanistic biomarkers that may guide precision oncology.

#5482 MethylFM: A DNA methylation foundation model for modeling epigenomic regulatory dynamics.

Limeng Pu, Xiang Chen

St. Jude Children's Research Hospital, Memphis, TN

DNA methylation regulates gene expression, differentiation, and disease, making it a key target for computational modeling in precision medicine. To integrate high-resolution whole-genome bisulfite sequencing (WGBS) data into a unified analytical framework, we developed MethylFM, a transformer-based foundation model that captures context-aware methylation patterns and supports multiple downstream tasks.We trained on the BLUEprint Epigenome dataset, comprising single-base WGBS profiles across diverse blood cell types with matched histone modification and transcriptome data. By focusing on ±100 CpG sites around transcription start sites (TSS), MethylFM targets regulatory regions central to gene expression and chromatin dynamics. Built on a BERT-style transformer with rotary positional embeddings and a masked-value prediction objective, it learns robust representations capturing both local and long-range dependencies in methylation.MethylFM demonstrated versatility across three downstream applications. For CpG-level imputation, it reconstructed high-resolution WGBS profiles from 450k array data with strong accuracy ($R^2 > 0.6$, MAE < 0.15). When benchmarked against METHimpute, evaluation was restricted to two samples due to METHimpute's intensive runtime; nonetheless, MethylFM achieved slightly higher accuracy ($R^2 = 0.518$ vs. 0.513), underscoring both precision and computational efficiency. In TSS-level H3K27ac prediction, the model reached $R^2 = 0.614$, matching the state-of-the-art M2A ($R^2 = 0.617$) and highlighting its capacity to infer promoter activity directly from DNA methylation. Finally, sample-level clustering based on predicted H3K27ac profiles accurately recapitulated hematopoietic lineages, surpassing experimental H3K27ac data (Silhouette = 0.47 vs. 0.30) and approaching RNA-seq-derived clustering performance (Silhouette = 0.51), demonstrating that MethylFM captures biologically meaningful epigenetic structure. Together, these results establish MethylFM as a generalizable and efficient framework for epigenomic modeling, enabling cost-effective methylation imputation, promoter activity prediction, and cellular identity characterization to advance biomarker discovery and precision medicine.

#5483 Revealing dynamic temporal trajectories and underlying regulatory networks with Cflows.

Shabarni Gupta[1], Xingzhi Sun[2], Alexander Tong[2], Manik Kuchroo[2], Dhananjay Bhaskar[2], Chen Liu[2], Aarthi Venkat[2], Beatriz P. San Juan[1], Laura Rangel[1], Vanina Rodriguez[1], John G. Lock[3], Christine Louise Chaffer[1], Smita Krishnaswamy[2]

[1]Garvan Institute of Medical Research, Darlinghurst, Australia,[2]Yale University, New Haven, CT,[3]University of New South Wales, Sydney, Australia

While single-cell technologies provide snapshots of tumor states, building continuous trajectories and uncovering causative gene regulatory networks remains a significant challenge. We present Cflows, an AI framework that combines neural ODE networks with Granger causality to infer continuous cell state transitions and gene regulatory interactions from static scRNA-seq data. In a new 5-time point dataset capturing tumorsphere development over 30 days, Cflows reconstructs two types of trajectories leading to tumorsphere formation or apoptosis. Trajectory-based cell-of-origin analysis delineated a novel cancer stem cell profile characterized by $CD44^{hi}EPCAM^{+}CAV1^{+}$, and uncovered a cell cycle-dependent enrichment of tumorsphere-initiating potential in G2/M or S-phase cells. Cflows uncovers ESRRA as a crucial causal driver of the tumor-forming gene regulatory network. Indeed, ESRRA inhibition significantly reduces tumor growth and metastasis in vivo. Cflows offers a powerful framework for uncovering cellular transitions and dynamic regulatory networks from static single-cell data.

#5484 Designing ATP-gated proteins for tumor selective drug delivery.

Angela Mei[1], Azim Dharani[2], Jody Mou[2], Benjamin Fry[2], Nicholas Polizzi[2]

[1]Departments of Computer Science and Chemistry and Chemical Biology, Harvard College, Cambridge, MA, [2]Department of Cancer Biology, Dana-Farber Cancer Institute, Boston, MA

Chemotherapy remains limited by lack of specificity in many existing treatments, motivating the need for therapeutic strategies that exploit molecular features unique to the tumor microenvironment (TME). A defining hallmark of the TME is the elevated concentration of extracellular ATP (eATP), which can rise ~1000-fold from nanomolar levels in healthy cells to ~100 μM in tumors. eATP promotes tumor growth and immune evasion, making it an attractive biochemical feature for tumor targeting. In this work, we used state of the art deep learning-based protein design methods to generate scaffolds capable of selectively binding ATP and experimentally validated their binding as an initial step toward developing ATP-gated systems for tumor-specific drug delivery. To accomplish this, we adapted our lab's Neural Iterative Selection and Expansion (NISE) workflow, which integrates deep learning-based sequence design and structure prediction. In this framework, ATP was first docked into candidate protein scaffolds to define the binding-site geometry. A sequence design model then generated amino acid sequences predicted to fold into stable structures accommodating the positioned ligand, after which a structure prediction network modeled the complex to assess self-consistency between the designed sequence and structure. The designed sequences were then filtered based on high structural similarity (indicating designability) and high confidence (reflecting complex plausibility), and top-performing designs were used as input for the next round of sequence generation. Across twenty NISE refinement cycles, the algorithm progressively enriched for protein-ATP complexes by optimizing the joint space of sequence, structure, and ligand conformation. The workflow ultimately produced ~2,600 candidate complexes, from which a small set of high-quality designs were selected for experimental validation. The designs were tested using NMR spectroscopy. One top construct displayed ^{1}H-chemical-shift perturbations upon ATP titration ($K_d \approx 250$ μM), consistent with the predicted isoleucine-adenine stacking interaction. Subsequent design rounds aimed to increase affinity by introducing features observed in natural ATP-binding proteins such as π-π stacking and expanded hydrogen-bonding motifs. In addition, the candidate protein structures were modified from 4-helix to 7-helix bundles to expand and solvate the binding pocket, enhancing hydrogen bonding, electrostatic complementarity, and water-mediated interactions. Together, these efforts represent the first step toward developing ATP-gated protein systems that can serve as tumor-selective drug delivery platforms, reducing the side effects commonly associated with chemotherapy in future applications.

: Machine Learning for Image Analysis
Poster Session

#5488 Inferring tissue element identities from sample-level compositional data in cancer.

Georgios Asimomitis[1], Kevin M. Boehm[1], Konstantinos Liosis[1], Armaan Kohli[1], Tom Pollard[1], Andrew Aukerman[1], Arfath Pasha[1], Anika Begum[1], Lora H. Ellenson[2], Jinru Shia[2], Hong A. Zhang[2], Nikolaus Schultz[1], Sohrab P. Shah[1], Francisco Sanchez-Vega[1]

[1]Halvorsen Center for Computational Oncology, Memorial Sloan Kettering Cancer Center, New York, NY,[2]Department of Pathology & Laboratory Medicine, Memorial Sloan Kettering Cancer Center, New York, NY

The relative abundance of cellular and structural components in cancer tissues reflects disease biology and outcomes. High-throughput technologies, e.g., digital pathology and single-cell transcriptomics (scRNA-seq), profile tissue regions or cells, revealing the heterogeneous building blocks (elements) that comprise bulk phenotypes. Yet, translational applications increasingly demand that models not only infer sample-level distributions but also provide element-level characterizations (e.g., of specific histology regions, cells) that explain tumor macroscopic behavior. Achieving such granularity from sample-level compositional data without laborious annotations remains a challenge, requiring models capable of connecting local properties to global phenotypes. Existing methods, using attention to weight element contributions to sample-level predictions, lack probabilistic grounding and biological interpretability; thus, have limited utility in clinical settings.

Here, we explicitly model sample-level compositional constraints with element-level assignments using Optimal Transport (OT). Particularly, we introduce *Composer*, a domain-agnostic dual-task machine learning model trained without element-level annotations to 1) estimate sample-level compositions, and, 2) importantly infer element labels as interpretable compositional allocations.

The model's performance was evaluated across data modalities, cancer types, and tasks. We highlight 3 concepts:

a) Tissue type classification on whole-slide images (WSIs): On 60 hematoxylin & eosin (H&E) WSIs from high-grade serous ovarian cancer (HGSOC, Boehm et al. 2022), *Composer* predicted the overall WSI tissue composition (Jensen-Shannon divergence (JSD): 0.26; mean absolute error: 0.11), classifying correctly (AUROC 0.98) the tissue type (tumor, stroma, necrosis, adipose, other) of individual regions within WSIs without training on regional annotations.

b) Tumor segmentation on WSIs: On 185 H&E WSIs spanning HGSOC, breast, and colorectal cancers (MSKCC), *Composer* estimated the overall tumor fraction per WSI (JSD 0.12; MAE 0.15), distinguishing efficiently tumor from non-tumor regions (AUROC 0.91) within WSIs.

c) Single-cell type annotation in scRNA-seq: Using 156 scRNA-seq HGSOC samples (Vazquez-Garcia et al. 2022), *Composer* not only inferred bulk cell type distributions (JSD: 0.15; MAE: 0.06), but also accurately classified (AUROC: 0.97) individual cells to their designated type (T cells, monocytes, fibroblasts, cancer cells, other).

In summary, the proposed OT-based weakly supervised framework provides an effective approach for linking element-level representations to sample-level compositional profiles in cancer. Its applicability across data analyses empowers spatial and molecular characterization of tumor ecosystems, biomarker quantification, and potential applications to precision oncology.

#5489 Multi-scale foundational AI descriptors enable accurate tumor localization in digitized renal cell carcinoma pathology.

Sahil Kapadia[1], **Brennan Flannery**[2], Satish Viswanath[3]

[1]Department of Neuroscience, University of North Carolina at Chapel-Hill, Chapel-Hill, NC,[2]Department of Biomedical Engineering, Case Western Reserve University, Cleveland, OH,[3]Department of Biomedical Engineering and Pediatrics, Emory University, Atlanta, GA

Background: Renal cell carcinoma (RCC) diagnosis relies on accurate tumor localization on pathology whole slide images, but suffers from substantial inter-observer variability, which can impact treatment selection. Recent advances in digital pathology AI tools have resulted in foundation models (FMs) that are trained on diverse H&E images to learn patterns of tissue morphology. However, the performance of these models has been evaluated at a single scale, whereas clinical pathology evaluation leverages multiple scales and magnifications. Our objective was to develop and validate multi-scale pathology FM signatures for tumor localization in renal cancers.
Methods: H&E-stained whole slide images of RCC were curated from a public repository. For each case, tissue regions were sampled at three histologic scales (5×, 10×, and 20× magnification). Using the pathology FM MUSK, quantitative representations of tissue morphology were generated from each region and at each scale, and a supervised classifier trained on available pathologist annotations was used to discriminate tumor from non-tumor tissue. A multi-scale signature was constructed by integrating feature representations across all three magnifications for each region. We confirmed our findings using additional FMs (CONCH, HOPTIMUS) and by comparing against models trained at individual magnifications.
Results: A total of 118 slides (2 institutions) were included, split by patient into training (n = 94) and hold-out validation (n = 24) sets. Slides were sampled to yield 300,000+ labeled tiles (~112,000 tumor and ~222,000 non-tumor). The multi-scale MUSK model yielded the best overall accuracy for discriminating tumor versus benign tissue in hold-out validation (AUC ~0.95; accuracy ~0.89). By comparison, MUSK models at individual magnifications performed markedly worse (AUC ~0.90 to 0.92; accuracy ~0.82 to 0.85). Models trained using CONCH and HOPTIMUS demonstrated similar trends, with multi-scale models achieving AUC ~0.94 and accuracy ~0.89 that were improved relative to single magnification models (AUC ~0.91, accuracy 0.81-0.84).
Conclusions: Integrating foundation model representations across multiple scales and magnifications yields accurate tumor localization of RCC on digital pathology. These findings will be validated in larger RCC cohorts and evaluated for impact on treatment selection.

#5490 Scalable and interpretable multimodal AI: Integrating imaging and genomics via image-based encodingfor cancer and disease classification.

Sakib Mostafa, Md. Tauhidul Islam

Radiation Oncology, Stanford University School of Medicine, Stanford, CA

The integration of disparate data modalities, such as medical imaging and genomics, is fundamental to modern oncology, capturing a holistic view of complex disease heterogeneity. Deciphering these multimodal relationships is critical for precision medicine, yet the diverse nature of the data represents a significant challenge for current computational methods. Traditional deep learning approaches for multimodal fusion, while powerful, often suffer from massive computational overhead and complex, resource-intensive architectures. To address this, we present a novel framework that transforms high-dimensional tabular omics data into a compact, two-dimensional image representation using Optimal Transport. This transformation recasts omics data as an additional image channel, enabling the use of a single convolutional neural network (CNN) to concurrently process both data streams, thereby overcoming critical limitations in computational efficiency. When evaluated on a multimodal cancer dataset integrating Whole Slide Images (WSI) and Spatial Transcriptomics (ST), our method achieved 96% accuracy, outperforming the 94% baseline using WSI alone. We further demonstrated the framework's generalizability on the ADNI Alzheimer's dataset, where it achieved 97.6% accuracy (vs. 93.4% for MRI-only). This framework thus provides a scalable, interpretable, and efficient approach for unified multimodal analysis, offering new opportunities for cancer diagnosis and the study of complex biological systems.<!--EndFragment-->

#5491 AI foundation model for single cell annotation from conventional histopathology images of cancer.

Xiangqi Bai[1], HoJoon Lee[1], Xiao Tan[2], Chaoyi Li[2], Anuja Sathe[1], Yan Wang[1], Quan Nguyen[2], Hanlee P. Ji[1]

[1]Stanford University, Stanford, CA,[2]The University of Queensland, Queensland, Australia

Spatial imaging technologies have revolutionized our understanding of the tumor microenvironment (TME) by delineating its molecular and cellular architecture. Some of these approaches characterize tissue at single cell resolution. These platforms enable precise cell type annotation and, when spatially registered, allow molecular label transfer onto conventional histopathology images with hematoxylin and eosin (H&E) staining. However, spatial imaging approaches require complex instrumentation and have a high-cost per assay. These limitations prevent the application of spatial analyses on large sets of cancers. In contrast, conventional cancer histopathology slides are widely available and can be imaged at low cost. However, single cell identification from these images remains a manual, semi-quantitative process that is difficult to scale up.To address these limitations, we developed an AI foundation model that enables single-cell characterization directly from conventional H&E images. Our approach uses either spatial proteomic data (e.g., immunohistochemistry - IHC) or spatial transcriptomic profiling. We use these spatial assays to generate molecularly defined labels for diverse cell populations, including epithelial, lymphocyte, macrophage, and stromal cells. For this study, the molecular labels were the basis for training a spatial multimodal classifier. There are two tiers, (1) single-cell H&E crops were embedded using the foundation model H-optimous to obtain high-dimensional representations, and (2) a Multi-Layer Perceptron (MLP) neural network was trained on those embeddings for supervised cell type classification.We trained our model on a set of colorectal cancers (CRC), consisting of 40 multiplexed IHC slides and five Xenium spatial transcriptomic slides. Overall, we had 34 million single cells for model training. The model achieved an overall accuracy of 87.1% and a macro-average area under the receiver operating characteristic curve (AUROC) of 96.1%. Independent validation on seven CRC samples (~8 million cells) yielded consistent performance with 87.2% accuracy and 95% macro-average AUROC.In summary, our multimodal model enables automated and scalable single-cell-level cell type annotation directly from H&E images. This approach provides a quantitative foundation for immune-tumor interactions for colorectal cancer. Furthermore, by integrating H&E-derived cell type maps with tumor-specific genomic alterations from matched TCGA datasets, the framework enables systematic analysis of important TME cell types such as tumor-infiltrating lymphocytes and their spatial cellular distributions, offering insights into colorectal cancer microenvironmental architecture.

#5492 Differential protein pattern analysis in highly multiplexed imaging.

Gourab Ghosh Roy, Peng Jiang

National Cancer Institute, Bethesda, MD

The recent progress in highly multiplexed protein imaging has advanced our ability to identify topological structures in tissue microenvironments associated with distinct clinical characteristics. However, a significant challenge with high dimensional imaging is how to systematically infer spatial features underlying different patient clinical groups, like cancer outcome groups or immunotherapy response vs resistance groups. We develop an artificial intelligence framework for identifying differential protein patterns between distinct groups from spatial proteomics images. Our image region-based framework does not need any prior manual or semi-automatic steps like cell segmentation and cell type annotation as required in existing spatial data analysis workflows, and therefore can capture essential features not defined by humans. The framework is also suitable for use with a low number of labeled samples, as is the case for exploratory spatial studies. We used the framework to identify differential protein patterns between different phenotypic groups from humans and mice. We expect that our proposed framework will be a useful tool for generating novel hypotheses regarding biomarkers or regulators of cancer therapy outcomes.

#5493 Patterns of acid-suppressive therapy prescriptions in cancer: Are we treating symptoms or fueling the disease?.

M. Payling[1], Bea Bakshi[2], Marta Sakal[1]

[1]Research, C the Signs, Boston, MA,[2]C the Signs Inc, Boston, MA

Background: Whether proton pump inhibitors (PPIs) or H_2 antagonists influence cancer risk remains uncertain, partly due to confounding by indication and reverse causation. We analyzed prescribing patterns in a large dataset to characterize lifetime and pre-diagnostic exposure to PPIs and H_2 antagonists across cancer types, with emphasis on upper gastrointestinal (GI) malignancies.
Methods: We examined 3,390,218 adults in the NHS with linked medication and cancer coding, identifying lifetime acid-suppressive use and, for cancer cases, exposure during the 5 years preceding diagnosis. Patients with oesophageal, stomach, pancreatic, or biliary tract cancers were specifically compared with cancer-free controls. Age-specific 10-year PPI and H_2 antagonist prevalence was calculated, and odds ratios (ORs) for ever-use were derived using cancer-free individuals as comparators.
Results: There were 1,078 oesophageal, 527 stomach, 696 pancreatic, and 130 biliary tract cancer patients. Lifetime PPI exposure differed markedly by cancer type: 93% of oesophageal cancer patients (OR=35.0), 89% of stomach cancer patients (OR=21.2), and 65-75% of other cancer types reported PPI use, compared with 3-55% among age-matched controls. H_2 antagonist use showed weaker associations (OR 1.6-2.0).
In the 5-year pre-diagnostic interval, PPI exposure was highest in oesophageal (93.0%), stomach (89.0%), pancreatic (88.6%), and biliary tract cancers (87.7%), with a median duration of 84 days. Duration of pre-diagnostic PPI use showed a strong gradient unique to upper-GI cancers; no similar gradient was seen for H_2 antagonists. Several non-GI cancers, including laryngeal cancer, also demonstrated elevated PPI use, though to a slightly lesser extent.
Conclusions: PPI exposure, both lifetime use and 5-year pre-diagnostic duration, was substantially higher among upper-GI cancer patients than among age-matched controls. While this may reflect symptom-driven escalation of therapy in the period preceding diagnosis, the consistently elevated exposure across multiple cancers raises the possibility that PPIs themselves may contribute to carcinogenic processes. The absence of comparable associations for H_2 antagonists suggests that acid suppression alone does not explain the observed patterns. Pronounced PPI enrichment in upper-GI cancers, weaker signals for H_2 antagonists, and detectable associations in selected non-GI cancers underscore the need for further work to determine whether PPIs act solely as markers of prodromal symptomatology or may exert independent effects relevant to cancer development.

#5494 Multiplex immunohistochemistry for immuno-oncology: A flexible approach to characterize the tumor microenvironment.

Elena Baranova[1], Sabine Iglesias[1], Amanda Finan-Marchi[1], Manon Motte[1], Renaud Burrer[1], **Rania Gaspo**[2], Marie Gerus-Durand[3]

[1]Cerba Research, Montpellier, France,[2]Cerba Research, Laval, QC, Canada,[3]Cerba Research Histalim, Montpellier, France

Background: In immuno-oncology (I/O), limited tissue availability underscores the need for precise characterization of the tumor microenvironment (TME). Comprehensive phenotyping of immune cell populations and novel biomarkers is critical for understanding pro- and anti-tumor dynamics and guiding immunotherapy strategies. Multiplex immunohistochemistry (IHC) offers a powerful approach to achieve this.

Methods: Cerba Research developed multiplex IHC protocols targeting key I/O markers, including macrophage phenotypes, myeloid-derived suppressor cells, cytotoxic T-cell status, and regulatory T cells. Protocols were optimized using Leica Bond Rx and Roche Discovery Ultra platforms with Akoya Opals and Roche Chromogens for detection. Panels were applied to normal and tumor tissues from lung, colon, and pancreas. Fluorescent images were analyzed using an internally validated workflow without deconvolution. Quantification of single markers and phenotypes was performed on whole-slide images or regions of interest (ROI) selected by a pathologist using Halo® (Indica Labs).

Results: Multiplex panels demonstrated versatility across multiple indications, enabling detailed comparisons of immune profiles between healthy and tumor tissues and across tumor types. Quantification of single-marker positivity and phenotypic combinations provided insights into spatial distribution of immune subsets within the TME. The study also evaluated benefits and limitations of ROI-based analysis versus whole-slide assessment.

Conclusions: Multiplex IHC is a robust and flexible tool for immune profiling in solid tumors, offering comprehensive characterization of I/O-related targets and their spatial context. This approach supports deeper understanding of tumor-immune interactions and informs precision immunotherapy development.

This text has been revised with the assistance of Microsoft Copilot to comply with the specified character limit.

#5495 AI-assisted Ki67 evaluation in solid tumors: Consistency and reliability compared to expert pathologists.

Rania Gaspo[1], Xavier Pichon[2], Maroua Tliba[2], Sabine Iglesias[2], Darshan Kumar[3], Renaud Burrer[2], Amanda Finan-Marchi[2], Marie Gerus-Durand[4]

[1]Cerba Research, Laval, QC, Canada,[2]Cerba Research, Montpellier, France,[3]Aiforia, Helsinki, Finland,[4]Cerba Research Histalim, Montpellier, France

Background: Ki67 is a key proliferation marker in solid tumors, particularly relevant for HR+/HER2- breast cancer when guiding adjuvant therapy. Despite its clinical importance, Ki67 immunohistochemistry (IHC) scoring lacks standardization. International guidelines aim to reduce variability among pathologists, and AI-driven image analysis solutions have recently emerged as rapid and reliable alternatives. This study compares Ki67 scoring using Aiforia® (AI platform) and Halo® (supervised image analysis software) against three independent pathologists across a large solid tumor cohort.

Methods: We stained 192 tumors of various origins, including breast and prostate, with Ki67 (clone 30-9). Pathologists were trained per International Ki67 Working Group (IKWG) recommendations and scored tissues accordingly. Aiforia®, based on deep learning, automatically quantified Ki67-positive tumor cells within minutes. Halo® employed a random forest classifier to segment tumor, non-tumor, and background regions, verified by a pathologist. After cell segmentation, Ki67 positivity was determined by thresholding.

Results: Ki67 scoring showed strong agreement between Aiforia® and Halo® across all solid tumors ($r^2 = 0.95$). Inter-pathologist correlations were weaker (A-B: $r^2 = 0.78$; A-C: $r^2 = 0.86$; B-C: $r^2 = 0.85$) despite standardized training, though still acceptable. Among 19 tumor types analyzed, only thyroid and stomach showed software correlation inferior to 0.75, with inter-pathologist agreement fair for stomach ($r^2 > 0.80$) and lower for thyroid ($r^2 = 0.65$-0.82). Organ-specific variability was notable among pathologists, while software scores remained consistent. For breast tumors (n = 16), Aiforia® and Halo® correlated strongly ($r^2 = 0.96$), whereas pathologist agreement ranged from $r^2 = 0.60$ to 0.87.

Conclusions: AI-based platforms like Aiforia® and supervised image analysis tools such as Halo® provide robust, reproducible Ki67 scoring and significantly reduce inter-observer variability. These technologies offer valuable assistance for IHC-based clinical analysis and may serve as arbitration tools or standardize Ki67 evaluation in solid tumors.

This text has been revised with the assistance of Microsoft Copilot to comply with the specified character limit.

: New Software Tools for Data Analysis
Poster Session

#5496 From transcripts to cells: Dissecting sensitivity, signal contamination, and specificity in Xenium spatial transcriptomics.

Mariia Bilous[1], Daria Buszta[1], Jonathan Bac[1], Senbai Kang[1], Yixing Dong[1], Stephanie Renaud-Tissot[2], Sylvie Andre[2], Marina Alexandre-Gaveta[2], Christel Voize[2], Solange Peters[2], Krisztian Homicsko[2], Raphael Gottardo[1]

[1]Biomedical Data Science Center, Lausanne University Hospital; University of Lausanne, Lausanne, Switzerland,[2]Department of Oncology, Lausanne University Hospital; Swiss Cancer Center Leman, Lausanne, Switzerland

Understanding cell states and interactions within tumors requires accurate spatial gene measurements. Spatial transcriptomics provides this capability by mapping gene expression directly within intact tissue, offering a powerful framework for studying tumor ecosystems. The purpose of this study was to systematically evaluate the performance of the Xenium platform in cancer samples and to develop an improved strategy for refining cell-level signals.We generated one of the largest Xenium datasets to date, comprising 41 breast and lung tumor sections from 27 donors and profiled using multiple targeted panels as well as the newer 5K panel. Using matched snRNA-seq, we assessed assay specificity, panel performance, segmentation strategies, and the prevalence of transcript spillover—a major source of technical variability in densely intermixed tumor ecosystems.We found that broader panel content increases biological coverage but reduces per-gene sensitivity. We further show that transcript spillover from adjacent cells significantly affects signal specificity, producing mixed profiles that obscure critical immune programs in cancer tissues. Building on these insights, we developed SPLIT (Spatial Purification of Layered Intracellular Transcripts), a method that combines snRNA-seq with deconvolution to correct spillover and recover cleaner cell-type signatures. SPLIT improved background correction, enhanced cell-type resolution, and revealed features such as T-cell exhaustion linked to local tumor-immune proximity that were not detectable using raw, contaminated data.In conclusion, our study provides a comprehensive performance assessment of Xenium in cancer contexts and introduces a scalable and interpretable approach for signal refinement, enabling more reliable inference of cellular programs and interactions within the tumor microenvironment. This dataset and methodology offer an important resource for designing, benchmarking, and interpreting spatial transcriptomics studies in cancer.

#5497 AI-augmented immersive 3D and 4D spatial analysis interface for cancer research.

Jonathan S. Kim[1], Minji Kim[2], Seock-Jin Chung[2], Inyeop Jang[2], Young-Won Cho[2], Jiwon Kim[3], Soonyoung Lee[3], Jongseong Jang[3], Eunyoung Choi[2], Tae Hyun Hwang[2]

[1]Cornell University, Ithaca, NY,[2]Vanderbilt University Medical Center, Nashville, TN,[3]LG AI Research, Seoul, Korea, Republic of

Background: Complex three-dimensional and time-resolved (4D) structures in cancer (cells, organoids, tissues, and drug distributions) are difficult to interrogate and discuss as a team. Our goal is to build an AI-augmented immersive interface that allows investigators to stand inside their data and explore it together in real time. We developed a multi-user VR/AR platform for volumetric microscopy that supports label-free holotomography (HT) (Tomocube HT-X1 Plus, 3D refractive-index images). The system enables interactive 3D segmentation, measurement, and annotation of subcellular and tissue-scale structures, including visualization of antibody drug conjugate (ADC) delivery. An integrated AI agent provides insight and can be augmented with domain-specific LLMs, including LG AI Research's EXAONE within a co-scientist AI agent framework.
Methods: We implemented a VR/AR environment where users can manipulate, segment, and annotate volumetric datasets in real time. The interface supports gesture-based selection, dynamic adjustment of 3D rendering parameters, and synchronized multi-user viewpoints. Users can query the AI assistant for literature context, analysis guidance, or suggestions for follow-up measurements inside the scene. The platform takes HT data as well as other multi-channel datasets for real-time multi-view rendering. We adapt LG's EXAONE's LLM-based chatbot and co-scientist agent architecture, which is trained on biomedical literature, to further enhance in-session analysis.
Results: We have validated the core visualization, interaction, and segmentation workflows and integrated the AI agent into the environment. Early demonstrations using 3D images of gastric cancer cell lines, organoids, and tissue sections allowed intuitive identification of nuclei, organelles, tumor glands, and stromal regions. Multiple users could concurrently explore morphology, annotate regions of interest, and derive quantitative metrics in real time. Ongoing data acquisition of gastric cancer cell lines, organoids, and tissues is coupled with manual annotation and AI-assisted segmentation to refine and benchmark performance.
Conclusion: We present an AI-augmented immersive interface for interactive analysis of volumetric cell and tissue datasets. By combining multi-user VR/AR, advanced 3D analysis tools, and a conversational AI agent, this platform enables detailed exploration of subcellular architecture and tumor microenvironments directly from HT or related volumetric and molecular data. Although our initial focus is gastric cancer and ADC delivery, the framework is disease and modality-agnostic and can be extended to other tumor types and therapeutic modalities.
Generative AI assistance was limited to language editing of this abstract. The scientific content, interpretation, and conclusions are the sole responsibility of the authors, who have reviewed and approved the final version.

#5498 Resolving phenotyping discordance with SPACEMAP, an integrated machine learning framework.

Arely Perez Rodriguez[1], Bassel Dawod[1], Sebastian Diegeler[1], Eslam A. Elghonaimy[1], Megan Wachsmann[2], Purva Gopal[2], David Hein[3], Paul H. Acosta[3], Andrew Jamieson[3], Gaudenz Danuser[3], Robert Timmerman[1], Satwik Rajaram[3], Todd A. Aguilera[1]

[1]Radiation Oncology, University of Texas Southwestern Medical Center, Dallas, TX,[2]Department of Pathology, University of Texas Southwestern Medical Center, Dallas, TX,[3]Lyda Hill Department of Bioinformatics, University of Texas Southwestern Medical Center, Dallas, TX

Introduction and Purpose: Multiplex imaging provides powerful insight into cellular organization, yet the complexity of these datasets requires robust analytical tools to extract meaningful biological information. The purpose of this study was to develop a unified analytical framework enabling reliable, high-resolution characterization of the tissue microenvironments in multiplex images. To achieve this, we developed SPACEMAP (Spatial Phenotyping And Classification with Enhanced Multiplex Analysis Pipeline), a comprehensive Python and Qupath-based platform that integrates image registration, cell segmentation, quality check, artifact removal, tissue and zone classification, spatial feature extraction, and a consolidated phenotyping approach into a single workflow.
Methods: To determine an optimal cell-classification strategy, we benchmarked our phenotyping method, RESOLVE, against three established approaches, Leiden clustering, Self-Organizing Maps, and SCIMAP. This evaluation revealed substantial inconsistencies among existing methods. To address this, SPACEMAP incorporates two complementary workflows: (1) a machine learning model trained on expert-annotated cells, and (2) a consensus-based model that integrates high-confidence cell assignments across methods, enabling robust classification even when manual references are limited.
Summary: We applied SPACEMAP to newly generated multiplex imaging datasets from colorectal tissue samples and further evaluated performance using a publicly available dataset. These analyses demonstrate that SPACEMAP improves classification consistency, reduces variability introduced by method selection, and supports reproducible extraction of spatial features for further downstream analysis.
Conclusions: SPACEMAP provides a standardized, high-fidelity workflow for spatial phenotyping that minimizes reliance on labor-intensive manual annotation and improves reproducibility in multiplex imaging studies. Its design supports adaptation to evolving imaging technologies and marker panels, enabling researchers to more effectively investigate tissue organization and generate biologically meaningful insights.

#5499 SpatialTopic exploring tumor ecosystem in 3D multiplexed imaging of melanoma.

Xiyu Peng[1], James Smithy[2], Mohammad Yosofvand[2], Caroline Kostrzewa[2], Fiona Ehrich[2], MaryLena Bleile[2], Jasme Lee[2], Michael A. Postow[2], Margaret K. Callahan[3], Katherine Panageas[2], Ronglai Shen[2]

[1]Texas A&M University, College Station, TX,[2]Memorial Sloan Kettering Cancer Center, New York, NY,[3]Univ. of Connecticut School of Medicine, Farmington, CT

Background: Advances in multiplexed imaging now profile cell phenotypes from 2D to 3D, creating new opportunities to analyze spatial organization in complex tissue. A 3D view of tissue architecture enables a re-examination of tumor-immune interactions in the tumor microenvironment, revealing spatially organized niches with direct biological and clinical relevance that may be obscured in 2D.

Methods: We developed SpatialTopic[1], a fast, scalable, unsupervised niche-detection method that identifies recurrent spatial patterns (“topics”) across multiplexed tissue images. SpatialTopic analyzes datasets with millions of cells within minutes using modest memory. With cell-type annotations as input, it applies to both spatial transcriptomics and proteomics (e.g., Xenium, CosMx, IMC and CODEX). Here, we extend SpatialTopic to 3D multiplexed images and demonstrate its applicability on a 3D CyCIF dataset from the melanoma invasive margin[2]. We also introduce a supervised framework of SpatialTopic that predicts spatial topic distributions using fixed, predefined topic compositions (“known topics”), enabling more scalable inference across multiple samples and facilitating links between spatial niches and clinical outcomes.

Results: SpatialTopic delineates four main topics along the vasculature-to-tumor-core axis at the melanoma invasive margin: (1) Vascular topic: endothelial cells with CD4 T cells and macrophages; (2) Immune topic: mainly including CD4 T cells, dendritic cells, as well as Regulatory T cells (Tregs), and B cells; (3) Tumor-immune boundary topic: tumor cells mixed with dendritic cells and CD4 T cells; and (4) Tumor core topic. In this dataset, relative to the prior publication[2], SpatialTopic more cleanly resolves vascular structures and reveals a graded shift in immune composition from vasculature toward the tumor boundary: decreasing macrophages and increasing CD4 T cells and dendritic cells at the invasive front of melanoma.

1.Peng, X. *et al.* Scalable topic modelling decodes spatial tissue architecture for large-scale multiplexed imaging analysis. *Nat. Commun.* 16, 6619 (2025). 2.Yapp, C. *et al.* Highly multiplexed 3D profiling of cell states and immune niches in human tumors. *Nat. Methods* 22, 2180-2193 (2025).

#5500 Morphology-aware profiling of highly multiplexed tissue images using variational autoencoders.

Gregory J. Baker[1], Edward Novikov[1], Shannon Coy[2], Yu-An Chen[1], Clemens Hug[1], Zergham Ahmed[1], Sebastian A. Cajas Ordonez[3], Siyu Huang[3], Clarence Yapp[1], Gaurav N. Joshi[4], Fumiki Yanagawa[4], Artem Sokolov[1], Hanspeter Pfister[3], Sandro Santagata[2], Peter K. Sorger[1]

[1]Laboratory of Systems Pharmacology, Harvard Medical School, Boston, MA,[2]Harvard Medical School/Brigham and Women's Hospital, Boston, MA,[3]Harvard John A. Paulson School of Engineering and Applied Sciences, Harvard University, Boston, MA,[4]Nikon Instruments, Inc., Cambridge, MA

Spatial proteomics (highly multiplexed tissue imaging) provides unprecedented insight into the types, states, and spatial organization of cells within preserved tissue environments. To enable single-cell analysis, high-plex images are typically segmented using algorithms that assign marker signals to individual cells. However, conventional segmentation is often imprecise and susceptible to signal spillover between adjacent cells, interfering with accurate cell type identification. Segmentation-based methods also fail to capture the morphological detail that histopathologists rely on for disease diagnosis and staging. Here, we present a method that combines unsupervised, pixel-level machine learning using autoencoders with traditional segmentation to generate single-cell data that captures information on protein abundance, morphology, and local neighborhood in a manner analogous to human experts while overcoming the problem of signal spillover. The result is a more accurate and nuanced characterization of cell types and states than segmentation-based analysis alone. We demonstrate the generality of this technique by applying it to a range of whole-slide, highly multiplexed human tissues acquired using platforms such as cyclic immunofluorescence (CyCIF), Lunaphore COMET, and Akoya PhenoCycler, and show that it can learn histological features across multiple spatial scales.

#5501 A quantum-enabled atlas-scale resource to study metabolic landscapes and heterogeneity in cancer TME.

Yinuo Zhao[1], Jiahe Yu[2], Min Yang[3], **Chi Zhang**[4]

[1]Middlesex School, Concord, MA,[2]Sierra Canyon School, Chatsworth, CA,[3]Oregon Health & Science University, Portland, OR,[4]Knight Cancer Institute, Oregon Health & Science University, Portland, OR

Metabolic networks are profoundly rewired in cancer, supporting uncontrolled proliferation, immune evasion, and therapy resistance. Although large atlas-level single-cell RNA-seq (scRNA-seq) datasets of cancer tumor microenvironments (TMEs) and normal human tissues are now available, there remains no systematic, genome-scale characterization of metabolic landscapes, shifts, heterogeneity, and cross-talk across cancer and normal cells using these data. Elementary flux modes (EFMs), representing the minimal sets of reactions that sustain steady-state flux, provide a principled basis for describing metabolic capabilities, yet identifying biologically feasible EFMs in genome-scale networks is a major bottleneck due to the combinatorial explosion of possible modes. We propose a quantum-enabled framework that leverages atlas-level scRNA-seq data to infer plausible EFM distributions and derive sample-specific metabolic fluxes, with the long-term goal of building a scalable resource of cancer metabolic landscapes. Both EFM discovery and flux prediction are formulated as Quadratic Unconstrained Binary Optimization (QUBO) problems solved on quantum annealing hardware. By exploiting the intrinsic parallel sampling capabilities of quantum devices, our approach efficiently explores high-dimensional solution spaces under stoichiometric, thermodynamic, and cancer-specific biological constraints. To handle genome-scale models relevant to oncology, we integrate tensor decomposition-based dimensionality reduction to yield tractable QUBO formulations while preserving key pathway structure. On simulated networks with up to 25 reactions, quantum sampling robustly enriches EFMs that satisfy stoichiometric balance, support minimality, and irreducibility, while structurally invalid modes are rarely sampled. When imposing distinct sample-specific constraints mimicking different tumor contexts, the high-frequency EFM sets shift systematically, demonstrating that the framework captures condition-specific flux distributions without explicit enumeration. We then apply this quantum-driven strategy to single-cell atlases of pancreatic, prostate, and breast cancer, and integrate these results with TCGA bulk RNA-seq in constraint-based models to generate a shared, extensible resource of cancer metabolic landscapes. We show that this resource can be used to map recurrent pathway vulnerabilities, prioritize metabolic intervention targets, and quantify condition-specific metabolic strategies within and across tumor types, treatment states, and patient cohorts. By bridging quantum optimization and systems biology, our work provides a practical and interpretable foundation for personalized metabolic modeling and hypothesis generation in cancer.

#5502 gOS: A total molecular oncology interpretation framework applied to repaired FFPE and heme whole genome and clinical targeted assays.

Kevin Hadi, Aditya Deshpande, Shihab Dider, Charalampos Xanthopoulakis, Johnathan Rafailov, Marcin Imielinski

NYU Langone Health Perlmutter Cancer Ctr., New York, NY

Cancer molecular diagnostics remain fragmented across multiple assays and disjointed software, leaving molecular pathologists to manually link QC, purity/ploidy, and variant classes before oncologists can act on recommendations. We address this with two complementary, genome-wide WGS assays—a repaired-FFPE solid tumor test and a blood-only heme test—that consolidate SNVs/indels, CNAs, SVs/fusions, LOH, and signatures into a single DNA workflow with panel-like performance. In parallel, we built the total genome Oncology System (gOS), which integrates WGS, targeted panels, methylation, and RNA fusions into a coherent browser with variant tiering, clinical validation, and discovery-oriented exploration.

At NYU, standard care comprises NYU-PACT (607-gene DNA panel), Illumina MethylationEPIC v2.0 for solid tumors, and Oncomine (40-gene DNA) plus Myeloseqer for driver heme fusions. To pilot a WGS drop-in for DNA/RNA panels, we used enzymatic shearing (Watchmaker Genomics) and a FFPE damage-repair step that improves coverage uniformity and lowers artifacts. We analyzed 23 mixed solid tumors with paired normals and 22 hematologic malignancies; seven solid FFPE were also prepped without repair for comparison. gOS processed all 55 cases via an integrated Nextflow pipeline and provided interactive WGS vs SoC comparison.

Unrepaired FFPE showed AT-rich dropout and megabase-scale coverage bias; repair restored uniformity and suppressed artifacts. In a BRCA1-mutant/LOH case, HRD was obscured in unrepaired WGS (HRDetect 0.004; B1+2 0.2) but recovered with repair (HRDetect 0.99; B1+2 0.78). Across 23 repaired FFPE solids, WGS vs NYU-PACT achieved 96% sensitivity (298/310 hotspots) and near-100% specificity (1/6,740 SoC–wild-type positions). Heme WGS showed 100% concordance with Myeloseqer fusions and Oncomine mutations.

Together, the complementary WGS assays and gOS deliver panel-like accuracy with broader, pan-variant coverage and a single, coherent interpretive view, supporting WGS as a practical replacement for fragmented DNA/RNA panels—especially in historically challenging FFPE tissue—and enabling expanded clinical utility through unified multi-omic interpretation.

#5503 Cancer epitope prediction tools & analysis pipelines in CEDAR.

Ibel Carri[1], Jason Greenbaum[2], Zhen Yan[2], Kevin Kim[2], Haeuk Kim[2], Ashmitaa Logandha Ramamoorthy Premlal[2], Daniel Marrama[1], Nina Blazeska[3], Hannah K. Carter[4], Morten Nielsen[5], Alessandro Sette[1], Bjoern Peters[1], Zeynep Kosaloglu-Yalcin[3]

[1]La Jolla Institute for Immunology, La Jolla, CA,[2]Bioinformatics Core, La Jolla Institute for Immunology, La Jolla, CA,[3]La Jolla Institute for Immunology, San Diego, CA,[4]UC San Diego, La Jolla, CA,[5]Department of Health Technology, Technical University of Denmark, Lyngby, Denmark

The identification of immunogenic cancer epitopes, including patient-specific neoepitopes and shared tumor-associated antigens (TAAs), is a central challenge for the development of effective cancer immunotherapies. To accelerate their discovery, the Cancer Epitope Database and Analysis Resource (CEDAR), a comprehensive resource for immuno-oncology, curates epitope data from the literature and develops tailored computational tools. Building on this foundation, we introduce the modular Next-Generation IEDB Tools (NGT) platform (nextgen-tools.iedb.org/) that integrates a wide array of cancer-focused computational tools.

The NGT platform allows users to construct, save, and share customized, reproducible, end-to-end computational pipelines for tumor antigen discovery. This architecture enables systematic prioritization of epitope candidates by applying multiple, sequential filtering criteria based on predicted and calculated relevant immune features, such as antigen expression, antigen presentation, self-similarity, and immunogenicity.

Key tools include the Mutated Peptide Generator (MPG), which translates genomic variants (e.g., SNVs, indels) into candidate neoepitope sequences; Peptide Expression Annotation (PepX), which integrates public RNA-Seq data from resources like TCGA and GTEx to quantify antigen-encoding transcript abundance in tumor tissue; the Patient-Specific Presentation Metric (PHBR), a metric that estimates the likelihood of a mutation being presented by a patient's specific MHC Class I alleles; ICERFIRE (via Peptide Variant Comparison, PVC), a robust immunogenicity model that predicts the T-cell recognition potential of neoepitopes; PEPMatch, a tool to filter out candidate neoepitopes that are highly similar to self-peptides, which can indicate potential tolerance or autoimmunity risks; and Cluster, which groups highly similar peptide sequences to reduce redundancy and focus on the most representative candidates for experimental validation.

The CEDAR computational tools and integrated pipeline architecture on the NGT platform provide cancer immunologists with a flexible, user-friendly, and state-of-the-art resource. This comprehensive framework accelerates the translation of genomic and transcriptomic sequencing data into clinically actionable epitope candidates. Here, we present how these integrated tools can be applied to patient-level analyses, enabling personalized identification and prioritization of tumor epitopes to guide cancer vaccine design and immunotherapy development.

#5504 CoMMpass Explorer: An interactive platform to explore clinical and genomic data from newly diagnosed multiple myeloma patients from the landmark CoMMpass observational study.

Wanxing Zhang[1], Chaitanya R. Acharya[1], **Steven M. Foltz**[1], David E. Avigan[2], Samir Parekh[3], Ravi Vij[4], Shaji Kunnathu Kumar[5], Taxiarchis Kourelis[5], Sagar Lonial[6], Hearn Cho[1], Ioannis S. Vlachos[2], Sacha Gnjatic[3], Li Ding[4], Manoj Bhasin[7], George Mulligan[1]

[1]Multiple Myeloma Research Foundation, Norwalk, CT,[2]Beth Israel Deaconess Medical Center, Boston, MA,[3]Icahn School of Medicine at Mount Sinai, New York, NY,[4]Washington University School of Medicine in St. Louis, St. Louis, MO,[5]Mayo Clinic, Rochester, MN,[6]Emory Winship Cancer Institute, Atlanta, GA,[7]Emory School of Medicine, Atlanta, GA

The CoMMpass study (NCT01454297) is a prospective, longitudinal observational study involving 1,141 newly diagnosed multiple myeloma (NDMM) patients. Bone marrow aspirates from the study participants were collected for comprehensive molecular characterization of tumor (using bulk RNA sequencing and whole genome sequencing) and tumor immune microenvironment using 3' single-cell RNA sequencing (scRNA-seq). To support exploration of this rich multi-omic dataset, we developed CoMMpass Explorer (CE), an intuitive interactive platform that enables real-time analysis of clinical and genomic data from CoMMpass.

A central feature of CE is cohort building, where users can filter and stratify patients by clinical, genomic, and survival data elements to create custom cohorts for analysis. CE provides five main views: Overall Summary for clinical feature distribution, Kaplan-Meier curves, and multivariate Cox proportional hazards models; Mutational Profile for visualizing and comparing somatic mutations; Tumor Profile for bulk differential expression and gene set enrichment; Immune Microenvironment for comparing cell type abundance and cell cycle dynamics between cohorts using scRNA-seq data; and Pseudo-Bulk, which aggregates single-cell expression by cell type to enable cohort-level comparisons of transcriptional programs using DEseq2.

CE reproduces prior CoMMpass studies, including WEE1 expression being associated with poorer progression-free survival (Simhal, et al.) and different mutation frequencies between African American and European American patients (Manojlovic, et al.).

We further demonstrate CE's utility by interrogating the 2025 Consensus Genomic Staging (CGS) risk classification system (Avet-Loiseau, et al). We compared CGS high-risk (HR, n=249) vs. CGS standard-risk (SR, n=573) patients. HR patients have significantly worse progression-free survival, overall survival, and time to second-line therapy compared with SR patients. Univariate models recapitulated expected differences in the clinical features that define CGS risk. Bulk tumor RNA-seq and ssGSEA highlighted a more proliferative and genomically unstable transcriptional program in HR group, with upregulation of angiogenesis and cell-cycle-related pathways. In the immune microenvironment, monocytes were more abundant in the SR group. Pseudo-bulk RNA-seq of plasma cells showed overexpression of ANXA1, NSD2, IGF1R, MAF and related genes in HR.

CE democratizes access to the CoMMpass multi-omic resource, allowing researchers to interrogate clinical and molecular heterogeneity. By enabling hypothesis generation and replication of published results, CE serves as a valuable tool for identifying prognostic biomarkers and meaningful patterns in gene expression, mutation profiles, and the immune microenvironment.

#5505 A unified framework for cross-platform spatial omics analysis and deep spatial profiling.

Yunhe Liu[1], Edoardo L. Draetta[1], Kayla R. Caughlin[2], Alexandria Lau[2], Andre Fonseca[3], Tian Chu[1], Kyung Serk Cho[2], Yibo Dai[2], Yang Liu[4], Jun Wang[2], Jiahui Jiang[2], Yinyin Yuan[4], Futreal Andrew[2], Mingyao Li[5], Linghua Wang[2]

[1]Department of Genomic Medicine, The University of Texas MD Anderson Cancer Center, Houston, TX,[2]Department of Translational Molecular Pathology,, The University of Texas MD Anderson Cancer Center, Houston, TX,[3]Instituto Metropole Digital (IMD), Universidade Federal do Rio Grande do Norte (UFRN), Natal, Brazil,[4]The University of Texas MD Anderson Cancer Center, Houston, TX,[5]University of Pennsylvania, Philadelphia, PA

Background: Spatial multi-omics has advanced rapidly in resolution, multiplexing, 3D modeling, and multi-modality. Platforms rely on distinct chemistries and assay architectures, yielding heterogeneous outputs but complementary strengths. These spatially indexed readouts enable neighborhood/niche inference, cell-cell communication, and 3D reconstruction, but demand rigorous normalization, uncertainty modeling, and scalable computation. Despite progress with foundation models for imputation and integration, a domain-specific suite that unifies these models for spatial omics is lacking.
Methods: We developed Spyrrow (Spatially Resolved Multi-omics Data Visualization and Analytic Framework), a Python toolkit for cross-platform analysis, visualization, multi-modality integration and enhancement, spatial registration, and 3D reconstruction (https://github.com/WangLab-ComputationalBiology/spyrrow). Spyrrow ingests heterogeneous outputs and standardizes them into a unified spatial data model. Modules span raw-data processing (cell segmentation to cell-level matrices; single-cell enhancement for Visium; Visium HD single-cell transformation using registered H&E), multimodal registration, and a foundation-model hub (UNI, KRONOS, LOKI) for panel expansion, imputation, and cross-modality retrieval. With harmonized data and z-axis registration, Spyrrow builds 3D models linking serial sections. On the unified object, we provide clustering, graph-based neighborhood retrieval and niche identification, region detection (tumor compartments, TLS), spatial label transfer, and a comprehensive cell-cell communication module. Visualization includes pseudo-H&E/pseudo-fluorescence, ligand-receptor quiver plots, and 3D voxel renderings.
Results: Spyrrow has been applied across multiple spatial-omics datasets and projects. The visualization suite produces clear, interpretable displays of niches, regions, and interaction patterns. Across benchmarks, integration with state-of-the-art models improves spatially aware clustering, label transfer, registration, and communication inference. Region-detection performance was corroborated by experimental validation. Together these results demonstrate robust performance, scalability, and cross-platform integration that are difficult to achieve with existing tools.
Conclusions: Spyrrow addresses a critical need in spatial multi-omics by providing a unified, adaptable, and cross-platform analytical framework. It facilitates both biological discovery and methodological innovation by supporting a wide range of spatial omics platforms. Importantly, it offers a scalable and interpretable approach to spatial data analysis—from broad tissue-level context to detailed subcellular features-empowering deeper insights into the tumor microenvironment and advancing immune-oncology research.

#5506 An ensemble machine learning approach to ALT detection revals therapeutic vulnerabilities in pediatric cancers lacking actionable drug targets.

Declan Bennett, Monika Weirdl, Lillian M. Guenther, Paul Geeleher

St. Jude Children's Research Hospital, Memphis, TN

Alternative lengthening of telomeres (ALT) maintains telomeres in 15-20% of cancers through a recombination-based mechanism associated with poor outcomes. ALT is frequently driven by ATRX/DAXX loss-of-function mutations and is enriched in pediatric malignancies including osteosarcoma, neuroblastoma, and soft tissue sarcomas—cancers with limited therapeutic options. Current ALT detection methods are low-throughput and not scalable to large cohorts, impeding systematic discovery of ALT-specific vulnerabilities. We developed ALTitude, a whole-genome sequencing (WGS)-based ensemble machine learning framework to predict ALT status. Using telomere-relevant genomic features extracted from >1,000 cancer cell lines in the Pediatric Cancer Dependencies Accelerator and Cancer Dependency Map (DepMap) resources. We trained and validated the model against orthogonal ALT detection methods. We integrated ALTitude predictions with genome-wide CRISPR loss-of-function screening data in DepMap to identify ALT-specific dependencies. ALTitude achieved high accuracy in ALT classification across diverse cancer types, providing the first scalable map of ALT in a densely functionally characterized cell line panel. Integration with CRISPR essentiality screens revealed SMARCAL1 as a top selective dependency in ATRX/DAXX mutant ALT - positive osteosarcoma, soft tissue sarcomas, and neuroblastoma. SMARCAL1 harbors a helicase domain distantly paralogous to ATRX and resolves stalled replication forks at telomeres during DNA damage response, suggesting that increased replication stress at ALT telomeres creates essentiality for SMARCAL1 function. This work establishes a scalable method to infer ALT status from WGS data and systematically connects ALT biology to therapeutic vulnerabilities in cancer cell line models. By identifying SMARCAL1 as selective dependency in ALT-positive cell lines, we nominate novel therapeutic targets for challenging pediatric cancer types. Our approach demonstrates how integrating features derived from genomic data with functional screening and other 'omics data can reveal novel insights into drivers across aggressive cancer subtypes.

#5507 A user-friendly, no-code, application for HIPAA-compliant automated analysis of tabular data at scale.

Paraic A. Kenny

Gundersen Medical Foundation, La Crosse, WI

Much research in clinical settings involves review of large quantities of often unstructured data in electronic medical records, which is time consuming and requires an educated workforce of clinical research coordinators, residents and/or fellows. Large language models, such as ChatGPT, have demonstrable capabilities for efficiently analyzing and summarizing large volumes of text, offering the potential to greatly accelerate chart review-based research in clinical settings. Concerns regarding leakage of personal health information (PHI) sharply limit the potential to utilize commercial chatbots for this purpose. Secure, fire-walled in-house LLM chatbots in a well-governed system can solve concerns related to PHI leakage. Although processing data for large studies one-prompt-at-a-time may offer substantial efficiency gains versus prior human-only processes, far greater efficiencies can be achieved by automating the prompt submission and retrieval process.

To address these concerns, we developed a user-friendly application for processing any form of tabular data at scale using an in-house implementation of ChatGPT 4o-mini on Emplify Health's Azure cloud environment. The application imports tabular data (in excel or text format), guides the user through a straightforward prompt engineering process and then automatically submits the data, row-by-row, to the LLM and retrieves and tabulates the returning data in the manner specified by the user.

The application was initially developed with the goal of rapidly reasoning through thousands of pathology reports to identify those which correspond to cancer cases and, for those cases, automatically extracting multiple cancer-related parameters. Following this early success, we developed a completely generalized data agnostic application which has found widespread utility within our research institute, being deployed on diverse data sources such as cancer registries, cardiology CT reports, imaging narratives and clinical encounter notes. In this way, the application has substantially accelerated research projects by dramatically reducing the time needed to retrieve data, enabling our personnel to spend more time on higher yield activities such as data analysis.

#5508 Bioinformatic method for the detection of micro copy number variations with exome sequencing data.

Jin Young Lee[1], Hyo Young Choi[2], D. Neil Hayes[1]

[1]Center for Cancer Research, University of Tennessee Health Science Center, Memphis, TN,[2]Department of Preventive Medicine, Division of Biostatistics, The University of Tennessee Health Science Center, Memphis, TN

Short-sized copy number variants (CNVs) account for a large proportion of the somatic cancer genome landscape. Analysis of CNVs from Pan-Cancer Analysis of Whole Genomes (PCAWG) Consortium showed that the sizes of copy number deletions and duplications have multimodal distributions with one of the major modes centering around 1kb [1]. Sensitive profiling of structural variants (SVs), which include CNVs, with long-read sequencing (LRS), showed that the median SV lengths range from 133bp to 1kbp by multiple SV callers [2]. However, existing CNV analysis tools for short-read sequencing data (SRS) are based on a binning approach, which limits the reliable detection of these short-sized CNVs. Exome sequencing data poses additional challenges of uneven read depth due to capturing efficiency differing between genomic positions. Therefore, we developed a methodology that uses read depth data available at every genomic position to discover short-sized CNVs, or Micro CNVs, from exome sequencing data. We employed an approach we named adaptive window extension, in which we extended the windows to identify genomic segments with read depths significantly deviating from control samples. Then, we fine-tuned the variant boundaries by searching for an optimal score in the base-level space. We evaluated our approach in our simulated data where we locally simulated 12 genomic loci containing well-known cancer genes, both tumor suppressors and oncogenes. We were able to obtain median sensitivity over 0.9 for 2-fold copy number deletions and duplications in 90% purity tumors as short as 300bp over the captured region, which corresponds to 1-2 exons involved in the variation. At 50% purity, similar performance was observed for simulated variants as short as 1kbp over the captured region, retaining high specificity. Given the current lower limit of sensitive detection of germ-line CNV (of 100% purity) is 3 exons (~750bp in the captured region) after comprising specificity [3], we believe our tool presents competitive results even in the lower purity settings and, when applied to a larger cancer exome cohort, will discover additional cancer driver genes and actionable genes.

---

1. Li, Y., et al., *Patterns of somatic structural variation in human cancer genomes.* Nature, 2020. **578**(7793): p. 112-121.

2. Liu, L., et al., *Performance of somatic structural variant calling in lung cancer using Oxford Nanopore sequencing technology.* BMC Genomics, 2024. **25**(1): p. 898.

3. Babadi, M., et al., *GATK-gCNV enables the discovery of rare copy number variants from exome sequencing data.* Nat Genet, 2023. **55**(9): p. 1589-1597.

#5509 A computational framework for reproducible analysis of cancer drug screening data.

Huiyi Yang[1], Jax Lubkowitz[1], Xiaomeng Huang[2], Gabor Marth[2], Samuel Cheshier[3], Philip Moos[4], Yi Qiao[1]

[1]Biomedical Informatics, University of Utah, Salt Lake City, UT,[2]Human Genetics, University of Utah, Salt Lake City, UT,[3]Huntsman Cancer Institute, University of Utah, Salt Lake City, UT,[4]Pharmacology and Toxicology, University of Utah, Salt Lake City, UT

Background: Screening therapeutic responses in patient-derived or model-based cancer cells provides a direct experimental strategy to evaluate treatment efficacy. These assays generate complex datasets that require scalable, standardized analysis pipelines to ensure reproducibility and cross-study comparability. However, current data management and analysis workflows remain fragmented, relying on manual curation and ad hoc scripts that hinder reproducibility. This study introduces an open-source computational framework that standardizes storage, analysis, and visualization of high-throughput screening (HTS) data, providing easy access to common analysis methods while maintaining reproducibility in clinical and academic settings.
Methods: We developed a Python framework that provides a coherent workflow for storing, processing, and analyzing high-throughput drug screening data. It enables efficient and uniform storage with consistent data structure across experiments and datasets. The framework integrates automated drug name standardization, standardized data preprocessing, and common dose-response modeling methods including IC50, EC50, and DSS calculations. In addition, the framework supports cohort-level summarization and treatment prioritization, allowing users to compare drug responses across patients. Together, these components create a reproducible and adaptable pipeline that transfers raw experimental measurements to interpretable biological and translational insights.
Results: To demonstrate its broad utility, we applied the framework to three use cases. With the imported GDSC2 dataset, our recomputed IC50 and AUC values were highly consistent with published data, while providing integrated visualization and more contextual insights. We re-analyzed a breast cancer PDX-derived organoid dataset and were able to evaluate batch effects and compare responses across multiple models. We also analyzed an ex-vivo drug screening data from an ongoing pediatric brain tumor precision oncology initiative. The outputs were used to aid in prioritizing treatment candidates for individual patients at molecular tumor board meetings, demonstrating applicability in translational contexts. Across all cases, the framework ensured consistent preprocessing, minimized manual data manipulation, and provided comprehensive cross patient and cross drug comparison for identifying personalized drug candidates.
Conclusion: Our framework provides a comprehensive, interoperable solution for managing cancer drug screening data. By minimizing manual data manipulation and enabling reproducible analysis, it bridges the gap between experimental data generation and actionable insight. Beyond personalized ex-vivo assays, this platform empowers systematic analysis across public and clinical datasets, facilitating translational research and personalized treatment selection.

#5510 Hunting for microsatellite instability in long-read data with Owl.

Zev Kronenberg[1], Khi Pin Chua[1], Mark J. P. Chaisson[2], Byunggil Yoo[3], Lisa Lansdon[3], William J. Rowell[1], Egor Dolzhenko[1], Kie Kyon Huang[4], Patrick Tan[5], Shruti S. Bhise[6], Everett Fan[6], Mark Mendoza[6], Emily O'donnell[7], Tomi Pastinen[7], Elizabeth R. Lawlor[8], Scott N. Furlan[6], Midhat S. Farooqi[3], Michael A. Eberle[1]

[1]Computational Biology, PacBio, Menlo Park, CA,[2]University of Southern California, Los Angeles, CA,[3]Children's Mercy Research Institute, Kansas City, MO,[4]Duke-NUS Medical School, Singapore, Singapore,[5]Prog. In Cancer & Stem Cells Bio., Duke-NUS Graduate Medical School, Singapore, Singapore,[6]Fred Hutch Cancer Center, Seattle, WA,[7]Children's Mercy Kansas City, Kansas City, MO,[8]Seattle Children's Research Institute, Seattle, WA

Background: Microsatellite instability (MSI) refers to the accumulation of somatic mutations in simple repeat regions and is a hallmark of mismatch repair deficiency as well as a predictive biomarker for immunotherapy response. Most existing MSI callers are built for short-read sequencing and typically require paired tumor-normal data or high sequencing depth. These methods quantify repeat-length variability and classify genomes as MSI high when 10-30 percent of markers are unstable. Long-read sequencing (LRS) enables haplotype-resolved repeat profiling, allowing accurate MSI detection from tumor-only genomes at standard (~30×) coverage.

Methods: We developed Owl, a MSI detection software tool for PacBio HiFi data. Owl interrogates more than 160,000 simple repeats using a wrap-around dynamic programming algorithm and calculates the coefficient of variation (CV) in repeat length across phased haplotypes. Genome-wide MSI scores are then reported as the fraction of markers exceeding a parametrically derived CV threshold (CV > 5).

Results: We first applied Owl to 131 healthy controls from the Human Pangenome Reference Consortium and observed that MSI-stable genomes typically fall between 2-6%. We then profiled 26 additional cancer genomes, all of which had Owl scores between 2-3%, consistent with microsatellite-stable profiles. Finally, we identified five MSI-high samples that exceeded our 10% threshold, with scores ranging from 15-18%. These included two gastric cancers, an astrocytoma sample, and two Ewing sarcoma cell lines. Only one sample had both HiFi and Illumina data available for comparison; in that astrocytoma sample, Owl (17.1%) and Illumina DRAGEN (20.0%) produced concordant MSI-high classifications.By measuring MSI at >160,000 repeats, we can also detect motif-specific instability in tumor samples. For example, the two Ewing sarcoma cell lines (TC32 and CHLA10) showed a two fold increase of GGAA motif instability (23-26% MSI) compared to other motifs, an interesting and potentially disease-relevant pattern. The EWS::FLI1 fusion is known to bind GGAA-rich regulatory elements, and the observed instability at these motifs suggests that repeat variation itself may play an important role in Ewing sarcoma biology.

Conclusions: Owl enables robust, quantitative detection of MSI from long-read whole-genome data, requiring only tumor samples. Integrated into the PacBio HiFi Somatic workflow, Owl extends MSI profiling to long-read sequencing, revealing motif-specific instability patterns not captured by short-read approaches.

#5511 Exacto: Accurate identification of mutant proteoforms and neoantigens using integrative long-read sequencing.

Jin Seok Lee[1], Maria J. Sambade[2], Jeremy Wang[3], Alex Rubinsteyn[1], Benjamin G. Vincent[1]

[1]University of North Carolina at Chapel Hill, Chapel Hill, NC,[2]UNC Lineberger Comprehensive Cancer Center, Chapel Hill, NC,[3]Department of Pathology and Laboratory Medicine, University of North Carolina at Chapel Hill, Chapel Hill, NC

Neoantigen discovery is essential for personalized immunotherapy, but current approaches are limited by a focus on small somatic variants identifiable by short-read sequencing. These variants often produce peptides that resemble self-antigens and are weakly immunogenic. Long-read sequencing enables more sensitive detection of large structural variants and full-length transcripts. Large mutations can generate neoantigens that are more dissimilar to self and thus more immunogenic. However, no method exists to identify a comprehensive set of somatic DNA and RNA variants, integrate these, and contextualize each amino acid using long-read data. To address this gap, we developed Exacto, a publicly available software program that uses long-read sequencing data to accurately characterize tumor genomes, transcriptomes, and mutant proteoforms. Exacto performs three main functions. First, it profiles reference-genome aligned long reads to identify major types of tumor-specific DNA variants (SNV, multi-nucleotide variant, insertion, deletion, duplication, inversion, and translocation) and RNA variants (SNV, multi-nucleotide variant, insertion, deletion, cryptic exon, intron retention, exon skipping / truncation, fusion gene, circular RNA, and unannotated intergenic isoforms). Second, it integrates RNA and DNA variants to predict the splicing consequences of somatic mutations. Third, it translates full-length RNA sequences and annotates each amino acid with underlying RNA and DNA variants. We have also developed a genome and transcriptome variation graph builder in Exacto to generate synthetic tumor and matched normal genomes as well as tumor transcriptomes. To perform a comprehensive benchmark study for mutant peptide identification, we developed VSTOL and Nexus. VSTOL introduces a new framework, called Occam's Variant Grammar, to characterize DNA and RNA variants in a unified representation for existing variant callers. Nexus is a Nextflow suite that runs over 50 tools for neoantigen discovery. Using synthetic samples generated from the variation graphs, we benchmarked somatic DNA variant calling with Exacto, ClairS, Nanomonsv, Savana, Severus, and SVision-pro. Exacto achieved the highest or tied-highest recall for all simulated variant types (SNV, deletion, insertion = 1.000; translocation and inversion = 0.983). It outperformed the next-best tools by substantial margins: for translocations and inversions, Exacto achieved 0.688 precision versus 0.205 for Savana (both with 0.983 recall); for deletions, 0.945 (Exacto) precision compared to 0.761 (Savana) with both methods obtaining 1.000 recall; and for insertions, 1.000 (Exacto) recall versus 0.901 (Nanomonsv) with both delivering 1.000 precision. Given this performance, we expect Exacto will become the standard method for discovery of immunogenic neoantigens using long-read DNA and RNA sequencing.

#5512 ProteoRon: High-fidelity proteome inference from transcriptomes.

Kaiqiang Hu, Wanyu Tao, Ye Yuan, Zhe Li, Yuxin Zhang, Pengwei Pan, Fang He

Pharmaron Beijing Co., Ltd., Beijing, China

Transcriptome profiling has become a routine and relatively low-cost component of drug discovery. In contrast, direct proteome measurement—although invaluable for assessing drug target engagement and pathway activity at the protein level—remains far less accessible, thereby limiting its use in high-throughput screening assays. To bridge this gap between transcriptome and proteome, we proposed ProteoRon, a deep learning model for proteome prediction. To support this transformation, we generated a foundational dataset of more than 800 cancer cell lines with paired transcriptome and proteome profiles using our in-house Illumina and Orbitrap Astral platforms. This internally curated resource encompasses expression data for more than 20,000 genes and the abundances of over 8,000 proteins. Building on our high-quality internal data and further augmented by public resources such as CPTAC and CCLE, ProteoRon functions as an accessible in silico surrogate for proteomics. Its architecture incorporates residual layers that explicitly model how post-transcriptional regulation modulates the quantitative relationship between baseline mRNA and its cognate protein. To evaluate ProteoRon's functional utility, we applied GSVA to both ProteoRon-predicted proteins and raw RNA-seq for drug response modeling. The ProteoRon-based features yielded significantly higher prediction accuracy, indicating a superior ability to capture functional pathway states. The model also correctly predicts the ISR-induced increase in ATF4 protein abundance despite minimal changes in its corresponding mRNA levels, underscoring its ability to capture non-transcriptional regulatory logic. Taken together, ProteoRon unlocks the latent proteomic potential of routine transcriptome data, thereby enabling deeper biological insight from existing RNA-seq resources.

#5514 BART-spatial: Predicting biologically significant transcriptional regulators from spatial omics data.

Jingyi Wang[1], Hongpan Zhang[1], Zhenjia Wang[2], Chongzhi Zang[1]

[1]Department of Genome Sciences, University of Virginia, Charlottesville, VA,[2]Department of Genome Sciences, University of Virginia, CHARLOTTESVILLE, VA

Transcription regulators (TRs), including transcription factors and chromatin regulators, are essential for maintaining cell identity and directing cell fate decisions by activating or repressing lineage-specific gene expression program and integrating environmental signals with intrinsic regulatory networks. Identifying active TRs is critical for understanding transcriptional regulation in both normal physiology and diseases like cancer. Emerging spatial omics technologies, such as 10x Visium and Visium HD and spatial ATAC-seq, enable simultaneous profiling of genomic information and spatial location at near-single-cell resolution, providing unprecedented opportunities to study transcription activities in the tissue microenvironment. However, inferring functional TRs from spatial omics data remains challenging due to data sparsity, high dimensionality, and the complex nature of transcriptional regulation. Here we present BART-spatial (Binding Analysis for Regulation of Transcription for spatial omics data), a computational method for identifying functional TRs from spatially resolved transcriptomics or epigenomics data. BART-spatial integrates spatial variability and pseudo-temporal dynamics of molecular profiles to generate biologically informed predictions of TR activity. It leverages public TR binding profiles to enhance prediction accuracy, without relying on TR expression levels. Applied to multiple real spatial transcriptomics datasets across different biological systems and platforms, BART-spatial successfully identifies TRs with region- or stage-specific activities, outperforming existing tools. Moreover, BART-spatial also works for other spatial omics data such as spatial ATAC-seq, enabling cross-validation between transcriptomic and epigenomic layers. Implemented as an open-source package, BART-spatial provides a useful computational tool for decoding spatial omics data and offers new insights into transcriptional regulation in various biological systems.

#5515 Accelerating minimal residual disease (MRD) detection through GPU-accelerated genomic analysis using NVIDIA Parabricks.

Zhuosheng Gu, Adam Harmon, Maciej Pacula, Megan Rivera, Zachary Costliow, Ashley Tellis, Seka Lazare, Xiaomin Zhao, Wendy Winckler

Droplet Biosciences, Cambridge, MA

Previously we demonstrated that ctDNA present in lymphatic exudate collected via surgical drains (“lymph”) outperformed plasma for detecting MRD in head and neck squamous cell carcinoma (HNSCC) patients through a targeted sequencing (TS) approach[1]. However, detecting ultra low frequency variants requires deep sequencing coverage and computationally intensive workflows, often resulting in long turnaround times. To enhance the performance of the TS approach, we implemented an MRD detection pipeline optimized with NVIDIA Parabricks[2] to accelerate computation and enable faster, scalable molecular analysis without compromising accuracy.

25 unique patients with HPV-independent HNSCC were included in the cohort to demonstrate the performance improvements by porting our MRD workflow from a CPU-based infrastructure to GPU-accelerated Parabricks. Clinical validity was assessed by testing those same 25 patients who each had a minimum of 1 year of clinical follow up data and using the determined mean variant allele fraction (VAF) to classify them as MRD-positive or MRD-negative. MRD classifications were compared to a CLIA / CAP-validated orthogonal tumor-informed whole-genome sequencing-based ctDNA MRD assay. Additionally, as artifacts introduced during library preparation and sequencing remain challenges to sensitive low VAF mutation detection, a base-error model (BEM) that reduces sequencing artifacts and maximizes ctDNA signal was built using a series of high-quality lymph reference samples to quantify the background noise of each tumor variant[3]. A GPU-accelerated pipeline was implemented for this step when generating the baseline. Tumor-derived variants in lymph samples were considered artifacts if the VAF was not greater than BEM cutoff controlled by false discovery rate.

We observed significant reduction in processing time and cost at the steps that implemented GPU acceleration. At alignment, we reduced processing time by 30% and computation cost by 15%. At tumor-informed variant calling, we reduced the average processing time from over 2 hours to 30 minutes per sample. For BEM, combined with optimization on VCF filtering, we have reduced processing time from over 5 hours to 45 minutes along with 60% reduction in computation cost. Furthermore, the comparison between our enhanced method and the CLIA / CAP-validated assay showed high concordance with p-val = 0.0005 using Fisher’s exact test. We achieved 84% percent agreement, indicating the accuracy of the GPU-accelerated pipeline.

We demonstrated that our GPU-accelerated MRD pipeline using NVIDIA Parabricks delivers clinical-grade accuracy with significant performance boost, enabling scalable, rapid molecular insights for adjuvant decision making. Given its advantages, we envision that GPU acceleration will prove useful to be a general strategy for deep sequencing applications.

#5516 Learning-based invariant feature engineering reveals symmetry-encoded fingerprints of cancers that facilitate drug discovery.

Cristina Correia[1], Choong-Yong Ung[2], Cheng Zhang[2], Shizhen Zhu[2], Hu Li[2]

[1]Department of Molecular Pharmacology and Experimental Therapeutics, Mayo Clinic College of Medicine, Mayo Clinic, Rochester, MN,[2]Mayo Clinic, Rochester, MN

Background: Symmetry principles, a long foundational framework in physics and chemistry, have rarely been applied to understand biological phenotypes especially in cancers. Here we examine whether symmetric relationships in gene expression can characterize and differentiate healthy from disease conditions.
Method: To test this concept, we built a hybrid machine-learning framework, Learning-Based Invariant Feature Engineering (LIFE), that applies two symmetric invariant feature functions, IFF1 and IFF2, to all possible gene pairs in bulk transcriptomic datasets to identify invariant feature genes (IFGs) - gene pairs whose transformed expression values by either IFF1 or IFF2 produce quasi-constant single-value outputs within a phenotype despite inter-individual variability.
Results: Using bulk transcriptomes from 25 normal organs (GTEx) and 25 cancer types (TCGA), we computed IFF values for all normally distributed gene pairs, selected the 1000 most stable pairs per phenotype, and evaluated their performance in multiclass classification with five-fold cross-validation and independent hold-out testing. IFGs generated >70% accuracy across organs and cancers, establishing the existence of robust phenotype-specific symmetry “fingerprints.” Mapping approved and experimental drug targets onto networks construction from IFGs (IF-Nets) showed strong enrichment of hubs in cancer networks and highlighted the use of IF-Nets as drug discovery platforms in cancer treatment.
Conclusion: Our findings demonstrate that gene-expression symmetry as a unifying organizing principle for phenotype definition and illustrate how IFGs and IF-Nets can guide biomarker design and symmetry-aware pharmacological intervention via “symmetry breaking.”

#5517 Standardizing global patient safety and site compliance in oncology trials using a configurable, technology-driven oversight model.

Ashley Herrick, Dmitri Berman, Elaina Haeuber, Sandy Shah, Salini Naidu

Oncology, Premier Research, Morrisville, NC

Background:
Variability in how adverse events (AE), protocol deviations (PD), and response assessments are reviewed across sites can delay detection of emerging issues in oncology trials—especially in global studies with dispersed teams. To address this, Premier Research implemented Remarque, a proprietary, technology-enabled data oversight platform to centralize trial intelligence, standardize review workflows, and provide near-real-time visibility into patient safety and data quality.
Methods:
Remarque integrates various clinical and operational data streams into a unified environment. Configurable analytics, dashboards, and built-in audit trails align clinical operations, data management, central monitoring, and medical/safety review on a single, traceable process. Key features include standardized review templates, data-driven alerts for AE clusters, customizable views of safety and efficacy data, and traceable documentation to support inspection readiness. Remarque was deployed across more than 30 oncology studies including novel therapeutics and first-in-class products, spanning different geographies.
Results:
Deployment of Remarque enabled earlier detection of common safety patterns, including clusters of low-grade toxicities and delayed AE entry. Studies using the platform achieved faster signal-to-action time and more consistent AE review. Near-real-time collaboration between central monitoring and medical monitoring allowed earlier flagging of potential eligibility concerns, decreasing eligibility-related non-compliance. Ability to trend data patterns within and across sites allowed for monitoring of site's execution of critical processes such as AE capture, reducing time to detection of AE underreporting from an average of 4-6 weeks down to 5-7 days. Notably, Remarque central monitoring identified 55% of PDs that occurred, with a 20% reduction in time from PD occurrence to identification. Centralized traceability strengthened data defensibility for regulatory review and facilitated proactive remediation of recurring data-quality findings. Overall, this resulted in cleaner data, efficient patient safety management, and improved patient retention.
Conclusions:
A technology-driven oversight model improved the reliability, transparency, and timeliness of data review in oncology trials. By replacing fragmented processes with a standardized framework, Remarque enabled earlier signal detection, reduced variability, and improved data quality. This approach reflects how integrated digital infrastructure enhances clinical and medical oversight and supports the goal of safeguarding patients while accelerating efficient delivery of effective cancer therapies globally.

#5518 Towards an accurate quantum support vector module for predicting cancer cell dynamics.

Amit Prakash

Illinois Mathematics and Science Academy, Aurora, IL

High dimensional cancer omics datasets capture molecular heterogeneity central to tumor progression and treatment resistance, yet classical methods often compress or obscure this structure when faced with nonlinear variation. Identifying computational frameworks that preserve oncogenic signals while distinguishing subtle phenotypic states remains a major challenge. To address this, we introduce QomiKS, a Quantum Oncological Kernel Suite designed to examine how quantum enhanced feature spaces recover biologically meaningful separation among cancer phenotypes.Using fidelity based quantum kernels, classical Gram matrices, and a lightweight NumPy angle encoding pipeline, we evaluate how separability among tumor derived samples shifts under different encoding schemes. Early PCA driven quantum models provided modest improvements but required substantial computational resources. In contrast, angle encoded QSVMs produced sharper discrimination among malignant and nonmalignant states while lowering computational cost, showing that quantum kernels can preserve high value oncogenic structure even with minimal features. Implementations using ZZFeatureMap and PauliFeatureMap revealed complementary sensitivities to pathway level nonlinearities linked to proliferation, immune evasion, or metabolic change.Across diverse datasets, we observe a consistent pattern. Classical SVMs dominate in extremely low data regimes due to their stability when oncogenic signal is sparse. As training sizes increase, QSVMs increasingly recover latent biological structures that classical kernels fail to resolve, ultimately surpassing classical baselines with statistically significant gains. This reflects a shift from noise limited to structure limited learning in which quantum feature spaces act as geometric projectors that amplify subtle differences in oncogenic programs, lineage states, or microenvironmental adaptation.These findings show that classical and quantum models encode cancer specific biology in fundamentally different ways. QomiKS provides a framework for understanding these differences and identifies conditions in which quantum kernels yield clearer discrimination of malignant phenotypes. As quantum hardware develops and multi omics cohorts grow, quantum kernel learning may offer a promising route for decoding complex molecular landscapes that govern tumor behavior and for supporting more precise classification and therapeutic stratification.

#5519 SOMaC: An interpretable and generalizable framework for integrating and clustering multimodal spatial omics to resolve cell states and immune niches in cancer.

Junming Shi, Md Tauhidul Islam

Stanford University School of Medicine, Stanford, CA

Spatial omics technologies, including spatial transcriptomics and multiplex spatial proteomics, provide unprecedented opportunities to characterize cellular organization, microenvironmental interactions, and functional states within intact tumor tissues. However, integrating these heterogeneous modalities and resolving spatially coherent cell states and immune niches remain major computational challenges. Existing approaches typically analyze individual modalities in isolation, rely on expression-based feature spaces that overlook higher-order molecular structure, and provide limited interpretability for biological discovery.

We present SOMaC, an interpretable and generalizable framework for integrating and clustering multimodal spatial omics data to resolve cellular and microenvironmental architecture in cancer tissues. SOMaC extends the OmicsMap paradigm by transforming each cell or spot into an image-like molecular interaction map that encodes pairwise gene or protein correlations, capturing regulatory structure beyond conventional expression matrices. These biologically grounded representations are jointly integrated with spatial topology using a convolutional autoencoder, graph neural network, and learnable-center clustering module, enabling end-to-end optimization of molecular-spatial embeddings for domain discovery.

Across 13 benchmark datasets spanning nine human and mouse tissues profiled by 10x Visium, Xenium, Slide-seqV2, Stereo-seq, imaging mass cytometry (IMC), and CODEX, SOMaC consistently outperformed leading methods such as GraphST and SEDR. SOMaC achieved significantly higher clustering quality, with an average Silhouette score of 0.21 (vs. 0.11 for GraphST) and more than a two-fold improvement in the Calinski-Harabasz Index, indicating tighter and more separable spatial domains. On multiplex proteomics datasets, including human colon cancer IMC, SOMaC demonstrated strong cross-modality generalization, achieving a Calinski-Harabasz Index of 40,541 and a Davies-Bouldin Index of 3.03. Notably, SOMaC resolved fine-scale tumor-immune interfaces, stromal barriers, and functional immune niches that were poorly captured by existing methods.

By jointly modeling molecular interaction structure and spatial architecture across transcriptomic and proteomic platforms, SOMaC provides a unified and interpretable framework for dissecting tumor ecosystems. This approach enables high-resolution discovery of spatially organized cell states, regulatory programs, and microenvironmental niches, offering new insights into cancer biology and therapeutic targeting.

#5520 Multi-modal integration in the NetFlow framework for comprehensive exploratory data analysis.

Rena Elkin, Jung Hun Oh, Anish K. Simhal, Joseph O. Deasy

Memorial Sloan Kettering Cancer Center, New York, NY

High-dimensional biomedical studies increasingly require comprehensive exploratory tools that jointly model, integrate, and visualize sample organization across modalities within a single, interpretable framework. We therefore developed NetFlow, a computational framework that constructs a Pseudo-Organizational StructurE (POSE) graph of sample relationships from high-dimensional and multimodal data, preserving both continuous variation and local neighborhoods while enabling downstream analytics in the same space. Glioblastoma (GBM) exhibits pronounced heterogeneity across transcriptomic, epigenomic, and miRNA profiles that complicates subtype discovery and interpretation. To demonstrate NetFlow's multi-modal integration capability, we applied it to TCGA GBM (n=213) with matched mRNA expression, DNA methylation, and miRNA profiles. Per-modality sample-sample distances were computed, each was transformed to a common range, and then fused into a unified similarity matrix. Next, diffusion-based, multi-scale metrics on the fused similarity seeded a lineage-tracing-inspired backbone augmented with mutual nearest neighbor edges to build the POSE. The NetFlow framework enabled POSE-aware clustering, survival analysis, and cross-omic differential feature testing. The POSE revealed a distinct lower-risk GBM subgroup with significantly improved overall survival (log-rank $P=1.19x10^{-5}$) that was not reproducible from any single modality alone. This subgroup exhibited a cross-omic signature including reduced mRNA expression of *EMP3* and *TIMP1*, *CRIP1* hypermethylation, and decreased *miR-222* expression. Additionally, the identified subgroup showed clinical correlates consistent with favorable prognosis including enrichment for *IDH1* mutation and younger age. We further quantified edge-level modality influence, which indicated balanced contributions from each modality, supporting genuine multi-modal integration rather than dominance by any single data type. These results establish that NetFlow yields an interpretable, modality-balanced POSE. They further demonstrate that its unified modeling, integration, visualization, and analysis enables discovery of prognostically relevant subgroups and cross-omic biomarkers. More broadly, NetFlow provides a practical, extensible framework for comprehensive exploratory data analysis in multi-modal oncology cohorts that generalizes beyond GBM to accelerate hypothesis generation and subtype refinement in diverse settings.

#5521 MeDOC-KB: Knowledge base for unraveling the metabolic links between obesity-related cancers.

Madhan Subramanian[1], Sam Rosin[1], Stephanie Hall[2], Nisha Grover-Fairchild[2], Kim Robien[3], Loretta DiPietro[3], Marinella Temprosa[1]

[1]Biostatistics and Bioinformatics, Milken Institute School of Public Health, George Washington University, Washington, DC,[2]George Washington University Biostatistics Center, Bethesda, MD,[3]Exercise and Nutrition Sciences, Milken Institute School of Public Health, George Washington University, Washington, DC

Metabolic Dysregulation and Obesity Cancer Risk Consortium (MeDOC) is an NCI-sponsored program using team science and transdisciplinary approach to elucidate mechanisms linking obesity, metabolic dysregulation, and cancer risk. Both obesity and metabolic dysregulation contribute to a cascade of derangements in adipocyte function, growth factors, inflammation, gut microbiome, immune function, sex hormones, lipid and glucose metabolism which, in turn, can disrupt several downstream signaling pathways related to cancer initiation and progression. Given this complexity, integrating multi-omic, mouse models and epidemiologic data is critical. The MeDOC-Knowledge Base (MeDOC-KB) is a comprehensive atlas cataloging associations to link obesity, metabolic dysregulation, and cancer risk from consortium studies and external literature. A large language model-based agent harmonized biomarkers derived from metabolomics, proteomics, and lipidomics platforms such as Nightingale, Olink, and Metabolon, standardizing nomenclature and resolving cross-platform synonyms into a unified vocabulary. MeDOC-KB uses a Neo4j graph database architecture to enable efficient traversal of complex relationships among the biomarkers, publications, cohorts, and cancer sites. Literature data are extracted into four core tables (Citation, Cohort, Methods, and Association) and transformed into a graph structure where nodes represent publication, cohorts, biomarkers, and cancer sites while edges denote their relationships. MeDOC-KB is accessible through an interactive R Shiny web application. The current version contains 42,838 nodes and 189,709 relationships with 21,945 being biomarker-cancer associations spanning 1,645 biomarkers and 15 cancer outcomes, including 11 of the 13 known obesity related cancers. For example, MeDOC-KB reveals that insulin-like growth factor binding protein-1 (IGFBP-1) shows inverse associations with endometrial, colorectal, and pancreatic cancers across multiple cohorts, suggesting shared metabolic mechanisms. The platform enables researchers to identify biomarker patterns associated with obesity-induced metabolic dysregulation across cancer types, compare findings across cohorts, and discover understudied biomarker-cancer relationships. MeDOC-KB provides a critical resource for hypothesis generation regarding mechanistic pathways, biomarker validation across populations, and identification of promising targets for cancer prevention strategies in high-risk metabolic populations. The knowledge base is publicly accessible and will be continuously updated with consortium findings and literature.

#5522 scSurvival: Single-cell survival analysis of clinical cancer cohort data at cellular resolution.

Tao Ren[1], Faming Zhao[2], Canping Chen[1], Lingyun Wu[3], Gordon B. Mills[2], Lisa M. Coussens[4], Zheng Xia[1]

[1]Oregon Health & Science University, Portland, OR,[2]OHSU Knight Cancer Institute, Portland, OR,[3]Academy of Mathematics and Systems Science, Chinese Academy of Sciences, Beijing, China,[4]OHSU Knight Cancer Institute, Lake Oswego, OR

Survival analysis is fundamental to cancer research. Advances in technology have enabled an increasing number of cohort-level cancer studies to incorporate single-cell sequencing while collecting clinical survival data. However, no effective strategy currently exists for directly modeling survival outcomes from single-cell data. To address this gap, we present scSurvival, an attention-based multiple-instance Cox regression framework that models each patient as a bag of cells to predict survival outcomes at both the patient and single-cell levels. To handle high dimensionality, sparsity, and batch effects, scSurvival integrates a variational autoencoder-based feature extraction module with generative modeling to enhance feature robustness and cross-batch generalizability. Comprehensive simulations demonstrate scSurvival's superior performance and scalability. In melanoma and liver cancer scRNA-seq cohorts, scSurvival accurately predicts patient outcomes and identifies the cell subpopulations most critical to survival. Overall, scSurvival enables robust prediction of patient survival while uncovering survival-associated cell subpopulations, advancing single-cell survival analysis in cancer research.

#5523 TNMplot 2.0: Stage-resolved and pan-cancer transcriptomic analytics for target discovery in oncology.

Aron Baratha, **Balazs Gyorffy**

Semmelweis University, Budapest, Hungary

BACKGROUND. TNMplot.com is a web-based resource that integrates RNA-Seq and gene-chip data from 56,938 samples, enabling differential gene expression analysis among normal, primary tumor, and metastatic tissues across 22 cancer types. Here, an updated version of the TNMplot database was established featuring new capabilities that advance pharmacological and translational oncology research.

METHODS. We implemented a stage-based expression module using 4,521 tumors from breast (n=2,331), colorectal (n=648), lung (n=1,399), skin (n=82), and prostate (n=61) cancer. We added pan-cancer dot-matrix visualization and extended multi-gene tools including density analyses, correlation matrices, correlation profiling, signature evaluation, and targetgram analysis. Using the integrated database, we performed parallel RNA-seq and microarray validation to identify druggable candidates.

RESULTS. The stage module was used to evaluate isolated genes linked to tumor progression and therapeutic timing. Multi-gene and pan-cancer functions enabled rapid mapping of druggable pathways and co-expression structures. Cross-platform filtering highlighted MET (p = 5.1e-69), FGFR4 (p = 1.59e-49), and EZH2 (p = 1.08e-54) as robust progression-associated candidates for repurposing in advanced colon cancer. A separate screening of dysregulated colon cancer genes identified 16 FDA-approved drug targets through ≥2-fold expression changes and ChEMBL matching, with LY6E and CDK1 each surpassing a 3-fold differential threshold. The complete combined database was integrated into our analysis platform available at www.tnmplot.com.

CONCLUSIONS. The upgraded TNMplot platform provides a unified, high-fidelity environment for progression analysis, biomarker discovery, and pharmacological target prioritization across multiple cancers. A unique feature of the database is the parallel analysis of RNA-seq and gene array cohorts, enabling robust cross-platform validation of candidate biomarkers.

#5524 Visualization and analysis of cancer genomics data using UCSC Xena.

Mary Goldman[1], Brian Craft[1], Cally Lin[2], Jingchun Zhu[1], David Haussler[3]

[1]UC Santa Cruz Genomics Institute, Santa Cruz, CA,[2]Stanford University, San Francisco, CA,[3]Investigator/Distinguished Professor, Ctr. For Bio. Sci. & Eng., UC Santa Cruz, Santa Cruz, CA

UCSC Xena (http://xena.ucsc.edu/) is a web-based visual integration and exploration tool for both bulk and single-cell multi-omic data, and associated clinical and phenotypic annotations. Researchers can easily view and explore public data, their own private data (bulk only), or both using the Xena Browser. Private data are kept on the researcher's computer and are never uploaded to our public servers. We support Mac, Windows, and Linux.

Questions Xena can help you answer:* Is overexpression of this gene associated with survival differences?* What genes are differentially expressed between these two groups of samples?* What is the relationship between mutation, copy number, expression, etc for this gene?

Xena visualizes seminal cancer genomics datasets from TCGA, the Pan-Cancer Atlas, GDC (a complete update from 2024, including new data from CPTAC3 and HCMI), PCAWG, ICGC, and more; a total of more than 1500 datasets across 50 cancer types. We support virtually any type of functional genomics data: SNPs, INDELs, copy number variation, gene expression, ATAC-seq, DNA methylation, exon-, transcript-, miRNA-, lncRNA-expression and structural variants. We also support clinical data such as phenotype information, subtype classifications and biomarkers. All of our data is available for download via python or R APIs, or using our URL links.

Our signature Visual Spreadsheet view shows multiple data types side-by-side enabling discovery of correlations across and within genes and genomic regions. We also have dynamic Kaplan-Meier survival analysis, powerful filtering and subgrouping, differential gene expression analysis, GSEA, charts, statistical analyses, genomic signatures, and the ability to generate URLs to live views.

We now visualize single-cell data, primarily gene, transcript, and protein expression, from spatially-resolved and disassociated single cell datasets. Using Xena, researchers can visualize 2D or 3D embedding views, such as tSNE and UMAP as well as the spatial imaging views, such as H&E, multiplex immunofluorescence, and co-registration of both. Crucially, we overlay genomic data — such as gene and protein expression, genomic signature scores, cell annotations, and label transfer information — on top of these images dynamically. We support a diverse range of data modalities ranging from 10x Chromium and Smartseq2 platforms for scRNA-seq and 10x scATAC-seq, to spatial transcriptomics platforms of Visium, Visium HD, Xenium, CosMx, and MERFISH/Vizgen, to imaging proteomics such as t-CycIF, CODEX, and MIBI-TOF. We showcase data from the HTAN data portal.

If you use us please cite our publication in Nature Biotechnology: https://www.nature.com/articles/s41587-020-0546-8

#5525 Aneuploidy prediction in the spatial domain.

Calogero Carlino[1], Valentina Giansanti[1], Giovanni Petri[2], Davide Cittaro[1]

[1]Universita Vita-Salute San Raffaele, Milano, Italy,[2]Network Science Institute, Northeastern University London, London, United Kingdom

Cancer emergence and progression are often driven by genomic instability and disruption of the tissue microenvironment. Insights on the prognostic values of genomic features have been reported in cohort of cancer patients, suggesting Copy Number Alterations (CNAs) signature as highly relevant in multiple cancer types [1,2]. Moreover, insights on the transcriptional state of the tumor microenvironment suggest the recurrence of spatially defined gene modules with functional significance among cancer states [3].Building on the above insights, we aim to study the topology of the spatial distribution of CNAs and its influence on the transcriptional state of the tumor microenvironment. To this end, we describe a workflow that enables the prediction of CNAs in spatially resolved transcriptomics data, and the construction of a topological signature from the CNAs prediction map of the tumor sample. The topological signature is then used as a topological descriptor of the tumor microenvironment.We ported to Python the Numbat algorithm [4] and expanded it with a custom implementation of personalized PageRank algorithm [5] on the diffusion map [6] of the CNAs feature, enhancing the spatial signal of the predicted CNAs. Superlevel set filtration is then applied to the CNAs predictions, obtaining a persistent homology signature of the CNAs spatial distribution [7].Experiments suggest that our method for including the spatial context in CNAs predictions produces simpler data topology (spatial smoothing) and, similarly to a recent report [8], that the resulting persistent homology signature of spatial CNAs can be used to discriminate between states of the tumor microenvironment.

References:

1. Smith JC, SheltzerJM. Genome-wide identification and analysis of prognostic features in human cancers. Cell Rep. 2022.
2. Steele, C.D., Abbasi, A., Islam, S.M.A. et al. Signatures of copy number alterations in human cancer. Nature 606, 984-991 (2022).
3. Barkley, D., Moncada, R., Pour, M. et al.Cancer cell states recur across tumor types and form specific interactions with the tumor microenvironment. Nat Genet54, 1192-1201 (2022).
4. Gao, T., Soldatov, R., Sarkar, H. et al. Haplotype-aware analysis of somatic copy number variations from single-cell transcriptomes. Nat Biotechnol 41, 417-426 (2023).
5. Page, L. and Brin, S. and Motwani, R. and Winograd, T. (1999). The PageRank Citation Ranking: Bringing Order to the Web. Technical Report. Stanford InfoLab.
6. R.R. Coifman, S. Lafon, F. Warner, & S.W. Zucker. Geometric diffusions as a tool for harmonic analysis and structure definition of data: Diffusion maps, PNAS. U.S.A. (2005).
7. Carlsson, G. E. (2009). Topology and data. Bulletin of the American Mathematical Society, 46(2), 255-308.
8. I. H.R. Yoon, R. Jenkins, C. Swanton, H. M. Byrne, E. Sahai. Deciphering the diversity and sequence of extracellular matrix and cellular spatial patterns in lung adenocarcinoma using topological data analysis. bioRxiv 2024.01.05.574362

: Bi- and Tri-Specific Antibody Therapies
Poster Session

#5529 Preclinical characterization of LY4336619, a novel ALPPL2xCD3 bispecific antibody, for the treatment of ovarian and endometrial cancer.

Colleen Burns[1], Julie Dobkin[1], Kevin Lindquist[2], Hee Rae Shin[1], Cindy Nguyen[1], Wei Yang[1], Xiaodong Huang[1], Marie Mutryn[1], Whitney S. Helms[3], Nicholas Arce[2], Yvonne Mak[2], Alexandra Antonoplis[2], Amelie Forest[1], Abraham Abouzeid[4], Marta Witek[4], Claire F. Friedman[1], Zhao Hai Lu[4], Mohan Srinivasan[2], Kyla Driscoll[1], Andrew Hass[4], Omar Duramad[2], Rikke Holmgaard[1], Kristin Bedard[2]

[1]Eli Lilly and Company, New York, NY,[2]Eli Lilly and Company, South San Francisco, CA,[3]Eli Lilly and Company, Silver Spring, MD,[4]Eli Lilly and Company, Indianapolis, IN

Development of CD3-bispecific antibodies has been challenging in solid tumors due to the difficulty identifying tumor antigens with high tumoral expression but with minimal or no expression in normal tissues. Placental-like alkaline phosphatase 2 (ALPPL2) is overexpressed in various solid tumors, including ovarian and endometrial carcinomas, while its expression in normal tissues is largely restricted to the placenta. This expression profile makes ALPPL2 a promising target for CD3-bispecific antibody therapies. We have developed a fully human common light chain-based ALPPL2×CD3 bispecific antibody, LY4336619, on an Fc-silenced IgG1 backbone designed to engage ALPPL2 on tumor cells and CD3 on T cells, facilitating targeted T cell-mediated cytotoxicity against ALPPL2-expressing tumor cells. LY4336619 was generated by pairing a novel anti-ALPPL2 monoclonal antibody, identified through a murine immunization strategy, with an anti-CD3 antibody. The binding, target selectivity, and cytotoxic activity of LY4336619 were evaluated using multiple ALPPL2-expressing cell lines. *In vivo* efficacy was evaluated using immunocompromised murine models engrafted with human tumor xenografts and human peripheral blood mononuclear cells (PBMCs). Additionally, a comprehensive proteomics analysis was performed to characterize ALPPL2 expression across tumor tissue specimens. LY4336619 specifically bound to ALPPL2-expressing cell lines but spared ALPI and ALPL, the other more widely expressed alkaline phosphatase family members; it also bound to the highly homologous ALPP family member, a protein with similar limited normal expression and association with similar tumor types. LY4336619 engaged with both CD3 and ALPPL2, and induced concentration-dependent T-cell activation and T cell-mediated cytotoxicity in co-culture assays with T cells and ALPPL2-expressing tumor cells. Furthermore, it demonstrated antitumor activity and relatively low cytokine release as a single agent in human PBMC-engrafted mice with human tumor xenografts representing a range of ALPPL2 expression levels. Additional preliminary studies revealed that the combination treatment with LY4170156, a clinical-stage anti-FRα antibody-drug conjugate (ADC), resulted in more sustained and pronounced tumor growth inhibition compared to either monotherapy alone. Our ALPPL2×CD3 bispecific antibody exhibited IgG-like pharmacokinetics and low immunogenic potential. These findings demonstrate that LY4336619 has target specificity, favorable functional activity, and a promising developability profile. LY4336619 has the potential as a first-in-class medicine to treat ALPPL2-positive solid tumors, including ovarian and endometrial cancers. An IND submission is anticipated for 2026.

#5530 Preclinical validation of the antitumor activity and safety of M0324, a novel MUC-1 conditional CD40 agonist, and its combination with immune checkpoint inhibitors (ICIs), for selective immune activation.

Weixiao Sha[1], Jing Ni[1], Anika Bergmann[1], Nathalie Duncan[1], Bo Marelli[2], Feng Jiang[2], Julia Marie Mueller[1], Sina Junkers[1], Christina Hubl[1], Ivana Durutovic[1], Sonia Jaramillo[1], Paul D. Lyne[2], Laura Helming[2]

[1]the healthcare business of Merck KGaA, Darmstadt, Germany,[2]EMD Serono, Billerica, MA

Background: MUC-1, a glycoprotein commonly overexpressed in various cancers, plays a pivotal role in tumor progression and immune evasion. M0324 is a novel MUC-1-conditional CD40 agonist designed to activate antigen-presenting cells in the presence of MUC-1-overexpressing tumor cells. Targeted CD40 activation could minimize systemic toxicity observed with first-generation unconditional CD40 antibodies.

Methods: The effect of M0324 on the activation of CD40 expressed on human dendritic cells (DCs) was assessed *in vitro* and benchmarked against anti-CD40 antibodies, using MUC-1 expressing HCC827 tumor cell line co-cultured with primary human monocyte-derived DCs. Co-culture of human primary B cells with human tumor cell lines with various MUC-1 expression was analyzed to further characterize MUC-1 dependent M0324 activity. *In vivo* efficacy was evaluated using M0324m, a mouse surrogate for M0324, as monotherapy or in combination with anti-PD-L1, in hMUC-1 expressing tumor models.

Results: *In vitro*, M0324 significantly enhanced DC activation in the presence of MUC-1 expressing tumor cells; no activity was observed in the absence of MUC-1 expressing cells. M0324 led to higher activation of IL-12p40 expression in DC HCC827 tumor cell co-cultures versus other agonistic anti-CD40 antibodies. Co-culture of human primary B cells with tumor cell lines with various levels of MUC-1 expression demonstrated that M0324-induced B cell activation was linked to MUC-1 expression levels on tumor cells. *In vivo*, a single dose of M0324m demonstrated robust tumor eradication in hMUC-1^{high} immune competent mouse tumor models (orthotopic Panc02-MUC-1 model: 93%; MC38-MUC-1 model: 100% tumor-free mice). The lack of body weight loss in mice after M0324m dosing indicated minimal off-tumor effects and increased therapeutic index due to the conditional activation of CD40 in the presence of MUC-1. In contrast, anti-mouse CD40 benchmark antibody induced body weight loss, and its marginally tolerable dose failed to control tumor growth. M0324m also demonstrated robust antitumor activity in hMUC-1^{int} tumor models (MC38, 4T1). Combination of M0324m with anti-PD-L1 in hMUC-1^{int} tumor model further improved tumor growth inhibition.

Conclusions: M0324 was shown to selectively activate DC and B cells only in the presence of MUC-1 expressing tumor cells, demonstrating superior *in vitro* and *in vivo* activity compared to anti-CD40 agonistic antibodies. M0324m further improved tumor control when combined with anti-PD-L1. M0324m was also well-tolerated *in vivo*. Overall, the preclinical data suggest that combination of M0324 with ICIs may maximize the rigor of *de novo* or pre-existing T cell responses. A Phase 1 study of M0324 as monotherapy and in combination with pembrolizumab and chemotherapy is ongoing (NCT07166601).

#5532 Bispecific antibodies targeting EGFR and HER2 for effective killing of solid tumor cells via a safe CD47-SIRPA modulation.

Eric Hatterer, Vanessa Buatois, Alizee Viandier, Emeline Rousset, Cecile Raymond, Adeline Lesnier, Pauline Lloveras, Christelle Mougin, Ulla Ravn, Pauline Malinge, Frederic Bollin, Limin Shang, Walter Ferlin, Nicolas Fischer, Jose Saro, Krzysztof Masternak

R&D, Light Chain Bioscience - Novimmune SA, Plan-Les-Ouates, Switzerland

INTRODUCTION: The CD47-SIRPα axis is a crucial immune checkpoint, allowing tumor cells to evade immune destruction. Initial efforts to target CD47 with monoclonal antibodies and SIRPa-Fc fusion proteins encountered significant hurdles due to ubiquitous and abundant CD47 expression in particular on blood cells (including RBC and platelets). To overcome the limitation of mono-specific CD47 targeting, we generate bispecific antibodies (bsAbs) that block CD47 selectively on tumor cells, upon co-engagement of a tumor-associated antigen (TAA) on the cell surface. Harboring an immunologically active Fc portion (human IgG1 Fc) these TAA/CD47 bsAbs mediate efficient tumor cell killing through antibody-dependent cellular phagocytosis (ADCP) and antibody-directed cellular cytotoxicity (ADCC). Importantly, this strategy has now been clinically validated: NI-1801, our mesothelin/CD47 bsAb, has demonstrated selective and safe CD47 targeting together with encouraging antitumor activity in heavily pretreated ovarian cancer patients (1).

METHODS: EGFR/CD47 and HER2/CD47 bispecific antibodies were assembled using the κλ-body technology/platform (2). For that goal, high affinity antibody arms specific to different regions of the extracellular domains of EGFR or HER2 were paired with a low affinity anti-CD47 arm. The resulting hIgG1 bsAbs were tested *in vitro* for activity in ADCP assays with TAA-positive tumor cells and monocyte-derived macrophages as effector cells, and in ADCC assays using unfractionated PBMCs as effector cells.

RESULTS: The EGFR/CD47 and HER2/CD47 bsAbs efficiently induce ADCP and ADCC of tumor cell expressing varying levels of EGFR or HER2, respectively, including low level-expressing cancer cell lines. Interestingly, we could observe that the killing activity depended not only on the affinity of the TAA arm, but also on the region of the ECD bound by the TAA arm, suggesting that the geometry of the antigen-co-engagement on tumor cell surface may affect the efficiency of the immunological synapse. This was particularly apparent when comparing the killing activity mediated by different HER2xCD47 bsAbs.

CONCLUSION: The “unbalanced affinities” design of TAA/CD47 bispecific antibodies effectively addresses the safety and pharmacokinetic liabilities observed with monospecific CD47 antibodies. Importantly, our clinical experience with NI-1801 (MSLN×CD47) validates both the safety and the potential clinical benefit of this tumor-restricted CD47-blocking strategy (1). Together, these findings support TAA/CD47 bsAbs as a valuable addition to the anti-cancer armamentarium, with the EGFR/CD47 and HER2/CD47 bsAbs described here representing promising development candidates. *(1) De La Motte Rouge T. ESMO 2025 (Abstract #1512O) (2): Fischer N. Nat Commun, 2015 Feb 12:6:6113*

#5533 VISTA×MSLN bispecific antibody-directed therapies as a biomarker-guided strategy for epithelioid malignant pleural mesothelioma.

Sang Moo Lee[1], Hee geon Park[2], Gyo-Jin Choi[1], Myeung Ryun Seo[1], Ji Eun Park[3], Seok Gyeong Yun[1], Na Eun Jeong[1], Soo Jin Ryu[1], Yeong Jeong Jeon[4], Yoon La Choi[5], Sung Youl Hong[6], Young Kee Shin[1]

[1]Department of Molecular Medicine and Biopharmaceutical Sciences, Seoul National University, Seoul, Korea, Republic of,[2]ABION INC., Seoul, Korea, Republic of,[3]Research Institute of Pharmaceutical Science, College of Pharmacy, Seoul National University, Seoul, Korea, Republic of,[4]Department of Thoracic and Cardiovascular Surgery, Samsung Medical Center, Sungkyunkwan University School of Medicine, Seoul, Korea, Republic of,[5]Department of Pathology and Translational Genomics, Samsung Medical Center, Sungkyunkwan University School of Medicine, Seoul, Korea, Republic of,[6]BitD Inc., Siheung, Korea, Republic of

Background Malignant pleural mesothelioma (MPM) is a rare, lethal cancer largely linked to asbestos exposure, with a 5-year overall survival <20%. Until the approval of nivolumab plus ipilimumab (CheckMate 743), platinum-based chemotherapy was the only systemic standard of care. The epithelioid subtype (~70% of cases) of MPM derives limited benefit from current ICIs, underscoring the need for biomarker-guided therapies. We identified co-expression of the immune checkpoint V-domain Ig suppressor of T-cell activation (VISTA) and the tumor-associated antigen mesothelin (MSLN) in epithelioid MPM and validated this axis by scRNA-seq, which demonstrated concordant VISTA and MSLN transcription within malignant epithelioid clusters. Based on this biomarker pair, we engineered an anti-VISTA×MSLN bispecific antibody (BsAb) and explored multiple modalities, including an IFN-β mutein immunocytokine and bispecific ADC concepts.
Method Anti-VISTA×MSLN BsAb formats were designed and screened for optimal binding/cell-surface coverage on VISTA/MSLN co-expressing cells. A stability/production/PK-enhanced IFN-β mutein relative to recombinant IFN-β was fused to the BsAb to generate a trispecific immunocytokine. In vitro binding, internalization, and effector assays were performed in human MPM cell lines. In vivo antitumor activity and TME modulation were tested in xenografts and a syngeneic mouse model; a subset used human IFNAR1/2 knock-in (hIFNAR1/2-KI) mice. To assess suitability for payload delivery, we analyzed antigen-dependent internalization and early bispecific ADC feasibility in vitro.
Results scRNA-seq confirmed VISTA/MSLN co-expression in malignant epithelioid populations, supporting VISTA×MSLN as a therapeutic axis. The anti-VISTAxMSLN BsAb showed enhanced binding to dual-positive cells relative to the parental monospecific antibodies and efficient, antigen-driven internalization. The trispecific immunocytokine retained BsAb targeting and induced type I IFN-dependent tumor-cell killing and immune activation in vitro. In vivo, it produced significant antitumor activity in MPM models, including in hIFNAR1/2-KI mice, and remodeled the TME consistent with enhanced antitumor immunity. Internalization/trafficking supported feasibility of developing anti-VISTA×MSLN BsAb ADCs as an additional therapeutic modality.
Conclusion VISTA/MSLN co-expression defines a biomarker-guided therapeutic axis in epithelioid MPM. The engineered anti-VISTAxMSLN BsAb is a versatile scaffold enabling multiple modalities — including an IFN-β mutein immunocytokine with in vivo efficacy and TME reprogramming—and exhibits internalization compatible with bispecific ADC development. Collectively, these findings support anti-VISTA×MSLN-based therapeutics as promising preclinical candidates for epithelioid MPM.

#5534 INCA036873, a first-in-class CD70×CD3 T cell-redirecting bispecific antibody, for the treatment of CD70-positive malignancies.

Yao-Bin Liu[1], Charlie Kang[1], Christina Stevens[1], Lifeng Zhang[1], Daniel Merenich[1], Emily Ren[1], Chifei Sun[1], Lu Huo[1], Taylor Getty[1], Heather Bullins[1], Zhiwan Dong[1], Zhiying Ji[1], Michelle Kinder[1], Jun Guan[1], Tessa Steevels[2], Femke Feenstra[2], Rinse Klooster[2], David Maussang-Detaille[2], Cynthia Timmers[1], Jonathan Rios-Doria[1], Horacio Nastri[1], Jeff Jackson[1], Patrick Mayes[1], Chryssa Kanellopoulou[1]

[1]Incyte Corporation, Wilmington, DE,[2]Merus NV, Utrecht, Netherlands

CD70 is a member of the tumor necrosis factor ligand superfamily, with CD27 being its sole receptor. Under normal physiological conditions, CD70-CD27 signaling promotes T-cell activation, survival, and differentiation. In normal tissues, CD70 expression is restricted to activated T, B, and dendritic cells. Aberrant CD70 expression is observed in various malignancies, including renal cell carcinoma (RCC), ovarian cancer, acute myeloid leukemia, and non-Hodgkin's lymphoma. This highly selective upregulation in tumor cells and restricted expression in normal tissues make CD70 an attractive therapeutic target.

INCA036873 is a novel Biclonics® bispecific antibody designed to redirect and activate T cells to specifically kill CD70-expressing tumor cells. INCA036873 binds CD70 with high affinity (K_D = 0.4 nM) and CD3 with moderate affinity (K_D = 115 nM), enabling selective T-cell activation, while minimizing systemic immune activation and cytokine release. INCA036873 induced potent CD70-dependent T cell-mediated cytotoxicity of tumor cells. In vitro, INCA036873 demonstrated robust killing across multiple CD70-expressing tumor cell lines as well as freshly disassociated primary patient-derived RCC tumor cells. In vivo, INCA036873 showed strong antitumor efficacy in multiple cell line xenograft models such as 786-O (RCC) and SKOV3 (ovarian cancer), as well as RCC patient-derived xenograft models in human CD34-positive humanized NSG mice. Importantly, INCA036873 exhibited a favorable safety profile, with limited cytokine release in human whole blood cytokine release assays and no adverse findings at doses up to 3.0 mg/kg (>15-fold above the projected therapeutic exposure) in a 4-week toxicology study in huCD70/huCD3EDG knock-in mice. INCA036873 also demonstrated desirable pharmacokinetics in cynomolgus monkeys.

Overall, these data support the advancement of INCA036873 as a promising, potential, first-in-class bispecific T-cell engager antibody for CD70-positive malignancies.

#5535 GPRC5D multispecific antibodies: Engineering for affinity, cross-species reactivity, and bi/trispecific engagement in multiple myeloma.

Hayley Roth, Trevor Barnes, Daniel Rogers, Ileine Sanchez, **Lewis Joe Stafford**, Valerie Firers, Breanna Tyrell, Amelia M. Snyder, Kyle Doolan, Benjamin J. Doranz, Ross Chambers, Joseph B. Rucker

Integral Molecular, Philadelphia, PA

Background: GPRC5D is a G protein-coupled receptor expressed on multiple myeloma cells but largely absent from healthy tissues, making it an attractive target for T cell-engaging multispecific antibodies. Antibodies that simultaneously engage GPRC5D and other molecules (e.g. BCMA and CD3) to activate T cells are anticipated to provide excellent efficacy as monotherapies. Multipass membrane proteins are valuable therapeutic targets but often inaccessible for antibody discovery due to structural complexity and high conservation. Using our membrane protein-optimized discovery platform (MPS), we generated a panel of GPRC5D antibodies and engineered them as bi- and trispecific molecules. We also developed a platform for comprehensive CDR-Scanning of our lead antibody for affinity maturation, developability, and cross-species reactivity for preclinical testing.
Methods: Antibodies against GPRC5D were isolated and formatted as GPRC5D×CD3 and GPRC5D×BCMA×CD3. These molecules were tested for in vitro and in vivo potency, cytokine release, and binding specificity. To further optimize our lead, we developed and optimized method for comprehensive CDR-Scanning where each residue across 6 CDR regions was substituted to all 19 other amino acid variants, generating 986 single residue variants. Variants were individually evaluated for expression and binding using ELISA and assessed for expression and reactivity against both human and cynomolgus GPRC5D. Beneficial substitutions (>200% wild-type binding) were combined using structure-guided and AI/ML-informed design strategies for further validation.
Results: We identified multispecific antibodies that exhibited potent T cell-mediated cytotoxicity with picomolar potency on multiple myeloma cell lines, a large window between cell killing and cytokine release and robust tumor control against multiple myeloma xenografts in a humanized mouse model. Antibody specificity profiling confirmed high specificity binding to the intended targets, without detectable off-target interactions across the membrane proteome. Saturating mutagenesis of the CDR regions of the GPRC5D-binding moiety of the lead antibody identified 14 variants with elevated binding to the human GPRC5D >200% WT, and 10 variants with elevated binding to cynomolgus GPRC5D. Combination yielded more than 20 variants with binding >4,000% WT.
Conclusions: GPRC5D multispecific antibodies hold promise as potent and safe therapeutics for multiple myeloma. Through CDR-Scanning, we are advancing a new generation of GPRC5D antibodies with enhanced attributes, including affinity improvements, pH sensitivity, reduced polyreactivity, improved half-life, and cross-reactivity in cynomolgus for preclinical development.

#5536 Preclinical immunotoxicity assessment of bispecific antibodies using an *ex vivo* circulating human whole blood assay.

Helena Harlin Laven[1], Louise Nilsson[1], Marika Pettersson[1], Gunilla Tornqvist[1], Erika Fletcher[1], Sakthi Ponandai-Srinivasan[1], Sara Mangsbo[2], **Alexander Kele**[1]

[1]Immuneed, Uppsala, Sweden,[2]Uppsala University, Uppsala, Sweden

The technologies for producing bispecific antibodies (BsAbs) are relatively new, and only recently have several BsAbs been approved for clinical use. However, they are often associated with a high risk of cytokine release syndrome (CRS) and other adverse events. Since many BsAbs target antigens unique to humans and given the need for new approach methodologies (NAMs) that comply with the 3Rs, it would be valuable to have an *in vitro* system for predicting immunotoxicity during preclinical development of novel BsAbs.

ID.Flow is an *ex vivo* system using circulating human whole blood at 37 °C, previously evaluated for predicting infusion reactions of monoclonal antibodies and oligonucleotide drugs. The system allows for simultaneous evaluation of multiple immune responses, such as cytokine release, complement activation, activation or depletion of platelets and white blood cells, and coagulation. By using clinically relevant controls, the relative levels of immunotoxicity can be assessed. ID.Flow was used here to evaluate glofitamab, a bispecific T cell engager approved for the treatment of diffuse large B cell lymphoma. Glofitamab is associated with cytokine release syndrome (CRS) including serious or fatal reactions. The efficacy and immunotoxicity of glofitamab were investigated in ID.Flow at concentrations similar to Cmax. As controls, the monoclonal antibodies (mAbs) obinutuzumab and alemtuzumab were used, both of which are associated with CRS in the clinic. Glofitamab resulted in B cell depletion with live B cell counts significantly reduced by 6 hours (60%) and most B cells (90%) depleted by 24 hours. In comparison, B cell depletion using the mAbs occurred with slightly faster kinetics (80-90% depletion by 6 hours). Activation of T cells and B cells was observed in samples treated with glofitamab, but NK cells, granulocytes, and monocytes were also activated. A population of double-positive $CD3^+$ $CD22^+$ events was observed, correlating with the mechanism of action of the drug.

Similar to what has been observed in the clinic, inflammatory cytokines (IFN-γ, IL-2, IL-6, IL-8, and TNF-α) were present at very high levels in circulating whole blood treated with glofitamab for 6 hours. IL-6 and IL-8 were induced to similar levels as those seen using alemtuzumab at Cmax, and for IFN-γ and TNF-α, the levels were even higher than those seen with alemtuzumab. IL-2 was, as expected, not produced in response to either obinutuzumab or alemtuzumab, but was induced to high levels (similar to an agonistic anti-CD28 antibody) in the presence of glofitamab. Neither obinutuzumab nor glofitamab had any effect on complement activation in ID.Flow, whereas alemtuzumab induced increased levels of C3a and C5a.

In conclusion, ID.Flow can be used to assess the immunotoxicity and potentially the efficacy of bispecific antibodies with glofitamab as a relevant clinical control.

#5537 A half-life extended PD-1×VEGFA bispecific antibody demonstrates potent anti-tumor activity in preclinical models.

Frank An, Weiqiu Lan, Baihong Liu, Yang Chen, Xi Yang, Jinhua Zhao, Gao An, Yi Yang

Biocytogen, Waltham, MA

Background PD-1 blockade reactivates T-cell-mediated tumor killing but faces resistance in "cold" tumors with poor immune infiltration. VEGF-A inhibition (e.g., bevacizumab) normalizes tumor vasculature, enhancing immune cell delivery and synergizing with PD-1 inhibitors. Simultaneously disrupts immune evasion (via PD-1) and tumor blood supply (via VEGF-A), addressing microenvironmental barriers. Currently, several PD-1/L1×VEGF-A bispecific antibodies have been developed and demonstrated superior antitumor activity.

Methods We developed a novel PD-1×VEGF-A bispecific antibody, BCG036, by fusing a fully human anti-VEGF-A VHH domain with an Fc-engineered IgG1 anti-PD-1 monoclonal antibody to extend its half-life. We used reporter cell lines to conduct blocking assays for PD-1 and VEGF-A. *In vivo* pharmacokinetic and efficacy studies were evaluated in FcRn humanized mice and xenograft mouse models bearing an established A375 tumor. Toxicology studies were conducted in cynomolgus monkeys to assess the safety and pharmacokinetic characteristics of the BCG036.

Results BCG036 demonstrated high affinity and specificity for both human PD-1 and VEGF-A, with superior blocking activity for both PD-1/PD-L1 and VEGF/VEGFR signaling pathway than the benchmark. *In vivo*, BCG036 exhibited an extended half-life in humanized FcRn mice and demonstrated potent antitumor efficacy than the benchmark. Importantly, BCG036 displayed a favorable safety and PK profile in cynomolgus monkeys after repeated dosing at 100 mg/kg.

Conclusions Our prolonged half-life version of the PD-1×VEGF-A bispecific antibody shows high affinity *in vitro* and has a strong ability to block the interactions of PD-1/PD-L1 and VEGFR2/VEGFA. It demonstrates strong antitumor activity in mouse models and has demonstrated good safety in cynomolgus monkeys, supporting a long-term dosing regimen.

#5538 Pan-αβ-T-cell reactive anti-TCR VHH bispecifics demonstrate potent cytotoxicity through novel constant region targeting.

Michael B. Battles

Antibody Engineering, Adimab, LLC, Lebanon, NH

Introduction: All approved T-cell engagers target CD3ε, but alternative engagement sites on the TCR complex may yield differentiated functional properties. We developed VHH-based T-cell-engaging (TCE) arms that bind a previously unexploited quaternary epitope formed at the TCRα/β constant-region interface. These binders exhibit pan-αβ-T-cell reactivity with inherent human-cynomolgus cross-reactivity.
Methods: Anti-TCR VHHs were identified using yeast-based selections against recombinant human and cynomolgus TCRα/β heterodimers, employing both synthetic libraries and llama immunization. Affinity optimization of VHHs maintained cross-species recognition. Epitope mapping was performed using TCR constant-region mutant libraries generated by error-prone PCR. Structures of VHH-TCR complexes were solved. Bispecifics incorporating anti-tumor associated antigen (TAA) domains were assessed in T-cell-dependent cytotoxicity (TDCC) assays across tumor models and benchmarked against clinical CD3 controls.
Results: Multiple VHH lineages that recognize a conserved quaternary epitope at the TCRα/β constant-region interface were isolated, providing TRBC1/C2 coverage and human-cynomolgus cross-reactivity. Structural analyses established the binding mode. Despite moderate monovalent affinities, anti-TCR bispecifics demonstrated potent TDCC activity comparable to or exceeding benchmark CD3 bispecifics and clinically active controls. Functional activity was confirmed in both human and cynomolgus assay systems, including preliminary cytokine readouts.
Conclusions: VHH-based bispecifics that target a quaternary epitope within the TCR constant region constitute an emerging class of T-cell-engagers with potent cytotoxic activity and broad αβ-T-cell coverage. The combination of TRBC1/C2 inclusivity, structural definition, and human-cynomolgus cross-reactivity positions TCR constant-region targeting as a promising alternative for next-generation T-cell-redirecting therapeutics.

#5539 The anti-tumor activity of BB-202, a novel anti-PD-1/anti-VEGF bispecific antibody.

Hongyan Zhong, Daniel Guo, Phuong Nguyen, Daniel Li, **Ming Yang**

Bright Biologics LLC, Sunnyvale, CA

Background: Immune checkpoint blockade targeting PD-1/PD-L1 and VEGF inhibition each modulates the tumor microenvironment, and their combination has shown synergistic anti-tumor effects in preclinical models. Clinically, combining anti-PD-1/PD-L1 antibodies with anti-angiogenic agents has improved outcomes across multiple cancers and led to several regulatory approvals. Bispecific antibodies that co-target PD-1 and VEGF within a single molecule represent a promising strategy to further enhance this synergy. While the anti-PD-1/anti-VEGF bispecific antibody ivonescimab (AK112) has demonstrated clinical benefit, we developed BB-202, a novel bispecific antibody with a distinct structure designed to improve potency and stability.
Methods:BB-202 was engineered using pembrolizumab-derived Fab regions and anti-VEGF VHH fragments fused to a human IgG1 Fc. PD-1 binding affinity was characterized using whole-cell binding assays. PD-1 and VEGFA blockade were assessed using cell-based reporter assays, and PD-1 functional blockade was further evaluated in mixed lymphocyte reaction (MLR) assays. In vivo efficacy and safety were examined in multiple mouse xenograft models, including PBMC-humanized mouse models.
Results:BB-202 demonstrated high PD-1 binding affinity equivalent to pembrolizumab. In PD-1/PD-L1 blockade assays, BB-202 showed potency similar to pembrolizumab and substantially greater than AK112 and LM-299. BB-202 also blocked VEGFA activity with potency comparable to bevacizumab (Avastin), AK112, and LM-299. In MLR assays, BB-202 induced robust human T-cell activation, exhibiting approximately 38-fold greater potency than AK112. The molecule also showed excellent accelerated and serum stability.In vivo, BB-202 demonstrated strong anti-tumor activity. In an NCI-H1975 PBMC-humanized mouse model, BB-202 achieved significantly greater tumor growth inhibition than an equimolar dose of pembrolizumab. Consistent results were observed in the NCI-HCC827 xenograft model, where BB-202 again outperformed pembrolizumab. No weight loss or observable toxicities were detected.
Conclusion:BB-202 is a potent, stable, and well-tolerated anti-PD-1/anti-VEGF bispecific antibody. Its superior in vitro potency and robust in vivo efficacy, together with a favorable developability profile, position BB-202 as a promising best-in-class therapeutic candidate among PD-1/VEGF-targeting bispecific antibodies.

#5540 SCR-M015, a PD-1/VEGF bispecific antibody exhibits potent anti-tumor efficacy in preclinical studies.

Qiong Wang, Yayuan Fu, Fengli Shan, Yanqiu Wang, Guimei Yang, Yan Wang, Xiaokang Qin, Renhong Tang

Simcere Zaiming, State Key Laboratory of Neurology and Oncology Drug Development. Simcere Pharmaceutical Group., Shanghai, China

Background: Combinations of PD-1 antibodies and anti-VEGF agents significantly improved clinical benefits over standards of care. The immune checkpoint and VEGF pathways has been demonstrated intrinsic mechanistic complementation, including VEGF effect on angiogenesis, immune cell infiltration, and dendritic cell maturation. We have developed a PD-1xVEGF bispecific antibody SCR-M015 and reported preclinical studies characterizing the functional activity.
Method: Binding affinity was assessed using Surface Plasmon Resonance, and the EC50 were determined using ELISA and FACS. Bioluminescent cell-based reporter assays were explored to measure VEGF/VEGFR2 or PD-L1/PD-1 signaling blockage function. Mixed lymphocyte reaction (MLR) assay was applied to evaluate anti-PD1 functional activity. Anti-VEGF bioactivity was determined in HUVEC proliferation assay. In vivo efficacy studies were conducted in CDX models with human tumor cell lines.
Result: SCR-M015 was constructed by fusing anti-PD-1 nanobody to the C-terminus of the heavy chain of an anti-VEGF-A antibody with a silent Fc, forming a 2+2 symmetrical structure. SCR-M015 exhibited specific and high-affinity binding to human PD-1 and VEGF. In vitro assays demonstrated that the anti-PD-L1/VEGF bispecific antibody exhibited more potent blockade activity against VEGF-A/VEGFR2 signaling and inhibition of HUVEC proliferation. In MLR assay, SCR-M015 showed dose-dependently increased IL-2 and IFN-γ secretion, which was comparable to benchmark antibody. In vivo, SCR-M015 demonstrated more robust anti-tumor activity than benchmark antibody in different xenograft models. Furthermore, compared to the combination of anti-PD-1 monoclonal antibody and anti-VEGF monoclonal antibody, SCR-M015 showed more potent anti-tumor efficacy.
Conclusions: SCR-M015 inhibits PD-1/PD-L1 signaling and VEGF-A/VEGFR2 signaling in vitro and shows potent and superior anti-tumor activity in vivo. These preclinical data demonstrates the promising potential for further clinical investigation in various types of tumors.

#5541 Characterization and functional evaluation of PF-08634404 (SSGJ-707) a tetravalent PD-1 x VEGF bispecific for the treatment of cancer.

Ryan A. Heiser[1], Meghan Zuck[1], Catalina Sakai[1], Eliana Moskovitz[1], Laila Shehata[2], Markus Carlson[1], Florian Heinkel[1], Sherif Abdelhamed[3], MIchelle Ulrich[1], Matt Rathgeber[1], Brian P. O'Connor[1], Joseph D. Dekker[1], Haomin Huang[4], Sharsti Sandall[1]

[1]Pfizer Oncology, Bothell, WA,[2]Pfizer Oncology, Seattle, WA,[3]Pfizer Oncology, Bothell, Bothell, WA,[4]3SBio Inc., Shanghai, China

PF-08634404 (formerly known as SSGJ-707) is an investigational anti-PD-1 and anti-VEGF bispecific antibody designed to simultaneously inhibit PD-1-mediated T cell dysfunction and VEGF-A-mediated tumor angiogenesis and immune suppression in the tumor microenvironment. PF-08634404 is a tetravalent 2+2 bispecific leveraging Common Light Chain Linear Fab x2 (CLF^2) technology with an IgG4 backbone. The PD-1 and VEGF-A binding arms of PF-08634404 are unique among the PD-1 x VEGF bispecific class. PF-08634404 has demonstrated promising clinical activity in NSCLC and CRC in clinical trials conducted in China. Here we present preclinical data demonstrating binding to and functional inhibition of PD-1 and VEGF-A by PF-08634404 in vitro. PF-08634404 displays nanomolar binding affinities for PD-1 and VEGF-A and can bind both targets simultaneously. The functional inhibition of VEGF by PF-08634404 is increased (~7.5-fold) compared to relevant benchmarks, and the inhibition of PD-1 is equivalent or superior to relevant benchmarks. Consistent with this class of bispecific molecules, PF-08634400 multimerizes in the presence of dimeric VEGF-A, increasing the avidity for PD-1 (>100-fold), driving rapid internalization of PD-1 on T cells, and improving the functional inhibition of PD-1 (>10-fold). Collectively, these data characterize core features of the bispecific mechanism and support the ongoing clinical investigation of PF-08634404 proof of concept and pivotal trials in multiple disease settings/tumor types.

#5542 Novel PD-1xVEGFxIL-2 trispecific immune modulator with superior safety and greater efficacy.

Lei Wu, Mengmeng Sun, Bowei Liao, Shuang Wang, Tengfei Yu, Jijie Gu

WuXi Biologics, Wuxi Shi, China

PD-1 antagonist antibodies have demonstrated significant success in the clinic. However, low response rate and high cancer recurrence requires the development of next-generation immunotherapies. Bispecific immune modulators PD-1xVEGF and PD-1xIL-2 molecules have shown promising clinical improvement over PD-1 antagonist antibodies, particularly in populations resistant to PD-1 monotherapy. VEGF, a soluble dimer enriched in the tumor microenvironment (TME), plays a crucial role in angiogenesis and tumor growth. Local enrichment of PD-1xVEGF bispecific antibodies by VEGF dimers could further potentiate the efficacy of PD-1 blockade. On the other hand, IL-2 of PD-1xIL-2 molecules can be cis-presented on PD-1-expressing T cells, expanding tumor-specific T cell populations and enhancing the functions of PD-1 antibodies. We therefore built a novel PD-1xVEGFxIL-2 trispecific immune modulator that combines the biologic functions of all three. We have optimized the trispecific format to retain the affinity and potency of both VEGF and PD-1 blockers. The proprietary IL-2 mutein has over 1000X attenuated IL-2Rβγ binding and muted CD25 binding to ameliorate systemic immunotoxicity on non-specific T and NK cells in the periphery. The sub-nanomolar anti-PD-1 antibody then directs IL-2 mutein to PD-1+ T cells and effectively replaces the natural function of CD25. Thus, proprietary IL-2 mutein specifically acts on PD-1-expressing tumor-specific T cells to expand effector populations. VEGF neutralization suppresses angiogenesis and potentiates the potency of PD-1 blockade. These creates a “super PD-1” next-generation immune modulator. PD-1xVEGFxIL-2 trispecific has been fully characterized. The potency of the trispecific for PD-1 and VEGF blockades were comparable to the respective monoclonal antibodies. The proprietary IL-2 mutein bound weakly to human IL-2Rβγ, with equivalent affinity to cynomolgus and mouse IL-2Rβγ. This IL-2 variant was inert on primary pan T cells and did not activate Treg cells, but induced potent activation of PD-1+ T cells. In addition, PD-1xVEGFxIL-2 enhanced immune activation of T cells induced by A375 tumor cells in a co-culture system. In an exploratory toxicity study, the attenuated IL-2 mutein supported a higher maximum tolerated dose for the trispecific than IBI363 in cynomolgus monkeys, which matched the optimal therapeutic doses for PD-1 and PD-1xVEGF antibodies. In mouse efficacy studies, PD-1xVEGFxIL-2 exhibited significantly greater efficacy than both PD-1xVEGF and PD-1xIL-2 in PBMC-engrafted CDX model and mouse syngeneic models. In summary, WuXi Biologics has developed a novel PD-1xVEGFxIL-2 trispecific molecule. This potent next-generation immune modulator shows great potential for further clinical investigation.

#5543 Mechanism-driven cell-based assays to screen & characterize bi-specific antibodies.

Venkatesh Chari, Surekha Bonasu, Luhan Yang, Jennifer Lin-Jones, Jane Lamerdin, Alpana Prasad, Gaurav Agrawal

Eurofins DiscoverX Products LLC., Fremont, CA

Recent advances in cancer immunotherapy using monoclonal antibodies have dramatically revolutionized the therapeutic strategy against advanced malignancies, inspiring the exploration of various types of therapeutic antibodies. Bispecific antibodies (BsAbs) are engineered molecules designed to target two different epitopes or antigens. The mechanism of action of BsAbs can be manipulated to create variable and novel functionalities, including linking immune cells with tumor cells or signaling pathway blockade. BsAb-based therapies have demonstrated significant preclinical and clinical potential, as evidenced by the regulatory approval of molecules like blinatumomab (CD19/CD3), amivantamab (EGFR/Her3), ivonescimab (PD-1/VEGF-A), and others.

Eurofins DiscoverX® provides a robust portfolio of cell-based assays for oncology targets and offers three primary assay formats to characterize BsAbs: (1) Cytotoxicity assays: To assess functional activity of BsAbs in *trans*, specifically for characterizing T-cell engagers (BiTEs) and similar molecules, (2) Dimerization assays: To record hetero dimerization of target receptors in *cis*, and (3) Pathway signaling assays: To evaluate the functional activity of each individual BsAb target arm

This presentation highlights case studies illustrating the use of these cell-based assays to monitor key BsAb MOAs targeting critical tumor antigens, including CD19, PD-1, and VEGF-A. Applications will demonstrate the evaluation of BsAb-mediated tumor cell killing, rank-ordering of antibody candidates, and assessment of the function and specificity of individual BsAb arms. These assays provide essential tools for the accelerated discovery and characterization of next-generation BsAb therapeutics.

#5544 Organoid-T cell co-cultures: A robust platform for bispecific antibody immunotherapy development.

Sonia Aristin Revilla, Cesar Oyarce, Sumeyra Mucuk, Javier Frias Aldeguer, Timo Voskuilen, Merel Derksen, Farzin Pourfarzad, Robert G. J. Vries, Sylvia F. Boj

HUB Organoids B.V., Utrecht, Netherlands

Recent advances in cancer immunotherapy have significantly improved patient survival across multiple indications. As new treatment strategies and druggable targets emerge, the number of patients eligible for immunotherapy continues to grow. However, translating promising preclinical findings into clinical success remains challenging, as conventional 2D cancer models offer limited predictive value. We developed an innovative alternative based on the ability of adult stem cells to form three-dimensional organotypic structures within an extracellular matrix. Patient-derived organoids, generated from normal and malignant tissues and stored in high-quality biobanks, yield highly reproducible results. HUB Organoids faithfully recapitulate the complexity of parental tissue, including molecular heterogeneity and morphological and functional traits. Over the last decade, bispecific antibodies (bsAbs) have gained significant attention in cancer treatment, leading to several approved therapies. Bispecific T-cell engagers (BiTEs), a subclass of bsAbs, bring T cells into close proximity with cancer cells and promote immunologic memory, enabling the immune system to more effectively recognize and eliminate tumor cells. To de-risk drug development and accelerate clinical translation, we developed an assay in which labeled tumor organoids are co-cultured with labeled PBMCs and exposed to BiTEs to assess immune cell-mediated cytotoxicity. Fluorescent dyes enable real-time evaluation of cytotoxic activity via high-resolution microscopy, complemented by cytokine secretion analysis to confirm immune cell activation. HUB's organoid co-culture system is robust and reproducible, providing a dynamic window to evaluate the activity of multiple BiTEs. Organoid-based cytotoxicity assays accurately reflect BiTE-mediated T cell killing, demonstrating that our model captures the expected mechanism of action. This platform offers a powerful tool for developing and validating cancer immunotherapies, helping to de-risk novel strategies through patient-derived models.

#5545 Collagen-binding anti-GITR antibody reshapes immunosuppressive microenvironment and prolongs survival in recurrent glioblastoma.

Jun Takei[1], Chuyi Wang[2], Ken Furudate[3], Opeyemi Iwaloye[1], Lewis Barr[1], Haruka Ichie[1], Shunsuke Tsuzuki[1], Jun Ishihara[2], Satoru Osuka[1]

[1]Department of Neurosurgery, University of Alabama at Birmingham, Birmingham, AL,[2]Department of Bioengineering, Imperial College London, London, United Kingdom,[3]Department of Genomic Medicine, UT MD Anderson Cancer Center, Houston, TX

Recurrent glioblastoma (rGBM) remains lethal with median survival under six months, due to immunotherapy resistance driven by immunosuppressive tumor microenvironment (TME) with elevated regulatory T cells (Tregs). Despite the development of Treg-targeting antibodies such as anti-GITR (Glucocorticoid-induced TNFR-related protein) antibody, their poor delivery to brain tumors has restricted therapeutic efficacy, necessitating novel drug delivery strategies. We aimed to identify anchors for selective antibody delivery to tumors and focused on Collagen type I and III (COLI&III), which are minimal in normal brain but highly upregulated in rGBM.We engineered a novel antibody, CBD-αGITR, by conjugating the COLI&III-binding domain (CBD) of von Willebrand Factor (vWF) to an anti-GITR antibody. vWF naturally binds to exposed collagen only at sites of vascular injury, inflammation, and tumor while sparing normal tissues, providing a potential mechanism for tumor-specific drug delivery. We investigated the tumor-selective accumulation, immunosuppressive microenvironment remodeling, and antitumor effects of CBD-αGITR using clinically relevant syngeneic rGBM mouse models, humanized mouse models, and patient-derived 3D tumor slice cultures.Using a fluorescently labeled biodistribution assay, CBD-αGITR selectively accumulated in rGBM tumors but not in normal brain or COLI/III-expressing organs. Single-cell RNA sequencing revealed that CBD-αGITR dramatically decreased GITR+ Tregs and exhausted CD8+ T cells (which express moderate levels of GITR), thereby reversing the immunosuppressive TME and promoting the recruitment of anti-tumor macrophages and type 1 conventional dendritic cells. CBD-αGITR treatment (300ug, i.v. 1x) achieved approximately 20% complete remission (CR) in two independent rGBM mouse models, while αGITR (non-CBD) antibody showed no survival benefit. Furthermore, combining CBD-αGITR with PD-1 inhibitor further enhanced antitumor efficacy, achieving 67% CR in rGBM mouse models. We have developed a humanized CBD-αGITR for clinical application, which demonstrated extended survival in humanized rGBM mouse models and significant human Treg reduction in patient-derived 3D tumor slice cultures.GITR antibody modified for COLI&III binding achieved selective tumor accumulation, immune reprogramming, and robust tumor control. This delivery strategy can be applied to other antibodies and has the potential to significantly advance treatment approaches for rGBM.

#5546 Rilvegostomig elicits greater immune activation and tumor inhibition than clinically approved anti-PD-1 monotherapy in models of HNSCC.

Jun Ren, Ngan Mitchell, Marie Boutet, Vladimir Roudko, Jeremy Ratiu, Jorge Blando, Sophia Varriano, Elizabeth Galery, Rebecca Halpin, Trevor Connor, Kanam Malhotra, Bartholomew Starich, Jessica Wagner, Yi Luan, Anna Huntley, Joseph Boland, Maurizio Scaltriti, Mark Cobbold, Simon Hollingsworth, Scott Hammond, Doug Palmer, Paul Chariou, Kristen Pollizzi, Daniela Dinulescu

Oncology, AstraZeneca, Gaithersburg, MD

Background: Rilvegostomig (AZD2936) is a monovalent, bispecific humanized IgG1 monoclonal antibody that targets human TIGIT and PD-1, engineered with a triple-mutation in its fragment crystallizable (Fc)-domain to prevent Fc-effector functionality. Rilvegostomig has shown promising anti-tumor activity in NSCLC patients in a Phase I/II clinical trial (NCT04995523) and is currently being investigated in multiple Phase III trials. Here, we report the enhanced anti-tumor activity of rilvegostomig compared to a clinically approved anti-PD-1 (αPD1) mAb in ex vivo and in vivo models of head and neck squamous cell carcinoma (HNSCC).
Methods: Primary HNSCC explants, derived from freshly resected patient tumors, were cultured ex vivo in a 3D platform for therapeutic agent testing. Ex vivo immune activity was assessed via IFN-γ quantification. Baseline tumor features—characterized by IHC, flow cytometry, scRNA-seq, and multiplex imaging—were used to stratify patient response and identify candidate biomarkers. A CD34+ humanized mouse model of HNSCC was developed to enable long-term engraftment of functional multi-lineage hematopoietic cells and used to investigate efficacy and effects of IO therapeutics on different components of the immune system.
Results: We investigated a cohort of 42 newly diagnosed HNSCC patient resected tumor samples. These samples represent the incidence of HNSCC by anatomical sites and share similar cohort attributes as those enrolled in KEYNOTE-689. Patient-derived tumor explants maintain tumor architecture and intact tumor microenvironment (TME), including tumor cells, immune cells, stroma cells, and extracellular matrix. αPD1 monotherapy elicited immune activity in 9.5% of HNSCC samples tested in our ex vivo platform, consistent with clinical observation of major pathological response in KEYNOTE-689. In contrast, rilvegostomig induced a significantly higher rate of ex vivo immune activity (28.6%). Rilvegostomig's activity was observed in samples derived from multiple anatomical sites, showing the highest response rate in oral cavity samples. Moreover, our analyses identified key baseline correlates that distinguish rilvegostomig activity from αPD1. Lastly, using a CD34-engrafted humanized mouse model of oral cavity HNSCC, we compared the therapeutic efficacy of αPD-1 monotherapy with rilvegostomig. In contrast to αPD-1, which produced modest effects on tumor growth, rilvegostomig induced significant tumor growth inhibition.
Conclusions: Rilvegostomig elicits greater immune cell activation and broader activity in samples derived from different anatomical sites of HNSCC compared to αPD1 monotherapy in a 3D ex vivo platform and a humanized mouse model of HNSCC. These results underscore rilvegostomig's potential as a promising treatment for newly diagnosed HNSCC and support its investigation in clinical trials.

#5547 Enhancing antibody-dependent cellular cytotoxicityin mesothelioma through concurrent EGFR and MET targeting withamivantamab.

Shinichiro Suzuki, Kaushal Parikh, Ezequiel Tolosa, Kuan-Li Wu, Jennifer Ayers-Ringler, Lin Yang, Katherine E. R. Smith, Farhad Kosari, Aaron S. Mansfield

Mayo Clinic, Rochester, MN

Background: Diffuse pleural mesothelioma (DPM) is a highly aggressive malignancy with limited treatment options and poor prognosis. Although immune checkpoint inhibitors have improved outcomes, particularly for non-epithelioid subtypes, there remains no approved targeted therapy for mesothelioma. EGFR and MET are receptor tyrosine kinases frequently overexpressed in DPM, suggesting susceptibility to targeted antibody therapy. Amivantamab is a bispecific EGFR/MET antibody, originally developed for EGFR-mutant lung cancer, that blocks growth signals and engaging immune mechanisms. Given the high levels of EGFR and MET expression in mesothelioma, we evaluated the therapeutic potential of amivantamab in preclinical models.
Methods: EGFR and MET transcript levels in DPM were analyzed using TCGA. Eight human mesothelioma cell lines were assessed by Western blotting and flow cytometry. Amivantamab binding, internalization, and signaling inhibition were examined using flow cytometry, confocal microscopy, and ligand-stimulated phosphorylation assays. Cytotoxicity and immune-effector activity were quantified using PBMCs, NK cells, and monocytes from healthy donors, along with an ADCC reporter assay. In vivo efficacy was tested in a DPM patient-derived xenograft (PDX) model in NOD/SCID-γ (NSG) mice supplemented with human NK cells and treated with amivantamab or control IgG.
Results: TCGA analysis showed frequent EGFR/MET co-expression in DPM. Mesothelioma cell lines expressed higher EGFR and MET levels compared with mesothelial cells. Amivantamab strongly bound both receptors, induced receptor internalization, and inhibited EGF- and HGF-stimulated phosphorylation of EGFR, MET, and downstream AKT/ERK signaling. Direct cytotoxicity was minimal; however, the addition of PBMCs or NK cells resulted in robust, dose-dependent tumor cell killing consistent with antibody-dependent cellular cytotoxicity (ADCC). Reporter assays demonstrated 7-11-fold Fcγ receptor activation in tumor cells compared with ~2-fold activation in non-malignant mesothelial cells. Co-culture with monocytes revealed amivantamab-induced trogocytosis, evidenced by loss of EGFR and MET from tumor-cell membranes. In the DPM PDX model, amivantamab produced 89.1% tumor-growth inhibition (TGI) relative to controls ($P < 0.0001$), with no overt toxicity observed in treated mice.
Conclusions: Dual EGFR/MET targeting with amivantamab produced potent antitumor effects in mesothelioma through coordinated receptor-signaling blockade, ADCC, and monocyte-mediated trogocytosis. These results support amivantamab as a promising targeted therapeutic strategy for EGFR/MET-positive DPM, particularly epithelioid subtypes that currently derive limited benefit from immunotherapy.

#5548 Unbiased discovery of novel macrophage-activating immunotherapies for ALK+ non-small cell lung cancer.

Carlota Pages-Geli[1], Thomas Wienclaw[1], Juliano Ribeiro[2], Matheus Silva[1], Kipp Weiskopf[1]

[1]Department of Medicine, Beth Israel Deaconess Medical Center, Boston, MA,[2]Harvard-MIT Health Sciences and Technology Program, Boston, MA

Non-small cell lung cancer (NSCLC) represents ~85% of all lung cancer cases and remains one of the leading causes of cancer-related mortality in the United States. Approximately 3-7% of NSCLC patients harbor ALK rearrangements, most commonly the EML4-ALK fusion. Although ALK+ tumors initially respond well to ALK tyrosine kinase inhibitors (TKIs), patients still develop resistance. Lorlatinib, a third-generation ALK inhibitor, achieves ~76% response rates in treatment-naïve patients; however, a substantial proportion experience disease progression within a few years, highlighting the urgency for new therapeutic strategies. The tumor immune microenvironment is increasingly recognized as a key contributor to resistance. Tumor-associated macrophages (TAMs) are the dominant immune population infiltrating NSCLC and can promote tumor growth, survival, and immune evasion. Here, we aimed to identify novel therapeutic strategies to stimulate macrophages to eliminate ALK+ lung cancer cells.Using in vitro co-culture assays, we found that macrophages markedly protect ALK+ lung cancer cells from lorlatinib, making the cancer cells significantly less responsive compared to cells cultured alone. We found that blocking macrophage immune checkpoints, such as the CD47/SIRPa axis, could restore macrophage activation and promote phagocytosis of the ALK+ lung cancer cells. Since systemic administration of anti-CD47 antibodies can result in dose-limiting hematotoxicity, we therefore developed a high-throughput bispecific antibody (bsAb) engineering platform to leverage the benefits of targeting CD47 while increasing specificity to the tumor microenvironment. We generated a library of bsAbs targeting CD47 with a second arm binding well-known tumor antigens including EGFR, EpCAM, HER2, TROP2, FOLR1, Nectin-1, Nectin-4, PD-L1, and CD71. Using live-cell imaging, we evaluated macrophage-mediated cytotoxicity for each bsAb across three ALK+ NSCLC cell lines. Among all constructs tested, a bsAb incorporating a low-affinity CD47-binding domain and a TROP2-targeting domain showed the strongest anti-tumor activity, significantly reducing tumor growth over time. This bsAb enhanced macrophage phagocytosis and decreased tumor area more effectively than lorlatinib alone. Importantly, combining the CD47×TROP2 bsAb with lorlatinib produced synergistic anti-tumor effects, offering a promising strategy to overcome or delay resistance. Overall, our study has identified novel bispecific antibodies that may be highly active for ALK+ lung cancer and our findings could be translated to the clinic to benefit patients in the future.

#5549 Non-clinical modeling the therapeutic window of HX044, a novel CTLA4xCD47 BsAb.

Hang Ke[1], Zihan Xu[2], Tao Yang[1], Cen Chen[1], Sheng Gao[2], Lei Zhang[1], Faming Zhang[1], **Henry Li**[1]

[1]Hanx Bio, Wuhan, China,[2]Crown Bioscience, Inc., Suzhou, China

MOAs of the CTLA4-mAb (*e.g.* Ipilimumab or Ipi) for anti-cancer efficacy include: 1) ADCC/the associated TIL-T_{reg}-depletion, 2) CTLA4-ligand (CD80/CD86) blockade/the associated T-cell activation in tdLN (tumor draning lymphonoda) (priming), and 3) Fc-mediated effector activities/the associated TME remodeling enhancing immunogenicity. Ligand-blockade is also blamed for the associated immunotoxicity (irAE). We previously described a bispecific CTLA4-antibody/SIRPα-fusion protein, HX044, where it is considered to be a next generation CTLA4-therapy with enhanced efficacy via increased ADCC on $CTLA4^{+++}CD47^{+++}$ TIL-T_{reg} and lowered irAE via reduced ligand-blockade over Ipi. Its design concept was based on the assuption that Til-T_{reg} have higher CTLA4/CD47 expression over those in peripheral in both levels and frequency. The present study assayed HX044 in various *in vitro/in vivo* experimental systems to approximately simulate its therapeutic window by modeling a variety of possible relevant parameters of pharmacokinetic exposures, irAE and efficacy. First, we surveyed available cancer patient T_{reg} scRNAseq-datasets, which indeed confirmed both higher frequencies and levels of CTLA4/CD47 expressions in TIL-T_{reg} over peripheral T_{reg}, a benefiting factor in term of less irAE, although their thresholds for irAE remained to be determined. Second, HX044 was confirmed to have significantly enhanced ADCC over Ipi in double-high cells, confirming greater potential in TIL-T_{reg} depletion, which is also confirmed along with associated enhanced antitumor efficacy in humanized syngeneic tumor models. Third, HX044's ligand-blockade in double-positive cells was determined to be slightly reduced (~50%) as compared to Ipi, while little ligand-blockade in CTLA4-single-positive cells, contrasting to potent blockade by Ipi, suggesting that HX044 could have reduced irAE if the dual receptor expression in peripheral are below the assumed thresholds. As a reference, blocking assay using recombinant CTLA4 protein revealed ~300x fold reduction of CD80-blocking for HX044 in comparison to Ipi. Fourth, NHP study of HX044 demonstrated excellent PK profile with long half-life and dose-proportional exposure as well as dose-dependent irAE, mostly seen in the highest dose level at 40mg/kg rather than lower dose levels at 1mg/kg and 6mg/kg, respectively. The data could not necessarily confirm significant better safety over Ipi in the 40mg/kg dose level, thus higher tolerable dose for irAE in the presence of sufficient double-positive T_{reg} cells in peripheral. Nevertheless, HX044 has significantly broadened therapeutic window over Ipi, via lower efficacious dose levels attributed to significantly enhanced ADCC activities.

#5550 T cell transcriptome is altered by Talquetamab in presence of GPRC5D on MM cells.

Umair Munawar[1], Alexander Leipold[2], Seungbin Han[1], Silvia Nerreter[1], Shilpa Kurian[1], Emma Besant[1], Nina Rein[1], Johanna Lehmann[1], Max Koeppel[1], Xiang Zhou[1], Ondrej Slaby[3], Hermann Einsele[1], Leo Rasche[1], Emmanual Saliba[2], Johannes Waldschmidt[1], Martin Kortuem[1]

[1]University Hospital Wuerzburg, Wuerzburg, Germany,[2]Helmholtz Institute for RNA-based Infection Research, Wuerzburg, Germany,[3]Masaryk University, Brno, Czech Republic

Background: G protein-coupled receptor class C group 5 member D (GPRC5D) has emerged as a promising immune target in multiple myeloma (MM). Talquetamab, a GPRC5D-directed bispecific antibody, has shown an efficacy of 70% in triple class refractory MM patients however, genomic loss mediated relapse is often observed. To better understand the interplay of talquetamab, GPRC5D loss and T cells within the immune microenvironment, we performed single cell sequencing on a coculture of GPRC5D loss models and healthy T cells in presence and absence of talquetamab.
Methods: GPRC5D mono- and biallelic knockout models were generated using CRISPR-Cas9 technology. Cocultures were established using healthy T cells with or without talquetamab for 24 hours. CITE-seq was performed. Cell hashing with TotalSeq-C antibodies enabled multiplexing. Pooled cells underwent 10x Genomics 5' GEM-X workflow and were sequenced on Illumina NovaSeq X Plus. Differential gene expression was assessed using the Wilcoxon rank-sum test, and interferon response scores were calculated using AddModuleScore.
Results: Pronounced transcriptomic changes in MM cells were observed with both mono- and bi-alleic loss of GPRC5D via CITE-seq. Based on the expression of canonical markers (*IL2RA, IRF4, TNFRSF4-18, TNF, IFNG*), CD4 and CD8 activated T cells were only observed in presence of talquetamab and GPRC5D^{+} cells and completely disappeared when stimulated with GPRC5D$^{Del/Del}$ models. A significant induction of interferon stimulated genes (*GBP2-4-5, IFI44, IFIT2, ISG15*) in presence of talquetamab with GPRC5D on MM cells (p-value < 0.001, absolute log2FC > 2) was observed across T cell subpopulations. Interferon signaling genes (*STAT1, IRF1*) were found to be upregulated in T cells by talquetamab alone even in absence of GPRC5D^{+} cells in coculture. Additionally, we also identified genes only upregulated in presence of GPRC5D and talquetamab, including *SOCS3, CD69, JUNB, BATF, CISH*, and *PRDM1*, indicating a unique activation status of these T cells. Gene set enrichment analysis performed on T cell sub types indicated an enrichment of IFN-γ and IFNA-signaling (NES>2.0, FDR 0,0) in CD4, CD8, Tcm and Treg populations. Additionally, IL2-STAT5 signaling and inflammatory response (NES>2.0, FDR 0.0) pathways were found to be enriched only in presence of talquetamab and GPRC5D^{+} cells. Of note, in the absence of talquetamab, T cells transcriptomic profile did not change in response to GPRC5D presence or absence on MM cells.
Conclusions: Our findings demonstrate that talquetamab upregulates the expression of interferon signaling genes in T cells even in the absence of GPRC5D and this response is enhanced when GPRC5D is present on MM cells. Moreover, talquetmab alters the activation profile across T cells subsets and both abundance and distribution of different T cells subpopulations is changed by GPRC5D status of the MM cells in coculture.

#5551 MHC class II targeted immunotherapy in the treatment of pancreatic cancer.

Reeder Robinson[1], Leticia Reyes[1], Samaneh Saberi[2], Lena Golick[2], Sandeep Gupta[1], Michael Ostrowski[2], **Nathan G. Dolloff**[1]

[1]Leukogene Therapeutics, Inc., Charleston, SC,[2]Medical University of South Carolina, Charleston, SC

Introduction: Pancreatic ductal adenocarcinoma (PDAC) is one of the deadliest tumor types, claiming approximately 50,000 lives per year in the United States and carrying a 5-year overall survival rate of only 13%. While immunotherapy has revolutionized therapy for certain cancer types, this has not been the case for PDAC, where there have been zero immunotherapy approvals. This is attributed to a variety of factors related to the PDAC tumor microenvironment (TME) including its dense desmoplastic stroma with high interstitial pressure and a prevalence of immunosuppressive cell types. In addition, genetic characteristics like microsatellite instability (MSI) and high mutational burden, which predict responsiveness to immune checkpoint inhibitors (ICIs), are absent or low in PDAC compared to more responsive tumor types. This suggests that effective anti-tumor immune responses depend on tumor-derived immunogenic signals, leading us to explore new strategies to stimulate immunity against PDAC-associated antigens. We developed a Major Histocompatibility Complex class II (MHCII) targeted approach to direct the immune system against PDAC associated antigens. MHCII is a major antigen presentation complex that directly educates CD4+ helper T cells, and studies have shown that MHCII-CD4 signaling is essential for effective anti-cancer immunity. Specifically, we developed a recombinant high affinity MHCII engager that is conjugated to mesothelin (MSLN), which is overexpressed in a high percentage of PDAC but not the normal pancreas.
Methods: To evaluate the preclinical efficacy of our MHCII targeted MSLN therapy (LTI-002), we injected KPC mouse PDAC cells orthotopically in syngeneic C57BL/6 mice. Tumor burden was measured at a predetermined endpoint or by survival analysis. Pharmacodynamic markers of immune response including anti-MSLN specific IgGs and antigen-specific T cell recall were also evaluated.
Results: This approach induced a polyclonal humoral response and antigen specific T cell response against mouse and human MSLN candidates. This led to a significant reduction in the size of orthotopic PDAC tumors and significantly improved animal survival. Anti-tumor responses were detected in therapeutic as well as prophylactic experiments and further demonstrated in the de novo KPF mouse PDAC model and in a model of PDAC metastasis. We observed synergy in combination with PDAC standard of care agents like gemcitabine, RAS(ON) inhibitors, and anti-PD1 immunotherapy. As a direct MHCII engager, LTI-002 induced internalization of MSLN into early endosomes where it was processed and loaded onto new MHCII molecules for presentation to CD4+ T cells. LTI-002 target engagement was independent of MHCII polymorphisms, which is an advantage given the diversity of HLA alleles found in different human populations.
Conclusions: This study demonstrates the therapeutic potential of targeting MHCII to stimulate anti-PDAC immunity.

#5552 MHC class II engager immunotherapy for the treatment of acute myeloid leukemia.

Lena Golick[1], Reeder Robinson[2], Leticia Reyes[2], Sandeep Gupta[2], **Nathan G. Dolloff**[2]

[1]Medical University of South Carolina, Charleston, SC,[2]Leukogene Therapeutics, Inc, Charleston, SC

Introduction: The treatment of acute myeloid leukemia (AML) remains a challenge due to disease heterogeneity and therapeutic resistance to traditional cytotoxic drugs and immunotherapy. To address this, we developed LTI-214, a novel recombinant Major Histocompatibility Complex class II (MHCII) engager linked with AML antigen sialic acid binding Ig-like lectin 3 (CD33). MHCII is a critical player in antigen presentation, and studies have shown that MHCII function is essential for effective cancer immunotherapy. MHCII directly educates CD4+ helper T cells against specific antigens. CD4+ T cells then orchestrate a coordinated immune response by communicating cytokine signals to virtually all immune effector cells including CD8+ cytotoxic T cells, B cells, NK cells, and others. CD33 is a myeloid cell surface glycoprotein highly expressed on AML blasts. However, while ~90% of AML cases express CD33, 50% of these patients harbor a single nucleotide polymorphism (SNP) that eliminates the antibody binding epitope for existing CD33-targeted antibody therapeutics such as gemtuzumab ozogamicin (Mylotarg®). Mylotarg® induces objective responses in AML patients, but its efficacy is limited by this splice variant. Therefore, while CD33 was validated as an actionable target in AML, more effective CD33-directed therapies are needed.
Methods: To demonstrate the therapeutic potential of LTI-214, we used the murine C1498 AML xenotransplant model in syngeneic and immunocompetent C57BL/6 mice. Animal survival was a primary endpoint along with pharmacodynamic markers of immune response including measurement of anti-CD33 specific IgGs and antigen-specific T cell recall.
Results: We found that LTI-214 (M2T-CD33) induced a robust polyclonal anti-CD33 humoral response characterized by induction of the full immunoglobulin repertoire. LTI-214 significantly improved animal survival in a CD4+ and CD8+ T cell dependent manner. The immune response was elicited against both the full length and spliced version of CD33, unlike existing anti-CD33 MAbs (gemtuzumab and lintuzumab), which bound exclusively to the IgV domain fragment. LTI-214 showed a favorable safety profile with no evidence of cytokine release syndrome or organ toxicity, and minimal impact on normal hematopoiesis at concentrations 40-fold higher than the efficacious dose. LTI-214 was enhanced by combinations with anti-PD-1 therapy potentially due to the inducible nature of PD-L1 expression of C1498 AML cells.
Conclusions: These experiments demonstrate the potential of LTI-214 in AML and emphasize the importance and targetability of MHCII in cancer immunotherapy.

#5553 Tumor-selective activation of 4-1BB receptor via bispecific antibody combinations.

Lucie Diby[1], Pauline Malinge[1], Valery Moine[1], Lise Nouveau[1], Laurence Chatel[1], Krzysztof Masternak[1], Limin Shang[1], Walter Ferlin[1], Nicolas Fischer[1], Jose Saro[1], Mikael Pittet[2], Vanessa Buatois[1], Eric Hatterer[1]

[1]Light Chain Bioscience - Novimmune SA, Plan-les-Ouates, Switzerland,[2]University of Geneva, Geneva, Switzerland

INTRODUCTION:
4-1BB (CD137) is an inducible co-stimulatory molecule that plays crucial roles in immune activation. Upon ligand binding, 4-1BB forms trimeric signaling complexes triggering receptor activation. However, therapeutic monoclonal antibodies targeting 4-1BB often face challenges due to peripheral toxicities arising from systemic receptor activation. To address this, bispecific antibodies (bsAbs) have been developed to selectively activate 4-1BB in a tumor-associated antigen (TAA)-dependent manner. This report investigates whether a combination of bsAbs, pairing 4-1BB and TAA targeting arms, can further enhance 4-1BB clustering and activation in the tumor microenvironment.
METHODS:
A panel of Fc-silent bsAbs targeting different domains on 4-1BB and HER2 were generated and tested in combination for optimal 4-1BB signaling. For that purpose, 4-1BB reporter cells were co-cultured with HER2-expressing tumor cells. Functional *in vitro* assays were conducted using primary human T cells isolated from peripheral blood mononuclear cells to assess cytokine production and their tumoricidal activity. *In vivo* efficacy was evaluated in PBMC-engrafted NOG mice inoculated with JIMT-1, a HER2-expressing tumor cell line.
RESULTS:
The simultaneous binding of two bsAbs to the same epitope on 4-1BB, while targeting distinct epitopes on HER2, markedly enhances 4-1BB signaling, compared to the single bsAbs. 4-1BB signaling triggered by the bsAbs is driven by HER2 expression, with strong IL-2 release observed only in the presence of HER2-positive cells. In JIMT-1 xenograft models, combination of the bsAb pair with a T cell engager (TCE) resulted in superior antitumor activity and enhanced $CD4^+$ and $CD8^+$ T-cell infiltration within the tumor microenvironment, compared to either single bsAb plus TCE or the TCE alone.
CONCLUSIONS: This study introduces a novel bsAb combination strategy that amplifies TAA-driven activation of $4\text{-}1BB^+$ T cells and may unlock similar opportunities to other TNFR superfamily targets such as OX40 and CD40.

#5554 Anti-human CTLA-4×TIGIT bispecific antibody: A novel immunotherapy specifically targeting tumor-infiltrating FOXP3+ regulatory T cells.

Soojin Ryu[1], Hee Geon Park[2], Sang Beom Bang[1], Ji Hye Nam[3], Ho Jin Lee[4], Ju Yeon Seo[1], Gun Yi Ahn[1], Myeung Ryun Seo[1], Sang Moo Lee[1], Yoon La Choi[5], Sung Youl Hong[6], Young Kee Shin[1]

[1]Department of Molecular Medicine and Biopharmaceutical Sciences, Seoul National University, Seoul, Korea, Republic of,[2]ABION INC., Seoul, Korea, Republic of,[3]Logone Bio-Convergence Research Foundation, Seoul, Korea, Republic of,[4]SNU Future Innovation Institute, Seoul National University, Seoul, Korea, Republic of,[5]Department of Pathology and Translational Genomics, Samsung Medical Center, Sungkyunkwan University School of Medicine, Seoul, Korea, Republic of,[6]BitD Inc., Siheung, Korea, Republic of

Background: Regulatory T cells (Tregs) are key drivers of immune suppression within the tumor microenvironment (TME). In multiple cancer types, increased numbers of Tregs are associated with poor prognosis in terms of both disease progression and patient survival. This includes lung, breast, pancreatic, hepatocellular, renal, gastric, and cervical cancers. Specifically, the subset of Forkhead box P3 (FOXP3)+ effector Tregs, distinguished by increased expression of immune checkpoint molecules Cytotoxic T-Lymphocyte-Associated Protein 4 (CTLA-4) and T cell Immunoreceptor with Ig and ITIM domains (TIGIT), plays a dominant role in mediating potent immunosuppression within the TME. Current anti-Treg therapies, such as the anti-CTLA-4 monoclonal antibody ipilimumab, show significant clinical efficacy but often induce severe systemic toxicity due to broad depletion of peripheral Tregs. This underscores the unmet medical need for novel agents that selectively target tumor-infiltrating effector Tregs while minimizing systemic adverse effects.
Methods: Multiplex Immunohistochemistry (mIHC) assays were performed to identify Tregs within non-small cell lung cancer (NSCLC) tumor samples from 10 donors, using markers including CD4, CD8, FOXP3, TIGIT, CTLA-4, and Pan-Cytokeratin (Pan-CK). TIGIT and CTLA-4 co-expression on tumor-infiltrating Tregs were analyzed by single cell RNA sequencing (scRNA seq) data from NSCLC tumor and normal lung in 12 datasets of 10X genomics and healthy PBMCs from Human Immune Health Atlas. We engineered various formats of anti-human CTLA-4×TIGIT BsAbs. In vitro efficacy was evaluated in hPBMCs and in hCTLA-4 and hTIGIT-expressing stable cell lines, while in vivo effects were assessed in hCTLA-4/hTIGIT double knock-in mice and additional mouse models. Ex vivo analyses were also conducted to characterize immune cell population changes.
Results: scRNA-seq analysis revealed that co-expression of CTLA-4 and TIGIT is significantly enriched in tumor-associated Tregs compared to peripheral Tregs. Notably, the frequency of CTLA-4 and TIGIT double-positive cells exceeded that of cells expressing either marker alone. Among inhibitory receptor genes, CTLA-4 and TIGIT exhibited the highest expression levels across T cell subpopulations within NSCLC tumors. The anti-human CTLA-4×TIGIT BsAbs demonstrated enhanced binding affinity under dual expression conditions and exhibited robust antibody-dependent cellular cytotoxicity (ADCC). Furthermore, these BsAbs maintained binding activity in acidic pH conditions and displayed potent antigen blocking efficacy.
Conclusions: These findings indicate that the anti-human CTLA-4×TIGIT BsAbs specifically targets tumor-infiltrating Tregs and represents a promising strategy for maximizing specificity while minimizing systemic effects.

: Oncogenic Pathways and Cancer Immunity
Poster Session

#5558 KRT6A mediates immune exclusion and anti-PD-1 resistance in head and neck squamous cell carcinoma.

Yi-Che Wu, Muh-Hwa Yang

Institute of Clinical Medicine, NYCU, Taipei, Taiwan

Head and neck squamous cell carcinoma (HNSCC) is one of the most common malignancies worldwide and is currently the third leading cause of cancer-related death among Taiwanese men. Immune checkpoint blockade (ICB) therapies, including the PD-1-blocking monoclonal antibodies pembrolizumab and nivolumab, have been approved as first-line and salvage treatments for PD-L1-positive recurrent or metastatic (R/M) HNSCC. However, only a minority of patients derive durable benefit from anti-PD-1 therapy. Both innate and acquired resistance to ICB remain major obstacles to effective treatment. In this study, we investigated potential mechanisms underlying ICB resistance using a syngeneic mouse HNSCC model, MOCL2-1. Serial in vivo and in vitro passaging under anti-PD-1 treatment pressure generated an anti-PD-1-resistant subline, L2-1-R. L2-1-R tumors were immunologically "cold," characterized by minimal $CD8^+$ T-cell infiltration and resistance to anti-PD-1 therapy. RNA sequencing of sequential sublines, along with the anti-PD-1-sensitive subline L2-1-S, revealed distinct transcriptional reprogramming in resistant tumors. *KRT6A*, a stress-induced keratin, was markedly upregulated in L2-1-R. Knockdown of *KRT6A* in resistant cells increased $CD8^+$ T-cell infiltration and restored responsiveness to anti-PD-1 therapy in vivo. Furthermore, analysis of a clinical cohort of HNSCC patients treated with pembrolizumab demonstrated that high *KRT6A* expression was associated with poor therapeutic response. Together, these findings identify KRT6A as a key mediator of immune exclusion and resistance to PD-1 blockade in HNSCC, suggesting that targeting KRT6A-related pathways may enhance immunotherapy efficacy.

#5559 Spatial neuroimmune crosstalk driving perineural invasion in head and neck squamous cell carcinoma.

Riya Chhabra[1], Alfred Kao[1], Suravi Bajaj[1], Reena Ding[1], Daniel John[1], Wei Tse Li[2], Jessica Y. Wang-Rodriguez[3], Weg M. Ongkeko[4]

[1]UC San Diego, La Jolla, CA,[2]School of Medicine, UC San Francisco, San Francisco, CA,[3]Professor, Dept. of Clinical Pathology, UCSD Moores Cancer Ctr., San Diego, CA,[4]Department of Otolaryngology- Head and Neck, UC San Diego, La Jolla, CA

Perineural invasion (PNI)—the infiltration of tumor cells within, around, or through nerve fibers—is a hallmark of aggressive tumor biology and an independent predictor of poor prognosis in head and neck squamous cell carcinoma (HNSCC). Despite its high prevalence, reported in up to 90% of cases, the molecular and spatial mechanisms enabling PNI remain poorly characterized. Here, we apply spatial transcriptomics to delineate the cellular, molecular, and microenvironmental features that drive PNI and its associated immune contexture. Spatial transcriptomic datasets (GSE300147, GSE252265, and GSE281978) were processed using standardized pipelines for quality control, normalization, and unsupervised clustering (UMAP). Cell populations were annotated based on canonical markers, identifying distinct epithelial, neural, Schwann, immune, and axon guidance-related clusters. Composite module scores were calculated to quantify PNI activity, neuronal and Schwann cell identity, axon guidance signaling, and immune infiltration. Correlation analyses and Gene Ontology (GO) enrichment were used to define key biological pathways associated with spatially resolved PNI phenotypes.

UMAP visualization revealed spatially distinct neural-enriched tumor clusters co-localizing with Schwann and axon guidance signatures, indicating a neural-like invasive niche. Correlation analysis demonstrated strong associations between PNI and neuronal ($r = 0.89$) and axon guidance ($r = 0.65$) programs, with moderate correlation to Schwann cell activity ($r = 0.49$). In contrast, PNI exhibited weak negative associations with T-cell ($r = -0.26$) and macrophage ($r = -0.12$) scores, consistent with an immune-excluded perineural microenvironment. GO enrichment further supported these trends. PNI-high regions showed activation of pathways involved in chemokine-mediated signaling, cellular adhesion, and fluid and lipid transport—processes that may facilitate neural infiltration and axon-tumor communication. PNI-low regions, by contrast, were enriched for immune-related functions including T-cell and B-cell receptor signaling, interleukin-2 production, and tumor necrosis factor regulation, consistent with active antitumor immunity. Collectively, these data reveal that PNI progression coincides with the emergence of a neural-dominant, immune-silent niche enriched for chemotactic and axon guidance signals. Together, these findings define the spatial neuroimmune landscape of PNI in HNSCC, implicating reciprocal nerve-tumor signaling and localized immune evasion as synergistic drivers of invasion. By integrating spatial resolution with transcriptomic profiling, this study provides mechanistic insight into how cancer cells remodel the perineural microenvironment to support invasion and immune escape.

#5560 KRAS^{G12D}inhibition stimulates antigen presentation and potentiates mRNA-based immunotherapy in pancreatic cancer.

Amanda Creech[1], Hailey Lee[2], Khalid Rashid[2], Tony Luu[2], Emma Lieberman[2], Michael Srienc[3], Alykhan Premji[3], Ahmad Kassem[1], Luyi Li[3], James Wohlschlegel[4], Timothy Donahue[1], Norbert Pardi[5], Caius Radu[1]

[1]Medicine, UCLA David Geffen School of Medicine, Los Angeles, CA,[2]Molecular and Medical Pharmacology, UCLA David Geffen School of Medicine, Los Angeles, CA,[3]Surgery, UCLA David Geffen School of Medicine, Los Angeles, CA,[4]Biological Chemistry, UCLA David Geffen School of Medicine, Los Angeles, CA,[5]Perelman School of Medicine, University of Pennsylvania, Philadelphia, PA

Inhibition of constitutively-active KRAS^{G12D}, a powerful oncogenic driver in pancreatic ductal adenocarcinoma (PDAC), has been shown to sensitize tumors to T-cell-mediated immunotherapy in preclinical models. However, the influence of KRAS^{G12D} inhibition on tumor cell antigen presentation remains unclear. Therefore, we employed a multi-omic profiling workflow to investigate alterations in the proteome and peptide MHC-I ligandome (immunopeptidome) following the treatment of HPAC human cancer cells with a RAS(ON) G12D-selective inhibitor RMC-9945 (representative of investigational agent zoldonrasib), and/or IFNɣ *in vitro*. KRAS^{G12D} inhibition induced a unique IFN response signature and potentiated the expression of proteins involved in antigen processing and presentation. Immunopeptidomic analysis revealed a two-fold increase in both ligand abundance and diversity, reflecting the differential expression of proteins induced by KRAS^{G12D} inhibition.

We hypothesized that KRAS^{G12D} signaling inhibition in preclinical models could augment immune responses initiated by immunization targeting tumor antigens *in vivo* via the following mechanism: the release of antigens from KRAS^{G12D}-induced cell death, coupled with increased MHC-I expression on remaining tumor cells, would enhance interactions with T cells activated by immunization. To test this, we orthotopically inoculated C57Bl/6 mice with a murine PDAC-KRAS^{G12D} cell line engineered to express the model self/tumor-associated antigen gp100. Mice were then immunized with either empty ionizable lipid nanoparticles (e-iLNPs) or iLNPs packaged with mRNA encoding full-length gp100 (gp100-iLNP). Prior to and during subsequent vaccine boost doses, mice were treated continuously with either KRAS^{G12D} inhibitor RMC-9945 or vehicle. Mice treated with both gp100 mRNA-iLNP immunization and KRAS^{G12D} inhibition exhibited significant tumor regression that was sustained over time compared to either treatment modality alone. This anti-tumor response was associated with a superior antigen-specific T cell response to subsequent immunizations, the retention of functional tumor antigen-specific cytotoxic T lymphocytes in both the tumor microenvironment and local secondary lymphoid organs, and sustained MHC-I and MHC-II surface expression on tumor cells.

These preclinical findings underscore the dynamic nature by which PDAC antigen presentation can be modulated by KRAS signaling inhibition and IFNɣ. Combining allele-specific KRAS inhibition with tumor antigen immunization resulted in sustained tumor regression *in vivo* and was associated with the retention and function of tumor antigen-specific T cells. This rationalizes the combination of both approaches for enhanced anti-tumor activity, offering a strategy that is worth exploring clinically for improving outcomes in pancreatic cancer treatment.

#5561 LILRB1 antibody targeting the LILRB1/HLA-G axis: Preclinical efficacy, pharmacokinetics, and safety supporting first-in-human trials.

Han Byoul Kim, Seok-Joo Kim, Younghoon Kim, Junhaeng Cho, Minsoon Kim, JungA Kim, Suji Hong, Heehang Kim, Shin-Young Kang, Kyungna Ko, Jun-Gyu Park, Hyungjin Cho, Jeeyeon Roh, Young Dok Son, Wooseok Ko

LG Chem, Seoul, Korea, Republic of

Background:LILRB1 is an inhibitory receptor expressed on T cells, B cells, NK cells, and monocytes. It binds to HLA class I molecules, with the highest affinity for HLA-G. This interaction delivers inhibitory signals that allow tumor cells to evade immune surveillance, impairing NK cell, T cell, and macrophage function. Disrupting the LILRB1/HLA-G axis is a promising strategy for restoring anti-tumor immunity. Additionally, LILRB1 may regulate T cell function independently of PD-1, suggesting potential to overcome resistance to PD-1 inhibitors.
Methods: Binding affinity and specificity of LG-LILRB1 antibody were assessed via surface plasmon resonance and flow cytometry. Competitive binding assays confirmed blockade of LILRB1/HLA-G interaction. Restoration of immune cell function was evaluated using flow cytometry and western blotting. Anti-tumor efficacy was tested in human LILRB1 transgenic mice. Pharmacokinetics and toxicokinetics were studied in cynomolgus monkeys, and safety was assessed through GLP-compliant toxicology and immunotoxicity studies.
Results:LG-LILRB1 antibody showed high-affinity, selective binding to LILRB1 and dose-dependent blockade of HLA-G. Functional assays revealed enhanced T cell proliferation, NK cell cytotoxicity, and macrophage phagocytosis. In vivo, LG-LILRB1 antibody significantly inhibited tumor growth (up to 88.8%) in transgenic mice bearing HLA-G-expressing tumors. Pharmacodynamic analysis showed increased infiltration and activation of $CD8^+$ T cells and NK cells. Combination with PD-L1 blockade yielded synergistic anti-tumor effects. In monkeys, LG-LILRB1 antibody exhibited dose-proportional exposure and a long half-life (>12 days). No treatment-related adverse findings were observed in 4-week GLP toxicity studies.
Conclusions:LG-LILRB1 antibody, a first-in-class LILRB1 blocker, restored anti-tumor immunity by disrupting the LILRB1/HLA-G axis. It enhanced immune cell function and showed strong efficacy in preclinical models. Favorable pharmacokinetics and safety support its clinical development. Combination with PD-L1 blockade further improved outcomes. These findings support LG-LILRB1 antibody as a promising candidate for cancer immunotherapy, with a Phase 1a trial currently ongoing (NCT06332755).

#5562 Antagonism of β-Catenin/BCL9 interaction suppresses polymorphonuclear myeloid-derived suppressor cell generation and maintenance.

Claudio Scuoppo, Julia Diehl, Rick Ramirez, Barry J. Kappel, Abi Vainstein-Haras, **Jim A. Rotolo**

Sapience Therapeutics, Tarrytown, NY

Myeloid-derived suppressor cells (MDSCs) are a heterogenous group of myeloid-lineage cells thought to play a role in the immunosuppressive cancer environment. Evidence indicates that in colorectal cancer (CRC) patients, MDSCs accumulate in peripheral blood (PB), secondary lymphoid organs and tumors. Further, nonclinical models have proved their contribution in suppressing anti-tumor T-cell responses. Thus, MDSCs have become an attractive target of therapeutic strategies aimed at reversing tumor-related immunosuppression and, as these cells can be readily assessed in PB fractions, as a pharmacodynamic biomarker to track therapeutic response and disease progression. Despite the great interest in MDSC biology, the genetic pathways responsible for their expansion and maintenance are poorly understood, in part due to the difficulty in defining MDSCs immunophenotype. ST316 is a clinical-stage peptide antagonist of the β-catenin/BCL9 protein complex that is currently being evaluated in a Phase 1/2 study (NCT05848739) in patients with advanced CRC. Consistent with literature, polymorphonuclear (PMN)-MDSCs were elevated in the PB of most evaluable patients in the Phase 1 part of the study (7 of 8 patients); strikingly, ST316 exposure resulted in statistically significant suppression of MDSCs in the PB of all patients who displayed baseline elevations (7 of 7 evaluated). Similar increases in PMN-MDSCs were observed at baseline in the immunocompetent APC^{min} and CT-26 CRC murine models, while exposure to ST316 resulted in dose-dependent decreases in their frequency. Mechanistically, ST316 prevented proliferation of immature MDSC precursor populations in the bone marrow while accelerating mature MDSC turnover in PB and splenic fractions. Transcriptomics analysis indicated that ST316 suppressed Wnt/β-catenin signatures in PMN-MDSCs. In addition, ST316 reduced expression of several myeloid markers associated with neutrophil differentiation, including CD101, CD300a, and Siglec-F, suggesting that these markers reflect β-catenin/BCL9 controlled dynamics of MDSCs generation. Overall, our results identify a new role for β-catenin/BCL9 signaling in MDSC generation and maintenance, and identify suppression of MDSCs as a consequence of ST316 exposure in nonclinical and clinical tumor settings.

#5563 Long noncoding RNAs networks as novel master regulators of cytotoxic immune cell exhaustion in triple-negative breast cancer.

Raquel Sanchez[1], Eduardo E. Chaib Lozano[1], Barbara Yang[1], Shrikanth S. Gadad[2], Enrique I. Ramos[1]

[1]The University of Texas at El Paso, El Paso, TX,[2]University of Texas Rio Grande Valley, El Paso, YT

Background: Breast cancer is the second leading cause of cancer-related deaths among women in the United States, with triple-negative breast cancer (TNBC) representing the most aggressive subtype. Although immune checkpoint inhibitors (ICI) and CAR-T therapy emerge as promising therapy options for TNBC patients, their overall effectiveness is limited. This therapeutic failure is strongly influenced by immunosuppressive tumor microenvironments, where chronic antigen exposure leads to exhaustion in cytotoxic lymphocytes. Exhausted $CD8^+$ T cells, NK cells, and NKT cells display diminished effector capacity and reduced persistence, ultimately impairing tumor clearance. Understanding the regulatory mechanisms that sustain exhaustion is critical for improving immunotherapies. Long non-coding RNAs (lncRNAs) have gained recognition as regulators of transcriptional and epigenetic programs in cancer biology; however, their contribution to immune cell exhaustion in TNBC remains unexplored.
Methods: We analyzed single-cell RNA-seq datasets (NCBI/GEO) from TNBC tumors, focusing on immune cell populations. We performed scRNAseq analysis and clustering to assess expression of specific exhaustion markers (TOX, TIGIT, PDCD1, LAG3, as well as differential gene expression to identify dysregulated lncRNAs in those exhausted $CD8^+$, NK, and NKT cell subsets.
Results/future directions: Preliminary data identified variable exhaustion-associated lncRNAs shared among CD8 T cells, NK, and NKT cells in TNBC samples. Some of these candidate lncRNAs were selectively enriched in certain immune populations. Signaling pathway analyses are in progress to evaluate the functions of these lncRNAs and their involvement in chromatin regulation, RNA-protein scaffolding, transcriptional activation/repression, and metabolic stress responses, all hallmarks of immune exhaustion. We will then functionally validate top candidate lncRNAs using RNA interference and overexpression models in primary human cytotoxic lymphocytes to assess their impact on exhaustion phenotypes and effector function.
Conclusion: In our study, we identified a previously unrecognized group of lncRNAs in TNBCs, which could potentially drive immune exhaustion across cytotoxic immune subtypes by regulating TNBC tumors physiology. These lncRNAs could be crucial for exhaustion progression, and reversing their effects through ASOs or gene silencing could reveal their influence towards recovering anti-tumor response by maintaining T cell persistence.

#5564 Crosstalk between ceramide and prostaglandin signaling mediates resistance to immune checkpoint blockade.

Wyatt O. Wofford, Elif Percin, Han G. Lee, Odai Darawshi, Bryan Granger, Lucy Mulligan, Natalia V. Oleinik, Mohamed F. Kassir, Chase Walton, Paramita Chakraborty, Stefano Berto, Raymond N. DuBois, Shikhar Mehrotra, Besim Ogretmen

The Medical University of South Carolina, Charleston, SC

Immunotherapy has revolutionized cancer treatment, yet only a fraction of patients develop durable responses to immune checkpoint blockade (ICB). Identifying tumor-intrinsic mechanisms driving αPD-1/αPD-L1 resistance remains critical to improving patient outcomes. We recently discovered that reduced ceramide synthase 4 (CerS4) activity and the subsequent loss of C18/20 ceramide impairs response to ICB through intracellular PD-L1/Caprin-1 signaling. To investigate this further, we generated an orthotopic, transplantable TNBC (E0771) model of ICB resistance through serial *in vivo* αPD-L1 exposure, yielding the 2RA cell line. 2RA tumors are refractory to both αPD-L1 and αPD-1 therapy, and transcriptomic signatures derived from this model strongly predict clinical ICB outcomes, supporting its relevance to human disease. Functionally, 2RA tumors display reduced CerS4 expression, diminished C18/20 ceramide, and increased intracellular PD-L1/Caprin-1 interaction. Bulk RNA-seq revealed marked enrichment in prostaglandin E_2 (PGE_2) signaling, a potent immunosuppressive pathway, in 2RA tumors. Mechanistically, we identified that CerS4 inversely regulates prostaglandin-endoperoxide synthase 2 (Ptgs2, COX-2) expression and PGE_2 production through the PD-L1/Caprin-1 complex, whereby ceramide directly interacts with PD-L1 to restrict Caprin-1 binding. Analysis of TCGA and ICB-treated patient datasets substantiated the CerS4/PD-L1/COX-2 axis across multiple solid tumor subtypes. Immune profiling via flow cytometry and snRNA-seq identified dysfunctional progenitor and effector $CD8^+$ T cells as central to impaired ICB response in 2RA tumors. Genetic or pharmacological disruption of the CerS4/PD-L1/PGE_2 axis, achieved through CerS4 restoration or TGF-β inhibition (LY2157299), restored ICB sensitivity, prolonged survival, and induced tumor rejection *in vivo*. Targeting PGE_2 production with celecoxib, but not aspirin, further enhanced responses when combined with LY2157299 and αPD-1 therapy. Targeted lipidomics and multiplex immunofluorescence (mIF) confirmed that this triple combination potently blocks the ceramide/PGE_2 axis and stimulated $CD8^+$ T cell responses to control tumor growth. Finally, mIF analysis of nivolumab-treated pre-surgical human HNSCC specimens (responders vs. non-responders) corroborated these findings by demonstrating reduced tumor ceramide abundance, elevated $PanCK^+COX\text{-}2^+ceramide^{lo}$ populations, and decreased intratumoral $CD8^+$ T cell density amongst non-responders. Collectively, these studies (1) establish a relevant model of ICB resistance, (2) define a mechanistic framework linking ceramide metabolism to prostaglandin-mediated immune suppression, and (3) highlight therapeutic strategies to target ICB resistance and improve patient outcomes.

#5565 C118S-mediated redox modulation of KRASG12D mutation reprograms immunometabolism to suppress obesity-driven pancreatic tumorigenesis.

Zahid Rafiq[1], Weiqin Lu[2]

[1]Biological Sciences, University of Texas at El Paso, El Paso, TX,[2]Department of Biological Sciences, University of Texas at El Paso, El Paso, TX

Background: Pancreatic ductal adenocarcinoma (PDAC) is frequently driven by oncogenic $KRAS^{G12D/+}$ and exacerbated by obesity-induced metabolic inflammation, driving immune suppression and metabolic reprogramming. The concurrent rise in global obesity and PDAC incidence demands mechanistic strategies specifically tailored to the unique biology of obesity-associated KRAS-mutant tumors. Redox-sensitive regulation of KRAS at cysteine118 (C118) plays a critical role in signaling activity, and mutation to serine (C118S) has been shown to attenuate KRAS function in other tumor models. However, the impact of C118S on the immunometabolism landscape of $KRAS^{G12D/+}$ driven PDAC particularly in the context of obesity remains unexplored. This study aims to characterize how the C118S mutation alters immune and metabolic dynamics in obese versus lean PDAC settings.

Methods &

Results: Using in-house genetically engineered mouse models ($KRAS^{G12D/+}$ and $KRAS^{G12D+C118S/+}$ on a KC (KrasCre) background) fed with high-fat or standard normal diets to examine tumor progression. We found changes related to the C118S modification in the KRAS-G12D allele slowed the progression of PDAC. H&E staining showed reduced high-grade PanIN lesion. Alcian Blue and Sirius Red staining revealed a marked reduction in mucin production and fibrosis, indicating an alleviation of the desmoplastic response. Immunohistochemistry for Ki67 showed decreased cell proliferation, CK19 staining confirmed reduced ductal marker expression, and MIST1 staining indicated preservation of acinar cell identity. We also examined the related immune infiltration ($CD8^+$ T cells, PD-1/PD-L1, myeloid cells), metabolic markers (GLUT1, CPT1A). We found that $KRAS^{G12D+C118S/+}$ tumors had improved antitumor Immune and Metabolic profile components of TIME, particularly under obese conditions. Elucidating the redox-dependent mechanisms linking $KRAS^{G12D+C118S/+}$ to immune-metabolic reprogramming. We quantified ROS and GTP-bound KRAS activity, and downstream signaling (PI3K/AKT/mTOR, ERK). We found that C118S reduced ROS-dependent KRAS activity, suppresses oncogenic signaling, and restore metabolic immune fitness.

Conclusion: This study pioneers a paradigm shift in pancreatic cancer research by combining redox-based KRAS mutation, metabolic stress (obesity), and immunometabolism signaling. It aims to show that targeting KRAS redox regulation can reshape the immune-metabolic microenvironment to impede tumor progression. Findings could lead to novel redox-immunometabolism therapeutic strategies for obesity-associated KRAS-driven cancers.

#5566 Molecular evolution reveals low-prevalence driver mutations, mutational synergies, and associated immune dynamics in ovarian cancer.

Julia McAdams, Nic Fisk

Cell and Molecular Biology, University of Rhode Island, Kingston, RI

Ovarian cancer remains significantly underrepresented in genomic studies despite its high mortality rate, highlighting the need to make the most of extant data. Traditional approaches focus on mutation prevalence, potentially overlooking rare but highly oncogenic driver mutations or mutational synergies that provide substantial evolutionary advantages to tumor cells, including those that may shape the cancer-immune landscape. In ovarian cancer, tumor mutational burden (TMB), immune checkpoint molecule expression (LAG-3, ICOS, CTLA-4), and regulatory T cell (Treg) infiltration have been associated with clinical outcomes, yet their relationship to underlying mutational selection pressures remains poorly understood. We applied cancereffectsizeR to quantify the evolutionary benefit of single nucleotide variants (SNVs) in ovarian cancer, analyzing whole-exome, whole-genome, and targeted panel sequencing samples pooled across studies. This approach distinguishes mutational selection from prevalence, enabling us to quantify not only the relative contribution of high-frequency mutations but also to uncover low-frequency yet highly-selected driver mutations. We then investigated epistatic selection patterns to infer mutational ordering and synergistic interactions between mutated genes. Finally, we examined correlations between quantified selection coefficients and immune phenotypes, developing a predictive model to associate patterns of evolutionary selection within individual tumors with clinically relevant immune characteristics. Our analysis revealed numerous low-prevalence driver mutations with significant selective advantages in ovarian cancer, including mutations in BCL10 and PSIP1. Epistatic analysis uncovered mutational synergies implying temporal ordering of mutational acquisition across several gene pairs, with multiple interactions unreported in STRINGdb, such as a positive synergy between mutant EBP and IGSF21. Our predictive model relating cancer effect size to immune phenotypes—including TMB, LAG-3/ICOS/CTLA-4 expression, and Treg infiltration—revealed that somatic mutations under strong positive selection are modestly predictive of the immune landscape in ovarian cancer, suggesting that evolutionary dynamics and immunogenicity are interconnected. These findings provide new insights into ovarian cancer evolution and identify potential biomarkers for immunotherapy response.

#5567 Combination therapies promote immune-mediated bystander killing of KRAS-G12C inhibitor resistant cells.

Mona Tomaschko, KangBo Ng, Christopher Moore, Claire E. Pillsbury, Sareena Rana, James Campbell, Saptaparna Mukherjee, Ania Mikolajczak, Panayiotis Anastasiou, Andrea de Castro, Alicia Alonso de la Vega, Sophie de Carne Trecesson, Nathan W. Goehring, **Miriam Molina-Arcas**, Julian Downward

The Francis Crick Institute, London, United Kingdom

Although initial clinical responses to KRAS-G12C inhibitors (G12Ci) have been encouraging, their efficacy is limited by the rapid development of resistance. To extend therapeutic benefit, strategies capable of limiting or preventing resistance are required. However, given the heterogeneity of resistance mechanisms identified, designing targeted combination therapies remains challenging. Here, we hypothesised that a more broadly applicable approach would be to exploit the ability of KRAS-G12C inhibition to partially relieve the KRAS-induced immunosuppressive tumour microenvironment, thereby promoting immune-mediated attack on the inhibitor-resistant cancer cells.

We developed a preclinical model to mimic development of resistance to G12Ci by co-engrafting reporter-traced isogenic cells harbouring KRAS-G12C (G12Ci-responsive) with a minor subpopulation of KRAS-G12D (G12Ci-resistant) cells. KRAS G12C inhibition as monotherapy using either the RAS(ON) G12C-selective inhibitor RMC-4998 or the KRAS G12C(OFF) inhibitor adagrasib, led to a rapid outgrowth of the G12Ci-resistant subpopulation. However, when combined with therapies that enhance anti-tumour immune responses, such as SHP2 inhibition or PD-1 blockade, the G12Ci-resistant cells were eliminated, even though these treatments do not affect their growth in the absence of G12Ci-sensitive cells. Notably, this bystander killing of G12Ci-resistant cells and the resulting complete responses were dependent on the adaptive immune system.

These combination therapies led to a profound remodelling of the tumour immune microenvironment, with an increase of inflammatory macrophages and an influx of NK and T cells, including $CD8^+$ T cells recognising the Emv2 endogenous retroviral protein, which represents the major tumour-associated antigen shared between the G12Ci-resistant and G12Ci-sensitive cancer cells. Moreover, transcriptional profiling suggested an enhanced interferon response in the G12Ci-resistant cells caused by the effect of G12Ci on the G12Ci-sensitive cells. Loss of IFNγ receptor rendered the resistant cells less susceptible to immune-mediated bystander killing, indicating that this process was at least partly dependent on their tumour cell–intrinsic ability to respond to IFNγ.

Overall, our preclinical results demonstrate that appropriate combinations can elicit anti-tumour immune responses capable of bystander elimination of G12Ci-resistant subclones, providing a paradigm for the development of therapeutic combinations with greater potential to prevent or counteract the emergence of inhibitor resistance.

#5568 PRTN3 suppresses cytotoxic immune-cell activation and antitumoral immunity through proteolytic cleavage of CXCL9 in KRAS mutant lung adenocarcinoma.

Rong Xiang[1], Yi Liu[2], Yunping Luo[3]

[1]Immunology and Oncology, Nankai University, Tianjin, China,[2]Nankai University, Tianjin, China,[3]Postdoctoral Fellow, Chinese Academy of Medical Sciences, Beijing, China

KRAS-mutant lung adenocarcinoma (LUAD) is largely refractory to immune-checkpoint blockade (ICB). Here, we define a novel immune evasion mechanism in KRAS-mutant LUAD mediated by tumor-secreted protease 3 (PRTN3), which proteolytically inactivates the T-cell chemoattractant CXCL9 to create an immune-cold microenvironment. Mechanistically, KRAS signaling transcriptionally upregulates PRTN3 via c-Myc. Secreted PRTN3 then cleaves and inactivates CXCL9 in the tumor microenvironment, thereby disrupting CXCL9/CXCR3 signaling and suppressing the recruitment and activation of cytotoxic NK and CD8+ T cells. In LUAD patients, high PRTN3 expression is associated with low CXCL9 activity. Crucially, genetic ablation of PRTN3 synergizes with anti-PD-1 therapy to restore antitumor immunity in vivo. Moreover, the application of a hydrolysis-resistant CXCL9 variant is sufficient to potently enhance T-cell-mediated killing in LUAD patient-derived organoids, establishing the therapeutic potential of targeting this axis. Our findings establish tumor-derived PRTN3 as a key mediator of immune suppression and a promising therapeutic target in KRAS-driven LUAD.

#5570 Multi-omics dissection of tumor-related leukocytosis in urothelial carcinoma identifies IL13RA2 as a key driver.

Harvey Yu-Li Su[1], Shih-Yu Huang[1], Chung-Wen Kuo[2], Chang-Ting Lin[3], Yi-Hua Chen[3], Ming-Chun Kuo[1], Hsuan-Ying Huang[4], Chih-Yen Chien[1]

[1]Kaohsiung Chang Gung Memorial Hospital, Kaohsiung City, Taiwan,[2]National Kaohsiung University of Science and Technology (NKUST), Kaohsiung City, Taiwan,[3]Kaoshiung Chang Gung Memorial Hospital, Kaoshiung City, Taiwan,[4]Pathology, Kaohsiung Chang Gung Memorial Hospital, Kaohsiung City, Taiwan

Background:
Tumor-related leukocytosis (TRL), driven largely by neutrophil overproduction, is associated with aggressive disease, treatment resistance, and poor survival across solid tumors. In metastatic urothelial carcinoma (mUC), patients with TRL experience particularly poor outcomes under immune checkpoint inhibitor (ICI) therapy, suggesting an immune-suppressive tumor microenvironment. However, the molecular basis linking TRL to ICI resistance remains unclear.
Methods:
We retrospectively evaluated mUC patients receiving ICIs to assess the prognostic role of TRL. RNA from 35 tumors underwent NanoString profiling to identify leukocytosis-associated genes. IL13RA2 and related candidates were validated across UC cell lines by qPCR, western blotting, and functional assays including proliferation, migration, cytokine analysis, and neutrophil chemotaxis. Transcriptional programs regulated by IL13RA2 were defined using Clariom S microarray.
Results:
Patients with baseline leukocytosis (WBC >10,000/μL) showed significantly worse overall survival, confirming TRL as a negative prognostic factor during ICI therapy. High-WBC tumors displayed a distinct inflammatory signature, with IL13RA2 among the most upregulated genes. IL13RA2 expression strongly associated with neutrophil enrichment in TCGA BLCA (Pearson $r = 0.41$; TIMER $\rho = 0.199$) and was validated in the ICI-treated GSE176307 cohort, where IL13RA2-high tumors exhibited increased neutrophil and myeloid fractions. Functionally, IL13RA2 knockdown reduced proliferation, migration, and wound-healing capacity in UMUC3 and T24 cells. Microarray analysis identified reproducible IL13RA2-regulated gene sets enriched for cytokine, inflammatory, motility, and chemotaxis pathways. Conditioned media from IL13RA2-expressing cells robustly induced migration of purified neutrophils, whereas IL13RA2 depletion markedly impaired neutrophil chemotaxis. IL13RA2 silencing suppressed JAK1/2-STAT3 activity and reduced multiple pro-inflammatory cytokines and chemokines, including CXCL5, CXCL6, CXCL8, CCL3, and CCL4.
Conclusions:
TRL is a potent negative prognostic factor in ICI-treated mUC. IL13RA2 emerges as a central driver linking leukocytosis to immune resistance by promoting inflammatory signaling, cytokine production, and myeloid recruitment. These findings identify IL13RA2 as a key mediator of TRL and a potential therapeutic target to overcome myeloid-driven ICI resistance in urothelial carcinoma.

#5571 Dynamic transcriptional remodeling and functional adaptation drive malignant progression in lymphoma.

Bandish Kapadia[1], Anirban Roychodhury[1], Forum Kayastha[1], Won Sok Lee[2], Nahid Nanaji[3], Jolene windle[1], Ronald B. Gartenhaus[1]

[1]Virginia Commonwealth University, Richmond, VA,[2]Richmond Department of Veterans Affairs, Richmond, VA,[3]Veterans Affairs Maryland Health Care System-Baltimore Division, Baltimore, MD

Background: Lymphoma progression is shaped by dynamic interactions between malignant B cells and the tumor microenvironment, generating marked transcriptional and functional heterogeneity. To define mechanisms driving this adaptive evolution, we developed a transplantable oncogene-driven lymphoma model enabling controlled tracking of clonal evolution, transcriptional remodeling, and functional adaptation across serial tumor passages.
Methods: Primary tumors from transgenic lymphoma-bearing mice were serially propagated into syngeneic hosts, generating early (P0), intermediate (P2), and advanced (P4) stages. Single-cell transcriptomics, CNV-inference (inferCNV), and pathway-level modeling (Seurat/Scanpy, GSVA, Enrichr, DrugBank-based prediction) were used to define malignant and microenvironmental evolution and emerging vulnerabilities.
Results: Serial propagation produced progressive transcriptional diversification consistent with malignant evolution. P0 tumors exhibited proliferative activation and metabolic priming, whereas P4 tumors developed immunosuppressive, angiogenic, and stress-adaptive programs mirroring hallmarks of advanced human B-cell lymphoma. A key finding was a unified stress-survival module in P4, marked by hypoxia-responsive, UPR-related, and metabolically rewired pathways, alongside reduced proliferative dependence. Sex-specific pathway biases including cytokine/chemokine signaling and metabolic checkpoint usage also emerged. Drug-response inference identified passage-specific vulnerabilities, with P4 showing heightened sensitivity to inhibitors of oxidative-stress buffering, lipid metabolism, and UPR nodes.
Future Directions: Multiparametric flow cytometry, immunohistochemistry, and spatial profiling are underway to validate lineage reprogramming, CNV-based malignant classifications, and pathway activation states.
Conclusions: Malignant progression in this model is driven by iterative transcriptional reprogramming and functional adaptation shaped by microenvironmental selection. P4 most accurately recapitulates transcriptomic and functional features of advanced disease, making it an optimal preclinical platform for studying therapeutic resistance and identifying emergent vulnerabilities in aggressive B-cell lymphoma.

#5572 Conservation of driver mutations and oncogenic pathway alterations revealed through a comparative genomic analysis of human angiosarcoma and canine hemangiosarcoma.

Lucas Rodrigues, Garrett Harvey, Gerald Post, Benjamin Lewis, Abigail Hull, Aubrey O'Grady, Lindsay Lambert, Christina Lopes, Thaddeus Allen

FidoCure - One Health Company, Palo Alto, CA

Angiosarcoma (AS) is a rare and aggressive endothelial malignancy, representing <2% of soft tissue sarcomas in humans. Progress in developing effective therapies has been hindered by its low incidence, genomic heterogeneity, and the scarcity of representative preclinical models.Integrative genomic analyses of two cBioPortal cohorts (n=131) identified recurrent alterations in TP53 (26%), KDR (17.6%), POT1 (17.6%), PIK3CA (14.5%), FLT4 (11.5%), PTPRB (11.5%), and NRAS (5.3%), highlighting pervasive disruptions of DNA damage response, PI3K/AKT/mTOR, and angiogenic receptor signaling. However, the rarity of AS limits functional validation and biomarker-driven therapy development.Canine hemangiosarcoma (HSA) is a biologically analogous vascular tumor that occurs spontaneously with far higher incidence, offering a unique opportunity to model AS in an immunocompetent host. Large-scale profiling of HSA from the FidoCure Precision Medicine Platform (n=1,177) revealed overlapping mutations in TP53 (54.9%), PIK3CA (29.9%), NRAS (15.3%), FLT4 (3.6%), PTEN (3.4%), and KDR (2.6%), mirroring the human landscape.Cross-species analyses showed striking molecular parallels. PIK3CA mutations in both species clustered in the helical and kinase domains, consistent with pathway activation. While mutation at the canonical hotspot (H1047R/L/Y) predominated in HSA, AS was found to harbor heterogeneous variants (P124L, T957P, M1043V/I). TP53 variants localized to conserved DNA-binding regions (human R175, R248, R273; canine R164H, C228R/Y, R263H, R272H), indicating convergent loss of tumor-suppressor function. KDR, NRAS, and PTEN alterations similarly disrupted VEGFR2, RAS/MAPK, and PI3K signaling pathways across species.Collectively, these findings reveal deep evolutionary conservation of molecular drivers in vascular sarcomagenesis. Canine HSA faithfully recapitulates the genetic complexity and therapeutic vulnerabilities of human AS, establishing a robust comparative platform for biomarker discovery, targeted therapy validation, and translational oncology research within an immunocompetent context.

#5573 Novel ASPORIN/CRABP2 axis drives cell-state plasticity from adenocarcinoma to neuroendocrine-like prostate cancer.

Parthasarathy Seshacharyulu, Shobhit Lall, Sushanta Halder, Sakthivel Muniyan, Zahraa Wajih Alsafwani, Ramakanth Chirravuri-Venkata, Moorthy P. Ponnusamy, Surinder K. Batra

Biochemistry and Molecular Biology, University of Nebraska Medical Center, Omaha, NE

Background: Prostate cancer (PCa) remains a highly lethal disease due to the rapid emergence of neuroendocrine (NE)-like variants from adenocarcinoma. It is predicted that *de novo* NEPC will emerge from 17% of localized PCa, while treatment-related NEPC will account for 20% of advanced PCa. Clinically, NEPC patients frequently harbor visceral metastasis (62%, P<0.001) compared with CRPC patients (24%), with poor overall survival of 12-17 months. Thus, exploring the unknown mechanism underlying cell-state transition from adeno to NEPC will help identify new targets to overcome lineage plasticity and improve PCa patient survival.

Methods: We developed a novel indolent and metastatic PCa mouse model by overexpressing cMyc and knocking out Pten with/without Mutant p53 (R172H). Global transcriptional profiling was performed in indolent and aggressive mice and ASPORIN (ASPN) knockdown (KD) to identify differential gene expression, biological, and pathway analyses. ASPN ectopic overexpression (OE) and KD clones confirmed ASPN biological function and on-target proteins/genes using RT-PCR and western blot analyses. ASPN *in vitro* function was analyzed in the Incucyte® live imaging system, colony growth assay, and proliferation assays.

Results: The novel **P**ten$^{fl/fl}$; Hi-Myc; **T**rp53$^{R172H/+}$; Rosa-26; PB-**C**re4^{+} (PCTP^{Luc}) mouse exhibits phenotypic resemblance to PCa visceral metastasis to the lung, liver, inguinal lymph node, and intestine with poor survival as compared with age-matched indolent **P**ten$^{fl/fl}$; Hi-Myc; Rosa-26$^{\mathbf{Luc}}$; **P**B-Cre4^{+} (PCP^{Luc}). Unbiased RNA-Seq analysis of PCa adenocarcinoma tissues from PCTP mice revealed a significant association between unique extracellular matrix (ECM) protein clusters and liver and lung metastasis. Asporin (ASPN) emerged as the top differentially expressed ECM protein among the top 25 genes. Consistently, ASPN knockdown and overexpression were directly associated with PCa cellular phenotypes of proliferation and colony growth. Mechanistically, ASPN modulation impacts pERK, CyclinD3, EMT proteins, and a neuroendocrine-like phenotype, as well as cell differentiation-related transcriptomes such as cellular retinoic acid-binding protein 2 (CRABP2), along with Chromogranin A (CHGA), NeuroD1, and INSM1. Using a publicly available TCGA database, we observed a significant overexpression of ASPN and CRABP2 in PCa tissues (N=497) relative to normal (N=52) (P<0.001). Finally, ASPN ectopic overexpression in immortalized RWPE-1 cells confirmed an aggressive *in vitro* phenotypes.

Conclusion: For the first time, we explored the influence of ASPN/CRABP2 and other signaling involved in luminal epithelial to neuroendocrine differentiation and validated CRABP2 as a novel target to prevent NEPC transdifferentiation. Our findings support ASPN's new role, mechanism(s) and as a target for PCa and other visceral metastasis disease.

#5574 Role of KMT2C and KMT2D in modulating tumor immune microenvironment of endometrial cancer.

Sanjeev Ganesh[1], Swornalata Pukhrambam[1], Juveria Ali[1], Savannah Hughes[1], Heather Marie Gibson[2], Michael Wilson[1]

[1]Wayne State University School of Medicine, Detroit, MI,[2]Oncology, Barbara Ann Karmanos Cancer Institute, Detroit, MI

BACKGROUND: Recent molecular classifications of Endometrial Cancer (EC) have enhanced prognostic accuracy and helped guide targeted therapies. Among frequently mutated factors are epigenetic regulators like lysine methyltransferases KMT2C and KMT2D which monomethylate H3K4 at enhancer sites and their loss of function (LOF) mutation is associated with genomic instability, altered chromatin accessibility and increased immune evasion. Although increased CD8+ T cells infiltration and high PDL1 expression in postmenopausal EC patients is linked to poor prognosis, the impact of epigenetic mutation on immune signaling remains poorly understood. Pan-cancer analysis by Cao et al suggests that low KMT2C expression may reduce immunosuppressive and better immunotherapy responses, with similar patterns seen in other cancers suggesting a potential role in modulating immune response.
METHODS: CRISPR technology was used to generated KMT2C and KMT2D knockouts in 12Z and HEC1a cells and whole cell lysates of these cells were used for immunoblotting analysis. Next, Immunohistochemistry on KMT2D KO mouse tissues were performed to look at specific immune markers. Finally, flow cytometry analysis was done to understand the makeup of the tumor microenvironment and explore the differences in the role of various immune cells.
RESULTS: TCGA database showed upregulation of immune factors like IFN-G and CTLA-4 when KMT2C is altered. Immunoblotting analysis of the CRISPR knockout cells showed upregulation of PDL1 expression in KMT2C knockout cells. Further, Immunohistochemistry of KMT2D KO mouse tissues showed decreased CD8+ expression. Following this, flow cytometry analysis of KMT2D KO mouse tissues showed increased myeloid derived suppressor cells and decreased CD8+ and CD4+ cells which indicates an immunosuppressive environment.
CONLCUSION: Overall, these findings highlight the role of KMT2C and KMT2D mutations on the tumor immune microenvironment and support their potential as predictive biomarker for ICI responsiveness in endometrial cancer. The mixed clinical efficacy of immunotherapies, it is critical to understand the intricacies of the tumor microenvironment. Future studies will focus on replicating the results in KMT2C KO mice and further understand the potential of KMT2C and KMT2D alteration in shaping the immune microenvironment.

#5575 Inhibition of immune evasion via targeting the dysregulated EZH2-RKIP axis in cancer cells.

Ryan McWhorter, Talia Festekedjian, Benjamin Bonavida

Microbiology, Immunologyn& Molecular Genetics, UCLA - University of California Los Angeles, Los Angeles, CA

Introduction: We have recently witnessed several milestones in the treatment of a subset of cancer patients with immunotherapy. However, the unresponsive subset is due, in part, to intrinsic factors in the cancer cells that regulate immune evasion. Thus, the identification of such resistant factors might be potential targets to restore the anti-tumor immune response.
Procedure: Two dysregulated gene products were identified, the overexpressed epigenetic enhancer of zeste homologue 2 (EZH2) , a promoter of immune evasion, and the underexpressed Raf kinase inhibitor protein (RKIP), an inhibitor of immune evasion.
Findings: Analyses of the signaling and cross-talk signaling pathways mediated by these two gene products established a dysregulated EZH2-RKIP axis in cancer cells that regulate immune evasion. For example, analysis of pancreatic ductal adenocarcinoma (PDAC) cancer cells overexpress EZH2 and it plays a central role in immune evasion and PDAC does not respond to check point inhibitors or various EZH2 inhibitors.
Conclusion: We propose that targeting the EZH2-RKIP axis by agents that can induce RKIP expression in cancer cells will lead to downregulation of EZH2 will inhibit immune evasion and will restore the unresponsive cancer cells to respond to immunotherapy. Such agents can be used alone or in combination with other therapies. The specific targeting directly to the tumor cells and sparing normal tissues remain challenging and require novel approaches .

#5576 BRD- and EHMT-dependent immunosuppressive transcriptome in triple-mutant Astrocytoma.

Qingzhu Gao, Leyi Xie, Gengchen Cai, Sophie Sall,Bachchu Lal, Lopez-Bertoni Hernando, John Laterra, **Yunqing Li**

Hugo W. Moser Research Institute at Kennedy Krieger, Baltimore, MD

Astrocytomas (WHO grade II and III) primarily occur in early-middle adult life and frequently progress to more aggressive secondary GBM despite best standard-of-care therapy. Developing more effective therapeutic strategies requires a more complete understanding of the mechanisms employed by astrocytoma cells to escape anti-tumor immunity. The majority (~80%) of grade II & III astrocytoma carry mutations in isocitrate dehydrogenase (e.g., $IDH1^{R132H}$), which typically occurs in combination with p53 mutation and ATRX inactivation (i.e., $IDH1^{R132H}/p53_{mut}/ATRX_{loss,}$ triple-mut for simplicity), indicating that this triple mutation background has an important role in tumor growth and tumor microenvironment reprogramming potentially including immune evasion mechanisms. Our recent findings show that triple-mut induces multiple pathways with anti-tumor immune modulating potential including checkpoint ligands, IFN-γ signaling insensitivity, down-regulation of MHC-I and -II antigen presentation pathways (MHC APP), and dysregulated cytokine/chemokine profiles that modulate the astrocytoma immune microenvironment. Furthermore, we found that the components of the immune-modulating transcriptome associated with triple-mut astrocytom are augmented by standard-of-care radiation (IR) and temozolomide (TMZ). Epigenetic mechanisms orchestrate the tumor cell and the immunosuppressive microenvironment. BET proteins as epigenetic readers regulate gene expression by binding to acetylated lysine residues and/or protein partners, while EHMT1/2 as histone-lysine-N-methyltransferases associated with epigenetic silencing of genes. We show that BRD- and EHMT-dependent histone modifications are elevated in triple-mut astrocytoma cells and together generate the immune-modulating transcriptome. Pan-BET bromodomain inhibitors (e.g., JQ1) significantly inhibited the immunosuppressive transcriptome associated with triple-mut astrocytoma and induced by IR/TMZ, and the pan -EHMT inhibitor UNC0642 significantly up-regulated MHC APP genes and IFN signaling-related genes. SIGNIFICANCE: our findings identify targetable epigenetic determinants that induce an immunosuppressive transcriptome associated with the immunosuppressive microenvironment in triple-mut astrocytoma.

#5577 LSD1 inhibition remodels the tumor microenvironment to enhance anti-PD1 immunotherapy in HNSCC.

Amit Kumar Chakraborty, Chumki Choudhury, Rajnikant Raut, Manish V. Bais

BU School of Medicine, Boston, MA

Background: The histone demethylase LSD1 (KDM1A), an epigenetic regulator implicated in tumor progression and immune suppression. Programmed cell death protein-1 (PD-1/CD279) marks exhausted CD8+ T cells and binds PD-L1 (CD274) in the tumor epithelium. Anti-PD-1 therapy has limited success in head and neck squamous cell carcinoma (HNSCC). We hypothesized that LSD1 inhibitor (SP2509), due to its specific mechanisms, shows superior anti-cancer activity in combination with anti-PD1 therapy.

Methods: We assessed SP2509's impact on the tumor microenvironment (TME) in a syngeneic 4MOSC1 oral squamous cell carcinoma (OSCC) model and 4NQO-induced progressive OSCC model. Anti-PD-1 monotherapy and anti-PD-1-SP2509 combination therapy were tested in a 4NQO model. Multiple methods like immunostaining, qRT-PCR, flowcytometry were employed to test the hypothesis. Ovalbumin overexpression assay followed by flowcytometry was used to determine the antigen presentation in every groups. ChIP-qPCR was used to determine the H3K4 and H3K9 methylation change status on HLA-A, HLA-B and PD-L1 gene locus. Public RNA-seq data (GSE153383) were analyzed to examine immune cell responses to anti-PD-1 and compared with our findings.

Results: SP2509 increased immune cell infiltration, including $CD8^+$ T cells, and reduced the frequency of $PD\text{-}L1^+$ epithelial tumor cells in both 4MOSC1 and 4NQO models. Anti-PD-1 monotherapy expanded $CD8^+$ T cells but did not alter PD-L1 + epithelial cells. Each treatment alone enhanced CD8+ T-cell IFN-γ production, consistent with the GSE153383 analysis showing elevated T-cell infiltration and IFN-γ in anti-PD-1 treated samples. Furthermore, we observed a significant increase in antigen presentation in anti-PD-1 and SP2509 combination group with ovalbumin assay. The combination regimen produced greater immune infiltration, particularly CD8+ T-cells with higher IFN-γ levels, a significant reduction in PD-L1+ epithelial cells, and more pronounced tumor regression than anti-PD-1 alone was observed *in vivo*. ChIP-qPCR results shows increase in H3K4me2 in HLA-A and HLA-B gene locus while H3K9me2 increase in PD-L1 gene locus was observed after SP2509 treatment. We also observed DC activation in SP2509 alona and in combination groups and absent in only anti-PD1 treatment group.

Conclusions: Targeting LSD1 with SP2509 enhances the anti-PD-1 efficacy in HNSCC by modulating the TME, augmenting $CD8^+$ T-cell-mediated antitumor immunity and antigen presentation via MHC class I activation, and reducing tumor PD-L1 expression, ultimately leading to a reduction in HNSCC growth.

#5578 Regulation and expression of transposable elements in ovarian cancer.

Reddick Russell Walker, Kevin Nestler, Melissa Hadley, Katherine B. Chiappinelli

The George Washington University, Washington, DC

Background: Transposable Elements (TEs) are highly repetitive DNA sequences that, when transcribed into RNA, bind immunogenic double-stranded RNA sensors. Through this, expression of TEs can induce type-I interferon (IFN) signaling which has shown potency in improving the response of tumors to immune-modulating therapies. We have published the R175H mutant p53 ovarian cancer cell lines activate chronic TE expression compared to wildtype p53 tumor cells. Despite this, activation of durable immune responses are not seen in R175H p53 tumors, indicating unknown tolerance mechanisms that dampen TE-induced IFN. To this end, we sought to characterize how p53 status alters the expression of TEs and influences downstream IFN signaling.
Methods: To determine the effect that direct binding of p53 has on TE transcription, we correlated p53-targeted chromatin immunoprecipitation sequencing (chIP-seq) with bulk RNA-sequencing expression. Next, we used phosphorylation status of MAVS/MDA-5 signaling mediators, IRF3/7, to determine disruptions in kinase activity downstream of dsRNA sensing.
Results: We found the majority of transcribed TEs did not display direct p53 binding, but rather were transcribed as a biproduct of intragenic insertion within downstream p53 target genes. Additionally, R175H mutant or null p53 bulk RNA sequencing results indicated the downregulation of many TE repressors including KRAB zinc finger proteins (ZNF43, ZNF93, and ZNF561) and DNA Methyltransferase 1 (DNMT1). This suggests TEs lose either DNA methylation and/or KRAB zinc finger silencing in mutant R175H or null p53 backgrounds. The assessment of IRF3/7 indicate R175H p53 cells have reduced phosphorylation levels as compared to wildtype p53 cells. We hypothesize that inactivation of TBK1 by the mutant R175H p53 protein prevents phosphorylation of IRF3 and thus prevents IFN stimulation despite higher TE expression.
Discussion: Overall, these data suggest DNA methylation/expression of KRAB zinc finger proteins are indirect mechanisms by which p53 status dysregulates TE transcription. We aim to characterize DNA methylation status of TEs in wildtype, R175H, or null p53 ovarian cancer cells using whole genome bisulfite sequencing. Additionally, we hope to profile the activation of antiviral response mediators using phosphorylated western blot analyses to determine the disruption of effector signaling in these same cell lines.

: T Cell Engagers 2 / Antibody-Drug Conjugates 1
Poster Session

#5582 Trispecific TCE with second signal boosts solid tumor response efficacy, durability and safety.

Yuanyuan Wang, Huijuan Lu, Hanmian Cai, Chun Liu, Liang Xiao, Peipei Hu, Chang Zhou, Yongting Huo, Di Lu

Guangdong Fapon Biopharma Inc., Guangdong, China

T-cell engager(TCE) drugs have demonstrated substantial clinical benefits in hematological malignancies, yet their application to solid tumor therapy remains challenging. Key hurdles include on-target off-tumor toxicity, inadequate immune cell infiltration into the tumor microenvironment, and T-cell exhaustion. Moreover, sustained stimulation of the first signal can induce T-cell anergy or apoptosis, underscoring an urgent need for safer and more effective next-generation TCEs.
Herein, we have developed FPE021, a triple-specific TCE targeting CD3, CD28, and CDH17. Through optimized affinities for the first and second signals combined with rational structural screening, FPE021 does not induce T-cell fratricide or non-specific activation, indicating a favorable safety profile. Notably, compared with bispecific TCEs, FPE021 exhibits stronger cytotoxicity in vitro and more potent tumor suppression in vivo. Furthermore, the integration of the second signal effectively enhances T-cell proliferation and mitigates T-cell apoptosis. Collectively, FPE021 represents a promising therapeutic strategy to overcome the current barriers limiting TCE efficacy in solid tumor treatment.

#5584 TCX-101, a trispecific T-cell engager (TcE) co-targeting a tumor-associated carbohydrate (TACA) antigen and a tumor-associated protein antigen (TAA) for the treatment of solid tumors with enhanced preclinical activity.

Karla E. G. Soto, Francesco Muraca, Stephan Grunwald, Wiebke Winkler, Carolin Lange, Jean Engela, Peter Sondermann, Matthias Ocker

Tacalyx GmbH, Berlin, Germany

Tumor-associated carbohydrate antigens (TACAs) are carbohydrate structures that result from aberrant glycosylation, a common feature of many cancers. Because TACA overexpression is associated with tumor progression, they represent attractive yet underexplored targets for cancer therapy.Tacalyx focuses on the generation of sophisticated antibodies against specific TACAs and successfully generated a high-affinity, humanized monoclonal antibody (mAb), TCX-101, targeting a TACA structure that is highly expressed across a broad range of cancer indications. Previously, our team demonstrated encouraging *in vitro* activity against breast and gastrointestinal (GI) cancers with TCX-101 as a bispecific T-cell engager (TcE) with a 2+1 CrossmAb format. To reduce off-tumor effects and enhance specificity, we explored a co-targeting approach by engineering a trispecific TcE comprising a CD3-engaging moiety and two tumor-targeting arms: one derived from the TCX-101 and another recognizing a tumor-associated protein antigen (TAA) overexpressed in epithelial tumors. This next-generation TcE demonstrated efficient *in vitro* cell binding and potent T-cell-mediated killing of cancer cells from multiple tumor indications expressing varying levels of the TACA and TAA, at very low effector-to-target ratios with human peripheral blood mononuclear cells (PBMCs), and in some models at picomolar concentrations. *In vivo* evaluation of this TcE format is currently investigated using cell-line derived xenograft models in humanized mice. In conclusion, these results highlight the feasibility of incorporating TCX-101 as a co-targeting arm in a TcE for solid tumors, enabling dual recognition of a TACA and a TAA. Preclinical studies provide proof-of-concept for this approach and support further investigation and development.

#5585 ARK102, a novel tri-specific T cell engager targeting TROP2, HER2, and CD3 for treatment of solid tumors.

Kyeongsik Min, Deukjoo Ahn, Sangwoo Park, Jaejin Jeon, Heeyeon Kim, Yongwon Jung, Yong-Boo Kuk, Jeongmin An, Taehwan Jeong, Seungwon Lee

ARKGENBioScions, Daejeon, Korea, Republic of

ARK102 is a novel trispecific T-cell engager in a fragment format lacking an Fc domain, engineered using proprietary platform technology to simultaneously target HER2 and TROP2 while recruiting CD3 T cells for potent redirected cytotoxicity. HER2 and TROP2 are clinically validated tumor-associated antigens that have demonstrated favorable outcomes across multiple therapeutic modalities. However, limited target expression in some tumors can restrict therapeutic efficacy. As HER2 and TROP2 are broadly co-expressed across diverse malignancies, dual targeting of these antigens offers an innovative strategy to enhance tumor binding through increased avidity and to overcome challenges such as tumor heterogeneity, antigen loss, and resistance to existing therapies.Comprehensive in vitro analyses showed that ARK102 effectively binds both target antigens, activates T cells, and mediates T-cell-dependent cytotoxicity in dual and single target-expressing cancer cell lines at sub-nanomolar concentrations. In vivo, ARK102 demonstrated robust, dose-dependent antitumor activity in human PBMC-reconstituted immunodeficient mice bearing HER2- and/or TROP2-expressing tumor xenografts, without dose-limiting toxicity at efficacious doses, and showed antitumor efficacy comparable to or greater than that of benchmark TROP2-ADC and HER2-ADC therapies.Together, these results highlight ARK102 as a potent and selective dual-targeting T-cell engager with the potential to expand treatment options for patients with solid tumors co-expressing HER2 and TROP2. The compelling preclinical efficacy and favorable safety profile strongly support its further clinical evaluation.

#5586 A next-generation CD8-selective tri-specific T cell engager targeting CDH17 with enhanced efficacy and reduced toxicity.

Jian Guo, Jiaojiao Ding, Tian Wang, Hanmian Cai, Liang Xiao, Peipei Hu, Chang Zhou, Yongting Huo, Di Lu

Guangdong Fapon Biopharma Inc., Guangdong, China

T cell engagers (TCEs) have already achieved remarkable clinical potential. However, severe toxicities such as cytokine release syndrome (CRS) have led to the failure of many TCE candidates in clinical trials. In addition, because Treg cells also express the TCR-CD3 complex, TCEs can inadvertently activate Treg cells, thereby substantially suppressing anti-tumor immune responses. To address these problems, a CD8-biased TCE has been developed that strongly activates CD8+T cells while minimally activating CD4+T cells and Treg cells, thereby reducing toxicity and improving therapeutic efficacy. However, CD8+T cell activation requires help from CD4+T cells; without this assistance, the effector function of CD8+T cells is limited.
Therefore, we have developed an first-in-class next-generation TCE based on NKG2D. NKG2D is highly expressed on CD8+T cells but is rarely expressed on CD4+T cells and Tregs, providing inherent selectivity for CD8+T-cell activation. Moreover, NKG2D delivers a costimulatory signal that restores the function of CD8+T cells without CD4+T-cell help. Here, we present a tri-specific TCE, CDH17×CD3×NKG2D (FPE026). FPE026 binds to and activates CD8+T cells, but not CD4+T cells or Treg cells. It effectively mediates T cell-driven killing of CDH17-positive tumor cells while inducing much lower levels of cytokines, such as TNF-α and IL-6, compared with traditional TCEs. In addition, compared with the CDH17×TCR×CD8 construct, FPE026 exhibits stronger cytotoxic activity. Furthermore, FPE026 demonstrates significant anti-tumor activity in the AsPC-1 subcutaneous xenograft model, with limited cytokine elevation in serum. Together, these findings highlight FPE026 as a promising next-generation TCE candidate that combines enhanced CD8+ T cell selectivity and potent anti-tumor efficacy with an improved safety profile.

#5587 VTS208: A first-in-class CD3/CLDN18.2/CDH17 Tri-specific T cell engager (TCE) for the treatment of gastrointestinal (GI) cancer.

Wei (Vivian) Wang[1], Xuekun Zhang[2], Man Xu[1], Yingchun Wang[2], Mei Yuan[2], Yanwei Wang[2], Liping Chen[2], Yanling Gong[2], Jing Li[1]

[1]VelaVigo (Hong Kong) Limited, Hong Kong, China,[2]VelaVigo (Shanghai) Limited, Shanghai, China

Zolbetuximab (Astellas' anti-CLDN18.2 mAb, approved) has validated CLDN18.2 as a promising tumor-associated antigen (TAA) for gastrointestinal (GI) cancer therapy. CLDN18.2-targeting T cell engagers (TCEs), including IBI389 (phase I) and ASP2138 (phase I), demonstrate anti-tumor activity in patients with low CLDN18.2 expression, indicating that the TCE modality is effective even with minimal TAA expression. However, short duration of response and drug resistance persist because tumor heterogeneity drives therapeutic limitations. Notably, CDH17 (Cadherin 17) has emerged as a novel biologic target, frequently overexpressed in GI cancers. CLDN18.2 and CDH17 exhibit highly complementary expression patterns (co-expressed or individually expressed) across multiple cancers with limited normal tissue expression, positioning them as ideal dual targets for trispecific TCE design that may address tumor heterogeneity and overcome antigen-loss resistance in single-target therapies.

We present VTS208, a first-in-class trispecific antibody featuring a proprietary CD3 arm that targets both CLDN18.2 and CDH17. It achieves potent on-target cytotoxicity with reduced concomitant T cell activation, thereby widening the therapeutic window. Its bi-paratopic CDH17-targeting design enhances binding avidity and efficacy against low-expression tumors. In human PBMC-reconstituted CDX models with variable CLDN18.2/CDH17 expression across gastric cancer (GC), pancreatic ductal adenocarcinoma (PDAC) and colorectal cancer (CRC), VTS208 demonstrated robust anti-tumor activity even at low doses. Preliminary cynomolgus monkey toxicity studies confirmed favorable tolerability under step-up dosing. Current development includes CMC process optimization and dose-range-finding (DRF) toxicity studies. With mini-pool fermentation titers of 4-6 g/L supporting targeted drug substance concentrations for subcutaneous administration, the IND application is scheduled for filing in H2 2026.

In summary, VTS208's unique trispecific design and differentiated features demonstrate promising efficacy and safety, positioning it as a compelling first-in-class TCE candidate for clinical development.

#5588 A next-generation tri-specific T cell engager targeting CDH17 with 4-1BB co-stimulation for the treatment of gastrointestinal cancers.

Shan Gao[1], Xiaoli Zhang[2], Yuanyuan Yang[2], Zhijian Cai[2], Feifei Cui[1], **Liu Yang**[1], Lei Fang[1]

[1]Excalipoint Biotechnology （Shanghai） Co.,Limited, Shanghai, China,[2]Lepu Biopharma Co., Ltd, Shanghai, China

Background: Cadherin-17 (CDH17), a membranous cell adhesion protein, is highly expressed in gastrointestinal (GI) cancers, particularly in colorectal cancer. In normal intestine tissue, CDH17 is restricted to the lateral side of the epithelial cells and remains largely inaccessible to antibody, making it a promising therapeutic target for GI malignancies. Our platform has demonstrated that incorporating 4-1BB costimulation can effectively convert immunologically "cold" tumors into "hot". This transformation is achieved by enhancing the infiltration of peripheral T cells into the tumor and systemically remodeling the tumor microenvironment. Moreover, this strategy elicits a durable T cell memory response and significantly prolongs survival. Given that GI cancer is a classic "cold" tumor, we have developed a novel tri-specific T cell engager (TCE) that targets CDH17 on cancer cells and engages CD3 and 4-1BB on T cells. This TCE is engineered to redirect and enhance T cell responses against CDH17-expressing tumor cells. With a manageable safety profile, this approach holds strong potential to improve clinical outcomes for patients with GI cancers.

Methods: The *in vitro* activities of the CDH17-CD3-4-1BB tri-specific TCE were evaluated in both CDH17-positive and -negative tumor cell lines. These assessments included T cell-mediated cytotoxicity, T cell activation, cytokine release and T cell proliferation. *In vivo* anti-tumor activity was investigated in two models: a humanized syngeneic mice model bearing B16F10-hCDH17 tumors and NCG-MHC-dKO mice with human PBMC bearing Lovo tumors. Cytokine release assay (CRA) was conducted to evaluate potential cytokine storm risk. Additionally, the toxicological profile was assessed in a pilot toxicity study in cynomolgus monkeys.

Results: CDH17-CD3-4-1BB tri-specific TCE demonstrated CDH17-dependent activation of CD3 and 4-1BB. It effectively induced tumor lysis in multiple CDH17+ tumor cell lines and significantly enhanced T cell activation, cytokine production and T cell proliferation in the presence of CDH17-expressing target cells. In humanized syngeneic tumor mouse model and human PBMC xenograft tumor mouse model, this molecule demonstrated robust tumor growth inhibition and prolonged survival rate. Furthermore, an *in vitro* CRA indicated lower IL-6 release compared to a clinical benchmark, indicating a more manageable risk of cytokine release syndrome (CRS). In the pilot tox study, no adverse effects were observed in clinical signs and histopathology.

Conclusion: CDH17-CD3-4-1BB tri-specific TCE represents a novel CDH17-targeted T cell engager with potent and durable anti-tumor activity. Collectively, these results underscore its potential as a novel therapeutic agent against GI cancers and support its advancement into clinical development.

#5589 A biparatopic DLL3-targeting trispecific T-cell engager delivered by mRNA-LNP drives potent anti-tumor activity *in vitro*and*in vivo*.

Xue Qiao[1], Qiang Zhang[1], Lushuai Jin[1], Yao Lv[1], Shaoli Liu[2], Xiaoju Zhang[1], Xiaoyun Ma[2], Hongya Han[1], **Wei Xu**[1]

[1]Metis TechBio, Hangzhou, China,[2]Metis TechBio, Beijing, China

Background: T-cell engagers (TCEs) targeting DLL3 show promising clinical activity in small cell lung cancer (SCLC), yet response rates, durability, and toxicities such as cytokine release syndrome (CRS) remain challenges. Because DLL3 is a low-abundance antigen, increased avidity can improve tumor cell killing. We developed an mRNA-lipid nanoparticle (mRNA-LNP) platform enabling sustained in vivo expression of a DLL3-targeting TCE, using the pharmacokinetic profile of mRNA to reduce CRS risk. To enhance penetration and avidity, we incorporated compact camelid VHH domains and a biparatopic design that engages two distinct DLL3 epitopes.

Methods: A trispecific T-cell engager was engineered by fusing two DLL3-binding VHHs, each recognizing non-overlapping epitopes, with a CD3 agonist domain via flexible peptide linkers. The mRNA expression was optimized using codon engineering to balance Codon Adaptation Index (CAI) and Minimal Free Energy (MFE) across the full transcript, including untranslated regions (UTRs) and the coding sequence (CDS). The optimized mRNA was formulated into a novel LNP delivery system to generate the therapeutic candidate MTS108. Cytotoxic activity was assessed using T cell-dependent cellular cytotoxicity (TDCC) assays with human PBMCs co-cultured with DLL3-expressing SHP-77 or MC38-DLL3 target cells. In vivo efficacy was evaluated in both subcutaneous and orthotopic lung tumor models, including a humanized CD3ε transgenic syngeneic model and a human PBMC-reconstituted cell-derived xenograft (CDX) model.

Results: In TDCC assays, MTS108 (mRNA-LNP) demonstrated potent tumor-killing activity against SHP-77 (low DLL3) and MC38-DLL3 (high DLL3) target cells. Against SHP-77 cells, MTS108 exhibited an EC_{50} more than 10-fold lower than that of the approved therapeutic Xaluritamig. It also showed significantly enhanced cytotoxicity against MC38-DLL3 cells relative to Xaluritamig. In vivo, MTS108 consistently and significantly outperformed the benchmark agent across both subcutaneous and orthotopic tumor models. Optimized mRNA design enabled robust expression in vitro and in mice, and both cell-culture supernatants and mouse serum containing mRNA-expressed TCEs displayed tumor-killing potency comparable to recombinant protein. In the subcutaneous MC38-DLL3 syngeneic model and the orthotopic SHP-77 lung cancer model, MTS108 achieved superior anti-tumor efficacy with an improved safety profile.

Conclusion: These data demonstrate that an mRNA-LNP platform can effectively deliver a biparatopic DLL3-targeting trispecific TCE with potent and superior anti-tumor activity and a favorable safety profile. MTS108 represents a promising therapeutic candidate and supports advancement of mRNA-encoded TCEs toward clinical evaluation.

#5590 BCG024: A novel DLL3×CD3×4-1BB trispecific T cell engager enhances T cell persistence and functionality in preclinical models.

Guan Wang, Baihong Liu, Liu Yang, Xue Li, Shuangshi Liu, Yu Qi, Jinhua Zhao, Yang Chen, Frank An, Yi Yang

Biocytogen, Waltham, MA

Background: CD3-based T cell engagers (TCEs) as powerful therapeutic agents have demonstrated clinical success in both hematologic malignancies and solid tumor indications. One major obstacle to TCE therapies in treating solid tumors is T-cell exhaustion due to conventional TCEs lacking co-stimulatory signaling, limiting their therapeutic durability. To address this challenge, integrating a co-stimulatory signal such as 4-1BB into TCEs could be an attractive approach to enhance T cell function and durability.

Methods: We developed a trispecific antibody (TriAb) targeting DLL3, CD3, and 4-1BB using a VHH 4-1BB agonist derived from RenNano® mice to achieve tumor antigen-dependent co-stimulation. *In vitro* assays included repeated stimulation assay and cytotoxicity against DLL3-positive small cell lung cancer (SCLC) cell line. *In vivo* efficacy and T cell proliferation were evaluated in xenograft mouse models bearing established SCLC tumors. The toxicity study was evaluated in CD3ε×4-1BB humanized mice.

Results: The DLL3 TriAb demonstrated significantly enhanced T cell proliferation while maintaining high cell viability and cytotoxicity following repeated stimulation. However, the benchmark and bsAb counterparts showed marked reductions in cell viability and activity. *In vivo*, mice treated with benchmark caused dose-dependent reductions in serum T cell number, whereas those treated with DLL3 TriAb maintained stable T cell populations. That indicated TCE integrated 4-1BB nanobody co-stimulation indeed enhances T cell durability and functionality. In SCLC xenograft models, DLL3 TriAb exhibited robust antitumor efficacy in a monovalent antigen-binding format rather than a bivalent antigen-binding format. Notably, contrasting with non-specific TriAb controls, DLL3 TriAb displayed favorable safety profiles in CD3ε×4-1BB humanized mice even at high doses, with no significant body weight loss or systemic cytokine elevation observed.

Conclusions: Our DLL3×CD3×4-1BB TriAb demonstrates tumor-dependent co-stimulation, enhanced T cell persistence and functionality, further exhibiting superior anti-tumor efficacy in preclinical SCLC model and good safety profiles at high dose. These findings highlight the DLL3 TriAb as a next-generation immunotherapy, offering enhanced T cell functionality and clinical translatability.

#5591 Development of a novel anti-CD19 x BCMA dual targeted T cell engager for the treatment of autoimmune diseases and B cell malignancies.

Lin Huan, Hao Ran, Shiyi Wang, Xiaoping Zhang, Bing Yang, Yang He, Dandan Liu, Chenpeng Su, Chuan Chen, Xiaoqian Chen, Kezhen Ye, Liang Tian, Jian Peng, Zhenping Zhu

Earendil Labs, Wilmington, DE

Rationale B cells and autoantibodies drive the progression of autoimmune diseases. Targeting B cells or plasma cells alone is often insufficient to eliminate both pathogenic B cells and autoantibody. Here, we generated HXN-1031, a novel trispecific T cell engager (TCE), simultaneously targeting CD19 and BCMA.
Methods Affinity, cell-binding and cytotoxicity were evaluated in vitro. In vivo efficacy was investigated in mice bearing $CD19^+$ or $BCMA^+$ tumor cells, and in non-human primates.
Results HXN-1031 has sub-micromolar CD3 affinity and nanomolar CD19/BCMA affinity. Against $CD19^+$ targets, it showed weaker potency (IC50) but similar maximum killing efficacy versus Blinatumomab, with significantly reduced T cell activation and cytokine release. For BCMA, HXN-1031 shows high potency in in vitro cytotoxicity. HXN-1031 effectively kills both $CD19^+$ and $BCMA^+$ cells simultaneously within a mixed cell population while maintaining moderate T cell activation and cytokine release. In contrast, CD19-TCE and BCMA-TCE only selectively target B cells ($CD19^+BCMA^-$) or H929 ($CD19^-BCMA^+$) cells, respectively. In vivo, HXN-1031 demonstrated superior efficacy to Blinatumomab against $CD19^+$ tumors, and significantly suppressed $BCMA^+$ tumor growth, matching Teclistamab analogue efficacy. In non-human primates, HXN-1031 potently depleted, both in peripheral and bone marrow, B cells and plasma cells, leading to significantly reduced serum immunoglobulin, for a prolonged period of times.
Conclusion HXN-1031 is an innovative TCE with finely tuned activity, designed to reset immune system by simultaneously depleting pathogenic B cells and plasma cells. It holds great potential in the treatment of various B cell and plasma cell related autoimmune diseases and malignancies.

#5592 QL535: A novel CD2-costimulating PSMA-targeted T-cell engager with dose-responsive efficacy in PDX models and a favorable GLP toxicology profile in NHP.

Xiao Liu

QLSF Biotherapeutics, South San Francisco, CA

Prostate cancer remains a major cause of cancer mortality, highlighting the need for better targeted immunotherapies. Prostate-specific membrane antigen is highly expressed in malignant prostate tissue, confirmed by immunohistochemistry in 77 patients. Earlier T-cell engagers show limited activity in solid tumors, prompting designs incorporating co-stimulation. Single-cell RNA sequencing of 2,170 tumor-infiltrating lymphocytes from 14 metastatic castration-resistant prostate cancer patients showed broader and higher CD2 expression than CD28, especially in CD8-positive T cells, supporting CD2 as an accessible co-stimulatory axis.QL535 is a trispecific PSMA × CD3 × CD2 T-cell engager engineered to provide optimized CD3 activation and CD2-mediated co-stimulation. *In vitro,* QL535 enhanced PSMA-dependent cytotoxicity compared to CD2-deficient controls and matched the potency of CD28-based trispecifics while reducing secretion of IL-6, TNFα, IFN-γ, and IL-8. Repeated-stimulation assays using patient peripheral blood mononuclear cells demonstrated preserved cytolytic activity and reduced exhaustion relative to CD28-based trispecifics and clinical benchmark analog.*In vivo,* QL535 produced clear dose-responsive tumor regression in prostate cancer patient-derived xenograft models. Good Laboratory Practice toxicology studies demonstrated favorable tolerability. Intravenous dosing from 1 to 10 mg/kg resulted in dose-dependent exposure. Cytokines increased transiently after the first dose, accompanied by reversible decreases in monocytes and lymphocytes and transient elevations in neutrophils and C-reactive protein. Circulating T cells declined at 24 hours and returned to baseline by Day 7. QL535 was overall well tolerated in non-human primates, with pharmacodynamic changes consistent with T-cell engager activity. These findings demonstrate that QL535 delivers potent PSMA-targeted cytotoxicity, sustains function under exhaustion-inducing conditions, drives dose-responsive antitumor activity in patient-derived xenograft models, and exhibits a favorable safety and pharmacology profile, supporting advancement toward clinical evaluation in PSMA-positive prostate cancer.

#5593 A CD19/BCMA dual-targeting VHH format T-cell engager with novel CD3 binder for enhanced potency and safety profile.

Fan Wu, Yongfeng Li, Liang Xiao, Chang Zhou, Peipei Hu, Jiya Shi, Tingchu Wu, Yue Huang, Mengying Liang, Chun Liu, Yuanyuan Wang, Yongting Huo, Di Lu

Guangdong Fapon Biopharma Inc., Guangdong, China

Recently, B cell depletion therapies targeting CD19 or BCMA, including chimeric antigen receptor T-cell (CAR-T) therapies and bispecific antibodies such as Blincyto and Tecvayli, have shown great potential in treating systemic lupus erythematosus (SLE) and other autoimmune diseases (AID). Targeting B cells and plasma blasts expressing CD19 is a key therapeutic strategy in autoimmune disease. However, in some patients, disease may also be anchored in long-lived plasma cells in the bone marrow expressing BCMA but not CD19.This means that the strategy of targeting CD19 alone has limitation in the therapy of B cell depletion.

Here, we have developed CD19/BCMA dual-targeting T cell engager(FPE024) to achieve more extensive depletion of pathogenic B cells. All components of FPE024, including the CD3 nanobody, exhibit excellent cross-species binding activity between human and cynomolgus monkey. This enables us to simultaneously conduct safety and efficacy tests on cynomolgus monkeys, facilitating better translational studies bridging to clinical trials. FPE024 exhibits strong cytotoxicity in tumor cells with different CD19 and BCMA expression patterns, and the level of cytokine release is comparable to that of Blincyto and Tecvayli, indicating that FP024 has a good safety profile. FPE024 induces relatively similar B-cell killing in PBMC from healthy volunteers and SLE patients. In conclusion, FPE024 is a highly potent, CD19/BCMA dual-targeting TCE with preclinical data providing a strong rationale for broad development in AID which benefits from B cell depletion.

#5594 Pharmacological integration of CD3 and CD2 signaling triggers formation of a CD2 corolla that boosts T cell activation.

Sergio Trombetta[1], Shengpan Zhang[2], Tanmay Mitra[2], Salvatore Valvo[2], Colleen Brown[3], Oksana Segreeva[3], Stella Martomo[3], Martin Preyer[3], Jay Fine[3], Jeremy Myers[3], Michael Dustin[2]

[1]EvolveImmune Therapeutics, Branford, CT,[2]Oxford University, Oxford, United Kingdom,[3]Evolveimmune Therapeutics, Branford, CT

Redirecting patient's endogenous T cells to safely and effectively eradicate tumors continues to offer compelling therapeutic opportunities. We found that EVOLVE, a trispecific antibody targeting a tumor-specific antigen together with integrated CD3 activation and CD2 costimulation, led to unique T cell activation profiles. Like the events observed with intact or artificial antigen presenting cells, these trispecific antibodies were sufficient to trigger the formation of a CD2 corolla surrounding the immunological synapse, independent of membrane CD58, on 95% primary human T cells, in a tumor-antigen dependent manner, compared to 20% observed with CD3-matched bispecifics. Trispecific antibodies demonstrated significant functional advantages over conventional bispecific antibodies, with corolla-associated signaling leading to a 1.6-fold amplification of T cell activation events. This resulted in an over 10-fold increase in killing potency against high-antigen-expressing tumor cells and a 20-fold enhancement of killing potency against low-antigen-expressing tumor cells. These findings provide fundamental insights into the CD2 tropism for corolla localization, even when the CD2 and CD3 ligands are covalently linked to each other, confirming the potential for EVOLVE to initiate CD2-costimulatory signaling at the T cell synapse, thereby enhancing the therapeutic efficacy of T cell engagers.

#5595 Development of EDP001, a tetravalent T Cell engager targeting CD19 and BCMA for B Cell lymphoma.

Qinglin Du, Zongjun Xia, Pan Du, Xing Wang, Xiaoman Wang, Feng Wang, Xueyan Yang, Yi Wu, **Shuhua Han**

Edding, Shanghai, China

Background: The current therapeutic landscape for B-cell lymphoma, while much advanced, still faces significant limitations primarily related to treatment resistance, toxicity and accessibility. This study describes a novel tetra-specific antibody, EDP001, that binds CD3, BCMA, and CD19 with two distinct epitopes. The biparatopic CD19 design greatly enhances antigen avidity, while the inclusion of BCMA enables dual-antigen targeting and further increases its efficacy. EDP001 is designed to maximize tumor cell killing, mitigate antigen escape, and sustain low cytokine secretion. Thus, EDP001 holds a great potential for the better treatment of various B cell malignancies.

Methods: Multiple rounds of screening and characterization of antibody candidates were performed by comprehensive evaluation including binding affinity, specificity and functional analysis. Specific target-killing activity was examined using multiple B cell lines expressing CD19 and/or BCMA. Cytotoxicity against primary B cells from different donors were also examined. In vivo B-cell depletion and anti-tumor efficacy were tested in hCD34+ reconstituted mice and a panel of B-cell malignant murine models, respectively.

Results: EDP001 exhibited high affinity for BCMA while demonstrating low affinity for CD3, as intended by design. Notably, its biparatopic anti-CD19 domains conferred an approximately 100-fold higher binding affinity for CD19 than clinically validated CD19/CD3 bispecific antibodies. EDP001 potently lysed target tumor cells expressing CD19, BCMA, or both antigens, outperforming CD3×CD19 or CD3×BCMA bispecific antibodies. In addition, it induced significantly more potent cytotoxicity against primary B cells from both healthy donors and SLE patients, with minimal cytokine release. In vivo studies showed that EDP001 mediated profound and sustained B-cell depletion in hCD34+ reconstituted mice and demonstrated superior anti-tumor activity across multiple B-cell malignant models with varying expression levels of CD19 or BCMA (e.g., Raji, NCI-H929, Jeko-1, WSU-DLCL2, NALM6-BCMA), surpassing CD3×CD19 and CD3×BCMA bispecific antibodies in all the animal models tested.

Conclusion: EDP001 is the first reported tetravalent TCE targeting CD19 and BCMA. The unique molecular design of EDP001 enables a deep depletion of primary B cells as well as various lymphoma lines in preclinical studies. EDP001 may represent a promising off-the-shelf therapeutics with a superior efficacy for the treatment of variety of B-cell lymphomas.

#5597 Plinabulin boosts antitumor efficacy of topoisomerase inhibitor-based antibody-drug conjugates without or with immune checkpoint inhibitor.

Yingjuan June Lu[1], Xiaoyan He[2], Weiwei Cheng[2], Zhengyan Zhang[2], James Tonra[1], Lan Huang[1]

[1]BeyondSpring Pharmaceuticals, Florham Park, NJ,[2]Pharmaron, Beijing, China

Background: Antibody drug conjugates (ADC) with topoisomerase inhibitors (TOP1-ADC) hold significant promise in cancer treatment. FDA-approved TOP1-ADC includes TROP2- or HER2-directed datopotamab deruxtecan (Dato-DXd) and trastuzumab deruxtecan (T-DXd), respectively. To boost ADC efficacy without overlapping toxicity, combination strategies including immune checkpoint inhibitors (ICI) are under active investigation. Plinabulin (Plin) is a first-in-class, differentiated tubulin binder that exerts anticancer activity primarily by activating GEF-H1-mediated pathways in dendritic cell (DC) maturation and T cell activation. In Dublin-3 phase 3 study, Plin/docetaxel outperformed docetaxel with significant OS/PFS/ORR benefits and doubling of 2- and 3-year survival rates, and reduced docetaxel induced neutropenia. In post-ICI settings given after radiation, Plin potentiates anti-PD-1 with significantly higher GEF-H1 immune activation in responders of mixed cancer types. Preclinically, Plin boosts irinotecan activity in human colon cancer models and reduces topotecan-induced neutropenia. Here we investigated Plin synergy with TOP1-ADC in-vitro, and with or without PD-1/L1 inhibitor pembrolizumab (Pembro) or atezolizumab (Atezo) in-vivo.

Methods: For combinations in-vitro, HER2+ KPL-4 breast cancer cells were treated with Plin (1.46 - 46.8 nM), T-DXd (0.105 - 3.37 μM) or both. For combinations in-vivo, MC38 mouse colon adenocarcinoma cells overexpressing hTROP2 (hTROP2-MC38) or hHER2 (hHER2-MC38), were inoculated in B-hPD-1 or B-hPD-1/hPD-L1/hHER2 mice respectively, and antitumor activities of Plin (7.5 mg/kg) plus Dato-DXd (5 mg/kg) ± Pembro (0.3 mg/kg) or T-DXd (3 mg/kg) ± Atezo (8 mg/kg) were evaluated.

Results: On HER2+ KPL-4 cells, Plin showed synergistic activity with T-DXd with median CI <1 at 1:1, 2:1 and 4:1 ratios (T-DXd:Plin). In hTROP2+ MC38 tumor model, Dato-DXd antitumor activity was significantly enhanced by Plin (doublet) and further boosted by Pembro (triplet) with complete response rates of 0%, 20% and 60% respectively. Compared to Dato-DXd plus Plin or Pembro groups, the triple combo most significantly delayed tumor growth (p=0.009 or 0.028) and improved animal overall survival, and was better tolerated than Dato-DXd+Pembro (10% vs. 40% mortality). In hHER2+ MC38 tumor model, only the triple combo group (T-DXd+Plin+Atezo) prolonged animal survival better than T-DXd alone (p=0.0256).

Conclusions: Plinabulin is a Phase 3 novel agent clinically validated to promote DC maturation and T-cell activation, which provides a durable response by strengthening the cancer-immunity cycle when combined with ICI and neutropenia-limiting agents such as docetaxel and ADCs. Clinical investigations assessing plinabulin safety and efficacy combined with TOP1-ADC alone or plus ICI are highly encouraged.

#5598 Exploiting electron transport chain dynamics to sensitize OXPHOS-dependent cancers to immunotherapy.

Haojie Dong[1], Guoyun Kao[2], Umesh P. Yadav[1], Lei Zhang[2], Arshad J. Ansari[2], Srinivasarao Singireddi[2], Bei Jia[3], Jianai Sun[4], Guohua Wu[1], Yini Wang[1], Xin He[1], Lei Zhang[1], Zheng Li[1], Ruiheng Wang[1], Wei Chen[1], Meng Liu[1], Shuaishuai Ge[1], Yang Li[1], Whitaker Cohn[2], Amandeep Salhotra[5], David B. Sykes[6], Jie Jin[4], Jianjun Chen[1], Guido Marcucci[1], Shoubao Ma[1], Hong Zheng[3], Yong Zhang[2], Ling Li[1]

[1]Beckman Research Institute of The City of Hope, Duarte, CA,[2]University of Southern California, Los Angeles, CA,[3]Penn State University, Hershey, PA,[4]Zhejiang University School of Medicine the First Affiliated Hospital, Hangzhou, China,[5]Department of Hematology and HCT, City of Hope Medical Center, Duarte, CA,[6]Massachusetts General Hospital, Boston, MA

Primary or acquired resistance to immunotherapies, including immune checkpoint inhibitors (ICIs) and CAR-T cells, remains a major clinical challenge. This resistance is particularly prevalent in "immune-cold" tumors like acute myeloid leukemia (AML), which are characterized by low immunogenicity, an immunosuppressive microenvironment, and immune escape by leukemia stem cells (LSCs). Activating the tumor-intrinsic cGAS–STING pathway to induce Type I interferon (IFN-I) responses is a promising strategy to convert "cold" tumors to "hot". However, achieving this selectively in cancer cells while sparing normal tissues remains a critical, unsolved barrier. We sought to identify novel mechanisms controlling innate immune signaling in OXPHOS-heightened cancers like AML to develop a strategy for overcoming immunotherapy resistance.We employed an inducible CRISPR-KO screen to identify regulators of mitochondrial homeostasis and cGAS-induced innate immunity. The screen identified a subset of minor mitochondrial dehydrogenases (including DHODH, SDHs) as critical regulators of mitochondrial redox balance and mtDNA integrity. We demonstrate that genetic or pharmacologic inhibition of these enzymes reroutes metabolic flux toward the Electron Transport Chain (ETC) Complex I (C-I). This paradoxically hyperactivates C-I, amplifying mtROS, inducing mtDNA instability, and causing mtDNA leakage into the cytosol. The cytosolic mtDNA is sensed by cGAS, leading to robust STING activation and systemic IFN-I responses in vivo. Crucially, this immune-stimulatory mechanism is independent of the canonical metabolic roles of these enzymes; for instance, this response after DHODH inhibition was not rescued by uridine supplement. In immunocompetent murine AML models, we found that while tumor-selective DHODH ablation was curative, systemically pharmacologic inhibition of DHODH was profoundly immunosuppressive, as it blunted T-cell proliferation essential for an anti-leukemia response. To overcome this toxicity-efficacy barrier, we developed "DHODHi-ADC", a first-in-class, immune-boosting ADC that achieves leukemia-selective delivery of a potent DHODH inhibitor (DHODH-IN16). The ADC preserves systemic immune function while inducing potent, tumor-intrinsic innate immune activation, a clear distinction from purely cytotoxic ADCs. In humanized AML models, our ADC synergized remarkably with both ICIs and CAR-T cell therapy, resulting in highly effective, durable leukemia clearance, including the eradication of LSCs.Our findings define a novel, therapeutically exploitable immune-metabolic axis where ETC homeostasis controls innate immunity via mtDNA dynamics. Disrupting this homeostasis through C-I hyperactivation provides a powerful and highly translational strategy to sensitize OXPHOS-dependent cancers to immunotherapy.

#5599 ATG-125, a novel B7H3 × PD-L1 bispecific antibody-drug conjugate, demonstrates potent antitumor efficacy by dual targeting of immune evasion and direct tumor killing.

Jishun Chen[1], Suya Bai[1], Yu Bai[1], Huiling Liu[1], Zaoshun Hu[1], Jay Mei[2], Peng Chen[3], **Bing Hou**[2]

[1]Antengene (Hangzhou) Biologics Co., Ltd, Hangzhou, China,[2]Antengene Corporation, Shaoxing, China,[3]Shanghai Antengene Corporation Limited, Shanghai, China

Background B7-H3 (CD276) and PD-L1 (CD274) are immune checkpoint molecules overexpressed in a wide range of solid tumors, often associated with immune evasion and poor prognosis. While monoclonal antibodies targeting PD-1/PD-L1 have shown clinical success, resistance remains a major challenge. B7-H3 is an emerging, highly promising target for antibody-drug conjugates (ADCs) due to its broad tumor expression and rapid internalization. Co-expression of B7-H3 and PD-L1 on tumor cells provides a rationale for dual targeting to enhance both direct cytotoxicity and immune activation. ATG-125 is a novel bispecific ADC designed to address this opportunity.

Methods ATG-125 is a B7-H3 × PD-L1 bispecific ADC (BsADC) engineered from a human IgG1 anti-B7-H3 antibody with C-terminally fused PD-L1-specific scFv. It is conjugated via a cleavable GGFG linker to the DNA topoisomerase I inhibitor, resulting in a drug-to-antibody ratio (DAR) of ~4. Binding affinity, cytotoxicity, internalization, lysosomal trafficking, bystander killing, and T-cell activation were evaluated in solid tumor cell lines with varying expression levels of B7-H3 and PD-L1. The *in vivo* antitumor efficacy of ATG-125 against the HCC827 human NSCLC model was evaluated in nude mice.

Results ATG-125 bound B7-H3 and PD-L1 with nanomolar affinity and demonstrated strong, antigen-dependent internalization in dual- and single-target positive tumor cells, enabling efficient intracellular release of the Dxd payload. ATG-125 exhibited potent, target-dependent cytotoxicity against multiple cancer cell lines (e.g., lung, breast, ovarian) that co-expressing B7-H3 and PD-L1. The parental naked antibody blocked PD1-PDL1 interaction and induced robust IL-2 and IFNγ production in a Mixed Lymphocyte Reaction (MLR) experiment. The BsADC induced significantly enhanced T-cell activation, as shown by a higher frequency of $CD69^+$ $CD3^+$ T cells in a co-culture with HCC827 cells and human PBMCs. *In vivo*, ATG-125 induced marked and sustained tumor regression in HCC827 xenograft models at well-tolerated doses. Its efficacy was significantly superior to that of single-target ADC comparators.

Conclusion ATG-125 represents a novel bispecific ADC that co-targets B7-H3 and PD-L1 to achieve synergistic IO+ADC antitumor efficacy. Its unique mechanism combines enhanced, dual-target-mediated internalization for superior payload delivery with potential restoration of anti-tumor immunity. The compelling preclinical profile of ATG-125 underscores its significant therapeutic potential and supports its advancement into clinical trials for patients with solid tumors.

#5601 LBL-061: A novel EGFR×PD-L1 targeted drug conjugate for the treatment of multiple solid tumors.

Yurong Qin, Yang Ye, Yujia Dang, Juan Tang, Peng Zhang, Yan Zhu, Shuijun Hu, Mi Ye, Xiaoxiao Liu, Xu Bao, Huan Lin, Wanting Wang, Guojin Wu, Jianming Sun, Hui Yuwen, Yuanzhi Lv, Jing Guan, Min Chen, Yue Zhao, Jordan Zhu, Charles Cai, **Xiao Huang**, Xiaoqiang Kang, Hong Ling

Leads Biolabs Co., Ltd., Nanjing, China

Background: EGFR is overexpressed in multiple solid tumors such as head and neck squamous cell carcinoma (HNSCC), non-small cell lung cancer (NSCLC), and nasopharyngeal carcinoma (NPC). Emerging antibody-drug conjugates (ADCs) targeting EGFR have demonstrated preliminary efficacy and safety in clinical trials. PD-L1, a clinically validated immune checkpoint, is frequently overexpressed in tumors including HNSCC and NSCLC, where it is often co-expressed with EGFR. Clinical evidence supporting the combination of ADCs and immune checkpoint inhibitors (ICIs) provides a rationale for developing an EGFR×PD-L1-targeting ADC. Here, we describe the preclinical development of LBL-061, a novel EGFR×PD-L1-targeting ADC composed of a 2:2 format bispecific antibody conjugated via our proprietary TOPiKinectics^{TM} linker-payload platform.

Methods: Cell binding activity of LBL-061 against tumor cells was assessed by flow cytometry. Cytotoxicity of LBL-061 against tumor cells and normal tissue cells was assessed by Cell Counting-Lite Luminescent Cell Viability Assay kit. PD-L1 blocking activity of LBL-061 was evaluated using a PD-1/PD-L1 reporter gene assay system. Bystander killing of LBL-061 was analyzed by flow cytometry. LBL-061 induced tumor cells immunogenic cell death (ICD) was assessed in PBMC-tumor cells co-culture systems. The anti-tumor activity of LBL-061 was evaluated in mouse syngeneic and cell line-derived xenograft (CDX) models. The safety profile and pharmacokinetics (PK) of LBL-061 were evaluated in a cynomolgus monkey dose-range finding (DRF) study.

Results: LBL-061 exhibited potent binding activity and cytotoxicity to different tumor cells. It also demonstrated robust PD-1/PD-L1 blocking activity. *In vitro*, LBL-061 showed minimal cytotoxicity to PD-L1 expressing dendritic cells (DCs) and macrophages. In PBMC-tumor cells co-culture systems, LBL-061 induced tumor cells immunogenic cell death (ICD). It also mediated potent bystander effect on EGFR negative tumor cells. *In vivo*, LBL-061 showed superior control of tumors' growth in syngeneic and xenograft mouse models. In a 6-week cynomolgus DRF study, it was well tolerated with a highest non-severely toxic dose (HNSTD) of 40 mg/kg following repeated intravenous infusion (Q3W dosing). LBL-061 exhibited a linear PK characteristic in cynomolgus monkeys at doses ranging from 10 to 40 mg/kg.

Conclusions: Our findings indicate that LBL-061, a novel bispecific EGFR×PD-L1-targeting ADC synergizes antitumor effects by combining direct cytotoxicity and immune activation. It showed a favorable PK profile and a good safety profile in cynomolgus monkeys. Taken together, these preclinical data strongly suggest that LBL-061 is a promising candidate worthy of further clinical investigation.

#5602 Novel ATR inhibitor payloads for antibody-drug conjugates targeting PD-L1.

Anne Roulston, Martin Duplessis, Francois Denis, Hugo Poirier, Shou Yun Yin, Sara Fournier, Roselyn Kryczka, Jessica Desjardins, Nancy Laterreur, Abira Rajah, Alexanne Bonneau-Fortin, Bingcan Liu, **Alejandro Alvarez-Quilon**, Philipe Mochirian, Ismael Samudio

DCx Biotherapeutics, Saint-Laurent, QC, Canada

Ataxia telangiectasia and Rad3-related kinase (ATR) is essential to the faithful replication of DNA in rapidly dividing cells such as cancer cell lines. ATR is activated in response to single-strand DNA breaks that result from increased replication stress caused by defects in DNA repair mechanisms and/or damaged DNA. ATR stabilizes and restarts the stressed replication forks, suppresses origin firing, activates cell cycle checkpoints, and facilitates DNA repair. In fact, ATR activity contributes to the tolerance of chronic replication stress in cells transformed by oncogenes rendering cancer cells more dependent on ATR activity for survival. Systemic exposure to ATR inhibitors (ATRis) in clinical studies have demonstrated dose-limiting toxicities that reduce their clinical utility. Therefore, precision antibody-drug conjugates (ADCs) for targeted delivery of ATR payloads could bypass the systemic toxicities associated with oral administration. There is significant overlap between cancers with ATRi sensitizing defects in DNA repair mechanisms with those expressing high levels of PD-L1 surface antigens including stomach, breast, lung and colon cancers. Our personalized antibody-drug conjugate approach couples surface targeted therapeutics to tumors with increased sensitivity to the delivered payload to improve the therapeutic index. We have discovered multiple derivatizable proprietary ATRis with desirable physicochemical properties that demonstrate low nM potency in cancer cell lines with ATRi sensitizing mutations. Furthermore, the ATRi payloads maintained *in vitro* cytotoxic potency in cells harbouring clinically relevant acquired resistance mutations in Topoisomerase 1, whereas exatecan did not. Once conjugated to the anti-PD-L1 monoclonal antibody, the resulting ADCs demonstrated selective picomolar cellular growth inhibition and excellent metabolic stability in mouse plasma. Preclinical *in vivo* studies in mice demonstrate robust efficacy and selectivity with PD-L1-ATRi as single agent relative to IgG-ATRi. The *in vitro* and *in vivo* data presented herein demonstrate the efficacy of an ADC with an ATRi mono-payload and illustrate the potential for combinations with standard of care chemotherapeutic agents such as gemcitabine or PARP inhibitors.

#5603 Targeting B7-H3 in the small cell lung carcinoma (SCLC) tumor-immune microenvironment (TIME).

Marco Campisi[1], Carla Stornante[1], Ian D. Dryg[2], Harrison Olszewski[3], Alan E. Bers[1], Ian Gillanders[1], Kathleen Pfaff[3], Robert Gentleman[2], Scott Rodig[3], Navin R. Mahadevan[4], David A. Barbie[1]

[1]Medical Oncology, Dana-Farber Cancer Institute, Boston, MA,[2]Department of Data Science, Dana-Farber Cancer Institute, Boston, MA,[3]Center for Immuno-Oncology, Dana-Farber Cancer Institute, Boston, MA,[4]Department of Pathology, University of Michigan, Ann Arbor, MI

Introduction: Despite incorporation of immune checkpoint blockade into first line treatment of SCLC, patients have a poor prognosis with limited treatment options. Recent profiling of the SCLC TIME has revealed distinct immunologic subtypes: non-neuroendocrine (non-NE) SCLC, which exhibits robust upregulation of MHC I and immune infiltration, and neuroendocrine (NE) SCLC subpopulations which downregulate MHC I and show an “immune desert” TIME. Therapeutic strategies targeting B7-H3 using the antibody-drug conjugate (ADC), ifinatamab deruxtecan (I-DXd), has shown recent promise in SCLC. In the IDeate-Lung01 trial, patients treated with I-Dxd after ≥1 prior line of chemotherapy showed a disease control rate of 87.6% (NCT05280470). Yet, the mechanism of action on the constituent cells of the SCLC TIME remains relatively unexplored. In this study, we aimed to determine the expression of B7-H3 in the SCLC TIME and consequent susceptibility to I-DXd, of SCLC subpopulations and stromal cells using a SCLC TIME 3D microphysiological system (MPS).

Methods: We initially profiled B7-H3 expression using a human SCLC cell line panel representative of the NE MHC I low (n=3) or non-NE MHC I high (n=4) phenotype, as well as stromal components (endothelial cells, fibroblasts) by flow cytometry. We validated these findings in patient SCLC samples (n=31) using a mIF panel. We then evaluated the direct cytotoxic effect of the I-DXd on SCLC cell lines and stromal components using 2D and 3D *in vitro* cytotoxicity assays. Further, we evaluated I-DXd in a model of vascular networks using an ex vivo MPS. Finally, using the MPS, we assessed the functional impact on vascular structure via permeability assays.

Results: NE MHC I low SCLC cell lines showed low/moderate levels of B7-H3 expression, while non-NE MHC I high SCLC upregulated B7-H3. B7-H3 was also highly expressed by stromal TIME components such as vascular endothelial cells (HUVEC) and human lung fibroblasts (hLFB). While SCLC expression of B7-H3 was more variable in patient samples, and did not show a clear correlation with tumor MHC I expression, stromal cells, particularly endothelial cells showed strong B7-H3 expression, and, in the majority of cases, were the major contributors of B7-H3 expression in the TIME. Non-NE SCLC cells showed sensitivity to I-DXd in a B7-H3 dependent manner in a 2D viability assay, while NE SCLC cells exhibited relative resistance. Experiments using vascular networks in the MPS demonstrated that I-DXd caused increased vascular permeability.

Conclusions: Our study suggests that B7-H3 expression is heterogenous in SCLC and may differ by immunologic subtype. Moreover, our findings suggest that B7-H3 may serve as a target on stromal components of the SCLC TIME. Our results suggest that in addition to the direct targeting of tumor cells, a potential mechanism of action underlying the efficacy of I-DXd may be an increase in vascular permeability.

#5604 TAK-188, an antibody-drug conjugate with a novel amanitin payload, disrupts immune suppression and leads to potent anti-tumor immunity through selective depletion of CCR8$^+$ intratumoral regulatory T-cells.

Cierra N. Casson[1], Eun-Ah Bae[1], Sarah B. Hesse[1], Carla Guarino[1], Rohan Diwanji[1], Tiquella Hatten[1], Adam Hinthorne[1], Jian Huang[1], Ajeeth K. Pingili[1], Judy Qiuju Shi[1], Natasha Iartchouk[1], Brandon Wilkinson[1], Jessica Riceberg[1], Aniko Palfi[2], Natalie Roy D'Amore[1], Torsten Hechler[2], Adnan O. Abu-Yousif[1]

[1]Takeda Development Center Americas, Inc. (TDCA), Cambridge, MA,[2]Heidelberg Pharma Research GmbH, Ladenburg, Germany

Regulatory T cells (Tregs) play a critical role in mediating tolerance to self-antigens and are a major contributor to an immunosuppressive tumor microenvironment (TME). The presence of Tregs in solid tumors is associated with poor prognosis and decreased overall survival in patients, as well as resistance to immunotherapy in several tumor types. CCR8 is a chemokine receptor identified to be highly expressed on tumor-infiltrating Tregs, with lower expression on peripheral Tregs and other cells, making it an attractive target for immunotherapy. Current CCR8-targeting therapeutics in development aim to achieve Treg depletion via Fc-enabled antibody-dependent cellular cytotoxicity, which relies on the presence of effector cells that can vary in frequency and may be functionally inhibited in the TME. In contrast, TAK-188 is a first-in-class anti-CCR8 antibody-drug conjugate designed to facilitate antitumor efficacy by direct cytotoxic depletion of intra-tumoral CCR8$^+$ Tregs using a novel amanitin payload that can kill both dividing and quiescent cells. The specificity and potency of TAK-188 was evaluated preclinically using CCR8-expressing cells, dissociated human tumor samples, and syngeneic tumor models in human CCR8 knock-in mice. The preclinical data showed that TAK-188 specifically bound to and killed CCR8$^+$ cells in vitro. TAK-188 also demonstrated dose-dependent anti-tumor activity in syngeneic tumor models and anti-tumor memory following tumor rechallenge in human CCR8 knock-in mice. TAK-188 selectively killed CCR8$^+$ Tregs in vivo, demonstrating a robust decrease in tumor Tregs and an increase in CD8$^+$ T cells that together resulted in an increased CD8/Treg ratio in the TME. In a mouse syngeneic tumor model, TAK-188 as a single agent was more efficacious than Fc-enabled anti-CCR8 antibodies and shifted the phenotype of immune cells in the TME to be more favorable for anti-tumor activity. Finally, TAK-188 potently and specifically depleted Tregs in dissociated human tumor samples while sparing conventional CD4$^+$ and CD8$^+$ T cells, supporting the mechanism of action of direct tumor Treg killing without the need for exogenous effector cells. In conclusion, TAK-188 robustly depletes CCR8$^+$ cells both in vitro and in vivo and demonstrates anti-tumor activity as a single agent in nonclinical models. Based on this promising preclinical data, a Phase 1 study of TAK-188 has been opened (NCT07205718).

#5605 Advanced dual payload antibody-drug conjugates for targeted chemoimmunotherapy.

X. Margaret Liu, Zhuoxin "Zora" Zhou

The Ohio State University, Columbus, OH

Antibody drug conjugates (ADCs) represent an effective therapeutic strategy for cancers, leveraging cancer-targeting monoclonal antibodies linked to potent payloads. Here, we report several novel conjugation platforms for dual-payload ADCs (DualADCs) that harness antibodies to co-deliver a chemotherapeutic agent, such as microtubule or topoisomerase I inhibitors, for direct tumor cell killing, alongside a toll like receptor agonist to enhance tumoral immunity. Aggressive triple-negative breast cancer was used as the model cancer for evaluating and comparing our DualADCs. Specifically, we developed advanced cysteine and lysine-based coconjugation technologies by linking chemotherapy and immunotherapy with one antibody, designing and optimizing linkers, increasing homogeneity, and refining reaction formulations to increase conjugation rate. The chemo-immunotherapy conjugation was validated with HPLC, and the drug to antibody ratios and drug to drug ratio were quantitated using advanced UPLC MS. The robustness and scalability of our optimal conjugation procedure was validated using spinner flask based reaction. *In vitro* characterizations revealed high cancer binding via flow cytometry, strong cancer specificity with minimal off target in normal human tissues, appropriate binding affinity, efficient drug internalization as revealed by confocal microscopy, and high cytotoxicity in cancer cell lines. *In vivo* evaluations demonstrated favorable tumor biodistribution, high plasma stability, low systemic toxicity, promising therapeutic efficacy in multiple xenograft mouse models, and immune modulation in tumor microenvironment. Collectively, this study establishes advanced dual-payload ADCs and innovative conjugation procedures for targeted chemo-immunotherapy of cancers.

: TCR and Autologous T Cell Therapies
Poster Session

#5609 Mechano-dynamic-principle-driven rational design of next-generation TCRs with high specificity and sensitivity.

Yushen Du[1], **Wei Hu**[1], Luying Liu[2], Suqiong Wang[2], Wei Chen[1]

[1]Zhejiang University, Hangzhou, China,[2]Hangzhou Mechanodynamic Biotechnology Co., Ltd, Hangzhou, China

Background: Naturally evolved T-cell receptors (TCRs) achieve extraordinary antigen specificity through a flexible binding interface that forms force-stabilized catch bonds with cognate peptide-MHC (pMHC) complexes. This critical mechano-regulatory feature is often lost in conventional high-affinity engineered TCRs, whose rigid interfaces can paradoxically cause cross-reactivity with self-antigens and off-target toxicity, a major barrier to safe TCR-based immunotherapies.
Purpose: Building on our prior elucidation of this mechano-regulation mechanism, we aimed to establish a novel engineering platform for designing next-generation TCRs—including TCR mimics, TCR-engineered cells (TCR-T), and T cell engagers (TCEs)—with enhanced specificity and sensitivity, using the KRAS-G12D neoantigen (presented by HLA-A*11:01) as a proof of concept.
Methods: Following an initial screen, top-performing TCR clones were selected for comprehensive characterization. We evaluated their biophysical binding and *in vitro* function (single-molecule force spectroscopy, kinetic-functional mapping, serial tumor killing, memory phenotype differentiation), *in vivo* anti-tumor efficacy (KRAS-G12D cell-derived xenograft models), and safety profile (whole-proteome cross-reactivity screening).
Results: Mechano-optimized TCRs exhibited ~40-fold higher antigen sensitivity in vitro compared to conventional high-affinity TCRs, with no detectable cross-reactivity to wild-type (WT) KRAS; TCR-T cells engineered with these optimized TCRs showed superior serial tumor killing, reduced exhaustion (37% lower PD-1 expression vs. controls), and enhanced differentiation into long-lived memory phenotypes (2.2-fold higher $CD62L^{+}CD44^{+}$ cells); In KRAS-G12D CDX models, mechano-optimized TCR-T cells achieved robust tumor clearance (mean tumor volume reduction of 82% vs. 41% in controls at day 21) and displayed a more infiltrative, less exhausted T-cell phenotype; Whole-proteome cross-reactivity screening confirmed exceptional specificity, with no off-target binding to 10,000+ human proteins.
Conclusions: Our study establishes a mechano-principle-driven paradigm for rational TCR engineering. By translating fundamental insights into TCR-pMHC mechanics into a practical design framework, we generated next-generation TCRs —including TCEs, TCR mimics, and TCR-T cells —with unprecedented specificity, sensitivity, and potency. This platform offers a promising route toward safer and more effective immunotherapies for solid tumors and leukemia. Our lead TCR-T candidate is currently advancing into IND-enabling studies, alongside a complementary in vivo TCR engineering program aimed at expanding the therapeutic reach of this mechano-principled approach.

#5610 Characterization of cancer-reactive T cells and neoantigen-specific T cell receptors.

Wei Sun, Si Liu, Bo Yu, Zhehao Zhang, Philip Bradley, Marie Bleakley

Fred Hutchinson Cancer Center, Seattle, WA

Not all tumor-infiltrating T cells are cancer-reactive (CR). Several studies have reported gene expression signatures associated with CR-T cells. To integrate these findings, we developed a computational workflow, CAT (Cancer-Associated T cells), which harmonizes existing CR-T cell signatures and applies them to identify CR-T cells across an atlas of one million T cells. Our findings reveal that the abundance of CR-T cells varies across cancer types and that baseline levels of CR-T cells predict patients' responses to immunotherapy. In parallel, we established a high-throughput computational platform, Neo-TCR, for systematic screening of neoantigen-specific TCRs and their cognate neoantigens. The efficacy of Neo-TCR is validated by cross-validation studies and replications in two independent datasets. Together, our findings suggest a new direction for developing biomarkers for cancer detection and monitoring: integrating CR gene expression signatures with neoantigen-specific TCRs.

#5611 Adoptive T cell transfer suppresses endogenous tumor-specific CD8$^+$ T cell recovery following lymphodepletion.

Rohan B. Chaudhari, Megan L. Burger

Oregon Health & Science University, Portland, OR

Adoptive T-cell transfer (ACT), where patients are infused with millions of tumor-specific effector T-cells, has proven to be highly effective in hematologic malignancies and is FDA approved as early as a first-line treatment for refractory disease. Unfortunately, extending the benefits of ACT to solid tumors has been largely hindered with challenges intrinsic to solid tumor microenvironments such as intratumoral heterogeneity, where the ACT target antigen is only expressed in a fraction of the tumor. Engaging the endogenous immune system alongside ACT may be one strategy to circumvent the issue of intratumoral heterogeneity by allowing for a broader, more synergistic T-cell response against the tumor. However, the role of endogenous cells in ACT remains poorly understood, and past clinical and preclinical research suggests that ACT does not engage anti-tumor endogenous responses. In this study, we investigated whether ACT and accompanying lymphodepletion may directly suppress the tumor-specific endogenous T cell response in a Kras/p53(KP)-driven autochthonous mouse model of lung adenocarcinoma expressing defined tumor-specific neoantigens, both ACT-targeted and non-targeted. Lung tumor-bearing mice were lymphodepleted (LD) with a standard dose of 150 mg/kg cyclophosphamide intra-peritoneally with or without transfer of 6 million tumor-specific ACT cells intra-vascularly. Our results demonstrate that LD alone depletes endogenous tumor neoantigen-specific CD8 T cells, but these cells largely recover by 3 weeks post-treatment. In contrast, adoptive cell transfer with LD resulted in sustained depletion of endogenous tumor-specific CD8 cells and these cells had reduced expression of effector markers Ki67 (proliferation) and Granzyme B (cytotoxicity). Adoptive cell transfer without LD did not result in a significantly decreased population of endogenous tumor-specific CD8 cells, however results were confounded by a significantly lower number of adoptively transferred cells infiltrating into the lung. These findings suggest that ACT may be playing a suppressive role against the endogenous tumor-specific T cell response when pre-conditioning mice with cyclophosphamide. Further research studying this suppression with lower doses of LD or homeostatic cytokine supplementation (e.g. IL-7/IL-15) could reveal if the suppression is intrinsic to the adoptively transferred cells or cyclophosphamide. Furthermore, future studies into finding ways to overcome this suppression and activate the endogenous immune system, such as neoantigen-targeted vaccination, could be critical to unlocking the full potential of ACT.

#5612 Antigen-specific T cells engineered with nanoparticle photothermal therapy demonstrate antitumor efficacy in an immunocompetent murine model of ovarian cancer.

Abigail V. Lee[1], Erin Grundy[2], Jose Colina[1], Elizabeth Sweeney[1], Rohan Fernandes[3], Nethaji Muniraj[4], Russell Y. Cruz[4], Katherine B. Chiappinelli[1]

[1]George Washington University Cancer Center, Washington, DC,[2]Emory University, Atlanta, GA,[3]Fischell Department of Bioengineering, University of Maryland, Baltimore, MD,[4]Children's National Research Hospital, Washington, DC

Ovarian cancer (OC) is the most lethal gynecological malignancy with less than a 10% response rate to immune checkpoint blockade. Personalized vaccination with tumor lysate-pulsed dendritic cells amplifies T cell responses, including neoepitope-specific T cells, but is not curative. Thus, amplifying the pre-existing tumor-specific T cell response is insufficient. We developed a novel method to expand T cells *ex vivo* for OC specificity using Prussian Blue nanoparticle-photothermal therapy (PBNP-PTT), and verified *in vivo* efficacy using a syngeneic murine model. PBNP-PTT -generated ID8 OC cell lysate was used to stimulate bone marrow-derived dendritic cells (BMDCs) isolated from healthy female C57Bl6 mice. Autologous splenic CD3+ T cells were cocultured *ex vivo* with BMDCs and assessed in vitro for tumor-specific activation and killing using IFNγ ELISpot and MTS cytotoxicity assays. Congenic mice bearing ID8B OC cells received either *ex vivo* expanded T cells or nonspecifically expanded T cells, and the accumulated ascites was profiled for cytokine composition. Adoptively transferred T cells were immunophenotyped with spectral flow cytometry.Ex vivo expansion of T cells with DCs primed using PBNP-PTT-generated OC cell lysate produced a pool of CD8+ T cells with enhanced IFNγ and TNFα secretion in tumor coculture compared to nonspecifically expanded T cells. PBNP-PTT-expanded T cells exhibited greater tumor cell killing at increasing effector-to-target ratios and did not demonstrate off-target IFNγ secretion. Tumor-bearing female C57Bl6 mice receiving OC-expanded T cells lived significantly longer and exhibited decreased tumor burden compared to mice receiving nonspecific T cells. Adoptively transferred T cells expanded with PBNP-PTT lysate also persisted longer in vivo with maintained activation in the ascites, and synergized with concurrent epigenetic therapy to further prolong survival. *Ex vivo* expansion methods using PBNP-PTT were also applied to healthy human blood donors to generate human T cells that demonstrate potent activation when challenged with human OC cell lines. In summary, we developed a novel method of engineering T cells *ex vivo* for specificity against ovarian cancer using nanoparticle photothermal therapy. This study is the first to harness PBNP-PTT *ex vivo* to demonstrate antitumor activity in vivo using an autologous mouse model of ovarian cancer.

#5613 RenTCR-derived MAGEA1-specific TCRs demonstrated superior peptide sensitivity and potent antitumor activity *in vitro* and *in vivo*.

Yi Yang, Yabo Zhang, Jiawei Yao

Biocytogen, Waltham, MA

Background: MAGEA1, a cancer-testis antigen, is broadly expressed in solid tumors such as HCC and NSCLC, but is restricted to the testis in normal tissues, making it an ideal therapeutic target. TCR therapies against MAGEA1 are in preclinical/early clinical stages. Conventional strategies for TCR discovery typically rely on isolation from donor PBMCs or patient TILs. In contrast, Biocytogen's proprietary RenTCR platform enables the generation of TCRs using TCR/MHC humanized mouse models. Lacking thymic negative selection to human antigens, this platform facilitates the identification of TCRs exhibiting higher reactivity and specificity.

Method: RenTCR mice (HLA-A*02:01) were immunized with full-length MAGEA1 mRNA. PBMCs or splenocytes were isolated and stimulated *in vitro* with artificially modified antigen-presenting cells (APCs) presenting MAGEA1. Activated antigen-specific CD8+ T cells were then sorted. Single cells were sorted by FACS for reverse transcription, amplification, and sequencing to obtain TCR sequences. Initial TCR screening used a Jurkat reporter assay for binding. Positive TCRs were transduced into primary human T cells and co-cultured with HLA-A2.1+/MAGEA1+ tumor cells to assess killing and cytokine release. Functional TCR candidates underwent off-target risk assessment, with final anti-tumor efficacy validated in CDX models using NDG mice.

Results: Immunization of 20 mice yielded a total of 80 binding-positive TCRs. The majority of these TCRs mediated potent cytotoxic activity *in vitro*. Assessment of functional avidity showed that TCRs derived from RenTCR mice recognized target peptides with superior sensitivity compared to human donor-derived TCRs. No cross-reactivity was detected in the candidate TCRs. All candidate TCRs demonstrated efficacy by inducing tumor regression in NDG mice bearing HLA-A2.1+/MAGEA1+ tumors.

Conclusion: The RenTCR platform enables the generation of T cell receptors (TCRs) with higher reactivity and specificity. TCRs derived from RenTCR mice exhibited better peptide sensitivity than human donor-derived TCRs. The candidate TCRs demonstrated excellent antitumor activity both *in vitro* and *in vivo*.

#5614 RenTCR-derived natural MAGE-A4-specific TCRs outperformed affinity-enhanced TCRs in antitumor efficacy.

Yi Yang, Yong Wang, Yabo Zhang, Jiawei Yao

Biocytogen, Waltham, MA

Background: MAGE-A4 is a clinically validated target highly expressed in multiple solid tumors, but its expression in healthy tissues is restricted to the testis and placenta. TCR-T cell therapies targeting MAGE-A4 show promising efficacy in synovial sarcoma but exhibit limited efficacy in other solid tumors. Biocytogen's proprietary TCR discovery platform, RenTCR, showed advantages including lower costs and higher efficiency in screening high-reactivity TCRs. Using this platform, we successfully identified TCRs against MAGE-A4 with high reactivity, high specificity, and superior anti-tumor activity.

Methods: TCRs targeting MAGE-A4 were identified using the RenTCR platform. Reporter cell lines were used to rapidly screen reactive TCRs, followed by TCR transduction into primary human T cells to evaluate cytotoxicity, IFN-γ release, and peptide sensitivity. Candidate TCRs underwent cross-reactivity screening and X-scan analysis for safety assessment. To assess *in vivo* antitumor efficacy, NDG mice bearing MAGE-A4^{+} HLA-A2.1^{+} human tumor xenografts were administered human primary T cells transduced via lentiviral vectors with candidate TCRs.
Results: The RenTCR platform identified TCRs targeting two distinct epitopes of MAGE-A4. Two TCRs demonstrated excellent cytotoxicity, IFN-γ release, and specificity *in vitro*. The candidate TCRs also induced tumor regression *in vivo*. RenTCR Platform-derived natural TCRs exhibited better antitumor activity than clinical-stage affinity-enhanced TCRs.
Conclusion: These findings highlight the therapeutic potential of two MAGE-A4-targeting TCR candidates as an effective strategy for treating melanoma, lung cancer, and other solid tumors expressing MAGE-A4.

#5615 ALK-specific TCR-T cells showed potent and specific activity in ALK-positive anaplastic large cell lymphoma.

Simone Piane[1], Carmen Mecca[1], Nirmala Tilija Pun[1], Ana Azambuja[1], Luca Alessandri[2], Phuc Bao Chi Nguyen[1], Elisa Bergaggio[1], Gabriele Saccu[1], Alessandro Gasparetto[1], Haley Ohlson[1], Claudia Voena[2], Marcos Simoes-Costa[1], Roberto Chiarle[1]

[1]Boston Children's Hospital, Boston, MA,[2]Dept. Biomedical Sciences and Human Oncology, University of Torino, Torino, Italy

Introduction: Anaplastic Lymphoma Kinase (ALK)-positive Anaplastic Large Cell Lymphoma (ALCL) is a rare subtype of T-cell lymphoma driven by nucleophosmin 1 (NPM1)-ALK fusion protein. Treatment with standard chemotherapy or ALK tyrosine kinase inhibitor crizotinib is highly effective; however, a significant portion of patients still experience relapses or refractory disease, highlighting the need for innovative therapeutic options. Our group has recently identified two ALK-specific T cell receptors targeting the human ALK peptide RPRPSQPSSL presented by HLA-B*07:02 (B7) and demonstrated specific and robust anti-tumor activity of ALK.TCR-T cells (ALK.TCR-T) in ALK+ non-small cell lung cancer [Mecca et al, Cancer res, 2024]. In this work, we aimed to address the efficacy of ALK.TCR-T in multiple models of ALK+ ALCL.

Methods: Two ALK-specific TCRs were retrovirally transduced into human CD3+ T cells to generate ALK.TCR-T1 and ALK.TCR-T2. The anti-tumor activity of ALK.TCR-T was tested both *in vitro* and *in vivo* against a panel of crizotinib-sensitive and crizotinib-resistant ALK+ ALCL models. The specificity of peptide-MHC recognition was evaluated by employing ALK+/B7+, ALK+/B7-, and ALK-/B7+ cells. For *in vivo* studies, NSG mice were injected intravenously with ALK+ ALCL cell lines, and, after engraftment, treated with ALK.TCR-T, alone or in combination with crizotinib. Mice received 50mg/kg crizotinib by oral gavage for 10 days. Tumor growth was evaluated weekly by bioluminescence imaging.

Results: *In vitro killing assays* demonstrated that both ALK.TCR-T selectively recognize and eliminate 80-100% of ALK+/B7+ ALCL, while no killing occurred in ALK+/B7- or ALK-/B7+ models, confirming that ALK.TCR-T specifically target the ALK peptide RPRPSQPSSL presented by HLA-B*07:02. Moreover, ALK-TCR-T were equally effective in killing crizotinib-resistant ALCL cells, independently of the mechanism driving the resistance to crizotinib. Interestingly, the combination of ALK.TCR-T and crizotinib potentiated the killing of crizotinib-sensitive ALK+ ALCL even at unfavorable E:T ratios (1:5 and 1:10).A single treatment with ALK.TCR-T significantly slowed tumor growth in an ALK+/B7+ systemic tumor model and increased the survival of mice, compared to treatment with irrelevant TCR-T cells. The combined treatment with ALK.TCR-T and crizotinib resulted in a further enhancement of tumor regression and mouse survival, with 50% (5/10) mice with no evidence of tumor 40 days after ALK.TCR-T injection.

Conclusions: We demonstrated that ALK.TCR-T show specific and potent anti-tumor activity against multiple ALK+ ALCL models both *in vitro* and *in vivo*. The combination of ALK.TCR-T and crizotinib further potentiate the ability of ALK.TCR-T to control tumor growth and extend the survival of mice. These results lay the basis for developing a novel immunotherapy strategy for patients with ALK+ ALCL.

#5616 Tumor necrosis factor-alpha armed TCR-T and CAR-T cells for solid tumors provide superior anticancer activity in the absence of toxicity.

Cole W. Peters[1], Miriam Valenzuela Cardenas[2], Moe Kawakami[2], Jaden Nguyen[2], Allison Flores[2], Andrew Dinh[2], Stephen Ma[2], Daniel G. Chen[3], Valerie Rezek[3], Scott Kitchen[3], Katie M. Campbell[1], Melissa Lechner[3], **Theodore Scott Nowicki**[2]

[1]UCLA - University of California Los Angeles, Los Angeles, CA,[2]Pediatric Oncology, University of California, Los Angeles, Los Angeles, CA,[3]University of California, Los Angeles, Los Angeles, CA

Background: TCR-T and CAR-T cells directed against tumor-specific antigens are associated with robust initial clinical responses which are often not durable against solid tumors, demonstrating an urgent need for more potent cell therapy products. We created TNF-alpha (TNF-a) armed variants of TCR-T and CAR-T cells to test their effectiveness and toxicity against a variety of solid tumors.
Methods: Lentiviral vectors encoding the TCR/CAR of interest with or without a supplemental copy of TNF-a were generated for NY-ESO-1 TCR, HPV-16 E7 TCR, and GD2 CAR. Mock, conventional TCR/CAR, and TNF-a armed TCR/CAR T-cells were co-cultured with nRFP-transduced tumor cells expressing the corresponding tumor antigen and appropriate HLA-A haplotype for the TCR-T cells (A375/M257-A2 melanoma cells for NY-ESO-1, 4050/CaSki cervical carcinoma cells for HPV-16 E7, and 143B/G292 osteosarcoma cells for GD2). Cells were subjected to repetitive stimulation assays to assess tumor killing efficiency in the setting of chronic antigen exposure. In parallel, in vivo tumor challenges were performed using humanized NSG mouse xenografts treated with mock, conventional TCR/CAR, or TNF-a-armed TCR/CAR T-cells. Mice were subjected to end of study necropsies to assess end-organ toxicity. T-cell phenotypes in circulation and intratumorally were assessed via flow cytometry, while serum cytokines were assessed weekly via multiplex sandwich ELISA. Tumors were also subjected to spatial transcriptomic analysis via CosMx.
Results: In vitro, TNF-a-armed TCR/CAR T-cells displayed significantly increased tumor cell killing and significantly increased secretion of TNF-alpha both initially and over time, exclusively in a tumor antigen-dependent manner. In vivo, TNF-a-armed TCR/CAR T-cells displayed superior tumor control and mouse survival compared to the corresponding conventional TCR/CAR. Importantly, this superior tumor control occurred in the absence of any systemic increases in TNF-a or IL-6, systemic toxicity (temperature, weight, body condition score), as well as without any differences in end-organ inflammatory damage/lymphocytic infiltration. Tumors treated with TNF-a-armed TCR/CAR T-cells displayed significantly increased T-cell infiltration, as well as significant reductions in intratumoral MDSCs, CD4 Tregs and Th2 cells and associated cytokines, while tumor cells displayed significant increases in TNF-a signaling, and significant decreases in IL-10 immunosuppressive pathways arising from the Tregs.
Conclusions: TNF-a-armed TCR/CAR-T cells possess superior antitumor efficacy against a wide variety of solid tumors, in the absence of any systemic toxicity, due to the antigen-dependent nature of the increased TNF secretion. This is due to both increased local TNF-a secretion and antitumor effector activity, as well as decreased Treg activity within the tumor.

#5617 Humanized antibody Fab-TCR T cells targeting GPC2 effectively regress neuroblastoma via enhanced TCR signaling and sustained cytotoxicity.

Mingyu Huo[1], Alex Quan[1], Dan Li[1], Laura E. Hutchins[1], Constanza Rodriguez[1], Jangsuk Oh[1], Hsi-En Tsao[1], Madeline Spetz[1], Elijah Edmondson[2], Dana Ashworth[3], Rui Zheng[3], Jing Zhou[3], Jinyun Chen[4], Jingbao Liu[4], Guangyan Xiong[4], Hongbing Zhang[4], Cheng Liu[4], Rosa Nguyen[1], Nan Li[1], Mitchell Ho[1]

[1]NIH/NCI, Bethesda, MD,[2]Frederick National Laboratory for Cancer Research, Frederick, MD,[3]Spatomics LLC, Guilford, CT,[4]Eureka Therapeutics Inc., Emeryville, CA

Background and Significance: Chimeric antigen receptor (CAR) T cell therapy has revolutionized the treatment of hematologic cancers but remains less effective against solid tumors, where heterogeneous antigen expression poses a major barrier to efficacy. Neuroblastoma, a pediatric solid tumor with poor survival rates in high-risk patients, often expresses glypican-2 (GPC2), a promising yet variably expressed surface antigen. To overcome these challenges, we engineered antibody-T cell receptors (AbTCRs) that combine antibody-based antigen recognition with the signaling machinery of γ/δ T cell receptors, aiming to promote more physiological activation and sustained antitumor activity in GPC2-positive neuroblastoma.
Methods: We developed AbTCRs containing anti-GPC2 Fab fragments (humanized CT3 or murine CT3) fused to γ/δ TCR constant regions and a co-stimulatory domain, CD30. Primary human T cells were transduced with these constructs and tested through in vitro tumor-killing assays, repeated cytotoxicity tests, western blotting, and in vivo xenograft models bearing GPC2 neuroblastoma (IMR5, NBEB, LAN1, and SH-SY5Y) tumors. The LAN1 and SH-SY5Y models have low GPC2 antigen density, enabling evaluation of efficacy under stringent antigen conditions.
Results: We found strong anti-tumor effects in humanized CT3 AbTCR-T cells, including significant tumor reduction and complete responses in multiple xenograft models. Tumors from mice administered with humanized CT3 AbTCR-T cells showed notably augmented infiltration of $CD8^+$ and $CD8^+CD27^+$ T cells, consistent with enhanced effector persistence. Humanized CT3 AbTCR-T cells demonstrated downregulation of exhaustion markers PD1, LAG3, and TIM3 and an enriched less-differentiated Tscm subset, as assessed by peripheral blood testing. These cells maintained lower PD1 levels after prolonged coculture with tumor cells, and retained cytotoxic activity in second- and third-round killing assays. Mechanistically, upon tumor engagement, hCT3 AbTCRs elicited more robust TCR signaling, evidenced by higher NFAT nuclear translocation and greater phosphorylation of key TCR pathway proteins.
Conclusion: Humanized CT3 AbTCR T cells exhibit durable and potent antitumor effects against low-GPC2 neuroblastoma by combining antibody specificity with physiological TCR signaling. Their enhanced TCR signaling, reduced exhaustion, and sustained cytotoxic ability suggest that AbTCR T cells represent a promising next-generation cellular therapy for solid tumors with heterogeneous or low antigen expression.

#5618 KRASG12V- and CTAG1B-targeted TCR-T cells from phage TCR library suppress colorectal and esophageal tumors.

Obed Boadi Amissah[1], Wenfang Chen[2], Zhiyuan Li[2], Gloria Bora Kim[1]

[1]Mayo Clinic Arizona, Scottsdale, AZ,[2]Guangzhou Institutes of Biomedicine and Health, Chinese Academy of Sciences, Guangzhou, China

Background: Colorectal cancer (CRC) remains a leading cause of cancer-associated mortality and is difficult to treat due to therapy resistance and limited durable responses. Esophageal cancer (EC) is similarly challenging, exhibiting highly aggressive and metastatic behavior that contribute to its poor prognosis. Adoptive TCR-engineered T cell (TCR-T) therapies show promise in these settings, but their efficacy is limited by suboptimal antigen specificity and an immunosuppressive tumor microenvironment (TME). To address these barriers, we isolated high-affinity TCRs from a phage-displayed TCR library targeting KRASG12V neoantigen in CRC and CTAG1B cancer/testis antigen (CTA) in EC.

Methods: KRASG12V$_{(8\text{-}16)}$/HLA-A11:01-restricted and CTAG1B$_{(157\text{-}165)}$/HLA-A02:01-restricted TCRs were isolated from an optimized phage-displayed TCR library generated from healthy donor CD8$^+$ T cells through high-throughput biopanning. Binders were screened against antigen-family peptides and irrelevant controls by phage ELISA to eliminate cross-reactivity. Binding affinities were measured by SPR. Antigen-specific TCRs (asTCRs) were cloned into lentiviral vectors and transduced into primary human T cells. TCR-T function was assessed using peptide-pulsed T2 cells and KRASG12V$^+$ or CTAG1B$^+$ tumor cells through LDH-release cytotoxicity and cytokine secretion assays. Normal human cells were used to evaluate off-target toxicity. *In vivo* antitumor activity was tested in NOD/SCID-IL2rγ$^{-/-}$ xenografts with histological confirmation of TCR-T infiltration.

Results: Next-generation sequencing confirmed that the 10^9-scale library contained >90% functional genes and >80% sequence diversity. Three high-affinity TCRs were identified for each antigen (K_D as low as 1.07 μM). These TCRs exhibited strict antigen specificity with no detectable cross-reactivity. TCR-T cells expressing asTCRs showed potent antigen-dependent cytotoxicity against KRASG12V$^+$/HLA-A11:01$^+$ colorectal and CTAG1B$^+$/HLA-A02:01$^+$ esophageal tumor cells (up to 80% lysis, $p<0.01$), accompanied by robust IFN-γ and TNF-α secretion (>1000 pg/mL, $p<0.01$). No killing was observed against any of seven healthy cell types. TCR-T cells remained effective at low effector-to-target ratios and maintained stable proliferation and effector-memory phenotypes. In xenograft models, KRAS- and CTAG1B-targeted TCR-T cells induced significant tumor regression compared to unmodified T cell controls ($p<0.05$), with increased effector TCR-T infiltration, and reduced antigen escape.

Conclusions: This work establishes a rapid and robust platform for isolating potent, safe, antigen-specific TCRs targeting both oncogenic driver mutation (KRASG12V) and an immunogenic CTA (CTAG1B). TCR-T cells demonstrated strong antitumor activity *in vitro* and *in vivo*, supporting the translational potential of this approach for solid tumor treatment.

#5619 First-in-class anaplastic lymphoma kinase (ALK)-specific TCR-T cells induce potent and selective antitumor immunity across ALK-driven human cancers.

Carmen Mecca[1], Simone Piane[1], Nirmala Tilija Pun[1], Ana Azambuja[1], Luca Alessandri[2], Rafael Blasco[1], Chi Nguyen Puc Bao[1], Elisa Bergaggio[1], Gabriele Saccu[1], Alessandro Gasparetto[1], Haley Ohlson[1], David A. Barbie[3], Ellis L. Reinherz[4], Marcos Simoes-Costa[1], Roberto Chiarle[1]

[1]Pathology, Boston Children's Hospital, Boston, MA,[2]Universita Degli Studi di Torino, Turin, Italy,[3]Lowe Center Thoracic Oncology, Dana Farber Cancer Institute, Boston, MA,[4]Department of Medical Oncology, Dana Farber Cancer Institute, Boston, MA

Introduction: Anaplastic Lymphoma Kinase (ALK) tyrosine kinase inhibitors (TKIs) have dramatically improved outcomes for patients with ALK-rearranged non-small cell lung cancer (NSCLC) and other ALK-positive (ALK+) cancer types. However, the near-universal emergence of resistance underscores an urgent need for new, durable therapeutic strategies. Leveraging our prior identification of the ALK-derived peptide RPRPSQPSSL presented by HLA-B*07:02 (PMID: 37430060), we aimed to develop ALK-specific TCR-engineered T cells (ALK.TCR-T) that can selectively recognize and eliminate ALK-driven tumors.

Methods: HLA-B*07:02 transgenic mice were vaccinated with the RPRPSQPSSL peptide. After two priming and two booster injections, $CD137^{+}/CD8^{+}$ T cells were sorted and subjected to single-cell sequencing for TCR discovery. The most expanded TCR clonotypes were then cloned and retrovirally transduced into human T cells to generate ALK.TCR-T cells. The anti-tumor activity of ALK.TCR-T cells was evaluated against various models of ALK+ tumors both *in vitro* and *in vivo*.

Results: From twelve dominant clonotypes, six ALK-specific TCRs were identified. Two (ALK.TCR-1 and ALK.TCR-2) demonstrated >95% ALK-dextramer binding. Notably, ALK.TCR-2 bound the ALK-dextramer also in $CD4^{+}$ T cells, indicating co-receptor-independent peptide-MHC recognition. Both TCRs mediated robust, antigen-specific cytotoxicity against ALK+/HLA-B*07:02+ cell lines, with no activity against mismatched targets. Engineering either EML4;ALK variant 3 or HLA-B*07:02 into non-expressing cells restored potent killing, confirming strict peptide-MHC specificity. *In vivo*, a single infusion of ALK.TCR-1 or ALK.TCR-2 markedly suppressed tumor growth and extended survival in a metastatic ALK+/HLA-B*07:02+ NSCLC model. Treated animals exhibited near-complete tumor clearance by day 7 post-ALK.TCR-T infusion, while control mice experienced progressive disease. Remarkably, in a metastatic ALK+/HLA-B*07:02+ neuroblastoma model, 70% (7/10) of mice achieved complete, durable responses (>100 days tumor-free) without evidence of on-target/off-tumor or off-target toxicity.

Conclusion: We report the first generation of ALK-specific TCR-T cells targeting the naturally presented ALK peptide RPRPSQPSSL in the context of HLA-B*07:02. ALK.TCR-T cells display potency, selectivity, and safety across multiple ALK-driven tumor models, providing a strong rationale for advancing ALK.TCR-T cell therapy into clinical development.

#5620 Development of T cell receptor (TCR) based cellular therapy for fibrolamellar HCC uncovers role of TCR in CD4 T cell differentiation.

Kayla J. Bendinelli[1], Allison M. Kirk[2], Marina Baretti[3], Abigail M. Gottschall[1], Heng-Chung Kung[1], Jeric Peter Hernandez[4], Waqar Arif[3], Julie Nauroth[3], Jennifer Durham[3], Christopher Thoburn[3], Amanda Huff[3], Neeha Zaidi[5], Alexei Hernandez[3], Hassan Jamaleddine[6], Timothy N. West[6], Justin McCallen[5], George Coukos[7], Alexandre Harari[8], Challice L. Bonifant[3], Elizabeth Jaffee[3], Won Jin Ho[3], Gregoire Altan-Bonnet[6], Paul G. Thomas[9], Mark Yarchoan[10]

[1]Johns Hopkins University School of Medicine, Baltimore, MD,[2]Department of Host-Microbe Interactions, St. Jude Children's Research Hospital, Memphis, TN,[3]Johns Hopkins University, Baltimore, MD,[4]JOHNS HOPKINS UNIVERSITY, Baltimore, MD,[5]Oncology, Johns Hopkins Hospital, Baltimore, MD,[6]National Cancer Institute, Bethesda, MD,[7]UNIL University of Lausanne, Lausanne, Switzerland,[8]Harari (Individual), Lausanne, Switzerland,[9]Fred Hutchinson Cancer Center, Seattle, WA,[10]Sidney Kimmel Comprehensive Cancer Center, Baltimore, MD

Background: Fibrolamellar carcinoma (FLC) is a rare and often lethal liver cancer that primarily affects children and young adults. There is no approved systemic therapy for FLC. The FLC transcriptome is defined by an in-frame fusion of exon 1 of *DNAJB1* with exons 2-10 of *PRKACA*, resulting in expression of the chimeric oncoprotein DNAJ-PKAc. Direct pharmacologic inhibition of this oncoprotein has been infeasible due to unacceptable on-target toxicity. However, the shared, tumor-specific expression of DNAJ-PKAc presents an opportunity for neoantigen-targeted immunotherapy.

Methods: We are conducting an ongoing clinical trial of a peptide vaccine targeting DNAJ-PKAc in combination with immune checkpoint inhibitors. We used single-cell sequencing and functional assays to identify DNAJ-PKAc-specific T cell receptors (TCRs) from peptide-expanded peripheral blood cells of trial participants. We characterized their HLA restriction, avidity, cytotoxicity, cytokine profiles, and differentiation phenotypes using co-culture systems.

Results: We identified seven $CD4^+$ TCRs that recognize DNAJ-PKAc in the context of HLA-DRB1*13:01 (n=2) or HLA-DRB3*01:01 (n=5). When introduced into healthy donor T cells and co-cultured with tumor cells expressing the corresponding HLA allele, these TCRs exhibited variable functional avidity, cytokine production, differentiation, and cytotoxic activity against DNAJ-PKAc-pulsed targets. Among them, JHU12-TCR2 (*HLA-DRB3*01:01-restricted*) mediated the strongest cytokine production and tumor cell killing despite only moderate avidity. Consistent with this, JHU12-TCR2 showed the greatest *in vivo* expansion in the original patient, who achieved a near-complete response to immunotherapy. In contrast, a fusion-specific TCR identified from a non-responder, JHU8-TCR2, that shares sequence similarities and clusters with JHU12-TCR2, demonstrated limited cytotoxicity *in vitro*. Interestingly, although all TCRs recognized the same antigen in matched donor T cells, they drove divergent helper T cell differentiation programs. For example, JHU12-TCR2 favored Th1/Th17 polarization with minimal Treg induction, whereas JHU8-TCR2 promoted a Th2-biased phenotype.

Conclusions: We identified and functionally characterized multiple $CD4^+$ TCRs specific for the DNAJ-PKAc oncoprotein, highlighting their potential utility as the basis for TCR-based therapy in FLC. A clinical trial of JHU12-TCR2-based TCR therapy for patients with FLC and HLA-DRB3*01:01 is in development. These findings also suggest that variation in vaccine-induced TCR repertoires may contribute to differences in clinical response, and that intrinsic biophysical or signaling properties of individual TCRs can shape the differentiation fate of $CD4^+$ T cells expressing them.

#5621 The GPC3-targeting hYP7 antibody-based gamma/delta TCR-T cell therapy for overcoming antigen mutation and heterogeneity in liver cancer.

Dan Li[1], Tianyuzhou Liang[1], Hsi-En Tsao[1], Zhijian Duan[1], Laura E. Hutchins[1], Madilyn Gaydos[1], Iris Yang[1], Elijah Edmondson[1], Xiaoshan Wang[2], Rui Zheng[2], Jing Zhou[2], Chin-Hsien (Emily) Tai[1], Jing Bian[1], Maggie Cam[1], Hongbing Zhang[3], Cheng Liu[3], Mitchell Ho[1]

[1]National Cancer Institute, Bethesda, MD,[2]Spatomics, Guilford, CT,[3]Eureka Therapeutics, Inc, Emeryville, CA

Antigen mutation and heterogeneous expression remain major barriers to effective antibody- and chimeric antigen receptor (CAR)-based immunotherapies for hepatocellular carcinoma (HCC). Glypican-3 (GPC3) exhibits variable surface density and epitope alteration in advanced or recurrent HCC tumors. To address these clinically relevant obstacles, we developed a modular antibody-based γ/δ T-cell receptor (γδAbTCR) platform that integrates antibody specificity with intrinsic TCR-CD3 signaling to enhance tumor recognition under conditions of antigen variation. Using two GPC3 antibodies recognizing distinct epitopes (hYP7 and HN3), we generated four γδAbTCR constructs—hYP7-hYP7, hYP7-HN3, HN3-hYP7, and HN3-HN3—and evaluated their functional properties in primary human T cells. Among these, hYP7-hYP7 γδAbTCR-T cells demonstrated the strongest antigen binding and cytotoxic activity against Hep3B and other GPC3$^+$ HCC models, particularly those with low or heterogeneous antigen density. In vivo, hYP7-hYP7 T cells showed superior tumor infiltration, persistence, and control of large, established xenografts compared with other configurations. Mechanistic studies revealed that the hYP7-hYP7 γδAbTCR architecture couples enhanced antigen-binding avidity with coordinated TCR-CD3 and CD30 signaling, leading to potent NF-κB and NFAT activation and rapid induction of caspase-mediated apoptosis in tumor cells. These findings establish hYP7-hYP7 as a lead γδAbTCR design that overcomes the limitations of antigen heterogeneity and mutation in liver cancer, providing a promising framework for next-generation T-cell therapies targeting liver cancer.

#5622 Development of allogeneic TCR-mimic activating gdT (TAG-T) cells targeting KRAS^{G12D}/HLA-A*11 pMHC for undruggable KRAS-mutated cancers.

Chia-Chun Chao[1], Hsin-Yu Chang[2], Wei-Ze Hong[1], Jhen-Yu Chen[3], Yi-Wen Jiang[3], K.S. Clifford Chao[3], Kevin Chih-Yang Huang[3]

[1]NDV Therapeutics Corp., HsinChu City, Taiwan,[2]National Yang Ming Chiao Tung University, HsinChu City, Taiwan,[3]China Medical University, Taichung City, Taiwan

The therapeutic antibodies are at the vanguard of the most promising cancer treatments. Whereas conventional therapeutic antibodies have been limited to extracellular antigens, T cell receptor mimic (TCRm) antibodies can target intracellular antigens presented by cell surface major histocompatibility complex (MHC) proteins. We successfully obtained KRAS^{G12D}/HLA-A*11-specific TCRm antibodies from a phage display using a human scFv library. The affinity and target binding specificity of TCRms was validated by SPR and flow cytometry. Then, the KRAS^{G12D}/HLA-A*11-specific TAG receptor was designed as a double-chain, TCR-based construct, with the KRAS^{G12D}/HLA-A*11-specific TCRm fused to the N-terminus of the human TCR-Cγ and TCR-Cδ chain with Furin-P2A linker sequence. *In vitro* and *in vivo* cytotoxicity assays demonstrated that the KRAS^{G12D}/HLA-A*11-specific TAG-T cells exhibited high cytotoxic activity against KRAS^{G12D}/HLA-A*11-positive cells. Furthermore, TAG-T cells engineered with a co-stimulatory domain and a chimeric switching receptor (CSR) showed the highest anticancer activity and proliferation both *in vitro* and *in vivo*. Therefore, our results demonstrate that the TCRm-based TAG-T platform targeting KRAS^{G12D}/HLA-A*11 represents a novel and promising allogeneic cell therapy strategy for patients with KRAS-G12D-positive cancers.

#5623 Novel mechanism for eliminating tumor collagens to boost efficacy by attIL12-TIL therapy in PDX sarcoma models.

Jiemiao Hu[1], Harjeet Singh[1], Yining Jin[1], Wendong Zhang[1], Jian Wang[1], Xueqing Xia[1], Neeta Somaiah[2], Richard Gorlick[1], Shulin Li[1]

[1]UT MD Anderson Cancer Center, Houston, TX,[2]Assistant Professor, UT MD Anderson Cancer Center, Houston, TX

Tumor-targeted T-cell therapies of various types have been booming, but T-cell therapy is limited by its inability to penetrate the collagen barrier that “stuffed” within tumors and surrounding tumors/tumor cells. Compared to normal human tissues, sarcoma tissues exhibited significantly higher density of collagens and extracellular matrix (ECM) determined via bulk RNAseq and Masson’s trichrome staining. The destruction of tumor collagen is significant because collagen does not only suppresse T cells but also contributes to the formation of the extracellular matrix. In this study, for the first time, we used three pairs of autologous sarcoma patient-derived xenograft (PDX) and autologous tumor infiltrating T cells (TILs) models to discover that CCKAR directly boosts collagen production by tumor cells in vitro and in vivo. attIL12-modified TILs disabled collagen production from CCKAR-high autologous tumor cells in vitro and in vivo. This attIL12-TILs induced disruption of tumor cell derived collagen production required a simultaneous interaction between two signaling pathways: 1) the CSV on autologous tumor cells, which is targeted by attIL12, and 2) HLA-TCR on attIL12-TILs; when either interaction was abrogated, collagen production and CCKAR expression were not shut down. Mechanistically, the dual signaling activation between attIL12-TILs and autologous tumor cells synergistically induced super high IFNγ production in tumors, which in combination with CCKAR downregulation reduced collagen expression through suppression of both TGFβ-stimulated SMAD activation and CCKAR-AKT signaling. Diminishing collagen expression from tumor cells significantly increased T-cell infiltration and improved tumor growth inhibition in PDX sarcomas. This study revealed for the first time that CCKAR, which is highly expressed in immunotherapy resistant sarcomas, may serve as a novel target for reducing tumor collagens. attIL12 modification mediated collagen disrupting reversed the lost tumor penetration function of TILs post ex vivo expansion, resulting in sarcoma tumor regression that TILs alone fail to achieve. Thus, this attIL12-TIL therapy holds great clinical potential for boosting T-cell infiltration in high-grade, collagen-rich tumors.

#5624 Clinical strategies to enhance the efficacy of tumor-infiltrating lymphocyte (TIL) therapy using preclinical models.

Asraa Ahmed[1], Jonathan F. Khan[2], Sadna Budhu[2], Jedd D. Wolchok[2], Taha Merghoub[2]

[1]Pharmacology, Weill Cornell Grad. School of Medical Sci., New York, NY,[2]Sandra and Edward Meyer Cancer Center, Weill Cornell Medical College, New York, NY

Advanced metastatic melanoma refractory to immune checkpoint blockade (ICB) remains exceedingly difficult to treat, highlighting the need for alternative immunotherapeutic strategies. Due to the immunosuppressive mechanisms within the tumor microenvironment (TME), the infiltration and effector function of tumor-associated antigen (TAA) and neoantigen-specific CD4+ and CD8+ tumor-infiltrating lymphocytes (TILs) are limited, allowing the tumor to escape immune surveillance and hinder the endogenous immune response. Adoptive cell therapy (ACT) of autologous, ex-vivo expanded TILs was recently approved as a second line of therapy for advanced metastatic melanoma patients refractory to ICB. Despite positive responses observed in a subset of patients, many fail to respond, highlighting the urgent, unmet need to identify strategies which improve TIL-ACT efficacy. We have shown that a lower precursor frequency of self-antigen-specific CD8+ T cells enhances the quality of the antitumor response, whereas self-antigen-specific CD4+ T cells are susceptible to exhaustion at the same frequencies. These preliminary findings suggest that clonal abundance plays a critical role in determining T cell functional state—an unexplored area in the context of TIL therapy efficacy. ICB reinvigorates exhausted T cells under certain conditions, however, whether ICB can also reprogram exhaustion that arises as a consequence of dysregulated precursor frequency or subset composition is unknown. We hypothesize the efficacy of TIL therapy is determined by antigen-specific precursor frequency and T cell subset composition, and combining TIL-ACT with ICB will reprogram the exhausted T cells to sustain the hostile TME. To investigate this, we transferred varied precursor frequencies of neoantigen and tumor associated antigen-specific CD4+ and CD8+ T cells into tumor-bearing mice. Preliminarily, we have found antigen-specific CD4+ T cells to modestly enhance the anti-tumor response to ACT, however, this effect is not mediated through effector function and tumor control. This suggests that antigen-specific CD4+ T cells provide a helper role in ACT products. Next, we have shown upregulated immune checkpoint expression on ex vivo expanded TILs using flow cytometry and aim to assess combinatorial strategies with ICB to improve anti-tumor immune response. Further, we aim to investigate how precursor frequency and CD8+/CD4+ T cell ratio impacts TIL-ACT response by spiking in exogenous transgenic, antigen-specific T cells in the TIL product at varied frequencies.

#5625 Epigenetic reprogramming of T cell exhaustion.

Tsunghan Hsieh, Ruomin Xin, Enchong Zhao, Xiao Tian

Sanford Burnham Prebys Med. Discovery Inst., La Jolla, CA

During tumor progression, T cells are recruited to the tumor microenvironment (TME), where T cells experience hypoxia, nutrient deprivation, immunosuppressive cytokines, and continuous stimulation by tumor antigens. These harsh conditions drive global epigenetic remodeling of T cells and promote their transition into a state of T cell exhaustion, characterized by impaired capacity in proliferation, reduced production of proinflammatory cytokines, and diminished self-renewal. Immune checkpoint blockade (ICB) treatment has revolutionized cancer therapy; however, it fails to reprogram the exhaustion-associated epigenetic landscape and therefore only partially restores T cell functions. Here, we aim to prevent T cell exhaustion by targeting this epigenetic landscape through ectopic expression of epigenetic reprogramming factors (ERFs). To this end, we first generated a mouse model with inducible ERF expression, isolated CD8+ T cells, and cultured them under hypoxic conditions with continuous stimulation, to mimic the TME. Under these conditions, ectopic expression of ERF factors significantly downregulates expression of exhaustion markers such as Tim3. We next assessed whether ERF-mediated reprogramming can restore the T cell function. In vitro, ERF-reprogrammed T cells exhibit increased durability compared to non-reprogrammed control T cells in response to exhaustion signals. In vivo, ERF-reprogrammed T cells, when transferred into tumor-bearing mice, significantly delays the tumor growth compared with transfer of non-ERF-expressing control T cells. Transcriptomics profiling further reveals that ERF reprogramming upregulates the genes involved in T cell activation, proliferation, and epigenetic remodeling. Collectively, these data support ERF-mediated reprogramming of T cells as a promising strategy to reshape the entrenched exhaustion-associated epigenetic landscape and restore T cell functions, with the potential to improve adoptive cell transfer (ACT)-based therapy such as Tumor-Infiltrating Lymphocytes (TIL) and Chimeric Antigen Receptor (CAR) T therapy.

#5626 Combination epigenetic therapy unmasks non-canonical neoantigens to improve adoptive T cell therapy in ovarian cancer.

Jose A. Colina[1], Katherine B. Chiappinelli[1], Erin E. Grundy[1], Conrad Russell Y. Cruz[2]

[1]The George Washington University, Washington DC, DC,[2]Children's National Health System, Washington, DC

Immunotherapy has revolutionized cancer treatment across a range of malignancies, yet its efficacy in ovarian cancer (OC) has remained limited due to low tumor mutational burden and limited neoantigen availability. While current immunotherapy strategies have struggled to achieve durable responses, adoptive T cell therapy (ATT) combined with epigenetic therapies that expand the antigenic landscape present a promising avenue to overcome the inherent challenges of immune resistance in OC. Epigenetic remodeling can increase tumor immunogenicity as well as de-repress “cryptic antigens”, that are normally transcriptionally silent yet selectively expressed in malignant cells. These cryptic antigens arise from mis-splicing, alternative open reading frames, and endogenous retroelements that generate HLA-restricted peptides recognizable by T cells. Their selective expression in cancer cells and immunogenicity highlight the actionability of these non-canonical targets for immunotherapy. We treated four OC cell lines with DNA methyltransferase and histone deacetylase inhibitors and identified a reproducible subset of upregulated protein-coding cryptic antigens, including endogenous retroviruses (ERVs) and other endogenous retroelements. We then generated an overlapping peptide library spanning the identified targets to prime and expand T cells from PBMCs of healthy donors. The resultant T cell products demonstrated robust proliferation, antigen-specific cytokine production, and high-avidity responses across multiple peptide pools. Functional avidity assays confirmed specific recognition of epigenetically induced antigen targets. These results demonstrate that epigenetic therapy can uncover a previously inaccessible tumor-specific antigen pool in OC and enable the generation of potent T cell products directed against these cryptic antigens. Leveraging epigenetic induction of cryptic antigen expression may thus provide path a to expand the target landscape for ATT and improve therapeutic efficacy in ovarian cancer.

#5627 Intermittent cyclophosphamide and vinorelbine combined with anti-PD-1 induce transferable T-cell-mediated antitumor immunity and long-term memory in TNBC mouse models.

Stefania Orecchioni[1], D'Ambrosio Lorenzo[2], Davide Lombardi[3], Anna Vaccari[3], Paola Nistico'[4], Francesco Bertolini[3], **Paolo Falvo**[3]

[1]European Institute Of Oncology, Milano, Italy,[2]Tumor Immunology and Immunotherapy Unit, IRCCS-Regina Elena National Cancer Institute, Rome, Italy,[3]IEO - European Institute of Oncology, Milan, Italy,[4]IRCCS-Regina Elena National Cancer Institute, Rome, Italy

Cell-based immunotherapies offer a powerful means to harness treatment-induced antitumor immunity for durable tumor control. We previously developed a Triple-Therapy (TT) regimen combining vinorelbine-mediated activation of antigen-presenting cells (APCs) with cyclophosphamide-driven induction of TCF1$^+$ stem-cell-like T cells (scTs), markedly enhancing anti-PD-1 efficacy in resistant tumor models. The TT protocol consists of three intermittent doses of vinorelbine, and cyclophosphamide administered every six days, together with five anti-PD-1 doses delivered every two days.In a Non-Hodgkin Lymphoma (NHL) model, TT not only achieved strong tumor regression but also conferred long-term immunological memory, as evidenced by protection upon tumor rechallenge. Extending these findings to triple-negative breast cancer (TNBC), TT induced comparable antitumor activity. To determine whether TT-elicited immunity could be adoptively transferred, immunocompetent BALB/c mice bearing 4T1 TNBC were treated with TT, and immune tissues—including blood, spleen, and lymph nodes—were collected and transferred into syngeneic BALB/c nude mice inoculated with the same tumor.Strikingly, transfer of peripheral blood from TT-treated donors significantly delayed tumor growth, indicating that circulating immune cells are sufficient to convey protection. In contrast, lymphocyte depletion abolished this effect. Selective ablation of CD4$^+$ or CD8$^+$ T cells—performed either by flow cytometric sorting or using neutralizing antibodies—also eliminated the therapeutic benefit, confirming their essential role in the transferable antitumor response.Overall, these findings demonstrate that TT induces systemic, memory-forming T-cell responses capable of mediating cell-transferable tumor control. Current work focuses on identifying the tumor antigens recognized by TT-induced T cells, with the ultimate goal of developing targeted therapeutic vaccines to extend these benefits to broader patient populations.

: Antibody-Drug Conjugates and Linker Engineering 4
Poster Session

#5631 TCX-201, a novel ADC targeting a specific tumor-associated carbohydrate antigen (TACA) with excellent preclinical efficacy, PK and safety profile in solid tumor models.

Matthias Ocker, Francesco Muraca, Stephan Grunwald, Wiebke Winkler, Karla E. G. Soto, Carolin Lange, Jean Engela, Peter Sondermann

Tacalyx GmbH, Berlin, Germany

Tumor-associated carbohydrate antigens (TACAs) are defined oligosaccharide structures that are expressed on the surface of cancer cells. They are derived from changes in glycosylation pathways associated with malignancy, which lead to overproduced or aberrant structures, and represent a still unexplored target class for cancer therapy. We have generated specific antibodies against several of these difficult to target antigens and obtained a high affinity, fully humanized monoclonal antibody (mAb), TCX-201, against one of these TACAs, highly expressed across a broad range of cancer indications, including various gastrointestinal cancer types as well as NSCLC. This mAb shows superior internalization, affinity, and specificity for the target compared to the available benchmark, as assessed by glycan array, flow cytometry, and immunohistochemistry or immunofluorescence. Three ADC-variants were created by conjugation with MMAE (DAR 4), Exatecan (DAR 8), and Deruxtecan (Dxd, DAR 8) via a cleavable linker and were subsequently analyzed regarding their potency. *In vitro* studies showed effective killing of various pancreatic and colon cancer cell lines expressing different levels of the TACA (e.g. HuP-T4 (high expressing, IC50 of 0.3 nM), Capan-2 (heterogeneous expression, IC50 of 1.03 nM), Colo-205 (high expressing, IC50 of 0.013 nM), LS180 (medium expressing, IC50 of 4.7 nM). Moreover, high efficacy was observed for the tested payloads in different xenograft models with weekly iv administration: Capan-2 pancreatic cancer (reaching T/C of 16% and 6% at 3 and 7 mg/kg MMAE, respectively and T/C of 27% with 7 mg/kg Dxd) and Colo-205 colorectal cancer reaching T/C of 3% with 7 mg/kg MMAE. In addition to CDX models, PDX *in vitro* screening on PDAC and CRC models showed highly effective killing in 5/8 PDAC PDX and 2/5 CRC PDX with TCX-201 MMAE. These results, coupled with a favorable PK and safety profile make this ADC a first-in-class molecule for the treatment of various solid tumors that express different levels of the target structure.In conclusion, our antibody represents a new promising treatment option for different cancer indications and can be effectively employed as an ADC using different payloads.

#5632 Enhancing dual-payload ADC discovery projects by overcoming heterogeneity and resistance through dual-payload innovation.

Ying Meng, Lili Chai, Wei Liu, Xue Yang, Min Kang, Rui Song, Zhengtai Li, Yan Zhang, Zhiwei Bao, Ying Bi, Yixiao Zhao, Wange Fan, Xiao Li, Li Li, **Tiejun Bing**

ICE Bioscience, Beijing, China

Dual-payload antibody-drug conjugates (ADCs) have emerged as an innovative promising next-generation ADC format, delivering two cytotoxic agents to enhance efficacy through synergistic effects, mitigate resistance, without an accompanying increase in toxicity risk, aiming to address the challenge of poor-responsive cancers and rapid patient relapses. The success of dual-payload ADCs hinges on the appropriate dual-payload combination.DNA-damage response (DDR) inhibitors are increasingly being evaluated as payloads for ADCs, with Topoisomerase 1 (Top 1) inhibitors being the most commonly used class. Top 1 inhibition traps DNA breaks at replication forks, simultaneously blocking the DDR pathway severs the repair escape route, leading to replication catastrophe and selective synthetic-lethal cell death.To identify a rationally designed dual-payload combination that overcomes tumor heterogeneity and conventional resistance of colorectal cancer (CRC), synergistic pairs of Top 1 inhibitors and a group of DDR inhibitors with different mechanisms were screened and evaluated. Single payload activities were first investigated in CRC cell panel, and dual-payload combination synergies were then assessed in some selected CRC cell lines and ADC-related drug-resistant cell lines. A pair of Top 1 inhibitor + CHK inhibitor combination showed significant potent synergy in CRC cell lines and ADC-related drug-resistant cell lines with 2D and 3D cytotoxicity evaluation models. Mechanistic studies of this combination were further explored with cell cycle and apoptosis studies, WB of biomarkers, as well as RNA-Sequencing, revealing that the synergy stemmed from coordinated cell cycle arrest and enhanced apoptosis induction, supported by transcriptomic profiling of DDR pathways. Critically, the dual-payload combination showed no increased toxicity in a group of healthy human cell lines and limited or additive hematotoxicity in the in vitro CD34+ HSPCs myeloid progenitor cell proliferation and differentiation assays, indicating a potentially improved therapeutic window. These study strategies and findings accelerate dual-payload ADC innovative research, especially in the stage of proof of concept for dual-payload combination as a promising strategy to overcome cancer heterogeneity and resistance

#5633 YB-811, a novel antibody drug conjugate targeting the tumor-selective human neuronal pentraxin receptor shows pronounced efficacy in experimental tumor models.

Peter Schiemann[1], Michel Janicot[1], Gunther Wennemuth[2], Mykola Lyndin[2]

[1]Ymmunobio AG, Riehen, Switzerland,[2]University Hospital Essen, Essen, Germany

The human neuronal pentraxin receptor (NPTXR) gene encodes a type II transmembrane protein that functions as a trans-synaptic organizer and anchors neuronal pentraxin complexes to plasma membranes in a subset of neuronal cells of the hippocampus and cerebral cortex. Beside its synaptic functions in the brain, NPTXR is not present in other organs and therefore does not have any physiological role; hence *NPTXR*$^{-/-}$mice showed no abnormalities in reproduction, development, metabolism, or motor function. Recent immunohistochemistry studies performed with a fully humanized monoclonal antibody (YB-800) targeting NPTXR with high affinity have revealed expression of membrane-associated NPTXR protein in a wide variety of solid tumors (but not in adjacent healthy tissues and healthy tissue samples) with a high prevalence (up to 98%) and H-scores (up to 300); e.g., in bladder, cervix, non-TNBC, NSCLC, and pancreas tumor samples. These results strongly support the rationale for the design of a YB-800-based antibody drug conjugate (ADC) as novel option for safe therapeutic intervention in Oncology. A novel ADC (YB-811) was engineered with YB-800 linked to 4 monomethylauristatin F molecules (*via* non-cleavable linkers), and 4 exatecan molecules (*via* cleavable linkers). YB-811 was evaluated in multiple experimental tumor models in both cell-based assays and *in vivo* tumor studies. Results clearly indicate concentration- and time-dependent effect on tumor cell proliferation and survival, as well as pronounced anti-tumor activity - tumor growth inhibition/regression - in established tumor-bearing athymic mice. Taken together, these results strongly support further exploration of the potential therapeutic benefit of YB-811.

#5634 KY102, a novel Glypican 3-targeting nanobody drug conjugate bearing a topoisomerase 1 inhibitor payload demonstrates compelling preclinical activity in hepatocellular carcinoma models.

Haikun Shi

Hangzhou kunyu pharmaceutical, Hangzhou, China

Background: Glypican-3(GPC3), a cell-surface oncofetal glycoprotein highly expressed in hepatocellular carcinoma (HCC) with minimal presence in normal adult tissues. KY102 is a nanobody-drug conjugate (NDC)targeting human GPC3, composed of a monovalent nanobody covalently conjugated to a topoisomerase 1 inhibitor, DXD. via a maleimide anchor and a glycyl glycyl phenylalanyl glycine (GGFG)- aminomethyl (AM) cleavable linker at a drug to nanobody ratio (DAR) of 3.
Materials and Methods: Extensive functional characterization was performed to assess the mechanism of action and therapeutic potential of the KY102 (NDC) at DARs of 3.
1.Nanobody binding to human,cynomolgus monkey rat and mouse GPC3 was assessed by biolayer interferometry (BLI) and flow cytometry(FACs).
2.Am assessment of off-target binding, and target specificity was conducted using 177-Lu labeled Nanobody in normal and cell line derived animalmodel.
3.KY102 nanobody internalization in GPC3-expressing tumor cell lines was assessed by flow cytometry.
4.In vitro KY102 (NDC) cytotoxicity against tumor monolayers was assessed in a panel of HCC cell lines.
5.Tumor cell co-culture assays were also performed to assess bystander-mediated cell killing by KY102.
6.Anti-tumor activity of KY102 was investigated in a panel of cell line-derived xenograft (CDX) and patient-derived xenograft (PDX) mouse models representing a range of GPC3 expression.
7.The tolerability of KY102 was assessed in a single dose and repeat-dose (4 doses; once every weeks) non-GLP toxicology study in a cell line-derived xenograft (CDX) in mice.
Results:
1.The KY102 nanobody backbone demonstrated pico-molar binding affinity to both human, cynomolgus monkey, rat and mouse GPC3, and strong binding to target-expressing cancer cell lines.
2.Rapid internalization of KY102 nanobody was observed in GPC3-expressing HCC cell lines.
3.KY102 exhibited potent and target-specific cytotoxicity in a panel of HCC cells cultured either in monolayer.
4.KY102 showed effective bystander-mediated killing of GPC3 negative cancer cells when in co-culture with GPC3 positive cancer cells.
5.A single administration of KY102 (2.5mg/kg and 5.0 mg/kg) resulted in robust tumor growth inhibition of a panel of CDX and PDX models representing a range of GPC3-expression.
6.A single dose and a repeat-dose mouse toxicology study of KY102 showed encouraging tolerability at 30, and 60 mg/kg dose levels.
7.A dose-dependent nanobody pharmacokinetics at 2.5 mg/kg, and 5 mg/kg dose levels, without the maximum tolerated dose (MTD) determined.
Conclusions: Overall, these results support the potential of KY102 as a novel therapeutic agent against GPC3-bearing cancers including HCC. An IND application is anticipated in 2026. No conflict of interest

#5635 Rational design of a bispecific ADC targeting ITGB4 and TROP2 for co-expressing solid tumors.

Mi Young Cha, **Jiyoung Lee**, Hyunkyung Yu, Hyunuk Kim, Youngeun Ha, Bu-Nam Jeon, Seungmin Byun, Kitae Park, Mira Kim, Han-Sol Kim, Wuhwui An, Hyonam Kim, Sang-Gyun Kim, Hansoo Park

Genome & Company, Suwon-si, Korea, Republic of

Integrin beta 4 (ITGB4) was identified as a promising tumor-specific antigen through the GNOCLE™ platform. ITGB4 is highly expressed in head & neck, colorectal, esophageal, and other solid tumors, but shows minimal expression in matched normal tissues by immunohistochemistry, supporting a favorable therapeutic window. ITGB4 promotes epithelial detachment, migration, and invasion, and its high expression is associated with therapy resistance and poor prognosis. Target profiling further revealed the frequent co-expression of ITGB4 and TROP2 in multiple cancers, including pancreatic, lung, bladder, and HER2-negative breast cancers, with minimal overlap in normal tissues, supporting the tumor-selective potential of ITGB4/TROP2 co-targeting. TROP2-targeting antibody-drug conjugates (ADCs) have been actively developed, with several already approved for the treatment of solid tumors. However, relatively high TROP2 expression in normal epithelia can drive on-target/off-tumor toxicity, thereby restricting the therapeutic index of TROP2-targeting ADCs. This highlights an unmet need for strategies that preserve the antitumor benefit of TROP2 targeting while improving tumor selectivity. Leveraging the complementary biology of ITGB4 and TROP2, we designed a bispecific ADC targeting ITGB4 and TROP2 to preferentially deliver cytotoxic payloads to dual-positive cancer cells, thereby increasing therapeutic effect and expanding the therapeutic window. To construct the bispecific antibody, we combined the variable region of sacituzumab with our humanized anti-ITGB4 antibody, GENA-120B17. Guided by target affinity and relative expression, we generated 1+1 and 2+2 valency formats to optimize efficacy and selectivity. The bispecific antibodies showed enhanced internalization in TROP2/ITGB4 double-positive cancer cells compared with sacituzumab or GENA-120B17, without increased uptake in target-negative cancer cells or normal cells. These bispecific antibodies were then conjugated, via a hydrophilic, cleavable linker (LinkerE) designed to reduce retro-Michael elimination, to either a topoisomerase I inhibitor or a microtubule inhibitor. The resulting bispecific ADCs exhibited superior in vitro cytotoxicity in double-positive cancer cell lines relative to the corresponding monospecific ADCs, while maintaining a safer profile in normal cells. In conclusion, this bispecific ADC design broadens the therapeutic index and offers a safer, more effective treatment approach that addresses key limitations of existing TROP2-targeted ADC therapies.

#5636 Preclinical evaluation of LM-338: An innovative anti-STn antibody drug conjugate for solid tumors.

Jin Li, Junwei Yang, Yuan Li, Te Du, Xia Qin, Da Fei, Lei Shi, **Wei Cao**

LaNova Medicines, Shanghai, China

Background: Sialyl-Thomsen-nouveau(STn)antigen is a truncated O-glycan generated by early sialylation of the Tn antigen. While with limited expression in normal tissues, STn is overexpressed in numerous human carcinomas, including ovarian, breast, bladder, cervical, colon, pancreatic and lung cancers. LM-338, a STn-targeted antibody-drug conjugate (ADC), is comprised of a humanized monoclonal antibody (LM-138) conjugated to a topoisomerase I inhibitor via a cleavable linker, with a drug-antibody ratio of 4.
Methods: Target binding activity of LM-338 was assessed by flow cytometry. Internalization was evaluated using a pH-sensitive dye. Binding specificity was evaluated using glycan array. Cytotoxic and bystander effects were measured using CellTiter-Glo luminescent cell viability assay. In vivo anti-tumor activity of LM-338 was examined in several STn-positive cell line-derived xenograft (CDX) and patient-derived xenograft (PDX) models. Immunohistochemistry was used to assess STn expression in tumor tissues. Toxicity was evaluated inrepeated-dose toxicity study in rhesus monkeys.
Results: LM-338 showed high binding activity and specificity to STn with minimal cross-reactivity to sialyl-T-antigen. LM-338 bound to and was internalized by STn-positive tumor cells in a dose-dependent manner, resulting in potent cytotoxic and bystander effects in vitro. *In vivo*, LM-338 (3 or 6 mg/kg) induced significan tumor growth inhibition or regression across multiple CDX and PDX models (ovarian, colorectal and lung cancers), with superior efficacy as compared to a DXd-conjugated comparator. LM-338 was well tolerated in non-human primates at dosed up to 60 mg/kg.
Conclusion: LM-338, an anti-STn ADC, demonstrated potent anti-tumor activityacross several solid tumor models with favorable preclinical tolerability. These findings support further clinical development of LM-338 for patients with STn-expressingmalignancies.
Keywords: STn, antibody-drug conjugate, LM-338, solid tuomrs, ovarian cancer, colorectal cancer, lung cancer
Disclosure: The study was funded by LaNova Medicines Limited, China.

#5637 A novel EGFR and B7H3 dual-targeted antibody-drug conjugate (ADC) for the treatment of solid tumors.

Mingkun Zhang[1], Xuguo Zhu[1], Jun Wang[2], Jing Zhao[1]

[1]NeoMab Biotechnology Co,. Ltd, Suzhou, China,[2]GemPharmatech LLC., San Diego, CA

Background: EGFR (also known as HER1) is an epidermal growth factor receptor involved in tumor progression, and its overexpression in approximately 70% of colorectal cancer (CRC), 60% of lung cancers, and over 90% of head and neck squamous cell carcinoma (HNSCC). B7H3 belongs to the B7 immunoregulatory family. B7H3 is overexpressed on a wide range of solid tumors such as lung cancers, gastrointestinal cancers and gynecological cancers, but its expression is absent or low in normal tissues. Therefore, dual targeting of both EGFR and B7H3 can achieve better therapeutical efficacy. EGFR/B7H3-ADCs are novel bispecific Antibody-drug Conjugates (ADCs), composed of fully human anti-EGFR/B7H3 bispecific antibodies (BsAbs) conjugated to TOP1i payload via cleavable linker.
Methods: the fully human monoclonal antibodies were derived from transgenic mouse model NeoMab mice. Flow cytometry was performed to examine binding of ADCs to tumor cells. In addition, we used pHrodo conjugated to ADCs to detect internalization activity in tumor cells. CTG (CellTiter-Glo®) assay was employed to measure cell viability. In immunodeficient mice, xenograft model was generated to assess the tumor growth inhibition of ADCs.
Results: EGFR/B7H3-ADCs showed stronger binding to tumor cells than EGFR-ADC and B7H3-ADC. Besides, EGFR/B7H3-ADCs displayed superior internalization activity. More importantly, our EGFR/B7H3-ADCs suppressed tumor growth more effectively than EGFR-ADC and B7H3-ADC in CDX mouse model.
Conclusion: our EGFR/B7H3-ADCs show potential therapeutic promise in patients with EGFR or B7H3 positive tumors. This study provides crucial rationale for supporting the further development of our novel dual-targeted Antibody-drug Conjugates (ADCs).

#5638 A first-in-class photo-responsive EGFR-ADC drives ROS-mediated, energy-dependent tumor eradication in preclinical models.

Wentao Shang[1], Hua Shang[2], Josie Cai[2], Vicky Qin[2], Lyan Chen[2], Xiaobo Zhang[1]

[1]School of Basic Medicine and Clinical Pharmacy, China Pharmaceutical University, Nanjing, China,[2]Shanghai Biophy Biological Pharmaceutical Co., Ltd., Shanghai, China

Light-activated antibody-drug conjugates (ADCs) represent an emerging class of precision therapeutics that enable spatial and temporal control of cytotoxicity. By restricting payload activation to illuminated tumor sites, this modality can enhance local potency while limiting systemic toxicity. We developed Cetuximab-I21-2, a next-generation EGFR-targeted ADC incorporating a Heloporfin-derived photosensitizer engineered for high singlet-oxygen yield, serum stability, and rapid photochemical activation upon exposure to red light near 650 nm. This architecture integrates receptor-mediated tumor localization with externally programmable activation, enabling precise, on-demand cytotoxicity.

In vitro studies were conducted across tumor cell lines with high, intermediate, and low EGFR expression, including A431, HCC827, Huh7, NCI-N87, and MIA-PaCa-2. Cetuximab-I21-2 exhibited minimal dark toxicity at concentrations up to several micrograms per milliliter, confirming that the payload remains inactive without illumination. Upon irradiation, the ADC produced potent, energy-dependent cytotoxicity consistent with singlet-oxygen-driven membrane injury and mitochondrial dysfunction. IC50 values were 0.05 μg/mL in A431 and 0.14 μg/mL in HCC827 at 5 J/cm², with substantially reduced potency in EGFR-low cells, demonstrating both antigen-dependent delivery and illumination-triggered activation. Fluorescent ROS probes showed an immediate burst of intracellular singlet oxygen and secondary reactive oxygen species within minutes of irradiation, accompanied by rapid loss of mitochondrial membrane potential and plasma membrane integrity, confirming the dual targeting-activation mechanism.

In vivo antitumor activity was evaluated in A431 xenograft-bearing B-NDG mice treated with a single 35.3 mg/kg intravenous dose followed by localized irradiation at 100 or 200 J. Cetuximab-I21-2 produced distinct, energy-dependent tumor suppression, achieving 22.2% inhibition at 200 J. Histopathology revealed focal necrosis and photodynamic vascular disruption, consistent with ROS-mediated tissue injury. Treated animals maintained stable clinical condition, and transient (<10%) weight loss resolved spontaneously without supportive care, with no evidence of systemic toxicity.

Collectively, these findings demonstrate that Cetuximab-I21-2 provides potent, selective tumor ablation through the integration of EGFR-targeted delivery, payload stability, and externally controlled photochemical activation. This first-in-class photo-responsive ADC platform offers a programmable therapeutic strategy that may improve therapeutic index, enable dose-sparing treatment, and expand precision oncology approaches for EGFR-expressing solid tumors.

#5639 HDP-103, a PSMA targeting amanitin-based ADC, is efficacious even in difficult to treat patient derived xenograft models with heterogenous PSMA expression.

Kristin Decker[1], Christian Orlik[2], Irina Dranova[2], Aniko Palfi[2], Torsten Hechler[2], Andreas Pahl[1], Michael Kulke[1]

[1]Heidelberg Pharma AG, Ladenburg, Germany,[2]Heidelberg Pharma Research GmbH, Ladenburg, Germany

Background
Antibody drug conjugates (ADCs) are increasingly used in the treatment of solid tumors. HDP 103 is an anti PSMA ATAC (amatoxin based ADC) targeting metastatic castration resistant prostate cancer (mCRPC). ATACs offer distinct advantages over conventional ADCs: i) inhibition of RNA polymerase II confers activity in both proliferating and quiescent cells; ii) there are no known resistance mechanisms; iii) ATACs are potent against target low cancer cells; and iv) ATACs show particular good efficacy in patients with 17p/TP53 deletion who have poor prognosis. This study presents preclinical data demonstrating HDP 103 efficacy and a favorable therapeutic window in difficult to treat mCRPC patient derived xenograft models with heterogeneous PSMA expression.
Materials and Methods
HDP 103: anti-PSMA ADC with site specific, cysteine conjugated amatoxin linker.
Immunofluorescence: IF on PDX tumors using HDP 103 antibody.
Efficacy: subcutaneous prostate cancer PDX models treated intravenously with HDP 103 q14d × 3.
Tolerability: cynomolgus monkeys dosed intravenously on days 1 and 22; PK sampling, necropsy, and histopathology performed.
PK/PD: two compartment model with parallel linear and Michaelis-Menten elimination.
Results
HDP 103 produced potent, durable tumor remissions and significantly extended survival in PDX models at doses ≤5 mg/kg, including models with del(17p) and heterogeneous PSMA expression. In cynomolgus monkeys, HDP 103 was well tolerated, causing only transient changes in serum chemistry and hematology, and exhibited a half life of approximately 5-10 days. No salivary gland toxicity was observed; microscopic adverse findings were limited to the kidney. Integrated PK/PD modeling of efficacy and tolerability predicted serum exposures and patient dose ranges consistent with a convenient therapeutic window.
Conclusion
HDP 103, an anti PSMA ATAC for the treatment of mCRPC, demonstrates robust and durable antitumor activity in PDX models representative of the target population, including tumors with heterogeneous PSMA expression and those harboring a del(17p). Combined with a favorable half life and a manageable safety profile in nonhuman primates, HDP 103 warrants further clinical development as a novel treatment option for mCRPC, particularly for patients with del(17p) with a high unmet medical need.

#5640 ZW439, a novel CLDN18.2-targeting pan-RAS inhibitor antibody drug conjugate for the treatment of RAS mutated pancreatic cancer.

Sam Lawn, Andrea Hernandez Rojas, Vidhi Khanna, Jodi Wong, Ambroise Wu, Matthew Bonderud, Victoria Harman-McKenna, Taixiang Wang, Allysha Bissessur, Kaylee Wu, Manuel Lasalle, Vincent Fung, Chayne L. Piscitelli, Dunja Urosev, Luying Yang, Graham A. E. Garnett, Raffaele Colombo, Jamie R. Rich, Stuart D. Barnscher

Zymeworks Inc., Vancouver, BC, Canada

Pancreatic cancer remains one of the most difficult to treat cancers, with 5-year survival rates of just 13%, and there is an urgent unmet need for novel, differentiated, and effective therapeutics. Recently, encouraging progress has been made through inhibition of RAS, a key oncogenic driver mutated in over 90% of pancreatic ductal adenocarcinoma (PDAC). Antibody drug conjugates (ADCs) have demonstrated clinical success at improving the effectiveness of multiple respective classes of small molecules. The full therapeutic potential of pan-RAS inhibitors (pan-RASi) has been limited by toxicities likely arising from on-target inhibition of wild-type RAS in normal tissues, as well as by the emergence of resistance. These challenges may be improved upon by enhancing delivery of a RASi via an antibody drug conjugate mechanism. Here, we seek to leverage the ability of ADCs to enhance the delivery of a novel pan-RASi payload to tumors for improved response, and to provide a differentiated safety profile that mitigates the toxicity limitations of current small molecule pan-RASi. To this end, the novel pan-RASi ADC ZW439 is directed to CLDN18.2, a clinically validated oncology target that is highly expressed in PDAC.

A novel potent pan-RAS inhibitor ADC platform was developed through synthesis, screening, and iterative optimisation of payloads and drug-linkers for favorable ADC biophysical properties, antitumor activity, tolerability and pharmacokinetics (PK). A novel CLDN18.2 targeted antibody was selected for optimal ADC properties including its binding and internalization to CLDN18.2 expressing cells. Tumor cell spheroids were utilized to determine the cytotoxicity of the pan-RASi ADC, and its bystander activity was determined in CLDN18.2 positive and negative tumor cell co-cultures. The antitumor activity and PK of ZW439 were evaluated in multiple mouse xenograft models.

The novel humanized IgG1 antibody of ZW439 features strong and exclusive binding to CLDN18.2 and demonstrates superior internalization to CLDN18.2 expressing tumor cells compared to a clinical benchmark CLDN18.2 targeted antibody. ZW439 demonstrates potent target-specific cytotoxicity to RAS-mutated tumor cells expressing a range of CLDN18.2 levels and drives effective bystander activity to antigen negative cells. In vivo, ZW439 demonstrates highly efficacious anti-tumor activity in multiple CLDN18.2 expressing xenografts and has a favourable PK profile. ZW439's pan-RASi ADC drug-linker platform demonstrates encouraging tolerability, with no significant toxicity observed following dosing up to 200 mg/kg in mice.

The encouraging preclinical profile of ZW439 supports its potential as a differentiated therapeutic for the treatment of Pancreatic cancer.

#5641 BCG037, a first-in-class anti-human ALPP/ALPG therapeutic ADC that inhibits tumor growth in pancreatic cancer and gastric cancer PDX models.

Yong Xie, Peiran Li, Ying Zhu, Yanan Guo

Biocytogen, Waltham, MA, MA

Placental (ALPP) and germ cell (ALPG) alkaline phosphatases, sharing 98% sequence homology, are tumor-associated antigens with a highly restricted expression profile. While largely absent in normal adult tissues, they are frequently overexpressed across a wide spectrum of malignancies, including pancreatic, gastric, ovarian, and lung cancers. Elevated ALPP/ALPG levels correlate with poor prognosis in gastric and ovarian cancers, making them compelling targets for antibody-based therapies. Here, we report the development of BCG037, a first-in-class, fully human IgG1 antibody-drug conjugate (ADC) targeting ALPP/ALPG. The antibody was generated from RenMab™ humanized mice and conjugated with the potent topoisomerase I (Top1) inhibitor payload, achieving a high drug-to-antibody ratio (DAR) of ~8. BCG037 exhibits high affinity (nanomolar range) and cross-reactivity to both human and cynomolgus monkey ALPP/ALPG, with no cross-reactivity to other ALP family members (ALPL, ALPI). Notably, the antibody component of BCG037 demonstrates superior binding affinity to tumor cells compared to the analog used in SGN-ALPV. *In vivo*, BCG037 treatment led to significant and superior tumor growth inhibition in both pancreatic and gastric cancer patient-derived xenograft (PDX) models, outperforming the benchmark ADC, SGN-ALPV-MMAE, and no treatment-related toxicity or weight loss was observed in mice. Collectively, these data validate ALPP/ALPG as promising therapeutic targets and position BCG037 as a highly novel and potent clinical candidate for treating ALPP/ALPG-positive malignancies, including refractory cancers with limited treatment options.

#5642 BCG040, a novel B7-H4-targeting biparatopic ADC, demonstrates superior preclinical efficacy in heterogeneous tumors.

Guan Wang, Peiran Li, Ying Zhu, Yanan Guo

Biocytogen, Waltham, MA, MA

B7-H4 (VTCN1) is overexpressed in many epithelial malignancies, particularly in ovarian, breast, biliary tract, and pancreatic cancers. These tumors are often resistant to both chemotherapy and immunotherapy, due to their aggressive nature and poor prognosis. Here, we present BCG040, a novel first-in-class, fully human IgG1κ biparatopic B7-H4 ADC. BCG040 binds to two non-overlapping B7-H4 epitopes and is conjugated to the potent topoisomerase I (TOP1) inhibitor BCPT02 (DAR≈8) via a hydrophilic protease-cleavable linker. *In vitro*, BCG040 showed nanomolar affinity for B7-H4, superior to Hu2F7 and SGN-B7H4V benchmark analogs, with fully human/cynomolgus cross-reactivity and no off-target binding to other B7 family members. BCG040 exhibited stronger binding and more rapid internalization than the two analogs in breast and ovarian cancer cells. *In vivo*, a single low dose of BCG040 showed durable tumor regressions (~40 days) in breast cancer PDX models and significant efficacy in pancreatic cancer PDX models, outperforming other ADCs such as Hu2F7, SGN-B7H4V, or FPA150 (conjugated with MMAE or BCPT02). This potent efficacy was achieved without observable toxicity and was supported by a favorable pharmacokinetic (PK) profile. Furthermore, this drug demonstrates excellent developability. The enhanced therapeutic activity of BCG040 is attributed to its unique biparatopic design, which promotes receptor clustering and accelerated intracellular trafficking, leading to enhanced delivery of payload. Notably, BCPT02-containing ADCs exhibited potent antitumor activity in heterogeneous PDX tumors, whereas MMAE-based conjugates were ineffective. These findings underscore the potential of BCG040 as a promising therapeutic candidate for the treatment of pancreatic, biliary tract, ovarian, and breast cancers.

#5643 Preclinical characterization of RC118 ADC and identification of its differential binding pattern relative to other anti-CLDN18.2 antibodies.

Lili Wang[1], Xiaoping Zhang[1], Mingyang Li[1], Xiao Wang[1], Yidan Xu[1], Xiaoli He[1], Shengle Ji[1], Shuya Ji[1], Shifu Wang[1], Yinghao Xin[1], Fanxue Bu[1], Yuelei Shen[2], Jianmin Fang[1], **Yuanhao Li**[1]

[1]RemeGen Co., Ltd., Yantai, China,[2]Biocytogen Pharmaceuticals (Beijing) Co., Ltd., Beijing, China

CLDN18.2 is a tight junction transmembrane protein normally buried in the gastric epithelium, rendering it largely inaccessible under physiological conditions. However, it is frequently overexpressed in malignancies such as gastric, gastroesophageal junction (GEJ), and pancreatic adenocarcinomas, where it becomes exposed and functions as a tumor-associated antigen suitable for targeted therapy. Structurally, CLDN18.2 has four transmembrane domains anchoring two extracellular loops (ECL1 and ECL2) that extend into the extracellular space. These loops form β-sheet-rich structures with conserved charged and polar residues critical for paracellular ion selectivity and tight junction integrity. Many therapeutic antibodies and ADCs exploit these extracellular regions to selectively target CLDN18.2-positive cancer cells through diverse mechanisms.

RC118 is an anti-CLDN18.2 antibody-drug conjugate (ADC) developed by RemeGen. It consists of a humanized anti-CLDN18.2 monoclonal antibody conjugated to the monomethyl auristatin E (MMAE) via a cleavable linker. RC118 exhibits strong and selective binding to CLDN18.2-positive cells, inducing rapid internalization and potent cytotoxicity in vitro. In multiple in vivo models, including patient-derived xenograft (PDX) models of gastric and pancreatic cancers, RC118 showed robust antitumor efficacy. Collectively, these findings support RC118 as a promising ADC candidate for gastric cancer therapy.

Structural modeling indicated that RC118 and zolbetuximab, a FDA-approved CLDN18.2 antibody drug, recognize a similar epitope within ECL1 around a loop structure at the end of the β-sheet, whereas a few other comparator antibodies target the side face of the β-sheet region. To further delineate epitope specificity among CLDN18.2-targeting antibodies, we engineered chimeric CLDN18.2/CLDN3-expressing cell lines exposing different extracellular loop configurations for comparative binding analysis. Targeted mutations of the Cys52-Cys62 disulfide motif within ECL1 were introduced to evaluate its contribution to antibody recognition. These studies revealed that RC118 shares a similar binding pattern with zolbetuximab, while differing from other investigational CLDN18.2 antibodies. Structural analyses further suggest that variations in ECL1 engagement may underlie differences in therapeutic activity among these antibodies.

RC118 is currently under evaluation in multiple clinical trials. At the 2025 ESMO meeting, combination data with immunotherapy showed encouraging results, supporting its potential in personalized treatment strategies for CLDN18.2-positive cancers. The emerging clinical outcomes, together with the structural insights into RC118-CLDN18.2 interactions, indicate that RC118 remains a strong and competitive candidate for continued clinical development.

#5644 DA-3501 (AT-211): Evaluation of immune-mediated antitumor activity and combination immunotherapy potential of a site-specific CLDN18.2-targeting antibody-drug conjugate (ADC).

Kyoung-Ho Pyo[1], Seong-Hyun Park[1], Dongsop Lee[2], Haneol Kim[2], Younggyu Kong[2], Younggeun Lee[1], Hojin Yeom[1], Sowon Aum[1], Sun Hee Park[1], Huijo Oh[1], Cheyeon Kim[1], Hyeonseok Jin[2], Hyeonseok Jin[2], Aera Lee[2], Hojeong Hong[2], Ju Hwan Kim[1], Hyungseok Choi[2], Mi-Kyung Kim[2], Taedong Han[1]

[1]AbTis Co., Ltd, Yongin, Korea, Republic of,[2]Dong-A ST Research Headquarter, Yongin, Korea, Republic of

Background: Claudin 18.2 (CLDN18.2) is a clinically validated therapeutic target in gastric and pancreatic cancers. However, acquired resistance to CLDN18.2-directed antibodies such as zolbetuximab and trastuzumab highlights the need for next-generation therapeutics with distinct mechanisms of action. DA-3501 (AT-211) is a CLDN18.2-targeting antibody-drug conjugate (ADC) developed using the AbClick® site-selective conjugation platform. The antibody component exhibits enhanced binding affinity, internalization efficiency, and molecular stability. This study aimed to evaluate the immune-mediated antitumor activity of DA-3501 and explore its potential for combination immunotherapy.
Methods: To assess efficacy in resistant disease contexts, immune organoids derived from gastric cancer patients with acquired resistance to trastuzumab and zolbetuximab were used to evaluate DA-3501 activity. Antitumor effects were analyzed in immune cell co-culture systems to assess cytotoxicity, CLDN18.2-dependent responses, and immune activation markers. Furthermore, in vivo efficacy studies incorporating immune checkpoint inhibitor (ICI) combination groups were conducted under immunocompetent conditions to investigate immune-mediated mechanisms and the combinatorial potential of DA-3501.
Results: DA-3501 demonstrated potent and selective cytotoxicity toward CLDN18.2-positive tumor cells and induced immune cell activation consistent with IgG1-mediated antibody-dependent cellular cytotoxicity (ADCC). In vivo, DA-3501 exhibited robust immune-mediated antitumor activity both as a monotherapy and in combination with ICIs, indicating complementary interactions between the ADC's direct cytotoxic payload and immune-modulatory mechanisms.
Conclusions: DA-3501 (AT-211) is a site-selectively conjugated CLDN18.2-targeting ADC that exerts strong immune-mediated antitumor effects, even in models derived from patients resistant to existing antibody therapies. These results highlight the dual mechanism of action of DA-3501—combining direct cytotoxicity and Fc-driven immune activation—and support the development of rational ADC-immunotherapy combinations as a promising strategy in the evolving landscape of ADC-based cancer treatment.

#5645 NW006-296, a novel ROR1 targeting ADC, demonstrates compelling anti-tumor efficacy in preclinical studies.

Zhaoyu Gou[1], Liqian Zhou[1], Li Liu[1], Zikuo Zhang[1], Gang Liu[1], Yiran Wu[1], Dan Mi[1], Jiabao Liu[1], Yaolan Dai[1], **Zhijian Li**[2], Wenting Luo[1], Bin Liu[1], Desi Pan[1], Zhigang Guo[1]

[1]Chengdu Chipscreen NewWay Biosciences Co., Ltd., Chengdu, China,[2]Chipscreen Biosciences (United States) Ltd, Somerset, NJ

Background: Receptor tyrosine kinase-like orphan receptor 1 (ROR1) was found broadly expressed in both hematological malignancies and solid tumors whereas its expression was largely absent from normal blood lymphocytes and adult tissues, making it an attractive tumor target being explored clinically via mAb, bi-specific abs, CAR-T and ADC. While several ROR1-targeting ADCs with different MoA payloads are in development, we engineered NW006-296, a novel ADC comprising a humanized anti-ROR1 antibody site-specifically conjugated to monomethyl auristatin E (MMAE), aiming to achieve a homogeneous and stable therapeutic agent. NW006-296 was assessed in vitro and in vivo to evaluate its therapeutic potential.

Methods: A library of ROR1-binding clones was screened for affinity, cell binding and internalization. Then the selected antibody is conjugated via cleavable linker to MMAE with drug-to-antibody ratio (DAR) of 4. The binding ability of the conjugates to human ROR1 is tested by enzyme-linked immunosorbent assay (ELISA). Finally, the anti-tumor efficacy of ROR1-targeting ADC is assessed in vitro through cell cytotoxicity assays and in vivo in multiple cell-line-derived xenograft (CDX) models. In detail, mice were treated with single (3 mg/kg, MDA-MB-231 and 5 mg/kg, U2932) and multiple (1 mg/kg or 3 mg/kg in HT-29; 3 mg/kg or 5 mg/kg in NAMALWA) doses of the ROR1-targeting ADC.

Results: The lead antibody showed low nanomolar affinity to human ROR1 (KD=3.9 nM), strong binding to ROR1-expressing cells (EC50=0.4 nM, 0.3 nM, 0.5 nM for MDA-MB-231, HT-29 and NAMALWA, separately) and robust internalization in ROR1-expressing cells. Conjugation to the payload did not compromise binding of the antibody to human ROR1. NW006-296 showed potent cytotoxicity against the previous ROR1-expressing cells in vitro cell cytotoxicity assays. Furthermore, NW006-296 demonstrated significant dose-dependent anti-tumor activity, with tumor regression observed in both in vivo models used. When compared to the benchmark ADC (MK-2140), NW006-296 demonstrated superior anti-tumor activity in all CDX models investigated. Intriguingly, NW006-296 remained potent anti-tumor efficacy more than 40 days after the drug withdrawal in the U2932 CDX model, while the tumor re-growth in the benchmark ADC treating group regressed during therapy. Additionally, NW006-296 was well tolerated in mice as indicated preliminarily by no body weight loss occurring.

Conclusions: NW006-296 has compelling anti-tumor efficacy and supports clinical development for ROR1-targeting ADCs across a broad spectrum of cancers. Further preclinical safety assessment, pharmacokinetics and IND-enabling studies are on-going with the goal to develop NW006-296 as a transformative therapeutic candidate for the treatment of colorectal cancer, breast cancer and hematological malignancies.

#5647 GS24-B057, a potential best-in-class Nectin-4- and Trop-2-directed bispecific ADC, for the treatment of urothelial carcinoma and other solid tumors.

Meihan Li[1], Fu Li[2], Qiuru Che[1], Xiaojing Huang[2], Dongxia Chu[1], Qiyang Zhang[1], Nan Li[2], Qingjuan Ma[2], Weiming He[2], Wenqiang Zhai[2], Yihui Lin[2], Xiaozhen Wang[2], Fanglong Yang[2], Siqing Wang[2], Lei Jin[2], John L. Xu[2]

[1]Changchun GeneScience Pharmaceutical Co., Ltd., Changchun, China,[2]Changchun GeneScience Pharmaceutical Co., Ltd., Shanghai, China

Background: Nectin-4 and Trop-2 are transmembrane proteins commonly co-overexpressed in various solid tumors and associated with tumor progression. ADCs targeting Nectin-4 or Trop-2 have shown promising therapeutic potential in urothelial carcinoma (UC), non-small cell lung cancer (NSCLC), and triple-negative breast cancer (TNBC). Notably, the combination of Padcev™ (a Nectin-4-directed ADC; also referred to as EV) and Trodelvy™ (a Trop-2-directed ADC; also referred to as SG) as second-line therapy for metastatic UC has demonstrated significantly improved efficacy, with the overall response rate (ORR) reaching 70%. However, the safety profile of this combination remains to be a concern, with ≥Grade 3 treatment-emergent adverse events (TEAEs) occurring in 78% of patients. To maintain clinical efficacy while minimizing toxicity, we developed GS24-B057, a dual Nectin-4- and Trop-2-targeting ADC with a drug-to-antibody ratio (DAR) of 6, integrating an optimally engineered bispecific antibody, a tailored topoisomerase I inhibitor payload, and site-specific conjugation.

Materials and Methods: The *in vitro* tumor cell binding activity of GS24-B057 was assessed by flow cytometry. For internalization analysis, Nectin-4- and Trop-2-expressing cells were incubated with pHrodo-conjugated ADC, followed by fluorescence intensity quantification. Cytotoxicity and bystander killing effect were assessed in a Cell Titer-Glo assay and in a luciferase assay, respectively. The *in vivo* anti-tumor efficacy of GS24-B057 was systematically examined in mouse models bearing human cancer cell line-derived xenografts (CDX) and patient-derived xenografts (PDX). Pharmacokinetics was studied in cynomolgus monkeys.

Results: In preclinical studies, GS24-B057 exhibited significantly stronger *in vitro* cell binding and internalization than the EV and SG combination, as well as robust direct cytotoxicity and bystander killing effect in tumor cell lines. GS24-B057 demonstrated potent anti-tumor activity across multiple CDX and PDX models of human cancer, including UC, TNBC, and NSCLC, with superior efficacy *versus* EV, SG, and SKB264 as single agent, and comparable efficacy to the EV and SG combination but at a lower dose level and administration frequency. Furthermore, GS24-B057 featured a favorable pharmacokinetic profile in cynomolgus monkeys.

Conclusion: These data suggest the potential of GS24-B057 as an effective therapeutic option for patients with UC and other solid tumors and support its further evaluation in IND-enabling studies.

#5648 Preclinical efficacy and safety of KIVU-305, a novel CEACAM5-targeting antibody-drug conjugate (ADC) for colorectal cancer (CRC).

Ann MacLaren, Natasja N. Viller, Tessie Ng, Liangyi Zhang, Xiaoyue Jiang, Mohit Trikha

Kivu Bioscience, San Mateo, CA

CEACAM5 (carcinoembryonic antigen-related cell adhesion molecule 5) is a cell-surface glycoprotein highly expressed in CRC, pancreatic ductal adenocarcinoma (PDAC), gastric cancer and non-small cell lung cancer (NSCLC), with minimal expression in normal adult tissues. Elevated CEACAM5 correlates with tumor burden and poor prognosis, making it an attractive ADC target. The first-generation CEACAM5 ADC labetuzumab govitecan demonstrated clinical feasibility but with limited efficacy at tolerable doses, highlighting the opportunity for an improved ADC with more stable linker payload to provide superior clinical benefit.KIVU-305 is a CEACAM5-targeting ADC composed of a humanized monoclonal antibody conjugated to SYNtecan E™ via the GlycoConnect®/ Hydraspace® (GC/HS) site-specific conjugation technology, delivering an exatecan-based topoisomerase I inhibitor payload at an average drug-to-antibody ratio (DAR) of 4. GlycoConnect® leverages the native Fc glycan for site-specific conjugation, while HydraSpace® introduces a hydrophilic spacer to reduce aggregation and systemic payload release, resulting in an ADC with improved manufacturability, plasma stability and pharmacokinetic profile to provide a superior therapeutic index. Upon binding CEACAM5, KIVU-305 undergoes efficient internalization and exatecan release to inhibit DNA topoisomerase I, causing DNA damage, cell cycle arrest and apoptosis. Notably, exatecan is more potent than deruxtecan and is a poor substrate for P-glycoprotein (P-gp), which may help overcome common drug resistance mechanisms in patients.In vitro, KIVU-305 demonstrated potent, target-specific cytotoxicity in vitro at low nanomolar concentrations and robust bystander activity resulting in killing of adjacent CEACAM5-negative cells. In vivo, KIVU-305 induced sustained tumor regressions in multiple CEACAM5-positive CRC and PDAC xenograft models, including models resistant to irinotecan. KIVU-305 exhibited high stability in human and cynomolgus plasma with no measurable DAR loss and minimal free payload release over 21 days. Pharmacokinetic studies in cynomolgus monkeys confirmed linker stability with high intact ADC and minimal systemic payload exposure. Tolerability studies in cynomolgus monkeys demonstrated that KIVU-305 was well tolerated with only mild reversible toxicities consistent with the expected profile of a topoisomerase I inhibitor payload. No on-target toxicities were identified, consistent with historical CEACAM5 ADC experience.Collectively, these data support KIVU-305 as a promising CEACAM5-directed ADC with a favorable safety profile that may provide an improved therapeutic index. A Phase I clinical trial in patients with advanced solid tumors is planned for 2026.

#5649 KIVU-107: A clinical-stage, best-in-class PTK7 antibody-drug conjugate (ADC) with favorable PK and an improved tolerability profile.

Natasja N. Viller, Liangyi Zhang, Xiaoyue Jiang, Ann MacLaren, Mohit Trikha

Kivu Bioscience, San Mateo, CA

PTK7 (protein tyrosine kinase 7) is a catalytically inactive receptor tyrosine kinase associated with tumor-initiating cells and overexpressed in multiple solid tumors, including ovarian, endometrial, lung, breast and gastric cancers. Overexpression of PTK7 is associated with poor prognosis, further exemplifying its pivotal role in carcinogenesis. PTK7 has previously been validated as an ADC target but development of first-generation PTK7 ADCs was limited by payload mediated toxicity, suggesting that an ADC with improved linker payload could improve clinical benefit. KIVU-107 is an antibody-drug conjugate (ADC) composed of a humanized IgG1 monoclonal antibody targeting protein tyrosine kinase 7 (PTK7), conjugated to the SYNtecan E™ linker-payload via the GlycoConnect®/ Hydraspace® (GC/HS) site-specific conjugation technology with a drug-to-antibody ratio (DAR) of 4. The GC/HS platform abolishes Fcγ receptor-mediated effector activity and utilizes a highly polar spacer to reduce hydrophobicity and aggregation, resulting in an exatecan ADC with improved stability to provide a superior pharmacokinetic and safety profile to expand the therapeutic index.KIVU-107 demonstrated rapid internalization and robust target-specific cytotoxicity across high and low-expressing tumor cell lines. The cleavable linker and cell permeable hydrophilic payload conferred potent bystander killing in PTK7-negative cells co-cultured with PTK7-positive cells, addressing tumor heterogeneity. In vivo, a single dose induced complete regression in multiple xenograft models, including patient-derived xenografts (PDXs) resistant to platinum-based chemotherapy and ADCs such as mirvetuximab soravtansine and datopotamab deruxtecan. KIVU-107 also exhibited enhanced efficacy and improved survival when combined with PARP inhibition, standard-of-care in ovarian, breast and prostate cancers, supporting combination strategies. KIVU-107 was highly stable in vitro, with no measurable DAR loss and minimal free payload release over 21 days in human or cynomolgus plasma. Nonclinical pharmacokinetic and safety evaluations in cynomolgus monkeys confirmed the stability of KIVU-107 with high exposure of intact ADC and minimal unconjugated payload levels and demonstrated favorable tolerability, with a highest non-severely toxic dose (HNSTD) of 60 mg/kg. Hematologic effects were mild, transient and reversible, consistent with the expected profile of a topoisomerase I inhibitor payload.Collectively, these data highlight KIVU-107 as a highly stable, next generation DAR4 exatecan ADC with potent anti-tumor activity, bystander effect and broad therapeutic potential. A Phase I clinical trial in patients with advanced solid tumors is ongoing (NCT07229313).

#5650 Preclinical development of LUA006: A bispecific EGFR/B7-H3 ADC with dual payloads to address tumor heterogeneity and resistance.

Shaojuan Zhao[1], **Ling Zhang**[1], Ying Huang[1], Qian Dong[1], Xiaofan Gu[1], Guoshun Tian[1], Xiaoman Li[1], Fanrui Meng[1], Wei Zheng[1], Xiaoshuang Yan[1], Xinmei Wang[2], Yazhi Yuan[2], Shuyong Zhao[2], Ken Qin[1], Yang Yang[1], Hua Ying[1], Weikang Tao[1]

[1]Shanghai QiLu Pharmaceutical Research and Development Center LTD., Shanghai, China,[2]QiLu Pharmaceutical Co., Jinan, China

Background: While antibody-drug conjugates (ADCs) have emerged as a transformative therapeutic class, their clinical utility is largely limited by either on-target, off-tumor toxicities or acquired drug resistance. EGFR and B7-H3 are clinically validated targets that are frequently co-expressed in a range of solid tumors including non-small cell lung cancer (NSCLC), especially lung squamous cell carcinoma (LUSC), esophageal squamous cell carcinoma (ESCC), and Head and neck squamous cell carcinoma (HNSCC), while exhibit rare co-expression in normal tissues. It has been revealed that both heterogeneous expression of a single target and acquired resistance to a single payload often compromise the efficacy of monospecific ADCs containing a single payload. To address these challenges, we generated LUA006, a bispecific ADC targeting both EGFR and B7-H3 with attenuated EGFR binding to reduce on-target, off-tumor toxicity and enhanced B7-H3 binding and internalization dynamics to improve anti-tumor efficacy, particularly in tumors with heterogeneous expression of a single target. Additionally, LUA006 incorporates two distinct payload classes, to achieve deep response and overcome payload-associated resistance.
Methods: A bispecific anti-EGFR/B7-H3 IgG was site-specifically conjugated to two payloads with complimentary mechanism of actions and well optimized DAR values. Meanwhile, the linkers for each payload were screened to enable sequential payload release. LUA006 demonstrated high DAR homogeneity and stability *in vitro*.
Results: LUA006 demonstrated superior internalization efficiency versus parental antibodies, indicating synergistic targeting. It achieved nanomolar-level cytotoxicity against diverse cancer cell lines with variable EGFR/B7-H3 expression, while showing minimal toxicity to normal human epidermal keratinocytes, resulting in a broader therapeutic window than clinical stage EGFR monospecific ADCs *in vitro*. *In vivo*, a single dose of LUA006 induced profound, durable tumor regression in cell-derived xenograft (CDX) models, surpassing combinations of mono-payload ADCs and monospecific ADCs. Critically, LUA006 maintained efficacy in CDX models with intrinsic low sensitivity to each payload used by LUA006 and in models overexpressing drug efflux pumps, demonstrating robust activity against diverse resistance mechanisms.
Conclusion: LUA006 is a novel bispecific ADC with dual payloads that may enhance efficacy in tumors with heterogeneous expression of a single target or with resistance toward either of dual payloads. Its potent efficacy, reduced toxicity profile and activity in resistant models support further development as a promising therapy for EGFR/B7-H3-expressing solid tumors.

#5651 Preclinical development of LUA005: A differentiated bivalent EGFR/cMET bispecific ADC displays strong anti-cancer efficacy and a wider therapeutic window.

Lei Han[1], Ken Qin[1], Ying huang[1], Xi Xiao[1], Zhebin Zhang[1], Wei Wang[1], Wei Zheng[1], Hai Wu[1], Xiaoshuang Yan[1], Dongdong Wu[1], Shuyong Zhao[2], **Ling Zhang**[1], Yang Yang[1], Hua Ying[1], Weikang Tao[1]

[1]Shanghai Qilu Pharmaceutical Research and Development Center LTD., Shanghai, China,[2]Qilu Pharmaceutical Co., Ltd., Jinan, China

Background Compensatory functions between EGFR- and cMET-mediated signaling contribute to resistance to either EGFR- or cMet-targeting agents such as osimertinib. The frequent co-expression of these two targets in solid tumors supports dual targeting strategy, evidenced by the approved bispecific antibody amivantamab. Several EGFR-cMET antibody-drug conjugates (ADCs) have entered clinical trials. While most bispecific ADCs targeting EGFR and cMET use a 1+1 format, we designed and generated LUA005 with bivalent arms for each target. It exhibits low affinity but high avidity to EGFR, coupled with high-affinity to cMET. This design aims to minimize on-target off-tumor toxicity while ensuring robust efficacy across heterogeneous tumors, including those with low EGFR expression. Here, we report the preclinical characterizations of LUA005 as an EGFR/c-Met bispecific ADC with differentiated properties. **Methods** LUA005 was built on the QILU's proprietary novel topoisomerase-1 inhibitor platform, conjugated via a hydrophilic cleavable linker to yield a uniform DAR 8 product. The payload displayed nanomolar activity across various cancer cell lines and much faster systematic clearance than Dxd *in vitro*, to reduce systematic toxicity. Benchmark ADCs were included for comparison. **Results** *In vitro*, LUA005 exhibited strong cytotoxicity against tumor cell lines but minimal killing of normal keratinocytes, indicating a wider therapeutic window than benchmarks. Meanwhile, LUA005 demonstrated superior antitumor activity compared to benchmarks across a spectrum of CDX models with different EGFR and cMET expression levels, highlighting its potential to address tumor heterogeneity. LUA005 also demonstrated remarkable efficacy in a series of patient-derived xenograft (PDX) models, including those resistant to osimertinib, cetuximab, or immunotherapy. Meanwhile, LUA005 was well tolerated in Cyno monkeys, with HNSTD up to 60 mpk Q3W for three times repeated dosing in NHP toxicity study, without obvious on-target toxicity or ILD, consistent with our molecule design. LUA005 demonstrated favorable PK profile in cyno monkeys, with high stability and limited free drug release in circulation. **Conclusions** LUA005, an EGFR/cMET bispecific ADC with differentiated molecular design, demonstrated superior antitumor efficacy with enhanced therapeutic index. Preclinical studies warranted its further development into clinical trials, which are anticipated to start in early 2026.

#5652 Preclinical development of LUA011, a novel CDH17/cMET bispecific ADC with enhanced antitumor efficacy and mitigated gastrointestinal toxicity.

Guoyin Huang[1], Ken Qin[1], Man Wu[1], Lei Han[1], Ying Huang[1], Wei Zheng[1], Xiaoshuang Yan[1], luchan deng[1], Hai Wu[1], Wenshu Huang[2], Shuyong Zhao[2], **Ling Zhang**[1], Yang Yang[1], Hua Ying[1], Weikang Tao[1]

[1]Shanghai Qilu Pharmaceutical Research and Development Center LTD.,, shanghai, China,[2]Qilu Pharmaceutical Co., Ltd.,, Jinan, China

Background: CDH17 is an emerging ADC target in gastrointestinal (GI) cancers due to its overexpression in colorectal, gastric and pancreatic tumors. However, CDH17-directed ADCs suffer on-target GI toxicities. cMET is a clinically validated target in GI malignancies with limited expression in some normal tissues. Expression profiling shows that CDH17 and cMET are frequently co-expressed in GI tumors, while seldomly co-expressed in normal tissues. Therefore, targeting both CDH17 and c-Met might improve therapeutic index and maintain or even enhance efficacy. Here we report the preclinical development of LUA011, a bispecific ADC targeting both CDH17 and cMET, with a proprietary TOPO1i payload conjugated to the antibody via a glycan-based platform.
Results: LUA011 was selected from a panel of bispecific ADC formats based on a comprehensive evaluation of pharmacokinetic properties, *in vivo* efficacy, and overall developability. Both LUA011 and its unconjugated bispecific antibody moiety exhibited strong binding to CDH17-positive and cMET-positive GI cancer cell lines, with EC50 values in the nanomolar range. Rapid internalization of the antibody component was observed in multiple GI cancer cell lines expressing CDH17 and/or cMET. *In vitro*, LUA011 demonstrated potent and specific cytotoxicity against cell lines positive for CDH17, cMET, or both targets, with enhanced activity compared to CDH17 mono-specific ADCs in CDH17 and cMet dual-positive cell lines. LUA011 demonstrated significantly superior antitumor efficacy over CDH17- and cMET-targeting monospecific ADCs across multiple gastrointestinal CDX and PDX models with varying target expression levels. This enhanced activity was consistently observed even when compared to its own CDH17-parental ADC and a benchmark CDH17-specific ADC conjugated with the same linker-payload, underscoring that the therapeutic advantage stems from the bispecific format and the synergistic effect of dual targeting CDH17 and cMET. LUA011 exhibited high stability in human and cynomolgus monkey plasma, with minimal payload release and maintained DAR. In cynomolgus monkeys, LUA011 displayed favorable pharmacokinetics and a promising safety profile, with a maximum tolerated dose exceeding 30 mg/kg.
Conclusions: LUA011 is a novel bispecific ADC targeting both CDH17 and c-Met with favorable physicochemical properties, strong target binding, cellular internalization and potent antitumor activity in preclinical GI cancer models. Its dual targeting activity, along with its optimized payload, conjugation method, and DAR value, contribute to its strong anti-tumor efficacy, improved therapeutic index, and reduced GI toxicities. Further investigation is warranted to advance this promising ADC into clinical development.

#5653 Preclinical characterization of LUA004, a novel 5T4-targeting ADC with improved therapeutic window.

Jinpeng Pei[1], Shaojuan Zhao[1], Ying Huang[1], Junfei Wang[1], Wei Zheng[1], Hai Wu[1], Jie Chen[1], Ke Li[2], Xinmei Wang[2], Shuyong Zhao[2], **Ling Zhang**[1], Yang Yang[1], Daqing Sun[1], Hua Ying[1], Weikang Tao[1]

[1]Shanghai Qilu Pharmaceutical Research and Development Center LTD, Shanghai, China, [2]Qilu Pharmaceutical Co., Ltd., Jinan, China

Background: Trophoblast glycoprotein (5T4), an oncofetal protein, is a member of the leucine-rich repeat family of proteins that is associated with intercellular connectivity, cell morphology and movement, and altering cell adhesion in embryonic development and cell differentiation. 5T4 is upregulated in several cancers, including esophageal, head-and-neck, and lung cancers, especially the squamous subtype, with low or absent expression in adult normal tissues. The high expression of 5T4 was notably correlated with poor survival in different cancer types, which makes it an attractive ADC target. The therapeutic potential of 5T4 as ADC modality was recently unraveled by several ADCs with preliminary clinical efficacy reported. In this study, we present the development of a novel 5T4-targeting ADC with Qilu's proprietary microtubule inhibitor as payload, LUA004, which exhibited excellent efficacy and expanded therapeutic window than vedotin ADC.

Method: LUA004 utilizes a novel microtubule inhibitor payload QLS8152 with a proprietary cleavable linker to achieve a homogeneous product with a drug-to-antibody ratio (DAR) of 8 through site-specific conjugation. The payload QLS8152 showed sub-nanomolar activity across a wide range of cancer cell lines *in vitro* and rapid systematic clearance in rodent models. Our next generation microtubule inhibitor platform QLS8153 demonstrated significantly improved therapeutic window than vedotin technology.

Result: LUA004 showed sub-nanomolar binding affinity and dose-dependent internalization in multiple tumor cell lines with different 5T4 expression levels. LUA004 showed strong (nM range IC_{50}) and comparable *in vitro* cytotoxicity to vedotin-ADC against a variety of 5T4-positive cancer cell lines. Meanwhile, LUA004 showed robust and dose-dependent tumor inhibition in different cell-derived xenograft (CDX) as well as patient-derived xenograft (PDX) models with various 5T4 expression, with comparable tumor inhibition as vedotin-ADC. Moreover, compared to vedotin-ADC, LUA004 exhibits more favorable plasma stability, preclinical pharmacokinetic, and toxicity profiles. LUA004 was well tolerated in cyno monkeys, with HNSTD up to 20 mpk Q3W x 4 in non-GLP toxicity study, indicating a tremendous increase in the therapeutic index compared to vedotin-ADC.

Conclusion: LUA004 represents a novel 5T4-targeting ADC with favorable anti-tumor activity and superior tolerability, which can address the high unmet needs in patients with cancers expressing variable levels of 5T4. The promising preclinical profiles of LUA004 warrant its further development into clinical trials.

#5654 Novel ALDC and ADC with TMEAlinker and eribulin payload demonstrate excellent safety and efficacy in preclinical evaluation.

Tao Chen, Cheng Liu, **Yuan Liu**

Affinity Biopharmaceutical Co., Ltd., Shanghai, China

Overexpression of extracellular legumain in the tumor microenvironment (TME) plays a critical role in tumor invasion and metastasis. TMEAlinkers (TME-activated linkers) are legumain-activated linkers with clinical proof-of-concept (POC) from the phase 3 study of legubicin (an albumin drug conjugate, ALDC). Leveraging this TMEAlinker platform, eribulin can be conjugated to albumin or antibodies via TMEAlinker to generate novel ALDCs and ADCs.

QHL-1848 is a TMEAlinker-based ALDC carrying eribulin as payload. In both in vitro and in vivo studies, QHL-1848 exhibited markedly improved safety data compared with the free payload. In human plasma at 37 °C, only ~0.5% of free eribulin was released after 7 days of incubation, indicating high plasma stability. The maximum tolerated dose (MTD) of QHL-1848 was 0.491 μmol/kg (QWx4) in dogs, displaying a significantly superior safety profile relative to eribulin (MTD = 0.054 μmol/kg, QWx3 in dogs). In murine HT1080 xenograft models, QHL-1848 achieved complete tumor regression of large (750 mm^3) tumors with a dosing regimen of 1 μmol/kg given 3 times.

IMD2128, a bispecific ADC targeting EGFR/c-Met, is conjugated with eribulin via TMEAlinker at a drug-to-antibody ratio (DAR) of 2. IMD2128 demonstrated potent curative antitumor activities across multiple xenograft models, including lung and pancreatic carcinomas, achieving complete tumor elimination with a single dose of 3.75 mg/kg. Remarkably, IMD2128 retained efficacy in models resistant to DXd-based ADCs. In cynomolgus monkeys, IMD2128 was well tolerated with a highest nonseverely toxic dose (HNSTD) over 16 mg/kg, showing a superior safety profile compared to VC linker-eribulin based ADCs (e.g., MORAb-202, HNSTD = 1.95 mg/kg). Pharmacokinetic studies in monkeys revealed a Cmax of 291.07 μmol/mL for IMD2128 ADC versus a Cmax of 0.0000823 μmol/mL for free eribulin (Cmax ratio ≈ 3.54×10^6 : 1), confirming strong linker stability in circulation. Together, these findings highlight the versatility of the TMEAlinker platform for developing both ALDCs and ADCs with eribulin payloads, demonstrating excellent safety and efficacy in preclinical evaluations.

#5655 YL252: A dual-functional PD-L1/VEGF-targeting ADC integrating immunotherapy, anti-angiogenesis, and cytotoxicity.

Wei Lian, Xinzhen Shi, Qing Zong, Hanwen Deng, Chun Deng, Tao Wang, Fang Xu, Shuaikun Wang, Tongtong Xue, Jiaqiang Cai

MediLink Therapeutics (Suzhou) Co., Ltd., Suzhou, China

The clinical success of combining immune checkpoint inhibitors with antibody-drug conjugates (ADCs), as well as the well-established synergy among immunotherapy, anti-angiogenic therapy, and chemotherapy, supports the development of multi-mechanistic therapeutic strategies. Based on this rationale, we developed YL252, a dual-functional ADC designed to simultaneously target PD-L1 and VEGF while enabling controlled payload release within the tumor microenvironment. YL252 is derived from Tumor Microenvironment-Activable Linker platform, incorporating a proprietary protease-cleavable tripeptide linker and a novel DNA topoisomerase I inhibitor payload. YL252 binds PD-L1 to modulate immune suppression, while also sequestering soluble VEGF, thereby exerting anti-angiogenic effects. The engineered drug-to-antibody ratio (DAR) is optimized to align with clinically relevant exposures of anti-PD-L1 and anti-VEGF monoclonal antibodies. We conducted a comprehensive nonclinical evaluation of YL252, including assessments of physicochemical properties, antitumor efficacy, pharmacokinetics, and safety. YL252 showed efficient internalization, potent cytotoxicity, and strong bystander effects in PD-L1-expressing tumor cells. In xenograft models, YL252 produced dose-dependent tumor growth inhibition, including complete regressions, without detectable toxicity. Mechanistic studies confirmed that YL252 effectively blocked PD-L1 signaling, consistent with immune activation alongside cytotoxic and antiangiogenic activity. Pharmacokinetic studies in cynomolgus monkeys demonstrated high systemic stability, as shown by overlapping total antibody and conjugated ADC profiles. Repeat-dose toxicology studies established a favorable safety profile, with a therapeutic index of approximately 100 and no drug-related adverse findings in major organs, including lung, liver, and kidney. In summary, YL252 is the first reported ADC that concurrently blocks PD-L1, inhibits VEGF-driven angiogenesis, and releases a cytotoxic payload in the tumor microenvironment, representing a single-agent approach that integrates immunotherapy, anti-angiogenic therapy, and chemotherapy mechanisms.

#5656 Characterization and translational development of novel pre|CISION® technology compounds delivering complementary dual payloads to the tumor microenvironment following FAP cleavage.

Victoria Juskaite[1], Tom Clough[1], Ellen Watts[1], Iva Zlatareva[1], Folake Orafidiya[1], Hanna Buist[1], Alexa Kennedy[1], Jannah Jeon[1], Greg Billenness[1], Douglas Sammon[1], Sophie Brown[1], Curtis Rink[1], Ruairidh Edwards[2], Vidicha Chunilal[1], Manuel Pinto[1], Dave Liebowitz[2], Francis Wilson[1], Michelle Morrow[1], **David Jones**[1]

[1]Discovery, Avacta Therapeutics, London, United Kingdom,[2]Clinical Development, Avacta Therapeutics, London, United Kingdom

The proprietary pre|CISION® technology incorporates a peptidic substrate that is specifically cleaved by Fibroblast Activation Protein α (FAP). FAP is a post-proline protease that is overexpressed on the surface of cancer associated fibroblasts (CAFs) in many solid tumors, and facilitates delivery of pre|CISION® medicines specifically to the tumor microenvironment (TME). AVA6103 is a pre|CISION®-enabled exatecan candidate in clinical development. AVA6103 consists of exatecan, a potent Topoisomerase I (TOP1) inhibitor, covalently linked to a dipeptide containing a cleaving sequence (D-Ala-L-Pro), which is susceptible to hydrolysis by FAP but is resistant to hydrolysis by other mammalian proteases. The exquisite selectivity of the pre|CISION® substrate for FAP results in release of exatecan payload in the TME, greatly increasing the therapeutic window and hence reducing systemic exposure and associated toxicities. Drug combinations are commonly used in cancer therapy to improve outcomes and overcome resistance, therefore we engineered two complimentary payloads into a single pre|CISION® molecule. This may offer similar benefits whilst minimizing systemic toxicity. To create dual payload pre|CISION® Peptide-Drug Conjugates (PDCs), a series of compounds have been engineered with modifications in the capping-group and linker portions. Using structure-based drug design, clear structure-activity relationships have been established for affinity to, and susceptibility of linker cleavage by FAP and subsequent payload release. We now demonstrate how the use of the pre|CISION® technology platform has been widened to selectively control the release of multiple payloads from a single molecule via a FAP cleavable linker. This includes TOP1 inhibitors and DNA damage response inhibitors as the dual payloads. Selective payload release has been demonstrated in kinetic studies showing the ability to tune the rate of payload release and in cellular studies showing potent cytotoxicity and bystander activity in cell-based assays including tumor cell-fibroblast 3D co-culture models. Synergistic activity of two potentiating payloads and downstream pharmacodynamic markers for each payload have also been evaluated in cancer cell-lines with specific gene expression profiles. This has provided translational evidence for potential biomarkers and clinical indications. Delivery of payloads to mouse tumors in vivo has also been confirmed. We show the potential of the technology to deliver a therapeutically relevant combination of payloads specifically to the TME while reducing systemic dose-limiting toxicities. This broadens the utility of the pre|CISION® platform in the delivery of novel medicines.

#5657 A novel bispecific ADC to treat solid tumors by removing immunosuppression in the tumor microenvironment.

Shiva Bhowmik[1], William Brady[2]

[1]Purdue University, West Lafayette, CA,[2]University of Washington, Seattle, WA

TNBC remains one of the most aggressive breast cancers, with limited success from current antibody and immuno-oncology regimens, largely due to the persistence of myeloid-derived suppressor cells (MDSCs) in the tumor microenvironment. We developed a novel dual-action bispecific antibody drug conjugate (ADC), TRIO-525, a first-in-class Tumor Immunogenicity Enhancing Antibody Conjugate (TIE-ADC) designed for tumor-selective, dual-targeted elimination of both cancer cells (via TROP2) and MDSCs (via CD33).Mechanistically, TRIO-525 utilizes a unique antibody format engineered for higher affinity to TROP2 and, tumor-selective engagement of CD33, enabling selective depletion of immunosuppressive MDSCs within the tumor while sparing hematopoietic and other immune cells. Preclinical studies confirmed TRIO-525's receptor-mediated cytotoxicity. It demonstrated superior potency and specificity compared to existing therapies, with effective and selective killing of both TNBC cells and MDSCs at nanomolar concentrations, restoration of T cell proliferation, and full preservation of healthy immune cells. TRIO-525 induces robust, dose-dependent tumor regression in xenograft models without any toxicity or off-target effects. TRIO-525 also displays exceptional plasma stability with no degradation species.These findings establish TRIO-525 as a ground-breaking solution to generate immunogenic tumors, directly overcoming TME-driven immunosuppression—an unmet need in TNBC and solid tumor therapy. The development of TIE-ADC drugs, as exemplified by TRIO-525, signals a paradigm shift in cancer immunotherapy through simultaneous, tumor-selective eradication of malignant and immunosuppressive cells, with broad implications for overcoming therapeutic resistance and improving patient outcomes.

#5659 Unveiling the PanCancer potential of dual-targeting uPAR-directed ADCs across cancers.

Virginia Metrangolo[1], Lars Henning Engelholm[1], Henrik Jessen Jurgensen[1], Sine Rosendal Syversen[1], Michaela Hansen Blomquist[2]

[1]PanTarg ApS, Copenhagen, Denmark,[2]The Finsen Laboratory/Biotech Research & Innovation Centre (BRIC), Copenhagen, Denmark

Antibody-drug conjugates (ADCs) are revolutionizing cancer therapy; yet, their impact in solid tumors remains limited, partly because most approved ADCs primarily target tumor-associated antigens on malignant cells. This tumor-centric approach is often insufficient in highly desmoplastic cancers such as pancreatic ductal adenocarcinoma (PDAC), where the dense, immunosuppressive stroma promotes tumor progression, restricts drug penetration, and contributes to therapeutic resistance. Targeting both malignant and stromal compartments is therefore a critical unmet need to enhance ADCs' efficacy in these refractory tumors. To address this gap, PanTarg is advancing a novel ADC that targets both the cancer and the surrounding stromal compartment. The ADC specifically targets the urokinase plasminogen activator receptor (uPAR), which is broadly overexpressed across tumor and stromal populations in aggressive cancers, particularly PDAC, while minimally expressed in normal tissues. This dual-targeting strategy aims to overcome stromal barriers and support a broader, potentially Pan-Cancer therapeutic approach. PanTarg's ADC leverages a proprietary uPAR antibody with optimal biophysical and ADC properties. In preclinical models of PDAC and other uPAR-positive tumors, PanTarg ADCs demonstrated potent anti-tumor activity across multiple payload classes. Mechanistic studies revealed stromal targeting, bystander killing of uPAR-negative cancer cells, and immune-modulatory effects promoting a more permissive tumor microenvironment. Moreover, the ADCs showed favorable tolerability consistent with uPAR's restricted expression profile. Overall, these findings validate uPAR as a clinically relevant dual-compartment ADC target and position PanTarg as a promising next-generation therapeutic candidate for PDAC and, more broadly, aggressive uPAR-positive cancers.

: Cell Death Pathways and Treatment
Poster Session

#5663 Chemotherapy-induced galectin-1 derives drug-tolerant persister state associated EMT in triple negative breast cancer with targetable vulnerability to ferroptosis inducers.

Shagufa A. Ehtesham Shaikh[1], Kedar Sharma[1], Dipti Bhattacharya[2], Vaibhav Kothari[2], Samruddhi Jadhav[2], Nandini Verma[1]

[1]Tata Memorial Centre-Advanced Centre for Treatment, Research and Education in Cancer (TMC-ACTREC) and HBNI, Mumbai, India,[2]Tata Memorial Centre-Advanced Centre for Treatment, Research and Education in Cancer (TMC-ACTREC), Mumbai, India

Triple-Negative Breast Cancer (TNBC) is the most aggressive and difficult-to-treat disease with high mortality rates. Therapeutic challenges are largely due to limited treatment options, disease heterogeneity, drug resistance, and metastasis to vital organs. Clinical studies established that non-genetic alterations derive chemoresistance and metastasis in TNBC. however, experimental studies investigating residual disease and metastatic recurrence in TNBC are limited. We derived subtype-specific TNBC Drug-Tolerant Persister (DTP) cellular models using taxol and platinum drugs and longitudinally characterized parental, mitotically quiescent and proliferating DTP cellular states to study the molecular basis of post-treatment aggressiveness. We observed that therapeutic agents induced autophagy and dysregulation of ferroptosis regulators including GPX4 and FSP1, irrespective of subtype and EMT largely in basal and luminal androgen receptor-positive TNBC cells. Since these phenotypes are known to be regulated by both intra- and extra-cellular signaling factors we profiled for differentially expressed soluble intracellular and secretome proteome in TNBC DTP cells using label-free quantitative mass spectrometry. Interestingly, we found that soluble factors IGFBP6, SERPINE1 and LGALS1 were among the most upregulated proteins in extracellular protein fractions of DTP cells, LGALS1 was also found significantly high in the cellular fraction. Integrative in-silico analysis of survival and expression data of TNBC patients under treatment accentuated that LGALS1 (Galectin-1) has strong clinical association with adverse prognosis and co-expression with EMT and ferroptosis-related genes. Further, conditioned medium experiment revealed that secretome from proliferating TNBC DTPs was capable of conferring multiple aggressive phenotypes including EMT, migration, invasion, proliferation, antioxidant pathway deregulation, autophagy in parental TNBC cells. These changes were collaborated with an increased activation of pSTAT3, pSrc and MAP kinase signaling pathways. Moreover, genetic and pharmacological targeting of Galectin-1 in TNBC DTP cells significantly attenuation proliferation, EMT, migration and invasion properties, with an increased susceptibility to ferroptosis inducers. Further, Galectin-1 knockdown resulted in downregulation of GPX-4 and FSP-1 in a NRF2-dependent manner, highlighting the therapeutic potential of targeting Galectin-1 in controlling EMT and inducing ferroptotic cell death. Most importantly, considering that tumor-secreted Galectin-1 can be detected in the blood it may serve as a theranostic biomarker for therapy resistance and poor prognosis as well as potential therapeutic target for overcoming chemo-tolerance and metastasis in TNBC patients.

#5664 Targeting cholangiocarcinoma with ferroptosis-inducing siRNA-based nanotherapeutics.

Peyton Classon[1], Danielle Marie Carlson[2], Jayla Millender[1], Irene Yan[3], Sumera Ilyas[1], Rory L. Smoot[4], TUSHAR PATEL[3], Gregory J. Gores[5], Davide Povero[1]

[1]Mayo Clinic, Rochester, MN,[2]Mayo Clinic Hospital-Rochester, Rochester, MN,[3]Mayo Clinic, Jacksonville, FL,[4]Surgery, Mayo Clinic, Rochester, MN,[5]Professor of Medicine, Mayo Clinic, Rochester, MN

Background: Cholangiocarcinoma (CCA) is a highly lethal epithelial cell malignancy of the hepatic biliary tract. Efficacy of current standard-of-care therapy is limited. Ferroptosis, an iron-catalyzed, caspase-independent cell death driven by phospholipid peroxidation, has emerged as a novel therapeutic target. Our goal is to develop a tumor-selective therapeutic approach targeting ferroptosis in CCA using siRNA-based nanotherapeutics.

Materials & Methods: Milk-derived nanovesicles (lactosomes) coated with EpCAM aptamer and packaged with siRNA against Glutathione Peroxidase 4 (siGPX4-lactosomes) and Ferroptosis Suppressor Protein 1 (siFSP1-lactosomes), were used to induce ferroptosis in murine CCA cells (FAC) and in syngeneic liver orthotopic CCA-bearing mice. *In vitro*, lactosome uptake and efficacy were assessed by fluorescence-based, cell-viability and molecular biology assays. *In vivo*, target engagement, tissue distribution, safety and efficacy were assessed.

Results: EpCAM (epithelial cell adhesion molecule expressed on CCA cells)-coated lactosomes showed robust uptake by FAC cells in a EpCAM-dependent manner. EpCAM knockdown via siRNA reduced lactosome uptake, confirming aptamer selectivity. Dose-dependent siGPX4/siFSP1-lactosome treatment led to GPX4/FSP1 knockdown and induced ferroptotic cell death in up to 60% of FAC cells after 72 hours ($p<0.001$ vs. siNC). In CCA-bearing mice, intravenous administration of siRNA lactosomes was well-tolerated with no liver or systemic toxicity observed and demonstrated robust tumor distribution compared to non-tumorous tissues. Efficacy studies demonstrated that siGPX4/siFSP1-lactosomes significantly reduced intratumor *Gpx4* and *FSP1* mRNA expression by 40-60% and induced significant upregulation of ferroptosis markers *Ptgs2* and *Acsl4* ($p<0.01$ vs. siNC). Ferroptosis in siRNA-lactosome treated tumors was confirmed by immunohistochemistry for phospholipid peroxidation markers oxPAPC and 4-HNE. Additionally, proliferation marker Ki67 was significantly downregulated in siGPX4/siFSP1-lactosome treated tumors ($p<0.05$ vs. siNC), indicating ferroptosis-mediated tumor suppression. Importantly, siGPX4/siFSP1-lactosomes reduced tumor burden and expression of CCA markers CK19/7 in treated mice, as compared to control mice.

Conclusions: siRNA-based nanotherapeutics targeting CCA can effectively and safely induce ferroptosis *in vitro* and *in vivo*, representing a potential therapeutic strategy for CCA treatment.

#5665 Levistolide A inhibits bladder cancer progression by suppressing GPX4 expression and activating ferroptosis.

Yixi Gong, Jihye Kim, Ingyu Lee, Xiaoyu Guo, Bomi Han, Eui Man Jeong

Jeju National University, Jeju Special Self-Governing Province, Korea, Republic of

Bladder cancer is the second most common malignant tumor of the urinary system worldwide, with high incidence and mortality rates. However, existing drugs for treating bladder cancer often cause many adverse reactions. Levistolide A (LA), a natural compound isolated from the traditional Chinese herb *Ligusticum chuanxiong Hort*, has been identified as an anti-cancer agent. However, its role in bladder cancer and underlying mechanisms remain largely unknown. In this study, we used the MTT assay and Annexin V/PI staining to detect the co-induced death of bladder cancer cell lines 5637 and T24 by LA and different cell death inhibitors. The rescue experiment show that ferrostatin-1 (Fer-1, ferroptosis inhibitor) could rescue the proliferation of bladder cancer cells prevented by LA or not other inhibitors of cell death. At the same time, through in vivo verification using a xenograft model, LA can effectively inhibit the proliferation of bladder cancer cell line 5637. Subsequent RNA-seq analysis, nude mouse tumor model, MDA detection, and Western blotting, demonstrated that LA-enhanced lipid peroxidation by up-regulating PTGS2 and down-regulating GPX4, accompanied by dysregulation of intracellular iron homeostasis. Furthermore, we also found that in in vivo experiments, co-treatment with LA and RSL3 (ferroptosis inducer) increased the inhibitory effect on bladder cancer cells 5637, highlighting its potential for clinical application. This provides a novel therapeutic strategy for eliminating bladder cancer cells.

#5666 Tambiciclib (SLS009), a CDK9 inhibitor, promotes apoptosis and suppresses MCL-1 levels in AML cell lines.

Elizabeth C. Trull, Philip C. Amrein

Cancer Center, Massachusetts General Hospital, Boston, MA

Background: Tambiciclib (SLS009) is a potent, selective CDK9 inhibitor that has shown promising results in Phase I clinical trials in hematological malignancies (NCT04588922). CDK9 is a critical regulator of transcription elongation through RNA polymerase II. Its inhibition results in downregulation of protein synthesis, thus decreasing the expression of short half-life molecules, such as MCL-1, MYC, E2F, and survivin, which leukemia cells, especially acute myeloid leukemia (AML) cells, depend on for survival. Here, we demonstrate the mechanistic effects of tambiciclib exposure correlated with apoptosis and cell death in AML cell lines.

Methods: We exposed the following cell lines to various concentrations of tambiciclib for 6 to 8 hours followed by washout: THP1 (p53 mutant, MLL-AF9 rearranged, NRAS mutant), NOMO1 (p53 mutant, MLL-AF9 rearranged, ASXL1 mutant), MOLM-13 WT (MLL-AF9 rearranged, NRAS mutant, FLT3 mutant), and MOLM-13 TP53 KO (MLL-AF9 rearranged, NRAS mutant, FLT3 mutant, p53 knockout). We performed viability assays on these cell lines using CellTiterGlo and examined protein expression using western immunoblotting and intracellular flow cytometry. Additionally, we stained cells with Annexin-V and a fixable viability dye before intracellular staining to correlate how protein expression levels change as cells undergo apoptosis and cell death.

Results: Treatment of AML cell lines with tambiciclib demonstrated cytotoxicity in the low nanomolar range and a dose-dependent decrease in cell viability after an 8-hour exposure. Repeated 8-hour exposures of tambiciclib consistently decreased IC50s, warranting further investigation into the mechanism through which this occurs. Our results show that when cells are exposed to 50 nM or 100 nM SLS009 for 6 hours, active caspase-3 levels increase and MCL-1 and survivin levels decrease. These changes in caspase-3 and MCL-1 expression are observed as early as 6 hours and are even more pronounced 24 hours after the completion of treatment. We observed that lower levels of MCL-1 and survivin correlate with increased apoptosis, suggesting that tambiciclib may lower the threshold for AML cell death and therefore may be useful in combination with existing therapeutic agents for leukemia treatment.

Conclusions: These results suggest that AML cell lines undergo cell death and apoptosis at low nanomolar concentrations of tambiciclib. Preliminary analysis of apoptotic molecules and pathways suggests a mechanism involving MCL-1 and survivin. With ongoing investigations into the dose and schedule of tambiciclib, our future directions include optimizing the use of tambiciclib in combination therapy to leverage the mechanistic effects of CDK9 inhibition and provide a novel therapeutic approach to treating patients with high-risk AML.

#5667 Ferroptosis necessitates caspase 5 dependent GSDME cleavage in ovarian cancer.

Mahmuda Akter, Lei Sun, Cheng Chi, Shuang Huang

University of Florida, Gainesville, FL

Ferroptosis, an intracellular iron-catalyzed form of programmed cell death (PCD) driven by lethal lipid reactive oxygen species (ROS)–induced membrane damage, is mechanistically uncharacterized in its execution process as a newly discovered PCD pathway. This study aimed to elucidate the molecular execution cascade of ferroptosis in ovarian cancer and to determine whether it uses common effector proteins shared with other PCD mechanisms. Mesenchymal-like ovarian cancer cells (OCC1, OVCAR8, ES2) were exposed to Erastin and ML162 with pathway-specific inhibitors, providing evidence that only the pyroptosis inhibitor YVAD reduced ferroptosis-induced death, supporting the association of pyroptotic executors. Lactate dehydrogenase (LDH) release and IL-1β secretion indicated that ferroptosis activates a pore-forming execution process, while both YVAD and gasdermin inhibitor disulfiram protected membrane damage. Ferroptotic cells exhibited cleavage of Gasdermin E (GSDME), whereas Gasdermin D was not processed. GSDME knockdown protected ovarian cancer cells from ferroptotic death, confirming its essential role in the execution phase. Our study further illustrated that ferroptosis does not follow the canonical inflammasome pathway by showing that caspase-1 remained inactive, and both NLRP3 inhibition (MCC950) and ASC knockdown did not affect ferroptotic sensitivity. Noncanonical pyroptotic PCD executors, specifically caspase-5 was activated during ferroptosis, but not caspase-4. Additionally, the siRNA Knockdown and CRISPR-Cas9 knockout of caspase-5 significantly suppressed ferroptotic death. The cell-free biochemical assay demonstrated that active caspase-5 directly cleaves full-length GSDME, confirming the interaction between caspase-5 activation and pore formation. Oxidized lipidomic profiling identified the accumulation of oxidized phosphatidylethanolamine (PE) species in ferroptotic cells, suggesting a potential upstream trigger for caspase-5/GSDME activation. Our data define a novel ferroptosis execution pathway mediated by caspase-5 activation and GSDME cleavage, revealing a mechanism with potential therapeutic relevance in ovarian cancer.

#5668 USP7 and ITCH/UBE4B ubiquitin ligase regulate the switch between apoptosis and necroptosis via Ku70 and c-FLIPL polyubiquitination in neuroblastoma.

Christophe Le Clorennec[1], Carla Sampaio[2], Peter E. Zage[2]

[1]UCSD Moores Cancer Center, La Jolla, CA,[2]Pediatrics, UCSD Moores Cancer Center, La Jolla, CA

Dysregulation of the Ubiquitin Proteasome System has been linked to many human diseases, including cancer. Expression of UBE4B ubiquitin ligase is associated with neuroblastoma patient outcomes and its functional roles in neuroblastoma pathogenesis are not known. We have recently identified an ubiquitin ligase complex ITCH/UBE4B which mediates ubiquitination of Ku70 and c-FLIPL proteins for proteasomal degradation allowing HDAC inhibitor-mediated caspase-8 dependent apoptosis. We also confirmed that the deubiquitinase USP7, critical player in tumor suppression and DNA repair, can be a potential therapeutic target for neuroblastoma. Highly selective USP7 inhibitors have demonstrated significant antitumor activity in preclinical models of adult cancer, and we reported that these inhibitors alone can be more effective against neuroblastoma tumor growth. Our hypothesis is that USP7 inhibition will be more effective against neuroblastoma tumors through destabilization of ITCH/UBE4B complex protein targets allowing a stronger induction of cell death in response to treatment for the children. To evaluate efficacy of USP7 inhibitors in combination with HDAC inhibitors or chemotherapy against neuroblastoma tumor growth, neuroblastoma cell lines depleted for UBE4B or USP7 were treated with increasing concentrations of USP7 inhibitors alone or in combination with chemotherapy or with HDAC inhibitors. Cell proliferation was measured using continuous live cell imaging and apoptosis by caspase cleavage and PARP cleavage detection by western blot. We have evaluated also, whether ubiquitination/deubiquitination and degradation rates of p53, Ku70 and c-FLIPL proteins could modulate induction of apoptosis and necroptosis. USP7 inhibition resulted in decreases in cell viability in p53 wild-type neuroblastoma cell lines via the induction of apoptosis and necroptosis by increasing phosphorylation of MLKL, RIPK3 and RIPK1. In UBE4B or USP7 depleted cells, a huge induction of necroptosis and a small rate of apoptosis were observed. We also identified USP7 as a deubiquitinase of Ku70 and c-FLIPL, stabilizing the Ku70/c-FLIPL/Bax “FLIPosome” complex. USP7 inhibition destabilizes ku70 and c-FLIPL for protein degradation leading to induction of apoptosis as well as necroptosis. UBE4B depletion in neuroblastoma inhibits HDAC inhibitors mediated caspase-8 mediated apoptosis but enhances necroptosis, notably because the stabilization of the FLIPosome can allow the blockade of caspase-8 activation and can trigger the activation of the necroptosome. Our data suggests that USP7 and ITCH/UBE4B can control the switch between apoptosis and necroptosis in response to USP7 and HDAC inhibitors. USP7 inhibition and ITCH/UBE4B activation by HDAC inhibitors could be a promising therapeutic strategy for children with high-risk and relapsed neuroblastoma.

#5669 Investigating the role of TRPM4 in the cancer cell death induced by ErSO and derivatives.

Brooke A. Bouwens[1], Michael P. Mulligan[2], Rowan Glover[2], Paul J. Hergenrother[2]

[1]Department of Biochemistry, University of Illinois at Urbana-Champaign, Champaign, IL,[2]Department of Chemistry, University of Illinois at Urbana-Champaign, Champaign, IL

The majority of breast cancers (BC) are hormone receptor positive (HR+/HER2-), and there remains a significant unmet need for alternative therapeutics for patients who become resistant to or no longer respond to endocrine therapy. Endocrine therapies primarily target estrogen receptor alpha (ERα) to inhibit tumor growth; however, acquired resistance and ERα mutations often limit the long-term efficacy of these treatments. Alternative therapeutic strategies that do not rely on endocrine pathways are critical for managing unresponsive breast cancers. Transient receptor potential cation channel subfamily M member 4 (TRPM4) is a calcium-activated monovalent ion channel that has emerged as a promising non-endocrine target in oncology. We have discovered a compound, called ErSO-TFPy, with potent cytotoxicity against TRPM4-positive (TRPM4+) cancer cells via a novel non-apoptotic mechanism. Notably, elevated TRPM4 expression correlates with increased sensitivity to ErSO-TFPy. To investigate the role of TRPM4 in the cell death induced by ErSO-TFPy, we performed studies including cellular thermal shift assays (CETSA) and cellular probe colocalizations. To assess the possibility of leveraging TRPM4 activation as a selective anticancer strategy, we looked at TRPM4 mutations, subcellular localization, temperature sensitivity, and cell viability in response to ErSO-TFPy and related compounds. Our data suggests TRPM4 plays a key role in the cell death induced by ErSO-TFPy.

#5670 Oxidative stress-mediated non-apoptotic, non-autophagic cell death: A mechanistically distinct strategy to overcome resistance in colorectal cancer cells.

Mati Ur Rehman[1], Almuayyad Gajani[1], Mahwish Fatima[1], Paras Jawaid[2], Arooj Shafiq[2], Azhar Hussain Rajabali[2]

[1]Biological and Biomedical Sciences, Aga Khan University - Karachi, Pakistan, Karachi, Pakistan,[2]Aga Khan University Hospital - Karachi, Pakistan, Karachi, Pakistan

Cancer remains a leading cause of mortality worldwide, with therapeutic failure often driven by apoptosis resistance a major hurdle that limits the efficacy of conventional anticancer therapies. Targeting alternative, caspase-independent cell death pathways has emerged as a promising strategy to overcome this resistance. In this study, we evaluated the effects of two mechanistically distinct small molecules a BCL-XL inhibitor and an NRF2 activator on colorectal cancer cell lines to investigate their ability to induce non-apoptotic cell death. Both agents reduced cell viability in a dose- and time-dependent manner. The NRF2 activator triggered cytoplasmic vacuolation at lower concentrations, characteristic of paraptosis, accompanied by endoplasmic reticulum (ER) dilation, oxidative stress, and downregulation of Alix, a key inhibitor of paraptosis. This mode of cell death required de novo protein synthesis and was independent of caspase activation, PARP cleavage, and DNA fragmentation. In contrast, the BCL-XL inhibitor displayed a dose-dependent switch between vacuolation-induced cell death and classical apoptosis, marked by phosphatidylserine externalization and DNA fragmentation. These findings underscore oxidative stress-mediated, vacuolation-associated non-apoptotic cell death as a mechanistically distinct and therapeutically relevant modality for targeting apoptosis-resistant cancer cells. This approach may pave the way for innovative cancer therapies that exploit tumor redox vulnerabilities while bypassing traditional cell death pathways.

#5671 Mitotic entry with DSB induces pyroptosis through 53BP1-mediated NLRP3 inflammasome activation.

Mengshi Luo[1], Yuewen Zhang[1], Wenjian Gong[1], Zhiqi Liao[1], Linghui Wang[1], Qiuyang Xu[1], Xingzhe Liu[1], Yijie Wu[1], Xuejiao Zhao[2], Gorden B. Mills[3], Ding Ma[2], Guangnian Zhao[2], Qinglei Gao[2], Yong Fang[2]

[1]Department of Gynecological Oncology, Tongji Hospital, Tongji Medical College, Huazhong University of Science and Technology, Wuhan, China,[2]National Clinical Research Center for Obstetrics and Gynecology,Department of Gynecological Oncology, National Clinical Research Center for Obstetrics and Gynecology, Department of Gynecological Oncology,Tongji Hospital, Tongji Medical College, Huazhong University of Science and Technology, Wuhan, China,[3]Department of Cell, Development and Cancer Biology, Oregon Health and Sciences University, Portland, OR

Background: Accumulated DNA double-strand breaks (DSBs), a key hallmark of cancer, are efficiently repaired during interphase to preserve proper mitotic progression, a process crucial for preventing genomic collapse. This protective strategy also represents a potential vulnerability for selectively eliminating tumor cells. However, when unrepaired DSBs persist into mitosis, the subsequent cellular fate and underlying mechanisms remain poorly understood. Using a cell model harboring under-repaired mitotic DSBs, we found that these mitotic DSBs robustly trigger NLRP3 mediated pyroptosis, an inflammatory form of cell death characterized by the release of inflammatory molecules, which has the potential to stimulate antitumor immunity within the tumor microenvironment. Mechanically, we identify 53BP1, an DNA repair associated protein, as a new regulator that drives mitotic pyroptosis.
Methods and Results: Using flow cytometry, western blot and immunofluorescence co-localization, a cell model in which DSBs prematurely enter into mitosis was established. Leveraging live-cell imaging and the H2B-mCherry system, we observed that DSBs in mitosis induces pyroptosis mediated by NLRP3 inflammation activation, as evidenced by characteristic pyroptotic morphologies, ASC foci formation and GSDMD cleavage. To elucidate the underlying mechanism of NLRP3 activation during mitosis, we employed liquid chromatography-mass spectrometry (LC-MS) combined with a DNA damage response (DDR) gene library analysis. This approach identified p53-binding protein 1 (TP53BP1) as the most abundant and intriguing candidate for NLRP3 interaction and activation in mitosis, which was further validated by molecular cloning, co-immunoprecipitation assays, and immunofluorescence co-localization. Furthermore, validation experiments across multiple cell models demonstrated that the phosphorylated 53BP1 during mitosis promoted NLRP3 inflammation activation and induced pyroptosis. This effect was consistent with the pyroptotic phenotype observed in a mouse model harboring a phosphorylated 53BP1 knock-in mutation.
Conclusion: Our work identifies 53BP1 as a novel NLRP3 regulator that activates NLRP3 inflammation during mitosis and induces pyroptosis, thereby revealing a new mechanism that compensates for the loss of NEK7-dependent NLRP3 activation during mitosis. This study provides an unprecedented insight into the crosstalk between the DNA damage response and the NLRP3 mediated pyroptosis, and offers a conceptual framework for the development of new therapeutic strategies.

#5672 PRMT5 inhibition enhances therapeutic vulnerability to Bcl-xL/Bcl-2 inhibitors in glioblastoma.

Shumpei Onishi[1], Ashis Chowdhury[1], Jean-Paul Bryant[1], Dragan Maric[2], Qi Li[3], Jing Wu[3], Yeshavanth Kumar Banasavadi-Siddegowda[1]

[1]Surgical Neurology Branch, NIH National Institute of Neurological Disorders & Stroke (NINDS), Bethesda, MD,[2]Flow and Imaging Cytometry Core Facility, NIH National Institute of Neurological Disorders & Stroke (NINDS), Bethesda, MD,[3]Neuro-Oncology Branch, NIH National Cancer Institute (NCI), Bethesda, MD

Glioblastomas are aggressive brain tumors characterized by heterogeneity and resistance to standard multimodal therapies. To address this challenge, we investigated potential vulnerabilities arising from the inhibition of protein arginine methyltransferase 5 (PRMT5), an epigenetic regulator critical for glioblastoma cell proliferation and survival. Although previous studies have demonstrate that PRMT5 inhibition induces a senescence-like state, the precise biological and therapeutic implications of this response in glioblastoma remain poorly understood.

Using patient-derived glioblastoma stem-like cells (GSCs), we performed a comprehensive screen of senolytic compounds in PRMT5-depleted GSCs. Among these compounds, the BCL-2/xL inhibitor navitoclax showed the most substantial reduction in cell viability, supporting its selection for subsequent combination studies. We then evaluated the therapeutic potential of combining PRMT5 inhibition, using the CNS-penetrant PRMT5 inhibitor LLY-283, with navitoclax. Treatment with LLY-283 induced G1 cell cycle arrest consistent with senescence induction. Western blot analysis showed that PRMT5 inhibition increased expression of the anti-apoptotic proteins BCL-2 and BCL-xL while reducing MCL-1 levels, indicating a shift in cellular dependency towards the BCL-2/xL axis. Quantitative drug-interaction analysis based on cell viability assay confirmed a synergistic effect between LLY-283 and navitoclax. The combination treatment enhanced the G1 cell cycle and led to a significant increase in cleaved PARP and γH2AX, indicative of enhanced apoptosis as evidenced by Annexin V assay. Mitochondrial functional assays demonstrated a substantial decrease in ATP production along with elevated mitochondrial reactive oxygen species (ROS), implicating mitochondrial dysfunction in the enhanced apoptotic and DNA-damage responses observed under dual inhibition.

In summary, our findings elucidate that PRMT5 inhibition creates a senescence-associated vulnerability in patient-derived glioblastoma cells, which can be effectively exploited through BCL-2/xL blockade. This combinatorial strategy offers a promising therapeutic avenue for overcoming the intrinsic resistance of glioblastoma.

#5673 Ferroptosis induction synergizes with KRAS inhibitors in *KRAS*-mutant lung adenocarcinoma.

Amirali Karimi[1], Yu Qian[1], David Molkentine[1], Alvaro Guimaraes Paula[1], Busra Ernhofer[2], David Hwa Peng[3], Monique B. Nilsson[1], John V. Heymach[1]

[1]Department of Thoracic, Head and Neck Medical Oncology, UT MD Anderson Cancer Center, Houston, TX,[2]Medical University of Vienna, Vienna, Austria,[3]Therapeutics Discovery Division, TRACTION Platform, UT MD Anderson Cancer Center, Houston, TX

Background: KRAS inhibitors hold substantial potential for the treatment of numerous malignancies harboring activating *KRAS* mutations, including non-small cell lung cancer (NSCLC). *KRAS* mutations are present in 25-30% of patients with non-squamous NSCLC, most commonly in the form of G12C mutations. Unfortunately, patients with inactivating mutations in *KEAP1*, which is frequently co-mutated with *KRAS* and *STK11*/LKB1, respond poorly to KRAS G12C inhibitors. *KEAP1* inactivation impairs NRF2 protein degradation, leading to enhanced antioxidant and ferroptosis response in the tumor cells. Whether ferroptosis resistance mediates resistance to KRAS G12C and G12D inhibitors in lung adenocarcinoma cells harboring these mutations is unknown.
Methods: DepMap was used to retrieve the drug sensitivity data for RSL3, erastin, ML162, ML210, sotorasib, and MRTX1133 as well as CRISPR and RNAi screen data in NSCLC human cell lines. A NSCLC ferroptosis resistance gene signature was constructed using genes that positively correlated (Pearson correlation z-score > 3) with resistance to both RSL3 and erastin in human NSCLC cell lines accessed from the Cancer Therapeutics Response Portal. We knocked-out *Keap1* and *Stk11* from murine LKR13 KRAS G12D and KRAS G12C cells using CRISPR-Cas9, to create isogenic models of $Kras^{MUT}$ (K), $Kras^{MUT}/Keap1^{KO}$ (KK), $Kras^{MUT}/Lkb1^{KO}$ (KL), and $Kras^{MUT}/Lkb1^{KO}/Keap1^{KO}$ (KLK) tumor cells. Lipid peroxidation was quantified by flow cytometry using BODIPY™ 581/591 C11.
Results: We determined that *KEAP1*-mutant, but not LKB1-mutant, NSCLC cell lines were resistant to ferroptosis inducers RSL3, ML162, ML210, and erastin. *KEAP1* deficiency also correlated with poor response to KRAS G12C inhibitors (sotorasib and adagrasib) and the KRAS G12D inhibitor MRTX1133 in human and murine cell lines, suggesting that ferroptosis resistance may contribute to KRAS inhibitor resistance. Treatment of KRAS mutant tumor cells with adagrasib or MRTX1133 induced lipid peroxidation- the biochemical defining feature of ferroptosis. In KRAS G12D mutant LKR13 cells, MRTX1133-induced cell death could be partially reversed by the ferroptosis inhibitor ferrostatin-1, but not by apoptosis or necroptosis inhibitors. Moreover, a higher NSCLC ferroptosis resistance gene expression signature correlated with reduced sensitivity to *KRAS* gene disruption in CRISPR and RNAi screens in *KRAS*-mutant NSCLC cell lines. Finally, ferroptosis inducers erastin and RSL3 synergized with adagrasib and MRTX1133 in LKR13 K cell lines.
Conclusions: KRAS inhibition induces ferroptosis in *KRAS*-mutant lung adenocarcinoma cell lines and ferroptosis resistance correlates with resistance to KRAS inhibitors. Combining ferroptosis induction strategies could potentially enhance the effectiveness of KRAS targeting treatments.

#5674 CD47 blockade induces necroptosis and complements the effects of BCL-2 inhibition in hematologic malignancies.

Stephen Jun Fei Chong[1], Rebecca Valentin[2], Jing Wang[2], Fen Zhu[2], Filip Garbicz[2], Kartini Iskandar[3], Brienne C. Y. Toh[4], Marisa Peluso[5], Jeremy Zhang[2], Liam Hackett[2], Benjamin H. Lee[5], Li Ren Kong[6], Catherine J. Wu[2], Wee Joo Chng[4], Shazib Pervaiz[3], Carsten U. Niemann[7], Ruben D. Carrasco[2], Matthew S. Davids[2]

[1]Physiology, Cancer Science Institute, NUS Centre for Cancer Research, National University of Singapore, Singapore, Singapore,[2]Dana-Farber Cancer Institute, Boston, MA,[3]Physiology, NUS Centre for Cancer Research, National University of Singapore, Singapore, Singapore,[4]Medicine, Cancer Science Institute, NUS Centre for Cancer Research, National University of Singapore, Singapore, Singapore,[5]Surface Oncology, Cambridge, MA,[6]Nanyang Technological University, Singapore, Singapore,[7]Institute of Clinical Medicine, University of Copenhagen, Copenhagen, Denmark

Introduction: CD47 is a macrophage checkpoint protein that acts as a "*don't-eat-me*" signal to prevent cell phagocytosis. Its blockade has shown promising results in clinical trials of lymphomas. Interestingly, CD47 blockade-induced cell death beyond phagocytosis, has also been reported, potentially contributing to the overall anti-tumor activity. This cell death mechanism has yet been well-characterized, thus warranting investigation to comprehensively unravel the mechanism of CD47 blockade and to facilitate the identification of optimal drug partners for combination therapy.
Method: Anti-CD47 monoclonal antibodies (mAb), SRF231, magrolimab, B6H12, were evaluated for cell death mechanisms such as apoptosis, autophagy or necroptosis. Techniques used include BH3 profiling, Annexin V, siRNA/CrisprCas9, Western blot and immunohistochemistry. Diffused large B-cell lymphoma (DLBCL) and acute myeloid leukemia (AML) cell lines were used. In vitro results were used to select for appropriate drug to combine with CD47 blockade. Results were validated ex vivo in leukemia patient samples and in vivo in cell line and patient-derived mouse models.
Result: Anti-CD47 mAbs consistently killed tumor cells from 10 cell lines, 24 patients, 3 mouse models by activating necroptosis, while sparing healthy immune cells. Necroptosis was confirmed via increased phospho(p)-RIPK and p-MLKL, which were rescued by necroptosis inhibitors or CD47/MLKL silencing. We further ascertained that PLCγ activation is upstream of necroptosis, as inhibiting PLCγ prevented p-MLKL and necroptosis. Moreover, apoptosis or autophagy was not involved, as inhibiting these pathways did not rescue SRF231-induced cell death. Given that necroptosis is the primary mechanism, we proceeded to leverage on apoptosis as an additional pathway to enhance cell death. Using BH3 profiling, a technique that informs cellular sensitivity to apoptotic inducers - BH3 mimetics, we identified the BCL-2 inhibitor venetoclax as an effective partner for SRF231 against hematologic malignant cells that depend highly on BCL-2 for survival (*i.e.* Cell survival: DMSO - 100%, (50nM) VEN - 71.39%, SRF231 - 57.01%, Combo - 19.53%, $P < 0.0001$). SRF231 and venetoclax combination completely eliminated tumor burden and prolonged progression free survival in BCL-2 dependent DLBCL and AML mouse models (*i.e.* Mice survival at day 70: Control - 0%, VEN - 0%, SRF231 - 58.3%, Combo - 100%; $P < 0.0001$). Importantly, SRF231 was equally effective against non-BCL-2 dependent, venetoclax-resistant DLBCL mouse models (*i.e.* Mice survival at day 200: Control - 0%, SRF231 - 62.5%, $P < 0.0001$).
Conclusion: Our study unravels a novel cell death mechanism of CD47 blockade through necroptosis, thereby permitting the inclusion of venetoclax-induced apoptosis, a complementary combination worthy of further study against BCL-2 dependent hematologic malignancies in the clinic.

#5675 MUC1-C-directed exatecan ADC induces genotoxic stress and transcriptional suppression of UPR-inflammatory pathways in metastatic colorectal cancer.

Surender Kharbanda[1], Deepak Raina[1], Rehan Ahmad[1], Changchuin Mao[1], Sourav Choudhary[2], Brian Lawney[1], Nandita Sreenivasalu[1], Govind Panchamoorthy[1], Ravi Jasuja[1]

[1]Research & Development, Xyone Therapeutics Inc, Canton, MA,[2]Research & Development, Birla Institute of Technology and Science, Hyderabad, India

Background:Metastatic colorectal cancer (mCRC) remains a major cause of cancer mortality and MUC1 is overexpressed in most tumors. However, no approved therapies target the tumor-anchored MUC1 antigen. The MUC1 oncoprotein consists of MUC1-N and MUC1-C, which form a heteromeric complex on the cell surface. The MUC1-N is shed into circulation and is highly heterogeneous in its glycosylation patterns across tumor types, creating both an antigen sink and unpredictable epitope presentation. This glycosylation variability can sequester MUC1-N-directed antibodies and significantly reduce consistent target engagement. In contrast, the membrane-anchored MUC1-C remains structurally accessible and uniform, representing a more reliable target for ADC development and addressing a critical unmet need in mCRC therapy.
Methods: We generated a first-in-class exatecan-based antibody-drug-conjugate (XYA02-8) recognizing the α4 helix within the extracellular domain of MUC1-C through a cleavable linker *. In vitro, cellular and patient-derived xenograft studies were perfomed to evaluate anti-tumor potency and safety of XYA02-8.
Results: The anti-MUC1-C monoclonal antibody displayed high-affinity binding to the MUC1-C extracellular domain and robust, ligand-driven internalization across multiple mCRC cell lines. Conjugation to exatecan via a cleavable linker yielded XYA02-8, an optimized ADC with >98% monomeric purity and a DAR of 8. XYA02-8 induced potent cytotoxicity in vitro, achieving low-nanomolar IC_{50} values across a panel of MUC1-expressing mCRC models. In SW620 xenografts, QW dosing x 3 at 7.5 mg/kg generated pronounced tumor growth inhibition without measurable body-weight loss or overt systemic toxicity. Transcriptomic profiling revealed a dominant exatecan-associated DNA-damage and replication-stress signature, repression of UPR regulators (DDIT4, STC2), and attenuation of pro-inflammatory signaling, concordant with increased γH2AX induction and PARP cleavage. In a MUC1-positive mCRC PDX, XYA02-8 produced substantial tumor regression with minimal toxicity, and efficacy was recapitulated in NCG mice treated at 5 mg/kg QW ×3. High-dose escalation (10× therapeutic level) resulted in negligible changes in hematologic or serum chemistry parameters, supporting a strong preclinical safety margin.
Conclusion: XYA02-8, a first-in-class MUC1-C-directed exatecan ADC, demonstrates potent and selective antitumor activity driven by efficient internalization, high DAR stability, and targeted induction of DNA-damage and replication-stress programs. Its robust efficacy across CDX and PDX models, coupled with minimal systemic toxicity at supra-therapeutic doses, positions XYA02-8 as a strong candidate for clinical translation in MUC1-positive mCRC.
* https://patents.google.com/patent/US20230265208A1/en

#5676 Bites that kill: Understanding cancer cell fate after macrophage mediated trogocytosis.

Ishwaree Datta[1], Meghan Morrissey[2], Annie Rogers[1]

[1]Molecular, Cellular and Developmental Biology, University of California, at Santa Barbara, Santa Barbara, CA,[2]University of California, Santa Barbara, Santa Barbara, CA

Macrophage therapies are an exciting avenue for targeted cancer cell killing in tumors. Macrophages phagocytose (that is, whole cell engulfment) of dying, dead, and abnormal cells. However, it's been observed that in solid tumors, macrophages primarily perform trogocytosis or nibbling, where they tear away portions of solid tumor cells. Trogocytosis in tumors is observed to be paradoxical: while it allows immune cells to strip away antigen from the cancer cell surface and thus allowing cancer progression. Conversely, it can cause cancer cell death, aiding immunotherapy. This dichotomous result raises the question of how to leverage trogocytosis in immunotherapy to be consistently lethal. We observe higher rates of trogocytosis compared to phagocytosis with Chimeric Antigen Receptor macrophages (CAR-M) when interacting with solid tumor cells. Our 3D tumor spheroid model constructed with SKOV3 cells shows a significant reduction in size with Her2CAR macrophages, with higher trogocytosis. I observe trogocytosed cancer cells to undergo apoptotic cell death via specific targeting by Her2CAR macrophages in 2D cell cultures. However, interestingly, death is not immediate in the co-cultures; instead, it happens following sustained trogocytic attack. In the first 2 hours of co-culture, when trogocytosis is significantly higher than phagocytosis, there's no cancer cell death. Our 3D tumor spheroid model also shows a reduction in spheroid diameter with Her2CAR macrophages after 5 days of co-culture. The cancer cell death can be blocked with a pan-caspase inhibitor Q-VD-Oph. The delayed cancer death suggests that trogocytosed cancer cells overcome initial, non-lethal loss of cell membrane; however, continual trogocytic attack renders cancer cells susceptible to apoptosis at later timepoints. Continuous loss of the cell membrane, followed by continual repair while maintaining homeostasis, is an energy-expensive process for the cancer cells. Thus accumulation of sustained stress in the trogocytosed cancer cells can ultimately push them to undergo apoptosis. I am currently investigating oxidative stress accumulation for activation of apoptosis in trogocytosed cells. Further, a change in transcriptomic profile for certain genes following 3-day co-culture with Her2CAR macrophages is also observed, suggesting the trogocytosed cells can alter their transcriptomic response to trogocytosis. Under current investigation is whether accumulated stress in trogocytosed cells causes this change in transcriptomic profile. CAR-M presents a promising avenue for targeting tumors. However, their efficacy in solid tumors needs to be improved. We observe continual trogocytosis pushes cancer cells to apoptosis at later timepoints. Thus, to make trogocytosis lethal in immunotherapy, understanding the trogocytosed cell response and investigating the fate of trogocytosed cells is essential.

#5677 GPX4-FTH1-ARNT signaling regulates iron efflux to suppress ferroptotic cell death and promote immune remodeling in osteosarcoma.

Md Abdullah[1], Donghee Lee[2], Jong Hyuk Kim[1]

[1]University of Florida, Gainesville, FL,[2]Small Animal Clinical Sciences,, University of Florida, Gainesville, FL

Osteosarcoma is the leading primary malignant bone tumor in children and young adults. Despite multimodal therapy involving surgery and multi-agent chemotherapy, patient survival rates have remained stagnant over the past four decades, necessitating the development of novel, effective therapeutic strategies. Ferroptosis, an iron-dependent programmed cell death, is a promising therapeutic target in osteosarcoma. Our recent findings indicate that osteosarcoma cells may circumvent GPX4-mediated ferroptosis by promoting iron detoxification through the ferroportin (FPN) exporter. This study was designed to define the molecular mechanisms by which osteosarcoma cells withstand redox stress associated with excess intracellular iron and to assess the potential impact of this regulation on the tumor immune microenvironment. First, we found that the TFRC gene, encoding the transferrin receptor responsible for cellular iron uptake, was associated with poor survival time in cervical cancer, glioblastoma, and liver cancer, and renal cancer in TCGA datasets. In contrast, SLC40A1 encoding FPN showed favorable clinical associations in liver cancer, pancreatic adenocarcinoma, and renal cancer. In human osteosarcomas (n = 88) from the Target Osteosarcoma database, SLC40A1 expression was positively correlated with overall immune gene scores ($r = 0.241$, $p = 0.024$) and M1 macrophage transcripts ($r = 0.340$, $p = 0.001$). Comparative transcriptomic analysis in canine osteosarcomas (n = 43) revealed that iron-related genes, including FTH1 ($r = 0.659$, $p < 0.0001$), SLC39A8 ($r = 0.665$, $p < 0.0001$), and ALAS1 ($r = 0.573$, $p < 0.0001$), were associated with immune scores. In DOUG canine osteosarcoma cells, treatment with the GPX4 inhibitor RSL3 significantly altered the expression signature of genes involved in tissue damage and remodeling, including those in in the ECM-receptor interaction, PI3K-AKT, and AGE-RAGE signaling pathway. Specifically, RSL3 treatment resulted in the marked upregulation of ARNT (encoding HIF-1β) and ALDH3A1, both critical components of detoxification and oxidative stress response pathways. Furthermore, Erastin, another ferroptosis inducer, substantially increased HMOX1, a key antioxidant defense gene, in both canine DOUG and COS31 and DOUG canine osteosarcoma cells. These data collectively suggest that osteosarcoma cells employ robust regulatory mechanisms governing iron detoxification and antioxidant defense, potentially influencing tumor immunity. Furthermore, our ongoing studies are investigating the mechanistic role of the GPX4-ARNT-FTH1 axis in immunomodulatory processes in osteosarcomas. This work will also seek to identify a conserved cross-species mechanism that regulates the interplay between iron metabolism and tumor immunity, enabling translational models using naturally occurring canine osteosarcoma.

#5678 Cuproptosis induction in TP53-mutated acute myeloid leukemia.

Yuju An, Xinghan Zeng, Brandy Perkins, Nour S. Naji, Yanyan Wang, Booseong Seo, Yashvi Hemani, Frederick Bunz, Theodoros Karantanos

Johns Hopkins University, Baltimore, MD

Patients with acute myeloid leukemia (AML) carrying *TP53* loss-of-function mutations exhibit extremely poor outcomes, partly due to intrinsic resistance to current treatments such as intensive chemotherapy and venetoclax-based regimens that depend on p53-mediated apoptosis. Developing therapeutic strategies capable of bypassing defective apoptotic pathways and eliminating *TP53*-deficient AML remains a critical need. Copper ionophores, including elesclomol—a compound previously evaluated in clinical trials—and its next-generation analog UM4118, trigger a mitochondria-dependent, nonapoptotic mode of copper-regulated cell death known as cuproptosis. Here, we demonstrate that inducing cuproptosis through these agents effectively targets AML cells in a p53-independent manner.Analysis of the BEAT AML 2.0 dataset revealed that the copper ionophore elesclomol exhibits the strongest anti-leukemic activity in *TP53*-mutated AML cells compared with *TP53* wild-type counterparts. Based on this observation, we hypothesized that cuproptosis induction could suppress AML cell growth and survival independent of p53 status. To test this, *TP53* was disrupted via CRISPR-Cas9 gene editing in 3 *TP53* wild-type human AML cell lines (MOLM13, MV4-11, and UKE-1) to generate isogenic *TP53* knockout derivatives, along with UKE-1 clones harboring heterozygous and homozygous *TP53* R273H mutations. Short-term viability and growth assays demonstrated a marked, dose-dependent reduction in viability 72 hours after treatment with copper ionophores, with comparable sensitivity across *TP53* wild-type, *TP53*-KO, and *TP53*-deficient (TF-1 and F36P) AML cells. In contrast, cytarabine, idarubicin, and venetoclax activity was substantially diminished in *TP53*-deficient cells, consistent with the known resistance of *TP53*-mutated AML to these standard therapies. Notably, combining low-dose elesclomol with the hypomethylating agent decitabine, which has established clinical efficacy in TP53-mutated AML, produced a synergistic increase in apoptosis in *TP53*-deficient AML cells.Together, these findings demonstrate that copper ionophores can bypass *TP53*-associated resistance to AML cell death by activating cuproptosis rather than relying on p53-dependent apoptotic pathways. The robust activity of copper ionophores across diverse *TP53*-deficient AML models, coupled with the enhanced efficacy observed in combination with decitabine, underscores cuproptosis induction as a promising therapeutic approach for *TP53*-deficient AML.

#5679 LIFR inhibition with EC359 triggers ferroptosis to overcome chemoresistance in endometrial cancer.

Emily Jean Aller[1], Baskaran Subramani[1], Xue Yang[1], Paulina Ramirez[1], Bindu Santhamma[2], Hareesh B. Nair[3], Edward Kost[1], Ratna K. Vadlamudi[1], **Suryavathi Viswanadhapalli**[1]

[1]UTHSA, San Antonio, TX,[2]Evestra, San Antonio, TX,[3]Texas Tech University Health Science Center, El Paso, TX

Background: Endometrial cancer (ECa), the most common malignancy of the female reproductive tract, has rising incidence and mortality, highlighting the need for better treatments. Targeting leukemia inhibitory factor receptor (LIFR) with EC359 shows promise by reducing viability and invasion in both Type I and II ECa. Since LIFR signaling is linked to ferroptosis, an iron-dependent cell death, this study explores whether EC359 induces ferroptosis and enhances chemotherapy, offering a novel therapeutic strategy for advanced ECa.
Methods: Chemotherapy-resistant ECa cell lines were established through prolonged exposure to chemotherapeutic agents and validated by RNA sequencing to confirm resistance-associated transcriptional profiles. The antitumor effects of EC359 were assessed in multiple established and patient-derived primary ECa cell models through colony formation assays, MTT-based cell viability assays, and apoptosis analysis. Mechanistic studies were conducted using Western blotting, RT-qPCR, transmission electron microscopy (TEM), and flow cytometry to evaluate ferroptosis-related markers and cellular changes. For preclinical validation, patient-derived organoids (PDO) and xenograft (PDX) models of ECa were employed to determine the therapeutic efficacy of EC359 in combination *in vivo*.
Results: RNA-seq analysis of taxol-resistant ECa cells revealed upregulation of pathways associated with cell proliferation, stemness, and LIFR signaling, along with downregulation of apoptotic pathways. EC359 significantly reduced cell viability in taxol-resistant advanced ECa models. Notably, the cytotoxic effect of EC359 was markedly attenuated when ferroptosis was pharmacologically inhibited using Ferrostatin-1, indicating that ferroptosis is a key mechanism of EC359-induced cell death. Mechanistic studies demonstrated that EC359 suppresses the glutathione antioxidant defense system, thereby promoting ferroptosis. Consistent with this, supplementation with extracellular cystine restored cell viability following EC359 treatment. Moreover, EC359 markedly reduced the expression of key anti-ferroptosis proteins. Flow cytometry confirmed increased lipid peroxidation in EC359-treated cells, while TEM studies revealed characteristic mitochondrial damage associated with ferroptosis. Importantly, EC359 combined with chemotherapy significantly decreased the viability of PDOs and robustly inhibited tumor progression in PDX models of advanced ECa.
Conclusion: Our studies suggest that EC359 induces ferroptosis by disrupting antioxidant defenses and synergizes with chemotherapy and that EC359 serve as a promising strategy to overcome chemoresistance in advanced ECa.

#5680 Hinokitiol targets metal and redox vulnerabilities in liver cancer.

Daniela Delgado[1], Anyssa Rodriguez[2], Subhash C. Chauhan[3], Nirakar Sahoo[1]

[1]School of Integrative Biological and Chemical Sciences, University of Texas Rio Grande Valley, Edinburg, TX,[2]University of Texas Rio Grande Valley, Edinburg, TX,[3]South Texas Center of Excellence in Cancer Research, University of Texas Rio Grande Valley, Edinburg, TX

Hepatocellular carcinoma (HCC) represents one of the most fatal forms of liver cancer, which accounts for most liver cancer deaths worldwide. The current medical treatments offer limited efficacy, especially in advanced stages, so there is a clear need for alternative therapeutic strategies. In recent years, natural compounds have gained attention as options for difficult-to-treat cancers. Hinokitiol (β-thujaplicin) is one such compound. Studies have shown that Hinokitiol possesses anti-cancer properties; interestingly, this compound is also known to bind and mobilize iron. However, the link between iron-mobilizing ability and the type of stress response or cell death pathway it activates in HCC cells remains unclear. Since HCC cells inherently carry more iron, how hinokitol interacts with iron-rich environments and what specific pathway it activates in HCC cells still needs to be elucidated. We used the liver cancer cell SK-HEP1 to characterize the effect of hinokitol. We assessed the cell responses through Western blotting, RT PCR, immunocytochemistry, and live-cell imaging to measure cell viability, lysosome activity, mitochondrial integrity, autophagy, and oxidative stress. Our results showed that the Hinokitiol markedly suppressed liver cancer growth in a time and dose-dependent manner with an IC_{50} ~5 μM at 96 hours; and concentrations at or above this level almost abolished clonogenic growth. At doses near IC_{50}, Hinokitiol enhanced autophagy and stress-related gene expression by roughly 2-4 fold. Western blot analysis also confirmed an increase in LC3 lipidation and lysosome markers, suggesting that Hinokitiol engages the autophagy-lysosome system rather than simple growth arrest. At the same concentrations, Hinokitiol induced the stress-response gene CHAC1 and decreased ferritin protein levels. The live-cell imaging results demonstrated that Hinokitiol treatment caused an increase in lipid peroxidation and expanded labile Fe^{2+} pool sizes in cells compared to control cells. The combined induction of CHAC1, loss of ferritin, and increased lipid damage suggest that Hinokitiol produces iron mediated oxidative stress. Taken together, these findings suggest that Hinokitiol causes cell death through an iron and lipid oxidation-driven mechanism that is independent of apoptosis and necroptosis, and is compatible with a ferroptosis-like form of cell death. By mobilizing excess intracellular iron, Hinokitiol activates ferroptosis-related pathways and takes advantage of iron and redox weaknesses in HCC cells, supporting its potential as a therapeutic agent.

#5681 Mechanism of mitochondria-independent cuproptosis.

Martin Mistrik[1], Martin Loffelmann[1], Petr Dzubak[1], Marian Hajduch[1], Josef Srovnal[1], Zdenek Skrott[1], Lucie Beresova[1], Tomas Pluhacek[2], Petr Tarkowski[2]

[1]Lekarska fakulta UP Olomouc, Olomouc, Czech Republic,[2]Univerzita Palackeho v Olomouci, Olomouc, Czech Republic

Copper is an essential trace element that functions as a cofactor for numerous metabolic and detoxification enzymes. In excess, however, copper exerts marked cytotoxicity in cancer cells and can induce a recently characterized form of regulated cell death termed *cuproptosis*. Currently, cuproptosis is believed to depend on mitochondrial activity, involving the reduction of bivalent copper ions to monovalent, leading to subsequent toxic effects via the oligomerization of lipoylated DLAT (dihydrolipoyl transacetylase) and the loss of iron-sulfur cluster proteins. Here, we evaluated several copper ionophores in their copper-complexed forms, including bis(diethyldithiocarbamate) (CuET), pyrithione, NSC319726, and 8-hydroxyquinoline, to assess their ability to induce cuproptosis. Surprisingly, their cytotoxic effects were comparable in oxidative-phosphorylation-dependent cancer cells and in glycolysis-driven counterparts. Consistently, neither chemical inhibition of individual mitochondrial complexes nor the use of mitochondrial DNA-deficient Rho0 cells revealed differential sensitivity. Instead, all tested ionophores induced aggregation and immobilization of the essential p97 cofactor NPL4, mirroring the mechanism previously reported for CuET. NPL4 dysfunction disrupts the p97/proteasome axis, and its aggregation strongly correlates with cytotoxic outcomes. Ionophore treatment also triggered canonical proteotoxic stress pathways, including the unfolded protein response, the heat-shock response, and accumulation of polyubiquitinated proteins. Importantly, additional treatment with the non-toxic, more potent divalent copper chelator, dibenzyldithiocarbamate, reversed NPL4 aggregation and ionophore-induced cytotoxicity. Together, these findings refine the mechanistic framework of copper-dependent cell killing by revealing a prominent proteotoxic component of bivalent copper associated with targeting the NPL4. This insight strengthens the rationale for targeting copper-regulated proteostasis pathways as a potential anticancer strategy.

#5682 Elucidating and overcoming therapeutic resistance in esophageal adenocarcinoma.

Naren Li[1], Jessica Ji[2], Jaylon C. Aggison[1], Siqi Wu[1], Francisco A. Molina-Pelayo[1], Cristian G. Medina[1], Ritika Raj[1], Yuan Xu[1], Robert T. Ripley[1]

[1]Baylor College of Medicine, Houston, TX,[2]Rice University, Houston, TX

Background: Esophageal adenocarcinoma (EAC) accounts for over 80% of esophageal cancers in the United States and remains a highly lethal malignancy with poor prognosis and rising incidence. Despite advances in therapy, recurrence occurs in most EAC patients, largely due to the emergence of therapeutic resistance. Resistance can be intrinsic or acquired from a rare subpopulation known as Drug Tolerant Persister (DTP) cells, which survive cytotoxic therapy through non-genetic adaptive mechanisms. Unlike genetic resistance, the drug-tolerant state is reversible upon drug withdrawal. This study aims to establish cisplatin-derived DTP(CDDP-DTP) and drug-resistant (CDDP-DR) EAC cell models to elucidate resistance mechanisms, identify therapeutic vulnerabilities, and develop strategies to overcome resistance and prevent recurrence in EAC.

Methods: CDDP-DTP cells were generated by exposing EAC cells to the IC_{80} of CDDP for four days, while CDDP-DR cells were developed via stepwise dose escalation based on the IC_{50}. Cytotoxic effects of compounds targeting ferroptosis, pyroptosis, and epigenetic regulation (RSL3, DMB, BIX-01294, and GSK3326595) were evaluated by MTS assays in four EAC cells (FLO-1, OE19, OE33, SK-GT-4). Drug synergy was analyzed using the Combenefit tool. BH3 profiling was performed to assess mitochondrial apoptotic priming and anti-apoptotic dependency. Seahorse assay was used to evaluate cellular metabolism. Cell cycle distribution and cell death were analyzed by propidium iodide (PI) and annexin V/PI staining. Gene and protein expression were measured by quantitative real-time polymerase chain reaction (RT-qPCR) and western blot.

Results: CDDP-DTP EAC cells exhibited reduced proliferation and upregulation of canonical DTP markers, while CDDP-DR cells displayed >2-fold increased resistance to CDDP, elevated ATF4 expression, an epithelial-to-mesenchymal transition (EMT) phenotype, and resistance to apoptosis accompanied by metabolic reprogramming. Among compounds targeting non-apoptotic, non-genetic adaptive mechanisms, RSL3, DMB and BIX-01294 effectively suppressed EAC cell growth compared with GSK3326595. Notably, BIX-01294 combined with CDDP and DMB combined with a Bcl-xL inhibitor exhibited synergistic cytotoxicity in EAC cells. The target proteins of these compounds—GPX4, GSDMD, and G9A—were upregulated in both TCGA datasets and EAC cells, further highlighting their potential roles as mediators of therapeutic resistance and as promising therapeutic targets.

Conclusions: This study successfully established CDDP-DTP and CDDP-DR models of EAC and revealed that targeting non-apoptotic, adaptive mechanisms can enhance therapeutic response. These findings lay the foundation for multi-omic characterization of resistant EAC populations and support exploration of non-apoptotic vulnerabilities to undermine recurrence and improve long-term outcomes in EAC.

: Mechanisms of Anticancer Drug Action
Poster Session

#5685 Mitotic error-tolerant survival following WRN inhibition is overcome by sustained spindle checkpoint activation.

Sungmin Cho[1], Joong-Bae Ahn[2], Sang Joon Shin[2]

[1]Yonsei University College of Medicine, Seoul, Korea, Republic of,[2]Division of Medical Oncology, Department of Internal Medicine, Yonsei Cancer Center, Seoul, Korea, Republic of

Background: Microsatellite instability-high (MSI-H) cancers are known to depend on the Werner (WRN) helicase, which resolves repetitive TA sequences. Recently, a selective WRN inhibitor, HRO-761, has shown to be highly effective in MSI-H cells, validating WRN as a promising therapeutic target. However, the cellular mechanisms by which WRN inhibition fails to completely eliminate tumor cells remain unclear. In this study, we uncovered a mitotic survival pathway activated upon WRN inhibition and propose a drug combination strategy with Vinblastine to suppress it.
Method: To examine the cellular state following WRN inhibition, we performed confocal microscopy after durg treatment and confirmed spindle assembly checkpoint (SAC) activation by Western blot. Drug sensitivity profiles were analyzed using GDSC2, and OmicsExpression and CRISPRGeneEffect from DepMap (25Q2) were analyzed. Combination effects were assessed using CCK-8 and colony formation assays in MSI-H colorectal cancer cell lines (HCT-116, LOVO, SNU-C2B).
Results: WRN inhibition in MSI-H colorectal cancer cells induced robust cell-cycle arrest and activated SAC, as evidenced by increased MAD2 re-localization (IF) and accumulation of Cyclin B1 and Securin (WB). Despite the initial SAC activation, we also observed subsequent SAC deactivation accompanied by abnormal morphological changes characteristic of mitotic error. These cells continued to survive while bearing persistent mitotic errors, representing an error-tolerant survival phenotype following WRN inhibition.
Transcriptomic analyses revealed that genes involved in kinetochore-microtubule attachment were significantly downregulated after WRN inhibition (NES < -2, adjusted $P < 0.05$). Using whole cell line expression and CRISPR Gene Effect data, we found that cells with reduced kinetochore gene expression exhibited increased dependency on α-tubulin and β-tubulin ($P < 0.05$), suggesting a complementary and potentially synthetic-lethal relationship between WRN loss and microtubule function.
We combined WRN inhibition with Vinblastine, a microtubule-targeting agent(MTA) known to prolong SAC activation, and observed reduced cell viability in CCK-8 and colony-formation assays. In HCT-116 cells, co-treatment with HRO-761 and Vinblastine (0.1 nM) decreased the IC_{50} from 1.058μM to 0.382 μM, demonstrating a clear synergistic effect of the combination.
Conclusion: Based on our findings, we identified a previously unrecognized mitotic error-tolerant survival pathway induced by WRN inhibition. We further demonstrated that Vinblastine, by sustaining spindle checkpoint activation, synergized with WRN inhibition to reduce cell viability and suppress escape mechanism. These results suggest that combining MTA with WRN inhibitors represents a promising therapeutic strategy in MSI-H cancers.

#5686 SF3B1 inhibition suppresses prostate cancer by disrupting ATRX splicing and inducing cell cycle arrest.

Linyue Li[1], Weijian Ding[1], Zhihao Nie[1], Congrong Jiang[2], Ruining Zhao[2], Siyuan Xia[1], **Baotong Zhang**[1]

[1]Southern University of Science and Technology, Shenzhen, China,[2]Department of urology, People's Hospital of Ningxia Hui Autonomous Region, The Third Clinical Medical College of Ningxia Medical University, Yinchuan, China

Prostate cancer is the most common malignancy in men in the United States, and dysregulated RNA splicing has emerged as a critical driver of prostate cancer progression. Although alternative splicing pathway genes are mutated in approximately 4% of prostate cancers, mutations in the core splicing factor SF3B1 represent a disproportionately high fraction (27.5%). However, whether and how SF3B1 inhibition suppresses prostate cancer progression remains unclear. Here, we demonstrate that the SF3B1 inhibitor Pladienolide B exerts robust antitumor activity in prostate cancer cell lines, cell-derived xenografts, and patient-derived xenografts. RNA-seq analysis revealed widespread splicing alterations enriched in pathways regulating cell-cycle arrest, which we validated using flow cytometry and live-cell imaging. Following double-thymidine synchronization, Pladienolide B-treated DU145 cells exhibited a markedly prolonged S phase, indicating that SF3B1 inhibition suppresses tumor growth primarily by inducing cell-cycle arrest. To elucidate the molecular basis of this arrest, we examined individual splicing changes and identified a key event in ATRX, which retained a 74-bp cryptic exon before exon 25 upon Pladienolide B treatment. This aberrant splicing disrupted the ATRX-MeCP2 interaction required for maintaining genome stability through repression of R-loop accumulation in heterochromatin. Interestingly, we further identified CDK12 as a previously unrecognized upstream kinase of SF3B1. CDK12 physically interacted with SF3B1, and its inhibition by THZ531 reduced SF3B1 phosphorylation at T313, induced cell-cycle arrest, and suppressed tumor growth. Given the therapeutic potential of SF3B1 inhibition, we evaluated combinatorial strategies with current prostate cancer treatments. Inhibition of SF3B1 activity by THZ531 or Pladienolide B conferred resistance to docetaxel, a first-line therapy for metastatic disease. Notably, Pladienolide B exhibited synergistic antitumor effects when combined with the PARP inhibitor olaparib. Collectively, our findings reveal how SF3B1 inhibition impairs prostate cancer progression through RNA splicing dysregulation, and they provide a rationale for integrating SF3B1-targeted therapies into prostate cancer treatment.

#5687 Targeting KIFC1 induces anaphase catastrophe in small cell lung cancer.

Minemichi Toda[1], Natsuki Nakagawa[1], Masakatsu Tokunaga[1], Mirei Ka[2], Takahiro Iida[3], Hiroaki Ikushima[1], Takahiro Ando[1], Akiko Kunita[4], Kousuke Watanabe[4], Xi Liu[5], Ethan Dmitrovsky[5], Hidenori Kage[1], Masanori Kawakami[1]

[1]Departments of Respiratory Medicine, Graduate School of Medicine, The University of Tokyo, Tokyo, Japan,[2]Division of Integrative Genomics, Graduate School of Medicine, The University of Tokyo, Tokyo, Japan,[3]Thoracic Surgery, Graduate School of Medicine, The University of Tokyo, Tokyo, Japan,[4]Next-Generation Precision Medicine Development Laboratory, Graduate School of Medicine, The University of Tokyo, Tokyo, Japan,[5]Frederick National Laboratory for Cancer Research, Frederick, MD

Cancer cells often possess more than two centrosomes, which is one of the hallmarks of cancer. By clustering these supernumerary centrosomes during mitosis, cancer cells can achieve bipolar division. We previously reported that in non-small cell lung cancer, CDK2 inhibition suppresses centrosome clustering, leading to multipolar cell division and apoptotic cell death—a phenomenon termed anaphase catastrophe. Because normal cells have only two centrosomes, anaphase catastrophe does not appreciably affect them, making it a promising therapeutic strategy for selectively eliminating cancer cells. However, as CDK2 inhibition also interferes with normal cell cycle progression, identifying therapeutic targets that can induce anaphase catastrophe preferentially is desirable. Motor protein KIFC1 has been implicated in centrosome clustering. Here, we investigated its potential as a novel therapeutic target to induce anaphase catastrophe in small cell lung cancer (SCLC). Owing to p53 inactivation, SCLC is expected to frequently harbor supernumerary centrosomes and be vulnerable to mitotic abnormalities, including anaphase catastrophe. First, in vitro experiments using multiple SCLC cell lines were conducted. Immunofluorescence staining for pericentrin confirmed that centrosome amplification occurs more frequently in SCLC cells than in normal human bronchial epithelial (NHBE) cells. Western blotting revealed that KIFC1 was overexpressed in SCLC cells as compared with NHBE cells. Functional analyses, both pharmacologic (using a specific inhibitor) and genetic (using siRNAs and the CRISPR-Cas9 system), demonstrated that inhibition of KIFC1 induced apoptosis and suppressed proliferation in SCLC cell lines, whereas these effects were largely absent in NHBE cells. Furthermore, immunostaining for α-tubulin, pericentrin, and DAPI showed a statistically significant increase in multipolar mitotic cells and a decrease in cells with clustered supernumerary centrosomes among dividing cells, implicating KIFC1 inhibition in conferring anaphase catastrophe in SCLC. These findings were validated and extended in the in vivo setting. In human SCLC cell-derived xenograft models, administration of KIFC1 inhibitor statistically significantly suppressed tumor growth. Staining of excised tumors for pericentrin revealed reduced numbers of cells with clustered supernumerary centrosomes and increased numbers undergoing multipolar mitosis, consistent with in vitro findings and indicative of anaphase catastrophe induction. Finally, potential combination therapies with other pharmacologic targets were explored and will be presented. In conclusion, inhibition of KIFC1 disrupts the clustering of supernumerary centrosomes and caused anaphase catastrophe, indicating its promise as a novel therapeutic target for SCLC.

#5688 Synthetic lethal targeting of TRIP13 and Aurora A induces mitotic DNA damage and concurrent pyroptotic-apoptotic cell death in Rb-deficient cancer cells.

Lacin Yapindi[1], Soma Ghosh[1], Li Shen[2], Lixia Diao[2], Jing Wang[2], Faye M. Johnson[1]

[1]Department of Thoracic/Head & Neck Medical Oncology, UT MD Anderson Cancer Center, Houston, TX,[2]Department of Bioinformatics and Computational Biology, UT MD Anderson Cancer Center, Houston, TX

There are currently no effective, biomarker-guided therapies specifically targeting cancers with functional loss of the Rb pathway, underscoring the urgent need to exploit their unique vulnerabilities. We previously demonstrated that combined inhibition of TRIP13 and Aurora A elicits a synthetic lethal effect specifically in Rb-deficient cancer cells. To dissect the underlying mechanism of this synthetic lethality, we employed live-cell imaging to monitor single-cell dynamics and found that the combination induces mitotic cell death by inducing prolonged mitotic arrest. These findings were validated using the orthogonal *in vitro* assays assessing apoptosis and cell cycle, which further revealed that the combination leads to DNA damage and concurrent apoptotic and GSDME-mediated pyroptotic cell death in mitotically arrested Rb-deficient cancer cells. The inhibition of mitotic entry using CDK1 inhibitor, RO-3306 abrogated these combination-induced lethal effects, further confirming the essential role of mitotic catastrophe in mediating this synthetic lethality. These *in vitro* findings were strengthened *in vivo*, as the combination of TRIP13 depletion and Aurora A inhibition achieved marked antitumor efficacy and provided a measurable survival benefit in Rb-deficient cell line xenograft model. TCGA analyses of head and neck and lung squamous cell carcinoma cohorts showed that Rb-deficient tumors have significantly higher *CASP3* expression but lower *GSDME* expression than Rb-proficient tumors. This suggests that Rb-deficient tumors may possess an inherent tendency toward stress-induced caspase-3 activation due to elevated baseline *CASP3* levels. The concurrent reduction of *GSDME* expression may therefore reflect an adaptive strategy to mitigate this potential vulnerability by limiting downstream caspase-3-mediated pyroptotic cell death. Here we report for the first time a detailed mechanism behind the synthetic lethal vulnerability of Rb-deficient cancer cells to dual inhibition of TRIP13 and Aurora A. This combination therapy offers new therapeutic avenues for Rb-deficient cancers and provides a rationale for exploiting mitotic vulnerabilities of Rb-deficient cancers.

#5689 Flow-cytometric analysis of cell-cycle arrest and apoptosis induced by a novel benzopyran derivative (SK6) in MCF-7 breast cancer cells.

Mariappan Gurusamy[1], Razia Shaika[2], Brijesh Sharma[2]

[1]Dept of Pharm Chemistry, St Mary's College of Pharmacy, Secunderabad, Telangana, India,[2]Dept of Pharm Chemistry, School of Pharmacy, Institute of Biomedical Education and Research, Mangalayatan University, (U.P.), India, Aligarh, India

Introduction: Breast cancer remains a major global health challenge, accounting for 2.3 million new cases and nearly 670,000 deaths in 2022. The limitations of current therapies, including drug resistance, toxicity, and reduced efficacy, highlight the urgent need for novel anticancer agents.

Purpose of the Study: The aim of this study was to evaluate the anticancer potential of a novel benzopyran derivative (SK6) using flow-cytometric analysis. After identifying SK6 as the most potent compound through MTT assay, its mechanism of action was investigated in MCF-7 cells. Flow cytometry was employed to assess SK6-induced apoptosis using Annexin-V/PI staining. Additionally, PI-based DNA content analysis was performed to determine the compound's effect on cell-cycle progression.

Experimental Methods: In continuation our research on synthesis of benzopyran derivatives, 5 molecules were synthesized and characterized using UV, IR, ^{1}HNMR, and mass spectrometry. Their cytotoxicity was evaluated against MCF-7 cells using the MTT assay. Consequently, SK6 was selected for mechanistic investigation. Flow cytometry (Beckman Coulter Gallios analyser, USA) was employed to assess its effects on the cell cycle and apoptosis in treated MCF-7 cells.

Results: All five benzopyran derivatives were successfully synthesized and structurally confirmed using spectral analyses. Among them, SK6 showed the lowest IC_{50} value i.e. 20.99µg/ml in the MTT assay, demonstrating the strongest antiproliferative activity against MCF-7 cells. Flow-cytometric Annexin-V FITC/PI analysis revealed that SK6 treatment induced a measurable apoptotic response in MCF-7 cells. Annexin-V FITC/PI staining revealed that SK6 induced a measurable apoptotic response. Quadrant analysis showed 78.44% viable cells, 8.40% in early apoptosis, 8.15% in late apoptosis, and 5.01% necrotic. Overall, SK6 induced 16.55% total apoptosis, confirming its ability to activate programmed cell death in MCF-7 cells. The SK6 compound caused a marked alteration in the cell-cycle profile, producing a dominant S-phase arrest. Treated cells showed a substantial increase in the S-phase population (54.33% vs. 13.05% in control) with a drastic reduction in G0/G1 cells (1.02% vs. 62.91%). A moderate rise in G2/M cells and minimal sub-G1 events indicate primarily cytostatic rather than DNA-fragmenting effects. These findings suggest that SK6 disrupts DNA replication and halts progression at the S-phase checkpoint.

Conclusion: SK6 demonstrated potent cytotoxic activity against MCF-7 cells and caused a pronounced S-phase arrest, indicating disruption of DNA replication. This was accompanied by a moderate induction of apoptosis, supporting its antiproliferative effect. Finally, these results highlight SK6 as a promising lead candidate for further development as a selective and effective therapeutic agent against breast cancer

#5690 Mechanisms of efficacy of endonuclease FEN1 inhibition in neuroblastoma.

Carla S. Sampaio[1], Eric Wu[2], Madison Cinelli[1], Erica Steen[1], Andrew Shiau[3], Richard Kolodner[4], Jean Wang[4], **Peter E. Zage**[5]

[1]Pediatrics, UCSD/Moores Cancer Center, San Diego, CA,[2]Cellular and Molecular Medicine, UCSD, San Diego, CA,[3]Cell and Developmental Biology, UCSD, San Diego, CA,[4]Cellular and Molecular Medecine, UCSD, San Diego, CA,[5]UCSD, San Diego, CA

Background: Children with high-risk and relapsed neuroblastoma (NB) need improved therapies, and recurrent cytogenetic abnormalities, such as MYCN oncogene amplification, represent candidate therapeutic targets. MYCN amplification and increased MYCN expression drive deregulated hyper-transcription that leads to development and growth of NB tumors, and MYCN amplifications, which can be found both within the linear genome (HSR) and on circular extrachromosomal DNA (ecDNA), are associated with significantly worse survival rates for children with NB. MYCN overexpression has been linked to an increase in replication stress (RS), and RS and subsequent genome instability are important drivers of tumor initiation and progression. Flap Endonuclease 1 (FEN1), a non-essential DNA replication enzyme, was identified as a synthetic lethal target in BRCA1/2-deficient cancers via induction of RS. Recent success of targeting RS-elevated cancers with replication enzyme inhibitors opens a new avenue to target MYCN-amplified NB.
Methods: The efficacy of FEN1 inhibition was assessed using live cell imaging and cell viability assays, comparing results in MYCN-amplified to -nonamplified NB cells and in NB cells with inducible MYCN expression and repression. Mechanisms of cell death and impacts on replication stress in cells treated with FEN1 inhibitors were evaluated by Western blots.
Results: FEN1 inhibition was effective against NB cells and was significantly more effective in MYCN-amplified NB cells causing reduced cell growth and viability. Increased MYCN expression also led to increased sensitivity to FEN1 inhibition, and reduced MYCN expression reduced sensitivity. FEN1 inhibition led to the induction of apoptosis and responses to FEN1 inhibition were associated with markers of replication stress.
Conclusions: We have discovered that MYCN-amplified NB cells are hypersensitive to FEN1 inhibition, suggesting that FEN1 inhibition may be a promising therapeutic strategy for children with high-risk and relapsed neuroblastoma.

#5691 Per and polyfluoroalkyl substances (PFAS) promote proliferation and migration in genetically distinct kidney cancer cell lines.

Rakesh Kumar Arya[1], Mia Sand[2], Sahab Ram Dewala[1], Can Aydogdu[3], Gabriela M. Diaz[3], Christopher Weight[3], Riccardo Autorino[3], Abhishek Chakraborty[4], Jacob M. Knorr[3], Joseph M. K. Irudayaraj[2], Laura Bukavina[3]

[1]Center for Immunotherapy and Precision Immuno-oncology, Cleveland Clinic Lerner Research Institute, Cleveland, OH,[2]Department of Bioengineering,, University of Illinois Urbana-Champaign, Champaign, IL,[3]Glickman Urological and Kidney Institute, Cleveland Clinic, Cleveland, OH,[4]Department of Cancer Biology, Cleveland Clinic Research, Cleveland, OH

Introduction and Objectives: Per- and polyfluoroalkyl substances (PFAS) such as GenX, PFOA, and PFOS are persistent environmental pollutants increasingly associated with renal carcinogenesis. Their direct effects on kidney cancer progression remain unclear. This study investigated whether PFAS exposure enhances proliferation and migration in two genetically distinct kidney cancer models-human RCC-ER (VHL-mutant) and murine Renca (VHL-wild type).

Methods: RCC-ER and Renca cells were treated with GenX, PFOA, or PFOS at physiologically relevant concentrations (0.5-40 nM). Proliferation was monitored over 72 h using the IncuCyte S3 system. Migration was assessed in ImageLock plates, where wounds were created after 24 h and imaged every 1.5 h for 72 h. Wound closure was quantified by percentage wound closure (WC) and relative wound density (RWD) using IncuCyte software. All experiments were performed in triplicate to assess dose dependency and statistical significance.

Results: PFAS exposure significantly enhanced both proliferation and migration in kidney cancer cells, with compound- and cell line-specific variations. RenCa cells exhibited strong proliferative responses to GenX and PFOS from 0.5-20 nM, peaking at 5 nM respectively, while PFOA showed cytotoxic effects at these doses. In contrast, RCC-ER cells demonstrated increased proliferation in response to PFOA (max at 40 nM) and PFOS (max at 5 nM), whereas GenX had minimal effect on proliferation at low doses. All three PFAS markedly accelerated wound closure and relative wound density in both cell lines, indicating enhanced migratory potential. Collectively, these data reveal that PFAS compounds augment pro-oncogenic behaviors across human and murine kidney cancer models.

Conclusion: PFAS compounds promote proliferative and migratory phenotypes in both murine and human kidney cancer models through distinct but convergent metabolic mechanisms. The conserved effects across VHL-wild-type and VHL-mutant systems underscore PFAS as a potential environmental accelerator of renal tumor progression and justify further mechanistic and translational studies.

#5692 Mechanism of antiproliferative activity of tolfenamic acid.

Fatima Rehman[1], Hesham Syed[2], Umesh T. Sankpal[1]

[1]University of North Texas Health Science Center, Fort Worth, TX,[2]University of Texas at Austin, Austin, TX

Non-steroidal anti-inflammatory drugs have been shown to exhibit anti-tumor activities primarily through the inhibition of cyclooxygenases (COX-2). Among them, tolfenamic acid (TA) has also demonstrated potent anti-cancer effects across multiple cancer cell lines but acts through COX independent pathways. The proposed mechanism of action of TA involves its ability to target specificity protein transcription factors (Sp1, Sp3, and Sp4) which in turn downregulate potential oncogenic proteins such as survivin, VEGF, and c-MET. Recent work from our laboratory demonstrated, in medulloblastoma cells, the ability of TA to induce DNA double-strand breaks (DSBs). In this study we investigated the DNA damaging effects of TA across multiple cancer cell lines (including neuroblastoma, ovarian, breast, pancreatic, and prostate) and examined the activation of the DNA damage response pathways. Cell lines representing various cancers were treated with increasing concentration of TA for 48h and DNA damage assessed by monitoring phosphorylation of histone variant H2AX (γH2AX) by Western blot analysis. Activation of the DSB response following TA treatment, in a medulloblastoma cell line was investigated by examining the activation of ATM / ATR and Chk1 / Chk2 by Western blotting. Apoptosis was detected by cleavage of PARP-1 protein. Consistent with our findings in medulloblastoma, we observed a dose dependent increase in γH2AX, following TA treatment for 48h, in all cancer cell lines tested. Levels of cleaved PARP also increased with TA treatment in all cell lines. Furthermore, in medulloblastoma cells, γH2AX was detected as early as 24h post-treatment. We also demonstrated a dose dependent increase in phosphorylation of ATM and Chk2 proteins. Taken together, these results suggest that TA treatment induces DNA DSBs in cancer cells resulting in the activation of ATM and Chk2, a major DNA damage response pathway, ultimately leading to cell death via activation of apoptosis. The results highlight TA's multi-targeted effects and the potential to develop effective combination strategies with other small molecules or drugs to achieve synergistic therapeutic outcomes.

#5693 Synergy of a CDK4/6 inhibitor and an HDAC inhibitor in pancreatic cancer overcomes autophagy.

Vikas Dukhande[1], Shraddha Bhutkar[2], Anjali Yadav[2]

[1]Pharmaceutical Sciences, St. John's University, Queens, NY,[2]St. John's University, Queens, NY

Pancreatic Ductal Adenocarcinoma (PDAC) is a malignant aggressive tumor with a poor prognosis and survival rate. Therapy resistance in PDAC is common and is attributed to metabolic plasticity, dense desmoplastic stroma, tumor heterogeneity, and immune evasion. Our previous study demonstrated synergy and efficacy of Panobinostat (Pan), a pan-HDAC inhibitor, and Abemaciclib (Abe), a CDK4/6 inhibitor, in PDAC cells. We aimed to identify the mechanism of these synergy effects as they can help in therapy efficacy and in overcoming resistance. Our mechanistic studies to understand the combination effects of Pan-Abe utilized transcriptomics and metabolomics experiments followed by Seahorse analysis. Abe treatment resulted in mitochondrial dysfunction whereas Pan treatment induced autophagy and lysosomal processes. We followed these studies using cell biological experiments assessing autophagy profile using fluorescence microscopy and western blotting. The Pan-Abe combination demonstrated metabolic dysfunction but did not induce robust autophagy response. Interestingly, the synergy of Pan-Abe from PDAC cells was confirmed in MIA PaCa-2 tumor xenograft model. Further studies are needed to understand the role of autophagic processes in the efficacy of Pan-Abe in PDAC.

#5694 SQLE inhibitor triggers ovarian cancer apoptosis by causing ER stress.

Cheng Chi[1], Lei Sun[2], Mahmuda Akter[1], Shuang Huang[1]

[1]University of Florida, Gainesville, FL,[2]University of Florida College of Medicine, Gainesville, FL

High-grade serous ovarian cancer (HGSOC) remains highly lethal due to late diagnosis and the high frequency of chemoresistance, underscoring the need to identify new metabolic vulnerabilities that can be therapeutically targeted. This study investigates the mechanism through which inhibition of squalene epoxidase (SQLE), a rate-limiting enzyme that converts squalene to 2,3-epoxysqualene in the cholesterol biosynthesis pathway, suppresses ovarian cancer cell growth, and evaluates the therapeutic potential of the SQLE inhibitor NB-598. Using ovarian cancer cell lines cultured under cholesterol-replete and cholesterol-depleted conditions, we performed cell growth assays, western blot analysis of ER-stress signaling pathways, and apoptosis assays. NB-598 selectively inhibited ovarian cancer cell growth under cholesterol-depleted conditions, and this effect was fully reversed by cholesterol supplementation. Notably, inhibition of upstream HMG-CoA reductase with atorvastatin abolished NB-598-induced growth suppression, suggesting that NB-598 cytotoxicity does not stem from cholesterol deprivation but instead from the accumulation of squalene. Consistently, activation of ER-stress markers and rescue by JNK and p38 inhibitors implicate ER-stress signaling in NB-598-induced toxicity. Apoptosis was confirmed by cell-cycle analysis, Annexin V/PI staining, and western blotting, demonstrating increased sub-G1 populations, elevated early and late apoptotic cells, and cleavage of PARP and caspase-3 in NB-598-treated cells. Together, these findings identify squalene accumulation, rather than cholesterol depletion, as the primary driver of NB-598-induced cytotoxicity in ovarian cancer cells. This work establishes SQLE as a mechanistically defined metabolic target in ovarian cancer and provides a strong rationale for developing SQLE inhibitors as a novel therapeutic strategy.

#5695 CyTOF analysis of targeted therapy in addition to standard of care against Ewing sarcoma tumor subpopulations.

Kaitlyn H. Smith, Lucy Endean, Kimberly Q. McKinney, Poornima Gourabathini, Kenzie Wells, Jeffrey Huo, Erin M. Trovillion, Javier Oesterheld

Atrium Health Wake Forest Baptist Comprehensive Cancer Center, Charlotte, NC

Introduction: The overall survival for Ewing sarcoma (ES) is ~70% after current standard of care (SOC) chemotherapy but outcomes remain dismal for relapsed or metastatic disease. SOC involves chemotherapy using alternating cycles of Vincristine, Doxorubicin, Cyclophosphamide (VDC) with Ifosfamide and Etoposide (IE). ES tumors are increasingly being studied in the context of the EWS:FLI1 fusion. Recent work has shown that the EWS:FLI1^{high} cells are more proliferative and sensitive to chemotherapy and the EWS:FLI1^{low} cells are more invasive and less sensitive to chemotherapy. Cancer stem cells are another population known to be chemoresistant. The invasiveness and decreased sensitivity of these various populations suggest they may contribute to chemoresistance, relapse, and metastasis, representing a major clinical problem. Previous work has shown that HDAC inhibition synergizes with SOC agents due to an accumulation of DNA damage, though the effect on specific subpopulations within tumors remains unknown. The purpose of this study was to identify effects of romidepsin combined with SOC treatment on specific subpopulations of ES cells.

Methods: For *in vitro* experiments, A673 ES cells were treated with vehicle, romidepsin, IE, or romidepsin+IE for 24 hours and then stained for CyTOF analysis. For *in vivo* experiments, A673 cells were injected subcutaneously into Nude mice. Once tumors were 150-200mm^3, mice were grouped and treatment with vehicle, romidepsin, ifosfamide/etoposide (IE), or romidepsin+IE began. Romidepsin was given on days 1 and 4 and IE was given days 2-4. Tumors were harvested and dissociated on day 5 for CyTOF analysis. The CyTOF panel used was designed to assess tumor subpopulations as well as mechanistic changes.

Results: *In vivo* and *in vitro,* the combination treatment led to a significant increase in pH2AX in the bulk tumor cells, indicative of DNA damage. *In vivo,* UMAP display of phenograph clustering, and associated heatmap of expression, revealed distinct changes in expression patterns among treatment groups. In the EWS:FLI1^{high} population both IE alone and IE in combination with romidepsin led to a significant increase in pH2AX. In the EWS:FLI1^{low} population, only the combination led to a significant increase in pH2AX. Furthermore, only the combination treatment led to a significant increase in pH2AX in the cancer stem cell population.

Conclusions: We have identified that the combination of romidepsin with IE, but not IE alone, leads to an increase in DNA damage in the EWS:FLI1^{low} and cancer stem cell populations. This suggests that the addition of romidepsin to SOC may improve treatment efficacy against subpopulations of tumor cells that are known to be chemoresistant. Further, this study highlights the use of CyTOF to assess treatment effects within ES tumor subpopulations to identify therapies that may be more effective against chemoresistant populations.

#5696 RAS(ON) multi-selective inhibitors stimulate the hydrolysis of RAS-GTP to RAS-GDP and drive synergistic combination benefit with KRAS(OFF) inhibitors in G12 mutant tumors.

Hiroyuki Matsubara[1], Alec Millner[2], Yu C. Yang[2], Jun Sun[2], Stephanie Change[2], Shelby L. Steele[2], Marini Thian[2], Miguel Sandoval[2], Zhican Wang[2], Mike Flagella[2], Mallika Singh[2], Jingjing Jiang[2], Jacqueline A. M. Smith[2], Ryan B. Corcoran[1], **Kyle J. Seamon**[2]

[1]Massachusetts General Hospital, Boston, MA,[2]Revolution Medicines, Redwood City, CA

KRAS mutations are among the most common oncogenic drivers across human cancers. Although RAS was long considered undruggable, recent advances have led to multiple classes of direct RAS inhibitors. KRAS(OFF) inhibitors preferentially target the inactive GDP-bound state whereas RAS(ON) tri-complex inhibitors selectively engage the active, GTP-bound form. In addition to suppressing RAS signaling by disrupting interactions with downstream effectors via steric occlusion, the RAS(ON) multi-selective inhibitor daraxonrasib (RMC-6236) and the preclinical tool compound RMC-7977 also activate RAS(ON) GTPase activity and promote the conversion of RAS(ON) to RAS(OFF). By stimulating formation of the inactive, GDP-bound state the RAS(ON) inhibitor enables potent target engagement by a KRAS(OFF) inhibitor and synergistic inhibition of oncogenic KRAS G12 mutant signaling. The inhibitory activity of the combination of daraxonrasib or RMC-7977 with representative mutant-selective KRAS(OFF) and pan-KRAS(OFF) inhibitors was evaluated in a series of KRAS G12 mutant cancer cell lines. In addition, real-time RAS-RAF complex disruption assays were used to monitor the kinetics of target engagement. As predicted, the RAS(ON) multi-selective inhibitors accelerated the rate of RAS-RAF disruption for KRAS(OFF) inhibitors. Consistent with this, a synergistic increase in potency of inhibition of KRAS signaling and cell viability was observed with the combinations. Synergy was dependent on the ability of the RAS(ON) inhibitors to convert RAS(ON) to RAS(OFF) and was abolished with the use of RAS(ON) inhibitors that do not stimulate GTP hydrolysis or the introduction of mutations in RAS that block GTP hydrolysis. *In vivo*, the combination of daraxonrasib and KRAS(OFF) inhibitors at well-tolerated doses drove deep and durable RAS pathway suppression and tumor regressions in various KRAS G12 mutant xenograft models, including models with reduced sensitivity to either single agent, e.g., those with mutant KRAS amplification. Overall, these preclinical findings provide a mechanistic rationale for, and experimental evidence in support of, the clinical evaluation of the combination of a RAS(ON) multi-selective inhibitor that stimulates the GTPase activity of oncogenic KRAS mutants with a KRAS(OFF) inhibitor as a potential therapeutic strategy to maximize RAS inhibition and enhance antitumor activity in RAS-addicted cancers.

#5697 EZH2 inhibition upregulates GD2 to enhance anti-GD2 immunotherapy in Ewing sarcoma.

Kenzie Wells, Kimberly Q. McKinney, Kaitlyn H. Smith, Poornima Gourabathini, Jeffrey Huo, Erin M. Trovillion, Javier Oesterheld

Atrium Health Wake Forest Baptist Comprehensive Cancer Center, Charlotte, NC

Introduction: Ewing sarcoma (ES) is a rare and aggressive malignancy of the bones and soft tissue for which substantial improvements in treatment options are desperately needed. ES cells heterogeneously express GD2, a surface marker for which there are targeted immunotherapies that are effective in other pediatric malignancies. The use of EZH2 inhibitors has been reported to increase expression of GD2 on the surface of sarcoma tumor cells. This study investigated the *in vitro* efficacy of an EZH2 inhibitor at increasing GD2 expression on ES cells with the aim of sensitizing them to anti-GD2 antibody treatment.

Methods: Both commercial and patient derived ES cell lines were treated with low dose tazemetostat for an extended period, up to 28 days, followed by a withdrawal from treatment for 7 days. GD2 expression, cell cycle, and markers of apoptosis were evaluated at regular timepoints using a novel mass cytometry panel (CyTOF). OMIQ was used for data analysis and visualization. Efficacy of naxitamab was examined using immune cell killing assays on an Incucyte S3.

Results: Tazemetostat treatment was found to increase GD2 expression on ES cells without significant impact on cell cycle or apoptosis. Elevation of GD2 expression was reversed upon withdrawal of drug. The addition of naxitamab displayed increased NK cell-mediated cell death in ES cells in response to increased GD2 expression. When pretreated with tazemetostat, GD2-low cell lines exhibit higher levels of apoptosis after treatment with naxitamab compared to untreated cells.

Conclusions: This data supports the use of the EZH2 inhibitor tazemetostat for ES tumors that express low or heterogeneous levels of GD2 to enhance the effectiveness of GD2-targeting immunotherapeutic approaches. This study demonstrates the capability of CyTOF to look at multiple markers simultaneously to achieve a comprehensive characterization of various samples.

#5698 Exploiting MYC Oncogenic Stress for Therapeutic Benefit in Lymphoma.

Smriti Kanangat, James D. Phelan, Louis Staudt

National Institutes of Health, Bethesda, MD

Diffuse Large B-cell Lymphoma (DLBCL) is the most frequently occurring form of Non-Hodgkin's Lymphoma. Gene expression profiling identified two types of DLBCL based on germinal center reaction cell-of-origin: germinal center B cell-like (GCB) or activated B cell-like (ABC) DLBCL. Though GCB patients respond better than ABC to the standard immunochemotherapy regimen, one subtype of GCB patients paradoxically exhibit the lowest response rates. These represent a clinically and genetically distinct subset of DLBCL with both MYC and BCL2 translocations and overexpression, known as 'double-hit' (DHIT)-GCB.

Recently, the ViPOR phase I/II clinical trial in relapsed/refractory DLBCL, designed to target survival pathways in ABC, demonstrated unexpectedly that DHIT-GCB had a 50% complete response (CR) rate. In vitro drug sensitivity studies revealed that venetoclax, a BCL2 inhibitor in ViPOR, is significantly more toxic in DHIT-GCB cell lines than in other BCL2 translocated GCB lines lacking MYC translocations. Thus, we hypothesized that inhibition of BCL2 renders DHIT-GCB malignant cells vulnerable to MYC-induced toxicity, explaining the selective sensitivity of DHIT-GCB lymphomas to venetoclax.

To test this, we employed the degradation tag (dTAG) system to controllably degrade MYC protein in malignant lymphoma cells. We used a knock-in approach to engineer GCB cell lines stably expressing a MYC-GFP-dTAG fusion protein from the endogenous MYC locus. BCL2 inhibition induced rapid apoptosis in these lines, but notably, concomitant degradation of MYC increased the proportion of live, non-apoptotic cells.

To investigate how MYC modulates response to BCL2 inhibition in DHIT-GCB, we performed unbiased transcriptomic and genomic profiling studies in the MYC-dTAG lines. RNA-seq of MYC degradation in a time-course in DHIT-GCB cells validated that MYC gene expression signatures were the most strongly downregulated but, interestingly, showed upregulation of signatures for B-cell differentiation and proliferation. Genome-wide CRISPR screens sorted on viable, non-apoptotic cells treated with venetoclax +/- MYC degradation demonstrated that the strongest genetic regulators of differential response to venetoclax were DNA replication and damage and cell cycle genes. These results indicated that disruption of these pathways could synergize with high MYC to promote sensitivity of DHIT-GCB cells to venetoclax.

Finally, functional assays with clinically available targeted therapies perturbing DNA damage and cell cycle highlighted how MYC levels relate to these processes in malignant B-cells and thus modulate response to BCL2 inhibition.

These studies may suggest drug combinations strategies that would harness the synergism between MYC and BCL2 in DHIT-GCB, and hopefully improve therapeutic outcomes for these DLBCL patients.

#5699 Tegavivint directly targets TBL1 to inhibit b-catenin nuclear oncogenic activity.

Aundrietta Duncan, Prashi Jain, Elena Ramirez, Julissa Simmons, Mahtab Youseffi, **Stephen Horrigan**

Iterion Therapeutics, Houston, TX

Tegavivint (BC2059) is a first-in-class small molecule that has demonstrated clinical activity in multiple cancer types including HCC and NSCLC. Tegavivint binds to TBL1 resulting in inhibition of Wnt/β-catenin oncogenic activity. To further define tegavivint's mechanism of action, we performed a series of biochemical, cell-based, and structural studies to characterize its interaction with TBL1 family members and β-catenin. TBL1, the human homologue of EBI, is a cancer driver gene and core component of the nuclear coactivator complex that regulates protooncogenic transcription factor activity. The TBL1 gene family consists of three highly conserved family members (TBL1x,TBL1xR1,TBL1Y) which are overexpressed and mutated in aggressive and invasive cancers. TBL1 deletion or silencing suppresses tumor cell growth, whereas overexpression induces invasion and EMT. Notably, TBL1 binds directly to nuclear β-catenin to form a regulatory complex on β-catenin target-gene promoters, positioning it as a critical node in Wnt/β-catenin signaling. To characterize the tegavivint-TBL1 interaction we have performed structural and functional studies using recombinant purified TBL1 proteins. TBL1 was observed to self-assemble into a functional dimer, creating the β-catenin binding site, and also spontaneously forming a larger multimeric complex of three dimers. Tegavivint binds directly to both TBL1x and TBLxR1 with nanomolar affinity. Binding of TBL1 to β-catenin was characterized, and a low nanomolar affinity binding region in β-catenin mapped within an armadillo domain. Cell-based studies across multiple cancer types confirmed tegavivint disrupts the TBL1/β-catenin transcriptional complex, selectively promotes degradation of nuclear b-catenin , and impairs β-catenin nuclear transcriptional activity. These studies also characterized the role of active WNT signaling in modulation of TBL1 function and tegavivint activity. An X-ray crystal structure of TBL1xR1 protein was resolved, enabling precise modeling of tegavivint's binding mode within the β-catenin-binding pocket of TBL1. Further structure-guided computational screens identified multiple new structurally diverse chemical series. Similar to tegavivint, these series bind directly to TBL1, disrupt the β-catenin/TBL1 interaction, inhibit β-catenin dependent transcription, and promote nuclear β-catenin degradation. These findings establish the oncogenic driver gene TBL1 as a novel, druggable target in the WNT/ β- catenin signaling pathway and highlight tegavivint as a differentiated therapeutic strategy for Wnt-driven cancers.

#5702 An image-based approach to visualize ADC internalization and cytotoxicity in patient-derived organoids.

Daniele Mori, Javier Frias Aldeguer, Rene Overmeer, Sylvia F. Boj

HUB Organoids B.V., Utrecht, Netherlands

Antibody-drug conjugates (ADCs) represent an emerging class of cancer therapies designed to address the limitations of traditional chemotherapy, particularly the toxicity that arises from healthy cells being exposed to cytotoxic agents. ADCs combine a target-specific monoclonal antibody with a cytotoxic payload, enabling selective delivery to cancer cells and significantly reducing adverse effects. HUB Patient-Derived Organoids (PDOs) are advanced 3D in vitro models derived from adult stem cells that faithfully replicate the architecture, genetics, and physiology of original patient tissues. By preserving patient-specific genetic and phenotypic traits, including surface marker expression, HUB has established a comprehensive and well-characterized biobank of tumor-derived PDOs. This biobank provides a powerful platform for translational research, drug discovery, and the development of targeted therapies. In this study, we present an organoid-based, image-based internalization assay that complements standard Cell Titer-Glo viability assays by enabling direct visualization of ADC internalization. This assay facilitates a deeper exploration of the mechanisms of action of ADCs. We pre-selected tumor-derived organoids based on HER2 expression, which was assessed using flow cytometry. After treating the organoids with FDA-approved HER2-targeting ADCs, we utilized the internalization assay to support the viability data and to define key parameters such as the timing of action, the effect of the payload, and whether cell death resulted from ADC internalization. Overall, these results reinforce the value of patient-derived organoids as a physiologically relevant preclinical platform for ADC development. They also highlight the suitability of the described image-based assay for investigating critical stages of ADC mechanisms, including internalization and payload activity.

#5703 Profiling osteosarcoma convergent evolution and molecular adaptations through patient-derived organoid drug-screening.

Kailee A. Rutherford, Jonathan N. Levi, Summer Norris, Alice Soragni

Department of Orthopaedic Surgery, David Geffen School of Medicine, University of California Los Angeles, CA, USA, Los Angeles, CA

Osteosarcoma is the most common primary bone malignancy in children and young adults, yet accounts for only 2% of cancers in this age group. Its rarity and extensive molecular heterogeneity have hindered biomarker discovery and therapeutic development for more than three decades. Chromosome instability (CIN) is a defining feature of osteosarcoma and contributes to both intratumoral and intertumoral genetic heterogeneity. Emerging evidence suggests that chromosome instability can promote convergent evolution, where distinct genetic alterations arise within shared pathways across subpopulations and may have common druggable vulnerabilities. Drug treatments impose selective pressures that may further influence convergence, although the resulting adaptations remain poorly understood. To investigate how therapeutics shape molecular evolution, we utilize our established high throughput patient-derived tumor organoid (PDO) drug screening platform. This system leverages unpassaged sarcoma organoids that retain all characteristics of the original tumor and shows promising concordance with clinical drug responses (Al Shihabi et al, Cell Stem Cell 2024). Our expanding osteosarcoma biobank comprises multi-sampled osteosarcomas from the same individuals across distinct clinical sites and timepoints, creating a rare resource to study evolutionary trajectories under drug exposure. To improve drug screen interpretability, we developed a quantitative PDO Response Integrated Scoring Model (PRISM) that integrates multiple viability metrics to classify sensitive and resistant phenotypes and allows reproducible comparisons across hundreds of compounds. Drugs are grouped by shared molecular targets and analyzed through pathway enrichment approaches to identify convergent patterns associated with resistance and vulnerability. We further perform single-cell RNA sequencing of organoids persisting post-treatment to directly characterize molecular profiles of resistant cells. Together, this work will establish a scalable map of adaptive molecular states and convergent vulnerabilities in osteosarcoma. Our goal is to define the pathways repeatedly selected under treatment pressure, identify resistant cell states that emerge and uncover molecular dependencies that can be targeted through rational drug combinations. This framework is intended to guide future precision medicine strategies for patients with osteosarcoma.

#5704 Preclinical studies reveal that protease-mediated payload release and immuno-oncology/immunomodulatory effects contribute to the antitumor activity of HLX43.

Lixin Feng, Jijun Yuan, Wan-Jen Yang, Chenqiang Jia, Ge Song, Qingyu Wang, Jun Zhu

Shanghai Henlius Biotech, Inc, Shanghai, China

HLX43 is an innovative PD-L1-targeted antibody-drug conjugate (ADC) designed for cancer treatment. It consists of HLX20, an engineered anti-PD-L1 humanized IgG1 antibody, conjugated via a protease-cleavable tripeptide linker to a potent camptothecin-derived topoisomerase I inhibitor (C24) at a drug-to-antibody ratio (DAR) of 8. Previously reported preclinical studies have demonstrated that HLX43 retains the binding affinity and internalization kinetics of the parental HLX20 antibody and exhibits favorable stability and potent antitumor activity.

The mechanism of action (MoA) of HLX43 is multifaceted, integrating immune checkpoint blockade with payload-induced cytotoxicity. The preclinical studies reported here show that, as an anti-PD-L1 agent, HLX43 effectively blocks PD-1/PD-L1 interaction and reactivates T-cell activity, evidenced by increased IL-2 and IFNγ secretion in mixed lymphocyte reaction assays. The direct cytotoxicity of HLX43 arises from inhibition of DNA repairing and induction of cell apoptosis as evidenced by cleaved PARP and increased γH2AX. In addition, HLX43 induces immunogenic cell death (ICD) marked by increased cell-surface calreticulin, contributing to its immunomodulatory effects. In parallel, protease-mediated cleavage of the linker within the tumor microenvironment (TME)—by enzymes such as matrix metalloproteinases (MMPs) and cysteine proteases—enables payload release independent of the PD-L1 binding. The extracellularly released payload exerts a bystander effect by diffusing into neighbor tissues and killing adjacent PD-L1-negative cancer cells, a feature that underlies HLX43's robust efficacy in patient-derived xenograft (PDX) models with heterogeneous PD-L1 expression. Beyond direct cytotoxicity, HLX43 also remodels the TME, with *in vivo* studies showing increased infiltration of cytotoxic $CD8^+$ T cells and reduced regulatory T cells (Tregs). These $CD8^+$ T cells display enhanced effector function, including elevated IFNγ and Granzyme B expression.

In summary, HLX43's convergent mechanisms—combining immune checkpoint inhibition, targeted cytotoxicity, and TME modulation—support its potential as both a monotherapy and in combination with other immuno-oncology agents, positioning HLX43 as a promising therapeutic candidate across diverse tumor types

#5705 Identifying androgen deprivation-induced responses in prostate cancer with single cell multiomic analysis.

Anni Peramaki[1], Iina Koivisto[1], Alfonso Urbanucci[1], Frank Claessens[2], Mikael Marttinen[1], Matti Nykter[1]

[1]Tampere University, Faculty of Medicine and Health Technology, Tampere, Finland,[2]KU Leuven, Leuven, Belgium

Understanding how cancer cells adapt to therapy and develop treatment resistance remains a major challenge. The main treatment for advanced primary prostate cancer is chemical castration, or androgen deprivation therapy (ADT), which reduces the activity of androgen receptor (AR) in cancer cells. Castration resistance is characterized by AR reactivation which is the main driver of disease progression. While currently available AR signaling inhibitors (ARSI) are effective, in long term treatment, resistance emerges. It has been proposed and tested in neoadjuvant settings to utilize ARSI in early-stage tumors with curative intent. While these trials have shown effectiveness in reducing tumor volume, some cancer cells manage to survive, thus reducing the benefit for patients. It is expected that mechanisms of resistance are patient specific.

To gain insight into how cells adapt in response to ARSI (here, apalutamide), we generated a single-cell multiomic dataset using the single-cell ultra-high-throughput multiomic sequencing assay (SUM-seq), from selected prostate cancer cell lines: 22Rv1, R1AD1, LNCaP, LNCaP-ResA, LAPC4, and VCaP, to observe cell states and aberrant regulatory interactions in detail. These cell lines exhibit distinct androgen responsiveness and resistance mechanisms, including genetic alterations such as AR mutations and amplifications as well as non-genetic mechanisms like AR splice variants. We focused on the direct response to ARSI and thus characterized the cells at 48 hours after treatment.

Multiplexing resulted in a total of 18,477 cells characterized, each with RNA and chromatin profiles. In all cell lines, the treated and control cells formed separate clusters, indicating that the data recapitulates the expected apalutamide response dynamics. More detailed analysis highlighted distinct treatment-associated molecular differences between the cell lines. ADT-responsive cell lines showed decreasing accessibility in sites enriched for AR, SOX, WNT, and MYC family motifs. Paired single-cell RNA and chromatin profiles are ideal for understanding the gene regulatory programs associated with treatment responses. We inferred the gene regulatory network for each cell line using single-cell Deep multi-Omic Regulatory Inference (scDoRI), highlighting distinct regulatory programs (topics) in response to treatment.

Our data underlines diverse responses to apalutamide treatment by prostate cancer cell lines. Integration with treatment response data from patient samples will help to address the role of these cell states and regulators in context of treatment resistance and provide a foundation for selecting appropriate model systems to validate mechanisms observed from the clinical cohorts.

#5706 Modeling the influence of Tumor Treating Fields (TTFields) treatment usage time and break patterns on therapeutic outcomes.

Rotem Engelman[1], Daria Gerasimova[1], Talya Borkum[1], Eyal Dor-On[1], Itai Tzchori[1], **Hila Fishman**[1], Adi Haber[1], Moshe Giladi[1], Uri Weinberg[2], Yoram Palti[1], Na Tosha N. Gatson[3]

[1]Novocure Ltd, Haifa, Israel,[2]Novocure GmbH, Baar, Switzerland,[3]Department of Neurology and Neurosurgery, Indiana University Health Medical Center, Indianapolis, IN and Department of Neurology, University of Arizona College of Medicine, Phoenix, TX

Introduction: Tumor Treating Fields (TTFields) therapy delivers low-intensity, alternating electric fields that disrupt cancer cell division and tumor growth. Clinical evidence indicates that device usage is directly correlated with patient outcomes. While the clinical recommendation for patients is to aim for maximal average monthly usage, there are no clear guidelines on how to manage treatment interruptions within the month. The aim of the current study was to examine the impact of treatment breaks, including their timing and duration, on TTFields efficacy in vitro.
Methods: Human NSCLC (A549) and GBM (U87 MG) cell lines were exposed to TTFields (150 and 200 kHz, respectively; 1 V/cm RMS) under varying treatment schedules incorporating intentional interruptions. Initially, continuous TTFields exposure for 48 or 72 hours was compared to a 48-hour cumulative exposure delivered within a 72-hour experimental window, including either a single 24-hour interruption at mid-treatment or three distributed 8-hour daily breaks. The effect of break timing was then evaluated by positioning a 24-hour interruption at the beginning, middle, or end of the 72-hour treatment period. Subsequently, the duration of the mid-treatment break was extended to 24, 48, or 72 hours (total experimental duration of 72, 96, and 120 hours, respectively), followed by an assessment of fractionating the 72-hour break across the 120-hour period. Treatment efficacy across all conditions was determined by measuring cell counts at experiment completion, expressed as a percentage relative to untreated time-matched controls.
Results: Implementing treatment breaks totaling up to 24 hours within a 72-hour experimental window yielded similar efficacy to uninterrupted TTFields exposure with the same cumulative treatment duration of 48 hours. Comparable results were observed whether the 24-hour interruption was delivered as a single continuous break or fractionated into three 8-hour intervals. Varying the timing of the 24-hour break - at the beginning, middle, or end - did not significantly influence efficacy. Extending the mid-treatment break from 24 (of 72) to 48 (of 96) to 72 (of 120) hours had little effect on TTFields response in U87 MG cells but markedly reduced efficacy in A549 cells when the interruption lasted 72 hours. Fractionating the 72-hour break for the A549 cells across the 120-hour total experimental duration partially restored efficacy.
Conclusions: These results indicate that TTFields efficacy is preserved under short or fractionated 24-hour interruptions but declines with extended continuous treatment breaks. Optimizing treatment adherence and defining tolerable interruption patterns may help sustain clinical efficacy while reducing device burden and improving patient quality-of-life.

#5707 Mechanism of action of GEM144, a POLA1-HDAC11 dual inhibitor, in colorectal cancer models.

Rana Abdel-Samad[1], Avery Lazaro[1], Maura Mack[1], Berthe Hayar[2], Claudio Pisano[3], Nadine Darwiche[2]

[1]Biology, Saint Mary's College, Notre Dame, IN,[2]American University of Beirut, Beirut, Lebanon,[3]Biogem, Centro Ricerche, Ariano Irpino (AV), Italy

Background and objectives: Colorectal cancer (CRC) initiation and progression are governed by complex molecular networks that regulate cell survival and the epithelial-to-mesenchymal transition (EMT). This malignancy remains one of the leading causes of cancer-related mortality worldwide, underscoring the need for novel therapeutic strategies. One promising approach involves the investigation of new molecular entities with enhanced anticancer properties. In this study, we investigated the mechanism of action of a novel hybrid therapeutic candidate, GEM144, which integrates a DNA polymerase-α (POLA1) inhibitor and a histone deacetylase 11 (HDAC11) inhibitor moieties, both reported to play crucial roles in CRC.

Methods: Using human CRC cell lines HCT116 and HT29, and “normal-like” human colon cells CCD-841-CoN, proliferation assays were performed to analyze the effect of GEM144 on cell survival *in vitro*. In addition, CRC xenograft mouse models were used to demonstrate the effect of GEM144 on tumor growth *in vivo*. Finally, SDS-polyacrylamide gel electrophoresis allowed the identification of molecular pathways that are targeted by GEM144.

Results: Our results revealed that GEM144 decreased CRC cell viability *in vitro*, sparing “normal-like” colon cells. This growth inhibition seemed to be partly relying on apoptosis induction, detected by an increase in the expression of the pro-apoptotic protein Bax when cells were treated with GEM144, at concentrations as low as 1 µM starting 24 hours post-treatment. In addition, GEM144 suppressed the EMT, as evidenced by the upregulation of E-cadherin expression, a key epithelial marker that maintains cell-cell adhesion and epithelial integrity. This was accompanied by a tumor burden reduction in HCT116 xenograft mouse models treated with GEM144.

Conclusion: Collectively, these findings provide new insights into the molecular mechanisms underlying the anticancer activity of GEM144 and support its potential as a promising therapeutic candidate for CRC treatment.

#5708 Dual targeting of PDPK1 and mutated BRAFV600E is synthetically lethal.

Tejinder Pal Khaket, Chandrayee Gosh, Zhongyue Yang, Electron Kebebew

General Surgery, Stanford University School of Medicine, Stanford, CA

Anaplastic thyroid cancer (ATC) exhibits near-uniform activation of the MAPK and PI3K/AKT/mTOR pathways, driving resistance to BRAF-targeted therapies. PDPK1, a key AGC-kinase activator downstream of PI3K, integrates multiple oncogenic and stress-response pathways and represents a critical resistance node. We investigated PDPK1 inhibition using BX795 alone and with BRAF inhibition (dabrafenib) in *BRAF*V600E mutant *in vitro* (8505C, SW1736), *ex vivo* (patient-derived ATC spheroids ATC-01, ATC-02), and orthotopic xenograft models. BX795 monotherapy reduced cellular proliferation and invasion, and in combination with dabrafenib produced strong synergistic anticancer activity (Combination Index <1), and led to ~55% tumor volume reduction *in vivo* without toxicity. Mechanistically, dual blockade of PDPK1Ser241 and MEK/ERK phosphorylation, prevented the compensatory upregulation of PI3K/AKT and MAPK pathways seen with monotherapy. The synthetic lethality of dual targeting of PDPK1 and *BRAF*V600E was due to induction of extensive DNA damage (γ-H2AX↑, ATM/CHK2↑), G_2/M cell-cycle arrest through suppression of CDC25C, CDK1, and cyclin A2, and triggering of mitochondrial hyperpolarization with impaired oxidative phosphorylation and increased ROS generation. Elevated mitochondrial ROS amplified DNA-damage signaling, culminating in BAD dephosphorylation, caspase-3 activation, and PARP cleavage. ROS scavengers (N-acetylcysteine, MitoQ) and CHK2 inhibition partially reversed apoptosis and cell cycle arrest, confirming a ROS-CHK2-dependent cell death mechanism. Together, these findings reveal that combined PDPK1 and BRAF inhibition is synthetically lethal in *BRAF*V600E-mutant cancer. PDPK1 represents a targetable vulnerability for enhancing *BRAF*V600E-targeted cancer therapy and in other MAPK/PI3K-coactivated cancers.

: Molecular Targets 2
Poster Session

#5712 Virtual screening identification of FDA approved drugs blocking the therapeutic action of tumor-specific amplitude-modulated radiofrequency electromagnetic fields.

Hugo Jimenez[1], Ping Dou[1], Aaban A. Azmi[1], Elyas Khan[1], Alhussein Elshebiny[1], Yusuf Fateh[1], Nathan Elias[1], Cameron Osenkowski[1], Liyue Zhang[1], Grayson Barker[1], Allan M. Johansen[1], Ravi Paluri[2], Janaka S. S. Liyanage[1], Mohammed N. Al Hallak[1], Anthony F. Shields[1], Muhammad W. Saif[1], Husain Y. Khan[1], Amro Aboukameel[1], Md Hafiz Uddin[1], Sahar F. Bannoura[1], Ramzi M. Mohammad[1], Alexandre Barbault[3], Boris C. Pasche[1]

[1]Oncology, Wayne State University School of Medicine, Barbara Ann Karmanos Cancer Institute, Detroit, MI,[2]Medicine, Atrium Health Wake Forest Baptist Hospital, Winston-Salem, NC,[3]TheraBionic GmbH, Ettlingen, Germany

Background: Amplitude-modulated 27.12 MHz radiofrequency electromagnetic fields (AM RF EMF) delivered via a spoon-shaped antenna placed on the patient's tongue result in shrinkage of the primary and metastatic tumors in patients with advanced hepatocellular carcinoma (HCC). Treatment is FDA-approved for patients with advanced HCC who fail 1stline and 2ndline therapy (H220001). The mechanism by which AM RF EMF has a direct antiproliferative effect depends on the influx of extracellular Ca^{2+} into the cancer cell via $Ca_V3.2$ (*CACNA1H*) T-type voltage-gated calcium channel (VGCC). Here we show that HCC-specific AM RF EMF's (HCCMF) therapeutic action is inhibited by drugs with the same binding profile as ethosuximide.
Methods: Computational docking study, using AlphaFold Protein Structure Database (AFDB accession: AF-O95180-F1-v4) showed that ethosuximide binds to an intracellular, hydrophobic pocket formed by amino acids (AAs) Val79 and Phe80 of the free N-terminal segment and Leu160 and Phe161 of S2-S3 linker of CACNA1H Domain 1. To confirm the ethosuximide binding-pocket (EBP) AAs [Val79, Phe80, Leu160, and Phe161] are important for the inhibition of HCCMF, we virtually screened (VS) the FDA library for drugs that would bind similarly to ethosuximide. Drugs predicted / identified via VS where then tested (colony formation, qPCR, and Fluo-4 Ca^{2+} dye) HCCMF-mediated cell proliferation in HCC cell lines.
Results: Tadalafil and abiraterone acetate are the first two drugs found, via VS and tested, to inhibit HCCMF. In the Huh7 cell line, tadalafil blocked HCCMF-mediated cell proliferation with respect to colony formation and Ki-67/Cyclin D1 expression. Tadalafil also blocked Ca^{2+}influx assessed by Fluo-4 in Huh7 and HepG2 cell lines. Interestingly, we found that sildenafil, while belonging to the same class of phosphodiesterase inhibitors as tadalafil, did not block HCCMF-mediated Ca^{2+}influx. This was shown via Fluo-4 Ca^{2+} staining in both Huh7 and HepG2. Specifically, mean fluorescent intensity (MFI) was higher in the HCCMF treated group even when sildenafil was present. HCCMF-MFI increased by 33.07% (*p*-value: 0.0162, n=5) in Huh7 and by 31.86% (*p*-value: 0.0012, n=5) in HepG2 compared to SHAM (no treatment control).
Conclusions: The availability of the EBP AAs is necessary for HCCMF-mediated inhibition of HCC cell proliferation. Theoretical modelling confirmed by laboratory experiments demonstrate that binding of drugs to this pocket interferes with Ca^{2+} influx and block the anti-cancer effects of HCCMF. These results support the use of computational modeling to predict and identify all FDA drugs which could be used during cancer therapy and should thereby be avoided in patients receiving HCCMF treatment.

#5713 Comparative performance of amplicon-based DNA and RNA NGS co-detection versus hybrid-capture DNA-NGS for SNV/INDEL profiling in Chinese NSCLC driver genes.

Zefeng Xie[1], Yuze Zhao[1], Haitao Li[1], Yu Li[1], Yulan Chen[2], Meilian Liu[3], Xuyuan Li[4]

[1]Department of Thoracic Surgery, First Affiliated Hospital of Shantou University Medical College, Shantou City, China,[2]Department of Oncology, The First People's Hospital of Zhaoqing, Zhaoqing City, China,[3]Department of Pulmonary Oncology, The Affiliated Hospital of Guangdong Medical University, Zhanjiang City, China,[4]Department of Oncology, Shantou Central Hospital, Shantou City, China

Background: Although amplicon-based DNA+RNA NGS co-detection has demonstrated clear advantages over hybrid-capture DNA-NGS for identifying gene fusions in non-small cell lung cancer (NSCLC), the clinical relevance of single-nucleotide variants (SNVs) and small insertions/deletions (INDELs) in NSCLC remains equally critical for precision oncology. However, whether amplicon-based DNA+RNA NGS co-detection provides comparable or improved performance for detecting NSCLC driver-gene SNVs/INDELs relative to hybrid-capture DNA-NGS has not been systematically evaluated.

Methods: We performed a comparative analysis of SNV and INDEL detection across 19 clinically relevant NSCLC driver genes, including AKT1, ALK, ARAF, BRAF, EGFR, ERBB2, FGFR1/2, HRAS, IDH1/2, KIT, KRAS, MAP2K1, MET, MTOR, NRAS, NTRK, PDGFRA, PIK3CA, and RET. Detection rates generated by a 35-gene amplicon-based DNA+RNA NGS co-detection assay (n = 2,242) were compared with those obtained using hybrid-capture DNA-NGS (n = 2,504).

Results: Amplicon-based DNA+RNA NGS co-detection demonstrated significantly higher detection rates for EGFR (50.68% vs 45.73%, $P < 0.05$), KRAS (12.25% vs 10.78%, $P < 0.05$), and KIT (0.40% vs 0.08%, $P < 0.05$) compared with hybrid-capture DNA-NGS. The increase in EGFR detection was primarily driven by improved identification of EGFR L858R (23.39% vs 20.01%, $P < 0.05$). For KRAS, differences were mainly contributed by KRAS G12C (4.12% vs 3.75%) and G12D (2.43% vs 1.80%), though these did not reach statistical significance. In contrast, hybrid-capture DNA-NGS showed a significantly higher detection rate for PIK3CA (6.11% vs 4.51%, $P < 0.05$). For all remaining genes, including AKT1(0.32% vs 0.28%), ALK(0.11% vs 0.12%), ARAF(0.12% vs 0.12%), BRAF(2.89% vs 2.6%), ERBB2(2.98% vs 3%), FGFR2(0.08% vs 0.08%), FGFR3(0.21% vs 0.16%), HRAS(0.08% vs 0.16%), IDH1(0.28% vs 0.28%), IDH2(0.12% vs 0.12%), MAP2K1(0.31% vs 0.48%), MET(0.52% vs 0.52%), MTOR(0.26% vs 0.32%), NRAS(0.41% vs 0.52%), NTRK(0.01% vs 0.04%), PDGFRA(0.12% vs 0.16%), RET(0.1% vs 0.12%), the mutation detection rates showed no significant difference between the two platforms.

Conclusion: This large-cohort comparison demonstrates that amplicon-based DNA+RNA NGS co-detection performs comparably to hybrid-capture DNA-NGS for most NSCLC driver-gene SNV/INDEL alterations, while offering significantly higher sensitivity for critical mutations in EGFR, KRAS, and KIT. These findings indicate that co-detection workflows integrating both DNA and RNA may improve mutation detection efficiency for key actionable NSCLC biomarkers, supporting their broader adoption in routine clinical genomic profiling.

#5714 Amplicon-based DNA and RNA co-detection improves ROS1 fusion identification across Chinese solid tumors compared with hybrid capture DNA-NGS.

Meiyi Li

Guangzhou Medical University Affiliated Qingyuan Hospital (Qingyuan People's Hospital), Qingyuan City, China

Background: ROS1 fusions are actionable drivers across many solid tumors, with multiple targeted therapies approved, yet conventional DNA assays show limited sensitivity. Although RNA-NGS improves fusion detection, the relative performance of amplicon-based DNA+RNA NGS co-detection versus hybrid-capture DNA-NGS for ROS1 fusion identification across diverse tumors remains unclear.

Methods: We analyzed a total of 16,424 solid tumor samples using a 35-gene amplicon-based DNA+RNA NGS co-detection assay, including BTC (n=310), COAD (n=3,839), ESCA (n=83), LIHC (n=123), NSCLC (n=11,242), SARC (n=61), and STAD (n=766). In parallel, 4,624 tumors were assessed using a hybrid-capture DNA-NGS assay, including BTC (n=398), COAD (n=857), ESCA (n=83), LIHC (n=269), NSCLC (n=2,504), SARC (n=67), and STAD (n=446). ROS1-positive cases were identified for each tumor type, and fusion orientation and partner genes were characterized to evaluate differences in fusion detection performance between the two sequencing strategies.

Results: Amplicon-based DNA+RNA NGS co-detection identified 217 ROS1-positive tumors, yielding detection rates of 0.32% in BTC (1/310), 0.10% in COAD (4/3,839), 2.41% in ESCA (2/83), 0.81% in LIHC (1/123), 1.82% in NSCLC (205/11,242), 3.28% in SARC (2/61), and 0.26% in STAD (2/766). All detected ROS1 fusions were canonical 5′-3′ events. Across all fusion-positive tumors, the predominant partner genes were CD74-ROS1 (46.08%), EZR-ROS1 (21.66%), SDC4-ROS1 (16.13%), SLC34A2-ROS1 (3.23%), CCDC6-ROS1 (3.23%), GOPC-ROS1 (2.30%), TPR-ROS1 (0.92%), EML4-ROS1 (0.46%), LRIG3-ROS1 (0.46%), PPFIBP1-ROS1 (0.46%), and ZCCHC8-ROS1 (0.46%). In contrast, hybrid-capture DNA-NGS identified only 43 ROS1-positive tumors, with detection rates of 0.75% in BTC (3/398), 0% in COAD (0/857), 0% in ESCA (0/83), 0.37% in LIHC (1/269), 1.56% in NSCLC (39/2,504), 0% in SARC (0/67), and 0% in STAD (0/446). All fusions detected by DNA-NGS were classical 5′-3′ rearrangements, and the dominant partner genes were CD74-ROS1 (53.49%), SDC4-ROS1 (18.60%), EZR-ROS1 (11.63%), GOPC-ROS1 (6.98%), TPM3-ROS1 (2.33%), ROS1-NT5DC1 (2.33%), ROS1-SLC34A2 (2.33%), and ROS1-TBC1D32 (2.33%). Overall, the co-detection strategy demonstrated substantially higher fusion detection rates and broader partner diversity, particularly in ESCA, NSCLC, and SARC.

Conclusion: Amplicon-based DNA+RNA NGS showed higher sensitivity and broader fusion-partner detection than hybrid-capture DNA-NGS for ROS1 rearrangements, underscoring the value of integrating RNA-based methods into routine testing to improve ROS1 fusion identification and support precision oncology.

#5715 Histone-modifying enzymes in androgen-deprived prostate cancer: EZH1 as a synergistic therapeutic target.

Tanaya Purohit[1], **Emily Schmitt**[1], Zachary Schultz[1], Marcelo Bigarella[1], Kayla Bahr[1], Mohammad Rizvi[1], Diana Garcia[1], Sean Sardeson[1], Erika Heninger[2], Shannon Reese[2], Jacob Popp[2], Joshua M. Lang[3], Karla Esbona[4], Wei Huang[4], Peter W. Lewis[5], John M. Denu[5], Bing Yang[1], David F. Jarrard[1]

[1]Department of Urology, University of Wisconsin-Madison, Madison, WI,[2]Department of Medicine, Division of Hematology-Oncology, University of Wisconsin-Madison, Madison, WI,[3]University of Wisconsin Carbone Cancer Center, Madison, WI,[4]Department of Pathology and Laboratory Medicine, University of Wisconsin-Madison, Madison, WI,[5]Department of Biomolecular Chemistry, University of Wisconsin-Madison, Madison, WI

Background: Androgen deprivation therapy (ADT) is the cornerstone of treatment for advanced prostate cancer (PC). While ADT induces apoptosis and senescence, residual tumor cells frequently persist and drive castration resistance. The initiation of ADT may create vulnerabilities that can be therapeutically exploited. We investigated the role of histone-modifying enzymes (HMEs) in supporting tumor cell survival after ADT, hypothesizing that their upregulation contributes to persistence and represents a target for synergistic therapy.
Methods: High-risk prostatectomy samples treated with 3 months of ADT were compared to untreated controls using bulk RNA sequencing (n=10 vs. 26). Publicly available datasets (Wyatt GSE550162; Sowalsky GSE1831003) were interrogated for validation. The expression of EZH1/2 and H3K27me3 was assessed in hormone-sensitive PC (HSPC) cell lines LNCaP, LAPC4 and VCaP treated with ADT (CSS: charcoal-stripped serum) at different timepoints by Western blotting. A tissue microarray was constructed to evaluate the protein expression of EZH1 in 30 ADT-treated and 29 untreated post-prostatectomy HSPC tumors using immunohistochemistry and automated VECTRA imaging and quantification. HSPC cell lines and patient-derived organoids were treated with bicalutamide or darolutamide in combination with dox-inducible EZH1 shRNAs or FDA-approved EZH1/2 inhibitor valemetostat to examine synergistic inhibition of cell growth.

Results: High-risk prostatectomy samples identified four consistently upregulated HMEs: EZH1, MECOM, SIRT1, and GCN5, KDM6B, PRDM5/6/16 after ADT. Among these, EZH1 and MECOM showed increased protein expression with ADT in a validation tissue microarray of 59 patients with EZH1 correlated with adverse clinical features including and PSA recurrence in the ADT-treated cohort. In LNCaP and VCaP cell lines EZH1 expression rose or persisted after early ADT, while EZH2 declined with increased H3K27 methylation levels. Total H3K27me3 levels increased. EZH1 expression positively associates with a subset of EMT and stem cell markers. EZH1 knockdown reduced survival of ADT-treated cells, and patient-derived organoid models showed synergistic cell death with combined either bicalutamide or darolutamide and EZH1/2 inhibition (valemetostat).
Conclusions: ADT induces EZH1 upregulation, which promotes prostate cancer cell persistence potentially through regulation of cancer stemness and epithelial-to-mesenchymal transition. These findings establish EZH1 as a mediator of survival after ADT and a promising target for synergistic therapeutic inhibition.
Funding Acknowledgements: This study was supported in part by DoD PC150211, UW Prostate SPORE P50CA269011, and NIH/NCIR01CA76184, P30 CA014520. COI: none

#5716 Establishing a drug-target relationship between doxycycline/methacycline and acetylated KLF5 in bone-metastatic prostate cancer.

Duo Zhang, Xinyuan Jiang, Yutian Ren, Yujing Qin, Shiqi Deng, Qifan Zhou, Yuanguang Chen, Zhiqian Zhang, Xumu Zhang, **Jin-Tang Dong**

Southern University of Science and Technology, Shenzhen, China

Advanced prostate cancers (PCa) often metastasize to the bone, where they eventually develop resistance to virtually all available therapies. We previously reported that TGF-β induces acetylation of the transcription factor KLF5 at K369, and acetylated KLF5 (Ac-KLF5) is essential for TGF-β to maintain EMT, promote osteoclast differentiation, and cause bone metastasis in prostate cancer. On the other hand, tetracycline derivatives doxycycline (D) and methacycline (M) can inhibit tumor growth and even metastasis, but their molecular targets remain undetermined. In this study, we screened 1987 FDA-approved drugs to identify those that selectively bind to the $KLF5^{K369Q}$ mutant, which mimics Ac-KLF5, using surface plasmon resonance assays. We identified D and M, but not their parent compound, tetracycline (T), as potential inhibitors of Ac-KLF5. Functionally, D and M but not T inhibited $KLF5^{K369Q}$-induced cell invasion, osteoclast differentiation, and osteolytic bone metastasis. RNA-seq and ChIP-seq analyses identified 22 genes transcriptionally regulated by KLF5K369Q via direct promoter binding, with transcription modulated by D and M but not T. One gene, PGK1, was shown to be responsible for D- and M-suppressed cell invasion, osteolytic differentiation, and bone metastasis. These findings suggest a drug-target relationship between doxycycline/methacycline and Ac-KLF5, providing a therapeutic strategy for treating prostate cancer bone metastases resistant to antiandrogen therapy and chemotherapy.

#5717 Identifying the regions responsible for isoaspartylation and aggregation of SCLC antigen ELAVL4.

Shiori Fukutome[1], Diego Alejandro Velarde[1], Chunli Yan[1], Whitaker Cohn[2], Nazarius Lamango[3], Ite A. Offringa[1]

[1]USC Norris Comprehensive Cancer Center, Los Angeles, CA,[2]USC Mann School of Pharmacy, Los Angeles, CA,[3]Professor, Florida A&M Univ. College of Pharmacy, Tallahassee, FL

Small cell lung cancer (SCLC) is the most aggressive type of lung cancer, with a 5-year survival of 9%. Despite the aggressive nature, therapy options are still limited, and there is a need for the development of new treatments. Pulmonary neuroendocrine cells (PNEs), the predominant cells of origin for SCLC, uniquely express embryonic lethal abnormal vision Drosophila-like 4 (ELAVL4) and are presented on surface of SCLC cells. Clinical research has identified that 15% of SCLC patients with naturally-occurring low titer antibodies against ELAVL4 show significantly better survival. Patients with high-titer antibodies can see complete regression but suffer from a paraneoplastic autoimmune syndrome. The characteristic expression of ELAVL4 in SCLC and the observed improved survival of patients with an immune response against ELAVL4 suggest this protein may be used as a new therapeutic target. Our previous work indicates that the anti-ELAVL4 immune response is triggered by isoaspartylation in the unstructured N-terminal region of ELAVL4 adjacent to the first RNA-recognition motif domain (RRM1). Isoaspartylation occurs when asparagine or aspartic acid side chains spontaneously form a cyclic intermediate with the peptide backbone, followed by hydrolysis, resulting in an isoaspartyl kink that can be antigenic. The N-terminal region contains 6 asparagine residues and 2 aspartic acid residues. Some are followed either by a glycine, serine, or histidine, which increases the likelihood of isoaspartylation. One characteristic of isoaspartylation-prone proteins is the formation of protein aggregates, a process that may play a role in triggering immunogenicity. Here, we aim to identify which residues undergo isoaspartylation and trigger aggregation. We have generated four deletion constructs of the amino acid 1-117 ELAVL4 region (comprising residues 1-13, 8-18, 16-29, and 28-38, fused to RRM1), each including isoaspartylation-prone sites. These constructs are incubated under isoaspartyl-inducing conditions (pH 7.4, 37ºC, 7 d, in K-HEPES). We will use Western blots and mass spectrometry to determine which constructs undergo isoaspartylation and aggregation. Understanding the sites of isoaspartylation and aggregation in ELAVL4 will help identify the optimal target for the development of anti-isoaspartylated ELAVL4 monoclonal antibodies, which may provide a novel, targeted immunotherapy for SCLC patients.

Supported by the Robert E. and May R. Wright Foundation Transformative Cancer ResearchGrant, USC's Undergraduate Research Associates Program, and the Norris ComprehensiveCancer Center core grant, award number P30CA014089 from the NIH/NCI. DAV, NSL and IAO are members of CaRE^2, the Cancer Research Education and Engagement Health Center, which is supported by NIH/NCI grants U54CA233396, U54CA233444, and U54233465.

#5718 Cbx5 as a potential target to enhance immunotherapy in small cell lung cancer.

Hong Cao[1], Yiting Li[1], Jiajia Gu[1], Yuan Hao[2], Ziyang Wang[1], Benjamin A. Nacev[1], Kwok-Kin Wong[2], **Hua Zhang**[1]

[1]Hillman Cancer Center, University of Pittsburgh Medical Center (UPMC), Pittsburgh, PA,[2]Laura and Isaac Perlmutter Cancer Center, New York University Langone Medical Center, New York, NY

Small cell lung cancer (SCLC) is a highly aggressive neuroendocrine carcinoma with a very poor prognosis and accounts for approximately 15% of all lung cancers. Although immunotherapy is now a key component of standard care for SCLC, the clinical benefits remain modest. Growing evidence indicates that epigenetic regulators play important roles in antitumor immunity and in controlling responses to immunotherapy response. In this study, we report Cbx5 as a potential epigenetic regulator of antitumor immunity in SCLC. Our preliminary data suggests that Cbx5 loss may enhance the responses of SCLC tumors to anti-PD-1 therapy in immunocompetent mice. Our preliminary analysis suggests that Cbx5 loss may activate immune response related genes/pathways, while its depletion may derepress endogenous retroviruses in SCLC. Cbx5 deficiency may potentially remodel the tumor microenvironment by converting SCLC from an immune-cold to an immune-hot state. In summary, our findings indicate that Cbx5 may function as a central epigenetic regulator of immune response and immune evasion in SCLC, revealing a potential epigenetic target to enhance responsiveness to immunotherapy. Additional studies are ongoing to validate these findings and further characterize the immunoregulatory mechanisms governed by Cbx5.

#5719 Contrasting roles of MSH2 and MLH1 in basal-like breast cancer.

Tanzia Islam Tithi[1], Jiao Mo[2], Nicholas Borcherding[3], Sung Jo[4], Heather R Kates[5], Chandra Maharjan[6], Seyedehalaleh Anvar[7], Richard L. Bennett[7], Jixiu Shan[8], Rohan A. Desai[7], Kailey E Cash[9], Masayoshi Honda[10], Lei Wang[7], Kawther K. Ahmed[11], Kalyanee Shirlekar[7], Li Chen[7], Katherine N. Gibson-Corley[12], Ronald Weigel[13], Jonathan D. Licht[7], Maria Spies7[13], Ryan Kolb[6], Weizhou Zhang[1]

[1]Department of Pathology, Immunology and Laboratory Medicine, University of Florida, Gainesville, FL,[2]Thermo Fisher Scientific, Alachua, FL,[3]Department of Pathology and Immunology, Washington University School of Medicine, St. Louis, MO,[4]Department of Pathology, University of Iowa Carver College of Medicine, Iowa City, IA,[5]University of Florida Health Cancer Institute, University of Florida, Gainesville, FL,[6]1. Department of Pathology, Immunology and Laboratory Medicine, University of Florida, Gainesville, FL,[7]University of Florida, Gainesville, FL,[8]University of Florida College of Medicine, Gainesville, FL,[9]University of Iowa, Iowa City, IA,[10]University of Iowa, Iowa, IA,[11]University of Baghdad College of Pharmacy, Baghdad, Iraq,[12]Vanderbilt University Medical Center, Nashville, TN,[13]University of Iowa, Iowa city, IA

Basal-like breast cancer (BLBC) is the most aggressive molecular subtype of breast cancer, characterized by high genomic instability. Because of higher mutational load and genetic heterogeneity in BLBC, cancer cells tend to upregulate DNA repair pathways. Therefore, DNA repair-based therapies are considered to have significant potential for BLBC patients. PARP (Poly (ADP-ribose) polymerase) inhibitors are approved by FDA to treat a subset of BLBC patients with *BRCA1/2* mutations. However, most BLBC patients have wildtype *BRCA1/2* and lack good therapeutic targets. We analyzed all available DNA repair genes and proteins using TCGA RNA-sequencing and RPPA (Reverse Protein Phase Array) data. Our investigation identified that mismatch repair (MMR) proteins MSH2 and MSH6 (referred to as MutSα) are highly elevated in BLBC and their higher expressions are correlated to poor survivals of BLBC patients. Conversely, MLH1 and PMS2 (referred to as MutLα), the second major component of the MMR machinery, are downregulated at the mRNA level and cannot predict patient survival in BLBC. In contrast to the known tumor suppressor functions of MMR proteins, our data indicates that MSH2 promotes BLBC metastasis; MLH1, on the other hand, is associated with decreased tumor progression and metastasis. The contrasting functions of MSH2 and MLH1 have never been reported. At the mechanistic level, our data strongly indicate that MSH2, in contrast to MLH1, regulates the expression of chemokines and tumor infiltrating immune cells. Further investigation at the genomic level suggests that MSH2 regulates the expression of interferon alpha/beta receptor 1 (*IFNAR1)*, which plays various roles in the tumor microenvironment (TME) for potential antitumor effects. Deletion of MSH2 initiates a chain of immune reactions via the upregulation of *IFNAR1* expression which explains a highly immune active TME in tumors with MSH2-deficiency. Our study supports the contrasting functions of MSH2 and MLH1 in BLBC progression are due to their distinct transcriptional regulation of immune related genes, not related to their canonical mismatch repair activity. These findings challenge the universal paradigm that all MMR proteins have similar effects on tumor progression or suppression.

#5720 High TROP2 expression is frequent and linked to nodal metastasis in head and neck cancer.

David Dum[1], Juliana Knief[2], Christoph Thorns[2], Morton Freytag[1], Florian Lutz[1], Waldemar Wilczak[1], Katharina Moller[1], Florian Viehweger[1], Fiete Gehrisch[1], Nina Schraps[1], Claudia Hube-Magg[1], Martina Kluth[1], Maria Christina Tsourlakis[1], Ronald Simon[1], Guido Sauter[1], Natalia Gorbokon[1], Munir Hamad[3], Nikolaus Mockelmann[3], Till Clauditz[1], Adrian Munscher[3], **Viktoria Chirico**[1]

[1]University Medical Center Hamburg-Eppendorf, Hamburg, Germany,[2]Pathologie-Hamburg, Medizinisches Labor Nord, Hamburg, Germany,[3]Marienhospital Hamburg, Department of Ear, Nose, and Throat Medicine, Head and Neck Tumor Center, Hamburg, Germany

Head and neck cancers constitute a highly heterogeneous group of malignancies exhibiting variable clinical outcomes. Despite advances in surgery, radiotherapy, and systemic treatments, more than 300,000 patients worldwide die annually from these cancers. The identification of novel molecular markers to improve patient stratification and to guide personalized treatment approaches is therefore urgently needed. The membrane glycoprotein Trophoblast cell surface antigen 2 (TROP2) is the molecular target of sacituzumab govitecan (SG), an antibody-drug conjugate that has been approved for the treatment of metastatic triple-negative breast cancer and advanced urothelial carcinomas. Additionally, it has shown promising clinical activity in other tumor types, such as non-small cell lung cancer, and gastrointestinal cancers. To evaluate the prevalence and potential clinical significance of TROP2 expression in head and neck cancer, we analyzed a total of 583 head and neck cancers by immunohistochemistry (IHC) in a tissue microarray format. H score analysis was used to define cancers as strongly positive (h-score 300), moderately positive (200-299), weakly positive (1-199), or negative (0). TROP2 expression was found to be strong in 53.7%, moderate in 18.8%, weak in 22.8%, and negative in 4.7% of 531 evaluable head and neck carcinomas. There was a marked variability of TROP2 expression between tumors of different localization. TROP2 expression was found to be strong in 61.2% of 336 carcinomas of the oropharynx, 48.0% of 25 cancers of the hypopharynx, 40.1% of 143 cancers of the larynx, 37.5% of 8 carcinomas of the oral cavity, and in 21.4% of 14 carcinomas of the nasopharynx (p=0.0028). Among 347 patients with data on the pN-stage, high TROP2 expression was associated with nodal metastasis (p=0.0002). However, the level of TROP2 expression was statistically unrelated to pT-stage (p=0.3206), histologic grade of malignancy (p=0.7732), presence of distant metastasis (M1, p=0.4024), L-status (p=0.2895), and V-status (p=0.6822). It is concluded from our data, that high level TROP2 expression is very common in head and neck cancers. Accordingly, many patients with these tumors could potentially benefit from SG treatment. Site specific differences in TROP2 expression levels are likely to be driven by location-specific risk factors for subtypes of head and neck cancers.

#5721 Aldehyde dehydrogenase inhibition as a strategy to overcome drug-refractory multiple myeloma.

Michael J. Ingling[1], Robert Chitren[1], Krishne Gowda[2], Shantu Amin[3], Subash C. Jonnalagadda[4], Tulin Budak-Alpdogan[5], Manoj Pandey[6]

[1]Department of Biomedical Sciences, Cooper Medical School of Rowan University (CMSRU), Camden, NJ,[2]Penn State College of Medicine, Hershey, PA,[3]Penn State University College of Medicine, Hershey, PA,[4]Department of Chemistry and Biochemistry, Rowan University, Glassboro, NJ,[5]MD Anderson Cancer Center at Cooper, Cooper University Health Care, Camden, NJ,[6]Rowan University, Glassboro, NJ

Multiple myeloma (MM) remains an incurable hematologic malignancy characterized by inevitable relapse and progressively therapy-resistant disease, despite the widespread use of combination regimens and autologous stem cell transplantation (ASCT). While only ~30% of patients achieve a complete response following initial therapy and ~40-50% with ASCT, the durability of these responses is limited, underscoring the persistence of highly drug-refractory cellular subpopulations. Increasing evidence implicates multiple myeloma stem-like cells (MMSLCs), a $CD138^{-}/ALDH^{+}$ phenotype enriched for self-renewal, metabolic plasticity, and intrinsic chemoresistance, as key drivers of relapse. Aldehyde dehydrogenases (ALDHs) promote MM survival by detoxifying cytotoxic aldehydes and sustaining retinoic acid-dependent stemness pathways, making them attractive therapeutic targets. We report the development and characterization of KS100, a novel pan-ALDH inhibitor, which potently eliminates both bulk MM cells and MMSLC populations in treatment-naïve and treatment-resistant models in vitro and in vivo. KS100 significantly reduces clonogenic growth, exhausts the ALDH-high compartment, and synergizes with standard MM therapies, including proteasome inhibitors and IMiDs, even in models with established resistance. These findings demonstrate that ALDH inhibition disrupts a universal resistance mechanism and position KS100 as a promising therapeutic strategy to eradicate stem-like reservoirs and improve long-term disease control in MM.

#5722 Protein regulator of cytokinesis 1 (PRC1) promotes Wilms tumor progression by orchestrating tumor-stromal crosstalk.

Qiushi Wang, Tianshun Zhang

The Hormel Institute, University of Minnesota, Austin, MN

Wilms tumor (WT) is the most common pediatric renal malignancy and a major cause of cancer-related morbidity in children. Despite advances in multimodal therapy, patients with high-risk histology, relapsed disease, or bilateral WT continue to experience poor survival and long-term treatment-related toxicity. The absence of effective targeted therapies highlights the urgent need to identify new oncogenic drivers and therapeutic vulnerabilities in WT. Using integrative systems biology approaches, including Weighted Gene Co-expression Network Analysis (WGCNA) and survival analysis across TARGET and GEO datasets, we identified Protein Regulator of Cytokinesis 1 (PRC1) as a gene significantly associated with unfavorable prognosis. PRC1, a critical mediator of spindle organization and cytokinesis, has been implicated in multiple adult cancers, yet its role in Wilms tumor remains undefined. We hypothesize that PRC1 drives Wilms tumor progression by dual mechanisms: (1) intrinsically promoting tumor cell proliferation via the β-catenin/WT1 axis, and (2) extrinsically reprogramming the tumor stroma through paracrine signaling between WT cells and cancer-associated fibroblasts (CAFs). These findings will provide new mechanistic insights into the role of PRC1 in pediatric kidney cancer and may inform future targeted therapeutic strategies to improve outcomes for children with aggressive or refractory Wilms tumors.

#5723 TMEM165-CLOCK fusion protein drives metastasis through enhanced lysosomal exocytosis.

Youngkeun Lee, Ji-yoon Choi, Min-jeong Kim, **Sung Wook Seo**

Samsung Medical Center, Seoul, Korea, Republic of

TMEM165-CLOCK is a chimeric protein identified in osteosarcoma, where its expression correlates with poor prognosis. The fusion incorporates CLOCK in reverse orientation without clear functional contribution but truncates the C-terminal transmembrane domain of TMEM165, potentially altering its subcellular localization and function. We investigated its clinical impact and underlying mechanisms. TMEM165-CLOCK expression was quantified by RT-qPCR in UPS and NSCLC cohorts and correlated with clinical outcomes. Subcellular localization was assessed by colocalization imaging. Calcium flux, lysosomal exocytosis, and cathepsin S secretion were compared between parental KHOS/NP cells and TMEM165-CLOCK-overexpressing KHOS/NP cells. Tumor aggressiveness was evaluated by migration, invasion, and a rat metastasis model. RT-qPCR analysis in the UPS cohort showed that higher TMEM165-CLOCK expression correlated with worse progression-free survival (HR: 2.71, p=0.040). In the lung cancer cohort, TMEM165-CLOCK expression significantly correlated with advanced tumor stage (p= 0.038) and nodal stage (p=0.014) at presentation, suggesting cross-cancer relevance. Colocalization imaging revealed a marked shift from Golgi localization to increased presence at lysosomes and the plasma membrane. His-tag imaging confirmed C-terminal exposure on the cell surface, rendering the fusion protein as a druggable target. Despite this redistribution, TMEM165-CLOCK did not alter Golgi glycosylation, as glycosylated LAMP2 levels remained unchanged. In contrast, TMEM165-CLOCK-overexpressing KHOS/NP cells displayed impaired ATP-induced calcium dynamics, with reduced peak amplitude and delayed recovery to baseline, consistent with disrupted calcium homeostasis. These cells showed enhanced lysosomal exocytosis, evidenced by increased surface LAMP1 exposure, and significantly elevated cathepsin S secretion. Functionally, TMEM165-CLOCK overexpression increased cell migration and invasion. siRNA-mediated knockdown of the fusion protein rescued the invasive phenotype, establishing causality. In vivo, rats injected with TMEM165-CLOCK-expressing UPS cells developed markedly greater metastatic burden compared to controls, confirming the fusion's pro-metastatic activity. TMEM165-CLOCK promotes tumor progression through mechanism involving subcellular relocalization, disrupted calcium homeostasis, and enhanced lysosomal exocytosis with cathepsin S release. Its association with aggressive disease across sarcoma and lung cancer identifies TMEM165-CLOCK as a driver of metastasis and potential therapeutic target.

#5724 HMGB1 overexpression is a strong and independent prognostic feature in ERG negative prostate cancer.

Neele Heckmann[1], Nicolas Hertzsprung[2], Christian Bernreuther[3], Eike Burandt[3], Florian Lutz[3], Clara Luhr[3], Clara von Bargen[3], Martina Kluth[3], Maria Tsourlakis[3], Nina Schraps[4], Fiete Gehrisch[4], Ronald Simon[3], Hans Heinzer[1], Alexander Haese[1], Henning Plage[2], Sarah Minner[3], Guido Sauter[3], Thorsten Schlomm[2], Markus Graefen[1], **Cosima Volkl**[3]

[1]Martini-Clinic, Prostate Cancer Center,University Medical Center Hamburg-Eppendorf, Hamburg, Germany,[2]Department of Urology, Charite - Universitatsmedizin Berlin, Berlin, Germany,[3]University Medical Center Hamburg-Eppendorf, Hamburg, Germany,[4]General, Visceral and Thoracic Surgery Department and Clinic, University Medical Center Hamburg-Eppendorf, Hamburg, Germany

High-mobility group box 1 (HMGB1) is a chromatin-associated protein with a key role in DNA damage repair and genome stability, involved in DNA replication, transcription, and chromatin remodeling. By impacting the activity of multiple signaling pathways HMGB1 contributes to critical characteristics of cancer cells including proliferation, migration and invasion, angiogenesis, and cellular energy metabolism. Depending on the tumor type, both increased and reduced expression of HMGB1 have been found to be linked to unfavorable tumor features and poor patient prognosis. To better understand the prevalence and clinical relevance of HMGB1 expression in prostate cancer, a tissue microarray containing 17,747 prostate cancer samples from patients with follow-up data was analyzed by immunohistochemistry (IHC). In normal prostate epithelium, HMGB1 expression was strong in basal cells but only weak in acinar cells which are considered the precursor cells of prostatic adenocarcinoma. HMGB1 IHC was interpretable in 13,642 cancers and was rated negative in 19.9%, weak in 56.1%, moderate in 22.4%, and strong in 1.6% of tumors. HMGB1 staining was significantly more frequent and more intense in cancers harboring the *TMPRSS2:ERG* fusion (91.6% positive) than in ERG fusion negative tumors (70.4% positive; $p<0.0001$). A comparison with clinico-pathological features revealed significant associations between high HMGB1 expression and advanced pT stage, high Gleason grade, high quantitative Gleason grade ($p\leq0.0001$ each), nodal metastases ($p=0.0038$), and early PSA recurrence ($p<0.0001$). A subgroup analysis of 3,854 ERG positive and 4,751 ERG negative cancers revealed that the prognostic impact of HMGB1 expression was entirely driven by the ERG negative group ($p<0.0001$) while the level of HMGB1 expression did not impact PSA recurrence in ERG positive cancers. Several different multivariate analyses considering either preoperatively available (cT, PSA, Gleason grade obtained on biopsies) or postoperatively available (pT, pN, Gleason grade obtained on the entire prostate, R status) parameters unanimously revealed an independent prognostic impact of HMGB1 expression in ERG negative cancers ($p<0.0001$) if compared to established prognostic parameters. It is concluded that HMGB1 overexpression is a potentially clinically useful prognostic feature of ERG negative prostate cancer which can be assessed by IHC. The striking impact of the ERG status on the prognostic role of HMGB1 expression could be identified due to high dimension of our patient cohort. It may be possible that other molecular key alterations also critically affect the impact of established prognostic markers in other cancer types.

#5725 Targeting Rac1 as a therapeutic vulnerability in T-cell lymphomas.

Lucero Alvarado[1], Maria M. Debernardi[1], Gonzalo Gonzalez[1], Helena Andrea Sterle[1], Valeria G. Sanchez[1], Silvina Palmer[2], Sofia Rivarola[2], Jorgelia Real[3], Barrozo Julio[3], Goergina A. Cardama[4], **Florencia Cayrol**[1]

[1]UCA Instituto de Investigaciones Biomedicas, Buenos Aires, Argentina,[2]Servicio de Hematologia, Hospital Britanico, Buenos Aires, Argentina,[3]Servicio de Patologia, Hospital Britanico, Buenos Aires, Argentina,[4]Centro de Oncologia Molecular y Traslacional (COMTra), Universidad Nacional de Quilmes-CONICET, Bernal, Argentina

T-cell lymphomas (TCL) are aggressive and heterogeneous neoplasms with limited therapeutic options and poor prognosis, underscoring the need for novel molecular targets. Here, we investigated Rac1, a Rho GTPase that regulates cytoskeletal dynamics, migration, and survival pathways, as a potential therapeutic vulnerability in TCL. Its central role in these tumor-promoting processes suggests that Rac1 inhibition could represent an innovative strategy to limit lymphoma growth and dissemination. We first evaluated the anti-lymphoma activity of the pharmacological Rac1 inhibitor 1A-116 in a panel of TCL cell lines (EL4, CUTLL1, OCI-Ly12, OCI-Ly13.2, HuT78, MJ, Karpas299). Cell viability was assessed by luminescence assay, and apoptosis by caspase-3/7 activity after 48 h of treatment. We found that 1A-116 markedly reduced cell viability in all models ($p<0.01$), with IC_{50} values ranging from 20 to 250 µM, and induced a 60-200% increase in caspase activity ($p<0.05$). Basal Rac1 expression was elevated compared with healthy murine lymph node controls, showing a 30-60% increase across cell lines ($p<0.05$). Consistently, basal phosphorylated PAK 1-3 levels, an indicator of Rac1 pathway activation, were significantly higher in most lines, except for HuT78 and Karpas299, the most resistant cells to Rac1 inhibition. To further validate the therapeutic potential of Rac1 targeting, we used a syngeneic mouse model bearing subcutaneous EL4 tumors. Daily intraperitoneal injections of 1A-116 (20 mg/kg) for nine consecutive days significantly reduced tumor growth, showing an average 80% reduction in tumor area under the curve ($p=0.0071$) and a 79% decrease in final tumor volume ($p=0.0175$), with no overt signs of toxicity. Finally, analysis of three independent TCL RNA-seq datasets (GSE113113, GSE168508, GSE58445) showed that increased expression of Rac1 activators such as VAV1 and TIAM2, and downstream effectors such as PAK2 and GSK3 correlates with advanced disease and poorer survival ($p<0.05$). In line with these findings, Rac1 immunostaining in 14 TCL biopsies revealed positive expression in all cases, underscoring the clinical relevance of Rac1 signaling in TCL. Together, these results identify Rac1 as a key molecular driver in TCL and establish its pharmacological inhibition as a promising and translationally relevant therapeutic strategy. Our study provides a strong rationale for further evaluation of Rac1 inhibitors, either alone or in combination regimens, to improve treatment outcomes in patients with T-cell lymphomas. Overall, these data identify Rac1 signaling as a promising target that may expand the currently limited treatment landscape for these aggressive malignancies.

#5726 Targeting canine bladder cancer with Nimbolide, a Neem (*Azadirachta indica*) limonoid.

Conner Suen[1], Eashan Sharma[2], Gabriel Gilchrist[2], Neelu Batra[3], Christopher A. Lucchesi[3], Kenneth A. Iczkowski[4], Robert B. Rebhun[5], **Paramita M. Ghosh**[3]

[1]Urological Surgery, University of California Davis, Sacramento, CA,[2]Research Service, VA Northern California Health Care System, Sacramento, CA,[3]Urological Surgery, University of California Davis School of Medicine, Sacramento, CA,[4]Pathology and Laboratory Medicine, University of California Davis School of Medicine, Sacramento, CA,[5]Surgical and Radiological Sciences, University of California Davis School of Veterinary Medicine, Davis, CA

Background: The 5-year relative survival rate for Bladder Cancer (BlCa) patients with distant metastases is about 9%. Hence, novel and innovative therapies for metastatic BlCa are required. Dogs were found to develop muscle-invasive BlCa (MIBC) spontaneously and 10% progress to distant metastases at the time of diagnoses. Currently most dogs with MIBC are treated with non-steroidal anti-inflammatory drugs (NSAIDs); however, <25% respond to them. Our quest was to identify low-cost natural compounds of low toxicity that can be used in dogs. Nimbolide, a limonoid extracted from *Neem* leaves, was found to have anti-tumor effects in human BlCa cell lines. Hence, we tested whether this natural product will be effective in canine BlCa cell lines.
Methods: We obtained two canine BlCa cell lines - K9TCC-PU-AXC (AXC), that formed tumors in nude mice and K9TCC-PU-Pu (PuPu), which did not, from Dr. Deborah Knapp, Purdue University. Cell viability was estimated by MTT assay and by live/dead cell staining on 3D-printed spheroids. Flow cytometry was used to estimate the rate of apoptosis. Autophagy was estimated by the expression of LC3B and p62 whereas EMT was estimated by the expression of vimentin, Snail-1, Snail-2, and cell migration was estimated by scratch assay using a Cytation 5 platform.
Results: Nimbolide was more effective in suppressing proliferation in PuPu cells (IC_{50} = 0.656 µM) compared to AXC cells (IC_{50} = 1.2 µM). Flow cytometric analysis showed that AXC did not undergo apoptosis in response to nimbolide whereas PuPu did; however, nimbolide caused autophagy in both cells. On the other hand, nimbolide prevented epithelial mesenchymal transition (EMT) and migration in AXC, but not in PuPu cells. These effects of nimbolide were not seen in human dermal fibroblasts, underlining the specificity and selectivity of nimbolide.
Conclusions: Based on these results, we intend to develop nimbolide as a therapeutic tool in the treatment of canine BlCa in future studies.
Acknowledgements: The content is solely the responsibility of the authors and does not necessarily represent the official views of the National Institutes of Health, the Department of Veterans Affairs or the United States Government. We are grateful for a generous award from the University of California Comprehensive Cancer Center (UCDCCC) Support Grant (P30CA093373) for this project.

#5727 MTAP deficiency is common in head and neck tumors but dependent on the site of tumor origin.

Juliana Knief[1], Christoph Thorns[1], Morton Freytag[2], Florian Lutz[2], Viktoria Chirico[2], David Dum[2], Waldemar Wilczak[2], Katharina Moller[2], Florian Viehweger[2], Fiete Gehrisch[2], Nina Schraps[2], Claudia Hube-Magg[2], Martina Kluth[2], Maria C. Tsourlakis[2], **Ronald Simon**[2], Guido Sauter[2], Natalia Gorbokon[2], Munir Hamad[3], Nikolaus Mockelmann[3], Till Clauditz[2], Adrian Munscher[3]

[1]Pathology-Hamburg, Medizinisches Labor Nord, Hamburg, Germany,[2]Institute of Pathology, University Medical Center Hamburg-Eppendorf, Hamburg, Germany,[3]Department of Ear, Nose, and Throat Medicine, Head and Neck Tumor Center, Marienhospital Hamburg, Hamburg, Germany

Head and neck cancers (HNCs) represent a heterogeneous group of malignancies with highly variable clinical outcomes. Despite advances in surgery, radiotherapy, and systemic treatments, more than 300,000 patients still die from HNC every year worldwide. S-methyl-5′-thioadenosine phosphorylase (MTAP) is encoded by the *MTAP* gene located at 9p21 and is often homozygously co-deleted in cancer together with cyclin dependent kinase 2A (*CDKN2A*). MTAP deficiency results in a critical vulnerability of cancer cells towards drugs targeting multiple pathways. Since MTAP is ubiquitously expressed and homozygous *MTAP* deletions result in a complete expression loss, MTAP immunohistochemistry (IHC) can be used for its detection. To evaluate the prevalence and clinical significance of MTAP expression loss in head and neck cancer, a total of 583 carcinomas were analyzed by immunohistochemistry (IHC) in a tissue microarray format. MTAP expression was lost (0+; MTAP deficiency) in 15.2%, weak (1+) in 31.2%, moderate (2+) in 29.7%, and strong (3+) in 23.9% of 508 interpretable head and neck carcinomas. The prevalence of MTAP deficiency varied markedly between tumors of different sites of origin. MTAP deficiency occurred in 36.0% of 25 cancers of the hypopharynx, 27.0% of 126 cancers of the larynx, 33.3% of 6 carcinomas of the oral cavity, 21.4% of 14 carcinomas of the nasopharynx, but only 8.6% in 336 carcinomas of the oropharynx ($p<0.0001$). MTAP deficiency tended to be more prevalent in tumors of high pT-stage ($p=0.0923$) and in patients with concomitant metastases (M1; $p=0.0625$) but these differences did not reach a level of statistical significance. MTAP deficiency was unrelated to histologic grade of malignancy, nodal metastasis, L-status, and V-status. Among 432 head and neck cancers lacking MTAP deficiency, the level of MTAP expression (1+ vs 2+ vs. 3+) was unrelated to parameters of cancer aggressiveness. It is concluded from our data, that MTAP deficiency occurs in a relevant fraction of head and neck cancers. Once anti-MTAP treatments should become safe and efficient and approved for patient treatment, many patients with these tumors could benefit. Moreover, IHC analysis for MTAP deficiency appears to have diagnostic utility in assessing dysplasia, given its high prevalence in grade 1 carcinomas.

#5728 Amplicon-based DNA and RNA NGS co-detection enhances ROS1 fusion detection and partner diversity compared with hybrid-capture DNA-NGS in Chinese NSCLC.

Yang Zebo

Cardiothoracic Surgery Department, Yichang Central People's Hospital, Yichang City, China

Background: ROS1 rearrangements are important actionable drivers in non-small cell lung cancer (NSCLC), yet traditional DNA-based assays show limited sensitivity for detecting these fusions. RNA-NGS has been demonstrated to outperform DNA-NGS in fusion detection; however, the relative performance of amplicon-based DNA+RNA NGS co-detection versus hybrid-capture DNA-NGS for identifying ROS1 fusions in large real-world NSCLC populations remains insufficiently characterized.
Methods: We retrospectively analyzed ROS1 fusion detection in NSCLC samples using two next-generation sequencing strategies: a 35-gene amplicon-based DNA+RNA NGS co-detection assay (n = 11,242) and a hybrid-capture DNA-NGS assay (n = 2,504). For both approaches, ROS1 fusion-positive cases were identified, and all confirmed rearrangements were annotated for fusion partners. Detection rates and partner diversity were compared to evaluate differences in analytical performance between the two platforms.
Results: Amplicon-based DNA+RNA NGS co-detection demonstrated a higher ROS1 fusion detection rate (1.82%, 205/11,242) than hybrid-capture DNA-NGS (1.56%, 39/2,504). Amplicon-based DNA+RNA NGS co-detection identified a wide variety of classical 5′-3′ ROS1 fusion partners, with CD74-ROS1 (46.34%), EZR-ROS1 (22.93%), and SDC4-ROS1 (16.10%) being the most prevalent, followed by less frequent partners such as TPM3-ROS1(10/205, 4.88%), SLC34A2-ROS1(7/205,3.41%), CCDC6-ROS1(5/205,2.44%), GOPC-ROS1(2/205,0.98%), TPR-ROS1(2/205,0.98%), and several rare events including EML4-ROS1(1/205,0.49%), LRIG3-ROS1(1/205,0.49%), PPFIBPI-ROS1(1/205,0.49%), and ZCCHC8-ROS1(1/205,0.49%). In contrast, hybrid-capture DNA-NGS detected a narrower spectrum of partners, dominated by CD74-ROS1 (58.97%), SDC4-ROS1 (20.51%), and EZR-ROS1 (12.82%), with only isolated occurrences of GOPC-ROS1, TPM3-ROS1, and a single ROS1-SLC34A2 event. All rearrangements detected by either method were classical 5′-3′ fusions.
Conclusion: In this large real-world cohort, amplicon-based DNA+RNA NGS co-detection outperformed hybrid-capture DNA-NGS by yielding a higher ROS1 fusion detection rate and uncovering a more diverse spectrum of ROS1 fusion partners. These findings highlight the importance of integrating RNA-based analysis into routine NGS workflows to enhance the detection accuracy of actionable gene fusions and support more precise therapeutic decision-making for patients with NSCLC.

#5729 Discovery of tumor-specific antigens in melanoma tissue biopsies via integrated proteogenomic analysis.

Arthur Viode[1], Daniel Gautheret[2], Anamarija Pfeiffer[1], Hughes Hermann[3], Sharane Muralli[3], Severine Roy[4], Antoine Meant[3], Amaury Lachaud[1], **Yuehan Feng**[1], Caroline Robert[3]

[1]Biognosys AG, Schlieren, Switzerland,[2]Institute of Integrative Biology of the Cell (I2BC), Universite Paris-Saclay, CEA, CNRS, Gif-sur-Yvette, France,[3]Biomarqueurs predicteurs et nouvelles strategies moleculaires en therapeutique anticancereuse, Universite Paris-Saclay, Gustave Roussy, Inserm, Villejuif, France,[4]Biomarqueurs predicteurs et nouvelles strategies moleculaires en therapeutique anticancereuse, Gustave Roussy, Inserm, Villejuif, France

Background
Despite significant progress in therapeutic outcomes, melanoma remains frequently resistant to immunotherapy. Efforts to improve response rates include the development of vaccines targeting tumor neoantigens; however, the optimal tumor-associated antigens (TAAs) to target remain uncertain. Recent evidence suggests that the most relevant TAAs may originate from non-mutated protein sequences, including those derived from the so-called dark proteome (1). In this study, we conducted an immunopeptidomic analysis of tumor samples obtained from patients with metastatic melanoma before initiation of systemic therapy
Methods
A total of 35 tumor biopsy samples from melanoma patients were subjected to native tissue lysis, followed by immunoaffinity purification of HLA class I complexes using a pan HLA class I antibody (W6/32) and subsequent elution of the bound immunopeptides. The isolated immunopeptides were analyzed using data-independent acquisition (DIA) mass spectrometry on an Exploris 480 mass spectrometer (Thermo Scientific) equipped with FAIMS Pro. Data analysis was performed using Spectronaut 20 (Biognosys) using directDIA.
For peptide identification, a customized human proteome database was constructed to enable the detection of tumor-associated antigens (TAs). This database included the canonical and isoforms human proteome, a previously reported TA reference dataset (1), and an in-house generated “dark genome” database derived from tumor RNA-sequencing data.
Results
Analysis of these 35 melanoma tissue samples yielded in total over 120,000 unique immunopeptides with an average of ~15,000 per sample, with notable inter-sample variability (ranging from ~6,000 to >28,000 identifications). All samples displayed the expected HLA class I length distribution, with a predominant population of 9-mer peptides. Across the cohort, approx. 70 previously reported tumor-associated antigens (TAs) were identified, spanning multiple categories including tumor-associated antigens (TAA), lineage-specific antigens (LSA), and aberrantly expressed tumor-specific antigens (aeTSA). These TAs originated from both annotated open reading frames (ORFs) and noncanonical translation events such as frameshifts, noncoding RNA (ncRNA), and 5′UTR-derived peptides.
From the RNA-seq-derived database, approximately 22 immunopeptides were mapped to sequences originating from both annotated genes (18 peptides) and previously uncharacterized genomic regions (4 peptides; dark genome).
Together, these results demonstrate that the applied proteogenomic immunopeptidomics workflow enables the detection of tumor-specific and neoantigenic peptides directly from clinical melanoma biopsy samples, underscoring its potential utility in translational immuno-oncology research.
Reference: (1) Apavaloaei et al. Nature Cancer, 2025

#5730 CDX1 binding to the *PVT1* exon 9-associated promoter drives oncogenic *PVT1* exon 9 overexpression in aggressive prostate cancer.

Chinedum C. Udekwu[1], Siti K. Nuraziza[1], Seidu Adams[1], Rachel E. Bonnaci[1], E. Oluwabunmi Olapade-Olaopa[2], Olorunseun O. Ogunwobi[1]

[1]Biochemistry and Molecular Biology, Michigan State University, East Lansing, MI,[2]Department of Surgery, University of Ibadan, Ibadan, Nigeria

This study elucidates a previously uncharacterized epigenetic-transcriptional regulatory axis involving the transcription factor CDX1 and the *PVT1* exon 9-associated promoter (PEAP) that governs *PVT1* exon 9 overexpression in aggressive prostate cancer. The long noncoding RNA (*lncRNA*) *PVT1*, located at the 8q24 oncogenic locus, has been implicated in prostate tumorigenesis and progression; however, the molecular mechanisms underlying its exon-specific transcriptional activation remains obscure. Through in silico motif discovery using FIMO analysis, we identified a high-affinity CDX1 consensus binding site within the PEAP sequence, suggesting a potential transcriptional regulatory role. DNA methylation profiling of matched prostate tumor and adjacent normal tissues from prostate cancer patients demonstrated promoter hypomethylation at PEAP, concomitant with a significant upregulation of *PVT1* exon 9. While siRNA-mediated CDX1 silencing in *PVT1* exon 9 overexpressing cells (MDA-PCa-2b and C22OH) attenuated *PVT1* exon 9 expression, CDX1 overexpression in RWPE-1 cells enhanced *PVT1* exon 9 transcription. Immunohistochemical and immunofluorescence analysis corroborated the nuclear localization and elevated expression of CDX1 in high-Gleason-grade tumors, underscoring its role as a transcriptional activator. Using digital PCR, CRISPR-mediated base editing of the CDX1 binding sequence on PEAP in MDA-PCa-2b and C22OH revealed drastic reduction in *PVT1* exon 9 copy number compared to scramble. Collectively, these findings delineate a CDX1-PEAP-PVT1 signaling axis that is dependent on CDX1 binding to PEAP, thereby driving oncogenic *PVT1* exon 9 overexpression. This mechanistic insight provides a novel framework for understanding *PVT1* exon-specific regulation and positions the CDX1-PEAP interaction as a promising molecular target for therapeutic interventions in *PVT1* exon 9 overexpressing prostate cancers.

#5731 ID4 maintains undifferentiated and immune-evasive states in aggressive triple-negative breast cancer and represents a novel druggable vulnerability.

Lautaro Rivera[1], Carla Toro[1], Juan Manuel Fernandez[2], Jochen Maurer[3], **Maria Teresita Branham**[1]

[1]IHEM-CONICET, Mendoza, Argentina,[2]FCM-UNCuyo, Mendoza, Argentina,[3]RWTH Aachen University Hospital, Aachen, Germany

Background: Inhibitor of Differentiation 4 (ID4) is overexpressed in triple-negative breast cancer (TNBC) and is essential for proliferation, anchorage-independent growth, and tumorigenicity of MDA-MB-231 cells. These findings position ID4 as a candidate driver of undifferentiated, aggressive TNBC phenotypes. However, its expression pattern across molecularly heterogeneous TNBC subtypes and its therapeutic potential remain undefined.

Methods: We integrated *in silico* analyses of clinically annotated TNBC cohorts with functional studies in ID4-high TNBC models. ID4 expression and co-expression patterns across TNBC subtypes were evaluated using bc-GenExMiner v5.2. ID4 was silenced by CRISPR-Cas9 or shRNA in three representative TNBC cell lines: MDA-MB-231 (mesenchymal stem-like, MSL), MDA-MB-468 (basal-like 1), and BT-549 (mesenchymal-like). Pharmacologic ID4 degradation was achieved using AGX51, a first-in-class pan-ID degrader. Proliferation was monitored by MTT assay and IncuCyte live-cell imaging. Drug response was further assessed in five patient-derived basal-like breast cancer stem cell (BCSC) cultures, with proliferation evaluated in all five and mammosphere formation in two.

Results: *In silico* analysis revealed that ID4 expression is significantly enriched in the two most aggressive, immune-suppressed TNBC subtypes: basal-like immune-suppressed (BLIS) and mesenchymal-like immune-altered/immunomodulatory (MLIA; formerly mesenchymal stem-like/MSL). In MLIA tumors, ID4 strongly co-expresses with mesenchymal, myoepithelial, and stemness programs (YAP/TAZ-Hippo, FOXC1, SOX10, ACTA2, and basal cytokeratins). Both genetic silencing and pharmacologic degradation of ID4 markedly impaired proliferation across all tested cell lines and BCSC cultures. Notably, AGX51 completely disrupted mammosphere formation and 3D structural integrity in the two BCSC models examined. Stable ID4-knockout and knockdown TNBC cell lines were successfully generated for ongoing RNA-seq and DNA-methylation profiling.

Conclusions: These data establish ID4 as a subtype-enriched, druggable vulnerability in the most aggressive and immune-suppressed TNBC subsets. Ongoing transcriptomic and epigenomic studies will elucidate the molecular circuits governed by ID4 and identify rational combination strategies for BLIS, MLIA, and mesenchymal stem-like TNBC. This abstract incorporates text revised with the assistance of artificial intelligence for language clarity and conciseness

#5732 Identification and functional analysis of chloride intracellular channel protein 1-binding peptide and its uses for ProTac-based cancer therapy.

Aryeong Lee, Byungheon Lee

Kyungpook National University, Daegu, Korea, Republic of

Targeted therapy using antibodies that treat only certain cancer cells is currently being studied because it causes less side effects on normal cells. Compared to antibodies, peptides are relatively smaller and have higher tissue penetration ability and lower immunogenicity. Chloride intracellular channel protein1 (CLIC1) is a metamorphic protein as it can exist in two forms: soluble globular protein in the cytoplasm or transmembrane protein. CLIC1 is related to cancer angiogenesis, cell migration and metastasis and is upregulated in various types of cancer, including hepatocellular carcinoma and lung cancer, presenting it as a promising therapeutic cancer target. In this study, we identified a peptide candidate (CLIC1pep) that binds to CLIC1 using phage display. The affinity and specific binding of CLIC1pep to CLIC1 was validated by SPR, ELISA, and pull-down assays. CLIC1pep linked to a cell-penetrating peptide (R7) (R7-CLIC1pep) showed an increased cell penetration and binding to CLIC1 in the cytoplasm, whereas it did not induce tumor cell death. However, R7-linked CLIC1pep inhibited the membrane insertion of CLIC1 and reduced the migration and invasion of cancer cells through reducing the p-ERK levels. Moreover, R7-CLIC1pep-linked E3 ligase peptide was synthesized for a ProTAC against CLIC1 and degraded CLIC1 in tumor cells. These results suggest that R7-CLIC1pep and R7-CLIC1pep-linked E3 ligase peptide hold a potential for a ProTac-based cancer therapy of CLIC1-high tumors.

#5733 Decoding ELAVL4 isoaspartylation in SCLC using engineered PCMT1: A strategy for uncovering immune triggers.

Davin Pan[1], Shiori Fukutome[1], Xuhan Zhou[1], Diego De Luna Moran[1], Chunli Yan[1], Diego Alejandro Velarde[1], Whitaker Cohn[2], Ite A. Offringa[1]

[1]USC Norris Comprehensive Cancer Center, Los Angeles, CA,[2]Department of Clinical Pharmacy, USC Mann School of Pharmacy, Los Angeles, CA

The 5-year survival rate for SCLC patients is only 9%-new therapies are urgently needed. Approximately 15% of SCLC patients develop a low-titer immune response against the neuronal protein embryonic lethal abnormal vision-like 4 (ELAVL4), exhibiting significantly improved survival. In the lung, ELAVL4 is uniquely expressed in pulmonary neuroendocrine cells, the primary cell of origin of SCLC. Prior research in our lab suggests that the anti-ELAVL4 immune response originates from an immunogenic type of post-translational damage called isoaspartylation. We previously mapped the isoaspartylation of ELAVL4 to the 38-amino acid N-terminal unstructured region, upstream of the RNA recognition motif domain (RRM1). Isoaspartylation can occur at asparagine and aspartic acid residues, most commonly when they are located in a flexible protein region and followed by a small amino acid (glycine, serine, or histidine). The asparagine or aspartate side chain reacts with the main chain, forming a cyclic succinimide intermediate that, in 70% of cases, resolves to an isoaspartate (isoAsp), thereby kinking the peptide backbone. Isoaspartylation is repaired by the enzyme protein-L-isoaspartate (D-aspartate) O-methyltransferase (PCMT1) in vivo. PCMT1 deficiency is invariably fatal in mice, illustrating the essential nature of this repair enzyme. PCMT1 utilizes the methyl donor S-adenosylmethionine (SAM) to initiate repair, producing S-adenosylhomocysteine (SAH), which can be quantified via ELISA and bioluminescent assays. Mapping the isoaspartylation site(s) in ELAVL4 is essential, as this will help identify the antigenic epitope used to design future targeted immunotherapies for SCLC patients. However, mapping of isoaspartylation sites is challenging due to minimal molecular weight differences between asparagine, aspartate, and isoaspartate residues. In the past, tritiated SAM has been used in conjunction with PCMT1 to label proteins and detect isoaspartylation. Here, we investigate whether PCMT1 can be utilized in conjunction with mass spectrometry to methylate and detect isoaspartylation in ELAV4. This method is site-specific and avoids the use of radioactivity. We will also assess substrate binding kinetics using a Bruker heliX biosensor. Improved detection and mapping of isoaspartylation sites in ELAVL4 can help identify therapeutic targets that leverage the anti-isoaspartylated ELAVL4 response for new SCLC treatments. Supported by the Robert E. and May R. Wright Foundation Transformative Cancer Research Grant, USC's Undergraduate Research Associates Program, and the Norris Comprehensive Cancer Center core grant, NIH/NCI P30CA014089. DAV and IAO are members of CaRE2 the Cancer Research Education and Engagement Health Center, supported by NIH/NCI grants U54CA233396, U54CA233444, and U54233465.

#5734 Targeting exportin 1 reduces cutaneous squamous cell carcinoma growth alone and in combination with 5-fluorouracil.

Moynul Islam, Justin Rudd, Louise Monga, James Grunkemeyer, Laura Hansen

Biomedical Sciences, Creighton University, Omaha, NE

Background: Cutaneous squamous cell carcinoma (cSCC) affects approximately 1.8 million people annually in the US with an increasing number of cases. Nuclear-cytoplasmic transport of proteins and RNA is vital for cellular homeostasis and becomes dysregulated in skin cancer. Exportins like Exportin 1 (XPO1) transport cargo from the nucleus to the cytoplasm and are upregulated in multiple cancer types. We found increased expression of XPO1 in premalignant actinic keratosis and cSCC. The Exportin 1 inhibitor Selinexor is FDA approved for the treatment of relapsed multiple myeloma and refractory large diffuse B cell lymphoma. This project aimed to determine whether XPO1 targeting could be a useful strategy for the treatment of cSCC, as well as to identify additional targets for combination therapy with XPO1 inhibition. Thymidylate synthase (TYMS) inhibitor 5-Fluorouracil (5-FU), used clinically for the treatment of actinic keratosis and superficial basal cell carcinoma was identified as a potential agent in combination with Selinexor.
Methods: XPO1-targeted or control shRNA was introduced into human cSCC cell line SCC-13 and validated. cSCC cells or subcutaneous tumors were treated with Selinexor or the vehicle. IC_{50}s were established for Selinexor in HaCaT, KerCt, SCC-13, SCC-12B.2, COLO-16, and SRB1 cells, and for other inhibitors in SCC-13 cells. Flow cytometry and Caspase-Glo assays were used for cell cycle and apoptosis analyses. Genome-wide CRISPRi screen was performed in SCC-13 dCas9-KRAB cells and analyzed by MAGeCK followed by GSEA. *In vitro* synergy between 5-FU and Selinexor was evaluated using SynergyFinder 3.0. In addition, we assessed the effects of XPO1 inhibition and of 5-FU-Selinexor combination treatment on TYMS and key DNA damage repair proteins (MLH1, MSH2, CHEK1) using immunoblotting.
Results: XPO1 knockdown or inhibition using Selinexor caused cell cycle arrest and apoptosis of SCC-13 cells. Selinexor was effective at killing cSCC cells with submicromolar IC_{50}s and significantly reduced tumor growth in SCC-13 xenografts. The genome-wide CRISPRi screen identified 293 genes that increased cSCC cell sensitivity and 70 genes that increased resistance to Selinexor. The sensitizers were enriched in DNA damage repair pathways. XPO1 inhibition decreased TYMS and key DNA damage repair proteins (MLH1, MSH2, and CHEK1). 5-FU and Selinexor together decreased the expression of these DNA damage repair proteins compared to Selinexor alone and caused synergistic cell death of SCC-13 cells.
Conclusions: Inhibition of XPO1 was effective at killing cSCC cells in culture and in xenografts. Our genome-wide CRISPRi screen, identified 293 potential sensitizers of Selinexor, one of which was TYMS, the target of 5-FU. 5-FU-Selinexor combination were more effective than either agent alone, suggesting this combination may have potential for the treatment of nonmelanoma skin cancer.

#5735 Imiquimod targets tankyrase 2 to suppress wnt-active colorectal cancer.

Philemon Ubanako[1], Ramesh Pandian[2], Adedapo Adeyinka[3], Bernice Monchusi[1], Clement Penny[1]

[1]Internal Medicine, University of the Witwatersrand, Johannesburg, South Africa,[2]Protein Structure and Function Unit, University of the Witwatersrand, Johannesburg, South Africa,[3]Chemical Sciences, University of Johannesburg, Johannesburg, South Africa

The Wnt/β-catenin signaling pathway is frequently upregulated in colorectal cancer (CRC), driving tumor progression and therapeutic resistance. Tankyrase (TNKS), a key regulator of this pathway, has emerged as a promising therapeutic target. XAV939, a small-molecule inhibitor of TNKS, has been widely used to study Wnt pathway inhibition. TNKS inhibitors suppress Wnt signaling by stabilizing Axin, a key component of the β-catenin destruction complex, which leads to enhanced degradation and thus a reduction in the cellular and nuclear levels of β-catenin. We investigated the anticancer potential of Imiquimod (IMQ), a Toll-like receptor 7 (TLR7) agonist, through its interaction with TNKS2. Molecular docking and dynamics simulations revealed that IMQ binds stably to the PARP catalytic domain of TNKS2, with a higher docking score than the co-crystallized ligand. Notably, IMQ formed critical interactions with residues Tyr1060 and Glu1138, located within the catalytic core of TNKS2, suggesting its ability to modulate Wnt/β-catenin signaling. Cytotoxicity and cell cycle analysis demonstrated differential sensitivity to IMQ and XAV939, across colorectal cancer and normal cell lines. Interestingly, confocal microscopy revealed that IMQ significantly reduced β-catenin expression in DLD1 CRC cells harboring wild-type β-catenin, while no significant decrease was observed in HCT116 CRC cells with mutant β-catenin. This study reveals a novel potential route for repurposing a clinically approved agent to suppress Wnt-driven oncogenesis. This is the first study to propose a mechanism by which IMQ may inhibit Wnt/β-catenin signaling.

#5736 BMAL2 maintains DNA integrity via regulating homologous recombination to promote ovarian clear cell carcinoma tumorigenesis.

Grace Yin Tze Tan, Pei-Yi Lin, Li-Tzu Cheng, Wendy Wenhua Hwang-Verslues

Genomics Research Center, Academia Sinica, Taipei, Taiwan

Ovarian cancer is the most lethal gynecologic malignancy worldwide. Among its subtypes, ovarian clear cell carcinoma (OCCC) is characterized by its intrinsic chemoresistance, poor prognosis, and lack of effective therapies. To date, only ARID1A mutant OCCC has shown modest sensitivity to PARP inhibitors, highlighting the urgent need for novel therapeutic targets. Here, we identified BMAL2, a circadian transcription as a critical DNA integrity regulator in OCCC cells. BMAL2 depletion downregulated RAD51, impaired homologous recombination-mediated DNA repair thereby inhibited cell survival and tumor growth. To pharmacologically target BMAL2, we performed structure-based virtual screening and identified GW-833972A as a small-molecule inhibitor that effectively bound and degraded BMAL2 protein. Mechanistically, GW-833972A mediated BMAL2 degradation impaired DNA repair and suppressed tumor growth *in vivo*. Collectively, these findings reveal the critical oncogenic role of BMAL2 in OCCC and demonstrate that BMAL2 inhibition offers a promising therapeutic strategy for this chemoresistant cancer.

#5737 Developing agents to target IL-8 signaling and intercept progression to esophageal adenocarcinoma.

Yun Zhang[1], Andrew Alt[2], Nick Santoro[2], Shari Barnett[1], Kiran Lagisetty[1], Jules Lin[1], Rishindra M. Reddy[1], Chigozrim Ekeke[1], Andrew Chang[1], David Odell[1], Laura A. Kresty[1]

[1]University of Michigan, Ann Arbor, MI,[2]Center for Chemical Genomics Members, Life Science Institute, Ann Arbor, MI

The goal of this research was to investigate whether agents targeting Interleukin (IL)-8 and its chemokine receptors (CXCR) 1 and 2 can be identified and exploited to intercept the progression of Barrett's esophagus (BE) to esophageal adenocarcinoma (EAC). Experimental approaches investigated circulating and transcript level changes in IL-8 and CXCR1/2 in EAC progressors and patients with BE, the only known precursor lesion, compared to non-cancer controls or normal tissue, respectively. Gene set enrichment analysis (GSEA) investigated the IL-8 signaling axis in esophageal tissues with progressive pathology changes from BE with low-grade dysplasia (BE.LGD) to BE with high-grade dysplasia (BE.HGD) and EAC. Deconvolution analysis further assessed immune cell alterations in this cohort. Finally, EAC and BE cell lines were employed to investigate various IL-8 assays and determine whether select agents targeting IL-8 signaling induced cell death in BE.HGD or EAC cells. Results showed that plasma IL-8 levels were 3.6-fold (p=0.039) higher in EAC patients compared to non-cancer controls. Moreover, significantly elevated tissue levels of IL-8, CXCR1 and CXCR2 were detected in BE.HGD or EAC compared to BE.LGD. GSEA further implicated the IL-8-CXCR-signaling axis by revealing that 60% of the up-regulated pathway maps during EAC progression contained IL-8 or its receptors (i.e., IL-8-dependent cell migration and adhesion, neutrophil chemotaxis and release of pro-inflammatory factors). Deconvolution analysis identified alterations in multiple immune cell populations with BE progression (BE.LGD to BE.HGD), including up-regulation of neutrophils, which secrete IL-8 and are an abundant cell type at sites of inflammation. Conversely, NK cells, which respond to cellular stress and mediate tumor killing, were downregulated. Proof-of-concept studies conducted in BE.HGD and EAC cell lines showed that a natural product, cranberry proanthocyanidins, as well as the drug lanraplenib, both significantly inhibited IL-8 secretion, followed by potent cell death induction. However, a recent clinical trial with lanraplenib resulted in unacceptable toxic side effects. Ultimately, these results support that IL-8 signaling is induced early during the transition from BE.LGD to BE.HGD and that elevated levels are sustained through EAC development. Thus, we plan to screen the NCI's natural product library for agents that inhibit the IL-8-CXCR-immune signaling axis and that, in turn, may offer efficacious options to intercept BE progression to EAC. This research was supported in part by NCI 1UG3CA299397-01, along with other funding sources.

#5738 Beyond bulk: Resolving RNASeq/mass spectrometry/IHC discrepancies with multiplexed spatial profiling and 3D cluster analysis to refine HER3 (bs)Ab and (bs)ADC therapeutic strategies.

Jeannette Fuchs, Christophe Mas, Eric Durandau, Diana Rocha Gomes, Min Ma, Antoine Attinger, Anna Pokorska-Bocci

Translational Medicine, Debiopharm International S.A., Lausanne, Switzerland

Assessment of target expression for mono- and bispecific antibodies (Ab/bsAb) and antibody-drug conjugates (ADCs/bsADCs) can be challenging due to poor correlation between bulk RNASeq, proteomics and immunohistochemistry (IHC) data. While IHC is sufficient to address single target expression levels at single cell level, multiplexing is required to assess spatial distribution and expression thresholds of multiple targets for bsAb and bsADC use.
To address these challenges, we performed a full characterization of (bs)ADC targets in patient-derived xenografts (PDX) across different omics platforms. Based on these outputs, we created a 3D biologics-tailored analysis tool which allows multifactorial target assessment to guide PDX model selection for evaluation of (bs)Ab/ADC sensitivity.
HER3 and other selected tumor-associated antigens (TAA) were investigated, showing different levels of mRNA/protein correlations and different levels of mass spec-derived proteomics versus IHC. Based on these results, PDX models with a pre-defined TAA expression spectrum were selected for multiplexed spatial proteomics to determine single cell expression intensities and co-localization of those TAAs. Our 3D biologics analysis tool facilitates a multifactorial, granular assessment of the selected targets.
The target-specific variability of correlation between the different analytes highlights once again the importance of proper omics/IHC platform selection depending on each individual target. Once the appropriate expression values are identified, the 3D analysis tool allows dynamic adjustment of expression thresholds of multiple targets with the potential to inform on the sample-specific most promising (bs)Ab/ADC treatment options.

#5739 Defining sodium channel isoforms in oral squamous cell carcinoma *in vitro.*

Kelly Jean Sherman[1], Alexis Gray[2], Dennis Paul[3]

[1]Pharmacology and Experimental Therapeutics, LSU Health New Orleans, New Orleans, LA,[2]Mount Carmel Academy, New Orleans, LA,[3]LSU Health New Orleans, New Orleans, LA

Overview: Sodium channels overexpression contributes to invasion and metastatic behavior and plays a functional role in cancer progression. Many knowledge gaps remain in voltage-gated sodium channels (VGSC's) subtype's role in metastasis, as well as distinguishing the difference of cancer progression of Oral Squamous Cell Carcinoma (OSCC) HPV(-) and HPV(+). Defining isoform-specific regulatory roles in OSCC may serve as potential targets for novel therapeutic treatments. The purpose of the study was to define VGSC isoforms regulating the cell growth, motility, and invasiveness in OSCC.
Methods: To access sodium channel expression patterns and comparisons of components of metastasis, we used two OSCC cell lines, Cal-27 HPV(-) and SCC-090 HPV(+). We measured motility in wound healing, area progression of invasiveness, cell proliferation over time treated with TNF-α, and compared VGSC isoforms and organelle expression patterns using microscopy.
Results: Motility rate for Cal-27 was significantly higher than SCC-090. When treated with TNF-α there was no significant difference relative to controls for either cell line. Invasiveness of Cal-27 exhibited significantly greater migration compared to SCC-090. Under low-glucose conditions, Cal-27 demonstrated a significant decrease in migration, whereas SCC-090 had no significant change. At 24 hours, there was no significant difference in cell growth of either cell line; however, by 48 hours, Cal-27 had a significantly higher growth. Both cell lines treated with TNF-α, demonstrated a concentration-dependent response, with SCC-090 showing a significant reduction in proliferation at higher concentrations. Immunofluorescence was performed for all VGCS isoforms (NaV1.1 - 1.9) and centrosome marker, anti-PCM-1. NaV1.6 and NaV1.7 display distinct expression patterns as punctate signals in both cell lines. In SCC-090 cells, PCM-1 expression closely resembled the NaV1.6/NaV1.7 localization.
Conclusion: Cal-27 cells exhibited greater migratory and proliferative capacity than SCC-090, particularly evident through higher motility at 24 hours, increased migration, and proliferation by 48 hours. While TNF-α did not alter migration in either cell line, it produced a concentration-dependent decrease in proliferation, most notably in SCC-090. Metabolic stress further differentiated between the two lines: low glucose significantly impaired migration in Cal-27 but had no effect on SCC-090. Immunofluorescence revealed that NaV1.6 and NaV1.7 exhibited distinct punctate localization patterns in both cell lines. In SCC-090, this pattern closely aligned with PCM-1 staining. Together, these findings highlight functional and phenotypic differences between Cal-27 and SCC-090.

: Multi-Axis Antineoplastic Agents
Poster Session

#5743 Discovery of a novel orally available microtubule-destabilization agent that targets the colchicine binding site and exhibits antitumor activity in *KRAS*-mutant models.

Yeni K. Romero, Joshua W. Large, Kylie Luther, Molly M. Hood, Ranjan Preet, Chase K. Crawley, Salim Javed, Yu Mi Ahn, Forrest A. Stanley, Bertrand Le Bourdonnec, Bryan D. Smith, Daniel L. Flynn, Jeffery D. Zwicker, Stacie L. Bulfer

Deciphera Pharmaceuticals, LLC, Waltham, MA

Background: Microtubules are essential for regulating cell growth, cell division, protein trafficking, and key cell signaling events. Alterations to the microtubule network affect cell survival, thus making microtubule-targeting agents desirable as cancer therapeutic agents. Currently, several tubulin modulators are approved for cancer treatment. However, development of additional microtubule-targeting agents is still needed to improve treatment outcomes, mitigate side effects, and overcome resistance mechanisms. Here, we describe compound A, a novel, orally available microtubule-destabilizing agent that targets the colchicine binding site and exhibits single-agent antitumor activity in *KRAS*-mutant models.

Methods: Inhibition of tubulin polymerization was measured using a recombinant polymerization assay and a cell-based microtubule sedimentation assay. Binding to the colchicine site of tubulin was determined by a binding competition assay using a BODIPY-colchicine probe. Disruption of tubulin formation was determined by immunofluorescence of microtubules in A549 cells. Compound binding to the tubulin complex was determined via X-ray crystallography. Cellular proliferation of *KRAS*-mutant and isogenic cell lines was measured using resazurin. *KRAS*-mutant mouse xenograft models were used to assess pharmacokinetics (PK), pharmacodynamics, and antitumor activity.

Results: Compound A binds to the colchicine site and destabilizes tubulin polymerization. Treatment resulted in single-agent inhibition of proliferation of *KRAS*-mutant cancer cell lines. Immunofluorescence of microtubules in A549 cells revealed disruption of the microtubule network and dysregulated spindle formation. Compound A exhibited a favorable ADME and PK profile. Oral treatment of compound A as a single agent resulted in 56% tumor growth inhibition in a subcutaneously implanted *KRAS*-mutant lung xenograft model.

Conclusions: Compound A is an orally bioavailable tubulin modulator that binds to the colchicine site and inhibits tumor growth in a *KRAS*-mutant model as a single agent. Our preclinical data provide proof of concept for the development of an orally available microtubule-destabilizing agent.

#5744 Robust anti-tumor activity of the novel KIF18A inhibitor, ATX-295, in preclinical models of chromosomally instable tumors.

Laura Ghisolfi[1], Maureen M. Lynes[1], April Greene-Colozzi[1], David Sutton[1], Jie Wu[1], Livia Shehaj[1], Brian A. Sparling[1], Inbal Gazy[2], Stuart J. Ince[1], Jason A. Sager[1], Serena J. Silver[1]

[1]Accent Therapeutics, Lexington, MA,[2]Imagene AI, Tel Aviv, Israel

KIF18A is a plus-end directed kinesin known to play a role in mitosis by facilitating chromosome alignment and spindle microtubule dynamics. TP53 mutant cells with ongoing chromosomal instability (CIN), such as a subset of aneuploid or whole genome doubled cells, are particularly vulnerable to disrupted mitosis upon KIF18A knockdown or knockout. These findings indicate that KIF18A is a compelling oncology target in the setting of tumors with high levels of chromosomal instability. Analysis of the Cancer Genome Atlas (TCGA) demonstrates that high grade serous ovarian cancer (HGSOC), triple negative breast cancer (TNBC), and squamous non-small cell lung cancer (sqNSCLC) have a high prevalence of CIN, and as such have the potential for therapeutic benefit from KIF18A inhibition. Accent Therapeutics has identified ATX-295, a highly potent and selective inhibitor of KIF18A. ATX-295 has robust *in vitro* anti-proliferative activity in HGSOC, TNBC, and sqNSCLC cell lines. Consistent with the role of KIF18A in orchestrating mitosis in CIN cells, ATX-295 treatment induces phospho-histone H3 (p-HH3) in sensitive cell lines. This corresponds to a dose-dependent increase in G2M arrest and apoptosis selective to CIN cell lines. To further validate the opportunity for ATX-295 in CIN tumor types, it was tested *in vivo* in patient-derived xenograft (PDX) studies in models derived from HGSOC and TNBC patients. Whole genome doubling (WGD) is a known correlate of CIN; robust and durable efficacy was achieved by ATX-295 treatment in WGD+ (positive) HGSOC and TNBC PDX models. These findings support CIN and WGD as predictive biomarkers for ATX-295 response. To assess clinical feasibility, an H&E-based WGD detection model was developed using Imagene AI's OI Suite and TCGA-labeled samples. The model achieved >0.8 AUC on a held-out test set within minutes, demonstrating proof-of-concept for AI-based WGD detection in clinical samples. ATX-295 is currently being evaluated in a first-in-human, Phase 1/2 open-label study assessing safety, pharmacokinetics, pharmacodynamics, and preliminary antitumor activity in patients with advanced solid tumors and ovarian cancer (NCT06799065).

#5745 Discovery of AZD4956, a potent and selective inhibitor of DNA polymerase theta, a clinical candidate for treatment of HRR-deficient tumors in combination with saruparib.

Bernard Barlaam[1], Josep V. Forment[2], Lee Mulderrig[2], de Renty Christelle[2], Harriet Southgate[2], Adina Hughes[2], Derek Barratt[3], Nina Akrap[4], Marcello Maresca[4], Oliver Turner[1], Dougles Ferguson[5], Andy Pike[6], Ross Hill[7], Lenka Oplustil O'Connor[7], Kainat Khan[8], Sonja Gill[8], Stefan Kavanagh[8], Susan Critchlow[2], Sabina Cosulich[9], David Wilson[10]

[1]Oncology Targeted Discovery Chemistry, AstraZeneca, Cambridge, United Kingdom,[2]Oncology Targeted Discovery Bioscience, AstraZeneca, Cambridge, United Kingdom,[3]Discovery Sciences, AstraZeneca, Cambridge, United Kingdom,[4]Discovery Sciences, AstraZeneca, Gothenburg, Sweden,[5]Oncology Targeted Discovery DMPK, AstraZeneca, Waltham, MA,[6]Oncology Targeted Discovery DMPK, AstraZeneca, Cambridge, United Kingdom,[7]Oncology Translational Medicine, AstraZeneca, Cambridge, United Kingdom,[8]Clinical Pharmacology and Safety Sciences, AstraZeneca, Cambridge, United Kingdom,[9]Early Oncology Programs Group, AstraZeneca, Cambridge, United Kingdom,[10]Oncology Targeted Discovery Chemistry and DMPK, AstraZeneca, Cambridge, United Kingdom

Deficiency in the homologous recombination repair (HRR) pathway, which is key for high-fidelity DNA double-strand break (DSB) repair, is prevalent across various cancers (including ovarian, breast, pancreatic, and prostate). It frequently arises from loss-of-function mutations in *BRCA1*, *BRCA2*, or other HRR-associated genes. PARP inhibitors (PARPi) have transformed the treatment landscape and survival outcomes in patients with HRR-deficient tumors. However, despite the remarkable efficacy of PARPi, clinical benefit is variable, and a significant number of patients develop resistance. Combinations of PARPi with targeted agents blocking the cellular DNA damage response have been pursued to improve efficacy of PARPi treatments, but enhanced myelosuppression has limited dosing and, consequently, efficacy of these approaches. DNA polymerase theta (Polθ; POLQ) is a key component of microhomology-mediated end joining (MMEJ) DSB repair pathway. Under HRR-deficient conditions, cellular DSB repair becomes increasingly dependent on POLQ-driven MMEJ. We report the identification and optimization of a novel chemotype of POLQ inhibitors, culminating in the discovery of the clinical candidate AZD4956. AZD4956 is a potent and selective inhibitor of the polymerase domain of POLQ (IC_{50} <10 nM) in biochemical assays. AZD4956 suppresses cellular MMEJ activity with single digit nanomolar potency (IC_{50} 3.95 nM) and shows potent antiproliferative activities (IC_{50} values between 3-10 nM) and induction of genomic instability (assessed by micronuclei quantification) in a wide range of HRR defective cell lines, with no measurable activity in HRR proficient genetic backgrounds. AZD4956 further enhances genomic instability and antiproliferative activity induced by the PARP1-selective inhibitor, saruparib, in multiple HRR defective cell lines, with no activity of the combination in HRR proficient settings. Additionally, combination of AZD4956 and saruparib does not exacerbate hematotoxicity of saruparib treatment in a 3D-bone marrow microphysiological system. Oral daily treatment of AZD4956 combined with saruparib drives sustained regression of the HRR deficient *BRCA2*$^{-/-}$ DLD-1 xenograft model, superior to the respective activities of the two agents as monotherapies. Increased efficacy of the combination can be pharmacodynamically tracked by increased accumulation of micronuclei in circulating red blood cells. The preclinical profile, spanning efficacy, safety, DMPK and physicochemical properties, supports clinical development of AZD4956 as a combination partner with saruparib in patients with HRR deficient cancers. Clinical evaluation of AZD4956 is ongoing in a first-in-human, open-label, multicenter, phase 1/2a study in patients with HRR deficient solid tumors (PARTHENON study) in combination with saruparib.

#5746 The risk of high-grade hyperglycemia with PI3K inhibitors-a meta-analysis.

Zhan Rong[1], Shenhong Wu[2]

[1]Department of Medicine, Stony Brook University Hospital, Stony Brook, NY,[2]Division of Medical Oncology, Department of Medicine, Stony Brook University Hospital, Stony Brook, NY

Background: Phosphoinositide 3-kinase (PI3K) inhibitors are a promising therapeutic class in cancer treatment and their clinical utility has been limited by toxicity, particularly high-grade hyperglycemia. Currently the overall risk of hyperglycemia in patients treated with PI3K inhibitors has not been well understood. We performed a meta-analysis on the risk of high-grade hyperglycemia in patients treated with PI3K inhibitors based on currently available published randomized control trial (RCT) data.
Methods: A systematic meta-analysis was conducted including phase II-III RCTs evaluating PI3K inhibitors in cancer patients. The primary endpoints were the incidence and relative risk of grade ≥3 hyperglycemia. Pooled effect sizes were calculated using random- or fixed-effects models based on the heterogeneity of included studies.
Results: A total of 4977 patients across 16 eligible RCTs were included for analysis. The overall incidence of high-grade hyperglycemia was 12.7% (637/4977). Compared to controls, PI3K inhibition was associated with a significantly increased risk of high-grade hyperglycemia (RR: 2.27; 95% CI, 1.74-2.80; $p < 0.001$), with moderate heterogeneity ($I^2 = 38.9\%$). Subgroup analyses revealed that control type significantly moderated toxicity risk ($p < 0.001$), with the greatest risk observed in trials with placebo controls (RR: 2.60; 95% CI, 2.05-3.15) and active controls (RR:1.50; 95% CI, 0.49-2.52). PI3K inhibitor subtype also moderated risk ($p < 0.001$). PI3K-α selective inhibitors were associated with the highest risk (RR: 3.80; 95% CI, 2.50-5.11), followed by pan-PI3K (RR: 2.15; 95% CI, 1.79-2.52) and PI3K/mTOR dual inhibitors (RR:1.46; 95% CI, 0.61-2.31). Class I α/β/δ inhibitors showed no significant elevation.
Conclusions: PI3K inhibitors substantially increased the risk of grade ≥3 hyperglycemia, with heterogeneity driven by control type and inhibitor subtype. The markedly elevated risk with PI3K-α selective agents highlights the need for vigilant metabolic monitoring and tailored management strategies in clinical use.

#5747 GenSci145: A mutant selective PI3Kα inhibitor overcoming brain metastasis treatment barriers.

Xing Fan, Sheng Zhao, Xiaojing Huang, Yihui Lin, Xiaozhen Wang, **Biao Lu**, Yuanfeng Xia, Fanglong Yang

Changchun GeneScience, Shanghai, China

Background: PIK3CA gene mutations are important targets in cancer treatment and are widely present in various solid tumors. Existing PI3Kα inhibitors lack sufficient selectivity for mutant subtypes, which can lead to dose-limiting toxicities such as abnormal glucose metabolism and skin toxicity, affecting patient tolerance and long-term efficacy. Moreover, PIK3CA mutations may increase the risk of central nervous system (CNS) metastasis in patients. Existing inhibitors have extremely poor permeability across the blood-brain barrier, making it difficult to effectively suppress brain metastases and allowing the CNS to become a “sanctuary” for tumor recurrence. Therefore, the development of highly selective PI3Kα mutation inhibitors with brain-penetrating capabilities has become a key research direction to improve the prognosis of such patients.

Methods: The activity of GenSci145 against PI3Kα mutant/wild-type cells was evaluated through in vitro experiments (CTG proliferation inhibition, HTRF detection of pAKT, kinase selectivity panel). In vivo experiments used CDX (T47D, CAL-33, GP2D), PDX (BR9466, etc.), and brain metastasis models (intracranial + subcutaneous transplantation) to analyze the anti-tumor effects of monotherapy or in combination with fulvestrant (TGI, CFB (change from baseline)).

Results: In *in-vitro* experiments, GenSci145 exhibited nanomolar-level inhibitory activity against PI3Kα mutants (H1047R, E545K, E542K) (IC_{50}: 20-162 nM). It significantly inhibited proliferation (T47D IC_{50}: 120.6 nM, selectivity 28.6-fold) and pAKT signaling (IC_{50}: 67.5 nM, selectivity 11.3-fold) in mutant cells, with no significant effects on other PI3K subtypes or off-target kinases.In *in-vivo* experiments, GenSci145 showed dose-dependent anti-tumor effects in HR-positive, HER2-negative breast cancer CDX/PDX models, with significant synergy when combined with fulvestrant. In the xxT47D-Luc brain metastasis + subcutaneous model, GenSci145 dose-dependently inhibited both subcutaneous and intracranial tumors. For intracranial tumors, the CFB was 4.78 at 25 mg/kg and 1.71 at 100 mg/kg, which was superior to STX-478 (100 mg/kg, CFB=9.56). The results indicated that GenSci145 has the potential to treat patients with brain metastases.

Conclusion: GenSci145 is a highly selective PI3Kα mutant inhibitor that mechanistically avoids the metabolic side effects of traditional inhibitors. Preclinical studies have shown significant anti-tumor effects in various PIK3CA mutant tumor models, with excellent blood-brain barrier penetration and effective inhibition of brain metastases. Overall, GenSci145 is expected to overcome the clinical limitations of existing PI3Kα inhibitors and provide a new treatment option for patients with PIK3CA mutations. It is currently being advanced to the IND application stage.

#5748 PM534, a novel tubulin inhibitor, has antitumor activity in patient-derived xenograft models of soft tissue sarcoma.

Agathe Bouju[1], Daniel Gorgels[1], Chao-Chi (Ally) Wang[1], Kimberly Verbeeck[1], Ulla Vanleeuw[1], Maria J. Guillen[2], Carmen Cuevas[2], Pablo M. Aviles[2], Agnieszka Wozniak[1], Patrick Schoffski[3]

[1]Department of Oncology, KU Leuven, Leuven, Belgium,[2]PharmaMar, S.A., Madrid, Spain,[3]Department of General Medical Oncology, University Hospitals Leuven, Leuven, Belgium

Objective: Soft tissue sarcoma (STS) is an heterogenous group of rare, malignant, mesenchymal tumors. Doxorubicin (DOX)-based chemotherapy is standard of care for advanced/metastatic disease, despite significant toxicity, low response rates and poor disease control. Trabectedin (TRA) is a second-line treatment for liposarcoma (LPS) and leiomyosarcoma (LMS), with clinical activity seen also in other subtypes. We explored the antitumor activity of PM534 (PharmaMar, Spain), a novel tubulin inhibitor, in patient-derived xenograft (PDX) models of STS.

Methods: Female NMRI *nu/nu* mice (n=92) were transplanted bilaterally with UZLX-STS149^{LMS}, UZLX-STS22^{LMS} (LMS) and UZLX-STS112^{DDLPS} (dedifferentiated liposarcoma - DDLPS). Mice were randomized to 4 treatment groups, receiving treatment once weekly *via* tail vein injection 1) vehicle (VEH) 5 mL/kg; 2) DOX 5 mg/kg; 3) trabectedin (TRA) 0.15 mg/kg; 4) PM534 4.75mg/kg. Treatment lasted 16 days and antitumor activity was assessed by tumor volume (TV) analysis, histopathology (markers for proliferation and apoptosis), validated by western blot. The Mann-Whitney U test was used to compare groups on the last day of experiment, the Wilcoxon test to compare the TV evolution during the experiment per group (day 1 *vs* day 16). Statistical significance was defined as $p < 0.05$.

Results: In UZLX-STS22^{LMS} and -112^{DDLPS} treatment with PM534 led to TV stabilization (growth to 156% and 133% on day 16 as compared to baseline). In UZLX-STS149^{LMS} the compound led to tumor growth delay (289% *vs* 644% in untreated controls; p=0.0039). The antitumor effect in all models was significantly better than in vehicle-treated mice, while in UZLX-STS22^{LMS} and -STS112^{DDLPS} PM534 outperformed DOX. Histopathology showed a high degree of necrosis in PM534-treated tumors, and the drug had strong anti-proliferative and pro-apoptotic activity, as assessed with hematoxylin and eosin staining. Both DOX and TRA led to a moderate inhibition of mitosis as compared to untreated controls. PM534 was well tolerated throughout the experiment at the dose administered, while TRA showed some degree of local toxicity at the site of administration. The completed histopathological analysis and western blotting will be reported at the meeting and the efficacy of PM534 will now be explored in additional models.

Conclusion: PM534 has strong antitumor effects in PDX models of LMS and DDLPS, outperforms the *in vivo* efficacy of treatment with standard agents and should be further evaluated in the preclinical and clinical setting.

#5749 DNA damage, apoptosis and cell cycle disruption: Antitumor effects of a novel tin(IV) complexes.

Shubham Sharma[1], Margret H. Ogmundsdottir[2], Helga M. Ogmundsdottir[3], Krishna Kumar Damodaran[1]

[1]University of Iceland, Reykjavik, Iceland,[2]BioMedical Center, University of Iceland, Reykjavik, Iceland,[3]University of Iceland Faculty of Medicine, Reykjavik, Iceland

Introduction: Platinum-based chemotherapeutics like cisplatin are widely used against cancer but are limited by toxicity and drug resistance. Organotin(IV) complexes offer a promising alternative with enhanced efficacy and distinct mechanisms. Here, we evaluated the anticancer activity of dibutyl and diphenyl organotin(IV) complexes and investigated their mechanisms of action across multiple cancer cell lines.

Material and Method: Synthesis of Organotin(IV) Complexes: Dibutyl and diphenyl organotin(IV) (Bu-Sn and Ph-Sn) complexes were synthesized following established protocols. The purity and structural confirmation of the complexes were verified using spectroscopic techniques. Anti-cancer activities: The following human cell lines were used in this study: T-47D (breast carcinoma), HCT116 (colorectal carcinoma), AsPC-1 (pancreatic adenocarcinoma), and MCF-10A (non-tumorigenic mammary epithelial). Following manufactures protocol MTT assay is utilized for the determination of half maximum inhibitory concentration (IC_{50}). The mode of cell death (apoptosis and necrosis) investigated in cell lines via flow cytometry using the Annexin V and propidium iodide (PI) staining method. Analysis of cell cycle with flow cytometry performed to determine the changes in the cell cycle for each cell lines utilizing cisplatin as a reference drug. Subcellular distribution of the organotin(IV) complexes was evaluated by ICP-MS. Treated cells were fractionated into major cellular compartments to determine the predominant localization of the complexes. DNA damage induced by the organotin(IV) complexes was assessed using the Comet assay, allowing quantification of treatment-related DNA strand breaks.

Results and Discussion: Bu-Sn exhibited strong cytotoxic activity across all tested cancer cell lines (IC_{50} < 3.00 μM), with particularly high potency against T-47D human breast cancer cells (IC_{50} = 0.53 μM). Importantly, it showed minimal toxicity toward non-cancerous MCF-10 cells, demonstrating a favorable level of selectivity. In contrast, Ph-Sn displayed only limited cytotoxic activity. Mechanistically, Bu-Sn induced G1 phase arrest and triggered dose-dependent apoptosis in T-47D cells. Subcellular analysis revealed predominant nuclear accumulation (32% for Bu-Sn, 24% for Ph-Sn), correlating with pronounced DNA damage observed in Comet assays, suggesting that nuclear targeting and genotoxic stress underlie its anticancer activity.

Conclusion: Two organotin(IV) complexes containing dibutyl and diphenyl groups were synthesized and fully characterized. The dibutyl complex exhibited strong cytotoxic activity across multiple cancer cell lines while sparing non-malignant cells. Mechanistic studies indicated that these tin complexes primarily target DNA, inducing cell cycle arrest and apoptosis, ultimately leading to cancer cell death.

#5750 Solid tumor cell-intrinsic function of PI3Kδ.

Sarah E. Conduit[1], Elena Lopez-Guadamillas[1], Daniele Morelli[1], Harriet Howard[1], Wayne Pearce[1], Cheryl Scudamore[2], Bart Vanhaesebroeck[3]

[1]University College London (UCL), London, United Kingdom,[2]Exepathology, Devon, United Kingdom,[3]Centre Lead, Centre for Cell Signalling, University College London Cancer Institute, London

PI3Kδ is a predominantly leukocyte-enriched class I PI3K consisting of the p110δ catalytic subunit (encoded by *PIK3CD*) and most commonly the p85α regulatory subunit (encoded by *PIK3R1*). PI3Kδ is an important regulator of B-cell function and has been the target of extensive drug development efforts for B-cell malignancies, with multiple inhibitors approved for this indication. Based on our pre-clinical studies, PI3Kδ inhibition is now also emerging as an immunotherapy approach for solid tumours. Regulatory T-cells (Treg) are exquisitely sensitive to PI3Kδ inhibition, therefore pharmacological PI3Kδ inhibitors preferentially target the Tregs, rebalancing the immune system in favour of an effector T cell-mediated anti-tumour immune response. This concept is currently under investigation in clinical trials in uveal melanoma and non-small cell lung cancer. Notably, we and others have also observed multiple solid tumour types including glioblastoma, melanoma, breast cancer, prostate cancer, neuroblastoma and hepatocellular carcinoma also express wild-type *PIK3CD*, often at much higher levels than their non-transformed cell types of origin. Some studies suggest PI3Kδ promotes proliferation in these tumour cells, but this remains unclear with the potential that inhibitors were used at non-PI3Kδ-specific concentrations, and these findings are not consistently confirmed with genetic approaches. This raises the questions of what function PI3Kδ plays in solid tumours and how the use of PI3Kδ inhibitors for immunotherapy will affect the tumour cells themselves via inhibition of cell-intrinsic PI3Kδ. Using highly-selective PI3Kδ inhibitors and CRISPR-Cas9-mediated *PIK3CD* deletion in solid tumour cell lines, we demonstrate that PI3Kδ inhibition does not affect cell proliferation in these models. However, through both *in vitro* and xenograft studies, we have identified cancer-relevant roles for PI3Kδ in solid tumours, the implications of which will be presented. Our data suggest the solid tumour cell-intrinsic PI3Kδ expression should be considered to inform PI3Kδ-targeting immunotherapy studies.

#5751 (E,E)-bisantrene silences *c-MYC* expression by stabilizing its promotor region G-quadruplex.

Sumit Sahni[1], Emily Ryan[1], Peter Cuthbertson[1], Feroz Ahmad[1], Kirsten Curnow[1], Nehad Elsalamouny[2], Qiang Zhu[2], Haibo Yu[2], Jinho Jang[3], Jonathan Dickerhoff[3], Danzhou Yang[3], Emma-Jayne Proctor[2], Martina Sanderson-Smith[2], Daniel Tillett[1], Michael Kelso[1]

[1]Race Oncology, Sydney, Australia,[2]University of Wollongong, Wollongong, Australia,[3]Purdue University, West Lafayette, IN

Background: G-quadruplex (G4) DNA and RNA are important non-canonical nucleic acid secondary structures that play key roles in many cellular processes. They regulate the expression and translation of several oncogenes, including the master cell growth regulator, MYC. Bisantrene is a small-molecule anticancer agent that has been shown to be safe and effective in >1500 clinical trial patients. This study characterized the binding and stabilization of a G4 region in the *c-MYC* promoter by the (E,E)-bisantrene isomer and silencing of *c-MYC* expression in cancer cells.
Methods: Circular dichroism spectroscopy established if (E,E)-bisantrene stabilizes the *c-MYC* promotor G4 structure, with surface plasmon resonance used to measure the binding affinity. Nuclear magnetic resonance spectroscopy provided structural insights into the binding interactions within the complex. Molecular dynamics simulations modelled the 3-dimensional structure of the complex. Changes in *c-MYC* gene expression were assessed across a range of cancer cell lines after treatment with (E,E)-bisantrene and RNA-seq with pathway analysis was performed.
Results: (E,E)-bisantrene was found to stabilize the *c-MYC* promoter G4 region, producing similar increases in melting temperature to other G4 ligands (i.e., pidnarulex and pyridostatin). NMR spectroscopy and molecular modelling suggests (E,E)-bisantrene binds with a 2:1 stoichiometry to the planar surfaces of the top and bottom G-tetrads. (E,E)-bisantrene potently inhibited *c-MYC* expression in multiple cancer cell lines. RNA-seq analysis showed (E,E)-bisantrene also decreased expression of other oncogenes containing G4 regions in their promoters, including *MET, TERT, VEGFA, ATF4* and *MDM2*. Pathway analysis of the RNA-Seq data demonstrated a transcriptomic profile similar to pidnarulex, a known G4-binding drug in early-stage clinical development.
Conclusion: (E,E)-bisantrene binds to and stabilizes the G4 structure contained within the *c-MYC* promotor region, leading to silencing of *c-MYC* gene expression. These studies support clinical evaluation of (E,E)-bisantrene as a new G4-targeting drug in MYC-driven tumors.

#5752 Bi-functional thiopurine-based oligonucleotides for AML cell-targeted telomere damage and immunostimulation.

Chunsong Yu[1], Elaine Y. Kang[1], Piotr Swiderski[1], Haiqing Li[1], Ya-Huei Kuo[2], Guido Marcucci[2], **Marcin Kortylewski**[1]

[1]Beckman Research Institute of The City of Hope, Duarte, CA,[2]City of Hope, Duarte, CA

Telomerase (TERT) is an enzyme commonly activated in human cancers and critical for maintaining cell survival. TERT expression and activation correlates with more aggressive, treatment-resistant disease, with the highest telomerase activity in relapsed acute myeloid leukemia (AML) patients. Telomerase inhibitors showed promise in preclinical studies on AML leading to leukemic stem cells (LSC) eradication. However, TERT inhibition in cancer cells faced challenges, such as the delayed clinical responses and on-target/off-tumor toxicities to hematopoietic stem cells (HSCs) or to activated T cells that result in cytopenias or immunosuppression, respectively. We previously developed clinically-relevant strategy for targeted delivery of therapeutic molecules into TLR9^{+} positive myeloid cells, such as AML cells including LSCs, using synthetic CpG oligodeoxynucleotides (CpG-ODNs) as a targeting domain. Here, we report generation of new CpG-conjugates for the delivery of a synthetic TERT substrate, 6-thio-2'-deoxy-guanosine (6tdG) into AML cells. CpG-6tdG oligonucleotides (CpG-6tdGOs) comprise multiple (5-10) 6tdG nucleosides in the 3' end of CpG-ODN. The CpG-6tdGOs retain serum stability, while allowing for slow release of the 6tdG nucleotides after uptake into target leukemic cells. *In vitro*, CpG-6tdG-oligonucleotides (CpG-6tdGOs) were selectively cytotoxic to human TLR9^{+}/TERT^{+} AML cells without affecting activated TLR9$^{—}$/TERT^{+} T-cells, HSCs or non-malignant TERT$^{—}$ cells. The liquid chromatography-tandem mass spectrometry (LC-MS/MS) analysis confirmed that 6tdG was effectively incorporated into chromatin of target cancer cells after *in vitro* and *in vivo* treatment using CpG-6tdGO. Repeated intravenous injections of CpG-6tdGO, but not 6tdG nucleoside, within days induced cytotoxic effects against xenotransplanted models of primary human AML with diverse genomic background in immunodeficient NSG mice and inhibited leukemia progression. CpG-6tdGO showed enhanced antitumor activity when tested *in vivo* against syngeneic *Cbfb/MYH11/Mpl* (CMM) and C1498 mouse AML models. In immunocompetent mice, treatment with CpG-6tdGO induced systemic, cancer cell-selective and CD8 T-cell-mediated antitumor immune responses that were at least partly dependent on TLR9- and STING-mediated signaling in response to CpG-6tdGO-induced cancer cell death. Importantly, the repeated treatments were well-tolerated in humanized hCD34/NOG mice. Except for the reduced percentage of human B-cells, CpG-6tdGO did not decrease the numbers of HSCs, myeloid cells, or T-cells. Overall, CpG-6tdGO offers an effective and safer strategy against aggressive TERT^{+} hematologic malignancies and potentially certain solid tumors.

#5753 Clinical-stage anticancer agent BOLD-100 demonstrates protective effects against chemotherapy-induced peripheral neuropathy.

Mark Bazett, Ashish Kumar, Josie C. Setiawan, E. Russell McAllister, Jim Pankovich

Bold Therapeutics Inc, Vancouver, BC, Canada

BOLD-100 is a first-in-class, ruthenium-based anticancer agent in Phase 2 clinical development for advanced gastrointestinal (GI) cancers in combination with the chemotherapy regimen FOLFOX (NCT04421820). BOLD-100 plus FOLFOX improves overall survival and progression-free survival in patients with advanced colon (mCRC), gastric (GC), and bile duct cancers (BTC). While FOLFOX is a standard-of-care therapy for GI cancers, its clinical utility is limited by acute and chronic peripheral neuropathies. However, a significantly lower incidence of oxaliplatin-induced peripheral neuropathy (OIPN) was observed in patients treated with BOLD-100 plus FOLFOX, including those who had been treated with FOLFOX in previous lines of therapy. Any-grade neuropathy was reduced compared to benchmark FOLFOX-alone patients; mCRC (14% vs 53%), BTC (36% vs 68%), and GC (19% vs 63%). To assess BOLD-100's neuroprotective effects *in vivo*, Sprague-Dawley rats received vehicle (10 mL/kg), oxaliplatin (1.5 mg/kg), paclitaxel (1.0 mg/kg), or BOLD-100 (40 mg/kg) alone, plus BOLD-100 in combination with oxaliplatin and paclitaxel. Cold allodynia was measured using the acetone spray test. Rats treated with oxaliplatin alone induced significant cold allodynia by Day 7, while co-treatment with BOLD-100 ameliorated OIPN development. Importantly, BOLD-100 administration starting on day 15 reversed developed OIPN, opening the possibility of BOLD-100 as a treatment option. BOLD-100 also mitigated the development of paclitaxel-induced cold allodynia, highlighting a broader application of BOLD-100. To elucidate the underlying mechanisms, *in vitro* models using primary dorsal root ganglion (DRG) neurons and differentiated PC12 neuronal cells were used to assess neurite outgrowth. In both models, oxaliplatin treatment reduced average neurite length and number, whereas co-treatment with BOLD-100 protected against oxaliplatin-induced neurotoxicity. Oxaliplatin activates stress pathways leading to neuronal damage, including the unfolded protein response (UPR) - pathways BOLD-100 is known to impact. Oxaliplatin treatment induced upregulation of UPR proteins ATF6 and GRP78, whereas BOLD-100 co-treatment attenuated this upregulation. Furthermore, phosphorylated γH2AX, a marker of DNA damage, was markedly elevated following oxaliplatin exposure, while BOLD-100 ameliorated this response. Chemotherapy-induced peripheral neuropathies have limited therapeutic options; these results demonstrate BOLD-100's potential for both neuroprotection and treatment via impacting important stress pathways. Ongoing clinical study BOLD-100-001 is assessing BOLD-100's neuroprotective effects and its ability to enhance patient outcomes and reduce neurotoxicity.

#5754 PM54 suppresses WNT/β-catenin signaling and synergizes with chemotherapy in gastric cancer models.

Francisco Javier Gutierrez Alvarez, Gema Santamaria, Marta Martinez Diez, Maria Jose Guillen, Pablo Aviles, **Marcelo L. Ribeiro**, Carmen Cuevas

Pharma Mar, S.A., Madrid, Spain

Background: PM54 is a lurbinectedin analog that binds CG-rich promoter regions, inducing transcriptional blockade, DNA double-strand breaks, and S-phase arrest culminating in apoptosis. In gastric cancer models, it drives early transcriptional reprogramming with repression of cell-cycle and DNA repair pathways and demonstrates potent single-agent antitumor efficacy in vivo. We aimed to evaluate the antitumor efficacy of PM54 in gastric cancer and to assess its potential synergy with standard chemotherapeutic agents

Methods: WNT/β-catenin activity was assessed in gastric cancer cell lines using TCF/LEF reporter assays and pathway biomarker analysis. Drug interactions with 5-fluorouracil (5-FU) and cisplatin were quantified by combination index analysis. In vivo efficacy was tested in gastric cancer xenografts treated with PM54, chemotherapy, or combinations, with tumor growth monitored over time.

Results: As a single agent, PM54 markedly inhibited the WNT/β-catenin pathway, reducing TCF/β-catenin-driven transcription by about 40% at 6 hours and over 70% at 18 hours post-treatment. In vitro, PM54 showed strong synergy with 5-fluorouracil (5-FU) in diffuse-type gastric cancer cell lines (HGC-27 and Hs746T) and with cisplatin in HGC-27 cells. In vivo, treatment with PM54 (0.9 mg/kg; days 0 and 7) of mice bearing HGC-27 xenograft tumors resulted in strong antitumor activity. On day 10 (last day of survival in the placebo-treated group), the median tumor volume in placebo-treated mice was 1612 mm^3, compared with mice treated with 5-FU (1375 mm^3), cisplatin (1423 mm^3), and PM54 (616 mm^3; $p = 0.019$). The combination of PM54 with 5-FU or cisplatin resulted in clearly superior performance to the corresponding therapies, with a median $\Delta T/\Delta C$ (%) of 29.4 (PM54), 84.2 (5-FU), and 15.0 (combination); a similar pattern was observed with cisplatin, with $\Delta T/\Delta C$ (%) 29.4 (PM54), 85.7 (cisplatin), and 21.5 (combination).

Conclusions: PM54 represses WNT/β-catenin signaling and enhances the efficacy of chemotherapy in gastric cancer models. These findings support its development in rational combination regimens to improve patient outcomes.

#5755 MTORC1/2 inhibition enhances STX-478, a *PIK3CA*^{H1047R} mutant inhibitor, in *PIK3CA*^{H1047R} mutant colorectal cancer.

Alexa E. Schmitz[1], Addison Zick[1], Cheri A. Pasch[1], Dustin A. Deming[2]

[1]Univ. of Wisconsin Madison Sch. of Med. & Public Health, Madison, WI,[2]University of Wisconsin Carbone Cancer Center, Madison, WI

Background: STX-478, a *PIK3CA* mutant selective inhibitor, that we have previously shown to have promise in treating *PIK3CA*^{H1047R} mutant colorectal cancer (CRC) models. A high throughput drug screen was performed and identified AZD2014, an MTORC1/2 inhibitor, to have enhanced response with STX-478. Here, we examine the combination of PI3K inhibition with MTORC1/2 inhibition in *PIK3CA*^{H1047R} mutant colorectal cancer (CRC).

Methods: CRC cell lines SW48 and SW48PK (Horizon Discovery; SW48 with a *PIK3CA*^{H1047R} mutation) were treated with varying concentrations of STX-478 (250-750 nM) and AZD2014 (20-250 nM) and viability measured by WST was performed. *PIK3CA*^{H1047R} mutant PDCOs were treated, imaged, and response was determined by measuring the change in longest diameter of the organoids over time. Glass's Delta was used as a statistical test to measure the effect size of the different treatment groups. Mouse derived cancer organoids (MDCOs) were derived from Fc[1] Apc$^{fl/+}$ Pik3ca^{H1047R} murine colon tumors. MDCOs/PDCOs and CRC cell lines were treated with 750 nM or 500 nM STX-478 and 100 nM AZD2014, respectively, and collected for immunoblotting for apoptosis and PI3K proteins.

Results: Both SW48 and SW48PK had a significant reduction in cell viability with treatment of single agent AZD2014 at 100 nM (SW48 $p<0.001$, SW48PK $p=0.005$). When treated with combination of STX-478 and AZD2014, both cell lines had a significant reduction in cell viability (500 nM STX-478 with 100 nM AZD2014; SW48 $p=0.002$, SW48PK $p<0.001$). For SW48PK, a significant reduction of phosphorylation of ribosomal protein S6 (RPS6; $p<0.001$), AKT ($p<0.001$), and 4EBP1 ($p=0.002$) were observed after treatment with the combination, while no significant difference was seen in SW48. MDCOs had a significant decrease in RPS6 compared to control and single agent STX-478 ($p<0.001$). In *PIK3CA*^{H1047R} mutant PDCOs, a significant reduction in relative change in diameter was observed in the combination treatment compared to control (relative change in diameter control versus combination: 30.2% vs -0.96%; Glass's Delta = 1.67). *PIK3CA*^{H1047R} mutant PDCOs also had a significant decrease in phosphorylation of 4EBP1 ($p<0.001$) and RPS6 ($p<0.001$).

Conclusions: The combination of STX-478 and AZD2014 enhanced response in both 2D and 3D *PIK3CA*^{H1047R} mutant CRC models and shows promise for combining MTORC1/2 with *PIK3CA* inhibition for *PIK3CA* mutant CRC. Future work should investigate STX-478 and MTORC1/2 inhibition in *PIK3CA* mutant CRC *in vivo*.

#5756 Preclinical evaluation of BH4601, a novel tetravalent PD-L1 and B7H3 bispecific antibody-drug conjugate (ADC) with Topo1 inhibitor for the treatment of solid tumors.

Jun Wang[1], Pengfei Rong[2], Jing Wang[1], Yang Liu[1], Mengrui Zhao[2], Jie Feng[1], Lijuan Li[1], Yue Wang[1], Aihong Zhang[1], Dongyang Li[1], Hongjuan Zhang[1], Jingmei Cai[1], Xiaochun Li[1], **Jiangcheng Xu**[1], Jiawang Liu[1], Hui Ding[2], Fangxing Ouyang[2], Kyoungwoo Lee[1]

[1]Beijing Hanmi Pharm. Co. Ltd., Beijing, China,[2]FDC Biotech Kunshan China, Kunshan, China

PD-L1 and B7-H3, members of the B7 superfamily, are frequently overexpressed across various tumor types. While antibody-drug conjugates (ADCs) targeting either PD-L1 or B7-H3 individually have demonstrated modest clinical efficacy, their co-expression in multiple malignancies presents a compelling rationale for dual-targeting strategies. This bispecific approach broadens the scope of tumor targeting and simultaneously alleviates T-cell suppression, potentially leading to enhanced therapeutic efficacy. The dual-targeting strategy addresses the compensatory upregulation observed between these targets—where suppression of B7-H3 leads to PD-L1 upregulation, and vice versa.

A novel bispecific antibody concurrently targeting PD-L1 and B7-H3 was conjugated with a topoisomerase I inhibitor (XYD-295) and BH4601 was generated. In vitro evaluations revealed that BH4601 exhibits excellent target binding and internalization activities, as well as potent PD-1/PD-L1 blockade. Effective tumor control was demonstrated in multiple in vivo models, accompanied by significant T-cell activation. All animals remained well-tolerated at efficacious dose levels.

By simultaneously engaging both PD-L1 and B7H3 pathways, BH4601 achieves enhanced tumor-specific distribution and efficient tumor cell internalization, potentially improving both efficacy and safety profiles compared to its parental ADCs.

#5757 Exatecan payload-based antibody-drug conjugates with a short hydrophilic beta-glucuronidase cleavable linker.

Vasu Jammalamadaka, **Jiang Liu**, Sunil Bhakta, Vidya S. Jonnalagadda, Jagath R. Junutula

Aarvik Therapeutics, Hayward, CA

Antibody-drug conjugates (ADCs) enable the specific targeting of a potent cytotoxic drug to cancer cells expressing a select antigen via the release of the cytotoxin covalently linked to a target-specific antibody. A classic ADC comprises three elements: (a) a target-specific antibody that enables the binding of the ADC to cells expressing the target antigen, (b) a potent cytotoxic drug (payload) that kills cells when released from the ADC, and (c) a linker that covalently links the payload to the antibody until pre-defined conditions cause release of the payload. One of the factors limiting the *in vivo* biological activity of an ADC is high hydrophobicity, which stems partly from the linker or spacer and partly from the payload. In the body, high hydrophobicity often leads to aggregation of the ADC molecules; these aggregates are then rapidly cleared from circulation by the liver. Several approaches investigated in the past to reduce the overall hydrophobicity of ADCs include (a) reducing the hydrophobicity of the payload itself, (b) positioning the (hydrophobic) payload in a shielded pocket of the antibody, and (c) modifying the linker structure by introduction of hydrophilic spacers such as polyethylene glycol (PEG), polysarcosine (PSAR), hydrophilic macrocycles or long hydrophilic XTEN peptides. However, all these linker modifications involve bulky spacers, which can impact permeability into tumor tissue. Our goal was to develop short, streamlined hydrophilic linkers that boost ADC solubility without adding significant bulk. We successfully synthesized and screened several linker-payloads, and validated a novel hydrophilic, lysosomal β-glucuronidase cleavable linker combined with a short sugar-based spacer (AV-L03). We synthesized an ADC comprising trastuzumab conjugated to an exatecan payload via this novel, short, stable, hydrophilic linker AV-L03 at a drug-to-antibody ratio (DAR) of 8 and compared it to Enhertu®, which comprises trastuzumab conjugated to a DXd payload via a (hydrophobic) tetrapeptide linker. The ADC with the novel AV-L03 linker showed superior hydrophilicity, *in vitro* cytotoxicity, improved plasma stability, and *in vivo* efficacy in a mouse xenograft model compared to Enhertu®. The AV-L03 linker makes possible the use of exatecan as a payload for ADCs, which is promising given that exatecan is a more potent inhibitor of TOP1 isomerase compared to DXd, with higher permeability and bystander activity, and is a poorer substrate for some MDR pumps. Moreover, the AV-L03 linker, the shortest hydrophilic linker reported to date, is compatible with diverse payloads, and thus opens up several avenues for the design of superior ADCs.

#5758 Single protein encapsulated SN38: Extremely effective anticancer drug with low toxicity.

C. J. Yu[1], leslie Wang[1], Kinsley Wang[1], Mengmeng Liu[1], Faqing Huang[2], Warren A. Chow[3], Xiaojiang Cui[4]

[1]Sunstate Biosciences, LLC, Pasadena, CA,[2]The University of Southern Mississippi, Hattiesburg, MS,[3]University of California at Irvine, Irvine,, CA,[4]Cedars-Sinai Medical Center, Los Angeles, CA

Purpose: SN38 is a potent antineoplastic agent, however, the poor water solubility prohibited its direct clinical applications. At present, only prodrug approach on SN38 has resulted in 2 types of therapeutics approved by the FDA, irinotecan/ONIVYDE and Trodelvy. Furthermore, the poor enzymatic conversion (2-8%) of irinotecan into the active metabolite SN38 severely limits its efficacy. Numerous attempts of drug delivery systems failed to achieve effective SN38 delivery. Therefore, novel approaches are urgently needed for effectively delivering SN38.
Methods: Our patented single protein encapsulation (SPE) platform, allowing encapsulation of small-molecule drugs by a single protein (albumins or globulins) without artificial nanoparticles and chemical modifications to drugs and proteins, has made the first drug product, SPEDOX-6 into human phase IB/IIA clinical trial (NCT0764018). The great success of SPEDOX-6 has prompted us to utilize the same SPE technology for encapsulation of SN38 by HSA to create SPESN38-5/8 complexes, which were characterized by membrane dialysis, HPLC, UV and dynamic light scattering. We conducted pharmacological evaluations with respect to MTD, PK, *in vitro* and *in vivo* efficacy against various cancers.
Results: Lyophilized SPESN38-5/8 complexes can be dissolved in water to form clear and stable solutions. PK of SPESN38-5 by IV at 55 mg/ kg yielded much higher mouse plasma AUC for SN38 and SN38G, producing a molar ratio of SN38G:SN38 = 1.5:1. We tested *in vitro* growth-inhibitory effect of SPESN38-8 against SK-ES-1 (Ewing Sarcoma), SK-LMS-1 (soft tissue sarcoma), A204 (rhabdomyosarcoma) and HT1080 (soft tissue sarcoma) with IC50 at 0.1079, 0.1526, 1.023, 1.087 uM, respectively, which is 7 to 60-fold lower than irinotecan. *In vivo* antitumor efficacy against 5 cancer models was evaluated: (1) SK-ES-1 model, SPESN38-8 at 35 mg/kg vs DOX at 3.0 mg/kg and Doxil at 4.0 mg/kg; led to 8/8 mice tumor free on Day 21, which were monitored for total 230 days, tumor relapse wasn't found for > 209 days, indicative of cancer eradication; (II) A204, SPESN38-8 at 35 mg/kg vs Doxil at 4.0 mg/kg, led to all 4 females free of tumor & 4 males almost tumor free, (III) SK-LMS-1, SPESN38-8 at 35 mg/kg vs DOX at 5.0 mg/kg, led to 6/7 mice free of tumor, indicative of SPESN38-8's superior anticancer efficacy; (IV) HCT-116 (colorectal cancer) model, SPESN38-5 at 55 mg/kg vs irinotecan at 50 mg/kg, SPESN38-5 was much effective to suppress HCT-116 than irinotecan; (V) A549 (non-small cell lung cancer) model, SPESN38-8 at 35 mg/kg vs irinotecan at 50 mg/kg, SPESN38-8 was extremely effective to inhibit A549 than irinotecan.
Conclusion: SPESN38 complexes provide a novel water soluble SN38 formulation. SPESN38-5 and SPESN38-8 demonstrate better PK values, lower toxicity and superior antitumor efficacy in mouse models, compared with irinotecan, DOX and Doxil. FDA has green-lighted SPESN38-8 (IND #: 164346) for clinical development.

#5759 Genome-wide CRISPR screen identifies GPX4 as a potential vulnerability in cells treated with PI3Kα-mutant selective inhibitor RLY-2608.

Fabiana Napolitano[1], Yuan Wang[1], Dan Ye[2], Jingxuan Lu[1], JINGXUAN CHEN[3], Khushi Ahuja[4], Pamela Luna[2], Yuki Matsunaga[5], Dylan Calhoon[1], Maria Rosario Chica-Parrado[1], Yasuaki Uemoto[1], Javier Garcia Bermudez[1], Jeon Lee[6], Chang-Ching A. Lin[5], Ariella B. Hanker[7], Carlos L. Arteaga[8]

[1]Harold C. Simmons Comprehensive Cancer Center, Dallas, TX,[2]Harold C. Simmons Comprehensive Cancer Center, Dallas, TX, United States, Dallas, TX,[3]Lyda Hill Department of Bioinformatics, Dallas, TX,[4]Medical College of Wisconsin, Milwaukee, WI,[5]UT Southwestern Medical Center, Dallas, TX,[6]Lyda Hill-Dept of Bioinformatics, Dallas, TX,[7]UT Southwestern Harold C. Simmons Comprehensive Cancer Center, Dallas, TX,[8]Director, Breast Cancer Program and Center for Cancer Targeted Therapies, UT Southwestern Simmons Comprehensive Cancer Center, Dallas, TX

Background/Objectives: Approximately 40% of HR+ breast cancers harbor PIK3CA mutations. The clinical efficacy of PI3Kα inhibitors has been limited by toxicity and a narrow therapeutic window. Recently, mutant-selective PI3Kα inhibitors, such as RLY-2608 (zovegalisib), have shown improved efficacy and tolerability. Here, we aimed to identify genetic modulators of response to RLY-2608 in *PIK3CA*-mutant breast cancer cells.

Methods: A genome-wide CRISPR-knockout (KO) screen (80,000 sgRNAs targeting ~20,000 genes) was performed in T47D cells to identify genes whose loss sensitizes to PI3Kα inhibition. Key candidates were validated with CRISPR-Cas9, and RNA-seq was used to assess transcriptomic changes upon treatment.

Results: Among enriched sgRNAs in vehicle-treated controls, *PTEN*, *NF2*, *TSC2,* and *TSC1* showed the highest differential scores, consistent with known resistance mechanisms to PI3K inhibitors, therefore validating the screening's robustness. Among the top depleted genes in RLY-2608-treated cells - potentially associated with increased sensitivity to PI3Kα inhibition - was *GPX4,* encoding the antioxidant enzyme glutathione peroxidase 4. GPX4 protects cells from lipid peroxidation and ferroptosis (iron-dependent cell death). Stable *GPX4*-KO MCF7 and T47D cells, established via CRISPR-Cas9, displayed a 2.5-3-fold increased sensitivity to RLY-2608, respectively. Bliss independence analysis revealed strong synergy between RLY-2608 and the GPX4 inhibitor RSL3. In T47D cells treated with RLY-2608, transcriptome profiling revealed broad upregulation of lipid-associated genes, including enzymes involved in fatty acid β-oxidation, lipid mobilization and membrane lipid metabolism. These data suggest a shift toward enhanced lipid turnover and oxidation. Ongoing BODIPY-C11 and lipidomic analyses aim to quantify resulting lipid peroxidation. Compared to cancer cells without PI3K pathway mutations, *PIK3CA*-mutant cells exhibit suppressed xCT-mediated cystine uptake to preserve NADPH for lipid synthesis. PI3Kα inhibition relieves this suppression, increasing cystine availability; however, the accompanying induction of lipid metabolic and oxidative pathways increases lipid peroxide burden. Thus, we speculated that treatment with a PIK3CA-mutant inhibitor increases dependence on the GPX4-mediated antioxidant system, creating a therapeutically exploitable vulnerability via combination with GPX4 inhibitors.

Conclusions: Genome-wide CRISPR KO screen identified GPX4 inhibition as a vulnerability in HR+/*PIK3CA*-mutant breast cancer cells treated with the PI3Kα-mutant selective inhibitor RLY-2608. These data support a mechanistic link between PI3Kα inhibition, lipid peroxidation, and ferroptosis, providing a rationale for clinical trials with the combination of PI3K pathway and GPX4 inhibitors.

#5760 Metabolic rewiring renders *KEAP1*-mutant lung cancers sensitive to AKR1C3-activated prodrugs.

Michela Ranieri[1], Matthew Cattle[1], Doyeon Jang[1], Kwok-Kin Wong[2], Charles M. Rudin[3], John Thomas Poirier[4]

[1]NYU Langone Health Perlmutter Cancer Ctr., New York, NY,[2]NYU Langone Health, New York, NY,[3]Memorial Sloan Kettering Cancer Center, New York, NY,[4]NYU Langone Health Perlmutter Cancer Ctr., Brooklyn, NY

The AKR1C1-3 family (aldo-keto reductase family 1, members C1-C3) comprises cytosolic NADPH-dependent oxidoreductases that catalyze the reduction of carbonyl groups on steroids, prostaglandins, and xenobiotics. Upregulation of AKR1C enzymes in certain cancers can contribute to resistance to chemotherapeutic agents and oxidative stress, making them key effectors in redox homeostasis and drug resistance. AKR1C3 expression has been exploited to convert inert prodrugs to their active form with tumor selectivity. ACHM-025 is a second-generation AKR1C3-activated prodrug that is reduced in a single enzymatic step to ACHM-025H, a nitrogen mustard that bis-alkylates DNA to form intra- and interstrand cross-links (ICLs) leading to stalled DNA replication fork progression and cell death. ACHM-025 was shown to have potent activity in preclinical models of T-ALL, a cancer that can express high levels of AKR1C3. Loss-of-function alterations in *KEAP1* occur frequently in lung cancer, often co-occurring with alterations in *KRAS*, *STK11*, and *TP53*, forming distinct molecular subgroups that influence therapeutic response. *KEAP1*-mutant tumors are typically resistant to immune checkpoint blockade and platinum doublet chemotherapy, leading to significantly worse clinical outcomes. Previously, we showed that *AKR1C1/2/3* are among the most significantly up-regulated genes in *KEAP1*-mutant lung cancers, which supports preclinical testing ACHM-025 as novel therapeutic agent in this subset of tumors.Using a series of isogenic lung adenocarcinoma cell lines, we found that lines deficient in KEAP1 express high levels of AKR1C3 and are sensitive to ACHM-025. Colony formation and cell viability assays demonstrated dose-dependent sensitivity to ACHM-025, which was positively correlated with the amount of AKR1C3 protein expressed. The *KEAP1*-mutant isogenic clones of H292 and H358 cell lines exhibited IC_{50} values of 171 nM (95% CI: 124-240 nM) and 466 nM (95% CI: 329-689 nM), respectively. Among the tested cell lines, H460 cells showed the greatest sensitivity to ACHM-025, with an IC_{50} of 4 nM (95% CI: 2-10 nM). Co-treatment with SN34037, a potent and selective AKR1C3 inhibitor, abolished ACHM-025 activity, which demonstrated selective activation. Clonal competition assays admixing KEAP1-mutant and wild-type human adenocarcinoma cell lines demonstrated rapid depletion of *KEAP1*-mutant cells with minimal bystander effect. Finally, we confirmed that the cytotoxic effect of ACHM-025 led to increased phosphorylated H2AX (γH2AX) which is consistent with a mechanism of action involving DNA damage.Taken together, our data support the rationale that metabolic rewiring in KEAP1-mutant tumors leads to enhanced sensitivity to ACHM-025 and, therefore, supports AKR1C3 mediated prodrug activation as a potential therapeutic strategy for this subset of lung cancer patients.

#5762 FMC-242, a highly potent and selective covalent inhibitor of the PI3Kα -RAS interaction, demonstrates robust anti-tumor activity as monotherapy and in combination with targeted therapies.

Kevin R. Webster, Ryan McFadden, Abdul Awol, Koli Basu, Barun Bhhatarai, Yu-Hsin Chao, John Conway, Jay Duffner, Dan Erlanson, Robert Everley, Susan Fong, Sarah Gilfillan, Johannes Hermann, Alessandra Ianari, Lata Jayaraman, Svetlana Kholodar, Nathan Lavey, Tiep Le, Laura Marholz, Bethany Parker, Snahel Patel, Emily Sabbey, Shefali Sabhlok, Shayna Simonstein, Luke Utley, John Vassiliadis, Weiru Wang, Yan Wang

Frontier Medicines, South San Francisco, CA

Activation of RAS and PI3Kα are the most frequent oncogenic events in cancer, playing a key role in many aspects of tumor cell physiology, including growth, survival, differentiation, and migration. While treatment options have recently emerged for a subset of KRAS mutant patients and inhibitors of PI3Kα catalytic activity have been approved, both approaches have been limited by drug resistance and in the case of PI3Kα, hampered by poor tolerability (e.g., hyperglycemia). An alternative therapeutic strategy that addresses drug resistance with improved tolerability is needed. Application of the FrontierTM platform, which integrates chemoproteomics, AI, and covalent fragment-based drug discovery, enabled the discovery of FMC-242, a potent, selective, and orally bioavailable covalent inhibitor of the PI3Kα -RAS family interactions disrupting oncogenic RAS and RTK signaling without impacting the insulin homeostasis. FMC-242 rapidly and selectively forms a covalent bond with cysteine 242 in the RAS Binding Domain (RBD) of PI3Kα resulting in allosteric inhibition of PI3Kα -RAS complex formation. This leads to inhibition of AKT activation in tumors with mutations in KRAS or PI3Kα, and where receptor tyrosine kinases, e.g., HER2, are activated. FMC-242 treatment of CDX and PDX models carrying HER2 amplification and/or KRAS mutation results in potent anti-tumor activity including regressions. FMC-242 is well tolerated in vivo, and inhibition of PI3Kα -RAS interaction does not impact insulin signaling or blood glucose level. Combination of FMC-242 with targeted therapies including EGFR inhibitors, KRASG12C inhibitors such as FMC-376, divarasib, olomorasib, or pan-RAS/KRAS agents results in enhanced efficacy and tumor regressions in vivo. Together, these data demonstrate the potential of FMC-242, a selective covalent inhibitor of PI3Kα -RAS interaction, to deliver improved outcomes for patients as monotherapy and in combination with targeted therapies in the clinic.

#5763 Roginolisib stabilizes inactive PI3Kdelta to deliver specific target blockade with reduced immune toxicity.

Giusy Di Conza[1], Oscar Vadas[2], Simon Tiede[3], Elise Solli[4], Maria Chaouki[5], Laura Tesmer[3], Shanlin Rao[3], Remy Visentin[2], Mathias Wenes[6], Denis Migliorini[6], Sigrid S. Skanland[4], Anne Quillet-Mary[5], Loic Ysebaert[5], Julie Guillermet-Guibert[5], Alessio Bevilacqua[1], Lars van der Veen[7], Michael Lahn[1], Kjetil Tasken[4], Gerhard Hummer[3]

[1]iOnctura SA, Geneva, Switzerland,[2]University of Geneva, Geneve, Switzerland,[3]Max Planck Institute for Biophysics, Frankfurt am Main, Germany,[4]Institute for Cancer Research, Oslo University Hospital, Oslo, Finland,[5]Centre de Recherches en Cancerologie de Toulouse, Toulouse, France,[6]Faculty of Medicine, University of Geneva, Geneve, Switzerland,[7]iOnctura BV, Amsterdam, Netherlands

Phosphoinositide 3-kinase (PI3K) is a key target in cancer therapy, but first-generation PI3K inhibitors were associated with toxicities limiting their clinical use. Roginolisib, a next-generation PI3Kdelta inhibitor, is currently being investigated across multiple cancer types. In contrast to previous PI3K inhibitors, roginolisib has shown a well-tolerated profile. We hypothesize that this improved safety is in part due to high selectivity, driven by its structural properties. Structural and biophysical analyses—including X-ray crystallography, molecular dynamics simulations, and hydrogen-deuterium exchange mass spectrometry—demonstrate that roginolisib, unlike the first-generation inhibitor idelalisib, stabilizes the catalytic C-terminal helix (k-alpha12) of PI3Kdelta. This stabilization is specific for PI3Kdelta and locks the enzyme in an inactive conformation, resulting in potent and sustained inhibition of PI3Kdelta activity. This inhibition profile is observed in tumor samples from patients with chronic lymphocytic leukemia (CLL) and in lymphoma cell lines. Although roginolisib and idelalisib exhibit similar potency in CLL cells, their effects on immune cells differ. Notably, high concentrations of idelalisib impair the cytotoxic activity of $CD8^+$ T cells and promote the differentiation of $CD4^+$ T cells towards Th17 and Th2 subsets. By contrast, roginolisib preserves $CD8^+$ T-cell function and does not alter CD4+ T-cell differentiation. This mechanism of inhibition, likely based on conformational stabilization of the inactive kinase, is novel for PI3K small-molecule inhibitors. Hence, our findings may enable the development of more effective and better-tolerated PI3K inhibitors.

#5764 Evaluating the molecular mechanism of axitinib response in head and neck squamous cell carcinoma.

Behirda Karaj, Jiayu Wang, Paul L. Swiecicki, An-Yun Teng, J. Chad Brenner

University of Michigan, Ann Arbor, MI

Head and Neck Squamous Cell Carcinoma (HNSCC), the 6th most common cancer with 800,000 new cases each year, is an extremely aggressive disease with poor overall survival that has remained unchanged for several decades. For patients that develop recurrent and metastatic (R/M) disease, treatment options are extremely limited, and despite the recent success of immune checkpoint inhibitor (ICI) therapies, overall response rates remain low. To overcome this gap in knowledge and improve survival, our team completed a Phase 2 clinical trial of the pan-VEGF inhibitor, axitinib, in R/M patients. Genetic analysis of tumors from this study revealed that 75% of patients with genomic aberrations in either *PIK3CA* or *PTEN* had a longer progression-free survival compared to 17% in those without a PI3K pathway alteration. Importantly, PI3K pathway aberrations are highly prevalent in HNSCC, accounting for 45-55% of all HNSCCs, suggesting the potential for a substantial clinical impact. In our genetically engineered mouse model (GEMM), axitinib significantly extended the overall survival of mice with K14:Pik3ca-H1047R, but not K14:control, tumors. Additionally, the use of in vitro cell proliferation and survival assays in HNSCC cell lines has shown that axitinib reduces cell numbers by 50%, increases γH2AX (DNA damage marker) protein levels as measured by western blots, and is more effective in *PIK3CA* mutant cell lines. Further, when testing the mechanism, we observed that axitinib, but not Lenvatinib (known VEGFR inhibitor), induced apoptosis in HNSCC cell lines. Deeper investigation showed that the HNSCC cell lines did not express any known axitinib targets, suggesting that axitinib may have an additional, unknown mechanism of action (MoA). To test for additional MoA, we used RNA sequencing of axitinib-treated HNSCC cell lines to compare the signal transduction pathways differentially regulated by axitinib compared to other VEGFR and PI3K inhibitors. Future studies will allow us to continue investigating axitinib's mechanism of action and its therapeutic potential in PI3K aberrant HNSCC. Our findings support clinical advancement of axitinib and use of PI3K genetic status as a predictive marker for therapeutic response for a large subset of HNSCC patients with limited therapeutic options.

#5765 Discovery of QLS1522, a mutant-selective allosteric PI3Kα inhibitor for the treatment of PIK3CA-mutant solid tumors.

Yuxing Zhang, Hua Qin, Jiasheng Fu, Naijie Fu, Difei Dong, Changliang He, Lan Zhang, Yu Zhang, Ling Li, Jun Mao, Jianping Chen, Weibo Zhu, Dong Yang, Xinghua Cheng, Guqin Shi, Jinxiao Bao, Ying Wang, Ping Chen, Su Qian, **Liang Xie**, Daqing Sun, Weikang Tao

Shanghai Qilu Pharmaceutical Research and Development Center LTD., Shanghai, China

Background: PIK3CA is a predominant oncogene in human cancers. While approved PI3Kα inhibitors like Alpelisib validate that PI3Kα blockade can suppress tumors and improve outcomes in PIK3CA-mutant ER+HER2- breast cancer, their major on-target toxicity against wild-type PI3Kα interferes with regulation of glucose metabolism which reduces their therapeutic index and limits clinical efficacy. Development of PIK3CA mutant selective inhibitors can significantly improve therapeutic window and anti-tumor efficacy by substantially reducing side effects.
Experimental procedures: The enzymatic activity was evaluated in biochemical and biophysical assays. Viability of cell lines was measured using CellTiterGlo®. Antitumor activity was evaluated in ER+ breast cancer cell line-derived xenograft (CDX) models with either kinase domain or helical domain mutations. The impact on glucose metabolism was analyzed using an oral glucose tolerance test (OGTT).
Results: QLS1522 is a potent, selective allosteric PI3Kα inhibitor designed to spare wild-type PI3Kα. It exhibited nanomolar potency against the PIK3CA H1047R mutation with high selectivity over wild-type PI3Kα and other isoforms (β, γ, δ). In a 447-kinase selectivity panel, QLS1522 showed outstanding specificity, with only Aurora-B kinase exhibiting >50% inhibition at 10 μM (IC_{50} of 7.8 μM for QLS1522 vs. 1.4 μM for STX-478). Cell panel studies revealed that QLS1522 exerted broad inhibitory effects across cancer cell lines carrying either kinase domain or helical domain mutations. In comparative analyses with other clinical-stage candidates such as STX-478 and RLY-2608, QLS1522 showed enhanced inhibition of pAKT in the T47D breast cancer cell line harboring the PIK3CA H1047R mutation. Notably, it maintained selectivity comparable to STX-478 and better than RLY-2608 in wild-type SKBR3 cells. *In vivo*, QLS1522 was well tolerated and exhibited potent antitumor efficacy in multiple ER+ breast cancer CDX models, without inducing significant glucose metabolism abnormalities. The combination of QLS1522 with standard-of-care (SoC) agents resulted in enhanced efficacy compared to monotherapy or SoC alone. QLS1522 demonstrated a favorable drug-like profile, characterized by superior solubility, permeability, and excellent pharmacokinetic properties across species, with a wide therapeutic window.
Conclusions: QLS1522 is a mutant-selective allosteric PI3Ka inhibitor and represents a promising therapeutic candidate for treating PIK3CA-mutant solid tumors. IND-enabling studies are currently in progress.

#5766 Network-level kinase activity associate with differential drug sensitivity in B-Cell lymphoma cell lines.

Simar Pal Singh, Laken Woods, Robin Keijzers, Gitanjali Dharmadhikari, Dora Schuller, Rik de Wijn

PamGene International B.V., 's-Hertogenbosch, Netherlands

Background: B-cell lymphomas display heterogeneous responses to kinase inhibitors, reflecting underlying variability in kinase activity and signaling network states. Understanding how baseline kinase activity and broader signaling network patterns relate to drug sensitivity could improve therapeutic stratification and uncover mechanisms of drug response.
Methods: Drug sensitivity data (IC_{50} values) for B-cell lymphoma cell lines were retrieved from the CancerRxGene database (Genomics of Drug Sensitivity in Cancer) and response variability for small-molecule inhibitors targeting serine/threonine kinase (STK) families was quantified using the standard deviation of its LN(IC_{50}) values across cell lines. For 11 B-cell lymphoma cell lines, kinase activity profiling was performed using KinomePro platform (PamGene International B.V.) and Upstream Kinase Analysis was used to predict kinases from the phosphorylation signatures. We conducted Multi-Omics Factor Analysis (MOFA) to integrate phosphorylation signatures and drug sensitivity data, identifying latent factors that capture correlations between kinases and drug responses.
Results: Drug responses showed substantial heterogeneity across cell lines: 7% of drugs were homogeneous (LN(IC_{50}) SD < 0.5), 41% moderately heterogeneous (SD 0.5-1), and 52% heterogeneous (SD > 1). In cell lines where drug sensitivity was observed, only 10-30% showed elevated activity of the drug target kinase, and this correlation was not statistically significant. Correlation analysis (MOFA) identified latent factors that mapped kinase activity to drug sensitivity and revealed two distinct sensitivity clusters: one comprising PI3K/AKT/mTOR, central to cell growth, survival, metabolism, and proliferation; and a second cluster including CDK, ATM/ATR, Wee1, AURKA, and MAPK, central to DNA damage response, cell cycle regulation and checkpoint signaling. Upstream Kinase Analysis validated that cell lines sensitive to AKT/PI3K/mTOR inhibitors exhibited relatively high AKT and RSK signaling activity, whereas cell lines sensitive to inhibitors targeting cell cycle pathway showed higher baseline CDK and MAPK family kinases.
Conclusions: Our integrative analysis of drug sensitivity and kinase-activity data demonstrates that B-cell lymphoma response is shaped not only by individual kinase activities but also by the architecture of signaling networks. The strong concordance between baseline kinase activity signatures and drug sensitivity highlights network-level determinants of response. Signal-network signatures associated with sensitivity may serve as biomarkers for stratification and provide mechanistic insight into heterogeneous drug responses. These findings lay a foundation for functional validation and the development of combination therapies guided by network-level dependencies.

#5767 Combining SUMO inhibition and irinotecan increases pancreatic cancer cytotoxicity.

Asimina Courelli, Leonie Ren, Herve Tiriac, Yuan Chen, Andrew Lowy

University of California, San Diego, La Jolla, CA

Introduction: Pancreatic cancer (PDAC) has a transient response to chemotherapy, motivating the need for improved treatment options. Irinotecan (IRI) is a standard of care agent for both 1st and 2nd line PDAC therapy. SUMOylation is a post translational modification on topoisomerase 1 (Top-1) that modulates its DNA binding. We hypothesized that combining IRI with Subasumstat (SST—a SUMOi agent) would synergize in reducing Top-1 efficacy, leading to augmented apoptosis.

Methods: *Human single cell RNA sequencing (scRNASeq)*: using the Human Pancreatic Cancer Single-Cell Atlas to identify SUMO2/3 expressing cancer cells after FOLFIRNINOX. *In Vitro Synergy*: KPC46, FC1245, FC1245-Gem Resistant murine PDAC cells treated with IRI and/or SST (1nM-500nM, 24hrs); viability assessed with cell titer glo; synergy plots generated using Combenefit.

Western Blots (WB): KPC46 and FC1245 cells treated with SST and/or IRI (100nM) for 24 hours; probed for Top-1 (chromatin protein fraction), γ-H2AX, and cleaved caspase-3 to validate apoptosis.

Survival Experiments: NSG mice underwent orthotopic KPC46 cell injections—IP injections with SST (15mg/kg q48h) and/or IRI (12.5mg/kg qwkly); tumor volume (TV) assessed with ultrasound.

Human PDAC Cultures: patient tumor slices incubated in 200nM SST and/or IRI for 5 days; flow Cytometry (FC) conducted for EPCAM and PanCK PDAC cell markers.

Results: scRNASeq showed SUMO2/3 is highly expressed PDAC primary tumor cells as compared to adjacent normal tissue and that SUMO2/3 expressing cancer cells persist after FOLFIRINOX treatment. Significant in vitro synergy between SST+IRI occurred as low as 50nM. WB showed the greatest increase in chromatin bound Top-1, total cell Y- H2AX, and cleaved caspase 3 (Band Intensity: IRI: 0.1, SST:0.15, SST+IRI: 0.52; p=0.009) occurred for SST+IRI. Synergistic cytotoxicity of SST+IRI treatment in vivo resulted in significantly improved survival (IRI:16, SST:17, SST+IRI=24 days; p=0.008) and reduced TV (after 2 wk-treatment; AvgTV: IRI=358mm3, SST [all mice dead], SST+IRI=132mm3; p=0.001). In human PDAC slices, SST+IRI treatment yielded the greatest decrease in PANCK+ and EPCAM+ cells (IRI:24.4%, SST:15.5%, SST+IRI:9.5%).

Conclusion: SST+IRI constitutes a promising combination treatment for PDAC with synergistic PDAC cytotoxicity observed in both murine and human models. Clinically, SST could serve as an adjunct to FOLFIRINOX or SST+IRI could be an alternative 2nd line treatment with potential to include a RAS inhibitor.

#5768 Repurposing veratridine, a previously used antihypertensive supplement, for effective treatment of metastatic colorectal cancer.

Morgan Eikanger, Khosrow S. Rezvani

University of South Dakota, Vermillion, SD

Despite significant advances in improving colorectal cancer (CRC) survival over the past decade, therapeutic challenges persist due to the rapid spread of primary tumors. The rising incidence of early-onset colorectal cancer (patients under age 50) across all ethnicities has created another major health concern, as these patients are often diagnosed with advanced, metastatic disease, leading to higher mortality rates. This highlights the urgent need to develop more effective targeted therapies to fight metastatic CRC. The mTORC2 signaling pathway plays a key tumorigenic role in CRC by driving processes such as metastasis and drug resistance. The objective of this study is to develop a selective mTORC2 inhibitor that prevents tumor growth and metastasis without harming normal cells. This project aims to advance Veratridine (VTD), a small plant-derived molecule that transcriptionally upregulates UBXN2A, a colon-specific tumor-suppressor protein. UBXN2A's E3 ubiquitin ligase partners enable it to specifically target and degrade mitochondrial HSP70 (mortalin) oncoprotein and Rictor protein in the mTORC2 pathway. This study demonstrates the dual-action mechanisms of the VTD-UBXN2A axis in patient-derived xenograft (PDX) cell lines. Acute and sub-chronic VTD treatment using both two-dimensional (2D) and three-dimensional (3D) PDX cells, assessed using real-time cell analysis via xCELLigence and Cytation visualizing technologies, revealed that VTD effectively suppresses cell migration and metastatic features of human CRC cells. Our genetic and pharmacological tools have established a platform for repurposing Veratridine, a previously used anti-hypertensive supplement, into a new generation of anti-metastatic drugs that function mechanistically through a ubiquitin-like protein, while simultaneously providing greater safety and therapeutic efficacy in patients with metastatic CRC.

#5769 A potent TOP2 poison with robust preclinical efficacy and a favorable therapeutic window supporting clinical evaluation in pancreatic cancer.

Krzysztof Grela, Stanislaw Skora, Izabela Fokt, Edd Felix, Zofia Zielinska, Mihai G. Iurascu, Mateusz Kwasnik, Rafal Zielinski, **Waldemar Priebe**

UT MD Anderson Cancer Center, Houston, TX

Background. Topoisomerase 2 alpha (TOP2A) is overexpressed in pancreatic ductal adenocarcinoma (PDAC) and its expression strongly correlates with poor prognosis and increased metastatic potential. Several TOP2A targeting drugs, including doxorubicin (DOX) are available, but none represent effective PDAC treatment modalities. Annamycin (ANN), a potent, non-cardiotoxic analog of DOX, but in contrast to DOX exhibits high accumulation in the pancreas and displays robust antitumor activity in orthotopic human PDAC models. It is currently being evaluated as a liposome formulation (L-ANN) in Phase 3 clinical trials in AML patients.

Objective. Our objective was to assess the preclinical anticancer efficacy of L-ANN using the syngeneic KPC cell line model for PDAC, and the potential impact of L-ANN on the tumor microenvironment.

Methods. In vivo efficacy of L-ANN was assessed in a KPC syngeneic model of PDAC in fully immunocompetent mice (C57BL/6). Tumor progression was measured using bioluminescence imaging (BLI) and ultrasound imaging (USI). ANN levels in plasma and tumors were assessed using LC/MS/MS. Immunohistochemistry analysis of residual tumor tissue were quantified using Aperio Image Scope.

Results. The KPC model is derived from genetically engineered mice, in general characterized by profoundly immunosuppressive tumor microenvironment. All mice were injected orthotopically with established KPC cells and showed consistent tumor growth with an average weight of 654.6± 83.8 mg at day 20. However, mice that received 3 weekly L-ANN injections at 4 mg/kg (IV, starting day 7) had significantly reduced tumors (103.5±34.1 mg), with 3 mice exhibiting complete regression. Tumor weight correlated with BLI and USI data and confirmed the dramatic inhibition of tumor growth in the L-ANN cohort. High levels of ANN were measured in residual tumor tissue 1h post injection (5.8±0.5 µg/kg) and were roughly 7-fold higher than the average plasma levels (0.83±0.1 µg/ml). Ex vivo analysis revealed increased levels of DNA damage in residual tumors when compared to vehicle-treated mice (pH2A gamma 35.3±5.4% vs. 5.8±0.3%, respectively). Immune profiling of the tumors revealed significant infiltration of CD8+ and CD4+ cells only in L-ANN treated mice, suggesting their contribution to the antitumor activity of ANN. T cell ablation experiments warrant verification of the role played by CD8+ T cells in the antitumor response.

Conclusion. Our preclinical studies demonstrate robust antitumor activity of L-ANN in different PDAC models, including prior human PDAC models and now an implantable syngeneic immunocompetent KPC model, that correlates with high tumor uptake of L-ANN. Along with low toxicity prolife of L-ANN (e.g. lack of cardiotoxicity) established in ongoing clinical trials, these data substantiate the clinical evaluation of L-ANN in PDAC patients.

#5770 Design, synthesis, and biological investigation of a new class of duocarmycin payloads for ADC development.

Goreti R. Morais, David Pajtas, Enric A. Picher, Sneha Smarakan, Robert A. Falconer, **Klaus Pors**

Institute of Cancer Therapeutics, University of Bradford, Bradford, United Kingdom

Introduction: The duocarmycins belong to a class of agent that has been in the interest of chemist and drug developers for over four decades. Their pico-molar cellular potency, unique mechanism of action, and efficacy against drug-resistant cancer cells makes them attractive as payloads for inclusion in antibody-drug conjugate (ADC) discovery approaches. However, despite great advances in fine-tuning biological activity through structure-activity relationship (SAR) studies, no duocarmycin-based therapeutic has reached clinical approval. Recent duocarmycin-based ADCs under clinical evaluation have been hampered by a narrow therapeutic index, which have inspired us to modulate the duocarmycin scaffold designed by nature. Here we present our design approach, synthesis and biological investigation of new duocarmycin chemotypes.
Methodology: Seco-duocarmycins derived from common scaffolds such as CBI and CPI are precursor molecules where the phenolic OH group essential for spirocyclisation was converted into a triflate. The latter was subjected to (i) Suzuki chemistry to generate novel aryl C-C linked compounds or (ii) or Buchwald-Hartwig reaction to generate aniline-linked duocarmycin target molecules. Subsequently, modulated compounds were studied for their ability to spirocyclise (LCMS), cause DNA damage using γ-H2AX as marker and produce antiproliferative effects in a panel of breast, colon, ovarian, prostate cancer and rhabdomyosarcoma cell lines (MTT assay).
Results: Biochemical assays revealed that these analogues exhibit a slower spirocyclization rate (2-48 hours) compared to the control compounds CPI-MI and CBI-MI (< 90 min). The library of duocarmycin payloads exhibited a wide range of cellular potencies in our panel of cancer cell lines (0.1 - 1000 nM), retaining antiproliferative activity in doxorubicin (MCF7adr) and docetaxel-resistant (PC3-D8) cancer cell lines whilst also be unaffected by the p53 status (HCT116 p53+/+ and p53-/-).
Conclusion: New duocarmycin chemotype design offers an opportunity to reduce spirocyclisation rate and DNA reactivity to fine-tune cellular potency. We hypothesise incorporation of these promising payloads into ADC therapeutics will improve tumour biodistribution, bystander effect and reduce normal tissue toxicity.

: Proximity-Induced Drug Discovery 2
Poster Session

#5774 Discovery of potent CDK8/CDK19 PROTAC degraders with superior anti-leukemia efficacy.

Li Zhang, **Jia Zheng**, Rebekah Martin, Jing Li, Zachary T. Mack, Hao Ji, Eugenia V. Broude, Igor B. Roninson, Campbell McInnes, Mengqian Chen

Drug Discovery and Biomedical Sciences, University of South Carolina, College of Pharmacy, Columbia, SC

Aggressive leukemias, including acute myeloid leukemia (AML), remain highly challenging diseases due to the lack of curative therapies. AML rapidly develops resistance to both conventional and targeted treatments, underscoring the urgent need for more effective therapeutic strategies. Recently, the transcription-regulating Mediator kinases CDK8 and CDK19 have emerged as promising targets, with CDK8/19 kinase inhibitors (CDK8/19i) now in clinical trials for leukemia. However, preliminary data from our laboratory demonstrate that leukemia cell lines exhibit heterogeneous and often incomplete responses to CDK8/19i, with many developing resistance after initial sensitivity. To test the hypothesis that direct depletion of CDK8/19 proteins in contrast to inhibiting kinase activity alone, may elicit more potent and durable anti-leukemia activity, we developed three series of PROteolysis TArgeting Chimeras (PROTACs) based on selective CDK8/19 inhibitors conjugated through diverse linkers to cereblon (CRBN)-recruiting ligands. After extensive optimization of both the kinase targeted warhead and composition of the linker, the most potent degrader obtained, SNX7886, induced efficient and simultaneous degradation of CDK8 and CDK19 across multiple cell types with a DC_{50} of 10 nM. When evaluated side-by-side with its cognate CDK8/19i (BI1347), SNX7886 consistently produced superior and sustained growth inhibition without the adaptive resistance observed with CDK8/19 kinase inhibitors in multiple leukemia lines. Notably, in an aggressive refractory AML cell line NOMO1, prolonged treatment with CDK8/19-PROTACs resulted in complete growth arrest, with no surviving cells detectable over extended exposure. Transcriptomic and proteomic analyses further revealed that CDK8/19-PROTACs engage both shared and distinct molecular pathways compared to CDK8/19i, indicating deeper disruption of transcriptional reprogramming circuits associated with AML survival and adaptation. These findings highlight targeted CDK8/19 degradation as a promising therapeutic strategy capable of overcoming key limitations of CDK8/19 kinase inhibitors in AML.

#5775 When CDK meets CIP: Linking target engagement to functional outcomes in CDK2 molecular glue and CDK-TCIP.

Qing Xue, Zhu Meng, Xue Yang, Qian Wang, Lili Chai, Wei Liu, **Tj (Tiejun) Bing**

ICE Bioscience, Beijing, China

Background: Cyclin-dependent kinases (CDKs) orchestrate cell cycle progression and transcriptional control, and their dysregulation is a hallmark of cancer. While conventional CDK inhibitors have shown utility, emerging modalities such as molecular glues (MGs) and transcriptional/epigenetic chemical inducers of proximity (TCIPs) offer novel mechanisms to modulate or utilize CDK activity. CDK2 MG promote selective degradation of CDK2 complexes, whereas CDK9 TCIP induce proximity-driven transcriptional rewiring. The purpose of this study was to demonstrate linkage of target engagement to cellular outcomes across these two modalities, thereby establishing mechanistic insights for next-generation CDK therapeutics.
Methods: We developed an integrated platform combining biophysical binder screening (Spectrum Shift, SPR, HTRF), cellular assays of CDK2 degradation and cell cycle control (proliferation, phospho-RB, flow cytometry), mechanism-of-action studies in CCNE-amplified and resistant models with drug combinations, CDK-TCIP engagement and transcriptional assays (NanoBRET, BCL6 reporter, qPCR), downstream functional profiling (viability, apoptosis, cancer cell panels, primary cell lines), and off-target evaluation by Western blotting, proteomics, and ICESTP safety panels.
Results: CDK2 MG induced robust CDK2/CRBN ternary complex formation and degradation of CDK2, leading to reduced proliferation, decreased phospho-RB, and G1 arrest. CCNE amplification conferred heightened sensitivity, while palbociclib resistant cell lines revealed CDK2 MG as a potential strategy to overcome drug resistance. In contrast, CDK-TCIP stabilized ternary complexes that drove nuclear translocation and transcriptional activation, evidenced by BCL6 reporter activation and target qPCR upregulation. Functional assays demonstrate broad vulnerability across cancer cell panels, with apoptosis induction in select primary cell lines. Off-target profiling confirmed high selectivity, with minimal liabilities detected across proteomic and ICESTP safety screens.
Conclusions: This study provides comprehensive profiling showing that CDK2 MGs and CDK-TCIPs achieve distinct biological outcomes through degradation versus transcriptional rewiring. By integrating biophysical, biochemical, and cellular analyses, we establish quantitative links between target engagement and phenotypic consequences. These findings define mechanistic frameworks for optimizing CDK-targeting modalities and inform rational design of selective, context-dependent interventions in oncology.

#5776 Discovery of an orally bioavailable AKT degrader with sustained *in vivo* efficacy and translational potential.

Seung Jae Jeong[1], Hyunsun Jo[2], Juyoung Jung[2], Hyunah Yoon[2], Aerim Hwang[2], So-Eun Son[2], Iljin Shin[1], Eun Seo Bae[1], Narkhyun Bae[1], Hyounmie Doh[1]

[1]Daewoong Pharmaceutical, Seoul, Korea, Republic of,[2]Pin Therapeutics Inc., Seongnam-si, Korea, Republic of

The PI3K-AKT signaling pathway is frequently dysregulated across solid tumors, including PIK3CA-mutant cancers. While several PI3K and AKT inhibitors have been approved for clinical use, therapeutic benefit remains limited by feedback reactivation and incomplete pathway suppression. We developed a novel, orally active small-molecule degrader designed to achieve sustained AKT removal and pathway inhibition.

Our AKT degrader lead molecule DWP221/PIN002 induced rapid and sustained degradation of AKT in tumor cells and demonstrated a strong correlation between systemic exposure and pharmacologic response after oral dosing in tumor-bearing mice. In vivo, the degrader achieved dose-dependent tumor growth inhibition and showed preferential distribution to tumor tissue. Exploratory combination with fulvestrant further improved tumor growth control, supporting potential therapeutic complementarity in hormone receptor-positive tumors. DWP221/PIN002 was well tolerated throughout the study period, without notable body-weight loss or overt signs of systemic toxicity, and maintained a favorable exposure-response relationship consistent with its drug-like properties.

This study demonstrates that an orally bioavailable AKT degrader can achieve durable target suppression and in vivo efficacy through sustained exposure and efficient target engagement. These findings support that targeted protein degradation may overcome key limitations of conventional kinase inhibition and provide a differentiated approach toward next-generation targeted therapies for PI3K-AKT-driven cancers.

#5777 Functional role of PLK1 in colorectal cancer progression and its potential to chemoresistance.

Kong Hyejeong[1], Baek MooJun[1], HyoWook Gil[1], Eunjung Yang[1], Kwangseock Kim[1], Taewan Kim[1], jaesung Ryu[1], Beamjun Park[1], Jeong Kyu Bang[2], **Seob Jeon**[1]

[1]Soonchunhyang University Cheonan Hospital, Cheonan, Korea, Republic of,[2]Division of Magnetic Resonance, Korea Basic Science Institute(KBSI), Ochang, Korea, Republic of

OBJECTIVE
Colorectal cancer is a cancer with high prevalence and mortality rates worldwide, treated with surgery, chemotherapy, and radiation therapy depending on the stage. Advanced colorectal cancer is mostly curable by surgical excision combined with chemotherapy remains the primary treatment for most patients with advanced colorectal cancer. Drug resistance is one of the major obstacles in colorectal cancer treatment, highlighting the need for new therapeutic targets. Polo-like kinase 1(PLK1), a key regulator of the cell cycle, is frequently overexpressed in colorectal cancer as well as various malignancies and associated with poor prognosis. To explore the mechanisms of chemoresistance in colorectal cancer and identify potential strategies to overcome it, we investigated the functional role of PLK1 and its impact on drug sensitivity.
METHODS
PLK1 was silenced using siRNA, and functional studies assessing proliferation, migration, invasion, and wound healing were conducted to investigate its role in colorectal cancer. To evaluate chemoresistance, colorectal cancer cells were treated with oxaliplatin. Additionally, we assessed the drug sensitivity of the oxaliplatin versus PLK1-PROTAC+oxaliplatin to evaluate its impact on cell survival. Subcutaneous implantation of CRC cell line-derived tumors was performed in BALB/c nude mice to assess tumor growth after drug treatment.
RESULTS
Suppression of PLK1 expression significantly impaired function of colorectal cancer. Colorectal cancer cells with low PLK1 expression exhibited significantly increased sensitivity to oxaliplatin. Compared to oxaliplatin alone, treatment with a PLK1-targeting PROTAC in combination with oxaliplatin significantly reduced colorectal cancer cell viability. In the in vivo study, PLK1-PROTAC exerted significantly enhanced suppression of tumor growth compared with Oxaliplatin.
CONCLUSION
Suppression of PLK1 expression led to a significant decrease in colorectal cancer cell function highlighting its essential role in sustaining tumor growth and metastatic functions. These findings suggest that PLK1 may serve as a potential therapeutic target for inhibiting colorectal cancer progression and overcoming chemoresistance.

#5778 RCZY-690: A tri-complex molecular glue pan-RAS (ON) inhibitor exhibiting best-in-class potential for RAS-addicted solid tumors.

Xiaojing (Celia) Chen[1], Lin Wang[1], Xiaohong Liu[1], Qiaoni You[1], Shenjun Li[2], Ling Wang[2], Shanshan Bi[2], Jing Jiang[2], Jianming Bao[1]

[1]Rongchang Pharmaceuticals, Ltd., Yantai, China,[2]RemeGen Co., Ltd., Yantai, China

The RAS family, including HRAS, KRAS, and NRAS, acts as a master molecular switch that regulates essential cellular processes, including cell growth, proliferation, survival, and differentiation, and is strongly implicated in cancer. As members of the small GTPase superfamily, RAS proteins cycle between an active (GTP-bound) state and an inactive (GDP-bound) state to control key signaling pathways such as the MAPK/ERK and PI3K/AKT. Oncogenic RAS mutations— mostly occur at codons 12, 13, and 61—impair intrinsic or GAP-stimulated GTP hydrolysis, and shifting the equilibrium toward the active, GTP-bound form of RAS. This persistent activation leads to constitutive downstream signaling, driving uncontrolled cell proliferation, enhanced survival, and tumorigenesis. RCZY-690 is a highly potent, orally bioavailable tri-complex molecular glue pan-RAS (ON) inhibitor with Best-in-Class potential. It specifically targets both mutant and wild-type RAS proteins in their active GTP-bound (ON) state, thereby blocking RAS engagement with downstream effectors and disrupting oncogenic signal transduction. In multiple RAS-mutant cell lines, RCZY-690 exhibited significantly greater inhibition of cell proliferation and more profound suppression of downstream p-ERK levels compared with RMC-6236. RCZY-690 has favorable ADME and PK properties, achieving higher exposure, an extended half-life ($T_{1/2}$), and a flat Cmax/Ctrough concentration-time profile consistent with an improved therapeutic index (TI). Compared to RMC-6236 and ERAS-0015, it shows higher degree of preferential tumor distribution in mouse models. These advantages enable RCZY-690 to achieve comparable tumor growth inhibition (TGI) at doses as low as 1/25th to 1/250th those of RMC-6236 and 1/3rd to 1/10th those of ERAS-0015 across KRAS-mutant CDX and syngeneic tumor mouse models. RCZY-690 demonstrates favorable PK/PD profiles, including more durable DUSP6 suppression than RMC-6236, alongside excellent in vivo tolerability and promising safety margins in preclinical toxicity studies. Taken together, these attributes position RCZY-690 as a promising pan-RAS(ON) inhibitor and support its advancement toward an Investigational New Drug (IND) filing planned for Q2 2026.

#5779 RCZY-869: A highly potent, selective, and orally bioavailable covalent KRAS^{G12D} (ON-state) inhibitor with robust antitumor activity in preclinical models of KRAS^{G12D}-driven solid tumors.

Xiaojing (Celia) Chen, Lin Wang, Xiaohong Liu, Dan Wang, Jianming Bao

Rongchang Pharmaceuticals, Ltd., Yantai, China

KRAS^{G12D} is the most prevalent oncogenic mutation in the RAS family. Among common solid tumors, it drives approximately 40% of pancreatic ductal adenocarcinoma (PDAC), 15% of colorectal cancer (CRC), and 5% of non-small cell lung cancer (NSCLC) cases, underscoring a significant unmet clinical need for targeted therapies. To date, no direct KRAS^{G12D} inhibitors have received global regulatory approval, highlighting the pressing demand for effective agents. In KRAS^{G12D}, the G12D substitution reduces RAS-bound GTP hydrolysis rate by ~2-fold compared to wild-type KRAS (and even more relative to KRAS^{G12C}), resulting in a higher proportion of KRAS^{G12D} existing in the GTP-bound conformation within cancer cells. This makes the “ON” state the dominant, therapeutically relevant form driving oncogenesis. Inhibiting this active, GTP-bound pool directly disrupts the core signaling activity, potentially yielding greater efficacy than targeting the transient “OFF” state. This mechanism supports targeting the GTP-bound conformation as a strategy with high clinical benefit potential. Emerging KRAS^{G12D} inhibitors target OFF, ON, or both states. Phase 1/1b data show ON-state inhibitor RMC-9805 and ON/OFF inhibitor VS-7375 (GFH375) have comparable objective response rates (ORR) and disease control rates (DCR) in NSCLC at their respective recommended Phase 2 doses (RP2D). In PDAC, VS-7375 had marginally higher ORR/DCR (52%/100% vs. 30%/80% for RMC-9805), but RMC-9805 had superior safety: low dose modification rates, no grade 4/5 TRAEs (predominantly grade 1 toxicities), and no DLTs. VS-7375 had a ~4-fold higher discontinuation rate, with 27.5% of patients experiencing grade 3/4 TRAEs. To address these challenges, Rongchang Pharmaceuticals has developed RCZY-869, a highly potent, selective, and orally bioavailable covalent tri-complex inhibitor that specifically targets the GTP-bound (ON) state of KRAS^{G12D}. It engages cyclophilin A (CypA) to form a stable ternary complex with KRAS^{G12D}(ON), blocking downstream effectors and suppressing MAPK signaling. RCZY-869 exhibits significantly greater in vitro antiproliferative activity than RMC-9805 across KRAS^{G12D}-mutant cell lines, favorable ADME properties, and superior oral PK in preclinical species. In KRAS^{G12D} xenograft models, it delivers dose-dependent antitumor effects at well-tolerated doses, achieving tumor growth inhibition (TGI) comparable to RMC-9805 but at substantially lower exposures. These findings position RCZY-869 as a novel ON-state-selective KRAS^{G12D} inhibitor with compelling preclinical potency and efficacy. Ongoing characterization advances its candidate package to support clinical development.

#5780 Discovery of ATH-007, a novel, potent and highly selective CCNE1 molecule glue shows robust anti-tumor activities and better safety profile.

Zhiyong Yu, Wenming Li, Yuyao Zhang, Wenwen Zhao, Youxi Chen, **Feng Zhou**

Atheron Therapeutics, Ltd., Shanghai, China

Cyclin E1 (CCNE1) is a key cell cycle regulatory protein and binds to cyclin-dependent kinase 2 (CDK2), forming a CCNE1-CDK2 complex, which is essential for driving the cell cycle progression to S-phase for subsequent DNA replication. Amplification of the *CCNE1* locus on chromosome 19q12 is prevalent in multiple tumor types, particularly in breast cancer, high-grade serous ovarian cancer, uterine tumors, and gastro-esophageal cancers. In breast cancer, amplification of CCNE1 is a potential cause of resistance to CDK4/6 inhibitor. CCNE1 amplification may also confer resistance to chemotherapy and is associated with poor overall survival. Therefore, there is a significant unmet medical need for tumors with CCNE1 amplification. Compared with CDK2 inhibitors, CCNE1 molecular glues exhibit better selectivity, thereby reducing the adverse effects caused by CDK2 inhibitors in clinical trials. Here, we report that ATH-007 is a highly selective CCNE1 degrader that demonstrates superior degradation selectivity and anti-tumor activity against CCNE1-amplified cells. ATH-007 strongly degrades CCNE1 with DC_{50} of <10 nM and achieves complete protein degradation (Dmax of >95%) and also shows 1000-fold degradation selectivity over other CRBN substrates, including GSPT1, CK1α, and IKZF1, etc. ATH-007 can effectively inhibit the proliferation of MKN1 cells with CCNE1 amplification, however, after the deletion of RB1 (a downstream substrate of CCNE1), the inhibitory effect of ATH-007 on MKN1-RB1-KO cells is abrogated. Across a panel of CCNE1-amplified tumor cell lines, ATH-007 potently inhibits proliferation with GI_{50} values ranging from 1 to 100 nM, similar to the potency of CDK2 inhibitors. In CCNE1-non-amplified cells, ATH-007 exhibits significantly superior selectivity compared to CDK2 inhibitors, rendering it the greater therapeutic window. In terms of *in vitro* hematotoxicity assay, ATH-007 shows no inhibitory effect on the differentiation of all lineages, while CDK2 inhibitors exhibits a strong inhibitory effect. Compared with existing CCNE1 molecular glues, ATH-007 exhibits weaker inhibition of hERG, indicating that it has potentially better safety. ATH-007 exhibits favorable PK properties, which enable us to advance this molecule to *in vivo* experiments. In tumor model with CCNE1 amplification, ATH-007 shows tumor suppression activity even at low doses and inhibit tumor growth in a dose-dependent manner. Furthermore, the inhibitory activity against tumors is correlated with the degradation of CCNE1.

#5781 CXB-7138, A novel GSPT1/ZFP91 dual molecular glue degrader, for targeted treatment of pancreatic ductal adenocarcinoma.

Jin-Hee Park, Jae-Seon Lee, Shin-Hae Lee, NamKyoung Kim, Sumin Kim, Chaeseon Kim, Yong Chan Kim, Eunbin Park, Jiah Kim, **Heung Sik Hahm**, Jung Beom Son, Nam Doo Kim, Hwan Geun Choi

CoBX Bio Co., Ltd, Seoul, Korea, Republic of

Background: Pancreatic ductal adenocarcinoma (PDAC) remains one of the most lethal malignancies, driven by profound intertumoral heterogeneity and a dense tumor microenvironment that limits the effectiveness of current therapies. GSPT1 (eRF3a), a translation termination GTPase historically considered “undruggable,” has recently become targetable through cereblon (CRBN)-mediated protein degradation. ZFP91, an atypical E3 ligase and transcriptional regulator, is also highly expressed in PDAC and correlates with poor clinical outcomes. Here, we present CXB-7138, a CRBN-recruiting molecular glue degrader built on a novel, nontraditional chemical scaffold, designed to induce selective degradation of both GSPT1 and ZFP91. To our knowledge, CXB-7138 represents the first dual-target GSPT1/ZFP91 degrader leveraging CRBN for therapeutic intervention in PDAC.
Methods: A panel of PDAC and non-PDAC cancer cell lines was treated with CXB-7138, and viability was assessed across genetically diverse models. Degradation of GSPT1 and ZFP91 was quantified by proteomics, Western blotting, and HiBiT-based assays. Antitumor activity was evaluated in a subcutaneous PDAC xenograft model following oral administration, with tumor volume and body weight monitored longitudinally.
Results: CXB-7138 exhibited potent antiproliferative activity across a broad spectrum of cancer cell lines—including but not limited to PDAC—with IC_{50} values in the sub-nanomolar to double-digit nanomolar range. Within PDAC models, a trend toward increased sensitivity was observed in cell lines harboring SMAD4 alterations, suggesting a potential genomic determinant of CXB-7138 responsiveness. Comparative proteomic profiling confirmed that the compound’s pharmacologic effects arise from selective and sustained CRBN-mediated degradation of both GSPT1 and ZFP91. In vivo, oral single-agent CXB-7138 inhibited tumor growth in a PDAC xenograft model, demonstrating potent antitumor efficacy with favorable tolerability.
Conclusions: CXB-7138 is a first-in-class CRBN-recruiting dual molecular glue degrader targeting GSPT1 and ZFP91 through a nontraditional scaffold. Its broad antiproliferative activity, molecularly defined sensitivity patterns, and strong in vivo efficacy position CXB-7138 as a highly promising therapeutic strategy for PDAC, a malignancy in urgent need of new treatment options.

#5782 Machine learning and structure-guided discovery of EP300-selective, orally bioavailable degraders for cancer therapy.

Ho Yeon Nam, Sun Young Jang, SeokJong Kang, Yongtaek Lee, Seongil Kang, Taegun Kim, Jooyun Byun, Gunwoo Lee, Wonjong Lee, Hobin Im, Haemin Chon, Yu-Yon Kim, Seunghwan Jung, Young Gil Ahn

Hanmi Pharmaceutical Co., Ltd., Hwaseong, Korea, Republic of

EP300 and CBP are closely related transcriptional co-activators with histone acetyltransferase (HAT) activity that regulate gene expression, cell proliferation, and differentiation. In normal tissues, EP300 and CBP compensate for each other; however, CBP-deficient tumor cells become selectively dependent on overexpressed EP300, creating a synthetic-lethal therapeutic window. Despite this opportunity, designing EP300-selective inhibitors has been challenging because the EP300 and CBP HAT domains share ~90% sequence identity. In this regard, targeted protein degradation (TPD) platform provides potential opportunity to achieve selective degradation. Recent findings indicate that even subtle structural variations, such as a single surface residue near the binding interface or the positioning of a lysine, amplify into significant differences in ternary complex stability and ubiquitination efficiency for proteolysis. Accordingly, we designed and synthesized heterobifunctional degraders that selectively degrade EP300 over CBP. Here, we report the discovery of orally bioavailable EP300 degraders and their evaluation *in vitro*, *in silico*, and *in vivo*. We identified early leads that selectively degrade EP300 over CBP, as confirmed by western blotting, thereby establishing proof-of-concept that TPD can confer EP300 selectivity. To further improve cellular potency, we optimized the initial lead using structure-guided design informed by molecular dynamics (MD) simulations; this analysis highlighted functionally important EP300 residues and guided modifications that increased the stability of the EP300-CRBN ternary complex relative to the starting scaffold. We applied a bioinformatics framework to identify solid tumor indications responsive to EP300 degradation. Using DepMap EP300 CRISPR scores integrated with RNA expression profiles, we developed and optimized a machine-learning model that accurately distinguished sensitive from resistant cell lines. Model-based prioritization identified several indications with the highest predicted sensitivity. Experimental validation confirmed that the optimized EP300 degrader induced robust EP300 degradation and potent growth inhibition across these tumor cell lines. In mouse xenograft models, it achieved high antitumor efficacy with lower toxicity than an EP300/CBP dual inhibitor, consistent with synthetic lethality. In conclusion, this study demonstrates that selective EP300 degradation can be achieved by applying TPD modality, enabling synthetic-lethal strategy and oral bioavailability. Structure-guided design and bioinformatics-driven indication selection provided an efficient path to preclinical candidates, underscoring the therapeutic potential of Hanmi's EP300 degraders for solid cancers.

#5783 HY809382, a PRC2 degrader with best-in-class properties, demonstrates efficacy across multiple tumors and overcomes EZH2 inhibitor clinical resistance caused by EZH2 genetic mutations.

Xin Li[1], Weixing Zhu[1], Ruwei Wang[1], Zengrong Li[1], Liming Zhang[1], Lei Chen[1], Sai Yang[1], Feng Xu[1], Qian Ma[1], Huangtao Jin[1], Xiaotian Huang[1], Ting Zhang[1], Xing Yu[1], Ming Weng[1], Xiaoxiao Wang[1], Xiaohong Hou[1], Manli Hu[1], Tingting Dai[1], **Ruowen Zhang**[2], Juan Du[1]

[1]Yangtze River Pharmaceutical (Group) Co., Ltd., Taizhou, China,[2]Medicilon USA Corp, Lexington, MA

The dysregulation of Polycomb repressive complex 2 (PRC2) is implicated in tumorigenesis across a spectrum of cancers, such as prostate cancer, non-small cell lung cancer, endometrial carcinoma, ovarian cancer, clear cell renal cell carcinoma and hematological malignancies. Furthermore, aberrant PRC2 activity is closely associated with tumor immune evasion and the development of therapy resistance, thereby influencing clinical outcomes. Given its critical role in tumor initiation and progression, the core PRC2 subunits EZH2 and EED have emerged as promising therapeutic targets. Among various EZH2 inhibitors under development, Tazemetostat (Tazverik) was the first to received FDA approval for the treatment of follicular lymphoma (FL) and epithelioid sarcoma (ES). Despite this progress, new challenges have emerged, including acquired resistance through EZH2 mutations and limited efficacy in tumors due to EZH1 compensatory mechanisms. Degradation of EED disrupts the assembly, stability, and activity of PRC2 complex, offering potential advantages over merely inhibiting EZH2 catalytic function. HY809382 is a potent and selective PRC2 degrader that targeted the EED subunit, designed with superior drug-like properties compared to existing EZH2 and EED inhibitors. HY809382 potently inhibited the proliferation of multiple tumor cell lines *in vitro*, including prostate cancer, endometrial carcinoma and gastric adenocarcinoma. Under identical experimental conditions, HY809382 exhibited greater potency than both PF-06821497 (an EZH2 inhibitor) and APG-5918 (an EED inhibitor). Once-daily oral administration of HY809382 demonstrated significant and dose-dependent tumor growth inhibition in xenograft models of prostate cancer, endometrial carcinoma, and gastric adenocarcinoma. Furthermore, HY809382 combined with enzalutamide synergistically suppressed tumor growth in a castration-resistant prostate cancer xenograft model. Clinically identified EZH2 mutations confer resistance to FDA-approved EZH2 inhibitors, whereas HY809382 remained effective in both cellular and *in vivo* xenograft models. Collectively, these data support HY809382 as a promising best-in-class PRC2 degrader candidate, warranting further development for the treatment of tumors exhibiting clinical resistance to EZH2 inhibitors.

#5784 Discovery of FX-111, a first-in-class heterobifunctional degrader of transcriptionally active androgen receptor (AR_{ON}), to treat patients with AR-driven prostate cancer.

Jennifer A. Mertz, Thomas H. Graham, Brian J. Golbourn, Yong Li, Alex P. Rossi, Marco Chiumiento, Phuong A. Nguyen, Jeremy W. Setser, Gregg Chenail, Rainer Wilcken, Jonathan T. Goldstein, Hannah Nguyen, Christina S. Henderson, Kaylyn E. Williamson, Byron DeLaBarre, Christopher M. Bailey, Miljan Kuljanin, Matthew C. Koehler, James E. Audia, Jonathan E. Wilson, Jacob I. Stuckey, Robert J. Sims

Flare Therapeutics, Cambridge, MA

Significant unmet need exists in metastatic castration resistant prostate cancer (mCRPC). As the disease progresses, mutations, amplification and overexpression of the androgen receptor (AR), often accompanied by elevated intratumoral androgen levels, become increasingly prevalent, with 85% of mCRPC cases remaining AR-dependent. Current therapies target the cytoplasmic, hormone-unbound AR (AR_{OFF}); however, rising AR levels as prostate cancer (PC) advances represent a primary mechanism of resistance to these therapies. Nuclear, hormone-bound, transcriptionally active AR (AR_{ON}) is the main driver of androgen signaling and tumor progression in AR-dependent PC. Here we report the discovery of a selective AR_{ON} degrader that utilizes a novel allosteric binding site revealed upon hormone binding. We identified multiple x-ray validated ligands that bind to this novel AR_{ON} pocket. Conversion and optimization of these ligands into Cereblon-based heterobifunctional degraders resulted in the identification of FX-111. FX-111 achieves rapid and sustained degradation of AR (DC_{50} = 10 nM) and displays exquisite selectivity, with no observed degradation of other steroid hormone receptors or other proteins using proteome-wide analysis in multiple cell lines. FX-111 degrades AR and silences AR target genes effectively irrespective of increasing hormone as it is non-competitive with androgen binding, in contrast to the loss of potency seen with orthosteric degraders with increasing hormone levels. FX-111 degrades AR_{ON} when alternative agonists are used to stimulate its activity and can effectively degrade clinically relevant mutant forms of AR. RNA-seq analysis in LNCaP and VCaP cells treated with FX-111 reveals complete inhibition of androgen-driven transcriptional changes, with minimal gene expression impact in hormone-depleted conditions, underscoring FX-111's specificity for AR degradation. In vivo, FX-111 induces robust AR degradation, prostate specific antigen suppression and significant tumor growth inhibition in VCaP xenograft models, with oral administration at 10 mg/kg BID. Addition of exogenous androgen in intact or castrated mice, mimicking intratumoral hormone, did not affect the pharmacodynamic profile or efficacy of FX-111, whereas orthosteric degraders lost both potency and the ability to suppress AR transcriptional activity. Potent suppression of AR function in prostate and testes tissues, with accompanying organ weight loss, was observed in mice. Targeting AR_{ON} in PC could potentially treat all forms of PC that are driven by AR signaling without the need for androgen deprivation. FX-111 is currently in IND-enabling studies with plans to initiate clinical studies in 2026.

#5785 RBM39 degrader anticancer activity against neuroblastoma: CDKN2A/B deletion as a biomarker.

James Finn[1], Imad salhab[2], Haihong Jin[3], Fei Liu[1], Dong Liu[1], Yunkai Zhang[1], Xing Liu[4], James Tonra[1], Lan Huang[1], **Dan Lu**[1]

[1]Seed Therapeutics, King of Prussia, PA,[2]Seed Therapeutics, New York, NY,[3]Vitsgen Therapeutics, Portland, OR,[4]Independent Consultor, King of Prussia, PA

Robust anticancer effects of molecular glue RBM39 degraders have been reported in human neuroblastoma models (DOI: 10.1126/sciadv.abj5405 and 10.1038/s41467-022-28907-3). In the present study we further explored the MOA underlying the potent activity of RBM39 degraders in neuroblastoma, utilizing SEED Therapeutics' optimized RBM39 degrader ST-00937, and its deuterium derivative ST-01156 that was recently cleared by the FDA for clinical testing (NCT07197554**)**. Method In vitro anticancer activity was profiled in 3D clonogenic assays utilizing tissue derived from 4 neuroblastoma patients and 6 human neuroblastoma tumor cell lines. In vivo anticancer efficacy was evaluated in nude mice bearing subcutaneous tumors established with SH-SY5Y human neuroblastoma cells. Cell lysates generated from 2D culture of neuroblastoma cell lines treated with ST-01156 were evaluated by TMT labeling mass spectrometry and Western Blot. Result ST-00937 treatment showed differential anticancer activity in 6 neuroblastoma cell lines and 4 patient-derived models. For the 6 neuroblastoma cell lines, the IC_{50} values ranged from 0.04 to 0.3μM among 5 sensitive cell lines, while SH-EP cells did not respond. The IC_{50} for colony formation ranged from 0.03 to 2.3μm in 4 patient-derived models. Notably, the most insensitive patient-derived model NB0277 has a homozygous CDKN2A/B deletion. In vitro activity was extended to in vivo activity utilizing SH-SY5Y cells. In vivo, complete tumor regressions were observed with 5-Days On/2-Days Off, twice daily oral treatment with ST-01156, without body weight loss. Proteomic analysis in vitro showed that ST-01156 decreased proteins involved in DNA damage and cell cycle control, and increased p53 signaling after 16h treatment. The divergent anticancer responses of SH-SY5Y and SH-EP subclones (both derived from SK-N-SH) warranted further investigation. Although both lines expressed similar levels of RBM39 and exhibited complete RBM39 degradation after treatment, distinct downstream effects were observed. In SH-SY5Y cells (adrenergic CDKN2A wild-type, cMYC amplified), cMYC expression was downregulated and the p21/p53 pathway was upregulated by ST-01156. In contrast, these changes were not detected in SH-EP cells (mesenchymal, CDKN2A/B deletion). This differential regulation may explain why cleaved caspase-3 (apoptosis) was not observed in ST-01156 treated SH-EP CDKN2A/B deleted cells, although DNA damage indicated by γH2AX was increased in both cell lines. Conclusion RBM39 degraders demonstrate differential potency in 6 neuroblastoma cell lines and 4 patient-derived models in vitro, and total tumor regression in SH-SY5Y in vivo. DNA damage and increased p53-mediated apoptosis are confirmed in the sensitive neuroblastoma model SH-SY5Y, while resistance in CDKN2A/B-deleted lines suggests CDKN2A loss may serve as a predictive biomarker of resistance to RBM39-targed therapy.

#5786 Novel non-CRBN based molecular glue identification and corresponding E3 ligase target deconvolution through multi-omics analysis.

Tongrui Hao, Yi Chen, Yan Gao, Jing Wen, Wenzhang Chen, **Zhongyao Ma**, Letian Kuai, Wenji Su

WuXi AppTec, Shanghai, China

Targeted Protein Degradation (TPD) is considered one of the new drug discovery strategies that could address previously “undruggable” disease targets through the ubiquitin-proteasome system (UPS). Although the current Target Protein Centric approach has proven successful in many cases, especially with well-validated E3 ligases such as CRBN and VHL, there is still a strong need to identify potential target protein degraders (PROTACs, molecular glues, etc.) through both target-centric and target-agnostic approaches. This would not only explore and identify potential tissue-specific novel E3 ligases but also greatly expand the range of potential degradable disease targets. In this study, we first developed a molecular glue-focused library consisting of approximately 5,000 compounds through various medicinal chemistry evaluations. A GSPT1-HiBit cell line and a GSPT1-CRBN-KO counter cell line were developed for primary hit screening purposes. More than 100 potential hits were identified through the initial screening, which included both CRBN-dependent and CRBN-independent hits. A GSPT1-based proximity labeling cell line was then constructed for further target deconvolution purposes via proteomics. Potential candidate E3 ligases were subsequently validated using an array-based expression manipulation strategy. Additionally, we tested novel synthetic lethal target discovery through both in vitro and in vivo screens, followed by omics-based target validation. Using a CRBN-focused glue library, we combined both transcriptomics and proteomics assays to evaluate potential “degradable” targets. To sum up, our study demonstrates that integrated target discovery and target deconvolution strategies could be useful for TPD drug discovery as well as other disease scenarios.

#5787 TRI-611, a development stage molecular glue degrader of ALK, promotes the degradation of TKI-resistant ALK fusion proteins and leads to regression of ALK TKI-refractory tumors.

Andrew R. Conery[1], Daniel S. La[1], Artyom A. Alekseyenko[1], David Marcoux[1], Aaron G. Bart[1], **Matt L. Harlow**[1], Patrick R. Arsenault[1], Nico R. Cantone[1], Rebecca L. Casaubon[1], Hari B. Kamadurai[1], Aravind Prasad Medikonda[1], Duncan E. Nunes[1], Tim J. Wigle[1], Maolin Yu[1], Aleksandra Zagulyaeva[1], Christine Zarate[1], Lauren Highfield[2], Nobuyuki Kondo[3], Aaron N. Hata[3], Kenneth Ngo[4], Jisu Lee[4], Prafulla C. Gokhale[4], Kathleen I. Seyb[1], Patrick Trojer[1], Vito J. Palombella[1]

[1]Triana Biomedicines, Lexington, MA,[2]Massachusetts General Hospital, Boston, MA,[3]Massachusetts General Hospital and Harvard Medical School, Boston, MA,[4]Dana-Farber Cancer Institute, Boston, MA

TRI-611 is a potent, brain-penetrant molecular glue degrader (MGD) of anaplastic lymphoma kinase (ALK) that represents the first development stage MGD of an oncogenic fusion protein. By engaging ALK via a novel degron that is distal from the orthosteric tyrosine kinase inhibitor (TKI) binding site, TRI-611 has the potential to promote the degradation of ALK proteins that are either wild-type or mutant in the kinase domain, the latter of which are an important mechanism of disease progression in patients treated with ALK TKIs. Here we show through in vitro biochemical and biophysical studies that TRI-611 is equally effective at promoting the interaction of CRBN with wild-type ALK and the ALK$^{L1196M/G1202R}$ compound mutant protein, as well as subsequent poly-ubiquitination. Through the use of Ba/F3 cells engineered to express 30 distinct alleles of EML4-ALK, we show that TRI-611 effectively targets all tested EML4-ALK mutant proteins in cells, including those that are refractory to ALK TKIs. The broad phenotypic activity of TRI-611 is further highlighted by potent anti-proliferation of cell line and patient-derived ALK+ NSCLC models with multiple ALK TKI resistance alleles. In mouse efficacy studies, TRI-611 leads to the regression of subcutaneous xenografts of CRISPR engineered EML4-ALK-mutant NCI-H3122 cells that do not respond to ALK TKIs. Finally, we show that TRI-611 leads to the regression of an EML4-ALK mutant primary patient-derived xenograft isolated from a patient that had progressed on prior alectinib and lorlatinib. These data demonstrate the potential of TRI-611 to address a key liability of ALK TKIs that all target the same site on ALK and support the development of TRI-611 in all ALK+ NSCLC patients, including patients with wild-type ALK kinase domain and those with acquired TKI resistance mutations.

#5788 Rational discovery of novel molecular glues.

Simon Woehrle[1], Andreas Blum[1], Beatrix Blume[1], Jorg Bomke[1], Hans-Peter Buchstaller[1], Vincenza Dragone[1], Isabella Ferrara[1], Alessia Gambardella[1], Jakub Gunera[1], Ulrich Gradler[1], Ingo Kober[1], Johannes Krieger[1], Birgitta Leuthner[1], Andrea Unzue Lopez[1], Oliver Schadt[1], Christina Schindler[1], Fiona J. Sorrell[1], Ana M. Esteves[2], Sandra P. Santos[2], Raquel L. Sousa[2], Margarida M. S. Silva[2], Ana R. Lemos[2], Pedro M. F. Sousa[2], Tiago M. Bandeiras[2], Maria Emanuela Cuomo[1]

[1]EMD Serono, Inc., The healthcare business of Merck KGaA, Darmstadt, Germany, Darmstadt, Germany,[2]Instituto de Biologia Experimental e Tecnologica (iBET), Oeira, Portugal

Purpose: We developed and applied a streamlined workflow to discover and optimize cereblon (CRBN)-mediated molecular glues.
Methods: We combine computational and structural approaches to define the CRBN target space with both CRBN-focused small molecule and DNA-encoded (DEL) libraries for high-throughput screening of novel molecular glues. Proximity based protein-protein interaction assays are applied to screen for induced CRBN proximity of novel glue degrader targets. Cell-based degradation methods can then drive lead optimization, with advanced biophysical and structural methodologies for structural and functional aided design.
Results and Conclusions: We have identified multiple leads from rational screening approaches inducing concentration-dependent target-CRBN proximity in TR-FRET and NanoBRET assays. Hits were orthogonally confirmed to induce ternary complex formation by biophysical methods including surface plasmon resonance (SPR) and size exclusion chromatography (SEC). Cellular readouts demonstrated degradation activity using HiBiT and immunofluorescence-based methods dependent on CRBN E3 ligase expression or activity and proteasomal degradation. This integrated workflow together with proteomics technologies for on-target and off-target selectivity, is a rapid, mechanism-centric discovery platform for CRBN molecular glues across diverse target classes taking advantage of advanced but readily available methodologies.

#5789 Discovery of a selective molecular glue degrader of CCNE1 for the treatment of CCNE1-amplified solid tumors and CDK4/6i-resistant HR+/HER2- breast cancers.

Benjamin M. Vincent, David Marcoux, Claudia Caligioni, Aaron G. Bart, Matt L. Harlow, Rosaline Y. C. Hsu, Prashant Singh, Rachel Badger, Andrew J. Ingersoll, Thomas B. Jordan, Hari B. Kamadurai, Christine Zarate, Nico R. Cantone, Aravind Prasad Medikonda, Artyom A. Alekseyenko, Duncan E. Nunes, Taras Dauzhenka, Anushka Bhagwat, David Y. Rhee, Patrick R. Arsenault, Andrew R. Conery, Alex Constan, Louis Plamondon, Tim J. Wigle, Daniel S. La, Kathleen I. Seyb, Patrick Trojer, Vito J. Palombella

Triana Biomedicines, Lexington, MA

Cyclin E1 (CCNE1) is a central regulator of the G1 to S-phase transition of the cell cycle and a key dependency in multiple solid tumor types, including ovarian and endometrial cancers, and promotes resistance to CDK4/6 inhibitors in HR+/HER2- breast cancer. CCNE1 lacks a druggable pocket or enzymatic activity, which has precluded attempts to develop drugs that inhibit its function. Efforts to inhibit CCNE1 activity indirectly with CDK2 kinase inhibitors have been hindered by poor selectivity and dose-limiting toxicities that prevent full pathway suppression. Here we report the discovery of a molecular glue degrader (MGD) that co-opts the $CRL4^{CRBN}$ E3 ubiquitin ligase to eliminate the CCNE1 protein. Single-particle cryo-electron microscopy identifies a novel non-G-loop degron on CCNE1 that drives direct recognition of CCNE1 by the MGD:CRBN:DDB1 complex without preventing CDK2 binding to CCNE1. In cell lines analyzed, MGD treatment triggers rapid, CRBN-dependent depletion of CCNE1 with complete selectivity over the rest of the proteome. MGD-induced CCNE1 degradation exerts potent and selective anti-proliferative effects, with over 500-fold greater potency in CCNE1 amplified lines compared to non-amplified lines, a substantial improvement relative to CDK2 inhibitors (~15-fold potency window). In HR+/HER2- breast cancer cell lines with evolved resistance to the combination of a CDK4/6 inhibitor and fulvestrant, co-treatment with the MGD restores sensitivity. Oral administration of the MGD drives robust CCNE1 reduction and antitumor activity in a CCNE1-amplified xenograft model. These data suggest that directly and selectively degrading CCNE1 could provide an effective targeted therapy for CCNE1-amplified solid tumors and overcome resistance to CDK4/6 inhibitors in HR+/HER2- breast cancer.

#5790 Next-generation PRMT5 activity modulation through directed degradation.

Jose C. Clemente, Xuqing Zhang, Brian Vidal, Aaron Stonberger, Sudeep Banjade, Cory T. Rice, Nathan M. Kendsersky, Curran A. Rhodes, Matthew Tudor, Qiaolin Deng, Bomie Han, Clemente Aguilar-Bonavides, Elham Behshad, Steven D. Knight, Corey Strickland, Larry J. Jolivette, Ryan G. Kruger

SK Life Science Labs, King of Prussia, PA

PRMT5 is a key epigenetic regulator that is responsible for symmetric demethylation (SDMA) of arginine residues on histones and non-histone proteins, leading to regulation of transcription, RNA splicing, and genome stability. PRMT5 activity is linked to a range of malignancies, making it an attractive therapeutic target. The therapeutic potential of SAM and protein substrate competitive PRMT5 inhibitors have been hampered by dose-limiting cytopenia leading to incomplete target coverage. In contrast, MTA-cooperative inhibitors exploit the accumulation of MTA, a SAM-competitive inhibitor of PRMT5, in MTAP-deleted tumors to achieve enhanced tumor selectivity. MTA-cooperative degraders offer the potential to eliminate both catalytic and non-catalytic functions of PRMT5 with improved depth and durability of target modulation. Here, we describe PRMT5-directed degraders that rapidly, potently, and selectively eliminate PRMT5. Our degraders exhibit potent and robust PRMT5 degradation within 6 hours of treatment, leading to marked suppression of SDMA. Mechanistic studies demonstrate that PRMT5 loss is strictly dependent on UPS, as pharmacological blockade of ubiquitination or proteasomal activity effectively abrogates degrader-induced PRMT5 turnover. Our data highlights the potential for PRMT5 targeted degradation, driving a rapid and selective silencing of PRMT5 activity that can overcome limitations of first-generation inhibitors and provide a differentiated therapeutic approach for PRMT5-driven cancers.

#5791 Preclinical characterization of NEO-811, a novel molecular glue degrader of ARNT for the treatment of clear cell renal cell carcinoma.

J. Scott Lee, Michelle S. Cruz, Isabella Tran, Kevin Chiu, Jennifer Griffin, Andres H de la Pena, Kurt Januszyk, Xiaoxi Liu, Bryan Lee, Anthony Burt, John Tellew, Mengyu Wu, Leslie Watson, Ana Dominguez-Andres, Ling Huang, Randy Soriano, Devin Knece, Molly FitzGibbon, Jake Fathman, Celin Sanchez, Nathalia Cruz, Zac Neiman, Ana Grant, Mary Matyskiela, Rohan Beckwith, Ben Wen, Klaus Wagner, Philip Chamberlain

Neomorph, Inc, San Diego, CA

A hallmark of clear cell renal cell carcinoma (ccRCC) is inactivation of the von Hippel-Lindau tumor suppressor gene (VHL). Deficiency in VHL results in aberrant stabilization and activation of hypoxia-inducible factors 1α and 2α (HIF-1α/2α) promoting cancer cell survival, metastasis, and angiogenesis. The therapeutic value of targeting hypoxia signaling in ccRCC has been clinically validated by the development of small molecule inhibitors of HIF-2α. However, subsequent studies have also uncovered susceptibility to the onset of resistance conferred by mutations in the small molecule binding pocket. As class I basic helix-loop-helix PER/ARNT/SIM (bHLH-PAS) proteins, HIF-1α/2α require heterodimerization with aryl hydrocarbon nuclear translocator (ARNT, also known as HIF-1β, a class II bHLH-PAS protein) to exert their transcriptional activity. Consequently, ARNT represents a viable alternative target for disrupting oncogenic HIF activity. While traditionally regarded as undruggable, here we highlight the preclinical characterization of NEO-811, a potent, selective, and orally bioavailable molecular glue degrader of ARNT. Consistent with its mechanism of action, NEO-811 induced rapid, cereblon (CRBN)-dependent ARNT depletion in multiple ccRCC cell lines in vitro and in vivo. Global proteomics analysis confirmed that NEO-811 was highly selective and did not degrade well-known neosubstrates. Transcriptomic profiling of NEO-811 activity across several VHL-deficient ccRCC cell lines confirmed suppression of HIF-2α target genes, including cyclin D and vascular endothelial growth factor (VEGF). NEO-811 also uniquely suppressed expression of target genes regulated by other Class I bHLH-PAS transcription factors, including HIF-1α and aryl hydrocarbon receptor (AHR). Critically, NEO-811 retained activity in HIF-2α inhibitor-resistant cells that harbored previously described mutations. In conclusion, our findings highlight the potential of ARNT degradation as a promising therapeutic modality for the treatment of VHL-deficient ccRCC.

#5792 Identification of first in class selective ARID1B degraders.

Madeleine Henley, Benjamin Adams, Richard Caldwell, Jozlyn Clasman, Silvia Escudero, Imran Hossain, Kana Ichikawa, Jamie Im, Alexia Kalogeropulou, Dipti Sadalge, Gabriel Sandoval, Cody Schwarzer, Laura Von der Porten, Nick Yang, Marina Nelen, Gromek Smolen, Kevin Wilson, Steven Bellon

Foghorn Therapeutics, Watertown, MA

ARID1B, a core component of the SWI/SNF chromatin remodeling complex, has long been considered undruggable due to the absence of known binders and lack of ligandable pockets. Striking dependency on ARID1B is observed across multiple cancer indications harboring ARID1A mutations, including endometrial, ovarian, and gastric cancers. This highlights the synthetic lethal relationship between the two paralogs and establishes ARID1B as a high value target for precision oncology. We report the discovery and optimization of first in class selective ARID1B degraders for the treatment of ARID1A mutant cancers. Using our platform and structure based design, we first identified several selective ARID1B binder series, which were then used to develop VHL and CRBN based molecules that induce robust ARID1B degradation via the ubiquitin-proteasome system. These compounds exhibit on mechanism activity, high selectivity, and downstream transcriptional modulation. This work establishes ARID1B degradation as a promising therapeutic strategy and provides a blueprint for targeting previously intractable chromatin remodelers.

#5793 First-in-class potent and selective oral KAT6A degrader development candidate, PRT13722, drives complete tumor regressions as a monotherapy with an improved pre-clinical hematological safety profile.

Monisha Sivakumar, Sarah Pawley, Corey Basch, Jimin Park, Justin Kurian, Anthony Reichelderfer, Yue Zou, Kirsten Gallagher, Miles Cowart, Joy Cote, Alexander Grego, Jessica Burtell, Amy Crossan, Michael Hulse, Anjana Agarwal, Arpita Mondal, Chun Chen, Vijay Devannah, Sina Rezazadeh, Quincy Lewis, Patrick Wen, Ken Ray, Raul Leal, Daniel Porreca, Ganfeng Cao, Neha Bhagwat, Shanthi Ganesan, Stefan Ruepp, Min Wang, Joseph Rager, Koichi Ito, Sandy Geeganage, Andrew Combs, Peggy Scherle, Andrew Buesking, **Jack Carter**

Prelude Therapeutics, Wilmington, DE

KAT6A is a member of the MYST family of histone acetyltransferases and is recurrently amplified in multiple cancer types, driving cancer cell growth. Targeting KAT6 has recently been clinically validated in ER+/HER2- breast cancer (BC) and is being evaluated in Phase 3 trials in combination with fulvestrant (FUL). Notably, MYST proteins (e.g. KAT6A/B, KAT7) co-regulate normal hematopoiesis and current clinical inhibitors co-target these proteins in addition to KAT6A, resulting in dose-limiting neutropenia. Further, KAT6A protein degradation has been shown to drive differential biology compared to inhibition and deeper efficacy than KAT6A/B inhibitors. With the goals of addressing the clinical incidence of neutropenia and improving efficacy, we sought to identify KAT6B-sparing KAT6A heterobifunctional degraders. Utilizing structure-based drug design, we engineered the first known bivalent TPDs to potently and selectively degrade KAT6A over KAT6B. Further optimization of the ADME and physicochemical properties provided our orally bioavailable KAT6A selective degrader development candidate, PRT13722. PRT13722(±) is a picomolar KAT6A degrader with exquisite selectivity over KAT6B (<5% D_{MAX}) and high oral bioavailability across species. Global proteomic and neosubstrate profiling confirmed the selectivity of PRT13722(±), including against other MYST proteins. Despite a lack of KAT6B degradation, we observed PRT13722(±) demonstrated superior (95% E_{MAX}) anti-proliferative activity in T47D ER+ BC cells compared to a KAT6A/Bi (43% E_{MAX}) and good breadth of efficacy. Unlike inhibitors, PRT13722 disrupted the KAT6A complex, driving deeper suppression of global oncogenic gene expression (e.g. *ESR1*, *PGR*, *MYC*). In numerous ER+ BC xenografts, PRT13722(±) safely drove deep and complete tumor regressions as a monotherapy (e.g. T47D TGI = 101%), unlike a clinical KAT6A/Bi plus FUL (T47D TGI = 71%), at low oral daily doses (<5 mg/kg). Repeat dose *in vivo* PD studies demonstrated robust KAT6A (>84%) and no KAT6B degradation at efficacious doses. Mice treated with PRT13722(±) had higher neutrophil counts than those treated with clinical exposures of a KAT6A/Bi. These findings potentially address a clinical limitation of KAT6A/Bi by reducing an overlapping toxicity with other therapeutic agents such as CDK4/6i. Indeed, PRT13722 demonstrated combinability *in vitro* and *in vivo* with CDK4/6i, PI3Ki, and endocrine therapies (ET), while maintaining activity in CDK4/6i- and ET-resistant, and *ESR1*/*PIK3CA* mutant models. In summary, our first-in-class potent and selective oral KAT6A degrader, PRT13722, demonstrates improved efficacy and the potential for reduced off-target neutropenia compared to certain clinically validated KAT6A/B dual inhibitors. IND filing for PRT13722 is on track for mid-2026.

#5794 Leveraging E2 ligases for induced proximity and modulation of novel cancer-relevant targets and neosubstrates.

Xiangrong Chen[1], Vittorio Katis[1], Qilong Wu[1], Lukas Scheibelberger[1], Jesper Hansen[1], Brian D. Dill[2], Oksana Zavidji[2], Maria-Dorothea Nastke[2], Tiffany V. Saunders[2], Clifford G. Phaneuf[2], Andrea Pierangelini[1], Darragh O'Brien[1], Alejandro Gonzalez Orta[1], Niven R. Narain[2], Stephane Gesta[2], Alex N. Bullock[1], Dinesh Chimmanamada[3], Paul Brennan[1], Kilian Huber[1], **Vivek K. Vishnudas**[2]

[1]University of Oxford, Oxford, United Kingdom,[2]BPGbio, Waltham, MA,[3]Coorg Biosciences, Arlington, MA

Ubiquitin-conjugating enzymes (E2s) govern ubiquitin chain topology and flux through the ubiquitin-proteasome system, thereby shaping proteostasis, DNA-damage responses, and oncogenic signaling. Although targeted protein degradation (TPD) has largely focused on E3 ligases, convergent evidence from recent chemical biology and oncology studies indicates that E2s are druggable nodes with dual therapeutic potential for reprogramming using bifunctional and molecular glue degraders. Here, we demonstrate that E2s can act as a recruitment engine for proximity-induced degradation when E3 access or cooperativity is limiting for a distinct set of targets. We introduce a first-in-class, selective, small-molecule-based bifunctional degrader platform that exploits E2 recruitment to degrade oncology-relevant targets, including nuclear receptors and kinases. In biochemical and cellular systems, the ligand engages its E2 target with high selectivity, induces proximity through ternary complex formation and degrades the protein of interest in a proteasome- and Cullen-dependent manner. We validated our approach by designing bifunctional degraders of ERα, coupling ERα and E2 ligands with short linkers, and demonstrating target degradation in MCF7, T47D, SH-SY5Y, and K562 cell lines. We demonstrate early degradation by 6 hours and maximal degradation at 24 hours with a D_{max} of 85% and DC_{50} of 83nM. Further, by conjugating 4 kinase inhibitor scaffolds with 2-6 linker designs, we screened the proteome to cover almost 500 potential kinase targets in K562 and MCF7. We demonstrated dose-dependent degradation of dozens of kinases, including kinases of potential therapeutic interest such as SYK, FYN, and MAPK2. We observed dramatically different sensitivity to degradation across the cell lines tested, and degradation activity was more robust at the 24h timepoint compared to 5h. Collectively, these findings validate E2 ligases as functional recruiters for TPD, expanding the degrader toolbox beyond canonical E3 ligases and establishing a complementary, generalizable framework for therapeutic development.

#5795 The discovery of BLU-020: A potent and selective degrader of CDK2 for the treatment of *CCNE1* aberrant cancers.

Phil Ramsden, Dean Zhang, Maria Iliou, Suhasini Parimi, Jeff Keats, Maxine Chen, Lakshmi Muthuswamy, Guangyan Du, Fereidoon Daryaee, Ben Barlock, James Baker, **Sue Spong**, Ken Kearney, Gramoz Kondakci, Deborah G. Conrady, Stella Li, Xavier Fradera, Yinghui Dai, Tina Tran, Tom Dineen, Chiara Conti

Blueprint Medicines Corporation, Cambridge, MA

Background: Cyclin E1 is the catalytic binding partner of CDK2, which becomes aberrantly activated when *CCNE1* is amplified and overexpressed, driving tumorigenesis. Tumors with aberrant cyclin E1 expression are highly dependent on Cyclin E1/CDK2 activity, presenting a distinct therapeutic opportunity. Selective degradation of CDK2 may limit off-target CDK family-driven toxicities commonly associated with pan-CDK inhibitors. We highlight the discovery of BLU-020, a potent, CDK2-selective, and kinome-sparing investigational degrader of CDK2.
Our efforts began with the design of CDK2-targeted heterobifunctional degraders leveraging Blueprint's proprietary inhibitor library, resulting in the identification of several potent compounds with moderate selectivity. Subsequent modifications led to improvement on both CDK family selectivity and improvement on ADME properties of the lead series. With additional efforts to optimize the degraders for projected human dose, a development candidate, BLU-020, was identified.
Results: BLU-020 is an orally bioavailable, kinome-sparing, CDK2-selective small molecule degrader that leads to potent and sustained pRb inhibition, significant and sustained G1 cell cycle arrest, strong and selective suppression of E2F targeted genes and inhibition of cell proliferation in CCNE1-aberrant CDK2-dependent tumor cell lines. In a screen against a panel of ~100 tumor cell lines, BLU-020's potency and selectivity was demonstrated by showing strong inhibition of CCNE1-aberrant tumor cells bearing the triple biomarker CCNE1 high/RB positive/p16 high, while completely sparing non-CDK2 dependent triple biomarker negative cell lines, with a selectivity ratio of over 500 fold. BLU-020 was able to sensitize tumor cell lines lacking p16 in combination with the CDK4/6i ribociclib. Finally, BLU-020 demonstrated robust and durable in vivo anti-tumor activity in preclinical models of *CCNE1*-amplified cancers such as OVCAR3 CDX model following once-daily oral administration.
Conclusion: With its potency on CDK2 and improved selectivity over other CDK family members and the kinome compared to previous reported CDK2 agents, BLU-020 has best-in-class potential for CCNE1-aberrant ovarian cancers.

#5796 Rpn13Pru targeting small molecules induce mitotic arrest in breast cancer..

Santwana K C[1], Xiuxiu Lu[2], Snehal M. Gaikwad[3], Venkata R. Sabbasani[4], Rolf Swenson[4], Beverly A. Mock[3], Kylie J. Walters[2], Deborah E. Citrin[1]

[1]Radiology Oncology Branch, National Cancer Institute, Bethesda, MD,[2]National Cancer Institute, Frederick, MD,[3]Cancer Biology and Genetics, National Cancer Institute, Bethesda, MD,[4]Chemistry and Synthesis Center, National Heart, Lung, and Blood Institute, Bethesda, MD

Proteolysis-targeting chimeras are heterobifunctional molecules that link a protein of interest (POI) to an E3 ubiquitin ligase, promoting ubiquitylation and degradation of the POI via the ubiquitin-proteasome system (UPS). XL44 is a structurally modified small molecule previously identified as a potent hRpn13^{Pru} degrader, that induces ubiquitin-dependent apoptosis in myeloma cells. and ubiquitin-independent cell cycle defects. Recently, we evaluated two more potent derivatives; XL69 and XL80 with a similar cell cycle arrest mechanism. Here, we evaluated that the anticancer activity of XL69 and XL80 mediated disruption of UPS function in the MCF-7 cell line. MCF-7 cells were treated with XL69 and XL80 for 24 h and the IC_{50} values were determined by MTT assay. For cell cycle analysis, cells were treated with 10 µM of each compound for 24 h and analyzed via flow cytometry. The spindle assembly checkpoint (SAC), and anaphase promoting complex/ cyclosome (APC/C) activity were assessed through western blotting and immunofluorescence microscopy. The MTT assay for XL69 and XL80 showed increased cytotoxicity at concentrations above 30 µM upon treatment but cells exhibited rapid detachment at lower concentrations. Detached, floating cells remained viable for the next 48-72 h post-treatment before cell death and exhibited marked variation in nuclear morphology and cytoskeleton organization. XL69 and XL80 treated MCF-7 cells accumulated in G2/M (65.7% and 54.1%, respectively vs DMSO- (25.2%; $p < 0.001$). In addition, elevated levels of phospho-histone 3 were detected 24 h post-treatment (31.5%, 32.5%, vs DMSO 10.7%, p-value <0.01) indicating robust mitotic arrest. Immunofluorescent detection of aurora B with DAPI nuclear staining confirmed prometaphase-metaphase arrest in treated cells. Western blot analysis showed upregulation of Bub1 and BubR1, confirming SAC activation post mitotic arrest. Activation of the SAC led to formation of the mitotic checkpoint complex, subsequently inhibiting the APC/C, as evidenced by the accumulation of cyclin B and securin. Furthermore, the inhibition of APC/C also prevented degradation of aurora B kinase, resulting in impaired tubulin assembly. Immunofluorescent images showed disordered organization of tubulin with XL69 and XL80 treatment, similar to Nocodazole, a microtubule polymerization inhibitor. These findings suggest that XL69 and XL80 induce mitotic arrest by targeting the APC/C pathway and disrupt microtubule dynamics. These studies demonstrate that the small molecules XL69 and XL80 effectively induce mitotic arrest, impair microtubule dynamics, disrupt cellular attachment leading to cell death in adherent MCF-7 cells. The treatment led to sustained cell cycle arrest, SAC activation, APC/C pathway inhibition and impaired microtubule organization. As such, the study highlights XL69 and XL80 as promising anti-cancer agents that target mitotic progression.

#5797 PK/PD and preclinical ADME characterization of TB-008, a first-in-class CDK9 degrader in xenograft models.

Narayana Narasimhan, Mahesh Koirala, Isabelle Dussault, Lindy Yan, Oscar Kashala, Zoser Mohamed, **Mario DiPaola**

Therabene, Inc., Norwood, MA

Targeted protein degradation (TPD) offers a promising therapeutic strategy by removing, rather than inhibiting, disease-driving proteins. Cyclin-dependent kinase 9 (CDK9) is a key oncogenic regulator implicated in multiple hematologic and solid tumors. TB008 is a rationally designed CDK9-targeting PROTAC developed using an AI-driven degrader platform to achieve high affinity, selectivity, and favorable pharmacologic properties. Preclinical studies have demonstrated potent, selective CDK9 degradation with downstream suppression of oncogenic targets such as c-MYC and MCL-1. TB008 has shown robust antiproliferative and pro-apoptotic activity across cancer cell lines and strong tumor growth inhibition >95% in triple negative breast cancer xenograft model which support further development of TB008 as a CDK9-directed therapeutic candidate. Pharmacokinetics in Balb/c-nude mice (efficacy study species) has shown that TB-008 is rapidly absorbed following an intraperitoneal dose with ~90% bioavailability and a half-life of 1 hr. Interestingly, *in-silico* PK and bioavailability analysis does predict that there is a 90% decrease in drug concentration in mouse plasma within the first hour after administration. Furthermore, also based on *in-silico* evaluation, it is also predicted that higher drug concentration will be in the GI tract, lungs, plasma, spleen and portal vein. Even with the relatively short half-life, the high tumor growth inhibition observed in xenograft studies confirms the potency and fast kinetics of TB-008 in effecting the degradation of the tumor CDK9. We have initiated studies in mouse xenograft models to better understand the PK/PD and design optimal dosing regimens. Also, we will report the efficacy of TB-008 in additional xenograft models. Additional preclinical ADME data and PK in higher nonclinical species will be reported.

#5798 Targeted protein degradation of cell surface proteins through peptide-induced clearance.

Hadir Marei, Sanjana Sen, Patrick Aouad, Victoria Pham, Christopher Rose, Wen-Ting Tsai, Sheil Kee, Eva Lin, Matthew Grimmer, Tim Sterne-Weiler, Xiaosai Yao, Mark Wang, Diana Wu, Russell Xie, Nicholas Agard, Stephen Miller, Robert Yauch

Genentech, Inc., South San Francisco, CA

In recent years, several modalities have emerged that enable the clearance of cell surface proteins. Contributing to the current toolbox, we previously reported the development of an antibody-based degrader platform that enables the repurposing of the Wnt-responsive cell surface E3 ubiquitin ligases, RNF43 and ZNRF3, for the degradation of plasma membrane proteins. In particular, through the design of recombinant bispecific antibodies that we termed Proteolysis Targeting Antibodies (PROTABs), we facilitate the tethering of RNF43 or ZNRF3 to the extracellular domains of different receptors, including IGF1R, HER2 and PD-L1. Consequently, this drives efficient “on demand” target degradation both *in vitro* and *in vivo*. We also demonstrate the broad applicability of this platform through the identification of additional E3 ubiquitin ligases that can be repurposed as cell surface protein degraders. Stemming from this work, we profiled the cell surface proteome in a panel of isogenic ‘Wnt-low’ and ‘Wnt-high’ Colorectal Cancer (CRC) cell lines. Focusing on differentially regulated proteins, we demonstrate that the Transferrin Receptor (TfR1) has increased cell surface expression under ‘Wnt-high’ conditions, a known hallmark of CRC. Consistently, several studies show that TfR1 is commonly upregulated in cancer, which is often attributed to its role in mediating iron uptake. Indeed, the Cancer Dependency Map (DepMap) Project reveals that the viability of a large number of cancer cell lines is dependent on TfR1, highlighting its therapeutic potential. To explore this, we generated anti-TfR1 PROTABs. In an exogenous ligase expression setting, anti-TfR1 PROTABs, induce target degradation, dependent on RNF43/ZNRF3 levels, concomitant with cell viability defects. Intriguingly, while non-targeting bivalent TfR1 bispecific antibodies drive minimal target clearance, treatment induces viability aberrations comparable to that seen with anti-TfR1 PROTABs. We, therefore postulated that TfR1 cell surface clustering might be sufficient to affect cell fitness. To investigate this, we explored alternative target clustering approaches. Excitingly, this led to the development of a multimeric peptide-based modality that mediates efficient target cell surface clearance and protein degradation. Importantly, through testing a large panel of cancer cell lines, we show a dose-dependent effect on cell viability that spans multiple indications beyond CRC. Together, this highlights the therapeutic potential of leveraging anti-TfR1 multivalent peptides as an alternative targeted protein degradation approach.

#5799 Lumit-based profiling of degrader dynamics reveals signaling-dependent, cell context-specific sensitivity to degraders.

Matthew Swiatnicki, Laurie Engel, Hicham Zegzouti

Promega, Madison, WI

While targeted protein degradation (TPD) offers a transformative approach for refractory disease, testing degraders in disease relevant models remains challenging. Determining degrader kinetics and potency often involves engineered cell systems, which despite their merits, are resource intensive and low throughput. To alleviate these issues, we used the Lumit® Immunoassay Cellular Systems (ICS) platform to develop quantitative, high-throughput luminescent immunoassays for TPD targets. These assays measure degrader potency, selectivity, and cell-line variability. Multiple target-degrader pairs have been validated, including BRD4-ARV-771, IKZF1-Iberdomide, and STAT3-SD-36. These validated assays demonstrate the platforms versatility and robustness in capturing diverse degradation mechanisms. Using Lumit to profile the STAT3 degrader, SD-36, across numerous cells lines, we uncovered an unexpected potency shift in A431 cells. This was evidenced by DC_{50} values in the µM range, compared to nM range for other cell lines tested. Multiple avenues were explored to uncover the cause of this shift, including discrepancies in degrader mechanism or the target protein. When looking across multiple cell lines including A431, no discrepancies in degrader membrane permeability, target ubiquitination, cereblon expression, STAT3 expression, or STAT3 turnover were found. However, we uncovered that higher expression of epidermal growth factor receptor (EGFR) correlated with reduced degrader efficacy. Furthermore, we found that degrading EGFR or inhibiting EGFR phosphorylation in A431 cells restored the potency of SD-36. Combined, these data establish EGFR signaling as a key modulator of STAT3 degradation response. This phenomenon was specific to STAT3 degradation, as degraders for other targets maintained comparable nanomolar DC_{50} values across cell lines, including A431. Further exploration also indicated that the PARylation and PERK pathways appear to contribute to the protection of STAT3, with the effect being more pronounced in A431 cells. The PARylation and PERK pathways have previously been shown to affect degradation of certain targets, while our findings point to an additional signaling pathway that seems to specifically regulate STAT3 degradation. While it has been traditionally thought that resistance to TPD therapies can occur due to changes in degrader mechanics or the target protein within the cell, we have demonstrated that intrinsic cellular pathways can impact degrader potency. This discovery may redefine TPD limitations to include signaling-regulated phenotypes.

#5800 Discovery of pan-KRAS molecular glue degraders via protein-first coevolution-guided E3 ligase recruitment.

Roman Timakhov, Haishan Li, Nikolay Savchuk, Alexander Khvat

Eilean Therapeutics, LLC, Dover, DE

Background: KRAS is one of the most frequently mutated oncogenes in human cancer; however, the absence of deep hydrophobic pockets renders it challenging to drug by conventional inhibitors. Molecular glue degraders (MGDs) that induce proximity between KRAS and an E3 ubiquitin ligase represent a promising modality to achieve loss of KRAS function through proteasomal degradation.
Methods: We employed proprietary MGD platform, which initiates with a protein-first, coevolution-driven selection of E3 ligases. Multiple sequence alignments of KRAS and human E3 ligases were analyzed to identify co-mutating amino acid pairs that preserve physiologically relevant protein-protein interaction (PPI) interfaces. Predicted KRAS-E3 complexes were modeled using state-of-the-art protein folding algorithms and molecular dynamics simulations. Ternary complex-compatible sites were then screened *in-silic*o against the commercially available chemical space using flexible, structure-based docking. Hit compounds were evaluated in HEK293T cells stably expressing HiBiT-tagged KRASWT, KRASG12D, KRASG12V, or KRASG13D. Target degradation was quantified by HiBiT luminescence, confirmed by automated capillary electrophoresis (Jess/WES) western blotting of both HiBiT-tagged and endogenous KRAS, and validated for proteasome dependence using MG132. Cytotoxicity was assessed in KRAS-dependent (AsPC-1) and KRAS-independent (RKO BRAFV600E) cell lines over 7 days.
Results: The platform delivered multiple chemically tractable series of small-molecule (<500 Da) MGDs capable of potent, proteasome-dependent degradation of KRAS. Lead compounds induced >70% degradation of HiBiT-tagged KRASWT, G12D, G12V, and G13D at 10 µM after 24 h, with DC50 values in the high-nanomolar to low-micromolar range. Degradation of endogenous untagged KRAS in wild-type HEK293T cells reached 30-40% at 10 µM after 18 h treatment. Rescue experiments with proteasome inhibitors fully reversed degradation, confirming a ubiquitin-proteasome mechanism. Selected degraders exhibited favorable selectivity profiles, with CC50 values >5 µM in long-term proliferation assays and minimal cytotoxicity in KRAS-independent lines.
Conclusions: Our coevolution-guided, protein-first MGD platform enables rapid discovery of small molecules that induce pan-KRAS degradation across major oncogenic mutants. These compounds achieve degradation of KRAS protein through a proteasome-dependent mechanism, distinguishing them from covalent KRASG12C inhibitors and RAS(ON) tri-complex inhibitors. The identified pan-KRAS molecular glue degraders represent a novel therapeutic modality with potential to address the majority of KRAS-driven cancers previously considered undruggable.

#5801 NRX-0305 is an orally bioavailable, pan-mutant BRAF degrader that exhibits single-agent and combination efficacy with MEKi or anti-EGFR across Class 1/2/3 BRAF-mutant cancers.

Ya-Wen Lu, Alexandra Borodovsky, Ge Peng, Karthik Arumugam, Paul L. Auger, Delia Bradford, Lilly G. Carlson, Scott K. Kimura, Daniel Medina-Cleghorn, Mariah J. Mesner, Davorka Messmer, Madeleine P. Nemchek, Ryan B. Rountree, Rusha M. Sardhara, Sangita Sridharan, Jennifer M. Stokes, Leslie Tong, Alexandra M. S. Trotier, Jennifer S. Tung, Ge Wei, Jeffrey Wu, Jordan Ye, Gwenn M. Hansen

Nurix Therapeutics, Inc., Brisbane, CA

Activating mutations in BRAF, a central kinase within the MAPK pathway, promote sustained pathway signaling and drive oncogenic transformation across multiple tumor types including melanoma, non-small cell lung cancer (NSCLC), and colorectal cancer (CRC). BRAF mutations are categorized into three functional classes: Class 1 (e.g., V600X), which are RAS-independent and targetable with approved BRAF inhibitors; Class 2, which signal as constitutive dimers; and Class 3, which are kinase-impaired and depend on upstream RAS activation. While approved BRAF inhibitors provide significant survival benefit to patients with Class 1 mutations, they are ineffective against tumors harboring Class 2 or 3 mutations, which remain refractory to current BRAF-targeted therapies. Motivated by the lack of therapeutic options for patients with Class 2 and 3 BRAF mutations, we developed NRX-0305, a potent and orally bioavailable pan-mutant BRAF degrader that selectively eliminates mutant BRAF while sparing the wild-type protein. In vitro, NRX-0305 potently degraded Class 1/2/3 mutant BRAF and suppressed downstream pERK1/2 signaling, resulting in strong antiproliferative effects across a diverse panel of Class 1/2/3 BRAF-mutant cell lines, including those expressing BRAF fusion proteins. In vivo, daily oral administration of NRX-0305 induced robust, dose-dependent BRAF degradation and pathway inhibition, producing marked single-agent efficacy in multiple Class 1/2/3 cell lines-derived xenograft and patient-derived xenograft models. Furthermore, combination studies of NRX-0305 with MEK inhibitor or anti-EGFR demonstrated enhanced antitumor activity, supporting its potential use in clinically relevant combination regimens. Collectively, these studies demonstrate NRX-0305 is a potent, mutant-selective BRAF degrader that can overcome the limitations of approved BRAF inhibitors, offering broad therapeutic potential both as a single agent and in combination with MEKi or anti-EGFR antibodies across Class 1/2/3 BRAF-mutant cancers.

#5802 Long acting injectable of pan-RAF-MEK molecular-glue: Metronomic exposure for the treatment of pancreatic ductal adenocarcinoma.

Drishti Rathod, Ketankumar Patel

St. John's University, Queens, NY

Pancreatic ductal adenocarcinoma (PDAC) remains one of the most lethal malignancies, with 5-year survival rates below 12%. KRAS mutations (95% of cases) driving aberrant MAPK signaling—yet MEK inhibitors have failed due to rapid resistance, off target inhibition, and poor pharmacokinetics. There is an urgent need of paradigm-shifting approach that blocks MAPK pathway beyond conventional inhibitors. NST-628 (NST) is a potent pan-RAF-MEK molecular glue that provide dual blockade by preventing the activation of MEK and by blocking the RAF proteins, thus enabling prolonged inhibition of MAPK oncogenic signaling pathway. NST's physicochemical properties make oral delivery suboptimal, limiting clinical translation, prompting for a sustained-release injectable formulation of NST to ensure therapeutic efficacy. We developed a self-injectable, biodegradable, sustained-release depot formulation of NST (DepNeST). This represents the first extended-release formulation of a molecular glue for cancer therapy. We aim to a) To evaluate anticancer efficacy in 2D and 3D PDAC models; b) To optimize and characterize DepNeST for sustained NST release kinetics. NST demonstrated potent *in-vitro* cytotoxicity with an IC_{50} of 183.8 nM in MIA PaCa-2 and showed concentration dependent increase in cell size. NST treatment induced concentration-dependent cytoskeletal disruption in MIA PaCa-2, characterized by actin filament accumulation and aberrant lamellipodia/filopodia formation. Acridine orange and Giemsa staining confirmed chromatin condensation and marked morphological remodeling, reflecting NST-driven antitumoral activity. NST triggered 2-fold G0/G1 arrest in MIA PaCa-2 and inducing 1.8- to 2.2-fold increases in apoptosis (acute vs. chronic), effectively blocking proliferation and driving cell death. Multicellular 3D spheroid models demonstrate superior cytotoxicity with ~50% reduction in spheroid area with NST compared to control. Live/Dead assays revealed extensive apoptosis in both regimens, with marked red fluorescence confirming cell death and validating NST's potency in clinically relevant 3D models. DepNeST was fabricated by dissolving biodegradable polymers in different concentrations in a biocompatible solvent, N-methyl pyrrolidone (NMP). Subsequently, NST was dissolved into a polymer-NMP solution. DepNeST formulation with constant PLGA and increasing Poloxamer 338 concentrations enhanced depot dissolution profile. The *in-vitro* release study demonstrated an initial burst release followed by a sustained release of NST from DepNeST over a period of 6 days. This first-ever investigation of NST-628 molecular glue in pancreatic cancer establishes DepNeST as a paradigm-shifting depot platform that delivers sustained MAPK suppression at reduced doses—potentially transforming therapeutic landscape for RAS/RAF-driven malignancies.

#5803 Discovery of a paralog selective p300 protein degrader with potent anti-cancer activity in hematological malignancies.

Marwa Asem, Yan Zhai, Xiaohong Song, Milad Rouhimoghadam, Sreenivas Punna, Fritz G Buchanan, Daniel T Cohen, Ryan McClure, Stephanie Sandoval, Anlu Chen, Shaun McLoughlin, Colin Woodford, Peter Kovar, Vlasios Manaves, Alla V Korepanova, Justin M Reitsma, Andrea Shergalis, Judith A Ronau, Yifei Kong, Yu Shen, Jurgen Dinges

AbbVie Inc., North Chicago, IL

The E1A-associated protein p300 (EP300) functions as a key regulator of oncogenic transcriptional programs, positioning it as an attractive therapeutic target in cancer. However, the high sequence homology between p300 and its paralog CREB-binding protein (CBP) has limited the development of selective inhibitors, often resulting in dose-limiting toxicities. In this study, we report the discovery of a highly potent and selective degrader of p300. Distinct from dual p300/CBP degraders, this compound exhibits enhanced formation and stability of the ternary complex with p300, drives stronger ubiquitination and proteasomal recruitment, and targets a unique lysine residue on p300 for degradation. Hematological malignancies including multiple myeloma, non-Hodgkin's lymphoma, and acute myeloid leukemia were particularly sensitive to p300-selective degradation, which elicited a cytotoxic response in cancer cells and demonstrated robust antitumor activity in xenograft models. Together, these findings establish selective p300 degradation as a promising therapeutic approach for hematologic cancers and a novel strategy to disrupt oncogenic transcriptional dependencies.

All Authors were or are employees of AbbVie. The design, study conduct, and financial support for this research were provided by AbbVie. AbbVie participated in the interpretation of data, review, and approval of the publication. No honoraria or payments were made for authorship.

: Radiopharmacuetical Platforms for Theranostic Precision Oncology
Poster Session

#5807 Synergistic integration of nanobodies and a specialized linker library: A novel radionuclide drug conjugate (RDC) platform paving the way for next-generation radiotherapeutics with optimal druggability and therapeutic index.

Chong Liu, Zengyan Mu, Sipeng Li, Qingsong Wu, Yajun Sun, Paul H. Song, Gang Qin

GeneQuantum Healthcare (Suzhou) Co., Ltd., Suzhou, China

Background: Radionuclide drug conjugates (RDCs) represent a promising approach in oncology, yet their development is hindered by the scarcity of targeting moieties possessing both high affinity and favorable pharmacokinetics, leading to intense competition for validated targets. To address this, we have developed a novel and differentiated RDC platform utilizing readily available nanobodies as targeting vectors. This platform incorporates our intelligent Ligase-Dependent Conjugation (iLDC) technology and a proprietary linker, which collectively enhance pharmacokinetic profiles and biodistribution. The platform's efficacy is validated by GR9001, a $^{64}Cu/^{177}Lu$-labeled anti-PSMA nanobody-based RDC, which has demonstrated superior tumor targeting and biodistribution, potent therapeutic efficacy, and a promising safety profile in both preclinical and first-in-human studies.
Results: In preclinical studies, ^{64}Cu-GQ9001 exhibits an enhanced pharmacokinetic profile, along with excellent biodistribution characterized by significantly higher tumor accumulation and retention and minimized kidney uptake. Meanwhile, ^{177}Lu-GQ9001 also demonstrates superior antitumor activity and shows great potential to overcome resistance to Pluvicto®. In mCRPC patients, ^{177}Lu-GQ9001 was well tolerated, and no severe adverse events were observed. SPECT images revealed an optimal circulation half-life of ^{177}Lu-GQ9001 in the blood, with high, increasing tumor uptake and low, rapidly clearing normal tissue uptake. Compared with published data for other PSMA-targeted radioligands (e.g., PSMA-617), ^{177}Lu-GQ9001 exhibited significantly higher normalized absorbed doses in tumor lesions and similar absorbed doses in normal organs. Consequently, this profile resulted in substantially superior tumor-to-background (T/B) ratios. Furthermore, ^{177}Lu-GQ9001 showed superior efficacy at lower doses, with a significant reduction in PSA levels.
Conclusion: By leveraging GQ's nanobody-based RDC platform, a potential best-in-class anti-PSMA RDC has been developed that demonstrates a comprehensively superior profile to Pluvicto®—including optimized half-life, enhanced tumor uptake, excellent safety, and potent efficacy in CDX models and mCRPC patients—thereby establishing a transformative paradigm that expands the promise of nanobody-based therapeutics beyond existing modalities to novel tumor targets.

#5810 [^{212}Pb]Pb-AG1206, A novel fibroblast activation protein-targeted radioligand therapy demonstrated excellent efficacy and safety profile.

Xin Gan[1], Tao Robert Wu[1], Miaomiao Song[2], Shaohua Xu[1], Guiyu Liu[1], Vivi Yang[1], Jinpeng Liu[1], Xuefei Li[1], Hu Li[3], Zhen Cheng[2], Maijing Liao[1]

[1]AlphaGen Therapeutics, Shanghai, China,[2]Shanghai Institute of Materia Medica, Chinese Academy of Sciences, Shanghai, China,[3]Eight Roads Ventures China, Shanghai, China

Fibroblast activation protein (FAP) is highly expressed in a wide range of solid tumors, making it an attractive target for agents designed to accumulate within the tumor microenvironment. Lead-212 (^{212}Pb) is highly effective for targeted alpha therapy causing localized tumor cell killing induced by double strand DNA breaks while sparing surrounding healthy tissue. [^{212}Pb]Pb-AG1206 is a novel macrocyclic peptide radioligand that is designed to bind to FAP selectively, and to have rapid and high tumor uptake and fast renal clearance. When conjugated with the radioisotopes ^{203}Pb (for imaging) or ^{212}Pb (for therapy), AG1206 enables theranostic applications. Preclinical studies demonstrated excellent in vitro and in vivo properties of [^{212}Pb]Pb-AG1206 supporting its clinical development.

Methods: Binding affinity and selectivity were assessed using surface plasmon resonance (SPR). Cell binding and internalization were evaluated in FAP-expressing cell lines. In vivo biodistribution, antitumor efficacy, and dosimetry were performed in subcutaneous mouse cell-derived xenograft (CDX) models that express FAP.

Results: [^{212}Pb]Pb-AG1206 exhibited FAP-specific cellular uptake and high binding affinity in the picomolar (pM) range. It showed rapid tumor accumulation and fast clearance, and robust tumor growth inhibition with an excellent safety profile. Dosimetry studies in preclinical models demonstrated low radiation absorption in normal organs, indicating a favorable safety margin that is translatable to humans. These findings underscore FAP-targeted radioligand therapy (RLT) as a promising strategy for treating a broad spectrum of solid tumors characterized by desmoplastic microenvironments.

Conclusions: In conclusion the data support clinical development of [^{212}Pb]Pb-AG1206 as a novel therapeutic for patients with FAP-expressing solid tumors.

#5811 Preclinical evaluation of [^{212}Pb]Pb-AG1002, a next generation SSTR2-targeting, non-agonist radiopharmaceutical.

Xuexiang Zhang, Xuefei Li, Shaohua Xu, Xiao Tang, Xiang Gu, Vivi Yang, Guiyu Liu, Maijing Liao, Tao Robert Wu, **Xin Gan**

AlphaGen Therapeutics, Shanghai, China

Somatostatin receptor 2 (SSTR2), overexpressed in neuroendocrine tumors and other solid malignancies, is a validated target for radioligand therapies (RLTs). Here, we present the preclinical evaluation of [^{212}Pb]Pb-AG1002, a next generation SSTR2 non-agonist theragnostic agent,with the alpha-emitter ^{212}Pb for therapeutic purposes.

Methods: In-vivo PET/CT imaging, biodistribution and efficacy studies were conducted in athymic nude mice bearing AR42J (SSTR2+) xenografts. The biodistribution of [^{212}Pb]Pb-AG1002 was analyzed by harvesting the organs of interest and measuring the radioactivity with gamma counter. In efficacy studies, [^{212}Pb]Pb-AG1002 was administrated comparing to [^{212}Pb]Pb-DOTAM-TATE. The tumor growth inhibition and median survival time were measured and analyzed at time intervals post dosing.

Results: [^{212}Pb]Pb-AG1002 achieved high radiochemical purities following radiolabeling. In biodistribution studies, it demonstrated a superior pharmacokinetic profile compared to [^{212}Pb]Pb-DOTAM-TATE and [^{212}Pb]Pb-TCMC-JR11, exhibiting higher tumor uptake and prolonged retention, and reduced kidney accumulation, giving rise to excellent tumor-to-kidney ratios. Efficacy studies in SSTR2-expressing models showed that mice treated with [^{212}Pb]Pb-AG1002 had robust tumor growth inhibition and a more durable response than those treated with [^{212}Pb]Pb-DOTAM-TATE. Preclinical dosimetry studies further revealed low radiation absorption in normal organs, indicating a favorable safety profile with strong translational potential to humans.

Conclusion: [^{212}Pb]Pb-AG1002 exhibits excellent radiolabeling efficiency, desirable pharmacokinetics, anti-tumor efficacy and favorable safety profile. Its robust preclinical pharmacological profiles support clinical development as a next generation α-therapeutic agent for SSTR2-positive tumors.

#5812 Preclinical evaluation of [177Lu]Lu-PSMA-617 and [225Ac]Ac-PSMA-617 in mice bearing castration-resistant prostate adenocarcinoma patient-derived xenografts.

Denis Beckford-Vera, Jaeho Lee, Kyle Monger, Erin Kosmowski, Kayla Cotton, Sebastian Brabetz, Markus Hippich, Sarah Maenhout, Paul Heverly, Maria Mancini

Champions Oncology (Rockville, MD), Rockville, MD

Background: Patient-derived xenograft (PDX) models are essential for radiopharmaceutical evaluation because they preserve the genetic and microenvironmental complexity of human tumors, offering a more clinically relevant platform than traditional cell lines. This enables more accurate prediction of drug distribution, target engagement, and therapeutic efficacy, reducing translational gaps in radiopharmaceutical development. This study presents a comprehensive preclinical evaluation of two PSMA-targeted radiopharmaceuticals, [177Lu]Lu-PSMA-617 and [225Ac]Ac-PSMA-617, in murine models bearing PDXs of metastatic, castration-resistant prostate adenocarcinoma. These models are deeply characterized across multiple layers, including in-depth molecular data such as phosphoproteomics.
Methods: PSMA-617 was successfully radiolabeled with lutetium-177 and actinium-225 using optimized protocols that ensured high radiochemical purity. Preclinical evaluation of [177Lu]Lu-PSMA-617 and [225Ac]Ac-PSMA-617 was conducted in mice bearing CTG-2428 (PSMA+) PDX tumors derived from a 67-year-old Caucasian male with metastatic, castration-resistant prostate adenocarcinoma, and CTG-3537 (PSMA-) PDX tumors derived from a 63-year-old African American male with metastatic, castration-resistant prostate adenocarcinoma. Biodistribution studies of [177Lu]Lu-PSMA-617 were performed in mice bearing PSMA+ and PSMA- PDX tumors. Mice received 0.3 mCi (11 MBq) [177Lu]Lu-PSMA-617, and tumors and major organs were collected, weighed, and measured for radioactivity 24 hours post-injection. Therapeutic efficacy of [177Lu]Lu-PSMA-617 and [225Ac]Ac-PSMA-617 was assessed in mice bearing CTG-2428 (PSMA+) PDX tumors. Mice received 1 mCi (37 MBq) of [177Lu]Lu-PSMA-617 or 1 µCi (37 kBq) of [225Ac]Ac-PSMA-617, and tumor size and body weight were measured twice weekly throughout the study.
Results: [177Lu]Lu-PSMA-617 and [225Ac]Ac-PSMA-617 were obtained with radiochemical purity greater than 98%, as determined by radio-TLC and radio-HPLC. The radiotracers demonstrated selective uptake in PSMA-positive tumors, with minimal accumulation in PSMA-negative PDX, confirming target specificity. Importantly, the radiotracers showed excellent tumor-to-tissues ratios. Both agents significantly inhibited tumor growth compared to controls in mice bearing PSMA-positive PDX tumors. Treatment was well tolerated, with no significant weight loss or acute toxicity observed.
Conclusions: Further studies are warranted to optimize dosing strategies and evaluate long-term safety. Importantly, this work underscores the critical role of PDX models in capturing real receptor expression and tumor heterogeneity, thereby enhancing the translational relevance of radiopharmaceuticals in preclinical development.

#5813 Mass dose effects of the immunotheranostic [^{89}Zr]Zr-LNTH-2403 by PET/CT and dosimetry in non-human primates.

Hansel Comas Rojas[1], Marcus Lindsey[1], David Ulmert[2], Abigail Hasson[3], Aseem U. Anand[4], Daniel L. Thorek[3], Reinier Hernandez[1]

[1]Medical Physics, University of Wisconsin-Madison, Madison, WI,[2]Molecular and Medical Pharmacology, UCLA, Los Angeles, CA,[3]Dept. of Radiology, Washington University in St. Louis, St. Louis, MO,[4]Lantheus, North Billerica, MA

Leucine-rich repeat-containing protein 15 (LRRC15) is a TGFB-driven cell surface protein overexpressed selectively on highly aggressive mesenchymal stem cell-derived cancers and on cancer-associated fibroblasts of several solid tumors. Herein, we characterized the in vivo biodistribution, dosimetry, pharmacokinetic (PK) profile, and preliminary safety [^{89}Zr]Zr-LNTH-2403 targeting LRRC15 in healthy non-human primates (NHPs) under different administered mass regimens. The humanized monoclonal antibody (mAb) LNTH-2403 (also known as DUNP-19) targeting and internalizing LRRC15 was conjugated to p-SCN-Bn-DFO at a 5 chelator-to-mAb molar ratio for radiolabeling with ^{89}Zr ($t_{1/2}$=3.3 d). [^{89}Zr]Zr-LNTH-2403 was synthesized with a 174 MBq/mg molar activity and 99% radiochemical purity, as confirmed by iTLC. Three cohorts of two adult male Rhesus Macaques received a single 13 MBq/kg [^{89}Zr]Zr-LNTH-2403 IV bolus at total mAb mass doses of 2, 4, or 8 mg. Serial PET/CT imaging was acquired at 4 time points up to 168 hours post-injection (p.i.). Blood samples were collected at baseline and at each imaging session for PK analysis and CBC and CMP assessments. Volume of interest analyses were performed using the Imalytics Preclinical 3.1. Image-based human dosimetry extrapolations were performed using OLINDA/EXM 1.1 VOI analysis of PET/CT images in the 2 mg cohort demonstrated that [89Zr]Zr-LNTH-2403 exhibited rapid blood-pool distribution, with increasingly prominent adrenal gland uptake, peaking at 27.24 SUV_{mean} at 168 h p.i. Other organs of uptake included the liver, spleen, kidneys, and bone marrow, with peak SUV_{mean} of 7.71, 8.56, 3.98, and 6.56, respectively. Notably, increasing the antibody mass dose to 4 or 8 mg had a significant effect on blood PK and tissue biodistribution, reducing [^{89}Zr]Zr-LNTH-2403 uptake by 3- to 4-fold in the adrenal glands and in the bone marrow, albeit to a lesser extent. The PK profile exhibited a biphasic pattern, with an initial fast distribution half-life of 8.59 hours and a terminal slow half-life of 20.54 hours in the 2 mg cohort. Notably, the slow elimination half-life progressively increased to 33.68 hours at an 8 mg mass dose, evidencing longer antibody circulation. Estimated human-equivalent organ-absorbed doses confirmed that the adrenals received the highest equivalent dose, 2.82 mSv/MBq, followed by the liver, with 1.63 mSv/MBq. The effective whole-body dose was 0.471 mSv/MBq, indicative of acceptable radiation exposure. Blood parameters remained within normal limits. These findings demonstrate a favorable safety and dosimetry profile for [^{89}Zr] Zr-LNTH-2403 in NHPs, supporting its advancement toward first-in-human imaging studies. Importantly, the administered mass of mAb significantly affected the radiotracer's blood and normal organ biodistribution, highlighting the value of preclinical mass-dose optimization in humans.

#5814 Towards treating prostate cancer with $^{188}ReO_4^-$ using an engineered human sodium/iodide symporter (NIS) protein.

Haswitha Sabbineni, Alejandro Llorente-Esteban, Alejandra Paola Torres-Manzo, Dila Karakas, David Lopez-Gonzalez, Vengatesh Kumar Raja, Mohammed Noor Tantawy, Todd Giorgio, Nancy Carrasco

Vanderbilt University, Nashville, TN

The sodium/iodide symporter (NIS) is the plasma membrane protein that mediates the active transport of iodide (I^-) and various clinically approved radiotracers used for imaging [such as pertechnetate ($^{99m}TcO_4^-$), radioiodide ($^{123}I^-$), and tetrafluoroborate ([^{18}F] BF_4^-)] and for therapeutic purposes [e.g., $^{131}I^-$ and preclinically approved perrhenate ($^{186/188}ReO_4^-$)]. For over 80 years, targeted internal radiation therapy (TIRT) has been used successfully to treat thyroid cancer: administered radioactive iodide ($^{131}I^-$) is selectively accumulated in the thyroid cancer cells by NIS. NIS-mediated TIRT is a promising approach to treating prostate cancer, the second deadliest cancer in men in the United States and Europe. About 1 in 8 men will be diagnosed with prostate cancer at some point in their life. Localized prostate cancer is typically treated with prostatectomy or definitive radiotherapy (RT), but these treatments *fail* to cure up to 20-40% of patients. For metastatic castration-resistant prostate cancer (mCRPC), there are only a very limited number of effective agents available with unique mechanisms: androgen receptor antagonists, inhibitors of androgen synthesis, cytotoxic chemotherapy, immune-cell transfer therapy, and bone-directed and prostate-specific membrane antigen (PSMA)-targeted radiopharmaceuticals, all of which improve survival *only modestly*, by ~4 months, in randomized trials for patients with mCRPC. In order for NIS-based TIRT to be successful, three challenges must be overcome: (i) thyroid protection from β-radiation, (ii) immune response mitigation, and (iii) tissue specificity. To overcome these limitations, we engineered a NIS molecule with 2 amino acid substitutions L253P and V254F: PF-NIS. PF-NIS selectively transport oxyanions but does *not* transport I^-. *In vitro* studies demonstrated that PF-NIS-expressing cells were selectively susceptible to $^{186}ReO_4^-$ + 100 μM I^- in contrast to WT-NIS cells, which survived in the presence of 100 μM I^-. To minimize immunogenicity, PF-NIS cDNA was delivered via polyplexes (*in vivo* jetPEI), and tissue specificity was ensured by the prostate-specific antigen (PSA) promoter. Building on these data, athymic nude mice with PF-NIS-bearing tumors were imaged by SPECT-CT, which revealed PF-NIS-mediated tracer accumulation in tumors after intratumoral or intravenous delivery of PF-NIS polyplexes, as well as an ~80% decrease in thyroidal signal following administration of 100 μM I^-. Treatment with $^{188}ReO_4^-$ markedly reduced tumor volume while the thyroids of the mice were protected, leveraging the higher energy and shorter half-life of ^{188}Re vis-à-vis those of ^{186}Re or ^{177}Lu (the radionuclide currently used in most PSMA targeted radiopharmaceuticals). This approach constitutes a novel strategy for NIS-based TIRT, selectively targeting prostate cancer cells while protecting the thyroid.

#5815 pH-targeted gadolinium-based nanoparticles for enhanced radiotherapy.

Jessica Wen, Yuwei Xue, Wu Liu, Guillem Pratx

Radiation Oncology, Stanford University, Palo Alto, CA

Gadolinium-based nanoparticles (GdNP) are sub-5 nm particles designed for radiosensitization and MRI contrast enhancement. The high atomic number of Gd (Z = 64) enables efficient X-ray absorption and dose deposition within tumors, with tumor accumulation facilitated by the enhanced permeability and retention effect. Previous clinical trials have provided preliminary evidence for the safety and potential therapeutic benefit of intravenous GdNP in patients with cervical cancer and brain metastases. To improve tumor specificity, we conjugated GdNP with pH-low insertion peptide (pHLIP), which targets the acidic tumor microenvironment through pH-dependent membrane insertion. Previous work demonstrated that pHLIP conjugated to GdNP enhanced gadolinium uptake and radiosensitization in vitro. In vitro experiments were performed with cultured A549 human lung adenocarcinoma cells at pH 6.2 (tumor-like) and pH 7.4 (physiologic) conditions. Clonogenic assays and ICP-MS analysis revealed that while pHLIP-GdNP (0.17 mM dose) did not significantly alter cell survival, it increased intracellular gadolinium levels by approximately 18-fold under acidic conditions compared to unconjugated GdNP. In vivo, mice bearing subcutaneously implanted A549 tumors received 10 Gy X-ray irradiation with or without unconjugated GdNP or pHLIP-GdNP pretreatment (300 mg/kg; n = 7 mice/group). All irradiated groups exhibited significant tumor growth delay compared to controls ($P < 0.013$), but no additional radiosensitization was observed in the nanoparticle-treated cohorts, despite Gd accumulation in the tumor. MRI T1 mapping demonstrated shortened T1 relaxation times following GdNP administration, with greater reduction following pHLIP-GdNP injection, indicating enhanced contrast agent delivery. These findings suggest that pHLIP conjugation improves gadolinium uptake and MRI visibility but does not enhance radiotherapeutic efficacy under current conditions. Departing from previous work, this study used a simpler covalent bond to conjugate pHLIP to GdNP rather than a disulfide bridge, which may explain the decreased efficacy. Reintroducing the disulfide linkage might be critical, as it allows the conjugate to remain stable in circulation while releasing nanoparticle cargo upon insertion into acidic tumor cells, potentially increasing therapeutic efficacy.

#5816 A novel NTSR1-targeting diagnostic radioligand SKL35502 for noninvasive solid tumor imaging.

Jungtae Na, Taeyun Lee, Seona Jeon, Hyunseok Lee, Sunghak Lee, Sungwan Hwang, Jungshin Park

SK Biopharmaceuticals Co., Ltd., Seongnam-si, Korea, Republic of

Background: Neurotensin receptor 1 (NTSR1) is highly expressed in several aggressive malignancies, including pancreatic ductal adenocarcinoma, colorectal cancer, esophageal cancer, gastric cancer, biliary tract cancer, and head and neck squamous cell carcinoma. Given its role in tumor progression, NTSR1 represents a compelling target for molecular imaging and for selecting patients for NTSR1-directed radionuclide therapy. SKL35502, an ^{111}In-labeled small-molecule NTSR1 ligand, was developed to enable sensitive and selective visualization of NTSR1-positive tumors. This study evaluates the preclinical pharmacology, biodistribution, and imaging performance of SKL35502.
Methods: The binding affinity of SKL35502 was determined using a cell-based saturation binding assay. Time-dependent uptake and internalization were assessed in HCT116 human colorectal carcinoma cells. In vivo biodistribution was evaluated in female mice bearing HCT116 or AsPC-1 xenografts by SPECT/CT imaging up to 168 hours post-injection, and ex vivo biodistribution and excretion were confirmed in HCT116 xenograft models up to 48 hours. Urine and feces were collected at 8, 24, 48, 72 and 96 hours post-dose.
Results: SKL35502 exhibited high binding affinity to HCT116 cells (KD = 0.37 nM). Cellular uptake was time-dependent and NTSR1-specific, reaching 31.5% at 90 minutes and remaining at 30.5% at 240 minutes. Internalization accounted for approximately 56% of total uptake at both time points.
In vivo SPECT/CT imaging revealed an initial widespread distribution followed by rapid clearance from non-target organs (heart, liver, kidney). Tumor uptake peaked at 4 hours post-injection and persisted through 168 hours. *Ex vivo* biodistribution confirmed strong tumor enrichment (44 %ID/g at 8 hours), with tumor exposure (AUC) approximately 22-fold higher than blood. By 96 hours (4 days) post-dose, the total excreted radioactivity was 84.12% of the administered dose
Conclusions: SKL35502 demonstrates high affinity and specific uptake in NTSR1-expressing tumor cells, together with rapid systemic clearance that minimizes nonspecific radiation exposure to healthy tissues. These properties support its potential as a highly sensitive and selective imaging agent for detecting NTSR1-positive tumors and guiding patient selection in NTSR1-targeted theranostic approaches.

#5817 A novel NTSR1-targeting alpha radiotherapeutic SKL35501 demonstrating potent anti-tumor efficacy in HCT116 colorectal tumor model.

Jungtae Na, Taeyun Lee, Seona Jeon, Hyunseok Lee, Sunghak Lee, Sungwan Hwang, Jungshin Park

SK Biopharmaceuticals Co., Ltd., Seongnam-si, Korea, Republic of

Background: Radiopharmaceutical Therapy (RPT) using the alpha-emitter Actinium-225 (^{225}Ac) is emerging as a promising therapeutic approach for advanced solid tumors. Neurotensin Receptor 1 (NTSR1), highly expressed in aggressive cancers such as pancreatic ductal adenocarcinoma, colorectal cancer, esophageal cancer, gastric cancer, biliary tract cancer, and head and neck squamous cell carcinoma, represents an attractive target for RPT. SKL35501, the ^{225}Ac-labeled NTSR1 ligand, was developed as the therapeutic agent. This study evaluated the preclinical characteristics of SKL35501 using the HCT116 cell line. Here, we demonstrate favorable *in vitro* pharmacology, *in vivo* biodistribution, and *in vivo* antitumor activity in a colorectal tumor model.

Methods: *In vitro* cellular uptake/internalization and cytotoxicity of SKL35501 were assessed in NTSR1-expressing HCT116 human colorectal carcinoma cells using uptake and colony formation assays. *In vivo* biodistribution and antitumor efficacy following a single intravenous administration were evaluated in HCT116 xenograft models across multiple dose levels (0, 7.5, 15, and 30 kBq). Safety was assessed by body weight and hematological parameters.

Results: SKL35501 demonstrated rapid and time-dependent, NTSR1-mediated uptake in HCT116 cells, with >90% of cell-associated activity internalized, and showed a dose-dependent colony formation inhibition in the colony-formation assay. *In vivo*, SKL35501 exhibited robust and sustained tumor accumulation (31 %ID/g at 24h, with retention through 168 hours) alongside rapid clearance from non-target organs. A single administration produced dose-dependent tumor growth inhibition, with partial tumor regression at doses ≥15 kBq by Day 75. All SKL35501 dose levels resulted in significantly prolonged survival compared with vehicle ($p=0.0005$).

Toxicity was transient and reversible, characterized by mild hematological suppression and <10% body weight loss, both of which recovered within several weeks.

Conclusions: SKL35501 is a highly effective, first-in-class, ^{225}Ac-labeled NTSR1-targeting alpha radiotherapeutic demonstrating excellent tumor selectivity, durable tumor retention, potent antitumor activity, and a favorable safety profile. These preclinical findings strongly support advancement to the FIH trial for patients with NTSR1-positive advanced solid tumors using the SKL35501.

#5818 *De novo* protein design of calreticulin binders for theranostic applications.

Luke Rathbun[1], Yuvasri Golivi[2], **Rachael Guenter**[2], J. Bart Rose[2], Benjamin Larimer[1]

[1]Radiology, University of Alabama at Birmingham, Birmingham, AL,[2]Surgery, University of Alabama at Birmingham, Birmingham, AL

Background: Calreticulin (CALR) is an endoplasmic reticulum (ER) protein that can translocate to tumor cell surfaces during partial ER stress. Surface CALR is largely absent on normal cells yet upregulated on many types of tumor cells undergoing stress, making it a tumor-specific target with potential ubiquity and application as a tumor-agnostic biomarker. Targeting surface CALR with theranostic agents could offer a novel strategy to visualize tumors and monitor treatment response. We hypothesized that *de novo* protein design could generate a novel CALR-specific theranostic agent.

Methods: We employed the *de novo* protein design platform BindCraft to generate small (<10kDa) high-affinity binders against CALR. A streamlined *in silico* to *in vitro* screening pipeline enabled isolation of CALR binders within two weeks. Binding affinity and specificity were validated by biolayer interferometry (BLI) and flow cytometry. For flow cytometry, human pancreatic cancer cells were treated with doxorubicin, a known surface CALR inducer. Cells were incubated with two CALR binders for 30 minutes, followed by staining with fluorescent antibody. In a Matrigel plug model, mice bearing CALR and control plugs were injected with 100 µCi of [^{64}Cu]Cu-NOTA-binder and imaged by dynamic PET for 1 hour followed by CT.

Results: BLI against CALR identified two high affinity binders, d4 and d6, with calculated dissociation constants of 83.2 nM (k_{on} = 512790 $M^{-1}s^{-1}$, k_{off} = 0.04265 s^{-1}) and 31.2 nM (k_{on} = 551797 $M^{-1}s^{-1}$, k_{off} = 0.01723 s^{-1}), respectively. Flow cytometry showed both CALR binders, d4 and d6, detected increases in surface CALR of 1.6-fold and 2.1-fold, respectively, on doxorubicin-treated cancer cells compared to vehicle. PET imaging revealed significantly higher uptake of [^{64}Cu]Cu-NOTA-d6 in CALR plugs compared to controls as early as 20 minutes post-injection, with sustained retention throughout the imaging period. At 1 hr post-injection, SUV_{mean} of the CALR plug was (0.882±0.270) compared to (0.344± 0.048) for the control plug (p = 0.0272). [^{64}Cu]Cu-NOTA-d6 was cleared renally with insignificant uptake in non-target organs compared to blood pool and an average blood ½-life of 4.2 minutes.

Conclusions: This study demonstrates the feasibility of *de novo* protein design to rapidly generate high-affinity CALR-targeted binders suitable for theranostic applications. Further *in vivo* studies will evaluate tumor-specific uptake and long-term retention of d6 in preclinical cancer models to support its translational development as a theranostic agent.

#5819 PD-L1 targeted radiotherapy can reduce tumor burden and delay tumor growth in a mouse model of triple-negative breast cancer.

Jonathan Moye, Hailey Houson, Sharmila Sridhar, Sherin James, Jason M. Warram, Suzanne E. Lapi, Anna G. Sorace

The University of Alabama at Birmingham, Birmingham, AL

Introduction: Due to lack of targeted therapies, triple-negative breast cancer (TNBC) accounts for 40% of breast cancer mortalities despite only comprising 10-15% of diagnoses. Combination of PD-1/PD-L1 inhibitors with radiation therapy have been shown to have synergistic effects in TNBC. Targeted radiotherapy (TRT), in which a targeting probe is attached to a cytotoxic radioisotope, has emerged as a promising technique to deliver a therapeutic radiation payload to cells expressing the protein of interest. This is advantageous when targeting proteins such as PD-L1, which is highly expressed in TNBC and strongly upregulated after radiation-induced cytotoxicity. The purpose of this study was to assess the efficacy and safety of a novel PD-L1 targeted radiotherapy to improve immunotherapy outcomes in TNBC.

Methods: The PD-L1-targeted antibody atezolizumab was radiolabeled with lutetium-177, a cytotoxic radioisotope, to selectively deplete PD-L1$^+$ cells. Athymic nude mice bearing high PD-L1-expressing MDA-MB-231 tumors were treated with saline (n=6), 250μCi (n=3) or 500μCi (n=5) of [^{177}Lu]Lu-atezolizumab. Mice were imaged with Single Photon Emission Computed Tomography (SPECT) on days 1, 3, and 7 post-treatment, informing on distribution of the tracer in the tissue. Mice were monitored for 60 days for changes in tumor volume and body weight. Upon reaching endpoints, mice were euthanized and relevant organs (tumor, spleen, liver, kidney) were collected. Clearance organs were stained with hematoxylin and eosin to assess gross pathological changes. One- and two-way ANOVAs were utilized to assess differences between tumor volumes and SPECT imaging metrics across time, and log-rank tests were used to assess differences in survival between treatment groups.

Results: Mice treated with 500μCi or 250μCi of [^{177}Lu]Lu-atezolizumab demonstrated a significant reduction in tumor volume compared to control by day 20 ($p < 0.05$) or day 24 ($p < 0.05$) post-treatment, respectively. Increased median survival was observed in both treated groups (35 days in control versus 52 and 60 days in 250μCi and 500μCi treated mice, respectively, $p < 0.01$). No weight loss was observed in any treated groups, and histology revealed minimal splenic and renal toxicity, with mild to moderate hepatotoxicity consistent with reversible changes. SPECT imaging revealed high uptake of [^{177}Lu]Lu-atezolizumab in the tumor by day 1 post treatment and high tumor to background ratios across all three imaging timepoints.

Conclusions: Utilizing TRT to selectively deplete PD-L1$^+$ cells resulted in decreased tumor volumes and increased survival in a mouse model of TNBC. Further, SPECT imaging validated high uptake of the PD-L1-targeted TRT within tumor tissue. These results validate [^{177}Lu]Lu-atezolizumab as a novel PD-L1-targeted radiotherapy which has the potential to improve outcomes of immunotherapy in TNBC patients.

#5820 Biodistribution analysis of Leutetium-177 radiopharmaceuticals in mammary, prostate, and glioblastoma models using Alpha-SPECT Mini and gamma counts.

Kathryn R. Meshaw, William F. Durham, Karsten E. Fynboe, Tyler Rowe, Jacob C. Hauser, Joseph P. Kolb, Kenneth A. Meshaw, Stephanie M. Fogerson, Beth A. Hollister

Powered Research, LLC, Durham, NC

Background: Radiopharmaceuticals play a pivotal role in both diagnostic imaging and targeted radionuclide therapy for cancer. With the increase in clinical use and expansion of oncology indications, accurate characterization of their biodistribution is essential to optimize tumor targeting and reduce systemic toxicity. This study utilizes two approaches, the Alpha-SPECT Mini imaging system and gamma counts, to evaluate the in vivo distribution of radiopharmaceutical agents across three clinically relevant tumor types: human mammary gland adenocarcinoma, prostate carcinoma, and glioblastoma. By utilizing these two methods we aimed to improve profiling of radioligand uptake and clearance patterns across various tumor types and radiopharmaceuticals.
Methods: Subcutaneous xenografts of MDA-MB-231 human mammary gland adenocarcinoma, 22Rv1 and LNCaP human prostate carcinoma, and orthotopic xenografts of U-87 MG-Luc2 human glioblastoma in athymic nude mice were treated with lutetium-177 (^{177}Lu) conjugated Anti-human CD44 (10 µCi), ^{177}Lu-Anti-human PSMA (20-22 µCi or 10 µCi), or ^{177}Lu-Anti-human EGFRvIII (10 µCi), respectively, at a mean start size of 300 mm^3 (subcutaneous) or 3 weeks post cell implant (orthotopic). Alpha-SPECT Mini imaging was performed at 24, 72 and 168 hours post-dose and tissues for gamma counts were collected at 4, 24, 48, 72, and 168 hours post-dose.
Results: Preferential uptake of the radioligand in the tumor was apparent by 24 hours post-dose in the LNCaP, 22Rv1 and U87 MG-Luc2 xenografts, while the MDA-MB-231 xenograft had lower concentrations in comparison to the liver, serum, spleen and whole blood. By 48 hours, only the liver and spleen had higher concentrations than the MDA-MB-231 tumor. Radioligand clearance was observed as early as 48 hours in the MDA-MB-231 tumors. Alpha-SPECT Mini showed similar biodistribution and dynamics of the radioligands to the gamma counts.
Conclusions: Alpha-SPECT Mini imaging and gamma counting provided complementary profiling of radiopharmaceutical biodistribution across tumor types. Tumor-specific uptake patterns were evident, differences in radioligand retention, clearance, and off-target accumulation were observed. These findings underscore the importance of tumor biology in radiopharmaceutical pharmacokinetics and highlight the value of multimodal approaches for accurate profiling and therapeutic optimization.

#5821 Utilize a soluble T-cell receptor TCR targeting tumor intracellular antigen PRAME to develop therapeutic and radioactive diagnostic agents for PRAME-positive tumors.

Yujun Huang[1], Xiao Liang[2], Yajuan Xue[2]

[1]Suzhou Hepius Therapeutics, Suzhou, China,[2]Suzhou Hepius Therapeutics Co, Suzhou, China

T-cell receptor (TCR)-based therapeutics and diagnostics hold great promise for targeting intracellular tumor antigens presented by HLA molecules. The preferentially expressed antigen in melanoma (PRAME) is expressed in many cancers, but is highly restricted in normal tissues, making it a good target for TCR-based therapy. We have established a proprietary high-efficiency TCR discovery platform, enabling rapid identification of antigen-specific TCRs from healthy donors and cancer patients. TCRs specifically targeting PRAME425-433 peptide/ HLA-A*02:01 complex were cloned from healthy donors. T cells transduced with lentivirus encoding PRAME-specific TCR exhibited robust IFN-γ secretion and cytolytic function in an antigen-specific manner. By engineering the constant regions of both TCR α and β chains, the soluble expression of monovalent and bivalent native TCRs was achieved. We developed an exclusive cell based TCR binding assay to screen and identify the soluble forms of native PRAME-specific TCRs with various affinities. Surface plasmon resonance (SPR) analysis demonstrated that the bivalent native TCR protein HP-002 binds PRAME425-433/HLA-A*02:01 with a KD of 1.08×10^{-7} M. The Bivalent native TCR was used to develop TCR-CD3 T cell engager and radioactive diagnostic agent for imaging. Iodine-125 (125I)-labeled bivalent native TCR protein HP-002 exhibited in vivo antigen-dependent tumor accumulation in xenograft tumor models by SPECT/CT imaging. These data highlight the capability of our discovery and molecular engineering platform to develop the soluble TCRs for therapeutics and radioactive diagnostics in cancer. Our ongoing work focuses on TCR affinity maturation and molecular optimization of HP-002 to improve its affinity and selectivity, aiming to achieve enhanced tumor accumulation for future diagnostic and therapeutic applications.

#5822 Efficacy of targeted radionuclide therapy Using ^{131}I-FAPi dimers labeled via tetrazine ligation in a human glioblastoma xenograft model.

Umberto Maria Battisti[1], Marcel Martin[2], Vladimir Shalgunov[2], Filipe Elvas[3], Alan Miranda[3], Andreas Jensen[2], Matthias Herth[1]

[1]University of Copenhagen, Copenhagen, Denmark,[2]Tetrakit Technologies ApS, Copenhagen, Denmark,[3]University of Antwerp, Antwerp, Belgium

The successful use of diagnostic radiotracers targeting the pan-tumor marker fibroblast activation protein (FAP) across numerous cancer types is well established; however, translating these agents into effective therapeutics remains challenging. Compared with monomeric FAP inhibitors (FAPi), FAPi dimers—containing two FAP-targeting vectors—exhibit enhanced tumor retention, resulting in higher tumor doses and encouraging preliminary clinical outcomes. Current therapeutic agents targeting FAP rely largely on chelator-based constructs, restricting their labeling to radiometals. To overcome this limitation, we previously developed FAPi dimers equipped for tetrazine ligation using the novel trans-cyclooctene T4CO, enabling selective formation of a single isomer. Our lead compound, (^{131}I)I-FAPi 5, was synthesized with high yield and purity and evaluated in tumor-bearing animals, where it demonstrated therapeutic effects comparable to the established agent (^{177}Lu)Lu-DOTAGA-Glu(FAPi)$_2$. These findings suggest that (^{131}I)I-FAPi 5 may offer a cost-effective and scalable radioligand therapy (RLT) option to meet the expanding demand for FAP-directed treatments.
(^{131}I)I-DUAL FAPi-5 was prepared by a two-step radiolabeling process using tetrazine ligation. First, a tetrazine-trimethylgermyl precursor was radioiodinated with ^{131}I. The resulting synthon was purified by HPLC and subsequently clicked with the T4CO-FAPi derivative, achieving complete ligation within 10 minutes without requiring further purification. The therapeutic effect was investigated in U87-MG tumor-bearing mice. When the tumors reached 64±4mm^3, the mice received a single intravenous injection of (^{131}I)I-FAPi 5 (30 or 60 MBq), (^{177}Lu)Lu-DOTAGA-Glu(FAPi)2 (30 MBq) or vehicle control (n=6/group). Tumor response was monitored every other day via caliper measurement and survival was assessed up to 70 days after the start of treatment. The mice were euthanized on reaching one of the predefined endpoint criteria.(^{131}I)I-FAPi 5 was obtained in two steps with a final radiochemical yield of 60 ± 5% (n=4), radiochemical purity ≥98% (n=4). In U87-MG xenograft models, the tracer exhibited high and sustained tumor uptake. Treatment with (^{131}I)I-FAPi 5 at both dose levels (30 MBq and 60 MBq) resulted in rapid tumor regression, with therapeutic performance comparable to that of (^{177}Lu)Lu-DOTAGA-Glu(FAPi)$_2$. Our dual-targeting FAPi compound labeled with ^{131}I demonstrated robust tumor uptake and retention, with renal clearance as the primary excretion pathway. These findings confirm the therapeutic efficacy of this agent in preclinical tumor models, showing marked tumor regression and improved survival. Collectively, the results support the potential of this compound as an effective and accessible FAP-RLT candidate.

#5824 First target disclosure for the preclinical development of ATNM-400, a first-in-class actinium-225 radioconjugate with pan-tumor efficacy in solid tumors.

Amanda S. Chin, **Sumit Mukherjee**, Jason Li, Karina Peregrina, Debbie Lewis, Le-Cun Xu, Dhiren Patel, Madhuri Vusirikala, Monideepa Roy, Adeela Kamal

Actinium Pharmaceuticals, Inc., New York, NY

Background: Therapeutic resistance is a major barrier to durable cancer control across solid tumors. We report the first disclosure of a novel membrane target and the preclinical development of ATNM-400, a first-in-class Actinium-225 (225Ac) antibody radioconjugate designed to selectively eradicate therapy-refractory cancer cells. This target is overexpressed and functionally linked to resistance mechanisms in prostate, lung, and breast tumors. We evaluated the pan-tumor efficacy, mechanism of action, and translational potential of ATNM-400 in preclinical models representing advanced and therapy-resistant disease.
Methods: A full-length antibody specific to the novel target was conjugated to p-SCN-Bn-DOTA and radiolabeled with the alpha-emitter 225Ac (>98% purity). Target expression, binding affinity, and cellular internalization kinetics were tested across therapy-resistant tumor models, including enzalutamide- and 177Lu-PSMA-617-resistant prostate cancer, osimertinib-resistant EGFR-mutant lung cancer, hormone positive (HR+) breast cancer, triple-negative breast cancer (TNBC) and tamoxifen- or trastuzumab-resistant breast cancer. In vivo biodistribution, tumor retention, and efficacy were evaluated as monotherapy or in combination with standard-of-care agents.
Results: ATNM-400 selectively bound and rapidly internalized into target-positive tumor cells, inducing robust alpha-particle mediated DNA double-strand breaks. Notably, tumors resistant to other standard of care therapies showed increased target expression, thereby sensitizing the resistant tumors to ATNM-400. In vivo, ATNM-400 demonstrated sustained tumor uptake with off-target exposure in normal tissues, driving potent anti-tumor activity in:
• Prostate cancer: ATNM-400 outperformed androgen receptor (AR) pathway inhibitor enzalutamide, 177Lu-PSMA-617, and 225Ac-PSMA-617, producing durable regressions and complete responses in enzalutamide- and 225Ac-PSMA-617-resistant models.
• EGFR-mutant lung cancer: ATNM-400 synergized with EGFR inhibitor osimertinib, achieving complete cures in animals, correlating with increased target expression in osimertinib-resistant models.
• Breast cancer: ATNM-400 exhibited tumor regressions in HR+ breast cancer, TNBC and combination activity in estrogen receptor (ER) inhibitor tamoxifen- and HER2 antibody trastuzumab-resistant tumors, correlating with increased target expression. No significant toxicity or weight loss was observed at therapeutic doses.
Conclusions: ATNM-400 exhibits robust pan-tumor activity, overcomes resistance to AR, EGFR, and HER2/ER-targeted therapies, and demonstrates a favorable safety profile. These findings support ATNM-400 as a next-generation 225Ac radiotherapeutic platform with broad potential across many refractory solid tumors.

#5825 Discovery of FL-261 as a theranostic RDC vector for the treatment of c-MET overexpression cancers.

Junyu Yang, Guangcheng Jiang, Jiajia Xia, Juan Zhang, Fa Liu

Full-Life Technologies Limited, Shanghai, China

Mesenchymal-epithelial transition factor (c-MET) is an important member in the receptor tyrosine kinase family that is overexpressed and abnormally activated in most malignant tumors, making it an attractive target for radionuclide drug conjugate (RDC) based therapy. Despite the clinical validation of the target by small molecule kinase inhibitors, EGFR/c-MET bispecific antibodies and antibody drug conjugates (ADCs), their efficacy is mostly observed in non-small cell lung cancer (NSCLC). With the aim of developing a novel c-MET targeting RDC vector for the diagnosis and treatment of broader c-MET overexpressing indications, we have applied our UniRDC^{TM} platform technologies and discovered the development candidate FL-261. The binding affinity and selectivity of FL-261 against c-MET was tested by surface plasmon resonance (SPR) protein binding assay. FL-261 was then labelled with ^{111}In and ^{225}Ac, and their radiochemical purity (RCP) was determined by radio high-performance liquid chromatography (radio-HPLC). Their *in vivo* performance, assessed via imaging, *ex vivo* biodistribution and efficacy studies, was evaluated in xenograft mouse models with varying levels of c-MET overexpression. FL-261 showed potent binding affinity against c-MET with a K_D value of 7.5 nM and demonstrated over 450-fold selectivity over structurally similar receptor tyrosine kinases. FL-261 was successfully labeled with ^{111}In and ^{225}Ac, with each achieving an RCP of over 95%. After administration of [^{111}In]In-FL-261 in mice implanted with EBC-1 non-small cell lung cancer (NSCLC) xenografts, SPECT/CT images revealed intense and sustained tumor uptake which was significantly higher than that of normal organs. In addition, the tumor uptake was nearly completely blocked when extra mass of unlabeled FL-261 was co-administrated in the imaging study, suggesting *in vivo* cMET-specificity of FL-261. Separately, *ex vivo* cut-and-count biodistribution studies were performed after administration of [^{225}Ac]Ac-FL-261 in c-MET overexpressing EBC-1 xenograft model, demonstrating persistent and high tumor uptake from 1-hour to 120-hour post-dosing and rapid clearance from normal organs. Furthermore, in multiple xenograft models with varying levels of c-MET expression and one PDX model derived from a patient who became refractory to c-MET ADC therapy, [^{225}Ac]Ac-FL-261 consistently exhibited significant anti-tumor activity resulting in marked tumor regression. In these studies, there were no notable changes in body weight observed, suggesting a favorable safety profile of [^{225}Ac]Ac-FL-261. In summary, FL-261 demonstrates high theranostic potential, with favorable imaging profile of [^{111}In]In-FL-261 and potent antitumor activity of [^{225}Ac]Ac-FL-261 across a diverse set of tumor models. This compelling data set supports the further development of FL-261 as a theranostic agent for c-MET overexpressing cancers.

#5826 RT01: A novel anti-TF, radionuclide drug conjugate (RDC) for theranostic precision oncology.

Yi Zhao, Huahua Hao, Xin Yang, Weiwei Pan, XinxinLiang, Quanai Zhang, Xiaoxia Liu, Jingting Cui, Elizabeth Wu, **Zhican Qu**

Nanolattix, Taiyuan, China

Tissue Factor (TF) is an attractive therapeutic target for various tumors. We developed RT01, a first-in-class, targeted radio-theranostic agent consisting of a humanized anti-TF antibody conjugated to the diagnostic 89Zr or therapeutic 177Lu radionuclide. In a xenograft tumor model, SPECT/CT imaging demonstrated rapid and specific tumor accumulation of RT01-177Lu (single 200μCi i.v. dose), with retention over 6 days and rapid non-target clearance (background decreased by 4 hours post-injection). The tumor-to-kidney ratio of radiation intensity uptake (%ID/cc) exceeded 9.2. This single 200μCi dose injection of RT01-177Lu demonstrated potent anti-tumor efficacy and excellent tolerability. Histopathology analysis of ten major organs (kidney, intestine, brain, lung, liver, femur, spleen, stomach, heart, and pancreas) revealed no observable abnormalities or serious toxicity. In conclusion, the RT01 theranostic pair provides superior tumor targeting, rapid non-target clearance, and a favorable toxicity profile, supporting its continued clinical development for TF-positive cancers.

#5827 Actimab-A, a CD33-targeted actinium-225 radioconjugate, drives mutation-agnostic anti-leukemic activity and synergizes with standard therapies in AML through transcriptional reprogramming.

Amanda S. Chin[1], Merve Sahin[2], Jason Li[1], Le-Cun Xu[1], Monideepa Roy[1], Madhuri Vusirikala[1], Kaitlyn H. Ko[2], Wenbin Xiao[2], Adeela Kamal[1], Sheng F. Cai[2]

[1]Actinium Pharmaceuticals, Inc., New York, NY,[2]Memorial Sloan Kettering Cancer Center, New York, NY

Introduction: Acute myeloid leukemia (AML) is a genetically heterogeneous and aggressive malignancy with limited durable treatment options. Actimab-A (lintuzumab-Ac225), a CD33-targeted antibody radioconjugate, delivers the alpha emitter actinium-225 (Ac-225) to AML cells, inducing potent, localized DNA damage. Clinical studies have shown encouraging responses when combined with CLAG-M chemotherapy in relapsed/refractory AML, including in patients with *TP53* mutations or venetoclax resistance. Previously, we have shown the anti-leukemic activity of lintuzumab-Ac225 in AML cells regardless of mutations (*FLT3*, *TP53*, *NPM1*, and *KMT2A*) in both *in vitro* and *in vivo* AML models. Here, we demonstrated in primary AML patient samples that lintuzumab-Ac225 has strong translational therapeutic potential both as monotherapy and in combination with other therapies. We also defined the transcriptional profiles of AML cells treated with lintuzumab-Ac225 combination therapies to understand the underlying molecular mechanisms of anti-leukemic activity of these combination treatments.

Methods: Lintuzumab was conjugated to p-SCN-Bn-DOTA and radiolabeled with Ac-225. To explore mechanisms of synergy, AML cell lines harboring common mutations (*FLT3*, *KMT2Ar*: MV-4-11, MOLM-13 cells, *NPM1c*: OCI-AML3, and mutant *TP53*: Kasumi-1, HL-60 cells) were treated for 24 hours with standard-of-care (SOC) therapies: FLT3 inhibitors (gilteritinib, quizartinib), menin inhibitors (revumenib, ziftomenib) or azacitidine alone or in combination with lintuzumab-Ac225. We performed RNA sequencing (RNA-seq), followed by comprehensive gene set enrichment analysis. The cytotoxic potency of SOC was evaluated as monotherapies and in combination with Lintuzumab-Ac225 in primary AML patient samples.

Results: Lintuzumab-Ac225 showed a robust, dose-dependent cytotoxicity in primary AML patient samples, irrespective of FLT3, KMT2A, NPM1, or TP53 status. Notably, combining SOC therapies with lintuzumab-Ac225 *in vitro* enhanced their growth inhibitory effects. Lintuzumab-Ac225 combination versus SOC alone produced significant downregulation of MYC, G2M checkpoint, E2F targets and MTORC1 signaling while activating p53-mediated apoptosis, underscoring the mechanistic rationale for clinical development

Conclusions: Lintuzumab-Ac225 shows broad mutation-independent anti-leukemic activity in AML cell lines and primary AML patient samples. When combined with standard therapies, it drives complementary transcriptional programs that enhance depth and durability of response. Together, these findings support the clinical evaluation of lintuzumab-Ac225-based combinations as a strategy to overcome resistance and enhance therapeutic efficacy in AML.

: Tumor Microenvironment, Multispecifics, and Immunomodulation
Poster Session

#5832 Development and utility of precision FISH/IF multiomic panel to elucidate T cell functionality in the tumor microenvironment.
Anushka Dikshit[1], **Chandler Callaway**[2], Sukhbir Lulla[1], Will Paces[2], Alan Busar[2], Sara Wells[3], Mandy Bell[2], Lauren Matelski[4], Sharel Figueredo[1], Lenka Sinik[4]

[1]ACD, a Bio-Techne Brand, Newark, CA,[2]Flagship Biosciences, Broomfield, CO,[3]Flagship biosciences, Bloomfield, CO,[4]Flagship Biosciences, Bloomfield, CO

Immunohistochemistry (IHC) is a widely utilized tool for visualizing biomarker expression in tissues of interest. However, not all biomarkers are amenable to investigation by IHC, including secreted factors, such as cytokines. In these cases, *in situ* hybridization (ISH) may be a suitable alternative. The combination of IHC and ISH approaches allows for investigation of protein and RNA targets in the same multiomic assay, offering greater utility and flexibility than traditional assays. Furthermore, image and spatial analyses can be applied to elucidate the colocalization, proximity, and spatial relationship of RNA and protein biomarkers in the same sample. Flagship Biosciences, in collaboration with Advanced Cell Diagnostics (ACD), is developing a multiplex IHC/ISH fluorescent, which aims to identify and characterize subsets of T lymphocytes in the context of cancer. Using the RNAscope™ Multiomic LS assay we detected CD8, CD3, and Ki67 proteins alongside *IL4*, *IFNG*, and *GZMB* RNA expression to assess the activation and functional state of different T cell subsets based on biomarker expression profiles. Here, we demonstrate the capacity of this analysis on a set of FFPE lung samples from healthy and non-small cell lung cancer subjects. Our approach and analysis highlights the potential of spatial multiomics assays to bridge immunobiology with cancer research. Data generated could prove useful for phenotyping tumors, monitoring therapy response, or better understanding immune cell dynamics within the tumor microenvironment.

#5833 Therapeutic targeting of adhesion receptor GPR56 for the treatment of triple-negative breast cancer.

Yueh-Ming Shyu[1], Joan Jacob[2], Carla Godoy[1], Treena Chatterjee[1], Zhengdong Liang[1], Kendra S. Carmon[1]

[1]UTHealth Houston, Houston, TX,[2]Baylor College of Medicine, Houston, TX

Triple-negative breast cancer (TNBC) is an aggressive subtype lacking durable targeted therapies, and resistance continues to drive poor clinical outcomes. The clinical success of antibody-drug conjugates (ADCs), which combine antibody specificity with potent cytotoxic payloads, highlights their growing clinical impact. Although the approved anti-TROP2 ADC, sacituzumab govitecan, provides clinical benefit, it causes toxicity in normal tissues, underscoring the need for more selective therapeutic strategies. Adhesion-mediated signaling through the FAK-SRC axis is a major survival pathway under therapeutic stress. Our previous study showed that GPR56, an adhesion G protein-coupled receptor (GPCR), activates the FAK-SRC pathway and that targeting GPR56 with an ADC elicited potent antitumor efficacy in colorectal cancer models. Given these results, we examined GPR56 as a potential therapeutic target in TNBC. While TROP2 is a validated ADC target in TNBC, its expression in normal tissues limits tumor selectivity. GPR56, by contrast, is highly expressed in TNBC and associated with poor prognosis, yet shows limited normal tissue expression, potentially conferring a superior therapeutic index for GPR56-targeted ADCs. Our first-generation anti-GPR56 ADC (10C7-Duo), incorporating the DNA-damaging payload duocarmycin, exhibited target-dependent cytotoxicity in GPR56-positive TNBC cell lines, confirming that GPR56 is a viable therapeutic target. However, the monoclonal antibody (mAb) 10C7 exhibited agonistic activity, which could limit its therapeutic potential. Thus, we developed 9E3, a non-agonist anti-GPR56 mAb that internalizes efficiently and traffics to lysosomes for payload delivery. 9E3 was conjugated to a more potent pyrrolobenzodiazepine (PBD) payload using site-specific chemistry, and analyses confirmed successful conjugation, stability, and preserved antigen binding. Functional studies in breast cancer models showed that GPR56 knockdown suppressed, while overexpression enhanced, FAK-SRC phosphorylation, tumor cell growth, and invasion. Currently, we are evaluating 9E3-PBD for in vitro cytotoxic potency and selectivity, as well as in vivo safety and antitumor efficacy in TNBC cell line xenografts and patient-derived models. These findings help establish GPR56 as a clinically relevant adhesion GPCR and introduce a novel ADC approach to target therapeutic resistance in TNBC. By integrating receptor biology with targeted payload delivery, this work lays the foundation for potentially safer and more selective therapeutic options for TNBC patients.

#5834 Dual targeting GLI1 and EZH2 for treatment of invasive breast cancer.

Jer-Yen Yang, Chun Ju Chang, Yu-Wa Lai

China Medical University, Taichung City, Taiwan

About 12% of breast cancers are invasive breast cancers, including triple-negative breast cancer (TNBC), which manifests early metastasis and recurrence with limited treatment options. Therefore, there is an urgent need to better understand key mechanisms governing invasive breast cancers to develop effective treatment strategies. Our clinical database analysis indicates that overexpression of EZH2 is often correlated with metastatic breast cancer, and high expression of the oncogenic GLI1-Hedgehog signaling is positively correlated with poor survival of invasive breast cancers. Our pilot findings indicate that deletion of the EZH2 gene results in reduced expression levels of GLI1 and its downstream target gene, cyclin D1. Previous literature also suggests that cMYC can activate GLI1, and the EZH2-cMYC complex can induce target gene expression in an atypical manner, promoting cancer. However, it is reported that the clinical use of either an EZH2 inhibitor alone or a GLI1 inhibitor alone cannot hinder tumor growth or metastasis. Our data suggest that EZH2 may regulate GLI1 expression, but its synergistic functionality has not been fully elucidated. We expect that EZH2 forms a complex with cMYC and GLI1 to synergistically activate the target genes involved in breast cancer progression (for example, GLI1 and Cyclin D1). As a result, a combination of EZH2 inhibitors and GLI1 inhibitors can synergistically suppress cancer cell growth and metastasis, serving as a new and effective therapeutic option for invasive breast cancers. Using a cell viability assay, the combination therapy was shown to be more effective in inhibiting TNBC cell viability compared to the single-drug treatment and the vehicle groups. The wound healing assay showed that combination therapy was more effective in suppressing TNBC cell migration. The CompuSyn for drug synergy analysis, both the Combination Index (CI) and Dose Reduction Index (DRI) indicated that the combination therapy exhibited significant synergistic effects, where Vismodegib could reduce the dose by ~52-fold, while GSK126 could reduce the dose by ~22-fold. Form the findings, we believe that dual targeting GLI1-EZH2 has potential to become a novel and effective combination treatment for invasive breast cancer in the clinical setting.

#5835 Treatment of pancreatic cancer cells with Tumor Treating Fields (TTFields) and KRAS inhibitors.

Hila Fishman[1], Lena Lifshitz[1], Helena Mumblat[1], Zeina Drawshy[1], Anat Klein-Goldberg[1], Yara Eid Mutlak[1], Hila Ene[1], Efrat Zemer-Tov[1], Tali Voloshin[1], Itai Tzchori[1], Adi Haber[1], Moshe Giladi[1], Uri Weinberg[2], Yoram Palti[1]

[1]Novocure Ltd, Haifa, Israel,[2]Novocure GmbH, Baar, Switzerland

Background: Pancreatic ductal adenocarcinoma (PDAC) remains a major cause of cancer-related mortality, with limited survival despite intensive chemotherapy regimens such as FOLFIRINOX or gemcitabine/nab-paclitaxel. KRAS mutations, present in approximately 90% of PDAC cases, are a central driver of tumor aggressiveness and therapeutic resistance, in part by activating and stabilizing (and often overexpressing) c-MYC—a key regulator of cell growth and metabolism. Tumor Treating Fields (TTFields), electric fields that disrupt cellular processes crucial for cancer cell viability, have recently been shown to suppress c-Myc at the transcript and protein levels in various cell lines. TTFields therapy was shown to improve survival in pancreatic cancer patients when used together with gemcitabine/nab-paclitaxel. The current study aims to examine the benefit of adding TTFields to KRAS inhibitors (KRASi) in PDAC preclinical models.
Methods: KPC pancreatic cancer cells harboring the KRAS G12D mutation were treated for 72 hours with TTFields (150 kHz, 1 V/cm RMS) using the inovitro system. The pan-KRAS inhibitor daraxonrasib (RMC-6236) was applied at varying concentrations, either alone or in combination with TTFields. Following treatment, cell count, colony formation, and apoptosis were quantified, and an overall effect score was derived from changes in cell count and colony formation. Expression of c-Myc was assessed by real-time PCR and Western blot analysis.
Results: Treatment of KPC cells with either TTFields or the KRAS inhibitor resulted in a dose-dependent reduction in cell viability and colony formation, along with increased apoptosis. The co-application of TTFields with RMC-6236 amplified these outcomes, demonstrating a synergistic interaction between the two modalities. Both TTFields and RMC-6236 independently reduced c-Myc expression, with a more pronounced downregulation observed upon co-treatment.
Conclusions: Concomitant application of TTFields and the pan-KRAS inhibitor in KRAS G12D pancreatic cancer cells produced a synergistic antitumor effect, potentially mediated by modulation of the master regulator c-Myc. Ongoing studies are exploring KRAS mutation-specific inhibitors, expanding the analysis to additional pancreatic cancer cell lines harboring diverse KRAS variants, and testing the in vivo efficacy of TTFields with KRAS inhibition.

#5836 Augmented antitumor activity of Tumor Treating Fields (TTFields) with anti-VEGFR and docetaxel treatment in a lung cancer mouse model.

Helena Mumblat[1], Yara Eid Mutlak[1], Yuval Shmueli[1], Ruslana Militsin[1], Catherine Tempel-Brami[1], Shay Cahal[1], Alexandra Volodin[1], Sara Jacobovitch[1], **Martin Gabay**[1], Itai Tzchori[1], Adi Haber[1], Moshe Giladi[1], Uri Weinberg[2], Yoram Palti[1]

[1]Novocure Ltd, Haifa, Israel,[2]Novocure GmbH, Baar, Switzerland

Introduction: Angiogenesis drives disease progression and poor outcomes in non-small cell lung cancer (NSCLC). Ramucirumab, an antibody targeting the vascular endothelial growth factor receptor (VEGFR), is approved as a second-line therapy in combination with docetaxel for metastatic NSCLC. By normalizing tumor vasculature, angiogenesis inhibitors enhance drug delivery and facilitate immune cell infiltration Tumor Treating Fields (TTFields) are electric fields that disrupt cellular processes critical for cancer cell survival. TTFields therapy is approved for metastatic NSCLC concomitant with immune checkpoint inhibitors or docetaxel following progression on/after platinum-based therapy. Here, we investigated the therapeutic impact of TTFields applied together with docetaxel and anti-VEGFR treatment in an orthotopic mouse model of NSCLC.

Methods: C57Bl/6 mice were orthotopically implanted with LL/2 lung carcinoma cells and allowed seven days for tumor establishment. Mice were then exposed continuously to TTFields (150 kHz) or sham (heat) treatment for eight days. The murine anti-VEGFR antibody DC101 (10 mg/kg) or vehicle was administered intraperitoneally on days 1, 4, and 7 of treatment. Docetaxel (3 mg/kg) or vehicle was administered intraperitoneally on days 2 and 6. The study included six treatment groups: control, docetaxel alone, docetaxel + DC101, TTFields alone, TTFields + docetaxel, and TTFields + docetaxel + DC101. At treatment completion, tumors were excised, weighed, and analyzed by immunohistochemistry using anti-CD31 for vessel staining, alongside additional functional markers.

Results: Treatment with TTFields together with docetaxel and DC101 led to a marked reduction in tumor volume compared with all other treatment groups. Tumor weights and MRI analysis consistently showed the strongest inhibition of tumor growth under this regimen. Histological analysis revealed elevated cell death in tumors from the TTFields + docetaxel + DC101 group, as indicated by TUNEL staining. CD31 and αSMA co-staining indicated that TTFields, when applied together with anti-VEGFR therapy, promoted vascular normalization characterized by pericyte coverage and a more organized vasculature. This remodeling of the tumor microenvironment was accompanied by enhanced infiltration of $CD8^+$ cytotoxic T cells, pointing to improved immune accessibility to the tumor core.

Conclusions: Collectively, these findings suggest that TTFields amplify the therapeutic activity of antiangiogenic and chemotherapeutic agents by stabilizing tumor vasculature, facilitating immune cell penetration, and potentiating treatment-induced cell death.

#5837 Tolvaptan as a potential anticancer and immunomodulatory treatment for triple-negative breast cancer.

Laura Naldi[1], Zhi Huang[1], Brionna King[1], Kimberly McCarter[1], Kelsey Gardiner[1], Alessandro Peri[2], Lucio Miele[1], Giulia Monticone[1]

[1]LSU Health New Orleans, New Orleans, LA,[2]University of Florence, Florence, Italy

Background: Triple-negative breast cancer (TNBC) is an aggressive breast cancer (BC) subtype characterized by rapid progression, high risk of recurrence and metastasis. Although immunotherapy has improved outcomes for some patients, treatment resistance remains a major challenge, highlighting the need for novel therapeutic targets and drug repurposing strategies. Hyponatraemia, defined by a serum sodium concentration <135 mEq/L, is the most common electrolyte disorder in cancer, affecting over one-third of BC patients. Tolvaptan, a G protein-coupled (GPC) vasopressin type 2 receptor (AVPR2) antagonist, is clinically used to treat hyponatremia in various settings, including cancer. Beyond its clinical use, *in vitro* and *in vivo* studies indicate that tolvaptan inhibits cancer cell proliferation, reduces invasiveness, and promotes apoptosis in several tumor types. Interestingly, database analysis revealed that TNBC has the highest expression of AVPR2 among all BC subtypes. Further, there is evidence of tolvaptan modulating T cells, and it is known that other GPC receptors can regulate T cell antitumor activity, although the underlying mechanism of tolvaptan immunoregulation remains unclear. This study aimed to investigate the potential anticancer and immunomodulatory effects of tolvaptan in TNBC models.
Experimental Procedures and Results: Tolvaptan treatment significantly reduced TNBC cell viability in MTT assays in murine (C0321) and human (MDA-MB-231, MDA-MB-436) TNBC cell lines from the lowest concentration of 1 nM, while non-tumorigenic MCF10A cells remained unaffected up to 10 µM. In contrast, treatment with the AVPR2 agonist desmopressin had no effect on the viability at any concentration used. In agreement, tumor-derived TNBC organoids treated with tolvaptan showed a significant increase in cell death and a higher number of infiltrating $CD8^+$ T cells compared to those treated with DMSO. Consistently, primary cultures of splenic murine $CD8^+$ T cells treated with tolvaptan exhibited increased expression of the activation marker CD69, as determined by flow cytometry. In an orthotopic syngeneic TNBC mouse model (C0321, FVB mice), tolvaptan treatment (10 mg/kg for 27 days) resulted in smaller tumors, whereas desmopressin (2 µg/kg) promoted tumor growth. Immunohistochemical analysis demonstrated increased cleaved caspase-3 expression and $CD8^+$ T cell infiltration in tolvaptan-treated tumors. Flow cytometry analysis confirmed a higher number of tumor-infiltrating $CD8^+$ T cells and an upregulation of Notch-1 and IFN-γ, markers of an effective antitumor immune response.
Conclusions: Overall, these findings indicate that tolvaptan exerts both direct cytotoxic and immune antitumor effects in TNBC models. The cytotoxicity toward TNBC cells, together with enhanced $CD8^+$ T cell responses, supports the potential use of tolvaptan as a novel therapeutic approach for TNBC.

#5838 QLS2401: A novel PSMA/STEAP1/CD3 tri-specific T-cell engager for the treatment of mCRPC.

Chenjun Tang[1], **Langyong Mao**[1], Jiaxin Yue[1], Moyan Hu[1], Shuyong Zhao[2], Hua Ying[1], Weikang Tao[1]

[1]Shanghai Qilu Pharmaceutical Research and Development Center LTD., Shanghai, China,[2]Qilu Pharmaceutical Co., Ltd., Jinan, China

Prostate cancer (PCa) is one of the most common malignancies in men worldwide. Approximately 10%-20% of PCa patients develop castration-resistant PCa (CRPC) within 5 years and subsequently progress to metastatic CRPC (mCRPC). Current approved therapies for mCRPC patients offer limited survival benefits with unsatisfied long-term remission, underscoring an urgent need for novel therapeutic options. Both STEAP1 (Six Transmembrane Epithelial Antigens of the Prostate 1) and PSMA (Prostate-Specific Membrane Antigen) are frequently co-expressed at high levels in mCRPC, presenting dual targeting opportunity to enhance efficacy. Here, we report the generation and preclinical development of QLS2401, a novel PSMA/STEAP1/CD3 tri-specific TCE engineered to have optimized CD3 affinity and tumor associated antigen (TAA)-binding valency to enhance T cell-mediated cytotoxicity and mitigate the resistance resulting from single antigen-loss. QLS2401 causes potent target-dependent and T cell-mediated cytotoxicity against prostate cancer cell lines and induces tumor regression in prostate cancer xenograft models, demonstrating superior or comparable efficacy to the xaluritamig analog. The avidity-driven activity of QLS2401 enables selectivity for tumor cells with higher STEAP1- and PSMA- expression than normal cells. QLS2401 was well-tolerated in a toxicity study in cynomolgus monkeys, with an HNSTD (Highest Non-Severely Toxic Dose) significantly higher than that of the xaluritamig analog. In conclusion, preclinical studies have demonstrated that QLS2401 exhibits an expanded therapeutic window, superior efficacy and improved tolerability compared to the xaluritamig analog.

#5839 Tumor-selective treatment of metastatic pancreatic cancer with an engineered, probiotic living drug.

Amanda R. Decker-Farrell[1], Stephen A. Sastra[2], Tetsuhiro Harimoto[3], Marie C. Hasselluhn[2], Carmine F. Palermo[2], Tanner C. Dalton[2], Llewelyn Levett[1], Edward R. Ballister[3], Michael A. Badgley[2], Tobias Janowitz[1], Tal Danino[3], Kenneth P. Olive[2]

[1]Cancer Center, Cold Spring Harbor Laboratory, Cold Spring Harbor, NY,[2]Herbert Irving Comprehensive Cancer Center, Columbia University Irving Medical Center, New York, NY,[3]Biomedical Engineering, Columbia University, New York, NY

Treating pancreatic ductal adenocarcinoma (PDAC) with intravenous chemotherapy has remained a challenge, due in part to the hypovascularized and poorly perfused nature of PDAC tumors, thus limiting drug accumulation. However, the features that impede systemic therapy in PDAC may favor bacterial therapies, as bacteria can actively migrate through tissues, thrive in hypoxic microenvironments, and exploit local immune suppression. Once colonized within the tumor niche, live bacteria can provide a stable source of anticancer compounds, rather than relying on repeated systemic doses. Here, we addressed the current drug delivery challenges of PDAC by developing a probiotic-based bacterial therapy. Through 2D monolayer and PDAC tissue-slice screens, we identified the pore-forming Theta toxin (from *C. perfringens*) as a potent candidate and expressed it in a probiotic strain of *E. coli*, Nissle 1917 (Nis). Intratumoral injections of live Nis-Theta bacteria into subcutaneous and genetically engineered mouse models of PDAC (KPC - Kras LSL.G12D/+; Tp53 LSL.R172H/+; PdxCre tg/+) resulted in significantly higher rates of complete tumor regression, reduced tumor growth kinetics, and extended median survival to 35.5 days, compared to 12 days for Vehicle or Gemcitabine controls and 16.5 days for non-toxic bacteria, Nis-GFP. We also thoroughly monitored systemic body response to bacterial treatment for safety. Bacterially treated mice did not exhibit any weight loss, body composition changes, or other infection-like symptoms compared to non-bacterial treatment (Gemcitabine) arms. Bacterial spread to healthy tissues (lung, liver, intestine, and diaphragm) was minimal with no increase in cellular damage in non-tumor tissues. Furthermore, mice systemically cleared the bacteria within several weeks of full tumor regression. Strikingly, while there was minimal spread of bacteria to non-tumor tissues, bacteria translocated to distant secondary tumor sites following injection of the primary pancreatic tumor. Histology showed bacterial co-localization with apoptotic tumor cells in both primary and metastatic lesions, suggesting a mechanism for targeting both known and unknown metastases following local administration. Histological and flow cytometry analyses demonstrated modest recruitment of anti-tumor immune populations in Nis-Theta treated tumors, suggesting potential synergy with immunotherapies. Together these data demonstrate potent preclinical activity of cytotoxic bacterial therapy as a novel drug delivery method to circumvent the challenges of systemic treatment of PDAC. These bacteria demonstrated preferred tumor colonization over healthy tissue with no systemic illness, targeted metastatic lesions, and significantly extended survival in a clinically relevant model of PDAC with only a single dose.

#5840 The development of minocycline-loaded microparticles and injectable alginate scaffolds composites to prolong release for the treatment of glioblastoma.

Florestella Rivera, Dorina A. Madrid, Samantha C. Davila, Serenade Trevino, Jorge L. De Leon, Sebastian Flores, Sue Anne Chew

Health and Biomedical Sciences, The University of Texas Rio Grande Valley, Brownsville, TX

Glioblastoma multiforme (GBM) is a Grade IV malignant brain cancer characterized by rapid progression and high recurrence. Minocycline (MINO), an antibiotic know to have antiangiogenic properties, has potential for GBM treatment ; however to address the limitations of current therapies, this project integrates two biomaterial-based delivery systems: 1) electrosprayed minocycline-loaded PLGA microparticles, which exhibited a 67-80% burst release within the first hour, and 2) injectable alginate scaffolds, which exhibited a 36-43% burst release within the first day. MINO-loaded MPs alone exhibit a significant burst release that limits sustained therapeutic exposure. The alginate (i.e. a biocompatible polysaccharide) injectable hydrogels are capable of decreasing the burst release compared to MPs and possibly increase the control release of drug. Combining both systems may therefore reduce burst release and extend overall delivery.Thus, the objective of this study was to investigate the drug release kinetics from MINO-loaded MPs, MINO loaded alginate scaffolds and MINO-loaded MPs in alginate scaffolds. MINO-loaded MPs were fabricated via vertical electrospraying using a 0.9 mL/ flow rate, 14kV voltage, and 20 cm distance. Polyethylene glycol (PEG) was incorporated to enhance MINO solubility, and the MPs were collected on copper /glass plates. Sodium alginate scaffolds (2.0 wt/vol%) were prepared by dissolving sodium alginate and calcium carbonate, homogenizing with glucono-delta lactone and with MINO or drug loaded MPs and injecting into 24-well plates to mold them uniformly. Release kinetics for MPs, MINO-loaded scaffolds (scaffold + MINO), and MINO-loaded MP scaffolds (scaffold + MINO-loaded MPs) were assessed in 1x DPBS by measuring MINO absorbance at 350 nm with a microplate reader. The drug release kinetics studied showed high burst release on Day 1 for the Mino-loaded MPs alone (45%), and a substantially reduced initial burst release for the other groups (16% for both scaffold + MINO and and scaffold + MINO-loaded MPs). On Day 2, 3 and 6, MINO-loaded scaffold released significantly more drug compared to MINO-loaded MPs and MINO-loaded MP scaffolds had a trend of having a lower percentage of cumulative release of drug compared to MINO-loaded scaffolds. In conclusion, the combination of MINO and PLGA MINO-loaded MPs with the injectable alginate scaffolds will prolong the release of the therapeutic agents and allow better control of the release kinetics compared to using MPs alone with the MINO-loaded MPs and scaffold combination having a trend of being a more promising for sustained released for localized GBM treatment. Future studies will focus on evaluating U87 cell viability following treatment with the different groups to determine whether the prolonged and controlled release results enhance the cytotoxic effect.

#5841 Targeting type XI collagen to facilitate elimination of cancer-associated fibroblasts?.

Annika Hettich, Cecilie Bager, Morten Karsdal, Nicholas Willumsen

Nordic Bioscience, Herlev, Denmark

Background: Fibrotic tumors pose a major therapeutic challenge due to the dense stromal barriers formed by myofibroblastic cancer-associated fibroblasts (myCAFs), which increase tissue stiffness and impede drug delivery. These myCAFs are characterized by elevated expression of type XI collagen, a key component of the fibrous cap. Antibody-drug conjugates (ADCs) offer a targeted approach by linking monoclonal antibodies to cytotoxic payloads, enabling selective delivery within the tumor microenvironment. Here, we present a novel ADC-based strategy that targets tumor-associated type XI collagen to selectively eliminate myCAFs. This approach combines CT11a1, an antibody recognizing a tumor-specific type XI collagen epitope, as the delivery vehicle, with PRO-C11, a circulating biomarker of type XI collagen for potential patient selection and treatment monitoring.
Methods: ELISAs were used to quantify CT11a1 and PRO-C11 collagen epitopes in serum from patients with various cancer types and healthy controls. Pancreatic cancer-associated fibroblasts (CAFs), normal fibroblasts (NFs), and co-cultures of CAFs with pancreatic cancer cells (BxPC3) were cultured in the SiaJ model for 12 days. On day 12, cultures were immunostained with CT11a1 or PRO-C11 antibodies. A CT11a1-ADC was developed and its effect on cell viability was quantified using the Alamar Blue assay.
Results: Among several tested collagen-based biomarkers, PRO-C11 demonstrated the highest diagnostic accuracy (AUC: 0.99) across all cancer types. In contrast CT11a1 was barely detectable in serum. Immunostaining with the CT11a1 antibody on day 12 of the SiaJ model revealed prominent type XI collagen deposition in wells containing CAFs while minimal to no signal was detected in wells with NFs. In contrast, staining CAFs with the PRO-C11 antibody did not result in any detectable signal, indicating limited accessibility or absence of the PRO-C11 epitope in the extracellular matrix (ECM). Staining of co-cultures with the CT11a1 antibody revealed that type XI collagen is localized in the fibrous cap-like structure positioned between the cancer cells and the fibroblasts. Initial treatments with CT11a1-ADC induced a dose-dependent decrease in CAF viability.
Conclusion: Type XI collagen is specific to myCAFs. The CT11a1 epitope is detectable in the CAF-derived ECM, but not in circulation, whereas the opposite is true for PRO-C11. The developed CT11a1-ADC demonstrates potential as an ADC specifically targeting type XI collagen produced by myCAFs. PRO-C11 may serve as a biomarker to identify patients with high type XI collagen production. Further exploration and validation are ongoing.

#5842 Combined KRAS pathway inhibition and liposomal irinotecan treatment enhances tumor regression, attenuates desmoplasia, and augments T cell infiltration in pancreatic ductal adenocarcinoma.

Hari Krishnareddy Rachamala[1], Fang Wei[1], Debabrata Mukhopadhyay[2], Hani M. Babiker[3]

[1]Department of Biochemistry and Molecular Biology, Mayo Clinic, Jacksonville, FL,[2]Mayo Clinic College of Medicine, Jacksonville, FL,[3]Mayo Clinic, Jacksonville, FL

Background: Pancreatic ductal adenocarcinoma (PDAC) is driven predominantly by oncogenic KRAS signaling and characterized by an immunosuppressive, fibrotic tumor microenvironment that limits therapeutic responses. RMC-6236, a pan-KRAS inhibitor, and liposomal irinotecan, an investigational anti-tumor agent, each demonstrate partial activity in KRAS-mutant cancers. However, their combined therapeutic potential in PDAC remains unexplored. Here, we evaluated the anti-tumor efficacy, survival benefit, and immunomodulatory effects of RMC-6236, liposomal irinotecan and irinotecan alone and dual combinations multiple in vitro and in vivo PDAC models.

Methods: In vitro cytotoxicity assays were performed using KPC, PANC-1, AsPC-1, and PANC-02 cell lines. In vivo therapeutic studies were conducted in orthotopic KPC and PANC-1 tumor models. RMC-6236 was administered orally at 10 mg/kg; liposomal irinotecan and irinotecan was administered intravenously at 5 mg/kg. Tumor growth inhibition, survival, collagen deposition, and immune cell infiltration were analyzed. Tumor microenvironment remodeling was quantified via immunohistochemistry for CD8, CD4, collagen I, and fibronectin.

Results: The combination of RMC-6236 and liposomal irinotecan elicited potent anti-tumor effects across all evaluated PDAC cell lines, achieving greater than 90% growth inhibition in vitro. In vivo, co-treatment resulted in more than 90% tumor regression in both KPC and PANC-1 xenograft models, markedly surpassing the efficacy of individual monotherapies and other dual-agent controls. Combination therapy significantly extended overall survival and produced sustained suppression of tumor progression. Mechanistic analyses revealed a substantial reduction in collagen and fibronectin deposition within the tumor microenvironment, consistent with attenuation of desmoplasia. Immune profiling demonstrated a robust enhancement of intratumoral $CD8^+$ and $CD4^+$ T-cell infiltration, along with a pronounced decrease in survivin expression. Importantly, no observable systemic toxicity was detected in treated animals.

Conclusions: RMC-6236 combined with liposomal irinotecan yields synergistic anti-tumor effects, remodels the fibrotic PDAC microenvironment, enhances T-cell infiltration, and significantly improves survival in aggressive pancreatic tumor models. These findings provide strong rationale for clinical evaluation of RMC-6236-based combination therapies for KRAS driven PDAC.

#5843 Beyond viability: Post treatment single cell and spatial transcriptomic profiling in mixtures of PRISM barcoded cancer cell lines.

Laura Doherty[1], Ashish B. George[1], Mustafa Kocak[1], Paul Lund[2], Andrew Kohlway[2], Andrew Boddicker[3], Ben Song[3], Carlos Ruiz Perez[3], Bryan Lajoie[3], Catarina D. Campbell[1], Matthew G. Rees[1], Jennifer A. Roth[1]

[1]Broad Institute of MIT and Harvard, Cambridge, MA,[2]10x Genomics, Pleasanton, CA,[3]Element Biosciences, San Diego, CA

PRISM is a highly multiplexed, genomic barcode-based cell line viability technology of nearly 1000 solid tumor and hematopoietic cell lines. The unique cell line barcodes enable the cell lines to be multiplexed into pools of dozens to hundreds of different cell lines per well or dish, which greatly reduces the time and costs required to profile the viability effects of compounds or biologics across 900+ cell lines. Leveraging underlying genomic characterization of these cell lines enables the discovery of biomarkers of sensitivity and resistance. In addition to enabling viability screening in 900+ cell lines at scale, the PRISM barcoding technology also enables us to profile post-perturbation RNA transcript and protein changes in mixtures of cell lines by adapting commercially available single cell sequencing (10x Genomics Flex v2) and spatial transcriptomic assays (Element Biosciences AVITI24). Expanding the phenotypic readout capabilities of the PRISM technology beyond viability to include gene and protein changes will provide deeper insight into drug mechanisms of action, resistance, off-target effects, and heterogeneity of response. Here we present our work developing multiomic phenotypic profiling assays in barcoded PRISM cell line pools. We leverage 10x Genomics Flex v2 (for genomewide RNA single cell sequencing and PRISM barcode identification) in conjunction with the Flex-compatible Proteintech Human Discovery antibody panel (to measure abundances of 300+ proteins) in response to perturbations. In a pilot of 100 cell lines spanning 20+ lineages, we reliably detect 99 cell lines, recovering on average ~7000 unique genes per cell. In parallel, we are exploring the potential of Element Biosciences AVITI24 for spatial transcriptomic readouts in pools of PRISM cell lines. In a pilot of 25 cell lines spanning 15 lineages, we detect each of the 25 cell lines and although we recover fewer counts per cell, we recover morphology features from 6 cell paint stains (membrane, nucleus, actin, mitochondria, golgi, and ER). In both assays, we treated with a pan-RAS inhibitor and observed a concordant gene signature in differentially expressed genes. The 10x Flex v2 assay has the benefit of depth (detecting more transcripts per cell), while the Element imaging workflow enables culturing cells directly on the flowcell and provides spatial and morphological features. Thus, the two assays are highly complementary. We identify commonalities as well as distinct insights obtained by the two technological approaches and identify cell line specific responses.

#5844 Novel inhibition of transcriptional cyclin-dependent kinases, CDK12/13, using CT7439 as a treatment for colorectal cancer with CDK12 upregulation.

Jason A. Somarelli[1], Wylie Katherine Watlington[1], Divya Dayanidhi[1], Mohammad Zokaasadi[1], John B. Mantyh[1], Pelumi D. Olawuni[1], Gabrielle Rupprecht[1], Jeremy Force[2], Shannon McCall[1], Ashwani K. Bahl[3], David S. Hsu[1]

[1]Duke University, Durham, NC,[2]Daiichi Sankyo, Inc., Bernards Township, NJ,[3]Carrick Therapeutics, Inc., Dublin, Ireland

Introduction: Cell proliferation is a hallmark of cancer growth, and regulation of transcription and translation is key to controlling proliferative capacity. A crucial connection between transcriptional regulation and the cell cycle occurs via transcriptional cyclin-dependent kinases (CDKs), CDK12 and its paralog, CDK13, which regulate transcription by phosphorylating the c-terminal domain of RNA polymerase II. Both CDK12 and CDK13 are often upregulated in solid tumors, rendering them compelling targets for therapeutic intervention.
Methods: A total of eight CDK12 or CDK12/13 inhibitors with different mechanisms of action (covalent, non-covalent, proteolysis-targeting chimera, and molecular glue) were screened against a panel of cancer cell lines spanning five solid tumor types (breast, colorectal, lung, ovarian, and prostate). Colorectal cancer patient-derived organoids (PDO) were used to validate the most efficacious agents, covalent binders (THZ531 and CDK12-IN-E9). In order to determine whether CDK13 plays a compensatory role for loss of CDK12 function, knockdown of CDK13 by siRNAs was employed, followed by CDK12-specific inhibition using a proteolysis-targeting chimera (BSJ-4-116). Finally, synergy was conducted to determine whether CDK12/13 inhibition increases sensitivity to poly-ADP ribose polymerase (PARP) inhibition. qPCR quantified the presence of short and long isoforms of BRCA1 following CDK12/13 inhibition to confirm whether transcription elongation in DNA damage repair genes was prevented.
Results: Covalent inhibition of CDK12/13 was the most efficacious across pan-cancer cell lines. Validation in colorectal cancer PDO showed greater inhibition by covalent inhibitors than standard of care chemotherapies for colorectal cancer (oxaliplatin, SN38, and 5-FU). CDK13 siRNA-mediated knockdown sensitized colorectal cell lines to the CDK12-specific inhibitor, BSJ-4-116, suggesting CDK13 may compensate for CDK12 loss of function. CDK12/13 inhibition led to downregulation of long isoforms of BRCA1, rendering cells susceptible to dual CDK12 and PARP inhibitors. These compelling data prompted evaluation of CT7439, a CDK12/13 inhibitor and cyclin K glue-degrader, which showed efficacy in the low nanomolar range for a panel of colorectal PDO.
Conclusions: Here we highlight CDK12/13 inhibition as a compelling target for colorectal cancers and other solid tumors and show the importance of CDK13 compensation during CDK12 inhibition. These findings support further evaluation of the novel CDK12/13 inhibitor, CT7439, for the treatment of solid tumors with CDK12/13 upregulation.

#5845 BCG010, a potentially best-in-class NKG2A blocker for cancer treatment.

Yong Xie[1], Peiran Li[1], Huichao Liang[1], Tao Wang[2], Yanan Guo[1], Rongjing Zhang[2], Zhe Shao[2]

[1]Biocytogen, Waltham, MA, MA,[2]Dragon Boat Biopharmaceutical, Shanghai, China

BCG010, a fully human IgG1κ monoclonal antibody, has been engineered with an Fc LALA (L234A/L235A) substitution to block the CD94-NKG2A inhibitory checkpoint engaged by HLA-E. This development addresses the limitations of first-generation NKG2A inhibitors, which have shown variable activity, particularly as monotherapy, highlighting the need for molecules with enhanced affinity, selectivity, pharmacokinetics (PK), and developability, as well as cynomolgus cross-reactivity to support clinical translation and combination therapies. BCG010 fulfills these requirements, exhibiting higher affinity for human NKG2A compared to a Monalizumab analog at the nanomolar level, full cross-reactivity with cynomolgus NKG2A, and no binding to human NKG2C or NKG2E. Mechanistically, BCG010 alleviates NKG2A-mediated inhibitory signaling and promotes NK-cell cytotoxicity against K562 targets *in vitro*, akin to the Monalizumab analog, while demonstrating favorable biophysical and developability properties under defined conditions. *In vivo*, BCG010 inhibited tumor growth in B-hNKG2A/hCD94 humanized mice bearing MC38-HLA-E cells, in the K562-bearing B-NDG mouse model when combined with adoptive NK-cell therapy, and in RMA-bearing B-hCD94/hNKG2A mice when combined with an Atezolizumab analog, without inducing weight loss across studies. Notably, BCG010 also exhibits a longer half-life than the Monalizumab analog in B-hNKG2A/hCD94 humanized mice. These data collectively support BCG010 as a promising, potentially best-in-class NKG2A blocker with high affinity, strict selectivity, encouraging efficacy and tolerability, and favorable PK and developability profiles, warranting clinical advancement and the exploration of combination strategies for cancer treatment. The development of the CMC cell line for BCG010 is ongoing.

#5846 AVA6103 is a FAP-enabled pre|CISION®peptide-drug conjugate delivering sustained release of exatecan in the tumor microenvironment with potent antitumor activity.

Curtis Rink[1], Tom Clough[1], Ellen Watts[1], Folake Orafidiya[1], Marine Houee[1], Sophie Brown[1], Victoria Juskaite[1], Gezim Lahu[2], Ruairidh Edwards[3], Karen Campbell[3], Dave Liebowitz[3], David Jones[1], **Francis Wilson**[1], Michelle Morrow[1]

[1]Discovery, Avacta Therapeutics, London, United Kingdom,[2]thinkQ2, Baar, Switzerland,[3]Clinical Development, Avacta Therapeutics, London, United Kingdom

AVA6103 is a novel peptide drug conjugate (PDC) based on proprietary pre|CISION® technology which incorporates a dipeptide that is specifically cleaved by Fibroblast Activation Protein α (FAP).

FAP is a post-proline protease that is overexpressed on the surface of cancer associated fibroblasts (CAFs) in many solid tumors, and facilitates delivery of pre|CISION® medicines specifically to the tumor microenvironment (TME). AVA6103 consists of exatecan, a potent Topoisomerase I payload, covalently linked to a dipeptide containing a cleaving sequence (D-Ala-L-Pro), which is susceptible to hydrolysis by FAP but is resistant to hydrolysis by other mammalian proteases.

Exatecan has been investigated in the clinic, however, its utility is limited by dose-limiting toxicities. The exquisite selectivity of the pre|CISION® substrate for FAP results in release of exatecan payload selectively in the TME, greatly increasing the therapeutic window and hence reducing systemic exposure and associated toxicities.

AVA6103 is a pre|CISION-enabled PDC that demonstrates FAP-dependent release of exatecan and kills cancer cells via a bystander mechanism. In multiple *in vivo* efficacy studies utilizing diverse cell and patient-derived models, AVA6103 achieved complete regressions and sustained, durable responses which remained until study termination. Biomarker assessment indicated on-target activity of the exatecan payload.

The PK profile of AVA6103 and released-exatecan were assessed in tumor-bearing mice, showing that released-exatecan levels in the plasma were undetectable after 4 hours, whereas in the tumor, released-exatecan persisted throughout the 5-day observation period of the study, indicating the potential for AVA6103 to deliver sustained exatecan to the tumor whilst minimizing systemic exposure of exatecan below clinically toxic levels.

To gain a greater understanding of patient populations that may be sensitive to AVA6103, co-expression of FAP and SLFN11, a gene linked to sensitivity to topoisomerase inhibitors, were evaluated using Tempus AI's LENS database. A positive correlation was observed between FAP and SLFN11 across multiple tumor types, further supporting the rationale for clinical development. Additional mechanistic studies demonstrated on-target activity and supported utility of AVA6103 in specific cancer indications to exploit genetic vulnerabilities.

This preclinical data package highlights the potential for AVA6103 to selectively target exatecan to the tumor microenvironment in a wide range of cancers. A Phase 1 dose escalation study designed to evaluate the safety, pharmacokinetics, and preliminary anti-tumor activity of AVA6103 in gastric, pancreatic, cervical and small cell lung cancers is anticipated to start in 1H 2026.

#5847 Development of a selective haem oxygenase-1 inhibitor for the immunotherapy treatment of cancer.

Emre Demirel[1], Alessia Marrocu[1], Meriem Bahri[2], Mark Laws[2], James N. Arnold[1], Khondaker Miraz Rahman[1]

[1]King's College London, London, United Kingdom,[2]University College London, London, United Kingdom

Immunotherapy has been hailed as a breakthrough for cancer therapy, however, only a fraction of patients respond in the clinic. The tumour microenvironment (TME) represents a major obstacle to the success of these treatments in solid tumours, of which, tumour-associated macrophages (TAMs) play a major role. A sub-population of perivascular TAMs express an enzyme called haem oxygenase-1 (HO-1), through which they have been demonstrated to subvert the anti-tumour response by immune suppression and exclusion of $CD8^+$ T cells. $HO\text{-}1^+$ TAM-containing tumours can therefore negate the immune-stimulating effects of chemotherapy to become treatment-resistant. Inhibiting HO-1 has been demonstrated to reverse this effect and re-sensitise tumours to immune-dependent cell death. However, there are no clinically available HO-1 inhibitors, and the current landscape of candidates suffer from undesirable pharmacokinetics and exhibit isoform promiscuity; blocking the activity of both HO-1 and the HO-2 isoform which maintains redox homeostasis in healthy tissues.This study has developed several novel, selective HO-1 inhibitors using a synthetic chemistry approach and validated activity with an *in vitro* microsomal system. We identified two lead compounds based on selectivity and potency for HO-1. A preliminary safety screen took place *in vitro* using non-malignant cells and confirmed a lack of general toxicity. Anti-tumour efficacy was evaluated *in vivo* using a murine model of fibrosarcoma, where administration of either lead HO-1 inhibitor synergised with standard-of-care chemotherapy to deliver durable tumour control and was associated with a re-invigorated lymphoid compartment. We utilised *in silico* modelling to predict lead compound pharmacokinetics, which are expected to be orally bioavailable. Unexpectedly, one of these candidates effectively penetrates the blood brain barrier, which is now under investigation for therapeutic utility in glioblastoma.

#5848 Targeting phosphodiesterase 10A by ADT-030 normalizes the tumor immune microenvironment by inhibiting RAS-MAPK signaling in both cancer cells and myeloid-derived suppressor cells.

Gazi Md Yeashin[1], Ogacheko David Okoko[1], Yan Ye[1], Xin Wang[1], Khalda Fadlalla[2], Adam Keeton[2], Yulia Maxuitenko[2], Xi Chen[2], Lynn Hedrick[1], Huidong Shi[1], **Gary A. Piazza**[2], Gang Zhou[1]

[1]Augusta University Medical Center, Augusta, GA,[2]Auburn University, Auburn, AL

Phosphodiesterase 10A (PDE10A), a cyclic nucleotide-degrading enzyme, is overexpressed in various human cancers. While PDE10A inhibition using small-molecule inhibitors or gene silencing suppresses tumor growth in xenograft models, its precise mechanism of action and immunological impact remain unclear. Here, we report that ADT-030, a novel PDE10A inhibitor, exhibits potent cytotoxicity against a broad range of murine tumor cell lines through suppression of RAS/MAPK signaling in both cancer cells and myeloid-derived suppressor cells (MDSCs). ADT-030 is orally bioavailable and effectively suppresses tumor growth in multiple syngeneic mouse models. Notably, its efficacy is significantly diminished in immunodeficient mice or upon CD8+ T cell depletion, highlighting a critical dependence on host immunity. The immunopotentiating effects of ADT-030 are further evidenced by its synergy with anti-PD-1 therapy, its ability to induce immunogenic tumor cell death and promote dendritic cell (DC) maturation in vitro, and its reliance on cDC1 to elicit antitumor effects in vivo. Comprehensive immune profiling in the 4T1 triple-negative breast cancer model, both in orthotopic and metastatic settings, revealed that ADT-030 selectively reduces tumor-associated neutrophils while restoring the presence and function of CD8+ T cells. These findings highlight PDE10A inhibition as a multi-faceted strategy that not only disrupts tumor-intrinsic oncogenic signaling but also reshapes the tumor immune microenvironment to unleash antitumor immunity.

#5849 Leveraging expression of tumor microenvironment GAGs to enhance platinum-based therapy in pancreatic adenocarcinoma.

Vashti L. Bandy[1], Erica Peterson[2], Nicholas P. Farrell[3], Jose G. Trevino[4], Praveen Bhoopathi[2], Vignesh Vudatha[2], Arunima Punjala[5], Dongyu Zhang[2], Jennifer Koblinski[2], Ada Beaudin[1], Thomas M. Clausen[2], Chunqing Guo[1], Larisa Litovchick[1], Nicholas Woods[6]

[1]VCU Massey Cancer Center, Richmond, VA,[2]Virginia Commonwealth University, Richmond, VA,[3]Professor, Dept. of Chemistry, Virginia Commonwealth University, Richmond, VA,[4]Div. of Surgical Oncology, VCU Massey Cancer Center, Richmond, VA,[5]Virginia Commonwealth University - VCU, Richmond, VA,[6]UNMC Eppley Institute, F&P Buffett Cancer Center, Omaha, NE

Pancreatic ductal adenocarcinoma (PDAC) is often diagnosed at an advanced stage, with most patients experiencing disease progression within 6-12 months following frontline FOLFIRINOX (5-fluorouracil, oxaliplatin, irinotecan, leucovorin), underscoring the need for more effective treatment strategies. Recent evidence suggests that overexpression of glycosaminoglycans (GAGs)—particularly chondroitin-4-sulfate (C4S)—contribute to the dense, fibrotic stroma characteristic of PDAC and tumor resistance to chemotherapy. C4S, a tumor-associated GAG linked to proteoglycans such as CD44, glypicans, and syndecans, is prominently expressed on the cell surface within the tumor stroma. Our studies demonstrate that C4S expression predicts PDAC tumor sensitivity to the Phase II polynuclear platinum agent, Triplatin (BBR3464). The highly cationic structure of Triplatin enhances its binding affinity for negatively charged GAGs, promoting drug accumulation and increased formation of platinum-DNA adducts. These findings provide a strong mechanistic rationale for re-evaluating Triplatin in tumors with high GAG expression, particularly C4S.

Our preliminary data shows that modulating GAG levels in PDAC cell lines alters both the cytotoxicity and cellular uptake of Triplatin. First, Triplatin exhibits greater cytotoxicity than oxaliplatin in the CHX1990 mouse cell line, an established model of PDAC derived from the Kras(G12D)/Trp53 null/Pdx1-cre (KPC) model. Second, a GAG-deficient CHX1990 cell line, B4GalT7 (CRISPR KO of β-1,4-galactosyltransferase 7), verified by reduced binding of the CS-binding peptide rVAR2-V5, shows a correlative loss in cytotoxicity. Finally, Triplatin significantly suppresses CHX1990 tumor growth *in vivo* with minimal changes in body weight relative to untreated controls. Collectively, these findings suggest that GAGs serve as a viable biomarker for Triplatin response in PDAC and may confer significant therapeutic advantage over oxaliplatin in this context.

To further support our studies, we are investigating Triplatin's mechanism of action through proteomic analyses that assess intracellular drug accumulation impacts on DNA repair proteins and apoptosis pathways. To complement this work, spatial transcriptomics will be used to map gene expression within the tumor microenvironment, providing insight into how Triplatin distribution corresponds with tumor cell responses. Additionally, synergy studies examining Triplatin in combination with standard-of-care therapies will help determine its therapeutic effectiveness. Together, these integrated approaches aim to advance Triplatin as a promising therapy for treatment of PDAC.

#5850 Novel platinum nanotherapeutics reprogram the tumor microenvironment to potentiate cancer immunotherapy.

Yongbin Liu[1], Xueying Ge[2], Busra Akay Hacan[1], Dongfang Yu[1], Junjun Zheng[3], Roderic I. Pettigrew[4], Ping-Ying Pan[3], Shu-Hsia Chen[3], Junhua Mai[5]

[1]Nanomedicine, Houston Methodist Academic Institute, Houston, TX,[2]School of Engineering Medicine/ENMED, Texas A&M University, Houston, TX,[3]Center for Immunotherapy Research, Houston Methodist Research Institute, Houston, TX,[4]School of Engineering Medicine, Texas A&M University, Houston, TX,[5]Houston Methodist Research Institute, Houston, TX

Background: Immune checkpoint inhibitors (ICIs)-based immunotherapy has transformed cancer treatment, but its efficacy is often limited by immune suppressive cells in the tumor microenvironment (TME), such as tumor-associated macrophages (TAMs). We recently developed a novel platinum therapeutic (carrier-Pt) that can induce cancer cell death through triggering rapid and robust intracellular reactive oxygen species (ROS) storm. Interestingly, ROS production was found to enhance anti-cancer immunity by inducing immunogenic cell death (ICD) and reprograming immunosuppressive TAMs. Thus, we aim to investigate its underlying mechanisms and potential synergy with immunotherapy.
Methods: CT26 and PyMT-N cells were inoculated into immunocompetent and immunodeficient nude mice, and tumor growth was compared. Immune cell populations were analyzed by imaging mass cytometry (IMC). CT26 cells were treated with carrier-Pt to assess ICD markers (CRT by flow cytometry, ATP by luminescence), while bone marrow-derived macrophages were evaluated for CD80/CD206 (flow cytometry) and TNF-α (ELISA). CT26 tumor-bearing mice received carrier-Pt alone or in combination with anti-PD-1 therapy, and tumor growth was monitored to evaluate therapeutic efficacy.
Results: Carrier-Pt at 4 mg(Pt)/kg significantly inhibited CT26 and PyMT-N tumor growth compared with the untreated group in both immunocompetent and immunodeficient nude mice ($P < 0.0001$). Notably, in immunocompetent mice, 3 out of 10 animals became tumor-free, whereas in immunodeficient nude mice, all tumors continued to grow, although at a slower rate, after carrier-Pt treatment. Carrier-Pt administration significantly increased the infiltration of $CD8^+$ T cells and macrophages in CT26 tumors ($P < 0.05$), with Pt signals predominantly enriched in macrophage and fibroblast populations within TME ($P<0.05$). Notably, carrier-Pt treatment also showed a trend toward increasing the frequency of $CD8^+PD\text{-}1^+$ T cells. M2 macrophages treated with carrier-Pt exhibited a marked upregulation of TNF-α and CD80 ($P < 0.0001$), indicating a shift toward the M1 phenotype. Additionally, CT26 cells exposed to carrier-Pt displayed elevated surface exposure of calreticulin and ATP release ($P < 0.0001$), indicative of ICD. Finally, the combination of carrier-Pt with anti-PD-1 therapy synergistically suppressed CT26 tumor growth compared with either treatment alone.
Conclusion: Carrier-Pt can reprogram the TME by repolarizing immunosuppressive TAMs toward an M1 phenotype and inducing ICD of tumor cells, thereby increasing $CD8^+$ T cell infiltration and enhancing the efficacy of anti-PD-1 immunotherapy. These findings position carrier-Pt as a promising nanotherapeutic to potentiate cancer immunotherapy.

#5851 (Common-light-chain-antibody+nano-body) × multi-matrix-immunization platform facilitates the development of antitumor multispecific antibody drugs.

Yi Gu, Xinde Liu, Peng Li, Feng He, **Feng Hao**, JInying Ning

Kyinno Biotechnology Co., LTD, Beijing, China

Multispecific antibodies represent one of the most advanced and promising therapeutic modalities in contemporary biopharmaceutical development. Among the various design strategies for multispecific antibody assembly, common light-chain(CLC) antibodies and nanobodies offer substantial advantages. They inherently avoid light-chain mispairing, thereby markedly reducing the complexity of subsequent process development. Kyinno's CLC mouse system is protected by global patent rights. Distinct from conventional approaches that introduce only partial heavy-chain germline elements into mice, Kyinno preserves the entire heavy-chain germline repertoire and pairs it with a fixed light-chain germline, which exhibits the highest compatibility with diverse heavy chains. This design minimizes the impact of genetic engineering on sequence diversity within the CLC system. For nanobody discovery, Kyinno operates a parallel system consisting of non-immunized alpaca and a heavy-chain-only mouse, ensuring both low off-target reactivity and high molecular diversity. In addition, Kyinno provides proprietary antigen optimization and immunization strategies that are particularly effective for challenging targets and the development of bispecific monoclonal antibodies. Thus, Kyinno's antibody library and antibody development services offer innovative solutions that overcome the limitations of traditional technologies, thereby accelerating the development of next-generation antibody therapeutics.

#5852 A novel CD33 and TRAIL-R2 targeting bispecific antibody to treat relapsed/refractory acute myeloid leukemia.

Shiva Bhowmik[1], William Brady[2], Kaitlyn Ko[1], Sheng Cai[3], William Grossman[3], Naval Daver[4], Jonathan Gerber[5], Herbert Kim Lyerly[6]

[1]Purdue University, West Lafayette, IN,[2]University of Washington, Seattle, WA,[3]Washington University, St. Louis, MO,[4]Leukemia, UT MD Anderson Cancer Center, Houston, TX,[5]John Hopkins University, Baltimore, MD,[6]Professor, Duke University (Columbus, OH), Durham, NC

Acute myeloid leukemia (AML) remains a challenging disease due to poor survival and high relapse rates as current therapies lack selectivity: cannot eradicate leukemic blasts without causing immune and hematopoietic toxicity, resulting in severe toxicities and low efficacy. Furthermore, current therapies such as hypomethylating agents (HMA) and venetoclax (Ven) fail in patients with TP53 mutations. There is a critical need for therapies that can selectively eliminate leukemic cells while sparing normal hematopoiesis.TRIO-863 is a first-in-class CD33 and TRAIL-R2 targeting bispecific antibody designed to trigger apoptosis selectively in AML blasts through dual engagement of CD33 and TRAIL-R2. By binding CD33 with high affinity and restricting TRAIL-R2 activation to CD33+ cells, TRIO-863 confines apoptotic signaling to leukemic cells minimizing off-target effects. Potency, selectivity, and mechanism of action were evaluated in AML cell lines, including high-risk TP53-mutant and HMA/Ven-refractory patient samples. Safety was assessed ex vivo using human liver microtissue and immune cells.TRIO-863 showed potent CD33-dependent killing of AML cells including high risk TP53-mutant and drug-resistant models, with over 3700-fold greater potency than Mylotarg. It synergized with HMA/Ven and eliminated blasts ex vivo from AML patients who are relapsed/refractory, heavily pre-treated, with unfavorable genetic mutations – including high risk biallelic TP53 mutations. TRIO-863 also exhibited statistically significant and dose-dependent inhibition of TP53-mutant leukemic cell growth in a xenograft model. Anti- leukemic activity of TRIO-863 *in vivo* requires dual engagement of CD33 and TRAIL-R2 suggesting TRIO-863 remains intact *in vivo* as a stable drug. CFU assays with non-leukemic CD34+ progenitors from healthy donors demonstrated TRIO-863 spared normal hematopoietic stem and progenitor cells. In contrast, Mylotarg, a CD33-targeting ADC currently approved for use in fit AML patients, killed non-leukemic hematopoietic progenitor cells. Ex vivo safety studies using primary human liver microtissues showed no liver toxicity by TRIO-863 in contrast to monospecific anti-TRAIL-R2 antibodies that showed high toxicity in the assay. Mechanistic studies confirmed apoptosis depends on dual engagement, overcoming resistance from TP53 inactivation and MCL1 upregulation. CD33 and TRAIL-R2 expression will serve as biomarkers for patient selection; analysis of blasts of AML patients exposed to Ven/HMA and 7+3 confirmed expression of the receptors.TRIO-863 represents a mechanistic breakthrough in AML therapy, selectively inducing apoptosis in malignant myeloid cells while preserving normal hematopoiesis. This approach addresses major limitations of current treatments. Clinical trials are planned for relapsed/refractory AML, including TP53-mutant and drug-resistant cases.

#5853 Bispecific and biparatopic antibodies targeting tumor-specific Tn-glycoepitopes on MUC1 and MUC4 enable broad, selective tumor coverage in epithelial cancers.

Nisha Shrestha, Boris Klebanov, Aaron C. Groen, Constantine Theodoropulos, Hans H. Wandall

GO Therapeutics, Natick, MA

Altered O-glycosylation in epithelial cancers generates tumor-specific Tn-glycoepitopes that are largely absent from normal tissues. Using advanced O-glycoproteomics, we have leveraged these neoepitopes to create a large suite of highly cancer-specific, humanized monoclonal antibodies targeting Tn-glycoepitopes in tumor-associated proteins. Here, we combine select Tn-targeting mAbs to develop two next-generation antibody-drug conjugates (ADCs): Tn-MUC1 biparatopic (M100A×M100B) and MUC1/MUC4 bispecific (M400×M100B) that broaden tumor coverage, increase avidity, while still maintaining the clean target profile with no reactivity to healthy tissue. Both designs were engineered as site-specific ADCs using an mc-vc-PAB-MMAE linker to generate homogeneous DAR2 conjugates. Biophysical analyses confirmed dual-epitope engagement and enhanced binding avidity: M100A×M100B bound two distinct Tn-MUC1 epitopes with sub-nanomolar affinity, mitigating epitope heterogeneity within MUC1, while M400 × M100B simultaneously recognized MUC1-Tn and MUC4-Tn, improving cross-mucin coverage in heterogeneous tumors. Immunohistochemistry demonstrated broad reactivity across breast, lung, ovarian, pancreatic, and gastrointestinal cancers with negligible binding to normal tissue. In vitro, both ADCs exhibited potent cytotoxicity against dual-positive tumor cell lines and sustained activity in mixed A+/B+ heterogeneity models. In vivo, M400 × M100B-vedotin and M100A × M100B-vedotin achieved tumor regressions comparable or superior to combinations of parental ADCs, while maintaining favorable tolerability in preclinical models. These data establish MUC1 and MUC4-targeted bispecific and biparatopic designs as powerful next-generation therapeutics for overcoming tumor heterogeneity and improving selectivity in solid tumors.

#5855 NECTIN4×PD-L1 bispecific antibody-drug conjugate integrating checkpoint blockade and targeted cytotoxicity for urothelial carcinoma and lung squamous cell carcinoma.

Kyoung-Ho Pyo[1], Seong-Hyun Park[1], Dongsop Lee[2], Haneol Kim[2], Younggyu Kong[2], Younggeun Lee[1], Hojin Yeom[1], Sowon Aum[1], Sun Hee Park[1], Huijo Oh[1], Cheyeon Kim[1], Hyeonseok Jin[2], Aera Lee[2], Hojeong Hong[2], Ju Hwan Kim[1], Hyungseok Choi[2], Mi-Kyung Kim[2], Taedong Han[1]

[1]AbTis Co., Ltd, Yongin, Korea, Republic of,[2]Dong-A ST Research Headquarter, Yongin, Korea, Republic of

Background: The first-line approval of enfortumab vedotin plus pembrolizumab validates the clinical rationale for combining ADCs with ICIs. However, administering two separate agents poses challenges in cost, compliance, toxicity management, and in achieving comprehensive coverage of target and immune heterogeneity. To address these limitations, we engineered a NECTIN4×PD-L1 bispecific ADC using Dong-A ST BsAb platform with an enhanced knob-into-hole (eKiH) interface that integrates NECTIN4-directed cytotoxic delivery with PD-L1 axis blockade in a single molecule. The molecule was designed to overcome resistance and spatial heterogeneity in locally advanced/metastatic urothelial carcinoma (la/mUC) and LUSC.
Methods: High-affinity NECTIN4 and PD-L1 antibody leads were identified and assembled into Dong-A ST BsAb platform. Site-selective conjugation was applied to generate ADCs bearing MMAE, exatecan, or dual-payload configurations. Functional characterization included: (i) binding affinity and competition to both targets, (ii) internalization and payload release in NECTIN4-positive cells, and (iii) PD-1/PD-L1 reporter assays and T-cell co-culture cytotoxicity. To support clinical translation, scRNA-seq and tissue microarray-based mIHC were performed on bladder cancer and LUSC cohorts to evaluate NECTIN4/PD-L1 co-expression, spatial heterogeneity, and correlations with immune infiltration and checkpoint pathways.
Results: scRNA-seq revealed intra-patient coexistence of NECTIN4-only, PD-L1-only, and co-expressing tumor subpopulations, with notable inter-patient variability. Multiplex IHC confirmed mosaic and cluster-type spatial heterogeneity. The bispecific ADC maintained high-affinity binding to both targets, exhibited efficient internalization and payload release in NECTIN4-positive cells, and preserved potent PD-1/PD-L1 blockade activity in reporter assays. ADCs carrying MMAE, exatecan, or dual payloads demonstrated consistent in vitro cytotoxicity across NECTIN4-high, PD-L1-high, and co-expressing tumor models, along with enhanced T cell-mediated tumor killing in co-culture. Preliminary in vivo studies showed dose-dependent tumor growth inhibition in bladder cancer and LUSC xenograft models with acceptable tolerability (detailed results pending final analysis).
Conclusions: This NECTIN4×PD-L1 bispecific ADC integrates targeted cytotoxicity (NECTIN4) and checkpoint blockade (PD-L1) into a single therapeutic agent, rationally designed to provide catch-all activity against target and immune microenvironment heterogeneity in la/mUC and LUSC. The preclinical data support evaluation as an early-line therapeutic strategy that could complement or substitute separate ADC+ICI combinations.

#5856 Hanjugator camptothecin platform: Effective, low-toxicity design maximizing antibody functionality and delivering potential best-in-class EGFR/cMet bispecific antibody-drug conjugate.

Rui Liu, Ge Song, Yushi Chi, Lingli Zhang, Fan Yang, Junjie Zhang, Boqi Gu, Chencheng Han, Xiayan Zhang, Wan-jen Yang, Xiaomu Cheng, Xiaoling Yuan, Yi Zhang, Zhiliang Lv, Qian Zou, Huixin Yan, Chen Hu, Jijun Yuan

Shanghai Henlius Biotech, Inc., Shanghai, China

Introduction: High toxin potency in antibody-drug conjugates (ADCs) limits clinical doses to those below optimal antibody levels, diminishing signal blockade potential and emphasizing chemotherapeutic effects. To address this limitation, we developed Hanjugator, a customizable, modular camptothecin-based linker-payload platform with tunable potency—from threefold lower than deruxtecan to comparable with exatecan—enabling a broader therapeutic window and preserving antibody functionality. We applied medium-potency payload to an EGFR/cMet bispecific ADC, a target combination known to require higher clinical doses for optimal receptor occupancy and efficacy.

Methods: Cytotoxicity of toxin candidates and ADCs was assessed via CellTiter-Glo (CTG) assay in immortalized cell lines. ADC binding and internalization were evaluated by flow cytometry on cells with varying antigen expression levels. Pharmacokinetics (PK) of LPA003-based ADC were determined in rats following single intravenous 5 mg/kg dosing. Bystander killing was quantified by co-incubating antigen-positive and -negative (Jurkat) cells, with Jurkat viability measured via CTG assay. *In vivo* efficacy of EGFR/cMet-LPA003 was tested in multiple xenograft models (LU387, SW48, HT29, NCI-H1975). For preliminary toxicology, cynomolgus monkeys were treated with three doses of 30 or 60 mg/kg of the test article, administered every three weeks (Q3W).

Results: The Hanjugator platform delivers a series of highly hydrophilic linker-payloads with excellent compatibility for non-standard, hydrophobic antibodies and superior thermal, plasma, and freeze-thaw stability. These conjugates exhibit bystander killing over 10-fold stronger compared with deruxtecan and outperform multiple clinical-stage linker-payload systems in efficacy studies, despite some competitors' higher intrinsic payload potency. The platform's wide toxin potency range broadens its applications. Medium-potency LPA003, conjugated to EGFR/cMet bispecific antibody, induced significant tumor regression at single 3 mg/kg doses in various xenograft models, outperforming AZD9592 in the HT29 CDX model. Preliminary toxicology shows EGFR/cMet-LPA003 is well tolerated in cynomolgus monkeys after 3 doses at 60 mg/kg Q3W.

Conclusion: We have developed Hanjugator, a versatile camptothecin-based linker-payload platform with tunable toxin potency. This modular design accommodates diverse targets and ADC programs, optimizing dosing regimens and broadening clinical applications. The LPA003-conjugated EGFR/cMet bispecific ADC exhibits a superior therapeutic index, maximizing antibody-mediated signaling blockade, and positions as best-in-class molecule with Investigational New Drug submission anticipated in Q1 2026.

#5857 LBL-054 TDC: A first-in-class CDH17 targeted T cell engager drug conjugate for the treatment of CDH17-positive gastrointestinal cancer.

Yang Ye, Yurong Qin, Xingxing Fang, Xiaoya Liu, Tingting Li, Chengze Ni, Peng Zhang, Chao Chu, Mi Ye, Huan Lin, Wanting Wang, Guojin Wu, Jianming Sun, Hui Yuwen, Yuanzhi Lv, Jing Guan, Min Chen, Yue Zhao, Jordan Zhu, Charles Cai, **Xiao Huang**, Xiaoqiang Kang, Hong Ling

Leads Biolabs Co., Ltd., Nanjing, China

Background: CDH17 is a member of the cadherin superfamily. In normal tissues, CDH17 is highly restricted to the lateral membrane and concealed within intestinal tight junctions, making it inaccessible to immune cell infiltration. In contrast, it is overexpressed and redistributed in 50% to 90% of gastrointestinal cancers, leading to its exposure on the cancer cell surface, therefore becoming more accessible. This unique feature makes CDH17 a promising target for T cell engagers or antibody-drug conjugates for GI cancer. Here, we have developed a novel T cell engager drug conjugate, LBL-054 TDC, targeting CDH17 and CD3 conjugated via our proprietary TOPiKinectics^{TM} linker-payload platform.

Methods: The binding and internalization activity of LBL-054 TDC to CDH17-expressing tumor cell lines and CD3+ T cells were assessed by flow cytometry. Cytotoxicity of LBL-054 TDC against tumor cells and T cells were assessed using Cell Counting-Lite Luminescent Cell Viability Assay kit. Cytotoxicity of LBL-054 TDC against tumor cell lines with varying endogenous expression levels of CDH17 were both evaluated in absence of T cells and in T cell dependent cellular cytotoxicity (TDCC) assay system. Bystander killing of LBL-054 TDC was performed in TDCC system by flow cytometry. The anti-tumor activity of LBL-054 TDC was evaluated in human CD3 transgenic mice bearing MC38/hCDH17 syngeneic model. The safety profile of LBL-054 TDC was evaluated in a cynomolgus monkey dose-range finding (DRF) study.

Results: LBL-054 TDC showed potent binding and internalization on tumor cells, but weak binding and no internalization on T cells. It demonstrated potent cytotoxicity against tumor cells, while has no cytotoxicity to naïve T cells. In TDCC assays, LBL-054 TDC induced potent cytotoxicity under various E:T ratios and CDH17 expression levels, along with lower cytokine release compared to conventional TCE. LBL-054 TDC also mediated potent bystander killing of CDH17^{neg} tumor cells while sparing T cells. In the MC38/hCDH17 syngeneic mouse model, LBL-054 TDC showed stronger anti-tumor effect than TCE and ADC. In a 4-week cynomolgus DRF study, LBL-054 TDC was well tolerated following repeated intravenous infusion.

Conclusions: Our results demonstrate that LBL-054 TDC combines the potent, direct killing of an ADC with the T-cell redirecting activity of a TCE both *in vitro* and *in vivo* while posing a lower cytokine release than a conventional TCE. It also exhibited good safety profiles in cynomolgus monkeys. Overall, LBL-054 TDC holds promise for treating gastrointestinal cancers with varying T-cell infiltration and CDH17 expression, potentially benefiting a broad patient population.

#5858 SCR-M030, an innovative and potential first-in-class trispecific T cell engager targeting PSMA and STEAP1 for mCRPC.

Changyan Chen, Yayuan Fu, Shumei You, Meijuan Gao, Kun Wang, Yi kuang, Chuanchuan Lu, Renhong Tang

State Key Laboratory of Neurology and Oncology Drug Development. Simcere Zaiming Pharmaceutical Co, Ltd., Shanghai, China

Metastatic castration-resistant prostate cancer (mCRPC) represents a highly aggressive and incurable disease, with limited therapeutic options and a dismal prognosis. Among the most promising molecular targets, prostate-specific membrane antigen (PSMA) and six-transmembrane epithelial antigen of the prostate 1 (STEAP1) are both markedly overexpressed in mCRPC, and their expression levels correlate positively with tumor aggressiveness and resistance to androgen-deprivation therapy. Notably, PSMA exhibits significant inter- and intratumoral heterogeneity, a factor that may underlie the heterogeneous clinical responses observed with PSMA-directed agents. In contrast, STEAP1 demonstrates a more uniform distribution across malignant cells, and its expression pattern partially complements that of PSMA in a subset of patients. Leveraging the complementary expression of STEAP1 and PSMA, we generated a first-in-class trispecific T-cell engager (TCE), SCR-M030, that concomitantly binds STEAP1 with high affinity, PSMA with moderate affinity, and CD3 with deliberately attenuated affinity. This avidity-optimized architecture drives preferential docking to double-positive tumor cells, conferring a marked binding advantage over single-target engagement. Functionally, SCR-M030 outperformed PSMA-CD3 and STEAP1-CD3 bispecific controls in vitro, eliciting superior lysis of medium-to-low antigen-expressing tumor cells while releasing minimal cytokines in target-negative conditions, forecasting a reduced risk of CRS. In PBMC-reconstituted prostate cancer xenograft mouse models, SCR-M030 demonstrated specific, dose-dependent antitumor activity. Notably, in the 22RV1 model, SCR-M030 exhibited more potent tumor suppression than the AMG509 analog. Finally, rat pharmacokinetic profiling revealed a long plasma half-life and full compatibility with both intravenous and subcutaneous dosing routes, supporting flexible clinical administration. In conclusion, the novel trispecific TCE SCR-M030 is a strategically designed therapy that demonstrates potent efficacy against challenging low-expression tumors by simultaneously targeting PSMA and STEAP1 with differential affinity. Its robust in vivo performance, favorable pharmacokinetics, and superiority over a relevant comparator underscore its strong potential as a next-generation therapeutic for prostate cancer.

#5859 Novel T cell engager targeting CD3 and CDH17 for the treatment of solid tumors.

Mingkun Zhang[1], Yuqiang Xu[1], Jun Wang[2], Jing Zhao[1]

[1]NeoMab Biotechnology Co,. Ltd, Suzhou, China,[2]GemPharmatech LLC., San Diego, CA

Background: Despite the success of T-cell engagers (TCEs) in hematologic cancers, their translation to solid tumors has been limited by key obstacles such as the immunosuppressive tumor microenvironment, inefficient T-cell trafficking, and antigen heterogeneity. The pursuit of suitable target antigens is therefore critical. Cadherin-17 (CDH17), which is highly expressed in many gastrointestinal malignancies but shows limited normal tissue expression, offers a compelling opportunity for next-generation TCE therapy.
Methods: A novel, bispecific T-cell engager (TCE) was engineered for concurrent binding to CD3 and cadherin-17 (CDH17). Its cytotoxic potency was quantified against a panel of CDH17-positive human cancer cell lines in co-culture assays with healthy donor peripheral blood mononuclear cells (PBMCs). T-cell activation (CD69+/CD25+ upregulation) and cytokine secretion were profiled by flow cytometry and immunoassay, respectively. In vivo antitumor efficacy was evaluated in immunodeficient mice bearing CDH17-positive gastric cancer cell-derived xenografts (CDX).
Results: The CDH17xCD3 T cell engager exhibited high-affinity binding to CDH17, coupled with a modulated affinity for CD3. *In vitro*, the molecule induced potent and specific lysis of CDH17-positive tumor cells in a dose-dependent manner, while sparing CDH17-negative controls. This targeted cytotoxicity was accompanied by a reduced cytokine release profile compared to a conventional CD3-engaging benchmark, *In vivo*, our TCE treatment led to enhanced tumor growth inhibition and marked regression in CDH17-high CDX models, with no significant systemic toxicity observed at efficacious doses.
Conclusion: The novel CDH17xCD3 bispecific T-cell engager exhibits potent and targeted anti-tumor activity, supporting its translational potential as an immunotherapeutic agent for CDH17-positive solid tumors. The favorable efficacy and safety profile observed warrants further clinical investigation.

: Tyrosine Kinase, Phosphatase, and Other Inhibitors
Poster Session

#5863 Enhanced antitumor activity of zipalertinib and amivantamab combination in EGFR mutant NSCLC models.

Kohei Hayashi, Yoshimi Aoyagi, Akihiro Hashimoto, Tomoaki Hitotsumachi, Shuichi Ohkubo

Taiho Pharmaceutical Co., Ltd., Tsukuba, Japan

Zipalertinib is a selective epidermal growth factor receptor (EGFR) tyrosine kinase inhibitor (TKI) that targets mutations in exon 20 insertions (ex20ins) and has demonstrated clinical efficacy in patients with EGFR ex20ins-positive non-small cell lung cancer (NSCLC), including those previously treated with amivantamab and chemotherapy. Currently, amivantamab plus platinum-based chemotherapy is the standard first-line treatment for NSCLC harboring EGFR ex20ins. However, efficacy of EGFR-TKIs combined with amivantamab in EGFR ex20ins positive patient remains unclear. In this preclinical study, we aimed to investigate the therapeutic potential of zipalertinib and amivantamab combination therapy.
EGFR mutant cell lines NCI-H1975, H1975insSVD (EGFR D770_N771insSVD), II-18 (EGFR L858R), and HCC827OR8 (EGFR del19 with MET amplification) were used for in vitro and in vivo experiments. The binding of amivantamab to the cell surface was quantified in the presence or absence of zipalertinib. An antibody-dependent cellular cytotoxicity (ADCC) assay was conducted using H1975insSVD cells cocultured with peripheral blood mononuclear cells (PBMCs) to assess amivantamab-mediated cytotoxicity with or without zipalertinib treatment. In vivo antitumor efficacy was evaluated using human cell-derived xenograft (CDX) mouse models, and tumor volumes were analyzed for statistical significance using the Aspin-Welch's t-test.
Zipalertinib treatment increased EGFR protein expression and enhanced amivantamab binding to the cell surface. Amivantamab induced ADCC in H1975insSVD cells cocultured with PBMCs, and zipalertinib co-treatment further potentiated this cytotoxicity. Additionally, compared to zipalertinib monotherapy, the combination of zipalertinib and amivantamab exhibited significant antitumor efficacy ($p < 0.05$) across all three CDX models, without notable changes in body weight. Complete tumor regression was observed in the H1975insSVD CDX model.
Zipalertinib upregulates EGFR protein expression and enhances amivantamab binding to the cell surface. These results provide mechanistic insights into the observed combinatorial efficacy of zipalertinib and amivantamab, both in vitro and in vivo. Further, our findings support the therapeutic potential of zipalertinib and amivantamab in EGFR-mutant NSCLC and further clinical investigations.

#5864 Taletrectinib, a next generation selective ROS1 inhibitor, demonstrates a differentiated profile in ROS1 fusion models.

Hitisha Patel, Laura Heller, Kevin Bowman, Zheyi Hu, Irma M. Grossi, Max Pan, Gary Hattersley

Nuvation Bio Inc., New York, NY

ROS1 fusions, present in approximately 2% of non-small cell lung cancer (NSCLC) patients, drive cancer cell growth and survival. FDA-approved tyrosine kinase inhibitors (TKI) for ROS1 fusion positive NSCLC include crizotinib, entrectinib, repotrectinib, and more recently, taletrectinib. However, resistance mechanisms such as secondary kinase-domain mutations (e.g., ROS1-G2032R) limit the efficacy of crizotinib and entrectinib, while repotrectinib can cause central nervous system (CNS) adverse reactions including dizziness, ataxia and cognitive impairment, attributed to the inhibition of tropomyosin receptor kinase B, TRKB. Taletrectinib is a potent, CNS-active, selective, next-generation ROS1 inhibitor for the treatment of patients with locally advanced or metastatic ROS1-positive NSCLC. Taletrectinib is currently approved by the US FDA and is also approved in China and Japan. As of Jun 7, 2024, pooled results from the TRUST-I and TRUST-II studies of taletrectinib demonstrated a confirmed objective response rate (cORR) of 88.8%, an intracranial cORR of 76.5%, a median duration of response (mDOR) of 44.2 months and a median progression free survival (mPFS) of 45.6 months in patients with advanced ROS1-positive NSCLC that have not previously received a ROS1 TKI. Durable responses were also reported in patients who had previously been treated with a TKI (Pérol M, et al. *J Clin Oncol*. 2025). Herein, we describe taletrectinib and its differentiated profile in comparison to other approved ROS1 inhibitors. At clinically relevant concentrations, taletrectinib demonstrated complete inhibition of ROS1 wild type and ROS1 G2032R in vitro and inhibited the growth of cell lines harboring single and double mutations in ROS1. Mechanistic studies revealed that taletrectinib inhibited the expression of key markers associated with the epithelial to mesenchymal transition (EMT) pathway and inhibited the migration of lung cancer cells indicating that taletrectinib could potentially inhibit the invasive capacity of lung cancer cells. Taletrectinib treatment also induced tumor regressions in several *in vivo* ROS1 fusion models, regardless of the fusion partner. In summary, our nonclinical data demonstrate that, at clinically relevant concentrations, taletrectinib exhibits activity in ROS1 wild-type and mutant-driven cancers and has a distinct profile that addresses the unmet needs of ROS1-positive NSCLC patients.

#5865 Developing COUPLrs, dual-warhead cysteine-reactive compounds, to target oncoproteins through interaction modulation and degradation.

Diane Yang[1], Stefan Andrew Harry[2], Harrison Byron Chong[2], Edwin Zhang[1], Natalie Shannon Nordenfelt[1], Stefan Kaluziak[1], Elizabeth Codd[1], Nicholas Chen[2], Samay Trivedi[2], Wenxin Yang[1], Abigail Elizabeth Smith[2], Alexander Daniel Carlin[2], Dawn R. Mitchell[1], Neha Khandelwal[2], Brian B. Liau[3], Liron Bar-Peled[2], A. John Iafrate[1]

[1]Department of Pathology, Massachusetts General Hospital, Boston, MA,[2]Krantz Family Center for Cancer Research, Massachusetts General Hospital,, Boston, MA,[3]Harvard University, Cambridge, MA

COUPLrs (COvalent Protein Ligators) are cysteine-reactive small molecules designed to dimerize or disrupt protein complexes, thereby modulating protein function. In our previous work, we identified COUPLrs that bind to the oncogenic fusion protein EML4-ALK in non-small cell lung cancer (NSCLC) cells. These compounds engaged the EML4 rather than the ALK kinase domain targeted by clinical inhibitors. This unconventional binding disrupted ALK signaling and induced proteasome-dependent degradation of the fusion protein, establishing proof of concept that COUPLrs can engage two protein partners simultaneously, altering their interactions and stability. These findings define COUPLrs as a new mechanistic class of molecules capable of bridging or disrupting protein complexes and driving selective degradation, offering opportunities to target proteins lacking conventional binding pockets.To systematically characterize COUPLrs' targets and interaction networks, we employed a two-pronged workflow combining Cysteine Druggability Mapping to identify reactive and accessible cysteine residues across oncogenic proteins, while SDS-PAGE and fractionation assays monitored changes in molecular weight, revealing COUPLr-involved protein complex formation. We synthesized a 32-member library of cysteine-reactive compounds with diverse scaffolds, warheads, and reactivities. Library characterization revealed proteome-wide COUPLr targets, including inter- and intramolecular protein coupling.To expand this analysis, we conducted a proteomic screen across 13 cancer cell lines representing diverse tissue origins, generating a comprehensive atlas of COUPLrs-targetable proteins. This screen revealed both shared and lineage-specific targets, including several proteins previously considered undruggable, such as transcription factors. Notably, some protein showed mutation-specific engagement by COUPLrs, suggesting potential to selectively target oncogenic variants resistant to existing therapies.Collectively, our work establishes COUPLrs as powerful tools for modulating protein-protein interactions. By integrating covalent chemistry with proteomic profiling, we delineated protein interactions stabilized or disrupted by COUPLrs. These findings open new avenues for therapeutic development against previously inaccessible targets in cancer biology.

#5866 Preclinical combination approaches with the pan-KRAS inhibitor AMG 410 in *KRAS*-mutant cancers.

Ying-Chu Chen[1], Tao Osgood[1], Kevin Gaida[1], Gilbert Diaz[1], Chun Su[2], Elissa Swearingen[2], Daniel Lu[2], Deanna Mohn[1], Anne Y. Saiki[1], Monica Leavitt[1], Upendra P. Dahal[2], Ryan P. Wurz[1], Brian A. Lanman[1], Jason DeVoss[2], Karen Rex[1], Paul E. Hughes[1], Rati Verma[1]

[1]Amgen, Thousand Oaks, CA,[2]Amgen, South San Francisco, CA

KRAS is the most frequently mutated oncogene in solid tumors. Covalent KRAS G12C-selective inhibitors have been approved for G12C-mutant non-small cell lung cancer (NSCLC). Despite their clinical success, the durability of response and emergence of resistance have tempered the efficacy of KRAS-targeted therapies, leading to the exploration of combination strategies to enhance clinical outcomes. AMG 410, currently in Phase 1, is a reversible pan-KRAS inhibitor capable of targeting KRAS mutants (e.g., G12D, G12V, and G12C) and wild-type amplification. These altered *KRAS* alleles are prevalent in multiple solid tumor indications, particularly colorectal cancer (CRC), pancreatic ductal adenocarcinoma (PDAC), and NSCLC. Preclinically, AMG 410 demonstrated significant tumor growth inhibition as a single agent in multiple cell line-derived xenograft (CDX) and patient-derived xenograft (PDX) models. Guided by reverse translation findings from the G12C-selective inhibitor sotorasib, we evaluated AMG 410 combination approaches in preclinical models to proactively mitigate potential primary and acquired resistance mechanisms. A large panel of diverse *KRAS*-mutant cancer cell lines representing three indications (NSCLC, CRC, and PDAC) was screened in combination with inhibitors of the RAS signaling pathway, DNA damage repair pathways, cell cycle regulators, and select chemotherapy agents. Robust synergistic effects on cell viability were observed with pan-HER kinase and PI3K/mTOR inhibitors. To further explore resistance mechanisms, an AMG 410-anchored genome-wide CRISPR screen was performed. The Hippo pathway and *YAP1* were identified as key modifiers of response to KRAS inhibition. Co-treatment with YAP/TEAD inhibitors demonstrated strong synergy in multiple *KRAS*-mutant cell lines. To assess whether these observations translated to improved efficacy in vivo, rational combinations were evaluated in tumor xenograft models. Consistent with the in vitro synergy observed with pan-HER inhibition, the combination of AMG 410 with panitumumab resulted in tumor regression in a CRC PDX model. Additionally, enhanced anti-tumor activity was observed when AMG 410 was combined with chemotherapy agents in CRC and PDAC xenografts. Building on the potential benefit of clinical KRAS G12C immune-oncology combinations, treatment with AMG 410 and PD-1 blockade in a *KRAS* G12D syngeneic CRC model led to tumor regression and significantly enhanced survival. Finally, co-treatment with a TEAD inhibitor enhanced durability of response to AMG 410 in vivo. Taken together, these findings support the clinical investigation of AMG 410 combination strategies to extend the therapeutic benefit of KRAS inhibition across diverse *KRAS*-mutant cancers.

#5867 IN10028, a next-generation FAK inhibitor discovered for the treatment of solid tumors.

Baoyuan Zhang[1], Hao Wang[2], Jiaming Gao[1], Fengmin Xi[1], Liyuan Liu[1], Leo Liu[1], Zaiqi Wang[1]

[1]Inxmed (Shanghai) Co., Ltd, Shanghai, China,[2]Pharmablock Sciences (Nanjing), Inc, Nanjing, China

The development of small-molecule inhibitors targeting Focal Adhesion Kinase (FAK) has been ongoing for several decades. In May 2025, the FDA approved a combination therapy involving FAK and MEK/RAF inhibitors for the treatment of low-grade serous ovarian cancer, marking a significant advancement in FAK-targeted therapies. In this study, we present IN10028, a second-generation FAK inhibitor that demonstrates enhanced efficacy in combination therapies and favorable safety profiles. IN10028 effectively targets both FAK1 and FAK2, exhibiting IC50 values of 0.2 nM and 60.1 nM, respectively, and significantly inhibits FAK-related signaling pathways. Compared to IN10018, a first-generation FAK inhibitor, IN10028 shows superior cancer cell cytotoxicity. Notably, IN10028 also demonstrates stronger target engagement than several first-generation FAK inhibitors. Through experiments conducted in animal models, IN10028 was evaluated in both monotherapy and combination therapy settings, consistently outperforming multiple first-generation FAK inhibitors in terms of tumor growth inhibition. Additionally, pharmacokinetic and toxicity studies necessary for Investigational New Drug (IND) filing have been completed, with the IND application anticipated in December 2025.

#5868 Proteomic analysis and efficacy evaluation reveal strong synergistic anti-leukemic activity of lasmotinib combined with menin inhibitors for AML.

An-Na Moon, Hee-sun Hwang, **Ky-Youb Nam**, KyungMin Cha, Sang Beom Lee, ChongChul Chai, Jinsun Kwon, Kyu-Tae Kim, June H. Han, Jeong Hyeok Yoon

Pharos iBio Co., Ltd., Anyang, Korea, Republic of

Acute myeloid leukemia (AML) is a genetically heterogeneous hematologic malignancy. The interaction between menin (*MEN1*) and mixed lineage leukemia 1 (*MLL1*, also known as *KMT2A*) is a critical dependency for KMT2A-rearranged (*KMT2A*-r*)* or nucleophosmin 1 (*NPM1*)-mutant AML, providing a strong rationale for therapeutic targeting. Here, we evaluated a novel combination strategy using lasmotinib (PHI-101), a clinical-stage FLT3 inhibitor, together with menin inhibitors that disrupt the menin-MLL interaction. To investigate synergy in leukemic cells harboring *FLT3*-Internal Tandem Duplication (ITD) mutation and *KMT2A*-r, MV4-11 and MOLM-13 cells were co-treated with lasmotinib and multiple clinical-stage menin inhibitors. Cell viability was assessed using the CellTiter-Glo assay, and the drug interaction profiles were quantified with SynergyFinder. Mechanistic studies of the lasmotinib-bleximenib combination in MV4-11 cells were conducted by Astral-based global proteomics, immunoblotting, and flow cytometry. *In vivo* efficacy of the combination was assessed using a mouse xenograft model of AML. The single-agent treatment with lasmotinib potently suppressed the growth of three AML cells (MV4-11, MOLM-13, and MOLM-14) bearing *FLT3*-ITD mutations, with IC_{50} values from 0.5 nM to 3 nM. Among five menin inhibitors, bleximenib induced strong cytotoxicity against three *KMT2A*-r AML cells, including MV4-11, MOLM-13, and MOLM-14, with IC_{50} values from 3 nM to 23 nM. After the drug combination, lasmotinib enhanced and accelerated the anti-leukemic effects of menin inhibitor bleximenib in both MV4-11 and MOLM-13 cells. SynergyFinder analysis demonstrated strong synergism across multiple menin inhibitors, with high synergy scores (>20) even at low drug concentrations. Global proteomics revealed that the lasmotinib-bleximenib combination substantially reduced expression of key AML oncogenic proteins including MEIS1, FLT3 and c-Myc. Immunoblotting confirmed complete suppression of downstream signaling pathways including p-FLT3, p-STAT5, p-AKT, and p-ERK, while Annexin V/PI flow cytometry analysis showed profoundly increased apoptosis. *In vivo*, combined lasmotinib and bleximenib treatment resulted in markedly synergistic anti-tumor effects. In conclusion, lasmotinib is identified as a highly promising combination partner for menin inhibitors in AML. The strong synergism observed, both in vitro and in vivo, supports further development of lasmotinib plus bleximenib as a compelling therapeutic strategy for *KMT2A-r* and FLT3 mutant leukemia.

#5869 Preclinical characterization of CGT4255, an EGFR sparing, pan-mutant HER2 clinical development candidate with potential best-in-class brain penetration.

Paul Larsen, Tanna Bettendorf, Abiezer Blandon, Karyn Bouhana, Richard K. Brizendine, Eric Brown, LouAnn Cable, Mark J. Chicarelli, Michelle Crow, Brad Fell, John Fischer, Jennifer Fulton, Anna Guarnieri, Jackie Harrison, Leyla Haygood, Ravi Jalluri, Vijay Kumar, Cori A. Malinky, Maralee McVean, Rob Rieger, John Robinson, Lee Stunkard, Francis Sullivan, John I. Trujillo, Logan E. Vine, Shannon Winski, Yeyun Zhou

Cogent Biosciences, Inc, Boulder, CO

HER2 alterations including amplification, overexpression, insertions, and point mutations are established oncogenic drivers across various solid tumor types. HER2 is amplified or overexpressed in 15-20% of breast cancer patients. In contrast, activating mutations are found in approximately 4% of cases with the L755S mutation commonly associated with drug resistance. Up to 50% of patients with HER2+ metastatic breast cancer may develop brain metastasis over the course of the disease, highlighting a critical need for brain penetrant HER2-directed therapies. In lung cancer, activating HER2 mutations occur in 2-4% of advanced cases and are linked to increased incidence of brain metastasis. The risk is especially high in patients whose tumors harbor an exon 20 YVMA insertion. Treating brain metastasis in this group of patients remains a clinical challenge, as most therapeutic options have limited CNS penetration. Herein, we describe the advanced preclinical profiling of CGT4255, an investigational drug targeting mutant and wild type HER2, which spares EGFR and demonstrates potential best-in-class brain penetrance. CGT4255 shows potent activity against commonly occurring point mutations such as L755S and exon 20 YVMA insertions. In vitro assays confirmed that CGT4255 is not a substrate of the P-gp or BCRP efflux transporters at the blood-brain barrier. In vivo pharmacokinetic studies with CGT4255 in mice and monkeys showed high drug levels in the CNS, predicting high human brain exposure. CGT4255 demonstrated robust efficacy in HER2 overexpressed and HER2 YVMA intracranial models. The CGT4255 and T-DXd combination demonstrated enhancement of ADC internalization, thus highlighting a biological rationale for combination therapy. In HER2-overexpressed, L755S, YVMA, and T-DXd resistant subcutaneous xenografts, CGT4255 demonstrated dose dependent TGI with tumor regressions observed at dose levels as low as 30 mg/kg.

#5870 Momelotinib: Unique polypharmacology and novel combination strategies for myelofibrosis and beyond.

Shane O'Brien[1], Shannon McKearnan[1], Ashley Lento[1], Jeffrey Guss[1], Anna Waszkiewicz[1], Bin Wu[1], Allison Hartman[1], Matthew Powell[1], Gabriella Cifelli[1], Maggie Connelly[1], Hoang Tran[1], Bryan Strouse[1], Dwaipayan Patnaik[2], Mary Antonysamy[1], Anthony Mazurek[1], Michael T. McCabe[1]

[1]GSK, Collegeville, PA,[2]GSK, Baar Onyx, Switzerland

Momelotinib (Ojjaara / Omjjara) is a clinically differentiated JAK inhibitor that improves key manifestations of myelofibrosis (MF), including anemia, splenomegaly, and constitutional symptoms. Its efficacy stems from dual inhibition of JAK1/JAK2, addressing pro-inflammatory signaling, and targeting Activin A Receptor Type I (ACVR1/ALK2), which alleviates anemia by suppressing hepcidin expression, increasing iron bioavailability, and improving red blood cell production. Herein, we report comprehensive profiling of momelotinib's kinome selectivity revealing a distinctive polypharmacology beyond ACVR1 that includes inhibition of rho-associated kinases (ROCK1/ROCK2), inhibitor of NF-κB kinases (IKKs), and interleukin-1 receptor-associated kinase 1 (IRAK1). Cellular reporter assays demonstrated that this unique profile enables momelotinib to inhibit NF-kB activity stimulated by either canonical or non-canonical pro-inflammatory cytokines. These findings establish a strong rationale for momelotinib's therapeutic potential beyond MF in pro-inflammatory conditions, such as Vacuoles E1 X-chromosome Autoinflammatory Somatic (VEXAS) syndrome, low-risk myelodysplastic syndrome (LR-MDS), and graft-versus-host disease (GvHD), where these pathways are significantly dysregulated and medical need remains high. Additionally, recognizing momelotinib's differentiated clinical benefit and well-characterized safety profile, drug combination screening was performed to identify combination partners that cooperate with momelotinib to further improve MF patient outcomes. Specifically, two high-throughput drug screens targeting malignant cell viability in $JAK2^{V617F}$ or MPL^{W515L} MF models and hepcidin suppression in a BMP6-stimulated liver cell line were conducted with over 650 small molecules in late-stage clinical development. The viability screen identified inhibitors of signaling pathways that function in parallel to JAK-STAT as promising combination partners to reduce the viability of malignant MF cells. The hepcidin screen identified inhibitors that cooperated with momelotinib to additively suppress hepcidin expression. Notably, the XPO1 inhibitor selinexor emerged as a combination partner that both inhibited malignant cell growth and deepened hepcidin suppression. These discoveries highlight momelotinib's unique activity, both as a monotherapy for expanded indications and as an ideal combination partner to more effectively control anemia and halt disease progression in MF patients.

#5871 Discovery and characterization of firmonertinib, a novel EGFR inhibitor with broad activity against both EGFR classical and exon 20 insertion mutations.

Huibing Luo[1], Qing Li[1], Qiufeng Liu[1], Huayong Zhou[1], Yuting Sun[1], Jerry Y. Hsu[2], Luna Musib[2], Marcin Kowanetz[2], Stuart Lutzker[2], **Zineb Mounir**[2]

[1]Allist Pharmaceuticals, Shanghai, China,[2]ArriVent Biopharma, Burlingame, CA

Background: Lung cancers harboring classical *EGFR* mutations are sensitive to approved EGFR tyrosine kinase inhibitors (TKIs) while those harboring *EGFR* exon 20 insertion mutations (ex20ins) show minimal sensitivity to approved EGFR TKIs and have limited treatment options. Firmonertinib is an investigational novel orally bioavailable and highly brain-penetrant irreversible EGFR TKI targeting classical and uncommon *EGFR* mutations including ex20ins. Firmonertinib received FDA Breakthrough Therapy Designation for first-line treatment of patients with advanced NSCLC with *EGFR* ex20ins mutations, and has now completed enrollment in a global phase 3 trial in these patients (NCT05607550). Here, we describe the structural and preclinical findings supporting the binding potency and anti-tumor activity of firmonertinib in *EGFR* ex20ins mutations.

Methods & Results: Using high resolution crystal structures, we uncover a unique structural attribute that differentiates firmonertinib from other EGFR TKIs and that provides firmonertinib with superior binding to mutant EGFR proteins including those harboring ex20ins. Our biochemical and cellular assay findings are in line with the structural observations and demonstrate that firmonertinib is a potent and mutant selective EGFR inhibitor. In a large cell line panel evaluating *EGFR* ex20ins mutations within different regions of exon 20 (far and near loop, helical domain), all ex20ins mutations evaluated demonstrated a high sensitivity profile to firmonertinib compared to other EGFR TKIs. In addition, firmonertinib was equally highly potent against far and near loop insertion mutations which is a differentiating characteristic from some EGFR TKIs previously tested in the clinic (Elamin et al. 2022). In animal models, our findings demonstrate that firmonertinib is a highly potent inhibitor of cell proliferation in tumors harboring both near and far loop *EGFR* ex20ins mutations.

Conclusions: Findings from this study support the structural mechanism of EGFR binding and inhibition by firmonertinib, eliciting strong anti-tumor activity in multiple *in vitro* and *in vivo* models harboring *EGFR* ex20ins mutations. These findings provide scientific support for the ongoing global Phase 3 study for first-line NSCLC patients with *EGFR* ex20ins mutations (NCT05607550).

#5872 CLK inhibitor BH-30236 synergizes with venetoclax in anti-leukemia activity via splicing modulation in preclinical AML and CLL models.

Wei Deng, Ping Jiang, Zhenping Wang, Yue Hu, Nancy Ling, Danan Li, Joshua Choi, Eugene Y. Rui, Zachary Zimmerman, Geoffrey Oxnard, J. Jean Cui

BlossomHill Therapeutics, Inc., San Diego, CA

Alterations of splicing patterns are increasingly recognized as a hallmark of cancer by promoting proliferation, evading apoptosis, changing cell signaling, and driving drug resistance through aberrantly spliced isoforms. In hematologic malignancies of both myeloid and lymphoid lineages, including myelodysplastic syndromes (MDS), acute myeloid leukemia (AML), and chronic lymphocytic leukemia (CLL), frequent mutations or overexpression of RNA splicing factors are associated with aberrant alternative splicing. CDC-like kinases (CLKs) regulate alternative splicing by phosphorylating serine/arginine-rich splicing factors (SRSFs) which are essential for splice site recognition and spliceosome assembly. Thus, targeting CLKs represents a promising therapeutic strategy, especially in hematologic malignancies with splicing dysregulation. BH-30236 is a novel, potent, orally bioavailable, ATP-competitive, small molecule kinase inhibitor of CLK1/2/4. BH-30236 inhibited the phosphorylation of SRSFs in cancer cells, leading to modulation of splicing patterns and RNA/protein expression of genes related to apoptosis and DNA damage response pathways, thereby promoting apoptosis. In addition, the expression of stem cell markers was downregulated by BH-30236 in AML cell lines. BH-30236 effectively inhibited the proliferation of hematologic cancer cell lines or leukemia cells from AML or CLL patients. In addition, effective anti-tumor activity of BH-30236 was observed in tumor models derived from AML cell lines or leukemia patients. A synergistic anti-cell proliferation effect between BH-30236 and venetoclax, a BCL2 inhibitor, was consistently observed across multiple hematologic cancer cell lines of diverse lineages. The synergy is likely driven by BH-30236 mediated suppression of anti-apoptotic and pro-survival proteins including MCL1, a pro-survival factor whose upregulation is associated with resistance to venetoclax. Moreover, the combination of BH-30236 and venetoclax synergistically induced complete tumor regression in the highly resistant MOLM13 cell-derived xenograft tumor model. This in vivo synergistic effect was observed even when BH-30236 or venetoclax was administered at low dose levels. Notably, modification of combinatory treatment regimen after achieving complete tumor regression to single agent BH-30236 treatment sustained tumor-free survival in mice and maintained tumor free for more than 80 days, even after treatment discontinuation. This finding is consistent with BH-30236 modulation of leukemia stem cells via regulation of alternative splicing. BH-30236 is currently under clinical investigation, either as a single agent or in combination with venetoclax, in adults with relapsed or refractory AML or higher risk MDS in a Phase 1/1b clinical trial (NCT06501196).

#5873 OB-001 boost the brain penetration of multiple TKIs.

Hitesh Mistry, **Jim Millen**, Josh Fleet, Mark Brimble

OncoBayesAlpha Ltd., London, United Kingdom

Background: Osimertinib, Adagrasib, Tucatinib, Mobocertinib and Lorlatinib all demonstrate clinically meaningful CNS activity across numerous cancer types. However, all four agents show incomplete and variable CNS penetration, with reported CSF:plasma or Kp,uu values typically well below unity, largely due to ABCB1/ABCG2 efflux at the blood-brain barrier. OB-001 is a novel KinetiSol amorphous solid dispersion first-in-class efflux transporter inhibitor. We evaluated whether OB-001 can selectively enhance the brain distribution of kinase inhibitors.
Methods: Male CD-1 mice received one of oral Osimertinib, Adagrasib, Tucatinib, Mobocertinib and Lorlatinib following 2-h pretreatment with vehicle or OB-001 (10 mg/kg). Plasma and perfused-brain concentrations were quantified to 24 h by LC-MS/MS. Pharmacokinetic parameters were derived by noncompartmental analysis, and fold-changes in area under the curve (AUC) between brain and plasma were compared.
Results: OB-001 led to a 4, 33, 5, 11 and 4 -fold increase in Brain AUC for Osimertinib, Adagrasib, Tucatinib, Mobocertinib and Lorlatinib respectively. No change in plasma AUC was observed for Osimertinib and Adagrasib with less than 2-fold increase obserevd for Tucatinib, Mobocertinib and Lorlatinb.
Conclusions: OB-001 selectively boosts brain exposure without substantially increasing systemic exposure. These data demonstrate that theoretically a pharmacokinetic window can be achevied with OB-001 whereby enhanced brain metatsases efficacy could be acheived for numerous kinase inhibitors without effecting systemic toxicity. These findings support OB-001 as a first-in-class CNS-targeted efflux modulating adjunct capable of elevating brain drug exposure beyond what is achievable by existing kinase inhibitors alone. OB-001 has strong translational rationale for combination development with Osimertinib, Adagrasib, Tucatinib, Mobocertinib and Lorlatinib—to further extend CNS disease control in numerous cancer types.

#5875 Multikinase inhibitor olverembatinib (HQP1351) is efficacious and synergizes with BTK inhibitor acalabrutinib in mantle cell lymphoma (MCL) preclinical models.

Bo Peng[1], Zhiyan Liang[2], Yan Xiong[1], Bingxing Wu[1], Shujie He[1], Zhou Yu[1], Guoqin Zhai[1], Dajun Yang[1], Yifan Zhai[2]

[1]Ascentage Pharma (Suzhou) Co., Ltd., Suzhou, China,[2]Ascentage Pharma Group Inc., Rockville, MD

Background: MCL is a rare, aggressive type of non-Hodgkin lymphoma. Although Bruton tyrosine kinase (BTK) inhibitors have transformed MCL treatment, response to monotherapy is limited, and efforts are underway to develop combination therapies. Olverembatinib, an investigational multikinase inhibitor (approved in China for chronic myeloid leukemia), inhibits Src-family kinase Lyn, which is essential for B-cell receptor (BCR) signaling and B-cell proliferation, differentiation, and activation. Hypothesizing that dual inhibition of Lyn and BTK pathways enhances antitumor effects, we evaluated olverembatinib combined with acalabrutinib in preclinical MCL models and explored potential mechanisms of action (MOAs).

Methods: MCL cell lines Mino and Rec-1 were selected for *in vitro* growth inhibition assessments. CellTiter-Glo® assays were conducted to evaluate antiproliferative activity. Apoptosis and cell cycle arrest were assayed by flow cytometry. MOAs were examined by tyrosine phosphoproteomic analysis and confirmed by western blotting. *In vivo* activity was evaluated in a subcutaneous cell-derived xenograft (CDX) mouse model.

Results: Olverembatinib potently inhibited MCL cell proliferation, with respective IC_{50} values of 15 and 25 nM in Mino and Rec-1 cells. When combined with acalabrutinib, olverembatinib showed synergistic antiproliferative effects in both cell lines (respective Loewe scores = 10.04 and 10.92). The combination also significantly increased percentages of apoptotic cells (Mino, $p < 0.001$; Rec-1, $p < 0.01$), and significantly induced G0/G1 cell cycle arrest versus either agent alone (Mino, $p < 0.01$; Rec-1, $p < 0.0001$). On tyrosine phosphoproteomic analysis, olverembatinib inhibited kinase activities of Lyn, Fyn, Lck, Syk, and BTK, leading to potent inhibition of BCR signaling. Acalabrutinib inhibited BTK and other Tec-family kinases (e.g., Tec, Itk). Combining both agents potentiated inhibition of BCR and NFkB pathways. These results were further confirmed by western blot analysis. Olverembatinib inhibited phosphorylation of Lyn and its downstream BTK, while the combination further downregulated NF-kB activity. The combination also significantly suppressed cell cycle-promoting protein CDK6 and increased apoptotic markers PARP and caspase-3. In the Mino CDX model, olverembatinib dose-dependently inhibited tumor growth, with a treatment-to-control (T/C) value of 35.35% at 15 mg/kg, while acalabrutinib (10 mg/kg) exhibited a T/C value of 73.37%. When coadministered, both agents further enhanced antitumor activity (T/C = 18.64%), achieving a synergistic index of 1.39.

Conclusions: Olverembatinib is efficacious and synergizes with acalabrutinib in preclinical MCL models. These data provide a rationale for further clinical evaluation of this novel combination therapy in patients with MCL.

#5876 Soluble TNF blockade as a strategy to enhance tyrosine-kinase inhibitor response and control metastatic burden in HER2-positive breast cancer.

Sofia Bruni[1], Marla Ladera[2], Camila Jencquel[2], Federico Waisberg[3], Martin A. Rivas[1], Roxana Schillaci[2], Maria Florencia Mercogliano[2]

[1]University of Miami Miller School of Medicine and Silvester Comprehensive Cancer Center, Miami, FL,[2]Instituto de Biologia y Medicina Experimental, Buenos Aires, Argentina,[3]Instituto Alexander Fleming

Tyrosine kinase inhibitors (TKIs), such as lapatinib and tucatinib, are used to treat metastatic HER2-positive breast cancer, especially those located in the brain, as they can cross the blood-brain barrier. Although both TKIs improve survival, there is still an urge to boost their efficacy and overcome resistance. We have demonstrated that soluble TNF (sTNF) blockade overcomes resistance to trastuzumab-based therapies targeting HER2 by downregulating mucin 4 (MUC4), which shields its epitope on the HER2 molecule. Now, we asked whether sTNF neutralization might overcome TKI-based therapy resistance or enhance its antitumor activity.We used the HER2+/MUC4+ JIMT-1 and its brain-tropic subline JIMT-1BR3-luc cell lines, resistant to lapatinib. For proliferation and cell migration assays, cells were treated with 1 µM lapatinib or 10 µM tucatinib, either alone or combined with 10 µg/ml of a dominant negative (DN) protein that neutralizes sTNF. For preclinical studies, female nude mice bearing JIMT-1 tumors received vehicle, 100 mg/kg lapatinib via oral gavage daily, 10 mg/kg DN i.p. twice a week, or the combination (n=5/group). For JIMT-1BR3-luc tumors, mice were treated with vehicle, 100 mg/kg tucatinib via oral gavage daily, DN twice weekly, or both (n=9/group). Tumor volume was measured biweekly for 21 days; metastases were detected *ex vivo* by IVIS luminescence.Neither lapatinib nor DN alone impacted JIMT-1 cell proliferation, but their combination reduced cell proliferation by 60%. For JIMT-1Br-luc cells, DN and tucatinib decreased cell proliferation by 35 % and 55%, respectively, and the combination enhanced the effect to 80%. Cell migration was significantly inhibited in both cell lines by their respective combo treatment, compared to the monotherapies.In preclinical studies, treatment with DN, lapatinib, or tucatinib did not affect the primary tumor growth, compared to the vehicle. However, the combination of DN and lapatinib reduced JIMT-1 tumor growth by 77% and, in the case of JIMT-Br-luc tumors, treatment with DN and tucatinib inhibited tumor growth by 68%, compared to the monotherapies. The percentage of JIMT-Br-luc tumor-bearing mice with lung metastases was 100% in the vehicle group, 75% in the DN group, 37.5% in the tucatinib group, and 12.5% in the combined group. Animals with brain and liver metastases accounted for 50% and 75% respectively, in the vehicle group, and were 90-100% reversed upon treatment with either tucatinib or DN, or the combination.These findings highlight that sTNF blockade can overcome lapatinib resistance and improve tucatinib inhibitory effect on cell proliferation, both *in vitro* and in *vivo*. In addition, DN was able to curb brain and liver metastasis and lung metastases in combination with tucatinib, underscoring the potential benefit of its use in combination with TKIs in advanced HER2-positive breast cancer patients.

#5877 BH-30643, a novel macrocyclic non-covalent, mutant-selective EGFR inhibitor, addresses the resistance and potency limitations of contemporary EGFR TKIs.

Ping Jiang, Wei Deng, Nancy Ling, Danan Li, Zhenping Wang, Yue Hu, Joshua Choi, Eugene Rui, Geoffrey Oxnard, Jean Cui

BlossomHill Therapeutics, Inc., San Diego, CA

Historical design of EGFR tyrosine kinase inhibitors (TKIs) left them vulnerable to recurrent resistance liabilities which curtail the durability of their clinical effect. These TKIs gain potency either by binding the EGFR kinase back pocket or by forming covalent bond with C797, rendering them susceptible to T790M or C797S resistance mutations. Limited potency or PK exposure of some TKIs also permits regrowth of residual tumor cells and thereby shortening their duration of clinical benefit. BH-30643 was designed as a macrocyclic, non-covalent, mutant selective OMNI-EGFR inhibitor targeting the disease-driven active conformation of mutant EGFRs, allowing super-potency against diverse EGFR oncogenic drivers and resistance mutations while sparing wildtype EGFR. Aiming to characterize how this novel, super-potent OMNI-EGFR inhibitor could address the resistance liabilities of contemporary EGFR TKIs, BH-30643 was studied alongside 10 contemporary EGFR TKIs, approved or in clinical studies with a panel of primary cancer or engineered Ba/F3 cell lines expressing classical *EGFR* mutation (ex19del or L858R) or compound resistance mutations (T790M, C797S, or both). *EGFR* C797S conferred resistance to 6 covalent EGFR TKIs, T790M rendered resistance to 4 EGFR TKIs with a structure motif in EGFR back pocket, while the triple compound mutations with C797S and T790M were resistant to all 10 contemporary EGFR TKIs, leaving BH-30643 as the only TKI capable of overcoming both C797S and T790M resistance mutations while maintaining super potency against classical *EGFR* mutations. Furthermore, BH-30643 and osimertinib were investigated in a long-term colony formation assay in cancer cells with *EGFR* classical mutations. BH-30643 demonstrated markedly prolonged suppression of cell proliferation compared to osimertinib at the same clinically relevant concentration not only under standard growth conditions, but also in the presence of EGF, which mimicked accelerated resistance. These data support the potential of BH-30643, as a super-potent OMNI-EGFR TKI for longer duration of treatment than osimertinib. Upregulation of growth factors are well recognized as a common resistance mechanism for receptor TKIs. Targeting the active EGFR kinase conformation is hypothesized to reduce vulnerability to growth factor-mediated EGFR TKI resistance (eg, EGF). In the presence of EGFR ligands, BH-30643 maintained cell potency in all cell lines, while potency of osimertinib steeply fell, particularly in cells with *EGFR* L858R mutation. The first-in-human trial of BH-30643 (SOLARA) is now enrolling globally, with a focus on advanced *EGFR*-mutant NSCLC either with TKI resistance or prior to targeted therapy exposure (NCT06706076).

#5878 Tumor Treating Fields remain effective in therapy-resistant glioblastoma with kinome shifts revealing novel therapeutic opportunities.

Taylor Lynn Schanel[1], Amber Jones[2], Rhea Pandit[1], Johsua C. Anderson[3], Patricia H. Hicks[1], Corinne Griguer[4], Braden C. Mcfarland[5], Christopher D. Willey[6], **Anita B. Hjelmeland**[1]

[1]University of Alabama at Birmingham, Birmingham, AL,[2]St Judes Children's Hospital, Memphis, TN,[3]Radiation Oncology, University of Alabama at Birmingham, Birmingham, AL,[4]University of Iowa, Iowa City, IA,[5]Postdoctoral Fellow, Dept. of Cell, Developmental and Integrative Biology, University of Alabama at Birmingham, Birmingham, AL,[6]O'Neal Comprehensive Cancer Center at UAB, Birmingham, AL

Glioblastoma (GBM) is the most common primary brain tumor in adults with a median survival of less than 15 months with maximal safe surgical resection, radiation, and the chemotherapy temozolomide. Addition of Tumor Treating Fields (TTFields), or alternating electromagnet fields therapy, to temozolomide was shown to extend the survival of GBM patients by approximately 4.9 months. TTFields disrupt mitosis to inhibit cell growth, but we also determined that TTFields alter the cellular kinome. Using a PamStation, we identified kinases that are predicted to be activated and repressed by TTFields treatment in newly diagnosed and recurrent GBM models that are sensitive or resistant to temozolomide or irradiation, respectively. While the growth of all GBM cells tested was significantly decreased by TTFields, there was a relatively limited set of kinases that were commonly altered in newly diagnosed and temozolomide-resistant GBM cells with little similarly across irradiation resistant GBMs. These kinase data are reminiscent of published data demonstrating kinome variability in radioresistant GBM xenografts. We did find that TTFields were predicted to activate PDGFRα in both newly diagnosed and temozolomide-resistant GBM cells: when combined with TTFields, a blood brain barrier penetrant PDGFR inhibitor, crenolanib, significantly decreased GBM cell growth. Subsequent studies have identified additional kinases to be evaluated in combination with TTFields in radioresistant GBM cells. Using the Novocure inovivo system, we plan to test these novel kinase inhibitor combinations with TTFields in mouse models bearing intracranial GBMs. We hope to identify a kinase inhibitor based treatment strategy that can be translated to the clinic to further improve TTFields mediated increases in patient survival.

#5879 Spleen tyrosine kinase as a novel target in medulloblastoma.

Veena Salvi[1], **Ganesh Naik**[2], Ajay Sharma[3], Nagendra K. Chaturvedi[4]

[1]Chemistry, College of Saint Mary, Omaha, NE,[2]Chemistry, University of Nebraska at Omaha, Omaha, NE,[3]Cancer research readuate program, University of Nebraska Medical Center, Omaha, NE,[4]University of Nebraska Medical Center, Omaha, NE

Background: Group 3 medulloblastoma (MB) is the most aggressive pediatric brain tumor, characterized by MYC oncogene amplification, poor prognosis, and resistance to standard chemoradiation, necessitating novel therapeutic targets. Spleen Tyrosine Kinase (SYK) is known as an important oncogene and signaling mediator in various hematologic and solid malignancies, contributing to proliferation and survival pathways. Because MYC proteins remain largely undruggable, we investigated SYK as a potential therapeutic target based on its reported cooperation with MYC-driven transcriptional programs in other malignancies.
Methods: Since MYC is undruggable, we explored targeting the Spleen Tyrosine Kinase (SYK), a component of MYC-dependent pathways. We used pharmacological inhibition (R406, Bay61, Fostamatinib) in MYC-amplified MB cell lines (HD-MB03 and D425) to assess cell viability and MYC protein levels via MTT assays and Western blotting. We also evaluated the therapeutic potential of SYK inhibition combined with cisplatin in D425 cells. Future work will elucidate the molecular mechanism (transcription/translation) in vitro (via shRNA knockdown, ChIP, RNA sequencing) and evaluate therapeutic efficacy in patient-derived xenograft (PDX) mouse models.
Data: SYK inhibition significantly reduced HD-MB03 cell viability in a dose-dependent manner (R406 reduced viability to ~18% at $5 μM) and caused distinct downregulation of MYC protein in both HD-MB03 and D425 cells. Crucially, the combination of SYK inhibitors with the standard chemotherapeutic agent cisplatin showed a synergistic effect in D425 cells, suggesting a potential chemo sensitization mechanism. These preliminary data strongly support the critical role of SYK in MYC-driven MB oncogenesis.
Conclusions: The preliminary findings support the hypothesis that SYK acts as a key regulator of MYC-driven tumorigenesis in aggressive medulloblastoma. The observed synergistic toxicity when combining SYK inhibitors with cisplatin in D425 cells highlights a prospective chemo-sensitization mechanism. Targeting the SYK-MYC axis using SYK inhibitors, especially in combination with existing chemotherapies, offers a powerful, clinically translatable strategy to overcome treatment resistance and significantly improve outcomes for patients with high-risk, MYC-driven medulloblastoma

#5880 A comprehensive approach to targeting PI3K and Hippo pathways in sarcomas.

Samuel Y. Yu, Keith Garcia, Ali Khan, Souradip Sinha, Colleen Fullenkamp, Munir R. Tanas

University of Iowa, Iowa City, IA

Sarcomas are heterogeneous cancers of mesenchymal origin with limited effective targeted therapies. One frequently dysregulated pathway in sarcomas is PI3K signaling, due to PTEN loss in 30–60% of patient samples. PI3K activation promotes tumor growth via the canonical Akt-mTORC1 axis and a parallel PI3K-TAZ/YAP-TEAD axis. TAZ/YAP are transcriptional co-activators that drive oncogenic gene expression and are regulated by the Hippo pathway consisting of the core kinases MST1/2 and LATS1/2. TAZ/YAP lack DNA binding domains and complex with TEAD transcription factors in the nucleus. The TAZ/YAP-TEAD axis is regulated by PI3K in a LATS1/2 dependent manner. In sarcomas, loss of Hippo kinases is seen in 30-50% of samples, leading to aberrant TAZ/YAP activation. Epigenetic silencing of MST1/2 and MAP4Ks via histone deacetylation may account for a significant subset of these cases. Preliminary data shows HDAC inhibition with Romidepsin restores MST1 expression and reduces TAZ/YAP transcriptional activity, suggesting a therapeutic opportunity. We propose dual inhibition of PI3K-Akt-mTORC1 signaling and TAZ/YAP transcriptional activity to reduce sarcoma proliferation and survival. We hypothesize that combination therapy will be more effective due to the convergence of these pathways on tumor growth.We used three cell lines: RD (embryonal rhabdomyosarcoma), A204 (malignant extrarenal rhabdoid tumor) and RH30 (alveolar rhabdomyosarcoma). Cells were treated with MK2206 (Akt inhibitor), Everolimus (mTORC1 inhibitor), Romidepsin (HDAC inhibitor) and VT-107 (TEAD inhibitor) alone or in combination. Proliferation was assessed via cell viability assays and clonogenic outgrowth was measured to evaluate cell survival. Western blotting was used to assess signal transduction.MK2206 reduced proliferation in A204/RH30 cells at concentrations greater than 1 μM, with corresponding decreases in phosphorylation of Akt-mTORC1 substrates. Clonogenic assays showed reduced colony formation in both lines. Combination treatment with MK2206, VT-107 and Everolimus further suppressed proliferation/clonogenic outgrowth, suggesting additive or synergistic effects. In RD cells, Romidepsin at 5nM significantly reduced proliferation/clonogenic outgrowth, consistent with increased MST1 protein levels and reduced TAZ/YAP activity.PI3K and Hippo pathways are frequently dysregulated in sarcomas and combination therapy targeting both can more effectively inhibit tumor growth. TEAD inhibition disrupts TAZ/YAP transcriptional activity downstream, while HDAC inhibition restores Hippo signaling and suppresses TAZ/YAP transcription, and PI3K pathway inhibitors reduce survival signaling. These findings provide rationale for further investigation into dual-pathway inhibition as a therapeutic strategy, including mechanistic studies and *in vivo* validation to define therapeutic windows and potential clinical applications.

#5881 Fragment-recombination design of a dual VEGFR2/TIE2 inhibitor with sarcoma-selective cytotoxicity.

Youngkeun Lee, Bo Kyoung Kim, Ji-yoon Choi, Min-jeong Kim, **Sung Wook Seo**

Samsung Medical Center, Seoul, Korea, Republic of

Sarcomas have limited systemic options beyond cytotoxic chemotherapy. VEGFR-directed multi-kinase inhibitors such as regorafenib provide modest benefit, but their broad RTK inhibition constrains the therapeutic margin. Because VEGFR2 and TIE2 are central regulators of tumor angiogenesis and vascular stability, we hypothesized that selective dual VEGFR2/TIE2 inhibition would improve potency while reducing off-target toxicity. We applied fragment recombination of validated RTK inhibitor scaffolds, combined with dual VEGFR2/TIE2 docking and phenotypic screening, to design candidate inhibitors with an improved potency-selectivity balance for sarcoma therapy. We computationally designed ~300 dual VEGFR2/TIE2 candidates via fragment recombination and synthesized 15 prioritized by docking and binding-site analyses. Antiproliferative activity was evaluated by MTS assay at 24 and 48 h (2.5-10 μM) in human osteosarcoma lines (143B, MG63, KHOS/NP, U-2 OS) and murine macrophages (RAW264.7) to assess myeloid cell toxicity. Lead compounds were compared with pazopanib, regorafenib, and sorafenib. At 2.5 μM (48 h), pazopanib, regorafenib, and sorafenib maintained ≥100% viability across all sarcoma lines. At 10 μM, pazopanib and regorafenib showed ≥80% viability, while sorafenib reduced 143B viability to 55% but spared other lines (≥80%). Among synthesized candidates, SMC-101-008 and SMC-101-011 showed early activity at 2.5 μM, reducing 143B and MG63 viability to 57-65% (24 h) and 47-84% (48 h). However, at 10 μM (48 h), both compounds also ablated RAW264.7 (1% viability), indicating loss of selectivity at higher doses. In contrast, SMC-101-017 exhibited time- and dose-dependent sarcoma-selective activity. At 2.5 μM, minimal activity was observed at 24 h (≥88% viability), but by 48 h, KHOS/NP and 143B viability dropped to 39% and 19%, respectively, while RAW264.7 remained unaffected (>100%). At 10 μM, SMC-101-017 showed moderate early suppression (66-72% viability across all lines at 24 h) but selectively eliminated KHOS/NP and 143B by 48 h (25% and 7%, respectively) while preserving RAW264.7 viability (>100%) SMC-101-017 demonstrated potent, time-dependent cytotoxicity against osteosarcoma while sparing myeloid cells across a 4-fold dose range, distinguishing it from approved multi-kinase TKIs. These findings nominate SMC-101-017 for target validation and in vivo evaluation, and support fragment-based design for developing kinase inhibitors with improved therapeutic windows.

#5882 Structure- and bioinformatics-driven development of a selective, orally bioavailable HER2 small molecule inhibitor (HM100714) for cancer therapy.

Ho Yeon Nam, Sun Young Jang, Jiyoung Jeon, HyungSeok Yoo, Jooyun Byun, Soonki Park, Soye Jeon, Haemin Chon, Yu-Yon Kim, Boram Kim, Young Gil Ahn

Hanmi Pharmaceutical Co., Ltd., Hwaseong-si, Korea, Republic of

HER2 alterations, encompassing overexpression, amplification, and activating or other mutations, occur across multiple solid tumors and can drive cancer cell growth and metastatic progression. To address these alterations, HER2-targeted therapeutics are under development and clinical evaluation for breast, gastric, cholangiocarcinoma, colorectal, bladder, and non-small-cell lung cancers. However, several existing HER2 inhibitors also inhibit wild-type EGFR, leading to EGFR-related toxicities such as skin rash and diarrhea. Collectively, these considerations support the development of HER2-selective inhibitors that spare wild-type EGFR. Herein, HM100714 covalently targeted HER2 Cys805 and selectively inhibited HER2 while minimizing EGFR-mediated toxicities. To elucidate the improved tolerability, we performed molecular dynamics (MD) simulations of the inhibitor-protein complex. Beyond the covalent linkage to Cys805, MD revealed interactions with HER2-specific residues that are absent in wild-type EGFR, providing a structural rationale for HER2 selectivity and reduced EGFR liability. We further explored potential clinical indications using a bioinformatics framework. We trained a machine-learning model using published *in vitro* datasets of HER2 inhibitors and transcriptomic information from the Cancer Cell Line Encyclopedia to predict sensitivity to the drug. Further *in vitro* validation was done using an in-house panel of 75 cell lines. Extrapolation of the model to patient-derived datasets allowed prioritization of cancer indications predicted to be effective. These results will inform the IND-enabling studies and documentation. HM100714 inhibited HER2-altered enzymes and cell lines and showed a DMPK profile compatible with oral dosing. Guided by bioinformatics-driven indication selection, we evaluated the antitumor activity as a single agent across multiple HER2-altered xenograft models. Oral administration of HM100714 resulted in statistically significant antitumor efficacy in the NCI-N87 xenograft model, which exhibits HER2 overexpression, and in the Ba/F3 xenograft model harboring the $HER2^{A775\_G776insYVMA}$ mutation. We further assessed efficacy in leptomeningeal metastasis and brain metastasis models and characterized the toxicity profile to define a safety margin in support of the IND-enabling studies. In conclusion, HM100714, an orally bioavailable small-molecule inhibitor, demonstrated robust efficacy against HER2-altered tumors with minimal EGFR-related toxicities. Moreover, structure-based analyses and bioinformatics provided key data that streamline clinical readiness. These preclinical results support HM100714 as a promising therapeutic candidate for HER2-altered cancers.

#5883 FAK inhibitor APG-2449 triggers immunogenic ferroptosis in gastric cancer via the AKT-FOXO1-ACSL4 axis.

Lin Zhang[1], Jing Xiao[1], Liqun Chen[1], Siyi Mao[2], Peiyao Song[3], Liqiong Yang[4], Runduan Lin[1], Miaozhen Qiu[5], Dajun Yang[4]

[1]Clinical laboratory, State Key Laboratory of Oncology in South China, Sun Yat-Sen University Cancer Center, Guangzhou, China,[2]Department of Breast Surgery, The First Affiliated Hospital of Guangzhou Medical University, Guangzhou, China,[3]Clinical Laboratory Science, Qingyuan Hospital of Traditional Chinese Medicine Affiliated to Guangzhou University of Traditional Chinese Medicine, Qingyuan, China,[4]Department of Experimental Research, State Key Laboratory of Oncology in South China, Sun Yat-Sen University Cancer Center, Guangzhou, China,[5]State Key Laboratory of Oncology in South China, Sun Yat-Sen University Cancer Center, Guangzhou, China

Gastric cancer remains a major clinical challenge worldwide with limited effective treatment options for advanced stages. APG-2449, an innovative multi-kinase inhibitor targeting FAK, ALK and ROS1, has demonstrated promising clinical potential in various malignancies, though its precise mechanism of action in gastric cancer requires further elucidation. This study aims to investigate the novel hypothesis that APG-2449 exerts its anti-tumor effects through inducing ferroptosis and subsequently activating anti-tumor immunity.Through comprehensive experimental approaches combining in vitro cell culture models and in vivo syngeneic mouse systems, we employed advanced techniques including Western blotting, chromatin immunoprecipitation, lipid peroxidation measurement, and multidimensional immune profiling.Our results demonstrate that APG-2449 effectively suppresses the FAK-AKT signaling pathway, resulting in FOXO1 dephosphorylation and nuclear translocation. Crucially, we provide direct evidence that FOXO1 binds to the ACSL4 promoter region, upregulating its transcription and subsequently driving lipid peroxidation that culminates in ferroptosis execution. Moreover, we establish that APG-2449-induced ferroptosis exhibits distinct immunogenic characteristics, triggering damage-associated molecular pattern release that promotes dendritic cell maturation and enhances CD8+ T cell infiltration and cytotoxic function within the tumor microenvironment. The therapeutic combination of APG-2449 with anti-PD-1 antibody generates significantly superior anti-tumor efficacy compared to either treatment alone.These findings illuminate a previously unrecognized dual mechanism of APG-2449 action: direct induction of ferroptosis via the FAK-AKT-FOXO1-ACSL4 axis coupled with potent activation of anti-tumor immunity, thereby providing a compelling rationale for clinical development of FAK inhibitor and immunotherapy combinations in gastric cancer management.

#5884 Targeting multivalent receptor tyrosine kinases to enhance the efficacy of anti-PD-1 immunotherapy in gastric cancer.

Melanie Genoula[1], SHOUMIN ZHU[2], Mohammed Soutto[2], Nadeem Sidiq Bhat[2], Marwah M. Al-Mathkour[2], Wael El-Rifai[2]

[1]Surgery, Miller School of Medicine, University of Miami, Miami, FL,[2]Surgery, Miller School of Medicine, University of Miami, Miami, FL

Background: Gastric cancer (GC) is the fifth most common cancer and the fifth leading cause of cancer-related deaths globally. The response to immune checkpoint blockade (ICB) therapy in GC is relatively poor with almost two thirds of the patients not responding due to the tumor's ability to maintain an immunosuppressive microenvironment and develop resistance to immunotherapy. Previously, we demonstrated that dovitinib, a multi-target receptor tyrosine kinases (RTKs) inhibitor, suppresses tumor growth and remodels the tumor microenvironment (TME) by facilitating the recruitment of CD8+ T cells into immune-suppressive types of mouse gastric cancer. This study aimed to assess whether dovitinib enhances the therapeutic effectiveness of PD-1 blockade.
Methods: ATP-GLO to measure cell viability in vitro. A syngeneic murine gastric tumor model with two distinct mouse GC cell lines was utilized to assess the synergistic effects of dovitinib and anti-PD-1 treatment. IF and flow cytometry to immunophenotyping.
Results: The combination of dovitinib and PD-1 blockade was significantly more effective than either treatment alone, leading to reduced tumor growth and increased animal survival in both models ($p<0.01$). IF analysis revealed that while dovitinib alone increased CD8+ T cell infiltration in the tumor core, the combination treatment further enhanced the infiltration of cytotoxic T cells (Perforin+ CD8+) compared to the other groups ($p<0.01$). Furthermore, multiparametric flow cytometry combined with FlowSOM clustering analysis showed an increase in CD4+ and CD8+ T cell clusters with higher activation (CD69+) and lower or absent expression of exhaustion markers (PD-1, CTLA-4). In contrast, dovitinib alone was associated with a more exhausted T cell phenotype. Notably, only the combination treatment increased the tumor killing capacity of the cytotoxic T cells.
Conclusion: Our findings demonstrate that the combination of dovitinib and PD-1 blockade is significantly more effective than either treatment alone, as the two therapies synergistically remodel the TME beyond their direct cytotoxic effects. This synergy is achieved by increasing the infiltration of activated tumor-infiltrating lymphocytes (TILs) and reducing the exhaustion phenotype typically seen with monotherapy. This study supports the rationale for combining multi-target RTKs inhibitors with immunotherapies as an effective therapeutic strategy for gastric cancer.

#5885 Targeting myeloid-derived suppressor cells (MDSCs) to restore antitumor immunity in non-small cell lung cancer (NSCLC) via SRC family kinase Inhibition with NXP900.

Bobby Kaghazchi[1], In Hwa Um[2], Amber Ortiz[3], Enrique Podarosu[4], David J. Harrison[2], Neil Carragher[1], Asier Unciti-Broceta[1]

[1]Cancer Research UK Scotland Centre, Institute of Genetics and Cancer, University of Edinburgh, Edinburgh, United Kingdom,[2]School of Medicine, University of St Andrews, St Andrews, United Kingdom,[3]Indica Lab, Albuquerque, NM,[4]Nuvectis Pharma Inc., Fort Lee, NJ

Background: Despite therapeutic advances, non-small cell lung cancer (NSCLC) demonstrates poor survival outcomes, with global 5-year rates of only ~ 16 - 19%. The tumor microenvironment (TME) critically influences NSCLC prognosis and treatment response through immune contexture (cell type, density, and spatial location). Elevated $CD4^+$ and $CD8^+$ T-cell tumor infiltration correlates with improved survival. Contrastingly, increased myeloid-derived suppressor cells (MDSCs) promote immune evasion, angiogenesis, and metastasis. NXP900 (eCF506) is a highly potent and selective SRC family kinase (SFK) inhibitor (IC_{50} of 0.47 nM against YES1) that locks SFKs in their inactive “closed” conformation (type 1.5), inhibiting both enzymatic and scaffolding activities of SFKs. Cancer models exhibiting hippo pathway modulators such as FAT1 or NF2 mutation or loss are associated with increased sensitivity to NXP900 *in vitro* and tumor growth inhibition and regression *in vivo*. Given MDSC dependence on SFKs and YAP/TAZ signaling required for immunosuppressive function, we hypothesized that NXP900 may suppress MDSCs, thereby reversing immune suppression, and enhance antitumor immunity in NSCLC.

Methods: Tumor and immune cell morphology were analyzed in 162 chemotherapy-naïve, early-stage NSCLC adenocarcinomas. Multiplex immunofluorescence (mIF) was performed on a subcohort (n=60) using lymphocyte (CD4, CD8 and CD20) and MDSC panels (CD11b, CD14 and CD15), with population and spatial analysis performed using HALO® software. Induced MDSCs (iMDSCs) were validated *in vitro* via flow cytometry and RT-PCR, treated with NXP900 for 48 hours, and immunostained for YAP1, YES1, phalloidin, and Hoechst and analyzed. Viability was assessed using Presto Blue assay.

Results: $Immune^{high}$ NSCLC patients showed longer overall survival compared with $immune^{low}$ patients (HR = 1.763; 95% CI, 1.098-2.830; *p = 0.03). Elevated MDSC populations negatively correlated with survival (HR, 0.5456; 95% CI, 0.2355-1.265; * p = 0.04) and exhibited contact-dependent suppression of effector T cells. NXP900 treatment depleted iMDSCs, reduced YAP1 phosphorylation and nuclear localization in a dose-dependent manner, and demonstrated pro-immune effects consistent with inhibition of hippo pathway modulation.

Conclusions: These findings identify MDSCs as a key immunosuppressive driver of prognostic significance in NSCLC. NXP900 currently in a Phase 1b study (NCT05873686) including in NSCLC patients with YES1 and FAT1 genomic alterations, effectively suppresses MDSC viability and YAP1 signaling in vitro, supporting its potential as a novel therapy in NSCLC.

#5886 *In vitro* profiling of IDRX-42 and NB003 against secondary and tertiary (AP/AL) mutations found in TKI-resistant GIST.

Michael C. Heinrich[1], Ajia Town[1], Marcelina Roberti[1], Sebastian Bauer[2]

[1]Medical Oncology, Portland VA HCS and OHSU Knight Cancer Institute, Portland, OR,[2]Sarcoma/Medical Oncology, West German Cancer Center, Essen, Germany

Approximately 70-75% of Gastrointestinal stromal tumor (GIST) harbor a KIT mutation and patients with KIT-mutant GIST have durable responses to front-line imatinib (IM). Over time, clinical resistance emerges due to secondary IM-resistance mutations. These secondary mutations are restricted to two regions of the KIT protein: the drug/ATP binding pocket (AP, exons 13 and 14) and the activation loop (AL, exons 17 and 18). Although additional TKI drugs are now approved for 2L-4L+ treatment these agents lack activity against the entire spectrum of known resistance mutations. For example, sunitinib (SU) is potent against AP mutations (V654A, T670I), but has minimal activity against AL mutations. Conversely, ripretinib (RIP) has minimal activity against AP mutations. Neither SU nor RIP has activity against KIT-mutant GIST with both AP and AL mutation paired with the original primary KIT mutation (AP/AL). Recently, two new agents, IDRX-42 and NB-003 have been tested in phase 1 studies of patients with TKI-resistant GIST and are initiating randomized phase 3 studies in the second- and third-line, respectively. However, the cellular potency of IDRX-42 and NB-003 against different primary, secondary, and AP/AL KIT mutations has not been comprehensively described. We assessed the biochemical potency of IDX-42 and NB-003 against cell lines with relevant primary, secondary, and AP/AL KIT mutations. To assess relative potency, we also profiled IM in the same cell line model. IM was potent against primary K11 mutations (K11 exon 11 deletion and K11 V560D) but was much less potent against K11 + secondary mutations, KIT exon 9 (K9) primary mutations, and K9 + secondary mutations. IDRX-42 was active against K11, K11 + V654A, K11 + AL, K9 primary, K9 + AP, K9 +AL mutations. IDRX-42 lacked potency against K9 or K11 with T670I mutations. NB003 was active against K11, K11 + AP, K11 + AL, and K11 + V654A + A829 P (AP/AL), K9 primary, K9 + AP, K9 +AL mutations. Notably, none of these drugs had activity against K11 + AP/AL or K9 + AP/AL mutant kinases. IDRX-42 and NB003 have superior biochemical potency against a panel of primary and secondary KIT mutations compared with IM. NB003 may lack potency against certain K9 + secondary mutations. Neither IDRX-42 or NB003 have activity against K9 + AP/AL or K11 + AP/AL mutations. Ideally, future development of these newer agents should focus on earlier lines of therapy, prior to the development of AP+ AL mutations. The pan-resistance of AP/AL mutations to existing TKIs indicates the need to develop new drugs to target these resistance mutations.

#5887 Profiling of reversible and covalent HER2 kinase inhibitors for anti-tumor activity and broader biological effects to evaluate selectivity and functional activity.

Luciano Galdieri[1], Steven Garner[1], Brogan Epkins[1], Emily Schultz[1], Daria Clucas[1], Pony (Yu-Ling) Lee[2], Chao-Di Chang[2], Chien-Chang Shen[2], Alastair J. King[1]

[1]Eurofins Discovery Services North America, LLC, Saint Charles, MO,[2]Pharmacology Discovery Services Taiwan, Ltd., New Taipei City, Taiwan

Hurman epidermal growth factor receptor 2 (HER2) is a member of the human epidermal growth factor receptor tyrosine kinase family that regulates cell proliferation, survival, and differentiation. Amplification or activating mutations of HER2 result in constitutive signaling through pathways such as PI3K/AKT and MAPK, driving oncogenic transformation and tumor progression in various cancers. This is particularly notable in breast and gastric cancers, making it an important therapeutic target for the treatment of tumors in these tissues. HER2-directed therapies, including monoclonal antibodies, antibody–drug conjugates, and small molecule tyrosine kinase inhibitors (TKIs), have markedly improved outcomes for HER2-positive malignancies. Among TKIs, lapatinib was the first dual HER2/EGFR inhibitor to be approved for clinical use. Its reversible inhibition of both kinases leads to broad pathway inhibition but also to off-target effects, limiting its use. Tucatinib, a third-generation reversible HER2 TKI, was designed for enhanced selectivity towards HER2 with minimal EGFR inhibition, reducing toxicity while preserving efficacy in HER2-driven tumors. Furthermore, tucatinib demonstrates clinical benefit in combination treatments, particularly for HER2-positive breast cancer with brain metastases, due to favorable CNS penetration. Zongertinib is a newly approved next-generation, highly selective covalent HER2 inhibitor with optimized pharmacologic and safety profiles. As such, it retains potent activity against HER2-amplified and HER2-mutant tumors while minimizing off-target kinase effects, which translates into improved tolerability and the potential for broader therapeutic use. We evaluated the activity and selectivity of lapatinib, tucatinib, and zongertinib *in vitro* across a panel of about 300 human tumor cell lines using the OncoPanel® cellular phenotypic platform. Potencies were determined from ten-point dose–response curves to calculate IC_{50} and EC_{50} values, thus allowing the identification of similarities and differences in potency, efficacy, and genomic biomarkers of sensitivity and resistance relating to each drug. Activities are also being assessed in a human tumor xenograft model of the HER2-positive NCI-N87 human gastric cancer cell line, to further enable the comparison and contrasting of these drugs *in vivo*. To complement these *in vitro* and *in vivo* analyses, these HER2 inhibitors were further characterized in the BioMAP® Diversity PLUS® panel of primary human cell systems to assess functional activities across a diverse range of tissue and immune biology contexts. Together, these studies define distinct biological and mechanistic profiles among HER2-targeted TKIs and highlight the evolution of this drug class with increasing selectivity, tolerability, and efficacy.

#5888 Quantitative phospho-proteomics uncovers CX-4945 effects on translational control and differentiation in neuroblastoma.

Marudhu Pandiyan Shanmugam, Muhammed Danial, Upendarrao Golla, Rifat Tasnim Juthi, Yasin Uzun, Hannah Valensi, Giselle Saulnier Sholler, Chandrika Gowda Behura

Pennsylvania State University College of Medicine, Hershey, PA

Introduction: Neuroblastoma is a third most prevalent pediatric cancer of the sympathetic nervous system, which is often diagnosed at a clinically advanced stage with primary or acquired resistance to conventional chemotherapy. Protein Kinase CSNK2A1 (CK2) is an intrinsically active, ubiquitously present serine-threonine kinase overactive in various pediatric solid cancers, including neuroblastoma (NBL) and Ewing sarcoma (EWS). Recurrent genetic alterations in CK2 were not observed in NBL, indicating that its oncogenic role is driven by dysregulated activity rather than mutation. CX-4945 (Silmitasertib) is a potent, ATP-competitive CK2 inhibitor with low-nanomolar Ki values and high selectivity, targeting 49 of 250 tested kinases. CX-4945 has demonstrated potent in vivo antitumor activity in solid tumors and leukemia, with favorable pharmacokinetics and good tolerability in human studies. It is currently under Phase I clinical evaluation for pediatric solid tumors. Here, we report the quantitative phospho-proteomic profiling of CX-4945 treated NBL cells

Methods: The susceptibility of NBL cell lines with and without MYCN amplification was tested against CX-4945. We performed label-free quantitative Phosphoproteomic profiling of 2 NBL cell lines (SMS-KCNR and SHSY5Y) following *in vitro* treatment with CX-4945 for 24 h. Trypsin digested peptides were enriched for phospho-peptides by using Titanium Ion-Metal Affinity Chromatography. Differentially expressed phospho-peptides and their corresponding phosphoproteins were identified using high-resolution LC-MS/MS, and functional enrichment analysis was conducted to map the affected signaling networks. We also performed transcriptomic analysis for comparing the commonly regulated proteins at mRNA and Protein level. For validation studies, WB and IHC-based quantification of selected phosphoproteins, and their associated pathways, was tested in pre-clinical model-derived tissue treated with CX-4945.

Results: Quantitative phospho-proteomics analysis revealed 4064 and 3131 downregulated phospho-proteins in CX-4945-treated NBL cell lines, SMS-KCNR and SHSY5Y, respectively. GPCR5C/IRS4-PI3K-AKT/MYC axis and EIF4A1/MYC axis are found to be downregulated in multi-omics approach. Network analysis highlighted the disruption of translation initiation, proliferation, and neuronal differentiation signaling, suggesting a mechanistic link between CK2 inhibition and altered signaling pathways. CK2 mediated cMYC signaling inhibition was validated using WB and IHC studies.

Conclusion: Protein kinase CK2 is intrinsically active and negatively impacts survival in HR-NBL patients. Phospho-proteomic analysis reveals, changes in multiple pathways which leads to reduced proliferation and increased neuronal differentiation.

#5889 Preclinical evaluation of EO1001 in EGFR-ECD mutant solid tumor models: Toward biomarker-directed therapy.

Jeffrey Bacha[1], Sophia Frentzas[2], Malaka Ameratunga[3], Sarath Kanekal[4], Ian Nisbet[5], Neil Sankar[1], Denni M. Brown[1], Jasmine Borroel[6], Rowan Prendergast[6]

[1]Edison Oncology Holding Corp., Menlo Park, CA,[2]Monash Health, Melbourne, Australia,[3]The Alfred Hospital - Monash Univ., Melbourne, Australia,[4]President, Regulatory Strategy Consulting, San Diego, CA,[5]Senz Oncology Ptd. Ltd., Melbourne, Australia,[6]Certis Oncology, San Diego, CA

Background: EGFR extracellular domain (ECD) mutations—including EGFRvIII, A289 substitutions, R108 variants, and related structural alterations—drive ligand-independent EGFR activation and highly aggressive tumor biology. These mutations are enriched in glioblastoma (GBM) and also occur in head and neck, lung, and gastrointestinal cancers, where they are associated with therapeutic resistance and poorer patient outcomes. EGFR-ECD mutations are intrinsically resistant to approved EGFR TKIs, including osimertinib, erlotinib, gefitinib, and afatinib, because the structural alterations lie outside the ATP-binding pocket and preserve receptor signaling despite drug engagement. EO1001 is an orally bioavailable, irreversible pan-ErbB inhibitor designed to target both wild-type and structurally altered ErbB receptors. Early signals of clinical benefit in EGFR-ECD mutant GBM patients have been observed in an ongoing Phase 1-2a study (ANZCTR: ACTRN12620000583943), underscoring the need for mechanistic validation. To address this, we initiated a focused preclinical program assessing EO1001 activity in patient derived (PDX) cell culture models harboring clinically relevant EGFR-ECD variants.
Methods: PDX GBM cell culture models were selected to evaluate EO1001 across representative EGFR mutation states. EO1001 is tested using a 9-point dose-response curve, run in triplicate at two timepoints. Cell viability and proliferation are quantified using CellTiter-Glo assays. Each plate includes a vehicle control, a DMSO cytotoxicity control, and an FDA-approved EGFR TKI as a positive control to benchmark EO1001 against a clinically used inhibitor known to be ineffective in ECD mutations. Primary endpoints include IC50 values and maximal inhibitory activity to determine whether EO1001 demonstrates direct antiproliferative effects in EGFR-ECD mutant GBM models.
Results: Study is ongoing, data will be presented at the AACR annual meeting. Planned analyses will define whether EO1001 demonstrates meaningful activity against EGFR-ECD variants, which represent a therapeutically intractable subgroup characterized by resistance to existing EGFR inhibitors and poor clinical outcomes.
Conclusions: This preclinical program will further explore mechanisms of EO1001's activity in EGFR-ECD mutant cancers, providing support for biomarker-guided clinical development.

: Functional Roles of Noncoding RNAs in Cancer Progression, Metabolism, and Therapy Response
Poster Session

#5894 Long non-coding RNA LINC01614 overexpression defines a ferroptosis-associated molecular signature in papillary thyroid cancer.
Danielle Quaranto[1], Michelle Carnazza[2], Nicole R. DeSouza[1], Sina Dadafarin[3], Augustine Moscatello[4], Humayun K. Islam[1], Codrin Iacob[5], Raj K. Tiwari[1], Jan Geliebter[1]

[1]Pathology, Microbiology, and Immunology, New York Medical College, Valhalla, NY,[2]General Nutraceutical Technology, LLC, Elmsford, NY,[3]Otolaryngology-Head and Neck Surgery, University of Washington, Seattle, WA,[4]Otolaryngology/Head and Neck Surgery, Westchester Medical Center, Valhalla, NY,[5]New York Eye and Ear Infirmary, Mount Sinai, New York, NY

Papillary thyroid cancer (PTC) is the most common endocrine malignancy, with incidence rising by approximately 3% each year. PTC disproportionately affects females of reproductive age, while male patients often exhibit more aggressive disease. Although overall survival is high, recurrence and metastasis remain significant clinical challenges that can persist for decades after initial diagnosis. Identifying reliable prognostic biomarkers and actionable therapeutic targets is therefore essential. Long non-coding RNAs (lncRNAs), a class of regulatory molecules with diverse roles in gene expression, display tissue- and cancer-specific expression patterns, making them promising candidates for biomarker discovery. Bioinformatic analysis of our PTC vs. normal thyroid genomic repository identified the lncRNA LINC01614 transcript as significantly 12-fold upregulated in PTC. Thus, we are studying LINC01614 as a potential PTC biomarker and/or therapeutic target. LINC01614 expression was found to be upregulated in multiple thyroid cancer cell lines. The PTC cell line K1 (~2 fold upregulated; BRAFV600E; male), was selected for in vitro study. CRISPR interference (CRISPRi) was used to transcriptionally repress LINC01614 in K1 cells. LINC01614 knockdown in K1 resulted in decreased migration (~20%), clonogenicity (~34%) and proliferation (~45%), indicating a role of this lncRNA in supporting malignant phenotypes. RNA sequencing analysis of a CRISPRi knockdown cell line vs. a CRISPRi control demonstrated reduced expression of key ferroptosis-related genes- SLC7A11 and SLC3A2. Both genes encode for the xCT system (cystine/glutamate reverse transporter) that regulates the uptake of cystine - a key precursor for glutathione (GSH) synthesis. GSH is a critical antioxidant defense against lipid peroxidation, further preventing ferroptosis. Thus, these findings suggested LINC01614 involvement in a ferroptosis-related mechanism. Consistent with this, total cell iron levels were quantified and found to be significantly higher in our LINC01614 knockdowns, signifying increased ferroptosis induction. Western blot analyses also showed decreased levels of ferroptosis-associated proteins such as GPX4, an important antioxidant enzyme that reduces lipid peroxidation to prevent ferroptosis. Current studies are ongoing to identify a LINC01614 mechanism of action within the ferroptosis pathway. These findings suggest that LINC01614 contributes to PTC pathogenesis through modulation of ferroptosis-related processes, highlighting its potential utility as a biomarker and/or therapeutic target.

#5895 The role of noncoding transcripts in glucose-dependent gene regulation in estrogen receptor-positive breast cancer.

Barbara Yang[1], Shreya Kolli[2], Melina J. Sedano[3], Enrique I. Ramos[1], Shrikanth S. Gadad[3]

[1]Biological Sciences, The University of Texas at El Paso, El Paso, TX,[2]TTUHSC El Paso, El Paso, TX,[3]Medicine and Oncology, UTRGV School of Medicine, McAllen, TX

Around seventy percent of breast cancers are of the estrogen receptor-positive (ER+) molecular subtype. Conventional treatments include endocrine therapy that antagonizes ER signaling with tamoxifen or aromatase inhibitors. However, over 50% of patients later develop resistance and relapse. Understanding the underlying molecular mechanisms by which ER drives breast cancer will provide new opportunities to diagnose and therapeutically target it. In this regard, we focused on the part of the genome that is pervasively transcribed to produce noncoding transcripts that are overexpressed in the presence of estrogen. These transcripts are advantageous for tracking disease progression due to their specific expression patterns. We resorted to understanding the function of an intergenic noncoding transcript, "long noncoding RNA 16 (*LNC16*)" that we previously characterized. Since ER can also be activated by specific signaling pathways in the absence of its ligand, investigating the role of *LNC16* in an estrogen-independent context could provide insights into the mechanisms underlying the development of resistance and/or the progression toward relapse. Metabolic reprogramming, especially the preference for undergoing glycolysis, is one of the hallmarks of cancer, and affects various signaling pathways, which could also have integral implications in the ligand-independent activation of ER. To study *LNC16*'s role in glucose-dependent gene expression in ER+ breast cancer in the luminal breast cancer cell line, using CRISPR, *LNC16* knockout MCF7 cells (KOs) were created and treated with glucose. We also introduced *LNC16* into MCF7 cells using a doxycycline-inducible overexpression system and treated them with glucose. Then we performed genome-wide transcriptomic analyses to identify the genes and pathways regulated. Gene ontology analysis of unique differentially expressed genes (DEGs) under normal glucose conditions showed plausible roles of *LNC16* in nucleosome assembly, in regulating cell-cell communication, adhesion, and junction, as well as in signaling pathways. Similarly, unique DEGs in higher glucose conditions predominantly have functions in adhesion, signaling, and chromatin remodeling. We also examined the expression of condition-specific DEGs in breast cancer tumors and identified the association with specific clinical outcomes. Currently, we are elucidating *LNC16*'s molecular mechanism by which it regulates gene expression to drive ER+ breast cancer biology using cell- and mouse-based experiments. Collectively, these results suggest that estrogen-regulated transcripts can regulate glucose-dependent gene expression to control ER+ breast cancer phenotypic outcomes.

#5896 Identification of lncRNAs associated with breast cancer prognosis from Latina America patients.

Xinhui Wang[1], Marcio L. Acencio[1], Flavia Rotea Mangone[2], Roger Chammas[3], Dirce Maria Carraro[4], Andrea S. Llera[5], Eliana Abdelhay[6], Nora Artagaveytia[7], Adrian Daneri-Navarro[8], Bettina Muller[8], Osvaldo L. Podhajcer[9], Carlos Velazquez[10], **Maria A. Nagai**[3]

[1]Luxembourg Centre for Systems Biomedicine,University of Luxembourg, Luxembourg, Luxembourg,[2]Inst. do Cancer do Estado de Sao Paulo (ICESP), Sao Paulo, Brazil,[3]Center for Translational Research in Oncology, University of Sao Paulo, Sao Paulo, Brazil,[4]A.C. Camargo Cancer Center - Brazil, Sao Paulo, Brazil,[5]Leloir Institute Foundation, Buenos Aires, Argentina,[6]Bone Marrow Transplantation Unit, Instituto Nacional de Cancer, Rio de Janeiro, Brazil,[7]Hospital de Clinicas, Facultad de Medicina Universidad de la Republica, Montevideo, Uruguay, Montevideo, Uruguay,[8]Universidad de Guadalajara, Guadalajara, Mexico,[9]Head, Gene Therapy Laboratory, Fundacion Institute Leloir, Ciudad de Buenos Aires, Argentina,[10]Universidad de Sonora, Hermosillo, Mexico

Breast cancer (BC) is the most common cause of female cancer-related death worldwide and is considered a public health problem. Many functional studies have shown that long noncoding RNAs (lncRNAs) play different roles in gene expression regulation, acting as epigenetic factors. Accumulating evidence indicates that lncRNAs modulate diverse biological processes, and their altered expression is associated with the development and progression of cancer, including BC. Here, aiming to identify lncRNAs associated with breast cancer, we performed a re-analysis of the expression data from 1,071 tumors of eligible patients in the project LACRN MPBCS (Latin American Cancer Research-Network - Molecular Profile of Breast Cancer Study). Using normalized data, we compared the expression profiles of triple-negative breast cancer (TNBC; 170 cases) and non-TNBC tumors (782 cases). A total of 59 differentially expressed lncRNAs (DElncRNAs) could be identified based on the criteria of $|\log2FC| > 1$ and FDR < 0.05, using the DESeq2 R package. In the Kaplan-Meier survival analysis, we identified DElncRNAs that affect disease-free survival and/or overall survival, with 8 in TNBC and 26 in non-TNBC patients. Further, we used multivariate Cox proportional-hazards models to evaluate independent predictors of survival. Two of those DElncRNAs, VLDLR-AS1 and PART1, were independent prognostic markers for TNBC patients, and seven, LINC00239, FAM30A, LINC00842, LINC01315, EGOT, LY6E-DT, and SLC25A21-AS1, were independent prognostic markers for non-TNBC patients. Our study identifies several lncRNAs that might participate in tumor progression and may serve as candidate biomarkers for BC.

#5897 piRNA-5939 drives lung cancer progression via PIWIL3-mediated post-transcriptional regulation.

Sudhir Kumar Rai[1], Yuanyuan Fu[2], Masaki Nasu[2], Zhuokun Feng[3], Li Ma[2], Asmita Pandey[4], Lauren Higa[2], Hua Yang[2], **Youping Deng**[2]

[1]Quantitative Health Sciences, John A. Burns Sch. of Med. Univ. of Hawaii at Manoa, Honolulu, HI,[2]University of Hawaii at Manoa, Honolulu, HI,[3]University of Hawaii, Honolulu, HI,[4]John A. Burns Sch. of Med. Univ. of Hawaii at Manoa, Honolulu, HI

Introduction: PIWI-interacting RNAs (piRNAs) constitute a distinct class of small non-coding RNAs initially described for their roles in germline transposon silencing. Recent evidence implicates somatic piRNAs in cancer-associated gene regulation; however, their mechanistic contribution to lung tumor progression remains poorly defined. In this study, we identify piRNA-5939 as a novel oncogenic regulator that enhances lung cancer cell proliferation and migration via PIWIL3-mediated post-transcriptional modulation of gene expression.
Methods: Human lung adenocarcinoma cell lines (A549, ABC1, and H522) were transfected with antisense oligonucleotides targeting piRNA-5939. Proliferation was assessed by MTT, Click-iT™ EdU incorporation, and colony formation assays; migration and invasion were analyzed by wound-healing and transwell assays; and apoptosis was quantified using Annexin V Alexa Fluor™ 488/Propidium Iodide flow cytometry. Global transcriptomic changes following piRNA-5939 knockdown were examined by RNA sequencing, and key targets were validated using qRT-PCR and Western blotting. Cytoplasmic and nuclear RNA fractionation determined piRNA-5939 subcellular localization and its impact on PIWIL family (PIWIL1-4) expression profiles.
Results: Subcellular fractionation revealed heterogeneous cytoplasmic and nuclear distribution of piRNA-5939 across lung cancer cell lines. Baseline profiling demonstrated that PIWIL3 transcripts are preferentially localized to the cytoplasm, and piRNA-5939 silencing led to a significant downregulation of PIWIL3 mRNA and protein expression. Functionally, loss of piRNA-5939 markedly reduced cell proliferation (~40%) and migration (~55%) relative to controls ($p < 0.01$). Transcriptomic analyses highlighted suppression of oncogenic signaling pathways, including those governing cell cycle progression, cytoskeletal remodeling, and RNA stability—all consistent with attenuated PIWIL3 activity.
Conclusions: These findings identify piRNA-5939 as a functional oncogenic piRNA that promotes lung cancer progression through PIWIL3-dependent post-transcriptional regulation of key growth and migration pathways. The piRNA-5939/PIWIL3 axis represents a previously unrecognized regulatory mechanism and a potential therapeutic vulnerability in lung cancer.

#5898 A novel role of snoRNAs in proteasome inhibitor induced apoptosis.

Alexei F. Kisselev, Olasubomi A. Akintola, Chandler R. Earley, Addison M. Wilson, Amit Kumar Mitra

Auburn University, Auburn, AL

Small nucleolar RNAs (snoRNA) are 60-300 nucleotide long RNAs that guide modification of rRNAs during ribosome biogenesis. Many of them have non-canonical functions, such as regulation of splicing, pseudouridylation, and 2'-O-methylation of specific mRNAs. We have made a serendipitous discovery that treatment of cells with proteasome inhibitors (PIs) induces expression of several snoRNAs, including SNORD3 and SNORA71 families. Two other agents that induce production of misfolded proteins, tunicamycin and thapsigargin, also induced these snoRNAs, but DNA-damaging agent doxorubicin did not. Knocking SNORA71D down reduced PI-induced apoptosis. These findings indicate a novel and unexpected role of snoRNAs in proteasome inhibitor induced apoptosis.

#5899 Characterization of prostate-derived glycoRNA in the context of cancer progression.

Esther Jones, Samantha McGuire, Spencer Moen, Julius Nyalwidhe, **Aurora Esquela Kerscher**

Virginia Health Sciences at Old Dominion University, Norfolk, VA

Noncoding RNA harbors a range of post-transcriptional modifications (m6A, pseudouridine, uridine tailing) important for RNA folding, stability, transport, and localization. Dysregulation of these RNA modifications is associated with human diseases, ex., cancer, inflammation, fibrosis, and viral infection. Noncoding RNA carrying a new class of glycosylation modifications was recently noted in cultured human cells metabolically labeled using bioorthogonal chemistry methods normally employed for glycosylated protein enrichment. Nothing is known about the clinical significance of glycoRNA in prostate cancer (PCa). As high-grade forms of PCa often lead to poor prognoses, it is imperative to improve patient stratification screening tools and treatment options to increase patient survivorship. We hypothesize that RNA requires carbohydrate modifications to maintain organ homeostasis and proper immune surveillance, and we predicted that the glycosylated state of RNA could serve as a biomarker correlating with prostate disease progression and patient prognosis. A clearer understanding of how PCa-associated glycoRNA is regulated during disease progression will provide valuable insight into its function in the prostate. We confirmed that prostate glycoRNA exists using a panel of human prostate cell lines that differed in androgen response and metastatic status. We employed a stringent RNA isolation workflow and validated the existence of carbohydrate-modified RNA using two independent approaches: metabolic labeling using azide click chemistry for biotin-tag detection & lectin northern blot analysis. Small (<200 nucleotide) noncoding RNA were found to carry both N-linked and O-linked sugars, with sensitivity to RNase, endoglycosidases (PNGase F, O-glycosidase) and glycosylation inhibitors. As predicted, glycoRNA expression correlated with PCa progression. GlycoRNA was preferentially enriched in human prostate cell lines and syngeneic panels with no/low malignancy compared to metastatic PCa lines. Subcellular fractionation studies showed glycoRNA localization at the plasma membrane of prostate cells, indicating a signaling role. LC-MS/MS analysis showed glycans containing core-fucosylation and α2-3/α2-6 sialylation. Several glycans displayed LacNAc and GalNAc extensions, suggesting lectin binding and biological function. We have profiled a large panel of glycosylation-associated enzymes in prostate cell lines to gain insight into glycoRNA regulation. This work will provide novel insight into how RNA modifications impact PCa progression and identify first-in-class clinical tools to improve patient outcomes.

#5900 LncRNA UCA1 regulates LDHA expression to drive Warburg metabolism and colorectal cancer progression.

Salique H. Shaham, Ricardo Pequeno Bracho, Kaylee Renteria, Manish Tripathi

Oncology and Medicine ISU, South Texas Center of Excellence in Cancer Research, The University of Texas Rio Grande Valley, McAllen, TX

Background: Colorectal cancer (CRC) is the third most common malignancy worldwide and the second leading cause of death in the US. In 2025, an estimated 154,270 new cases of colon cancer will be diagnosed. In the US, colorectal cancer ranks as the second most common cause of cancer-related deaths, with an expected 52,900 deaths in 2025. Urothelial cancer-associated 1 (UCA1), a long noncoding RNA (lncRNA), has been found to be dysregulated in CRC and to promote tumor growth. Unlike carcinogenic colon cells, we have observed that the lncRNA UCA1 is significantly expressed in metastatic CRC cells. Its expression is also linked to glucose metabolism factors, including glucose transporter 1 (Glut1) and lactate dehydrogenase (LDHA). LDHA is essential for the rapid production of ATP in cancer cells, thereby supporting their progression.
Methods: Cell migration, invasion, and proliferation assays were conducted on isogenic CRC cells (SW480 and SW620), as well as on cells overexpressing UCA1 (SW480+UCA1; OE) and those with UCA1 knockdown (SW620+shUCA1; KD). Anoikis induction was examined using the isogenic, OE, and KD cell lines. RT-PCR, Western blot, and immunofluorescence techniques were employed for RNA and protein analysis of YAP1, Glut1, and LDHA. Glucose and lactose levels in CRC cells were also assessed.
Results: LncRNA UCA1 showed significantly higher expression in metastatic CRC (SW620) cells compared to carcinogenic CRC (SW480) cells. After 36 hours under anoikis conditions, UCA1 expression became exponentially higher. UCA1 levels, along with Glut1 and YAP1, are also elevated in metastasis (SW620 cells) compared to carcinogenic (SW480 cells). In UCA1-overexpressing SW480 cells, the gene expression levels of Glut1 and YAP1 increased significantly, indicating that UCA1 plays a role in regulating glucose metabolism. In the Warburg effect, cancer cells convert Pyruvate into lactate even in the presence of oxygen, rather than using it for the TCA cycle. We found that the gene expression of LDHA, the enzyme converting pyruvate to lactate, was significantly higher in metastatic CRC cells compared to carcinogenic CRC cells. UCA1-overexpressing cells also showed significantly increased LDHA expression, suggesting that UCA1 influences LDHA enzyme activity. LDHA correlated with GLUT1 and YAP1, highlighting the crucial role of LDHA during Warburg glucose metabolism and CRC cell progression. Inhibiting LDHA reduces Glut1 levels within the cell and limits tumor cell growth.

#5901 Using chimeric eCLIP to uncover ancestry-related noncoding RNAs in head and neck cancer.

Chayil C. Lattimore, Lu Li, Lauren Gay, Rolf Renne, Mingyi Xie, Kristianna M. Fredenburg

University of Florida, Gainesville, FL

Introduction: Chimeric enhanced cross-linking and immunoprecipitation (eCLIP) is a high-throughput method that enables direct mapping of Argonaute (Ago)-mediated RNA interactions. To our knowledge, this method has never been used to investigate ancestral differences in cancer outcomes. We performed chimeric eCLIP in African and European-ancestry head and neck cancer cell lines, with the goal of identifying canonical and non-canonical RNA interactions that may underscore differences in tumor behavior and therapeutic response related to ancestry.
Methods: We abstracted gene expression data from patients in the Cancer Genome Atlas (TCGA) head and neck cancer cohort with different ancestral backgrounds. Differential expression analysis (edgeR) was used to identify differentially expressed genes (FDR < 0.05, -1 < log((FC)) > 1) and KEGG pathway analysis was performed to identify pathway enrichment (p adj. < 0.05). miRNA-target predictions were generated using miRnet. Admixture analysis was used to validate ancestry from head and neck cancer cell lines. Chimeric eCLIP protocol was performed on these cell lines. Briefly, Ago proteins were covalently cross-linked to their native RNA interaction partners. Ago immunoprecipitation was performed. RNA fragments were phosphorylated and ligated to generate RNA-RNA chimeras. Libraries were reverse transcribed, PCR amplified, and size selected to limit adapter dimer contamination. Paired-end sequencing (150 bp reads) was performed via Illumina NovaSeq.
Results: Higher expressed genes in patients with self-reported African ancestry were enriched for drug metabolic pathways ($p= 8.31E^{-10}$), while lower expressed were enriched for actin cytoskeletal function ($p= 3.22E^{-52}$). miRnet predicted genes associated with drug metabolism and actin cytoskeletal function to be regulated by miR-200, miR-99, and miR-143/145 family members, which play a role in cell growth and survival, epithelial-mesenchymal transition, and cytoskeletal integrity. Preliminary eCLIP data supports this prediction, highlighting miRNA-mRNA pairings such as miR-100-5p/ABCF2, miR-200c-3p/CDK6, and miR-141-3p/ITGB8.
Conclusion: We present evidence of ancestry-related noncoding RNA regulation associated with head and neck cancer. Future analyses will involve differential binding analysis, pathway enrichment analysis, and genetic overlay with SNPs to determine associations with ancestry. Overall, this methodology may be used to uncover pathways in other cancers with differing outcomes. ChatGPT was used for language editing and text refinement of this abstract.

#5902 Long non-coding RNA RFX5-AS1 exhibits upregulated expression in early stages of ovarian cancer.

Alya Juma Al Handhali[1], Shika Malgundkar[2], Ikram Burney[3], Aikou Okamoto[4], Yahya Tamimi[5]

[1]SQU, Al Khodh, Oman,[2]Sultan Qaboos University, Muscat, Oman,[3]Sultan Qaboos Comprehensive Cancer Care and Research Center (University Medical City), Muscat, Oman,[4]Associate Professor, Dept. of Ob/Gyn, Jikei Univ. School of Medicine, Tokyo, Japan,[5]Biochemistry, Sultan Qaboos University, Muscat, Oman

Ovarian cancer (OC) is a significant global health challenge to women's health worldwide, leading to high rates of morbidity and mortality. Early detection of OC remains a serious challenge since it is asymptomatic, and the conventional biomarkers (CA125 and HE4) often lack sufficient sensitivity and specificity in the initial stages. Long non-coding RNAs (lncRNAs) have emerged as promising molecular indicators due to their regulatory roles in tumorigenesis. Previously, bioinformatics analysis using the GEPIA database identified the upregulation of *RFX5-AS1* in OC compared to healthy individuals, suggesting its potential as a biomarker and highlighting its role in OC pathophysiology and tumor progression. The current study investigated the possibility of early detection potential of *RFX5-AS1* as a marker for OC, emphasizing the need for further investigation of this lncRNA to improve diagnosis, prognosis, and therapies. The expression levels of *RFX5-AS1* were analyzed by quantitative real-time PCR (qRT-PCR) in well-characterized ovarian tissue samples obtained from OriGene Technology, USA, encompassing a spectrum of disease stages. Rigorous normalization to housekeeping (β-actin) was performed to ensure reproducibility and accuracy. Statistical analyses were conducted to evaluate differential expression across stages. *RFX5-AS1* was significantly upregulated in early-stage ovarian cancer tissues, with elevated expression observed in stage IIA ($p = 0.0490$) and stage IIB ($p = 0.0113$). Importantly, *RFX5-AS1* expression remained consistently high in advanced disease, with significant increases detected in stage IIIB ($p = 0.0156$) and stage IV ($p = 0.0286$). These findings suggest that *RFX5-AS1* is not only detectable at early stages but also maintains relevance in later progression, underscoring its potential utility as a robust biomarker across the disease continuum. The consistent overexpression of *RFX5-AS1* in both early and late stages of ovarian cancer highlights its promise as a reliable biomarker for early detection and disease monitoring. Incorporation of *RFX5-AS1* into diagnostic workflows may improve sensitivity in identifying OC at stages where current markers are limited, thereby contributing to earlier intervention and improved patient outcomes.

#5903 TUG1-mediated replication stress regulation as a potential vulnerability in bladder cancer.

Akinobu Ishiyama[1], Miho Suzuki[1], Keiko Shinjo[1], Shusuke Akamatsu[2], Yutaka Kondo[1]

[1]Graduate School of Medicine, Department of Cancer Biology, Nagoya University, Nagoya, Japan,[2]Graduate School of Medicine, Department of Urology, Nagoya University, Nagoya, Japan

Bladder cancer (BCa) displays marked genomic instability driven by APOBEC mutational processes, recurrent alterations in TP53, RB1, ERCC2, and ATM, and chronic replication stress (RS). Such RS-rich genomes require mechanisms that buffer R-loop accumulation and replication-associated DNA damage to sustain proliferation. We have previously demonstrated that the long non-coding RNA (lncRNA) Taurine upregulated gene 1 (TUG1) is a RS-responsive lncRNA induced by ATR-CHK1 signaling and essential for maintaining genome stability across multiple cancer types. Our prior work revealed that TUG1 promotes R-loop resolution and supports tumor cell survival under genotoxic conditions. Given that BCa is intrinsically defined by APOBEC-driven mutagenesis, DNA repair defects, and persistent RS, we hypothesized that BCa cells may rely on TUG1-mediated R-loop regulation. To evaluate this possibility, we analyzed TCGA-BLCA and found significantly elevated TUG1 expression in tumor tissues compared with adjacent normal urothelium. RNA-FISH of clinical BCa specimens further confirmed higher expression of TUG1 within malignant epithelial compartments. Functional assays using a TUG1-targeting antisense oligonucleotide (TUG1-ASO) demonstrated efficient depletion of endogenous TUG1, reduced cell viability, and downregulation of cell-cycle-related transcripts. Loss of TUG1 also induced replication stress and DNA damage markers, including pRPA32 and γH2AX, and sensitized BCa cells to RS-inducing conditions.Taken together, these findings indicate that BCa cells depend on TUG1 to maintain proliferation under high RS pressure. Therapeutic depletion of TUG1 disrupts this adaptive mechanism and impairs tumor cell growth, supporting TUG1 as a potential therapeutic target in BCa.

#5904 Long noncoding RNA, *RAMS11,* promotes DNA damage response in colorectal cancer.

Yesol Kim, Shilpa Hebbar, Nicole White, Amy Ly, Christopher A. Maher

Washington University School of Medicine in St. Louis, Saint Louis, MO

Colorectal cancer remains a leading cause of cancer-related mortality worldwide, with approximately 30% of patients developing resistance to standard chemotherapy. Tumors that exhibit defects in DNA damage response (DDR) and DNA repair pathways exhibit increased genomic instability, which can manifest as resistance, underscoring the clinical significance of therapeutic targeting of DDR. While protein-coding drivers in colorectal cancer have been extensively characterized, persistent therapeutic challenges emphasize the necessity of elucidating novel mechanisms driving cancer development. Here, we found that the long noncoding RNA (lncRNA) *RAMS11* is significantly upregulated in metastatic colorectal cancer, particularly in tumors harboring p53 mutations, as revealed by analyses of The Cancer Genome Atlas (TCGA) datasets. p53-mutant metastatic CRC, a population normally reliant on the ATR/Chk1 checkpoint for survival. However, from small-molecule drug screening, we discovered that high *RAMS11* cells showed resistance to ATR and CHK1 inhibitors. While *RAMS11* drives a state of high replication stress, as evidenced by increased RAD51 foci in RAMS11-overexpressing cells, it simultaneously confers profound resistance to ATR and CHK1 inhibitors. Mechanistically, we resolve this paradox by demonstrating that *RAMS11* attenuates the checkpoint response, leading to a blunted pChk1 activation even under replication stress. We find these cells are now critically dependent on an alternative repair pathway, Homologous Recombination (HR), to resolve the DNA damage. Indeed, our functional studies confirm that knockdown of *RAMS11* significantly impairs HR repair capacity. This work identifies that *RAMS11* reroutes DDR dependencies in cells, revealing a new mechanism of intrinsic chemoresistance and suggesting a synthetic lethal strategy targeting the HR pathway. Collectively, these findings suggest that aberrant overexpression of *RAMS11* disrupts the DDR and promotes DNA replication stress, thereby leading to chemoresistance. Elucidating the mechanism of *RAMS11* will provide critical insights into chemoresistance in colorectal cancer.

#5905 Comparative analysis of lncRNA detection using qPCR and ddPCR technologies in breast cancer research.

Srikanth Perike, Nish Kumar, Cynthia Shu, Andrew Prantner, Angelica P. Olcott, Elizabeth Jordan Dreskin

Bio-Rad Laboratories, Pleasanton, CA

Long noncoding RNAs (lncRNAs) are a diverse class of RNA molecules (>200 nucleotides) with limited protein-coding potential. Thousands of lncRNAs have been identified, however, most remain functionally uncharacterized. These molecules play critical roles in gene regulation, chromatin remodeling, and epigenetic control. When dysregulated, they are linked to cancer and other diseases. Their tissue-specific expression makes them promising biomarkers. But their low abundance compared to mRNAs creates significant challenges for detection. Sensitivity is a major obstacle, since lncRNAs are typically expressed at levels much lower than mRNAs, making accurate quantification difficult.

Conventional quantitative PCR (qPCR) has been widely used for gene expression analysis; however, its sensitivity and precision can be limiting when detecting low-abundance targets such as lncRNAs. Droplet digital PCR™ (ddPCR™), by contrast, offers absolute quantification without reliance on standard curves and demonstrates superior sensitivity and reproducibility, particularly for rare transcripts.

In this study, we compared qPCR and ddPCR platforms for profiling breast cancer associated lncRNAs using an assay panel of up to seven targets in the MCF7 estrogen receptor-positive (ER$^+$) cell line and its Tamoxifen-resistant derivative (MCF7-TAMR), including reference genes (HPRT1, RPL13a) from validated panels. We evaluated sensitivity, multiplexing, and workflow efficiency. Droplet Digital PCR consistently outperformed qPCR, providing more accurate measurements of gene expression for low-abundance lncRNAs. The ddPCR platform reliably achieved absolute quantification at levels as low as 0.5 copies per µL. It also detected subtle changes in expression, even those below two-fold differences.

Superior sensitivity and multiplexing capabilities make ddPCR technology especially well-suited for the early detection and monitoring of breast cancer. These results demonstrate Droplet Digital PCR as a highly reliable tool for biomarker validation and translational research. Its advanced capabilities make it valuable for detecting rare transcripts such as lncRNAs. Selecting the right method is crucial for accurately measuring new RNA targets and Droplet Digital PCR offers the reliability needed for absolute quantification.

#5906 Analysis of metabolic dysfunction-associated transcripts in hepatocellular carcinoma.

Karla Perez[1], Frida Mariana Delgadillo[2], Subramanian Dhandayuthapani[1], Murali M. Yallapu[1], Subhash Chauhan[1], Enrique Ramos[2], SHRIKANTH GADAD[1]

[1]The University of Texas Rio Grande Valley, McAllen, TX,[2]The University of Texas at El Paso, El Paso, TX

Hepatocellular carcinoma (HCC) is the primary form of liver cancer, because early symptoms may be absent, it is often detected late, resulting in a median survival of less than a year. Metabolically-dysfunction-associated steatotic liver disease (MASLD), previously known as non-alcoholic fatty liver disease (NAFLD), has been identified as the fastest-growing cause of HCC globally, including in the United States. Vitellius et al. reported that MASLD may account for 35% of HCC cases. Furthermore, Younossi et al. mentioned it is estimated that by 2040, MASLD will be present in 55% of the population. Therefore, understanding the molecular mechanisms by which MASLD progresses to HCC is critical.

In this study, we leveraged the existing whole-transcriptomic data from over 200 patients with MASLD or Metabolic Dysfunction-Associated Steatohepatitis (MASH) to identify all differentially expressed transcripts, compared to normal liver tissue. We examined the expression of unique noncoding transcripts that are associated with metabolism in HCC. To explore their potential functions, we used the Genomic Regions Enrichment of Annotations Tool (GREAT). Currently, we are employing various molecular and phenotypic based assays to identify their function in HCC. We will link their functions to HCC patient outcomes using RNA in situ hybridization in human tissues.

The analysis identified differentially expressed transcripts in MASLD and MASH. We observed overlapping gene expression patterns across both conditions, along with distinct transcriptomic profiles unique to each stage. In MASLD, 4,403 genes were significantly upregulated and 4,411 downregulated compared to controls. Similarly, in MASH, 4,702 genes were upregulated and 4,433 downregulated. Comparative analyses revealed substantial overlap between the two cohorts, while also highlighting transcripts unique to each condition. These findings suggest that as metabolic liver disease progresses from fatty liver to steatohepatitis, many transcriptional alterations are conserved and become increasingly dysregulated. GREAT analyses indicate that these may be linked to various cellular processes known to play critical role in HCC, such as long-chain fatty-acyl-CoA and fatty-acyl-CoA metabolism, cellular catabolism, apoptosis, and kidney development, including mesonephros. Notably, many of these transcripts exhibit distinct expression patterns in HCC, suggesting their potential as diagnostic and therapeutic markers. We have begun elucidating their mechanism of action using loss- and gain-of approaches in HCC and how their expression is regulated in patient tissue samples.

#5907 Splicing of 3'UTR contributes to colon cancer progression.

Jiunn Fung Cheong[1], Xiaonan Fan[2], Xiao Hong Chew[2], Yvonne Tay[1]

[1]National University of Singapore, Singapore, Singapore,[2]Cancer Science Institute Singapore, Singapore, Singapore

The 3′ untranslated regions (3′UTRs) of messenger RNAs (mRNAs) play crucial roles in regulating gene expression. These regions have been found to be involved in important processes, including mRNA stability, localization, and translation. It is shown that 3'UTR splicing is widespread in many cancers and dysregulated 3′UTR splicing leads to cytoplasmic localization of the spliced 3'UTR (3'SP) transcript variant, resulting in increased protein expression, thus contributing to tumor progression. Currently, little is known about the functional mechanism of 3'UTR splicing in the progression of colon cancer and its implications for treatment outcomes. To address this, we integrated short-read RNA sequencing (RNA-seq) data from The Cancer Genome Atlas (TCGA) colorectal cancer cohort, in-house patient samples, single-cell PacBio long-read sequencing, short-read fractionation RNA-seq data of colon cancer cell lines, and in-house patient sample mass spectrometry data. We shortlisted four candidates that have upregulated 3'SP transcript expression in the tumor samples for further validation. Additionally, our fractionation RNA sequencing in colon cancer cell lines showed that the 3'SP isoforms were significantly more enriched in the cytoplasm compared to the nucleus. Further mechanistic studies are ongoing to identify the corresponding splicing and transport factors, which will determine the mechanism controlling the localization of spliced 3'UTR transcripts and how they are linked to dysregulated 3'UTR splicing.

#5908 PCGEM1 overload: Triggering lethal stress responses in castration-resistant prostate cancer.

Sabrina Ledesma-Bazan[1], Pablo Sanchis[1], Rocio Seniuk[2], Gaston Pascual[2], Maria Jimena Rada[2], Manuel Agulleiro[2], Camila Russo[2], Pia Valacco[3], Elba Vazquez[2], Geraldine Gueron[2], Javier Cotignola[2]

[1]1 Laboratorio de Inflamacion y Cancer, IQUIBICEN-CONICET, Buenos Aires, Argentina. 2 Universidad Argentina de la Empresa (UADE), Instituto de Tecnologia (INTEC), Buenos Aires, Argentina,[2]Laboratorio de Inflamacion y Cancer, IQUIBICEN-CONICET, Buenos Aires, Argentina,[3]CONICET-Universidad de Buenos Aires, Instituto de Quimica Biologica de la Facultad de Ciencias Exactas y Naturales (IQUIBICEN), Buenos Aires, Argentina

Metastatic castration-resistant prostate cancer (mCRPC) represents the most advanced stage of the disease, with no curative treatments. lncRNAs are emerging regulators of prostate cancer (PCa) biology and the lncRNA *PCGEM1* has been linked to tumorigenesis and c-Myc activity in AR positive cells, but its role in an androgen independent context is less characterized. PCGEM1 expression across ISUP grades was assessed by linear trend testing, and its association with progression-free survival was evaluated by Kaplan-Meier analysis in the TCGA-PRAD cohort. PC3 cells were transfected with a PCGEM1 expression plasmid or empty vector and validation by qPCR and MTS assays were performed at 24, 48 and 72 h. Clonogenic, hanging drop, and wound healing assays were conducted at 72h. To assess cell morphology, DAPI/phalloidin staining and fluorescence microscopy were performed. ER-stress and EMT programs were examined by RT-qPCR. Proteomic profiling of PC3 transfected cells was performed by LC-ESI-MS/MS followed by GSEA analysis, and pathway enrichment patterns were further evaluated in the MD Anderson PDX and SU2C cohorts. PCGEM1 expression declined with increasing ISUP grade, and higher levels correlated with longer progression-free survival in the TCGA-PRAD cohort. In PC3 cells, PCGEM1 overexpression reduced cell viability at 72 h, markedly impaired clonogenic growth, and decreased spheroid size. Transfected cells displayed an elongated morphology with increased cell area and reduced circularity, but both *CDH1* and *CDH2* expression were reduced whereas *FN1* and *TWIST1* had no changes. Furthermore, PC3-overexpressing cells had migration impaired at all times assessed (3, 6 and 24 h). ER-stress markers (HSPA5, XBP1, DDIT3) were upregulated, indicating activation of stress-response pathways. Proteomic analysis of PC3 transfected cells with PCGEM1 revealed repression of translational and ribosomal-biogenesis programs and downregulation of MYC-target pathways. Finally, the evaluation of MYC-core proteins in PDX models segregated AR-positive adenocarcinomas from poorly differentiated or AR-low tumors, whereas clustering in the SU2C cohort was more heterogeneous. *PCGEM1* is reviewed in literature as an oncogenic lncRNA and its overexpression in AR-positive PCa cells is associated with a more aggressive phenotype. Nevertheless, its overexpression in an androgen-independent context induced ER-stress programs, suppressed protein biosynthetic and MYC-related pathways, and impaired key malignant traits. This response suggests that excessive *PCGEM1* activation becomes incompatible with cellular homeostasis, inducing a hyperactivation-induced lethality mechanism. These findings highlight a previously unrecognized regulatory role for *PCGEM1* and suggest that exploiting lncRNA hyperactivation may uncover a therapeutic vulnerability in advanced, therapy-refractory PCa.

#5909 Functional characterization of specific non-coding transcripts involved in chemo-resistant triple negative breast cancer.

Melina J. Sedano[1], Barbara Yang[2], Subramanian Dhandayuthapani[1], Murali Yallappu[1], Subhash Chauhan[1], Shrikanth Gadad[1]

[1]Division of Cancer Immunology and Microbiology, Medicine and Oncology Integrated Service Unit, The University of Texas Rio Grande Valley School of Medicine, McAllen, TX,[2]Department of Biological Sciences, The University of Texas at El Paso, El Paso, TX

Triple-negative breast cancer (TNBC) accounts for many new breast cancer cases, with poorer outcomes than other molecular subtypes. Compared to other subtypes of breast cancer, TNBC is typically associated with larger, higher-grade tumors and decreased overall and recurrence-free survival rates. Treatment for this type of cancer is often aggressive and includes chemotherapeutic agents like anthracyclines, such as doxorubicin. However, it is not always effective due to dose-limiting toxicity and the development of resistance to doxorubicin over time. There are many theories behind the mechanism of resistance, possibly due to changes at the genetic level, transcriptome, cellular pathways, or epigenetic modifications, warranting further investigation. To study the mechanism of resistance, we developed doxorubicin-resistant MDAMB231 and HCC1143 TNBC cell lines that were engineered using physiological or low-dose doxorubicin concentrations with gradual increments of doxorubicin. We performed integrated genomic analyses to identify transcripts that are potentially contributing to the resistance mechanisms and also drive cancer progression. These transcripts range from coding RNAs, microRNAs, pseudogenes, divergent transcripts, and long noncoding RNAs. We focused on the intergenic long noncoding RNAs that are differentially expressed compared to non-resistant TNBC cells. We analyzed these RNAs by interrogating their neighborhood based on their chromosomal location, revealing that they could be involved in cellular plasticity, which allows cancer cells to adjust to the presence of doxorubicin, possibly through transcriptional reprogramming. A subset of them are localized to chromatin and the nucleus, which have the potential to reprogram the epigenetic landscape and drive resistance-specific genes and cellular pathways, and currently we are studying them for their role in chromatin organization. Additionally, we are also assessing their clinical utility using in vivo xenograft mouse models with genetically engineered chemo-sensitive and chemo-resistant cells, linking outcomes to changes observed in patient samples and associated with clinical prognosis. Collectively, our studies provide insights into mechanisms driving doxorubicin resistance in TNBC, which may offer new avenues for the development of diagnostic markers and targeted therapies.

: Genetic and Transcriptomic Dissection of Cancer Evolution
Poster Session

#5913 Integrative transcriptomic profiling reveals stromal activation patterns in gastric cancer beyond HER2 status.

Woo Sun Kwon[1], Chan Hee Park[1], Sejung Park[1], Choong-Kun Lee[2], Poh Zhong Wee[3], Jia Hui Liew[3], Jingming Chew[3], Sun Young Rha[1]

[1]Yonsei University College of Medicine, Seoul, Korea, Republic of,[2]Yonsei University Health System, Seoul, Korea, Republic of,[3]Auristone Pte. Ltd, Singapore, Singapore

Advanced gastric cancer (AGC) continues to show suboptimal outcomes despite therapeutic progress. Among TCGA-defined subtypes, the genomically stable (GS) subtype remains particularly challenging due to the absence of actionable drivers and its limited responsiveness to immune checkpoint inhibitors. GS tumors frequently exhibit stromal activation—characterized by cancer-associated fibroblasts, desmoplastic fibrosis, and angiogenic remodeling—which contributes to immune exclusion and therapeutic resistance. Although recent clinical activity of trastuzumab deruxtecan has refined HER2 classification, biological determinants of treatment response in non-HER2-driven subtypes, especially GS-like disease, remain poorly understood. Fibrosis- and angiogenesis-related transcriptional scores may capture key tumor-microenvironment programs relevant to AGC biology. We analyzed bulk RNA sequencing data generated from pre-treatment FFPE tumor samples of 120 patients diagnosed with stage IV AGC at Yonsei Cancer Center between 2015 and 2024 (IRB no. 4-2014-0349), categorized into HER2 positive (n=62) and negative (n=58). Differential expression analysis (DEG) and GSVA-based pathway enrichment were used to characterize transcriptomic differences across HER2 groups. Fibrosis and angiogenesis scores were computed and compared among the subgroups, and key findings were validated in the TCGA GC cohort. Across the entire AGC cohort, fibrosis scores (median 29.72, range 0-100) and angiogenesis scores (median 17.92, range 0-98.06) exhibited broad interpatient variability and showed a strong positive correlation ($R^2 = 0.501$, $p < 0.0001$). When samples were mapped to TCGA molecular subtypes, fibrosis scores were highest in GS-likely and were significantly elevated compared with CIN-likely ($p = 0.04$), a trend reproduced in the TCGA cohort. Low PD-L1 expression was associated with lower angiogenesis scores ($p = 0.0059$), indicating a relationship between angiogenic activation and immune phenotype. No significant differences in stromal scores were observed across HER2 subgroups, suggesting that stromal activation is largely independent of HER2 status. Within HER2-defined subgroups, HER2-low showed distinct transcriptomic programs characterized by KRAS pathway activation, loss of SNF-related tumor-suppressor activity, enrichment of proliferation-related signaling, and a marked reduction in inflammatory and interferon-related pathways compared with the other two groups. Stromal remodeling, represented by fibrosis and angiogenesis scores, is a major biological feature of AGC and is particularly enriched in GS-like tumors, independent of HER2 status. These findings suggest that fibrosis- and angiogenesis-based stromal programs may improve biological stratification and identify tumor-microenvironment-driven vulnerabilities in advanced gastric cancer.

#5915 Utility of long-read RNA-sequencing for isoform and fusion discovery in lung cancer.

Kevin Levine[1], Colette Felton[2], Tanvi Damle[1], Christina Baik[1], Angela Norie Brooks[2], **Alice H. Berger**[1]

[1]Fred Hutchinson Cancer Center, Seattle, WA,[2]UC Santa Cruz, Santa Cruz, CA

Isoform expression is frequently dysregulated in lung cancer via cis-acting splice site mutations or trans-acting mutations in splicing factors such as U2AF1, RBM10, and SF3B1. While prior studies have sought to characterize the isoform landscape in cancers, the short reads of next-generation sequencing platforms, ranging in length from 50-150 bp, preclude the accurate phasing of alternative splicing events across the full transcript length (typically exceeding 1 kb). To provide a more comprehensive and accurate view of expressed isoforms in lung cancer, we performed long-read RNA-sequencing on 32 matched tumor/normal pairs of early stage resected lung adenocarcinoma, four biopsies from tumors that had progressed on targeted therapy treatment, and 14 non-small cell lung cancer cell lines. RNA was isolated from fresh frozen tissue specimens and cDNA prepared using the PacBio Kinnex full-length isoform method. PacBio HiFi data were generated per manufacturer's recommendations at the University of Washington Long Reads Sequencing Center or UC Davis DNA Technologies core. Libraries were sequenced on the PacBio Revio system to a read depth of >10M HiFi reads per sample, providing >80% saturation of known isoforms. FLAIR3 was used to identify and quantify isoforms, including novel isoforms, and phase isoform expression with somatic mutations including SNVs and insertion/deletion mutations. Analysis of alternative splicing patterns in RAS-pathway genes identified increased expression of the minor *KRAS* isoform, *KRAS4A*, in tumors compared to normal samples. Phasing of somatic variants enabled integration of *KRAS* mutation with *KRAS* isoform expression and validated the previously identified role of KRAS Q61 variants on aberrant *KRAS* splicing. In addition, we identified deletions predicted to inactivate tumor suppressor genes and identified novel rearrangements in clinically actionable oncogenes including *EGFR*. Together these data demonstrate the utility of long-read RNA sequencing for accurate and complete isoform characterization in cancer.

#5917 Single-cell profiling of NK cells in chronic myeloid leukemia identifies distinct cell states with gene regulatory signatures associated with differential outcomes after imatinib discontinuation.

Santoshi Borra[1], Da Yan[2], Robert S. Welner[3], **Zongliang Yue**[4]

[1]Department of Bioinformatics, Indiana University, Bloomington, IN,[2]Department of Computer Sciences, Indiana University, Bloomington, IN,[3]Department of Medicine, University of Alabama at Birmingham, Birmingham, AL,[4]Department of Health Outcomes Research and Policy, Auburn University, Auburn, AL

Background: Treatment-free remission (TFR) is an emerging therapeutic goal in chronic myeloid leukemia (CML), achieved by ~40% of patients who discontinue tyrosine kinase inhibitor (TKI) therapy after maintaining a deep molecular response. However, the immunogenomic mechanisms that distinguish sustained remission from molecular relapse remain incompletely defined. Previous single-cell RNA (scRNA-seq) and TCR sequencing studies revealed that CML is characterized by an expanded population of activated CD56dim natural killer (NK) cells and anti-PR1 T cells that mediate anti-leukemic immunity.
Methods: Building on these findings, we reanalyzed NK cell transcriptomes from six CML patients, two with early relapse, two with late relapse, and two maintaining durable TFR, using an integrated computational framework combining unsupervised clustering, pseudotime trajectory inference, gene regulatory network (GRN) reconstruction, and artificial intelligence-assisted gene panel discovery. Longitudinal samples collected at TKI discontinuation and at 6- and 12-month post-therapy were analyzed to delineate transcriptional dynamics and regulatory drivers of immune outcomes.
Results: Comparative GRN modeling revealed distinct transcription factor modules governing NK cell activation, differentiation, and exhaustion. Patients maintaining TFR exhibited higher activity in RUNX3, EOMES, ELK4, and REL regulons, whereas relapse cases showed modules enriched for FOSL2 and MAF with inflammatory/translational targets. Pseudotime analysis revealed altered state-transition kinetics between functional NK subtypes, with accelerated exhaustion trajectories in relapsing patients. An AI-guided gene prioritization model further identified a gene NK cell regulatory panel, including previously uncharacterized transcriptional mediators that robustly separated TFR, late relapse, and early relapse groups. Pathway enrichment linked these genes to IFN-γ signaling, metabolic reprogramming, and immunoregulatory feedback networks.
Conclusions: This integrative reanalysis highlights transcriptional control and regulatory network rewiring as key determinants of immune persistence versus exhaustion following TKI cessation. The AI-derived gene panel provides a scalable framework for exploratory biomarker discovery and mechanistic stratification of CML remission outcomes. Together, these findings advance our understanding of the immune architecture underlying successful TFR and identify candidate transcriptional targets to improve remission durability in CML.

#5918 Single cell functional characterization of cancer mutations and their cellular phenotype.

Huiyun Sun, Dongin Lee, HoJoon Lee, Susan M. Grimes, Raegan Wood, Hanlee P. Ji

Stanford University, Stanford, CA

Many cancer driver mutations lead to proteins with amino acid substitutions which dramatically affect their function. This class of cancer mutations play a critical biological role in cancer progression and maintenance of nearly all malignancies. However, the effect of substitution mutations is mostly inferred computationally rather than functionally tested. As a result, there is practically no biological information about their functional consequences for these substitutions except for a small number.We developed a high-throughput single cell approach to systematically investigate the functional effects of reported cancers substitutions. This system provides parallel, highly scalable testing of many cancer mutations across multiple genes in a single experiment. It uses CRISPR base editors to introduce specific cancer mutations into the genome, identifies the newly introduced mutation genotype among individual cells and determines each mutation's transcriptional phenotype per a given cell. Specifically, long-read targeted sequencing is applied to single cell cDNAs. Single cell long read sequencing identifies the presence of an engineered mutation in each cDNA assigned to an individual cell. To determine phenotype of the mutation, we integrate the short-read transcriptome profile from the same single cells. This integrative approach enables single-cell direct genotyping of the introduced genetic variant and matching phenotype from the same cell.We chose a set of mutations that occur with high frequency as reported in the TCGA's pan-cancer atlas. All the possible gRNAs were designed based on the location of the C/A bases in the oncogenic mutations' sequence context. We detected the engineered mutations by linking actual mutation genotype determined by long-read sequencing with corresponding transcriptome change detected by short-read sequencing in one single experiment.These results demonstrate how combining single cell genomics and direct genome engineering method increase the scale for characterizing diverse cancer-associated mutations. In the future, we will evaluate in parallel large sets of different cancer mutations, how they alter gene expression and changes in the cellular states. Importantly, characterizing the function of novel oncogene mutations may lead to the discovery of new targeted therapeutics for cancers.

#5919 Dissecting gene regulation of cellular states in glioblastoma using single-cell multi-omics.

Min Yang[1], Nicolas L. Gonzalez Castro[2], Alexander Jucht[1], Sophia Kovatsis[1], Channing Pooley[1], Sydney Dumont[1], Kevin Johnson[3], Julie Laffy[4], Bo Xia[1], Roel Verhaak[3], Itay Tirosh[5], Mario Suva[1]

[1]Department of Pathology and Krantz Family Center for Cancer Research, Massachusetts General Hospital and Harvard Medical School, Boston, MA,[2]Center for Neuro-Oncology, Dana-Farber Cancer Institute, Boston, MA,[3]Yale School of Medicine, Department of Neurosurgery, New Haven, CT,[4]Broad Institute, Boston, MA,[5]Department of Molecular Cell Biology, Weizmann Institute of Science, Rehovot, Israel

Glioblastoma (GBM) is an incurable and aggressive brain cancer characterized by profound intra- and intertumoral heterogeneity and remarkable cellular plasticity. Single-cell transcriptomic analyses have revealed several major cell states, including NPC-like, OPC-like, GPC-like, AC-like and MES/Hypoxia-like. However, the cis-regulatory networks that govern GBM cell state transitions remain poorly understood. In this study, we performed single-cell chromatin accessibility profiling and multi-omics analysis on 35 GBM IDHwt samples. Firstly, we developed a new scATAC-seq data analysis framework and reconstructed six malignant consensus cis-regulatory element (CRE) modules. Four of these modules were specifically associated with malignant cell states corresponding to the MES/Hypoxia-like, AC-like, OPC-like, and NPC-like identities. Interestingly, cycling cells exhibited broadly open chromatin across all four CRE modules, while GPC-like cells showed accessibility in both the AC-like and OPC-like states, suggesting a role as an intermediate or hybrid regulatory state. Further epigenetic information quantification revealed that NPC-like malignant cells harbor higher regulatory information content compared with other cell states. Master regulator enrichment analysis identified AP-1 transcription factors as key regulators of differentiated (MES/AC-like) malignant state-associated CRE modules, whereas neuronal-development transcription factors were enriched in stem-like (NPC/OPC-like) state-associated modules. Through in vitro gain- and loss-of-function experiments, we screened and validated several transcription factors that modulate malignant cell-state transitions. Additionally, our scATAC-seq-based copy number alteration (CNA) analysis captured hallmark GBM genomic events at high resolution, including EGFR focal amplification, CDKN2A/B deletion, and CDK4 and MDM2 amplifications. Leveraging these CNA profiles, we successfully constructed a high-resolution phylogenetic tree, capturing the clonal architecture and evolutionary trajectory of GBM. By integrating transcriptomic, chromatin accessibility, and genetic CNA data, we elucidated the evolutionary landscape of GBM progression and cellular plasticity. Our findings provide significant insights into the regulatory architecture of GBM and establish a foundational framework for precision therapies targeting distinct cell states.

#5921 Cell type-specific mapping of endometrial cancer risk genes using single-nucleus multi-omics.

Preety Bajwa, Carly Chapman, Dylan Glubb, Tracy O'Mara

QIMR Berghofer Medical Research Institute, Brisbane, Australia

Endometrial cancer is a common gynecological malignancy with more than 410,000 new cases diagnosed worldwide in 2020. Endometrial cancer genome-wide association study (GWAS) have identified 21 robust susceptibility regions, most of which lie in non-coding regions and are presumed to act through cell type-specific regulatory elements. However, bulk tissue and cell-line models cannot fully resolve these regulatory programs. This project uses single-nucleus multi-omic (RNA+ATAC) profiling, enabling simultaneous measurement of chromatin accessibility and gene expression within the same nucleus, to generate cell type-specific enhancer-gene maps in endometrial tumors. By integrating these maps with GWAS data, we aim to identify a comprehensive set of candidate endometrial cancer risk genes. We used the 10X Multimodal GEX+ATAC single nucleus sequencing kit to map open chromatin and gene expression profiles in archival endometrial tumors available through the Australian National Endometrial Cancer Study (ANECS), a population-based case-control study of endometrial cancer with extensive clinical data. Libraries were sequenced on the NextSeq2000 platform before data processing using Cell Ranger, Seurat and Signac for cell-type-resolved enhancer-gene mapping. Exploratory enhancer-gene mapping was performed using co-accessibility and gene expression correlation analysis in Signac. Credible risk variants from 21 endometrial cancer GWAS loci were intersected with enhancers to identify candidate causal risk variants and corresponding target genes. Approximately 25,000 nuclei were successfully profiled and clustered into major endometrial cell types, including epithelial (ciliated and unciliated), fibroblast and immune cells. Initial enhancer-gene mapping using Signac co-accessibility analysis identified endometrial cancer risk variants at the 13q22.1 locus residing within epithelial cell enhancers that correlate with *KLF5* expression. We have generated the first single-nucleus multimodal map of endometrial cancer, enabling direct linkage of endometrial cancer risk variants to cell type-specific regulatory elements and target genes, including *KLF5*, a transcription factor that regulates uterine epithelial remodeling and promotes endometrial cancer cell proliferation in experimental models. This work represents an ongoing pilot study, with further tumors and loci being analyzed to reveal cell type-specific endometrial cancer risk genes.

#5922 Single-cell mapping of the colon epithelium reveals a pre-malignant stem cell that defines early transformation risk.

Yujin Lee[1], Moray J. Campbell[2], James C. Fleet[1]

[1]Dept. of Nutritional Sciences, The University of Texas at Austin, Austin, TX,[2]Karmanos Cancer Institute, Wayne State University, Detroit, MI

Intestinal stem cells (ISC) are viewed as the origin of colorectal cancer (CRC), but the early stages of carcinogenesis are unclear. We hypothesize that early, non-transforming mutations reprogram ISCs into a preneoplastic state that increases the risk of transformation. We performed single-cell RNA sequencing (scRNA-seq) on colon epithelial cells from Car1-Cre (CAC) mice, which express Cre specifically in colon epithelial cells. CAC mice were crossed to those with floxed oncogene alleles to generate mice with one ($Apc^{+/-}$, AC) or two ($Apc^{+/-}$; $Kras^{G12D/wt}$, AKC) non-transforming mutations. AC mice had normal crypt morphology and low adenoma incidence, while AKC mice exhibited crypt elongation by 4 weeks and multiple adenomas by 8-10 weeks. Cells from distal colonic crypts (n=7) and from tumors (n=3) representing phenotypes ranging from normal to malignant were profiled using the 10X Genomics Chromium. Processing and clustering with Cell Ranger and Seurat yielded 58,906 cells from crypts and 36,327 from tumors. Initial clustering identified epithelial, immune, endothelial, and cancer groups. The epithelial group was subclustered and visualized by UMAP. Cells from CAC crypts followed the classic differentiation path: Stem, Progenitor, Transit-amplifying, Absorptive epithelial cell, Goblet, Tuft, and Enteroendocrine. Stem cell clusters were classified as Normal (CAC), Abnormal 1 (young AKC), or Abnormal 2 (older AKC). The abnormal ISC states in the crypt structures are distinct from the cancer stem cells found in the cancer group. Trajectory analysis revealed that each stem cell population follows a distinct differentiation sequela, with abnormal ISC giving rise to transcriptionally divergent epithelial lineages. This was validated by integrating scRNA-seq data with spatial transcriptomics data from the same lines, showing that abnormal epithelial populations progressively overtake the normal crypt epithelium while retaining crypt structure. Differential gene expression analysis and Gene Set Enrichment Analysis showed that normal ISC was enriched for classic stemness markers (e.g., Lgr5, Lrig1, Smoc2). Abnormal 1 ISC began to lose these features and instead exhibited increased expression of cell-cycle regulators (e.g., Ccna2, Aurkb) and markers of oxidative stress (e.g., Prdx4, Gsta3, Gpx2). Gene expression profiles in Abnormal 2 ISC showed enrichment of pathways controlling p53 (e.g., Cdkn1a, Smad7), RAS/MAPK (e.g., Map2k1, Epha2), and PI3K/Akt/mTOR signaling (e.g., Akt3, Pik3r3, Mtor), as well as for an inflammatory response (e.g., Fos/Jun, Nfkbiz, Il18). Collectively, these findings show that early, non-transforming mutations push ISC into preneoplastic states marked by increased proliferation and stress response signaling favorable for malignant progression.

#5923 Optical pooled CRISPR screening coupling multiplexed guide RNA detection and single-cell spatial multi-omics.

Yi Cui[1], Marena I. Trinidad[2], Nurel Arriaran[2], Isabel Lee[1], Chia-Ying Lee[1], Shanshan He[1], Timothy Riordan[1], Joseph Beechem[1], Alexander E. Ehrenberg[2], Hanqin Li[2]

[1]Bruker Spatial Biology, Seattle, WA,[2]Innovative Genomics Institute, Berkeley, CA

Optical pooled screening (OPS) enables high-throughput measurement of cellular responses to genetic perturbations directly in situ. However, most sequencing-by-synthesis (SBS)-based OPS approaches remain limited to single-gene perturbation readouts or narrow phenotypic panels, restricting their ability to resolve the full complexity of perturbation-driven cellular states. In contrast, multiplexed in situ hybridization-based platforms offer an orthogonal detection strategy capable of simultaneously measuring multiple gRNAs and rich multiomic phenotypes within the same cell. We establish a framework for large-scale pooled CRISPR screening using the CosMx® Spatial Molecular Imager (SMI), enabling spatially resolved, single-cell whole-transcriptome profiling integrated with multiplexed gRNA detection. We evaluated diverse vector architectures expressing barcoded gRNAs to minimize guide-barcode decoupling, a major obstacle in pooled optical screens. Using a reporter-based functional assay, we identified an optimized vector design that preserves Cas9 activity while enabling sensitive, accurate, high-fidelity detection of barcoded gRNAs in situ. We further demonstrate seamless coupling of gRNA detection with high-dimensional RNA and protein profiling at subcellular resolution within the standard CosMx workflow. This provides a practical and scalable path to pooled optical combinatorial CRISPR screening with omics-level phenotypes. By leveraging whole-transcriptome spatial readouts, this approach captures global gene expression changes, emergent cell states, microenvironment-dependent phenotypes, and spatially coordinated transcriptional responses not detected using targeted phenotyping or dissociated single-cell methods. Importantly, spatially resolved whole-transcriptome OPS enables knockouts to be interpreted in their native architectural context, revealing how genetic perturbations influence cell-cell communication, signaling cascades, neighborhood formation, and ligand-receptor interactions. These capabilities position CosMx-enabled pooled CRISPR OPS as a transformative platform for cancer research. It allows investigators to map causal genetic mechanisms within complex in vitro and ex vivo models, uncover cryptic phenotypes that manifest only in spatially organized environments, and identify therapeutic targets invisible to conventional pooled screens. Together, these results establish a strong foundation for next-generation multimodal spatial CRISPR screening. The ability to perform pooled perturbations with unbiased, spatially resolved whole-transcriptome readouts will accelerate discovery of cancer-relevant pathways, support mechanism-of-action and resistance studies, and enable development of spatially aware functional genomics atlases and AI-driven predictive models of tumor biology.

#5924 Single-cell full-length transcriptome of lung cells reveals genetic effects on isoform regulation beyond eQTL.

Bolun Li[1], Thong Luong[2], Elelta Sisay[3], Jinhu Yin[4], Zixuan Zhang[5], Ju Hye Shin[6], Jinyoung Byun[7], Yoon Soo Chang[6], Maria Teresa Landi[8], Nat Rothman[9], Erping Long[10], Qing Lan[11], Christopher I. Amos[7], Tongwu Zhang[12], Jianxin Shi[13], Nicholas Mancuso[14], Haoyu Zhang[15], Jin Gu Lee[16], Eon Young Kim[6], Jiyeon Choi[17]

[1]NIH-NCI, Bethesda, MD,[2]National Cancer Institute, Rockville, MD,[3]NCI, Rockville, MD,[4]DCEG, National Cancer Institute, Rockville, MD,[5]Perelman School of Medicine, University of Pennsylvania, Philadelphia, PA,[6]Yonsei University College of Medicine, Seoul, Korea, Republic of,[7]University of New Mexico Comprehensive Cancer Center, Albuquerque, NM,[8]Senior Investigator, Dceg, NCI-DCEG (Division of Cancer Epidemiology and Genetics), Bethesda, MD,[9]NCI-DCEG, BETHESDA, MD,[10]Chinese Academy of Medical Sciences and Peking Union Medical College, Beijing, China,[11]NCI Div. of Cancer Epidemiology & Genetics, Bethesda, MD,[12]DCEG, National Cancer Insititute, Rockville, MD,[13]National Cancer Insititute, Potomac, MD,[14]Keck School of Medicine, University of Southern California, Los Angeles, CA,[15]National Cancer Inst. Div. of Cancer Epidemiology & Genetics, Bethesda, MD,[16]Department of Thoracic and Cardiovascular Surgery, Yonsei University College of Medicine, Seoul, Korea, Republic of,[17]NCI, Bethesda, MD

Background: Lung cancer is one of the most prevalent and life-threatening cancers worldwide. Genetic factors contribute to lung cancer risk in smokers and non-smokers, and genome-wide association studies (GWAS) identified > 50 genomic loci from diverse populations. Expression quantitative trait loci (eQTL) and splicing QTL (sQTL) analyses can reveal distinct genetic effects on gene- or transcript isoform-level regulation contributing to GWAS signals to identify target genes and elucidate etiology. However, current sQTL studies using short-read sequencing of bulk tissues fail to capture full-length and novel isoforms or cell-type-specific splicing events contributing to tumorigenesis.**Methods**: We present an isoform-level lung cell atlas from 129 never-smoking Korean women using single-cell long-read RNA-sequencing. Epithelial cells, where lung cancer originate, were enriched by FACS sorting. Isoform signatures of each lung cell type were identified by differential analysis. We mapped isoform-level QTLs (isoQTLs) using jaxQTL negative binomial model of pseudo-bulk counts. Colocalization and transcriptome-wide association study (TWAS) with GWAS were performed to prioritize susceptibility isoforms.**Results:** We identified 325,865 full-length isoforms from 360,133 lung cells, where 83% are novel isoforms not annotated in GENCODE v32. We identified isoform-level signatures of 37 lung cell types, where 67.2% of differential isoforms display larger differences than in gene levels. Isoform-QTLs (isoQTLs) identified unreported genes in bulk tissue-based sQTL studies attributed to cell-type-specific and unannotated isoforms. Compared to the barcode-matched short-read expression data, 46% of isoQTLs did not colocalize with eQTLs in the same cell type. Consistently, isoQTLs were distinctly enriched in the functional elements of splicing and post-transcriptional regulation. Colocalization of isoQTLs with lung cancer and trait GWAS signals nominated candidate isoforms, where 69% were previously unreported at the gene level. Moreover, 71% of GWAS-colocalized isoforms were independent from eQTLs, including *PPIL6-207* for lung cancer. TWAS of ancestry-matched lung adenocarcinoma identified 12 isoforms from the sub-threshold GWAS regions, which include lineage or cell-type-specific genes.**Conclusions:** We established an isoform-level lung cell atlas using single-cell long-read sequencing and detected isoQTLs that are cell-type-specific and independent from eQTLs. This isoform-level resource advances our understanding of cell-type-specific isoform regulation and its contribution to lung cancer and diseases.

#5925 Diagnostic concordance of WHO 2021 standards, WGS, and DNA methylation classification in diffuse gliomas: A single-center cohort study.

Jungyu Kim[1], Yongjae Lee[1], Jeong Seok Lee[1], Tae Hoon Roh[2], YOUNG SEOK JU[1]

[1]Korea Advanced Institute of Science and Technology, Daejeon, Korea, Republic of,[2]Neurosurgery, Ajou University School of Medicine, Daejeon, Korea, Republic of

Background: Diffuse gliomas exhibit significant clinical and molecular heterogeneity. However, the real-world concordance among WHO 2021 clinical diagnoses, whole-genome sequencing (WGS), and DNA methylation-based classification remains to be fully characterized.

Methods: We retrospectively analyzed 111 glioma patients treated at Ajou University Hospital (2013-2022). Following strict quality control (excluding low tumor fraction <20%, sample swaps, and recurrent-only cases), 93 patients (104 tumors) underwent WGS, enzymatic methyl-seq (EM-seq), and bulk RNA sequencing. Clinical diagnoses were updated to WHO 2021 standards using routine immunohistochemistry and targeted panel sequencing (astrocytoma, n=14; glioblastoma, n=76; oligodendroglioma, n=14). WGS was utilized to refine classifications based on *IDH* mutation, *TERT* promoter mutation, *EGFR* amplification, and chromosome 7 gain/10 loss. Methylation classes (e.g., GBM RTK I/II, Mesenchymal, MID, HGNET-BCOR) were assigned using an AI-driven classifier trained on Illumina array data (~20,000 CpGs). We evaluated the diagnostic concordance across these three layers.

Results: Diagnostic concordance was 100% for *IDH*-mutant astrocytomas and oligodendrogliomas across clinical, WGS, and methylation layers. In contrast, discrepancies emerged in cases clinically diagnosed as glioblastoma. One case was reclassified as *pediatric-type diffuse hemispheric glioma, H3 G34-mutant*. Another tumor in a 13-year-old patient, harboring complex alterations (*ATRX, PTEN, TP53, PIK3R1, PTPRD, CDKN2A*), was assigned non-GBM methylation labels (CONTR/INFLAM), precluding definitive subclassification. Among tumors classified as GBM RTK I (9/10), GBM RTK II (18/18), or Mesenchymal (15/16) by methylation, nearly all fulfilled molecular glioblastoma criteria (*IDH*-wildtype, TERTp mutation, *EGFR* amp, chr7+/10-). Conversely, tumors in the MID and non-GBM methylation classes frequently lacked these canonical features (17/21). Notably, WGS identified a *BCOR::EP300* translocation in a sample with an HGNET-BCOR methylation profile—a fusion undetected by routine clinical testing—expanding the spectrum of *BCOR*-altered CNS tumors beyond canonical internal tandem duplications.

Conclusions: Integrated WGS and methylation profiling in this single-center cohort demonstrate that DNA methylation-based classification refines WHO 2021 diagnoses, particularly for tumors routinely diagnosed as glioblastoma. This approach uncovers rare entities, such as pediatric-type gliomas and *BCOR*-altered tumors, that may be missed by targeted panels alone. Our findings support the implementation of a multi-omics framework to capture biological heterogeneity obscured by limited molecular markers.

#5926 Overcoming low SEPTIN14 expression to detect EGFR-SEPTIN14 fusion in RNA sequencing.

Suhyun Hwangbo, Sungyoung Lee

Department of Genomic Medicine, Seoul National University Hospital, Seoul, Korea, Republic of

EGFR-SEPTIN14 fusion is a rare but clinically significant oncogenic event, occurring in approximately 3-4% of glioblastoma (GBM) cases. This fusion retains the tyrosine kinase domain of EGFR fused to the coiled-coil domain of SEPTIN14 but is often undetected by RNA sequencing (RNA-seq) due to minimal SEPTIN14 expression outside the testis. To overcome this limitation, we developed a novel detection approach that leverages soft-clipped reads mapped to EGFR with perfect matches to SEPTIN14 sequences, enabling detection even in the absence of SEPTIN14 transcript reads. Using this method, we identified EGFR-SEPTIN14 fusion in positive controls, samples with DNA-based evidence, and additional previously undetected cases in the SNUH cohort. These GBM samples exhibited characteristic oncogenic mutation profiles, including TERT promoter mutation, EGFR amplification, and CDKN2A/B deletions, which may as markers indirectly indicating fusion presence. Notably, one fusion-positive patient treated with erlotinib showed a partial response, suggesting potential sensitivity to EGFR tyrosine kinase inhibitors. Application of our approach to the TCGA-GBM dataset also identified novel positive samples with similar mutation profiles, demonstrating scalability to whole transcriptome data. Overall, our strategy increased detection sensitivity 66.7%, addressing a key limitation of current RNA-seq fusion detection tools and supporting recognition of EGFR-SEPTIN14 fusion as an additional actionable oncogenic driver in solid tumors.

#5927 Integrative analysis of EMT and hippo pathway activity in gastric cancer peritoneal metastasis.

Juin Park[1], Woo Sun Kwon[2], Chan Hee Park[2], Tae Soo Kim[2], Jingmin Che[2], Sun Young Rha[3]

[1]Department of Medicine, Yonsei University College of Medicine, Seoul, Korea, Republic of,[2]Song-Dang Institute for Cancer Research, Yonsei University College of Medicine, Seoul, Korea, Republic of,[3]Yonsei University College of Medicine, Seoul, Korea, Republic of

Gastric cancer (GC) is one of the most aggressive malignancies, with poor patient outcomes often due to frequent peritoneal metastasis. Epithelial-mesenchymal transition (EMT) plays a pivotal role in this metastatic process. Recent studies highlight the involvement of the Hippo signaling pathway in regulating EMT and tumor progression. However, the molecular interplay between Hippo signaling components and *ARID1A*, a key chromatin remodeling factor frequently mutated or lost in GC, remains poorly understood. This study investigates the relationship between Hippo pathway dysregulation and *ARID1A* alteration in gastric cancer peritoneal metastasis (GCPM). Genomic and molecular profiling were performed on 47 GCPM cell lines of CIN and GS-like subtypes. Hierarchical clustering classified the cell lines into EMT and non-EMT groups, as well as into Hippo and non-Hippo groups. EMT and Hippo pathway activity scores were calculated using single-sample gene set enrichment analysis (ssGSEA). Expression of genes related to EMT, Hippo pathways, and *ARID1A* was analyzed at mRNA and protein levels. Invasiveness was evaluated by transwell invasion assays, and sensitivity to the YAP inhibitor CA3 (CIL56) was assessed using cell viability assays. Hierarchical clustering divided the cell lines into EMT (n=34) and non-EMT (n=13) groups. The EMT group was enriched in gene sets related to EMT, YAP, and TGF-β pathways and exhibited significantly higher EMT and Hippo pathway scores ($p < 0.05$). These molecular features were accompanied by markedly higher invasive capacity. CA3 sensitivity varied widely across PMGC cell lines, with a mean IC_{50} of 0.65 μM (range, 0.07-1.98 μM). No significant differences in CA3 sensitivity were observed across TCGA molecular subtypes, EMT, or Hippo subgroups. Notably, *ARID1A*-altered cell lines demonstrated significantly enhanced sensitivity to the YAP inhibitor CA3 compared with *ARID1A*-wild-type lines, suggesting a dependency on YAP activity in *ARID1A*-deficient tumors. Together, these findings indicate that *ARID1A* alterations enhance Hippo-YAP pathway dependence and confer increased sensitivity to YAP inhibition in GCPM. *ARID1A*-deficient tumors may therefore benefit from therapeutic strategies targeting the Hippo-YAP axis.

#5929 Global mRNA 3'UTR lengthening in small-cell neuroendocrine carcinoma.

Yi Zhang[1], Xiaofan Zhao[1], Ya-Mei Hu[1], Xiao-Xin Sun[2], Faming Zhao[3], Nicole Andeen[2], Rosalie C. Sears[2], Jonathan R. Brody[3], Joshi J. Alumkal[4], Gordon B. Mills[3], Mushui Dai[2], Zheng Xia[2]

[1]Biomedical Engineering, Oregon Health & Science University, Portland, OR,[2]Oregon Health & Science University, Portland, OR,[3]OHSU Knight Cancer Institute, Portland, OR,[4]Rogel Cancer Center, Ann Arbor, MI

Small-cell neuroendocrine carcinoma (SCNC) is a rare but highly malignant tumor subtype, primarily arising in the lung and prostate. The convergence of SCNCs across diverse tissues enables their identification through conserved SCNC-specific molecular markers, facilitating tumor subtype classification. As a critical post-transcriptional regulatory mechanism, alternative polyadenylation (APA) is involved in various biological processes, especially in tumor progression. However, its role across tumor subtypes remains unclear. Here, we revealed a global 3'UTR lengthening pattern due to APA in the SCNCs. We identified a set of conserved lengthening 3'UTR events across SCNCs originating from different tissues, showing a high association with neural development and related signaling pathways. More broadly, we developed a prediction model using a neural network framework to identify SCNCs based on the SCNC-specific APA signatures as additional molecular markers. Our work provides new insights into the post-transcriptional landscape of SCNCs and establishes APA as a potential biomarker for SCNC identification.

#5930 Spatial transcriptomics of colonic neoplasia presenting mucinous adenocarcinoma with genetically-engineered mouse model.

Haruki Sada[1], Hiroaki Niitsu[2], Hikaru Nakahara[2], Masashi Miguchi[3], Hirotaka Tashiro[1], Hideki Ohdan[4], Takao Hinoi[2]

[1]Surgery, NHO Kure medical center, Kure, Japan,[2]Clinical and Molecular Genetics, Hiroshima University Hospital, Hiroshima, Japan,[3]Department of Gastroenterological Surgery, Hiroshima Prefectural Hospital, Hiroshima, Japan,[4]Gastroenterological and Transplant Surgery, Hiroshima University,, Hiroshima, Japan

Background: We previously established a genetically engineered mouse model in which Apc and Tgfbr2 are specifically knocked out in the colonic epithelium (CDX2P-G19Cre; $Apc^{flox/+}$; $Tgfbr2^{flox/flox}$). In this model, 40% of mice developed mucinous adenocarcinoma (MAC) in the colon, while 25% exhibited non-mucinous high-grade dysplasia with the same genotype. The mucinous tumors invaded beyond the muscularis mucosae, and nuclear localization of β-catenin was observed in the deep invasive lesion. To elucidate the mechanisms underlying the development of mucinous colorectal carcinoma, we previously performed transcriptomic analysis comparing MAC and non-mucinous dysplasia. In the present study, we conducted spatial transcriptomic analysis to characterize the spatial distribution of gene expression, cellular composition, and cell-cell interactions within MAC tissues.**Methods:** Tumors diagnosed as MAC by H&E staining were obtained from CDX2P-G19Cre; $Apc^{flox/+}$; $Tgfbr2^{flox/flox}$ mice. FFPE tissue blocks were sectioned to prepare libraries and sequencing was performed using the NovaSeq platform. Data were analyzed using Space Ranger software and visualized in Loupe Browser (10x Genomics).**Results:** Spatial transcriptomic profiling revealed heterogeneous tumor microenvironments within the same MAC lesion. In the deepest invasive lesion, increased infiltration of SPP1 (secreted phosphoprotein 1)-positive macrophages was identified, suggesting the presence of a localized immunomodulatory niche associated with invasion.**Conclusions:** Spatial transcriptomic analysis demonstrated distinct intratumoral regions characterized by unique cellular compositions and gene expression profiles. These findings provide novel insights into the spatial heterogeneity and progression mechanisms of mucinous colorectal carcinoma, potentially informing future therapeutic strategies.

#5931 Modeling of bladder cancer evolution from field effects by multi-platform spatial mapping on the whole-organ scale.

Bogdan A. Czerniak[1], Sangkyou Lee[1], Khanh Ngoc Dinh[2], Huiqin Chen[3], Yishan Wang[3], Jiansong Chen[3], June Goo Lee[1], Sung Yun Jung[4], Nagireddy Putluri[5], Neema Navai[6], David McConkey[7], Charles Chuanhai Guo[1], Peng Wei[3], Marek Kimmel[8]

[1]Department of Pathology, UT MD Anderson Cancer Center, Houston, TX,[2]Irving Institute for Cancer Dynamics & Department of Statistics, Columbia University, New York, NY,[3]Department of Biostatistics, UT MD Anderson Cancer Center, Houston, TX,[4]Molecular & Cellular Biology, Baylor College of Medicine, Houston, TX,[5]Metabolomic Core, Baylor College of Medicine, Houston, TX,[6]Department of Urology, UT MD Anderson Cancer Center, Houston, TX,[7]Department of Urology, University of Rochester, Rochester, NY,[8]Department of Statistics, Rice University, Houston, TX

Introduction: Understanding the mechanisms driving evolution of the mucosal field effects to invasive cancer is not possible unless they are analyzed in the context of their geographic distribution in the entire organ. Bladder cancer is an ideal model disease for such studies as it effects an anatomically simple organ permitting the multi-platform analysis of the affected mucosa on the scale of whole organ.

Methods: We performed comprehensive multi-platform analyses on nine cystectomies with invasive bladder cancer comprising of 433 mucosal tissue samples analyzed by bulk whole-exome and mRNA sequencing, genome-wide copy number variation and methylation profiling complemented with proteomics, metabolomic and single cell sequencing spatial mapping. The data from multi-platform profiling were geographically annotated to microscopically normal urothelium (NU) and low-grade intraurothelial neoplasia (LGIN; n=243), high-grade intraurothelial neoplasia (HGIN; n=90), and invasive urothelial carcinoma (UC; n=100).

Results: We identified ~16000 non-silent mutations per cystectomy. In two maps the hypermutator phenotypes with ~48000 and ~57000 mutations were detected. The mutational analysis identified three types of mutations based on the variant allele frequency and geographic distribution referred to as α, β, and Ƴ. Time modeling by a parsimonious time-continuous Markov model incorporating cell migration (immigration) and growth (branching) revealed that bladder carcinogenesis takes approximately three decades and can be divided into dormant and progressive phases. Low selection α mutations were private and most frequent. They continuously developed over 30 years primarily in the dormant phase of carcinogenesis. β mutations clonally expanded regionally and signified the advent of progressive phase of carcinogenesis which lasted five years. Ƴ mutations were the ultimate drivers of the progressive phase and emerged 2-3 years before the final progression to invasive bladder cancer. The mutational landscape developed on the background of severely dysregulated urothelial differentiation and increased immune infiltration with T-cell exhaustion. The proteomic and metabolomic changes involved a wide-spread disorganization of glycolipid energy metabolism with downregulation of mitochondrial oxidative phosphorylation.

Conclusion: Dysregulated mitochondrial energy metabolism converging on anerobic glycolysis and oxidative phosphorylation with Warburg phenotype emerged as the leading mechanism driving the progression of mucosal field effects to invasive cancer.

#5932 Cell free DNA based genomic analysis revealed the distinct whole genome landscape and chronology of intravascular large B cell lymphoma.

Takuto Mori[1], Kazuyuki Shimada[2], Kaito Mimura[1], Suguru Fukuhara[3], Koji Izutsu[3], Daisuke Kawauchi[4], Yoshitaka Narita[4], Akiko Miyagi Maeshima[5], Ryosuke Koyamada[6], Nobuhiro Hiramoto[7], Hirona Maeda[8], Nobuyuki Kakiuchi[8], Ai Okada[9], Kenichi Chiba[9], Yuichi Shiraishi[9], Akifumi Takaori–Kondo[10], Seishi Ogawa[8], Akihiro Tomita[11], Kenichi Yoshida[1]

[1]Division of Cancer Evolution, National Cancer Center Research Institute, Tokyo, Japan,[2]Department of Hematology and Oncology, Nagoya University Graduate School of Medicine, Nagoya, Japan,[3]Department of Hematology, National Cancer Center Research Institute, Tokyo, Japan,[4]Department of Neurosurgery and Neuro-Oncology, National Cancer Center Research Institute, Tokyo, Japan,[5]Diagnostic Pathology, National Cancer Center Research Institute, Tokyo, Japan,[6]Department of Hematology, St. Luke International Hospital, Tokyo, Japan,[7]Department of Hematology, Kobe city medical center general hospital, Kobe, Japan,[8]Department of Pathology and Tumor Biology, Kyoto University, Kyoto, Japan,[9]Division of Genome Analysis Platform Development, National Cancer Center Research Institute, Tokyo, Japan,[10]Department of Hematology, Kyoto University, Kyoto, Japan,[11]Department of Hematology, Fujita Health University School of Medicine, Tokyo, Japan

The scarcity of tumor cells in biopsies has hampered genomic analysis of intravascular large B-cell lymphoma (IVLBCL), an aggressive lymphoma characterized by selective tumor growth within vessels. The utility of cell-free DNA (cfDNA) for genomic studies, demonstrated in our previous work, may help reveal the genetic alterations of IVLBCL, which might differ from those of related subtypes of lymphoma subtypes, such as immune-privileged large B-cell lymphoma (IP-LBCL).To comprehensively characterize the mutational landscape of IVLBCL, we performed whole-genome and whole-exome sequencing of 36 IVLBCL samples, which are derived from cfDNA (n = 32) and patient-derived xenografts (n = 4), as well as 25 biopsy or surgical samples from IP-LBCL, including 12 central nervous system and 13 testicular lymphomas, and compared their genomic profiles.The majority of cfDNA from IVLBCL was derived from tumor cells (median, 88.8%; range, 55-98%). Most frequently mutated genes were *PIM1*, *MYD88, CD79B, TBL1XR1, MPEG1*, and *ETV6*. Mutational signature analysis showed that clustered mutations, such as kataegis, were caused by activation-induced cytidine deaminase (AID). However, in general, driver mutations such as *MYD88* mutations were not affected by AID activity. Copy number (CN) analysis showed recurrent arm-level changes such as loss-of-heterozygosity (LOH) of 9p and 3p, gain of 1q, and deletion of 6q. As for focal CN changes and/or structural variants (SVs), deletions involving *CDKN2A, TOX, PRDM1*, and *CD58*, as well as focal amplification or multiple types of SVs involving *CD274/PDCD1LG2*, were frequently observed in IVLBCL. Timing analysis indicated that *MYD88* mutations and 9p LOH targeting *CDKN2A* were acquired at early stages of tumor evolution.Comparing IVLBCL and IP-LBCL, most genetic abnormalities, including early *MYD88* mutations and 9p changes, were shared, but several lesions differed significantly between the two. *RAC2* coding mutations were enriched in IVLBCL (33% vs 0%). As for immune pathway, one of the notable differences was the frequency of *CD274/PDCD1LG2* abnormalities, which were observed in about 40% of IVLBCL but were rarely detected in 4% of IP-LBCL. In contrast, *B2M* abnormalities were more frequent in IP-LBCL than IVLBCL. Although the earliest driver mutations and CN abnormalities in IVLBCL are similar to those in IP-LBCL, our findings suggest that the immune-evasion-related genetic alterations uniquely observed in IVLBCL may reflect its distinct interactions with the tumor microenvironment and could help distinguish IVLBCL from IP-LBCL.

#5933 Whole-genome sequencing of lung neuroendocrine neoplasms reveals a *TP53*^{WT} / *RB1*^{WT} subtype with *CCND* amplification.

Minjun Ha[1], Kwon Joong Na[2], Soyeon Kim[3], Miso Kim[4], Bhumsuk Keam[5], Tae Min Kim[5], Dong-Wan Kim[5], Jeonghwan Youk[4], Young Tae Kim[2]

[1]Cancer Research Institute, Integrated Major in Innovative Medical Science, Seoul National University College of Medicine, Seoul, Korea, Republic of,[2]Cancer Research Institute, Department of Thoracic and Cardiovascular Surgery, Seoul National University Hospital, Seoul National University College of Medicine, Seoul, Korea, Republic of,[3]Cancer Research Institute, Biomedical Research Institute, Seoul National University Hospital, Seoul National University College of Medicine, Seoul, Korea, Republic of,[4]Cancer Research Institute, Department of Internal Medicine, Seoul National University Hospital, Seoul National University College of Medicine, Seoul, Korea, Republic of,[5]Cancer Research Institute, Integrated Major in Innovative Medical Science, Department of Internal Medicine, Seoul National University Hospital, Seoul National University College of Medicine, Seoul, Korea, Republic of

Background: Lung neuroendocrine neoplasms (LNENs) comprise a spectrum of entities, including typical/atypical carcinoid, large cell neuroendocrine carcinoma (LCNEC), and small cell lung cancer (SCLC). Data from both whole-genome sequencing (WGS) and targeted panel sequencing show that SCLC is typically associated with biallelic inactivation of *TP53* and *RB1* in 91% of cases. While SCLC has been extensively profiled using WGS, other LNEN subtypes have largely been investigated using targeted panels or whole-exome sequencing, limiting comprehensive genomic characterization. To advance the understanding of early-stage LNEN biology, we performed WGS on a surgically resected cohort spanning the full spectrum of LNENs.

Methods: We analyzed ~30× WGS data from 58 surgically resected LNENs at Seoul National University Hospital (carcinoid n=11; LCNEC n=22; SCLC n=25). Somatic single-nucleotide variants (SNVs), structural variants (SVs), copy-number profiles, and mutational signatures were evaluated.

Results: Across the cohort, median SV/SNV burdens were 0.015 [28/1,929] for carcinoids, 0.006 [186/28,954] for LCNECs, and 0.002 [62/36,181] for SCLCs. Three SCLC samples exhibited markedly elevated SV/SNV ratios compared with other SCLCs (patient #135: 0.092 [345/3,750]; patient #144: 0.158 [331/2,098]; patient #147: 0.031 [94/3,053]; other SCLCs: 0.000-0.005). This pattern was absent in LCNECs but was detected in one carcinoid sample (patient #126: 0.024 [50/2,128]). These four cases (three SCLCs, one carcinoid) uniformly lacked tobacco-associated mutational signatures and were *TP53*^{WT}/*RB1*^{WT}. Two samples from patients #126 and #135 demonstrated chromothripsis involving chromosomes 3 and 11, whereas the remaining two from patients #144 and #147 showed dense rearrangements between chromosomes 12 and 20 with prominent copy-number oscillations. These alterations converged on amplification of *CCND1* (chr11) or *CCND2* and *CDK4* (chr12), with shared losses involving *FHIT*, *TGFBR2*, and additional copy-number alterations on partner chromosomes. Pathologic review further revealed coexisting atypical carcinoid and SCLC components in one SCLC case (patient #135).

Conclusions: All four cases displayed convergent *CCND*-*CDK4* pathway activation and characteristic complex SV-driven genome remodeling. Together with the histological coexistence of atypical carcinoid and SCLC in patient #135, these data raise the possibility that *CCND*-dependent SCLC may evolve from a carcinoid precursor. The observation of one carcinoid in patient #126 provides independent evidence of *CCND*-dependent tumorigenesis. Although limited by sample size, our findings highlight a distinct, early-stage LNEN subset defined by catastrophic SV events and G1-S checkpoint dysregulation, suggesting potential therapeutic vulnerability to cell-cycle-targeted strategies.

#5934 Genomic signatures of chromosomal instability from a pan-cancer landscape of haplotype-specific copy-number alterations.

Chunyang Bao[1], Matthew Leventhal[2], Hansol Park[1], Gang-Hee Lee[1], Ryul Kim[1], Won-Chul Lee[1], Jonghoon Lee[1], Yoonsuh Lee[1], Beomki Lee[3], David Lehotzky[4], Ron Solan[4], Antonia Kowalewski[4], Xavi Loinaz[4], Vasuki Narasimha Swamy[4], David I. Heiman[4], Samantha Van Seters[4], Saveliy Belkin[4], Sam Wiseman[4], Andrew D. Cherniack[4], Luis Antonio Corchete Sanchez[4], Brian P. Danysh[4], Zachary Everton[4], Chip Stewart[4], Haruna Tomono[4], Gengchao Wang[4], Esther Rheinbay[4], Gad Getz[4], Cheng-Zhong Zhang[2], Young Seok Ju[1]

[1]Inocras Inc., San Diego, CA,[2]Department of Data Science, Dana-Farber Cancer Institute, Boston, MA,[3]Graduate School of Medical Science and Engineering, Korea Advanced Institute of Science and Technology, Dajeon, Korea, Republic of,[4]Cancer Program, Broad Institute of MIT and Harvard, Cambridge, MA

Whole-chromosome and segmental copy-number changes are nearly ubiquitous in human cancers. Here, we present the first pan-cancer landscape of haplotype-specific somatic copy number alterations (SCNAs) in nearly 9,000 cancers across 30 cancer types from The Cancer Genome Atlas (TCGA) whole-genome sequencing (WGS) data. This analysis was primarily carried out with CancerVision, a proprietary bioinformatic workflow for detecting both somatic and germline variants in cancer samples developed by Inocras. The haplotype-specific copy-number analysis provides three pieces of information not available from previous analysis. First, the haplotype-specific SCNAs enables a more accurate assessment of aneuploidy, i.e., the fraction of the cancer genome with copy number alterations. Second, the haplotype resolution directly resolves interactions between germline variant genotypes and SCNAs. Finally, haplotype-specific SCNAs directly inform the instigating mechanisms of chromosomal instability. In this study, we provide examples demonstrating each scenario. Notably, we observed a diverse range of haplotype-specific SCNA patterns, each reflecting a distinct mechanism of chromosomal instability, including arm-level alterations related to WGD, segmental changes indicative of breakage-fusion-bridge (BFB), complex rearrangements displaying signatures of successive BFB cycles and chromothripsis, as well as focal amplifications consistent with extrachromosomal DNA (ecDNA) formation. Our analysis of haplotype-specific SCNAs in TCGA suggests a mechanism-based classification of copy-number patterns linked to chromosomal instability. Extending this framework to treatment-exposed samples could provide new insights into synthetic lethality dependencies, with potential diagnostic and therapeutic implications for cancer precision medicine.

#5935 Accurate detection of DNA variants and ecDNA from prostate FFPE biopsies using LinkPrep.

Shiting Li[1], Alexander Fortuna[2], Rahul Mannan[1], John Zachary Sanborn[3], Yuping Zhang[1], Xuhong Cao[1], Natalie Fredriksson[2], Lisa Munding[2], Saravana M. Dhanasekaran[1], Marcin Cieslik Cieslik[1], Arul M. Chinnaiyan[1]

[1]University of Michigan, Ann Arbor, MI,[2]Cantata Bio, LLC, Scotts Valley, CA,[3]Dovetail Genomics, Scotts Valley, CA

Detecting genomic variants and structural rearrangements in formalin-fixed paraffin-embedded (FFPE) tumor biopsies simultaneously remains challenging and lacks comprehensive clinical utility assessments. Here we performed the novel Dovetail®-FFPE (LinkPrep), an *in vitro* transposition Hi-C assay free from restriction enzyme bias to 20 prostate cancer samples. These included 5 normal adjacent to tumor (benign), 10 primary localized, and 10 metastatic castration-resistant prostate cancer (mCRPC) patient samples. By leveraging patient and site-specific in-house matched fresh-frozen (FF) whole-genome sequencing (WGS), exome capture sequencing, transcriptomics sequencing, and a publicly available cohort of 80 mCRPC FF Hi-C samples data, we performed a comprehensive evaluation on FFPE LinkPrep library preparation and sequencing performance. Our evaluation covered multiple aspects including 3D genome contact detection, single nucleotide variant (SNV)/indel calling, copy number variation analysis, structural variant (SV) detection, ecDNA detection and compartments definition.Our analysis shows that FFPE sample achieves good contact capture efficiency that is slightly lower but comparable performance (Wilcoxon test p=0.33) to the FF Hi-C data for mCRPC tumors. For SNV/INDEL calling, using FF WGS or exome capture sequencing as the gold standard, the assay reached a mean recall rate of 97% across five samples based on two different variant- calling algorithms. By comparing with 2 FF WGS, 4 transcriptomic and 80 external Hi-C data, we further demonstrated that FFPE samples can accurately identifies whole-genome copy number variations and chromatin compartments. Additionally, we developed a robust SV-calling pipeline with carefully designed denoising steps suitable for FFPE samples that accurately detected common structural variants in prostate cancer, such as TMPRSS2-ERG fusions (6/7) and FOXA1mutations (2/2). Lastly, by applying the new developed Hi-C specific pipeline for extrachromosomal DNA (ecDNA) detection, we identified AR ecDNA in one sample, which was supported by matched FF WGS AmpliconSuite result. Overall, the comprehensive analysis and performance evaluation demonstrates that FFPE LinkPrep accurately captures DNA-level variants and holds strong potential for application in FFPE clinical samples.

#5936 Massively parallel installation and evaluation of cancer coding mutations.

Xiaoyu Zhao[1], Isabella Panagiotou[1], Rachel Collier[1], Catalina Fogg[1], Katherine Licon[1], John J. Y. Lee[1], Dylan Fong[1], Jing Chen[1], Paulina Rios[2], Ondine Atwa[2], Samuel I. Gould[2], Ingoo Lee[1], Jiahao Gao[1], Francisco J. Sanchez-Rivera[2], **MARCUS R. KELLY**[1], Trey Ideker[1]

[1]Medicine, University of California San Diego School of Medicine, La Jolla, CA,[2]Koch Inst. for Integrative Cancer Research at MIT, Cambridge, MA

Most cancer coding mutations are of unknown function, limiting their biological and therapeutic interpretation. While prime editing enables precise genomic alterations, mutations often reside in sequence contexts unfavorable to current prime-editing guide RNA (pegRNA) designs. Here we develop CodonPrime, a prime-editing framework that exploits codon degeneracy surrounding a mutation site to substantially expand its targeting set of pegRNAs. We use this approach to screen ~2500 coding mutations spanning 298 cancer genes, yielding a 9.2-fold increase in amino-acid editing efficiency over conventional prime editing. Approximately 10% of coding mutations enhance cell growth, recovering known oncogenic hotspots and revealing oncogenic potential for previously uncharacterized mutations (e.g. $HNF1A^{R272C}$). Our analysis uncovers dominant effects in paralogous genes (e.g. RHOBTB1/2) and organization of mutant phenotypes in pathways (e.g. PI3K-MTOR signaling). We formulate a general-purpose transformer for design of CodonPrime pegRNAs, enabling scalable interrogation of human coding variants.

#5937 Panorama of chromosomal instability in 1209 lung cancer genomes.

YANG YANG[1], Tongwu Zhang[2], **Lixing Yang**[1], Maria Teresa Landi[2]

[1]University of Chicago, Chicago, IL,[2]National Cancer Institute, Bethesda, MD

Lung cancer is the leading cause of cancer death worldwide in both men and women. It is a highly heterogeneous disease primarily driven by tobacco smoking. About 20% of lung cancers occur among never smokers. There are major differences between lung cancers in patients who have never smoked (LCINS) and who have smoked in patient ancestry, sex, tumor histology and clinical features. LCINS occur more frequently in Asians and females and are predominantly adenocarcinomas. *EGFR* mutations are enriched in LCINS, whereas *KRAS* and *TP53* mutations are more common in tumors from patients who have smoked. Our understanding of the etiology of LCINS is still limited. Here, we perform a comprehensive study in 1,209 whole-genome sequenced lung cancers collected from 30 different locations across four continents through Sherlock-Lung Project as well as published studies. Among these tumors, 1024 of them are adenocarcinomas and 864 are LCINS. This cohort represents the largest genomics cohort in lung cancer to date. Our study focuses on somatic structural variations (SVs) which are large-scale chromosomal rearrangements. In total, we detect 182,429 somatic SVs in 1209 tumor samples with an average of 151 SVs per sample. Complex SVs, such as chromothripsis, are studied separately from simple SVs because they arise through one-time catastrophic chromosome shattering and rejoining. About two-thirds of the SVs in our cohort are part of complex events. We deconvolute a total of 8 complex SV signatures based on event topology and 8 simple SV signatures using non-negative matrix factorization. They likely represent divergent molecular mechanisms. Among these, chromatin bridge signature, driven by dicentric chromosomes, is the most abundant complex SVs; and median size deletion is the most common simple SVs. SVs are more abundant in tumors from patients who have smoked; however, they are more complex and play more important roles in tumorigenesis in LCINS. The SV breakpoints have distinct distributions across the genome depending on the signatures due to combined effects of mutagenesis and positive selection. Many established cancer-driving genes are recurrently rearranged by multiple SV signatures suggesting functional convergence of these genome instability mechanisms. *EGFR* mutations and *KRAS* mutations profoundly and independently shape the SV landscape. *EGFR* mutant tumors have higher SV burden and more cancer-driving SVs. In contrast, *KRAS* mutations are associated with lower SV burden and fewer driver SVs. Our study has deepened our understanding of genomic landscape and etiology of lung cancer.

#5938 High-resolution multi-omic dissection of bone marrow in TP53-mutant acute myeloid leukemia.

Gonzalo Lopez Garcia[1], Felix Andreas Radtke[2], Sagnik Banerjee[3], BIJAY JAISWAL[4], Daiane Hemerich Brennan[5], Yilin Zhao[6], Verena Korber[7], Marlen Metzner[7], Rachel Moore[7], Bilyana Stoilova[7], Junfei Zhao[5], Bettina Nadorp[1], David Cruz Hernandez[7], Batchimeg Usukhbayar[7], Aimee O'Donohue[8], Maria Ortiz Estevez[9], Daniel Lopes de Menezes[4], Rajasekhar NVS Suragani[10], Paresh Vyas[11], Anita Gandhi[8]

[1]Informatics and Predictive Sciences, Bristol Myers Squibb, Cambridge, MA,[2]Weatherall Institute for Molecular Medicine, Headington,[3]Informatics and Predictive Sciences, Bristol Myers Squibb, San Diego, CA,[4]Translational Development, Bristol Myers Squibb, Brisbane, CA,[5]Informatics and Predictive Sciences, Bristol Myers Squibb, Summit, NJ,[6]Informatics and Predictive Sciences, Bristol Myers Squibb, Seattle, WA,[7]University of Oxford, Oxford, United Kingdom,[8]Translational Development, Bristol Myers Squibb, Summit, NJ,[9]Informatics and Predictive Sciences, Bristol Myers Squibb, Sevilla, Spain,[10]Translational Development, Bristol Myers Squibb, Cambridge, MA,[11]University of Oxford, Department of Biochemistry, Oxford, United Kingdom

TP53-mutated (*TP53*m) AML is a distinct biological entity with adverse prognosis, characterized by prominent clonal heterogeneity; cells within a patient may exhibit wild type, monoallelic, or biallelic *TP53* status, alongside co-occurring genomic alterations and transcriptomic heterogeneity. This complexity poses challenges in accurately aligning genotypes with transcriptomic and epigenomic profiles at single-cell resolution.

To address this, we integrated single-cell RNA-seq (10x and long-read Oxford Nanopore, ONT) with open chromatin profiles (scATAC-seq) and whole-genome sequencing (WGS) to capture structural variants (SV), copy number alterations (CNV), and single nucleotide variants (SNV) from bone marrow samples taken from a cohort of 47 *TP53*m, 7 *TP53* wild-type (wt) AML patients, and 4 healthy donors.Cell type annotation for scRNA-seq (335K cells) utilized a bone marrow reference dataset, while scATAC-seq (130K cells) was annotated using the ArchR label-transfer method. Cell type proportions were concordant across modalities (median correlation, $\rho = 0.76$).

SV and CNV profiles showed that *TP53*m samples displayed frequent loss of Chr5q (72.5%), Chr17p (52.5%), and Chr7q (40%); chromothripsis was present in 16 (40%) samples. All these events were reported to occur in under 3% of *TP53*wt AMLs. In contrast, *TP53*m samples showed relative paucity of SNV co-mutations.We leveraged CNV profiles to map genetic gain/loss effect in scRNA and scATAC-seq compared to healthy donors, providing a clear separation of cells with abnormal CNV profiles. In TP53m AML, apart from mature lymphoid populations, >80% of cells including lymphoid progenitors (LMPP), displayed abnormal CNV status. Abnormal CNV cell fractions by sample strongly correlated with orthogonal tumor purity estimations from WGS for scRNA ($\rho = 0.81$) and ATAC-seq ($\rho = 0.84$).Single-cell SNV mapping was attempted with the standard 10x pipeline, where we detected driver hotspot mutations in only ~3% of non-lymphoid cells. To improve mutation calling, we developed a new SNV pipeline using long-read ONT chemistry on full-length cDNA. SNV calling rates rose to 15% in non-lymphoid cells. Mature lymphoid cells showed low alteration rates: SNVs (1-2%), CNVs (5%), while expressing lineage-specific markers, confirming cell-type assignment.

Long-read *TP53* transcript sequencing also enabled phased variant genotyping. Combined with WGS SV and CNV profiles, we observed that *TP53* loss-of-function dosage distinctly associates with the genomic architecture: biallelic loss of *TP53* was associated with extensive intrachromosomal breaks and chromothripsis, whereas monoallelic loss primarily induced numerical chromosomal changes.

This multi-omic framework enables high-resolution characterization of somatic genomic alterations at the single-cell level in *TP53*m AML, providing a powerful platform for mechanistic interrogation of disease biology.

#5939 A large-scale sequencing study identifies a novel non-coding structural variant as a high-penetrance susceptibility variant for melanoma.

Linh T. Bui-Raborn[1], Lorenza Pastorino[2], Donato Calista[3], Huu Phuc Hoang[1], Bruna Dalmasso[4], Jessica Scales[1], Sophie Papiernik[1], Xiaoyu Wang[1], Rohit Thakur[1], Stefania Pellegrini[5], Mai Xu[1], Joshuah Yon[1], William Bruno[2], Tongwu Zhang[1], Zaida Garcia-Casado[6], Enrica Teresa Tanda[7], Francesco Spagnolo[8], Monia Di Prete[9], Irene Bottillo[10], Siranoush Manukian[11], Maria Chiara Scaini[5], Katerina P. Kypreou[12], Lucia Di Nardo[13], Miriam Potrony[14], Paula Aguilera-Peiro[15], Nesreen Shahrour[1], Tam-Anh Tran[1], Weiyin Zhou[1], Wen Lou[1], Aurelie L. Vogt[1], Jia Liu[1], Kristine Jones[1], Monica Rodolfo[16], Irene Stefanaki[12], Cristina Pellegrini[17], Carlo Cota[9], Chiara Menin[5], Maria Concetta Fargnoli[9], Ketty Peris[18], Susana Puig[14], Eduardo Nagore[19], Paola Grammatico[20], The Melanostrum Consortium, Jianxin Shi[1], Paola Ghiorzo[2], Kevin M. Brown[1], Maria Teresa Landi[1]

[1]Division of Cancer Epidemiology and Genetics, National Cancer Institute, Rockville, MD,[2]Department of Internal Medicine and Medical Specialties, University of Genoa; IRCCS Ospedale Policlinico San Martino, Genoa, Italy,[3]Department of Dermatology, Maurizio Bufalini Hospital, Cesena, Italy,[4]IRCCS Ospedale Policlinico San Martino, Genoa, Italy,[5]Immunology and Molecular Oncology Unit, Veneto Institute of Oncology (IOV-IRCCS), Padua, Italy,[6]Laboratory of Molecular Biology, Instituto Valenciano de Oncologia, Valencia, Spain,[7]Department of Internal Medicine and Medical Specialties, University of Genoa, Genoa, Italy,[8]Medical Oncology 2, IRCCS Azienda Ospedaliera Metropolitana, Genoa, Italy,[9]Dermatopathology Research Unit, San Gallicano Dermatological Institute IRCCS, Rome, Italy,[10]Laboratory of Medical Genetics, Experimental Medicine Department, San Camillo-Forlanini Hospital, Sapienza University, Rome, Italy,[11]Unit of Medical Genetics, Department of Medical Oncology and Hematology, Fondazione IRCCS Istituto Nazionale dei Tumori, Milan, Italy,[12]1st University Clinic of Dermatological and Venereal Diseases, Andreas Syggros Hospital, School of Medicine, National and Kapodistrian University of Athens, Athens, Greece,[13]Immunology Research Core Facility - Gemelli Science and Technology Park (GSTeP), Fondazione Policlinico Universitario Agostino Gemelli IRCCS, Rome, Italy,[14]Biochemistry and Molecular Genetics Department, Hospital Clinic of Barcelona, IDIBAPS, Barcelona, Spain,[15]Dermatology, Hospital Clinic de Barcelona, Barcelona, Spain,[16]Unit of Translational Immunology, Department of Experimental Oncology, Fondazione IRCCS Istituto Nazionale dei Tumori, Milan, Italy,[17]Department of Biotechnological and Applied Clinical Sciences, University of L'Aquila, L'Aquila, Italy,[18]Dermatologia, Dipartimento Universitario di Medicina e Chirurgia Traslazionale, Universita Cattolica del Sacro Cuore, Rome, Italy,[19]Dermatology, Instituto Valenciano de Oncologia, Valencia, Spain,[20]Experimental Medicine Department, Laboratory of Medical Genetics, Sapienza University of Rome, San Camillo-Forlanini Hospital, Rome, Italy

Approximately 10% of cutaneous malignant melanoma cases are familial. Variants in *CDKN2A* account for ~40% of melanoma-prone families, with 10% more explained by other established genes. Strikingly, many unexplained families nonetheless show genetic linkage to chromosomal band 9p21, which harbors *CDKN2A*, suggesting that high-penetrance non-coding variants in the region may contribute to familial risk.As a part of a large-scale study of high-risk melanoma families from the Mediterranean region, we conducted germline whole-genome sequencing (WGS) on a melanoma case from a four-case family from Genoa, Italy, that is negative for variation in known susceptibility genes. We identified a novel 100kb deletion mapping to 9p21 205kb from *CDKN2A* and verified cosegregation in the two other available cases. The deletion is not protein-coding but contains annotated melanocyte enhancer elements and open chromatin that we find to interact with the promoters of the p16 and p14 transcripts of *CDKN2A* in melanocytes using H3K27Ac Hi-ChIP.To identify additional deletion carriers in whole-exome sequencing (WES) data, we searched for nearby exonic variants that cosegregate in the discovery family to serve as a proxy of the deletion, identifying a rare cosegregating missense variant in *MTAP* (rs755147810; chr9: 21,802,755:T:G; p.Ser3Ala; gnomADv4.1 Non-Finish European MAF: $3.4x10^{-6}$). We assessed this variant in WES data from 3,574 high-risk Mediterranean melanoma patients and 2,673 controls, identifying 17 additional Italian melanoma cases (mostly from Genoa) and a single control, and subsequently confirmed all carriers of rs755147810 harbored the deletion. We verified cosegregation of the deletion in all available cases from four additional families (3/3, 2/2, 2/2 and 2/2 cases). The association of the *MTAP* variant with melanoma risk was highly significant when considering unrelated individuals from Italy, Spain, and Greece (3,219 cases and 2,266 controls; $P = 4.34 \times 10^{-4}$; OR = 13.88) as well as Italian samples alone (2,170 cases, 1,888 controls; $P = 4.14 \times 10^{-4}$; OR = 14.01). Analysis of a shared haplotype among carriers suggests a founder haplotype with the most recent common ancestor (MRCA) dating approximately 26 generations, *i.e.* the 17th century, when Italy was repeatedly struck by devastating outbreaks of plague that profoundly affected major urban and commercial centers. The coincidence of the estimated MRCA timeframe with this major population collapse suggests that the demographic effects of the plague epidemic may have contributed to the persistence of this genetic variant in modern populations.In conclusion, our study provides evidence of a distant high-penetrance non-coding variant conferring melanoma susceptibility, with potential translational impact on facilitating screening and early-detection efforts in high-risk individuals.

#5940 Chromosome-level phasing to resolve haplotypes using multiomic data in multiple myeloma reveals complex distal interactions between chromosomes that impacts epigenetic states and gene expression.

Nathan J. Becker[1], Enze Liu[1], J. Zachary Sanborn[2], Attaya Suvannasankha[3], Kelvin Lee[3], Dickran Kazandjian[1], Benjamin Diamond[1], Abhishek Pandey[1], Rafat Abonour[1], Ola Landgren[1], Elizabeth M. Munding[2], Aneta Mikulasova[4], Brian A. Walker[1]

[1]University of Miami, Miami, FL,[2]Dovetail Genomics, Scotts Valley, CA,[3]Indiana University, Indianapolis, IN,[4]University of Edinburgh, Edinburgh, United Kingdom

Introduction: Linking markers together into large phase-blocks, and examining the interaction of different sequencing modalities, allows complex genomic and epigenomic states to be integrated to generate true multiomic haplotypes at the chromosomal level.
Methods: Fourteen multiple myeloma patient-derived xenografts were used to generate multiomic data including short- (Illumina) and long-read (PacBio) whole genome sequencing (WGS) to identify single nucleotide variations (SNVs), copy number (CN) abnormalities, structural variation (SV), and DNA methylation, as well as expression, chromatin states (Cut&Tag-IT), and Micro-C/LinkPrep (Dovetail Genomics) to identify 3D chromatin architecture. Chromosome-scale haplotypes of SNVs, SVs, CNVs, DNA methylation, expression, and chromatin marks were generated.
Results: For the first time, complete haplotype-resolved assemblies at the chromosomal level have been generated in multiple myeloma. A 100x coverage genome Micro-C/LinkPrep libraries we were able to phase the long and short arms of each chromosome, resulting in an average 94.3% haplotype phasing per autosome - thereby generating chromosome length haplotypes up to 241.9 Mb. Haplotype-specific heatmaps were generated allowing us to examine the interaction of complex SVs across chromosomes. In one sample, we identified a primary t(11;14) and additional SV events linked to the t(11;14) including a t(3;14), t(11;17), and t(3;17) which created a cyclical pattern. We found that 70-83.5% of reads support specific combinations of haplotype interactions, and that all four SV events were linked and involved the same haplotypes on each chromosome. The pattern of interactions combined with breakpoint analysis in this case indicated a four-way complex reciprocal translocation between chromosomes 3,11,14 and 17. Integration of epigenetic data in this complex SV showed DNA hyper-methylation 17 kb upstream of *CCND1* next to the t(11;14) breakpoint as well as increased H3K27ac marks on the same haplotype, indicating spreading of the activating broad domain from the *IGH* super-enhancer on chromosome 14. Equally, the hypomethylated DNA marks at the *IGH* promoter are spread to chromosome 3, via the t(3;14), resulting in over-expression of the proto-oncogene *SKIL*. The same is true for the t(3;17), which shows hypomethylation on both sides of the breakpoint, compared to the non-translocated allele.
Conclusion: We have generated the first chromosome scale haplotype-resolved genomes in multiple myeloma and integrated them with epigenetic states to identify interactions across chromosomes and resolve complex SVs as well as their epigenomic consequences to understand the intricate nature of how the genome is organized.

#5941 Large-scale analysis reveals distinct molecular subtypes in real-world gastric cancer data.

Akul Singhania[1], Swati Kaushik[1], Brandon L. Mapes[1], Lee F. Langer[1], Kayla R. Bastian[1], Samantha Cowher[1], Yaakov E. Stern[1], Bo Hu[2], Gonzalo Lopez[2], Ruslan Novosiadly[2], Maria Ortiz-Estevez[2], Kai Wang[2], Nick Callamaras[1], Richard A. Klinghoffer[1], Justin Guinney[1], Radia M. Johnson[1]

[1]Tempus AI, Inc., Chicago, IL,[2]Bristol Myers Squibb, Princeton, NJ

Introduction

Gastric cancer (GC) remains a global health concern, with limited outcome improvement despite targeted therapy. Here, a large real-world dataset of diverse disease stages and tumor sites was used to profile the molecular and clinical landscape of GC.

Methods

De-identified clinico-genomic records from GC patients profiled with Tempus xT (DNA) and xR (RNA)-seq assays were analyzed. Molecular subtyping used non-negative matrix factorization on xR data from primary tumors of the stomach and esophagus (n=1,385; 89.9% Stage III/IV). A classifier trained on tumor-intrinsic features was applied to metastatic sites (n=640; 99% Stage III/IV) and samples with low subtype probability were excluded (n=159). Real-world overall survival (rwOS), from first-line therapy to death was evaluated in patients with available data (31.5%). Sensitivity analysis for delayed entry included prospective-like patients with samples received/sequenced before treatment. Only subtypes with ≥20 patients contributing rwOS data were reported.

Results

To enhance interpretability and biological relevance, nine clusters were identified and merged into seven molecular subtypes with prognostic differences (p=0.01) based on centroid distance. The G1 subtype (25.6%; median OS 12.2 months, 95% CI 6.4-16.1) was associated with chromosomal instability (CIN) (78% CIN-High), Stage IV (91%), liver site samples (26%), microsatellite stability (MSS; 97%), and low tumor mutation burden (TMB<10; 97%). G1 exhibited *TP53* mutations (81.9%), *CCNE1* amplifications (16.7%), and *CDKN2A*/*B-MTAP* deletions (~15%). The G2 subtype (21.8%; median OS 20.6 months, 95% CI 14-22.2) had the highest TMB (TMB≥10; 21%), microsatellite instability (MSI; 20%), frequent *ERBB2* (14.3%) and *FGFR2* (5.9%) amplifications, and lower *TP53* mutations (62.6%). The G3 subtype (21.8%; median OS 18.1 months, 95% CI 11.6-27.4) had diffuse histology (58%), *CDH1* mutations (21.2%), low TMB (94%), and stomach site enrichment (54%). The G4 subtype (5.6%) was enriched for *KRAS* mutations (11.4%) and amplifications (9.6%), *TP53* mutations (75.4%), and CIN (62%, trending significance). The G5 subtype (6.4%) had the highest PD-L1 (CPS≥10; 40%), EBV positivity (16%), high TMB (17%), and low CIN (55%). G5 exhibited *ARID1A*/*B* (41.9%/9.3%), *PIK3CA* (21.7%), and *KRAS* mutations (18.6%), and had the lowest *TP53* mutation proportion (46.5%). The G6 subtype (4.9%) was enriched for Stage III (22%) and *CDKN2A*/*B-MTAP* deletions (~13%). The G7 subtype (17.1%; median OS 20.6 months, 95% CI 7.6-15.5%) was associated with diffuse histology (67%), *CDH1* mutations (23.9%), MSS (97%), low TMB (97%), and low CIN (53%).

Conclusions

This study shows that real-world data integration enables identification of clinically relevant, biologically distinct GC subtypes with prognostic differences. These findings provide a foundation for tailoring therapeutic strategies and improving patient outcomes.

#5942 Longitudinal liquid biopsy profiling in breast cancer patient: Clinical utility and guidelines.

Aurelia Robert[1], Alexandre Xu-Vuillard[1], Thomas Grinda[1], Antoine Italiano[2], Christophe Massard[2], Elie El-Rassy[1], Adrien Mouren[2], Alessandro Viansone[1], Barbara Pistilli[1], Joana Mourato-Ribeiro[2], Cyril Roussel-Simonin[2]

[1]Departement de Medecine Oncologique, Gustave Roussy, Villejuif, France,[2]Departement des Innovations Therapeutique et des Essais Precoces (DITEP), Gustave Roussy, Villejuif, France

Background:The clinical impact of repeated liquid biopsies in metastatic breast cancer have not been fully established. While circulating tumor DNA (ctDNA) profiling provides actionable insights, its value after an initially positive test is uncertain. We evaluated the clinical relevance of serial ctDNA analyses according to the initial biopsy result.
Methods:Patients from the prospective STING trial (NCT04932525) who underwent ≥2 plasma-derived ctDNA next-generation sequencing assays were analyzed. Somatic variants were classified according to the ESMO Scale for Clinical Actionability of Molecular Targets (ESCAT). Mutational burden, clonal evolution, and emergent actionable alterations were compared between the first (BL1) and subsequent (≥BL2) biopsies. Clinical trial and off-label therapy access were recorded.
Results:Among 152 patients, 77% had hormone receptor-positive and 19% triple-negative disease. The number of liquid biopsies ranged from 2 to 6 (median = 2). Fifty-nine patients (38.8%) had a non-contributive first biopsy; 38 became contributive at BL2 and 3 at BL3, while 14 remained non-contributive. The total number of mutations did not differ significantly between BL1 and later biopsies ($p = 0.274$) but showed a strong correlation (Spearman $\rho = 0.65$). Newly emergent variants mostly involved clonal hematopoiesis-related (*TP53, DNMT3A, TET2*) or resistance-associated genes (*RB1, BR*CA). Eighty-six patients accessed a clinical trial or off-label targeted therapy; 68 (79%) were guided by alterations already detected at BL1 and 14 (9%) by emerging mutations. Only 10 patients developed new ESCAT I-III alterations, including 7 with ESR1 mutations; others involved ERBB2, PTEN, and somatic BRCA2. Four patients acquired ESCAT IV alterations.
Conclusions:Serial liquid biopsies are most relevant in patients with an initially non-contributive assay, with a conversion rate of 64%, as repetition frequently yields actionable findings. In contrast, repeating full-panel sequencing after a contributive biopsy provides limited added value, except for ESR1 mutation monitoring after aromatase inhibitor exposure, which could be performed using lower-cost targeted assays. These results underline that the choice of re-biopsy should balance potential clinical impact and cost-effectiveness.

: Mechanisms and Dynamics of Gene Expression
Poster Session

#5946 Proteomics at the guanylin gene locus reveals Wnt/β-catenin regulatory factors underlying GUCY2C hormone silencing in colorectal cancer.

Adi Caspi[1], Ariana A. Entezari[1], Jasmine R. Alvarez[1], Annie K. Londregan[1], Thomas J. M. Kuret[1], Jeffrey A. Rappaport[2], Adam E. Snook[1], Scott A. Waldman[1]

[1]Pharmacology, Physiology, and Cancer Biology, Thomas Jefferson University, Philadelphia, PA,[2]Department of Medicine, Johns Hopkins University, Baltimore, MD

Guanylin (GUCA2A) is a paracrine hormone expressed in the colonic epithelium that activates the transmembrane receptor guanylyl cyclase C (GUCY2C). Activated GUCY2C promotes fluid secretion, genome stability, barrier integrity, and homeostasis through cGMP signaling. In early colorectal cancer (CRC), guanylin expression is universally suppressed, silencing the GUCY2C signaling cascade and contributing to tumorigenesis. Repression of guanylin is mediated transcriptionally by aberrant Wnt/β-catenin/TCF4 signaling at a Wnt-sensitive enhancer upstream of the *GUCA2A* gene. Using unbiased proteomics in Wnt-inducible CRC cell lines, we sought to directly identify regulators that mediate Wnt sensitivity to guanylin expression and control its transcriptional silencing in the context of tumorigenesis. sgRNAs targeting the *GUCA2A* regulatory element, consisting of the promoter and enhancer, were coupled to a dCas9-APEX2 fusion protein to capture the desired DNA locus. ChIP-qPCR and ChIP-seq confirmed sgRNA effectiveness and specificity in targeting *GUCA2A*. APEX2-mediated proximity biotinylation was performed to label proteins associated with the targeted site. Streptavidin affinity pulldown followed by LC-MS/MS-based proteomics revealed candidate regulatory proteins differentially enriched at the *GUCA2A* promoter under Wnt-on and Wnt-off conditions, including the previously identified Wnt-modulated guanylin activator p38α (MAPK14). Additionally, other candidates were enriched at the promoter irrespective of Wnt status, suggesting regulation of guanylin that is either Wnt-independent or requires post-translational control downstream of Wnt signaling. Potential regulators of guanylin expression identified in this analysis are undergoing validation using a knockdown screen in combination with a *GUCA2A* luciferase reporter with the goal of identifying the regulatory machinery underlying guanylin loss in CRC. As GUCY2C functions as a tumor suppressor, new insights into the mechanism of guanylin transcriptional silencing will provide an opportunity to inform prevention and treatment strategies to repair the signaling pathway and oppose disease.

#5947 LSD1 performs demethylase-independent and context-specific functions in Ewing sarcoma.

Rachel D. Dreher, Cenny C. Taslim, Ira Miller, John W. Sherman, Ariunaa Bayanjargal, Emily R. Theisen

Nationwide Children's Hospital, Columbus, OH

Ewing sarcoma (EwS) is an aggressive malignancy afflicting adolescents and young adults. A chromosomal translocation fusing the *EWSR1* gene to the *FLI1* gene (EWSR1::FLI1) causes 85% of cases. Due to the inability to target EWSR1::FLI1, the field has attempted to target critical co-regulators to disrupt oncogenesis. One candidate is Lysine specific demethylase 1 (LSD1), which is overexpressed in EwS, colocalizes with the fusion, and inversely correlates with patient prognosis. LSD1 inhibitors have shown mixed activity in EwS. Noncompetitive LSD1 inhibitors have potent cytotoxic activity, but these effects are not seen with irreversible inhibitors. Recent work from our group suggests the activity of noncompetitive inhibitors is likely LSD1-indpendent. This has left the precise function of LSD1 in EwS unclear. We hypothesize that LSD1 has important nonenzymatic functions in EwS. We have developed a suite of genetic and pharmacological tools to deplete LSD1 and define its nonenzymatic functions. Genetically, we knocked out LSD1 via CRISPR genome editing. Pharmacologically, we degraded full-length LSD1 protein with UM171. We assessed proliferation and transformation capacity and identified differentially expressed genes with RNA sequencing. To distinguish between enzymatic and nonenzymatic functions, we also used genetic and pharmacological approaches. We engineered a full length, wild type LSD1 (LSD1wt) and a K661Q/A539E mutant enzymatically dead LSD1 (LSD1ed). Pharmacologically, we treated parental cells with irreversible inhibitor OG-L002. RNA-sequencing was used to define genes regulated by enzymatic and nonenzymatic functions. Surprisingly, LSD1 KO does not impair proliferation or anchorage independent growth. In contrast, degradation of LSD1 protein caused a pronounced, cell line-dependent reduction in colony formation. This cell line-specific reduction in colony formation was recapitulated with OG-L002 treatment. Overlap and pathway analysis found that LSD1 has both shared and cell line-specific targets. Across all cell lines, LSD1 consistently represses genes involved in neurotransmitter functioning and e-cadherin targets. In A673 cells, LSD1wt and LSD1ed demonstrated highly overlapping expression profiles. In addition, OG-L002 treatment showed no phenotype, suggesting that LSD1's enzymatic activity is dispensable for core functions in A673. When we define nonenzymatic functions pharmacologically, we see that LSD1 performs core functions through both enzymatic and nonenzymatic means. Interestingly, repression of e-cadherin target genes is consistently a nonenzymatic function. Our results demonstrate that LSD1 has a core set of functions that it regulates via cell line dependent mechanisms. In addition, the changes seen in 3D assays with LSD1 inhibition and depletion suggest LSD1 plays a more important role in 3D growth and that future studies should prioritize 3D assays.

#5948 EGR1 Expression and Perineural Invasion in Salivary Duct Carcinoma: A comparison of SDCDN and SDCXPA.

Airi Sakyo[1], Eijitsu Ryo[2], Seiichi Yoshimoto[3], Go Omura[3], Chihiro Fushimi[3], Toshihiko Sakai[3], Yoshifumi Matsumoto[1], Azusa Sakai[3], Kohtaro Eguchi[3], Yo Suzuki[1], Kazuki Yokoyama[4], Yoshitaka Honma[4], Yasushi Yatabe[5], Fumihiko Matsumoto[1], Taisuke Mori[5]

[1]Otorhinolaryngology, Juntendo University Faculty of Medicine, Tokyo, Japan,[2]Division of Molecular Pathology, National Cancer Center Research Institute, Tokyo, Japan,[3]Head and Neck Surgery, National Cancer Center Hospital, Tokyo, Japan,[4]Department of Head and Neck, Esophageal Medical Oncology, National Cancer Center Hospital, Tokyo, Japan,[5]Diagnostic Pathology, National Cancer Center Hospital, Tokyo, Japan

Salivary duct carcinoma (SDC) is primarily categorized as de novo (SDCDN) or ex pleomorphic adenoma (SDCXPA). Previous reports indicate a higher frequency of HMGA2 and PLAG1 fusion events in SDCXPA. Surgical resection remains the main intervention due to limited guidance on new treatment strategies. However, frequent recurrence and challenging management of metastasis highlight the necessity for innovative treatments. This study aimed to investigate SDC characteristics, including perineural invasion (PNI), and elucidate its carcinogenic mechanisms and adverse prognostic factors. We analyzed 52 patients with SDC diagnosed in the National Cancer Center Hospital from 2014 to 2023. To compare gene expression profiles, we performed immunohistochemical staining, including Her2, androgen receptor (AR), PLAG1, and HMGA2, followed by human epidermal growth factor receptor 2 (HER2) in situ hybridization and RNA sequencing of 30 cases. Differential analysis identified genes subjected to immunohistochemical staining and statistical analysis. Based on histologic classification using PLAG1 and HMGA2, 52 cases were classified as 26 cases (50%) SDCDN and 26 cases (50%) SDCXPA. Compared with SDCXPA, SDCDN showed higher perineural, venous, and lymphatic invasion rates ($P = .0005$, .0294, and .0044, respectively). Genetic expression profiling revealed clustering tendencies between these subtypes. Focusing on PNI, gene expression was decreased in early growth response 1 in tumor portions infiltrating perineural tissues, indicating a negative correlation ($P < .0001$). Similarly, ARID1A expression was elevated in tumor regions of cases with perineural invasion; however, immunohistochemical analysis showed no difference between perineural and non-perineural areas. Furthermore, RNA sequencing identified three novel fusion genes in SDC. In conclusion, clinical disparities between SDCDN and SDCXPA based on molecular and pathological features were observed. We found early growth response 1-brain-derived neurotrophic factor-linking crosstalk between cancer cells and nerves for PNI in SDC, offering insights into future treatment and prognostic factors.

#5949 Targeting SLC25A13 sensitizes melanoma to treatment and reduces tumor aggressiveness via metabolic rewiring.

Beatriz Cristina Biz Tonin[1], Ana Luisa P. Auyb[1], Jeremie Nsengimana[2], Hatylas Azevedo[1], Beatriz Kopel[3], Nadja C. Souza-Pinto[3], Frank John Slack[4], Miriam G. Jasiulionis[1]

[1]Federal University of Sao Paulo (UNIFESP), Sao Paulo, Brazil,[2]Newcastle University and NIHR Newcastle Biomedical Research Centre, Newcastle, United Kingdom,[3]Universidade de Sao Paulo (USP), Sao Paulo, Brazil,[4]Professor, Harvard Medical School, Boston, MA

Therapy resistance is one of the main challenges for melanoma treatment, prompting the investigation of new therapeutic targets to elucidate novel therapeutic approaches and molecular insights. In this melanoma study, we have investigated the role of SLC25A13 which in humans encodes citrin, a mitochondrial carrier protein with a well-characterized function in metabolic diseases. We demonstrated that SLC25A13 upregulation in tumors is associated with poor survival in two large melanoma cohorts with long follow-up. Functional assays revealed that overexpression of SLC25A13 alters the level of key metabolites, leading to a metabolic syndrome-like state that is essential for the survival of metastatic melanoma cells. We propose that SLC25A13 functions as a key metabolic node promoting melanoma aggressiveness by enhancing proliferation, invasion, and tumor progression. Notably, we show that silencing *Slc25a13* in aggressive mouse melanoma cells sensitizes them to both dacarbazine and MEK inhibition, highlighting its potential as a therapeutic target. Thus SLC25A13 is a key biomarker and a promising target for overcoming therapy resistance in metastatic melanoma.

#5950 Dynamic low-complexity domain interactions of PAX3::FOXO1 mediate endogenous pathological transcriptional hub formation in alveolar rhabdomyosarcoma.

Yanghao Zhong, Michael Di Martino, Shasha Chong

Division of Chemistry and Chemical Engineering, California Institute of Technology, Pasadena, CA

Rhabdomyosarcoma (RMS), a cancer of skeletal muscle tissue, is the most common pediatric soft tissue sarcoma with 5-year survival rate less than 30% in high-risk RMS, despite advances in prognosis and treatment over the past few decades. PAX3::FOXO1 (P3F1) is a fusion oncoprotein found in 60% cases of alveolar RMS (aRMS), the most aggressive subtype of RMS, and has been thought to drive oncogenic transcription in aRMS. However, the molecular mechanisms by which P3F1 regulates transcription remain poorly understood, and the extent to which these transcriptional changes contribute to tumorigenesis is unclear. In the current study, we first demonstrated exogenously expressed P3F1 exhibited neomorphic hub formation propensity which is not observed for its parental proteins. Using CRISPR/Cas9-based gene editing method, we endogenously labeled P3F1 with a fluorogenic HaloTag in patient-derived aRMS cells, allowing us, for the first time, to visualize P3F1 at its native pathological environment. We discovered that endogenous P3F1 forms transcriptional hubs at its target genes, and the average hub size is ~117 nm characterized by photoactivatable localization microscopy. Single particle tracking experiment showed that P3F1 molecules have longer chromatin bound residence time in the hubs compared to those outside the hubs, suggesting an important role of P3F1 hubs in target gene transcription. We found disrupting the intrinsically disordered low complexity domains (LCDs) of P3F1 impaired its hub formation propensity, target gene transcription and its ability to recruit coactivator p300. Using a phase-separation-induced interactome detection (PhaseID) method, we mapped unique interacting proteins that P3F1 hubs recruit and utilize to influence oncogenic transcription. In summary, our results uncover a neomorphic hub formation behavior of pathological P3F1 and provide a strong rationale of targeting P3F1 hub formation as new therapeutics for aRMS.

#5951 Hypertrophic chromatin condensates govern oncogene control in cancer.

Bjorn Stolte, David Pease, Max Slotnik, Anna Pertl, Nancy Hannett, Tong Ihn Lee, Richard Young

Whitehead Institute For Biomedical Research, Cambridge, MA

Summary: This study shows that hypertrophic transcriptional condensates are the defining regulatory architecture for oncogenes in diverse cancers, describes mechanisms that lead to their assembly and regulation, and suggests therapeutic concepts that may be broadly applicable to cancers with dysregulated transcription.
Pertinent experimental procedures: We investigate oncogenic transcriptional condensates using an integrated cell-biological, genomic, and biochemical framework. Alterations of protein, DNA, and RNA constituents of transcriptional condensates and dependencies on these components are analyzed in public and experimentally generated datasets. Condensate dynamics are quantified using microscopy approaches, such as fluorescence recovery after photobleaching (FRAP) and single particle tracking (SPT) with acute genetic and pharmacologic perturbations of condensate constituents. Interactions between oncogenic transcription factors (TFs) and cis-regulatory elements are assessed by chromatin immunoprecipitation and complementary methods and combined with chromatin-accessibility mapping. Key molecular interactions are identified by approaches including co-immunoprecipitation, proximity labeling, and mass spectrometry.
Description of the new, unpublished data: Hypertrophic transcriptional condensates, defined as exceptionally large pathogenic assemblies of transcription apparatus with specialized physicochemical properties, are assembled at driver oncogenes in a broad spectrum of cancers. These transcriptional condensates differ from those in most normal cells in their exceptional size, the genetic and biochemical mechanisms involved in their assembly, and their components' dynamics. Some hypertrophic transcriptional condensates incorporate a disproportionately large portion of the transcription apparatus, encompass nearly a megabase of DNA, remain assembled longer than typical transcriptional condensates, and arrest the properties that produce condensate dissolution in normal cells. Some of the properties of the hypertrophic condensates are amenable to new approaches that concentrate drugs within the pathological assembly.
Conclusions: Driver oncogenes in cancers share a unifying theme: their transcription is controlled by hypertrophic transcriptional condensates, which differ from normal transcriptional condensates in terms of their exceptional size, the genetic and biochemical mechanisms involved in their assembly, and their components' dynamics. We present common features to this condensate architecture and describe mechanisms that lead to their assembly and unusual regulatory behaviors. The concept that hypertrophic transcriptional condensates evolve to serve oncogenic drivers, and evidence of their specialized physicochemical environments, offers new opportunities for antineoplastic drug discovery.

#5952 A unifying mechanism for shared splicing aberrations in splicing factor mutant cancers.

Rahul Roy, Prajwal C. Boddu, Manoj M. Pillai

Yale School of Medicine, New Haven, CT

Cancer-associated mutations in splicing factors (SFs) such as SF3B1, U2AF1, and SRSF2 generate well-recognized cis-acting alterations in splice site choice, specific to each mutational subtype. However, there is substantial overlap in alternative splicing (AS) defects across these genetically distinct mutation groups which has remained unexplained. We hypothesized that this convergence reflects a shared trans-regulatory mechanism. To answer this, we profiled global transcriptomes to delineate AS programs across SF-mutant states using a cohort of 395 patients with SF-mutant clonal myeloid disorders and 64 healthy donors. While the majority of AS alterations were mutation-specific, we identified a robust subset of shared events, strongly enriched for retained intron (RI) signatures. These RI defects were bidirectional (both increase and decrease in RI) yet strikingly concordant across SF3B1, U2AF1, and SRSF2 mutants. Given that RNA binding proteins (RBPs) are the primary regulators of AS, we compared these SF-mutant RI to those in cells with loss of 356 individual RBPs (ENCODE). SF-mutant RI closely mirrored RI in resulting from SRSF1 loss of function. Phosphoproteomics revealed that SF-mutant cells have hypophosphorylation of RS domains in SRSF1, impairing its splicing activity. This reduction stemmed from a shift in the AMPKα-AKT signaling balance, which suppressed the AKT-SRPK1-SRSF1 phosphorylation axis. We next traced this signaling imbalance to an upstream trigger: R-loop-associated transcriptional stress, which activates a DNA damage response (DDR). DDR activation enhanced AMPKα signaling while diminishing AKT activity, thereby reducing SRPK1-mediated phosphorylation of SRSF1. Pharmacologic DDR activation recapitulated SRSF1 hypophosphorylation, decreased AKT/SRPK1 activity, and induced RI defects resembling those in SF-mutant cells. Conversely, relief of DDR signaling restored AKT/SRPK1 activity, normalized SRSF1 phosphorylation, and corrected RI abnormalities. These results were confirmed in SF-mutant clonal myeloid cells from patients using RNAseH over-expression to reverse R-loops and quantifying effect on colony formation by CFU assays. Together, our findings demonstrate that, beyond distinct cis-acting splice site changes, SF-mutant cancers share a stress-driven, trans-acting splicing program coordinated through DDR-mediated rewiring of SRSF1 activity. This unified mechanism links replication stress, kinase signaling, and RNA processing across diverse clonal states, and highlights novel actionable nodes (DDR, AMPK/AKT balance, and SRPK1-SRSF1 coupling) with therapeutic potential.

#5953 Unlocking new frontiers in mouse research by exploring the whole-transcriptome in space and time with mouse embryo stages E11 - E14.

Michael Patrick, Liang Zhang, Isabel Lee, Shanshan He, Martin Shelton, John Lyssand, Joseph M. Beechem

Bruker Spatial Biology, Seattle, WA

Bruker Spatial Biology introduces the CosMx® Mouse Whole Transcriptome Assay: a 21,242 gene panel that covers the entirety of the protein-coding mouse transcriptome. CosMx Spatial Molecular Imager (SMI) is a first-in-class instrument that offers spatially resolved, single-cell transcriptomic analysis at a scale an order of magnitude greater than any other commercially available system. This study profiles four FFPE mouse embryo sections - E11, E12, E13, and E14 - using a development lot of CosMx Mouse Whole Transcriptome (WTX) Assay. Each slide was stained with a 5-channel segmentation cocktail of PanCK, CD3, CD45, CD298/B2M, and DAPI prior to RNA profiling. Cells are segmented according to presence of DAPI and a combined overlay of all four segmentation markers using a machine learning algorithm based on the open-source platform CellPose, trained on staining information collected on over a dozen human and mouse tissue types on CosMx SMI. RNA transcripts are decoded using a multiplexed barcoding strategy where individual ISH probes are assigned unique barcode across 39 reporter sequences, a strategy that is key to allowing over twenty-thousand targets to be detected simultaneously in space. The CosMx Mouse WTX Assay unveils an unprecedented depth of information on each mouse sample. Cell typing was performed on each embryo to identify each developing organ, and niche analysis was used to identify spatial neighborhoods unique to each timepoint. The development of specific organs during these timepoints, such as the retina, liver, gonads, and heart, are interrogated in detail by comparing localized gene expression across the whole transcriptome throughout timepoints, offering a unique four-dimensional window (three spatial dimensions, one time dimension) into embryonic development with the unparalleled resolution of spatial transcriptomics. Capitalizing on the high number of genes available per cell, single cell pathway scores were assigned to each slide, and differential expression was used to quantify which pathways are upregulated at each timepoint. Unbiased spatial algorithms such as Insitucor were used to identify localized gene module expression based on normalized expression across nearby cells, and disease/control perturbation algorithms such as Insitudiff revealed spatial domains defined by gene perturbations of later timepoints relative to E11. CosMx Mouse WTX Assay delivers a first-of-its-kind opportunity to examine the development of mouse embryos in four dimensions using >20,000 spatially resolved genes. This study on mouse embryo development provides a first look at the limitless applications that a whole-transcriptome mouse panel can unlock for researchers including cancer research.

#5954 Enabling single-cell transcriptomics from samples with degraded and low-input RNA using TempO-LINC.

Kevin White[1], Albus Kilili[2], Hanna Ha[2], Dennis Eastburn[1], Nathan Jayne[1], Salvatore Camiolo[2], Zhoutao Chen[1], Bruce Seligmann[1]

[1]BioSpyder Technologies, Inc., Carlsbad, CA,[2]BioClavis, LTD, Glasgow, United Kingdom

Background: Single-cell RNA sequencing (scRNA-seq) technologies enable characterization of cellular heterogeneity and rare cell types, and mapping of cell states in complex tissues. However, scRNA-seq performance in clinical samples is limited by RNA degradation, fragmentation, or inherently low RNA abundance. Peripheral blood mononuclear cells (PBMCs) are a common low RNA, heterogeneous sample, while formalin-fixed paraffin-embedded (FFPE) tissues, an invaluable archive of human samples, often contain degraded RNA of poor quality/quantity, due to tissue processing. Thus, TempO-LINC, a targeted, instrument-free single-cell transcriptomics assay, was designed for high-throughput gene expression profiling with strong tolerance to low RNA integrity. Here, we report that TempO-LINC enables robust gene expression profiling and rare cell subtype detection in human PBMCs and dissociated FFPE tissues from human and mouse.
Methods: The TempO-LINC assay is a scalable, combinatorial split-pool barcoding approach to uniquely index RNA molecules in fixed cells/nuclei. Cryopreserved PBMCs from three donors were fixed using the TempO-LINC Fixation Kit and profiled with the TempO-Seq human whole transcriptome v2.1 probe set. FFPE blocks from human lung and mouse brain were sectioned, two 30µm thick sections per block, deparaffinized, enzymatically dissociated, filtered, and then processed with the TempO-LINC Fixation Kit. TempO-LINC scRNA-seq was performed on FFPE lung and brain using the human whole transcriptome v2.1 and mouse whole transcriptome v1.1 probe sets, respectively. Data processing and visualization were performed using the open-source Python Scanpy and R Bioconductor packages.
Results: Analysis of 12,027 PBMCs revealed 16 transcriptionally distinct cell populations, including major classes of blood/immune cell subsets, and rarer cell populations of hematopoietic stem/progenitor cells and proliferating CD4+ T cells, demonstrating high sensitivity in low-RNA contexts. TempO-LINC successfully generated FFPE single-cell expression profiles with mean mapping rates from 71-93% and ~1,000 genes detected per cell. UMAP data shows clearly defined cell subtypes from dissociated FFPE lung and brain tissues.
Conclusion: The TempO-LINC scRNA-seq assay enables high-resolution gene expression profiling across heterogenous, low-RNA PBMCs and FFPE samples. These results highlight the assay's high sensitivity in determining rare cell types from samples with degraded RNA. Applying TempO-LINC scRNA-seq on FFPE specimens unlocks new opportunities in precision medicine, biomarker discovery, and mechanistic toxicology.

#5955 Dissecting the enhancer logic in breast cancer metastasis through transcriptional, chromatin accessibility profiling and footprint-inferred transcription factor activity.

Frances Heredia Negron[1], Homer W. Fogle[1], Michael R. Kelly[2], Kamila Wisniewska[2], Lisa A. Carey[2], Hector L. Franco[1]

[1]Comprehensive Cancer Center of the University of Puerto Rico, San Juan, PR,[2]Lineberger Comprehensive Cancer Center, University of North Carolina at Chapel Hill, Chapel Hill, NC

Breast cancer metastasis remains a major clinical challenge, highlighting the need to dissect the molecular mechanisms involved. In this project, we generated a multi-omic resource consisting of RNA-seq and ATAC-seq profiles from ER-positive primary breast tumors and matched liver and lung metastases. We collected samples from four patients collected at diagnosis and eight patients collected at autopsy following cancer-related death, enabling a comprehensive assessment of metastatic regulatory programs. We hypothesized that breast cancer metastasis is driven by tissue-specific enhancer networks, in which differential transcription factor (TF) motif activity coordinates distinct gene regulatory programs across metastatic sites. Towards this end, RNA-seq reads were aligned using STAR, quantified with HTSeq, and analyzed with DESeq2 to identify differential gene expression between primary and metastatic tissues. ATAC-seq reads were processed with the PEPATAC pipeline, and differentially accessible chromatin regions were identified using DiffBind. Peak-to-gene correlation analyses integrating ATAC-seq and RNA-seq data revealed putative metastasis-driver genes including 99 liver specific genes and 9 lung specific genes. Notably, there were 23 shared genes across both metastatic sites, including CCNF, SPINT1, and SLC2A1. The majority of these genes were associated with three or more enhancers in metastases but not in primary tumors, suggesting enhancer rewiring as a key mechanism of metastatic progression. To identify TFs that may drive these regulatory changes, we applied TOBIAS footprinting to infer TF occupancy by integrating motif information with chromatin accessibility. By combining footprint scores with gene expression correlations, we uncovered tissue-specific TF activity: KLF5, KLF12, SP3, and KLF10 predominated in lung metastases, whereas SP5, SP1, SP4, KLF14, and KLF15 dominated liver metastases. Most chromatin accessibility peaks exhibited differential TF motif usage between tissues, further supporting distinct enhancer regulatory programs in liver versus lung metastases. Only a minority of peaks shared the same top motifs across tissues, and some peaks contained motifs in one tissue but not the other, underscoring both shared and tissue-selective regulatory mechanisms that likely shape metastatic adaptation. By analyzing TF motif activity utilizing patient-specific depth of coverage across peaks allowed us to refine transcription factor binding predictions in ways that reflect individual tumor biology. Prioritizing TFs based on activity within these regulatory landscapes may ultimately improve the development of targeted therapeutic strategies to combat metastatic breast cancer.

#5956 Effect of the evolutionary selected Andean Aymara *NFKB1* polymorphisms on inflammatory and HIF-dependent gene expression in endometrial and ovarian cancer.

Jihyun Song[1], Soo Jin Kim[1], Anthony Panarelli[2], Linus Chuang[3], David Doo[3], Leslie Andriani[3], Shatovisha Dey[2], Syeda Rashid[2], Steven Sieber[4], **Sabina I. Swierczek**[2]

[1]Division of Hematology and Hematological Malignancies, School of Medicine University of Utah/Huntsman Cancer Institute, Salt Lake City, UT,[2]Rudy Ruggles Research Institute, Nuvance Health, Danbury, CT,[3]Gynecologic Oncology, Nuvance Health, Danbury, CT,[4]Pathology, Nuvance Health, Danbury, CT

JS,SS-corresponding authors; SJK, AP-equal contributionGynecological cancers cause ~132/1 million deaths in women /year worldwide (PMID: 39148469). Endometrial cancer (EC) is the most common gynecological cancer, while ovarian cancer (OC) is the most lethal, with a 5-year US mortality ~51% overall and less than 30% in advanced stage of disease. NF-κB signaling contributes to progression, chemoresistance, and relapse in both EC and OC. The evolutionary selected Aymara *NFKB1* variant (rs230511; CC, CT, TT genotype), existing in ~30% Europeans, Asians, and Hispanics, correlates with expression of inflammatory and hypoxia-inducible factor (HIF)-regulated genes (PMID:39971917). Because inflammation and hypoxia promote tumor growth, invasion, metastasis, and resistance to treatment, this variant may influence EC/OC biology and clinical outcomes. We investigated role rs230511 genotypes in inflammatory and HIF-dependent gene expression in EC and OC.Genomic DNA from blood mononuclear cells from EC (n=103), OC (n=108) and benign controls (n=86) was genotyped for rs230511. Tumors samples from treatment naïve patients (25 OC, and 20 EC) and normal tissues from (ovary n=6; endometrium n=9) were collected. RNA was extracted and gene expression analysis of HIF-targeted genes (*VEGFA, SLC2A1, LDHA)* and inflammatory genes *(IL6, P2RY2, CCR7, CXCL8, IL1B, NFKB1*, *TNF*), with *GAPDH* as the housekeeping gene evaluated. No differences in allele frequencies or genotype distributions of rs230511 were observed among EC, OC, and benign groups, indicating that this *NFKB1* variant does not predispose to OC/EC. In EC tumors, *NFKB1* mRNA were significantly lower than in normal endometrium (p=0.004) *NFKB1* expression in EC positively correlated with the expression of HIF-targeted genes (*VEGFA*, *SLC2A1*) and inflammatory genes (*IL6, P2RY2, TNF*). Patients carrying the *CT* genotype had lower expression of *IL6* and *P2RY2* than the *CC*, suggesting less aggressive tumors.; the expression of other inflammatory genes (*CCR7, CXCL8, IL1B, TNF)* also trended lower but were not significant. The *CT* genotype was associated with lower white blood cell counts than *CC*, consistent with reduced inflammation. In OC, *NFKB1* mRNA was lower than in normal ovary. OC patients with the *CT* and *TT* genotype had lower *NFKB1* mRNA than *CC* carriers. In OC inflammatory genes (*CCR7, CXCL8, IL1B*, *TNF*) were highly expressed but did not correlate with *NFKB1* mRNA levels and genotypes. HIF-target genes positively correlated with inflammatory gene levels, suggesting HIF, not NFKB1, drives inflammation in OC. *NFKB1* genotype-dependent variation and its downstream pathways appear to influence EC but not OC, potentially contributing to differences in tumor aggressiveness and prognosis. The effect of the *NFKB1* genotype is undergoing analysis of overall survival, tumor aggressiveness and treatment response.

#5957 Transcriptional alterations in neoplastic transformation.

Usman Hyder, Nova Fong, Benjamin Erickson, David Bentley

University of Colorado Anschutz Medical Campus, Aurora, CO

Genetic alterations aberrantly turn on oncogenic transcription programs, thereby driving cellular transformation and tumor progression. Transcription comprises multiple steps, including initiation, promoter-proximal pausing, pause release, elongation, and termination. Because these steps are essential in both normal and cancer cells, targeting transcription has historically lacked therapeutic specificity. To address this problem, a key unmet need for the field is to identify differential features of transcription between normal and transformed cells to then exploit factors that regulate those distinctions. In line with this goal, we have identified two distinct changes in global transcription dynamics in normal breast cells undergoing oncogenic transformation. First, oncogenic transformation is associated with global increases in transcription elongation rate, or the speed by which RNA Polymerase II (Pol II) travels in gene bodies. This heightened rate is not just observed at genes inducible upon transformation, suggesting that oncogenic signaling may exploit elongation control to globally alter the transcriptome to advance cellular transformation. Second, oncogenic transformation is associated with decreases in promoter proximal pausing, implying that one of two potential mechanisms is elicited once cells undergo this cell state change: (i) increased premature termination to evict Pol II off promoters, and/or (ii) decreased Pol II recruitment. Given these findings, I hypothesize that oncogenic transformation requires global alterations to multiple transcription steps, and that perturbation of factors that selectively regulate these steps may obstruct the transformation process without killing normal cells, enabling the identification of targetable therapeutic approaches.

#5958 APOBEC4, a novel regulator of p53-dependent tumor suppression.

Dipesh Thapa[1], Atul Ranjan[2], Alejandro Parrales Briones[2], Elizabeth Thoenen[3], Shigeto Nishikawa[4], Jay Vivian[2], Tomoo Iwakuma[2]

[1]The University of Kansas Medical Center, Kansas City, KS,[2]Children's Mercy Research Institute, Kansas City, MO,[3]Washington University in St. Louis , St. Louis, MO,[4]Kyoto University, Kyoto, Japan

Introduction: The tumor suppressor protein p53 (p53) functions as a transcription factor that activates downstream target genes such as *p21*, *PUMA, NOXA, BAX,* and *GADD45α* to induce cell cycle arrest, senescence, apoptosis, and other biological processes. However, p53 activity is frequently compromised during tumorigenesis, with approximately half of human cancers harboring TP53 mutations. Even in tumors retaining wild-type p53 (wtp53), it gets degraded or inhibited through various mechanisms, including the overexpression of its E3 ubiquitin ligase MDM2. MDM2 antagonists such as Nutlin-3a are promising strategies to restore p53 function and inhibit tumor growth. Yet, factors/biomarkers regulating the efficacy of MDM2 antagonists and p53-mediated tumor suppression remain poorly understood. Identifying such factors and understanding their functions are essential for optimizing p53-targeted therapies.
Experimental Procedures: Using a human whole-genome shRNA library screen, we sought to identify factors regulating p53-dependent tumor suppression in osteosarcoma U2OS cells treated with Nutlin-3a. This screening and subsequent validation revealed APOBEC4 as a critical factor for p53-mediated colony suppression following Nutlin-3a treatment. Deletion of *APOBEC4* attenuated Nutlin-3a-induced p53 transcriptional activation and reduced p53-dependent cell cycle arrest and apoptosis across multiple p53-proficient cancer cell lines. To investigate the underlying mechanism, we performed co-immunoprecipitation (Co-IP) and proximity ligation assays (PLA), which revealed APOBEC4 binds to p53. Furthermore, cellular senescence induced by H_2O_2 and oncogenic $HRAS^{G12V}$, was also reduced upon *APOBEC4* knockdown. Importantly, APOBEC4 deletion significantly attenuated Idasanutlin-mediated tumor suppression *in vivo*.
Conclusion: Our findings identify APOBEC4 as a novel regulator of p53-dependent cell cycle arrest, senescence, apoptosis, and tumor suppression, highlighting its potential as a biomarker for p53-targeted therapies.

#5959 Therapeutic targeting of HuR using a specific small-molecule inhibitor in triple negative breast cancer.

Arundhathi Dev J R[1], Ajay Gogia[1], Sandeep R. Mathur[2], Ashutosh Mishra[3], Chandra Prakash Prasad[1]

[1]Medical Oncology, All India Institute of Medical Sciences New Delhi, New Delhi, India,[2]Pathology, All India Institute of Medical Sciences New Delhi, New Delhi, India,[3]Surgical Oncology, All India Institute of Medical Sciences New Delhi, New Delhi, India

Human Antigen R (HuR/ELAVL1) is an RNA-binding protein that interacts with U/AU-rich elements in target mRNAs, and its aberrant cytoplasmic accumulation have been observed in multiple cancers. HuR modulates the expression of key oncogenic and survival-related transcripts, thereby driving tumor progression, metastasis, and therapeutic resistance. Given this central role, HuR represents a compelling molecular target for cancer therapy. The present study specifically evaluates the potential of CMLD2, a highly selective small-molecule inhibitor of HuR, in the context of Triple-Negative Breast Cancer (TNBC). Comparative assessments were conducted using CMLD2 and DHTS across *in silico* and *in vitro* models. Immunohistochemical analysis of 71 TNBC samples revealed HuR overexpression in 66% of cases, along with elevated expression of HuR downstream target MMP9 (56%). Furthermore, in silico analysis established significant association between HuR overexpression and poor patient survival ($p = 0.028$). Functional assays in TNBC cell lines MDA-MB-231 and MDA-MB-468 demonstrated that both inhibitors suppressed proliferation, invasion, and clonogenicity; however, CMLD2 exhibited markedly higher specificity and consistency in inhibiting HuR function. Mechanistically, CMLD2 treatment downregulated HuR and its downstream effectors MMP9 and β-catenin, while reversing epithelial-mesenchymal transition (EMT) marker expression (E-cadherin, N-cadherin and Vimentin). Immunofluorescence and cell fractionation confirmed effective cytoplasmic HuR inhibition. Moreover, CMLD2 distinctly suppressed aerobic glycolysis, evidenced by reduced extracellular acidification and downregulation of key glycolytic mediators—PFKP, LDHA, and MCT4—validated at both transcript and protein levels. HuR silencing by siRNA supported the role of HuR in glycolytic regulation and TNBC progression. *In vivo*, CMLD2 significantly impaired tumor-forming ability in female BALB/c mice. Together, these findings underscore the therapeutic promise of CMLD2 as a specific and potent HuR inhibitor, providing strong experimental rationale for its further development as a targeted intervention in Triple-Negative Breast Cancer.

#5960 CRISPR-Cas engineering of allogeneic regulatory T cells reveals an essential role for steroid receptor coactivator 3 (SRC-3) in maintaining FOXP3 expression and suppressive function.

Subhashree Pradhan, Bryan Nikolai, Aiden Lynn Moser, Davis Alexander Graham, Lanz Rainer, Bert W O'Malley, David Lonard

Baylor College of Medicine, Houston, TX

Genetically engineered allogeneic regulatory T cells (Tregs) represent a promising off-the-shelf therapy to prevent graft-versus-host disease and transplant rejection, but their clinical utility is constrained by immune rejection and alloreactivity. Using CRISPR-Cas editing, we generated hypoimmunogenic human Tregs through multiplex knockout of B2M (reducing HLA class I), TCRα/β (eliminating receptor-mediated alloreactivity), and SRC-3 (a transcriptional coactivator linked to Treg stability). In prior murine studies, SRC-3 disruption enhanced tumor clearance, but in human Tregs, its deletion impaired suppressive function, underscoring SRC-3's role in maintaining lineage identity. Functionally, SRC-3 knockout Tregs failed to suppress effector T cell proliferation, a defect mirrored in triple knockout (TCR+B2M+SRC-3) cells. Co-culture with unedited Tregs restored suppression, suggesting functional compensation. FOXP3 protein levels were markedly reduced in SRC-3 and triple knockout Tregs, consistent with destabilized lineage commitment. These findings highlight SRC-3, TCR, and B2M as central regulators of transcriptional and antigen-presentation pathways shaping Treg identity. RNA sequencing revealed that triple knockout Tregs exhibited increased transcript diversity compared to controls. SRC-1/NCOA1 and SRC-2/NCOA2 were upregulated in SRC-3 and triple knockout samples, while B2M and TRAC were strongly downregulated in triple knockouts. Chemokine transcripts were elevated in SRC-3 and triple knockout Tregs, with triple knockouts also showing diverse cytokine upregulation. Collectively, these results demonstrate that while genome editing can enhance allogeneic compatibility, SRC-3 is indispensable for human Treg stability and suppressive function. Effective engineering of universal Tregs must therefore balance hypoimmunogenic design with preservation of functional integrity for adoptive cell therapy.

#5961 The roles of METTL3 in colorectal cancer.

Hung Mai, Sidi Zhao, DEBANJAN SAHA, Jace Webster, Li Lin, Emily Rozycki, Ashna Agarwal, Muheng Liao, Christopher Maher

Department of Medicine, Washington University, St. Louis, MO

Colorectal cancer (CRC) is a leading cause of cancer-related mortality worldwide, accounting for 10% of all cancer deaths. Metastatic disease occurs in half of all CRC cases, with a 5-year survival rate of 14%. Thus, understanding molecular mechanisms of CRC progression is important for improving diagnostics and therapies. Recent studies identified the m6A (N6-methyladenosine) RNA methyltransferase-METTL3 as a key oncogene in CRC, suggesting the important role of epitranscriptomic regulation in cancer. M6A modification affects multiple aspects of RNA metabolism, including degradation, export, and translation. However, the precise mechanisms of METTL3 in CRC remain undefined. We identified YTHDF1, an m6A reader, as the most upregulated reader in CRC patients. Yet, the METTL3-YTHDF1 interplay in CRC progression is unclear. This study aims to define how METTL3 and YTHDF1 act together to promote CRC progression via m6A modifications, and to identify novel, clinically relevant m6A targets. To achieve this, we performed Nanopore direct RNA-seq in METTL3-knockdown cells to map METTL3-dependent m6A sites across the CRC transcripts. To identify genes whose m6As are read by YTHDF1, we conducted short-read RNA-seq in METTL3- and YTHDF1-knockdown cells to determine shared transcriptional changes associated with RNA methylation. Integrating these datasets with patient data revealed clinically relevant transcripts regulated by METTL3 and YTHDF1. m6A enrichment on selected candidates were validated by MeRIP-qPCR. Comparison with two existing m6A databases confirmed overlapping sites and uncovered previously unannotated sites. Among these, *TRIB3*, a known oncogene in CRC, consistently emerged as a top m6A target across datasets, with expression significantly reduced upon METTL3 or YTHDF1 knockdown. Thus, TRIB3 was selected as a conceptual target for further studies. Using RNA immunoprecipitation, we found YTHDF1 interacts with *TRIB3*, and this interaction is reduced upon METTL3 depletion. Knockdown of METTL3 or YTHDF1 reduces *TRIB3* RNA stability and polysome occupancy causing decreased transcript and protein levels. To directly remove m6As on *TRIB3*, we used dCasRX conjugated to ALKBH5, an m6A demethylase, and coupled with sgRNAs targeting *TRIB3*. Dual sgRNAs effectively removed m6As on *TRIB3* and reduced its expression, confirming functional roles of m6As in regulating TRIB3 level. TRIB3 overexpression rescued migration and invasion defects in METTL3 knockdown cells, while m6A removal on *TRIB3* by dCasRX-ALKBH5 suppressed these phenotypes, indicating METTL3 and YTHDF1 promote CRC invasion and migration through TRIB3 regulation. Our study highlights the role of the YTHDF1-TRIB3 axis in cooperating with METTL3 to promote CRC. Additionally, our unbiased analyses reveal several other potential m6A targets in CRC. These findings provide new insights into CRC progression and highlight potential therapeutic paths targeting the m6A regulatory network.

#5962 METTL1-mediated m7G modification of valine tRNAs drives pancreatic ductal adenocarcinoma progression.

jiabei zhu[1], Qi Zhang[2], Rui Su[3], Qiuhui Pan[2], Ajay Goel[1]

[1]Department of Molecular Diagnostics and Experimental Therapeutics, Beckman Research Institute of City of Hope, Monrovia, CA,[2]Department of Clinical Laboratory, Shanghai Children's Medical Center, Shanghai, China,[3]Department of Systems Biology, Beckman Research Institute of City of Hope, monrovia, CA

Background: Transfer RNA (tRNA) modifications play a critical role in regulating codon-specific mRNA translation and supporting tumor cell adaptation. The RNA methyltransferase METTL1 installs N7-methylguanosine (m7G) modifications on tRNAs, shaping their codon usage landscape and influencing protein synthesis. However, the function and mechanism of the METTL1/tRNA axis in pancreatic ductal adenocarcinoma (PDAC) remain poorly understood. This study examines the role of METTL1-mediated m7G tRNA modification in the progression of PDAC and its associated metabolic reprogramming.

Methods: METTL1 expression was analyzed using transcriptomic data from The Cancer Genome Atlas (TCGA) and validated in an independent PDAC tissue cohort by qRT-PCR. METTL1-knockout PDAC cell lines were generated via CRISPR/Cas9. Cellular proliferation and migration were assessed through MTT, colony formation, and wound-healing assays, while tumor growth was evaluated in xenograft models. Global tRNA m7G levels were measured using dot blot, and qRT-PCR was used to quantify specific tRNA abundances. Polysome profiling identified METTL1-dependent translational targets, and mitochondrial function was assessed by Seahorse Mito Stress testing.

Results: METTL1 was significantly upregulated in PDAC ($p < 0.001$) and correlated with poor patient survival ($p < 0.05$). METTL1 knockout suppressed PDAC cell proliferation, migration, and tumor growth ($p < 0.001$) in vitro and in vivo. Mechanistically, METTL1 loss decreased the abundance of m7G-modified valine tRNAs, particularly Val-AAC, Val-CAC, and Val-TAC (all $p < 0.001$), leading to reduced translation of valine codon-enriched oxidative phosphorylation genes. Consequently, METTL1 deficiency impaired mitochondrial respiration and energy production. Consistently, valine tRNA expression was elevated in PDAC tissues ($p < 0.01$), and selective knockdown of these tRNAs inhibited proliferation and migration ($p < 0.001$) by disrupting mitochondrial function. Reintroduction of Val-AAC, Val-CAC, and Val-TAC restored growth ($p < 0.001$) and migratory capacity ($p < 0.01$) in METTL1-deficient cells.

Conclusions: METTL1-mediated m7G modification of valine tRNAs promotes PDAC progression by reprogramming the translational landscape to support mitochondrial metabolism. This METTL1-tRNA-mitochondrial axis represents a novel metabolic vulnerability and a promising therapeutic target in pancreatic cancer.

#5963 mTORC1-eIF4A1 dependent translational regulation of oncogenic fatty acid desaturases.

Yujin Chun[1], Joohwan Kim[1], Izabelle Le[2], Cuauhtemoc B. Ramirez[1], Won-Suk Song[2], Cholsoon Jang[2], Gina Lee[1]

[1]Department of Microbiology & Molecular Genetics, University of California, Irvine, School of Medicine, Irvine, CA,[2]Department of Biological Chemistry, University of California, Irvine, School of Medicine, Irvine, CA

Cells actively remodel their lipid composition to support membrane integrity, organelle function, and signaling as environmental and nutrient condition changes. While transcriptional control of lipogenesis has been extensively studied, how these pathways are controlled at the translational level remains incompletely defined. Our prior works identified transcriptional and post-transcriptional regulation of de novo lipogenesis. Here, we found that the mTORC1-eIF4A1 axis selectively enhances the translation of the oncogenic fatty acid desaturases stearoyl-CoA-desaturase 1 (SCD1) and fatty acid desaturase 2 (FADS2), which together supply monounsaturated fatty acids (MUFA). Across multiple mTORC1-hyperactive cancer cell lines, eIF4A1 inhibition by siRNA or small molecules (silvestrol and zotatifin) reduced the desaturase protein abundance while other lipogenic enzymes were unchanged. Using polysome assay and 5'UTR luciferase assays, we confirmed that the translational regulation is via their unique 5'UTR structures. In addition, to investigate how eIF4A1 perturbation affects cellular lipidome, we applied ^{13}C-isotope tracing to examine newly synthesized fatty acids and related lipids. eIF4A1 inhibition lowered cellular MUFA content, shifted phospholipids toward more saturated fatty acids and induced ER stress and lipid peroxidation. This impaired fatty acid balance and lipid composition led to decreased cell proliferation upon eIF4A1 inhibition and was partially rescued by MUFA supplementation. Extending these findings in vivo, zotatifin treatment in a Tsc2$^{+/-}$ kidney tumor mouse model, where loss of Tsc2 hyperactivates mTORC1, reduced tumor burden, decreased desaturase expression, and increased lipid peroxidation. Together, these data establish a direct link between translational control and fatty acid desaturation in cancer cells, and support eIF4A1-targeted strategies to simultaneously suppress two oncogenic fatty acid desaturases in mTORC1-hyperactive tumors.

#5964 Single-cell multi-omics profiling unveils the regulatory mechanisms of small cell lung cancer.

Charny Park[1], Namhee Yu[1], Jung-Hyun Kim[1], Sehwa Hong[1], Mihwa Hwang[1], Bo Ram Song[1], Sunshin Kim[1], Soo Young Cho[2], Beung-Chul Ahn[1], Ji-Youn Han[3]

[1]National Cancer Center - Korea, Goyang-si, Korea, Republic of,[2]Hanyang University, Seoul, Korea, Republic of,[3]National Cancer Center - Korea, Goyang-Si, Korea, Republic of

Small cell lung cancer (SCLC) is a highly aggressive lung cancer with an extremely poor prognosis. The mechanisms underlying its tumor progression and therapeutic strategies remain poorly understood. To address this clinical challenge, we utilized single-cell ATAC-RNA multiomic profiling to investigate clonal progression and its regulatory mechanisms. Patient-derived cells (n=73,546) were collected from pleural effusions (n=22) and categorized into tumor, stromal, lymphoid, and myeloid populations. Tumor cells exhibited progression along two clonal trajectories, characterized by *ASCL1*+ and *NEUROD1*+ subtypes. *ASCL1*+ cells, derived from *KEAP1*-mutated patients, activated the NRF2-KEAP1 pathway and ferroptosis. Notably, patients with *KEAP1* mutations were diagnosed with both large-cell neuroendocrine carcinoma and SCLC. In contrast, *NEUROD1*+ cell evolution was associated with upregulation of G protein signaling and Rho GTPase pathways, along with neuronal development. Tumor progression regulators were identified in both *ASCL1*+ (*FOXA1*, *KLF2*, *NR2C1*, *NRF1*) and *NEUROD1*+ (*PITX1*, *RORB*) subtypes. The mechanisms of these transcription factors identified target genes, which consistently reflected tumor cell progression along distinct trajectories. Among TME cells, exhausted T cells and *TREM2*+ macrophages were more prevalent in longer-survival and post-treatment patients. Cell-cycle-associated cancer fibrosis was abundant in progression and shorter-survival patients. When investigating cell-cell interactions, *ASCL1*+ tumor clusters predominantly interacted with myeloid and stromal cells through the GAS6 and SPP1 signaling networks, while NCAM and NEGF pathways enhanced the function of *NEUROD1*+ tumor cells by promoting communication within neuroendocrine tumor cells. This study delineates distinct clonal trajectories in SCLC, with *ASCL1*+ and *NEUROD1*+ subtypes driving tumor progression through specific regulatory pathways. Key transcription factors were identified as pivotal drivers of tumor evolution. Immune and stromal profiles suggest that immune exhaustion and fibrosis significantly impact patient survival, underscoring potential targets for therapeutic strategies and post-treatment interventions.

#5965 Plk1-BRN2 signaling axis drives lineage plasticity in castration-resistant prostate cancer.

Fatemeh Seilani[1], Meng Wu[1], Jia Peng[2], Mohammad Esfini Farahani[1], Xinyi Wang[1], Jinghui Liu[1], Yanquan Zhang[1], Ruixin Wang[1], Xiaoqi Liu[1]

[1]University of Kentucky, Lexington, KY,[2]Univ. of Kentucky College of Medicine, Lexington, KY

Prostate cancer frequently acquires resistance to androgen receptor (AR)-targeted therapies through lineage plasticity, leading to neuroendocrine prostate cancer (NEPC), an aggressive and therapy-resistant subtype. BRN2 (POU3F2) is a key transcription factor that drives this transition and is normally repressed by AR signaling; however, the upstream mechanisms that activate BRN2 during therapy resistance remain poorly defined. We identify Polo-like kinase 1 (Plk1), a mitotic kinase upregulated in advanced disease, as a previously unrecognized upstream regulator of BRN2. Plk1 directly phosphorylates BRN2 at a conserved motif, enhancing its transcriptional activity and promoting downstream neuroendocrine reprogramming. Disruption of this phosphorylation markedly diminishes neuroendocrine marker expression and inhibits cellular plasticity. RNA-seq analysis further revealed suppression of EMT-associated transcriptional programs as a major downstream consequence of impaired BRN2 phosphorylation. In vivo, using a robust NEPC mouse model, inhibition of Plk1-dependent BRN2 activation reprograms tumor histology and molecular phenotype toward an AR-positive prostate adenocarcinoma (ARPC) state, indicating inhibition of lineage plasticity. These findings identify Plk1-mediated BRN2 phosphorylation as a critical driver of neuroendocrine transdifferentiation and highlight the Plk1-BRN2 axis as a promising therapeutic target to prevent NEPC progression in castration-resistant prostate cancer.

#5966 Barcoded cell state specific transcription factors screen identifies SIX1 as a critical regulator of neuroblastoma plasticity and drug resistance.

Xingyu Liu[1], Ying Wu[2], Haiyan Lei[1], Wendy Fang[1], John Shern[1], Zhihui Liu[1], Carol Thiele[1]

[1]Cell and Molecular Biology Section,, Pediatric Oncology Branch, Center for Cancer Research, National Cancer Institute, National Institutes of Health, Bethesda, MD,[2]Advanced Biomedical Computational Science, Frederick National Laboratory for Cancer Research, Frederick, MD

Neuroblastoma (NB) is characterized by intratumoral heterogeneity, consisting of at least two distinct cell types: adrenergic (ADRN) and mesenchymal (MES). These cell states can spontaneously interconvert, potentially driven by changes in super-enhancer landscapes and transcription factor (TF) networks. This interconversion presents a significant therapeutic challenge, as MES NB cells are less differentiated, more migratory, and drug-resistant, emerging during treatment and contributing to relapse. Therapeutic strategies targeting one state (like ADRN) may leave behind or select for more chemoresistant MES cells, complicating treatment efforts. Understanding the mechanisms behind the plasticity between the ADRN and MES states is critical for developing more effective treatments that prevent therapy resistance, tumor relapse, and improve patient outcomes. This MES cell state exhibits resistance to standard cytotoxic treatments and is associated with a more aggressive, migratory phenotype, contributing to poor therapeutic outcomes in NB. Additionally, NOTCH3 signaling drives the transition from ADRN to MES, with PRRX1 acting as a key reprogramming driver that reshapes the super-enhancer and mRNA landscapes of ADRN cells toward a MES state. However, what are the other TFs are involved with the transdifferentiation between ADRN and MES? What are the other TFs are responsible for the resistance of the cytotoxic therapies remain unclear. Furthermore, the most effective strategies to therapeutically target these pathways to prevent MES transition and overcome therapy resistance remain unknown.

#5967 Overexpression of the transcription factor gene TGIF1 inhibits proliferation in NRAS-driven acute myeloid leukemia cells.

Michael Roberts[1], Herryung Choi[2], Chase Mitchell Weizer[3], Helena Holley[4], Mishra Pranav[5], Ellsa Hritz[6], Jeffrey Forrester[1]

[1]Dickinson College, Carlisle, PA,[2]Biology, Dickinson College, Carlisle, PA,[3]Dana-Farber Cancer Institute, Boston, MA,[4]Molecular Medicine, University of Maryland, Baltimore, MD,[5]Yale University, New Haven, CT,[6]Data Analytics, Dickinson College, Carlisle, PA

The relatively few oncogenic driver mutations in most acute myeloid leukemia (AML) cells signifies that the numerous phenotypic hallmarks of cancer are established through the dysregulated expression of normal genes, by creating a leukemic transcriptome. We have sought to identify key transcriptional regulators that have the capacity to reprogram the AML transcriptome in ways that promote more normal cell behavior. The AML cell line HL-60 is responsive to treatment with phorbol esters, such as phorbol 12-myristate 13-acetate (PMA), that activate Protein Kinase C (PKC) and result in cell cycle arrest, myeloid differentiation, and eventual apoptosis. Through DNA microarray and RNA sequencing gene expression assays, we have identified approximately 100 genes encoding transcriptional regulators that significantly change in expression level during the PMA response. Among them, the TALE homeobox protein TGIF1 is up-regulated and serves as an expression prognostic marker demonstrating greater overall survival for patients expressing high levels compared to low expression samples by Kaplan-Meier survival plot analyses. Here we show that overexpression through transfection of TGIF1 in AML cell lines inhibits proliferation, as measured by Ki67 and DNA content levels using flow cytometric assays. These findings confirm a tumor suppressor role for TGIF1 in certain AML subtypes as has been previously described in pancreatic cancer. We also provide evidence that the mechanism for TGIF1 proliferation inhibition includes transcriptional repression of MYC and CCND1 expression. A more complete understanding of how TGIF1 directs the AML cell transcriptome is currently in progress using RNA sequencing to identify differentially expressed genes defining TGIF1 targets.

#5968 *FOXM1* as a key regulator of metastatic outgrowth in brain metastasis of breast cancer.

Shannon Cartay Kalsi[1], Lara Luzietti[1], Aoibheann Dowd[1], Aoibhin M. Powell[1], Gabriela Gomez[1], Jason McGrath[2], Nicola S. Cosgrove[3], Hian Hui Young[2], Arnold D. K. Hill[3], Stefan Prekovic[4], Leonie S. Young[2], Damir Vareslija[1]

[1]School of Pharmacy and Biomolecular Sciences, Royal College of Surgeons in Ireland (RCSI), Dublin, Ireland,[2]Department of Surgery, Royal College of Surgeons in Ireland (RCSI), Dublin, Ireland,[3]Department of Surgery, Beaumont RCSI Cancer Centre, Dublin, Ireland,[4]Center for Molecular Medicine, University Medical Center Utrecht, Utrecht, Netherlands

INTRODUCTION: Brain metastases occur in approximately 20% of breast cancer patients. These secondary lesions exhibit distinct phenotypic and genomic alterations compared to primary breast tumours, often driven by specific transcription factors. Identifying such factors may reveal novel therapeutic targets for treating brain metastases. We investigate FOXM1 as a key regulator in breast cancer brain metastasis, highlighting it as a potential prognostic and therapeutic marker.

MATERIALS AND METHODS: We performed RNA sequencing on 45 paired patient samples of primary breast tumours and corresponding brain metastases. Gene co-expression network analysis was conducted to identify preserved modules, focusing on the FOXM1-driven module. FOXM1 expression levels were assessed across patient cohorts to evaluate their correlation with survival outcomes and enrichment in tumours that progressed to brain metastasis. The impact of FOXM1 silencing on tumorigenicity and metastatic potential was investigated using breast-to-brain metastatic cell lines and *in vivo* models, with subsequent analysis of metastatic cluster formation and cellular proliferation.

RESULTS: The FOXM1-driven gene module was conserved in brain metastases and associated with poor clinical outcomes, including reduced overall survival. High FOXM1 expression was notably enriched in tumours that relapsed in the brain and correlated with diminished recurrence-free survival. Genetic and pharmacological inhibition of FOXM1 significantly impacted proliferation across multiple models of breast cancer brain metastasis representing all major subtypes. Transcriptomic analysis following FOXM1 silencing revealed the regulation of key pathways, including mTOR, TGF-β, EGFR, and epithelial-mesenchymal transition (EMT). Genetic silencing of FOXM1 *in vivo* models significantly inhibited the formation and size of brain metastasis clusters, reducing both proliferation and metastatic capacity.

CONCLUSION: FOXM1 is a critical regulator of breast cancer brain metastasis. Inhibition of FOXM1 hinders metastatic growth in the brain and improves survival-related outcomes. Targeting FOXM1 may signify a promising therapeutic strategy for patients with breast cancer brain metastasis. These findings underscore the importance of FOXM1 in brain metastases progression and suggest that targeting it could offer a novel therapeutic avenue.

#5969 Splicing variability and oncogenic isoforms: Transforming our understanding of HNSCC biology.

Daria Gaykalova[1], Madeleine Ndahayo[2], Ishita Gupta[3]

[1]Otorhinolaryngology, University of Maryland, Baltimore, Baltimore, MD,[2]University of Maryland, Baltimore, Baltimore, MD,[3]University of Maryland School of Medicine, Baltimore, MD

Head and neck squamous cell carcinoma (HNSCC) remains a cancer type with limited effective targeted therapies, currently restricted to anti-EGFR (Cetuximab) and anti-PD1 agents (Nivolumab and Pembrolizumab), and only one clinically established biomarker (HPV or its surrogate p16, applicable to ~30% of patients). Despite extensive genomic sequencing efforts, no new targeted therapy or biomarker has been approved for HNSCC in the past two decades. Our research addresses this critical gap by focusing on alternative splicing events (ASEs), which can profoundly alter gene function independently of mutations and represent an underexplored mechanism of oncogenesis. We hypothesize that ASEs in HNSCC contribute to tumor progression and can serve as biomarkers and therapeutic targets. To test this, we analyzed RNA-Seq data from The Cancer Genome Atlas (TCGA) and institutional cohorts, identifying 110 recurrent ASEs, including those in AKT3, PIK3R1, and HOXC6. These isoforms frequently originate from alternative transcription start sites (TSS) and display a strong inverse correlation between promoter DNA methylation and ASE expression, coupled with a positive correlation between H3K27ac enrichment and ASE expression. Together, these findings implicate chromatin architecture as a critical regulator of cancer-specific splicing programs. Functional validation revealed that these isoforms are frequently upregulated in tumors and drive oncogenic phenotypes such as increased proliferation and migration through activation of PI3K/AKT and other signaling pathways. To systematically characterize splicing variability and its immunogenic potential, we developed Splice Expression Variability Analysis (SEVA), enabling detection of differential isoform usage across tumor subtypes, and SpliceMutr, a computational pipeline for predicting splicing-derived neoantigens. These tools have uncovered splicing-driven vulnerabilities that may inform immunotherapy strategies and precision oncology. In conclusion, our findings created a map of ASE in HNSCC and established ASEs as a major contributor to HNSCC oncogenesis, independent of coding mutations, and highlighted the interplay between epigenetic regulation and RNA processing. Detection of oncogenic isoforms offers a path toward novel biomarkers, while targeting isoform-specific mechanisms could lead to innovative therapeutic strategies. This work introduces a paradigm shift in understanding HNSCC biology and opens new avenues for biomarker discovery and treatment development.

#5970 Rescuing VHLD missense mutations to prevent or treat renal cell carcinoma.

Shabnam Pirestani

Drexel University College of Medicine, Philadelphia, PA

Von Hippel-Lindau disease (VHLD) is an autosomal dominant cancer syndrome caused by germline mutations that occur throughout the *VHL* gene, affecting approximately 1 in 36,000 individuals. VHLD most commonly results in clear cell renal cell carcinoma (ccRCC) but can cause pancreatic neuroendocrine tumors and central nervous system hemangioblastomas, depending on the site of mutation. Somatic mutations in VHL are also common features of spontaneous ccRCC. The VHL protein (pVHL) serves as the substrate recognition component of the VCB E3 ubiquitin ligase complex (Elongin B/C, Cullin-2, and Rbx1), which targets hydroxylated HIF-α for proteasomal degradation under normoxic conditions. When *VHL* is mutated or oxygen is limited, HIF-α accumulates, activating genes such as *VEGFA* and *TGFα* that promote angiogenesis and proliferation. pVHL also has HIF-independent functions that are less understood but may contribute to VHLD pathogenesis. Belzutifan, which inhibits HIF-2α activity, has emerged as a valuable treatment for VHLD and spontaneous ccRCC, but not all patients respond, possibly due to cancer-promoting, HIF-independent consequences of VHL loss. This suggests the potential value of targeting pVHL directly.To evaluate how distinct missense mutations affect the canonical HIF-degradation role versus non-canonical functions, we analyzed public databases to identify common *VHLD* mutations associated with ccRCC versus other VHLD syndromes. We selected mutations distributed across the protein surface, including those disrupting interactions with VCB or HIF. We then generated lentiviruses encoding wild-type, null, and 10 VHLD-associated mutations, and used these to establish a series of isogenic models in *VHL*-null 786-O cell line. Cell models were characterized for pVHL and HIF-2a expression, as well as a series of non-canonical VHL-regulated phenotypes including control of mitotic integrity and spindle checkpoint activity. We then compared the ability of belzutifan and three pVHL-targeting drugs (VH298, CP4, CP4.29) to reverse phenotypes associated with VHLD mutations or loss. Whereas VH298 disrupts the VHL:HIF interaction interface, the recently described CP4 and its derivative CP4.2 bind a cryptic pocket near Asp197 in pVHL, stabilizing the structure and potentially restoring multiple protein functions. We will discuss activity of these compounds in rescuing essential VHL activities across diverse VHLD mutations, for canonical and non-canonical pathways. The goal of this work is to develop a new therapeutic approach for VHLD patients.

#5971 MYC cooperatives with KDM7A to repress SIDT2 and dampens dsRNA-mediated anti-tumor immunity.

Tae-Won Lee[1], Kyung-min Lee[1], Carlos L. Arteaga[2], Ariella B. Hanker[3], Seung Han Son[1]

[1]Life Science, Hanyang University College of Natural Sciences, Seoul, Korea, Republic of,[2]Director, Breast Cancer Program and Center for Cancer Targeted Therapies, UT Southwestern Simmons Comprehensive Cancer Center, Dallas, TX,[3]UT Southwestern Harold C. Simmons Comprehensive Cancer Center, Dallas, TX

MYC is a proto-oncogene frequently amplified in various cancers and is well known for its transcriptional activation functions, yet the mechanisms by which MYC mediates transcriptional repression remain poorly understood. Through integrative multi-omics analysis, we identified *SIDT2* as a novel direct target repressed by MYC. Analysis of public single-cell RNA sequencing datasets revealed mutually exclusive expression patterns between MYC and *SIDT2*, and their expression levels were inversely correlated across tumor transcriptome datasets. Loss of *SIDT2* reduced cytoplasmic double-stranded RNA (dsRNA) levels, leading to decreased expression of inflammatory chemokines including *CXCL9*, *CXCL10*, *CXCL11* and *CCL5*, resulting in impaired T cell recruitment. Inhibition of *DDX58* and *IFIH1*, two dsRNA sensors essential for innate immune signaling, abrogated the cytokine reduction caused by *SIDT2* loss, demonstrating that *SIDT2*-dependent cytokine expression is mediated through the dsRNA pathway. Consistent with its functional role, *SIDT2* expression correlated positively with cytotoxic T lymphocyte infiltration and was associated with favorable outcomes in patients receiving immune checkpoint blockade therapy. To identify factors that facilitate MYC-mediated transcriptional repression, we examined genes directly bound and suppressed by MYC and found substantial overlaps with gene targets regulated by KDM7A, a histone demethylase. Mechanistically, KDM7A functions as a transcriptional cofactor that enables MYC to repress *SIDT2* transcription. MYC and KDM7A co-occupied the regulatory region of *SIDT2*, forming a cooperative repressive complex, and loss of KDM7A abolishes MYC-dependent downregulation of *SIDT2*. ATAC-seq analysis further supported this mechanism by showing that MYC knockdown markedly increases chromatin accessibility at the *SIDT2* locus, whereas this chromatin remodeling does not occur when KDM7A is inhibited or depleted, indicating that KDM7A is essential for maintaining the repressive chromatin state imposed by MYC. Together, these findings reveal a previously unrecognized MYC-KDM7A cooperative mechanism that silences *SIDT2*, providing a mechanistic basis for MYC-mediated transcriptional repression and clarifying how oncogenic MYC suppresses dsRNA-driven anti-tumor immune responses.

#5972 Transcriptional dysregulation of pediatric B-ALL derived from Hispanic/Latino patients with and without high-risk genetic structural variants.

Joseph Schramm, **Brindangnanam Pownraj**, Bing He, Yali Ding, Daniel Bogush, Singh Chingakham, Katarina Dovat, Diwakar Bastihalli Tukaramrao, Sinisa Dovat

Penn State College of Medicine, Hershey, PA

Childhood Acute Lymphoblastic Leukemia (ALL) is the most common cancer diagnosis in children and teens. Relapsed ALL still contributes to leading cancer mortality in children and teens with ALL given it is highly prevalent. Hispanic/Latino (H/L) patients are a vulnerable population due to higher incidence of diagnosis and mortality compared to NHW despite correction for socioeconomic risk factors. H/L children have a higher incidence of high-risk genetic structural variants such as BCR-ABL1 translocations. IKZF1-del occurs more frequently and is frequently accompanied by other high-risk translocations or deletions such as CRLF2. CRLF2 translocations along with JAK2 alterations result in high-risk Ph-like B-ALL. We analyzed H/L leukemia samples from 42 H/L children and 18 NHW children using transcriptomics derived from RNAseq to uncover dysregulated regulatory pathways for childhood H/L ALL. We compared these two patient groups based on wildtype IKZF1 status or IKZF1 deleted status. Using ranked gene set enrichment analysis we found increased representation of dysregulated pathways for multiple genome maintenance pathways that affect replication, repair, and histone modification in H/L B-ALL with IKZF1 deletion. When comparing samples from H/L and NHW with wildtype IKZF1, gene set enrichment analysis showed downregulated showed increased dysregulated expression of DNA repair, cell cycle regulation, as well as amino acid metabolism pathways. Reduced representation bisulfide sequencing analysis of equal H/L and NWH B ALL samples (n = 16) showed altered methylation signatures for H/L patients in comparison to NHW for genes represented in cytoskeletal structure, vesicle trafficking, cancer cell signaling, amino acid response pathways, and long noncoding RNAs associated with cancer. The data show that there are some fundamental differences in the transcriptomics and transcriptomic regulation of B-ALL derived H/L patients compared to that of NWH. This was observed even in the absence of high-risk genetic structural variants. The H/L B-ALL results suggest that further research into the mechanisms of this transcriptional dysregulation will result in new approaches for risk adapted therapy to address this vulnerable population.

: RAS/MAPK Signaling, KRAS Targeting, and Adaptive Resistance
Poster Session

#5976 Spatiotemporal control of RAS-RAF signaling at the single-molecule level.

Rodrigo E. Caceres-Gutierrez[1], Rebika Shreshta[1], Jean Castillo-Badillo[1], Vanessa Wall[1], Scott Eury[1], Katie Powell[1], William Burgan[1], Min Hong[1], Peter Frank[1], Dwight V. Nissley[1], Frank McCormick[2], Thomas Turbyville[1]

[1]Frederick National Laboratory for Cancer Research, Frederick, MD,[2]UCSF Helen Diller Family Comprehensive Cancer Center, San Francisco, CA

RAS GTPases are central drivers of proliferation, differentiation, morphology, and apoptosis, yet oncogenic RAS remains largely untreatable: only two KRAS G12C–specific therapies are approved, benefit a minority of patients, and face clinical resistance. A key unresolved problem is how RAS activates its main effector, RAF, inside cells. Bulk affinity measurements show strong RAS–RAF binding but obscure the lifetimes of individual encounters and their spatial context. Here we integrate single-molecule with both *in vitro* and live-cell approaches to quantify the spatiotemporal dynamics of RAS–RAF binding. To directly visualize one-to-one RAS–RAF and RAF–RAF interactions in a TIRF microscope, we conducted dynamic single-molecule pulldowns: we built artificial 2- or 8-lipid membranes on coverslips (supported lipid biolayers) with tethered recombinant human RAS proteins. Then, BRAF or CRAF proteins from crude human cell lysates were captured by the membrane-bound RAS. This system allowed us to quantitate the biophysical parameters of RAS-RAF complexes diffusing on a lipid bilayer in real time. Strikingly, most individual RAS-RAF encounters only lasted a few tens of milliseconds. These short-lived interactions are consistent with constant interaction turnover detected in conventional co-immunoprecipitation assays. In live cells, we built upon a human HEK cell line devoid of endogenous H/N/KRAS and A/B/CRAF genes (6 KOs), to stably express halo-KRAS4b and snap-CRAF at stoichiometric, low levels. Then, we imaged single-molecule halo-KRAS4b and snap-CRAF using simultaneous two-color TIRF video acquisition, and analyzed the dynamics of the RAS/RAF interaction. Similar to our *in vitro* results, we observed that CRAF exhibits very short membrane dwell times in live cells, which increased upon MAPK pathway activation with soluble EGF. By bridging millisecond-scale binding kinetics with MAP kinase pathway activation, our work outlines how transient RAS–RAF contacts are regulated in space and time. This could reveal potential vulnerabilities for therapeutic intervention beyond current RAS inhibitors.

#5977 mTOR inhibition activates the EGFR-MAPK network by a novel AKT-initiated feedback loop promoting adaptive resistance.

Keiichi Koshizuka[1], Hiroki Izumi[2], Tomohiko Ishikawa[3], Kuniaki Sato[3], Jean-Philippe Coppe[4], J. Silvio Gutkind[3]

[1]Moores Cancer Center, University of California, San Diego, San Diego, CA,[2]National Cancer Center Hospital East, Kashiwa-shi, Japan,[3]University of California, San Diego, San Diego, CA,[4]UCSF - University of California San Francisco, San Francisco, CA

Head and neck squamous cell carcinoma (HNSCC) is the sixth most common cancer globally, resulting in more than 300,000 deaths each year worldwide. Treatment options for HNSCC patients include surgery, radiation, chemotherapy, and molecularly targeted therapies, and although immunotherapies have recently revolutionized the treatment landscape, <20% of HNSCC patients respond to immune checkpoint blockade (ICB) therapies. The survival rate of HNSCC patients has changed only modestly over the past decades, and therefore, HNSCC is a significant global health problem with high mortality and morbidity. Genomic alterations converging on persistent activation of the PI3K/mTOR pathway (>80% of cases) represent one of the most frequently altered signaling circuits in HNSCC. This overreliance on PI3K/mTOR signaling for tumor growth may expose a cancer vulnerability that can be therapeutically exploited, as revealed by recent clinical trials of mTOR inhibitors (mTORi) in HNSCC in the adjuvant and neoadjuvant settings. However, mTORi are ineffective in patients with advanced HNSCC, highlighting the urgency of elucidating the mechanisms underlying mTORi resistance. By combining the power of systems biology and computational approaches, including a high-throughput kinase activity mapping strategy, CRISPR/Cas9 synthetic lethal screening, CRISPR-guided GFP-tagging of endogenous EGFR, and the analysis of the spatiotemporal activation of intracellular ERK pools, we have now identified the activation of EGFR-MAPK signaling induced by mTORi in HNSCC as a major adaptive compensatory resistance pathway. Mechanistically, we found that mTOR inhibition activates the EGFR-MAPK pathway by disrupting a novel AKT-regulated feedback loop that inactivates EGFR. Ultimately, our findings suggest that the adaptive activation of EGFR represents a new mechanism of mTORi resistance, and that EGFR co-targeting may be a potent therapeutic option for HNSCC. These findings may be relevant to a large number of cancer types that depend on PI3K/mTOR signaling but fail to respond to mTORi therapies as single agents.

#5978 SPR2015, a highly potent and selective KRAS G12D (on) inhibitor, exhibits favorable pharmacokinetic behavior and significant anti-tumor efficacy against colorectal cancer as monotherapy in preclinical models.

Yi Qian, Zirong Zhang, Zhifei Fu, Kai Zhou, Meibi Dai, Shuqin Liu, Yang Zhang, Tao Hu

SciBrunch Therapeutics Co., Ltd, Shanghai, China

Colorectal cancer (CRC) is the third most common malignancy and the second leading cause of cancer-related deaths worldwide. To date, effective treatments for CRC remain limited. About 40% of colorectal patients harbor KRAS mutations, with KRAS G12D mutation accounting for the largest population. Although many KRAS G12D (off or on) selective inhibitors are currently in clinical development, with several reported promising clinical results in pancreatic ductal adenocarcinoma (PDAC) and non-small cell lung cancer (NSCLC) patients, none have demonstrated clinically meaningful efficacy in CRC patients as monotherapy. SPR2015 is a highly potent and selective KRAS G12D (on) inhibitor with nanomolar proliferation inhibitory activities in various KRAS G12D cell lines while with good selectivity over KRAS wild type. Co-crystal structure showed that SPR2015 formed tri-complexes via binding tightly with cyclophilin A (CypA) and forming a covalent bond with G12D. SPR2015 exhibited longer CypA residence time and improved target engagement kinetics in both human and mouse CypA binding assays. Oral administration of SPR2015 in mice—alone or together with another G12D (on) inhibitor (cassette PK) — clearly confirmed target-mediated drug disposition (TMDD) PK behaviors of this type inhibitors. SPR2015 outperformed the other G12D (on) inhibitor achieving rapid and sustain target engagement via enhanced CypA competitive binding. In mouse PDAC/NSCLC xenograft models, SPR2015 effectively inhibited tumor growth at 10 mg/kg (oral, q.d.) and achieved tumor regression at 30 mg/kg (oral, q.d.). Accompanying PK/PD studies in these models established the correlation between tumor growth inhibition efficacy, downstream PD inhibition on DUSP6 mRNA, and drug exposures in blood, tumor, and other tissues. Furthermore, a mouse head-to-head clinical trial was evaluated between SPR2015 and another G12D (on) inhibitor in over 15 CRC cell-derived xenograft (CDX) or patient-derived xenograft (PDX) models, using a single dose at 100 mg/kg (oral, q.d.). SPR2015 showed significantly superior efficacy in these in vivo CRC xenograft models, achieving a 64.7% objective response rate (ORR) and 94.1% disease control rate (DCR) as monotherapy. On the safety part, SPR2015 demonstrated favorable in vitro safety profiles and was well-tolerated in a 28-day rodent repeat dosing tox studies. SPR2015 is currently under IND-enabling and is expected to advance to human Phase 1 study by the end of 2026.

#5979 RASurgence: ARF6 boosts RAS oncoprotein synthesis and accelerates tumor progression..

Gwen Kramer[1], Deja M. Brooks[2], Joshua Tay[3], Prachi Gupta[2], Sheri L. Holmen[3], Thomas Jacob[2], **Allie H. Grossmann**[2]

[1]Providence Portland Medical Center, Portland, OR,[2]Providence Cancer Institute, Providence Portland Medical Center, Portland, OR,[3]University of Utah Huntsman Cancer Institute, Salt Lake City, UT

Oncogenic mutations in *RAS* genes occur in approximately twenty percent of all cancers and drive lethal malignancies such as lung, pancreatic, colorectal carcinoma and melanoma. Despite decades of research, *RAS*-mutant cancers remain difficult to treat and resistance to emerging RAS targeted therapies is a major clinical challenge. The small GTPase ADP-Ribosylation Factor 6 (ARF6), a member of the RAS superfamily, is critical for endomembrane trafficking, cytoskeletal remodeling, and production of phosphatidylinositol 4,5-bisphosphate (PIP_2), a substrate for PI3K and PLC lipid signaling. We have previously shown that ARF6 mediates invasion, metastasis and adaptive immune suppression in BRAF-mutant melanoma. Here we present preliminary data suggesting that ARF6 supports survival of *RAS*-mutant cancer cells and accelerates RAS-driven tumor progression by augmenting oncoprotein expression. In human *NRAS*-mutant melanoma and *KRAS*-mutant carcinoma cells, inhibition or knockdown of *ARF6* significantly reduces viability. In genetically engineered, immunocompetent mice bearing $NRAS^{Q61R}$ melanomas, tumor-specific deletion of *Arf6* delays tumor onset, slows tumor growth and prolongs overall survival. Mechanistically, activation of ARF6 stimulates PI3K-AKT-mTOR signaling and increases expression of RAS, BRAF and PI3K oncoproteins, at least partly through mTOR-mediated protein translation. Together these data suggest that oncogenic RAS signaling relies on ARF6 to fortify expression of key oncoproteins in the RAS pathway and enhance tumor progression.

#5980 AUBE00: A novel cyclic peptide pan-KRAS inhibitor targeting KRAS-activated cancers including KRAS-mutant cancers and wild-type colorectal cancer.

Kana Takei[1], Mayuki Ueda[1], Toshiaki Tsunenari[1], Ai Shinoda[1], Munehiro Yuki[1], Hitoshi Sase[2], Saki Michisaka[1], Yukako Tachibana[1], Masami Hasegawa[1], Toshihiko Fujii[1], Shino Kuramoto[1], Miho Nagayasu[1], Mengxuan Gao[1], Kazuhiro Ohara[1], Keisuke Oki[1], Mikito Owa[1], Seiya Hirai[1], Haon Futamata[1], Takuya Torizawa[1], Hatsuo Kawada[1], Mirai Kage[1], Mikimasa Tanada[1], Takuya Shiraishi[1], Hitoshi Iikura[2], Takehisa Kitazawa[1], Hiroshi Tanaka[1]

[1]Chugai Pharmaceutical Co., Ltd., Yokohama, Japan,[2]Chugai Pharmaceutical Co., Ltd., Tokyo, Japan

KRAS represents the most frequently mutated oncogene in human cancers, with mutations occurring in approximately 30% of all malignancies. Significant progress has been made in RAS-targeted therapies over recent years. These include the FDA approval of G12C inhibitors such as sotorasib and adagrasib that target the OFF state of RAS, as well as the ongoing development of various non-G12C inhibitors and ON-state RAS inhibitor.

Here we present AUBE00, a novel cyclic peptide that selectively binds to the OFF state of KRAS. AUBE00 demonstrates equivalent binding affinity across a broad spectrum of KRAS mutations. In vitro studies revealed potent antiproliferative activity against cancer cell lines harboring various KRAS alterations.Pharmacokinetic evaluation across multiple species demonstrated favorable oral bioavailability of AUBE00. Oral administration resulted in robust in vivo antitumor efficacy in preclinical models.

The intracellular equilibrium between ON and OFF states of the KRAS protein is thought to vary depending on mutation types. Wild-type RAS predominantly exists in the OFF state under physiological conditions. The G13D mutant retains higher susceptibility to NF1-dependent hydrolysis compared to G12X mutants, suggesting a relatively higher proportion of OFF-state conformation. Based on this biological insight, we compared efficacy of AUBE00 with RMC-6236, a pan-RAS(ON) inhibitor among models with various KRAS alterations. Our findings demonstrate that AUBE00 exhibits superior antitumor activity against cancers with KRAS wild-type amplification or KRAS G13D mutations compared to RMC-6236.

Notably, RAS wild-type colorectal cancers typically show high dependency on EGFR signaling, with anti-EGFR antibodies established as standard therapy. This clinical observation suggests that downstream activation of wild-type RAS signaling significantly contributes to cancer proliferation and progression. Our investigations revealed that AUBE00 demonstrates significant antitumor activity in RAS wild-type colorectal cancer models. Furthermore, combination treatment with cetuximab and AUBE00 exhibited synergistic antiproliferative effects in vitro.

In conclusion, our preclinical data establish AUBE00 as a promising therapeutic option for cancers harboring KRAS mutations as well as RAS wild-type colorectal cancer. AUBE00 is currently being evaluated in a Phase 1 dose escalation study to assess its safety, tolerability, and preliminary efficacy in patients with advanced solid tumors.

#5981 Metabolic stress conditions dictate MAPKAPK2-dependent efficiency of MEK1/2 inhibition in colorectal carcinoma.

Niti Kumari[1], Xu Chen[2], Amber M. Baldwin[1], Kristin I. Clemons[1], Mohammad Alharakeh[1], Lilian Calisto[1], Balawant Kumar[3], Qiaoqiao Zhang[4], Jiang Min[5], Bin Xiao[6], Amar B. Singh[3], Bin Wang[2], **Brian J. North**[1]

[1]Biomedical Sciences, Creighton University School of Medicine, Omaha, NE,[2]Daping Hospital, Chongqing, China, Chongqing, China,[3]Department of Medicine, Division of Gastroenterology, Hepatology and Motility, Kansas University Medical Center, Kansas City, KS,[4]Jinfeng Laboratory, Chongquing, China,[5]Gastrointestinal Surgery Department, The First Affiliated Hospital of Chongqing Medical University, Chongqing, China,[6]Chongqing Medical University, Chongqing, China

The kinase MAPKAPK2 regulates cell survival, proliferation, and death, and is upregulated in colorectal carcinoma (CRC) where it is associated with tumor growth and progression. However, how it regulates tumor progression in conjunction with other signaling pathways, such as MEK/ERK, remains elusive. Solid tumors are often subjected to metabolic stress, notably glucose deprivation. Here we demonstrate that MAPKAPK2 protein levels in CRC regulate cell fate decision during stress conditions, such as glucose deprivation and therapeutic treatment. While MAPKAPK2 expression is a limiting factor for CRC growth *in vitro*, depleting MAPKAPK2 or inhibiting its activity pharmacologically provides a survival advantage to CRC cells under glucose limiting conditions. Subjecting CRC cells to low glucose resulted in an ERK1/2-mediated decline in MAPKAPK2 to promote survival. Additionally, cells with reduced MAPKAPK2 activity were less sensitive to trametinib under glucose limiting conditions. Utilizing transcriptomic profiling, we found that glucose deprivation and MAPKAPK2 depletion activate pathways associated with survival during metabolic stress. This relationship was also observed in CRC patients (TCGA), where tumors with low MAPKAPK2 expression had higher ERK1/2 activation and upregulated stress-induced pathways, leading to poor survival. Finally, MAPKAPK2 modulated growth of CRC organoids, subcutaneous tumors, and patient-derived xenografts (PDX), and reduced MAPKAPK2 levels decreased efficacy of trametinib, *in vitro* and *in vivo*. Overall, this study identifies an interrelationship between MEK/ERK and p38/MAPKAPK2 signaling pathways during glucose deprivation to support cell survival and features MAPKAPK2 loss as a possible mechanism leading to reduced efficacy of trametinib-based anticancer therapy and poor patient outcomes in CRC.

#5982 Eradicating metastatic cancers by targeting a major tumor vulnerability of the K-RAS pathway: Seven in absentia homolog (SIAH).

Jonathan M. Baker[1], Emanuel Frank Petricoin[2], Julia Wulfkhule[2], Andrew Howell[3], Ashleigh Hannah[3], Amy H. Tang[4]

[1]Biomedical and Translational Sciences, Macon & Joan Brock Virginia Health Sciences Eastern Virginia Medical School at Old Dominion University, Norfolk, VA,[2]George Mason University, Manassas, VA,[3]Eastern Virginia Medical School, Norfolk, VA,[4]Old Dominion University, Norfolk, VA

Background: Persistent activation of the K-RAS pathway is multipotent: its downstream signaling networks promote tumorigenesis, drug resistance, relapse, and metastasis. Despite newly developed state-of-the-art therapies, none have yet to achieve durable antitumor efficacy. Seven in absentia homologues (SIAHs) are a conserved family of RING-domain E3 ubiquitin ligases that function as the most downstream signaling gatekeepers in the K-RAS pathway. Our preclinical studies demonstrated that SIAH inhibition leads to a tumor eradication phenotype of multiple stage IV human cancer cell lines both in vitro and in vivo.

Aims: We propose SIAH is a major tumor vulnerability and actionable drug target for inhibiting K-RAS pathway activation. In this study, we aim to elucidate the molecular mechanisms underpinning the antitumor efficacy of our potent SIAH inhibitor, $SIAH_2^{PD}$, as a new targeted therapy to achieve tumor eradication.

Methods: Reverse phase protein arrays (RPPAs) and principal component analysis (PCA) were used to quantify statistically significant fold-changes of 294 signaling proteins and phospho-proteins in response to SIAH blockade in five stage IV cell lines. RPPAs were performed in triplicate on MiaPaCa, MDA-MB-231, MDA-MB-468, HeLa, and A459 cell lines in which $SIAH_2^{PD}$ expression was controlled by a doxycycline (DOX)-inducible Tet-ON/OFF system. Four experimental conditions were used: Tet-ON vector control cells without DOX (**group A**) and with DOX induction (**group B**); Tet-ON-$SIAH_2^{PD}$ experimental cells without DOX (**group C**) and with DOX induction (**group D**). The ratios of each group were calculated in a pairwise comparison after normalization to GAPDH as an internal control. To validate putative targets of interest, immunofluorescence (IF), flow cytometry (FC), and Western blots (WB) were performed on cells for **group C** and **D** at 3-, 5-, and 7-days post-DOX-induction. Adherent and single cell suspensions were used respectively for cell-based assays in biological triplicates and normalized to α-Tubulin. Target protein expression was quantified and validated, and statistical analyses were performed by one-way ANOVA and T-tests using GraphPad Prism software.

Results: The altered expression of NFκB, Caspase-3, Caspase-7, Cofilin, and PARP in response to SIAH blockade were independently validated by RPPA, WB, FC, and IF, demonstrating the roles of heightened cellular stress, apoptosis, and dysfunctional DNA damage and repair pathways induced by $SIAH^{\text{loss of function}}$ as mechanistic, synergistic to kill cancer cells and prevent tumor growth.

Conclusions: RPPA cancer pathway mapping provides invaluable molecular insights into cancer network rewiring in response to SIAH blockade, revealing a major tumor vulnerability. This study supports the design of anti-SIAH-based, anti-EGFR/K-RAS targeted therapies to control and eradicate incurable human cancers.

#5983 Functional characterization of the RAS processing enzyme Rce1.

David Van Dongen

Memorial Sloan Kettering Cancer Center, New York, NY

Proteins containing a C-terminal CaaX motif undergo post-translational modifications required for their localization to membrane surfaces and biologic functions. These post-translational modifications consist of: lipidation by a protein prenyltranferase, endoproteolytic cleavage by RAS-converting enzyme 1 (Rce1), and carboxyesterification by isoprenylcysteine carboxymethyltransferase (ICMT). These enzymatic processes are possible targets for cancer therapeutics, as they are necessary for the signaling function of RAS GTPases and other oncoproteins. However, difficulties associated with the biochemical purification and characterization of membrane embedded proteins have limited our understanding of the enzymatic mechanism of Rce1, which resides within the ER membrane. To address this, we identified a biochemically tractable ortholog of Rce1 from *Drosophila melanogaster* and developed a strategy to purify the enzyme in its catalytically active form. Purified Rce1 recapitulates known enzymatic properties, including a requirement for its substrates to contain an attached prenyl lipid. Characterization of the enzyme's kinetic properties reveal slow enzymatic turnover (~ 20 hr^{-1}), which is consistent with other integral membrane proteases. We find that Zn^{2+} and the lipid PA inhibit Rce1, raising the possibility these factors may regulate its catalytic activity *in vivo*. Mass spectrometry analysis of the purified protein indicates that the enzymatic mechanism does not utilize metal ions. We hypothesize that conserved histidine and glutamate amino acids have catalytic roles, which differentiates Rce1 from most other proteases. This study provides insights into the catalytic mechanism of the enzyme, which could be useful for developing mechanism-based inhibitors.

#5984 Small molecule induced KRAS activation triggers ferroptosis in mutant KRAS expressing PDAC.

Haiyuxin Zhu[1], Kartini Iskandar[1], Nur Syafiqah B. Suleiman[1], Benedict J. Leong[1], Hanqing Pang[1], Alessandro Carrer[2], Anne-Sophie ARMAND[3], Franck Oury[4], **Shazib Pervaiz**[1]

[1]National University of Singapore, Singapore, Singapore,[2]University of Padua, Padua, Italy,[3]University of Paris Cite, Paris, France,[4]Institut Necker, Paris, France

Pancreatic ductal adenocarcinoma (PDAC) is the most prevalent histological subtype of pancreatic cancer with limited treatment options and poor prognosis. More than 90% of PDAC harbor mutations in the oncogene *KRAS* and are dependent on downstream pro-survival and/or proliferative factors such as AKT, MEK and MAPK. As such, targeting these downstream pathways has been employed as a therapeutic strategy, however, recent success in developing KRAS-specific inhibitors has added an important dimension in the management of PDAC. The clinical efficacy of the direct KRAS inhibitors has been less than optimal, which circumvents the need for identifying new therapeutic strategies. To that end, we recently described a novel approach using a small molecule that induced KRAS activation-dependent, ROS-mediated, execution of mutant *KRAS* driven cancer cells (*Iskandar, K. et al. Autophagy 2024*). Here we investigated the effect of this small molecule (merodantoin; C1) on mutant *KRAS* expressing PDAC. Results show that C1 selectively targets PDAC cells (cytotoxicity, colony formation and spheroid formation) harboring *G12 KRAS* mutation compared to wild-type *KRAS* expressing cells. Mechanistically, C1 treatment led to significant increase in both intracellular and mitochondrial reactive oxygen species (ROS), increase in labile iron levels due to increased transferrin receptor 1 (TfR1) and decreased ferritin heavy chain (FTH1), and disruption of the glutathione-based antioxidant system by reducing cystine uptake and decreasing Glutathione peroxidase 4 (GPX4) expression. These changes together triggered lipid peroxidation, a key sign of ferroptosis. Experiments using ferroptosis inhibitors, iron chelators, and ROS scavengers restored cell viability, confirming that C1 triggered cell death in PDAC cells by ferroptosis. Importantly, genetic and pharmacological modulation of *KRAS* provide evidence that mutant *KRAS* is upstream of ferroptotic cascade. Moreover, *KRAS* mutations were shown to make PDAC cells more sensitive to ferroptosis by naturally lowering their antioxidant defences and iron storage capacity. This was evident in the reduced baseline expression of GPX4 and SLC7A11, along with decreased cystine uptake in mutant *KRAS* expressing cell lines compared to wild-type controls. Beyond *in vitro* validation, C1 demonstrated strong effectiveness in patient-derived PDAC organoids and significantly limited tumor growth in a orthotopic PDAC mouse model. Evidence presented here strongly argue in support of targeting ferroptosis vulnerability of KRAS-mutant PDAC as a novel treatment strategy.

#5985 *GNAS*^{R201C} enhances peritoneal carcinomatosis in K*RAS*^{G12D}-driven gastrointestinal cancer models.

Ichiaki Ito, Saikat Chowdhury, John Paul Shen

UT MD Anderson Cancer Center, Houston, TX

Background*KRAS*^{G12D} and *GNAS*^{R201C} co-mutations are common in low-grade appendiceal mucinous neoplasms and promote peritoneal metastasis. We examined the role of *GNAS*^{R201C} in tumor progression using syngeneic mouse models.

Methods We generated *cdx2-Cre;LSL-Kras*^{G12D}*;Rosa26R-LSL-rtTA;TetO-Gnas*^{R201C} (cdx2-Kras/Gnas) mice, where *KRAS*^{G12D} is constitutively active and *GNAS*^{R201C} is doxycycline (dox)-inducible in the intestine. Protein levels were compared in RPPA between dox- and dox+ appendiceal organoids (cdx2-Kras/Gnas) generated from cdx2-Kras/Gnas mice. Pancreatic IPMN cells (p48-Kras/Gnas) were tested in a syngeneic peritoneal carcinomatosis model. Tumor burden, signaling, and survival were assessed.

Results In cdx2-Kras/Gnas mice, phospho-p44/42 MAPK Erk1/2 was robustly increased in cecum and colon without histologic abnormalities after 3-9 months of dox administration. In cdx2- Kras/Gnas organoids, dox induced *GNAS*^{R201C} expression (>3000-fold) and increased phosphorylated PKA substrates, accelerating organoid growth (doubling time: 78.5 h in dox+ vs. 121 h in dox−). In RPPA, proteins related to 1) survival and anabolic signaling (AKT2 pS474), 2) ER stress response and amino acid biosynthesis (PERK, Calnexin, and ASNS), and 3) glycolytic and lipid metabolism (Hexokinase II, ACSL, and UGT1A) were increased in dox+ vs. dox− organoids. To test the role of *Gnas*^{R201C} in peritoneal carcinomatosis, cdx2-Kras/Gnas and p48-Kras/Gnas cells were IP implanted in C57BL/6 mice. No peritoneal tumor formation was detected in mice after cdx2-Kras/Gnas cell IP implantation, whereas p48-Kras/Gnas cells formed pancreatic tumor, and extensive peritoneal and visceral metastases including liver and mesenteric lymph nodes in dox+ mice, reducing median survival to 11.5 days (log-rank p = 0.0368). Dox− mice implanted with p48-Kras/Gnas cells showed minimal disease. $CD3^+$ immune cells were locally enriched in dox+ pancreatic tumors, whereas minimal infiltration was observed in dox− tumors.

Conclusion *GNAS*^{R201C} cooperates with *KRAS*^{G12D} to promote peritoneal metastasis and alter the tumor microenvironment, suggesting GNAS signaling as a therapeutic target.

#5986 Deletion of AKT1 inhibits PTEN-loss induced intrahepatic cholangiocarcinoma but not hepatocellular carcinoma development in mice.

Ielyzaveta Slarve[1], Yining Ding[1], Yushan Wang[1], Zifei Xu[1], Lina He[1], Bangyan L. Stiles[2]

[1]USC - University of Southern California, Los Angeles, CA,[2]Assistant Professor, USC School of Pharmacy, Los Angeles, CA

Liver cancer is the third most common cause of cancer-related mortality worldwide, with hepatocellular carcinoma (HCC) and intrahepatic cholangiocarcinoma (ICC) representing the two most common subtypes. Mice lacking the tumor suppressor PTEN in the liver (*Pten*$^{loxP/loxP}$; albumin [*Alb*]-*Cre*$^{-/+}$; LiPten) display gradual, age-dependent development of hepatosteatosis and combined HCC-ICC. *Pten* loss results in activation of the serine/threonine kinase AKT. Of the three AKT isoforms identified to date, AKT1 isoform is implicated in regulation of cell growth, proliferation, and survival. In the present study, we investigated the role of AKT1 in mediating PTEN-loss induced liver cancer development by generating a novel double knockout mouse model (*Pten*$^{loxP/loxP}$; *Akt1*$^{loxP/loxP}$; *Alb-Cre*$^{-/+}$; LiPtenA1). Compared to 6-month-old control animals (*Alb-Cre*$^{-/-}$), LiPten mice fed normal chow developed marked hepatomegaly and diffuse steatosis. Loss of AKT1 in LiPten animals was unable to reverse steatosis, and LiPtenA1 animals did not exhibit any differences in body or liver weights. At 12 months old, LiPten mice developed tumor nodules on their livers, with microscopic features of steatosis, ductal proliferation and ectasia, HCC, and ICC. Like LiPten mice, all LiPtenA1 animals developed tumor nodules by 12 months of age. Microscopically, livers of LiPtenA1 mice displayed features of fatty nodules and HCC. Our preliminary analysis of expression of ICC-related genes and immunohistochemical staining of livers for ICC markers revealed significant reduction of ICC phenotype in LiPtenA1 mice. The induced phenotypic switch from combined HCC-ICC in LiPten mice to predominantly HCC in LiPtenA1 mice suggests a role for AKT1 in ICC development and contributes to the understanding of the role of AKT isoforms in regulating liver tumorigenesis.

#5987 Dual targeting of Pyk2/FAK and MEK/ERK pathways enhances growth suppression in glioblastoma.

Emely Morales-Colon[1], Kevin A. Rosa- Gonzalez[1], Lilia Kucheryavykh[2]

[1]Biochemistry, Universidad Central del Caribe, Bayamon, PR,[2]Universidad Central del Caribe, Bayamon, PR

Glioblastoma (GBM) is a highly aggressive brain tumor characterized by strong resistance to both chemotherapeutic and targeted therapeutic interventions. Our previous studies demonstrated that pharmacological inhibition of Focal Adhesion Kinase (FAK) and Proline-rich Tyrosine Kinase 2 (Pyk2) signaling in mouse glioma models significantly reduces tumor growth but results in only a modest increase in overall survival, suggesting the development of compensatory resistance mechanisms. Additionally, compensatory activation of the MEK/ERK signaling pathway was observed following the inhibition of FAK/Pyk2. We therefore hypothesized that concurrent targeting of FAK/Pyk2 and MEK/ERK signaling pathways could overcome MEK/ERK activation and enhance the therapeutic efficacy of FAK/Pyk2 inhibition in GBM.

Western blot analysis of primary human GBM cell lines and the GL261 glioma model in C57BL/6 mice revealed increased phosphorylation of MEK and ERK following treatment with the dual Pyk2/FAK inhibitor defactinib (5 μM in vitro; 50 mg/kg in vivo) for 72 hours. Combinatorial treatment with the MEK/ERK inhibitor avutometinib (1 μM in vitro; 0.3 mg/kg in vivo) abolished this compensatory activation, resulting in a 10-fold reduction in ERK phosphorylation in vitro and a 3-fold reduction in vivo. Cell cycle analysis demonstrated an accumulation of cells in the G2/M phase and induction of apoptosis following 72-hour treatment with defactinib, indicating cell cycle arrest. In contrast, avutometinib treatment for 72 hours resulted in cell accumulation in the G0 phase, accompanied by a decrease in cyclin D1 expression, as confirmed by Western blot analysis, consistent with a cytostatic effect. Combined treatment induced cell cycle arrest at both the mitotic (G2/M) and G0 phases, reflecting the additive effects of both inhibitors. Cell viability assays supported these findings, showing that defactinib and avutometinib monotherapies induced approximately 50% and 20% cell death, respectively, together with 60% and 25% reductions in live cell populations compared to untreated controls.

In conclusion, combined inhibition of Pyk2/FAK and MEK/ERK signaling produced an additive anti-tumor effect in glioma cells, suppressing compensatory MEK/ERK activation and enhancing growth inhibition.

#5988 MEK1/2 degraders uncover kinase-independent role of MEK1/2 in CRAF stabilization and maturation.

Jason S. Wasserman[1], Alison M. Kurimchak[1], Carlos Herrera-Montavez[1], Glenn A. Doyle[1], Brandon D. Fox[1], Ishadi K. M. Kodikara[1], Jian Jin[2], **James S. Duncan**[1]

[1]Fox Chase Cancer Center, Philadelphia, PA,[2]Icahn School of Medicine at Mount Sinai

The mitogen-activated protein kinase (MAPK) cascade is an evolutionarily conserved signaling pathway comprised of RAS GTPases, and downstream effector kinases (RAF, MEK, and ERK) that promote cell growth and survival. MEK1 and MEK2 (MEK1/2) are ubiquitous members of the dual-specificity MAP2K kinase family that phosphorylate and activate ERK1/2, controlling cellular proliferation. MEK1/2 paralogs share highly similar kinase domains, including their activation loops, which are phosphorylated by the upstream RAF family of kinases ARAF, BRAF, and CRAF. The activation of MEK1/2 by RAF is thoroughly described; RAF directly interacts with and phosphorylates MEK1/2, resulting in MEK1/2 kinase activation and subsequent phosphorylation of ERK1/2. In contrast, how the upstream RAF kinase, particularly CRAF, is activated is highly complex, involving an orchestration of chaperones, phosphorylation, and RAF dimerization, ultimately resulting in the phosphorylation of MEK1/2. The recognized CRAF signaling cascade has MEK1/2 functioning solely as a substrate of CRAF, binding to CRAF after RAS binding and RAF dimerization. However, there is evidence that MEK1 can directly regulate CRAF activity independent of RAS, suggesting that MEK1 has additional functions in the CRAF cycle. Here, using MEK1/2 proteolysis targeting chimeras (PROTACs), we discovered that MEK1/2 have kinase-independent functions in the regulation of CRAF protein stabilization, maturation, and kinase activation. Our findings reshape the current view of the CRAF activation cycle, establishing MEK1/2 binding to CRAF as an early required stabilizing event preceding CRAF-RAS engagement. Thus, MEK1/2 functions as both an activator and substrate of CRAF.

#5989 Targeting SHOC2 and GAB2 in acral melanomas driven by RAS-GTP.

Rony Andre Francois[1], Nick Lertwiriyapiti[2], Lucy C. Young[1], Matthew J. Sale[1], Frank McCormick[1]

[1]UCSF Helen Diller Family Comprehensive Cancer Ctr., San Francisco, CA,[2]University of California San Francisco, San Francisco, CA

Acral and cutaneous melanomas both rely on sustained mitogen-activated protein (MAP) kinase pathway activation for growth, however, unlike cutaneous melanoma, acral melanomas harbor distinct genomic drivers. These include frequent amplifications of *GAB2*, loss of function mutations in *NF1*, activating mutations in the KIT receptor tyrosine kinase (RTK), and mutations in canonical RAS (often codons 12 or 13 of NRAS). These mutations may occur separately or co-occur, and converge to increase RAS-GTP, resulting in oncogenic MAPK signaling.RAS-driven cutaneous melanomas have recently been found to be particularly dependent on SHOC2 for sustained MAPK signaling, however the extent to which RAS-driven acral melanomas rely on SHOC2 and/or GAB2 for sustained MAPK signaling has not extensively studied to date. To determine the extent to which SHOC2, GAB, and RAS-GTP contribute to MAPK signaling in acral melanoma, we used targeted si-RNA to SHOC2, GAB1, GAB2, or a combination of these, to determine the necessary RAS/MAPK pathway components critical for pathway activation. In parallel, we also utilized the RAS-ON inhibitor RMC-6236 (Daraxonrasib), the MEK inhibitor Trametinib, or a combination of both agents in RAS-driven acral melanoma cell lines. We found that the *NRAS* G12-mutant acral melanoma cell lines HS852T and Ma-Mel-27 were markedly sensitive to SHOC2 knockdown, with concurrent SHOC2/GAB1/GAB2 knockdown conferring the greatest inhibition of MAPK activity. Similarly, both cell lines were sensitive to RAS-GTP inhibition with RMC-6236, with the addition of Trametinib resulting in the greatest decrease in MAPK activity.These results demonstrate that RAS-driven acral melanomas rely on components upstream of RAS that activate MAPK signaling, such as GAB, as well as components downstream of RAS such as SHOC2 for maximal MAPK pathway activation. In keeping with this, pharmacologic inhibition of RAS-GTP with RMC-6236 combined with the MEK kinase inhibitor Trametinib resulted in maximal pathway inhibition. Therefore, targeting RAS/MAPK signaling using a vertical inhibition approach warrants further exploration in RAS-driven acral melanomas.

#5990 UBE3A and SV2A modulate GBM progression through MAPK pathway regulation..

Lee Eunju[1], MIN-JEE KIM[2], Peter CW Lee[2]

[1]Department of Biochemistry & Molecular Biology, Brain Korea 21 Project, University of Ulsan College of Medicine, Asan Medical Center, Seoul, Korea, Republic of,[2]Department of Biomedical Sciences, University of Ulsan College of Medicine, Seoul, Korea, Republic of

Glioblastoma (GBM) is the most aggressive and common primary brain tumor in adults, yet effective therapeutic strategies remain limited. In this study, we integrated transcriptomic and clinical data from the Chinese Glioma Genome Atlas (CGGA) and found that high UBE3A expression is significantly associated with poor prognosis in GBM. As an E3 ubiquitin ligase within the ubiquitin-proteasome system (UPS), UBE3A plays a crucial role in maintaining protein homeostasis and cellular processes. Functional assays in GBM cell lines demonstrated that UBE3A knockdown markedly reduced cell proliferation, colony formation, migration, and invasion. Mechanistically, UBE3A physically interacted with SV2A and promoted its ubiquitination, indicating that SV2A is one of its potential substrates. Either UBE3A depletion or SV2A overexpression reduced ERK and p38 phosphorylation, indicating suppression of MAPK signaling, and was accompanied by increased apoptotic signaling (enhanced PARP cleavage and caspase-3 activation). These findings indicate that UBE3A and SV2A drive GBM progression mainly via MAPK pathway regulation. Although additional studies of the UBE3A-SV2A axis and downstream MAPK signaling are needed, this axis may represent a promising therapeutic target in glioblastoma.

#5991 p53-induced FBXL20 suppresses the PP2A regulatory subunit PR55α.

Alison L. Camero[1], Michel Ouellette[2], Keith Johnson[3], Ying Yan[4]

[1]Genetics, Cell Biology, & Anatomy, University of Nebraska Medical Center, Omaha, NE,[2]Internal Medicine, University of Nebraska Medical Center, Omaha, NE,[3]Oral Biology, University of Nebraska Medical Center, Omaha, NE,[4]Radiation Oncology, University of Nebraska Medical Center, Omaha, NE

Background:Protein phosphatase 2A (PP2A) is a major serine/threonine phosphatase that regulates cell survival and proliferation. Each PP2A holoenzyme consists of a scaffolding subunit, a catalytic subunit, and a regulatory subunit, with the regulatory subunit determining substrate specificity and cellular localization. Work from our group and others has shown that the PR55α regulatory subunit promotes oncogenic signaling through YAP, c-Myc, β-catenin, and ERK pathways. Despite its established role in supporting tumorigenesis and progression, the upstream mechanisms controlling PR55α expression and activity remain poorly understood. Pancreatic cancer (PC), one of the most lethal human cancers, is characterized by frequent loss of p53 function, with mutations occurring in more than 75% of cases. We recently discovered that p53 induces the F-box protein FBXL20, which in turn reduces PR55α stability and expression. This finding reveals a previously unrecognized mechanism whereby p53 restrains PR55α through SCF-mediated ubiquitination and proteasomal degradation. Defining this regulatory interaction is essential for understanding how p53 loss enhances PR55α-driven oncogenic signaling in PC.
Methods:To identify the FBXL20 interaction site on PR55α, we generated Myc-tagged PR55α truncation constructs and performed co-immunoprecipitation assays. Additional immunoprecipitations are underway to determine whether FBXL20 engages PR55α within an assembled SCF complex by assessing SKP1 and CUL1-4 association. To evaluate functional consequences, we are generating PR55α point mutations that disrupt FBXL20 binding and will examine their biological effects on PR55α stability and downstream signaling pathways.
Results:Mapping studies indicate that FBXL20 binds to a region between WD40 domains 5-6 of PR55α, potentially involving an α-helical linker. FBXL20 also associates with the heterotrimeric PR55α-PP2A complex, suggesting that PR55α engagement with PP2A does not block its recognition by the SCF ligase. Ongoing experiments are testing whether core SCF components co-precipitate with PR55α, which will determine whether a functional ubiquitin ligase complex forms. Parallel studies using PR55α point-mutation constructs are examining how loss of p53/FBXL20 interaction alters PR55α stability and downstream signaling.
Conclusions:Our findings establish a novel mechanism by which p53 constrains PR55α abundance through FBXL20-mediated ubiquitination and proteasomal degradation. Identifying the FBXL20 recognition site on PR55α provides a foundation for defining the phosphodegron required for its turnover and significance on PR55α stability and oncogenic activity. Understanding this regulatory pathway offers insight into how p53 loss through mutations enables unchecked PR55α/PP2A-driven oncogenic signaling in PC and other malignancies and may uncover new PR55α-based therapeutic strategies.

#5992 A hotspot phosphorylation site on SHP2 drives oncoprotein activation and drug resistance.

Prashath Karunaraj[1], Remkes Scheele[2], Malcolm L. Wells[2], Ipek S. Gokulu[1], Lila Taylor[1], Ruchita Rathod[2], Sophia Abrahamson[2], Lamia Chowdhury[2], Abiha Kazmi[2], Weixiao Song[3], Anum Glasgow[2], Neil Vasan[1]

[1]NYU Langone Health Perlmutter Cancer Ctr., New York, NY,[2]Columbia University Irving Medical Center, New York, NY,[3]WuXi AppTec, Suzhou, China

SHP2, a protein phosphatase encoded by *PTPN11*, is a critical mediator of receptor tyrosine kinase (RTK)-driven RAS/mitogen-activated protein kinase (MAPK) signaling and is targeted by allosteric inhibitors that stabilize its autoinhibited conformation. Despite promising preclinical data, SHP2 inhibitors have shown minimal clinical efficacy (monotherapy response rate ~0%), with no defined mechanisms of primary resistance in patients. Here, we elucidate phosphorylation of SHP2 at tyrosine 62 (pY62) as a hotspot phosphorylation site enriched across normal cells and tissues, cancer cells, and varied RTK-driven tumor types in patients. We demonstrate that SRC family kinases (SFKs) directly phosphorylate SHP2 at Y62, downstream but not directly phosphorylated by RTKs. Using biochemical and biophysical analyses, we show that SHP2 pY62 enforces an open, active conformation, resulting in constitutive phosphatase activation that is sufficient to activate MAPK signaling and confer resistance to allosteric SHP2 inhibitors. These findings establish SHP2 pY62 as a phosphorylation hotspot phenocopying mutational activation, as a mechanism of primary resistance to SHP2 inhibitors, and as a cancer drug target distinct from wildtype SHP2.

#5993 The Rho-GEF ECT2 links Rho GTPases to MEK/ERK pathway activation in pancreatic ductal adenocarcinoma.

Dania Al-Qasrawi[1], Nayya N. Murray[1], Ryan A. Argo[1], Alicia K. Fleming Martinez[1], Prita Pandya[1], Anaya Y. Clarke[1], Kayla C. Winter[1], Murli Krishna[2], Peter Storz[1], Nicole R. Murray[1], **Verline Justilien**[1]

[1]Cancer Biology, Mayo Clinic Florida, Jacksonville, FL,[2]Pathology/Lab Medicine, Mayo Clinic Florida, Jacksonville, FL

Pancreatic ductal adenocarcinoma (PDAC) remains one of the most lethal human malignancies due to its silent clinical onset, rapid progression, and limited responsiveness to current treatment options. These features underscore the urgent need for early detection strategies and for new molecular targets that can be exploited therapeutically. Epithelial Cell Transforming Sequence 2 (ECT2) is a Rho family guanine nucleotide exchange factor that was originally identified as an oncoprotein and later shown to regulate cytokinesis. In this study, we examined the clinical relevance of ECT2 expression in PDAC and determined its functional contribution to transformed growth and tumorigenicity. Our analyses revealed that ECT2 expression increases at the earliest stages of PDAC development, remains persistently elevated during disease progression, and associates with reduced overall patient survival. Furthermore, a substantial fraction of ECT2 is aberrantly localized to the cytoplasm of PDAC cells. Functional studies demonstrated that depletion of ECT2 suppresses three-dimensional growth, invasive behavior, and tumor formation in vivo, while having little impact on PDAC cell cytokinesis. Mechanistically, we found that ECT2 is required for activation of Rac1 and RhoA and downstream MEK/ERK and ROCK signaling, respectively. Consistent with these results, analyses of PDAC patient datasets revealed a strong positive association between ECT2 expression and Rho GTPase as well as MEK/ERK and ROCK pathway signatures. Together, our data identify ECT2 as an early driver of PDAC transformation and highlight it as a promising therapeutic target.

#5994 Mechanism of oncogenicity induced by overexpression of the PRL phosphatases.

Jingmei Yu[1], Frederick Nguele Meke[1], Yunpeng Bai[1], Meaghan Maureen Broman[2], Haoran Zhang[1], Abhinanda Kar[1], Zhong-Yin Zhang[1]

[1]Borch Department of Medicinal Chemistry and Molecular Pharmacology, Purdue University, West Lafayette, IN,[2]Department of Comparative Pathobiology, Purdue University, West Lafayette, IN

The phosphatases of regenerating liver (PRL) phosphatases are frequently overexpressed in a wide variety of human cancers and are correlated with cancer progression, metastasis, and poor patient outcomes. Although PRLs appear to be linked to oncogenesis, it is not yet fully understood whether PRL overexpression is sufficient to drive spontaneous tumorigenesis *in vivo* or the mechanisms by which PRLs contribute to cancer. To address this gap, we developed a novel genetically modified mouse model that conditionally overexpresses PRL2 in the prostate epithelium, mimicking the onset of human cancers. Our findings indicate that transgenic overexpression of PRL2 leads to a multifocal low-grade prostatic intraepithelial neoplasia (LGPIN) phenotype, with a rare occurrence of malignancy in older mice. Furthermore, elevated PRL2 promotes significant acceleration and progression from high-grade prostatic intraepithelial neoplasia (HGPIN) to prostatic adenocarcinoma mediated by PTEN heterozygosity, whereas PRL2 overexpression is dispensable for PTEN-loss-mediated transformation. The initiation and progression of prostate cancer following PRL2 overexpression correlate with decreased PTEN levels and upregulation of AKT/mTOR pathways. Taken together, these findings elucidate the pivotal role of proto-oncogenic PRL2 in promoting tumorigenesis through the downregulation of PTEN. Therefore, PRLs are compelling therapeutic targets for cancer drug discovery, and PRL2 inhibition may be a novel approach for cancer treatment through PTEN augmentation in both PTEN-deficient and wild-type backgrounds.

#5995 Pterostilbene enhances dabrafenib activity in BRAF mutant melanoma through synergistic MAPK suppression and apoptotic induction.

Joshua Steven Fraser[1], Jordan Bury[1], Colt Summers[1], Jennifer Meyer[2], Gennie Lynne Parkman[3]

[1]Chemistry, Utah Tech University, St George, UT,[2]Utah Tech University, St George, UT,[3]Weber State University, Ogden, UT

Resistance to BRAF inhibitors limits durable responses in melanoma. Pterostilbene (PTB), a dietary polyphenol, has anti-proliferative and pro-apoptotic properties and may augment targeted therapy. We evaluated whether PTB enhances the activity of the BRAF inhibitor dabrafenib (DAB) in BRAF-mutant melanoma cells. IC_{50} values for PTB and DAB were determined in A375 and HT144 melanoma cells following 48 h treatment. Synergy studies were conducted in HT144 cells using 5×5 fixed-ratio matrices based on experimentally determined IC_{50} values, and synergy was quantified using Loewe additivity, Bliss independence, ZIP synergy, and Combination Index models. Mechanistic effects were assessed by Western blot analysis of key markers of MAPK signaling and apoptosis. In A375 cells, IC_{50} values were ~12 nM for DAB and ~60 μM for PTB. In HT144 cells, IC_{50} values were ~3 nM for DAB and ~45 μM for PTB. Multiple PTB+DAB combinations in HT144 produced strong synergy, with the most synergistic doses (e.g., PTB ~12 μM + DAB ~0.8-3 nM) showing Loewe CI < 0.7 and corresponding Bliss/ZIP synergy. Synergistic treatment decreased MAPK pathway activation and increased apoptotic markers relative to single agents, consistent with enhanced signaling suppression and apoptosis induction. PTB enhances DAB efficacy in BRAF-mutant HT144 melanoma cells, producing robust synergy and mechanistic evidence of MAPK pathway inhibition and apoptosis. These findings support further evaluation of PTB as a low-toxicity adjuvant to improve responses to BRAF-targeted therapy in melanoma.

#5997 Network based mapping reveals mechanistic drivers and targetable hubs contributing to Sotorasib resistance in KRAS G12C lung cancer.

Atish Ranjan Mohanty[1], Baiyi Quan[2], Dana Do[1], Ting-Yu Wang[2], Tsui-Fen Chou[2], Prakash Kulkarni[1], Ravi Salgia[1]

[1]City of Hope National Medical Center, Duarte, CA,[2]California Institute of Technology, Pasadena, CA

KRAS mutations are among the most common oncogenic drivers in lung adenocarcinoma, present in 30% of NSCLC cases. Most occur at codon 12, impairing KRAS's intrinsic GTPase activity and locking it in a constitutively active state. Although KRAS was long considered "undruggable," the development of covalent inhibitors, such as sotorasib, which bind to the KRAS G12C GDP-bound form, marked a significant therapeutic advance. However, the clinical responses remain limited, as many patients exhibit intrinsic resistance or eventually develop acquired resistance. These limitations highlight that cancer cells expressing KRAS G12C were not solely dependent on KRAS signaling for survival. Instead, they adapt to therapeutic pressure by rewiring their underlying gene regulatory and protein-protein interaction networks. These networks are highly complex, coordinated, and dynamic in nature rather than fixed. Environmental cues, drug exposure, and intrinsic signaling programs can reshape network topology, generating new regulatory states that sustain tumor survival and drive resistance. Therefore, a systems-level examination of these topological transitions is essential for identifying the mechanistic basis of KRAS inhibitor resistance and identifying the upstream nodes that may serve as therapeutic vulnerabilities. Methods: Mass-spectrometry-based proteomic and phosphoproteomic profiling was performed on parental and isogenic resistant NCI-H23 cells, with and without sotorasib treatment. Network-based analyses were conducted to identify signaling alterations associated with the development of resistance. Results and Conclusion: The integrated analysis suggests that tolerance to KRAS G12C inhibition is not mediated by a single pathway, but rather by a coordinated network of mitotic, replication stress, RNA processing, and chromatin remodeling mechanisms. Upregulation of mitotic regulators (FOXM1, MELK, PLK4, NEK2), replication-stress proteins (RRM2, RFC3, MCM5/6, RPA2/3), and splicing/chromatin factors (CLK1, SRPK1, SRSF1&3, SUZ12, EED) creates a robust stress-adaptation network that enables survival under KRAS-G12C inhibition. This coordinated pathway maintains cell proliferation, stabilizes stalled forks, supports chromatin plasticity, and promotes the emergence of drug-tolerant persisters. Together, these data support a model in which sotorasib-exposed cells adapt by coupling mitotic and replication-stress programs with RNA and chromatin remodeling, thereby maintaining viability in a chromosomally unstable state that can give rise to drug-tolerant persisters and, ultimately, fully resistant clones. In addition, these findings also highlight a set of actionable vulnerabilities within the mitotic and replication-stress machinery that may be targeted to prevent or delay resistance to KRAS G12C inhibitors.

: Senescence and Cell Stress
Poster Session

#6000 Transglutaminase 2 mediates the p53-dependent senescence-associated secretory phenotype.
Xiaoyu Guo[1], Jihye Kim[1], Yi-Xi Gong[1], Ingyu Lee[1], Bomi Han[1], Ki Baek Lee[2], In-Gyu Kim[2], Eui Man Jeong[1]

[1]Jeju National University, Jeju, Korea, Republic of,[2]Seoul National University, Seoul, Korea, Republic of

Senescent cells secrete a variety of NF-κB-dependent proteins, collectively known as the senescence-associated secretory phenotype (SASP), which promotes paracrine senescence, resistance to apoptosis, and chronic sterile inflammation. To clarify the role of SASP in both tumorigenesis and age-related diseases, we investigated the mechanism underlying NF-κB activation in senescent cells. Here, we demonstrate that transglutaminase 2 (TG2) functions as an effector enzyme that activates NF-κB in response to DNA damage-induced stress. In normal cells, senescence inducers upregulated TG2 expression in a p53-dependent manner, thereby enhancing SASP. In contrast, in p53-inactivated cells, senescence inducers further elevated TG2 expression through a positive feedback loop, accounting for the paradoxical increase in SASP. Both TG2 knockdown and pharmacological inhibition reduced SASP. Moreover, TG2 promoted apoptotic resistance in senescent cells by inhibiting caspase-3 activity. Consistently, TG2-deficient mice exhibited reduced Ras-induced cytokine production and inflammation, while tissue-specific TG2 expression increased with age. Collectively, these findings identify TG2 as a key regulator of SASP and suggest its contribution to age-related pathologies.

#6001 Senescence-inhibitory Δ133p53α mitigates accelerated ageing in mice.

Leo Yamada, Huaitian Liu, Natalia Von Muhlinen, Curtis C. Harris, Izumi Horikawa

National Cancer Institute, National Institutes of Health, Bethesda, MD

Hutchinson-Gilford progeria syndrome (HGPS), a premature aging disorder caused by a de novo LMNA G608G mutation, is characterized by the accumulation of DNA damage and persistent inflammation, which drive accelerated aging and lead to severe clinical manifestations, including skin atrophy, alopecia, and progressive deterioration of the aortic wall due to loss of vascular smooth muscle cells, resulting in severely shortened lifespan. Mouse models of HGPS recapitulate these pathological aging phenotypes, including cardiovascular defects, increased cellular senescence, DNA damage accumulation, systemic inflammation, and shortened lifespan.The human p53 isoform Δ133p53α, which lacks the N-terminal 133 amino acids, is a naturally occurring truncated variant with distinct biological functions. In HGPS patient-derived fibroblasts, Δ133p53α suppresses cellular senescence, reduces pro-inflammatory IL-6 production, limits DNA-damage accumulation, and extends replicative lifespan. These findings suggest that Δ133p53α selectively attenuates p53-mediated cell-cycle arrest and senescence while preserving DNA-repair functions.Here, in a heterozygous HGPS mouse model, we show that transgenic expression of Δ133p53α reproduces these in vitro-observed effects across multiple organs in vivo and extends median lifespan by approximately 10% (387 vs. 358 days, P = 0.0235). In the aorta and skin, Δ133p53α mitigates progeria-associated pathological changes and preserves tissue integrity. Δ133p53α also mitigates spinal kyphosis characteristic of the HGPS mouse phenotype. RNA-sequencing analysis suggests that Δ133p53α promotes mitochondrial function and metabolic fitness. The effects of Δ133p53α in naturally aging mice are under investigation. Our human expression database analysis shows an age-associated downregulation of Δ133p53α in multiple human tissues, including aorta and skin.This study suggests not only a Δ133p53α-based therapeutic approach for HGPS but also broader interventions for preventing or delaying aging.

#6002 The lncRNA TUG1 enhances helicase-mediated R-loop resolution through RNA-protein interaction.

Shuya Mimura[1], Jingqi Xie[1], Miho M. Suzuki[2], Yutaka Kondo[3]

[1]Nagoya University, Nagoya, Japan,[2]Nagoya Univ. Graduate School of Medicine,[3]Nagoya City University Medical School, Nagoya, Japan

Long non-coding RNAs (lncRNAs) are emerging regulators of genome stability. Taurine upregulated gene 1 (TUG1) is highly expressed in cancer cells and rapidly induced by ATR-CHK1 signaling under replication stress. We previously showed that TUG1 interacts with replication protein A and the DEAE/DEAD-box helicase DHX9, enabling the resolution of pathogenic R-loops and supporting cancer cell proliferation. To expand our understanding of TUG1 function, we comprehensively profiled its interacting proteins using a CRISPR-based RNA-protein detection approach coupled with proteomic analysis. A conserved set of R-loop-associated factors, including RNA helicases, was enriched under replication stress, suggesting dynamic remodeling of TUG1-protein interactions in response to R-loop accumulation. Structural and biochemical analyses further suggested that TUG1 promotes helicase-mediated R-loop resolution through direct RNA-protein association. Collectively, our findings uncover a replication stress-responsive TUG1-helicase axis that maintains genome integrity by promoting R-loop resolution. Given that TUG1-targeting antisense oligonucleotides are already advancing into clinical trials, this study provides a mechanistic foundation supporting TUG1 as a promising therapeutic target for cancer treatment.

#6003 Modulation of cytokine-induced senescence in melanoma cells by JAK inhibitor: A possible way to improve therapeutic efficacy of immune checkpoint inhibitor.

Min You[1], Niramol Savaraj[1], Ying-Ying Li[2], Chunjing Wu[2], Mano Nagarajan[1], Medhi Wangpaichitr[1], Lynn G. Feun[1]

[1]University of Miami Miller School of Medicine, Miami, FL,[2]Miami VAMC, Miami, FL

Apart from the direct blocking of immunosuppressive checkpoint signaling, a prominent feature of immune checkpoint inhibitors (ICIs) is the enhancement of cytokine production by immune cells to facilitate anti-cancer immunity in the tumor microenvironment. Prolonged cytokine stimulation may also lead to immune suppression. On the other hand, it is known these cytokines can act on cancer cells to induce cellular senescence (cytokine-induced senescence, CIS). It has also been recognized that cellular senescence is intertwined with stemness or cell plasticity, and these phenotypic changes can be adopted by cancer cells to evade the anticancer effect of therapeutics agents including ICIs, resulting in resistance to treatment and or relapse post treatment. In this study, we attempt to investigate whether senomorphics such as JAK inhibitors can ameliorate CIS in melanoma cells and whether this reduction is accompanied by changes in the stemness and senescence-associated secretory phenotype (SASP). Melanoma cell line SK-MEL-28 was treated with INF-γ and TNF-α to establish CIS as indicated by SA-β-gal staining and detected with flow cytometry. Ruxolitinib (Ruxo) as a JAK1/2 inhibitor was then used to treat the cells, and at the end of the treatment the expression of stemness markers, SASP components, and immune checkpoint ligands was measured with qPCR. We observed that Ruxo was able to partially reduce the SA-beta-gal fluorescence in SK-MEL-28 (express PD-L1) at 10 nM and to the levels comparable of non-senescent control with non-senescent cell morphology at 10 μM. Furthermore, the expression of SASP component IL-1β and stemness markers CD271 was upregulated (about 4-fold) in the CIS state. Subsequent Ruxo treatment (10 μM) could partially attenuate the upregulation of IL-1β (by about 23%) and CD271 (by about 40%). However, Ruxo was unable to downregulate the increased expression of the stemness marker CD133 (1.77-fold from control); on the contrary, further upregulation (by about 31%) was noted. In addition, the expression of immune checkpoint ligands PD-L1 and PD-L2 showed moderate increase (by about 37% and 61%, respectively) in CIS and was not largely altered by Ruxo (increased by about 3% and 13%, respectively) while the increase of TIGIT ligand CD155 in CIS (by about 43%) could virtually be reverted by Ruxo. In summary, Ruxo could revert the senescent morphology and elevated SA-β-gal activity in the CIS of SK-MEL-28. Moreover, it could attenuate the expression of some stemness markers and SASP component elevated during CIS in melanoma cells. Further expansion of this study such as inclusion of more molecular markers and mechanism(s) is underway. Clinical study to include JAK inhibitor with ICI will also be initiated. This work is supported by the fund from Woman Cancer Association. Sylvester Comprehensive Cancer Ctr, U. of Miami and Miami VA Med. Ctr.

#6004 A link between the nuclear envelope protein LEM2 and an endoplasmic reticulum stress signaling pathway provides new insight into features of tumor development.

Natasha O. Saik[1], Maho Niwa[2], Katharine S. Ullman[1]

[1]Oncological Sciences, Univ. of Utah Huntsman Cancer Inst., Salt Lake City, UT,[2]Molecular Biology, University of California San Diego, School of Biological Studies, San Diego, CA

Cancer is often associated with reduced levels of certain nuclear envelope (NE) proteins, which contributes to irregularly shaped nuclei or nuclear dysmorphia. Nuclear dysmorphia can reflect compromised nuclear integrity and impaired DNA repair, which together can drive genomic instability and tumor development. Accordingly, expression levels of NE proteins—including LEM-domain proteins—are emerging as informative biomarkers for tumor detection, classification, and patient prognosis. Given that LEM2, an NE-associated LEM-domain protein, is altered in multiple cancers, we explored the effects of LEM2 depletion on phenotypic outcomes associated with cancer progression. Traditionally, the role of NE proteins in cancer phenotypes has been studied within the context of their canonical nuclear roles. However, hints from the literature suggest LEM2 contributes to the regulation of a physically connected organelle, the endoplasmic reticulum (ER). Despite the functional coupling and the physical continuity between the membranes that enclose the nucleus –the NE– and the ER, how changes originating in the nucleus influence ER organization and homeostasis remains poorly understood. Therefore, we examined whether disrupting LEM2 affects ER homeostasis—an important regulator of cancer progression. When ER homeostasis is disrupted, the unfolded protein response (UPR) pathway relays ER stress signals to the nucleus via transcriptional programs to alleviate ER stress and promote cell survival. Cancer cells often exploit the adaptive features of the UPR, and UPR components have emerged as promising biomarkers for predicting treatment response and prognosis. Here, we identify a novel mechanism of nucleus-to-ER communication in which loss of LEM2 triggers non-canonical activation of a specific branch of the UPR. Rather than responding to classic proteotoxic stress, the UPR activated by LEM2 depletion appears to arise from alterations in specific lipids. Our findings define a novel nucleus-to-ER signaling axis through which the NE modulates lipid-mediated UPR activity in the ER. Ongoing work aims to determine how this nucleus-to-ER pathway affects additional cancer phenotypes and to dissect how NE perturbations alter ER lipid homeostasis to activate the UPR. More broadly, uncovering the inter-organelle regulatory mechanisms of NE-ER communication provides a novel framework for gaining insight into tumor development.

#6005 Human DEAH-box RNA helicase 8 regulates HSF1-mediated stress response and cancer-associated pre-mRNA splicing.

Jennifer R. Tall, Robert Te Poele, Alexandra Vasile, Pradeep Ramagiri, Caitlin Davies, Marissa Powers, Toby Roe, Deivendran Sankaran, Konstantinos Mitsopoulos, Bissan Al-Lazikani, Robert L. Van Montfort, Emmanuel de Billy, Paul Workman, **Paul A. Clarke**

Centre for Cancer Drug Discovery, The Institute of Cancer Research, Sutton, London, United Kingdom

Background: Heat Shock Factor 1 (HSF1) drives stress tolerance, oncogenic transformation, and survival in diverse human cancers. Although pharmacologic inhibition of HSF1 remains challenging, identifying druggable upstream regulators of HSF1 offers a promising alternative strategy to disrupt stress adaptation in tumours.
Methods: A focused siRNA screen targeting 7,598 druggable genes was performed in human osteosarcoma cells to identify modulators of HSF1-activation. Transcriptomic, RNA immunoprecipitation (RIP), and enhanced CLIP (eCLIP) analyses were used to define the function and RNA-binding sites of the DEAH-box RNA helicase 8 (DHX8). Genetic rescue with wild-type versus ATPase- and RNA-binding-defective DHX8 mutants validated the mechanistic requirements for HSF1 mRNA processing. Functional assays (viability, cell cycle, apoptosis) assessed the effects of DHX8 depletion across tumorigenic and non-tumorigenic cell lines.
Results: DHX8 was identified and validated as a potent regulator of the HSF1 stress response. DHX8 silencing led to the accumulation of intron-retained HSF1 transcripts, decreased HSF1 protein levels, and suppression of HSF1 target genes. Genome-wide RNA-seq revealed broad DHX8-dependent splicing changes, dominated by intron retention, affecting>1,300 mRNAs. eCLIP profiling identified DHX8 binding between the lariat branch site and 3′ splice junction, consistent with its role in late-stage mRNA splicing. Rescue experiments demonstrated that both ATPase and RNA-binding activities are essential for HSF1 mRNA maturation. Acute degradation of DHX8 using a dTAG system phenocopied siRNA knockdown, confirming on-target effects. Functionally, DHX8 depletion in tissue culture experiments was generally tolerated by non-tumorigenic lines, but induced G_2/M arrest, apoptosis, and loss of viability in cancer cells.
Conclusions: DHX8 is a key regulator of HSF1 mRNA processing and cancer-associated splicing programs. Loss of DHX8 disrupts the oncogenic stress response, suppresses heat shock gene induction, and preferentially kills tumour cells. These findings establish DHX8 as a potentially druggable node linking RNA splicing to HSF1-driven cancer-survival pathways, offering a new therapeutic entry point for targeting stress resilience in malignancy.

#6006 Discovery of nuclear p62-PI4,5P$_2$ colocalization suggests a new regulatory layer in cancer proteostasis.

Alexandra Gebbia, Oisun Jung, Suyong Choi

Eppley Institute for Research in Cancer and Allied Diseases, University of Nebraska Medical Center, Omaha, NE

Aggrephagy, the selective autophagic clearance of protein aggregates, is essential for maintaining cellular homeostasis, particularly in cancer cells undergoing metabolic or proteotoxic stress. This process is mediated by the cargo receptor p62 (sequestosome-1, SQSTM1), which canonically recognizes ubiquitinated protein aggregates in the cytoplasm and delivers them to autophagosomes for lysosomal degradation. Intriguingly, p62 is also detected within nuclear condensates, a phenomenon that remains poorly understood given that autophagy has traditionally been regarded as a strictly cytoplasmic pathway.

Within the Phox and Bem1 (PB1) domain of p62, we identified a putative polybasic motif (PBM) capable of binding nuclear phosphoinositides, as well as a ZZ domain previously implicated in DNA binding. Because nuclear phosphoinositides and the kinases that generate them, such as phosphatidylinositol 4-phosphate 5-kinase type 1 alpha (PIP5K1A), regulate transcription, DNA repair, and other spatially organized nuclear processes, we hypothesized that p62 may engage lipid-defined microenvironments within the nucleus.

To test this hypothesis, we examined the nuclear interplay of p62 with the signaling lipid phosphatidylinositol 4,5-bisphosphate (PI4,5P$_2$) generated by PIP5K1A. We identified a previously unrecognized nuclear colocalization of p62 and PI4,5P$_2$ in breast cancer cell lines, a pattern not observed in pancreatic ductal adenocarcinoma (PDAC) models, suggesting that nuclear lipid-p62 regulation is highly cell-type specific. Nutrient deprivation reduced both p62 puncta and total p62 protein abundance, indicating that p62 levels are tightly coupled to metabolic status. Notably, genetic loss of PIP5K1A decreased total p62 levels independent of nutrient conditions, revealing that phosphoinositide signaling and metabolic cues converge to control p62 expression.

Together, these findings uncover a novel nuclear interaction between p62 and PI4,5P$_2$ and point to a regulatory axis involving PIP5K1A that may influence nuclear condensate formation and p62-dependent stress responses. Ongoing studies using proximity ligation assays, lysosomal activity measurements, and pharmacologic perturbation aim to define the functional significance of this pathway, which may represent an unrecognized therapeutic vulnerability in cancers dependent on p62-mediated proteostasis.

#6007 Fibroblast-driven IGF1 signaling suppresses CD44 and promotes tumor cell senescence at the invasive front of colorectal cancer.

Tae Jun Park[1], Hee Young Kang[1], Jang Hee Kim[1], Seok Yun Kang[1], Hyun Woo Lee[1], Sang Wun Kim[2], Hong Seok Kim[3], Soon Sang Park[1]

[1]Ajou University School of Medicine, Suwon, Korea, Republic of,[2]Yonsei University College of Medicine, Seoul, Korea, Republic of,[3]Inha University School of Medicine, Incheon, Korea, Republic of

Senescent tumor cells are cancer cells that undergo cell-cycle arrest in response to diverse intrinsic and extrinsic stresses. In our previous study, we observed that senescent tumor cells are preferentially enriched at the invasive front of colorectal cancer, where they display a marked global reduction in CD44 expression—including both standard and variant isoforms—an important hyaluronic-acid receptor associated with stress tolerance and redox resistance. Single-cell RNA-seq-based ligand-receptor interaction analysis revealed that senescent tumor cells are highly active in both sending and receiving intercellular signals. Among these, IGF1-IGF1R signaling between fibroblasts and senescent tumor cells was prominently upregulated.Mechanistically, activation of IGF1R triggered downstream AKT signaling, which suppressed CD44 transcription in tumor cells. Loss of CD44, a major regulator of cellular oxidative stress buffering, led to increased intracellular ROS levels. Elevated ROS subsequently downregulated DNMT1 expression, resulting in reduced methylation of the $p16^{INK4a}$ promoter and robust induction of $p16^{INK4a}$, thereby driving tumor cells into a senescent state. Consistent with this mechanism, in vitro treatment with recombinant human IGF1 or co-culture with fibroblasts induced AKT activation, decreased CD44 levels, increased ROS, and ultimately promoted p16 expression.Together, these findings identify a previously unrecognized tumor-stromal crosstalk in which fibroblast-derived IGF1 activates the IGF1R-AKT-CD44-ROS-DNMT1-$p16^{INK4a}$ axis to promote tumor cell senescence at the invasive front. This stromal-driven process suggests that the invasive front is not merely a region of physical invasion but an active signaling niche where fibroblasts dictate tumor cell fate. Our study highlights this signaling cascade as a key regulatory mechanism shaping senescence, redox biology, and phenotypic plasticity in colorectal cancer progression.

#6008 Defining PON2 as a metabolic immune checkpoint of iron redox balance and ferroptotic defense in lung adenocarcinoma.

Yonatan Amzaleg[1], Angel Perez-Hunt[1], Chi Li[2], **Aaron M. Neely**[1]

[1]Integrative Translational Sciences, Beckman Research Institute of The City of Hope, Duarte, CA,[2]Brown Cancer Center-University of Louisville, Louisville, KY

Lung adenocarcinoma (LUAD), the predominant subtype of non-small cell lung cancer, survives persistent oxidative stress through adaptive remodeling of mitochondrial and metabolic networks. Redox equilibrium therefore dictates whether LUAD cells withstand oxidative pressure or succumb to ferroptosis; a lipid peroxidation driven form of regulated cell death[1]. The mitochondrial enzyme paraoxonase 2 (PON2) functions as an intrinsic antioxidant that detoxifies lipid peroxides and sustains respiratory integrity[2]. In LUAD, chronic activation of NRF2 (NFE2L2); frequently through loss of KEAP1, drives constitutive antioxidant programs involving glutathione synthesis and GPX4, FSP1, and PON2 dependent ferroptosis defenses[3-4]. These redox insulated states promote metabolic resilience, suppress immunogenic cell death (ICD), and reinforce immune excluded tumor architectures[4-5].We identify PON2 as a metabolic immune checkpoint that integrates NRF2/KEAP1 driven redox adaptation with ferroptosis resistance and immune escape. Integrative genomic, spatial, and functional analyses reveal that PON2 expression stratifies LUAD by ferroptotic vulnerability; aligns with antioxidant and iron handling networks (TFRC, FTH1, FTL); and that PON2 loss increases lipid peroxide burden, disrupts mitochondrial flux, and heightens ICD signaling in patient derived LUAD models.These findings delineate how PON2 enforces ferroptosis resistance and immune invisibility, revealing targetable redox metabolic bottlenecks that could be leveraged to restore tumor immunogenicity[6].

#6009 Mitochondrial glutathione reductase as a redox vulnerability in KEAP1/NRF2-mutant non-small cell lung cancer.

Yun Huang[1], Chao Ting[1], Jing-Chun Lin[2], Ryan Martin[1], Duy T. Nguyen[1], Jose Serrano-Velez[1], Yun Pyo Kang[3], Nathan P. Ward[4], Ana P. Da Silva Gomes[1], Mingxiang Teng[1], **Chang Jiang**[1]

[1]H. Lee Moffitt Cancer Center, Tampa, FL,[2]H Lee Moffitt Cancer Center and Research Institute, Tampa, FL,[3]Seoul National University, Seoul, Korea, Republic of,[4]H. Lee Moffitt Cancer Center, Wesley Chapel, FL

Non-small cell lung cancer (NSCLC) accounts for 85-90% of lung cancers. NRF2 is a master transcription factor that orchestrates antioxidant defense. Under basal conditions, KEAP1 binds NRF2, promoting its ubiquitination and degradation. Oxidative stress alters KEAP1 conformation, preventing NRF2 binding and enabling NRF2 nuclear accumulation and activation of cytoprotective genes. NSCLC frequently harbors KEAP1 or NRF2 mutations—often within the KEAP1 Kelch domain or the NRF2 Neh2 domain—that impair KEAP1-mediated turnover and drive constitutive NRF2 activation. Such tumors are resistant to chemo-, radio-, and immunotherapy, yet direct NRF2 inhibitors remain elusive due to the absence of catalytic pockets and concerns about systemic toxicity. To identify synthetic-lethal targets that heighten ROS-induced death in NRF2-active NSCLC, we performed negative-selection CRISPR/Cas9 screens using a focused antioxidant-enzyme sgRNA library. Cells were treated with a sublethal dose of the NQO1-bioactivatable ROS-generating prodrug β-lapachone. As expected, NQO1 was the top sensitizing hit, and TXNRD1/TXN were enriched among resistant hits, consistent with the protective thioredoxin pathway. Unexpectedly, genes required for de novo glutathione synthesis (GCLM, GCLC, GSS) showed minimal dropout, indicating limited contribution of GSH biosynthesis to β-Lap sensitivity. Instead, the NRF2 target gene GSR—responsible for reducing GSSG to GSH—emerged prominently, suggesting that GSR loss uniquely impairs survival under oxidative stress. Across multiple ROS-inducing agents, GSR knockout strongly sensitized KEAP1/NRF2-mutant cells but not KEAP1/NRF2-intact cells. Importantly, toxicity was not driven by global GSH depletion. Rather, we found that mitochondrial GSR is essential: cytosolic-only GSR could not rescue GSR-deficient cells, whereas forced mitochondrial localization fully restored viability. Mechanistically, GSR loss caused severe mitochondrial fragmentation, compromised electron transport chain (ETC) integrity, and reduced ETC activities. GSR-deficient cells accumulated mitochondrial ROS and showed decreased expression of iron-sulfur cluster-containing proteins, collectively driving mitochondrial dysfunction and cell death. In vivo, GSR deletion triggered redox collapse and dramatically sensitized KEAP1-mutant tumors to chemotherapy. Together, these findings reveal an unrecognized mitochondrial redox dependency in KEAP1/NRF2-mutant NSCLC and identify GSR as a promising therapeutic vulnerability for overcoming NRF2-mediated ROS resistance.

#6010 Cellular senescence in the cancer microenvironment.

Subhiksha Meenakshisundaram, Robyn Laura Kosinsky, Dominik Saul

Robert Bosch Centre for Tumor Diseases, Stuttgart, Germany

Cellular senescence is a stress-induced state of stable cell cycle arrest accompanied by sustained metabolic activity. In the context of cancer, senescence acts as a double-edged sword, halting cell growth while simultaneously creating conditions that favor tumor advancement. To understand the pro-tumorigenic effects of senescence, we analyzed publicly available single-cell RNA-seq datasets of six major cancers, with a refined and robust definition of cellular senescence based on cell-cycle arrest and senescence-associated secretory phenotype (SASP) gene signatures. We quantified senescent cell burden in six cancers and observed a significant enrichment in colorectal and pancreatic tumors compared to healthy controls. Comparative genomic and transcriptomic analyses revealed that senescent tumor cells exhibit distinct molecular features, reflecting a reprogrammed senescence biology within tumors. Trajectory inference analysis demonstrated that senescence represents a terminal cellular state, indicating that tumor-associated senescence constitutes a reprogrammed, terminal fate. Having characterized senescence at the single-cell level, we next examined the spatial impact of its SASP. Spatial transcriptomic analysis revealed that SASP signaling acts as a key mediator of local inflammation and promotes bystanding cells across the tumor microenvironment. By inducing cellular senescence in colorectal and pancreatic cancer cell lines *in vitro*, we confirmed the senescence induction using telomere associated foci (TAF) staining and profiled their molecular signatures. Given the pro-tumorigenic effects of senescent cells, we subsequently evaluated the impact of senolytic drugs and treated these senescent cells with senolytics, namely Dasatinib and Quercetin (D+Q) as well as fisetin. Both senolytic treatments effectively reduced the expression of senescent markers, confirming selective clearance of senescent cells. The treatment also significantly reduced tumor proliferation. Collectively, our findings refine the molecular and spatial characterization of tumor-associated senescence and highlight senolytics as a promising therapeutic strategy to mitigate its tumor-promoting effects and controlling tumor growth in distinct tumor entities.

#6011 Treatment-induced senescence in metastatic colorectal adenocarcinomas: implications for single-cell biology and therapeutic intervention.

Antoine Hollebecque[1], Marine Aglave[2], Mohamed-Amine Bani[3], Trang Nguyen[1], Ludovic Bigot[4], Thierry Mathieu[5], Florence Lhospice[5], Benjamin Le Calve[5], Eric Angevin[6]

[1]Drug Development Department (DITEP), Gustave Roussy, Villejuif, France,[2]Bioinformatics facility, Gustave Roussy, Villejuif, France,[3]Biopathology Department, Gustave Roussy, Villejuif, France,[4]Research Division, Gustave Roussy, Villejuif, France,[5]Starkage Therapeutics, Lille, France,[6]Clinical Research Division, Gustave Roussy, Villejuif, France

In cancers, the harmful effect of senescence is now well recognized and mediated by the local production of pro-inflammatory cytokines, soluble immunosuppressive factors and metalloproteinases, called 'SASP' phenotype. Many chemotherapy and radiation regimens can induce senescence of tumor cells and a deleterious microenvironment that promote tumor growth, invasion and neoangiogenesis leading to treatment resistance, relapse and poor prognosis, especially at advanced stages. Senescence biomarkers, such as dipeptidyl-peptidase 4 (DPP4/CD26), a membrane glycoprotein involved in chemotactic and inflammatory responses, is frequently constitutively expressed and/or overexpressed on primary tumors and metastases, including in colorectal adenocarcinoma (mCRC). A study aimed at dissecting the pathophysiology of senescence induced by standard of care (SoC) treatments is currently underway on a large series of mCRC, as well as other digestive cancers and hepatic carcinomas. The pre- and post-SOC scoring of DPP4 expression is assessed by immunohistochemistry and will be correlated to clinical annotations and other senescence features on primary tumors and liver metastases (n=100 samples). A comprehensive bioinformatic study is conducted on a large pan-tumor bulk RNA sequencing database (n=1155 samples) assessing the expression of a broad panel of candidate genes and signatures relevant to senescence pathways, including DPP4, and signaling signatures of interest from MSigD, CellMarker2.0, panglaoDB and SenNet. The same evaluations are conducted on a large set of single cell RNA sequencing (scRNASeq) data from different mCRC cohorts (n=105 patients) in which pre- and post-SoC treatment samples were collected on treatment-naïve primary tumor or liver metastatic samples (n=72) and post-SoC biopsies (n=54), including MSI-high tumors (n=16). Bioinformatics pipelines were designed to address correlations of candidate genes and molecular signatures to cellular heterogenicity, context, biology and clinical outcomes. To our knowledge, this study will be the first to highlight at the protein and scRNASeq levels the deleterious impact of senescence in a large series of patients with mCRC during the progression and treatments of cancer. This could have important implications for the development of innovative therapies targeting senescence biomarkers and related signaling pathways for cancer cell elimination in refractory tumors.

#6013 TUSC2 drives NK cell maturation and aging-associated functional decline.

Salvador Gonzalez Ochoa[1], Metin Aksu[2], Karan Lagisetty[3], Edward J. Hughes[2], Thanigaivelan Kanagasabai[1], Muna A. Mohammed[4], Alla Ivanova[1], Anil Shanker[5]

[1]Department of Biochemistry, Cancer Biology, Neuroscience and Pharmacology, Meharry Medical College, Nashville, TN,[2]Department of Clinical Sciences, Meharry Medical College School of Medicine, Meharry Medical College, Nashville, TN,[3]Undergraduate Summer Intern Program, Meharry Medical College, Nashville, TN,[4]Department of Biomedical Sciences, Meharry Medical College School of Graduate Studies, Meharry Medical College, Nashville, TN,[5]The Office for Research and Innovation, Meharry Medical College, Nashville, TN

Background: Aging is a biological process that drives metabolic and functional decline across physiological systems, including immune system. Natural killer (NK) cells, key mediators of tumor and viral surveillance, have emerged as a promising immunotherapeutic tool; however, the molecular and metabolic pathways that shape NK-cell function during aging remain poorly defined. We show that expression of Tumor Suppressor Candidate 2 (TUSC2), a mitochondrial protein with structural features consistent with a calcium sensor, steadily declines across multiple human tissues with age. We investigated further how the loss of TUSC2 impacts NK-cell development and the differentiation of distinct functional NK-cell subsets.
Methods: Phase 1: Human single-cell RNA-seq data from harmonized datasets of healthy blood NK cells and tissue-resident or tumor-associated NK cells were analyzed. Core functional programs including interleukin signaling, metabolic pathways, and developmental signatures were examined. Differential expressions between TUSC2high and TUSC2low NK cells were assessed and integrated with these programs. Phase 2: Splenocytes were collected from young (1-3 months) and aged (18-21 months) Tusc2 wild-type (WT) and knockout (KO) mice. Single-cell immune suspensions were stained with NK lineage and maturation markers: CD122, CD49b, CD11b, and NKp46 to delineate developmental stages I-IV. Following surface staining, cells were labeled intracellularly to identify transcription factors and functional mediators.
Results: TUSC-2 expression strongly correlated with the maturation of NK1C (effector-terminal) population, as well as with cytotoxic and metabolic programs in these functional subsets. NK cells at early developmental stages (I-III) showed comparable frequencies between WT and KO mice, indicating preserved early progenitor commitment. However, absence of Tusc2 generates an inappropriate downregulation of Tcf7/Tcf1 and Gata3 with age, suggesting their persistent stem-like state that impaired maturation. Aged Tusc2-KO NK cells also exhibited elevated expression of IL15Rα, FasL, and CX3CR1 at early stages, reflecting heightened activation potential and migratory responsiveness, yet failed to acquire effector markers such as CD16, indicating uncoupling between activation, licensing, and effector differentiation. Consistent with this impaired progression, the frequency of Stage IV (mature NK) populations markedly declined with age in KO mice, whereas WT mice maintained Stage IV NK-cell frequency.
Conclusion: These findings indicate that TUSC2 is required for proper coordination of developmental transcriptional programs and for the acquisition of effector and metabolic competence during NK-cell aging, particularly within terminal effector subsets.

#6014 From metal to malignancy: How ROS and inflammatory cytokines accelerate cadmium-induced prostate carcinogenesis.

Kunj Bihari Gupta[1], Truett Taylor[1], Siva S. Panda[2], Vinata B. Lokeshwar[3], Bal L. Lokeshwar[1]

[1]Georgia Cancer Center, Augusta University, Augusta, GA,[2]Department of Chemistry and Biochemistry, Augusta University, Augusta, GA,[3]Department of Biochemistry and Molecular Biology, Augusta University, Augusta, GA

Cadmium (Cd) is a toxic metal ubiquitous in nature and an industrial pollutant. Exposure to elemental Cd or its salts lead to their high accumulation in tissues and clears very slowly, biological half-life; >30 years. Abnormally high levels of Cd are reported in human prostate tissues. The studies on rodents have shown that their exposure causes prostate cancer. The mechanism of carcinogenesis caused by Cd remains unclear. This study tested the hypothesis that continuous low-dose exposure to Cd induces chronic inflammation driven by high levels of Reactive Oxygen Species (ROS) which promote sustained up-regulation of proinflammatory cytokines and accelerating the transformation of healthy prostate epithelial cells to tumorigenic cells. We used two non-transformed prostate epithelial cell lines (RWPE-1 and NHPrE-1) and exposed to 10μM of Cadmium Chloride ($CdCl_2$) continuously up to one year. The $CdCl_2$ exposed cells and culture media were regularly analyzed for changes in oxidative stress, inflammatory cytokines, elevated carcinogenesis markers. Cd exposure significantly increased the cellular ROS levels beginning in the first week of exposure and remained elevated. Analysis of a repertoire of cytokines, pro-tumorigenic growth factors and several transcription factors using ELISA, qPCR, cytokine array and transcriptomic RNA-seq analysis showed a strong correlation with exposure time and an increase in the levels of key cytokines and transcription factors. We found IL-8 was the first cytokine to increase when exposed to $CdCl_2$, followed by activation of NF-κB (p65-rel), VEGF-A, & B and other factors. Further, IL-1β, IL-6, IFN-γ, and TGF-β and IL-8 receptors CXCR1, and CXCR-2 were also elevated with prolonged exposure to Cd. In addition, when compared to unexposed cells, we observed activation of Nuclear Factor-kB (NF-κB), and pro-tumorigenic growth factors involved in angiogenesis vascular endothelial growth factors VEGF-A and B); all at RNA and protein levels. The inflammatory cytokine array analysis also supported the occurrence of a “cytokine storm” in the $CdCl_2$-exposed RWPE-1 and NHPrE-1 cells. Neutralizing oxidative stress with ROS scavenger [e.g. N-Acetyl cysteine (NAC)], significantly reduced the mRNA levels of cytokines and pro-inflammatory chemokines. RWPE-1 and NHPrE-1 cells exposed to $CdCl_2$ for a year were fully transformed into tumorigenic cells and formed subcutaneous tumors in less than 30 days in male NOD/SCID mice. In summary, IL-8 and NF-κB mediated signaling axis is critical for Cd-induced carcinogenesis and controlling this axis is a potential strategy to prevent metal-induced toxicity and carcinogenesis.

#6015 Senescence-associated secretory phenotype drives PGCC's lifecycles and blastomere-like reprogramming to promote therapeutic resistance.

Zhiqian Zhang[1], Xiaoran Li[2], Xinxin Tian[1], Limin Deng[1], Jin-Tang Dong[1], **Jinsong Liu**[2]

[1]Southern University of Science and Technology (SUSTech Shenzhen), Shenzhen, China,[2]UT MD Anderson Cancer Center, Houston, TX

Background: Polyploid giant cancer cells (PGCCs) are stress-responsive tumor subpopulations linked to treatment resistance and poor prognosis. While prior studies have characterized their senescent-like phenotypes and capacity for developmental reprogramming, two core questions remain poorly understood, including the temporal dynamics governing PGCC's lifecycle progression and the precise mechanistic role of senescence in shaping their biology.
Methods: We induced PGCC formation using vincristine (VCR), a mitotic destabilizer, and tracked their lifecycle via live-cell fluorescence imaging. We assessed proliferative activity, EMT, blastomere-like features, and differentiation potential *in vitro*, alongside tumorigenicity *in vivo*. Mechanistically, we interrogated SASP cytokines using genetic silencing and pharmacologic inhibition.
Results: VCR activated an endoreplication-based lifecycle in PGCCs, replacing canonical mitosis. PGCCs progressively exhibited reduced proliferation but enhanced EMT, progressive blastomere-like stemness, and multilineage differentiation. Both PGCC populations and their progeny acquired time/dose-dependent malignant traits and tumorigenic capacity. PGCCs partially adopted senescence, marked by elevated SASP cytokines. Silencing IL1β/IL6/IL8 or inhibiting their receptors suppressed PGCC formation, budding, EMT, and stemness, thus identifying SASP as critical for PGCC homeostasis and fate.
Conclusion: Our work delineates PGCCs' lifecycle evolution and establishes SASP as a key driver of their lifecycle and the emergence of aggressive, therapy-resistant progeny, bridging senescence, developmental reprogramming, and cancer progression.

#6016 Identification of a novel non-flavonoid senolytic agent from natural resources targeting oncogene- and DNA damage-induced senescence.

Jihye Kim, Xiaoyu Guo, Yi-Xi Gong, Ingyu Lee, Bomi Han, Eui Man Jeong

Jeju National University, Jeju, Korea, Republic of

Senolytics represent a promising therapeutic strategy for age-related diseases by selectively eliminating senescent cells. In this study, we screened a library of 101 extracts derived from natural resources indigenous to Jeju Island to identify potential senotherapeutics. We evaluated their senolytic activity using two distinct models of cellular senescence: Oncogene-Induced Senescence (OIS) in human diploid fibroblasts and DNA Damage-Induced Senescence (DIS) in A549 lung cancer cells. Through this screening, we identified a specific extract that exhibited significant selective cytotoxicity against senescent cells while sparing proliferating cells. Following bioassay-guided fractionation, we isolated an active compound, designated as ACE. Interestingly, ACE-induced cell death was significantly attenuated by pretreatment with Z-VAD (a pan-caspase inhibitor) and Necrostatin-1, suggesting that ACE exerts its senolytic effect via regulated cell death pathways, primarily apoptosis. Flow cytometry and Western blot analyses confirmed that ACE treatment significantly reduced Senescence-Associated β-galactosidase (SA-β-gal) activity and downregulated key senescence markers, including p16, p21, and p53, in a dose- and time-dependent manner. Mechanistically, ACE activated the p38 MAPK signaling pathway, leading to the accumulation of reactive oxygen species (ROS). Notably, chemical analysis revealed that ACE is a non-flavonoid compound. Collectively, these findings suggest that ACE is a novel senolytic candidate derived from Jeju natural resources with potential clinical applications.

#6017 BET inhibition potentiates salvage chemotherapy response through TXNIP upregulation in osteosarcoma.

Keiko E. Kreklau[1], Niknam Riyahi[2], Ryli E. Justice[1], M. Reza Saadatzadeh[3], Erika A. Dobrota[1], Harlan E. Shannon[1], Rada Malko[4], Christopher Davis[1], Khadijeh Bijangi-Vishehsaraei[3], Sara Covin[1], Melissa A. Trowbridge[5], Kathy Coy[5], Felicia M. Kennedy[5], Anthony L. Sinn[5], Christopher D. Collier[6], Steven P. Angus[3], Karen E. Pollok[3], Pankita H. Pandya[3]

[1]Herman B Wells Center for Pediatric Research, Indiana University School of Medicine, Indianapolis, IN,[2]Department of Biochemistry & Molecular Biology, and Pharmacology, Indiana University School of Medicine, Indianapolis, IN,[3]Department of Pediatrics, Division of Pediatric Hematology/Oncology, Indiana University School of Medicine, Indianapolis, IN,[4]Department of Medical and Molecular Genetics, Indiana University School of Medicine, Indianapolis, IN,[5]Preclinical Modeling and Therapeutics Core, Indiana University Melvin and Bren Simon Comprehensive Cancer Center, Indianapolis, IN,[6]Department of Orthopaedic Surgery, Indiana University School of Medicine, Indianapolis, IN

Osteosarcoma (OS) is an aggressive bone cancer in pediatric adolescent and young adult patients. Survival rate for metastatic and relapsed OS patients remains dismal at <30%. Additionally, no effective standardized salvage therapy currently exists for these patients, in part due to genomic complexities arising from moderate levels of replication stress (RS). Bromodomain and extra-terminal domain protein inhibitors (BETi) are an underexplored option to target RS, as BET inhibition creates an imbalance between transcription-replication kinetics thereby exacerbating oncogenic RS and cell death. BETs (BRD2,3,4) are epigenetic readers that play a role in regulating gene expression networks as well as DNA replication and repair. We hypothesized that BET inhibition with AZD5153 would suppress OS growth by inducing tumor suppressive mechanisms that exacerbate DNA damage and sensitize tumors to DNA-damaging chemotherapeutic agents. AZD5153 monotherapy significantly suppressed OS tumor growth compared to vehicle ($p<0.05$) in female and male patient-derived xenografts (PDXs) established from both treatment-naïve (PDX96, PDX115, PDX112) and metastatic OS (PDX77-TT2). Mechanistic evaluation showed increased γ-H2AX and p-RPA2 S8 following AZD5153 exposure in PDX96, indicative of enhanced RS. RNA-seq and protein analyses revealed dysregulation of DNA damage response genes, including upregulation of TXNIP, a tumor suppressor that promotes DNA damage and apoptosis, and downregulation of PDGFRA. Similar TXNIP upregulation and PDGFRA suppression were observed in AZD5153-treated PDX115. Increased TXNIP expression was also evident in vitro when BET/BRD4 activity was inhibited in OS cell lines by siRNA, PROTAC-mediated degradation, or disruption of BRD4-histone interactions via AZD5153. These effects were accompanied by elevated c-PARP levels, a marker of cell death. Ongoing studies suggest BRD4 inhibition elevates TXNIP via AKT pathway suppression, as indicated by reduced phospho-AKT in AZD5153-treated tumors. In vitro combination studies showed additive-to-synergistic effects between AZD5153 and a variety of salvage agents (etoposide, SN38, and topotecan). In particular, AZD5153 in combination with topotecan resulted in enhanced apoptosis, increased TXNIP, decreased AKT, and elevated RS markers (γ-H2AX, comet assays). In vivo, dose finding studies indicated that PDX77-TT2 was resistant to salvage agents ifosfamide and SN38 but moderately sensitive to topotecan. Furthermore, AZD5153 alone or in combination with topotecan improved survival compared to single agents ($p<0.05$) and was well tolerated. Collectively, these data support BET inhibition alone or with salvage therapy as a promising therapeutic approach for aggressive OS, potentially mediated through TXNIP upregulation and AKT pathway suppression.

#6018 Reactive oxygen species (ROS)-sensitive SOX4 signaling mediates ferroptosis in esophageal adenocarcinoma.

Heng Lu[1], Farah Ballout[2], Dunfa Peng,[2], Lei Chen[3], Zheng Chen[2], Wael El-Rifai[2]

[1]Surgery, University of Miami, Miami, FL,[2]University of Miami Miller School of Medicine, Miami, FL,[3]University of Miami, Miami, FL

Introduction: Esophageal adenocarcinoma (EAC), a malignancy largely driven by gastroesophageal reflux disease (GERD), remains highly resistant to chemotherapy, resulting in poor clinical outcomes. Ferroptosis is an iron-dependent, non-apoptotic form of regulated cell death characterized by lipid peroxidation and oxidative membrane injury. SOX4, a critical transcription factor, has been broadly implicated in tumorigenesis and the maintenance of cancer stemness. This study investigates SOX4-mediated anti-ferroptosis as a mechanism of chemoresistance in EAC, focusing on the reactive oxygen species (ROS)-sensitive APE1-redox-STAT3-SOX4 signaling axis, with the goal of identifying novel therapeutic strategies.

Methods: Public datasets and multiple experimental models were employed, including 3D organotypic cultures, patient-derived organoids, and tumor spheres. *In vivo* validation was performed using a patient-derived xenograft (PDX) model.

Results: Analysis of EAC public datasets revealed significant enrichment of the SOX4 transcriptional signature in tumor tissues. SOX4 activation was induced by elevated ROS and APE1 protein under reflux-mimicking conditions (acidic bile salt exposure, ABS), while treatment with a ROS scavenger, N-acetyl-l-cysteine (NAC), blocked ABS-induced SOX4 upregulation. Chromatin immunoprecipitation (ChIP) assay identified a STAT3 binding site within the SOX4 promoter, indicating that STAT3, an APE1 redox-sensitive transcription factor, directly regulates SOX4 expression. Silencing of APE1 or pharmacological inhibition of STAT3 suppressed SOX4 expression under both reflux conditions and oxaliplatin treatment. Single-sample gene set enrichment analysis (ssGSEA) demonstrated a strong correlation between ferroptosis-related signaling and the SOX4 signature in the TCGA EAC cohort. Notably, SOX4 knockdown reduced GPX4 expression and sensitized both intrinsically resistant SK-GT-4 cells and acquired oxaliplatin-resistant FLO-1 cells to oxaliplatin. These findings were validated in PDX tumors treated with the APE1 redox-specific inhibitor APX2009 in combination with oxaliplatin.

Conclusion: ROS/APE1-dependent activation of SOX4 plays a crucial role in anti-ferroptosis and chemoresistance in EAC. Targeting the redox function of APE1 represents a promising therapeutic approach to overcome SOX4-mediated ferroptosis resistance and enhance chemotherapy efficacy in EAC.

#6019 Fatty acid exposure promotes age-related mammary tissue alterations with pro-tumorigenic potential.

Mariana Bustamante Eduardo[1], Abul B.M.M.K. Islam[2], Curtis W. McCloskey[3], Maria Paula Zappia[2], Ashok Z. Samuel[4], Maxim V. Frolov[2], Rama Khokha[5], Rohit Bhargava[4], Elizaveta V. Benevolenskaya[2], Seema A. Khan[1], Susan E. Clare[1]

[1]Northwestern University, Chicago, IL,[2]University of Illinois at Chicago, Chicago, IL,[3]University of Pittsburgh, Pittsburgh, PA,[4]University of Illinois at Urbana-Champaign, Urbana, IL,[5]Princess Margaret Cancer Centre, Toronto, ON, Canada

Introduction. Exposure of non-transformed breast cells and breast microstructures to the medium-chain (MC) fatty acid (FA) octanoic acid (OA) induces a metabolic shift toward the serine, one-carbon, glycine and methionine pathways (SOG/methionine), enhancing epigenetic plasticity, increasing reactive oxygen species (ROS), promoting cell survival and disrupting cell-cell communication. Similarly, the aged mammary gland is characterized by disrupted cell-cell communication, epigenetic plasticity and increased ROS. We hypothesize that FA-induced metabolic reprogramming leads to biological aging of the mammary gland, contributing to pro-tumorigenic alterations observed during chronologic aging.

Methods. MCF-10A cells were exposed to OA for proteomics. Breast microstructures exposed to ± OA were analyzed by scRNAseq. Breast microstructures and 3D mammary spheres derived from primary cells were embedded in Matrigel, exposed to ± OA for 7 days, stained for luminal and basal markers, F-actin, and nuclei, and imaged by confocal microscopy to assess migration/invasion. Migratory cell populations enriched in OA-containing media were identified with scRNAseq. Raman spectroscopy (RS) was used to characterize the lipid content in normal breast tissue.

Results. OA treatment induced changes previously reported in aging and tumorigenic contexts, including: (1) upregulation ($p < 0.01$) of aging-related genes (*GDF15, MDK, PLIN2*), and downregulation ($p < 0.01$) of lineage markers and *MMP7*, a gene whose downregulation promotes mammary epithelial aging; (2) upregulation ($p < 0.01$) of Senescence-Associated Secretory Phenotype (SASP) genes, including *AREG* (reprogramming) and *ANGPTL4* (migration); (3) increased secreted signaling via *AREG*, *GDF15*, and *MDK;* and (4) reduced extracelular matrix (ECM)-receptor and cell-cell interactions. *Ex vivo*, OA altered tissue architecture disrupting the basal barrier and promoting cellular migration. BMYO1, LASP1, and LHS1 epithelial subtypes were among the migratory cells in OA media and expressed SASP, cancer (*MYC*, *EGFR*, *SREBF1*), migration (*S100A4*, *NCAM1*), aging and SOG/methionine genes. FB1 fibroblasts dominated in vehicle media, but OA favored ECM-disassembling FB2 cells. RS analysis demonstrates the presence of both saturated and unsaturated FAs and revealed the presence of MCFAs, such as OA, with higher intensities observed in the postmenopausal tissue supporting the *in vivo* plausibility of our *in vitro/ex vivo* findings.

Conclusions. Our data supports a model suggesting that chronological and biological aging processes increase the release of free FAs, due to elevated GDF15-induced lipolysis. The rise in FAs drives mammary gland remodeling and accelerates aging of the gland. Chronological and biological aging increase vulnerability to breast cancer. This model suggests potential preventive strategies such as targeting GDF15 and SOG/methionine.

#6020 Cargo profiling of extracellular vesicles from senescent glioblastoma identifies small nucleolar RNAs as candidate liquid biomarkers for therapy-induced senescence.

Valerie DeLuca[1], Nathaniel Hansen[1], Priya Digumarti[1], Nanyun Tang[1], Karen Fink[2], George J. Snipes[2], Patrick Pirrotte[1], Michael E. Berens[1]

[1]TGen (The Translational Genomics Research Institute), Phoenix, AZ,[2]Baylor Scott & White Medical Center, Dallas, TX

Therapy-induced senescence (TIS) in glioblastoma (GBM) is an undesirable cell fate that contributes to GBM treatment resistance and tumor outgrowth. While emerging senescence-targeting drugs called senotherapies may be beneficial for patients who undergo TIS following standard of care, identifying candidate patients with an appreciable TIS burden is difficult. Current methods to measure TIS are tissue based and require repeated, sequential biopsies for robust analysis. The impracticality of such an effort for GBM patients therefore necessitates the development of novel, less-invasive approaches that can detect TIS clinically over time. To this end, we aimed to identify candidate extracellular vesicle (EV) liquid biomarkers for TIS by profiling senescence-associated cargo changes within GBM EVs. Using a panel of GBM patient derived cell lines, we show that radiation induces TIS across GBM models and that this is associated with a reprogramming of the cargo in the corresponding senescent-derived EVs (senEVs). In particular, senEV transcriptomes have an increased abundance of senescence-associated RNA species and enrichment of senescence-associated gene sets. Most striking, however, was the observed enrichment of small nucleolar RNAs (snoRNAs), which represented over 50% of the top 20 most upregulated species in senEVs. This signature was conserved in 4/5 GBM models of TIS and was validated by qRT-PCR. Interestingly, the increased snoRNA abundance in EVs is not a simple function of increased cellular content, as whole cells did not show consistent upregulation upon TIS. We further found that snoRNAs are likely packaged with their partner proteins, as mass spectrometry of senEVs revealed an increased abundance of snoRNA-associating proteins. Notably, a GBM model of temozolomide-induced stress that does not result in prominent senescence failed to promote increased snoRNA cargo, supporting snoRNA enrichment as a TIS-selective finding. Ongoing work is focused on identifying whether this senEV profile is conserved across tumor types and senescence-inducing stimuli, and whether nucleolar stress during TIS plays a mechanistic role in snoRNA EV packaging. Finally, to determine the feasibility of detecting these candidate biomarkers in patient biofluids, we employed a small patient cohort of matched pre-operation and post-standard of care plasma samples. Promisingly, we identified increased senescence-associated RNA such as *CDKN2B* and *GLB1* and the snoRNA *SNORA49* in post-standard of care EVs. This data suggests that senEV RNA species, specifically snoRNAs, are strong candidates for TIS biomarker development.

: Fibroblasts as Architects of the Tumor Microenvironment
Poster Session

#6024 Decoding new mechanisms of stromal-driven inflammation in breast cancer.

Fernanda G. Kugeratski[1], Lisa Neilson[2], Adrian Kacperczyk-Perdyan[3], Juan R. Hernandez-Fernaud[2], Sergio Lilla[2], Jakub Mieczkowski[3], Sara Zanivan[1]

[1]Department of Experimental Therapeutics, The University of Texas MD Anderson Cancer Center, Houston, TX,[2]CRUK Scotland Institute, Glasgow, United Kingdom,[3]Medical University of Gdańsk, Gdańsk, Poland

Cancer-associated fibroblasts (CAFs) are an abundant cell population of the breast tumor microenvironment (TME). Several CAF phenotypes exist in tumors, being the inflammatory type (iCAF) characterized by the high expression of interleukin 6 (IL-6). Hypoxia promotes the iCAF phenotype and is linked to poor prognosis of breast cancer patients. However, the molecular mechanism driving the iCAF program upon hypoxia exposure remains elusive. We analyzed the changes in the proteome and secretome of patient-derived CAFs exposed to hypoxia and identified a Leucine Rich Repeat Containing Protein (LRRC) as one of the most up-regulated proteins. Further analyses revealed that LRRC in induced by hypoxia at transcriptional level in a HIF1α-dependent manner. Histological analyses show that LRRC is uniquely expressed in CAFs across species, in both human and murine breast tumors. Stromal specificity of LRRC was further confirmed by single-cell RNA sequencing of breast cancer patients. Through loss-of-function approaches in CAFs we uncovered that LRRC is an upstream regulator of IL-6, a key driver of pathological angiogenesis and inflammation in cancer. Notably, LRRC$^+$ CAFs activate STAT signaling in cancer and TME cells. Supporting similar roles in tumors, increased STAT phosphorylation was also observed in tumors of breast cancer patients with high expression of LRRC, in proteomics data from TCGA. Thus, by regulating IL-6, LRRC may function as a driver of pathological angiogenesis and inflammation in breast cancer. Indeed, we observed that LRRC promotes endothelial sprouting angiogenesis and an inflammatory transcriptional program in CAFs and TME cells. Suggesting tumor-promoting roles of LRRC, high levels of LRRC correlate with worsened survival of breast cancer patients in TCGA datasets. To determine the influence of LRRC$^+$ CAFs on the surrounding TME, we are utilizing spatial proteomic analysis of breast cancer patient tissues. Together, our findings position LRRC as a central regulator of inflammatory signaling in breast cancer. By functioning upstream of IL-6 and driving activation of STAT, LRRC emerges as a key molecular nexus linking hypoxia to the iCAF phenotype and its tumor-promoting functions. The discovery of microenvironmental factors that fuel breast cancer inflammation is a sought-after milestone in the field since it may lead to the development of novel therapeutic interventions aimed at disrupting stromal-driven inflammation and tumor progression.

#6025 Transgelin-positive cancer-associated fibroblasts promote pancreatic cancer progression.

Keiko Shinjo[1], Xingxing Wang[1], Kohei Kumegawa[2], Reo Maruyama[2], Shinji Mii[3], Yukihiro Shiraki[1], TATSUNORI NISHIMURA[1], Yoshiteru Murofushi[1], Miho Suzuki[1], Atsushi Enomoto[1], Yutaka Kondo[1]

[1]Nagoya University, Nagoya, Japan,[2]Japanese Foundation for Cancer Research, Tokyo, Japan,[3]Department of Pathology, Hiroshima University, Hiroshima, Japan

Pancreatic ductal adenocarcinoma (PDAC) is characterized by a pronounced desmoplastic reaction, predominantly composed of cancer-associated fibroblasts (CAFs), including a major population of myofibroblastic CAFs (myCAFs). This study was designed to elucidate the biological significances of CAFs in PDAC tumorigenesis. We performed a single-cell assay for transposase-accessible chromatin with high-throughput sequencing (scATAC-seq) on pancreas tissues from KPC mice (*LSL-Kras*$^{G12D/+}$; *LSL-Trp53*$^{R172H/+}$; *Pdx-1-Cre*). Epigenetic profiling uncovered substantial heterogeneity within the myCAF population, revealing distinct subclusters characterized by specific transcription factor (TF) motifs, such as those associated with Srf, Cebpb, Prrx1, and Smad4. Parallel single-cell RNA sequencing (scRNA-seq) further identified three transcriptionally distinct myCAF subtypes, each enriched for unique TF-associated signaling pathways, validating the TF motifs identified in the scATAC-seq analysis. Among the identified myCAF subtypes, Transgelin (Tagln), an actin-binding protein highly expressed in activated fibroblasts, emerged as a potential functional driver. In an orthotopic PDAC mouse model, *Tagln* knockout mice exhibited significantly reduced PDAC tumor burden compared to wild-type controls. Analysis of TCGA data revealed that high *TAGLN* expression in PDAC samples was significantly associated with poor overall survival. These findings highlight the functional heterogeneity of myCAFs and identify TAGLN-expressing myCAFs as critical mediators of tumor progression, providing the evidence that targeting stromal TAGLN may represent a promising therapeutic strategy for PDAC.

#6026 Iron metabolism underlies the activation of cancer associated fibroblasts.

Kedi Huang, Minh Duc Pham, Chang-il Hwang

Microbiology and Molecular Genetics, UC Davis, Davis, CA

Pancreatic ductal adenocarcinoma (PDAC) has one of the highest mortality rates among major cancers with a 5-year survival rate of 13%. This malignant disease is characterized by a dense, fibrotic stroma primarily driven by cancer-associated fibroblasts (CAFs). However, little is known about the molecular mechanism underlying the activation of CAFs. Our analysis of ATAC-seq conducted on in vitro myofibroblasts/inflammatory CAF (myCAFs/iCAFs) models suggest that a distinct landscape of chromatin accessibility underlies the activation of pancreatic stellate cells into both myCAFs and iCAFs. Here, we show that pharmacologic inhibition of the p300/CBP histone acetyltransferase complex with A485 suppresses activated CAF morphology, CAF transcriptional signatures, as well as the growth of tumor organoids in co-culture systems. Interestingly, RNA-seq analysis revealed an upregulation of heme metabolism that coincides with A485 treatment for both myCAFs and iCAFs, suggesting the potential dependency of CAF activation on iron metabolism. Both iCAFs and myCAFs also showed significantly reduced viability and CAF marker expression upon iron chelation compared with quiescent PSCs, and iron supplementation rescued this phenotype. Together, these findings suggest a link between epigenetics and iron metabolism in the context of CAF activation. Targeting the iron metabolic pathway for CAFs in PDAC may therefore serve as a promising strategy to reduce stromal remodeling and improve therapeutic interventions.

#6027 Cancer associated fibroblasts-derived PDE3A promotes lipid raft-regulated IGF-1R translocation and immunotherapy resistance in triple negative breast cancer.

Na Hao

The First Affiliated Hospital of Xi'an Jiaotong University, Xi'an, China

Objective: Immunotherapy resistance remains a significant clinical challenge in the treatment of triple-negative breast cancer (TNBC). Cancer-associated fibroblasts (CAFs)-mediated induction of an immunosuppressive tumor microenvironment (TME) is a key contributing mechanism, but the underlying molecular regulatory networks are inadequately understood. This study aims to systematically elucidate the specific role and molecular mechanisms of PDE3A-expressing CAFs (PDE3A+CAFs) in TNBC immunotherapy resistance, and to assess the safety and therapeutic efficacy of a PDE3A-targeted degrader combined with immunotherapy.
Methods: Single-cell sequencing analysis was performed on tumor tissues from TNBC patients undergoing immunotherapy to identify CAF subpopulations associated with immunotherapy resistance. Functional experiments were conducted to evaluate the effects of PDE3A+CAFs on the infiltration of myeloid-derived suppressor cells (MDSCs) and the function of T cells. Mechanistic investigations included assessments of the interaction between PDE3A and Cbl-b, the lipid raft translocation of insulin-like growth factor 1 receptor (IGF-1R), and the activation of signal transducer and activator of transcription 3 (STAT3) signaling axis. Additionally, experiments such as chromatin immunoprecipitation (ChIP) were used to verify the regulatory relationship between STAT3 and PDE3A transcription.
Results: A specific subpopulation of PDE3A+CAFs was identified as a pivotal mediator of TNBC immunotherapy resistance. Functional experiments confirmed that PDE3A+CAFs significantly promoted MDSC infiltration into TNBC tumors while suppressing T cell function and activity. Mechanistically, PDE3A in CAFs inhibited the negative regulator Cbl-b in a phosphodiesterase-independent manner, thereby facilitating IGF-1R lipid raft translocation and activating the STAT3 signaling axis. Activated STAT3 further recruited MDSCs via upregulating C-X-C motif chemokine ligand 12 (CXCL12) secretion, fostering an immunosuppressive TME. Moreover, STAT3 directly regulated PDE3A transcription, forming a positive feedback loop that sustained pathway activation.
Conclusion: PDE3A+CAFs play a critical role in driving TNBC immunotherapy resistance through the PDE3A-Cbl-b-IGF-1R-STAT3-CXCL12 axis and the STAT3-PDE3A positive feedback loop. Targeting PDE3A combined with immunotherapy holds promising potential as a novel therapeutic strategy to overcome immunotherapy resistance and improve TNBC treatment outcomes, providing a solid theoretical foundation for clinical translation.

#6028 The impact of CAF-derived ANKRD1 on the lung cancer tumor microenvironment.

Kazuhiro Okada, Ken Suzawa, Shunsuke Mori, Kenta Manabe, Ryunosuke Fujii, Kousei Ishimura, Ryota Fujiwara, Kazuya Hisamatsu, Ryo Yoshichika, Atsushi Matsuoka, Yuma Fukumoto, Hidejiro Torigoe, Kazuhiko Shien, Shinichi Toyooka

Okayama Univ. Graduate School of Med., Dentistry & Pharm. Sci., Okayama, Japan

Background: Cancer-associated fibroblasts (CAFs) constitute a major component of the tumor microenvironment (TME) and are key drivers of cancer progression, therapeutic resistance, and malignancy. To improve treatment outcomes in lung cancer, it is essential to identify stromal factors that contribute to tumor aggressiveness.
Methods: RNA sequencing was performed to compare gene expression profiles between normal fibroblasts (NFs) and CAFs. Clinical databases were analyzed to determine the prognostic significance of ANKRD1 expression in lung cancer. We investigated whether cancer-derived stimuli activate ANKRD1 in NFs by exposing them to cancer cell-derived growth factors. NFs with overexpressed ANKRD1 were established and used to evaluate the effects of ANKRD1 on migration ability and treatment resistance through migration assays and colony formation assays. The effects on angiogenesis were assessed by measuring VEGF secretion and performing HUVEC (Human Umbilical Vein Endothelial Cells) tube formation assays.
Results: ANKRD1 was significantly overexpressed in CAFs compared to NFs and was associated with poor prognosis, particularly in lung adenocarcinoma. TGF-β stimulation induced ANKRD1 expression in NFs. ANKRD1-overexpressing NFs exhibited enhanced migratory ability and increased therapeutic resistance. Conditioned medium from ANKRD1-overexpressing NFs promoted VEGF secretion by cancer cells and enhanced angiogenic activity in HUVECs, suggesting that ANKRD1 activation contributes to angiogenesis both indirectly and directly.
Conclusions: ANKRD1 activation in fibroblasts within the lung cancer TME promotes tumor progression, angiogenesis, and treatment resistance through fibroblast-cancer cell crosstalk. These findings highlight ANKRD1 as a promising therapeutic target for modulating the TME and improving lung cancer outcomes.

#6029 SFRP4+ cancer-associated fibroblasts drive IL-6/STAT3-mediated EMT and immunosuppressive tumor microenvironment in hepatocellular carcinoma.

Hyo Jung Cho[1], Sujin Kim[1], Hye Ri Ahn[1], Minsu Kwon[2], Myungchan Park[3], Tae Jun Park[1]

[1]Ajou University School of Medicine, Suwon, Korea, Republic of,[2]Ulsan University School of Medicine, Seoul, Korea, Republic of,[3]Inje University College of Medicine, Busan, Korea, Republic of

Background: Secreted frizzled-related protein 4 (SFRP4) is a Wnt modulator, and SFRP4$^+$ fibroblast subsets have recently been identified across various cancer types. However, evidence that SFRP4$^+$ cancer-associated fibroblasts (CAFs) directly mediate immunosuppression and therapeutic resistance in hepatocellular carcinoma (HCC) remains limited. This study aimed to elucidate how SFRP4$^+$ CAFs reprogram the tumor microenvironment (TME) to drive immune suppression and treatment resistance in HCC.

Methods: Whole-transcriptome sequencing (WTS) was performed on eight matched CAF and paracancer fibroblast (PAF) pairs from HCC patients, and five publicly available HCC datasets were integrated to identify candidate genes. Cell-cell interactions in the TME were analyzed using CellChat analysis in the GepLiver database. Functional validation was conducted through *in vitro* coculture assays using primary CAFs and HCC cell lines, as well as *in vivo* xenograft and humanized mouse models. Transcriptomic profiling of tumors from atezolizumab-bevacizumab (Atezo/Beva) responder and non-responder groups was further performed to assess clinical relevance.

Results: SFRP4$^+$ CAFs exhibited an inflammatory phenotype characterized by marked induction of *IL6* and *NECTIN2* expression. Coculture of HCC cells with SFRP4$^+$ CAFs increased phosphorylated STAT3 and CD44 expression, enhancing proliferation, invasion, and stemness, while these effects were abrogated by SFRP4 knockdown. In the immune compartment, SFRP4$^+$ CAFs promoted regulatory T-cell (Treg) infiltration via NECTIN-TIGIT interactions and induced M2 macrophage polarization, establishing an immunosuppressive milieu.
In the humanized mouse model, tumors co-implanted with SFRP4$^+$ CAFs showed increased Treg infiltration and M2 polarization based on enrichment score analysis. Clinically, Atezo/Beva non-responder tumors exhibited upregulation of SFRP4, IL6-STAT3/CD44, and NECTIN-TIGIT pathways, accompanied by reduced *CD8A* and *GZMA* expression.

Conclusions: SFRP4$^+$ CAFs orchestrate a multifaceted pro-tumor program through IL6-STAT3/CD44 signaling, NECTIN-TIGIT-mediated Treg recruitment, and M2 macrophage polarization. High SFRP4 expression correlates with impaired cytotoxic immunity and poor response to Atezo/Beva therapy in HCC. Targeting SFRP4$^+$ CAFs may represent a promising therapeutic strategy to overcome stromal-mediated immune resistance in liver cancer.

#6030 Gli2 increases Osteopontin expression to alter cancer associated fibroblast behavior.

Zenaida Fuentes, Rachel Mangano, Jade Miller, Erik Beadle, Julie Rhoades

Cancer Biology, VANDERBILT UNIVERSITY - NASHVILLE - TN, Nashville, TN

Breast cancer is known to often metastasize into the bone. Among the subtypes, triple negative is the most aggressive. Once the cancer spreads to the bone it activates a positive feedback loop known as the vicious cycle of bone metastasis. In this cycle, Parathyroid hormone-Related protein (PTHrP) is released from tumor cells which activate osteoblasts inducing their expression of Receptor Activator of Nuclear factor Kappa-B Ligand (RANKL). RANKL binds to Receptor Activator of Nuclear factor Kappa-B Ligand (RANK) expressed on osteoclasts, thereby activating the osteoclasts to induce bone resorption subsequently releasing growth factors that fuel the tumor. This can lead to increased risk in bone fractures from the tumor indirectly activating osteoclasts. Chemotherapy is commonly given to patients with breast cancer such as paclitaxel, however, drug resistance often occurs, and treatment becomes less effective, particularly in metastatic disease. Fibroblasts are cells that are responsible for wound healing in normal circumstances. However, in cancer they can transform into Cancer Associated Fibroblasts (CAFs) capable of producing extracellular matrix proteins that surround the tumor which prevents drugs and immunotherapies from reaching the tumor. Our recent studies indicate that a transcription factor from hedgehog signaling known as GLI2 binds is upregulated in response to the chemotherapeutic, paclitaxel. RNA-sequencing analyses showed that increased expression of Gli2 increases genes associated with CAFs including osteopontin (OPN), a secreted glycoprotein. Furthermore, using the JASPAR transcription binding software, we found that Gli2 is predicted to bind to the SPP1 promoter (gene name for OPN) on chromosome 4 at a potential Gli2 binding element. Therefore, we hypothesize that osteopontin secretion is directly regulated by GLI2 in the tumor cells through direct binding of the SPP1 promoter. To test this, we knocked out GLI2 expression in bone metastatic breast cancer cell lines and showed a reduction in OPN secretion. Additional studies with a Gli2 small molecule inhibitor Hedgehog Pathway Inhibitor 1 (HPI-1) showed a 75% reduction in SPP1 by QPCR and a significant reduction of OPN secretion by ELISA. Furthermore, we showed direct changes in the production of collagens and other matrix proteins both by QPCR and immunohistochemistry. In the future, we will directly examine changes in the surrounding fibroblast phenotypes and investigate the impact on drug resistance that CAFs may play in bone metastatic tumors. Taken together, this suggests that Gli2 expressing tumors can increase OPN secretion and this may alter the production of extracellular matrix proteins by the surrounding CAFs.

#6031 The Treg-fibroblast axis shapes the immunosuppressive tumor microenvironment in colorectal cancer.

Liqian Ma[1], Mingying Bi[2], Bonnie Huang[2], Lilian Ho[2], Hin Ching Lo[1], Min Liao[2], Gaurav Mehta[2], Nicole Belmar[2], Michelle Chen[2], Tifani Anton[1], Areej Ammar[1], Haiyan Li[2], Kyle Halliwill[1], Kate MacDonald[2]

[1]Quantitative Medicine & Genomics, Genomic Research Center, AbbVie Bay Area, South San Francisco, CA,[2]Oncology Discovery Research, AbbVie Bay Area, South San Francisco, CA

The tumor microenvironment (TME) is a critical regulator of cancer progression and therapeutic response. Cancer-associated fibroblasts (CAFs) are a heterogeneous and significant component of the TME. Among CAFs, the subset marked by leucine-rich repeat containing 15 (LRRC15) is enriched in tumors and has been implicated in immune suppression and resistance to immunotherapy. However, the functional interactions of LRRC15+ CAFs within the TME, particularly with regulatory T cells (Tregs), remain incompletely understood. While it has been reported that LRRC15+ CAFs are induced by TGFβ signaling, we show in murine models that blockade of TGFβ pathways does not reverse LRRC15 expression, indicating that maintenance of LRRC15+ CAFs in the tumor microenvironment is not solely dependent on TGFβ. Using multi-omics and spatial analysis of human tumor samples, we define the specific molecular profile of LRRC15+ CAFs, which strongly correlates with Treg abundance and shows frequent proximity to Tregs within the TME. Finally, functional studies in mouse models demonstrate that Treg depletion leads to pronounced remodeling and reduction of the LRRC15+ CAF compartment. Together, these findings reveal a Treg-LRRC15+ fibroblast axis that actively shapes the immunosuppressive landscape of colorectal cancer via Treg maintenance of CAF phenotype and suggest that targeting this interaction may disrupt stromal-mediated immune evasion in immuno-oncology.

AbbVie Disclosure Statement: All authors are employees of AbbVie. The design, study conduct, and financial support for this research were provided by AbbVie. AbbVie participated in the interpretation of data, review, and approval of the publication.

#6032 Subtypes of cancer-associated fibroblasts, myCAF, iCAF, and apCAF, might be associated with adverse prognostic signature of patients with gastric cancer.

DONGHENG MA, Hinano Nishikubo, Tomoya Sano, Daiki Imanishi, Takashi Sakuma, Canfeng Fan, Yurie Yamamoto, Masakazu Yashiro

Osaka Metropolitan University, Osaka, Japan

Background: It has been reported that the tumor microenvironment (TME) may play an important role for the progression of various carcinomas, including gastric cancer (GC). The cancer-associated fibroblast (CAF) is one of major stromal components of TME. CAF includes 3 subtypes such as myofibroblastic CAF (myCAF), inflammatory CAF (iCAF), and antigen-presenting CAF (apCAF). In this study, we investigated the clinicopathologic significance of 3 CAF subtypes in GC.
Methods: A total of 1330 GC specimens was collected in this study. Immunohistochemical study was performed using 3 antibodies against myCAF, iCAF, and apCAF. Staining level of fibroblasts was scored using a semi-quantitative combined score (from 0 to 6) which was obtained by the addiction of intensity score (0 to 3) and the proportion score (0-3).
Results: myCAFs were found significantly ($p<0.05$) frequent in GC patients with advanced T stage, high lymphatic invasion, and high venous invasion. apCAFs were found significantly ($p<0.05$) frequent in GC patients with advanced T stage, lymphatic metastasis, distant metastasis, and postoperative recurrence. In contrast, iCAF showed significantly ($p<0.05$) lower in GC patients with tumor infiltration and few postoperative recurrence. Univariable Cox indicated that myCAF+ showed significantly shorter overall survival (OS; HR 1.97, 95%CI 1.34-2.90, $p<0.001$), iCAF+ showed significantly shorter OS (HR 1.29, 1.04-1.61, $p=0.022$), and apCAF+ showed significantly shorter OS (HR 1.26, 1.03-1.54, $p=0.027$). After adjustment for age, sex, T/N/M stage, histology, cytology, and lymphatic invasion, only myCAF+ remained to be independent prognostic factor for OS (HR 1.56, 1.04-2.34, $p=0.032$), whereas iCAF+ and apCAF+ were not ($p>0.05$). The triple-positive signature of myCAF, iCAF, and apCAF+) conferred significantly ($p<0.001$) high risk for OS (univariable Cox HR 2.98, 95%CI 1.83-4.83; multivariate Cox HR 2.48, 95%CI 1.51-4.06).
Conclusions: In this GC cohort, myCAF, iCAF, and apCAF are individually associated with lower survival, and myCAF, iCAF, and apCAF defined an independent adverse prognostic signature. Cooperative stromal programs might provide rationale for CAF subtype status as a prognostic factor. CAF subtypes might be associated with adverse prognostic signature of GC patients.

#6033 Different roles of cancer-associated fibroblasts in pancreatic cancer and biliary tract cancers cancer-associated fibroblasts as a tumor suppressor in biliary tract cancers.

Ryota Tanaka, Kenjiro Kimura, Naoki Tani, Shimpei Eguchi, Daisuke Inoue, Takuto Yasuda, Changgi Ahn, Koichi Nakanishi, Kosuke Hatta, Shigeaki Kurihara, Jun Tauchi, Sadaaki Nishimura, Masahiko Kinoshita, Kohei Nishio, Hiroji Shinkawa, Takeaki Ishizawa

Department of Hepato-Biliary-Pancreatic Surgery, Osaka Metropolitan University Graduate School of Medicine, Osaka, Japan

Background and aims: Cancer-associated fibroblasts (CAFs) are a major component of the tumor microenvironment and can exhibit cancer-promoting functions; however, recent studies indicate that CAFs can also inhibit cancer growth and progression. In this study, we identified CAFs that act in an inhibitory manner in biliary tract cancer and elucidated their mechanisms.
Materials and Methods: We retrospectively evaluated alpha-smooth muscle actin (αSMA) expression in CAFs from 114 cases of pancreatic ductal carcinoma (PDAC) and 154 cases of biliary tract cancers (BTCs) who underwent surgical treatment at our institution from 1996 to 2017. The BTC cell lines, PDAC cell lines, and CAFs were isolated from resected specimens of BTC and PDAC were used to evaluate the proliferative potential of cancer cells. Conditioned media (CM) were prepared from CAFs (CM-CAF). Protein array analysis of CM-CAFs was conducted to identify candidate factors responsible for growth suppression.
Results: PDAC patients with positive αSMA expression showed significantly shorter overall survival and recurrence-free survival than αSMA-negative patients ($p = 0.003$, $p = 0.009$, respectively). On the other hands, BTC patients with positive αSMA expression showed better recurrence-free survival than αSMA-negative patients ($p = 0.03$). CM-CAF suppressed the proliferation of cancer cells only in BTC cancer cell lines, not in PDAC cell lines. Protein arrays of CM-CAFs revealed that IL-6 and IL-8 were key suppressive factors on BTC cancer cell proliferation. The inhibitory effects on BTC cell proliferation were abolished upon neutralization of IL-6 and IL-8.
Conclusions: CAFs serve as a favorable prognostic factor in BTC but not in PDAC. We demonstrated the presence of tumor-suppressive CAFs in BTC, which exert their anti-proliferative effects through the secretion of IL-6 and IL-8. These findings suggest a novel, context-dependent role for CAFs in the tumor microenvironment of biliary tract cancers.

#6035 Non-immune stromal reprogramming shapes breast cancer immunotherapy resistance: insights from mouse models.

Yujia Yue, Stephanie Mittman, Rohit Reja, Julia Lau, Minyi Shi, Ana Xavier-Magalhaes, Jonathan Paw, Carolina De Amat Herbozo, Marco De Simone, Yan Qu

Genentech, Inc., South San Francisco, CA

Background: PD-1/PD-L1 blockade benefits only a subset of breast cancer patients.While tumor and immune cells have been extensively studied, the role of non-immunestroma such as endothelial cells (ECs) and cancer-associated fibroblasts (CAFs) intherapeutic resistance is less understood.
Methods: We performed single-cell RNA sequencing of $CD45^-$ cells from threesyngeneic breast cancer models with divergent ICB responses (4T1: resistant, EMT6:partial responder, EO771: responder). Stromal composition, functional programs (GOBiological Process), and tumor-stroma paracrine communication (CellChat) wereanalyzed. Findings were compared with published human breast and lung cancerdatasets (Cell Res 30, 745-762 (2020)).
Results: Distinct stromal states were linked to ICB outcomes. 4T1 were enriched forfibroblast- and extracellular matrix-dominant stroma with immune-silent endothelium,while EMT6 tumors showed endothelial expansion and interferon-active CAFs. EO771tumors displayed pericyte-stabilized, quiescent vasculature and immune-stimulatoryfibroblast programs. Pathway-level analysis highlighted conserved modes of stromalcommunication and identified fibroblast-associated signatures that correlated withdisease stage in human cohorts. Pathway-level analysis highlighted conserved modesof stromal communication and identified fibroblast-associated signatures that correlatedwith disease stage in human cohorts.
Conclusions: Stromal reprogramming contributes to ICB resistance. Cross-speciesanalysis highlights endothelial and fibroblast states as potential biomarkers andtherapeutic entry points to enhance immunotherapy efficacy.

#6036 Antigen-presenting cancer-associated fibroblasts in murine pancreatic tumors differentially control regulatory T cell phenotype and function via CCL22.

Saumya Maru[1], Meredith Wetzel[2], Jacob Mitchell[2], Nicole Gross[2], Lalitya Andaloori[3], Kathryn Howe[3], Emma Kartalia[4], Guanglan Mo[3], James Leatherman[4], Won Jin Ho[2], Elana Judith Fertig[5], Luciane Tsukamoto Kagohara[6], Edward J. Pearce[4], Elizabeth M. Jaffee[4]

[1]Fox Chase Cancer Center, Philadelphia, PA,[2]Convergence Institute, Johns Hopkins University School of Medicine, Baltimore, MD,[3]Department of Oncology, Johns Hopkins University School of Medicine, Baltimore, MD,[4]Johns Hopkins University School of Medicine, Baltimore, MD,[5]University of Maryland School of Medicine, Baltimore, MD,[6]Johns Hopkins University, Baltimore, MD

Pancreatic ductal adenocarcinoma (PDAC) is characterized by an immunosuppressive tumor microenvironment (TME), where cancer-associated fibroblasts (CAFs) play pivotal roles in shaping therapeutic responses. Among these, MHC-II-expressing antigen-presenting CAFs (apCAFs) modulate CD4 T cell activity, yet their contribution to the antitumor immune response remains unclear. Using tumor clones of the KPC murine PDAC model differing in sensitivity to immune checkpoint blockade (ICB), we show that immunosensitive (sKPC) tumors exhibit greater apCAF infiltration than resistant (rKPC) tumors. Depletion of apCAFs in sKPC tumors impaired responsiveness to ICB, highlighting their role in mediating effective antitumor immunity. Ex vivo assays revealed that apCAFs from both models activate CD4 T cells and induce regulatory T cell (Treg) differentiation. However, single-cell transcriptomics revealed that rKPC apCAFs promote Tregs with heightened immunosuppressive signatures, driven by distinct chemokine signaling. Notably, we identified elevated CCL22 expression and signaling in rKPC-derived apCAFs as a contributor to enhanced Treg-mediated suppression. Functional blockade of CCL22 reduced TGFβ secretion by rKPC apCAF-induced Tregs, supporting a mechanistic role for this pathway in fostering an immunosuppressive TME. These findings position apCAFs as regulators of CD4 T cell antitumor immunity in PDAC, and suggest that modulating apCAF-T cell interactions could offer strategies to enhance immunotherapy efficacy.

#6037 An immune-activating and tumor-suppressive subtype of cancer-associated fibroblasts identified in gastric cancer.

HUAITAO WANG, Takashi Semba, Atsuko Yonemura, Takatsugu Ishimoto

Japanese Foundation for Cancer Research, Tokyo, Japan

The tumor microenvironment (TME) is a critical determinant of progression and therapy resistance in advanced gastric cancer (GC), with cancer-associated fibroblasts (CAFs) being a key component. While protumorigenic CAFs have been extensively characterized, the identity and regulatory mechanisms of tumor-suppressive CAF subsets remain elusive. To address this, we analyzed single-cell RNA sequencing (scRNA-seq) datasets derived from gastric cancer (GC) samples and identified fibroblast subclusters characterized by high expression of antitumor-associated genes such as CXCL10 and ASPN. Further analysis revealed that RARRES2, encoding Chemerin, was one of the signature genes defining this CAF subpopulation. Chemerin is a multifunctional protein exhibiting chemotactic and metabolic functions. Accumulating evidence indicates that Chemerin mediates the recruitment of multiple immune cell types, thereby influencing immune surveillance and inflammatory processes. However, its precise roles within the tumor microenvironment have yet to be fully elucidated. Functionally, recombinant Chemerin potently induced CD8+ T cell migration in vitro. Through co-culture models and mechanistic dissection, we demonstrated that tumor cells actively suppress RARRES2/Chemerin expression in CAFs by activating the Jag1-Notch2-HDAC5 signaling axis, leading to epigenetic silencing. Crucially, CAF-specific overexpression of RARRES2 in vivo was sufficient to attenuate tumor growth and profoundly augment the recruitment of CD8+ T cells into tumors. Our findings definitively identify Chemerin+ CAFs as a pivotal stromal subset that orchestrates antitumor immunity by recruiting cytotoxic T cells. Furthermore, we unveil a dynamic and therapeutically targetable crosstalk wherein tumor cells subvert this stromal defense mechanism via Jag1-Notch2-HDAC5 signaling, thereby identifying a novel immune-evasion pathway in GC.

#6038 Cancer associated fibroblast subtype heterogeneity in colorectal cancer influences primary tumor invasion.

Bethany Haliday[1], Carly Strelez[2], Eileen Fung[2], Shannon M. Mumenthaler[2]

[1]University of Southern California, Los Angeles, CA,[2]Ellison Medical Institute, Los Angeles, CA

The influence of the tumor microenvironment (TME) on cancer progression has become a major area of study, driven in part by the continual advances in single-cell and spatial technologies that reveal the TME to be highly heterogeneous. Cancer associated fibroblasts (CAFs), a major component of the tumor stroma, have been classified into several subtypes, each with distinct functionality and influences on the tumor progression. Among these, inflammatory CAFs (iCAFs) and myofibroblastic CAFs (myCAFs) are typically defined by characteristic biomarker profiles and have been shown to have distinct spatial distributions within the tumor. However, the specific functions of these subtypes in contributing to cancer progression, particularly metastasis, is largely unknown. With metastatic disease having poor prognoses, it is vital to elucidate the roles these CAF subtypes play within the metastatic cascade. To address this gap, we have built a diverse biobank of CRC patient-derived tissue samples and matched CAF lines. Single cell RNA-sequencing of patient tissues identified distinct CAF subpopulations. These transcriptional signatures were then applied to bulk RNA-sequencing of the patient-derived CAF lines, which revealed expression patterns consistent with iCAF and myCAF profiles. Flow cytometry and secretome analysis further confirmed expression of subtype-specific markers, suggesting that each CAF line retains features of the originating subtypes.To investigate how these different CAFs influence tumor cell invasion, we developed a CRC organ-on-chip co-culture model. Specifically, this microfluidic device simulates gut-relevant biomechanical cues, including fluid flow and peristalsis-like motion, and is composed of two extracellular matrix-coated overlapping channels separated by a porous membrane, allowing biochemical and cellular exchanges between compartments. Patient-derived CAFs and GFP-labelled CRC tumor cells are cultured together in the top “epithelial” channel, while the endothelial cells line the bottom “vascular” channel. Using time-lapse confocal microscopy, GFP+ tumor cells intravasating into the vascular channel are tracked and quantified, providing real time invasion rates. We observed patient-specific differences in CAF-induced CRC invasion when exposing human CRC cells on-chip to CAF-conditioned media and in physical co-cultures. Interestingly, a myCAF-enriched line promoted invasion in only physical co-culture conditions, suggesting contact-dependent signaling. Additionally, each CAF line displayed distinct morphology and invasion patterns on-chip with the myCAF-enriched line invading before the CRC cells. Collectively, these results suggest that there may be specific CAF phenotypes that induce tumor invasion which could give insight into determining the invasive potential of a primary CRC tumor at diagnosis.

#6039 Cancer cell-driven HIF-1α activation enhances the motility of cancer-associated fibroblasts in the lung tumor microenvironment.

Jihye Park[1], Sieun Lee[1], Jonathan M. Kurie[2], Young-Ho Ahn[1]

[1]Ewha Womans University College of Medicine, Seoul, Korea, Republic of,[2]Professor, Dept. of Thoracic & H&N Onc., UT MD Anderson Cancer Center, Houston, TX

Cancer-associated fibroblasts (CAFs) display significant phenotypic heterogeneity driven by dynamic interactions within the tumor microenvironment. To investigate motility-driven CAF heterogeneity, we utilized a 3D culture system and the photoconvertible fluorescent protein Dendra2, to isolate ‘motile’ and ‘static’ CAF subpopulations. Transcriptomic analyses revealed that motile CAFs upregulated hypoxia- and glycolysis-related genes, which are downstream targets of HIF-1α. In line with these findings, HIF-1α activation enhanced CAF motility, while the knockdown of its downstream targets, ALDOA and LDHA, significantly reduced CAF motility. Notably, mesenchymal-like lung cancer cells enhanced both HIF-1α activity and motility in CAFs through secretory factors. Using mass spectrometry, we identified ceruloplasmin (CP) as a key secretory protein from these lung cancer cells, whose transcription was regulated by the EMT-inducing transcription factor ZEB1. Functionally, CP knockdown abolished the ability of lung cancer cells to promote CAF motility in vitro and to metastasize in vivo. Collectively, these findings demonstrate a novel mechanism where lung cancer cell-secreted CP facilitates HIF-1α signaling in CAFs, thereby driving their motility and promoting metastasis.

#6040 Targeting EP3$^+$FAP$^+$ stromal reprogramming uncovers a therapeutic vulnerability in early recurrent hepatocellular carcinoma.

guiqi zhu[1], guan zhiqi[1], yinghong shi[1], weiren liu[1], zheng tang[1], Kang Wang[2], jia fan[1]

[1]Zhongshan Hospital Fudan University, Shanghai, China,[2]Karolinska Inst. Cancer Ctr., Stockholm, Sweden

Early recurrence after curative therapy remains a major obstacle in hepatocellular carcinoma (HCC), yet the stromal determinants of early relapse are poorly defined. Across integrated mouse and human datasets, this stromal program was consistently associated with early relapse. Integrating bulk, single-cell and spatial transcriptomics with functional assays from primary and relapse HCC, we identify a recurrence-enriched cancer-associated fibroblast (CAF) population marked by FAP and EP3. A CAF- and neutrophil-derived high-risk gene signature predicted early relapse and was accompanied by expansion of FAP$^+$EP3$^+$ CAFs, immunosuppressive neutrophils and stem-like tumor epithelial cells in relapsed lesions. Lineage and perturbation studies indicate that CD36$^+$ lipid-associated CAFs are reprogrammed by tumor-derived PGE_2 into FAP$^+$EP3$^+$ matrix CAFs, linking stromal plasticity to recurrence. Mechanistically, FAP physically associates with EP3 on CAFs to potentiate PGE_2-induced EP3 signaling, thereby amplifying downstream cAMP-PKA activation. This FAP-EP3 complex drives a proline-metabolic, senescent and inflammatory CAF phenotype characterized by PYCR1-dependent proline production and SASP factors including IL-6 and TIMP1. PGE_2-FAP-EP3-cAMP/PKA signaling engages the chromatin reader BRD9 and pioneer factor FOXA1 to establish super-enhancer landscapes at IL6, FAP, PYCR1 and TIMP1, locking EP3$^+$FAP$^+$CAFs into a relapse-permissive state and sustaining SASP output. Imaging mass cytometry and spatial analyses revealed that EP3$^+$FAP$^+$ CAFs organize relapse-associated niches enriched for neutrophils, CD44$^+$/CD133$^+$ stem-like tumor cells, FOXP3$^+$ Tregs and CD163$^+$ macrophages, in close apposition to invasive tumor fronts. In autochthonous HCC models, genetic deletion of EP3 in fibroblasts or pharmacologic blockade of EP3 or BRD9 reduced tumor burden, decreased pro-tumoral neutrophils and exhausted CD8$^+$ T cells, and enhanced effector CD8$^+$ differentiation. Combined EP3 inhibition and anti-PD-1 therapy produced superior tumor control, indicating that stromal targeting can sensitize HCC to immune checkpoint blockade. In human HCC cohorts, EP3$^+$FAP$^+$ CAF signatures correlated with T cell exhaustion, high PTGES expression and poor survival, validating the clinical relevance of this stromal program. Together, our data uncover a PGE_2-FAP-EP3-cAMP/PKA-BRD9-FOXA1 axis that epigenetically locks CAFs into a relapse-permissive, metabolically active SASP state and remodels the immune microenvironment. Targeting EP3$^+$FAP$^+$ CAFs or their epigenetic circuitry represents a promising strategy to limit HCC recurrence and improve responsiveness to immunotherapy.

#6041 Fidaxomicin targets PDGFR$^+$ cancer-associated fibroblast to restrain colorectal cancer progression.

Haoxiang Zhang, Xudong Zhu, Chang Li, Yinping Jiang, Yuning Zhou, **B. Mark Evers**, Qingding Wang

UK Markey Cancer Center, Lexington, KY

Background: Colorectal cancer (CRC) features a stroma-rich, immunosuppressive tumor microenvironment (TME) where activated fibroblasts drive tumor progression and correlate with poor prognosis. PDGFR$^+$ cancer-associated fibroblasts (CAFs)—including PDGFRα$^+$ inflammatory CAFs (iCAFs) and PDGFRβ$^+$ myofibroblastic CAFs (myCAFs)—are proportionally increased and serve as key hubs of intercellular communication in CRC. High PDGFR$^+$ CAF signatures are associated with unfavorable outcomes. Fidaxomicin, an FDA-approved oral antibiotic which selectively eliminates pathogenic *Clostridioides difficile*, inhibits ileal fibrosis and suppresses PDGFR expression in intestinal fibroblasts. The purpose of this study was to define the mechanisms by which PDGFR$^+$ CAFs promote CRC progression and to evaluate the anti-tumor effects of fidaxomicin targeting PDGFR.
Methods: We performed R-based analyses of datasets from human CRC and matched normal tissues to compare cellular subpopulation proportions, functional enrichment, cell-cell communication, and virtual cell states. Effects of fidaxomicin on the proliferation of CRC cells and CAFs were assessed *in vitro* using 2D and 3D cultures and *in vivo* using an orthotopic colon cancer model (MC38 co-implanted with mCAF cells). CAF-neutrophil interactions were examined through 3D co-culture, multicolor immunofluorescence, and flow cytometry.
Results: Analysis of datasets from single-cell transcriptomics revealed markedly activated fibroblasts and increased monocyte-macrophage and neutrophil populations within the TME of CRCs. Tumor-enriched CAF subsets, including PDGFRα$^+$ iCAFs and PDGFRβ$^+$ myCAFs, expressed high levels of PDGFR and neutrophil-attracting chemokines such as CXCL1 and CXCL14. ssGSVA scores of CAF signature genes strongly correlated with poor prognosis. Treatment of CAFs with fidaxomicin significantly reduced PDGFR expression at both mRNA and protein levels, inhibited STAT3 phosphorylation, and downregulated CXCL1 and CXCL14 transcription. Moreover, oral fidaxomicin administration suppressed MC38 tumor growth. Mechanistically, fidaxomicin inhibited the transcriptional activity of the NOTCH-RBPJ-HDAC1/HDAC3 complex, leading to PDGFR downregulation and blocking PDGFR-mediated STAT3 activation and nuclear translocation that drives CXCL14 transcription and immune evasion.
Conclusions: Our results demonstrate that PDGFR$^+$ CAF subsets play a critical role in CRC progression. Fidaxomicin disrupts PDGFR$^+$ CAF-neutrophil interactions, remodels the TME, and inhibits tumor growth. Importantly, our findings suggest a potential usage of fidaxomicin, which maintains a favorable safety profile with minimal systemic toxicity, for CRC treatment.

#6042 Targeting GABA signaling in cancer associated fibroblasts to reduce immunosuppression in pancreatic cancer.

Ariana Musa de Aquino[1], Myree Graves[2], Kyra Langley[3], Peter Sajjakulnukit[4], Ian Loveless[5], Nina Steele[6], Julie Clark[1], Alexander Muir[7], Costas Andreas Lyssiotis[4], Ralph Francescone[8], Debora B. Vendramini-Costa[3], Guilaume Cognet G[7], David Kwon[9]

[1]Pancreatic Cancer Center, Henry Ford Health, Detroit, MI,[2]Department of Surgery- Pancreatic Cancer Center, Henry Ford Health, Detroit, MI,[3]Department of Surgery - Pancreatic Cancer Center, Henry Ford Health, Detroit, MI,[4]University of Michigan, Ann Arbor, MI,[5]Henry Ford Health System, Bexley, OH,[6]University of Cincinnati, Cincinnati, OH,[7]University of Chicago, Chicago, IL,[8]Department of Surgery-Pancreatic Cancer Center, Henry Ford Health, Detroit, MI,[9]Department of Surgery, Pancreatic Cancer Center, Henry Ford Health, Detroit, MI

Pancreatic ductal adenocarcinoma (PDAC) is a devasting disease with few therapeuticoptions. This is due, in large part, to the expansion of the non-tumor cellular compartmentknown as the stroma. Cancer-associated fibroblasts (CAFs) are one of the major celltypes that populate the stroma of PDAC tumors and are extremely immunosuppressivebecause they produce large amounts of cytokines, growth factors and metabolites. Thus,understanding how CAFs impart severe immunosuppression in the tumormicroenvironment is critical to make PDAC amenable to immunotherapies. Using a novel3D culturing method, our data support the notion that PDAC CAFs produce the glutamatemetabolite and inhibitory neurotransmitter gamma aminobutyric acid (GABA), *de novo*,and we detected GABA (~27μM) in tumor interstitial fluid (TIF) isolated from patient tissue(10 patients). Surprisingly, CAFs lacked expression of glutamate decarboxylase, thecanonical enzyme responsible for converting glutamate into GABA, which led us toexplore alternative, non-canonical pathways for GABA synthesis. We found that CAFsderived from patient PDAC tumors expressed the enzymes of the non-canonicalsynthesis pathway (ODC1, DAO, ALDH1A1 and ALDH9A1), and to a greater degreewhen compared to normal fibroblasts. In parallel, we demonstrated that, by exploringparacrine signaling, GABA treatment of CAFs resulted in changes in expression of p-p70,p-JNK, p-MTOR and p-AKT proteins, key signaling hubs involved in overcomingmetabolic stress in PDAC. In addition, GABA treatment increased the production of pro-tumor cytokines, such as TGFβ, IL8, and IL6, by CAFs. In preclinical orthotopic murinetumor models of PDAC, inhibition of GABA synthesis through ALDH1A1, and GABAsignaling through GABAB receptor inhibitors, reduced tumor burden, increased influx ofanti-tumor T and NK cells, and blocked production of pro-tumor cytokines in tumorexplants. Translationally, we have acquired patient matched plasma, TIF, and tissue from10 patients, and will compare their metabolic, immune, and spatial transcriptomic profileswith well annotated clinical parameters, in order to develop improved diagnostic tests.Overall, we have uncovered a novel signaling circuit driven by GABA that plays a role incontrolling the extremely immunosuppressive PDAC microenvironment.

#6043 Deactivating liver metastatic colorectal cancer-associated fibroblasts with all-trans retinoic acid.

Brandon Choi[1], Ken Huang[2], Yuyuan Zhou[2], Seungil Kim[2], Eileen Fung[2], Shannon M. Mumenthaler[2]

[1]Keck School of Medicine, University of Southern California, Los Angeles, CA,[2]Ellison Institute, LLC, Los Angeles, CA

Cancer-associated fibroblasts (CAFs) are a prominent component of the tumor microenvironment (TME) and are known to support tumor growth and disease progression. Reprogramming the stroma, particularly targeting the pro-tumorigenic functions of CAFs, has emerged as a promising therapeutic intervention to disrupt the supportive environment tumors rely upon. An in-house drug screen of FDA-approved oncology therapies was conducted on patient-derived colorectal cancer CAFs and tumor organoids (PDTOs) to identify compounds that may be repurposed as stroma targeting agents. This preliminary screen identified all-trans retinoic acid (ATRA) as a potential candidate that selectively inhibited CAF proliferation without affecting PDTO viability. ATRA is an active metabolite of vitamin A and can inhibit canonical transforming growth factor beta (TGF-β) signaling, a primary means of CAF activation and maintenance of the pro-tumorigenic TME. To investigate the mechanism underlying ATRA-mediated CAF deactivation, patient-derived liver metastatic CAFs were treated with ATRA for 5 days and analyzed at the transcriptional, protein, and metabolic level. qPCR was performed to assess the expression of glycolytic enzymes, CAF activation markers, and ATRA signaling genes. Western blots quantified expression of SMAD 2/3 and α smooth muscle actin (αSMA), a biomarker of CAF activation. ATRA-mediated alterations to CAF secretomes were validated with ELISAs probing for the following CAF activating cytokines: TGF-β, stromal derived factor 1 (SDF-1), and IL-6. Finally, alterations to the metabolic activity in response to ATRA was measured using Fluorescence Lifetime Imaging Microscopy (FLIM), providing a functional readout of TME normalization. All three patient-derived CAF lines treated with ATRA showed increased expression of retinoic acid receptor β (RARβ), a documented indicator of active ATRA signaling. Similarly, αSMA and TGF-β signaling were reduced across all lines in response to treatment. Secretome profiling was also consistent across patient lines, with ATRA lowering the quantities of TGF-β, SDF-1 and IL-6 released from CAFs. However, qPCR analysis revealed heterogeneity in transcriptional response: two CAF lines showed broad downregulation of CAF activation and glycolytic markers, but one line showed variable results. Finally, at a single-cell resolution, FLIM analysis revealed an ATRA-driven shift in metabolism away from aerobic glycolysis, a metabolic state associated with activated CAFs. Overall, these results suggest that ATRA effectively reprograms CAFs toward a deactivated phenotype but also highlights the inherent heterogeneity of CAFs and the impact this may have on drug response.

#6044 Immunosuppressive role of DKK1 and cancer-associated fibroblasts across molecular subtypes of endometrial cancer.

Alessandro Canella[1], Danielle Glassman[1], Keith Brownewell[1], Caprice Eisele[2], Aharon Gideon Freud[2], **Casey Cosgrove**[1]

[1]Division of Gynecologic Oncology, Department of Obstetrics and Gynecology, The Ohio State University Wexner Medical Center, James Cancer Hospital and Solove Research Institute, Columbus, OH,[2]Department of Pathology, The James Cancer Hospital and Solove Research Institute, The Ohio State University, Columbus, OH

BACKGROUND. Endometrial Cancer (EC) is the most diffuse and leading cause of gynecologic cancer-related mortality in the United States. Unlike many other cancers, EC mortality has continued to rise over the past two decades. Although recent advances in immunotherapy, particularly immune checkpoint inhibitors, most EC patients have limited or modest responses to current immunotherapies. The TCGA classification stratifies EC into four molecular subtypes: POLE-mutated, mismatch repair-deficient (MMRd), no specific molecular profile (NSMP), and p53-abnormal (p53abn). Each subgroup differs in tumor biology, immune cell infiltration, and prognosis. A deeper understanding of immune evasion across these subtypes and tumor grades is critical for improving targeted immunotherapies. Dickkopf-1 (DKK1), a secreted inhibitor of the canonical WNT pathway, has emerged as a key immunosuppressive regulator in several solid tumors. High DKK1 levels correlate with increased infiltration of myeloid-derived suppressor cells (MDSCs) and suppression of CD8+ T and NK cell cytotoxicity in breast and colorectal cancer. A recent study in breast cancer identified stromal fibroblasts as major contributors to extracellular DKK1, leading to suppression of NK cell cytotoxicity.
METHODS. We analyzed fresh and FFPE tumor samples across molecular subtypes from newly diagnosed, ICI-naïve EC patients who underwent surgical staging at The Ohio State University. Total RNA was extracted and analyzed using bulk RNAseq, single-cell RNAseq (scRNAseq), GSEA, and immune deconvolution. The tumor immune and stromal microenvironment was investigated by immunofluorescence (IF), multiplex IF, and DSP.
RESULTS. High-grade EC tumors showed significant upregulation of genes and pathways associated with tumor proliferation, invasion, WNT signaling, immunosuppression, and stromal fibroblasts proliferation. DKK1 expression was significantly higher in the tumor microenvironment (TME) of high-grade EC tumors, with spatial colocalization of DKK1 and perivascular CAF polarization. No DKK1 expression was detected in EC cells. scRNAseq confirmed exclusive upregulation of DKK1 in CAFs. Analysis of the TCGA-UCEC dataset confirmed significant upregulation of DKK1, and a positive correlation between DKK1+CAFs, immunosuppressive myeloid cells, and exhausted NK cells.
CONCLUSIONS. Our findings highlight CAF-derived DKK1 as a key immunosuppressive factor in high-grade and aggressive EC, suggesting that targeting DKK1 may enhance cytotoxic immune cell activation and improve immunotherapeutic outcomes.

#6045 Exploring surface interactors promoting viability of CLL cells in contact with stromal fibroblasts.

Uday Aditya Sarkar[1], Domenico Maisano[1], Stacey M. Fernandes[1], Kiyomi Mashima[1], Colin Mcnulty[1], Nikhil C. Munshi[1], Jennifer R. Brown[1], Fabiana Perna[2], Eugenio Morelli[3], Paolo P. Ghia[1]

[1]Department of Medical Oncology, Dana-Farber Cancer Institute, Boston, MA,[2]Department of Blood and Marrow Transplant and Cellular Immunotherapy, Moffitt Cancer Center, Tampa, FL,[3]Candiolo Cancer Institute, Candiolo (TO), Italy

INTRODUCTION

Survival and expansion of chronic lymphocytic leukemia (CLL) B cells are strongly shaped by interaction with the tissue microenvironment. This pro-survival activity is sustained by indirect and direct interactions, through soluble and surface factors, respectively. In this study, we aimed at exploring the lesser-known direct cell-to-cell surface interactions between CLL cells and their microenvironmental stroma that support the increased viability in CLL cells.

METHODS

Primary CD19+/CD5+ cells from 20 untreated patients with CLL (16 with unmutated IGHV) were cultured in the presence or absence of HS-5, a human bone marrow derived fibroblast cell line, that was also grown alone, as control. After 72 hours, viability of the primary CLL cells was assessed and HS-5 cells were harvested from the 2 culture conditions, with and without CLL cells, respectively, to be processed for RNA sequencing. Cell surface protein annotation method was used to identify the most prominent proteins expressed on the cell surface. These genes were used to design the CRISPR/Cas9 screening library encapsulated in lentiviral particles to infect HS-5 cells.

RESULTS

As expected, direct cellular contact with stroma increased the viability of CLL B cells by ~30% at day 3 ($p < 0.0001$) compared to CLL cells cultured alone. Using the method of surface protein annotation, we analyzed the RNA-Seq data obtained from HS-5 cells grown in co-culture and identified a list of 120 genes, likely coding for surface proteins, that were differentially expressed as compared to HS-5 cells cultured alone. Pathway enrichment analysis of these genes, particularly including notable names like *ALCAM*, *DDR2*, *TM4SF1*, *ITGB8* & *GJA1* etc., identified few vital cellular activities such as cell-adhesion, extracellular matrix protein binding, integrin binding and kinase binding. We have created a CRISPR/Cas9 library to enable functional testing directly in HS-5 cells to selectively remove each gene of interest. These modified HS-5 cells will be used for co-culture with primary CLL B cells to identify specific genes whose removal may show a significant impact on leukemic viability in our *in vitro* model.

CONCLUSIONS

In our work, we focused on the surface interactions, occurring between CLL and stromal cells, supporting the contact-dependent survival of the leukemic clone. By combining RNA-seq-based surface protein annotation with a targeted CRISPR screen, we establish a functional approach to identify a number of surface molecules on stromal cells that are potentially involved in direct surface interactions. This strategy may expose microenvironmental vulnerabilities that can be targeted to disrupt CLL-stroma interactions. Therapeutically, this study may pave the way to define the stromal interface as a tractable target to exploit novel treatment strategies for CLL in future.

#6046 Spatial transcriptomic profiling of cancer-associated fibroblast niches in extrahepatic cholangiocarcinoma.

Giulia Petroni[1], Simone Romagnoli[2], Daniele Lavacchi[3], Giulia Massaro[3], Francesca Rizzo[4], Elena Alexandrova[4], Costanza Winchler[3], Alfonso Carleo[4], Gian Luca Grazi[1], Daniele Rossini[1], Luca Messerini[5], Matteo Benelli[2], Serena Pillozzi[2], Lorenzo Antonuzzo[1]

[1]Department of Experimental and Clinical Medicine, Universita degli Studi di Firenze - UniFI (University of Florence), Firenze, Italy,[2]Department of Experimental and Clinical Biomedical Sciences 'Mario Serio', Universita degli Studi di Firenze - UniFI (University of Florence), Firenze, Italy,[3]Clinical Oncology Unit, Careggi University Hospital, Firenze, Italy,[4]Department of Medicine, Surgery and Dentistry "Scuola Medica, Salernitana", University of Salerno, Salerno, Italy,[5]Department of Experimental and Clinical Medicine, Pathology Unit, Universita degli Studi di Firenze - UniFI (University of Florence), Firenze, Italy

Background. Cholangiocarcinoma (CCA) is a rare and highly lethal malignancy characterized by a dense desmoplastic stroma containing cancer-associated fibroblasts (CAF). While CAF have been extensively studied in intrahepatic CCA, their impact on TME remodeling and chemo-immunotherapy (CIT) efficacy in extrahepatic (e) CCA remains largely unexplored. A comprehensive characterization of CAF in eCCA is needed to identify therapeutic strategies able to improve the CIT efficacy, that, so far, is limited in these patients.

Methods. Spatial transcriptomics was performed on treatment-naive tumor specimens from 8 patients with advanced eCCA treated with durvalumab + cisplatin/gemcitabine. A total of 126 microregions were profiled with the GeoMx Digital Spatial Profiler and classified based on pan-CK and ACTA2/αSMA straining, as follow: tumor ($CK^+\alpha SMA^-$), distant and peritumor CAF-enriched stroma ($CK^-\alpha SMA^+$) or peritumor αSMA-negative stroma ($CK^-\alpha SMA^-$).

Results. αSMA staining revealed marked stromal heterogeneity across all eCCA, with some tumor nests surrounded by a dense CAF-enriched stroma and others by αSMA^- cells within the same sample. Based on CD45 staining all samples were classified as immune-desert or -excluded, with no intratumoral immune infiltration. GSEA showed a positive enrichment of epithelial-mesenchymal transition (EMT) signatures, coupled with the downregulation of immune activation and IFN response pathways, in both CAF-enriched regions and tumor cells surrounded by αSMA^+ cells. Interestingly, genes encoding matrix metalloproteinase 11 (MMP11) and secreted phosphoprotein 1 (SPP1) were found overrepresented in CAF-enriched regions adjacent to tumor nests, as compared to distant CAF regions, suggesting CAF as major source of stromal MMP11 and SPP1. Finally, receptor-ligand interaction modeling performed using the CellChat tool showed that CAF-enriched regions exhibited significant interactions with adjacent tumor cells, throughout the secretion of factors involved in EMT-remodeling, tumor progression and immunosuppression (i.e., POSTN, HGF, WNT5A, TGFB1, INHBA, SPP1).

Conclusions. Our findings suggest that $MMP11^+SPP1^+$ CAF may promote desmoplastic barrier formation in eCCA, thereby hindering intratumoral recruitment of immune cells and limiting CIT efficacy. Ongoing analyses aim to further characterize CAF states and CAF-tumor crosstalk to support the development of strategies to enhance CIT responsiveness in eCCA.

#6047 CTHRC1-TGFb crosstalk between myofibroblasts and tumors drives invasion in early-stage lung adenocarcinoma.

Abhilasha Sinha, SEUNGYEUL YOO, Nanzeeba Faraby, Thinh Nguyen, Hideo Watanabe, Alexander Tsankov, Jun Zhu, Charles A. Powell

Icahn School of Medicine at Mount Sinai, New York, NY

Background Despite significant improvements in lung cancer detection, lung cancer remains leading cause of cancer related deaths in both men and women in United States. This is due to high heterogeneity in tumor microenvironment (TME). Cancer associated Fibroblasts (CAFs) are essential components of TME and are associated with tumor progression. Recently, single-cell RNA profiling of LUAD tumors has identified heterogenous CAF subpopulations. However, their role in early-stage tumor invasion is largely unclear.
Methods We performed unsupervised clustering of 53 esLUAD tumors and examined their association with invasiveness. We investigated enrichment of pro-invasive and indolent signatures and key drivers of the invasive subnetworks (Sinha and Yoo 2022) in different cell populations from 3 LUAD scRNA seq datasets and spatial gene expression dataset from Kras/TP53 (KP) tumors. We co-cultured conditioned media (CM) from human lung fibroblasts (HLF) and LUAD cells (HCC78 and HCC2209) and used techniques such as immunofluorescence, ELISA, co-culture migration/invasion assay, neutralization assays and bulk RNA sequencing to investigate crosstalk between cancer cells and myofibroblasts.
Results Unsupervised clustering of 53 esLUAD tumors identified four groups (G1-G4), capturing a linear progression of invasiveness which correlated with their histology. Key drivers of COL1A2 subnetwork, COL1A1 and CTHRC1, were significantly upregulated in G2 (LPA) vs G1 (AIS/MIA), indicating early ECM activation. Invasiveness programs were localized to tS2 tumor cells and myofibroblast subsets. Within fibroblasts, CTHRC1+ CAFs exhibited higher COL1A2 subnetwork scores than CTHRC1- CAFs and normal fibroblasts in all 3 LUAD scRNA seq datasets. Spatial analysis of KP tumors displayed focal Cthrc1 and high pro-invasion/COL1A2 programs in Tgfbr2-KO. Our in vitro data revealed that exposure to LUAD cells CM transforms fibroblasts into myofibroblasts leading to elevated CTHRC1 secretion. The CM from myofibroblasts induced significant increase in migration and invasion phenotype in LUAD cells, which was attenuated on blocking TGFb signaling. Our RNA seq data revealed that exposure to CM from
myofibroblasts induces EMT signature in LUAD cells. Additionally, exposure to recombinant CTHRC1 to HCC78 LUAD induced increased migration and invasion phenotype and enrichment of Wnt/b-Catenin signaling.
Conclusion Taken together, our data indicates that Tgfb-CTHRC1 crosstalk between LUAD tumors and myofibroblast plays important role in development of invasive features in esLUAD tumors. This data suggests the clinical importance of myofibroblast in LUAD invasiveness and potential value of CTHRC1 as target for combination therapy for invasive esLUAD tumors.

#6048 CAF-secreted periostin promotes tumor aggressiveness in BRAF-mutant papillary thyroid carcinoma by upregulating MMP1.

ZHUORAN LIU, JINYUE LIU, JIE KUANG, WEIHUA QIU

Rujin Hospital, SHANGHAI, China

Papillary thyroid carcinoma (PTC) harboring the *BRAF* V600E mutation sometimes demonstrates higher invasiveness and an increased risk of metastasis; however, the underlying mechanisms are not fully elucidated. Cancer-associated fibroblasts (CAFs) are key components of the tumor microenvironment. This study aims to investigate the role and molecular mechanisms of CAFs in promoting invasiveness in *BRAF*-mutant PTC. Bioinformatic analysis suggested that high expression of the stromal protein periostin (*POSTN*) is associated with poor prognosis in *BRAF* V600E-mutant PTC. We demonstrated that the *BRAF* mutation, via activating the MAPK signaling pathway, promotes the secretion of IL-1β by PTC cells, which stimulates CAFs to express *POSTN*. Functional assays further revealed that CAF-secreted *POSTN* significantly enhances the migration and invasion capabilities of PTC cells by upregulating matrix metalloproteinase-1 (MMP1). Animal experiments further confirmed that the combination of a *BRAF* inhibitor (encorafenib) with knockdown of *POSTN* in CAFs most effectively suppressed lung metastasis of PTC and prolonged mouse survival. This study uncovers a novel signaling axi—*BRAF* mutation/IL-1β/CAFs/*POSTN*/*MMP1*—that plays a critical role in enhancing the aggressiveness of PTC. Thus, a combined therapeutic strategy targeting *BRAF* and inhibiting CAF-secreted *POSTN* represents a promising strategy to improve the prognosis of aggressive *BRAF*-mutant PTC.

#6049 Cartilage oligomeric matrix protein, cancer-associated fibroblast phenotypes, and versican proteolysis modulate CD8+ T cell infiltration in colorectal cancer.

Cadence E. Brown[1], Ruchi Shah[1], Cindy Wuerz[1], Isoline M. Donohue[1], Katherine A. Johnson[1], Cheri Pasch[1], Dustin A. Deming[2]

[1]Univ. of Wisconsin Madison Sch. of Med. & Public Health, Madison, WI,[2]University of Wisconsin Carbone Cancer Center, Madison, WI

Background: Cytotoxic T cell infiltration in colorectal cancers (CRCs) is critical for immunotherapy response and is regulated by various tumor microenvironment (TME) factors. Cartilage oligomeric matrix protein (COMP), a large pentameric glycoprotein involved in extracellular matrix (ECM) organization and stability, has been implicated in elevated fibrosis and immunomodulation in CRC. Likewise, myofibroblastic and inflammatory cancer-associated fibroblasts (myCAFs and iCAFs) regulate ECM remodeling and immunomodulation in the TME. Versican (VCAN) and its proteolysis product, versikine (Vkine) also impact CD8+ T cell infiltration. Here, we evaluate the impact of COMP on CD8+ Tumor-infiltrating lymphocyte (TIL) abundance alone and in combination with CAF phenotypes and VCAN proteolysis status.

Methods: Immunohistochemistry was performed on CRC samples from 243 patients to evaluate COMP, myCAF, αSMA, TAGLN, PDPN, ICAM1, CD8, VCAN, and Vkine. CD8+ TILs were quantified per high-power field (HPF). COMP was scored from 0-3 based on staining abundance and intensity in the cancer epithelium, CAFs, immune cells, ECM, and the total stromal compartment. All other stains were scored from 0-3 based on stromal abundance and intensity. αSMA and TAGLN scores were averaged to calculate a myCAF score, and PDPN and ICAM1 were averaged to calculate an iCAF score. CAF and VCAN status was assigned as per previous.

Results: Abundant COMP was observed in the cancer epithelium (80%), CAFs (77%), immune cells (76%), ECM (36.2%), and stroma overall (64%). High stromal COMP expression is more prevalent in myCAF high cancers (25%) relative to iCAF high (8%) cancers. High stromal COMP expression is more prevalent in VCAN proteolytic weak (VPW, percent of samples 41%) vs VCAN/Vkine low (VVL, 15%) and VCAN proteolytic predominant (VPP, 19%) cancers. CD8+ TIL abundance increased with COMP expression across all compartments. A trend of higher CD8+ TIL abundance in stromal COMP high cancers relative to stromal COMP low cancers for iCAF high was observed (mean CD8+ TILs/HPF in COMP low cancers 8, COMP high cancers 10), while myCAF high cancers were comparable (5, 5). Interestingly, CD8+ TIL abundance was significantly higher in iCAF high cancers with high CAF COMP expression vs low CAF COMP (high CAF COMP mean CD8+ TILs/HPF 12, low CAF COMP 3, p=0.0488), though myCAF high cancers exhibit the opposite trend. CD8+ TIL abundance was also higher in stromal COMP high VPP cancers and VVL cancers vs VPW cancers (mean CD8+ TILs/HPF 19, 8 vs 4, respectively, p=1.398e-05).

Conclusion: COMP is abundant in the CRC TME and can vary with other TME features. The presence of COMP correlates with enhanced CD8+ T cell infiltration in the setting of a pro-inflammatory TME, including VPP and iCAF high cancers. Mechanistic studies are needed to evaluate how COMP may enhance T cell infiltration.

#6051 Pancreatic tumor expressed growth factors activate a neural-like program in human fibroblasts which is associated with poor prognosis.

Myriam Iliana Ibanez Rios, Maelle Batardiere, Alexandre Archambault-Marsan, Elham Dianati Ajibisheh, Vincent Quoc-Huy Trinh, David J.H F. Knapp

Institute for Research in Immunology and Cancer (IRIC), Montreal, QC, Canada

Pancreatic ductal adenocarcinoma (PDAC) is one of the most aggressive cancers, with a 5-year survival of less than 14%. The tumor microenvironment (TME) plays a central role in PDAC progression and is composed primarily of cancer-associated fibroblasts (CAFs), together with smaller populations of tumor, nerve, and immune cells. Recently, a population of stromal cells exhibiting a neural-like program has been identified within the PDAC TME, and its presence correlates with poor outcomes and chemoresistance. However, the origin of these neural-like cells and their role in tumor progression remain unclear. In a related project using Xenium spatial transcriptomics, we found that some CAFs express this neural-like program and often cluster near tumor cells. Based on this, we hypothesized that this program can be activated in CAFs through exposure to growth factors secreted by PDAC cells.To validate our Xenium findings, we performed cyclic immunofluorescence on 32 macrodissected PDAC samples across disease stages, staining for tumor, fibroblast, and neural markers. These analyses showed that a subset of CAFs expresses a neural-like program. Unbiased clustering further demonstrated that higher densities of neural-program-activated CAFs, as well as their closer proximity to tumor cells, are associated with disease progression. Next, we investigated in vitro the relationship between tumor cells and the neural-like program in human cell line fibroblasts. When co-cultured with PDAC cells, fibroblasts promoted tumor growth and activated neural markers even without added growth factors, indicating that tumor cells can drive this reprogramming. After gemcitabine treatment, neural-program-activated fibroblasts survived better than normal fibroblasts, while tumor cells remained sensitive. This suggests that the neural-like program enhances fibroblast survival rather than directly promoting tumor chemoresistance, potentially supporting the proliferation of residual tumor cells, although this requires further validation.Finally, we aimed to identify the mechanisms underlying neural-like program activation. Xenium data highlighted several neural-associated growth factors as candidates. Exposing human fibroblast cell lines to combinations of these factors showed that two of them were sufficient to induce neural markers. Re-analysis of mass cytometry data identified the downstream signaling pathways involved, and the use of inhibitors confirmed these findings.Overall, our work shows that PDAC cells can activate a neural-like program in fibroblasts through growth factor-mediated signaling and implicates this plasticity as a contributor to tumor progression and treatment resistance. Further dissecting this process could reveal new intervention points to limit CAF support for the tumor and enhance chemotherapy effectiveness in PDAC.

: In Vivo Models 2: Genetically Engineered Mouse Models, PDXs, Syngeneic Models
Poster Session

#6055 Targeting CEP55 as a universal oncogenic dependency: Integrating spatial multi-omics and targeted therapy across translational preclinical cancer models.

Behnam Rashidieh[1], Pirjo Apaja[2], Quan Nguyen[3], Nigel McMillan[4], Kum Kum Khanna[1]

[1]Mater Research, University of Queensland, Brisbane, Australia,[2]SAHMRI, University of Adelaide, Adelaide, Australia,[3]QIMR Berghofer Medical Research Institute, Brisbane, Australia,[4]Griffith University, Gold Coast, Australia

CEP55 is an emerging oncogenic driver that is overexpressed across diverse cancers. It promotes genomic instability, and hyperactivates PI3K/AKT signaling, contributing to aggressive, metastatic, and therapy-resistant cancers. However, the mechanistic basis of CEP55-driven tumor progression and its potential as a therapeutic target have remained unresolved. To dissect Cep55 function across the evolutionary trajectory of transformation, we developed a hierarchical mouse embryonic fibroblast (MEF) cell lines encompassing primary (non-malignant), SV40-immortalised (early-transformation), and E1A/Ras-transformed (fully oncogenic) states with Cep55 deletion. This unbiased platform enabled stage-specific mapping of CEP55-controlled pathways. In parallel, we generated an inducible Cep55 KO mouse and interrogated CEP55 dependency *in vivo* using PTEN-deficient Cre^{ERT2} system and $KRAS^{LSL\text{-}G12D}$; $TP53^{fl/fl}$ (KP) lung adenocarcinoma GEMMs. We integrated quantitative proteomics, spatial transcriptomics, histopathology, and functional assays, with additional validation using human cancer datasets. Finally, to overcome the “undruggable” nature of CEP55, we deployed a CEP55-targeted antisense oligonucleotide encapsulated in tumor- antigen targeted lipid nanoparticles (ASO-LNP). Inducible Cep55 deletion was well tolerated in adult tissues, indicating Cep55 is non-essential for adult homeostasis but critical for tumorigenesis. Cep55 loss profoundly impaired oncogenic traits most strikingly in E1A/Ras MEFs, reducing proliferation, adhesion, migration, and invasion. In vivo, Cep55 ablation delayed tumor onset and progression, and significantly extended survival in both PTEN-deficient and KP GEMMs. Spatial transcriptomics revealed extensive CEP55-dependent remodeling of the tumor microenvironment, including disrupted extracellular matrix architecture, altered collagen networks, impaired integrin expression and trafficking, and collapse of focal-adhesion-PI3K/AKT-ERK signaling axes. Stress-response and anti-proliferative pathways were concomitantly activated. Proof-of-concept therapeutic studies showed that CEP55-targeting ASO-LNP suppressed tumor growth in vitro, providing a foundation for optimization and evaluation of CEP55 inhibition using precision RNA-based therapies in preclinical models. CEP55 is a fundamental oncogenic dependency that coordinates ECM remodeling, integrin signaling, and multiple oncogenic pathway activation during tumor initiation and progression. Its genetic ablation suppresses transformation, delays tumor growth, and prolongs survival across multiple cancer models. Together, these findings validate CEP55 as a compelling therapeutic target and establish ASO-LNP delivery as a promising strategy for targeting this previously undruggable node.

#6056 The KSHV genome, devoid of the essential immediate early transactivator RTAORF50, induces angiosarcoma in transgenic mice.

Dirk P. Dittmer, Kyle Shifflett, Eason B. Anthony, Su Huanjuan, Zhigang Zhang, Blossom Damania

Lineberger Comprehensive Cancer Center, University of North Carolina at Chapel Hill, Chapel Hill, NC

Kaposi Sarcoma-associated herpesvirus (KSHV) extensively alters host cell signaling to induce a variety of malignant and premalignant phenotypes, including Kaposi sarcoma (KS). The mechanisms by which KSHV initially induces KS remain unclear due to a lack of animal models, as the human pathogen KSHV does not productively infect rodents or non-human primates. Our lab has recently developed a small-animal model of KS by integrating the entire 160-kb KSHV viral genome into the germline of mice, thereby circumventing rodent barriers to viral replication. KSHV transgenic mice develop a murine angiosarcoma indistinguishable from human KS by histology and transcriptional profile; however, deletion of the viral miRNA locus was required for the transgene founder animals to produce offspring. This yielded the FVBNJ-Tg(HHV8)197DtmrMmnc line (Cell Host Microbe. 2024 32(5):755-767). We have now generated another KSHV transgenic mouse line that carries all viral miRNAs but lacks the immediate-early transactivator RTA/ORF50, which is necessary and sufficient to induce lytic gene transcription. Without RTA/ORF50, the viral miRNAs are compatible with embryonic development. The intact transgene is transmitted in Mendelian fashion, and homozygous animals are viable. The Tg(HHV8dRta) mice have significantly higher overall survival but still develop angiosarcoma. The dispensability of RTA for murine KS has significant implications for the role of viral replication in KSHV oncogenesis. Pending further studies, we hypothesize that RTA-dependent genes are not required for tumor formation. Alternatively, transcripts that are classified as strictly lytic in other herpesviruses may have alternative modes of regulation in KSHV. Tumor cell lines derived from HHV8dRta murine KS tumors grow indefinitely in culture, providing a powerful new tool for KSHV research. A detailed comparison of tumor biology in KSHV transgenic mice with or without the essential immediate early transactivator will be presented.

#6057 The IKZF1 N159Y partial tandem duplication mutant drives chromatin remodeling, B-cell developmental defects and leukemia initiation.

Ruth W. Wang'ondu, Devanand Bondage, Qiong Zhang, Yiming Wu, Baranda Hansen, Chun Shik Park, Prady Baviskar, Emily Backhaus-Wagner, Ilaria Iacobucci, Surbhi Sona, Huiyun Wu, Qingsong Gao, Wojciech Rosikiewicz, Beisi Xu, Hongjian Jin, Ti-Cheng Chang, Stanley Pounds, Laura Janke, Trevor Cunningham, Kristine R. Crews, Jun J. Yang, Shondra Pruett-Miller, Charles G. Mullighan

St. Jude Children's Research Hospital, Memphis, TN

IKZF1 N159Y, present as a partial tandem duplication (hereafter N159Y), defines a distinct subtype of B-cell precursor acute lymphoblastic leukemia (B-ALL). The mechanistic basis of leukemogenesis of this mutation, in contrast to diverse IKZF1 alterations present across the spectrum of B-ALL, is unknown. Here we elucidate mechanisms of N159Y. We generated cell lines with heterozygous or hemizygous N159Y expression. Motif enrichment, luciferase assays, and AlphaFold3 modeling were used to evaluate altered DNA interactions. Inducible knock-in mouse models and in vitro colony-forming assays assessed developmental and self-renewal phenotypes. Cell fitness and cytotoxicity assays assessed epigenetic dependency. N159Y leukemia cells displayed a characteristic gene expression signature with activation of non-B lineage pathways and repression of B-cell identity genes. N159Y bound both canonical IKZF1 motifs and neomorphic bHLH motifs. Downregulated genes were associated with super-enhancer-linked B-cell developmental regulators. ChromHMM revealed gain of active and poised enhancers driven by N159Y. In IKZF1-null NALM6 cells, N159Y bound more sites than WT. In 293T cells, N159Y repressed the ETS motif-containing MCL1 promoter. N159Y leukemia cells showed dependency on *EP300* and *CREBBP*, and sensitivity to A-485, JQ1, and vorinostat. In mouse models, N159Y caused a marked reduction of mature B cells with expansion of aberrant B-cell precursors, and was associated with leukemia development, while also conferring abnormal self-renewal capacity in vitro. We show that N159Y is a chromatin-remodeling transcription factor mutant with neomorphic chromatin-binding. It disrupts B cell development and induces B-ALL.

#6058 Tumor suppressor gene inactivation shapes the landscape of EGFR-mutant lung adenocarcinoma progression with therapeutic implications.

Mariana Do Carmo[1], Matthew Martin[2], Michael Rosen[3], Lily Blair[3], Anna Tribe[2], Keita Maemura[1], Giorgia Foggetti[4], Francisco Exposito[1], Zeynep Ugur[1], Lafia Sebastian[3], Vy Tran[3], Ian Lai[3], Alyna Katti[3], Ian Winters[3], Dmitri A. Petrov[5], Nicolas Floc'h[2], Monte M. Winslow[6], Katerina A. Politi[7]

[1]Yale School of Medicine, New Haven, CT,[2]Bioscience, Oncology R&D, AstraZeneca, Cambridge, United Kingdom,[3]D2G Oncology, Mountain View, CA,[4]Comprehensive Cancer Center, IRCCS San Raffaele Scientific Institute, Milan, Italy; Vita-Salute San Raffaele University, Milan, Italy, Milan, Italy,[5]Department of Biology, Stanford University, Stanford, CA,[6]Asst. Professor, Dept. of Genetics, Stanford University School of Medicine, Stanford, CA,[7]Yale Cancer Center, New Haven, CT

Oncogenic alterations in exons encoding the kinase domain of the Epidermal Growth Factor Receptor (e.g. EGFR L858R mutations) occur frequently in lung adenocarcinomas (LUADs) and promote tumor growth. EGFR tyrosine kinase inhibitors (TKIs), like osimertinib, have greatly improved lung cancer outcomes, yet EGFR TKI resistance remains inevitable. In addition to mutations in oncogenes, co-occurring genomic alterations in tumor suppressor genes (TSGs) have emerged as core determinants of LUAD tumor fitness and therapeutic response. Moreover, recent work suggests that the oncogenic driver dictates the effect of putative TSG inactivation on the fitness landscape of tumorigenesis. To study the effects of co-occurring TSG mutations *in vivo*, we leveraged autochthonous, immunocompetent genetically engineered mouse models (GEMMs) of EGFR L858R-driven LUAD, in *Trp53* proficient and deficient settings, carrying a conditional *Cas9* allele for CRISPR-Cas9 genome editing. We investigated the effect of inactivation of 58 putative TSGs on EGFR-driven LUAD tumor growth, tumor initiation, and osimertinib sensitivity. In parallel, we also induced tumors using the same lentiviral pool in models of Kras G12D, Kras G12D;*p53*-deficient, and Kras G12C-driven LUADs. In mutant EGFR-driven tumors, we identified genes that when inactivated: (i) promote tumor growth, (ii) suppress tumor growth, and (iii) reduce sensitivity to osimertinib. Inactivation of *Tsc1* or *Tsc2*, negative regulators of mTOR-complex signaling, and the ubiquitin ligase associated genes *Cul3* and *Rnf43* significantly promoted tumor growth in addition to *Apc*, *Rbm10*, *Rb1* described in a prior screen. Surprisingly, we also identified a set of genes, enriched in chromatin modifiers, that decreased tumor fitness in mutant EGFR-driven LUADs, including *Crebbp* and *Smarca4*. Conversely, loss of these same genes did not affect the growth of Kras G12C and G12D-driven tumors, suggesting that fitness effects of gene inactivation can vary across oncogenic contexts, even within what is conventionally considered a linear signaling axis. Indeed, loss of *Setd2*, *Kmt2d*, *Ep300*, and *Stk11* all had significant detrimental effects on tumor growth in an EGFR context but had significant effects promoting tumor growth in a Kras G12C context. Through this screen we also identified genes that when inactivated contribute to reduced osimertinib sensitivity in mutant EGFR-driven tumors including *Nf1*, *Kmt2d*, and *Pten* in *Trp53* proficient and deficient settings, whereas loss of *Nf2* and *Kdm6a* only reduced sensitivity in a *Trp53* deficient setting. These results inform the biology of tumor growth and reveal new genetic interactions in EGFR-driven LUADs with therapeutic implications.

#6059 Vertical MAPK pathway targeting is required for tumor regression in novel human and mouse models of NF1-inactivated melanoma.

Olvania-Danyca Hilaire[1], Alexis M. Jones[1], Moriah H. Nissan[1], Sebastien Monette[1], Jordan Eichholz[1], Cailian Liu[1], Xia Yang[1], Ayana Sawai-Frantz[1], Elisa de Stanchina[1], Taha Merghoub[2], Neal Rosen[1], David B. Solit[1], Aphrothiti J. Hanrahan[1]

[1]Memorial Sloan Kettering Cancer Center, New York, NY,[2]Weill Cornell Medicine, New York, NY

Inactivating, oncogenic alterations in the tumor suppressor neurofibromin 1 (*NF1*), a RAS-GTPase, have been identified in approximately 4% of all cancers and in a significant subset of melanomas, nerve sheath tumors, and gliomas. While the MEK inhibitor selumetinib has been FDA approved for pediatric patients with Neurofibromatosis type 1 with benign plexiform neurofibromas arising from germline *NF1* mutation, MEK inhibitors and other therapies targeting the MAPK pathway have had limited clinical benefit in patients with tumors driven by *NF1*-inactivation. In melanoma, inactivation of *NF1* is insufficient to induce tumorigenesis. Sequencing data from 1,912 melanoma tumor/normal pairs generated as part of MSK-IMPACT identified oncogenic mutations in *TP53* as the most significant event common to *NF1*-inactivated melanoma, with oncogenic *BRAF* mutations frequently co-occurrent. Given the lack of models for studying NF1 loss, a cohort of genetically engineered mice were generated with melanocyte-restricted conditional loss of $Nf1^{fl/fl}$ and/or $Trp53^{fl/fl}$, and/or conditional gain of oncogenic BRAF V600E ($Braf^{CA}$). Combined *Nf1/Trp53* knockout induced hyperpigmentation and melanoma formation with features common to the human disease including pigmented melanocytic and amelanotic spindle-shaped neoplasms and S100-positive staining in most. Other genetic cohorts developed were $Braf^{CA}/Nf1^{fl/fl}/Trp53^{fl/fl}$ and $Braf^{CA}/Trp53^{fl/fl}$ (faster onset, high penetrance) and $Braf^{CA}/Nf1^{fl/fl}$ (latent onset, lower penetrance) mice. To facilitate preclinical and functional studies, 22 mouse tumor-derived, syngeneic, immunogenic cell lines were generated. As anticipated, loss of *Nf1* conditioned the response to treatment with a BRAF monomer inhibitor (vemurafenib). While *Nf1*-inactivated cells were more sensitive to MEK inhibition (trametinib), or combined BRAF/MEK inhibition, as seen by suppression of ERK phosphorylation (pERK), cyclin D1 and DUSP6 expression, and cell proliferation, levels of pERK quickly rebounded. BRAF V600E/NF1/TP53-mutant cells were also transiently sensitive to combined inhibition of BRAF and the positive RAS adaptor SHP2 (using SHP099); with the rebound of pERK mitigated only by MEK, not upstream BRAF/SHP2, inhibition. In mice with established $Braf^{CA}/Nf1/Trp53$-null tumors as well as in a genetically similar PDX of human melanoma (SK-MEL-1273A), combination strategies such as the triple regimen of RAF/MEK/SHP2 inhibitors induced more durable suppression of pERK and tumor regression. Studies evaluating vertical MAPK targeting strategies that include direct inhibition of RAS or inhibition of parallel survival pathways are ongoing in this molecularly defined cohort.

#6060 Patient-derived models of primary breast cancer for preclinical evaluation of neoadjuvant therapies.

Stefan J. Hutten[1], Xue Chao[1], Madelon Badoux[1], Timo Eijkman[1], Michael Sheinman[2], Roebi de Bruijn[1], Andrea Herencia-Ropero[3], Alba Llop-Guevara[3], Catrin Lutz[1], Jelle Wesseling[1], Violeta Serra[3], Jacco Van Rheenen[1], Colinda LGJ Scheele[4], Jos Jonkers[1]

[1]Netherlands Cancer Institute, Amsterdam, Netherlands,[2]Weizmann Institute of Science, Tel Aviv, Israel,[3]Vall D'Hebron Institute of Oncology, Barcelona, Spain,[4]VIB-KU Leuven Center for Cancer Biology, Leuven, Belgium

Targeted therapies are important for invasive breast cancer (IBC) treatment but are generally not standard-of-care in the neoadjuvant setting. To identify therapies with the potential to improve neoadjuvant treatment response, it is essential to develop patient-derived preclinical models that faithfully reflect the diversity of primary IBC subtypes in patients. Here, we collected data of all breast cancer patients (N=1675) diagnosed in the Antoni van Leeuwenhoek hospital (AVL) for a period of three years, while simultaneously receiving tissue samples of 314 patients to establish a collection of mouse-intraductal patient-derived xenograft (MIND-PDX) models fully recapitulating the heterogeneity of primary IBC. Serial transplantation of lesions resulted in the first large-scale cohort of 60 transplantable IBC-MIND models, comprising 31 luminal (i.e., ER+/HER-), 5 HER2+ and 24 TN models, as well as 7 matching PDX organoid (PDXO) models. We show that our IBC-MIND cohort can serve as a platform for preclinical evaluation of experimental neoadjuvant treatments. For triple-negative IBC, we demonstrate that neoadjuvant treatment does not benefit from addition of a PARP inhibitor, while for estrogen receptor (ER) positive IBC the combination of a CDK4/6 inhibitor and fulvestrant improves neoadjuvant treatment response. Our work provides a valuable resource of primary IBC models to study breast cancer biology and develop novel neoadjuvant treatments.

#6061 Development of pancreatic and colon patient-derived xenograft (PDX) tumor microarrays (TMAs) from the NCI patient derived models repository.

Cindy R. Timme[1], Lindsay Dutko[2], Sayak Ghatak[2], Ting-Chia Chang[2], Alice P. Chen[3], Li Chen[2], Biswajit Das[2], Tara Grinnage-Pulley[3], Shahanawaz Jiwani[2], Kaci Paulus[2], Chris A. Karlovich[2], Sergio Alcoser[3], Yvonne Evrard[1], Melinda G. Hollinghead[3], James H. Doroshow[4]

[1]Frederick National Laboratory for Cancer Research, Advanced Development Research Directorate, Leidos Biomedical Research, Inc., Frederick, MD,[2]Molecular Characterization Laboratory, Frederick National Laboratory for Cancer Research, Leidos Biomedical Research, Inc., Frederick, MD,[3]Biological Testing Branch, Developmental Therapeutics Program, National Cancer Institute at Frederick, Frederick, MD,[4]Division of Cancer Treatment and Diagnosis, National Cancer Institute, NIH, Bethesda, MD

The National Cancer Institute's Patient Derived Models Repository (NCI PDMR; https://pdmr.cancer.gov) has developed a national repository of Patient-Derived Models (PDMs) currently comprised of over 1000 patient-derived xenograft (PDX), 450 organoid (PDOrg), 500 tumor cell culture (PDC), and 425 cancer associated fibroblast (CAF) models. Over 450 PDXs have matched PDOrg and/or PDCs allowing for complimentary/parallel in vivo/in vitro studies. These PDMs are clinically annotated with molecular information available in a public database for the extramural community with additional molecular features including OncoKB annotated mutations, microsatellite instability (MSI), human leukocyte antigen (HLA) typing, and clinically relevant fusions. Researchers can use these clinical and molecular features or perform their own independent analyses using the public data to aid in their selection of preclinical models. Due to the large number of NCI PDMR models within histologies and research community interest, we have developed histology-based PDX TMAs to further facilitate the selection of models for cancer research. Each TMA panel includes up to 60 unique PDX models, with two 1.5mm cores/model plus murine control tissue. Quality control (QC) assessment of the TMA cores is performed by a pathologist. Each core is reviewed with an initial pass/fail threshold set to ≥10% human tumor/core area with ≥500 tumor cells. TMA slides pass QC if they meet these criteria and ≥75% of the models have at least one passing core. TMA blocks are QC'd at regularly set intervals to ensure all distributable slides meet these requirements. The first PDX TMA panel available for distribution this year (PANC I) contains 60 pancreatic cancer PDXs (predominantly pancreatic adenocarcinoma [PAAD]) derived from primary and metastatic lesions from treatment naïve through heavily pretreated patients. *KRAS* mutated models include 28 G12D, 15 G12V, 10 G12R, 3 G12C, 1 Q61H, and 3 *KRAS* wildtype. Other genes frequently mutated in pancreatic cancer are also found in this cohort including *TP53*, *SMAD4*, and *CDKN2A*. Also in development are four colorectal cancer TMAs panels: (1) a general set of colon adenocarcinomas (COAD) with features including early onset, non-European ancestry, and MSI-High; (2) *KRAS* mutated COAD; (3) Treatment naïve COAD and wildtype *APC* COAD; and (4) Rectal adenocarcinoma models. These TMAs can be used to stratify models by therapeutic target, develop predictive markers or classify differential signaling in disease subtypes, integrative analysis of genomic and protein expression, and discover or validate biomarkers of disease in an efficient and cost-effective way. Targeted model selection is of high importance to better understand the biology of these cancers and improve preclinical drug testing and screening design to translate novel therapeutics from bench to clinic.

#6062 The role of sex hormones and sex chromosomes in urethane-induced lung carcinogenesis.

Maksat Babayev[1], Carolyn D. Ekpruke[1], Omar Borges Sosa[1], Shikha Sharma[2], Dustin Rousselle[1], Chukwudike Igwe[1], Patricia Silveyra[1]

[1]Environmental & Occupational Health, Indiana University, Bloomington, IN,[2]Forensic Science, University of New Haven, Bloomington, IN

Lung cancer is the leading cause of cancer-related deaths worldwide and remains among the top ten causes of mortality in the United States. Non-small cell lung cancer (NSCLC) constitutes approximately 85% of all lung cancer cases, with lung adenocarcinoma (LUAD) being the most prevalent subtype. Intriguingly, sex differences in lung cancer incidence and mortality have been observed, particularly among non-smokers, where LUAD is more common in females. Understanding the sex-specific mechanisms underlying LUAD progression is critical for developing targeted therapeutic strategies. In this study, we used the “four core genotypes” (FCG) ArnoJ (C57BL/6J background) mice in which gonadal sex is decoupled from the sex chromosome complement. We applied urethane-induced lung cancer protocol (a well-established mimic of human LUAD), to investigate the roles of gonadal hormones and sex chromosomes in lung tumor progression. Mice of 6-8 weeks of age received urethane (1 g/kg body mass, weekly for 10 weeks) or the same volume of PBS (control) injections and were evaluated after a 20-week tumorigenesis period. We assessed cytological changes in bronchoalveolar lavage fluid (BALF), changes in mice body weights, histological/immunohistochemical (IHC) analysis in fixed lung tissue. All animals experienced increased BALF total counts and weight loss after urethane treatment (vs. control). When comparing animals of different genotypes, we found that the XXM (female chromosomes, male gonads) displayed the most prominent weight reduction between urethane and control groups. When combining mice with the same chromosomes treated with urethane vs. PBS, animals with XX composition displayed a greater difference in weight than those with XY chromosomes. In contrast, when comparing animals with the same gonads, mice with male gonads showed a stronger effect in weight reduction than those with female gonads. Overall, BALF from urethane-treated mice had higher total cell counts than PBS-treated mice. Differences across genotypes were also noted. Our preliminary analysis indicates that mice with female gonads experienced a more prominent increase in cell counts than mice with male gonads. No apparent differences were noted when comparing animals with XX or XY chromosomes. The IHC analysis with anti-Ras (Q61R) antibody (Abcam) revealed that sex hormones have a statistically significant ($p=0.00178$) effect on mutated RAS (Q61R) levels independent of genotype. The IHC analysis on cell proliferation rate (Ki-67, CST) did not reveal significant differences between groups. In conclusion, our preliminary analysis of this pilot experiment revealed a potential contribution of sex hormones and sex chromosomes to urethane-induced weight loss and BALF counts. Further analysis of histological and molecular markers in these mice will reveal additional information that could help us understand sex-specific mechanisms of carcinogenesis.

#6063 MICAL2 promotes oncogenic *Kras*-induced pancreatic cancer initiation by regulating acinar to ductal metaplasia.

Nirakar Rajbhandari, Evangeline Mose, Mojgan Hosseini, Deepa Sheik Pran Babu, Herve Tiriac, Andrew Lowy

UC San Diego, La Jolla, CA

Background: Pancreatic ductal adenocarcinoma (PDAC) is a deadly form of pancreatic cancer with the poorest 5-year survival rate among all solid cancers. Therefore, identifying effective therapeutic strategies is crucial for treating this disease. Using a genome-wide screening approach to find novel and targetable factors in human PDAC, we identified MICAL2 (microtubule-associated monooxygenase, calponin, and LIM domain containing 2) as a gene uniquely enriched in PDAC patients. Our research has shown that MICAL2 is highly expressed in human PDAC and is linked to a worse prognosis for patients. Additionally, tumor growth and distant metastasis are reduced in PDAC tumors silenced for MICAL2. Although these findings establish MICAL2 as a key regulator in PDAC, its role in pancreatic cancer initiation and progression remains poorly understood.

Methods: We utilized a genetically engineered mouse model of early pancreatic tumorigenesis (LSL-Kras$^{G12D/+}$, Pdx1-Cre, i.e. KC), where we conditionally deleted the Mical2 gene (Mical2$^{flox/flox}$) specifically in the pancreas to understand the importance of MICAL2 (M) in the early tumor initiation. We performed comparative histological analysis and in vitro biochemical studies to identify early tumor lesions and understand the underlying differences in the wild-type (KC) and the Mical2-deficient KC (KCM) mice.

Results: Our preliminary studies indicate that deleting MICAL2 in a genetically engineered mouse model (GEMM) of pancreatic cancer functionally delays PDAC initiation and progression. Biochemical and histopathological analysis show that removing MICAL2 impairs oncogenic KRAS-induced acinar to ductal metaplasia (ADM), which involves a significant cytoskeletal rearrangement and is linked to PDAC initiation. Additionally, extensive biochemical studies, gene expression analyses, and immunostaining reveal a significant decrease in RAC1 and ARP2 expression, along with reduced EGFR and PI3K/AKT activity when MICAL2 is inhibited during KRAS-driven pancreatic duct neoplasia.

Conclusions: Our observations indicate that MICAL2 plays a crucial role downstream of oncogenic Kras during the early stages of pancreatic cancer initiation by regulating RAC1 and ARP2, as well as EGFR and PI3K/AKT activity, which are necessary for Kras-induced ADM. This suggests that inhibiting MICAL2 could be a viable target for prevention and therapeutic strategies in PDAC.

#6064 The *in vivo* impact of UBTF tandem duplications on hematopoiesis and leukemia development.

Lisett Contreras, Juan Martin Barajas, Tamara Westover, Melvin Thomas III, Emily Xiong, Catherine Callahan, Chandra Rolle, Masayuki Umeda, Michael Walsh, Jing Ma, Laura Janke, Jeffery Klco

St. Jude Children's Research Hospital, Memphis, TN

This study aims to investigate hematopoietic and leukemic development in a physiological UBTF-tandem duplication (TD) model to better understand the biology underlying this subtype-defining alteration of acute myeloid leukemia (AML). UBTF-TDs are characterized as somatic, heterozygous, in-frame tandem duplications (TDs) within exon 13 of *UBTF* (upstream binding transcription factor). These alterations are associated with an overall inferior outcome. We developed a conditional knock-in mouse in which Ubtf-TD is expressed from the endogenous *Ubtf* locus after recombination by Cre recombinase driven by the hematopoietic *Vav* promoter, recapitulating the somatic mutation observed in patients. We first assessed the self-renewal potential of hematopoietic stem progenitor cells (HSPCs) from 8-10-week mice using colony-forming unit (CFU) assays. To assess leukemic burden, we monitored peripheral blood using flow cytometry and complete blood cell count. The hematopoietic compartments (bone marrow and spleen) from mice that progressed to terminal disease were examined by RNA sequencing (RNA-Seq) to characterize the expression profiles. Tumors that developed were transplanted into sub-lethally irradiated recipient mice to assess their engraftment potential. To investigate hematopoietic development in Ubtf-TD mice, we performed a comprehensive cellular and molecular characterization using multiparameter flow cytometry. We then performed single-cell RNA-seq to examine pre-leukemic progression. Finally, to explore functional dependencies of murine Ubtf-TD tumor cells, we conducted *in vitro* CRISPR knockout (KO) screens of 210 genes prioritized from RNA-seq data, UBTF-TD cord-blood CD34 (cbCD34) functional studies, and key UBTF-TD AML genes. Murine HSPCs expressing Ubtf-TD exhibit increased self-renewal capacity both *in vitro* and *in vivo*. Ubtf-TD expression induces a myeloid leukemia by 45 weeks of age. Clinical features include elevated white blood cell counts, anemia, and splenomegaly. Phenotypically, these leukemias exhibit high levels of CD11b and Gr-1 expression, are serially transplantable, and have dysregulated *Hoxa/Hoxb* gene expression. Flow cytometry further reveals increases in the granulocyte-monocyte progenitor (GMP) and multipotent progenitor (MPP3) populations in Ubtf-TD mice. Dependency screens revealed that Ubtf-TD cells rely on *Xpo1*, *Men1, Kmt2a,* and *Meis1*. Collectively, our work demonstrates that UBTF-TD is sufficient to drive leukemia development *in vivo* and that this model recapitulates key phenotypes observed in UBTF-TD AMLs. This mouse model provides a platform for evaluating leukemia initiation, progression, and therapeutic vulnerabilities, including XPO1 inhibition (eltanexor) and Menin inhibition (revumenib), both of which have demonstrated efficacy in cbCD34 and patient-derived xenograft (PDX) UBTF-TD models.

#6065 Decoding KRAS signaling intensity: A key driver of tumor aggressiveness and response to RAS inhibition in pancreatic cancer.

Mehrnaz Salehi[1], Sara Raji[1], Mohammadreza Ranjouri[1], Fengming Chen[2], Ashley Fletcher[1], Peter J. Allen[3], **Zahra Kabiri**[1]

[1]Surgery, Duke University School of Medicine, Durham, NC,[2]Pathology, Duke University School of Medicine, Durham, NC,[3]Duke University School of Medicine, Durham, NC

Background: Pancreatic ductal adenocarcinoma (PDAC) is a highly aggressive malignancy, with KRAS mutations present in near 90% of cases, most frequently in codons 12 and 61. Increased KRAS copy number, resulting in elevated KRAS signaling intensity, correlates with poor prognosis and limited chemotherapy response. However, the role of KRAS signaling intensity in PDAC initiation, progression, and response to treatment remains unclear due to the lack of suitable *in vivo* models.

Methods: We developed a unique set of pancreatic cancer mouse models ranging from low to high levels of KRAS signaling by crossing the *Pdx1-CreER*$^{(+)}$/*Trp53*$^{(fl/fl)}$ mice with Cre-inducible *Kras*-LSL^{G12D} or *Kras*-LSL^{Q61R} alleles that either express these oncogenic alleles with native codons (low expression) or optimized codons (high expression). Tumor onset, progression, metastasis, and survival were systematically assessed. Additionally, 24 murine PDAC cell lines were established from these models, and eight human PDAC cell lines were classified into low- and high-intensity KRAS signaling groups to evaluate therapeutic response to the pan-RAS inhibitor RMC-6236.

Results: KRAS signaling intensity profoundly influences the timing of PDAC onset, disease progression, and metastatic potential. Mice with high, intermediate, and low KRAS signaling developed PDAC at approximately 4-5, 12-16, and 16-24 weeks of age, respectively. Survival analysis over a 52-week period revealed striking differences in overall survival, with median survival times of 8 weeks (high), 23 weeks (intermediate), and 41 weeks (low). Notably, the high-intensity group exhibited significantly higher rates of distant metastases to the lung and liver compared with the intermediate- and low-intensity groups. In vitro treatment suggested that cells with lower KRAS signaling intensity tended to be more sensitive to RMC-6236, highlighting its potential as a biomarker for patient stratification and therapeutic decision-making.

Conclusions: KRAS signaling intensity is a key determinant of PDAC initiation, progression, metastasis, and overall clinical outcomes. Moreover, it may serve as a predictive biomarker for response to RAS-targeted therapies. Collectively, these findings suggest that quantifying KRAS signaling intensity could enable precision medicine approaches and guide therapeutic decision-making in PDAC.Generative AI tools were used to assist with text editing and improvement of this abstract.

#6066 A model of spontaneous brain metastasis in small cell lung cancer undergoes epithelial-to-neuronal transition.

Shreoshi Pal Choudhuri[1], Thomas Salisbury[1], Mantre Dehnad[1], Bratati Mukherjee[1], Braeden Freitas[1], Kyle May[1], Seth Hamilton[1], Shruti Raghavan[1], Victor Stastny[1], Kimberley Avila[1], Jui Wan Loh[1], Urooba Nadeem[1], Luc Girard[1], Jeon Lee[1], Michael S. Lawrence[2], Genevieve Konopka[1], James Kim[1], Benjamin J. Drapkin[1]

[1]UT Southwestern Medical Center, Dallas, TX,[2]Broad Institute of Harvard and MIT, Cambridge, MA

Brain metastases (BrMs) occur in 40-60% of small cell lung cancer (SCLC) patients, causing significant morbidity and mortality. Although most patients present with extracranial metastases (EMs) at diagnosis, approximately two-thirds of BrMs arise after diagnosis and could be prevented by effective and tolerable therapies. However, SCLC models rarely form BrMs in mice, hindering translational research. We report patient-derived xenograft (PDX) models of SCLC that form recurrent, spontaneous, and symptomatic BrMs. By refining a surgical approach to generate solitary orthotopic primary (OP) tumors within the margins of the left lung parenchyma, six PDX models developed diffuse EMs within 8 weeks of OP detection by MRI. In a model harboring therapy-induced subclonal mutations, we confirmed that these EMs arose spontaneously from the left lung OP tumors, and further validated this finding with a lentiviral DNA barcode library. Model MGH1564-1A, derived from a relapsed SCLC patient shortly after the emergence of small BrMs, produced delayed ataxia and hydrocephalus in 70% of mice (median onset ~100 days). Whole brain sectioning of these mice consistently revealed BrMs up to 2 mm in diameter, whereas in mice without neurologic symptoms, BrMs were not detected. Intriguingly, when compare with the OP tumors, these spontaneous BrMs demonstrated an epithelial-to-neuronal transition (ENT) in global transcription that was confirmed by immunohistochemistry. This transition was absent from EMs within the same animals, suggesting that ENT is a BrM-specific adaptation. Two additional PDX models demonstrated recurrent BrMs, suggesting brain tropism as a property of some PDX models but not others. To our knowledge, these are the first models of human SCLC to reliably develop spontaneous BrMs that limit animal survival, providing a preclinical system for investigating the drivers of brain organotropism in SCLC and for evaluating anti-BrM therapies.

#6067 HPV+ and HPV- head and neck cancer patient-derived models in the NCI Patient-Derived Models Repository.

Yvonne A. Evrard[1], Ting-Chia Chang[2], Jasmine B'Lanton[1], Gareth Bliss[1], Alice Chen[3], Li Chen[2], Kevin Cooper[1], Kristin Cox[1], Natalie Czarra[1], Isabella Czernia[1], Biswajit Das[2], Kelly Dougherty[1], Aarin Dreyer[1], Lindsay Dutko[2], Katie Frey[1], Marion Gibson[1], Tara Grinnage-Pulley[4], Shahanawaz Jiwani[2], Poorva Juneja[2], Keegan Kalmbach[1], Tamikia Lamb[1], Eva Loewenstein[1], Candace Mallow[1], Chelsea McGlynn[1], Justine Mills[1], Michael Mullendore[1], Matthew Murphy[1], Sandra Navas-Reyes[1], Michelle Norris[1], Jessica Park[2], Kaci Paulus[2], Kevin Plater[1], Tia Shearer[1], Jessica Steed[1], Luke Stockwin[1], Howard Stotler[1], Ruth Thornton[2], Cindy R. Timme[1], Shannon Uzelac[1], Dianne L. Newton[1], Chris A. Karlovich[2], Melinda G. Hollingshead[4], James H. Doroshow[3]

[1]Frederick National Laboratory for Cancer Research, Frederick, MD,[2]Molecular Characterization Laboratory, Frederick National Laboratory for Cancer Research, Frederick, MD,[3]Division of Cancer Treatment and Diagnosis, National Cancer Institute, Bethesda, MD,[4]Biological Testing Branch, Developmental Therapeutics Program, National Cancer Institute-Frederick, Frederick, MD

Head and neck (HN) cancers are a rare set of cancers defined by their anatomical point of origin including mouth, sinus, throat, or nose. Human papilloma virus (HPV) infection plays a pathogenic role in HN cancers resulting in distinct clinical and molecular characteristics from those that are HPV-. The National Cancer Institute's Patient-Derived Models Repository (NCI PDMR; https://pdmr.cancer.gov) has developed a national repository of patient-derived models (PDMs) comprised of patient-derived xenografts (PDXs), organoids (PDOrg), tumor cell cultures (PDCs) and cancer associated fibroblasts (CAFs). These models are clinically annotated with molecular information available in a public database for the extramural community. To date, 361 patient HN tumor specimens have been received from 351 unique patients across a range of histologies including lip/oral, pharyngeal, laryngeal, salivary and sinonasal with an overall PDX take rate of 48% (322 assessable specimens). The NCI PDMR currently has 200 public HN PDX, PDOrg, and PDC models from 124 unique patients. Thirty-three models (PDX, PDOrg, PDC) from 20 unique patients are positive for HPV16 or 18 (one double positive) as detected by PCR and one sinonasal PDOrg model is positive for HPV33 identified in NextGenSeq data. As has been reported in the clinical literature, *TP53* and *CDKN2A* mutations are found predominantly in PDX models that are HPV- (84% and 65%, respectively) but not HPV+ (0%; 0%) and *PIK3CA* is more commonly mutated in HPV+ models (47% vs 25%). No significant difference in loss of heterozygosity is observed in the models. However, significant differences in chromosome arm copy number changes (copy gains in 7p, 11p and 12p and copy losses in 3p, 9p and 18q [P-value<0.05; Wilcoxon Rank-Sum test]) are observed in HPV- compared to HPV+ models. Gene set enrichment analysis (GSEA) suggest the E2F_TARGETS, G2M_CHECKPOINT, and DNA_REPAIR gene sets are significantly up-regulated in HPV+ while the APOPTOSIS gene set is significantly down-regulated using MSigDB Hallmark dataset (P-value<0.05). In all analyses, differences are consistent whether examining *in vivo* PDX models or *in vitro* PDC/PDOrg models indicating the fidelity of the models. These preclinical models recapitulate the molecular differences reported in HPV+ versus HPV- clinical cases providing an important tool for the development of novel therapeutics for HN cancers. Funded by NCI Contract No. HHSN261200800001E

#6068 The double-edged role of anti-inflammatory drugs in ovarian carcinosarcoma, in a *Trp53;Brca2;Pten* genetically engineered mouse model.

Einav Bangiev Girsh[1], Roba Gabesh[1], Eden Gal[1], Amir Basis[1], Sharona Tornovsky-Babeay[2], Gwo Yaw Ho[3], Dimitri Goncherovsky[4], Morad Zayoud[5], Paul Zannou[1], Inna Naroditsky[6], Tamar Klienberger[1], Liron Berger[1], Oren Parnas[2], Ruth Perets[1]

[1]Technion-Israel Institute of Technology, Haifa, Israel,[2]The Hebrew University of Jerusalem, Jerusalem, Israel,[3]Monash University, Wantirna South, Australia,[4]Bnei-Zion Medical center, Haifa, Israel,[5]Ziv Medical Center, Safed, Israel,[6]Rambam Health Care Campus, Haifa, Israel

Introduction: Ovarian carcinosarcoma (OCS) is a rare and deadly subtype of ovarian cancer, characterized by an admixture of epithelial and mesenchymal components. The limited understanding of its pathogenesis and the lack of effective therapies highlight the need for pre-clinical OCS models. In particular, the role of inflammation in OCS pathogenesis remains unknown.
Methods: We generated an inducible genetically engineered mouse model of OCS by deleting relevant tumor suppressor genes, namely Trp53, Brca2 and Pten, in the ovarian surface epithelium and fallopian tube epithelium. To assess the role of NSAIDs in OCS, mice were treated with indomethacin starting shortly after tumor induction. We performed single-cell RNA sequencing (scRNA-seq) analysis of tumors and metastases and validated key findings using immunohistochemistry and flow cytometry. Finally, we created murine OCS cell lines and conducted an in vivo omentum migration assay and bulk RNA-seq, to distinguish the effects of NSAIDs on tumor cells versus the tumor microenvironment (TME).
Results: Mice in our model developed ovarian tumors that recapitulated the dual epithelial-mesenchymal morphology of OCS and expressed clinically relevant OCS markers. Deletion of Trp53 and Pten was essential for tumor formation, whereas Brca2 deletion had only a minimal effect on survival. Tumors with combined Trp53, Brca2, and Pten deletion demonstrated high macrophage infiltration within the TME, mirroring human OCS and supporting the model's suitability for investigating the role of inflammation in this disease. Indomethacin-treated mice developed markedly smaller primary tumors and exhibited prolonged survival, yet showed a significant increase in metastatic burden, highlighting the double-edged role of inflammation in OCS. scRNA-seq analysis revealed that indomethacin affected both cancer cells and the TME. Indomethacin-treated cancer cells expressed lower levels of genes associated with angiogenesis and extra cellular matrix turnover. Indomethacin led to a marked reduction in macrophages abundance within primary tumors, accompanied by decreased CD4 and CD8 T cells and an increase in T regulatory cells. An in vivo omentum migration assay demonstrated a metastasis-suppressing effect on the pre-metastatic niche, alongside a direct metastasis-enhancing effect on the tumor cells. Finally, bulk RNA-seq of mOCS cells treated with indomethacin revealed a dramatic upregulation of cholesterol homeostasis pathways, potentially mediating the pro-metastatic effect on cancer cells.
Conclusions: We developed a reproducible OCS model that faithfully mirrors key pathological and molecular features of the human disease. While the tumor-suppressive effects of NSAIDs were discussed in other cancer types, we caution that NSAIDS might have contradictory and complex roles in specific tumor types.

#6069 Mutant BRAF and AKT cooperate to induce melanoma formation.

Camden VanTassell[1], MiKaela N. Field[2], Boyd Griffiths[1], Landen Barnett[1], Madison Hawkins[1], Joshua Knight[1], Katie Culver[2], Allison Stevens[1], Sheri L. Holmen[2], Gennie Lynne Parkman[1]

[1]Weber State University, Ogden, UT,[2]University of Utah Huntsman Cancer Institute, Salt Lake City, UT

Genetic studies have greatly advanced our understanding of the molecular and genetic drivers underlying the steps of melanomagenesis. Although activation of the mitogen-activated protein kinase (MAPK) signaling pathway—specifically in the form of a single driver mutation in the oncogenes BRAF or NRAS—triggers melanocyte proliferation in over 60% of cases, mutations in the RAS pathway alone are not sufficient for melanoma formation. However, the addition of activating tumorigenic mutations or loss of tumor suppressor functions in the phosphoinositide 3-kinase (PI3K) pathway promotes the escape from oncogene-induced senescence, leading to the formation of malignant melanomas. While dysregulation of the PI3K lipid signaling cascade in melanoma is conventionally believed to occur through activation of AKT, it has not been shown whether constitutively active AKT can substitute for mutationally activated PI3K or loss of PTEN in mutant BRAF melanomagenesis in the absence of Cdkn2a loss.In this study, we investigated the potential of aberrant MAPK signaling through mutational activation of BRAF to cooperate with dysregulated AKT signaling to drive melanoma tumor formation and observed that genetic alterations in both BRAF and Akt1 are sufficient to promote melanomagenesis. Using an established autochthonous melanoma mouse model, we evaluated the ability of constitutively active Akt1 to promote tumor initiation and progression and found that Akt1 was sufficient to initiate tumorigenesis with an average tumor onset of 130.5 ± 32.5 days and a median overall survival of 178 ± 2.70 days. We have previously established the potential of myrAkt1 to enhance tumor activity and metastasis with additional genetic events such as loss of the tumor suppressors Pten and Cdkn2a. We now demonstrate that Akt1 not only drives melanoma progression and promotes metastasis but also plays a role in melanoma initiation. Furthermore, proteomic analysis of tumors using reverse-phase protein array (RPPA) revealed an upregulation of total FAK protein in the Pten samples, a finding that we are currently investigating further. Results from this study establish a role for Akt1 in melanoma initiation and highlight the ability of multiple alterations in the PI3K/AKT signaling pathway to influence BRAF mutant melanoma initiation, progression, and metastasis.

#6070 Clinical and genomic determinants of PDX engraftment across solid tumors.

Leva Gorji[1], Kurt W. Evans[2], Xiaofeng Zheng[3], Erkan Yuca[2], Ran Zhang[2], Hung Le[2], Gabriela Raso[4], Argun Akcakanat[2], Ana Galan Cobo[2], Timothy P. DiPeri[1], Milind Javle[5], Burak Uzunparmak[2], Funda Meric-Bernstam[2]

[1]Surgical Oncology, The University of Texas at MD Anderson Cancer Center, Houston, TX,[2]Investigational Cancer Therapeutics, The University of Texas at MD Anderson Cancer Center, Houston, TX,[3]Bioinformatics and Comp Biology, The University of Texas at MD Anderson Cancer Center, Houston, TX,[4]Translational Molecular Pathology, The University of Texas at MD Anderson Cancer Center, Houston, TX,[5]GI Medical Oncology, The University of Texas at MD Anderson Cancer Center, Houston, TX

Introduction: Patient-derived xenograft (PDX) models support investigation of tumor biology and treatment response, yet determinants of successful engraftment and the extent to which PDXs retain patient tumor genomic features remain incompletely defined. This study evaluated clinical and actionable genomic characteristics associated with PDX establishment across solid tumors.
Methods: Tumor specimens from biopsies in 529 patients (555 tumors) were implanted into immunodeficient mice and classified as take or no-take based on successful implantation. Clinical diagnoses and histologic subtypes were recorded. Matched patient tumors and PDXs underwent sequencing to assess mutations, amplifications, deletions, and composite alteration events across actionable genes.
Results: Of the 555 implanted tumors, 266 PDXs were generated (~47% take rate). We generated PDXs from 250 patients across more than 27 tumor types; 14 patients contributed two models, and one contributed three longitudinal models. Pancreatic and esophageal tumors demonstrated higher engraftment frequencies, while peritoneal and appendiceal tumors showed lower frequencies. Among breast cancers, engraftment was higher in triple-negative tumors compared with hormone receptor-positive or HER2-positive subtypes (52% TNBC, 39% HR+, 36% HER2+). Engraftment was more common in tumors bearing *TP53* alterations; however, significance was not retained after adjustment for multiple testing (62.6% vs 50.2%; p=0.007, adjusted p=1). Sequencing of 114 PDXs were compared to clinical sequencing in matched patients. Patients harbored alterations in 159 actionable genes; 157 were also detected in PDXs. All PDXs harbored at least one shared actionable alteration, and 36 PDXs retained all actionable alterations present in their matched patient tumor. Additionally, 88 actionable alterations were detected in at least one PDX but not in patients, and 106 PDXs harbored at least one such alteration. All PDXs acquired additional actionable alterations relative to their matched patient tumors.
Conclusions: PDX engraftment is feasible from biopsies in advanced cancer; engraftment success varies across tumor types. Sequenced PDXs broadly preserved patient tumor actionable alterations but may also have acquired additional events.

#6072 Characterization of the immunological responses in a mouse model expressing humanized FcγR/FcRn.

Angela Pappalardo[1], Julie Donaghey[2], Danielle Huggins[2], Patrick Kirby[2], **Fabiane Sonego**[1], Gaelle H. Martin[1], Kader Thiam[1]

[1]genOway, Lyon, France,[2]Merida Biosciences, Cambridge, MA

Therapeutic antibodies have revolutionized cancer treatment by leveraging immune mechanisms such as Fc-effector functions, which depend on interactions between IgG and Fcγ receptors (FcγRs). However, preclinical evaluation of antibody pharmacokinetics (PK) and pharmacodynamics (PD) remains challenging due to species-specific differences in FcγR and FcRn expression and function. We previously reported a FcγR humanized mouse model that expresses a human-like pattern of FcγRs (including FcγRI, FcγRIIA, FcγRIIB, FcγRIIIA, and FcγRIIIB - genO-hFcγR). These receptors are functional and enable accurate evaluation of Fc-effector functions such as ADCC and B-cell depletion. The model demonstrated Fc-dependent activity of therapeutic IgG, allowing differentiation between antibodies with regular versus enhanced FcγR binding, and supports ranking of Fc-engineered antibodies in preclinical studies. Herein we describe a model expressing human FcRn in addition to humanized FcγRI, FcγRIIA, FcγRIIB, FcγRIIIA, and FcγRIIIB. As the FcRn is involved in IgG recycling and transport, this model was developed to enhance the translatability of PK studies by enabling human FcRn-mediated IgG recycling, while maintaining PD assessment of Fc-engineered therapeutic antibodies**.** We now aim to characterize the immunological competence of the humanized genO-FcγR/FcRn model in the context of inflammation and humoral immunity. Specifically, we investigated whether the immune responses of these mice are comparable to those of wild-type (WT) mice when exposed to defined immunological challenges. We assessed cytokine profiles and cell activation following lipopolysaccharide (LPS) stimulation. Upon LPS challenge, genO-hFcγR/hFcRn mice secreted inflammatory cytokines at levels comparable to WT controls. Additionally, CD25 and CD69 were upregulated on NK and T cells. Similarly, treatment with anti-mouse CD3 antibody triggered a rapid immune response characterized by elevated production of multiple cytokines in both genO-hFcγR/hFcRn and WT mice. Finally, to evaluate humoral responses, we performed a T-cell dependent antibody response assay using Keyhole Limpet Hemocyanin (KLH) as immunogen. genO-hFcγR/hFcRn mice successfully produced antigen-specific IgG and IgM antibodies in response to treatment with KLH, confirming functional cooperation between T and B cells, as observed in WT mice. In summary, these results demonstrate that genO-hFcγR/hFcRn mice are immunologically competent and respond physiologically to immune challenges. This model is a robust and reliable tool for studying Fc-engineered therapeutic antibodies in a context that preserves native immune functionality. The genO-hFcγR/hFcRn model is also being improved to enable tolerability to hIgG1 antibodies, and flexibility of therapeutics testing through expression of human immune checkpoints.

#6073 Establishment and characterization of a panel of EGFR-mutant lung XPDX models representing naïve, chemotherapy, and targeted therapy-resistant patient populations.

Christopher Nelson[1], Mia Lopez[1], Amy Fredrickson[1], Alyssa Simonson[1], Natalia Banos Herraiz[1], Shaquille Johnson[1], Ian Sturgill[1], Guillermo Sanz Martin[1], Jim Lund[1], Jennifer Garcia[1], Kyriakos P. Papadopoulos[2], Victor Moreno Garcia[3], Chris Takimoto[2], Michael J. Wick[2]

[1]The START Center for Cancer Research- XenoSTART, San Antonio, TX,[2]The START Center for Cancer Research, San Antonio, TX,[3]The START Center for Cancer Research- Madrid, Madrid, Spain

Background: Epidermal growth factor receptor (EGFR) mutations represent clinically actionable driver alterations in non-small cell lung cancer (NSCLC), defining a molecular subset with distinct biology, therapeutic vulnerabilities, and patterns of resistance. While common activating mutations including exon 19 deletions (19del) and L858R substitutions have well-characterized responses EGFR tyrosine kinase inhibitors (TKIs), the landscape of EGFR-driven disease is increasingly complex. Uncommon EGFR variants (e.g., D761Y, Y801C, G863C) and acquired compound mutations such as T790M and C797S as well as other resistance mechanisms drive resistance and disease progression. These biologically diverse contexts underscore the need for translational research platforms that accurately represent clinical heterogeneity and enable evaluation of therapeutic strategies across the evolving spectrum of EGFR-mutant disease. To this end, we have established and characterized a panel of EGFR-mutant lung PDX models representing naïve, chemotherapy, and targeted therapy-resistant patient populations. These models were characterized for receptor expression, genomic alterations, and in vivo drug sensitivity to relevant therapies.
Methods: XPDX models representing EGFR 19del and L858R-mutated lung cancer were established from primary or metastatic samples collected from naïve or pretreated patients; additional lung XPDX models harboring uncommon EGFR mutations were also established. Resulting models were passaged and further developed until growth stabilization. Resulting models were characterized using histopathology, WES and RNA_{seq} and in vivo drug sensitivity studies. For in vivo studies, single agent osimertinib or afatinib were evaluated at standard treatment regimens. Study endpoints included tumor volume and time from treatment initiation with %T/C values and tumor regression reported at study completion.
Results: Histopathology confirmed models as similar to patient in most cases. Sequencing identified EGFR co-mutations including T790M, C797S, and several uncommon mutations including D761Y (ST5185B), Y801C (ST6984), G863C (STM225C), and an A767ASVG inframe insertion (ST6963). Several EGFR 19del and L858R-mutated models from naïve patients were sensitive to osimertinib or afatinib while most models from patients treated with one or more EGFR inhibitors were resistant to single agent therapies. ST5185B, ST6963, and STM225C were insensitive to either therapy; however, afatinib but not osimertinib was active towards ST6984.
Conclusion: We have established and characterized a panel of EGFR-mutated lung XPDX models representing naïve, chemotherapy, and targeted therapy-resistant patients. These models can be utilized as a valuable tool in better understanding EGFR-mutated lung cancer.

#6075 Lentiviral vector induced modeling of low grade glioma in the minipig spinal cord.

Kecheng Lei[1], Angeliki Mela[2], Thais Federici[1], Muhibullah S. Tora[1], Marybeth Yonk[1], Yuliya Lakhina[1], Brett Henshey[1], Melissa Danielle Babbitt[1], Roy Raheb Khelo[1], Jeffrey N. Bruce[2], Peter Canoll[2], Nicholas M. Boulis[1]

[1]Emory University, Atlanta, GA,[2]Columbia University, New York, NY

Gliomas represent a diverse spectrum of central nervous system tumors, ranging from aggressive high-grade gliomas (HGG) to less aggressive low-grade gliomas (LGG). Our group previously developed a high-grade glioma model in the minipig spinal cord using PDGFB, HRAS, and TP53. We now report the development of a minipig low-grade glioma model. Lentiviral vectors gene expression of PDGFB, BRAF V600E, and TP53 were used to generate the low-grade glioma model. Disease progression was monitored through behavioral assessment, MRI imaging for lesion detection, and histopathological analysis. Unlike the previously characterized high-grade phenotype, these models demonstrated a distinct, less aggressive low-grade phenotype. Both groups developed spinal cord lesions with divergent histological features: Group 1 (PDGFB + shTP53) displayed diffusely infiltrative gliomas with uniform tumor cells, edema, and minimal necrosis, while Group 2 (PDGFB + BRAF V600E + shTP53) exhibited heterogeneous lesions combining diffuse gliomatous and spindle cell components with increased atypia, apoptosis, and greater axial involvement. These spindle cells appear to originate from myeloid rather than glial lineage. This work establishes the first minipig low-grade glioma model, providing a clinically relevant large animal system for investigating low-grade glioma biology and developing novel therapeutic interventions for spinal cord tumors.

#6076 Preclinical models of cancer cachexia: Bridging the gap to clinical applications.

Hongyan Sun, Dan Zhou, Yunlong Jiang, Yujing Zhang, Jianming Xu, Jing Zhao, Xiang Gao

GemPharmatech Co., Ltd., Nanjing, China

Cancer cachexia (CC) is a multifactorial syndrome affecting up to 80% of advanced cancer patients. Characterized by unintentional weight loss, skeletal muscle wasting, and fat depletion, CC significantly impairs quality of life, treatment tolerance, and patient survival. Despite its prevalence, effective therapeutic options remain limited, underscoring the urgent need for preclinical models that closely mimic clinical symptoms to support drug development. Towards this end, we developed and validated a CC preclinical model with HT-1080 xenograft in NCG mice, which demonstrated hallmark CC features, including body weight loss, fat and muscle loss, as well as impaired physical performance. The tumor-bearing mice also displayed elevated hGDF15 levels (undetectable in non-tumor-bearing (NTB) mice), and significantly reduced cumulative food intake. In this study, we used Ponsegromab (anti-GDF15 monoclonal antibody) as a positive treatment for CC starting when mice had lost ~7% body weight. At the end of the study, mice in hIgG1-treated control group suffered over 15% body weight loss, while the Ponsegromab treatment restored body weight to baseline levels. Although Ponsegromab treated mice remained lighter than NTB PBS controls, our data suggested that Ponsegromab treatment could significantly improve food intake and increase survival rates. Fat and muscle tissue weights, including gonadal, peri-renal, and inguinal subscapular white fat, as well as gastrocnemius and soleus muscles, were significantly reduced in the hIgG1-treated control group compared to baseline controls. Ponsegromab treatment preserved fat and muscle weights to levels similar to the baseline group. Motor function assessed via rotarod performance, and grip strength showed coordination and strength impairments in tumor-bearing mice, while Ponsegromab significantly improved grip strength and physical performance in comparison to the hIgG1-treated control group. In conclusion, our validated preclinical cachexia models closely align with clinical CC manifestations, providing a robust platform for the evaluation of novel therapeutic strategies. These models enable detailed exploration of CC mechanisms and support the development of effective interventions to mitigate cachexia and improve patient outcomes.

#6077 A natural antibody response associated with improved survival of SCLC patients can be actively induced in a SCLC mouse model and leads to significantly improved survival.

Diego Alejandro Velarde[1], Joseph Valdes[2], Chunli Yan[1], Sarah Elmalh[3], Hannah Lee[4], Daniel James Mullen[3], Angie Moreno[1], Matthew A. Gladstone[3], JONATHAN CASTILLO[5], Crystal N. Marconett[6], Nicky Nie[3], Ming Li[3], W. Martin Kast[7], Ite A. Offringa[1]

[1]USC/Norris Comprehensive Cancer Center, Los Angeles, CA,[2]University of California San Diego, San Diego, CA,[3]USC - University of Southern California, Los Angeles, CA,[45]City of Hope Beckman Research Institute, Duarte, CA,[6]Beckman Research Institute of The City of Hope, Glendale, CA,[7]Keck School of Medicine of USC, Los Angeles, CA

BACKGROUND: Small cell lung cancer (SCLC) has a 5-year survival of 8%, killing over 20,000 Americans annually. New therapies are urgently needed. ~15% of SCLC patients exhibit a natural “anti-Hu” antibody response against ELAVL4 and show improved response to therapy with significantly better survival. Rare SCLC patients develop a severe and sometimes lethal autoimmune response to ELAVL4 and can show complete SCLC regression. We determined that the antigenic epitope consists of ELAVL4 that is isoaspartylated in its unstructured N-terminal region (aa 1-38). Isoaspartylation is an immunogenic type of protein damage that is normally repaired but appears to be abnormally present in ELAVL4 in SCLC. IsoAsp-ELAVL4 constitutes a cancer-specific neo-antigen. ELAVL4 has been shown to be expressed on the outside of SCLC cells. In rare cases the anti-ELAVL4 antibody response can lead to autoimmunity through epitope spreading.
METHODS: Here we tested whether actively inducing an immune response against recombinant isoaspartylated Elavl4 (isoAsp-Elavl4) in a mouse SCLC model improves survival. We used a $Trp53^{fl/fl}$; $Rb1^{fl/fl}$ inducible SCLC mouse model to examine: 1) Whether immunization with isoAsp-Elavl4 prior to SCLC induction is protective, and 2) Whether immunization with isoAsp-ELAVL4 following completion of cisplatin+etoposide therapyincreases survival. Mice were immunized with a recombinant N-terminal fragment of Elavl4 (isoAsp-Elavl4, aa 1-117) generated in Clear Coli and incubated under isoaspartyl-inducing conditions (7 days in PBS at 37°C), then emulsified in incomplete Freund’s adjuvant (IFA). The negative control was PBS in IFA; Elavl4 naturally undergoes isoaspartylation even after short periods under physiological conditions, preventing its use as a negative control. The trajectories of mice were closely monitored with a detailed body metric score, and serum was collected from blood draws every 2 weeks to monitor the anti-Elavl4 antibody response. The tumor immune microenvironment of ELAVL4 and control-immunized mice was examined using Visium HD spatial transcriptomics.
RESULTS: ELISA data showed that all isoAsp-Elavl4-immunized animals became immune responsive against isoAsp-Elavl4, and just as in human SCLC patients, a small fraction of control-immunized animals spontaneously developed anti-Elavl4 reactivity. Immunization alone before SCLC induction in the absence of chemotherapy did not improve survival. In contrast, immunization following cisplatin+etoposide therapy significantly increased survival ($p < 0.001$). Visium HD analyses will be presented.
CONCLUSIONS: An immune response against isoAsp-Elavl4 can be actively induced, and when given after chemotherapy can significantly improve SCLC survival in a mouse model. We are leveraging these observations for the development of a new SCLC therapy.

#6078 Integrating patient-derived systems to model metastatic prostate cancer and decode therapy resistance.

Agustina Sabater[1], Pablo Sanchis[2], Jun Yang[3], Jiabin Dong[3], Peter Shepherd[3], Nicolas Anselmino[3], Christopher J. Logothetis[3], Geraldine Gueron[4], Estefania Labanca[3]

[1]Universidad de Buenos Aires (UBA) - IQUIBICEN - CONICET - Universidad Argentina de la Empresa (UADE), CABA, Argentina. UT MD Anderson Cancer Center, Houston, TX, [2]Universidad de Buenos Aires (UBA) - IQUIBICEN - CONICET - Universidad Argentina de la Empresa (UADE), Buenos Aires, Argentina, [3]UT MD Anderson Cancer Center, Houston, TX, [4]Universidad de Buenos Aires (UBA) - IQUIBICEN - CONICET, Buenos Aires, Argentina

Prostate cancer (PCa) lethality is driven by treatment-refractory disease and skeletal metastases, yet progress in understanding these processes has been hindered by the lack of physiologically relevant models. To address this gap, we developed an integrated platform of MD Anderson PCa Patient-Derived Xenografts (MDA PCa PDXs) and PDX-derived organoids, that recapitulate the heterogenous biology of advanced PCa. These models enable genetic manipulation and mechanistic interrogation of metastasis, therapeutic resistance and microenvironment influence. Our PDX series comprises over 150 models with molecular characterization. When engrafted intrafemorally, these models reproduce hallmark osteogenic phenotypes observed clinically, as monitored by multi-modal imaging and bone histomorphometry analyses. Particularly, MDA PCa PDX 118b, a double-negative PDX, generates bone even when injected subcutaneously. Moreover, we performed intracardiac injections of luciferase engineered cell lines and PDXs. This approach allowed us to explore their metastatic potential and tropism using *in vivo* imaging systems (IVIS), providing a model to study therapeutic approaches that could mitigate progression. Through cross-species molecular profiling and spatial analysis, we contrasted subcutaneous and intrabone tumors. This revealed how epithelial-stromal interactions and transcriptional reprogramming at the bone-tumor interface drive niche-specific adaptations. Building on these observations, we investigated molecular drivers of skeletal colonization. We have previously identified Fibroblast Growth Factor Receptor 1 (*FGFR1*) signaling as a key driver of skeletal colonization. Thus, we tested Erdafitinib, a pan-FGFR inhibitor, using intrabone PDX models with different FGFR status. We observed significant changes on both tumor growth and, mainly, in bone compartment architecture, highlighting the importance of the metastatic niche in supporting tumor growth. Beyond skeletal colonization, we also sought to model relapse trajectories. Using relapsed PDXs, we uncovered metabolic rewiring upon castration resistance, including enhanced ketone body utilization. In our *in vitro* and *in vivo* models, targeting the ketogenic enzyme ACAT1 emerged as a promising strategy to counteract therapy-induced metabolic plasticity. Together, these therapeutic insights complement our platform's broader utility. Collectively, these models bridge clinical observations with experimental systems, enabling functional studies of metastatic tropism and therapeutic escape. The combination of PDXs, organoids, different engraftment approaches, and in vitro studies, integrated with ongoing clinical feedback, iteratively refines experimental strategies and enhances model accuracy of disease complexity.

#6080 Multi-omics analysis revealed clonal evolution of sarcoma patient-derived xenografts.

Kentaro Gosho[1], Shigehiro Yagishita[1], Kaito Mimura[1], Takahiro Ebata[2], Nobuyuki Kakiuchi[3], Kotoe Katayama[4], Seiya Imoto[4], Yoshitaka Narita[5], Akihiro Yoneda[5], Mitsuya Ishikawa[5], Yukihide Kanemitsu[5], Kan Yonemori[5], Akira Kawai[5], Shun-ichi Watanabe[5], Ayumu Arakawa[5], Toshikazu Ushijima[2], Seishi Ogawa[3], Akinobu Hamada[1], Kenichi Yoshida[1]

[1]National Cancer Center Research Institute, Tokyo, Japan,[2]Hoshi University, Tokyo, Japan,[3]Kyoto University Graduate School of Medicine, Kyoto, Japan,[4]The University of Tokyo, Tokyo, Japan,[5]National Cancer Center Hospital, Tokyo, Japan

Patient-derived xenografts (PDXs) are used in translational research and are particularly valuable for studying rare cancers such as sarcomas. Although it is critical to understand how accurately they reflect the genetic and phenotypic features of the original tumor, comprehensive analyses that access changes in both single-nucleotide variants (SNVs) and copy number variants (CNVs) during the establishment and passaging of PDXs remain scarce. In addition, as previous studies have focused on those derived from early-stage tumors or major cancer types, it remains unclear how genomic features are preserved in PDXs derived from advanced, treatment-resistant sarcomas.

Here we performed whole-exome sequencing, RNA-seq and DNA methylation analysis of 144 sarcoma PDXs established from 39 patients, along with their matched primary tumors when available. The cohort was enriched for highly recurrent cases (n = 29) and included not only major sarcoma types, such as osteosarcoma (n = 11), but also ultra-rare sarcomas, including alveolar rhabdomyosarcoma (n = 4) and *CIC*-rearranged sarcoma (n = 2). PDXs were successfully established from a wide range of molecular subtypes, including fusion-driven tumors, *TP53*-mutated cases, and hypermutated types associated with microsatellite instability. Targetable genomic alterations, including amplifications of *CCNE1* or *MDM2* and deletions of *MTAP*, were identified in 55% of cases. Several PDXs harbored mutations associated with resistance to molecular targeted agents and immunotherapies.

The vast majority of somatic alterations detected in the primary tumors were retained in the PDXs (97% for SNVs, 99% for CNVs). Moreover, mutational signature analysis suggested that mutations detected exclusively in PDXs likely represent low-frequency mutations already present in the original tumors. Extrachromosomal DNAs involving oncogenes such as *MYC*, *CDK4*, and *MDM2* were also identified in 28% of PDXs and were retained in 83% of cases during serial PDX passaging. Despite overall genomic stability, clonal architecture changed during establishment and passaging, with highly diverse patterns, and clonal shifts were observed in 53%, 65%,71% of cases based on SNVs, CNVs, and both combined, respectively. Interestingly, clonal shifts were observed in all models derived from diagnostic samples (n = 9) and primary tumors (n = 8), which was much more frequent than in models derived from relapsed or metastatic tumors (62%). In addition, gene expression and methylation clustering revealed distinct clusters within each cancer type and individual cases, suggesting that key tumor characteristics were preserved during PDX establishment and passaging.

Our data reveal the genetic and phenotypic stability of sarcoma-derived PDX models during their establishment and passaging, and provide new insights into their clonal evolution, which we believe will contribute to the clinical utility of PDX models.

#6081 Development of a lung cancer orthotopic transplantation model for investigating the TME and evaluating anticancer agents for preclinical studies.

Chiyoko Nishime, Eiko Nishinaka, Hitomi Satou, Toshio Imai, Masayuki Komatsu, Misa Mochizuki, Taichi Yamamoto, Masami Suzuki

Department of Development Research, Central Institute for Experimental Medicine and Life Science, Kawasaki, Japan

Heterotopic subcutaneous (SC) tumor transplantation models are widely used in cancer research owing to their technical simplicity and ease of tumor monitoring. However, these models fail to recapitulate the native tumor microenvironment (TME). To overcome this limitation, we developed a bronchoscopy-based orthotopic (ORT) lung cancer model in mice and compared its TME and drug response with those of the SC model.Three luciferase-expressing lung adenocarcinoma models were used: A549-Luc, RERF-LC-KJ-Luc, and LC-58-Luc (a cell line derived from a patient-derived xenograft, CIEM-established). In the ORT model, 3% lauryl-10 solution was administered via bronchoscopy to the left lung lobule three days prior to transplantation, followed by instillation of 1×10^5 cells in 20 µL medium containing 10% Matrigel. SC tumors were established by subcutaneous injection of the same cells (1×10^5 cells in 100 µL with 50% Matrigel). Tumor growth was monitored via bioluminescence (ORT) or caliper measurements (SC). Mice received carboplatin (CBDCA, 50 mg/kg, i.p., 3 doses at 5-day intervals) and paclitaxel (PTX, 15 mg/kg, i.p., 5 doses at 3-day intervals). VEGF inhibitor combination chemotherapy was also evaluated. RNA sequencing was performed using 150 bp paired-end NovaSeq, with the reads processed using TrimGalore, Xenogsort, STAR, and RSEM. The human–mouse interactome was analyzed using MultiNicheNet. CBDCA and PTX showed significant antitumor effects in both SC and ORT models. In the SC tumors, combination chemotherapy with the VEGF inhibitor significantly reduced the number of mCD31-positive endothelial cells, which is consistent with the anti-angiogenic response. By contrast, no such effect was observed in the ORT tumors, highlighting the TME-dependent differences in vascular responses. RNA sequencing showed ORT-specific upregulation of surfactant genes (*SFTPA1*, *SFTPB,* and *SFTPC*), indicating lung-specific adaptation. MultiNicheNet analysis revealed ORT-enriched ligand–receptor pairs linked to perineural invasion and adhesion, underscoring enhanced host–tumor crosstalk. This ORT model better mimics clinical TME dynamics and enables a more translationally relevant evaluation of anticancer agents.
Bronchoscopy-based ORT lung cancer models recapitulate physiologically relevant tumor–host interactions and TME-dependent drug responses. By incorporating VEGF inhibitor response and transcriptomic profiling, this model provides a better preclinical platform for evaluating antitumor agents and improving translational predictability compared with SC models.

#6082 IFNα polarizes granulocytic MDSCs from neutrophils by inducing protein translation.

Juanita L. Merchant, Lin Ding

Medicine, Univ. of Arizona Health Sciences Ctr., Tucson, AZ

The extensive heterogeneity in the tumor immune microenvironment is a problem plaguing immune-based treatment failures for solid tumors because it prevents defining the specific vulnerabilities of the various cells to develop treatments with greater precision. Myeloid-derived suppressor cells (MDSCs) are a heterogenous collection of immunosuppressive monocytes and granulocytes (neutrophils) whose link to poor cancer survival is not well understood. Most MDSCs exhibit features of immature granulocytes (Gr-MDSCs) and exert their T cell suppression by secreting reactive oxygen and nitrogen species (RONS). Gr-MDSCs can survive for days by recruiting mechanisms to protect protein translation despite generation of RONS. One MDSC subtype of interest is defined by their polarization in response to type 1 interferon (IFNα) that we previously identified in chronic *Helicobacter*-infected mice with gastric metaplasia, suggesting that a *Helicobacter*-infected stomach polarizes neutrophils to acquire an immunosuppressive phenotype. We hypothesize that IFNα initiates neutrophil reprogramming by increasing protein synthesis required to alter their metabolic activities as they acquire the Gr-MDSC phenotype. We performed scRNA-Seq on biopsies from 5 groups of patients referred for endoscopy and showed no gastric abnormalities, were *H. pylori*+ (Hp), had intestinal metaplasia (IM) or gastric adenocarcinoma (GAC) and identified that the IFN-polarized MDSC population initially present in IM increased substantially in GACs but was not detected in normal and *Hp*-infected patients, confirming the polarization of IFN-polarized Gr-MDSCs once IM appears. We showed that the IFN-polarized Gr-MDSCs re-programmed from neutrophils in vitro and required induction of protein translation. To analyze translation, we treated primary cultures of granulocytes from mouse bone marrow or human PBMCs with IFNα and quantified protein translation by flow cytometry after incubating the cultures with 20μM O-propargyl-puromycin (OPP) and proliferation with EdU. In vivo analysis was performed by administering OPP to mice before euthanization. In the in vitro neutrophil cultures, about 28% of the polarized neutrophils were $CD11b^{+}Gr\text{-}1^{+}$ MDSCs, and 85% of these Gr-MDSCs induced their protein synthesis coincident with increased proliferation. scRNA-Seq analysis of both mouse and human gastric tissues demonstrated induction of mediators of the unfolded protein response (UPR), e.g., CHOP. In summary, polarization of Gr-MDSCs by type 1 IFNs from neutrophils requires induction of protein translation, revealing possible metabolic pathways that may be targeted to reprogram the immunosuppressive tumor microenvironment.

#6083 Intracarotid injection-based brain metastasis models without disrupting the blood-brain barrier for preclinical drug evaluation.

Arianna Bandini[1], Gojko Bijelic[2], Melanie Heisler[2], Pia Norz[2], Philipp Metzger[2], Cynthia Obodozie[2], **Holger Weber**[2]

[1]Department of Translational Research and New Technologies in Medicine and Surgery, University of Pisa, Pisa, Italy,[2]Reaction Biology Europe GmbH, Freiburg, Germany

Brain metastases are one of the most common and serious complications of solid tumors, affecting 20-40% of patients. They are common in lung, breast, and melanoma cancers and are associated with a poor prognosis and limited treatment options. Key challenges include the blood-brain barrier (BBB), which restricts penetration of many therapeutic agents, and the brain's historically immune-privileged status, limiting immune responses against tumor cells. Establishing in vivo models that accurately replicate the natural metastatic process to the brain is essential for understanding disease mechanisms and advancing therapeutic research.

Most current preclinical brain metastasis models rely on intracranial implantation of tumor cells directly into the brain or systemic delivery via intracardiac injection. Although intracranial implantation enables rapid local tumor formation, this approach disrupts the BBB integrity and limits physiological relevance for studying natural metastatic progression and evaluating compounds with specific BBB-crossing properties. In contrast, intracardiac injection allows systemic dissemination of tumor cells and can lead to brain metastases in ~50% of cases using MDA-MB-231 cells and 70%-80% using JIMT-1 cells while likely preserving BBB integrity. However, these models are limited by suboptimal brain metastasis rates or early euthanasia due to aggressive extracranial tumor growth, hindering study of brain-specific disease progression over time.

In this study, we present a more physiologically relevant brain metastasis model based on intracarotid injection. This approach enhances the targeted delivery of tumor cells to the brain while preserving BBB integrity, increasing translational relevance. We report take rate and intracranial tumor growth kinetics of human breast cancer cell lines following intracarotid injection and compare these outcomes with those from conventional intracardiac injection. The intracarotid technique yields a high rate of brain metastasis and confines tumor growth to the brain region. To further validate the model, we evaluate efficacy of standard-of-care (SOC) therapies within this system, providing insights into therapeutic responsiveness under conditions closely mimicking clinical scenarios. Additionally, we present data on the growth of 4T1 syngeneic tumor cells in the brain, enabling the study of immune-tumor interactions in an immunocompetent host. This syngeneic model adds another dimension by allowing exploration of immunological mechanisms and testing of immunotherapies in a controlled, biologically relevant setting.

In conclusion, these findings suggest that the intracarotid injection model is a valuable tool for preclinical evaluation of novel therapies targeting brain metastases.

: Mechanisms of Metastasis
Poster Session

#6087 SOX2-LGR5 signaling mediates ovarian cancer cell survival in response to loss of anchorage..

Shriya Kamlapurkar[1], Amal T. Elhaw[2], Mythreye Karthikeyan[3], Nadine Hempel[1]

[1]University of Pittsburgh School of Medicine, Pittsburgh, PA,[2]Penn State University, Hershey, PA,[3]University of Alabama at Birmingham, Birmingham, AL

Ovarian cancer (OVCA) primarily metastasizes through the transcoelomic route, where tumor cells detach, passively disseminate through the peritoneal cavity and establish metastatic niches in the abdominal cavity. A feature of transcoelomic spread is the development of malignant ascites, which is characterized by tumor cells that adapt to survive anchorage-independence (a-i) by evading detachment-induced cell death, known as anoikis. Malignant ascites are frequently observed in advanced stage and recurrent patients and are associated with tumor aggressiveness and therapy resistance. We previously reported that OVCA cells manipulate their transcriptomic profile to promote the expression of anoikis resistance genes in a-i and identified SOX2 as a key detachment-responsive transcription factor necessary for OVCA cell survival in a-i and metastasis. However, the key factors downstream of SOX2 transcriptional regulation in a-i remain unknown. Here, we identified the leucine-rich G-protein coupled receptor, LGR5, as a novel SOX2 regulated gene that is specifically under the control of SOX2 in a-i conditions. LGR5 is a marker of cancer stemness known to promote cancer cell motility, epithelial-to-mesenchymal transition, and tumor formation by potentiating Wnt signaling upon binding with its ligand, R-spondin1 (RSPO1), which is abundant in OVCA ascites. We demonstrate that LGR5 expression is critical for OVCA cell a-i survival. Interestingly, the effects of LGR5 are not driven via canonical Wnt/beta-catenin signaling but are associated with widespread transcriptional repression. In addition, we find that LGR5 knock-down leads to upregulation Wilms' Tumor-1 (WT1) regulated transcription. These studies show for the first time that SOX2 has context specific functions as a transcription factor in a-i conditions, and that OVCA cells may compensate for inhibition of SOX2 or LGR5 by upregulating WT1 signaling. Current studies are focused on understanding the SOX2-LGR5-WT1 regulatory axis further and its impact on driving ovarian cancer cell survival and metastasis. In addition, using transcriptomics and CUT&RUN sequencing analysis we are exploring the context-specific SOX2 transcriptome and role of SOX2 on the epigenome in a-i. Although SOX2 remains a hard-to-drug target in cancer, identifying novel downstream pathways facilitating a-i survival and potential resistance mechanism to SOX2 inhibition are critical for therapeutic targeting of metastatic disease.

#6088 USP15 promotes ovarian cancer progression by modulating cell cycle checkpoints and DNA damage signaling.

Ayokunnumi Sewanu Ogunsanya, Noel Amadu, Achuth Padmanabhan

Biology, University of Maryland, Baltimore County, Baltimore, MD

Ovarian cancer remains one of the deadliest gynecologic malignancies and the sixth leading cause of cancer-related death among women in the United States. Poor clinical outcomes are largely driven by late diagnosis and limited therapeutic options for metastatic disease. Therefore, there is an urgent need to identify molecular drivers of ovarian cancer progression and develop strategies to target them. Analysis of tumor gene expression datasets revealed that the deubiquitinase USP15 is significantly upregulated in metastatic ovarian tumors compared to normal tissues. Elevated USP15 expression also correlates with decreased progression-free survival in patients. Although USP15 has been shown to promote tumorigenesis in several cancer types, its role and the mechanisms regulating its levels in ovarian cancer remain poorly understood.

We hypothesize that elevated USP15 promotes ovarian cancer progression and metastasis, and that its depletion sensitizes tumors to chemotherapeutic agents. To test this, we generated stable USP15 knockdown ovarian cancer cell lines and assessed metastatic properties using in vitro assays and in vivo xenograft models. Mechanistic studies examined cell-cycle and DNA damage responses via flow cytometry and western blotting.

USP15 knockdown significantly reduced cell proliferation, migration, and invasion of ovarian cancer cells. In xenograft models, USP15 depletion suppressed metastasis, confirming its role in promoting ovarian tumor progression. Cell-cycle analysis revealed a G2/M arrest phenotype in USP15-depleted cells, consistent with impaired cell-cycle progression or checkpoint activation. Western blotting also showed altered expression of key cell-cycle regulators and increased activation of DNA damage markers.

Collectively, these findings indicate that USP15 regulates ovarian cancer cell-cycle progression, checkpoint control, and DNA damage responses. Targeting USP15 may therefore represent a promising strategy to inhibit ovarian tumor progression and metastasis.

#6089 Comprehensive analysis of NR2F2 functions during tumor initiation and progression in a genetically engineered mouse model of high-grade serous ovarian carcinoma.

Miranda Mansolf[1], Danqi Liao[2], Samantha Goncalves Novo[1], Tobias M. Hartwich[1], Jasmine Jathan[1], Kevin Yang[1], Viktoriia Kolesnyk[1], Smita Krishnaswamy[2], Yang Yang-Hartwich[1]

[1]Yale School of Medicine, New Haven, CT,[2]Yale University, New Haven, CT

High-grade serous ovarian carcinoma (HGSOC) is often diagnosed at late stages when tumors have metastasized in the peritoneal cavity. We know HGSOC can originate from fallopian tube secretory epithelial cells, yet the molecular and cellular processes controlling tumor metastasis from the origin are still unclear. Using a genetically engineered mouse model (GEMM) and patient-derived cell lines, we aim to understand the molecular mechanism of tumor progression and metastasis in HGSOC with a focus on the orphan nuclear receptor NR2F2, which was identified as a potential transcriptional regulator in a subpopulation of fallopian tube secretory epithelial cells with tumor forming ability. Inhibition of NR2F2 has shown therapeutic effects in prostate and breast cancer preclinical models. A better understanding of NR2F2 functions in HGSOC is a critical step in developing therapeutic approaches to target oncogenic NR2F2.

Method: Distal oviducts collected from BPRN mice at different timepoints of ovarian tumor formation (2, 4, 6, and 8 months) were analyzed using single cell RNA-sequencing and deep learning AI tools (PHATE and MIOFlow). Bulk RNA sequencing was subsequently used to evaluate gene expression changes in murine and human ovarian cancer cell lines expressing inducible shRNA targeting NR2F2 or scramble shRNA. Co-immunoprecipitation and mass spectrometry (Co-IP/MS) were performed to identify NR2F2-interacting proteins in human ovarian cancer cells overexpressing NR2F2 or treated with a small molecule inhibitor of NR2F2. Chromatin immunoprecipitation sequencing (ChIP-seq) was used to characterize genes and related pathways regulated by NR2F2 and its co-factors.

Result: Trajectory analysis of single cell RNA-sequencing data identified that NR2F2 and its target genes are enriched in a subpopulation of oviduct epithelial cells. The upregulated NR2F2 pathway is associated with tumor development and gene signatures of metastasis. Bulk RNA sequencing of human and mouse cancer cell lines with inducible NR2F2 knockdown demonstrated that NR2F2 regulates signaling pathways involved in cell cycle, cytokine signaling, and extracellular matrix/integrin interactions. Co-IP/MS results show that NR2F2 interacts with several key regulators of tumor progression including PARP1, beta-catenin, and menin 1. ChIP-seq results identified genes directly regulated by NR2F2 and its co-factors.

Conclusion: Through comprehensive analyses of NR2F2 functions in the GEMM, we identified genes and co-transcriptional factors that are regulated by NR2F2. This knowledge will advance our understanding of NR2F2's role in regulating HGSOC initiation and metastasis from the fallopian tubes. Our findings support the rationale of evaluating the therapeutic potential of NR2F2 inhibitors in preventing metastatic recurrence after debulking surgery.

#6090 Characterization of eIF3h as a driver of triple negative breast cancer progression.

Tiffany J. Rios-Fuller

Ponce Health Sciences University, Ponce, PR

Background: Triple-negative breast cancer (TNBC) has a worse prognosis than other breast cancer subtypes, leading to a 5-year relative survival rate of just 15% if metastasized. TNBC is aggressive and challenging to treat, as it lacks estrogen, progesterone, and HER2 receptors. It also exhibits a high rate of proliferation and chromosome instability and is extremely metastatic. Unfortunately, there are limited effective therapy options for TNBC. In breast and other cancers, tumor cells often alter how they translate genetic signals from mRNA into proteins, allowing them to adapt and become more aggressive. This understudied mechanism is crucial for continuous cell proliferation, survival under physiologic stress, and metastasis. Eukaryotic translation initiation factors (eIFs) are among the master players of protein synthesis and are involved in the formation of large pre-initiation complexes (PICs) containing 40S ribosome subunits and mRNA. PICs, including the eIF3 complex, specifically eIF3h, are involved in mRNA translation and regulate the key processes of translation initiation, including recruitment and disassembly of ribosomes. In metastatic breast tumors, eIF3h is up-regulated, and it forms the basis of cell growth and survival; nevertheless, inhibition decreases cell viability and inhibits colony formation. Nonetheless, its specific function in TNBC metastasis remains relatively unexplored, suggesting that inhibiting eIF3h function may be a potential therapeutic target.
Objective/Hypothesis: We hypothesize that increased expression levels of eIF3h are the primary driver of TNBC progression and metastasis, resulting from the activation of oncogenic pathways that promote high-grade TNBC growth, leading to poor overall, relapse-free, and metastasis-free survival.
Results: Unpublished preliminary data support this hypothesis. First, survival analyses performed on several large public datasets (GEO, EGA, TCGA) show that high eIF3h expression correlates with reduced overall survival ($p = 0.0038$), distant metastasis-free survival ($p = 0.018$), and relapse-free survival ($p = 0.0012$). Second, transcriptomic data from normal, tumor, and metastatic breast tissues (GDC, GTEx, GEO) revealed significantly increased eIF3h expression in both tumors and metastases ($p < 0.0001$). Third, genomic profiling conducted using cBioPortal (TCGA) identifies repeated co-alterations in eIF3h-high tumors that modulate the action of anti-apoptotic, autophagic, cell cycle progression, angiogenic, and epithelial-to-mesenchymal transition (EMT) pathways, which mediate tumor progression and metastasis.
Conclusions: These findings collectively demonstrate that eIF3h overexpression is a significant negative prognostic risk factor and a contributor to TNBC progression, therapy resistance, and metastasis through the induction of a potent regulatory mechanism for oncogenic translation.

#6091 Neuronal architect Pax6 orchestrates stemness and brain metastatic progression.

Laiba Anwar[1], Asad Ur Rehman[1], Md Arafat Khan[1], Mohammad Abbas Ali Zaidi[1], Zahraa Wajih Alsafwani[1], Nivedeta Krishna Kumar[1], Mahek Fatima[1], Aatiya Ahmad[1], Parvez Khan[1], Moorthy P. Ponnusamy[1], Metin Uz[2], Juan A. Santamaria-Barria[3], Surinder K. Batra[1], Mohd Wasim Nasser[1]

[1]Biochemistry and Molecular Biology, University of Nebraska Medical Center, Omaha, NE,[2]Chemical and Biomedical Engineering, Cleveland State University, Ohio, OH,[3]Department of Surgery, Division of Surgical Oncology, University of Nebraska Medical Center, Omaha, NE

At the time of breast cancer (BC) diagnosis, many patients have already seeded disseminated tumor cells in the brain, where these cells can persist in a dormant, clinically silent state for years before reactivating to form devastating brain metastasis (BrM). The molecular programs and signals that enable dormant cells to awaken in the neural microenvironment remain an area of limited understanding. Yet this transition is thought to rely heavily on the acquisition of stem cell-like properties. To decipher its mechanism, we performed integrative analyses of publicly available paired primary tumor and brain metastatic transcriptomic patient datasets to identify genes that may be involved in neuronal mimicry. We identified Pax6 as one of the most consistently upregulated genes in metastatic lesions, which was further confirmed through BCBrM tissue microarray. Pax6 is a key neuronal developmental transcription factor that orchestrates CNS specification and sustains neural stem cell identity during embryogenesis. Functional studies using CRISPR/Cas9-mediated Pax6 knockout (KO) in BCBrM cell lines revealed profound reductions in proliferation, migration, and wound closure. Pax6 loss also diminished core stemness programs, including suppression of OCT4, NANOG, and KLF4 expression, diminished CD44+/CD24- tumor initiating cell populations, and impaired mammosphere formation and side populations, a phenotype consistent with a collapse of stem-like potential. Consistently, genes previously linked to BrM were elevated upon Pax6 overexpression (OE) in primary BC cells and were downregulated in Pax6 KO models, further supporting Pax6 as an upstream regulator of BrM - associated transcriptional programs. To critically examine if the observation holds true in preclinical setting, we performed intracardiac injection of Pax6 KO BrM cells in athymic nude mice. We observed that Pax6 KO cells failed to form significant brain macro metastasis, demonstrating the importance of Pax6 in establishing BrM outgrowth. Conversely, Pax6 OE in primary BC cells induced a BrM-like phenotype with increased cell proliferation, migration, and induction of stemness-associated markers, supporting a causal role of Pax6 in promoting metastatic reprogramming. Together, these findings identify Pax6 as a developmental stem cell regulator hijacked by BC cells to escape dormancy and acquire the functional plasticity necessary for growth within the brain microenvironment. By showing that Pax6 plays a key role in driving BCBrM, this work highlights a potential targetable weakness and suggests that therapeutic targeting of Pax6 or its associated pathways may offer a new therapeutic strategy to limit brain metastatic progression and improve clinical outcomes.

#6092 STAT5 modulates STAT3 and the aggressive behaviors of triple negative breast cancer.

Alexandra E. Temple, Emily C. Armlin, **Sarah R. Walker**

University of New Hampshire, Durham, NH

Triple Negative Breast Cancer (TNBC) is an aggressive subtype of breast cancer that accounts for about 15-20% of cases and often has high rates of metastasis. Signal transducer and activator of transcription 3 (STAT3) is constitutively active and highly associated with TNBC. Alternatively, STAT5 expression is often lost or reduced in TNBC and metastasis. STAT5 activation in breast cancer is generally associated with more differentiated tumors and better response to therapies. Interestingly, breast tumors with concurrent activation of STAT3 and STAT5 generally have improved prognostic outlooks compared to tumors with activation of STAT3 alone, suggesting that STAT5 can attenuate some of the aggressive characteristics associated with STAT3 activity. Therefore, understanding how STAT5 can modulate these aggressive phenotypes associated with STAT3 could improve therapies for individuals with TNBC or metastatic breast cancer. STAT3 and STAT5 are latent transcription factors that reside in the cytoplasm. Upon phosphorylation of a specific tyrosine residue, these STATs can enter the nucleus and regulate transcription of target genes. To characterize STAT3 and STAT5 activity in breast tumor subtypes, activity scores were calculated for patients from the Cancer Genome Atlas. STAT3 activity was found to be highest in basal tumors, whereas STAT5 activity was lowest in basal tumors. Furthermore, epithelial to mesenchymal (EMT) scores were calculated for each patient using gene set variation analysis and STAT5 activity was negatively correlated with EMT. Additionally, relapse free survival was improved in patients with high levels of STAT5 and low levels of STAT3 in basal breast tumors. To determine if STAT5 directly modulated EMT and STAT3 in TNBC, a doxycycline-inducible constitutive STAT5 construct was introduced into the TNBC cell line, MDA-MB-231, which contains constitutively active STAT3. It was determined that constitutive STAT5 activation can reduce the viability of these cells. Moreover, preliminary results suggest that STAT5 can affect response to drug treatment and may modulate expression of certain genes involved in EMT. Lastly, in rare cases, breast cancer can metastasize to the peritoneal cavity. Using a mesothelial clearance assay adapted for breast cancer, we found that constitutive STAT5 activation in TNBC cells reduced mesothelial clearance, which is an important step in peritoneal metastasis. Moreover, activation of constitutive STAT5 and concurrent inhibition of STAT3 reduced mesothelial clearance with a greater effect compared to activation of STAT5 or inhibition of STAT3 alone. Therefore, activation of STAT5 can potentially reduce the aggressive behaviors of TNBC. These findings have potential implications in treating patients with TNBC and metastatic breast cancer.

#6093 Investigating the role of stress induced nuclear relocalization of SIPA1 in breast cancer metastasis.

Nirupama S. Kotian[1], Kent W. Hunter[2]

[1]Center for Cancer Research, National Cancer Institute, NIH, Bethesda, MD,[2]National Cancer Institute, Bethesda, MD

Breast cancer is the most commonly diagnosed cancer among women in the U.S., and metastasis is the leading cause of deaths in breast cancer patients. This disease presents with an 87.2% 5-year (2015-2021) survival rate in regional tumors which drops to 32.6 % in metastasized cancers. The goal of Hunter laboratory is therefore to understand the dynamics of cancer progression by identifying mechanisms of metastasis. In this study, we hypothesize that when breast cancer cells are under stress during metastasis, the relocalization of metastasis susceptibility proteins to the nucleus is essential for metastatic progression. Previous work in the laboratory revealed that metastasis susceptibility genes were present in the nucleolus, a central stress sensor. During stress, cytoplasmic proteins are sequestered in the nucleolus and the size of the nucleolus increases. We showed that SIPA1 (Signal Induced Proliferation-associated 1), one of the first metastasis susceptibility genes identified in the laboratory, relocalizes to the nucleus under stresses mimicking metastasis. SIPA1 is a mitogen-induced GTPase activating protein predominantly known to be present in the perinuclear region. However, SIPA1 can relocalize to the nucleus, a phenotype associated with poor prognosis in breast cancer patients. In current experiments, we observed that SIPA1 relocalizes to the nucleus in response to stress conditions like heat shock, nutrient deprivation, hypoxia and low dose chemotherapy drugs. This stress-induced relocalization is primarily in nuclear speckles, a splicing factor storage site, and partially in the nucleolus. Additionally, SIPA1 also binds to higher order repeats near the centromeric regions of multiple chromosomes. Through spectral karyotyping, we observed that knocking down SIPA1 in breast epithelial cells alters chromosomal stability. Future experiments involve assays to determine the mechanism of nuclear relocalization of SIPA1 under stress and proximity assays to identify the interacting proteins in the proximity of SIPA1. Revealing mechanisms that control the relocation of SIPA1 in the nucleus, will further clarify the pathways responsible for stress response in breast cancer cells during metastasis.

#6094 Caveolin-1 modulates stemness and chemosensitivity in triple negative breast cancer.

Shreya Pokharel[1], Naveen Chintala Ramulu[1], Biplov Sapkota[1], Dhirendra Pratap Singh[2], Abhishek Pandit[1], Shilpa Thota[1], Rizwana Begum[1], Shobhit Srivastava[3], Yuxio Yo[1], Shang Su[1], Dayanidhi Raman[3], Joseph Francis[1]

[1]Louisiana State University, Baton Rouge, LA,[2]Radiology and Imaging Science, Indiana University, Indianapolis, IN,[3]University of Toledo, Toledo, OH

Triple-negative breast cancer (TNBC) is the most aggressive subtype of BC, characterized by a therapy-refractory phenotype, higher propensity to early metastases, and worse prognosis. TNBC has a high expression of cancer stem-like cells (CSC), contributing to a poor clinical outcome. Notably, an upregulation of caveolin-1 (CAV-1), a major structural protein of caveolae within the plasma membrane, is associated with TNBC. In agreement, the Kaplan-Meier survival analysis predicted that patients with high CAV-1 expression have a significantly worse survival than those with low expression. Consistently, immunoblot analysis of PDX tumor samples revealed inter-tumor variation with high CAV-1 expression, supporting the role of dysregulated CAV-1 expression in TNBC progression. Previously, we have shown that CAV-1 knockout (Cav-1 KO) mitigated BC metastasis to the lungs via integrin alpha3 in a 4T1 syngeneic 4T1-murine model of TNBC. Upon further investigation, we observed a significant downregulation of pluripotent transcription factors such as SOX2, OCT-4, and NANOG when CAV-1 was depleted in mouse 4T1 and human SUM159PT cells. We hypothesized that CAV-1 regulates TNBC stemness through focal adhesion kinase (FAK)/ c-Myc signaling. Consistently, depletion of CAV-1 altered the levels of pY397FAK and c-Myc, confirming CAV-1-dependent suppression of CSC-like traits to be associated with FAK/c-Myc signaling. Next, we observed that CAV-1 KO cells exhibited enhanced chemosensitivity to paclitaxel (PTX) as compared to the corresponding 4T1 control cells (PTX IC_{50}: 24.51nM in Cav-1 KO vs 30.82nM in 4T1 at 48h). The observed chemosensitivity was due to the downregulation of multidrug resistant protein 1 (MRP1/ABCC1) and P-glycoprotein (ABCB1). Importantly, CAV-1 expression was significantly higher in PTX-resistant human Pac200 cells as compared to the naïve SUM159PT cells. Collectively, these findings indicate that CAV-1 loss impairs major drug efflux pathways and promotes chemosensitivity. Overall, our study proposed a putative role for CAV-1 in TNBC stemness and multidrug resistance through FAK/c-Myc dependent modulation of the stemness pathway and ABC efflux transporters. Therefore, targeting CAV-1 provides a therapeutic strategy to enhance chemotherapy efficacy and overcome drug resistance in TNBC. Since CAV-1 lacks enzymatic activity or ligand-binding pockets, small-molecule targeting may not be a feasible approach. Hence, selective degradation of Cav-1 by (CAV-1)targeting PROTAC offers an innovative first-in-class therapeutic strategy to abrogate cancer stemness and effectively treat metastatic TNBC.

#6095 Breast cancer metastasis to the liver; a new mouse model system.

Jesus Garcia-Lerena, **Eran Andrechek**

Michigan State University, East Lansing, MI

While 30% of breast cancer metastasis occurrs in the liver, the majority of genetically engineered mouse models only metastasize to the lungs. Using a bioinformatic approach and human TCGA data, we predicted genetic pathways that were involved in metastasis to other locations and examined these genes in mouse model systems. We repeatedly observed a role for the E2F5 transcription factor loss in metastasis. We therefore generated a conditional knockout of E2F5 in the mammary epithelium and this alone was sufficient for development of mammary tumors after a long latency that were highly metastatic, including metastases to the lymph, liver and lung among other sites. Using a serial transplantation approach, we enriched for either lymph or liver metastasis and examined these tumors through RNAseq to determine which genetic pathways were involved with liver specific metastasis. Our gene expression analysis revealed a concerted alteration to the primary tumor cells through multiple mechanisms, both metabolomic and genetic, to allow the tumor cells to use the coagulation cascade to drive liver metastasis. We observed that the E2F5 transcription factor normally repressed several genes in the coagulation cascade and with the conditional knockout, these coagulation genes were derepressed. This resulted in a striking ability of these tumor cells to induce a fibrin clot in an *in vitro* clotting assay with human pooled plasma. However, expression of the clotting cascade genes alone is insufficient to induce a fibrin clot and we noted that the tumor cells could clot due to a negative charge on the membrane, were also positive for external phospholipids and had altered lipid uptake and reactive oxygen species. To definitively test whether clotting was essential for breast cancer liver metastasis, we treated mice with low molecular weight heparin as we implanted a metastatic tumor into the fat pad. In several lines, this resulted in a near complete blockage of liver metastasis. To test whether this treatment and pathway might also be functional in human cancer, we turned to the Truveta electronic health record data. This revealed that human pancreatic cancer patients that had been administered heparin for other reasons had a 40% reduction in liver metastasis rates. Thus, our work suggests that inhibition of the clotting cascade on the fibrin side may also be beneficial for prevention of breast cancer liver metastasis.

#6096 Characterization of a novel doxycycline inducible model of EZH2 overexpression in mammary glands.

Ahmad Eido[1], **Maria E. Gonzalez**[1], LiJyun Syu[2], Andrzej A. Dlugosz[3], Celina G. Kleer[4]

[1]University of Michigan, Ann Arbor, MI,[2]MM Dermatology, University of Michigan, Ann Arbor, MI,[3]Professor, Dept. of Dermatology, University of Michigan, Rogel Cancer Center, Ann Arbor, MI,[4]Harold A. Oberman Collegiate Professor, Dept. of Pathology, University of Michigan Medical School, Ann Arbor, MI

Background: Enhancer of Zeste Homolog 2 (EZH2) is a histone methyltransferase and catalytic subunit of the Polycomb Repressive Complex 2 (PRC2), responsible for trimethylating histone H3 at lysine 27 (H3K27me3). In human breast cancer, EZH2 overexpression is an independent prognostic marker and is significantly associated with negative ER and PR expression. However, the timing and functional significance of EZH2 overexpression in breast cancer development is still unclear. Towards this, we generated a conditional model of EZH2 overexpression to the mammary gland in FVB mice.

Methods: We generated a doxycycline-inducible transgenic mouse model MMTV-rtTA;TetO-EZH2 and appropriate controls in an FVB background to enable targeted overexpression of EZH2 within mammary epithelial cells. We administered doxycycline (2 mg/mL) in the drinking water to 10-week-old female mice for 96 hours and in chow for 6 months, to induce EZH2 overexpression. At this age, the mammary glands are mature. At study endpoints, mammary glands were resected and analyzed using whole-mount carmine alum staining to assess ductal architecture. Mammary glands were embedded in paraffin and studied by histopathology and immunostaining using anti-EZH2 antibodies.

Results: Induction of EZH2 expression in adult mice for 96 hours led to increased numbers of ductal branches compared to induced and uninduced controls. Long-term EZH2 induction also resulted in a hyperbranching phenotype and development of mammary epithelial nodules observed in carmine alum stains of whole glands, which were not present in the controls. Additional studies, including histopathological evaluation, immunostaining, and spatial analyses are underway to further characterize the biological and molecular consequences of EZH2 induction.

Conclusions: We present the development and initial characterization of a novel inducible EZH2 overexpression model in the mammary glands of adult mice. Preliminary studies show that EZH2 overexpression results in intraductal epithelial hyperplasia and ductal hyperbranching recapitulating human preneoplastic lesions. Future studies will combine this novel model with other breast cancer mouse models to explore the consequences of EZH2 overexpression on tumor initiation and progression.

#6097 In vivo CRISPR knockout screen reveals ribosome biogenesis as a driver and a potential therapeutic target for melanoma metastasis..

Anna Fakhardo[1], Chethana Gowda[1], Emily Johnson[1], Ricardo Petroni[2], Vivek Tomar[2], Zhenqiu Liu[3], Andres Blanco[2], Jacob Janssen[1], Irina Elcheva[1], Matthew Lanza[1], Serge Fuchs[2], Vladimir Spiegelman[1]

[1]Penn State University, Hershey, PA,[2]University of Pennsylvania, Philadelphia, PA,[3]Radiation Effects Research Foundation, Hiroshima, Japan

Metastatic melanoma is a highly aggressive cancer that spreads rapidly, with a five-year survival rate below 15%. Despite advancements in treatment options, patient outcomes remain poor, highlighting the urgent need for novel therapeutic approaches. Here, we have applied *in vivo* CRISPR KO screening to uncover new genes involved in metastasis and identified Polr1a as one of the drivers of melanoma metastasis. Polr1a is a major subunit of RNA polymerase I (Polr1), which is responsible for the transcription of 47S rDNA, resulting in the generation of 5.8S, 18S, and 28S rRNA needed for ribosome formation. Pharmacological and genetic inhibition of Polr1a impaired migration of melanoma cells, leading to the hypothesis that moderate inhibition of Polr1a preferentially suppresses the translation of genes needed for the metastatic spread. Indeed, genetic inhibition of Polr1a significantly decreased the invasion ability of melanoma cells. Importantly, pharmacological inhibition with CX-5461 (Polr1 inhibitor) significantly slowed down the primary tumor growth and dramatically decreased the number of lung metastases. Also, CX-5461 treatment significantly suppressed metastasis when used in combination with primary tumor resection, demonstrating an impressive metastasis-specific effect independent of primary tumor growth inhibition. To identify the potential mechanism by which Polr1a regulates melanoma metastasis, we have conducted in parallel RNA seq and Ribo seq analysis in Polr1a KD melanoma cells. Inhibition of Polr1a did not affect global translation; however, KEGG enrichment analysis has revealed the non-canonical NF-κB signaling pathway as one of the most strongly impacted on the translational level. Indeed, western blot analysis of the cells with Polr1a KD confirmed that a decrease in Polr1a level is associated with the decrease of p52 and RelB, which are the key proteins responsible for the activation of the non-canonical NF-κB pathway. Re-expression of RelB in the cells with Polr1a KD rescued the migration phenotype, demonstrating that Polr1a regulates melanoma migration ability in an NF-κB-dependent manner.Overall, these results suggest Polr1a as a prospective new target for the treatment of metastatic melanoma and shed light on a potential mechanism responsible for the pro-metastatic effect of this gene.

#6098 Signature surface glycan architecture promotes galectin-8-mediated vascular adhesion and metastatic dissemination of human melanomas.

Jose Souchak[1], Basilio Garcia[2], Norhan B. B. Mohammed[2], Lee Seng Lau[3], Ismaray Govea[2], Brandon Fernandez[2], Charles J. Dimitroff[2]

[1]Herbert Wertheim College of Medicine, Florida International University, Miami, FL,[2]Florida International University, Miami, FL,[3]Herbert Wertheim College of Medicine (FIU), Miami, FL

The molecular mechanisms enabling circulating melanoma cells to adhere to the vascular endothelium and disseminate systemically remain poorly defined. Prior data by our laboratory indicate that, as melanocytes progress to aggressive melanoma cells, they display signature surface glycan features defined by loss of I-branched poly-N-acetyllactosamines (poly-LacNAc) and a gain of galectin (Gal)-8-binding i-linear poly-LacNAcs. Here, we investigated how Gal-8-binding i-linear poly-LacNAcs remodeling influences melanoma metastasis. Flow cytometry and parallel-plate flow chamber assays were used to assess expression of canonical vascular endothelial (E)-selectin-binding glycans, sialyl Lewis$^{X\ or\ A}$, and of E-selectin-mediated adhesion and Gal-8-binding pathways; RT-qPCR was used to evaluate glycosyltransferase expression necessary for canonical E-selectin binding glycans; and experimental metastasis xenograft assays were used to examine metastatic colonization. Data showed that human melanoma cells lacked E-selectin-binding glycans and expression of α1,3 fucosyltransferases essential for sialyl Lewis$^{X\ or\ A}$ biosynthesis, though they possessed an abundance of Gal-8-binding glycans, which supported robust Gal-8-mediated vascular endothelial adhesion under physiological blood flow conditions. Furthermore, in experimental metastasis assays designed to model metastatic colonization potential and our flow-based adhesion assays, exogenous rhGal-8 facilitated significantly more systemic dissemination of human i-linear poly-LacNAc^{high} melanoma cells than control I-branched poly-LacNAc^{high} melanoma cells. These findings support the hypothesis that Gal-8 can bridge vascular endothelial cells to i-linear poly-LacNAc^{high} melanoma cells to support intravascular melanoma cell adhesion, implicating the Gal-8 - Gal-8-binding poly-LacNAc axis as a novel therapeutic target for disrupting systemic dissemination.

#6099 Identification of key pathways regulating colorectal cancer stemness and metastasis through compound screening.

Teruaki Fujishita, Yanqing Niu, **Masahiro Aoki**

Pathophysiology, Aichi Cancer Center Research Institute, Nagoya, Japan

Distant metastasis is the leading cause of mortality in patients with advanced colorectal cancer (CRC), underscoring the need for novel therapeutic targets. Although cancer stem cells are thought to contribute to metastatic progression, the regulatory mechanisms governing CRC stemness remain incompletely understood. Using an autochthonous metastatic mouse model harboring sporadic mutations in *Ctnnb1*, *Kras*, *Trp53*, and *Smad4* genes (CKPS mice), together with CRC cell lines derived from these mice (CKPS cells), we previously demonstrated that the cAMP/PKA/CREB signaling promotes CRC stemness and metastasis partly by inducing the stemness markers ALCAM (CD166) and PROM1 (CD133).To further elucidate pathways sustaining CRC stemness, we performed a compound screen of approximately 500 agents using CKPS spheroid cultures. Among them, QNZ—an inhibitor reported to target NF-κB—significantly downregulated ALCAM and PROM1 and markedly suppressed liver metastasis. Unexpectedly, genetic analysis revealed that these effects were independent of canonical NF-κB signaling. Integrating proteomic and RNA-seq analyses, we identified transcription factors GRHL2 and SOX9 as candidates linking spheroid-induced transcriptional changes to QNZ responsiveness. *Grhl2* knockout reduced ALCAM expression in CKPS spheroid cultures and impaired liver metastasis. On the other hand, *Sox9* knockout or *Ctnnb1* knockdown attenuated PROM1 induction in CKPS spheroids, consistent with SOX9 functioning downstream of Wnt/β-catenin signaling.Collectively, these findings reveal the involvement of multiple pathways—including GRHL2- and Wnt/SOX9-mediated regulation—in maintaining CRC stemness and metastatic potential, providing new insights into therapeutic vulnerabilities of metastatic CRC.

#6100 MYADM drives RhoA-dependent amoeboid plasticity and chromatin remodeling to promote metastasis.

Tai-Lung Cha[1], Yi-Ta Tsai[2], En-Ting Liu[2]

[1]National Institute of Cancer Research, National Health Research Institutes (NHRI), Zhunan, Taiwan,[2]School of Life Science, National Defense Medical University, Taipei, Taiwan

Metastasis relies on the ability of cancer cells to adopt amoeboid migration, yet the upstream regulators of this highly plastic phenotype remain incompletely defined. We identified MYADM, a transmembrane protein normally expressed during myeloid maturation, as a central driver of amoeboid migration and metastatic competency. Cancer cells hijack MYADM to mimic leukocyte-like trafficking, enabling RhoGDI interaction and RhoA activation, which induce leukocyte trafficking-associated genes, membrane blebbing, invasiveness, and anoikis resistance. Multi-omics profiling further revealed that MYADM remodels chromatin accessibility (CA) to control intermediate filament dynamics and establish a pro-metastatic transcriptional state. Loss of MYADM activates CA-driven cell-death pathways and completely suppresses metastasis—an effect selective for cancer cells but not monocytes. These results identify MYADM as a master regulator linking RhoA signaling, cytoskeletal plasticity, and chromatin remodeling, and establish MYADM inhibition as a promising therapeutic strategy to block amoeboid migration and metastatic progression.

#6101 Spectrin SPTAN1 loss triggers genome instability and tumor growth in bladder cancer.

Jim Sheu, Chun-Yu Su

National Sun Yat-sen University, Kaohsiung, Taiwan

Spectrin αII (SPTAN1) is a cytoskeletal protein which plays important roles in actin filament organization and chromosome segregation. Alterations in spectrin network was found to influence cell division and enhance tumor progression. By analyzing cancer genomics data from TCGA databank, silent mutations in spectrin gene *SPTAN1* and its down-regulation were frequently detected in patients with muscle invasive bladder cancer (MIBC), the most aggressive cancer type of bladder cancer. To investigate the possible role of spectrin αII loss in MIBC development, we established stable MB49 cell clones (SPTAN1-KD) which constitutively express SPTAN1-specific shRNAs, leading to down-regulation of SPTAN1 expression. Multinucleated cells with micronuclei were found in SPTAN1-KD cells which were associated with strong staining of γ H 2AX and pCHK2, suggesting DNA damage and genome instability triggered by SPTAN1 loss. Interestingly, these cells can escape the genome crisis-induced cell death by down-regulating the cGAS-STING pathways, a mechanism frequently found in metastatic cancer cells with genome instability. Cell proliferation assay by MTT assay revealed enhanced growth rate in SPTAN1-KD cells as compared to control cells transfected with pLKO empty vector or the parental cells. Xenografted tumor model also confirmed higher tumor growth rate in lesions formed by SPTAN1-KD cells Transcriptome analysis indicated up-regulation of several pathways involved in T cell exhaustion, lipid metabolism and ECM remodeling in SPTAN1-KD cells, which associated with down-regulation of pathways related to immune surveillance. Our study therefore suggests that SPTAN loss functions as a driving force to promote cancer progression by inducing genome instability and cell proliferation. SPTAN loss can also enhance cancer survival by triggering immune editing through transcriptional reprograming.

#6102 *In vivo* CRISPR screening of chromatin regulators reveals p53-dependent drivers of lung metastasis in esophageal cancer.

Raul Navaridas[1], Gizem Efe[1], Ali Iftikhar[2], Karen J. Dunbar[1], Katherine Cunningham[1], Emily Esquea[2], Noriyuki Noriyuki[1], Constanza Tapia Contreras[1], Alice E. Shin[1], Francisco J. Sanchez-Rivera[3], Chao Lu[2], Anil K. Rustgi[1]

[1]Herbert Irving Comprehensive Cancer Center, Vagelos College of Physicians and Surgeons, Columbia University Irving Medical Center, New York, NY,[2]Herbert Irving Comprehensive Cancer Center, Department of Genetics and Development, Columbia University Irving Medical Center, New York, NY,[3]Koch Inst. for Integrative Cancer Research at MIT, Cambridge, MA

Metastatic esophageal cancer exhibits a strong predilection for dissemination to the lungs. Lung metastases are associated with poor survival outcomes, therapeutic resistance, and limited treatment options, underscoring the urgent need to identify targetable mechanisms driving lung colonization. Yet, these molecular mechanisms driving lung-specific tropism remain poorly understood, which serves as the basis for our novel approaches. Herein, we employed state-of-the-art *in vivo* CRISPR-Cas9 knockout screens using a sgRNA library targeting chromatin regulators to identify epigenetic modulators of lung metastasis in esophageal cancer. This screen targeted 600 genes with a pooled sgRNA library enriched for epigenetic regulators and chromatin remodelers. The library, containing 6 sgRNAs per gene and appropriate non-targeting controls, was transduced into isogenic cells with either mutant *Trp53*$^{R172H/-}$ (a frequently detected hotspot *Trp53* mutation in the DNA binding domain) or its depletion at a low multiplicity of infection to ensure single sgRNA integration per cell. The transduced cells were injected orthotopically or via tail-vein into mice, and comparative abundance analysis was performed between the pre-implantation pool and lung metastatic lesions. Our screen uncovered key chromatin regulators that selectively promote lung colonization in the presence of mutant p53, including histone methyltransferases and demethylases (Kmt2d, Kdm1b, Kdm4d), histone deacetylases (Hdac4), and additional DNA and chromatin modifiers (Eya2, Prmt8, Parp14, Tox4, Eny2, and Gata2a). To elucidate the mechanisms by which these epigenetic regulators contribute to metastatic potential, we are performing comprehensive histone methylation and acetylation profiling in the corresponding KO clones, in combination with ATAC-seq and RNA-seq. This integrative approach will enable us to correlate histone modification landscapes with chromatin accessibility and gene expression programs, delineating how mutant p53 cooperates with specific chromatin regulators to reprogram enhancer networks and drive pro-metastatic transcriptional states. Collectively, these studies will define epigenetic mechanisms underlying lung tropism in esophageal cancer and identify actionable vulnerabilities for therapeutic targeting, with broader implications for TP53-mutant cancers.

#6103 Extrachromosomal circular DNA-mediated NOSIP amplification drives OXPHOS-dependent metastasis in hepatocellular carcinoma.

Xiaorong Lin, Yusheng Luo, Yuxi Pan, Guofei Deng, Yuqing Lin, Yuzhi Zhang, Jiancheng Wang, Shuo Fang

The Seventh Affiliated Hospital, Sun Yat-sen University, Shenzhen, China

Background: Distant metastasis is the major cause of cancer-related mortality in hepatocellular carcinoma (HCC), yet the molecular determinants that confer metastatic competence remain poorly defined. Extrachromosomal circular DNA (eccDNA), a non-chromosomal genetic element capable of amplifying oncogenes and promoting tumor evolution, has recently gained attention. However, the functional landscape of eccDNA-carried genes in HCC and their mechanistic roles in metastatic progression remain undefined.
Methods: Paired primary and metastatic HCC tissues were analyzed using Circle-seq to identify metastasis-associated eccDNAs. Candidate drivers were further evaluated through integrated multi-omics analyses and validation using public datasets. Functional studies were performed in HCC cell lines with stable NOSIP overexpression or knockdown, followed by migration and invasion assays. Protein interactors were identified by immunoprecipitation-mass spectrometry. Cellular bioenergetic function was evaluated using Seahorse XF analysis, and the mechanistic relevance of identified interactions was further examined in vitro and in vivo.
Results: NOSIP-containing eccDNA was markedly enriched in metastatic HCC samples, and elevated NOSIP expression correlated with poor overall survival. NOSIP overexpression significantly enhanced cell migration and invasion, while knockdown suppressed these phenotypes. Proteomic profiling identified pyruvate dehydrogenase E1 subunit beta (PDHB) as a major NOSIP-binding partner. NOSIP upregulation increased oxygen consumption rate and activated oxidative phosphorylation (OXPHOS), indicating enhanced mitochondrial metabolic activity. These findings demonstrate that eccDNA-mediated NOSIP amplification promotes metastatic traits by engaging PDHB-dependent mitochondrial metabolic reprogramming.
Conclusion: In conclusion, this study identifies NOSIP-containing eccDNA as a previously unrecognized molecular driver of OXPHOS-dependent metastatic adaptation in HCC. The proposed eccDNA-NOSIP-PDHB axis reveals a mechanistic link between non-chromosomal genetic amplification and mitochondrial metabolic remodeling, offering a potential metabolic vulnerability for therapeutic intervention in advanced HCC.

#6104 STK11 loss enhances stress-adaptive programs supporting shear resilience in circulating tumor cells from KRAS-driven lung adenocarcinoma.

Anna Showalter[1], Princess Rodriguez[1], David Joseph Seward[2], Paula B. Deming[1], **Melissa Nicole Scheiber**[1]

[1]University of Vermont, Burlington, VT,[2]University of Vermont Medical Center, Burlington, VT

Lung adenocarcinoma (LUAD) remains the leading cause of cancer-related mortality, with the KRAS/STK11 (LKB1) co-mutant subtype displaying marked therapeutic resistance and metastatic potential. Metastatic success depends on the ability of circulating tumor cells (CTCs) to withstand the oxidative and mechanical challenges of blood flow, yet the contribution of STK11 loss to fluid shear stress (FSS) tolerance is not fully defined. Using our embryonic zebrafish xenograft model with KRAS-mutant parental and STK11-null LUAD lines, we conducted longitudinal imaging of CTC behavior in physiologic circulation. Under glutamine-deprived conditions that simulate metabolic stress, STK11-null cells exhibited higher micrometastatic burden and increased frequency of extravasation at four days post-injection compared with parental controls. RNA-seq performed under glutamine deprivation and analyzed using Reactome GSEA revealed enrichment of broad stress- and stimulus-response pathways. An FSS-specific gene panel further demonstrated enrichment of shear-adaptive programs, notably NRF2-mediated antioxidant responses, highlighting the need to define these programs directly in vivo. Our data support a model in which STK11 loss facilitates CTC persistence and outgrowth through NRF2-driven survival mechanisms engaged under oxidative and mechanical strain. Ongoing studies leverage high-speed confocal imaging (200–500 fps) and Fiji/ImageJ velocity quantification to map the relationship between shear forces and CTC survival, with planned pharmacologic tuning of cardiac output to modulate intravascular FSS. Future directions include defining molecular programs mediating shear-adaptive survival through candidate panels assessing NRF2 oxidative stress targets, YAP/TEAD outputs, and NF-κB/survival regulators. Collectively, this work identifies NRF2-mediated shear adaptation as a potential mechanism driving metastasis in KRAS/STK11 LUAD and a targetable vulnerability in shear-tolerant tumor cells.

#6105 Cholecystokinin-B receptor epigenetic regulation and targeted therapy in hepatocellular carcinoma.

Martha Gay, Hong Cao, Wenqiang Chen, Jill P. Smith

Medicine, Georgetown University, Washington, DC

Background: Metabolic dysfunction and dietary saturated fat contribute to rising hepatocellular carcinoma (HCC) rates. The cholecystokinin-B receptor (CCK-BR) is upregulated in HCC, yet the upstream mechanisms driving its expression remain undefined. Emerging evidence suggests that microRNA dysregulation and DNA methylation may promote oncogenic receptor signaling. This study investigates whether saturated fat induces CCK-BR expression through epigenetic repression of miR-148a and evaluates whether CCK-BR antagonism suppresses HCC progression in vivo.
Methods:
Epigenetic Regulation: HCC cells were treated with palmitic acid for 8, 24, and 48 hours. qRT-PCR quantified miR-148a and CCK-BR mRNA expression. To validate miRNA-dependent regulation, Hepa1-6 cells were transiently transfected with miR-148a mimics or negative controls using Lipofectamine 2000. To assess diet-induced DNA methylation, genomic DNA from livers of high-fat diet (HFD) and control mice was bisulfite-converted and amplified across CpG-rich regions of the miR-148 promoter. PCR products were cloned into pCR2.1-TOPO vectors and sequenced using PyroMark MD instrument and bisulfite pyrosequencing. To test reversibility, HCC cells are treated with 5-azacytidine, and expression of miR-148a and CCK-BR reassessed.
In Vivo Therapeutic Targeting: Luciferase-expressing RIL-175 HCC cells are orthotopically injected into C57BL/6 mouse livers. After recovery, mice (N=10/group) received either proglumide-treated or untreated water. Tumor growth and metastasis were monitored weekly via IVIS imaging. At week 5, serum α-fetoprotein (AFP) was assessed by ELISA, and livers were analyzed for tumor burden and metastatic spread.
Results: Palmitic acid is expected to suppress miR-148a and increase CCK-BR expression, with miR-148a mimic transfection reversing this effect. HFD livers are predicted to show hypermethylation of the miR-148 promoter correlating with elevated CCK-BR. 5-azacytidine should restore miR-148a and downregulate CCK-BR. In vivo, proglumide therapy is anticipated to reduce tumor flux, AFP levels, tumor size, and metastasis.
Conclusions: These studies define an epigenetic mechanism linking saturated fat exposure to CCK-BR upregulation in HCC and provide preclinical evidence supporting CCK-BR antagonism as a therapeutic strategy for metabolically driven liver cancer.

#6106 Targeting intracellular Galectin-3 disrupts BRAF^{V600E} mutated dormant cell dissemination and restores chemosensitivity in thyroid cancer.

Chiara Modica[1], Vincenzo Davide Pantina[1], Francesco Verona[2], Roberta Drago[1], Giulia Bozzari[1], Matilde Todaro[2], Giorgio Stassi[1]

[1]Department of Precision Medicine in the Medical, Surgical and Critical Care Areas, University of Pa, University of Palermo, Palermo, Italy,[2]Department of Health Promotion, Mother and Child Care, Internal Medicine and Medical Specialties (PR, University of Palermo, Palermo, Italy

Introduction: Papillary Thyroid Carcinoma (PTC) often exhibiting local invasion and the capacity for distant metastasis. While Galectin-3 (Gal-3) is a well-established diagnostic marker, absent in normal thyroid tissue and benign lesions, its intracellular functional role in thyroid cancer remains largely unknown. This study aimed to determine whether cell-autonomous Gal-3 in **BRAF^{V600E}** mutated cells contributes directly to tumor aggressiveness by activating an invasive and metastatic program.

Experimental procedures: We profiled Gal-3 expression in well-differentiated, poorly differentiated, and metastatic TC samples and used genetic modulation in TC cells to test its impact on proliferation, migration, invasion, and cell cycle. Transcriptomic and proteic profile characterization investigated the dormancy pathway and the interaction of Gal-3 with CD44v6 signaling axis to uncover intra and extra-cellular cooperative mechanisms in thyroid carcinoma progression. Synergistic anti-cancer effects of Gal-3 knockdown in combination with chemotherapy were tested both in vitro and in vivo trough ortothopic mouse models, to understand the intracellular Gal-3's impact on primary tumor growth, metastasis and chemosensitivity.

New data: Our data establishes Gal-3 as a pivotal molecular character in PTC pathogenesis. Elevated Gal-3 expression is a hallmark of high-grade disease, showing a striking correlation with poorly differentiated and metastatic tumors compared to their well-differentiated counterparts, underscoring its prognostic significance. Mechanistically, the CD44v6 signaling cascade acts upstream, promoting the intracellular accumulation of Gal-3. This accumulation triggers a transcriptional program that simultaneously dictates cell cycle arrest, fuels enhanced migration and invasion, and crucially, activates a disseminated-dormant phenotype.Remarkably, disrupting Gal-3 via knockdown fundamentally destabilizes this dormant state, forcing dormant TC cells to exit quiescence and undergo outgrowth. This vulnerability translates directly into a therapeutic opportunity: combining Gal-3 silencing with standard chemotherapy profoundly sensitizes these slow-cycling, metastatic cells, achieving a synergistic enhancement of therapeutic efficacy.

Conclusions: These findings unequivocally position Gal-3 as a functional driver of both invasive potential and the elusive dormant phenotype in TC. Furthermore, its modulation represents a highly promising strategy to re-sensitize slow-cycling, treatment-refractory metastatic TC cells, offering a novel avenue for treating patients with advanced disease.

#6107 Activation of NF-κB signaling drives pro-metastatic programs in STK11-deficient lung adenocarcinoma.

Allison R. Racela[1], Shannon M. Prior[1], Sean M. Lenahan[2], Cole M. Royer[1], David Joseph Seward[3], Paula B. Deming[1]

[1]University of Vermont, Burlington, VT,[2]Dana-Farber Cancer Institute, Boston, MA,[3]University of Vermont Medical Center, Burlington, VT

Lung cancer remains the leading cause of cancer-related deaths worldwide and is characterized by marked clinical aggressiveness, including high rates of therapy resistance and metastatic progression. Although recent therapeutic advances have modestly improved 5-year survival in lung cancer, overall response rates remain low (~25%), and effective treatments for metastatic disease are limited. A particularly strong genotype-phenotype correlation predicting broad treatment resistance, early disease dissemination, and poor overall survival in KRAS-driven lung adenocarcinomas (LUADs) is loss of the Serine/Threonine kinase 11 (STK11) tumor suppressor. Patients with STK11-deficient tumors commonly present with advanced-stage disease, exhibit enhanced metastatic potential and experience an especially aggressive clinical course. Despite these well-established clinical associations, the molecular mechanisms driving this aggressive, treatment-refractory phenotype remain largely undefined. We performed whole transcriptome and pathway enrichment studies comparing a KRAS-driven/STK11-competent LUAD (K) cell line with KRAS-driven/STK11-null (KS) cell line and identified STK11-loss-dependent activation of the NF-kappa B (NF-κB) signaling pathway in response to glutamine deprivation. Kmeans clustering of the RNA transcripts highlighted 36 genes induced upon glutamine depletion in KS cells. These genes were subsequently downregulated in the absence of the NF-κB transcription factor (p65) through genetic ablation or pharmacological inhibition (using *PS-1145*), with corresponding decreases in protein expression of candidate oncogenes and anti-apoptotic markers. These findings indicate that NF-κB activation is essential for transcriptional induction of survival, proliferation, and premetastatic genes under glutamine stress. We then showed that p65 consistently accumulates in the nucleus of KS cells following the removal of glutamine, suggesting transcriptional regulation through NF-κB signaling. Following pharmacological inhibition of NF-κB and glutamine depletion, p65 was unable to translocate into the nucleus and was sequestered in the cytoplasm of KS cells. To assess whether glutamine stress and NF-κB signaling promote metastasis we used a 3D spheroid model. Spheroid models more closely mimic the microenvironment of *in vivo* tumors, in which nutrients and oxygen become restricted. Glutamine deprivation enhanced ameboid-like single-cell invasion in KS spheroids, an effect markedly reduced by p65 knockout or PS-1145 treatment. Using a combination of transcriptomic analyses and *in vitro* invasion assays to model metastasis, these results suggest that STK11 loss in KRAS driven lung adenocarcinoma promotes an NF-κB-dependent metastatic phenotypes.

: Metastasis and Organ-Specific Microenvironmental Evolution
Poster Session

#6110 Systemic inflammation induced by calprotectin (S100A8/S100A9 complex) triggers reactivation of dormant cells in mouse models of breast cancer.

Ahmet B. Caglayan[1], Ying Xin[1], Aysun Caglayan[1], Shruti Nagaraja[1], Deeksha Sharma[1], Cody Hager[1], Fulya Koksalar-Alkan[2], Hilmi K. Alkan[2], Monika Burness[1], Hasan Korkaya[2], Max S. Wicha[1]

[1]Internal Medicine Hematology/Oncology, University of Michigan, Ann Arbor, MI,[2]Department of Oncology, Karmanos Cancer Institute and Wayne State University, Detroit, MI

Breast cancer is the most common cancer in women in the developed countries. Cancer stem cells play key roles in tumorigenesis, dormancy and recurrence in breast cancer, yet they are resistant to many treatments. Despite recent advances in the field in terms of imaging and adjuvant therapies, disseminated dormant tumor cells (DTCs) resistant to these therapies are major cause of late metastatic relapse. However, the mechanisms by which the dormancy maintenance and reactivation, particularly within bone and lung niches remain poorly understood, due in part to limited preclinical models. There is a need for better mouse models to study breast cancer dormancy to mitigate the risk of late metastatic recurrence. Systemic inflammation is increasingly recognized as a trigger of dormancy escape but its mechanistic role in awakening DTCs in vivo is not fully explored. To address this, we evaluated two murine breast cancer syngeneic models in mice to establish a tractable platform for studying tumor dormancy and its awakening. Using orthotopic implantation of EMT6-Luci cells followed by surgical resection in BALB/c mice and intracardiac injection of D2.0R-Luci cells, we examined whether systemic inflammatory cytokines, including IL-1b, G-CSF or Calprotectin (S100A8-S100A9 heterotetramer) promote escape from dormancy. Beginning 30 days post-resection of EMT6-Luci or post-injection of D2.0R-Luci cells, mice received intraperitoneal treatment of indicated cytokines. We monitored the dormancy awakening longitudinally using IVIS bioluminescence imaging as well as the peripheral immune profile assessed by flow cytometry. D2.0R-luci cells demonstrated a robust sensitivity to inflammatory cues. Treatment with Il-1b, G-CSF or calprotectin all markedly increased the frequency of mice exhibiting bioluminescent reactivation of dormant cells compared to the control vehicle mice. Notably, calprotectin induced reawakening in 100% of treated mice versus 33% in control animals highlighting its potent pro-inflammatory and pro-metastatic role. In contrast, disseminated EMT6-luci cells remined below the detection threshold in lung and bone marrow following resection, indicating differences in dormancy biology. Our findings reinforce emerging evidence that systemic inflammation is a critical driver of dormant tumor cell awakening. Our work provides a robust syngeneic dormancy platform for dissecting systemic and microenvironmental regulators of metastatic reactivation and establishes calprotectin as strong candidate mediating dormancy escape. Ultimately, these models will facilitate the development of therapeutic strategies to eliminate dormant cells and prevent late metastatic relapses in breast cancer patients.

#6111 Opposite regulation of brain and lung metastases by endothelial FAK deletion.

Shoko Noda-Narita, Atsu Aiba

The University of Tokyo, Tokyo, Japan

Introduction: In lung metastasis, tumor-derived factors, such as VEGFs and TNF-α, activate focal adhesion kinase (FAK) in vascular endothelial cells (ECs). Activated FAK promotes VE-cadherin phosphorylation and facilitates the extravasation of cancer cells. In contrast, cerebral blood vessels possess much stronger intercellular adhesion, supported by surrounding pericytes and astrocytes. This highly restrictive barrier, known as the blood-brain barrier (BBB), is regulated differently from the endothelial barrier in trunk ECs, and the role of endothelial FAK in brain metastasis remains unclear. In this study, we investigated the function of the cerebral endothelial FAK and compared its contribution to brain metastasis with lung metastasis.

Methods: We generated tamoxifen-inducible, EC-specific FAK knockout (FAK-cKO) mice (*VEcad-Cre^{ERT2}; FAK-flox/flox*) and established brain metastatic (BrM) and lung metastatic (LuM) cell lines from Ex3LL murine lung cancer cell line. BrM cells were intracardially injected into FAK-cKO mice, and brain metastases were analyzed using the CUBIC tissue-clearing system. Lung metastases were also evaluated following tail vein injection of LuM cells.

Results: While endothelial FAK deletion reduced lung metastasis, it conversely increased brain metastasis. The number of brain metastases increased in FAK-cKO mice, whereas the size of individual lesions remained unchanged. These findings suggest that endothelial FAK deletion promotes the initiation of brain metastasis but does not enhance the proliferation of metastatic tumors in the brain. FAK-cKO mice showed no difference in adhesion molecule expression or BBB permeability compared with control mice. However, primary brain ECs from FAK-cKO mice sporadically exhibited internalization of PECAM-1 and VE-cadherin, suggesting endothelial-to-mesenchymal transition (EndoMT). BrM cells co-cultured with these ECs preferentially localized to the dysregulated ECs. This increased susceptibility of FAK-deficient brain ECs to BrM cells suggests that brain endothelial FAK plays a critical role in maintaining BBB integrity and suppressing brain metastasis.

Conclusion: Endothelial FAK deletion exacerbated brain metastasis, while reducing lung metastasis. These findings suggest that endothelial FAK differentially regulates vascular barrier functions in the brain and lung, thereby exerting opposing effects on cancer metastasis. Further investigation is required to elucidate the mechanisms by which endothelial FAK preserves BBB integrity and prevents brain metastasis.

#6112 Inflammatory niche remodeling by metastatic breast cancer stem cells.

Claire Engstrom[1], Jessica Pham[2], Wenxue Ma[2], Emma Klacking[3], Kendale Wirtjes[2], Patrick Chang[1], Inge van der Werf[2], Catriona H. M. Jamieson[4]

[1]UCSD, San Diego, CA,[2]UCSD, La Jolla, CA,[3]UCSD Medical Ctr., San Diego, CA,[4]UCSD Moores Cancer Center, La Jolla, CA

Metastatic breast cancer (MBC) remains one of the leading causes of cancer-related mortality among women in the United States. Cancer stem cells (CSCs), which are characterized by immune evasion, self-renewal, and regenerative potential, are thought to be critical drivers of metastasis and recurrence.Here, we performed single-cell RNA sequencing on eight MBC samples from accessible secondary tumor sites with diverse hormone receptor and HER2 status, including three pleural effusions, one ascites, and five breast to bone metastases. To investigate the relationship of these metastatic cells to their microenvironment, we utilized the package CellChat which uses expression of receptor-ligand pairs to infer communication between populations.Across all samples, we identified a rare population of non-immune ($CD45^-$ $CD24^-$) cells that consistently formed a distinct transcriptional cluster and expressed canonical stemness and cancer markers, including *CD44*, *CD47*, *ALDH1A3*, *MET*, *HER3*, *THY1*, and *PROCR*. Notably, they exhibited elevated expression of the RNA- and DNA-editing enzymes ADAR1 and APOBEC3C which are deaminases previously implicated in mutagenesis, splicing dysregulation, and cancer progression. This population also showed consistent downregulation of retrotransposable elements, a proposed mechanism of immune evasion in leukemia stem cells and consistent with upregulation of base deaminases, which are known repressors of retroelement activation. We uncovered a high degree of autocrine and paracrine signaling from this CSC population, particularly via the IL-6 pathway which is a known inducer of ADAR1 and APOBEC3C, and we performed downstream in vitro and in vivo analysis in patient-derived xenograft mice and nanobioreactor tumor organoid models to investigate the inflammatory and base deaminase activation through cytokine arrays and flow cytometry.Our findings highlight a conserved metastatic niche remodeling CSC-like population across MBC patients that may drive metastasis through base editing, inflammatory signaling, and retroelement repression, and targeting these pathways could offer new avenues for diagnostics and intervention.

#6113 ccRCC lung metastases harbor cancer associated fibroblast lymphocyte exclusion sites that form a confined TME as revealed by single cell and spatial multi-omics.

Yufei Wang[1], Jae-Won Cho[2], Yasmin Nabil Laimon[2], Wenxin Xu[1], Kun Huang[1], Aseman Bagheri Sheshdeh[2], Nithyassree Murugan[1], Hsien-Chi Yuan[1], Jon Wee[2], David Alexander Braun[3], Toni K. Choueiri[1], Catherine J. Wu[1], Sabina Signoretti[2], Gordon J. Freeman[1], Martin Hemberg[2], Wayne A. Marasco[4]

[1]Dana-Farber Cancer Institute, Boston, MA,[2]Brigham and Women's Hospital, Boston, MA,[3]Yale School of Medicine, New Haven, CT,[4]Associate Professor, Dana-Farber Cancer Institute, Boston, MA

Tumor progression and metastasis is driven by interplays between cancer cells and their surrounding tumor microenvironment (TME). Investigating the spatiotemporal transcriptomic and proteomic profile of primary and metastatic tumors sheds light on how differences in spatial architecture shape the TME and promote tumor metastasis. Here, we profiled six primary clear cell renal cell carcinoma (ccRCC) specimens and their lung metastases using three different spatial transcriptomic and proteomic platforms: CosMx, Xenium and CODEX. After cell segmentation and annotation, we incorporated the cellular context and spatial information to identify niches by identifying spatial regions with similar cell type composition. This revealed 12 distinctive niches including cancer, stroma, alveolar, and tertiary lymphoid structure (TLS) niches, formed by 25 different cell types. Furthermore, we analyzed cell-cell communication and architecture were analyzed to understand the intercellular interplay and spatial organization in primary and metastatic ccRCC. The architecture analysis showed that the metastatic lesion has a distinct architecture compared to the primary tumor which we refer to as Cancer Associated fibroblaST Lymphocyte Exclusion Sites (CASTLES). The key characteristic of CASTLES is that malignant cells surrounded by cancer associated fibroblasts (CAFs), endothelial cells as well as tumor associated macrophages (TAMs), constituting a physical barrier. In contrast, primary ccRCC cells were accessible to tumor infiltrating leukocytes (TILs). This difference in spatial organization supports the aggressive characteristics of metastatic cancer cells. Our results show the impact of spatial architecture on primary and metastatic ccRCC, as well as the relation between spatial organization of the cellular context and cell-cell communication. In addition, it suggests that cancer-associated fibroblasts (CAFs) and immune cells are essential components of the ccRCC TME. Their interaction constitutes a major factor not only for tumor progression but also limiting therapy response in metastatic ccRCC.

#6114 Integrated single-cell and spatial atlas of tumor-draining lymph nodes reveals metastasis-associated stromal and immune remodeling.

Enshuo Zhang[1], Lu Zhang[2], Haitang Yang[1], Feng Yao[1]

[1]Department of Thoracic Surgery, Shanghai Chest Hospital of Shanghai Jiao Tong University of Medicine, Shanghai, China,[2]Shanghai Chest Hospital of Shanghai Jiao Tong University of Medicine, Shanghai, China

Introduction: Tumor-draining lymph nodes (TDLNs) are critical sites for anti-tumor immunity and important targets of immunotherapy. However, they are also early sites of tumor dissemination, and lymph node-resident metastatic tumors exhibit reduced responsiveness to immunotherapy compared with their primary counterparts. How metastasis reshapes TDLN stromal-immune ecosystems remains underexplored.
Methods: We built a pan-cancer TDLN atlas, which consists of >1 million cells from healthy lymph nodes (hLN), non-metastatic TDLNs (nLN), and metastatic TDLNs (mLN) across 15 cancers and 70 donors using single-cell RNA sequence (scRNA-seq) and spatial transcriptomics (ST). Key findings were validated in independent patient specimens and mouse models.
Result: Our integrated analysis constructed a public resource named PanTDLN, which identifies myeloid cells, stromal cells, and T cells as the most altered populations after metastasis, with characteristics including hypoxia, activation, and exhaustion. Spatially, four cross-cancer niches that form after metastasis are identified: naïve-enriched, tumor-reactive, peritumoral, and metastatic tumor, each with distinct cellular compositions and ligand-receptor networks. Naïve-enriched zones are filled with naïve T/B cells and PD-1+ CXCL13+ T helper cells with enrichment of immune-recruiting and activating chemokine axes. Peritumoral niches are built by a unique barrier-forming fibroblastic reticular cell (FRC) with the strongest extracellular matrix remodeling program, which spatially segregates the tumor-reactive niche, rich in antigen-presenting cells and cytotoxic lymphocytes, from the tumor mass. Within the tumor niches, hypoxia-associated macrophages and monocytes (HAMs) are specifically enriched, leading to an intratumoral immune desert. Meanwhile, these HAMs promote regulatory T cells (Tregs) within tumor-reactive niches toward terminally differentiated phenotypes via the TNF-TNFR axis, resulting in dysfunction of activated cytotoxic T/NK cells in the tumor-reactive niche. Animal models prove that targeting barrier-forming FRCs and the communication between HAMs and Tregs can disrupt the stromal-immune remodeling and enhance immunotherapy response in mLNs.
Conclusion: PanTDLN decodes the spatiotemporal stromal-immune remodeling during TDLN metastasis and provides potential cross-cancer therapeutic targets, facilitating the treatment of lymph node-positive cancer patients.

#6115 Deciphering tumor microenvironment dynamics in tumorigenesis and lymph node metastasis of esophageal squamous cell carcinoma using single-cell and spatial transcriptomics.

Tae Hee Hong[1], Hansoll Na[1], Chung Lee[2], Young Ho Yang[1], Ha Eun Kim[1], Byung Jo Park[1], Min Hee Hong[3], Hye Ryun Kim[3], Hyun Ki Kim[2], Dae Joon Kim[1]

[1]Department of Thoracic and Cardiovascular Surgery, Yonsei University College of Medicine, Seoul, Korea, Republic of,[2]Department of Pathology, Yonsei University College of Medicine, Seoul, Korea, Republic of,[3]Division of Medical Oncology, Department of Internal Medicine, Yonsei Cancer Center, Yonsei University College of Medicine, Seoul, Korea, Republic of

Esophageal squamous cell carcinoma (ESCC) is an aggressive malignancy with late diagnosis and high propensity for lymph node (LN) metastasis. Given the major prognostic and therapeutic impact of LN involvement, defining the cellular and molecular features distinguishing metastatic LNs from primary tumors is imperative. We aimed to delineate tumor microenvironment (TME) dynamics between primary tumors and metastatic LNs integrating single-cell RNA/TCR sequencing (scRNA/TCR-seq) with high-resolution spatial transcriptomic validation.

We performed scRNA-seq on 344,790 cells from 58 upfront surgical specimens of 18 stage T1-2N0-1M0 ESCC patients. Samples included paired tumor mucosa (TM), normal mucosa (NM), tumor-associated LNs (TLN), and normal LNs (NLN). scTCR-seq in 8 patients delineated clonal trajectories and functional T-cell states. Additionally, spatial transcriptomics using the CosMx 6K platform profiled 3,493,957 cells across 34 specimens (NLN, TLN, and TM) from 13 patients, enabling in situ validation of compartment-specific cellular interactions.

Our analysis revealed marked divergence between TM and TLN immune landscapes. TM showed an immunosuppressive milieu dominated by regulatory T cells (T_{REG}s) and sharp loss of cytotoxicity in CD8 exhausted T cells (T_{EXH}s). In contrast, TLN retained partially functional T_{EXH}s following two trajectories: a pre/intermediate-exhausted path with sustained *GZMB* and *PRF1* expression, and a terminally-exhausted path showing steep functional decline—prominent in TM but attenuated in TLN. TCR clonotype analysis supported this, as shared TM-TLN clones preserved cytotoxicity whereas TLN-restricted clones displayed weaker effector programs, suggesting antigen-driven trafficking from primary tumor. Myeloid profiling showed *TREM2*^{high} macrophages (M) enrichment in TLN, while TM featured T_{REG}-dendritic cell (DC) interactions. Spatial transcriptomics validated these compartmentalized suppressive circuits, demonstrating colocalization of *TREM2*^{high} Ms with T_{REG}s or T_{EXH}s in TLN. SPP1-mediated signaling between these populations appeared exclusively in TLN, highlighting niche-specific immunoregulatory interactions within metastatic sites.

This integrated single-cell and spatial transcriptomic study highlights distinct immunoregulatory programs driving ESCC progression and LN metastasis. While TLNs contained T_{EXH}s with preserved cytotoxicity and reinvigoration potential, TMs exhibited abrupt functional collapse. We identified compartment-specific suppressive networks—TREM2^{high} M-mediated axes in TLN and DC-mediated axes in TM—validated by spatial analysis. These findings offer mechanistic insight into LN metastasis and may inform biomarker development, neoadjuvant treatment optimization, and tailored immunotherapy in ESCC.

#6116 Spatial multi-omics dissection of colorectal cancer micrometastasis.

Yang Liu, Akshaya S. Jadhav, Yuwen Pan, Jianlong Liao, Isha Khanduri, Yunhe Liu, Riham Katkhuda, Wei Lu, Kyung Serk Cho, Tieling Zhou, Baohua Sun, Mei Jiang, Sharia D. Hernandez, Idania Carolina Lubo Julio, Patrick Brennan, Guangsheng Pei, Kai Yu, Yibo Dai, Tian Chu, Fuduan Peng, Khaja Khan, Saxon Rodriguez, Ling Xia, Youming Guo, Alicia Mejia, Zhiming Tong, Sean W. Barnes, Ou Shi, Shreeya Indulkar, Alaa Mohamed, Natalie Wall Fowlkes, Timothy Newhook, Yun Shin Chun, Van K. Morris, David G. Menter, Dadi Jiang, Jean-Nicolas Vauthey, Ruoyan Li, Humam Kadara, Luisa M. Solis Soto, Scott Kopetz, Linghua Wang, Dipen M. Maru

The University of Texas MD Anderson Cancer Center, Houston, TX

Background: Colorectal cancer (CRC) metastases frequently recur due to minimal residual disease (MRD) and persisting micrometastases after therapy. However, the spatial and molecular features underlying micrometastatic persistence and CRC recurrence remain poorly defined.
Study design and methods: We performed integrative spatial multi-omics profiling—including Visium spatial transcriptomics (ST), Visium HD ST, laser-capture microdissection with whole-genome sequencing (LCM-WGS), and PhenoCycler-Fusion multiplex imaging—across 49 tumors from 19 patients with paired primary CRC, liver (CLiM), and lung (CLuM) metastases. The analysis encompassed 341,328 Visium spots and approximately 3.8 million Visium HD bins. Non-negative matrix factorization (NMF) was applied to identify conserved and distinct spatial metaprograms across CLiM, CLuM, and primary CRC using Visium ST datasets. For Visium HD ST data, StarDist-SMURF segmentation was used to transform subcellular bins into single-cell-level data. Cross-modality alignment and Jaccard similarity analyses integrated spatially resolved DNA, RNA, and protein profiles across both corresponding and independent tissue blocks, enabling multi-layer characterization of tumor evolution and microenvironmental organization.
Results: Spatial phylogenetic and molecular analyses delineated distinct evolutionary trajectories of primary and metastatic CRC, revealing early clonal divergence and stem-like phenotypes in liver micrometastases (CLiMi) across DNA, RNA, and protein levels. Spatial profiling uncovered stromal interactions in both CLiM and CLuM, with macrophages enriched in CLiM and lymphocytes predominating in CLuM. Micrometastases exhibited pronounced immunosuppression and T cell exhaustion, potentially mediated by PGE2/PTGES2-PTGER4 and NECTIN2/3-TIGIT signaling interactions. A CLiMi-specific six-gene signature predictive of micrometastasis was identified and validated, correlating with disease-free survival (DFS) and MRD-DFS in the MDACC cohort (n = 117), and with DFS and overall survival (OS) in TCGA (n = 610) and GSE17538 (n = 232).
Conclusions: Our integrative spatial multi-omics analysis provides a comprehensive atlas of CRC micrometastases, revealing their evolutionary and immune landscapes. These findings illuminate the molecular and spatial determinants of micrometastatic persistence and identify potential therapeutic vulnerabilities for preventing CRC recurrence.

#6117 Fibroblast-derived extracellular vesicles promote organ-specific tumor growth and chemoresistance in pancreatic cancer liver metastasis via ptch2 downregulation.

Mahsa Pahlavanneshan[1], Weikun Xiao[2], Eileen Fung[2], Chae Young Eun[2], Chang-Il Hwang[3], Shannon Mumenthaler[2], Reginald Hill[2]

[1]Alfred E. Mann Department of Biomedical Engineering, University of Southern California, Los Angeles, CA,[2]Ellison Medical Institute, LLC, Los Angeles, CA,[3]Department of Microbiology and Molecular Genetics, University of California Davis, Davis, CA

Pancreatic ductal adenocarcinoma (PDAC) is the 3rd leading cause of cancer death in USA with a 5-year survival rate of only 13%. Early diagnosis is very difficult and 53% of patients are diagnosed after metastasis has already occurred, with liver being the most frequently affected site. Both primary tumors and metastases have dense desmoplastic stroma, which contributes significantly to chemoresistance. However, the mechanisms by which primary and metastatic fibroblasts influence tumor behavior remain understudied. This study aims to investigate the contributions of fibroblasts-derived extracellular vesicles (EVs) at the primary versus metastatic sites. To achieve this, we developed tunable 3D biomimetic models that replicate aspects of the tumor microenvironment (TME) of primary PDAC and the liver metastatic niche (LMN). We used matched primary PDAC and liver metastatic (LM) organoids derived from the *Kras*$^{+/LSL\text{-}G12D}$*; Trp53*$^{+/LSL\text{-}R172H}$*; Pdx1-Cre* genetically engineered mouse model of PDAC, combined with either primary PDAC or liver fibroblasts. We hypothesized that primary and metastatic site derived fibroblasts possess distinct properties influenced by their different TMEs, that lead to organ-specific effects on tumor growth and chemoresistance. Supporting this hypothesis, fibroblasts enhanced tumor growth and chemoresistance to gemcitabine, only when paired with the organoids from the same site. Fibroblast-derived EVs were identified as critical drivers of this site-specific tumor support. Mechanistically, we found that expression of *Ptch2*, a tumor suppressor in the Sonic Hedgehog (SHH) signaling pathway, is significantly decreased in organoids exposed to site-matched fibroblasts or their EVs, while EV depletion restores *Ptch2* expression. Finally, we pharmacologically modulated the SHH pathway via a small molecule *Ptch2* agonist, Robotnikinin, which appeared to reduce organoid growth and chemoresistance in our models, indicating a potential role for SHH pathway targeting. These findings suggest that site-specific fibroblast-derived EVs may carry distinct *SHH* ligands that differentially interact with *Ptch2* in tumor cells of the corresponding site, which is currently under investigation. Taken together, our findings underscore the importance of developing models to elucidate the pivotal role of the organ-specific microenvironment in driving tumor progression. Our tunable 3D biomimetic model faithfully recapitulates the tumor-stroma interactions and provides a platform to evaluate therapeutic strategies aimed at disrupting fibroblast-tumor crosstalk. Defining how SHH signaling contributes to tumor growth and chemoresistance driven by fibroblast-derived EVs in an organ-specific manner can potentially uncover novel therapeutic strategies for targeting the metastatic niche in pancreatic cancer.

#6118 Spatially resolved SEED (stromal-enriched metastatic decider) niches integrate tumor, stromal, and immune ecosystems to enable lymph node dissemination in LUAD.

Junghan Oh[1], Hoyeon Jeong[1], Yoon La Choi[2], Donggun Lee[1], Misook Lee[1]

[1]Samsung Advanced Institute of Technology, Seoul, Korea, Republic of,[2]Samsung Advanced Institute for Health Sciences and Technology, Seoul, Korea, Republic of

Purpose Lung adenocarcinoma (LUAD) displays substantial intratumoral heterogeneity, but the precise primary-tumor subregions that give rise to lymph-node metastasis remain unclear. We aimed to identify metastasis-competent SEED regions and characterize their microenvironmental context using paired single-cell-resolution spatial transcriptomics.
Methods Formalin-fixed tissues from 17 LUAD patients were profiled using the 10x Genomics Xenium 5K panel, generating paired datasets from primary tumors and matched lymph-node metastases. Spatial and transcriptional integration was performed using Seurat and SpatialData, and metascores and differential expression analyses were computed with Scanpy.
Results Integrated primary-lymph node analysis revealed a recurrent tumor-cell cluster whose transcriptional state aligned most closely with lymph-node profiles, representing a metastasis-competent SEED population. SEED regions showed elevated metascores and enrichment of invasion and hypoxia-associated programs, including robust HIF1A upregulation. The surrounding microenvironment was spatially distinct: fibroblasts immediately adjacent to seed clusters exhibited high POSTN expression, forming a dense stromal shell, while CXCR4-high B-cell aggregates accumulated peritumorally. In contrast, T-cell distribution remained relatively uniform across regions, indicating that SEED-associated remodeling was driven by specific stromal and B-cell interactions rather than general immune infiltration. Together, these spatially coordinated patterns delineate a niche in which HIF1A-high tumor cells interface with POSTN-rich fibroblasts and CXCR4-expressing B cells to support metastatic competence.
Conclusions Paired single-cell spatial mapping identifies discrete metastasis-prone SEED niches within LUAD primary tumors. These niches are defined by HIF1A-high tumor cells embedded in a POSTN-rich stromal compartment and surrounded by CXCR4-high B-cell aggregates. This spatial ecosystem provides a mechanistic framework for how only specific primary-tumor regions acquire the capacity for lymph-node dissemination and suggests niche-level targets for metastasis interception.
AI Disclosure (AACR-required) This abstract includes text revised with the assistance of generative AI.

#6119 Immune-vascular profiles in primary tumors and paired liver metastases of colorectal cancer.

Alfonso Martin-Bernabe[1], Tove Bekkhus[2], Elisabet Rodriguez-Tomas[2], Reetta Peltonen[3], Pauliina Reijonen[3], Emerik Osterlund[4], Caj Haglund[5], Jaana Hagstrom[3], Helena Isoniemi[3], Bengt Glimelius[1], Tobias Sjoblom[1], Arne Ostman[2], Ari Ristimaki[3], Teijo Pellinen[5], Pia Osterlund[6]

[1]Uppsala University, Uppsala, Sweden,[2]Karolinska Institutet, Stockholm, Sweden,[3]Helsinki University Hospital and University of Helsinki, Helsinki, Finland,[4]The University of Texas MD Anderson Cancer Center, Houston, TX,[5]University of Helsinki, Helsinki, Finland,[6]Tampere University Hospital and Karolinska Institutet, Tampere/Stockholm, Finland

Background: The immune and vascular features of the tumor microenvironment influence outcomes of patients with colorectal cancer liver metastases (CRLMs). However, comparative analyses of these features, and their interactions, between primary colorectal tumors and their matched CRLMs, as well as their treatment-driven remodeling are limited.
Methods: We analyzed 1-3 TMA cores per tumor (1 mm) from 50 matched primary tumors and CRLM (15 untreated, 35 neoadjuvant-treated with cytotoxic ±VEGF-/EGFR-targeted agents before liver resection). We used multiplex immunofluorescence to quantify T-cell densities (CD3, CD4, CD8, PD1, FOXP3, TIM3, Ki67), vessels (claudin-5) and perivascular (PV) subset (αSMA, PDGFRβ) fractions. Statistical analyses included non-parametric tests (Wilcoxon, Mann-Whitney, Spearman) and Intraclass Correlation Coefficient (ICC) for concordance.
Results: Comparisons of untreated paired primary tumors and CRLMs identified significantly lower densities of CD3+CD8+Ki67+, CD3+CD4+Ki67+, CD3+CD4+FOXP3+, and CD3+CD8+PD1+ cells (all p≤0.006) in CRLMs. Regarding vessels, CRLMs showed a lower fraction of αSMA+PDGFRβ+ PV subset (p=0.001), higher fraction of αSMA+PDGFRβ- PV subset (p<0.001), and increased vessel density (p=0.01). Analyses contrasting untreated and treated CRLM showed reduced vessel size (p=0.002) in treated CRLM. Analysis of immune-vascular co-occurrence patterns of potential functional significance was also performed. In untreated primaries, the αSMA-PDGFRβ+ PV subset correlated positively with densities of CD3+CD8+FOXP3+ (r=0.66, p=0.008), CD3+CD8+Ki67+ (r=0.61, p=0.016), and CD3+CD4+PD1+ (r=0.59, p=0.002) cells. In contrast, in untreated CRLMs, the αSMA+PDGFRβ+ PV subset correlated with CD3+CD4+Ki67+ (r=0.56, p=0.03) and CD3+CD4+PD1+ (r=0.62, p=0.013) cell densities. Furthermore, in CRLMs, larger vessel size was uniquely associated with higher CD3+CD4+ cell density (r=0.54, p=0.04). Treatment-exposed CRLMs lacked the associations of untreated CRLMs and instead displayed new associations such as αSMA-PDGFRβ+ PV subset and CD3+CD8+Ki67+ cells (r=0.40, p=0.018). Finally, ICC analyses of inside-case concordance regarding marker status in untreated primary, and CRLM showed that vascular metrics were more stable within patients (αSMA-PDGFRβ+ PV subset ICC=0.60; vessel size ICC=0.36), than T-cell densities (mean ICC=0.02).
Conclusion: These exploratory analyses indicate that CRLM is characterized by lower immune cell densities and a different PV stroma compared to primary tumors. Treatment appears to have a stronger impact on CRLM vessel features than on immune features. Furthermore, immune-vascular co-occurrence patterns are site specific and modulated by treatment. Collectively, these preliminary results identify immune-vascular features for further exploration regarding biomarker and drug target potential.

#6120 Histologic growth pattern dictates immune cell spatial topography in liver metastases.

Artur Mezheyeuski[1], Gemma Garcia-Vicien[2], Nuria Ruiz[2], Jose C. Ruffinelli[3], Kristel Mils[4], Maria Banuls[4], Natalia Molina[5], Miguel A. Pardo[4], Laura Llado[6], Patrick Micke[7], David G. Mollevi[8]

[1]Vall d'Hebron Research Institute (VHIR), Barcelona, Spain,[2]IDIBELL, L'Hospitalet de Llobregat, Barcelona, Spain,[3]Institut Catala d'Oncologia, L?Hospitalet de Llobregat, Spain,[4]Institut Catala d'Oncologia, Barcelona, Spain,[5]IDIBELL, Barcelona, Spain,[6]Hospital Universitari de Bellvitge, Barcelona, Spain,[7]Uppsala University, Uppsala, Sweden,[8]Laboratori de Ricerca Translacional, Institut Catala D'Oncologia, Barcelona, Spain

Background: Hepatic metastases from colorectal cancer represent one of the leading causes of mortality associated with this disease, and their management remains a clinical challenge that requires increasingly precise diagnostic and therapeutic strategies. We have previously reported colorectal liver metastases (CRCLM) with desmoplastic histological growth pattern (dHGP) to have more cytotoxic immune environment, enriched by $CD8^+$ lymphocytes over tumor nests. $FoxP3^+$ cells followed the $CD8^+$, but $CD4^+FoxP3^+$ (Tregs) did not demonstrate difference. Here we focused on rare lymphocyte subset: $CD8^+FoxP3^+$ cells.

Methods: We applied multiplex IHC panel with immune cell markers for tissue samples from 100 patients with CRCLM, characterized by HGP. Cell classes included Cytokeratin (CK)-positive cells, CD8, CD4, $CD4^+FoxP3^+$, $CD8^+FoxP3^+$, $CD20^+$ and HSA (Hepatocyte specific antigen). Cell density defined as number of cells per mm^2. To resolve spatial patterns, we computed neighborhood enrichment (ENR) and the pair correlation function (PCF). ENR, evaluated distance to k-nearest neighbors (k=5-100), and quantified attraction or avoidance between cell classes while controlling for cell density. PCF, computed over radial distances (10-50 µm).

Results: The initial cell density analysis demonstrated that $CD8^+FoxP3^+$ cells were significantly more abundant in dHGP (p=0.003), following similar arrangement of larger CD8+ cell set (p=0.007). Spatial analysis, adjusted to cell density, demonstrated more complex patterns. **First**, $CD8^+FoxP3^+$ showed strong spatial attraction to CD8 cells in non-dHGP, while in dHGP, where both cell types were significantly more abundant, they tended to disperse (confirmed by agreement across five spatial metrics, with k=5-50, r=50, p=0.01-0.004). **Second,** In dHGP, the $CD8^+FoxP3^+$ cells had strong tendency to neighbor to $CD20^+$ (B-cells) (confirmed by agreement across five spatial metrics, with k=5-25, p=0.05-0.005). **Third,** $CD8^+FoxP3^+$ cells demonstrated attraction to cancer cells, in dHGP, detected by ENR at k=5-25 (p=0.01), indicating nearest vicinity or direct contact.

Conclusions: The neighboring tendencies observed between $CD8^+FoxP3^+$ and $CD8^+$ cells in non-dHGP, suggest either a strong biological interaction between these two T-cell subsets or dynamic conversion between states of $CD8^+$ linage. In dHGP, $CD8^+FoxP3^+$ cells were instead redirected toward $CD20^+$ B-cell rich areas and showed nearest-neighbor attraction to CK-positive tumor cells, consistent with positioning in or near tertiary lymphoid structure (TLS)-like niches and at the tumor-stroma interface. Altogether, this provides the first spatially resolved description of $CD8^+FoxP3^+$ cells in CRCLM and highlights their abundance and neighborhood context as potential contributors to the distinct immune architectures and clinical behavior of dHGP versus non-dHGP liver metastases.

#6121 Hippo/YAP1 mediated interplay of tumor-stromal-immune suppressive TME through IL6/gp130/STAT3 axis in advanced gastric cancer.

Junsong Zhao[1], Xiaodan Yao[1], Yibo Fan[2], Dipti Athavale[1], Yanting Zhang[1], Francis Spitz[3], Generosa Grana[3], Shilpa S. Dhar[2], Jaffer A. Ajani[2], Shumei Song[1]

[1]Coriell Institute for Medical Research, Camden, NJ,[2]UT MD Anderson Cancer Center, Houston, TX,[3]Camden Cancer Research Center, Camden, NJ

Abstract

Background: Peritoneal metastases (PMs) occur in ~45% of patients with advanced gastric cancer (GC) and are associated with debilitating symptoms and median survival of less than six months, yet the tumor-stromal–immune mechanisms sustaining the immune suppressive metastatic niche in GC with PM (GCPM) remain poorly defined. Single-cell RNA sequencing of patient-derived PMs revealed that, in addition to tumor epithelial clusters, a subset of activated cancer-associated fibroblasts (CAFs) expresses high levels of the Hippo pathway coactivator YAP1, which associates with CAF activation programs and poor survival. We hypothesized that YAP1^{high} CAFs orchestrate an IL-6-dependent immunosuppressive metastatic niche that can be therapeutically targeted.

Methods: Primary CAFs were established from GCPM implants and malignant ascites. YAP1 was genetically ablated using CRISPR/Cas9, and effects on the CAF secretome were assessed by cytokine arrays, multiplex ELISA, and qPCR. Co-culture assays with GC cell lines and CAFs with YAP1^{hgih} or YAP1^{KO} to determine the effects of YAP1 in CAFs on tumor cell malignant behaviors including tumor invasion, growth and tumor sphere formation; Co-culture of CAFs with YAP1^{hgih} or YAP1^{KO} with PBMC from peripheral blood or malignant ascites-derived CD45^{+} immune cells were used to evaluate the effects of YAP1 in CAFs on T-cell function. In vivo, genetic and pharmacologic YAP1 inhibition were tested in YAP1^{high} patient-derived xenograft (PDX) and patient-derived orthotopic (PDO) models and in the KP-luc2 syngeneic GC model using the TEAD inhibitor VT00278, the STAT3 inhibitor WP1066, and their combinations with anti-PD-1.

Results: YAP1 knockout in CAFs reduced invasion and growth of co-cultured tumor cells in vitro and enhanced T-cell activation in co-culture with PBMC. Secretome profiling by cytokine array identified interleukin-6 (IL-6) as the most strongly YAP1-dependent cytokine, IL-6 was highly expressed in YAP1^{high} CAFs and enriched in malignant ascites, whereas IL6R/gp130 were upregulated in exhausted CD4^{+}/CD8^{+} T cells, fibroblasts, and tumor cells within PM samples. YAP1 depletion decreased IL-6 expression and secretion, and pharmacologic blockade of the IL-6/gp130/STAT3 axis partially phenocopied the effects of YAP1 loss on tumor and T-cell function. Ongoing PDX, PDO, and KP-luc2 studies are evaluating dual YAP1/TEAD and STAT3 inhibition, with or without PD-1 blockade, as a strategy to remodel the PM microenvironment.

Conclusions: These data support a model in which YAP1^{high} CAFs drive an IL-6/gp130/STAT3–dependent immunosuppressive metastatic niche in GCPMs. Dual targeting of YAP1/TEAD and IL-6/STAT3, potentially combined with immune checkpoint blockade, represents a rational novel therapeutic strategy that will be prioritized for clinical translation in GC patients with PM.

#6122 Organ-specific immune and metabolic programs shape spatial microenvironments in MSS colorectal cancer metastases.

Jian Ye[1], Colt A. Egelston[2], Chongkai Wang[3], Marwan Fakih[4]

[1]Department of Medical Oncology and Therapeutics Research, City of Hope National Medical Center, Duarte, CA,[2]Department of Immuno-Oncology, Beckman Research Institute of the City of Hope, Duarte, CA,[3]City of Hope National Medical Center, Department of Medical Oncology and Therapeutics Re, CA,[4]City of Hope National Medical Center, Duarte, CA

Background: Our previous spatial analysis of MSS metastatic colorectal cancer (mCRC) revealed organ-specific differences in immune infiltration across metastatic sites (Ye et al., *Cancer Res Commun*, 2023). Building on that work, we expanded the cohort and applied high-plex spatial transcriptomic and proteomic platforms to characterize region- and organ-dependent microenvironmental programs.

Methods: Spatial transcriptomic profiling using the GeoMx WTA (70 specimens) was performed across malignant, stromal, invasive-margin, distal, and TLS-associated regions. A 56-plex CODEX spatial proteomic panel (120 specimens) was used for whole-tumor multiplex imaging to visualize immune and stromal architecture.

Results: Spatial compartment was the primary driver of transcriptional variation, with malignant epithelial regions from different organs clustering closely together and separating distinctly from normal colon villus epithelium and stroma. Liver outer-margin and distal regions formed a separate transcriptomic cluster from analogous regions in other organs, indicating a strong liver-associated imprint. Within this region-defined structure, GSEA revealed coherent organ-specific archetypes. Primary colon generally showed intermediate immune and metabolic programs. Liver metastases showed broad metabolic activation across regions, including lipid and amino-acid metabolism, mitochondrial and peroxisomal activity, and complement-related signatures, reflecting a metabolically conditioned liver niche. Lung metastases were associated with immune-enriched stromal, margin, and distal regions, marked by strong NK-cell cytotoxicity, T cell differentiation, cytokine signaling, mucosal-like immune networks, and antiviral pathways. Peritoneal metastases showed metabolically and immunologically quiet tumor cores, while outer and distal regions were enriched for lipid and steroid metabolism, and ECM and mesothelial activation, consistent with a lipid-rich, immune-poor peritoneal niche. Preliminary CODEX observations were broadly consistent with these patterns. Lung metastases often showed abundant T-cell infiltration; liver metastases showed lymphocytes accumulating at tumor boundaries with myeloid-enriched tumor centers; and peritoneal metastases displayed dense stromal or fibrotic architecture with limited intratumoral lymphocytes.

Conclusions: High-plex spatial profiling reveals distinct organ-imposed microenvironmental programs in MSS mCRC. Liver metastases adopt a highly metabolic and complement-associated niche, lung metastases display strong peritumoral immune activity, and peritoneal metastases develop within a lipid-rich but immune-low environment. These findings highlight how each organ shapes metastatic ecology and may guide site-adapted therapeutic strategies.

#6123 TNBC-derived lipocalin-2 potentiates metastasis by inducing immunologic reprogramming of premetastatic and metastatic microenvironments.

Gabriela Ortiz-Soto[1], Joshua Gamez[2], Carolyn Rentz[1], Raynah Cheng[1], Francesca Sanchez[3], Abigail Terry[1], Peter Gray[4], Mary Lauren Benton[1], Jonathan Kelber[1]

[1]Baylor University, Waco, TX,[2]Biology, California State University - Northridge, Northridge, CA,[3]California State University - Northridge, Northridge, CA,[4]Independent Research Consultant, Los Angeles, TX

Triple negative breast cancer (TNBC) is distinguished by the absence of estrogen/progesterone receptors and HER2 overexpression. Generally, the median survival for metastatic TNBC is a dire 8-10 months, representing a sharp drop from the five-year survival for metastatic breast cancer of other subtypes (~40%) or non-metastatic TNBC (~75%). Metastatic TNBC is associated with anti-inflammatory tumor immune microenvironments (TIMEs) and little is known about how primary and secondary tumors communicate with one another during disease progression. The Lipocalin-2 gene (LCN2) encodes a cytosolic and secreted protein (Lcn2) that regulates receptor trafficking, inflammation, microbiome dynamics and iron homeostasis. Previous work from our group and others has shown that LCN2/Lcn2 promotes tumorigenesis; however, questions persist regarding the specific contexts in and mechanisms by which it functions to potentiate cancer progression. To define the molecular and cellular factors that govern LCN2-mediated tumor progression, we developed the Py230-C57Bl/6 syngeneic experimental metastasis model for interrogating mechanisms by which tumor cell-secreted factors condition premetastatic lung tissue to potentiate TNBC cell seeding/expansion. Using this model and TCGA data, we identify LCN2/Lcn2 as a molecular candidate that is upregulated in lung-tropic Py230 cells and other human TNBC cells, and that predicts poor TNBC patient outcomes. We demonstrate that TNBC cell-secreted Lcn2 potentiates premetastatic lung reprogramming to increase tumor cell seeding and expansion. Our analyses of global transcriptome and single-cell spatial proteome data in premetastatic lung tissue collected from mice systemically educated by mock media or breast cancer conditioned media from Py8119 (Lcn2-low), Py230-IgG2a (Lcn2-hi) or Py230-αLcn2 (Lcn2-blocked) cells reveal novel gene set enrichments affiliated with oxidative phosphorylation and proliferating B cells. Further single-cell spatial proteome analyses on Lcn2-potentiated lung metastases indicate an increase in proliferating regulatory T cells (FoxP3-pos) indicating that Lcn2-mediated reprogramming of the tumor-naïve lung microenvironment suppresses inflammation to support increased tumor burden. Finally, by using single-cell spatial transcriptomics on matched primary and metastatic TNBC samples, we determine that LCN2 expression localizes to a subpopulation of epithelial and hybrid EMT cells near T cells within primary tumor sites. Notably, within corresponding matched metastatic TNBC samples, we find immune cells that are enriched for genes affiliated with oxidative phosphorylation and anti-inflammatory signaling. Taken together, we report a novel immunologic reprogramming role for LCN2 in TNBC that may be targeted to block or reverse disease progression and improve patient outcomes.

#6124 TIM3⁺tumor associated M2 macrophages impair antitumor T cell immunity and promote gastric cancer progression and peritoneal metastasis.

Xiaodan Yao[1], Junsong Zhao[1], Yibo Fan[2], Yanting Zhang[1], Dipti Athavale[1], Curt Balch[1], Mikel Ghelfi[1], Anthony Pompetti[1], Jiankang Jin[2], Yong Ki Hong[3], Jamin Morrison[3], Madeline Torres[3], Francis Spitz[3], Generosa Grana[3], Shilpa S. Dhar[2], Linghua Wang[2], Jaffer A. Ajani[2], Shumei Song[1]

[1]Coriell Institute for Medical Research, Camden, NJ,[2]UT MD Anderson Cancer Center, Houston, TX,[3]Cooper University Hospital, Camden, NJ

Background: Peritoneal metastases (PM) are the leading cause of cancer-related death in gastric cancer (GC), with typical survival of <9 months and no effective targeted or immune therapies available. T-cell immunoglobulin and mucin domain-3 (TIM3) was initially identified on the surface of T helper 1 (Th1) cells and cytotoxic (CTL) lymphocytes as an immunosuppressive molecule that interacts with its ligands (GAL-9, CEACAM1, HMGB1, and PtdSer), and its expression is associated with advanced cancer stage. However, its functional role in promoting GC-associated PM (GCPM) and its clinical relevance in advanced GC remain unclear.

Methods: multiple profiling and functional assays including scRNA-seq, CyTOF, qRT-PCR, cytokine arrays, kinase arrays, ELISA, and Western blotting were used to evaluate gene expression and secretion. TIM3 was genetically ablated using CRISPR/Cas9 in in macrophages to determine its functional role in tumor cells and T cells by co-culture system. *In vivo*, genetic and pharmacologic inhibition of TIM3 in macrophages co-innovation with tumor cells were tested in $TIM3^{high}$ vs $TIM3^{KO}$ macrophages on tumor growth in patient-derived xenograft (PDX) and patient-derived orthotopic (PDO) models and in the KP-luc2 syngeneic GC model.

Results: We demonstrate that TIM3 and its ligands increased along the GC continuum and are associated with poor survival. Integrated omics analyses, multi-flow and co-immunofluorescent staining revealed that TIM3 is highly enriched in $CD163^{+}$ tumor associated M2 immunosuppressive macrophages, which significantly increased tumor cell invasion *in vitro*, and promoted tumor growth *in vivo*. TIM3 depletion in macrophages reduced tumor cell malignant phenotypes and enhanced T-cell immunity from PBMCs or $CD45^{+}$ immune cells isolated from malignant ascites in co-culture assays. Cytokine and kinase array analyses showed that TIM3 depletion in macrophages reduced production of key cytokines and chemokines from M2 macrophages. We further identified the RSK/CCL20/CCR6 axis as essential for the pro-tumor activity of $TIM3^{+}$ macrophages. Finally, we show that TIM3 blockade or genetic knockout exhibits strong antitumor effects, especially when combined with anti-PD-1/PD-L1 immunotherapy or mitomycin C (MMC) chemotherapy. Together, these findings reveal a critical role for TIM3 in tumor associated macrophages and highlight the potential of TIM3 targeted immune therapy in GC patients with PM.

Conclusion: TIM3 is highly enriched in tumor associated macrophages in GC with PM and plays a pivotal role in promoting GC progression and suppressing T-cell function. Thus, targeting TIM3 especially in combination with anti-PD1/PD-L1 or chemotherapy MMC may provide a novel therapeutic strategy for advanced GC patients with PM.

#6125 Osteosarcoma exploits macrophage VCAM1-VLA4 signaling axis to facilitate pulmonary metastasis.

Daniel Kingsley, Sung Hee Choi, Jay Myers, Alex Y. Huang

Case Western Reserve University, Cleveland, OH

Osteosarcoma (OS) is an aggressive bone cancer primarily found in children and young adults with a five-year survival rate that drops significantly in patients with metastatic disease. At diagnosis, around 20% of patients have lung metastases, reducing survival from 70% to 30%. We believe that an indicator of metastatic potential is the aberrant expression of Vascular Cell Adhesion Molecule 1 (VCAM-1) on the tumor surface as human OS tissues have been shown to overexpress this molecule; however, its precise role remains unclear. We hypothesize that the interaction between VCAM-1 on OS cells and its receptor, the α4β1 integrin (VLA-4) on macrophages, contributes to the ability of OS to metastasize. Our preliminary evidence suggests that tumorigenic effects of VCAM-1 are isoform dependent, and truncated VCAM-1 is critically important to metastasis. Our research model uses bone marrow-derived macrophages exposed to murine OS cell lines K7 and K7M2, the latter being highly metastatic. Early data show that VCAM-1-VLA-4 binding induces a pro-tumoral macrophage phenotype, upregulating Arginase 1, an M2 macrophage marker. Currently, we are investigating whether this effect is specifically driven by the truncated isoform and exploring the role it plays in the PI3K-AKT signaling pathway. We plan to evaluate this hypothesis by looking at expression of the proteins in this signaling axis on bone marrow derived macrophages (BMDMs) that have been influenced by the aforementioned osteosarcoma cell lines. By elucidating how VCAM-1-VLA-4 interactions drive macrophage polarization, we aim to identify novel therapeutic targets that could shift macrophage behavior and improve treatment outcomes in OS.

#6126 Multiomics integration unveils a shifted balance in the sphingosine-1 phosphate/ceramide rheostat fueled by macrophage immunosuppression in metastatic colorectal cancer.

Michelle M. Maurin[1], Siddabasave Gowda B. Gowda[2], Divyavani Gowda[3], Heiman Wang[1], Michael Nebozhyn[4], Ramani Soundararajan[1], Mckayla Carr[1], Punith M Sundaraswamy[5], Ashley Alden[1], Carolina Martinez[1], Robert David Bennett[1], Allen Chudzinski[1], Andreas Karachristos[1], Timothy M. Nywening[1], Paul M. Cavallaro[1], Matthew Linley Anderson[1], Robert J. Coffey[6], Michael Schell[7], Jorge Marcet[1], Richard Jacobson[1], Andrey Loboda[4], Ganesh V. Halade[8], Mingli Yang[1], Lance Pflieger[9], Warren Jackson Pledger[10], Shu-Ping Hui[3], Timothy J. Yeatman[1]

[1]Department of Surgery, University of South Florida, Tampa, FL,[2]Graduate School of Global Food Resources and Faculty of Health Sciences, Hokkaido University, Sapporo, Japan,[3]Faculty of Health Sciences, Hokkaido University, Sapporo, Japan,[4]Director, Informatics&Analysis, Merck & Co., Inc., Boston, MA,[5]Graduate School of Global Food Resources, Hokkaido University, Sapporo, Japan,[6]Vanderbilt University Medical Center, Nashville, TN,[7]Biostatistics and Bioinformatics Department, Moffitt Cancer Center, Tampa, FL,[8]Department of Internal Medicine, University of South Florida, Tampa, FL,[9]Buck Institute for Research on Aging, Center for Phenom Health., Novato, CA,[10]Tampa General Hospital and Department of Molecular Medicine, University of South Florida, Tampa, FL

Background Thirty years ago, a S1P/ceramide “sphingosine rheostat” model was proposed based on ceramide’s pro-apoptotic *vs.* sphingosine-1 phosphate (S1P) pro-survival role, where in cancer, the rheostat tilts towards enhanced synthesis of S1P from ceramides, increasing the ratio. Human tumor data supporting the hypothesis, however, are very limited.
Objective To leverage quantitative multi-omics to explore the balance in the synthesis of lipids within the S1P/Ceramide metabolic pathway in a large set (n = 629) of human colorectal cancers (CRC).
Design Quantitative LC-MS/MS analysis was performed on 525 primary and 104 metastatic CRC (mCRC). An integrative multi-omics analysis combining quantitative lipidomics with whole transcriptomics, quantitative RT-PCR of selected genes and clinical data was completed.
Results We demonstrated that mCRC versus primary specimens are relatively enriched in S1P and sphinganine-1-P (Sa1P), whereas the long chain ceramides (24:1) are relatively decreased. Gene-expression analysis of a large (n = 2200) CRC patient dataset and qRT-PCR of CRC revealed that S1P/Sa1P-synthesizing enzymes and their receptors are enriched in mCRC and are linked to poor prognosis. scRNA-seq analysis showed that their expression prevailed in myeloid cells. Finally, a three-gene S1P macrophage-associated signature correlated with stage and patient survival.
Conclusion Our findings define an imbalance in the synthesis of S1P/Ceramide linked to poor prognosis and cancer progression, and attributable to proinflammatory macrophages in the tumor microenvironment, validating the sphingosine rheostat hypothesis in mCRC.

#6127 Hepatic niche driven metabolic-epigenetic reprogramming mediates metastatic colonization through liver progenitor like plasticity.

Ajit Kumar SHARMA[1], Nobuyuki Takahashi[2], Sophie Zhuang[3], Amira Kazi[3], Michael Nirula[3], Abhinav Joshi[3], Yingying Cao[4], Rajesh Kumar[4], Kanak Parmar[3], Christopher Schultz[5], Parth Anil Desai[6], Samantha Nichols[3], Linda Sciuto[3], Yue Huang[7], Chiori Tabe[3], Yang Zhang[3], Sanghvi Neel[1], Nishanth Ulhas Nair[4], Christopher A Febres Aldana[1], Nir Friedman[8], Simone Difilippantonio[9], Thorkell Andresson[3], Eytan Ruppin[3], Stephen M. Hewitt[3], Anish Thomas[4]

[1]NIH/National Cancer Institute, Bethesda, MD,[2]National Cancer Center Hospital East, Kashiwa, Japan,[3]National Institutes of Health, Bethesda, MD,[4]National Cancer Institute, Bethesda, MD,[5]Department of Medical Oncology, Fox Chase Cancer Center, Philadelphia, PA,[6]Fox Chase Cancer Center, Philadelphia, PA,[7]Developmental Therapeutics Branch, NIH/National Cancer Institute, Bethesda, MD,[8]The Hebrew University of Jerusalem, Rehovot, Israel,[9]Leidos Biomedical Research, Inc., Frederick, MD

Background
Liver metastasis is a major cause of mortality in small cell lung cancer (SCLC), but the organ-specific cues that enable metastatic colonization are poorly understood. We hypothesized that the hepatic microenvironment promotes a stem-like, high-plasticity state required for metastatic outgrowth.
Methods
We analyzed patient-derived SCLC liver metastases using RNA-seq, ATAC-seq, and metabolomics, combined with spatial transcriptomics and orthotopic liver colonization models. Regional hypoxia, HIF1α signaling, and metabolic flux were assessed by protein quantification and 13C-glucose tracing. Functional studies included pharmacological ACLY inhibition (SB204990) and CRISPR-mediated ACLY knockout in vivo.
Results
Across patient specimens and in vivo models, metastatic SCLC cells in the liver adopted a distinct stem-like transcriptional state, marked by activation of regenerative programs and chromatin accessibility at stemness loci (HNF1A, HNF4A, SOX9, ATF3). Spatial profiling revealed that tumor cells adjacent to hepatocytes experienced localized hypoxia, resulting in HIF1α stabilization and the transcriptional induction of ACLY, a key enzyme that generates nuclear acetyl-CoA. ATP-citrate lyase (ACLY)-dependent generation of nuclear acetyl-CoA, driving histone hyperacetylation and chromatin remodeling at liver-lineage transcription factors HNF1A, HNF4A, and SOX9. Liver-metastatic cells undergo glycolytic reprogramming, a metabolic shift that parallels hepatocyte regeneration during liver injury, providing acetyl-CoA and biosynthetic precursors to support epigenetic remodeling and lineage adaptation. Similar progenitor-like hepatic plasticity is observed across other epithelial cancers with liver tropism, including breast, colon, and non-small cell lung cancers, indicating a conserved mode of metastatic adaptation. ALY activity mediated histone hyperacetylation and epigenetic remodeling required for the stem-like state. ACLY was functionally essential. Pharmacologic ACLY inhibition blocked the induction of stem-like programs, reduced histone acetylation, and growth rate of liver metastatic cells. CRISPR-ACLY knockout prevented the acquisition of the reprogrammed phenotype. Similar hepatic niche-induced stemness signatures were observed in liver metastases from breast, colon, and NSCLC, suggesting a conserved mechanism across epithelial cancers.
Conclusions
The liver microenvironment actively promotes metastatic competency by inducing a HIF1α-ACLY-acetyl-CoA-driven stem-like state in disseminated tumor cells. ACLY inhibition disrupts this metabolic-epigenetic reprogramming and markedly suppresses liver metastatic outgrowth, highlighting ACLY as a tractable therapeutic target for liver metastasis.

#6129 Microenvironmentally-driven dynamic deposition of histone H3.3 controls entry and exit from dormancy in disseminated cancer cells.

Stanislav Drapela[1], Cristina Megino-Luque[2], Rojan Chimeh Rad[1], Devesh Raizada[1], Nadir Sarigul[1], Didem Ilter[3], Brian J. Czerniecki[4], Javier J. Bravo-Cordero[2], Ana P. Da Silva Gomes[1]

[1]Department of Tumor Microenvironment and Metastasis, Moffitt Cancer Center, Tampa, FL,[2]Department of Medicine, The Tisch Cancer Institute, Icahn School of Medicine at Mount Sinai, New York, NY,[3]Moffitt Cancer Center, Tampa, FL,[4]Department of Breast Oncology, Moffitt Cancer Center, Tampa, FL

Breast cancer metastases can go undetected for long periods of time, are highly resistant to therapy, and are the cause for more than 90% of breast cancer mortality. Dormancy is a critical step in the metastatic cascade, whereby disseminated cancer cells (DCCs) enter a non-proliferative state at distal sites until they reactivate and give rise to overt metastasis, often years after disease remission. As such, dormancy represents a major clinical obstacle in breast cancer patient care. Chromatin remodeling serves as a foundation for the cellular reprogramming required to drive cell fate transitions. However, little is known about the nature of this remodeling in dormancy. Here, we hypothesize that differential deposition of histone H3.3 determines whether DCCs enter and remain dormant in secondary organs or proliferate and form overt metastases. We used a combination of H3.3 deposition sensors and genetic tools to manipulate H3.3 and its cognate chaperone, HIRA, *in vitro* and *in vivo* to track H3.3 deposition through the metastatic cascade and evaluate its importance for dormancy. Our data demonstrates that H3.3 incorporation at secondary sites is heterogenous, revealing a subset of DCCs with low H3.3 in chromatin. Blocking H3.3 deposition onto chromatin leads to a reversible arrest in G0/G1 which tracks with the activation of canonical dormancy signaling. To define mechanism of regulation, we used a combination of whole genome sequencing (ChIP-seq, ATAC-seq and RNA-seq) followed by in-depth analysis and functional validation. Our data supports a model where blocking H3.3 incorporation into chromatin directly represses the expression of SKP2, the main regulator of progression through the restriction point of cell cycle via regulation of p27 degradation. SKP2 suppression in turn leads to the accumulation of p27 thereby causing cell cycle arrest in G0/G1 and dormancy establishment. We traced this H3.3-mediated regulation of dormancy through the dynamic regulation of H3.3 histone chaperone, HIRA, whose levels inversely correlate with dormancy in experimental models as well as in patient samples. Moreover, we found that HIRA levels respond to the metastatic microenvironment where fibrotic conditions induce HIRA expression and trigger metastatic outgrowth in an H3.3-dependent manner. Together, our work unveils for the first time a patient-relevant epigenetic mechanism, impinging on H3.3 deposition and HIRA as its driver, as a major regulatory point of DCCs' cell fate at secondary organs controlling both entry of DCC's into dormant state as well as their reactivation and thriving as overt metastasis.

#6131 BDNF-TrkB.T1 receptor signaling modulate an immunosuppressive tumor microenvironment and epithelial-mesenchymal transition in gliomas.

Leyre Merino-Galan[1], **Jin-Yih Low**[1], Sergio Ortiz-Espinosa[2], Hawa L. Jagana[1], John M. Hemmenway[1], Ashmitha Rajendran[1], Mathew R. Hattaway[1], Taylor S. Jackson[1], Maryam Shabar[1], Noemi Reche-Ley[1], Sonali Arora[2], David Johnson[1], Daniel A. Kuppers[2], Patrick J. Paddision[2], Siobhan S. Pattwell[1]

[1]Ben Towne Center for Childhood Cancer and Blood Disorders Research, Seattle Children's Research Institute, Seattle, WA, [2]Division of Human Biology, Fred Hutchinson Cancer Center, Seattle, WA

Introduction: Gliomas are the most common and aggressive brain tumors in children and adults. The tumor microenvironment (TME), including neurons, glial cells, blood-brain barrier, and immune components, plays a key role in glioma progression and therapy resistance. Brain-derived neurotrophic factor (BDNF) and its receptor, tropomyosin receptor kinase B (TrkB), encoded by NTRK2, are emerging as central players in glioma biology. Among TrkB isoforms, truncated TrkB.T1 is the most abundantly expressed variant in human gliomas and various adult and pediatric tumors. Recent studies show TrkB.T1 is the predominant isoform during embryogenesis and organogenesis, with high expression along mesenchymal trajectories, suggesting a role in glioma epithelial-mesenchymal transition (EMT). Previously, we showed TrkB.T1 overexpression in human neural stem cells downregulated genes in the MHC Class II and interferon-gamma signaling pathways, both essential for antigen presentation and cytotoxic T cell recruitment. This study aims to elucidate BDNF-TrkB.T1 signaling in modulating glioma TME and EMT phenotype.
Approaches: We performed in silico analyses using publicly available single-cell RNA sequencing data (GSE182109), stratified into NTRK2 high, medium, and low clusters, and correlated with PTPRC (CD45) expression. Using the PDGFB RCAS-tva model, we generated in vivo gliomas via intracranial RCAS-PDGFB + RCAS-TrkB.T1 injection in Nestin/tv-a;Ink4a/Arf-/- mice at postnatal day 1-2. Tumors were collected at 3.5-5 weeks post-injection for immunofluorescence and flow cytometry. We also created a TrkB.T1 knockout (KO) mouse model and performed blood immune profiling. For in vitro studies, we used 448T (TrkB.T1 high) and 559T (TrkB.T1 low) glioma stem cells (GSCs) to assess BDNF-TrkB.T1 signaling effects on cytokine profiles and neutrophil chemotaxis. EMT changes were examined via western blot and transwell migration assays.
Results: NTRK2 expression in gliomas was inversely correlated with PTPRC, and higher NTRK2 levels were linked to reduced immune cell infiltration. In vivo, TrkB.T1 expression reduced classical dendritic cells and T cell-activating cytokines, while increasing microglial density and neutrophil infiltration, indicating an immunosuppressive TME. Conversely, TrkB.T1 KO mice showed increased effector CD8+ T cells. In vitro, BDNF-TrkB.T1 signaling promoted chemokine release linked to neutrophil recruitment and T-cell inactivation, and enhanced neutrophil migration in GSC-BDNF chemotaxis assays. BDNF stimulation also increased N-cadherin and GSC migration, indicating an EMT phenotype.
Conclusion: These findings reveal the role of BDNF-NTRK2 splice variant TrkB.T1 in promoting immunosuppressive TME and EMT in gliomas, suggesting a therapeutic opportunity to target TrkB.T1 in future translational and clinical studies.

#6132 Linking metabolic reprogramming to JAK-STAT signaling in triple-negative breast cancer brain metastasis.

Jayshree Mishra[1], Narendra Kumar[2]

[1]Pharmaceutical Sciences, Texas A&M University, KINGSVILLE, TX,[2]Texas A&M University, Kingsville, TX

Introduction: Triple-negative breast cancer (TNBC) is an aggressive breast cancer subtype disproportionately affects younger patients and associated with high recurrence rates and rapid disease progression. TNBC cells that colonize the brain undergo extensive metabolic reprogramming to survive in this specialized microenvironment. Understanding the mechanisms by which TNBC cells adapt their metabolism and signaling networks to thrive in the brain niche is critical to uncovering novel vulnerabilities for therapeutic intervention.
Materials and Methods: To address this knowledge gap, we conducted integrated metabolomic and transcriptomic analyses utilizing a TNBC brain metastasis (BM) xenograft mouse model, with validation in human patient-derived tissues. Metabolite profiling was performed using liquid chromatography-mass spectrometry equipped with an ACQUITY UPLC BEH C18 column. Matched samples from primary tumors, brain metastases, and serum were analyzed. Metabolite deconvolution employed AMDIS software, and compound identification was cross-referenced with NIST and HMDB spectral databases. Unique metabolites enriched in brain metastases and serum were identified and subjected to pathway enrichment analysis using MetaboAnalyst. To integrate metabolic findings with gene expression, pathway-associated genes were cross-referenced against transcriptomic datasets (GEO GSE76714), enabling network analysis of metabolite-gene interactions.
Results: Our integrative analyses revealed that RNF125, an E3 ubiquitin ligase involved in immune regulation and oncogenesis, functions as a central regulatory node connecting metabolic pathways to the JAK-STAT signaling axis. RNF125 upregulation was inversely correlated with JAK3 activity, suggesting a role in modulating cytokine signaling to promote TNBC cell adaptation within the brain microenvironment.
Conclusion: This study identifies RNF125 as a novel biomarker and potential therapeutic target in TNBC brain metastasis.

#6133 Horizontal mitochondria transfer stimulates pro-tumorigenic astrocyte reprogramming in glioblastoma.

Jonathan Mitchell[1], Brandon Leon[1], Oriana Teran Pumar[1], Asmita Pathak[1], Carolina De La Pena Fernandez[1], Pedro Assenza Tavares Coroa[1], Ogechukwu Mbegbu[2], Yi-An Chen[2], Floris P. Barthel[2], Justin Ruiz[1], Irem Karaman[1], Anna Lasorella[1], Antonio Iavarone[1], Defne Bayik[1], Dionysios C. Watson[1]

[1]University of Miami Miller School of Medicine, Miami, FL,[2]The Translational Genomics Research Institute, Phoenix, AZ

Glioblastoma (GBM), the most aggressive primary brain tumor, co-opts astrocytes in the tumor microenvironment (TME) to facilitate growth, immunosuppression, and therapeutic resistance. However, the signaling mechanisms driving these pro-tumorigenic astrocyte states are poorly defined. We previously showed that astrocytes donate mitochondria to GBM cells to augment GBM metabolism and self-renewal, but the role of mitochondria transfer in astrocyte biology and TME signaling remains unclear. To assess mitochondria transfer to astrocytes, we transduced patient-derived GBM cells (PDCs) with mitochondria-localized GFP (mito-GFP) and co-cultured them with human astrocytes, revealing that GBM cells transfer mitochondria to astrocytes in a cell type-dependent manner, with rates approaching 40% in some models. To additionally validate transfer, we performed deep mitochondrial DNA (mtDNA) sequencing of co-cultured astrocytes and detected transfer of unique PDC mtDNA variants to astrocytes. To evaluate transfer in the tumor microenvironment, we intracranially implanted mito-GFP PDCs in an orthotopic mouse model and found that tumor-associated astrocytes contained GBM-derived mitochondria at similar frequencies to in-vitro observations. Initial survival studies demonstrated that co-implantation of astrocytes with PDCs increased tumorigenesis, and we subsequently showed that co-implantation of astrocytes harboring GBM mitochondria further accelerated tumor growth. To characterize the functional consequences of GBM mitochondria transfer, we assessed transfer-positive astrocyte phenotypes and observed increased cell cycling, proliferation, cellular ROS, and altered oxidative metabolism. Critically, we found that astrocytes acquiring GBM mitochondria increased secretion of the chemokine CCL2 and facilitated enhanced recruitment of immunosuppressive myeloid cells. Collectively, these results suggest that GBM mitochondria transfer to astrocytes is both a pro-tumorigenic mechanism and a therapeutic vulnerability in the GBM TME. Ongoing studies will define the astrocyte signaling networks activated by mitochondria acquisition and identify molecular regulators of transfer initiation to enable therapeutic intervention.

#6134 Immunomodulatory *PIGR*$^{+}$*RORC*$^{+}$dendritic cells (PRDCs) are enriched in malignant ascites.

Steven M. Blum[1], Thomas L. Chan[1], Neal P. Smith[1], Courtney Ambrose[1], Katherine H. Xu[1], Alice Tirard[1], Nandini Samanta[1], Sidney Martin[1], Roya Best[1], Elizabeth Tuttle[1], Christopher T. Stueber[1], Vaishnavi R. Yalala[1], Haley Barnes[1], Sean T. Bannon[1], Yuhui Song[1], Benjamin Y. Arnold[1], Mushriq Al-Jazrawe[2], Joseph J. Zhao[3], Kamil Slowikowski[1], Jessica Tantivit[1], Kasidet Manakongtreecheep[1], Lukas M. Altenburger[1], Simon Knott[4], Matthew R. Strickland[1], Michael G. Drage[1], Linda T. Nieman[1], Jesse S. Boehm[2], Raghav Sundar[5], Gary Reynolds[1], Samuel J. Klempner[1], Alexandra-Chloe Villani[1]

[1]Massachusetts General Hospital, Boston, MA,[2]Koch Inst. for Integrative Cancer Research at MIT, Cambridge, MA,[3]Yong Loo Lin School of Medicine, Singapore, Singapore,[4]Cedars-Sinai Medical Center, Los Angeles, CA,[5]Yale University School of Medicine, New Haven, CT

Background: Peritoneal carcinomatosis and malignant ascites are frequently caused by solid tumors, and the presence of ascites is associated with a poor prognosis and resistance to immune checkpoint inhibitors. While some immunosuppressive features of ascites have been described, the role of dendritic cell (DC) subsets in this microenvironment is unknown. Recently, a subset of DCs that express *RORC* have been found in normal mouse and human tissues, and they have been linked to tolerance of gut antigens. However, this DC population has not previously been associated with cancer or well characterized in humans.

Methods: We performed single-cell RNA sequencing (scRNA-seq) with paired surface proteomics (CITE-seq), and secreted proteomics (n = 109 analytes) on ascites (n = 23) and matched peripheral blood (n = 15) from patients with gastric and gastroesophageal adenocarcinoma (GEA; n = 523,322 total cells). Allogeneic mixed lymphocyte reactions (MLRs) were performed using DCs from GEA and pancreas cancer patients with ascites. *In vitro* differentiation experiments leveraged cDCs from healthy donors and cultured them in media supplemented with ascites supernatant or paired plasma from GEA patients.

Results: We identified a DC subset expressing *PIGR* and *RORC* (PRDCs) that were transcriptionally distinct from canonical DC subsets and similar to tolerogenic cell subsets. Analysis of >1x10^{7} cells from public datasets suggest that PRDCs are found in other human tissues but enriched in malignant ascites from both GEA and ovarian cancers. Sorted PRDCs stimulated T-cell proliferation in MLRs. However, scRNAseq of T cells stimulated by PRDCs showed that those T cells were less effectively polarized due to reduced expression of effector cytokine genes (*e.g.*, *IFNG*, *IL5*, *IL13*) compared to T cells stimulated by cDC2s. Spatial transcriptomics confirmed the presence of PRDC-like cells in human lymphoid tissues, and neighboring, proliferating CD4 T cells similarly showed reduced polarization signatures. Features of the PRDC transcriptional program could be induced by culturing blood-derived cDC1s from healthy donors in supernatant from patients with malignant ascites, suggesting that PRDCs are induced in the ascites microenvironment.

Conclusions: PRDCs represent a conserved, immunomodulatory DC subset enriched in malignant ascites. PRDCs are capable of modulating T-cell responses and may represent a tolerogenic state induced by the ascites microenvironment. Targeting PRDCs or their differentiation pathways may offer new strategies to enhance anti-tumor immunity in patients with peritoneal metastases.

#6135 Amyloid-β accumulation in glioblastoma is driven by vascular remodeling and APP-processing pathways.

Felix Y. Narvaez Irizarry, Alondra M. Bermudez Adorno, Lilia Kucheryavykh

Biochemistry, Universidad Central del Caribe, Bayamon, PR

Background: Glioblastoma (GBM) is an aggressive brain tumor with a poor prognosis.Identifying biomarkers for targeted therapies remains a major challenge in GBM treatment.Recently, we demonstrated that amyloid-β (Aβ), a peptide classically associated with neurodegenerative diseases, accumulates in GBM tumors. This study aims to investigate the mechanism underlying Aβ accumulation in GBM tissues.
Methods: Immunohistochemical analysis and confocal imaging were performed to assessAβ localization in human GBM tissue sections. Glial fibrillary acidic protein (GFAP), ionizedcalcium-binding adaptor molecule 1 (Iba1), and CD31 were used as markers of astrocytes, microglia, and blood vessels, respectively. Western blot analysis was performed toevaluate the expression of Aβ and amyloid precursor protein (APP), along with matrixmetalloproteinases 2 and 9 (MMP-2 and MMP-9), presenilin-1, nicastrin proteins involved inAβ production and vascular endothelial growth factor (VEGF). Pearson correlation analysis was conducted to assess relationships among Aβ, VEGF, MMP-2/9, presenilin-1, and nicastrin.
Results: Confocal imaging revealed robust Aβ accumulation in blood vessels and in tumor regions with high vascularization, as well as strong Aβ accumulation in microglia and, to alesser extent, in glioma cells. Western blot analysis showed strong correlations betweenAβ levels and factors such as VEGF, MMP-2, and presenilin-1, indicating complex regulatory interactions driving Aβ accumulation.
Conclusion: These findings demonstrate that Aβ accumulation in GBM is closely linked to tumor vascularization and microglial involvement. The strong correlations with VEGF, MMP-2, and presenilin-1 suggest that both vascular remodeling and proteolytic processing contribute to Aβ buildup.This study was supported by: NIH Grants 1R15CA287203 and 1R16GM153522

#6136 Macrophages support the growth of pediatric posterior fossa ependymoma type A.

Gabrielle L. Persad[1], Kaitlin Kharas[1], Andrea Ribeiro[2], Alexandra Rasnitsyn[1], Michael D. Taylor[3], Lincoln David Stein[2]

[1]University of Toronto, Toronto, ON, Canada,[2]Ontario Institute for Cancer Research, Toronto, ON, Canada,[3]Baylor College of Medicine, Houston, TX

Posterior fossa type A ependymoma (PFA), the most prevalent of the nine ependymoma molecular subtypes, predominantly affects the hindbrain of infants and young children and has a five-year overall survival of only 56%. PFA harbors few genetic mutations, aside from H3K27M (2-4% of cases) and chromosome 1q gain (~20%). Instead, PFA displays hypoxia-dependent metabolic and epigenetic regulation. *In vitro*, even transient exposure of PFA cells to normoxia results in irreversible toxicity and rapid senescence.

To investigate microenvironmental support, we applied single-cell and spatial transcriptomics to primary PFA tumors. Metabolic pathway analysis revealed that macrophages upregulate glycolysis-related programs. Both macrophages and hypoxic tumor cells exhibited elevated inflammation and glycolysis signatures, suggesting a shared metabolic niche. Spatial mapping revealed a regional hypoxic microenvironment consisting of proliferating PFA cells in close apposition to macrophages.

Functional studies using co-culture and conditioned media experiments revealed a high-molecular weight diffusible factor in macrophage-conditioned media that enhances PFA cell growth under hypoxia and, strikingly, enables their growth under normoxic conditions, where PFA cells are otherwise non-viable.

These findings uncover a critical functional interaction between PFA cells and macrophages that supports tumor growth beyond the hypoxic conditions. Exploring and leveraging intercellular crosstalk between PFA and its microenvironment could open up new avenues for novel therapeutic intervention. Additionally, as there are currently no reliable mouse models to study PFA, understanding how the tumor grows could enable the development of the cells and conditions required for successful patient-derived xenograft models.

#6137 Multi-omicsinpostoperative lymphatic exudate in HPV-negative head and neck cancer.

Zachary Costliow[1], Seka Lazare[1], Zhuosheng Gu[1], Adam Harmon[1], Maciej Pacula[1], Megan Rivera[1], Aadel A. Chaudhuri[2], Jose P. Zevallos[3], Jessalyn Marie Ubellacker[4], Wendy Winckler[1]

[1]Droplet Biosciences, Inc., Cambridge, MA,[2]Mayo Clinic, Rochester, MN,[3]University of Pittsburgh Medical Center, Pittsburgh, PA,[4]Harvard T.H. Chan School of Public Health, Boston, MA

Our team has demonstrated that lymphatic exudate collected via surgical drains (“lymph”) is a proximal biofluid rich in ctDNA and prognostic of recurrence in HPV-independent Head and Neck Cancer (HPV- HNSCC). Other analytes such as proteins, metabolites, and cells are also abundant in lymph. To understand the liquid tumor microenvironment (TME) immediately after tumor resection, we characterized lymph at 24 hrs in HNSCC. We performed a multi-omic survey, demonstrating that lymph is distinct from plasma and represents a largely unexplored source of biomarkers relevant to immune modulation and metastasis.Metabolomics and proteomics were run on lymph supernatant and plasma. Proteomic screening was performed via Olink and normalized to internal standards for quantitative analysis. Metabolomic samples were assayed via LC-MS and normalized. 16s libraries were sequenced utilizing Illumina and analyzed in QIIME. 16s sequencing on 6 patients indicated an array of bacterial genera present in post-surgical lymph with consistency across patients. The distribution consisted primarily of microbes native to the oral cavity, suggesting post-surgical lymph may reflect the native microbiome prior to surgery. Pathogenic blooms were observed in a subset of patients. Ongoing analysis will correlate microbiome data with both cancer and surgical outcomes.Metabolite profiling was performed on post-surgical lymph and matched plasma from 4 patients, including 3 who recurred within 1 year of surgery. The metabolite profile in lymph of all 4 patients was more diverse than plasma with higher metabolite abundance per mL. 13% of identified metabolites were >2-fold enriched in lymph. Lymph from recurred patients showed high levels of saturated and monounsaturated fatty acids, reported to be associated with metastasis. Post-surgical lymph has a unique and largely uncharted metabolome to mine for biomarkers associated with recurrence.Proteomes were compared between lymph and plasma from 44 HPV-HNSCC patients. This cohort consists of 25 recurred (REC) and 19 patients with no evidence of disease (NED) with >1 year of follow up. Lymph and plasma displayed highly non-overlapping protein repertoires. The mean absolute volcano score was 25.2, indicating a strong global difference between lymph and plasma. Lymph was significantly enriched in 91 proteins (p range 4.1e-47 to 0.037), many associated with inflammation. REC lymph was also enriched in inflammatory markers compared to NED, including IL-1a, TNF, and TSLP (p = 0.002, 0.015, 0.003, respectively), which have been implicated in cancer metastasis, invasion, and angiogenesis. Lymph hits were largely non-overlapping with plasma, indicating the opportunity for novel biomarker discovery in this fluid.
Analysis of the microbiome, metabolome, and proteome of post-surgical lymph reveals a rich and differentiated tumor-adjacent biofluid to study biomarkers relevant to metastasis and the TME.

#6138 Profiling the unique resident immune cell compartment in acral skin and its implications for acral melanoma tumor immunity.

Joshua K. H. Tay[1], Emilio Cortes-Sanchez[2], Amanda Jiang[3], Anastasia Prokofyeva[3], Robert Judson-Torres[4], Melissa Q. Reeves[1]

[1]Microbiology & Immunology, Huntsman Cancer Institute, Salt Lake City, UT,[2]Surgical Oncology, Huntsman Cancer Institute, Salt Lake City, UT,[3]Oncological Sciences, Huntsman Cancer Institute, Salt Lake City, UT,[4]Dermatology, Huntsman Cancer Institute, Salt Lake City, UT

Acral melanoma is a rare and understudied form of melanoma that arises in either glabrous skin or the nail matrix and bears distinct characteristics from other cutaneous melanoma subtypes. The purpose of our study is to investigate biological underpinnings that may explain why acral melanomas have worse prognosis and worse response to therapy, including immunotherapy, when compared with other cutaneous melanoma subtypes in patients. It has been previously reported that the tumor microenvironment in acral melanoma is less infiltrated by T cells compared with other cutaneous melanomas subtypes. We hypothesized that the resident immune cells in non-tumor bearing skin may differ between skin sites and could help explain the downstream immune response to a tumor. To test this hypothesis, we obtained paired sets of non-tumor bearing glabrous (acral) and non-glabrous skin from a human donor and enzymatically treated them to enable mechanical separation of the epidermis from the dermis. We then profiled the resident immune cells in the epidermis and dermis separately by flow cytometry. We quantified T cells, macrophages, dendritic cells, and Langerhans cells and discovered a distinct cadre of immune cells at each site. We observed a dramatic reduction in the abundance of Langerhans cells in the epidermis at glabrous sites. Langerhans cells are skin-resident antigen presenting cells that play a critical role in immune surveillance, and reside in the epidermis, the same layer of the skin as melanocytes, the cell of origin of melanoma. These findings open new avenues for future investigation into how early immune surveillance by Langerhans cells to nascent melanomas may directly influence long-term tumor immunity in acral melanoma and its response to immunotherapy.

#6139 Development of a flow cytometry panel for microglia and immune cell populations in a brain tumor model.

Helen Ketteringham[1], Cheryl Davis[2], Mollie McArthur[1], Corrine Silvio[3], Shannan Paul[3], Ben Hoerner[3], Victoria Caruso[3], Liz Bailey[4], Chris Holding[5], Aliccia Koznecki[5], Dawn Lusk[3], Shorena Nadaraia-Hoke[3]

[1]Reaction Biology Corp, Malvern, PA,[2]Reaction Biology Europe GmbH, Freiburg im Breisgau, Germany,[3]Reaction Biology Corp, Hummelstown, PA,[4]Reaction Biology Corp, Boston, MA,[5]Reaction Biology Corp, Hershey, PA

Accurate characterization of microglia and infiltrating immune cell populations is essential for understanding the immunological landscape of brain tumors and for evaluating therapeutic responses. Here, we report the development and optimization of a multicolor flow cytometry panel tailored to discriminate resident microglia from peripheral myeloid and lymphoid subsets within an experimental brain tumor model. Marker selection was guided by tissue-specific expression profiles, leveraging differential levels of CD45, CX3CR1, and P2RY12 to resolve microglia, while incorporating canonical markers for infiltrating macrophages, dendritic cells, neutrophils, and T cells. Enzymatic dissociation conditions, viability dye selection, and gating hierarchy were systematically optimized to preserve epitope integrity and maximize signal resolution. Validation using tumor-bearing and control brain tissues demonstrated robust separation of microglial and infiltrating populations with reproducible quantification across biological replicates. This workflow provides a reliable and scalable approach for immune profiling in brain tumor research, enabling deeper insight into neuroimmune interactions and immunotherapy-driven changes within the tumor microenvironment.

: Metastatic Niches and Microenvironment
Poster Session

#6143 Tumor exosome-initiated neutrophil IRG1/itaconate axis awakens dormant tumor cells and promotes lung metastasis.

Yue Deng, Jialin Lu, Xiao Yang, Lingyi Kong, Chao Wan, Kunyu Yang

Cancer Center, Union Hospital, Tongji Medical College, Huazhong University of Science and Technology, Wuhan, China

Purpose/Objective(s): Tumor cell dormancy and metabolic reprogramming are critical events in metastatic relapse. However, the mechanisms, particularly how the lung pre-metastatic niche and its associated metabolic alterations awaken dormant disseminated tumor cells (DTCs), remain elusive. This study aims to decipher the cascade from primary tumor-derived exosomes to DTC reactivation in the pre-metastatic lung, specifically identifying the key metabolite-mediated pathway driving this process.

Materials/Methods: We employed multiple mouse models of spontaneous lung metastasis (e.g., B16-F10, Lewis). To comprehensively profile the pre-metastatic niche, we performed untargeted metabolomics on lung tissues to identify differentially enriched metabolites, and single-cell RNA sequencing (scRNA-seq) to delineate the cellular source of *Irg1*. Other key techniques included: *in vivo* imaging and H&E staining for metastasis tracking; generation of $Irg1^{flox/flox}$ mice with Mrp8-Cre for neutrophil-specific *Irg1* deletion; RNA-seq of sorted alveolar macrophages; co-immunoprecipitation and Western blotting for itaconate-mediated LATS2 alkylation validation; chromatin immunoprecipitation (ChIP) for YAP1 nuclear translocation.

Results: We delineated a sequential pathway driving metastatic reactivation in the lung. Initially, primary tumor-derived exosomes educated $SPP1^{+}$ alveolar macrophages to bolster the production of CXCL2 and ensue neutrophil recruitment. Subsequently, these lung-infiltrating neutrophils specifically expressed *Irg1*, resulting in a marked accumulation of the metabolite itaconate within the pre-metastatic niche. Mechanistically, itaconate directly alkylated dormant DTCs at the C910 and C911 site of the key upstream kinase LATS2 in the Hippo pathway. This modification inhibited the LATS2's capacity to phosphorylate YAP1, thereby promoting the nuclear translocation of unphosphorylated YAP1 to activate a pro-proliferative transcriptional program, forcing DTCs to exit dormancy. Crucially, this entire axis was disrupted by either neutrophil-specific genetic ablation of *Irg1* or pharmacological inhibition of CXCR2, both of which significantly reduced tumor lung metastasis.

Conclusions: Our work unveils a novel paradigm in which the tumor exosome-neutrophil axis drives metastatic reactivation via metabolite-mediated protein alkylation. We pinpoint the neutrophil-IRG1-itaconate axis as a pivotal signaling cascade in this process, and our findings demonstrate that therapeutic targeting of this axis, either upstream at CXCR2 or at the metabolite itaconate, represents a viable strategy to prevent tumor lung metastasis.

#6144 A site-specific microenvironmental program in plantar skin confers heightened metastatic capacity to acral melanomas.

Marie Elena Portuallo[1], Tyler Aprati[2], Limin An[1], Steffanus Pranoto Hallis[3], Kuai Yu[1], MiKaela N. Field[4], Sheri L. Holmen[4], David Liu[2], Vito Rebecca[1]

[1]Johns Hopkins University, Baltimore, MD,[2]Dana-Farber Cancer Institute, Boston, MA,[3]Johns Hopkins Bloomberg School of Public Health, Baltimore, MD,[4]University of Utah Huntsman Cancer Institute, Salt Lake City, UT

Acral melanoma is an aggressive melanoma subtype with a predilection for metastasis and poor clinical outcomes, yet no FDA-approved therapies are tailored specifically for this population. Progress has been hindered by limited clinico-genomic data and a lack of orthotopic preclinical models. Here, we integrate genomic profiling and longitudinal clinical annotations from 29 patients with metastatic acral melanoma—alongside a comparison cohort of 455 patients with cutaneous melanoma—revealing an enhanced metastatic capacity in acral disease. We further show that the plantar skin microenvironment fosters a human acral melanoma, pro-metastatic cell state through elevated matrix stiffness, and identify a matrix stiffness-induced FAK-SRC-YAP vulnerability as a therapeutically actionable axis to combat distant metastasis. This work establishes the first series of orthotopic models of metastatic acral melanoma and uncovers tractable drivers of distant organ metastasis, offering new avenues for tailored therapeutic strategies.

#6145 Regulation of small extracellular vesicle production by sirtuin 1 as a determinant of breast cancer metastasis.

Yu-Wei Chang[1], Michael Guo[1], Aidan M. Quinn[1], Anthony M. Chen[1], James J. Mullmann[1], Andrew D. Miller[2], Richard A. Cerione[3], Marc A. Antonyak[4], Robert S. Weiss[1]

[1]Department of Biomedical Sciences, Cornell University, Ithaca, NY,[2]Department of Population Medicine and Diagnostic Sciences, Cornell University, Ithaca, NY,[3]Department of Molecular Medicine & Department of Chemistry and Chemical Biology, Cornell University, Ithaca, NY,[4]Department of Molecular Medicine, Cornell University, Ithaca, NY

Metastatic breast cancer remains a major clinical challenge and the primary cause of breast cancer-related mortality. Increasing evidence points to a role for tumor-derived small extracellular vesicles (EVs) secreted by cancer cells in preparing distant sites for metastasis. Sirtuin 1 (SIRT1), a metabolic and epigenetic regulator frequently downregulated in advanced breast cancer, influences key cellular processes, including lipid metabolism and autophagy, both of which are implicated in EV biogenesis. However, the mechanisms by which SIRT1 loss alters small EV production and function to promote breast cancer metastasis remain unclear. In this study, we investigated how SIRT1 expression influences the production and cargo of small EVs released by breast cancer cells, and how these changes affect aggressiveness. First, using triple-negative breast cancer (TNBC) cell lines with genetically altered SIRT1 levels, we observed that SIRT1 loss increased small EV secretion. Second, incubation of recipient breast cancer cells *in vitro* with small EVs derived from SIRT1-deficient cells enhanced their migration and invasiveness to a greater extent than with small EVs from SIRT1-proficient control cells. *In vivo*, inhibition of SIRT1 by genetic or small molecule approaches led to the development of larger tumors in both orthotopic transplantation and MMTV-PyMT mouse mammary tumor models. Moreover, animals preconditioned with small EVs derived from SIRT1-deficient cells, followed by tail vein injection of mammary tumor cells, showed increased lung colonization and metastatic outgrowth compared to those preconditioned with EVs derived from control cells, suggesting that SIRT1 regulation of EV cargo contributes to shaping a pro-metastatic microenvironment. In conclusion, this work identifies a novel link between SIRT1 status in breast cancer cells and their small EV-mediated signaling potential. Our findings position SIRT1 as a key regulator of small EV content and underscore the therapeutic potential of targeting SIRT1-dependent pathways that drive small EV-mediated metastasis in breast cancer.

#6146 Analysis of potential drivers of tungsten-enhanced breast cancer metastasis: A longitudinal study of bone marrow adipocytes.

Charlotte Marie McVeigh[1], Jennifer A. Tjung[1], Jorge L. Moreno[1], Sydnee J. Yazzie[2], Lauren K. Heine[1], Grace A. Picha[1], Guy W. Herbert[1], Sebastian Medina[1], Alicia M. Bolt[1]

[1]Pharmaceutical Sciences, University of New Mexico Health Sciences Center, Albuquerque, NM,[2]Pathology, University of New Mexico Health Sciences Center, Albuquerque, NM

Tungsten (W) is classified as an emerging environmental toxicant due to increased human exposure and lack of knowledge of the health risks. Epidemiological and *in vivo* studies reveal exposure to W contributes to the carcinogenic process, but molecular mechanisms are poorly defined. Due to a cohort of breast cancer patients accidentally exposed to W during intraoperative radiotherapy, our lab is investigating the effects of W on breast cancer progression and metastasis. W is known to store in the bone, causing long-term exposure and toxicity. Previous research in our lab has shown in multiple triple-negative breast cancer orthotopic models, W enhances breast cancer metastasis to the bone niche. Bone marrow adipocytes (BMA) play an important role in metastasis through secretion of adipokines/cytokines that drive tumor cells homing, colonization, and growth by changing the microenvironment. Understanding changes throughout metastasis is crucial to uncover adipokines/cytokines that could drive colonization and proliferation of tumor cells in the bone niche after W exposure. 6-8 week old female BALB/c or C57BL/6 mice were exposed to 15ppm W in drinking water or tap water for 4 weeks. After 4 weeks, mice had orthotopic injections of 4T1 (BALB/c) or E0771-Luc (C57BL/6) cells into the mammary fat pad. Longitudinal time points were taken to track changes with no tumor cell injection (0 week; 0W), 2 week post injection (2 week; 2W), and 3 week post injection (3 week; 3W). At the end, femurs were used for immunohistochemistry staining of Perilipin-1+ (Plin1+) adipocytes in bone marrow. Bone marrow from tibiae was cultured to select for mesenchymal stromal cells (MSC), which were then differentiated into BMA. Cell supernatant and RNA were collected from both MSCs and BMA to profile changes in adipokines/cytokines. Both models had increased metastasis to the bone after W exposure, 4T1 induced greater systemic inflammation compared to E0771-Luc. Adiponectin levels remained unchanged in E0771-Luc, but increased after W exposure at 2W and 3W in 4T1. CXCL2 expression was increased after W exposure at 0W and 2W and trending at 3W in 4T1 and increased at 3W in E0771-Luc. Plin-1+ staining revealed E0771-Luc has more adipocytes compared to 4T1, regardless of exposure. Some analytes did not change with W exposure or weekly, suggesting that those may not be not the main drivers of metastasis. Analytes like Adiponectin showed changes after W exposure, but were dependent upon the model. This suggests that there are differences between models and W might do slightly different things in each one, including systemic inflammation that we observed more in the 4T1 compared to the E0771-Luc. CXCL2 was increased in both models, suggesting a common key player in enhanced metastasis to the bone. This study provides insights into adipokine/cytokines that might be crucial players in W enhanced breast cancer metastasis to the bone.

#6148 GPR35 as a therapeutic target to halt breast cancer progression and osteolytic bone metastasis.

Gunjan Sharma, KM Abdullah, Seema Singh, Ajay Singh, Jawed Siddiqui

Cell and Molecular Biology, UMMC Cancer Center and Research Institute, Jackson, MS

Bone metastasis is a frequent and devastating complication of breast cancer (BC) and causes severe skeletal-related events, reduced quality of life, and poor overall survival. BC cells engage in bidirectional interactions with the bone microenvironment by modulating the expression of various chemokines and their receptors, thereby promoting metastatic colonization and niche formation. Numerous G protein-coupled receptors (GPCRs) are implicated in oncogenic processes. Among them, G protein-coupled receptor 35 (GPR35), the cognate receptor for CXCL17, has recently been identified as a key regulator of tumor progression and metastasis. Nevertheless, its precise role in cancer progression, metastatic spread, and modulation of the bone microenvironment remains poorly understood. GPR35 is overexpressed in BC patients, and its elevated expression is strongly associated with reduced overall survival. Consistently, our study also demonstrates elevated GPR35 expression in breast cancer bone-metastatic (BC-BoneMet) cell lines, further supporting its potential role in driving bone metastatic progression. To functionally validate these observations, we generated GPR35 knockout (KO) BC-BoneMet cell lines using the CRISPR/Cas9 system. GPR35 deletion significantly reduced cell migration, invasion, and colony-forming ability *in vitro*. *In vivo* studies showed that loss of GPR35 in breast tumor cells led to significantly reduced primary tumor growth in syngeneic mice, supporting a critical role for GPR35 in driving tumor progression. To evaluate the therapeutic benefits of targeting the GPR35, we employed a highly selective GPR35 inhibitor (GPR35i). In functional studies, GPR35i markedly reduced the proliferation, migration, and clonogenicity of BC-BoneMet cells even under CXCL17 stimulation. Furthermore, flow cytometry revealed that GPR35i significantly induces apoptosis and cell cycle delay in BC-BoneMet cells. Given that most BC bone metastases are osteolytic (bone-destructive) and osteoblasts regulate osteoclast functions, we also investigated the effects of the tumor secretome on bone cells. The secretome of GPR35-deficient tumor cells failed to promote bone cell differentiation. Similar effects were observed when the secretome of GPR35i-treated BC-BoneMet cells was applied to osteoblast and osteoclast differentiation assays. Conclusively, these findings demonstrate that GPR35 plays a key role in breast cancer bone metastasis by remodeling the bone microenvironment and supporting the formation of a metastatic niche. These findings highlight GPR35 as a promising therapeutic target for preventing osteolytic progression and reducing metastatic burden in bone.

#6149 Oncogenic ASPP2*kappa* exerts a regulatory role within the tumor microenvironment and promotes metastasis in TNBC models.

Cornelia Wincek[1], Alessia Ruiba[1], Wenfeng Liu[2], Sakthi Kembu Chettiar Ravichandran[1], Marcus M. Schittenhelm[1], **Kerstin Maria Kampa-Schittenhelm**[1]

[1]Med. Oncology and Hematology, HOCH Health Ostschweiz, St. Gallen, Switzerland,[2]HOCH Health Ostschweiz, St. Gallen, Switzerland

Breast Cancer is the most common cancer in woman to date. While cure rates in localized stages are relatively good, tumor-associated death rates increase dramatically in the distant metastatic stage. Composition of the tumor microenvironment plays a decisive role therein. Metastasis is a complex, multistep process involving a multitude of intracellular steps of transformation, as well as interactions of tumor cells with the surrounding environment. The mechanisms underlying these processes are only partially understood. We have evidence that ASPP2*κ*, a novel, oncogenic isoform of the p53-related tumor suppressor ASPP2, is involved in this process. ASPP2*κ* is highly expressed in breast cancer and characterized by loss of the p53- as well as BCL-2 and NFκB-binding sites, impairing major pathways controlling cellular fate. We have demonstrated, that ASPP2*κ* promotes a more aggressive tumor biology and shorter patient survival. We now show that ASPP2*k* exerts a pro-tumorigenic role within the tumor microenvironment, facilitating neo-angiogenesis and early metastasis. To study the role of ASPP2*κ* in a tissue context, we established a TNBC *ASPP2κ* knock-down (KD) NOD/SCID as well as an immunocompetent BALB/C orthotopic *ASPP2k* knock-in mouse model, employing the human TNBC MDA-MB-231 and the murine 4T1 cell lines. ASPP2*k* KD and KI primary and metastatic lesions, as well as the respective controls, were explanted and analyzed on the transcriptional and translational level. Proteome arrays and bulk RNA sequencing was performed on TNBC cell models. Results were confirmed by qPCR, WB, FACS and ELISA assays. All conducted analyses confirme a driving role of ASPP2*k* in angiogenesis and early metastasis as well as a tumor promoting role in the microenvironment. Comprehensive analyses of our bulk RNA sequencing data identified significant differential expression patterns of genes clustered within the GO terms “angiogenesis”, “EMT” and “immune response” (149/200 genes within GO:0001525 angiogenesis, 33/43 genes associated with GO:0001837 EMT and 134/194 genes linked to the GO:0006955 Immune Response). Pathways involved in metastasis, angiogenesis and pro-inflammatory signaling were studied in detail in dependency of ASPP2*κ* expression. ELISA readouts confirmed secretion of pro-angiogenic growth factors (eg. VEGF, Angiogenin or PDGF) in dependency of ASPP2*κ* expression (KD cells: VEGF 247.2 ± 97.8 pg/mL vs. 535.9 ± 60.8 pg/mL in controls). TNBC tumoroid models confirme inhibition of invasive growth in ASPP2*κ* attenuated models. Differences in vascularization were confirmed by immunohistochemistry and confocal microscopy.

We here demonstrate, that ASPP2*κ* exerts a regulatory role on key hallmarks of metastasis and the tumor microenvironment, promoting tumor progression and metastasis. Therapeutic inhibition of ASPP2*κ* might provide a completely new approach to combat metastasis in the future.

#6150 Cathepsin G as a central regulator of tumor plasticity and osteolytic metastasis in breast cancer.

Ridhi Bhola[1], Reegan Sturgeon[2], Gabriel Tonucci[1], Rakesh K. Singh[3]

[1]Pathology, Microbiology, and Immunology (PMI), University of Nebraska Medical Center, Omaha, NE,[2]University of Nebraska Medical Center, Omaha, NE,[3]Professor, Dept. of Microbio. & Path., University of Nebraska Medical Center, Omaha, NE

Breast cancer frequently metastasizes to bone, where osteolytic lesions drive substantial morbidity. We identified Cathepsin G (CTSG), a serine protease expressed by both tumor cells and neutrophils, as being highly upregulated at the tumor-bone interface. However, the distinct contributions of tumor- versus neutrophil-derived CTSG remain poorly defined. To examine the role of CTSG in modulating malignant phenotype, we treated breast cancer cells with recombinant CTSG (rCTSG), which reduced proliferation, induced cell cycle arrest, promoted homotypic aggregation and collective migration; and induced a luminal to basal shift. Modeling tumor-derived CTSG through stable overexpression reproduced these effects and, in vivo, suppressed tumor growth yet paradoxically enhanced osteoclast activation and bone destruction. Immunohistochemical analysis indicated that tumor-derived CTSG reduced proliferation, did not significantly affect apoptosis, and altered epithelial characteristics, particularly at the tumor-bone interface. To assess neutrophil-derived CTSG, we co-cultured breast cancer cells with neutrophils, which similarly inhibited proliferation, promoted aggregation and migration, implicating a paracrine role. Together, our findings position CTSG as a central regulator of tumor phenotype and bone-tumor interactions and highlight it as a potential therapeutic target in breast cancer bone metastasis.

#6151 ESR1 mutations rewire TGF-B and hedgehog signaling to drive endocrine resistance and osteolytic bone metastasis in estrogen receptor-positive breast cancer.

Erykah J. Coe[1], Julie Rhoades[2]

[1]Program in Cancer Biology, Vanderbilt University School of Medicine, Nashville, TN,[2]Department of Medicine, Vanderbilt University Medical Center, Nashville, TN

Endocrine therapy-resistant ER+ breast cancer frequently acquired activating *ESR1* mutations (e.g. Y537S) conferring ligand-independent ER activation and aggressive bone metastasis, yet underlying mechanisms remain unclear. We hypothesized that *ESR1* mutations promote bone colonization by simultaneously dysregulating TGF-β/SMAD and Hedgehog/Gli2 pathways. Wild-type and mutant (Y537S) MCF7 and T47D cells with ERE-luciferase reporters showed Y537S cells maintained elevated basal PTHrP transcription independent of estrogen while responding to TGF-β. Intratibial xenografts demonstrated Y537S tumors induced greater osteolytic lesion burden than wild-type, with TGF-β neutralization significantly reducing lesion formation. RNA-seq revealed Y537S cells exhibited dramatic Gli2 and PTHLH upregulation. Critically, ligand-stimulation activated Gli2/PTHLH in mutant but not in wild-type cells. CRISPR-mediated Gli2 knockout reduced PTHrP production while Gli2 overexpression maximized osteolytic potential. These results demonstrate that *ESR1* mutations reprogram ER to activate dual bone-remodeling pathways (TGF-β/SMAD and Hedgehog/Gli2) explaining aggressive bone metastatic phenotypes and identify ER, TGF-β/SMAD, and Gli2 as rational combination therapeutic targets.

#6154 A single-cell atlas reveals a tumor microenvironment-dominated ecosystem in breast cancer brain metastasis.

Chuanbao Zhang[1], Wang Jia[2], Lei Xing[1], Md Tauhidul Islam[1]

[1]Stanford University, Stanford, CA,[2]BEIJING TIANTAN HOSPITAL, CAPITAL MEDICAL UNIVERSITY, Beijing, China

Purpose. Brain metastasis in breast cancer is a major cause of mortality, yet the cellular heterogeneity and dynamic evolution of the tumor microenvironment (TME) during metastatic progression remain poorly defined. The aim of this study was to elucidate the transcriptional and microenvironmental reprogramming that accompanies breast cancer metastasis to the brain.
Experimental Design. We integrated single-cell RNA sequencing data from primary breast tumors, lymph node metastases, and brain metastases (n=65) to construct a comprehensive single-cell transcriptomic atlas. We performed Non-negative Matrix Factorization to identify malignant cell metaprograms and applied multi-layered analyses to assess genomic instability, subtype plasticity, and cell-cell communication within the TME. We further validated the results in bulk RNA sequencing data (N=1184).
Results. Metastatic progression was associated with increased genomic instability and amplification of brain-metastasis-specific genes, including UBE2M, which correlated with poor prognosis. At single-cell resolution, we observed marked transcriptional plasticity of clinical subtypes, with ER$^+$ tumors frequently converting to more aggressive intrinsic subtypes in the brain. Ten malignant metaprograms were defined, with conserved inter-program interactions but sample-type-specific activity; notably, hypoxia and oxidative phosphorylation programs were enriched in brain metastases. The TME underwent profound remodeling, becoming depleted of stromal and immune infiltrates but developing a dense, autonomous intercellular signaling network dominated by myeloid and endothelial cells.
Conclusions. This study delineates the co-evolution of tumor-intrinsic states and the TME during metastatic dissemination, revealing that the brain microenvironment becomes an independent signaling hub that supports colonization. These findings underscore the pivotal role of the TME in shaping metastatic adaptation and suggest new avenues for therapeutic intervention in advanced breast cancer.

#6155 S-Nitrosylated COX-2 is a microenvironment-regulated breast cancer biomarker of mesenchymal phenotypes.

Reuben J. Hoffmann[1], AeSoon Bensen[1], Mark Dane[2], Jane Arterberry[1], Rebecca Smith[2], James Korkola[2], Pepper Schedin[1]

[1]CDCB, OHSU Knight Cancer Institute, Portland, OR,[2]BME, OHSU Knight Cancer Institute, Portland, OR

COX-2 is an inducible enzyme key to the production of inflammatory prostaglandins. COX-2 also has tumor intrinsic oncogenic activity in mouse models of breast cancer. Previously, we reported that increased expression of Cys-526-nitrosylated COX-2 (SNO-COX-2), but not non-nitrosylated COX-2, associated with progression of early-stage human breast cancer to invasive ductal carcinoma. Here, we used a 3D culture model of early-stage human breast cancer (MCF10DCIS cells) to investigate the relationship between SNO-COX-2 expression and mesenchymal/invasive tumor cell morphology. We find that SNO-COX-2, but not non-nitrosylated COX-2, closely associated with mesenchymal phenotypes induced by fibrillar type I collagen. Interestingly, invasive phenotypes did not associate with induction of classic epithelial-to-mesenchymal transition (EMT) markers including *SNAIL*, *CDH2* (N-cadherin), and *VIM* (vimentin). By contrast TGFβ-1 strongly induced EMT-related transcripts, but not SNO-COX-2 protein expression nor mesenchymal phenotypes. These observations suggest that in MCF10DCIS cells, SNO-COX-2 associates with mesenchymal phenotypes more strongly than non-nitrosylated COX-2 protein or expression of classic EMT transcripts. Supporting these observations *in vivo*, a heterogeneous mouse breast tumor model (D2A1 cell injection) demonstrates that invasive mesenchymal tumor regions also have increased SNO-COX-2 expression compared to epithelial tumor regions. Further, using a microenvironment microarray to test MCF10DCIS.com cells 300 distinct tumor microenvironment conditions we find SNO-COX-2 protein expression is driven by inflammation, wound resolution, and cancer-associated factors. Standouts include TNC, SPP1, decorin, fibrillar type I and III collagens, INF-γ, and IL-4/13, with evidence for specific extracellular matrix-ligand interactions driving both high and low SNO-COX-2 expression. In sum, in MCF10DCIS cells, expression of SNO-COX-2 is highly microenvironment-dependent and strongly associated with invasive/mesenchymal growth, indicating potential for SNO-COX-2 as a biomarker to assess risk of early-stage breast cancer progression.

#6156 Omega-6 lipid-gene module linked to colorectal cancer pre-metastatic niche.

Ramani Soundararajan[1], Lance Pflieger[2], Gunjan Upadhyay[3], Michelle M. Maurin[1], Mingli Yang[1], Michael Schell[4], McKayla Carr[1], Ahalya Sekhar[1], Rachel Kenis[1], Heiman Wang[1], Michael Nebozhyn[5], Andrey Loboda[6], Aejaz Nasir[7], W. Jack Pledger[8], Ganesh V. Halade[3], Timothy J. Yeatman[9]

[1]Surgery, University of South Florida, Tampa, FL,[2]Buck Institute for Research on Aging, Novato, CA,[3]Internal Medicine, University of South Florida, Tampa, FL,[4]Biostatistics and Bioinformatics, Moffitt Cancer Center, Tampa, FL,[5]Merck Research laboratories, Boston, MA,[6]Director, Informatics&Analysis, Merck Research laboratories, Boston, MA,[7]BJ's Diagnostic and Precision Oncology, Tampa, FL,[8]Molecular Medicine, University of South Florida; Tampa General Hospital Cancer Institute, Tampa, FL,[9]Surgery, University of South Florida;Tampa General Hospital Cancer Institute, Tampa, FL

Introduction: We recently reported (Soundararajan *et. al.*, GUT, 2024) a strong pro-inflammatory lipid mediator bias in colorectal cancer (CRC), possibly related to the omega-6 rich fatty acid preponderance in western-style diets. The current project expands on those findings, linking omega-6 fatty acids to expression of inflammatory genes in human CRC and mouse models.
Method: We performed an integrative, multi-omics, weighted gene co-expression network analysis (WGCNA) of 25 quantified arachidonic acid-derived lipid mediators with whole transcriptomes from 293 primary and 77 metastatic human CRCs, to identify a lipid-gene module significantly associated with metastasis. In mice fed omega-6:omega-3 (10:1 w/w) *vs.* control (1:1 w/w) diets, we analyzed syngeneic CRC subcutaneous tumors using whole transcriptome RNA-sequencing. THP1-derived gene expression signatures for M0, M1 and M2 macrophages were correlated with the lipid-gene module.
Results: In the human tumors using an *unsupervised* analysis, we identified a pro-inflammatory lipid-gene module, linked to the clinical feature of metastasis (P< 1.1e-42), with prominence of "hallmark" genes linked to coagulation, complement, inflammation and EMT/tumor progression and associated with M1 macrophages. Analysis of murine tumors derived from animals fed a diet enriched with omega-6 fatty acids revealed a significant (p < 3.7329E-06), shared enrichment of 18 coagulation and EMT related genes --orthologous to those identified in the pro-inflammatory human lipid-gene module. Among the 18 genes, *SerpinA1b*, *SerpinA1d*, *SerpinA3k*, *Ambp* and *Plg* with anti-inflammatory and coagulation- *inhibitory* properties were *downregulated* in omega-6 fed mice. Moreover, we observed a dramatic *decrease* in *Serpina1* protein expression in the hepatic sinusoids in omega-6 mice.
Conclusion: A human tumor pro-inflammatory lipid-gene module was identified, and its gene expression was shared with tumors derived from mice fed with an omega-6-rich diet. Hallmark gene analysis found inflammation and deranged coagulation prominent. In omega-6 fed mice, decrease in *Serpina1* protein expression in liver sinusoidal endothelial cells---the first target of metastasizing cells---suggests localized inflammation with enhanced coagulation. Collectively, these data suggest omega-6 enriched murine and human western diets may foster the development of an inflammatory, coagulopathic pre-metastatic liver niche, with M1 macrophages as the main contributors of CRC inflammation.

#6157 Single-cell characterization of tumor niches driving liver metastasis in colorectal cancer.

Jinho Jang[1], Yoojeong Seo[1], Kyung Pil Ko[1], Jie Zhang[1], Sohee Jun[1], Jae-Il Park[2]

[1]UT MD Anderson Cancer Center, Houston, TX,[2]Asst. Professor, Exp. Radiation Oncology, UT MD Anderson Cancer Center, Houston, TX

Metastasis has been linked to the tumor microenvironment, but the cellular interaction networks that organize metastatic niches in microsatellite-stable colorectal cancer are not fully characterized. We performed single-cell RNA sequencing of colon normal tissue, primary colorectal tumors, liver metastases, and matched liver normal tissue to define microenvironmental remodeling with a focus on T-cell and fibroblast compartments. Tumor-associated fibroblasts showed broad upregulation of collagen genes, enrichment of apical junction and surface-related pathways, increased communication among fibroblast subsets, and the emergence of metastasis-associated fibroblast populations. In parallel, liver metastases exhibited depletion of $CD8^+$ T cells and NK cells compared with liver normal tissue, accumulation of regulatory T cells and $CD8^+$ exhausted T cells and strengthened fibroblast-$CD8^+$ T-cell interactions. Ligand-receptor analysis revealed CLEC signaling between fibroblasts and T cells across multiple conditions, with selectively enhanced CLEC-mediated interactions in liver metastases compared with liver normal tissue. Galectin-mediated communication was restricted to tumor settings and, while broadly distributed across fibroblast clusters in primary tumors, became selectively intensified within a specific fibroblast subset in liver metastases. Fibroblasts in liver metastases also preferentially engaged $CD8^+$ exhausted T cells through NRXN signaling. Together, these data delineate fibroblast-centered, site-specific signaling circuits that shape immune composition and function during metastatic progression and nominate fibroblast-T-cell communication hubs as candidate targets for modulating the tumor niche in microsatellite-stable colorectal cancer.

#6158 Senescent tumor-associated macrophages promote peritoneal metastatic niche formation in gastric cancer.

Tadahito Yasuda[1], Mayu Yasuda[1], Atsuko Yonemura[2], Fabio de Mello[1], Feng Guo[1], Boping Jing[1], Hudie Li[1], Takatsugu Ishimoto[2], Yaoqi Alan Wang[1]

[1]Indiana University School of Medicine, Indianapolis, IN,[2]The Cancer Institute, Japanese Foundation for Cancer Research, Tokyo, Japan

Peritoneal metastasis represents a major clinical challenge in gastric cancer (GC), yet the mechanisms underlying metastatic niche formation remain poorly understood. In particular, the specific tumor-associated macrophage (TAM) subsets that drive peritoneal dissemination remain poorly characterized. Here, we identify a subset of senescent macrophages that promote metastatic niche propagation in GC. Using a newly established GC cell line, GAN-KPC (harboring a $Kras^{G12V}$ mutation with Trp53 and Cdh1 knockout), and a syngeneic gastric wall transplantation model in C57BL/6 mice, we investigated the cellular landscape of metastatic niche formation. High-resolution spatial transcriptomics (10x Visium HD) revealed macrophages within metastatic niches exhibiting transcriptional features of cellular senescence. Pharmacologic clearance of senescent cells with the senolytic agent ABT263 markedly reduced peritoneal tumor formation, and macrophage-specific $p16^{INK4a}$ knockout further confirmed the essential role of senescent macrophages in metastatic niche formation. Complementarily, single-cell mass cytometry (CyTOF) of ascitic fluid from GC patients with peritoneal metastasis revealed a macrophage subset expressing p16 and SASP-associated factors. These findings uncover a previously unrecognized role of senescent macrophages in peritoneal metastatic niche formation and suggest that targeting senescent cells may represent a promising therapeutic strategy to limit peritoneal dissemination in GC.

#6159 Co-evolution of cancer cells and their microenvironment of primary and lymph node metastatic prostate cancer under androgen deprivation therapy.

Ping Xu[1], Yuehui Zhao[1], Yun Yan[1], Rui Ye[1], Chenling Tang[1], Emi Sei[1], Shanshan Bai[1], Tuan Tran[1], Cole Ruoff[1], Christine Ly[2], Keyi Zhu[2], Miao Zhang[2], Bila A. Siddiqui[3], Sumit K. Subudhi[3], Paul Corn[3], Christopher J. Logothetis[3], Patricia Troncoso[2], Amado J. Zurita-Saavedra[3], Nicholas Navin[1]

[1]Department of Systems Biology, UT MD Anderson Cancer Center, Houston, TX,[2]Department of Pathology, UT MD Anderson Cancer Center, Houston, TX,[3]Department of Genitourinary Medical Oncology, UT MD Anderson Cancer Center, Houston, TX

Prostate cancer (PC) is the most commonly diagnosed malignancy and the second leading cause of cancer-related death among men in the United States. The presence of lymph node (LN) metastases is a strong prognostic indicator of progression. Although LNs are the second most frequent metastatic site after bone, they are the first site of detectable metastasis in patients. Currently, the molecular and microenvironment transitions from primary tumors to LN metastases remain poorly understood. Prior bulk sequencing studies have provided important insights into metastatic tumors but failed to resolve the cellular heterogeneity and spatial organization in the tumor microenvironment (TME). We hypothesized that both cancer cell-intrinsic transcriptional programs and their interactions with the TME drive LN metastasis and resistance to androgen deprivation therapy (ADT). To test this, we integrated single-nucleus RNA sequencing with multiple spatial transcriptomic platforms (10x Visium, Vizgen MERSCOPE, and Xenium) to profile primary prostate tumors and matched LN metastases. Spatial analyses revealed site-specific remodeling of the TME between cancer and adjacent normal regions in both the prostate and LN. Despite being distinct organs, the prostate and LN also exhibit overlapping enrichment of specific immune and stromal cell populations within tumor regions, reflecting conserved functional roles across these environments. Non-negative matrix factorization identified recurrent cancer cell metaprograms (MPs), including an androgen receptor (AR) associated program enriched in LN metastases. By integrating MP activity with TME composition through ecotype analysis, we defined distinct ecotypes representing combinations of cancer states and their microenvironment cell types. One ecotype characterized by AR signaling and protumorigenic TME components was preferentially enriched in LN metastases. Ecotype-based stratification of primary tumors identified a ‘pre-metastatic’ subgroup, which showed ecotype contributions similar to those of LN metastases, and a ‘non-metastatic’ subgroup, which displayed different ecotype profiles. Primary tumors characterized by pre-metastatic ecotypes were linked to significantly poorer clinical outcomes. Collectively, these findings delineate the co-evolution of prostate cancer cells and their microenvironment during LN metastasis. Our study establishes ecotypes as a framework for linking cancer-intrinsic programs with TME remodeling, providing new biomarkers of progression and resistance and offering opportunities for precision therapeutic intervention.

#6160 TRPV6/CXCR4 signaling complexes as therapeutic targets to prevent osteoblastic bone metastasis in castration-resistant prostate cancer.

Clement Cordier[1], Aurelien Haustrate[1], Adriana Mihalache[2], Erika Duval[2], Emilie Desruelles[1], Corentin Spriet[3], Lofti Slimani[4], Baptiste Casel[4], Laurent Allart[1], Pierre Gosset[2], Natalia Prevarskaya[1], V'yacheslav Lehen'kyi[1]

[1]Inserm U1003, Phycel, Physiology Cellulaire, University of Lille, France, Lille, France,[2]Pathology Department, Saint Vincent de Paul Hospital, Hospital Group of Catholic Institute of Lille (GHICL), Lille, France, Lille, France,[3]University of Lille, CNRS, Inserm, CHU Lille, Institut Pasteur of Lille, US 41 - UAR 2014 - PLBS, Lille, France, Lille, France,[4]University of Paris Cite and Sorbonne Paris Nord, Inserm UMR1333, Oral Health, Montrouge, France, Lille, France

Background: Bone metastasis is a leading cause of morbidity and mortality in advanced prostate cancer, affecting up to 90% of patients with castration-resistant prostate cancer (CRPC). Around 85% of these lesions are osteoblastic. The calcium channel TRPV6 is absent in healthy prostate tissue but produced de novo during malignant transformation, with higher expression in advanced and castration-resistant stages. TRPV6 regulates calcium influx and downstream signalling pathways that promote proliferation, invasion and survival. Previous studies have shown that TRPV6 promotes epithelial-mesenchymal transition (EMT), migration, invasion and metastatic dissemination, particularly to bone, and forms functional complexes with the chemokine receptor CXCR4, a key mediator of tumour cell homing to bone. Here, we investigated how the TRPV6-CXCR4 axis contributes to osteoblastic bone metastases and whether its pharmacological inhibition could be therapeutically beneficial.

Methods: TRPV6 and CXCR4 expression and co-localization were analyzed in human prostate cancer tissues and bone metastases. Functional assays using TRPV6-overexpressing or TRPV6-knockout cells evaluated osteoblast-mediated migration, invasion and activation. In vivo studies assessed the effect of targeting TRPV6 and CXCR4, individually or in combination, with monoclonal antibodies on metastatic burden and bone lesion phenotype.

Results: TRPV6 expression strongly correlated with tumor aggressiveness and metastatic progression in clinical samples. TRPV6 activation triggered CaMK2 phosphorylation, NF-κB nuclear translocation and upregulation of EMT-associated transcription factors (Twist, Snail, Slug), enhancing migratory and invasive phenotypes. Concurrently, TRPV6 promoted stable CXCR4-TRPV6 complex formation, amplifying pro-metastatic signalling. In co-culture assays, TRPV6-expressing cells markedly increased osteoblast activation markers (ALP, RUNX2, OPN) and matrix mineralisation, indicating functional tumour-osteoblast crosstalk driving osteoblastic niche formation. In vivo, TRPV6-positive tumors primarily produced osteoblastic bone lesions, and dual targeting of TRPV6 and CXCR4 reduced the incidence of metastases, attenuated pathological bone remodeling, and prolonged overall survival.

Conclusions: These results highlight the TRPV6-CXCR4 complex as a key regulator of osteoblastic bone metastasis in CRPC. Dual targeting of TRPV6 and CXCR4 provides a proof-of-concept therapeutic strategy to prevent or limit bone metastasis in prostate cancer.

#6161 Ybx1 correlates with an immunosuppressive microenvironment in bone-metastatic lung adenocarcinoma.

Yongsheng Wang[1], Liyun Miao[2]

[1]Respiratory Diseases, Nanjing Drum Tower Hospital, Nanjing, China,[2]Nanjing Drum Tower Hospital, Nanjing, China

Bone metastasis in lung cancer is frequently associated with immunotherapy resistance, yet its underlying mechanisms remain elusive. Here, we demonstrate that the transcription factor YBX1 orchestrates both bone metastasis and immunosuppressive microenvironment formation in non-small cell lung cancer (NSCLC) through IL6 and CCL5 signaling, respectively. Mechanistically, YBX1 protein stability is regulated by glycosylation-dependent mitophagy, wherein O-GlcNAc transferase (OGT)-mediated glycosylation at T271 enhances its mitochondrial membrane localization and subsequent autophagic degradation. Notably, reduced YBX1 glycosylation was observed in highly bone-metastatic NSCLC cells. Through drug screening, we identified Icaritin(iac) as a small molecule that potentiates YBX1 glycosylation, accelerates its degradation, and consequently suppresses bone metastasis while reversing immunosuppression. Our findings unveil YBX1 as a dual-functional therapeutic target for simultaneously inhibiting NSCLC bone metastasis and sensitizing tumors to immunotherapy.

: Pediatric Cancer Models
Poster Session

#6165 Matrix density shapes early invasion and EWSR1::FLI1 protein dynamics in Ewing sarcoma.

Manon Watzky, James Amatruda

Children's Hospital Los Angeles, Los Angeles, CA

Ewing sarcoma (EwS) is a pediatric bone and soft tissue cancer driven by chromosomal translocations generating fusion oncogenes, primarily EWSR1::FLI1. Metastasis is the most adverse prognostic factor, associated with persistently low survival rates. The low mutational burden in EwS suggests that tumor progression relies more on how cells adapt to their environment than on genetic selection. Invasion represents the first transition where cells leave the primary tumor and face new environmental constraints that can shape their metastatic potential. This study aims to establish a model that captures early EwS adaptation during invasion and to determine how extracellular matrix (ECM) parameters influence this process. To study EwS adaptation, we use cell lines derived from primary tumors or metastases to generate 3D spheroids embedded in collagen I matrices of defined densities, allowing us to monitor invasion and its associated morphological and molecular changes. We notably focus on EWSR1::FLI1 dynamics and its regulatory mechanisms during invasion onset, as this transcription factor is essential for EwS transformation and proliferation, yet reduced activity has been suggested in metastatic contexts. The ECM-embedded spheroid model shows that active invasion is restricted to metastasis-derived cells. Spheroids from primary tumors expand or sense the matrix but display rare cell detachment, whereas metastasis-derived spheroids show robust invasion with elongated, amoeboid, and collective behaviors captured by high-resolution microscopy. Increasing collagen density gradually reduces invasion, highlighting the strong influence of matrix properties. This prompted us to examine EWSR1::FLI1 dynamics, with immunohistochemistry revealing a spatial decrease at spheroid edges and within invading cells. Low heterogeneity is detectable before spheroid embedding, but the extent of EWSR1::FLI1 downregulation markedly expands during invasion. Time-course analyses show that this downregulation precedes active detachment. Moreover, fewer EWSR1::FLI1-low cells are observed at the edge of spheroids embedded in invasion-restrictive high-density matrices, further linking matrix density with invasive behavior and EWSR1::FLI1 dynamics. RNAscope shows that spheroid-edge and invading cells retain high EWSR1::FLI1 transcript levels, suggesting that the regulation occurs at the protein level. In line with this, proteasome inhibition with MG132 prevents invasion onset without inducing major cell death, supporting proteasome-dependent regulation of early EwS invasion. Taken together, these findings identify an ECM-associated EWSR1::FLI1-low state as an early adaptive feature during invasion onset. Our model enables dissection of this regulation -from matrix sensing to active detachment- and suggests a role for proteasome-mediated mechanisms in shaping early metastatic traits in Ewing sarcoma.

#6166 Next-generation models to advance pediatric solid cancer treatments.

Emon Nasajpour[1], Dena Panovska[2], Ruolun Wei[3], Conrado Soria[4], Calvin J. Kuo[5], **Rachana Agarwal**[4]

[1]Neurology and Stanford Cancer Model Development Center, Stanford University, Stanford, CA,[2]Neurology, Stanford University, Stanford, CA,[3]Neurosurgery, Stanford University, Stanford, CA,[4]Frederick National Laboratory for Cancer Research, Leidos Biomedical Research, Inc., Frederick, MD,[5]Stanford University, Stanford, CA

Drug development is notoriously inefficient, slow, and expensive. In oncology, only 5% of new compounds identified during the drug discovery phase successfully progress to clinical trials. This high attrition rate is attributed to patient intra- and inter-tumor heterogeneity, as well as an over-reliance on 2D cell cultures and animal models, which often fail to accurately replicate patient tumor biology and physiology. The adoption of advanced, clinically relevant preclinical models at earlier stages of drug development is essential for better identifying and prioritizing agents with a higher likelihood of success in clinical trials. The Human Cancer Models Initiative (HCMI) is a global initiative founded by the National Cancer Institute (NCI), in collaboration with the Cancer Research UK, Wellcome Sanger Institute, and the foundation Hubrecht Organoid Technology. The mission is to generate patient-derived next-generation cancer models from diverse tumor types as a community resource. Unlike traditional cancer models, the new models are cultured under optimized, predominantly 3D conditions that better preserve the characteristics of the parental tumors than historical culture conditions. This preservation is validated through phenotypic and molecular analyses of tumor tissue and models, which are shared with the community alongside standard operating procedures, informed consent templates, and associated clinical and molecular data. To contribute towards the goal of the HCMI, several Cancer Model Development Centers (CMDC) have been generating cancer models from a variety of tumor types. This includes the Stanford CDMC which is currently dedicated to models of pediatric solid tumors, emphasizing central nervous system (CNS) tumors, the leading cause of cancer-related death in children. We developed a standardized bioprocessing pipeline which yielded a functional tumor bank, achieving a 60-70% success rate in establishing next-generation cancer models for long-term passaging. We have successfully generated and submitted 85 pediatric cancer models along with case-associated clinical and biospecimen data, as well as internal QC data validating the derived cancer models, for further characterization and distribution via the HCMI pipeline. Our next-generation cancer models partially capture the heterogeneity of pediatric CNS tumors, neuroblastoma, hepatoblastoma, Wilms tumor, and brain metastases from neuroblastoma and rare sarcoma-related cancers. Longitudinal biobanking has identified and characterized novel onco-fusion proteins, rare tumor entities, and recurrences, and therapeutic vulnerabilities through multi-omics. In summary, next-generation cancer modeling overcomes known challenges by benchmarking models and creating standardized protocols and procedures, thereby enhancing their predictive capabilities, therapeutic efficacy and promoting personalized treatment strategies.

#6167 Modeling the impact of chemotherapy and small molecule inhibitors on the 3D microenvironment of pediatric bone sarcomas.

Allison Haley Reno[1], Joshua Kelley[2], Reid Barker[3], Jamie Silverman[3], Jack Hyland[3], Cameron Bumbleburg[4], Elizabeth Maahs[3], Anna Tingler[4], Denis C. Guttridge[4], Melinda A. Engevik[4], Yongren Wu[2], Casey Langdon[4]

[1]Pediatrics, The Medical University of South Carolina, Charleston, SC,[2]Clemson-MUSC Bioengineering, Clemson University, Charleston, SC,[3]Biology, The College Of Charleston, Charleston, SC,[4]Medical University of South Carolina, Charleston, SC

One of the main types of pediatric sarcomas is primary bone sarcoma (PBS) where the sarcoma initially occurs in the bone matrix. PBS includes osteosarcoma and Ewing sarcoma, both of which are primarily seen in pediatric populations. Treatment for osteosarcoma often includes amputation or limb salvaging surgery, along with pre- and post-operative chemotherapy, both of which are significant surgeries for adolescents. These surgeries can significantly limit their long-term mobility, altering their quality of life. These sarcomas produce osteoid and a porous, mineralized matrix like that of native bone tissue. In this work, we have designed pediatric sarcoma 3D cell culture models by creating custom hydrogel materials to match the ECM properties of bone sarcomas such as osteosarcoma and Ewing sarcoma. We refined the composition of this material using nanoscale mechanobiology analysis to assess the nanoscale stress, strain, compression, and Young's modulus to match the mechanical properties of the native bone sarcoma ECM. We have cultured organoids in this material using imaging to track and quantify the ECM remodeling by the 3D culture tumor model. Like what is seen in literature we have found that with tumor proliferation and progression comes increased collagen, collagen remodeling for increased mechanical stiffness, and overall ECM stiffness increased to create a denser, mechanically stiffer tumor. We hypothesize that chemotherapies and small molecule inhibitors may be able to weaken the dense tumor formation and ECM remodeling seen in our 3D cell culture models as the drugs penetrate through the hydrogel induce apoptosis in the cells and lead to a decrease in ECM components and cell-matrix bonding. Both AKT and proteasome inhibitors block the pathways associated with collagen type I, III, and IV driving tumor progression through the pERK and PI3K/AKT pathways. The goal is to test these targeted therapies on our sarcoma 3D cell culture models to see if they would then slow or inhibit the effects of collagen on driving tumor growth and progression in pediatric solid tumors where collagen plays such a vital role. Additionally, in immune "cold" tumors such as Ewing sarcoma collagen functions as an important immunosuppressive signaling molecule so inhibiting collagen in signaling helps to turn Ewing sarcoma and other pediatric sarcomas into more immune "hot" tumors by taking away the role collagen plays in keeping this an immune "cold" tumor. We anticipate our novel 3D culture models can model the complex relationships between tumor, microenvironment, and therapeutic response.

#6168 Investigating the mechanism of oncogenesis of BCOR-CCNB3 fusion positive sarcomas.

Victoria Ann Pete[1], Ryota Shirai[1], Sydney Hakim[1], Joshua Broadman[1], Naoki Oike[2], Andrew E. Goodspeed[3], **Masanori Hayashi**[1]

[1]The University of Colorado School of Medicine, Aurora, CO,[2]Niigata Univ. School of Medicine, Niigata, Japan,[3]University of Colorado Cancer Center, Aurora, CO

BCOR-CCNB3 sarcomas (BCS) are a subtype of small cell sarcomas that represent a recently recognized group of solid tumors identified by rearrangements of BCOR. Gene expression profiles of patient samples demonstrate a very similar profile to other BCOR rearranged solid tumors, such as BCOR-MAML3 fusion sarcomas, and CCSK with BCOR ITD. BCOR is a corepressor of the transcription factor BCL6 and is a critical member of the non-canonical polycomb repressive complex (PRC), PRC1.1, which mediates transcriptional repression through epigenetic modifications. In stem cells, PRC1.1 complexes are recruited to the chromatin through binding of KDM2B to nonmethylated CpG islands, catalyzing the ubiquitination of the histone H2A (at Lys119) via the RING-PCGF1 enzymatic core, leading to the repression of target genes. Through this process, the PCGF1-interacting PUFD region of BCOR is critical for the BCOR-PRC1.1 interaction. Despite this evolving understanding of the diagnostic profile of BCS, preclinical and mechanistic investigations of BCOR rearranged sarcomas have been limited due to the lack of models. Here, using two distinct BCS model systems, we investigated the mechanism of how BCOR-CCNB3 contributes to the oncogenesis of BCS. First, BCOR was knocked down in NBC-1, a patient-derived BCOR-CCNB3 cell line, and confirmed by western blotting and qRTPCR. Next, we created a vector transposon system to create isogenic cell lines expressing FLAG-tagged BCOR-CCNB3 or wild type BCOR. Interestingly, in NBC-1 cells, while the knockdown of the fusion gene did not lead to a statistically significant change in proliferation or survival, RNA-seq analysis identified that BCOR-CCNB3 knockdown led to a significant decrease of the expression of HOX family genes. Furthermore, co-IP identified that the fusion BCOR-CCNB3 was not bound to PRC1.1 components, including KDM2B, RING1, and PCGF1. In the isogenic cell model, we were able to establish an inducible BCOR-CCNB3 expression model, and demonstrate that the exogenous expression of BCOR-CCNB3 leads to increased cell proliferation.These results indicate that the BCOR-CCNB3 oncogenesis occurs through the disruption of the PRC1.1 complex function, and cannot be reversed by fusion gene targeting. Future work is currently ongoing to define the interaction of BCOR-CCNB3 with the various subunits of PRC1.1 through co-immunoprecipitations, IP-mass spectrometry and CUT&Tag analysis.

#6169 Evaluating TCR mimetic CAR T cell preclinical therapeutics in an immunocompetent MYCN-driven murine neuroblastoma allograft model.

Elisabeth Posthill[1], Minu Samanta[1], David Groff[1], Colleen Casey[1], Tina Acholla[1], Anna Maria Giudice[1], Kristopher R. Bosse[1], Ruoning Wang[2], Timothy T. Spear[1], John M. Maris[1]

[1]Center for Childhood Cancer Research, Division of Oncology, Children's Hospital of Philadelphia, Philadelphia, PA,[2]Nationwide Children's Hospital, Columbus, OH

Background: Tractable immunocompetent murine models for adoptive cellular therapies could fill a critical gap in preclinical evaluations. Peptide-centric (PC) chimeric antigen receptor (CAR) T cells targeting pMHC of a 9mer peptide derived from the neuroblastoma intracellular oncoprotein PHOX2B presented by HLA-A*24:02 (A24) is now in Phase 1 clinical trial for relapsed neuroblastoma (NCT07007117). To study therapeutic limitations and enhancement strategies, we developed a syngeneic model of PHOX2B/A24-targeting murine (m)PC-CARs.

Methods: C57BL/6 (BL/6)-penetrant TH-MYCN-derived allografts and cell lines were engineered with a chimeric human/murine MHC HLA-A*24:02/H-2K^{b} to present conserved PHOX2B 9mer peptide. MSCV retroviral vectors encoding second-generation mPC-CARs containing the clinical scFv conjoined to murine CD28 or 4-1BB with CD3ζ were used to create stable GPE86 producer cell lines. Truncated mCD19 or luciferase was included to monitor transduction efficiency and *in vivo* trafficking. BL/6 splenocytes were activated and transduced *ex vivo* with human (h)IL-2, and expanded in hIL-7/15. Multiplex functional assays were performed using flow cytometry, ELISA, real-time cell impedance, and O-link proteomics.

Results: Transduction efficiency reproducibly ranged from 40-60%. mPC-CAR-T cells expanded 15 to 20-fold over 14 days while maintaining balanced memory and effector immunophenotypes with minimal exhaustion markers post-manufacture. Against PHOX2B-A24-H-2K^{b}-expressing cell lines, mPC-CAR-T cells with CD28ζ or 4-1BBζ costimulatory domains exhibited robust IFN-γ, IL-2, and TNFα secretion and potent cytotoxicity down to an effector:target ratio of 0.5:1 up to 14 days post-manufacture and after cryopreservation. CD28ζ mPC-CAR T cells maintained 100% cytotoxicity upon serial tumor rechallenge, whereas cytotoxicity of 4-1BBζ was limited to 50% after 3 challenges. In the absence of exogenous cytokine support, tumor exposure induced CD44^{+}IL7Rα^{-} terminal effector phenotype and upregulation of exhaustion markers CD39, CTLA-4, and Tim-3. *In vivo* studies to assess anti-tumor potency, persistence, and barriers to efficacy are ongoing and will be reported.

Conclusion: We created a tractable MHC hybrid TH-MYCN-derived neuroblastoma allograft model in BL/6 mice. This model is currently being deployed to study various PC-CAR enhancement strategies such as mRNA encoded epitope vaccination and cytokine armoring with accompanying spatial transcriptomics that will inform further clinical development of our PHOX2B-directed PC-CAR T cells.

#6170 Development and characterization of 3D osteosarcoma models recapitulating tumor heterogeneity and bone microenvironment.

Margaux Chantoiseau[1], Pierre Khneisser[2], Birgit Geoerger[3], Nathalie Gaspar[3], Maria Eugenia Marques da Costa[3], Antonin Marchais[1]

[1]Anti-tumor immunology and cancer immunotherapy, Gustave Roussy, Villejuif, France,[2]Department of Medical Biology and Pathology, Gustave Roussy, Villejuif, France,[3]Department of Pediatric and Adolescent Oncology, Gustave Roussy, Villejuif, France

Introduction: Osteosarcoma is the most common primary bone cancer in adolescents and young adults. It is characterized by high heterogeneity and a hostile bone microenvironment shaped by osteoclasts, endothelial cells, and immunosuppressive myeloid populations, underscoring the need for innovative models to evaluate novel therapeutic strategies. Objective: This study aims to develop and characterize novel three-dimensional (3D) culture models that recapitulate the complexity and the microenvironment of osteosarcoma.
Methods: Tumor samples from patient-derived xenografts (PDXs) established from patients with osteosarcoma at relapse or treatment failure were processed to generate 3D tumor cultures. Tumor tissues were mechanically and enzymatically dissociated into single-cell suspensions and seeded into round-bottom plates with very low adhesion to promote spontaneous formation of 3D tumoroids. Culture conditions were optimized using medium supplemented with specific growth factors to support cell viability and proliferation. Morphology and growth of the tumoroids were monitored over time. The resulting 3D models were characterized by histology (H&E and specific immunostaining like SATB2, SPP1, SOX9⋯), and by RNA sequencing and Whole exome sequencing (WES) to assess transcriptional stability relative to the parental primary/PDX tumors. In addition, these 3D tumoroid models were used for drug testing to evaluate therapeutic responses and identify potential treatment sensitivities.
Results: We established five 3D osteosarcoma models from PDX with an establishment rate of 83%. The tumoroids formed spontaneously under low-adhesion conditions within approximately 7 to 30 days, (depending on the derived sample) and remained viable and morphologically stable during this culture period. Histological analysis revealed that the 3D tumoroids recapitulated key features of the parental PDX tumors and the patient tumors, including cellular heterogeneity, hypoxic regions, and osteoid-like matrix deposition. RNA sequencing and drug testing studies to evaluate therapeutic responses are currently ongoing.
Conclusions: Patient-derived 3D osteosarcoma models faithfully preserve tumor heterogeneity and microenvironmental features, providing a robust and scalable system for preclinical drug testing. This approach holds a strong potential to accelerate the development of personalized combination therapies targeting both tumor cells and their supportive bone microenvironment in osteosarcoma.

#6171 Patient-derived pediatric glioblastoma models provide key insights into IDH1-driven drug resistance.

Stephen Friend, Matthew Graziano, Ruby E. Thamert, Heather Branscome, Utsav Sharma, Abhay Andar, **Carolina Lucchesi**

Microphysiological Systems, American Type Culture Collection (ATCC), Manassas, VA

Background: Pediatric glioblastoma (GBM) is a rare, aggressive brain cancer with molecular characteristics distinct from adult GBM. IDH1 mutations, which occur more frequently in pediatric cases, are associated with unique clinical outcomes and resistance mechanisms. Despite its severity, GBM remains incurable, with limited treatment options. Pediatric populations rarely participate in clinical trials, making clinically relevant in vitro models critical for preclinical research and therapeutic development. The Human Cancer Models Initiative (HCMI) has developed patient-derived brain tumor models, including organoids and spheroids, annotated with comprehensive clinical and molecular data. These models offer a platform to study tumor biology and drug response in IDH1-mutant GBM.

Methods: Patient-derived glioblastoma models from the HCMI biobank—representing primary and recurrent tumors—were genomically profiled for key pediatric GBM mutations (IDH1, ATRX, TP53, KRAS, RELA). Histopathology confirmed IDH1 status and supported molecular classification. Genomic data were compared to patient records and The Cancer Genome Atlas (TCGA) to validate model fidelity. A subset of models was exposed to a panel of four compounds, including standard and experimental drugs. Drug sensitivity was assessed via 12-point dose curves, with IC50 values calculated. Cytotoxicity was measured using live/dead staining and ATP-based viability assays. This integrated approach links genomic alterations to drug resistance, supporting the development of targeted therapies for high-risk pediatric GBM.

Results: Patient-derived GBM organoid models were sequenced and confirmed to carry key mutations, including IDH1 p.R132H, ATRX p.C1590Y/p.R1739, TP53 p.R273C, KRAS Q22R/G13R, and RELA rearrangements. Drug screening across a 10-compound panel revealed variable responses based on genotype and dosage. Taxanes and platinum agents showed broad cytotoxicity, while PARP and KRAS inhibitors exhibited limited effects except at high concentrations. Viability was assessed via fluorescent staining and ATP-based assays, demonstrating the utility of these models for genotype-informed therapeutic screening in pediatric GBM.

Conclusion: HCMI-derived pediatric GBM models recapitulate IDH1-driven genomic features and reveal mutation-specific drug responses. These 3-D platforms support high-throughput screening and integrated genomic-pharmacologic profiling to inform targeted therapy development for high-risk pediatric GBM. Importantly, these preclinical models bridge a critical gap by providing insights from patient populations that cannot participate in clinical trials, reinforcing their role in precision oncology.

#6172 The transcription factor DMRTA2 regulates radial glial maintenance and tumorigenicity of pediatric high-grade glioma.

Hitomi N. Royston[1], Autumn B. Hampton[1], Elissa G. Oliver[1], Jayden Jackson[1], Ibukunoluwa Florence Tella[1], Miriam D. Emerson[1], Dhruv Bhagat[1], Daijiro Konno[2], Kosuke Funato[1]

[1]University of Georgia, Athens, GA,[2]Kindai University, Higashiosaka, Japan

Brain tumor is the leading cause of cancer-related death in children. Among them, pediatric-type diffuse high-grade glioma (HGG) accounts for 40% of brain tumor deaths in children. Diffuse hemispheric glioma (DHG), H3 G34-mutant (DHG-H3G34), represents a highly malignant subtype of HGG with a poor prognosis. Although dysregulated developmental programs have been implicated in these tumors, the exact mechanisms that drive subtype-specific tumorigenesis remain unclear. DMRTA2, a member of the Doublesex-mab3-related (DMRT) transcription factor family, has been linked to the proliferation and maintenance of neural progenitor cells. However, its functions in human brain development and pediatric glioma are not yet fully understood.

To address this gap, we first analyzed previously published single-cell RNA-seq datasets from human fetal brains and cerebral organoids. We found robust *DMRTA2* expression in neural progenitor populations, particularly in radial glial (RG) cells. To investigate the functional role of DMRTA2 in human brain development, we knocked out the *DMRTA2* gene using CRISPR-Cas9 genome editing in human embryonic stem cell (hESC) lines and differentiated them into cerebral organoids. *DMRTA2* KO organoids exhibited reduced size, decreased proliferation, and a marked depletion of RG cells, suggesting an important role of DMRTA2 in early cortical development.

We next examined *DMRTA2* expression in DHG-H3G34 patient tumors and observed its high and specific expression compared to other subtypes of pediatric brain tumors. To investigate the role of DMRTA2 in DHG-H3G34, we knocked out *DMRTA2* in hESC-based DHG-H3G34 model cells that we developed. Loss of *DMRTA2* resulted in a significant decrease in RG-like population and a marked increase in differentiated cells. In our mouse xenograft studies using luciferase-labeled *DMRTA2* WT and KO cells, loss of *DMRTA2* significantly reduced tumor growth in vivo. KO tumors also displayed reduced proliferation and fewer RG-like cells.

Together, our findings suggest that DMRTA2 is a key regulator of radial glial cells in human cortical development and promotes tumorigenicity in pediatric DHG-H3G34 tumors.

#6173 Developing zebrafish avatars for pediatric sarcomas to support functional precision oncology.

Karoline Felisbino, Jonathan Tyler Kinder, Colin Williams, Andrew Gaines, Jessica Blackburn

Molecular and Cellular Biochemistry, University of Kentucky, Lexington, KY

Pediatric sarcomas, including rhabdomyosarcoma (RMS) and osteosarcoma, remain associated with poor outcomes in relapsed or high-risk disease, highlighting the need for rapid functional models to guide patient-specific therapeutic decisions. Zebrafish patient-derived xenografts (zPDX “avatars”) provide a low-cost, scalable in vivo platform to test drug responses within days. As a foundation for pediatric sarcoma avatars, we optimized zebrafish xenografts using human RMS cell lines (RD, embryonal; RH30, alveolar) prior to introducing primary patient samples. GFP-labeled RD cells injected into the dorsal perivitelline space (PVS) of 48-hours-post-fertilization larvae produced approximately 60% larval survival, nearly 100% engraftment at 1 day postinjection (dpi), and stable tumors through 4 dpi, enabling reproducible conditions for standardized tumor size and short-term drug testing. CellTiter-Glo assays at 34 °C, the incubation temperature required for zPDX experiments, confirmed that RD cells retain drug sensitivity under these conditions: dactinomycin (DAC) significantly reduced RD viability at low nanomolar concentrations (≥10 nM), whereas vincristine (VIN) was effective at 2-10 nM. Parallel larval toxicity assays indicated that both drugs were generally well tolerated by zebrafish larvae at concentrations ≤200 nM for 72 h, establishing a practical exposure window for in vivo testing. As a proof-of-concept for drug response assessment, GFP+ RD cells were injected into 48 hpf larvae and tumor burden (fluorescence intensity) and dissemination were evaluated following treatment with VIN and DAC at 15 nM. At this concentration, no statistically significant differences were observed versus control, although a trend was noted toward reduced tumor size and dissemination. In contrast, RH30 cells did not persist beyond 1-2 dpi when injected in simple carriers (PBS or HBSS + 1-2% FBS), prompting systematic optimization of the injection medium. Guided by media described for zPDX, we developed an enriched medium containing HEPES, glutamine, MEM-NEAA, B27, nicotinamide, ITS, Y-27632, SB202190, N-acetylcysteine, and EGF/FGF with reduced serum. Using this formulation, we achieved approximately 100% tumor-positive larvae up to 4 dpi, indicating that medium composition, particularly exogenous growth factors, are critical for xenograft retention. Together, these preliminary data define robust survival and engraftment parameters for RMS xenografts in zebrafish, validate the feasibility of this platform for rapid chemotherapy response readouts, and establish an optimized injection medium that enables even challenging sarcoma subtypes to persist in vivo. These advances provide the foundation for extending this platform to primary pediatric sarcomas, including osteosarcoma, to generate zebrafish avatars for functional precision oncology.

#6175 Development of a human neuroblastoma organoid model.

Simon Tusnady[1], Eva Bakos[2], Anna Lovrics[2], Katalin Monostory[2], Jozsef Tovari[3], Andras Furedi[2], Kornelia Szebenyi[2]

[1]Semmelweis University, Budapest, Hungary,[2]Institute of Molecular Life Sciences, HUN-REN Research Centre for Natural Sciences, Budapest, Hungary,[3]KINETOLab Biotechnology, Budapest, Hungary

Neuroblastoma (NB) is the most prevalent solid malignancy in infants, with approximately 20% of cases classified as high-risk due to amplification of the MYCN oncogene - a marker associated with aggressive tumor behavior and poor prognosis. Despite therapeutic advances, relapsed high-risk NB accounts for nearly 15% of pediatric cancer-related mortality. Studies using non-human models may yield misleading results due to species-specific differences in sympathoblast development -the fetal precursors of NB cells - which differ markedly between mice and humans. To address this, we developed and characterized an iPSC-derived human neuroblastoma organoid model that enables the study of early tumorigenesis in a tissue-like context.
First, we developed a differentiation protocol to generate human neural crest (NC) organoids from hiPSCs. Key neural crest markers, detected by fluorescent microscopy and Western Blot, were used to characterize the cell types present in the organoids. We then engineered transgenic iPSCs harboring a removable STOP cassette upstream of the MYCN gene (MYCN-GFP hiPSCs) and control iPSCs lacking MYCN (GFP hiPSCs). We verified the success of genomic integration by PCR and differentiated NC organoids from the transgenic hiPSCs using the previously established protocol. Then NC organoids were transduced with a Cre-expressing adeno-associated virus (AAV) that induced MYCN expression in a sympathoblast-specific manner. Changes in organoid size and GFP expression were observed over time with flow cytometry and fluorescent microscopy. The resulting neuroblastoma-like (NB) organoids were characterized by fluorescent microscopy and bulk RNA-sequencing. NB organoids were also treated with chemotherapeutics and were implanted subcutaneously into mice.
Successful generation of NC organoids from wild type and transgenic iPSC lines was validated by the expression of neural crest markers. The formation of tumor tissue was observed in organoids generated from MYCN-GFP hiPSC lines after AAV-mediated MYCN overexpression in targeted cells. The resulting NB organoids displayed hallmark features of high-risk NB and were sensitive to clinically relevant chemotherapeutics. NB organoids could also engraft and expand in vivo in mice.
We have created a hiPSC-based three-dimensional human neuroblastoma organoid model that includes tumor cells as well as healthy cells of neural crest origin forming the tumor environment. This innovative human organoid model of high-risk neuroblastoma provides a platform to study tumor initiation and investigate resistance mechanisms emerging after repeated chemotherapy cycles. Its application in drug screening may facilitate the discovery of novel, more effective therapies tailored to aggressive NB subtypes.

#6176 Embryonic reprogramming of neural crest cells drives the development of Ewing sarcoma.

Elena Vasileva[1], Claire Arata[2], Yongfeng Luo[1], Gage Crump[2], James Amatruda[1]

[1]Children's Hospital Los Angeles, Los Angeles, CA,[2]Keck School of Medicine, University of Southern California, Los Angeles, CA

Ewing sarcoma (ES) is a pediatric cancer of the bone and soft tissues with poor outcomes for patients with metastatic or relapsed disease. Ewing sarcoma cells are characterized by the presence of a driver fusion oncogene, most commonly EWSR1::FLI1. In the absence of a genetic animal model due to the severe toxicity of the oncofusion, the developmental aspects of ES initiation, including its cellular origin, have remained poorly understood. To address these questions, we developed a stable zebrafish transgenic model enabling tissue-specific expression of the human EWSR1::FLI1 oncofusion in neural crest cells, one of the proposed cell of origin for ES (Vasileva et al., Cell Reports 2025). Using this model, we demonstrated that expression of human EWSR1::FLI1 oncofusion in neural crest cells can lead to their transformation and the development of tumors in vivo. Single-cell analysis of tumor initiation shows that EWSR1::FLI1 reprograms neural crest-derived cells to a mesoderm-like state, strikingly resulting in ectopic fin formation throughout the body. Such hijacking of the limb development program led to abnormal activation of developmental signaling pathways in EWSR1::FLI1-induced outgrowths, resulting in dysregulation of the FGF signaling cascade and HOX gene expression. EWSR1::FLI1 reprograms neural crest cells by hijacking developmental enhancers and upregulating the expression of mesodermal regulators. One such regulator is tbxta (Brachyury or T), a key transcription factor controlling mesodermal specification. Notably, tbxta/TBXT expression was maintained in a subset of zebrafish and human tumors. Our model provides a mechanism by which a neural crest cell lineage can be transformed into Ewing sarcoma, a malignancy with predominant mesenchymal features. Taken together, these findings show how a single mutation can disrupt normal developmental trajectories, driving neural crest cells reprogramming and initiating malignant transformation.

#6177 Targeted posterior fossa A ependymoma therapy using a tumor-selective nanoparticle drug delivery approach.

Jon D. Larson[1], Darren Finlay[1], Yan Yuen Lo[1], Rabi Murad[1], Ming Zhao[1], Antony MichaelRaj[2], Sachin A. Kumar[3], Kristen Vogt[4], Ian Pass[1], Charles Handley[1], Bryan K. Li[5], Robert J. Wechsler-Reya[6], Michael D. Taylor[7], Kristiina Vuori[1], Michael Jackson[1], Daniel A. Heller[4], G. Praveen Raju[8], Lukas Chavez[1]

[1]Sanford Burnham Prebys Medical Discovery Institute, La Jolla, CA,[2]University of Pittsburgh, Pittsburgh, PA,[3]Boston Children's Hospital, Harvard Medical School, Boston, MA,[4]Molecular Pharmacology Program, Memorial Sloan Kettering Cancer Center, New York, NY,[5]Department of Pediatrics, University of California, San Diego, La Jolla, CA,[6]Herbert Irving Comprehensive Cancer Center and Department of Neurology, Columbia University Medical Center, New York, NY,[7]Cancer and Hematology Center, Texas Children's Hospital, Houston, TX,[8]Department of Neurosciences, University of California, San Diego, La Jolla, CA

Ependymoma (EPN) is the third most common malignant pediatric brain tumor. The most frequent and aggressive EPN subgroup, posterior fossa ependymoma group A (PFA-EPN), occurs predominantly in younger children with a 5-year progression-free survival of 33%. In the absence of recurrent mutations, PFA EPN tumors are driven by EZHIP overexpression resulting in global loss of the gene repressive chromatin mark H3K27me3. Despite progress in EPN molecular characterization, the standard treatment remains surgery with adjuvant radiation therapy. As such, identifying novel therapies for PFA-EPN is an important unmet medical need. To define therapeutic sensitivities for PFA-EPN, we performed a drug screen using multiple drug libraries: (i) a 120 drug FDA-Approved Oncology collection (ODL3), (ii) a CTD^2 Informer Set of 320 tool compounds, and (iii) a 336 drug Epigenetics Drug Collection on three patient-derived PFA-EPN cell lines. We found that these PFA-EPN cell lines were sensitive to several clinically relevant drugs, including those targeting epigenetic regulators. Multiple histone methyltransferase, proteasome, BCL2, and BET domain inhibitors were also identified as high-value drug candidates. These results warrant further PFA-EPN functional evaluation *in vivo*, but dose-limiting toxicity and limited blood-brain barrier (BBB) penetration are known limitations for many of the identified compounds. To overcome these limitations, we are applying a novel P-selectin-targeted fucoidan-based nanoparticle (FiNP) technology recently shown as a viable approach for effective BBB drug penetration specifically at brain tumor sites *in vivo*. As proof of principle, we have successfully fucoidan-encapsulated BET domain inhibitor drugs including a BRD2/3/4 PROTAC degrader (dBET6) providing improved pharmacological properties. Our preliminary results show P-selectin expression on treatment-naive human PFA-EPN tumor vasculature with current studies underway to assess effects of low dose ionizing radiation on P-selectin tumor vasculature expression enhancement, FiNP tumor localization throughout the tumor space, as well as therapeutic assessment in PFA-EPN PDX mouse models. Collectively, these findings provide new putative therapeutic approaches in these rare yet aggressive tumors.

#6178 Establishment and analysis of spontaneous metastatic PDX models of Ewing sarcoma.

Ali Mokhtar Mahmoud, Unsun Lee, Arnulfo Mendoza, Christine M. Heske

Pediatric Oncology Branch, Center for Cancer Research (CCR), NCI, NIH, Bethesda, MD

Although improvements in local therapy have increased the 5-year survival rate for localized Ewing sarcoma (EWS) from less than 20% to 70%, little progress has been made in the treatment of metastatic disease, which has a 5-year survival rate of less than 30%. A major challenge in the field is a lack of preclinical models that can recapitulate spontaneous metastatic disease and can be used to better understand the disease and identify new vulnerabilities. In this study, we present and characterize a murine model of spontaneous distant EWS metastasis derived from human patient-derived xenografts (PDX) in two different mouse backgrounds that mimics the clinical progression of the human disease. A panel of seven molecularly diverse patient-derived xenograft (PDX) models (SJ18, SJ17, S049, NCH1, NCH4, PDMR-098, PDMR-077) were injected orthotopically into the gastrocnemius muscle in the left hind leg of athymic nude and NOD SCID gamma (NSG) mice. Once primary tumors reached 1500 mm^3, hind limb amputation survival surgery was performed, and we observed animals for the development of distant spontaneous metastases. EWS PDXs formed spontaneous macrometastases in multiple sites including lymph nodes, lung, liver, and kidney in both NSG and nude mice. Each PDX model exhibited a distinct pattern of macrometastasis formation, based on site, metastasis frequency, and mouse strain. Immunohistochemical analysis for CD99 positivity revealed the presence of micrometastases in some locations where no macrometases were evident. The highest frequency of distant metastases (macro- plus micro-) was seen in PDMR-098 and SJ18 models in NSG mice (75% and 73.3% respectively); SJ18 most frequently metastasized to lung, whereas PDMR-098 most frequently metastasized to liver and mesenteric lymph nodes. Comparing results in NSG versus nude mice, we observed variations in metastasis frequency and site preference, with NSG mice demonstrating a higher rate of metastasis overall. Here we describe a preclinical model of spontaneous distant EWS metastasis that recapitulates the characteristics of human disease. The site and frequency of metastases vary based on the specific PDX model as well as the mouse background, highlighting that modeling metastasis formation is a multifactorial process driven by complex interactions between the tumor and host. Metabolomic profiling conducted to compare primary and macrometastatic tumors between models and metastatic sites revealed differences in multiple metabolic pathways. Future studies will focus on identifying potentially targetable metabolic vulnerabilities that could be used in the development of treatments for metastatic EWS.

#6179 Differential sensitivity of paired FUS-TFCP2+ RMS PDX models developed from tumor specimens obtained prior to and after ALK inhibitor therapy.

Erika Dobrota[1], M. Reza Saadatzadeh[1], Barbara Bailey[1], Keiko Kreklau[1], Gabe Mervis[1], Kathy Coy[2], Felicia Kennedy[2], Melissa Trowbridge[2], Anthony Sinn[2], Christopher Davis[1], Steven Angus[1], Michael Ferguson[3], Pankita Pandya[4], Karen Pollok[4]

[1]Wells Center for Pediatric Research, Indiana University School of Medicine, Indianapolis, IN,[2]Preclinical Modeling and Therapeutics Core, Indiana University Simon Comprehensive Cancer Center, Indianapolis, IN,[3]Department of Pediatrics, Division of Pediatric Hematology/Oncology, University of Louisville, Louisville, KY,[4]Indiana University Simon Comprehensive Cancer Center, Indianapolis, IN

FUS-TFCP2-positive rhabdomyosarcoma (FUS-TFCP2+ RMS) is a rare subtype of spindle cell/sclerosing RMS with a craniofacial predilection. These tumors are highly aggressive, quick to metastasize and evade conventional chemotherapies. FUS-TFCP2 fusion results in a gain of function transcription factor that promotes proliferation and activates survival pathways while blocking myogenic differentiation and inhibiting DNA repair. Currently, there is no effective standard of care, surgery can be difficult due to location and patients typically succumb to the disease within 15 months of diagnosis. Overexpression of downstream target, Anaplastic Lymphoma Kinase (ALK), is characteristic of FUS-TFCP2+ RMS. However, while case reports of targeted treatment with ALK inhibitors (ALKi) have shown modest results, resistance always emerges. In collaboration with the Pediatric Cancer Precision Genomics Program at the Riley Hospital for Children, we developed a paired set of FUS-TFCP2+ RMS patient-derived xenografts (PDXs). ALKi-sensitive PDX174 was derived from a patient tumor sample obtained prior to an 11-month ALKi (lorlatinib) regimen. Subsequently, a second sample was acquired following disease progression from which ALKi-resistant PDX199 was established. RT-PCR validated the fusion site in both models. In vivo studies confirmed PDX174 sensitivity and PDX199 resistance to lorlatinib (0.1mg/kg and 1mg/kg). Concordant with FUS-TFCP2+ characterization, transcriptome analysis showed significantly increased expression of ALK in both PDX174 (14.9-fold) and PDX199 (11.1-fold). Western blot analysis revealed robust overexpression of ALK isoforms in PDX174, whereas ALK expression in the ALKi-resistant PDX199 was only barely detectable. Instead, PDX199 exhibited increased levels of TERT, CDK4/6, and BET proteins. To further compare the models, we utilized two complementary approaches to evaluate the activated kinome of ALKi-resistant PDX199 compared to ALKi-sensitive PDX174. Kinase activity profiling using PamGene peptide microarrays revealed a statistically significant increase in kinase activity of components involved in PI3K/AKT pathway and cell cycle CDKs (CDK1,2,4), with concomitant suppression of kinase activity of JNK/p38 MAPKs, indicating a shift toward PI3K/mTOR-driven pro-survival signaling and potential vulnerability to PI3K/AKT and CDK inhibition. Global kinome analysis using multiplexed inhibitor beads also showed an increase in CDK4/6 activation in ALKi-resistant PDX199 versus ALKi-sensitive PDX174. Pre-clinical models such as these provide a platform to connect molecular signatures with targeted therapy, increase our mechanistic understanding of tumor adaptive responses and design therapies that will mitigate the emergence of therapeutic resistance.

#6180 Gene editing in the mouse reveals functional mechanisms of ASPS-TFE3 induced translocation renal cell carcinoma.

Gopinath Prakasam, Alana Christie, Lisa Kinch, Jeffrey Miyata, Quyen Do, Mylinh Nguyen, Robert Hammer, Payal Kapur, James Brugarolas

UT Southwestern Medical Center, Dallas, TX

Translocation renal cell carcinoma (tRCC) is an aggressive form of kidney cancer that predominantly affects children and young adults. With no specific FDA-approved therapies, it remains an unmet clinical need. Patients often present with metastatic disease and median overall survival is less than two years. tRCC is driven by oncogenic fusion proteins involving transcription factors of the MiTF family, most commonly TFE3, yet the mechanisms by which these fusion proteins promote tumorigenesis remain poorly understood. To investigate tRCC tumorigenesis, we expressed human ASPS-TFE3, the most prevalent oncogenic fusion, in postnatal renal proximal tubule cells generating the first tRCC mouse model faithfully reproducing the human disease. These mice developed aggressive tRCC with complete penetrance and short latency. In addition, they also developed ASPS and PEComas, illustrating a shared pathogenesis that goes beyond MiTF fusion oncoproteins. Through integrated histologic, ultrastructural, transcriptomic, proteomic and functional analyses, we found that ASPS-TFE3 simultaneously activates mTORC1 signaling and lysosomal pathways. To dissect the role of ASPS-TFE3 in tumor initiation, we employed CRISPR-mediated gene editing. Structural modeling, mutagenesis, and localization studies identified a bHLH domain mutant [ASPS-TFE3(2RA)] that retains nuclear localization but fails to bind DNA and lacks transactivation activity. Unlike wild-type fusions, ASPS-TFE3(2RA) failed to induce tRCC, demonstrating that DNA binding is essential for tumorigenesis. Furthermore, its broader expression in renal epithelial cells compared to ASPS-TFE3 (despite the same driver) illustrates oncogene-induced protective mechanisms expanding our ex vivo studies. Interbreeding experiments coupled with phenotypic and functional studies revealed a context-dependent lineage-specific dominant-negative effect modulating tumor spectrum and latency. Together, these findings provide insight into ASPS-TFE3 tRCC pathogenesis and establish a genetically tractable platform to dissect fusion-driven oncogenesis and evaluate therapeutic strategies.

#6181 Development of a clinically relevant *in vitro* model of ETMR and implications for drug efficacy studies.

Evangelos Liapis, Adele Ponzoni, Lea Anne T. Maristela, Claire L. Carter, Derek Hanson

Hackensack Meridian Center for Discovery and Innovation, Nutley, NJ

Background: Patient-derived 3D models of pediatric brain tumors are increasingly used in preclinical drug screening due to their greater clinical relevance. However, no guidelines or widely adopted methods exist, and most drug screening studies still rely on small tumorspheres. The primary ETMR line, BT183, retains key molecular features, including C19MC amplification and LIN28A overexpression, yet its conventional tumorsphere format fails to recapitulate the characteristic multilayered rosettes observed in patients, lacks cellular complexity, and remains size-restricted for functional studies and drug screening. To overcome these limitations, we established a more clinically relevant 3D pseudo-organoid model by optimizing the culture medium, promoting growth from 700-3000 µm in diameter, and co-culturing with non-tumor cell populations, including blood brain barrier (BBB) and immune cells.
Methods: BT183 cells were cultured as tumorspheres in NeuroCult (NC) or as pseudo-organoids in tumor stem cell medium (TSM). Rosette abundance was quantified in H&E sections, while rosette architecture and size were assessed by 3D multiplex immunofluorescence (mIF) of optically cleared whole pseudo-organoids followed by confocal imaging and morphometric analysis. Drug screening was performed across multiple sizes and drug penetration was evaluated by mass spectrometry imaging (MSI). Multicellular BBB pseudo-organoids were generated by staged seeding of tumor, microglia, neuronal, endothelial, and pericyte populations in ratios reflecting ETMR patient samples; Integration and layering were evaluated by mIF. Large (> 2 mm) organoids were produced with or without Matrigel under constant agitation.
Results: Pseudo-organoids grown in TSM contained significantly more rosettes compared to tumorspheres grown in NC. There was a divergence in the size of the spheroids once they reached 500 µm, with the rosette forming model growing to larger sizes faster than the conventional model. Notably, the rosettes forming pseudo-organoid model demonstrated drug-dependent enhanced chemoresistance to clinically relevant agents compared to the standard model. MSI provided quantification of drug penetration and spatial distribution across models to correlate with efficacy. BBB pseudo-organoids showed successful incorporation of cell populations, including endothelial cells and pericytes. Prolonged culture under agitation, coupled with Matrigel dome embedding, further supported the formation of large, structurally complex organoids.
Conclusions: Our ETMR pseudo-organoid model recapitulates the multilayered rosette architecture characteristic of patient tumors. Ongoing work is being carried out to further refine this system into multicellular, large-scale 3D organoids that further advance preclinical modeling and therapeutic testing in embryonal tumors with multilayered rosettes.

#6182 Post-transcriptional silencing of p14ARF drives retinoblastoma malignant conversion in CRISPR-engineered retinal organoids.

Jinlun Bai, David S. Koos, Kevin Stachelek, Bhavana Bhat, Susan Asatrian, Patrick Belen, Sunjum Sanghari, Kayla Stepanian, Scott Fraser, Rex A. Moats, David Cobrinik

Children's Hospital Los Angeles, Los Angeles, CA

Purpose: This study aims to elucidate the molecular mechanisms driving malignant transformation from pre-malignant lesions, leveraging a CRISPR-engineered human retinoblastoma retinal organoid (RBRO) model that recapitulates the cone cell-of-origin and timing of multi-step retinoblastoma genesis.

Background: Most retinoblastomas arise from maturing cone photoreceptor precursors (CPs) following biallelic *RB1* inactivation. The process can be recapitulated in explanted fetal retina, where pRB-depleted CPs proliferate, followed by a 3-5 month indolence phase and emergence of retinoblastoma-like masses at tissue ages mirroring in vivo disease. CRISPR engineered retinal organoids (ROs) provide a promising model with which to define mechanisms that underlie malignant progression.

Methods: We generated *RB1* knockout iPSC lines through CRISPR editing of the GNAT2-EGFP cone reporter (Bai *et al*., PMID 37902188). Chimeric RBROs were produced by mixing *RB1* knockout and unedited parental iPSCs. Proliferation dynamics, cell identities and cell state changes of EGFP+ $RB1^{-/-}$ cones were evaluated by live imaging of hydrogel-embedded RBROs, immunofluorescent (IF) staining, and deep full-length scRNA-seq. Additional CRISPR edits were introduced to test candidate drivers of indolence entry and escape.

Results: In *RB1* WT ROs, EGFP specifically, robustly and innocuously labeled post-mitotic cones. In RBROs, live imaging and IF staining revealed initial EGFP+ $RB1^{-/-}$ cone proliferation followed by a pre-malignant indolence phase starting at ~d120. Most of the initially proliferating cones become Ki67-negative, with some adopting mature cone morphology. Retinoblastoma-like foci composed of cells co-expressing EGFP, cone markers, and Ki67 formed after ~d280, a tissue age that equates to the first post-natal month when retinoblastomas emerge. Single-cell transcriptomic profiling at different tumorigenesis stages revealed distinct $RB1^{-/-}$ cell proliferation, cell differentiation, and cell stress states with high expression of $CDKN2A^{ARF}$ RNA and p14ARF protein. In contrast to initially proliferating pre-indolence CPs, the later proliferating post-indolence retinoblastoma-like cells expressed $CDKN2A^{ARF}$ RNA but not p14ARF protein, consistent with post-transcriptional silencing of p14ARF as a mechanism underlying indolence escape. RBROs lacking p14ARF exhibited sustained initial cone proliferation similar to indolence-escaped p14ARF-WT RBROs.

Conclusion: We established a human retinoblastoma organoid model that recapitulates the cell-of-origin, developmental context, and temporal sequence of multi-step retinoblastoma genesis. This system uncovers stage-specific molecular signatures and highlights p53 pathway regulation – particularly p14ARF post-transcriptional silencing – as a key driver of the indolence-malignancy transition.

#6183 MIAC51 cells induce rapid-onset leukemia across multiple rat strains: A novel and reproducible model of Chloroleukemia.

Joel Costoya[1], Joaquin J. Jimenez[2]

[1]Department of Biochemistry and Molecular Biology, University of Miami Miller School of Medicine, Miami, FL,[2]Dr. Phillip Frost Department of Dermatology and Cutaneous Surgery, University of Miami Miller School of Medicine, Miami, FL

The American Cancer society states leukemia as the most prevalent form of pediatric cancer, nearly 1 in 5 cases of childhood leukemia are acute myeloid leukemia (AML). Advances in risk-group stratification, and chemotherapeutic regimens, have improved clinical outcomes for pediatric patients such that 5-year survival rates are at around 70%. Significant challenges remain in their treatment of leukemia, considering as many as 30% of patients relapse and the expected survival rate is drastically lower. Efforts to understand the mostly unknown etiology of childhood leukemia have been greatly improved by animal modeling which can simulate biological multi-system involvement and a more accurate disease state. We aim to document a new viable animal model in the limited repertoire of AML models using MIAC51 cells, a rat Chloroleukemia cell line. Multiple strains of rat pups, at 7 days old, were injected intraperitoneally with MIAC51 rat cells and compared to respective control groups who received saline solution. All pups had 50 µL of blood drawn at both 7- and 14-days post-injection via tail snip method. Complete blood count (CBC), and differential staining were performed to detect presence of leukemia. At 14 days post-injection, all breeds tested: Wistar, Sprague Dawley, Long Evans, Brown Norway, and Fischer 344, developed leukemia with 100% success rate. Chloroleukemia blasts were found in peripheral blood, indicative of AML as confirmed by Wright stain and CBC. Established here is a novel and reproducible young-rat leukemia model using MIAC51 cells, demonstrating consistent engraftment and leukemic transformation across all tested breeds. Induction of leukemic-state was confirmed by the presence of Chloroleukemia blasts in peripheral blood staining and CBC abnormalities. This model will accelerate translation of hematological science research by providing a platform for studying leukemogenesis, and leukemic pathophysiology in a young-host, with relevance to childhood acute myeloid leukemias. Inquiry into the mechanistic basis for Chloroleukemia induction, and further genetic analysis of the leukemia model will help define its fidelity to human pediatric AML and determine its utility in downstream pre-clinical application.

#6184 Site-specific tumor modeling: DIPG and meningioma in mice.

Melissa Tran[1], Cheryl Davis[2], Ben Hoerner[1], Victoria Caruso[1], Helen Ketteringham[3], Corrine Silvio[4], Shannan Paul[3], Chris Holding[3], Aliccia Koznecki[3], Dawn Lusk[4], Shorena Nadaraia-Hoke[4], Delaney McCormick[1], Jocelyn Saurbaugh[1]

[1]Reaction Biology Corp, Malvern, PA,[2]Reaction Biology Europe GmbH, Freiburg im Breisgau, Germany,[3]Reaction Biology Corp, Hershey, PA,[4]Reaction Biology Corp, Hummelstown, PA

Diffuse intrinsic pontine glioma (DIPG) and meningioma are central nervous system tumors where anatomical location critically influences disease behavior and therapeutic response. To investigate this impact, we have developed and compared preclinical models using SF8628-GFP$^+$/Luc$^+$ (DIPG) and Ben-Men-1-Luc (meningioma) across three inoculation sites: (1) clinically relevant locations (pons for DIPG; skull base for meningioma), (2) general intracranial sites, and (3) subcutaneous sites. Tumor progression was monitored longitudinally using bioluminescence imaging and confirmed by histopathology. This study sought to determine how site-specific microenvironments affect growth kinetics, infiltration patterns, and imaging characteristics. Understanding these differences is essential for drug development, as orthotopic models better replicate blood-brain barrier constraints, tumor vascularization, and local tissue interactions that influence therapeutic delivery and efficacy.

: Spatial Niches and Functional Boundaries within the Tumor Microenvironment 2
Poster Session

#6187 Elevating bulk sequencing with high-resolution spatial transcriptomics: A paired-data analysis of clinically-relevant spatial niches in CRC and NSCLC.

Yajas Shah, Tianyou Luo, Christine M. Hoeman, Luca Lonini, Stanislaw Szydlo, Eduardo Diaz, Rossin Erbe, Matthew B. Maxwell, Michelle M. Stein, Andrew J. Sedgewick, Nicholas Rachell, Zachary Chelsky, Sonal Khare, Ryan D. Jones, Kate Sasser, Richard A. Klinghoffer, Justin Guinney, Chi-Sing Ho

Tempus AI, Chicago, IL

Background. Bulk RNA-next generation sequencing (RNA-NGS) is a standard tool for the molecular characterization of solid tumors and is used in clinical practice to guide therapy selection. However, the spatial organization of the tumor microenvironment (unobservable in bulk RNA-NGS) plays an important role in clinical phenotypes and therapy response. While spatial transcriptomics (ST) overcomes the limitations of bulk sequencing, the relationship amongst ST, bulk NGS, and clinical phenotypes in real-world cancer patients has not been explored. To address this, we generated and analyzed a large multimodal, real-world cohort of colorectal (CRC) and non-small cell lung cancer (NSCLC) tumors profiled with ST, bulk RNA-NGS and targeted DNA-NGS data from the same biospecimen.
Methods. Gene expression data from 3.7 million cells, sourced from 42 NSCLC (16 metastatic) and 19 CRC (6 lung and 6 liver metastases) patients were generated at whole-transcriptome level using 10X Genomics Visium HD platform. Cells were integrated using scVI and annotated using SCimilarity. Spatially-informed clusters were generated using CellCharter. Association testing between spatial, clinical, and biomarker features, including the Tempus Immune Profile Score (IPS) were performed using linear models adjusted for clinical (tumor type, stage, histology, metastasis) and molecular features (TMB) as appropriate.
Results. Visium HD pseudo-bulk showed high correlation with paired bulk RNA, with a median Spearman correlation of 0.79 (IQR: 0.78-0.81). Spatial clustering of gene expression revealed six distinct spatial niches: two enriched for epithelial cells, one for stromal cells, and three for immune cells (myeloid-rich, lymphoid-rich, and tumor-immune mixed regions). Among NSCLC tumors sourced from the lung, we found that the myeloid, lymphoid and stroma-rich niches were enriched for Stage I, II and IV cases respectively ($p < 0.05$). Spatial niches were associated with key oncogenic alterations in NSCLC (lymphoid-, myeloid- and stroma-rich, *CDKN2A*, *KEAP1*, *RBM10*, $p < 0.05$) and CRC (lymphoid- and myeloid-rich, *KRAS*, *TP53*, $p < 0.05$). Patients with higher IPS scores were associated with an enrichment of lymphoid and tumor-immune mixed niches ($p < 0.05$), while cells from tumor-immune mixed regions had higher expression of immune infiltration and exhaustion markers than the lymphocyte-rich regions (*IKZF2*, *TOX2*, *PTPRC*, *CD69*).
Conclusion. Our work profiles the genomic and transcriptional features contributing to spatial heterogeneity, revealing distinct molecular patterns associated with immune cell infiltration. This dataset provides a powerful foundation for understanding tumor microenvironment-driven phenotypes and translating spatial-only insights into scalable biomarkers, empowering future translational discovery in precision oncology.

#6188 Decoding the archetypes and ecotypes of triple-negative breast cancer in responses to chemotherapy.

Yun Yan[1], Yiyun Lin[1], Tapsi Kumar[1], Shanshan Bai[1], Aatish Thennavan[1], Jianzhuo Li[1], Tuan Tran[1], Min Hu[1], Mitchell Rao[1], Anna Casasent[1], Elizabeth Ravenberg[1], Gaiane Margishvili Rauch[1], Alyson Clayborn[1], Debu Tripathy[1], Alastair Thompson[2], Bora Lim[1], Lei Huo[1], Lei Huo[1], Stacy Moulder[1], Clinton Yam[1], Nicholas E. Navin[1]

[1]UT MD Anderson Cancer Center, Houston, TX,[2]Baylor College of Medicine, Dan L. Duncan Cancer Center, Houston, TX

Triple-negative Breast Cancer (TNBC) is an aggressive subtype of breast cancer. The pillar of treatment is chemotherapy, but only half of the patients have a complete response and good survival. To resolve inter- and intra-tumoral heterogeneity and determine their clinical associations, we performed single-cell RNA-sequencing and spatial transcriptomics experiments (including Xenium, Visium HD, and Visium) on treatment-naïve samples of TNBC patients in the ARTEMIS clinical trial. We find that TNBC is classified into 4 major archetypes at patient level: luminal secretory-like, basal-like, interferon responsive, and androgen receptor-enriched. At cell level, cancer cells exhibited intratumoral heterogeneity in 13 gene expression metaprograms. The TNBC tumor microenvironment (TME) consisted of 49 distinct immune and stromal cell states, many of which were reprogrammed relative to normal breast tissues from disease-free women. We further identified 8 ecotypes of cancer cells and TME cell states that co-occurred among patients and were associated with specific archetypes and chemotherapy response groups. Using the Xenium data, we identified 10 distinct spatial niches based on the co-localization of cancer and TME cells, including the tertiary lymphoid structure (TLS) niche, the immune-'hot' niche enriched for interferon signaling, and the EMT-associated niche characterized by the angiogenic and ECM-remodeling macrophages together with the hypoxic, EMT-related cancer cells. In contrast to previous work on T-cells, our data showed the importance of macrophage cell states and cancer cell metaprograms for interferon signaling, HLA expression and cell cycle activity that were associated with chemotherapy response. To facilitate a clinical application, we developed a 13-gene-based model of response prediction, which was validated using public TNBC cohorts. Collectively, this study provides new insights into the natural biology of untreated TNBC tumors and their association with chemotherapy response.

#6189 *ERBB2* expression and the immune landscape shape the tumor microenvironment and influence prognosis in esophageal adenocarcinoma brain metastases.

Nora M. Lawson[1], Ines Martin-Barrio[1], Lingqun Ye[1], Bo Zhao[1], Thomas Mitchell[2], Mesut Unal[1], Chae Yun Cho[1], Andrew Futreal[3], Kadir C. Akdemir[1]

[1]Neurosurgery, UT MD Anderson Cancer Center, Houston, TX,[2]Genetics, UT MD Anderson Cancer Center, Houston, TX,[3]Genomic Medicine, UT MD Anderson Cancer Center, Houston, TX

Esophageal adenocarcinoma (EAC) is a prevalent and fatal malignancy, ranking sixth globally in cancer-related deaths. Brain metastases from EAC are rare, occurring in only 2-6% of cases, and little is known about the molecular drivers or tumor microenvironment (TME) characteristics that underpin this metastatic spread. To investigate drivers of brain metastasis, we analyzed a test cohort of frozen primary and brain metastasis pairs (n = 8) and an expansion cohort of 60 FFPE brain metastases from surgeries performed at MD Anderson Cancer Center (2010-2018).To characterize molecular determinants of EAC brain metastases, we performed multi-omics profiling, integrating whole-genome sequencing, fluorescence in situ hybridization (FISH), and single-cell spatial transcriptomics (10x Genomics Xenium). *ERBB2* amplification emerged as a recurrent and potentially targetable alteration, present in 90% of brain metastases versus 20-25% of primary and extracranial tumors, suggesting an early and frequent driver event. The cohort included 12 long-term survivors (LTS; >3 years), including one patient alive 17 years post-diagnosis, whereas most patients succumbed within one year. Several received HER2-targeted therapy with variable clinical responses, underscoring the need to elucidate factors distinguishing LTS from short-term survivors (STS; <1 year). Single-cell spatial transcriptomics revealed distinct tumor-immune ecosystems associated with *ERBB2* copy number. LTS tumors with high *ERBB2* amplification exhibited immune-active microenvironments enriched in macrophages, T cells, and endothelial cells, with fewer cycling tumor cells, indicative of effective immune surveillance. In contrast, low-*ERBB2* tumors were proliferative and immune-poor. Across all cases, *ERBB2* expression correlated with T cell infiltration and tertiary lymphoid structures (TLS). Differential gene expression confirmed LTS tumors up-regulated immune activation and T cell persistence genes (*IGH1, IGH3, IGH4, IL2RB, TOX*), whereas STS tumors expressed pro-tumor, inflammatory, and angiogenic genes (*MUC5AC, REG4, CXCL1, CXCL3, RGS5, ACE2*). These findings indicate that *ERBB2* amplification and immune contexture jointly shape the tumor microenvironment and prognosis in EAC brain metastases, suggesting that *ERBB2*-directed therapies combined with strategies to enhance immune activity may improve outcomes in this patient population.

#6190 Spatial architecture analysis reveals disrupted lymphotoxin signaling gradients associate with recurrence in high-grade serous ovarian cancer.

Zhewei Zhang, Tat San Lau, Chi Chiu Wang

The Chinese University of Hong Kong, Shatin, Hong Kong

Background: Recurrence drives mortality in ovarian cancer patients, with tumor-stromal signaling interactions playing critical roles in disease progression. Lymphotoxin family signaling, operating through lymphotoxin-LTBR interactions between tumor and stromal compartments, orchestrates chemokine-mediated immune cell recruitment. However, existing studies have focused on expression levels rather than spatial organization of these signaling networks. We aimed to characterize spatial gradient patterns of lymphotoxin signaling in high-grade serous ovarian cancer (HGSC) and determine whether spatial organizational features distinguish recurrent from non-recurrent disease.
Methods: We integrated publicly available subcellular spatial transcriptomics datasets spanning multiple independent cohorts, comprising >100 HGSC patients and >2.5 million spatially resolved cells. Patients were stratified by 2-year progression-free survival into recurred versus non-recurred groups. We quantified spatial expression gradients using neighborhood-based approaches, calculating spatial autocorrelation and tumor boundary-associated expression patterns for lymphotoxin family genes (LTA, LTB, LTBR) and related chemokines.
Results: Recurrent HGSC exhibited disrupted spatial organization of lymphotoxin signaling despite comparable expression levels. LTB displayed reduced spatial autocorrelation in recurrent tumors (-0.254 vs -0.320, $p=0.029$), indicating loss of organized spatial expression patterns. LTBR showed attenuated tumor boundary gradients in recurrent samples (Spearman $\rho=-0.121$ vs -0.178, $p=0.034$), suggesting disrupted spatial signaling architecture at tumor-stromal interfaces. LTB also demonstrated diminished tumor boundary enrichment in recurrent cases ($\rho=-0.010$ vs 0.070, $p=0.055$). Cellular composition and overall gene expression showed no significant differences, confirming that spatial organization rather than abundance drives these findings.
Conclusion: Disrupted LTB/LTBR spatial gradients in recurrent HGSC indicate that immune evasion involves spatial disorganization of tumor-stromal signaling beyond expression-level changes. These findings suggest that interventions restoring spatial chemokine gradients—such as engineered lymphotoxin delivery or spatially-targeted stromal reprogramming—may enhance immune infiltration and warrant investigation as strategies to prevent ovarian cancer recurrence.

#6191 Decoding the interactions between cancer cells and monocyte-derived macrophages in a co-culture model using flow cytometry and bead-based multiplexing immunoassay panels.

Amy Zhao, Anugraha Gandhirajan, Michael Hunegnaw, Anil Kumar Jaiswal, Jessie Ni

BioLegend, San Diego, CA

Macrophages play a pivotal role in the immune response and in the maintenance of tissue homeostasis. It is well known that many tumors recruit monocytes from circulation and transform them into an immunosuppressive subset called Tumor-Associated Macrophages (TAMs). TAMs are highly plastic and can alter their phenotypes between M1 pro-inflammatory and M2 anti-inflammatory according to their location and surrounding cytokine milieu in the tumor microenvironment. M1 macrophages are associated with the recognition and destruction of cancer cells whereas M2 macrophages are thought to promote proliferation, angiogenesis, and metastasis of cancer cells. In this study, monocytes-derived THP1 macrophages were cultured with conditioned medium collected from various cancer cell lines, such as colon cancer cell line HT29, lung cancer cell line A549 and breast cancer cell line MDA-MB-231, to study the influence of cancer cells and their secreted factors on the activation and differentiation of monocyte-derived macrophages. The phenotypes of the macrophages in the culture were characterized by flow cytometric analysis of macrophage surface markers including CD86, CD206, CD163, CD274, CD11b, CD14 and CD40, and the soluble factors produced by them including the M1 and M2 markers were measured using the LEGENDplex ™ Human Macrophage Panel and Human Tumor-Associated Macrophage Panel. In a parallel study, macrophages were activated and polarized into M1 and M2 phenotypes, followed by co-culture with cancer cells. The proliferation and viability of cancer cells were measured at the end of the incubation by flow cytometry to assess the distinct influences of M1 and M2 macrophages on cancer cell cultures. Our data suggests that cancer cells could release soluble factors to actively influence the phenotypes of monocyte-derived macrophages. Moreover, the study demonstrated that M1 and M2 macrophages may have different impact on cultured cancer cell's viability and proliferation. This *in vitro* study enhances our understanding of the interplay between cancer cells and tumor-associated macrophages, underscoring the utility of LEGENDplex^{TM} panels in studying tumor-associated macrophages.

#6192 Multi-omics reveals the diversity of CAF in ESCC lymph node metastasis.

Licheng Tan[1], Beilei Liu[2], Shuang Zhang[3], Jiayi Huang[4], Bowen Yao[4], Xin-Yuan Guan[4]

[1]Department of Clinical Oncology, University of Hong Kong, Hong Kong, Hong Kong,[2]City University of Hong Kong, Hong Kong,[3]University of Hong Kong, Shenzhen Hospital, Shenzhen Shi, Hong Kong,[4]University of Hong Kong, Hong Kong, Hong Kong

1. Introduction Esophageal squamous cell carcinoma (ESCC) is among the most common and lethal malignancies in China, accounting for the fifth-highest rate of cancer-associated mortality. Cancer-associated fibroblast (CAF) plays an important role in tumor microenvironment (TME). Lymph node metastasis is a key risk factor that leads to worse prognosis of ESCC patients. However, the initiation and mechanism of lymph node metastasis is still uncertain. Our previous study has revealed that CAF can promote ESCC lymph node metastasis through secreting MFGE8 to activate AKT/STAT3 signaling. Thus, we decided to further explore the role of CAF in ESCC lymph node metastasis.
2. Materials and methods We collected ESCC tumor samples for spatial transcriptome sequencing. Combined with our single-cell RNA sequencing data and published single-cell sequencing cohort, we performed multi-omics spatiotemporal analysis to reveal the diversity of CAF in ESCC. We also performed multi-plex immunohistochemistry (mIHC) to verify the subtype in ESCC samples. We collected fresh ESCC samples from patients and murine models to isolate CAF from tumor for in vitro and in vivo experiment. Sirius red staining was performed for collagen composition analysis. KYSE30, KYSE180, KYSE410, KYSE520, and mouse mEC25 cell lines were cultured for in vivo and in vitro experiments.
3. Results We integrated our single-cell RNA sequencing data (GSE203067) and another published cohort (GSE160269), which contained 64 ESCC patients. After unsupervised clustering, we got 6 subclusters of fibroblast (including pericyte and smooth muscle cell). Tissue distribution showed that MMP11+ Fib was enriched in primary tumor and metastatic lymph node, while PI16+ Fib was enriched in normal esophagus. Then we analyzed spatial transcriptome sequencing data via deconvolution algorithm, and revealed the spatial distribution of different fibroblast subtypes in ESCC tumor. MMP11+ Fib showed a higher proportion in primary tumor of patients with lymph node metastasis. Gene Set Enrichment Analysis indicated pathways with extracellular matrix and epithelial-mesenchymal transition were upregulated in MMP11+ Fib. Western blot and immunofluorescent staining verified the expression of MMP11 in CAF from ESCC patients and murine ESCC model. Cell-cell interaction analysis, based on spatial localization, indicated the POSTN-(ITGAV/ITGB5) ligand-receptor signaling was significantly activated between MMP11+ Fib and tumor cell.
4. Conclusion CAF in ESCC showed a huge diversity, and the MMP11+ Fib is a pro-tumor and pro-metastasis subtype of CAF, which is a potential target for ESCC treatment.

#6193 Spatial remodeling of immune and stromal microenvironments in sentinel lymph nodes during melanoma progression.

Shankar Suman[1], Wendy K. Nevala[1], Noah A. Stueven[1], Raymond M. Moore[1], Chathu L. Atherton[1], Jeffrey E. Johnson[1], Ray Guo[2], James W. Jakub[2], Svetomir N. Markovic[1]

[1]Mayo Clinic, Rochester, MN,[2]Mayo Clinic, Jacksonville, FL

The sentinel lymph node (SLN) is often the first site of melanoma spread and a critical immune checkpoint that determines local tumor dissemination to systemic metastasis. Although lymph nodes are central to antitumor immunity, the mechanisms that render them permissive to metastasis remain poorly understood. This study used spatial imaging to characterize immune and stromal phenotypic alteration in tumor-negative SLNs (SLN^-) and tumor-positive SLNs (SLN^+) from patients with cutaneous melanoma, compared to non-melanoma-associated normal lymph nodes (NLN). We performed multiplex immunofluorescence (MxIF) analysis of formalin-fixed, paraffin-embedded lymph node tissues from patients with cutaneous melanoma and control subjects, including two subjects per group (NLN, SLN^-, and SLN^+). Furthermore, quantitative single-cell segmentation and classification using QuPath generated median fluorescence intensities for immune, stromal, and tumor markers across LN, SLN^- and SLN^+ regions of interest. In addition to the initial analysis, we employed spatial neighborhood analysis to characterize markers expression profiles surrounding target immune population. This approach quantified local microenvironment based on marker normalized intensity-based co-expression pattern and stromal remodeling signatures. We grouped these markers based on the functional panels representing T-cell activation and exhaustion, myeloid polarization, tumor interaction, stromal remodeling, and apoptosis pathways providing insights into how prometastatic niche evolve within SLN.

Normalized data, via centered log ratio (CLR) transformation and Gaussian Mixture Model (GMM) gating was analyzed using principal component analysis, UMAP/tSNE embedding, and hierarchical clustering in in python. Progressive immune remodeling was observed from normal NLN to SLN^+, including expansion of regulatory T cells, enrichment of exhausted T cells as well as myeloid-derived suppressor cells (MDSC), and transition toward an M2-like macrophage phenotype. The spatial data from SLN^- samples showed an early sign of immune suppression, with reduced cytotoxic capacity. These results show that SLN gets features of peripheral immune tolerance for melanoma early, prior to pathological dissection of metastatic spread supporting the existence of a pre-metastatic niche that facilitates lymphatic colonization of tumor cells. This work provides insights into early immune escape and may inform strategies for immunotherapy and early intervention in melanoma.

#6194 Spatial architecture of immunochemotherapy response in pleural mesothelioma.

Harim Chun[1], Yeoun Eun Sung[2], Sook Hee Hong[3], Sangjeong Ahn[4], Sung Hak Lee[2]

[1]Department of Medical Science, Graduate School, The Catholic University of Korea, Seoul, Korea, Republic of,[2]Department of Hospital Pathology, Seoul St. Mary's Hospital, The Catholic University of Korea, Seoul, Korea, Republic of,[3]Division of Oncology, Department of Internal Medicine, Seoul St. Mary's Hospital, The Catholic University of Korea, Seoul, Korea, Republic of,[4]Department of Pathology, Korea University Anam Hospital, College of Medicine, Korea University, Seoul, Korea, Republic of

Introduction: Pleural mesothelioma (PM) is a rare and aggressive malignancy originating from the mesothelial cells of the pleural lining, with a well-established etiological association with asbestos exposure. Although immunochemotherapy is being applied as a first-line treatment, most patients fail to respond to the therapy. Previous single-cell RNA sequencing studies on PM have revealed cellular heterogeneity but lack spatial resolution and comparative analyses of immune checkpoint inhibitor (ICI) responses, limiting understanding of tumor microenvironment (TME)-mediated resistance mechanisms. This study aims to comprehensively identify the cellular composition and spatial architecture of the TME, as well as mechanisms responsible for ICI resistance in PM.
Methods: Spatial transcriptomics analysis using the Xenium Prime 5K platform was conducted on baseline samples from 21 mesothelioma patients who received neoadjuvant immune checkpoint inhibitors (nivolumab/pembrolizumab), stratified as Responders (CR/PR, n=7) and Non-responders (PD/SD, n=14). Transcript-aware cell segmentation was performed with Proseg, followed by clustering and downstream analysis using Scanpy and Seurat. Copy number variations (CNV) were inferred with insituCNV, and pathway analysis was conducted via PROGENy and KEGG. Conserved spatial niches were identified using the BuildNicheAssay() function in Seurat v5.
Results: Spatial transcriptomics identified distinct 36 cell clusters, including mesothelial, immune, stromal, and normal alveolar cells. Mesothelial cells exhibited chromosome 22 deletions, with CNV scores inversely correlating with treatment response. Mesothelial cells of non-responders displayed “Active & Proliferative” phenotype with the high MAPK/PI3K/VEGF activities, whereas responders demonstrated “Stressed & Adaptive” state with elevated p53/TRAIL pathway activities. Responders demonstrated increased B cells, proliferating T cells, CD8 effector memory T cells, and exhausted T cells (CD8 Tex), whereas non-responders showed elevated tumor-associated macrophages. Among the 12 recurrent spatial niches, two tumor-reactive immunity niches of CD8 Tex and B cell-enriched tertiary lymphoid structure-like regions were prominent in responders. Immunosuppressive niches featuring mesothelial cells and SFRP2+ cancer-associated fibroblasts with active TGFβ pathways predominated in non-responders.
Conclusion: This study defines the TME architecture, mesothelial cell functional states, and cell type proportions associated with therapeutic response in PM. Cell type proportions and spatial niche composition featuring tumor-reactive immunity in responders versus TGFβ-driven immunosuppression in non-responders demonstrate predictive value for treatment outcomes and establish novel therapeutic targets to enhance immunotherapy responses.

#6195 Spatial transcriptomics analysis reveals tumor cell plasticity and diverse tumor microenvironments in Ewing sarcoma.

Heng Luo[1], Clemence Henon[2], Gleb Rukhovich[1], Stefanie Kutschmann[2], Nina Wilhelm[1], Wolfgang Hartmann[3], Uta Dirksen[4], Duncan T. Odom[5], Thomas G. Grunewald[2], Moritz Gerstung[1]

[1]Division of Artificial Intelligence in Oncology, DKFZ German Cancer Research Center, Heidelberg, Germany,[2]Division of Translational Pediatric Sarcoma Research, DKFZ German Cancer Research Center, Heidelberg, Germany,[3]Gerhard-Domagk-Institute of Pathology, Munster University Hospital, Muenster, Germany,[4]Pediatrics III, University Hospital Essen, West German Cancer Center, NCT West, Essen, Germany,[5]Division of Regulatory Genomics and Cancer Evolution, DKFZ German Cancer Research Center, Heidelberg, Germany

Objective

Ewing sarcoma (EwS) is a highly aggressive fusion-driven cancer of childhood and adolescence that can arise in both bone and soft tissue.In EwS, the tumor microenvironment (TME) is composed of cell types from the mesenchymal and hematopoietic lineages. Complex interactions between tumor cells and their TME are believed to shape the TME structure and the tumor cell plasticity in EwS. There have been existing efforts to characterize the fusion related tumor cell heterogeneity in EwS using bulk RNA-seq. In contrast, the TME of Ewing sarcoma remains largely underexplored at both single-cell and spatial level due to limited accessibility to patient samples and the constraints of contemporary staining methods. The aim of this project is to chart the EwS tumor cell heterogeneity and to characterize the interaction between the EwS tumor cells and the cells from the TME.

Methods

We performed single-cell FFPE sequencing (scFFPEseq) on four EwS tissue blocks. By utilizing the scFFPEseq data, we developed a probe panel comprising 480 genes. This refined selection includes cell type markers, differentially expressed genes (DEGs), highly variable genes (HVGs), hallmarks of tumor heterogeneity, pathway signatures, and specific receptor-ligand pairs, enabling precise in situ profiling of gene expression. We then performed spatially-resolved single-cell transcriptomics (10x Xenium) on 1 whole-section EwS sample and 137 EwS core sets from archived tissue microarrays.

Results

We generated a spatially-resolved single-cell dataset of 138 Ewing sarcoma patient samples, comprising 3.14 million cells. Meta program analysis on this dataset revealed 5 transcriptional states shared among EwS tumor cells across samples. These states include cell cycle, protein regulation, hypoxic stress, interferon response and high EWSR1-FLI1 fusion activity. The EwS TME consists of four stromal cell types and eight immune cell types. Spatial analysis showed that the EwS tumor cell states co-localize with distinct TME cells, giving rise to 8 recurrent niches.In the necrotic regions, SPP1+ macrophages and NK cells are found enriched in close proximity to hypoxic tumor cells. In regions with lymphocytic infiltration, co-localization with C1QC+ macrophage is associated with increased interferon response and JAK-STAT pathway activity in the EwS tumor cells.Finally, spatial single-cell interaction analysis suggests that lower EWSR1::FLI1 signature levels in the EwS tumor cells may be attributed to FGFR1 signaling stimulated by proximal fibroblasts.

Conclusion

In this project, we defined 5 shared tumor cell programs and 8 recurrent spatial neighborhoods across 138 EwS patient samples. The interplay between EwS tumor cells and fibroblasts via FGFR1 was found to be associated with lower EWSR1::FLI1 fusion signatures. This finding will lead to a potential therapeutic value of FGFR1 in the EwS treatment.

#6196 Neutrophil extracellular traps is involved in ovarian cancer-associated venous thrombosis.

Gaku Yamamoto[1], Mahiru Kawano[1], Mina Sakata[1], Michiko Bun[2], Aasa Shimizu[1], Erika Nakatsuka[1], Yasuto Kinose[3], Kenjiro Sawada[1], Michiko Kodama[1]

[1]Graduate School of Medicine Osaka University, Osaka, Japan,[2]Osaka Kaisei Hospital, Osaka, Japan,[3]Sakai City Medical Center, Osaka, Japan

Aims: Ovarian cancer patients have increased risk of venous thrombosis. However, the responsible mechanism of ovarian cancer associated venous thrombosis is not fully understood. This study aimed to investigate the formation of neutrophil extracellular traps (NETs) and its pathologic role in ovarian cancer patients. Methods: Human neutrophils were isolated from peripheral blood by density gradient centrifugation. Neutrophils were incubated in various conditions and tested for NETs formation in vitro. NETs formation was quantified by observing neutrophils stained with DNA-binding dye under fluorescent microscope. Several benign tumor sera and ovarian cancer sera were analyzed by cytokine array and ELISA. Serum NETs levels were measured by sandwich ELISA using anti-neutrophil elastase (NE) and anti-double strand DNA antibody. Clinical records of ovarian cancer patients who underwent surgery at our institution were retrospectively reviewed to evaluate the association between serum NETs levels and clinical. Immunohistochemistry with NETs marker, citrullinated histone H3 (CitH3) and myeloperoxidase (MPO), was performed for the samples of intravascular thrombosis in ovarian cancer patient. Results: Neutrophils could be isolated from peripheral blood with high purity. Conditioned media collected from OVCAR8 and OVKATE induced neutrophils to form NETs strongly. Serum from ovarian cancer patient predisposed neutrophils to form NETs more strongly than that from benign tumor patient (Median of index: 0.55 vs. 1.64; $p < 0.05$). Serum granulocyte-colony stimulating factor (G-CSF) levels from ovarian cancer patients were significantly higher than those from benign patients (Mean [pg/mL]: 4.5 vs. 9.9; $p < 0.05$). The stimulation with recombinant G-CSF induces neutrophils to form NETs. By cytokine array, Insulin-like Growth Factor 1 (IGF-1), C-C motif chemokine ligand 5 (CCL5), Angiogenin and Epidermal Growth Factor (EGF) were upregulated in ovarian cancer serum. However, when we verify CCL5 levels using multiple samples, there were no significant differences between benign tumor and ovarian cancer. Neutrophils isolated from ovarian cancer patients form NETs more greatly than neutrophils from benign tumor patients (Mean of index: 1.12 vs. 2.34; $p < 0.05$). Serum NETs level was significantly higher in ovarian cancer patients than in benign tumor patients (Median index: 0.0318 vs. 0.0667; $p < 0.05$). High NETs concentration was related to poor prognosis, increased neutrophil count, high platelet count, elevated CA125 level, advanced stage and venous thrombosis. Among them, thrombosis was significantly related to high NETs concentration in multi-variate analysis. Immunohistochemical analysis revealed NETs foci in thrombosis in ovarian cancer patients. Conclusion; It is suggested that ovarian cancer predisposed neutrophils to form NETs, which might have a causal effect on venous thrombosis.

#6197 Spatial transcriptomics reveal distinct tumor microenvironment associated with clinical response in thymic epithelial tumors after neoadjuvant therapy.

Hyunsu Kim[1], Jinyong Kim[1], Hyun-Ae Jung[1], Jong-Mu Sun[1], Se-Hoon Lee[1], Jin Seok Ahn[1], Myung-Ju Ahn[1], Yeong Jeong Jeon[2], Junghee Lee[2], Jong Ho Cho[2], Hong Kwan Kim[2], Yong Soo Choi[2], Seong Yong Park[2], Woong-Yang Park[3], Yoon-La Choi[4], Sehhoon Park[1]

[1]Division of Hematology-Oncology, Department of Medicine, Samsung Medical Center, Sungkyunkwan University School of Medicine, Seoul, Korea, Republic of,[2]Department of Thoracic and Cardiovascular Surgery, Samsung Medical Center, Sungkyunkwan University School of Medicine, Seoul, Korea, Republic of,[3]Department of Health Sciences and Technology, Samsung Advanced Institute of Health Sciences and Technology, Sungkyunkwan University, Seoul, Korea, Republic of,[4]Department of Pathology & Translational Genomics, Samsung Medical Center, Sungkyunkwan University School of Medicine, Seoul, Korea, Republic of

Background: Thymic epithelial tumors (TETs) are rare malignancies, mostly treated with surgical resection as the standard approach. However, recurrence rates remain high and immunotherapy can lead to immune-related adverse events, highlighting the need for improved therapies and predictive biomarkers. In this study, TET patients were administered three cycles of neoadjuvant immunochemotherapy prior to surgery. We aimed to characterize the tumor microenvironment (TME) to identify the association with treatment response.
Methods: We performed 18 single-cell RNA sequencing and 15 spatial transcriptomics on surgical specimens from 19 patients treated with neoadjuvant immunochemotherapy. Major pathological response (MPR) was defined as less than 10% viable tumor cells in resected specimens. Patients were stratified into three pathological response groups — thymic carcinoma (TC) with MPR, TC non-MPR, or thymoma (TM) non-MPR.
Results: Analysis of cell composition and ligand-receptor interaction networks revealed distinct TME differences according to pathological response group. In TC, tumors with MPR were characterized by extensive immune infiltration, tertiary lymphoid structures (TLS) formation, and prominent malignant cell necrosis. This immunologically hot TME featured robust interactions between lymphocytes and dendritic cells (DCs). Conversely, the TC non-MPR TME was dominated by thymic epithelial cells (TECs). Within the tumor core, these TECs orchestrated a localized immunosuppression by promoting the exhaustion of infiltrating CD8+ T cells and driving the polarization of tumor-associated macrophages into an M2-like state. This suppressive niche was further compounded by a scarcity of DC. In the context of TM, the non-MPR tumors was defined by scattered cortical TECs (cTECs) and thymocytes, alongside a sparse infiltration of effector T cells. Notably, cTECs maintained an immature TME by promoting thymocyte survival and retention while concurrently impairing the tumor-killing functionality of CD8+ T cells. Detailed cell-to-cell interaction results that further elucidate these TME dynamics will be presented.
Conclusions: Our findings that responses to neoadjuvant therapy in TETs are closely associated with distinct spatial characterization of the TME. Leveraging integrated single-cell and spatial multi-omics data, this study provides valuable insights into the TME and may inform a rationale for therapeutic strategies to improve clinical outcomes in TETs.

#6198 Single cell spatial multi-omic characterization of the tumor microenvironment in transformed follicular lymphoma.

Shaocheng Wu[1], **Eric Lee**[1], Anne-Sophie Fratzscher[1], Andrew Lytle[1], Spencer D. Martin[2], David G. Huntsman[1], David W. Scott[1], Christian Steidl[1], Andrew Roth[1]

[1]BC Cancer Agency, Vancouver, BC, Canada,[2]University of British Columbia, Vancouver, BC, Canada

Histological examination of follicular lymphoma (FL) biopsies remains the cornerstone for diagnosis and staging of FL. Single cell sequencing approaches, while transcriptomically rich, require tissue dissociation and therefore lose the native spatial context that may underpin FL progression and transformation to a high-grade lymphoma, typically diffuse large B cell lymphoma (DLBCL). By single cell spatial profiling, we aimed to characterize the spatiotemporal heterogeneity and interplay between malignant B cells and the tumor microenvironment (TME) during transformation from FL to DLBCL histology.

Single cell spatial transcriptomics (Nanostring CosMx) and proteomics (Cell DIVE) were performed on FFPE tissue cores of 14 tFL patients with paired FL (tFL-FL) and DLBCL (tFL-DLBCL) timepoints, and 13 FL patients without evidence of progression or transformation (non-tFL; >6y of follow-up). Spatial omics confirmed malignant B cell dominated follicular structures in non-tFL and tFL-FL while absent in tFL-DLBCL, consistent with pathologic classification. Follicles were then delineated (defining intra-follicular, peri-follicular and extra-follicular regions) and enriched proliferation and exhaustion features were observed in intra-follicular regions compared to extra-follicular counterparts. Moreover, differential spatial interaction patterns were observed, amongst which Galectin-9 crosstalk components were identified as being differentially expressed and exhaustion-related pathways were more prevalent in intra-follicular and peri-follicular regions in non-tFL and tFL-FL timepoints. Macrophage phenotypes also markedly shifted across spatial regions with progression: intrafollicular FOLR2$^+$ and IL4I1$^+$ macrophages present in non-tFL progressively diminished, while CD163$^+$, SPP1$^+$, and NLRP3$^+$ macrophages became increasingly enriched in extra-follicular regions in tFL-DLBCL. Cell neighborhood analysis showed differential abundance among non-tFL, tFL-FL, and tFL-DLBCL timepoints. For B-cell-predominant cell neighborhoods (CNs), the germinal center (GC) score was higher in non-tFL than tFL-FL, whereas tFL-FL and tFL-DLBCL shared similar GC score levels. Within CNs of similar cell type compositions, T cells were more exhausted and macrophages were more polarized towards anti-inflammatory phenotypes in the transformed state. Subsequent single cell proteomics validated the differential follicular Galectin-9 signaling and macrophage-related gene expression patterns among spatial regions.

In summary, we delineated the spatial landscape of both indolent and transformed FL. We identified a spatiotemporal shift in TME composition, spatial interactions, and cell neighborhoods. This study provides novel insights into the spatial lymphoma architecture associated with FL transformation, contributing to a refined disease evolution model.

#6199 Spatially revealed malignant and microenvironment ecosystems in PanIN- and IPMN-derived PDAC.

Tengyu Zhang[1], Assya Legrini[1], Mari-Claire McGuigan[1], Stephan B. Dreyer[1], Ghazal Latifi[1], Claire Kennedy Dietrich[1], Hannah Morgan[1], Eva Verkolf[2], Virginia Padoan[2], Yoana Doncheva[1], Joao Da Silva Filho[3], Michail Doukas[4], Bas Groot Koerkamp[2], Joanne Edwards[1], Nigel Jamieson[1]

[1]School of Cancer Science, Univ. of Glasgow, Glasgow, United Kingdom,[2]Department of Surgery, Erasmus Medical Center, Rotterdam, Netherlands,[3]School of Infection and Immunity, Univ. of Glasgow, Glasgow, United Kingdom,[4]Pathology and Clinical Bioinformatics, Erasmus Medical Centre, Rotterdam, Netherlands

Introduction: Pancreatic ductal adenocarcinoma (PDAC) arises from distinct precursor lesions, mainly pancreatic intraepithelial neoplasias (PanINs) and intraductal papillary mucinous neoplasms (IPMNs), which differ in genetics, differentiation ecosystem, and clinical behavior. PanIN-derived PDAC typically demonstrate more molecular and spatial heterogeneity, with pronounced classical-basal divergence. IPMN-derived adenocarcinomas display different histologic types: intestinal-type lesions often develop colloid carcinoma, where adenocarcinomas arising from pancreatobiliary(PB)-type IPMN resemble conventional PanIN-derived PDAC. Defining how precursor origin shapes malignant states, spatial microenvironment ecosystems are essential for PDAC classification.

Method: Single-cell spatial transcriptomics was performed by CosMx SMI (Bruker) in whole transcriptome and 6K-panel. Two different Tissue Microarrays (TMAs) cohorts were used (1.5-mm cores) include PanIN-origin PDAC (15 patients) and IPMN-origin PDAC (10 patients). Cell Segmentation performed by *CellPose* and strict quality control (QC) thresholding yielded 459,195 high-quality cells. Data was log-normalized and integrated with *scVI* using patient-level correction. Hierarchical annotation was performed by combining expert histopathological alignments with Leiden-based refinements. Downstream spatial analysis used Python based methods including Squidpy.

Results: Cross-cohort integration revealed marked origin-dependent divergence in the malignant spatial atlas. Malignant epithelium in PanIN-PDAC exhibited higher heterogeneity with more diverse and dispersed cell states. In contrast, the tumor cells in IPMN-derived PDAC presented obvious differentiation features for each carcinoma type. Intestinal-type IPMN PDAC developed unique malignant program that exhibiting typical goblet-like subtype, which was not observed in either other IPMN-type PDAC or PanIN-derived PDAC. However, the PB-type IPMN-PDAC showed substantial similarity with PanIN-PDAC, sharing multiple malignant programs, primarily including pEMT, progenitor cell-like and ADM-like subtypes. Furthermore, PanIN-PDAC retained specific tumor programs as exocrine-like, squamous, and inflammatory-association basal-like. Notably, although PB-type in IPMN PDAC and PanIN-PDAC share similarities in some tumor states, further analysis revealed significant differences in the spatial patterns and cell communication between tumor and microenvironments (TME). This suggests potentially different evolution of microenvironments.

Conclusion: Precursor origin fundamentally shapes PDAC malignant states and stromal-immune ecosystems. Together, this work establishes a spatial framework for understanding PDAC heterogeneity and highlights the importance of origin-aware stratification in clinic and biology.

#6200 Single-cell spatial CRISPR screen for tumor microenvironment.

Boyoung Jeong, Xuejiao Zhao, David Kilburn, Kang Jin Jeong, Soon Young Park, Hongli Ma, Gordon B. Mills

OHSU Knight Cancer Institute, Portland, OR

The tumor microenvironment (TME) comprises diverse cell types, including mesenchymal, endothelial, adipocyte, stromal, and immune cells. Among them, cancer-associated fibroblasts (CAFs) represent one of the most abundant and functionally active components. CAFs play a crucial role in tumor progression through bidirectional communication with cancer cells. They originate from various sources, such as normal fibroblasts, endothelial cells, and mesenchymal cells, and once activated, promote tumor cell invasion and metastasis. Recent studies have revealed that CAFs consist of multiple subpopulations with distinct phenotypic and functional properties. This heterogeneity of CAFs has provided new insights into tumor biology and has become a key focus in the development of novel targeted therapeutic strategies across different cancer types. CRISPR/Cas9 is a powerful genome-editing tool widely used for knock-out (KO) gene studies to investigate gene function. To overcome the limitations of conventional phenotyping and bulk analysis, a barcoding system known as Perturb-map was developed by the Brown laboratory that allows KO of genes in tumor cells and facilitates identification of effects of the KO on the TME. Perturb-map utilizes triplet combinations of linear epitope protein barcodes (Pro-codes) that enable the identification of cells expressing distinct CRISPR guide RNAs (gRNAs). In this study, we applied the Perturb-map approach to perform parallel CRISPR KO of 34 genes closely associated with CAF function in the TME in a syngeneic mouse breast cancer model. This approach allowed us to simultaneously assess the functional roles of multiple TME-related genes in tumor cells, providing a comprehensive understanding of their contributions to tumor progression. Pro-code-expressing tumors were analyzed using cyclic immunofluorescence (CycIF), a highly multiplexed proteomics imaging platform that enables spatial and single-cell level analysis. We developed, validated, and applied mouse antibody panels targeting approximately 100 proteins, allowing comprehensive profiling of tumor heterogeneity, cellular states, fibroblast, and immune cell activities. Through this approach, we identified potential therapeutic targets in tumor cells that confer growth advantages and contribute to remodeling of the TME. Furthermore, we identified effects of the KOs on CAF subtypes with distinct functional states. CD274 and IL11Rα1 KO tumors exhibited accelerated tumor growth accompanied by an increased abundance of myofibroblastic CAFs (myCAFs). In contrast, Snai2 KO tumors showed a marked enrichment of inflammatory CAFs (iCAFs). Our findings demonstrate the power of integrating functional genomics with high-dimensional proteomics to characterize TME dynamics at single-cell resolution.

#6201 PaintScape™ enables multiomic in-situ direct visualization of spatial 3D genome architecture of single cells in intact fresh frozen Glioblastoma tissue in native tumor microenvironments.

Matija Snuderl[1], Yuxiu Wang[1], Neha Dhasmana[1], Pamela Flatley[2], Stacy Elliott[2], Douglas Werner[2], Jude Dunne[2], **Huy Nguyen**[2], Shyamtanu Chattoraj[2]

[1]NYU Langone Health, New York, NY,[2]Bruker Spatial Genomics, San Jose, CA

The 3D organization of genome structure, which plays a critical role in regulating gene expression and cellular function, is often restructured in many different cancers including Glioblastoma (GBM). Characterized by extreme molecular and phenotypic diversity, GBM is the most aggressive and lethal form of brain cancer and often show clonal and sub-clonal variations across genomic, epigenomic, transcriptomic, and proteomic signaling networks within distinct tumor microenvironments. Structural aberrations such as copy number variations (CNVs), structural variations (SVs), and topological changes rewire the 3D genome allowing aberrant activation of oncogenes, repression of tumor suppressors and dysregulation in gene expression. Current methods such as WGS or Hi-C provide bulk-level understanding of dysregulation but lack single-cell spatial resolution and do not provide insight into spatial distribution and association between molecular subclones and microenvironment in intact tissue. Since tumor heterogeneity drives therapy resistance and hinders successful GBM treatment, understanding the molecular mechanism in a heterogenous spatial context demands state-of-the-art in-situ single cell and spatial technologies that can provide deeper insight into early detection and disease progression.

In this study, we present a novel multiomic jebFISH™ protocol on the PaintScape™ platform that can be used to analyze and directly visualize 3D chromatin architecture of fresh frozen GBM cells in different tissue microenvironments such as perinecrotic, perivascular, infiltrative, at single-cell, sub-population and population level. Using the ChromoPaint™ PanChromo MPX Panel, which visualizes over 400 loci across all chromosomes, we show disruption in 3D folding of individual chromosomes such as re-organization of chromosome territory, differential p-q arm interaction, intra and inter-chromosomal proximity at single cell and sub-population level in intact GBM tissue. By combining jebFISH with multiplexed immunofluorescence proteomic detection of hypoxia and microvasculature, we show how different tissue microenvironment e.g. hypoxic vs normoxic regions within the same GBM tissue section have different 3D genome aberrations and structural organization in the cancer cell sub-populations. We characterize chromosomal instability, CNVs and SVs of different GBM cancer cell and immune cell states at sub-chromosomal level in-situ within the tissue.

The PaintScape system will enhance understanding of glioblastoma disease progression by providing deeper insight into the 3D genomic heterogeneity of single cancer cells and sub-populations with unique spatial context within intact tissue microenvironments, potentially guiding better cancer treatment design in the future.

#6202 Integrated multiomic atlas of pancreatic solid pseudopapillary neoplasms suggests acinar cells as a potential cell-of-origin.

Biren Reddy, Maria Korah, James P. Agolia, Rosyli Reveron-Thornton, Maggie Lam, Deshka Foster, Michael T. Longaker, Daniel Delitto

Stanford University, Stanford, CA

Introduction:
Solid pseudopapillary neoplasms (SPNs) of the pancreas are rare, low-grade tumors that typically affect young women and occasionally recur or metastasize. While the histological features and mutational profile of SPNs are well documented, their cell-of-origin and spatial organization remain incompletely understood. The purpose of this study was to delineate the development and spatial transcriptomic landscape of SPNs.

Methods:
Regions of interest from 10 surgically resected SPN specimens collected between 2020 and 2025 were profiled using the G4X Singular In Situ Multiomic platform. Gene expression data were integrated and analyzed to generate spatial embeddings, followed by unsupervised clustering. Cell types were annotated using canonical markers, and proteomic data were integrated for further resolution.

Results:
Spatial transcriptomic profiling of 30 SPN sections from 10 patients yielded 3.6 million high-quality cells. The cohort was entirely female, with a median age of 31.5 years. Integrated analysis demonstrated a heterogeneous tumor microenvironment composed of exocrine pancreatic cells, immune cells, fibroblasts, endothelial cells, and tumor cells. Tumor cells demonstrated intra- and inter-tumoral heterogeneity, with five distinct subpopulations: (1) CPB1$^+$ tumor cells, (2) MYH11$^+$ tumor cells, (3) FN1$^+$ VIM$^+$ MMP2$^+$ tumor cells, (4) IGHG1$^+$ FCGR1A$^+$ TBX21$^+$ tumor cells, and (5) STAT1$^+$ TAP1$^+$ CD74$^+$ tumor cells. Mapping these tumor transcriptional states back onto the tissue sections revealed distinct microenvironmental niches. IGHG1$^+$ FCGR1A$^+$ TBX21$^+$ tumor cells and MYH11$^+$ tumor cells were the most prevalent tumor cells across samples. STAT1$^+$ TAP1$^+$ CD74$^+$ tumor cells, characterized by elevated antigen-presentation and interferon-signaling programs, were localized in areas with high immune-infiltration, which was further corroborated and delineated proteomically. CPB1$^+$ tumor cells showed relatively increased expression of acinar cell markers and formed spatial gradients at tumor-acinar interfaces, suggesting that SPN tumor cells may arise from an acinar lineage.

Conclusion:
We present the first multiomic analysis of SPNs of the pancreas, establishing a high-resolution atlas of their cellular and spatial architecture. We identify conserved tumor transcriptional and proteomic states that occupy distinct spatial niches. Spatial gradients in CPB1$^+$ tumor cells suggest a potential acinar origin for SPN tumor cells, warranting further lineage-focused investigation. These findings collectively refine our understanding of SPN tumor biology.

#6203 Spatial transcriptome mapping identifies endothelial anergy and CD4⁺ T cell stress as key drivers of immune escape in colorectal cancer liver metastasis.

Peter Kok-Ting Wan[1], Ranchu Cheng[1], Len Seymour[1], Kerry Fisher[1], Alex Gordon-Weeks[2]

[1]Department of Oncology, University of Oxford, Oxford, United Kingdom,[2]Nuffield Department of Surgical Sciences, University of Oxford, Oxford, United Kingdom

Background

Colorectal liver metastasis (CRLM) remains poorly responsive to immunotherapy, yet the mechanisms underlying its immune-resistant microenvironment are not fully understood. To address this, we generated a single-cell spatial transcriptomic atlas from four replacement-only, microsatellite-stable CRLM treated with neoadjuvant FOLFOX chemotherapy, representing the most common clinical scenario. Our dataset spans intratumoral, peritumoral, and adjacent normal liver, comprising 1,930,656 cells. In parallel, we performed thirteen whole-slide multiplexed immunohistochemistry to dissect the spatial cellular and molecular interactions shaping the immune landscape in CRLM.

Results

We identified a progressive shift in endothelial phenotypes across regions: from a non-inflamed state in the normal liver, to a highly inflamed peritumoral endothelium characterized by TNFα, NFκB, STING and inflammasome signature enrichment, and finally to an anergic, angiogenic endothelial population within CRLM. This anergic endothelial state was defined by reduced expression of adhesion molecules required for T cell extravasation, including SELE, SELP, ICAM1 and VCAM1, in contrast to the more immune-permissive peritumoral endothelium. In line with these endothelial differences, the peritumoral region contained a high density of T cells, most of which were TCR-reactive yet displayed features of exhaustion. The intratumoral region contained far fewer T cells (p <0.01), and those present were predominantly CD4⁺ cells adopting a stress-response phenotype, characterized by an upregulation of genes related to integrated stress response, unfolded protein response, and heat-shock protein pathways. These intratumoral CD4⁺ T cells lacked cytokine expression, showed minimal TCR activity, and localized to hypoxic niches. Their transcriptional profile reflected a hypoxia- and PGE2-driven stress programme rather than classical exhaustion, suggesting that CD4⁺ T cell dysfunction in CRLM is driven by stress-induced pathways. Fibroblasts also demonstrated marked regional variation. In CRLM, fibroblasts secreted neutrophil-attracting chemokines CXCL1 and CXCL8, and produced ECM-remodeling factors such as LOXL2 and TNC. This cancer-associated fibroblast population showed strong spatial correlation with ‘glial-like’ cells, which were found almost exclusively within CRLM (p <0.0001). These glial-like cells expressed neural ligands, including NGF and NPY, supporting a glial-fibroblast signaling axis that may reinforce fibroblast activation and matrix deposition.

Conclusions

Together, these findings reveal key mechanisms driving immune exclusion in CRLM, highlighting endothelial anergy, intratumoral CD4⁺ T cells in a stress-response state, and a glial-fibroblast axis as central features of its immunosuppressive landscape.

#6204 Spatial transcriptomic dissection of TSC-associated angiomyolipoma reveals microenvironmental programs driven by mTORC1 dysregulation.

Ryuta Watanabe[1], Kensuke Shishido[1], Shota Nobumori[1], Naoya Sugihara[1], Keigo Nishida[1], Haruna Arai[1], Takatora Sawada[1], Shunsuke Haga[1], Osuke Arai[1], Tomoya Onishi[1], Kenichi Nishimura[1], Tstsuya Fukumoto[1], Noriyoshi Miura[1], Mie Kurara[2], Riko Kitazawa[3], Yuki Miyauchi[1], Tadahiko Kikugawa[1], Takashi Saika[1]

[1]Department of Urology, Ehime University Graduate School of Medicine, Toon, Japan,[2]Department of Analytical Pathology, Ehime University Graduate School of Medicine, Toon, Japan,[3]Division of Diagnostic Pathology, Ehime University Hospital, Toon, Japan

Background
Tuberous sclerosis complex-associated angiomyolipoma (TSC-AML) frequently presents in young patients with multifocal and large tumors, leading to clinical complications such as hemorrhage and renal dysfunction. Although mTORC1 activation due to TSC1/TSC2 loss is recognized, the spatially organized transcriptional architecture and differences from sporadic AML remain unclear. This study applied spatial transcriptomics to characterize molecular features underlying TSC-AML structure.
Methods
Formalin-fixed, paraffin-embedded sections from one case each of TSC-AML, sporadic AML, and renal cell carcinoma (RCC) were analyzed using the 10x Genomics CytAssist Visium platform. Clustering, differential expression, and pathway analyses were performed to identify spatial transcriptional patterns and TSC-AML-specific signatures.
Results
Spatial gene expression maps showed that TSC-AML and sporadic AML shared the classic triphasic architecture of vascular, smooth muscle, and adipose components, consistent with a PEC lineage origin, whereas RCC displayed a distinct epithelial profile.TSC-AML demonstrated reduced TSC1/TSC2 expression with mild upregulation of MTOR, MLST8, and RPTOR, indicating mTORC1 pathway dysregulation.Comparative analysis identified 42 genes specifically upregulated in TSC-AML, including neurodevelopment-related (GRIA2, ASTN1), lipid metabolism-associated (FABP4, APOC1), structural (LDB3, SYNM), and immune-regulatory (IL33, ABCC8) genes. These transcriptional differences represent potential molecular features distinguishing TSC-AML from sporadic AML.Spatial mapping further highlighted intratumoral heterogeneity and structural component-dependent variation in gene expression.
Conclusions
Despite the single-case limitation, this study provides a detailed spatial transcriptomic profile of TSC-AML, revealing transcriptional programs linked to TSC1/TSC2 dysfunction and identifying TSC-AML-specific gene signatures. These findings offer candidate biomarkers and therapeutic targets and establish a foundation for future multi-case studies aimed at refining molecular characterization and improving clinical management of TSC-associated renal tumors.

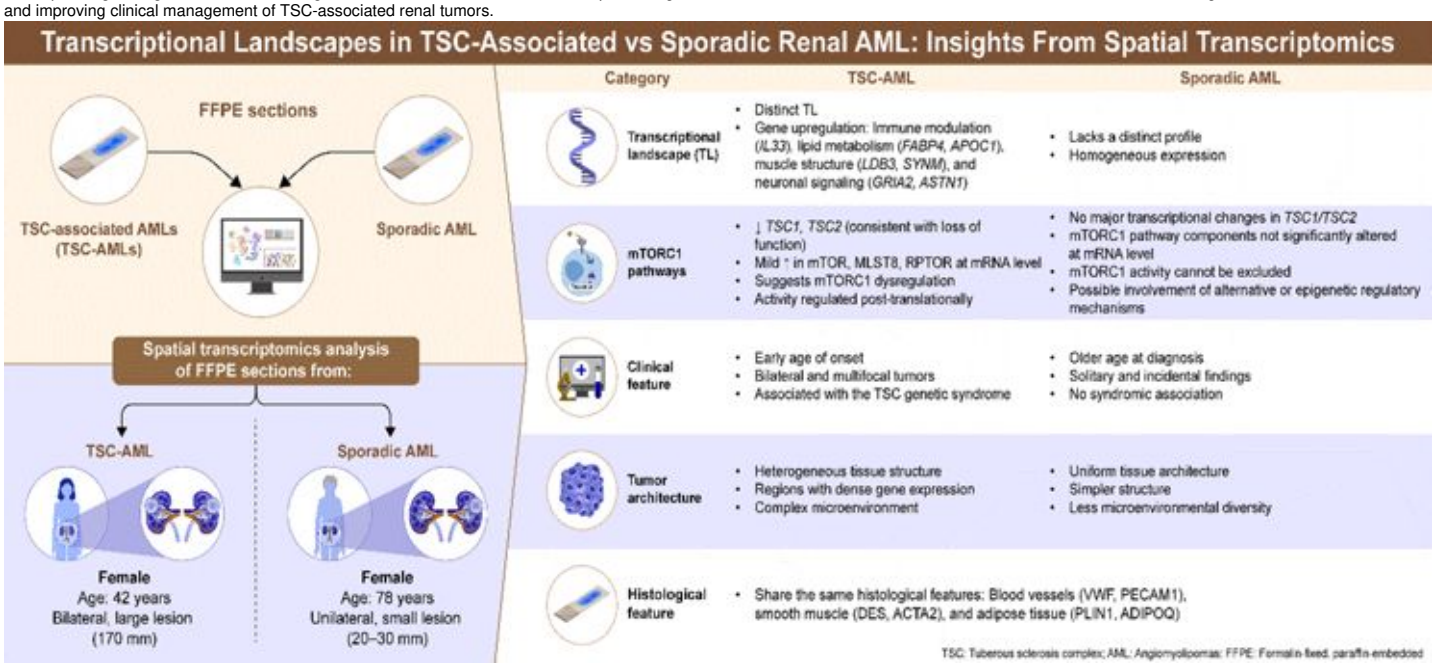

#6205 Establishing reproducibility standards for Xenium spatial transcriptomics through multi-replicate validation and cross-sectional analysis.

Tommy Tran, JingHao Tian, Elim Cheung, Rikita Gakhar, Vidyodhaya Sundaram

BioChain Institute, Inc., Newark, CA

Spatial transcriptomics technologies such as Xenium are rapidly gaining relevance in translational and clinical research, yet there remains a lack of standardized reproducibility benchmarks and quantitative quality-control (QC) metrics. Establishing technical validation frameworks is essential for ensuring cross-run, cross-section, and eventually cross-site comparability as the field moves toward regulated environments.

Methods: We conducted a multi-replicate validation study using eight sections derived from a single FFPE block containing four human carcinoma tissues (lung, breast, colon, and stomach). Each slide included four tissue regions, yielding 32 total spatial transcriptomic datasets generated with the Xenium Human Multi-Tissue and Cancer Gene Expression Panel (10x Genomics). Sections at defined depths (X3-4, X14-15, X16-17, X20-21) enabled evaluation of technical reproducibility across both slide-to-slide and depth-dependent variation. Technical reproducibility metrics—including cross-replicate correlation, coefficient of variation, spatial pattern consistency, cell-type abundance stability, and gene-level variance—were assessed to define preliminary QC thresholds suitable for multi-replicate benchmarking.

Results:Initial analyses demonstrate high reproducibility across replicates, with consistent gene expression profiles, stable spatial organization of major cell populations, and low variance across serial depths. Spatial pattern concordance remained robust across all carcinoma types, and variance decomposition suggests minimal depth-related technical drift. Ongoing analyses include expanded statistical modeling and evaluation of QC thresholds that could serve as standardized criteria for platform validation.

Conclusions: This study establishes a practical framework for defining reproducibility and QC standards for Xenium spatial transcriptomics. By integrating multi-replicate evaluation with cross-sectional comparisons, we outline a foundation for reproducible spatial data generation that supports clinical translation, regulatory readiness, and harmonization across studies and institutions.

#6206 Spatially resolved cell-cell architecture in WHO grade 4 *IDH*-wildtype glioblastoma revealed by CosMx 6K discovery panel.

Dexter Wing Lun Lee[1], Kaiyan Xu[2], Parker Li[3], Joshua Jing Xi Li[4], Wei Dai[1], Karrie Kiang[5], Gilberto Ka-Kit Leung[5], Aya El Helali[1]

[1]Department of Clinical Oncology, School of Clinical Medicine, The University of Hong Kong, Hong Kong, Hong Kong,[2]Centre for Oncology and Immunology, Hong Kong Science Park, Hong Kong, Hong Kong,[3]School of Biomedical Sciences, LKS Faculty of Medicine, The University of Hong Kong, Hong Kong, Hong Kong,[4]Department of Pathology, School of Clinical Medicine,, The University of Hong Kong, Hong Kong, Hong Kong,[5]Department of Surgery, School of Clinical Medicine, The University of Hong Kong, Hong Kong, Hong Kong

Background: *IDH*-wildtype glioblastoma is well-known for its intratumoral heterogeneity, with malignant, immune, and stromal populations coexisting in shared microenvironment that may shape hyper-progression and therapeutic resistance. These could be highly localized while spot-resolution spatial assays probably mask the underlying cellular architecture. Targeted single-cell spatial transcriptomics, like CosMx SMI now provide confident cells segmentation for delicate patient-specific interaction networks across GBM.

Methods: GBM tissues were profiled using the CosMx 6K Human Discovery Panel. Standardized preprocessing, including RNA QC, batch harmonization, and multi-reference cell typing were completed with Seurat v5. Cells underwent stepwise cleanup, which are the removal of AtoMx-flagged cells and those below the first quartile of number of detected genes and total transcript counts and further exclusion of fields of view (FOVs) retaining <50% of cells after cell filter. SCTransform, PCA and UMAP were applied on raw counts using AtoMx-recommended parameters with Giotto v4. Spatial networks and neighborhood were built using radius-based and k-nearest neighbor criteria. Co-localization was evaluated with Ripley's K-function. L-R networks were inferred with CellChat v2. All computation and analysis were with reference to AtoMx manual v2.1 (MAN-10162-10) under R 4.4.1 located at HPCF2, CPOS, HKU.

Results: After the stringent filtering, 297,125 confident cells across 413 FOVs in 23 TMA cores were retained for studying cell-cell communication. Pearson correlation of 0.99 indicated that cell density did not bias per-core analyses. Radius-based spatial network revealed extensive intratumoral heterogeneity between and within patient. Of notes, Patient #025 showed a marked shift, with a stem-like/mesenchymal-like cluster dominating one core and differentiated-like cells predominating in another, given both cores extracted from the same FFPE block resected at primary diagnosis. k-nn modeling showed reproducible tumor-tumor and tumor-vascular adjacency, while myeloid and lymphoid cells remained spatially diffuse across the cores, which was further confirmed significantly with Ripley's K function. Next, highly heterogeneous L-R pairs were inferred across patients, with a mean of 546 highly variable ligand-receptor pairs per core. A set of canonical GBM interaction pathways, like NCAM1-, CD99-, and JAG1-mediated signaling was conserved across cores. Apart from the homotypic network within tumoral and vasculature, there are extensive patient-specific L-R, like CNTN1-NOTCH1 networking in patient # 011.

Conclusions: By resolving cell-cell interaction, CosMx exposed distinct ligand-target dependencies across patients, which is a basis for designing bespoke neoantigen-directed vaccines or ligand-target bispecific antibody approaches.

#6207 Spatial organisation of tumor-infiltrating B cells in Claudin 18.2-expressing advanced gastric cancer predicts response to immune checkpoint inhibition.

Joseph J. Zhao[1], Choong-Kun Lee[2], Allison Si-Yu Chan[3], Wenyi Luo[4], Li Chang[5], Woo Sun Kwon[6], Sejung Park[6], Minkyu Jung[7], Joe P. Yeong[8], Anand Devaprasath Jeyasekharan[1], Maria Rodriguez Martinez[5], Sun Young Rha[6], Raghav Sundar[4]

[1]National University of Singapore (NUS), Singapore, Singapore,[2]Yonsei University Health System, Seoul, Korea, Republic of,[3]Cancer Science Institute of Singapore, Singapore, Singapore,[4]Yale University School of Medicine, New Haven, CT,[5]Biomedical Informatics and Data Science, Yale University School of Medicine, New Haven, CT,[6]Yonsei University College of Medicine, Seoul, Korea, Republic of,[7]Yonsei University Cancer Center, Seoul, Korea, Republic of,[8]Singapore General Hospital, Singapore, Singapore

Background: Claudin 18.2 (CLDN18.2), a tight junction protein aberrantly expressed during malignant transformation of gastric cancer (GC), has emerged as a key therapeutic target. This study seeks to understand the role of CLDN18.2 in shaping the tumor microenvironment (TME).

Methods: This single-center study included 99 patients with advanced gastric cancer treated first-line immune checkpoint inhibition (ICI) agent(s) with chemotherapy. CLDN18.2 expression was determined using immunohistochemistry (VENTANA 43-14A, Roche) on FFPE biopsies, reported as % 2+/3+. To enable a balanced representation of CLDN18.2 status, a median split approach was employed. Samples were also stained with multiplex-IHC (CK, CD4, CD8, FOXP3, CD68 and CD20) to elucidate the corresponding TME. Orthogonal validation was undertaken through independent analyses of whole transcriptome sequencing (WTS) data from 6 cohorts comprising 1,098 GC tumor samples. Cellular neighbourhood (CN) analyses were conducted using a *k*-nearest neighbors' algorithm. Survival analyses were conducted with a Cox-proportional hazards model.

Results: We retrieved CLDN18.2 status through median-split of CLDN18.2 expression (25.1%), yielding 44 CLDN18.2^{high} samples and 45 CLDN18.2^{low} samples. We observed an increase in CD20^{+} B cell density in CLDN18.2^{high} samples (p=0.042), whereas no significant differences in cell density were observed in CD4^{+}/CD8^{+} T cells, CD68^{+} macrophages and FOXP3^{+} Tregs. These findings were orthogonally validated utilizing immune cell deconvolution (xCell, Epic & MCP-counter) across the 6 independent WTS cohorts. CLDN18.2 status alone did not predict for response or survival (overall survival [OS], HR=1.02, p=0.947). GCs with increased CD20^{+} B cell density was found to confer a greater magnitude of benefit from first-line ICI (OS, HR=0.71, p=0.196), but the benefit was largely conserved amongst CLDN18.2^{low} tumors and not in CLDN18.2^{high} tumors (OS interaction p=0.109). We identified 4 B cell related CNs: B-TumorInfiltrating, B-MacrophageNiche, B-LA/TLS (Lymphoid Aggregate/Tertiary Lymphoid Structure) and B-ImmuneNiche. In CLDN18.2^{high} tumors, we observed a relative increase in CD20^{+} B cell abundance within B-TumorInfiltrating and B-MacrophageNiche CNs and a relative decrease in B cell abundance within B-LA/TLS and B-ImmuneNiche CNs in comparison to CLDN18.2^{low} tumors. While B-ImmuneNiche and B-LA/TLS conferred ICI sensitivity, the relative enrichment of B cells within a B-TumorInfiltrating CN compared to a B-ImmuneNiche CN conferred ICI resistance, particularly in CLDN18.2^{high} tumors (OS, HR=2.60, p=0.040).

Conclusions: The CLDN18.2^{high} gastric cancer microenvironment is characterized by an enriched humoral response. Intra-tumoral B cell infiltration confers ICI resistance in a CLDN18.2^{high} microenvironment.

#6208 Subcellular imaging of murine models of metastatic colorectal cancer using a whole transcriptome spatial molecular imaging panel.

Liang Zhang[1], Isabel Lee[1], **Shanshan He**[1], Martin Shelton[1], Owen J. Sansom[2], Joseph M. Beechem[1]

[1]Bruker Spatial Biology, Seattle, WA,[2]Cancer Research UK Scotland Institute, Glasgow, United Kingdom

Spatial transcriptomics enables in situ characterization of molecular and cellular heterogeneity within complex tissues. However, such high-plex subcellular resolution analysis has not previously been available for mouse models, which are central to cancer biology and therapeutic development. To address this gap, we have developed a new mouse Whole Transcriptome (WTX) assay containing over 20,000 targets, enabling comprehensive subcellular imaging with potential for future multiomic integration. Using the CosMx Spatial Molecular Imager (SMI), we profiled formalin-fixed paraffin-embedded (FFPE) primary and metastatic colorectal cancers from advanced murine models of Kras-mutant colorectal cancer. Each slide was processed according to standard CosMx workflow. UMAP and clustering analyses were performed to identify spatially resolved cell populations. Cell type annotation was guided by canonical marker genes. Transcriptional heterogeneity and adaptive plasticity of the tumour epithelium and supporting micro-environment in response to targeted KRAS inhibition was interrogated in both primary colonic cancers and in hepatic metastases. The CosMx mouse WTX assay demonstrated robust detection sensitivity and dynamic range across both liver and colon cancer samples. Distinct cellular niches were identified within tumor and stromal compartments, revealing transcriptionally unique clusters corresponding to hepatocytes, immune cells, and fibroblast subtypes. In the colon tumor, spatially distinct tumor regions exhibited divergent gene expression patterns, suggesting differential microenvironmental influences. Transcriptional adaptation to therapeutic challenge was observed across tumour compartments in both primary and secondary disease, highlighted novel, exploitable avenues to drive improved therapeutic response. We present the first application of a mouse Whole Transcriptome assay on the CosMx platform, enabling subcellular spatial resolution across >20,000 targets. This new capability opens avenues for multiomic integration, allowing comprehensive investigation of tumor-stroma interactions and immune microenvironments in mouse models. Together, these advances bridge preclinical and translational spatial biology, providing a new foundation for spatially resolved discovery in cancer research.

#6209 Gynecologic carcinosarcomas beyond epithelial-mesenchymal transition: Morpho-transcriptomic evidence of an immune gradient in the tumor microenvironment.

Amel Kime[1], Julie Berthet[1], Juliette Renard[1], Antoine Gaudet Chardonnet[2], Pierre Laurent-Puig[1], Jerome Alexandre[3], Bruno Borghese[2], Guillaume Beinse[3]

[1]MEPPOT Team, Cordeliers Research Center, Paris, France,[2]Gynecologic Surgery Unit, APHP - Cochin Port-Royal Hospital, Paris, France,[3]Oncology Unit, APHP - Cochin Port-Royal Hospital, Paris, France

Introduction: Gynecologic carcinosarcomas (GynCS) are rare, aggressive uterine and ovarian cancers with a median survival under two years. Their biology is marked by epithelial-mesenchymal transition (EMT), driving dissemination and a biphasic carcinoma-sarcoma morphology. However, the molecular drivers of intratumoral heterogeneity beyond EMT remain poorly understood. This study seeks to clarify these mechanisms by characterizing the transcriptomic landscape of GynCS.
Methods: Hematoxylin-eosin-saffron (HES) slides from 35 uterine and ovarian carcinosarcomas were reviewed by a gynecologic pathologist. A total of 251 tumoral tissue sectors, including carcinoma, sarcoma and mixed components, were selected for morphological assessment and bulk RNA sequencing (RNA-seq) using the SMARTer library preparation kit.
Results: Among 35 tumors included in cohort, 33 (94%) were TP53-mutated, 2 (4%) had no specific molecular profile, 1 (2%) was mismatch repair-deficient and none was POLE-mutated. EMT expression signature correlated with histological features despite 26% of histologicaly sarcomatous sectors being reclassified as epithelial based on RNAseq (WISP classifier). Gene set enrichment analysis (GSEA) in all carcinoma sectors compared to all sarcoma sectors revealed a depletion in the response to inflammation and immunity as the main mechanism alongside EMT. Both cell-type deconvolution on RNA-seq data and immunohistochemical CD3 staining on FFPE slides suggest an enrichment in T cells, particularly cytotoxic T cells, in the tumor microenvironment of carcinoma sectors compared to sarcoma sectors. Within-tumor immune gene set analysis in a subset of tumors (n=15) revealed heterogeneous microenvironmental switch across patients, with 53% of tumors (n=8) shifting from a hot-to-cold microenvironment while most others (47%; n=7) remained immune-deprived. Gene expression profiles revealed the sustained activation of non-canonical NFκB pathway by cGAS-STING as a potentially leading cause of immune exhaustion and associated with EMT. Spatial RNAseq (Visium2) of 4 representative cases confirmed inflammation response as among most spatially variable features.
Conclusion: This study suggests that chromosomal instability, acting through the cGAS-STING pathway, plays a dual role in driving immune exhaustion and promoting EMT as key biological features, despite notable inter-tumor variability in this process. These findings are consistent with existing literature on the non-canonical NFκB pathway. This work highlights potential therapeutic opportunities, including the emerging STING-targeted treatments and personalized immunotherapeutic strategies tailored to the unique immune landscape of each tumor.

#6210 Spatial compartmentalization of tumor and immune cellular architecture defines opposing prognostic roles in prostate cancer.

Ahmed Elsehemy[1], Xinpei Ci[2], Magnus Lam[3], Matthew Ramotar[2], Alejandro Berlin[4], Theodorus van der Kwast[5], Housheng Hansen He[5]

[1]Radiation Oncology, Medical Biophysics, University of Toronto, Toronto, ON, Canada,[2]Medical Biophysics, University Health Network, Toronto, ON, Canada,[3]Medical Biophysics, University of Toronto, Toronto, ON, Canada,[4]Radiation Oncology, University of Toronto, Toronto, ON, Canada,[5]University Health Network, Toronto, ON, Canada

Background:
Understanding the role of immune cells in prostate cancer (PCa) remains challenging, with conflicting reports on immune infiltration's prognostic value. We hypothesized that spatial localization, rather than immune cells absolute bulk abundance, drives their association with clinical outcomes. To test this, we generated a clinical cohort of PCa patients integrated with multiplex IHC from spatially profiled immune cells in both the tumor and surrounding stroma (n=41).

Methods:
IHC multiplex assay was utilized to assess CD3+, CD8+, CD20+, FoxP3+, and CD68+ cells within cytokeratin-positive (CKpos; epithelial nests) and cytokeratin-negative (CKneg; stroma) compartments. Cell counts, densities, and ratios were correlated with time to metastasis (TTM), biochemical recurrence (BCR), BMI, tumor burden, intratumoral heterogeneity, PSA, and TMPRSS2:ERG/ETV4 fusions. After data collection validation and curation, statistical analysis of correlations between continuous variables was done using Spearman's or Pearson's correlation, while Chi square test was used for categorical variables.

Results:
Our association analysis revealed a pattern where immune infiltration within CKpos tumor nests (cancer cells) showed consistently favorable associations with clinical outcome (r=0.36-0.52, $P < 0.001$), with CD8+ T-cells showing the strongest correlation with prolonged TTM and delayed BCR. In contrast, the same immune populations in CKneg compartment (stroma) demonstrated opposite correlations (r=-0.31 to -0.47, $P < 0.05$), with stromal FoxP3+ T-cells most strongly associated with accelerated metastasis. Interestingly, identical immune subsets displayed opposite prognostic directions within the same patient samples, despite strong cross-compartment correlations (r=0.66-0.79, $P < 0.001$), indicating coordinated recruitment but compartment-specific roles. Higher BMI correlated exclusively with increased stromal (non-protective) lymphocytic infiltration (r=0.39-0.59, $P < 0.05$). Tumor burden inversely correlated with intratumoral T-cell and stromal macrophage ratios. TMPRSS2:ERG and ETV4/TMPRSS2 fusions were significantly associated with elevated stromal CD8+ infiltration, and higher pre-treatment PSA correlated with stromal CD68+ density, linking tumor biology with macrophage recruitment.

Conclusion:
This work demonstrates that the spatial location of immune cell populations determines their association with outcomes in PCa. Notably, our data indicate that high-burden aggressive tumors might be associated with suppression in protective intratumoral immunity. Our current work is aimed at validating these observations in a larger cohort. These findings highlight the need for a shift towards spatially-resolved tumor microenvironment and immune biomarkers for risk stratification and patient selection for immunotherapies.

#6211 AI-guided spatial multi-omics integration reveals immune and stromal heterogeneity underlying population disparities in prostate cancer..

Samuel Mwakisha Mwamburi, Jevon Layne, Niki Talebian, Ezra G. Baraban, Ashley Kiemen, Clayton C. Yates

Pathology, Johns Hopkins University School of Medicine, Baltimore, MD

Prostate cancer disproportionately affects African American (AA) men, who experience higher incidence and mortality rates than European American (EA) men. The purpose of this study was to develop and apply an artificial intelligence (AI)-based framework to investigate biological mechanisms contributing to these disparities through spatial characterization of the tumor microenvironment (TME). We employed CODA, a computational method that reconstructs large tissues at subcellular resolution from serially sectioned hematoxylin and eosin (H&E)-stained slides, for histological segmentation and multi-omics integration.CODA was trained on 600 H&E-stained prostate tumor sections from AA and EA patients using a deep convolutional neural network optimized for pixel-level classification of nine compartments, including tumor, stroma, vasculature, and inflammation. Model performance, evaluated using a confusion matrix, achieved over 90% classification accuracy and generalized robustly across cohorts. CODA segmentation maps were aligned with 10x Genomics Visium HD spatial transcriptomic data to generate biologically annotated domains such as luminal secretory, stromal, inflammatory epithelial, and immune regions.Functional analysis revealed distinct TME niches, including adaptive immune, myeloid-rich, cytotoxic, fibroblast, and luminal-epithelial compartments. AA tumors demonstrated higher immune infiltration and inflammatory activity than EA tumors, characterized by dense lymphoid aggregates and cytokine signaling enrichment. Integration with spatial proteomics data from the AKOYA IO60 panel (60 immune and stromal markers) confirmed immune clusters (CD20+, CD3e+, CD68+, CD8+) and revealed a level of discordance between transcript expression and protein signaling, suggesting context-dependent regulation.Three-dimensional reconstructions from serially sectioned tumors (one AA, one EA) visualized compartment continuity and immune-stromal interfaces. Collectively, these findings provide new evidence of population-specific immune and stromal heterogeneity that may contribute to prostate cancer disparities and demonstrate the utility of AI-guided spatial multi-omics for advancing equitable precision oncology.

#6212 Spatial immune and vascular remodeling defines recurrence in oligodendroglioma.

Julia Louw[1], Kenan Zhang[1], Anna Corcoran[1], Elizabeth Owens[1], Jodie Jepson[1], Jose R. Conejo-Garcia[2], David M. Ashley[3], Kanish Mirchia[4], David R. Raleigh[5], Mustafa Khasraw[6]

[1]Duke University, Durham, NC,[2]Duke University School of Medicine, Durham, NC,[3]Duke University Medical Center, Durham, NC,[4]UCSF, San Francisco, CA,[5]University of California San Francisco, San Francisco, CA,[6]Duke Cancer Institute, Durham, NC

Introduction/Rationale: Oligodendrogliomas recur after therapy but how spatial immune architecture changes during recurrence is poorly understood.
Methods: Visium Spatial Transcriptomics (ST) from primary and matched recurrent tumors (n = 14 patients) were processed with SpaceRanger. Cell-type deconvolution was performed using SpaCET's low-grade glioma model, generating spatial immune and stromal distributions. Cell-type fractions were normalized using Centered Log-Ratio transformation and clustered (k = 5, Euclidean distance) to define niches. Immune subsets were compared to assess niche-specific remodeling. Propensity score matching was used to control for baseline differences between treated and untreated tumors.
Results: Five spatial niches were identified, including immune-enriched perivascular regions and infiltrative tumor-immune interfaces. Recurrent tumors showed contraction of adaptive immunity, with downregulation of $CD4^+$ T-helper subsets, Th1, Th2, Th17, and Tfh ($log_2FC \approx -3$), and depletion of total $CD4^+$ T cells (-2.9). This reduction was greatest in previously treated patients suggesting therapy-associated collapse of adaptive immune niches. Myeloid cells including macrophages and microglia, were preserved or increased, indicating a shift toward myeloid-dominant, immunosuppressive microenvironment. Perivascular immune regions demonstrated reduced T-helper diversity and enhanced myeloid signaling, consistent with immune exclusion and vascular remodeling. These patterns persisted after propensity score matching, with treated recurrences enriched for myeloid-driven immunosuppressive niches ($p < 0.05$). Applying cNMF-derived activity programs, treated recurrent tumors showed upregulation of systemic inflammatory genes (IL1B, OSMR, CXCL8) but downregulation of microglial inflammatory genes (CXCR4, CX3CR1, JUN, EGR1), reflecting partial loss of lymphocyte related pathways. Complement-associated immunosuppressive programs were mildly increased, while scavenger receptor-associated programs were slightly reduced, indicating therapy-related myeloid shifts. Untreated recurrences had upregulation of inflammatory and immunosuppressive programs, reflecting activated and suppressive immune states. Validation with Xenium and CODEX will be presented.
Conclusion: Recurrent tumors undergo remodeling marked by collapse of adaptive immune niches, loss of $CD4^+$ T-helper diversity, and a shift toward myeloid-dominant signaling. Treated recurrences show weaker microglial inflammatory activity and partial transition to a myeloid-driven immunosuppressive state, whereas untreated recurrences display activation of inflammatory and suppressive programs. These findings identify therapy-associated depletion of adaptive immunity and enrichment of suppressive myeloid niches, a features that can be exploited to identify therapeutic targets.

#6213 Single cell imaging uncovers a coordinated tumor-immune-stroma spectrum with genomic associations in pancreatic ductal adenocarcinoma.

Ferris Nowlan[1], Noor Shakfa[1], Sibyl Drissler[1], Tan Tiak Ju[1], Elizabeth Sunnucks[1], Edward LY Chen[1], Cassandra J. Wong[1], Brendon Seale[1], Zhen Yuan Lin[1], Michelle Chan-Seng-Yue[2], Amy Zhang[2], Sabiq Chaudhary[2], Chengxin Yu[1], Golnaz Abazari[1], Michael Geuenich[1], Matthew Watson[1], Jiaxi Peng[1], Somaieh Afiuni-Zadeh[1], Ayelet Borgida[3], Ricardo Gonzalez[1], Sheng-Ben Liang[4], Klaudia Nowak[4], Miralem Mrkonjic[5], Anna Dodd[4], Julie M. Wilson[2], Kieran Campbell[1], Jenn Gorman[1], Barbara Grunwald[6], Robert C. Grant[2], Jennifer J. Knox[7], Anne-Claude Gringas[1], Faiyaz Notta[8], Steven Gallinger[9], Grainne O'Kane[10], Hartland Jackson[1]

[1]Lunenfeld-Tanenbaum Research Institute, Toronto, ON, Canada,[2]Ontario Institute for Cancer Research, Toronto, ON, Canada,[3]Pancreatic Cancer Canada, Toronto, ON, Canada,[4]University Health Network (UHN), Toronto, ON, Canada,[5]Mount Sinai Hospital, Toronto, ON, Canada,[6]West German Cancer Center, Essen, Germany,[7]Princess Margaret Cancer Centre, Toronto, ON, Canada,[8]Postdoctoral Fellow, Princess Margaret Cancer Centre, Toronto, ON, Canada,[9]Professor of Surgery, Div. of General Surgery, University of Toronto University Health Network, Toronto, ON, Canada,[10]St. Vincent's University Hospital, Dublin, Ireland

Pancreatic ductal adenocarcinoma (PDAC) has consistent genomic drivers and established classical and basal transcriptional subtypes, but despite this, there exist many intermediate state tumors, a multiplicity of copy number aberrations and low frequency mutations, and a complex, spatially heterogeneous tumor microenvironment. These elements are not random; they are evidence of coordinated biological programs and evolving signaling networks that underlie tumor progression. Merging data from these varied molecular and spatial layers is essential to clinically define and therapeutically target a) tumors that fall into the ‘grey zone’ of pancreatic cancer subtyping and b) specific collusive epithelial-stromal niches.To identify the in situ interdependencies between distinct tumor cell states, fibroblast phenotypes, deposited extracellular matrix, immune infiltrate, and vasculature, we performed imaging mass cytometry on three serial sections of a PDAC tissue microarray (221 resected tumors, ~4 cores each), generating >800 multiplexed images (40-43 channels) each focused on deeply profiling a different cell lineage. We captured 76 immune and stromal cell types and states, as well as six cancer cell types that recapitulated the classical and basal PDAC signatures, plus four discrete “intermediate” states with distinct associations to RNA subtype (n = 92), tumor ploidy (n = 192), and patient outcome. We clustered our immune and stromal cell populations to define 8 recurrent microenvironments, and found the microenvironment dominated by CD105+ CAFs was significantly spatially associated to classical tumor cells with strong epithelial differentiation transcription factor expression (pairwise Fisher’s exact test, odds ratio = 3.7), ECM-rich microenvironments were proximal to basal tumor cells (odds ratio = 4.3), and pMLC2+ CAFs were enriched near the poor-prognosis, low-ploidy S100A4+ tumor phenotype (odds ratio = 4.2). We additionally denote a specific fibroblast-centric microenvironment associated with neoadjuvant treated tumors (n = 26). Using matched 30X whole-genome sequencing (n = 192), we found specific mutations and copy number changes that were associated changes in tumor and microenvironment composition, and performed Lasso-based machine learning to determine the most important cross-omic features for overall survival prediction. Together, our findings define a phenotypic and molecular framework of PDAC from genome to tumor-microenvironment, provide insight into the connection between tumor phenotype and stromal niches, and offer a refined basis for patient stratification.

#6214 Mapping the tumor landscape: spatial multiomics reveals immune and stromal heterogeneity across early and late-stage NSCLC.

Gaurav N. Joshi, Nicholas Sciascia, Michael Yang, Brenna Fearey, Junya Yoshioka, Fumiki Yanagawa

Nikon Bioimaging Lab, Nikon Instruments Inc, Lexington, MA

Background: Lung cancer accounts for 12% of all cancers and 20% of cancer-related deaths. Rapid advances in spatial biology are uncovering mechanisms of disease, patient-to-patient variability, and immune biomarkers predictive of response to immunotherapy. Using a combination of spatial multiomics approaches and data analysis in the same section, we characterized the spatial distribution, phenotypes, and functional states of tumor, immune, and stromal cells between stage IA (early) and IIIA (late) non-small cell lung cancer (NSCLC).
Method: 5 µm formalin-fixed paraffin-embedded (FFPE) tissue sections were prepared from stages IA and III A human NSCLC with confirmed histology of adenocarcinoma. Same sections were analyzed using two complementary platforms, (1) multiplex immunofluorescence (mIF) with a 30-antibody panel on Lunaphore COMET system and (2) spatial transcriptomics using 10x Genomics Visium CytAssist. Protein-level data were processed using HORIZON, and transcriptomic data were analyzed in Loupe Browser. Unbiased clustering (Leiden) and cellular phenotyping were performed to identify region-specific cell populations and marker co-expression patterns.
Results: In early NSCLC tumor, CD8+, CD4+ T cells were more concentrated within the tumor core. In addition, fewer Tregs, immunosuppressive macrophages, and cells expressing immune checkpoint were observed. There were less stromal remodeling, fibrosis and angiogenesis and more TLSs in stage IA tumor. On the other end, late NSCLC tumor showed an increased expression of markers associated with immunosuppression/evasion and stromal remodeling, including an increase in Treg cells, TAMs, CAFs and immune checkpoint expression. A difference in the gene expression signature between early and late-stage NSCLC support observations from protein expression. Early-stage tumor was enriched for genes associated with immune surveillance and active cytotoxic response, whereas late-stage tumor was enriched for immune suppression and stromal remodeling genes. Spatial analysis also highlighted changes in various chemokines and cytokines between the two tumor types.
Conclusions: The integration of multiomics technologies on the same section helped identify diverse processes and transcriptional changes associated with a varied tumor and immune landscape between early and late-stage NSCLC. Cellular phenotyping triaged cell types based on marker expression in pathologist annotated regions. These findings highlight intra and inter-tumor changes, the biology within and helped with the identification of potential biomarkers for immunotherapy response and intervention.

#6215 Spatial biology tools identify distinct spatially localized fibroblasts in adenomacarcinoma lung cancer predictive of survival.

Calum MacAulay, Paul Gallagher, Martial Daniel Guillaud

BC Cancer Research Institute, Vancouver, BC, Canada

Predicting overall patient survival from excised lung cancer tissue is a challenging task. We applied spatial biology tools to define 10 cell types using unsupervised clustering and using the spatial distributions of these 10 cell types and unsupervised clustering to define 8 cell neighborhoods to over 400 Adenocarcinoma TMA spots.
The unsupervised cell type clustering identified 4 types of tumour/epithelial cells, 4 types of immune like cells and 2 types of potentially CAF cells. The frequencies of the cell types within the TMA spots correlated with a host of clinical variables such as stage, tumor size, differentiation degree, EGFR mutation status, patient sex, etc. As did the frequencies of the cells in the 8 neighborhoods. Collapsing the 8 neighborhood types into 3 neighborhoods (tumor, stroma and cells boarding tumor and stroma) and selecting the 2 types of CAF cells identified we calculated the frequency and density of CAF cells in the three neighborhoods.
We found that the density and frequency of CAFs in the stroma neighborhood was highly predictive of overall survival in early stage (< 1B) Non smokers (p=0.0005 females, p=0.00007 males) but not as strong in early stage smokers. For Late stage lung cancers (>=1b) the frequency of a type of large tumor cell combined with the density (number of stromal cells per mm2) was highly predictive (p=0.000005) of outcomes for late stage current smokers in both males and females.
Key to the success of this analysis was the exact segmentation of the all the DNA specific stained nuclei, even in areas of highly overlapping nuclei, using a novel deep learning enabled segmentation that allow pixels to belong to more than one nucleus.

#6216 Novel whole transcriptome spatial transcriptomics technology reveals CAF/TAM-mediated basement membrane remodeling at the invasive front.

Amanda Janesick, McKenzi Toh, Syrus Mohabbat, Stephanie Kravitz, 10X Genomics Development Team

10x Genomics, Inc., Pleasanton, CA

Introduction:
A precise understanding of the Tumor Microenvironment (TME) requires comprehensive, high-resolution transcriptomic profiling that can classify the functional states of numerous cell types and map their interactions with neighboring cells. In this study, we use novel technologies to investigate TME-mediated basement membrane (BM) remodeling in lung, kidney, breast, and ovarian cancers. We identify key proteases and laminins enriched in the tumor periphery surrounding hypoxia-adapted cancer cells and the invasive front.

Methods:
Formalin-fixed, paraffin-embedded (FFPE) tissues were stained for H&E on Superfrost slides, then analyzed using spatial transcriptomics and subsequent cytoplasmic/cell membrane marker-based segmentation. Data were visualized using a 10x Genomics interactive workspace, which enables the subcellular mapping of transcripts overlaid on morphology images, alongside integrated capabilities for normalization, clustering, and differential gene expression analysis. We employed a spatial neighborhood approach and ROI export to quantify BM and TME marker expression. These molecular findings were subsequently correlated with the local cell type composition of the tumor region.

Results:
Spatial transcriptomic analysis demonstrated significant changes in the expression of laminins and metalloproteases in close proximity to the tumor's invasive front. These remodeling activities were found adjacent to proliferating cancer cells expressing oncogenes known to function in angiogenesis, glycolysis, and invasion. Critically, in breast cancer, we observed alterations to BM markers even where the myoepithelial layer remained histologically intact, suggesting that traditional markers are insufficient to capture early tumor progression. Hypoxia-adapted cancer cells expressing VEGFA and chemokines recruited Cancer-Associated Fibroblasts (CAFs) and Tumor-Associated Macrophages (TAMs), which were identified as the primary source of metalloprotease secretion. Furthermore, T-cells in these regions exhibited an exhausted phenotype, indicating a robust immune-evasive pathway.

Conclusions:
By employing high-resolution spatial transcriptomics, this study provides a comprehensive, spatially-resolved analysis of molecular heterogeneity within the TME, precisely localizing BM-remodeling activity to the invasive front. We successfully demonstrated the capacity of this technology to enable the discovery of novel, spatially-defined biomarkers and provide mechanistic insight into cancer progression.

: Tumor-Neuron Interactions and Neuro-Regulation of Cancer
Poster Session

#6220 Stromal SPARC drives tumor-nerve-stroma crosstalk and perineural invasion in pancreatic ductal adenocarcinoma.

Satoru Furuhashi[1], Ryuta Muraki[2], Yoshifumi Morita[1], Daiki Nishiwaki[1], Akio Matsumoto[1], Yuji Shimizu[1], Tomohiro Murakami[1], Makoto Takeda[1], Hirotoshi Kikuchi[1], Yoshihiro Hiramatsu[1], Hiroya Takeuchi[1]

[1]Hamamatsu University School of Medicine, Hamamatsu, Japan,[2]Shizuoka General Hospital, Shizuoka, Japan

Background: Perineural invasion (PNI) is frequent in pancreatic ductal adenocarcinoma (PDAC) and contributes to poor outcomes. However, the stromal-neural mechanisms that underlie tumor neurotropism remain poorly understood. We hypothesized that soluble factors secreted by stromal fibroblasts, in cooperation with nerves and cancer cells, drive PNI-related tumor aggressiveness.
Methods: A vertical transwell tri-culture system was established using human PDAC cells (MIA PaCa-2) in the upper chamber and neonatal mouse dorsal root ganglia (DRG) with human pancreatic stellate cells (PSCs) in the lower chamber. PDAC cell migration was quantified after 24 h. Conditioned media from each condition (control, DRG, PSC, DRG + PSC) were analyzed by LC-MS/MS with intensity-based quantification; candidate proteins were selected by correlation with migration (Pearson $r \geq 0.95$) and ≥ 2-fold enrichment in DRG + PSC. Clinical significance was assessed using TCGA-PDAC and GTEx datasets. Cell-of-origin was inferred by CIBERSORTx deconvolution and single-cell RNA-seq analysis. Stromal versus epithelial SPARC protein expression and its association with PNI were evaluated by immunohistochemistry and semi-automated QuPath scoring in 81 resected PDACs.
Results: Tri-culture with DRG + PSC significantly enhanced PDAC migration compared with control or either single-cell condition (all $p < 0.001$). Proteomic profiling identified Secreted Protein Acidic and Cysteine-Rich (SPARC) as one of the most enriched proteins in DRG + PSC condition, with abundance strongly correlating with migratory activity. In transcriptomic datasets, SPARC was markedly upregulated in PDAC relative to normal pancreas, and high SPARC expression was associated with shorter overall survival. CIBERSORTx and single-cell analyses localized SPARC expression primarily to fibroblast/cancer-associated fibroblast (CAF) populations. In clinical specimens, SPARC protein was concentrated in the desmoplastic stroma and significantly higher than in tumor epithelium ($p < 0.0001$). Stromal SPARC levels were elevated in PNI-positive versus PNI-negative tumors in our institutional cohort ($p < 0.0001$), with consistent results in TCGA-PDAC ($p = 0.032$).
Conclusions: A nerve-stroma-conditioned microenvironment accelerates PDAC cell migration, with CAF-derived SPARC serving as a pivotal driver of tumor-nerve crosstalk and PNI. Through extracellular matrix remodeling and promotion of neural infiltration, SPARC emerges as a promising biomarker and therapeutic target for stroma-directed, anti-PNI strategies in PDAC.

#6221 Senescent cancer-associated fibroblasts drive perineural invasion and pain in pancreatic ductal adenocarcinoma.

Jinpeng Lu[1], Ziyi Tu[1], Shuncang Zhu[1], Hongyi Lin[1], Yinhao Chen[1], Yiting Chen[2], Zuwei Wang[1], Haoxiang Zhang[1], Shi Chen[1]

[1]Shengli Clinical Medical College of Fujian Medical University, Fuzhou, China,[2]College of Biological Science and Engineering, Fuzhou University, Fuzhou, Fujian 350108, People's Republic of China, Fuzhou, China

Background Pain in pancreatic ductal adenocarcinoma (PDAC) correlates with perineural invasion (PNI), severely impairs quality of life, and predicts poor prognosis. The mechanisms driving this PNI-pain axis, particularly the role of senescent cancer-associated fibroblasts (senCAFs), and effective therapies remain elusive.
Methods We correlated pain scores (NRS) with PNI (IHC/IF) in two PDAC cohorts. Single-cell/spatial transcriptomics and lipidomics were performed and cross-validated with external datasets. Human/murine senCAFs were co-cultured with tumor cells, dorsal root ganglion (DRG) neurons, and patient-derived organoids (PDOs), with neuronal activity assessed via patch-clamp electrophysiology. In vivo studies utilized orthotopic models with fibroblast-specific knockouts, evaluated by behavioral and nociceptive analyses.
Results Higher pain grades strongly correlated with increased PNI, nerve density, and poor prognosis. scRNA-seq and spatial analyses revealed p16+ senCAFs enriched near nerves, confirmed by flow cytometry in painful tumors. Orthotopic co-inoculation with senCAFs induced nociceptive hypersensitivity prior to differences in tumor burden. Mechanistically, senCAFs activated an IL-6-JAK2/STAT3 feedback loop, sensitizing DRG neurons. JAK2 blockade normalized neuronal excitability and reduced pain behaviors. This neural-stromal crosstalk was bidirectional: senCAFs sensitize DRGs via IL-6-JAK2/STAT3, while activated DRGs release ATP, triggering P2RX7-mediated tumor cell depolarization to promote invasion. This loop is stabilized by tumor-derived, SPHK2-dependent S1P signaling via S1PR2 on CAFs, reinforcing the senescent phenotype. In vivo, JAK2 inhibition combined with nab-paclitaxel/gemcitabine significantly improved pain control and overall survival.
Conclusion p16+ senCAFs orchestrate a vicious cycle by activating the IL-6-JAK2/STAT3 pathway, enhancing neuronal firing and pain; this in turn amplifies ATP/P2RX7-driven tumor cell depolarization and progression. This cycle is stabilized by tumor-derived sphingolipid reprogramming of CAFs. Targeting this senCAF-driven neural-stromal axis via JAK2 inhibition, combined with standard chemotherapy, provides a translationally potent therapeutic strategy for PDAC-related pain.

#6222 Microbiotas activate a tuft cell-sensory neuron feedback loop to promote esophagogastric junction (EGJ) tumorigenesis.

Yi Zeng[1], Feijing Wu[1], Puran Zhang[1], Ruhong Tu[1], Xiaofei Zhi[2], Biyun Zheng[1], Jin Qian[1], Hualong Zheng[1], Shuang Li[1], Hiroki Yi Kobayashi[1], Yosuke Ochiai[1], Masahiro Hata[1], Juli Lin[1], Junya Arai[1], Leah B. Zamechek[1], Zaisheng Ye[3], Timothy C. Wang[1]

[1]Columbia University Irving Medical Center, New York, NY,[2]Nantong University, Nantong, China,[3]Fujian Cancer Hospital, Fuzhou, China

Background Esophagogastric junction (EGJ) adenocarcinoma is rising in developed countries. While diet and reflux contribute, microbial-neuronal mechanisms remain poorly defined.

Methods Metabolomic and 16S rRNA sequencing were performed on 40 paired human EGJ tumors and adjacent tissues, and single-cell RNA sequencing on five pairs. Mechanistic studies used the pL2-IL1B mouse model of Barrett's esophagus, Cck2r-CreERT2 mice to label EGJ progenitors, and crosses to $p53^{R172H}$; pL2-IL1B to provide a tumor-prone background. Dclk1-CreERT2 targeted Tuft cells, while Trpv1-Cre, hM3Dq, and Ramp1 flox examined sensory signaling. Additional lines (Cck2r-CreERT2; $Ramp1^{flox/flox}$, Dclk1-CreERT2; $Cox1^{flox/flox}$; $Cox2^{flox/flox}$, Pou2f3-CreERT2; DTA) dissected the Tuft-neuron-epithelial circuit. P. melaninogenica colonization and deoxycholic acid (DCA) supplementation modeled microbial-metabolic effects. Calcium imaging, phospho-ERK staining, and Tuft-neuron co-cultures assessed functional signaling.

Results EGJ tumors were enriched in *Firmicutes/Bacteroidota* and *Prevotella*, while adjacent tissues contained *Proteobacteria* and *Helicobacter*. *Prevotella* abundance correlated positively with arachidonic-acid and negatively with tryptophan metabolites. Single-cell data showed epithelial, immune, and metabolic clusters, with bile- and fatty-acid pathways enriched in proliferative cells. *P. melaninogenica*, linked to bile-acid-rich, cancer-prone environments, was selected for mechanistic study. DCA alone enhanced EGJ dysplasia in pL2-IL1B mice. Oral *P. melaninogenica* colonized the EGJ, further increased by DCA, forming a bile-acid niche. Colonization amplified $CGRP^+$ neuronal signaling, expanded Tuft cells, and aggravated dysplasia. Tumor-prone Cck2r-CreERT2; p53R172H; pL2-IL1B mice showed more Tuft-$CGRP^+$ contacts, and pseudotime analysis indicated enhanced $Cck2r^+$-to-Tuft differentiation. In ex vivo organoids, activation of $Dclk1^+$; $hM3Dq^+$ Tuft cells elevated PGE_2/NGF secretion, strengthened Tuft-nerve contacts, and induced calcium influx in co-cultured $Trpv1^+$; $GCaMP6s^+$ DRG neurons. $Trpv1^+$ neurons co-expressed CGRP and EP4. Combined DCA + CNO treatment in Trpv1-Cre; hM3Dq; pL2-IL1B mice further increased dysplasia. Tuft ablation (Pou2f3-CreERT2; DTA), Tuft-specific Cox1/2 loss, or Ramp1 deletion in $Cck2r^+$ cells suppressed *P. melaninogenica*-induced dysplasia, demonstrating that blocking the Tuft-neuron-progenitor axis halts tumor progression.

Conclusions We define a microbiota-bile-acid-Tuft-neuron feedback loop driving EGJ tumorigenesis. *P. melaninogenica* and DCA activate Tuft cells to release PGE_2/NGF, stimulating EP4-CGRP/Ramp1 signaling and promoting epithelial dysplasia. Disrupting this circuit suppresses tumor growth, highlighting a metabolic-neuronal target for EGJ cancer prevention.

#6223 Characterize the role of cholinergic signalling in pancreatic cancer liver metastasis.

Xiaotong Long[1], Christine Chio[2], Tak W. Mak[3]

[1]Medical Biophysics, Univ. of Toronto Faculty of Medicine, Toronto, ON, Canada,[2]Columbia University, New York, NY,[3]UHN Princess Margaret Cancer Centre, Toronto, ON, Canada

Cholinergic signalling, traditionally attributed to the parasympathetic nervous system, is increasingly recognized as an immunoregulatory pathway in diverse disease contexts. Acetylcholine, the primary neurotransmitter in cholinergic signalling, is reported to be secreted by immune cells and plays an important role in hepatocellular carcinoma, liver regeneration, and metabolic dysfunction-associated steatohepatitis. However, whether immune cell-derived ACh influences cancer metastasis to the liver remains unknown. Pancreatic ductal adenocarcinoma (PDAC) frequently metastasizes to the liver, providing a relevant model to interrogate the neuroimmune mechanisms that shape the metastatic microenvironment. Using a spontaneous liver metastasis model generated by orthotopic or splenic injection of murine pancreatic cancer cells, we observed a marked induction of the ACh-synthesizing enzyme choline acetyltransferase (ChAT) in immune cells during liver metastatic progression, suggesting that immune cells contribute to a local immune-derived cholinergic niche. These findings identify a previously unrecognized cholinergic-immune axis in the pancreatic cancer metastatic niche, where immune-derived ACh increases during liver metastasis. Targeting neuroimmune pathways may offer new strategies to modulate the liver metastatic microenvironment in PDAC.

#6224 Neurotrophic receptor GFRα2 drives pro-metastatic programming of Kupffer cells in liver metastases.

Jintian CHEN, **Jingying Zhou**

School of Biomedical Sciences, Chinese University of Hong Kong, Hong Kong, China

Gastrointestinal cancers such as colorectal, gastric and pancreatic cancers frequently metastasize to the liver, contributing significantly to cancer-related mortality and resistance to immune checkpoint inhibitors (ICIs). Recent multidisciplinary studies have highlighted a functional and mechanistic interplay between the nervous and immune systems in cancers, termed as neuroimmune axis. Given the rich hepatic innervation, we investigated whether neuroimmune signaling contributes to liver metastasis by analyzing the expression profiles of 217 known receptors involved in efferent signal transmission using single-cell omics datasets from colorectal cancer liver metastasis (CRLM) patients, among which glial cell line-derived neurotrophic factor (GDNF) family receptor alpha 2 (GFRα2) was identified due to its reproducibly and exclusively elevated expression on CRLM adjacent livers compared with healthy livers from transplantation donors. Using scRNA-seq, high-dimensional flow cytometry and multiplex-immunofluorescence analysis in mice and patients with CRLM, we further confirmed that GFRα2 was selectively expressed and upregulated on Kupffer cells (KCs). Notably, GFRα2$^+$KCs were found in close proximity to liver-infiltrating nerve fibers in CRLM, whereas chemical liver denervation led to reduced expression of GFRα2, suggesting a possible neural regulation on GFRα2$^+$KCs. Functionally, lentiviral shRNA-mediated *Gfra2* knockdown significantly suppressed liver metastasis without affecting primary colorectal tumor growth, which could be abolished by KCs depletion using liposomal clodronate. Mechanistically, GFRα2$^+$KCs displayed impaired antigen presentation capacity, but enhanced pro-angiogenesis and neutrophil recruitment, suggesting a reprogrammed, metastasis-promoting phenotype. Notably, *Gfra2* knockdown significantly reduced neutrophil accumulation and angiogenesis, but increased MHCII$^+$KCs. Taken together, our findings pinpointed that GFRα2 upregulation reprograms KCs towards a pro-metastatic state, thereby facilitate liver metastasis.

#6225 Spatial biomarker related to PNI and LVI in stage II colon cancers.

Hanqing Hu[1], Hongzhe Sun[2], Lin Zhu[2], Shuo Han[2], Zhifu Zhang[2], Enkai Zhang[3], Na Li[3], **Guiyu Wang**[1]

[1]Department of Colorectal Surgery, the Second Affiliated Hospital of Harbin Medical University, Haerbin, China,[2]Beijing PhenoVision Bio Co., ltd, Beijing, China,[3]Hangzhou PhenoVision Bio Co., ltd, Hongzhou, China

Multiple retrospective studies and meta-analyses have shown that presence of lymphovascular invasion (LVI) and/or perineural invasion (PNI) is associated with significantly worse disease-free and overall survival in stage II colorectal cancer (CRC), and these features are commonly considered when deciding whether to recommend adjuvant chemotherapy for stage II disease. Current study reviewed 32 stage II CRC patient archived FFPE samples to investigate immune cell features among LVI, PNI or no-invasion groups. IHC control, multiplex immunofluorescence (mIF) panel control and the followed mIF staining were conducted using PN 7-Plex Detection Kit (PhenoVision Bio Co., ltd) targeted CD68, CD3, CD20, panCK, PD-1, PD-L1 and CD68, panCK, CD3, CD8, CD163, αSMA, respectively. The QC procedures made sure each marker from mIF results exhibited identical location and density of the same marker from IHC staining. The 64 staining slides were scanned, tumor areas were lined out by pathologist based on H&E staining from the serial section of each sample. Non-tumor region, tumor invasive margin (IM) , which was defined as 360μm within and outside of tumor boundary *i.e.* total 720μm, tumor parenchyma, tumor stromal, 30μm region inside and outside of tumor parenchyma boundary were analyzed using PhenoVision mIF AI analysis system trained from Oncotopix Discovery system (Visiopharm). Positive cell percentage were analyzed for further analysis. Statistical analysis exhibited correlation of CD20 and CD20+/PD-1- cell percentage to PNI condition (p=0.046 and 0.046, respectively) in tumor invasive region and CD68+/CD163- cell percentage to PNI (p=0.048) of 30μm outside tumor parenchyma based on binary logistic regression. There were higher CD20+ positive cell percentage and CD20+/PD-1- cell percentage in PNI group *vs.* non PNI group (p=0.013 and 0.013, respectively) at tumor invasive region. Whereas lower CD68+CD163- cell percentage was observed in PNI group *vs.* non PNI group of 30μm outside of tumor parenchyma region (p=0.01). There was significant more panCK cell percentage in LVI positive group at tumor parenchyma region compared to non LVI group (p=0.000). Current study indicates that spatial biomarkers are correlated to PNI and LVI in tumor invasive margin and tumor parenchyma region of stage II colon cancers which may be related to stage II CRC prognosis. Increased sample number of the spatial marker distribution feature to disease prognosis analysis are scheduled.

#6226 Integrative multi-omic analysis identifies neuronal reprogramming and vascular remodeling as hallmarks of recurrent high-grade serous ovarian carcinoma.

Ilaha Huseynli[1], Gregory Gibson[1], Benedict B. Benigno[2], Stephen N. Housley[1]

[1]School of Biological Sciences, Georgia Institute of Technology, Atlanta, GA,[2]Ovarian Cancer Institute, Atlanta, GA

Background: High-grade serous ovarian carcinoma (HGSOC) is the most common and aggressive subtype of epithelial ovarian cancer, with over 80% of patients experiencing recurrence after initial therapy. Recurrent disease is typically chemoresistant and remains the leading cause of gynecologic cancer mortality, yet the molecular changes driving recurrence, particularly at the cell type-specific level, are poorly understood.
Objective: To define cell type resolved transcriptional programs that distinguish late primary from recurrent disease, to place these programs into a stage aligned cellular context from benign tissue through recurrence, and to nominate robust biomarkers with external replication and genomic concordance.
Methods: Matched late primary and recurrent HGSOC specimens were profiled by snRNAseq with additional benign and early tumors included for stage contextualization. Paired pseudobulk differential expression between late primary and recurrence was performed using DESeq2 and limma voom with patient blocking, low expression filtering, trimmed mean normalization, and false discovery rate control. Replication of 46 significant genes was assessed in four external cohorts. In addition, somatic variant and copy number profiles from late primary tumors generated by whole exome sequencing were compared with transcriptional effects at panel loci. A transcriptional signature was related to time to recurrence using exact rank statistics with bootstrap assessment of robustness.
Results: snRNAseq of matched late primary and recurrent HGSOC revealed a recurrence program that maps to tumor associated endothelium and to a neuronal lineage state in malignant epithelium. *FLT1 STC1* and *CA2* and selective suppression of the endothelial long noncoding RNA *MEF2C AS1; FLT1* and *CA2* together with *MEF2C AS1* constitute novel recurrence associated endothelial markers in this disease. Malignant cells exhibited a novel neuronal reprogramming signature defined by induction of *NTM* and *KCNQ5* with reciprocal downregulation of *PEG3*, and stromal compartments showed reduced *ABCA8* and the novel marker *PLCXD3*. Whole exome copy number profiling of late primary tumors provided directional concordance with the transcriptome, including deep loss at *KCNQ5*, late stage copy number reduction at *FLT1*, *ESM1,* and *NTM* aligned with their induction at recurrence, and late stage gain at *C7* and *PLCXD3* aligned with its suppression at recurrence.
Conclusion: Our integrative multi-omic analysis reveals that recurrent HGSOC is characterized by coordinated vascular remodeling in tumor-associated endothelium and neuronal reprogramming in malignant epithelium, accompanied by stromal reconfiguration. These findings nominate cell-state-specific biomarkers and pathways for prospective validation and therapeutic targeting in recurrent disease.

#6227 Cancer-associated enteric glial cell abundance as a prognostic marker in gastric cancer revealed by single-cell analysis.

Carolyn R. DePinho[1], Jianming Zeng[2], Xiling SHEN[2], Sandra W. Ryeom[1]

[1]Columbia University Irving Medical Center, New York, NY,[2]MD Anderson Cancer Center, Houston, TX

Enteric glial cells (EGCs), essential regulators of gastrointestinal barrier function, immune responses, and neuro-epithelial homeostasis, remain largely unexplored in the context of gastric cancer (GC). EGCs are a specialized population of peripheral neuroglia that, along with enteric neurons, make up the enteric nervous system. While neural innervation in GC has been increasingly recognized, the presence and functional significance of cancer-associated EGCs (CAEGCs) within the gastric tumor microenvironment (TME) remain undefined.

In this study, we utilized integrative single-cell transcriptomic analysis of human GC to identify a rare but distinct population of CAEGCs residing within the stromal compartment. Defined by consistent expression of canonical glial markers, this CAEGC population emerged as a robust and reproducible signature across six independent datasets. To evaluate clinical relevance, we then applied LASSO-Cox regression modeling to The Cancer Genome Atlas Stomach Adenocarcinoma (TCGA-STAD) cohort to establish a GAEGC-derived glial signature that stratified GC patients into high- and low-risk groups with significant survival differences ($p < 0.001$) and distinct molecular features. This GAEGC-derived glial signature also aligned with established molecular subtypes and predicted response to therapy.

Our findings reveal a prognostically relevant and previously underappreciated population of CAEGC-like stromal cells within the GC TME. This GAEGC-derived glial signature offers a way to predict GC relapse risk and survival, and it highlights neuro-glial interactions as a potential site of therapeutic intervention in GC.

#6228 Reactive oligodendrocytes promote glioblastoma progression through CCL5/CCR5-mediated glioma stem cell maintenance.

Nicholas Mikolajewicz[1], Kui Zhai[2], Anish Puri[2], Petar Miletic[2], Nazanin Tatari[2], jiarun Wei[1], Neil Savage[2], Zhi Huang[3], Qian Huang[3], Seon Yong Lee[1], Mahta Jan-Ahmadnejad[4], Roseanne Nguyen[4], David Chen[1], Tiegan Korman[2], Daniel Mobilio[2], Maxwell Topley[2], Jack Qinyu Lu[2], Matthew R. Voisin[2], Zsolt Zador[2], Shawn C. Chafe[2], Chitra Venugopal[2], Kevin R. Brown[1], Gelareh Zadeh[5], Hong Han[2], Julien Muffat[4], Shideng Bao[3], Sheila K. Singh[2], **Jason Moffat**[1]

[1]Genetics and Genome Biology, Sick Children's Hospital, Toronto, ON, Canada,[2]McMaster University, Hamilton, ON, Canada,[3]Cancer Biology, Cleveland Clinic, Cleveland, OH,[4]Neurosciences and Mental Health, Sick Children's Hospital, Toronto, ON, Canada,[5]University Health Network, Toronto, ON, Canada

Glioblastoma (GBM) evolves within a microenvironment abundant in oligodendrocyte-lineage (OL) cells. In this study, we utilized single-cell and spatial transcriptomics from primary and recurrent GBM tumors, immunohistochemistry, cytokine profiling, and migration assays to show that GBM cells recruit OLs to the tumor border via CXC3L1/CXC3R1 signaling. A pan-disease human OL meta-atlas and syngeneic mouse models reveal an interferon-induced reactive OL state, akin to those seen in demyelinating inflammatory and traumatic injury, which is enriched in CNS malignancies. These reactive OLs secrete pro-tumorigenic cytokines, notably CCL5, that promote GBM tumor cell growth through CCR5 signaling. CCR5 is preferentially expressed in glioma stem-like cells (GSCs) and upregulated at recurrence. Targeting CCR5 with genetic knockdown or FDA-approved drug Maraviroc impairs GSC stemness and prolongs survival in GBM models. Our work highlights the functional interplay between OLs and GBM cells and positions the CCL5/CCR5 axis as a druggable target in GBM.

#6229 Neighborhood analyses in nerve fiber-associated tumor regions in hereditary diffuse gastric cancer.

Idania Carolina Lubo Julio[1], Yunhe Liu[1], Sharia Hernandez[1], Alejandra G Serrano[1], Wei Lu[1], Larisa Kostousov[1], Sean Barnes[1], Khaja Khan[1], Karen Colbert[1], Yanshuo Chu[1], Yang Liu[1], Rebecca Waters[1], Jeremy L. Davis[2], Paul F. Mansfield[1], Linghua Wang[1], Luisa Maren Solis Soto[1]

[1]UT MD Anderson Cancer Center, Houston, TX,[2]University of Maryland School of Medicine, Baltimore, MD

Background: In carcinomas**,** perineural invasion and tumor-nerve niches are increasingly recognized as associated with cancer progression. In Hereditary Diffuse Gastric Cancer (HDGC), the molecular programs behind these interactions are not fully understood. In this study, we aim to depict multicellular neighborhoods and spatial transcriptomics programs associated with tumor-nerve interactions in patients with HDGC.

Methods: Six FFPE specimens from five patients with invasive HDGC were sectioned at 5-um thickness. Histological sections from ≥T3 tumors were analyzed using Spatial Gene Expression of a capture area of 11 x 11 mm. Histological spot-level annotations were performed to identify niches enriched for nerve fibers. Granular annotations identifying tumor cells and their microenvironment (TME) were conducted. Tumor cells were categorized by morphology as signet-ring, intermediate-stage, moderately differentiated/tubular and undifferentiated cells. Immune cells, connective tissue, smooth muscle, and vessels were annotated to define the TME. Integration with markers of both nerve tissue and potentially altered genes was conducted. Using identified nerve tissue as epicenter we measured the distance between spots (approximately 900 um). We then conducted comprehensive analysis of these areas for cell type enrichment, gene profile and intercellular crosstalk in the nerve neighboring tumor region.

Results: The spatial mapping of nerve fibers showed that they were distributed in the submucosa and predominantly in myenteric layers; nerve-enriched niches were highly associated with undifferentiated, and moderately differentiated cells/tubular patterns. Non-nerve niches were enriched with signet ring cells or intermediate-stage cells. Connective tissue, smooth muscle, and vessels were not enriched in nerve-niches. Differential gene expression (DGE) analysis of tumor cells in the nerve-niches showed upregulation of genes related to cell integrity (*MYOC, CLDN17*), metabolic programs (*ADIPOQ, PLIN1*), cell cycle regulation (*FAM83D*), and inflammatory response (*CCL3*). Also, transcription factors related to neural survival were upregulated (*NR4A1, NR4A2, NR4A3, EGR2*). Importantly, DGE in the TME annotations showed that nerve-niches had upregulation of immune enriched pathways associated with chemokines, immune cell adhesion and immune cell migration *(CXCL13, CXCL14, ITGB2, ITGB4, ITGB6, ITGBP6, ITGBP7, CD46, CD79B, CD14, XRCC6, CCL5, CD74).*

Conclusions: Spatial transcriptomic profiling in HDGC delineated distinct morphological domains and transcriptomic signatures linked to tumor-associated nerve niches pointing to tumor-nerve-TME interaction programs that may act as critical modulators of cancer aggressiveness, offering novel insights into vulnerabilities that could be leveraged to impede gastric cancer progression.

#6230 Tumor nuclear uPA: A transcriptional modulator of perineural invasion in PDAC.

Yun HE, Zonghua Su, Feng Ding, Zheng Chen, Xinxing Cui, **Liu Yang**, Shuangying Qiao, Yaru Hou, Aiping Lu, Fangfei Li

Hong Kong Baptist University, Hong Kong, Hong Kong

Perineural invasion is highly prevalent in pancreatic ductal adenocarcinoma and correlates with poor outcomes; clinical approaches to inhibit PNI remain limited. Using integrated transcriptomic analyses of PDAC parenchymal cells with escalating nerve-invasive potential, we identified PLAU (uPA) as a key determinant of PNI capacity. Patient single-cell datasets showed that high tumor PLAU expression is associated with enrichment of Schwann cells in the tumor microenvironment and strengthened ductal cell-Schwann cell communication. Functionally, nuclear uPA in PDAC parenchymal cells activates Schwann cells in a coculture perineural invasion model. Mechanistically, chromatin profiling revealed that nuclear uPA occupies a compact set of genomic sites enriched near transcription start sites and linked to genes governing neural development and neuronal signaling. Motif analysis, biolayer interferometry (BLI), and co-immunoprecipitation showed that uPA binds c-Jun; the uPA-c-Jun complex engages DNA and serves as a co-regulator that drives pro-neurogenic transcriptional programs. Together, these findings establish nuclear uPA as a central mediator of tumor-nerve crosstalk in PDAC and highlight targeting its nuclear function as a promising strategy to inhibit perineural invasion.

#6231 Schwann like reprogramming of cancer associated fibroblasts remodels the tumor neural niche in pancreatic ductal adenocarcinoma.

Liu YANG, Xinxing Cui, Shuangying Qiao, Yun HE, Zonghua Su, Zheng CHEN, Feng DING, Aiping LU, Fangfei Li

Hong Kong Baptist University, Hong Kong, China

Pancreatic ductal adenocarcinoma (PDAC) has a significantly higher incidence of peripheral neuropathy compared to other cancers, which is associated with local recurrence and a poor prognosis for PDAC patients. Notably, Schwann cells, the principal glia of peripheral nerves, are critically involved in this process due to their multifaceted roles in tumorigenesis and neural remodeling. Nevertheless, the biological sources of the increased Schwann cell population and overall increased neuronal density in PDAC are still mainly unknown. Here by employing an integrative approach combining single-cell RNA sequencing, immunofluorescence, and functional assays, we revealed a novel neural reprogramming of cancer-associated fibroblasts (CAFs) in PDAC: the Fibroblast-Schwann Transition (FST), through which a subset of CAFs directly transdifferentiates into Schwann-like states. The FST was confirmed by pseudotime trajectory analysis, which showed a cell fate transition from CAFs to Schwann-like cells. Multiplex immunofluorescence of patient tumors identified transitional interface cells co-expressing canonical Schwann and CAF markers, which is consistent with the computational inference. Furthermore, in the co-culture of tumor cells and CAFs, CAFs developed Schwann-like features, with upregulation of Schwann-cell genes, highlighting their profound plasticity. To figure out the regulatory driver of this process, SCENIC analysis identified key fibroblast-specific transcription factors as critical regulators of the FST program. Additionally, a Schwann-like phenotype was induced in vitro by overexpressing the candidate transcription factor in CAFs, as evidenced by decreased CAF-associated gene expression and increased Schwann-cell markers.Overall, our findings suggest that the FST is a biological process associated with the increased neuronal density observed in PDAC. This study identifies a previously unknown cellular plasticity mechanism in the tumor microenvironment and proposes that targeting FST could be a potential therapeutic strategy for treating peripheral neuropathy in PDAC.This work is supported by the Hong Kong RGC Theme-based Research Scheme (No. T12-201/20-R, HongKong, China), Hong Kong General Research Fund (No. 12102722, HongKong, China), and the 2020 Guangdong Provincial Science and Technology Innovation Strategy Special Fund (No. 2020B1212030006, GuangDong, China).

#6233 Proximity-based gene expression profiling identifies multi-pathway activation in perivascular, perineural, and pseudo-capsule adjacent human prostate cancer cells.

Rafael Sainz[1], Kelvin W. Pond[1], Beatrice S. Knudsen[2], Gregory C. Rogers[1], Noel E. Warfel[1], Anne E. Cress[1]

[1]University of Arizona Cancer Center, Tucson, AZ,[2]University of Utah, Salt Lake City, UT

Prostate cancer (PCa) progression is critically driven by the tumor microenvironment (TME), which imposes selective pressures and dictates specialized invasive behaviors, such as perineural and lymphovascular invasion. We hypothesized that heterogeneity within the tumor allows for the selection of functionally specialized cancer cell clones based on their proximity to TME niches. Using Spatial Transcriptomics, we profiled cancer cell populations at three critical invasive fronts: near nerves, vessels, and the prostatic pseudo-capsule from 55 human prostate tissue datasets. Differential expression analysis revealed distinct, niche-specific functional signatures: neurotropic clones near nerves exhibited a loss of prostate identity and a gain of neural adhesion genes (e.g., NCAM1, NTN1) consistent with perineural invasion; perivascular clones showed upregulation of ECM remodeling and an EMT-like state (e.g., ANXA2, CCN1), suggesting priming for intravasation; and pseudo-capsule-adjacent clones displayed a highly proliferative phenotype (e.g., CCND1, CDK4). These results demonstrate that the TME drives the functional specialization of PCa cells, refining our understanding of invasion and nominating several niche-specific pathways as potential therapeutic targets. Studies are currently ongoing to validate these signatures, refine heterogeneity scoring, and cross-link the identified genes with pharmacological databases for future in-vitro inhibition assays.

#6234 Characterizing the competitive interactions between glioblastoma and oligodendrocyte progenitor cells.

Lindsey A. Dudley[1], Sunlan Lu[2], Beatrice O'Brien[2], Carol Watkins[3], Travis Perryman[4], Riki Kawaguchi[1], Steve A. Goldman[5], Kunal S. Patel[4], Harley I. Kornblum[6]

[1]The Intellectual and Developmental Disabilities Research Center, UCLA, Los Angeles, CA,[2]UCLA, Los Angeles, CA,[3]CIRM Bridges Program, California State University, Northridge, Northridge, CA,[4]Department of Neurosurgery, UCLA, Los Angeles, CA,[5]Center for Translational Neuromedicine, University of Rochester Medical Center, Rochester, NY,[6]Professor Psychiatry, Pharmacology and Pediatrics, UCLA David Geffen School of Medicine, Los Angeles, CA

Resection of glioblastoma (GBM) often only includes the contrast-enhancing (CE) solid portion of the tumor and radiation therapy also targets this region. These therapies leave behind infiltrating tumor cells that lay beyond the CE border in the non-enhancing region (NE) with the capacity to propagate the tumor following therapy. Non-transformed cell types in the brain have been shown to promote GBM progression via a variety of mechanisms. We performed single nucleus RNA-sequencing (snRNA-seq) on 17 biopsies from the NE and CE regions of seven different primary IDH WT glioblastoma tumors during maximal resection surgery. While some oligodendrocyte progenitor cells (OPCs) are present in the NE region, they are almost absent in the CE region, a finding corroborated by our prior study of recurrent tumors. OPCs, the most common cycling cells in the brain, share many genes with GBM and the interaction between the two cell types has yet to be described on a single cell level. Prior work has demonstrated that in the developing and adult brain young, more fit OPCs can outcompete older OPCs leading us to hypothesize that brain tumor cells can compete with non-transformed OPCs. To explore possible interactions between GBM and OPCs we utilized predictive cell-cell interaction software, finding that OPCs express transcripts that are predicted to respond to GBM signals to induce proliferation, migration and differentiation. Compared to snRNA-seq of healthy OPCs, the OPCs from our biopsies were more likely to be proliferative, migratory, and differentiated. To assess possible enrichment of pathways associated with a more competitive state, we performed differential expression between OPCs contained in our biopsies and GBM cells. This revealed a significant enrichment of the YAP1 pathway which is associated with a more competitive state. GBM cells were predicted to be activated by OPCs to proliferate, migrate and have increase synaptic activity. To investigate how soluble factors secreted by OPCs and GBM cells influence each other by culturing each cell population in conditioned media (CM) derived from the opposite cell type. OPCs treated with GBM CM have shown increased proliferation and GBM cells treated with OPC CM have shown decreased proliferation, possibly due to younger nature of OPCs that were differentiated from iPSCs. Our findings support the hypothesis that there are complex and possibly competitive interactions between OPCs and GBM cells, extending the concept of “cancer neuroscience”. Further studies are ongoing to establish the nature and mechanisms of these interactions.

#6235 Smoking behavior is associated with increased tumor-associated neurogenesis in prostate cancer.

Kunwar Somesh Vikramdeo[1], Shashi Anand[1], Amod Sharma[1], Muhammad Tahir[2], Varsha Manucha[3], Seema Singh[1], Ajay Pratap Singh[1]

[1]Department of Cell and Molecular Biology, Cancer Center and Research Institute, University of Mississippi Medical Center, Jackson, MS,[2]Department of Pathology, UW Medicine-University of Washington Medical Center, Seattle, WA,[3]Department of Pathology, Cancer Center and Research Institute, The University of Mississippi Medical Center, Jackson, MS

Tumor-associated neurogenesis is being increasingly recognized as a contributor to cancer progression and therapeutic resistance. While tobacco smoking is known to influence inflammation and microvascular remodeling, its relationship with tumor neurobiology remains poorly understood. In this study, we investigated whether smoking behavior is associated with alterations in nerve density within the prostate cancer microenvironment. Prostatectomy specimens from prostate cancer patients with documented smoking history were selected (n=53), and smoking status was categorized as never (n=24), former (n=18), or current (n=11) smoker. The tumor tissues were sectioned and subjected to immunohistochemistry for S100B (Schwann cells) and TUBB3 (neuronal axons). Nerve density was quantified by measuring the number of neural clusters in five random fields, and an average value was calculated for each tumor. The difference in nerve density was compared between current, former, and never smokers using Kruskal-Wallis non-parametric test. Current smokers and former smokers exhibited significantly higher ($p < 0.001$) intratumoral nerve density compared to never-smokers. However, the difference was not significant ($p=0.268$) between current smokers and former smokers. In grade-wise comparisons, a significant difference ($p < 0.001$) between never smokers and current /former smokers was observed in low/medium (Gleason's score ≤7) grade tumors but not in high-grade tumors (Gleason's score >7). Interestingly, nerve mini-bundles at tumor edges were also more frequent in current smokers than in never smokers or former smokers. Altogether, our data demonstrate that the smoking behavior is associated with enhanced neural remodeling in prostate cancer, characterized by increased nerve density and Schwann cell/axon clustering at tumor margins. These findings suggest that host exposure to tobacco smoke promotes a neurotrophic tumor microenvironment, which may be linked to prostate cancer aggressiveness and a higher risk of recurrence.

: Environmental and Occupational Risk Factors, Infection, and Aging
Poster Session

#6239 Military cancer outcomes research (MilCan): A sub-study of the Millennium Cohort Study.

Erin L. Richard[1], Sheila F. Castaneda[1], Anna Baccetti[1], Anna C. Rivera[1], Rudolph P. Rull[1], Aaron Auerbach[2], Diego A. Vicente[1]

[1]Naval Health Research Center, San Diego, CA,[2]Joint Pathology Center, Silver Spring, MD

Background: Cancer remains a leading cause of death in the US, and US service members and veterans have higher rates of certain cancers than the US general population. Military-specific occupational exposures, such as aviation-related ultraviolet radiation exposure, chemical toxicants, and blasts leading to immune system dysregulation have been hypothesized to have long-term implications for cancer risk.
Methods: The Millennium Cohort Study (MCS) is a large-scale, prospective cohort study designed to examine the long-term health effects of military service. Over 260,000 US service members were enrolled between 2001 and 2021, and follow-up of participants is planned through 2068. As the cohort matures, there is increased focus on age-related diseases such as cancer. The MCS has collected longitudinal survey data on well-established cancer risk and protective factors, such as tobacco and alcohol use, physical activity, and obesity. The Military Cancer Outcomes Research (MilCan) initiative aims to develop a military cancer data warehouse platform that will link data from various military and civilian data sources (eg, electronic health records, military environmental exposures, lifestyle behaviors, and tumor biology, pathology, and imaging).
Results: Preliminary analyses of available survey and medical record data suggest there are at least 11,000 occurrences of cancer in the MCS. The study team is in various stages of linking with the (1) Department of Defense Cancer Registry, a centralized database of patients diagnosed with cancer in the Military Health System; (2) Virtual Pooled Registry Cancer Linkage System, a web-based, streamlined process for researchers to conduct minimal risk linkage studies with the nationwide resource of Central Cancer Registries; (3) Joint Pathology Center, which is part of the Defense Health Agency and maintains the world's largest collection of human pathology specimens; and (4) Individual Longitudinal Exposure Record, which includes historical deployment information and occupational exposures.
Conclusion: The planned data and specimen linkages with MCS survey data will allow MilCan to conduct population-based research on a wide range of military occupational, environmental, and behavioral exposures on the etiology of cancer among post-9/11 service members and veterans and could inform the development of policies and programs to prevent cancer.

#6240 Serum concentrations of per- and polyfluoroalkyl substances and mosaic chromosomal alterations in the Prostate, Lung, Colorectal and Ovarian (PLCO) Cancer Screening Trial.

Jongeun Rhee[1], Cynthia Rebecca Robbins[1], Vicky C. Chang[2], Weiyin Zhou[2], Mitchell J. Machiela[2], Jonathan N. Hofmann[2], Mark P. Purdue[2], Sonja I. Berndt[2]

[1]Center for Prostate Disease Research, Murtha Cancer Center Research Program, Uniformed Services University of the Health Sciences, Bethesda, MD,[2]Division of Cancer Epidemiology and Genetics, National Cancer Institute, Rockville, MD

Per- and polyfluoroalkyl substances (PFAS) are persistent organic pollutants detectable in the serum of most U.S. adults. Some PFAS are established or possible human carcinogens. Mechanistic studies in human cells and animals suggest PFAS may have genotoxic effects through indirect DNA damage caused by oxidative stress or other pathways; however, evidence from human populations remains limited. We investigated the relationship between serum PFAS concentrations and mosaic chromosomal alterations (mCAs), including autosomal mCAs among both men and women and mosaic loss of chromosome Y (mLOY) among men, as biomarkers of genotoxicity and genomic instability. We analyzed blood-derived DNA from 2,377 men and 696 women in three nested case-control studies within the PLCO Cancer Screening Trial. mCAs were detected using high-density genotyping array intensity data for the autosomes in men and women and separately in the male-specific region of the Y chromosome for mLOY. Pre-diagnostic serum concentrations of four PFAS [perfluorooctanoate (PFOA), perfluorooctane sulfonate (PFOS), perfluorohexane sulfonate (PFHxS), perfluorononanoate (PFNA)] were measured. Using study-specific multivariable logistic regression, we estimated odds ratios (ORs) and 95% confidence intervals (CIs) for the associations between serum PFAS concentrations and any detectable autosomal mCA, any mLOY, and mLOY affecting ≥10% of cells (expanded mLOY) among cancer cases and cancer-free controls, separately. Study- and case-control-specific results were summarized using random effects meta-analyses. Overall, autosomal mCAs were detected in 7% of men and 8% of women. Among men, 22% had mLOY, including 8.3% with expanded mLOY. 2% of men had both autosomal mCAs and mLOY. We found a suggestive positive association between serum PFOS concentrations and autosomal mCAs (per doubling in serum concentration, summary $OR_{continuous}$=1.43, 95%CI=0.93-2.21; I-squared=49%, P-heterogeneity=0.08). Among men, serum PFHxS was marginally positively associated with mLOY (any mLOY, summary $OR_{continuous}$=1.14, 95%CI=0.83-1.40; I-squared=59%, P-tenerogeneity=0.03), and the magnitude of the association was stronger for those with a higher proportion of affected cells (expanded mLOY; summary $OR_{continuous}$=1.19, 95% CI=0.89-1.59; I-squared=58%, P-tenerogeneity=0.03). No associations were observed for other PFAS. In conclusion, in this large population-based study, we observed suggestive evidence of a positive association between elevated serum PFOS concentrations and autosomal mCAs among men and women, and between serum PFHxS and mLOY among men. As the first study to evaluate PFAS in relation to mCAs, our findings, if confirmed, may provide new insights into PFAS-related effects on genome maintenance that are relevant to cancer development.

#6241 High-throughput screening for cancer-relevant chemicals in hair relaxer products sold in Kenya.

Elissia T. Franklin[1], Alexis A. Schaefer[2], Sstuti D. Mehra[3], Tabitha C. Hardin-Zollo[2], Karthik Mahakala[4], Jasmine A. McDonald[5], Mary Beth Terry[2], Beatrice N. Irungu[6], Cecilia Kimani[6], Esther Matu[6], Adana A. M. Llanos[2]

[1]Silent Spring Institute, Newton, MA,[2]Epidemiology, Columbia University Mailman School of Public Health, New York, NY,[3]Data Science, Columbia University, New York, NY,[4]Columbia University, New York, NY,[5]Columbia University Irving Medical Center, New York, NY,[6]Kenya Medical Research Institute, Nairobi, Kenya

Introduction: Hair relaxer use is associated with increased risks of several hormone-related cancers, including uterine, ovarian, and breast cancer. Given the high prevalence of relaxer use among Black women and women of African ancestry, unequal exposure to toxicants in these products might contribute to observed disparities in cancer incidence and mortality. Although recent regulatory efforts have targeted specific chemicals such as formaldehyde and formaldehyde releasers, hair relaxers may contain additional unregulated chemicals and chemical mixtures of concern. Comprehensive data on the chemical composition of these products remain limited.

Methods: As part of a larger investigation, we identified commonly used hair relaxers among women in two counties in Kenya (Embu and Nakuru) and purchased 19 products (11 cream relaxers and 8 multi-component relaxer kits) from local retailers and beauty shops between May and July 2024. Non-targeted two-dimensional gas chromatography-high-resolution mass spectrometry (GCxGC-HRMS) was used to identify and semi-quantify semi-volatile compounds in sample extracts. Inductively coupled plasma-mass spectrometry (ICP-MS) and atomic absorption spectroscopy were employed to screen for heavy metals and mercury, respectively. The Highlight™ machine learning system and a search of the National Institute of Standards and Technology library facilitated data processing and suspect screening. Tentatively identified chemicals were cross-referenced with authoritative hazard databases, including the European Union's Cosmetics Regulation (EC) No 1223/2009 lists of prohibited (Annex II) and restricted (Annex III) chemicals, which align with the Kenya Bureau of Standards cosmetic regulations.

Results: We detected 353 individual features across all samples and identified 83 chemicals with medium-to-high identity confidence, including multiple known or suspected carcinogens. Over 50% of samples contained at least one chemical appearing on an established hazard list. Notably, lead and radioactive uranium—both banned in EU cosmetics—were detected in nearly 10% of the samples.

Conclusions: This study provides the first high-throughput chemical characterization of commercially available hair relaxers commonly used by Black women and women of African ancestry in Kenya. The detection of numerous carcinogenic and restricted substances highlights an urgent need for strengthened regulatory oversight, policy action, and evidence-based interventions to reduce exposure to hazardous chemicals in hair and personal care products, emphasizing the importance of evidence-based policies and interventions to eliminate hazardous exposures and advance equitable cancer prevention globally.

#6242 Hair products usage and breast cancer among Latinas living in Puerto Rico: The HERSAFE Study.

Nancy Raquel Cardona-Cordero, Brenda Gonzalez, Ana Patricia Ortiz

University of Puerto Rico Comprehensive Cancer Center, San Juan, PR

Introduction. Hair products are widely used for aesthetic enhancement, yet their prolonged usage raises concerns about potential health risks. Many shampoos, conditioners, mascaras, dyes, among other products, contain ingredients that have been linked to endocrine disruption and possible carcinogenic effects. This study aims to assess the use of hair products across the lifespan of Latina women and breast cancer risk.

Materials and Methods. The ongoing “HERSAFE” case-control study examines the relationship between beauty product use and breast cancer among Hispanic women in Puerto Rico. Participants were recruited from Comprehensive Cancer Hospital and Radiotherapy Center. Data collection included a 45-60-minute survey on socio-demographics, lifestyle, maternal health, and beauty product usage. Data was stored in RedCap. STATA was used for demographics and logistic regression analysis (95%CI).

Results. Participants (n=105) mean age was 55.4 (SD±11.5). Only 28% of participants live below poverty levels (<$20,000) and 87% had at least one child. Around 23% of the participants reported a darker skin tone, compared to the lightest color. Participants reported the use of permanent and semi-permanent products during their lifetime; with 57% and 16% of the participants reporting over 10 years of permanent dye and semi-permanent dye. A non-significant trend of increased risk of breast cancer was observed among users of semi-permanent dye (AOR 1.65 95%CI:0.64-4.21). Similar results were observed for those who used permanent dye.

Conclusion. This research aims to enhance awareness of cosmetic safety, encourage informed consumer choices, and advocate for stricter regulations on harmful ingredients in beauty care products. Further research with larger samples and additional variables is needed to better understand potential influences on breast cancer risk for this population.

#6243 Mapping risk: spatial analysis of 2,4-D herbicide emissions and colorectal cancer.

Danny Baxter[1], Dan Dixon[1], Andrew Morris[1], Tongzhang Zheng[2], **Yong Zhu**[1]

[1]University of Arkansas for Medical Sciences, Little Rock, AR,[2]Brown University, Providence, RI

Colorectal cancer (CRC) incidence remains disproportionately high in rural agricultural regions, including Arkansas, where environmental exposures may contribute to persistent cancer disparities. Yet, ambient community-level herbicide exposures have been minimally studied as potential CRC risk factors, representing an important knowledge gap. To identify candidate environmental contributors, we integrated county-level air pollutant emission estimates from the EPA AirToxScreen dataset with age-adjusted CRC incidence from the National Cancer Institute State Cancer Profiles. Screening 133 pollutants in Arkansas identified 2,4-dichlorophenoxyacetic acid (2,4-D), one of the most widely used herbicides in U.S. agriculture, as the exposure most strongly correlated with CRC incidence (Spearman $\rho = 0.338$, $p = 0.003$). Linear regression indicated that each one-log-unit increase in 2,4-D emissions corresponded to 6.28 additional CRC cases per 100,000 population ($p = 0.001$), with similar associations in rural and urban strata. Extension to 2,555 U.S. counties demonstrated a consistent association nationally ($\beta = 5.94$, $p < 0.001$). Spatial error regression improved model fit and confirmed the association after accounting for geographic autocorrelation ($\beta = 2.55$, $p = 0.001$). Adjustment for county-level poverty modestly strengthened the association ($\beta = 2.81$, $p < 0.001$), suggesting that both socioeconomic conditions and herbicide exposure may jointly contribute to CRC burden in agricultural regions. While ecological and not causal, this study is among the first to evaluate ambient, population-level 2,4-D exposure rather than occupational exposure, and demonstrates a spatial epidemiologic approach for identifying environmental carcinogen candidates relevant to precision public health and rural cancer equity. These findings support the need for follow-up studies integrating individual-level exposure biomarkers, mechanistic data, and targeted CRC screening strategies in high-exposure regions.

#6244 Agricultural glyphosate use and early-onset colorectal cancer mortality in the United States.

Jiayu Lin[1], Malia Cortez[1], Caroline Nondin[1], Seigi Karasaki[2], Sam L. S. Chao[3], Trang VoPham[1]

[1]Epidemiology Program, Public Health Sciences Division, Fred Hutchinson Cancer Center, Seattle, WA,[2]Fred Hutchinson Cancer Center, Seattle, WA,[3]Public Health Sciences Division, Fred Hutchinson Cancer Center, Seattle, WA

PURPOSE Early-onset colorectal cancer (CRC) (diagnosis before age 50 years) incidence has risen dramatically. Individuals born in the 1990s compared to the 1960s have a four-fold higher risk for early-onset CRC. Recent evidence suggests that risk factors experienced in early life and/or emerging in relatively later generations may play an etiologic role in early-onset CRC. One environmental exposure potentially contributing to the surge in early-onset CRC is glyphosate, the most widely utilized herbicide in the world that substantially increased in usage following the introduction of glyphosate-resistant crops in 1996. Glyphosate is hypothesized to promote colorectal carcinogenesis through mechanisms such as gut microbiome dysbiosis. Our objective was to conduct an epidemiologic study examining the association between agricultural glyphosate use and risk for early-onset CRC-specific mortality in the United States.

METHODS We extracted mortality and sociodemographic data from death certificates of all individuals in the United States who died from early-onset CRC (defined as death before age 50) (ICD-9 153.0-153.4, 153.6-154.1; ICD-10 C18.0, C18.2-C18.9, C19, C20) from 1989-2023 from the National Center for Health Statistics. Annual average glyphosate use was estimated by linking nationwide agricultural pesticide application data from the United States Geological Survey with the year and county of residence at death. Quasi-Poisson regression with robust standard errors was used to estimate mortality rate ratios (MRRs) with 95% confidence intervals (CIs) for the association between glyphosate use and early-onset CRC-specific mortality risk adjusted for individual-level age, sex, race, ethnicity, year, marital status, and education level, and county-level socioeconomic status.

RESULTS A total of 108,315 deaths from CRC among those <50 years old were included in this study. We observed a statistically significant dose-response relationship, in which higher annual average glyphosate use was associated with incremental increases in risk for CRC-specific mortality (adjusted MRR highest quintile (>5.74 kg/km2) vs. lowest quintile (<=0.08 kg/km2): 1.10, 95% CI 1.06-1.13; p trend <0.0001).

CONCLUSIONS Higher agricultural glyphosate use was associated with increased risk for early-onset CRC-specific mortality in the United States. Future research should further explore the role of glyphosate in early-onset CRC through examining incidence outcomes and life-course exposures using residential address histories.

#6245 Lead Bioaccumulation Drives Genomic Instability and Apoptotic Resistance in Human Breast Cancer.

Rita Bonfiglio, Anatomical Pathology Tor Vergata, Manuel Scimeca

Experimental Medicine, University of Rome Tor Vergata, Rome, Italy

Introduction: Lead (Pb) is a widespread environmental toxicant classified by IARC as a probable human carcinogen, yet its mechanistic involvement in breast cancer remains poorly defined. Epidemiological studies suggest an association between Pb exposure and breast cancer risk, but tissue-level data linking Pb accumulation to molecular cancer features are limited. Understanding whether Pb bioaccumulates within breast tumors and influences key cancer hallmarks may reveal overlooked environmental determinants of breast cancer progression.
Methods: Formalin-fixed paraffin-embedded breast cancer samples from 26 female patients. Lead concentration was quantified using inductively coupled plasma mass spectrometry (ICP-MS). Whole-genome sequencing and RNA-seq were performed on frozen tumor aliquots (n = 21), enabling assessment of Tumor Mutational Burden (TMB), Microsatellite Instability (MSI), mutational signatures, and PAM50 molecular subtypes. Spearman correlation, bootstrap confidence intervals, and non-parametric tests assessed relationships between Pb concentration and clinicopathological or molecular variables.
Results: Lead was detected in 100% of breast cancer samples, with a mean concentration of 18.2 ± 16.2 mg/kg (range: 0.2-310 mg/kg). Lead levels showed no association with age or classical pathological features, including histologic grade ($p = 0.8$) and lymph-node metastasis ($p = 0.6$). Notably, Pb concentration was independent of PAM50 subtypes, suggesting that Pb accumulation reflects a biological dimension distinct from established intrinsic classifications.A significant relationship emerged between Pb accumulation and genomic instability. Lead concentration strongly correlated with TMB ($\rho = 0.87$; $p < 0.0001$) and MSI ($\rho = 0.79$; $p < 0.0001$). Tumors with the highest Pb levels also harbored TP53 missense mutations and frameshift deletions, underscoring a link between Pb burden and DNA repair pathway dysregulation. These findings support a model in which Pb bioaccumulation promotes mutational processes, potentially via disruption of mismatch repair mechanisms.Pb concentration was also positively associated with expression of BCL2 ($\rho = 0.66$; $p = 0.001$) and p53 ($\rho = 0.65$; $p = 0.002$), pointing toward enhanced resistance to regulated cell death.
Conclusion: Data here reported highlighted the need to incorporate environmental metal burden into breast cancer risk assessment particularly for patients exhibiting elevated TMB/MSI who may benefit from immunotherapy.

#6246 Associations between natural radionuclides in borehole water and cancer risks: A comprehensive population-based study from Finland.

Peng Li[1], Pekka Martikainen[2], Mikko Myrskyla[1]

[1]Max Planck Institute for Demographic Research (MPIDR), Rostock, Germany,[2]University of Helsinki, Helsinki, Finland

Background:
Carcinogenic effects of radioactive elements in environmental background for all cancer types have not been fully investigated.
Methods:
This paper assesses the associations between radioactive elements in borehole water and all cancer types based on total Finnish population. National registries of the general population living continuously in Finland during 1987-2016 were linked to annual municipality-level concentrations of uranium (Ur) and radon (Rn) in borehole water. Average radiation exposures over 30 years were calculated individually based on residential location annually. Newly diagnosed cancers were followed from 2017 until 2021 based on national cancer registry. Associations between exposures and cancer incidences were assessed via Cox proportional hazards models, adjusted for pre-existing health conditions and socio-economic factors. Multiplicity was adjusted using Bonferroni correction.
Results:
Totally 1,013,054 men and 1,101,589 women with non-missing municipality-level exposures were included. During follow-up period, totally 62,085 cancer cases of 70 sub-types were diagnosed in men and 57,627 cancer cases of 73 sub-types were diagnosed in women respectively. Significant associations between environmental radiation exposures and elevated risks of cancer were observed in men (Ur: hazard ratio [HR] 1.05, 95% confidence interval [CI] 1.03-1.07; Rn: 1.04, 1.02-1.05) and women (Ur: 1.07, 1.05-1.09; Rn: 1.05, 1.03-1.07). After correction of multiplicity, significantly elevated risks were observed for cancers of uncertain lymphoid and hematopoietic tissue (1.66, 1.39-1.97), mesothelioma (1.48, 1.18-1.86), myeloma (1.36, 1.18-1.57), melanoma (1.31, 1.22-1.40), leukemia lymphoid (1.28, 1.12-1.48) in men with higher exposure to Ur; and Polycythemia vera (1.79, 1.30-2.45), uncertain lymphoid and hematopoietic tissue (1.61, 1.36-1.91), myeloma (1.52, 1.32-1.75), melanoma (1.22, 1.14-1.31) and bladder (1.20, 1.08-1.32) with higher exposure to Rn. Significantly elevated risks were observed for uncertain lymphoid and hematopoietic tissue (1.78, 1.52-2.08), leukemia lymphoid (1.48, 1.24-1.77), melanoma (1.33, 1.24-1.44), lung (1.26, 1.19-1.34) and breast (1.07, 1.04-1.10) in women with higher exposure to Ur; and uncertain lymphoid and hematopoietic tissue (1.73, 1.48-2.03), Polycythemia vera (1.72, 1.26-2.35), myeloma (1.51, 1.30-1.75), melanoma (1.28, 1.19-1.38) and lung (1.21, 1.14-1.29) with higher exposure to Rn. In sensitivity analysis, similar patterns were observed in samples who only lived in houses during 1987-2016. Dosage-response trends were observed for total cancer risks in men and women respectively.
Interpretation:
High environmental radiation exposures were significantly associated with elevated total cancer risks and several sub-types in the general population.

#6248 Long-term air pollution and lung cancer incidence by histological subtypes.

Sun-Young Kim, Jeongho Park, Miyoun SHIN, Yoon-Jung Choi

National Cancer Center, Goyang, Korea, Republic of

Background: There is mounting evidence of long-term exposure to air pollution and incidence of lung cancer based on large cohort studies worldwide. A few subsequent studies have suggested that the association may vary by histological subtypes, although findings have been inconsistent. This study aimed to investigate whether air pollution affects a specific histological subtype of lung cancer more than the others using a population-representative cohort including 2 million adults.
Methods: Our study population includes 2,346,332 adults who were aged 30 years or over in 2007, participated in health examinations for 2005-2007, and were retrospectively followed-up until 2020 in the National Health Insurance Services database linked with the Korea Central Cancer Registry of South Korea. We identified lung cancer incidence of three histological subtypes, including adenocarcinoma (AD), squamous cell carcinoma (SqCC), and small cell carcinoma (SCC), based on the International Classification Diseases for Oncology. Individual-level long-term exposures to particulate matter ≤ 2.5 $\mu g/m^3$ in diameter ($PM_{2.5}$) and nitrogen dioxide (NO_2) were 5-year average concentrations estimated at district-level home addresses by previously-validated exposure prediction models. Then, we applied time-varying Cox proportional hazard model to estimate hazard ratios of lung cancer incidence for 10 $\mu g/m^3$ and 10 ppb increases in $PM_{2.5}$ and NO_2 respectively.
Results: For 20,811 new lung cancer cases occurred over 13 years, AD, SqCC, and SCC made up 52, 21, and 10 %, respectively. We found no association of total lung cancer incidence for both pollutants ($PM_{2.5}$: HR=1.065, 95% CI=0.957–1.186; NO_2: 0.980, 0.957–1.004). However, $PM_{2.5}$ was associated with SqCC (1.353, 1.054 –1.738), but not associated with AD (0.892, 0.722–1.038) and SCC (1.148,0.818–1.609). In contrast, NO_2 showed the association for AD (1.064, 1.027–1.102) but not for SqCC 0.905 (0.861 – 0.951) and SSC 0.956 (0.888 – 1.029).
Discussion: Our findings of different associations by pollutants and histological subtypes suggest different mechanistic roles in lung cancer development depending on the pollutant.

#6249 PM2.5 and black carbon levels associated with increased mortality in lung cancer patients.

Victoria A. Chu[1], Xianhong Xie[1], Kith Pradhan[1], George S. Downward[2], Thomas E. Rohan[1], Haiying Cheng[3], Brendon Stiles[4], Xiaonan Xue[1], Tamar Nobel[5], Aditi Shastri[6], H. Dean Hosgood[1]

[1]Department of Epidemiology and Population Health, Albert Einstein College of Medicine, Bronx, NY,[2]Department of Population Health Sciences, Utrecht University, Utrecht, Netherlands,[3]Departments of Oncology and Medicine, Albert Einstein College of Medicine, Bronx, NY,[4]Departments of Oncology, Medicine, Cardiothoracic & Vascular Surgery, Albert Einstein College of Medicine, Bronx, NY,[5]Departments of Epidemiology and Population Health, Cardiothoracic & Vascular Surgery, Albert Einstein College of Medicine, Bronx, NY,[6]Departments of Oncology, Medicine, Developmental & Molecular Biology, Albert Einstein College of Medicine, Bronx, NY

Lung cancer is the leading cause of cancer mortality in the United States. Over recent years, lung cancer incidence among never-smokers has been rising. Additionally, heterogeneity in treatment responses among patients with lung cancer have not been fully elucidated. Outdoor air pollution (OAP) is a known lung carcinogen, but little is known about the effects of OAP on lung cancer survival and prognosis. Therefore, this study aimed to assess the association between OAP exposure and lung cancer survival. A retrospective cohort study was conducted by gathering patient and clinical data from a cohort of 8,793 non-small cell lung cancer (NSCLC) patients from the Montefiore Einstein Comprehensive Cancer Center (MECCC) in the Bronx, NY. Environmental exposure to OAP was estimated based on the patients' geo-coded addresses. Pollutants were estimated by combining Aerosol Optical Depth retrievals from different instruments with the GEOS-Chem chemical transport model. The data were calibrated to regional ground-based observations using a geographically weighted regression. Quantitative analyses were performed using Kaplan-Meier curves and Cox proportional hazard models. Stepwise regression model selection for confounding variables, including smoking, sex, age, histology, stage, treatment (transplant, surgery, chemotherapy, radiation), and other pollutants (NH_4, organic matter, SO_4) was used. Exposure to >9ug/m^3 of PM2.5 and >median levels of Black Carbon at the time of diagnosis were associated with an 8% and 6% decrease in overall lung cancer survival, respectively ($p<0.0001$). PM2.5 was associated with decreased lung cancer survival by 5-9% in all sex, smoking, and histology groups ($p<0.0001$). Black Carbon was associated with a 4-9% decrease in lung cancer survival in male ($p=0.01$), female ($p<0.0001$), never ($p=0.05$) or ever ($p<0.0001$) smoker, and Adenocarcinoma ($p<0.0001$) subgroups. Consistent with previous studies, we observed an association between PM2.5 exposure and decreased lung cancer survival. Black Carbon, not tested in previous studies, was also associated with decreased lung cancer survival. Future research is needed to explore the relationship(s) between additional geospatially correlated exposures, OAP, and lung cancer survival.

#6250 Chemical composition of fine particulate matter and mortality of older lung cancer patients.

Jiaowei Gong[1], Edgar Castro[2], Min Zhang[3], Robert O. Wright[3], Christine C. Ekenga[4], Joel D. Schwartz[2], **Yaguang Wei**[3]

[1]Department of Global Health and Population, Harvard T.H. Chan School of Public Health, Boston, MA, [2]Department of Environmental Health, Harvard T.H. Chan School of Public Health, Boston, MA, [3]Department of Environmental Medicine, Icahn School of Medicine at Mount Sinai, New York, NY, [4]Emory University, Rollins School of Public Health, Atlanta, GA

Importance: Lung cancer mortality remains elevated despite advances in treatment. Although ambient fine particulate matter ($PM_{2.5}$) has been identified as Group 1 carcinogen for lung cancer, which increases the incidence, the role of chemical components in mortality of lung cancer patients and the identification of harmful components and susceptible groups remain unclear.
Objective: To evaluate whether long-term exposure to $PM_{2.5}$ chemical components is associated with all-cause mortality among lung cancer patients, and whether the associations differ by histology and stage at diagnosis, demographics, and comorbidity.
Design, Setting, and Participants: This cohort study derived from the SEER-Medicare database that identifed 495,339 adults aged ≥65 years with lung cancer diagnosed between 2000 and 2019. Patients were followed annually from diagnosis until death, loss to follow-up, or the end of 2019 (mean follow-up, 4.1 years). The SEER-Medicare database provided longitudinal residential ZIP code, demographics, cancer-specific characteristics, and comorbidities.
Exposures: Annual exposures to 15 $PM_{2.5}$ chemical components were estimated from 2000 to 2019 using high-resolution spatiotemporal models and linked to each patient based on residential ZIP code in each year.
Main Outcome: The primary outcome was the relative risk of all-cause mortality, measured from the year of lung cancer diagnosis until death or the end of follow-up. We used generalized weighted quantile sum regression to estimate both cumulative effects of annual exposure to all components and individual contributions for each component, adjusted for demographic, cancer-specific characteristics (histology, stage, treatment), comorbidities, and neighborhood-level covariates.
Results: Joint exposure to $PM_{2.5}$ components was associated with increased all-cause mortality, with relative risk [RR] being 1.012 (95% confidence interval [CI], 1.011-1.014) per decile increase in all components. Iron contributed most strongly (8.3% of total effects), followed by organic carbon, vanadium, ammonium, bromine, and silicon. Associations were stronger among patients with non-small cell lung cancer, particularly squamous cell carcinoma, as well as among women and those with regional-stage disease.
Conclusions and Relevance: Long-term exposure to $PM_{2.5}$ components was linked to greater mortality among patients with lung cancer, especially in those diagnosed with non-small cell and squamous cell carcinoma, women, and with advanced stage. Chemical components that contributed most to this effect emitted from traffic, power generation, biomass burning, and heavy fuel oil, highlighting the need for targeted emission reductions to improve outcomes in high-risk populations.

#6251 Long-term exposure to wildfire smoke $PM_{2.5}$ and survival of older lung cancer patients.

Min Zhang[1], Juan P. Wisnivesky[2], Minghao Qiu[3], Mahdieh Danesh Yazdi[4], Rosalind J. Wright[5], Joel D. Schwartz[6], Christine C. Ekenga[7], Robert O. Wright[1], **Yaguang Wei**[1]

[1]Environmental Medicine, Icahn School of Medicine at Mount Sinai, New York, NY,[2]Medicine, Icahn School of Medicine at Mount Sinai, New York, NY,[3]School of Marine and Atmospheric Sciences, Stony Brook University, Stony Brook, NY,[4]Family, Population, and Preventive Medicine, Stony Brook University, Stony Brook, NY,[5]Public Health, Icahn School of Medicine at Mount Sinai, New York, NY,[6]Environmental Health, Harvard T.H. Chan School of Public Health, Boston, MA,[7]Emory University, Rollins School of Public Health, Atlanta, GA

Importance Fine particulate matter ($PM_{2.5}$) is a key risk factor of lung cancer incidence and mortality. However, the specific effect of $PM_{2.5}$ originating from wildfire smoke, an increasingly important contributor to total $PM_{2.5}$ in the US driven by climate change, on mortality of patients with lung cancer remain unclear.

Objective To explore the effect of long-term exposure to wildfire smoke versus non-smoke $PM_{2.5}$ on all-cause mortality of older lung cancer patients.

Design, Setting, and Participants This cohort study included patients ≥65 years with primary diagnosis of lung cancer from the SEER-Medicare database from 2006 to 2019 linked with estimates of exposure to wildfire smoke and non-smoke $PM_{2.5}$ based on patients' residential zip codes.

Exposures Three-year moving average exposures to wildfire smoke and non-smoke $PM_{2.5}$.

Main Outcomes and Measures The study outcome was all-cause mortality after primary lung cancer diagnosis. A time-varying Cox proportional hazards model was applied to estimate hazard ratios (HRs) for mortality risk.

Results Among 503,409 patients with 1,542,491 person-years of follow up, each 1-μg/m³ increase in wildfire smoke $PM_{2.5}$ was associated with a 9.3% increased mortality risk (HR: 1.09, 95% CI: 1.08-1.11), substantially greater than that of non-smoke $PM_{2.5}$ (HR: 1.020, 95% CI: 1.018-1.022). The number of smoke days and of smoke waves, reflecting duration and frequency of wildfire smoke $PM_{2.5}$ exposure, were also positively associated with mortality risk. Larger effect of wildfire smoke $PM_{2.5}$ was observed among women, patients with lung cancer other than non-small cell lung cancer, patients with comorbidities, and those not receiving first course treatment after diagnosis.

Conclusions Wildfire smoke posed a substantially larger risk in older lung cancer patients than non-smoke $PM_{2.5}$. Under a changing climate, strengthening wildfire management and reducing wildfire smoke exposure in clinical care could improve survival of older lung cancer patients.

HR for mortality and corresponding annual excess deaths associated with smoke and non-smoke PM2.5

Three-year moving average wildfire smoke $PM_{2.5}$ exposure	Hazard ratio (95% CI)	Annual excess deaths (95% CI)
Concentration, per 1-μg/m^3 increase		
Smoke $PM_{2.5}$	1.0927 (1.0801, 1.1055)	2,908 (2,513, 3,310)
Non-smoke $PM_{2.5}$	1.0202 (1.0182, 1.0222)	634 (571, 696)
Smoke-event duration and frequency, per day/event increase		
Number of smoke days	1.0040 (1.0037, 1.0043)	125 (116, 135)
Number of smoke waves	1.0209 (1.0185, 1.0233)	656 (580, 731)

#6253 Spatial association between thyroid cancer incidence and environmental carcinogen emissions in Korea.

Taehoon Kim, Sangjun Lee, Sue K. Park

Department of Preventive Medicine, Seoul National University, Seoul, Korea, Republic of

Background: Thyroid cancer is the most commonly diagnosed cancer in Korea, with a recent resurgence in incidence since 2016. Environmental and occupational exposures—including air pollutants such as nitrogen dioxide (NO_2), particulate matter (PM2.5), ozone (O_3), and industrial chemicals such as toluene and mercury—have been reported as potential risk factors. This study examined whether regional variation in thyroid cancer incidence across Korea can be explained by differences in community-level carcinogenic emissions.
Methods: An ecological study was conducted across 229 districts in Korea, using thyroid cancer incidence (ICD-10: C73) from 2014-2018 as the outcome. Exposure variables were district-level annual emissions of carcinogenic substances reported in the Pollutant Release and Transfer Register (PRTR), aggregated into three latency-reflective periods (2004-2008; 2009-2013; 2004-2013). Missing emission values were spatially interpolated using Bayesian spatial assumptions. Covariates included demographic (sex ratio, proportion aged 25-44), behavioral (smoking, obesity), and socioeconomic indicators (number of physicians per 1,000 population, basic livelihood recipient rate). Bayesian hierarchical Poisson models with BYM2 spatial structure were fitted using Integrated Nested Laplace Approximation (INLA). Model fit was assessed using WAIC, and relative risks (RRs) were estimated for each exposure period.
Results: Higher district-level carcinogen emissions were associated with increased thyroid cancer incidence. In baseline models, a 1-unit increase in log-transformed emissions corresponded to RRs ranging from 1.037 to 1.051 across exposure periods. Spatially interpolated emission datasets showed similar associations (RR 1.037-1.041). In adjusted models controlling for demographic, behavioral, and socioeconomic factors, associations remained directionally consistent, with RRs between 1.023 and 1.028 for raw emission data and 1.024-1.025 for interpolated data. Spatial clusters of high relative risk were identified in urbanized and industrialized regions.
Conclusions: Districts with higher emissions of carcinogenic substances exhibited increased thyroid cancer incidence after accounting for spatial dependence and community-level covariates. These findings support the hypothesis that environmental pollution from industrial facilities contributes to regional disparities in thyroid cancer and that latency windows of 5-10 years are relevant. Future research should incorporate refined exposure assessments at the individual level, improved temporal matching, and linkage to targeted prevention or screening strategies for high-risk regions.

#6254 Pre-diagnosis green space exposure and survival in women diagnosed with ovarian cancer.

Jaileene Perez-Morales[1], Hari S. Iyer[2], Jaime E. Hart[3], Francine Laden[4], Laura D. Kubzansky[5], Joshua M. Moreau[1], Guillermo Armaiz-Pena[6], Shelley Tworoger[1], **Charlotte Roscoe**[1]

[1]Division of Oncological Sciences, OHSU Knight Cancer Institute, Portland, OR,[2]Rutgers Cancer Institute of New Jersey, New Brunswick, NJ,[3]Channing Division of Network Medicine, Department of Medicine, Brigham and Women's Hospital and Harvard Medical School, Boston, MA,[4]Department of Environmental Health, Harvard T.H. Chan School of Public Health, Boston, MA,[5]Department of Social and Behavioral Sciences, Harvard T.H. Chan School of Public Health, Boston, MA,[6]Cancer Biology and Women's Health Divisions, Ponce Health Sciences University School of Medicine, Ponce, PR

Background: Despite treatment advances, the five-year relative survival is 50% for patients with invasive ovarian cancer. Increasing literature demonstrates that distress, depression, and other psychosocial stressors negatively influence survival. Exposure to green spaces - e.g., parks, gardens, forests and street trees - has been associated with lower stress hormone levels and reduced risk of depression. Thus, our objective was to evaluate if greenness exposure, pre-diagnosis, was associated with improved ovarian cancer survival among cases in the Nurses' Health Study (NHS) and NHSII cohorts.

Methods: Greenness exposure was assessed seasonally within nearby (270m) and walkable (1230m) distance buffers surrounding NHS and NHSII cohort participants' residential addresses (updated biennially from 1988 to 2018) using the Normalized Difference Vegetation Index (NDVI; $30m^2$ resolution)-a satellite-derived indicator of photosynthetic vegetation cover. We used time-varying Cox proportional hazards models to assess cumulative, pre-diagnosis, maximum average NDVI exposure and ovarian cancer specific survival among confirmed cases. Models were adjusted for age and calendar time, US region, population density, and pre-diagnosis factors associated with ovarian cancer survival, including menopause status, family history of breast or ovarian cancer, and parity. Time-varying depression - self-reported antidepressant use or clinician diagnosed depression - was additionally adjusted to evaluate potential mediation of the relationship between greenspace exposure and survival.

Results: Analyses included 1,052 women with confirmed ovarian cancer. We observed a suggestive decrease in ovarian cancer mortality risk for a 0.1 unit (10%) increase in cumulative pre-diagnosis 270m NDVI exposure (aHR 0.92; 95% CI 0.79, 1.07) when adjusting for all factors except depression. Adding depression led to a slightly stronger inverse association (aHR 0.90 95% CI 0.76, 1.07), although it did not reach statistical significance. No association was observed for cumulative pre-diagnosis 1230m NDVI exposure.

Conclusions: Pre-diagnosis near-residence greenness exposure was suggestively associated with improved survival among ovarian cancer cases. Adjusting for depression status slightly strengthened the inverse association, indicating that the association of greenness with survival is unlikely to be fully explained by depression status; other potential mechanistic pathways (e.g., pollution and temperature reduction, improved sleep quality, physical activity, vitamin D levels and immune function) should be explored. On-going analyses will assess associations by histologic subtype. Future studies are needed to assess the type and quality of nature exposure, including but not limited to green spaces, with risk and survival among patients, with stratification by geographic and ecological regions.

#6255 Occupation and breast cancer risk in the Long Island Breast Cancer Study Project cohort.

Hannah M. Thompson[1], Susan L. Teitelbaum[1], Yaguang Wei[1], Zoey Laskaris[2]

[1]Environmental Medicine, Icahn School of Medicine at Mount Sinai, New York, NY,[2]Barry Commoner Center for Health and the Environment, Queens College, New York, NY

Purpose: Work is a modifiable risk factor that may influence breast cancer incidence, yet the role of specific occupations is understudied. We evaluated associations between longest held job and breast cancer incidence in the well-characterized Long Island Breast Cancer Study Project (LIBCSP).
Methods: The LIBCSP, a population-based case-control study, enrolled women with first primary invasive and in situ breast cancer diagnosed between 1996-1997. Frequency matched controls were identified via random digit dialing and Health Care Finance Administration rosters. Socioeconomic (race, ethnicity, and education), reproductive (parity, age at first birth, lactation, age of menarche, family history of breast cancer, and use of oral contraceptives and hormone replacement therapy), and lifestyle (body mass index, alcohol use, and smoking status) factors were collected via interviewer-administered questionnaires. Self-reported occupational histories were coded using the 1980 Standard Occupational Classification (SOC) and 1987 Standard Industrial Classification systems, then crosswalked to the 2018 SOC and 2017 North American Industry Classification System codes. Participants without at least one occupation held for >1 year were excluded. Multivariable logistic regression estimated the odds ratio (OR) for breast cancer using longest held minor occupation group as the exposure and other longest held minor occupation groups as the reference, adjusting for key factors as above. Effect modification by menopausal status was examined.
Results: Analyses included 3001 study participants (1468 cases and 1533 controls). Most participants were non-Hispanic White. Cases were older at first birth ($p=0.03$) and more likely to have a first degree relative with breast cancer ($p <0.001$). The average duration of the longest held job was 13.0 years among cases and 12.2 among controls. Most occupations were not associated with breast cancer risk. However, elevated risks were observed for financial clerks (OR=1.54, 95% confidence interval [CI] 1.10-2.14) and personal appearance workers (OR=2.02, 95%CI 1.07-3.78) compared with all other occupations when controlling for socioeconomic, reproductive, and lifestyle factors. Stratified analyses indicated increased risk among pre-menopausal financial clerks and post-menopausal personal appearance workers.
Conclusions: Specific occupations, financial clerk and personal appearance worker, were independently associated with increased risk of breast cancer. Future work will seek to better understand the relationship between work and breast cancer risk by evaluating industry and occupation types based on exposure, which may further delineate why certain jobs are associated with an increased risk of breast cancer. Incorporating occupational history into population-based cancer research may identify important cancer risk prevention opportunities.

#6256 Leveraging the Healthy Oregon Project (HOP) to evaluate environmental exposures during critical reproductive periods and young-onset breast cancer risk.

Charlotte Roscoe[1], **Sofia I. Chapela Lara**[2], Wesley Stoller[1], Marit Simmons[1], Hailey Brack[1], Jackilen Shannon[1], Pepper J. Schedin[1], Zhenzhen Zhang[1]

[1]Division of Oncological Sciences, OHSU Knight Cancer Institute, Portland, OR,[2]School of Public Health, Oregon Health & Science University, Portland, OR

Background: Young-onset breast cancer (YOBC), diagnosed before age 50, has twice the mortality of cases diagnosed ≥50. In the US, YOBC diagnoses increased by 1.4% annually from 2012-2021, with higher increases in non-metropolitan vs. metropolitan areas in western states. Geographic disparities may be influenced by environmental factors, such as neighborhood socioeconomic context, limited healthcare access, and exposure to environmental hazards (e.g., pesticides, per- and polyfluoroalkyl substances [PFAS]-contaminated water, wildfire smoke), which have been associated with breast tissue inflammation and increased breast cancer risk. Shifts in critical reproductive periods (e.g., menarche, delayed childbirth, menopause) and parity or nulliparity, which may be shaped by these environmental factors, may also affect risk and interact synergistically with environmental stressors. Our objective was to assess environmental exposures during critical reproductive periods to evaluate YOBC risk in a western US state with strong urban-rural environmental exposure contrasts.
Methods: We used the Healthy Oregon Project (HOP) - a statewide prospective cohort of >50,000 Oregonians - to assess rurality of residential addresses of enrolled females, 18-49 years old, diagnosed with YOBC. Cases were identified via self-report on the HOP baseline questionnaire. Baseline residential addresses were linked to the USDA Economic Research Service's Rural Urban Commuting Area (RUCA) codes, and classified as Urban (codes 1-3), Rural (codes 4-9), or Frontier (code 10). A supplementary reproductive lifecourse questionnaire, including residential addresses during critical reproductive windows, is in development to allow us to link spatial datasets (e.g., fine particulate air pollution [$PM_{2.5}$], wildfire smoke, temperature, PFAS in water, land cover, agricultural pesticides) to YOBC cases and matched controls.
Results: HOP has consented 51,978 Oregonians (~1.5% of the state's 3.4 million adult residents). On baseline questionnaires, 37,695 (72.5%) identified as female at birth, and 615 reported a YOBC diagnosis. Overall, participants resided in Urban (72.5%), Rural (13.5%) and Frontier (1.9%) areas, with 12.1% missing. Those diagnosed with YOBC showed a similar distribution (79.8%, 13.5% and 2.3%, respectively; 4.4% missing).
Conclusion: Rurality of HOP participants' residences was similar across those with YOBC and the overall cohort; this distribution is representative of Oregon's urban-rural composition. Future analyses will link historic residential addresses during critical reproductive windows across the lifecourse to spatiotemporally aligned environmental and socioeconomic exposure data to evaluate how cumulative, and potentially synergistic, environmental exposures contribute to YOBC risk.

#6257 Associations of area level deprivation with survival outcomes among patients with newly diagnosed colorectal cancer considered across the lifespan.

Jessica R. Burns[1], Maria F. Gomez[2], Stephanie Hogue[1], Esther Jean-Baptiste[1], Julaxis Love[1], Erin Siegel[2], Adetunji T. Toriola[3], Christopher I. Li[4], Jane C. Figueiredo[5], Nicole C. Lorona[5], Biljana Gigic[6], David Shibata[7], Seth Felder[8], Patricia A. Erickson[9], Mmadili N. Ilozumba[9], Ildiko Strehli[9], Megan Mclaws[9], Victoria Damerell[6], Shaneda Warren Andersen[10], Caroline Himbert[9], Cornelia M. Ulrich[9], Sheetal Hardikar[9], Doratha A. Byrd[2]

[1]Non-Therapeutic Research Office, Moffitt Cancer Center, Tampa, FL,[2]Department of Cancer Epidemiology, Moffitt Cancer Center, Tampa, FL,[3]Siteman Cancer Center, Washington University School of Medicine in St. Louis, St. Louis, MO,[4]Division of Public Health Sciences, Fred Hutchinson Cancer Center, Seattle, WA,[5]Department of Medicine at Samuel Oschin Comprehensive Cancer Institute, Cedars-Sinai Medical Center, Los Angeles, CA,[6]Department of General, Visceral and Transplantation Surgery, Heidelberg University Hospital, Heidelberg, Germany,[7]Department of Surgery, University of Tennessee Health Science Center, Memphis, TN,[8]Department of Gastroenterological Oncology, Moffitt Cancer Center, Tampa, FL,[9]Huntsman Cancer Institute, Salt Lake City, UT,[10]University of Wisconsin, Madison, WI

Background: Colorectal cancer (CRC) is the second overall leading cause of cancer-related deaths in the United States (US). The Area Deprivation Index (ADI), a neighborhood socioeconomic disadvantage measure, reflects multiple CRC survival-related exposures including access to resources, healthcare, quality of life, and other opportunities for economic mobility. These exposures may vary by birth cohort, making it important to examine ADI across age of onset. The purpose of this study is to investigate the associations of ADI with overall (OS) and disease-free survival (DFS) by age of onset (early: <50 years (EO), average: 50-64 years (AO), older: ≥65 years (LO)) in the ColoCare Study.

Methods: We included US data from the ColoCare Study, a prospective multicenter cohort study of newly diagnosed stage I-IV CRC patients. National- and state-level ADI were calculated using residential addresses captured at study entry. We compared ADI across ages of onset and estimated hazard ratios (HRs) and 95% confidence intervals (95% CI) for the associations of ADI with OS and DFS using multivariable Cox proportional hazard models, overall and stratified by age of onset, race, and ethnicity.

Results: There were 2,477 participants from the ColoCare study with ADI data, with a median follow-up time of 3.6 years (SD=2.5) starting at the date of diagnosis and ending at the date of death, last follow-up, or censored at 5 years. On average, individuals in the LO group had higher national ADI (mean=4.08 [2.81]) compared to the AO group (mean=3.93 [2.85]; P<0.001) and early onset group (mean=3.49 [2.72]; P<0.001]). Survival associations of the ADI based on national percentiles tended to be stronger than those based on the state. Considered per 10-percentile increase in national-level ADI, there was an 8% (95% CI=1.01, 1.15; P=0.02) and 10% (95% CI= 1.01, 1.21; P=0.03) higher overall mortality risk among LO and EO groups, respectively. After adjusting national-level ADI for race, there was a 6% and 3% higher overall mortality risk among the LO and AO groups, respectively. Among average onset individuals, the association of the ADI measures with OS was closer to the null and not statistically significant. Associations of ADI with DFS were weaker and not statistically significant among the EO and LO groups, but the ADI was positively associated with DFS among the AO groups (HR_{DFS} =1.09; 1.01-1.16; P=0.02). Though not statistically significant, the associations of ADI with OS and DFS were strongest among Non-Hispanic Black individuals (HR_{OS} = 1.12; 95% CI=0.92, 1.36; P=0.27; and HR_{DFS} =1.14; 0.93-1.40; P=0.20).

Conclusion: We observed that older CRC survivors tended to live in more deprived areas; however, across the lifespan, area level determinants of health were associated with poorer CRC survival outcomes.

#6258 Age at menopause, epigenetic aging, and cancer risk: A secondary analysis of the PLCO Trial.

Tiffany Y. Pei[1], Ting Zhai[2], Jinyoung Byun[1], Vernon S. Pankratz[1], Shuguang Leng[1]

[1]Department of Internal Medicine, University of New Mexico, Albuquerque, NM,[2]Department of Environmental Health, Harvard T.H. Chan School of Public Health, Boston, MA

Background: Our previous studies have linked early menopause (early-M, <45 years) with increased risks of lung-related morbidities and mortalities. However, its relationship with other cancer types and the underlying biological and causal mechanisms remains unclear. **Aim**: To conduct a secondary analysis evaluating the associations between early-M and blood-based epigenetic aging biomarkers, and cancer risks and mortalities using the prospective Prostate, Lung, Colorectal, and Ovarian (PLCO) cancer screening trial.
Methods: Genome-wide DNA methylation (DNAm) profiles were available from baseline blood samples in 1,517 PLCO participants who subsequently developed breast cancer or who remained cancer-free. Epigenetic age acceleration was estimated using four established DNAm clocks, HorvathAge, HannumAge, PhenoAge, and GrimAge, as well as DNAm-based telomere length. An epigenome-wide association study (EWAS) was performed followed by pathway enrichment analysis and exploratory analyses integrating immune marker data. For cancer risk and mortality analyses, we included all postmenopausal women of European ancestry with natural menopause from the full PLCO cohort with genotype and phenotype data available (n = 31,022). A polygenic risk score (PRS) for age at natural menopause was constructed using 154 genetic variants identified from the NHGRI-EBI GWAS Catalog, after quality control based on imputation quality, minor allele frequency, Hardy-Weinberg equilibrium, linkage disequilibrium, and ambiguity filtering. The associations between this PRS and cancer incidences and mortalities were modeled using Cox proportional hazards regression.
Results: Phenotypic early-M was associated with higher GrimAge acceleration (0.57 years, 95%CI=0.04, 1.10) in the 1,517 PLCO participants. EWAS and pathway analyses identified CpG sites enriched in estrogen response and immune regulation pathways, consistent with immune marker profiling that revealed upregulation of immune-related proteins among women with early-M. In the full trial, genetically predicted younger age at natural menopause (per 1 SD change) was associated with lower risks of breast cancer incidence (HR=0.14, 95%CI=0,12, 0.16) and longer survival (HR=0.27, 95%CI=0.19. 0.40), and lower risk for incidence of ovarian (HR=0.07, 95%CI=0.04, 0.11) and lung (HR=0.30, 95%CI=0.17, 0.50) cancers. In contrast, a higher incidence of bladder cancer (HR=3.34, 95%CI=1.05, 10.61) was observed. No significant associations were found for colon, melanoma, or hematologic malignancies.
Conclusion: Early-M is associated with accelerated biological aging and distinct immune and hormonal regulatory patterns, with the potential to contribute to heterogeneous cancer risk profiles across cancer types.

#6259 Circadian disruption from time zone position and risk of colorectal cancer precursors in women.

Bethsaida Cardona[1], Trang VoPham[2], Kyriaki Papantoniou[3], Eva Schernhammer[4], Jaime E. Hart[5], Mingyang Song[6], Andrew T. Chan[1]

[1]Clinical and Translational Epidemiology Unit, Department of Medicine, Massachusetts General Hospital, Boston, MA,[2]Fred Hutchinson Cancer Center, Seattle, WA,[3]Barcelona Institute for Global Health (ISGlobal), Barcelona, Spain,[4]Department of Epidemiology, Center for Public Health, Medical University of Vienna, Vienna, Austria,[5]Department of Environmental Heath, Harvard TH Chan School of Public Health, Boston, MA,[6]Department of Epidemiology, Harvard TH Chan School of Public Health, Boston, MA

Background/Aims: Research on the link between circadian disruption, particularly from night shiftwork, and colorectal cancer (CRC) has been limited and inconsistent. Few studies have investigated whether other sources of circadian disruption may be associated with CRC or its precursors. One source is solar jetlag that leads to residents in the western vs. eastern part of a time zone to receive less light exposure in the morning and greater light exposure at night, likely suppressing melatonin release and reducing sleep propensity and sleep duration. The objective of this study was to examine the association between solar jetlag and CRC precursors in the United States.
Methods: Our study consisted of Nurses' Health Study (NHS) II participants who received one or more lower endoscopies between 1991-2015. Cases self-reported colorectal polyps in biennial questionnaires and were confirmed by medical record review. As a proxy for solar jetlag, we calculated the distance from the time zone meridian (TZM), based on participant's geocoded residential address histories, which was modeled as a per 5-degree increase in longitude moving east to west within a time zone. Time-varying multivariable-adjusted logistic regression models for clustered data estimated odds ratios (OR) and 95% confidence intervals (CI).
Results: Over a 24-year follow-up period, 72,612 NHSII participants received at least one lower endoscopy; 4,450 conventional adenomas and 4,873 serrated polyps were diagnosed. We found no statistically significant association between distance to TZM and conventional adenomas (OR=1.03; 95% CI=0.99,1.07) or serrated polyps (OR=0.98, 95% CI= 0.95,1.02). Results were similarly null in analyses stratified by age at endoscopy (<50 vs. ≥ 50 years), polyp size, anatomical location, malignant potential, or reason for endoscopy. We observed statistically significant effect modification in which positive associations were observed in the Mountain time zone, among those never engaging in rotating night shift work, areas with higher ultraviolet radiation, and lower latitudes.
Conclusions: Although we did not observe an association between distance to TZM and CRC precursors, we found significant effect modification in the association by various covariates determined a priori. These findings require further research into the mechanisms of action and confirmation in other cohorts.

#6260 Proteomic aging clock (PAC) is cross-sectionally associated with frailty in cancer survivors: The Atherosclerosis Risk in Communities (ARIC) study.

Shuo Wang[1], Anne H. Blaes[1], Josef Coresh[2], Corinne E. Joshu[3], James S. Pankow[1], Bharat Thyagarajan[1], Weihua Guan[1], Sanaz Sedaghat[1], Anna Kucharska-Newton[4], Elizabeth A. Platz[3], Anna Prizment[1]

[1]University of Minnesota, Minneapolis, MN,[2]New York University Grossman School of Medicine, New York, NY,[3]Johns Hopkins Bloomberg Sch. of Public Health, Baltimore, MD,[4]University of North Carolina, Chapel Hill, NC

Background: Accelerated aging induced by cancer and its treatment contributes to a higher prevalence of frailty in cancer survivors than individuals without cancer. Frailty in cancer survivors poses significant challenges for healthcare providers, as it increases the risk of adverse health outcomes and leads to high rates of hospitalization. However, current frailty assessments often require in-person evaluations in clinics, which can be time-consuming and difficult to perform, particularly in older cancer survivors. Therefore, a biomarker that could predict frailty is needed to facilitate risk stratification in this population. Our previous study suggested that PACs could capture accelerated aging in cancer survivors; however, no previous studies have tested PACs' associations with frailty in cancer survivors. This study examined the cross-sectional associations of a previously validated PAC (Wang et al. [2025]) with frailty in cancer survivors in the ARIC study.
Methods: ARIC is an ongoing cohort of White and Black men and women initiated in 1987. At Visit 5 (2011-13), 5,000 plasma proteins were measured using SomaScan in 3,699 participants without a history of cancer (cancer-free) and 806 cancer survivors, all aged 66-90. We previously created a PAC in 67% of randomly selected cancer-free participants and validated it internally in ARIC and externally in another large cohort. We calculated age acceleration after regressing PAC on chronological age (PAC-accel). At Visit 5, ARIC assessed frailty using the cumulative frailty index (FI) and the Fried Frailty Phenotype (FFP). We examined the cross-sectional associations of PAC-accel with frailty in cancer survivors (after cancer diagnosis), using linear regression for FI and logistic regression for FFP (Frail & Pre-frail vs. Robust). All associations were adjusted for chronological age, sex, race, education, BMI, smoking status, diabetes, cardiovascular disease, and eGFR.
Results: In our study, cancer survivors had a mean FI (SD) of 0.21 (0.10), and 57.8% of them were either frail or pre-frail. Considering the most common cancers (lung, colorectal, breast, prostate), both mean FI and the proportion of frail & pre-frail cancer survivors were highest among lung cancer survivors (0.28 (0.10) and 80%). In all cancer survivors, PAC-accel (per 5 years) was cross-sectionally associated with both FI (difference = 0.04, 95% CI 0.03-0.05) and FFP (OR = 2.56, 95% CI 1.77-3.70). Limited sample size precluded examining associations with frailty by cancer type.
Conclusion: Our findings suggest a cross-sectional association of PAC with frailty. Our next step is to examine whether PAC is associated with future frailty risk. This research will help determine whether PAC holds promise as a tool for frailty risk stratification among older cancer survivors in clinical settings.
Funding: NHLBI, NCI, NPCR

#6261 Inflammation-related exposures and histotype- specific ovarian cancer risk in the Ovarian Cancer Association Consortium (OCAC).

Maxwell Akonde[1], Britton Trabert[2], SHELLEY TWOROGER[3], Allan Jensen[4], Kathryn L. Terry[5], Joshua Sampson[6], Hoda Anton-Culver[7], David Bowtell[8], Elisa V. Bandera[9], Angela Brooks-Wilson[10], Andrew Berchuck[11], Daniel William Cramer[12], Linda S. Cook[13], Julie M. Cunningham[14], Jennifer A. Doherty[15], Ellen L. Goode[16], Marc T. Goodman[17], Holly Ruth Harris[18], Susanne K. Kjaer[19], Nhu Le[20], Alice Wen-Ron Lee[21], Francesmary Modugno[22], Kirsten B. Moysich[23], Celeste Pearce[24], Malcolm C. Pike[25], Harvey A. Risch[26], Mary A. Rossing[27], Joellen M. Schildkrau[28], Daniel O. Stram[29], Rebecca Sutphen[30], David Van Den Berg[31], Penelope M. Webb[32], Anna Wu[33], Argyrios Ziogas[34], Nicolas A. Wentzensen[35]

[1]Division of Cancer Epidemiology and Genetics, National Cancer Institute, Rockville, MD,[2]University of Utah Huntsman Cancer Institute, Salt Lake City, UT,[3]Oregon Health and Science University, Knight Cancer Institute, Portland, OR,[4]Department of Lifestyle, Reproduction and Cancer, Danish Cancer Society Research Center, Copenhagen, Denmark,[5]Asst. Professor, Dept. of OB/GYN, Brigham and Women's Hospital, Boston, MA,[6]Division of Cancer Epidemiology and Genetics, National Cancer Institute, Rocville, MD,[7]Chair & Professor, Dept. of Epidemiology, Department of Medicine, Genetic Epidemiology Research Institute, University of California, Irvine, Irvine, CA,[8]Cancer Genetics Laboratory, Research Division, Peter MacCallum Cancer Center, Melbourne, Australia,[9]Rutgers Cancer Institute of New Jersey, New Brunswick, NJ,[10]Head, Cancer Genetics, BC Cancer Research Centre, Vancouver, BC, Canada,[11]Duke University Medical Center, Durham, NC,[12]Obstetrics and Gynecology Epidemiology Center, Brigham and Women's Hospital and Harvard Medical School, Boston, MA,[13]Epidemiology, School of Public Health, University of Colorado, Aurora, CO,[14]Mayo Clinic College of Medicine and Science, Rochester, MN,[15]Huntsman Cancer Institute, Department of Population Health Sciences, University of Utah, Salt Lake City, UT,[16]Mayo Clinic, Rochester, MN,[17]Cedars-Sinai Medical Center, Los Angeles, CA,[18]Fred Hutchinson Cancer Center, Seattle, WA,[19]Department of Virus, Lifestyle and Genes, Danish Cancer Institute, Copenhagen, Denmark,[20]Cancer Control Research, BC Cancer Agency, 675 West 10th Avenue, Vancouver, BC, Canada,[21]California State University, Fullerton, Fullerton, CA,[22]Womens Cancer Research Center, Magee-Womens Research Institute and Hillman Cancer Center, Pittsburgh, PA,[23]Professor, Dept. of Epidemiology, Roswell Park Cancer Institute, Buffalo, NY,[24]Univ. of Michigan School of Public Health, Ann Arbor, MI,[25]Department of Epidemiology and Biostatistics, Memorial Sloan Kettering Cancer Center, New York, NY,[26]Professor, Dept. of Epidemiology & Public Health, Yale Univ. School of Medicine, New Haven, CT,[27]Program in Epidemiology, Division of Public Health Sciences, Fred Hutchinson Cancer Center, Seattle, WA,[28]Department of Epidemiology, Rollins School of Public Health, Emory University, Atlanta, GA,[29]Department of Preventive Medicine, University of Southern California, Los Angeles, CA,[30]Epidemiology Center, College of Medicine, University of South Florida, Tampa, FL,[31]Department of Preventive Medicine, Keck School of Medicine, University of Southern California, Los Angeles, CA,[32]Queensland Institute of Medical Research, Herston, Australia,[33]Department of Population and Public Health Sciences, University of Southern California, Los Angeles, CA,[34]Department of Medicine, Genetic Epidemiology Research Institute, University of California, Irvine, Irvine, CA,[35]NCI Div. of Cancer Epidemiology & Genetics, Bethesda, MD

Background: Chronic inflammation is implicated in ovarian carcinogenesis, but how different inflammation-related exposures individually or jointly affect histotype-specific associations remains unclear. Materials and Methods: We pooled data from 16 case-control studies in the Ovarian Cancer Association Consortium to evaluate associations of eight inflammation-related factors (anti-inflammatory: aspirin use, tubal ligation (TL); pro-inflammatory: endometriosis, obesity, lifetime ovulatory cycles (LOC), smoking, pelvic inflammatory disease (PID), polycystic ovary syndrome (PCOS)) with epithelial ovarian cancer (OvC) by histologic subtype. We examined individual associations and clustering of risk factors across histotypes and computed population attributable risk (PAR) for each factor. We assessed additive and multiplicative interactions for exposure combinations. Results: Associations with OvC risk differed by histotype (e.g., high-grade serous: aspirin: OR=0.90; 95%CI 0.82, 0.99; TL: OR=0.80; 95%CI 0.73, 0.88; overall serous: endometriosis: OR=1.17; 95%CI 1.03, 1.31; high LOC: OR=1.42; 95%CI 1.28, 1.58; obesity (low-grade serous): OR=1.50; 95%CI 1.14, 1.98). Clustering analyses showed highly correlated risk profiles in endometrioid and clear cell (r=0.91). High-grade serous and mucinous profiles were moderately correlated with endometrioid and clear cell (r=0.60) tumors. The profile for low-grade serous (r=0.36) tumors was distinct from other histotypes. PAR estimates suggested modifying aspirin use, TL, and LOCs could substantially reduce burdens of endometrioid, clear cell and mucinous tumors. Out of 28 exposure combinations tested in overall OvC and 189 by histotype, we observed 12 interactions. Not using aspirin regularly showed positive additive interactions with obesity and high LOCs, particularly in endometrioid tumors (obesity relative excess risk due to interaction (RERI)=0.74, 95%CI 0.31, 1.18; P_{int}=0.001 for; LOCs RERI=0.80, 95%CI 0.03, 1.56; P_{int}=0.04). Not using aspirin regularly also showed a positive additive interaction with endometriosis in clear cell tumors (RERI=1.77, 95%CI 0.03, 3.52; P_{int}=0.05). Lack of TL showed positive interactions with obesity in endometrioid (RERI=0.86, 95%CI 0.17, 1.53; P_{int}=0.01) and mucinous (RERI=1.10, 95%CI 0.23, 1.97; P_{int}=0.01) tumors, while negative additive interactions were observed for smoking and endometriosis in endometrioid tumors (RERI=-1.12, 95%CI -2.19, -0.05; P_{int}=0.04). A multiplicative interaction was observed between obesity and endometriosis in mucinous tumors (P_{int}=0.01). Conclusion: The findings suggest ovarian tumorigenesis is strongly shaped by pro- and anti-inflammatory pathways that act largely independently. Further examining these pathways may clarify the origins of histotype heterogeneity and guide prevention strategies.

#6262 Intraprostatic inflammation and FoxP3, a marker of Regulatory T cells, increase with age in benign prostate biopsies irrespective of clinical indication: placebo arm of the Prostate Cancer Prevention Trial (PCPT).

Zhike Lin[1], Lauren M. Hurwitz[2], Ibrahim Kulac[3], Berrak Gumuskaya[4], Javier Alonso Baena-Del Valle[5], Ines Benedetti Padron[6], Kathryn B. Arnold[7], M. Scott Lucia[8], Ian M. Thompson[9], Charles G. Drake[10], William B. Isaacs[11], William G. Nelson[12], Christopher M. Heaphy[13], Alan K. Meeker[14], Angelo M. De Marzo[14], Elizabeth A. Platz[1]

[1]Epidemiology, Johns Hopkins Bloomberg School of Public Health, Baltimore, MD,[2]National Cancer Inst. - Bethesda Campus, Rockville, MD,[3]Department of Pathology, Koc University School of Medicine, Istanbul, Turkey,[4]Department of Pathology, Ankara City Hospital, University of Health Sciences, Ankara, Turkey,[5]Fundacion Santa Fe de Bogota University Hospital, Bogota, Colombia,[6]Department of Basic Sciences, Universidad de Cartagena School of Medicine, Cartagena, Colombia,[7]SWOG Statistics and Data Management Center, Fred Hutchinson Cancer Center, Seattle, WA,[8]Department of Pathology, University of Colorado Denver, Aurora, CO,[9]Department of Urology, CHRISTUS Santa Rosa Medical Center Hospital, San Antonio, TX,[10]Columbia University Irving Medical Center, New York, NY,[11]The James Buchanan Brady Urological Institute, Johns Hopkins University School of Medicine, Baltimore, MD,[12]Sidney Kimmel Comprehensive Cancer Center, Baltimore, MD,[13]Department of Medicine, Boston University Chobanian & Avedisian School of Medicine and Boston Medical Center, Boston, MA,[14]Department of Pathology, Oncology, and Urology, The Sidney Kimmel Comprehensive Cancer Center at Johns Hopkins and the James Buchanan Brady Urological Research Institute, Baltimore, MD

Background: Intraprostatic inflammation is suspected to contribute to prostate cancer pathogenesis. Prostate cancer has the steepest age-related rise in incidence in solid cancers, and inflammation is thought to increase with age. But prostate tissue is typically obtained only from men with clinical indications, e.g., elevated plasma prostate-specific antigen (PSA). Associations between age and inflammation could be biased, given that PSA concentration increases with age, prompting biopsy. Thus, we used benign prostate tissue collected irrespective of indication to assess the association between age and intraprostatic inflammation and abundance of immune cells.

Methods: We performed a cross-sectional analysis in a subset of men of the PCPT placebo arm. Using slides containing biopsy cores (mean 4) from protocol-prompted end-of-study prostate biopsies at Year 7, we visually assessed the presence and extent of inflammation and quantified immunohistochemistry staining for CD4 (CD4+ T cells), CD8 (CD8+ T cells), CD68 (macrophages), FoxP3 (T regulatory cells), and c-KIT (mast cells) using a score (0: none - 4: extensive). Scores were weighted by total number of cores per man. Associations between age (continuous or quartiles) and inflammation measures (any core inflamed vs none; all or some cores inflamed vs none; mean percent tissue inflamed ≥3% or <3% vs 0%) were estimated using logistic regression. Associations between age and immune cell marker scores (continuous) were estimated using linear regression. Estimates were adjusted for race, BMI, smoking, physical activity, education, diabetes, statin use, and aspirin use.

Results: Participants (N=357) were 62 to 85 years of age at biopsy (median 70, IQR 65-74). Older age was associated with presence of inflammation [Q4 of age vs Q1: OR, 2.3; 95% CI, 1.1-4.9, p-trend across age, 0.003]. Positive associations were also observed with having some [Q4 OR, 2.1; 95% CI, 1.0-4.3] or all cores inflamed [Q4 OR, 7.8; 95% CI, 2.0-30.6]. Age was also associated with having ≥3% mean tissue with inflammation [Q4 OR, 2.6; 95% CI, 1.2-6.0, p-trend, 0.006]. Age was positively associated with FoxP3 score [p-value, 0.01], but not with any other immune cell markers. Associations were slightly attenuated when excluding men with PSA >4 ng/mL, diagnosed with prostate cancer, or who received for-cause biopsy.

Conclusion: Age is associated with increasing presence and extent of intraprostatic inflammation in biopsies taken irrespective of indication. Consistent with findings in circulation, prevalence of T regulatory cells in prostate biopsies increased with age. Findings may inform the etiologic pathway, mediated by inflammation, between increasing age and prostate cancer. Funding: P50 DK082998, U01 CA182883, UG1CA189974, T32 CA09314, R01 CA255349, DOD.

#6263 Association of tumor infiltrating lymphocytes and proinflammatory biomarkers with breast cancer molecular subtypes: Analysis of the MEND study..

Jovita Byemerwa[1], Drew Neish[1], April Deveaux[1], Lukeman Forgah[2], Omolola Salako[3], Adetola Daramola[3], Olusegun Alatise[4], Gabriel Olabiyi Ogun[5], Tomi Akinyemiju[1]

[1]Population Health Sciences, Duke University School of Medicine, Durham, NC,[2]Chicago Medical School, Chicago, IL,[3]Lagos University Teaching Hospital, University of Lagos College of Medicine, Lagos, Nigeria,[4]Obafemi Awolowo University Teaching Hospital, Ile-Ife, Osun State, Nigeria,[5]University College Hospital, University of Ibadan, Ibadan, Nigeria

Background: The tumor microenvironment is characterized by tumor-infiltrating lymphocytes (TILs) and proinflammatory biomarkers/cytokines, factors that inform therapeutic options and predict treatment response and tumor progression. Breast tumors in Nigerian women are relatively more aggressive; however no prior study has characterized the landscape of TILs and proinflammatory biomarkers across molecular subtypes in this population.

Materials and Methods: A total of 436 newly diagnosed, treatment-naïve BC patients from Nigeria were included in the study. BC molecular subtyping was determined by immunohistochemistry (IHC), and TILs were quantified on H&E-stained tumor slides using the International TILs Working Group criteria. Serum levels of proinflammatory biomarkers (IL-6, IL-8, IL-1B, TNF-α, and leptin) were assessed using immunoassays by Meso Scale Discovery. Descriptive statistics were used to evaluate the distribution of study covariates, and Spearman correlation was used to test the association of each proinflammatory biomarker and TILs. Multivariable logistic and multinomial regression models were used to estimate adjusted odds ratios (aOR) and 95% confidence intervals (95% CI) for the association of TILs and proinflammatory biomarkers with molecular subtype.

Results: The median age of study participants was 49, and 52.8% and 28.9% were diagnosed with grade 2 or 3 tumors respectively. The majority of BC tumors were of triple-negative subtype (43%), compared with 31% luminal A, 12% luminal B and 15% HER2-enriched subtype. Overall, BC patients had a median (Q1, Q3) TIL (%) of 10.0 (4.0, 21.0), with 49% categorized as low TIL (<10%), 41% categorized as intermediate TILs (10% ≤ TIL < 40%) and 10% categorized as high TIL (≥ 40%). Among a subset of 109 patients with proinflammatory biomarkers' data, TNF-α significantly correlated with TILs (ρ: 0.21; p = 0.026). Patients in high TIL category (vs low TIL category) were approximately 5-fold (OR: 5.03, 95% CI: 1.01, 24.94) more likely to be diagnosed with TNBC, while each standard deviation increase in TNF-α levels was significantly associated with 3.5-fold higher odds of TNBC (OR: 3.42, 95% CI: 1.32, 8.86) after adjusting for age, BMI, menopausal status, and all proinflammatory biomarkers. Other proinflammatory biomarkers showed no significant associations.

Conclusion: Our study, first to our knowledge to characterize the TME by molecular subtype in Nigerian women, reveal strong associations of high TIL levels and TNF-alpha with TNBC subtype, highlighting opportunities for immunotherapy and the prognostic significance of TNF-α in this population.

#6264 Familial gastric conditions indicating helicobacter pylori infection and risk of childhood leukemia.

Julia E. Heck[1], Yu Chen[2], Johnni Hansen[3]

[1]University of North Texas, Denton, TX,[2]NYU Langone Medical Center, New York, NY,[3]Danish Cancer Institute, Copenhagen, Denmark

Background: *Helicobacter pylori* (*H. pylori*) is a cause of gastric cancer and B-cell MALT lymphoma. Cancer may arise from bone-marrow derived hematopoietic stem cells. *H. pylori* antigens are linked to B-cell proliferation, secondary to T cell response and the release of cytokines. However, *H. pylori* may inhibit T-cell proliferation. *H. pylori* is genotoxic and promotes chronic inflammation and oxidative stress. Infection is typically acquired in childhood, resulting from close personal contact with infected family members. Infections are suspected to play a role in the etiology of childhood leukemia. However, an earlier study found mixed results for any association between maternal *H. pylori* IgG and IgM antibodies. The purpose of this study was to investigate parental and childhood *H. pylori*-related diagnoses of peptic ulcer and gastritis in relation to risk for childhood leukemia. *H. pylori* colonizes the stomach lining and is a major cause of gastritis and peptic ulcer disease. As the study was based on registry data, we used these diagnoses as proxy for *H. pylori* infection.

Methods: The study was based upon Danish national registers (births 1968-2013). We extracted *H. pylori*-related diagnoses of peptic ulcer and gastritis (ICD8 codes: 531-534; ICD-10 codes: K25-K28) and gastritis (ICD-8 code: 535; ICD-10 code: K29) from the National Patient Register for the parents and children. We linked these to childhood leukemia diagnoses from the Cancer Registry. Controls were 20:1 matched and selected at random from the Central Person Register. Conditional logistic regression was used to estimate associations between *H. pylori*-related diagnoses and childhood acute lymphoblastic leukemia (ALL), with adjustment for covariates.

Results: We observed 3.1% of mothers and 4.2% of fathers had ever been diagnosed with gastric conditions. Maternal lifetime diagnosis with gastric conditions was not notably related to offspring ALL (OR=1.21, 95% CI 0.89-1.65). When we examined maternal gastric conditions diagnosed prior to the child's cancer diagnosis, risks increased (OR=1.74, 95% CI 1.11-2.73). There was no association with paternal lifetime history of gastric conditions (OR=1.10, 95% CI 0.83-1.45). Children's lifetime diagnosis of gastric conditions was associated with ALL (OR=1.87, 95% CI 1.08-3.23).

Conclusions: Maternal and childhood *H pylori*-related diagnoses of peptic ulcer and gastritis are related to increased risk of childhood leukemia, perhaps related to aberrant immune responses. The child's increased risk may reflect heightened medical surveillance in cancer survivors and should be taken with caution. The findings warrant replication using serologic data.

#6265 Association of Area Deprivation Index with immune functioning and history of abnormal cervical screening among Appalachian young women.

Chloe M. Hery[1], Yesung Kweon[1], Mohamed I. Elsaid[1], Cecilia DeGraffinreid[1], Mack T. Ruffin[2], Electra D. Paskett[1]

[1]The Ohio State University, Columbus, OH,[2]Pennsylvania State University, Hershey, PA

Introduction: High chronic stress can influence immune response; therefore, we aimed to examine how residing in areas of high deprivation (marker for high stressor) is associated with Epstein-Barr Virus (EBV) reactivation, a proxy measure of immune function, and abnormal Papillomavirus (Pap) smear tests among young women in Appalachia.
Methods: Baseline data were available for 145 women aged 18-26 who were enrolled in the Community Awareness, Resources, and Education (CARE II) initiative, Project 3, which focused on reducing cervical cancer in the Ohio Appalachian. Area Deprivation Index (ADI) was geocoded from U.S. Census Block Group data to identify high- and low-deprivation areas based on the highest deprivation quartile. EBV was grouped into low/negative or medium/high levels, with the latter suggesting poor immune functioning. Participants were also asked if they ever had an abnormal Pap test (yes/no). Generalized Estimating Equations models with robust variance were fitted using a modified Poisson regression for binary outcomes: EBV reactivation and abnormal Pap test. All models were adjusted for age group, race, education, smoking status, marital status, and insurance.
Results: Average age of participants was 22.8 years, most had some college education (53.3%), and were never married (65.4%). The proportion of women with medium/high EBV reactivation was significantly higher among those residing in areas of high deprivation (89.5% vs. 69.1%, P=0.01). Similarly, living in high deprivation areas was associated with an over 2-fold increase in reporting a history of abnormal Pap tests (46.7% vs. 22.7%, P=0.01). Those living in high-deprivation areas had a 31% increased risk of medium/high EBV reactivation compared with those in low-deprivation areas (RR: 1.31, 95% CI: 1.11-1.54). This association remained significant after multivariable adjustment (aRR: 1.29, 95% CI: 1.06-1.56). Additionally, those living in high deprivation areas had 2.08 times the risk of reporting a past abnormal Pap test compared to those living in low deprivation areas (RR: 2.08, 95% CI: 1.22-3.53), and this remained significant after adjustment (aRR: 2.11, 95% CI: 1.12-3.99).
Conclusions: Our study found that residing in areas of high deprivation was associated with an increased risk of EBV reactivation, a proxy measure of poor immune functioning, and history of abnormal Pap tests. Stress caused by where one lives may have a significant impact on immune response and should be further examined to better implement cervical cancer control efforts.

#6266 Functional Class I, Class II, and nonclassical HLA variation drives lymphoma and myeloma risk in the all of us research program.

Lara Sucheston-Campbell[1], Saanika Tambe[1], Lian Zuo[1], Alyssa Clay-Gilmour[2], Vijai Joseph[3], Benjamin Tycko[4], Wendy Cozen[5]

[1]Wayne State University, Barbara Ann Karmanos Cancer Institute, Detroit, MI,[2]Epidemiology and Biostatistics, University of South Carolina, Columbia, SC,[3]Memorial Sloan Kettering Cancer Centre, New York City, NY,[4]Hackensack Meridian School of Medicine, Nutley, NJ,[5]UCI School of Medicine, Irvine, CA

Background: HLA-mediated immune surveillance involves classical, non-classical, and class I-like pathways. Because lymphoma and myeloma rely on different immune mechanisms, we evaluated HLA class I/II, non-classical, and class I-like loci across ancestries using allele-level amino acids(AA), heterozygosity (HET), evolutionary divergence (HED), IEDB-derived peptide-binding breadth (PBW; 9-mer binding entropy), and positional amino-acid heterozygosity (residue mismatch).
Methods: Hodgkin lymphoma (HL), NHL and subtypes, and multiple myeloma (MM) in All of Us Cohort were identified using ICD/SNOMED; controls lacked hematologic malignancy. HIBAG-imputed allele with n>20 cases were analyzed in EUR, AFR, and AMR. Models adjusted for age, sex, PCs, and admixture proportions tested ORs, 95% CIs, and FDR<0.1. We used joint PRS-HLA models to test whether HLA metrics contributed risk information beyond the lymphoma PRS.
Results: We replicated EUR HET and/or HED class I/II associations with NHL (N=1668), DLBCL (N=490), HL (N=393), and FL (N=435), and extended these patterns using PBW and AA-level metrics. In NHL, we confirmed that HET-C reduced risk (p=0.027) and found greater PBW was protective (OR=0.49; p=0.09). Similarly, in CLL, we replicated the HET-A association (p=0.027), identified PBW-A effect (OR=0.25; p=.03), and a positional signal at A-163 (OR=.83, p=0.015) that also appeared in NHL(p=.015). Neither locus showed HED effects.Novel MM associations with HET-B and -C (OR≈0.74; p<0.03), were supported by a positional hit at B-42 (OR=0.77; P=0.033) and a PBW-C effect (OR≈0.24; p=0.01), while HED remained null. In contrast, DLBCL showed protection across all class I metrics as well as at MICB (OR=0.75; p=0.006) and MHC-like HET (OR=0.73; p=0.084). In EUR DLBCL, A*01:01 (OR=1.23; p=0.076) and A26:01 (OR=1.56; p=0.051) showed risk effects consistent with some prior reports reinforced by multiple A-locus positional signals (P<0.02).Novel AFR-specific findings included A*68:02 in: HL (OR=2.88; $p=1.8\times10^{-5}$), mirrored by a positional hit at A-30 (OR≈3.0, p=.0004), NHL at B*07:02 (OR=1.69; p=0.018) and for C1-motif alleles C07:01 (OR=1.51, p=.04) and C*07:02 (OR= 2.02, p=.00017) consistent with a KIR-C1 mechanism.The DLBCL PRS replicated (which includes an HLA-B variant) in EUR (OR=1.25, 95% CI 1.15-1.36; $p=7.3\times10^{-7}$) and joint models showed HED (p=0.0028) and HET (OR=0.86, 95% CI 0.80-0.93, $p=7.0\times10^{-5}$) remained significant when combined with PRS. AIC identified HET + PRS with covariates as the best model. The PRS did not replicate in AFR or AMR.
Conclusion: We replicated classical HLA associations and identified novel non-classical and functional HLA features that shape B-cell malignancy risk across ancestries. Furthermore, adding orthogonal HLA metrics provided substantial, independent information beyond the PRS.

#6267 Advancing cancer prevention through policy: State-level variation in HPV vaccine mandate in the United States.

Grace Kwakyewaa Kyei[1], Esther Nana Kwaning[1], Evans F. Kyei[2]

[1]Umass Boston, Boston, MA,[2]Capstone College of Nursing, The University of Alabama, Tuscaloosa, AL

Purpose: Human papillomavirus (HPV) vaccination remains a cornerstone of cancer prevention, yet adolescent coverage in the United States is inconsistent. According to the National Conference of State Legislatures (NCSL), five jurisdictions - Hawaii, Puerto Rico, Rhode Island, Virginia, and the District of Columbia - require the HPV vaccine for school attendance, although mandate scope and enforcement vary. This study examined policy determinants influencing mandate adoption to inform equitable cancer prevention strategies.
Methods: Guided by Kingdon's Multiple Streams Framework and Policy Diffusion Theory, a comparative qualitative policy analysis was conducted across eight purposively selected states representing variation in HPV vaccine mandate status and coverage. Data sources included state statutes, legislative records, health department documents, and CDC immunization data. A theory-driven coding and state-by-variable matrix identified patterns in mandate design, exemption structures, diffusion mechanisms, and implementation barriers.
Results: Jurisdictions with HPV vaccine mandates achieved higher adolescent vaccination coverage compared with non-mandate states. Effectiveness was influenced by the scope of mandates, enforcement mechanisms, and availability of medical and nonmedical exemptions. Non-mandate states with high vaccination rates demonstrated comparable outcomes through robust public health infrastructure, provider engagement, and school-based education initiatives. Policy diffusion of mandates remains limited due to ideological resistance, politicization of adolescent vaccines, and the absence of coordinated federal or interstate incentives.
Conclusions: HPV vaccine mandates can increase coverage when designed with clear enforcement provisions, limited exemptions, and strong public communication. Comparable progress may also be achieved through mandate-equivalent policies that strengthen provider engagement and community outreach. Findings highlight actionable strategies for policymakers, nursing leaders, and cancer prevention advocates to accelerate HPV vaccination and reduce HPV-related cancer disparities across U.S. states.

: Genetic Epidemiology 2: Pathway Analysis, Sequencing, Functional Genetics / Family and Hereditary Studies
Poster Session

#6272 Enhancing variant interpretation through multi-database and systematic variant classification: Reducing uncertainty in clinical genomics.

Bharat Sinha Bhosale[1], Sandhya Iyer[2], Mina Darooei[2], Madhura Basavalingegowda[2], Anay walunjkar[2], Mohan Uttarwar[2], Kanchan Hariramani[2], Aarthi Ramesh[2], **Gowhar Shafi**[3]

[1]BB Precision Oncology, Mumbai, India,[2]OneCell Diagnostics India Private Limited, Pune, India,[3]1Cell.Ai, Pune, India

BackgroundInterpretation of Variants of unknown significance (VUS) is one of the major challenge in the era of comprehensive genomic profiling (CGP) in precision oncology. With several broad genomic panels hitting the oncology market, most struggle with VUS and its clinical utility. Thus, it is critical to understand and interpret VUS in patient context for utmost utility. Utilizing large language models and automated systems for VUS reclassification is on the rise. This will certainly impact several aspects including patient management, treatment surveillance, prophylactic opportunities, and preventing disease inheritance. Here, we describe the utility of our machine model system for effective interpretation and reclassification of VUS in patient context to reduce uncertainty and achieve high clinical utility.
MethodsCGP was performed on patients using next-generation sequencing (NGS) with the OncoIndx® panel. Variant reclassification was performed through our in-house automated precision classification and interpretation system.
ResultsUsing our computational molecular oncology workflow, a precision classification and interpretation system has been developed for the confirmation of variants of uncertain significance (VUS). The system when tested on several VUS intronic based on *in silico* evidence (PP5, PM2, BP4) and low evolutionary conservation scores (-0.423), ended up being reclassified as likely pathogenic. The system also investigates for the presence of conditions like Lynch-syndrome and its associated genomic findings including high microsatellite instability, loss of MSH2 protein on IHC. Functional consequences of the computational predictions such as weakening of the native acceptor site, and functional RNA studies are also utilized to confirm functionality. Finally, the patient and family history act as critical parameters. Using these combined evidence, the precision classification system generates a final verdict of reclassification.
ConclusionWhen complementary lines of evidence pertaining to functional loss of a variant (PS3), its identification in affected individuals (PS4_supporting), segregation-consistent family history (PP1), rarity in population databases (PM2), and supportive *in silico* predictions (PP3/BP4)—are integrated, a coherent and biologically consistent explanation can be generated for disease causation. Our automated machine system in-built with robust and essential criteria for variant classification, thus can be optimally utilized to reclassifiy VUS and improve clinical outcomes.

#6273 Clinicopathological and genetic features of Algerian patients with suspected Li-Fraumeni Syndrome: Implications in genetic screening and testing.

Farid Cherbal[1], Chiraz Mehemmai[1], Djamel-Eddine Seddik[1], Mouchira Saidi[1], Mohammed Oukkal[2], Fatiha Gachi[3]

[1]Molecular Genetics Research Team, LBCM-Tamayouz, Faculty of Biological Sciences, University of Science and Technology Houari Boumediene (USTHB), Algiers, Algeria,[2]Clinic of Medical Oncology Amine Zirout, Issad Hassani University Hospital, Beni-Messous, University of Health Sciences, Algiers, Algeria,[3]Children's Cancer Center, Lamine Debaghine University Hospital, Bab-El-Oued, School of Medicine, University of Health Sciences, Algiers, Algeria

Background: Li-Fraumeni Syndrome (LFS) is a rare hereditary cancer predisposition syndrome. LFS is an autosomal dominant disease caused by heterozygous germline pathogenic variant in *TP53* gene and frequently predisposes to a broad spectrum of cancers including early-onset cancers. Because of the rarity of LFS, data on clinical and genetic features in Algerian patients are limited. Our study aimed to report clinicopathological and genetic features in 25 families with suspected LFS.

Patients and Methods The present study investigated 25 patients and 22 relatives from 25 families with suspected LFS. Patients and relatives were referred through Children's Cancer Center and medical oncology services in two University hospitals. Clinical and pathological information was extracted from medical records of the patients with particular attention to age of diagnosis and updated Chompret clinical criteria such presence of adult rare tumors, childhood rare tumors and early-onset breast cancer. Family history of LFS was obtained from interviews of adult patients and relatives, pedigree and chart review of patients. TP53 exons 2-11 were screened in 25 patients and 22 high risk relatives using PCR-Sanger sequencing, respectively.

Results We identified various primary cancers in our study. The following"Core"cancers were observed in 25 patients, early- onset breast cancer, adult sarcomas and rare childhood tumors including: rhabdomyosarcoma, osteosarcoma and adrenocortical carcinoma, respectively. In addition, we observed early-onset colorectal cancer in relatives from 9 LFS families. Rhabdomysarcoma was most frequently observed (N=12) in children. The median age at diagnosis for early-onset breast cancer, adult sarcomas and childhood cancers was 30.5 years, 38 years and 6.8 years, respectively. The genetic analysis identified 11 individuals (23.4%) with TP53 germline variants. The TP53 common germline variant c.215C>G/p.Arg72Pro has been identified in eight patients. Interestingly, the rare germline TP53 c.314G>T/p.Gly105Val has been identified in 4-year old girl (the index case) who developed rhabdomyosarcoma at age 3 years and secondary cancer in the right lung at age 4 years after radiotherapy. Her mother is also a carrier of this rare variant, she developed an early-onset breast cancer at age 30 years. To date, the TP53 c.314G>T has been initially classified as a Variant of Uncertain Significance in the ClinVar database. Interestingly, our present study reclassifies the variant as"likely Pathogenic" (Class 4) based on ACMG criteria, which directly impacts patient care, risk assessment, and management.

Conclusions Our study highlights the importance of understanding clinical features of LFS and germline genetic variants of TP53 gene in underrepresented populations, such as Algeria, where clinical and genomic features of LFS are largely unknown.

#6275 Multidimensional analyses of pedigree, epidemiologic, and molecular data provide etiologic clues for myalgic encephalomyelitis/chronic fatigue syndrome.

Roxana Moslehi[1], Anil Kumar[1], Amiran Dzutsev[2]

[1]University at Albany, Albany, NY,[2]National Cancer Institute, Bethesda, MD

Background: Myalgic encephalomyelitis (ME)/chronic fatigue syndrome (CFS) is a complex disabling disorder with no known etiology or approved treatment. Estimates of the prevalence suggest that up to 3.4 million Americans may be afflicted and emerging evidence indicates that the COVID-19 pandemic may lead to a significant increase in ME/CFS cases globally. We conducted a molecular epidemiologic study to identify risk factors and biologic mechanisms for ME/CFS.

Methods: Our clinic-based case-control study involved 60 carefully selected ME/CFS patients and 61 appropriately matched healthy controls. We compared cases and controls with respect to the following: 1. prevalence of autoimmune disease (AID) and cancer among their first-degree relatives, 2. prevalence of epidemiologic factors, 3. serum levels of 48 cytokines, and 4. whole-blood RNA-seq gene expression data. We used conventional and machine learning approaches to calculate associative and predictive metrics, and to identify cytokine and gene expression profiles of ME/CFS.

Results: First-degree relatives of ME/CFS cases were more likely than those of the controls to have AID [Relative Risk (RR)=3.52, p=0.0014) and early-onset (diagnosed <60 years of age) cancer (RR=2.24, p=0.034) including blood cancers (p=0.047). Comparison of epidemiologic factors identified several risk factors such as history of allergies requiring medication [Odds Ratio (OR)=6.00, p<0.0001), exposure to contaminants (OR=4.35, p=0.0002), history of illness requiring hospitalization (OR=4.33, p=0.0004), ≥4 episodes of significant illness requiring hospitalization (OR=24.36, p<0.0001), and ≥2 episodes of significant stress (OR=3.07, p=0.03). The most common self-identified perceived *causes* of ME/CFS reported by cases in response to an open-ended question were Infectious Illness (27.3%), Infectious Agents (15.9%), and Stress (15.9%).

We identified a cytokine signature of ME/CFS, which classified patients with AUC>0.75, sensitivity>80%, and specificity>70% at an optimized threshold in all three tested machine learning models: XGBoost, k-nearest neighbors, and Support Vector Machines. Key cytokine predictors included IL-27, IP-10, RANTES, and Fractalkine among others. Whole blood RNA-seq analysis identified 115 differentially expressed genes with FDR<0.25 belonging to biologic pathways relevant to infectious diseases and neurologic disorders.

Conclusions: Our multidimensional analysis identified previously unreported risk factors for ME/CFS, links with AID and early-onset cancer, a dysregulated immune profile, and potential biologic mechanisms—such as neuronal injury—thus providing etiologic clues and druggable targets for treatment.

#6276 Predictors of engagement on a closed social support network for individuals with Hereditary Breast and Ovarian Cancer syndrome and Lynch syndrome.

Patrick Boyd, Yi Xiao, Sandra Davey, Jenna R. Hoopes, Cassiel Suarez, Justin Martinez, Alex Capasso, Kathryn Reyes, Ilana Solomon, Stacy W. Gray

City of Hope National Medical Center, Duarte, CA

Background: Genomic testing is increasingly used in cancer care, but patients often receive results without formal psychosocial support. Many social support platforms for patients exist, but few are embedded within genomic results portals while also focusing on providing support for populations with hereditary cancer risk. To address this, we developed a closed Social Support Network (SSN) at City of Hope integrated in a program (HOPE-Genomics) that delivers patient-friendly genomic results. This SSN was piloted with patients with pathogenic/likely pathogenic (P/LPs) variants associated with Hereditary Breast and Ovarian Cancer syndrome (HBOC) and Lynch syndrome. We examined engagement patterns and predictors of SSN use to inform future implementation of the SSN in broader populations for patients with hereditary risk for cancer.
Methods: 120 patients from City of Hope were invited to use the SSN for 4-6 months. Participants completed baseline and follow-up surveys that included psychosocial indicators (e.g., social isolation and cancer fatalism) and the Feelings About genomiC Testing Results (FACToR) scale. A subset of users participated in qualitative interviews following their participation in the pilot (n=9). SSN activity (logins, posts, likes, page views) was tracked. Patients who logged in at least once were classified as users. Chi-square/Fisher's exact tests and multivariable logistic regression were used to compare users vs. non-users across demographic and psychosocial variables.
Results: 68.3% (n=82) completed the baseline survey, 50.8% (n=61) logged in at least once, and 45.0% (n=54) completed the follow-up survey. Across all participants, there were 1081 page views, 51 posts, and 82 likes. The first discussion thread topic, "Living with a Genomic Change," had the most activity, indicating the importance of discussion thread topic placement over content. Page views peaked approximately halfway through the pilot (i.e., 3 months). Ethnicity was a significant predictor of SSN use whereby having a Hispanic/Latino identity was associated with a lower likelihood of being a user relative to not having a Hispanic/Latino identity (OR=0.40; 95% CI=0.16-0.99; p=.047). In interviews, all participants recommended the use of the platform to others with similar P/LPs, however, most participants described useability issues such as difficulty sub-commenting and navigation obstacles on smartphones (vs. desktops or laptops)
Conclusion: A closed SSN integrated in a genomic results portal achieved moderate uptake and engagement. Thread visibility drove activity. The ethnicity gap in user status indicates a need to understand decreased uptake among Hispanic/Latino participants in future research. Qualitative interviews highlighted needs for smartphone optimization, sub-commenting, and private messaging capabilities.

#6277 Determinants of Cancer Risk in Hereditary Cancer-Prone Individuals: The eGene Study.

Zhengwei Zhang[1], Lou Romanens-Renard[2], Li Zhang[3], Pamela N. Munster[2]

[1]Department of Epidemiology and Biostatistics, University of California San Francisco, San Francisco, CA,[2]Helen Diller Family Comprehensive Cancer Center, University of California San Francisco, San Francisco, CA,[3]Department of Medicine, University of California San Francisco, San Francisco, CA

Background: Individuals with genetic cancer predisposition have higher risks of cancer. However, the role of lifestyle, environmental factors, and health history in modifying cancer risk in these individuals is not well defined. The eGene study was designed to address this gap by utilizing large-scale self-reported data.**Methods**: The 216-item eGene questionnaire was used to assess environmental, behavioral, and medical history factors that may influence cancer risk among individuals with or without hereditary cancer gene variants. Participants were recruited through Eureka and MyChart. To assess the association between each factor and cancer risk, Odds Ratios (OR) with 95% Confidence Intervals (CI) obtained by univariable logistic regression models were reported.**Results**: Among all 1603 participants, the median age was 52, 68% were females, 82% were white, 27% had a personal history of cancer, and 60.5% had a family history of cancer. Among 615 individuals who had genetic testing, 354 tested positive for a pathogenic variant (PV) and 185 tested negative. For PV carriers, 60% never had cancer, 19% had breast cancer history, 5.4% had non-melanoma skin cancer history, and 3.8% had prostate cancer history. For no PV carriers, 62% never had cancer, 14% had breast cancer history and 3.4% had prostate cancer. PV incidence rate was higher in black (58.6%) and mixed populations (58.8%) compared with Asian (42.9%) and American Indian (33.3%). The most common PVs in both cancer cases and controls were in *BRCA1*, *BRCA2* and *ATM* genes. Table 1 summarizes the list of variables statistically significantly associated with cancer incidence within PV carriers and no PV carriers. **Conclusion**: These findings suggest increased environmental susceptibility in PV carriers. Ongoing analyses will further examine associations between medical, lifestyle, and environmental factors and cancer incidence in the general population in a multivariable fashion and explore possible gene-environmental interactions.

Table 1: list of variables statistically significantly associated with cancer incidence

Variable	Level	PV OR (95% CI)	No PV OR (95% CI)
Medication			
Hormone therapy	Yes	16.2 (6.01, 43.7)	28.6 (9.54, 85.80)
Thyroid	Yes	2.61 (1.36, 5.00)	2.44 (1.22, 4.86)
Steroids	Yes	3.21 (1.65, 6.24)	1.82 (0.94, 3.49)
Vitamin D	Yes	2.93 (1.61, 5.37)	2.04 (1.08, 3.86)
Calcium	Yes	2.33 (1.44, 3.79)	2.18 (1.30, 3.65)
Lifestyle			
Strengthening exercise (ref: 0 hour)	0-1 hours	0.56 (0.24, 1.17)	1.19 (0.56, 2.58)
	1-2hours	0.31 (0.11, 0.79)	1.41 (0.57, 3.43)
	2-4 hours	3.23 (0.59, 16.11)	2.28 (0.79, 6.54)
	>4 hours	0.45 (0.12, 1.48)	1.47 (0.41, 5.23)
Lived with a smoker for at least a year	Yes	1.97 (1.18, 3.27)	1.37 (0.83, 2.26)
Age of starting drinking alcohol once a week (ref: < 25)	25-29	2.25 (0.96, 5.34)	1.44 (0.66, 3.08)
	30-39	1.04 (0.31, 3.08)	2.43 (0.94, 6.36)
	40-49	1.66 (0.40, 6.53)	5.15 (1.34, 25.0)
	50-59	12.5 (2.06, 239)	5.51 (1.13, 39.9)
	≥ 60	2.08 (0.08, 53.2)	2.94 (0.62, 15.6)
Still drinking more than once a week	Yes	0.55 (0.31, 0.97)	2.22 (1.12, 4.39)
Medical			
Hepatitis B	Yes	3.09 (1.46, 6.86)	5.81 (2.70, 13.2)
Measles	Yes	3.72 (1.42, 10.9)	3.83 (1.79, 8.51)
Meningococcal	Yes	2.58 (1.33, 5.06)	3.36 (1.67, 6.92)
Mumps	Yes	3.30(1.35, 8.62)	4.10 (2.03, 8.58)
Rubella	Yes	2.48 (0.96, 6.67)	3.62 (1.52, 8.93)
Smallpox	Yes	0.49 (0.24, 0.95)	0.38 (0.14, 0.94)
Colonoscopy (ref: No)	Yes, once	2.55 (1.38, 4.74)	3.07 (1.66, 5.79)
	Yes, > 1	4.67 (2.63, 8.44)	3.55 (1.89, 6.82)
PSA (ref: No)	Yes, once	1.00 (0.04, 10.8)	3.00 (0.53, 17.8)
	Yes, >1	7.20 (1.93, 35.4)	5.19 (1.49, 21.7)
Environmental			
Chemicals, Acids, Solvents	Yes	2.49 (1.22, 5.24)	0.89 (0.42, 1.83)
Diesel Engine Exhaust	Yes	7.70 (1.22, 149)	0.68 (0.14, 2.49)
Gasoline Exhaust	Yes	3.45 (1.32, 10.1)	0.55 (0.17, 1.49)
Pesticides Herbicides	Yes	4.71 (1.37, 21.6)	2.78 (0.67, 13.8)
Wood Dust	Yes	4.71 (1.37, 21.6)	1.63 (0.50, 5.34)

#6278 Unraveling the missing heritability of unexplained familial cancers with germline genome sequencing.

Noah Fields[1], Ryan Collins[1], Seunghun Seunghun Han[1], Erin Shannon[1], Ryan Buehler[1], Deborah Wood Neklason[2], Jihye Park[1], Junne Kamihara[1], Judy Garber[1], Riaz Gillani[1], Saud H. AlDubayan[1], Eliezer Van Allen[1]

[1]Dana-Farber Cancer Institute, Boston, MA,[2]University of Utah Huntsman Cancer Institute, Salt Lake City, UT

While established predisposition genes account for syndromes like Cowden and Lynch syndrome, cancers frequently cluster in families without any identifiable pathogenic variant (PGV). We hypothesized that other germline factors beyond established PGVs might partially explain the large fraction of familial cancer cases with no known PGV. In this study, we systematically assessed potential genetic risk factors in 2,721 germline whole genomes from individuals with no recognized PGV, comparing 1,389 familial cancer cases across 18 cancer types to 1,332 controls with no family history of cancer in the NIH AllofUs Biobank. We performed genome-wide germline variant discovery using GATK-HC and GATK-SV to capture the full spectrum of rare and common SNVs, indels, and structural variants (SVs), notably including a total of 309,848 high-confidence SVs (9,639 SVs per genome). We first examined the rates of rare germline structural variants (SVs) predicted to cause loss-of-function of established predisposition genes, finding elevated rates of these likely pathogenic SVs in most cancer types compared to cancer-free controls, with neuroendocrine, colorectal, and ovarian cancer patients harboring notably high rates of these SVs (ORs: neuroendocrine 2.9; colorectal 3.1; ovarian 2.4). We also observed a small fraction of breast cancer patients carrying structural variants overlapping the BRCA1 promoter. We next tested for enrichment of rare missense variants of uncertain significance in established predisposition genes and found significant enrichment in endometrial, hematologic, prostate, and neuroendocrine cancer patients ($p < 0.05$). To search for potential new predisposition genes, we performed rare variant association tests for all 18,544 autosomal protein-coding genes, which nominated several candidate predisposition genes driven by rare damaging variants, such as BRAT1 in breast cancers (p=3.99e-5) and TSTD2 in thyroid cancers (p=3.26e-5). Finally, we assessed common-variant contributions and found that polygenic risk, long recognized in sporadic cancers, strongly contributed to familial cases in 11 of 15 cancer types with existing polygenic scores. Notably, polygenic risk scores were higher in patients from families with multiple occurrences of the same cancer type compared to patients whose own diagnosis was the only instance of that cancer in their family; conversely, in families with clusterings of a given cancer type, unaffected probands had polygenic risk scores for that cancer type on par with individuals who were both cancer-free and had no family history. Collectively, we estimate that 1-8.8% of unexplained familial cancers can be attributed to germline genetic factors detectable by genome sequencing but missed by routine gene panels, underscoring the potential clinical and diagnostic value of high-resolution germline testing for hereditary cancer patients and their families.

#6279 Socioeconomic and geographic disparities in germline genetic testing for Korean male breast cancer.

Jun-Ha Jang[1], Eun Gyeoung Lee[2], Hyun-Jin Kim[3], Kong Sun-Young[4]

[1]Public Health & AI, National Cancer Center Graduate School of Cancer Science and Policy, Goyangsi, Korea, Republic of,[2]Center for Breast Cancer, National Cancer Center, Goyangsi, Korea, Republic of,[3]National Cancer Control Institute, National Cancer Center, Goyangsi, Korea, Republic of,[4]Laboratory Medicine, National Cancer Center, Goyangsi, Korea, Republic of

Introduction: Male breast cancer (MBC) accounts for <1% of all breast cancers. Germline genetic testing (GT) is recommended for all MBC patients for treatment and family risk assessment. In Korea, reimbursed GT initially focused on BRCA1/2 then expanded to multigene panel testing (MGPT) in 2017. Nationwide data demonstrate a 2.6-fold increase in MGPT utilization from 2019 to 2023; however, 89.7% of tests were performed in tertiary centers raising concerns about equitable access. We aimed to examine time trends in GT utilization and quantify socioeconomic and geographic disparities in access among Korean MBC patients.

Methods: We assessed time trends, determinants and survival outcomes according to GT receipt using the Cancer Public Library Database in K-CURE (Korea-Clinical data Utilization network for Research Excellence), a nationwide registry linking cancer incidence, insurance claims, and mortality data. Total of 774 MBC cases (ICD-10 C50) diagnosed between 2014 and 2019 were identified after applying a 2-year washout period, with follow-up available through 2021. GT was defined as BRCA or MGPT within 12 months of diagnosis. Time trends and associated factors (income level, hospital type, and region) of GT receipt was evaluated. Survival according to GT receipt was explored using Cox proportional hazards models with propensity score matching and inverse probability weighting.

Results: Overall, 360 patients (46.5%) received GT, and the proportion undergoing testing increased significantly from 7.0% in 2014 to 68.9% in 2021 ($p<0.001$). This trend was driven predominantly by BRCA testing, which accounted for 92.3% of the overall increase, whereas MGPT contributed only 7.7%. GT receipt was significantly lower among medical aid recipients than among patients in the highest income quintile (20.0% vs. 51.4%, $p<0.01$), and in small hospitals compared to tertiary centers (25.0% vs. 52.6%, $p<0.01$). Geographic centralization was prominent that 42.8% of GT was performed in Seoul, among them 48.0% were non-Seoul residents. Higher income ($p=0.013$) and residence in Seoul ($p=0.023$) were independently associated with higher GT receipt, while hospital type was not significant ($p=0.087$) in multivariable models. For overall survival (OS), GT receipt was associated with improved OS [adjusted HR 0.55 (95% CI 0.36-0.83); $p<0.01$].

Conclusion: Despite sustained increases in GT utilization, marked socioeconomic and geographic disparities in access indicate that precision oncology for Korean MBC remains inequitable. These findings highlight gaps between national reimbursement policies and the real-world delivery of guideline-concordant care. Further targeted interventions to reduce income- and region-based barriers to GT would be needed. (This study was supported by grants from the National Cancer Center, Korea Grant No. NCC2410821 & NCC2510430)

#6280 Leveraging RNA and long-read DNA to improve genetic etiology identification in individuals with elevated cancer risk: A pilot study in individuals with Li-Fraumeni-like phenotype.

Yewon Kim[1], Anvith Kakkera[1], Asher Bryant[1], Sharon A. Savage[2], Michael C. Dean[3], Payal Khincha[4], Misha Kolmogorov[1], Sheila Rajagopal[1]

[1]Cancer and Data Science Laboratory (CDSL), National Cancer Institute (NCI), Bethesda, MD,[2]NCI Div. of Cancer Epidemiology & Genetics, Rockville, MD,[3]National Cancer Institute - Cancer Genomics Research Laboratory (CGR), Rockville, MD,[4]Clinical Genetics Branch, National Cancer Institute (NCI), Rockville, MD

Individuals with clinical Li-Fraumeni Syndrome (LFS) are at hereditary risk of developing multiple cancers in their lifetime. Among those meeting classic LFS criteria, about 10% do not have a germline mutation identified in *TP53*. Long-read DNA sequencing identifies complex and structural variants (SVs) missed on short-read sequencing. Clinical germline testing labs also recently began using short-read RNA-seq to characterize alternative splicing events. This project aims to explore underlying genetic etiology of those with LFS and no identifiable germline *TP53* variant using long-read DNA-seq and RNA-seq.

We performed germline Oxford Nanopore long-read DNA-seq and Illumina short-read RNA-seq on blood samples from 21 individuals participating in the NCI's Li-Fraumeni Syndrome Study. Selected individuals had a personal history of cancer and/or at least 2 1st degree relatives diagnosed with cancer and no known pathogenic germline *TP53* variant. Insertion-deletion variants (indels) in the long-read DNA-seq were called using Clair, and SVs were called using Severus. Annotation was performed using AutoGVP (indels) and LRGenotate (SVs). Variants were excluded if they were designated as benign/likely benign or if they were common (>1% for indels, >0.1% for SVs) in GnomAD populations. Variants were prioritized if they were designated as "pathogenic" or "likely pathogenic" or if they were predicted to have functional effects. We used RNA-seq to compare relative expression levels of candidate associated genes versus housekeeping genes as compared to control blood samples from the GTEx dataset. We also used rMATS to calculate a Percent Spliced In index (PSI) for splicing variants to parallel commercial labs.

We identified 21 indels in 11 genes classified as pathogenic/likely pathogenic and confirmed by IGV. The genes most affected by these prioritized variants were *ATXN3, ADCY2, KRT10*, *ITPKB, CCDC103, TBP, MUC5B, KRT81, MPO* and *GBE1*. Two related individuals (one diagnosed with cancer, one not) had a *TP53* variant of uncertain significance (c.845G>A) and two unrelated individuals had variants in *ATM*: c.9023G>A and c.8147T>C. We identified 2,453 SVs, with one deletion within *DHX32* and other SVs most often involving *SOS2*, *DICER1*, *NTHL1*, *TSC2*, *RUNX1*, *WAS*, and *GPC3*. We did not observe any significant difference in expression levels of *TP53* compared to housekeeping genes when comparing our samples to GTEx. We did not observe any family-specific PSI patterns.

Long-read DNA-seq and RNA-seq can help characterize the familial cancer syndromes without established genetic etiology. In this pilot study, we are actively evaluating potential causal genes related to clinical presentations of LFS with no identifiable pathogenic germline *TP53* variant.

#6281 Germinal pathogenic variants in Chilean early-onset gastric cancer patients.

Graciela Adriana Molina Fuentes[1], Enrique Norero Munoz[2], Ana Patricia Estrada-Florez[3], Paul Lott[4], Guillermo Lay-Son[5], Paulina Gonzalez Canales[6], Carol Parra[7], Osvaldo Torres[8], Jose Miguel Martinez[9], Cedric Adelsdorfer[10], Glyn Llewelyn[10], Alejandro H Corvalan[11], Luis G. Carvajal-Carmona[3]

[1]Facultad de Ciencias de la Salud. Carrera de Medicina, Universidad Autonoma de Chile, Providencia, Santiago, Region Metropolitana, Chile,[2]Esophagogastric Surgery Unit, Digestive Surgery Department, Hospital Dr Sotero del Rio, Pontificia Universidad Catolica de Chile, Puente Alto, Santiago. Region Metropolitana, Chile,[3]Genome Center and Department of Biochemistry and Molecular Medicine, School of Medicine, UC Davis, Davis, CA,[4]Genome Center and Department of Biochemistry and Molecular Biology, UC Davis, Davis, CA,[5]Unidad de Genetica en el Hospital Dr. Sotero del Rio, Pontificia Universidad Catolica de Chile. Hospital Sotero del Rio, Puente Alto, Santiago, Region Metropolitana., Chile,[6]Esophagogastric Surgery Unit, Digestive Surgery Department., Hospital Dr Sotero del Rio, Puente Alto, Santiago. Region Metropolitana, Chile,[7]Laboratorio de Investigacion en Nutricion y Alimentos (LINA), Departamento de Salud, Comunidad y Ges, Universidad de Playa Ancha, Valparaiso, Chile,[8]Servicio de Cirugia digestiva alta, Hospital Regional Dr. Guillermo Grant Benavente de Concepcion, Servicio de Salud Concepcion, Concepcion, Chile,[9]Hospital Dr. Eduardo Pereira. Servicio de Salud Valparaiso-San Antonio, Valparaiso, Chile,[10]Servicio de Cirugia, Hospital Dr. Gustavo Fricke, Servicio de Salud Vina del Mar-Quillota, Vina del Mar, Chile,[11]Departamento de Hematologia y Oncologia, Facultad de Medicina, Pontificia Universidad Catolica de Chile. Advanced Center for Chronic Diseases, Santiago, Region Metropolitana, Chile

Aim: This study aims to identify and describe the pathogenic/likely pathogenic (P/LP) germline variants found in 159 Chilean patients with early-onset gastric cancer (EOGC).
Introduction: Early-onset gastric cancer (EOGC), diagnosed before the age of 45 or 50, is increasingly recognized as a distinct clinical entity. Familial gastric cancer, which clusters within families often with early onset, is associated with specific genetic syndromes. Hereditary gastric cancer (HGC) accounts for about 10% of all gastric cancer cases, with mutations in the CDH1 gene being the most frequently observed in HGC. A previous report from our group described a Chilean family with hereditary diffuse gastric cancer (HDGC) harboring a pathogenic CDH1 variant, suggesting a lower frequency of pathogenic variants in this population.
Methods: Gene panel analysis was performed on 124 patients, and whole-exome sequencing (WES) was conducted on 35 patients using the Agilent SureSelect Human All Exome V7 kit. Alignment and variant calling were performed using Dragen v3.8, and variants were annotated with Illumina Nirvana and Annovar. Genotyping of index patients and their relatives was done using PCR and Sanger sequencing.
Results: Nine P/LP germline variants were identified across five genes in 11 patients. No P/LP pathogenic variants were found in the **CDH1** gene, consistent with prior findings. A P/LP variant in the **CTNNA1** gene (c.531T>G, p.Tyr177Ter) was found in one patient. Additionally, a high CAAD score variant of uncertain significance (VUS) (c.293G>A, p.Arg98Gln) was found in a large HDGC family. Two **BRCA2** P/LP variants were identified: c.4740_4741dupTG (p.Glu1581fs) in two unrelated patients and c.5439delT (p.Leu1813_Val1814insTer) in one patient, both variants having been previously described in Chilean hereditary breast cancer patients. Three **ATM** P/LP variants were identified, including c.3381_3384del (p.Gln1128fs) in a family with three affected individuals, and c.3894dup (p.Ala1299fs) and c.8122G>A (p.Asp2708Asn) in other unrelated patients. A **RUNX1** variant (c.1270T>G, p.Ser424Ala) was found in three independent cases, and a **POT1** variant (c.1087C>T, p.Arg363Ter) was identified in a family with multiple gastric cancer cases.
Conclusion: These families exhibited incomplete penetrance and multi-organ cancers. This is the first report of P/LP variants in the **RUNX1** and **POT1** genes in hereditary gastric cancer. **RUNX1** is associated with hereditary myeloid malignancies, and **POT1** with hereditary colorectal cancer. This study provides new insights into the genetic basis of early-onset gastric cancer in the Chilean population, highlighting the need for further investigation of these variants in familial gastric cancer syndromes.
Funding: Beca Chile Postdoctorado 74190063, CONICYT-FONDAP 15130011 /ANID-FONDAP apoyo 1523A0008, FONDECYT 1231773, NIH R01CA223978, R21CA199631, U54CA233306, and P30CA093373.

#6282 Evidence for pathogenicity of inherited biallelic *MSH3* variants causing early-onset colorectal cancer.

Yuki Aisu, Minoru Koi, John M. Carethers

Medicine, UC San Diego, La Jolla, CA

Background. We previously reported on an individual from a fourth family worldwide with early-onset colorectal adenocarcinoma with germline compound heterozygous *MSH3* variants (c.2436-1G>A / c.3265A>T). Tumor DNA from this individual demonstrated microsatellite instability-low (MSI-L) and elevated microsatellite alterations at selected tetranucleotide repeats (EMAST) suggestive that both alleles were pathogenic. Additionally, tumor cells exhibited MSH3 in the cytoplasm, with some cells showing loss of MSH6 that might be suggestive of at least one MSH3-expressing allele having a dominant-negative effect on MSH2, which binds to both MSH3 and MSH6 for their stability. Here, we aimed to prove that both *MSH3* variants are pathogenic as well as to assess effects on other mismatch repair proteins.

Methods. Both *MSH3* variants, c.2436-1G>A and c.3265A>T, were introduced individually into SW620 cells using CRISPR/Cas9. Presence of each variant was confirmed by Sanger sequencing. Western blotting (WB) and fragment analysis were performed on variant clones and compared with parental SW620 cells.

Results. We successfully established *MSH3* variant clones with homozygous c.2436-1G>A and clones with homozygous c.3265A>T. WB analysis revealed complete loss of MSH3 protein in cells containing homozygous c.2436-1G>A. However, variant MSH3 protein was detected in cells containing homozygous c.3265A>T, although the amount of protein was less than that of wild-type (WT) MSH3 expressed in parental SW620. These results suggest that the transcription rate of variant c.3265A>T may be reduced and/or variant-generated protein may be less stable than WT MSH3. Expression levels of MSH2, MSH6 and MLH1 in these 2 variant cell lines were similar to expression in parental SW620 cells. MSI-L/EMAST was detected in 18.8% (6/32) of subclones isolated from each variant indicating loss of MMR function, whereas no subclones (0/32) from SW620 showed MSI-L/EMAST.

Conclusions. We established cell models of two germline *MSH3* variants (c.2436-1G>A and c.3265A>T) which had been identified in an early-onset colorectal cancer patient. Cells with each variant exhibited MSI-L/EMAST indicating loss of MSH3 function, proving that these two germline variants are pathogenic. As we did not observe any change in cell MSH6 expression, further studies are in progress to generate cells that are compound heterozygous for these two variants and to further elucidate the pathological effects of the combinations of these variants.

#6284 Putative pathogenic germline variants associated with hereditary cancer syndromes identified through clinical tumor-only sequencing.

Sheehyun Kim, Suhyun Hwangbo, Sungyoung Lee, Hongseok Yun

Seoul National University Hospital, Seoul, Korea, Republic of

Background: Clinical tumor sequencing using next-generation sequencing (NGS) is widely applied to identify targetable variants and molecular biomarkers in cancer patients. Due to time and cost constraints, most institutions perform targeted gene panel sequencing only on tumor tissue, rather than on both tumor and matched normal samples. However, tumor-only sequencing cannot reliably distinguish true germline variants carried by the patient, particularly those associated with hereditary cancer syndromes.
Methods: We retrospectively collected clinical tumor-only sequencing data from cancer patients at Seoul National University Hospital (SNUH) between December 2022 and May 2025. All data were generated using targeted NGS with a customized SNUH FiRST Cancer Panel consisting of 336 cancer-related genes. Potential pathogenic germline variants (PPGVs) were classified based on the recommendations of the ESMO Precision Medicine Working Group and the patient's clinical and family history. Finally, we confirmed true pathogenic germline variants using Sanger sequencing or targeted NGS methods with normal genomic DNA from peripheral blood mononuclear cells.
Results: A total of 2,513 tumor samples underwent clinical targeted cancer panel sequencing during the examined period. Of those samples, 239 PPGVs were identified in 221 samples (8.8%) of various cancer types. While most cancers were breast or ovarian, different types of cancer were also associated with PPGVs, including those of the colon, pancreas, bladder, kidneys, prostate, bile ducts, and uterus. Of the 239 PPGVs, 129 (54.0%) were validated through germline confirmation testing. Of those, 88 (68.2%) were confirmed as true pathogenic germline variants, while the remaining 41 (31.8%) were somatic. Most germline variants were found in genes involved in homologous recombination repair (HRR), such as BRCA1, BRCA2, PALB2, BRIP1, RAD51D, CHEK2, and RAD50; or in genes involved in mismatch repair (MMR), such as MLH1, MSH6, MSH2, and PMS2. Among the PPGVs, 85.0% of BRCA1 variants were confirmed as germline, whereas only 12.5% of PTEN variants were verified to be germline. The germline variants showed an average variant allele frequency (VAF) of 58.1%, which is sufficiently high to be considered germline. However, the somatic variants exhibited a mean VAF of 51.5%, making them difficult to distinguish from true germline variants without additional confirmatory testing.
Conclusions: Clinical tumor-only sequencing can not only identify therapeutically actionable mutations but also infer PPGVs associated with hereditary cancers. Therefore, careful attention to PPGVs is essential when interpreting tumor-only sequencing results for the accurate diagnosis and prevention of hereditary cancer syndromes.

#6285 A novel functional cell line model for high throughput assessment of SDHA VUS for pathogenicity.

Michael C. Heinrich, Christine Robbins, Ajia Town

Medical Oncology, Portland VA HCS and OHSU Knight Cancer Institute, Portland, OR

Pathogenic (P), loss-of-function (LOF) SDHA germline mutations are associated with an increased risk of developing GI stromal tumors, paraganglioma/pheochromocytoma, or renal cell carcinoma. Although the penetrance of SDHA germline mutations appears less than for other SDH complex members, international guidelines recommend surveillance of germline pathogenic mutation carriers for early detection of SDH mutant cancers using a combination of laboratory testing, routine medical examinations, and periodic imaging. The number of SDHA VUS far exceeds the number of mutations that are classified as benign (B), likely benign (LB), likely pathogenic (LP), or pathogenic (P). As of November 2025, of the 1531 missense SDHA mutations in ClinVar, 1412 (92%) are VUS. We previously generated a CRISPR KO Hap1 cell line with integration of a single genomic copy of a landing pad cassette. Using targeted recombination of individual SDHA variants and measurement of SDHA enzymatic activity measurements, we determined that 19/20 control P/LP variants met the criteria for PS3strong evidence and 16/20 control benign B/LP variants met the criteria for BS3supporting (6 variants) or BS3moderate (10 variants). Using this model we functionally profiled 21 VUS and combined the weight of evidence with pre-existing population frequency data and computational predictions. Using this functional data, we were able to definitively classify 17/21 VUS as either LB (1) or LP (16) with only 4 remaining as VUS. Despite the utility of this model to functional profile and classify individual VUS, the throughput of this system is too limited to meaningful profile large numbers of VUS. Notably, these cell lines have metabolically adapted to culture conditions, and we cannot select against loss-of-function (LOF) variants. To enable metabolic selection against LOF variants, we developed a novel system where parental HAP1 cells with intact genomic SDHA are stably “pre-rescued” by lentiviral SDHA cDNAs that have mutation of the PAM and sgRNA binding sites for our most efficient SDHA sgRNA. The cDNAs encode for variants of interest (WT, VUS, control B and P variants). Stably expressing cells are then transduced with an SDHA sgRNA that edits the genomic SDHA gene but not the cDNA transgene. Parental or empty vector cells are nearly eliminated after transduction of SDHA sgRNA due to efficient editing of the essential genomic SDHA gene, whereas SDHA WT cDNA transduced cells are minimally depleted at 10-14 days after transduction. To date we have profiled 18 P and 18 B control variants in both systems and had 100% agreement between the assay systems. Overall, we profiled 79 variants in our depletion assay system and compared the results to those from our landing pad system and found excellent agreement with a r^2=0.89. This system is suitable for deep mutational scanning (DMS) as LOF variants are efficiently depleted. Pilot DMS experiments are currently in progress.

#6286 Functional assessment of RECQL4 missense variants identified in *RECQL4*genetic disorder-associated osteosarcomas.

Brian Rodemoyer, Samuel Brito, Thales C. Nepomuceno, Alvaro N. Monteiro

Cancer Epidemiology, Moffitt Cancer Center and Research Institute, Tampa, FL

Pathogenic germline mutations in *hRECQL4*, a member of the highly conserved family of RecQ DNA helicases, are associated with three rare genetic disorders: Rothmund-Thomson Syndrome type II (RTS type II), Baller-Gerold Syndrome (BGS), and RAPADILLINO. All three disorders predispose patients to an array of cancers including osteosarcoma, breast, ovarian, and lymphoma. While most known pathogenic mutations found in *RECQL4*-associated disorders lead to premature protein termination, a subset of patients also display missense variants, making their clinical classification more challenging. Moreover, some missense variants of unknown significance (VUS), are present in the general population, however, their contribution to disease prevalence has remained mostly unexplored. To assess the functional impact of RECQL4 missense VUS, we selected 15 missense variants identified in *RECQL4*-associated disorders from the ClinVar and genomAD databases. Our dataset includes three known benign, three known pathogenic, nine VUS, and the helicase-dead K508M variant. Here, we utilize immunochemical and fluorescence microscopy techniques to assess the functional impact of these 16 RECQL4 missense variants. Using a *pcDNA5-FRT-eGFP-RECQL4* construct, we generated missense variants by site-directed mutagenesis followed by transient transfection into endogenous *RECQL4*-silenced U2OS osteosarcoma cells in triplicate. Missense variants were analyzed by Western blotting for alterations in protein expression compared to the wildtype. While the benign variants p.(E71G) and p.(E267D) displayed expression like the wildtype as expected, pathogenic variants p.(P466L) and p.(S1079I) showed markedly reduced expression levels. Interestingly, VUS p.(L566P), p.(V768A), and p.(R1058G) also displayed reduced protein expression as compared to the wildtype, indicating a possible mechanism of pathogenicity. Furthermore, we performed fluorescence microscopy to assess the effect of the variants on subcellular localization under basal conditions and in the presence of the oxidative DNA damaging agent Streptonigrin. The pathogenic p.(P466L) variant, which is located in the nuclear localization signal (NLS), failed to localize to the nucleus, however, VUS p.(L566P), which is located downstream of the NLS, also impaired nuclear localization. Even under oxidative DNA damage conditions, which targets RECQL4 to the nucleolus, neither pathogenic p.(P466L) nor VUS p.(L566P) were capable of nuclear localization. In summary, we have successfully generated 16 *RECQL4* missense variant constructs and evaluated them for both protein expression and subcellular localization under normal and oxidative DNA damaging conditions, identifying a VUS that behaves similarly to a known pathogenic variant.

#6287 Ancestry-enriched *ACKR1* germline variant and its functional impact on normal and breast cancer biology.

Stephanie Adama[1], Adedeji Adebayo[2], Sedat Kacar[3], Poornima Bhat-Nakshatri[4], Jiang Guanglong[5], Cihat Erdogan[5], Bryan P. Schneider[6], Kathy D. Miller[6], Harikrishna Nakshatri[7]

[1]Translational Cancer Biology, Indiana University Melvin and Bren Simon Comprehensive Cancer Center, Indianapolis, IN,[2]Winship Cancer Institute, Emory University, Atlanta, GA,[3]Center for Computational Biology and Bioinformatics, Indiana University School of Medicine, Indianapolis, IN,[4]Surgery, Indiana University School of Medicine, Indianapolis, IN,[5]Center for Computational biology and Bioinformatics, Indiana University School of Medicine, Indianapolis, IN,[6]Division of Hematology/Oncology, Indiana University School of Medicine, Indianapolis, IN,[7]Surgery, Indiana University School of Medicine/ VA Roudeboush Medical Center, Indianapolis, IN

Atypical chemokine receptor 1 (*ACKR1*) gene, harbors single nucleotide polymorphisms in its regulatory and coding regions. The regulatory region variant rs2814778 is enriched in African and Arab populations and it confers protection against malarial infection. However, it is responsible for the Duffy-Null (CC) /heterozygous (C/T) phenotype, characterized by a significant reduction in *ACKR1* expression in epithelial and non-epithelial cells. *ACKR1* functions as a decoy receptor for several chemokines including the breast cancer metastasis-associated CXCL12, to regulate immune/ inflammatory pathways. There is a growing interest to include Duffy genotyping in clinical trial design to account for normal biological differences underlying aggressive breast cancer outcomes in black women. We seek to investigate the potential influence of *ACKR1* variant on breast cancer outcomes, with a long-term goal of identifying therapeutic vulnerabilities. We established a model system by generating immortalized breast epithelial cell lines with functional *TT* (wild type that express *ACKR1* -African and European ancestry), heterozygous (*C/T*) and homozygous (*CC*), using breast tissues from the institutional resource of Komen Normal Tissue bank. Cell lines with TT expressed higher *ACKR1* mRNA levels relative to *C/T* or *CC* in the regulatory region. We hypothesized that reduced *ACKR1* expression alters chemokine signaling which may influence intrinsic and extrinsic signaling to activate downstream oncogenic pathways. To test this, we investigated WNT/GSK-3β signaling and observed that *ACKR1* variant influences differential phosphorylation of β-catenin, facilitating nuclear translocation. We sought to explore further the effect of cytokines including inflammatory IL-6 secreted as a result of *ACKR1* variant on downstream oncogenic pathways. We observed increased phosphorylation of STAT3, a surrogate of IL-6 activity in breast epithelial cells of *ACKR1 CC* and *C/T* cells compared to *TT*. Our analysis of the UALCAN database further revealed that reduced *ACKR1* expression in breast cancer correlates with progression to brain metastases. Consistent with this, our results demonstrate enrichment of CD271-high populations; indicative of cancer stem-like properties in *ACKR1 CC* and *C/T* cells. These findings suggest that reduced *ACKR1* expression may promote acquisition of stem-like and metastatic properties. In vivo studies are underway to evaluate the effect of *ACKR1* status on distinct tumor characteristics including cancer stem cell properties, increased metastatic potential and response to targeted and conventional chemotherapy. A positive outcome from this study will have a transformative impact, establishing *ACKR1* germline variants as determinants of breast cancer biology and highlight the need to integrate ancestry-informed genotypes into clinical trial design and therapeutic decision-making.

#6288 Rational pairing of tumors with off-patent targeted therapies (TT): Next^3 generation sequencing with global applications for the unprivileged patients!.

Farah Mazahreh, **Liyan Mazahreh**, Ahmad Mazin Safar

University of Arkansas for Medical Sciences, Little Rock, AR

Since the success of imatinib as the inaugural TT, attempts to identify rational targets for similar approaches have gained prime importance. Cancer is defined by genomic alterations producing constantly activated oncogenes (O). Classically, this was inferred by clonal DNA alterations in proto-oncogenes which became the basis for identifying actionable changes in Next Generation Sequencing (NGS) platforms (successful in <25% of cases). Mutations, translocations and amplifications generate 'constant' pathologic state but this can also result from DNA amplification of transcription factors (TF) or ligands (for receptor Os). TTs are priced beyond the reach of uninsured or impoverished populations. Few TTs are off-patent, however, with affordable formulations enabling access to such agents even in underprivileged communities. We hypothesized that a substantial portion of cancers might be rationally paired to off-patent TTs if extended, but scientifically sound, criteria were used to identify therapeutic targets. Methods: We examined The Cancer Genome Atlas for cases that are wild type but over-expressed for an inclusive O list. We report on amplifications of the TF or ligand of receptor Os. We then examined the list for cases that could benefit from unpatented TTs. We also report on cases with increased transcriptional O activity. All histologies/stages were included when >5 cases were available. Results: Table reports the findings per type of tumor examined. Conclusions: Our method provides underprivileged patients with affordable TTs that wouldn't have otherwise been considered with classic NGS in 9-60% of genomically defined Os. Pairing Os with effective TT should extend beyond the classic NGS criteria. Relevant DNA events in TFs and ligands seem to play a variable role in O-wild type cancers depending on histology (0% in pancreas, kidney, thyroid and glioma). In others, the finding is noted in 13-100% of cases.

#6289 Targeted sequencing of common cancer susceptibility genes reveals germline variants in African prostate cancer patients.

Abimbola F. Onyia[1], Freeman Okwuchi[1], Opeyemi C. De Campos[1], Sylvester Divine[1], Olutola Olasehinde[1], Ayinde Yahaya[2], Ayo Salako[3], Aminu Zakari[4], Iya Bassey[5], Nicholas Titiloye[6], Bernard Petershie[6], Isidore GANDAHO[7], Luc Brun[7], Tore Sanni[7], Safiatou Coulibaly[8], Noel Coulibaly[9], Michael Fakayode[8], Coulibaly Issoufou[10], Valerie Gbonon[8], Kouame Benjamin[10], Yao Evrard[9], Peter Coleman[11], Ayun Cassell[11], Victor Ajumbo[12], Lilac Wattanga[13], Benson Ochieng Nyambega[12], Folakemi T. Odedina[14], **Solomon Rotimi**[1]

[1]Covenant University, Ota, Ogun State, Nigeria,[2]iCCaRE for Black Men Consortium, Ogun, Nigeria,[3]Obafemi Awolowo Teaching Hospital Complex, Ile Ife, Osun State, Nigeria,[4]Aminu Kano Teaching Hospital, Kano, Nigeria,[5]University of Calabar Teaching Hospital, Calabar, Nigeria,[6]Kwame Nkrumah University of Science and Technology, Kumasi, Ghana,[7]Parakou Teaching Hospital, Parakou, Benin,[8]Pasteur Institute of Cote d'Ivoire, Abidjan, Cote D'Ivoire,[9]Teaching Hospital of Treichville, Abidjan, Cote D'Ivoire,[10]Teaching Hospital of Cocody, Abidjan, Cote D'Ivoire,[11]John F. Kennedy Memorial Hospital, Monrovia, Liberia,[12]Maseno University, Maseno, Kenya,[13]Jaramogi Oginga Odinga Teaching & Referral Hospital, Kisumu, Kenya,[14]Mayo Clinic Florida, Jacksonville, FL

Background: Prostate cancer (PCa) is the leading cause of cancer-related deaths globally and disproportionately affects men of African ancestry. African men often present at younger ages and with more aggressive disease, and approximately half of the PCa risk has been attributed to genetic factors. Africa is the most genetically diverse region of the world, and even within the continent, populations show important differences in allele frequencies and patterns of pathogenic variation. Despite this diversity, African men remain underrepresented in genomic studies, creating significant gaps in knowledge that limit precision medicine efforts.

Methods: A total of 182 prostate cancer patients were recruited from teaching hospitals in Benin, Côte d'Ivoire, Ghana, Kenya and Nigeria. 50 cancer susceptibility genes using the Aviseq ONCO50 panel and the Illumina MiSeq platform. Variant calling was performed using an in-house Snakemake workflow, followed by additional bioinformatic steps to distinguish true PMS2 variants from PMS2CL-related artifacts. Pathogenicity assessment relied on annotations from ClinVar and LOVD databases.

Results: Pathogenic and likely pathogenic variants were detected in 31.3% of the study group identified in 26 genes. The five most frequently altered genes were RAD50, PTCH1, MSH6, MUTYH, and NF1. Nigerian patients accounted for 52.6 percent of all pathogenic variants, with recurrent alterations observed in MSH6, MUTYH, NF1, and PTCH1. In contrast, pathogenic BRCA1 and BRCA2 variants were observed primarily in patients from Kenya, Benin, and Côte d'Ivoire. Several frameshift, nonsense, and splice-site variants identified in this study have not been previously reported in African populations.[SR1]

Conclusion: This study provides one of the most detailed assessments of inherited cancer susceptibility gene variants in African PCa patients. The findings reveal substantial regional variation in the spectrum of pathogenic variants and highlight population-specific genomic signatures that may contribute to the unequal burden of PCa in men of African ancestry. These data emphasize the importance of expanding genomic research efforts within Africa to strengthen precision oncology and reduce global PCa disparities.

#6290 Next-generation sequencing utilization among U.S. Veterans with metastatic cancer in the VA Healthcare System.

John R. Bihn[1], Aditi Hazra[1], Kaelyn Nannini[1], Cassidy Kenny[2], Rachel E. Ward[1], Jennifer La[1], Nathanael R. Fillmore[1], Gieira S. Jones[2], J. M. Gaziano[1]

[1]VA Boston Healthcare System, Boston, MA,[2]Merck and Co., Inc, Rahway, NJ

Background: Access to molecular and genetic testing enables the delivery of precision oncology and improved cancer outcomes. However, patterns of testing utilization among U.S. Veterans remain understudied. This study evaluated the receipt of FoundationOne next-generation sequencing (NGS) testing for metastatic patients across three common cancers. We assessed demographic, clinical, and social determinants of health (SDOH) correlates of testing within the nationwide Veterans Affairs (VA) healthcare system.

Methods: We conducted a retrospective cohort study of U.S. Veterans recorded in the VA Cancer Registry with metastatic lung, colorectal, or prostate cancer and treated in the VA system from 2019 - 2023. We evaluated the utilization of FoundationOne NGS panels (CDx and Liquid) by year and cancer type as accessed through the National Precision Oncology Program (NPOP) database; for this study period other NGS platforms were beyond the scope of this study. Associations of testing frequency with SDOH, including self-reported race, ethnicity, age, sex, rurality, and socioeconomic status, were examined using descriptive statistics, with standard mean differences (SMD) >0.1 considered significant.

Results: Among 71,569 cancer patients, 17.4% (n = 12,465) had metastatic disease. Of these, 4,743 patients received FoundationOne NGS testing (38.1%) including 514 colorectal cancer patients, 2,519 lung cancer patients across histologies, and 1,710 prostate cancer patients. Tested patients were younger than non-tested patients (median age of 71.5 vs. 72.8, SMD = 0.26). Differences in racial distribution were observed (SMD = 0.14); for example, 27.7% of tested patients were Black or African American compared to 22.4% of non-tested patients. Tested patients were more likely to be non-frail (36.6% vs. 31.8%) and less likely to be severely frail (4.2% vs. 6.0%, SMD = 0.15) than non-tested patients, while no substantial disparities were found across sex (SMD = 0.053) or ethnicity (SMD = 0.04). The proportion of rural patients was lower for tested colorectal (20.2% vs. 24.7%, SMD = 0.11) and lung cancer patients (29.3 % vs. 34.3%, SMD = 0.12) versus non-tested patients; tested patients also resided closer to VA facilities for colorectal (median of 24.6 km vs. 31.9 km, SMD = 0.13) and prostate cancer (25.6 km vs. 32.1 km, SMD = 0.11).

Conclusion: Among Veterans with common metastatic cancers, we identified differences in FoundationOne NGS testing utilization for some demographic and clinical factors, while other factors showed similar testing rates. Future directions include evaluating additional NGS platforms utilized in the VA, as well as NGS testing through community care. Continued investment in interventions such as tele-oncology and targeted outreach may help increase NGS testing and ensure all Veterans benefit from precision cancer care.

#6291 Clonal hematopoiesis and incident hematologic and myeloid malignancy in ARIC.

Elizabeth A. Platz[1], Hidetaka Uryu[2], Vernon A. Burk[1], Meng Ru[1], Sergiu Pasca[3], Lukasz P. Gondek[3], Katherine Y. King[4], Anna E. Prizment[5], Corinne E. Joshu[1], Pradeep Natarajan[6], Margaret A. Goodell[4], Christie M. Ballantyne[4], Koichi Takahashi[2]

[1]Johns Hopkins Bloomberg School of Public Health, Baltimore, MD,[2]UT MD Anderson Cancer Center, Houston, TX,[3]Johns Hopkins University School of Medicine, Baltimore, MD,[4]Baylor College of Medicine, Houston, TX,[5]University of Minnesota, Minneapolis, MN,[6]Massachusetts General Hospital, Harvard Medical School, Boston, MA

Background: Clonal hematopoiesis (CH), defined using mutations in myeloid-lineage driver genes (N=74 [classic], Bick et al. *Nature* 2020), is a risk factor for hematologic malignancy (HM). Bernstein et al. (*Nature Genetics* 2024) identified 17 additional genes with mutations that are positively selected in the population, and documented a positive association with HM. Continuing to refine CH mutations that convey risk is critical for clinical use and research on modifiable drivers of CH to HM. Thus, we developed a CH-calling pipeline that detects CH from population-based sequencing data using an expanded gene list as well as a variant pathogenicity score based on Google AlphaFold 3. We investigated associations between CH called by the new pipeline and HM risk in a community-based cohort with long follow up.

Methods: We conducted a prospective analysis of 9,365 participants in the Atherosclerosis Risk in Communities study aged 44-80 years, without a cancer history, and with whole exome sequencing data. 410 HMs (147 myeloid) were ascertained mainly by cancer registry linkage in a median follow up of 21 years. Follow up is longer than in the original well-known CH studies. With a mean depth of 100x, mutations with a variant allele frequency (VAF)>3.8% were considered for CH. We classified definitive CH as mutations in classic CH genes and truncating mutations in genes additionally identified by Bernstein et al. For missense mutations in the additional genes, we applied AlphaFold 3 to predict pathogenicity and called probable if score≥0.9. We estimated hazard ratios (HR) and 95% confidence intervals (CI) for the association of small (3.8<vaf<10%) and="" large="" (vaf≥10%)="" ch="" (both="" vs="" no="" ch)="" with="" incident="" hm="" myeloid="" malignancy="" adjusting="" for="" age,="" sex,="" race.="" comparison,="" we="" ran="" the="" same="" analyses="" using="" classic="" (bick="" et="" al.="" defined="" vaf≥2%).</vaf<10%)>

#6292 Comprehensive whole-Genome profiling reveals Cooperative PI3K-TP53-RB1-ATRX pathway alterations and immune-modulatory drivers in myxoid liposarcoma.

Jonathan Gonzalez[1], Hayde Caro-Sanchez[1], Dorian Y. Garcia-Ortega[1], Andrea Ramirez[1], Rodrigo Cruz-Nieto[1], Claudia Garcia-Cuellar[1], Diddier Prada[2]

[1]Innstituto Nacional de Cancerologia, Mexico City, Mexico,[2]Icahn School of Medicine at Mount Sinai, New York, NY

Background: Myxoid liposarcoma (MLS), a genetically stable soft-tissue sarcoma driven by FUS-DDIT3 fusions, harbors additional somatic alterations contributing to progression and microenvironmental adaptation. These remain underexplored in non-European populations.
Methods: We conducted whole-genome sequencing (WGS) on tumors from 56 Mexican MLS patients using a standardized pipeline (BWA-MEM2 alignment, GATK Mutect2 variant calling, VEP annotation). We analyzed somatic SNVs/indels, mutational signatures, gene-specific clustering (OncodriveCLUST), and co-occurrence patterns via cohort-level MAF files. Results were visualized with oncoplots and positional analyses.
Results: Tumors exhibited moderate mutational burden (median 6.4 × 104 variants/sample), dominated by missense substitutions and C>T transitions (SBS1 and SBS5 signatures). Recurrent alterations enriched in structural genes (e.g., *MUC3A*, *MUC4*, *MUC5AC*, *MUC16*, *AHNAK2*, *FLG*, *TTN*, *ZNF*) suggested extracellular and cytoskeletal remodeling. Key oncogenic hits included *PIK3CA* (89%; activating p110α variants), *TP53* (98%; DNA-binding loss-of-function), *RB1* (87%; RB_A/RB_B disruptions), and *ATRX* (98%; helicase/ADD domain mutations), implicating PI3K-TP53-RB1-ATRX pathway cooperation and telomere instability. Co-occurrence clustered in adhesion/matrix genes without exclusivity, while OncodriveCLUST hotspots (*DEFB4A*, *DEFB107A*, *USP17L17*, *FOXD4L4*) pointed to immune and epigenetic modulation.
Conclusions: Beyond FUS-DDIT3 fusions, MLS features coordinated PI3K-TP53-RB1-ATRX alterations, structural remodeling, and immune hotspots. This first WGS study in Mexican (and one of few in Latin American) MLS patients establishes a genomic atlas for diverse populations, informing targeted therapies like PI3K inhibitors.

#6293 Distinguishing radiation-induced from sporadic thyroid cancers after the Chornobyl nuclear power plant accident.

Danielle M. Karyadi[1], Tetiana I. Bogdanova[2], Stephen W. Hartley[1], Vladimir Drozdovitch[1], Sergii Masiuk[3], Belynda Hicks[4], Kristine Jones[4], Amy Hutchinson[4], Petra Lenz[4], Maria Brown[4], Aaron M. Rozeboom[4], Elizabeth K. Cahoon[1], Mykola Chepurny[3], Liudmyla Yu Zurnadzhy[2], Vibha Vij[1], Cari M. Kitahara[1], Michael Dean[1], Gayle E. Woloschak[5], Dale A. Ramsden[6], Mykola D. Tronko[7], Stephen J. Chanock[8], **Lindsay M. Morton**[1]

[1]National Cancer Inst. Div. of Cancer Epidemiology & Genetics, Bethesda, MD,[2]2 Laboratory of Morphology of the Endocrine System, V.P. Komisarenko Institute of Endocrinology and Metabolism of the National Academy of Medical Sciences of Ukraine, Kyiv, Ukraine,[3]Radiological Protection Laboratory, State Institution National Research Center for Radiation Medicine Hematology and Oncology of the National Academy of Medical Sciences of Ukraine, Kyiv, Ukraine,[4]Cancer Genomics Research Laboratory, Leidos Biomedical Research, Frederick National Laboratory for Cancer Research, Frederick, MD,[5]Northwestern University Feinberg School of Medicine, Chicago, IL,[6]98 Department of Biochemistry and Biophysics, Lineberger Comprehensive Cancer Center, University of North Carolina at Chapel Hill, Chapel Hill, NC,[7]109 Department of Fundamental and Applied Problems of Endocrinology, V.P. Komisarenko Institute of Endocrinology and Metabolism of the National Academy of Medical Sciences of Ukraine, Kyiv, Ukraine,[8]Sect. Head & Director, CGF/ATC, National Cancer Institute, Rockville, MD

Radioactive fallout from the 1986 Chornobyl accident increased papillary thyroid carcinoma (PTC) risk after childhood exposure. Radiation-induced versus sporadic tumors cannot be distinguished by clinical characteristics, histologic features, or known COSMIC signatures. A recent analysis examined the pattern of DNA damage that generated PTC oncogenic drivers from Chornobyl-exposed and unexposed individuals because such patterns reflect DNA repair mechanisms, e.g., healthy cells engage efficient DNA double-strand break (DSB) repair without substantial DNA loss. PTC with fusion/structural variant (SV) drivers generated from two breakpoints and <20 basepairs (bp) breakpoint gain/loss (Fusion$^{2B<20bp}$) were consistent with having been caused by radiation (higher frequency with increasing radiation dose, even distribution by sex), whereas fusion/SV-driven PTC with ≥3 breakpoints and ≥1000 bp breakpoint loss (Fusion$^{3B\geq1000bp}$) and *BRAF*^{V600E}-driven PTC exhibited no radiation dose association and strong female predominance. To investigate radiation dose and sex distributions for additional fusion/SV driver categories and replicate the previous report, we reconstructed thyroid radiation doses and sequenced 244 histologically-confirmed PTCs (Table). Radiation doses were significantly higher for all fusion/SV-driven PTC with <1000 bp breakpoint loss (P=0.0084 to 7.1×1^{-10}), regardless of the number of fusion/SV driver breakpoints, compared with *BRAF*^{V600E}-PTC, while doses were comparably low for fusion/SV-driven PTC with ≥1000 bp breakpoint loss, albeit based on small numbers. Only the Fusion$^{2B<20bp}$-PTC replication group had a lower female predominance compared with *BRAF*^{V600E}-PTC (67.1% vs. 79.0%, P=0.068). These results provide evidence that the amount of gain/loss at the fusion/SV driver breakpoint is a more informative feature than the number of DNA DSBs for distinguishing radiation-induced from sporadic tumors in this dose range.

Distribution of sex and radiation dose by PTC oncogenic driver category

		Sex			Thyroid radiation dose (mGy)								
		Female	Male		Unexposed	1-99	100-199	200-499	500-999	≥1000			
Driver category	**Total**	**N (%)**	**N (%)**	**P***	**N (%)**	**N (%)**	**N (%)**	**N (%)**	**N (%)**	**N (%)**	**Mean**	**Median**	**P***
2 breaks, <20 bp at both breakpoints (Previously published)	66	35 (53.0%)	31 (47.0%)	1.34×10^{-4}	3 (4.5%)	15 (22.7%)	14 (21.2%)	20 (30.3%)	6 (9.1%)	8 (12.1%)	315.2	207.7	8.39×10^{-8}
2 breaks, <20 bp at both breakpoints (Replication)	73	49 (67.1%)	24 (32.9%)	0.068	0 (0.0%)	22 (30.1%)	15 (20.5)	16 (21.9%)	9 (12.3%)	11 (15.1%)	361.7	185.5	7.10×10^{-10}
2 breaks, <1000 bp at both breakpoints (New category)†	34	26 (76.5%)	8 (23.5%)	0.72	6 (17.6%)	9 (26.5%)	8 (23.5)	5 (14.7%)	3 (8.8%)	3 (8.8%)	230.4	130.5	5.46×10^{-4}
2 breaks, ≥1000 bp loss at ≥1 breakpoint (New category)	7	5 (71.4%)	2 (28.6%)	0.60	1 (14.3%)	4 (57.1%)	2 (28.6%)	0 (0.0%)	0 (0.0%)	0 (0.0%)	58.9	58.2	0.42
≥3 breaks, <20 bp at all breakpoints (New category)	4	3 (75.0%)	1 (25.0%)	0.87	0 (0.0%)	2 (50.0%)	0 (0.0%)	1 (25.0%)	0 (0.0%)	1 (25.0%)	360.8	203.4	0.0084
≥3 breaks, <1000 bp at all breakpoints (New category)†	13	11 (84.6%)	2 (15.4%)	0.60	1 (7.7%)	4 (30.8%)	3 (23.1%)	1 (7.7%)	2 (15.4%)	2 (15.4%)	341.6	127.2	4.21×10^{-5}
≥3 breaks, ≥1000 bp loss at ≥1 breakpoint (Previously published)	32	30 (93.8%)	2 (6.3%)	0.075	12 (37.5%)	15 (46.9%)	4 (12.5%)	0 (0.0%)	1 (3.1%)	0 (0.0%)	62.1	35.6	0.12
≥3 breaks, ≥1000 bp loss at ≥1 breakpoint (Replication)	5	4 (80.0%)	1 (20.0%)	0.99	1 (20.0%)	3 (60.0%)	0 (0.0%)	1 (20.0%)	0 (0.0%)	0 (0.0%)	77.5	52.1	0.70
Large deletion (≥1000 bp) (New category)	13	10 (76.9%)	3 (23.1%)	0.87	3 (23.1%)	5 (38.5%)	1 (7.7%)	0 (0.0%)	2 (15.4%)	2 (15.4%)	273.3	86.1	0.0017
BRAF^{V600E} (Previously published)	162	124 (76.5%)	38 (23.5%)	Reference	30 (18.5%)	88 (54.3%)	28 (17.3%)	11 (6.8%)	2 (1.2%)	3 (1.9%)	93.6	48.9	Reference
BRAF^{V600E} (Replication)	95	79 (83.2%)	16 (16.8%)		11 (11.6%)	55 (57.9%)	17 (17.9%)	6 (6.3%)	5 (5.3%)	1 (1.1%)	114.9	52.1	

* P-values were derived from a polytomous logistic regression model including covariates for sex, thyroid radiation dose, and age at PTC.† includes ≥1 breakpoint with 20-999 bp gain/loss

#6294 Rare germline variants in key pathways contribute to hepatocellular carcinoma risk in Hispanics.

Xiangnan Li, Spiridon Tsavachidis, Priya B. Shetty, Yanhong Liu, Aaron P. Thrift

Baylor College of Medicine, Houston, TX

Background: Hepatocellular carcinoma (HCC) is the sixth most common cancer and the third leading cause of cancer-related death. The primary cause of HCC is shifting from viral hepatitis infections to metabolic dysfunction-associated steatotic liver disease (MASLD). In the U.S., Hispanics have the highest incidence of HCC. Furthermore, MASLD-related HCC occurs more frequently in Hispanics compared to non-Hispanic Whites and Blacks. These disparities suggest population-specific genetic mechanisms underlying HCC development. While genome-wide association studies have uncovered genetic risk factors for HCC, most studies have focused on East Asian and European ancestry populations and common variants, which often confer small effect sizes. Rare variants can exert larger effects than common variants and may provide novel biological insights, particularly in underrepresented Hispanics.
Methods: We performed whole-exome sequencing on blood samples from 719 Hispanic individuals, including 455 HCC cases and 264 controls. Analyses focused on 576 genes previously implicated in HCC and MASLD. We prioritized rare, protein-altering variants with minor allele frequency ≤ 0.01 in both our controls and the Admixed American (AMR, primarily Hispanic/Latino ancestry) population from the Genome Aggregation Database (gnomAD). Only variants present in ≥ 3 HCC cases and predicted to be deleterious (with a scaled Combined Annotation Dependent Depletion (CADD) score ≥ 15) were considered. Associations were evaluated using single-variant allelic analysis and gene-based burden tests. Allele counts from gnomAD AMR population controls (n = 30,019) were integrated into the analysis to improve the estimation of odds rations (ORs) and 95% confidence intervals (CIs).
Results: Among 576 genes examined, we identified 27 rare deleterious variant candidates across 24 genes significantly enriched in HCC cases. Top candidate variants included those in immune response genes such as HLA-DRB1 (W38X; OR 15.13, 95% CI 4.91-39.90) and in cell growth genes such as SIK3 (A1272V; OR 7.19, 95% CI 1.85-20.11). Several lipid metabolism genes also showed enrichment, including *PLB1* V417L (OR 21.95, 95% CI 3.81-88.18), *ADAMTS9* S1638L (OR 3.09, 95% CI 0.98-7.47), *TM6SF2* R138W (OR 2.66, 95% CI 1.55-4.28). These genes also showed significant aggregation of rare variants in the burden test. Notably, *TM6SF2* R138W significantly enriched in HCC cases born in the US and in HCC cases with alcohol liver disease and MASLD etiologies (OR = 3.30, 95% CI: 0.98-14.27, P = 0.040).
Conclusion: These results highlight that rare, deleterious variants across immune, cell-regulatory, and lipid-metabolic pathways contribute to elevated HCC risk in Hispanics. These findings further suggest potential gene-environment interactions that may underlie HCC disparities and provide a genetic basis for future targeted prevention strategies in high-risk populations.

#6295 Mutational processes in esophageal and gastroesophageal junction adenocarcinomas across geographical regions.

Laura Torrens[1], Sarah Moody[2], Jiali Pang[2], Behnoush Abedi-Ardekani[1], Ayesha Noorani[2], Haoran Zhang[3], Pilar Gallego-Garcia[4], Valerie Gaborieau[1], Thomas Cattiaux[1], Priscilia Chopard[1], Stephen Fitzgerald[2], Calli Latimer[2], Christine Carreira[5], Marcos Diaz-Gay[4], Laura Humphreys[2], Ludmil B. Alexandrov[3], Michael R. Stratton[2], Sandra Perdomo[1], Paul Brennan[1], on behalf of the MUTOGRAPHS project

[1]Genomic Epidemiology Branch, International Agency for Research on Cancer (IARC/WHO), Lyon, France,[2]Cancer, Ageing and Somatic Mutation, Wellcome Sanger Institute, Cambridge, United Kingdom,[3]Moores Cancer Centre, University of California San Diego, San Diego, CA,[4]Digital Genomics Group, Cancer Genomics Program, Spanish National Cancer Research Center (CNIO), Madrid, Spain,[5]Evidence Synthesis and Classification Branch, International Agency for Research on Cancer (IARC/WHO), Lyon, France

Esophageal adenocarcinomas (EAC) and gastroesophageal junction cancers (GEJ) share multiple risk factors such as reflux disease, obesity, and tobacco smoking. Despite their anatomical proximity and overlapping etiology, they are often considered as esophageal and gastric tumors, respectively. This study aims to decipher the mutational processes that have been operative in EAC and GEJ cancer development and determine whether these are shared across tumor sites and geographical regions.

Whole-genome sequencing data were generated from 520 EAC/GEJ cases (159 EAC and 361 GEJ) from eight countries (China, Iran, United Kingdom, Canada, Kenya, Malawi, Brazil, and Colombia), with available demographic, lifestyle, and environmental exposure data. Mutational signatures were extracted using SigProfilerExtractor and decomposed into reference signatures. Associations between the mutational signatures and epidemiological or molecular features were assessed using multivariate regression models.

Our analysis revealed 17 reference signatures from the COSMIC catalogue, and three signatures described in previous cancer datasets. EAC/GEJ tumors exhibited high burdens of SBS17a and SBS17b, linked to acid reflux, accounting for 26.8% of the median signature burdens. Signature SBS-D, which has been speculated to be caused by DNA repair infidelity, was the second most abundant signature (12% median relative burden), suggesting a relevant role in EAC/GEJ carcinogenesis. EAC and GEJ cancers shared a highly similar mutation, driver, and copy number profile, pointing to shared mutagenic processes, with the exception of SBS-D, which showed enrichment in cancers from the lower and distal esophagus. Signatures SBS17a/b were positively associated with obesity (p-value<0.0005), particularly in EAC cases, supporting the epidemiological notion that obesity may exacerbate reflux disease. We observed no differences in signature burdens with other risk factors, such as tobacco, suggesting its carcinogenic effect in this cancer type could be promotional rather than mutagenic. Finally, we found an association between age-standardized incidence and the signatures SBS5, SBS8, and SBS-D, suggesting a potential dysregulation of endogenous cellular functions in high-risk populations.

This study delineates the mutational forces driving GEJ/EAC cancers. Our results show an overall shared mutational profile across tissues and suggest that obesity enhances the presence of reflux-related mutagenesis. The observed differences across countries could provide relevant information to aid in the development of global prevention strategies.

#6296 Deciphering the promotional determinants of esophageal cancer in countries with varying incidence.

Laura Torrens[1], Raquel Blanco[2], Joanna C. Fowler[3], Ana Carolina de Carvalho[1], Behnoush Abedi-Ardekani[1], Valerie Gaborieau[1], Priscilia Chopard[1], Christine Carreira[4], Abel Gonzalez[2], Jeffrey Reina[5], Anna Martinez-Casals[5], Augusta Jensen[6], Rui Manuel Reis M. Reis[7], Abdolreza Fazel[8], M. Iqbal Parker[9], David Zaridze[10], Patricia Ashton-Prolla[11], Maria P. Curado[12], Mats Nilsson[6], Emma Lundberg[5], Philip H. Jones[3], Nuria Lopez-Bigas[2], Paul Brennan[1], on behalf of the PROMINENT project

[1]Genomic Epidemiology Branch, International Agency for Research on Cancer (IARC/WHO), Lyon, France,[2]Institute for Research in Biomedicine (IRB Barcelona), The Barcelona Institute of Science and Technology, Barcelona, Spain,[3]Wellcome Sanger Institute, Hinxton, United Kingdom,[4]Evidence Synthesis and Classification Branch, International Agency for Research on Cancer (IARC/WHO), Lyon, France,[5]Department of Bioengineering, Stanford University, Department of Bioengineering, Stanford University, Palo Alto, CA,[6]SciLifeLab Department of Biochemistry and Biophysics, Stockholm University, Stockholm, Sweden,[7]Barretos Cancer Hospital, Barretos, Brazil,[8]Golestan Research Center of Gastroenterology and Hepatology, Golestan University of Medical Sciences, Gorgan, Iran, Islamic Republic of,[9]University of Cape Town, Cape Town, South Africa,[10]Department of Clinical Epidemiology, N. N. Blokhin National Medical Research Centre of Oncology, Moscow, Russian Federation,[11]Hospital de Clinicas de Porto Alegre, Porto Alegre, Brazil,[12]A.C. Camargo Cancer Center, Sao Paulo, Brazil

Esophageal squamous cell carcinoma (ESCC) incidence varies widely across the world, correlating with exposure to known risk factors like alcohol, smoking, and hot liquids. It has traditionally been assumed that such exposures lead to malignant cell transformation by directly or indirectly causing DNA mutations. However, recent evidence revealed that most ESCC risk factors do not elicit distinct mutation profiles, suggesting that these carcinogens may act as non-mutagenic tumor-promoting agents. This study aims to investigate the role of exogenous exposures in promoting the clonal expansion of pre-initiated cells in normal esophageal tissue, leading to ESCC.

To address this, we are examining the clonal structure of 200 esophageal epithelium samples from ESCC patients and non-cancer donors across nine geographical regions in China, Iran, Malawi, South Africa, Russia, Brazil, and Canada, with age-standardized ESCC incidence rates ranging from 1 to 84 per 100,000. Detailed demographic, lifestyle, and exposure information, including tobacco, alcohol, and hot liquids, is available. Esophageal epithelial tissues are dissected and analyzed by NanoSeq for mutational signature and mutation burden evaluation, and by 500x whole-exome sequencing to identify mutant genes under positive selection. Spatial proteomics and transcriptomics are ongoing to profile the phenotype of premalignant cells and their microenvironment niches.

Preliminary analyses of 97 cases from high- and intermediate-risk regions revealed a strong mutagenic effect of alcohol and tobacco on normal esophageal tissue. Alcohol-related mutational signatures SBS16 and ID11 were detected in 73% of drinkers (22/30), and were enriched in cases exposed to both alcohol and tobacco. In contrast, hot liquid consumption was not related to distinct mutation profiles. dN/dS analysis in 47 cases with available WES data identified 11 genes under positive selection, including *NOTCH1*, *TP53*, *FAT1*, and *PPM1D*. Cases exposed to tobacco presented higher fractions of mutated epithelia in several of these cancer genes. Notably, the fraction of *NOTCH1*-mutant epithelia was inversely associated with ESCC incidence, suggesting a reduction of clones harboring this protective mutation in high-risk populations.

These findings shed light on the complex interplay between mutagenic and promotional processes in ESCC development and provide insights into the role of known and suspected risk factors in clonal selection. This work may ultimately guide preventive strategies targeting the earliest stages of esophageal carcinogenesis.

: Advances in Survivorship
Poster Session

#6300 How do healthcare providers approach breast cancer diagnoses in young women? Findings from the BRAVE Study.

Alice W. Lee[1], Mojgan Sami[1], Peyton Fisher[2], Diana Aguilar-Cruz[1], Thien-Y Do[1], Melissa Vargas[1], Aleah La Flair[2], Nicole Wells[2]

[1]California State University, Fullerton, Fullerton, CA,[2]The Young Breast Cancer Project, Chula Vista, CA

Background: Young women face unique challenges when it comes to breast cancer. Not only are they more likely to be diagnosed with late stage tumors and have poorer prognoses relative to older women, but they are also more likely to experience diagnostic delays. Given the complexity of delays and how they can stem from both the patients themselves as well as the healthcare system, we sought to better understand the barriers and facilitators to a timely diagnosis of breast cancer in young women from the perspectives of primary care and obstetrics/gynecology (OB/GYN) providers who often serve as the first point-of-contact for health issues for female patients.
Methods: As part of the Breast Cancer in Young Women: Awareness, Views, Experiences (BRAVE) Study, we conducted one-on-one interviews with four primary care and three OB/GYN physicians, who routinely see young female patients in their California-based practice, to understand their perceptions, approaches, and procedures to diagnosing a young woman with breast cancer. Each interview was recorded, transcribed, coded, and analyzed using NVivo 15, and emergent themes were identified. A survey that included demographic, medical training, and practice-related questions was also administered.
Results: The average age of the providers was 47 years with most identifying as Asian American (57%). Four key themes emerged from the interviews. First, there appeared to be a distinction between provider autonomy versus healthcare system constraints with providers in private practice having greater flexibility to deliver more personalized care. Second, we noted how provider-led education could facilitate early detection of breast cancer by reducing stigma surrounding feminine bodily self-awareness. Third, providers acknowledged how there were insurance and financial barriers, which often prevented coverage for diagnostic tests or problem-based visits and left women unable to access needed care. Fourth, it seemed like the diagnostic process was often impacted by providers having to balance screening guidelines with patient anxiety.
Conclusions: When it comes to the diagnosis of breast cancer in young women, structural, institutional, and provider-specific factors play critical roles. Providers working in institutions that allow them more clinical autonomy often have the flexibility and time to deviate from standardized guidelines and deliver more personalized care. Clinical autonomy may facilitate timely diagnosis particularly in young women under age 40 whose case may not conform to standardized screening and diagnostic recommendations. Given that a timely diagnosis can be attributed to factors related to patients as well as providers, our study is currently exploring this topic from both perspectives. Focus groups with young breast cancer survivors have already been conducted, and additional interviews with providers are planned.

#6301 Coronary atherosclerosis as an incidental finding within the lung cancer screening program.

Edoardo Sostero[1], Kathrin Chiffi[1], Lisa Jungblut[2], Vanessa Englmaier[2], Thomas Frauenfelder[2], Isabelle Opitz[3], **Sven Hillinger**[1]

[1]Thoracic Surgery, University Hospital, Zurich, Switzerland,[2]Radiology, University Hospital, Zurich, Switzerland,[3]Thoracic Surgery, University Hospital Zurich, Zurich, Switzerland

Purpose: Smoking is a leading cause of preventable morbidity and mortality worldwide, contributing to lung cancer, COPD, stroke, and coronary heart disease. Lung cancer remains the deadliest malignancy, with smoking as its main etiologic factor. Early detection via low-dose computed tomography (LDCT) reduces mortality. Since 2019, a national feasibility study on LDCT-based lung cancer screening (LCS) has been conducted at University Hospital Zurich. Because smoking also increases coronary atherosclerosis risk, this study aimed to determine the prevalence, severity, and clinical significance of coronary artery calcification (CAC) as an incidental finding in LCS participants and assess its relationship with age and smoking exposure.
Methods: 201 participants from the Swiss LCS cohort were retrospectively analyzed. All were current or former heavy smokers meeting national screening criteria. LDCT scans were assessed by two thoracic radiologists using the SHEMESH score, grading calcification in LM, LAD, LCx, and RCA from 0 (absent) to 3 (severe), with total CAC scores 0-12. Relationships between CAC, age, and smoking exposure (pack-years) were analyzed using a generalized linear mixed model. Participants with CAC > 4 were advised to undergo stress testing and followed for four years for cardiologic evaluation or cardiovascular events.
Results: CAC was detected in 55.7% (112/201): 30.8% mild (1-3), 15.9% moderate (4-6), and 8.9% severe (7-12). CAC correlated significantly with age ($p = 0.032$) and pack-years ($p = 0.011$). Among 50 participants with CAC > 4, one was lost to follow-up; two did not undergo evaluation due to palliative care or non-cardiac death; 18 are under assessment. Eight (19.5%) had prior cardiac events; 18 had negative stress tests. Three (6.3%) had positive tests or symptoms, leading to angiography and stent placement; in two cases, the treated vessel matched the highest CAC score. Most calcifications were in LAD and RCA. Nine of 49 reported exertional dyspnea or atypical chest discomfort, prompting further evaluation.
Conclusions: Incidental CAC was highly prevalent in smokers undergoing LDCT screening, with severity linked to age and cumulative tobacco exposure. CAC detection during LCS offers an opportunity for cardiovascular risk assessment without added radiation or scan time. Integrating CAC evaluation into LDCT protocols could enhance early identification of at-risk individuals, support preventive cardiology, and improve outcomes. This study supports LDCT screening as a dual-purpose tool against lung cancer and coronary atherosclerosis, aligning with precision preventive medicine strategies.

#6302 Impact of biological aging due to chemotherapy on breast cancer survivorship.

Swarnavo Sarkar[1], Mina S. Sedrak[2], Judith E. Carroll[2], Clyde Schechter[3], Hyman B. Muss[4], Jeanne S. Mandelblatt[1]

[1]Georgetown University, Washington, DC,[2]UCLA - University of California Los Angeles, Los Angeles, CA,[3]Albert Einstein College of Medicine, Bronx, NY,[4]University of North Carolina, Chapel Hill, Chapel Hill, NC

Background: Chemotherapy improves breast cancer survival, but also increases the accumulation of senescent cells in breast cancer survivors. Excess accumulation of senescent cells increases inflammation and tissue damage, which leads to premature onset of age-related diseases (biological age acceleration) in breast cancer survivors.

Objective: We integrate a systems biology model of accumulation of senescent cells with chronological age and a well-established Cancer Intervention and Surveillance Modeling Network (CISNET) breast cancer simulation model to estimate the impact of biological age acceleration on survivorship outcomes.

Methods: We used published data on senescence biomarker expression level ($p16^{INK4a}$ mRNA expression) in chemotherapy recipient breast cancer survivors to simulate the elevated senescence expression level in the remaining lifetime of breast cancer survivors. The difference in the senescence expression level in the chemotherapy group was evaluated against the expression level in the general female population to quantify the biological age acceleration after chemotherapy. The biological age, instead of chronological age, was used to determine the hazard of non-breast cancer mortality in chemotherapy recipient breast cancer survivors. We used CISNET breast cancer simulation model to simulate multi-birth cohorts of US females diagnosed with breast cancer to estimate survivorship outcomes after chemotherapy. Outcomes included remaining life years after breast cancer diagnosis, absolute number of non-breast cancer deaths, and time-point of transition to dominant risk of non-breast cancer mortality.

Results: Biological age acceleration after anthracycline-based regimens caused a greater loss of life years than anthracycline-free regimens for women diagnosed at ages 30-39 years (median of 17.7 years vs. 2.8 years lost). Within the anthracycline group, life years lost varies from 10.4 years to 23.3 years, depending on the level of biological age acceleration. The loss in life years diminished with increasing age at diagnosis (median of 7.5 years vs. 2.2 years lost for 70-79 year old women). The risk of non-breast cancer mortality exceeded breast cancer mortality up to 10-15 years earlier than expected based on chronological age, especially after anthracycline-based regimens.

Conclusions: Including biological age acceleration as a factor in breast cancer life history simulation models can help to identify subgroups of breast cancer survivors who need targeted survivorship care for non-breast cancer mortality. Biological age acceleration is a crucial factor especially for the long-term care of younger chemotherapy recipient breast cancer survivors.

#6303 Designing an integrative theoretical framework for predicting endocrine toxicity in a large prospective cohort of cancer patients treated with immune checkpoint inhibitor therapy.

Hala Awad[1], Mostafa Mohamed[2], Michelle C. Janelsins[3], Jeremy Jonathan McGuire[4], Lisa Danish[1], Song Yao[5], Charles Kamen[4]

[1]Department of Surgery, Univ. of Rochester School of Medicine & Dentistry, Rochester, NY,[2]Department of Public Health Sciences, Univ. of Rochester School of Medicine & Dentistry, Rochester, NY,[3]Postdoctoral Fellow, Dept. of Radiation Onc., Univ. of Rochester Cancer Ctr., Rochester, NY,[4]University of Rochester, Rochester, NY,[5]Postdoctoral Res. Associate, Dept. of Cancer Prev. & Control, Roswell Park Cancer Institute, Buffalo, NY

Immune checkpoint inhibitors (ICI) are associated with immune-related adverse events (irAEs) involving the endocrine system. The rate of endocrine irAEs can vary significantly depending on the agent used, with an average all-grade occurrence of 23% and a severe-grade occurrence of 19%. Unlike other irAEs, endocrinopathies frequently persist after ICI treatment discontinuation, highlighting the need for risk stratification and predictive monitoring. The current understanding of endocrine irAEs is limited, and there are no reliable methods to identify individuals who are most at risk of developing these complications prospectively or to stratify risk at the initiation of treatment. The current study presents an theoretical framework for systematically investigating underlying mechanisms and risk factors for endocrine irAEs. The primary objective is to generate hypotheses and advance methodological approaches for subsequent predictive modeling and clinical trials, thereby supporting the development of tailored strategies for the early detection and management of these irAEs. Within this framework, we propose that endocrine irAEs are complex and result from multidimensional interactions among various clinical, biological, and lifestyle determinants. We examine endocrine irAE risk through a multifaceted approach encompassing: (1) clinical and treatment factors (ICI agent selection, dosing schedules, treatment sequencing), (2) biomarkers of immune dysregulation (CBC-derived indices and lymphocyte/neutrophil counts), (3) inflammatory mediators (IL-6, IFN-γ, TNF-α, IL-8, TGF-β), (4) genetic predisposition, and (5) behavioral and environmental exposures (nutrition, physical activity, tobacco use, comorbid diseases). Sex is also hypothesized to be a critical effect modifier, specifically influencing the predictive utility of specific CBC indices for immune dysregulation parameters for susceptibility to irAEs. Using a systems biology framework informed by mechanistic data and current empirical evidence, we develop an integrative approach that combines quantitative biomarkers with patient-reported assessments of behavioral and environmental exposures. Robust predictive models, we propose, require integration of clinical, biological, modifiable risk, and environmental factors, stratified by sex. This approach seeks to move toward a systems-based approach rather than biomarker assessment, providing a structured foundation for subsequent empirical validation and integration into clinical trial methodology. By integrating clinical, biological, and lifestyle factors, this framework supports the development of predictive models and tailored surveillance protocols that can be implemented in future clinical trials and oncology practice.

#6304 Predictors of engagement and healthcare resource utilization in chemotherapy patients using a text message response system.

Suma Sri Chennapragada, Yang Wang, Jay Carlson, Aswanth Reddy

Mercy Hospital, Fort Smith, AR

Background: Patients receiving chemotherapy face a high risk of treatment-related complications, often leading to increased healthcare resource utilization (HCRU). Mercy Hospital, St. Louis, implemented a text message response system (TRS) to proactively capture patient-reported symptoms and facilitate timely nursing interventions. We evaluated demographic and clinical factors associated with TRS engagement and their relationship to HCRU.

Methods: We analyzed data from 3,899 patients across hospitals in three states (January-July 2025), including 2,750 TRS responders and 1,149 non-responders. Variables assessed included age, sex, ethnicity, comorbidities (cerebrovascular disease [CVD], chronic obstructive pulmonary disease [COPD], renal disease), cancer type, and HCRU (emergency department [ED] visits, inpatient [IP] admissions). Statistical analyses employed Welch t-tests, Pearson χ^2 tests, odds ratios (OR) with 95% confidence intervals (CI), and Holm correction for multiple comparisons.

Results: Responders were slightly younger than non-responders (mean age 67.22 vs. 67.91 years, p=0.111). Female patients were more likely to respond (73.2% vs. 67.5%; OR=1.31, 95% CI 1.15-1.51, p=0.00010). Response rates did not differ significantly by ethnicity or comorbidities. Cancer type showed modest variation (χ^2=19.77, p=0.011, Cramér's V=0.065), though no pairwise differences remained after correction. ED utilization was higher among responders (14.33% vs. 10.71%; OR=1.39, 95% CI 1.12-1.73, p=0.0014), while IP admission rates were similar (15.96% vs. 16.10%, p=0.915). Leading IP diagnoses included sepsis (41.94%) and anemia (38.4%), while pain (48.41%) and nausea (14.96%) dominated ED visits.

Conclusions: TRS engagement was higher among female and younger patients, while older adults were less likely to respond, suggesting the need for alternative outreach strategies such as direct telephone calls. Responders demonstrated greater ED utilization, primarily for pain and nausea, but comparable IP admission rates. These findings underscore the importance of targeted interventions—such as infusion center support and palliative care integration—to proactively manage chemotherapy-related symptoms and reduce HCRU in the outpatient setting.

#6305 Prostate cancer chronotherapy: Influence of treatment timing on radiation efficacy and quality of life.

Andrea A. Almeida, Jiji Jiang, Sally Elsamanoudi, Carrie Cheung, Ayaan Hussein, Tracy Pletcher, Faisal Del, Fouad Mumayiz, Arwa Fallatah, Gregory T. Chesnut, Ayesha A. Shafi

Center for Prostate Disease Research, Bethesda, MD

Circadian-controlled genes influence numerous physiologic processes, including hormone regulation. Emerging evidence across cancer types suggests that aligning therapy delivery with circadian cycle (chronotherapy) may optimize efficacy and reduce toxicity. Given the hormone-sensitive nature of prostate cancer (PCa) and frequent use of androgen deprivation therapy (ADT) combined with external beam radiation therapy (EBRT), the timing of EBRT relative to circadian phase may modulate treatment response. Thus, we investigated whether time-of-day (TOD) of EBRT delivery is associated with PCa outcomes overall and by ADT status. Patients with localized PCa enrolled in the Center for Prostate Disease Research Multicenter National Database Study (2007-2023) were eligible for inclusion if treated with EBRT. TOD of EBRT was categorized as morning (≥80% of sessions before 10AM), afternoon (≥80% of sessions after 10AM), or mixed. Clinical endpoints included biochemical recurrence (BCR), metastasis, and death. Quality of life was longitudinally evaluated over 36 months via the Expanded Prostate Cancer Index Composite (EPIC). Cox proportion hazards regression models estimated hazard ratios (HR) and 95% confidence intervals (CI) for associations between TOD of EBRT and PCa outcomes. Kaplan-Meier analyses were used to examine survival. Among 339 included patients, 156 received morning EBRT, 137 afternoon EBRT, and 46 mixed TOD EBRT. On average, patients were 69.9 years old, had clinical stage T1 disease (78.8%), and had a PSA of 9.0 ng/mL at EBRT initiation. ADT was more often administered to afternoon (55.5%) and mixed TOD patients (58.7%) than morning patients (38.5%). Afternoon EBRT was not associated with death (HR=1.24, 95% CI 0.66-2.33) or BCR/metastasis (HR=1.37, 95% CI 0.66-2.85) relative to morning EBRT. Results were similar when stratified by ADT status. There were no differences in BCR-free, metastasis-free, or overall survival by TOD or ADT status. Overall, morning and afternoon patients reported similar EPIC scores; sexual function and bother scores were notably lower than other scores. Among those who received ADT, afternoon patients reported worse urinary bother (UB) and sexual bother (SB) scores (*p-values*: UB month 36=0.04; SB month 18=0.01; SB month 30=0.04) than morning patients. Scores were similar among morning and afternoon patients who did not receive ADT. Within an equal-access healthcare setting, TOD of EBRT was not associated with oncologic outcomes for localized PCa. However, the combination of ADT and afternoon EBRT was associated with worse urinary and sexual quality of life, suggesting potential interaction between circadian regulated hormone signaling, ADT, and treatment timing. This study provides evidence that ADT may interact with TOD of PCa therapy and that further research in circadian biology, ADT timing, and chronotherapeutic optimization in PCa is warranted.

#6306 Novel application of the iCCaRE consortium virtual reality assistant (ViRA) to support Black men at the point of prostate cancer diagnosis.

Folakemi T. Odedina[1], Che Ngufor[2], Christopher Williams[3], Mary Ellen Young[4], Floyd Willis[5], Adam M. Kase[1], Arnold Merriweather[6], Emelina Asto-Flores[1], Dee M. Glaser-Boivin[5], Jada Melton[1], Monica L. Albertie[7], Michelle Fudge[1], Quincy Wimberly[1], Inclusive Cancer Care Research Equity (iCCaRE) Consortium, Prostate Cancer Transatlantic Consortium (CaPTC)

[1]Mayo Clinic Florida, Jacksonville, FL,[2]Mayo Clinic, Rochester, MN,[3]Urological Assoc Inc, Jacksonville, FL,[4]University of Florida College of Public Health & Health Professions, Gainesville, FL,[5]Mayo Clinic, Jacksonville, FL,[6]Black Male Prostate Coalition of Florida, Jacksonville, FL,[7]Cancer Services, Mayo Clinic, Jacksonville, FL

Background: Black men carry a disproportionate prostate cancer (CaP) burden and often experience significant psychosocial distress at the point of prostate cancer diagnosis (PPCD). Many report emotional shock, uncertainty, and limited access to culturally competent guidance, which can negatively affect treatment decisions and long-term survivorship. To address these needs, we developed the PPCD Virtual Reality Assistant (ViRA), an immersive, AI-enabled intervention co-designed with Black CaP survivors. ViRA delivers tailored psycho-oncology support, emotional guidance, and navigation of social determinants of health (SDOH) within virtual reality environments. This study evaluated the feasibility, acceptability, and usability of the PPCD ViRA (NCT06535802).
Methods: ViRA was developed through a structured, seven-step co-design process with survivors, integrating mobile immersive technologies, SDOH navigation, and culturally grounded psycho-oncology content. Personalization was enabled through AI-driven predictive analytics and a recommendation engine. Alpha testing assessed initial usability and acceptability among 10 participants (seven team members and three Black CaP survivors). Beta testing with 24 Black men in Florida examined feasibility and preliminary efficacy.
Results: A demonstration of ViRA is available (https://www.youtube.com/watch?v=1mI-HS5R6sk). Alpha testing indicated strong usability, positive emotional engagement, and clear promise for enhancing support at the PPCD. In Beta testing, participants varied in age; most were married (58.3%), held a bachelor's degree (45.8%), were retired (45.8%), and had a family history of cancer (83.3%). ViRA use was associated with increased engagement and reduced distress across participants. Overall, 74% rated ViRA as “excellent,” while the remainder rated it as “good” or “very good.” More than 90% reported being “very satisfied,” with the rest indicating satisfaction.
Conclusions: Findings demonstrate high feasibility, acceptability, and cultural relevance of the PPCD ViRA for supporting Black men at diagnosis. Lessons learned highlight the need for culturally embedded design, emotional timing, community co-creation, flexible delivery formats, and strong community partnerships to advance digital health equity. The refinement and larger-scale validation to establish clinical utility and readiness for implementation is ongoing (NCT07126548).

#6307 Feasibility of a survivorship app for black prostate cancer survivors: Results from a 12-week mHealth pilot study.

Gaurav Kumar[1], Parisa Ghasemi[1], Yan D. Zhao[1], Zsolt Nagykaldi[1], Kathleen A. Dwyer[1], Andrew G. McIntosh[1], Ernie Kaninjing[2], Mary E. Young[3], Dickey Sabrina[4], Daniel Morton[1], Opeyemi Bolajoko[5], Darla E. Kendzor[1], Motolani Ogunsanya[1]

[1]The University of Oklahoma Health Campus, Oklahoma City, OK,[2]Georgia College & State University, Milledgeville, GA,[3]Mayo Foundation for Medical Education and Research, Jacksonville, FL,[4]Florida State University, Tallahassee, FL,[5]Mayo Clinic Florida, Jacksonville, FL

Introduction: Black prostate cancer (CaP) survivors experience unique quality-of-life (QoL) and recovery challenges after treatment compared with their White counterparts. Smartphone-delivered mobile health interventions offer promising avenues for symptom tracking and lifestyle changes; but their feasibility, user engagement, and acceptability in this population remain unclear. This study assessed the feasibility, engagement, and preliminary impact of the Survivorship App for Ethnically Diverse Black Prostate Cancer Survivors (SAFE-CaPS), designed to improve self-monitoring behaviors and health outcomes.

Methods: Nine Black CaP survivors (seven U.S.-born, one African-born, and one Caribbean-born) participated in a 12-week pilot study of SAFE-CaPS. The app provided daily prompts for symptoms (pain, sleep, fatigue, sexual function, anxiety, depression) and behavior tracking (physical activity, diet), brief self-management support, and physician alerts for severe symptom reports. Mental health (GAD-7 and PHQ-9) and QoL (FACT-P) were assessed at baseline and after 12 weeks. Feasibility was evaluated based on adherence rates (i.e., ≥70% of daily diary entries). Engagement and acceptability were assessed via app analytics and qualitative interviews on usability and cultural relevance. Participants were compensated up to $125 via Greenphire ClinCard. Surveys were analyzed with SPSS v29, and interviews with Atlas.ti v23.

Results: Participants' median age at diagnosis was 56 years; six had a positive family history of CaP, and four had undergone radical prostatectomy. Four participants met the feasibility threshold, and eight completed the study. Most daily entries reflected mild pain, fatigue, bowel and urinary issues, and generally good sleep. Several participants frequently reported severe sexual dysfunction, and most diary responses indicated <20 minutes of physical activity per day. Fruit/vegetable intake was low, with about half of daily responses showing 1-2 servings. At baseline, eight participants had minimal anxiety, while five had moderate depression. Overall, QoL improved from week 1 to week 12 in physical, emotional, and functional well-being, while social well-being declined over time. Interviews emphasized the app's user-friendly design, ease of navigation, and acceptability as key strengths, with several participants highlighting its simplicity and ease of use, with recommendations to reduce repetitive items and address minor technical issues.

Conclusions: SAFE-CaPS was feasible and well accepted. Sexual dysfunction, low physical activity, and moderate depression emerged as key concerns, heightening the need for integrated mental health, activity support, and stronger engagement strategies in future mHealth interventions.

#6308 Adhesive capsulitis vs. metastasis: Comparative frequency in oncology patients with hip pain.

Laasya Madana[1], Avneesh Chhabra[2], Alireza Eajazi[2]

[1]UT Southwestern Medical Center, Dallas, TX,[2]Musculoskeletal Radiology, UT Southwestern Medical Center, Dallas, TX

Background: Adhesive capsulitis (AC) is defined as the gradual, progressive loss of range of joint motion due to inflammation, adhesions, and capsular thickening. Shoulder AC is well established with a prevalence of 2-5% in the general population, but the prevalence of hip AC remains unknown, likely due to underdiagnosis. Existing literature suggests shared risk factors between shoulder and hip AC—including diabetes, thyroid disease, trauma, and surgery. In addition, while AC has been studied in the general population, its prevalence has not been extensively evaluated in the oncologic population. Oncologic patients with hip pain frequently undergo contrast-enhanced MRI to exclude metastasis, yet the relative frequency of tumor infiltration versus adhesive capsulitis remains unclear. Prior (few) studies have only used non-contrast, fat-suppressed T2W MRIs, making it challenging to differentiate the capsule from the iliofemoral ligament clearly. CEMR incorporates non-contrast sequences, allowing assessment of key AC features—including capsular and iliofemoral ligament thickening or enhancement, as well as preferential fluid pooling in the posterior recess or iliopsoas bursa.
Purpose: To determine the frequency of AC in patients with known primary malignancy undergoing CEMR of hip joint at a tertiary care academic center.
Methods: In this cross-sectional retrospective analysis, from 01/2021 to 01/2025, CEMR studies of hip joints were identified, yielding 57 eligible examinations. Adult patients (>18) with a known primary malignancy were included. Exclusions comprised non-contrast MRIs, absence of confirmed malignancy, significant artifacts, recent trauma, or known inflammatory or infectious conditions. Prospectively, reports were generated by fellowship-trained MSK radiologists in our center. Studies were subsequently re-reviewed by an additional radiologist to evaluate for features of AC, including capsular thickening, capsular enhancement, fluid pooling in synovial recesses, and/or presence of tumor lesions in the imaged hips.
Results: Preliminary analysis yields AC in 9/57(16%) cases. 48/57 (84%) MRIs demonstrated a malignant lesion, non-AC condition. Further analyses will assess how often hip adhesive capsulitis occurs across age groups, genders, and malignancy types. Quantitative measures of capsular thickening, enhancement, and joint recess distention will help refine characterization of these imaging findings.
Conclusion: Though occurring at a smaller frequency, AC can present as hip pain in patients with known primary malignancy. Recognizing this pattern can help clinicians direct appropriate management and prevent unnecessary concern for metastatic disease.

#6309 Perturbations in gut liver axis functions are associated with chemotherapy induced nausea and fatigue in patients with breast cancer.

Komal Preet Singh[1], Brenda J. Ernst[1], Jun Chen[2], Surendra Dasari[2], Felipe Batalini[1], Cindy Tofthagen[3], Kathryn J. Ruddy[4], Keenan Pituch[5], Linda Chlan[6]

[1]Mayo Clinic Cancer Center Arizona, Phoenix, AZ,[2]Health Science Research, Mayo Clinic, Rochester, MN,[3]Mayo Clinic Cancer Center, Jacksonville, FL,[4]Mayo Clinic Cancer Center, Rochester, MN,[5]Arizona State University, Phoenix, AZ,[6]Mayo Clinic Rochester, Rochester, MN

Background: Up to 50% of patients with breast cancer experience chemotherapy-inducednausea (CIN) and 95% experience fatigue. A comprehensive understanding of biological mechanisms remains elusive. Herein, we evaluated the association of CIN and fatigue with clinical and multi-omics features, including serum and stool metabolites before (T1) to after chemotherapy (T2).
Methods: Patients with breast cancer (n=36) who were to receive chemotherapy, provided symptom assessment using the Memorial Symptom Assessment Scale, stool and blood samples at T1 and T2. Patients provided dietary intake data using a Dietary Screener Questionnaire at T1. Descriptive and univariate analyses evaluated associations of co-occurringsymptoms and diet with CIN and fatigue at T2. Gut microbiome was sequenced using shotgun metagenomics. Targeted metabolomics was performed on stool and serum. Shift in the abundance of taxonomic groups and metabolite levels from T1 to T2 were evaluated in association with CIN and fatigue.
Results: Approximately 64% of the patients experienced CIN and 94% experienced fatigue atT2. Three gastrointestinal symptoms co-occurred with CIN and fatigue. Higher daily average intake of calcium ($p=0.013$) and dairy ($p=0.035$) were associated with CIN. Levels of hexosylceramides, ceramide, phosphatidylcholine and sphingomyelins were significantly perturbed in association with CIN and fatigue ($p<0.05$).
Conclusion: CIN and fatigue are associated with perturbation in the sphingolipid turnover pathway, which negatively impacts functions in the gut-liver axis that include apoptosis activity and change in bile acid levels. Confirmatory studies are warranted to support the development of interventions to alleviate CIN and fatigue in patients with breast cancer receiving chemotherapy.Keywords: breast cancer; chemotherapy-induced nausea; fatigue; metabolites; sphingolipids

#6310 Reduction of infections with intravenous immunoglobulin in chronic lymphocytic leukemia: A single-center retrospective analysis.

Nirja Shah, Tulsi Patel, Thomas J. Kipps, Michael Y. Choi

UCSD Medical Ctr., San Diego, CA

Hypogammaglobulinemia is common in chronic lymphocytic leukemia (CLL). Guidelines recommend Intravenous Immunoglobulin (IVIG) prophylaxis for patients with recurrent, serious infections (e.g., those requiring IV antibiotics or hospitalization) and IgG < 500 mg/dL. Prior trials showed reduced infections with IVIG without survival benefit, but predate modern CLL therapy. This study evaluates infectious outcomes in CLL patients who received IVIG between 2005 - 2022.

This was a single-institution retrospective cohort study of CLL patients. Patients were identified by IVIG receipt and excluded if IVIG was given for other indications (e.g., autoimmune hemolytic anemia). Infection frequency and severity were assessed during the year prior to and the year following IVIG initiation. Treatment history, concurrent therapy, and baseline immunoglobulin levels were also collected.

Of 79 patients identified with IVIG treatment, 48 met inclusion criteria of IVIG use for hypogammaglobulinemia and infections, based on charts available for close review. The median age at IVIG initiation was 58 years; mean time from CLL diagnosis to IVIG initiation was 10.5 years. At initiation, 52% had Rai stage 0-II disease and 48% had Rai stage III - IV disease. Baseline mean IgG prior to IVIG was 411 mg/dL (range 93 - 894 mg/dL) and baseline mean IgA was 42 mg/dL (range 4 - 177 mg/dL).

Pre-IVIG: 73% of patients experienced at least one grade 2 or 3 infection in the year prior to initiation of IVIG. Most patients had recurrent infections; the average number of grade 2 or higher infections was 1.6 (range 0 - 4). Only two patients had a grade 3 infection in the year prior to IVIG initiation, though notably 15 others had prior grade 3 infections since they were diagnosed with CLL. In total, 17 patients (35%) had a grade 3 infection at any time prior to IVIG.

Post-IVIG: Only 12 patients (25%) experienced a grade 2 or higher infection in the year following IVIG initiation, with a mean of 0.375 infections (range 0 - 4). Two of these patients (4%) had grade 3 infections, which were multifocal pneumonia and cellulitis. This represents a 66% relative risk reduction, and a Number Needed to Treat (NNT) of 2.1 to prevent grade 2 or higher infections in the year following IVIG initiation (RR 0.34, P = 0.0001, 95% CI: 0.20 - 0.58). No significant differences were observed between patients with and without post-IVIG infections in prior CLL treatment (75% vs. 83%, p = 0.57), baseline IgG (p = 0.91) or IgA levels (p = 0.93).

To conclude, IVIG prophylaxis significantly reduced both moderate (grade 2 or higher) infections, consistent with prior data. While IVIG is recommended primarily for patients with severe infections (2025 NCCN guidelines), our findings suggest IVIG may also meaningfully reduce grade 2 infections and improve quality of life. Future IVIG studies should incorporate quality of life metrics to define the role of IVIG in modern CLL care.

: Genomics, Proteomics, Biomarkers, and Risk Stratification
Poster Session

#6315 High prevalence of clonal hematopoiesis in biopsy-proven MASH and implications for cancer care.

Sourat Darabi[1], Brian T. Lee[2], Tse-Ling Fong[2], Benjamin H. Goldenson[1], Carlos E. Zuazo[1], John S. Cupp[3], Michael J. Demeure[1], Patrick Lee[2], David R. Braxton[1]

[1]Hoag Family Cancer Institute, Newport Beach, CA,[2]Liver Program, Hoag Digestive Health Institute, Newport Beach, CA,[3]Pathology, Hoag Memorial Hospital Presbyterian, Newport Beach, CA

Background: Metabolic dysfunction-associated steatohepatitis (MASH) is a systemic disease increasingly recognized for its oncologic relevance. Patients with MASH face elevated risks of visceral malignancies, including hepatocellular, colorectal, and endometrial cancers. Age-related clonal hematopoiesis (CH)—defined by somatic mutations in peripheral blood cells—is associated with inflammation, cardiovascular disease, malignancy, and therapy-related myeloid neoplasms. Recent studies suggest CH contributes to MASH pathogenesis, yet its prevalence and clinical impact remain unclear. We evaluated the prevalence of CH in biopsy-proven MASH patients within a community hepatology cohort.
Methods: We conducted a cross-sectional study of 20 patients with biopsy-confirmed MASH who underwent next-generation sequencing using a commercial hematologic malignancy panel. CH was defined as the presence of somatic mutations with variant allele frequency (VAF) ≥2.5%. Demographic, metabolic, and hepatic (including transient elastography with FibroScan® and histologic characteristics) parameters were analyzed for association with CH.
Results: Among 20 patients (13 female, 7 male; mean BMI 29; mean age 57.0 ± 15.5 years, range 25-84), CH was detected in 5 (25%; mean age 59.4 ± 12.4 years, range 45-75). Compared with the expected population prevalence of 10% at age 70, the relative risk of CH was 2.5, with an indirect age-adjusted relative risk of 3.07. Detected driver mutations (VAF%) included *ASXL1* (8.2), *ATRX* (3.6), *CBL* (2.7), *DNMT3A* (3.7), and *KMT2C* (4.1). All CH-positive patients were low risk by clonal hematopoiesis risk score (CHRS) and none reported tobacco use. ALT was significantly lower in CH-positive vs CH-negative patients (median 36.5 vs 70 U/L; p = 0.048). No significant differences were observed in age, BMI, AST, NAFLD activity score, fibrosis stage, liver stiffness measurement, or peripheral blood counts.
Conclusions: CH is enriched in biopsy-proven MASH, independent of fibrosis or disease severity. Given its oncologic implications, CH testing may help identify MASH patients at increased risk for cancer and therapy-related complications. Integration of CH screening into hepatology-oncology workflows could enhance risk stratification and inform treatment planning for this high-risk population.

#6316 Accumulation of p21+ cells and enrichment of growth arrest signature in persistent high-grade premalignant lesions.

Alexis Assante[1], Khosbayar Lkhagvadorj[1], Hyunmin Kim[2], Kimberly R. Jordan[3], Daniel T. Merrick[4], Robert L. Keith[1], York E. Miller[5], Moumita Ghosh[1]

[1]Pulmonary, Allergy and Critical Care Medicine, University of Colorado, Aurora, CO,[2]Genetic and Genome Sciences, Case Western University, Cleveland, OH,[3]Department of Immunology and Microbiology, University of Colorado, Aurora, CO,[4]Department of Pathology, University of Colorado, Aurora, CO,[5]Rocky Mountain Regional Veteran Affairs Medical Center, Aurora, CO

Introduction: Lung squamous cell carcinoma is preceded by premalignant lesions (PML) or dysplasia that may persist, progress, or regress. Individuals with persistent PMLs have a significantly higher risk of incident cancer compared to those whose lesions regress. Mechanisms that control dysplasia fate, therefore, could be important for early detection and prevention. Epithelial basal progenitors are critical for maintaining a healthy airway, but their role in determining PML fate has not been studied before.
Methods: Basal progenitors grown from endobronchial biopsies collected from high-risk individuals were assayed for their cardinal features of self-renewal and multipotent differentiation. A combination of cellular, functional, and molecular analyses, including mutations and single-cell (sc) RNAseq, was used to investigate progenitor function and their roles in determining PML fate.
Results: Progenitor function decreased with worsening dysplasia grade, and poor progenitor self-renewal predicted dysplasia persistence and progression to cancer. Mutational analysis of high- and low-self-renewing progenitors did not detect any meaningful difference in overall mutational burden, including oncogenic mutations. Interestingly, there were increased numbers of cells expressing cyclin-dependent kinase inhibitor (CDKN1A) or p21 in the progenitors with low self-renewal compared to those with high self-renewal. Single-cell (sc) RNA-seq of biopsies revealed enrichment of p21-expressing basal cells in lesions with low progenitor self-renewal. VECTRA multiplexed immunofluorescence staining of PMLs confirmed significantly greater numbers of p21+ cells in persistent lesions, and the abundance of p21+ cells increased over time. Integration of the multiplexed immunostaining images with the VISIUM spatial transcriptomic profiles generated from serial sections of the same biopsies allowed for direct alignment of p21 protein expression and the corresponding transcriptomic features. A spot-level differential analysis between six $p21^{high}$ and $p21^{low}$ regions from four PMLs revealed the enrichment of specific pathways (primary cilium, cell-cycle arrest, DNA damage responses, metabolic rewiring, and immune engagement) in $p21^{high}$ spots.
Conclusions: p21 is a key determinant of cell cycle progression, and increased expression of this molecule indicates growth arrest by induction of a transient G0 state. The discovery of p21+ cells in PMLs containing low self-renewing progenitors and spatial analyses confirming the presence of a cell-cycle arrest signature in the $p21^{high}$ areas in multiple high-grade PMLs indicated a role of these pathways in determining PML fate. Future studies will focus on analyzing these signatures in independent PMLs with a known natural history of persistence, progression, and regression.

#6317 A reference-free PCR assay for absolute quantification of cancer methylation biomarkers.

Ziming Li, **Huichuan Yu**

The Sixth Affiliated Hospital of Sun Yat-sen University, Guangzhou, China

Background:DNA m5C methylation is a valuable resource for disease biomarkers widely applied in diagnosis. However, current qPCR methods rely on reference assays of genes or repetitive elements (e.g., ACTB, ALU-C4) for data normalization, which may bring inaccuracy and false negatives. To overcome these limitations, we developed a reference-free qPCR technology, MeRFPCR, that enabled accurate and absolute quantification of m5C methylation without external normalization.
Methods: MeRFPCR utilized uncomplementary sense and antisense DNA strands yielded from C-to-T conversion in bisulfite treatment, allowing the design of two sets of primers and fluorescent probes targeting the methylated CpGs in the sense strand and the adjacent CpG-free region in the antisense strand. An absolute methylation level was quantified as the ratio of the methylated signal to the CpG-free signal following PCR amplification, eliminating the need for external reference normalization. We evaluated specificity, sensitivity, and reproducibility across multiple loci, and benchmarked MeRFPCR against quantitative methylation-specific PCR (qMSP) with external reference normalization and bisulfite pyrosequencing. The assay was further applied to detect cancer methylation biomarkers in both tissue and liquid biopsy samples.
Results: MeRFPCR preserved robustness under challenging conditions, yielding reproducible methylation percentages across technical replicates (CV <5%) with inputs as low as 2 ng and fragment sizes ranging from 80 to 200 bp. In 20 matched tumor and adjacent normal tissues from colorectal cancer patients, *SEPT9* methylation measured by MeRFPCR showed excellent concordance with pyrosequencing (R^2 = 0.97) and distinguished all tumors from normal tissues. In contrast, qMSP showed lower concordance (R^2 = 0.73) and failed to resolve tumor-normal differences in several cases (sensitivity 90%). Of note, the workflow of MeRFPCR is faster, easily accessible and more cost-effective compared with pyrosequencing. In addition, MeRFPCR accurately detected methylated *SEPT9* in circulating cell-free DNA from as little as 300 µL of plasma in metastatic CRC patients. These findings support the technical accuracy and advantages of MeRFPCR resulting from the reference-free methods, highlighting its specific diagnostic potential in compromised samples and across laboratory settings where reference-based assays are limited.
Conclusion: The MeRFPCR technique is a fast, accurate, cost-effective, and reference-free method for absolute quantification of DNA methylation. It holds promise for reducing batch effects across platforms and improving detection in challenging clinical samples, including liquid biopsy and stool DNA. These findings highlight the potential of MeRFPCR as a basic and valuable tool for facilitating noninvasive detection of cancer methylation biomarkers and broader epigenetic applications.

#6318 Distinct molecular signatures in dense breast tissue as potential drivers of breast cancer development.

Jay William Fox[1], Natalia Dworak[2], Patcharin Pramoonjago[3], Christopher A. Moskaluk[4], **Ana Karina de Oliveira**[3]

[1]Assoc. Director, University of Virginia Cancer Center, Charlottesville, VA,[2]Spatial Biology Core, University of Virginia School of Medicine, Charlottesville, VA,[3]Department of Pathology, University of Virginia School of Medicine, Charlottesville, VA,[4]Assoc. Professor, Dept. of Pathology, University of Virginia Health System, Charlottesville, VA

Breast density is a significant independent risk factor for breast cancer; women with dense breasts have a 4-6-fold increased risk of the disease compared to women with non-dense breasts. It has been suggested that 30% of all breast cancer cases occur in women with > 50% dense areas. Breast density reflects variations in breast tissue composition. It is characterized by high proportions of stroma, containing collagen and other ECM proteins, fibroblasts, endothelial cells, and immune cells, suggesting a pro-tumor inflammatory microenvironment. To investigate molecular differences between dense and nondense breast tissue and their association with triple-negative breast cancer (TNBC), we used the PanCancer IO 360 panel to explore RNA expression and signaling pathway regulation across the samples. We observed differences in RNA expression among subjects, thereby identifying distinct molecular groups in dense breasts. The subjects were clustered into 3 subtypes with distinct molecular signatures and biological pathways. We identified a group (G1) with increased expression of genes involved in inflammatory processes, but still maintains a closer association with the phenotype of non-dense breasts. We also identified two other groups (G2 and G3) that are more distinct regarding the non-dense group and different from each other. These groups are related to reorganization and cellular architecture in the microenvironment (G2) and to proliferative regulation, cancer pathways, and increased gene expression in tumor development (G3). These groups do not seem to correlate with age or menopause stage in this first screen; instead, they resemble more subtypes of density or stages of density development. Additionally, analyzing RNA expression in TNBC samples, we identify an association with dense G3 samples that express more RNAs related to DNA repair, with upregulation of pathways in DNA damage, epigenetic regulation, apoptosis, and metabolic stress. At the same time, the pathways such as interferon signaling, immune cell adhesion and migration, and NF-kappa-beta are downregulated. These results suggest that specific density subtypes with distinct molecular signatures may promote tumor development more than others. To better understand this association and determine whether there are similarities in the resident cells of dense breast and TNBC samples, we are conducting spatial biology analyses to explore their microenvironments. The accurate classification of these subtypes has the potential to impact breast cancer prevention strategies and early diagnosis. Further investigations with a larger cohort are underway to understand better how molecular alterations in dense groups contribute to tumor development.

#6319 Using paired germline genome to predict the age of onset in pediatric cancer.

Kai Ren Chen[1], Safa Majeed Grant[1], Brianne Laverty[1], Ashby Kissoondoyal[1], Adam Shlien[2], David Malkin[3]

[1]Genetics and Genome Biology Program, The Hospital for Sick Children, Toronto, ON, Canada,[2]Pediatric Laboratory Medicine, The Hospital for Sick Children, Toronto, ON, Canada,[3]Division of Hematology/Oncology, The Hospital for Sick Children, Toronto, ON, Canada

Background: Germline events play a role in influencing the age of onset of pediatric cancers, but their specific contribution remains incompletely understood. Approximately 18% of children with cancer harbor a germline gene mutation associated with a Cancer Predisposition Syndrome (CPS). However, this fraction is believed to be an underestimation, given that a substantially larger proportion of childhood cancers is thought to have a genetic basis due to the limited environmental exposure in children compared with adults. Carriers of cancer predisposition gene mutations typically undergo clinical surveillance for early tumor detection. However, many children carry germline risk that would not be recognized by their cancer or family cancer phenotypes and are therefore not identified for surveillance, reflecting a major gap in leveraging whole genomic data for individual prediction. One notable example of a monogenic CPS is Li-Fraumeni Syndrome (LFS), caused by germline mutations in the *TP53* tumor suppressor gene. Our lab has demonstrated that additional (epi)genetic events that modify the LFS phenotype and enable more precise prediction of tumor onset, underscoring the need for a better understanding of the contribution of germline events to age of onset across pediatric cancers. In this study we analyze a broad range of pediatric cancer types, using their paired germline genomes to develop machine learning (ML) models that predict age of onset, uncover genomic predispositions, and support earlier tumour detection.
Methods: Whole genome sequencing data from the SickKids Cancer Sequencing (KiCS) program's initial cohort of poor-prognosis childhood cancer patients (n=333), ~18% of whom meet CPS criteria, were analyzed. After grouping germline variants by gene and pathogenicity according to ACMG guidelines, these variants were used as input features for UMAP and random forest models to classify the age of onset. Generative AI was used solely to modify code, refine written content, and identify relevant journal articles. All AI-assisted content was verified.
Results and Conclusion: Preliminary models achieved an average AUROC of ~0.63 in classifying onset before versus after various selected ages (1-17). These findings suggest that genomic profiles are dependent on developmental stages. The UMAP performed on the same variants led to the observation that one cluster contained a higher proportion of pediatric-enriched cancer subtypes (75%) compared to the other clusters (58%). Preliminary findings suggest that genomic profiles that are more consistent with hereditary cancer can be separated from genomic profiles that are more consistent with sporadic cancer. Integrating genomic data with predictive modelling may improve our understanding of how germline events collectively influence age of onset across pediatric cancer types, which could inform risk stratification in clinical surveillance protocols.

#6320 Plasma proteomics of cancer risk in patients with chronic kidney disease.

Lucas A. Mavromatis[1], Aditya Surapaneni[1], Carina Flaherty[1], Peter Ganz[2], Lawrence J. Appel[3], Morgan E. Grams[1]

[1]Department of Medicine, NYU Grossman School of Medicine, New York, NY,[2]Department of Medicine, University of California, San Francisco, San Francisco, CA,[3]Welch Center for Prevention, Epidemiology and Clinical Research, Johns Hopkins University, Baltimore, MD

Background Patients with chronic kidney disease (CKD) have higher cancer risk and worse cancer outcomes than the general population. Although circulating proteins are important biomarkers of incident and recurrent cancer, CKD profoundly remodels the proteome. High-throughput proteomic assays enable systematic interrogation of protein-phenotype associations and can disentangle CKD-specific proteomic biomarkers and pathways of cancer risk.

Methods We analyzed 4,091 plasma proteins measured by SomaScan (v4) at the year 1 visit of the Chronic Renal Insufficiency Cohort study (CRIC). The cohort included participants without prior cancer and with complete baseline covariates. For each protein, we fit Cox models for time-to-event (breast, colon, head & neck, leukemia, lung, lymphoma, prostate, and overall cancer). Fully adjusted models included age, sex, race, eGFR, smoking history, alcohol use, urine albumin-to-creatinine ratio, body mass index, diabetes, prior cardiovascular disease, and socioeconomic indicators. We reported Benjamini-Hochberg FDR-significant proteins and flagged “nominal” associations ($P < 0.001$ and HR per SD ≥ 1.5 or ≤ 0.67). Downstream analyses assessed overlap between proteomic signatures across cancer types. Hallmark and KEGG enrichment analyses highlighted biological pathways associated with oncologic endpoints.

Results Among the 2,975 participants who met study inclusion criteria (median age 59.5 years, 45.2% female), 395 developed cancers over a median of 12.5 years. Across cancer types, 78 proteins were FDR significant in demographics-adjusted models. In fully adjusted models, 37 met the nominal significance threshold and 12 remained FDR-significant, spanning colon, leukemia, lung, and prostate cancers. Many identified proteins were biologically plausible: higher soluble CD163—a marker of tumor-associated macrophages—was associated with colon cancer; Gremlin-2, a DAN-family BMP antagonist implicated in hematopoietic dysregulation, was associated with leukemia; RAN-binding protein 3, a regulator of nuclear export and TGF-β signaling, was associated with lung cancer; and cystatin C, a kidney filtration marker, was inversely associated with prostate cancer risk. Cancer types displayed distinct protein signatures, but pathway enrichment overlapped across outcomes, highlighting shared biological processes including epithelial-to-mesenchymal transition, KRAS signaling, inflammatory signaling, and cell adhesion.

Conclusions Plasma proteomics revealed early circulating biomarkers associated with future cancer in CKD. Many identified proteins have established or mechanistically plausible roles in cancer biology. Protein-cancer associations were cancer type-specific; however, the proteomic signatures of different cancers converged on known oncogenic pathways. Identified proteins, if replicated, might facilitate earlier detection of cancer in CKD.

#6321 Characterizing plasma protein LEG1 homolog, a novel potential risk factor for post-menopausal breast cancer.

Vernon A. Burk, **Elizabeth A. Platz**

Johns Hopkins Bloomberg School of Public Health, Baltimore, MD

Background: We previously identified and confirmed a positive association between plasma protein LEG1 homolog and post-menopausal breast cancer risk in 2 cohort studies in models adjusted for breast cancer risk factors. This evolutionarily conserved protein is understudied. We now aim to characterize the protein's within-person variation over time, its correlates and residual association after accounting for correlates.

Methods: We analyzed data from the Atherosclerosis Risk in Communities study, in which we first identified the protein (Syleouni M et al. *JNCI* 2025). We included 4,403 post-menopausal women (74% not taking hormone replacement therapy [HRT]) without cancer. Plasma proteins were previously measured by SomaScan® 5K at Visits 2, 3 and 5 (3, 18 years apart). We used demographic, anthropometric, lifestyle, and reproductive data collected by interview or measured by trained staff. Previously, plasma estradiol and testosterone were measured. We assessed within-person variation over time (ICC) and identified correlates of LEG1 after $\log_2$ transformation (linear regression). We re-analyzed the LEG1-breast cancer association stratifying by or adjusting for the correlates using multivariable-adjusted Cox regression. For highly correlated factors, we first regressed LEG1 on each correlate and then modeled LEG1 residuals.

Results: The ICC for LEG1 was 0.52 across the 3 time points. LEG1 was highly correlated with prolactin-inducible protein (r=0.95) and extracellular glycoprotein lacritin (r=0.86); these correlations were almost identical by age, race, HRT use, BMI, and diabetes. The remaining 4,709 proteins had $r< |0.35|$, including weak correlations for kidney function (albumin, ALT, AST) and inflammation (CRP) markers. LEG1 was only weakly correlated with estradiol (measured 3 years apart, N=316, r=0.13, p=0.02) and testosterone (measured 3 years apart, N=3,134, r=0.05, p=0.02). LEG1 declined modestly with age (p<0.0001). Adjusting for age, level was notably higher in Black than White women (p<0.0001). Adjusting for both age and race, LEG1 level was lower in women with higher BMI and diabetes. Direction of the association appeared to differ by race for HRT use (level was higher in users in White women only) and reproductive factors. The residuals of LEG1 after regression on prolactin-inducible protein (p=0.0001) or extracellular glycoprotein lacritin (p=0.015) were statistically significantly positively associated with breast cancer. Associations for LEG1 were stronger in women not using HRT, ≥median BMI, and with diabetes; we previously reported no difference in the association by race.

Conclusions: This study provides continued support for plasma protein LEG1 homolog as a risk factor for post-menopausal breast cancer. This protein should be considered for its utility in current risk stratification tools. Mechanistic studies are needed. Support: NHLBI, NCI, NPCR

#6322 Uncovering causal protein markers in prostate tissue for prostate cancer: A proteome-wide association study and functional validation.

Jingjing Zhu[1], Pramod KC[1], Sweaty Koul[1], Yijun Tian[2], Hua Zhong[1], Thomas G. Beach[3], Hyeyoon Kim[1], Athena A. Schepmoes[4], Karl K. Weitz[4], Tyler Sagendorf[4], Tao Liu[4], Maarit I. Tiirikainen[5], Lucio Miele[1], Nicholas Mancuso[6], Timothy R. Rebbeck[7], David V. Conti[6], Christopher A. Haiman[8], the PRACTICAL/ELLIPSE consortium, Chong Wu[9], Liang Wang[2], Hari K. Koul[1], Lang Wu[1]

[1]Louisiana State University Health Sciences Center, New Orleans, LA,[2]Moffitt Cancer Center, Tampa, FL,[3]Banner Sun Health Research Institute, Sun City, AZ,[4]Pacific Northwest National Laboratory, Richland, WA,[5]Associate Specialist/Genomics Shared Resource, University of Hawaii Cancer Center, Honolulu, HI,[6]University of Southern California, Los Angeles, CA,[7]Dana-Farber Cancer Institute, Boston, MA,[8]Co-Director, USC Genomics Ctr., USC Norris Comprehensive Cancer Center, Los Angeles, CA,[9]UT MD Anderson Cancer Center, Houston, TX

Background: Prostate cancer (PCa) is the second most frequently diagnosed malignancy among men. While multiple protein markers have been implicated in PCa, findings from conventional studies are often inconsistent due to methodological limitations such as selection bias and uncontrolled confounding. The proteome-wide association study (PWAS) design leverages genetic instruments to identify protein biomarkers with potential causal roles in diseases. Although candidate causal proteins in blood have been identified for PCa in our previous work, few studies have focused on prostate tissue.

Methods: We conducted the first prostate tissue-based PWAS using data from the PRACTICAL/ELLIPSE consortia, comprising 122,188 PCa cases and 604,640 controls. Proteomic and genomic data were generated from 201 frozen prostate tissue samples without PCa, quantifying 11,575 proteins. We used data of 195 unrelated subjects for model building. Prediction models for protein abundance were built using nearby unambiguous SNPs of potentially associated variants, applying BLUP, LASSO, elastic net, and top1 methods. Association testing was performed for genetically predicted protein levels with PCa risk and aggressiveness. For one of the identified proteins eIF4G1, we performed knockdown of its gene expression in androgen-sensitive (LNCaP), enzalutamide-resistant LNCaP (NO-LNCaP-ENZR), and castration-resistant (22RV1) PCa cell lines, and investigated the effects on multiple phenotypes. Survival analysis was also performed using TCGA primary PCa RNA-seq data.

Results: A total of 1,034 protein models achieved cross-validated $R^2 > 0.01$ and were retained for association testing. Fifty-six proteins showed significant associations with PCa risk, including 18 associated with advanced disease and seven distinguishing advanced from non-advanced cases. One of the top novel proteins, EIF4G1, is required for the initial steps of translation. Disrupting eIF4F complex activity via *EIF4G1* knockdown reduced cell proliferation, colony formation, and spheroid culture growth, and decreased cell migration and invasion. *EIF4G1* knockdown also sensitized LNCaP cells to enzalutamide treatment and inhibited clonogenic potential of enzalutamide-resistant cells. Pharmacological inhibition of eIF4F with SBI-756 reproduced these effects and induced G1 phase cell cycle arrest. Polysome profiling revealed decreased mRNA loading onto polysomes, indicating that knockdown of *EIF4G1* impaired cap-dependent translation. Elevated expression of *EIF4G1* in tumors was also associated with shorter disease-specific survival.

Conclusions: Our study reveals novel prostate tissue proteins putatively causally linked to PCa risk and aggressiveness. Our functional work suggests that a novel protein, eIF4G1, presents a new target for limiting PCa progression and overcoming therapy resistance.

#6323 Plasma proteomic profiling reveals shared biomarkers for MASLD-related hepatocellular carcinoma and gastrointestinal cancers in the UK Biobank.

Qing Wang, Yacong Zhang, **Ke-Xin Chen**

Tianjin Medical Univ. Cancer Inst. & Hospital, Tianjin, China

Background: Metabolic dysfunction-associated steatotic liver disease (MASLD) is a major global health challenge and markedly elevates the risk of hepatocellular carcinoma (HCC) and extrahepatic gastrointestinal (GI) cancers. Reliable biomarkers for early detection in MASLD populations remain lacking. We leveraged large-scale plasma proteomic profiling from the UK Biobank to identify circulating protein markers for MASLD-related HCC and GI cancers.
Methods: We performed a nested case-control study within the UK Biobank. Differentially expressed plasma proteins were identified and evaluated using Gene Ontology, Kyoto Encyclopedia of Genes and Genomes (KEGG) pathway enrichment, and protein-protein interaction (PPI) network analyses. Overlapping dysregulated proteins between cancer types were mapped to determine shared pathways.
Results: The UK Biobank cohort included 19,341 MASLD patients with proteomics data (mean age 61.1 ± 6.3 years), comprising 40 MASLD-HCC cases and 589 MASLD-GI cases. After excluding samples with protein data missing rates exceeding 30%, the study included 33 MASLD-HCC cases and 516 MASLD-GI cancer cases, matched 1:3 by age and sex to 99 and 1,548 MASLD controls, respectively.Quantitative proteomics identified 45 significantly dysregulated (44 upregulated and 1 downregulated) proteins in MASLD-HCC compared to MASLD, including established HCC-related keratins (e.g., KRT8, KRT18) and novel candidates (e.g., SPINT3, ADGRG1). Enriched pathways highlighted lipid metabolic dysfunction and xenobiotic metabolism. IL-6 and AGXT emerged as central hub genes in the PPI network. In MASLD-GI cancers, 24 proteins were significantly altered. Notably, 14 proteins were consistently dysregulated across both MASLD-HCC and MASLD-GI cancers, including CDHR2, INSL3, GPRC5C, FGF21, MME, CES1, KRT18, ADGRG1, HAO1, KLK3, GAST, and FOLR3.
Conclusion: This large prospective proteomic study delineates distinct and overlapping plasma protein signatures of MASLD-related cancers. The shared biomarkers map to a unified "metabolism-damage-inflammation" axis, suggesting common mechanisms underlying carcinogenesis in MASLD. These findings provide a promising biomarker panel with potential utility for multi-cancer early detection and risk stratification in MASLD populations.

#6324 A proteomics-based model improves the accuracy of upper gastrointestinal cancer prediction.

Xinyu Liu, Zhangyan Lyu, **Kexin Chen**

Tianjin Medical University Cancer Institutet and Hospital, Tianjin, China

Background: Upper gastrointestinal cancers (UGI), including esophageal cancer (EC), gastroesophageal junction cancer (GEJ), and gastric cancer (GC), pose a major global health burden, with prognosis heavily dependent on early diagnosis. Current screening strategies inadequately identify high-risk individuals. While advances in proteomics offer promise for risk assessment and early detection, their application in UGI cancer screening remains underexplored.
Methods: We conducted a prospective analysis within the UK Biobank. Participants were randomly divided into training and testing sets at a 7:3 ratio. Among proteins measured using the Olink Explore 3072 panel, those with >30% missing values were excluded, resulting in a final analysis set of 2,920 proteins. The associations of proteins with UGI cancer were identified by Cox proportional hazards models (FDR < 0.05). L1-penalized LASSO-Cox regression with ten-fold cross-validation was then applied to select candidate proteomic biomarkers. Then, two risk prediction models (a simple model based on epidemiological factors and an integrated model that further incorporated proteins) were developed and internally validated. The discrimination of the models was assessed using the area under the curve (AUC) and compared via DeLong's test.
Results: After excluding participants with baseline cancer or missing data, 48,366 individuals were included (median follow-up: 14.7 years; 261 UGI cancer cases). We identified 912 proteins significantly associated with UGI cancer (830 risk-related, 82 protective). LASSO-Cox regression refined this set to 46 proteins (31 risk, 15 protective), including five novel risk-related proteins—TEX101, MYBPC1, KIR2DL3, CLSTN2, and ADAMTS4—while the remaining 41 have been previously reported in the literature. Compared to the traditional model, which incorporated a novel high-risk status variable (defined as age ≥45 years plus at least one of: smoking history, heavy alcohol consumption, precancerous lesions, *Helicobacter pylori* infection, or an unhealthy diet), the integrated model demonstrated superior diagnostic performance, with significantly higher AUCs in both the training set (0.83 [95% CI: 0.80-0.86] vs. 0.70 [0.67-0.73]) and the testing set (0.81 [95% CI: 0.77-0.85] vs. 0.69 [0.65-0.74]; DeLong's test, $p < 0.05$).
Conclusion: We developed an integrated model that combines 46 plasma protein biomarkers with traditional epidemiological factors. This approach demonstrated superior performance over the traditional model in identifying UGI cancer. Further prospective studies in diverse regions and populations are needed to validate the generalizability of this promising early screening strategy.

#6325 Smoking and sex specific proteomic markers of lung cancer: A prospective cohort study.

Zhangyan Lyu, Xinyu Liu, Kexin Chen

Tianjin Medical University Cancer Institute and Hospital, Tianjin, China

Background While circulating proteins hold promise for elucidating lung cancer (LC) etiology, large-scale studies comprehensively assessing their associations with LC risk are limited. Crucially, the roles of these proteins across different sexes and smoking statuses, particularly in females and non-smokers who constitute a significant proportion of LC cases with distinct etiology, remain poorly characterized.

Methods We integrated observational analyses from the UK Biobank (UKB) cohort (N=49,370 cancer-free at baseline; 444 incident LC cases; median follow-up 11 years) with two-sample Mendelian randomization (MR). Plasma levels of 2,920 proteins were measured at baseline. Cox regression identified proteins associated with incident LC, with stratified analyses by sex and smoking status. MR used cis-pQTLs from UKB-PPP and deCODE studies as instruments for proteins and LC GWAS data from FinnGen, TRICL, and Pan-UKBB. Robust causal evidence was defined by a significant MR result (IVW $P<0.05$) combined with either a colocalization posterior probability (PPH4) > 0.75 or a significant SMR result (HEIDI $P>0.01$).

Results Sex-stratified analysis revealed 532 significant proteins in males and 375 in females. Among these, 271 were male-specific (e.g., C1R, HR=5.48, 95%CI: 2.23-13.50) and 114 were female-specific (e.g., SMAD5, HR=4.53, 95%CI: 2.39-8.58). Only 261 proteins were shared between sexes. Smoking-stratified analysis identified 683 significant proteins in smokers and 39 in non-smokers. A vast majority (657 proteins) were smoker-specific, including top risk protein SERPINA1 (HR=24.62, 95%CI: 5.65-107.39) and top protective protein GSN (HR=0.15, 95%CI: 0.09-0.27). In contrast, only 13 proteins were non-smoker-specific, such as risk protein CYTL1 (HR=3.46, 95%CI: 1.11-10.82) and protective protein CNTN4 (HR=0.17, 95%CI: 0.07-0.45). MR analysis provided genetic support for IL19 for LC among smokers (OR=1.18, 95%CI: 1.03-1.35 from cis-MR; OR=1.12, 95%CI: 1.01-1.23 from SMR).

Conclusion This study unveils strikingly distinct proteomic signatures of LC risk by sex and smoking status, predominantly in males and smokers, with genetic validation for key candidates like IL19. These findings underscore etiological heterogeneity and support stratified approaches to LC risk prediction and prevention, pending external validation in diverse populations.

#6326 Pregnancy, lactation, and involution-induced remodeling and cell state changes in breast tissues of healthy women.

Poornima Bhat-Nakshatri[1], Cihat Erdogan[1], Hongyu Gao[1], Yunlong Liu[1], Rana German[1], Michele L. Cote[2], **Harikrishna Nakshatri**[1]

[1]Indiana University School of Medicine, Indianapolis, IN,[2]IUPUI Fairbanks School of Public Health, Indianapolis, IN

Pregnancy, lactation, and involution have opposing effects on breast cancer incidence and tumor aggressiveness. While breast feeding and subsequent involution protects against breast cancers, pregnancy-associated breast cancers (breast cancers diagnosed during pregnancy and within 2 years postpartum) are associated with poor outcome. Clear understanding of these opposing effects of reproductive cycle needs single cell resolution of breasts during pregnancy, lactation and involution. We recently reported a reference single nucleus chromatin accessibility and transcriptome atlas of breast tissues of women of diverse genetic ancestry and reported 10 major cell types in the breasts. These include three epithelial cell types [luminal hormone sensing (LHS), luminal adaptive secretory precursors (LASP), and basal-myoepithelial cells (BM)], two adipocyte subtypes, two endothelial cell subtypes, T cells, macrophages, and fibroblasts. In this study, we generated single nucleus atlas of breast tissues of healthy women collected during pregnancy, lactation, and involution. Pregnancy, lactation, and involution are associated with dramatic changes in cell type proportions and cell state shifts within a cell type. LASP cell numbers increased from 24% in the normal reference breasts to 71% during pregnancy, 63% during lactation but returned to 25% during involution. There is also a dramatic shift in LASP cell states during pregnancy, lactation and involution. While the LASP cells in the normal reference breasts and breasts during pregnancy were in both LASP-basal-luminal (LASP-BL) and LASP-alveolar (LASP-AP) states, LASP-AP cells were dominant in lactating and involuting breasts. Increase in LASP cells during pregnancy and lactation is at the expense of BM cells, which reduced from 27% in the normal reference breasts to 7-9% during pregnancy and lactation. While T cell proportion was similar between normal reference and pregnant breasts (2-3%), it increased to 7-8% during lactation and involution, which a recent study has suggested to be responsible for breast feeding-associated protection against breast cancer. Increase in T cells during lactation and involution is likely due to expansion of tissue resident T (T_{RM}) cells as T cells of lactating and involuting breasts expressed higher levels of T_{RM} cell markers CD69 and CXCR6. We present pregnancy, lactation and involution-associated chromatin accessibility and transcriptome changes at individual gene and cell type levels. Several biomarkers associated with these changes have been identified, which will be a useful resource to mechanistically evaluate evolution of breasts during reproductive history and breast cancer development.

#6327 Translation of lung cancer biomarkers from nanoparticle-based LCMS to enzyme-linked immunosorbent assay.

Nga Ho, Jinlyung Choi, Guanhua Shu, Alicia Furlan, Ghristine Bundalian, Arcel Cunanan, Janelle Dela Vega, Jacob Waiss, Zachary Yanagihara, Joon-Yong Lee, Robert Zawada, Chinmay Belthangady, Brian Koh, Manway M. Liu, Bruce Wilcox

PrognomiQ Inc, San Mateo, CA

Lung cancer is the leading cause of cancer-related mortality in the United States. Newly diagnosed lung cancer patients generally have poor prognoses, in large part due to being diagnosed at later stages of disease. Earlier diagnoses, enabled by more effective screening, are expected to reduce morbidity and mortality. In pursuit of this, we previously reported on an unbiased, multi-omics discovery study to identify blood-based biomarkers for lung cancer that may be developed into a more effective screening test. A machine-learned model trained on nanoparticle-based LCMS measurements could achieve a specificity of 74% at a sensitivity of 85% across all lung cancer stages and sensitivity of 74% on stage-1 lung cancer alone. These results illustrate the power of unbiased LCMS plasma proteomics to identify proteins with high disease discrimination; however, there is limited demonstration of translating findings from nanoparticle-based unbiased LCMS proteomics to immunoassays. Here, we report on the translation of 8 of the most cancer discriminative, plasma proteins identified from our discovery study to enzyme-linked immunosorbent assay (ELISA). On a set of 404 subjects (110 cancer and 294 non-cancer) from the discovery study, a machine-learned model trained on nanoparticle-based LCMS measurements of these 8 proteins achieved an AUROC of 0.93 (95% CI 0.90-0.96) and $\geq$ 80% specificity at 87.5% sensitivity. The corresponding model trained on ELISA measurements of the same 8 proteins achieved an AUROC of 0.90 (95% CI 0.86-0.94) and $\geq$ 70% specificity at 87.5% sensitivity. The directionality and magnitude of the fold-changes between cancer and non-cancer subjects were preserved for each of the 8 proteins between the two assays. Statistically significant (adjusted p-value $\leq$ 0.05) and positive Spearman correlations were also observed between measurements of each of the 8 proteins on these two assays across the 404 subjects. These results demonstrate the feasibility of translating from nanoparticle-based LCMS to immunoassays while preserving lung cancer discriminative signals and set the foundation for the development of an immunoassay-based Lab Developed Test (LDT) for lung cancer detection.

#6328 Expression of hypoxia-inducible factor 1-alpha in diverse histological types of uterine cervical carcinoma and correlation with the aggressiveness of tumor type: An immunohistochemical study.

Conwell Ngobeni[1], Meshack Bida[1], Benny Mosoane[1], Rahaba Marima[2], Tebogo Marutha[2], **Zodwa Dlamini**[2], Tebogo Medupe[1]

[1]Department of Anatomical Pathology, University of Pretoria, Pretoria, South Africa,[2]Pan African Cancer Research Institute (PACRI), University of Pretoria, Pretoria, South Africa

Background:
Cervical cancer is the fourth leading cause of cancer-related deaths in women worldwide, with high prevalence in South Africa. High-risk human papillomavirus (HPV), along with genetic and epigenetic alterations, drives cervical carcinogenesis. Hypoxia-inducible factor 1-alpha (HIF-1α) is frequently expressed in cervical carcinoma and other solid tumors. Under normoxia, HIF-1α is degraded via the Von Hippel-Lindau pathway, while hypoxia stabilizes it, inducing angiogenic factors. HIF-1α immunohistochemistry has been proposed as a prognostic and therapeutic marker; however, previous studies are limited by small cohorts, single-center designs, and variable histology. This study assessed HIF-1α expression across cervical carcinoma subtypes and its association with tumor aggressiveness.
Methods:
We conducted a retrospective study of cervical carcinoma cases diagnosed at the University of Pretoria (2017-2022). Archived formalin-fixed paraffin-embedded tissues were retrieved, yielding 63 cases. HIF-1α immunohistochemistry was performed, and three pathologists independently scored staining using a modified quick Allred system, classifying cases as positive if the combined score exceeded zero.
Results:
HIF-1α expression was positive in 19/63 cases (30%) and negative in 44/63 (70%). Basaloid squamous cell carcinoma accounted for 26% of positive cases, CIN III-like and papillary squamous-urothelial carcinomas each 21%, adenoid basal, papillary squamous, and clear cell carcinomas 10% each, and adenosquamous carcinoma 5%. No adenoid cystic, small cell, or villoglandular carcinomas were positive. Positivity within subtypes was highest in papillary squamous-urothelial (57%) and clear cell (50%) carcinomas, followed by basaloid squamous cell (38%), adenoid basal (33%), CIN III-like and papillary squamous cell (28.5%), and adenosquamous (25%).
Conclusion:
HIF-1α is expressed in a subset of cervical carcinomas, predominantly in histological variants associated with aggressive behavior, suggesting a potential link with poorer prognosis. Limited sample size and single-center design warrant caution. Larger multicenter studies with clinical follow-up are needed to clarify whether HIF-1α can guide prognostic assessment or targeted therapy in cervical carcinoma.

#6329 Improved sensitivity in high-risk HPV genotype detection via processor-mediated PCR.

Niloufar Mertz, Eric K. Pomaranski, Adam McCoy, Vladimir Makarov

Signal Bioscience, Ann Arbor, MI

High-risk human papillomavirus (hrHPV) genotypes, particularly HPV16 and HPV18, drive the majority of cervical and several anogenital and oropharyngeal cancers. Although molecular screening assays have grown more sensitive, major limitations remain. Current NGS-based methods offer genotype resolution but are costly, slow, and difficult to implement in routine screening. Digital PCR (dPCR) provides absolute quantification, but most assays target only one or two conserved regions, making it difficult to distinguish transforming infections from transient or non-oncogenic HPV. Additionally, HPV DNA in patient samples is often fragmented, integrated, or present at low abundance, complicating amplification and reducing both sensitivity and specificity. We developed a Processor-Mediated PCR that decouples amplification from fluorescent readout using a universal processor oligo and tunable universal probes. This enables high multiplexing regardless of instrument channel count. To improve specificity, we created iProbes, multi-domain probes that trigger fluorescent response only when their full target sequence is present, allowing discrimination between oncogenic and non-oncogenic HPV even within highly conserved regions. Using HPV16 as a model, we built a multi-fragment assay that detects 10 genomic regions (<90 bp each), including E6/E7 oncogenic segments, in a single dPCR or qPCR reaction. Processor-Mediated PCR is tunable to multiple applications and supports either multichannel or single-channel fluorescent readouts, ensuring compatibility with instruments with limited channel capacity. This broad molecular coverage enhances detection of fragmented or partially degraded viral genomes. Together, Processor-Mediated PCR and iProbe-based multiplexing provide sensitive, high-specificity detection of cancer-associated HPV fragments in one assay, addressing key limitations of current NGS and PCR methods and improving HPV screening and triage.

#6330 Evaluating targeted versus universal BRCA testing in Asian women with ovarian cancer.

Boon Hong Ang[1], Sook-Yee Yoon[2], Joanna Lim[3], Nur Tiara Hassan[2], Mei-Chee Tai[1], Zhi Lei Wong[1], Jo Yi Chow[1], Xin Wen Lee[1], Meow-Keong Thong[4], Gaik-Siew Ch'ng[5], Jamil Omar[6], Chee-Meng Yong[7], Ismail Aliyas[8], Rozita Abdul Malik[9], Suguna Subramaniam[10], Wee-Wee Sim[11], Chun-Sen Lim[12], Saw-Joo Lee[13], Keng-Joo Lim[14], Mohamad Nasir Shafiee[15], Fuad Ismail[16], Mohd Pazudin Ismail[17], Mohamad Faiz Mohamed Jamli[18], Suresh Kumarasamy[19], John Seng Hooi Low[20], Ahmad Muzamir Ahmad Mustafa[21], Mary Jenifer Makanjang[22], Shahila Tayib[23], Nellie Lay Chin Cheah[24], Chee-Kin Fong[25], Kean-Fatt Ho[26], Azura Deniel[27], Soo-Fan Ang[28], Ahmad Radzi Ahmad Badruddin[29], Lye-Mun Tho[30], Boon-Kiong Lim[9], Yin Ling Woo[9], Weang-Kee Ho[31], Soo-Hwang Teo[1]

[1]Cancer Prevention and Population Science, Cancer Research Malaysia, Subang Jaya, Malaysia,[2]Genetic Counselling, Cancer Research Malaysia, Subang Jaya, Malaysia,[3]Core Laboratory, Cancer Research Malaysia, Subang Jaya, Malaysia,[4]University of Malaya Medical Centre, Kuala Lumpur, Malaysia,[5]Penang Hospital, Penang, Malaysia,[6]Institut Kanser Negara, Kuala Lumpur, Malaysia,[7]Hospital Ampang, Ampang, Malaysia,[8]Hospital Sultanah Bahiyah, Alor Setar, Malaysia,[9]University of Malaya, Kuala Lumpur, Malaysia,[10]Hospital Wanita Dan Kanak-Kanak Sabah, Kota Kinabalu, Malaysia,[11]Hospital Umum Sarawak, Kuching, Malaysia,[12]Hospital Sultan Ismail, Johor Bharu, Malaysia,[13]Hospital Raja Permaisuri Bainun, Ipoh, Malaysia,[14]KPJ Johor Specialist Hospital, Johor, Malaysia,[15]Hospital Universiti Kebangsaan Malaysia, Cheras, Malaysia,[16]Universiti Kebangsaan Malaysia Medical Centre, Kuala Lumpur, Malaysia,[17]Hospital Universiti Sains Malaysia, Kota Bahru, Malaysia,[18]Hospital Tuanku Ja'afar Seremban, Seremban, Malaysia,[19]Gleneagles Penang, Penang, Malaysia,[20]Pantai Hospital Kuala Lumpur, Kuala Lumpur, Malaysia,[21]Hospital Tengku Ampuan Afzan, Kuantan, Malaysia,[22]KPJ Sabah Specialist Hospital, Kota Kinabalu, Malaysia,[23]Penang General Hospital, Georgetown, Malaysia,[24]Loh Guan Lye Specialist Centre, Penang, Malaysia,[25]Subang Jaya Medical Centre, Subang Jaya, Malaysia,[26]Mount Miriam Cancer Hospital, Tanjong Bungah, Malaysia,[27]KPJ Ampang Puteri Specialist Hospital, Ampang, Malaysia,[28]Penang Adventist Hospital, Penang, Malaysia,[29]Dr. A. Radzi's Integrated Oncology Clinic & Daycare Centre, Johor Bahru, Malaysia,[30]Beacon Hospital Sdn Bhd, Petaling Jaya, Malaysia,[31]Univ. of Nottingham Malaysia, Semenyih, Malaysia

Background: Germline genetic testing for BRCA1 and BRCA2 pathogenic variants (PVs) is recommended for all ovarian cancer patients, as identifying PVs informs treatment planning and facilitates family cascade testing. However, in resource-limited settings, high testing costs often limit feasibility and uptake. An alternative approach is to use predictive models to prioritize patients with a higher likelihood of carrying PVs, optimizing resource allocation. Existing models are largely Western-derived and underperform in Asians; while we have a validated model for breast cancer, no equivalent model currently exists for ovarian cancer.
Methods: Using data from a multi-center study of 1,126 Asian ovarian cancer patients (including 147 BRCA PV carriers), we developed predictive models incorporating routinely collected information such as cancer history and clinicopathological features to estimate likelihood of carrying BRCA PVs. We evaluated model performance in terms of discrimination, calibration, overall accuracy, sensitivity, and specificity, and compared the associated genetic testing volumes and costs to those of universal testing.
Results: Our final model demonstrated good calibration and strong discriminatory power, with an area under the curve of 0.80 (95% confidence interval: 0.74-0.87). Factors included in the model were age at diagnosis, ethnicity, personal and family cancer history, and clinicopathological features. At the optimal threshold, the model achieved 77% accuracy (73% sensitivity and 73% specificity), compared with 13% accuracy for universal testing (100% sensitivity but 0% specificity). In practice, this translates to identifying one carrier for every three patients tested, versus one in eight under universal testing, reducing the genetic testing cost per carrier identified from USD 4,000 to USD 2,000. From a budget perspective, even when we need to detect every carrier, as in universal testing, the model reduces testing volume by 15%, yielding potential savings of USD 70,000 for every 800 patients screened annually.
Conclusions: Targeted testing using a mutation prediction model offers a more efficient alternative when universal testing is not feasible, with adjustable risk thresholds that can be tailored to local resources to optimize impact in resource-limited settings.

#6331 A translational framework for high-plex spatial profiling and complexity reduction toward diagnostic assay development in colorectal polyps.

Ettai Markovits[1], Joanne Edwards[2], Gerard Patrick Lynch[3], Ofir Rimer-Cohen[1], Aidan Lynch[4], Aula Ammar[2], Luke McNickle[2], Claire Kennedy-Dietrich[2], Amna Matly[2], Meir Azulay[1], Lina Sakhneny[1], Noori Maka[5], Lewis Irvine[2], Pamela McCall[6], Ken Bloom[1], Grainger Greene[1], Stephen McSorley[2], Nigel Jamieson[2]

[1]Nucleai, Tel Aviv, Israel,[2]University of Glasgow, Glasgow, United Kingdom,[3]Institute of Cancer Sciences, University of Glasgow, Glasgow, United Kingdom,[4]School of Cancer Sciences, University of Glasgow, Glasgow, United Kingdom,[5]NHS Scotland, Edinburgh, United Kingdom,[6]College of MVLS, Univ. of Glasgow Inst. of Cancer Sciences, Glasgow, United Kingdom

Background:
Accurate risk stratification of colorectal polyps is essential for reducing unnecessary surveillance while ensuring that high-risk patients receive timely intervention. Pathology workflows rely on morphology from H&E slides, while emerging immune-profiling techniques such as multiplex immunofluorescence (mIF) offer deeper biological resolution but are often too complex and costly for routine clinical deployment. To address this, we propose a diagnostic-assay development framework that integrates high-plex spatial profiling with computational complexity-reduction strategies to derive a clinically practical biomarker panel.
Methods:
We designed a 20-plex mIF panel to characterize immune cell populations and spatial interactions within colorectal polyp microenvironments. Corresponding H&E whole-slide images were analyzed to extract epithelial, stromal, and architectural features using area-based models and computational morphology descriptors. These multimodal data were integrated into a unified predictive modeling pipeline for stratifying patients into low- and elevated-risk groups. To support translation into a deployable assay, we implemented a complexity-reduction framework incorporating iterative feature selection, redundancy elimination, model pruning, and simulation of assay-ready marker subsets.
Results:
An initial dataset of 200 mIF and H&E slides was used for model fine-tuning, biomarker feature extraction, and preliminary integration of immune and morphological signatures. Early-stage mIF-based models captured >10 immune cell populations, distinguished epithelial subtypes, and localized key microenvironmental interactions. H&E-based models identified colorectal compartments, stromal-epithelial organization, inflammatory patterns, and dysplasia-related features. This groundwork enabled refinement of feature sets, assessment of model stability, and establishment of the multimodal fusion strategy guiding downstream predictive modeling and assay simplification later to be verified on a larger ~1000 sample cohort.
Conclusions:
We present a scalable framework that unifies high-plex mIF discovery with H&E-based computational morphology to support biomarker identification, feature reduction, and diagnostic assay development for colorectal polyp risk stratification. This platform provides the foundation for forthcoming clinical validation and deployment within colorectal surveillance programs.

#6332 nELISA high-throughput protein profiling applied to the RADIOHEAD cohort: Insights from the largest plasma proteomics study of patients receiving checkpoint inhibitor therapy.

Amy R. Johnson[1], Nathaniel Robichaud[2], Samantha I. Liang[3], **Jens Eberlein**[1], Grant Ongo[1], Enjun Yang[3], John CONNOLLY[3], Milad Dagher[1]

[1]Nomic Bio, Montreal, QC, Canada,[2]Nomic Bio, Montreal, QC, Canada,[3]Parker Institute for Cancer Immunotherapy, San Francisco, CA

Background Proteomics holds great promise for cancer immunotherapy, with intensive efforts being exerted for early disease identification, patients selection, and adverse event prediction. Despite this potential, the high cost and low throughput of existing tools to profile circulating proteins render such studies prohibitively slow and costly, limiting their wide-spread application. As a result, proteomics studies in the field have been constrained to sample sizes in the 10s and 100s, restricting the power to discover key biomarkers.

Methods The Nomic platform is a highly multiplexed immunoassay technology that enables the profiling of hundreds of proteins across 1536 samples per instrument daily, at significantly reduced costs. The method miniaturizes sandwich immunoassays by placing antibody pairs on the surface of color-coded microparticles, which can then be analyzed via high-throughput flow cytometry. RADIOHEAD is a prospective study of 1070 immunotherapy naive pan-tumor patients on standard of care immune checkpoint inhibitor (ICI) therapy regimens from community oncology clinics. Longitudinal samples were collected pre- and post-ICI, as well as following irAEs.

Results We previously reported leveraging the nELISA protein profiling platform to quantify 600 circulating proteins across 3000 samples from the RADIOHEAD cohort, resulting in the identification of greater than 200 proteins associated with response to ICI and greater than150 proteins associated with the development of irAEs. Here, we further dissect the dataset to capture treatment-specific biomarkers. Specifically, analysis of clinical data identified factors impacting response to ICI, including age, smoking, chemotherapy, radiotherapy, systemic corticosteroids, opioids, etc. We will present biomarkers associated with each of these factors, and their impact on response to ICI.

Conclusions Pairing nELISA protein profiling of these longitudinal samples with associated demographic metadata and clinical outcomes provides an opportunity to identify clinically actionable mechanisms to guide ICI therapeutic approaches. Here, we highlight biomarkers and protein signatures related to patient outcomes, to reveal additional insights and further accelerate research in the field of cancer immunotherapy.

#6333 Serum protein signatures specific to breast cancer in treatment-naive African American women identified using integrated proteomics and multivariate pattern analysis.

Padma P. Tadi Uppala[1], Hyun J. Kwon[2], Elmer C. Rivera[2], Sharon S. Lum[3]

[1]School of Population Health, Nutrition & Wellness, Andrews University, Berrien Springs, MI,[2]Department of Engineering, Andrews University, Berrien Springs, MI,[3]Department of Surgery, Loma Linda University Health, Loma Linda, CA

Background: Breast cancer is the leading cause of morbidity and mortality among African American women. Identifying population-specific serum biomarkers is essential for early detection and risk stratification. To address limitations of traditional univariate analyses, we developed an integrated platform combining classical proteomics (2D-DIGE, MALDI-TOF/TOF, LC-MS/MS) with Random Forest (RF) and cumulative distribution function (CDF)-based analyses to robustly discover and validate serum biomarkers.
Population: Two cohorts of treatment-naïve African American women were examined following depletion of high-abundance proteins. The primary cohort included eleven breast cancer patients median age 50 years, range 29-74, and 11 age-matched healthy controls analyzed by 2D-DIGE and MALDI-TOF/TOF. An independent cohort of 6 patients and 6 controls was assessed by LC-MS/MS (MudPIT). Patients represented both pre- and postmenopausal status and diverse tumor subtypes and receptor profiles. Controls were healthy women without a cancer history.
Methods: Proteomic analysis using 2D-DIGE gels combined with MALDI-TOF/TOF allowed the detection and identification of differentially expressed serum proteins. LC-MS/MS data were analyzed with RF (1,000 bootstrap iterations) using Gini importance to rank peptide relevance, and the CDF evaluated distribution differences using an S statistic derived from 1,000 permutations (S threshold greater than or equal to 3). The combination of RF and CDF enabled the detection of relevant signals under conditions of high dimensionality, collinearity, and potentially non-Gaussian distributions.
Results: The integrated approach revealed multiple differentially expressed serum proteins in breast cancer. Representative biomarkers included Ceruloplasmin, Complement C3; Alpha-1B-glycoprotein, angiotensinogen precursor, Insulin-like growth factor-binding protein complex acid labile subunit, Hemopexin precursor, and vitamin D binding protein. Complementary 2D-DIGE and MALDI-TOF/TOF analyses allowed direct determination of these differential protein patterns, while LC-MS/MS combined with RF and CDF prioritized peptides with high discriminatory power and independently confirmed their statistical significance.
Conclusion: The integration of classical proteomics techniques (2D-DIGE and MALDI-TOF/TOF) with LC-MS/MS combined with RF and CDF analysis enables reliable detection and prioritization of serum biomarkers. This approach combines the sensitivity of multivariate proteomics with non-parametric statistical rigor, making it suitable for small, high-dimensional cohorts, and demonstrates potential for identifying biomarkers specific to underrepresented populations, supporting precision oncology applications in breast cancer.

#6334 *CervicalMethDx:*A precision tool to enable at-home sampling and expand access to cervical cancer prevention while reducing unnecessary biopsies in the United States and Puerto Rico..

Ashley Ramos Lopez[1], Yanira Gonzalez Rodriguez[1], Amanda Garcia Negron[1], Paola Quinonez Mendez[1], Guie Beeu Guerrero Hunt[2], Adhi Guerrero Thillet[1], Mariana Brait[2], Teresa Diaz-Montes[3], Josefina Romaguera[4], Lourdes Fernadez[5], David Sidransky[2], Rafael E. Guerrero-Preston[1]

[1]LifeGene-Biomarks, Inc, Toa Baja, PR,[2]Oncology, Johns Hopkins Medical Insts., Baltimore, MD,[3]Gynecologic Oncology Center, Mercy Medical Center, Baltimore, MD,[4]Obstetrics and Gynecology, University of Puerto Rico School of Medicine, San Juan, PR,[5]Harvard University, Cambridge, MA

CervicalMethDx is a molecular precision tool designed to expand access to cervical cancer prevention through self-collection while reducing unnecessary biopsies. Two cohorts were analyzed: women from Salud Integral en la Montaña (SIM, *n* = 82) and the University of Puerto Rico School of Medicine (UPR, *n* = 105) cervical cancer clinics who participated in an IRB-approved study comparing *CervicalMethDx* and Human Papilloma Virus (AmpFire, Atila BioSystems) test results in physician-collected (PreservCyt, Hologic) and self-collected vaginal swabs (MSwabs, Copan). Participants completed structured questionnaires assessing demographics, reproductive and screening histories, and experiences using the LifeGene BioMarks self-collection kit. Acceptability and preference of sampling methods were evaluated using Likert scales. Cramér's V was used to measure associations between sample collection preference and participant characteristics. Additional acceptability data of self-sampling were collected through 300 structured interviews with women from Puerto Rico, the United States, and Latin America attending Bad Bunny's *Residencia* concerts in Puerto Rico and through an online market study of 2,800 statistically representative women from seven municipalities in rural Puerto Rico served by SIM. Health-economic modeling used biopsy data from UPR clinics (2022-2024, *n* = 422) and BRFSS data (2016-2020) to estimate cost savings from reduced unnecessary biopsies. Self-collection was highly acceptable: 88-94% "would do at home," 87-95% "satisfied," and >95% "recommend to others." SIM participants more often preferred self-collection (52%) than UPR participants (42%), where physician collection remained preferred (48%). Employment and education showed modest influence on preference (Cramér's V = 0.27 and 0.16, respectively). Community market study revealed 86% willingness to self-test if validated, affordable, and endorsed by physicians. In the online sample, 72% expressed intent to use at-home kits. Motivators included convenience (50%), privacy (49%), and time savings (48%), while concerns centered on accuracy (50%) and correct use (45%). Pharmacies were the preferred distribution channel (73%). Health-economic modeling showed that applying *CervicalMethDx* rule-out thresholds could reduce unnecessary biopsies from 81% to 10-25%, translating into potential savings of $16.7-23.2M annually in Puerto Rico and $2.0-2.7B in the U.S. *CervicalMethDx* demonstrates high acceptability across diverse settings and potential to reduce unnecessary procedures and healthcare costs, supporting its integration into cervical cancer screening algorithms.

#6335 Temporal profiling of the EGF-induced transcriptional cascade in PC3 prostate cancer cells reveals biphasic oncogenic reprogramming.

Amit Kumar Tripathi, Jamboor K. Vishwanatha

College of Biomedical and Translational Sciences, UNT Health Science Center, Fort Worth, TX

The Epidermal Growth Factor (EGF) signaling pathway is a potent driver of prostate cancer progression, yet a comprehensive, time-resolved understanding of its transcriptional dynamics remains incomplete. This study employed temporal RNA-sequencing on PC3 prostate cancer cells to profile the transcriptomic landscape at critical intervals (0, 30 min, 1 h, 6 h) following EGF stimulation. Our analysis reveals a **biphasic oncogenic reprogramming**. The initial phase, evident within 30-60 minutes, is characterized by a rapid surge of immediate-early genes (*FOS, JUN, EGR* family) and the coordinated activation of pathways promoting cell migration, inflammation (NF-κB, IL-17), and early signaling (MAPK). This is followed by a distinct secondary phase at 6 hours, where the transcriptome pivots to strongly enrich processes dedicated to sustained growth and survival, including cell cycle progression, DNA replication, and the PI3K-AKT-mTOR signaling axis. Having established this kinetic map, we demonstrate that the previously characterized L-peptide inhibitor, LA3IK, effectively suppresses this program. Co-treatment with EGF and LA3IK for 6 hours resulted in significant inhibition of genes across these critical pathways, including PI3K-AKT, MAPK, and cell cycle. To overcome the proteolytic limitations of the L-peptide, we then employed its D-enantiomer, D-LA3IK, which yielded **superior results**, driving a more profound and comprehensive reversal of the EGF-induced transcriptome and exhibiting enhanced efficacy in functional assays. This work delineates the phased transcriptional cascade orchestrated by EGF and establishes targeted peptide inhibition, particularly with the stable D-isomer, as a potent strategy to disrupt this oncogenic program.

#6336 AmbientcfRNApreservation: standardized extraction reveals superior stability in a multi-analyte tube.

Emily Medina[1], Tony Baker[1], Kamran Syed[2], Jason Saenz[2], Cameron Van Dieren[2], Carlos Hernandez[2], Daniel Cedeno[2], Mayer Saidian[2], Nafiseh Jafari[2]

[1]Truckee Applied Genomics, Reno, NV,[2]nRichDX, Irvine, CA

Introduction: Liquid-biopsy readouts are highly sensitive to pre-analytical variability: cellular lysis and nuclease activity can inflate background, suppress rare signals, and impair reproducibility. Concurrent stabilization of multiple targets at the time of collection, paired with a controlled extraction workflow, is therefore critical. We assessed two blood-collection tubes—a single-tube matrix designed for multi-analyte stability—using the magnetic bead-based chemistry, focusing on cfRNA signal integrity and compatibility with downstream RT-qPCR.
Methods: Whole blood from healthy donors was drawn into Tube-A (TAG FLEX-LB™) and Tube-B (Streck Nucleic Acid BCT) aliquots were spiked with purified total RNA from H441 cells (KRAS G12V) at a fixed concentration per mL. Tubes were stored at ~21-25 °C and processed at T0 and T7. cfRNA was isolated using silica-magnetic bead Revolution cfTNA Max 20 Kit. Endpoints: allele-specific RT-qPCR for KRAS G12V (Ct; ΔCt = T7-T0; amplification efficiency and recovery), hemolysis proxy hsa-miR-16 (ΔCt), and RNA integrity (RIN; 18S/28S).
Statistics: paired tests with 95% Confidence Intervals.
Results: With one extraction workflow across both tubes, KRAS G12V amplified consistently at T0. After 7 days at room temperature, Tube-A showed minimal degradation, preserved efficiency, and maintained high recovery. Tube-B exhibited greater degradation and reduced efficiency in recovery. Hemolysis signal was lower in Tube-A: Day-7 miR-16 abundance was lower than Tube-B. RNA integrity remained stable in Tube-A but declined in Tube-B. Assay QC pass rate were higher for Tube-A.
Conclusions: Under a realistic 7-day ambient hold, cfRNA targets remained quantifiable when stabilization was adequate. In this head-to-head study, the multi-analyte stabilizing tube better preserved KRAS-G12V detectability, showed lower hemolysis, and maintained RIN/18S-28S metrics relative to a different tube, using an identical extraction workflow. These findings support cfRNA workflows and underscore the need for standardized pre-analytics—spanning both preservation and extraction.

#6337 Single-reaction KRAS variant profiling via processor-mediated PCR: Enhanced SNV discrimination using the iProbe.

Eric K. Pomaranski, Adam M. McCoy, Karl Spork, Niloufar Mertz, Vladimir Makarov

Signal Bioscience, Ann Arbor, MI

Accurate discrimination of single-nucleotide variants (SNVs) remains a major limitation of quantitative PCR (qPCR) and digital PCR (dPCR). Even with optimized hydrolysis probes, subtle thermodynamic differences between alleles often lead to cross-reactivity, reduced sensitivity near the limit of detection, and the need for multiple singleplex reactions. These constraints are particularly problematic for oncology applications requiring detection of low-frequency variants across closely spaced mutation sites. KRAS mutations in codons 12 and 13 represent clinically actionable drivers in multiple solid tumors, influencing prognosis and response to targeted therapies. However, the extreme proximity of these variants makes simultaneous, highly specific detection difficult; most current PCR-based assays require separate reactions or exhibit off-target signal among neighboring alleles. We developed processor-mediated PCR, a detection architecture that decouples target amplification from readout using a universal “processor” oligo and universal fluorescent probes. This chemistry supports high multiplexing, reduced assay cost, and tunable specificity independent of fluorophore channel limitations. In parallel, we engineered a modular multi-domain probe structure, iProbe, that generates signal only upon complete hybridization to a target variant, enabling exceptional SNV discrimination. To demonstrate this platform, we created a single-tube KRAS G12/G13 assay combining processor-mediated PCR with domain-engineered iProbes. In dPCR, the assay simultaneously detected all major KRAS codon 12 and 13 mutants with no detectable cross-reactivity. Sensitivity studies confirmed reliable detection at allele frequencies down to 0.01% (1:10,000 mutant:wild-type) with clean digital separation. Processor-mediated PCR with iprobes provides a powerful solution to longstanding specificity and multiplexing barriers, enabling cost-effective, highly selective detection of clinically relevant SNVs in a single reaction.

#6338 Clinical validation of a multi-gene blood test for kidney cancer screening and stratification.

Taigo Kato[1], Koji Hatano[2], Yohei Okuda[3], Dharam P. Chauhan[4], Norio Nonomura[5], Rajvir Dahiya[6]

[1]Urology, The University of Osaka Graduate School of Medicince, Suita, Japan,[2]Urology, Osaka Univ., Suita, Japan,[3]The University of Osaka Graduate School of Medicince, Suita, Japan,[4]Geneverify Inc, Hayward, CA,[5]Professor, Osaka University Graduate School of Medicine, Suita, Japan,[6]UCSF School of Medicine, San Francisco, CA

Background: Kidney cancer remains one of the most aggressive and fatal urological malignancies. To address this issue, we developed and clinically validated the Geneverify blood-based, cell-free mRNA test, a cutting-edge liquid biopsy platform that enables real-time, non-invasive genomic profiling. By quantifying circulating tumor-derived transcripts in plasma, this next-generation assay delivers rapid and precise molecular insights, paving the way for precision screening, early diagnosis, and treatment monitoring.
Methods: In this prospective clinical study, we evaluated real-time expression levels of 30 kidney cancer associated genes in plasma samples from 51 subjects (41 suspected cancer cases and 10 healthy controls). The primary objective was to assess the diagnostic and prognostic performance of a blood-based multi-gene expression panel developed by Geneverify Inc. Log_2 fold-change values were calculated for each gene and integrated to generate a composite Geneverify risk score for each subject. Geneverify scores were compared with biopsy-confirmed diagnoses to determine assay sensitivity and specificity. Additional statistical analyses assessed correlations between Geneverify scores and pathological grade as well as clinical stage.
Results: All cancer samples demonstrated Geneverify scores greater than 10. Using an optimized threshold of 10, the assay achieved 100% sensitivity in detecting cancer cases. Specificity could not be determined because the study cohort did not include benign or non-cancer subjects; therefore, AUC relative to non-cancer controls was also not estimable. Baseline Geneverify scores from healthy volunteers served as the reference for comparison. Most patients in the cohort had T1a (early-stage) kidney cancer. Elevated Geneverify scores showed clear correlations with tumor stage, grade, and treatment status. In the majority of late-stage metastatic cases receiving systemic therapy, Geneverify scores decreased significantly, suggesting a favorable treatment response.
Conclusions: This study provides the first real-time clinical validation of a blood-based, cell-free mRNA genomic assay for kidney cancer detection. The Geneverify test demonstrated high diagnostic accuracy, strong concordance with biopsy results, and robust prognostic value, establishing it as a powerful non-invasive alternative for early detection. Its adoption in clinical workflows may reduce surgical biopsies, improve patient stratification, and accelerate personalized oncology care.

#6339 Methylation profiling of a novel donor-derived reference material using methylation-sensitive restriction enzyme digestion and droplet digital PCR.

Daniel Wasik[1], Yves Konigshofer[2], Mona Shahbazian[1], Adam Corner[1], Eddy vanCollenburg[1], Jayanthi Ramprakash[2], Nish Kumar[1], Andrew Anfora[2], Mai Ho[1]

[1]Bio-Rad Laboratories, Hercules, CA,[2]LGC Clinical Diagnostics, Gaithersburg, MD

Aberrant DNA methylation, along with other epigenetic modifications, are important indicators in the development of cancer. Unique tissue-specific patterns of hyper-methylated genes have been linked to certain cancer types and are increasingly leveraged to identify tumor type and monitor disease progression including minimal residual disease (MRD) and ongoing cancer surveillance. Accurate DNA methylation analysis relies on robust reference standards to validate assay performance and ensure clinical relevance. Traditionally, methylation standards are produced by mixing fully methylated DNA and non-methylated DNA at defined ratios. While these mixtures provide a convenient benchmark for quantitative linearity, they fall short of capturing the complex methylation heterogeneity found in patient samples, which can diminish the utility of these standards for translational research and clinical diagnostics. To address this gap, our study evaluates a novel, differentially methylated DNA standard, specifically engineered to mimic physiologically relevant methylation patterns and better reflect the complexity observed in real-world patient samples.

In this study, methylation-sensitive restriction enzymes (MSRE) are utilized in conjunction with droplet digital PCR (ddPCR) to establish a platform characterized by high sensitivity and precision for the quantitative analysis of DNA methylation. Compared to bisulfite conversion, MSRE digestion requires substantially less input material and eliminates the need for depurination, reducing the risk of DNA degradation; and when paired with ddPCR, it enables a streamlined, target-specific methylation detection in a single-tube workflow.

We assessed methylation at seven colorectal cancer gene loci across three reference materials: enzymatically methylated DNA standard, non-methylated DNA standard, and the differentially methylated standard. Consistent with manufacturer's stated performance, the enzymatically methylated standard showed consistently high methylation, while the non-methylated standard exhibited low background methylation. In contrast, the differentially methylated reference material displayed locus-specific methylation heterogeneity, with targets ranging from non-methylated to partially methylated, and none were found to be completely methylated. These results demonstrate that Bio-Rad's ddPCR platform reliably detects methylation heterogeneity, supporting both research and assay development across both contrived and physiologically relevant control materials.

(For Research Use Only)

#6340 Detection of ectopic phosphorylated PDGFRA antibodies in the serum samples of HCC patients.

Jian-Hua Luo, Muhamuda Kader, Yan-Ping Yu

University of Pittsburgh, Pittsburgh, PA

Hepatocellular carcinoma (HCC) is one of the most lethal cancers for humans. Early diagnosis of HCC can significantly enhance the treatment outcomes and reduce disease mortality. MAN2A1-FER is one of the most frequent oncogenic fusion genes in HCC. Our previous studies showed that MAN2A1-FER ectopically phosphorylated the extracellular domain of PDGFRA. The present study aimed to examine the diagnostic utility of antibodies specific for the ectopically phosphorylated PDGFRA generated by MAN2A1-FER in HCC patients' serum samples. In this study, 130 serum samples from HCC (65) patients and non-HCC (65) patients were analyzed. Our results showed that the antibody levels specific for the ectopically phosphorylated PDGFRA were 3.5- to 10-fold elevated in the serum samples from HCC patients in comparison with individuals without liver cancers and negative for MAN2A1-FER gene fusion. The higher titers of anti-ectopic-pPDGFRA-N-terminus in the serum samples correlated with the HCC diagnosis and outperformed the serum alpha-fetal protein for the diagnosis of HCC. The presence of these antibodies was also highly correlated with the levels of MAN2A1-FER mRNA in these serum samples. We concluded that the elevated serum levels of anti-pPDGFRA-N-terminus antibodies are highly predictive of liver cancer and can be utilized as a potential diagnostic marker for HCC.

#6341 High-fidelity detection and classification of ovarian cancer from histopathological images using Artificial Intelligence.

Elangovan Krishnan[1], Jansi R. Sethuraj[2], Sophia Ahmed[3], Gowrishankar Palaniswamy[4], Muhammad Waqas Khan[4], Aravind Raghavan[4], Tayyiba Wasim[3]

[1]AIMDOCTOR, Thiruverkadu, India,[2]Texas Heart Institute at St. Luke's Episcopal Hospital, Houston, TX,[3]Allama Iqbal Medical College, Lahore, Pakistan,[4]The Medical University of South Carolina, Charleston, SC

Introduction: Ovarian cancer is a lethal gynecological malignancy with a substantial economic burden. Accurate histopathological subtype classification is critical for precision therapy and prognostication. Traditional pathological diagnosis relies on subjective interpretation, which is vulnerable to significant interobserver variability. Convolutional neural networks leveraging residual architectures enable automated, objective feature extraction from histopathological images. This study investigates ResNet18-based ovarian cancer subtype classification to accelerate diagnostic accuracy and support evidence-based clinical decision-making.

Methods: Anonymized histopathological images from the University of British Columbia Ovarian Cancer Subtype Classification dataset encompassing five ovarian cancer subtypes (n=513) were procured. The dataset was randomly proportioned into training (60%), validation (20%), and testing (20%) cohorts. Images underwent comprehensive preprocessing and augmentation prior to training using the ResNet18 architecture. The diagnostic performance was assessed using accuracy, precision-recall, F1 and F2-scores, and area under the receiver operating characteristic curve (AUROC) on both validation and test sets. The trained model was deployed in a universally accessible, cross-platform application for expert validation globally.

Results:

ResNet18 demonstrated robust discriminative capability across ovarian cancer subtypes, achieving >98% training accuracy and >82% validation accuracy. Precision-recall analysis showed excellent performance, especially for the endometrioid subtype (0.95). These results indicate ResNet18's potential to augment histopathology workflows, facilitating equitable ovarian cancer subtype stratification.

Conclusion: ResNet18-based analysis provides automated, accurate ovarian cancer diagnosis. High validation accuracy and strong AUROC scores across histological subtypes indicate efficacy in standardizing diagnostic interpretation. Integration into clinical workflows could reduce diagnostic variability and support precision-guided therapy. Further validation in prospective multicenter cohorts will translate this into an effective diagnostic tool.

#6342 Performance of longitudinal cancer screening in Li-Fraumeni syndrome.

Payal P. Khincha[1], Sophia Ty[2], Siddharth Roy[3], Jessica N. Hatton[1], Ashkan Malayeri[4], Megan N. Frone[1], Margarita Aryavand[1], Phuong Mai[5], Paul Albert[3], Sharon A. Savage[6]

[1]Clinical Genetics Branch, Division of Cancer Epidemiology and Genetics, National Cancer Institute, Bethesda, MD,[2]Oden Institute for Computational Engineering and Sciences, The University of Texas at Austin, Austin, TX,[3]Biostatistics Branch, Division of Cancer Epidemiology and Genetics, National Cancer Institute, Bethesda, MD,[4]Department of Radiology and Imagi, Fairfax radiology Centers, Fairfax, VA,[5]Magee-Womens Hospital, University of Pittsburgh Medical Center, Pittsburgh, PA,[6]NCI Div. of Cancer Epidemiology & Genetics, Rockville, MD

Li-Fraumeni syndrome (LFS), a cancer predisposition syndrome caused by germline [likely] pathogenic (P/LP) *TP53* variants, confers elevated multi-organ cancer risks from infancy and high lifetime risk of multiple primary cancers. The heterogeneous cancer spectrum necessitates multi-modal lifelong cancer screening to facilitate early detection. The study included 145 individuals (62% female) with a germline P/LP *TP53* variant who enrolled in the National Cancer Institute's IRB-approved longitudinal LFS study (NCT01443468) and received cancer screening at the NIH Clinical Center including annual whole-body MRI (WBMRI), brain MRI, breast MRI (females>20 years), mammography (females>40 years), bloodwork, triennial colonoscopy (>25 years), and abdominal ultrasound every 4 months (age 3-16 years). Median age was 34 years (range 3-68) at the first screening visit. In all, 772 annual screening visits were completed (median 5 visits per participant, range 1-10) and 3956 screening tests performed at a compliance of 92.8%. Screening tests led to 545 follow-up tests. WBMRI led to at least one follow-up test in 29.1% scans (n=225/772). Invasive biopsies comprised 8.3% (n=45/545) of all follow-ups, 48.9% (n=22/45) of which resulted in a cancer diagnosis. WBMRI led to 62% (n=28/45) of all biopsies, of which 42.8% (n=12/28) resulted in a cancer diagnosis. Of the 72 cancers/pre-cancers diagnosed during the study, 75% (n=54) were screen-detected (32/54, 59% from WBMRI). The 18 (25%) interval cancers were diagnosed at a median of 8 months (range 3-13) after last screening test. Prevalence of asymptomatic cancer was 7% at first visit, varying between 4% and 11% at subsequent visits. The screening protocol had a sensitivity of 71.7%, specificity 89%, false positive rate (FP) 11%, negative predictive value (NPV) 99.1%. Diagnostic properties of each screening test for screen-detectable cancers were analyzed using logistic regression with generalized estimating equations. WBMRI sensitivity was 94%, specificity 94.8% (between 91.6% for thoracic cancers and 97.6% for upper extremity), FP 27%, NPV 99.9%. Brain MRI had sensitivity of 85.7%, specificity 98%, FP 2%, NPV 99.9%. Breast MRI had sensitivity of 88.9%, specificity 83.6%, FP 16.3%, NPV 98.9%. Neither germline *TP53* variant nor age significantly affected specificity. A previous cancer diagnosis in an anatomical region reduced specificity of WBMRI (OR=0.12, 95% CI 0.06-0.25, <0.001). A previous false positive finding in an anatomic region increased the probability of additional false positive findings in that region (p<0.001). This largest longitudinal LFS cancer screening study to date shows that multi-modal screening performs well with most reported cancers being screen-detected. FP rate is high but lower than previously reported. While further research on alternative screening strategies and cancer prevention is needed, screening is clinically crucial to early cancer detection in LFS.

#6343 Integrative analysis of proteomic, transcriptomic, and FACS-based surface marker data for ADC target discovery in cancer cell lines.

Nadine Obier[1], Vincent Vuaroqueqeaux[2], Johannes Krumm[3], Anne-Lise Peille[2], Daniel Feger[1], Sarah Ulrich[1], Johanna Wallner[3], Hannes Hahne[3], **Jan E. Ehlert**[1]

[1]Reaction Biology Europe GmbH, Freiburg im Breisgau, Germany,[2]Apex OncoSience SAS, Mulhouse, France,[3]Omicscouts GmbH, Munich, Germany

In the preclinical space of cancer drug discovery, multi-omics characterization of cancer models is essential for model selection, understanding mechanisms of action, and early biomarker discovery. We launched a panel of 160 cell lines (CL Proliferation Panel) to study drug responses across a large variety of cancer types and validated their molecular characteristics at both the transcriptomic and genomic levels. Recently, we characterized this set of models at the proteomic level using mass spectrometry, identifying a total of more than 15.000 proteins. In the present work, we aim to investigate the relevance of this new dataset in the daily practice of cancer model utilization. First, we demonstrated the robustness of the established proteomic profiles, showing high concordance among duplicate samples. Using a multiomics comparison and dimensionality reduction approaches, we curated the proteomic dataset to remove outlier and irrelevant protein profiles, ensuring high data quality. Next, unsupervised hierarchical clustering of the proteomic profiles revealed accurate classification of models according to their tumor type of origin, confirming the relevance of the data. Given the growing importance of proteomic information in the context of antibody-drug conjugate (ADC) development, we further assessed the relevance of our dataset for evaluating the expression of top 20 ADC targets such as ERBB2 and TACSTD2, among others. We also established a multi-omics strategy integrating transcriptomic and proteomic data to enhance target characterization. Finally, we explored the relationship between protein expression of the targets and drug sensitivity by analyzing ADC targets in the context of responses to clinically approved ADCs, including trastuzumab emtansine (Kadcyla), and sacituzumab govitecan.

: Science and Health Policy 2
Poster Session

#6346 How case based education elevated clinical performance in metastatic breast cancer management: A study for TROP2 directed antibody drug conjugates.

Meghan Coulehan[1], Serena Welch[1], Komal Jhaveri[2], Lavanya Anantharaman[1], Emily Kitterman[1], Aisha Suhail[1]

[1]Answers in CME, New York, NY,[2]Memorial Sloan Kettering Cancer Center, Scarsdale, NY

Background: The treatment landscape of metastatic breast cancer (mBC) has advanced with antibody-drug conjugates (ADCs), notably the TROP2-directed agents sacituzumab govitecan and datopotamab deruxtecan. These options have extended treatment potential for patients with HER2- mBC. However, rapid updates pose challenges for clinicians in adopting evidence-based, personalized strategies.
Objective: To assess whether a digital, case-based, short-format CME activity could address knowledge and competence (K/C) gaps regarding the evidence-based use of TROP2-directed ADCs in HER2- mBC.
Methods: A 15-minute, case-based, accredited online activity ("Opportunities to Personalize Care: Making the Case for TROP2-Directed ADCs in HR+, HER2- mBC") launched March 28, 2025. Global academic and community oncologists completed pre-/post-assessments measuring K/C outcomes. A qualitative follow-up questionnaire, 4 weeks post-launch, evaluated practice changes and implementation behaviors.
Results: As of June 3, 2025, 4,073 learners participated. Post-activity data showed a 20% mean improvement in K/C scores. Participants improved notably in identifying appropriate patients and applying ADCs in alignment with clinical evidence. The lowest baseline knowledge area—patient identification—showed marked gains, though further reinforcement may optimize impact in practice. Notably, 73% reported practice changes attributable to the activity. Post-education assessment revealed increased implementation of personalized and evidence-based treatment decision-making and adverse event management (Table 1).
Conclusion: This case-based CME activity effectively improved clinician K/C regarding TROP2-directed ADCs for HER2- mBC and supported sustained practice change. Personalized, digital education formats may accelerate integration of newly available and emerging therapies into oncology care.

Table 1: Impact of Education on Practice Change

Change in practice	Initial analysis, %; n=33	4 week F/U after participation, %; N=55
Identify appropriate patients with HR+, HER2-negative mBC who are candidates for TROP2-directed ADCs	58	71
Recognize appropriate characteristics to select between ADCs for patients with HR+, HER2-negative mBC	64	85
Proactively implement best practices to manage AEs for patients with mBC on TROP2-directed ADCs	39	69
Apply guideline recommendations to select TROP2 directed ADCs for patients with HR+, HER2-negative metastatic breast cancer	48	56

#6347 Cancer Voices: A community-engaged approach to transform cancer disparities through verbatim theater.

Azlan G. Smith, Craig A. Richard, Zeynep Madak Erdogan

Cancer Center at Illinois, Urbana, IL

Cancer outcome disparities persist among underserved populations in central Illinois, yet traditional research approaches often fail to capture lived experiences or engage affected communities in meaningful partnerships. This project employs verbatim theater, a documentary performance methodology, to address cancer disparities through storytelling, qualitative research, and community engagement, aiming to increase representation of historically excluded groups, identify barriers to patient-centered research, and foster collaboration among patients, caregivers, researchers, and clinicians. Building on 50+ interviews with cancer survivors, family members, healthcare providers, and researchers across central Illinois. Interview transcripts are being transformed into a verbatim theater script that authentically documents cancer treatment experiences and illuminates structural barriers to equitable care. Through partnerships with University of Illinois Cancer Research Advocacy Group, Prairie Dragon Paddlers, Carle-Mills Breast Cancer Institute, Station Theater, and other community organizations, we will present two live performances (April-May 2026) projected to reach 500+ community members, with digital distribution extending impact to broader audiences. Pre- and post-performance surveys coupled with facilitated discussions will assess changes in audience understanding of cancer disparities, research engagement intentions, and perceived barriers to care. Preliminary findings reveal significant therapeutic and educational value. Interview participants consistently report that sharing their narratives through this qualitative process has been healing and supportive. Both survivors and clinicians express enthusiasm for seeing diverse cancer experiences represented collectively in an accessible format they have never previously encountered. Participants identify isolation, fragmented communication, and silence as pervasive challenges during cancer treatment. Many view this verbatim theater intervention as a critical mechanism to bridge divides between stakeholder groups and foster new collaborations in cancer research and care delivery. This approach uniquely combines immediate quality-of-life benefits for participants with long-term structural change potential. By centering community voices and creating accessible science communication, this model offers a replicable framework for other institutions addressing cancer disparities through patient advocacy, community engagement, and implementation science strategies. (The trailer can be found at https://ipmnewsroom.org/u-of-i-funding-to-help-showcase-cancer-research-through-theater/)

#6348 Cover stories: How journal front pages amplify cancer research reach.

Ekaterina Zvorykina, Ella Marushchenko, Aleksandr Tokarev

Ella Maru Studio, Mount Pleasant, SC

Nowadays online communication and social media have become powerful amplifiers of scientific visibility and influence. Increasingly, scientists rely on decentralized networks and social media, such as X (formerly Twitter), YouTube, and other online platforms. They're used to disseminate findings, build collaborations, and engage broader audiences beyond traditional institutional channels. Emerging evidence suggests that scholarly work promoted online attains greater visibility and citation impact, underscoring the growing role of strategic digital engagement in shaping research dissemination and recognition.In this study, we investigated whether visual prominence through cover selection in Nature Cancer predicts enhanced article visibility and impact. We analyzed all publications from the six volumes of Nature Cancer (2020-present), comparing engagement metrics between articles featured on the journal's cover and those that were not. Metrics included article accesses, Altmetric scores, and citation counts. Altmetric data were further used to quantify public engagement through mentions in news outlets, policy documents, and online platforms.Statistical comparisons revealed that cover-featured articles persistently achieved significantly higher engagement across all dimensions: readership ($t = 3.78$, $p = 0.00026$), online attention ($t = 2.49$, $p = 0.014$), and scholarly citations ($t = 3.57$, $p = 0.00055$). Strong positive monotonic correlations were observed among accesses, Altmetric attention, and citations (Spearman $\rho = 0.68$-0.80), indicating that articles attracting online attention tend to be more widely read and cited. Temporal analyses from 2020 to 2024 showed that the "cover advantage" persisted annually and was most pronounced between 2021 and 2023, coinciding with the journal's rapid audience expansion. Even after accounting for citation-time bias, cover-selected papers consistently exhibited approximately twice the citation rate, 1.6× higher Altmetric scores, and 1.7× more accesses compared to non-cover articles.Our findings demonstrate that visual prominence through cover selection predicts measurable scientific impact. The results highlight a robust and sustained "cover advantage," suggesting that visibility-enhancing editorial decisions can substantially amplify both digital and scholarly reach. Future work should examine potential confounders, such as article type and topicality, to further elucidate the mechanisms linking visual presentation to scientific influence.

#6349 Engaging communities in cancer research: Outcomes from the CaRE^2 health center's 2025 community scientist ambassador program.

Carolina Aristizabal[1], Fern Webb[2], Sandra Suther[3], John Luque[3], Eduardo Ibarra[4], Ileana Guzman[5], Brooke Vintilla[6], Janet Rodriguez[7], Rosa Barahona[4], Mariana C. Stern[8], Jennifer Tsui[9], Lourdes Baezconde-Garbanati[9]

[1]USC Norris Comprehensive Cancer Center, Los Angeles, CA,[2]University of Florida College of Medicine - Jacksonville, Jacksonville, FL,[3]Florida A&M University, Tallahassee, FL,[4]University of Southern California, Los Angeles, CA,[5]University of Florida, Orlando, FL,[6]Universtiy of Florida, Gainesville, FL,[7]USC Norris Comprehensive Cancer Center, Ontario, CA,[8]Associate Professor, Dept. of Prev. Medicine, USC Norris Comprehensive Cancer Center, Los Angeles, CA,[9]Keck School of Medicine of USC, Los Angeles, CA

Background: Collaborative relationships between communities and scientists are essential for ensuring inclusivity and relevance in cancer research. The Florida-California Cancer Research, Education, and Engagement (CaRE^2) Health Center established the Community Scientist Research Ambassador (CSRA) Program to train community members to become informed about cancer research. The program, now in its eight years, aims to increase knowledge about cancer and ongoing research, improve confidence in community research engagement, and expand two-way communication between community members and researchers to promote full participation in cancer studies. Recruitment occurs primarily through community organizations, the CaRE^2 registry, and personal networks.

Methods: The CSRA program is implemented over ten weeks using a hybrid learning model that includes 90% virtual sessions and one in-person laboratory experience. The curriculum addresses topics such as cancer health differences, social determinants of health, policy, ethics, genomics, and community-based participatory research. All materials and sessions are available in English and Spanish with human interpreters. Participants complete pre- and post-program surveys to assess their knowledge, self-efficacy, and satisfaction, and complete an individual project. Descriptive and inferential analyses were conducted using Wilcoxon signed-rank tests.

Results: Of the 21 participants in 2025, 85.7% were female, 93.3% identified as Black/African American, and 35.0% identified as Hispanic/Latino. Most participants (66.7%) held a university degree or higher. Cancer knowledge scores significantly increased by program end (mean proportion correct 0.73 ± 0.08 pre-program vs. 0.81 ± 0.09 post-program; p=0.001), indicating higher understanding of cancer research concepts. Self-efficacy scores also improved (mean 4.39 ± 0.69 pre vs. 4.75 ± 0.45 post; p=0.032), reflecting increased confidence to share cancer research information with others and engage in advocacy. Participant satisfaction was uniformly high (mean satisfaction score 4.91 ± 0.20; evaluation score 4.79 ± 0.31), with nearly all respondents affirming that they gained new knowledge, improved their support skills, and intended to share information with others in their communities.

Conclusions: The CaRE^2 Community Scientist Research Ambassador Program effectively enhanced cancer research literacy and self-efficacy among community members completing the program. The CSRA program is responsive to community needs, fosters community capacity, strengthens communication with scientists, and promotes participation in cancer research. Sustaining and scaling this program advance cancer research by bridging gaps between community engaged ambassadors and the scientific enterprise.

#6350 Social media and technology preferences among colorectal cancer patients.

Itzya B. Ulloa[1], Daisy Hernandez[2], Charite N. Ricker[2], **Elena Taylor**[2], Rosa Barahona[3], Blanca Ovalle[2], Bo Y. Wang[2], Caryn Lerman[2], Julie O. Culver[2], Juan P. Lewinger[3], Mariana C. Stern[4], John D. Carpten[5], Heinz Josef Lenz[2], Lourdes Baezconde-Garbanati[2]

[1]USC Norris Comprehensive Cancer Center, Los Angeles, CA,[2]Keck School of Medicine of USC, Los Angeles, CA,[3]USC, Los Angeles, Los Angeles, CA,[4]Associate Professor, Dept. of Prev. Medicine, USC Norris Comprehensive Cancer Center, Los Angeles, CA,[5]City of Hope, Duarte, CA

Background: Knowledge, attitude, and beliefs impact participant engagement in genetics and genomics research. However, there is still room to better understand how information is disseminated within the community. The widespread use of smartphones has made health information more accessible, but understanding the devices and platforms used, as well as usage frequency is essential for effective health education.

Methods: A cross-sectional survey was conducted among 57 colorectal cancer (CRC) patients aged 18+ recruited at two Los Angeles area hospitals. The survey assessed knowledge, attitudes, and beliefs regarding cancer genetics/ genomic testing, as well as social media and technological device usage and preferences. Recruitment and survey administration were based on each participant's preferred language.

Results: The average age of participants was 53.96 years (SD = 10.38). Most, 66.7%, reported using social media at varying frequencies, while 33.3% reported never using social media. Among daily social media users, Facebook was the most popular platform (48.7%), followed by WhatsApp (36.8%), TikTok (35.1%), and Instagram (24.3%). Regarding access to technology, all participants reported owning a smartphone, while only 26% had access to a tablet and 22% had access to a laptop or desktop. Notably, 64% of participants reported needing assistance to access Zoom. The majority (63%) of participants were male, and 64.9% reported an annual household income of less than $25,000.

Conclusion: These findings indicate that smartphones are the primary device utilized by study participants to access online educational materials and videos. Social media platforms could be effective to disseminate health education materials (as 66.7% used it). However, relying solely on this would exclude the one in three participants who reported not using social media at all. While Zoom offers an alternative to overcome transportation and accessibility barriers, 64% of participants require assistance to use it, highlighting the need for dedicated support from research staff. Future research should explore how patients seek information through social media to develop effective health education materials.

#6351 Leveraging artificial intelligence and short educational videos to expand accessible cancer education for diverse communities.

Bianca Rosales[1], Yaneth L. Rodriguez[2], Rosa Barahona[2], Letech Caldera-Huerta[2], Samantha Verganza[2], Lourdes Baezconde-Garbanati[3]

[1]USC Norris Westside Cancer Ctr., Inglewood, CA,[2]USC, Los Angeles, Los Angeles, CA,[3]Keck School of Medicine of USC, Los Angeles, CA

Background: Colorectal cancer (CRC) is the second leading cause of cancer death in the United States, yet many adults lack knowledge about screening, symptoms, and genetic risk. Traditional materials often do not reach diverse socioeconomic and cultural groups because of low health literacy and differences in media use. Many Americans, especially younger and lower income adults, spend several hours each day on screens. This creates an opportunity for mobile friendly and visually engaging education. Artificial intelligence (AI) offers a rapid way to create accessible and adaptable cancer information that fits current media habits.

Methods: We created an early stage framework that uses AI to produce scalable and culturally adaptable cancer education. The approach uses generative video platforms, AI assisted scriptwriting, simplified language, and multilingual narration to create short films on prevention, screening, and genetic testing. The framework aims to increase knowledge and early detection behaviors, reduce production time and cost, support mobile and screen based viewing, and adapt content across languages, cultures, and socioeconomic settings. Initial prototypes include videos on lifestyle risk reduction, family history, genetic testing, and timely screening.

Results: Our team produced AI assisted scripts for a storyboard, a storybook concept, and a film to educate African American (AA) communities about CRC. Four focus groups with a total of 27 AA and African immigrant adults were conducted in person and on Zoom through the AltaMed patient network. Participants reported that the script was clear, easy to understand, and communicated the main ideas. Community specific statistics were motivating and relevant. Participants asked for more information about the screening experience and reassurance to reduce fear. Their feedback informed the development of a script board with key message cards that address barriers and essential CRC information for AA audiences.

Conclusions: AI assisted workflows can support the creation of culturally relevant CRC education materials while maintaining clarity and community alignment. This approach shows strong potential for producing high quality materials for populations underserved by traditional communication. The next phase will assess feasibility, acceptability, comprehension, and intent to seek CRC screening among diverse audiences, with planned use in community outreach, patient navigation, and digital education programs.

#6352 Strengthening guideline compliant care delivery in a safety net hospital through artificial intelligence (AI) enabled technology solutions.

Vishesh Khanna[1], Nagashayana Gampalahalli[2], Naresh Ramarajan[2], Anand Bhagat[3], Ajay Punpale[4], Pramod Kalidas Tike[5], Brijmohan Zawar[6], Ramya B[2], Nikhil Ghadyalpatil[7]

[1]Medical Oncology, Stanford University, California, CA,[2]Navya Care, Bangalore, India,[3]Surgical Oncology, Anand Cancer and Multispeciality Hospital, Nanded, Maharashtra, India,[4]Surgical Oncology, Latur Superspeciality Hospital Pvt Ltd, Latur., Maharashtra, India,[5]Consultant Radiation Oncologist, Vivekanand Cancer Hospital, Latur, Maharashtra, Maharashtra, India,[6]Consultant Surgical Oncologist, Vivekanand Cancer Hospital, Latur, Maharashtra, Maharashtra, India,[7]Medical Oncology, Apollo Cancer Centre, Hyderabad, Hyderabad, India

Background: Concordance with guideline-based cancer care is often low in resource-constrained settings, leading to under- or over-treatment and delays in care. Navya Earthshot is a validated AI-enabled decision support system that matches patient records to standard-of-care cancer treatment guidelines to generate evidence-based recommendations. This study evaluated the implementation of Navya Earthshot at a safety-net hospital in India to assess improvement in concordance with National Cancer Grid (NCG) guidelines and reduction in delays to care.
Methods: A prospective pre-post observational study conducted over six months at a safety net cancer center in the public health system of India. Baseline data prior to Navya Earthshot integration were collected for comparison. Key outcomes included concordance of treatment decisions and average number of hospital visits per treatment decision. Navya Earthshot was integrated into routine workflows. The system matched patient-specific information to NCG guidelines to generate treatment options, which were reviewed by treating oncologists and discussed in daily tumor boards. Diagnostic testing was streamlined by eliminating non-mandatory investigations, reinforced through digital care navigation and structured follow-up by lay cancer navigators.
Results: During the study period, 892 patients presented to the hospital for a first cancer visit. Among 537 patients requiring active treatment decisions (290 pre-implementation; 247 post-implementation), 411 were evaluable (210 pre; 201 post). Guideline concordance improved from 67% (140/210; 95% CI +/-6%) at baseline to 87% (175/201; 95% CI +/-5%) after Navya Earthshot integration—a 20% absolute increase. Integration of Navya Earthshot, combined with digitally enhanced care navigation, reduced the average number of patient visits before treatment initiation of care from an average 3.45 to 2.5 visits (0.95 visits, 27.5% reduction), primarily due to elimination of non-mandatory report-review visits. Care initiation moved forward from 6 weeks at baseline down to 4 weeks after intervention (2 weeks, 33% reduction).
Conclusion: Implementation of Navya Earthshot improved adherence to standard-of-care guidelines and reduced time to treatment in a resource-constrained setting. Integrating validated AI decision support tools into oncology workflows can strengthen cancer care delivery and enable broader adoption of guideline-based treatment in resource-constrained health systems.

#6353 Age-related differences in lung cancer patients' and caregivers' perceptions and challenges: 2025.

Joan Schiller[1], Dhru Deb[2], Alexandre Reuben[3], Peixin Jiang[3], Amy Cipau[4], Hildy Grossman[5], Marc Muskavitch[6], Sara Patton[7], **Mary Lisa Spain**[8]

[1]OUCH - International, Richmond, VA,[2]Lung Cancer Research Foundation, Philadelphia, PA,[3]The University of Texas MD Anderson Cancer Center, Houston, TX,[4]Lung Cancer Initiative, Raleigh, NC,[5]Upstage Lung Cancer, Brookline, MA,[6]ALK Positive, Atlanta, GA,[7]International Association of the Study of Lung Cancer, Denver, CO,[8]Rexanna's Foundation, Prosper, TX

Background Studies have been conducted looking at aspects of patient experiences with lung cancer, but a comprehensive assessment of how challenges may differ by age of US patients is missing. The Research team within the LungCAN organization conducted this project. LungCAN is a collaborative group of lung cancer advocacy organizations that work together to raise public awareness about the realities of lung cancer.

Methods 2055 surveys were sent out with 46% returned (63.39% patients, 45.09% caregivers). The cohort was stratified by age (44 and under vs. 45 and over) to determine if age influenced perspectives in fears or concerns about living with or supporting someone with lung cancer, and challenges faced with medical care or treatment. Chi-square test of independence was used to identify significant differences in fears, concerns, and challenges between age groups.

Results Statistical analysis suggested a significant disparity in fears concerning lung cancer between the two cohorts (p-value = 1.24e-09). Major concerns of the younger cohort (≤44) were psychosocial and emotional impact (19.2%) and social stigma (4.4%). The older cohort (≥45) was preoccupied with clinical and practical issues including disease progression and recurrence (24.3%) and insufficient information and support (11.3%).

Significant age-based divergence was observed in the challenges faced with medical care and treatment (p-value < 2.2e-16). The cost of care was the predominant concern across participants, but prevalence was substantially higher among participants aged 44 and below (67.3%) compared to the older group (46.9%). The younger cohort viewed transportation as a challenge with significantly greater frequency (41.5% vs. 30.5%) while job related issues were more prominent among the elder cohort (16.9% vs. 9.1%).

Conclusions Age reveals differences in how patients and caregivers perceive the challenges associated with lung cancer. Age-sensitive approach to support strategies are warranted.

Fears and Challenges faced with living with or supporting someone with lung cancer.

		Total N (%)	N (%)	N (%)
		Total 842* (%)	44 and under 364 (%)	45 and over 478 (%)
Fears	Disease progression & recurrence	149(17.7%)	33(9.1%)	116(24.3%)
	Death	193(22.9%)	98(26.9%)	95(19.9%)
	Physical Symptoms, Side Effects, and QOL	177(21.0%)	79(21.7%)	98(20.5%)
	Emotional & Psychological Impact	128(15.2%)	70(19.2%)	58(12.1%)
	Financial & Emotional Impact on Family	155(18.4%)	70(19.2%)	85(17.8%)
	Inadequate Information and Lack of Support Systems	69(8.2%)	15(4.1%)	54(11.3%)
	Social Stigma & Isolation	30(3.6%)	16(4.4%)	14(2.9%)
Challenges	Transportation to and from appointments	297(35.3%)	151(41.5%)	146(30.5%)
	Cost of care and payment	469(55.7%)	245(67.3%)	224(46.9%)
	Scheduling issues	270(32.1%)	117(32.1%)	153(32.0%)
	Access to trials or alternative therapies	293(34.8%)	132(36.3%)	161(33.7%)
	Language Barriers	76(9.0%)	50(13.7%)	26(5.4%)
	Availability of treatments in my geographic area	168(20.0%)	79(21.7%)	89(18.6%)
	Job related issues	114(13.5%)	33(9.1%)	81(16.9%)
	Other	112(13.3%)	6(1.6%)	106(22.2%)

*The participants include patients, their close and extended family members, and staff from health care providers.

#6354 Unpacking clinical trial referral processes: A qualitative study of community and academic oncologists.

Carma Bylund[1], Naomi Parker[1], Kelsey Lunsford[1], Jonathan Thomas[1], Margo Michaels[2], Tithi Amin[1], Stephanie Staras[1]

[1]College of Medicine, University of Florida, Gainesville, FL,[2]Health Care Access & Action, Boston, MA

Purpose: The purpose of this study was to examine how oncology clinicians, particularly those in community settings where the majority of patients receive care, navigate referrals to academic centers, including for clinical trial enrollment, by identifying factors that influence their referral practices, with the ultimate goal of improving partnerships between community and academic centers.
Methods: We conducted semi-structured interviews (N=23) with community oncology clinicians (oncologists, n=8; nurse practitioner, n=1; physician assistant, n=1) and academic oncologists at an NCI-designated cancer center (n=13) to examine their experiences and perspectives across the referral process to academic centers, including connecting patients to appropriate clinical trials. Both groups were included to capture the diverse contexts in which trial referrals occur and to understand how organizational environments shape referral practices. Transcripts were thematically analyzed.
Results: Oncology clinicians described three key considerations shaping the clinical trial referral process: (1) reasons to refer to academic centers, or reasons referrals were received to academic centers; (2) perceived barriers to referrals, such as logistical and financial barriers, and lack of communication; and (3) referral facilitators, including institutional support, scheduling efficiency, and strong communication between oncologists and trial teams. Oncology clinicians concluded by providing suggestions for improvement, such as streamlining referral pathways, reducing logistical or structural barriers, and improving patient education on clinical trials.
Conclusions: Oncology clinicians' engagement in the academic center referral process, including referrals to clinical trials, is shaped by multiple interrelated factors, including motivations, barriers, and facilitators for referrals. The oncology clinicians in our sample outlined several opportunities for improvement in the referral process. Understanding these considerations across both community and academic settings can inform strategies to streamline referrals, enhance trial participation, and improve patient access to novel therapies. Our findings highlight the importance of addressing context-specific barriers to enhance trial accessibility and participation. Strengthening communication channels and providing tailored institutional support may strengthen alignment between community and academic settings, thereby expanding equitable access to oncology clinical trials.

#6355 Building the first comprehensive research ecosystem and preclinical model platform for myoepithelial carcinoma.

Jamie Barber, Naomi Natale, **Michael Casaus**

cureMEC, Albuquerque, NM

Myoepithelial carcinoma (MEC) is an ultra-rare, clinically aggressive malignancy (incidence 0.013/100,000) that affects both children and adults and arises in diverse anatomic sites, most commonly the salivary gland and soft tissues. Despite its severity, MEC remains profoundly understudied, with no established therapeutic standards and historically limited access to biospecimens, molecular data, or disease-relevant models. Although recurrent gene fusions, most frequently involving EWSR1 with partners such as ATF1, KLF15, KLF17, PBX1, and POU5F1, define a subset of pediatric and young adult cases, MEC overall exhibits substantial biological heterogeneity that has yet to be systematically characterized. To address longstanding barriers to progress, cureMEC: The Myoepithelial Carcinoma Project was launched in 2022 as a patient-driven research initiative dedicated to building the foundational infrastructure required to study MEC across molecular subtypes. In partnership with the Rare Cancer Research Foundation (RCRF) and Pattern.org, cureMEC has established the first dedicated MEC biorepository and integrated clinical-molecular data platform, supporting systematic specimen acquisition, multiomic profiling, and open-access research engagement. MEC biospecimens are now incorporated into large-scale programs spanning transcriptomics, proteomics, and high-throughput drug-screening pipelines. Early achievements include creation of the first coordinated MEC biobanking network and establishment of two novel MEC cell lines have been developed and identification of a patient-derived xenograft (PDX) molecularly confirmed to harbor EWSR1-KLF15. These models will support mechanistic studies of EWSR1-driven oncogenesis, surface-protein mapping to identify therapeutic targets, and high-throughput drug-repurposing screens across fusion-defined contexts. Together, these efforts establish the first integrated research ecosystem for MEC, combining patient partnership, biospecimen infrastructure, and proteogenomic discovery. This model demonstrates how patient-driven collaborations can rapidly build foundational scientific resources for ultra-rare cancers, creating the tools necessary to elucidate disease mechanisms and accelerate the development of targeted therapies.

#6356 MATCHMAKERS Cancer Grand Challenge Team: Partnership and purpose to maximize patient research advocate involvement in collaborative preclinical research.

Annie Ellis[1], Luciana Holtz[2], Michele Rakoff[3], Tracy Solak[4], Matheus O. de Souza[5], Michael Birnbaum[5]

[1]Ovarian Cancer Research Alliance / SHARE Cancer Support, New York, NY,[2]Instituto Oncoguia, Sao Paolo, Brazil,[3]Breast Cancer Care and Research Fund, Los Angeles, CA,[4]Advocate, National Breast Cancer Coalition, Washington, DC,[5]Massachusetts Institute of Technology (MIT), Cambridge, MA

Objectives Patient research advocate (PRA) involvement in clinical trials has increased, yet involvement in pre-clinical research remains limited because pathways for incorporating patient perspectives are not always clear. MATCHMAKERS seeks to build models for effective PRA participation in pre-clinical science.
Background Cancer Grand Challenges (CGC), founded by NCI and CRUK, supports global interdisciplinary teams advancing cancer research and requires patient advocate involvement to ensure real-world impact. Launched in 2024, CGC Team MATCHMAKERS includes researchers from 10 institutions across six countries working to crack the code of how T cells recognize cancer cells using structural biology, high-throughput screening, and artificial intelligence to inform predictive immunotherapy tools.
Methods Four PRAs from the USA and Brazil contribute lived cancer experience and advocacy expertise. PRAs attend monthly research meetings, PRA meetings, CGC advocate sessions, and annual CGC and MATCHMAKERS summits. The Lead PI and Program Manager attend PRA meetings and coordinate interactions with trainees and investigators to facilitate bidirectional learning and involvement.
Results PRAs have partnered with five trainees from four labs, co-developing shared language, context, and communication tools. PRA involvement has strengthened understanding of MATCHMAKERS research goals, while trainees report appreciation of patient needs and translational relevance. Key activities and trainee reflections are summarized in the Table.
Conclusions Early experience demonstrates that structured PRA involvement fosters mutual respect, trust, and more patient-centered scientific thinking. Next steps include expanding PRA-trainees partnerships across institutions and contributing to CGC-wide best-practice development for PRA involvement in pre-clinical research.

PRA goals, key outputs, and trainee reflections

Category	
PRA Goals	Bring patient perspective into research; support trainee education; share MATCHMAKERS science with patient communities; develop best practices for pre-clinical advocacy
Outputs	Glossary; lay summaries; lay TCR overview; education module for advocates; lab-visit video series
Trainee Reflections	“I think more about applicability beyond fundamental research.” “Advocacy input keeps me focused on clinical translation.” “Engagement helps me see the broader purpose and communicate better.”

#6357 *Surprising myself of how much more confident I got in being able to share my voice*: A qualitative study exploring patient and public engagement in cancer research.

Piotr Teodorowski[1], Joi Miner[2], Jonathan B. Green[2], Daniel G. Garza[2], Marcus Arana[2], Beth Maclin[3], Edward Duncan[1], Jonine Figueroa[3], Liz Forbat[1], Sarah S. Jackson[3]

[1]University of Stirling, Stirling, United Kingdom,[2]Community Advisory Board, University of Stirling, Stirling, United Kingdom,[3]National Cancer Institute, Bethesda, MD

Background Patient and public engagement is becoming recognised as important to strengthen cancer research. This means that research is conducted with, rather than to, about, or for, members of the public. When done in a non-tokenistic way, engagement has the potential to improve the quality and relevance of research findings. However, there is limited methodological guidance and understanding of how to deliver meaningful engagement at every stage of the research process. This study aims to address these gaps by exploring the experiences of cancer researchers and members of the public engaged in cancer research in the United States.

Methods Qualitative interview design involving semi-structured interviews with cancer researchers (n=15) and members of the public engaged in cancer research (n=15), exploring how engagement is delivered, barriers, facilitators and its impact. Data were analysed using reflexive thematic analysis, supported by NVivo 20. A community advisory board comprising four lived experience experts who were previously involved in cancer research served as co-researchers. They come from diverse communities and have lived experience of cancer. Their contribution was throughout the entire study process, from design (including topic guides development) through data analysis and reporting.

Results The findings capture the experiences of researchers and members of the public around patient and public engagement in cancer research. They identify the enablers (e.g., institutional support) and barriers (e.g., financial) to public engagement in cancer research, capture existing strategies to mitigate these barriers, and examine the impact of engagement activities on the research project, researchers and members of the public. This study offers new insights into establishing and delivering effective engagement activities. First, it highlights the importance of identifying suitable community representatives who can advise researchers on selecting appropriate members for the advisory boards. Second, it describes how the public can contribute to research throughout the engagement process, and how researchers can support them to ensure everyone has confidence to contribute fully. Third, it suggests options for public engagement when financial resources are limited.

Conclusion Genuine patient and public engagement in cancer research is still evolving in the United States, with various approaches currently in use; however, there is a growing consensus that researchers should adapt their work to include public voices. This study will provide further understanding and guidance for cancer researchers on how to involve patients and the public in cancer research in an inclusive and impactful way.

#6358 Project CoMMunity: A local learning network deployed to address multiple myeloma care gaps in two communities.

Cesar Rodriguez[1], John T. Mckay[2], Abdur Rahman Jabir[2], Alex Lieberman-Cribbin[3], Sean Paul Ormond[1], **Kimberly Brunisholz**[4], Kristi Cohn[5], Dianna S. Howard[5]

[1]Mount Sinai Health System, New York, NY,[2]Atrium Health Wake Forest Baptist Comprehensive Cancer Center, Winston-Salem, NC,[3]Tisch Cancer Institute, Mount Sinai Health System, New York, NY,[4]Johnson & Johnson, Salt Lake City, UT,[5]Petauri Kinect, New York, NY

Introduction Treatment advances in multiple myeloma (MM) have resulted in five-year survival improvements. However, gaps remain in access and adoption of standard of care (SOC) and novel therapies. As a result, variation in care persists. Project CoMMunity is a multi-center, local learning network to detect unmet needs, understand barriers impacting SOC treatment access, and address care gaps through innovative oncology partnerships and targeted interventions.

Materials/Methods A multi-method approach was used to implement an integrated local learning network among academic and community oncology practices within New York City, NY and Winston-Salem, NC. A needs assessment and co-creation session to identify barriers and solutions was performed through community roundtables with diverse stakeholders. Electronic medical record data of patients with MM were compared across communities. Clinician-reported barriers and root causes limiting access and adherence to SOC treatments were solicited through 1:1 interviews.

Results Among 12 clinicians and 4 social workers/patient advocates that participated in the roundtables, common barriers were health literacy/socioeconomic factors, limited community/academic clinical relationships, cultural/racial issues and low patient trust, complex patient priorities/medical conditions, and limited clinical trial exposure. Stakeholders indicated opportunities to support education and awareness, improve care continuity transitions among community and academic sites, and development of educational materials. Of 332 patients (NY 237; NC 95), quantitative analysis highlighted clinical variation in time from diagnosis to specialist visit (NY: 34 vs NC: 62 days), frontline therapy (1LOT) count (quadruplet, NY: 62.3% vs NC: 11.6%; triplet, NY: 34.3% vs NC: 79.0%) and stem cell transplantation incidence (NY: 30.8% vs NC: 50.5%). Time from diagnosis to 1LOT and proportion of patients referred to sub-specialists were consistent among sites. Overall, few patients (5.1%) received innovative therapies (eg, CAR-T, bispecific antibodies). Among 10 interviews, clinician-reported barriers and root causes limiting access to SOC treatment included patient characteristics, care barriers, referral/treatment protocols, and community engagement/support resources.

Conclusion Local communities vary in needs, capacity, stakeholders, and existing healthcare infrastructure. Programs striving to improve access and adoption of SOC and novel therapies need to be multi-faceted and designed with local implementation in mind. A local learning network with regional participants provides a robust framework to efficiently transfer insights and clinical best practices while deploying local interventions that are responsive to needs of a diverse community. A one size fits all model will not succeed given unique setting and community needs.

#6359 Lineberger Excellence in Advocacy Program (LEAP): Implementation and evaluation of a comprehensive patient and community engagement program at the University of North Carolina to improve patient centered research.

Patricia A. Spears[1], Jennifer A. Potter[1], Veronica Carlisle[1], Hayley Morris[1], Barbara Alvarez Martin[2], Stephanie B. Wheeler[3], Marjory Charlot[4]

[1]Community Outreach and Engagement, UNC Lineberger Comprehensive Cancer Center, Chapel Hill, NC,[2]Community Outreach and Engagement, Population Science, UNC Lineberger Comprehensive Cancer Center, Chapel Hill, NC,[3]UNC Gillings School of Global Public Health, Community Outreach and Engagement, UNC Lineberger Comprehensive Cancer Center, Chapel Hill, NC,[4]Community Outreach and Engagement, Patient Engaged Research, UNC Lineberger Comprehensive Cancer Center, Chapel Hill, NC

Introduction: Engagement of advocates in cancer research ensures research is patient centered. However, engagement of advocates has been inconsistent in some cases and lacks equitable representation across cancer types. Some researchers find it challenging to identify advocates to engage in research and advocates feel underutilized and underrepresented. Lineberger Comprehensive Cancer Center (LCCC) has established a comprehensive advocate engagement framework called Lineberger Excellence in Advocacy Program (LEAP). By creating a comprehensive program through the office of Community Outreach and Engagement, LCCC can maintain meaningful and sustainable relationships between community members, patients and researchers.
Methods: LEAP began in 2022 and is an umbrella program that centralizes key components necessary to maintain adequate bi-directional involvement between community members, patients, and researchers. LEAP entails recruitment, training, advocate-researcher matching, compensation guidance (pre and post award), and evaluation. A Patient Advocate Learning Portal was developed to support LEAP members. The portal offers on-demand access to training videos (e.g., grant review, plain language), webinars (e.g., ASPIRE program), and supplementary resources, including key articles and websites, to enhance member knowledge and engagement. Advocate-researcher matching is accomplished through a simple process. Researchers submit a LEAP member request form in Qualtrics and a request email is sent to LEAP members. We track requesters, opportunity, time to fill the request, and advocates who volunteer in Excel. We also evaluate meaningful engagement of advocates and researchers through surveys and interviews, respectively. Advocate evaluations are conducted annually using a 31-item survey assessing demographics, activities, perceived value, decision-making, and engagement opportunities. LEAP facilitates recruitment and sustained engagement through an email listserv.
Results: LEAP has over 92 members of which 72 identify as 53% white, 27% Black/African American, 4% other and 20% unknown. There have been 86 requests from researchers since 2023. These have resulted in 257 LEAP engagements in research projects among the 92 members. Advocate-researcher matches were not made in 6% of the requests due in part to the specificity of the request (e.g., rare cancers). LEAP evaluations from 2024 and 2025 demonstrated that over 90% of advocates indicated high satisfaction on a 5-point Likert scale with feeling valued, respected and heard.
Conclusion: LEAP has increased the engagement of patient and community members in LCCC research, enhanced advocate-researcher satisfaction and improved the alignment of advocates with researchers' specific projects.

#6360 Project Cure CRC: A patient-powered ecosystem uniting data, discovery and accelerating cures for colorectal cancer.

Kim Newcomer, Travis Hyams, Tina Zeff, Marc Mason, David Fenstermacher, Michael Sapienza, Erin Siegel

Colorectal Cancer Alliance, Washington, DC

Background: Colorectal cancer (CRC) remains a leading cause of cancer mortality despite significant advances in molecular and immunologic science. Progress is limited by fragmented research infrastructure, underrepresentation of diverse populations, and a lack of coordinated translation between discovery and clinical care. The Colorectal Cancer Alliance launched Project Cure CRC in 2023 to build a national ecosystem that unites patients, investigators, and partners through research acceleration, data integration, patient empowerment, and collaborative partnerships. Project Cure CRC's goal is to improve overall survival from colorectal cancer and advance new therapies.

Methods: Project Cure CRC has several components that have never been combined before for colorectal cancer: 1) K-SPY, an adaptive platform trial evaluating perioperative, neoadjuvant, and minimal residual disease (MRD) interventions in colorectal cancer; 2) BlueLake, a data and real-world evidence platform connecting clinical, genomic, and patient-reported outcomes data to inform research and care delivery; 3) BlueHQ, a digital patient support, navigation, and engagement hub enabling patients to connect with each other and patient navigators, contribute longitudinal data, access tailored educational resources, and participate in research opportunities; and 4) A competitive request for proposals (RFPs) focused on accelerating translational progress towards a cure: Early-Career Investigator Awards, Senior Investigator Awards, Pilot Awards, and Team Science Awards. Each proposal is peer-reviewed and designed to feed forward into ongoing K-SPY and BlueLake efforts, ensuring rapid translation of discovery into clinical utility.

Results: Since its launch, Project Cure CRC has received 525+ proposals and has distributed over $15 million in funding across 33 projects, advanced multicenter biomarker and equity studies, and finalized governance frameworks for K-SPY submission to the FDA. More than 150 academic investigators, 20 industry partners, and patient participants are now engaged, forming the largest philanthropic CRC research network in the United States. In 2025, the Alliance launched a patient advisory council consisting of a diverse group of colorectal cancer patients to provide feedback on the ecosystem.

Conclusions: Project Cure CRC demonstrates a scalable, patient-powered model that connects discovery research, adaptive clinical trials, and real-world data within a single coordinated ecosystem. By aligning research acceleration, data integration, patient empowerment, and collaborative partnerships, the initiative is transforming colorectal cancer research and accelerating cures.

#6361 Patient and patient group engagement in cancer clinical trials in low- and middle-income countries.

Linsey Eldridge[1], Annette Galassi[2], Satish Gopal[1], Ophira Ginsburg[1], Mishka Kohli Cira[1]

[1]National Cancer Institute, Bethesda, MD,[2]Leidos Biomedical Research, Inc, Gaithersburg, MD

We conducted qualitative focus group discussions (FGD) with cancer patients and patient groups in low- and middle-income countries (LMICs) to understand their role in the cancer clinical trial ecosystem and identify strategies to improve engagement. These FGDs are part of a broader mixed-methods effort led by the National Cancer Institute to better characterize the clinical trial landscape in LMICs. Participants from six WHO regions were recruited through partner organizations, which disseminated email invitations including a link to a recruitment form collecting demographic and clinical trial experience information. Individuals in LMICs who have lived experience with cancer were invited to attend. Nine 90-minute semi-structured FGDs were conducted with 45 participants from 25 countries. Interviews were recorded, transcribed, and double-coded in Dedoose using directed content analysis. Most participants reported their primary role as a cancer patient advocate or person with cancer or survivor (33/45). Most participants said that patients and patient groups are not systematically involved in clinical trials, citing limited awareness about value of engagement and perceived researcher resistance as the greatest challenges. Limited availability of trials in LMICs and poor standard of care emerged as major challenges. When involved, engagement activities included educating patients about clinical trials and supporting recruitment. Participants described an ideal role that included serving as a bridge between patients and researchers, with involvement sought by researchers from design through dissemination. Participants noted several facilitators to increase patient engagement, including knowledge about the clinical process, access to information about specific clinical trials, capacity building for both patient groups and researchers, and implementing a formal process and compensation for engagement. Improving cancer care quality and access emerged as an important priority for many. This study provides an initial assessment of patient and patient group involvement in cancer clinical trials in LMICs from the perspective of people with lived experience. Findings reveal a gap between current and ideal levels of patient and patient group engagement, driven by limited awareness, structural barriers in LMICs, and perceived researcher resistance. Strengthening awareness, capacity, and structured mechanisms for involvement may enable patient groups to serve as effective bridges between communities and researchers and help improve patient-centered cancer care globally.

#6362 Optimization of outreach and engagement of patients/survivors and community supporters to reduce the cancer burden.

Lourdes Baezconde-Garbanati[1], Sandra Suther[2], Fern Webb[3], John Luque[2], Jennifer Tsui[1], Carolina Aristizabal[4], Brooke Vintilla[5], Ileana Guzman[6], Eduardo Ibarra[7], Rosa Barahona[7], Janet Rodriguez[8], Pastor Rhonda Holbert[1], Mariana C. Stern[9]

[1]Keck School of Medicine of USC, Los Angeles, CA,[2]Florida A&M University, Tallahassee, FL,[3]University of Florida College of Medicine - Jacksonville, Jacksonville, FL,[4]USC Norris Comprehensive Cancer Center, Los Angeles, CA,[5]University of Florida, Gainesville, FL,[6]University of Florida, Orlando, FL,[7]University of Southern California, Los Angeles, CA,[8]USC Norris Comprehensive Cancer Center, Ontario, CA,[9]Associate Professor, Dept. of Prev. Medicine, USC Norris Comprehensive Cancer Center, Los Angeles, CA

Introduction

Cancer deaths from prostate, lung, and pancreatic cancers remain highest in low-income communities. Survivors and caregivers report that these losses stem not only from disease, but from gaps in communication, trust, access, and culturally relevant information. Their lived experiences are essential for shaping solutions. The CaRE2 Health Center views patients and survivors as partners whose insights ensure scientific progress reaches those most affected.

Procedures

To elevate patient leadership, the CaRE2 Community Outreach Core (CaRE2-COC) uses an engagement model guided by a Florida-California Tri-Institutional Community Advisory Committee (CAC). The 13-member CAC—largely survivors and caregivers—meets quarterly to set priorities and ensure research reflects patient needs. Two training programs, the Community Supporters Academy (CSA) and the 10-week Community Scientists Research Academy (CSRA), build cancer knowledge, research literacy, and advocacy skills so participants can guide research and engage others. They co-create culturally tailored materials distributed at community events and online. A Community Contact Registry tracks willingness to join research, clinical trials, and biospecimen donation; low biospecimen comfort prompted creation of a patient-friendly biorepository video. Partnerships, a podcast, and public events expand opportunities for survivors to share stories and access information.

Results

The CAC ensures patient and survivor perspectives guide CaRE2-COC programs. Since 2019, the CSA has trained 150 ambassadors, and 80 community scientists completed the CSRA with stipends to lead local projects. Pre/post assessments show gains including increased confidence engaging other survivors and improved cancer-screening knowledge. A Cancer Community Conference reached 527 participants, and 5,000 community members received tailored educational materials. Registry data show strong willingness to complete surveys but lower biospecimen comfort, reinforcing education needs. The survivor-story podcast reached 240 listeners, and social media engagement exceeded 28,000 impressions. Events such as an Orlando Magic partnership brought cancer information into trusted community spaces.

Conclusions

CaRE2-COC strengthens patient, survivor, and community leadership by ensuring their experiences guide communication and research priorities. By training trusted influencers and embedding engagement into screening, prevention, and research, CaRE2-COC builds stronger community-academic partnerships, increases research participation, and advances its mission to reduce cancer burdens in California and Florida.

#6363 Supportive community and patient-centered spaces for discussing health concerns throughout the cancer journey.

Elena B. Nieves[1], Rosa Barahona[2], Marya Shegog[3], Dana Dornsife[3], Erin Miller[3], Lourdes Baezconde-Garbanati[4]

[1]USC Norris Comprehensive Cancer Center, Los Angeles, CA,[2]University of Southern California, Alhambra, CA,[3]Lazarex Cancer Foundation, Danville, CA,[4]Keck School of Medicine of USC, Los Angeles, CA

Background: Through purposeful collaboration with USC NCCC, the Lazarex Cancer Foundation established the Lazarex Cancer Wellness HUBs pop-up model to offer a supportive, welcoming space that reflects and responds to the cultural needs and unique cancer challenges of the diverse and vulnerable communities we serve. Advancing cancer health equity means partnering with our communities to create spaces that reflect who they are and provide culturally and language-specific guidance. With this purpose, the HUB ensures equitable access to cancer programs and support that strengthen outcomes across the full cancer-care continuum.

Methods: The Wellness Hubs have maintained a steady presence across Los Angeles County, partnering with various community and faith-based organizations—including the Chinatown Service Center, Black Men's Wellness Day, the Alhambra Lunar New Year Festival, and Macedonia Baptist Church of LA and at local YMCAs. We expanded our offerings with mindfulness workshops that help participants cultivate calm, emotional balance, and resilience throughout the cancer journey. Our speaker series, featuring scientists and expert guests, has continued to bring the community up-to-date information on cancer research, treatment options, and available support services.

Results: Our approach emphasizes active community participation. We have shared critical cancer information with over 11,000 individuals from diverse racial and ethnic backgrounds. Our speaker series has drawn more than 3,000 attendees and explored topics such as brain cancer, current research, access to care, and breast and cervical health. In addition, 86 community members have participated in our mindfulness workshops, using mind-body techniques to enhance emotional and physical well-being.

Conclusion: Our community outreach approach ensures that we remain present and engaged within Los Angeles County's diverse communities, providing culturally and locally tailored information. We offer education and connections to cancer support services, so individuals feel supported before, during, and long after their cancer journey. This includes sharing screening guidelines, emphasizing the need for diversity in cancer clinical trials, promoting self and patient advocacy, and directing community members to trusted sources. Through this work, we are actively helping to reduce cancer disparities.

#6364 A qualitative evaluation of storytelling narratives designed as strategy to increase uptake of lung cancer screening for veterans.

Hannah Brooks[1], Anna Gallion[1], Carolyn Audet[1], Rebecca Selove[2], Sally York[3], Fred Hendler[4], Drew Moghanaki[5], Robert Dittus[1], Christianne Roumie[1], Jennifer Lewis[1], Lucy B. Spalluto[1]

[1]Vanderbilt University Medical Center, Nashville, TN,[2]Tennessee State University, Nashville, TN,[3]VA Tennessee Valley Healthcare System, Nashville, TN,[4]Rex Robley VA Medical Center, Louisville, KY,[5]VA Greater Los Angeles, Los Angeles, CA

INTRODUCTION: Lung cancer screening with low-dose computed tomography (LDCT) reduces lung cancer mortality. However, LDCT utilization remains low, including in the Veterans Health Administration. Personal storytelling narratives are an evidence-based strategy to influence healthy behaviors like lung cancer screening. However, little is known about how Veterans might respond to narratives. We aimed to develop 3 preliminary digital (video) narratives about lung cancer screening and elicit feedback from Veterans about the narratives.
METHODS: In partnership with StoryCenter, we worked with three Veterans (i.e., Storytellers) to develop preliminary personal digital storytelling narratives about their lung cancer screening experiences. To elicit feedback, we recruited Veterans (i.e. interviewees) at a single Veterans Affairs Medical Center between January 14, 2025, and June 13, 2025 to view the narratives and participate in an interview. Guided by the Learner Verification and Revision technique, we conducted semi-structured interviews. We analyzed and organized qualitative data by constructs of the Learner Verification and Revision technique including: i) visual and auditory appeal of the tool (Attraction); ii) whether the tool is socially agreeable (Acceptability); iii) how well the viewer understood the central message of the tool (Comprehension) and whether the message compels the viewer to complete the suggested action (Persuasion); and iv) how confident the viewer is they are able to complete the suggested action (Self-efficacy).
RESULTS: Interviewees (n=30) generally perceived the videos as having compelling visual and auditory elements, noting the importance of subtitles and high-quality images (Attraction). Interviewees found few aspects of the narratives unacceptable, although casual language and discussion topics were noted as potentially off-putting (Acceptability). Narratives that displayed the CT scanner and portrayed Storytellers' screening experiences were most informative, reduced anxiety and built trust. Interviewees connected with narratives that reflected shared experiences such as smoking history, military service, and family responsibilities, viewing these as motivational to pursue screening. Nevertheless, some aspects of the narratives were less well-liked due to personal histories and experiences (Comprehension/Persuasion). Several interviewees stated the videos motivated them for screening, but noted the videos did not adequately describe next steps (Self-efficacy). Interviewees suggested future narratives emphasize the ease and benefits of screening, while integrating relatable and motivating messages.
CONCLUSIONS: Leveraging Veteran feedback to modify preliminary personal digital storytelling narratives can inform and improve future iterations of narratives for broader implementation.

#6365 Prostate cancer awareness and car show: An initiative to increase prostate cancer screening.

Vivian Carter, Doreatha Heard

Psychology and Sociology, Tuskegee University, Tuskegee, AL

Introduction: While data reflect that Prostate Cancer is lower in rural areas this can be misleading as rural communities also have higher death rates and higher rates of Prostate Cancer reoccurrence compared to urban areas. Macon County Alabama has one of the highest Prostate Cancer Mortality rates in the nation. Macon Means a Cancer Support Nonprofit Organization partnered with local health advocacy organizations, Civic organizations and Universities to support a health initiative specifically for men in rural communities.
Summary: The initiative was to sponsor a men's health fair alongside a car show. The combination of the health fair with the car show would bring more men out to the event and provide an opportune time for a one stop informational about their health and the necessary check ups they should have and provide access to the screening service on site. mobilize Macon County communities in the fight to eliminate prostate cancer racial disparity. The Prostate Cancer Awareness Health Fair and Car Show with Free PSA Screening was held on September 28, 2024, in Downtown Tuskegee.
Conclusion: The event united organizations throughout the state to raise awareness about critical health issues, forty-three (43) vendors delivered essential health services to over 275 people in attendance. Forty-seven (47) men received free PSA screenings; fourteen percent (14%) required further follow-up.

: Drug Delivery
Poster Session

#6370 Targeted polymeric nanoconjugates for BBB penetration and time specific delivery of PDL1 blocking small peptides via LRP1 targeting in melanoma brain metastases.

Saurabh Sharma[1], Prabhjeet Singh[2], Jay Chadokiya[3], Amanda R. Kirane[1]

[1]Stanford University School of Medicine, Stanford, CA,[2]Stanford University, Stanford, CA,[3]General Surgery, Stanford University School of Medicine, Stanford, CA

Background: Melanoma brain metastases (MBM) show high CNS tropism with limited benefit from single-agent ICB; a combination regimen with an AXL inhibitor may improve responses but carry substantial toxicity. The brain TiME features scarce T cells, abundant TAMs, and glial PD-L1, promoting immune evasion and poor ICB efficacy. BBB penetrant strategies via peptide-based Immuno-Nano-Conjugates (INCs) are under development, though intrathecal delivery has not improved survival. LRP-1-mediated INCs delivery may enable BBB transport and TAM-TiME reprogramming. Here, we report a targeted nanoplatform that crosses the BBB and delivers PD-L1-blocking peptides to the TiME.
Methods: Immuno-Nano-Conjugates (INCs) were synthesized by conjugating a biocompatible malic acid polymer conjugated with (i) P-12, a PD-L1 blocking peptide, and (ii) Angiopep-2 (AP2), a ligand for LRP-1 mediated transcytosis. Therapeutic efficacy, safety, toxicity, and biodistribution studies were assessed using an *in vitro* static BBB-on-a-chip brain tumor model and *in vivo* in established murine cancer models. Clinical transcriptomic correlation data from metastatic melanoma (TCGA-SKCM, n = 471) were analyzed via the GDC legacy archive to construct Kaplan-Meier survival curves.
Results: The INCs traversed the BBB and demonstrated penetration in a BBB-on-a-chip brain tumor model. Upon delivery, INCs were selectively internalized by the activated TiME environment, thereby promoting antitumor immune cell activation and proliferation. *In vivo* efficacy, safety, toxicity, and biodistribution revealed superior brain accumulation of INCs relative to ICB agents and significant efficacy and a better safety profile. Clinically, high AXL expression correlated with nonresponse to ICB in Stage IV melanoma and aligned with immunosuppressive myeloid signatures, demonstrating an association with reduced survival in patients with brain metastases. In subcutaneous melanoma models, the combination of P-12 (anti-PD-L1)- based peptides with the AXL inhibitor Bemcentinib yielded greater tumor burden reduction than anti-PD-1 monotherapy, suggesting the potential to circumvent ICB resistance in MBM settings.
Conclusion: Our data indicate that BBB transcytosis of INCs via LRP-1 mediates enhanced delivery of PD-L1 blocking peptides to the TiME, supporting improved therapeutic exposure for MBM. AXL emerges as a critical therapeutic target and a rational axis for combination strategies with targeted nanoplatforms to treat resistant MBM. Ongoing studies across additional MBM-relevant models aim to validate these findings and further optimize second-generation bispecific INCs approaches.

#6371 Enhanced therapy for triple-negative breast cancer (TNBC) using combinatorial drug delivery.

Santosh K. Singh[1], Melad Dababneh[2], Brian M. Rivers[1], Rajesh Singh[1]

[1]Morehouse School of Medicine, Atlanta, GA,[2]University of Alabama at Birmingham, Birmingham, AL

Breast cancer (BrCa) is the most common cancer among women. Although there has been progress in early detection and specific therapies, long-term success is still limited, especially for triple-negative breast cancer (TNBC). This challenge arises from issues such as recurrence, drug resistance, and side effects associated with treatments. Chemoprevention, which involves using natural compounds to delay, suppress, or prevent cancer development in individuals at high risk, shows promise, but clinical success is limited by poor bioavailability. Hedgehog (Hh) signaling pathways are being studied for the growth and metastasis of BrCa; thus, targeting Hh represents a promising therapeutic strategy. To address these challenges, we studied the effects of combining two drugs: honokiol (HNK), a natural compound derived from *Magnolia officinalis*, alongside the chemotherapy drug docetaxel (DTX) for treating TNBC. For this purpose, we employed gold nanoparticles (AuNPs). Our results show that dual drug delivery (HNK+DTX), combined with sonic hedgehog (Shh) DNA aptamer (AP32)- conjugated AuNPs, effectively targets the Hh pathway in TNBC cells that express it at high levels. We characterized the formulated AuNPs, including a Zetasizer for charge and size analysis, Transmission Electron Microscope (TEM), Fourier-Transform Infrared Spectroscopy (FTIR), Nuclear Magnetic Resonance (NMR), and Nanoparticle Tracking Analysis (NTA), before applying them to TNBC cells (MDA-MB-468 and MDA-MB-231). A cell viability/ cytotoxicity assay was performed to determine the IC_{50} values and assess drug combination synergy. Additionally, 3D cell models confirmed the internalization of AuNPs and the efficacy of combination AuNPs compared to single-drug or scramble aptamer AuNPs (control). Mechanistic studies using immunofluorescence, flow cytometry, qRT-PCR, and Western blot analysis show that Shh-targeted delivery suppresses the expression of downstream signaling molecules, Gli1 and Ptch1, induces cell cycle arrest at the G_0/G_1 phase, and triggers apoptosis. Furthermore, results from molecular dynamics simulations suggest that HNK influences both NF-κB-driven transcription and Shh-mediated signaling, subsequently affecting tumor cell-environment interactions. These findings highlight the potential of combination AuNPs for pathway-specific intervention in addressing TNBC, providing a foundation for further research in this area.

#6372 Regulating epithelial-to-mesenchymal transcription-driven metastatic capacity with molybdenum disulfide (MoS2) nanoparticles.

Samantha Michelle Foster, Kanwar A. Singh, John Soukar, Olajumoke Ogunlusi, Christian Nguyen, Subiksha Sankar, Anna Keller, Tapasree Roy Sarkar, Irtisha Singh, Akhilesh Gaharwar

Texas A&M University, College Station, TX

Epithelial-to-mesenchymal transition (EMT) is the process by which stationery, tightly connected epithelial cells transform into more mobile, flexible phenotype. This plays a significant role in allowing cancer cells to detach from the original tumor, invade surrounding tissues and spread throughout the body. While EMT plays a role in significant physiological functions such as wound healing, the development of a mesenchymal phenotype within the tumor microenvironment is detrimental, promoting cancer cell escape into circulation and subsequent development of the pre-metastatic niche. EMT is a major contributor to the risk and progression of metastatic cancers and targeting and blocking EMT presents a potential therapeutic intervention for preventing the development of metastases. Here, we introduce molybdenum disulfide (MoS_2) nanoparticles as a potential drug-free inhibitor of EMT, which is advantageous over traditional chemotherapy-type drugs due to lack of adverse off-target effects in distant tissues. This study investigates the impact of MoS_2 nanoparticles on epithelial-to-mesenchymal transition in highly metastatic triple-negative breast cancer both *in vitro* and *in vivo*. Treatment of MoS_2 nanoparticles decreased migratory capacity of *in vitro* and *in vivo* models of ER+ and triple negative breast cancer, demonstrating the anti-metastatic motility property of MoS_2. *In vitro*, MoS_2-treated breast cancer cells observe decrease in focal adhesion proteins and genes associated with cellular motility. Furthermore, cells show decrease in TGFβ signaling and expression of EMT markers after 72h of exposure, indicating that MoS_2 nanoparticles inhibited EMT progression mediated through cellular motility and TGFβ signaling. This effect was further demonstrated with functional 3D mammosphere assays, which indicated reduced mammosphere formation and size. Similarly, clonogenicity was significantly reduced in cells following treatment with MoS_2 nanoparticles. *In vivo*, direct injection of MoS_2 into 4T1 mouse mammary tumors significantly decreased primary tumor growth and burden as well as the number of metastatic foci in the lung. Our work demonstrates that MoS_2 nanoparticles inhibit integrin activity as well as the TGFβ signaling cascade pathway, blocking the transition of cells to a mesenchymal-like phenotype. These findings suggest that MoS_2 nanoparticles hold promise for drug-free cancer therapeutic applications in reducing metastatic potential.

#6373 Development of a lipid nanoparticle formulation of the bifunctional PARP and HDAC inhibitor kt-3283.

Sarah Truong[1], Samar Alsudir[2], Laila Al-Alwan[2], Beibei Zhai[1], Louise Ramos[1], Mona Marzban[1], Fariba Ghaidi[1], Haidar Almubarak[2], Qassem Alalaiwi[2], Aljohara Albabtain[2], Kally Singh[3], John Langlands[3], Dennis Brown[3], Ali H. Alhasan[2], Jeffrey Bacha[3], Mads Daugaard[4]

[1]Vancouver Prostate Centre, Vancouver, BC, Canada,[2]NanoPalm, Riyadh, Saudi Arabia,[3]Rakovina Therapeutics Inc., Vancouver, BC, Canada,[4]University of British Columbia, Vancouver, BC, Canada

Poly(ADP-ribose) polymerase (PARP) plays a major role in DNA repair and PARP inhibitors (PARPi) have shown clinical benefit in a number of tumor indications. Deacetylation of histones, controlled by histone deacetylases (HDACs) is a key regulatory event in DNA repair and inhibition of HDACs has been shown to reduce tumor growth *in vitro* and *in vivo*. PARPi combined with HDAC inhibition has demonstrated enhanced efficacy in pre-clinical studies in various tumor indications, and in patients with metastatic breast cancer. However, combination therapies can be limited in clinical utility due to overlapping toxicities and different pharmacokinetic profiles. kt-3283 embodies synthetic lethality by integrating two synergistic mechanisms—PARP inhibition and HDAC-mediated chromatin remodeling—into a single compound thereby eliminating the need for simultaneous or staggered drug combination regimens and the risk of overlapping toxicities. Previous studies have demonstrated strong inhibition of PARP1/2 and HDAC enzymes *in vitro*, inhibition of cell cycle arrest and DNA damage marker upregulation, significant inhibition of cell viability across multiple tumor types, and inhibition of metastatic seeding in an *ex vivo* pulmonary metastasis assay. While kt-3283 has demonstrated potent anti-tumor activity in vitro, its clinical viability is limited by low bioavailability and poor metabolic stability. Lipid nanoparticles (LNPs) are nanocarriers for oncology drugs, offering superior encapsulation efficiency, with the ability to incorporate hydrophobic and hydrophilic payloads, protecting them from degradation and targeting for tumor selectivity. Patterned LNPs (pLNPs) designed using the EnsaliX AI platform are novel class of LNPs enable superior targeting, stability and safety through highly ordered structures. Kt-3283 is being encapsulated into the EnsaliX-designed pLNPs to produce pLNP/kt-3283. Physicochemical parameters of kt-3283 (solubility, pKa, thermal behavior, and metabolic stability) are being integrated for optimal pLNP/kt-3283 fabrication supporting enhanced encapsulation efficiency, and superior in vitro cell uptake, stability and bioavailability. Development of pLNP/kt-3283 uniquely combines design, formulation, and evaluation of a DDR-targeting compound, overcoming metabolic instability, and off-target limitations, and improving the therapeutic index.

#6374 Sodium chloride nanoparticles as urinary bladder cancer therapeutics.

Xinning Lai

University of Georgia, Athens, GA

In 2025, bladder cancer ranks sixth in incidence and tenth in cancer mortality in the United States, with an estimated 84,870 new cases and 17,420 deaths. Surgical transurethral resection of bladder tumors (TURBT) is the first step in standard bladder cancer treatment, followed by adjuvant intravesical chemotherapy or immunotherapy to eliminate existing or residual tumors. Local-regional therapy is particularly effective for bladder cancer because it targets superficial cases and maximizes therapeutic exposure, resulting in improved anticancer effect. Ion homeostasis is critical for maintaining cellular integrity and ensuring proper cell function. The balance between ion influx and efflux is tightly regulated by ion channels and transporters. While several strategies have been developed to target ion homeostasis as potential anticancer agents, including channel blockers and ionophores, the sodium chloride nanoparticle strategy may offer additional advantages in the context of cancer therapy.Immunogenic cell death (ICD) is a unique form of regulated cell death that promotes an anti-tumor immune response and contributes to the success of several cancer therapies such as cisplatin and mitoxantrone (MTX). ICD is characterized by damage-associated molecular patterns (DAMPs), including calreticulin (CRT), ATP, and HMGB1, which engage pattern-recognition receptors on antigen presenting cells, promoting dendritic-cell maturation and cross-presentation to T cells. Nanoparticle platforms that trigger ICD have shown promise in augmenting conventional therapies. We recently found that sodium chloride nanoparticles (SCNPs) not only kill bladder cancer cells but also induce ICD, positioning them as competitive immunotherapeutics. In this study, we presented a novel approach using phospholipid-coated sodium chloride nanoparticles (PSCNPs) as a potential treatment for bladder cancer. We synthesized and characterized SCNPs of various sizes and coated them with a layer of DSPE-PEG(2000) Amine, resulting in PSCNPs that can be stably dispersed in aqueous solutions. We investigated the degradation, endocytosis, and effects of PSCNPs on cellular ion homeostasis, as well as their effects on cell viability and cell death mechanisms. Furthermore, we evaluated the ability of PSCNPs to induce ICD and their impact on the tumor microenvironment (TME) and major organs. Finally, we evaluated the therapeutic efficacy of PSCNPs in subcutaneous tumor models, both as a single treatment and in combination with αPD1. Our results suggest that PSCNPs hold promise as a novel and effective treatment for bladder cancer, with the potential to boost immunity and transform the tumor microenvironment without causing systemic toxicity.

#6375 Tardigrade Dsup mRNA nanoparticles reduce chemotherapy-induced normal tissue toxicity.

Ian C. Sutton, Pascal Cuhat, Ashley Cooney, James D. Byrne

University of Iowa, Iowa City, IA

Bleomycin is a commonly used chemotherapeutic in the treatment of lymphomas and germ-cell tumors, yet its utility can be restricted by dose-limiting pulmonary toxicity. Bleomycin-induced generation of reactive oxygen species (ROS) causes significant damage to the alveolar epithelium. This leads to alveolar cell death, senescence, and maladaptive crosstalk with stromal cells, ultimately driving irreversible pulmonary fibrosis. Despite the clinical need, no approved strategy directly protects the lung epithelium from bleomycin toxicity. Certain natural organisms, namely tardigrades, can tolerate high levels of ROS-driven cellular damage. This tolerance is partially attributed to the tardigrade-specific Damage suppressor (Dsup) protein which interacts with chromatin and shields DNA from ROS. Our laboratory has recently shown that Dsup expression can protect other types of epithelia from radiation-induced injury. Because bleomycin and radiation share a common cytotoxic mechanism, we believe that Dsup could similarly protect alveolar epithelium. To this end, we developed a KC2/cholesterol/PEG/DOPE lipid nanoparticle (LNP) formulation optimized for Dsup mRNA delivery to human airway epithelium. This formulation was optimized to achieve >95% transfection efficiency in human small airway epithelial cells (HSAECs) and A549 cells with minimal impact on viability or clonogenicity. Transient Dsup expression significantly attenuated bleomycin-induced DNA damage in A549 and HSAECs, reducing γ-H2AX foci by ~50% and decreasing alkaline comet % tail DNA by ~25% relative to controls. Dsup expression also mitigated epithelial cell senescence (detected via β-galactosidase assay) after bleomycin treatment. In A549 and HSAECs, β-gal-positive cells were reduced by ~40% at 16 days post-bleomycin treatment. To support translational feasibility, we evaluated the compatibility of our LNP formulation with nebulization and demonstrated that the LNPs retained particle size, polydispersity, and transfection efficiency after nebulization. We further assessed delivery in physiologically relevant models that typically resist nonviral mRNA transfection. In human and pig airway air-liquid-interface (ALI) cultures, multiple LNP formulations generated robust reporter (luciferase) expression. Additionally, dilution of LNPs in 4.5% NaCl further enhanced reporter expression by ~100-fold in our ALI models compared with isotonic conditions, highlighting an additional strategy to improve airway transfection. Collectively, these data demonstrate that Dsup expression substantially reduces bleomycin-induced DNA damage and senescence in airway epithelial cells and establishes that our LNP formulation can effectively deliver mRNA to human airway epithelium in vitro. This work provides a mechanistic foundation for the development of a novel approach for preventing bleomycin-induced pulmonary fibrosis.

#6376 Magnetoelectric MOFs for ferroptosis-driven and immune-enhanced glioblastoma therapy.

Huiwen Lien[1], Shang-Hsiu Hu[1], Alan Yueh-Luen Lee[2]

[1]National Tsing Hua University, Hsinchu City, Taiwan,[2]National Institute of Cancer Research, National Health Research Institutes, Miaoli County, Taiwan

This study explores the innovative application of magnetoelectric metal-organic frameworks (MOFs) for inducing ferroptosis in glioblastoma (GBM), aiming to transform both therapeutic precision and diagnostic efficacy. MOFs, with their tunable chemical and physical properties, serve as versatile platforms for precision oncology. Here, magnetoelectric MOFs are engineered to harness electromagnetic fields, regulating intracellular iron redox states to elevate reactive oxygen species (ROS) production and drive lipid peroxidation—the hallmark of ferroptosis, a distinct iron-dependent form of programmed cell death.To enhance tumor specificity, these MOFs are conjugated with extracellular vesicles (EVs), enabling selective delivery to GBM cells and minimizing off-target toxicity. This targeted system not only improves therapeutic efficacy but also reduces side effects. Moreover, the magnetoelectric MOFs are MRI-compatible, allowing real-time tumor imaging and precise localization. This dual diagnostic-therapeutic capacity offers a powerful, non-invasive treatment strategy.Beyond direct cytotoxicity, MOF-induced ferroptosis promotes the release of tumor-associated antigens, triggering immune activation and potentially initiating immunogenic cell death (ICD). This immunomodulatory effect broadens therapeutic benefit by reshaping the tumor microenvironment. Collectively, this multifunctional MOF-based platform integrates diagnostics, therapy, and immunogenic modulation, representing a paradigm shift for treating one of the most aggressive and therapy-resistant cancers.

#6377 Intranasal delivery of lipid-based nanoparticle encapsulating CXCR7 agonist improves PD-L1 blockade efficacy in glioblastoma.

Chan-Chuan Liu[1], Yao-Wei Yeh[2], Cheng-Lin Wu[2], Tsung-Lin Tsai[2], **Kwang-Yu Chang**[3]

[1]National Health Research Institutes (NHRI), Zhunan, Taiwan,[2]National Cheng Kung University, Tainan, Taiwan,[3]National Health Research Institutes, Tainan, Taiwan

[Background] Glioblastoma (GBM) is characterized by limited treatment options and poor survival outcomes. Glioblastoma-associated macrophages (GAMs) are crucial factors that tailor the immunosuppressive tumor microenvironment (TME). Our previous study revealed that VUF11207 (VUF), a CXCR7 agonist, effectively recaptured the efficacy of the anti-PD-L1 antibody (αPD-L1) in GBM-bearing mice through inhibited CXCL12 release from tumor to transmit signals to GAMs. However, the efficacy of VUF may be hindered by poor brain delivery due to the blood-brain barrier (BBB).

[Methods] To optimize the drug delivery, we developed lipid-based nanoparticle (LNP) formulations with a non-invasive naso-to-brain delivery manner by spray. We applied an *in vivo* brain-penetration evaluation platform to assess their ability to bypass BBB. The effect of LNP-encapsulated VUF (VUF@LNP) was then assessed by observing its molecular effect and the response to αPD-L1 treatment in the animal model.

[Results] The particle size, surface charge, and shape structure of the lipid nanoparticles was controlled by mixing lipids. Studies of LNP formulations encapsulated with Evans blue (EB) have shown that the highest brain penetration efficiency is achieved with LNPs exhibiting a positive charge when synthesized at a 1,2-Dioleoyl-3-trimethylammonium-propane (DOTAP) to 1,2-Dioleoyl-sn-glycero-3-phosphocholine (DOPC) ratio of 1:4. Next, the *in vivo* bioluminescent and fluorescent imaging confirmed that DiL-labelled VUF@LNP with intranasal delivery was able to accumulate in brain tumor sites. Comparing with systemic and intranasal administration of VUF, intranasal delivery of VUF@LNP significantly improved the survival outcome of GBM-bearing mice. Intranasal delivery of VUF@LNP combined with αPD-L1 treatment markedly prolonged survival in comparison with intranasal delivery of free VUF with αPD-L1 treatment. No significant body weight changes were observed, supporting the biosafety of VUF@LNP. In terms of biological aspects, intranasal-administrating VUF@LNP significantly reduced CXCL12 and pERK1/2 levels in TME, leading to PD-L1 downregulation in GAMs and increased $CD8^+$ T-cell infiltration in comparison with systemic-administrating VUF and intranasal-administrating LNP control.

[Conclusion] Together, these findings indicated that intranasal VUF@LNP provides a BBB-bypassing, non-invasive strategy for delivering CXCR7 agonists to reprogram the immune TME. This approach may be a potential nanotherapeutic platform for combinatorial immunomodulation against GBM.

#6379 Gadolinium-based nanocomposite as a theranostic agent for triple-negative breast cancer: Synergistic radiosensitization, immune modulation, and image-guided therapy.

Yue Wang, Jiazhuo Yan, Yihan Xu, Zhengkun Cai, Zhiyong Yuan

Tianjin Medical Univ. Cancer Inst. & Hospital, Tianjin, China

Purpose: Triple-negative breast cancer (TNBC) is an aggressive malignancy with limited therapeutic options and frequent radiotherapy (RT) resistance. This study developed a novel gadolinium-based nanocomposite (GdB) with dual functions—radiosensitization and immune modulation—to establish a diagnostic-therapeutic integrated approach for precision RT in TNBC.
Methods: GdB nanoparticles were characterized structurally (TEM, XRD, EELS) and functionally (peroxidase-like activity). Cytotoxicity and radiosensitization were assessed in vitro using CCK-8, colony formation assays, apoptosis (flow cytometry, JC-1 staining), ROS generation, and DNA damage (γ-H2AX immunofluorescence and Western blot). Biocompatibility was evaluated in vivo using blood biochemistry, histopathology, and fluorescence imaging. The mechanism of immune activation was verified by measuring immunogenic cell death markers (CRT, ATP, HMGB1 release) and identifying activated pathways through transcriptomic analysis and qPCR. Immune responses were tracked in vitro (co-culture, cytokine secretion) and in vivo. Immune cell infiltration, cytokine levels (ELISA), and the immune landscape of primary and distant tumors were comprehensively analyzed using flow cytometry and single-cell RNA sequencing.
Results: GdB formed uniform spherical crystalline nanoparticles exhibiting excellent peroxidase-like activity. Mechanistically, GdB significantly enhanced radiosensitivity by promoting DNA damage and apoptosis. GdB induces ICD and activates the cGAS-STING pathway, leading to Type I interferon production, providing a robust basis for immune enhancement. GdB demonstrated excellent biocompatibility in vivo at experimental doses. Functionally, GdB served as an MRI contrast agent, enhancing tumor contrast for precise GTV delineation and facilitating real-time monitoring of tumor response to RT. Therapeutically, the combination of GdB with RT markedly inhibited tumor growth by reprogramming the tumor microenvironment from an immunosuppressive "cold" state to an immune-activated "hot" state. This conversion was marked by increased infiltration of key effector immune cells and elevated levels of anti-tumor cytokines. Crucially, the combination treatment generated a systemic anti-tumor immune response, resulting in the inhibition of distant metastases.
Conclusion: GdB is a highly effective theranostic platform for precision radiotherapy in TNBC, as its dual functions of radiosensitization and cGAS-STING pathway-mediated immune modulation substantially enhance RT efficacy and systemic anti-tumor response. Furthermore, its function as an MRI contrast agent integrates precise diagnosis with enhanced therapeutic outcomes, supporting its strong potential for clinical translation in image-guided radiotherapy.

#6380 Targeted delivery of RNA using synthetic bacterial spores.

Federico Machinandiarena, Domenico D'Atri, David J. Fitzgerald, Kumaran S. Ramamurthi

NIH-NCI, Bethesda, MD

Background: RNA therapy holds increasing promise for the treatment of various diseases. Delivering RNA, however, typically requires encapsulation in lipid nanoparticles, and a limitation of this technology is achieving tissue specificity beyond the liver and kidneys. We previously reported synthetic bacterial spore-like particles, termed “SSHELs,” for targeted cargo delivery [1]. SSHELs, composed of defined, biocompatible materials, were shown to specifically bind to HER2-positive cancer cells and accumulate in tumors [2]. This study explores whether SSHELs can deliver RNA to tissue-specific locations, focusing on HER2-positive cells.
Methods: The experimental approach involved protein purification, SSHEL assembly, mRNA and siRNA loading, and assessing RNA delivery specificity via confocal microscopy and flow cytometry. In vitro and in vivo assays were conducted to assess the production of EGFP and luciferase in target cells. Experimental models included cell cultures and mice.
Results: By decorating SSHELs with anti-HER2 affibodies and modulating lipid composition, we achieved specific mRNA and siRNA delivery to HER2-positive cells, resulting in selective protein induction or silencing. Loading SSHELs with RNA was highly efficient (~95%), yielding thousands of transcripts per particle. In further investigations, we observed a distinctive feature of SSHELs made with DOTAP: they did not elicit or suppress inflammatory cytokine production (e.g., TNF-α, IL-6). This characteristic is noteworthy, as it suggests the biocompatibility and immunologically inert nature of SSHELs formulated with DOTAP. Ongoing in vivo experiments are assessing the efficacy of mRNA-loaded SSHELs in delivering cargo to HER2-positive tumors.
Conclusions: SSHELs represent a novel approach in RNA therapeutics due to their unique characteristics. These particles, which mimic the structure of bacterial spores, provide a biocompatible and versatile platform for the targeted delivery of myriad therapeutics, such as small molecules, peptides, and RNAs.
References:

1. Wu, I.-L., et al. (2015). A versatile nano display platform from bacterial spore coat proteins. *Nature Communications*, 6, 6777.
2. Kong, M., D’Atri, D., et al. (2023). Cell-specific cargo delivery using synthetic bacterial spores. *Cell Reports*, 42(1), 111955.

#6381 Extracellular vesicle-mediated co-delivery of FSL-1 and LY2157299 for immunotherapy of small-cell lung cancer liver metastases.

Yue Huang, Amira Kazi, Rajesh Kumar, Kanak Parmar, Chiori Tabe, Ajit Kumar Sharma, Anish Thomas

National Institutes of Health, Bethesda, MD

Small-cell lung cancer (SCLC) frequently metastasizes to the liver, where macrophage-dominated immunosuppression sustains tumor outgrowth. Bioinformatic analyses of SCLC liver metastases implicate macrophage metabolism as a driver of hepatic progression. We engineered extracellular vesicles (EVs) co-delivering FSL-1 (TLR2/6 agonist) and LY2157299/galunisertib (TGF-βRI inhibitor) to reprogram macrophages. In vitro, dual-loaded EVs more efficiently shifted macrophages toward pro-inflammatory, antigen-presenting states. In vivo, EVs efficiently targeted intrahepatic tumor sites, decreased liver tumor growth, and prolonged mouse survival. These data support EV-mediated co-delivery of FSL-1 and LY2157299 as a macrophage-centric strategy for SCLC liver metastasis.

#6382 Temozolomide co-encapsulated radioPDT nanoparticles possess effective cytotoxicity for the treatment of glioblastoma.

Muhammad Rafiq[1], Deepak Dinakaran[2]

[1]Biological Science Platform Sunnybrook Research Institute, Toronto, ON, Canada,[2]Department of Medical Biophysics, Temerty Faculty of Medicine, University of Toronto, Toronto, ON, Canada

Introduction: Radiation-activated photodynamic therapy (radio-PDT) has emerged as a promising approach to overcome the limitations of conventional photodynamic therapy, particularly the poor tissue penetration of external light sources. This study focuses on the synthesis, characterization, and evaluation of the effect of temozolomide co-encapsulated radio-PDT nanoparticles for the treatment of glioblastoma.

Material and Methods: An inorganic nanoscintillator was synthesized, and its comprehensive physicochemical characterization was assessed using electron dispersive x-ray spectroscopy (EDS), Transmission Electron microscopy (TEM), and X-ray diffraction (XRD) to evaluate the evolution of composition, size, and structure. The nanoscintillator was encapsulated with the photosensitizer protoporphyrin IX (PPIX), in combination with Temozolomide (TMZ), in a nanocarrier of PEG-PLGA. The characteristics of nanoparticles was assessed using TEM, Dynamic light scattering (DLS), and zeta potential was recorded. The tumor cytotoxicity of these nanoparticles was evaluated in vitro by using the U251 cell line. Furthermore, the molecular mechanism was elucidated using western blot.

Results:Our results showed the size of 15±5 for nanoscentilator, which was encapsulated with PPIX and temozolomide in the nanocarrier PEG-PLGA. The final nanocomposite was 100±10 with a Zeta potential (ZP) of -21.5. These nanoparticles demonstrated significant cytotoxicity against tumor cells compared to the control condition. Western blot analysis showed, decrease in the expression of AKT, PERK, and BCL2, while an increased expression of cleaved caspase 3 in radioPDT and TMZ Co-encapsulated radioPDT with a low dosage of irradiation.

Conclusion: Our results support the use of TMZ Co-encapsulated radioPDT and radioPDT with radiation can be used as an efficient approach for deep-seated tumors in particularly radio-resistant glioblastoma. These nanoparticles exhibited excellent biocompatibility, effective cytotoxicity towards tumor cells, and potential for translation into an in vivo tumor study.

#6383 Targeted co-delivery of paclitaxel and honokiol using MUC1-aptamer PBM-NP encapsulation for enhanced breast cancer treatment.

Briana Kinnel[1], Amit Kumar Srivastava[2], Santosh K. Singh[1], Rajesh Singh[1]

[1]Morehouse School of Medicine, Atlanta, GA,[2]School of Forensic Sciences, Uttar Pradesh State Institute of Forensic Sciences, Lucknow, India

Despite advancements in breast cancer (BrCa) treatments, dose-limiting toxicities caused by off-target exposure to healthy tissues remain a significant barrier to effective treatment options. This study aimed to enhance the anticancer properties of paclitaxel (PTX) and honokiol (HNK) through encapsulation in planetary-ball milled nanoparticles (PBM-NP) and coating with MUC1-aptamer (S2.2) for targeted delivery. Both *in silico* and *in vitro* methods were used to evaluate the efficacy of the encapsulation of PTX and HNK in aptamer-conjugated PBM-NPs (PTX-S2.2-PBM NP and HNK-S2.2-PBM NP). Pharmacokinetic simulations demonstrated the potential advantage of using PTX and HNK in combination while targeting MUC1 for BrCa treatment. Tissue microarray analysis confirmed the expression of MUC1 in BrCa tissues. It was found that MUC1 tissue expression was stage-dependent, with the highest MUC1 expression observed in Stage IV BrCa tissue (93.9%) compared to Stage III (36.5%), Stage II (11.3%), and Stage I (0.4%), respectively. NHS coupling was utilized to synthesize PTX-S2.2 and HNK-S2.2 PBM-NPs. Dynamic light scattering (DLS), FTIR, and HPLC were utilized to characterize the NPs. Cytotoxicity was assessed using MTT and Live/Dead cell assays. DLS analysis revealed that the NPs have a desirable size and zeta potential that are suitable for systemic circulation and improved therapeutic outcomes. Successful encapsulation and conjugation were confirmed through FTIR and HPLC analysis. Cell viability and proliferation studies demonstrated that PTX-S2.2-PBM NPs and HNK-S2.2-PBM NPs, when used individually, exhibited cytotoxicity comparable to or greater than that of free PTX and HNK, respectively. When combined, a synergistic effect was observed. Utilizing copolymers (PCL/PEG) and aptamer conjugation, PTX has the potential for improved bioavailability and reduced off-target effects compared to its free drug counterparts. Based on these findings, we believe that PTX-S2.2 and HNK-S2.2 PBM NP could represent a promising treatment option for BrCa.

#6384 Nanoparticle mediated disruption of tumor-nerve crosstalk enhances pancreatic cancer treatment and pain mitigation.

Songyu Wu[1], Lei Zhu[2], Weiping Qian[2], Tongrui Liu[2], Lisa Sudmeier[1], Charles A. Staley[2], Lily Yang[3]

[1]Emory Winship Cancer Institute, Atlanta, GA,[2]Emory University, Atlanta, GA,[3]Emory University School of Medicine, Atlanta, GA

Introduction: Pancreatic ductal adenocarcinoma (PDAC) is a highly aggressive malignancy with a dismal prognosis. Dense fibrous tumor stroma creates a drug delivery barrier, cultivates aggressive tumor biology and immunosuppression in PDAC. A well-recognized hallmark of PDAC is nerve infiltration into tumors and cancer cells invading neurons, which correlate with local invasion and poor survival. Neural invasion leads to severe and intractable pain in PDAC patients, due to release neurotransmitters and pro-inflammatory responses. Sympathetic nerves release catecholamines interacting with β-adrenergic receptors (β-AR) to stimulate tumor cell proliferation and invasion, induce immunosuppression and increase pain sensation. Clinical studies revealed treatment with β-AR inhibitors improved survival of PDAC patients. In this study, we have developed tumor cell, stroma, and cancer nerve targeted hyaluronic acid nanoparticles (HANPs) carrying SN-38 and β-AR blocker (Propranolol, Pro) for targeted therapy of PDAC and mitigation of neuropathic pain.
Methods: To enhance targeted delivery, we leveraged the biological properties of upregulation of urokinase plasminogen activator receptor (uPAR) and MMP14 in invasive tumor cells to developed a biomimetic nanoparticle drug delivery platform targeting to uPAR with MMP14 for stroma-penetration and drug delivery. The hydrophobic SN38 (an active metabolite of irinotecan) and Pro, were encapsulated into HANPs by self-assembling, resulting HANP/Pro+SN38 (HANP/PS). A uPAR targeted stroma penetrating recombinant ligand, ATFmmp14 was conjugated to HANP/PS to produce ATFmmp14-HANP/PS (AM-HANP/PS). Targeted delivery and therapeutic response were evaluated in an orthotopic PDAC patient derived xenograft model.
Results: Our results showed that NIR 830 dye labeled-AM-HANP/PS led to a high tumor accumulation (46%) in a PANC XXIV PDX model. AM-HANP/PS treatment by co-delivery of SN38 (4 mpk) and Pro (10 mpk) resulted in significantly stronger inhibition of tumor growth (67%) compared with single drug delivery (40%) or free SN38+Pro (46%). Histological analysis revealed nearly complete elimination of sympathetic and sensory nerves in treated tumors, while other formulations showed a moderate level of nerve reduction. Pain evaluation showed decreased pain in AM-HANP/PS treated mice. The level of pain neurotransmitter, substance P, was significantly reduced in tumors. These findings support AM-HANP/PS as an effective tumor and nerve targeted therapy.
Conclusion: AM-HANP/PS that targets PDAC tumor cells and cancer neurons achieved a high level of tumor accumulation. Co-delivery of SN38 and Pro significantly inhibits tumor growth, reduces density of sympathetic and sensory nerves, and relieves cancer-related pain. This dual-targeted strategy exhibited both antitumor efficacy and neuropathic pain mitigation in PDAC PDX model.

#6385 Targeted delivery of suicide gene to tumor cells using PD-L1-targeted extracellular vesicles for cancer therapy.

Geuna Park[1], SeokMin Lee[1], Eun Jung Park[2], Byungheon Lee[1]

[1]Kyungpook National Univ. School of Med, Daegu, Korea, Republic of,[2]National Cancer Center, Goyang, Korea, Republic of

Herpes simplex virus-thymidine kinase (HSV-TK) gene, a well-known suicide gene, causes cell death in rapidly dividing cells when treated with ganciclovir (GCV). The HSV-TK activates GCV and makes GCV-triphosphate. Insertion of activated GCV-triphosphate in elongating DNA by cellular DNA polymerases interferes DNA duplication and eventually leads to cell death. The suicide gene therapy, however, has been limited by non-specific cytotoxicity in off-target cells such as normal cells. In this study, we explored PD-L1-targeted extracellular vesicles (EVs) carrying the HSV-TK mRNA to deliver the HSV-TK selectively into tumor cells. HEK 293FT cells were transduced using lentivirus with the GFP-tagged, HSV-TK gene containing a sequence that is recognized by EV-trafficking RNA-binding protein. Stable HEK 293FT cells expressing the HSV-TK gene were established. EVs were isolated from the stable cells and labeled with a PD-L1-binding peptide (CVRARTR) using click chemistry to target PD-L1-high tumor cells. Delivery of the HSV-TK mRNA after incubation of cells with the EVs was validated by observing the fluorescence of GFP tag under a microscope. The PD-L1-targeted EVs carrying the HSV-TK mRNA exerted an efficient cytotoxicity in PD-L1-high MDA-MB-231 tumor cells. On the other hand, the EVs showed low levels of cytotoxicity in PD-L1-low tumor cells and normal cells. Systemic administration of the EVs inhibited the growth of MDA-MB-231 tumor xenografts in mice. These results demonstrate that the PD-L1-targeted EVs containing the HSV-TK mRNA provide a new avenue for the targeted delivery of a suicide gene. Keywords: HSV-TK; Peptide; PD-L1; Suicide gene therapy

#6386 Small bowel obstruction and short bowel syndrome may impair the efficacy of Avutometinib and Defactinib in recurrent low grade serous ovarian cancer: A case report.

Sarah Ottum[1], Luca Palmieri[2], Victoria Ettorre[1], Tobias Hartwich[1], Cem Demirkiran[1], Namrata Sethi[1], Stefania Bellone[1], **Alessandro D. Santin**[1]

[1]Department of Obstetrics, Gynecology, and Reproductive Sciences, Yale University, New Haven, CT,[2]Gynecologic Oncology Unit, Department of Woman and Child Health and Public Health, Fondazione Policlinico Universitario A. Gemelli IRCCS, Universita Cattolica del Sacro Cuore, Rome, Italy

The treatment of recurrent low grade serous ovarian cancer (LGSOC) is a challenge, but when complicated by recurrent small bowel obstructions (SBO) and/or major small bowel resections, the decreased absorption/efficacy of oral medications must be considered. We report the case of a patient with recurrent LGSOC previously treated with multiple debulking surgeries, neoadjuvant and adjuvant carboplatin/paclitaxel, and maintenance aromatase inhibitor therapy. A few weeks after initiating treatment within the RAMP-201 trial with the combination of Avutometinib (MEK inhibitor) and Defactinib (FAK inhibitor), two drugs recently approved by the FDA for the treatment of adult patients with KRAS-mutated LGSOC, she developed a small bowel obstruction that ultimately required extensive bowel resections, resulting in short bowel syndrome. Whole-exome sequencing (WES) of the recurrent LGSOC collected at the time of the bowel resection revealed copy number gains in multiple key genes within the RAS/RAF/MEK/ERK and FAK pathways, conferring potential tumor sensitivity to MEK/FAK inhibitors. In agreement with the WES results, the matched patient-derived xenograft (PDX) model established from the recurrent LGSOC demonstrated a remarkable sensitivity to the avutometinib/defactinib combination in vivo. Despite the high sensitivity of the PDX model, the patient progressed on the drug combination and had to be removed from the clinical trial. The experimental PDX results combined with our patient's clinical data strongly suggest that recurrent SBO and/or major bowel resections may represent unrecognized causes of resistance to avutometinib and defactinib significantly impairing the absorption of the oral drugs and decreasing the effectiveness of the regimen in recurrent heavily pretreated LGSOC patients. An earlier use of the novel oral drug combination in recurrent LGSOC is warranted.

#6387 Optimizing GPC3 gene editing in liver cancer: A comparison of Cas9 RNP and mRNA nanoliposome delivery systems.

Joshua Nieves-Reyes, Pablo E. Vivas-Mejia

Biochemistry, University of Puerto Rico - Medical Sciences Campus, San Juan, PR

Primary liver cancer ranks as the third leading cause of cancer-related deaths worldwide and has one of the lowest survival rates among all cancers. Late-stage detection and resistance to first-line therapies underscore the urgent need for novel treatment approaches. Glypican-3 (GPC3), a heparan sulfate membrane proteoglycan that is often overexpressed in hepatocellular carcinoma (HCC), is associated with a worse prognosis. As it is absent from healthy adult liver, it makes an attractive therapeutic target. Clustered Regularly Interspaced Short Palindromic Repeats (CRISPR)-Cas9 gene editing offers a versatile method to disrupt genes overexpressed in cancer, such as GPC3. The purpose of this study was to compare the efficiency of nanoliposomes carrying CRISPR-Cas9 ribonucleoproteins (RNPs) versus nanoliposomes carrying Cas9 mRNA for GPC3 targeting liver cancer cells. Nanoliposomes were designed using various lipid formulations and loaded either with Cas9-GFP RNPs or Cas9-GFP mRNA. We performed liposome-mediated Cas9-GFP RNP and mRNA internalization experiments in liver cancer cells, followed by fluorescence microscopy to compare delivery efficiency, while particle size distribution was determined using Dynamic Light Scattering (DLS). GPC3 knockout efficiency was evaluated using immunoblotting. Preliminary observations indicate that both RNP-loaded and mRNA-loaded nanoliposomes successfully enter liver cancer cells, with notable differences in internalization and intracellular GFP distribution between distinct lipid compositions. Initial comparisons also suggest that further optimization is required to achieve effective GPC3 protein reduction. This study demonstrates that both Cas9 RNP and Cas9 mRNA-loaded nanoliposomes show potential for delivering CRISPR components to liver cancer cells, with each approach offering distinct advantages for gene silencing. These results provide the bases for future therapeutic experiments in liver cancer mouse models.

#6388 Subcutaneous ANtibody-conjugated microGel platform enabling combination immunotherapy for refractory solid tumors.

Jongseong Kim, Yun Jin Chae, Yeobin Kim, Jaehee Lim

R&D center, Oncolab Co., Ltd., Goyang, Korea, Republic of

Background: Drug delivery systems (DDSs) are increasingly utilized to enhance the precision and durability of biologics in oncology. However, current cancer immunotherapies show limited efficacy in solid tumors due to profoundly immunosuppressive tumor microenvironments, underscoring the need for innovative delivery platforms. We developed the ANtibody-conjugated microGel (ANGel), a deformable hydrogel-based submicron particle engineered to deliver combination monoclonal antibodies (mAbs) targeting both the PD-1/PD-L1 axis and co-stimulatory pathways.
Methods: ANGel formulations were generated by surface affinity loading of multiple mAb types. In vitro studies assessed therapeutic synergy between two anti-PD-1/PD-L1 mAbs and two co-stimulatory mAbs when formulated with ANGel. Lead combinations were evaluated in vivo using triple-negative breast cancer (TNBC) mouse models. Subcutaneous administration was performed at peritumoral sites to assess local delivery, antitumor activity, and survival. Dose sensitivity and formulation parameters were fine-tuned to identify optimal therapeutic regimens.
Results: ANGel significantly enhanced in vitro synergy between PD-1/PD-L1-targeting and co-stimulatory mAbs compared with free-antibody mixtures. In TNBC models, subcutaneous peritumoral delivery of combination ANGel (dANGel) formulations produced marked tumor-growth delay relative to free-combination mAbs, including combinations with hyaluronidase. Antitumor efficacy of dANGel formulations demonstrated strong dose-dependent and regimen-dependent sensitivity, enabling optimization for maximal therapeutic output. Notably, dANGel treatment extended progression-free survival to 204 days, compared with 23 days achieved by anti-PD-L1 plus anti-CTLA-4 mAbs formulated with hyaluronidase.
Conclusions: These results demonstrate ANGel as a potent local delivery platform capable of overcoming key barriers to solid-tumor immunotherapy. By enabling subcutaneous peritumoral administration of synergistic mAb combinations, ANGel provides a novel therapeutic strategy with the potential to substantially improve outcomes in refractory solid tumors. Preclinical findings support dANGel as a strong candidate for clinical translation.

#6389 Maximizing systemic LNP-DNA delivery for cancer-activated expression of immunotherapy agents using nanoprimer technology.

Nadege Morisot[1], Blaine McCarthy[1], Sushil Lathwal[1], Jayalakshmi Ramani[1], Ajda Rojc[1], Francis Mpambani[2], Laurence Poul[2], Julie Devalliere[2], Matthieu Germain[3], Dang Dang[1], Robby Chandra[1], Xiaobin Wu[1], Moataz Reda[1], Badriprasad Ananthanarayanan[1], David Suhy[1]

[1]Earli Inc, Redwood City, CA,[23]Nanobiotix, Paris, France

Earli is developing a platform technology that utilizes lipid nanoparticle (LNP)-delivered recombinant DNA constructs containing cancer-activated synthetic promoters that drive the selective expression of therapeutic proteins such as cytokines to treat the tumor. Our approach demonstrated robust therapeutic impact in vivo via tumor-specific secretion of IL-2 and IL-12 which are uniquely produced in cancer cells, but not normal tissues to control syngeneic tumors growth. While LNP-DNA vehicles often offer advantages over viral vectors, their efficacy can be limited by rapid clearance via the mononuclear phagocyte system (MPS). Although modifications to the surface of LNPs, like pegylation, can extend circulation time, the hepatic clearance remains a challenge that reduces LNPs systemic bioavailability, hinders tumor accumulation, and can contribute to toxicity. In addition, LNP-DNA may produce transient acute inflammation primarily via the intracellular activation of the cGAS/STING pathway, a major host defense mechanism. To address this challenge, Nanobiotix's Nanoprimer technology, engineered biocompatible lipid-based nanoparticles that transiently occupy MPS clearance pathways, was utilized to extend blood circulation time of subsequently administered therapeutics. We investigated the impact of Nanoprimer pre-treatment on the pharmacokinetics , biodistribution, and tolerability of two Earli proprietary extrahepatic LNP formulations, longer-circulating FRM177 and fast clearing FRM146, which encapsulate a recombinant DNA comprised of a strong constitutive promoter to drive firefly luciferase expression in tumor naive mice. The pre-treatment improved the blood bioavailability of FRM146-DNA by 8-fold, while having a minor effect on the delivery of FRM177-DNA. Furthermore, a 2-fold decrease in hepatic DNA accumulation at 48h post dose for both LNP-DNA was observed as well as reduced hepatotoxicity as evidenced by normal levels of liver enzymes. Finally, both LNP-DNA produced a transient mouse body weight loss and serum cytokine elevation, effects that were ameliorated by the Nanoprimer, revealing improved tolerability. Our data demonstrates that the Nanobiotix technology can be a successful strategy to significantly improve the extrahepatic biodistribution and tolerability of LNP-DNA, even those already engineered for extrahepatic delivery. These results expand the known potential of the compound in MPS blockade for clinically relevant LNP-DNA constructs for cancer immunotherapy applications and confirms the relevance of further clinical development for systemically administered LNP-nucleic acid therapeutics. Ongoing studies are focused on determining the impact of Nanoprimer on the anti-tumor efficacy of our cancer-activated cytokine-expressing DNA constructs in syngeneic cancer models.

#6390 Nanoprimer technology for enhanced efficacy of intravenously administered vaccines.

Matthieu Germain, Maxime Bergere, Francis Mpambani, Jordan Da Silva, Andromeda Savary, Sebastien Paris, Laurence Poul, Julie Devalliere

Nanobiotix, Paris, France

The efficacy of intravenously (IV) administered therapeutic agents is often limited by hepatic clearance, resulting in reduced accumulation at the target site and in potential hepatotoxicity. Nanobiotix's innovative Nanoprimer technology aims to shift the balance of therapeutics' bioavailability and toxicity. The Nanoprimer is a biocompatible, engineered liposome that transiently occupies cells of the mononuclear phagocyte system, responsible for the clearance of nanoparticles. Administered shortly before the therapeutic agent, the Nanoprimer reduces the early elimination and increases bioavailability during the agent's critical window of activity. proofs of concept were realized with multiple modalities including nucleic acid-based products. Our latest research has expanded the evaluation of the Nanoprimer for enhancing the efficacy of cancer vaccines. The Nanoprimer's effect on antigen-specific CD8⁺ T cell responses was evaluated using 2 vaccine platforms: mRNA-loaded lipoplex encoding an ovalbumin epitope and ovalbumin peptide-loaded liposomes. *De novo* priming of CD8⁺ T cells was assessed 7 days post-immunization. To evaluate the functional activity of generated CD8⁺ T cells, splenocytes were restimulated *ex vivo* with the antigenic peptide for 24 hours, and IFN-γ production was quantified. In a single-dose immunization study, using peptide-loaded liposomes, pre-treatment with the Nanoprimer resulted in a 6-fold increase in antigen-specific CD8⁺ T cells and a marked elevation of IFN-γ production by splenocytes, indicative of a strong effector function. Similar studies using a single dose of mRNA-lipoplex demonstrated that the Nanoprimer dramatically enhanced the generation of antigen-specific CD8⁺ T cells, reaching up to 20% of the total CD8⁺ T cells. The expansion of antigen-specific CD8⁺ T cells was correlated with increased IFN-γ secretion, consistent with functional cytotoxic activity. For the evaluation of the memory immune response, animals received a primary vaccination (three repeated injections of the vaccine at days 0, 7 and 14), and memory response was assessed on day 73 by measuring the frequency of antigen-specific CD8+ T cells, 3 days after the booster immunization. The Nanoprimer increased antigen-specific CD8+ T cell responses, reaching up to 54% of total CD8+ T cells for mRNA-lipoplex (compared to 27% with vaccine alone) and up to 27% for peptide-liposome (with no detectable response observed in the vaccine alone group). These findings demonstrate that the Nanoprimer can enhance acute and memory cellular immune responses across multiple vaccine modalities. Its ability to increase antigen-specific CD8⁺ T cell quantities and functional cytokine responses underscores its potential to improve the therapeutic index of cancer immunotherapies. Overall, Nanoprimer technology represents a promising strategy to unlock the full clinical potential of innovative therapies.

#6391 Development of a stabilized Z-endoxifen topical formulation for breast cancer prevention.

Alison Wissmann, Travis Belknap, Lindsey Lafal, **Quentin Lawrence**, Jonathan White

MRIGlobal, Kansas City, MO

Purpose: The primary objective of this work was to develop a pharmaceutically stable, transdermal delivery strategy for Z-endoxifen, the highly potent and bioactive metabolite of tamoxifen.
Methods: Four distinct topical formulation types were prepared. Each formulation type was evaluated with a control and four different antioxidants, allowing for the assessment of both water-soluble and lipid-soluble antioxidant effects across various bases. Each prepared formulation was stored at both refrigerated conditions and ambient temperature for a period of up to 6 months. Formulations were evaluated for visual appearance and isomeric purity over time. Isomeric purity was determined by high-performance liquid chromatography.
Results: Our study identified specific antioxidant combinations that mitigated Z-endoxifen isomerization. Combined with reduced temperature storage, these strategies led to the successful development of a stable topical formulation of Z-endoxifen.
Conclusion: Instability challenges of Z-endoxifen in a topical formulation were overcome by adding specific antioxidants into varied formulation bases and controlling storage temperature. This advancement enables the development of a more potent and potentially safer localized breast cancer prevention therapy by delivering the highly bioactive Z-isomer and minimizing systemic exposure. Future work will involve in vivo pharmacokinetic/pharmacodynamic studies to confirm localized breast tissue delivery and minimal systemic absorption, paving the way for advanced clinical trials aimed at providing an improved preventative treatment for women at high risk for breast cancer.

#6392 Harnessing facial neuronal pathways via iontophoresis for targeted intradermal delivery of bimodal spherical nucleic acids to the brain for anti-glioma effect.

Akanksha S. Mahajan[1], **Davin Hickman-Chow**[2], Gaelen Clayton[3], Seunghyun Kim[1], Rachel Jarvis[1], Emma Shen[1], Clara Foltz[1], Cao Dai Phung[1], Eric Leuthardt[4], Alexander Stegh[5]

[1]Taylor Family Department of Neurosurgery, The Brain Tumor Center, Washington University in St. Louis, Saint Louis, MO,[2]Department of Biomedical Engineering, Washington University in St. Louis, Saint Louis, MO,[3]Department of Mechanical Engineering,, Washington University in St. Louis, Saint Louis, MO,[4]Department of Neuroscience, Neurosurgery, Mechanical Engineering, Biomedical Engineering, Washington University in St. Louis, Saint Louis, MO,[5]Taylor Family Department of Neurosurgery, The Brain Tumor Center, Department of Neuroscience, Washington University in St. Louis, Saint Louis, MO

Background: Glioblastoma (GBM) remains one of the most aggressive brain tumors due to barriers in drug delivery across the blood-brain barrier (BBB) and its profoundly immunosuppressive tumor microenvironment (TME). These limitations restrict therapeutic penetration into tumor sites. While intranasal strategies exploit trigeminal/olfactory routes, mucociliary clearance and off-target exposure have limited clinical translation. Here, we developed a facial dermal iontophoresis-based system to deliver immune-modulating nanoparticles through the facial neuro-lymphatic network to bypass the BBB and reprogram the TME.

Methods: To overcome delivery barriers affecting immunotherapies intended to modulate tumor-associated and peripheral immunity, we integrated two approaches. First, we established iontophoresis as a minimally invasive method to bypass the BBB and enhance the transport of therapeutics delivered via facial intradermal (i.d.) injection. Second, we engineered a bimodal Spherical Nucleic Acid (bi-SNA) platform that activates cGAS and inhibits STAT3. Bi-SNAs consist of a 15-nm gold core functionalized with a hairpin oligonucleotide with STAT3-decoy sequences, enabling simultaneous cGAS activation and STAT3 sequestration. Bi-SNAs elicit potent antitumor immunity in multiple HGG models and outperform cGAS-agonist monotherapies. A dedicated iontophoresis device was designed for preclinical assessment using murine GBM models, and iontophoretic parameters (current density, waveform, electrode placement) were optimized for controlled transdermal SNA transport. Biodistribution was measured by 3D fluorescence CT-IVIS with ICG-labeled SNAs, gold levels by ICP-MS, and immune modulation by multispectral flow cytometry.

Results: I.d. Bi-SNA delivery with iontophoresis significantly suppressed tumor progression, depleted immunosuppressive myeloid cells, and increased recruitment/activation of effector T cells. IVIS imaging showed a two-fold increase and faster kinetics of SNA trafficking from facial planes to the brain without detectable systemic spread, with preferential accumulation along maxillary-olfactory and temporomandibular conduits. ICP-MS revealed ~20-fold higher gold deposition in the brain and trigeminal nerve within 12 hours compared with passive i.d. delivery.

Conclusions: Iontophoresis-enhanced i.d. delivery provides a powerful non-invasive strategy for brain-targeted immunotherapy, leveraging neuronal pathways to bypass the BBB and reprogram the GBM TME. This establishes a foundation for patient-adaptable, at-home nanotherapeutic delivery for brain tumors.

#6393 Polo-like kinase 4 inhibition enhances radiosensitivity in non-small cell lung cancer via apoptosis and epithelial-mesenchymal transition regulation.

Hye Won Lee[1], Shin Kim[2], Jeong-Woo Hwang[2], Eun-Young Gong[1], Hyowon Hong[3], SangJun Byun[1], Sung Uk Bae[1]

[1]Keimyung University School of Medicine, Daegu, Korea, Republic of,[2]Keimyung University, Daegu, Korea, Republic of,[3]Keimyung University Dongsan Medical Center, Daegu, Korea, Republic of

Non-small cell lung cancer (NSCLC) remains one of the leading causes of cancer-related mortality worldwide. Radiotherapy (RT) is a mainstay of treatment; however, the frequent development of radioresistance limits its therapeutic efficacy. Polo-like kinase 4 (PLK4), a master regulator of centriole duplication and centrosome integrity, has been implicated in chromosomal instability, DNA damage responses (DDR), and epithelial-mesenchymal transition (EMT). Therefore, targeting PLK4 may represent a novel strategy to overcome radioresistance. In this study, we investigated the effects of the selective PLK4 inhibitor CFI-400945 in NSCLC cells exposed to RT. CFI-400945 treatment significantly reduced cell viability and clonogenic survival in combination with RT compared to either treatment alone. Mechanistically, CFI-400945 amplified apoptotic signaling, with marked upregulation of p53 and cleaved PARP1. In addition, PLK4 inhibition promoted G2/M cell cycle arrest by reducing RT-induced p-AKT and cyclin B1 expression level. Furthermore, PLK4 inhibition enhanced RT-induced DNA damage as indicated by increased γH2AX expression. Importantly, RT alone promoted EMT progression, characterized by reduced E-cadherin and increased N-cadherin and vimentin expression, as well as enhanced migratory capacity. These effects were significantly reversed by CFI-400945, indicating that PLK4 inhibition attenuates RT-induced EMT progression. Collectively, these findings demonstrate that PLK4 inhibition with CFI-400945 sensitizes NSCLC cells to RT by augmenting DNA damage and apoptosis while suppressing RT-induced EMT. Our results highlight PLK4 as a critical regulator linking centrosome abnormalities, DDR, and EMT, and suggest that combining PLK4 inhibition with RT may provide a promising therapeutic approach to overcome radioresistance in NSCLC.

#6394 Ferroptosis amplified by a tumor-targeted artesunate nano-derivative for effective colon cancer treatment.

Jianing Li, Dake Song, Qiutong Guan, **Zhenhua Li**

China Medical University,School of Pharmacy, Shenyang, China

Background: Artesunate (ART), a proven antimalarial drug, is promising but has limited antitumor activity because of its poor stability, low potency, and lack of tumor selectivity. While its effect is linked to ferroptosis, an iron-dependent form of cell death driven by lipid peroxidation, clinical translation in oncology requires enhanced drug delivery and targeting. We hypothesized that engineering a tumor-targeted nanoparticle of an ART prodrug could amplify ferroptosis induction and therapeutic efficacy against colorectal cancer (CRC).
Methods: We systematically designed and synthesized six amino acid-modified ART derivatives. The most potent conjugate was further functionalized with 3-aminophenylboronic acid (PBA) to create the final prodrug, AAP. AAP self-assembled into nanoparticles (AAP NPs) via a one-step precipitation method. The size, PDI, and morphology of the NPs were characterized. Efficacy was evaluated in multiple CRC cell lines (CT26, HCT116, SW480, SW620) and a hepatoma cell line (Huh7) via CCK-8 assays. Cellular uptake was visualized via coumarin-6-loaded NPs. The antitumor effect, systemic safety, survival benefit, and mechanism of AAP NPs were comprehensively investigated in a BALB/c mouse model bearing CT26 tumors.
Results: AAP demonstrated superior in vitro cytotoxicity compared with native ART, with IC50 values 1.77- to 2.09-fold lower across CRC and hepatoma cells. The resulting AAP NPs were monodisperse spheres with a uniform size of 174.44 ± 9.97 nm and a low PDI of 0.046. Compared with ART or ART-AA (no PBA), the completed AAP NPs exhibited significantly stronger, dose- and time-dependent cytotoxicity against all cancer cells tested ($P < 0.05$) and were effectively internalized by CT26 cells. In vivo, AAP NPs achieved the most potent tumor growth inhibition, reducing the tumor volume and weight to 531.29 ± 132.20 mm^3 and 483.14 ± 118.91 mg, respectively, significantly outperforming the control, ART, and ART-AA NP groups ($P < 0.05$). Critically, AAP NPs significantly prolonged mouse survival ($P < 0.05$) . Mechanistically, AAP NP treatment led to significant accumulation of ROS in tumor tissues, confirming the induction of ferroptosis.
Conclusion: We developed a dual-targeted ART nanoprodrug that leverages PBA-mediated active targeting and the EPR effect. This strategy potently inhibits CRC growth by triggering ferroptosis and exhibits an excellent safety profile, offering a compelling approach to repurpose ART for targeted cancer therapy.

#6395 Enhanced antitumor efficacy of berbamine dihydrochloride nanomedicine via apoptosis induction in colorectal cancer.

Chan Zhang, Qiutong Guan, **Zhenhua Li**

School of Pharmacy, China Medical University, Shenyang, China

Background: Berbamine dihydrochloride (BBM), a natural bisbenzylisoquinoline alkaloid, exhibits broad antitumor activity. However, its clinical translation is hampered by nonspecific tissue distribution, poor bioavailability, and dose-limiting toxicity. Bovine serum albumin (BSA) nanoparticles represent an ideal drug delivery platform because of their biocompatibility, low immunogenicity, and inherent tumor-targeting capability. This study aimed to develop BBM-loaded BSA nanoparticles (BBM-BSA-NPs) to enhance drug targeting and antitumor efficacy against colorectal cancer (CRC).

Methods: BBM-BSA-NPs were prepared and characterized. In vitro cytotoxicity was assessed against CRC cell lines (CT26, HT29) and other cancer lines (AGS, CAOV3, HepG2) via CCK-8 assays. Selectivity was evaluated by comparing the effects on cancer cells with those on normal 293 cells. Apoptosis induction was measured by flow cytometry. In vivo antitumor efficacy and systemic safety were investigated in a murine CT26 tumor model.

Results: Compared with native BBM, BBM-BSA-NPs significantly increased the cytotoxicity to CT26 and HT29 cells in a concentration- and time-dependent manner ($P < 0.05$). The formulation showed selective toxicity toward cancer cells, with markedly greater inhibition in HepG2 cells ($P < 0.05$) and minimal effects on normal 293 cells at 24 h and 48 h. Notably, BBM-BSA-NPs effectively induced morphological changes and apoptosis in CT26 cells, with apoptosis rates significantly exceeding those of native BBM at all concentrations tested ($P < 0.05$). In vivo, BBM-BSA-NP treatment resulted in a remarkable reduction in tumor volume (279.19 ± 46.75 mm^3) and weight (0.13 ± 0.04 g), significantly outperforming native BBM (456.75 ± 54.64 mm^3; 0.29 ± 0.04 g; $P < 0.05$). No significant changes in body weight or systemic toxicity were observed, confirming the safety of the treatment. The blank BSA-NPs showed no antitumor activity, confirming that the efficacy and safety benefits were attributable to the nanoformulation.

Conclusion: We successfully developed a novel BBM-BSA nanoparticle system that significantly enhances the selective cytotoxicity and apoptotic induction of BBM against colorectal cancer while improving its therapeutic efficacy in vivo. This study provides a compelling rationale for leveraging albumin nanoparticles to repurpose BBM as a potent and safe therapeutic agent for CRC.

#6396 Next-generation sabizabulin nanoformulation for cervical cancer treatment.

Vivek Kumar Kashyap[1], Prashanth KB Nagesh[2], Qinghui Wang[3], Upendra Nayek[1], Tusha Sharma[1], Bilal B. Hafeez[1], Duane D. Miller[4], Wei Li[5], Murali M. Yallapu[1], Subash Chauhan[1]

[1]Division of Cancer Immunology and Microbiology, University of Texas Rio Grande Valley, McAllen, TX,[2]Laboratory of Signal Transduction, Memorial Sloan Kettering Cancer Center, New York, NY,[3]Department of Pharmaceutical Chemistry, University of California, San Francisco, CA,[4]Professor, Chair and Associate Dean, University of Tennessee Health Science Center - College of Medicine, Chattanooga, Memphis, TN,[5]University of Tennessee Health Science Center, Memphis, TN

Background: Cervical cancer (CC) remains a significant global health burden in women, with intrinsic and acquired chemotherapy resistance limiting therapeutic efficacy. Sabizabulin (VERU-111) is an orally bioavailable colchicine-binding site inhibitor that offers a new way to treat cancer by targeting microtubule dynamics and changing the HPV-driven CC phenotype. However, optimization of its pharmaceutical formulation is critical to maximize efficacy while minimizing systemic toxicity and improving tumor-specific drug accumulation. In this study, we engineered and evaluated a next-generation nanoparticle formulation of sabizabulin to enhance its bioavailability, improve tumor-targeted delivery, and overcome chemotherapy resistance in CC models.
Methods: We engineered a multi-layered Pluronic F127 and polyvinyl alcohol stabilized and poly-L-lysine coated Sabizabulin-loaded poly(lactic-co-glycolic acid) nanoparticle formulation (PSab-NPs). PSab-NPs were characterized for physicochemical properties, stability, and drug loading efficiency by TEM, FT-IR, DSC, TGA, and HPLC. Cellular internalization was assessed after 6 hours of incubation with PSab-NPs in CC cells. To determine the therapeutic efficacy of PSab-NPs, we performed various in vitro (MTS, wound healing, Boyden chamber, real-time xCELLigence, and apoptosis assays) and in vivo xenograft mouse models using CC cells. We evaluated the effect of PSab-NPs on various key oncogenic signaling pathways using Western blot, immunohistochemistry (IHC), confocal microscopy, and qRT-PCR.
Results: Our novel PSab-NPs formulation provided an average size of 120-150 nm in dynamic light scattering (DLS) and exhibited -10.46 to -12.73 mV zeta potential with an outstanding loading efficiency. Cellular uptake and internalization studies demonstrate that PSab-NPs efficiently evade lysosomal degradation, facilitating strong endosomal release into the cytosol. PSab-NPs showed remarkable anti-cancer potential in various CC cells (HeLa, SiHa, CaSki, and C33A). Mechanistically, PSab-NPs more effectively modulate the PI3K/AKT/MDM2 signaling pathway and suppress HPV E6 and E7 in vitro and CaSki cell-derived xenografts in athymic nude mice.
Conclusions: Taken together, our findings suggest that PSab-NPs represent a novel, promising nanoparticle platform that has more anti-cancer potential than free sabizabulin. PSab-NPs may reduce the toxicity and improve the bioavailability of free sabizabulin and could be used for the effective management of CC.

#6397 Immunogenic eradication of melanoma via ultrasmall lactoferrin-ICD inducer nanoconjugates integrated with BRAF-inhibitory liposomes.

Ahmad Ziada[1], Mousa El-Sayed[2], Asmaa Reda[2], Leo Ren[3], Cuiyan Xin[4], Ahmed Elzoghby[2]

[1]Amherst College, Amherst, MA,[2]Engineering in Medicine, Brigham and Women's Hospital, Harvard Medical School, Boston, MA,[3]Rice University, Houston, TX,[4]Renal Medicine, Brigham and Women's Hospital, Harvard Medical School, Boston, MA

Approximately 50% of human melanoma is driven by B-Raf protooncogene mutation (BRAF-mutant). Tumors with such mutation are highly immunosuppressive, and often resistant to immune checkpoint inhibitor (ICI) therapies. Blocking the BRAF-MAPK pathway in the BRAF-mutant melanoma cells markedly increases the tumor antigen expression and hence enhances the ability of T cells to recognize autologous BRAFV600 mutant melanoma cells. In parallel, induction of immunogenic cell death (ICD) of melanoma cells can overcome immunosuppression and enhance the antigen presenting capacity of dendritic cells (DCs). Therefore, our goal is to engineer a novel nanomedicine for combined delivery of BRAF inhibitor and ICD inducer drugs for immunogenic eradication of melanoma cells and thus boost the efficacy of ICI therapy. First, we engineered liposomes encapsulating dabrafenib (DFN, BRAF inhibitor) and selumetinib (SLM, MEK inhibitor). To ensure their stability, we coupled DFN and SLM to cholesterol via pH-responsive carbamate and ester bonds, respectively prior to incorporation into liposomes. The liposomes showed uniform size, high drug loading and excellent physical stability as well as high internalization and cytotoxicity against A375 melanoma cells. Moreover, the expression of MHC I & II by A375 cells was enhanced after treatment with liposomes. Second, we synthesized ultrasmall lactoferrin (LF) nanoconjugates with ICD inducer drugs including doxorubicin (DOX), shikonin and bortezomib via a pH-responsive hydrazone bond to induce ICD of melanoma cells. The LF-DOX nanoconjugate showed a small size (38.4 nm) with efficient internalization into A375 cells resulting in high cytotoxicity. The engineered nanoconjugate successfully induced ICD of melanoma cells as evidenced by increased surface exposure of CRT and reduced intracellular expression of HMGB1 in A375 cells. Moreover, the ICD inducing nanoconjugate induced remarkable degree of apoptosis (33%) of A375 melanoma cells compared to control non-treated cells (5.7%). Finally, we encapsulated the ultrasmall ICD inducing LF-drug nanoconjugate into the aqueous core of the pH-responsive DFN/SLM liposomes decorated with αPD-L1 antibody. A mouse syngeneic melanoma model with BRAF mutation was established by subcutaneously implanting YUMM1.7 Melanoma cells (1×10^5) in the flanks of 4-6 weeks old C57BL/6 mice. The intravenously injected nanomedicine markedly increased the antitumor efficacy with significant reduction of tumor volume relative to vehicle treated group and mice treated with αPDL1 alone. In conclusion, the combined delivery of BRAF inhibitory and ICD inducing nanomedicine into one platform could boost the antitumor immune response to αPDL1 therapy and hence overcome the immune resistance of melanoma cells.

: Screening and Technology Advances for Probe and Drug Discovery
Poster Session

#6401 A translational screening platform with AI integration for clinically predictive discovery of safe and effective macropinocytosis-dependent cancer therapeutics.
Qiuming Chu, Antonio Bonanno, **Yanping Kong**

Kongs Pharmaceutical, Lowell, MA

Background: Macropinocytosis-dependent cancers rely on nutrient-scavenging pathways to sustain tumor growth under stress. Current therapies rarely provide durable control, underscoring the need for strategies that stabilize cancer progression as a chronic condition. Although extensive clinical data exist for approved drugs—linking mechanisms of action (MoAs), safety, and efficacy—clinically translatable, macropinocytosis-relevant cell-based screens remain limited. We developed an AI-driven translational discovery platform integrating phenotypic screening with clinical correlation to identify safe, mechanistically meaningful, and clinically predictive therapeutic candidates.
Methods: An automated image-based cytometry assay was optimized to quantify macropinocytosis in cancer cells with minimal human bias. FDA-approved drugs and proprietary compounds were screened with this medium throughput method. AI algorithms correlated *in vitro* phenotypes with retrospective clinical data, integrating MoA, toxicity, and efficacy metrics. Mechanistic clustering identified shared therapeutic pathways among clinically effective agents. AI modeling also predicted clinical performance and generated rational combination hypotheses emphasizing safety and translational potential.
Results: AI validation confirmed strong concordance between phenotypic results and clinical safety/efficacy profiles from 892 FDA-approved cancer and non-cancer drugs, demonstrating high translational fidelity. Mechanistic clustering revealed a convergent signaling axis associated with durable benefit and low toxicity. Several novel in-house compounds exhibited comparable inhibition profiles and AI-predicted clinical potential. AI modeling proposed synergistic combinations between approved and proprietary agents with underexplored mechanisms, prioritizing safe, durable therapeutic responses.
Conclusions: This platform unites bias-free phenotypic assays with AI-guided clinical validation, enabling early identification of therapeutically meaningful and translatable drug candidates. Discovery of a shared mechanistic target and AI-predicted novel compounds demonstrates a clinically grounded, data-driven model for developing safe, effective, and chronic disease-oriented cancer therapies.
Keywords: Phenotypic screening; macropinocytosis; AI drug discovery; translational oncology; clinical validation; mechanistic clustering; combination therapy; drug repurposing; safety profiling

#6402 Identification of novel CRBN molecular glue ternary binders from a highly diverse CRBN MG library.

Qingbo Xu, Hailong Yang, Yongqiang Wang, **Zhenyu Wu**, Hongbo Zhang

HitChem, Wilmington, DE

High-throughput screening (HTS) of cereblon (CRBN) molecular glue (MG)-biased libraries remains a key strategy for proof-of-concept studies and hit identification against emerging targets. Because the CRBN binding pocket and its induced interface can adopt multiple conformations, and the substrate binding pocket is often unpredictable at the early stages of discovery, the structural diversity of both CRBN binders and substrate-recognition motifs is crucial to screening efficiency.In this work, we constructed a high-quality, CRBN MG-biased library derived from more than 40 validated CRBN binders. To further enhance chemical diversity, we introduced novel fragments using a tailored AI-based molecular generation model, designed to maximize variations in substrate-binding motifs. HTS case studies demonstrated that this library effectively identified CRBN-substrate ternary binders and degraders with unique scaffolds, representing promising starting points for further optimization.

#6403 High-content morphology profiling identifies autophagy-modulating compounds and their off-target activities.

Petr Dzubak[1], Alzbeta Srovnalova[2], Pavel Polishchuk[3], Anna Siskova[1], Martin Mistrik[4], Matthew Lacey[4], Marian Hajduch[4]

[1]Insititute of Molecular and Translational Medicine, Palacky University and University Hospital in Olomouc, Olomouc, Czech Republic,[2]Institute of Molecular and Translational Medicine, Palacky University and University Hospital in Olomouc, Olomouc, Czech Republic,[3]Faculty of Medicine and Dentistry,, Palacky University and University Hospital in Olomouc, Olomouc, Czech Republic,[4]Institute of Molecular and Translational Medicine, Palacky University and University Hospital in Olomouc, Olomouc, Czech Republic

Background: Autophagy gives many tumors a way to cope with stress, adjust their metabolism, and weather therapy. Compounds that interfere with this process, therefore, attract considerable interest. To efficiently spot such compounds, we rely on screening methods that detect subtle shifts in cell structure. The Cell Painting assay offers this possibility: by capturing rich morphological snapshots, it lets us see how different compounds alter organelles and pathways involved in autophagy.
Methods: We exposed HepG2 cells for 24 hours to several well-characterized autophagy inhibitors—chloroquine, bafilomycin A1, dauricine, daurisoline, and dorsomorphine—as well as two established activators, rapamycin and PP242. MCOPPB and its derivatives MS107 and MS108 were included in the same panels, alongside JUMP-target controls. After staining, we imaged the cells on a Yokogawa CV8000 microscope, recording four channels across nine fields per well. From these images, we extracted and normalized 1,065 single-cell features using pycytominer. Dimensionality reduction (UMAP) and correlation analyses were performed in R, and autophagy markers (LAMP2B, p62/SQSTM1, and LC3) were assessed by immunofluorescence.
Results: The morphological profiles separated inhibitors from activators with a clear margin, each group forming tight clusters. Inhibitors produced the expected signatures: a fragmented Golgi apparatus, swollen mitochondria, and expanded ER structures, all indicative of impaired autophagic flux. Compounds with known mechanisms behaved as anticipated. Strikingly, MCOPPB—usually classified as a NOP receptor agonist—fell directly into the inhibitor cluster. Follow-up staining corroborated this pattern: disrupted autophagosome-lysosome fusion, p62 accumulation, and LC3 changes all pointed toward autophagy inhibition.
Conclusion: Cell Painting proved effective at distinguishing autophagy-modulating compounds through their characteristic organelle-level effects. The unexpected behaviour of MCOPPB highlights a previously overlooked mechanism. Combining morphological profiling with marker-based validation provides a practical framework for identifying new modulators of autophagy with potential oncological relevance.
This work was supported by the Technology Agency of the Czech Republic project PERMED: T2BA (TN02000109). We also acknowledge the contributions from infrastructural projects CZ-OPENSCREEN (LM2023052), EATRIS-CZ (LM2023053), IGA_LF_2025_21, and the SALVAGE project (CZ.02.01.01/00/22_008/0004644) supported by OP JAK, with cofinancing from the EU and the State Budget.

#6404 A robust organoid-based platform for high-throughput screening and drug discovery.

Rene Overmeer, Mariana Martins Costa Silva, Gerben ten Hag, Mayke Doorn, Yasmine Abouleila, Ricardo Korporaal, Francisco Morales Rodriguez, Merel Derksen, Carla Verissimo, Robert G. J. Vries, Sylvia F. Boj

HUB Organoids B.V., Utrecht, Netherlands

Patient-derived organoids (PDOs), or HUB Organoids®, are advanced 3D models generated from adult stem cells of normal and malignant epithelial tissues and stored in high-quality biobanks to ensure reproducibility. HUB Organoids faithfully recapitulate the physiology, molecular heterogeneity, and morphological and functional characteristics of the original tissue, effectively mimicking patient response and bridging the gap between laboratory research and clinical application—bringing the “patient into the lab.” The rapid development of Petosemtamab (MCLA-158) exemplifies the value of organoid technology in drug development, as this target could not have been identified using conventional 2D models. Further supporting this, recent publications highlight the ability of organoids to predict treatment response in metastatic colorectal cancer. Here, we present our capabilities for medium- to high-throughput screening, enabling the evaluation of over 6,000 compounds across multiple organoid models in parallel. Available readouts include plate reader-based viability assays (CellTiter-Glo 3D) and imaging-based assays (CyQuant). Beyond initial large-scale screening, rapid iterations of follow-up structure-activity relationship (SAR) studies or expanded screening across diverse patient models are facilitated by the precision and reproducibility of our platform. In summary, we offer a robust, clinically relevant, and cost-effective platform to support drug development from early-stage compound screening to advanced validation studies.

#6405 Small-molecule screening of HiBiT-tagged PAX3::FOXO1 rhabdomyosarcoma cell lines identifies eltanexor as a potent therapeutic agent against fusion-positive rhabdomyosarcoma.

Soumili Dey[1], Yong Y. Kim[2], Katrina Jia[1], Mehal Churiwal[1], Michele Ceribelli[1], Teresa S. Hawley[1], Raj Chari[1], David Milewski[1], Young K. Song[1], Xinyu Wen[1], Hsien-Chao Chou[1], Vineela Gangalapudi[1], Jun S. Wei[1], Craig Thomas[1], Robert G. Hawley[3], Javed Khan[1]

[1]National Cancer Institute, NIH, Bethesda, MD,[2]Stanford University, Palo Alto, CA,[3]Anatomy & Regenerative Bio., The George Washington University, Washington

Introduction: Rhabdomyosarcoma (RMS) is a highly malignant soft tissue sarcoma. An aggressive subtype, fusion-positive RMS (FP-RMS), which is driven by PAX3/7::FOXO1 translocations, has a dismal 5-year overall survival rate of 13% for patients with metastatic disease. We hypothesized that targeting the oncogenic driver PAX3::FOXO1 with small molecules would be an effective treatment. To test this, we developed cell lines with endogenous PAX3::FOXO1 tagged with HiBiT epitope and performed a drug screen to identify drugs that downregulate PAX3::FOXO1 protein. **Study Design:** Using CRISPR-Cas9, we endogenously tagged PAX3::FOXO1 with HiBiT in two RMS cell lines (RH4 and SCMC), enabling the monitoring of PAX3::FOXO1 protein levels. We performed a drug screen using the Mechanism Interrogation Plate (MIPE) library of 2,480 compounds, of which 53% are FDA-approved or in clinical trials. NanoGlo Luciferase assays monitored levels of HiBiT-tagged PAX3::FOXO1, while CellTiterGlo measured cell viability at 24 hours. We selected hits that showed a difference in area under the curve (AUC) between the two readouts of ≥ 90 for drugs that preferentially reduce the fusion protein level over general cytotoxicity. We investigated whether inhibitors led to nuclear accumulation and reduced total protein levels using Western blot and immunofluorescent imaging. Candidates were validated in the parental cells and *in vivo* studies. **Results and Conclusions:** The screen identified 183 hits, including Eltanexor, an XPO1 inhibitor. XPO1 exports over 200 proteins from the nucleus by recognizing their nuclear export sequences (NESs). Since the fusion gene retains the NES of FOXO1, a known XPO1 target, we tested whether PAX3::FOXO1 is a substrate. We observed that Eltanexor enhanced PAX3::FOXO1 nuclear accumulation at 6 hours in RH4, and at 2 hours in SCMC, followed by protein downregulation at 24 hours by Western blotting. Furthermore, Eltanexor induced p53 nuclear accumulation, detectable at 6 hours in SCMC, suggesting that early accumulation of PAX3::FOXO1 may drive cytotoxicity. At 24 hours, RNA-seq in Eltanexor-treated cell lines demonstrated downregulation of PAX3::FOXO1 and MYCN signatures, components of the core regulatory network in FP-RMS. Preliminary *in vivo* studies also showed Eltanexor induces delays in tumor progression in an RMS xenograft model. Furthermore, Eltanexor in combination with Mivebresib, a validated BRD4 inhibitor, demonstrated significant synergy against FP-RMS cells. We will perform site-directed mutagenesis studies to disrupt PAX3::FOXO1's NES and validate combination with Mivebresib *in vivo*. In conclusion, we identified Eltanexor, an XPO1 inhibitor, as a novel therapeutic agent that suppressed PAX3::FOXO1 activity and levels, induced nuclear accumulation and led to cytotoxicity in incurable FP-RMS.

#6406 Accelerating selective cancer ligand discovery through an accessible phage display analysis suite.

Stephen Lees[1], Monica Shokeen[2], KIMBERLY KELLY[3]

[1]Biomedical Engineering, University of Virginia, Charlottesville, VA,[2]Washington University in St. Louis, St. Louis, MO,[3]University of Virginia, Charlottesville, VA

Identifying novel druggable targets remains a major challenge in cancer research. Of the approximately 5,000 potentially druggable cancer genes found through various sequencing techniques, 94% are well characterized, yet only 14.3% have approved drugs. This gap highlights the limitations of indirect, sequence-driven approaches, which infer targets rather than directly measuring functional binding. Direct discovery platforms like phage display help overcome this barrier by screening ligands in biologically relevant contexts. Phage display is a high-throughput screening technology that presents vast libraries of randomized peptides or proteins on bacteriophage surfaces to identify ligands that selectively bind cancer associated targets. Broader use of this technique is limited by restricted access to high-diversity libraries and the absence of standardized, user-friendly pipelines for analyzing next-generation sequencing (NGS) phage screen data. These barriers make it difficult to distinguish true binders from artifacts caused by non-specific binding, amplification bias, or sequencing noise. These challenges are especially pronounced in whole-cell and tissue-based screens, where identifying true binders is critical for discovering targets in authentic cancer environments. To address these limitations, we developed a high-diversity ($>10^8$), disulfide-constrained, variable-loop-length peptide library optimized for cancer target discovery, along with a unified phage screen NGS analysis pipeline. The library design supports high-affinity binders and enables analysis of sequence and loop-size biases across targets. The software pipeline provides a standardized processing workflow which directly influences downstream analysis. Machine-learning-based denoising and robust motif discovery further improve identification of enriched sequences and true binders. The platform has been validated with established protein-target screens and successfully used to identify ligands selective for known protein targets in multiple myeloma. These results provide a strong foundation for ongoing whole-cell panning on drug-resistant multiple myeloma lines to discover ligands with therapeutic and diagnostic potential. Our long-term aim is to build a community-driven database of phage screens processed with this unified pipeline, analogous to TCGA for RNA-seq, allowing cross-study comparisons and in-silico identification of ligands or binding motifs selective for cancer instead of surrounding healthy tissue. This standardized platform lowers barriers to actionable ligand discovery in cancer research and accelerates the development of selective agents for cancer therapeutics.

#6407 Deep learning-driven image analysis for tracking nucleolar morphology.

Leif E. Lindberg[1], Katelyn R. Alley[1], Sylvia M. Kennerly[1], Ian Reynolds[1], Ryan W. Holly[2], Jongtae Yang[2], Chris L. Vonnegutt[2], John C. Rogers[2], Victoria J. DeRose[1]

[1]Chemistry and Biochemistry, University of Oregon, Eugene, OR,[2]Thermo Fisher Scientific, Eugene, OR

Introduction: The nucleolus, a membraneless nuclear organelle responsible for ribosome production, is highly sensitive to stress. A subset of chemotherapeutic drugs induce nucleolar stress, which could influence their apoptotic mechanisms. However, tracking morphological changes of the nucleolus during treatment remains challenging due to its amorphic state and nanoscale organization. A major bottleneck for drug screening and mechanistic studies is the reliance on time-intensive manual imaging and immunostaining to identify nucleolar stress. To overcome this we have developed a suite of image analysis models to rapidly identify and classify cells.

Methods: The mechanisms that lead to nucleolar stress by small molecules and mechanisms that allow the nucleolus to recover from reversible stress remain unclear. To facilitate time-dependent morphological studies as well as general drug screening for nucleolar defects, we developed deep learning models leveraging Thermo Fisher Scientific's RNA-selective dyes to automatically detect and quantify nucleolar stress from microscopy images. Using osteosarcoma cells, we successfully classified stressed and unstressed populations with SYTO™ RNASelect™ Red, a novel RNA-selective dye developed by Thermo Fisher Scientific. This dye can be implemented into rapid high-throughput imaging methods for cancer detection and drug screening. Using these deep-learning models we can rapidly screen for novel chemotherapeutics and study the efficacy of current nucleolar stress-causing drugs.

Results: Osteosarcoma cells labeled with SYTO™ RNASelect™ Red and treated with chemotherapeutics display distinct nucleolar staining enabling precise segmentation and quantitative analysis. Under chemotherapeutic treatment nucleoli decrease in size and become more rounded. Our deep learning models not only identify which cells are experiencing nucleolar stress but also determine the specific stage of stress for each cell. These results have been validated through current known methods to identify nucleolar stress such as immunocytochemistry and RNA production assays. This platform now allows us to investigate how cells recover from reversible nucleolar stress, providing a high-throughput approach to dissect nucleolar function, resilience, and responses to chemotherapeutic treatment.

Conclusions: SYTO™ RNASelect™ Red is an effective RNA dye because it provides a bright stain for the nucleolus, enabling clear segmentation and quantitative analysis using machine learning. Its compatibility with immunocytochemistry allows for high-resolution, dynamic studies of RNA biology and cellular stress responses, making it a versatile tool for both single cell and population-level investigations. This dye, coupled with our deep-learning methods, opens the door to broad screening protocols, allowing for a spectrum of drug candidates to be tested rapidly.

#6408 Unlocking the unlockable: AS-MS for swift hit identification against challenging targets.

Renaud Renaud

Edelris SAS, Lyon, France

Affinity selection-mass spectrometry (AS-MS) is a label-free, high-throughput platform that can be used to screen small-molecule ligands by incubating them with biomolecular targets, separating bound complexes via size-exclusion or ultrafiltration, and detecting binders using high-resolution mass spectrometry. This approach bypasses the need for chemical modifications, fluorescent tags, or functional assays, thereby preserving native binding interactions and minimizing artifacts. As a label-free method, it allows for the rapid evaluation of large libraries and ranking of binding affinities without requiring functional data. Additionally, the flexibility of AS-MS enables diverse hit identification strategies, including exploration of combinatorial libraries while remaining agnostic to binding sites or mechanisms, thus uncovering novel allosteric and orthosteric ligands.In particular, the versatility of AS-MS enables adaptation of affinity selection methods to target particularities by relying on SEC-based, filter-based, or pull-down techniques. These orthogonal selection modalities can be fine-tuned—by adjusting buffer conditions, SEC polymers and volume, incubation times, wash volumes, or competitive inhibitors—to modulate assay sensitivity and selectivity, thereby maximizing enrichment for ligands with desired on/off rates. In conjunction with chemically diverse libraries, it is a powerful and highly effective approach to identify agents with innovative mechanisms of action.As an illustration of how AS-MS accelerates drug discovery by accessing challenging or “undruggable” targets lacking enzymatic activity or favorable binding pockets, we present here several case studies. In these, we have utilized AS-MS screening technology in the search for novel molecular glues and targeted protein degraders (on the VHL-BRD3 pair and other undisclosed targets), and against a wide range of challenging targets, including transcription factors (such as TEAD), RNAs, and membrane proteins such as GPCRs or ion channels (P2X4 receptor), either as isolated targets or embedded in membrane preparations.In summary, AS-MS accelerates discovery against intractable targets, compressing timelines and delivering validated, mechanism-rich hits for optimization. Its integration with downstream biophysics (e.g., SPR, NMR) and structural biology further validates hits, paving the way for next-generation therapeutics against previously intractable disease drivers.

#6409 AI-accelerated discovery of B7-H3 and DLL3-targeted cyclic peptide radioligands: From library design to preclinical validation.

Tj (Tiejun) Bing

ICE Bioscience, Beijing, China

Background: Radiopharmaceutical drug conjugates (RDCs) represent a transformative paradigm in precision oncology, yet target-specific ligand discovery remains a critical bottleneck. We developed an integrated AI-augmented platform to rapidly identify cyclic peptide binders for two emerging RDC targets: B7-H3 (immune checkpoint) and DLL3 (Notch ligand).
Methods: A structurally diverse phage display library (1.5×10^{11}capacity; 8-17 aa macrocycles) was engineered with NGS-validated complexity. Recombinant 4Ig-B7-H3 (2Ig-B7-H3 as off-target counterscreens), DLL3 (and counterscreens DLL1/DLL4) underwent orthogonal biophysical characterization by SPR and Spectral shift assay (SPS). Hit triangulation employed: (1) Deep sequencing-driven consensus motif analysis, (2) AlphaFold3 multimer modeling of peptide-target complexes, and (3) Parallel SPR/spectral shift assays (10^{-7} M affinity threshold). Top candidates were Cy5-labeled for real-time binding and internalization kinetics in engineered tumor lines.
Results: Discovery: 15/40 phage clones demonstrated target binding - AI optimization: AlphaFold3 predictions revealed a conserved β-turn motif in 7/15 top hits that anchors to a cryptic pocket in targets - Validation: Hit peptide were synthesized and showed: (i) KD 8.2×10^{-7} M (SPR), (ii) >3-fold selectivity over homologous target proteins (iii) showed binding on cells
Conclusions: This platform addresses critical challenges in RDC development by providing a streamlined solution for hit discovery, optimization, and validation. The integration of AI-driven structural prediction with high-throughput experimental validation compresses traditional hit discovery timelines This platform will significantly accelerate the RDC development pipeline—especially for hit binder identification for neo tumor antigens or other validated surface proteins like GPCRs, transporters, to accelerate RDC drug discovery using cyclic peptide as the modality.

#6410 mtKO: A dedicated guide RNA library for mitochondria redox biology research.

Karambir Kaur[1], Fengchao Lang[1], **Chunzhang Yang**[2]

[1]NIH-NOB (Neuro-Oncology Branch), Bethesda, MD,[2]NIH-NOB (Neuro-Oncology Branch), Bethesda, Maryland, MD

Mitochondria are multifunctional organelles essential for both physiological regulation and pathological progression. In malignant cancer cells, mitochondrial reprogramming establishes a metabolic foundation that supports tumor growth, which is essential for cancer cells to overcome intrinsic metabolic abnormalities and stress. To uncover key mitochondrial pathways involved in cancer development, we developed mitochondrial Knockout (mtKO) — a robust, flexible, and unbiased CRISPR/Cas9 guide RNA screening platform designed to systematically identify critical mitochondria-associated functions. The mtKO library target genes involved in diverse mitochondrial-guided processes, including biosynthesis, transmembrane transport, oxidative phosphorylation, and redox regulation. Through a mtKO dropout screen, we identified the mitochondrial antioxidant enzyme superoxide dismutase 2 (SOD2) as indispensable for the fitness and survival of cancer cells harboring oncogenic mutations in isocitrate dehydrogenase 1 (IDH1). Mechanistically, SOD2 mitigates mitochondrial reactive oxygen species (ROS) generated by dysfunctional Krebs cycle activity in IDH1-mutant glioma and chondrosarcoma cells. Functionally, SOD2 maintains redox homeostasis and preserves mitochondrial integrity thereby controlling disease manifestation both *in vitro* and *in vivo*. Overall, our study introduces a powerful functional genomics approach to interrogate mitochondrial biology and uncovers a selective mitochondrial redox vulnerability in Krebs cycle-deficient cancers, highlighting mitochondrial redox imbalance as a potential therapeutic target.

#6411 A high content live cell cancer toolbox uniquely enabled by high throughput imaging.

Matthew Boisvert, Lydia Hernandez

Araceli Biosciences Inc., Portland, OR

Live cell imaging assays are essential for in vitro cancer biology, enabling interrogation of cellular state over time, tracking changes in growth and phenotype. High content imaging (HCI), where resolution and multiparametric quantification is key to extracting insight from cellular features, is stymied by slow imaging times, preventing live cell screens at scale. However, the Araceli Endeavor® newly enables live cell high throughput high content imaging, capturing the majority of cells in a 1536-well plate in <6 minutes in 5 channels with submicron resolution. Here, we apply this speed to cancer biology, scaling up the subcellular detail of HCI to live cell screening over a multi-day time-course. We first examine cell growth and quantify where cells are in the cell cycle based on DNA content and morphology, showing changes over time in response to drug treatment. Using fluorescent dyes, we further assess changes in cell death, mitochondrial function and cellular morphology, as well as evaluate cell proliferation. High resolution brightfield imaging, added to fluorescent imaging here in <30 seconds/run, provides a dynamic, unbiased look into off-target effects and generates the detailed image features needed for machine-learning-based analysis.

Both proliferation and cell cycle measurements are traditionally done with fixed endpoint flow cytometry but these assays have limited insight. Live assays are far more revealing and vital to drug development. For instance, potential therapeutics may appear to suppress cancer in vitro, only for growth to rebound hours later, or this fixed endpoint may miss the window where a treatment is effective altogether. Unlike traditional HCI, Endeavor's speed ensures that the first well is the same state as the last, not hours older. Overall, live cell HCI offers exquisitely detailed insight over time: here correlating cell growth, death, location, morphology, and mitochondrial dynamics in a single assay, at the speed and scale required for modern screening.

#6412 Development of a high-throughput assay platform for the screening of selective integrin inhibitors in cancer.

Ziwei Zhang, Yu Zhou, **Peichuan Zhang**, Zhonghua Yan

WuXi AppTec, Shanghai, China

Integrins are critical mediators of cancer progression, facilitating cancer cell invasion, survival in circulation, and metastatic outgrowth. Integrins result in cancer progression by activating pro-survival signaling pathways and remodeling the cancer microenvironment, and thus represent promising targets for anticancer treatments. To accelerate the discovery of novel integrin-targeted therapeutics, we developed an integrated platform of high-throughput screening assays for the evaluating integrin inhibitors of diverse modalities, including small molecules, peptides, antibodies, and antibody-drug conjugates. In this study, we developed a panel of cell-free fluorescence polarization (FP) assays in 384-well plate format using a Cy3B-RGD probe to screen compounds against multiple RGD-binding integrins (αvβ1, αvβ3, αvβ5, αvβ6, αvβ8 and α8β1). In addition, we generated HEK293 cell lines stably overexpressing integrins such as α8β1, and developed ELISA as well as IncuCyte based α8β1-Mfge8 competition binding assays for compounds screening in cell-based assays. The assay results were further validated using cancer cell lines endogenously expressing high levels of integrins such as α8β1, confirming compound binding and activity in a more physiologically relevant model. In summary, we have created a robust high-throughput screening platform that combines cell-free and cell-based assays. This integrated integrin assay platform enables the efficient evaluation of selective integrin inhibitors, accelerating the development of novel integrin inhibitors for target-based cancer treatment.

#6413 Cellular DNA-Encoded Library (DEL) Screening Coupled with MICRO-TAG Real-Time Cellular Target Engagement Enables Discovery of Novel Therapeutics.

Ivan Babic, **Elmar Nurmemmedov**

CellarisBio, San Diego, CA

Transcription factors are challenging drug targets that require the native cellular environment for interrogation of direct engagement with potential therapeutic candidates. The transcription factor β-catenin is a therapeutically valuable yet challenging drug target, serving as signaling hub of the complex and highly interconnected WNT signaling network. Its central role and extensive pathway crosstalk have complicated efforts to distinguish effectors that bind β-catenin directly from those acting indirectly through upstream WNT components. This mechanistic distinction is critical for guiding rational drug discovery. We applied the MICRO-TAG® Cell Target Engagement technology to interrogate 25 reported β-catenin/WNT effectors. Using a novel direct target engagement system employing real-time temperature series, we quantified ligand-dependent stabilization of β-catenin across multiple doses, profiling their cellular target engagement potencies, under cellular conditions. Parallel functional assays, including TOPFlash reporter activity and WNT-responsive surface markers, integrated direct binding with downstream signaling readouts. This integrated approach distinguished direct β-catenin binders from effectors acting indirectly through upstream pathway components. By coupling cellular target engagement with functional readout, the MICRO-TAG® system enables scalable, mechanism-resolved drug discovery system for complex signaling pathways. This approach establishes a new paradigm for functionally interrogating therapeutic candidates through integrated target engagement and functional readout, within a unified, quantitative, and biologically relevant framework that is readily translatable to other challenging drug targets.

#6414 Ultra-sensitive structural biomarker discovery for TNBC and pancreatic cancer using a deep VHH repertoire (IBMET): A translational platform for tissue-agnostic target identification.

Akihiro Imura[1], Ryota Maeda[1], Hiroyuki Yamazaki[1], Tsuyoshi Inoue[2], Sadako Aakashi-Tanaka[3], Hiroko Tsukada[3]

[1]COGNANO INC., Kyoto, Japan,[2]Pharmaceutical Sciences, Osaka University, Suita, Japan,[3]Breast Surgery, Tokyo Women's Medical University, Tokyo, Japan

Background: In cancers with substantial unmet medical need (UMN), the limited availability of reliable and tumor-selective surface biomarkers continues to hinder therapeutic development. This challenge is particularly evident in triple-negative breast cancer (TNBC) and pancreatic ductal adenocarcinoma (PDAC), where currently available targets often show insufficient specificity or restricted applicability across patient subgroups.
Methods: We established the Inverse Biomarker Exploration Technology (IBMET), a systematic framework designed to detect pathological structural alterations on tumor cells. IBMET utilizes a large alpaca-derived VHH antibody repertoire as highly sensitive structural probes. Alpacas were immunized with multiple tumor cell lines, and the resulting VHH library was analyzed using phage display and next-generation sequencing. Candidate antibodies were selected based on statistical enrichment and evaluated by IHC/IF across an extensive panel of tumor and normal tissues. Antigen identification was performed by cross-linking immunoprecipitation, SDS-PAGE, and LC-MS/MS. Clinical relevance was examined using a breast cancer biopsy cohort (n = 106).
Results: IBMET identified several structural biomarker candidates relevant to TNBC and PDAC. The lead antibody, VHH89, selectively recognized a previously uncharacterized low-molecular-weight isoform of ALCAM (approximately 70 kDa; designated ALCAM70). VHH89 showed lesion-selective staining in tumor tissues with minimal reactivity in normal organs, indicating a high degree of tumor specificity. In clinical breast cancer specimens, VHH89 demonstrated positivity in more than 20% of TNBC cases. In addition, subsets of pancreatic cancer and cholangiocarcinoma specimens also showed VHH89 positivity, suggesting that this isoform may represent a structurally altered antigen present across multiple tumor types.
Conclusion: IBMET offers a reproducible and scalable approach for identifying structurally defined biomarkers that may not be detectable using genomic or transcriptomic analyses alone. By systematically excluding antibodies that react with normal tissues and enriching for tumor-associated conformational epitopes, IBMET broadens the spectrum of actionable targets for aggressive cancers. These findings support the potential integration of IBMET-derived antibodies into the development of next-generation antibody-drug conjugates, radioligand therapies, and companion diagnostics. To facilitate broader validation, COGNANO will make eight PDAC-selective VHH antibodies available for research use at AACR 2026.

#6415 Champions: Scalable chem-seq and functional-seq platforms for profiling chemical and genetic perturbations in patient-derived organoids.

Devin Porter[1], BanuPriya Sridharan[2], Gervaise Henry[1], Kakajan Komurov[1], Yamini Nallana[1], Brandon Walling[1]

[1]Champions Oncology (Rockville, MD), Rockville, MD,[2]Champions Oncology, Inc. (Hackensack, NJ), Hackensack, NJ

Background :
Large-scale functional drug screening has been limited by low throughput reliance on simple 2D systems and a lack of high-resolution mechanistic readouts. To address these challenges, we implemented Chem-Seq and Functional-Seq, scalable transcriptomic profiling platforms that enable high-content screening of both chemical and genetic perturbations in clinically relevant cancer models.
Methods :
Experiments were conducted across six tumor models, including cell lines and four patient-derived xenograft organoids from Champions Oncology's proprietary Patient-Derived Xenograft Organoid (PDXO) bank, which preserves tumor heterogeneity and 3D architecture. We applied Chem-Seq to 44 standard-of-care (SOC) oncology therapeutics spanning diverse pathways, including MAPK, PI3K/AKT/mTOR, CDK, EGFR/HER2, MET, AMPK, proteasome, and topoisomerase inhibition. Compounds were tested at various concentrations to capture dose-dependent transcriptional changes and pathway-specific effects. Functional-Seq was performed in parallel using siRNA-mediated knockdown of selected drug targets to generate loss-of-function signatures that anchor interpretation of Chem-seq profiles. This also serves as a proof-of-concept for using a predefined siRNA signature bank to match unknown compounds in larger screens.
Results :
Chem-Seq produced robust transcriptional signatures with high reproducibility across replicates. SOC compounds targeting the same pathway (e.g., MEK, PI3K, EGFR) clustered cohesively, while structurally distinct inhibitors of related pathways were separable. Functional-Seq knockdowns phenocopied chemical inhibition of select targets, confirming on-target activity. Dose-response profiling revealed concentration-dependent separation of cytotoxic versus pathway-selective signatures, demonstrating sensitivity and dynamic range.
Future Directions and Conclusions:
Following validation, the workflow will scale to ~50,000 perturbations per week. Combined with the PDXO bank, this high-dimensional dataset will be leveraged to support mechanistic insight, compound prioritization, and toxicity prediction. Additionally, machine-learning tools can be applied to predict compound responses and guide de novo compound generation for desired traits. By integrating high-throughput transcriptomics with patient-derived 3D biology and AI-driven analytics, this platform offers a powerful, scalable tool for accelerating preclinical drug discovery and advancing personalized therapeutic strategies.

#6416 DEL-chemomics approach for the discovery of targeted protein degraders for cancer therapy.

Ying Zhang[1], Anthony D. Keefe[2], Matthew A. Clark[1], Marie-Aude Guie[2], John Guilinger[1]

[1]X-Chem Pharmaceuticals, Waltham, MA,[2]X-Chem, Inc., X-Chem, Inc., MA

DNA-encoded chemical library (DEL) technology has become a powerful tool for hit identification, enabling the efficient screening of large collections of encoded compounds with advantages over traditional high-throughput screening in terms of library size, cost, and resource efficiency. The high chemical diversity and encoding fidelity of DELs yields extensive data that can support computational approaches such as machine learning (ML), 3D pharmacophore generation and structure-based discovery. This DEL-chemomics approach has been applied to the discovery of novel E3 ligase receptor ligands, expanding the repertoire of E3 ligands beyond the traditional CRBN and VHL for degradation of drug targets. A case study of the discovery of DCAF1 ligand and its application in PROTACs that targeted WDR5 for degradation will be presented.

#6417 High-throughput peptide screening for radioligands by DNA encoded libraries.

Yihui Xie

BioDuro, Irvine, CA

Targeting ligands play a critical role in radiopharmaceuticals for cancer diagnosis and therapy. Due to their excellent binding affinity and specificity, peptides have been widely used to conjugate with radionuclides for delivery to cancer cells in targeted lesions. Current high-throughput de novo peptide hit finding heavily relies on phage display and mRNA display. While efficient, the generation of those peptide libraries is still limited by the biological translation process. As an emerging peptide screening approach, DNA encoded library technology (DELT) offers a higher degree of chemical flexibility. Unnatural amino acids and a variety of cyclization strategies that are inaccessible to display technologies can be readily incorporated into DEL peptides, leading to improved pharmacokinetic profiles including prolonged retention time and increased in vivo stability. Here we report our efforts in developing billion-member peptide libraries and primary screening for radioligand discovery through DELT, followed by high-throughput solid-phase synthesis that accelerates hit confirmation and affinity maturation.

#6418 Adapting the SAR-MAP chemical biology platform to target tumor immune checkpoints.

Hannah L. Thirman[1], Stephanie Medina[1], Jonathan M. Irish[2]

[1]Vanderbilt University, Nashville, TN,[2]University of Colorado, Aurora, CO

A major challenge in preclinical drug discovery is adapting deep cellular profiling of complex primary human cells to scalable small-molecule screening and subsequent structure-activity relationship (SAR) studies. This is especially the case when the goal is to target an intercellular interaction, such as a tumor immune checkpoint. We previously developed Structure-Activity Relationships by Multiplexed Activity Profiling (SAR-MAP; PMC12313981), a single cell chemical biology platform that quantitatively maps how small structural changes in compounds can drive distinct functional responses within human cells. SAR-MAP integrates phospho-specific flow cytometry with fluorescent cell barcoding to efficiently profile dozens of key intracellular signaling nodes, surface markers, and cell states in parallel. This platform revealed previously unrecognized mechanistic heterogeneity for the rocaglate natural product family, including a structural feature that confers selective anti-leukemia activity. Here we adapted SAR-MAP to primary human macrophages and established a scalable screening assay capable of dissecting IFN-γ responsive pathways, immune checkpoint regulation, and fundamental immune-relevant signaling nodes within a single experiment. Monocytes were isolated from peripheral blood, differentiated, and polarized to an M1-like proinflammatory state using IFN-γ in a fluorescently barcoded 96-well format suited for screening and iterative SAR. Multiplexed activity profiling quantified key functional and surface markers including PD-L1, CD14, CD206, and CD32, confirming that IFN-γ polarization robustly induces PD-L1 relative to baseline macrophages. This adaptation enables simultaneous evaluation of multiple mechanisms regulating immune checkpoint expression, including direct PD-L1 blockade, modulation of IFN-γ, and JAK-STAT1 or mTOR pathway interference. Small molecules that selectively modulate these pathways not only have translational relevance but may also illuminate previously unrecognized targets and mechanisms governing immune regulation. Together, these studies further establish SAR-MAP as a scalable, high-content approach for linking chemical structure to immune regulation in primary human cells.

#6419 Automated culture and AI-enabled image analysis of compound responses in patient-derived colorectal cancer organoids.

Oksana Sirenko[1], Prathyushakrishna Macha[1], Zhisong Tong[1], Nikki Carter[2], Felix Spira[1]

[1]Molecular Devices, LLC, San Jose, CA,[2]Molecular Devices, LLC (Moldev), San Jose, CA

Organoids transformed biomedical research by providing physiologically relevant models for cancer studies, essential for investigating disease mechanisms and drug responses. However, manual organoid culture processes are labor-intensive and prone to variability, limiting widespread adoption. Additionally, extracting information from complex biological systems remains a major challenge in organoid research. Here, we present the development of methods for automated culture, expansion, and end-point assays using patient-derived organoids, combined with machine-learning approaches for image-based analysis of compound responses. Patient-derived colorectal cancer (CRC) organoids were cultured in Matrigel domes using the CellXpress.ai automated cell culture system, which enables automated seeding, media exchanges, imaging, and passaging. Imaging and media exchanges were set periodically, while passaging was either triggered by users or automatically, based on image analysis and phenotypes of organoids. Using this system, we successfully maintained organoid cultures for over a month and expanded them to quantities sufficient for multiple 96-well assay plates. Cultured organoids were treated with a panel of anti-cancer drugs representing diverse mechanisms of action. Dose-dependent effects on organoid morphology and cell viability were evaluated using automated confocal high-content imaging. Following drug treatment, organoids were either stained live with viability dyes or fixed and stained with a panel of markers for nuclei, cytoskeleton, mitochondria, and RNA content. Images were analyzed using a deep learning model in IN Carta analysis software. Machine learning tools offer an unbiased and comprehensive approach to analysis by automatically identifying organoids and scoring them as intact or damaged. The analysis protocol extracted a panel of quantitative features per organoid. These included morphological descriptors, intensity metrics across three fluorescent channels, textural features, and spatial distribution patterns. Features were extracted enabling multidimensional phenotypic profiling of organoid populations. Classification was performed using a combination of unsupervised and supervised machine learning. Unsupervised clustering grouped organoids into phenotypic clusters based on feature similarity, which were then curated into biologically relevant categories using user-defined criteria. The classification allowed evaluation of compound effects in a concentration-dependent manner. Unlike single-parameter readouts, this approach incorporates a broad morphological context. In summary, we demonstrated a fully automated workflow for evaluation of compound effects using 3D human organoids. The described approach enables AI-driven phenotypic profiling for assessing drug-induced effects in organoid models.

#6420 Monitoring S-adenosylmethionine (SAM) and S-Adenosyl homocysteine (SAH) using a homogeneous luminescent assay.

Said Goueli[1], Dareen Mikheil[2], Nathan H. Murray[3], Kevin Hsiao[4], Hui Wang[5], Matt Larsen[5]

[1]Promega, Madison, WI,[2]Research and development, Promega Corp., Madison, WI,[3]Research, Promega Corp., Madison, WI,[4]Research and Development, Promega Corp., Madison, WI,[5]Promega Biosciences, San Louis Obispo, CA

Methylation is the enzymatic process of transferring a methyl group (-CH_3) to a substrate molecule (DNA, RNA, proteins, lipids, small metabolites). The universal substrate and product for these methyltransferases are S-Adenosyl Methionine (SAM) and S-Adenosyl homocysteine (SAH) respectively. SAH is a competitive inhibitor of many methyltransferase reactions. Thus, high SAH leads to reduced methylation capacity. More recently, there's an immunometabolic angle where tumor cells can out-compete CD8+ T cells for SAM/SAH availability, impairing T-cell survival; and supplementing SAM improved T-cell effector function and reduced tumor growth in vivo. Other cancers such as hepatic cancer were reported to have reduced SAM/SAH ratio because SAM production is impaired and/or SAH accumulates, leading to disturbed methylation and potentially contributing to oncogenes. One-carbon metabolism (methionine cycle, folate cycle, trans-sulfuration) is tightly integrated with cellular signaling and metabolic status thus, nutrient supply, amino acid availability, redox state, methyl donor availability all influence signaling pathways. The SAM/SAH ratio is therefore a "metabolic sensor" to some degree. Thus, it is apparent that the "ratio" of SAM to SAH is often used as a surrogate metric for cellular "methylation potential" or "methylation index". Thus, development of an assay that monitors the concentration of SAM and SAH and thus SAM/SAH ration determination is needed to investigate the role of SAM/SAH ratio in normal and abnormal physiological processes. Current methods to monitor these metabolites include LC-MS/MS, or ELISA in some cases in the relevant cellular/tissue context. We have found ELISA not to be reliable assay for SAM since all commercially available assays do not measure SAM and LC-MS/MS requires technical expertise and expensive equipment. Towards this goal we embarked on the development of homogenous assay that is simple and amenable to high throughput formatting. The assay relies on the complementation of nanoluc luciferase fragments that are linked to two interacting molecules. We use an SAM selective aptamer that is biotinylated, and Streptavidin linked to nanoluc large fragments. In the presence of SAM linked to the small nanoluc fragment, the proximity of the two fragments results in complementation of nanoluc luciferase and upon addition of Fumerazine substrate, light is generated. However, in the presence of free SAM, it competes with SAM linked to the small fragment (sensor) and thus no complementation of nanoluc occurs and no light. A decreasing signal indicates high SAM concentration and high signal indicates the absence or low SAM. Similar strategy was followed to develop a SAH sensor. The assays are homogenous, sensitive and easy to use and selective for SAM and SAH and we demonstrate it utility in monitoring SAM/SAH ratio changes in different physiological models.

#6421 Enabling phenotypic high-throughput drug screening with patient-derived organoids.

Abraham Lin[1], Maxim Le Compte[1], Rebecca Stone[2], Tyler Gilcrest[2], Edgar Cardenas De La Hoz[3], Geert Roeyen[4], Jeroen M. H. Hendriks[5], Filip Lardon[1], Christophe Deben[1]

[1]Center for Oncological Research, University of Antwerp, Wilrijk, Belgium,[2]Orbits Oncology, Palo Alto, CA,[3]Industrial Vision Lab, University of Antwerp, Antwerp, Belgium,[4]Department of Hepatobiliary Transplantation & Endocrine Surgery, University Hospital Antwerp, Wilrijk, Belgium,[5]Thoracic and Vascular Surgery, University Hospital Antwerp, Wilrijk, Belgium

Patient-derived organoids (PDOs) can recapitulate patient tumors in the lab, making them more realistic models compared to traditional *in vitro* cell cultures. However, challenges in reproducibility, standardization, and analysis have limited the use of PDOs in drug discovery, especially for high-throughput screening (HTS) applications. To address this, we have developed an efficient workflow, using automation equipment and interoperable computational platforms to facilitate the adoption of PDOs for HTS applications[1]. Our protocol leverages live-cell imaging techniques to capture the dynamic, complex PDO-drug interactions for more comprehensive analysis. Using label-free detection of organoids from brightfield images, we integrated growth-rate-based drug response metrics[2] with drug synergy metrics to significantly improve the identification of synergistic drug interactions[3]. Here, we screened 10 distinct drug combinations on 10 PDOs, sourced from healthy lung, non-small cell lung cancer, and pancreatic ductal adenocarcinoma. In particular, we focused on repurposing the Thioredoxin reductase inhibitor, Auranofin. This screen required a total of 20 384-well plates and resulted in 37,000 images captures. With lab automation, organoid seeding only took 1 hour, and with analysis automation, all 37,000 images were analyzed in under 8 hours. Altogether, we identified drug candidates that can synergistically enhanced the efficacy of Auranofin in a tumor selective manner. Our study highlights the advantage of combining lab automation with computational automation to enable HTS with PDOs. The implementation of our method supports the current push by the FDA to reduce animal experimentation for the discovery of effective therapeutic strategies. We are now further investigating streamlined integration techniques between different lab automation systems.

[1] Le Compte, M., et al *JoVE* 190 (2022) [2] Deben, C., et al *Communications Biology* 1612 (2024) [3] Deben, C., et al *Journal of Experimental & Clinical Cancer Research* 88(2024)

#6422 A 3D bioprinted vascularized tumor tissue model of non-small cell lung cancer: A model for drug screening.

Fahimeh Shahabipour[1], Yuchi Chen[1], Yen-Ting Tung[2], Min Jae Song[2], Marc Ferrer[3]

[1]NIH-NCATS (National Center for Advancing Translational Sciences), Bethesda, MD,[2]NIH-NCATS (National Center for Advancing Translational Sciences), Rockville, MD,[3]NCAT/NIH, Rockville, MD

Lung cancer remains the leading cause of cancer-related death worldwide, with non-small cell lung cancer (NSCLC) accounting for 80-85% of all cases. There is therefore a need for new, effective treatments for lung cancer. A major challenge in preclinical drug development is the lack of assay platforms that accurately recapitulate the tumor microenvironment (TME), thereby enabling the investigation of cell-cell interactions between the tumor and surrounding stroma cells. To address this gap, we have developed a 3D-bioprinted vascularized lung cancer tissue model in a 96-well format that incorporates human NSCLC cells within a physiologically relevant TME. The TME tissue model includes GFP-expressing lung endothelial cells, pericytes, and fibroblasts that form a vascular network, surrounded by RFP-expressing NSCLC cells (A549, H1975, or H460). Using this platform, we conducted quantitative fluorescence cell imaging to assess vascular morphology, including angiogenesis and tumor growth. Our results revealed distinct tumor morphologies for each of the three NSCLC cell lines used, with H1975 cells showing migration toward the vessels and forming irregular tumor shapes. In contrast, H460 cells formed spheroidal tumors, with no migration to the vessels. We are currently conducting single-cell RNA sequencing on these tissue models and will apply a pharmacogenomics approach to identify novel therapeutic targets based on cancer cell-tumor microenvironment (TME) interactions. This engineered 3D lung cancer model provides a scalable, clinically relevant approach to discovering new treatments for NSCLC patients.

#6423 DNA-encoded chemical library screening for glue discovery for oncology targets.

Anthony D. Keefe, Paolo A. Centrella, Zhen Chen, Matthew A. Clark, Paige Dickson, Marie-Aude Guie, John P. Guilinger, Ying Zhang

X-Chem Inc., Waltham, MA

There is considerable interest in the discovery of novel molecular glues that induce proximity between oncology targets and their modulators. Induced proximity can be used to degrade proteins by a range of mechanisms, including ubiquitination and trafficking to the proteasome. DNA-Encoded Chemical Library screening can readily be adapted to the discovery of glues, and we will describe case studies that exemplify how carefully designed screening campaigns with highly diverse encoded compound libraries can identify small molecules capable of inducing proximity. Case studies will include a small molecule discovered in a DEL screen against ATAD2 that is able to inappropriately dimerize ATAD2 thereby reducing its ability to bind to acetylated histones and an activator of the integrated stress response pathway that only binds to the eIF2b complex, not its isolated components, thereby stabilizing it.

#6424 MICRO-TAG® cell target engagement redefines GPCR drug discovery with functional relevance.

Ivan Babic, Elmar Nurmemmedov

CellarisBio, San Diego, CA

G protein-coupled receptors (GPCRs) form the largest and most pharmacologically important family of membrane proteins, translating extracellular cues into intracellular signaling cascades. As master regulators of cell metabolism, differentiation, growth, neurotransmission, and sensory perception, GPCRs remain among the most valuable yet technically challenging therapeutic targets. Discovery of drugs targeting these receptors is a challenge in early drug discovery. Conventional biophysical methods that rely on recombinant or purified proteins have achieved limited success, as they poorly capture the structural and functional relevance of GPCRs outside of their native cellular context. Here, we present the MICRO-TAG® Cell Target Engagement platform as a cellular and translatable assay system capable of identifying and functionally validating compounds that directly bind GPCRs in their native membrane environment. Using GPR75 — a receptor implicated in obesity, cancer, and metabolic syndrome—as a model, we demonstrate the ability of MICRO-TAG® to: (1) detect direct ligand-receptor binding, (2) monitor downstream GPCR signaling, and (3) provide sensitive reporter-based readouts of agonist or antagonist activity. By integrating direct target engagement with functional pathway interrogation in a cellular environment, MICRO-TAG® enables scalable and physiologically relevant drug discovery for some of the most challenging drug target classes in biology.

#6425 High throughput screening identifies novel drugs for calreticulin surface translocation in pancreatic ductal adenocarcinoma.

Yuvasri Golivi[1], Steven D. Forsythe[1], Rachael Guenter[1], Faris Zaibaq[1], Michele Ceribelli[2], Craig Thomas[2], J. Bart Rose[1]

[1]University of Alabama at Birmingham, Birmingham, AL,[2]Lymphoid Malignancies Branch, National Cancer Institute, NIH, Bethesda, MD

Background: Pancreatic ductal adenocarcinoma (PDAC) is currently the fourth leading cause of cancer-related deaths in the United States and is projected to increase within the next decade due to its poor prognosis and increasing incidence. There is an urgent need to develop more effective therapeutic options and detection strategies to improve survival outcomes for PDAC patients. Calreticulin (CALR), an endoplasmic reticulum protein, is known to translocate to the cell surface following cellular stress. Surface-expressed CALR holds promise for cancer detection or therapeutic delivery. To explore this potential, we performed high-throughput screening to identify compounds which induce surface CALR expression.

Methods: Two human PDAC cell lines (Panc1, MIA Pa Ca-2) were engineered using the Nano-Glo HiBiT Extracellular Detection System to stably integrate HiBiT into the *CALR* gene. A high throughput screen for surface CALR-inducing compounds was performed at the National Center for Advancing Translational Sciences (NCATS). Cell lines expressing HiBiT-CALR were treated with approximately 3,000 drugs from the Mechanism interrogation PlatEs (MIPE) library for 24 or 48 hours and then assessed for cell viability using CellTiter-Glo and surface CALR levels by luminescence. Surface HiBiT-CALR and cell viability signals were quantified using a ViewLux microplate imager and automated processes utilizing the XTS Staubli UniVAL robotic system. The top ten drugs demonstrating high CALR signal (AUC) with minimal toxicity were validated for surface CALR induction by flowcytometry. Cells were also analyzed for viability using MTT assay, with $P < 0.05$ considered significant.

Results: Out of the compounds evaluated, 102 compounds showed increased CALR surface expression and were selected for secondary screening, from which ten were further chosen for in-lab validation. Among these, bisindolylmaleimide IV and AEM1 were identified to reliably increase CALR. Flow cytometry analysis confirmed significant increases in live surface CALR+ cells, with bisindolylmaleimide IV (1.1μM) increasing CALR by 1.7-fold in MIA Pa Ca-2 and 1.32-fold in Panc1, while AEM1 (10μM) increased CALR by 7-fold in MIA PaCa-2 and 3.7-fold in PANC-1. Viability assays confirmed low cytotoxicity for bisindolylmaleimide IV (1.1 μM), with 77% and 84% cell viability observed in MIA PaCa-2 and PANC-1 cells, respectively. Similarly, AEM1 (10 μM) showed 81% viability in MIA PaCa-2 and 76% in PANC-1 cells.

Conclusion: Our results identified the potential of two novel drugs, bisindolylmaleimide IV and AEM1, as promising candidates for enhancing surface CALR expression, offering new avenues for PDAC detection and tumor specific delivery of therapies.

Keywords: Calreticulin, pancreatic ductal adenocarcinoma, drug discovery, therapeutic delivery, HiBiT-CALR.

#6426 Development and validation of HTS assays for discovery of SMARCAL1 ATPase inhibitors.

Matthew Blackburn, **Robert Lowery**

BellBrook Labs, Madison, WI

SWI/SNF-related matrix-associated actin-dependent regulator of chromatin subfamily A-like protein (SMARCAL1) is an ATP-dependent SNF2 motor protein family annealing helicase that maintains genomic stability during DNA replication by catalyzing fork regression and Holliday junction migration. Loss of SMARCAL1 and the attendant DNA damage has been shown to increase tumor immunity via stimulation of the cGAS/STING pathway and suppression of PDL-1 expression, making it an attractive target for cancer immunotherapy. Here we describe development of HTS-compatible assays for screening and profiling SMARCAL1 inhibitors using the Transcreener ADP^2 Assay to measure DNA-dependent ATPase activity. The Transcreener ADP^2 Assay directly detects ADP in a competitive immunoassay with far-red, fluorescence polarization (FP), fluorescence intensity (FI) or time-resolved Förster-resonance-energy-transfer (TR-FRET) readouts. This format is homogenous (mix-and-read), compatible with diverse DNA substrates, and resistant to interference from screening compounds. A human SMARCAL1 construct comprising the core catalytic domain plus the HARP1, HARP2 domains, produced in BaV-infected insect cells, showed robust ATPase activity in initial testing with synthetic forked DNA (fDNA) and sheared salmon sperm DNA (sssDNA); hydrolysis of ATP was completely dependent on the presence of DNA. The K_m for ATP with either substrate was 110 µM, and the K_m values for sssDNA and fDNA were 30 ng/ml and 38 pM, respectively. The enzyme showed remarkable catalytic rates (kcat) of 58.6 s^{-1} and 81.1 s^{-1} with the two respective DNA substrates, enabling the use of less than 100 pM enzyme to produce a robust signal under initial velocity conditions. The kinetic parameters determined using the three different assay readouts (FP, FI and TR-FRET) were in concordance. The FP assay was validated for HTS by screening a collection of 1280 bioactives, yielding a Z' > 0.9 and identification of hits that were confirmed in dose response experiments.

#6427 BRETTSA: A BRET-based assay for ultra-sensitive measurement of target engagement through protein denaturation in live cells.

Cesear Corona[1], James Vasta[2], Matthew B. Robers[3], Michael Beck[4], Inhong Hwang[1], Min Zhou[5], Ani Michaud[6], Wenhui Zhou[7], Mei Cong[6]

[1]Discovery, Promega Corporation, San Luis Obispo, CA,[2]Promega Corporation, Madison, WI,[3]Research and Development, Promega, Fitchburg, WI,[4]R&D, Promega Corporation, Madison, WI,[5]Research Scientist, Research & Development, Promega Corp., San Luis Obispo, CA,[6]Promega, Madison, WI,[7]Promega Corp, San Luis Obispo, CA

Understanding ligand-target interactions within the native cellular environment is a persistent challenge in early drug discovery. Conventional thermal shift assays (TSAs) enable evaluation of target engagement in cells with minimal prior knowledge of the target, but their reliance on protein aggregation limits both sensitivity and scalability for high-throughput screening (HTS). We introduce a novel bioluminescence resonance energy transfer-based thermal shift assay (BRETTSA) that detects ligand-protein interactions in intact cells by monitoring protein denaturation events. In this approach, cell-permeable, denaturation-sensitive dyes report on the unfolded state of a NanoLuc-tagged target protein following a controlled thermal challenge. Ligand binding is quantified as a shift in the protein's thermal stability profile, observed as a dose-dependent decrease in BRET signal within live cells. BRETTSA is broadly applicable and has been successfully deployed to assess ligand binding for more than 100 targets spanning 20 protein families and six subcellular compartments, including transcription factors and integral membrane proteins. The method exhibits a wide dynamic range, enabling detection of ligand interactions across at least five orders of magnitude—surpassing the performance of aggregation-based TSAs. Beyond classical small-molecule binding, BRETTSA can also characterize molecular glues, bifunctional degraders, and cooperative ternary complexes. Together, these results establish BRETTSA as a robust, sensitive, and scalable platform for quantifying ligand engagement directly in living cells, offering a powerful tool for hit discovery and target validation in drug development.

#6428 DiscoveryDirect: Extending direct-to-biology paradigms to accelerate oncology drug discovery.

Allan Michael Jordan[1], Daniel Clare[2], Kam Chohan[1], Rick Davies[2], Jonathan Finlayson[2], Euan Fordyce[2], Clare Hammond[2], Philip MacFaul[2], Christopher Pearce[1], Raquel Faba Rodriguez[2], Alexandra Stowell[2], Denise Swift[3], Megan Thompson[2], Graeme Walker[2], Terence Wu[2]

[1]Sygnature Discovery, Nottingham, United Kingdom,[2]Sygnature Discovery, Macclesfield, United Kingdom,[3]Sygnature Discovery, Nottingham

The average timeline from project initiation to preclinical candidate delivery in oncology drug discovery is approximately four years. To compress these timelines, direct-to-biology strategies are increasingly employed to expedite early decision-making and compound progression. However, conventional approaches often remain limited to biophysical off-rate assessments of crude reaction mixtures (CRMs), restricting their utility. To overcome these constraints, we have expanded this paradigm through integrated methodologies, including Direct-to-Crystallography (D2C), to validate hits and elucidate structure-activity relationships (SAR), enabling pre-candidate delivery in as little as 18 months.

Harnessing our Hit Synergy platform which combines complementary screening technologies, we rapidly generated novel, high quality and structurally diverse hits for a challenging and clinically relevant oncology target. Early deployment of D2C, using existing HTS liquid stocks, delivered ligand-bound structures without delays associated with hit re-synthesis or re-acquisition. These structures confirmed target engagement and revealed novel binding interactions. Orthogonal hit validation employed direct-to-biology approaches such as off-rate screening, alongside tailored biochemical and cellular assays on purified samples.

Integration of structural insights and biological data accelerated hit expansion *via* high-throughput chemistry (HTC) and complementary direct-to-biology assays validated for both pure compounds and CRMs. Robust D2C determinations from CRMs yielding as little as 15% product further streamlined SAR generation and hypothesis testing, influencing medicinal chemistry design and decision making and compressing the design-make-test cycle. Generative AI-driven idea generation and direct-to-physicochemical assays further supported optimization for developability.

Together, this fully integrated, multi-modal workflow enabled rapid, holistic decision-making at critical project stages, delivering pre-candidate quality derivatives in a significantly truncated timeframe. By embedding direct-to-discovery methodologies throughout the pipeline, we successfully accelerated progression from hit identification to candidate selection, advancing novel therapeutics toward the clinic with unprecedented efficiency.

#6429 NMR assessment of ternary complex formation by targeted protein degraders.

Emily M. Grasso, David Fry, Nabin Panth, Zachary Sparta, Madhavi Latha S. Chalasani, Adam Haidi, Steven Murkli, Nareshkumar Jain

NJ Bio, Inc., Princeton, NJ

Targeted protein degradation (TPD) is an increasingly prominent therapeutic strategy for targeting systems previously thought to be undruggable. Unlike typical small molecule inhibitors or agonists, TPDs induce the degradation of specific proteins by forcing them into proximity with the cell's native proteasomal degradation machinery. Many companies are rapidly developing new TPDs, and several degraders have reached clinical trials. From a chemistry standpoint, there are three main aspects of a TPD to study and optimize: 1) a ligand that binds and recruits a target protein, 2) a ligand that binds an E3 ligase, and 3) a linker that orients the two ligands and their associated proteins at the correct geometry for degradation. TPDs present a more complicated case of lead optimization than traditional programs since they bind simultaneously to two proteins forming a non-native protein:protein complex. The formation of these target protein-TPD-E3 ternary complexes is of particular interest in the field. As in any drug development program, knowing structural details of how TPDs bind to their target proteins provides critical information that may offer new and unique insights into future TPD design. Further, ideal TPDs allow for turnover of the degradation machinery, meaning that these molecules act catalytically to degrade more target protein at low concentrations, which complicates the desired kinetics for the formation and dissolution of ternary complexes. Recent work has shown that these complexes may be fundamentally dynamic and involve non-optimal interactions.

Nuclear magnetic resonance (NMR) spectroscopy is uniquely poised to study these TPD complexes since it can be used to study both the structure and dynamics of molecules in solution. We report our use of NMR to characterize ternary complexes consisting of a TPD bound to both its target protein and the E3. Using isotopically labeled proteins, we first study the TPD binary complexes to establish how each end of the TPD binds before assessing additional changes that occur in ternary complexes. With this approach, we have the capacity to discriminate between changes due to ligand binding and those due to novel protein-protein interactions between the target protein and the E3. We find that the presence of the second protein in the ternary complex affects how the TPD binds to each protein, suggesting that these experiments report on the cooperativity of binding and the possible structural basis of this cooperativity. We further explored the use of NMR data acquired across a series of TPDs with different linkers to guide our understanding of the idealized ternary complex structural ensemble when combined with traditional assays for degradation. The study of ternary complex dynamics using NMR offers a new strategy to allow for the design and optimization of the next generation of TPDs. We will be disclosing all the structures related to this study.

: Biostatistics in Clinical Trials / Surgical Oncology
Poster Session

#6434 Affective trajectories during adaptive pharmacotherapy for smoking cessation: Insights from EMA data.

Hadeel Al-Sahli[1], Ferdous Qudus[2], George Kypriotakis[3], Paul Cinciripini[3], Yong Cui[3]

[1]UT Health Houston McGovern Medical School, Houston, TX,[2]Philadelphia College of Osteopathic Medicine, Philadelphia, PA,[3]University of Texas MD Anderson Cancer Center, Houston, TX

Background: Medications such as varenicline and combination nicotine replacement therapy (NRT) have demonstrated efficacy in promoting smoking cessation. However, the underlying psychological mechanisms that drive successful abstinence are less well understood. This study used Ecological Momentary Assessment (EMA) to evaluate the impact of cessation medications and adaptive treatment phases on affect among adults undergoing a two-phase smoking cessation trial.

Methods: Adult smokers (N=490) were randomized to receive varenicline (VAR) or nicotine replacement therapy (NRT) in a two-phase study. At the end of *6-week Phase* 1, non-abstinent participants were re-randomized for the 6-week Phase 2 to continue, switch, or augment their pharmacotherapy, while abstinent participants continued with their initial pharmacotherapy. Participants provided daily ecological momentary assessment (EMA) data on positive and negative affect, which were averaged by week and phase. Linear mixed effects models were used to examine the effects of medication group, treatment phase, and weeks since quit date on positive and negative affect, allowing the effect of phase to vary randomly by subject.

Results: Several trends emerged when examining the affect trajectories over time. Visual inspection of the data suggests that participants on augmented medication tended to show greater improvements in affect scores compared to those remaining on standard NRT or varenicline alone. For positive affect, individuals in the augmented varenicline and augmented NRT groups showed an upward trajectory in Phase 2, with mean positive affect increasing steadily in the weeks following adaptation of their medication regimen. In contrast, participants in the standard NRT and varenicline groups demonstrated relatively stable or only modest increases. For negative affect, participants who were augmented in Phase 2 exhibited sharper decreases in negative affect, while those in the non-augmented medication showed more variable or persistent negative affect scores across both phases.

Conclusion: Adaptive pharmacotherapy strategies for smoking cessation show greater improvement in positive affect and reduction in negative affect over time. Importantly, there was substantial heterogeneity in affective response, suggesting that individual characteristics such as age and sex may influence emotional adjustment during smoking cessation. Clinicians should consider evaluating and, when appropriate, adjusting medication regimens to support desirable affective trajectories throughout the quitting process. Future studies should investigate how changes in affect are linked to abstinence outcomes and explore how personalized medication strategies can optimize both affect and quit rates in diverse populations.

#6435 Dose optimization in multi-indication oncology basket trials: Leveraging Bayesian borrowing to identify OBD.

Danny Lu[1], Yutao Liu[1], Yanning Wu[2], Nelson Liu[3], Jayne Marshall[4], Cindy Lu[3]

[1]AstraZeneca, Mississauga, ON, Canada,[2]Case Western Reserve University, Cleveland, OH,[3]AstraZeneca, Waltham, MA,[4]AstraZeneca, Cambridge, United Kingdom

Introduction: Project Optimus encourages early identification of the Optimal Biological Dose (OBD) by balancing efficacy and safety, moving beyond the maximum tolerated dose paradigm. For programs spanning multiple indications, a key challenge is that the OBD may differ by indication. We propose a basket trial strategy that formally borrows information across indications to improve dose selection efficiency, aiming to reduce per_indication sample size and time to decision while maintaining robust inference when OBDs are heterogeneous.
Methods: We assume a basket trial design to address dose optimization up front within a single trial rather than multiple separate cohorts. We apply a utility based, three outcome decision rule (recommend low dose, consider, or high dose) integrating efficacy-toxicity tradeoffs. We compare three strategies: fully exchangeable Bayesian hierarchical modeling (BHM-EX) that borrows across all indications, latent cluster hierarchical modeling (BHM-LC) that borrows within data driven clusters, and no borrowing (NB) analyzing indications independently. We evaluate operating characteristics and sample size efficiency via simulations across varying sample sizes and true OBD heterogeneity.
Results: When indications share the same true OBD, borrowing improves correct dose selection and enables fewer patients per indication to reach decisions; BHM-EX performs best, particularly under uneven enrollment. NB shows higher misselection risk with small samples. When true OBDs differ, BHM-EX underperforms due to full pooling, whereas BHM-LC is more robust, maintaining improved accuracy without overborrowing.
Conclusions: Bayesian borrowing in basket trials can reduce sample size while maintaining the same probability of correct OBD selection and time to decision, especially when indications share OBDs or have imbalanced enrollment. Clinical, preclinical, and clinical pharmacology insights should guide assumptions about similarity across indications and the choice of borrowing strategy, with prespecified sensitivity analyses to support regulatory confidence.

#6436 Carmel Awadallah , MD.

Carmel Awadallah[1], Myer Marc Warshawsky[2]

[1]St. John's Episcopal Hospital, Far Rockaway, NY,[2]Hematology and Oncology, St. John's Episcopal Hospital, Far Rockaway, NY

Background: Pancreatic ductal adenocarcinoma (PDAC) remains one of the most lethal malignancies despite adjuvant chemotherapy. Immunotherapy has transformed adjuvant therapy in other solid tumors, yet its role in PDAC is undefined. We aimed to characterize the landscape of adjuvant systemic trials in resected PDAC, with a focus on immunotherapy, to identify progress and barriers to clinical impact.
Methods: We queried ClinicalTrials.gov for interventional phase 2-3 adjuvant trials in resected PDAC registered between January 2000 and January 2025. Trials were categorized as immunotherapy, targeted therapy, other novel systemic strategies, or traditional chemotherapy. Phase, enrollment, sponsor type, and endpoints were extracted and summarized descriptively.
Results: Thirty-six eligible trials were identified. Most were phase 2 (n=27, 75%), with only two phase 3 studies (6%). Enrollment was modest: 27 trials (75%) included fewer than 50 patients, while only three (8%) enrolled ≥200. Overall survival was the most common endpoint (n=35, 97%), followed by safety/toxicity (n=23, 64%) and disease-free survival (n=10, 28%); surgical endpoints were rare, including R0 resection (n=6, 17%) and pathologic complete response (n=2, 6%). Sponsorship was predominantly academic (n=28, 78%), with limited industry-led (n=3, 8%) or mixed (n=5, 14%) involvement. Immunotherapy approaches were mainly vaccines (GVAX, TG-01, ELI-002) and immune modulators, with only one small trial testing a checkpoint inhibitor (CT-011).
Conclusions: Over two decades, adjuvant immunotherapy in PDAC has not advanced beyond small, exploratory studies. Trials were underpowered, academic-led, and focused largely on vaccine-based strategies, with minimal checkpoint inhibitor evaluation and no definitive phase 3 programs. Adequately powered, industry-supported phase 3 trials are urgently needed to establish effective adjuvant immunotherapy strategies in resected PDAC.

#6437 Comparative efficacy of adjuvant CDK4/6 inhibitors in early breast cancer: A hazard ratio-based network meta-analysis using the NetMetaEasy platform.

Janos Tibor Fekete, **Balazs Gyorffy**

Semmelweis University, Budapest, Hungary

BACKGROUND: Adjuvant CDK4/6 inhibitors have shown variable results across phase III trials in hormone receptor-positive, HER2-negative early breast cancer, and no direct comparisons exist to clarify their relative efficacy. Network meta-analysis (NMA) enables the integration of direct and indirect evidence to compare multiple treatments simultaneously. In this study we applied a hazard ratio-based NMA to evaluate the comparative effectiveness of abemaciclib, ribociclib, and palbociclib using invasive disease-free survival (iDFS) as the primary endpoint. Endocrine therapy (ET) served as the standard-of-care reference across trials.

METHODS: Data from four randomized phase III trials (case n=17,741) were analyzed. Treatment nodes included abemaciclib+endocrine therapy (ET), ribociclib+ET, palbociclib+ET, and ET alone. Analyses were performed using the NetMetaEasy platform (https://www.metaanalysisonline.com/netmetaeasy), an R/Shiny-based implementation supporting binary, continuous, and summary-effect inputs. A frequentist random-effects NMA was conducted using the inverse-variance method with the DerSimonian-Laird estimator for between-study variance (τ^2). Standard NMA outputs were generated, including forest plots, network geometry, treatment ranking (P-scores), inconsistency assessments, and funnel plots.

RESULTS: Ribociclib+ET showed the strongest effect versus ET (HR 0.72; 95% CI 0.62-0.83). Abemaciclib+ET also improved iDFS (HR 0.73; 95% CI 0.66-0.82). Palbociclib+ET did not differ significantly from ET (HR 0.89; 95% CI 0.79-1.00). Indirect comparisons yielded HR 0.82 (95% CI 0.70-0.97) for abemaciclib versus palbociclib, HR 1.25 (95% CI 1.03-1.50) for palbociclib versus ribociclib, and HR 1.03 (95% CI 0.85-1.23) for abemaciclib versus ribociclib. P-scores ranked ribociclib+ET highest (0.86), followed by abemaciclib+ET (0.80) and palbociclib+ET (0.33). Funnel-plot inspection did not indicate small-study effects.

CONCLUSIONS: In this hazard ratio-based NMA, abemaciclib and ribociclib significantly improved iDFS compared with endocrine therapy, whereas palbociclib did not. Our findings illustrate the utility of NMA for comparative evaluation in the absence of head-to-head trials.

#6438 Unfinished stories: Consequences of melanoma clinical trial discontinuation and non-publication.

Hadeer Hafez[1], Abdelrahman Hagag[1], Mohamed Ashraf Mohamed[2], Mohamed Saad Rakab[3], Ismail Zakaria Ismail[4], Aya Jamal Elkenani[5], Nada Elmetwally Ahmed[1], Abdelrahman M. Hafez[6], Doaa Mashaly[1], Ali Tarek Lasheen[2], Mohamed Abdelsalam[1]

[1]October 6 University, Faculty of Medicine, Giza, Egypt,[2]Misr University for Science and Technology, Faculty of Medicine, Giza, Egypt,[3]Faculty of Medicine, Mansoura University, Giza, Egypt,[4]Faculty of medicine, Misr University for Science and Technology, Giza, Egypt,[5]Faculty of Medicine, Mansoura University, Mansoura, Egypt,[6]Faculty of Medecine, Damietta University, Damietta, Egypt, Damietta, Egypt

Background: Melanoma is a major cause of skin cancer-related death, and clinical trials are essential for advancing melanoma treatment options. However, many trials either are terminated prematurely or are never published, eaving critical data unreported. These “unfinished stories”, hinder scientific progress, waste resources, and limit informed clinical decision-making. Therefore, understanding how many and what factors predict unpublished or discontinued melanoma trials is key to improving the transparency of research and advancing best care for patients.
Objective: To identify the extent, characteristics, and variables related to Discontinuation and Non-Publication melanoma clinical investigations.
Methods: We systematically searched ClinicalTrials.gov for Melanoma studies up to March 1, 2025. Studies completed within the past 24 months were excluded to account for potential delays in the peer review process. Publication status was identified using NCT numbers. Data on participant gender, age, study design, funding source, type of intervention, sample size, and trial location were collected and analyzed. Multiple logistic regression was used to identify factors associated with trial discontinuation or non-publication. All statistical analyses were conducted using Jamovi version 2.6.24.
Results: In total, there were 2,144 trials, with 712 (33.2%) published, 1,215 (56.7%) non-published, and 217 (10.1%) unknown. Of the discontinued trials (516, 24.1%), just 59 (11.4%) were published. Non-publication status was noted to be significant among trials of genetic interventions (OR = 0.104, 95% CI: 0.027-0.401, p=0.001), procedural interventions (OR = 0.262, 95% CI: 0.121-0.567, p<0.001), and in a multicenter trial (OR = 0.185, 95% CI: 0.123-0.278, p<0.001). Also, a study was considerably more probable to be discontinuation if smaller-sized (≤500 participants, p<0.001) or earlier (Phase 1/2, p<0.001).
Conclusions: The high frequency of Discontinuation and Non-Publication trials record highlights the importance of efforts toward completing and/or fully publication melanoma clinical investigations, particularly those for genetic and/or procedural treatments and/or smaller trials.

#6439 Growth rate of fastest-growing lesion predicts survival better than growth rate of RECIST 1.1 sum of diameters: A real-world retrospective study of 84 NSCLC patients over multiple treatment lines.

Dean C. Bottino[1], Jayant Narang[2], Michael Hanley[1], Maria Guzman Castillo[3], Heidi Loponen[3], Risto Kesavuori[4], Juha Mehtala[3], Mark Lin[1]

[1]Takeda Development Centers America, Cambridge, MA,[2]Imaging, Takeda Development Centers America, Cambridge, MA,[3]MedEngine Oy, Helsinki, Finland,[4]University of Helsinki, Helsinki, Finland

Background: Sum of Diameters (SoD) of up to 5 target lesions is the continuous metric used for Response Evaluation Criteria In Solid Tumors (RECIST) classifications. As demonstrated in many studies, RECIST based outcomes such as progression free survival and response rate do not always correlate well with overall survival, warranting the need to explore alternative ways of assessing response, particularly in the setting of novel therapies. Many studies have correlated SoD rates of change to overall survival (OS) in solid tumor indications such as non-small cell lung cancer (NSCLC). To test the hypothesis that a patient's survival could be influenced more strongly by their most poorly responding or quickly progressing lesion, we compared the ability of SoD growth rate and the growth rate of the fastest growing target lesion to predict OS.

Methods: CT scans from 84 adult (18+) stage III/IV NSCLC patients with varying baseline mutation status (N=19 non-Exon-20 EGFR mutation, 15 ALK rearrangements, 5 other mutations, 44 No driver mutation), treated in Finland in secondary care setting were analyzed by a radiologist to identify and track the diameters of up to 5 target lesions in each patient. Lesion diameters from the last two CT scans of each treatment line (representing 224 distinct patient-lines of treatment: 78 1st Line, 63 2nd Line, 99 3rd -6th Line, 4 unknown) were analyzed in two ways: EGRmax = max of the (signed) exponential growth rates (EGR) of target lesions; EGRSoD = EGR of SoD of target lesions. EGRmax and EGRSoD values were then clustered into three categories: low (L), medium (M) and high (H). Kaplan-Meier (KM) and Cox Proportional Hazards (CPH) analyses were then performed to determine the correlation of EGRmax or EGRSoD categories to OS.

Results: Clustering analysis (independent of OS) resulted in EGRmax cutoffs of 0.06/month between L and M and 0.25/month between M and H (resulting in N=137/75/12 patient-lines in L/M/H categories), and EGRSoD cutoffs of -0.015/month between L and M and 0.095/month between M and H (resulting in N=46/151/27 patient-lines in L/M/H). Directionally, the KM analysis was as expected, with higher EGRs correlating with lower OS. However, KM analysis revealed consistent separation between L, M, and H categories for EGRmax (median OS of 33, 17.8 and 15.4 months respectively), while the KM curves for EGRSoD were overlapping for L and M and only separated for H (median OS of 19.5, 27.7, and 17 months respectively). Accordingly, CPH analysis indicated a spread of statistically significant hazard ratios (HRs) for EGRmax (HR = 1.97 for M/L and 3.28 for H/L), while only significant differences between H and L for EGRSoD (HR = 0.98 for M/L and 1.99 for H/L).

Conclusions: In this population of NSCLC patients across several treatment lines, EGRmax appears to be a better predictor of OS than RECIST-based EGRSoD.

#6440 Effects of cumulative tobacco exposure on lung cancer genomic profiles in Latin Americans.

Javiera Garrido[1], Evelin Gonzalez[2], Alejandro Blanco[2], Gonzalo Sepulveda-Hermosilla[2], Matias Freire[3], Solange Rivas[2], Katherine Marcelain[4], Gareth I. Owen[5], Carolina Ibañez[6], Alejandro H. Corvalan[5], Marcelo Garrido[7], Rodrigo Assar[3], Rodrigo Lizana[3], Javier Caceres-Molina[3], Diego Ampuero[3], Liliana Ramos[3], Paola Perez[8], Osvaldo Aren[9], Sara Chernilo[10], Cristina Fernandez[10], Maria Loreto Spencer[11], Jacqueline Flores[12], Giuliano Bernal[13], Monica Ahumada Olea[14], German Rasse[15], Carolina Sanchez[16], Maria Galli de Amorim[17], Emmanuel Dias-Neto[17], Helano C. Freitas[17], Ricardo Armisen[2]

[1]Universidad Mayor, Santiago, Chile,[2]Universidad del Desarrollo, Santiago, Chile,[3]CORFO Center of Excellence in Precision Medicine, Pfizer, Santiago, Chile,[4]Universidad de Chile, Santiago, Chile,[5]Pontificia Universidad Catolica de Chile, Santiago, Chile,[6]Advanced Center for Chronic Diseases, Santiago, Chile,[7]Centro de Oncologia de Precision, Universidad Mayor, Santiago, Chile,[8]NIDCR, National Institute of Health, Bethesda, MD,[9]Centro de Investigacion Clinica Bradford Hill, Santiago, Chile,[10]Instituto Nacional del Torax, Santiago, Chile,[11]Hospital Clinico Regional de Concepcion Dr. Guillermo Grant Benavente, Concepcion, Chile,[12]Departamento de Salud Publica, Facultad de Medicina, Universidad Catolica del Norte, Antofagasta, Chile,[13]Departamento de Ciencias Biomedicas, Facultad de Medicina, Universidad Catolica Del Norte, Antofagasta, Chile,[14]Servicio de Oncologia, Departamento de Medicina Interna, Hospital Clinico de la Universidad de Chile, Santiago, Chile,[15]Hospital de Puerto Montt, Puerto Montt, Chile,[16]Centro de Genomica y Bioinformatica, Universidad Mayor, Santiago, Chile,[17]Laboratory of Medical Genomics, A. C. Camargo Cancer Center, Sao Paulo, Brazil

Motivation: Tobacco exposure is a major determinant of tumor genomic landscapes in non-small cell lung cancer (NSCLC). Two of the most clinically relevant actionable genes in lung cancer, EGFR and KRAS, show opposite patterns, with smokers exhibiting a higher prevalence of alterations in KRAS and never-smokers in EGFR. Yet, the dynamic and evolution of genomic changes as a function of cumulative tobacco exposure has received limited attention. Here, we examine how tumor genomic profiles vary according to smoking intensity, duration, and time since cessation (TSC). Our study focuses on an underrepresented population of Latin American patients, where additional research is needed to better characterize tumor heterogeneity.

Methodology: The population was obtained from the protocol *Characterization and Validation of Molecular Diagnostic Technologies for Lung Cancer Patients from Chile, Brazil, and Peru*. Participant recruitment was between July 2015 and October 2018 across 37 different centers. Primary or metastatic NSCLC specimens were analyzed, and genomic profiles were generated with the Oncomine Focus Assay (OFA). A total of 1,864 participants yielded QC-approved genomic profiles. Covariates of interest were assessed at enrollment. Cumulative tobacco exposure, including smoking intensity (cigarettes per day), duration, and TSC, was quantified using the Comprehensive Smoking Index (CSI). In addition, smoking status (current vs. never) was recoded as a function of TSC in order to identify the time period during which major genomic alterations (GA) are most likely to occur. Descriptive statistics, generalized linear models, and generalized additive models were used to evaluate the association between CSI and the prevalence of GA across genes. All models were adjusted for potential confounders, including country, age, sex, NSCLC subtype, cancer stage and history of cancer.

Results and Conclusions: A total of 1100 patients had complete genomic and tobacco exposure information. Among current smokers, median smoking intensity and duration were 20 cigarettes per day and 48 years, respectively, compared with 30 cigarettes per day and 47 years among former smokers. Ninety percent of former smokers had ceased tobacco use at least 10 years prior to diagnosis, with a median TSC of 1 year. CSI analysis identified 14 genes significantly associated with genomic alteration status, including EGFR, PIK3CA, ALK, MTOR, ERBB3, and RET. Higher CSI values (4th quartile) showed approximately double the frequency of genomic alterations compared with the lowest CSI quartile for ALK (16.2% vs. 8.7%), RET (12.8% vs. 6.9%), and MTOR (15% vs. 6.9%). Mid-range CSI values exhibited the lowest prevalence of alterations in EGFR (12.6% vs. 31%) and PIK3CA (6.9% vs. 14.5%). Overall, these findings support the value of CSI in refining exposure-genotype associations and the need for improves risk stratification efforts in diverse populations.

#6441 Safety profile of post-CDK4/6 treatments in HR+/HER2– metastatic breast cancer (mBC): A network meta-analysis.

Martina Pagliuca[1], Roberto Buonaiuto[1], Michelino De Laurentiis[2], Carmine De Angelis[1]

[1]Scuola Superiore Meridionale, Napoli, Italy,[2]Istituto Nazionale Tumori IRCCS "Fondazione G.Pascale", Napoli, Italy

Several treatments (tx) are available for HR+/HER2- mBC; however, choosing subsequent tx after progression on first-line CDK4/6 inhibitor + endocrine therapy (ET) remains challenging. Assessing the safety profiles of these options is crucial for guiding tx selection. We performed a network meta-analysis (NMA) to compare the safety of systemic tx approved for this setting. Tx strategies were retrieved through a systematic review of randomized phase II-III trials published from January 2014 to October 2025 (PROSPERO CRD420251234039) and only FDA- and/or EMA-approved tx were included. Each tx was compared with standard ET or chemotherapy (CT). A frequentist random-effects NMA was performed using the netmeta package in R. Risk ratios (RRs) for safety outcomes (grade[G] ≥3 adverse events [AEs], any grade AEs, and AEs leading to discontinuation) were calculated from each trial using pairwise comparisons and pooled using a random-effects model estimated by restricted maximum likelihood. Results were shown as forest plots with 95% confidence intervals (CI), and tx ranked based on P-scores. The NMA included 16 trials. Among ET-based strategies, the lowest RRs were observed for: imlunestrant alone (0.98, 95% CI 0.92-1.05) for any G AEs; camizestrant 75 mg (0.81, 0.36-1.83) for G≥3 AEs; elacestrant (1.45, 0.66-3.16) for AEs leading to discontinuation. While among antibody-drug conjugates (ADCs) the lowest RRs were observed for: sacituzumab govitecan (SG) for any G AEs (1.00, 0.99-1.01); datopotamab deruxtecan (Dato-DXd) (0.47, 0.37-0.59) for G≥3 AEs; SG (0.83, 0.26-2.66) for AEs leading to discontinuation. The estimated RRs and P-scores are shown in table. Among ET-based options, novel mono-ETs (oral SERDs and PROTACs) showed the lowest risk of discontinuation and G≥3 AEs. Among ADCs, TROP2-directed agents had fewer discontinuations, while ADCs with DXd as a payload showed higher rates of any G AEs but (except for DESTINY-Breast06) lower G≥3 AEs risk than other tx strategies.

Trial	Treatment strategy	Control arm	RR (95% CI) any grade AEs	P-score any grade AEs	RR (95% CI) G≥3 AEs	P-score G≥3 AEs	RR (95% CI) AEs leading to discontinuation	P-score AEs leading to discontinuation
SERENA-2	Camizestrant 75mg	ET	1.12 (0.92-1.37)	0.44	0.81 (0.36-1.83)	0.86	4.93 (0.24-101.00)	0.47
SERENA-2	Camizestrant 150mg	ET	1.32 (1.11-1.57)	0.09	1.55 (0.78-3.07)	0.58	NA	NA
EMBER-3	Imlunestrant	ET	0.98 (0.92-1.05)	0.90	0.83 (0.60-1.14)	0.90	3.47 (1.15-10.42)	0.57
EMBER-3	Imlunestrant+abemaciclib	ET	1.16 (1.11-1.22)	0.29	2.35 (1.82-3.03)	0.38	5.06 (1.67-15.32)	0.44
EMERALD	Elacestrant	ET	1.07 (1.00-1.14)	0.60	1.32 (0.95-1.83)	0.66	1.45 (0.66-3.16)	0.82
VERITAC-2	Vepdegestrant	ET	1.07 (1.00-1.14)	0.61	1.71 (1.25-2.36)	0.65	4.47 (0.97-20.53)	0.48
SOLAR-1	Alpelisib+ET	ET	1.07 (1.03-1.10)	0.61	2.13 (1.75-2.58)	0.44	5.98 (3.32-10.78)	0.36
CAPItello-291	Capivasertib+ET	ET	1.17 (1.11-1.24)	0.26	3.11 (2.30-4.23)	0.22	5.67 (2.72-11.84)	0.39
postMONARCH	Abemaciclib+ET	ET	1.19 (1.11-1.28)	0.22	2.76 (2.01-3.79)	0.28	23.51 (1.40-395.96)	0.17
PALMIRA	Palbociclib+ET	ET	1.07 (0.96-1.19)	0.61	4.00 (1.82-8.78)	0.18	NA	NA
PACE	Palbociclib+ET	ET	NA	NA	22.16 (3.14-156.38)	0.05	NA	NA
BOLERO-2	Everolimus+ET	ET	NA	NA	NA	NA	5.04 (2.59-9.81)	0.44
MAINTAIN	Ribociclib+ET	ET	NA	NA	NA	NA	4.92 (0.59-40.83)	0.46
TROPION-Breast01	Datopotamab deruxtecan	CT	1.08 (1.03-1.14)	0.02	0.47 (0.37-0.59)	1.00	1.01 (0.44-2.29)	0.67
DESTINY-Breast04	Trastuzumab deruxtecan	CT	1.04 (1.01-1.08)	0.56	0.81 (0.70-0.93)	0.80	2.05 (1.18-3.56)	0.12
DESTINY-Breast06	Trastuzumab deruxtecan	CT	1.04 (1.01-1.06)	0.25	1.19 (1.03-1.37)	0.22	1.53 (1.05-2.23)	0.32
EVER-132-002	Sacituzumab govitecan	CT	1.00 (0.99-1.01)	0.83	1.18 (1.04-1.33)	0.25	0.83 (0.26-2.66)	0.75
TROPiCS-02	Sacituzumab govitecan	CT	NA	NA	1.23 (1.08-1.39)	0.14	1.44 (0.69-3.01)	0.40

#6442 Persistent elevation of plasma Neuropilin-1, a tumorigenic protein, during the first month after minimally invasive colorectal cancer resection.

Chandana S. K. Herath Mudiyanselage[1], Yi-Ru Chen[2], Neil Mitra[2], Monica S. Naparst[2], Elizabeth Nilsson Sjolander[2], Vesna Cekic[3], Richard L. Whelan[2]

[1]Surgery, Northwell Health, Lenox Hill Hospital, New York, NY,[2]Department Surgery, Northwell Health, Lenox Hill Hospital, New York, NY,[3]Department Surgery, Northwell Health, Lenox Hill Hospital, Ney York, NY

Introduction: Neuropilin-1 (NRP1), also known as CD304, is a transmembrane glycoprotein that functions as a co-receptor for VEGF, PLGF, TGF-B1 and other ligands. NRP1 is expressed in various tissues and in endothelial cells (EC), tumor and immune cells. NRP1 upregulation is closely associated with enhanced angiogenesis in tumors and can promote EC proliferation, migration, and neovascularization. NRP-1 also plays a role in the tumor microenvironment by stabilizing regulatory T cells, which suppress the immune response. NRP1 is overexpressed in various tumors including colorectal cancer (CRC) and elevated plasma levels are linked to tumor progression, higher tumor grades, and poor clinical outcomes. NRP-1 also plays a role in the tumor microenvironment by stabilizing regulatory T cells,that suppress the immune ability. NRP1 regulates VEGF-driven wound angiogenesis, with peak vascular growth followed by regression that restores normal capillary density. Surgery's impact on blood levels of NRP1 levels is poorly studied. This study's purpose was to measure plasma NRP1 levels before and during the first month after minimally invasive colorectal resection (MICR) for CRC.

Method: This study included CRC patients from an IRB-approved data/plasma bank who underwent MICR for whom sufficient plasma samples were available. Clinical data were reviewed, and blood was collected preoperatively (preop) and at defined postoperative (postop) intervals. Plasma was stored at -80°C and late samples were grouped into 7-day bundles intervals. NRP1 levels were measured in duplicate using ELISA (ng/ml) and reported as mean± SD mean ± SD. The paired t-test was used for statistical analysis (significance $p<0.05$).

Results: Preop and 1 or more late postop plasma sample were available for 92 MICR patients (colon 71%; rectal 29%; 47 male /45 female, mean age 64.3± 14.1years). The mean incision length was 8.3± 3.6 cm and mean length of stay was 6.8 ± 4.2 days. The final cancer stage breakdown was; Stage I, 30%, Stage II, 30%, stage III, 35% and stage IV, 5%. The mean Preop NRP1 level was 296.0± 68.8 ng/m; in comparison, mean postop levels were significantly elevated ($p<0.0001$) on postop day (POD) 3 (384.3±96.6, n=88), POD7-13 (405.4±111.9, n=73), and POD14-20 (380.4±101.7, n=28) , POD 21-27(346.8±87.9, n=16,p-0.01) and on POD 28-41 (342.8± 84.3, n=18; $p<0.001$).

Conclusion: Following MICR for CRC, plasma NRP1 levels were significantly increased from POD3 through POD 28-41. The rise in NRP1 levels may reflect enhanced shedding from EC and circulating tumor cells, potentially driven by angiogenesis related processes associated with wound repair and regeneration. Surgery-induced inflammatory signaling likely contributes to increased NRP1 expression and release. Elevated levels of NRP1 may promote angiogenesis in residual tumor deposits after surgery. Further investigation is warranted.

#6444 Prognostic impact of ctDNA status and multi-site disease burden for patients with peritoneal metastases from appendiceal or colorectal cancer.

Justin M. Bader[1], Kelsey LaBella[1], Nicole Aguirre[1], Kwasi Ofori[1], Princy Gupta[1], Anup Sharma[2], Huxley Smart[1], Alexander Kim[1], Robert Tseng[1], SANGWON YUN[1], Michael Cecchini[2], Raghav Sundar[2], Kiran Turaga[1]

[1]Yale New Haven Hospital, New Haven, CT,[2]Yale School of Medicine, New Haven, CT

Purpose: Circulating tumor DNA (ctDNA) is prognostic for patients with metastatic appendiceal and colorectal cancer (CRC), however, its impact on therapy considerations and surgical candidacy is unclear. Current randomized trials are exploring approaches to locoregional therapy for management of multi-site oligometastatic disease. We investigate the role of ctDNA-guided locoregional therapies in the management of peritoneal metastases (PM) with or without multi-site disease.

Methods: The study cohort included high-grade appendiceal or CRC patients with single site (peritoneum) or multi-site metastases (peritoneum plus liver, lung, or distant lymph node involvement) who had curative intent surgical interventions for PM between 2023-2025. ctDNA testing was performed in the pre- and post-operative setting. Univariate and multivariate analysis of demographics, pathological, and ctDNA dynamics were performed. Overall survival (OS) was analyzed using Kaplan-Meier (KM) curves to evaluate prognostic impact of ctDNA status and presence of multi-site disease.

Results: Of the 61 patients in the study, 67% (n=41) had CRC and 33% (n=20) had high-grade appendiceal cancer. Median postoperative follow up was 18 months with 82% of patients alive at last follow up. Prior to surgery, 33% (n=17) of patients were ctDNA positive with 13% clearing their ctDNA postoperatively initially. However, none of these patients maintained durable negative ctDNA as all converted back to ctDNA positive within 6 months. Of those with negative ctDNA preoperatively, 32% converted to ctDNA positive postoperatively - including 91% converting to positive within 1 year. Patients with ctDNA negative status preoperatively had KM-estimated 2-year OS of 91.2%.

History of multi-site disease was present in 39% (n=24) of patients at time of surgery including 50% (n=12) with active multi-site disease and 50% (n=12) with previously treated disease. KM-estimated 2-year OS was excellent for ctDNA negative patients regardless of multi-site disease involvement (2-year OS = 83.3%) or peritoneal-only metastases (2-year OS = 95.6%).

Conclusion: This study analyzed the prognostic impact of ctDNA status and multi-site disease for patients with PM from CRC or appendiceal cancer who underwent locoregional therapy. ctDNA appears to be prognostic in patients undergoing curative intent surgical resection for peritoneal metastases. Furthermore, patients with multi-site disease who have negative ctDNA and undergo surgery for peritoneal metastases appear to have survival comparable to patients with peritoneal only metastases. With variable approaches and conflicting guidelines for the management of patients with PM and oligometastatic disease, ctDNA could augment treatment selection, surgical eligibility, and clinical trial enrollment.

#6445 Clinical benefits of perioperative chemotherapy for patients with stage I-II large cell lung cancer: A SEER database analysis.

Wongi Woo[1], Seoin Kim[2], Jongwoo Kim[2], Yoonjin Cha[3], Duk Hwan Moon[4], Sungsoo Lee[4], Young Kwang Chae[5]

[1]St Joseph's Medical Center Stockton, Stockton, CA,[2]Metrowest Medical Center, Framingham, MA,[3]Yonsei University College of Medicine, Seoul, Korea, Republic of,[4]Gangnam Severance Hospital, Seoul, Korea, Republic of,[5]Northwestern Univ. Feinberg School of Medicine, Chicago, IL

Background: Large cell lung cancer (LCLC), a neuroendocrine subtype of non-small cell lung cancer, remains an aggressive malignancy with limited therapeutic options. Even early-stage disease shows high recurrence rates and suboptimal survival after resection. Evidence guiding the role of perioperative chemotherapy (CTx) in stage I-II LCLC is limited. This study evaluated the association between perioperative CTx and survival outcomes in surgically resected LCLC using a nationally representative dataset.

Methods: Patients with stage I-II LCLC diagnosed between 2000-2021 were identified from the Surveillance, Epidemiology, and End Results Program (SEER) 17 registries. Inclusion criteria were pathologically confirmed LCLC, surgical resection, and American Joint Committee on Cancer (AJCC) 7th/8th edition staging. Demographic, clinicopathologic, and socioeconomic variables were collected. Overall survival (OS) and cancer-specific survival (CSS) were compared between surgery alone and surgery plus perioperative CTx using Kaplan-Meier analysis. Multivariable Cox regression was performed to identify independent predictors of CSS among stage II LCLC.

Results: A total of 1,894 patients met inclusion criteria, including 489 who received neoadjuvant and/or adjuvant CTx . Patients receiving neoadjuvant and/or adjuvant CTx were younger (median 65 vs. 70 years, $p<0.001$), had more advanced T and N stages, and more frequently had advanced stages ($p<0.001$). Socioeconomic factors were not significantly different between groups. Perioperative CTx was significantly associated with improved CSS (Hazard ratio (HR) 0.71, 95% confidence interval (CI) 0.60-0.85, $p<0.001$) and OS (HR 0.67, 95% CI 0.58-0.78, $p<0.001$) with a more pronounced benefit among patients with nodal involvement. On multivariable analysis among stage II LCLC, perioperative CTx independently predicted better CSS (HR 0.79, 95% CI 0.57-0.86, $p<0.001$); age over 75 (HR 1.76), male sex (HR 1.26), and N1 nodal status (HR 2.10) were also associated with higher mortality.

Conclusions: In this large SEER cohort, neoadjuvant and/or adjuvant chemotherapy was associated with significantly improved cancer-specific survival in patients with resected stage I-II LCLC, with the greatest benefit observed among patients with nodal disease. Although information on surgical extent and mediastinal lymph node dissection was limited, these findings support consideration of perioperative CTx for early-stage LCLC and underscore the need for prospective studies to define optimal treatment strategies.

#6446 Molecular profiling to predict the first site of recurrence in pancreatic cancer patients receiving neoadjuvant therapy followed by surgery.

Luigi Liguori[1], Marco Ventin[1], Liti Zhang[1], Erica Daniels[1], Giulia Cattaneo[1], Chiara Camillo[1], Maoyang Qi[1], Enrica Quattrocchi[1], Eduardo Tejeda-polanco[1], Arsen Osipov[1], Alexandra Gangi[1], Andrew Hendifar[1], Nicholas Nissen[1], Kambiz Kosari[1], Francesco Sabbatino[2], Cristina R. Ferrone[1]

[1]Cedars Sinai Medical Center, Los Angeles, CA,[2]University of Salerno, Baronissi, Italy

Pancreatic ductal adenocarcinoma (PDAC) remains one of the most lethal cancers, with a five-year survival rate of only 13%. Although neoadjuvant chemotherapy and radiotherapy have improved resectability and survival outcomes, most patients ultimately experience disease recurrence. Identifying biomarkers that can stratify recurrence patterns is therefore critical for optimizing patient selection and tailoring postoperative management. We retrospectively analyzed data from PDAC patients who underwent neoadjuvant therapy followed by surgery at Cedars Sinai Medical Center between May 2013 and November 2024. Uni- and multivariable binary logistic regression including clinicopathologic variables and NGS-based molecular features was used to predict the first site of recurrence. Among 244 patients receiving neoadjuvant therapy for PDAC, 138 had complete clinicopathologic and NGS-based molecular data. Most common mutated genes included *TP53* (69.6%), $KRAS^{G12D}$ (43.5%), $KRAS^{G12V}$ (31.2%), *CDKN2A* (24.6%), *SMAD4* (20.3%), $KRAS^{G12R}$ (12.3%), *CDKN2B* (10.1%), $KRAS^{Q61X}$ (7.2%), *ATM* (5.1%), and *BRCA2* (4.3%). First-site recurrence patterns were locoregional (25.5%), liver (32.6%), lung (21.0%), peritoneum (14.5%), and bone (7.2%). Molecular features independently and significantly predicted the first site of recurrence. Specifically, $KRAS^{Q61X}$ mutation was associated with increased risk of locoregional recurrence (OR, 5.6, 95% CI 1.4-22.4, p=0.01), CDKN2B mutations with liver recurrence (OR, 4.4, 95% CI 1.2-16.2, p=0.02), ATM mutations with both lung (OR, 7.7, 95% CI 1.3-44.9, p=0.02) and peritoneal recurrence (OR, 5.0, 95% CI 1.0-24.4, p=0.04), and BRCA2 mutations with bone recurrence (OR, 7.7, 95% CI 1.2-48.9, p=0.03). Our study demonstrates that molecular profiling can predict the first site of recurrence in PDAC patients who have undergone neoadjuvant therapy followed by surgery. While prospective validation in larger cohorts is warranted, this work provides a foundation for developing risk-adapted postoperative surveillance strategies in PDAC.

#6447 FOLFIRINOX plus nivolumab promotes plasma cell production from intra-tumoral lymphoid aggregates in borderline resectable pancreatic adenocarcinoma.

Serena Zheng[1], Jason Link[1], Alykhan Premji[1], Michael Srienc[1], McKensie Hammons[2], Shineui Kim[2], David Dawson[3], Zev Wainberg[4], Timothy Donahue[1]

[1]Surgery, UCLA Medical Center, Los Angeles, CA,[2]UCLA David Geffen School of Medicine, Los Angeles, CA,[3]Pathology, UCLA Medical Center, Los Angeles, CA,[4]Medicine, UCLA Medical Center, Los Angeles, CA

Background: Combination chemotherapy and immune checkpoint inhibitors have shown limited benefit in pancreatic ductal adenocarcinoma (PDAC) despite their success in other solid tumors. However, most studies were conducted in advanced disease. In a phase 1b/2 investigator-initiated clinical trial, we evaluated immunologic effects of neoadjuvant FOLFIRINOX (FFX) plus nivolumab (nivo) in patients with borderline-resectable (BR) PDAC.

Methods: Resected tumor tissue was analyzed by bulk RNA sequencing with CIBERSORT leukocyte deconvolution, immunohistochemical (IHC) quantification of plasma cells and characterization of lymphoid aggregates (LAs), and 10x Xenium spatial transcriptomics (ST) to investigate LA organization. In parallel, tumor draining lymph node (TDLN) cores from untreated, FFX-only, and FFX+nivo cohorts were profiled with Xenium ST.

Results: Across paired pre- and post-treatment samples, intra-tumoral CD8 T cells and plasma cells increased concurrently. Compared with historical FFX controls, nivo-treated tumors had significantly higher plasma cell abundance ($p=0.002$) and a modest CD8 T cell increase ($p=0.037$). IHC revealed that plasma cell abundance correlated with dense intra-tumoral LAs lacking germinal center-like structures ($p<0.001$), consistent with extrafollicular B cell differentiation. ST identified irregular LAs within the tumor bed with high plasma cell to B cell ratios (PBRs) enriched for terminally exhausted CD8 T cells and de-enriched for progenitor exhausted CD8 T cells and central memory CD4 T cells. In TDLN follicles from nivo-treated patients compared to historical FFX controls, plasma cells were again enriched ($p=0.049$), and PBR was significantly higher ($p=0.035$). However, CD8 T cell and memory B cell density decreased within the lymph node follicles ($p<0.001$ and $p=0.005$, respectively). T follicular helper (Tfh) cells provide a critical link between antigen-specific B cells and CD8 T cells; accordingly, IL-21 expression was de-enriched in TDLN Tfh cells from patients treated FFX+nivo compare to FFX alone ($p<0.0001$).

Conclusion: Neoadjuvant FFX plus nivo in BR PDAC is associated with disorganized intra-tumoral LAs, extrafollicular-like plasma cell differentiation, and accumulation of terminally exhausted CD8 T cells within the tumor bed. TDLN follicles in nivo-treated patients also showed plasma cell-skewed, high-PBR architecture, but with reduced CD8 T cell and memory B cell density and selective loss of IL-21 expression in Tfh cells. These features may represent barriers to effective anti-PD-1-based chemoimmunotherapy in PDAC.

#6448 The obesity paradox in pancreatic cancer.

Jacob Lambdin[1], Charlotte Burch[1], William Royster[1], Adam Khader[2], Leopoldo Fernandez[1], Raphael Louie[1], Ricardo Bello[1], Jose G. Trevino[3]

[1]VCU Massey Comprehensive Cancer Center, Richmond, VA,[2]U.S. Department of Veterans Affairs, Richmond, VA,[3]Div. of Surgical Oncology, VCU Massey Cancer Center, Richmond, VA

Introduction: The “obesity paradox,” in which higher body mass index (BMI) appears to confer a survival advantage despite its role in carcinogenesis, has been reported in several solid tumors, but its relevance across racial groups in patients with pancreatic cancer is unclear. We performed a retrospective database study using TriNetx, a multinational deidentified dataset, to identify patients with pancreatic cancer and to examine associations between BMI, race/ethnicity, survival, and post operative complications.

Methods: Using the TriNetx database, we identified patients with pancreatic cancer and stratified the cohort by BMI at time of diagnosis: underweight (UW) (BMI < 18.5 kg/m²), healthy weight (HW) (18.5-24.9 kg/m²), and overweight (OW) (≥25.0 kg/m²). Subgroups were created of Black, Hispanic, and White patients within each BMI cohort to evaluate for racial/ethnic differences in BMI associated outcomes. The primary outcome was overall survival with secondary outcomes of post-operative complications. Propensity score matching was performed for age, sex, stage, comorbidities, and type of surgical resection performed. Kaplan-Meier curves and multivariable Cox models were used to evaluate survival across BMI categories overall and within racial strata. Multivariable logistic regression was used to evaluate associations between BMI category and postoperative complications.

Results: We identified 247,150 patients with pancreatic cancer, including 51,057 (87%) OW, 3241 (6%) HW, and 3815 (7%) UW patients. In propensity matched models, BMI category was found to be associated with overall survival. Compared with HW, OW was associated with a longer 5-year median survival (895 vs 493) and reduced hazard of death (HR = 0.76, 95% CI (0.70-0.82)), while UW was associated with worse survival than HW (HR = 1.24, 95% CI 0.74-0.87)). The magnitude and direction of these associations differed by race/ethnicity with OW Black (HR = 0.69, 95% CI (0.59-0.85)) and OW Hispanic patients (HR = 0.88, 95% CI (0.62-1.25)) deriving more substantial survival benefit over HW when compared to their OW White counterparts (HR = 0.80, 95% CI (0.73-0.86)). Among propensity matched surgical patients, OW was associated with increased risk intraabdominal abscess (10.2% vs 5.1%, RR = 2, p = 0.02), and increased odds of AKI (19.7% vs 12.9%, RR = 1.53, p = 0.026) compared with HW individuals. No significant difference in postoperative pancreatic leak was identified between the OW and HW cohorts. (11.5% vs 11.8%, RR = 0.97, p = 0.89).

Conclusions: In this large, real-world cohort of patients with pancreatic cancer, BMI and race were significant determinants of survival and postoperative morbidity, with patterns consistent with an obesity paradox. These data may refine risk stratification and motivate studies of adiposity and pancreatic cancer biology across diverse populations.

#6449 Adenosine blockade combined with FOLFIRINOX chemotherapy enhances T follicular helper cell function in pancreatic adenocarcinoma draining lymph nodes from mice and humans.

Michael K. Srienc[1], Serena Zheng[1], Jason Link[2], Alykhan Premji[1], McKensie Hammons[3], Shineui Kim[3], Evan Abt[1], Caius G. Radu[3], David W. Dawson[1], Zev A. Wainberg[4], Timothy R. Donahue[5]

[1]UCLA Health, Los Angeles, CA,[2]UCLA Dept of Surgery, Los Angeles, CA,[3]UCLA David Geffen School of Medicine, Los Angeles, CA,[4]UCLA Medical Center Santa Monica, Santa Monica, CA,[5]Assistant Professor, Dept. of General Surg., UCLA David Geffen School of Medicine, Los Angeles, CA

Over 90% of all pancreatic cancer cases are pancreatic ductal adenocarcinoma (PDAC), an aggressive disease with poor prognosis and limited treatment options. Chemotherapy and immunotherapy efficacy are both limited by the immunosuppressive PDAC tumor microenvironment (TME). Treatment-related tumor cell death leads to accumulation of extracellular adenosine, a potent immunosuppressive metabolite in the PDAC TME; accordingly, we investigated the effects of blocking adenosine during chemotherapy treatment. In an orthotopic murine model of PDAC, CD73 - the primary enzyme responsible for extracellular adenosine - inhibition in combination with FOLFIRINOX reduced tumor size by 57% (P=0.04) and significantly increased survival compared to treatment with FOLFIRINOX alone. FOLFIRINOX+CD73i significantly decreased suppressive SPP1+ tumor-associated macrophages, increased Type I and Type II interferon signaling of multiple cell types in the TME, and was CD4+ and CD8+ T cell dependent. To track antigen-specific CD4+ T cells, we engineered expression of an MHC-II restricted epitope in orthotopically implanted tumor cells and found that FOLFIRINOX+CD73i treatment increased follicular helper T (Tfh) cells in tumor-draining lymph nodes but that these cells were not enriched for tetramer-positive, tumor antigen-specific cells. In contrast, Treg cells in the TME were enriched for tetramer-positive cells suggesting that CD73i may drive antigen-reactive T cells toward a suppressor phenotype. Targeting activated T cells by adding anti-CCR8 to FOLFIRINOX+CD73i significantly decreased tumor masses compared to FOLFIRINOX+CD73i alone (P=0.02).
To investigate the effect of CD73i on adaptive immune responses in PDAC patients, we performed Xenium image-based spatial transcriptomics on 53 tumor-draining lymph nodes from patients treated with neoadjuvant FOLFIRINOX+anti-PD-1+CD73i, FOLFIRINOX+anti-PD-1, FOLFIRINOX alone, or untreated. In line with our mouse model, we found a significant CD73i-dependent increase in intra-follicular antigen-experienced B cell density (P=0.037) with a concomitant increase in intra-follicular CD8+ T cell density (P<0.001), which could be explained by enhanced function of Tfh cells. Accordingly, we found enrichment in IL-21 expressing Tfh cells in tumors treated with FOLFIRINOX+anti-PD-1+CD73i compared to FOLFIRINOX+anti-PD-1. These results indicate that CD73i may drive distinct immune remodeling in PDAC, boosting Tfh cell function in draining lymph nodes but favoring antigen-specific Treg enrichment in the tumor microenvironment.

: Clinical Correlates of Immunotherapy
Poster Session

#6453 Serum pharmacodynamic biomarkers of IPI/NIVO/RELA plus sarilumab in Stage III-IV melanoma: Stage 1 results of a Simon Phase II trial (NCT05428007).

Teruyuki Mizutani[1], Amrutesh Puranik[1], Inderjit Mehmi[2], Judith Goldberg[1], Maya Dimitrova[1], Perla Arriola[1], Stanzin Idga[1], Xiaochun Li[1], Benjamin Levinson[1], Justine Cohen[3], Elizabeth I. Buchbinder[3], Donald Lawrence[4], Alissa Kalyan[1], Morgan Simons[1], F. Stephen Hodi[3], Ryan J. Sullivan[4], Omid Hamid[2], Michelle Krogsgaard[1], Janice M. Mehnert[1]

[1]NYU Langone Health Perlmutter Cancer Ctr., New York, NY,[2]The Angeles Clinic and Research Institute, Los Angeles, CA,[3]Dana-Farber Cancer Institute, Boston, MA,[4]Harvard Medical School/Massachusetts General Hospital, Boston, MA

Background: Assessing biomarkers to predict response is crucial for optimizing melanoma treatment with immune checkpoint inhibitors (ICIs). In this context, monitoring cytokine dynamics over time provides a rational strategy to determine whether IL-6R inhibition with sarilumab is biologically active and to identify pharmacodynamic signatures associated with clinical outcomes. Here, we focus on longitudinal serum cytokine profiling using Luminex assays to explore pharmacodynamic biomarkers for response in a phase II trial combining nivolumab (3 mg/kg), ipilimumab (1 mg/kg), the IL-6 receptor inhibitor sarilumab (150 mg), and the LAG-3 antibody relatlimab (160 mg) (INR + S) in patients with unresectable or advanced melanoma.
Methods: We analyzed serum cytokines from 33 melanoma patients treated with INR + S using samples from baseline, week 4, week 6, week 12, week 18, and week 28 (final timepoint after discontinuation of sarilumab), and categorized patients according to response and toxicity. Patients were classified into PR/CR, SD, and PD groups, as well as grade 1-2 versus grade 3 or greater toxicity. Serum cytokines were profiled using Luminex assays, measuring 23 analytes. In total, 152 samples from 33 patients were analyzed. Statistical analyses were conducted using Mann-Whitney U test, paired t-test, and Kruskal-Wallis test, with the significance level set at 0.05.
Results: The best overall response rate was 63.6%. Grade 3-5 irAEs occurred in 12% of patients by week 24. At baseline, no pretreatment predictive factors for either treatment response or > grade 3 irAEs were identified. Across all patients, several significant post-treatment patterns that correlated with clinical benefit were observed compared with baseline at one or more time points for IL-6, IL-6R, OSM, CXCL10, IL-4, IL-10, G-CSF, and M-CSF. Notably, PR/CR patients showed increased IL-6 and decreased IL-6R levels over time, which returned to baseline levels after discontinuation of sarilumab. When comparing baseline with week 4, progressive disease was associated with marked increases in OPN, and IL-8, whereas PR/CR patients showed decreases in IL-6R, IL-4, and G-CSF.
Conclusion: Longitudinal analyses in the present study revealed increased IL-6 and decreased IL-6R levels. These dynamics likely reflect a more active mode of IL-6R blockade and may have contributed to improved clinical outcomes. The next phase of the trial is a randomized comparison of INR +/- S, and biospecimens from this randomized comparison will be analyzed to build on our findings.

#6454 Enhanced monocyte activation and T cell cytotoxicity underlie the benefit of neoadjuvant durvalumab plus gemcitabine-cisplatin (D+GP) in localized biliary tract cancer (BTC): Phase 2 DEBATE study.

Changhoon Yoo[1], Hyung-Don Kim[1], Chang Yeon Kim[2], Joon Oh Park[3], Hyehyun Jeong[1], Kyu-Pyo Kim[1], Jung Yong Hong[4], Sang Hyun Shin[4], Tae Jun Song[1], Dongwook Oh[1], Woohyung Lee[1], Jae Hoon Lee[1], Dae Wook Hwang[1], Jeong Seok Lee[5]

[1]University of Ulsan College of Medicine, Seoul, Korea, Republic of,[2]Seoul National University College of Medicine, Seoul, Korea, Republic of,[3]Associate Professor, Dept. of Hem./Onc., Samsung Medical Center, Seoul, Korea, Republic of,[4]Samsung Medical Center, Seoul, Korea, Republic of,[5]Korea Advanced Institute of Science and Technology, Daejeon, Korea, Republic of

Introduction: The prognosis of localized BTC remains poor despite surgery. The role of neoadjuvant therapy in BTC has not been well established.
Methods: DEBATE is a multicenter, randomized, non-comparative phase 2 trial enrolling treatment-naïve patients (pts) with localized BTC. Pts were randomized (2:1) to receive 4 cycles of neoadjuvant D+GP or GP alone. Those undergoing surgery received 6 cycles of adjuvant durvalumab. The primary endpoint was the R0 resection rate. Biomarker analyses included single-cell RNA sequencing (scRNA-seq) of peripheral blood mononuclear cells (PBMCs), and plasma proteomics (baseline and cycle 1 day 8 [C1D8]).
Results: A total of 45 pts were enrolled (D+GP, n=31; GP, n=14). Surgery was performed in 64.5% vs. 42.9%, and R0 resection rates were 48.4% vs. 42.9% in the D+GP and GP arms, respectively. In the D+GP group, the objective response rate was 38.7%, median PFS 19 months (1-sided 80% CI, 15-21), and OS 28 months (24-43), versus 14.3%, 6 months (3-11), and 30 months (23-44) in the GP group. Biomarker data were available in 98% (n=44). scRNA-seq showed a significant enrichment of classical monocytes with pro-inflammatory signatures in the D+GP group, especially among responders, along with increased CXCL10 expression in both scRNA-seq and plasma proteomics. Responders in the D+GP group also exhibited increased CD8+ T cell cytotoxicity, CD4+ Terminally differentiated effector memory T (TEMRA) cells, and IL12RB2 expression. TIGIT expression in CD4+ TEMRA cells decreased from baseline to C1D8 only in responders treated with D+GP.
Conclusion: Neoadjuvant D+GP was feasible and demonstrated encouraging efficacy in localized BTC. Integrated biomarker analyses suggest that enhanced monocyte activation and T cell responses contribute to the added benefit of durvalumab. Current study provide the rationale of adding anti-TIGIT to D+GP in BTC (NCT04308174).

#6455 Cytotoxic T-cell signatures underlie therapeutic response to 177Lu-DOTATATE plus pembrolizumab in well-differentiated gastroenteric neuroendocrine tumors.

Naoki Mizutani[1], Shloka Shukla[1], Nicholas Fidelman[2], Bridget P. Keenan[2], David Y. Oh[2], Kira Chan[2], Li Zhang[2], Emily K. Bergsland[2], Thomas Hope[2], Lawrence Fong[1]

[1]Translational Science and Therapeutics Division, Fred Hutchinson Cancer Center, Seattle, WA,[2]University of California San Francisco, San Francisco, CA

Background

Peptide receptor radionuclide therapy (PRRT) with 177Lu-DOTATATE is an established treatment for well-differentiated neuroendocrine tumors (WD-NETs). PD-1 blockade with pembrolizumab has been investigated in NETs; however, radiographic responses are limited when used as monotherapy. As such, we investigated the combination of PRRT and pembrolizumab as an investigational approach to enhance antitumor immunity and efficacy in 26 patients with grade 2 or 3 WD-NET (NCT03457948). The overall response rate (ORR) by RECIST 1.1 was 34.6% (9/26), but the systemic immune changes induced by this combination remain incompletely understood. We now report the results of our investigation of peripheral immune remodeling and T-cell clonal dynamics using single-cell (sc) transcriptomic and TCR repertoire profiling of PBMCs.

Methods

A total of 111 PBMC samples were collected longitudinally from 26 patients treated with PRRT plus pembrolizumab. scRNA sequencing and TCR sequencing were performed using the 10x Genomics platform. Major immune populations were annotated, and transcriptional and clonal characteristics were analyzed in relation to treatment response. Patients were stratified into pancreatic NET (pNET, N=14; 5 responders [36%, PR] and 9 non-responders [64%; 7 SD, 2 PD]) and extrapancreatic NET (epNET, N=12; 4 responders [33%, PR] and 8 non-responders [67%; 7 SD, 1 PD]), with the latter including tumors of intestinal, pulmonary, and unknown primary origin. Statistical analysis was performed with Mann-Whitney U test.

Results

In epNET responders, the frequency of $CD8^+$ T cells increased across timepoints compared with epNET non-responders ($p<0.05$). Further subclustering of T cells revealed that both $CD4^+$ and a subset of $CD8^+$ cytotoxic T cells were significantly elevated ($p<0.05$) and exhibited prominent clonal expansion in epNET responders, particularly post treatment. Non-responders showed an enrichment of immunosuppressive subsets, including $CD4^+$ regulatory T cells (Treg) and $CD4^+$

Th2 cells ($p<0.05$). Differential gene expression analysis demonstrated that several cytotoxic genes (*NKG7*, *CCL5*, *GNLY*, and *GZMH*) were upregulated in both $CD4^+$ and $CD8^+$ T cells in the responders compared with non-responders. In contrast to epNET, systemic immune remodeling was generally limited in pNET patients regardless of response status.

Conclusions

Integrated single-cell and TCR analysis revealed distinct systemic T-cell activation profiles between responders and non-responders to PRRT plus PD-1 blockade, but this effect varied by site of origin. Responding patients with epNET exhibited prominent clonal expansion and upregulation of cytotoxic genes. These findings highlight key differences in peripheral immune dynamics associated with treatment response in WD-NETs and may inform strategies to optimize combination therapy.

#6456 Pan-tumor investigation of peripheral biomarkers of excellent response to anti-PD(L)1-based therapy.

Howard L. Li[1], Soren Charmsaz[2], Chester Kao[1], Carlotta Pazzi[1], Madelena Brancati[1], James Leatherman[1], Nicole E. Gross[1], Royce P. Lee[1], Xiyu Zhao[3], Christopher Thoburn[1], Jeannie Hoffman-Censits[1], Evan J. Lipson[1], Yasser Ged[1], Marina Baretti[1], G Scott Chandler[4], Rajat Mohindra[4], Laura Tang[5], Sanjay Bansal[5], Aditi Guha[5], Elizabeth Jaffee[1], Daniel J. Zabransky[1], Won Jin Ho[1], Mark Yarchoan[1], Mari Nakazawa[1]

[1]Sidney Kimmel Comprehensive Cancer Center, Baltimore, MD,[2]Johns Hopkins University School of Medicine, Baltimore, MD,[3]The Johns Hopkins Hospital, Baltimore, MD,[4]Roche, Basel, Switzerland,[5]Genentech, South San Francisco, CA

Background: Immune checkpoint inhibitors (ICIs) have transformed contemporary cancer care, yet few patients experience objective responses. There is a need for novel peripheral biomarkers that can not only identify patients likely to respond but also distinguish those with excellent, durable benefit to enable improved patient selection, therapeutic monitoring, and target discovery.
Methods: We prospectively collected serial blood samples from patients with advanced/metastatic solid tumors treated at Johns Hopkins on anti-PD(L)1-based therapy from 2021-2024. Patients with complete or durable partial response with progression-free survival (PFS) greater than one year were classified as excellent responders (ERs); other patients were classified as non-ERs. Peripheral blood mononuclear cells were analyzed using CyTOF to quantify 28 immune cell clusters with associated functional markers, and plasma samples were analyzed using a Luminex multiplex assay to quantify concentrations of 39 cytokines at baseline and early-on-treatment (month 1 or 2).
Results: Our total cohort included 123 patients, 30 of whom were classified as ERs. The most common tumor types were HCC, head and neck cancer, RCC, and bladder cancer. Our cytokine cohort included 118 patients. At baseline, ERs had significantly elevated Th17-associated cytokines, IL-17F, IL-21, and IL-23 compared to non-ERs (Wilcoxon rank-sum, $p<0.05$). Non-ERs had elevated baseline IL-8 concentrations ($p<0.05$). These results persisted early-on-treatment, with the addition of elevated on-treatment IL-6 being associated with non-ER ($p<0.05$). Patients with greater than median IL-17F concentrations at baseline demonstrated improved PFS ($p=0.075$), while greater than median IL-6 and IL-8 baseline concentrations demonstrated worse OS ($p=0.053$ and $p<0.001$). Our CyTOF cohort included 116 patients. As compared to non-ERs, ERs were associated with greater early-treatment expansion of NK cells and double negative (CD4-CD8-) T-cell as well as multiple Th2-central memory clusters ($p<0.05$). Th17 cells were also increased in ERs as compared to non-ERs, although this result did not reach significance ($p=0.06$). Immune cell functional marker analysis in non-ERs shows that Th17 cells had increased proliferation of exhausted T-cells (Ki67+TIGIT+) from baseline to early-on-treatment (Linear mixed model, $p < 0.01$), which was not present in ERs.
Conclusions: In a prospective, pan-tumor cohort, we find that Th17 cytokines, IL-17F, IL-21, and IL-23, as well as Th2-central memory cells are associated with excellent ICI response, in addition to re-demonstrating the negative prognostic implications of Th17 cytokine, IL-6, as well as IL-8. Our study highlights the Th17 pathway as a polarizing determinant of excellent ICI response and represents a comprehensive exploration of other peripheral cytokines and immune cells in mediating durable ICI benefit.

#6457 Phase I study of STA551 (STA) a tumor-selective CD137 agonist, as monotherapy and in combination with atezolizumab (atezo) using CD8 PET imaging to assess pharmacodynamic effects.

Udai Banerji[1], Diogo Silva[1], Joshua Ting[1], Zoulikha Zair[2], Prakash Manoharan[2], Toshihiko Doi[3], Shigehiro Koganemaru[3], Noboru Yamamoto[4], Takafumi Koyama[4], Seiichi Ikeda[5], Yuki Kanai[5], Michiyasu Inatani[5], Hitomi Takeshita[5], Akiko Hashimoto[6], Yoshitaka Ogita[5], Yuma Takano[5], Kei Higashikawa[5], Fiona Thistlethwaite[2]

[1]The Institute of Cancer Research; The Royal Marsden Hospital, London, United Kingdom,[2]The Christie NHS Foundation Trust, Manchester, United Kingdom,[3]National Cancer Center Hospital East, Chiba, Japan,[4]National Cancer Center Hospital, Tokyo, Japan,[5]Chugai Pharmaceutical Co., Ltd., Tokyo, Japan,[6]Chugai Pharma Europe Ltd., London, United Kingdom

Background: CD137 is a promising costimulatory receptor for cancer immunotherapy. Several CD137 agonist antibody biologics have been developed, but none show clear promising clinical potential due to severe toxicity. STA, an ATP-dependent switch antibody, is designed to selectively activate CD137 within tumors, and minimize systemic toxicity. We conducted a phase I study of STA alone or the combination of STA and atezo to evaluate tolerability, PK and pharmacodynamics using CD8 PET imaging, in patients with advanced solid tumors.

Methods: The Phase 1 study includes dose escalation and CD8 PET cohorts. For the dose escalation cohorts, patients were treated with either STA monotherapy IV q3 weekly or STA in combination with atezo (1200 mg) q3 weekly. For the CD8 PET cohort, patients received STA q3 weekly for two cycles as monotherapy, followed by combination therapy with atezo 1200 mg from cycle 3 onwards. Zr-89 crefmirlimab berdoxam (a minibody targeting CD8, labeled with Zr-89) was used as the tracer of CD8 PET scan. CD8 PET scans were done at baseline, after two STA doses (Cycle 2 Day 9), and after two combination doses (Cycle 4 Day 9).

Results: A total of 94 patients were treated in the dose escalation cohorts (41 patients in monotherapy and 41 patients in the combination) and in the CD8 PET cohort (12 patients). The most common treatment related adverse events (≥10%) were AST increased (17.1%), fatigue (14.6%), and ALT increased (12.2%) in mono cohorts; ALT increased (22.6%), AST increased (18.9%), infusion related reaction (IRR) (15.1%), nausea (13.2%), diarrhoea (11.3%) and fatigue (11.3%) in combination and CD8 PET cohorts. No severe adverse events related to Zr-89 crefmirlimab berdoxam were reported. No dose limiting toxicities were observed up to STA 1200 mg alone. The maximum tolerated dose was 450 mg of STA in combination with 1200 mg of atezo administered q3 weekly. The PK analysis showed STA increased in a dose proportional manner. In the CD8 PET cohort, 10 patients were evaluable for efficacy and CD8 PET analyses. One partial response (PR) was observed in a heavily pretreated patient with triple negative breast cancer. Five patients had stable disease. Increased tracer accumulation in tumor lesions was indicated in a subset of patients. Notably, in the patient who achieved a PR, clear increased accumulation was observed in all evaluable lesions. No clear increase in the tracer accumulation was observed in the spleen which has been reported with other systemic CD137 agonists.

Conclusions: STA demonstrated a manageable safety profile both as monotherapy and in combination with atezo. CD8 PET analysis suggested STA increased intratumoral $CD8^+$ T cell levels in a subset of patients, with limited effects in normal organs. These findings potentially support the tumor-selective mechanism of action of STA as a CD137 agonist.

#6458 Harnessing tumor-informed B cell receptors for discovery and antibody-based immunotherapy in sarcoma.

Varshini Arunkumar, Manoj Chelvanambi, Joshua B. Plummer, Monika Zelazowska, Fabiana J. Veguilla, Elise Nassif Haddad, Noha M. Osman, Wei-Lien Wang, Davis Ingram, Khalida M. Wani, Angela Bhalla, Sharon M. Landers, Keila E. Torres, Jennifer A. Wargo, Bin Liu, Alexander Lazar, Neeta Somaiah, Christina L. Roland, Kevin McBride, Emily Z. Keung

UT MD Anderson Cancer Center, Houston, TX

Background: Soft tissue sarcomas (STS) are rare and heterogenous cancers, with limited effective treatments and poor prognosis. While some patients with STS respond to immune checkpoint blockade (ICB), the majority do not benefit. This highlights an urgent need to elucidate mechanisms of response and resistance to ICB and develop novel immunotherapeutic approaches for patients with STS. We and others have shown that tumor infiltrating B cells (TIL-Bs), particularly those in tertiary lymphoid structures (TLS) are associated with response to ICB and longer survival. However, the antigen specificity, mechanisms of action, and therapeutic potential of these TIL-Bs and their B cell receptors (BCRs) remain unknown.
Methods: We recently completed a phase 2 clinical trial evaluating ICB administered in the neoadjuvant setting in patients with resectable undifferentiated pleomorphic sarcoma (UPS) of the extremity/trunk or dedifferentiated liposarcoma (DDLPS) of the retroperitoneum (Roland et al. *Nature Cancer* 2024). Leveraging a unique biospecimen resource from this trial, we reconstructed intratumoral BCR heavy and light chain (V_H and V_L) repertoires using pre-treatment baseline tumor biopsies (n = 27), RNA-sequencing, and an in-house pipeline including TRUST4. We then performed single intratumoral B cell immunoglobulin sequencing using cell suspensions from 4 TLS-positive tumors to reconstruct and express 105 recombinant BCR antibodies (rBCR Abs) as IgG1. Flow cytometry (FC) was performed to characterize the binding features of a subset of 20 rBCR Abs with human DDLPS (LPS224, LPS246) and UPS cell lines (UPS186, RIS819.1). Binding was quantified as the ratio of the mean fluorescent intensity (MFI) of the antibody to the MFI of the isotype control for each cell line. Abs with an MFI ratio ≥ 1.2 were classified as binders and tumor surface binding was further assessed by live cell microscopy. Antibody-dependent cellular cytotoxicity (ADCC) assays were performed to assess the functional capacity of this cohort of rBCR Abs to mediate NK-cell dependent tumor killing. The anti-tumor efficacy of 1 lead rBCR Ab was assessed using an MCA205 immunocompetent murine STS model.
Results: Of 105 rBCR Abs screened, 23 (22%) exhibited reproducible surface binding to at least one sarcoma cell line by FC. Among these, 13 (12%) bound LPS lines and 18 (17%) bound UPS lines. To date, 20 rBCR Abs have been confirmed to bind the surface of sarcoma cell lines by live cell staining of which 5 mediated tumor cell killing in vitro. One candidate rBCR Ab has been evaluated in vivo, localizing to tumor and synergized with PD-1/PD-L1 blockade to suppress tumor growth when administered intraperitoneally.
Conclusion: These findings highlight the potential of rBCR Abs to serve as a novel therapeutic strategy and as tools to elucidate the roles of B cells and the BCR repertoire within the tumor immune microenvironment of patients with STS.

#6459 Development of FL115, a novel IL-15 superagonist, as subcutaneous injection for cancer immunotherapy.

Qinghua Wu, Quanxiao Li, **Dong Wei**

Forlong Biotechnology, Suzhou, China

Background: FL115 is an engineered IL-15/IL15Rα-Fbody fusion protein, in which Fbody is a single-chain Fc designed to eliminate classical Fc effects including ADCC/CDC/ADCP while retaining FcRn engagement. In Phase I clinical studies in patients with advanced solid tumors, FL115 administered as weekly IV infusion (dose range: 3-90 μg/kg) demonstrated favorable safety profile and preliminary clinical efficacy including 2 confirmed PR. Dose-proportional pharmacokinetics was observed, with on-target pharmacodynamic activities including sustained significant expansion of NK and CD8+ T cells. Strong transient induction of IFN-γ in plasma was observed, with peak concentration at over 3000 pg/ml compared to IL-6 at ~1 pg/ml at 3 μg/kg dose. Prior IL-15 therapeutic agents have shown significant profile enhancement when administered as subcutaneous injection compared to IV infusion. Here we present the preclinical data supporting further development of FL115 as subcutaneous injection.

Methods: In an SD rat study, a single dose of FL115 was injected subcutaneously at 0.1,0.3 or 1.0 mg/kg or via IV at 0.3 mg/kg, and pharmacokinetic parameters were assessed. In a Cynomolgus monkey study, a single dose of FL115 was injected via IV at 0.23,0.43 or 1.02 mg/kg or subcutaneously at 0.43 mg/kg, and pharmacokinetic parameters were assessed. In a subcutaneous irritation study in New Zealand white rabbits, FL115 was injected subcutaneously at 0.1 ml/kg (FL115 concentration: 21.1mg/ml) per injection site at Day 1 and Day 7, and local injection site reaction was assessed.

Results: In the Cynomolgus monkey study, FL115 of 0.43 mg/kg via IV injection resulted in serum C_{max} of 9350-9360 ng/ml and T_{max} of 0.08 hours, while 0.43 mg/kg via subcutaneous injection resulted in serum C_{max} of 350-436 ng/ml and T_{max} of 4 hours as well as bioavailability of 54.7-65.8%. In the SD rat study, FL115 of 0.3 mg/kg via IV injection resulted in serum C_{max} of 4370 ng/ml and T_{max} of 0.08 hours, while 0.3 mg/kg via subcutaneous injection resulted in serum C_{max} of 223 ng/ml and T_{max} of 6 hours as well as bioavailability of 67%, . A single dose subcutaneous injection at 0.1,0.3 or 1.0 mg/kg in rat also showed good linearity. In the rabbit study, from Day 1 to 24, skin irritation at gross observation was at Grade 0 (no abnormality). At Day 10, histopathological assessment showed mild inflammatory cell infiltration under the skin and in muscle, which was fully resolved at Day 24.

Conclusion: Compared to IV injection, subcutaneous FL115 in rats and monkeys showed a significant delay (up to 4-6 hours) and drastic lowering of C_{max} (up to 26.7×) with bioavailability at ~60% as well as good linearity in PK file. FL115 at approximately 9 mg per injection site in rabbits showed no significant gross skin irritation. These results support continuing development of FL115 as subcutaneous injection for cancer immunotherapy.

#6460 Immunologic and transcriptional features associated with long-term response and resistance to immune checkpoint inhibitors in non-small cell lung cancer checkpoint inhibitors in non-small cell lung cancer.

Yoshihiro Masui[1], Tatsuya Yoshida[1], Jun Miyakoshi[1], Ryoko Higashiyama[1], Akiko Tateishi[1], Yuki Shinno[1], Tomonori Mizutani[1], Yusuke Okuma[1], Hidehito Horinouchi[1], Kouya Shiraishi[2], Takashi Kohno[2], Yasushi Goto[1]

[1]Thoracic Oncology, National Cancer Center Hospital, Tokyo, Japan,[2]Division of Genome Biology, National Cancer Center Research Institute, Tokyo, Japan

Background: Immune checkpoint inhibitors (ICIs) have markedly improved outcomes in non-small cell lung cancer (NSCLC), yet durable benefit is achieved in only a minority of patients. The biological mechanisms underlying tumor response to ICIs—including primary resistance (PriR), acquired resistance (AcqR), and long-term response (LTR)—remain poorly understood.
Methods: We reviewed patients with advanced or recurrent NSCLC who initiated first-line ICI monotherapy at the National Cancer Center Hospital (Japan) between 2015-2020. Patients were classified as LTR (defined as progression-free survival ≥48 months), AcqR (initial disease control followed by progression <48 months), or PriR (best response PD). Clinical characteristics were characterized across these groups. Pretreatment tumor RNA-seq data were subjected to transcriptomic analyses. Differential pathway activity was evaluated using Hallmark and Reactome GSEA, and immune-cell composition was inferred using CIBERSORT.
Results: A total of 216 patients were included in the clinical cohort. Pretreatment tumor RNA-seq data were available for 46 patients (LTR, n=10; AcqR, n=23; PriR, n=13). Compared with responders (LTR + AcqR), PriR tumors showed marked enrichment of inflammatory and immunosuppressive programs, including IL6-JAK-STAT3, TNFα/NF-κB, complement, glycolysis, and hypoxia pathways, suggesting a metabolically stressed and suppressive microenvironment that hinders initial immune activation. In contrast, responders exhibited higher interferon-γ (IFN-γ) signaling and T-cell activation signatures. In a direct comparison between LTR and AcqR, LTR tumors uniquely preserved strong IFN-γ-driven inflammation, intact MHC class I antigen-presentation machinery, and robust cytotoxic and memory T-cell programs. AcqR tumors showed attenuation of antigen-presentation and effector-immune pathways, suggesting that reduced immunogenicity contributes to progression after an initial response. Among PD-L1-high tumors, LTR cases again maintained intact antigen-presentation machinery and sustained IFN-γ-driven cytotoxic T-cell activity, whereas AcqR tumors demonstrated attenuation of these programs.
Conclusion: Compared with PriR and AcqR tumors, LTR tumors showed higher IFN-γ activity, preserved antigen-presentation activity, and sustained effector T-cell signaling. PriR tumors were characterized by inflammatory and metabolically stressed immunosuppressive programs, whereas AcqR tumors showed loss of antigen-presentation and effector-immune activity after the initial response. These features may help identify patients likely to achieve durable ICI benefit and suggest potential targets to overcome resistance.

#6461 Comprehensive cytokine, chemokine and immune marker evaluation in plasma samples of primary, non-metastatic high grade serous ovarian cancer patients to estimate outcome and platinum resistance.

Sabine Kasimir-Bauer[1], Buesra Eser[1], Yipeng Wang[2], Gordon Vansant[2], Stefanos I. Moukas[1], Rainer Kimmig[1], Fabinshy Thangarajah[1]

[1]Department of Gynecology and Obstetrics, University Hospital Essen, Essen, Germany,[2]LuminoDx, San Diego, CA

Background: Ovarian cancer (OC) still has the highest mortality rate of all gynecological malignancies, diagnosed mostly at advanced stages, resulting in a generally poor outcome. Radical tumor debulking, followed by platinum-based chemotherapy with/without bevacizumab and with/without PARP inhibitors is the standard of care in advanced OC. However, the majority of patients will ultimately relapse due to the development of platinum resistance. Efforts to apply immunotherapy has been less successful, however, immunologic processes play an important role in tumorigenesis and therapy response. Little is known about immune-marker, cytokine and chemokine expression in OC. In view of biomarker research to identify patients at high risk for relapse, we here determined cytokine/chemokine/immune-related marker levels in blood samples of primary, non-metastatic, high grade serous (HGS) OC patients before and after therapy to estimate their value with regard to progression-free survival (PFS), overall survival (OS) and platinum resistance.

Patients and Methods: Plasma samples of 53 HGSOC patients were collected prior (n=53) and following platinum-based chemotherapy (n=27) with/without bevacizumab. Cytokine/chemokine/immune-related marker levels were quantified using the Olink Target 48 Cytokine panel and Immune Surveillance Panel (LuminoDx, San Diego, USA), which includes total 89 immune-related proteins and requires only one µL of sample. Results were correlated between cytokine/chemokine/immune related marker levels and PFS and OS using the Cox proportional hazards model and Log-rank test as well as platinum resistance applying the student`s t-test.

Results: Associations between cytokine/chemokine/immune-related marker levels and patient outcomes were evaluated using Cox proportional hazards models. At baseline, lower IL19 levels and higher FASLG and CEACAM5 levels were significantly associated with an improved PFS ($p<0.01$). Lower IL17A, IL19, VEGFA, IL27 and higher FASLG levels were significantly associated with a longer OS ($p<0.01$). Decreases in FASLG and CEACAM5 levels over the course of treatment correlated with a longer PFS while increasing VEGFA levels were significantly associated with a longer OS. Additionally, high baseline IL19 and IL6 levels and low CXCL12 and IL18 levels were significantly associated with the development of platinum resistance ($p<0.05$). IL19 was the only marker demonstrating statistical significance ($p<0.05$) for both, PFS and platinum resistance.

Conclusion: Here we demonstrate the potential value of cytokine, chemokine and immune-related marker plasma levels to better estimate PFS, OS as well as platinum resistance in HGSOC. These prognostic and predictive markers may be further developed into clinical assays to support patient management.

#6462 Baseline peripheral immune signatures associate with toxicity to immunotherapy in melanoma.

Iluja Gautam[1], Patricia Rayman[1], Nickolas Stabellini[1], Jennifer Powers[1], Adam Moen[1], Brian Race[1], Paul Pavicic[1], Mona Patel[1], Alberto J. Montero[2], C. Marcela Diaz-Montero[1]

[1]Cleveland Clinic Research, Cleveland, OH,[2]University Hospitals, Cleveland, OH

Background: Adjuvant immune checkpoint inhibitors (ICIs) improve recurrence-free survival in high-risk melanoma. Despite this, a subset of patients do not respond to ICIs while other experience immune-related adverse events (irAEs) without therapeutic benefits. Predictive biomarkers remain undefined, and grouping patients without accounting for irAE status may obscure meaningful immune correlates. We hypothesized that comprehensive immune profiling of baseline peripheral blood mononuclear cells (PBMCs) may help identify predictive immune signatures associated with both response and toxicity to adjuvant ICI.

Methods: Blood samples were collected from a total of 22 melanoma patients undergoing adjuvant ICI therapies at baseline and on-treatment. PBMCs were isolated using standard density gradient centrifugation and stained using two comprehensive immunophenotyping panels. Data was acquired on FACS symphony A5. FlowJo's built-in UMAP plugin was used to visualize immune cell clustering and further characterized using Marker Enrichment Modeling. Response to therapy was determined retrospectively. Immune subsets were compared between responders and non-responders at the two time points and was further stratified by occurrence of irAEs.

Results: At baseline, responders demonstrated enrichment of central memory T cells and terminally differentiated effector memory T cells, consistent with a primed yet regulated immune state poised for rapid activation. In contrast, non-responders had elevated CD16+ MDSCs, which further expanded on treatment, indicating a suppressive peripheral milieu. Among responders, those developing irAEs demonstrated increased memory-like T cells and CD14+CD62P+ myeloid populations compared to those with no irAEs. Among non-responders, irAE-positive patients displayed higher CD45RA+CD4+CD62L+ memory and CD8+CD57+ effector T cell populations. Within the myeloid compartment, CD62P+ cells were increased in both responders and non-responders with irAEs highlighting platelet-myeloid activation. Non-responders without irAEs showed globally low activation, consistent with an immune quiescent state. No significant treatment induced changes distinguished response categories, underscoring the importance of baseline immune context.

Conclusions: Baseline peripheral immune composition reflects distinct states of immune readiness in melanoma patients receiving adjuvant ICI. Responders display a primed immune profile whereas non-responders exhibit myeloid driven suppression. These findings highlight peripheral immune features that may predict therapeutic efficacy and toxicity in melanoma patients in the adjuvant ICI setting. Importantly, stratifying patients by irAE status is essential to reveal true immune correlates of efficacy and toxicity, as pooled analyses risk conflating biologically distinct activation and suppression states.

#6463 Longitudinal single-cell atlas of GD2-CAR T cell therapy in H3K27M-mutant diffuse midline glioma identifies humoral and cellular anti-CAR immunity.

Yiyun Chen, Kun-Wei Song, Moksha H. Desai, Ying-Wen Huang, Nadya Iswari, Zachary J. Ehlinger, Hossein Daghagh, Maximilian R. A. Koch, Kevin Reynolds, Kelvin C. Mo, Kristin C. Y. Tsui, Skyler Rietberg, Mark P. Hamilton, Snehit Prabhu, Sonia Partap, Jasia Mahdi, Emily Egeler, Steven A. Feldman, Sabine Heitzeneder, Sean A. Yamada-Hunter, Elena Sotillo, Bita Sahaf, Zinaida Good, Michelle Monje, Sneha Ramakrishna, Crystal L. Mackall

Stanford Cancer Institute, Stanford, CA

GD2-CAR T cell therapy has demonstrated clinical benefit in a high fraction of patients with H3K27M-mutant diffuse midline glioma (DMG), but the durability of response is limited in some patients. To define mechanisms underlying loss of response and immune adaptation during repeated CAR T infusions, we performed longitudinal single-cell RNA and TCR sequencing of over 1.4 million cells from apheresis, CAR T products, and serial cerebrospinal fluid (CSF) samples collected from 13 DMG patients enrolled in the Arm A of Phase I trial of GD2-CAR T cell therapy (NCT04196413). Our analysis showed that GD2-CAR T cells exhibited poor persistence in vivo, with minimal detection after six infusion cycles. Endogenous lymphocytes, rather than CAR T cells, dominated the CSF immune compartment over time. Regulatory T cells were significantly enriched in non-responders, suggesting a suppressive immune milieu that limits CAR T activity. Among four patients who initially achieved sustained responses for over 12 months, three eventually relapsed after repeated infusions. Flow cytometry detected presence of anti-CAR antibodies in plasma and CSF these three patients, accompanied by an increase in CSF B cells at the time of relapse, indicating a humoral anti-CAR immune response. Complementing this, single-cell TCR-seq revealed that endogenous T cell repertoires stabilized toward the end of treatment in these relapsed responders, with hyper-expanded clonotypes exhibiting activated, cytotoxic, and exhausted transcriptional programs. In contrast, two durable responders maintained a dominant tissue-resident memory-like T cell program, which is associated with sustained disease control. Altogether, we generated a comprehensive longitudinal collection of single-cell sequencing and other omics data, and identified co-existing humoral and cellular mechanisms of anti-CAR immunity that emerge during prolonged GD2-CAR T cell therapy. These findings illuminate correlates of response and resistance and underscore the immunogenic potential of CAR constructs. Future approaches to reduce host immunoreactivity could improve CAR T cell efficacy and durability in solid tumors.

#6464 Surgery-induced expansion of myeloid-derived suppressor cells and loss of cytotoxic lymphocyte function predict poor survival in pancreatic cancer.

Olivia Johnsson[1], Malin S. Nilsson[1], Roberta Kiffin[1], Johan Bourghardt Fagman[2], Caroline Vilhav[2], Svein Olav Bratlie[2], Peter L J Naredi[2], Kristoffer Hellstrand[3], Anna Martner[1]

[1]TIMM Laboratory, Sahlgrenska Center for Cancer Research, Department of Microbiology and Immunology, Institute of Biomedicine, University of Gothenburg, Gothenburg, Sweden, [2]Department of Surgery, Institute of Clinical Sciences, University of Gothenburg, Gothenburg, Sweden,[3]TIMM Laboratory, Sahlgrenska Center for Cancer Research, Department of Infectious Diseases, Institute of Biomedicine, University of Gothenburg, Gothenburg, Sweden

Pancreatic cancer remains a highly lethal malignancy, with high recurrence rates even after curative-intent resection. Evidence suggests that surgical stress triggers inflammation and immunosuppression, potentially facilitating tumor recurrence. Myeloid-derived suppressor cells (MDSCs) and dysfunctional natural killer (NK) cells are mediators of this process. We hypothesized that surgery-induced immune dysregulation, driven by NOX2-derived reactive oxygen species, impairs immunity and worsens outcomes.

Peripheral blood mononuclear cells from 33 pancreatic cancer patients enrolled in the IPEP trial (ethical no. 057-18) were collected pre- and postoperatively (days 1 and 3-5). Single-cell multiomic profiling (BD Rhapsody) was used to characterize immune populations and activation. Frequencies of immune cells and surface receptor expression were analyzed longitudinally and correlated with patient outcome.

Analysis of 445,152 cells revealed major postoperative shifts in circulating leukocytes (Table 1). $NOX2^+$ monocytic MDSCs (M-MDSCs) expanded markedly on postoperative day 1 and remained elevated through day 3-5. Conversely, cytotoxic T and NK cells significantly declined after surgery, and postoperative NK cells showed reduced expression of the activating receptor NKp30. High postoperative M-MDSC frequencies were associated with poorer overall survival (P = 0.017, n=29, log-rank test).

Pancreatic cancer surgery induces profound immune remodeling characterized by M-MDSC expansion and cytotoxic lymphocyte suppression. These changes associate with adverse outcomes, suggesting that postoperative immune dysfunction may promote recurrence. Targeting NOX2-dependent immunosuppressive pathways may help preserve antitumor immunity and improve postoperative survival.

[1]Mean ± SD[2]Median CLR-normalized protein expression[3]Mixed-effects model with Šídák correction. P values compared with pre-op.

Table 1. Perioperative immune cell subsets in healthy donors and pancreatic cancer patients.

	Healthy donor (n=13)	**Pre-op. (n=33)**	**Post-op. day 1 (n=29)[3]**	**Post-op. day 3-5 (n=29)[3]**
M-MDSC (% of all cells)[1]	0.3 ± 0.6	2.7 ± 3.3	23.3 ± 12.6 (P < 0.0001)	20.2 ± 12.2 (P < 0.0001)
$CD8^+$ T cells (% of all cells)[1]	16.5 ± 12.1	20.5 ± 17.5	14.8 ± 14.5 (P < 0.01)	14.9 ± 12.3 (P < 0.05)
NK cells (% of all cells)[1]	18.9 ± 12.3	14.2 ± 10.5	6.3 ± 7.4 (P < 0.001)	7.9 ± 6.6 (P < 0.001)
$NKp30^2$ on NK cells[1]	0.4 ± 0.2	0.5 ± 0.2	0.3 ± 0.2 (P < 0.001)	0.4 ± 0.2

#6465 Validating tumor-infiltrating lymphocyte classification in primary cutaneous melanoma using cytokine immune scores: Addressing biomarker disparities in underserved populations.

Meshack Bida[1], Rodney Hull[2], Thabiso Miya[2], Tebogo Marutha[2], **Zodwa Dlamini**[2]

[1]Department of Anatomical Pathology, University of Pretoria, Pretoria, South Africa,[2]Pan African Cancer Research Institute (PACRI), University of Pretoria, Pretoria, South Africa

Background: Immunotherapy has transformed melanoma treatment, but its promise is not equitably distributed. Biomarker disparities-particularly in tumor-infiltrating lymphocyte (TIL) classification may limit access to precision treatment among patients from low-resource settings. Visual histopathologic scoring of TILs into brisk, non-brisk, or absent categories remains standard practice, but this subjective method is prone to interobserver variability and lacks standardization. This is especially problematic in underrepresented African populations, where diagnostic tools and molecular profiling resources are limited. We aimed to validate conventional TIL classification using cytokine-based immune scoring and explore its implications for biomarker equity in melanoma care.
Methods: A total of 205 formalin-fixed, paraffin-embedded (FFPE) primary cutaneous melanoma samples from South African patients were categorized histologically based on AACR-defined TIL criteria. Immunohistochemical (IHC) staining for tumor necrosis factor-alpha (TNF-α) and interferon-gamma (IFN-γ) was performed using an automated platform. Cytokine expression was quantified using a modified Allred scoring system, which combines staining intensity and proportion of positive cells. Concordance between histologic TIL classification and cytokine-based immune scores was assessed through positive predictive value (PPV) and negative predictive value (NPV) analysis.
Results: In the brisk TIL group, TNF-α and IFN-γ immune scores showed PPVs of 0.68 and 0.79, respectively, suggesting moderate to strong correlation between histologic appearance and cytokine activation. In the absent TIL group, NPVs were 0.84 (TNF-α) and 0.91 (IFN-γ), indicating reliable association with immunologically quiescent tumors. However, a subset of histologically “TIL-absent” tumors demonstrated strong cytokine expression, highlighting biologic heterogeneity and potential misclassification. These discordances have real-world implications, especially where visual interpretation is the only method available to guide treatment.
Conclusion: Our findings underscore the value of cytokine-based immune scoring in validating and standardizing TIL classification. In underserved settings, where access to advanced genomic assays is limited, incorporating affordable and accessible IHC-based immune profiling may improve diagnostic accuracy and expand equitable access to immunotherapy. As immunotherapy eligibility increasingly depends on biomarker evidence, such approaches are essential to closing gaps in precision oncology and addressing global cancer care disparities.

#6466 Preliminary results of a phase 2 study of leronlimab in combination with TAS-102 and bevacizumab in previously treated metastatic colorectal cancer.

Pashtoon M. Kasi[1], Ari Baron[2], Arvind Chaudhry[3], Laura Tenner[4], Daniel L. Adams[5], Alexis B. Duffy[6], Hallgeir Rui[7], Patrick Vittner[8], Joseph Meidling[8], Jacob P. Lalezari[8]

[1]City of Hope Comprehensive Cancer Ctr., Duarte, CA,[2]Division of Hematology Oncology, Sutter/California Pacific Medical Center, San Francisco, CA,[3]Summit Cancer Centers, Spokane, WA,[4]University of Nebraska Medical Center, Fred and Pamela Buffett Cancer Center, Omaha, NE,[5]Creatv MicroTech, Monmouth Junction, NJ,[6]Creatv MicroTech, Inc., Rockville, MD,[7]Thomas Jefferson University, Philadelphia, PA,[8]CytoDyn Inc., Vancouver, WA

Background: CCR5 promotes recruitment of immunosuppressive myeloid populations and contributes to immune evasion in metastatic colorectal cancer (mCRC). Leronlimab is a humanized monoclonal antibody targeting CCR5 with immune-activating effects. TAS-102 plus bevacizumab is a standard regimen in refractory mCRC. This study evaluates the safety of leronlimab in combination with TAS-102/bevacizumab and if this combination enhances objective response rates via immune activation.
Methods: This ongoing multicenter Phase 2 trial will enroll up to 60 previously treated mCRC patients. Leronlimab will be initially dosed 350 mg SC QW with TAS-102/bevacizumab at standard doses. CCR5 expression and PD-L1 CPS is assessed by immunohistochemistry on tumor samples at baseline. PD-L1 and CCR5 is assessed in circulating tumor cells (CTCs) and cancer associated macrophage-like cells (CAMLs) from blood samples.
Results: Among all pre-screened patients with evaluable archival samples, 33/33 (100%) demonstrated CCR5 expression. As of 11/17/ 2025, 10 patients have been enrolled across 6 sites, with preliminary baseline and biomarker data in Table 1. At the City of Hope site, 4/4 patients (with data) had clinical and/or biomarker responses, i.e. declines in CEA, CA19-9, and/or ctDNA, despite refractory liver-metastatic disease. Serial kinetics showed an increase in PD-L1 on CTCs and CAMLs after 1 week on treatment, while the number of CAMLs and CTCs lowered in responders. Leronlimab has been well tolerated, with no unexpected safety signals. This preliminary trial report, which is enrolling ahead of pace, reflects a high unmet need in mCRC disease.
Conclusions: Leronlimab combined with TAS-102 and bevacizumab is feasible, showing promising early biomarker and clinical activity in heavily pretreated mCRC. Universal CCR5 positivity supports CCR5 as a potential therapeutic target. Updated outcomes and correlative data will be presented.

Table

Parameter	Result
Ethnicity (N=10)	Hispanic n=1; Non-Hispanic n=9
Sex (N=10)	Male n=6; Female n=4
Mean age (N=10)	54.3 years
Mean weight (N=10)	100.2 kg
CTCs at baseline: median (range)*	0 (0-2)
CAMLs at baseline: median (range)*	47 (1-67)
CTCs at follow-up: median (range)*	0 (0-4)
CAMLs at follow-up: median (range)*	31 (1-87)
PD-L1 increase in CAMLs or CTCs*	60% (n=3/5)
* 5 patients with both baseline and Week 1 data	

#6467 Myeloma cells with therapy-induced senescence-like phenotype are associated with resistance to CAR-T therapy.

Sofia Arbelaez[1], Andre De Menezes Silva Corraes,[1], Gabriel Alvares Borges[1], Chen Wu[2], Christoph Schaefers[3], Malvika Gupta[1], Zuoyi Shao[1], Kevin Regan[3], Rayaan Kamal[3], Angelo Jose Guilatco[1], Neal I. Sannuli[3], Ying Li[3], Taxiarchis Kourelis[1], Wilson Gonsalves[1], Moritz Binder[1], Melinda Tan[4], Nadine Abdallah[1], Megan Weivoda[1], Yi Lin[1]

[1]Mayo Clinic, Rochester, MN,[2]Mayo Clinic College of Medicine and Science, Rochester, MN,[3]Mayo Clinic Cancer Center, Rochester, MN,[4]Mayo Clinic Cancer Center Minnesota, Rochester, MN

Background: Patients (pts) with myeloma (MM) receiving CAR-T therapy have usually been exposed to many prior therapies. Melphalan (HDM) and other chemotherapies can induce cellular senescence. It has recently been shown that MM cells can also exhibit features of therapy-induced senescence (TIS). TIS tumor cells are associated with resistance to therapy and relapse. To investigate the presence of TIS MM cells prior to CAR-T and association with response, we examined the transcriptome and phenotype of MM prior to CAR-T.
Method: We used scRNA-seq data from bone marrow (BM) MM cells: Boiarsky, et al. (GSE193531, dbGaP: phs001323.v3.p1) newly diagnosed MM (NDMM) pts; Dhodapkar, et al. (GSE210079), pre- and post CAR-T; pts who received CAR-T at Mayo Clinic, pre- (N=10) and post- (N=2). To evaluate TIS, single-cell gene set enrichment analysis (scGSEA) for several gene sets (PMID: 40164720): SenUp (Senescence Upregulated), SenGA (Senescence Growth Arrest), and SCAPs (Senescent Cell Anti-apoptosis Pathways); and a Plasma Cell Senescence (PCSen) gene set (GSE5900, GSE47552). To assess TIS and myeloid phenotype, BM MM cells (CD138+) were stained for CD14, CD16, KLRG1 and GPNMB and analyzed by CytoFlex and Kaluza.
Results: In the integrated dataset, scGSEA showed significantly higher enrichment of PCSen, SenUp, SenGA, and SCAPs in late-stage MM cells (both pre- and post-CAR-T) compared to NDMM and healthy donors ($p<0.05$, Kruskal-Wallis with Dunn's posttest). Conversely, the Normal gene set was significantly enriched in healthy plasma cells relative to MM ($p<0.05$). Expression of CDKN2A, which encodes the senescence marker p16, was also increased in late-stage MM relative to NDMM or healthy plasma cells. Notably, in our newly generated scRNA-seq samples collected within 6 months before CAR-T, a significant inverse correlation between senescence marker expression and progression free survival (PFS) post-CAR-T was seen, suggesting that MM cells exhibiting TIS may be more resistant to T cell mediated cytotoxicity. We found that 62.5% (25/40) of pts had >1% MM cells that were CD14+. Among them, the median CD14+ MM cells were 5.5% (1-71%); and median CD14+CD16+ MM cells were 2.14% (0.4-67%). Among 7 pts with available samples for KLRG1 and GPNMB assessment, 100% (7/7) had KLRG+ MM cells (median: 59% (24-99%)) and 57% (4/7) had GPNMB+ MM cells (median: 15% (3.9-30%)), and KLRG1+GPNMB+ MM cells (median: 9.6% (3.8-17%)).
Conclusion: Our study shows that late-line MM cells exhibit transcriptional and phenotype profiles consistent with TIS. This senescent phenotype may contribute to resistance to immunotherapies, including CAR-T. Additional phenotype data is collected and will be presented. A phase II clinical trial is ongoing (NCT06940297) to assess for the combined treatment with senolytic drugs dasatinib and quercetin peri-CART to deepen clinical response.

#6468 Biopsy site-specific variation in immune signatures identified by RNA profiling in breast cancer.

Smruthy Sivakumar[1], Ericka Ebot[1], Douglas I. Lin[1], Meagan Montesion[1], Jeffrey S. Ross[1], Lee A. Albacker[1], Garrett M. Frampton[1], Michelle Marie Williams[2], Ethan S. Sokol[1]

[1]Foundation Medicine, Inc., Boston, MA,[2]University of Pittsburgh School of Medicine, Pittsburgh, PA

Background: Breast cancer is generally considered to be immune cold; however, emerging data indicate heterogeneity in its immune landscape. Triple negative and HER2-positive tumors typically show higher immune cell infiltration than hormone receptor-positive (HR+) tumors. Additionally, the local microenvironment at the biopsy site may influence the immune profile of the tumor, contributing to distinct immunophenotypes. In this study, we used gene expression profiling to evaluate biopsy site-specific patterns of immune activity in breast cancer.

Methods: Tumor tissue from 1,009 patients with breast cancer (all-comers) underwent targeted RNA profiling using a laboratory-developed test, FoundationOne®RNA, as part of routine clinical care. Scores for immune and stromal gene sets were generated using a single-sample gene set enrichment analysis (ssGSEA) using a research use algorithm. K-means clustering of Z-normalized scores identified two immunophenotypes: immune-high and immune-low. Samples with a negative silhouette width were classified as unknown phenotype.

Results: The most common sample sites were breast (n=363), liver (n=142), lymph node (n=120), bone (n=81), and lung (n=55). Immune ssGSEA scores varied significantly by sample site. Brain biopsies (n=23) exhibited the lowest immune scores, with only 5% (1/23) classified as immune-high, whereas lymph node and lung biopsies showed higher immune scores, with 42% (51/120) and 47% (26/55) classified as immune-high, respectively ($p<0.05$). Among local breast samples, 26% (96/363) were immune-high. Although liver metastases are typically considered to be immune cold, 12% (17/142) in this cohort were immune-high. Consistent with reports of lower immune activity in HR+ tumors, ESR1 expression was significantly higher in immune-low tumors compared to immune-high tumors (median expression 4,872 vs. 986 transcripts per million; $p < 10^{-4}$). Furthermore, distinct immune cell populations and gene signatures also showed site-specific patterns. IFN-γ scores were above median in 60% of breast biopsies, compared with 17% of brain, 39% of liver, and 62% of lung metastases. T-cell and CD8+ T-cell scores were typically higher in lung (65%, 62% above median) and lymph node metastases (66%, 62%), intermediate in breast biopsies (53%, 56%), and lowest in liver (32%, 37%) and brain metastases (17%, 22%). In contrast, dendritic cell scores were highest in liver metastases (83% above median), compared with breast samples (48%).

Conclusion: Immunophenotypes in breast cancer vary substantially by sample site, reflecting-heterogeneity of the local microenvironment. These site-specific immune signatures may have important implications for immunotherapy selection, prognostic assessment, and vaccine development strategies.

#6469 Longitudinal loss of microbiome stability is associated with poor response to immune checkpoint inhibitors in lung cancer and melanoma.

Yujie Zhao[1], Jarushka Naidoo[1], Michael Conroy[2], Jacqueline T. Ferri[1], Joell J. Gills[1], Krista Y. Chen[1], James R. White[3], Sara Glass[1], Willaim O. Assan[1], Kimberly Peloza[1], Megan D. Schollenberger[1], William H. Sharfman[4], Kristen Marrone[5], Patrick M. Forde[6], Julie R. Brahmer[7], Valsamo (Elsa) Anagnostou[6], Drew M. Pardoll[8], Joseph Murray[1], Evan J. Lipson[9], Cynthia L. Sears[1], **Fyza Y. Shaikh**[1]

[1]Johns Hopkins University School of Medicine, Baltimore, MD,[2]Johns Hopkins School of Medicine, Baltimore, MD,[3]Resphera Biosciences, Baltimore, MD,[4]Medical Director, Dept. of Med. Oncology, Johns Hopkins Sidney Kimmel Comp. Cancer Center, Lutherville, MD,[5]Johns Hopkins Hospital, Baltimore, MD,[6]Johns Hopkins University, Baltimore, MD,[7]Sidney Kimmel Comprehensive Cancer Ctr., Baltimore, MD,[8]Johns Hopkins Bloomberg-Kimmel Inst. for Cancer Immunotherapy, Baltimore, MD,[9]Johns Hopkins University School of Medicine, Baltmore, MD

While immune checkpoint inhibitors (ICI)-based regimens and chemo-immunotherapy combinations (chemo-ICI) are now first-line therapy for patients with metastatic non-small cell lung cancer (NSCLC), the number of patients who experience a sustained response to treatment remains limited. The majority of patients will eventually develop progressive disease. Microbiome-based biomarkers offer an opportunity to identify patients who may have a poor response to ICI-based regimens using non-invasive methods, and potentially, the microbiota may be amenable to therapy-enhancing alteration. However, a deep understanding of the longitudinal dynamics of gut microbial features in patients treated with ICIs in NSCLC, a feature of likely importance for microbiome-based therapeutics, remains limited. In this study, we show that patients with NSCLC who experience a poor response to an ICI-based regimen show a loss of intra-individual microbiome stability in the first 4 months during treatment with an ICI-based regimen, independent of antibiotic exposure. Longitudinal loss of microbiome stability was also associated with poor response in patients with melanoma. To identify key microbial species associated with progression, recursive feature elimination with random forest classifiers was used to identify temporally-associated microbial species associated with disease progression. An index of these progression-associated species was able to predict clinical outcomes based on pre-treatment fecal samples, with validation on an independent lung cancer cohort. Together, our data show that microbial instability may be an early indicator of ICI-resistance in patients with NSCLC and melanoma, with the potential to be developed into biomarkers of primary resistance to ICI-based regimens.

#6470 Spatial remodeling of the tumor microenvironment by IL-18-armored CD19 CAR T cells is associated with durable remission in relapsed or refractory lymphoma.

Nakial C. W. Cross[1], Yael A. Day[1], Sonia Ndeupen[1], Vanessa E. Gonzalez[1], Zhen Miao[1], Sam I. Kim[1], Rachel M. Leskowitz[1], Amy Marshall[1], Julie K. Jadlowsky[1], Gabriela Plesa[1], Donald L. Siegel[1], Elizabeth O. Hexner[1], Jakub Svoboda[1], Stephen J. Schuster[1], Nancy R. Zhang[2], Joseph A. Fraietta[1], Andrew J. Rech[1], Carl H. June[1]

[1]Perelman School of Medicine Univ. of Pennsylvania, Philadelphia, PA,[2]Statistics & Data Analysis, Wharton School Univ. of Pennsylvania, Philadelphia, PA

Patients with relapsed or refractory B-cell lymphoma who experience disease progression after CD19-directed CAR T-cell therapy have poor outcomes and few effective treatment options. Subsequent therapies provide only modest benefit, with complete remission (CR) rates near 20% and limited durability. huCART19-IL18, an IL-18-secreting CD19 CAR T-cell product, produced an overall response rate of 81% and a CR rate of 52% after prior anti-CD19 CAR T failure in a phase I trial, but the spatial determinants of durable response within the tumor microenvironment (TME) remain incompletely defined.

We performed multimodal spatial profiling of paired pre- and post-huCART19-IL18 lymph node biopsies from 11 patients (6 with CR, 5 without CR) enrolled in the phase I study. GeoMx whole-transcriptome atlas and protein profiling were integrated with CosMx 6000-plex single-cell spatial imaging to map transcriptional and cellular remodeling across tumor, myeloid, and lymphoid compartments. CoPro, a computational framework for detecting coordinated progression of cell states in space, was applied to identify spatially coordinated gene expression programs within and between myeloid and T-cell compartments.

Post-infusion samples from responders showed increased T-cell and NK-cell infiltration, frequent tertiary lymphoid structures, and induction of interferon (IFN)- and tumor necrosis factor-responsive chemokine and immune effector programs, including enhanced antigen presentation, together with coordinated loss of B-cell identity and signaling. These changes localized to regions enriched for CAR T cells, effector memory $CD4^+$ and $CD8^+$ T cells, and IFN-polarized macrophages, consistent with IL-18-driven recruitment and reprogramming of myeloid and T-cell compartments. Pre-infusion TMEs in responders showed baseline myeloid chemokine signatures associated with clinical response. CoPro revealed that myeloid functional heterogeneity is organized along spatial gradients that are independent of lineage identity and coordinated with T-cell effector programs in CAR T-infiltrated regions.

These findings support a model in which IL-18 armoring promotes spatially organized remodeling of the TME through coordinated myeloid and T-cell activation associated with durable remission after CD19 CAR T failure, nominating myeloid recruitment, antigen presentation, and T-cell exhaustion programs as critical biomarkers and rational engineering targets for next-generation armored CAR T strategies in lymphoma.

#6471 Immune correlates post MMF omission lead to accelerated immune reconstitution without increased graft versus host disease risk signatures for allogenic stem cell transplant (OmitMMF trial).

Vanshika Chauhan, Joseph Lownik, Larry Milshteyn, Haein Kim, Ronald Paquette, Akil Merchant

Cedars-Sinai Medical Center, Los Angeles, CA

Mycophenolate mofetil (MMF) has been a standard practice of care used in combination with post-transplant cyclophosphamide (PTCy) in graft-versus-host-disease (GvHD) prophylaxis regimen. This study evaluated the safety and potential benefits of eliminating MMF in patients receiving reduced-intensity (RI) and myeloablative (MA) conditioning with fludarabine and total body irradiation (FluTBI) prior to peripheral blood stem cell transplants (PBSCT) from matched or haploidentical related, or match unrelated, donors. The outcomes of 60 study subjects were compared to time-matched historical control patients. As we have previously presented, relapse-free survival at 1 year and viral reactivation by day +100 was not different in OmitMMF patients and control patients. While there were no significant clinical differences between treatment arms, we explored whether omitting MMF had significant effects on immune reconstitution. We used a 42-color spectral flow cytometry to characterize T-cells, NK-cells, B-cells, and monocytes. High dimensional clustering was performed using Phenograph to identify T-cell activation state clusters and other granular cell populations. OmitMMF patients had a higher number of T-cells at days +15 and +30, but lower by day +60. This increase was due to increased CD4+ T-cells in the OmitMMF patients and not CD8+ T-cells. Effector CD4+ T-cells were significantly higher while naïve CD4+ T-cells were not different. NK-cells were not significantly different between the two groups, contrasting the published effects of MMF on NK-cell function suggesting an anti-proliferative effect. While NK-cells were higher in the control arm at day 60, this was after MMF was removed and may represent a rebound affect. B-cells were not significantly different between the two groups. Omitting MMF led to faster CD4+ recovery as MMF suppresses CD4+ T-cell proliferation without adding greater risk of developing GvHD. Within the OmitMMF cohort, immune recovery was compared between patients who developed GvHD and those who did not. No distinct early immune correlates, such as a higher CD4+ T-Cells or different NK-cell count, were observed in the patients who developed GvHD, suggesting that omitting MMF reduces immunosuppression without leading to the T-cell signatures that are associated with a higher GvHD risk. Interestingly, the rate of grade II-IV aGVHD was significantly higher in the OmitMMF patients who received MA conditioning than the control group; this is dependent on preconditioning and is being further evaluated with the flow cytometry data. In conclusion, MMF can be safely eliminated in patients receiving RI and MA FluTBI conditioning regimens with the PTCy+tacro prophylaxis, and allows for quicker early T-cell recovery without causing harmful immune overactivity.

#6472 Tumor-cell NY-ESO-1 expression predicts poor response to PD-1/PD-L1 blockade in NSCLC.

Adele Lerue[1], Jean-Philippe Guegan[2], Christophe REY[2], Sophie Cousin[3], Benjamin Besse[2], Fabrice Barlesi[4], Christophe Massard[5], David Planchard[6], Alban Bessede[7], **Antoine Italiano**[8]

[1]Gustave Roussy, Villejuif, France,[23]Cousin (Individual), Bordeaux, France,[4]INSERM U1030 - Gustave Roussy Institute (Molecular Radiotherapy), France,[5]Institute Gustave Roussy, Villejuif, France,[6]Medical Oncology, Gustave Roussy, Villejuif, France,[7]ImmuSmol, Pessac, France,[8]Institute Bergonie, Bordeaux cedex, France

Background: NY-ESO-1 is an immunogenic cancer-testis antigen and a therapeutic target for TCR-based strategies. Its significance as a baseline biomarker in non-small cell lung cancer (NSCLC) treated with PD-1/PD-L1 inhibitors is not well established. Because NY-ESO-1 has biological relevance only when expressed by tumor epithelial cells, we focused our analysis specifically on NY-ESO-1 expression within $CK7^+$ tumor cells and evaluated its association with clinical outcomes in patients receiving immune checkpoint blockade.
Methods: Baseline FFPE tumor samples from 195 patients with advanced NSCLC treated with PD-1/PD-L1 inhibitors were profiled using a validated multiplex immunofluorescence panel including CD8, CD68, CD103, CK7, HLA-ABC, cMAF, NY-ESO-1, and pSMAD3. Digital image analysis was performed using Vectra Polaris imaging, QuPath segmentation, and FlowJo-based phenotyping after signal normalization. Tumor-specific NY-ESO-1 expression was defined by $CK7^+$/$NYESO1^+$ co-localization. Associations with RECIST response, durable clinical benefit (DCB), progression-free survival (PFS), and overall survival (OS) were assessed using Wilcoxon tests, chi-square tests, and cutpoint-based survival modeling. CK7→CD8 and CK7→CD68 intercellular distances were also computed.
Results: Higher $CK7^+$/$NY\text{-}ESO\text{-}1^+$ tumor cell levels were significantly associated with non-response to PD-1/PD-L1 blockade ($p=0.011$), and increased NY-ESO-1 expression intensity also associated with non-response ($p=0.044$). Tumor-restricted NY-ESO-1 was strongly predictive of shorter survival. Patients with high $CK7^+$/$NY\text{-}ESO\text{-}1^+$ tumor expression had a median PFS of 1.8 months, compared with 8.1 months in the low-expression group ($p=7.2\times10^{-5}$). Median OS was similarly reduced, with 11.0 months in the high-expression group versus 33.5 months in the low-expression group ($p=3.9\times10^{-3}$). High tumor NY-ESO-1 also correlated with substantially reduced durable clinical benefit (χ^2 $p=0.013$). Independently of NY-ESO-1, greater CK7→CD8 and CK7→CD68 distances predicted inferior PFS and OS, although no direct association between NY-ESO-1 levels and spatial distances was assessed.
Conclusions: Tumor-cell NY-ESO-1 expression is a robust adverse biomarker in NSCLC treated with PD-1/PD-L1 inhibitors. High $CK7^+$/$NY\text{-}ESO\text{-}1^+$ tumor burden identifies patients with dramatically reduced PFS and OS, lower response rates, and poor likelihood of achieving durable clinical benefit. These findings support the role of tumor-restricted NY-ESO-1 as a clinically meaningful negative baseline predictor of immunotherapy outcome and may help refine patient selection for NY-ESO-1-targeted therapies.

#6473 Clonal consolidation and transcriptional re-programming define non-small cell lung cancers resistant to immune checkpoint inhibitors.

Natalie Vokes[1], Arvind Ravi[2], Mark M. Awad[3], Patrick M. Forde[4], Marta Luksza[5], Benjamin Dylan Greenbaum[6], Adam Jacob Schoenfeld[6], John V. Heymach[7], Alice T. Shaw[8], Pasi A. Janne[9], Jedd D. Wolchok[10], Matt Hellman[11], Gad Getz[12], JUSTIN GAINOR[13]

[1]MD Anderson Cancer Center, Houston, TX,[2]DFCI/Harvard Medical School, Boston, MA,[3]Memorial Sloan Kettering, New York City, NY,[4]Johns Hopkins University, Baltimore, MD,[5]Icahn School of Medicine at Mount Sinai, New York, NY,[6]Memorial Sloan Kettering Cancer Center, New York, NY,[7]UT MD Anderson Cancer Center, Houston, TX,[8]Dana-Farber Cancer Institute, Cambridge, MA,[9]Dana-Farber Cancer Institute, Boston, MA,[10]Weill Cornell, New York City, NY,[11]AstraZeneca, Cambridge, United Kingdom,[12]Massachusetts General Hospital, Charlestown, MA,[13]Massachussetts General Hospital, Boston, MA

Analysis of pre-treatment non-small cell lung cancers (NSCLCs) has helped identify predictors of response to immune checkpoint inhibitors (ICI), including low PD-L1 expression, targetable drivers alterations (*EGFR*, *ALK*), and *STK11*/*KEAP1* mutations. To-date, however, few samples at treatment resistance have been studied, and consequently less is known about the mechanisms contributing to ICI resistance.Methods: Building on our previous analysis Stand Up 2 Cancer-Mark Foundation (SU2C-MARK) Cohort, we identified patients with on or post-treatment samples and performed whole exome (WES) and/or RNA-sequencing, based on tissue availability and quality. Genomic and transcriptomic features in post vs pre-treatment samples were compared. Subclonal evolution in paired samples was assessed using PhylogicNDT, and immune phenotypes were inferred using published gene signatures and deconvolution methods (CIBERSORTx).Results: Building on the original n=393 cohort, 41 patients with on and/or post-treatment samples were identified, with n=45 WES and n=35 RNA-seq on-treatment/post-treatment samples passing QC, for a total of n=445 samples included in the updated cohort, SU2C-MARKv2. N=28 patients had paired samples across treatment time, ranging from 2-5 time points. Only 3 samples had acquired mutations in *B2M* or *JAK2*; more commonly, post-treatment tumors showed persistence of clones containing *STK11*, *KEAP1*, and/or *ARID1A*/*SMARCA4* alterations. The proportion of subclonal alterations decreased at resistance, suggesting elimination of passenger-rich antigenic subclones (median 7.9% vs1.9%, p<0.001). Acquired copy number loss in antigen presentation genes in 6p21 (*STAT1/HLA/TAP1/TAP2*) were observed in 5 treatment pairs, and amplification in 9p24.1 (JAK2/PD-L1/PD-L2) in 4 pairs. In the transcriptional space, resistant tumors demonstrated increased expression of gene sets associated with tumor-intrinsic biology, including MYC, oxidative phosphorylation, and EMT, and decrease in DNA repair genes (ATM). Alterations in immune gene sets were most prominent in on- rather than post-treatment specimens, with increase in T, B and myeloid cell signatures in both responding and non-responding tumors, though numbers were low (n=5). Immune clustering into hot, intermediate, and cold phenotypes confirmed an increase in hot tumors in on-treatment specimens, while post-treatment tumors had predominantly 'intermediate' immune phenotype.Conclusions: Integrated genomic/transcriptomic analysis of the expanded SU2C-MARKv2 cohort suggests that ICI resistance emerges through elimination of immunogenic subclones and selection for resistant subclones that maintain immune-suppressive transcriptomic phenotypes. Further integration of spatial and single-cell data will define the tumor-immune architecture and identify potential treatment targets.

#6474 Robust and precise rare event analysis for immunotherapy clinical trials.

Chengsen Xue[1], Thomas W. Mc Closkey[1], Andew Roche[2]

[1]Biomarker & Diagnostic Assay Development, ICON Laboratory Services, Farmingdale, NY,[2]Scientific Affairs, ICON Laboratory Services, Dublin, Ireland

Modulating the human immune system has become a lifesaving option for selected malignancies. Biomedical approaches with both engineered cytotoxic T cells and cancer vaccines that boost antigen-specific cytotoxic T cells (CTLs) continue to advance the field. Both rely on rare event analysis, detecting and quantifying interactions between uncommon biomarkers and common leukocyte antigens. Flow cytometry is essential for today's clinical research and is the gold standard for identifying and phenotyping very low-frequency events in large mixed cell populations. Careful assay design is required for success, taking into consideration background, brightness, resolution, frequency, and donor to donor variation. We established a practical framework for robust, precise rare event analysis. First, define the rare events of interest—such as CAR T cells in peripheral whole blood, antigen-specific CTLs, circulating tumor cells (CTC), minimal residual disease (MRD), or T lymphocyte stem cells. Sample volume to be tested is critical in order to achieve an appropriate level of precision. For example, achieving about 20% CV (coefficient of variation) at a target frequency of 1 in 100,000 typically requires roughly 2.5 million leukocytes. Inadequate sample volume may yield false negative results and often be a cause of a failed assay. Key performance limits—Lower Limit of Quantitation (LLOQ), Limit of Detection (LOD), and Limit of Blank (LOB)—must be part of the performance characterization of the method. In CAR T immunophenotyping, we assess LLOQ to find a linear, reliable range, then spike CAR T cells across serial dilutions in triplicate. The lowest dose with $\leq$ 35% CV across donors defines the LLOQ. Because rare event work can be computationally heavy, concentrating the target population helps, for example, removing 80% of neutrophils during export of raw flow cytometry fcs data and using a dump channel containing with CD19, CD4, and CD56 focuses the analysis on antigen-specific CTLs within the CD8 subpopulation cells. In summary, our approach improves precision of rare event analysis by addressing data imbalance, statistical bias, and sample inefficiency.

#6475 Myeloma cells with therapy-induced senescence-like phenotype have increased resistance to killing by T cell directed therapies.

Christoph Schaefers[1], Angelo Jose Guilatco[2], Sofia Arbelaez[2], Gabriel Alvares Borges[2], Chen Wu[3], Andre de Menezes Silva Corraes[2], Malvika Gupta[2], Zuoyi Shao[2], Kevin Regan[2], Rayaan Kamal[2], Neal I. Sannuli[2], Ying Li[4], Taxiarchis Kourelis[2], Wilson Gonsalves[2], Melinda Tan[5], Nadine Abdallah[2], Yi Lin[2], Megan Weivoda[2]

[1]Hematology, Mayo Clinic Rochester, Rochester, MN,[2]Mayo Clinic, Rochester, MN,[3]Mayo Clinic College of Medicine and Science, Rochester, MN,[4]Mayo Clinic, Jacksonville, FL,[5]Mayo Clinic Cancer Center Minnesota, Rochester, MN

Background: Therapy-induced senescence (TIS), a tumor cell state associated with distinct gene expression patterns and implicated in therapy resistance, may be activated in Multiple Myeloma (MM) patients (pt) by genotoxic chemotherapies, such as high-dose melphalan (HDM). We investigated whether TIS is activated in MM cells following chemotherapy and linked to resistance to T-cell directed therapies.

Method: We integrated scRNA-seq data from healthy donors (CNTRL) and MM pts (newly-diagnosed (NDMM), pre/post-CAR-T) bone marrow plasma cells (PCs) using two public datasets (Boiarsky, et al.; Dhodapkar, et al.) and a newly generated pt dataset. Senescence was evaluated using scGSEA with published gene sets (SenUp, SenGA, and SCAPs). For in vitro MM cytotoxicity assay, human H929 MM cells were treated with vehicle (Veh) or HDM (3μM, IC90) for 6h and examined for TIS features. H929VEH or H929HDM were co-cultured with CNTRL T cells with or without teclistamab (Tec, 10 nM) or with day 14 PBMCs from MM pts post-CAR-T (E:T 5:1). CAR+ T cells were high among the day 14 PBMC (median±SD: 93.4±7.2% of CD3+ cells, n=6).

Results: scGSEA revealed significantly higher enrichment of SenUp, SenGA, and SCAPs in late-stage MM cells compared to NDMM and CNTRL ($p<0.05$). Expression of CDKN2A, encoding the senescence marker p16, was also increased in late-stage MM relative to NDMM/CNTRL PCs. Of interest, cells enriched for senescence also exhibited enrichment for myeloid markers (TET2, CEBP family). Notably, in pre-CAR-T, increased baseline senescence or myeloid marker expression showed an inverse association with CAR-T progression-free survival (PFS), suggesting TIS confers resistance to T cell mediated cytotoxicity. This may be due to myeloid plasticity. TIS MM cells generated in vitro, H929HDM, exhibited a distinct morphology characterized by increased cell size and enhanced cytoplasmic granularity. Increased CD14 expression was seen in 4 of the 6 experiments (median, range % increase: 11.2%, 2.5%-21%), consistent with myeloid plasticity; Increased KLRG1 expression was seen in 5 of the 7 experiments (median MFI ratio, range: 3.7, 1.3-471). No significant change was seen in GPNMB expression. Compared to H929VEH, H929HDM had a reduction in killing by CAR-T cells (median±SD: 22.8±32.94% n=6, p=0.016, Wilcoxon paired test). Similarly, H929HDM had a 10.69% decrease in Tec-mediated T-cell killing compared to H929VEH (n=8, p=0.02, Wilcoxon paired test).

Conclusions: Late-stage MM cells exhibit transcriptional signatures consistent with TIS, which can be associated with decreased PFS to CAR-T. We report an in vitro model of TIS MM cells for testing of resistance to T cell killing. Based on these findings, a phase II trial (NCT06940297) is underway to test the hypothesis that peri-CAR-T senolytic therapy with dasatinib and quercetin will deepen responses by targeting this resistant TIS MM population.

#6476 Microbiome modulation via CBM588 dampens T cell exhaustion in patients with metastatic renal cell carcinoma on dual immune checkpoint blockade.

Colt A. Egelston[1], Miguel Zugman[1], Hedyeh Ebrahimi[1], Regina Barragan Carrillo[2], Nazli Dizman[1], Salvador Jaime-Casas[1], Xiaochen Li[1], Daniela V. Castro[1], Benjamin Mercier[1], Marice Alcantara[1], Motomichi Takahashi[3], Atsushi Hayashi[3], Tom Parks[4], Sumanta Kumar Pal[1], Peter P. Lee[1], Alexander Chehrazi-Raffle[1]

[1]City of Hope National Medical Center, Duarte, CA,[2]Salvador Zubiran National Institute of Health Science & Nutrition, Mexico City, Mexico,[3]Miyarisan Pharmaceuticals, Tokyo, Japan,[4]Osel Inc, Mountain View, CA

Background: Immune checkpoint inhibitors (ICIs) are well-described to augment T cell responses and boost anti-tumor immune responses, with increased survival benefits of patients with a number of different indications treated with a variety of PD-1, PD-L1, or CTLA-4 targeting monoclonal antibodies. While the combination of nivolumab (nivo) and ipilimumab (ipi) is currently one of the standard-of-care treatments for patients with metastatic renal cell carcinoma (mRCC), the majority of patients still suffer disease progression. CBM588 is a live biotherapeutic product that has previously demonstrated ability to enhance clinical responses to nivo+ipi treatment in patients with mRCC. In our current study, we sought to explore immune correlatives of patients treated with nivo+ipi alone as compared to those treated with CBM588+nivo+ipi.

Methods: Peripheral blood was collected from patients with mRCC treated across two clinical trials: the initial CBM588+nivo+ipi study (NCT0382911) and an ongoing CBM588 dose finding study of patients with (NCT06399419). Both trials enrolled treatment-naïve patient with mRCC with clear cell and/or sarcomatoid histology. The initial trial enrolled patients with or without CBM588 co-treatment at a 2:1 ratio. The initial trial enrolled patients treated with or without CBM588 at 4×10^8 CFU/dose, while the dose escalation study followed a 3+3 design with three dose levels of CBM588 (4×10^8 CFU, 1.2×10^9 CFU, and 4×10^9 CFU). Cryopreserved blood was thawed and analyzed by high parameter spectral flow cytometry for overall immune composition and detailed T cell phenotyping.

Results: No significant differences were observed in myeloid cell or innate lymphocyte changes between patients treated with or without CBM588. Increased frequencies of proliferating CD8+ T cells (Ki-67+) were observed across all patients from baseline to Cycle 3 Day 1. The expansion of proliferating CD8+ T cells was significantly less accelerated in patients treated with CBM588+nivo+ipi as compared to those treated with nivo+ipi alone. Notably, the expanding Ki-67+ CD8+ T cell population identified demonstrated features of T cell exhaustion with less expression of CD127 (IL-7R) and higher expression of CD38, KLRG1, TIM-3 relative to other circulating CD8+ T cell populations.

Conclusions: Our results suggest that CBM588 may improve patient responses to ICIs by restraining CD8+ T cell amplification and attenuating features of T cell exhaustion. The CBM588+nivo+ipi dose escalation study is still ongoing with further immune correlative analyses pending.

#6477 Peptide-based tumor-associated antigen vaccine in glioblastoma: Correlative results of the ETAPA Phase I clinical trial.

Elizabeth Owens, Kelly M. Hotchkiss, Pamela Norberg, Evan Buckley, Katayoun Ayasoufi, Stevie Threatt, Justin T. Low, Madison L. Shoaf, Melody Goldston, Kristen Batich, Margaret O. Johnson, James E. Herndon, Smita K. Nair, Kent Weinhold, Henry S. Friedman, David M. Ashley, Annick Desjardins, John H. Sampson, Mustafa Khasraw

Duke University School of Medicine, Durham, NC

Introduction/Rationale: Immunotherapy has yet to yield benefit in glioblastoma (GBM), in part due to inadequate T-cell priming and insufficient $CD4^+$ helper support. To enhance coordinated $CD4^+$ and $CD8^+$ activation, the ETAPA phase 1 trial (NCT05283109) evaluated P30-EPS, a peptide vaccine linking three class I tumor-associated antigens (CMV pp65, Survivin, EphA2) to the universal class II tetanus toxoid epitope P30 (TVSFWLRVPKVSASHLE). This design aims to broadly recruit $CD4^+$ T-cell help and augment cytotoxic responses.
Methods: Adults with newly diagnosed, MGMT-unmethylated GBM (n = 18) received seven post-radiation intramuscular vaccinations with Hiltonol (20 μg/kg) and either 300 μg (n = 6) or 400 μg (n = 12) of P30-EPS. Peripheral blood mononuclear cells (PBMCs) were analyzed longitudinally by IFN-γ ELISpot, high-parameter spectral flow cytometry, and 5′ scRNA TCR sequencing to quantify antigen-specific cytokine production, helper and cytotoxic phenotypes, lineage distribution, clonal expansion, and repertoire diversity. Paired single-cell V(D)J TCR sequencing of PBMCs was used to resolve $CD4^+$ and $CD8^+$ subsets, define activation and memory-associated transcriptional programs, and map clonotype-specific trajectories. Baseline and on-treatment tumors are being profiled using spatial transcriptomics (ST) and spatial proteomics (SP) to localize vaccine-responsive T-cell populations within the tumor microenvironment.
Results: The vaccine was well tolerated in all 18 patients, with all adverse events ≤ grade 2. P30-EPS induced antigen-specific IFN-γ responses in 11 patients, with stronger recall responses at the 400-μg dose. Patients with longer progression-free survival exhibited higher baseline frequencies of naïve $CD4^+$ T cells and fewer terminally differentiated effector-memory ($CD45RA^+CCR7^-$) cells, indicating a more plastic helper pool capable of sustaining $CD8^+$ priming. Longitudinal TCR sequencing demonstrated expansion of vaccine-associated clonotypes after boosting, including emergence of new low-frequency clones and persistence of dominant clones, consistent with durable memory formation. Early single-cell transcriptomic and paired TCR analyses revealed coordinated activation signatures in helper and cytotoxic compartments that paralleled peripheral clonotype expansion. Pre- and post-vaccination tumor ST and SP analyses will be presented.
Conclusion: ETAPA achieved its primary objectives, demonstrating safety and correlative findings indicating that a universal $CD4^+$ helper epitope can enhance cytotoxic and memory responses in GBM. Integration of PBMC scRNA/TCRseq with tumor ST and SP profiling will define intratumoral correlates of systemic vaccine-induced immunity. These insights now support development of our next epitope-linked personalized vaccine for patients with glioblastoma.

#6478 Temporal dynamics of T cell reprogramming associate with clinical response to ICI-based combination therapy in metastatic renal cell carcinoma.

KyuTae Hwang[1], Seowoo Kim[2], Mi Zhou[3], William Y. Kim[2], Minyong Kang[4]

[1]Department of Health Sciences and Technology, Samsung Advanced Institute of Health Sciences and Technology (SAIHST), Seoul, Korea, Republic of,[2]UNC Lineberger Comprehensive Cancer Center, Chapel Hill, NC,[3]UNC Chapel Hill, Cary, NC,[4]Department of Health Sciences and Technology, Samsung Advanced Institute of Health Sciences and Technology (SAIHST)Samsung Medical Center, Seoul, Korea, Republic of

Immune checkpoint inhibitor (ICI) based therapy, including dual ICI (anti-PD-1 + anti-CTLA4) and anti-PD-1 plus tyrosine kinase inhibition (TKI), has improved outcomes for metastatic renal cell carcinoma (mRCC). While tumor-based immunologic determinants of response have been explored, predictive biomarkers/early changes in peripheral blood mononuclear cells (PBMCs), have not. To understand mechanisms of response and resistance to first line ICI-based therapy, we prospectively collected longitudinal PBMCs at baseline (T0, n = 20) and multiple post-treatment time points (T1-T3: T1 = 1-2 wks post treatment initiation, n = 17; T2 = time of surgery for patients undergoing cytoreductive nephrectomy, n = 11; T3 = at progressive disease (PD), n = 7), as well as paired tumor samples at T0 (n = 20) and T2 (n = 9). scRNAseq and scTCRseq of PBMCs and tumors were used together with single-cell spatial transcriptomics (Xenium 5K, T0, n = 31; T2, n = 26) to define dynamic PBMC and intratumoral immune changes. Few differences at baseline were found in the intratumoral immune contexture or PBMCs of R (responders) and NR (non-responders). Only baseline intratumoral CD56-high NK cells were significantly higher in R and no PBMC immune cell subsets were different. Differential gene expression analysis of CD8+ exhausted T cells showed upregulation of stress response genes (e.g. *HSPA1A*) and the *DUSP1* phosphatase in R. In contrast, there were dynamic temporal changes seen with ICI at T1. In particular a significant increase in the proportion of circulating proliferative T and NK cells in R, which had upregulation of cytotoxicity (*GZMB*, *PRF1*) and effector markers (*CX3CR1*, *FGFBP2*). Furthermore, analysis of multiple $CD8^+$ T cell subsets associated with ICI response demonstrated activation of NF-κB and MAPK module scores in R at T1. Intratumoral scRNAseq profiling at T2 revealed that $CD8^+$ T cells from R had lower exhaustion related genes (*TOX*, *LAG3*, *CD38*) and higher AP1 transcription factor (TF) activation including JUN/FOS, whereas NR accumulated terminally exhausted $CD8^+$ T cells with high level of *BATF* activity. These findings indicate that *JUN/FOS* signaling associates with T cell activation in R, while *BATF* drives terminal exhaustion and NR. Finally, tumor spatial transcriptomics demonstrated significant enrichment of C1QC tumor-associated macrophages (TAM) in the cellular neighborhoods of exhausted CD8+ T cells at T2 of R (but not T0 or in NR). The role of C1QC macrophages in ICI response remains debated. In total, these data demonstrate there is limited discrimination between R and NR at baseline (PBMCs or tumor) but identify early (1-2-week post-treatment) PBMC changes in R (increased proliferative T cells) as well as differences in spatially organized immune trajectories post-treatment tumors of R. The increase in proliferative T cells in PBMCs could serve as a very early biomarker of R.

#6479 Immunotherapy and microbiota interventions as potential treatment options for anaplastic thyroid cancer.

Jocelynn G. Colunga Minutti[1], Naimah Turner[2], Synat Keam[2], Roza Nurieva[1]

[1]UT MD Anderson Cancer Center, Houston, TX,[2]Immunology, UT MD Anderson Cancer Center, Houston, TX

Anaplastic thyroid cancer (ATC) is a rare and aggressive malignancy that accounts for approximately 50% of all thyroid cancer-related deaths despite its low incidence. While it is known that thyroid cancer has a higher incidence in women and a worse prognosis in men, age itself is an independent negative prognostic factor. Despite the median patient age for ATC being 65 years, no animal studies have accounted for age in this type of cancer, which represents a vital gap that must be addressed. Therefore, this research aims to investigate the impact of age and sex on ATC outcomes and treatment response. A Kaplan-Meier survival analysis demonstrated that younger female ATC patients had better survival odds than young males. However, aged patients had poorer overall survival, regardless of sex, suggesting that aging changes the biological mechanisms that confer better survival in younger females. Like ATC patients, our murine ATC model shows that young males display accelerated ATC growth compared to females, while older mice have similarly high growth rates regardless of sex. We correlated worse ATC outcomes in young male mice and aged mice with similar immunosuppressive tumor microenvironments (TMEs) that highly express immune co-inhibitory checkpoint molecules such as PD-1, PD-L1, TIM-3, LAG-3, and CTLA-4. In fact, ATC mice positively respond to combinatorial immune checkpoint inhibitors (anti-PD-1/anti-CTLA-4) regardless of sex or age, when given early in tumor development. In addition, we found that young mice of opposite sexes have very distinct gut microbial communities at baseline compared to aged mice, and this difference is associated with tumor growth outcomes. Moreover, targeting the microbiota through fecal microbial transplant (FMT) resulted in an antitumor benefit for aged groups disregard of sex. Together, these results reveal sex- and age-related immune mechanisms driving ATC progression and highlight the potential for immunotherapy and microbiota interventions.

: Combination Targeted Therapy
Poster Session

#6483 Convergent CDK4/6 and PI3K/mTOR pathway hyperactivation defines a targetable axis in osteosarcoma across RB1-proficient and RB1-deficient contexts.

Lauren K. Stevens[1], M. Reza Saadatzadeh[2], Farinaz Barghi[3], Erika A. Dobrota[4], Harlan E. Shannon[4], Rada Malko[3], Ryli Justice[4], Christopher Davis[4], Keiko Kreklau[4], Melissa A. Trowbridge[5], Kathy Coy[5], Felicia M. Kennedy[5], Anthony L. Sinn[5], Kyle W. Jackson[2], George Sandusky[6], L. Daniel Wurtz[7], Christopher D. Collier[7], Dana Mitchell[4], Ed Greenfield[7], Emma H. Doud[8], Amber L. Mosley[8], Steven P. Angus[2], Pankita H. Pandya[2], Karen E. Pollok[2]

[1]Indiana University Melvin and Bren Simon Comprehensive Cancer Center, Indiana University School of Medicine, Indianapolis, IN,[2]Department of Pediatrics, Division of Pediatric Hematology/Oncology, Indiana University School of Medicine, Indianapolis, IN,[3]Department of Medical and Molecular Genetics, Indiana University School of Medicine, Indianapolis, IN,[4]Herman B Wells Center for Pediatric Research, Indiana University School of Medicine, Indianapolis, IN,[5]Preclinical Modeling and Therapeutics Core, IUSCCC, Indiana University School of Medicine, Indianapolis, IN,[6]Department of Pathology and Laboratory Medicine, Indiana University School of Medicine, Indianapolis, IN,[7]Department of Orthopaedic Surgery, Indiana University School of Medicine, Indianapolis, IN,[8]Department of Biochemistry & Molecular Biology, Center for Proteome Analysis, Indiana University School of Medicine, Indianapolis, IN

Osteosarcoma (OS) in pediatric, adolescent, and young adult (AYA) patients is an aggressive malignancy with limited therapeutic progress. About 40% of OS patients develop metastases over time with 15-20% of OS patients already exhibiting metastases at initial diagnosis. Thus, there is a critical need to develop better therapeutics. Genomic analyses from our institution and others highlight recurrent alterations in CDKN2A and CDK4/6, suggesting that CDK4/6 inhibition (CDK4/6i) is a rational therapeutic vulnerability. Although RB1 proficiency (RB1+) is considered essential for CDK4/6i response, over 70% of OS tumors are RB1-deficient (RB1–), raising questions about the utility of CDK4/6i in these patients. Emerging evidence in other solid tumors and in our preliminary OS studies, suggests that CDK4/6i may retain antitumor activity in RB1– contexts. Compounding this complexity, pharmacologic CDK4/6 blockade induces compensatory PI3K/mTOR signaling, which can restore cyclin D–CDK4/6 activity and drive resistance.
We hypothesized that co-targeting PI3K/mTOR would enhance CDK4/6i efficacy irrespective of RB1 status by suppressing adaptive signaling. We evaluated palbociclib, voxtalisib, and the combination across RB1+ and RB1- OS models, using cell lines, patient derived xenografts (PDXs), and an experimental metastasis model. In vitro drug interactions (Chou–Talalay, Bliss) and mechanistic assays (cell cycle, senescence, autophagy) were complemented by in vivo tumor growth kinetics and pharmacodynamic profiling through histopathology, kinome, and proteomic analyses.
In RB1+ OS cells in vitro, palbociclib induced G1 arrest and senescence, accompanied by increased PI3K/AKT phosphorylation consistent with adaptive feedback. Voxtalisib suppressed this response, reinforced autophagic signaling, and maintained pathway inhibition. In vivo, combination therapy was well tolerated and produced significant tumor growth suppression in treatment-naïve and metastatic PDXs. In the RB1+ lung-colonization model, CDK4/6i alone reduced metastatic burden, with combination therapy achieving comparable control.
To interrogate RB1 as a biomarker, CRISPR-engineered human and mouse RB1– OS clones (MG63.3, K7M2) were generated and characterized. As expected, voxtalisib response was RB1-independent, and palbociclib sensitivity was reduced in RB1- cells. However, RB1- cells still exhibited growth inhibition at higher palbociclib concentrations. Notably, combination therapy of palbociclib+voxtalisib produced additive-to-synergistic growth inhibition regardless of RB1 status. In vivo validation studies are ongoing. These findings identify convergent CDK4/6–PI3K/mTOR hyperactivation as a targetable axis in OS and support further evaluation of CDK4/6i-based strategies, including in RB1-deficient disease.

#6484 Divergent roles of SPOP and CHD1 in ACSL4 regulation reveal context-dependent vulnerabilities for targeting ferroptosis in prostate cancer.

Feiyu Chen, Qidong Li, Qianlin Gu, Javier Leo, Xin Liang, Naayaa Mehta, Yin Wang, Francisco R. Saenz, Maya M. Phillips, Wei Shi, Chenling Meng, Jie Zhang, Boyi Gan, Di Zhao

The University of Texas MD Anderson Cancer Center, Houston, TX

Background: Genetic heterogeneity fundamentally shapes therapeutic responses in prostate cancer (PCa). Among the most recurrent alterations, SPOP mutations and CHD1 loss define molecularly distinct PCa subtypes that respond differently to androgen signaling-directed therapies. Ferroptosis, an iron-dependent form of cell death driven by unchecked lipid peroxidation, has recently emerged as a promising therapeutic vulnerability; however, the genetic determinants that govern ferroptosis responsiveness in PCa remain poorly defined.
Methods: We integrated engineered human cell lines, 3D organoid systems, genetically engineered mouse models (GEMMs) and isogenic xenografts to dissect how SPOP mutation and CHD1 deletion modulate ferroptotic sensitivity. Ferroptosis induction and GPX4 dependence were assessed using pharmacologic GPX4 inhibitors (RSL3, ML162, and JKE1674), lipid peroxidation assays, and ferroptosis rescue controls. Transcriptomic, lipidomic, and biochemical analyses, together with ChIP-seq, ChIP-qPCR, and ACSL4 promoter-luciferase reporter assays, were used to delineate how SPOP mutations and CHD1 deletion modulate the MYC-ACSL4 transcriptional axis.
Results: We uncover opposing roles for SPOP and CHD1 in regulating ferroptosis. SPOP mutations markedly sensitize PCa cells and tumors to GPX4 inhibition, whereas CHD1 loss abrogates this vulnerability and confers ferroptosis resistance. Mechanistically, SPOP mutation enhances, while CHD1 deletion suppresses, activation of the MYC-ACSL4 axis. SPOP mutation promotes, and CHD1 loss diminishes, MYC occupancy and transcriptional activation of ACSL4, a key enzyme governing polyunsaturated fatty acid metabolism and ferroptotic lipid peroxidation. Given our prior discovery that CHD1 loss upregulates cholesterol biosynthesis, we asked whether inhibiting this pathway could reverse ferroptosis resistance. Notably, pharmacologic blockade of cholesterol biosynthesis reinstates ACSL4 expression and restores ferroptosis sensitivity in SPOP-mutant/CHD1-deficient tumors in vivo, identifying a targetable metabolic checkpoint underlying ferroptosis resistance.
Conclusions: These findings define SPOP mutation and CHD1 loss as antagonistic genetic determinants of ferroptosis and uncover a MYC-ACSL4-dependent mechanism that governs GPX4 reliance. Pharmacologic inhibition of cholesterol biosynthesis overcomes CHD1-driven ferroptosis resistance, enabling a biomarker-guided combination strategy that couples ferroptosis induction with cholesterol-pathway blockade. This work establishes a precision strategy for exploiting ferroptosis-based combination therapies in genetically stratified PCa.

#6485 Combination of the GCN2 activator HC-7366 with VEGFR-TKI results in greater efficacy than VEGFR-TKI alone or VEGFR-TKI/HIF-2i combinations in ccRCC.

Weiyu Zhang, Kathryn Bieging-Rolett, Ashley LaCayo, Ben Harrison, Jeremy Drees, **Crissy Dudgeon**, Nandita Bose, Eric S. Lightcap

HiberCell, Roseville, MN

Current standards of care for metastatic clear cell renal cell carcinoma (ccRCC) include immune checkpoint inhibitors (ICIs), VEGFR-tyrosine kinase inhibitors (VEGFR-TKIs), or the combination of both. Recently, the HIF-2α inhibitor belzutifan was approved for 2L+ metastatic ccRCC patients and its combination with ICIs or VEGFR-TKIs is being studied in clinical trials. Despite the initial efficacy of these SOCs, most patients eventually relapse. Relapse after VEGFR-TKIs can be due to diverse mechanisms such as activation of non-VEGF angiogenic pathways, stromal remodeling, apoptosis evasion, and HIF upregulation. Therefore, novel therapeutic approaches are needed. HiberCell has developed HC-7366, a GCN2 activator that initiates the integrated stress response, leading to translation inhibition, cell-cycle arrest, HIF-1α suppression, and apoptosis in cancer cells. Based on these effects, we explored the potential of HC-7366 to overcome resistance to VEGFR-TKIs in RCC models. In the 786-O ccRCC xenograft model, HC-7366 treatment at multiple doses corresponding to exposures below the MTD in humans yielded robust combination efficacy with either cabozantinib or lenvatinib. HC-7366 alone achieved 63% tumor growth inhibition (TGI), whereas cabozantinib alone induced 30% regression (1/8 PR) and lenvatinib alone produced 95% TGI. When combined, HC-7366 significantly enhanced responses, achieving 71% regression with cabozantinib and 44% regression with lenvatinib (7/8 and 2/8 PRs, respectively). The combination of belzutifan and VEGFR-TKI was inferior to the HC-7366/VEGFR-TKI doublet, with only 36% regression (1 PR) for lenvatinib/belzutifan and 53% regression (5/8 PRs) for cabozantinib/belzutifan. The triplet combination using HC-7366/belzutifan/VEGFR-TKI was more beneficial than any doublet, further improving TGI and responses. Furthermore, in a single mouse trial of 10 RCC PDX models, addition of HC-7366 to axitinib improved outcomes in 8/10 PDX models and was superior to the belzutifan/axitinib doublet in multiple models. Analysis of xenografts showed the combination of HC-7366 and lenvatinib reduced HIF signaling and broadly suppressed cell cycle, growth factor, and angiogenic signaling while simultaneously inducing pro-apoptotic pathways. Our data reveal that combination of HC-7366 with any VEGFR-TKI may be an effective treatment strategy for RCC patients and has the potential to be superior to a VEGFR-TKI/HIF-2 inhibitor combination. A phase 1b clinical trial is now ongoing to evaluate the safety, tolerability, and efficacy of both HC-7366/belzutifan and HC-7366/cabozantinib doublets in metastatic ccRCC (NCT06234605). These results will form a foundation for future evaluation of triplet combinations that integrate HC-7366, VEGFR-TKIs, and HIF-2 inhibitors.

#6487 Exploratory study of camrelizumab combined with chemotherapy as second-line treatment for advanced esophageal squamous cell carcinoma.

Linlin Wang, Bingjie Fan, Bing Zou, Aiqin Gao, Shijiang Wang, Chunni Wang, Qian Shao, Yishan Yu, Hong Zhao, Jinzhi Wang, Yan Yi, Qingxi Yu

Shandong Cancer Hospital and Institute, Shandong First Medical University and Shandong Academy of Medical Sciences, Jinan, Shandong, China

Background: Patients with advanced esophageal squamous cell carcinoma (ESCC) face a poor prognosis and limited options after first-line therapy failure. This study aims to evaluate the efficacy and safety of camrelizumab combined with chemotherapy as a second-line treatment in patients who with or without prior immunotherapy exposure.
Method:This single-center, multi-cohorts, phase II exploratory clinical trial enrolled patients with locally recurrent or metastatic ESCC who had either failed or were intolerant to first-line treatment. Patients were stratified into two cohorts: those who had previously received immunotherapy (Cohort 1) and those who had not (Cohort 2). All patients received camrelizumab (Q3W, up to 2 years) combined with nab-paclitaxel or fluorouracil based chemotherapy (Q3W, 4-6 cycles).The primary endpoint was progression-free survival (PFS).
Results: Between May 2021 and September 2025, 40 patients were enrolled, with 20 patients in each cohort. The median age was 67 years in Cohort 1 and 66 years in Cohort 2.The median age was 67 years in Cohort 1 and 66 years in Cohort 2. The cohorts comprised 18 (90%) and 15(75%) males;15(75%) and 15(75%) with an ECOG performance status of 1; 10% and 15% with pulmonary metastases; and 55% and 45% with lymph node metastases, respectively. According to RECIST 1.1, among the 15 and 18 evaluable patients in Cohorts 1 and 2, the objective response rate (ORR) was 33.3% and 50.0%, and the disease control rate (DCR) was 93.3% and 88.9%, respectively. The median progression-free survival (mPFS) was 4.5 months(95%CI 2.13-6.8) in Cohort 1 and 9.5 months(95%CI 2.7-16.4) in Cohort 2. The median overall survival(mOS) was not reached.The most common adverse events (AEs) were lymphocyte count decreased (90% and 75%), anemia (85% and 70%), and decreased neutrophils (50% and 40%), which were grade 1-3. No grade 4 or 5 AEs occurred.The most common immune-related AEs (irAEs) was reactive cutaneous capillary endothelial proliferation(64.% and 57.1%), which was grade 1-2 in all cases.
Conclusion: Camrelizumab combined with chemotherapy showed good antitumor efficacy and safety in advanced ESCC as second-line treatment, regardless of whether the patients have previously received immunotherapy.

#6488 Dual targeting of PARP and RAS enhances antitumor activity in pancreatic cancer.

Chani Stossel, Gali Altman, Dikla Atias, Yulia Glick Gorman, Hanita Ovadia, Liora Chouchan, Elina Haimov-Talmoud, Maria Raitses-Gurevich, Tamar Beller, Talia Golan

Sheba Medical Center, Tel Hashomer, Israel

KRAS is the most frequent oncogenic mutation in PDAC. KRAS drives tumorigenesis and enhances mechanisms of DNA-damage repair (DDR). Specifically, KRAS upregulates HR and non-homologous end joining (NHEJ), which are critical pathways for DNA repair. Dual inhibition of these two driver pathways in BRCAmut PDAC, the MAPK/KRAS and the DDR, may have a promising therapeutic effect. However, this effect may be also exploited in the general PDAC population. PARP and RAS combined inhibition may extend and deepen therapeutic effect and delay emergence of therapeutic resistance.Our main goal was to examine the therapeutic effect of PARP and RAS(ON) combined inhibition on tumor growth in BRCAmut and BRCA-WT preclinical models. We established pre-clinical patient derived xenografts (PDX) models (n=160), PDX derived cells (n=37) and 3D organoids (n=11). Models were analyzed by WGS and RNAseq. We tested the effect of PARPi (olaparib) in combination with two RAS inhibitors: A tool RAS(ON) -multi-selective inhibitor RMC-7977 and a tool RAS(ON) G12D-selective inhibitor RMC-9945 (RM-044) in-vitro and in-vivo, utilizing specific models' systems based on BRCA and KRAS status (n=12).In vitro, PDCs were treated with olaparib, RMC-7977, RMC-9945 and combinations for 5 days. A dose response curve was observed for each cell line, with a variability of response between cell lines. Combination of RAS(ON)i and olaparib exhibited significant additive effect. In 3D organoids, combinational treatment of olaparib and RMC-7977 demonstrated a profound effect on viability. This effect was noted on BRCAmut and BRCA-WT cell lines. In-vivo experiment in a platinum sensitive BRCA2 mutated PDX model both RMC-7977 and RMC-9945 significantly attenuated tumor growth rate compared to control ($p<0.05$). The combination demonstrated a comparable effect to PARPi monotherapy. Yet, a tendency towards an enhanced response was observed by ex-vivo tumor volume and tumor weight. We hypothesize that a longer duration of experiment (currently being performed) will enhance response and delay the emergence of therapeutic resistance. In parallel mechanistic functional assays are being performed. Overall, we demonstrate a superior effect of the combination of PARPi and RAS(ON)i on PDAC using patient-derived models in-vitro (BRCAmut and BRCA WT) and in-vivo (BRCAmut). Notably, most models were generated from tumors obtained from patients at clinical resistance to standard of care treatment reflecting models with aggressive biology. Thus, these findings support further evaluation of combinational treatment of both RAS(ON) and PARP inhibition in this population.

#6489 Metabolic molecular subtyping of ovarian cancer reveals the role of oleic acid-CD36 in facilitating cisplatin resistance.

Jiagui Song

Peking University Third Hospital, Beijing, China

Current histopathological classification systems for ovarian cancer cannot adequately predict platinum chemotherapy response, hindering personalized therapeutic strategies. Here, through integrative analysis of multiple datasets from TCGA, ICGC and GEO databases, we stratify patients into metabolic associated chemotherapy-refractory and chemotherapy-sensitive types (MCRT, MCST for short) with distinct prognosis by 20 genes. Lipidomic profiling of ascites from patients with ovarian cancer further identifies oleic acid as a hallmark metabolite in MCRT cases. Oleic acid treatment facilitates the resistance to cisplatin in ovarian cancer cells and patient-derived organoids. Mechanistically, oleic acid activates and promotes nuclear translocation of YAP through CD36. Inhibition of SCD1—genetically or pharmacologically—synergizes with cisplatin in 26 patient-derived organoids and suppresses tumor growth in xenograft models. Our study proposes a new metabolic classification of ovarian cancer that can predict chemotherapy sensitivity. Moreover, it discovers the role of the oleic acid-CD36-YAP signaling axis in promoting cisplatin resistance. These findings shed light on how oleic acid facilitates the resistance to cisplatin in ovarian cancer and provide a potential therapeutic strategy for treating patients with ovarian cancer.

#6490 MEK inhibition overcomes stromal-mediated resistance to a MERTK targeted therapy in AML co-cultures and vascularized mesenchymal organoids.

Chloe Hope[1], Katherine Minson[1], Eleana Vasileiadi[2], Madeline G. Higgins[3], Alejandro De Janon[4], Shuichi Takayama[4], Xiaodong Wang[5], Steven Frye[5], H. Shelton Earp[5], Douglas K. Graham[1], Deborah DeRykere[1]

[1]Aflac Cancer & Blood Disorders Center, Children's Healthcare of Atlanta, & Department of Pediatrics, Emory University, Atlanta, GA,[2]Division of Pediatric Infectious Diseases, University of Pittsburgh Medical Center, Pittsburgh, PA,[3]Department of Surgery, University of Colorado Anschutz Medical Campus, Aurora, CO,[4]Georgia Institute of Technology & Emory University, Atlanta, GA,[5]University of North Carolina Chapel Hill, Chapel Hill, NC

MERTK receptor tyrosine kinase mediates pro-survival signaling and therapeutic resistance and is a potential therapeutic target in acute myeloid leukemia (AML); however, like many therapies, AML interactions with the bone marrow stroma confer resistance to MERTK inhibition, limiting therapeutic efficacy. Rational combination strategies that suppress compensatory signaling in physiologically relevant model systems are needed to overcome microenvironment-driven drug resistance in AML. Here, we demonstrate stromal-mediated ERK activation as a mechanism of resistance to the MERTK inhibitor, MRX-2843. Co-culture with stromal cell lines (Hs27 or Hs5 fibroblasts) or mesenchymal stem cells (MSCs) protected AML cell lines (NOMO-1, OCI-AML5, KASUMI-1) from induction of cell death in response to treatment with MRX-2843 (e.g. no co-culture vs. co-culture: Kasumi-1 + Hs27: 67.6% vs. 31.6% dead, OCI-AML5 + Hs5: 79.4% vs. 36.6%, NOMO-1 + MSC: 77.2% vs. 34.5%). Induction of γH2AX, an indicator of cell death, was also decreased in stromal co-cultures treated with MRX-2843 compared to AML mono-cultures. Mechanistically, MERTK expression was increased in AML cells cultured with stromal cells. ERK phosphorylation was also induced in stromal cell co-cultures and was refractory to inhibition by MRX-2843. Moreover, treatment with the MEK inhibitors PD0329501 or pimasertib in combination with MRX-2843 abrogated ERK phosphorylation and restored induction of γH2AX and anti-leukemia activity in the presence of stromal cells, confirming dependence on MEK/ERK signaling in AML cells for stromal-mediated survival. To better model the impact of the bone marrow microenvironment on anti-leukemia activity, we utilized a novel three-dimensional vascular mesenchymal organoid system that has greater stromal cell complexity and recapitulates many features of the bone marrow observed in human AML (e.g. architecture, cell-cell interactions, cytokine/chemokine production). Combined treatment with MRX-2843 and pimasertib significantly enhanced therapeutic efficacy in organoids established from NOMO-1 and KASUMI-1 AML cell lines, as evidenced by increased γH2AX expression compared to MRX-2843 or pimasertib monotherapies. Notably, these findings were recapitulated in organoids established from a MERTK-expressing patient-derived AML xenograft, reinforcing the translational relevance of the combination therapy. In preliminary dose-finding studies, concurrent treatment with MRX-2843 and pimasertib was well-tolerated in mice. Collectively, these data identify MEK/ERK signaling as a mechanism of stromal-mediated resistance to MERTK inhibition and establish combined treatment with MRX-2843 and a MEK inhibitor as a promising strategy for effective treatment of AML.

#6491 Co-treatment with FAK and PARP inhibitors for the treatment of homologous recombination-proficient high grade serious ovarian cancer.

Caree Carson, Breana Hill, Aarya Ghosalkar, Marjaana Ojalill, Antonia Boyer, Xiao Lei Chen, David Schlaepfer, Dwayne Stupack

UCSD Moores Cancer Center, La Jolla, CA

High grade serous ovarian cancer (HGSOC) - the most common subtype - accounts for the greatest number of patient deaths due to late detection and frequent recurrence. Treatment for HGSOC patients begins with cytoreductive surgery followed by platinum/taxane chemotherapy and adjuvant/maintenance therapy, the latter being specific to whether tumors are homologous recombination-proficient (HRP) or homologous recombination-deficient (HRD). HRD cancers are treated with PARP inhibitors (e.g. Niraparib) while HRP cancers are treated with bevacizumab, an anti-angiogenesis agent. Either regimen can be extended into maintenance therapy. Over 70% of HGSOC tumors present with amplifications or gains in the *PTK2* gene that codes for the focal adhesion kinase (FAK) protein, a key regulator of tumor cell migration, adhesion, and chemotherapy resistance that also regulates the endothelial cell response to VEGF. FAK-targeting drugs have been approved for use in the clinic for the treatment of low grade serious ovarian cancer, but their role in HGSOC is less clear. We have previously shown that FAK inhibition compromises several cell survival pathways, among them, a suite of key DNA repair enzymes. Unexpectedly, we find that FAK inhibition imbues PARP sensitivity on HRP cells. *In vivo*, an enhanced anti-tumor effect was observed with suboptimal doses combinations of FAK and PARP inhibitors. Notably, an even greater effect was observed when combining FAK and PARP inhibitors in a maintenance therapy model for chemoresistant HGSOC. FAK inhibition through treatment with narmafotinib impacts PARP1 protein expression, cleavage, and overall PARylation levels, implicating functional interaction between FAK and PARP pathways within the cell. These results provide an unexpected avenue to evaluate PARP inhibition as a viable therapy for HRP tumors.

#6492 Targeting phospholipase D1 overcomes platinum resistance and enhances cisplatin efficacy in ovarian cancer.

Shin-Wha Lee[1], Sung Wan Kang[1], Dong Woo Kang[1], Yu-na Noh[1], Young-Jae Lee[1], Min-Seo Lee[1], Yong-Man Kim[2]

[1]Asan Medical Center, University of Ulsan College of Medicine, Seoul, Korea, Republic of,[2]CHA Bundang Medical Center, CHA University School of Medicine, Seongnam, Korea, Republic of

Background: Platinum-based chemotherapy is the standard treatment for high-grade serous ovarian cancer (HGSOC), yet the development of platinum resistance remains a major barrier to effective therapy. Phospholipase D1 (PLD1) has been implicated in tumor progression and stress response pathways, but its potential as a therapeutic target in platinum-resistant ovarian cancer (OC) has not been clearly defined. This study investigated whether targeting PLD1 can restore platinum sensitivity and improve therapeutic efficacy in resistant disease.
Methods: The impact of PLD1 inhibition was evaluated using OC cell lines, patient-derived primary tumor cells, and both cell line-derived and patient-derived xenograft models. Functional assays measured clonogenic survival, proliferation, invasion, sphere formation, apoptosis, and DNA damage. Cisplatin responsiveness was assessed following genetic PLD1 knockdown or treatment with a PLD1 inhibitor.
Results: PLD1 suppression significantly reduced survival, proliferation, and invasiveness in platinum-resistant OC cells, while inducing apoptosis and accumulation of DNA damage. Importantly, PLD1 inhibition restored cisplatin sensitivity across multiple resistant models, leading to a marked reduction in clonogenic survival. In vivo, combined PLD1 inhibition and cisplatin treatment markedly suppressed tumor growth, prolonged survival, and reduced metastatic burden in xenograft and PDX models, with greater therapeutic benefit observed in platinum-resistant tumors.
Conclusions: PLD1 is a key survival determinant in platinum-resistant OC and contributes directly to treatment failure. Targeting PLD1 enhances the antitumor efficacy of cisplatin and provides strong preclinical rationale for PLD1-directed combination therapy in refractory HGSOC.

#6493 Azvudine combined with Doxitinib, a potential therapy for EGFRm⁺ NSCLC.

Jianmei Zhang, Shufang Zhang, Yujie Wang, Limin Jia, Ying Li, Pan Li, Feng Luo, Jinfa Du

Genuine Biotech Co., Ltd., Beijing, China

Osimertinib, a third-generation EGFR tyrosine kinase inhibitor (EGFR-TKI), is the current standard first-line therapy for patients with EGFR-mutant non-small cell lung cancer (NSCLC). Although Osimertinib significantly improves progression-free survival (PFS), some patients exhibit intrinsic resistance, and nearly all eventually develop acquired resistance.

Doxitinib, a deuterated analog of Osimertinib, retains potent EGFR inhibitory activity while significantly reducing the formation of toxic metabolites by up to 80% in preclinical models, suggesting an improved safety profile and the potential for enhanced therapeutic efficacy through higher tolerated dosing. In a phase 1/2 clinical study (ChiCTR2000039281), Doxitinib demonstrated a favorable safety profile without dose-limiting toxicities (DLTs) across doses ranging from 20 to 240 mg daily in patients previously treated with EGFR TKIs. Encouraging clinical activity was observed, including antitumor responses in brain metastases. The ongoing expansion phase is further evaluating Doxitinib in EGFRm⁺ NSCLC patients naïve to EGFR-TKI therapy.

To overcome resistance and enhance antitumor efficacy, we combined Doxitinib with Azvudine (FNC), a fluorinated nucleoside analog with dual antitumor mechanisms. FNC inhibits tumor cell proliferation via its active triphosphate metabolite, which incorporates into DNA or RNA to disrupt nucleic acid synthesis, induce replication stress, and arrest tumor growth. Moreover, FNC modulates the tumor immune microenvironment (TIME) by suppressing myeloid-derived suppressor cell (MDSC) differentiation and infiltration while enhancing $CD8^+$ T cell and NK cell activation, thus shifting the TIME from immunosuppressive to immunoreactive—an essential factor in overcoming EGFR-TKI resistance. In vitro, the combination of FNC and Doxitinib additively inhibited the proliferation of NCI-H1975 (EGFR L858R/T790M/C797S) triple-mutant NSCLC cells. In vivo, the combination achieved superior tumor growth inhibition compared to either monotherapy in the NCI-H1975 (EGFR L858R/T790M) xenograft model.

Collectively, these findings suggest that the combination of FNC and Doxitinib represents a promising therapeutic strategy to enhance efficacy and overcome acquired resistance in EGFRm⁺ NSCLC. Based on these preclinical and clinical findings, a phase 1/2 clinical trial will be initiated to evaluate the safety and efficacy of this combination therapy in EGFR-mutant NSCLC patients.

#6494 The selective YAP/TEAD inhibitor TY-1054 enhances the efficacy of KRAS inhibitors or Trop2-ADC in multiple solid tumors.

Shengli Dong, Zhengfei Guo, Zhiyong He, Apeng Liang, Meihua Li, Guangbin Liu, Chao Zhou, Yu Yu, Xinlong Yang, Hongqiang Li, Chengshan Niu, Shaoqing Chen, Jun Li, Yusheng Wu

TYK Medicines, Inc., Changxing, Zhejiang, China

Introduction: KRAS is one of the most common somatic mutations associated with human cancers. YAP/TEAD activation is a major cause of resistance to various targeted therapies. Recently, YAP/TEAD signaling has been identified as a synthetic lethal target that can enhance the efficacy of KRAS G12C inhibitors. TY-1054 is a potent YAP/TEAD inhibitor developed by TYK Medicines Inc. Results: 1. TY-1054 not only enhanced the efficacy of FDA-approved KRAS G12C inhibitors, Adagrasib and Sotorasib, in Non-Small Cell Lung Cancer (NSCLC) H1373 and H2122 cells, but also enhanced the efficacy of Divarasib (GDC-6036) and pan-KRASi Daroxonrasib (RMC-6236) in NSCLC H1972 and H2122 cells. 2. TY-1054 not only enhanced the efficacy of KRAS G12Di RMC-9805 in SU.86.86 (PDAC, KRAS G12D) in vitro and in vivo, but also enhanced the efficacy of pan-KRASi Daraxonrasib in SU.86.86 in vitro and in vivo. 3. TY-1054 enhances cetuximab efficacy in head and neck squamous cell carcinoma (HNSCC) Cal33 cells. 4. TY-1054 enhances the efficacy of Trop2-ADC (SKB264/Sac-TMT) in triple-negative breast cancer (TNBC) (MDA-MB 231 and HCC1806), NSCLC (H1975 and HCC827), and trastuzumab-resistant breast cancer (JIMT-1) cells. In summary, TY-1054 has a potentially wide therapeutic window and is currently being evaluated in patients in China. IND clearance from the US FDA was received in 2024. This study provides a strong rationale for testing the combination therapy of TY-1054 and KRAS inhibitors or Trop2-ADC in human clinical trials. The successful execution of the TY-1054 clinical trial will provide a powerful solution for precision oncology.

# Shengli Dong and Zhengfei Guo contributed equally to this work.
* Correspondence to: Shengli Dong, Ph.D.; TYK Medicines Inc.; Block D, No. 778 Huaxi Avenue, Changxing, Zhejiang, P. R. China, 313100. Tel: 86 17772745590; e-mail: shengli.dong@tykmedicines.com.

#6495 NXP900, a Phase 1b, first-in-class YES1/SRC inhibitor demonstrates potent synergy with KRAS inhibitors in KRASi sensitive and resistant NSCLC models.

Boback Kaghazchi[1], Enrique Podarosu[2], Asier Unciti-Broceta[1], **Neil O. Carragher**[1]

[1]Institute of Genetics and Cancer, University of Edinburgh, Edinburgh, United Kingdom,[2]Nuvectis Pharma Inc., Fort Lee, NJ

Background: NXP900 (eCF506) is a novel potent and selective SRC family kinase (SFK) inhibitor, (IC_{50} of 0.47 nM against YES1). NXP900 first-in-class mode-of-action locks its target into its native "closed" conformation, thereby inhibiting both kinase activity and scaffolding function with protein signaling partners (Temps et al. Cancer Res 2021). In contrast, other clinically available inhibitors, lock SRC in the active "open" conformation promoting the association of SFK and signaling partners via allosteric facilitation (Higuchi et al. Cell Rep 2021). G12C mutant-selective KRAS inhibitors (KRASi) have been FDA-approved and several mutant-selective, pan-mutant-KRAS, and pan-RAS inhibitors are in development. However, KRASi monotherapy results in limited clinical benefit and face the rapid development of acquired resistance. YAP1 activation is associated with drug resistance to KRASi and promotes the survival of drug-tolerant persister cells after therapy. Induction of YAP1 nuclear localization by SRC/YES1 mediated tyrosine phosphorylation of YAP1 and LATS1 is inhibited by NXP900 in NSCLC cell lines at a low nM concentration. A FIH, dose escalation study, demonstrated that NXP900 potently inhibits the activity of SRC kinase at well tolerated doses (Falchook et al. Cancer Res 2025). Moreover, no CYP3A induction was observed in a drug-drug interaction study in humans indicating the potential of NXP900 to be combined with KRASi to overcome primary and acquired resistance and improve clinical benefit to patients with KRAS mutated cancers.
Materials and methods: Resistant cell lines to the KRASi sotorasib were generated from NCI-H23 cells.
Cell proliferation assay - Cells were diluted in the corresponding ATCC recommended medium and dispensed in a 384-well plate, depending on the cell line used, at a density of 100 - 6400 cells per well. Cells were treated with KRASi and or NXP900 for 120 h and underwent ATPlite viability assay. Drug combination effects were studied using the Bliss independence principle.
Results: NXP900 potently inhibited the activating SRC autophosphorylation, YAP1 nuclear localization and demonstrated synergy in combination with sotorasib in sotorasib-sensitive and resistant cell lines.
Conclusions: Development of effective and tolerable combination therapies are needed to overcome resistance and maximize the clinical impact of RAS-targeted therapy. NXP900 can potently inhibit cell proliferation of KRAS mutated cell lines in combination with a KRASi in NSCLC models. The combination was synergistic both in KRAS sensitive and resistant models. The data suggests that NXP900, currently in a Phase1b expansion in patients with *FAT1, YES1* and other genomic alterations in solid tumors (NCT05873686), is an attractive and translatable combination partner that could synergize with KRASi.

#6496 Methylseleninic acid enhances anti-FN14 CAR-T cell effector function and redirects cytotoxicity against TGF-β-rich kidney, prostate, and brain tumors.

Gloria B. Kim[1], Obed B. Amissah[1], Casey R. Ager[2], Yousef Zakharia[3], Youcef M. Rustum[4]

[1]Mayo Clinic Arizona, Scottsdale, AZ,[2]Mayo Clinic Arizona, Phoenix, AZ,[3]Mayo Clinic Arizona, Pheonix, AZ,[4]Chair, Dept. of Cancer Biology, Roswell Park Cancer Institute, Buffalo, NY

Background: Clear cell renal cell carcinoma (ccRCC), metastatic castration-resistant prostate cancer (mCRPC), and glioblastoma (GBM) are treatment-refractory tumors marked by high TGF-β1, a master suppressor of antitumor immunity and antigen presentation. Pharmacologic methylseleninic acid (MSA) potently inhibits TGF-β1, PD-L1, and VEGF without significant off-target toxicity. FN14, the TWEAK receptor and a metastasis driver, is selectively overexpressed in these malignancies, making it a high-specificity CAR-T target.
Methods: We developed second-generation anti-FN14 CARs with CD28 or 4-1BB costimulation and CD3ζ signaling and lentivirally transduced them into human $CD4^+$/$CD8^+$ T cells. Cytotoxicity against $FN14^+$ ccRCC, mCRPC, GBM lines and patient-derived tumors was measured using LDH release and xCELLigence assays. Effector function was assessed by intracellular cytokines, phenotyping, and multiplex analysis. MSA was tested at physiologic concentrations to evaluate effects on CAR-T viability, metabolism, function, and tumor susceptibility.
Results: Anti-FN14 CAR-T cells mediated rapid, antigen-specific lysis across all tumor types, achieving >50% specific lysis at an E:T ratio of 1:1. MSA (2.5-5 μM) reduced tumor PD-L1 and TGF-β by >40% and improved CAR-T metabolic activity, enhancing IL-2 and IFN-γ secretion. Manufacturing CAR-T cells with MSA (2.5 μM) increased cytotoxicity and persistence versus controls ($p < 0.01$). MSA's effects were dose- and schedule-dependent at clinically compatible concentrations without detectable off-target toxicity.
Conclusion: MSA augments anti-FN14 CAR-T cytotoxicity, metabolic fitness, and sustained effector function by suppressing tumor-derived TGF-β1 and PD-L1 and directly enhancing CAR-T activity. As a clinically relevant TGF-β1 inhibitor and active seleno-L-methionine metabolite, MSA represents a readily translatable strategy to reduce CAR-T exhaustion and improve efficacy in TGF-β-rich solid tumors.

#6497 Synergistic disruption of KRAS and FAK pathways: A preclinical pipeline for PDAC therapy optimization.

Jaeger Moore[1], Taylor Bargenquast[1], Tithi Ghosh Halder[1], Serina Ng[1], Erkut Borazanci[1], Sara A. Byron[2], Cherie Wesley[2], Raffaella Soldi[1], Sunil Sharma[1]

[1]HonorHealth Research Institute, Phoenix, AZ,[2]TGen (The Translational Genomics Research Institute), Phoenix, AZ

Background: KRAS mutations are among the most prevalent oncogenic drivers across solid tumors, with particularly high incidence in Pancreatic Ductal Adenocarcinoma (PDAC). Despite their clinical relevance, direct targeting of KRAS has historically been difficult. The advent of KRAS G12C-specific inhibitors has marked a breakthrough in targeted therapy, yet acquired resistance remains a major challenge. RMC-6236 (daraxonrasib), a noncovalent RAS(ON) inhibitor, targets the active GTP-bound form of both mutant and wild-type RAS isoforms and has shown potent antitumor activity, especially in codon 12 KRAS-mutant cancers. In a Phase 1 trial for metastatic PDAC, RMC-6236 extended progression-free survival to approximately eight months. Recent studies suggest that KRAS inhibition may sustain focal adhesion kinase (FAK) activation, implicating the FAK-YAP axis and tumor-associated fibrosis in resistance. FAK, a key regulator of survival and DNA damage repair, has emerged as a promising co-target, with evidence of synergy between FAK inhibition and KRAS blockade, as well as enhanced sensitivity to PD-1 checkpoint inhibitors and radiation. We hypothesize that dual targeting of KRAS and FAK pathways will yield synergistic therapeutic effects in PDAC by disrupting oncogenic signaling and promoting cell death. To test this, we employ patient-derived organoid (PDO) cultures that preserve tumor architecture, heterogeneity, and stromal structure, enabling physiologically relevant evaluation of drug combinations.
Methods: Patient-derived cells were treated with RMC-6236, defactinib, and ifebemtinib, alone and in combination, in 2D and 3D viability assays. Organoids were generated by co-culturing tumor cells and fibroblasts (1:1) for 72 hours, then treated with an 8-point, 2-fold serial dilution of drugs for another 72 hours. Synergy was assessed using Bliss analysis via Combenefit, and 2D dose responses were analyzed in GraphPad Prism using Student's t-test. Western blotting was performed to evaluate RAS-MAPK pathway inhibition and apoptosis markers.
Results: Preliminary data from four KRAS-mutant PDOs (G12D, G12V, G12R) revealed robust synergy between RMC-6236 and either FAK inhibitor, with up to 10-fold and 100-fold increases in efficacy for defactinib or ifebemtinib and RMC-6236, respectively. Western blot analysis confirmed suppression of RAS-MAPK signaling, downregulation of c-MYC, and increased apoptotic markers including cleaved PARP and activated Caspase-3. These findings support the potential of KRAS-FAK co-targeting strategies in PDAC and lay the groundwork for future clinical development. These findings underscore a mechanistic interplay between KRAS and FAK signaling pathways, suggesting that dual targeting may overcome resistance and enhance cell death in KRAS-mutant PDAC, to improve outcomes in KRAS-driven pancreatic cancers.

#6498 Combination of MDM2 inhibitor and lipophilic gemcitabine: Strong synergism in lung cancer, while antagonism in brain cancer.

Bhoomi Mukeshbhai Dholariya, Akanksha S. Patel, Ketankumar Patel

St. John's University, Queens, NY

Cancer remains the leading cause of mortality worldwide, even in the post-COVID-19 era. Lung and brain cancers account for a substantial proportion of these deaths. Although multiple anticancer agents are available, single-agent therapies often fail to achieve durable responses due to limited efficacy or the development of drug resistance. Combination therapy is therefore recognized as a powerful strategy to enhance therapeutic efficacy and delay resistance.In this study, we investigated the synergistic potential of Idasanutlin (Ida), a second-generation MDM2 inhibitor, and Gemcitabine Elaidate (Gem Eli), a lipophilic prodrug of Gemcitabine, for the treatment of non-small cell lung cancer (NSCLC) and glioblastoma (GBM). Both molecules exhibit hydrophobic characteristics, prompting their incorporation into the lipid bilayer of liposomal carriers. Using a modified hydration method, we developed a liposomal nanoformulation co-loaded with Ida and Gem Eli (IG). A major challenge was the rapid insoluble precipitation of Ida, a brick-dust molecule. To address this, we introduced the cationic ionizable lipid DLin-DMA to enable the formation of a charge-tunable complex between anionic Ida and cationic DLin-DMA. Ionizable lipids remain neutral at physiological pH but acquire a positive charge in acidic conditions (e.g., the tumor microenvironment, pH ~5.5), which facilitates tumor-targeted delivery while minimizing systemic toxicity. The IG formulation was evaluated in NSCLC cell lines (A549 and H460) and a GBM cell line (U-87), all harboring wild-type p53. Strong synergism was observed in NSCLC, with combination index values of 0.07 (A549) and 0.3 (H460). In contrast, U-87 cells demonstrated no synergism; instead, Gem Eli displayed antagonistic behavior, with a ~7-10-fold increase in IC_{50} when combined with Ida across ratios ranging from 1:1 to 1:20. A 3D spheroid assay further confirmed antagonism in GBM, after 10 days of alternate-day treatment, IG, Gem Eli, and Ida reduced spheroid area by 81%, 61.9%, and 81%, respectively, compared to controls. Synergism in NSCLC was further validated using Combenefit analysis, which demonstrated robust synergy in 3D synergy maps. The optimized IG liposomes exhibited a particle size of 131.1 ± 0.68 nm, a PDI of 0.172 ± 0.13, and pH-responsive zeta potentials of -2.06 ± 0.06 (pH 7.4) and +8.88 ± 0.31 (pH 5.5), supporting their suitability for tumor-targeted delivery. Hemocompatibility testing in mouse red blood cells showed <1% hemolysis at concentrations up to 100 µM. Cryo-electron microscopy confirmed uniform particle morphology with no evidence of aggregation. Ongoing studies are focused on elucidating the cellular mechanisms underlying the observed antagonism in GBM.

#6499 Targeting BCR-ABL1-independent mechanisms of resistance in chronic myeloid leukemia.

Mark Pusung[1], Christopher A. Eide[1], Jessica Gibbs[1], Daniel Bottomly[2], Haijiao Zhang[1], Brian J. Druker[3]

[1]Hematologic Malignancies, OHSU Knight Cancer Institute, Portland, OR,[2]Division of Bioinformatics and Computational Biology, OHSU Knight Cancer Institute, Portland, OR,[3]Director, JELD-WEN; Chair of Leukemia Research and Investigator, OHSU Knight Cancer Institute, Portland, OR

Tyrosine kinase inhibitors (TKIs) targeting the BCR-ABL1 fusion gene in chronic myeloid leukemia (CML) have improved patient prognosis. While newer drugs have made inroads against BCR-ABL1-dependent TKI resistance, patients who develop resistance through pathways independent of BCR-ABL1 feature heterogeneous, poorly characterized molecular mechanisms and present a challenge for application of combination targeted therapy. To identify genes contributing to BCR-ABL1-independent resistance, we performed CRISPR/Cas9 genome-wide screens using Ba/F3 BCR-ABL1 cells cultured in the presence of DMSO, imatinib, and asciminib. After 10 days, cells were harvested and analyzed for gene-level enrichment/depletion of sgRNAs. Among candidate resistance genes (whose knockdown was enriched following TKI treatment), independent sgRNA guides for five genes were induced by lentiviral CRISPR/Cas9 knockout in Ba/F3 BCR-ABL1 cell line models for validation studies. Cell lines were evaluated for in vitro sensitivity to a panel of approved ABL1 TKIs and profiled against an expanded inhibitor panel spanning a range of drug targets. Expression levels of candidate resistance genes were compared by RNAseq in primary specimens from CML patients. CRISPR screening revealed varying subsets of genes enriched in TKI-treated cultures. Five candidate genes were selected for validation studies: *Chic2, Stub1* and *Pten* from the imatinib-treated cells and *Fbxo3* and *Ptar1* from the asciminib-treated cells. In Ba/F3 BCR-ABL1 cell line models, knockout of each of these genes resulted in varying degrees of reduced sensitivity to a panel of ABL1 TKIs (2-45-fold increase in IC_{50} compared to wild-type cells). For example, knockout of *Pten* and *Chic2* demonstrated increased IC_{50} values for imatinib of 12,714 and 914 nM, respectively, compared to 277 nM for wild-type cells. Profiling of cell lines using an expanded drug panel revealed differential sensitivities to inhibitors targeting multiple pathways. For example, *Chic2, Stub1* and *Fbxo3* knockout showed greater sensitivity (relative to wild-type cells) to inhibitors of WNT, proteasome, histone deacetylase, bromodomain, and/or nucleoside analog pathways. Lastly, analysis of RNASeq data highlighted differences in expression levels in patient samples. For example, expression levels of both *Ptar1* and *Pten* were reduced in patients with BCR-ABL1-independent resistance to imatinib relative to newly diagnosed patients, and expression of *Fbxo3* and *Chic2* were decreased with disease progression (blast vs chronic phase). Taken together, our results identify genes implicated in tumor suppression (*Pten*), ubiquitination (*Stub1, Fbxo3, Chic2*), and post-translational modification (*Ptar1)* with contributing roles for BCR-ABL1-independent TKI resistance and map these to potential actionable pathways amenable to novel combination targeted therapy approaches.

#6501 Preclinical evidence for synergistic activity of alectinib and everolimus in ALK-positive non-small cell lung cancer.

Hamadi Madhi[1], Habib Serhan[1], Rachel Mercer[1], Benjamin Levy[1], Anna Rottinghaus[1], Liwei Bao[1], Xu Cheng[1], Sharon R. Pine[2], Ross Camidge[2], Angel Qin[1], Nathan M. Merrill[1], Sofia D. Merajver[1], Matthew B. Soellner[3]

[1]Internal medicine, University of Michigan, Ann Arbor, MI,[2]University of Colorado, Aurora, CO,[3]Chemistry, University of Michigan, Ann Arbor, MI

Introductory Sentence: This study investigates the therapeutic potential of dual alectinib and everolimus inhibition to prolong the clinical benefit of alectinib in ALK-positive non-small cell lung cancer.
Pertinent experimental procedures: ALK-rearranged NSCLC cell lines (CUTO8, CUTO9, CUTO29.1, CUTO39, CUTO41, CUTO43, CUTO46) obtained from the University of Colorado; DFCI032 from Dana-Farber; NCI-H2228 and NCI-H3122 from ATCC; and SNU2292 and SNU2535 from Seoul National University were screened using a high-throughput drug-combination platform to identify synergistic interactions between alectinib and a curated library of 1,600 approved and experimental compounds. Functional validation in NCI-H3122 included colony-formation and Glo-Caspase 3/7 apoptosis assays with therapeutically relevant concentrations of everolimus (Cmax and Caverage) plus 100 nM alectinib, ~ten-fold lower than reported Cmax/Caverage. Apoptotic activation was further confirmed by Western blot for cleaved PARP, cleaved caspase-3, and the pro-survival protein MCL-1. In parallel, ex vivo screening was conducted on ALK167-T-01, an ALK-positive PDX model harboring the p.Leu1196Met ALK mutation.
Summary of new unpublished data: High-throughput screening identified a consistent synergistic response to alectinib combined with multiple mTOR inhibitors across all the ALK-rearranged models tested. Synergy was assessed by the Chou-Talalay method, with CI <1 in most ALK-positive cell lines tested. In NCI-H3122, the combination significantly reduced clonogenic potential (alectinib alone VS combo Caverage; $p<0.01$ and alectinib alone VS combo Cmax; $p<0.001$) and induced apoptosis, evidenced by increased Caspase 3/7 activity (alectinib alone VS combo Caverage; $p<0.01$ and alectinib alone VS combo Cmax; $p<0.001$) and significant PARP and caspase-3 cleavage. Ex vivo PDX screening using ALK167-T-01 with Glo-Caspase 3/7 assays at therapeutically relevant everolimus concentrations plus 100 nM alectinib showed higher apoptosis vs single agents (alectinib alone VS combo Caverage; $p<0.001$ and alectinib alone VS combo Cmax; $p<0.0001$), confirming synergy is not exclusive to sensitive lines.
Statement of the conclusions: Dual ALK and mTOR targeting with alectinib and everolimus produces synergistic antitumor activity in vitro and ex vivo, reflected by significantly increased apoptosis vs single agents. These findings support further investigation in in vivo models, including alectinib-sensitive and -resistant tumors.
AI disclosure: AI was used for language editing only; content was verified by the authors.

#6503 Investigating synergistic effects with CK2 and C-KIT inhibition in B-ALL.

Daniel Bogush, **Stephanie Buczkowski**, Rabab Husain, Sameer Ahmed Bhat, Yen Teng Tai, Avinash Kundadka Kudva, Sinisa Dovat

Penn State College of Medicine, Hershey, PA

Survival for pediatric pre-B cell acute lymphoblastic leukemia (B-ALL) has improved substantially, yet high-risk (HR) subgroups continue to experience significant morbidity and mortality. One molecular feature common in HR ALL is deletion of IKZF1, which reduces the tumor-suppressive activity of the transcription factor IKAROS. Casein kinase 2 (CK2), frequently upregulated in ALL, phosphorylates IKAROS and diminishes its DNA-binding capacity, impairing transcriptional regulation. Prior studies show that pharmacologic CK2 inhibition with CX-4945 can restore IKAROS function. Among IKAROS-regulated targets is the receptor tyrosine kinase c-KIT, which is often overexpressed in cancer. These observations suggest that restoring IKAROS-mediated repression of c-KIT may enhance the activity of c-KIT-targeted therapies such as imatinib. This study evaluated whether CX-4945 synergizes with imatinib in B-ALL cells. Nalm6 cells were treated with imatinib for 72 hours to establish the half-maximal inhibitory concentration (IC50), which was then used to guide concentration ranges for combination testing with CX-4945 in a 72-hour cytotoxicity synergy analysis. Cell viability was assessed using a WST-1 assay, and synergy was defined as a combination index <0.85 using Calcusyn. Experiments were repeated with multiple drug concentrations to refine the synergy window. The IC50 of imatinib as a single agent was 25 μM, while CX-4945 showed an IC50 of 4 μM. When CX-4945 was fixed at 4 μM and imatinib was applied across varying doses, multiple combinations demonstrated synergistic cytotoxicity. These results indicate that CK2 inhibition with CX-4945 enhances the therapeutic efficacy of the c-KIT inhibitor imatinib in B-ALL cells, supporting a cooperative mechanism involving restoration of IKAROS function. Given that imatinib is clinically used for Philadelphia chromosome-positive (Ph+) ALL, future work will assess CX-4945/imatinib synergy in Ph+ B-ALL, where an even more potent effect is anticipated. This combination approach may offer a promising therapeutic avenue for HR ALL subtypes characterized by IKZF1 alteration and chemotherapy resistance.

#6505 Combination therapy with selective SMARCA2 (BRM) inhibitor HD-11273 for treatment of SMARCA4 (BRG1)-deficient cancers.

Hyuntae Kim, MinOu Choi, Jongwoo Park, Goeun Yang, Min-Ah Park, Hyo Sun Choi, Yukyung Kim, Doo-Young Kim, Daehoon Kim, Seong Heon Kim, Suk Ho Lee

Hyundai pharmaceutics, Suwon, Korea, Republic of

SMARCA2 (BRM) and SMARCA4 (BRG1) are the catalytic subunits of SWI/SNF chromatin remodeling complexes, functioning in a mutually exclusive manner to regulate nucleosome composition via their ATPase domains. Pan-cancer analysis indicates that SMARCA4 mutations occur at all cancers, in particular, SMARCA4 mutations are found in 8-10% of non-small cell lung cancer (NSCLC) cases, suggesting SMARCA2 as a potential synthetic lethal target. Several studies reported that the co-mutation frequency of KRAS and SMARCA4 in NSCLC is approximately 7.7-10%, with about 39-47% of these SMARCA4-mutant patients harboring KRAS mutations. And patients with SMARCA4-mutant NSCLC generally demonstrate poor responses to conventional chemotherapy. We selected HD-11273 as a preclinical candidate, which showed improved physicochemical properties through the preparation of a specific salt of HD-10991, a selective SMARCA2 inhibitor. Here, we report a combination study of HD-11273 with standard chemotherapy and KRAS inhibitors currently in development. HD-11273 monotherapy significantly inhibited growth of SMARCA4-del A549 CDX model as well as patient derived cancer organoid (PDO) models. Combination therapies targeting multiple pathways are considered essential for overcoming monotherapy limitations, including resistance arising from prolonged treatment. To evaluate the therapeutic benefit, we tested our selective SMARCA2 inhibitor in combination with KRASG12C (storasib, adagrasib), KRASG12D (RMC9805), and pan-KRAS (Draxonrasib) inhibitors in cancers harboring KRAS and SMARCA4 co-mutations. Each combination exhibited robust synergy, suggesting that dual targeting of SMARCA2 and KRAS could be a promising therapeutic strategy. Additionally, we investigated the combinatory effect of a SMARCA2 inhibitor with standard chemotherapy agents for NSCLC; combination with oxaliplatin, docetaxel, or pemetrexed showed partial synergy, indicating that SMARCA2 inhibitors may serve as promising candidates for combination chemotherapy. In conclusion, the combination of HD-11273 with KRAS targeted therapy showed synergistic anti-tumor effect in preclinical models of SMARCA4 and KRAS co-mutated NSCLC. Also, the combination of HD-11273 with standard care for NSCLC chemotherapy significantly enhances anti-tumor activity in preclinical models of SMARCA4-mutated NSCLC.

#6506 Antitumor synergy of AOH1996 and next-generation caPCNA Inhibitors in combination with targeted and chemotherapeutic agents.

Robert G. Lingeman[1], Long Gu[1], Caroline Li[1], Pouya Haratipour[2], Robert J. Hickey[3], Linda H. Malkas[4], Maryam Zangi[3]

[1]Beckman Research Institute of The City of Hope, Duarte, CA,[2]City of Hope Comprehensive Cancer Ctr., Duarte, CA,[3]City of Hope National Medical Center, Duarte, CA,[4]City of Hope National Medical Center, Sylmar, CA

Background: AOH1996 is a small molecule that selectively targets the cancer-associated isoform of proliferating cell nuclear antigen (caPCNA), disrupting DNA replication and repair, and promoting DNA strand breaks through inhibition of effective resolution of transcription-replication conflicts. Building on its promising preclinical efficacy, we are also developing and testing next-generation caPCNA inhibitors with improved potency and druglikeness. We have developed two new inhibitors that exhibit up to 10-fold higher cellular potency relative to the parent compound, and an inhibitor with similar potency as the parent compound but 2.4-fold more soluble. Given PCNA's diverse role in processes that cancer cells depend upon for survival, e.g., coordinating DNA synthesis, damage tolerance, cell cycle control, chromatin assembly, and stress response signaling, it is hard to predict what other anticancer drugs would combine productively with AOH1996 and next-generation inhibitors. To that end, we screened a panel of 179 anticancer drugs with AOH1996 and three next-generation inhibitors to identify potential combinations that exhibit synergy.
Methods: A systematic combination drug screen was performed using AOH1996 and next-generation inhibitors and a drug panel of 179 different anticancer drugs.

- Synergy evaluation: We performed initial screens using the human neuroblastoma cell line SK-N-AS. We assessed the synergy of the combinations using the Chou-Talalay method for drug combination analysis. For favorable drug combinations, we tested additional cell lines including cancer cell types where the drug identified would be used clinically in a treatment regimen.
- Mechanistic studies: We analyzed cell cycle effects and apoptosis by flow cytometry. We also assessed DNA damage and checkpoint activation by using immunoblotting and immunofluorescence to measure γH2AX, cleaved PARP, and phospho-Chk1.

Results: Both AOH1996 and its next-generation analogs demonstrated synergy with some DNA-damaging and repair inhibiting agents such as cisplatin. Tyrosine kinase inhibitors (TKIs) in particular EGFR TKIs synergized well with AOH1996 and next-generation inhibitors. Inhibitors of the mitochondrial apoptosis pathway (e.g., venetoclax) also synergized as well.
Conclusions: AOH1996 and its next-generation analogs exhibit potent synergistic activity with targeted therapies and DNA repair inhibitors, supporting PCNA inhibition as a promising strategy to enhance therapeutic efficacy and overcome resistance. These findings provide a preclinical rationale for clinical development of AOH1996 combination regimens, as well as continued optimization of caPCNA-targeting analogs with superior potency and tolerability.

#6507 Genomic characterization of lung cancer: ERRFI1 and NKX2-1 mutations and CLU expression.

Metamia Ciampricotti[1], Yingying Yu[1], Stamatina Fragkogianni[1], Jyoti Patel[1], **Christine M. Lovly**[2]

[1]Tempus, Chicago, IL,[2]City of Hope Comprehensive Cancer Ctr., Duarte, CA

Introduction: Altered expression of *ERRFI1* (Epidermal Growth Factor Receptor Feedback Inhibitor 1), *NKX2-1* (also known as TTF1), and *CLU,* play a role in the response to targeted therapies and immune checkpoint inhibitors (ICI) in lung cancer. Here, we evaluate the prevalence of *ERRFI1* and *NKX2-1* mutations, changes in their RNA levels, and CLU RNA levels prior to therapy (PT) and upon disease progression (UP), focusing on *EGFR* and *ALK* tyrosine kinase inhibitors (TKIs).

Methods: De-identified records of 34,362 patients (pts) with a primary diagnosis of lung cancer and subjected to Tempus xT/xR NGS were identified. Gene expression levels of *ERRFI1, NKX2-1*, and *CLU* were compared between NSCLC vs. SCLC, squamous vs non-squamous histology, and sample collection time (PT vs UP). The somatic landscape was assessed for *ERRFI1* and/or *NKX2-1* pathogenic/likely pathogenic (P/LP) or variants of unknown significance (VUS) somatic mutations. Somatic differences were compared using Pearson's Chi-squared test or Fisher's exact test, as appropriate. The median log2 (TPM+1) gene expression was compared between groups using the Wilcoxon rank sum exact test.

Results: Among the total cohort, NSCLC had significantly higher expression levels of *ERRFI1* (7.8 vs 6.5, p<0.001) and CLU (7.3 vs 6.3, p<0.001) compared to SCLC, while *NKX2-1* levels were higher in SCLC (6.7 vs 5.5, p<0.001). *ERRFI1, NKX2-1*, and *CLU* expression were higher in non-squamous NSCLC compared to squamous NSCLC (p<0.001). *CLU* expression was significantly higher in UP samples with EGFR TKI (p=0.024), ALK TKI (p=0.033), and ICI treatments (p=0.048) compared to PT samples. *NKX2-1* expression was significantly lower in UP samples for EGFR TKI (p<0.001), ALK TKI (p=0.002), and ICI treatments (p<0.001) compared to PT samples. *ERRFI1* expression was also lower in UP samples with ALK TKI (p=0.013) but not EGFR TKI or ICI treatments. Of those samples, 1% (403/34,362) had somatic mutations in *ERRFI1* only, 6% (1,980/34,362) in *NKX2-1* only and 0.01% (39/34,362) in both. The top co-mutated genes in *ERRFI1* and/or *NKX2-1* mutated tumors included *TP53* (64%), *KRAS* (36%), *FOXA1* (25%), *CDKN2A* (24%), *NFKBIA* (24%) and *EGFR* (21%). *EGFR* co-mutated tumors from pts with a history of TKI had a significantly higher number of *NKX2-1* amplifications compared to those without (p<0.001), while *NKX2-1* deletions were more prevalent in the TKI naive cohort (p=0.002).

Conclusions: Lung cancers with *ERRFI1* and/or *NKX2-1* mutations exhibit distinct genomic profiles, with significant variations in *ERRFI1*, *NKX2-1*, and *CLU* expression across different subtypes. *CLU* expression was higher UP after EGFR TKI, ALK TKI, and ICI, while *NKX2-1* and *ERRFI1* expression were lower UP. Understanding the dynamic expression across disease states may inform knowledge of resistance mechanisms and putative treatment strategies. This could be particularly informative as clusterin inhibitors are undergoing evaluation in clinical trials.

: Diagnostic Biomarkers 2
Poster Session

#6512 Exploring clinical actionability of expanded liquid biopsy in advanced breast and colorectal cancers.

Keelia Clemens, Leslie Bucheit, Shaun Forbes, Hashem Alshurafa, Amar Das, Helmy Eltoukhy

Guardant Health, Palo Alto, CA

Background: Liquid biopsy via plasma circulating tumor DNA (ctDNA) analysis is used to aid in targeted therapy selection. While advanced lung cancer has a number of biomarkers with FDA-approved targeted therapies, advanced breast (mBC) and colorectal (mCRC) cancers have fewer targets. As biomarkers expand and technology evolves, it is important to balance broad ctDNA analysis with clinical actionability (CA). This study explored the potential CA of an integrated liquid biopsy leveraging genomic and epigenomic elements.
Methods: Results of mBC (n=2149) and mCRC (n=1345) patients who had genomic and epigenomic ctDNA testing (Guardant360 Liquid) as part of routine clinical care from June 1 - July 16, 2025, were retrospectively queried; only one test per patient was analyzed. Result components were categorized by CA: immediate (guides current therapy selection); expanded (may inform further work-up or future line decision); other (novel biomarkers that may influence care over time). Each patient was classified into one group. Availability of pharmacogenomic (PGx) results was assessed independently.
Results: >85% of mBC and mCRC patients had CA results with >50% classified as immediate (Table 1). For mBC, 99.9% of patients had PGx results, dramatically higher than published testing rates (<10%). Nearly 1 in 2 mBC patients had a blood-based molecular breast subtype (MBS) which may inform additional workup for hormone receptor and HER2 status. 270 mCRC patients had biomarker negative (BN) results with ≥95% confidence in the absence of FDA-approved targets, enabling rapid therapy selection. For mCRC, 99.9% had PGx results, doubling published testing rates (30-50%). Novel features such as MBS and >95% BN increased CA by 6.3% in mBC and 43.7% in mCRC.
Conclusions: A liquid biopsy with both genomic and epigenomic features broadens potential CA in tumors with few targeted therapy options. This data supports use of a multifaceted assay to guide first- and later-line decisions.

Table 1. Result actionability and availability in mBC and mCRC

	mBC (n=2149)	**mCRC (n=1354)**
RESULT ACTIONABILTY		
Total Actionable Findings	1841 (85.7%)	1215 (89.7%)
Immediate: *On-label or resistance alteration, Germline or HRD/GIS (mBC only), ≥90% Confident biomarker negative (mCRC only)*	1080 (50.3%)	939 (69.4%)
Expanded: *Clinical trial or off-label option, Molecular breast subtyping only (mBC only)*	611 (28.4%)	203 (15.0%)
Other: *Tumor fraction >0.05%*	150 (7.0%)	73 (5.4%)
RESULT AVAILABILITY		
Pharmacogenomics	2146 (99.9%)	1352 (99.9%)
Molecular Breast Subtyping	1013 (47.1%)	N/A
≥90% Confident Biomarker Negative	N/A	321 (23.7%)

#6513 Detection of bladder cancer in patients with gross hematuria using Oncuria-Detect, a urine-based multiplex immunoassay.

Sunao Tanaka[1], Yair Lotan[2], Makito Miyake[3], Edward M. Messing[4], Arnold I. Chin[5], Menghan Liu[6], Ian Pagano[7], Toru Sakatani[1], Yingye Zheng[8], Zhen Zhang[9], Charles Joel Rosser[1], Hideki Furuya[1]

[1]Cedars-Sinai Medical Center, Los Angeles, CA,[2]Associate Professor of Urology, UT Southwestern Medical Ctr., Dallas, TX,[3]Nara Medical University, Nara, Japan,[4]Chairman & Professor, Dept. of Urology, University of Rochester Cancer Center, Rochester, NY,[5]Assistant Professor, Dept. of Urology, University of California (UCLA), Los Angeles, CA,[6]Fred Hutchinson Cancer Center, Seattle, WA,[7]UHCC, Honolulu, HI,[8]Fred Hutchinson Cancer Research Ctr., Seattle, WA,[9]Associate Professor, Dept. of Pathology & Oncology, Johns Hopkins University School of Medicine, Baltimore, MD

Background - Cystoscopy is standard of care in evaluating patients with gross hematuria for bladder cancer with hematuria being the primary sign of bladder cancer. Oncuria-Detect, a liquid biopsy to detect *de novo* bladder cancer from a single voided urine sample demonstrated favorable performance.

Methods - To investigate whether Oncuria-Detect, a multiplex immunoassay that detects a urothelial cancer associated diagnostic signature composed of 10 proteins in voided urine could improve detection of urothelial cancer while evaluating participants with gross hematuria. From September 2016 through July 2025, 9 academic, private practice, and hospital facilities in the US and Japan prospectively enrolled 450 participants with gross hematuria into this urothelial cancer evaluation study. Diagnosis of urothelial cancer was based on cystoscopy (or ureteroscopy) with biopsy, which is accepted as the reference standard. Prior to the cystoscopic/ureteroscopic evaluation, participants provided a urine sample for analysis of Oncuria-Detect and BladderChek (analyzed in a blinded manner) as well as urine cytology. The performance of Oncuria-Detect was compared with BladderChek and urine cytology as an aid to detect de novo urothelial cancer with cystoscopy/ureteroscopy and histological evaluation.

Results - Urothelial cancer was diagnosed in 97 participants (4 of whom had upper tract urothelial carcinoma and 93 with urothelial carcinoma of the bladder). The Oncuria-Detect assay was positive in 80 of 97 participants with cancer resulting in a sensitivity of 82.6% (95% CI, 74.9%-89.6%) with a specificity of 33.3% (95% CI, 28.7%-38.7%) and 88.4% adjusted negative predictive value (NPV) (95% CI, 83.8%-93.0%). BladderChek results were positive in 16 of 97 participants resulting in a sensitivity, 16.4% (95% CI, 10.0%-23.5%) with a specificity of 99.2% (95% CI, 98.0%-100.0%) and 82.6% adjusted NPV (95% CI, 81.5%-83.7%), whereas cytology test results were positive in 35 of 97 participants with a noted sensitivity of 35.7% (95% CI, 26.5%-46.1%) at a specificity of 99.7% (95% CI, 99.1%-100.0%) and 86.1% adjusted NPV (95% CI 84.4-88.1). Oncuria-Detect sensitivity remained high for low-grade 81.7% (95% CI, 67.2%-94.7%) *vs.* high grade 82.7% (95% CI, 74.2%-90.9%) and NMIBC 82.9% (95% CI, 74.4%-90.8%) *vs.* MIBC 79.8% (95% CI, 61.3%-94.7%).

Conclusions - In this large prospective trial, Oncuria-Detect, had a substantially superior sensitivity compared to both BladderChek and urinary cytology in detecting *de novo* urothelial cancers, allowing it to effectively rule out approximately 30% of individuals presenting for gross hematuria evaluation.

#6514 Detection of bladder cancer in patients with microscopic hematuria using Oncuria-Detect, interim analysis of an international prospective study.

Sunao Tanaka[1], Yair Lotan[2], Makito Miyake[3], Edward M. Messing[4], Arnold I. Chin[5], Menghan Liu[6], Ian Pagano[7], Yingye Zheng[8], Charles Joel Rosser[1], Zhen Zhang[9], Hideki Furuya[1]

[1]Cedars-Sinai Medical Center, Los Angeles, CA,[2]Associate Professor of Urology, UT Southwestern Medical Ctr., Dallas, TX,[3]Nara Medical University, Nara, Japan,[4]Chairman & Professor, Dept. of Urology, University of Rochester Cancer Center, Rochester, NY,[5]Assistant Professor, Dept. of Urology, University of California (UCLA), Los Angeles, CA,[6]Fred Hutchinson Cancer Center, Seattle, WA,[7]UHCC, Honolulu, HI,[8]Fred Hutchinson Cancer Research Ctr., Seattle, WA,[9]Associate Professor, Dept. of Pathology & Oncology, Johns Hopkins University School of Medicine, Baltimore, MD

Background - Microscopic hematuria occurs in up to 10% of the general population and initiates costly evaluation to ensure no bladder cancer exists. Oncuria-Detect is a 10-plex immunoassay that detects *de novo* bladder cancer by generating a protein biomarker signature from a single voided urine sample. This report details the interim analysis of our prospective study that compares the diagnostic performance of the multiplex Oncuria-Detect assay to that of the single-analyte (*i.e.*, NMP22) BladderChek urine assay and urine cytology for identifying bladder cancer in patients with microscopic hematuria.

Methods - From September 2018 through July 2025, 9 medical facilities in the US and Japan prospectively enrolled 292 eligible patients (~30%) of the proposed 900 patients with microscopic hematuria into this study. The bladder cancer diagnostic reference standard was cystoscopy with biopsy. Pre-cystoscopy, patients provided a urine sample for analysis by Oncuria-Detect and BladderChek (analyzed in a blinded manner) as well as urine cytology.

Results - Bladder cancer was diagnosed in 22 patients (7.5%). The Oncuria-Detect assay had the following performance characteristics 82.0% sensitivity, 37.8% specificity, 97.5% adjusted negative predictive value (NPV) compared to BladderChek (9.3% sensitivity, 99.6% specificity, 95.4% adjusted NPV) and cytology (44.8% sensitivity, 99.3% specificity, 97.2% adjusted NPV). Oncuria-Detect displayed better sensitivity than BladderChek and cytology for identifying early- and late-stage cancer.

Conclusions - In this interim analysis of an international prospective trial, Oncuria-Detect performed favorably in the non-invasive evaluation of bladder cancer presence in patients presenting with microscopic hematuria.

#6515 High-throughput, 96-well plate-based single-cell TCR sequencing for scalable chain-pairing and immunophenotyping of cancer-associated T cells.

Alex Chenchik, Tianbing Liu, Dongfang Hu, Kitt Paraiso, Lester Kobzik, Khadija Ghias, Paul Diehl

Cellecta, Inc., Mountain View, CA

We present a streamlined, plate-based single-cell adaptive immune receptor (AIR) profiling technology that enables the discovery and detailed characterization of disease-relevant TCR clonotypes in cancer-associated T cells. Using a scalable 96-well plate workflow, flow-sorted single cells are individually isolated for multiplex RT-PCR of TCR α β chains together with 36 immunophenotyping genes, followed by Illumina NextSeq sequencing. The approach leverages MiXCR and RCEM software pipelines to deliver full-length paired TCR sequences, high-resolution clonotype frequency data, and a profile of key gene expression markers. Applied to longitudinal samples from T-cell large granular lymphocytic leukemia (T-LGL) patients, this method identified both dominant and rare clonotypes--with functional annotation--across multiple timepoints, including a case with a single expanded cytotoxic effector-memory T-cell clone (n=35 wells, with elevated NKG7 and CCL5 levels). High-throughput, “mini-bulk” configurations (approx. 100 cells/well) allow broader repertoire screening of ~10,000 cells/plate, detecting thousands of unique β chains and α β pairs, and facilitating the identification of rare, disease-associated clonotypes missed by bulk or lower-throughput methods.This rapid, cost-effective (<$0.10/cell), single-day workflow supports large-scale translational studies, providing direct access to paired receptor and phenotypic signatures from a variety of samples without reliance on microfluidics platforms or complex barcoding techniques. The technology significantly expands capacity for immunogenomic discovery and functional immunophenotyping, making it suited for biomarker validation, immunotherapy development, and real-time immune monitoring in cancer research.

#6516 Novel liquid biopsy epigenomic molecular tumor typing in carcinoma of unknown primary (CUP).

Axel Grothey[1], **Daniel Hintz**[2], Jayati Saha[2], Sheila R. Solomon[2], Nicole Zhang[2], Jack Tung[2]

[1]The West Clinic, Memphis, TN,[2]Guardant Health, Palo Alto, CA

Introduction: CUP is diagnostically complex commonly with treatment delays and poor outcomes. Diagnosis integrates clinical, radiologic, and pathologic data, but limited or exhausted tissue can restrict accuracy. Interrogation of cancer-derived epigenomic signatures provides insights that may support CUP adjudication. The Guardant360 Liquid (Guardant Health, Palo Alto, CA) Molecular Tumor Typing predictor (MTT) applies methylation signatures to predict cancer signal of origin with graded confidence across 14 solid tumors. This study describes MTT predictions and genomic landscapes in CUP vs non-CUP (NCUP) patients (pts) and examines real-world (RW) outcomes in CUP pts predicted to have lung cancer. Using InfinityAI Data Library, a database of claims data, treatment outcomes were examined in selected pts with MTT high confidence predictions.

Methods: CUP and NCUP pts with Guardant360 Liquid (LB) testing were identified from InfinityAI Data Library. Pts with high confidence MTT prediction (≥80% confidence) were included (n= 28,712). LB assessed alterations of >700 genes and thousands of differentially methylated regions. RW time to treatment discontinuation (RWTTD) and time to next treatment (RWTTNT) were evaluated as surrogate markers for RWOS and RWPFS, respectively, for CUP pts with MTT-predicted lung cancer vs NCUP pts with lung cancer on test requisition form (TRF). Pts were stratified by first line therapy post LB. Log rank test was used for time-to-event analyses.

Results: Of eligible pts, 1,145 had CUP and 27,641 had NCUP recorded on TRF. MTT with high confidence was generated for 74.7% of CUP and 71.7% of NCUP patients. MTT most often predicted lung (29.4%), biliary (15.5%), and gastroesophageal (10.5%) primaries in CUP, whereas lung (22.4%), breast (17.2%), and colon (18.7%) predominated in NCUP. In CUP pts with MTT predicted lung cancer, common alterations included *TP53* (69.1%), *KRAS* (31.7%), *EGFR* (28.4%), *KEAP1* (28.0%), and *STK11* (25.1%), while NCUP predicted as lung showed *TP53* (77.8%), *EGFR* (28.7%), *KRAS* (28.1%), *ATM* (26.4%), and *PIK3CA* (12.3%). In addition, there was no statistical difference in *KRAS* G12C ($p<0.1813$) and *EGFR* exdel19 ($p=0.273$) between the 2 cohorts. Treatment outcomes were available for 146 CUP-lung and 9,489 NCUP-lung pts. In the first 4 months (mo) RWTTNT was not statistically significant different, though favored targeted therapy. RWTTD was significantly longer in CUP-lung vs NCUP-lung ($p<0.0001$): median 3.7 vs 4.2 mo for non-targeted therapy, and 3.0 vs 8.0 mo for targeted therapy.

Conclusions: This study demonstrated RW pt outcomes after applying a plasma-based epigenomic MTT high confidence predictor. CUP-lung pts with targeted therapy had better survival outcomes vs pts with non-targeted treatment and have unique genomic profiles. This data is encouraging for MTT concordance with patient therapy selection and outcomes.

#6517 A decade-ahead signal of lung cancer from circulating exosomal sncRNAs.

Zhuokun Feng[1], Masaki Nasu[2], Lauren Higa[2], Isam M. Ibrahim[2], Loic L. Marchand[3], Youping Deng[1]

[1]Department of Quantitative Health Sciences, John A. Burns School of Medicine, University of Hawaii at Manoa, Honolulu, HI,[2]John A. Burns School of Medicine, University of Hawaii at Manoa, Honolulu, HI,[3]University of Hawaii Cancer Center, University of Hawaii at Manoa, Honolulu, HI

Lung cancer remains the leading cause of cancer-related mortality worldwide, yet current screening criteria focusing on heavy smoking overlook a significant portion of at-risk individuals. To develop a robust predictive biomarker, we profiled circulating exosomal small non-coding RNAs (sncRNAs, including miRNAs, piRNAs, tiRNAs, and tRFs) in a prospective discovery cohort (UHCC; n = 202 smokers, with up to 16-year follow-up) and an independent validation cohort (CHTN; n = 186) including healthy individuals or patients with either malignant or benign tumor of the lung. A rigorous 5×5 nested cross-validation pipeline integrating differential expression, correlation pruning, and eight classifier comparisons identified a 31-sncRNA panel. Random forest was selected as the optimal model and yielded excellent discrimination in UHCC (AUC=0.97), with sensitivity 0.93 and specificity 1.00 at the Youden-optimized threshold. In the independent validation cohort, the signature demonstrated moderate performance, particularly in discriminating diagnosed cancer patients from healthy controls (AUC=0.73; AUPRC=0.85). Furthermore, the resulting risk score was strongly associated with incident lung cancer in the UHCC cohort, independent of demographic and smoking factors (multivariable OR=13.19, 95% CI 6.83-25.45), and predicted a shorter time-to-diagnosis in a Fine-Gray competing risks model (sHR=4.73, 95% CI 3.61-6.21) with a significant non-linear dose-response. Landmark and time-dependent analyses confirmed robust discrimination up to a decade pre-diagnosis, although precision was attenuated at longer intervals. At last, pathway analysis of the signature's targets implicated key oncogenic pathways, including the PI3K-Akt, p53, MAPK, ErbB, and mTOR signaling pathways. This work establishes a panel of novel exosomal sncRNA signatures as a powerful risk prediction biomarker for lung cancer, enabling early risk stratification and creating a critical window for timely clinical intervention.

#6518 Integrating machine learning to optimize FFPE variant calling in a comprehensive genomic profiling assay for hematologic malignancies.

Grant Hogg[1], Tong Liu[1], Helen Cao[1], Adib Shafi[1], Amanda Williamson[2], Ashraf Shabaneh[1], Kimberly A. Holden[1], John Howitt[2], Xiaojun Guan[1], Michael Mooney[3], Li Cai[2], Eric A. Severson[2], Maria-Fernanda Senosain[4], Erik Vanroey[4], Shakti Ramkissoon[2], Anjen Chenn[2], Robert Daber[5], Marcia Eisenberg[6], Brian Caveney[6], Eyad Almasri[1], Taylor Jensen[2], Jon Williams[1]

[1]Oncology, Labcorp, San Diego, CA,[2]Oncology, Labcorp, Durham, NC,[3]Women's Health and Genetics, Labcorp, Durham, CA,[4]Oncology, Labcorp, Buffalo, NY,[5]Oncology, Labcorp, Metropark, NJ,[6]Labcorp, Burlington, NC

Optimal clinical management of lymphoma and other hematological malignancies require assessment of somatic mutations across a subset of clinically relevant genes. However, most lymphoma specimens are received after being formalin fixed and paraffin-embedded (FFPE), a process that can induce DNA damage leading to reduced specificity when assayed with next generation sequencing (NGS). Here we present the analytical validation results of a targeted NGS panel of 141 clinically relevant genes for pan-heme indications using FFPE samples. We also describe an analysis pipeline that performs additional filtering steps for FFPE specimens. The analysis pipeline is designed to analyze FFPE and non-FFPE samples (blood/bone marrow samples from myeloid or lymphoid malignancies) sequenced on the same flow cell with specific analysis performed for each specimen type automatically. FFPE has distinct variant calling parameters compared to blood/bone marrow and an additional random forest machine learning (ML) model to filter variants associated with FFPE artifacts. The FFPE NGS panel interrogates all coding exons of the 141 genes to detect single nucleotide variants (SNVs) and insertions/deletions (indels) up to 50bp at variant allele frequency ≥ 5%. The custom hybrid capture-based assay utilizes genomic libraries created from 50-182.5 ng gDNA extracted from FFPE tissue, followed by sequencing on Illumina® instruments. Concordance studies were performed on clinical samples previously assessed using orthogonal NGS-based assays for SNVs/indels. In total, 198 FFPE samples including 72 unique clinical FFPE samples were assessed. Analysis of concordance demonstrated a positive percent agreement (PPA) of 93.9% for SNV/indels (388/413) and false discovery rate (FDR) of 4.9% (20/408). Assay precision was determined using three replicates of 5 clinical FFPE samples at minimal DNA input for both intra and inter-assay precision. Overall precision was 95.9% (394/411). Minimal DNA input was established to be >50ng of input material based on results obtained from 6 clinical FFPE samples. Analytical specificity was >99.99% for SNVs/indels based on 5 replicates of FFPE NA12878. Analytical sensitivity was 3.7% VAF for SNV/indels based on a hit rate dilution series. The ML model removed 10 putative FPs throughout the study. Performance on an independent test set of 44 clinical FFPE analysis showed concordance of 95.5% (445/466) compared to 89.5% (445/497) without the ML model. These data describe the FFPE performance of an assay that enables a comprehensive evaluation of genomic alterations in hematologic malignancies from all major specimen types and indications using one laboratory workflow. The workflow includes a flexible pipeline with an optional ML model to successfully filter artefacts associated with FFPE DNA damage.

#6519 *In silico* discovery of fusion-specific RNA biomarkers in pediatric leukemias.

Elizabeth Tsuying Chang, Sean Lee

Tulane University School of Medicine, New Orleans, LA

Purpose: Pediatric leukemia remains a leading cause of cancer-related mortality in children, with fusion-driven subtypes such as KMT2A-rearranged and ETV6-RUNX1 leukemias accounting for a significant proportion of high-risk cases. Despite improvements in overall survival, fusion-positive leukemias are associated with poorer outcomes, suboptimal therapeutic response, and elevated relapse risk. A persistent challenge in pediatric oncology is delayed relapse diagnosis. Although minimal residual disease testing and bone marrow aspiration remain standard for diagnosis and monitoring, these approaches are invasive, costly, and often fail to capture dynamic oncogenic changes. Oncogenic chimeric transcription factors (OCTFs), formed by abnormal gene fusions, are key molecular drivers in many pediatric leukemias. Emerging transcriptomic data suggest that OCTF-driven tumors produce unique noncanonical RNA transcripts termed neogenes which may be highly cancer-specific and represent a promising new class of RNA biomarkers. The purpose of this study is to identify and characterize neogene transcripts in fusion-driven pediatric leukemias with the goal of evaluating their potential as subtype-specific RNA biomarkers for early detection and disease monitoring.
Methods: We assembled a modular transcriptome pipeline to identify neogene candidates in fusion-driven pediatric leukemias. Publicly available RNA-seq datasets were aligned to the human reference genome using STAR (Spliced Transcripts Alignment to a Reference), followed by transcript assembly with Scallop. Unannotated transcripts were identified via Gffcompare and quantified post-normalization. Candidate neogenes were filtered based on novelty, cross-sample recurrence, and biological plausibility. Parallel quantification of non-leukemic fusion-positive and fusion-negative cancers and normal tissues were performed to assess for neogene specificity.
Results: Seven pediatric leukemia subtypes were profiled: AML, AMoL, APL, CML, T-ALL, and preB/proB-cell leukemia. Preliminary analyses reveal that each subtype exhibits a distinct neogene signature not observed in non-leukemic fusion-positive cancers (Ewing sarcoma, rhabdomyosarcoma, and Desmoplastic Small Round Cell Tumor) or in common fusion-negative pediatric malignancies (neuroblastoma, nephroblastoma, and hepatoblastoma). Chromatin accessibility and histone modification markers at neogene loci provide evidence for active transcription and supports biological relevance of transcripts.
Conclusion: In silico findings support the existence of subtype-specific neogene signatures in fusion-driven pediatric leukemias. These transcripts may serve as novel biomarkers for early detection, subtype classification, and treatment monitoring. Further validation is underway to assess clinical utility and translational potential.

#6520 Development and first clinical experiences of a phage display derived bicyclic peptide for EphA2-specific PET imaging.

Ann-Christin Eder[1], Mohamed A. Omrane[1], Christoph-Ferdinand Wielenberg[1], Mohamed El Fakiri[1], Aikaterini Klotsotyra[1], Katia Bruggemann[1], Heiko Becker[1], Michael Quante[1], Michael Mix[1], Anusha Regupathy[2], Ben Blakeman[2], Francesca Wood[2], Gemma E. Mudd[2], Matthias Eder[1], Philipp T. Meyer[1], Martin T. Freitag[1]

[1]University Medical Center Freiburg, Freiburg, Germany,[2]Bicycle Therapeutics, Cambridge, United Kingdom

Background: Erythropoietin-producing hepatocellular receptor A2 (EphA2) is a tyrosine kinase receptor overexpressed in multiple solid tumors including pancreatic, bladder, head and neck, breast, colon, prostate, and lung cancers. EphA2 is associated with increased severity, metastatic disease and poor clinical prognosis. Following successful preclinical optimization of a phage display-derived EphA2-specific bicyclic peptide[1], this study outlines the first in-human application of EphA2-targeting [^{68}Ga]Ga-BCY18469 in PET/CT imaging.

Methods: Preclinical characterization of the EphA2-targeting bicyclic peptide BCY18469 was conducted by assessing stability, binding affinity, internalization, biodistribution and µPET/MR imaging in EphA2^{+} HT1080 and EphA2^{-} MCF-7 xenograft tumor-bearing nude mice. For clinical translation, seven patients with histologically confirmed pancreatic cancer (5 metastatic, 2 newly diagnosed) underwent [^{68}Ga]Ga-BCY18469-PET/CT (compassionate use). Four patients were examined at 15, 30, 45, 60, and 180 min p.i. for biodistribution and dosimetry assessment, three additional patients at 45 min p.i. (172±42 MBq). Time-activity curves were fitted monoexponentially, and dosimetry calculations were done using IDAC-Dose-Software.

Results: [^{68}Ga]Ga-BCY18469 demonstrated EphA2-specific binding and internalization, proteolytic stability up to 72 hours, and rapid background clearance with high tumor uptake, thereby enhancing imaging contrast within 30 minutes in mice. In clinical cases, [^{68}Ga]Ga-BCY18469 demonstrated rapid tumor uptake and was predominantly excreted via the kidneys. Notably, hepatic uptake remained favorably low (SUVmean 0.9±0.3 at 45 min p.i). Mean absorbed doses were 0.49 ± 0.24 mGy/MBq (kidneys), 0.14 ± 0.08 mGy/MBq (salivary glands), and 0.016 ± 0.003 mGy/MBq (liver). EphA2-targeted PET imaging successfully detected 13 liver metastases (SUVmax 6.9±3.4), 2 bone lesions (SUVmax 6.1±0.5), 13 lymph node metastases (SUVmax 5.0±1.1), and 2 peritoneal lesions (SUVmax 5.1±0.8). Primary tumor uptake was observed in 6 of 7 patients, albeit with lower intensity compared to liver metastases (SUVmax 4.8±1.6). Two pulmonary foci and 7 liver lesions identified on CT as morphologically consistent with metastases showed no uptake on EphA2-PET.

Conclusion: This first-in-human application of EphA2-targeting [^{68}Ga]Ga-BCY18469 demonstrates the feasibility for visualization of EphA2-expressing primary tumors and metastases, which is in line with the preclinical findings. These initial clinical results support further investigation of [^{68}Ga]Ga-BCY18469 as a diagnostic tool with potential to improve tumor characterization and patient management strategies in EphA2-positive cancers.

Reference:

[1]El Fakiri M, et al. Theranostics. 2024 Aug 6;14(12):4701-4712.

#6521 Actionable fusions and rearrangements can be efficiently identified by Hi-C whole genome sequencing in lung tumors.

Alex R. Hastie[1], Kristin Sikkink[1], Matija Snuderl[2], Darren S. Sigal[3], Sid Selvaraj[1], Anthony Schmitt[1]

[1]Arima Genomics, San Diego, CA,[2]NYU Langone Health, New York, NY,[3]Scripps Clinic and Scripps Cancer Center, La Jolla, CA

Introduction: Molecular testing in lung and other solid tumors has led to the identification of driver mutations that can be effectively targeted by new therapeutics. In addition to single point mutations that activate signaling proteins such as EGFR and KRAS, the presence of various gene fusions that lead to activation of key oncogenic drivers have become prominent drug targets. Detection of these fusions by RNA sequencing is the current gold standard but evidence suggests that fusions are still missed for various reasons. This study aims to improve detection rate of targetable fusions and rearrangements in solid tumors using a new method called Hi-C sequencing.

Methods: Hi-C sequencing is a novel whole genome DNA-sequencing assay for detection of structural variation based on unique Hi-C chemistry which leverages sequencing of linked pairs of reads which occur nearby one another in 3-dimensional and linear space, from FFPE samples. Linking reads amplifies the rearrangement signal by providing many more read pairs spanning the breakpoint and also overcoming masked fusions resulting from breakpoints in non-unique sequences.

Results: In a set of 139 NSCLC samples, Hi-C sequencing demonstrated 100% concordance with FISH and/or RNA sequencing results in cases with known fusions (19/19, including 11 *ALK*, 2 *MET*, 2 *ROS*, 2 *MET*, 1 *NTRK*, 1 *NRG1* and 1 *RET* fusions). The next cohort of 97 samples were previously determined by standard DNA and RNA sequencing to be negative for drivers such as *EGFR* and *KRAS* mutations and fusions of *ALK, MET, NTRK, RET,* and *ROS*. In this cohort, we have detected biomarkers related to drug sensitivity in 16 cases. These include targetable fusions such as *NTRK2* (1), *NRG1* (1), *PRKCA* (1), and *ERBB2* (*1*). Furthermore, we detected loss of function variants indicating sensitivity to checkpoint inhibitors (2 cases), or PARP inhibitors (6). In addition, noncanonical fusions were detected in *NRG1* (1), and *ALK* (1), both retaining their functional domains and potentially indicating sensitivity to inhibitors.

Conclusions: Encouraging results from this study suggest that Hi-C sequencing may be a valuable tool in the molecular classification of NSCLC and other solid tumors and could lead to improvement in patient care. Hi-C can detect gene fusions and rearrangements that are known to drive cancer and may be used for therapy selection, including in cases which were negative by standard genetic testing.

#6522 Novel serum biomarkers that detect ovarian cancer recurrence earlier than CA125.

Cuipeng Qiu[1], Hailing Yang[1], Zhen Lu[1], Joseph Celestino[1], Ridge T. Rogers[1], Karen H. Lu[2], Eleftherios P. Diamandis[3], Ioannis Prassas[4], Robert C. Bast[1]

[1]UT MD Anderson Cancer Center, Houston, TX,[2]Moffitt Cancer Center, Tampa, FL,[3]Lunenfeld-Tanenbaum Research Institute (LTRI) Sinai Health System, Toronto, ON, Canada,[4]University of Toronto, Toronto, ON, Canada

Despite a complete clinical response to primary surgery and chemotherapy, 80% of patients with advanced stage (III-IV) ovarian cancer recur. The serum biomarker CA125 is widely used to monitor patients for recurrence. Doubling of CA125 outside the normal range detects recurrent ovarian cancer in 70% of cases with a lead time of 3 - 4.8 months. Here we report novel biomarkers that detect recurrence missed by CA125 and that detect recurrence at an earlier interval than elevation of CA125. Novel biomarkers for recurrent OC were measured with the Olink multiplexed proximity extension assay. In a previous study, >1,196 Olink biomarkers were screened to identify 21 that detected disease recurrence including MUC16 (CA125), HE4 and 19 novel candidates (Ren et al., *Cancer Research* 80.16_Supplement (2020): 5144-5144). The 21 biomarkers were measured in 309 serial serum samples from 51 OC patients with advanced stage ovarian cancer who had been placed in complete clinical remission with primary surgery and chemotherapy and then monitored for recurrence with CA125 for an average of 4 years (range 1 - 8).Among the 51 OC cases, recurrence was observed in 31 cases with 17 exhibiting elevated CA125 (>35 U/mL) at the time of recurrence and 14 experiencing recurrence without CA125 elevation. Overall, 20 cases remained in remission during the observation period. We identified four biomarkers (DEFB4A, SULT1A1, TBCB, and TCL1A) that detected OC recurrence more than three months prior to clinical confirmation. In cases where biomarkers increased, TCL1A was elevated 131 days, TBCB 104 days, SULT1A1 242 days and DEFB4A 265 days prior to clinical recurrence. A combination of the four markers detected 14 of 31 (45%) recurrent cases at least three months earlier than standard clinical diagnosis. The four-biomarker combination identified 6 of 14 (43%) CA125-negative recurrent cases more than three months in advance. In summary, this study identifies a four-biomarker serum panel that improves early detection of OC recurrence compared to CA125 alone. The panel offers a more than three months lead time for detection of recurrence and detected patients with normal CA125 levels.

#6523 High-purity isolation of tumor-derived extracellular vesicles via SEC-immunoaffinity integration improves diagnostic sensitivity in breast cancer.

Young Kim, Min Woo Kim, Sol Moon, Su Ji Lee, Joon Ye Kim, Seung Il Kim, Jee Ye Kim

Yonsei University College of Medicine, Seoul, Korea, Republic of

Background: Extracellular vesicles (EVs) provide a non-invasive approach for liquid biopsy due to their enriched molecular cargo and structural stability. However, EV heterogeneity and contamination of current EV isolation methods by non-vesicular extracellular particles (NVEPs), particularly lipoproteins, remain substantial obstacles to reliable biomarker analysis. Reports showing that several proposed EV biomarkers are enriched in NVEP fractions underscore the need for high-purity EV isolation.
Methods: To improve plasma-derived small EV (sEV) purification, we systematically evaluated size-exclusion chromatography (SEC) resins using purified control materials representing sEVs, large EVs, lipoproteins (HDL, LDL, VLDL) and albumin. Fraction distribution patterns were mapped to predict NVEP co-elution during plasma processing. Based on these observations, SEC was combined with apoB100-based immunoaffinity depletion to reduce lipoprotein contamination. Tumor-derived EVs (tdEVs) were then enriched using immunocapture targeting breast cancer-associated surface epitopes, enabling downstream multi-omics analysis.
Results: CL-6B generated sharp peaks for individual control materials but showed convergence of VLDL and a portion of LDL in fraction 6, indicating a high likelihood of overlap with sEV-associated fractions when applied to plasma. In contrast, CL-4B produced broader elution patterns, with LDL largely absent from sEV-associated fractions and VLDL distributed across fractions 5-15, reducing the degree of overlap with sEVs. These findings indicate that CL-4B provides more favorable separation characteristics for plasma sEV purification. ApoB100-mediated immunoaffinity depletion further reduced VLDL and HDL signals while maintaining sEV recovery. The resulting fractions showed improved particle-to-protein ratios, decreased ApoA1/ApoB signatures, and retention of canonical sEV markers. Breast cancer-specific immunocapture enriched tdEVs carrying elevated levels of an oncogenic miRNA signature previously reported in our cohorts. Notably, this tdEV-focused miRNA panel demonstrated improved diagnostic sensitivity compared with our earlier total-EV-based approach, suggesting that high-purity tdEV enrichment more accurately reflects tumor-derived molecular profiles.
Conclusion: We developed an analytically stable EV purification workflow that combines optimized SEC with sequential immunoaffinity strategies to minimize NVEP interference while preserving sEV integrity. This high-purity, tumor-focused platform enables reliable multi-omics profiling of circulating tdEVs and supports the development of clinically applicable biomarkers for early breast cancer detection and disease monitoring.

#6524 Identification of diagnostic and prognostic extracellular vesicle biomarker signatures in inflammatory breast cancer.

Serena Lucotti[1], Mara Serena Serafini[2], Eleonora Nicolo[2], Letizia Pontolillo[2], Charles Warren[3], Brenno Pasto[2], Caterina Gianni[2], Nadia Bayou[2], Jacob B. Geri[4], Carolina Reduzzi[2], Massimo Cristofanilli[2], David Lyden[1]

[1]Departments of Pediatrics and Meyer Cancer Center, Weill Cornell Medicine, New York, NY,[2]Department of Medicine, Division of Hematology-Oncology, Weill Cornell Medicine, New York, NY,[3]Tri-Institutional PhD Program in Chemical Biology (TPCB), New York, NY,[4]Department of Pharmacology, Weill Cornell Medicine, New York, NY

Background: Inflammatory breast cancer (IBC) is a rare and aggressive type of BC with a very poor prognosis and accounts for 10% of BC-related deaths. Diagnosis of IBC is particularly challenging, as its symptoms resemble mammary infection and the tumor often presents with metastases at the time of diagnosis. Despite growing body of work, tools for identification and risk stratification of patients with IBC are lacking. Small extracellular vesicles (sEVs) mediate cell-to-cell communication and are released in the blood circulation, thus potentially serving as predictive and prognostic biomarkers. We have previously shown that sEVs are functional determinants of BC progression, but their role in IBC outcomes is not known.
Methods: sEVs were isolated from longitudinal plasma samples collected from patients with IBC (n=20), matched non-IBC patients (n=11), and healthy controls (HC, n=15) by ultracentrifugation and liquid chromatography mass spectrometry. Statistical analyses were conducted in R: (a) Kruskal-Wallis tests, followed by pairwise Wilcoxon rank-sum tests with Benjamini-Hochberg false-discovery rate (FDR) correction (IBC vs. non-IBC and HC); (b) Spearman's correlation with FDR correction for multiple testing (association with clinical parameters); (c) receiver operating characteristic (ROC) curve analysis (diagnostic performance); (d) Kaplan-Meier survival analysis with log-rank testing and Cox proportional hazards regression (association with overall survival [OS]).
Results: Out of the 2540 sEV proteins detected, we have identified a signature of 20+ proteins enriched more than 2-fold in plasma sEVs from IBC patients compared to non-IBC or HC and associated with immune response pathways. In univariate analysis, a total of 10 sEV biomarkers achieved an area under the curve (AUC) > 0.88, including MARCKSL1, which demonstrated the highest discriminatory power for IBC vs. non-IBC (AUC = 0.955, confidence interval [CI]: 0.878-1.000, sensitivity 100%, specificity 81.8%). When sEV proteins were compared with clinicopathological features, 998 significant associations were identified (FDR < 0.05 and p-value < 0.05), with the strongest associations observed for Ki67 proliferation index, tumor grading, and OS. Exploratory survival analyses identified a set of 20+ overrepresented sEV proteins in patients with IBC and worse OS. High composite scores of the top three sEV biomarkers (correlation > 0.81, $p < 0.0001$) showed a trend toward increased mortality with good prognostic discrimination (C-index = 0.705).
Conclusions: Our comprehensive proteomic analysis revealed extensive and robust associations between circulating sEV protein biomarkers, IBC detection, and clinical parameters, suggesting potential clinical utility as “liquid biopsy” biomarkers for IBC diagnosis and prognosis. Further validation in larger independent cohorts is warranted.

#6525 Real-time clinical validation of the Geneverify blood mRNA test for breast cancer screening and diagnosis.

Sudhir Rawal[1], Smreti Vasudevan[1], Samson Mani[1], Vishvak Chanthar[1], Dharam P. Chauhan[2], **Rajvir Dahiya**[3]

[1]Rajiv Gandhi Cancer Institute & Research Centre, New Delhi, India,[2]Geneverify Inc, Hayward, CA,[3]UCSF School of Medicine, San Francisco, CA

Background: Early detection remains the cornerstone of successful breast cancer management. We conducted a real-time clinical validation of the plasma cell-free mRNA-based Geneverify test for early screening and detection of breast cancer. This next-generation approach offers rapid, precise, and non-invasive results, potentially transforming the current diagnostic landscape by reducing dependence on surgical biopsies and enhancing early diagnosis.

Methods: We evaluated the real-time expression of 30 different breast cancer associated genes in plasma samples collected from 51 subjects (41 cases and 10 Controls). Eligible participants were selected based on the availability of paired blood and surgical tissue specimens from cases suspected of breast cancer. We assessed the diagnostic and prognostic potential of a multi-gene expression panel developed by Geneverify Inc. using blood samples. The $\log_2$-fold change in gene expression was calculated and used to generate a risk score for each subject. To determine the test's diagnostic performance and discriminatory power, we constructed receiver operating characteristic (ROC) and calibration curves. The Geneverify scores were compared against biopsy-confirmed results to calculate sensitivity and specificity. Geneverify scores were evaluated with respect to the patient's stage, grade, and metastasis.

Results: A total of 51 subjects were evaluated, including 41 suspected breast cancer cases and 10 healthy controls. The Geneverify Dx genetic risk score effectively distinguished breast cancer patients from benign controls. The area under the ROC curve (AUC), indicating acceptable discriminatory performance. Using a risk score cutoff of 17 yielded 100% sensitivity. Calibration analysis demonstrated that the probability of breast cancer increased progressively with higher Geneverify Dx scores, reaching 100% positivity at scores 35. Spearman's rank correlation revealed a significant positive association between the risk score and clinical stage, as well as pathological grade. Furthermore, metastatic cases exhibited significantly higher scores compared to non-metastatic cases. Benign subjects showed markedly reduced gene expression levels and substantially lower risk scores.

Conclusions: This prospective clinical study represents the first real-time validation of a blood-based, cell-free mRNA Geneverify test for screening and early detection of breast cancer. The test demonstrated exceptional diagnostic precision, reduce reliance on invasive biopsies, and ultimately improve patient management.

#6526 Integrated disc-fluidic platform for high-throughput extracellular vesicle processing in liquid biopsy.

Hakho Lee[1], Hyun-Kyung Woo[1], Cesar M. Castro[1], Jun Seok Park[2], Yoon-Jeong Choi[1]

[1]Harvard Medical School/Massachusetts General Hospital, Boston, MA,[2]Kyungpook National University Medical Center, Daegue, Korea, Republic of

Extracellular vesicles (EVs) represent a promising class of cancer biomarkers, enabling repeated and minimally invasive access to tumor-derived molecular information. A major challenge, however, is that EVs are embedded in complex and variable biological matrices, making the purification and standardized processing of these particles essential for reliable clinical analysis. Existing EV isolation methods are slow, labor-intensive, and prone to variability; limitations that hinder widespread adoption in translational cancer research. Here, we present an integrated centrifugal disc-fluidics platform designed for automated, high-throughput EV processing. The system incorporates key innovative features, including plasma separation, chromatographic EV purification, centripetal liquid transfer, and bead-based EV capture and immunolabeling. These modules operate seamlessly to execute a complete EV workflow on a single disposable disc. Using whole blood inputs, the developed system enriched plasma EVs within 8 minutes while removing >96% of lipoprotein contaminants. It further enabled multiplexed immunolabeling for 16 EV protein targets, completing the entire workflow in <75 minutes. In a pilot clinical study (n = 221 plasma samples), we applied the prototype device for multi-panel (30-marker) EV protein profiling. The resulting signatures robustly distinguished cancer from non-cancer samples and further stratified tumor types. By combining automation, standardization, and throughput, this disc-fluidic platform provides a scalable route toward reproducible EV analytics and has strong potential for advancing EV biomarkers into clinical oncology applications.

#6527 High-sensitivity whole-transcriptome sequencing of FFPE tumors enables immune profiling and predictive biomarker discovery.

Hang Dong[1], **Haoran Tang**[1], Feng Xie[1], Yue Zhang[1], Juanbai Shang[2]

[1]Huidu (Shanghai) Medicine Ltd., Shanghai, China,[2]Shanghai Medical College, Fudan University, Shanghai, China

Background: Immune-based biomarkers are essential for predicting therapeutic response in cancer patients, yet transcriptomic profiling of formalin-fixed paraffin-embedded (FFPE) tissues remains limited by RNA degradation and low input availability. PredicineWTS is a high-sensitivity whole-transcriptome sequencing (WTS) assay optimized for FFPE specimens, designed to support immuno-oncology research and precision therapy development.

Methods: PredicineWTS underwent analytical validation for FFPE inputs, assessing accuracy, precision, linearity, and reproducibility at low RNA quantities. The assay maintains high accuracy and precision at a 30 ng RNA input, enabling reliable transcriptome-wide profiling of challenging FFPE samples. A comprehensive bioinformatics analysis framework was established to perform quality control and characterize gene expression. Differential expression analysis, immune cell infiltration estimation, and HLA typing were performed to profile the tumor immune microenvironment and patient-specific immunogenomic features.

Results: The assay was applied to a clinical cohort of 24 urothelial carcinoma patients with paired pre- and post-treatment FFPE samples to identify transcriptional changes associated with therapeutic response. With 44 out of 48 samples achieving a unique alignment rate >80% and an average exonic rate of 86.9%, the assay demonstrates robust capture of high-quality RNA molecules for expression estimation. Comparative expression analysis revealed five immune-related genes—CD80, OASL, IDO1, HAVCR2 (TIM-3), and GZMB—that were significantly downregulated in responders ($p < 0.01$). These genes have been reported to be immune-associated regulators that reduce immune activation and shift immune contexture during effective therapy. We observed a significant 10% decrease in tumor purity following treatment in responders ($p = 0.03$), while no significant changes were observed in non-responders. These findings implicate a role for the tumor microenvironment in treatment efficacy. The patient-specific HLA typing analysis demonstrated substantial inter-individual variability in antigen presentation capacity, underscoring its relevance for guiding personalized immunotherapy strategies.

Conclusions: PredicineWTS enables highly sensitive, low-input whole-transcriptome profiling of FFPE tumor tissues, supporting robust immunogenomic characterization in clinical research settings. In this clinical cohort, decreased expression of five key immune genes and differential immune infiltration patterns were associated with treatment response. Integration of transcriptomic profiling, immune landscape assessment, and HLA typing provides a comprehensive framework for immunotherapy biomarker discovery and personalized treatment planning.

#6528 Evaluating molecular tumor type predictions for identifying new primary malignancies - A real-world clinical genomics analysis.

Elmira Forouzmand, Jack Tung, Nicole Zhang, William W. Young Greenwald, **Yupeng He**

Guardant Health, Palo Alto, CA

Background: Accurately distinguishing secondary malignancies from metastatic progression is critical in cancer surveillance, as each carries distinct prognostic and therapeutic implications. However, this distinction is often limited by overlapping radiologic features and the need for tissue biopsy. Methylation-based molecular tumor typing (MTT) of circulating tumor DNA (ctDNA) enables inference of tumor origin from blood and could support non-invasive and early identification of secondary malignancies.
Method: The MTT algorithm was developed to differentiate methylation signals across 14 cancer types. For each evaluable sample, MTT reports top predictions and associated confidence scores. We evaluated concordance between MTT predictions and clinical evidence of secondary malignancies in samples tested with the Guardant Reveal (Guardant Health, Palo Alto, CA) assay for MRD detection.
Insurance claims data from GuardantINFORM identified patients with evidence of multiple primary malignancies. Eligible patients had distinct primary cancers supported by sufficient ICD-10 codes and at least one evaluable Reveal sample within ±180 days of the second primary diagnosis. When multiple samples were available, the one closest to the second diagnosis was analyzed. To evaluate the effect of disease timeline on MTT performance, samples were stratified by interval since initial diagnosis: early (<=3 years) and late (>5 years). Second primary diagnoses in the early group were considered more likely to represent diagnostic refinement or recurrence, whereas those in the late group were presumed to reflect biologically independent new primaries.
Results: Of the 101 eligible patients, 82 had a high confidence MTT prediction (81%). Among these 82, 88% (72/82) of top MTT predictions matched either the initial diagnosis or the second diagnosis. MTT results tended to reflect the new primary with longer intervals between initial and secondary diagnoses: For samples collected >5 years after the original diagnosis (late category), MTT matched the second primary in 68% (19/28) and the first in 14.3% (4/28) of cases. In comparison, among samples in the early category, MTT matched the second and first primary in 45% (19/42) and 47.6% (20/42) of cases, respectively. Among the 9 late cases whose MTT prediction did not match the second diagnosis, 4 had MTT aligned with the original primary, and the MTT predictions of another 3 were biologically related to the second diagnosis (e.g., uterine predicted as ovarian; colorectal predicted as gastroesophageal).
Conclusions: This analysis demonstrates the potential of noninvasive epigenomic-based molecular tumor typing to identify evidence of new primary cancers during MRD assessment. This blood-based approach for MTT prediction could enable seamless integration of recurrence monitoring with the detection of new primaries.

#6529 Vaginal microbiome dynamics and clinical outcomes in cervical cancer patients undergoing radiotherapy.

Yogita Mehra[1], Julia Chalif[2], Elizabeth LaPlante[3], Laura Flora[3], Caroline Dravillas[1], January Kim[3], Jessica Aduwo[3], Naa Korley[3], Nyelia Williams[3], Rebecca Hoyd[1], David O'Malley[2], Elizabeth K. Arthur[3], Allison M. Quick[2], Daniel Spakowicz[1], Laura Chambers[2]

[1]The Ohio State University Comprehensive Cancer Center, Columbus, OH,[2]The Ohio State University Wexner Medical Center, Columbus, OH,[3]The Ohio State University, Columbus, OH

Advanced and recurrent cervical cancer (CC) is one of the major causes of death worldwide. Despite the advent of novel therapies and increasing utilization of immune checkpoint inhibitors, patients with advanced or recurrent CC have a poor prognosis, limited treatment options, and significant treatment-related toxicities. Limited evidence suggests that the vaginal microbiome (VM) may predict treatment outcomes and toxicity. Studies of the VM following radiotherapy (RT) using 16S amplicon sequencing observed a reduction in *Lactobacillus* and an increase in *Prevotella*. However, significant gaps remain in our understanding of the functional activities of these communities and their interactions with the host. To fill this gap, we initiated the “vaGinal hEalth in women ReceivinG pelvic radiation” (GEORGIA) trial to assess VM dynamics in CC patients undergoing RT and to investigate whether baseline microbiome composition predicts post-treatment outcomes. The GEORGIA trial (NCT04713618) enrolled 31 patients with CC who received pelvic RT. Vaginal swabs were collected at baseline and up to 24 months post-treatment. We assessed the metatranscriptome (metaT) using 2×150 bp sequencing libraries (>50 million reads per sample) to evaluate microbial abundance, activity, and human gene transcription. Longitudinal mixed-effects models (lme4 in R) and differential abundance analysis (ANCOM-BC2) were used to correlate microbial data with clinical variables, including recurrence status. A total of 27 patients had complete demographic information and longitudinal sequencing data. Over one-third were current smokers (35.5%), while 38.7% had never smoked, and 45.2% were post-menopausal at the time of treatment. Vaginal swab RNAseq reads aligned to human and microbe reference genomes in approximately equal numbers. Pelvic RT significantly altered the VM, driving a shift toward higher alpha diversity, as evidenced by increases in the Shannon ($p = 0.001$) and Simpson ($p = 0.002$) indices over time. When stratified by recurrence status, no significant differences in alpha diversity trajectories were observed. Differential abundance analysis revealed significant enrichment of taxa previously associated with HPV persistence and CC recurrence in VM studies, including *Fusobacterium hominis* ($p = 0.02$) and *Fusobacterium gonidiaformans* ($p = 0.03$), suggesting a potential role in disease progression. These findings underscore the possible influence of the VM on clinical outcomes and highlight its emerging role as a predictive factor in CC recurrence. Ongoing analysis will explore functional profiling and advanced longitudinal modeling to identify early microbial shifts preceding recurrence. We will use predictive modeling, integrating microbial and clinical features, to construct a recovery model and generate hypotheses for underlying biological mechanisms that can be tested experimentally.

#6530 Molecular biological differences between breast and cutaneous apocrine carcinomas.

Kei Kawashima[1], Eleanor A. Fallon[1], Kohei Chida[1], Mahato Sasamoto[2], Masanori Oshi[2], Akimitsu Yamada[2], Itaru Endo[2], Kazuaki Takabe[1]

[1]Roswell Park Comprehensive Cancer Center, Buffalo, NY,[2]Yokohama City University, Yokohama, Japan

Background: Breast apocrine carcinoma (BAC) and cutaneous apocrine carcinoma (CAC) are both adenocarcinomas with apocrine morphology. BAC is a mammary epithelial adenocarcinoma with apocrine metaplasia, whereas CAC arises from cutaneous apocrine glands. The axilla is not only rich in apocrine glands but can also contain ectopic breast tissue, allowing both tumors to arise. Despite different treatments and prognoses, they share highly similar histologic features, and no reliable diagnostic markers exist. We hypothesized that transcriptomic analyses could clarify the biological differences between BAC and CAC and provide molecular insights for distinguishing them.
Methods: We utilized clinical and transcriptomic data from the ORIEN cohort (breast carcinoma, n = 1,797 including 4 BACs; skin cancers, n = 331 including 2 CACs) and YCU (BAC, n = 5; CAC, n = 2). We compared BAC and CAC in terms of clinicopathologic features, gene expression profiles, and pathway analyses. In addition, we developed a diagnostic score based on differentially expressed genes (DEGs) between the two tumor types.
Results: In both the ORIEN and YCU cohorts, CAC showed worse recurrence and survival outcomes than BAC. In transcriptomic analyses, CAC demonstrated significant upregulation of Hallmark pathways related to cell proliferation such as E2F targets, G2M checkpoint and MYC targets v1/v2, and the expression level of Ki67, a proliferation marker gene, was also higher in CAC, although this was not statistically significant. Pathways related to immune responses were also upregulated in CAC; however, infiltration levels of individual immune cell types showed no clear differences between the two groups. We compared the expression of genes corresponding to ten immunohistochemical markers previously reported to distinguish BAC from CAC (positive in BAC: adipophilin, GATA3, mammaglobin, calretinin; positive in CAC: CK5/6, podoplanin, p63, CD14, CK17, and PAX5). CK5/6 and podoplanin showed higher expression in CAC in both cohorts, which was consistent with previous reports, although the differences did not reach statistical significance . The remaining markers showed either no consistent differences between cohorts or exhibited patterns inconsistent with previous reports. We then developed a score to distinguish BAC from CAC using the ORIEN cohort. To create this score, we first built a LASSO regression model using DEGs that separated all breast cancers from all skin cancers, then added a second component based on DEGs between BAC and CAC. By combining these two DEG-based components, we generated the distinguishing score. Validation using the YCU cohort demonstrated 100% sensitivity and specificity, accurately distinguishing BAC from CAC.
Conclusions: CAC exhibited higher cell proliferative activity and poorer prognosis compared with BAC. The transcriptomic score accurately distinguished BAC from CAC.

#6531 Immunoaffinity-enriched extracellular vesicles reveal tumor-derived DNA mutations for breast cancer detection.

Jee Ye Kim, Young Kim, Min Woo Kim, Sol Moon, Su Ji Lee, Joon Ye Kim, Seung Il Kim

Yonsei University College of Medicine, Seoul, Korea, Republic of

Background: Extracellular vesicle-derived tumor DNA (etDNA) has recently gained attention as a potential analyte for liquid biopsy; however, the biological origin and stability of EV-associated DNA remain controversial. These uncertainties highlight the need for size-independent, molecularly specific EV isolation approaches to rigorously evaluate tumor-derived DNA signals. To address this challenge, we isolated breast cancer-derived EVs (BEVs) using EPCAM-targeted immunoaffinity capture and assessed whether etDNA mutations accurately reflect tumor genotypes in both experimental models and clinical samples.
Methods: Mutational targets frequently observed in breast cancer were identified using the TCGA dataset, and four high-prevalence substitutions (PIK3CA p.H1047R, PIK3CA p.E545K, TP53 p.R175H, TP53 p.R273H) were selected. BEVs were isolated from plasma using magnetic beads conjugated with anti-EPCAM antibodies. EV identity was confirmed via nanoparticle tracking analysis and immunoblotting. etDNA was extracted from the isolated BEVs and analyzed by digital droplet PCR (ddPCR). Analytical validation included mutation profiling of breast cancer cell lines, 1D/2D droplet cluster analysis, and limit of detection (LOD) assays. Clinical concordance was assessed using matched tumor tissue sequencing results from breast cancer patients.
Results: In vitro studies demonstrated that etDNA mutations corresponded precisely to the genomic alterations of parental breast cancer cell lines. ddPCR yielded clear separation of mutant and wild-type droplets, and the assay showed high analytical sensitivity with an LOD of 0.08 copies/μL. Among 98 breast cancer patients, tumor tissue sequencing identified target mutations in 27 cases (28%). Of these, 19 had available plasma samples, and 11 patients (58%) harbored a concordant etDNA mutation in BEVs. PIK3CA p.H1047R was the most prevalent mutation in both tissue and etDNA. These findings indicate that EPCAM-enriched BEVs retain tumor-specific genetic alterations and that etDNA detection is feasible even at low DNA input, supporting potential applicability to early-stage or low-shedding disease.
Conclusion: This study demonstrates that etDNA extracted from immunoaffinity-isolated BEVs reliably reflects the mutational landscape of breast cancer. The combination of EPCAM-based BEV capture and ddPCR provides a sensitive and specific workflow for mutation detection, independent of size-based EV purification. These results support the utility of etDNA as a clinically informative biomarker and highlight its potential to enhance the diagnostic performance of liquid biopsy, particularly in early-stage breast cancer or settings with low variant allele frequency.

: Immune Checkpoint Blockade
Poster Session

#6535 Enhancing NSCLC susceptibility to anti-PD-1 - PD-L1 therapy trough PD-L1 ligand-Ir(III) complex conjugates.

Valentina Pagliara[1], Giulia Assoni[2], Giovanna Polcaro[1], Luigi Liguori[1], Pierfausto Seneci[3], Francesco Saverio Di Leva[4], Vincenzo Maria D'Amore[4], Cristina R. Ferrone[5], Stefano Pepe[1], Luciana Marinelli[4], Daniela Arosio[6], Francesco Sabbatino[1]

[1]University of Salerno, Baronissi, Italy,[2]University of Trento, Trento, Italy,[3]University of Milan, Milan, Italy,[4]University of Naples, Naples, Italy,[5]Cedars-Sinai Medical Center, Los Angeles, CA,[6]Consiglio Nazionale delle Ricerche (CNR), Milan, Italy

Immune checkpoint inhibitors (ICIs) targeting the PD-1-PD-L1 axis have revolutionized cancer therapy. However, their limited clinical success and the emergence of resistance mechanisms highlight the need for novel strategies to enhance anti-PD-1-PD-L1 immunotherapy. In this context, Iridium (III) complexes (Ir(III) complexes), have gained increasing attention for their potent anticancer activity and favorable safety profile. They are shown to induce immunogenic cell death (ICD) in non-small cell lung cancer (NSCLC), boosting tumor immunogenicity and improving response to conventional therapy. Here, we investigate whether Ir(III) complexes can synergize with anti-PD-L1 therapy and consequently synthetize a small array of triazine-based PD-L1 ligand-Ir(III) complexes by conjugating our previously reported anti-PD-L1 ligand (compound 10) with a bis-phenyl-pyridine-Ir(III) complex 2. The antitumor and immunomodulatory activity of Ir(III) complex 2 and PD-L1 inhibitor compound 10, as well as of four other PD-L1 ligand-Ir(III) complex conjugates 3-6, was tested in NSCLC cell lines expressing different levels of PD-L1, as well as in co-culture assays with peripheral blood mononuclear cells (PBMCs). Ir(III) complex conjugate 3 significantly enhanced anti-PD-L1-mediated PBMC tumor cell recognition and elimination, by increasing ER stress-mediated calreticulin (CRT) exposure, mitochondrial ROS production, and immunogenic signal release (ATP, HMGB1). More importantly, these effects were abrogated in PD-L1 knockout NSCLC cells incubated with the PD-L1 ligand-Ir(III) complex conjugate 3, validating a PD-L1-mediated selective delivery and dependent mechanism. These findings provide strong evidence that Ir(III) complexes potentiate anti-PD-L1 therapy in NSCLC, supporting the clinical implementation of PD-L1 ligand-Ir(III) conjugates as a novel combinatorial immunotherapeutic strategy for enhancing anti-PD-L1 therapy.

#6536 A novel multi-modal PD-L1xVEGF-ADC, HX116, could be a new potent candidate treatment for pan-solid tumors.

Hang Ke[1], Tao Yang[1], Feiyu Peng[1], Jialin Li[1], Cen Chen[2], Lei Zhang[1], Faming Zhang[1], **Henry Li**[2]

[1]Hanx Biopharmaceuticals, Ltd, Wuhan, China,[2]Hanx Bio, Wuhan, China

PD-L1 is an immune-checkpoint frequently over-expressed in many tumor cells as compared to normal tissues, while VEGF is an angiogenesis growth factor widely present within solid tumor microenvironment (TME). Therefore, both are also considered “tumor-associated antigen (TAA)” targetable by ADC modality, in addition to being druggable by mAbs against PD-L1-mAb (ICI) or VEGF that both are standard cancer treatments. Furthermore, multi-modal bispecific antibody (BsAb) simultaneously against PD-L1xVEGF has recently demonstrated impressive therapeutic benefit against different cancers in clinics, superior to single modal treatments or their combo treatments. It is therefore reasonable to hypothesize that a PD-L1xVEGF BsAb-ADC, HX116, with additional modalities of TOPO-I inhibitor, could become an even more powerful next-generation treatment of cancers than the naked BsAb. We thus tested HX116 for its anti-tumor activity in preclinical settings, in parallel to naked antibodies of HX116-and those against VEGF and PD-L1, respectively, so enabling assessing the roles of each modality of HX116. First, although the naked HX116 BsAb specifically binds to several PD-L1$^+$ tumor cells with high affinity, it exhibited poor internalization in PD-L1$^+$ cells. As a result, HX116 showed poor cytotoxicity in these cells as compared to SGN-PDL1V, a PD-L1-MMAE-ADC that is internalized efficiently. In contrast, HX116 demonstrated as robust cytotoxicity as much as, if not more, as SGN-PDL1V in these two PD-L1$^+$ 3D-tumor organoids *in vitro*, contrasting to the very poor cytotoxicity induction seen in the 2D-cell culture. It also showed robust anti-tumor activity in multiple PD-L1$^+$ human tumor xenograft models *in vivo*, including the ones with poor in vitro cytoxicity induction, and also superior to the naked BsAb, confirming the contributions of the additive ADC modality. Secondly, the parallel VEGF-mAb and naked HX116 BsAb in the same xenografts also demonstrated equal and robust tumor responses, suggesting the contribution of anti-angiogenesis modality. Thirdly, the pharmacology evaluation in human PBMC humanized xenograft model is currently ongoing, its superior activity over naked HX116 BsAb and PD-L1mAb would confirm its ICI contribution to the anti-tumor activity. Considering that the clinical dose for the similar PD-L1xVEGF BsAb needs to be high as 20~30 mg/kg to fully deploy their immune-checkpoint and anti-angiogenesis modalities in human, we have specifically selected a payload with moderate-potency as well as an optimal DAR value that will be tolerated in such high clinical doses. The high safety and tolerability of HX116 will also be confirmed in NHP model. If all are confirmed, HX116 would become a powerful new candidate for future cancer treatment.

Reference: *A living biobank of matched pairs of patient-derived xenografts and organoids for cancer pharmacology.* PLoS One, 2023. 18(1): p. e0279821.

#6537 Tumor IDO1 drives resistance to adoptive cell transfer by suppressing T cell recruitment and effector function.

Mamadou Alpha Bah[1], Rachana Maniyar[2], Jonathan F. Khan[2], Anais Assouvie[2], Sadna Budhu[2], Parwiz Abrahimi[2], Inna Serganova[2], Gabrielle A. Rizzuto[3], Taha Merghoub[4], Jedd D. Wolchok[1]

[1]Immunology and Microbial Pathogenesis, Weill Cornell Medicine, New York, NY,[2]Weill Cornell Medicine, New York, NY,[3]Memorial Sloan Kettering, New York, NY,[4]Weill Cornell Medical College, New York, NY

Adoptive cell transfer (ACT) has demonstrated potent anti-tumor efficacy in melanoma, yet therapeutic resistance frequently emerges within immunosuppressive tumor microenvironments. Indoleamine 2,3 dioxygenase 1 (IDO1) is a tryptophan catabolizing enzyme that generates kynurenine (Kyn), an immunomodulatory metabolite known to suppress effector T cell function. Here, we show that tumor overexpression of IDO1 undermines ACT efficacy through dual mechanisms of T cell exclusion and cytotoxic impairment. Using murine B16 melanoma cells engineered to overexpress IDO1 (B16IDO1), we observed elevated Kyn levels, reduced CXCL9/10 and CCL5 chemokine expression, and decreased intratumoral T cell infiltration. In vitro, IDO1 expressing tumor cells exhibited resistance to killing by activated CD8 PMEL T cells, a phenotype dependent on soluble factors in conditioned media and reversible with pharmacologic IDO1 inhibition. In vivo, adoptive transfer of either PMEL or TRP1 T cells, CD4 T cells specific for tyrosinase-related protein 1, failed to control B16IDO1 tumors, correlating with decreased infiltration, function, and survival. Pharmacologic blockade of IDO1 enhanced T cell infiltration and improved ACT mediated tumor control. Together, these findings identify IDO1 as a regulator of ACT resistance by suppressing T cell trafficking and effector activity. Complementary analyses of patient TIL, tumor, and serum samples are underway to assess correlations between IDO1/Kyn levels and immune cell burden, underscoring clinical relevance. Further studies extend this framework to human models, including IDO1^{+} melanoma xenografts and CAR T cells, to explore the translational potential of targeting the IDO1-Kyn-AHR axis to enhance cellular immunotherapy efficacy.

#6538 A phase-separation mechanism underlying PD-1-mediated T-cell inhibition via Shp2 condensation.

Takeya Masubuchi[1], George Wen[1], Xiaoxian Song[1], Haian Shao[2], **Enfu Hui**[2]

[1]UCSD, La Jolla, CA,[2]UCSD, San Diego, CA

Microcluster formation is a hallmark of PD1 engagement, but its physical basis and functional impact have remained unclear. We show that ligand-bound PD1 triggers Shp2 self-association and liquid liquid phase separation, generating dynamic condensates whose liquidity depends on Shp2 catalytic activity. Mutations that disrupt Shp2 self-association weaken PD1 microclusters and reduce inhibitory signaling. These findings identify Shp2 phase separation as a fundamental organizing mechanism of the PD1 pathway, linking enzymatic activation, substrate selectivity, and higher-order assembly to suppress T cell responses. This work reveals a biophysical mechanism of PD1-mediated immune regulation with implications for improving checkpoint blockade therapies.

#6539 Characteristics and predictors of multi-system immune-related adverse events in a large pan-cancer cohort: A retrospective analysis.

Julia G. Contini[1], Min Jung Koh[2], Charmi Trivedi[2], Mackenzie Adams[2], Jacqueline J. Chu[2], Sapana R. Gupta[2], Curtis Petruzzelli[2], Kanika Malani[2], Rebecca Steuer[2], Sandeep Jain[2], William Park[2], May Min[2], Matthew J. Hadfield[2]

[1]The Warren Alpert Medical School of Brown University, Providence, RI,[2]Brown University Health, Providence, RI

Background: Immune checkpoint inhibitors (ICI) can cause complex, multi-system immune-related adverse events (irAEs) that remain poorly described. This study characterizes their frequency and clinical features in a large institutional cohort.

Methods: Retrospective cohort of 2,134 metastatic cancer patients treated with ≥1 ICI at Brown University Health (2015-2025). IrAEs were identified and categorized by affected organ system. Multi-system irAEs were defined as ≥2 affected organ systems. Frequency was stratified by sex, cancer type, and treatment regimen. Fisher's exact tests assessed subgroup differences, and multivariable logistic regression identified independent predictors, reported as odds ratios (OR) with p-values.

Results: Of 2,134 patients, 24.8% (n=530) developed an irAE; 22.4% (n=119) had multi-system involvement, most commonly with two organs (16.8%, n=89) and less commonly three or more (5.7%, n=30). Common pairings included dermatitis + endocrine (10%, n=12), colitis + dermatitis (9.2%, n=11), and colitis + pneumonitis (5.9%, n=7), with clustering across dermatologic, gastrointestinal, pulmonary, and endocrine systems. Multi-system irAEs differed significantly by treatment regimen (5.1% in monotherapy vs. 4.7% in "ICI + chemo/targeted" vs. 13.9% in dual-ICI; p<0.001), but not by sex (p=0.6). They were more frequent in melanoma/skin cancers (p=0.004) and genitourinary cancers (p=0.03). On multivariable logistic regression adjusting for treatment regimen, melanoma/skin cancers remained significantly associated with higher odds of multi-system irAEs (OR: 1.92, p=0.03), while the association with genitourinary cancers was attenuated (OR: 1.37, p=0.2).

Conclusions: Multi-system irAEs comprised nearly one-quarter of all irAEs and were more frequent in melanoma/skin and genitourinary cancers, and among patients who received dual-ICI therapy, supporting the need for closer monitoring in these groups.

Uni- and multivariate logistic regression model predicting risk of multi-system vs. single/no irAE

	Univariate OR (p-value)	**Multivariate OR (p-value)**	
Treatment regimen			
ICI monotherapy	**0.33 (<0.001)**	**0.36 (<0.001)**	**0.37 (<0.001)**
ICI + chemo/targeted	**0.30 (<0.001)**	**0.35 (0.002)**	**0.36 (0.002)**
Dual ICI (reference group)			
Sex			
Male	0.89 (0.5)		
Female (reference group)			
Cancer type			
Thoracic (ref: non-thoracic)	0.80 (0.3)		
Melanoma/Skin (ref: non-melanoma/skin)	**2.43 (0.002)**		**1.92 (0.03)**
GU (ref: non-GU)	**1.62 (0.02)**	1.37 (0.2)	
GI (ref: non-GI)	0.58 (0.08)		
Head & Neck (ref: non-head & neck)	0.66 (0.3)		

#6540 Dissecting mechanisms of tumor immune checkpoint blockade resistance due to host genetic variation within Adam17.

James P. Heiserman[1], Darren Li[1], Ons Mamai[2], Tanuja Desai[1], Rosemary J. Akhurst[3], Szu-Ying Chen[1]

[1]UCSF Medical Ctr., San Francisco, CA,[2]UCSF, San Francisco, CA,[3]Professor in Residence, UCSF Helen Diller Family Comp. Cancer Center, San Francisco, CA

Clinical application of anti-PD-1 or anti-PDL-1 antibodies, also known as immune checkpoint blockade (ICB) therapy, has shown potential as an anti-cancer treatment. However, currently only 10 to 30 percent of cancer patients respond to ICB. Successful ICB treatment depends on a variety of factors including tumor mutation burden, cancer subtype, and patient germline genetics. Therefore, there is a clear need to understand how host genetics influences ICB clinical success to improve patient outcomes. Our laboratory primarily focuses on the study of transforming growth factor-beta (TGF-β) signaling across a variety of disease contexts. We have generated two paired congenic NIH/Ola mouse strains that harbor either NIH/Ola or C57Bl/6J across the *Tgfbm3b* locus on proximal chromosome mouse 12. *Tgfbm3b* is known to modulate TGFβ signaling and encompasses genetic variants of tumor necrosis-alpha converting enzyme (TACE, also known as ADAM17). Utilizing these congenic mice implanted with syngeneic cancer cells, we generated preliminary data suggesting that the C57 “hypoactive” allele of *Adam17*, with amino acid variation at D113N, I613V, correlates with better response to ICB compared to congenic mice that harbor the active NIH allele, which are resistant to ICB treatment. Considering that inheritance of hypoactive *Adam17* enhances ICB response, we employed a highly specific small molecule inhibitor of TACE (TMI-2) finding that it sensitizes ICB-resistant tumors to immunotherapy across two in vivo syngeneic squamous cell carcinoma (SCC) models, suggesting that ADAM17 activity may suppress ICB efficacy. We have detailed the immune cell infiltrate on ICB sensitive and resistant mouse models, with and without ICB, using both flow cytometry and RNA sequencing techniques, and have found differences in myeloid and T cell infiltrate into the tumor microenvironment, suggesting that ADAM17 may regulate the tumor microenvironment landscape. We also have in vitro data suggesting that hypoactive variants of ADAM17 may reduce immune cell secretion of Tumor Necrosis Factor Alpha (TNFα) and TNFα induced cell death in specific immune cell types. TMI-2 is safe in humans, and this study provides support for targeting ADAM17 as a therapeutic target for patients who harbor ICB resistant cancers. The study also provides invaluable insights into the cell-type specific consequences of ADAM17 activity in tumor biology and highlights the need to consider patient genetics when applying ICB therapy.

#6541 Time-of-day of first checkpoint inhibitor dose influences clinical outcomes and immune responses in hepatocellular carcinoma.

Howard L. Li[1], Soren Charmsaz[2], Benjamin J. Reisman[1], Franshisca Hayek[1], Madelena Brancati[1], James M. Leatherman[1], Carlotta Pazzi[1], Royce P. Lee[1], Xiyu Zhao[3], Eric Christenson[3], Waqar Arif[1], Jeric P. Hernandez[1], Caroline Ellis[1], Nicole E. Gross[1], Christopher Thoburn[1], G Scott Chandler[4], Rajat Mohindra[4], Sanjay Bansal[5], Laura Tang[5], Aditi Guha[5], Chi V. Dang[1], Neeha Zaidi[3], Elizabeth M. Jaffee[1], Daniel A. Laheru[2], Daniel J. Zabransky[1], Marina Baretti[1], Won Jin Ho[1], Mark Yarchoan[1], Mari Nakazawa[1]

[1]Sidney Kimmel Comprehensive Cancer Center, Baltimore, MD,[2]Johns Hopkins University School of Medicine, Baltimore, MD,[3]The Johns Hopkins Hospital, Baltimore, MD,[4]Roche, Basel, Switzerland,[5]Genentech, South San Francisco, CA

Background Although immune checkpoint inhibitors (ICIs) have long half-lives, preclinical and early clinical studies across multiple tumor types suggest that the time-of-day of ICI infusion may influence therapeutic efficacy by aligning initial drug exposure with circadian peaks in T-cell responsiveness. However, the impact of initial drug infusion timing on outcomes has not been established. The immunologic basis of improved outcomes in early-day infusions and its clinical relevance in hepatocellular carcinoma (HCC) also remain unknown. **Methods** We prospectively followed patients with advanced/metastatic HCC receiving ICI therapy at Johns Hopkins from 2021-2025, classifying them into the morning group (first infusion before 12:00) or the afternoon group (first infusion after 12:00). We assessed clinical outcomes and compared immunologic responses from baseline to early-on-treatment (month 1 or month 2) by profiling 28 immune cell clusters in peripheral blood mononuclear cells using Cytometry by Time-of-Flight (CyTOF) and 39 plasma cytokines using a Luminex multiplex assay. **Results** Our cohort included 85 patients, 40 of whom received their first infusion in the morning. There were no statistically significant differences in baseline demographic or clinical characteristics between patients initiating therapy in the morning versus afternoon. The morning group had superior progression-free survival (multivariable HR 0.49, 95% CI 0.29-0.82, adjusted $p<0.01$) and higher odds of objective treatment response (multivariable OR 3.26, 95% CI 1.08-10.90, adjusted $p<0.05$), with no significant increase in immune-related adverse events. The timing of subsequent infusions after the first dose had no impact on survival outcomes. Immunologic responses diverged after the initial dose, with morning-treated patients showing reduced IL-6 levels (Wilcoxon rank-sum, $p<0.01$) and greater expansion of cytotoxic central memory CD8+ T-cells (Wilcoxon rank-sum, $p=0.01$) and cytotoxic effector CD8+ T-cells (Wilcoxon rank-sum, $p<0.05$) compared to afternoon-treated patients. **Conclusions** Morning first-dose infusion of ICIs in HCC was associated with improved clinical outcomes and distinct immune responses, including reduced IL-6 signaling and expansion of cytotoxic central memory and effector CD8+ T cells. These findings suggest that the timing of the initial infusion can imprint an immunologic program that shapes subsequent anti-tumor immunity, providing a mechanistic rationale for strategically scheduling ICI administration.

#6542 Targeting ITGB3 reverses terminal T cell exhaustion to enhance therapeutic efficacy in esophageal squamous cell carcinoma.

Beilei Liu[1], Xin-Yuan Guan[2], **Bowen Yao**[2], Hongyu Zhou[3], Licheng Tan[2], Jiayi Huang[2], Shuang Zhang[2]

[1]City University of Hong Kong, Hong Kong, Hong Kong,[2]The University of Hong Kong, Hong Kong, Hong Kong,[3]Shanghai Cancer Center, Shanghai, China

Terminal T cell exhaustion represents a critical barrier limiting the efficacy of immune checkpoint blockade therapies in solid tumors, yet the underlying mechanisms remain to be fully elucidated. Based on the esophageal squamous cell carcinoma (ESCC) mouse cell line mEC25 established in our previous work, we successfully constructed an immunocompetent ESCC mouse CDX (cell-derived xenograft) model that effectively reflects the immune dynamics of ESCC. Single-cell sequencing analysis of this dynamic subcutaneous ESCC model delineated 17 T cell subpopulations, revealing the transition of T cells from activated and effector states to exhaustion and terminal exhaustion. Among these subsets, ITGB3+ T cells exhibited moderate cytotoxicity and moderate exhaustion levels. Pseudotime analysis confirmed that ITGB3+ T cells reside at a critical node in the transition of T cells toward terminal exhaustion, potentially bridging effector and exhausted states through integrin signaling modulation. To address this, we utilized ITGB3-neutralizing antibodies. In vitro tumor-T cell co-culture assays showed that treatment with these antibodies restored T cell proliferation, upregulated the secretion of IFN-γ and granzyme A, and enhanced tumor-killing capacity. In vivo studies demonstrated that neutralizing ITGB3, when administered during early tumor formation, effectively reduces ESCC tumor growth, promotes T cell infiltration into the tumor microenvironment, and diminishes the exhausted T cell pool. Additionally, combination therapy with PD-1 inhibitors further amplified these effects: in vivo experiments showed synergistic tumor suppression, with enhanced T cell cytotoxicity and prolonged survival in treated mice. Further multiplex immunohistochemistry staining on tissue microarrays confirmed that elevated ITGB3 expression in PD-1+ IFN-γ+ double-positive T cells correlates with tumor progression and poor patient prognosis in ESCC, highlighting ITGB3 as a biomarker of T cell dysfunction. These findings uncover a molecular basis for T cell therapy resistance in ESCC and provide a novel strategy to improve the efficacy of immunotherapy for solid tumors.

#6543 NTX1088 demonstrates the first-ever clinical restoration of DNAM1, defining a novel immune-oncology axis.

Anas Atieh[1], Alon Vitenshtein[1], Akram Obiedat[1], Simona Chechik[1], Rivki Cashman[1], Guy Cinamon[1], Keren Paz[1], Paola Kučan Brlić[2], Tihana Lenac Rovis[2], Lea Hirsl[2], marija mazor[2], ema bellulovich[2], Stipan Jonjic[2], Ofer Mandelboim[3], **Pini Tsukerman**[1]

[1]Nectin Therapeutics, Jerusalem, Israel,[2]Center for proteomics, MEDRI, Rijeka, Croatia,[3]HUJI, Jerusalem, Israel

NTX1088, a first-in-class anti-PVR (CD155) monoclonal antibody, is currently being evaluated in a Phase 1, open-label, multi-center study (NCT05378425) as monotherapy and in combination with pembrolizumab in patients with advanced solid malignancies. Preliminary clinical data, for the first time, demonstrate restoration of DNAM1 (CD226) expression and function on peripheral T and NK cells following PVR blockade by NTX1088. This mechanistic breakthrough is robustly observed across multiple dose levels and distinguishes NTX1088 as a unique immunotherapeutic agent, unlike all anti-TIGIT strategies, which have not achieved DNAM1 restoration in clinical settings. Clinical biomarker analyses confirm significant upregulation of DNAM1 across NK cells, CD4+, and CD8+ T cells, effectively reversing PVR-mediated DNAM1 downmodulation, a recognized mechanism of immune escape and resistance to checkpoint inhibition. In contrast to TIGIT blockade, which fails to restore DNAM1, NTX1088 drives a favorable shift in the TIGIT/DNAM1 ratio and expands potent effector subsets, directly enhancing antitumor immune activity. To further dissect the translational impact and molecular mechanisms, extensive in vitro work was performed, using PBMCs from healthy volunteers and Jurkat cell line. In these in-vitro assays, simultaneous engagement of DNAM1 with CD3 signaling resulted in increased induction of activation markers, unique changes in exhaustion profiles, and robust cytokine secretion, functional signatures which showed DNAM1 co-signaling is distinct from conventional CD28-mediated costimulation. Concordant findings in humanized mouse models reveal that much of NTX1088's tumor growth inhibition and immune effector activation are DNAM1-dependent, and DNAM1 positive cells are significantly more activated and primed for anti-tumor activity compared to cells that did not upregulate DNAM1. Collectively, these data establish NTX1088 as the first immunotherapy to achieve clinical restoration of DNAM1, validating both DNAM1 induction and TIGIT/DNAM1 ratio remodeling as actionable biomarkers for drug effect, patient selection, and future immune-oncology combinations. The concurrent restoration of DNAM1, alongside blockade of other PVR inhibitory receptors like TIGIT, CD96, and KIR2DL5A, positions NTX1088 as an attractive therapeutic agent for synergistic IO/IO combinations, charting a transformative course for next-generation anticancer immunity

#6544 Immune checkpoint inhibitor therapy in kidney transplant recipients: Real-world outcomes of antitumor activity and graft rejection risk.

Ali Rezazadeh Roudkoli[1], Elena Barbir[2], Shahin Kavousi[1], Mohamed A. Aboelatta[1], Claudia-Denise Haivas[1], Byron H. Smith[1], Aleksandra Kukla[1], Arkadiusz Z. Dudek[1]

[1]Mayo Clinic, Rochester, MN,[2]University of Alberta, Edmonton, AB, Canada

Background: Kidney transplant recipients (KTRs) have a markedly elevated risk of aggressive malignancies, yet the use of immune checkpoint inhibitors (ICIs) in this population remains limited by concerns for allograft rejection and the absence of prospective evidence. We evaluated real-world antitumor activity, graft safety, and immunosuppression-related outcomes of ICI therapy in KTRs with advanced cancers.

Methods: We retrospectively analyzed 57 KTRs with locally advanced unresectable or metastatic malignancies treated between 2018-2025 at a single tertiary center. Thirty-three received ICIs and 24 received non-ICI systemic therapy. Outcomes included objective response rate (ORR), clinical benefit rate (CBR), progression-free survival (PFS), overall survival from diagnosis (OSd), overall survival from treatment initiation (OSt), acute allograft rejection, and immune-related adverse events (irAEs). Tumor response was assessed by RECIST v1.1.

Results: ICI-treated patients achieved higher ORR (40.0% vs 26.1%) and CBR (60.0% vs 33.3%) compared with non-ICI therapy. Median OSd was 35.8 vs 23.3 months, and median PFS was 4.3 vs 3.5 months (both not statistically significant). Median OSt was significantly longer with ICIs (15.1 vs 7.9 months; p=0.012). Acute rejection occurred in 12.1% of ICI-treated patients (3% irreversible) versus 4.2% with systemic therapy; rejection events were heterogeneous in timing (3 weeks-14 months) and largely responsive to pulse-dose corticosteroids. IrAEs occurred in 27.3% of ICI patients, with grade ≥2 events in 12.1%, and no treatment-related deaths. In the cutaneous squamous cell carcinoma (cSCC) subgroup (n=33), ICI therapy produced an ORR of 47.4% and CBR of 63.2%, with trends toward improved survival relative to controls.

Conclusions: ICIs produced clinically meaningful antitumor activity in KTRs, particularly in cSCC, with a manageable rate of allograft rejection under carefully tailored immunosuppression. Despite higher historical concerns, irreversible graft loss was uncommon. These findings support the feasibility of ICI therapy in selected transplant recipients and highlight the importance of immunosuppression strategy in balancing antitumor efficacy and graft safety. Prospective, biomarker-integrated studies are needed to define optimal immunosuppression during PD-1 blockade in this high-risk population.

#6545 Characterizing ATF6 activation-driven mechanisms improving ICB efficacy.

Sanjay Adhikary[1], Jacob Edmondson[1], Daniel Fil[2], Duah H. Alkam[3], Megan R. Reed[1], Billie Heflin[1], Katherine Bronson[1], Sydnye Shuttlewoth[1], Katherine F. Wallis[1], Nathan Avaritt[1], Sean Taverna[1], Brian S. Koss[1], Alan Tackett[1]

[1]University of Arkansas for Medical Sciences, Little Rock, AR,[2]Biochemistry and Molecular Biology, University of Arkansas for Medical Sciences, Little Rock, AR,[3]UAMS Winthrop P. Rockefeller Cancer Institute, Little Rock, AR

Melanoma is the most fatal skin cancer and incidence continues to rise, particularly among young people. Among the current clinical standards of care for advanced melanoma, immune checkpoint blockade (ICB) therapy has been the most successful for improving the survival of melanoma patients. However, the benefits of ICB therapy are limited to a subset of melanoma patients, with only 50% of melanoma patients responding ICB due to primary resistance. Using a genetic model of activating transcription factor 6 (ATF6), our laboratory has found that constitutively active ATF6 improved ICB efficacy in multiple preclinical, ICB resistant mouse melanoma models and increased T cell mediated-killing (TCK) of melanoma tumor cells *in vitro*. As a translational strategy we used a previously reported small molecule ATF6 activator, AA147, and found an AA147-mediated increase in TCK *in vitro* and an improvement of ICB efficacy in preclinical ICB resistant subcutaneous and metastatic mouse melanoma models. To identify ATF6-dependent mechanisms improving anti-tumor immune response, we performed FactorPath (Active Motif) chromatin immunoprecipitation coupled with sequencing (ChIP-seq) to map the binding of FLAG-ATF6 at a genome-wide scale. We found that the constitutively active form of ATF6 binds to the promoter region of anti-tumor immune regulatory genes. In parallel with ChIP-seq findings, we found constitutively active ATF6 significantly upregulates the protein expressions of anti-tumor immune regulatory genes as determined through quantitative mass spectrometry. These findings indicate that ATF6 is a transcriptional regulator of anti-tumor immune regulatory genes in melanoma tumor cells and upregulation of these pathways leads to enhanced anti-tumor immune response and improved ICB efficacy.

#6546 Beyond density: Topography-aware spatial metrics predict immunotherapy outcomes.

Artur Mezheyeuski[1], Neda Hekmati[2], Ina Hrynchyk[3], Amanda Lindberg[2], Jakob Friedrich[2], Johanna Mattsson[2], Miklos Gulyas[2], Klas Karre[4], Johan Isaksson[2], Carina Strell[5], Patrick Micke[2]

[1]Vall d'Hebron Institute of Research (VHIR), Barcelona, Spain,[2]Uppsala University, Uppsala, Sweden,[3]City Clinical Pathologoanatomic Bureau, Minsk, Belarus,[4]Karolinska Institutet, Stockholm, Sweden,[5]Uppsala University, Dept of Immunology, Genetics and Pathology, Uppsala, Sweden

Background: Accumulating evidence suggests that the spatial organization of tumor-immune ecosystems determines the benefit of checkpoint inhibitors. Therefore, topography-aware metrics that adjust for baseline cell abundance are better suited to quantify spatial immune patterns, such as attraction, repulsion, and clustering, across scales. We hypothesized that such multiscale spatial metrics would outperform immune cell density alone for explaining therapy benefit and survival in advanced non-small cell lung cancer (NSCLC) patients.

Methods: We applied a multiplex immunofluorescence pipeline on diagnostic tissue of 54 NSCLC patients treated with checkpoint inhibitors. Annotated cell classes included cancer cells, $CD8^+$, $CD8^+FoxP3^+$, M1 and M2 macrophages (-/+PDL1), $CD68^-CD163^+$ cells and stromal non-immune cells. To spatially resolve the immune patterns, we computed neighborhood enrichment (ENR) and radial local enrichment (RLE). ENR was computed over k-nearest neighborhoods (k=5-100) and provided information about the attraction tendency between two cell classes, independent from cell density. RLE was evaluated over 10-50 µm radii and reflected the spatial cell clustering tendency. The spatial metrics were associated with therapy response and overall survival.

Results:

$CD8^+FoxP3^+$ cells stratify risk. Responders demonstrate neighboring of $CD8^+$ or $CD8^+PD1^+$ cells to $CD8^+FoxP3^+$ at different scales (ENR k=5-100, p=0.04-0.007), strongest at shorter distances. In the survival analysis, $CD8^+FoxP3^+$ cells were associated with shorter survival when they were closer to PDL1+ cancer cells (ENR: HR 3.7-7.5, p=0.01-0.04).

CD8 geometry in stroma tracks response but not survival. Increased clustering of $CD8^+PD1^+$ associated with higher response to therapy (ENR k=10-100, p=0.05- 0.002). Notably, $CD8^+PD1^-$ cells did not show such associations. This positive impact on therapy response did not translate into a longer overall survival in this cohort.

Tumor purity and compactness is associated with shorter survival. Local enrichment of cancer cells within 10-50 µm was associated with poor response and shorter OS, (RLE: HR 2.2-2.5, p=0.03-0.007), pointing to denser, homogeneous tumor nests as a risk factor.

Conclusion: Topography-aware spatial metrics capture clinically meaningful organization beyond simple density. These findings supported the cellular context-dependent evaluation of biomarkers. Furthermore our findings also provide in situ evidence for a focused evaluation of a rare, hitherto poorly described subtype of $CD8^+FoxP3^+$ immune cells.

#6547 Phase II single arm study of tremelimumab and durvalumab (MEDI4736) (T300+D) in advanced hepatocellular carcinomas with Child-Pugh-B cirrhosis (STRIDE in CP-B).

Sukeshi Patel Arora[1], Lorena Fuentes[1], James Denno[1], Jennifer Moseley[1], Brittany M. Altermatt[1], Elizabeth Diaz[1], Joshua Ray Smith[1], Joel Michalek[2], Lei Zheng[3]

[1]University of Texas Health San Antonio, Mays Cancer Center, San Antonio, TX,[2]UT Health San Antonio, San Antonio, TX,[3]Mays Cancer Center, UT Health Science Center at San Antonio, San Antonio, TX

Background: In registration phase 3 studies, most patients enrolled had Child-Pugh (CP)-A cirrhosis, with CP-B cirrhosis are often excluded from clinical trials, yet in clinical practices, patients are often treated with new agents without efficacy or safety data. Therefore, there is an unmet need to evaluate the efficacy and safety of therapeutics in patients with HCC and CP-B cirrhosis. Based on results from the HIMALAYA trial, tremelimumab and durvalumab (T300+D) is FDA-approved for HCC. In this trial, grade 3/4 treatment-related adverse events (TRAEs) occurred in 25.8% (T300+D), 12.9% (durvalumab), and 36.9% (sorafenib) of patients. Therefore, we hypothesize that T300+D will be safe and tolerated in CP-B patients with HCC, and the safety of efficacy of T300+D in patients with CP-B cirrhosis should be investigated. **Purpose:** Results from this study may establish T300+D as a first-line therapy for CP-B patients with HCC, and therefore, could be practice-changing and set precedence for future studies dedicated to investigating newer agents for CP-B with HCC. **Methods:** Single-arm, phase II study of patients with advanced HCC who are eligible for first-line treatment with T300+D [NCT06526104]. Priming dose of tremelimumab 300 mg intravenously (IV) once (Cycle 1, Day 1 only) with durvalumab 1500 mg IV on Day 1 of each 4-week cycle. Primary Objective: compare the percentage of grade 3 or higher TRTE-AEs with T300+D in patients with CP-B cirrhosis with historical controls of VEGF-targeting therapies. Secondary Objective(s): objective response rate (ORR), overall survival (OS), progression-free survival (PFS), associations of baseline albumin-bilirubin (ALBI) grade with PFS/OS and grade 3/4 AEs with T300+D. Exploratory endpoint: evaluate QOL at baseline and during treatment with T300+D, EORTC-QLQ-C30 and QLQ-HCC18 questionnaires. Inclusion criteria: Patients diagnosed with HCC based on pathologic diagnosis from biopsy or radiographic diagnosis on CT liver or MRI liver (i.e., Barcelona Clinic Liver Cancer (BCLC) stage B and not candidate for locoregional therapies or BCLC stage C), no prior systemic therapies, Child-Pugh-B7 or -B8 liver cirrhosis, and ECOG 0-1. . This study will achieve 80% power for testing H_o: $p_{D300+T}=p_{Historical}$ versus H_1: $p_{D300+T}\neq p_{Historical}$ at $\alpha=0.05$ with n=30 subjects. **Progress:** The study began enrollment in 12/2024, with 13 patients enrolled to the date of abstract submission. Three sites are opening soon with planned completion of enrollment at the end of 2026. **Conclusion:** After 15 patients are enrolled, enrollment will be held pending further review if there is sufficient evidence to suggest that the true probability of (possibly, probably, or definitely) treatment-related, grade 3-5 adverse events exceeds 60%. Results will be presented soon after.

#6548 A human multiorgan microphysiological system for modeling immunotherapies tumor clearance and normal tissue immune injury.

John Collins, Henry C. Wong, Alyssa J. Villegas, Johar Kohana, Harpreet S. Saluja

Biopico Systems Inc, Irvine, CA

Despite the clinical success of CTLA-4 blockade, immune checkpoint inhibitors can trigger immune-related adverse events (irAEs) that remain difficult to predict preclinically, in part because conventional in vitro and animal models lack the capacity to simultaneously evaluate ECM-dependent T-cell infiltration, tumor cytotoxicity, and normal tissue immune tolerance. We developed a multiorgan system to quantify how fibrin matrix density, T-cell donor identity, HLA compatibility, and ipilimumab dose collectively shape immune cytotoxic responses across tumor and normal tissues. Imaging experiments compared fibrin concentrations from 2.5-10 mg/mL to assess physical barrier effects on immune infiltration. Brain (SK-N-SH/HMC3), gut (T84) tumor spheroids, or human primary hepatocyte spheroids with or without Kupffer cells were embedded in a defined fibrin hydrogel (6 mg/mL fibrinogen, 4 U/mL thrombin). Tumor models used two T-cell donors, while the liver model was perfused with either matched or mismatched $CD8^+$ T-cell donors. Ipilimumab was applied from 0-10 µg/mL. Spheroid density, derived from fluorescence-based viability measurements, was plotted against antibody concentration.T-cell penetration into spheroids was strongly dependent on fibrin density with low-to-moderate matrix (2.5-6 mg/mL) supported deep infiltration, whereas high-density fibrin (8-10 mg/mL) restricted immune access and created an immune-excluded phenotype. CTLA-4 blockade overcame this barrier in part, enabling infiltration even through dense matrices. Dose-response analysis demonstrated robust tumor killing in both brain and gut spheroids, exhibiting a steep viability decline beginning at 1 µg/mL and reached near-complete loss at 10 µg/mL.Response magnitude varied between donors, reproducing clinically observed heterogeneity in immune potency. In contrast, normal hepatocyte spheroids remained intact under matched donor conditions across all doses. However, mismatched T cells produced clear dose-dependent injury that was significantly amplified in the presence of Kupffer cells, revealing a macrophage-dependent mechanism of immune-mediated hepatotoxicity.This multiorgan platform recapitulates fibrin-driven immune exclusion, checkpoint-enhanced infiltration, effective tumor cytotoxicity, and HLA mismatch-dependent normal tissue injury, mirroring key therapeutic and toxic outcomes observed in patients. We evaluated antigen-specific T cells, bispecific antibodies, and antibody-drug conjugates to assess on-target efficacy, off-target toxicity, and bystander effects. These findings support the use of human microphysiological systems as predictive tools for immunotherapy, enabling mechanistic dissection of efficacy-toxicity trade-offs prior to clinical testing and supporting FDA-aligned strategies to reduce non-human primate use in monoclonal antibody safety testing.

#6549 Integrating functional biosignatures and same-cell spatial multiomics to predict synergistic benefit of combination checkpoint therapy in head and neck cancer.

Yi Cui[1], Moumita Nath[2], Michael Emilio Patrick[1], Claire Williams[1], Daniel McGuire[1], Jobin K. Paul[2], Kowshik Jaganathan[2], Biswajit Das[2], Mohit Malhotra[2], Shanshan He[1], Joseph M. Beechem[1], Satish Sankaran[2]

[1]Bruker Spatial Biology, Seattle, WA,[2]Farcast Biosciences India, Bengaluru, India

Effective immune checkpoint blockade (ICB) requires coordinated activation, spatial organization, and functional cross-talk among immune populations within the tumor microenvironment (TME). Farcast TruTumor™ platform preserves viable tumor, stromal, and immune compartments in their near-native architecture, aligning with the FDA's New Approach Methodologies (NAM) framework for human-relevant cancer models. The model has shown that in head and neck squamous cell carcinoma (HNSCC) anti-PD-1 response is associated with cytotoxic T-cell (CTL) infiltration into tumor nests, and that moderate responders may be rescued by adding anti-CTLA-4, accompanied by increased spatial separation between CTLs and T regulatory (Treg) cells. Here, we integrate TruTumor's functional characterization with the CosMx® Spatial Molecular Imager (SMI) using same-cell spatial multiomics (64-plex IO protein panel plus whole-transcriptome RNA) to elucidate the dynamics of improved efficacy with nivolumab (N) plus ipilimumab (I) leading to predictors of ICB responses with greater accuracy. Patient-derived HNSCC explants were cultured on the TruTumor histoculture platform and treated for 72 hours with N or N+I. Treatment effects were assessed using histopathology, cleaved caspase-3 IHC, multiparameter flow cytometry, and NanoString nCounter bulk transcriptomics. Spatial profiling was performed using the CosMx SMI same-cell multiomic assay, enabling subcellular quantification of immune checkpoints, activation and exhaustion markers, costimulatory molecules, and whole-transcriptome signatures within intact tissue architecture. Analyses included spatial clustering, cell-cell neighborhood modeling, immune-tumor interface mapping, and ligand-receptor interaction inference. CosMx multiomics revealed treatment-dependent remodeling of immune states and spatial niches not captured by bulk assays. N+I responders exhibited: (i) expansion potential of cytotoxic and proliferative CTLs; (ii) depletion or spatial exclusion of suppressive Tregs from tumor nests; (iii) enhanced antigen-presentation and IFN-γ-response programs in tumor and myeloid cells; and (iv) rewired immune checkpoint and costimulatory ligand-receptor networks at tumor-immune borders. Same-cell integration of protein and RNA markers defined discrete CTL activation and exhaustion trajectories and uncovered microenvironments uniquely sensitized to combination therapy. Combining functional response metrics with spatial features yielded a mechanism-driven biosignature predictive of treatment outcome. Integrating the TruTumor histoculture models with CosMx SMI same-cell spatial multiomics establishes a scalable, NAM-aligned translational platform that enables discovery of predictive biomarkers for next-generation immuno-oncology therapies.

#6550 *In vitro* characterization of fully human antagonistic anti-BTLA monoclonal antibodies.

Bruce L. Daugherty[1], Hsunhui Yang[2], Subhra Mahapatra[2], Yadong Yu[2], Christine L. Hsieh[2], Brian A. Zabel[2], Seth Lederman[1]

[1]Tonix Pharmaceuticals, Inc., Chatham, NJ,[2]Curia Global, Inc., Hayward, CA

Introduction: B and T lymphocyte attenuator (BTLA) is an immune checkpoint receptor essential for immune homeostasis and tolerance. Unlike PD-1 or CTLA-4, BTLA is broadly expressed on lymphoid and some myeloid cells, including T cells, B cells, dendritic cells, and macrophages. Engagement with its ligand HVEM (herpesvirus entry mediator) transmits inhibitory signals that suppress immune activation. Within tumors, BTLA contributes to immune evasion by dampening anti-tumor responses. Given its unique expression profile and regulatory function, we developed monoclonal antibodies (mAbs) targeting BTLA as an immunotherapeutic strategy to enhance anti-tumor immunity.

Methods: Fully human anti-BTLA mAbs identified by hybridoma screening were reformatted as huIgG4 (S228P/L235A) and transiently expressed using Curia's TunaCHO® platform. The S228P mutation prevents Fab-arm exchange, stabilizing mAb structure, while L235A minimizes FcγR binding and effector functions. Binding potency was determined by ELISA; kinetics by Octet® biolayer interferometry (BLI) against human and cynomolgus BTLA. BLI also assessed FcγR, FcRn (at pH 6.0 vs 7.2), and C1q binding to evaluate recycling potential and complement activation. Neutralization of HVEM binding to BTLA was quantified by modified ELISA and cell-based reporter assays.

Results: Six fully human anti-BTLA mAbs and a clinical candidate comparator JS004 displayed similar ~1 nM binding potencies (IC_{50}) values to human and cyno BTLA by ELISA. Clone 13-F7-A exhibited the highest affinity (K_d < 1 nM) for both human and cyno BTLA among all 7 mAbs tested. Four mAbs and the comparator JS004 were high affinity binders to human and cyno BTLA (K_d 1-32 nM). All six fully human mAbs exhibited reduced FcγR binding relative to JS004. Each bound FcRn at pH 6.0 but not at 7.2, consistent with normal endosomal recycling. None bound C1q, whereas a positive-control IgG1 did bind to C1q as expected. In an ELISA-based biofunctional assay, all mAbs blocked HVEM binding to BTLA with similar IC_{50} values (~1 nM).

Conclusions: We generated potent, high affinity, human/cyno cross-reactive, fully human antagonistic anti-BTLA mAbs. Targeting BTLA offers promising opportunities for cancer immunotherapy and may demonstrate strong synergy when combined with other checkpoint antagonists, potentially overcoming resistance mechanisms and improving clinical outcomes.

#6551 Mifepristone-mediated induction of PD-L1 expression in hormone receptor positive breast tumors.

Mariana Salatino, Magali Berton, Joaquin Merlo, Andres M. Elia, Tomas Dalotto Moreno, Claudia Lanari, Gabriel Rabinovich

IBYME-CONICET (Institute of Biology and Experimental Medicine), Buenos Aires, Argentina

Luminal breast cancer has been associated with a poor response to immunotherapy with immune checkpoint blockade (ICB). The selection of patients with high chances of response and the combination of ICB with other therapies, with the ability to turn a 'cold' into a 'hot' tumour, may have a broad impact on the management of this highly frequent type of breast cancer.We previously demonstrated that an endocrine therapy with Mifepristone (MIFE), an antagonist of the classical progesterone receptor, can foster a complete remodeling of the immune landscape in hormone receptor-positive tumours, promoting immune cell infiltration, immunogenicity and activating transcriptional programs associated with response to ICB both in mouse models and patients.Here, we aim to evaluate the effect of MIFE on the expression of the ICB response predictor biomarker PD-L1 in luminal breast human tumour samples derived from the MIPRA clinical trial (NCT02651844). The MIPRA trial enrolled 20 breast cancer patients harbouring HR+ tumours that were treated with MIFE for 14 days before surgery (orally administration of 200mg/day of MIFE). Response to MIFE (reduction in percentage of Ki67 proliferation marker > 30%) was documented in 14 of the 20 patients; however, all patients presented remodeling in the tumour microenvironment. We observed that treatment with MIFE in HR+ luminal breast tumours reorganizes the ECM and the stroma, including the enrichment in lymphocyte infiltration. Immunohistochemistry (IHC) assessment of PD-L1 expression in tumour slides from patients was analyzed in the Ventana BenchMark ULTRA using the anti-PD-L1 (SP263 VENTANA).Twenty untreated luminal tumours with similar clinical characteristics were included as controls. IHC analysis of tumour slides from 20 patients enrolled in the MIPRA trial showed that after MIFE treatment, 47% presented any staining for PD-L1, as compared to newly diagnosed untreated luminal tumours, where only 20% showed PD-L1 staining. Notably, the PD-L1 staining observed was primarily located in the stroma and surrounding the infiltration area (images taken with an Aperio SC2 scanner). We scored the staining on a scale of 0-5, with 5 being the highest area stained and 0 indicating no staining detected. MIPRA trial-participating patients exhibit a significant increase in the score of PD-L1 detection after MIFE treatment ($p<0.05$).These results suggest that endocrine therapy with MIFE can reprogram the immune landscape of luminal breast tumours in patients, promoting a "hot" TME, increasing TILs and PD-L1 expression. This MIFE-mediated immune fitness may sensitize luminal tumours to ICI therapy and open new therapeutic avenues for this prevalent breast cancer subtype.

#6552 Nonresponders to PD-1 therapy share a combined OXPHOS and neuronal-like resistance program in melanoma.

Otilia Menyhart, Janos Tibor Fekete, **Balazs Gyorffy**

Semmelweis University, Budapest, Hungary

BACKGROUND: Immune checkpoint inhibitors (ICIs) targeting PD-1 have transformed melanoma therapy, yet only a subset of patients derive durable benefit. The molecular programs underlying responsiveness remain incompletely defined. We aimed to identify gene-expression patterns that distinguish responders from nonresponders by focusing on alterations specifically related to transformed cancer hallmarks.

METHODS: We compiled pretreatment transcriptional profiles from 17 independent studies, pooling data for 551 melanoma patients, including 233 responders to anti-PD-1 therapy. ROC analyses evaluated the discriminative potential of individual genes. Genes with high AUC and expression values in both responders and nonresponders were identified. Hallmark enrichment was assessed using cancerhallmarks.com, and gene ontology analyses were conducted to characterize the underlying biological programs. Significant differences were based on a fold change ≥ 1.4 and a $p<0.05$.

RESULTS: In responders, 467 overexpressed genes revealed a highly coordinated immune-inflamed state, with enriched Fc-gamma receptor signaling ($p = 3.97\times10^{-82}$), classical complement activation ($p = 1.42\times10^{-81}$), and T- and B-cell receptor signaling ($p = 3.47\times10^{-4}$, 3.06×10^{-4}). GO terms highlighted T-cell activation, lymphocyte-mediated immunity, and a strong IFN-gamma response. Cancer hallmark enrichment analysis identified “Evasion of Immune Destruction” as the only significant hallmark ($p < 0.0001$), emphasizing that clinical benefit arises from a pre-existing immune-activated microenvironment rather than tumor-intrinsic programs, such as proliferation, metabolic rewiring, or differentiation state. The 685 overexpressed genes in nonresponders converged on a metabolically amplified and lineage-rewired tumor state. Reactome analysis revealed a strong upregulation of mitochondrial programs, including mitochondrial RNA processing ($p = 1.47 \times 10^{-12}$) and respiratory electron transport ($p = 2.92 \times 10^{-2}$), defining a high-OXPHOS phenotype that can suppress antitumor immunity. Complementary GO terms related to myelination, oligodendrocyte differentiation, and trans-synaptic signaling highlighted a neuronal-like dedifferentiation program linked to reduced antigen presentation and T-cell exclusion, creating a multilayered barrier to immune recognition.

CONCLUSION: ICI nonresponders consistently exhibit high-OXPHOS metabolism and neuronal-like dedifferentiation, resulting in immune silence. The co-occurrence of these two resistance programs across multiple independent cohorts reveals a combined transcriptional barrier to PD-1 response.

#6553 A comprehensive analysis of HMGB1 as a biomarker for predicting immunotherapy efficacy in small cell lung cancer.

Bohui Zhao, Chaoqi Zhang, Peng Wu, Dongyu Li, Xuanyu Gu, Hengjia Tu, Nan Sun, Jie He

Cancer Hospital, Chinese Academy of Medical Sciences, Beijing, China

Background: High mobility group box 1 protein (HMGB1) is known to be associated with progression and poor prognosis of several solid tumors. However, its role in small cell lung cancer (SCLC) remains unclear. Therefore, we intend to provide the first systematically analysis of HMGB1 as a prognostic and immunotherapy predictive biomarker in SCLC.
Methods: Public datasets and self-tested transcriptomic/proteomic data from SCLC surgical samples were integrated to screen target molecules through differential analysis. HMGB1 expression was validated in multicenter cohorts using qPCR and tissue microarray immunohistochemistry (IHC). Public data and in-house data were utilized to investigate the association between HMGB1 and SCLC transcriptional subtypes as well as clinicopathological features. The impact of HMGB1 on the tumor immune microenvironment was evaluated through transcriptomic enrichment analysis, single-cell sequencing and IHC. In the NCC cohort of over 180 SCLC patients treated with immune checkpoint inhibitors (ICIs), the relationships between HMGB1 and ORR, PFS, and OS were analyzed, with a prediction model constructed. Finally, serum HMGB1 levels were measured by ELISA to assess its value as a secreted protein biomarker.
Results: Multi-omics screening and clinical validation confirmed that HMGB1 was significantly overexpressed in SCLC tumor tissues, and high expression was associated with shorter OS and DFS. HMGB1 expression showed no significant association with the four SCLC subtypes but correlated with high-risk factors such as advanced tumor stage. Transcriptomic enrichment and single-cell analyses revealed that high HMGB1 expression correlated with an immunosuppressive "cold tumor" microenvironment. In the ICIs-treated cohort, patients with high HMGB1 expression exhibited significantly shortened PFS and OS. ROC analysis demonstrated that HMGB1 outperformed traditional markers in predicting treatment response. Multivariate Cox regression confirmed HMGB1 as an independent predictor of immunotherapy efficacy in SCLC. Serum HMGB1 levels were consistent with tumor tissue expression, validating its liquid biopsy potential.
Conclusions: HMGB1 is an independent risk factor for SCLC prognosis. Its high expression shapes an immunosuppressive microenvironment and mediates resistance to immunotherapy. HMGB1 shows a good potential to serves as a novel biomarker for predicting immunotherapy efficacy in SCLC, with clinical applicability for both tissue-based and blood-based detection.

#6554 A bispecific TROP2/PDL1 antibody-drug conjugate demonstrates enhanced antitumor activity and favorable safety profile.

Chuan Chen, Yue Wu, Chenpeng Su, Dandan Liu, Jiyuan Tian, Yujuan Li, Yongxin Shang, Xiaoqian Chen, Rongmei Yan, Liang Tian, Jian Peng, Zhenping Zhu

Earendil Labs, Wilmington, DE

Purpose
This study aimed to develop and characterize a bispecific antibody-drug conjugate (ADC) targeting both TROP2 and PDL1, to address the limitations of current single-target therapies in advanced cancers.
Methods
We engineered a humanized bispecific antibody (bsAb) against TROP2 and PDL1 (α TROP2/PDL1), and subsequently produced the bispecific ADC using an optimized hydrophilic linker and TOP1 inhibitor payload. Comprehensive *in vitro* characterization encompassed binding affinity, internalization efficiency, and PDL1 degradation assays. *In vivo* efficacy was assessed across multiple xenograft models, while safety assessment was conducted in transgenic mice and non-human primates.
Results
α TROP2/PDL1 demonstrated potent bispecific activity, featuring efficient cellular binding and rapid internalization. The bsAb induced significant PDL1 internalization and degradation, and showed marked tumor growth inhibition in MC-38-huTrop2/PDL1 model. The bsAb TOP1i conjugated ADC (α TROP2/PDL1-TOP1i) exhibited enhanced potency, characterized by robust cytotoxicity against multiple Trop2/PDL1-expressing cell lines, potent bystander killing effects, and tumor regression in multiple CDX models. Notably, the ADC showed excellent stability and tolerability in cynomolgus monkeys, with no significant adverse effects observed in safety studies.
Conclusion
α TROP2/PDL1-TOP1i represents a promising therapeutic strategy for treatment-resistant cancers, effectively combining PD1/PDL1 immune checkpoint blockade with TROP2-targeted cytotoxic payload delivery while maintaining a favorable safety profile, supporting its advancement to clinical development.

#6555 BTN1A1 blockade with Nelmastobart potentiates cisplatin-induced tumor suppression in NSCLC.

Seung-Hoon Lee, Jong-Su Park, Young-Seung Kim, Chunai Wu, Bong-Ki Hong, Andrew H. Park, **Stephen S. Yoo**

STCube Pharmaceuticals Inc., Rockville, MD

Background: Butyrophilin 1A1 (BTN1A1) is a novel immune-regulatory checkpoint protein expressed in various solid tumors, including non-small cell lung cancer (NSCLC), where it modulates T-cell activation. We previously demonstrated that BTN1A1 inhibition by Nelmastobart enhances immune-mediated tumor suppression. In this study, we evaluated whether combining Nelmastobart with cisplatin could further potentiate anti-tumor immune responses in NSCLC.
Methods: A549 NSCLC cells, stably expressing RFP, were cultured as 3D spheroids and co-incubated with human peripheral blood mononuclear cells (PBMCs), Nelmastobart, cisplatin, or their combinations. Anti-tumor immune activity was assessed by monitoring spheroid size reduction and RFP intensity loss. To evaluate translational safety, zebrafish embryos were exposed to Nelmastobart alone, cisplatin alone, or both agents at clinically relevant concentrations. Developmental endpoints, including embryo survival, hatching success, axial and craniofacial morphology, pericardial edema, spinal curvature, cardiac rhythm, and early organogenesis of the eye, heart, and somite structures, were systematically evaluated according to established zebrafish developmental toxicity guidelines.
Results: Combination treatment with Nelmastobart and cisplatin induced the strongest PBMC-mediated cytotoxic effect, resulting in substantial reductions in spheroid volume and marked disruption of RFP signals compared to the monotherapies. These findings suggest that BTN1A1 blockade enhances immune recognition, increasing tumor susceptibility to chemotherapy. Zebrafish developmental toxicity testing revealed no significant abnormalities with either Nelmastobart alone or cisplatin alone at clinically relevant exposure ranges. Importantly, no additive or synergistic developmental toxicity was observed in the combination group.
Conclusion: BTN1A1 inhibition by Nelmastobart significantly enhances cisplatin-driven immune-mediated cytotoxicity in A549 3D spheroid models while maintaining a strong safety margin in vivo. These data support the continued clinical advancement of Nelmastobart, both as a monotherapy and in combination with standard chemotherapeutic agents.

#6556 The role of VISTA in the lung tumor microenvironment of metastatic melanoma.

Carly M. Fielder[1], Qianni Hu[2], Hyundong Yoon[1], Raymond Zhang[1], Anjali Raman[3], Megan L. Tigue[1], Chi Yan[2], Vivian L. Weiss[4], Douglas B. Johnson[5], Jin Chen[6], Tae Kon Kim[3]

[1]Cancer Biology, Vanderbilt University, Nashville, TN,[2]Immunology, University of Manitoba, Winnipeg, MB, Canada,[3]Medicine, Vanderbilt University Medical Center, Nashville, TN,[4]Pathology, Microbiology, and Immunology, Vanderbilt University Medical Center, Nashville, TN,[5]Vanderbilt Ingram Cancer Center, Nashville, TN,[6]Cell and Developmental Biology, Vanderbilt University Medical Center, Nashville, TN

Metastatic melanoma remains a significant clinical challenge despite recent advances with immune checkpoint inhibitors (ICIs) like anti-programmed cell death-1 (PD-1), which show variable efficacy across metastatic organ sites. The lung is a frequent site of metastasis, and while complete responses to ICIs occur more often in pulmonary lesions than in other organs, up to 60% of patients with lung metastases fail to respond. Pulmonary metastases are also a leading cause of death in patients with metastatic melanoma. This suggests that we will need to comprehensively understand the tumor immune microenvironments of pulmonary metastatic melanoma including the expression of alternative immune checkpoint targets. V-domain immunoglobulin suppressor of T cell activation (VISTA) is an emerging checkpoint molecule predominantly expressed in myeloid cells that suppresses immune activation. We found that VISTA was highly expressed in human pulmonary metastatic melanoma while PD-L1 expression was not significantly elevated. To investigate the role of VISTA in pulmonary metastatic melanoma, we utilized a variety of mouse models with B16-F10 murine melanoma. VISTA knock-out (KO) mice develop significantly fewer lung metastases than wild-type (WT) controls (lung-to-body weight ratio: VISTA WT = 0.05 ± 0.018, VISTA KO = 0.02 ± 0.011; p = 0.0012), with no difference in subcutaneous tumor growth (p = 0.1625). We assessed the immune cell infiltration in these mice. VISTA KO mice had significantly more proinflammatory monocytes (2.78% ± 1.50 vs. 0.52% ± 0.54; p = 0.0003) and macrophages (14.27% ± 6.18 vs. 6.75% ± 4.27; p = 0.006) in the metastatic lung tissue compared to WT mice. These data suggest that myeloid cell VISTA promotes lung metastasis of melanoma. We also demonstrated that $Rag1^{-/-}$ mice, which lack T and B lymphocytes, showed increased melanoma lung metastases compared to $Rag1^{-/-}$ $VISTA^{-/-}$ mice, suggesting that the metastatic phenotype is independent of T and B lymphocytes ($Rag1^{-/-}$ = 0.03 ± 0.008, $Rag1^{-/-}$ $VISTA^{-/-}$ = 0.01 ± 0.002; p = 0.0008). Mechanistically, VISTA-deficient bone marrow-derived macrophages (BMDMs) produce more TNFα and nitric oxide compared to WT BMDMs, indicating that VISTA suppresses macrophage activation as a mechanism of immune suppression (TNFα: 1.2-fold-change, 1166 vs. 946.3 pg/ml; p = 0.0001; nitric oxide: 3.2-fold-change, 29.42 vs. 9.089 µmol/L). Our findings establish VISTA as a critical regulator of immune suppression in pulmonary melanoma metastases. Ongoing mechanistic studies will clarify its potential as a therapeutic target, leading to improved treatment strategies and patient outcomes.

#6557 Combined PARP inhibition and immune checkpoint blockade elicit differentially improved survival in BRCA1, BRCA2 vs CHEK2, ATM deficient breast cancer by promoting an anti-tumor immune response through tertiary lymphoid structure formation.

Sibapriya Chaudhuri[1], Alberto Emata[1], Scott Thomas[2], Pamela N. Munster[1]

[1]UCSF - University of California San Francisco, San Francisco, CA,[2]Postdoctoral Fellow, Dept. of Hem./Onc., UCSF, San Francisco, CA

Introduction: Breast cancer affects over 2 million women globally every year despite advances in knowledge of disease biology, genomic assessment of disease profile and development of novel therapies. Preclinical and clinical studies suggest a benefit of combining PARP inhibitors (PARPi) and immune checkpoint inhibitors (ICi) in patients with homologous recombination proficient as well as deficient triple negative breast cancers. However, similar to the varied benefits of either drug class as single agent, the benefits of the combination therapy are strongly dependent on tumor mutation landscape. In this study, we identify which homologous recombination deficiency mutation respond best to PARPi and ICi combination therapy and explore the underlying mechanisms driving this sensitivity.

Methods: We used CRISPR engineering to individually repress BRCA1, BRCA2, ATM, CHEK2 in both murine and human breast cancer cell lines (EMT6, 4T1, MDA-MB231). The engineered murine cells were implanted in the mammary fat pad of Balb/cJ mice and subsequently treated with PARPi, ICi and drug combination. We evaluated how single agent and combined treatment affected tumor growth and overall survival. Using different biochemical techniques including spectral flow-cytometry, immunohistochemistry and spatial transcriptomics, we analyzed different immune cell populations in the tumor microenvironment.

Results: In EMT6 tumor models, the repression of BRCA1 or BRCA2 led to both reduced tumor growth and increased survival with either single agent or combination treatment. However, with ATM or CHEK2 repression, single agent ICi both reduced tumor growth and improved survival compared to untreated tumors, but no benefit was observed with PARPi addition. Spatial transcriptomics analysis suggested the formation of tertiary lymphoid structures (TLS) in combination therapy-responsive EMT6 tumors with repressed BRCA1. TLS formation was marked by higher CXCL13 expression, increased regions of B cells expressing CD19 and CD20, which were surrounded with $CD3^+$ T cells. We also observed inward migration of $CD45^+$ and $CD3^+$ cells from the tumor periphery. PDL1 expression was also higher in these tumors. Furthermore, in vitro olaparib treatment resulted in a substantial increase in surface PDL1 expression in EMT6 BRCA1-repressed cells, which was more moderate in EMT6 BRCA2-repressed cells. In 4T1 cells, repression of the HRD genes led to a modest change in PDL1 upregulation upon olaparib treatment.

Conclusion: Our findings mimic findings in the clinic and suggest that TLS formation may correlate with better response to the combination therapy of PARPi and ICi. TLS formation in the therapy responsive tumors might be maintaining the microenvironment necessary for anti-tumor immune response.

#6558 Selenium dependent regulation of immune checkpoint control in acute myeloid leukemia.

Deborpita Sarkar, Fenghua Qian, Robert F. Paulson, K.Sandeep Prabhu

Penn State University, State College, PA

Acute myeloid leukemia (AML) is a hematologic malignancy with a 5-year survival rate of ~27 % among individuals aged 20 years and older. Despite advances in immune checkpoint inhibitor (ICI) therapies such as PD-1/PD-L1 blockade, leukemic cells still evade immunity, leading to relapse. PD-L1 on AML cells binds PD-1 on cytotoxic (CD8+) T cells, driving immune exhaustion and suppression. Given the link between low serum selenium (Se) and poor outcomes in hematologic malignancies, we investigated the mechanisms underlying the anti-leukemic effects of Se in a murine model of human AML. Supplementation with graded levels of dietary Se (as selenite at 0.08 ppm and 0.4 ppm of Se) led to a dose-dependent decrease in PDL1 and PD-1 expression in leukemic stem cells (LSCs) and CD8+ T-cells, respectively, mitigating T-cell exhaustion, resulting in better prognosis when compared to the AML mice on a Se-deficient diet. The effect of Se was mediated, in part, through the activation of GPR44, a GPCR, by prostaglandin J2, an endogenous ligand produced via Se-dependent eicosanoid class-switching mechanisms. Our studies highlight a novel dietary intervention strategy with Se supplementation that could potentially complement existing ICI therapy in AML.

#6559 Investigating the transcriptomic signature of B7-H7-mediated activation of NK cell activity.

Michael Gomez[1], Deepthi Chowbene[2], Nahuel Perrot[2], Nikolaos Kalavros[2], Shuoshuo Wang[2], Antonella Arruda de amaral[2], David F. McDermott[3], Gordon J. Freeman[1], Ioannis S. Vlachos[2], Kathleen M. Mahoney[2]

[1]Dana-Farber Cancer Institute, Boston, MA,[2]Beth Israel Deaconess Medical Center, Boston, MA,[3]Beth Israel Deaconess Medical Center, Milton, MA

Determining how antibodies that target immune checkpoints alter lymphocyte functions can improve our understanding of immune checkpoint inhibitors responses in patients. HERV-H LTR-associating 2 (HHLA2, B7-H7) is an immune checkpoint expressed by many tumors. Our group previously found that B7-H7 has an inhibitory receptor, KIR3DL3, in addition to having an activating receptor, TMIGD2. Both B7-H7 receptors are expressed by subsets of T cells and NK cells. However, little is known about how different subsets of lymphocytes are affected by B7-H7 engagement of these receptors, and multiple B7-H7:KIR3DL3 blocking antibodies are currently enrolling cancer patients in Phase I clinical trials (NCT05824663, NCT06240728).In this study, we explored the effect of tumors expressing B7-H7 on NK cells *in vitro* by single cell RNA sequencing (scRNAseq). NK cells were isolated from peripheral blood and co-cultured with K562 cells or K562 cells overexpressing B7-H7 for 2hr. Co-cultures were performed in the presence of different B7-H7 blocking antibodies or isotype controls. 133,017 cells passed quality control, with 9 distinct NK cell populations being identified. Primary NK cells not co-cultured with tumor cells were mainly composed of two TXNIP+ CD96 hi NK cell clusters that had low expression of cytotoxic and inflammatory genes. Additionally, these two clusters had the highest expression of TMIGD2, suggesting that these populations represent resting NK cells. Co-culture with K562 or K562-B7-H7 cells increased the proportion of highly cytotoxic and inflammatory NK cell clusters. However, XCL2, CSF2, IFNγ and IL3 were higher in NK cells co-cultured with K562-B7-H7 than with K562, suggesting B7-H7 on K562 cells is proinflammatory in this early activation model. Notably, only a small subset of peripheral blood NK cells expressed the inhibitory receptor KIR3DL3, as expected in early NK activation. Furthermore, all antibody treatments regardless of the Fc isotype were associated with increased proportions of CRTAM+ IL2RA+ TNFRSF9+ NK cell clusters, compared to NK cells cultured without antibody. Differential gene expression analysis between B7-H7 antibody clones 6F10 and 2C4 by respective Fc (IgG1 or IgG4) suggested blocking TMIGD2 with the dual receptor blocking B7-H7 antibody (6F10) reduces the extent of activation of the NK cells compared to the B7-H7 antibody (2C4) that blocks KIR3DL3 but not TMIGD2.Our work suggests the importance of selecting B7-H7 therapeutics that spare the interaction of B7-H7:TMIDG2 to maintain any NK-dependent antitumor benefit of B7-H7 expression.

#6560 Targeting fitness surveillance restores T-cell immunity and sensitizes solid tumors to immune checkpoint inhibitors.

Amit Kumar[1], Antonio Palma[2], Praveen Bhoopathi[3], Esha Madan[3], Rajan Gogna[2]

[1]VCU Massey Comprehensive Cancer Center, Richmond, VA,[2]Cellular Molecular and Genetic Medicine, Virginia Commonwealth University, Richmond, VA,[3]Surgery, Virginia Commonwealth University, Richmond, VA

Immune checkpoint inhibitors (ICIs) fail in most solid tumors despite their transformative success in a minority of patients. Here, using integrated human tumor profiling and humanized patient-derived xenograft (PDX) models, we identify Flower-mediated fitness elimination as a dominant, conserved mechanism of T-cell attrition that limits ICI efficacy across epithelial cancers. Stromal compartments in high-grade serous ovarian cancer, non-small-cell lung cancer, colorectal cancer, hepatocellular carcinoma, and pancreatic ductal adenocarcinoma exhibit high Flower-Lose expressioncoupled to severe $CD8^+$ T-cell exclusion. Tumor-infiltrating T-cells themselves acquire a “loser” state marked by elevated Flower-Lose, rendering them vulnerable to competitive elimination by the stromal niche.

Across five orthotopic humanized PDX tumor types and three independent cohorts, ICIs alone produced minimal T-cell restoration, persistent metastatic dissemination, and negligible survival benefit (e.g., median ≈42 days). In contrast, pharmacologic blockade of Flower signaling increased intratumoral T-cell density by 5-7-fold (MixedLM $P < 10^{-15}$), reduced metastatic burden by 54-75%, suppressed tumor growth by >90%, and produced durable survival benefit across all models, with median survival not reached and strong meta-analytic significance ($Z = 10.56$, $P < 10^{-25}$).

Together, these findings reveal Flower-mediated fitness surveillance as a pan-cancer, tissue-level barrier to immunotherapy and establish Flower blockade as a universally effective strategy to restore T-cell persistence and unlock durable ICI responses across historically immune-cold solid tumors.

#6561 Rational design of a B7-H3/PD-L1 bsADC combining checkpoint blockade with targeted cytotoxicity for improved antitumor efficacy.

Zhangyi Song[1], Jie Chen[2], Huifang Zong[2], Zhen Li[2], Shusheng Wang[1], Jianwei Zhu[1], Xiaodong Xiao[1]

[1]Jecho Laboratories, Frederick, MD,[2]Jecho Institute, Shanghai, China

B7-H3 (CD276) is a transmembrane glycoprotein of the B7 family aberrantly overexpressed across diverse solid tumors with limited expression in normal tissues, making it an appealing therapeutic target. In addition to potential immunosuppressive effects on T cells, B7-H3 possesses non-immune regulatory functions in enhancing tumor proliferation, angiogenesis, and therapy resistance, which contribute to aggressive disease progression and poor prognosis. PD-L1, another member of the B7 family with clinically validated immune checkpoint function, is frequently co-expressed with B7-H3 in multiple tumor types. Although B7-H3-targeted antibody-drug conjugates (ADCs) and PD-1/PD-L1 checkpoint inhibitors have shown clinical benefit, therapeutic resistance and limited efficacy in “cold” tumors remain challenges. Co-expression of B7-H3 and PD-L1 creates an opportunity to pair targeted cytotoxic delivery with checkpoint blockade. Moreover, the ability of ADCs to induce immunogenic cell death provides additional rationale for integrating ADCs with immune-oncology therapy to enhance antitumor immunity.

Guided by this rationale, we developed a bispecific ADC (bsADC), JLC062, that engages both B7-H3 and PD-L1. Several anti-B7-H3 antibodies were identified from our fully human naïve phage library, recognizing different epitopes with varying affinities and internalization rates. Fast-internalizing anti-B7-H3 antibodies were formatted as IgGs to enable efficient intracellular delivery, which results in potent *in vitro* cytotoxicity across cancer cell lines with varying B7-H3 expression. A high-affinity PD-L1 binder, also isolated from our library, was fused to the C-terminus of the anti-B7-H3 IgG Fc as an scFv. It exhibited robust PD-1/PD-L1 blocking activity and induced IL-2 and IFN-γ secretion levels comparable to the clinical benchmark avelumab in a mixed lymphocyte reaction assay. Importantly, this anti-PD-L1 arm was intentionally selected as an antibody with minimal internalization to limit toxicity toward immune cells. In a syngeneic mouse model, JLC062 demonstrated significantly greater antitumor efficacy than either parental monotherapy, anti-PD-L1 antibody or anti-B7-H3 ADC, with no observed body weight loss. These findings highlight JLC062 as a promising therapeutic modality that integrates immune checkpoint inhibition with targeted cytotoxic delivery to yield deep and durable antitumor responses.

#6562 Identifying vulnerabilities to immune checkpoint inhibitors of oncogene-addicted non-small cell lung cancer subgroups..

Ines Diaz-Cano[1], Jose Gracia[2], Patricia Cozar[2], Belen Revuelta[2], Nuria Carrizo[2], Laura Garcia-Redondo[2], Joan Russo[2], Rita Manzano[2], Jose Garrido-Mesa[2], Daniel Meraviglia-Crivelli[1], Juan Dubrot[3], Luis Paz-Ares[4], Itziar Otano[1]

[1]H12O-CNIO Lung Cancer Clinical Research Unit, Spanish National Cancer Research Center (CNIO)/Biomedical Research Foundation Hospital 12 de Octubre (FIBH12O)/Spanish Center for Biomedical Research Network in Oncology (CIBERONC), Madrid, Spain,[2]H12O-CNIO Lung Cancer Clinical Research Unit, Spanish National Cancer Research Center (CNIO)/Biomedical Research Foundation Hospital 12 de Octubre (FIBH12O), Madrid, Spain,[3]Solid Tumors Program, Division of Oncology, Center for Applied Medical Research (CIMA), University of Navarra, Pamplona, Spain,[4]H12O-CNIO Lung Cancer Clinical Research Unit, Spanish National Cancer Research Center (CNIO)/Biomedical Research Foundation Hospital 12 de Octubre (FIBH12O)/Spanish Center for Biomedical Research Network in Oncology (CIBERONC)/Complutense University, Madrid, Spain

Purpose: Even though the treatment with PD-(L)1 axis blockers induces tumor response in approximately 20% of unselected lung cancer patients with advanced Non-Small Cell Lung Cancer (NSCLC), patients harbouring *EGFR* alterations or *ALK*-rearrangements have a poor response to immunotherapy. Tyrosine Kinase Inhibitors (TKIs) is the standard of care for these patients. However, resistance to TKIs is almost inevitable. The different clinical response to Immune Checkpoint Inhibitors (ICIs) in the different oncogene-addicted NSCLC subgroups may be explained by the composition and quality of the TME. Thus, we propose to investigate potential vulnerabilities and opportunities to overcome primary resistance to ICIs conferred by oncogene addiction.
Methods: To identify mechanisms involved in the restricted immune response of these subgroups, we performed a sub-genome-scale *in vivo* CRISPR/Cas9 screening, using a lentiviral vector system that allowed selective CRISPR antigen removal (SCAR) from tumor cells after genome editing. Genetically engineered mouse models were used to isolate cell lines bearing *Egfr* exon 19 deletion, *Egfr* L860R missense mutation or the *Eml4-Alk* oncogene fusion. Modified cell lines with the CRISPR/Cas9 sgRNA library were implanted subcutaneously into the flank of immunodeficient NOD-scid IL2Rg^{null} and immunocompetent wild-type (WT) mice. A group of WT mice received ICI treatment at different days post-tumor challenge and sgRNA abundances between the different groups were compared.
Results: As expected, both *Egfr* murine cell lines were sensitive to an EGFR-specific TKI, showing a decrease in phospho-Y1068-EGFR, demonstrating the oncogenic dependence on *EGFR* signaling for growth. However, when these cell lines were injected subcutaneously into immunocompetent mice, these tumors were resistant to PD1 blocking, mirroring the lack of response to human EGFR-mutant NSCLC to immunotherapy. To ensure an optimal coverage of the sgRNA library for *in vivo* studies, we estimated that around 55 mice for each experimental condition were necessary. Based on this estimation, an *in vivo* screen was performed and sgRNAs abundance are being analyzed to determine mechanisms of immune evasion in an *Egfr* oncogenic specific context. Cell lines bearing *Eml4-Alk* gene fusion were positive for TTF1 and SpC and negative for p63, confirming a lung adenocarcinoma phenotype. Phosphorylation of Stat3, Erk1/2 and Akt were also observed. The next steps include genetic modification of *Eml4-Alk* fusion cell lines with the CRISPR/Cas9 sgRNA library, followed by *in vivo* screening.
Conclusion: We expect to identify new resistance mechanisms that could result in novel treatment strategies for these NSCLC subgroups. The identification of these targets will provide the opportunity to reprogram the TME and to improve the efficacy of immunotherapy in a subset of patients with lung adenocarcinoma.

#6563 Immune and clinical determinants of response to immune checkpoint blockade (ICB) rechallenge after perioperative chemoImmunotherapy in gastroesophageal cancer.

Jeremy M. Tchack, Samuel L. Cytryn, Steven B. Maron, Patrick Evans, Jessica Posada, Geoffrey Y. Ku, Jessica Yang, Ryan B. Sugarman, Ping Gu, Laura H. Tang, Amitabh Srivastava, Vivian E. Strong, Daniela Molena, Yelena Yuriy Janjigian

Memorial Sloan Kettering Cancer Center, New York, NY

Background: The addition of perioperative ICB to chemotherapy improves survival in localized gastroesophageal adenocarcinoma (GEA), but optimal treatment at recurrence remains undefined. A key question is whether prior perioperative ICB influences clinical response or immune sensitivity to subsequent ICB in the metastatic setting. We evaluated clinical outcomes and immune correlatives in patients who recurred after perioperative chemo-immunotherapy and underwent ICB rechallenge.
Methods: We retrospectively analyzed patients with localized MSS GEA treated at Memorial Sloan Kettering (2020-2025) with curative intent perioperative chemo-immunotherapy (anti-PD-1 or anti-PD-L1). Patients treated on clinical trials were excluded. Clinical endpoints included RECIST response to ICB rechallenge at recurrence and progression-free survival (PFS) on rechallenge. Correlative studies (ongoing) include immune profiling and TCR clone-tracking from paired baseline and recurrence tumor biopsies and serial PBMCs in a subset of patients.
Results: Among 66 patients with localized gastric (n=26) and esophagus/GEJ (n=40) cancer, 33 received neoadjuvant ICB (anti-PD-1 + FLOT, n=17; anti-PD-1 + FOLFOX/CAPEOX followed by surgery and adjuvant chemo/ICB, n=28; or non-operative management, n=5), and 33 received chemotherapy alone followed by surgery and adjuvant ICB only. Eighteen of 66 patients (27%) experienced disease recurrence or progression; of these, 55% (10/18) were rechallenged with ICB plus chemotherapy at recurrence (4 with prior neoadjuvant ICB; 6 with adjuvant-only ICB). Rechallenged patients had a longer interval from completion of perioperative therapy to recurrence compared with those not rechallenged (6.30 vs 1.27 months; p=0.315). Among rechallenged neoadjuvant-exposed patients, all four experienced tumor regression or disease stabilization with chemo-ICB (1 CR, 2 PRs, 1 SD). Among rechallenged patients who received adjuvant-only ICB, disease progression occurred in 50% (3/6), and two had short-lived responses; all ultimately progressed, including two deaths. Overall, median PFS from time of ICB rechallenge was 6 months (95% CI 4.27-NR): NR (0 events) in the neoadjuvant-exposed group versus 5 months (95% CI 4.14-NR) in the adjuvant-only group (log-rank p=0.056).
Conclusions: In this perioperative chemo-immunotherapy cohort, prior neoadjuvant ICB exposure did not preclude - and may be associated with improved - response to ICB rechallenge at recurrence. Neoadjuvant-exposed patients showed numerically higher response rates and longer PFS on rechallenge compared with those who received adjuvant-only ICB. Ongoing correlative analyses of tumor and PBMC specimens aim to define immune determinants and TCR-based signatures associated with benefit from ICB rechallenge in MSS GEA.

#6564 Spatially resolved immunologic hallmarks of response to neoadjuvant immune checkpoint blockade in metastatic melanoma.

Zichao Liu[1], Xiaofei (Sophia) Song[2], Jodi A. Balasi[2], Wei-Shen Chen[3], Jiang He[4], Justin He[4], Jonathan Nguyen[2], Carlos M. Moran-Segura[2], Joseph O. Johnson[2], Chaomei Zhang[2], Jane L. Messina[2], Zena Sayegh[2], Douglas C. Marchion[5], Sean J. Yoder[2], Vernon K. Sondak[2], Jeffrey H. Chuang[1], Pei-Ling Chen[2]

[1]The Jackson Laboratory, Farmington, CT,[2]Moffitt Cancer Center, Tampa, FL,[3]University of South Florida, Tampa, FL,[4]Vizgen, Cambridge, MA,[5]Research Scientist, Moffitt Cancer Center, Tampa, FL

Background: The recent groundbreaking neoadjuvant immune checkpoint blockade (NICB) clinical trials in melanoma have demonstrated decisively that the administration of ICB prior to intent-to-cure surgeries will become the new standard-of-care for metastatic melanoma and beyond. The paradigm shifts from radiographic to pathologic response assessment also presents an unparalleled “window of opportunity” for the acquisition of abundant “on-treatment” tissues to elucidate the mechanisms and biomarkers of response and for guiding post-surgery personalized therapy decisions. To date, single-cell/bulk RNA studies have demonstrated that TCF7+ stem-like CD8+ T cells and tertiary lymphoid structures (TLS) are positive predictors of ICB response. However, how these immune cells organize and communicate within the spatial context of the neoadjuvant tumor microenvironment remains poorly understood.

Methods: We investigated a unique cohort of 91 FFPE biospecimens from 87 patients with stage III metastatic melanoma, including 60 treated with NICB (31 complete response, 7 partial response, 22 non-response) and 27 treatment-naïve. We deployed state-of-the-art technologies, including multiplexed error-robust fluorescent *in situ* hybridization (MERFISH), single cell sequencing of FFPE blocks, and multiplexed IF for this rich digital resource. Importantly, to analyze these challenging high dimensional spatial datasets, we developed 3 novel computational algorithms, including SCIRA, a scalable quantification method for spatial receptor-ligand (R-L) interactions; GC-SCAN, a graph-based clustering method to detect Germinal Center (GC)/TLS structures in single cell spatial data; and PathNet, an end-to-end AI algorithm for automated GC/TLS detection on H&E slides.

Results: Here, we interrogated ~5.6 million cells and showed that increased GC/mature TLSs, TCF7+ stem-like CD8 and CD4 T-cells, exhausted CD8 T-cells, plasma cells and myeloids in spatially distinct cellular neighborhoods are significantly associated with positive response. Our spatial (R-L) analyses further identified preferential chemokine R-L interactions between GC-B cells and follicular helper T-cell, and TCF7+ stem-like T-cells with CCL19+/CCL21+ fibroblasts in organizing these immune hubs. Lastly, Our PathNet GC/TLS detection algorithm outperforms recent state-of-the-art methods in both specificity and sensitivity, proven potential utility in facilitating clinical response assessment.

Conclusions: We leveraged cutting-edge spatial-omics technologies and novel computational methods to resolve the immunologic hallmarks of NICB response in metastatic melanoma. We believe our approach provides a model for how to precisely identify spatially intricate immune interactions that underline treatment response in the rapidly advancing era of standard of care neoadjuvant immunotherapy.

: Inflammation, Immunity, and Cancer
Poster Session

#6569 Single-cell transcriptomics reveal functional interaction between CD4+ T cells and B cells driving the activated peripheral immune phenotype in healthy women living with germline pathogenic *BRCA1* variants.

Vince Kornel Grolmusz[1], Klaudia Horti-Oravecz[1], Istvan Kelemen[1], Istvan Liko[1], Aniko Bozsik[1], Timea Pocza[1], Janos Papp[1], Szonja Polett Posa[1], Lorinc S. Pongor[2], Henriett Butz[1], Attila Patocs[1]

[1]National Institute of Oncology Hungary, Budapest, Hungary,[2]Hungarian Center of Excellence for Molecular Medicine, Szeged, Hungary

Our previous, mass cytometry-based results signalled an enrichment of peripheral activated CD4+ T and B cells in healthy women living with germline pathogenic *BRCA1* variants (gpath(*BRCA1*)) and in triple-negative breast cancer (TNBC) patients. Our aim was to assess the transcriptional background of this activation and investigate the interrelation between these two cell populations. Peripheral blood mononuclear cells were isolated from five healthy women living with gpath(*BRCA1*), seven women with treatment-naive TNBC living with gpath(*BRCA1*) and seven, age-matched healthy women living without hereditary cancer predisposition (control group). Viable single-cell suspensions were subjected to single-cell transcriptomic library preparation using the Chromium Controller. Libraries were sequenced on a Novaseq 6000 instrument. Bioinformatic analyses were performed using the CellRanger, Seurat, AUCell, CellChat and Monocle3 packages. Following quality control, 100 132 cells were analyzed. CD4+ T cells, CD8+ T cells, NK cells, B cells and monocytes were annotated and subclustered to subpopulations. B cell frequencies in gpath(*BRCA1*) study groups were decreased compared to controls. A pro-inflammatory B cell subpopulation was more frequent in healthy gpath(*BRCA1*) carriers while an activated Th17-polarized CD4+ T cell subpopulation was elevated in both healthy and TNBC-bearing gpath(*BRCA1*) study groups. Ligand-receptor interaction network analysis between these two subpopulations revealed a striking increase in interaction strength in gpath(*BRCA1*) carriers and identified multiple inflammatory cytokines which mediate the observed activated peripheral immune phenotype. Our results confirm the activated peripheral immune profile of healthy women living with gpath(*BRCA1*). This activated peripheral immune phenotype and the functional interactions between CD4+ T cells and B cells might serve as targets during precision prevention approaches in women living with gpath(*BRCA1*).

#6570 Assessment of multiplexed human and mouse cytokines in humanized mouse samples.

Andrew McDermott[1], Amanda Hrabovsky[1], Olivia Williams[1], Eric Bruder[1], Daniel Shoufler[1], Tina Raeber[2], Brooke Gilliam[3], Sineej Madathil[3], Kathryn MacPherson[4]

[1]Immunology and Immunotoxicology, Labcorp, Madison, WI,[2]Millipore Sigma, St. Louis, MO,[3]MilliporeSigma, St. Louis, MO,[4]Immunology and Immunotoxicology, Labcorp, Greenfield, IN

Humanized mice represent a critical model for the evaluation of advanced therapeutics targeting cancer, including chimeric antigen receptor T cell (CAR-T) therapies. Myriad humanized mouse models exist, each with varying levels of immunodeficiency present in the murine immune system and varying levels of immunocompetence engendered by the human graft cells. Furthermore, CAR-T cells themselves can produce human cytokines once transferred into a mouse, and murine stromal cells can release cytokines in response to cancerous cells and therapies . As such, a significant challenge to evaluating immunological responses in humanized mice is detecting and differentiating human and murine cytokines within relatively small sample volumes.

We evaluated the ability of the MILLIPLEX® Humanized Mouse Magnetic Bead Panel to detect 17 human or mouse cytokines in murine serum and plasma. Briefly, human or murine PBMCs were isolated from whole blood and stimulated overnight in the presence of lipopolysaccharide, eBioscience™ cell stimulation cocktail, and Rapid-Act T Cell Activation Kit (mouse or human). Resulting cell culture supernatants were diluted into murine serum and plasma individually and in combination to generate murine serum and plasma samples rich in human, murine, or human and murine cytokines *ex vivo*. These samples were then evaluated for murine IL-2, IL-5, IL-6, GM-CSF, IFNγ, IL-1β, IL-17A, TNFα and human IL-2, IL-5, IL-6, GM-CSF, IFNγ, IL-1β, IL-17A, TNFα, and IL-10 using the MILLIPLEX® Humanized Mouse Magnetic Bead Panel on the Bio-Plex 200 platform.

The MILLIPLEX® Humanized Mouse Magnetic Bead Panel was able to detect human and murine cytokines in samples spiked with human and/or murine PBMC supernatant. Additionally, the kit was able to distinguish between human and murine cytokines within spiked samples. On average, the level of human cytokines detected in serum spiked with human supernatant was 694-fold higher than human cytokine levels detected in serum spiked with murine supernatant alone, while the level of murine cytokine detected in serum spiked with murine supernatant alone was 261-fold higher than serum samples spiked with human supernatant alone. Similar results were seen in plasma samples.

These data demonstrate the utility of the MILLIPLEX® Humanized Mouse Magnetic Bead Panel to evaluate human and murine cytokines within humanized mouse samples. These data demonstrate this kit can detect and distinguish key mediators of inflammation between human and mouse, including IL-2, IFNγ, and TNFα, within small sample volumes. Collectively, this work suggests that this platform is suitable for evaluating human and murine cytokine responses within murine samples, allowing for reliable cytokine analysis across a variety of humanized mouse formats and experimental designs.

#6571 Proliferative T cell infiltration is associated with colorectal cancer molecular subtypes and cancer specific survival.

Yasutoshi Takashima[1], Claire Elizabeth Thomas[2], Andressa Dias Costa[1], Sushma Thomas[3], Evertine Wesselink[4], Conghui Qu[3], Steven Gallinger[5], Robert C. Grant[6], Li Hsu[3], Marios Giannakis[7], Jeroen Huyghe[8], Daniel D. Buchanan[9], Shuji Ogino[10], Riki (Ulrike) Peters[2], Amanda I. Phipps[3], Jonathan A. Nowak[11]

[1]Department of Medical Oncology, Dana-Farber Cancer Institute, Boston, MA,[2]Fred Hutchinson Cancer Center, Seattle, WA,[3]Public Health Sciences Division, Fred Hutchinson Cancer Center, Seattle, WA,[4]Department of Molecular Pathology, The Netherlands Cancer Institute. Antonie van Leeuwenhoek hospital, Amsterdam, Netherlands,[5]Lunenfeld Tanenbaum Research Institute, Mount Sinai Hospital, University of Toronto, Toronto, ON, Canada,[6]Division of Medical Oncology and Hematology, Princess Margaret Cancer Centre, University Health Network, Toronto, ON, Canada,[7]Dana-Farber Cancer Institute, Boston, MA,[8]Public Health Sciences Division, Fred Hutchinson Cancer Research Center, Seattle, WA,[9]University of Melbourne, Kallangur, Australia,[10]Brigham and Women's Hospital, Boston, MA,[11]Department of Pathology, Brigham and Women's Hospital and Harvard Medical School, Boston, MA

The immune microenvironment is a critical regulator of colorectal cancer (CRC) biology and represents a clinically targetable tumor feature in a subset of patients. T cells are one of the most common cell types in the CRC immune microenvironment and exist in a broad variety of subtypes and activation states. Proliferation status represents a general measure of T cell activity that is applicable to many subtypes. Evidence from other tumor types suggests that proliferating cytotoxic T cells may mediate adaptive immunity in cancer. However, T cell proliferation in CRC is incompletely characterized. To investigate the role of proliferating T cells in CRC, we developed a multiplexed immunofluorescence assay assessing CD3, CD4, CD8, FOXP3, PTPRC (CD45RA and CD45RO), MKI67 (Ki67), and KRT (cytokeratin) expression, and assessed 1,610 primary resected CRC specimens from four US/Canadian cohort studies. Digital imaging and pathologist-supervised machine learning were used to decompose image data into single-cell level information. The Kaplan-Meier method was used to describe CRC-specific survival (CSS) and multivariable Cox proportional hazards models were used to examine associations of proliferating and non-proliferating T cell densities with CSS. Multivariable ordinal logistic regression was used to adjust for confounding factors (age, cancer site, sex, and study batch) in analyses of T cell densities and tumor features. Across one million T cells, 4.5 % were classified as proliferating, as defined by positive MKI67 expression. While higher densities of both proliferating and non-proliferating T cells were positively associated with microsatellite instability (MSI), a CpG island methylator high phenotype, *BRAF* mutant status and *KRAS* wildtype status, these associations were stronger for proliferating T cells (e.g., adjusted odds ratio (OR) 2.09, CI 1.62-2.70, p<0.0001 for MSI and higher proliferative T cell density versus adjusted OR 1.40, CI 1.08-1.81, p=0.01 for MSI and higher non-proliferative T cell density). Higher proliferative and non-proliferative T cell densities were both positively associated with CSS (adjusted hazard ratio (HR) 0.75, CI 0.55-1.03, comparing highest versus lowest quartile of proliferative T cell densities (Ptrend=0.018) and adjusted HR 0.42, CI 0.31-0.57, comparing highest versus lowest quartile of non-proliferative T cell densities (Ptrend<0.001). Despite comprising a minor subset of total T cell infiltration in the CRC microenvironment, proliferative T cells are more strongly associated with specific molecular subtypes and are also associated with CSS. These results, across a large series of primary human tumors, suggest that proliferation marks a subset of functionally distinct subset of T cells in the CRC microenvironment.

#6572 Obesity shapes a reversible immune microenvironment that fosters breast cancer growth.

Tao Zhang[1], Shimeng Liu[1], Yi Zhang[2], Alva Yijia Jiang[1], Zachary Sandusky[1], Na Zhang[1], Tara Akhshi[1], Nicole Traphagen[1], Jack Yueyang Wang[1], Lucas Tian[1], Esme Wheeler[1], Yingtian Xie[1], Rong Li[1], Buraq Ahmed[1], Genevra Kuziel[1], Capucine Heraud[1], Mohammed Mutaher[1], Henry Long[1], Kornelia Polyak[1], Myles A. Brown[1]

[1]Dana-Farber Cancer Institute, Boston, MA,[2]Duke University, Durham, NC

Obesity is linked to breast cancer risk and severity, yet the underlying mechanisms remain unclear. Using single-cell RNA sequencing, we identified a role for C1q+ macrophages in mammary tumors and adipose tissues in mouse obesity and breast cancer models. Macrophage-derived C1q promotes the clearance of obesity-associated apoptotic adipocytes, enhancing lipid metabolism and leading to an immunosuppressive tumor microenvironment via the production of prostaglandin E2 (PGE2). Moreover, the tumor-associated macrophages (TAMs) engage tumor cells in a feedforward loop by inducing the production of monocyte-recruiting cytokines further suppressing the anti-tumor immune response. Blockade of C1q, TNF-α, and PGE2 synthesis reduced tumor growth in obese mice. Importantly, weight loss via dietary changes or glucagon-like peptide-1 receptor (GLP-1R) agonism decreased C1q expression and suppressed obesity-driven tumor growth. Interference with the immunosuppressive environment and the feedforward loop may be viable strategies for improving the outcomes of breast cancer patients with obesity.

#6573 Assessment of the T cell receptor repertoire in racially diverse prostate cancer patients.

Paula O. Cooper, Laila N. Scroggins, Sally Elsamanoudi, Amina Ali, Picabo Binette, Beatriz German Falcon, Leigh Ellis, Gregory T. Chesnut, Shyh-Han Tan, Cara C. Schafer

Surgery, Center for Prostate Disease Research, Bethesda, MD

Background: Prostate cancer (PCa), the second leading cause of cancer-related death for US men, gains limited benefits from immune therapies. Interestingly, African American (AA) men respond far better to Sipuleucel-T and undergo different T cell responses than Caucasian American (CA) PCa patients. Growing evidence suggests that variations in TCR diversity may serve as a biomarker for cancer progression and response to immune therapy; however, the extent of the TCR repertoire's contribution to PCa progression and disparate racial responses to treatment remains unclear, highlighting the need for further study.
Purpose: The rapid development of Next Generation Sequencing and single-cell transcriptomics provides a unique opportunity to examine the TCR repertoires of PCa patients in greater depth than previously possible. By examining TCR sequences in a racially diverse cohort from an equal-access Military Health System, we aim to identify how differences in AA and CA repertoires may contribute to variations in PCa initiation, progression, and response to therapy.
Methods: Bulk TCR-seq was performed on 25 AA and 30 CA treatment-naïve tumor biopsies to compare the percent of dominant and unique TCRs (D50) from each sample. Next, peripheral blood lymphocytes (PBLs) were isolated from 4 AA and 4 CA men undergoing radical prostatectomy for diagnosed PCa with no prior treatment, matched for age, Gleason score, and PSA. 10X Genomics V(D)J and GEX technologies were used to produce libraries of individual cell TCRs and transcriptomes. These were compared using previously described bioinformatics pipelines and may be assessed for co-expression of activation, exhaustion, and anergy markers.
Results: TCR-seq revealed significantly higher D50 scores in CA than AA tumors. We also found that men that developed biochemical recurrence and metastasis had significantly higher D50s than those that did not. Single cell V(D)J and RNA seq identified key differences in the TCR sequences of PBLs isolated from AA and CA PCa patients.
Conclusions/future directions: These data may be used to help guide therapeutic options based on predicted responsiveness of an individual. The V(D)J data will be used as a reference set to generate a panel for 10X Genomics Xenium. This will provide spatial data to examine the distribution of identified TCR clones in PCa tumor biopsies.
Disclaimer: The contents of this publication are the sole responsibility of the authors and do not necessarily reflect the views, opinions, or policies opinions of the USUHS, HJF, the DoW or the Departments of the Army, Navy, or Air Force. Mention of trade names, commercial products, or organizations does not imply endorsement by the U.S. Government.

#6574 NK cell therapy enhances the efficacy of CDK4/6i in breast cancer.

Yinchong Wang, Evdokiya Reshetnikova, Nar Bahadur Katuwal, Anna Vilgelm

Ohio State University, Columbus, OH

Cyclin-dependent kinase 4/6 inhibitors (CDK4/6i) are routinely used for patients with estrogen receptor-positive metastatic breast cancer. Abemaciclib is a CDK4/6 inhibitor that blocks cancer cell proliferation by preventing progression through the cell cycle. However, these drugs primarily inhibit cancer cell growth and do not typically induce complete tumor elimination. Combining CDK4/6i with a synergistic therapeutic modality could enable regression of metastatic breast cancer tumors and dramatically improve patients' outcomes. Adoptive cell therapy is a type of cancer therapy where effector immune cells, such as T and NK cells, are transferred into the patient's body to eliminate malignant cells. We found that CDK4/6i-treated tumor cells secrete NK cell-attracting chemokines and express stress ligands on their surface, which are known to trigger NK cell cytotoxic activity. This indicates that pre-CDK4/6i treatment increases tumor vulnerability to NK cells. Therefore, we hypothesized that CDK4/6i efficacy could be improved by combining it with NK cell therapy, resulting in the elimination of tumor cells.

Methods: We used human MCF7 and mouse PYMT-B6 cell line to evaluate the effect of CDK4/6 inhibition on chemokine production in tumors and NK cell migration toward the tumor. We used spectral cytometry to test the surface expression of NK cell-activating stress ligands on breast cancer cells and patient-derived organoids (PDO). PDOs were co-cultured with NK cells to investigate patient-to-patient differences in CDK4/6 inhibitor-mediated NK cell recruitment and tumor recognition. We performed patient-derived xenograft (PDX) implantation in huIL-15 mouse to test Abema and NK combination treatment *in vivo*.

Results and conclusions: We found that abemaciclib induced the expression of NK cell-attracting chemokines, including CCL5 and CXCL10, by tumor cells. We also found that therapeutic NK cells expressed the corresponding chemokine receptors, suggesting enhanced chemotactic potential. Pre-treatment of tumor cells with abemaciclib significantly increased the expression of stress ligands on the surface of breast cancer cells and PDOs. This stress ligands are recognized by NKG2D receptors on the NK cells that trigger their cytotoxicity. In NK&PDO co-culture assay, pre-treatment with CDK4/6i promoted the killing and infiltration of human NK cells to PDOs. Additionally, NK cells co-cultured with pre-treated tumor cells displaced activated functional phenotype with increased cytotoxicity and cytokine secretion. We conducted patient-derived xenograft (PDX) implantation in mice and observed slower tumor growth and improved survival following treatment with CDK4/6 inhibitors and NK cell infusion.

Significance: This research can provide a pre-clinical basis for the further development of CDK4/6i and immunotherapy combinations that could improve the outcomes of metastatic breast cancer treatment.

#6575 Investigating the role of glucocorticoid-induced leucine zipper (GILZ) in triple-negative breast cancer.

Devyn Aniya Hill[1], Jennifer B. Jacob[2]

[1]Michigan State University, East Lansing, MI,[2]Wayne State University School of Medicine, East Lansing, MI

Breast cancer is one of the leading causes of death for American women, with 1 in 8 expected to develop the disease in their lifetime. Breast cancers that lack the expression of hormone receptors (estrogen/progesterone) and the HER2 receptor are known as triple negative breast cancer (TNBC). TNBC accounts for about 15-20% of all breast cancer cases in American women, and is commonly characterized by a complex tumor microenvironment that often exhibits increased inflammation and immune suppression. This makes TNBC resistant to many treatments, resulting in an overall lower five-year survival rate than other breast cancer subtypes.Evidence found in our lab demonstrates that the gene TSC22D3 is correlated with longer survival in patients with TNBC. TSC22D3 encodes the immunomodulatory protein Glucocorticoid-Induced Leucine Zipper (GILZ). GILZ expression is induced by glucocorticoid binding to hormone response elements in the nucleus and is thought to be one of the first transcripts synthesized after GR activation. GILZ is known to directly inhibit inflammation and cell proliferation by preventing downstream phosphorylation or activation events of enzymes such as mitogen-activated protein kinases (MAPKs), and proteins like rat sarcoma protein (Ras) and hypoxia inducible factor 1 alpha (HIF1a) to suppress inflammatory signaling.While the function and effects of the GILZ protein have been previously studied in many systems including the renal system, central nervous system and digestive system, its expression and effects have not been explicitly observed in breast cancer studies. Furthermore, the mechanism by which GILZ inhibits inflammation is variable with oxygen availability and the biological reason for this also remains unknown. The goal of this project is to 1) identify a potential chemical compound to modulate GILZ expression to better observe the activity in vitro and, 2) investigate key protein-protein interactions that influence GILZ action in variable oxygen availability states in TNBC cells. This work seeks to explore and clarify the specific immunomodulatory effects of GILZ in adaptable tumor microenvironments by investigating existing compounds that can reduce or overexpress GILZ protein levels and examining potential biased protein binding across different environments. All told, characterizing the activity and role of GILZ in varying conditions will potentially lead to the development of targeted therapeutic treatment for inflammation-driven diseases such as triple negative breast cancer.

#6576 Integrative spatial transcriptomics reveals EMT-driven immune regulatory programs underlying metastasis in HNSCC.

Chih-Hung Chung, Han-Hsun Yu, Muh-Hwa Yang

National Yang Ming Chiao Tung University, Taipei, Taiwan

Head and neck squamous cell carcinoma (HNSCC) is a globally prevalent malignancy. Standard treatment typically involves surgical resection, radiotherapy, and chemotherapy. However, for patients with recurrent or distantly metastatic disease for whom surgery or radiation is no longer feasible, systemic therapy consisting of targeted agents combined with chemotherapy or immune checkpoint inhibitors (ICI) becomes the mainstay of management. Despite these advances, clinical outcomes remain suboptimal, underscoring the urgent need to elucidate how immune cell composition and functional states are altered within the tumor microenvironment (TME) of aggressive or metastatic tumors. Such insights are essential for improving the therapeutic effectiveness of ICIs in HNSCC. The objective of this study was to characterize TME compositional changes across diverse HNSCC specimens. We employed the GeoMx Digital Spatial Profiler (DSP) to perform high-resolution, imaging-guided spatial transcriptomic profiling. By comparing EMT-related gene signatures enriched at the invasive tumor front, we identified significant upregulation of canonical EMT markers—including FN1, CD44, and ITGB1. To further dissect the regulatory programs associated with ITGB1-high tumor cells, we applied Single-Cell Regulatory Network Inference and Clustering (SCENIC), which revealed distinct regulon activities. Notably, IRF-associated signaling emerged as a major downstream regulatory pathway in ITGB1-high EMT tumor populations. Subsequently, we analyzed HNSCC tissues using integrative spatial-omics (10x Visium and 10x Xenium) approaches and identified a clear transcriptional trajectory of tumor EMT states. To directly assess how EMT-high tumor cells modulate surrounding immune cells, we performed NicheNet ligand-receptor analysis, which revealed pronounced alterations in ligand-receptor interactions shaping the immune landscape of malignant HNSCC. Collectively, these findings provide mechanistic insights into EMT-driven immune suppression and highlight actionable TME features that could guide personalized therapeutic strategies for patients with head and neck cancer.

#6577 A potential role of NRF-2, MDR-1, and TET-2 in inflammatory bowel disease and colorectal carcinoma: An *in vitro* study.

Jessica Saliba[1], Ali Amhaz[2], Batoul Moussa[3], Souraya Ismail[3], Abdullah Shaito[4], Marwan El-Sabban[5]

[1]Department of Public Health, Faculty of Health Sciences, University of Balamand, Beirut, Lebanon,[2]Department of Medical Laboratory Sciences, Faculty of Health Sciences, University of Balamand, Beirut, Lebanon,[3]Department of Biology, Faculty of Sciences, Lebanese University, Beirut, Lebanon,[4]Biomedical Research Center and Biomedical Sciences, Qatar University, Doha, Qatar,[5]Department of Anatomy, Cell Biology and Physiological Sciences, Faculty of Medicine, American University of Beirut, Beirut, Lebanon

Study purpose: Inflammatory Bowel Disease (IBD) is partly attributed to cytokine storm and infiltrating immune cells. As part of the cell defensive mechanisms, a transcription factor called nuclear factor erythroid 2-related factor 2 (NRF-2) activates genes encoding antioxidant enzymes. Additionally, NRF-2 has recently emerged as an important contributor to chemo-resistance in colon neoplasms, by upregulating multi-drug resistant protein 1 (MDR-1). In addition, epigenetic factors have been shown to influence the onset of IBD and of colorectal cancer. One of these epigenetic factors is the interplay between DNA methylation status. A DNA demethylating enzyme, coded by the ten-to-eleven translocation 2 [tet2], yields the methylcytosine dioxygenase TET-2. Recent studies have demonstrated a potential association between TET-2 and NRF-2 in IBD-associated colon cancer. This study aims to understand the alteration in the expression and activity of these markers under inflammatory conditions.
Experimental procedures: NRF-2, MDR-1, and TET-2 expression level was evaluated in parental HT-29 cells and in HT-29 cells downregulated for TET-2 (HT-29shTET-2) and exposed to an inflammatory milieu; at the transcriptional level by quantitative real-time polymerase chain reaction (qPCR). Markers of the epithelial-to-mesenchymal transition (EMT, E-cadherin and N-cadherin) were also evaluated by qPCR and Western blotting.
Summary of results: Under inflammatory conditions, NRF-2, MDR-1, and TET-2 expression levels increased. However, NRF-2 and MDR-1 expression levels were downregulated in HT-29shTET-2 cells. Interestingly, N-cadherin levels were higher in HT-29shTET-2 exposed to inflammatory media compared to parental HT-29.
Conclusions: NRF-2 and MDR-1 expression levels increase upon exposure of HT-29 cells to inflammation. On the other hand, their expression is downregulated when TET-2 is downregulated, suggesting a potential demethylating role of TET-2 in activating NRF-2 and MDR-1 gene expression.

#6578 Heat shock protein inhibitors suppress cytokine-induced DUOX2 mRNA and protein expression in human pancreatic cancer cells in a JAK, STAT dependent manner.

Yongzhong Wu[1], David J. Mallick[2], Allan Di[2], Smitha Antony[2], Jennifer Meitzler[1], Mariam M. Konate[2], Becky Diebold[1], Krishnendu Roy[2], James H. Doroshow[1]

[1]DTB, National Cancer Institute, Bethesda, MD,[2]Department of Cancer Treatment and Diagnosis, National Cancer Institute, Bethesda, MD

Dual oxidase 2 (DUOX2), one of the seven NADPH oxidases family members, plays a critical role in both host defense and chronic inflammation-associated cancer in the gastrointestinal system. In vitro, pro-inflammatory cytokines, such as IFN- y, IFNα/β, IL-4 and IL-17A, enhance DUOX2/DUOXA2 expression through activation of STATs and NF-kB signaling pathway proteins; in vivo, DUOX protein and mRNA levels are substantially upregulated in chronic pancreatitis, pre-malignant pancreatic intraepithelial neoplasms and the early stages of pancreatic cancer patients compared to histologically normal pancreatic tissues. In pancreatic adenocarcinoma, increased DUOX2 expression is adversely correlated with overall patient survival. Heat-Shock Protein 90 (Hsp90), an important molecular chaperone involved in tumorigenesis, invasion and metastasis of cancer cells, is critical in folding, maturation and stability of many oncogenic client proteins, including kinases such as AKT and JAK1/2, and transcription factors, such as STAT3 and HIF-1α. Several STAT family members, along with Hsp90, are overexpressed in human pancreatic carcinomas. Using a panel of human pancreatic cancer cell lines (BxPC-3, AsPC-1 and CFPAC-1), we found that two different Hsp90 inhibitors, Tanespimycin (17-AAG) and Ganetespib (STA-9090), inhibit JAK1 and JAK2 kinases, blocking cytokine-induced, JAK-regulated STAT phosphorylation. Additionally, these Hsp90 inhibitors suppress cytokine-induced DUOX2, VEGF-A, MMP-7 and PD-L1 expression in human pancreatic cancer cell lines with varying sensitivity. Furthermore, the JAK1/2 inhibitor Ruxolitinib inhibits IL-4 induced and JAK-mediated STAT6 phosphorylation, and DUOX2 mRNA and protein expression in BxPC-3 cells. Similar results were observed with JAK1, STAT1, 2 and STAT6 specific siRNA knockdown. However, simultaneous knockdown of both isoforms of Hsp90, Hsp90α and Hsp90β, with specific siRNA did not inhibit JAK1 activity, cytokine-induced DUOX2 mRNA or protein expression. Either remaining Hsp90 protein or other isoforms of Hsp90 in cells may compensate decreased Hsp90 function after siRNA knockdown. Our data suggests that Hsp90 inhibitors, through blocking the cytokine-activated JAK-STATs oncogenic signaling pathway and their downstream genes such as DUOX2, VEGF-A, MMP-7 and PD-L1expression, may be a valuable therapeutic approach for inflammation-associated pancreatic cancer.

#6579 Investigating the role of signal peptide peptidase in tumor immune evasion via Qa-1-mediated peptide presentation.

Roya Solhi[1], Clara Wolfe[2], Hu Chen[1], Achintya Perumal[1], Kyle Ockerman[2], Grant Brennan[1], Jiayao Ye[1], Adrienne H. Long[2], Marc Schwartz[2], Susan Klaeger[2], Steven A. Carr[2], Thorbald van Hall[3], Jon A. Weidanz[4], Soroush Ghaffari[4], Kathleen B. Yates[2], Robert T. Manguso[2], Qin Ma[1], **Hakimeh Ebrahimi-Nik**[1]

[1]The Ohio State University, Columbus, OH,[2]Broad Institute of MIT and Harvard, Cambridge, MA,[3]Leiden University Medical Center, Leiden, Netherlands,[4]The University of Texas at Arlington, Arlington, TX

Canonical leader peptides, derived from the signal sequences of classical MHC class I molecules, are presented by HLA-E in humans and Qa1 in mice. These peptides serve as ligands for the NKG2A/CD94 receptor complex on NK cells and $CD8^+$ T cells, promoting immune homeostasis. Disruptions of this inhibitory axis—such as during viral infection—can lead to the display of novel peptides that override this inhibition and activate immune responses. However, the mechanisms controlling canonical peptide presentation remain unclear. To better understand how Qa1-restricted inhibitory peptide presentation is regulated, we targeted Signal Peptide Peptidase (SPP), an ER-resident protease that cleaves signal peptides. SPP was knocked out in two tumor models: YUMMER melanoma and KPC pancreatic adenocarcinoma. Changes in Qa1-bound peptides were evaluated using mass spectrometry, and tumor growth was assessed in vivo. Loss of SPP markedly reduced canonical peptide loading in both tumor models. SPP-deficient melanoma tumors were strongly rejected in vivo, while pancreatic tumors lacking SPP showed no such reduction, despite similar decreases in canonical inhibitory peptide levels. Interestingly, the dominant Qa1-bound peptide in both models remained the canonical peptide, indicating that alternative, SPP-independent mechanisms can liberate and generate this peptide for presentation. In the KPC model, novel peptides with potential inhibitory properties were identified. Ongoing studies aim to determine whether these peptides can sustain immune suppression in the absence of the canonical peptide. Our findings demonstrated that even in the absence of SPP, alternative mechanisms maintain inhibitory peptide presentation in tumor cells. Ongoing studies targeting other SPP family members and newly identified candidate inhibitory peptides aim to elucidate these compensatory pathways. A clearer definition of the Qa1/HLA-E inhibitory pathway will help determine whether this axis can be more effectively disrupted to improve anti-tumor immune responses.

#6580 A novel regulator of T-cell motility: Fhl2 controls CD8⁺ T-cell migration and infiltration.

Achintya Perumal[1], Grant Brennan[1], Jiayao Ye[1], Hu Chen[1], Roya Solhi[1], Omar I. Avila[2], Kathleen B. Yates[2], Robert T. Manguso[2], Stanley C. Huang[1], Haoxin Zhao[1], Giovanni Nigita[1], Zihai Li[1], No-Joon Song[1], Hazem E. Ghoneim[1], Ava Lowin[1], Kelley Ptak[1], Qin Ma[1], **Hakimeh Ebrahimi-Nik**[1]

[1]The Ohio State University, Columbus, OH,[2]Broad Institute of MIT and Harvard, Cambridge, MA

For tumor immunotherapy to succeed, CD8⁺ T cells must efficiently migrate into tumor sites, yet the molecular pathways controlling this critical step of T-cell trafficking remain only partially understood. Using a novel reverse-engineered strategy—starting from antigen-experienced CD8⁺ T cells that either robustly rejected tumors in vivo or completely failed to do so despite comparable functional profiles—we identified Fhl2 (Four-and-a-half LIM domains 2) as a novel positive regulator of T-cell migration and infiltration, consistent with its role as a LIM-domain adaptor protein that integrates cytoskeletal and signaling inputs. Fhl2-deficient CD8⁺ T cells exhibited reduced migratory capacity, accompanied by impaired cytoskeletal remodeling and CXCR3-mediated chemotaxis. High-resolution confocal microscopy revealed that Fhl2-wild-type CD8⁺ T cells formed significantly more dendrite protrusions than knockout counterparts, consistent with enhanced motility. These findings were further supported by RNA-seq and Functional Proteomics Reverse Phase Protein Array (RPPA) analyses: RNA-seq revealed higher expression of several chemokine receptors in Fhl2-wild-type cells, including CXCR3 and CXCR6, while RPPA showed positive enrichment of multiple cell-migration-associated pathways in wild-type cells compared to the knockout. Importantly, transwell chemotaxis assays demonstrated that Fhl2-wild-type CD8⁺ T cells exhibit superior chemokine-driven migration compared with Fhl2-deficient cells—both in polyclonally activated populations and in SIINFEKL-stimulated OT-I cells. This enhanced migratory capacity of Fhl2-wild-type CD8⁺ T cells was also reflected in vivo. Collectively, these results establish Fhl2 as a key orchestrator of CD8⁺ T-cell motility and reveal a previously unappreciated molecular pathway that could be harnessed to improve tumor immune surveillance and T-cell-based therapies.

#6581 Reprogramming microglial and GAMs phenotype and function, with HDAC inhibitors to overcome immune suppression in glioblastoma.

Sonia Sebaoui

Georgetown Lombardi Comprehensive Cancer Ctr., Washington DC, DC

Glioblastoma multiforme (GBM) stands as the most aggressive form of primary tumor in the central nervous system, primarily affecting older male individuals. The immune landscape in GBM is significantly influenced by Glioma-associated microglia and infiltrating macrophages (GAMs), which together account for up to 45% of the tumor mass. These cells are highly plastic and can shift their phenotype between tumor-fighting, pro-inflammatory (M1-like) and tumor-supportive, anti-inflammatory (M2-like) states in response to different environmental cues. Epigenetic regulation of this plasticity has emerged as a promising therapeutic strategy to reprogram innate immunity within the TME. Here, we demonstrated that selective class IIb HDAC inhibitor treatment reprograms primarily macrophages and microglia toward a pro-inflammatory, phagocytic, and tumor-killing state. Using the BV2 microglial cell line and bone marrow-derived macrophages, we found that HDAC class IIb inhibitors increased M1 markers, decreased M2 phenotype, and enhanced phagocytosis. Interestingly, they enhanced microglial migration in both M1-like and M2-like cells, potentially reflecting the innate migratory capacity of these resident immune cells in the brain, which are constantly surveilling and rapidly responding to environmental cues. In contrast, these class IIb inhibitors reduced macrophage migration, underscoring the functional divergence between these cell types. To further validate our findings in a physiologically relevant system, we optimized a robust high-purity primary microglia isolation protocol from murine brains. Future work includes transcriptomic profiling and in vivo studies to assess therapeutic efficacy and immune remodeling. Our results support HDAC class IIb inhibition as a promising strategy to modulate immune responses in GBM and suggest that targeting myeloid cell plasticity may enhance the efficacy of immunotherapeutic responses in GBM.

#6582 Cell surface plectin as a master regulator of tumor-immune interactions in pancreatic cancer.

Cody L. Wolf[1], Roxanne K. Ruiz[2], Sokchea Khou[3], Robert Cornelison[4], Edward Stelow[4], Karl M. Kowalewski[5], Matthew J. Lazzara[1], Amanda Poissonnier[6], Timothy N. J. Bullock[4], Lisa M. Coussens[6], Kimberly A. Kelly[1]

[1]Department of Biomedical Engineering, University of Virginia, Charlottesville, VA,[2]Department of Molecular Physiology and Biological Physics, University of Virginia, Charlottesville, VA,[3]OHSU Knight Cancer Institute, Portland, OR,[4]Department of Experimental Pathology, University of Virginia, Charlottesville, VA,[5]Department of Chemical Engineering, University of Virginia, Charlottesville, VA,[6]Department of Cell, Developmental, & Cancer Biology, OHSU Knight Cancer Institute, Lake Oswego, OR

Pancreatic ductal adenocarcinoma (PDAC) is the third deadliest cancer in the United States, with a five-year survival rate of only 13%, and is projected to become the second leading cause of cancer-related mortality by 2030. Despite advances in personalized medicine, therapeutic options for PDAC remain extremely limited, underscoring the need for new, clinically actionable targets. In 2008, *Kelly et al.* utilized a phage-display-based functional proteomics platform that identified plectin, a cytolinker protein normally restricted to the cytoplasm, as aberrantly mislocalized to the plasma membrane of PDAC cells. This cell-surface form of plectin (CSP) has since been detected across multiple malignancies, including PDAC, ovarian carcinoma, and cholangiocarcinoma, while remaining cytoplasmic in normal tissues. Functional studies using an anti-CSP monoclonal antibody (mAb) revealed that CSP supports pro-tumorigenic behaviors such as proliferation, migration, and invasion. A recent early-phase clinical trial (NCT05074472) evaluating an anti-CSP mAb in CSP-positive cancers demonstrated that CSP-targeted therapy is both safe and clinically feasible. To further resolve the molecular and immunologic roles of CSP, we analyzed transcriptomic data from human PDAC bulk and single-cell RNA-sequencing datasets. CSP-high tumors exhibited suppression of pro-inflammatory immune pathways and reduced infiltration of cytotoxic immune populations—hallmarks of the immune-cold PDAC microenvironment. Anti-CSP mAb treatment in vivo promoted infiltration of $CD4^+$ and $CD8^+$ T cells, reduced tumor burden, and generated a durable effector-memory response capable of preventing tumor re-challenge. Collectively, these findings provide the first direct evidence that CSP functions as an immune suppressor in PDAC. Moreover, therapeutic blockade of CSP can restore anti-tumor immunity in this notoriously immunoresistant cancer, offering a promising avenue for personalized treatment strategies for patients with historically few effective options.

#6583 Genetic characterization of KLRC2 deletion in racially diverse prostate cancer patients.

Laila Scroggins, Paula O. Cooper, Stefan DiFazio, Kun-Lin Ho, Sally Elsamanoudi, Jiji Jiang, Shyh-Han Tan, Ayesha A. Shafi, Cara C. Schafer

Surgery, Center for Prostate Disease Research, Bethesda, MD

Natural Killer (NK) cells are key mediators of anti-tumor immunity through direct tumor cell lysis. Emerging evidence suggests significant immune microenvironment differences in prostate tumors between African American (AA) and Caucasian American (CA) men; however, the contribution of NK cell-associated genes to these disparities remains incompletely understood. The NK cell receptor gene *KLRC2* is of particular interest because prior research within our patient cohort demonstrated significantly lower *KLRC2* expression in AA prostate tumors compared to CA tumors. Given that germline *KLRC2* deletion polymorphisms differ across global populations, including those with East and West African ancestry, investigating its deletion status may provide insight into downstream expression differences and associated immune variation. This study aims to gain a deeper understanding of immunobiological differences between AA and CA men with prostate cancer (PCa) by evaluating an NK cell-relevant gene, *KLRC2*, in racially diverse genomic datasets. We hypothesized that germline deletion may contribute to its variability in downstream expression in tumor tissues and ultimately contribute to observed racial disparities in PCa. Understanding germline deletion variations may provide insight into mechanisms driving tumor immune microenvironment differences and strategies to reduce these disparities in PCa outcomes. We analyzed germline, whole genome sequencing data from a large Center for Prostate Disease Research (CPDR) cohort including African American (AA, n=259) and Caucasian American (CA, n=272) men. Bioinformatics workflows were applied to accurately infer *KLRC2* deletion status, including copy-number calling and quality control filtering. We identified a significant difference in the heterozygous deletion status of *KLRC2* between AA and CA men in this robust CPDR cohort. These findings suggest population-level variation in *KLRC2* copy number that may account for reduced KLRC2 expression previously observed in AA prostate tumors. Germline *KLRC2* deletions may influence NK cell-mediated activity within the prostate tumor microenvironment, particularly among African America men. Our findings provide foundational evidence that *KLRC2* status may play a role in racial immune disparities. These findings place *KLRC2* as a promising biomarker and potential candidate for NK cell-based immunotherapeutic strategies.

#6584 Spatial mapping and significance of IL12 signaling in non-small cell lung cancer.

Juan Guiza[1], Lucy Zheng[1], Barani Kumar Rajendran[1], Luciene Borges[2], Sandra Martinez-Morilla[2], Jillian M. Prendergast[2], Reniqua House[2], Kurt A. Schalper[1]

[1]Yale University, New Haven, CT,[2]Boehringer Ingelheim, Ridgefield, CT

Background: Immunostimulatory therapies targeting T-cell co-inhibitory receptors have transformed the management of patients with non-small cell lung cancer (NSCLC) and revealed the potential of harnessing adaptive immunity to treat aggressive malignancy. However, only ~20-30% of patients with advanced NSCLC show clinical benefit to such therapies, highlighting the need for additional developments. Activation of IL-12 signaling in the tumor microenvironment (TME) induces prominent immunostimulatory responses and anti-tumor effect in pre-clinical models and early clinical trials. Understanding the expression, biological role and clinical significance of the IL-12 pathway in human NSCLC could be used to support optimal therapeutic developments.
Strategy: We established multiplexed quantitative immunofluorescence (mQIF) panels to measure and spatially map the IL-12 pathway (DAPI/CK/IL12Rβ1/pSTAT4/CD8), major tumor associated macrophage subpopulations (TAMs; DAPI/CK/CD14/CD68/CD206), dendritic cells (DCs; DAPI/CK/CD11c/XCR1/HLADR) and tumor-infiltrating lymphocytes (TILs; DAPI/CK/CD8/CD4/CD20) in consecutive sections from >600 primary NSCLCs from 4 independent cohorts represented in tissue microarrays. Western blot analysis and flow cytometry from cultured cell preparations of PC-9 human lung adenocarcinoma cell line stimulated for 48 hours with human recombinant IL-12 or IL-23 were used to assess functional responses and support analytical assay validations.
Results: Membranous IL12Rβ1 expression was seen in >95% of primary NSCLCs (mean 1519 ± 83.22 cell/mm^2), with continuous distribution across cases, predominant location in the (intratumoral) stromal compartment and association with pSTAT4 expression and adenocarcinoma histology. No consistent association was seen with other clinicopathologic variables, major oncogenic driver mutations and 5-year overall survival. Elevated abundance of IL12Rβ1/pSTAT4 expressing cells was consistently associated with higher density of M2/3-like polarized TAMs, DCs and CD4+, CD8+ and CD20+ TILs. Notably, 13.2-29.2% of NSCLCs across the cohorts showed IL12Rβ1 expression in cancer cells associated with increased pSTAT4 and reduced expression of pancytokeratin. Treatment of IL12Rβ1+ lung adenocarcinoma cells with human recombinant IL-12 or IL-23 reduced the levels of the epithelial marker EpCAM and increased Ki-67. Supporting enhanced proliferation.
Conclusions: IL-12 pathway expression and activation occurs in most primary NSCLCs with variable levels and is associated with adenocarcinoma histology and a favorable immune TME composition. IL12Rβ1 is expressed in cancer cells from ~23% of tumors and associated with enhanced oncogenic properties, supporting a dual role in immune evasion and malignant progression. These results can support optimal development of IL-12 directed therapies and patient selection strategies.

#6585 DUOX2 is finely tuned by synergism between cytokines IL-6, IL-22, IL-17A, and TNFα in colon cancer.

Becky A. Diebold[1], Agnes Juhasz[1], Mariam M. Konate[2], Jiamo Lu[1], Guojian Jiang[1], Jennifer L. Meitzler[1], Yongzhong Wu[1], Smitha Antony[2], David J. Mallick[2], Krishnendu K. Roy[2], James H. Doroshow[2]

[1]NCI Developmental Therapeutics Branch, Bethesda, MD,[2]NCI Division of Cancer Treatment and Diagnosis, Bethesda, MD

Gastrointestinal inflammation is associated with an increased risk for colorectal cancer (CRC) and is associated with elevated expression of NADPH oxidase (NOX) isoforms, NOX1 and DUOX2, which catalyze the synthesis of superoxide anion radical ($O_2^{\cdot-}$) and hydrogen peroxide (H_2O_2), respectively. To explore the mechanisms that regulate DUOX2, we investigated the effects of a combination of IL-6 and IL-17A on DUOX2 expression in CRC patient-derived cells (PDC) (T-280R, F725, F1126) vs. normal colon cell lines (CCD-112, CCD-841, CCD-18). DUOX2 mRNA levels were generally higher across CRC PDCs relative to the normal colon cell lines. Treatment of PDCs with IL-6 plus IL-17A for 4-6 days resulted in significant upregulation of DUOX2 mRNA and protein. This agrees with data demonstrating elevated DUOX2 levels in CRC tumors relative to corresponding non-malignant tissues. Treatment of HT-29 and Ls513 colon cancer cell lines with IL-6 plus IL-17A for 8-15 days yielded greater-than-additive increases in DUOX2 mRNA, protein, and DUOX2-dependent H_2O_2 production as measured by Amplex Red assays. RNA-Seq analysis of cytokine-treated HT-29 cells indicated that STAT3 and NFkB signaling pathways mediated the IL-6/IL-17A-induced DUOX2 expression. We also investigated the regulation of DUOX2 using a triple-cytokine cocktail of IL-6, IL-17A, and TNFα. The inclusion of TNFα increased the expression of DUOX2 50-fold more than treatment with IL-6 plus IL-17A in HT29 cells, and even more in LS513 cells. There were also substantial increases in DUOX2 activity. In addition, the triple-cytokine treatment shortened the time course of mRNA and protein expression from several days to 24-48 h. When IL-22 was substituted for IL-6 in the triple-cytokine treatment, the fold-increase was even greater. The STAT3 pathway was activated by IL-6 or IL-22, and the NFkB pathway was activated by IL-17A and TNFα in these cell lines. Silencing of STAT3 or RELA by siRNA nearly abolished DUOX2 expression. The triple-cytokine treatments could also induce cell death within 48-72 h, as well as DNA damage as evidenced by phosphorylation of γ-H2AX. In summary, DUOX2 expression and DUOX2-dependent H_2O_2 production in HT-29 and LS513 cells and PDCs could be finely tuned by synergism amongst several pro-inflammatory cytokines known to be overexpressed in CRC.

#6586 CCL3+ tumor cells orchestrate immune equilibrium and stemness maintenance in ESCC via IDE+ M2 macrophages and CCR3+ CAFs.

Beilei Liu[1], Licheng Tan[2], Jiayi Huang[2], Bowen Yao[2], Shuang Zhang[3], Mengsu Yang[4], Xin-Yuan Guan[5]

[1]City University of Hong Kong, Hong Kong, China,[2]the university of hong kong, the department of clinical oncology, China,[3]University of Hong Kong, Shenzhen Hospital, Shenzhen Shi, China,[4]city university of hong kong, BMS, China,[5]The University of Hong Kong, Hong Kong

Immune regulation plays a crucial role in tumor occurrence and development, yet the underlying mechanisms remain largely unclear. By constructing a mouse model to track tumor immune status and utilizing single-cell sequencing technology to dissect the interactions between tumor cells and the tumor microenvironment at different stages, we found that ESCC tumor progression undergoes four key phases: ① immune recognition phase (enhanced CXCL10/H2-K1 antigen presentation signaling); ② immune equilibrium phase (enrichment of PD-1 T cells/CD44 dormant tumor cells); ③ immune escape phase (proliferation of PD-L1+ EMT tumor cells); ④ immune suppression phase (dominated by M2 TAMs/Tregs). Cell communication analysis revealed that intercellular interactions in the tumor primarily occur among tumor cells, macrophages, fibroblasts, and T cells, with tumor cells serving as the core regulatory factor. Further GO analysis of tumor cell subtypes showed enrichment in keratin-reinforced type (Cnfn+), enhanced autophagy type (Plk5+), immunosuppressive type (Ccl3+), and metastasis-enhanced type (Krt8+). Among them, Ccl3+ tumor cells are highly enriched in the immune equilibrium phase and interact with Ide M2 macrophages and Ccr3+ CAFs. In vitro co-culture studies confirmed that tumor cells overexpressing Ccl3 can regulate macrophage polarization toward M2 and promote T cell exhaustion; however, these functions no longer change after knocking down the Ide gene in macrophages. On the other hand, when tumor cells overexpressing Ccl3 are co-cultured with Ccr3-knockout CAFs and control CAFs, the control group significantly enhances the stemness of Ccl3+ tumor cells. These studies confirm that Ccl3+ tumor cells remodel the tumor microenvironment through Ide M2 macrophages and Ccr3+ fibroblasts, thereby regulating stemness and surviving in the immune equilibrium phase. In vivo, neutralizing antibodies targeting Ccl3 effectively inhibit subcutaneous tumor formation and enhance immune effects. This study reveals the key regulatory role of Ccl3 in the immune evolution of ESCC tumors, providing an important molecular basis and potential clinical strategies for overcoming immunotherapy resistance and developing novel targeted therapies.

#6587 Characterizing the autoreactome in thymoma-associated myasthenia gravis.

Rohan Maniar[1], Taylor Bauman[2], Patricia Sikorski[2], Karli Gilbert[3], Patrick J. Loehrer[1], Henry Kaminski[2], Linda Kusner[2]

[1]Indiana University Simon Comprehensive Cancer Center, Indianapolis, IN,[2]George Washington University, Washington DC, DC,[3]George Washington Universtiy, Washington DC, DC

Thymic epithelial tumors (TETs), including thymomas (TMMs), are rare anterior mediastinal malignancies arising from the thymus, an organ essential for early-life T-cell maturation. Paraneoplastic autoimmune disorders (ADs) frequently accompany TMMs, likely due to the tumor's retained, but dysregulated capacity for T-cell processing, leading to defective negative selection and emergence of autoreactive T cells. Myasthenia gravis (MG) occurs in approximately 30-50% of patients with TMM, and nearly all individuals with TMM-associated MG (TAMG) harbor acetylcholine receptor (AChR) antibodies, often accompanied by reactivity against additional skeletal muscle proteins such as titin and ryanodine receptors. Although TAMG is characterized by a complex network of autoreactive immune elements, the breadth and functional relevance of associated autoantibodies remain poorly understood. We hypothesized that TAMG patients exhibit greater diversity of circulating autoantibodies compared with non-autoimmune controls.

Using biospecimens from the Indiana University Simon Comprehensive Cancer Center and the George Washington University Myasthenia Gravis Research Laboratory, we performed autoreactome profiling of sera from TAMG patients and age-matched healthy controls. Samples were interrogated using Molecular Indexing of Proteins by Self-Assembly (MIPSA; Infinity Bio), a high-throughput DNA-barcoded antigen display platform. The screening encompassed >16,000 full-length proteins and ~400,000 peptide sequences.

Autoreactome analysis was completed for 40 TAMG patients and 14 controls. The TAMG cohort had a mean age of 58.7 years; 22 (55%) were female. Twenty-six (65%) patients were AChR-antibody positive, none had MuSK antibodies, one (2.5%) was seronegative, and 13 (32.5%) had unknown serologic status. WHO TET subtypes included A (2.5%), AB (15%), B1 (12.5%), B2 (40%), B3 (20%), metaplastic (2.5%), and unknown (7.5%). Overall, 4,724 proteins and 6,553 peptides were identified as autoantibody targets, with 2,688 proteins and 4,890 peptides uniquely enriched in TAMG. Although TAMG patients demonstrated a higher number of unique autoantibodies than controls, this difference did not reach statistical significance. Notably, interferon-alpha (IFN-α) autoreactivity was observed in 23 (57.5%) TAMG subjects, including 14 with corresponding IFN-α peptide reactivity. Among 20 patients with IFN-α antibodies, we identified novel reactivity against P2X4 receptor and TRIM46, proteins implicated in immune regulation and neuromuscular signaling. These findings suggest a broader and previously unrecognized autoantibody landscape in TAMG. Ongoing studies will evaluate the specificity of these signatures, incorporate TMM patients without MG, and correlate autoreactive patterns with MG-related clinical features.

#6588 Exploring biomarker profiles in canine oncology using multiplex immunoassays.

Joseph B. Hwang, Tina Raeber, Brooke Gilliam, Anthony Saporita

R&D, MilliporeSigma, St. Louis, MO

Canine oncology has garnered significant attention due to the unique role of dogs as companion animals that often develop naturally occurring cancers, mirroring human disease processes. Common types of cancer in dogs include lymphoma, osteosarcoma, mast cell tumors, and hemangiosarcoma, with each presenting distinct clinical challenges. This predisposition to cancer highlights the importance of studying canine oncology not only for the purposes of veterinary medicine but also for advancing human cancer therapies. Dogs present an invaluable opportunity as test subjects for new therapeutic strategies, providing insights into tumor biology and treatment responses that may be applicable to human oncology. We have previously developed a multiplex immunoassay for the measurement of cytokines, chemokines, and growth factors in canine serum and plasma. These immune proteins play a crucial role in the pathophysiology of canine cancers, influencing tumor growth, metastasis, and the host immune response. Additional protein biomarkers, including immuno-oncology targets such as PD-1, PD-L1, and CTLA4 can potentially extend our understanding of tumor progression and the immune response in canine patients. Here we detail the development of a novel multiplex immunoassay which we then use to measure proteins in cell culture supernatant and tissue lysate, as well as serum and plasma samples from healthy and diseased dogs. Multiplex immunoassays offer a powerful platform for the simultaneous measurement of multiple canine cancer biomarkers in plasma and serum, enabling more comprehensive monitoring of disease progression and treatment efficacy. By utilizing this technology, researchers can evaluate the complex interplay of cytokines and other biomarkers, providing a deeper understanding of canine oncology and reinforcing the significance of dogs in comparative oncology research.

#6589 Nrf2 as a therapeutic target to improve T cell function in muscle invasive bladder cancer (MIBC).

Aprajita Tripathi, Nadine Santana-Magal, Jared Rack, Debolina Dasgupta, Benjamin L. Woolbright, Kalyani Pyaram

Cancer Biology, University of Kansas Medical Center, Kansas City, KS

Introduction: Bladder cancer is the seventh most common malignancy in the United States, with an estimated 16,840 deaths in 2024. Despite advances in surgical management and chemotherapy, muscle invasive bladder cancer (MIBC) remains associated with poor survival outcomes. Only ~20% of MIBC patients show durable responses to immune checkpoint inhibitors. Thus, there remains a critical unmet need to understand the mechanisms of immune resistance within MIBC tumor microenvironment and to develop therapies that can enhance T cell functions to improve patient outcomes. Nuclear factor erythroid 2-related factor 2 (Nrf2) is a transcription factor, regulated by Kelch-like ECH-associated protein 1 (Keap1), which protects against oxidative stress. However, its role in modulating the immune microenvironment, particularly the T cells in MIBC, remains poorly understood. Recently, it was reported that Nrf2-mediated oxidative stress response pathway is upregulated in tumor-infiltrating T cells compared to circulating T cells in bladder cancer patients. We and others have reported that loss of Nrf2 in T cells elevates IFN-γ and Granzyme B expression, supporting a cytotoxic phenotype, while Nrf2 activation exerts the opposite effect by repressing these key effector molecules. Based on these observations, we *hypothesized* Nrf2 inhibition will suppress MIBC progression by enhancing T cell-mediated anti-tumor immunity.
Methods: We used mice with T cell-specific deletion of Nrf2 (Nrf2-KO) or constitutive activation of Nrf2 by deleting its negative regulator Keap1 (Keap1-KO) to evaluate the T cell-intrinsic role of Nrf2 in MIBC. *In vivo*, we assessed tumor growth of BBN963 cells in a syngeneic bladder cancer model. *In vitro*, we performed tumor-killing assays by coculturing $CD8^+$ T cells, treated with the Nrf2 inhibitor ML385 and with BBN963 cells.
Results: BBN963 tumors implanted in Nrf2-KO mice (with Nrf2-depleted T cells) exhibited remarkably reduced tumor growth compared to wildtype mice while Keap1-KO mice (elevated Nrf2 in T cells) displayed significantly larger tumors. Pharmacological inhibition of Nrf2 using ML385 improved the tumor-killing ability of $CD8^+$ T cells against BBN963 bladder cancer cells *in vitro*.
Conclusions: Together, these findings identify a previously unrecognized T cell intrinsic role of Nrf2 in suppressing antitumor immunity and promoting bladder cancer progression. Our work highlights Nrf2 as an immune checkpoint for T cells and indicates its targeting as a promising therapeutic strategy, especially in synergy with current immunotherapies, to improve MIBC patient outcomes.

#6590 Investigation of carcinogenic effects of polystyrene microplastic on human bladder cancer cells.

Sahab Ram

Cleveland Clinic Lerner Research Institute, Cleveland, OH

Plastic pollution has become a global environmental problem. Humans are increasingly exposed to microplastics (MPs) and nano-plastics (NPs) through ingestion, inhalation, and skin contact. These particles may affect organs such as the brain, liver, kidneys, and bladder by triggering inflammation, altering immune responses, and disrupting the urothelial barrier-an established risk factor for bladder cancer and interstitial cystitis. We investigated the uptake of micro (0.5 µm) and nano-plastic (0.03 µm) polystyrene microplastics by human bladder cancer cell lines (SW-78 and UMUC-3). Both cell lines showed altered proliferation compared with controls. SW-78 cells responded significantly to 8,000, 16,000, and 32,000 p/mL, while 64,000 p/mL was toxic to cell proliferation. In UMUC-3 cells, proliferation increased at all concentrations in a time-dependent manner. Moreover, cell migration in UMUC-3 cells was not significantly influenced by 0.03 µm PS particles compared with controls, whereas 0.5 µm PS particles affected migration. In SW-78 cells, migration was significantly induced by lower concentrations of 0.03 µm particle but was significantly reduced at 64,000 p/mL. We also confirmed that higher doses of plastic particles caused significant DNA damage and ROS production in a concentration-dependent manner. PS particles showed strong attachment of MPs to the cell surface in live-cell imaging, while confocal imaging confirmed uptake, cytoplasmic accumulation, and nuclear translocation of the PS particles. Our findings suggest that PS microplastics influence bladder cancer cell proliferation and migration in a dose- and size-dependent manner, consistent with mechanisms involved in cancer progression. The presence of microplastics in the cytoplasm is likely to disrupt cellular metabolic processes, warranting further investigation. Given the rise in plastic pollution, microplastics may represent emerging risk factors for bladder cancer, underscoring the need for thorough toxicological and epidemiological studies.

#6591 Cross platform same slide multi-omics reveals Treg heterogeneity and links to spatial niche variability in pre-cancerous colonic inflammation.

Daniel Jimenez-Sanchez[1], Matthew H. Ingalls[1], Sanghamithra korukonda[2], Brian J. Lane[1], Isabella Marie Peshek[3], Patrick Danaher[2], Prajan Divakar[2], Oliver Braubach[1]

[1]Bruker Spatial Biology, St. Louis, MO,[2]Bruker Spatial Biology, Seattle, WA,[3]Division of Gastroenterology, Northwestern University, Chicago, IL

Introduction: FOXP3+ regulatory T cells (Tregs) maintain immune tolerance, and their dysfunction contributes to autoimmunity, chronic inflammation, and cancer. Treg heterogeneity is well documented in ulcerative colitis, where dysregulated Tregs can promote colon cancer. Treg heterogeneity is often defined by transcriptional profiles, which can include technical artifacts due to inherent biological differences between transcript and protein levels. Using cross-platform same-slide multi-omics with CellScape™ proteomics and CosMx™ transcriptomics, we aimed to assess whether quantitative FOXP3 protein improves definition of Treg transcriptional heterogeneity within the colonic microenvironment.
Methods: Eight FFPE intestinal biopsies from a pre-cancerous condition (ulcerative colitis) were profiled with CellScape™ (34-plex VistaPlex), followed by CosMx™ Human Universal Cell Characterization Panel (1K-plex) on the same slide. Whole-slide multimodal alignment used shared morphology markers and WsiReg to generate affine registrations. Segmentation masks were harmonized for pixel-level correspondence, enabling direct integration of protein and RNA per cell. CD4+ T cells were classified into $FOXP3_{neg}$, $FOXP3_{low}$, $FOXP3_{high}$ groups via quantitative automatic cell typing. Spatial neighborhoods (k=15) yielded 25 FOXP3-defined niches, and both protein and RNA features were included in neighborhood and state enrichment analyses.
Results: Quantitative spatial proteomics revealed reproducible $FOXP3_{low}$ and $FOXP3_{high}$ populations with corresponding transcriptomic variation. Neighborhood analysis showed two recurring contexts: (1) $FOXP3_{low}$ cells in innate- and vascular-associated neighborhoods, and (2) $FOXP3_{high}$ cells in adaptive immune-rich and proliferative niches. Integration with CosMx™ enabled transcriptional characterization of $FOXP3^+$ cells and neighbors.
Conclusion: Immune regulation relies on balanced Treg activity and their response to local microenvironmental changes. In ulcerative colitis rectal tissue, $FOXP3_{low}$ and $FOXP3_{high}$ T cells occupy distinct recurrenting spatial niches, indicating multiple $FOXP3^+$ regulatory states within inflamed tissue. Integrating same-slide CellScape™ proteomics with CosMx™ transcriptomics revealed microenvironment-linked patterns that were not evident from either modality alone. These findings underscore the power of spatial neighborhood analysis to expose context-dependent T-cell states in immune-mediated disease and the value of cross-platform multi-omics.

#6592 *In vitro* neutrophil assays to support immuno-oncology drug development.

Christoph Schifflers, Martijn Vlaming, Sofie Pattyn

IQVIA Laboratories, Gosselies, Belgium

Neutrophils play important roles in cancer progression. The presence of tumor-associated neutrophils can promote tumor growth, invasion, angiogenesis, and the formation of metastasis. On the other hand, neutrophils have also been associated with multiple anti-cancer functions, such as killing of antibody-opsonized cancer cells, trogocytosis, or indirectly through the release of cytotoxic mediators. Thereby, Neutrophils represent a target of interest for the development of novel cancer immunotherapy approaches. Here, we report a variety of *in vitro* assays allowing to evaluate the putative impact of drug candidates on neutrophil functions such as antibody-dependent cell-mediated cytotoxicity (ADCC), Neutrophil Extracellular Traps (NET) formation and the release of Reactive Oxygen Species (ROS) by flow cytometry and live-cell imaging. Furthermore, multiplex cytokine and peroxidase release analysis after activation and stimulation of neutrophils can be evaluated using ELISA or Luminex technology. Co-cultures of freshly isolated human neutrophils and fluorescent-labeled tumor cells can be used to screen the potency of candidate therapeutics to enhance anti-cancer neutrophil functions. Lastly, the toxicity of drug candidates on Neutrophils can be evaluated. Key factors to obtain reliable and reproducible results are the access to fresh blood as well as optimized protocols for purifying and culturing untouched neutrophils. Taken together, functional *in vitro* assay using fresh primary human Neutrophils provide cost-effective tools for the characterization and lead selection of drug candidates targeting Neutrophils.

#6593 B-cell guided inflammatory cascade perpetuates ICI-mediated colitis.

Roza Nurieva, Naimah Turner, Synat Keam, Jocelynn Colunga

UT MD Anderson Cancer Center, Houston, TX

Immune checkpoint inhibitor (ICI) therapy is often accompanied by inflammatory toxicities including ICI-colitis. Therapeutic options are limited because the mechanisms that predict its onset are unclear. We uncover a role for B cells in triggering the intestinal inflammatory cascade following ICIs. An increase in circulating B cells, particularly those with gut-homing markers, antigen-presenting capacity, and proinflammatory cytokine production, are found in both asymptomatic patients and mice which are susceptible to ICI-colitis. Furthermore, lack of B cells at the asymptomatic stage abrogates ICI-colitis by reducing the number of pathogenic intestinal T cells in mice. We find that latent microbial dysbiosis may underlie the B cell dysfunction in the asymptomatic stage that predisposes mice to the development of colitis following ICI therapy. Thus, our study examines the immunologic evolution underlying ICI-colitis and proposes B cell dysregulation as a critical initiating factor in this process and a potential biomarker for toxicity risk.

#6594 Establishing *ex vivo* models for targeting leukemic stem cells to investigate relapse and refractory pediatric leukemias.

Sashi Kandel, Jacqelyn M. Nemechek, Tykeem Manor, John N. Maina, John M. Perry

Children's Mercy Hospital, Kansas City, MO

Despite advancements in therapies for leukemia, relapses and refractory cases remain a significant clinical challenge largely due to persisted dormant leukemic stem cells (LSCs) and evade treatment. LSCs represent a rare cell population, making their isolation, culture, and expansion difficult and limiting our ability to study their functional properties. Developing an *ex vivo* model to culture and expand LSCs would enable detailed analysis of their role in drug resistance and relapses. Traditional 2D cultures fail to replicate the complexity of the bone marrow (BM) microenvironment, and animal models are limited by interspecies differences. To overcome these limitations, we are developing BM organoids derived from iPSCs, which are expected to better mimic the native BM architecture and function.In this study, we are establishing an *ex vivo* system for LSC culture and expansion. In previous studies, we demonstrated that mice with hematopoietic stem cell-specific (HSC-SCL-Cre-ER^T) loss of the tumor suppressor Pten and activation of the oncogene beta-catenin develop leukemia by expansion of normal stem cells with transformation to LSCs. BM cells from HSC-SCL-Cre-ER^T+ $Pten^{fl/fl}$ $dBC^{fl/wt}$ mice were harvested and cultured in media supplemented with mTPO and mSCF and treated with 1 μM 4-OHT during serial passaging to induce recombination. Cultures were analyzed at multiple time points (3, 6, 13, and 18 days) using flow cytometry to quantify hematopoietic stem cells (HSCs: Lin^- $CD3^-$ $cKit^+$ $Sca1^+$), LSCs (Lin^- $CD3^+$ $cKit^+$), and blast cells (Lin^- $CD3^+$ $cKit^-$). Preliminary results indicate that HSCs and blast cells increased by day 18 (62.1% and 0.65%, respectively) compared to day 13 (19.3% and 0.22%), whereas LSC frequency declined (0.14% vs. 0.25%). These findings suggest that LSC enrichment peaks around day 13, making this time point optimal for LSC culture. Ongoing work focuses long-term transformation of pre-leukemic HSCs to LSCs with subsequent expansion and maintenance of LSC phenotype and function. Concurrently, we are developing BM organoids. iPSCs were cultured to form embryoid bodies EBs), after which mesodermal induction and subsequent promotion of hemogenic endothelium Sprouting in hydrogel matrix was stimulated by supplementing different cytokines at different stages of culture. Finally, sprouted EBs were harvested and individually seeded into low-attachment 96-well plates. Mature BM organoids were analyzed using flowcytometry, immunofluorescence and PCR. Following organoid formation, LSCs will be engrafted to enable chemoresistance screening. Together, these approaches aim to establish a robust platform for LSC expansion to support immunocompetent functional assays, including co-culture studies, and develop new treatments targeting therapy-resistant leukemia.

#6595 Memory B cell Responses Ignite Anti-Tumor Immunity by Activating CD8+ T cell Cytotoxicity.

Kendrick Nguyen[1], Monika Quackenbush[1], Georgia Lattanzi[1], Daniel Hollern[1], Sara Basbous[1], Haley Rodriguez[1], Daniela Boassa[1], Jingting Yu[1], Asona Lui[2], April Wehner[2], Aatish Thennavan[3], Peter H. Watson[4]

[1]Salk Institute, La Jolla, CA,[2]UC San Diego, La Jolla, CA,[3]UT MD Anderson Cancer Center, Houston, TX,[4]Chief Physician, BC Cancer Agency Vancouver Island Ctr., Victoria, BC, Canada

Immunotherapies aimed at leveraging T cell responses have revolutionized cancer care with demonstrated effectiveness in a myriad of cancers. Yet, challenges remain in patients with solid tumors such as triple negative breast cancer (TNBC) that fail to generate and sustain a durable anti-tumor T cell mediated immune response. Numerous reports demonstrate opportunities to improve upon these treatments by leveraging B cells. Tumor infiltrating B cells have been shown to predict responses to chemo and immunotherapies across cancers. B cells within the tumor have also been experimentally shown to be intimately involved in controlling anti-tumor immune responses and markers for their interactions with T cells have immense prognostic value. However, experimental demonstration of how B cell responses to tumors are regulated and function remains a key gap in research, which limits leveraging B cells in future immunotherapies. Thus, we sought to understand the role of tumor antigen and activation signals of B cell-driven anti-tumor immunity. Our study has revealed that activating the CD40 pathway of B cells in the presence of neo-antigen can directly incite a robust non-germinal center (GC) memory B cell response that is able to facilitate powerful anti-tumor immune responses in mouse models of TNBC. Leveraging single cell sequencing in combination with microscopy approaches we have found that these memory B cells can participate in an anti-tumor response by promoting CD8+ T cell infiltration, organization, and stimulation of CD8+ T cells to promote tumor cell killing. These findings advance the canonical models of B cell and CD8+ T cell regulation along with function. Furthermore, these results showcases novel routes to leverage B cells to promote anti-tumor immunity.

#6596 Understanding DAP12-independent antitumor activation in KIR-based CAR T cells.

Qian Zhang, Kevin Zhou, Zhongze Sun, Chen Zhang, Marta Chebotar, Michael C. Milone

University of Pennsylvania, Philadelphia, PA

We previously described a chimeric killer immunoglobulin (KIR)-like receptor (cKIR) approach to modifying T cell antigenic specificity that mimics the multichain design of natural KIR immunoreceptors (Wang E et al. Cancer Immunol Res 2014). T cells modified to express a cKIR with the natural ITAM-containing adaptor, DAP12 that associates with activating KIRs, show significantly enhanced anti-tumor activity acrossmultiple solid tumor models when compared to traditional CD3z-based chimeric antigen receptors (CARs). However, unlike TCR, where assembly with ITAM-containing CD3 family members is required for plasma membrane expression, natural and chimeric KIR exhibit membrane expression in the absence of DAP12. We show that cKIR engineeredT cells also produce IFN-g and retain cytotoxic activity in the absence of DAP12, revealing previously unrecognized DAP12-independent signaling pathways. This is associated with phosphorylation of ERK, JNK and STAT3 at early time points (30-60 mins) following cKIR engagement with target antigen. Although the cytoplasmic domain of KIR2DS2 used in cKIR is short and lacks canonical signaling motifs, we hypothesized that this domain plays a functional role in T cells by recruiting alternative adaptors to promote noncanonical signaling in the absence of DAP12. Immunoprecipitation of cKIR in T cells lacking DAP12 identified GRB2 as an associated adaptor protein. CRISPR- mediated GRB2 knockout selectively abolished ERK activation, establishing GRB2 as a crucial link to the Ras/MAPK pathway in cKIR-activated T cells. Structure-functionanalysis of the KIR2DS2 cytoplasmic tail, containing one tyrosine, one threonine, and four serine residues, revealed that progressive truncation of these residues had minimal effect on membrane expression, but increasingly impaired cytotoxicity, cytokine production, proliferation, and downstream signaling with a > 25-fold loss of IFN-g andcytotoxicity observed with the truncation of C-terminal to serine residue 3. Collectively, these results suggest that DAP12-independent signaling by cKIR, mediated through GRB2 and likely other yet-to-be-identified adaptors, contribute to diverse signaling in T cells and may contribute to the enhanced anti-tumor function observed with KIR-based CAR T cells compared with conventional CAR designs.

: Radiation and Photodynamic Therapy Response Modifiers
Poster Session

#6600 Triad-SL: A new synthetic lethality paradigm combining two distinct DNA damage response pathway inhibitors and particle radiotherapy.

Neele Haxel, Ivana Dokic, Mahmoud Moustafa, Carmen Klein, Juergen Debus, Amir Abdollahi

Translational Radiation Oncology, National Center for Tumor Diseases (NCT), Heidelberg University Hospital (UKHD) and German Cancer Research Center (DKFZ), Heidelberg, Germany

Current synthetic lethality (SL) strategies in cancer therapy utilize tumor-specific deficiencies in the DNA damage response (DDR)—such as homologous recombination deficiency (HRD) from BRCA1/2 mutations—to selectively eradicate malignant cells by inhibiting backup repair pathways, most notably using PARP inhibitors. However, these vulnerabilities occur in only a small subset of patients, as many tumors exhibit complex or mosaic mutational profiles that only partially resemble classical BRCAness. To overcome this limitation, we propose that engineered synthetic lethality can be achieved by inducing spatially and temporally controlled DNA damage with high-precision particle radiotherapy (RT), combined with dual targeting of distinct DDR pathways. To this end, we systematically evaluated the effect of RT with a combinatorial matrix of potent small-molecule inhibitors targeting ATM, ATR, DNA-PK, and PARP, establishing the Triad-SL paradigm as a framework for next-generation cancer treatment. Single and dual drug concentrations causing minimal or no toxicity when used alone were established by titration experiments to ensure effective cell killing occurs only in the presence of RT and synergistic dual DDR inhibition. Interestingly, we found that conventional viability assays underestimated DDR-dependent effects, especially when combined with RT. When assessed using clonogenic survival assays, the same Triad-SL combinations exhibited up to 1000-fold greater sensitivity. Within their respective pathway classes, DDR inhibitors demonstrated comparable efficacy and synergized effectively with photon- or carbon ion irradiation, respectively. Of note, combined treatment with PARP- and ATM inhibitors produced strong, cell line-specific cytotoxicity, substantially reducing survival fractions even in the absence of irradiation, indicating combined cytotoxic potential. Among all combinations tested, ATM, DNA-PK, and PARP inhibitors yielded the most promising outcomes, producing strong radiosensitizing effects across multiple DDR inhibitor pairings. By leveraging DDR inhibitors with differing biodistribution, pharmacokinetics, and target selectivity, potent synergistic effects may be achieved at reduced doses—particularly when combined with focused irradiation. In conclusion, the multimodal Triad-SL strategy, integrating selective DDR inhibition with tailored radiation quality, represents a promising approach to enhance therapeutic efficacy and broaden the applicability of synthetic lethality in cancer treatment.

#6601 Activation of STING in response to partial-tumor radiation exposure.

Mickael Mathieu[1], Sadna Budhu[2], Prerna R. Nepali[3], James Russell[4], Simon N. Powell[5], John L. Humm[4], Joseph O. Deasy[4], **Adriana NA Haimovitz-Friedman**[1]

[1]Memorial Sloan Kettering Cancer Center, New york, NY,[2]Immunology, Memorial Sloan Kettering Cancer Center, New York, NY,[3]Memorial Sloan Kettering Cancer Center, Fort Lee, NJ,[45]Memorial Sloan Kettering Cancer Center, New York, NY

Purpose: To determine the mechanisms involved in partial volume radiation therapy (RT)-induced tumor response.
Methods and Materials: We investigated 67NR murine orthotopic breast tumors in Balb/c mice and Lewis lung carcinoma (LLC cells; WT, Crispr/Cas9 Sting KO and Atm KO) injected in the flank of C57Bl/6, cGAS or STING KO mice. RT was delivered to 50% or 100% of the tumor volume using a 2X2 cm collimator on a microirradiator allowing precise irradiation. Tumors and blood were collected at different time points post-RT and assessed for cytokine measurements.
Results: There is a significant activation of the cGAS/STING pathway in the hemi-irradiated tumors as compared to control and to 100% exposed 67NR tumors. In the LLC model, we determined that an ATM-mediated non-canonical activation of STING is involved. We demonstrated that the partial exposure RT-mediated immune response is dependent on ATM activation in the tumor cells and on the STING activation in the host, while cGAS is dispensable. Our results also indicate that partial volume RT stimulates a different cytokine expression as compared to 100% tumor volume exposure.
Conclusion: Partial volume RT induces an anti-tumor response by activating STING which stimulates a specific cytokine signature as part of the immune response. However, the mechanism of this STING activation, *via* the canonical cGAS/STING pathway or a non-canonical ATM-driven pathway, depends on the tumor type. Identifying the upstream pathways responsible for STING activation in the partial RT-mediated immune response in different tumor types would improve this therapy and its potential combination with immune checkpoint blockade and other anti-tumor therapies.

#6602 Venetoclax enhances radiation-induced anticancer immunity in breast cancer.

Emma Guilbaud, Ai Sato, Lorenzo Galluzzi

Fox Chase Cancer Center, Philadelphia, PA

Estrogen receptor-positive (ER+) breast cancer (BC) lesions are poorly infiltrated by lymphocytes (immunologically "cold") and are therefore insensitive to immune checkpoint inhibitors (ICIs). Radiation therapy (RT) represents a clinically promising partner for ICIs, as RT converts immunologically "cold" ER+ BC into "hot" lesions, reflecting the ability of RT to elicit BAX/BAK-initiated mitochondrial permeabilization (MOMP) in cancer cells, culminating with cytosolic mtDNA accumulation, CGAS/STING signaling and type I IFN secretion, which supports anticancer immunity. We hypothesized type I IFN signaling could be further enhanced by exacerbating mitochondrial damages with Venetoclax, the FDA-approved BCL2 inhibitor. *In vitro*, Venetoclax treatment in mouse models of ER+ BC amplified RT-induced mtDNA release, increased RT-driven type I IFN production, and upregulated interferon-stimulated gene (ISG) expression. Type I IFN signaling was abrogated by the pharmacologic inhibition of CGAS or STING, as well as in STING-deficient cells or in mtDNA-depleted (Rho0) cells, confirming that Venetoclax enhances RT-driven type I IFN production via the CGAS/STING pathway. *In vivo*, Venetoclax significantly improved RT-mediated tumor control, an effect that was further enhanced by CTLA4 blockage. However, RT also triggered the removal of damaged mitochondria in a dose- and time-dependent manner. This process was suppressed by genetic deletion of the essential autophagy genes *Atg5* or *Atg7*. Moreover, RT-induced mitophagy depended on BAX/BAK-mediated MOMP, as Venetoclax further enhanced RT-induced mitophagy, whereas BAX/BAK-deficient cells failed to activate mitophagy in response to RT and were unresponsive to Venetoclax. By investigating the mechanistic link between mitophagy (which degrades permeabilized, mtDNA-releasing mitochondria) and mtDNA-dependent type I IFN production, we observed that 1) blocking mitophagy with *Atg5*-/- cells increased cytosolic mtDNA accumulation and type I IFN production whereas 2) activating mitophagy with Urolithin A reduced cytosolic mtDNA accumulation and type I IFN production. These findings strongly suggest that mitophagy modulates type I IFN signaling. In summary, RT-driven BAX/BAK-dependent MOMP mediates both mtDNA release, which activates type I IFN signaling and enhances anticancer immunity, but also mitophagy, which limits type I IFN signaling and may therefore constrain anticancer immunity. To maximize MOMP-dependent type I IFN production, it is crucial to uncouple these mechanisms. Collectively, our findings identify both BCL2 and mitophagy as immune checkpoints that suppress RT-induced immune responses. **These pathways represent actionable targets for novel therapeutic strategies to overcome immunotherapy resistance not only in ER+ breast cancer, but also in other "cold" tumor types.**

#6603 MCT4-driven lactate shuttle in the irradiated tumor microenvironment upregulates neutrophils PD-L1 expression for immunosuppression in lung cancer.

Wenqian Yuan[1], Yijun Wang[1], Lingyi Kong[1], Minqi Zhou[1], Yuhan Sheng[2], Yajie Sun[1], Kunyu Yang[1]

[1]Cancer Center, Union Hospital, Tongji Medical College, Huazhong University of Science and Technology, Wuhan, China,[2]OHSU Knight Cancer Institute, Portland, OR

Purposes: Although tumor metabolic heterogeneity is known to shape tumor microenvironments (TME), the metabolic consequences of radiotherapy remain poorly defined. Thus, this study aims to elucidate the radiation-induced metabolic alterations in the TME, delineate their functional roles in radioresistance, and identify targetable metabolic vulnerabilities.
Methods: Metabolic perturbations were investigated through metabolomic profiling of lung cancer patients serum 5 days after radiotherapy and tumor interstitial fluid collected at 48h post-irradiation. Glycolytic flux was assessed via $^{13}C_6$-glucose-based metabolic flux analysis. Lactate dynamics were assessed through extracellular acidocation rate (ECAR) measurements. Spatial scRNA sequencing was conducted on tumors from Lewis models. All the histone modification antibodies available were used to identify the lactylation site of neutrophils. Cut&Tag assay was performed to elucidate the downstream genes.
Results: Metabolomic profiling of patients serums and irradiated tumors revealed a significantly elevation of lactate. Subsequent functional analyses demonstrated that radiation induces metabolic reprogramming in NSCLC cells, characterized by amplified glycolytic flux, elevated ECAR, and enhanced lactate secretion. Proteomic screening identified MCT4 as the most prominently upregulated glycolytic regulators post-irradiation. MCT4 blockade attenuated radiation-induced glycolytic potentiation and suppressed lactate efflux. Further investigation into the regulatory mechanism revealed that radiation triggers RAB3B expression, which competes with HSC70 for binding to MCT4, inhibiting the HSC70-mediated autophagy of MCT4. In vivo, Gene depletion of Mct4 reversed radiation-induced lactate-enriched TME. Spatial scRNA sequencing further revealed that irradiation induced an immunosuppressive neutrophil phenotype, which was effectively reversed by MCT4 inhibition. Mechanistically, tumor-derived lactate was internalized by neutrophils via MCT1, driving histone H4 lysine 5 lactylation, which subsequently promoted PD-L1 transcription and impaired $CD8^+$ T cells functions. Blocking lactate efflux from tumor reversed histone lactylation and PD-L1 expression in neutrophils, thereby potentiating radiotherapy efficacy.
Conclusion: Our study demonstrates that radiation reprograms tumor metabolism by enhancing glycolytic capacity and lactate efflux. This lactate surge drives PD-L1 expression of neutrophils and suppress the activity of $CD8^+$ T cells. Our findings propose that targeting MCT4 exerts dual therapeutic effects: reversing radiation-induced metabolic adaptation and disrupting immunosuppressive neutrophil remodeling, thereby providing a strategy to amplify radiotherapy efficacy.

#6604 Aurora kinase B inhibition enhances radiation response and activates type 1 interferon signaling in triple-negative breast cancer.

Meirola Amgad Endraws[1], Kassidy M. Jungles[2], Caroline Bishop[2], Cydnee Wilson[2], Priyanka S. Rana[1], Benjamin Hauk[3], Camila Diedrich[1], Vesna Markovic[1], Ethan Hochmuth[4], Breanna Nicole McBean[2], Meilan Liu[2], Lori Pierce[2], James M. Rae[5], Corey W. Speers[1]

[1]Radiation Oncology, University of Alabama at Birmingham, Birmingham, AL,[2]University of Michigan, Ann Arbor, MI,[3]Case Western Reserve University School of Medicine, Cleveland, OH,[4]Radiation Oncology, Case Western Reserve University, Cleveland, OH,[5]University of Michigan Medical School, Ann Arbor, MI

Purpose: Triple-negative breast cancer (TNBC) is an aggressive subtype with limited targeted therapies and poor response to radiotherapy[1]. Aurora kinase B (AURKB), a key regulator of chromosomal segregation during mitosis, is overexpressed in TNBC and correlates with poor recurrence-free survival following radiation[2]. Because radiation-induced DNA damage can promote innate immune activation through type I interferon (T1IFN) signaling[3], we hypothesized that AURKB inhibition would enhance radiosensitivity while amplifying T1IFN-mediated antitumor immune responses in TNBC.

Methods: AURKB expression was analyzed across breast cancer datasets and correlated with clinical outcomes. Pharmacologic inhibition of AURKB using ATP-competitive (barasertib-HQPA) and noncompetitive (SP-96) compounds was evaluated in multiple human and murine TNBC cell lines. Clonogenic survival assays quantified radiosensitization, and DNA damage was assessed by γH2AX and micronuclei formation. Type I interferon (T1IFN) activation was measured using IFN-β reporter assays, quantitative PCR for CXCL10 and PD-L1, and flow cytometry for surface MHC-I and PD-L1 expression. In vivo efficacy of AURKB inhibition combined with radiotherapy was evaluated in syngeneic TNBC models.

Results: AURKB expression was significantly elevated in TNBC and associated with poor outcomes in radiotherapy-treated patients. AURKB inhibition enhanced radiosensitivity in TNBC cell lines in vitro and reduced tumor growth in vivo. Combined AURKB inhibition and radiation increased micronuclei formation, consistent with genomic instability and cytosolic DNA accumulation. This combination also induced a robust T1IFN response, evidenced by increased reporter activity, upregulation of CXCL10 and PD-L1 transcripts, and elevated MHC-I and PD-L1 expression. These effects were observed following both single-dose and fractionated radiation regimens.

Conclusions: AURKB inhibition potentiates the efficacy of radiotherapy in TNBC by augmenting DNA damage and activating antitumoral T1IFN signaling. These findings identify AURKB as a dual radiosensitizing and immune-stimulatory target in TNBC, providing a strong rationale for clinical evaluation of AURKB inhibitors in combination with radiotherapy.

References:

1. Chandler BC, Moubadder L, Ritter CL, Liu M, Cameron M, Wilder-Romans K, et al. TTK inhibition radiosensitizes basal-like breast cancer through impaired homologous recombination. J Clin Invest. 2020;130(2):958-73.

2. Chang HHY, Pannunzio NR, Adachi N, Lieber MR. Non-homologous DNA end joining and alternative pathways to double-strand break repair. Nat Rev Mol Cell Biol. 2017;18(8):495-506.

3. Fuertes MB, Woo S-R, Burnett B, Fu Y-X, Gajewski TF. Type I interferon response and innate immune sensing of cancer. *Trends in immunology*. 2013;34(2):67-73.

#6605 USP3 stabilizes STING to enhance radiosensitivity and antitumor immunity of NSCLC.

Zeyuan Cheng, Zhengkun Cai, Yihan Xu, jiazhuo yan, Zhiqiang Wu, Zhiyong Yuan

Tianjin Medical University Cancer Institute & Hospital, National Clinical Research Center for Cancer, Tianjin, China

Purpose: Although radiotherapy (RT) is a predominant treatment for non-small cell lung cancer (NSCLC), radioresistance remains a major challenge and is strongly linked to dysregulated tumor immune microenvironments (TIME). Immunoradiotherapy has shown improved therapeutic activity by promoting antitumor immune responses and modifying the TIME. Recent studies positions STING activation as a potent catalyst of this immune reprogramming. Therefore, identifying upstream regulators capable of enhancing STING-mediated immune activation is critical for developing strategies to overcome radioresistance in NSCLC.
Methods: Ubiquitin-specific protease3 (USP3) expression patterns, immune infiltration profiles, and pathway enrichment analyses were performed using public datasets and institutional sequencing data. Prognostic value was evaluated via TCGA datasets and validated in a clinical cohort of 105 NSCLC patients (Tianjin Medical University Cancer Institute & Hospital, 2013-2015). Subsequently, we investigated the interaction between USP3 and STING and the effects of USP3 on RT-induced STING/type I interferon (IFN-Is) signaling through co-immunoprecipitation and immunofluorescence. Finally, we evaluated the effects of USP3 on RT-induced T cell infiltration in tumor and sensitivity to RT and radioimmunotherapy.
Results: USP3 expression was significantly downregulated in NSCLC specimens compared to normal tissues. High USP3 expression correlated with prolonged overall survival in public datasets and our independent clinical cohort. Functionally, USP3 overexpression enhanced the radiosensitivity of NSCLC cells and induced a pro-inflammatory phenotype. Mechanistically, USP3 physically interacted with STING, removed K48-linked polyubiquitin chains, and thereby prevented proteasomal degradation of STING. This stabilization amplified cGAS-STING signaling and downstream IFN-Is production. In vivo, USP3 overexpression remodeled the post-irradiation tumor immune microenvironment, as evidenced by increased infiltration of effector $CD8^+$ T cells and enhanced systemic antitumor immunity.
Conclusion: USP3 deubiquitinates STING and blocks its proteasomal degradation, thereby stabilizing the STING protein, potentiating the cGAS-STING axis and type I interferon signaling. These results highlight USP3 as a promising prognostic biomarker and a potential therapeutic target for overcoming radioresistance and improving radiotherapy-based treatment strategies.

#6606 Overcoming reduced efficacy of fractionated radiotherapy in obese mice.

Logan Vahid Vick[1], Yao-Hui Sun[1], Ming Fan[2], Julian R. Perks[1], Jian-Jian Li[2], Sean James Judge[3], Robert J. Canter[3], William J. Murphy[4], Arta M. Monjazeb[1]

[1]Radiation Oncology, UC Davis Comprehensive Cancer Center, Sacramento, CA,[2]Radiation Oncology, UC Davis School of Medicine, Sacramento, CA,[3]Surgery, UC Davis Comprehensive Cancer Center, Sacramento, CA,[4]Dermatology, UC Davis School of Medicine, Sacramento, CA

Purpose/Objective(s): Obesity is a medical condition of excess adiposity characterized by chronic inflammation and connected to comorbidities including metabolic disorders and cancer. Identifying how to best treat the growing number of obese cancer patients is paramount particularly as clinical data has implicated poorer outcomes following radiotherapy (RT) in obese patients. We observed using preclinical diet induced obesity (DIO) models that obesity promotes resistance to local fractionated RT; the aims of the current study were to identify the drivers mediating this resistance and if through altered dosing strategies it may be overcome.

Materials/Methods: In vivo obesity models consisted of C57BL/6 diet induced obese (DIO) alongside age matched controls. A syngeneic tumor model(3LL) was utilized for these studies in combination with local RT administered to anesthetized mice (per IACUC guidelines). RT was performed on a 5cm water block with tumors centered in a 2 cm electron light field cutout using a 5mm bolus and treated using 6MeV electron at the desired dose (3x 4Gy fractions or 1x12Gy). In collection studies tumor tissues were harvested either immediately after irradiation or at least a week following treatment regimen for additional analysis including immunofluorescence, RNA, and protein analysis.

Results: We observed that DIO mice demonstrated resistance to a fractionated local RT regimen (4Gy x 3) with no significant change in tumor burden while lean mice had significantly decreased compared to untreated controls. To evaluate if obesity associated resistance could be overcome in DIO mice, we administered a single ablative dose of 12Gy. We observed that a single dose of 12Gy was effective in both DIO and lean mice with a comparable significant decrease in tumor burden. Notably, DIO mice only responded to ablative RT doses while lean mice responded to both fractionated and ablative RT doses. Analysis of yH2AX immunofluorescence staining of treated and untreated tumors demonstrated that DIO mice had increased DNA damage and repair at baseline and following treatment. RNA sequencing of tumors confirmed increases in oxidative stress and DNA repair mechanisms

Conclusion: We identified that DIO mice are resistant to fractionated RT demonstrating reduced treatment efficacy when compared to lean counterparts. However, using a single ablative dose DIO mice demonstrated significant reductions in tumor burden. The observation that tumors from DIO mice had greater baseline levels of yH2AX illustrates increased DNA repair mechanisms, likely secondary to increased baseline oxidative stress in the obese setting, which we hypothesize is diminishing lower dose fractionated RT efficacy. These data have direct implications for patient care as understanding how obesity impacts RT response may assist in developing strategies to overcome RT resistance and improve outcomes in patients with obesity.

#6607 HDAC6 inhibition modulates macrophage function in the post-radiation therapy tumor microenvironment.

Xintang Li[1], Satish K. Noonepalle[1], Sonia Sebaoui[2], Manasa Suresh[2], Marie Durr[1], Bryan Weselman[2], Vidhi Sharma[1], Danae K. Boikos[1], Zazing Mawi[1], Gabriella Rigoli[1], Armijo Marisol. E[1], Scott Grindrod[3], Anatoly Dritschilo[3], Alejandro Villagra[1]

[1]Tumor Biology, Georgetown University, Washington, DC,[2]Georgetown Lombardi Comprehensive Cancer Ctr., Washington,[3]Shuttle Pharmaceuticals, Gaithersburg, MD

Historically, radiation therapy (RT) is the mainstay of cancer therapy, with more than half of the cancer patients receiving RT during the course of their treatment. Besides killing cancer cells by DNA damage, RT also induces immunogenic tumor cell death and reshapes the local antitumor immune response. Often, tumor-associated macrophages (TAMs) play a key role in regulating the innate antitumor immune response within the tumor microenvironment (TME). Post-RT, due to their phenotypic plasticity, TAMs often shift between a pro-inflammatory M1-like phenotype and immunosuppressive tumor-promoting M2-like state. Furthermore, these M2-polarized TAMs recruit circulating monocytes and tissue-resident macrophages into the tumor. This results in negating the therapeutic benefit of RT by promoting tumor growth and metastasis. Therefore, strategies to reprogram TAMs are critical to the success of RT. Our lab has reported that targeting Histone Deacetylase 6 (HDAC6) with isoform-specific inhibitors in macrophages can suppress the M2-like phenotype within the TME. We explored one of several molecular mechanisms underlying the interplay among tumor cells, macrophages, and tumor-infiltrating immune cells.First, we demonstrated that M2-like macrophages migrate toward irradiated tumor cells at a significantly higher rate than M1-like macrophages, a migration that was suppressed by the HDAC6 inhibitor SP-2-225. To unravel the factors involved in the macrophage migration, we analyzed a panel of 38 cytokines and chemokines from the co-culture assay. The data revealed that macrophages irradiated with a single dose of 6Gy significantly increased the expression of CCL5 chemokine. Also, co-culture with irradiated macrophages promoted the proliferation of 4T1 breast cancer tumor cells. In addition, qPCR and flow cytometry analyses showed that SP-2-225 suppressed the expression of CCL5 receptor, CCR5, on macrophages, providing a potential mechanism for the reduced migration. Furthermore, the in vivo combination of SP-2-225 and 6Gy of RT on the syngeneic murine 4T1 triple-negative breast cancer model demonstrated that mice receiving the combination therapy exhibited improved tumor control and delayed post-RT relapse. Overall, these findings suggest that targeting the CCL5-CCR5 axis with an HDAC6 inhibitor in TAMs post-irradiation may enhance the therapeutic efficacy of radiation therapy.

#6608 WNC0901 is a novel DNA-PK inhibitor and potent radiosensitizer of otherwise radioresistant solid tumors.

Jessica L. Abraham[1], Ann C. Mladek[1], Sonia Jain[1], Shiv K. Gupta[1], Paul A. Decker[2], Matthew L. Kosel[2], Katrina K. Bakken[1], Brett L. Carlson[1], Lauren L. Ott[1], Danielle M. Burgenske[1], Jeanette E. Eckel-Passow[2], Wei Zhong[3], Jann N. Sarkaria[1]

[1]Radiation Oncology, Mayo Clinic Hospital-Rochester, Rochester, MN,[2]Quantitative Health Sciences, Mayo Clinic Hospital-Rochester, Rochester, MN,[3]Wayshine Biopharm Inc., Corona, CA

Therapeutic resistance limits the efficacy of radiation therapy in many tumors and provides a compelling rationale to develop novel treatments to enhance radiation sensitivity. DNA-dependent protein kinase (DNA-PK) is a major mediator of DNA repair following radiation, and DNA-PK inhibitors are effective radiosensitizers. WNC0901 is a potent DNA-PK inhibitor in both a cell-free kinase assay (IC50 = 0.073 nM) and a cell-based assay (IC50 = 76 nM). WNC0901 has a 30-fold specificity for DNA-PK relative to other PI3K-related kinases. In a broader kinome screen (363 kinases), 1 μM WNC0901 resulted in >25% inhibition of only five other kinases. There is robust inhibition of radiation-induced DNA-PK autophosphorylation (Ser-2056), as analyzed by Western blotting, with maximal effect at 300 nM WNC0901 in A549 (lung carcinoma), U2OS (osteosarcoma), and HT29 (colorectal) cells. The efficacy of WNC0901 as a radiosensitizer was evaluated in clonogenic assays across these same three radioresistant tumor models. Following treatment with graded concentrations of WNC0901 (0-1000 nM) combined with 2.5 Gy radiation, maximal effects were observed at a 300 nM concentration in A549 (88-fold reduction in relative clonogenic survival compared to RT alone, $p<0.001$), U2OS (5.8-fold decrease, $p=0.002$), and HT29 (59-fold decrease, $p=0.008$) In a full radiation clonogenic, the sensitizer enhancement ratio at 10% survival (SER10) was 3.8 (A549), 2.3 (U2OS), and 1.8 (HT29). In vitro metabolism studies have identified demethylated WNC0901 (WNC0901-M) as a major metabolite. Similar to the parent drug, WNC0901-M is a potent DNA-PK inhibitor with maximal radiosensitizing effects of the metabolite observed at 300nM with SER10 of 2.4 (A549), 1.9 (U2OS), and 1.8 (HT29). The in vivo efficacy of 50 mg/kg WNC0901 combined with 8 Gy was evaluated and compared to another DNA-PK inhibitor, 50 mg/kg peposertib, in A549 tumor heterotopic xenografts. Compared to placebo (median time to endpoint 63 days) or RT alone (median 72 days), the combination of WNC0901 and RT significantly delayed tumor regrowth (median 169 days; $p=0.002$ compared to RT). Interestingly, peposertib + RT was ineffective (median 83 days; $p=0.332$ compared to RT). In a second study, similarly robust sensitizing effects of WNC0901 was observed in HT29 xenografts (placebo - median 45 days; RT - median 75 days; RT + WNC0901 - median >110 days; $p=.03$ relative to RT). Together, these findings demonstrate the robust radiosensitizing effects of WNC0901 in radioresistant tumors and provide a rationale for continued development of this drug.

#6609 Targeting pancreatic cancer with combination RAS inhibition and radiation therapy.

Candise L. Tat[1], Kimal Rajapakshe[2], Emma Rodriguez[2], Vincent Bernard-Pagan[2]

[1]The University of Texas MD Anderson Cancer Center UTHealth Houston Graduate School of Biomedical Sciences, Houston, TX,[2]The University of Texas MD Anderson Cancer Center, Houston, TX

Background
Radiation therapy (RT) is a key treatment modality for locally advanced PDAC, yet PDAC is characterized by intrinsic and acquired radioresistance. Our preliminary data suggest that PDAC radioresistance is driven in part by defenses against cuproptosis, a copper-dependent, oxidative phosphorylation- (OXPHOS) linked cell death pathway. KRAS-mutant PDAC is strongly dependent on mitochondrial OXPHOS and becomes even more cuproptosis-prone with KRAS inhibition. We find that this vulnerability can be exploited therapeutically, with KRAS inhibitors synergizing with RT to amplify copper driven cell death and mitigate radioresistance.
Methods
KPC cancer cells were orthotopically injected into the pancreas of mice and subjected to RT at clinically relevant doses (40 Gy in 5 fractions). Tumors were harvested either immediately post-radiation (day 6 post-stereotactic body radiation therapy, or SBRT) or at the time of recurrence and euthanasia (~day 40), and gene expression changes were identified through single-cell RNA sequencing.
MIA PaCa-2 and PANC-1 cells were treated with a pan-RAS inhibitor (iRAS) to evaluate effects on viability and protein expression, and cuproptosis defense genes were genetically modified to delineate pathways mediating RAS inhibition-induced cell death.
Results
In the recurrent KPC tumors, we found that therapy refractory PDAC tumors consistently overexpress metallothioneins (Mt1 and Mt2). Notably, the expression of Mt1 and Mt2 progressively increases from treatment-naïve status to post-SBRT, and further to the time of recurrence. These metallothioneins play a key role in sequestering intracellular copper, resulting in lower free copper pools in the radioresistant lesions. This sequestration preserves lipoylated enzymes, contributing to tumor cell resistance to RT. Treatment of PDAC cells with iRAS resulted in an increase in lipoylated protein levels at 24 hours. Overexpression of CTR1, a copper importer, in PDAC cells increased susceptibility to RT in the presence of copper and iRAS.
Conclusions
Targeting cuproptosis may be a viable option for therapy-resistant cancers such as PDAC. We have identified that cells upregulate genes related to copper defense upon development of radioresistance, and that iRAS therapy could serve as a primer to sensitize PDAC cells to cuproptosis.

#6610 Gut microbiome modulation shapes tumor responses to radiation in oral cavity carcinoma.

Seyedamirabbas Parizadeh, Elvin Canseco, Angelina Park, Andrew Ortega, Kit Cheung, Stephen L. Shiao, Julie K. Jang

Cedars-Sinai Medical Center, Los Angeles, CA

Tumor associated macrophages (TAMs) are key regulators in the tumor microenvironment (TME) and play an important role in the response to radiation therapy (RT). Therefore, there is a need to better understand the different factors that influence the response to RT. To this end, we used broad-spectrum antibiotics (Abx) to target the microbiome of the gut and oral cavity. We hypothesize that the gut and oral cavity microbiome are key in reshaping the TME after RT. We injected the syngeneic MOC1 cell line orthotopically into the buccal mucosa of C57BL/6 mice. Tumor-bearing mice were treated with an Abx cocktail of ampicillin, imipenem, cilastatin, and vancomycin once tumors reached a volume of 100 mm3. Tumor-bearing mice were focally irradiated (8Gy x 1) using the X-RAD SmART irradiator. At a week post RT, we magnetically isolated CD45+ leukocytes from tumors and performed high-dimensional profiling of the TME using flow cytometry and single-cell RNA sequencing (scRNA-seq). Macrophage polarization can provide insight into targetable pathways of myeloid inflammation to improve prognosis. By scRNA-seq and flow-cytometry, we found that treatment with Abx prior to RT reprograms the TME, leading to an increase in SPP1+ TAMs ($P<0.05$). By multiparametric flow-cytometry, we found that treatment with Abx prior to RT leads to an increase in anti-inflammatory ARG1+F4/80+ macrophages ($P<0.05$). The microbiome regulates the response to RT in OCSCC tumors. Strategies targeting the microbiome can have implications for better understanding the interplay between the TME and the microbiome.

#6611 Ferroptotic vulnerability in M1 and M2 macrophages is associated with adaptive radiation resistance in esophageal adenocarcinoma.

Sadhna Aggarwal[1], Rui Ye[2], Jared K. Burks[3], Steven H. Lin[1]

[1]Radiation Oncology, UT MD Anderson Cancer Center, Houston, TX,[2]Systems Biology, UT MD Anderson Cancer Center, Houston, TX,[3]Hematopoietic Biology & Malignancy, UT MD Anderson Cancer Center, Houston, TX

Background: Radiation resistance remains a critical barrier to enhancing cures after chemoradiation therapy (CRT) in esophageal adenocarcinoma (EAC). Ferroptosis, a lipid peroxidation-driven cell death pathway, is increasingly recognized as a regulator of tumor-immune interactions. We investigated how ferroptotic susceptibility of macrophages might differ in radiation responders (GR) and non-responders (NR) in EAC patients using both single cell sequencing and spatial proteomic analysis.
Methods: scRNA-seq and sequential multiplex-IF using Lunaphore COMET were performed on patient biopsies before, during and after CRT to characterize cellular subsets and ferroptosis markers at single-cell resolution. In vitro ferroptosis assays were performed in THP-1, and human PBMC-derived M1/M2 macrophages following 0-12 Gy radiation ± RSL3 or ferrostatin. Ferroptotic activity was assessed by CellTiter-Glo, BODIPY-C11 oxidation, and GPX4 staining (Confocal, flowcytometry).
Results: scRNA-seq confirmed robust myeloid cell expansion in both GR and NR and revealed that pro-ferroptosis gene programs (BH4 biosynthesis, iron utilization and glycolysis pathway) were upregulated in NR both at baseline and during CRT, particularly in the myeloid population, which greatly expands during CRT. Conversely, anti-ferroptosis pathways (GPX4) were enriched in GR and suppressed in NR. COMET profiling revealed that non-responders (NR) displayed higher baseline M2 macrophage density and significantly elevated ferroptosis marker 4-HNE in both M1 and M2 subsets. During CRT, NRs exhibited a further increase in M2 macrophage infiltration, reinforcing an immunosuppressive TME, whereas good responders (GR) maintained higher M1 representation. In vitro, radiation significantly potentiated RSL3-induced ferroptosis in both human and murine macrophage-like cells; ferrostatin rescued viability, confirming ferroptotic cell death. Human macrophages displayed polarization-dependent susceptibility: M2 macrophages were sensitive to radiation-induced ferroptosis, while M1 macrophages were resistant
Conclusion: CRT response appears to relate to macrophage polarization and ferroptosis susceptibility. Non-responders are characterized by (i) M2-dominant macrophage landscapes, (ii) elevated lipid peroxidation, (iii) expansion of ferroptosis-primed myeloid subsets, and (iv) persistent activation of pro-ferroptosis pathways. Collectively this data ascribes macrophage ferroptosis as a potential targetable axis for radio-sensitization in EAC.

#6612 Targeting CPT-1-mediated fatty acid oxidation causes radiation sensitization in glioblastoma.

Kenneth M. Austin[1], Tingting Huang[2], Todd Miller[3], Kelli B. Pointer[4]

[1]Hampton University, Hampton, VA,[2]Radiation Oncology and Applied Sciences, Tingting Huang, Lebanon, NH,[3]Pharmacology & Toxicology and Pathology, Medical College of Wisconsin, Milwaukee, WI,[4]Radiation Oncology and Applied Sciences, Dartmouth Cancer Center, Lebanon, NH

Background: Glioblastoma (GBM) is the most common primary brain tumor in adults and has a median survival of less than two years despite surgery, chemotherapy, and radiotherapy. A subpopulation of glioma stem-like cells (GSCs) survives radiation and repopulates the tumor. Recent studies have shown that GSCs rely heavily on mitochondrial fatty-acid oxidation (FAO) for ATP production, NAD^+ regeneration, and redox balance. Carnitine-palmitoyl-transferase-1 (CPT-1) catalyzes the rate limiting step of FAO by shuttling long-chain fatty acids into the mitochondrial matrix. We therefore hypothesized that pharmacologic inhibition of CPT-1 will limit GSC metabolism and sensitize GSCs to radiation.

Methods: Human GBM cell line U-118 and a patient-derived GSC line (GNS144) were treated for 72 h with perhexiline (5 μM), etomoxir (10 μM), or vehicle control.Cells then received a single fraction of 0, 2, 4, 6, or 8 Gy. Cell viability was measured 48 h later. Sphere formation assays were performed 7-14 days after radiation; sphere number and mean diameter were recorded. Immunoblotting was performed to evaluate for stem cell markers CD44, Nestin, and Vimentin. All experiments were performed in triplicate; statistical significance was assessed by two-way ANOVA with Tukey post-hoc test ($p < 0.05$).

Results: Perhexiline + radiation and etomoxir + radiation produced a dose dependent decline in cell viability compared with radiation alone ($p < 0.001$). Combination treatment reduced sphere number by 55-70 % across the 4-8 Gy range ($p \leq 0.005$) and lowered mean sphere diameter by 30 % ($p \leq 0.005$). Immunoblotting analysis showed a 2-fold reductions in CD44, Nestin, and Vimentin expression in the drug + radiation arms versus radiation alone ($p < 0.01$).

Conclusions: These results suggest that inhibition of CPT-1-mediated FAO with perhexiline or etomoxir enhances radiation induced cell death, suppresses sphere forming capacity, and downregulates key GSC markers in both standard and patient-derived GBM models. These findings should be investigated further and suggest that CPT-1 blockade could be integrated with current standard of care regimens to overcome stem cell driven radiation resistance.

#6614 Targeting the G2/M checkpoint as a radiosensitizing strategy in BRAF wild-type anaplastic thyroid cancer.

Linlin Yang[1], Eric Perez[1], Andrew Hu[2], Rebecca Packard[2], Terence M. Williams[1]

[1]Radiation Oncology, City of Hope, Duarte, CA,[2]The Ohio State Univeristy, Columbus, OH

Background/Purpose: Genomic profiling of aggressive thyroid cancer, particularly anaplastic thyroid cancer (ATC) revealed high frequency of mutations in RAS-RAF pathway. A phase II trial showed that dual inhibition of BRAF and MEK in BRAF mutant ATC leads to high response rates and improved clinical outcomes. However, non-BRAF mutant ATC accounts for ~ 60-70% of cases, underscoring the necessity for targeted strategies to enhance radiosensitivity in BRAF wild-type ($BRAF^{WT}$) ATC. Aside from RAS-RAF variants, ATC exhibits mutations in DNA damage response and cell cycle checkpoints, including inactivating mutation of TP53 (~60-70%). Tumor cells with dysfunctional TP53 have aberrant genome surveillance at the G1/S checkpoint, causing cells to depend on the intact G2/M checkpoint for DNA damage repair after genotoxic therapies. Therefore, we hypothesize that treating TP53 mutant ATC cells with inhibitors of G2/M checkpoint related proteins, such as ATR and WEE1, will enhance the efficacy of radiation therapy (RT).

Materials/Methods: VX970 and AZD1775, which are highly potent and selective inhibitors of ATR and WEE1 respectively, were investigated individually as radiosensitizers in $BRAF^{WT}$ ATC cell lines. IC50s of VX970 and AZD1775 were assessed by AlamarBlue cytotoxicity assay, and the radiosensitizing effects of these drugs were evaluated by radiation clonogenic assays. The biological outcomes of a combination treatment of ATR or WEE1 inhibition and RT were determined by immunoblotting, propidium iodide flow cytometry, and mitotic catastrophe assay. Additionally, mouse heterotopic and orthotopic thyroid tumor models with CT-guided radiation were generated to evaluate the *in vivo* radiosensitizing effects of VX970 and AZD1775.

Results: In TCGA thyroid cancer data, CHEK1/WEE1/CDK1 gene expressions were significantly upregulated in thyroid cancer compared to normal tissues. The IC50 values of VX970 and AZD1775 in the tested ATC cell lines were ~400nM and ~3000nM, respectively. Both VX970 and AZD1775 significantly enhanced the radiosensitivity of 5 $BRAF^{WT}$ ATC cells lines, 4 of which harbor the TP53 mutations. However, no synergy was found with concurrent ATR and WEE1 inhibition compared to single kinase inhibition. Mechanistically, both drugs suppressed p-$CDK1^{Tyr15}$ expression, attenuated radiation-induced G2/M cell cycle arrest, increased DNA damage and enhanced mitotic catastrophe following RT. *In vivo* studies further validated the role of VX970 and AZD1775 as potent radiosensitizers in ATC tumors by heterotopic and orthotopic tumor models.

Conclusion: Targeted inhibition of G2/M checkpoint by ATR/WEE1 inhibitors markedly sensitizes $BRAF^{WT}$ ATC to radiotherapy in both *in vitro* and *in vivo*. Our findings support that ATR/WEE1 inhibition is a promising new strategy to improve the radiotherapy efficacy for BRAF wild-type ATC patients and warrants further clinical exploration.

#6616 Limiting O-GlcNAcylation support prostate cancer radiation sensitivity through metabolic and epigenetic reprogramming.

Manish Thiruvalluvan, Sandrine Billet, Saravana Kumar Kailasam Mani, Joshua Watson, Neil A. Bhowmick

Cedars-Sinai Medical Center, Los Angeles, CA

Background: Prostate cancer (PCa) frequently develops resistance to radiation therapy (RT), driven in part by DNA repair mechanisms. We previously found that glutamine (L-Gln) enables protein O-GlcNAcylation post-translational modifications linked to DNA repair and therapy resistance. This is highly relevant to irradiation of PCa metastatic sites like the bone and liver microenvironments that have markedly high concentrations of L-Gln and accordingly poor response to irradiation. Here, we investigated whether pharmacologic glutamine depletion using sodium phenylbutyrate (SPB) disrupts this axis and enhances radiosensitivity.

Methods: Radio-resistant 22Rv1 and ARCaP$_M$ lines were generated by iterative chronic irradiation. Subcutaneous and liver xenografts were treated with vehicle, SPB, RT, or SPB+RT. Tumors analyzed by bulk RNA-seq, proteomics, and immunoblotting revealed the importance of NDRG1 and PRDX1 o-glycosylation. CRISPR/Cas9 mutagenesis was used to generate O-GlcNAc-deficient NDRG1 and PRDX1 variants. DNA-damage repair, cell-cycle dynamics, and mitochondrial function were assessed by γH2AX staining, flow cytometry, and Seahorse assays.

Results: SPB+RT produced the greatest tumor reduction and significantly reduced circulating and intratumoral glutamine, compared to either RT or SBP alone. Transcriptomic and proteomic analyses showed downregulation of amino-acid transport, fatty-acid metabolism, and histone demethylase activity, indicating broad metabolic and epigenetic reprogramming. Mass spectrometry identified NDRG1 and PRDX1 as radiation-induced O-GlcNAc targets suppressed by SPB. CRISPR-engineered O-GlcNAc-deficient NDRG1 and PRDX1 variants exhibited greater RT sensitivity as a result of persistent γH2AX foci, prolonged G2/M arrest, reduced nuclear localization, and decreased protein stability. RNA-seq of these variants showed enrichment of p53 signaling, endoplasmic reticular (ER) stress with metabolic compensation through increased c-Myc activity, and oxidative phosphorylation. Nucleoside supplementation did not reverse SPB-mediated radio-sensitization, indicating that SPB's effects extended beyond nucleotide depletion. Instead, the data suggested the role of L-Gln addiction in irradiated PCa tumors was due to NDRG1 and PRDX1 in ER stress-response proteins and activating the unfolded protein response.

Conclusions: O-GlcNAcylation of NDRG1 and PRDX1 stabilizes stress-response proteins to support DNA-repair and metabolic fitness after irradiation. SPB disrupts this L-Gln-driven O-GlcNAcylation axis, to impair protein translation supporting significant radio-sensitization. As SPB is used for chronic management of urea cycle disorders, repurposing to overcome radiation resistance provides a near-term therapeutic translation opportunity for PCa patients.

#6617 Targeting the PLK1-PRMT5 axis enhances radiosensitivity in prostate cancer.

Jia Peng, Xinyi Wang, Daheng He, Jianlin Wang, Qianjin Li, Fatemeh Seilani, Xiongjian Rao, Meng Wu, Jinghui Liu, Ruixin Wang, Pingli Mo, Min Zhang, Sai Wu, Yanquan Zhang, Zhiguo Li, Izumi Tadahide, Xiaoqi Liu

Univ. of Kentucky College of Medicine, Lexington, KY

Prostate cancer remains the most frequently diagnosed cancer and the second leading cause of cancer-related death among men in the United States. We previously demonstrated that Polo-like kinase 1 (PLK1) phosphorylates PRMT5 at the S470 site, a modification required to maintain PRMT5 enzymatic activity and to promote DDR in prostate cancer cells. Here, we further uncover the functional consequences of this phosphorylation on cell cycle regulation and radiosensitivity. RNA-seq analysis revealed that PLK1-associated phosphorylation at S470 influences cell cycle-related pathways. Flow cytometry showed that the phospho-deficient PRMT5 mutant (S470A) accumulates in S and G2 phases compared to wild-type cells. Consistently, ChIP-qPCR analysis demonstrated increased binding of H4R3Me2s to genes inducing cell cycle arrest and decreased association with genes driving cell cycle progression in S470A cells. Importantly, both PLK1 inhibition (Onvansertib) and PRMT5 inhibition (Onametostat) synergized with ionizing radiation (IR) to suppress tumor growth in vitro and in vivo. These findings highlight a previously unrecognized role of PLK1-mediated PRMT5 phosphorylation in cell cycle control and radiosensitivity, suggesting that targeting the PLK1-PRMT5 axis may serve as a promising therapeutic strategy to enhance radiotherapy efficacy in prostate cancer.

#6618 Investigation of 8-O-acetylharpagide induced G2/M arrest and radiosensitization effects on hypopharyngeal cancer.

Wan-Yu Yang, Yi-Jang Lee

National Yang Ming Chiao Tung University, Taipei, Taiwan

[Purpose] AT-1 (8-O-acetylharpagide) is a natural compound purified from the endemic Taiwanese plant *Ajuga taiwanensis* and has been reported to possess anti-aging, anti-inflammatory, and anti-cancer properties, such as skin, liver and breast, but its potential role in Hypopharyngeal squamous cell carcinoma (HPSCC) remains unclear. This study aimed to systematically characterize the cellular responses to AT-1 in human hypopharyngeal carcinoma cells (FaDu) versus normal human periodontal ligament fibroblasts (PDL) and to evaluate its selective cytotoxic and radiosensitizing potential.

[Methods] Cell viability was assessed using the MTT assay. Flow cytometry was performed to analyze cell-cycle distribution and apoptosis. DNA damage was evaluated by immunofluorescence staining and comet assay. Western blotting was used to detect changes in cell cycle- and apoptosis-related proteins. Radiation sensitivity was examined following AT-1 pretreatment and subsequent X-ray exposure.

[Results] AT-1 selectively reduced the viability of FaDu cells while exerting minimal cytotoxicity in PDL cells and induced pronounced G2/M phase arrest in FaDu, accompanied by abnormal upregulation of Cyclin B1 and modulation of cell cycle regulators. Apoptosis analysis revealed that AT-1 triggered cell death through downregulation of pro-survival proteins including AKT, p-AKT, and Bcl-2. Intracellular reactive oxygen species levels did not significantly increase, suggesting that oxidative stress was not directly responsible for AT-1-induced cytotoxicity. Immunofluorescence and comet assays confirmed the presence of DNA double-strand breaks in AT-1-treated FaDu cells, which may underlie the observed G2/M arrest and apoptosis. Furthermore, AT-1 pretreatment enhanced the radiosensitivity of FaDu cells, whereas PDL cells remained relatively resistant to AT-1 alone and to the combination treatment. AT-1 inhibits the growth of hypopharyngeal carcinoma cells by perturbing the cell cycle, inducing DNA damage, and promoting apoptosis, and it acts as a selective radiosensitizer in this model.

[Conclusions] These data demonstrate that AT-1 (8-O-acetylharpagide) induces G2/M arrest and selectively radiosensitizes hypopharyngeal cancer cells while sparing normal cells. AT-1 may represent a promising low-toxicity radiosensitizer candidate for head and neck cancer, and further in vivo and mechanistic studies are warranted to define its impact on DNA damage response.

#6619 Inhibition of PLK4 overcomes radioresistance in locally advanced rectal cancer through genomic instability and apoptotic cell death.

Sung Uk Bae[1], Jeong-Woo Hwang[1], Hyewon Lee[2], Hyowon Hong[2], Sang Jun Byun[2]

[1]Surgery, Keimyung University Dongsan Hospital, Daegu, Korea, Republic of,[2]Keimyung University Dongsan Medical Center, Daegu, Korea, Republic of

Background: Polo-like kinase 4 (PLK4), a key regulator of centrosome duplication, has been implicated in cancer progression and therapeutic resistance. Although PLK4 overexpression is frequently observed in various malignancies, its functional contribution to radiotherapy (RT) response in colorectal cancer (CRC) remains poorly understood.
Methods: To investigate whether PLK4 inhibition enhances radiosensitivity, CRC cell lines HCT116 (p53 wild-type) and HT29 (p53 mutant) were treated with the selective PLK4 inhibitor CFI-400945, RT or their combination. Cell viability and clonogenic assays were performed to evaluate cytotoxicity. DNA damage responses were assessed by γH2AX immunofluorescence and Western blot analysis of p-ATM, p-CHK2, and DNA-PKcs. Cell-cycle profiles and centrosomal abnormalities were examined by flow cytometry and γ-tubulin staining, respectively. Apoptosis was determined through cleaved PARP-1 and caspase-3 expression levels.
Results: CFI-400945 treatment reduced cell viability in a dose- and time-dependent manner and significantly enhanced the cytotoxic effects of RT in both CRC cell lines. Combined treatment markedly increased γH2AX foci formation and upregulated DNA damage response proteins, including p-ATM, p-CHK2, and DNA-PKcs. PLK4 inhibition also induced centrosome amplification, micronuclei formation, and multinucleation, indicating mitotic defects leading to genomic instability. Furthermore, the combination therapy enhanced G2/M arrest and apoptosis, as evidenced by elevated levels of cleaved PARP-1 and caspase-3.
Conclusions: PLK4 inhibition sensitizes colorectal cancer cells to radiation by promoting DNA damage accumulation, mitotic catastrophe, and apoptotic cell death. These findings suggest that targeting PLK4 may serve as a potential therapeutic strategy to overcome radioresistance in CRC.

#6620 CYLD induces ferroptosis through ALOX12B to enhance radiosensitivity in non-small cell lung cancer.

Yihan Xu, Jiazhuo Yan, Huiwen Yu, Lu Zhang, Jinpu Yu, Zhiyong Yuan

Tianjin Medical Univ. Cancer Inst. & Hospital, Tianjin, China

Background: Radiotherapy is is a pivotal treatment for locally advanced or inoperable non-small cell lung cancer (NSCLC), however its efficacy is limited by radioresistance. Approximately 44%-46% of patients develop recurrence or metastasis after chemoradiotherapy, with stage III patients showing a 30%-40% local recurrence rate within five years. Identification of effective therapeutic targets to enhance radiosensitivity remains a critical challenge in NSCLC management. This study aims to elucidate the molecular basis of radioresistance and develop novel approaches to enhance tumor radiosensitivity.
Methods: Through RNA transcriptome sequencing of treatment-naive NSCLC patients (n=87) stratified by RECIST into radiotherapy-sensitive (n=55) and -resistant (n=32) cohorts, and based on histopathological and clinical diagnostic data from Tianjin Medical University Cancer Hospital (2015-2020), we analyzed the association between CYLD expression and radiotherapy outcomes through RNA sequencing and tissue microarrays. The impact of CYLD on radiosensitivity was assessed through flow cytometry and colony formation assays, and further verified in nude mouse xenograft models. To investigate CYLD-related pathways, we performed next-generation sequencing and examined its role in ferroptosis through Western blotting, qPCR, glutathione assays, malondialdehyde measurements, lipid peroxidation assessment, and transmission electron microscopy. Potential CYLD-interacting proteins were identified via mass spectrometry, immunofluorescence, and co-immunoprecipitation assays, while CYLD-mediated deubiquitination of ALOX12B was characterized using ubiquitination immunoprecipitation.Furthermore, we combined database predictions with Western blot, qPCR, chromatin immunoprecipitation, and luciferase reporter assays to establish EGR1 as a transcriptional regulator CYLD expression.
Result: Our findings identify CYLD as a positive regulator of radiosensitivity in NSCLC, We demonstrate that CYLD enhances radiation sensitivity in NSCLC by stabilizing ALOX12B. Mechanistically, CYLD enhances ALOX12B protein stability by deubiquitinating K63- and K48-linked ubiquitin chains, thereby suppressing its proteasomal degradation. This stabilization potentiates cellular ferroptosis and consequently increases radiosensitivity. Furthermore, we identified EGR1 as an upstream transcriptional activator of CYLD that promotes ferroptosis in a CYLD-dependent manner.
Conclusion: Our study demonstrates that CYLD, driven by its transcriptional activator EGR1, promotes ferroptosis and enhances radiosensitivity in NSCLC by mediating the deubiquitination and stabilization of ALOX12B. This study identifies CYLD as both a valuable prognostic biomarker and a potential molecular target for radiosensitization in NSCLC.

#6621 Riluzole as a dual targeted radiosensitizer for osteosarcoma: Targeting tumor cells and angiogenic vasculature to enhance single high dose radiotherapy efficacy.

Pooja P. Rao[1], Adriana Haimovitz-Friedman[2], Charis Herbert[3], Syeda Maryam Azeem[4], Raisa Munira[5], Elena Garay[3], Hadi Askarifirouzjaei[2], Shahana Mahajan[1]

[1]Biochemistry, The Graduate Center, CUNY, New York, NY,[2]Radiation Oncology, Memorial Sloan Kettering Cancer Center, New York, NY,[3]Medical Laboratory Sciences, Hunter college, CUNY, New York, NY,[4]Biology, The Graduate Center, CUNY, New York, NY,[5]Biology, Hunter College CUNY, New York, NY

Osteosarcoma (OS), a highly aggressive bone cancer prevalent among young adults, poses significant challenges in treatment, particularly due to its intrinsic resistance to conventional radiation therapy. This necessitates the development of efficacious radiosensitizers to enhance treatment outcomes. Single high-dose radiation therapy (SDRT) has emerged as a promising strategy for combatting radioresistant sarcomas, particularly those characterized by extensive vascularity. However, its use in OS is constrained by potential toxicity to surrounding normal tissues. Radiosensitizers facilitate effective tumor eradication at reduced radiation doses, limiting normal tissue toxicity and optimizing the therapeutic window. Tumor microvasculature and intrinsic tumor cell mechanisms combinedly drive OS radioresistance. Anti-angiogenic therapies have largely failed as radiosensitizers due to compensatory signaling and cross-talk between surviving endothelial and tumor cells, which reinforces radioresistance. These observations highlight the urgent need for strategies that concurrently target both tumor cells and angiogenic vasculature to enhance the efficacy of SDRT. Riluzole, an FDA-approved drug for Amyotrophic Lateral Sclerosis, is currently under investigation for repurposing in OS treatment. By inhibiting glutamate release and downregulating xCT/SLC7A11, Riluzole increases reactive oxygen species production, promotes DNA damage and induces apoptosis in tumor cells. In parallel, it has shown to inhibit vascular endothelial growth factor A (VEGFA) induced endothelial cell proliferation and abnormal vessel formation. These combined mechanisms positions Riluzole as a promising dual-target radiosensitizer capable of overcoming key limitations of current therapies. In this study, we hypothesize that Riluzole increases the radiosensitivity of OS tumors to SDRT by targeting radioresistance mechanisms in both tumor cells and angiogenic vasculature. Our preliminary results demonstrate that Riluzole significantly reduced the survival fraction of irradiated OS cells compared to cells only exposed to SDRT, signifying potent radiosensitization. Combination treatment markedly increased apoptosis relative to either treatment alone. Mechanistically, Riluzole significantly inhibited the activity of DNA repair enzyme PARP1, and increased radiation induced ROS levels, resulting in enhanced radiation induced DNA damage. Additionally, pre-treatment with Riluzole reduced VEGFA levels in OS cells, suggesting its potential anti-angiogenic activity. In the long term, our objective is to translate these laboratory discoveries into pre-clinical and clinical studies, potentially offering a novel therapeutic approach of radiation therapy for OS patients.

#6622 Novel selective binders for gastrointestinal DCLK1 isoforms.

Uzma Uzmi[1], Shahid Umar[2], Prashanthi Karyala[3], **Rao VL Papineni**[4]

[1]Surgery, PACT and Health, Branford, CT,[2]University of Kansas Medical Center, Kansas City, KS,[3]Applied Sciences, MS Ramaiah, Bengaluru, India,[4]Surgery, University of Kansas Medical Center, Kansas City, KS

Doublecortin-like kinase 1 (DCLK1) is a microtubule-associated protein kinase that plays a critical role in the maintenance of gastrointestinal (GI) epithelial integrity and regeneration. Emerging evidence highlights the functional divergence of its isoforms—particularly the long and short forms—which are differentially expressed during homeostasis and disease. In healthy GI tissue, DCLK1-long primarily maintains stem cell quiescence and epithelial repair. Conversely, DCLK1-short is markedly elevated in several GI malignancies and is associated with oncogenic transformation, invasion, and poor prognosis. We are investigating compounds that modulate DCLK1 isoforms to mitigate irradiation-induced gastrointestinal acute radiation syndrome (GI-ARS). Our research demonstrates that 2-deoxyglucose (2DG) and its non-metabolizable analogue differentially regulate crypt and colonoid growth in ex vivo systems. Treatment with 2DG results in selective suppression of the DCLK1-short isoform while sparing or modestly enhancing the DCLK1-long variant, suggesting a potential therapeutic window for targeting tumor-specific isoform expression. To further identify molecular binders capable of modulating DCLK1 activity, we employed a structure-based virtual screening approach using a focused library of 100,000 small molecules. High-throughput in silico docking enabled the identification of several high-affinity lead compounds with potential isoform-selective binding. The strategy of small-molecule screening offers a promising approach for selective intervention in DCLK1-driven pathologies in GI tissue repair.

#6623 Stem cell transdetermination is a targetable driver of therapeutic response to neoadjuvant chemoradiotherapy in rectal cancer.

Nick Li[1], Petra Vlckova[1], Alistair Wilkinson[1], Ewa Basiarz[1], Aurelie Dobric[1], Corinne Molyneux[1], Rhianna O'Sullivan[1], Shauna Crampsie[1], Benoit Bilanges[1], Bart Vanhaesebroeck[2], Maria A. Hawkins[3], Chris Tape[1]

[1]University College London (UCL) Cancer Institute, London, United Kingdom,[2]Centre Lead, Centre for Cell Signalling, University College London Cancer Institute, London, United Kingdom,[3]Department of Physics and Biomedical Engineering, University College London (UCL), London, United Kingdom

Neoadjuvant chemoradiotherapy (nCRT) is used in about one third of rectal cancer cases in the UK, but treatment response is heterogeneous, leading to difficulties in response prediction and sensitization. Phenotypic plasticity, driven by both cell-intrinsic mutations and cell-extrinsic signals from the tumour microenvironment (TME) has been shown to influence therapy resistance in colorectal cancer. This study explores the role of proliferative cancer stem cells (proCSCs) and revival cancer stem cells (revCSCs) in CRT response, and how phenotypic plasticity can be targeted to improve CRT sensitivity.

Patient-derived organoids (PDOs) from a cohort of 10 patients with microsatellite-stable rectal cancer were subject to combinatorial perturbations of radiation, chemotherapy, exploratory radiosensitizers, and co-culture with cancer associated fibroblasts (CAFs). PDOs were analysed 3 hours and 48 hours after radiation in triplicate, totalling 2,400 experimental conditions. PDOs were analysed using single-cell thiol-organoid barcoding *in situ* mass cytometry (TOB*is* MC), enabling high-dimensional characterisation of CSC states, DNA damage responses, canonical signalling pathways, cell cycle, and apoptosis.

PDOs displayed heterogeneous, patient-specific responses to CRT, and could be classified in the following manner: 1) high signalling response, high apoptosis; 2) high signalling response, low apoptosis; and 3) low signalling response, low apoptosis. Therapy-induced apoptosis did not correlate with on-target DNA damage, but instead strongly aligned with baseline stem cell index (SCI), a metric that describes the relative proCSC-revCSC ratio of each PDO. Higher rates of apoptosis were seen in PDOs that were proCSC-dominant at baseline (high-SCI), whereas revCSC-dominant PDOs (low-SCI) were more resistant apoptosis after treatment. In certain low-SCI PDOs, the proCSC population could be enriched using a PI3Ka activator before radiation, resulting in increased apoptosis after radiation with little toxicity. After CRT, a significant reduction in SCI was seen across the cohort. Blockade of revCSC transdetermination with a YAP/TEAD1 inhibitor also resulted in increased radiation-induced apoptosis. Highly plastic PDOs exhibiting large differences SCI following CRT were identified by high DACH1 expression.

This study suggests that the initial level of on-target DNA-damage following CRT does not dictate cell death, rather, it is due to what state the cancer cell is in when the damage occurs. We find that rectal cancer cells in a proCSC state typically enter apoptosis in response to DNA damage, whereas cancer cells in the revCSC state survive therapy. We also find that pharmacologically enriching proCSCs and blocking access to the revCSC state can sensitize PDOs to CRT, and may have therapeutic importance in treating rectal cancer.

#6624 Exploiting radiation-induced tumor vulnerabilities via targeted antibody-drug conjugates.

P.M. Quan Mai[1], Prapannajeet Biswal[1], Prudhvi Chand Mallepaddi[1], Ngoc Tuyet Tra[1], Sai Kumar Samala[1], Shafqat Ehsan[2], Bhoomika Muruvekere Lakshmisha[1], Khadijeh Koushki[1], Muhammad A. Shohayeb[1], Lydia WT Cheung[1], Geraldine Vijay[1], Sunil Krishnan[1]

[1]Vivian L. Smith Department of Neurosurgery, University of Texas Health Science Center at Houston, Houston, TX,[2]University of Texas MD Anderson UTHealth Houston Graduate School of Biomedical Sciences, Houston, TX

Background: Antibody-drug conjugates (ADCs) demonstrate potent anti-cancer activity but may cause on-target off-tumor toxicity in normal tissues if the target antigen is not strictly tumor-specific. To address this, we leverage on radiation therapy (RT), a main pillar in gastric (GC) and colorectal cancer (CRC) treatment, to kill cancer cells while simultaneously triggering a cancer-specific response that relocates Heat Shock Protein A5 (HSPA5). HSPA5 is intrinsically localized to the endoplasmic reticulum (ER). The ability of RT to promote HSPA5 translocation from ER to the cell surface (cs) opens an opportunity to target cancer cells with anti-HSPA5 ADC. We seek to understand RT-induced csHSPA5 biology and target it via ADC.
Methods: We mined the TCGA data for HSPA5 expression in normal and GC or CRC tissues and for its correlation with patient prognosis. Irradiated human (AGS and MKN45) and murine (YTN16) GC, human (HCT116 and HT29) CRC cells were subjected to flow cytometry (FC) and immunofluorescence (IF) for csHSPA5 levels. csHSPA5+ cells' tumorigenicity was examined by co-staining the cells with HSPA5 and Ki67 (proliferation), CD44 (stemness), N-cadherin (EMT) via FC. To examine the involvement of O-glycosylation in HSPA5 cell-surface presentation, we performed co-immunoprecipitation to detect potential O-glycosylation regulators and inhibited O-glycosylation in AGS (+/-RT). To assess HSPA5 antibody biodistribution, we injected GC/CRC nude mice with anti-HSPA5 antibody-Alexa Fluor 647 dye prior to imaging, with the tumors and organs harvested for FC and IF. Lastly, Annexin V/PI staining was performed with AGS and HUVEC cells treated with RT+anti-HSPA5 ADC.
Results: Expression levels of HSPA5 are higher in GC and CRC against their normal counterparts and are correlated with worse patient prognosis. We detected RT-induced elevation of csHSPA5 in all GC/CRC cells, notably not in normal HUVEC or GES1. csHSPA5+ population is enriched for Ki67+, CD44+, and N-cadherin+ cells compared to csHSPA5- population, indicating the tumorigenic phenotypes of csHSPA5+ cells. Interestingly, our data revealed the cancer-specific csHSPA5 translocation mechanism, in which HSPA5 binds to N-acetylgalactosaminyltransferase 2 (GALNT2) and N-acetylgalactosamine (O-GalNAC) only in cancer cells but not normal cells. Inhibiting O-glycosylation blocks RT-induced HSPA5 cell-surface translocation. The *in vivo* models showed a significant accumulation of HSPA5 antibody in radiated tumors compared to non-irradiated tumors or healthy organs. Moreover, RT+ADC significantly decreased %live cells compared to RT or ADC alone. RT+ADC caused no decreased viability of the normal HUVEC cells, reflecting the low toxicity in healthy cells.
Conclusion: The overexpression of HSPA5 in cancer, coupled with radiation-induced cell-surface expression, renders it a promising ADC target for achieving high anti-tumor specificity.

#6625 Photodynamic activation of CX-5461 enhances its anti-tumor efficacy.

Jakub Trojnar[1], Marta Dudek[1], Kai-Wei Hsueh[2], Ping-Yen Huang[2], **Marco Deiana**[1]

[1]Wrocław University of Science and Technology, Institute of Advanced Materials, Wrocław, Poland,[2]Senhwa Biosciences Inc., New Taipei City, Taiwan

Introduction: CX-5461 (Pidnarulex) is the first selective inhibitor of RNA Polymerase I (Pol I) and a potent stabilizer of DNA G-quadruplexes (G4s), with additional activity as a TOP2 poison. Beyond its transcriptional inhibition, CX-5461 induces cell-cycle arrest, apoptosis, and DNA double-strand breaks, exhibiting broad anti-proliferative effects across diverse cancer models. Clinically, CX-5461 shows promising efficacy in advanced hematologic and solid tumors, such as breast, pancreatic, and ovarian cancers, with phototoxicity as the main adverse effect, manageable through sun protection. G4 structures are guanine-rich and inherently prone to oxidative modification, which has recently positioned them as promising targets for light-activated therapeutics. CX-5461 is known to be light-sensitive and capable of inducing phototoxic reactions; however, in this study we leverage this property as a functional advantage rather than a limitation. We show that CX-5461 acts as an efficient photosensitizer: upon UV irradiation, it generates reactive oxygen species (ROS), leading to enhanced oxidative DNA damage and an approximately ten-fold increase in cytotoxicity relative to its dark state, at concentrations that are otherwise minimally toxic. These findings reveal a photo-responsive mechanism of action for CX-5461, in which G4 binding and light-induced ROS generation converge to potentiate its anti-tumor activity.

Materials and Methods: CT26 and B16F10 cells were treated with a serial dilution of CX-5461, with or without UV exposure. DNA damage, ROS levels, and cell viability were analyzed. In the CT26 syngeneic model, CX-5461 was administered at 25 mg/kg, iv, weekly, alongside UV exposure (10 J/cm^2) for the first three days. B16F10 models received CX-5461 at 25 or 50 mg/kg, iv, weekly, with UV exposure (5 J/cm^2) on Day 1. Tumor size and survival were measured.

Results: CX-5461 exhibits strong absorbance in the UV region and generates both type I and type II reactive oxygen species (ROS), including superoxide anion, hydroxyl radicals, and singlet oxygen, upon UV irradiation. This exposure increased oxidative damage to 8-oxoG, raised ROS levels, and enhanced cytotoxicity in CT26 and B16F10 cells. In vivo studies confirmed that the combination of CX-5461 and UV light significantly inhibited tumor growth in the B16F10 model, with a tumor growth inhibition (TGI) of approximately 100% on Day 12, and in the CT26 model, with a TGI of around 74% on Day 14.

Conclusion: CX-5461 is a photosensitizer that produces both type I and type II ROS, which increases its cytotoxic effects in vitro when exposed to UV light. The efficacy of CX-5461 in combination with UV treatment has been demonstrated in syngeneic models like CT26 and B16F10. These findings suggest that the phototoxic properties of CX-5461 could represent a novel therapeutic strategy for treating of cancers that are amenable to UV light exposure.

#6626 Atomically precise NHC-stabilized gold nanoclusters for enhanced photodynamic and X ray activated cancer therapy.

Hetvi Shah[1], Angus Isaac Sullivan[2], Juan Chen[2], Gang Zheng[2]

[1]Pharmaceutical Sciences, University of Toronto, Toronto, ON, Canada,[2]Princess Margaret Cancer Centre, Toronto, ON, Canada

Gold nanoclusters (AuNCs) are atomically precise, ultrasmall (<2 nm) nanoparticles that exhibit favorable biocompatibility and renal clearance properties[1-2]. N-heterocyclic carbene (NHC) functionalized gold nanoclusters (NHC-AuNCs) are a new class of nanomaterials with high chemical stability, structural tunability, and strong potential to amplify radiation-induced cytotoxicity [3-4]. We have synthesized bis-N-heterocyclic carbene (NHC)-protected Au_{13} nanoclusters that display intrinsic photoluminescence quantum yields, making them attractive candidates for cancer theranostics. Our objective is to improve their therapeutic performance by enhancing their distribution, increasing their tumor-targeting capability, and employing them as sensitizers for photodynamic therapy and/or radiotherapy (RT). In this work, we developed novel NHC-AuNCs with ~20-30% reactive oxygen species (ROS) production efficiency, a key property for inducing ROS-mediated DNA damage in cancer cells. We performed *in vitro* studies, including cytotoxicity, cellular uptake, and PDT potency evaluation, to assess their effectiveness as PDT agents. ICP-MS analyses verified efficient cellular uptake across multiple pancreatic cancer cell lines. Upon PDT irradiation at 10 and 20 J/cm^2, treatment with 5 µM NHC-AuNCs induced over 90% cell death, whereas negligible cytotoxicity was observed in both non-AuNC-treated and no-light-treated control groups. These NHC-AuNCs show high PDT efficacy at half the concentration compared to previously tested AuNCs, making them a potent PDT agent. Ongoing work focuses on refining the nanocluster framework to enhance tumor specificity. The incorporation of surface azide groups enables click-chemistry conjugation of targeting peptides to improve tumour targeting. In parallel, *in vivo* studies assessing biodistribution, PDT efficacy, and survival outcomes in tumor-bearing models are underway to establish the therapeutic potential of these NHC-stabilized AuNCs.The ability of these nanoclusters to act as potent PDT agents provides a powerful nanoplatform for advancing cancer targeted therapy. The ability of various NHC-AuNCs with different photophysical and chemical properties to act as PDT agents will be discussed.

References [1] Huang, Y etc., *Nat. Nanotechnol.* 2023, *18* (6), 637-646. [2] Zhang, X.-D. etc., Enhanced Tumor Accumulation of Sub-2 Nm Gold Nanoclusters for Cancer Radiation Therapy. *Advanced Healthcare Materials* 2014, *3* (1), 133-141. [3] Kulkarni, V. etc., Impact of ligand Structure on Biological Activity and Photophysical Properties of NHC-Protected Au13 Nanoclusters. *J. Am. Chem. Soc* 2025, 147 (5) 4017-4025. [4] Sullivan, A. etc. Diving into Unknown Waters: Water-Soluble Clickable Au13 Nanoclusters Protected with N-Heterocyclic Carbenes for Bio-Medical Applications. *J. Am. Chem. Soc* 2025, 147 (5) 4230-4238.

#6627 Integrating padeliporfin vascular-targeted photodynamic therapy with enfortumab vedotin and immune checkpoint blockade in urothelial cancer models.

Abraham R. Meyerson[1], Daniel V. Rodriguez[1], Fengshen Kuo[2], Sanaz Firouzi[1], Sadna Budhu[3], Kwanghee Kim[1], Jonathan Coleman[1]

[1]Urology, Memorial Sloan Kettering Cancer Center, New York, NY,[2]Memorial Sloan Kettering Cancer Center, New York, NY,[3]Weill Cornell Medical College, New York, NY

Vascular-targeted photodynamic therapy (VTP) has demonstrated efficacy in the ongoing phase III trial for low-grade upper tract urothelial carcinoma (UTUC), achieving a 78% complete response rate (NCT0420239). VTP is a local ablation therapy where light activated padeliporfin occludes tumor blood vessels, causing tumor necrosis while sparing healthy urothelium. VTP induces systemic antitumor immunity and was reported to potentiate PD-1/PD-L1 immune checkpoint blockade (ICB) while preventing lung metastases in kidney and bladder cancer models. Enfortumab vedotin (EV), an antibody-drug conjugate targeting Nectin-4, with pembrolizumab (Pembro), improved overall and progression-free survival versus chemotherapy in locally advanced or metastatic urothelial carcinoma, with a 30.4% complete response rate (Phase III EV-302/KEYNOTE-A39, NCT04223856). Given the local ablation and immune activities of VTP, its combination with EV+Pembro may improve UTUC responses.

To better understand how patients with UTUC might benefit from such combination strategies, we investigated antibody drug conjugate (ADC) and ICB target expression using bulk RNA-seq from a UTUC patient cohort at MSKCC (n=100). A correlative study of patient PBMC samples from the VTP Phase-1 trial (NCT03617003) was performed to assess immune-modulatory activities. The effects of VTP on ADC and ICB expression were assessed using preclinical and patient tissue. Therapeutic activities of VTP in combination with ICB or EV in urothelial cancer were evaluated using both syngeneic and patient-derived xenograft (PDX) models.

ADC targets (Nectin-4, Trop2, and ERBB2) were expressed higher in patients with luminal papillary compared to variant histology such as basal and squamous subtypes. ICB targets (PD1, PDL-1, CTLA-4) were higher in aggressive UTUC cases. A PDX model (UCC14) with luminal papillary characteristics and high Nectin-4 demonstrated tumor regression with 3 doses of EV. Flow cytometric analyses of patient PBMCs and preclinical data using the MB49 bladder cancer model demonstrated $CD8^+$ T cell-driven immune modulation, leading us to hypothesize that VTP may complement EV and anti-PD1 by converting immune-desert tumors into more inflamed, treatment-responsive phenotypes. UCC14 and an MB49 high-Nectin-4 model are currently being evaluated to determine whether combining VTP with EV and/or Pembro enhances immune infiltration and response durability, providing translational rationale for integrating VTP with EV+Pembro in UTUC.

#6628 Cancer photodynamic therapy: Silicon quantum dots as therapeutic nanomaterials.

Dorra Gargouri, Artjima Ounkaew, David Antoniuk, Jonathan Veinot, Xuyang Liu

Applied Quantum Materials, Inc., Edmonton, AB, Canada

Cancer photodynamic therapy (PDT) is a minimally invasive cancer treatment that uses photosensitizers to generate reactive oxygen species (ROS) and induce selective tumor cell death. Conventional PDT agents, including organic dyes and metal-based nanoparticles, face significant limitations such as photobleaching, poor tissue penetration, toxicity, and limited photostability which restrict their clinical effectiveness. Silicon quantum dots (SiQDs) offer a new alternative of photosensitizers that can overcome these limitations. The nanomaterials have already shown strong potential in cancer detection and diagnostics. In addition, SiQDs are also ideal PDT agents because they are heavy-metal-free, non-toxic, biocompatible, photostable, and exhibit tunable optical properties with customizable surfaces for targeted delivery, enhanced precision and therapeutics. Applied Quantum Materials Inc. (AQM) synthesizes SiQDs that are highly-pure, have a narrow-size-distribution and showcase exquisite control over surface modifications (including biomolecule conjugation of 8-150 kDa). These nanomaterials display bright, size-dependent luminescence across the visible-NIR spectrum. Biocompatibility studies show >90% cell viability at concentrations up to 500 µg/mL after 24 h incubation, indicating SiQDs have great potential for clinical translation. AQM's recent advances have shown enhanced material uptake into cancer cells along with improved light-triggered therapeutic activity. Under low-level NIR laser irradiation, findings exhibited significantly reduced cancer cell viability, correlating with increased intracellular ROS generation. Initial results indicate cancer cells destruction in 10 minutes. These outcomes offer great potential for SiQDs as effective photosensitizers for PDT.

: Real World Data to Provide Real World Evidence
Poster Session

#6632 Trends in treatment and survival among patients with glioblastoma in the United States, 2000 to 2020: A population-based SEER analysis.

Jianan Chen, Qiong Wu, Catherine Boldig, Rob J B Macaulay, Arnold Etame

Moffitt Cancer Center, Tampa, FL

Background: Population-level patterns in the real-world use of initial treatment combinations for glioblastoma remain poorly characterized. We evaluated national trends in treatment uptake over two decades and examined their associations with survival outcomes.
Methods: We assessed temporal trends (2000-2020) in treatment and survival among 46,186 patients with glioblastoma in the SEER registry. Logistic regression modeled treatment utilization, and Cox regression estimated survival.
Results: Among 46,186 patients (50.0% aged 40-65; 43.0% aged ≥65; 58.0% male), 43.5% underwent gross total resection (GTR), 32.0% subtotal resection, and 24.5% no surgery; 71.8% received radiotherapy and 61.3% received chemotherapy. From 2000 to 2020, utilization increased for any surgery (OR/year 1.03, 95% CI 1.028-1.036), radiotherapy (1.01, 1.010-1.017), and chemotherapy (1.08, 1.081-1.088), whereas the likelihood of GTR vs subtotal resection declined (0.92, 0.915-0.922). Triple therapy increased modestly (1.01, 1.005-1.012) but plateaued at 30%. Older age, non-lobar tumors, unmarried status, and lower income predicted lower odds of triple therapy; after adjustment, calendar year showed a marginal decline (aOR/year 0.99, 0.99-1.00). Median overall survival improved from 6.0 to 10.0 months, with gains in fixed-time survival.
Conclusion: Standard triple therapy conferred the greatest survival benefit; however, GTR rates did not rise in recent years, and substantial disparities in receipt of standard care persisted. Efforts to expand equitable access and prioritize maximal safe resection are essential to achieve greater population-level survival gains.

#6633 PD-L1 expression-dependent efficacy of first-line immune checkpoint inhibitor plus chemotherapy in advanced gastric and gastroesophageal junction adenocarcinoma: A systematic review and meta-analysis of phase III trials.

Jialun Lyu[1], Zhenzhen Zhang[1], Krishnapriya Thangaretnam[1], Md Obaidul Islam[1], Jason Tang[2], Sabine Denize[3], Nadeem Bhat[1], Shoumin Zhu[4], Heng Lu[5], Dunfa Peng[1], Wael El Rifai[1], Zheng Chen[1]

[1]University of Miami Miller School of Medicine, Miami, FL,[2]American Heritage Schools, Plantation, FL,[3]Doctors Charter School of Miami Shores, Miami Shores, FL,[4]University of Miami - Sylvester Comprehensive Cancer Center, Miami, FL,[5]University of Miami, Miami, FL

Background: Immune checkpoint inhibitors (ICIs) have transformed the first-line management of advanced gastric and gastroesophageal junction adenocarcinoma. Several phase III trials have evaluated adding an ICI to chemotherapy, yet results have been heterogeneous. This study aimed to determine the efficacy and safety of first-line ICI plus chemotherapy versus chemotherapy alone and to define a clinically meaningful PD-L1 expression threshold through a systematic review and meta-analysis of randomized phase III trials.
Methods: PubMed, Embase, and the Cochrane Registry of Clinical Controlled Trials were systematically searched up to September 2025. The studies included in this analysis were Phase III randomized controlled trials that compared immune checkpoint inhibitors (ICI) combined with chemotherapy to chemotherapy alone in the treatment of patients with advanced or metastatic gastric cancer or GEJ adenocarcinoma. The combined hazard ratios (HRs) and 95% confidence intervals (CIs) for overall survival (OS) and progression-free survival (PFS) were calculated using a random-effects model. Subgroup analyses were conducted based on the PD-L1 combined positive score (CPS), age, gender, ECOG performance status score (ECOG), geographical region, liver metastasis and tumor location. Safety was assessed through the combined hazard ratio (RR) of grade ≥3 adverse events (AEs) and serious adverse events (SAEs).
Results: Eight phase III trials involving 7,127 patients with previously untreated, HER2-negative, advanced or metastatic gastric or GEJ adenocarcinoma were included. The pooled analysis showed significant improvement in OS (HR = 0.79, 95% CI 0.75-0.83) and PFS (HR = 0.71, 95% CI 0.65-0.79) with ICI plus chemotherapy versus chemotherapy alone. Treatment benefit increased with higher PD-L1 CPS: OS HRs were 0.90 (CPS < 1), 0.76 (CPS ≥ 1), 0.75 (CPS ≥ 5), and 0.65 (CPS ≥ 10); similar trends were seen for PFS (0.87, 0.73, 0.65, 0.63, respectively). Efficacy was consistent across major subgroups (all interaction $p > 0.05$). Combination therapy modestly increased grade ≥3 AEs (RR = 1.16, 95% CI 1.09-1.23) and SAEs (RR = 1.54, 95% CI 1.35-1.77) compared with chemotherapy alone.
Conclusions: First-line ICI plus chemotherapy significantly prolongs OS and PFS in advanced gastric and GEJ adenocarcinoma, with manageable toxicity. The magnitude of benefit is mainly driven by PD-L1 expression, supporting CPS as a clinically meaningful biomarker for treatment selection. ICI-based combinations should be considered a new standard of care across clinically relevant subgroups.

#6634 Real-world comparative outcomes of nivolumab + ipilimumab vs. atezolizumab + bevacizumab in advanced hepatocellular carcinoma: A TRINETX study.

Sameh Gomaa[1], **Abdelrahman Omara**[1], Hatem Ahmed[1], Imad Alabdul Razzak[1], Potdar Rashmika[1], Kuang-Yi Wen[2]

[1]Towerhealth Phoenixville Hospital, Phoenixville, PA,[2]Jefferson Health Sidney Kimmel Comprehensive Cancer Center, Philadelphia, PA

Hepatocellular carcinoma (HCC) is the second leading cause of cancer-related death. Atezolizumab plus Bevacizumab (ATZ+BEV) has transformed the treatment landscape for advanced HCC and is now a first-line option following the IMbrave150 trial. The Checkmate 040 randomized controlled trial has shown that Nivolumab plus Ipilimumab (NIVO+IPI) has improved long-term survival benefit. This study aims to compare outcomes of both treatment modalities for advanced HCC. Methods This is a retrospective cohort study utilizing the TriNetX database. Criteria included adult patients >18 years of age with Advanced HCC recently initiating (ATZ+BEV) or (NIVO+IPI). Outcomes are overall survival, the most recent AFP, AST, ALT, Bilirubin, INR, and Platelet count levels. Time to AFP to reach 0-40 ng/ml. Risk of developing hepatic encephalopathy or coma, hospitalization, and adverse events. Propensity score matching (PSM) was performed for demographics, lab results, MELD and ECOG scores, and confounding comorbidities. Results were expressed in the form of risk difference (RD) with 95% CI. Time to event endpoints using Kaplan-Meier curves and Cox proportional hazards models are reported as hazard ratios (HR) and log-rank P values. Results After matching, the cohort included 1979 patients in the (ATZ+BEV) group and 1973 patients in the (NIVO+IPI) group. (ATZ+BEV) showed significantly increased median survival 997 vs 504 days (HR 0.67, 95 % CI 0.61-0.74 log-rank $p < 0.0001$). However, mean AFP differed statistically (ATZ+BEV) 7,746 vs (NIVO+IPI) 17,495 $p = 0.006$. The time to normalization of AFP to below 40 was not significant ($p = 0.196$). (ATZ+BEV) Recipients experienced a high risk of inpatient visits (RD 2.08%, 95% CI -3.089, 7.257, $P = 0.43$). The risk of developing predefined adverse events was similar between regimens with nonsignificant RD. In conclusion, this real-world matched cohort (ATZ+BEV) conferred superior overall survival but was associated and greater healthcare utilization, while adverse event rates were comparable between treatments.

#6635 Evaluation of stage IV PTCL, NOS of the liver and gastrointestinal tract using a large national cancer database.

Olivia Davis[1], Taha Al-Juhaishi[2], Ryan Wilcox[3]

[1]Department of Internal Medicine, University of Michigan, Ann Arbor, MI,[2]Department of Internal Medicine, Division of Hematology/Oncology, University of Oklahoma, OU Health, Oklahoma City, OK,[3]Department of Internal Medicine, Division of Hematology/Oncology, University of Michigan, Ann Arbor, MI

Introduction: Peripheral T-cell lymphoma, not otherwise specified (PTCL, NOS) is a heterogeneous group of PTCL for which extranodal involvement is common and outcomes are poor. Previous research has suggested that primary disease site may impact overall survival (OS) for early-stage PTCL, NOS with worse outcomes for patients with gastrointestinal/genitourinary involvement. Little is known about the role of primary disease site in advanced stage disease and the impact of discrete gastrointestinal organ involvement. The purpose of this study was to investigate outcomes for stage IV PTCL, NOS with extranodal involvement using a national cancer database.
Methods: Patient and disease characteristics for individuals diagnosed with PTCL, NOS between 2000 and 2015 were extracted from the Surveillance, Epidemiology, and End Results (SEER) database. Patients with extranodal stage IV PTCL, NOS were isolated and included in the final analysis to reflect cases of extensive extranodal involvement. Primary disease sites were grouped into 11 distinct categories based on the most common primary sites identified. Our main primary disease sites of interest were liver and luminal GI tract, but other primary disease sites were analyzed as well with spleen serving as the comparison group. Patient and disease characteristics were analyzed using summary statistics. Survival analyses were performed using the Kaplan-Meier method and Cox proportional hazards models. Treatment status was identified for each case, and survival was compared between chemotherapy and non-chemotherapy groups for each primary disease site.
Results: A total of 464 patients were included in the final analysis. Median age was 63.0 years. Most patients were non-Hispanic white (60.8%) or male (62.3%). Thirteen cases (2.8%) involved primary disease of the liver while 70 cases (15.1%) involved the GI tract. Median OS for stage IV PTCL, NOS involving the liver was 1 month (95% CI (0-4)]. Median OS for stage IV PTCL, NOS of the GI tract was 4 months [95% CI (3-5)]. Primary disease of the liver was associated with worse lymphoma-specific survival [HR=2.400, 95% CI (1.081-5.328); p-value=0.0314]. Primary disease of the GI tract was associated with worse lymphoma-specific survival [HR=2.090, 95% CI (1.220-3.579); p-value=0.0073] and overall survival [HR=1.797, 95% CI (1.121-2.881); p-value=0.0149]. No statistically significant difference in overall survival or disease-specific survival was detected between treatment groups for PTCL, NOS of the liver [HR=0.780, 95% CI (0.185-3.287); p-value=0.7354].
Conclusions: Stage IV PTCL, NOS of the luminal GI tract was associated with worse OS and disease-specific survival. Stage IV PTCL, NOS of the liver was associated with worse disease-specific survival and may be considered a chemotherapy-resistant compartment.

#6636 Clinical outcomes of stage IV mucinous adenocarcinoma based on primary sites.

Wongi Woo[1], Seoin Kim[2], Jongwoo Kim[2], Vincent Lopez[1], Yeena Lee[1], Kirun Chohan[1], Young Kwang Chae[3]

[1]St.Joseph's Medical Center Stockton, Stockton, CA,[2]Metrowest Medical Center, Framingham, MA,[3]Northwestern Univ. Feinberg School of Medicine, Chicago, IL

Background: Mucinous adenocarcinoma (MAC) is an uncommon adenocarcinoma subtype that arises in multiple organs. Its biology and prognosis vary by site, and evidence supporting treatment benefit in stage IV MAC is limited. This study compared clinical features and survival outcomes of stage IV MAC across primary sites with emphasis on pulmonary MAC.
Methods: Clinical data were extracted from the Surveillance, Epidemiology, and End Results (SEER) 17 registries from 2000 to 2021. Patients initially diagnosed with stage IV MAC using the seventh or eighth TNM classification were included. Four major primary sites were analyzed: colorectal, lung, pancreas, and stomach. Exclusions were adenocarcinoma in situ, minimally invasive adenocarcinoma, stage I to III, and missing survival information. Demographic and clinicopathologic variables including age, sex, tumor stage, and socioeconomic factors were assessed with Cox proportional hazard regression to evaluate risk factors for overall survival. Survival differences by treatment were compared across sites by Kaplan Meier lwith log-rank test.
Results: A total of 1,036 patients were included: colorectal (n = 489), pulmonary (n = 160), pancreas (n = 331), and stomach (n = 56). Median age differed across sites ($p < 0.001$), with pulmonary MAC presenting at the oldest age and showing the highest proportion of advanced nodal disease ($p < 0.001$). Survival varied by primary site: Compared with colorectal MAC, pulmonary MAC (hazard ratio [HR] 1.66; 95% confidence interval [CI] 1.31-2.11; $p < 0.0001$) and stomach MAC (HR 1.64; 95% CI 1.13-2.37; $p = 0.009$) had worse outcomes, while pancreatic MAC had the poorest prognosis (HR 2.78; 95% CI 2.36-3.29; $p < 0.0001$). Surgery plus chemotherapy improved survival compared with chemotherapy alone in most sites (colorectal, HR 0.38, $p < 0.001$; lung, HR 0.49, $p = 0.024$; pancreas, HR 0.66, $p = 0.003$). Additionally, Higher income level was associated with better survival (HR 0.61; 95% CI 0.44-0.85; $p = 0.003$).
Conclusions: Stage IV MAC shows marked site specific survival differences. Pulmonary MAC has more favorable outcomes than pancreatic MAC, particularly with multimodal therapy. Tumor related macro/microenvironmental features and molecular profiles may contribute to these differences. The benefit of surgery plus chemotherapy was observed in most MAC. Prospective studies that integrate genomic and treatment related data are needed to guide personalized management.

#6637 Real world outcomes for patients with *KRAS G12D*-mutated non-small cell lung cancer: A University of California Health Data Warehouse retrospective analysis.

Jingtong Liang[1], Tali Azenkot[2], Sandip Patel[2]

[1]Department of Microbiology, Immunology, and Molecular Genetics, University of California Los Angeles - UCLA, Los Angeles, CA,[2]University of California San Diego - Moores Cancer Center, San Diego, CA

Background: KRAS is the most common driver mutation in non-small cell lung cancer (NSCLC), with *G12C* and *G12D* among its most frequent point mutations. Patients with *KRAS G12D* mutations are more likely to be never-smokers with worse response to immune checkpoint inhibitors (ICI) compared to those with *KRAS G12C*. As *KRAS G12D*-targeted therapies are under development, a greater understanding of real-world outcomes associated with current standard-of-care treatments is warranted.

Methods: We retrospectively analyzed NSCLC patients with and without *KRAS* mutations in the University of California Health Data Warehouse. Time on treatment (ToT) of first-line ICIs was estimated, and ICI-related overall survival (OS) was defined as the time from the first ICI infusion until death or loss to follow up. Kaplan-Meier analysis, Cox proportional hazards model, and student's t-test were applied.

Results: We identified 3,391 NSCLC patients, including 158 patients (5%) with *KRAS G12D*, and 735 (22%) with other *KRAS* mutations. Patients had a median (range) age of 64 (20-89) upon diagnosis and 57% were female (Table). Among 842 patient (25%) who received ICIs, 58% were treated with pembrolizumab, 20% with nivolumab (including 5% with ipilimumab), and 8% with either atezolizumab or durvalumab. Compared to patients with other *KRAS* mutations, there were more Hispanic patients with *KRAS G12D* (20 versus 36 patients, $p < 0.01$). When adjusting for age, race, and ethnicity in a Cox model, patients with *KRAS G12D* had similar ToT of ICIs (4.3 versus 4.8 months; $p = 0.25$; HR, 95%CI: 1.30, 0.83-2.04) and ICI-related OS (9.4 versus 14.0 months; $p = 0.36$; HR, 95%CI: 1.23, 0.79 - 1.92) as those with other *KRAS* mutations.

Conclusion: Harnessing the power of a structured, multicenter data collective, we describe real-world outcomes from patients with *KRAS G12D*-mutated NSCLC.

Table. Patient Characteristics.

		KRAS G12D NSCLC patients (n=158)	*KRAS NON-G12D* NSCLC patients (n=735)	P value	All NSCLC patients (n=3391)
Sex	Female	95 (60%)	431 (59%)	0.798	1932 (57%)
	Male	63 (40%)	304 (41%)		1458 (43%)
Age at diagnosis	Median (range)	67 (24-86)	61 (24-89)		64 (20-89)
Ethnicity	Hispanic	20 (13%)	36 (5%)	<0.001	259 (8%)
	Non-Hispanic	136 (86%)	665 (90%)		2994 (88%)
	Unknown	2 (1%)	34 (5%)		138 (4%)
Race	Asian	100 (63%)	512 (70%)	<0.01	1934 (57%)
	Black/African American	4 (3%)	44 (6%)		144 (4%)
	White	25 (16%)	95 (13%)		896 (26%)
	Others	26 (16%)	56 (4%)		325 (10%)
	Unknown	3 (2%)	28 (7%)		92 (3%)
Smoking	Never smoker	10 (6%)	36 (5%)	0.2337	342 (10%)
	Former smoker	8 (5%)	56 (8%)		189 (6%)
	Regular smoker	1 (1%)	20 (2%)		40 (1%)
	Unknown	139 (88%)	623 (85%)		2820 (83%)
ICI ToT (months)	Median	4.3	4.8	0.25	
ICI-related OS (months)	Median	9.4	14.0	0.36	

#6638 Real-World evidence of eflapegrastim (efla) usage in patients with gastrointestinal (GI) malignancies.

Howard Franklin[1], Jeffrey Crawford[2], John H. Baird[3], Kenneth Crist[1], Vincent Marino[4], Neil Shah[4], Lee S. Schwartzberg[5]

[1]Assertio Holdings, Inc., Lake Forest, IL,[2]Duke University Medical Center, Durham, NC,[3]City of Hope National Medical Center, Duarte, CA,[4]Atropos Health, Palo Alto, CA,[5]Renown Health-Pennington Cancer Institute, Reno, NV

Background: Long-acting granulocyte colony-stimulating factors (GCSFs) such as efla and pegfilgrastim (peg) are routinely used to prevent neutropenia in patients (pts) with cancer undergoing neutropenia-inducing chemotherapy. Registration studies compared efla to peg in pts with breast cancer; efla use in GI cancers is not as well characterized. We used real-world data to assess demographics, comorbidities, and clinical outcomes in pts receiving efla or peg and undergoing chemotherapy for various GI malignancies.
Methods: We conducted a retrospective, cross-sectional cohort analysis of pts with GI cancers (ie, malignant neoplasm of the anus, biliary tract, colon, rectum, esophagus, gall bladder, stomach, liver/intrahepatic ducts, pancreas, or small intestine) who received ≥1 dose of efla or peg with chemotherapy. Information was extracted from electronic health records of >60 million US pts in the Atropos Health Apollo data source (v1.1.0) between 2023 and 2025. Clinical outcomes measured through 15 (D15) and 30 (D30) days post-GCSF included febrile neutropenia (FN), absolute neutrophil count (ANC), platelet count, and adverse events (AEs; thrombocytopenia, back and bone pain, myalgia, GI and nontraumatic head bleeding, acute respiratory distress syndrome, and localized skin reaction).
Results: Pts (N=3353) receiving chemotherapy were identified (efla, n=106; peg, n=3247). Cancer types (>5%) in the efla and peg groups included pancreatic (36% each), colon (27% each), esophagus (10% vs 7%), rectum/rectosigmoid (9% vs 18%), gastric (8% vs 9%), and liver/intrahepatic ducts (7% vs 9%). Chemotherapy regimens included FOLFIRI (35% vs 21%) and FOLFOX (48% vs 34%). Pts receiving efla were older and had a higher burden of comorbidities than those receiving peg: mean (SD) age was 70.5 (8.3) vs 64.9 (12.3) y, respectively, and mean (SD) Charlson Comorbidity Index score was 12.0 (4.0) vs 10.5 (4.3), respectively. FN incidence was similar between pts receiving efla or peg through D15 (0.9% vs 1.3%) and D30 (0.9% vs 1.8%), with higher mean ANC observed with efla vs peg: 10.6 vs 6.4 x 10^9/L, respectively, through both D15 and D30. Thrombocytopenia occurred more frequently with efla than with peg (9.4% vs 7.8% through D15, 16.0% vs 11.0% through D30), with lower mean platelet counts through D15 (173 vs 216 x 10^3/μL) and D30 (188 vs 219 x 10^3/μL). Similar, low rates of AEs were reported through D30 with efla and peg.
Conclusions: Pts receiving chemotherapy for GI malignancies who were treated with efla were older and had a higher burden of comorbidities than those treated with peg. The incidence of FN was similar and low between treatments. Other AEs were also comparable between the two groups. These real-world findings suggest the safety and efficacy of efla in adult pts with GI malignancies receiving diverse chemotherapy regimens.

#6639 Impact of preexisting heart disease on survival and postoperative outcomes in pancreatic cancer: A TriNetX analysis.

Charlotte Burch[1], Jacob Lambdin[1], William Royster[1], Adam Khader[2], Leopoldo Fernandez[1], Raphael Louie[1], Ricardo Bello[1], Jose G. Trevino[3]

[1]VCU Massey Comprehensive Cancer Center, Richmond, VA,[2]U.S. Department of Veterans Affairs, Richmond, VA,[3]Div. of Surgical Oncology, VCU Massey Cancer Center, Richmond, VA

Background: Cardiovascular comorbidity is common among patients with pancreatic ductal adenocarcinoma (PDAC) and may influence both long-term survival and perioperative risk, yet its impact in contemporary practice is not well defined. We performed a retrospective database study using TriNetx, a multinational deidentified dataset, to identify patients with PDAC and to examine associations between heart disease, survival, and complications of pancreaticoduodenectomy (PD).
Methods: Using the TriNetx database, we identified patients with PDAC and stratified the cohort by presence or absence of heart disease (ischemic, structural, heart failure). Subgroup analysis was performed of patients who underwent PD. The primary outcome is overall survival, and secondary outcome is rate of post-PD complications. Propensity score matching was performed for age, sex, stage, and comorbidities. Kaplan-Meier curves and log-rank testing were used to determine survival between the groups and multivariable logistic regression was used to evaluate associations between heart disease and postoperative complications. Among patients undergoing PD, secondary outcomes include postoperative pancreatic leak, myocardial infarction (MI), acute kidney injury (AKI), surgical site infection (SSI), and venous thromboembolism (VTE), rates were evaluated using multivariable logistic regression.
Results: We identified 226,966 patients with PDAC, of whom 45,936 (20%) had preexisting heart disease and 181,030 (80%) did not; 12,840 underwent PD. Propensity matched median overall 5-year survival was 703 days for patients without heart disease versus 611 days for those without (HR = 0.90, $p < 0.0001$). In the matched surgical cohort, preexisting heart disease was associated with increased risk of post-operative myocardial infarction (RR = 3.34, $p < 0.0001$) and acute kidney injury (RR = 1.34, $p < 0.0001$) but not associated with post-operative pancreatic leak (RR = 1.11, $p = 0.18$), abscess (RR = 1.15, $p = 0.16$), or surgical site infection (RR = 1.13, $p = 0.16$). Among propensity matched cohorts of patients with PDAC and heart disease who did and did not undergo PD, those who underwent PD had significant improvement in 1-year overall survival (82% vs 63%, $p < 0.0001$).
Conclusions: In this large, real-world cohort of patients with PDAC, preexisting heart disease was an important determinant of overall survival and perioperative morbidity, with clinically meaningful differences in median survival and postoperative complication profiles. The benefit of PD does not seem to be lost to patients with cardiac risk factors, with significant improvement in overall survival seen in the group who underwent PD. These findings may inform risk stratification, treatment selection, and perioperative optimization strategies for this high-risk population.

#6640 Geriatric nutritional risk index at diagnosis predicts survival in pancreatic cancer.

Christina Grinstead, Saunjoo Yoon

University of Florida, Gainesville, FL

Introduction: Pancreatic cancer (PC) is one of the deadliest cancers with decreased overall survival due to cachexia and malnutrition. Early detection of nutritional risk is essential to improve treatment outcomes. Reliable and valid tools that are easily applicable in clinical settings will benefit to resolve this issue. The Geriatric Nutritional Risk Index (GNRI) utilizes commonly available clinical measures to assess nutritional risk, which may be useful in detecting risk as early as at diagnosis. Despite support for the GNRI in oncology, more research is needed to validate its use in PC. The purpose of this study was to examine the predictive value of the GNRI at diagnosis on survival in PC, controlling for demographics and cancer stage.
Methods: 924 adult patients with primary PC, visited between January 1, 2012, and July 31, 2020 were included in the retrospective study using de-identified data from the UF Health electronic health record. GNRI calculated using the Lorenz formula for ideal weight (Wlo). Weight and serum albumin closest to diagnosis within 120 days used. GNRI = [1.489 x albumin (g/L)] + [41.7 x (weight/Wlo)]. Scores categorized into 3 groups: high (<92), low (92-98), no risk (>98). Survival: days between diagnosis and death with censoring. Covariates: age, race, sex, stage. Multiple imputation used for GNRI missing data (290 patients, 31.4%). Statistical analysis: descriptive statistics, survival analysis using accelerated failure time (AFT) models.
Results: Results (Table 1) show GNRI at diagnosis, age, and stage predict survival, but not race or sex.
Conclusion: Higher GNRI scores at diagnosis predicted longer survival in PC, after controlling for other influential variables. With patients at low and no risk having over twice the survival compared to those at high risk, the GNRI is effective in early detection for need of proactive nutritional interventions. Further research is needed to investigate the long-term effects of changes in GNRI score on survival.

Table 1. Descriptive statistics and Survival analysis results

Variables		Total Sample(n=924)	GNRI groups			Univariate Results		Multivariate Results	
			High Risk (n=202)	Low Risk (n=129)	No Risk (n=303)	p-value	AF (95%CI)	p-value	AF (95%CI)
GNRI groups	High risk					Ref.	Ref.	Ref.	Ref.
	Low Risk					**0.0019**	2.26 (1.4-3.8)	**0.0046**	2.04 (1.25-3.34)
	No Risk					**<0.0001**	3.24 (2.1-4.9)	**<0.0001**	2.66 (1.77-4.00)
Survival (days)	Mean	1047	833	1091	1248				
	Median	654	278	717	968				
	Range	1-3164	5-3154	17-3128	8-3164				
Age (years)	Mean	71.7	72.7	69.7	71.0	**0.0031**	Per 1 year	**0.0057**	Per 1 year
	Median	73	73	72	72		0.98 (0.96-0.99)		0.98 (0.97-0.99)
	Range	27-101	27-94	34-93	30-98				
Sex	Male	501(54.2%)	105(52.0%)	65(50.4%)	166(54.8%)	Ref.	Ref.		
	Female	423(45.8%)	97(48.0%)	64(49.6%)	137(45.2%)	0.2196	1.23 (0.89-1.70)		
Race	White	741(80.2%)	168(83.2%)	103(79.8%)	251(82.8%)	Ref.	Ref.		
	All Other	183(79.8%)	34(16.8%)	26(20.2%)	52(17.2%)	0.8755	1.03 (0.69-1.56		
Stage	Early: 1-2	480(51.9%)	91(45.0%)	64(49.6%)	182(60.1%)	Ref.	Ref.	Ref.	Ref.
	Late: 3-4	444(48.1%)	111(55.0%)	65(50.4%)	121(39.9%)	**<0.0001**	0.27 (0.19-0.36)	**<0.0001**	0.29 (0.22-0.40)
Note: GNRI: Geriatric Nutritional Risk Index, AF: Acceleration Factor, CI: confidence interval									

#6642 Metabolic predictors of chemotherapy response in pancreatic cancer.

Parnian Naji, Jordan Winter

Surgery, Cleveland University Hospitals, Cleveland, OH

INTRODUCTION: Chemotherapy response in pancreatic cancer (PC) varies and is monitored by CA 19-9. Since PC is linked to metabolic dysregulation, this study evaluates how patient baseline metabolic status (glucose, HbA1c, and BMI) relates to the longitudinal trend of CA 19-9 over six months in non-surgical PC patients.
METHODS: A TriNetX-based study design was employed to analyze longitudinal CA 19-9 trends over six months (representing the optimal chemotherapy response window) in PC patients who did not undergo surgical intervention. Patients were categorized into distinct strata based on (1) glucose levels: <150 mg/dL, 150-250 mg/dL, 251-350 mg/dL; (2) HbA1c levels: <7%, 7-10%, 10%-13.5%; and (3) BMI ranges: 20-25, 25-30, 30-35, 35-40.
RESULTS: For Glucose: Baseline CA 19-9 levels correlated positively with increasing glucose strata. Only the highest glucose group (251-350 mg/dL) showed a statistically significant CA 19-9 reduction during chemotherapy ($p<0.05$). Significant differences emerged when comparing this group to both lower groups ($p<0.05$). Across disease stages, higher glucose levels were consistently associated with greater CA 19-9 declines, indicating enhanced chemotherapy response. This association was most pronounced in locally advanced stages (2,3). For HbA1c: Baseline CA 19-9 values were lower in the high HbA1c group (10%-13.5%). Although within-group declines were not significant, between-group comparisons at six months indicated a significantly greater CA 19-9 reduction in the highest HbA1c group compared with both the <7% and 7-10% groups ($p<0.05$). For BMI: Baseline CA 19-9 levels did not differ across groups. During treatment, only the highest BMI group (35-40) demonstrated a significant decline in CA 19-9 ($p<0.05$), while lower BMI groups (20-35) did not. Patients with BMI 35-40 responded more favorably compared with lower BMI categories ($p<0.05$).
CONCLUSION: This study demonstrates that baseline metabolic factors modulate chemotherapy response in non-surgical PC patients. Higher glucose and BMI, as well as elevated HbA1c, were associated with greater CA 19-9 declines during chemotherapy, suggesting that metabolic status may influence treatment efficacy. These findings highlight the need for further studies and supportive metabolic interventions to optimize chemotherapy outcomes in pancreatic cancer.

#6643 Incidence and outcomes of brain metastasis in ER-low breast cancer: Insights from a National Cancer Database (NCDB).

Aanika B. Warner[1], Sarah Darmon[2], Jeremy Perkins[3], Matt Nealeigh[4], Craig D. Shriver[5], Stan Lipkowitz[6], Kangmin Zhu[7], Takeo Fujii[1]

[1]Women's Malignancies Branch, National Institutes of Health, Bethesda, MD,[2]The Henry M. Jackson Foundation for the Advancement of Military Medicine Inc.,[3]Walter Reed Medical Center, Bethesda, MD,[4]Memorial Sloan Kettering, New York City, NY,[5]Uniformed Services University, Bethesda, MD,[6]National Cancer Institute, Bethesda, MD,[7]Professor, Walter Reed National Military Medical Center, Rockville, MD

Background: Brain metastases (BrM) are aggressive and life-limiting complications that occur more frequently in triple-negative and HER2-positive breast cancers. The optimal cut-off value of estrogen receptor (ER) positivity has been under discussion for over a decade. Emerging data suggest that ER-low (1-10% ER staining) breast cancers exhibit clinical and biological features closer to ER-negative tumors, underscoring the need to investigate the incidence of brain metastasis among ER-low tumors to better identify high-risk populations and optimize patient selection for future clinical trials.

Methods: A retrospective cohort study was performed using the 2022 NCDB Participant User File. We collected patients with de novo stage IV breast cancer from 2018-2022, as 2018 was the first year that ER was defined as a continuous variable allowing categorization of ER. ER status was categorized as ER <1% (negative), 1-10% (low), and >10% (positive). Demographic, clinicopathologic, and treatment variables were compared across ER groups using chi-square or Fisher's exact tests for categorical variables and t-test or Kruskal-Wallis tests for continuous variables. Associations between ER status and brain metastases (BrM) at diagnosis (yes vs no) were evaluated using univariate logistic regression. Overall survival (OS) was assessed using cox proportional hazards model for patients who had BrM.

Results: A total of 18,783 patients were included in the analysis. Most were aged 60-69 years (30.5%), 77.0% were White, 85.0% had infiltrating ductal carcinoma, and 51.7% had grade 3 histology. ER status was negative in 23.0%, low in 3.1%, and positive in 73.9%. HER2 status was negative in 70.2%, low in 10.7%, positive in 14.5%, and unknown in 4.6%. Overall, 7.3% of patients had BrM at baseline. BrM were higher in ER-negative (12.0%) and ER-low (10.0%) tumors vs ER-positive disease (5.7%) [Odds ratio: ER-negative; 2.24 (95% CI: 2-2.52), ER-low; 1.82 (95%CI: 1.38-2.41) compared to ER-positive] in univariate logistic regression. OS among patients with BrM was similar between groups (ER-negative; HR 0.93 [0.71-1.22], ER-low; HR 0.91 [0.43-1.93] compared to ER-positive).

Conclusions: The proportion of BrM at diagnosis in ER-low breast cancer was more similar to ER-negative than ER-positive disease. However, the OS in patients with brain metastasis was similarly poor across all ER subtypes, suggesting that once brain involvement occurs, underlying histology has limited prognostic impact. These findings highlight the similar clinical features of ER-low and ER-negative disease, reinforce prompt evaluation of neurologic symptoms, and encourage greater inclusion of this subgroup in BrM-specific clinical trials.

#6644 Adjuvant dose-dense chemotherapy is not associated with improved recurrence-free survival in early-stage, node-negative, HER2-negative breast cancer.

Jonathan Shpigelman[1], Tasnem Alsebai[1], Kathy Robinson[2], Aum Nimavat[3], Ricardo Cossyleon[2], Krishna Rao[2]

[1]Department of Internal Medicine, SIU School of Medicine, Springfield, IL,[2]Department of Hematology/Oncology, Simmons Cancer Institute at SIU School of Medicine, Springfield, IL,[3]University of Illinois Urbana-Champaign, Urbana, IL

Introduction: Adjuvant dose-dense (DD) chemotherapy improves outcomes in early-stage, node-positive breast cancer and is often extrapolated to node-negative disease despite limited evidence and increased toxicity. Whether DD chemotherapy confers benefit in this low-risk population remains unclear.

Methods: Females aged ≥ 18 years with T1-T2, node-negative, HER2-negative breast cancer who received adjuvant DD or non-DD chemotherapy were retrospectively identified. Recurrence-free survival (RFS) was defined as the time from definitive surgery to first documented recurrence; patients without recurrence were right-censored at their last disease-free clinical or imaging assessment. Median follow-up duration was estimated using the reverse Kaplan-Meier method. RFS was compared using log-rank tests, and adjusted hazard ratios (HRs) were estimated using multivariable Cox proportional hazards regression.

Results: A total of 139 patients were included, 50 (36%) of whom received DD chemotherapy. Patients treated with DD chemotherapy were younger (50 vs. 56 years, $P < 0.001$) and had higher rates of T2 tumors (48% vs. 27%, $P = 0.012$), with no significant differences in hormone receptor status, tumor focality, or lymphovascular invasion. Over a median follow-up duration of 9.9 years (95% CI: 9.0-11.2), 17 patients (12%) developed recurrence (7/50 [14%] in the DD group and 10/89 [11%] in the non-DD group). There was no difference in RFS between DD and non-DD groups ($P_{\text{log-rank}} = 0.509$). After adjustment for age, hormone receptor status, T stage, tumor focality, and lymphovascular invasion, DD chemotherapy was not associated with reduced recurrence risk (HR: 0.97 [95% CI: 0.26-3.26], $P = 0.961$). These findings were consistent across T stages, with no difference in RFS in either T1 ($P_{\text{log-rank}} = 0.947$) or T2 ($P_{\text{log-rank}} = 0.755$) subgroups, and no significant interaction between treatment regimen and T stage ($P_{\text{interaction}} = 0.512$).

Conclusions: DD chemotherapy was not associated with a reduction in recurrence risk among patients with early-stage, node-negative, HER2-negative breast cancer, even after adjustment for clinical and pathological characteristics. Although limited by a low number of recurrence events, these findings suggest that routine use of DD chemotherapy in this low-risk population may not be justified. Larger prospective studies are needed to identify whether any subset of patients derives meaningful benefit.

#6645 Practice patterns impacting relative dose intensity of adjuvant capecitabine among triple negative breast cancer patients with residual disease following neoadjuvant chemotherapy.

Andrea House, Pratik Thakur, Blair Hoeting, Ruth Johnson, Brittany Sandoval, Julie Stephens, Daniel G. Stover, Sagar Sardesai, Tanun Jitwatcharakomol, Sasha Beyer, Arya M. Roy, Nerea Lopetegui-Lia, Dionisia M. Quiroga, Ashley P. Davenport, Gilbert Bader, Nicole O. Williams, Robert Wesolowski, Margaret E. Gatti-Mays, **Kai C. C. Johnson**

The Ohio State University - James Comprehensive Cancer Center, Columbus, OH

Background: This study aims to identify real-world practice pattern factors in capecitabine prescribing and assess which factors lead to higher relative dose intensity (RDI) to help address the variability in dosing strategies that limits the ability to assess the real-world effectiveness of adjuvant capecitabine.
Methods: This institutional retrospective study involved patients diagnosed with triple negative breast cancer from 1/1/2016 to 12/31/2023 who had residual disease following neoadjuvant chemotherapy and received ≥1 dose of adjuvant capecitabine. Our objective was to examine factors that influence the achievement of an RDI >66%, with standard dosing based on a total of 8 cycles of capecitabine over 21-day cycles. Factors included radiation therapy, dose reductions, prescribing schedule, age, race, tumor grade, nodal status, tumor size, residual cancer burden, lymphovascular invasion, and neoadjuvant pembrolizumab & carboplatin. We also examined whether RDI impacts invasive disease-free survival (iDFS) and overall survival (OS) using pre-defined percentiles (0-66%, 67-92%, & 93-100%).
Results: Of the 83 total patients, 45 were RDI≤66, 29 were RDI>67-92, & 9 were RDI≥92-100. Among all clinicopathologic factors listed above, only the use of a 7-day prescribing schedule for capecitabine (28-day cycle) had a meaningful reduction on one's ability to reach an RDI of >66% (p=0.0234). When examining univariate iDFS, no statistically significant difference was noted between RDI percentiles (p=0.667) but a trend towards improved iDFS was noted among higher RDI groups. The 5-year iDFS was 78.4% for RDI≤66, 77.9% for RDI>67-92, & 88.9% for RDI>93-100. Similarly for OS, no statistically significant difference was noted between RDI percentiles (p=0.395), but a trend towards improved OS was noted when RDI exceeded 66%. The 5-year OS was 82.1% for RDI≤66, 92.7% for RDI>67-92, & 88.9% for RDI>92-100.
Conclusion: Real world practice patterns can differ, but the implementation of weekly capecitabine dosing frequency has been shown in this study to significantly influence the ability to achieve higher RDI values. While no statistical difference in iDFS or OS was noted, a trend towards worsening outcomes was recorded for those with an RDI≤66%.

#6646 Impact of histology subtypes (ductal, lobular, and mixed ductal/lobular) on pathological complete response (pCR) following neoadjuvant chemotherapy (NAC) and chemoimmunotherapy (NACI) for estrogen receptor low (ER-low) HER2-negative breast cancer.

Kai C. C. Johnson, Brandon Slover, Yengeniya Gokun, Dionisia M. Quiroga, Sagar Sardesai, Sachin Jhawar, Nerea Lopetegui-Lia, Arya M. Roy, Gilbert Bader, Ashley P. Davenport, Nicole O. Williams, Robert Wesolowski, Margaret E. Gatti-Mays, Daniel G. Stover

The Ohio State University - James Comprehensive Cancer Center, Columbus, OH

Background: Little is known regarding mixed ductal/lobular histology subtypes of breast cancer in terms of how they influence the likelihood of pathologic complete response (pCR) following neoadjuvant chemotherapy (NAC) & chemoimmunotherapy (NACI). Similarly, there is no literature on how estrogen receptor (ER) expression percentiles influence the likelihood of pCR after NACI among this mixed histology subgroup.

Methods: We examined data within the National Cancer Database on those diagnosed with HER2-negative breast cancer between 2018-2022. We categorized patients based on histology subtype (ductal, lobular, & mixed) and ER percentiles, including ER-low (1-10%). Binary logistic regression was used to examine the relationship between pCR & histology type among patients with ER-low disease, adjusting for age, race, ethnicity, tumor grade, tumor size, nodal status, progesterone receptor percentiles, immunotherapy use, endocrine therapy use, & lymphovascular invasion (LVI). Additionally, adjusted Cox proportional hazards regression was fitted between overall survival (OS) and histology subtype.

Results: A total of 58072 ductal, 1330 mixed, & 3500 lobular cases with available residual disease data following neoadjuvant therapy were examined. Among those with ER-low expression (ductal: 3319, mixed: 35, lobular: 80), it was shown that 46.7% (n=1549), 31.4% (n=11), & 12.5% (n=10) of patients, respectively, achieved pCR, which was a significant difference on univariate analysis ($p<0.001$). On adjusted analysis, the difference in pCR between patients with mixed & ductal ER-low disease was non-significant (aOR 0.69, 95%CI 0.27-1.77, reference: ductal). However, lobular patients were associated with 79% lower odds of achieving pCR compared to ductal patients (aOR 0.21, 95%CI 0.08-0.54). On multivariate analysis, variables that significantly improved the odds of achieving pCR were histology type ($p=0.004$), younger age ($p=0.010$), smaller tumor size ($p<0.001$), use of immunotherapy ($p<0.001$), and absence of LVI ($p<0.001$). For OS, larger tumor size ($p<0.001$), positive nodal status ($p<0.001$), & presence of LVI ($p<0.001$) were associated with worsened OS whereas the receipt of endocrine therapy ($p=0.003$) significantly improved OS. Histology subtype was not significantly associated with differences in OS ($p=0.238$).

Conclusion: Tumors of mixed ductal/lobular histology behave more similarly to ductal disease in terms of NACI response, including ER-low subgroups. Additional factors, such as tumor size, LVI, and receipt of immunotherapy play a stronger role in predicting pCR, but the histology subtype remains an important variable to consider when deciding how best to sequence treatment for those with HER2-negative ER-expressing disease.

#6647 MCM2 and the origin licensing complex: A putative node of ER+/HER2- breast cancer therapy resistance.

Alekya Raghavan[1], Rosemary N. Plagens[2], Cynthia X. Ma[3], Stephanie Graff[4], Maryam Lustberg[5], Andrew Elliott[2], George W. Sledge[2], C. Kent Osborne[1], Mothaffar F. Rimawi[1], Ahmed Elkhanany[1], Rachel Schiff[1]

[1]Lester & Sue Smith Breast Center; Dan L Duncan Comprehensive Cancer Center; Department of Medicine, Baylor College of Medicine, Houston, TX,[2]Caris Life Sciences, Irving, TX,[3]Siteman Cancer Center, Washington University at St. Louis, St. Louis, MO,[4]Brown University Health Cancer Institute, Providence, RI,[5]Yale Cancer Center, New Haven, CT

Background: The use of CDK4/6 inhibitors (CDK4/6i) in combination with endocrine therapy (ET) has revolutionized treatment practices for advanced and high-risk ER+/HER2- breast cancer (BC) via effective inhibition of cell cycle activation. However, the vast majority of patients eventually progress on these therapies, underscoring the need for new treatment strategies to select patients, monitor response, and target novel therapeutic vulnerabilities. We previously reported that high expression of *MCM2* and its origin licensing complex (LC) is enriched in primary tumors refractory to CDK4/6i (SABCS22-P2-03-10). LC factors are transcriptionally regulated by E2F/MYC-driven programs, which are activated by diverse drivers of resistance. We propose that *MCM2*/LC expression may be a biomarker reflecting multiple ET and CDK4/6i resistance mechanisms, due to its role in cell cycle activation.

Methods: A retrospective review was conducted on a real-world, treatment-naive ER+/HER2- BC cohort of 1,960 largely metastatic patients with biopsies from breast or other sites (~50% each) that underwent NGS profiling (DNA: 592-gene panel/whole-exome; RNA: whole-transcriptome) at Caris Life Sciences. Tumors were stratified by *MCM2* or LC gene set mRNA into Q4 (high) versus Q1 (low; n=490 each), balanced for ET/CDK4/6i exposure, MSI-H, and TMB-H. Histology, PAM50, mutations (^{mut}), gene amplifications(^{amp}) and deletions(^{del}), and differential gene expression were analyzed. Chi-square, Fisher's Exact, or Mann-Whitney U tests were performed with Benjamini-Hochberg FDR for molecular variables (q<0.05).

Results: *MCM2*-high vs -low tumors were LumB-dominant (LumB 85.5% vs 39.8%; LumA 5.3% vs 56.3%, p<1e-63) with less lobular histology (6.1% vs 17.1%, p=0.0001). Transcriptomically, PI3K/AKT/mTOR, E2F/MYC targets, G2M checkpoint, and DNA repair hallmark pathways were enriched in *MCM2*-high (all FDR q<0.05). Genomically, *MCM2*-high harbored a higher frequency of *TP53*^{mut} (32.6% vs 16.6%, q=4e-6), *RB1*^{mut} (5.8% vs 1.2%, q=0.052), *CCND1*^{amp} (26% vs 6%, q=4.5e-11), *FGF3*/*4*/*19*^{amp} (~25% vs ~6%, q≤2.2e-10), *MYC*^{amp} (5.4% vs 0.8%, q=0.0136), and *CDKN2A*/*B*^{del} (*CDKN2A* 29.3% vs 15.5%, q=6.9e-4; *CDKN2B* 17.5% vs 7.3%, q=1.38e-3). Notably, *MCM2* and *MKI67* gene expression were highly correlated (Spearman's ρ=0.77, p<0.05). Very similar results were found for LC-high vs -low tumors.

Conclusions: In ER+/HER2- BC, high *MCM2*/LC is associated with LumB subtype, E2F/MYC and cell cycle activation, selection of *TP53* and *RB1* mutations, and *CCND1*/*MYC*/*FGF* amplifications. Our findings suggest that *MCM2* or LC mRNA may act as a surrogate marker for a network of oncogenic pathways previously identified to drive endocrine and CDK4/6i resistance. Future studies will evaluate *MCM2*/LC beyond proliferation, as a predictive biomarker for CDK4/6i-based regimens, as we have previously shown in the primary ET-treated setting (SABCS24-P1-03-20).

#6648 Association between area deprivation index (ADI) and treatment persistence (TP) with CDK4/6 inhibitors (CDK4/6i)in HR+/HER2- breast cancer.

Michelle L. Caetano[1], Jessica Liu[2], Britny R. Brown[1], Guannan Gong[3], Sameer Pandya[2], Salma Taghzout[1], Mariah Ramos[1], Edward Tupper[4], Annette Hood[5], Michael Zummo[5], Robert Legare[3], Jing Du[3], Maryam Lustberg[3]

[1]Pharmacy Practice and Clinical Research, University of Rhode Island College of Pharmacy, Kingston, RI,[2]Yale University, New Haven, CT,[3]Yale Cancer Center, New Haven, CT,[4]School of Pharmacy and Physician Assistant Studies, University of Saint Joseph, West Hartford, CT,[5]Department of Pharmacy, Yale New Haven Health, New Haven, CT

Background: CDK4/6i improve invasive disease-free and progression-free survival in HR-positive/HER2-negative breast cancer, yet real-world treatment persistence is suboptimal. ADI is a validated composite of neighborhood socioeconomic disadvantage that has been linked to worse medication adherence and health outcomes. Evaluating the association between ADI and persistence with CDK4/6i may identify equity-sensitive targets for intervention. The primary objective was to assess the association between ADI and TP in early (EBC) and metastatic (MBC) breast cancer.
Methods: We conducted a retrospective cohort study of patients prescribed CDK4/6i at Yale New Haven Health from February 2018 through December 2024. Artificial intelligence and natural language processing were used to extract structured electronic health record data. TP was defined using Epic Beacon treatment plan start and end dates and analyzed separately for EBC and MBC cohorts. Analyses used Python and R. Residential addresses at initiation were batch processed in R (ezADI), geocoded to 12-digit census block group GEOIDs via the U.S. Census Geocoder, and linked to 2020 Neighborhood Atlas ADI percentiles. Records with suppressed or missing ADI were excluded. ADI was dichotomized at the cohort median (above-median = more deprived; below-median = less deprived). Cox proportional hazards models, adjusting for medication, age, and gender were used to estimate hazard ratios (HR) for therapy discontinuation. Kaplan-Meier analyses summarized TP by ADI and CDK4/6i.
Results: A total of 1,363 patients were included in the MBC cohort and 298 in the EBC cohort. The median ADI across both cohorts was 30, which was used as the deprivation cutoff. In MBC, median ADI values were 19 (IQR 11-25) for the less-deprived groups and 47 (IQR 39-62) for the more-deprived groups across agents (abemaciclib, palbociclib, ribociclib). In multivariable Cox models adjusting for medication, age, and gender, higher deprivation was not significantly associated with earlier therapy discontinuation (HR = 0.97; 95 % CI, 0.86-1.08; p = 0.56). Older age was associated with shorter TP (HR = 1.01 per year; 95% CI, 1.00-1.01; $p < 0.001$).
In EBC, median ADI values were 19 (IQR 14-25) versus 47 (IQR 39-63) among abemaciclib-treated patients, and median ADI was 16 (IQR 10-22) versus 50 (IQR 41-59) among ribociclib-treated patients. ADI was not associated with increased discontinuation (HR = 0.98; 95 % CI, 0.78-1.22; p = 0.83).
Conclusions: In this large, real-world cohort, TP with CDK4/6i did not differ by neighborhood socioeconomic deprivation. Further work incorporating individual-level social determinants of health may better elucidate drivers of adherence and persistence disparities.

Acknowledgment: ChatGPT (OpenAI) was used to assist with text revision and editing for clarity.

#6649 Comparative risk of secondary central nervous system metastases in metastatic non-small cell lung cancer: A real-world propensity-matched analysis of pembrolizumab vs atezolizumab monotherapy conducted on TriNetX.

Umer Rizwan[1], Athar Nawab[2], Syed Najafi[2], Karandeep Bawa[3], Fnu Muhibullah[2], Christian Kaftanic[2], Sunanda Tah[2], Sabir Hussain[4]

[1]Jefferson Einstein Philadelphia Hospital, Philadelphia, WV,[2]Internal Medicine Residency, West Virginia University Camden Clark Medical Center, Parkersburg, WV,[3]West Virginia School of Osteopathic Medicine, Lewisburg, WV,[4]Hematology and Oncology, West Virginia University Camden Clark Medical Center, Parkersburg, WV

Background: Bone and bone-marrow metastases significantly worsen morbidity in metastatic non-small cell lung cancer (mNSCLC). Comparative real-world data assessing skeletal metastatic progression between pembrolizumab and atezolizumab monotherapy remain limited.
Methods: We performed a retrospective cohort analysis using the TriNetX US Collaborative Network (69 HCOs). Stage IV mNSCLC patients treated with first-line pembrolizumab or atezolizumab monotherapy were identified. Propensity score matching (1:1) produced balanced cohorts (n=7,768 each). Outcomes were assessed over 365 days following treatment initiation. The primary endpoint was new-onset secondary bone/bone-marrow metastases (ICD-10 C79.51, C79.52, C79.5). Patients with prior skeletal metastases were excluded from outcome analyses.
Results: Following exclusions, 5,277 atezolizumab and 5,780 pembrolizumab patients were analyzed. Atezolizumab was associated with a significantly higher incidence of bone/bone-marrow metastases compared with pembrolizumab (16.5% vs 10.8%; RR 1.53; 95% CI 1.39-1.68; p<0.001). Kaplan-Meier analysis demonstrated reduced metastasis-free survival with atezolizumab (79.5% vs 86.8%, Log-Rank p<0.001). Hazard of metastatic progression was significantly higher with atezolizumab (HR 1.62; 95% CI 1.46-1.80). Atezolizumab also demonstrated a greater mean number of metastatic instances (0.93 vs 0.55; p<0.001).
Conclusions: In this large real-world matched cohort, atezolizumab monotherapy was associated with a significantly greater 1-year risk of secondary bone or bone-marrow metastases compared with pembrolizumab. These findings suggest clinically meaningful differences in skeletal metastatic progression between ICIs and warrant further prospective and mechanistic investigation.

#6650 Safety and efficacy of belzutifan for Von Hippel-Lindau disease-associated tumors.

Peixi Ge[1], Mohamed Atta[2], Nityasree Srialluri[2]

[1]Zanvyl Krieger School of Arts and Sciences, Johns Hopkins University, Baltimore, MD,[2]Johns Hopkins Medicine, Baltimore, MD

Background: Von Hippel-Lindau (VHL) disease is a rare autosomal dominant hereditary syndrome. Patients with VHL disease have a lifelong risk of developing clear-cell renal cell carcinoma (RCC), pancreatic neuroendocrine tumors (pNET), and hemangioblastomas of the central nervous system (CNS). Belzutifan, a hypoxia-inducible factor-2α inhibitor, received FDA approval in 2021 for adults with VHL-associated RCC, pNET, or CNS hemangioblastomas. Phase 2 data demonstrated objective response rates of 49%, 91%, and 30% by RECIST v1.1, respectively. However, real-world clinical outcomes remain limited. We evaluated the safety and efficacy of belzutifan in a real-world cohort.

Methods: We performed a retrospective review of adult patients (≥18 years) at Johns Hopkins Hospital between January 2016 and December 2024 who were genetically or clinically confirmed to have VHL and received belzutifan treatment. Eligible participants had at least one VHL-associated lesion and an available imaging following therapy. Patient demographics and clinical data were collected from EMR. Tumor and cyst characteristics at baseline and during follow-up were evaluated using CT or MRI. The sum of the longest diameters of evaluable lesions—including lesions < 1 cm—was used to assess tumor response. Secondary outcomes included duration of therapy, adverse events (AEs), and reasons for treatment discontinuation.

Results: Fourteen patients were included (mean ± SD age, 36 ± 14 years; 71% female). Among 10 patients with kidney lesions, 4/10 (40%) had ≥30% decrease over a median treatment duration of 18.5 months (range 12 - 27). All 3 (100%) patients with pNET had a ≥30% decrease, with a median follow-up of 24.7 months (range 12-32). Among 9 patients with CNS hemangioblastomas, 7/9 (78%) had ≥30% decrease over a median treatment duration of 18.1 months (range 7-28). The most common AEs were anemia (35%), dizziness (21%), and headache (21%). One patient discontinued treatment due to anemia, and another due to pregnancy planning.

Conclusion: In this real-world cohort of patients with VHL-associated lesions, belzutifan demonstrated clinical activity and a favorable safety profile across various VHL-associated neoplasms. Compared to phase II data, kidney lesions had lower response rates, while pNET and CNS hemangioblastomas showed higher responses. These differences may reflect variations in baseline imaging timing, small patient numbers, or occasional treatment interruptions due to insurance issues or missed doses. These findings support the continued use of belzutifan in VHL disease and highlight the need for larger studies to guide long-term management of VHL-associated tumors.

#6651 Characterizing the risk of infections with T-cell engagers in multiple myeloma.

Lindsay Fogel[1], Harsh Parmar[2], Shucen Wan[3], Adolfo Aleman[2], Pooja Phull[2], David Vesole[2], David S. Siegel[2], Rena Feinman[4], Claire L. Carter[1], Noa Biran[2]

[1]Hackensack Meridian School of Medicine, Nutley, NJ,[2]John Theurer Cancer Center, Hackensack Meridian Health, Hackensack, NJ,[3]Penn State Health Hershey Medical Center, Hershey, PA,[4]Center for Discovery and Innovation (Hackensack Meridian Health), Nutley, NJ

Background: T-cell engagers (TCE) have demonstrated remarkable efficacy in pts with heavily pretreated multiple myeloma; however, they are associated with a higher risk of infections which can contribute to increased morbidity and mortality. Here, we report our experience with infectious complications in relapsed/refractory MM pts receiving TCEs, characterizing their incidence, severity and risk factors.

Methods: This is a single-center retrospective study of 79 consecutive MM pts who received teclistamab (Tec), elranatamab (Elra) or talquetemab (Talq) between 1/2023-9/2025. Demographics, baseline disease characteristics, prior therapies, and toxicities were collected from electronic records. Infections were graded according to CTCAE version 5.0. Overall survival (OS) and progression-free survival (PFS) were estimated using Kaplan-Meier curves. Pts were separated into those with any grade infection versus those without. Univariate Cox proportional hazards regression was performed to identify variables associated with OS or PFS, with significant predictors ($p<0.05$) included in multivariable analysis.

Results: Seventy-nine pts received at least one dose of tec (n=29, 37%), talq (n=40, 51%), or elra (n=10, 13%). Median age was 68 yrs (range 39-86), 56% were female, and pts had a median of 5 prior lines of therapy (range 2-18). 44 pts (56%) had received prior BCMA-directed therapy. High risk cytogenetics were present in 36 pts (46%). A total of 109 infectious events were reported, with pts experiencing a median of 1 infectious event (range 0-12). Grade 1-2 CRS occurred in 58 pts (73%). 48 pts (61%) developed infections with rates varying by TCE: tec 19/29 (66%), talq 19/40 (48%), elra 8/10 (80%). Grade 3-4 infections occurred in 28 pts (35%). 10pts (13%) required intensive care, primarily due to bacterial pneumonia or sepsis. Four pts (5%) discontinued TCE due to infectious complications. 11 pts (14%) experienced infection related mortality while receiving or shortly after discontinuing TCE. At median follow-up of 11.9 mos (95% CI 10.1-14.0), mPFS was 5.5 mos (95% CI 3.7-11.3) and mOS was 16.3 mos (95% CI 7.9-21.6) for the entire cohort. Pts with infections had inferior outcomes compared to those without: PFS 4.2 vs 7.1 mos ($p=0.3$); OS 6.4 vs 17.4 mos ($p=0.027$). IVIG use was associated with improved PFS (14.6 vs 5.7 mos, $p=0.0002$) and OS (21.6 vs 7.9 mos, $p=0.0003$). On MVA, infection (HR 2.14, $p=0.030$) and IVIG (HR 0.28, $p=0.009$) were independent predictors of OS, while only IVIG significantly impacted PFS (HR 0.27, $p=0.0002$).

Conclusion: In this single-center analysis of heavily pretreated MM pts receiving TCEs, infectious complications were frequent, occurring in 61% pts. Infections were independently associated with inferior OS, while use of IVIG was associated with a 72% reduction in risk of death. Prospective studies are required to establish optimal timing and use of IVIG to demonstrate its efficacy in pts receiving TCEs.

#6652 Viral hepatitis paradox: Better outcomes in geriatric HCC transplant patients.

Ewan Kim[1], **Sungsu Park**[2], Amy Choi[3]

[1]Herricks High School, New Hyde Park, PA,[2]Daegu Catholic University School of Medicine, Daegu, Korea, Republic of,[3]Penn State College of Medicine, Hershey, PA

Hepatocellular carcinoma (HCC) causes significant mortality among elderly patients requiring liver transplantation. Traditional assumptions suggest viral hepatitis worsens transplant outcomes. We hypothesized that viral status would significantly influence survival outcomes, with potential interactions between HBV/HCV co-infection and metabolic comorbidities. We analyzed 7,890 geriatric patients (≥65 years) from the United Network for Organ Sharing database who received liver transplants for HCC, stratifying them by hepatitis B virus (HBV) and hepatitis C virus (HCV) status. Contrary to expectations, HCV-positive patients demonstrated significantly superior 5-year survival rates, with HBV+/HCV+ patients achieving 33.9% survival versus 27.3% for HBV-/HCV- patients. Mean survival time was 182 days longer for HBV+/HCV+ patients compared to HBV-/HCV- patients (1,361 vs. 1,179 days, $p<0.001$). Diabetes mellitus showed complex associations with outcomes, with particularly poor survival in coinfected diabetic patients (6.2% vs. 45.0% for non-diabetics). Age showed negative correlations with survival in all groups, relatively high in co-infected patients ($r=-0.160$). These findings challenge current transplant evaluation paradigms, suggesting viral status complexity requires reassessment in geriatric populations. Our results indicate that HCV should not automatically exclude elderly patients from transplant consideration, while diabetes requires careful management, especially in co-infected patients.

#6653 Hepatosplenic T-cell lymphoma gamma-delta versus alpha-beta: A comparative study of clinicopathologic features and outcomes.

Philip A. Haddad[1], Sireesha Vutukuri[2], Ankita Gupta[2]

[1]LSUHSC-S/ Overton Brooks VAMC, Shreveport, LA,[2]Overton Brooks VAMC, Shreveport, LA

Introduction: Hepatosplenic T-cell lymphoma (HSTCL) is an aggressive rare extranodal T-cell lymphoma. It is most commonly derived from γδ T cells, though an αβ variant has been increasingly recognized. While γδ HSTCL is considered the prototypic form and accounts for the majority of cases, the clinical significance, biological behavior, and prognostic impact of αβ versus γδ T-cell receptor (TCR) expression remain poorly defined due to the scarcity of comparative data. We conducted this study to compare the clinicopathological characteristics of both subtypes.
Methods: To study the clinicopathologic characteristics, prognostic factors, and overall survival (OS), we compiled a pooled database of HSTCL cases. Patients were stratified into two groups based on TCR expression: γδ-HSTCL and αβ-HSTCL. Descriptive statistics were used to summarize baseline characteristics. Continuous variables were compared using t-test, and categorical variables by χ^2 test. Survival outcomes were analyzed using Kaplan-Meier methodology.
Results: A total of 226 patients with HSTCL were identified, 52 αβ and 174 γδ. The median age at diagnosis was similar between subgroups (30 vs 34 years), with a slight male predominance in both, more pronounced in the γδ cohort (59% vs 72%). A history of immune suppression was frequent in both groups (76% αβ vs 71% γδ), with comparable durations of exposure (median 4.7 vs 5 years) and latency to lymphoma onset (4 vs 5 years). Both cohorts had high rates of hepatosplenomegaly (100% αβ vs 99% γδ) and marrow infiltration (100% in both). Cytopenias were common and showed no significant differences: anemia (90% vs 95%), leukopenia (66% vs 61%), and thrombocytopenia (86% vs 88%). Median LDH levels were elevated in both subtypes (797.5 vs 968 U/L). Median overall survival was similarly poor—10 months in αβ and 11 months in γδ HSTCL. Immunophenotypically, the two subtypes shared high expression of CD2, CD3, CD7, CD16, CD38, and CD56. However, CD5 was more frequently expressed in αβ cases (39% vs 14%, $P = 0.001$) as well as CD8 positivity (57% vs 31%, $P = 0.005$) and CD57 (41% vs 5%, $P = 0.01$). Trisomy 8 (33% vs 36%) and i/r 7 (72% vs 75%) were prevalent and comparable between groups.
Conclusion: In this large comparative cohort, αβ and γδ HSTCL demonstrated strikingly similar clinical features, patterns of immune suppression, cytopenias, organ involvement, cytogenetic abnormalities, and dismal overall survival. However, significant immunophenotypic differences—most notably higher expression of CD5, CD8, and CD57 in αβ HSTCL—suggest underlying biologic divergence between the two TCR-defined subtypes. These findings highlight that while both forms remain clinically indistinguishable at presentation and equally lethal, their distinct immunoprofiles may have diagnostic relevance and could inform future exploration of targeted therapeutic strategies.

#6654 Assessing skin cancer risk in systemic sclerosis patients with organ transplantation: A cohort study.

Ruhi Kanwar[1], Ellen Anshelevich[2], Goranit Sakunchotpanit[3], Kevin Fettel[4], Vinod E. Nambudiri[1]

[1]Cutaneous Oncology Program, Dana-Farber Cancer Institute, Boston, Massachusetts, Harvard Medical School, Boston, MA,[2]Hackensack Meridian School of Medicine, Nutley, NJ,[3]Tufts University School of Medicine, Boston, MA,[4]Harvard Medical School, Boston, MA

Systemic sclerosis (SSc) is an autoimmune condition characterized by fibrosis of the skin and organs. Cancer is a well-known association of SSc, with a higher incidence in men, and with particular evidence of elevated lung, breast, and melanoma incidence. In addition, non-melanoma skin cancer (NMSC) has been reported to have increased incidence, with one study showing higher incidence in women compared to men. The impact of solid organ or hematopoietic transplantations - known to confer increased risk of NMSC - on skin cancer risk have not been specifically characterized in the SSc population. We sought to explore skin cancer incidence in SSc patients with a history of kidney, bone marrow (BM), or lung transplantation.

The Research Patient Data Registry of Mass General Brigham was queried from 1979 to 2024 for SSc and lung, kidney, or BM transplantation in clinical documentation. For the unexposed cohort, patients with SSc and no transplantation (2:1 controls per case) were matched by age, sex, and race. For each exposed patient, up to one matched unexposed patient was included in the analysis. Among 178 exposed and 374 unexposed extracted, 48 SSc patients with transplant and 45 SSc patients without transplant were included after chart review. NMSC risk was calculated with either basal cell carcinoma (BCC) or squamous cell carcinoma (SCC).

We observed an increased association of skin cancer with transplantation (relative risk (RR) 5.31, 95% p=0.0047), specifically with NMSC (RR 4.69, p=0.0097), compared to non-transplantation. In addition, when examining only skin cancers that emerged after transplantation, there was an increased risk compared to controls (RR 3.75, p=0.0306), specifically with SCC (RR=4.69, p=0.0384). Subsequent subgroup analysis of transplanted patients by sex showed that females had an increased risk of skin cancer (RR 3.7, p=0.0298) and NMSC (RR 3.33, p=0.0468), while males did not.

Cutaneous malignancy amongst SSc patients remains understudied, and characterizing the contribution of transplantation to observed increased risks is necessary. Our results suggest that patients with SSc undergoing transplantation -- specifically females -- may have an increased risk of developing both NMSC and skin cancers compared to those without transplantation. Limitations include our study's retrospective nature and limited generalizability due use of one health system.

#6655 Characterization of adverse cutaneous effects in the setting of ponatinib, bosutinib, andasciminib for chronic myeloid leukemia patients.

Ruhi Kanwar[1], Juna Khang[2], Goranit Sakunchotpanit[3], Ruhi Nayak[2], Nicole R. LeBoeuf[1], Vinod E. Nambudiri[1]

[1]Cutaneous Oncology Program, Dana-Farber Cancer Institute, Boston, Massachusetts, Harvard Medical School, Boston, MA,[2]Harvard Medical School, Boston, MA,[3]Tufts University School of Medicine, Boston, MA

BCR-ABL tyrosine kinase inhibitors (TKIs) are used in the treatment of chronic myeloid leukemia (CML) and include second- and third-generation agents: ponatinib, bosutinib, and asciminib. While cutaneous adverse events (cAEs) of first-generation TKIs such as imatinib are well-documented, real-world reports involving newer agents remain limited and poorly described. We therefore aimed to characterize the range of cAEs in patients with CML receiving ponatinib, bosutinib, or asciminib.

We conducted a retrospective chart review queried from the Research Patient Data Registry of Mass General Brigham from 1979 to 2024. We excluded patients without CML or medication use. 291 patients met inclusion criteria, with 92 (32.3%) receiving ponatinib, 182 (62.5%) receiving bosutinib, and 111 (38.1%) receiving asciminib. 37 (12.7%) patients developed a documented cAE, with 1 patient developing 2 different cAEs. There were 38 total discrete cAEs, including rashes (cAEs=38), pruritus (cAEs=20), xerosis (cAEs=5), hyperpigmentation (cAEs=2) and squamous cell carcinoma (SCC) (cAEs=1). All drugs resulted in acneiform eruptions and maculopapular or papular eruptions. Ponatinib also induced pityriasis rubra pilaris-like, keratosis pilaris-like, petechial, and ichthyosiform eruptions. Photosensitive rashes occurred on ponatinib and bosutinib, while pustular eruptions, plaques, and eczematous eruptions occurred on bosutinib and ascimnib. cAEs were treated with topical steroids (cAEs=14), emollients (cAEs=10), and antihistamines (cAEs=9); TKI dose was held or discontinued for 17 events.

The median duration of cAE ranged from 35 days with asciminib to 91.5 days with bosutinib. 60.5% of events presented within 90 days of medication initiation. No patients required hospitalization for the cAEs; the majority were grade 1 severity (57.2%). There was a significant association between female sex and cAE development (OR 3.30, p=0.003), but no association for age, race, ethnicity, prior CML treatments, and initial dosage.

We present a detailed characterization of real-world presentations of cAEs developing on ponatinib, bosutinib, and asciminib, with observed incidence rates of 16.3%, 8.8%, and 6.3%, respectively. The significantly increased risk in females aligns with prior literature, possibly due to differences in body type, medication adherence, or reporting. Our limitations include retrospective design and single institution use.

: Spatial Proteomics and Transcriptomics 3
Poster Session

#6659 Spatial proteo-transcriptomic profiling of pancreatic adenocarcinoma unveils distinct malignant subtype-associated immune and stromal functional states.

Beatrice Wendler Awasthi[1], Nicole A. Lester[1], Deniz Guney Olgun[2], Yi Cui[3], Gabriel Francisco Pozo Mattos Pereira[1], Nicholas Caldwell[1], Mari Mino-Kenudson[1], Maria Ganci[1], Manisha Madhavan[1], Sierra Mckinzie[4], Jung Woo Bae[1], Xunqin Yin[1], Shanshan He[4], PRAJAN DIVAKAR[3], Martin Hemberg[5], Joe Beechem[3], William L. Hwang[1]

[1]Massachusetts General Hospital, Boston, MA,[2]University of Virginia, Charlottesville, VA,[3]Bruker Spatial Biology, Seattle, WA,[4]Bruker Spatial Biology, Seattle, MA,[5]Brigham and Women's Hospital, Boston, MA

Pancreatic adenocarcinoma (PDAC) remains one of the leading causes of cancer mortality. It has become increasingly clear that the spatial architecture of tumors can drastically influence treatment response and prognosis. Advances in large-scale spatial profiling have enabled detailed in situ mapping of cell types and states, which has unveiled multicellular neighborhoods and interactions associated with distinct clinicopathologic features. For example, we previously applied whole-transcriptome spatial molecular imaging (WT-SMI; ~19,000 protein-coding genes) to a prospective cohort of matched pre- and post-chemoradiation PDAC specimens (DF/HCC 18-469) and identified consistent treatment-induced transcriptional shifts in the tumor microenvironment (TME) that were linked to specific ligand-receptor interactions within distinct multicellular neighborhoods. However, many immune cell populations are poorly characterized at the transcriptional level and are better captured using proteomics. To address this gap, we leveraged a recently commercialized multi-omic SMI platform developed by Bruker Spatial/NanoString Technologies that enables concurrent WT and 64-plex protein analysis of a single tissue section to profile a human PDAC tissue microarray (TMA). Transcriptome-level data was used to assign broad cell type labels, and protein stains guided nested subtyping of immune cells by applying HieraType. This approach enabled the annotation of >450,000 cells at a coverage of >1000 transcripts and >750 unique genes per cell, in addition to quantitative staining of 64 protein targets per cell. Using spatial non-negative matrix factorization, we established cellular signatures for distinct neighborhoods composed of malignant cells, stromal cells and immune cells. Preliminary analyses suggest that different transcriptional neighborhoods correlate with distinct survival outcomes. We then used spatial proteomics data to guide functional annotation of immune cells within cellular neighborhoods. This enabled detailed differentiation of immune subtype populations and their interactions with other cells in the TME, which may uncover new mechanisms of immune evasion and therapeutic resistance. This study highlights a novel spatial multi-omics approach that enables more accurate characterization of key multicellular neighborhoods associated with treatment response and clinical prognosis.

#6660 CellScape Quality Control (CSQC): A tissue- and protein-agnostic platform for spatial proteomics quality assessment.

Daniel Jimenez-Sanchez[1], Brian J. Lane[1], Matthew H. Ingalls[1], Charles Eldon Jackson[1], Steven T. Lott[1], Adam Northcutt[1], Arne Christians[2], Anke Brix[2], Jennifer Brooks[2], Oliver Braubach[1]

[1]Bruker Spatial Biology, St. Louis, MO,[2]Bruker Spatial Biology, Hanover, Germany

Introduction: Spatial proteomics is an emerging diagnostic tool for precision oncology, yet data reproducibility across tissue sections and batches remains a major obstacle towards achieving robust biomarker discovery and clinically actionable results. Variability in tissue quality, tissue preparation, antibody performance, and imaging conditions all introduce artifacts that compromise quantitative accuracy. Manual quality control of imaging data is thus essential, but it is very time consuming and subjective. A standardized, automated, and quantitative quality control framework is therefore essential to support realistic adoption of spatial proteomic workflows in precision oncology.
Methods: We developed CellScape Quality Control (CSQC), a machine learning-based framework for automated stain quality assessment and tissue vetting. CSQC was trained on >100 samples from >20 tissue types from ten CellScape™ precise spatial phenotyping instruments across laboratories. The dataset included more than 50 biomarkers representing nuclear, membrane, and cytoplasmic targets across multiple antibody clones, stain protocols, and imaging magnifications (10x and 20x). Expert annotations were used as ground truth for model training and validation.
Results: CSQC achieved a mean IoU >0.7 for background, artifact, and usable tissue detection, showing strong concordance with expert annotations. The system automatically flagged suboptimal staining and batch-level artifacts, thereby enabling harmonization across instruments and sites. The deployment of CSQC reduced manual review time from several hours to minutes per sample, and thereby allowed rapid scaling of downstream analyses to dozens of slides and proteins analyzed by a single operator in a given time frame. In addition, we observed a noticeable improvement in downstream marker quantification and reproducibility following CSQC vetting.
Conclusion: CSQC provides a standardized, quantitative, and scalable approach to stain and tissue quality control, supporting robust multisite spatial proteomics workflows on the CellScape precise spatial phenotyping platform. This framework facilitates assay harmonization, benchmarked reproducibility, and reliable spatial biomarker discovery for clinical translation.

#6661 High quality whole transcriptome RNA-sequencing from challenging clinical samples.

Pieter Mestdagh, Lisa Van Den Bossche, Thomas Van Wunsel, Hilke Spooren, Emmanuel Riviere, Jan Van de Velde, Ana Carolina Elisa Fierro Gutierrez, Nathalie Bernard, Lien Heyrman, Dirk Goossens, Jurgen Del Favero

CellCarta, Antwerp, Belgium

RNA sequencing (RNA-seq) of clinical specimens poses several challenges due to limited sample material, RNA fragmentation, and high fractions of ribosomal RNA (rRNA) and globin RNA. These factors often result in elevated PCR duplication rates and reduced library complexity, compromising transcriptome data quality and downstream analyses. We evaluated the Watchmaker Genomics RNA library prep with Polaris Depletion workflow and compared its performance to a standard RNA-seq and exome capture workflow. Performance was assessed across a range of sample types, including reference materials, whole blood, and tumor FFPE samples with varying RNA integrity.The Polaris Depletion workflow achieved efficient depletion of both rRNA (< 5%) and globin RNA (< 1% in whole blood), compared to > 5% rRNA and > 50% globin RNA observed with the standard exome capture workflow. PCR duplication rates were approximately twofold lower with the Polaris Depletion workflow (30.2%) versus the standard exome capture approach (62.5%). Notably, the Polaris Depletion workflow demonstrated robust performance across samples of differing RNA quality, provided sufficient RNA input was used for library preparation. Overall performance of the Polaris Depletion workflow was highly reproducible, as confirmed through inter-operator and inter-laboratory experiments.In summary, the Watchmaker Genomics RNA library prep with Polaris Depletion workflow enables the generation of high-quality RNA-seq libraries with efficient rRNA and globin depletion, reduced PCR duplication, and reliable quantification of both coding and non-coding transcripts. These results demonstrate that RNA sequencing of challenging clinical samples can be effectively performed without the need for costly and time-intensive exome capture, thereby improving both sensitivity and workflow efficiency.

#6662 Spatial genomics reveals microenvironmental programs associated with organ-specific metastatic propensity in prostate cancer.

Maryam Ranjpour, Mohamed Omar

Cedars-Sinai Medical Center, Los Angeles, CA

Metastatic prostate cancer (PCa) exhibits pronounced organotropism, particularly to bone, yet the spatially resolved molecular features within primary tumors that correlate with organ-specific dissemination patterns remain poorly characterized. Although bulk and single-cell transcriptomic studies have highlighted microenvironmental heterogeneity in PCa, no validated spatial genomic signatures currently exist that link intratumoral ecosystems to metastatic risk and organotropism. To address this gap, we apply high-resolution spatial genomic profiling with Xenium (10x Genomics) across human tissues and genetically engineered mouse models (GEMMs) that recapitulate PCa initiation, progression, and metastatic competence. GEMMs were used to characterize spatially resolved transcriptional programs and tumor microenvironment (TME) interactions across defined biological stages, enabling controlled dissection of the stromal, epithelial, immune, and neurovascular states associated with metastatic readiness. In parallel, we profile paired primary tumors and anatomically distinct metastatic lesions from PCa patients enrolled in the Cedars-Sinai Molecular Twin Project, including metastases to lymph nodes, bone, liver, and soft tissues. Integrative analyses demonstrate organ-associated spatial gene expression programs and multicellular niches within the primary tumor that mirror the molecular landscapes of their eventual metastatic destinations. These include bone-associated niches enriched for osteomimicry programs, ECM-remodeling fibroblasts, and osteotropic ligand-receptor signaling; nodal-associated niches defined by immune-evasive epithelial states, lymphoid-interacting stromal programs, and chemokine circuits guiding lymphatic dissemination; and visceral-associated niches characterized by metabolic rewiring, hepatotropic signaling modules, and endothelial states predisposing to vascular invasion. These spatially resolved niches highlight shared biological modules that mediate, or are associated with, organ-specific metastatic behavior. Notably, several site-specific programs are detectable within the primary tumor prior to clinical metastasis, suggesting that metastatic organotropism is encoded early through stable TME-tumor interactions. Collectively, this work establishes a cross-species framework for mapping microenvironmentally encoded metastatic trajectories and identifies spatial genomic biomarkers with potential clinical utility for predicting organ-specific metastatic risk. These findings has the potential for identifying new therapeutic strategies aimed at disrupting early metastatic niches before dissemination occurs.

#6663 Integrated spatial transcriptomic and proteomic profiling reveals tumor-immune niches driving heterogeneity and resistance in clear cell renal cell carcinoma.

Qanber Raza, **Nick Zabinyakov**, Lauren Tracey, Liang Lim, Christina Loh

Standard BioTools, Markham, ON, Canada

Clear cell renal cell carcinoma (ccRCC) is a biologically heterogeneous malignancy shaped by complex tumor immune microenvironment interactions. Single-modality profiling often fails to capture this complexity. Spatial transcriptomics enables high-resolution mapping of gene expression, but proteins mediate functional states, signaling and therapeutic targets. Sequential integration of Imaging Mass Cytometry™ (IMC™) technology after spatial transcriptomics on the same tissue section adds a critical layer by quantifying protein expression and post-translational markers while preserving spatial context. Unlike fluorescence-based multiplexing, IMC technology avoids spectral overlap and autofluorescence, making it ideal for post-transcriptomic analysis. This multi-omic approach enables direct correlation of transcriptomic signatures with protein-level functional states, uncovering mechanisms of immune evasion and therapeutic resistance that remain hidden using transcriptomics alone. FFPE tumor sections from Stage 3 ccRCC patient were analyzed using spatial transcriptomics (Xenium 5K assay) followed by hematoxylin and eosin (H&E) staining and IMC with a 43-marker immuno-oncology panel. Data was coregistered for single-cell resolution integration of RNA, H&E and protein expression. Integrated analysis provided unprecedented resolution of the ccRCC microenvironment: Functional subtyping identified metabolically active tumor cells (high LDHA, GLUT-1), TIM-3+ tumor populations with angiogenic potential, and spatially organized immune niches such as tertiary lymphoid structures (TLS) containing B cells, activated T cells and macrophages. Combined profiling revealed spatial proximity and interaction of immune cells (CD4, CD8, CD20, CD38, TCF1, CD11c), stromal components (αSMA, vimentin, fibronectin), and vascular features (CD34, PLVAP) associated with tissue remodeling and dysfunctionality. Unsupervised clustering of RNA and protein data revealed robust immune activation in TLS and differentiated tumor cell states with metastatic potential. IMC analysis after spatial transcriptomics enables pathologist-in-the-loop evaluation, advancing diagnosis from morphology-based to molecularly informed and spatially precise interpretation of tumor heterogeneity and disease progression. Spatial multi-omic profiling delivers unprecedented resolution of tumor and immune landscapes in ccRCC, supporting development of spatially informed biomarkers and targeted therapies. Clinically, this approach could potentially refine patient stratification, identify resistance-associated niches, and guide combination strategies targeting both tumor and immune compartments. *For Research Use Only. Not for use in diagnostic procedures.*

#6664 Single-cell spatial proteomics of 1200+ protein targets in tumor microenvironments from diverse cancers using GeoMx Discovery Proteome Atlas.

Terence C. Theisen, Alexa E. Lasley, Giang Ong, Megan Vandenberg, Brian Filanoski, Lori Hamanishi, Erin Piazza, Sayani Bhattacharjee, Courtney Anderson, Mirko Corselli, Prajan Divakar, Margaret L. Hoang, Joseph M. Beechem

Research and Development, Bruker Spatial Biology, Seattle, WA

The tumor microenvironment (TME) is a heterogeneous landscape where immune cells interact with malignant cells to influence cancer progression and therapeutic response, but to date, dissecting the spatial proteomic signature of the TME has been limited by plex and resolution. Here we introduce the GeoMx® Discovery Proteome Atlas (DPA), a high-plex antibody-based spatial proteomic assay, and use it to characterize, for the first time, the 1200+ plex spatial proteomes of hundreds of individually selected cells from more than 8 FFPE cancer samples. GeoMx DPA includes 130+ Post-Translational Modification-targeting antibodies, allowing for the interrogation of phosphorylation, glycosylation, and ubiquitination modifications missed by transcriptomics or other proteomic methods. We developed and optimized a protocol to collect Regions of Interest (ROIs) at single-cell resolution with segmentation strategies on the GeoMx® Digital Spatial Profiler (DSP) platform (e.g., CD45+ leukocyte and CD3+ T cell markers). We mapped immune infiltration patterns and activation states within distinct tumor niches by comparing ROIs encompassing single cells and ROIs with hundreds of cells. Our analyses revealed tissue- and cancer-specific proteomic signatures, including differential expression of checkpoint molecules (PD-1, CTLA-4, LAG3), kinases, and inflammatory mediators. We examine the expression profiles of tumor infiltrating lymphocytes (T cells, B cells, and neutrophils) in different cancers and the dependency upon tumor spatial proximity. We also compare the single-cell proteomes from cancer tissues to single cell DPA data from more than 30 cell lines to identify protein targets differentially expressed based on cancer or cell line lineage. By integrating high-plex protein data with spatial segmentation strategies, we are providing the field with a critical tool to find more predictive biomarkers to drug response (e.g., PD-L1). The ability to resolve the spatial proteomic patterns of more than 1200 targets within tumor microenvironments, right down to the level of single cells, will enable deeper insights into cellular interactions and inform new approaches for patient treatment.

#6665 Validation of two melanoma biomarkers and two novel ready-to-use multiplex immunofluorescence panels for spatial profiling of the stromal and vascular compartments in the tumor microenviroment.

Paula Juricic, Francois Rivest, Clara Sinthon, Jade Nguyen, Isabelle Blanc, Bastian Nicolai, Alexandre Kehren, **Saska Brajkovic**

Lunaphore, a Bio-Techne brand, Tolochenaz, Switzerland

The use of multiplex immunofluorescence (mIF) to study the tumor microenvironment (TME) has significantly advanced our understanding of spatial dynamics within tumors. This technique has emerged as a valuable tool for identifying biomarkers and therapeutic targets. Despite its growing adoption, mIF protocols remain complex and technically demanding. Their manual execution and reliance on dedicated reagents make them time-consuming and expensive. Additionally, concerns persist regarding their reproducibility and transferability across different tissue types. Ready-to-use, validated antibody panels, such as the SPYRE™ Core Panels, help address these challenges.

In this study, we demonstrate the development and validation of two new antibody panels covering relevant stromal and vessel biomarkers to enable spatial analysis of the TME on the COMET™ platform across various tissue types as well as two additional antibodies against SOX10 and S100B optimized for melanoma studies. The stroma panel enables simultaneous detection of Vimentin, E-Cadherin, Collagen I, and FAP, while the vessel panel contains CD31, CD34, Podoplanin, and LYVE-1. Formalin-fixed paraffin-embedded human tissue sections from a 24-cores multi-organ tissue microarray and whole-section melanoma samples were stained on COMET™ by fully automated sequential immunofluorescence (seqIF™, PMID: 37813886). Staining and detection are done via indirect immunofluorescence using unlabeled primary antibodies and fluorophore conjugated secondary antibodies. Both panels were developed and validated on several tumoral and non-tumoral tissues at the same time. The sections retrieved from COMET™ after seqIF™, were stained by a histology facility with standard immunohistochemistry (IHC) established for pathological diagnosis to compare seqIF™ and IHC staining patterns and verify antibody specificity. All markers demonstrate accurate detection with specific seqIF™ staining, comparable to gold-standard IHC counterparts, as well as robust performance across multiple tissues. Protocols were optimized to achieve high staining quality for all ten markers in terms of sensitivity and signal-to-background ratio. The repeatability and reproducibility of the automated stainings on the COMET™ platform was verified by day-to-day tests on one instrument and tests among multiple ones.

Our validated SPYRE™ Stroma and Vessel Focus panels, along with melanoma-specific antibodies, deliver highly specific and reproducible results across diverse tissues. Ready-to-use on the COMET™ platform and designed as modular extensions of the SPYRE™ Core Panels, they enable quantitative marker detection, combination with custom antibodies, and empower researchers with robust and scalable workflows for advanced spatial biology studies.

#6666 Deriving high-fidelity, low-plex clinical signatures from ultra-high-plex spatial data for immunotherapy response prediction.

Raymond Yan[1], Brian Falkenstein[1], A. Burak Tosun[1], Filippo Pullara[1], **S. Chakra Chennubhotla**[2]

[1]PredxBio, Inc., Pittsburgh, PA,[2]PredxBio, Inc. / University of Pittsburgh, Pittsburgh, PA

Background: Ultra-high-plex multiplex immunofluorescence (mIF) imaging enables detailed characterization of the tumor microenvironment (TME), yet translating these rich datasets into clinically deployable, low-plex biomarkers remains a major barrier for precision immuno-oncology. Existing predictive models rely heavily on high-dimensional features or broad phenotypic panels, limiting scalability, interpretability, and routine pathology integration. A systematic framework is needed to compress spatially resolved molecular information into minimal, clinical-plex, yet highly informative signatures capable of predicting immunotherapy response.
Methods: Our SpaceIQ™ platform is a multi-omic analysis tool that integrates spatial proteomics data with optimized feature selection algorithms to distill molecular signatures. We employ unbiased cell typing and microdomain discovery to identify a differentially expressed network of spatial interactions between these unbiased cell types, utilizing pointwise mutual information (PMI) analysis. Each interaction (either pairwise or higher-order cliques) within this network represents a potential spatial prognostic model capable of predicting patient response. A key component of our approach is the identification of a subset threshold cell population that is enriched for a given unbiased cell type using a low-plex panel. The final prognostic model for a differential clique combines a spatial proximity score with these low-plex marker intensities.
Results: Analysis of ultra-high-plex (=51 markers) spatial data from trial specimens of checkpoint-treated cutaneous T-cell lymphoma patients demonstrated that tumor-immune and immune-immune interactions emerge as microdomains with minimal signatures of 6-8 markers and high prediction accuracies (AUC = 0.87, 95% CI (0.865-0.881)).
Conclusions: The SpaceIQ platform enables the extraction of compact, clinically practical biomarker panels from ultra-high-plex mIF datasets without sacrificing predictive power. By linking spatial microdomain biology to sparse signature derivation, this framework supports scalable deployment of precision immunotherapy biomarkers and enhances patient-selection strategies in clinical practice.

#6667 Integrated spatial transcriptomics and proteomics workflows for high-resolution multiomics analysis.

Cindy Pamela Ulloa Guerrero[1], Michele Bortolomeazzi[1], Pooja Sant[1], Laura Schutze[1], Laura Giese[1], Denise Keitel[1], Julia Boehl[2], Robin Reschke[2], **Jan-Philipp Mallm**[1]

[1]Single-cell Open Lab, DKFZ German Cancer Research Center, Heidelberg, Germany,[2]Max-Eder Research Group Reschke, University Hospital Heidelberg, Heidelberg, Germany

High-resolution tissue profiling increasingly relies on integrated spatial multiomic approaches that unify spatial transcriptomics and antibody-based proteomics to reveal coordinated molecular patterns within complex tissues. This enables a detailed exploration of spatial niches, cell-cell interactions, and tissue microenvironments. However, these modalities are often performed on consecutive sections, limiting precise correlation between molecular and spatial features. Here, we present optimized workflows that combine high-plex imaging and sequencing-based spatial transcriptomic assays with antibody-based proteomics from the same tissue section in a coordinated and customizable manner.

We developed and evaluated experimental adaptations to ensure high data quality and optimal tissue handling across multiple platforms, including Xenium, Visium, and COMET. Quality control procedures were implemented to assess antigen retrieval compatibility, as these conditions can be antibody dependent. We examined the balance between epitope exposure, tissue integrity, and background signal, providing specific recommendations tailored to different research objectives.

We further compared the sensitivity of these technologies and offer guidance on selecting and combining commercially available transcriptomic and proteomic workflows in a controlled, flexible setup. As in all multiomic approaches, signal loss can occur, particularly in the second readout of consecutive analyses. For proteomics, photobleaching and antigen retrieval are key considerations, especially for low-abundance or difficult-to-detect targets. Transcriptomic data can be enhanced by using HiPlex RNAscope Pro on COMET to detect lowly expressed transcripts. For data integration, we employed a straightforward pipeline that includes cell segmentation based on protein data, image registration using nuclear staining and/or segmentation masks, and extraction of single-cell transcript counts and pixel intensity data for downstream analyses within the SpatialData framework.

We applied these workflows to tonsil, skin, and colon tissues using immuno-oncology-focused panels. The combined approach improved molecular resolution and reduced data sparsity, enabling more precise definition of cell states, spatial neighborhoods, and functional niches. These spatial multiomics workflows expand the analytical capabilities and facilitate deeper biological interpretation across diverse tissue contexts.

#6668 Spatial and transcriptomic remodeling of the tumor microenvironment following neoadjuvant atezolizumab in urothelial carcinoma: Insights from the ABACUS Study.

Robbin Nameki[1], Jennifer Kinong[1], Chao-Hui Huang[1], Michelle Saul[1], Aakash Sur[1], Mehmet Tekman[1], Alexander Trageser[1], Wenjing Yang[1], Daniel Chawla[1], Greg Szeto[1], Arne Schmidt[2], Alberto Megina Gonzalo[2], Srishti Munjal Mehta[2], Nina Kozar-Gillan[2], Rosemarie Krupar[2], Sophie Laturnus[2], Cornelius Bohm[2], Marija Pezer[2], Gloria H.Y. Lin[1], Diane Fernandez[1], Keith Ching[1], Jadwiga R. Bienkowska[1], Thomas Powles[3], Craig B. Davis[1]

[1]Pfizer, Inc., San Diego, CA,[2]Aignostics, Berlin, Germany,[3]Experimental Cancer Medicine Centre, Barts Cancer Institute, London, United Kingdom

The ABACUS study was a single-arm, phase II trial evaluating neoadjuvant atezolizumab in operable urothelial carcinoma. Paired baseline and post-treatment tumor specimens were analyzed to identify biomarkers associated with treatment response. Initial bulk transcriptomic and immunohistochemistry analyses suggested links between immune activation, tissue remodeling and resistance pathways were associated with clinical outcome. To further characterize spatial and phenotypic changes at high resolution, artificial intelligence-assisted digital image analysis of hematoxylin & eosin sections and Visium spatial transcriptomics were performed on paired samples. Post-treatment specimens showed extensive remodeling of the tumor microenvironment with marked immune infiltration, stromal expansion, and altered endothelial-tumor proximity. Such alterations were associated with distinct clinical outcomes between stable disease and relapse. These findings indicate that atezolizumab reshapes the tumor microenvironment by enabling immune infiltration and remodeling stromal architecture; however, robust tumor and endothelial activity may sustain immune exclusion and drive resistance despite immune expansion. Spatial and phenotypic biomarkers identified here may inform rational combination strategies for immune checkpoint inhibitor-refractory urothelial carcinoma.

#6669 Spatially resolved multiplex immunofluorescence profiling of antibody-drug conjugate targets in bladder cancer using an AI-powered end-to-end workflow.

Christoph Kuppe[1], Markus Eckstein[2], Samaneh Samiei[1], Katharina Dornblut[3], Niklas Klumper[4], Fabian Schneider[5], Moritz Widmaier[3], Florian Leiss[3]

[1]RWTH Aachen, Aachen, Germany,[2]FAU Erlangen-Nurnberg, Nurnberg, Germany,[3]ZEISS Microscopy GmbH, Jena, Germany,[4]University of Bonn,[5]Mindpeak GmbH, Hamburg, Germany

Background: Bladder cancer is one of the most common malignancies, with significant morbidity and mortality rates. Emerging antibody-drug conjugates (ADC) are promising treatment options for this challenging disease. However, insight about the location and presence of different ADC target molecules is needed to guide treatment decisions. Multiplex immunofluorescent (mIF) offers the opportunity to investigate multiple biomarkers and their spatial distribution at the same time, enabling detailed spatial analysis of ADC targets within a tissue section.
Methods: We utilized a novel mIF reagent system to analyze formalin-fixed, paraffin-embedded (FFPE) bladder cancer samples from a patient cohort by staining clinically relevant ADC target molecules. Slides were imaged using the ZEISS Axioscan 7 spatial biology system and SlideStream automation for high-throughput, standardized acquisition. Image analysis was performed using Mindpeak PhenoScout integrated to the automated workflow, which employs pre-trained AI models for tissue region segmentation, single cell detection, biomarker positivity, and phenotype classification based on multichannel signal integration.
Results: We established an mIF assay to investigate different ADC targets in bladder cancer samples. This information, in combination with AI-based analysis, was used to generate an ADC sensitivity profile for each patient.
Conclusions: Spatially resolved mIF analysis of bladder cancer revealed clinically relevant biomarker signatures, highlighting its potential for patient stratification. The integration of automated imaging and AI-driven analysis ensures robust, reproducible spatial profiling, accelerating the translation of multiplex tissue imaging into precision oncology and personalized treatment approaches.

#6670 Automated co-detection of small RNAs, RNAs and proteins in tumor tissues with Roche DISCOVERY™ULTRA.

Renzo S. Adilardi, Rose Delvillar, Manvir Sambhi, Emerald Doolittle, Sonali Deshpande, Anushka Dikshit, Debia Wakhloo, Henry Lamparski

Advanced Cell Diagnostics, a Bio-Techne brand, Newark, CA

Advances in precision medicine utilizing antisense oligonucleotides (ASOs) and small interfering RNAs (siRNAs) as therapeutic platforms have brought promising solutions for various neurodegenerative/neuromuscular disorders and rare diseases. Currently, 20 oligonucleotide drug products have been commercially approved by the FDA and EMA, and many more are in clinical phase I-III trials. The FDA has issued recommendations to generate nonclinical biodistribution (BD) data for gene therapy products to evaluate and interpret nonclinical pharmacology and toxicology findings before initiating human clinical trials. *In situ* hybridization (ISH) and immunohistochemistry (IHC) are increasingly used to spatially visualize the delivered therapeutic, target gene, transgene, and/or cell markers and complement information gathered from molecular technologies such as quantitative polymerase chain reaction (qPCR) and digital PCR. Direct visualization of oligonucleotides can also monitor the risk of off-target events by studying BD of potential therapies in various organs. A new RNAscope™ ISH assay enabling the detection of ASOs, siRNAs, microRNAs (miRNAs), and other small RNAs was developed on the Roche DISCOVERY™ ULTRA System. This fully automated assay allows the co-detection of small RNAs, RNAs and proteins within the same formalin-fixed paraffin-embedded sections of tissues. This workflow includes protease-free RNA detection to prevent disruption of protease-sensitive epitopes. Multiple RNA species and protein targets can be visualized either chromogenically or fluorescently at the single-cell level, leveraging translucent chromogens or TSA-fluorophores. We investigated the expression profile of miR-21, a microRNA implicated in cancer proliferation and progression, in the human cancer TMA tissue. MicroRNA detection was combined with *PTEN* RNA to assess the impact of miR21 on the expression of *PTEN*, a tumor suppressor that regulates cell growth, proliferation, and survival. Ki67, and CD31 proteins were co-detected in the same sample to correlate with tumor cell proliferation, and neo-angiogenesis, respectively. This new automated ISH assay showed high sensitivity and specificity for the detection of small RNAs with different expression profiles, and subcellular resolution in intact tissue context. This novel assay will be particularly valuable for the study of ASO/siRNAs delivery, biodistribution, stability, and expression profile of their associated RNA targets for the development of new oligonucleotide therapeutics.

#6671 Actionable resistance mechanisms in osteosarcoma uncovered by the elucidate spatial biomarker platform.

Gulpreet Kaur[1], Jason Weirather[1], James Perna[1], Sizun Jiang[2], Will Singleterry[1]

[1]Elucidate Bio, Medford, MA,[2]Harvard Medical School, Cambridge, MA

Same-slide spatial multiomics enables comprehensive characterization of the tumor microenvironment (TME) by integrating high-plex spatial proteomics and whole-transcriptome on the same slide. For patients whose tumors have progressed or metastasized despite standard-of-care therapies, understanding the specific mechanisms active within their tumor becomes essential for guiding next-line treatment decisions. This requires resolving cell identity, state, morphology, and the organization of immune-tumor interactions within spatial neighborhoods. A systematic, multimodal approach is therefore necessary to reveal clinically actionable mechanisms of resistance directly within intact tissue architecture.

Methods

We developed the Elucidate Biomarker Platform using a same-slide spatial multiomics workflow combining 50-plex spatial proteomics and whole-transcriptome spatial transcriptomics. Model-guided annotation was applied for high-fidelity cell detection, quality control, and neighborhood-level analysis. Proteomic data identified phenotypic and spatial features associated with therapeutic response, while transcriptomic profiling on the same slide elucidated molecular pathways underlying these tissue-level patterns.

Results

Application of this platform to an osteosarcoma patient sample uncovered two actionable mechanisms of therapeutic resistance:

1.FAP-mediated T-cell exclusion: Excess fibroblast activation protein (FAP) expression on tumor-associated stromal cells formed a physical and immunoregulatory barrier preventing T-cell infiltration. Clinical treatment of the patient with a FAP-targeted radioligand inhibitor resulted in a positive therapeutic outcome.

2.$CD163^+$ macrophage survival pathway: Same-slide multiomic analysis identified a survival mechanism specific to $CD163^+$ tumor-associated macrophages via PAQR6, which was targetable using mifepristone, suggesting a second actionable therapeutic avenue.

These findings demonstrate that same-slide spatial multiomics, combined with model-guided annotation, delivers a systematic approach for revealing clinically actionable biomarkers and therapeutic targets to guide precision therapy and drug development.

#6672 Expanding the boundaries of spatial proteomics with a universal antibody labeling strategy and EpicIF™ multiplexing chemistry.

Thore Boettke, Jannik Boog, Charles Eldon Jackson, Matthew H. Ingalls, Arne Christians, **Oliver Braubach**

Bruker Spatial Biology, St. Louis, MO

Highly multiplexed immunofluorescence (mIF) has transformed cancer research by enabling the simultaneous visualization of dozens of biomarkers and cell types within the spatial context of the tumor microenvironment (TME). However, mIF assays often require custom antibody content, which is difficult to attain with inflexible or proprietary chemistries. Alternative detection systems provide partial workarounds but frequently rely on harsh conditions that can compromise tissue integrity and reduce assay reproducibility. To overcome these barriers, we developed a universal antibody-labeling strategy compatible with the CellScape™ Precise Spatial Proteomics platform and EpicIF™ multiplexing chemistry. This workflow enables low-volume fluorophore labeling of virtually any IgG antibody, independent of antibody buffer formulations, using standard organic fluorophores in minutes and without specialized instrumentation. The resulting labeled antibodies integrate seamlessly into CellScape workflows for custom, high-quality mIF imaging. In this study, we demonstrate how our universal labeling approach enables the seamless transfer of IHC-validated antibodies to the CellScape Platform without compromising staining quality or specificity. We first compared standard IHC-P DAB and immunofluorescence stains using several well-characterized and routinely applied antibodies. The results show that our universal labeling strategy allows a straightforward transition of these antibodies to multiplexed immunofluorescence staining. Next, we expanded our commercially available VistaPlex Kits with antibodies designed to provide deeper insights into the TME. Our final modified panel includes additional markers for immune infiltration, stromal activation, cellular metabolism, and checkpoint regulation. Applying this panel to whole-section tumor biopsies and tissue microarrays generated unprecedented single-cell-level data describing not only the composition of the TME but also the proteomic states of individual cells. Linking these data with patient treatment regimens and outcomes further revealed quantifiable spatial phenotyping signatures. This study details how a universal labeling strategy can easily expand mIF studies to better understand the TME. Presented here in its sum, our study marks a significant step toward fully user-driven, high-plex mIF assay development, which will accelerate discovery, expand biological insights, and redefine how complex cancer ecosystems are studied *in situ*.

#6673 MERFISH 2.0 enables high-sensitivity, customizable spatial transcriptomics for resolving immune and tumor programs in human cancers.

Renchao Chen, Bin Wang, Bing Yang, **Manisha Ray**, Justin He, Timothy Wiggin, Lizi Maziashvili, Alexander Genshaft, Peter Reinhold, Angela Vasaturo, Jiang He

Vizgen, Cambridge, MA

High-plex, imaging-based spatial transcriptomics with single-cell resolution has substantially advanced our understanding of how heterogeneous tumor ecosystems shape immune architecture and function, target expression, and cell-cell interface dynamics within the human tumor microenvironment (TME). By measuring gene expression directly in intact human tissues, spatial transcriptomics provides detailed insights into immune-cell identity, spatial organization, and molecular programs that govern antitumor activity or immune suppression. Resolving transcripts in situ enables precise delineation of immune-cell states, spatial interactions, and regulatory circuits underlying antitumor responses and context-dependent cellular phenotypes. A key limitation of current spatial transcriptomics approaches is the ability to sensitively detect transcripts across complex and heterogeneous human tumors, particularly when studies require focused interrogation of specific pathways or cellular programs. MERFISH 2.0 overcomes these constraints with an enhanced chemistry and streamlined sample-processing workflow that delivers substantially higher transcript detection efficiency in both frozen and FFPE tissue, enabling robust profiling of panels up to 1,000 genes. Building on these improvements in sensitivity and workflow performance, MERFISH 2.0 also provides the flexibility to add up to 100 custom genes to Pre-designed Panels (PdP), enabling researchers to tailor experiments to specific hypotheses, tumor-intrinsic biology, or emerging clinical signatures. In this study, MERFISH 2.0 was applied to human tumor specimens using an 815-gene PdP with an immune-oncology focus, supplemented with custom gene content selected to capture key biological processes across diverse tumor types and disease stages. Implementation on MERSCOPE® Ultra™ slides generated high-resolution spatial maps that resolved the distribution of specific cell populations, the localization of surface and intracellular markers of interest, and the complex organization of immune infiltrates, stromal architecture, and tumor-intrinsic transcriptional programs within intact tissue environments. The ability to augment MERFISH 2.0 panels with tailored gene sets further expands its utility for dissecting molecular features and spatial patterns of the TME that influence pathway engagement and functional activity. By integrating enhanced sensitivity with customizable panel design, MERFISH 2.0 provides a powerful platform for resolving spatial determinants of immune function and tumor behavior, supporting mechanistic discovery and informing the development of next-generation precision medicine strategies.

#6674 Metabolic reprogramming in advanced renal tumors contributes to a dysfunctional immune response and immune exhaustion within the tumor microenvironment.

Lakshmi Chandramohan, Kirsteen Maclean, Sergio Hernandez, Brigitte Lovell, Courtney Todorov, Harry Nunns, Jiong Fei, Judy Kuo, Erinn A. Parnell, Qingyan Au

NeoGenomics, Fort Myers, FL

Background: Renal cell carcinoma (RCC), a malignancy arising from renal tubular epithelial cells, represents 2-3% of global cancer diagnoses and 85% of all kidney neoplasms with the most common histological subtype being clear cell renal cell carcinoma (ccRCC), an immunologically and histologically diverse tumor associated with poor clinical outcomes. While significant progress has been made in the development of immunotherapy for ccRCC, there are still many unanswered questions regarding mechanisms of immune evasion and resistance, and the development of predictive biomarkers for optimal treatment strategies for individual patients. Emerging evidence suggests that metabolic reprogramming marked by dynamic shifts in nutrient utilization that extend beyond canonical Warburg physiology to include lipid anabolism, nutrient scavenging, catabolic pathways and microenvironment-driven metabolic plasticity, is central to overall ccRCC pathogenesis. This orchestrated rewiring of cellular dynamics has been suggested to sustain tumor proliferation under hypoxia while fostering immunosuppression through metabolite-mediated T cell exhaustion. We therefore investigated the phenotype, functional states, and metabolic competencies of RCC immune cell populations, evaluating their potential associations with tumor clinicopathological features and stage-specific metabolic conditions.

Methods: To investigate the complex interplay between the immunogenic nature of ccRCC tumors and metabolic reprogramming, we performed an integrative multi-omic analysis, combining transcriptomic and spatial proteomic data. We profiled 16 ccRCC patient samples representative across all clinical TNM stages (Stages I-IV) to define the potential changes in metabolic processes and infiltrating immune cells that correlated with advancing disease. Specifically, we incorporated the *new* Paletrra™ end to end spatial proteomic multiplexed immunofluorescence (mIF) workflow (NeoGenomics Laboratories, Inc.) and qualified a panel that includes: CD3, CD4, CD8, FoxP3, CD68, CD80, CD163, CD206, CA9, CD31, LAG3, PD1, PanCK. NanoString nCounter® Metabolic Pathways Panel testing was performed on these samples to investigate metabolic reprogramming, cellular stress, and their relationship to TME composition in advancing disease progression in ccRCC.

Results and Conclusions: We identified substantial TME-driven changes, notably the presence of immunosuppressive immune cells in advanced ccRCC disease, coupled with identification of several metabolism-related genes showing strong correlations with immune infiltration in ccRCC. Identifying and understanding these metabolic alterations within the different staging of RCC will help in designing new targeted therapies and improving diagnostic tools to improve care for patients with this disease.

#6675 An end-to-end quality control pipeline for spatially resolved molecular imaging data in the multi-omic SpaceIQ™ platform.

Brian Falkenstein[1], A. Burak Tosun[1], Raymond Yan[1], S. Chakra Chennubhotla[2], Filippo Pullara[1]

[1]PredxBio, Inc., Pittsburgh, PA,[2]PredxBio, Inc. / University of Pittsburgh, Pittsburgh, PA

Background: The rapid expansion of mIF imaging has increased the need for rigorous, standardized quality control. Variability introduced during sample prep, staining, and image acquisition can obscure biological signals and compromise downstream analysis. Common issues include batch effects that distort foreground-background contrast, acquisition errors causing over/underexposure or low contrast, and physical artifacts such as bubbles, debris, or deparaffinization defects. More difficult to detect is non-specific antibody binding, which can appear in unexpected structures or cell types. These challenges require a human-in-the-loop QC system capable of detecting, correcting, and documenting quality deviations across diverse tissues and platforms.
Methods: Using a pan-tissue real-world mIF dataset, we evaluated the SpaceIQ™ QC pipeline across the most frequent image quality failure modes. QC begins with raw pixel data: a nuclear-derived tissue mask defines foreground/background regions for estimating and correcting batch effects. Channel-level parametric models detect blurring, saturation, bubbles, and other acquisition-related artifacts. Spatial modeling quantifies uneven illumination across tissue areas. A library of expected staining patterns is used to identify non-specific binding. Segmentation outputs are used to flag biologically impossible co-expression events (e.g., PanCK/CD45) as indicators of staining or acquisition issues. Each QC module generates a 0-3 score, from low quality/not-usable to no-artifacts, enabling a simple, interpretable quantitative assessment. All QC outputs are visualized in the SpaceIQ™ interface, which highlights artifact-containing ROIs and enables user confirmation or override.
Results: The pipeline reliably detected and excluded regions affected by blurring, saturation, and uneven illumination. Applying standardized QC steps significantly altered cell counts and subtype distributions by correcting batch effects and removing regions affected by non-specific staining, demonstrating the importance of systematic QC before quantitative analysis.
Conclusions: The SpaceIQ™ QC pipeline provides a platform- and tissue-agnostic framework for automated yet interpretable quality assessment of mIF imaging. By integrating artifact detection, batch correction, and biological validity checks, it improves accuracy, reproducibility, and user confidence, ensuring results reflect true biological signal rather than technical variability.

#6676 Spatial proteomics and AI-driven analysis uncover therapeutic landscapes within the glioblastoma microenvironment.

Nadine Nelson[1], Hoyin Lai[2], Sophie Struble[2], Richard A. Heil-Chapdelaine[2], Natasha F. Diaz Granados[2], **Arindam Bose**[2]

[1]Abcam, Cambridge, United Kingdom,[2]Leica Microsystems, Waltham, MA

Glioblastoma (GBM) is a highly aggressive and spatially heterogeneous brain tumor with limited treatment options and poor prognosis. Effective therapeutic targeting requires a deeper understanding of the tumor microenvironment (TME), particularly the spatial relationships between malignant, immune, and stromal compartments. To address this, we employed the Cell DIVE™ multiplex immunofluorescence platform to perform high-plex spatial proteomic profiling of FFPE glioblastoma tissue section. A customized panel of directly conjugated recombinant antibodies from Abcam was optimized to interrogate markers relevant to tumor biology, immune modulation, and stromal architecture. Following iterative staining and imaging cycles, multi-channel, high-resolution images were analyzed using Aivia, an AI-powered image analysis platform. The workflow enabled accurate segmentation of tissue regions and quantification of spatial protein expression patterns across distinct anatomical zones within GBM. Spatial relationships among protein expression patterns revealed region-specific immune infiltration and phenotypic transitions at tumor-stromal interfaces. Co-localization and proximity analysis further identified potential immune evasion signatures and microenvironmental structures associated with resistance phenotypes. This integrative approach provides a scalable and clinically compatible method for spatially resolved proteomic analysis of complex tumor tissues. The combination of Cell DIVE™ multiplex imaging, Abcam direct-conjugate antibodies, and Aivia-based analysis offers a powerful platform for dissecting the spatial biology of glioblastoma. The translational relevance of this study lies in its potential to inform biomarker development, guide spatially targeted therapies, and support precision medicine strategies in GBM. This methodology is well positioned for integration into clinical research workflows and large-scale translational studies, with potential to inform personalized treatment strategies across neuro-oncology and other solid tumors.

#6677 Multiplexed imaging and AI-guided analysis reveal immune landscape diversity across multiple cancer types.

Lynne Turnbull, Michael J. Smith, Sophie Struble, Vasundhara Agrawal, Debayon Paul, Richard A. Heil-Chapdelaine, Natasha F. Diaz Granados, **Arindam Bose**

Leica Microsystems, Waltham, MA

Understanding the interplay between tumor and host tissues within the tumor microenvironment (TME) is critical for guiding drug development. Immuno-oncology features of the TME can determine whether cancers progress or respond to immunotherapies. Mapping the TME by characterizing the phenotype, functional state, and proliferative status of immune and cancer cells can advance drug discovery. Because of the considerable number of cell types and biomarkers present in cancer samples multiplexed imaging approaches are often required to capture this complexity, while AI-guided analysis platforms can extract meaningful insights from these data-rich experiments. Owing to intra-tumor heterogeneity and expression differences across cancer types, a multi-tumor workflow that examines biomarker panels in diverse tissue sections provides additional value, by enabling differential biomarker profiling, co-expression analysis, and cancer signature discovery. To this end, we utilized the Cell DIVE multiplexed imaging platform to perform multiplex imaging across several cancer types using a novel dye-conjugation strategy with validated antibody panels and specialized dyes. Biomarker expression profiles and phenotypic classifications across the tumor samples were subsequently analyzed using Aivia. In addition, both supervised and unsupervised clustering analysis revealed distinct cancer signatures across tumor types. By combining the high-throughput capabilities of the Cell DIVE platform with newly developed specialized panels and staining reagents, the immune-oncology researcher can gain a comprehensive understating of the biological processes occurring within cancer samples and identify key molecular targets. This integrated workflow provides deeper insight into tumor-immune dynamics, bridging basic research and clinical applications to accelerate the discovery of actionable biomarkers and therapeutic targets.

#6678 Ultra-high-plex immunofluorescence analysis of the tumor-immune microenvironment with EpicIF technology on the CellScape platform.

Arne Christians[1], Thore Boettke[1], Jannik Boog[1], Charles Eldon Jackson[1], Matt Ingalls[1], Brian J. Lane[1], Daniel Jimenez Sanchez[1], Christoph Rocken[2], Niclas Christian Blessin[2], Oliver Braubach[1]

[1]Bruker Spatial Biology, St. Louis, MO,[2]Dept. of Pathology, University Medical Center Schleswig-Holstein, Kiel, Germany

Spatial biology continues to transform cancer research by revealing the intricate molecular and cellular architecture of tissues. Yet, our understanding of the complex processes in the tumor microenvironment is still incomplete, partly because single-cell *in situ* proteomic data remain challenging to achieve. Most high-plex imaging approaches rely on complex and indirect detection schemes that restrict accessibility and decouple detection from direct visualization. To overcome these limitations, we developed EpicIF™ technology for the CellScape platform for precise spatial phenotyping. EpicIF™ technology is a novel multiplex immunofluorescence (mIF) method that employs a proprietary signal-removal chemistry to efficiently eliminate fluorophores between imaging cycles while preserving tissue morphology and antigenicity. This allows repeated rounds of staining and imaging with fluorophore-labeled primary antibodies, thereby eliminating the need for barcoding, oligo labeling, or sequencing-based decoding. Using this chemistry, we first determined biomarker and tissue integrity after 50 EpicIF-based signal removal cycles to ensure feasibility of an ultra-high plex assay. Of 30 representative markers tested, only 2 showed reduction in signal intensities, while the majority of biomarkers showed little or no significant reduction at all. We then performed direct cyclic immunofluorescence imaging of more than 200 protein targets within a single FFPE tissue section. Our antibody panel was entirely sourced from commercially available fluorophore-conjugated antibodies, and it targets a broad spectrum of biomarkers to profile tumor cells, immune cell subsets, the tissue architecture, and key signaling pathways. This broad immune-oncology focused antibody panel was used to stain more than 200 tumor tissues, including breast cancer, lung cancer, melanoma, glioma, colorectal cancer, and other cancer types. The practical realization of this 200-plex immunofluorescence assay was made possible through key enhancements to the CellScape platform, enabling higher imaging throughput, and sustained stability across extended acquisition runs. This platform establishes a new benchmark for spatial proteomics by combining assay innovation with high-throughput instrumentation to deliver rapid, reliable, and ultra-high-plex imaging at single-cell resolution. This approach provides a powerful framework for dissecting the complex cellular and molecular landscape of the TME and opens new avenues for biomarker discovery, therapeutic stratification, and mechanistic insights into tumor-immune dynamics.

#6679 Decoding immune and tumor niches through high-plex spatial multi-omics in human cancer tissues.

Bin Wang, Kevin Hwang, Yijia Sun, Cassandra Kysilovsky, Angela Vasaturo, Jiang He

Vizgen, Cambridge, MA

The tumor microenvironment (TME) is defined by extensive spatial and molecular heterogeneity, and single-biomarker assays fail to capture the complexity of cellular interactions that drive tumor progression and therapeutic response. To overcome these limitations, we present a spatial multi-omics strategy that integrates Vizgen's spatial transcriptomics and proteomics technologies to enable deeper characterization of the TME. The MERSCOPE® Ultra™ Platform, powered by MERFISH 2.0, currently supports high-resolution spatial profiling of up to 1,000 genes and 6 proteins in a single assay. Here, we introduce an expanded multi-omics workflow that increases protein detection capacity up to 30 targets while maintaining simultaneous spatial detection of up to 1,000 RNA transcripts. The workflow is initiated by staining with conjugated antibodies linked to optimized oligonucleotide tags, engineered to ensure high sensitivity and minimal background noise, followed by MERFISH 2.0 RNA imaging. The integrated spatial multi-omics approach seamlessly couples high-plex protein detection with MERFISH 2.0 transcriptomics. The robustness and utility of these integrated methodologies were extensively validated across a broad range of indications and antibody panels. We applied this multi-omics assay to cancer specimens, achieving simultaneous quantification of an up to 30-plex immuno-oncology (IO) protein signature and a comprehensive, pre-designed 815 IO transcript inventory which supports its powerful application in translational oncology. Our results demonstrated robust performance, characterized by high detection sensitivity and minimal background interference for both molecular modalities. A key advantage of the presented assay is the full user customization of both the protein biomarker panels and RNA transcripts, enabling researchers to optimally tailor panel design to specific mechanistic inquiries. Leveraging the subcellular resolution of the MERSCOPE Ultra Platform, we executed granular single-cell spatial profiling, successfully delineating cellular neighborhoods and characterizing cell-to-cell communication within the tumor microenvironment. The resulting multi-omic datasets allowed us to characterize the specific gene signatures and immune cell subsets enriched within distinct tumor regions, illuminating the spatial determinants governing tumor-immune interactions. Therefore, this integrated, expanded spatial multi-omics solution represents a powerful framework to enable comprehensive co-profiling of immune and tumor biomarkers within a single tissue section. By simultaneously capturing protein and RNA expression at single-cell resolution, it provides an unparalleled framework for dissecting cellular interactions, identifying spatially organized biomarkers, and accelerating translational studies aimed at predicting therapeutic response.

#6680 Decoding the tumor microenvironment with triple-omics: Automated spatial analysis of protein-protein interactions, RNA, and protein markers on the same section.

Alice Comberlato[1], Arec Manoukian[1], Pino Bordignon[1], Ge-Ah Kim[2], Sonali Deshpande[2], Florent Jeanpetit[1], **Alix Failletaz**[1], Li-chong Wang[2], Alexandre Kehren[1], Saska Brajkovic[1]

[1]Lunaphore, a Bio-Techne brand, Tolochenaz, Switzerland,[2]Adavanced Cell Diagnostics, a Bio-Techne brand, Newark, CA

Understanding the complexity of the tumor microenvironment (TME) requires simultaneous insight into multiple biological domains. Studying the molecular interactions that govern intercellular and intracellular signaling in combination with the analysis of cell phenotypes and transcriptional states, can guarantee an improved comprehension of key pathways driving tumor growth or the response of anti-cancer therapies. Protein-protein interactions (PPIs), such as PD-1/PD-L1, are central to immune evasion and targets of important immunotherapies. Despite the success of PD-1/PD-L1 and other checkpoint inhibitors, patient stratification for these therapies has been challenging, and marker expression alone has shown to not fully capture functional engagement or predict an efficient drug response. Here, we present a fully automated workflow that combines three omics layers on the same tissue section: protein-protein proximity, RNA, and protein expression, enabling a more comprehensive view of cellular interplay in cancer and modeling of treatment outcomes. The multiomics assay runs on the COMET™ platform. It allows the co-detection of: (i) RNA profiling via RNAscope™ HiPlex Pro, (ii) Protein expression through sequential immunofluorescence (seqIF™, PMID: 37813886), (iii) Protein-protein proximity detection using oligonucleotide-conjugated secondary antibody pairs and RNAscope™ amplification chemistry. Proximity signals are interpreted as probabilistic indicators of molecular interactions and supported by multiple controls to ensure their specificity: from the colocalization of seqIF™ signals to negative controls run on the same section. In this study, we demonstrated that it is possible to combine the detection of proximity signals for the analysis of intercellular interactions controlling anti-tumoral immune responses, alongside protein markers for cell phenotyping and RNA targets for functional markers and cell activation status. In detail, across multiple human FFPE tumor samples, PD-1/PD-L1 interaction was detected in combination with multiple proteins, for immune and stromal phenotyping, and RNA transcripts responsible for the expression of key secreted molecules like cytokines and chemokines. Furthermore, we showed that multiple iterative cycles allow the detection of more than one PPI on the same FFPE section. Tumor progression, immune evasion, and therapy resistance are not driven by single molecules but by complex interaction networks among proteins, signaling pathways, and cellular types. This automated spatial multiomics workflow incorporating protein-protein proximity as a third dimension, can help reveal how these processes are regulated. By combining RNA, protein, and proximity data, the assay offers a powerful approach to support biomarker discovery and improved patient stratification.

#6681 Innovative 10x Genomics technologies enable clinical-scale cancer research and AI-driven biomarker discovery.

Hiroshi M. Sasaki[1], Seayar H. Mohabbet[2], Ian T. Fiddes[3], Francesca Meschi[1], 10x Genomics Development Team

[1]Spatial Biology, 10x Genomics, Inc., Pleasanton, CA,[2]Histopathology Core, 10x Genomics, Inc., Pleasanton, CA,[3]Computational Biology, 10x Genomics, Inc., Pleasanton, CA

Background:
Spatial and single-cell omics are transforming cancer research, offering unprecedented resolution into tumor heterogeneity and microenvironment dynamics. However, the adoption of these powerful tools for large-scale clinical studies and subsequent integration into AI-driven diagnostic pipelines remains hampered by persistent challenges, including high cost, complex workflows, low sensitivity and specificity, and limited scalability and throughput. Addressing these bottlenecks is critical for accelerating the identification and validation of robust cancer biomarkers, especially for early detection.
Methods:
We introduce technology innovations that address the historic compromises inherent in existing spatial and single-cell technologies. These approaches are designed to deliver superior specificity, sensitivity and plex at significantly reduced cost and with streamlined, high-throughput workflow capabilities. Leveraging a novel integration of advanced chemistry and computational analysis, these technologies enable simultaneous, single-cell resolution profiling of both tissue morphology and gene expression signatures across clinically relevant sample scales.
Results:
Application of the technology innovations to clinically archived tumor specimens demonstrates their potential for clinical-scale studies. We achieved robust, high-plex molecular profiling with unprecedented efficiency. Critically, the data generated is inherently low-noise, high-resolution, and scalable, making it immediately amenable to machine learning and AI algorithms. Preliminary analysis highlights its utility in identifying novel biomarkers predictive of therapeutic response and supporting early detection. The simplified workflow dramatically reduces time-to-result, positioning this solution as a key enabler for population-scale cancer research.
Conclusion:
These technology innovations overcome major workflow, cost, and sensitivity limitations, paving the way for the clinical-scale deployment of spatial and single-cell omics. By generating high-quality, AI-ready data across large cohorts, this solution will accelerate biomarker discovery, drive the next generation of early cancer detection strategies, and fully support the ongoing AI revolution in cancer research.

#6682 Chimeric antibodies in oncology research: Properties and application in low-multiplexing assays.

Tom Bright, Nadine Nelson, Antonella Galli, Will Howat, Silvia Sbacchi

Abcam Limited (UK), Cambridge, United Kingdom

Chimeric antibodies, engineered by fusing the variable (antigen-binding) domains of one species (e.g. rabbit) with the constant domains of a different species (e.g. human, chicken), represent a significant advancement in antibody technology. This approach preserves the original antibody's specificity and affinity while introducing desirable features from the second species. Beyond therapeutics, the distinctive characteristics of chimeric antibodies offer notable benefits in *in vitro* diagnostic and research applications, for example in low-multiplexing assays. In particular, chimeric antibodies offer significant advantages in multiplexed assays, where their species-specific constant regions allow for the simultaneous use of multiple primary antibodies with minimal cross-reactivity. The use of chimeric antibodies is compatible with diverse experimental setups allowing researchers to leverage existing secondary antibodies systems. Here we demonstrate the advantage of using chimeric antibodies for building immunohistochemistry (IHC) panels for the co-detection of cancer protein markers and the study of tissue micro environment (TME) in formalin-fixed paraffin-embedded (FFPE) human tumor tissues. By leveraging antibodies derived from multiple host species, including mouse, rabbit, and chicken, we achieved robust and specific staining in both normal and tumor samples. Our results highlight the potential of chimeric antibodies to streamline complex IHC workflows and improve the resolution of multiplexed tissue analyses in cancer research.

#6683 Streamlined high-plex imaging with InSituPlex®and ZEISS Axioscan 7 for spatial phenotyping.

Kevin Hwang[1], Mike Woerdemann[2], Lars Loetgering[2], Moritz Widmaier[2], Cassandra Kysilovsky[1], Sherry Derakhshani[2], Jiang He[1], Angela Vasaturo[1]

[1]Vizgen, Cambridge, MA,[2]Zeiss, Jena, Germany

Multiplex immunofluorescence (mIF) provides a powerful means to visualize complex biomarker signatures with spatial context. Yet, most high-plex mIF approaches depend on repeated cycles of staining and imaging, which introduce workflow complexity and necessitate either labor-intensive manual handling or sophisticated instrumentation capable of automating these multistep procedures. Vizgen's InSituPlex assay supports rapid, multiplexed detection of up to 12 protein biomarkers in a single staining step, leveraging signal amplification to achieve robust detection of both abundant and lowly expressed targets using standard fluorescence filter configurations. When combined with the Axioscan 7 spatial biology platform, engineered for fully automated, high-throughput slide scanning with additional fluorescent channels, this workflow enables higher-plex, single-round imaging without the need for spectral unmixing. Here, we demonstrate the power of this integrated approach to streamline assay development, expand biomarker panel design flexibility, and deliver efficient, scalable multiplexed protein imaging. A next generation InSituPlex® assay was developed to increase the simultaneous detection of markers using the Axioscan 7 spatial biology system. A panel of fluorophores was carefully selected to minimize spectral overlap and maximize detection specificity, ensuring clear distinction of all fluorescent channels without requiring spectral unmixing to deconvolute signals. Signal quality was analyzed using the STARVUE image analysis pipeline which precisely determined positive cell signal intensity and density. The increased number of fluorophores showed excellent signal to noise ratio and no crosstalk between fluorescent channels. The expanded channel capacity of InSituPlex assay allows for a simplified workflow while increasing the number of biomarkers that can simultaneously be detected in tumor samples. This capability further enhances flexibility for InSituPlex panel design and streamlines the assay development process. The integration of the novel InSituPlex fluorescent dye panel and the Axioscan 7 spatial biology platform delivers a superior, high throughput mIF workflow. This combination enables higher-plex imaging while significantly reducing manual steps, leveraging the established reproducibility and throughput of both technologies. We anticipate this integrated platform will empower researchers to unlock deeper, high resolution spatial insights into cancers and their complex environments.

#6684 Spatial multi-omics profiling of clear cell renal cell carcinoma (ccRCC) pre-and post-immunotherapy identifies new druggable targets.

Navneet Kaur[1], Wadih Issa[1], Ze Yu[2], Hua Zhong[3], Aleksandra Weronika Nielsen[4], Jay Jasti[4], Shahed Abdullah[1], Libin Yan[1], Damla Gunenc[1], Qinhan Zhou[1], Andrew DeVilbiss[1], Satwik Rajaram[4], Payal Kapur[3], Chao Xing[5], Liwei Jia[3], Andrew Z. Wang[6], Tian Zhang[1]

[1]Department of Internal Medicine (Division of Hematology-Oncology), Harold C. Simmons Comprehensive Cancer Center, UT Southwestern Medical Center, Dallas, TX,[2]Eugene McDermott Center for Human Growth and Development, UT Southwestern Medical Center, Dallas, TX,[3]Department of Pathology, UT Southwestern Medical Center, Dallas, TX,[4]Lyda Hill Department of Bioinformatics, UT Southwestern Medical Center, Dallas, TX,[5]Lyda Hill Department of Bioinformatics; O'Donnell School of Public Health, Eugene McDermott Center for Human Growth and Development, UT Southwestern Medical Center, Dallas, TX,[6]Department of Radiation Oncology, Harold C. Simmons Comprehensive Cancer Center, University of Texas Southwestern Medical Center, Dallas, TX

Introduction: Immunotherapy (IO) and VEGF targeting TKIs have transformed outcomes of patients with advanced ccRCC. However, much less is known about treatment resistance mechanisms after IO therapy.

Methods: 15 patients (pts) with advanced ccRCC who had tumor samples pre- and post-treatment (Tx, IO-IO or IO-TKI) were included in this study. Tumors were profiled using the Nanostring GeoMx spatial profiling platform. 4 to 12 regions of interest (ROIs) were selected for each patient, and the ROIs were further segmented into tumor (PanCK+), immune (CD45+), and stroma (PanCk-, CD45-) compartments. Differentially expressed genes and proteins were assessed with Gene Set Enrichment Analysis (GSEA). Bulk gene expression was further deconvoluted to profile immune cell subsets using CIBERSORT. Deep learning algorithms analyzed H&E slides for angiogenic, immune gene signatures, and non-negative matrix factorization (NMF) clustering.

Results: In the tumor compartment (PanCK+), several clinically druggable targets such as Axl, HER2, TROP-2, GITR, HIF-1α, and FGFR2 were significantly upregulated after IO. Interestingly, Trop-2 expression was upregulated in IO-IO (Log2FC 0.038, $p<0.01$) post-Tx but not after IO-TKI (Log2FC -0.070, $p<0.01$). Some patients who received IO/TKIs had decreased tumor angiogenic expression post-Tx. NMF clustering classified post-Tx as NMF4 in 6/15 patients (4 of 10 in IO-TKI cohort and 2 of 5 in IO-IO cohort). NMF cluster 3 remained post-IO in most patients.While most pre-IO samples had moderate to high immune infiltration, post-IO samples had even higher levels. Notably, CIBERSORT profiling revealed post-IO proportion of immune suppressive regulatory T cells were decreased (IO-TKI, $p <0.01$), while cytotoxic CD8+ T cells were increased (IO-TKI, $p <0.01$) with both Tx cohorts. However, resting NK cells were increased ($p=0.29$), while activated NK cells were decreased ($p <0.01$) significantly only in IO-IO treated subsets.

Conclusion: Molecular gene expression changes in RCC after IO-based therapy identified clinical targets in residual tumors. NMF cluster 4 persistence, CD8+ infiltration, and reduction in Treg proportion suggests an expansion or persistence of immune cells post-IO. NMF cluster 3 and increased proportion of resting NK cells may explain the resistance of residual tumor post-IO. Given the heterogeneity in RCC, it is imperative to profile individual tumors to improve IO therapy outcomes. Ongoing analyses include IHC target validation.

#6685 Integrated high-throughput multimodal spatial profiling of RNA, protein, and morphology in FFPE sections with the G4X™ Spatial Sequencer.

Michael Lawson[1], Kenneth Gouin[1], Sabrina Shore[2], Yuji Ishitsuka[2], Richard Que[2], Eli Glezer[2], Daan Witters[2]

[1]Singular Genomics, San Diego, CA,[2]Singular Genomics, LA JOLLA, CA

Comprehensive characterization of the tumor microenvironment (TME) benefits from simultaneous measurement of transcripts, proteins, and morphology at single-cell resolution in clinically relevant samples. The G4X Spatial Sequencer is a high-throughput in-situ platform that delivers co-registered RNA, protein, and morphological readouts from the same FFPE section, supporting up to 40 cm^2 of tissue per run and flexible panel customization.We designed four targeted ~300-gene RNA panels for kidney, lung, colon, and breast tissues. Each includes 150 shared immuno-oncology genes, 50 stromal genes, and ~100 tissue-specific targets. A paired 16-plex immuno-oncology protein panel provides spatially resolved multiplexed proteomics measurements. All analytes were acquired from single 5 µm sections and directly aligned with fH&E™, a fluorescent analog of standard H&E.

Sections were processed via the TissuStamp™ transfer workflow in large (ten 10 × 10 mm^2/flow cell) or small (thirty two 4.5 × 4.5 mm^2/flow cell) arrays through antibody staining, padlock probe hybridization, amplification, and sequencing-by-synthesis (SBS). Per-cell detection ranged from 50-200 transcripts and 20-50 unique genes, with dynamic ranges exceeding 500 transcripts in high-expressing cells. RNA false discovery rates were ≤0.5% (typically <0.1%), and genomic DNA FDRs were 0.5-5%, with transcript detection unaffected by concurrent protein imaging.

Protein data quality matched single-plex immunofluorescence, and integration of protein abundance with gene-expression programs improved cross-modal specificity beyond single-gene comparisons.

In addition to curated panels for transcripts and proteins, G4X enables the inclusion of custom targets. The sequencing-based readout preserves probe-level resolution, enabling efficient optimization of custom RNA panels without loss of information, demonstrated across mouse, bone marrow, and pancreas datasets. Two additional custom protein targets were successfully incorporated into the curated 16-plex panel.

To highlight scalability, G4X is deployed in ongoing atlas-scale lung and colorectal cancer studies with academic partners and has been used for 3D reconstruction across serial sections.

Together, these results position G4X as a unified, scalable workflow for multiplexed spatial transcriptomic, proteomic, and morphological profiling of FFPE tissues, enabling large-cohort, integrative analyses of the TME.

#6686 Direct-Seq™ enables spatially resolved *in situ* sequencing of IgH and TCRβ transcripts in FFPE tissue at subcellular resolution.

Michael Lawson[1], Tung T. Le[2], Ryan Shultzaberger[2], Ashley Tsue[1], Zane Hiatt[2], Nathan Ing[1], Kenneth Gouin[2], Eli Glezer[2], Daan Witters[2]

[1]Singular Genomics, San Diego, CA,[2]Singular Genomics, LA JOLLA, CA

Spatial multi-omics is transforming our understanding of the tumor microenvironment, immune responses, and disease mechanisms. A critical gap remains in the ability to sequence highly variable transcript regions in situ at single-cell and subcellular resolution, essential for mapping B- and T-cell clonotypes in their native tissue context.

Here, we present Direct-Seq™, a novel in situ sequencing approach built on the G4X™ in situ multiomic platform, enabling high-resolution profiling of RNA variable regions. Direct-Seq employs probes targeting the V and J regions flanking the diverse CDR3 domain of IgH and TCRβ transcripts, allowing sequencing of both the J and CDR3 regions. The workflow integrates in situ reverse transcription, amplification, and sequencing-by-synthesis chemistry.

We applied Direct-Seq to 5-µm FFPE tonsil and renal cell carcinoma (RCC) sections and 10-µm fresh frozen tonsil sections. Up to 9% of B cells were profiled in FFPE tonsil, and ~20% of B and T cells in fresh frozen tissue. Extensive CDR3 diversity was detected, with clonally expanded B cells carrying highly similar CDR3 sequences localized within germinal centers, demonstrating the high-resolution clonotyping capacity of Direct-Seq.

In Renal Cell Carcinoma (RCC), nine serial FFPE kidney sections revealed clonally expanded B-cell populations enriched around tumor regions and T-cell clones with persistent expansion. One dominant T-cell clone was consistently detected across serial sections, highlighting the method's robustness and ability to track clonal populations spatially.

Direct-Seq was combined with multiplexed protein detection on the same sections, confirming spatial concordance between transcript identity and protein phenotype.

Together, these results establish Direct-Seq as a high-resolution, scalable approach for spatial immune repertoire mapping in both FFPE and fresh frozen tissue, enabling detailed studies of clonality, immune architecture, and translational immunology.

: Vaccines and Other Immunomodulatory Agents
Poster Session

#6690 Unfavorable early progression-free survival of immunotherapy compared to chemotherapy in bladder cancer: A meta-analysis of randomized trials.

Donghwi Choi, Hangyul Lee, Jinha Kim, Young Kwang Chae

Northwestern Univ. Feinberg School of Medicine, Chicago, IL

Introduction: Platinum-based chemotherapy has long served as the first-line standard for advanced urothelial carcinoma. However, the advent of immune checkpoint inhibitors (ICIs) has spurred efforts to evaluate their suitability as initial therapy, especially in patients with strong PD-L1 expression or those who cannot tolerate cisplatin. Early results from randomized controlled trials (RCTs) suggest that ICI-only regimens may produce inferior short-term progression-free survival (PFS) compared with chemotherapy, potentially due to delayed immune activation, lack of rapid tumor shrinkage, or hyperprogressive disease in select cases. To characterize this time-dependent efficacy pattern, we performed a meta-analysis comparing ICI-only regimen with chemotherapy in advanced bladder cancer.
Methods: A comprehensive search of PubMed, Embase, and the Cochrane Library identified phase II-III RCTs comparing first-line ICI-only regimen(Durvalumab, Durvalumab+Tremelimumab, Pembrolizumab) and platinum-based chemotherapy for advanced bladder cancer. Studies conducted exclusively in first-line treatment settings were selected for inclusion. Kaplan-Meier PFS curves from eligible trials were extracted and digitized, and reconstructed patient-level survival data were generated using the Guyot algorithm. Combined Kaplan-Meier estimates were produced from pooled data, and hazard ratio (HR) values comparing immunotherapy with chemotherapy were calculated at 3, 6, 9, and 12 months to evaluate temporal changes in treatment effect. HRs were obtained through two-stage meta-analysis, incorporating study-specific weights to account for differences in sample size and variance across trials.
Results: Three immunotherapy regimens in two RCTs met the inclusion criteria. ICI-only regimens demonstrated worse early PFS outcomes compared to chemotherapy, with HRs of 4.08(95% CI, 2.85-5.82) at 3 months, 2.87(2.23-3.70) at 6 months, 2.05(1.80-2.33) at 9 months and 1.92(1.63-2.25) at 12 months. HRs gradually decreased throughout the 12-month period, indicating slow convergence of survival trajectories. Pooled KM curves showed that immunotherapy exhibited reduced short-term benefit compared to chemotherapy that gradually improved with longer follow-up and ultimately crossed over at 10 months.
Conclusion: In advanced bladder cancer, first-line ICI-only regimen underperforms relative to chemotherapy in the early phase. Survivability slowly improves with follow-up and benefits are apparent around 10 months as the KM curves cross over. These findings underscore the need for vigilant early assessment and support combination or sequential treatment strategies to offset early progression while preserving long-term immunologic benefit.

#6691 Pattern of inferior early progression-free survival with immunotherapy versus chemotherapy in head and neck cancer: A meta-analysis of randomized trials.

Donghwi Choi, Hangyul Lee, Jinha Kim, Young Kwang Chae

Northwestern Univ. Feinberg School of Medicine, Chicago, IL

Introduction: Platinum-based chemotherapy combined with immunotherapy has long been the standard first-line treatment for advanced head and neck squamous cell carcinoma (HNSCC). Recently, pembrolizumab-based regimens guided by PD-L1 expression have introduced immunotherapy-only approaches as viable options for selected patients. However, early data from randomized trials suggest that immunotherapy may result in inferior short-term progression-free survival (PFS) compared with chemotherapy, likely due to delayed immune activation or possible hyperprogression of the disease. To clarify these time-dependent effects, we performed a meta-analysis comparing the early efficacy of immunotherapy versus chemotherapy in advanced HNSCC.
Methods: We systematically searched PubMed, Embase, and the Cochrane Library for phase II-III RCTs evaluating first-line immunotherapy(Pembrolizumab, Nivoluab+Ipilimumab, Durvalumab, Durvalumab+Tremelimumab) with platinum-based chemotherapy in advanced HNSCC. Eligible trials were required to have Kaplan-Meier PFS curves for immunotherapy and chemotherapy arms. Trials including post-first-line settings were excluded. Kaplan-Meier PFS curves were digitized, and reconstructed individual patient data were derived via the Guyot method. Pooled Kaplan-Meier survival curves were then generated, and hazard ratio (HR) values comparing immunotherapy and chemotherapy arms were calculated at 3, 6, 9, and 12 months to assess changes in treatment effect over time. Hazard ratios (HRs) were estimated through a two-stage meta-analytic method, with each study weighted according to its sample size and variance to accommodate inter-trial differences.
Results: Three eligible RCTs were identified. Immunotherapy exhibited a pronounced early disadvantage in PFS compared with chemotherapy, with HRs of 3.77 (95% CI, 3.17-4.48) at 3 months and 2.20 (95% CI, 1.80-2.68) at 6 months. This gap narrowed over time but was still statistically significant by the 9th (HR 1.86; 95% CI, 1.62-2,13) and the 12th month (HR 1.73; 95% CI, 1.49-2.01). Pooled Kaplan-Meier PFS curves mirrored these findings, showing inferior short-term performance of immunotherapy followed by gradual convergence of both arms, with the immunotherapy arm ultimately crossing over the chemotherapy arm around the 12th month.
Conclusion: Among patients with metastatic HNSCC, first-line ICI monotherapy initially shows inferior outcomes compared to chemotherapy, but the survival benefit becomes evident around the 12th month as the delayed effects of immunotherapy emerge. These results highlight the importance of close early monitoring and lend support to combination or sequential regimens to counteract early disease progression while maintaining long-term benefit.

#6692 Self-adjuvanting α-helical polypeptide simultaneously delivers neoantigen mRNAs and activates dendritic cells to eradicate tumors.

Jiadiao Zhou

University of Illinois at Urbana-Champaign, Champaign, IL

mRNA-based vaccines have demonstrated tremendous success during the era of COVID-19, but their therapeutic potential for treating cancer, especially poorly immunogenic solid tumors, remains under-achieved. Herein we report a class of self-adjuvanting α-helical polypeptides that can markedly improve the antitumor efficacy of tumor neoantigen-encoding mRNAs. Ideal carriers for antigen-encoding mRNAs should not only facilitate antigen expression in DCs but also activate DCs and induce effective processing and presentation of expressed antigens. Herein we report the development of cationic α-helical polypeptides as a self-adjuvanting delivery vehicle for antigen-encoding mRNAs.

The α-helical polypeptides facilitate intracellular delivery of mRNAs into dendritic cells (DCs) via temporary membrane disruption, simultaneously activate DCs by regulating NF-κB and IRF pathways, and improve the ability of DCs to process and present mRNA-encoded neoantigens. The cationic polypeptide condenses and stabilizes mRNAs, promotes internalization via its cell-penetrating property, and increases the expression of activation markers (CD86, MHCII, CD40, and CCR7) on DCs by upregulating NF-κB, IRF, and STING pathways. Molecular docking and simulation confirm the stable complexation between mRNA and α-helical polypeptides.

Upon subcutaneous administration, the polyplex migrates to draining lymph nodes, where it transfects and activates DCs, eliciting a strong neoantigen-specific cytotoxic T lymphocyte (CTL) response in vivo. Compared to mRNA-SM102 lipid nanoparticles or Lipofectamine 3000 lipoplexes, the polyplex enhances antigen expression and presentation by DCs, leading to significantly improved priming of antigen-specific $CD8^+$ T cells in vitro and in vivo. The polyplex achieves 83.3% and 33.3% tumor-free survival in E.G7-OVA lymphoma and 4T1 triple-negative breast cancer (TNBC), respectively. This is far exceeding the 0% tumor-free survival of conventional formulations. Polyplexes composed of α-helical L-PPOB50-G and mRNAs encoding 4T1 TNBC neoantigens elicit potent neoantigen-specific $CD8^+$ T cell responses while showing no detectable toxicity in major organs.

The polyplex also reprograms the immunosuppressive tumor microenvironment by enriching DCs, M1-phenotype $CD86^+$ macrophages, and $CD8^+$ T cells in tumors. We also observed increased PD-1 expression on intratumoral $CD8^+$ T cells and PD-L1 on 4T1 tumor cells after polyplex treatment and demonstrated synergistic effects between the polyplex vaccine and anti-PD-1 therapy. Our polyplex system provides a facile and generalizable approach to developing robust mRNA-based cancer vaccines.

#6693 KLRG1^{+}PD-1^{+} CD8^{+} T cells drive potent antitumor immunity induced by a systemic STING nanovaccine.

Shuang Chen[1], Shuyue Ye[1], Qiang Feng[1], Gang Huang[1], Animesha Krishnamurthy[1], Baran Devrim Sumer[2], Jinming Gao[3]

[1]UTSW, Dallas, TX,[2]UT Southwestern Medical Center, Dallas, TX,[3]UT Southwestern, Dallas, TX

Activation of the stimulator of interferon genes (STING) pathway enhances dendritic-cell priming and cytotoxic T-cell immunity, yet systemic STING agonists are limited by off-target toxicity. We recently developed a dual-stimuli-responsive STING nanovaccine that co-delivers HPV E7 antigen and a polymer-conjugated STING agonist, enabling safe systemic activation of antitumor T cells.[1, 2] Despite the strong induction of E7-specific CD8^{+} T cells, the phenotypic and functional heterogeneity of vaccine-elicited T cells remains incompletely understood. Identifying the dominant effector population responsible for tumor clearance is critical for rational vaccine optimization and for developing combination strategies with adoptive or checkpoint-based immunotherapies.[3] To address this, we analyze the splenic immune cells in C57BL/6 tumor-bearing mice after intravenous administration of the dual-stimuli-responsive STING nanovaccine. A distinct KLRG1^{+}PD-1^{+} CD8^{+} T-cell population emerged and was isolated by fluorescence-activated cell sorting for adoptive transfer into naïve, tumor-bearing recipients. Vaccination induced robust activation of dendritic cells (CD86^{+}MHC-II^{+}) in the spleen and lymph nodes, accompanied by expansion of E7-specific CD8^{+} T cells. Within this compartment, the KLRG1^{+}PD-1^{+} subset exhibited high expression of granzyme B and IFN-γ, consistent with a cytotoxic-effector phenotype. Adoptive transfer of these double-positive cells significantly delayed tumor growth and prolonged survival relative to unsorted or untreated controls, confirming their potent antitumor activity. Expansion of this subset correlated with spleen-targeted biodistribution and STING-dependent activation of myeloid cells.These data identify a functionally dominant KLRG1^{+}PD-1^{+} CD8^{+} T-cell subset as a key mediator of systemic STING nanovaccine efficacy. The findings support a mechanistic link between STING-driven myeloid activation and effector-T-cell differentiation. Ongoing single-cell and spatial transcriptomic analyses will define the lineage trajectories and molecular circuitry underlying their generation and persistence, informing future combinations of STING nanovaccines with adoptive-cell or checkpoint immunotherapies for durable systemic tumor control.

Keywords: STING nanovaccine, CD8^{+} T cells, KLRG1, PD-1, adoptive transfer, single-cell RNA-seq, spleen, immunotherapy

Reference1.Chen, S. et al. Stimuli-responsive STING nanovaccine for systemic therapy of HPV-induced cancers. *Proc. Natl. Acad. Sci. U.S.A.* 122, e2409570122 (2025).2.Li, S. et al. Prolonged activation of innate immune pathways by a polyvalent STING agonist. *Nature Biomedical Engineering* 5, 455-466 (2021).3.Giles, J.R., Globig, A.-M., Kaech, S.M. & Wherry, E.J. CD8+ T cells in the cancer-immunity cycle. *Immunity* 56, 2231-2253 (2023).

#6694 Monocyte-derived dendritic cells for antigen-specific T cell activation.

Kaitlin Hsu, Jessica Voce, Amy Zhao, Jessie Ni

BioLegend, San Diego, CA

This study describes an efficient workflow to generate functional dendritic cells (DCs) from human peripheral blood monocytes and their application in antigen-specific T cell activation assays. Monocytes were differentiated into mature DCs expressing high levels of co-stimulatory molecules and MHC molecules. When pulsed with specific antigens and co-cultured with autologous T cells, these DCs effectively activated CD4+, CD8+, and regulatory T cell populations, as demonstrated by proliferation assays and cytokine profiling. The differential activation kinetics between T cell subsets provided insights into the temporal dynamics of antigen-specific immune responses. Our workflow demonstrates a standardized approach that offers a reliable research platform to investigate DC-T cell interactions, evaluate vaccine candidates, and assess antigen-specific T cell responses. Furthermore, our reproducible workflow may serve as a valuable tool for applications in immunology research, including vaccine development, cancer immunotherapy, and autoimmune condition studies.

#6695 Early progression disadvantage of immunotherapy-only treatment versus chemotherapy in NSCLC: A meta-analysis of randomized controlled trials.

Jinha Kim, Hangyul Lee, Donghwi Choi, Young Kwang Chae

Northwestern Univ. Feinberg School of Medicine, Chicago, IL

Introduction : Immune checkpoint inhibitors (ICIs) have become a cornerstone in the treatment of advanced non-small cell lung cancer (NSCLC). However, across several randomized controlled trials (RCTs), immunotherapy-only arms have demonstrated an early disadvantage in progression-free survival (PFS) and overall survival when compared with chemotherapy or chemo-immunotherapy combinations. This early decline may reflect multiple factors, including lack of cytoreduction, delayed onset of immunotherapy efficacy relative to chemotherapy, or the phenomenon of hyperprogression. To better define this pattern, we conducted a meta-analysis of RCTs comparing immunotherapy-only regimens with chemotherapy in first-line NSCLC to determine whether this early disadvantage is consistent and generalizable.

Methods: We systematically searched three databases (PubMed, Cochrane Library, and Embase) for phase II and III RCTs evaluating an immunotherapy-only regimen (Nivolumab plus Ipilimumab, Pembrolizumab, Atezolizumab, Avelumab, Nivolumab, Durvalumab, Durvalumab plus Tremelimumab, Cemiplimab) in the first-line treatment of advanced NSCLC. Trials limited to later-line therapy were excluded. Eligible studies required Kaplan-Meier curves for PFS. Twelve RCTs met inclusion criteria. Survival curves were digitized, and individual patient data were reconstructed using the Guyot algorithm. Combined Kaplan-Meier estimates were generated from pooled data, and hazard ratios (HRs) comparing immunotherapy-only vs platinum-based chemotherapy were obtained through two-stage meta-analysis with study-specific weights. Area under the curve (AUC) values were calculated to evaluate temporal changes in treatment effect.

Results : Across 12 RCTs, immunotherapy-only regimens showed a clear early disadvantage in PFS. At three months, the hazard ratio for PFS was 2.03 (95% CI 1.77-2.32), indicating a significantly higher risk of progression in the immunotherapy arms. This persisted at six months (HR 1.36, 95% CI 1.18-1.57), but diminished by nine months (HR 1.13) and 12 months (HR 1.08). Over the full follow-up, immunotherapy ultimately outperformed chemotherapy (HR = 0.86, 95% CI 0.74-0.99, p = 0.048), showing a delayed benefit. AUC analysis confirmed an inferior cumulative PFS benefit during the first 6 months, followed by a gradual catch-up.

Conclusion : First-line immunotherapy-only treatment in NSCLC shows an early PFS disadvantage relative to chemotherapy, followed by superior long-term outcomes. This pattern underscores the need for early monitoring and optimized combination strategies to prevent early progression while maintaining immunotherapy's durable benefits.

#6696 A senescent whole-cell vaccine platform derived from conditionally reprogrammed primary tumor cells primes potent T-cell immunity and overcomes ICI resistance in murine breast cancer models.

Sara Rasouli[1], Chongwen Cao[2], Weiyi Gong[1], Haichang Li[3], Bei Liu[4], Anna Vilgelm[2], Jenny Li[2], Xuefeng Liu[2]

[1]Comprehensive Cancer Center, Biomedical Sciences Graduate Program, The Ohio State University, Columbus, OH,[2]Comprehensive Cancer Center, Department of Pathology, The Ohio State University, Columbus, OH,[3]The Ohio State University College of Veterinary Medicine, Columbus, OH,[4]Molecular, Cellular and Developmental Biology Program, Comprehensive Cancer Center, Ohio State University, Columbus, OH

Background: Aggressive cancers, including breast cancer, face challenges of therapeutic resistance and recurrence. Autologous cancer vaccines are limited by difficulties in obtaining sufficient primary tumor material. Our lab uses the Conditional Reprogramming Cell (CRC) method to enable long-term in vitro expansion of primary tumor cells. We are developing a novel vaccine strategy based on cellular senescence, a highly immunogenic state. We hypothesize that irradiated, senescent whole-tumor cells (SWCs) generated via CRC will function as potent, poly-antigenic vaccines to prime robust anti-tumor T-cell responses, synergize with immune checkpoint inhibitors (ICIs), and establish long-term immune memory.
Experimental method: Senescence was induced in murine breast cancer lines by γ-irradiation. Immune priming was assessed by injecting SWCs into naïve syngeneic mice, quantifying systemic T-cell activation ($CD4^+$, $CD8^+$, $CD69^+$, PD-1^+) in spleens and lymph nodes via flow cytometry. Therapeutic efficacy will be evaluated in orthotopic, tumor-bearing mice treated with SWC vaccine + CpG adjuvant, +/- dual ICI blockade (anti-PD-L1/anti-CTLA-4). Endpoints include tumor regression and survival. Vaccine efficacy will also be tested in prophylactic and post-surgical anti-recurrence models (simulating R1/R2 residual disease).
Summary of new data: In vivo immune-priming experiments (four weekly injections) demonstrated that senescent tumor cells elicited a robust, systemic adaptive immune response. Compared to controls, SWC-treated mice showed a marked expansion of both $CD8\alpha^+$ and $CD4^+$ T-cell populations in spleens and lymph nodes. Flow cytometry revealed an activated effector phenotype with elevated CD69 and cytotoxic markers in $CD8^+$ T cells. These findings confirm SWCs are highly immunogenic and induce systemic T-cell activation.
Conclusion: Senescent whole-tumor cells derived via the CRC method are a feasible and potent poly-antigenic vaccine platform. Our preliminary data demonstrate that this strategy breaks immune tolerance, inducing robust T-cell activation. This provides a strong rationale for advancing this personalized, autologous vaccine to overcome immune resistance and prevent recurrence in aggressive solid tumors.

#6697 Pelareorep combined with atezolizumab and chemotherapy shows immune conversion activity in advanced pancreatic cancer: Biomarker results of cohort 1 of the GOBLET trial.

Hendrik Schurmann[1], Sven-Thorsten Liffers[2], Richard Trauger[3], Thomas Heineman[3], Dirk Arnold[4], Jens T. Siveke[2]

[1]Department of Medical Oncology, University Hospital Essen, Essen, Germany,[2]Bridge Institute of Experimental Tumor Therapy, University Hospital Essen, Essen, Germany,[3]Oncolytics Biotech, San Diego, CA,[4]Asklepios Tumorzentrum Hamburg, AK Altona, Hamburg, Germany

Introduction: Pancreatic cancer features a profoundly immunosuppressive microenvironment and no approved immunotherapy to date. Pelareorep (REOLYSIN®) is a wildtype oncolytic reovirus that preferentially replicates in RAS upregulated tumor cells. In cohort 1 of the phase 1/2 GOBLET trial, patients with advanced pancreatic cancer were enrolled to receive first line (1L) pelareorep combined with atezolizumab and gemcitabine/nab-paclitaxel yielding a previously reported confirmed objective response rate (ORR) of 54% (7/13) and disease control rate (DCR) of 85% (11/13).
Methods: In an exploratory biomarker analysis, routine serum markers (CA19-9, CEA, CRP) and 172 circulating proteins quantified via proximity extension assay (PEA; Olink®) were integrated with selected T cell receptor (TCR) sequencing and clinical outcomes. Linear mixed effects models and semi supervised clustering were applied to identify protein patterns reflecting immune and inflammatory activity.
Results: Early on-treatment effects included increased abundance of adaptive immune (e.g. IFN-gamma, CXCL11, TNF) or cytotoxicity associated proteins (e.g. GZMB/H/A) and reduced tumor/stroma-associated proteins (MUC-16, MMP12). A 14-protein signature linked to oncolytic activity (IFN γ signaling, CD8+ and NK cytotoxic functions) stratified patients at week 4 into “hot” versus “cold” immune phenotypes relative to baseline. Despite small numbers, the ‘hot’ phenotype was associated with significantly longer median progression free survival (n=6; mPFS; 7.5 mo, 95% CI: 7.1-14.3) compared with “cold” (n=6; mPFS 5.6 mo, 95% CI: 1.7-6.0; log rank p<0.005).
Conclusion: Pelareorep combined with atezolizumab and gemcitabine/nab-paclitaxel demonstrated promising activity in 1L pancreatic cancer. A hot/cold immune signature detectable after 4 weeks may serve as an early stratification biomarker, supporting identification of patients likely to achieve durable benefit

#6698 EpitopeMiner: Scalable knowledge mining for evidence-driven personalized cancer vaccine design.

Agamjyot Singh Chadha[1], Isaac Jiasheng Cheong[2], Marcia Zhang[2], Wei Kit Tan[2], Wei Lin Tang[1], Jing Quan Lim[3], Solomonraj Wilson[1], Choon Kiat Ong[3], Bernett Lee[4], Chwee Ming Lim[5], Olaf Rotzschke[1], Mai Chan Lau[1]

[1]Singapore Immunology Network Lab, A*STAR - Agency for Science, Technology and Research, Singapore, Singapore,[2]Bioinformatics Institue, A*STAR - Agency for Science, Technology and Research, Singapore, Singapore,[3]Lymphoma Translational Research Laboratory, Division of Cellular and Molecular Research, National Cancer Centre Singapore, Singapore, Singapore,[4]Lee Kong Chian School of Medicine (LKCMedicine), Nanyang Technological University Singapore, Singapore, Singapore,[5]Surgery Academic Clinical Programme (Surgery ACP), Duke-NUS Medical School, Singapore, Singapore

Background: Personalized cancer vaccines hold great promise by eliciting tumor-specific immune responses [1-3]. A key challenge is identifying the right targets — immunogenic protein sequences, or epitopes, presented on tumor cells. While computational pipelines can predict epitope candidates from tumor sequencing, experimental validation is costly and slow. Leveraging literature and database knowledge could bridge this gap by enabling evidence-driven selection of high-confidence targets, but is constrained by fragmented information across journals and immunology databases [4-5]. We introduce EpitopeMiner, which integrates sequence-based candidate screening with evidence-driven knowledge retrieval for epitope prioritization.

Methods: A total of 25,966 tumor-specific epitopes were predicted from whole-genome sequencing of tumor-PBMC pairs from nine patients (including lung, sarcoma, NKTL, DLBCL) using a standard workflow: HLA typing (OptiType), variant calling (Strelka with wANNOVAR), MHC binding prediction (NetMHCpan) and RNA-supported protein-altering filtering. EpitopeMiner combines OpenAI's Large Language Model (LLM) with an in-house Retrieval Augmented Generation (RAG) database comprising (a) 78,461 full-text research articles from PMC, PLOS One, and Europe PMC and, (b) ~2.6 million unique epitopes from IEDB, dbPepNeo, SystemMHC, TANTIGEN, and caAtlas database. EpitopeMiner includes: (i) a screening module that processes an epitope list, detecting exact or ≥ 7 amino acid partial matches from the in-house database, and (ii) a reporting module that analyses each top-ranked hits, defined by highest sequence similarity and evidence density, to generate an LLM response covering 28 immunology keywords with citations.

Results: Among the 25,966 epitopes predicted from the nine patients, EpitopeMiner found 7 exact matches, and 17.6% had ≥ 6 partial matches; mean processing time per epitope was 0.97 seconds. In benchmarking with 3 lung cancer driver-gene epitopes (KITDFGRAK, ITDFGRAKL, TDFGRAKLL), EpitopeMiner outperformed ChatGPT and Gemini, returning the highest amount of relevant immunological information — summarized as (total responses, % with evidence) — (18, 100%), (8, 100%), and (2, 100%) respectively, compared to ChatGPT's (10, 70%), (4, 50%), (6, 33%) and Gemini's (7, 0%), (1, 0%), (1, 0%). In addition, EpitopeMiner retrieved ≥10 partial matches for each epitope, whereas ChatGPT retrieved total of 3 and Gemini none.

Conclusion: We built EpitopeMiner, a computational framework for sustainable literature and database curation. In a 9-patient dataset, EpitopeMiner retrieved experimentally and clinically validated epitope evidence at a scale and speed infeasible with manual analysis. EpitopeMiner outperformed general-purpose LLMs with cited responses, achieving 100% evidence coverage on benchmarks, reducing hallucinations and improving reliability.

#6699 Novel preclinical immunocompetent mouse model for assessment of immunotherapies targeting cGAS-STING axis.

Angela Pappalardo, Philippe De La Rochere, Patricia Isnard-Petit, Gaelle H. Martin, **Fabiane Sonego**, Kader Thiam

genOway, Lyon, France

The cyclic GMP-AMP synthase-stimulator of interferon genes (cGAS-STING) signaling axis represents a pivotal immunostimulatory pathway and an attractive pharmacological target in oncology. Its activation within the tumor microenvironment promotes cross-priming of tumor-associated antigens and enhances infiltration of effector T lymphocytes. Owing to its potent antitumor activity, the cGAS-STING pathway offers significant promise for the development of cancer vaccines, immunotherapeutic strategies such as antibody-drug conjugates, and interventions against virus-driven malignancies. However, translating preclinical findings to clinical applications has been challenging due to species-specific differences between human and mouse cGAS and STING. A model expressing human STING only has been previously reported and showed to be a valuable tool to investigate the activity of STING agonist in different tumor types. Herein, we report an immunocompetent mouse model expressing both human cGAS and human STING (genO-hcGAS-hSTING). Humanization of cGAS and STING did not alter immune cell composition in the spleen, blood and bone marrow when compared to WT mice. Expression of human cGAS has been confirmed in brain and lung by Western Blot, while hSTING expression was confirmed in immune cells in the spleen and blood by flow cytometry. Functionality of cGAS was investigated through activation of splenocytes with the non-human-specific cGAS agonist G3-YSD, which induced IFN-α, IFN-γ, and TNF-α secretion. Similarly, functionality of STING has also been investigated by activating splenocytes with diABZi and DMXAA. While diABZi activates both human and mouse STING, DMXAA activates specifically mouse STING. Indeed, diABZi induces the secretion of IFN-β, CXCL10, and IL-6 in cells from both WT genO-hcGAS-hSTING mice, wherein DMXAA induced cytokine secretion in WT only. These data indicate that human STING expressed in genO-hcGAS-hSTING mice is functional and mouse STING is no longer expressed in these mice. These humanized models provide valuable tools for assessing the efficacy and specificity of compounds targeting human cGAS and STING pathways, potentially streamlining drug discovery and enhancing our understanding of innate immune responses in human health and disease.

#6700 A fully integrated set of *in vitro* and *in vivo* tools for utilization of micro-organisms as new therapeutic weapons against cancer.

Guillaume Serin, Lucie Demontoux, Elizabeth Bertrand, Marie Leblanc, Sylvie Maubant, Ismahene Benzaid, **Marc Hillairet De Boisferon**

Oncodesign Services, Dijon, France

In the dynamic landscape of oncology, innovative approaches are constantly emerging to tackle complex challenges. One such promising avenue gaining attention is the development of micro-organisms like viruses or bacteria to destroy cancer cells and leverage the host immune system to enhance the effect. The combination of loss of intracellular viral and bacterial resistance to increase survival and proliferation pathways, profound changes of tumor microenvironment leading to inactivation of immune response and favored tumor accumulation of small particles by EPR enables microorganisms to massively and selectively colonize and attack the cancer cells. Genetic engineering is added to reduce their natural virulence and tropism and enhancing their therapeutic potential, often by expression of chemokine or antigens to (re)activate the immune response or expression of antibodies or proteins that can trigger T cell engagement or other physiological modification. Alone or combined with specific adjuvants and other therapeutic agents, oncolytic viruses or bacteria have shown significant reduction to even full remission of primary and metastatic tumors.At Oncodesign Services, we have hundreds orthotopic and subcutaneous rodent or human CDX and PDX tumor models readily available to study the activity and mechanism of action of micro-organisms in syngeneic, xenogeneic or humanized immune reconstituted models. Viruses and bacteria can be manipulated in BSL2 and BSL3 status. With 30 years of experience and thousands of studies performed, Oncodesign Services has also the know-how to provide support for testing combinations with other chemo, immuno-onco (ICI, ADC, BiTEs, CAR-T cells) or irradiation therapy to further increase the activity of micro-organisms.In addition to continuum of assays allowing us to evaluate the impact of microorganisms on tumor and/or immune cells (e.g. phenotyping of immune infiltrate, cytokine/chemokine profiling, tumor burden), we have developed assays to detect, quantify, identify and localize live microorganisms (e.g. qPCR, mass spectrometry, bioluminescence) in simple or complex samples.In this poster, we will highlight some results obtained in a cancer context such as the immunostimulatory properties of modified micro-organisms, the selective infection of tumor tissue or the benefits in delivery of therapeutic proteins or antigens.

#6701 Re-engineering cancer vaccines: Bria-OTS+ integrates innate and adaptive immunity for broad and persistent anti-tumor responses.

Miguel A. Lopez-Lago, Pravin Kesarwani, Vikas Bhardwaj, Xiaoyi Zheng, Ying Liu, Sagarika Pachhal, Patience cournoo, Renee Cortez, George Woodfield, Charles Wiseman, William V. Williams

BriaCell Therapeutics Corp., Philadelphia, PA

Background: Despite major advances in immuno-oncology, achieving durable tumor control remains difficult because of tumor heterogeneity, immune evasion, and limited coordination between innate and adaptive immune responses. Whole-cell cancer vaccines offer broad antigenic coverage but have historically lacked potency and persistence. Bria-OTS+ is a next-generation, genetically engineered whole-cell cancer vaccine platform designed to overcome these limitations by integrating innate and adaptive immunity. Bria-OTS+ is composed of genetically reprogrammed tumor cells that naturally display a broad antigen repertoire, while being engineered to express immune-stimulatory cytokines (GM-CSF, IFN-α, IL-12, IL-7), co-stimulatory molecules (CD80, CD86, CD40, 4-1BBL), and diverse HLA-A and HLA-DR alleles, supporting potent immune activation and broad semi-allogeneic compatibility (>99 % population coverage).
Methods: Irradiated Bria-OTS+ cells representing breast, prostate, lung, and melanoma lineages were co-cultured with human PBMCs in a four-phase in vitro vaccination assay (priming, resting, boosting, effector) designed to model sequential immune activation, memory formation, and recall response. Immune activation, proliferation, and cytotoxicity were quantified by flow cytometry and ELISA. Mechanistic dissection employed blocking antibodies to CD86, IL-12, NKp46, and HLA-I/II molecules to define signaling dependencies.
Results: Bria-OTS+ induced coordinated activation of $CD4^+/CD8^+$ T, NK, NKT, dendritic, and B cells, with strong IFN-γ/TNF-α release and up-regulation of CD69/CD25. CD80/CD86 increased on dendritic and B cells, indicating enhanced antigen-presenting potential. NK-cell cytotoxicity dominated early responses and was amplified by IL-12 and CD86 signaling. Upon recall, T and NK cells exhibited amplified cytokine release, proliferation, and tumor-cell killing together with a memory phenotype and controlled checkpoint profile (low PD-1/TIM-3, moderate LAG-3), indicating persistent effector competence without exhaustion. Bria-OTS+ activated PBMCs killed both homologous and heterologous tumor targets, supporting shared antigen recognition and/or NK activity and reduced Immuno-evasion risk.
Conclusions: Bria-OTS+ functions as a modular, immune-educating platform that integrates trained innate and adaptive immunity within a scalable, semi-personalized framework. By coupling multi-cytokine signaling and co-stimulation with HLA-guided antigen presentation, Bria-OTS+ achieves persistent immune activation, broad tumor recognition, and is readily manufacturable for off-the-shelf clinical deployment.

#6702 A *Cxcl10* mRNA-LNP adjuvant enhances immune checkpoint inhibitor responses in melanoma models.

Kaitlyn M. Landreth[1], Katherine Lee[1], Emel Sen Kilic[2], Joshua Chapman[1], Mary Garland-Kledzik[3], F. Heath Damron[1], Tracy W. Liu[1]

[1]MICB, West Virginia Univ. School of Medicine, Morgantown, WV,[2]Embry-Riddle Aeronautical University, Daytona Beach, FL,[3]Department of Surgery, West Virginia Univ. School of Medicine, Morgantown, WV

Immunotherapies have become standard of care in the treatment of melanoma; however, about 50% of patients are immunotherapy resistant. This can be caused by an immunosuppressive tumor microenvironment that has a low infiltration of immune cells, especially T cells. Tumors with high T cell infiltration demonstrate better responses to immune checkpoint therapy, making modulation of the tumor microenvironment to enhance T cell recruitment and activation a critical unmet need. In this study, we hypothesize that using an mRNA encoded “genetic adjuvant” can increase the infiltration of T cells into the tumor microenvironment and improve immunotherapy response. The chemokine CXCL10 plays a key role in T cell recruitment and activation, signaling via the CXCR3 receptor expressed by activated T cells. Consistent with this mechanism, analysis of melanoma patient serum samples showed significantly higher Cxcl10 levels in immunotherapy responders compared to non-responders. To directly enhance CXCL10, we developed a Cxcl10-encoded mRNA lipid nanoparticle (Cxcl10 LNP). A significant increase in CXCL10 levels in the sera and inguinal lymph nodes of C57BL/6J wild-type mice was observed post intramuscular administration of Cxcl10 LNP. Our data shows that intramuscular injection of Cxcl10 LNP significantly reduced the volume of established subcutaneous B16F10 murine melanoma tumors. Cxcl10 LNP treatment lead to a significant increase of CD8+ T cells within the tumor microenvironment at 48 hours assessed by flow cytometry and intravital imaging. Phenotypic profiling further revealed significant increases of TRP-2 tumor specific CD8+ T cells and CD107a+ cytotoxic effector CD8+ T cells 48hrs post intramuscular administration of Cxcl10 LNP. When combined with dual anti-PD-1 and anti-CTLA-4 immune checkpoint inhibitor antibodies, Cxcl10 LNP improved long-term survival and significantly decreased subcutaneous tumor growth, with 20% of mice tumor-free at day 100. Moreover, in our spontaneous metastatic melanoma model, mice received Cxcl10 LNP 24h post primary tumor resection followed by dual anti-PD-1 and anti-CTLA-4 immune checkpoint inhibitors for a total of 3 doses. Adjuvating immune checkpoint inhibitors with Cxcl10 LNP significant reduced lung and lymph node metastasis, with 80% of mice showing no detectable metastases. These findings demonstrate that using Cxcl10 LNP is an effective genetic adjuvant that enhances CD8+ T cell infiltration and cytotoxic function, resulting in improved efficacy of immune checkpoint inhibitors and reducing tumor burden and metastases.

#6703 Rg002: An mRNA-LNP-based immunotherapy targeting HPV-16/18-related malignancies.

Shan Cen[1], Lan Zhu[2], Fei Chen[2], Wei Wang[3], Lihua Qiu[4], Hua Yang[2], Yijie Dong[5], Weiguo Zhang[5], Huizhen Zhang[5], Jing Wang[5]

[1]Institute of Medicina Biotechnology, Chinese Academy of Medical Sciences, Beijing, China,[2]Peking Union Medical College Hospital, Beijing, China,[3]The Second Hospital of Shanxi Medical University, Taiyuan, China,[4]Renji Hospital, Shanghai Jiao Tong University School of Medicine, Shanghai, China,[5]RinuaGene Biotechnology Co., Ltd., Suzhou, China

Prophylactic vaccines against oncogenic human papillomaviruses (HPVs) are effective in preventing HPV infection but not in treating existing HPV infection and cervical intraepithelial neoplasia (CIN). Current treatments for CIN are often ablative and may lead to long-term reproductive morbidity. Thus, there is a tremendous need for therapies that can treat the millions living with persistent oncogenic HPV infection and CIN and the risk of HPV-related cancers. RG002 is a mRNA-based therapeutic treatment targeting the E2, E6, and E7 proteins of HPV-16/18 with a targeted LNP for selective delivery to spleen and dendritic cells, which demonstrated excellent efficacy and safety in preclinical studies. In the phase I and expanded clinical studies, we evaluated the safety, efficacy, and immunogenicity of RG002 in 12 women with HPV 16/18 associated CIN2/3. Patients receive intramuscular administrations of 25, 75, 150, or 300 μg of RG002 at weeks 0, 2, and 4. RG002 does not cause any serious vaccine-related adverse events at any of the administered doses. Notably, all patients have exhibited complete regression of lesions and viral clearance within 17 weeks after the first dose, along with unprecedented E2/E6/E7 specific IFN-γ-producing T-cell response with clear dose-responses relationships. These initial data demonstrate the strong potential of RG002 as a first-in-class, non-surgical treatment for HPV-16/18-associated CIN2/3 to prevent progression to invasive carcinoma.
Note on Study Status: *The initial cohort (n=12; 3 per dose) is nearing completion. Based on promising early results, the protocol has been amended to enroll an additional 15-30 patients by January 2026. Updated results from over 40 patients, including Week 17 efficacy data for at least 20 patients, are expected in mid-April 2026.*

#6704 Exercise attenuates anti-PD-1-induced adventitial macrophage inflammation in the aorta of aged melanoma-bearing mice.

Jonghae Lee, Sumedha Pareek, Truong Lam, Fei Wang, Guanshu Liu, Jared K Burks, Jun-ichi Abe, Keri Schadler

University of Texas MD Anderson Cancer Center, Houston, TX

Immune checkpoint inhibitors (ICI) improve cancer outcomes but can induce vascular toxicity, potentially threatening long-term survivorship. In our pilot data using young male mice with tumors, anti-PD-1 increased vimentin, an endothelial-to-mesenchymal transition (EndMT) marker linked to early atherosclerosis, in laminar-flow regions of the aorta, and exercise attenuated this response. Given the rapid growth of our melanoma model and the greater vulnerability of aged mice to ICI-associated vascular injury, we used aged mice to capture early vascular responses and determine whether exercise modifies anti-PD-1-induced vascular inflammation. One-year-old female C57BL/6J mice were injected subcutaneously with BP melanoma cells. Once tumors became measurable, mice were assigned to three treatment groups: control IgG (N=12), anti-PD-1 (aPD-1, 150 μg × 5 doses = 750 μg total; N=9), or anti-PD-1 plus moderate treadmill exercise (aPD1+Ex, N=8) for two weeks. Tumor growth was monitored every other day. Thoracic aortas were collected, embedded as FFPE tissue microarrays, and scanned by multiplex immunofluorescence, and analyzed in Visiopharm for tissue segmentation (intima, media, adventitia), cell identification, and immune/vascular phenotyping. Exercise plus aPD-1 suppressed tumor growth significantly better than aPD-1 alone (~60% reduction vs. IgG; $p = 0.04$). Across cross-sectioned aortic rings containing ~706 total cells on average (19,069 cells across 29 vessels), whole-vessel counts of $CD4^+$, $CD8^+$, and $B220^+$ cells were uniformly low across groups. $B220^+$ cells showed a polarized pattern in the aPD-1 group, with elevated counts in only a subset of mice. In contrast, aPD-1 increased adventitial $F4/80^+$ macrophages more than 2.5-fold relative to IgG (N.S.), consistent with early adventitial-driven vascular inflammation. Importantly, exercise significantly reduced adventitial infiltration accumulation ($p=0.03$). Additional spatial analyses of vascular inflammation and immune-vascular interactions are ongoing. In aged tumor-bearing mice, anti-PD-1 induces early aortic vascular toxicity characterized by adventitial macrophage inflammation, paralleling early inflammatory patterns reported in early human large-vessel vasculitis associated with ICI therapy. Exercise markedly attenuates this adventitial macrophage-driven vascular response without compromising antitumor efficacy, suggesting its potential as a non-pharmacologic strategy to mitigate early ICI-associated vascular injury.

#6705 A versatile coacervate based delivery system to overcome engineering barriers in immune cells.

Renxia Zhang[1], **Peipei Zhu**[1], Manman Lu[2], Qing Zhang[1], Lihong Jiang[2], Xiaowen Fei[2], Xiaofei Gao[1]

[1]Westlake University, Hangzhou, China,[2]Nanoportal Biotech, Hangzhou, China

The clinical translation of immune cell engineering (e.g., CAR-T, TCR-T) and functional genomics research in hematologic malignancies are significantly hampered by the limitations of existing gene delivery systems. Viral vectors raise safety and cost concerns, while conventional non-viral methods often suffer from low efficiency and high cytotoxicity, particularly in primary immune cells and refractory hematopoietic cell lines. To overcome these barriers, we developed ProteanFect, the first endogenous protein-based coacervate delivery system. This platform is designed for high-efficiency delivery of diverse genetic payloads, including mRNA, DNA, siRNA, and CRISPR/Cas9 components (mRNA or RNP), enabling robust gene expression and precise gene editing. In primary human immune cells, ProteanFect achieved >90% mRNA transfection efficiency (e.g., GFP mRNA in T cells) with sustained transgene expression and maintained over 90% cell viability. It enabled the generation of functional anti-CD19 CAR-T cells that effectively suppressed tumor growth in vivo. Furthermore, ProteanFect demonstrated high-precision gene editing, achieving 88% knockout efficiency at the TRAC locus in primary T cells via Cas9 mRNA/sgRNA delivery. The platform also showed broad applicability, attaining >70% and >65% transfection efficiencies in natural killer (NK) cells and B cells, respectively, and robust performance in mouse primary immune cells. Simultaneously, ProteanFect effectively addressed transfection challenges in hard-to-transfect hematopoietic cell lines (e.g., Jurkat, K562, THP1, HL-60, Raji, Kasumi-1). It achieved 70-90% RNA and 40-70% DNA transfection efficiency, supported large plasmid (~15.7 kb) delivery with >50% efficiency, and enabled ~70% siRNA-mediated knockdown and ~80% CRISPR/Cas9-mediated knockout in Jurkat cells. Even in more refractory lines, RNA transfection efficiency reached ~80%. The system also facilitated co-transfection and multiplexed gene editing, highlighting its versatility. In summary, ProteanFect represents a transformative non-viral platform that uniquely synergizes high-efficiency nucleic acid delivery with precise gene editing capabilities, all while maintaining minimal cytotoxicity and demonstrating broad applicability across primary human and mouse immune cells as well as challenging hematologic cell lines. Its versatile support for diverse payloads—from mRNA and large plasmids to CRISPR RNP complexes—positions this technology as a pivotal tool that not only accelerates the production of engineered cell therapies but also expands the frontiers of basic research, functional genomics, and therapeutic development in immunology and hematology.

#6707 Developing oncolytic measles virus expressing MG53 for the treatment of lung cancer.

Zhongguang Li[1], Cheng Chih Hsu[1], Fei Jiang[1], Matthew Bu[1], Ellica Leong[1], Umme Lubaba[1], Xuefeng Liu[2], Jianrong Li[1], **Haichang Li**[1]

[1]Ohio State Univ. College of Veterinary Med., Columbus, OH,[2]The Ohio State University, Columbus, OH

Background: Despite advances in lung cancer therapy, effective strategies that simultaneously eradicate tumors and stimulate antitumor immunity remain limited. Oncolytic virotherapy (OV) has emerged as a viable clinical approach for cancer immunotherapy option. Engineered attenuated measles virus strains offer several advantages: excellent safety profiles, tumor selectivity, lack of genotoxicity, and ease of genetic manipulation. MeV replicates preferentially in malignant cells and mediates anti-tumor effects not only on the cellular level by lytic infection of tumor cells, but also on the systemic level by priming anti-tumor immune responses. TRIM72, also known as Mitsugumin 53 (MG53), is a TRIM family protein secreted by muscle tissue and plays an anti-tumor role. In this study, we developed a recombinant measles virus expressing MG53 (rMeV-MG53) and investigated its dual ability to induce tumor cell death and activate antitumor immunity, as well as its potential synergy with immune checkpoint blockade in lung cancer models.

Methods: An attenuated measles virus (MeV) Edmonston vaccine strain was engineered to express MG53, generating rMeV-MG53. A measles virus encoding the mCherry reporter gene served as control. Human lung cancer cell lines were used for *in vitro* studies to evaluate viral infectivity, oncolytic activity, pyroptosis induction, and inflammatory signaling, with Western blotting performed to assess caspase-3/GSDME activation. For *in vivo* studies, mouse lung cancer cells were engineered to express human CD46, rendering them susceptible to rMeV-MG53. hCD46-overexpressing cells were implanted into immunocompetent mice, followed by intratumoral administration of rMeV-MG53 alone or combined with anti-PD-L1 antibody.

Results: *In vitro*, rMeV-MG53 efficiently infected human lung cancer cells and exhibited potent oncolytic activity. Western blot analysis demonstrated enhanced caspase-3/GSDME-mediated pyroptosis compared with rMeV alone. rMeV-MG53 also activated inflammatory signaling pathways, suggesting a role in promoting antitumor immunity. *In vivo*, CD46-overexpressing mouse lung cancer cells were highly sensitive to rMeV-MG53-mediated oncolysis. Intratumoral administration of rMeV-MG53 significantly suppressed tumor growth, with a more pronounced effect than rMeV alone. Combination therapy with rMeV-MG53 and anti-PD-L1 antibody further augmented antitumor efficacy.

Conclusion: These findings demonstrate that rMeV-MG53 exerts robust antitumor effects through direct induction of pyroptosis and activation of inflammatory signaling while synergizing with immune checkpoint blockade. rMeV-MG53 represents a promising oncolytic platform that integrates tumor cell killing with immune activation, offering translational potential as a novel therapeutic strategy for lung cancer.

#6708 Neoadjuvant pembrolizumab with therapeutic DNA vaccine reshape intratumoral immunity in a phase 2 trial of HPV-positive HNSCC.

Hye Ryun Kim[1], June-Young Koh[2], Chang Gon Kim[1], Min Hee Hong[1], Hyun Jun Hong[1], Dahee Kim[1], Nam Suk Sim[1], Sun Och Yoon[1], Gamin Kim[1], Wonrak Son[1], Yeju Kim[2], Chang Geol Lee[1], Kyung Hwan Kim[1], Jeong Seok Lee[2], Chan-Young Ock[3], Yoon Woo Koh[1]

[1]Yonsei University College of Medicine, Seoul, Korea, Republic of,[2]Inocras Inc., San Diego, CA,[3]Lunit Inc., Seoul, Korea, Republic of

Therapeutic cancer vaccines are a promising strategy for inducing antigen-specific T-cell immunity, but their efficacy in solid tumors remains limited by inadequate magnitude, persistence, and functional quality of vaccine-elicited responses. These challenges have intensified efforts to identify adjuvants that can strengthen durable antitumor immunity. Interleukin-7 (IL-7), a cytokine essential for T-cell survival and memory formation, provides a mechanistically grounded strategy for enhancing vaccine responses. To evaluate this in a defined viral antigen setting, HPV-associated head and neck squamous cell carcinoma offers an ideal tumor model for dissecting vaccine immunity and adjuvant mechanisms. We first tested long-acting IL-7 in an HPV16 E6/E7-expressing TC-1 model. IL-7 improved the efficacy of HPV DNA vaccination with PD-1 blockade, producing superior tumor control and enhancing stem-like and memory-associated transcriptional programs within intratumoral $CD8^+$ T cells—features consistent with strengthened long-term responsiveness. Guided by these results, we conducted a phase 2 neoadjuvant trial combining pembrolizumab, HPV DNA vaccine (GX-188E), and long-acting IL-7 (GX-I7) in patients with resectable HPV-positive HNSCC. Major pathologic responses occurred in 63.6% of patients, including 36.4% complete responses. Paired single-cell RNA/TCR sequencing and spatial AI analysis revealed coordinated reshaping of the intratumoral immune landscape. A $GZMK^+$ effector-memory $CD8^+$ population expanded prominently, displaying early memory priming, lymph node-to-tumor recirculation potential, and enrichment of tumor-reactive programs. Increased tertiary lymphoid structures correlated with reduced exhaustion among tumor-reactive $CD8^+$ T cells and appeared to facilitate entry and renewal of $GZMK^+$ $CD8^+$ T cells within tumors. Higher $GZMK^+$ $CD8^+$ abundance corresponded with greater TCR diversity among tumor-reactive clones, indicating sustained replenishment of antitumor specificities. To reconfirm upstream regulatory pathways, foundation-model-based in silico perturbations showed that knockout of IL7R or STAT5 markedly diminished GZMK-directed differentiation, supporting an IL-7-dependent mechanism underlying this effector-memory programming. Analyses of independent HPV-positive HNSCC cohorts aligned with these observations, showing that tumors enriched for GZMK-programmed $CD8^+$ states exhibit stronger antitumor immunity and improved long-term outcomes. Taken together, these comprehensive preclinical, clinical, and exploratory analyses reveal that IL-7 amplifies a $GZMK^+$ effector-memory $CD8^+$ T-cell program driving sustained recirculation, diversification, and renewal of tumor-reactive $CD8^+$ T cells, highlighting a mechanistic axis with potential to enhance the durability of cancer vaccine responses.

#6709 Temporal trends in biomarker utilization across 24,000+ immuno-oncology trials.

Fahad Benthani, Samik Upadhaya, Cynthia L. Neben, Kellie R. McDonald, Alicia Y. Zhou

Cancer Research Institute (CRI), New York, NY

As immuno-oncology (IO) matures beyond the checkpoint inhibitor era, understanding how biomarker-informed trial design is evolving along with therapeutic diversification is important for optimizing future development decisions. The Cancer Research Institute (CRI) has built a comprehensive IO clinical trial database, capturing global activity across cancer types and therapeutic modalities [1]. Here, we leveraged this resource to analyze temporal trends in IO therapeutic development and biomarker adoption to reveal how the field is evolving over time.

We curated over 24,000 interventional IO clinical trials (data cut-off: June 2025), extracting therapeutic modality, molecular targets, cancer indication, trial phase, sponsor type, and biomarker data. We analyzed temporal trends in trial initiation, modality, and biomarker usage. Biomarkers (n=9,849) were classified by molecular type, functional role, and indication-specific usage patterns.

The IO landscape shows clear maturation with over 10,000 currently active trials dominated by phase II studies. While checkpoint inhibitors remain dominant, IO drug target diversity has significantly increased, driven primarily by multi-target combinations designed to overcome resistance. Furthermore, biomarker strategies show striking differences across cancer types. Hematologic malignancies lead in biomarker usage, with about 65% adoption and 31% dual selection/monitoring use, compared to solid tumors (58% and 23% respectively). Among solid tumors, respiratory cancers show the highest adoption at around 66%, driven by established markers like PD-L1 and driver mutations, while gastrointestinal cancers lag at about 50% despite representing the largest trial volume. Protein biomarkers dominate at over 80% of total, with tumor mutational burden and microsatellite instability markers emerging as pan-cancer standards. Notably, biomarker usage dropped below 50% in 2024 for the first time since 2012. This may reflect how the field's strategy is shifting: pursuing broader patient populations while also developing smarter multi-marker approaches for specific indications, representing an important turning point in IO development.

The updated CRI IO landscape database, which integrates global IO clinical trial activity and biomarker utilization, gives the research community a unique look into how immunotherapy is evolving, helping investigators and sponsors see where their work fits in the bigger picture, spot emerging trends, and identify areas where biomarker development hasn't kept pace with new therapies. These landscape insights are important for making better decisions about where to invest resources and effort to have the greatest patient impact.

Reference 1. Benthani F, Upadhaya S, Zhou A. Cancer cell therapies: Global clinical trial trends and emerging directions. Nature Reviews Drug Discovery.

#6710 Development of T cell activating nucleic acid fusion vaccine to prevent metastatic uveal melanoma establishment.

Vitali Alexeev[1], Mizue Terai[1], Sergei Koshkin[1], Takami Sato[2]

[1]Medical Oncology, Thomas Jefferson University, Philadelphia, PA,[2]Thomas Jefferson University, Philadelphia, PA

Uveal melanoma (UM) is the most common intraocular malignancy in adults. Primary tumor treatment with brachytherapy achieves approximately 80% five-year survival rate, however, later in life nearly half of patients develop predominant liver metastases, resulting in a five-year survival rate of 16% and a median overall survival (OS) of only 3.9 months. Systemic therapy with a new T cell engager Tebentafusp (Kimmtrak) increases median OS to 21.7 months, an objective response rate remains low at about 9%. Given that UM may metastasize to the liver early and remain dormant, we hypothesize that vaccine-based activation of T cell immunity in primary UM patients could prevent the establishment of metastatic disease. Our initial data showed that GNAQ/GNA11 epitopes harboring Q209L tumor driver mutation with mutated leucine in a P9 and anchoring modification at P2 positions of the nonamer activates epitope-specific T cells response. To develop a nucleic acid vaccine, we engineered a plasmid backbone containing 5′ and 3′ untranslated regions, VP22, PADRE, *Tetanus toxoid* P2 epitopes, and an MHC class I trafficking domain. DNA encoding either a single anchor-modified mutant GNAQ epitope or a fusion with MART-1, Tyrosinase, and MC1R epitopes generated two vaccine constructs that activated mtGNAQ-specific T cells *ex vivo*. Activation was confirmed by IFN-γ secretion and cytotoxicity assays using mtGNAQ peptides and UM cells as targets. Solid-phase enrichment of UM-reactive T cells on mtGNAQ peptides further enhanced cytolytic activity. To improve vaccine efficacy, we identified additional immunogenic UM-associated epitopes. Comparative analysis of UM-specific gene expression revealed approximately 50 differentially expressed genes, with four—PMEL17, TYRP1, PRAME, and SLC45A2—showing markedly higher expression in UM compared to cutaneous melanoma or melanocytes. Regions within these antigens enriched for HLA-A*01, -A*02, and -A*03 putative binders were incorporated into the established construct to produce a multiepitope vaccine. cDNA coding for CCL21 chemokine was transcriptionally linked to the open reading frame via a P2A ribosomal skipping peptide to enhance vaccine immunogenicity. T cells activated by the vaccine *ex vivo* exhibited a fourfold increase in UM cell targeting compared to two other constructs. *In vivo* testing in HLA-A2/Kb transgenic mice confirmed that vaccinated animals generated T cells capable of recognizing UM-derived peptides and exerting cytolytic activity against melanocytic cells mimicking human UM.

Overall, these findings indicate that the engineered multiepitope vaccine effectively activates UM-specific T cells. Future work will focus on identifying the most immunogenic epitopes and evaluating whether vaccination can prevent metastatic UM development and progression in relevant animal models of MUM micrometastases.

#6711 Investigating MyD88 and NLRP3 pathway modulation in a TLR4 and TLR9 driven immunotherapy in a murine model of ovarian cancer.

Ania V. Klas, Rita E. Serda

Internal Medicine, University of New Mexico Health Sciences Center, Albuquerque, NM

Ovarian cancer remains one of the most devastating gynecologic malignancies, partly due to an immunosuppressive tumor microenvironment (TME) that limits immunotherapy efficacy. Our previous work showed that syngeneic cancer cell-based immune therapy containing monophosphoryl lipid A (TLR4 agonist) and CpG (TLR9 agonist) stimulates cancer-specific immune responses. Both receptors signal through MyD88 to activate NF-κB and pro-inflammatory cytokine production. These pathways also intersect with the NLRP3 inflammasome, which amplifies inflammation through IL-1β and IL-18. Controlled activation may enhance antitumor immunity, whereas dysregulated inflammasome signaling can promote chronic inflammation and immune suppression. Understanding how MyD88 and NLRP3 shape vaccine efficacy is therefore essential.This study evaluates how inhibition of MyD88 and NLRP3 affects the therapeutic efficacy of our ovarian cancer immune therapy. FVB mice bearing ovarian tumors received TLR-agonist silicified cancer cell immunotherapy with or without the NLRP3 inhibitor MCC950 (10 mg/kg) or the MyD88 inhibitor TJM-2010 (50 mg/kg). Inhibitors were administered around each immune-therapy dose. Ascitic immune cells were analyzed by spectral flow cytometry to assess immune subsets and activation markers.Blockade of the NLRP3 pathway accelerated ovarian cancer growth, while TLR-agonist immune therapy blocked tumor progression and cleared existing tumors. NLRP3 inhibition reduced therapeutic efficacy, tumor size decreased but complete clearance was not achieved. On Day 12, the immune-therapy group showed a significant reduction in tumor burden compared to PBS ($p = 0.0034$). The immune-therapy + NLRP3-inhibited group also differed from PBS but with diminished benefit ($p = 0.0091$). By Day 16, both BR5 immune-therapy and BR5 + inhibitor groups showed highly significant reductions in tumor burden compared to PBS ($p < 0.0001$).These findings demonstrate that NLRP3 signaling contributes critically to TLR4/TLR9-mediated antitumor responses. Ongoing studies will clarify how MyD88 and NLRP3 coordinate innate immune activation and guide future combination strategies to enhance immunity and overcome suppression within the ovarian TME.
AI Disclosure:ChatGPT was used to assist with editing and wording of this abstract. All scientific content, study design, and interpretation were generated and verified by the authors.

#6712 Promoting improved agnostic cross presentation of tumor antigens with an oncolytic adenovirus expressing bispecific macrophage engagers.

Ahmet Hazini[1], Margarida Rei[2], Natanya Cartwright[1], Ricardo A. Fernandes[3], Kerry Fisher[1], Len Seymour[1]

[1]Department of Oncology, University of Oxford, Oxford, United Kingdom,[2]Ludwig Institute, University of Oxford, Oxford, United Kingdom,[3]Nuffield Department of Medicine, University of Oxford, Oxford, United Kingdom

Background: Non-specific ('agnostic') cross-presentation of tumor antigens (TAA) is essential for generating adaptive immune responses against cancer. APCs uptake TAA by phagocytozing proteins from cancer cells and present them on HLA molecules to activate T cells.To induce cancer cell uptake by the APCs, we aimed develop a bispecific macrophage engager (BiME) that can bring cancer cells and APCs into close proximity, and we hypothesized that oncolytic viruses could be used to express BiMEs in the tumor microenvironment.
Methods: We generated an oncolytic adenovirus expressing a BiME (Ad-BiME) designed to bind a tumor-associated antigen on cancer cells and an activating receptor on APCs, thereby promoting interaction and triggering APC activation. The expressed bispecific protein efficiently bound ligands on both APCs and cancer cells. Co-culture assays evaluated phagocytosis, macrophage activation, and antigen cross-presentation. To analyse cross-presentation, we engineered NY-ESO-1-expressing HLA-A2-negative cancer cells and co-cultured them with HLA-mismatched HLA-A2-positive APCs. NY-ESO-1(157-165) peptide-loaded HLA-A2-specific 1G4 TCR primary T cells detected cross-presentation. Finally, freshly dissected colorectal tumor and normal colon biopsies were used to assess cancer-specific virus replication, BiME generation, and macrophage activation.
Results: The BiME significantly enhanced phagocytosis of cancer cells by macrophages, surpassing the clinically tested anti-CD47 antibody. It further activated macrophages, upregulating CD86 and CD80 expression. Notably, Ad-BiME induced the strongest macrophage activation. Tumor antigen cross-presentation by macrophages was markedly increased following BiME treatment. Ex vivo experiments showed that oncolytic viruses replicated and produced BiME exclusively in colorectal tumor biopsies, where they induced endogenous macrophage activation, unlike in normal tissues. Elevated IL-1β, TNF, IL-6, CXCL10, and IFN-γ were detected only in tumor samples, indicating targeted BiME expression. Interestingly, free BiME treatment markedly increased CCL17, a chemokine attracting regulatory T cells (Tregs). In contrast, Ad-BiME did not elevate CCL17, likely due to gradual in situ BiME generation. Bulk RNA analysis further revealed that Ad-BiME uniquely upregulated macrophage pathways linked to antigen cross-presentation and T-cell chemotaxis.
Conclusion: We generated the first oncolytic virus expressing a BiME and demonstrated its potential as a promising mechanism for antigen-agnostic cross-presentation in developing cancer vaccines for solid tumors.

#6713 Engineering a hydrogel-based vaccine to prevent recurrence in pancreatic ductal adenocarcinoma.

Peter Yuxin Xie[1], James P. Agolia[2], Rosyli F. Reveron-Thornton[2], Chuner Guo[2], Maria Moozhiyil Korah[2], Andrea Delitto[2], Deshka Foster[2], Ovijit Chaudhuri[1], Daniel Delitto[2]

[1]Mechanical Engineering, Stanford University, Stanford, CA,[2]School of Medicine, Stanford University, Stanford, CA

Purpose: Surgical resection remains the only curative treatment for pancreatic ductal adenocarcinoma (PDAC), yet only 15% of patients are resectable at diagnosis and up to 40% of patients present with locally advanced tumors involving vital vasculature. Even among those who undergo resection, recurrence rates exceed 60%. To address this, we conceived the idea of a locally implantable hydrogel (PancVax) capable of sustained release of an adjuvant therapeutic over a week post-operative to induce a sustained immune response in a murine model pancreatic cancer involving incomplete resection.

Materials and Methods: We engineered a mechanically tough interpenetrating network consisting of carboxyethyl chitosan with dynamic covalent crosslinks and ionically crosslinked alginate. Hydrogel biocompatibility was assessed incubating hydrogel components with RAW264.7 macrophage cell line and assessing markers for apoptosis and maturation. Release assays were conducted by assessment of the hydrogel supernatant following incubation. Compression failure testing was performed to assess the compression toughness. Our murine model for incomplete resection of pancreatic cancer involved orthotopically implanting a KPC-embedded collagen hydrogel at D0 and performing an incomplete tumor resection and implantation of PancVax at D12. Treatment response to adjuvant therapeutics embedded in the PancVax was monitored through tumor volume, collagen staining, and immune profiling.

Results: Individual hydrogel components were incubated for 24 hours with RAW264.7 macrophages, demonstrating >97% cell viability and <1% MHC-II+ demonstrating cytocompatibility and minimal macrophage activation. The hydrogel released albumin-FITC as a model of cytokines and peptides over a week with a sustained release profile. Hydrogels were microporous, showed a compression toughness of 60.8 kJ/m^3, and maintained structural integrity during suture fixation. Implantation of PancVax with encapsulated adjuvants after tumor resection resulted in a significant reduction in tumor volume compared to resection alone ($p<0.01$).

Conclusion: We successfully developed a hydrogel-based vaccine vehicle with properties of sustained release, high mechanical toughness suitable for suture fixation, and sufficient microporous structure permissive for cell trafficking. This work presents a novel perioperative hydrogel-based immunotherapy platform with the potential to shift the treatment paradigm for PDAC by improving post-surgical tumor control and expanding the pool of patients eligible for curative-intent surgery.

#6714 Humanized SLE mouse model for evaluating B-cell CAR-T therapy efficacy and safety.

Ruowen Zhang, Thi Minh Thi Ho, Bo Peng, Hongjing Qu, Qi Jiang, Benjamin Wei, Qingcong Lin

Medicilon, Lexington, MA

Systemic lupus erythematosus (SLE) is a complex autoimmune disease marked by dysregulated B-cell activation, autoantibody production, and systemic inflammation. Therapy development is limited by species-specific immune differences, poor modeling of human pathology in conventional mice, and low clinical predictive value. Similarly, immune-related adverse events (IRAEs), such as cytokine release syndrome (CRS), remain a major challenge in cell-based cancer immunotherapies like CAR-T. To address these issues, we developed a humanized preclinical SLE mouse model that mirrors human immune responses and serves as a platform to evaluate B-cell-targeted CAR-T therapies and immune toxicity.The SLE phenotype was induced by imiquimod (IMQ), a Toll-like receptor 7 agonist that activates plasmacytoid dendritic cells and B cells. In $CD34^+$ humanized mice, IMQ induced a humanized SLE-like phenotype, allowing human immune cells to respond to TLR7 stimulation and closely modeling human disease.CAR-T cells were delivered in vivo using lipid nanoparticles (LNPs) conjugated with anti-CD5 antibodies to target $CD5^+$ T cells. LNP internalization delivers DNA encoding a CD19-specific CAR, and transfected T cells were characterized by flow cytometry and digital droplet PCR. LNP pharmacokinetics were analyzed via LC-MS/MS, and tissue distribution was assessed by CAR gene detection.T-cell activation and CRS were monitored via multiplex assays for cytokines (IFN-γ, TNF-α, IL-2, IL-4, IL-6, IL-10) and chemokines (MCP-1, CCL5). Anti-drug antibody responses were evaluated by anti-PEG ELISA and anti-CAR MSD assays. CAR-T efficacy was assessed using serum anti-dsDNA antibodies and urinary lipocalin-2, key biomarkers of SLE activity.In summary, this humanized SLE model with integrated analytical panels provides a physiologically relevant platform for evaluating therapeutic efficacy and immune toxicity, accelerating preclinical development of human-targeted therapies for autoimmune disease and cancer immunotherapy.

#6715 Safety, tolerability, and early immune responses in the safety run-in of an HER2 multi-epitope vaccine combined with T-DM1 in residual HER2-positive breast cancer.

Saranya Chumsri[1], Sharmila Giri[2], Andy J. Ness[2], David W. Hillman[2], Nadine Norton[3], Davitte Cogen[3], Brian M. Necela[3], Aziza Nassar[3], Donald W. Northfelt[4], Pooja Advani[1], Rohit Rao[1], Alvaro Mareno-Aspitia[1], Brenda Ernst[4], Kathryn J. Ruddy[5], Matthew P. Goetz[5], Keith L. Knutson[3]

[1]Mayo Clinic Florida, Jacksonville, FL,[2]Department of Quantitative Health Sciences, Mayo Clinic, Rochester, MN,[3]Mayo Clinic, Jacksonville, FL,[4]Mayo Clinic, Phoenix, AZ,[5]Mayo Clinic Cancer Center, Rochester, MN

Background: Patients with residual invasive disease after neoadjuvant chemotherapy (NAC) for HER2-positive breast cancer remain at high risk for recurrence even with standard adjuvant trastuzumab emtansine (T-DM1). H2NVAC, a multi-epitope HER2 peptide vaccine, has previously demonstrated the ability to elicit robust and durable immune responses. Here, we assessed the safety and early immunogenicity of H2NVAC in combination with T-DM1 in this high-risk population.

Methods: Patients with stage II-III HER2-positive breast cancer and residual invasive disease following NAC and HER2-directed therapy received standard adjuvant T-DM1 alongside six priming doses of H2NVAC administered every 3 weeks. The primary endpoint was the occurrence of dose-limiting toxicity (DLT) within 21 days of the first vaccination, with adverse events graded per CTCAE v5.0. Immunogenicity assessments included HER2-specific T-cell responses measured by IFNγ ELISpot and HER-specific serum antibodies measured by ELISA at baseline and 30 days after the sixth priming dose.

Results: 20 patients were enrolled. H2NVAC plus T-DM1 was well tolerated with no DLTs observed. All treatment-emergent AEs were grade 1-2, with fatigue (grade 1 60%, grade 2 5%), peripheral sensory neuropathy (grade 1 35%, grade 2 10%), elevated alkaline phosphatase (grade 1 40%), nausea (grade 1 35%, grade 2 5%), arthralgia (grade 1 30%), and injection-site reactions (grade 1 50%) being most common. Robust vaccine-specific T-cell responses by ELISpot were observed in 94% of evaluable patients, who mounted HER2-specific T-cell responses at 30 days after the sixth priming dose, with a mean 197-fold increase over baseline. Further CYTOF analysis showed a significant decrease in exhausted T-cell phenotypes, with reduced LAG3 and TIM3 expression on both $CD4^+$ and $CD8^+$ T cells. For antibody responses by ELISA, 26% of patients developed HER2 protein-specific antibody responses at this time point. There was no significant increase in antibodies to H2NVAC peptides or to unrelated tumor antigens (p53, IGFBP2, TERT, myoglobin) at 30 days after the sixth vaccine. Ongoing correlative analyses will assess the evolution of immune responses at later time points following completion of T-DM1 therapy.

Conclusions: Concurrent administration of H2NVAC with T-DM1 was safe and did not increase toxicity beyond single-agent T-DM1. To our knowledge, this is the first study to demonstrate that a cancer vaccine can be delivered concurrently with an antibody-drug conjugate without increasing adverse effects while still eliciting robust T-cell responses. Ongoing analyses will further define the kinetics and durability of vaccine-induced antibody and T-cell responses at later time points, as well as evaluate the efficacy of H2NVAC in reducing recurrence risk in the randomized phase 2 trial.

#6716 ALK-mRNA vaccine as a new Immunotherapy for ALK+ cancers.

Gabriele Saccu[1], Alessandro Gasparetto[1], Carmen Mecca[1], Elisa Bergaggio[1], Simone Piane[1], Taek-Chin Cheong[2], Nirmala Tilija Pun[1], Roberto Chiarle[1]

[1]Boston Children's Hospital, Boston, MA,[2]Harvard Medical School, Boston, MA

Anaplastic lymphoma kinase (ALK)-driven cancers, including ALK$^+$ lymphoma and non-small cell lung cancer (NSCLC), are treated with ALK tyrosine kinase inhibitors (TKIs), yet resistance and relapse remain major challenges. Vaccine-based immunotherapy has emerged as a promising approach. Our group previously developed DNA- and peptide-based vaccines that extended survival in NSCLC mouse model. However, their clinical translation is limited. The success of SARS-CoV-2 lipid nanoparticle (LNP)-mRNA vaccines has generated interest in this platform, demonstrating effective antigen delivery and strong T-cell activation. These findings support the evaluation of a new ALK-mRNA vaccination and the direct comparison with the peptide-based strategy. We designed a codon-optimized ALK cytoplasmic domain (exons 20-29) mRNA and formulated it with LNPs using Moderna technology as standard (F#1). Two additional ionizable lipids (F#2 and F#3) were tested to assess delivery efficiency. *In vitro,* ALK protein expression and immunogenic peptide presentation was evaluated in 293T cells (1 µg single dose) in 293T HLA-B*07:02 cells using ALK.TCR-T cell killing assay. *In vivo*, 1 or 10 µg ALK-mRNA or peptide vaccine was administered intramuscularly or subcutis, respectively, in three biweekly doses in BALB/c mice. ALK-specific CD8$^+$ and CD4$^+$ response, T cell immunophenotypes, and anti-tumor activity were evaluated. Moreover, we tested ALK peptide presentation upon ALK-mRNA vaccination in HLA-B*07:02 transgenic model. We demonstrate that the ALK-mRNA vaccine enables the delivery of the expected ALK protein (~65 kDa) without detectable phosphorylation, and antigen presentation was confirmed using an ALK.TCR-T cell killing assay in HLA-B*07:02 cells *in vitro. In vivo*, 1 or 10 µg ALK-mRNA vaccinations induced robust anti-ALK-specific CD8$^+$ T cell responses (40-60%) against immunogenic ALK portion PGPGRVAKI in BALB/c mice, markedly surpassing peptide-based vaccines, particularly with the F#1. The 10-µg dose further elicited a CD4$^+$ ALK-specific response by ELISPOT and promoted CD4$^+$ and CD8$^+$ T cell expansion with increased effector CD44$^+$CD62$^-$ expression. Notably, both ALK-mRNA doses slowed tumor growth and extended survival in a preventive low MHC-I ALK$^+$ lung syngeneic tumor model. Additionally, ALK-mRNA vaccine elicited superior anti-ALK^{RPRPSQPSSL}-CD8$^+$ responses in HLA-B*07:02 mice compared to the peptide vaccine. No adverse effects were observed. Here, we identified F#1 as the best formulation and demonstrated that ALK-mRNA vaccine induces ALK-specific CD8$^+$ and CD4$^+$ strong, non-toxic immune response with an effector immunophenotype *in vivo*. In a preventive setting, ALK vaccination delayed tumor growth in a lung MHC-I-low ALK$^+$ model. Overall, these results outperformed the peptide vaccine and supported further investigation of the ALK-mRNA vaccine in therapeutic settings within ALK$^+$ malignancies for a future Phase I/II clinical trial.

#6717 Preclinical study of armored claudin 18.2 nanobody CAR NK cells targeting gastric cancer.

Byeong-Hyeok Choi[1], Ga-Ram Hwang[1], Morgan Flaherty[1], Vincent M. DeStefano[1], Masayuki Wada[1], Kevin Pinz[2], Jennifer E. Chow[2], Nabil Hagag[2], Yu Ma[3], Jing Luo[3], Yupo Ma[1]

[1]iCell Gene Therapeutics Inc., Stony Brook, NY,[2]iCell Gene Therapeutics, Inc, Stony Brook, NY,[3]iCAR Bio Therapeutics Ltd, Zhongshan, China

Introduction:
Claudin 18.2 (CLDN18.2) is highly expressed in gastric cancer with minimal expression in normal tissues, making it an attractive target for engineered cell therapies. CAR NK cells offer a potentially lower risk of inciting inflammatory cytokines and may be easily sourced for allogeneic or “off-the-shelf” use. However, conventional CAR NK approaches often show limited persistence and reduced activity when engaging with solid tumors. To enhance antitumor activity and persistence, we developed CLDN18.2 nanobody-based CAR NK cells incorporating IL-15/IL15sushi armoring. This study evaluated the antitumor efficacy and persistence in vitro and in vivo of the armored CLDN18.2 CAR NK cell construct generated via a feeder-independent NK expansion platform.
Methods:
Alpacas were immunized with recombinant human CLDN18.2 extracellular domain protein. Peripheral blood mononuclear cell (PBMC) mRNA was extracted and converted into a VHH (nanobody) to generate a library. The library was panned against CLDN18.2 antigen to enrich for high-affinity binders, which were identified through ELISA screening and cellular binding analysis by flow cytometry. VHH clone sequencing were used to generate our cCAR.A CLDN18.2-specific nanobody was identified through screening and used to generate an armored CLDN18.2 CAR NK cell construct. NK cells were isolated from cryopreserved cord blood and expanded using a feeder-independent NK expansion platform. CAR expression was measured by flow cytometry. Cytotoxicity was assessed using SNU-601 and REH-C18.2xp target cells. NSG mice received CAR NK cells.
Results:
The armored CLDN18.2 CAR NK cells displayed strong CAR expression following NK cell transduction. CLDN18.2 CAR NK cells demonstrated remarkable in vitro cytotoxicity across multiple effector-to-target ratios, eliminating CLDN18.2-positive targets rapidly and completely. In vivo, the armored CLDN18.2 CAR NK cells were observed to impart strong anti-tumor activity resulting in regression in SNU-601 xenografts. In NSG mice, armored CLDN18.2 CAR NK cells resulted in rapid tumor reduction and measurable NK persistence in mouse peripheral blood.
Conclusions:
Armored CLDN18.2 nanobody CAR NK cells generated via a feeder-independent NK expansion platform showed strong antitumor activity and improved in-vivo performance in CLDN18.2-positive tumor models. CAR NK cells also demonstrated sustained persistence following infusion. Together, these findings support future clinical investigation of our platform in patients with CLDN18.2-positive gastric cancer.

#6718 Identifying new cell surface markers of T-cell reactivity through single cell transcriptomic analysis.

Abraham A. Hakim[1], Lisa Kenney[2], Nivedita Mohan Ratnam[3], Jared J. Gartner[4], Ian S. Goldlust[5], Aarushi Bhasin[6], Brian Bui[6], Nicholas D. Klemen[6], Steven A. Rosenberg[3], Frank J. Lowery[3]

[1]NIH-NCI, Bethesda, MD,[2]Laboratory of Integrative Cancer Immunology (LICI), Center for Cancer Research, Bethesda, MD,[3]National Cancer Institute, Bethesda, MD,[4]National Institutes for Health, Bethesda, MD,[5]Surgery Branch, NIH-NCI, Bethesda, MD,[6]Surgery Branch, National Cancer Institute, Bethesda, MD

Background: Adoptive transfer of selected tumor infiltrating lymphocytes (SEL-TIL)+ pembrolizumab has yielded clinical responses of 23.5% in a phases 2 trial.[1] Following expansion in IL-2, TIL cultures are selected for treatment based on in vitro reactivity assays in which TIL are co-cultured with candidate autologous tumor targets, (peptides, tandem minigenes (TMGs), and autologous tumor organoid). Detection of neoantigen reactivity currently relies on 4-1BB, OX40, and interferon-γ (IFN-γ) upregulation.[2] Clinical administration of more neoantigen reactive CD4+ TIL is associated with improved responses.[1] However, there may be additional reactivity markers that would allow for detection of neoantigen relevant fragments and more diverse final treatment products in both CD4+ and CD8+ T-cells.

Methods: Initial screening and selection of neoantigen reactive TIL completed using standard screening via upregulation of 4-1BB, and OX40 by flowcytometry and IFN-γ by ELISpot. These samples with known reactivity were then selected for transcriptomics. scRNA sequencing was performed using 10x Genomics Chromium platform on known tumor-reactive fragments to organoid and negative controls. Conditions were tracked with barcode hashing of TCRs. CITE-Seq, and TCR-seq were also used. Clustering and analysis completed using Seurat.

Results: Upregulation of *TNFRSF9* (4-1BB) and *IFNG* (IFN-γ) were found in a single cluster. An additional larger cluster was found expressing additional genes including *TNFRSF18* (GITR). This activation of GITR, and other markers was not seen in negative control conditions. In additional validation samples, GITR was successfully observed by flow cytometry equal to or greater than 4-1BB when tested as a cell surface marker of activation for CD8 T-cells against autologous organoid.

Conclusions: The methodology of using scRNA transcriptomic analysis is a successful and viable method for identifying new markers of upregulation. GITR is a potential marker of CD8+ T-cell tumor reactivity, however, it requires further validation in additional samples and evaluation of antitumor effects.

: Aging Micro- and Macro-Environments in Tumor Progression and Therapy
Minisymposium

#6820 Age-related clonal hematopoiesis drives immune remodeling that promotes lung cancer and alters neoadjuvant chemo-immunotherapy outcomes.

K. Park[1], E. Kim[1], M. Sierra-Rodero[2], Y. Byun[1], T. McPherson[1], S. Kapadia[1], D. Bayer[1], J. Yoo[1], S. Ramalingam[1], W.-Y. Park[3], B. Bosch[4], N. Reguart[5], B. massuti_[6], A. Cruz-Vermudez[2], M. Provencio[2], **J. Woo**[1];

[1]Winship Cancer Institute of Emory University, Atlanta, GA, [2]Hospital Univ. Puerta de Hierro Majadahonda, Madrid, Spain, [3]Translational Genomics Center, Samsung Medical Center, Seoul, Korea, Republic of, [4]Medical Oncology, Institut Catala d'Oncologia, Hospital Universitari Dr. Josep Trueta and Precision Oncology Group (OncoGIR-Pro), Institut d'Investigacions Biomediques de Girona (IDIBGI-CERCA), Girona, Spain, [5]Hospital Clinic i Provincial de Barcelona, Barcelona, Spain, [6]Hospital General Dr. Balmis, Alicante, Spain

More than 20% of individuals ≥70 harbor clonal hematopoiesis (CH) mutations without overt malignancy. CH has been linked to elevated risk of non-hematologic cancers, particularly lung cancer, although causality remains unresolved. The TRACERx study showed that CH in blood and tumor predicts higher recurrence and mortality in NSCLC, and recent reports suggest that TET2-mutant CH may enhance immunotherapy responsiveness. However, how CH shapes lung tumorigenesis and modulates neoadjuvant immunotherapy outcomes in early-stage lung cancer remains unclear. We performed integrated analyses in murine models and NSCLC patients, identifying a CH-driven immunosuppressive program. To test whether age-associated Tet2-mutant hematopoiesis accelerates lung cancer, KP (KrasG12D;Trp53-/-) lung cancer cells were orthotopically implanted into young (8-week) and aged (30-week) Tet2-null (Tet2fl/fl;VavCre), Tet2-heterozygous (Tet2fl/+;VavCre), and WT mice. Aged Tet2-deficient mice developed tumors earlier and with greater burden compared to young counterparts. Spleen and tumor profiling showed expansion of CD11b+ myeloid cells, Tregs, and PD-1+ T cells, with profound NK-cell depletion in older Tet2-deficient mice, indicating enhanced immune suppression in aged Tet2-deficient hosts. We next profiled PBMCs from 59 NSCLC patients using scRNA-seq. Individuals with TET2-mutant CH (n=5) exhibited enrichment of MDSCs, Tregs, effector and exhausted T cells, along with significant reductions in naïve T cells and activated NK cells compared with CH-negative patients (n=45). Long-read variant calling from scRNA-seq further revealed that within CH-positive individuals, both wild-type and CH-mutant immune cells adopted similarly aberrant immune states, unlike those from CH-negative individuals. Ligand-receptor modeling indicated that myeloid cells predominantly drove CD4 T-cell alterations, whereas CD8 T-cell remodeling arose from B- and T-cell interactions—highlighting global immune rewiring triggered by limited CH-derived clones through repeated immune synaptic interactions. Finally, in the real-NADIM cohort treated with neoadjuvant immunotherapy (n=161), patients with CH mutations showed comparable response rates but improved cancer-specific and overall survival compared with CH-negative patients, with this preliminary evidence supporting the idea that CH-induced immune alterations can be therapeutically reprogrammed. Conclusion: age-associated TET2-mutant CH remodels systemic immunity to create tumor-promoting microenvironments. These effects appear reversible with immunotherapy. Ongoing work is evaluating combination strategies targeting both myeloid and T-cell pathways to intercept CH-mediated immune escape in age-associated Tet2-deficient CH and includes spatial transcriptomic analysis of early-stage NSCLCs.

#6821 The temporal dynamics and molecular impact of clonal hematopoiesis in non-small cell lung cancer.

A.-M. Leppa[1], O. Pich[1], J. R. M. Black[1], M. Zagorulya[1], E. Bernard[2], S. Ward[1], A. Rowan[1], H. Slawinski[1], L. Y. Liu[1], C. Grieco[1], R. Slama[3], C. Martinez Ruiz[1], A. Huebner[1], T. Karasaki[1], C. Naceur-Lombardelli[4], S. Veeriah[4], TRACERx Consortium, M. Jamal-Hanjani[4], A. M. Frankell[5], A. Mead[3], C. Swanton[1];

[1]The Francis Crick Institute, London, United Kingdom, [2]Gustave Roussy, Villejuif, France, [3]Medical Research Council Weatherall Institute of Molecular Medicine, University of Oxford, Oxford, United Kingdom, [4]University College London Cancer Institute, London, United Kingdom, [5]Early Cancer Institute, University of Cambridge, Cambridge, United Kingdom

Clonal hematopoiesis (CH) is a common age-associated phenomenon whereby blood cells derived from a somatically mutated hematopoietic stem cell expand, in the absence of hematological disorders. CH is linked to an increased risk of hematological and non-hematological malignancies, including lung cancer. We recently identified tumor-infiltrating CH (TI-CH) as a promoter of non-small cell lung cancer (NSCLC) progression, but its temporal dynamics and effects on the tumor microenvironment remain undefined. To address this gap, we integrated whole exome sequencing and longitudinal cell-free DNA sequencing with single-cell multimodal analyses to characterize CH dynamics in NSCLC patients. Using pre-surgical blood samples from over 800 patients in the TRACERx cohort, we detected CH-associated mutations in 32% of patients through whole exome sequencing, most frequently in DNMT3A and TET2. Of these patients, 46% had TI-CH. Patients with TI-CH exhibited reduced disease-free survival compared to patients without CH (HR = 1.53, 95% CI = 1.20-1.95, p = 0.0006) and to patients with blood-only CH (HR = 1.41, 95% CI = 1.04-1.90, p = 0.03). In 424 patients with longitudinal cell-free DNA from blood plasma samples, we tracked single-nucleotide variants (SNV) across a median of six timepoints per patient using patient-specific liquid biopsy panels. 38 SNV-CH mutations in 35 patients were covered through variant calling. Mixed-effects modeling revealed a modest but significant global expansion of CH clones (Estimate = 0.00022, p = 0.027), with ASXL1 and TET2 mutations showing the strongest positive trends. Adjuvant therapy modestly attenuated clone growth. To extend our analysis to molecular mechanisms, we used two single-cell multimodal frameworks to gain a detailed view of lung tumor microenvironments in the presence and absence of TI-CH. We examined lung tumor immune infiltrates from two early-stage NSCLC patients with mutations in TET2 using TARGET-seq, integrating gene expression and high sensitivity genotyping at single-cell resolution. Additionally, in six patients (3 with TI-CH and 3 without CH) we employed DOGMA-seq to profile gene regulation in single cells across three distinct modalities, including chromatin accessibility, mRNA levels and cell surface proteins. While differences between mutated and non-mutated cells were nuanced, genes involved in inflammasome activation and regulation were upregulated in $TET2^{Mut}$ mononucleated phagocytes compared to those that were $TET2^{WT}$. Collectively, these data show that CH clones expand over time in NSCLC and reshape the tumor immune microenvironment toward an inflammatory state that may potentiate disease progression.

#6822 TFF2 deficiency amplifies IL-1β-driven inflammation and promotes aging-associated gastric tumor progression.

Shuang Li[1], Hualong Zheng[1], Jin Qian[1], Puran Zhang[1], Feijing Wu[1], Yi Zeng[1], Biyun Zheng[1], Juli Lin[1], Hiroki Kobayashi[1], Yosuke Ochiai[1], Mashahiro Hata[1], Arai Junya[1], Leah B. Zamechek[1], Bruce Daugherty[2], Seth Lederman[2], Timothy C. Wang[1]

[1]Columbia University Irving Medical Center, New York, NY,[2]Tonix Pharmaceuticals, Inc, Chatham, NJ

Background: Aging is associated with a chronic low-grade inflammatory state that profoundly influences tumor development and progression, known as inflammaging. While this is due to increased myelopoiesis, the exact mechanisms leading to increased myeloid production and the effects on the gastric tumor microenvironment remain poorly understood.
Methods: We conducted comprehensive analyses of young (3 months) and aged (18 months) Hdc-GFP mice, evaluating expression of the peptide trefoil factor family 2 (TFF2) and abundance of GFP+ MDSCs in the stomach, circulation and other sites. The ACKP orthotopic model and Mist1^{CreERT}; RhoA^{Y42C}CDH1^{ff}; Hdc-GFP mouse (GEM) model were used to test whether aging promotes gastric cancer progression and to explore the underlying mechanisms. TFF2-MSA was given by i.p. injection twice weekly for 2 weeks before ACKP tumor inoculation, to test whether pretreatment could reverse the aging-related pro-tumor effects.
Results: Aging led to a significant reduction in TFF2 levels in both the stomach and circulation, as confirmed by IHC, ELISA, and qPCR. The decline in circulating TFF2 was accompanied by elevated IL-1β expression in bone marrow, peripheral blood, and gastric neutrophils, together with increased circulating IL-1β levels. Enhanced IL-1β signaling contributed to a myeloid-biased hematopoietic phenotype, leading to the increased GFP$^+$ MDSCs in the stomach, spleen, and peripheral blood. Elevated IL-1β in the aged stomach induced fibroblast activation with a senescence-associated secretory phenotype (SASP)-like profile, including increased IL-6, CXCL1 and CXCL2 expression. In the ACKP orthotopic and model and GEM model, with tumorigenesis initiated at 3mo or 18mo, aging significantly accelerated tumor growth and shortened survival. Immunofluorescence analyses of aged ACKP tumor identified an increased subset of IL-1R1$^+$ cancer-associated fibroblasts (CAFs) and CGRP+ sensory nerves. Functionally, pretreatment with TFF2-MSA prior to ACKP tumor implantation decreased IL-1R1$^+$ CAF and sensory nerves, reduced MDSC accumulation and IL-1β expression, and suppressed gastric tumor growth in aged mice.
Conclusion: Our findings uncover a systemic aging axis linking reduced gastric TFF2 production to myelopoiesis and thus to gastric cancer susceptibility. Aging-associated IL-1β signaling from expanded myeloid cells reprograms gastric fibroblasts toward a pro-inflammatory SASP phenotype, fostering immune suppression and tumor growth. Restoring youthful TFF2 levels may provide effective strategies to mitigate the aging-related tumor risk and other associated inflammaging syndromes.

#6823 The role of aging in immune mediated reactivation from metastatic dormancy.

Mitchell Fane, **Kelly Coutant**, Jhon Pasamonte, Pulkit Datt, Anastasia Burtseva

Fox Chase Cancer Center, Philadelphia, PA

Age is the strongest prognostic risk factor for melanoma-related death, and metastasis remains the primary driver of mortality. Yet despite this clear link, the mechanistic basis for why melanoma progression and metastatic outgrowth disproportionately worsen in older adults (>65 years) remains poorly understood. A key gap lies in the field's reliance on young (~8-week-old, equivalent to 20 human years) mouse models, which fail to capture the age-related dynamics such as immune dysfunction that shape metastatic behavior. Moreover, most studies have focused exclusively on lung metastasis, despite melanoma commonly metastasizing to sites such as the liver, which are more resistant to immune checkpoint inhibitors. To address these limitations, we developed novel syngeneic models of melanoma metastasis and colonization in young (8 weeks), middle-aged (12-16 months), and geriatric (22-26 months) mice, targeting metastases specifically to the lung or liver. Strikingly, both lung and liver metastases were increased in middle-aged mice, whereas young and geriatric mice showed limited outgrowth, recapitulating human data where melanoma incidence is low in young adults (<50 years), peaks between ages 65-79, and decreases thereafter (79+). These aging mouse models allow us, for the first time, to systematically assess immune surveillance pathways associated with age-induced melanoma reactivation (middle-aged) and dormancy (young and geriatric). Of the various immune subsets profiled, we found that γδ T-cells are decreased in the lungs and livers of middle-aged mice with metastatic disease but are elevated in young and (surprisingly) geriatric mice. Depletion of γδ T-cells in both young and geriatric mice reawakened dormant melanoma cells and promoted aggressive metastasis. We next assessed cytokine-specific changes in the pre-metastatic lung and liver that might explain this altered γδ T-cell phenotype. We found the cytokine ARG1 was markedly increased by $CD11b^+$ myeloid cells in the middle-aged lung and liver only. r-ARG1 treatment in young mice was sufficient to induce metastatic reactivation, reduce γδ T-cell abundance, promote γδ T-cell exhaustion, and also reduced human Vγ9Vδ2 T-cell killing of human melanoma cells ex-vivo. Finally, in vivo treatment with the ARG1 inhibitor CB-1158 reduced metastatic outgrowth in both the lung and liver of middle-aged mice, with no effect in young or geriatric hosts. Treatment was associated with increased γδ T-cell abundance, enhanced activation, and reduced exhaustion within the metastatic TME of middle-aged mice. These findings uncover a previously unrecognized age-specific ARG1-γδ T-cell immunoregulatory axis that drives melanoma reactivation and metastatic progression selectively in middle-aged hosts. This work underscores the critical need for age-appropriate modeling and identifies ARG1 and γδ T-cells as a promising therapeutic target in elderly melanoma patients.

#6824 Old age uncovers FGFR-dependent metabolic dependencies in TNBC lung metastasis with therapeutic potential.

S. Drapela, R. Chimeh Rad, S. Chang, V. Rubio, N. Sarigul, D. Ilter, P. Rodriguez, A. P. Da Silva Gomes;
Moffitt Cancer Center, Tampa, FL

The clinical manifestation of metastasis in a vital organ is the final stage of breast cancer progression, and the main culprit of breast cancer related mortality. This remain especially problematic in the case of triple negative breast cancer (TNBC), the most aggressive type of breast cancer, often diagnosed in its metastatic form and for which chemotherapies are still the major therapeutic option. Typically, TNBC is seen as a disease of younger women, however, 20% of TNBCs occur in patients aged 65 and older, whose prognosis is equally staggering. Unfortunately, due to co-morbidities, tolerability of chemotherapies, as well as severe reduction in quality of life, majority of women above age 65 can't or decide not to receive chemotherapy ultimately cutting their lives short. Metastatic outgrowth is largely dictated by the ability of TNBC disseminated cancer cells (DCCs) to thrive distal organs and is largely dependent on the physiology of the specific organs. However, how the aging process, a major driver of changes in organismal physiology, affects the interaction between the host organ and TNBC DCCs remains unknown. Here, we adapted several traditional syngeneic models of TNBC metastasis to old mice of different strains and coupled with RNA-seq to unveil molecular adaptations of TNBC DCCs to the aging lung. We show that the changes that occur in the lung with aging drives an increase in mitochondrial fitness in TNBC DCCs, an adaptation that is necessary for metastasis to thrive in the old lung environment. Mechanistically, our data show that the expression of FGF19, a gut hormone not normally expressed in TNBC DCCs, drives this increase in mitochondrial fitness in the old lung through an autocrine signaling axis impinging on activation of FGF-19 cognate receptor family, FGFRs. Inhibition of FGF19-FGFR signaling using an FDA-approved FGFR inhibitor not only blocks the age-induced increase in mitochondrial fitness but also effectively abolishes lung metastasis in old, but not in young, immune competent and immune compromised mice. We traced this to age-specific metastatic adaptation of TNBC lung metastasis to the increase in bile acids, the canonical regulators of FGF19 expression, in the old lung environment. Together, our work demonstrates an important contribution of age-driven metabolic reprogramming of the host to the traits that enable metastasis to thrive in the lung and provides rationale for the use of FDA-approved FGFR inhibitors for the treatment of breast cancer lung metastasis in the most vulnerable of stage IV metastatic TNBC patients, the elderly.

#6825 Age-stratified therapeutic strategies targeting tumor cell subclones that drive chemoresistance and immunosuppression in triple-negative breast cancer.

M. Spasic[1], M. Dolan[1], A. M. Parsons[2], B. Koca[2], D. Lineker[1], J. Hawk[1], H. Starobinets[3], R. A. Freedman[2], E. Mittendorf[2], P. van Galen[1], S. S. McAllister[4];
[1]Harvard Medical School/Brigham and Women's Hospital, Boston, MA, [2]Dana-Farber Cancer Institute, Boston, MA, [3]Mass General Brigham, Boston, MA, [4]Harvard Medical School, Boston, MA

Age is the biggest risk factor for developing most forms of cancer, including breast cancer. While over 50% of cancer cases occur in patients over 65, fewer than 25% of patients enrolled in clinical trials are in this age group. Furthermore, most preclinical models use young mice, together indicating that preclinical research and clinical trials may not appropriately reflect the age of patients most affected by cancer. Triple negative breast cancer (TNBC) is an aggressive subtype of breast cancer that has high rates of recurrent, chemoresistant disease and poor outcomes. Moreover, older patients do not tolerate chemotherapy well, so alternatives are needed.

We used a preclinical mouse model that reflects clinical progression with age, whereby young (~8 week old) and aged (12-16 month old) FVB/NJ mice were orthotopically injected with syngeneic Met1 TNBC cells. Mice were treated with standard therapy consisting of chemotherapy (paclitaxel, PTX) and immunotherapy (anti-PD-L1). Relative to young mice, aged mice did not benefit from combination therapy over monotherapy, which was at least partially due to signs of immune dysregulation and CD8+ T cell exhaustion. RNA sequencing revealed that in response to PTX or combination therapy, tumors from young mice became enriched for immune and inflammatory response hallmark programs, making the young mice look transcriptionally old. Aged mice, however, did not exhibit any response to chemotherapy, - underscoring the lack of response to treatment with age and need for chemotherapy alternatives.

The Met1 TNBC cells used here contain heritable, non-immunogenic, DNA barcodes through which we identified a unique subclone of tumor cells that is resistant to PTX, both in vitro and in vivo. Among minor clones comprising <15% of the tumor cells, this clone expands with age and PTX, drives an EMT-like phenotype, and displays features of immunosuppression. A drug screen using a library of FDA-approved compounds identified histone deacetylase inhibitors (HDACi) as a potent class of drugs that kill this chemo-resistant clone. Finally, we treated young and aged mice with Panobinostat, a pan-HDACi that was the top hit in the screen, in combination with anti-PDL1. This combination led to a more significant therapeutic benefit in aged mice by reducing tumor burden and significantly extending survival compared to young.

We have identified age-tailored therapies that improve TNBC outcomes in both young and aged mice, without the need for chemotherapy in aged mice. Further, specific subclones of tumor cells can drive transcriptional programs impacting age-associated differences in tumor progression, but they can be therapeutically targeted. This work sets the stage for the development of age-stratified therapeutic strategies that do not rely on toxic chemotherapy to improve outcomes for TNBC patients of all ages.

#6826 Age-dependent neuro-immune changes in glioblastoma shape therapeutic response and reveal senescent microglia as a targetable vulnerability.

M. Penco-Campillo[1], O. de Dios[2], M. Callender[3], K. L. Lauing[1], O. Odum[1], T. Koch[1], L. Zhai[1], V. C. Prabhu[1], D. E. Anderson[1], A. V. Germanwala[1], J. P. Thakkar[1], P. Bommi[1], P. Sanchez-Gomez[2], F. Varn[3], D. Wainwright[1];

[1]Loyola University Chicago Stritch School of Medicine, Maywood, IL, [2]Institute de Salud Carlos III (ISCIII-UFIEC), Madrid, Spain, [3]The Jackson Laboratory, Bar Harbor, ME

Background: Glioblastoma (GBM) is the most common aggressive primary brain tumor, with a median overall survival (OS) of ≈15-18 months despite standard of care (SOC). Aging is a major negative prognostic factor, with older adults showing worse OS. Senescent cells accumulate with age and contribute to poorer outcomes. Senolytics clear senescent cells and may improve responses in older hosts. While tumor-intrinsic molecular features appear age-independent, the aging brain microenvironment impact on GBM progression and immunity remains unclear.
Objective: To define age-associated senescence patterns in tumor core and peritumoral (PT) brain in GBM patients and mouse models and assess whether senolytic enhance treatment responses in aged syngeneic and humanized GBM models.
Methods: MRI-guided tumor core and PT biopsies from GBM patients (<65 vs. ≥65) underwent transcriptomic and single-cell analyses to assess age-related neuro-immune and senescence changes. Senescence across tumor regions was examined in young (7-9 weeks) and aged (97-104 weeks) C57BL/6 and INK-ATTAC mice with intracranial SB28 tumors (n=5/group). Flow cytometry quantified β-gal+ senescent populations among neurons, astrocytes, oligodendrocytes, microglia, and immune infiltrates from tumor core and extratumoral brain. Mice received brain radiation, anti-PD-1, and IDO enzyme inhibition, alone ± senolytics (dasatinib+quercetin) or AP compound-induced clearance *p16INK4A+* senescent cells. A human GBM aging model was developed by depleting CD4+, CD8+, CD19+, and NK1.1+ cells in young and aged C57BL/6 mice, prior to patient-derived GBM43 (PDX) intracranial engraftment, followed by SOC radiotherapy + temozolomide ± senolytics.
Results: Transcriptomic profiling showed minimal age-related changes in tumor core but marked alterations in older PT tissues. Aged PT microglia exhibited a senescent phenotype with an upregulation of senescence-associated secretory phenotype (SASP) genes. Senolytics or AP compound significantly reduced extratumoral β-gal+ microglia and synergized with radio-immunotherapy to extend OS in aged mice ($p<0.05$). In the humanized immunodepleted GBM43 PDX model, young and aged mice developed tumors, with faster mortality in older hosts. Therapeutic responses to SOC ± senolytics are ongoing.
Conclusions: The PT brain is a key site of age-dependent immune dysfunction in GBM. Senescent microglia may create an immunosuppressive niche that limits the immunotherapy efficacy in older adults. Senolytics may restore treatment efficacy and improve outcomes in older GBM hosts. We developed a novel immunodepleted GBM PDX model to mechanistically evaluate the role of aging in human tumor progression and therapy resistance. **Keywords:** glioblastoma, peritumoral brain, aging, immunotherapy, senescence, microglia

: Genomic Approaches to Understanding Tumor Evolution
Minisymposium

#6793 Clinico-genomic characteristics of multiple primary cancers in TRACERx.

L. Y. Liu[1], **C. Grieco**[1], A. Salcedo[2], T. Karasaki[1], C. Naceur-Lombardelli[2], O. Shutkever[2], A. Huebner[1], C. Martinez Ruiz[1], S. Waise[2], A.-M. Leppa[1], O. Lucas[2], T. Pandya[1], S. Veeriah[2], S. Ward[1], K. Haase[2], A. A. Azizi[1], W. Z. Zhang[3], E. Hazelwood[3], A. M. Frankell[3], TRACERx Consortium, A. Hackshaw[2], N. McGranahan[2], D. A. Moore[2], M. Jamal-Hanjani[2], C. Swanton[1];
[1]Francis Crick Institute, London, United Kingdom, [2]University College London Cancer Institute, London, United Kingdom, [3]Early Cancer Institute, University of Cambridge, Cambridge, United Kingdom

Management of multiple primary tumours is an increasing clinical burden as the population of cancer survivors rises globally. Despite standard-of-care histological, radiological and panel sequencing diagnostics, identifying multiple primary cancers remains clinically challenging. We characterize multiple primary tumours in the TRACERx study. We integrate baseline and follow up clinical data, centrally-reviewed histopathological assessments with whole-exome sequencing (WES) to identify patients with multiple primary tumours from lung and other sites. Where multi-region sample collection was available, we assessed the genomic relatedness of multiple lesions from the same patient through shared clonal mutations.
205 (24% of 844) TRACERx patients had clinically-diagnosed or genomically-discovered multiple primary cancers. Of these, 82 patients had a prior cancer diagnosis, 56 patients had synchronous primaries at study enrollment, and 95 developed new primaries during follow up. Lung was the most common organ site for additional primaries, with 98 patients having two or more lung primary tumours, including the lung tumour profiled for the TRACERx study.
High resolution tumour WES revealed clinical misclassification in 21 of 138 patients (15.2%) with multiple sequenced lesions. At baseline, clinical classification favoured relatedness between lesions: two patients diagnosed with intrapulmonary metastases actually had independent primary lung cancers. In addition, eight patients with lesions staged histopathologically as single tumours, some with microscopic evidence of histological heterogeneity, were confirmed through WES to be collision tumours composed of 2 to 3 independent lineages. One patient was discovered to have had synchronous lung primaries, undetectable clinically, through WES sequencing of lymph node metastases. During follow up, clinical classification tended to favour independent primary designation, with 6 of 10 discrepancies due to clinically-diagnosed metachronous primary tumours found through WES to be metastases.
Together, the TRACERx multiple primary cohort represents one of the largest multi-region cohorts of multiple primary lung cancers analyzed to date. These data demonstrate the clinical utility of WES in diagnosing independent primary cancers. Ongoing analysis will investigate the association between history of multiple primary cancers and germline cancer susceptibility and patient outcome. Deep, multi-region molecular characterization, available for 58 patients with multiple primary lung cancers, will also allow detailed exploration of the molecular mechanisms driving the evolution of multiple primary cancers, informing potential biomarkers to highlight patients with elevated risk of secondary primary tumours and improve subsequent clinical management.

#6794 The mouse cancer cell line atlas reveals core principles of tissue-specific cancer evolution.

S. Mueller[1], N. de Andrade Kratzig[1], M. Tschurtschenthaler[1], M. G. Silva[1], C. Thordsen[1], R. Trozzo[1], P. Simon[1], F. Saab[1], T. Kaltenbacher[1], M. Zukowska[1], D. Lucarelli[1], R. Ollinger[1], J. Griger[1], N. Gro?[1], T. Groll[1], L. R. Schomig[2], S. Baerthel[1], C. Falcomata[1], A. Strong[3], C. Brandt[3], M. Najajreh[4], A. Papargyriou[4], R. Maresch[1], U. Jungwirth[5], M. Reichert[4], G. S. Vassiliou[3], D. F. Alonso[6], P.-L. Lollini[7], J. J. Zhao[8], L. Chesler[9], C. M. Isacke[10], A. Riedel[11], C. J. Braun[12], M. Sos[13], F. Beleggia[14], H. C. Reinhardt[15], M. Musteanu[16], M. Barbacid[17], M. Quante[2], M. Schmidt-Supprian[1], G. Schneider[18], S. Clare[3], T. D. Lawley[3], G. Dougan[3], K. Steiger[1], N. Conte[3], A. Bradley[3], L. Rad[1], D. Saur[1], R. Rad[1];

[1]TUM Klinikum Rechts der Isar, Munich, Germany, [2]Universitätsklinikum Freiburg, Freiburg, Germany, [3]Wellcome Trust Sanger Institute, Cambridge, United Kingdom, [4]TU Munich, Garching, Germany, [5]Newcastle University, Newcastle, United Kingdom, [6]National University of Quilmes (UNQ), Buenos Aires, Argentina, [7]University of Bologna, Bologna, Italy, [8]Dana-Farber Cancer Institute, Boston, MA, [9]The Institute of Cancer Research, Sutton, United Kingdom, [10]The Institute of Cancer Research, London, United Kingdom, [11]University Hospital of Wurzburg, Wurzburg, Germany, [12]LMU University Hospital, Munich, Germany, [13]German Cancer Research Center (DKFZ), LMU Munich, Munich, Germany, [14]Faculty of Medicine and University Hospital Cologne, Cologne, Germany, [15]University Hospital Essen, Essen, Germany, [16]Centro de Investigacion Biomedica en Red de Cancer, Instituto de Salud Carlos III, Madrid, Spain, [17]Spanish National Cancer Research Ctr. (CNIO), Madrid, Spain, [18]University Medical Center Gottingen, Gottinger, Germany

Oncogenes like *KRAS* display striking tissue specificity in their oncogenic potential, genetic interactions and phenotypic effects, but the underlying determinants remain largely unresolved.
To address such fundamental questions, we developed the Mouse Cancer Cell line Atlas (MCCA), a broad utility resource encompassing 590 comprehensively characterized models from a wide spectrum of entities. Comparative and functional studies using the MCCA resource, human cohorts and mouse models uncovered general principles guiding *KRAS*-initiated cancer evolution. We describe how tissue context affects diverse aspects of evolution, including the role of mutant *KRAS* gene dosage variation, the relevance of collaborating cancer pathways, or the sequential order of genetic alterations.
Mechanisms governing tissue-specific evolution transpired at different levels: First, we show that mutant *KRAS* dosage increase through allelic imbalance exerts cell type-specific effects, such as reactivation of developmental programs in the pancreas. Selection of such dosage-sensitive processes defines the timing of *KRAS* imbalance and its phenotypic outcomes in individual entities. Second, we highlight how tissue- and stage-specific evolutionary requirements, such as block of differentiation in the intestine, select for *KRAS*-collaborating alterations. Third, we uncovered tissue-specific epistatic interactions between *KRAS* imbalance and tumor suppression - as demonstrated for *CDKN2A*, which displays distinct levels of chromatin repression in different cell types. We show that resulting reciprocal dosage sensitivities dictate the entity-specific patterns of tumor suppressor alterations in human cancers, explaining their frequency, extent/zygosity and acquisition chronology.
These findings thus highlight how the interplay of pre-existing and acquired determinants instructs cancer evolution along deterministic trajectories in different tissues - with predictable quantitative molecular patterns, temporal dynamics and phenotypic outcomes. Our study provides major advances towards a mechanistic understanding of cancer genomes.

#6795 The Genomics England 100,000 genome programme: Allele-specific KRAS mutational signatures define distinct subtypes in lung adenocarcinoma.

L. C. Woodhouse[1], A. Hawari[1], A. Tapinos[1], A. Gruber[2], A. J. Cornish[3], Genomics England Research Consortium, D. C. Wedge[1], **C. R. Lindsay**[1];
[1]Division of Cancer Sciences, The University of Manchester, United Kingdom, [2]Department of Biology, University of Konstanz, Germany, [3]The Institute of Cancer Research, London, United Kingdom

Background: Lung cancer is the leading cause of cancer mortality worldwide. Somatic RAS mutations are the most common oncogenes in human cancer, and KRAS mutations are the largest molecular subset of lung adenocarcinoma (LUAD). Each cancer genome accumulates a unique combination of somatic mutations, and these mutational signatures provide a genetic imprint of mutational processes that have occurred during tumorigenesis. Mutational signatures provide information on tumor aetiology/maintenance and could inform potential therapeutic targets or early detection strategies.
Methods: Paired tumor and germline WGS data were obtained through the 100 000 Genomes Project (Genomics England). KRAS mutations were annotated using Ensembl Variant Effect Predictor (VEP) v109.0. Single base substitution (SBS), doublet base substitution (DBS), small insertion and deletions (ID), structural variant (SV) and copy number (CN) mutational signature extraction was performed using SigProfiler (COSMIC version 3.4). Survival analysis was performed using multivariate cox-proportional hazard models, adjusting for clinical stage and patient age at diagnosis. Statistical analyses and plotting were performed in R (version 4.2.1), with two-tailed p-values <0.05 considered statistically significant.
Results: 680 LUAD patients were included; 301 KRAS mutant (44%) and 379 KRAS wild type (56%). 64 mutational signatures were extracted from the LUAD cohort, comprising 23 SBS, 10 DBS, 12 Indel, 9 CN and 10 SV signatures. Unsupervised clustering revealed three distinct mutational signature subsets, reflecting different mutagenic origins and biological pathways: a smoking-associated cluster (cluster 2), an APOBEC non-smoking-associated cluster (cluster 3) and a clock-like non-smoking-associated cluster (cluster 1). As anticipated, cluster 2 was strongly associated with KRAS mutation. However, KRAS allele-specific profiling revealed striking variation of smoking impact: G12C and G13C variants displayed strong tobacco-derived mutational signatures, including direct probabilistic associations inferred at the individual KRAS somatic variant level. G12D was more commonly associated with clock-like related mutational processes and RBM10 mutation. G12A was enriched for normal diploid segments (CN1). Finally, CN6, SV2 and SV9 signatures were independently associated with inferior overall survival in a KRAS-dependent context.
Discussion: This is the largest study to date to profile KRAS mutant LUAD mutational signatures using whole genome sequencing (WGS) data. KRAS allele-specific profiling reveals distinct mutational and co-mutation contexts that define biologically and clinically meaningful subtype heterogeneity. Many KRAS-mutant subtypes in LUAD are not a direct consequence of smoking.

#6796 AI enabled imaging and single cell multiomics reveal how gene amplification architecture shapes gene expression.

Y. Wang[1], J. Chen[2], O. Cope[1], A. Mehta[1], D. Fleifel[1], C. Gutierrez-Ford[1], P. Behnamie[1], S. Haase[1], S. Gulec[1], T. C. Elston[1], P. M. Spanheimer[2], C. Tomblin[3], A. Rojas[3], T. Tate[3], J. E. Purvis[1], J. Wang[4], J. M. Dahl[3], S. Wolff[1], J. Cook[1], **E. C. Brunk**[1];

[1]University of North Carolina at Chapel Hill, Chapel Hill, NC, [2]UNC School of Medicine, Chapel Hill, NC, [3]Bioskryb Genomics, Durham, NC, [4]UNC School of Medicine, NC

Cancer cells often carry large gene amplifications that can arise through very different structural mechanisms. In some tumors, amplified oncogenes reside on circular extrachromosomal DNA, or ecDNA. In others, the same oncogenes reside within chromosomes in homogeneously staining regions, or HSRs. While HSRs propagate through conventional chromosomal segregation, ecDNA replicates and divides unevenly, creating extreme variation in oncogene dosage from cell to cell. These architectural differences are increasingly linked to aggressive tumor behavior, therapeutic resistance, and rapid evolution, yet their functional and molecular consequences remain poorly understood. Traditional bulk sequencing cannot distinguish ecDNA from HSRs, and imaging based detection has relied on manual, low throughput workflows, limiting our ability to assess amplification architecture across cell populations. To address this challenge, we developed AI based imaging tools that automatically identify ecDNA and HSRs in fluorescence microscopy images and classify amplification architecture across hundreds of nuclei per experiment. In parallel, we created computational approaches that infer amplification architecture directly from single cell sequencing data, using the characteristic copy number patterns generated by ecDNA versus HSR based amplification. These automated tools provide scalable, reproducible structural profiling of cancer cells. We integrated these structural assignments with 10x Genomics single cell multiome data and BioSkryb ResolveOME, which provides whole genome and whole transcriptome profiles from the same individual cells. We applied this framework to six human cancer cell lines, three dominated by ecDNA and three dominated by HSR amplifications. Across these models, the frequently amplified oncogenic locus PVT1 offered a shared point of comparison. The data revealed striking differences between the two amplification types: Genes amplified on ecDNA showed broad spreads of expression and distinct isoform usage, including a consistent PVT1 isoform whereas HSR amplifications produced tighter, more predictable transcriptional profiles. These findings suggest that ecDNA enables tumors to access a wider range of transcriptional states that may support bet hedging and drug resistant phenotypes. HSRs may stabilize expression programs, emerging through ecDNA reintegration under selective pressure. Together, these results demonstrate how AI enabled imaging and computational inference, combined with single cell multiomics, can uncover the hidden architecture of oncogene amplification in cancer and link it directly to transcriptional output. This framework provides a scalable path for understanding how genome organization drives tumor evolution, therapeutic resistance, and cancer aggressiveness.

#6797 Basal-state origins and genotype-specific trajectories of neuroendocrine plasticity in lung cancer.

M. Wang[1], A. Sabet[1], S. Rakhade[2], E. Spanos[1], L. Morrill Gavarro[1], R. Giri[1], P. Manoj[1], H. A. Yu[1], A. Quintanal-Villalonga[1], J. T. Poirier[3], E. Redin[1], D. Pe'er[1], C. M. Rudin[1], **J. M. Chan**[1]; [1]Memorial Sloan Kettering Cancer Center, New York, NY, [2]Herbert Irving Comprehensive Cancer Ctr., New York, NY, [3]NYU Langone Health Perlmutter Cancer Ctr., Brooklyn, NY

Neuroendocrine (NE) lineage plasticity is a unifying mechanism of therapeutic resistance across lung cancers, enabling adenocarcinomas (LUAD) to evade targeted therapies (e.g. EGFR, KRAS) and adopt high-grade NE histologies, including small cell lung cancer (SCLC) and large cell neuroendocrine carcinoma (LCNEC). The conserved early states and genotype-specific trajectories driving NE plasticity remain unclear.We integrated targeted DNA sequencing, 10X single-cell transcriptomics (75 samples, 52 patients), and Xenium spatial imaging (22 samples, 16 patients) across NE-transformed lung cancers. Both *EGFR*-mutant (mut) and -wildtype (wt) transformed SCLC showed recurrent chromosomal instability and PI3K/AKT activating mutations. *EGFR*-mut cases were enriched for *RB1* loss, whereas *EGFR*-wt had more *CDKN2A* loss as well as *KRAS*, *STK11*, and *KEAP1* mutations. Single-cell data showed greater NE subtype diversity in transformed versus *de novo* NE cancers as well as dynamic transitions between NE and non-NE states. Our computational approaches (scDeBussy pseudotime alignment, factor analysis) converged on a conserved basal-like precursor enriched for JAK/STAT and NF-κB signaling that seeds multiple terminal outcomes, including NE, squamous, and mesenchymal fates. To identify regulators of the basal-to-SCLC transition, we compared transformed and *de novo* SCLC and found *PHOX2B*as the transcription factor most correlated with NE state. *PHOX2B* overexpression in *EGFR*-mut LUAD cells with *TP53/RB1* co-mutations induced NE markers, amplified by *MYC* activation and *REST* suppression. Although insufficient for full SCLC morphology, *PHOX2B* suppressed MAPK signaling (ERK/pERK), consistent with plasticity promoting EGFR independence. Recognizing *STK11/KEAP1* co-mutations as an alternate route to NE plasticity, we analyzed NE tumors with these mutations. LCNEC showed highest frequency of *STK11* and *KEAP1* loss (28-31%) exceeding LUAD or SCLC (10-11%, 1-4%). Regulatory network analysis in LCNEC found a *FOXA2-HNF1/4A* axis reactivating a hepatic developmental program alongside NRF2-aldoketoreductase (AKR)-driven redox adaptation. Spatial imaging uncovered intratumoral zonation of immune-hot and -cold NE states, shaped by immunosuppressive cell-cell interactions (*FGL1-LAG3*, *VEGFA-VEGFR*).Together, these studies delineate a shared basal precursor to NE plasticity with later divergence shaped by genotype. *PHOX2B* represents a late molecular event inducing early NE induction and MAPK bypass in *EGFR*-mut tumors, while *STK11/KEAP1*-mut LCNEC coopts a distinct hepatic-NE program linked to metabolic and immune remodeling. This framework reveals biomarkers and vulnerabilities across early and late stages of LUAD-to-NE transformation, including inflammatory precursors, signaling bypass, metabolic rewiring, and immune evasion, offering multiple points for intervention across NE lung cancers.

#6798 Mechanistic dissection of regulators of cancer plasticity using high-content optical pooled screens at clonal resolution.

M. Godzik[1], R. Walton[1], M. Bogaev[2], L. Bi[3], J. Dilly[1], M. Jankowiak[3], E. Donnard[3], D. T. Ting[4], N. Hacohen[5], E. S. Lander[3], P. Blainey[1], A. Mehta[6];
[1]Massachusetts Institute of Technology, Cambridge, MA, [2]Harvard University, Cambridge, MA, [3]Broad Institute of MIT and Harvard, Cambridge, MA, [4]Massachusetts General Hospital, Charlestown, MA, [5]Harvard Medical School, Cambridge, MA, [6]Column Group, San Francisco, CA

Cancer treatment failure is often attributed to two processes: selection for pre-existing resistant cells and cellular plasticity that allows drug-sensitive cells to become resistant. Plasticity is a hallmark of cancer, but we still lack a clear definition and a mechanistic understanding of how it is controlled in tumors. These gaps are especially problematic in pancreatic ductal adenocarcinoma (PDAC), where epithelial-to-mesenchymal plasticity (EMP) is thought to drive metastasis, tumor initiation, and resistance to therapy. Causally dissecting plasticity requires large-scale perturbation studies that systematically target many genes and measure how they reshape cell-state dynamics at single-cell resolution over weeks to months. Such studies must follow enough cells to observe rare state transitions and clonal heterogeneity, yet current methods force a tradeoff between (i) sufficient molecular phenotyping, (ii) temporal duration, and (iii) cellular throughput, limiting our ability to map regulators of plasticity at scale.

We set out to address both issues by (1) developing a screening platform that overcomes major limitations in existing paradigms to (2) enable discovery of the mechanistic underpinnings of cellular plasticity in pancreatic cancer. Using an engineered patient-derived PDAC model, we performed a paired single-cell CRISPRi transcriptomic screen (Perturb-seq) and high-throughput imaging-based optical pooled screen (OPS) of EMP across a panel of chromatin and transcriptional regulators. We identified factors responsible for distinct plastic behaviors by quantifying state transitions from a FACS-defined initial state linked to high-content imaging phenotypes for 150,000 clones, across 1000 genetic perturbations and 22 million cells after two weeks of sustained perturbation in culture. Crucially, this framework sorted regulators into distinct functional classes of plasticity control, including “maintenance” genes stabilizing the starting state, “transition” genes that biased state switching in one direction, and “catalytic” genes that regulated switching bidirectionally. Our methodology recapitulated many genes previously implicated in EMP and uncovered novel candidate “catalytic” targets that converge on H3K9me3-associated epigenetic reprogramming. This work clarifies how cell state is regulated at clonal resolution, identifies potential vulnerabilities in plastic tumor cells, and establishes a platform that can be extended to studies of cellular plasticity in other biological contexts.

#6799 Dissecting the epigenetic inter- and intra-tumor heterogeneity of glioma at single-cell resolution.

Y. Wu[1], J. Zhou[2], Z. Deng[1], K. Komandur[1], K. L. Hung[3], Q. Zheng[4], A. bartlett[4], J. Nery[4], R. G. Castanon[4], T. Beaumont[5], J. Dixon[4], J. R. Ecker[6];
[1]Salk Institute for Biological Studies, La Jolla, CA, [2]Arc Institute, Palo Alto, CA, [3]Scripps Research, La Jolla, CA, [4]Salk Institute, La Jolla, CA, [5]UC San Diego Health, San Diego, CA, [6]Salk Institue for Biological Studies, La Jolla, CA

Adult diffuse gliomas include IDH-mutant astrocytomas and oligodendrogliomas, as well as IDH-wildtype glioblastomas (GBM), the latter marked by extreme cellular plasticity. Bulk genomic studies from TCGA defined molecular subtypes, but how epigenetic programs coordinate state transitions within tumors remains unresolved. In this study, we applied single-nucleus methylome and 3D genome profiling (snm3C-seq) to 40 human gliomas and interrogated the heterogeneity of DNA methylation and chromatin structure within tumor and across donors. We assigned DNA methylation and chromatin conformation (Hi-C) cell states to individual cells. We reported the following results: 1) Cross-modal state mapping: Most tumors contain large fractions of OPC-like or Astro-like cells with strong concordance between methylation (mC) and Hi-C states. However, certain clusters of cells have discordant mC and Hi-C states, indicating transitional phenotypes. 2) Temporal discrepancy: We observe asynchronous remodeling, where chromatin architecture often shifts towards more differentiated states before DNA methylation during lineage transitions. For example, many cells are OPC-like in methylation and AC-like in chromatin conformation, suggesting 3D genome reorganization as an early indicator of fate change. 3) Copy number alterations in tumor associated normal cells: we detected CNV mosaicism in a large proportion of non-malignant cells, yet their methylation profiles are more similar to normal cells than cancer cells. 4) Clonal evolution and structural variants (SV): Clonal analysis by copy number reveals that some new malignant clones arise with global methylation loss. In contrast to the heterogenous copy number changes in cancer cells, structural variants are often shared by the majority of cancer cell proportions. However, the occurrence of new SV drives cell state transition more strongly than copy number changes. Lastly, we observed that extrachromosomal DNA (ecDNA) are frequently found in WT GBM and they are associated with local epigenetic rewiring at amplified loci. These insights nominate epigenetic states as a biomarker of plasticity and a potential guide for patient-specific interventions.

: Immunotherapy: Mechanisms and Responses
Minisymposium

#6740 Selective immune activation of antigen activated T cells with STK-012, an a/b IL-2 receptor biased partial agonist, with pembrolizumab and chemotherapy in 1L PD-L1 negative non-squamous NSCLC.

S. Punekar[1], A. J. Schoenfeld[2], E. B. Garon[3], S. Y. Kim[4], K. He[5], J. Marks[6], B. S. Henick[7], S. V. Liu[8], N. Seetharamu[9], A. Spira[10], J. Gainor[11], T. Larson[12], T. A. Leal[13], C. Oswalt[14], B. Izar[15], A. Marangoz-Stager[16], V. Danh[16], G. Lunardi[16], K. Bach[16], N. A. Rizvi[16], A. Azrilevich[16], A. Mehta-Damani[16], M. Oft[16];
[1]NYU, New York, NY, [2]Memorial Sloan Kettering Cancer Center, New York, NY, [3]University of California (UCLA), Santa Monica, CA, [4]Yale, New Haven, CT, [5]The Ohio State University Wexner Medical Ctr., Columbus, OH, [6]DFCI, Boston, MA, [7]Columbia University, New York, NY, [8]Georgetown University, Washington, DC, [9]Northwell Health, Great Neck, NY, [10]Virginia Cancer Specialists, Fairfax, VA, [11]Mass General Hospital, Boston, MA, [12]HealthPartners, Minneapolis, MN, [13]Emory University, Atlanta, GA, [14]Duke University, Durham, NC, [15]Columbia University Irving Medical Center, New York, NY, [16]Synthekine, Menlo Park, CA

Background: STK-012 is a first-in-class α/β-IL-2R biased partial agonist that drives antitumor activity by selectively stimulating CD25+ antigen-activated T-cells and avoids hallmark IL-2 toxicities by sparing pleiotropic activation of lymphocytes including NK cells. In this phase 1a/b study, STK-012 is combined with standard of care pembrolizumab + chemotherapy (PCT) in 1L PD-L1 negative NSQ NSCLC where PCT alone has poor outcomes (ORR 32% and median PFS 6.2 months).
Methods: 1L NSQ NSCLC subjects received STK-012 SC Q3W + PCT. Serial blood samples were analyzed for changes in cytokines in chemoluminescence assays, T cell proliferation and activation markers were analyzed in spectral flow cytometry, and T cell clonality was analyzed by TCR sequencing. Data are shown for a cohort of 22 efficacy-evaluable 1L NSCLC subjects (N=18 PD-L1<1%, N=4 PD-L1=1%) which was enriched for loss-of-function tumor suppressor gene (LoF TSG) mutations (n=11; STK11, KEAP1, SMARCA4) or mucinous histology (n=5) associated with a “cold” TME and primary immune resistance.
Results: STK-012 + PCT demonstrated an ORR of 55% in all efficacy evaluable patients; 50% in patients with PD-L1<1% tumors; 55% in LoF TSG mutations; and 80% in mucinous histology. STK-012 + PCT induced sustained proliferation of CD8+ and CD4+ T cells (13X and 5x increase from baseline, respectively), proliferation of antigen activated T cells including PD-1+ CD8+ (14X) and 4-1BB+ CD8+ (14X) and re-invigoration and proliferation of previously exhausted CD39+ (11x) and TIM3+ (18x) CD8+ T cells. After the first cycle, 3.35% of the total T cell repertoire were T cell clones which were newly detected or expanded ≥10x (n=12). STK-012 + PCT induced key cytokines IFNγ and IL-18 characterizing an activated CD8+ T cell response and increased IP-10 which is associated with enhanced T cell trafficking into tumor tissues (13x,14x and 23x mean increase from baseline, respectively). Sustained elevation of cytokines across treatment cycles (IFNγ median peak of 71, 95, 96 pg/mL in C1, C2 and C6) was observed, supportive of the emerging durability of the combination. Induction of cytokines TNFα and IL-6 was limited (median peak 4, 6 pg/mL), consistent with limited activation of naïve T cells and NK cells and the lack of capillary leak syndrome with STK-012.
Conclusions: STK-012 + PCT led to robust cytokine induction, proliferation and expansion of antigen activated T cells, proliferation of previously exhausted T cells, and remodeling of the T cell repertoire. The addition of STK-012 to PCT has the potential to overcome resistance in immune excluded populations including PD-L1<1% tumors, LoF TSG mutations and mucinous histology. A global, randomized Phase 2 study, SYNERGY-101, of STK-012 + PCT vs. PCT in 1L PD-L1<1% NSQ NSCLC is ongoing (NCT05098132).

#6741 Tertiary lymphoid structure (TLS)-associated immune circuits define response to durvalumab, trastuzumab, and pertuzumab (DTP) in HER2-enriched early breast cancer.

M. Li[1], X. Hoi[1], J. Deng[1], J. Zheng[1], R. Hashmani[1], R. Bayraktar[1], W. Qian[1], J. Zhou[1], J. Guan[2], K. Sun[2], H. Mai[2], T. Sheu[2], S. Haley[2], M. Schwartz[2], S. Mathur[1], S. T. Wong[2], F. Nikolo[1], K. Chan[1], P. Niravath[2], J. C. Chang[1];

[1]Houston Methodist Research Institute, Houston, TX, [2]Houston Methodist Hospital, Houston, TX

Background: Chemotherapy-free regimens combining HER2-targeted therapy with immune checkpoint blockade are emerging as promising strategies in HER2-Enriched breast cancer. In our Phase II trial of durvalumab, trastuzumab, and pertuzumab (DTP), ER-negative, PR-negative, HER2-Enriched tumors (BluePrint®) achieved a 49% Pathologic Complete Response (pCR) rate, suggesting an immunologically responsive subset. To define the cellular mechanisms underlying response and resistance to this chemotherapy-free approach, we performed single-nucleus RNA sequencing and spatial transcriptomic profiling on paired tumor samples.

Methods: Paired pre-treatment and surgical biopsies (n=37) underwent snRNA-seq to profile immune composition, functional states, and lineage dynamics. Patients were stratified by Residual Cancer Burden (RCB), with RCB-0 considered Responders (n=18) and RCB-2/3 as Nonresponders (n=6). Cell identities were label-transferred to Xenium 5K spatial transcriptomic data to assess cellular localization and interactions within the tumor microenvironment.

Results: We recovered 470, 997 high quality nuclei, including 168,516 immune cells. Pre-treatment Responder samples were enriched for CD4+ T follicular helper cells ($CD4^+CXCL13^+PD\text{-}1^+$ Tfh), CD8+ tissue-resident memory T cells (CD8+ Hobit+ Trm), and CD8+ exhausted T cells (CD8+Tim3+PD-1+ Tex), along with higher frequencies of LAMP3+ mature dendritic cells (mDCs), and naïve B-cells. Spatial mapping revealed co-localization of Tfh, mDCs, and B-cell subsets within tertiary lymphoid structures (TLS) spanning multiple maturation stages. CellChat analyses demonstrated Responders exhibiting a coordinated Tfh-mDC-B-cell communication network enriched in CXCL13-mediated B-cell recruitment, CD40 and CD28 costimulation, and cytokine programs supporting TLS maturation. In contrast, Nonresponders engaged predominantly inhibitory signaling pathways, marked by CD22-mediated suppression, BTLA-HVEM immune dampening, and reduced chemokine guidance, consistent with abortive B-cell activation.

Conclusions: Integrated single-nucleus and spatial transcriptomic profiling identifies coordinated Tfh-B-cell and dendritic-B-cell interactions, spatially organized within TLS, as dominant determinants of response to DTP therapy in HER2-Enriched early breast cancer.

Clinical trial information: NCT03820141.

Research Sponsors: Houston Methodist Hospital and AstraZeneca.

#6742 Nonsense-mediated mRNA decay inhibition augments *in vitro*, *in vivo*, and *ex vivo* anti-tumor immunity.

Hongchang Fu[1], Roberto Vendramin[1], Shanila Fernandez Patel[1], Yue Zhao[1], Danwen Qian[1], Lorena Ligammari[1], Osnat Bartok[2], Polina Greenberg[2], Ronen Levy[2], Andrea Castro[1], Krupa Thakkar[1], Jun Murai[3], Wei-ting Lu[4], Christopher C. T. Sng[1], Chen Weller[2], Gordon Beattie[5], Amandeep Bhamra[6], Roc Farriol-Duran[7], Despoina Karagianni[1], Marcellus Augustine[1], Krijn Djikstra[8], Christopher L. Pinder[1], Benjamin S. Simpson[1], Gordon Weng-Kit Cheung[9], TRACERx Consortium, Felipe Galvez Cancino[10], Petra Vlckova[11], Silvia Surinova[6], Manuel Rodriguez-Justo[12], Mansi Shah[13], Nicholas McGranahan[1], Jeremy G. Carlton[14], Eva Camilla Gronroos[4], Sergio Quezada[15], James Luke Reading[9], Samra Turajlic[16], Yardena Samuels[2], Charles Swanton[4], Kevin Litchfield[1]

[1]Department of Oncology, University College London Cancer Institute, London, United Kingdom,[2]Department of Molecular Cell Biology, Weizmann Institute of Science, Rehovot, Israel,[3]Drug Discovery Technology Laboratories, Ono Pharmaceutical Co. Ltd., Osaka, Japan,[4]The Francis Crick Institute, London, United Kingdom,[5]CRUK City of London Centre Single Cell Genomics Facility, University College London Cancer Institute, London, United Kingdom,[6]Proteomics Research Translational Technology Platform, University College London Cancer Institute, London, United Kingdom,[7]Barcelona Supercomputing Center (BSC), Barcelona, Spain,[8]Department of Molecular Oncology and Immunology, The Netherlands Cancer Institute, Amsterdam, Netherlands,[9]Department of Hematology, University College London Cancer Institute, London, United Kingdom,[10]Nuffield Department of Medicine, Immune Regulation Lab, University of Oxford, Oxford, United Kingdom,[11]Organoid Translational Technology Platform, University College London Cancer Institute, London, United Kingdom,[12]Department of Research Pathology, University College London Cancer Institute, London, United Kingdom,[13]CRUK City of London Explant and Patient-Derived Xenograft Core, London, United Kingdom,[14]School of Cancer & Pharmaceutical Sciences, King's College London, London, United Kingdom,[15]University College London Cancer Institute, London, United Kingdom,[16]CRUK Manchester Institute, Manchester, United Kingdom

Introduction: Neoantigens from somatic tumor mutations are essential for effective anti-tumor immune responses. Frameshift insertions and deletions (fs-indels) represent a rare but highly immunogenic mutation subtype, as they create novel open reading frames (neoORFs) that generate peptides that are significantly distinct from self-antigens. Nevertheless, fs-indels often introduce premature termination codons, leading to transcript degradation via the nonsense-mediated mRNA decay (NMD) pathway, leading to loss of immunogenic neoantigen.
Approach: For the first time, we pharmacologically inhibited SMG1, a core component of the NMD pathway, across a range of preclinical models, including human and mouse cancer cell lines, patient-derived tumor organoids (PDTOs), patient-derived tumor fragments (PDTFs), and syngeneic mouse xenografts. We analyzed the changes in transcriptome, proteome, and immunopeptidome following SMG1 inhibition (SMG1i) and peptide reactivity in *in vitro* priming experiments. We then combined tumor-T cell co-cultures and PDTFs to assess the anti-tumor immunogenicity induced by SMG1i. *Ex vivo* and *in vivo* immunological responses were assessed by high-dimensional flow cytometry, cytometric bead array, and single-cell RNA- and TCR-sequencing.
Results: Using multi-omic and checkpoint inhibitor (CPI) response data from over 1,000 patients, we show that decreased expression of the key NMD mediator, SMG1, correlates with improved CPI response. Inhibiting SMG1 *ex vivo* and *in vivo* activates and expands tumor-reactive T cells and sensitizes CPI efficacy. Mechanistically, SMG1 inhibition stabilizes frameshift-derived transcripts, increasing the abundance and surface presentation of immunogenic neoantigens. This results in an increase in neoepitope burden in tumors, similar to that seen in tumors with high tumor mutational burden (TMB), without inducing DNA damage. Co-culturing tumor cells and PDTOs with $CD8^+$ T cells after SMG1i results in strong MHC class I antigen-dependent T cell activation and tumor cell killing.
Conclusion: Our findings highlight SMG1 inhibition as a promising strategy to exploit an untapped source of highly immunogenic peptides. It enhances anti-tumor immunogenicity without introducing DNA mutations, regardless of tumor type or TMB status, providing translational evidence for sensitizing ICB responses.

#6743 Peripheral immune profiling from the DIET trial - A randomized double blinded dietary intervention study in melanoma patients receiving immunotherapy.

Yufan Qiu, Yan Jiang, Nazli Dizman, Courtney Nicholas, Yuwei Zhang, Sreyashi Basu, Elizabeth Burton, Michael A. Davies, Nadim J. Ajami, Padmanee Sharma, Jennifer A. Wargo, Jennifer L. McQuade, **Carrie R. Daniel**

UT MD Anderson Cancer Center, Houston, TX

Background: Dietary fiber intake is associated with improved response to immune checkpoint blockade (ICB) in melanoma. The phase II Diet and Immune Effects Trial (DIET, NCT04645680) was conducted in melanoma patients receiving ICB testing the effects of a high fiber diet intervention vs. healthy control diet. Our early results revealed that the high fiber diet intervention is feasible with promising improvements in treatment outcomes. Herein we report the secondary objective of the effects of dietary intervention on systemic immunity by arm.
Methods: Patients were randomized (2:1) to either a high fiber diet (30-50 g/d ramped-up fiber) or healthy control diet (20 g/d fiber). Cryopreserved paired (pre vs post dietary interventions) peripheral blood mononuclear cells (PBMC) were collected longitudinally and used for NanoString gene expression profiling and CyTOF mass cytometry analyses. For translational human-to-mouse fecal microbiota transplant (FMT) studies, mice received patient stool collected either pre or post high fiber intervention, followed by melanoma inoculation and anti-PDL1 treatment. Endpoint peripheral leukocytes and spleen specimens were collected for CyTOF mass cytometry.
Results: Using NanoString, we were able to identify decreased abundance scores of circulating macrophages (p=.018) and neutrophils (p=.035) (by cell type deconvolution) as well as classical monocytes (p=.06) and dendritic cells (p=.06) (Signature from Lam et al. Cell 2021) within week 5-8 of dietary intervention in high fiber (n=11) vs control arm (n=4). Pathway analysis showed higher transcriptional levels of T cell activation gene signature and T cell receptor signaling in the high fiber arm versus a higher level of Toll-like receptor signaling and type-1 interferon signaling in the control arm. These findings were validated at the protein level by CyTOF, which demonstrated reduced circulating classical monocytes (p=.0059) and increased frequency of effector-memory T cells (p=.01 in CD8+, p=.032 in CD4+) in the high fiber vs control arm within week 5-8 of dietary intervention. Within the high fiber arm, these findings were more prominent in those receiving combination nivolumab + ipilimumab (n=3) compared to those receiving pembrolizumab or nivolumab monotherapy (n=7). Human-to-mouse FMT studies also revealed an improved ICB response with lower frequency of monocytes and dendritic cells in post-high fiber diet stool recipients in the circulation and spleens.
Conclusion: Our analyses suggested microbiome-dependent benefits of a high fiber diet in reducing circulating monocytes and potentially enhancing T cell activation in the peripheral blood. Circulating monocyte levels are known to negatively correlate with ICB response, warranting further mechanistic study on dietary fiber mediated regulation of peripheral immunity during immunotherapy.

#6744 Persistent neuro-antigen-reactive Th17 cells drive IL-17-dependent neurotoxicity in CNS immune-related adverse events.

Yifei Ma[1], **Jingyao Zhang**[2], Fadian Ding[1], Ao Zhang[3], Jun Lv[4], Xinjia Wang[5], Weidong Wang[5], Guangmin Jian[4], Pengfei Zhu[4], Yue Ma[6], Jiacai Lin[7], Denghan Zhang[1], Guanqing Zhong[3], Rui Li[8], Haizhou Liu[1], Shangeng Weng[1]

[1]Fujian Medical University, Fuzhou, China,[2]Danbury Hospital, Danbury, CT,[3]Sun Yat-sen University Cancer Center, Guangzhou, China,[4]the First Affiliated Hospital of Zhengzhou University, Zhengzhou, China,[5]Cancer Hospital of Shantou University Medical College, Shantou, China,[6]Taiyuan Central Hospital of Shanxi Medical University, Taiyuan, China,[7]Hainan Hospital of Chinese PLA General Hospital, Sanya, China,[8]Institute of Neuroscience, Fujian Medical University, Fuzhou, China

Background: Immune checkpoint inhibitors (ICIs) have transformed cancer outcomes but can induce immune-related adverse events (irAEs) that limit therapy. Central nervous system irAEs (irAE-CNS) are rare, often corticosteroid-refractory, and lead to disabling neurological sequelae. Their immunopathogenesis remains poorly understood, hindering effective interventions. We aimed to define the immune mechanisms underlying irAE-CNS and identify therapeutic targets using multi-omics profiling and longitudinal clinical correlation.
Methods: We analyzed cerebrospinal fluid (CSF) from three independent irAE-CNS cohorts and controls (autoimmune encephalitis, CNS infection). Multi-omics profiling integrated OLINK proteomics, single-cell secretome and transcriptome analysis, and paired VDJ-TCR repertoire sequencing with FDG-PET/CT imaging, neurofunctional testing, and 15-month follow-up. Unsupervised clustering (Seurat) and clonotype mapping (CellRanger/IGBLAST) were used to define cell phenotypes and track longitudinal persistence. Neuroantigen reactivity was validated via MHC-multimer sorting and peptide libraries derived from neuronal surface proteins, including NMDAR1. Functional assays assessed T-cell-mediated neuronal cytotoxicity and the effects of IL-17 blockade.
Results: We identified a distinct population of $CD4^+CD137^+PD\text{-}1^+$ effector-memory T-helper cells ($Poly6^+$ Th cells) enriched in irAE-CNS, co-secreting IL-17A, TNFRSF9, CCL11, MCP-1, MCP-4, and Granzyme B, defining a polyfunctional Th17-like signature. $Poly6^+$ Th-cell frequency correlated with intracranial FDG-PET hypermetabolism especially within limbic regions, and with cognitive decline. Single-cell RNA-seq revealed stable $RORC^+IL23R^+GZMB^+$ transcriptional profiles, and VDJ analysis showed persistent, antigen-driven clonal expansion. Dominant clonotypes targeted NMDAR1 epitopes (notably EERITGINDPRLRNP), confirming neuroantigen-specific persistence. In co-culture assays, $Poly6^+$ Th cells induced neuronal apoptosis via IL-17-dependent mechanisms. In patients treated with IL-17 blockade, neurological symptoms and intracranial inflammation improved significantly without reducing ICI antitumor efficacy.
Conclusions: irAE-CNS is driven by persistent, NMDAR1-reactive Th17-like effector-memory cells that mediate IL-17-dependent neurotoxicity. These findings reveal a mechanistic basis for selective cytokine blockade to alleviate CNS autoimmunity while maintaining checkpoint efficacy, providing a framework for biomarker-guided management of ICI-associated toxicities.

#6745 NAT10-MYC loop induces MHC-I loss through autophagy to promote immune evasion and immunotherapy resistance in colorectal cancer.

J. Weng[1], T. Xiong[2], Z. Ye[3], Z. Shan[3], R. Su[4], J. Yu[5], M. A. Caligiuri[2], X. Li[3], A. Goel[6];

[1]Beckman Research Institute of The City of Hope, Duarte, CA, [2]City of Hope National Medical Center, Duarte, CA, [3]Fudan University Shanghai Cancer Center, Shanghai, China, [4]Beckman Research Institute of City of Hope, Monrovia, CA, [5]UC Irvine, Irvine, CA, [6]City of Hope, Duarte, CA

Background: Immune checkpoint inhibitors (ICIs) have significantly improved therapeutic outcomes in colorectal cancer (CRC), particularly for metastatic tumors with microsatellite instability-high (MSI-H) or deficient mismatch repair (dMMR). While patients with metastatic CRC have a median overall survival of only 21 months, MSI-H/dMMR patients treated with ICIs can achieve durable responses and even long-term survival. However, the vast majority are microsatellite-stable (MSS) and remain profoundly resistant to immunotherapy, underscoring a critical unmet clinical need. Therefore, elucidating and overcoming the mechanisms that drive immune resistance is essential to broaden the therapeutic benefit of immunotherapy.

Methods: We investigated the role of the RNA acetyltransferase NAT10, responsible for N4-acetylcytidine (ac^4C) modification, in mediating immune escape in CRC. MYC-mediated transcriptional regulation and NAT10-dependent mRNA stabilization were analyzed. The stability of autophagy-related transcripts and MHC class I expression was assessed. The effects of NAT10 inhibition, achieved through genetic knockdown or pharmacological Remodelin treatment, on immune cell infiltration and response to immune checkpoint blockade were evaluated.

Results: *NAT10* was found to be significantly upregulated in CRC across multiple cohorts, with higher expression in MSS tumors compared to MSI-H tumors (p<0.01-0.001). Elevated *NAT10* expression correlated with immune-cold phenotypes, poorer predicted immunotherapy response, and was negatively associated with T-cell activation genes (p<0.01). NAT10 positively regulated autophagy-lysosome genes, including *BECN1*, *ATG3*, and *ATG5*, through direct ac^4C modification, enhancing their mRNA stability (p<0.05). NAT10 knockout reduced autophagic flux (p<0.001), increased MHC-I expression (p<0.01), and promoted infiltration and activation of $CD8^+$ and $CD4^+$ T cells, leading to enhanced tumor cytotoxicity and suppressed tumor growth, effects that were abrogated by CD8 depletion. A combination of NAT10 knockout with anti-PD-1 therapy resulted in 80% complete tumor regression. MYC was identified as an upstream activator of NAT10, with *MYC* mRNA itself modified by ac^4C. MYC deletion reduced NAT10 expression, global ac^4C levels, and autophagy. Remodelin synergized with anti-PD-1 treatment, underscoring NAT10 as a druggable epitranscriptomic-autophagy checkpoint.

Conclusion: Our findings reveal a novel NAT10-MYC-autophagy axis that drives MHC-I degradation and orchestrates tumor immune evasion and resistance to immunotherapy in CRC. Targeting NAT10 represents a promising therapeutic strategy to overcome immune resistance and enhance the efficacy of immunotherapy in CRC.

#6746 Biomarker-driven restoration of tumor provisional matrix signaling network reverses resistance to checkpoint inhibition immunotherapy.

D. J. Lagal[1], D. Hong[1], A. Papadas[2], E. Geatches[1], G. Yacu[1], S. Naik[1], A. Gibbons[3], A. Cicala[4], K. Pestonjamasp[3], P. Toth[5], K. Matkowskyj[6], D. A. Deming[7], F. Asimakopoulos[1];
[1]Rush University Medical Center, Chicago, IL, [2]Ohio State University, Columbus, OH, [3]University of California, San Diego, La Jolla, CA, [4]Cold Spring Harbor Laboratory, Cold Spring Harbor, NY, [5]University of Illinois at Chicago, Chicago, IL, [6]Mayo Clinic, Rochester, MN, [7]University of Wisconsin Carbone Cancer Center, Madison, WI

Specialized immune niches located in the stroma-tumor junction promote interactions between tumor-resident antigen-presenting cells and effector lymphocytes that are required for immunotherapy efficacy. We have hypothesized that this stromal-based immune crosstalk may be regulated by provisional extracellular matrix signals, analogous to the early-stages of wound healing where provisional matrix hosts robust immune activity. A cardinal provisional matrix remodeling event, the regulated proteolysis of the large proteoglycan versican (VCAN) generates an immunomodulatory fragment (matrikine), versikine, that engages adaptive immunity. We have previously shown that VCAN proteolysis correlates with T-cell infiltration across multiple solid and liquid cancers with the most immune-evasive cancers showing low to negligible rates of VCAN proteolysis (e.g., 0% in pancreatic adenocarcinoma). A recent clinical trial generated informative prospective data linking VCAN proteolysis with immunotherapy outcomes: patients whose metastatic colorectal tumors categorized as VCAN proteolysis-weak (VPW, 60% of cases) demonstrated inferior responses to checkpoint inhibition (CPI, pembrolizumab) and worse outcomes compared to VCAN proteolysis-predominant (VPP, 40%) cases. Leveraging these prospective trial data, we hypothesized that versikine therapy may rationally reverse the immunosuppression associated with the prevalent VPW phenotype. To tailor versikine therapy to specific human biomarker-stratified tumor phenotypes, we studied experimental models replicating partially T-permissive VPW-VCAN^{lo} human cancers and poor-prognosis, immune-exclusionary VPW-VCAN^{hi} cancers. Across VPW-like tumors, versikine promoted the stromal accumulation of CD40lg^{hi}Icos^{hi}Foxp3^{neg} Tfh-like CD4+ T cells that engaged dendritic cells (DC) and CD8+ T cells in “immune triads” even at baseline (prior to CPI), concurrently with the intratumoral expansion of activated CD8+ T cells expressing cytolytic molecules (granzymes, perforin). In VPW-VCAN^{lo} tumors, versikine delivered as LNP-mRNA or recombinant protein demonstrated monotherapy activity, dependent on Batf3-lineage DC and CD8+ T cells. When combined with single-agent CPI, versikine cured most VPW-VCAN^{lo} tumors with memory to tumor re-challenge. In VPW-VCAN^{hi} tumors, versikine synergized with combination immunotherapy modulating “mature DCs enriched in immunoregulatory molecules” (mregDC). Our data provide mechanistic rationale for the biomarker-stratified, therapeutic restoration of a provisional matrix-regulated immune signaling network to reverse resistance to CPI. Moreover, the data highlight the need to reevaluate prior approaches to globally disrupt tumor stroma in favor of biomarker-driven, pathway-focused harnessing of stromal signals that modulate anti-tumor immunity.

: Inflammation and Immunity in Cancer Progression
Minisymposium

#6785 Evasion of hepatic ILC1 immunosurveillance drives breast cancer liver metastasis.
P. Li, J. Li, A. Cornish, J. Zhang, X. Zhang, M. Li;
Memorial Sloan Kettering Cancer Center, New York, NY

Metastasis is a complex biological process and the principal cause of cancer-related mortality. With dual blood supply and fenestrated sinusoids, the liver's haematogenous route uniquely favors seeding by circulating tumor cells (CTCs). Nonetheless, while portal drainage promotes frequent liver metastases from proximal gastrointestinal cancers such as colorectal carcinoma, hepatic colonization by systemically disseminated CTCs, including those originating from breast cancer, is highly inefficient. The cellular barriers and evasion mechanisms that govern this selective vulnerability remain poorly understood. Here we show that hepatic type 1 innate lymphoid cells (ILC1s) are selectively required for the immunosurveillance of breast cancer liver metastasis, the evasion of which is driven by both cancer cell-intrinsic and microenvironment-associated immune mechanisms. In a large patient cohort, liver metastasis occurred at a relatively later stage and was associated with poorer survival, with body mass index (BMI) above the WHO optimal range associated with higher risk. This metabolic vulnerability was recapitulated in a murine preclinical model, in which breast cancer CTC colonization of the liver—but not the lung—was promoted by a high-fat diet that induced hepatic steatosis. Mechanistically, NK cells expanded and activated in response to CTC challenge and employed both lytic granule and death receptor 5 (DR5, encoded by *Tnfrsf10b*) pathways for cancer cell clearance, hepatic ILC1s preferentially utilized DR5-mediated mechanisms and required high DR5 expression in cancer cells. Notably, loss of heterozygosity of *TNFRSF10B* in breast tumours was associated with a predisposition to liver metastasis, and poorer patient prognosis. Conversely, metabolic dysfunction-associated steatotic liver disease (MASLD), a pathological risk factor for breast cancer liver metastasis, correlated with depletion of hepatic group 1 innate lymphoid cells—a phenomenon recapitulated in high-fat diet-fed mice. Importantly, the high-fat diet-induced reduction in hepatic ILC1s and enhancement of breast cancer liver metastasis were reversed by treatment with glucagon-like peptide-1 (GLP-1) receptor agonists. Collectively, these findings reveal that breast cancer liver metastasis is primarily restrained by liver-resident ILC1s rather than circulating NK cells. Evasion of this immunosurveillance can arise from cancer cell-intrinsic genomic alterations that compromise DR5 sensitivity or from microenvironmental metabolic perturbations that diminish ILC1 function. Restoration of hepatic ILC1 activity by GLP-1 receptor agonists highlights a potential translational opportunity to extend these agents beyond metabolic disease into oncology, with innate lymphocyte-mediated cancer immunosurveillance as a distinct mechanism of action

#6786 Neutrophil extracellular trap inhibition mitigates tumor necrosis and metastasis in colorectal cancer.

E. Gazzara[1], A. Jose[2], S. Dziadowicz[1], S. Han[1], A. Liu[1], Z. Aminzada[1], N. Bhandari[1], V. Shirue[3], B. Shergill[3], M. Curtis[3], S. C. George[3], A. Cicala[1], A. Rishi[4], C. Devoe[4], H. Huang[5], M. Weiss[4], E. Lou[6], D. A. Tuveson[1], S. Beyaz[1], P. M. Westcott[1], M. Egeblad[7], **S. Gholami**[8];

[1]Cold Spring Harbor Laboratory, Cold Spring Harbor, NY, [2]The Francis Crick Institute, London, United Kingdom, [3]University of California Davis, Sacramento, CA, [4]Northwell Health, New Hyde Park, NY, [5]The Feinstein Institutes for Medical Research, Manhasset, NY, [6]University of Minnesota Medical School, Minneapolis, MN, [7]Johns Hopkins University School of Medicine, Lutherville-Timonium, MD, [8]Cold Spring Harbor Labortory, Cold Spring Harbor, NY

Neutrophils (polymorphonuclear cells, PMNs) have been shown to directly induce necrosis through the formation of neutrophil extracellular traps (NETs) in murine models of breast and lung cancer. Although necrosis is a well-recognized predictor of poor outcomes in cancer, it is typically regarded as a passive and non-targetable process. To determine whether NETs actively drive necrosis in colorectal cancer (CRC), we evaluated the pathogenic impact of NET formation in human CRC specimens and complementary preclinical models.In blood samples from patients with CRC, we identified elevated populations of neutrophils primed for NET formation, including an expanded $CD177^{Low}$ subset that retained strong NET-forming capacity with reduced extravasation ability. Histologic and immunofluorescent analyses of human CRC and colorectal liver metastases demonstrated abundant NET accumulation within necrotic regions, forming intravascular deposits. The extent of necrosis correlated with metastatic disease, independent of tumor size. Single-cell RNA sequencing and spatial transcriptomic profiling of human primary CRC and liver metastases showed that NET-rich necrotic tumors activate transcriptional programs associated with myelopoiesis (CSF1, CXCL2, CXCL12), hypoxia signaling, migration, and epithelial-to-mesenchymal transition—features linked to increased metastatic potential. In a mismatch-repair-proficient orthotopic CRC model using AKPS (APC^{KO} $KRAS^{G12D}$ $P53^{KO}$ $SMAD4^{KO}$) organoids implanted via colonoscopic injection, tumor progression was marked by rising circulating PMNs, bone marrow skewing toward myelopoiesis, and increasing NET deposition within necrotic tumor regions. Genetic and pharmacologic inhibition of NET formation reduced intratumoral necrosis and significantly decreased metastatic burden. Collectively, these findings demonstrate that NETs are active drivers of necrosis and metastatic evolution in CRC, reframing necrosis as an immunopathologic process rather than an unavoidable consequence of tumor growth. Targeting NET formation represents a promising translational strategy to improve disease control and oncologic outcomes for patients with CRC.

#6787 Metabolic reuse of tumor-derived signals coordinates dendritic cell function.

M. Belabed[1], C. Y. Moon[1], M. D. Park[1], C. Blouin[2], S. Balan[1], M. krishnamurthy[1], G. Freed[1], M. Quijada-lamo[1], J. Le Berichel[1], S. Ghosh[3], C. Rothlin[3], T. U. Marron[4], E. Wagenblast[1], N. Bhardwaj[4], C. Lamaze[2], D. J. Puleston[1], M. Merad[1];

[1]Icahn school of medicine at Mount Sinai, New York, NY, [2]Institut Curie, Paris, France, [3]Yale University School of Medicine, New Haven, CT, [4]The Tisch Cancer Institute, New York, NY

Dendritic cells (DCs) are central initiators of antitumor immunity, requiring not only the efficient acquisition of tumor antigens but also the activation of maturation programs that license them to prime T cells. Beyond capturing cellular debris, DCs can repurpose tumor-derived metabolites to support these immunogenic functions, yet how this metabolic reuse shapes DC behavior within the tumor microenvironment remains unclear. We show that DCs mobilize cholesterol recovered from tumor cells (together with newly synthesized pools) to reorganize their plasma membrane and assemble lipid nanodomains that potentiate signaling pathways essential for full maturation. In parallel, polyamines enriched in the tumors act as complementary metabolic cues that facilitate the capacity of DCs to internalize antigens through a Rac-dependent mechanism. Together, these findings reveal that DCs integrate multiple tumor-derived metabolites to tightly couple antigen acquisition with the structural and signaling transitions that drive their maturation. This metabolic cross-talk between tumors and DCs emerges as a key determinant of effective immune priming and highlights cholesterol flux and polyamine pathways as potential targets to enhance DC-mediated antitumor immunity.

#6788 Spatial single-cell analysis reveals stage-dependent mechanisms of anti-IL-1β therapy in lung adenocarcinoma.

B. Zhu[1], M. Aminu[2], Y. Tian[1], S.-W. Lu[1], O. Shi[1], W. Lu[1], H. Chen[2], H. Li[1], Z. Wei[1], M. B. Nilsson[1], L. Solis Soto[1], F. P. Andrew[1], D. L. Gibbons[1], J. V. Heymach[1], C. Cheng[3], J. Wu[1], J. Zhang[1]; [1]UT MD Anderson Cancer Center, Houston, TX, [2]The University of Texas MD Anderson Cancer Center, [3]Baylor College of Medicine, Houston, TX

Introduction: Lung adenocarcinoma (LUAD) is a leading cause of cancer mortality, with IL-1β-driven inflammation playing a central role in tumor progression. Although IL-1β blockade shows promising antitumor effects, its efficacy varies across tumor stages, and the mechanisms behind this stage-dependent response remain unclear. Here, we investigate how tumor-immune interactions and microenvironmental remodeling shape differential responses to anti-IL-1β therapy during LUAD progression.
Methods: We performed spatial single-cell analysis of the immune microenvironment using Visium HD on human (10 adjacent normal, 17 AAH, 12 IAC) and mouse samples (21 adjacent normal, 57 hyperplasia, 13 IAC). Integrating these data with stage-matched scRNA-seq, we mapped IL-1β-IL1R1-mediated cell-cell interactions across LUAD stages. Long-term anti-IL-1β treatment was evaluated in two mouse models—C57BL/6 Kras^G12D (early: 4-14 weeks; late: 20-30 weeks) and 129S4 urethane-induced (early: 4-14 weeks; late: 30-40 weeks)—with efficacy and mechanisms assessed via scRNA-seq and Xenium 5K. Short-term treatments (0, 6, 30 weeks) in C57BL/6 Kras^G12D were performed to further explore mechanisms.
Results: In human tissues, IL-1β-IL1R1 interactions (“IL-1βnets”) occurred primarily between myeloid cells and fibroblasts, epithelial, and endothelial cells, a pattern conserved in mouse tissues. Long-term anti-IL-1β treatment was effective only at the early stage. Early-stage scRNA-seq showed enhanced antitumor immunity and a marked reduction in interactions between IL1R1+ fibroblasts and IL-1β+ myeloid cells (monocytes, macrophages, cDCs, neutrophils), whereas late-stage tissues showed minimal changes. Spatial analysis with Xenium 5K confirmed reduced IL1R1+ cell fractions within IL-1βnets at the early stage, with IL-1βnet number and size largely unchanged. Short-term treatment at the early stage reduced interactions between IL1R1+ epithelial cells and neutrophils and attenuated NF-κB signatures in fibroblasts and epithelial cells; late-stage treatment had no significant effects.
Conclusion: Spatial single-cell profiling revealed the IL-1β-IL1R1 interaction landscape across LUAD progression in humans and mice. Anti-IL-1β therapy was effective in early-stage LUAD, disrupting key interactions between myeloid and fibroblast/epithelial cells, but was largely ineffective at later stages. These findings suggest that fibroblast and epithelial remodeling are critical determinants of stage-dependent anti-IL-1β efficacy.

#6789 Gut commensal dysbiosis modulates the lung microenvironment to promote breast tumor metastasis in a mast cell dependent axis.

M. Poblete, A. Putelo, S. Bajgai, C. Hatzinger, A. Mirani, M. Perusina Lanfranca, A. Feng, U. Miagkov, M. Rutkowski;
University of Virginia School of Medicine, Charlottesville, VA

This study aims to investigate the impact of the gut microbiome as a host-intrinsic factor in breast cancer metastasis to the lungs. The 5-year survival rate of metastatic breast cancer is 31%, however little is known as to what places patients at risk for metastatic disease. Here, we provide evidence that gut commensal dysbiosis, an inflamed and unbalanced microbiome, modifies the lung tissue microenvironment to promote the growth of hormone receptor-positive (HR+) breast tumor cells in a mast cell-dependent mechanism. This work uses a published model of dysbiosis, where we treat mice with oral broad-spectrum antibiotics for 2 weeks, before allowing 4 days of rest to promote optimal growth of antibiotic-resistant species. Non-dysbiotic controls were given vehicle treatment. The HR+ breast tumor cells PyMT were then administered intravenously (IV) to female C57BL/6 mice, mimicking circulating tumor cells to evaluate metastatic growth within the lungs. Mice with pre-established dysbiosis had significantly enhanced lung tumor burden and reduced survival. Pathology score of the lungs of mice challenged with IV tumors showed that at the same time-point dysbiotic mice display elevated tumor grade and inflammation. Furthermore, Luminex screen showed that the lungs of non-tumor-bearing mice displayed significantly elevated IL-6, a pleiotropic cytokine that has been shown to enhance tumor growth in the lungs. Single-cell RNA sequencing identified that mast cells are the main contributor of IL-6 to the lung environment of dysbiotic mice. Finally, to investigate the role of mast cells in promoting the vulnerability of dysbiotic mice to metastatic growth in the lungs, we treated dysbiotic mice with ketotifen, a mast cell stabilizer, before challenging them with PyMT cells as before. Kaplan-Meier analysis showed that dysbiotic mice treated with ketotifen had significantly improved survival compared to vehicle-treated controls. These findings highlight the significant and under-explored connection between the gut microbiome, the immune system, and tumor metastasis, and provoke future questions to investigate the impact of gut microbiome health as a host-intrinsic factor in breast cancer outcomes.

#6790 Myeloid IFN-γsignaling regulates immunosuppressive and fibrotic tumor microenvironment in PDAC liver metastasis.

T. Tanaka, E. Ivleva, A. Savas, K. Chojnacka, S. Grivennikov;
Cedars-Sinai Medical Center, Los Angeles, CA

Background; Pancreatic ductal adenocarcinoma (PDAC) remains one of the most lethal malignancies, and liver metastasis is the leading cause of mortality. Within the tumor microenvironment (TME), macrophages play central roles regulating inflammation and antitumor immunity. However, the specific contribution of macrophage-intrinsic IFN-γ signaling to metastatic progression remains poorly understood.

Methods; To investigate the role of IFN-γ signaling in macrophages, we established a portal vein injection model of PDAC liver metastasis using *Ifngr2*$^{flox/flox}$ LysM-Cre mice. Tumor burden was quantified by gross morphology and histology. Flow cytometry was used to assess macrophage and other immune cell abundance and phenotypes/activation states. Bulk RNA sequencing (Bulk RNA-seq) on whole liver metastases and single-cell RNA sequencing (scRNA-seq) on immune cell types were performed to examine the effect of myeloid-specific IFN-γ signaling on metastatic TME.

Results; We found that IFNgr2 myeloid specific deletion led to a marked increase in metastasis number and overall tumor load compared with WT controls. Flow cytometric analysis demonstrated that tumor associated macrophages (TAMs) in IFNgr2$^{\Delta Mye}$ mice showed increased Arg1 and CD206 expression and reduced MHC-II, CD80, and CD86, indicating a shift toward an immunosuppressive phenotype. Bulk RNA-seq revealed down-regulation of IFN-γ response, antigen presentation, and inflammatory pathways in metastases from IFNgr2$^{\Delta Mye}$ mice. ScRNA-seq analysis further uncovered profound remodeling of macrophage compartment with elevation in TREM2 high lipid-associated macrophages and angiogenic TAMs, accompanied by enhanced TGF-β signaling and fibrotic matrix gene expression.

Conclusions; Loss of macrophage-intrinsic IFN-γ receptor signaling drives the expansion of TREM2 high and angiogenic TAM subsets, promoting an immunosuppressive and fibrosis-prone TME that facilitates PDAC liver metastasis. These findings highlight the IFN-γ-macrophage axis as a critical regulator of metastatic progression and a potential therapeutic target in PDAC.

#6791 Target chronic inflammation in cancer and fibrosis with engineered immune cells.

Z. Zhang[1], Y.-J. Ho[1], X. Fang[2], M. Li[1], M. Kim[1], C. Hinterleitner[1], S. Haubner[1], F. Kogel[1], E. Pratt[1], A. FILLIOL[1], M. Sadelain[3], S. W. Lowe[1];
[1]Memorial Sloan Kettering Cancer Center, New York, NY, [2]Mount Sinai School of Medicine, New York, NY, [3]Columbia University Irving Medical Center (CUIMC), New York, NY

Background: Chronic inflammatory disorders contribute to over 30% of global mortality and underlie major diseases such as cancer, fibrosis, and autoimmunity. Fibrosis is a hallmark of chronic inflammation following tissue injury that drives progressive organ dysfunction and cancer progression. Existing anti-fibrotic therapies are limited by modest efficacy and systemic toxicity. We hypothesize that the selective elimination of fibrogenic and inflammatory effector cells can disrupt self-perpetuating cycles of injury and inflammation, providing a targeted therapeutic avenue for chronic disease. **Methods:** Using proximity-based surface proteomics, we identified the urokinase plasminogen activator receptor (uPAR) as broadly upregulated in senescent and chronically injured tissues across cancer and fibrotic contexts. This was corroborated by a meta-analysis of eight senescence-focused and sixteen cancer transcriptomic datasets, as well as immunohistochemical validation on patient tissue microarrays. uPAR, a GPI-anchored membrane protein central to wound healing and tissue remodeling, is consistently elevated during chronic inflammation in cancer and fibrosis. In a somatic tissue-engineered syngeneic mouse model of ovarian cancer, we demonstrated the anti-tumor efficacy of murine uPAR-targeted CAR T cells. We then generated clinical-grade human uPAR-targeting single-chain variable fragments (scFvs) through phage display and hybridoma screening, and validated their ability to eradicate both orthotopic and metastatic xenograft tumors. **Results:** uPAR-targeted CAR T cells selectively eliminated senescent cells and attenuated fibrosis in preclinical models of liver and lung injury. In cancer, uPAR expression marks aggressive tumor cells undergoing epithelial-to-mesenchymal transition (EMT) and senescent stromal cells embedded in immunosuppressive niches. In multiple solid tumor models, including immune-excluded settings, human uPAR CAR T cells exhibited potent and durable anti-tumor activity. In an ovarian cancer model, adjuvant administration of uPAR CAR T cells post-surgical debulking effectively prevented metastatic recurrence. Therapeutic efficacy was tracked via noninvasive biomarkers, including circulating soluble uPAR and uPAR-targeted PET imaging. Despite detectable expression in subsets of myeloid cells, treatment with uPAR CAR T cells did not induce sustained myelodepletion in mice with a humanized immune system. **Conclusions:** These findings establish uPAR-targeted CAR T cells as a promising therapeutic strategy across cancer, fibrosis, and degenerative diseases by eliminating shared pathological cell states that sustain chronic inflammation and tissue dysfunction.

: KRAS-Targeted Therapies: Overcoming Resistance and Novel Combinations
Minisymposium

#6767 Defining a molecular signature for KEAP1-NRF2 mediated resistance to KRAS inhibition in KRAS-mutant pancreatic and lung cancer.

W.-H. Chang[1], A. J. Vaughan[2], M. Mancini[3], A. G. Stamey[1], M. Hayashi[2], R. Yang[1], R. Robb[1], J. A. Klomp[1], A. M. Waters[1], A. Schaefer[1], D. Andrussier[4], K. L. Bryant[1], A. D. Cox[1], F. M. Simabuco[3], A. J. Aguirre[5], K.-K. Wong[4], C. A. Stalnecker[1], T. Papagiannakopoulos[2], C. J. Der[1];
[1]University of North Carolina at Chapel Hill, Chapel Hill, NC, [2]NYU Langone Health, New York, NY, [3]Federal University of Sao Paulo, Sao Paulo, Brazil, [4]New York University, New York, NY, [5]Dana-Farber Cancer Institute, Boston, MA

Mutational activation of KRAS is critical for driving the tumorigenic growth of pancreatic ductal adenocarcinoma (PDAC) and lung adenocarcinoma (LUAD). Recent approval of inhibitors of one KRAS mutation (G12C) supports the therapeutic value of targeting mutant KRAS in PDAC and LUAD. However, clinical efficacy is hindered by both primary and treatment-associated acquired resistance. With resistance mechanisms still incompletely established, we performed a CRISPR loss-of-function screen to identify genes that modulate the sensitivity of PDAC cells to KRAS inhibition. We determined that loss of *KEAP1* and activation of the transcription factor NRF2 drove resistance to the $KRAS^{G12D}$-selective inhibitor MRTX1133 and the RAS(ON) multi-selective inhibitor RMC-7977. RNA-sequencing analyses revealed that *KEAP1* loss protected cancer cells from oxidative stress and cell cycle arrest induced by KRAS inhibition. Building upon our transcriptomic analyses, we established a PDAC KEAP1-deficient (PKD) gene signature. The PKD signature was prevalent in preclinical models and patients insensitive to KRAS inhibitor treatment. This signature was also distinct from transcriptional changes associated with other mechanisms driving KRAS inhibitor resistance (ERK, MYC, and YAP/TAZ-TEAD). Finally, we observed that *KEAP1*-deficient cells exhibited elevated glutamine metabolism, and combination treatment with the clinical candidate glutamine antagonist DRP-104 (sirpiglenastat) strongly enhanced KRAS inhibitor-mediated growth suppression in KRAS-mutant PDAC and NSCLC tumors in vivo. In summary, our studies established a gene signature for *KEAP1* loss-driven resistance and validated a therapeutic strategy to overcome KEAP1-NRF2-driven RAS inhibitor resistance.

#6768 Selective ULK1/2 inhibitors enhance KRAS pathway blockade and uncover stress-adaptive programs.

S. Bayle, S. Chin Chan, M. Lamptey, M. Teng, A. Monastyrskyi, D. Duckett;
Moffitt Cancer Center, Tampa, FL

KRAS is the most frequently mutated member of the RAS family in lung adenocarcinomas such as NSCLC. Although KRAS pathway inhibition can reduce tumor growth, resistance arises and thwarts its clinical potential. Prior work has suggested that the autophagy pathway is an exploitable vulnerability for mutant RAS-driven tumors. ULK1 is a central upstream regulator of the autophagy pathway, and its inhibition is a promising strategy to abrogate autophagy and improve RAS-driven tumor sensitivity to approved therapeutics. Through structure-based drug design, we generated a 7-azaindole-derived series of ULK1/2 inhibitors and characterized their structure-activity relationships. Biochemical potency was measured via ULK1/2 enzymatic assays, and intracellular target engagement was evaluated using a ULK1 NanoBRET assay. Cellular analyses were performed in KRAS mutant models using viability assays, autophagy flux measurements under starvation or treatment with MEK inhibitor. Combination studies with RAF-MEK-ERK pathway inhibitors were assessed in subcutaneous xenograft models. In order to assess the type of resistance arising from KRAS treatment, we used a combination of DNA barcode technology and transcriptomic studies to distinguish between resistance arising from clonal expansion vs adaptive, reversible survival programs consistent with drug-tolerant persister (DTP) biology. We identified potent, selective ULK1/2 inhibitors, favorable physicochemical profiles, and strong cellular target engagement. The lead analog, MR-2088, inhibited stimuli-induced autophagic flux and displayed pharmacokinetics appropriate for in vivo studies. In cells, MR-2088 enhanced the activity of MEK/ERK inhibitors and produced synergistic reductions in viability. The synergistic effect was observed in vivo. DNA barcode analysis revealed that resistance emerging after KRAS pathway inhibition was not associated with expansion of distinct clonal populations, suggesting a non-genetic adaptive mechanism. Transcriptomic profiling showed enrichment of stress-adaptive pathways, including cell-cycle remodeling, metabolic rewiring, oxidative phosphorylation, and MYC-regulated targets; patterns consistent with previously described drug-tolerant persister-like programs. This study describes a new chemotype of selective, ULK1/2 inhibitors that robustly engage the target, inhibit autophagic flux, and enhance the effectiveness of RAS pathway inhibitors. By disrupting autophagy-supported adaptive programs that arise following KRAS pathway inhibition, ULK1 blockade may enhance therapeutic responses and limit stress-induced survival states relevant to treatment tolerance. These findings support further investigation of ULK1 inhibition as a strategy to augment targeted therapy in KRAS-driven malignancies.

#6769 Modeling of acquired resistance to the multi-RAS inhibitor RMC6236 in KRAS mutant pancreatic ductal adenocarcinoma.

Di Zhan, Jiajia Mei, Jing Yang, Ya Xu, Qikuan Chen, Yuzhou Xu, Yun Zhang, Yinfei Yin

Shanghai ChemPartner Co., Ltd., Shanghai, China

Mutations in the Kirsten rat sarcoma viral oncogene homologue (KRAS) are among the most prevalent oncogenic events in human cancers, with KRAS G12D being the dominant driver in pancreatic ductal adenocarcinoma (PDAC). While covalent KRAS G12C inhibitors have demonstrated clinical efficacy, the absence of effective therapies for non-G12C variants underscores the need for broader KRAS-directed approaches. The recent development of RMC6236, a RAS-MULTI(ON) inhibitor, has shown promising activity in KRAS G12D-driven PDAC, emphasizing the importance of understanding mechanisms underlying acquired resistance to this class of agents. To enable investigation of KRAS resistance pathways, we have established a panel of KRAS G12D PDAC cell models with acquired resistance to RMC6236 using a combination of CRISPR-Cas9-mediated genome editing and advanced engineering techniques. In addition, KRAS-mutant tumor models with engineered inhibitor resistance have been established to support pharmacology and efficacy evaluations. Genomic and functional characterization of these models reveal diverse mechanisms contributing to resistance, including secondary KRAS mutations (Y64C/D/H), BRAF alterations, and MAP2K1 variants, each associated with reactivation of the RAF-MEK-ERK signaling cascade. Beyond genetic adaptations, transcriptional profiling and phenotypic assays indicate the involvement of non-genetic mechanisms such as pathway rewiring and adaptive signaling plasticity. These resistance models provide a controlled experimental framework for dissecting the molecular determinants of multi-RAS inhibitor resistance, and enable comparative evaluation of resistance mechanisms across KRAS alleles, supporting rational development of combination strategies to sustain KRAS pathway inhibition. Collectively, these studies advance our understanding of adaptive resistance to next-generation KRAS inhibitors and inform translational strategies for KRAS G12D-mutant pancreatic cancer.

#6770 Combining RAS inhibitors with the clinical RNR inhibitor BBI-825 to prevent the emergence of extrachromosomal DNA (ecDNA)-driven resistance to RAS-targeted therapies in colorectal cancer.

S. Palladino[1], J. Lange[2], N. Catalano[1], S. Garcia[2], R. Hansen[2], H. Zhao[1], P. Kokate[1], E. De Stanchina[1], C. Hassig[2], R. Yaeger[1];
[1]Memorial Sloan Kettering Cancer Center, New York, NY, [2]Boundless Bio, San Diego, CA

Introduction: The advent of new RAS inhibitors provides an exciting chance to extend targeted therapy to the half of colorectal cancers (CRC) with *KRAS* mutations. However, the rapid development of resistance limits the clinical benefit of this approach. Focal and ecDNA-driven amplifications are a common mechanism of resistance; in the phase 1 trial of daraxonrasib (RAS multi ON), acquired mutant *KRAS* amplifications occurred in 30% of patients. *In silico*, ecDNA$^+$ tumor cells show a strong survival dependence on ribonucleotide reductase (RNR), the rate-limiting enzyme in the *de novo* synthesis of deoxyribonucleotide triphosphates (dNTPs). BBI-825, an oral and selective small molecule inhibitor of RNR, has entered clinical trials. We investigated whether BBI-825, in combination with different RAS inhibitors, can delay or overcome the development of acquired resistance in CRC. Based on the vulnerability of ecDNA$^+$ cells to BBI-825, we anticipated response may vary by tumor microsatellite status and evaluated microsatellite stable (MSS) and instable (MSI) CRC models.
Methods: Human cancer models were treated with combined RAS and epidermal growth factor receptor (EGFR) antibodies. We used parental and resistant models generated from murine and human cancer cell lines, cell derived xenografts (CDX) and patient derived xenografts (PDX) to compare the effect of RAS inhibition alone and in combination with BBI-825 on tumor growth, signaling and acquired resistance. RAS inhibitors used were MRTX1133 and zoldonrasib (*KRAS*^{G12D}), sotorasib and adagrasib (*KRAS*^{G12C}) and daraxonrasib. Metaphase fluorescence in-situ hybridization (FISH) was used to evaluate ecDNA presence.
Results: The addition of BBI-825 to RAS inhibitor (plus anti-EGFR antibody in human cells) delayed or prevented the emergence of resistance in the MSS parental cell lines, CDX and PDX. This combination suppressed the emergence of ecDNA-driven *KRAS*, *RAF1* and *MYC* amplifications. In MSS CRC models that had already acquired resistance to RAS inhibitors, the addition of BBI-825 to RAS plus EGFR inhibition slowed tumor growth and reduced the copies of putative resistance gene amplifications. In contrast, in the MSI model, acquired resistance was likely mediated by new mutations in *KRAS*, and addition of BBI-825 did not significantly impact acquired resistance or tumor growth.
Conclusions: We show in multiple models of MSS CRC that the selective RNR inhibitor BBI-825 combined with RAS inhibitors delayed or prevented RAS targeted therapy-acquired resistance in a novel approach that subverts the emergence of resistance. The selective sensitivity of MSS CRC models, particularly those that harbor ecDNA, further supports the distinct mechanism of action of BBI-825 and this potential new and important strategy to improve RAS inhibitor efficacy.

#6771 Targeting the JAK-STAT pathway sensitizes KRAS-mutant cancer to KRAS inhibitors.

Y. Zhao, Y. Cao, Y. Bao, B. Shen;
Ruijin Hospital Affiliated to Shanghai Jiao Tong University School of Medicine, Shanghai, China., Shanghai, China

Targeting KRAS is promising in KRAS-mutant cancers. However, primary and acquired resistance to KRAS inhibitors impedes their clinical use. We conducted a Phase IIa clinical trial enrolling 7 patients with resectable PDAC bearing KRAS^G12D mutations, who received standard neoadjuvant chemotherapy plus KRAS inhibitors. Genomic analyses revealed acquired mutations in KRAS and other cancer-related. Single-cell transcriptomic profiling showed significant differences in cancer-associated fibroblast (CAF) populations between responders and non-responders. Kinome CRISPR library screening and FDA-approved compound library screening nominated the JAK-STAT pathway as critical for response to KRAS inhibition. Cell lines resistant to KRAS inhibitors have activated JAK-STAT pathway. In vitro and in vivo, STAT3 inhibition synergized with KRAS inhibition, altered cytokine secretion by cancer cells, and modulated CAF status. These findings demonstrate that activation of the JAK-STAT pathway is a common mechanism of resistance to KRAS inhibitors in diverse KRAS-mutant cancers and suggest that dual targeting of KRAS and STAT3 may enhance therapeutic efficacy.

#6772 VEGFR2 blockade overcomes acquired KRAS G12D inhibitor resistance driven by PI3Kγ activation.

S.-H. Hwang[1], M. Bae[2], J.-W. Kim[3], S. Hyun[4], K.-J. Kim[5], J. Choe[6], M. Kim[7], J. Park[8], S. Jeong[7], S. Choi[1], W. Park[1], J. Seo[1], H. Chae[1], M. Kang[9], E. Jung[3], K. Suh[3], S. Kim[10], J. Kim[10], Y. Kim[3], J. Kim[10], H. Park[11], A. J. Aguirre[12], E. Lee[6], J.-L. Ku[13], K.-W. Lee[3];

[1]Seoul National University Bundang Hospital, Seongnam-si, Korea, Republic of, [2]Boston Children's Hospital, Harvard Medical School, Boston, MA, [3]Department of Internal Medicine, Seoul National University Bundang Hospital, Seoul National University College of Medicine, Seongnam-si, Korea, Republic of, [4]Seoul National University, Seoul, Korea, Republic of, [5]Seoul National University Bundang Hospital, Seongnam-si, [6]Broad Institute of MIT and Harvard, Cambridge, MA, [7]Department of Surgery, Seoul National University Hospital, Seoul National University College of Medicine, Seoul, Korea, Republic of, [8]Seoul National University Hospital, Seoul, Korea, Republic of, [9]Seoul National University Bundang Hospital, Seoul, [10]Seoul National University Bundang Hospital, Seongnam, Korea, Republic of, [11]DFCI/Harvard Medical School, BOSTON, MA, [12]Dana-Farber Cancer Institute, Boston, MA, [13]Seoul National University Cancer Research Institute, Seoul, Korea, Republic of

KRAS G12D mutation is a prevalent oncogenic driver in gastrointestinal (GI) cancer. Recently, novel KRAS inhibitors have shown promise in KRAS-mutant cancers. However, acquired resistance inevitably emerges, limiting clinical efficacy. Nevertheless, their resistance mechanisms and overcoming strategies remain largely undefined. We established nine human GI cancer models of acquired resistance to MRTX1133, a KRAS G12D selective inhibitor: two gastric (AGS and SNU-601), two pancreatic (AsPC-1 and PANC-1), and two colorectal cancer cell lines (SNU-C2A and SNU-C2B), and three colorectal cancer patient-derived organoids (SNU-4646S1-TO, SNU-6325-TO, and SNU-6330-TO). Single-cell RNA sequencing analysis of resistant and parental SNU-4646S1-TO (GSE290526) revealed enrichment of angiogenesis, hypoxia, and epithelial-mesenchymal transition (EMT) signatures in resistant models compared to parental cells. In line with this, all nine resistant models showed markedly elevated VEGFA expression and VEGFR2 activation, which we traced to AKT-mediated nuclear translocation of the transcription factor SP1. Mechanistic investigation revealed that oncogenic KRAS in the resistant state formed a complex with p110γ and p101, subunits of PI3Kγ, leading to hyperactivation of PI3Kγ. This, in turn, established the autocrine VEGFA-VEGFR2 signaling loop via AKT and SP1 activation that reinforced EMT and sustained the resistant phenotype. In the resistant models, disrupting VEGFA-VEGFR2 signaling using KDR knock-out and ramucirumab treatment restored MRTX1133 sensitivity and reversed EMT in resistant cells. Inhibition of hyperactivated PI3Kγ using eganelisib, a selective p110γ inhibitor, also replicated the same results. Indirect co-culture experiments of cancer cells and human large vessel endothelial cells (HUVECs) identified that cancer-endothelial paracrine crosstalk in resistant models further amplified angiogenesis, hypoxia, and EMT signatures (GSE290487) in cancer cells and concurrently promoted endothelial cell proliferation, suggesting a microenvironment-mediated feedback loop. In a mouse xenograft model of MRTX1133-resistant PANC-1 cells, anti-VEGFR2 antibody (DC101) treatment combined with MRTX1133 rechallenge more effectively reduced tumor growth and angiogenesis than either agent alone, without significant changes in body weight. Our study revealed a novel mechanism of acquired resistance to KRAS G12D inhibition in GI cancers: a KRAS-PI3Kγ interaction-driven autocrine and paracrine VEGFA-VEGFR2 signaling axis that fosters EMT and therapeutic escape. Importantly, co-targeting this axis with VEGFR2 or PI3Kγ inhibitor restored sensitivity to KRAS inhibition. These findings provide a rationale for further biomarker-guided clinical trials of combined VEGFA-VEGFR2 and KRAS inhibition in patients experiencing acquired resistance after KRAS inhibitor treatment.

#6773 Targeted therapy-induced chromosomal instability dictates mitotic dependency on Aurora kinase A.

C. Li[1], V. Nangia[2], M. Vieira[1], A. Nimbalkar[1], C. Graser[3], J. Chang[4], M. Syed[1], Y. Shen[1], R. Koranne[1], L. Zou[5], F. Michor[6], S. L. Spencer[7], A. N. Hata[8];
[1]Mass General Cancer Center, Harvard Medical School, Boston, MA, [2]University of Colorado Boulder, Boulder, CO, [3]Dana-Farber Cancer Institute, Cambridge, MA, [4]University of California San Francisco, San Francisco, CA, [5]Duke University School of Medicine, Durham, NC, [6]Dana-Farber Cancer Institute, Boston, MA, [7]Univ. of Colorado Denver School of Medicine, Aurora, CO, [8]Massachusetts General Hospital, Charlestown, MA

Targeted therapies are designed to eliminate cancer cells by directly inhibiting oncogenic driver proteins. In addition to their primary inhibitory effects on oncogenic signaling, these agents frequently impose collateral cellular stresses, such as DNA damage. KRAS-targeted therapies, particularly KRAS G12C inhibitors (G12Ci), represent a major therapeutic advance but remain limited in efficacy. Previous reports of targeted therapy-induced DNA damage, including studies of TKIs and MAPK inhibitors, have primarily been based on cytotoxic dosing conditions. Far less is known about whether DNA damage can also be induced by targeted therapies in less sensitive cancer models, particularly under sublethal doses that better mimic clinical responses. Failure to repair DNA damage can lead to chromosomal instability (CIN) and chromosomal aberrations. CIN is widely recognized to promote tumor evolution by enhancing cellular plasticity and adaptability, thereby contributing to therapeutic resistance and metastatic progression. However, it remains unknown how KRAS G12C inhibition influences CIN and whether G12Ci-induced CIN might generate unique, exploitable vulnerabilities.

In this study, we profiled 15 KRAS G12C-mutant NSCLC cell lines representing diverse mutational backgrounds. We treated these models with the KRAS G12Ci LY3499446 and comprehensively assessed their DNA damage responses, CIN phenotypes, and sensitivity screening to combination therapies with agents that perturb chromosomal stability. We observed heterogeneous induction of DNA damage and CIN across these cell lines. Notably, we identified the strongest correlation between G12Ci-induced CIN and synergistic interaction with the Aurora kinase A inhibitor (AURKAi) LSN3321213. Machine learning-based single-cell image tracking and DNA barcoding analyses revealed that AURKA inhibition alone causes mitotic arrest followed by mitotic slippage, allowing cells to evade death, whereas combined G12Ci and AURKAi treatment triggers catastrophic mitotic cell death. Mechanistically, we found that G12Ci stabilizes Cyclin B1 through mitotic activation of ATR/ATM DNA repair signaling, thereby prolonging mitotic arrest. Under conditions of combined inhibition of KRAS G12C and AURKA, in which Cyclin B1 degradation is impaired, cells fail to exit mitosis and undergo catastrophic cell death. Together, our findings identify CIN as a predictive marker of response to combined KRAS G12C and AURKA inhibition, providing mechanistic rationale to enhance the therapeutic window of AURKA inhibitors when used with targeted therapies.

: Machine Learning Approaches for Cancer Diagnosis and Treatment Prediction
Minisymposium

#6722 CUPAI-2: A collaborative multi-agent large language model framework for diagnosis of cancer of unknown primary.
Junhan Zhao[1], Juejie Zhang[2], Lingjie Fan[3], Anzhi Chen[4], Zheyi Ji[5], Zanmei Xu[6], Yannan Zhu[6], **Kai Wang**[7]

[1]The University of Chicago, Chicago, MI,[2]University of Science and Technology of China, Hefei, China,[3]Sichuan University, Chengdu, China,[4]Columbia University, New York, NY,[5]Chongqing University, Chongqing, China,[6]OrigiMed, Shanghai, China,[7]OrigiMed, Boston, MA

Background: Cancers of unknown primary (CUP) accounts for 2-5% of cancers but remains a leading cause of death, as failure to identify the primary site blocks targeted therapy and trial access. We developed CUPAI-2, a multi-agent LLM framework with a website that integrates genomic data to predict CUP primary site.
Methods: CUPAI-2 implements a Molecular Tumor Board (MTB)-inspired architecture comprising (i) domain specialist models and (ii) a meta-decision layer for consensus integration. The specialist tier comprises three LLMs (Qwen-2.5-0.5B, Qwen-3-0.6B, Llama-3.2-1B), each fine-tuned on modality specific corpora including single nucleotide variants, copy number alterations , and chromosomal translocations to produce independent primary site likelihoods and rationales. Their outputs (class probabilities, uncertainty scores, and rationale embeddings) feed a statistical coordinator that performs stacked generalization, employing an XGBoost model as a non-linear meta-learner to arbitrate and integrate predictions. A final oversight agent (DeepSeek) functions as the MTB manager, auditing discordant cases against structured genomic contexts and literature-derived priors, and issuing an adjudicated prediction. We analyzed 20,483 next generation sequencing (NGS) profiled tumors spanning 19 cancer types, and benchmarked CUPAI-2 against experienced oncologists on test sets.
Results: CUPAI-2 achieved robust diagnostic performance with Top1 accuracy of 76.93% and Top3 of 92.82%. Performance exceeded that of oncologists on 190 uniformly distributed cancer cases (Top1: 71.05% vs. 68.42%; Top3: 83.15% vs. 80%), and inter-model reliability within the CUPAI-2 was high as reflected by Jaccard similarity coefficients. Compared with traditional machine learning (Top1/Top3: 60.38%/79.77%), CUPAI-2 achieved substantial improvements of 17.83 and 12.33 percentage points (pp) , respectively. It also delivered additional gains of ~3-5 pp compared with non-collaborative, individually fine-tuned LLMs (75.27%/87.55%). CUPAI-2 further surpassed the current best published voting-based model, establishing a new state-of-the-art for CUP origin prediction while maintaining clinically acceptable computational efficiency. A prototype (https://cupai.origimed.com) enables uploading of NGS reports for CUP prediction and is not intended for clinical decision making.
Conclusions: CUPAI-2, a coordinated MTB-inspired multi-agent LLM architecture, synthesizes heterogeneous genomic features to predict CUP primary sites with greater accuracy, calibration, and interpretability than individual LLMs, conventional models, or human experts. These findings highlight the feasibility and value of multi-agent LLM systems for high dimensional genomic reasoning and suggest a promising clinical decision making direction for improving cancer primary site inference.

#6723 Multisite analysis of a deep learning model for prediction of palbociclib response in patients with ER+ HER2- advanced breast cancer.

A. Singhal[1], X. Zhang[2], K. T. Yeung[2], T. Ideker[3];

[1]University of California, San Diego, La Jolla, CA, [2]Moores Cancer Center, La Jolla, CA, [3]UC San Diego, La Jolla, CA

Deep learning is a powerful methodology that is beginning to impact many aspects of cancer care, including the prediction of therapeutic response. These models, consistent with advances in machine learning, are showing increasingly improved performance on preclinical datasets. For successful clinical deployment of these models, a key step (and frequent barrier) is rigorous evaluation on real-world patient populations. We address this translational gap through several advances. First, we collect two distinct, real-world cohorts of ER+ HER2- advanced breast cancer treated with palbociclib to enable gold-standard evaluation of precision oncology models. These include a novel cohort of 139 patients treated at the University of California, San Diego (UCSD), for which we track demographics, treatment duration, progression-free survival (PFS), and overall survival (OS). We supplement this dataset with a larger independent real-world cohort of 459 patients treated at the Memorial Sloan Kettering Cancer Center (MSK). Second, we the use of these cohorts to provide a full retrospective evaluation of a recently published interpretable deep learning model of palbociclib response. Model analysis results in accurate stratification of PFS (UCSD: HR = 0.38, $P = 0.01$; MSK: HR = 0.60, $P = 2 \times 10^{-3}$) and OS (UCSD: HR = 0.38, $P = 0.05$; MSK: HR = 0.74, $P = 0.05$). Third, model interpretation identifies a collection of rare and common genetic alterations underlying drug resistance in 18 molecular pathways, including RTK signaling, DNA damage response, and cell cycle regulation. Finally, we showcase a visualization schema to augment personalized diagnostic reports for individual patients. Together, these results build evidence to motivate future prospective studies exploring the predictive efficacy of precision oncology models.

#6724 OncoTwin: A multimodal digital twin framework for predicting treatment response and guiding trial design in ALK-rearranged non-small-cell lung cancer.

H. Xu, Y. Y. Elamin, L. Hong, K. Concannon, M. Saad, X. Xu, M. Amgad, H. Li, K. Qin, X. Han, S. Ismail, Y. Kitsel, S. Gandhi, M. B. Antonoff, C. C. Wu, B. W. Carter, G. Shroff, S. Heeke, X. Le, T. Cascone, N. Vokes, M. Altan, D. L. Gibbons, D. Jaffray, J. Chang, Z. Liao, D. Rice, A. Vaporciyan, S. G. Swisher, J. Lee, J. Zhang, J. V. Heymach, J. Wu;
University of Texas MD Anderson Cancer Center, Houston, TX

Introduction: Despite advances with next-generation tyrosine kinase inhibitors (TKIs), response and progression patterns in ALK-rearranged NSCLC vary widely, and currently no reliable biomarkers can predict individualized outcomes under alternative therapies. Digital-twin models offer a solution by integrating real-world evidence to reconstruct patient-specific counterfactual disease trajectories for single-arm trials and evaluation of escalation strategies.

Methods: We integrated real-world and clinical-trial datasets of ALK-rearranged NSCLC treated with TKIs, including MDACC cohort (n = 103, GEMINI database) for model development, Phase III randomized ALTA-1L (n = 207) for external validation, and Phase II BrightStar (n = 32) for clinical application. Tumor burden was quantified at whole-body and organ levels using CT-derived 3D volumetrics, combined with longitudinal routine blood test and demographic variables. Two digital twin models were developed through machine learning: OncoTwin-2D, a parsimonious model based on serial sum of longest diameters (SLD) and demographics, and OncoTwin-3D, an advanced model integrating longitudinal 3D volumetric, blood, and demographic features. Models were evaluated on MDACC and ALTA-1L cohorts by hazard ratio (HR) and log-rank test. The calibrated OncoTwin-3D was further applied to the single-arm BrightStar trial to simulate a counterfactual brigatinib-only control arm and evaluate the added benefit of local consolidation therapy (LCT).

Results: Early tumor response patterns and long-term outcomes differed by TKI generation, with second-generation TKIs showing greater overall and organ-level responses and longer median PFS (29 vs 10 months; HR = 0.45; $p < 0.001$) than first-generation TKI. For our digital twin framework, OncoTwin-2D achieved robust risk stratification (HR = 1.8, $p = 0.034$ in MDACC cohort; HR = 2.1, $p < 0.001$ for external ALTA-1L cohort). Furthermore, model predicted survival outcomes aligned consistently with observed outcomes in ALTA-1L for first- and second-generation TKI. The advanced OncoTwin-3D further improved prognostic accuracy with significant risk stratification in MDACC cohort (HR = 3.9, $p < 0.0001$) and separately for individual TKI subgroups ($p = 0.006$ and $p < 0.001$ for first- and second-generation TKI). In the prospective BrightStar phase II trial, OncoTwin-3D was applied to simulate a counterfactual brigatinib-only control arm, which revealed a significant benefit from adding LCT (median PFS 66 vs. 22 months; HR = 2.8, $p = 0.002$).

Conclusion: We introduced OncoTwin, an AI-driven multimodal digital twin for individualized response prediction and novel escalation evaluation. This scalable framework extends beyond thoracic disease, offering a generalizable paradigm that bridges real-world data and clinical trials to accelerate precision oncology.

#6725 AI-derived H&E biomarkers predict differential survival under immunotherapy vs chemotherapy in phase-3 metastatic NSCLC study NEPTUNE.

C. Parmar[1], V. Roudko[1], V. Muckerson[1], J. Blando[2], J. Daniel[2], J. Diez[3], S. Gunda[4], A. Mendoza Alcala[3], A. Franco[5], I. Stambolic[6], C. Benchea[3], R. Stewart[5], Z. Lai[1], J. S. Reis-Filho[7], M. Scaltriti[8], D. Palmer[9];

[1]AstraZeneca, Waltham, MA, [2]AstraZeneca, Gaithersburg, MD, [3]AstraZeneca, Barcelona, Spain, [4]Astrazeneca, Chennai, India, [5]AstraZeneca, Cambridge, United Kingdom, [6]AstraZeneca, Munich, Germany, [7]AstraZeneca US, Gaithersburg, MD, [8]AstraZeneca - MedImmune, LLC, Gaitherburg, MD, [9]AstraZeneca Oncology, Gaithersburg, MD

Background: Immunotherapy outcomes in metastatic NSCLC are variable, and existing biomarkers (PD-L1, TMB) incompletely predict benefit. Routine H&E slides are widely available and capture spatial tumor microenvironment (TME) context. We applied AI-Pathology to convert H&Es into quantitative, interpretable TME features and assessed whether they predict survival benefit with immunotherapy (IO) versus chemotherapy.

Methods: We conducted a retrospective analysis of H&E slides from NEPTUNE (a phase 3, study in metastatic NSCLC comparing durvalumab+tremelimumab (D+T) vs chemotherapy (CTX)). Slides from 426 patients (D+T n=154; CTX n=272) were processed using models trained independently on external, non-NEPTUNE datasets (>6,000 pathologist-annotated H&Es). Fifteen features (immune, cancer, fibroblast densities/ratios) were extracted in cancer-associated stroma and cancer regions. Overall survival (OS) was analyzed by fitting univariate Coxph regression models with Benjamini-Hochberg FDR control. Treatment × marker interaction terms evaluated predictiveness. Routinely used markers followed cutoffs (PD-L1 ≤25%; bTMB ≤20 mut/Mb) as described in the NEPTUNE study (de Castro Jr G et al., J Thorac Oncol, 2023;18:106-119).

Results: Higher stromal fibroblast density was associated with inferior OS in both arms (D+T HR=1.60 [1.14-2.25]; CTX HR=1.36 [1.05-1.76]) with no treatment interaction (nominal p_interaction=0.82), indicating a prognostic effect. Higher stromal immune density was associated with improved benefit for D+T (HR=0.64 [0.45-0.90]; median OS difference +5.8 months; FDR p=0.04) but not CTX (HR=0.84 [0.65-1.08], FDR p=0.38), with a significant treatment interaction (nominal p_interaction=0.03), supporting a predictive effect. Overall, AI-H&E features showed comparable or stronger stratification of D+T outcomes than established routine markers in this dataset, including PD-L1 (HR=0.67 [0.46-0.96], FDR p=0.08), bTMB (HR=0.78 [0.48-1.26], FDR p=0.45), and ECOG (HR=0.74 [0.52-1.07], FDR p=0.19).

Conclusions: NEPTUNE did not meet its primary endpoint. The observed prognostic fibroblast signal and predictive immune signal from AI-derived H&E features suggest the potential for enriched selection or stratification to improve detection of checkpoint blockade benefit. These assay-free, interpretable biomarkers warrant prospective validation for clinical application.

#6726 A translational deep learning platform predicts metabolic pathway activity from routine H&E slides to enable patient stratification.

Salim Arslan[1], Julian Schmidt[1], Cher Bass[1], Foivos Ntelemis[1], Oscar Maiques[2], Vishali Sharma[1], Jakob Nikolas Kather[3], **Pahini Pandya**[1]

[1]Panakeia Technologies, Cambridge, United Kingdom,[2]Queen Mary University of London, Barts Cancer Institute, London, United Kingdom,[3]Technische Universitat Dresden, Dresden, Germany

Background: Metabolic reprogramming is a hallmark of cancer and a potential therapeutic target, yet clinical assessment remains challenging. We hypothesized that functional metabolic states could be inferred from routinely collected H&E-stained whole-slide images (WSIs), offering a scalable approach to biomarker discovery and patient stratification. We developed a multi-omics platform integrating histomorphology with transcriptomic and metabolic modelling data, applying it across 21 cancer types to identify digital biomarkers predictive of pathway-specific metabolic activity.
Methods: We derived binary biomarkers for 32 pathways using personalized genome-scale metabolic models and transcriptomic data from The Cancer Genome Atlas (TCGA). Pathway activity was inferred by comparing sample-specific gene expression profiles to a generalized metabolic network, with statistical significance determined by t-tests and Benjamini-Hochberg correction (FDR < 0.05). Deep learning models were trained to learn the morphological features predictive of these metabolic states, with cohort sizes ranging from 41 to 887 WSIs per biomarker. Model performance was validated using three-fold cross-validation and evaluated by the area under the curve (AUC), with ± showing standard deviation across folds.
Results: The approach identified robust morphological patterns predictive of key metabolic pathways across diverse tumor types. High predictability was achieved for nucleotide metabolism in testicular germ cell tumors (AUC = 0.85 ±0.13) and pancreatic adenocarcinoma (AUC = 0.79 ±0.08). Strong morphological signals of nuclear transport were observed in colon adenocarcinoma (AUC = 0.79 ±0.05), skin cutaneous melanoma (AUC = 0.75 ±0.06), and lung squamous cell carcinoma (AUC = 0.71 ±0.07). Pathways related to fatty acid beta-oxidation showed consistent predictability (AUC > 0.65) across thyroid carcinoma (AUC = 0.73 ±0.07), liver hepatocellular carcinoma (AUC = 0.70 ±0.05), pancreatic adenocarcinoma (AUC = 0.69 ±0.02), stomach adenocarcinoma (AUC = 0.68 ±0.04), and ovarian serous cystadenocarcinoma (AUC = 0.67 ±0.05).
Conclusions: This study demonstrates the potential of a multi-omics platform for decoding functional metabolic states from routine pathology slides. The platform can identify patient populations with specific metabolic dependencies (e.g., nucleotide metabolism) or pathway dysregulations (e.g., nuclear transport), thereby enabling targeted patient stratification for clinical trials. By translating complex histomorphology from standard H&E slides into actionable molecular insights, this technology offers a scalable and cost-effective solution to accelerate biomarker-driven drug discovery in precision oncology.

#6727 Enhancing lung cancer risk prediction with longitudinal fusion of LDCT data.

H. Ajami[1], A. W. Waqas[1], J. Templeton[2], M. B. Schabath[1], G. Rasool[1];
[1]Moffitt Cancer Center, Tampa, FL, [2]University of South Florida, Tampa, FL

Background: Lung cancer is the leading cause of cancer death, and better early detection is critical to lowering its burden. Sybil, a deep learning model, predicts 6-year lung cancer risk from a single low-dose CT (LDCT). Yet screening patients typically receive annual LDCTs that capture temporal changes in nodules and disease. We hypothesized that fusing longitudinal imaging features across scans would improve long-term risk prediction and generalizability over single-timepoint models.
Methods: We re-implemented Sybil's backbone and feature embedding layers to enable the extraction of intermediate feature representations while preserving the original inference behavior by loading the publicly released pretrained checkpoints unchanged. We developed six longitudinal deep learning architectures trained on the National Lung Screening Trial (NLST; n = 3,977participants, n = 991 cancers over 6 years): (1) Bi-Fusion (MLP and Transformer), integrating baseline + year-1 LDCTs; (2) Tri-Fusion (MLP and Transformer), integrating baseline, year-1, and year-2 LDCTs; (3) Hybrid (Temporal Hybrid and Masked Hybrid), combining CNN backbone, vision transformer, and temporal transformer modules and supporting up to three timepoints with missing scan handling. All models estimated time-to-lung-cancer using a hazard layer and were evaluated using time-dependent AUCs at yearly prediction horizons and Harrell's C-index. External evaluation used Moffitt Lung Screening data (n = 1876 participants, n = 469 cancers). For Hybrid models, only the hazard head was fine-tuned on a Moffitt adaptation subset, followed by evaluation on a held-out external test set.
Results: Hybrid longitudinal models demonstrated the highest performance and stability across follow-up horizons. During internal testing of the NLST, the Masked and Temporal Hybrid models achieved near-perfect discrimination at Year 1 (time-dependent AUC ≈ 0.99), gradually decreasing to 0.91 and 0.90 by Year 6, with a C-index of 0.75 (95% CI: 0.73-0.78). After external fine-tuning and evaluation, Hybrid models generalized robustly to Moffitt, with an AUC of 0.89 at Year 1, declining to 0.81 at Year 6, and a C-index of 0.81 (0.74-0.87). Tri-Fusion architectures peaked at an AUC of ~0.92 at Year 3 and declined to 0.86 by Year 6 in NLST, but demonstrated limited generalizability (0.63 to 0.57, C-index 0.60 [0.53-0.67]). Bi-Fusion performance was intermediate (AUC 0.83 to 0.77 in NLST; ~0.70-0.62 on Moffitt).
Conclusion: Longitudinal fusion of LDCT scans improves risk prediction vs single-timepoint models. Hybrid models using up to three scans show superior accuracy, robust external performance, and may enable more precise risk-based care while reducing unnecessary imaging and invasive procedures; clinical utility will be tested via decision-curve and implementation analyses.

#6728 Predicting gastric cancer response to anti-PD-1 first-line treatment based on multi-modal data: A multi-center study.

J. Wang[1], P. Kuang[2], Y. Lin[3], Y. Liu[1], K. Zheng[2], Y. Jiang[4], G. Yu[4], Y. Ding[1], Y. Hou[1], T. Liu[5];

[1]Zhongshan Hospital Fudan University, Shanghai, China, [2]The First Affiliated Hospital of Nanchang University, Nanchang, China, [3]Zhongshan Hospital (Xiamen), Fudan University, Shanghai, China, [4]Yangtze River Delta Guozhi (Shanghai) Intelligent Medical Technology Co., Ltd., Shanghai, China, [5]Zhongshan Hospital, Fudan University, Shanghai, China

Objectives: Excepted for PD-L1 expression, no predictive maker for immunotherapy has been identified in gastric cancer. Our study aimed to develop a multimodal deep learning model by integrating clinical features, CT-derived radiomics, and H&E-based pathomics to accurately predict the efficacy of first-line immunotherapy in gastric cancer.

Methods: This multicenter diagnostic study retrospectively enrolled 477 gastric cancer patients from 5 centers. Whole-slide images (WSIs) underwent a weakly supervised computational pathology pipeline: CLAM extracted patch-level representations, which were organized into spatially coherent structures for histological pattern aggregation; handcrafted pathomics features (morphological, textural, color) were also extracted to complement deep learning pathology embeddings. Contrast-enhanced CT images were segmented via a nnU-Net cascade. The nnU-Net encoder generated deep radiological embeddings, while handcrafted radiomics features (first-order statistics, texture matrices, shape descriptors) were computed from segmented regions to quantify tumor heterogeneity. A Transformer-based architecture integrated the above pathology/imaging features and patient metastatic information via cross-modal self-attention, enabling synergistic multimodal learning.

Results: The dataset was allocated into training (n = 322, Center 1) and validation cohort (n = 115, Center 2-5). The integrated clinical-radio-pathomic (CRP) model demonstrated strong performance (Validation AUC = 0.857, Test set AUC=0.917, C-index = 0.746 for PFS prediction and C-index = 0.864 for OS prediction) and emerged as an independent prognostic biomarker for PFS (hazard ratio [HR] = 4.29, 95% confidence interval [CI],1.20-15.35, p = 0.025) and OS (HR = 8.39, 95% CI, 1.47-47.75, p = 0.017) controlling for other clinical variables (i.e., age, sex and PD-L1 CPS). Importantly, the CRP model outperformed unimodal models derived from radiology (Test AUC = 0.7583,Validation AUC = 0.759) or pathology (Test AUC = 0.83;Validation AUC = 0.796) alone, as well as PD-L1 CPS.

Conclusion: Our findings highlight the promise of multimodal deep learning in precisely identifying patients who are most likely to benefit from first-line immunotherapy.

: Metabolic Signaling and Therapeutic Vulnerabilities in Cancer
Minisymposium

#6802 Metabolite signaling drives oncogenic neuron-glioma crosstalk.

K. G. Abdullah[1], K. Miki[1], C. Edgar[2], S. Wu[2], Y. Xiao[2], M. R. Savani[2], M. T. Ghoche[1], J. I. Traylor[3], H. Yuan-Tai[4], D. D. Shi[5], M. Tang[2], S. Oken[1], N. Manoj[1], V. T. Puliyappadamba[2], P. Kaphle[2], T. Shipman[2], R. E. West III[6], S. Ma[2], T. Nolin[6], P. O. Zinn[1], L. G. Zacharias[2], T. P. Mathews[2], J. Gibson[4], K. Huber[4], S. Chamberland[7], R. J. DeBerardinis[2], S. K. McBrayer[2];
[1]Department of Neurosurgery, University of Pittsburgh School of Medicine, Pittsburgh, PA, [2]UT Southwestern Children's Medical Center Research Institute, Dallas, TX, [3]Department of Neurological Surgery, University of Texas Southwestern Medical Center, Dallas, TX, [4]Department of Neuroscience, University of Texas Southwestern Medical Center, Dallas, TX, [5]Department of Radiation Oncology, Dana-Farber/Brigham and Women's Cancer Center, Harvard Medical School, Boston, MA, [6]Department of Pharmacy and Therapeutics, University of Pittsburgh, Pittsburgh, PA, [7]Department of Neuroscience, University of Pittsburgh, Pittsburgh, PA

Our knowledge of the metabolic alterations that modulate glioma-neuron interactions is limited. Therefore, we performed unbiased metabolite profiling on 91 high grade gliomas, lower grade gliomas, brain metastases, and non-malignant brain tissues. Accumulation of guanidinoacetate (GAA), an intermediate in the creatine synthesis pathway, was a hallmark of high grade gliomas, displaying a nearly 100-fold increase in these tumors versus non-malignant brain tissues. However, creatine and related metabolites were not enriched, suggesting that GAA may play a non-canonical role. We found that glioma stem-like cell (GSC) lines robustly synthesize GAA but secrete this metabolite rather than using it to produce creatine.
This finding has a correlate in GAMT deficiency, an inborn error of metabolism in which GAA accumulates and causes neuronal hyperexcitability, neurological deficits, and seizures. These effects are also observed in glioma patients, but the mechanisms underlying neuronal hyperactivity in this context are not fully understood. We hypothesized that high grade gliomas reprogram the creatine synthesis pathway to generate and release GAA, which signals to surrounding neurons, drives local electrochemical activity and promotes glioma aggressiveness.
We found that GAA accumulation excites local, but not distal, neurons in xenografted brain slices. In patch-clamp recording studies, GAA decreased neuronal input resistance by acting as a $GABA_A$ receptor agonist. Although GABA signaling is inhibitory in the adult brain, we found that chloride dysregulation in the glioma microenvironment triggers excitatory GABAergic neurotransmission in response to GAA stimulation. Treating glioma-infiltrated brain tissue with a KCC2 chloride transporter agonist abolished GAA-induced hyperexcitability. Although genetic ablation of GAA synthesis had no effect on GSCs grown in vitro or in subcutaneous xenografts, inhibiting GAA production in orthotopic xenografts reduced local neuronal activity and extended survival of tumor-bearing mice. Collectively, our work nominates GAA as a targetable signaling metabolite that drives oncogenic crosstalk between glioma cells and neurons.

#6803 Targeting mitochondrial complex I overcomes adaptive response to chemotherapy in advanced pancreatic cancer.

S. Attanasio[1], F. Citron[1], R. Shah[1], F. Saj[1], Z. Liu[1], I.-L. Ho[1], E.-Y. Yen[1], C. Dyke[1], H. Kwon[1], L. Cecchetto[1], Z. Chen[1], E. Granato[1], S. S. Sainani[1], S. Loponte[1], Y. Chu[1], M. Seoung[1], L. Perelli[1], S. Jiang[1], P. Dutta[1], P. Bhattacharya[1], H. Wang[1], L. Wang[1], M. P. Kim[1], G. Genovese[1], C. A. Lyssiotis[2], D. G. Menter[1], G. F. Draetta[1], S. Kopetz[1], A. Maitra[3], S. Pant[1], A. Viale[1];
[1]UT MD Anderson Cancer Center, Houston, TX, [2]University of Michigan, Ann Arbor, MI, [3]Perlmutter Cancer Center, New York, NY

Chemotherapy remains the mainstay for treatment in patients with advanced pancreatic ductal adenocarcinoma (PDAC), but acquired therapeutic resistance remains a major challenge to sustaining responses. Here, we leveraged a high complexity barcoding technology to identify and isolate clonal lineages showing different sensitivity to chemotherapy *in vivo* in PDAC. Using transcriptomic profiling of chemotherapy sensitive and non-sensitive clonal lineages, we developed a prognostic gene signature named as chemo-type that enables the stratification of patients survival and predicts their response to chemotherapy in two independent datasets including n=301 human PDAC patients. We applied the chemo-type signature to stratify n=36 patient-derived xenograft models of PDAC based on their sensitivity to chemotherapy and to investigate vulnerabilities. We found that Oxidative Phosphorylation (OxPhos) is an adaptive stress response to chemotherapy in a subset of PDAC xenograft models which can potentially benefit from OxPhos inhibition and can be predicted by the chemo-type signature. We demonstrated that a combinatorial approach targeting OxPhos in addition with chemotherapy in PDAC xenograft models eradicates chemotherapy-resistant clones, thereby suppressing tumor relapse and prolonging survival, using a new inhibitor of the mitochondrial complex I named as IM156, which is currently under evaluation in a phase Ib clinical trial for patients with advanced pancreatic cancer.

#6804 Estrogen therapy alleviates cancer-associated cachexia in mouse models of both sexes.

V. T. Pham, V. Sanchez, S. Fu, Y. Nie, K. Liu, Y. Luan, L. Jin, G. Huang;
UT Health San Antonio, San Antonio, TX

Cancer-associated cachexia (CAC) is a multifactorial wasting syndrome marked by progressive loss of skeletal muscle and adipose tissue, affecting up to 80% of patients with advanced cancers and directly contributing to 20-30% of cancer-related deaths. It not only reduces quality of life but also impairs tolerance to therapy and worsens prognosis. Despite its prevalence and impact, CAC remains under-investigated, and although several agents are under clinical evaluation, no FDA-approved treatments exist. The lack of effective therapies represents a critical unmet medical need, as current supportive measures offer little benefit once tissue wasting begins. Clinically, male patients experience more severe and frequent CAC than female patients, suggesting a protective role for female-specific factor(s). To explore this, C57BL/6 mice were inoculated subcutaneously with B16F10 melanoma or KPL ($Kras^{G12D/+}$; $p53^{-/-}$; $Lkb1^{-/-}$) lung cancer cells, our two established models that recapitulate CAC features including severe anemia, muscle wasting, and adipose atrophy. Consistent with patients' data, male mice inoculated with cancer cells also developed significantly more severe CAC features than female mice. To determine whether gonadal hormones influenced this difference, mice of both sexes underwent gonadectomy before tumor implantation. Interestingly, ovariectomy in females markedly worsened CAC symptoms and abrogated female protection, while castration in males produced no effect on severity of CAC, indicating that ovarian factors likely help protect against tissue wasting. Among these factors, 17β-estradiol (E2) was identified as a key candidate due to its known metabolic and tissue-preserving effects. Importantly, when male and ovariectomized female mice were treated with controlled-release E2 pellets before tumor challenge, E2 supplementation preserved skeletal muscle and subcutaneous white adipose tissue, though it had minimal impact on visceral fat and failed to reverse CAC-associated anemia. Thus, these new findings suggest that E2 signaling plays a protective role in CAC progression and could represent a novel therapeutic target. Given the availability of FDA-approved agents that modulate E2 pathways, further studies combining E2 with treatments such as erythropoietin (EPO) may offer new opportunities to address the urgent need for effective CAC therapies and improve outcomes for patients suffering from this devastating condition.

#6805 A ketogenic diet sensitizes pancreatic cancer to metabolic therapies.

O. Hajihassani[1], A. Roichman[2], J. A. Boyer[1], M. MacArthur[2], R. Cordova[2], P. Sunita[1], G. Dey[1], P. Rezvani[1], A. Loftus[3], C. Boutros[1], J. Hue[1], P. Naji[1], N. Manzoor[1], A. Buch[1], H. J Graor[1], J. D. Rabinowitz[2], J. M. Winter[3];

[1]Case Comprehensive Cancer Center, Case Western Reserve University, Cleveland, OH, [2]Ludwig Institute for Cancer Research, Princeton University, Princeton, NJ, [3]UH Cleveland Medical Center, University Heights, OH

Background: Pancreatic cancer is the third leading cause of cancer-related death in the United States, and current chemotherapy options provide limited benefit. Recent studies have shown that a ketogenic diet (KD) can exert anti-tumor effects by reprogramming tumor metabolism and exposing new therapeutic vulnerabilities[1]. Efforts to target glutamine metabolism—an essential pathway in many cancers—have shown promise in preclinical models but have not translated into significant clinical success.

Methods: A ketogenic diet was administered to mice, along with a normal diet in control mice. Pancreatic cancer xenografts were monitored for growth and harvested for biochemical analyses. Tumors were analyzed for metabolites and histone modification by LC/GC-MS and for oxidative stress by measuring the levels.

Result: Here, we show that a KD increases tricarboxylic acid (TCA) cycle activity and elevates reliance on glutamine-related metabolites in murine pancreatic cancer models and in vitro under KD-mimicking conditions. This metabolic adaptation is in response to increased tumor dependence on glutamine-mediated anaplerosis to compensate for reduced glucose availability. Additionally, we examined the impact of a ketogenic diet on redox homeostasis and found that tumors from ketogenic-diet-fed mice exhibited a marked increase in ROS levels. This redox imbalance provides further rationale for combining TCA-cycle inhibition with ROS-inducing agents to amplify metabolic and oxidative stress in PDAC tumors. We demonstrate that combining glutamine metabolism inhibitors, such as CB839 or 6-diazo-5-oxo-L-norleucine (DON), with a KD leads to robust anti-tumor effects in preclinical models of pancreatic cancer. Moreover, the combination of ivosidenib and a ketogenic diet caused a synergistic rise in intratumoral ROS and yielded a 50% survival benefit in treated mice.

Conclusion: Together, these findings demonstrate that a ketogenic diet exposes a metabolic and redox vulnerability in PDAC by increasing reliance on glutamine-driven anaplerosis and elevating intratumoral ROS. Exploiting this state with targeted metabolic inhibitors—alone or in combination with ROS-inducing agents—produces potent anti-tumor responses and highlights a promising therapeutic strategy for pancreatic cancer.

#6806 Metabolic changes associated with senescence in CAFs regulate fibrosis in pancreatic cancer.

D. Sen[1], J. I. Belle[1], B. L. Knolhoff[1], G. Qian[2], P. P. Provenzano[2], D. G. DeNardo[1];
[1]Washington University School of Medicine in St. Louis, Saint Louis, MO, [2]University of Minnesota, Minneapolis, MN

Pancreatic Ductal Adenocarcinoma (PDAC) remains one of the deadliest solid malignancies, with only 13% of patients surviving beyond five years. This dismal prognosis is largely attributed to the metastatic nature of the disease and its resistance to both cytotoxic and immune-based therapies. The treatment-refractory nature of PDAC has been linked to its tumor microenvironment, characterized by a dense fibrotic stroma and impaired immune surveillance. Cancer-associated fibroblasts (CAFs) and the extracellular matrix (ECM) are prominent components of the PDAC stroma. However, CAFs are functionally and phenotypically heterogeneous and thus can harbor both pro- and anti-tumorigenic effects. PDAC contains several subpopulations of CAFs, including *1)* antigen-presenting fibroblasts (apCAFs), *2)*inflammatory fibroblasts (iCAFs), and *3)* myofibroblasts (myCAFs). Although heterogeneity in CAF phenotypes has been investigated, it remains unclear whether CAF subtypes differ in their metabolic profiles and how this metabolic diversity impacts the fibroinflammatory microenvironment of PDAC. Recently, we identified a subset of myofibroblasts in PDAC that have undergone senescence, which we termed “senescent CAFs” (senCAFs). Using a genetic mouse model of spontaneous PDAC with inducible senescent cell depletion {*LSL-KRAS^{G12D}; p53^{flox}; p48-CRE; INK-ATTAC* (KPPC-IA)}, we demonstrated that senCAFs support tumor growth by inducing fibrosis and compromising anti-tumor immunity. In this study, we aimed to determine whether senescence in CAFs is accompanied by metabolic reprogramming and if these metabolic changes are required for the profibrotic property of senCAFs. To address this, we first assessed the architecture of the ECM deposited by senescent fibroblasts using immunofluorescence imaging and found that the collagen fibers deposited by senescent fibroblasts are thicker compared to those from non-senescent fibroblasts. Moreover, transcriptomic and metabolomic analysis on senescent and non-senescent fibroblasts showed an increase in glycolysis and impaired tricarboxylic acid (TCA) cycle flux and mitochondrial function in the senescent fibroblasts. Interestingly, these metabolic changes associated with senescence in fibroblasts led to the accumulation of cellular α-ketoglutarate, a key metabolite required for prolyl 4-hydroxylase and lysyl hydroxylase-dependent collagen hydroxylation and subsequent triple-helix formation. Transcriptomic analysis also revealed high gene expression of collagen prolyl 4-hydroxylase (*P4ha2*, *P4ha3* & *P4hb*) and lysyl hydroxylase (*Plod1*) in senCAFs compared to myofibroblasts. Together, our current data demonstrate differences in the metabolism and architecture of the ECM deposited by senescent CAFs and myofibroblasts. Future experiments will test whether these metabolic alterations in senCAFs impact fibrosis and the progression of PDAC.

#6807 Mitochondrial genome alterations as early drivers of lung adenocarcinoma evolution.

Alvaro Gutierrez[1], Ido Sloma[2], Adrian Daniel Schubert[3], Karthik Suresh[4], Mohammad Obaidul Hoque[3], Carmen Gloria Ili[1], Evgeny Izumchenko[5], Santanu Dasgupta[6], David Sidransky[7]

[1]Center of Excellence in Translational Medicine (CEMT- BIOREN), Universidad de la Frontera, Temuco, Chile,[2]Champions Oncology, Rockville, MD,[3]The Sidney Kimmel Comprehensive Cancer Center, Johns Hopkins University School of Medicine, Baltimore, MD,[4]Division of Pulmonary Critical Care Medicine, Johns Hopkins University, Baltimore, MD,[5]Department of Medicine, Hematology & Oncology, University of Chicago, Chicago, IL,[6]Department of Pathology, University of South Alabama, Mobile, AL,[7]Department of Otolaryngology-Head and Neck Surgery, Johns Hopkins University School of Medicine, Baltimore, MD

Lung adenocarcinoma (LUAD) is thought to arise gradually, beginning as atypical adenomatous hyperplasia (AAH) and advancing through adenocarcinoma in situ (AIS) toward minimally invasive adenocarcinoma (MIA). Although this progression is well-described, the biological events that trigger and sustain these early transitions remain unclear Mitochondrial DNA (mtDNA) is present in many copies, lacks histone protection, and is continually exposed to oxidative stress, making it more prone to mutation than nuclear DNA. Consequently, alterations in the mitochondrial genome may provide an opportunity to identify and classify potentially aggressive preneoplastic lesions long before they reach an invasive stage. We analyzed 109 lesions from 37 non-small-cell lung cancer (NSCLC) patients, encompassing the continuum of AAH, AIS, MIA, and ACA. Whole mitochondrial genome (16.5kb) was sequenced from formalin fixed paraffin embedded (FFPE) tumor and matched normal samples using an amplicon-based Illumina NextSeq approach. Variant detection was performed with a custom pipeline (BWA, SAMtools, GATK Mutect2). We observed that somatic mtDNA alterations arise very early in the neoplastic sequence, with AAH lesions carrying numerous changes across the non-coding tRNA, rRNA, and D-loop regions, as well as repeated nonsynonymous variants in OXPHOS coding genes such as MT-ND5, MT-ATP8, and MT-CYB. Several of these mutations appeared in lesions located in different areas of the same lung, pointing to an early clonal expansion rather than isolated, random events. As lesions advanced into AIS and then MIA, the number of mitochondrial alterations increased steadily. MIA, in particular, showed the greatest accumulation of non-coding changes, and coding variants such as A8860G (ATP6) were frequent across most cases, suggesting that these alterations are not simply incidental. The expression data followed a similar trend. Specifically, in AAH and AIS, numerous mtDNA encoded OXPHOS genes showed higher expression, reflecting an early compensatory response to emerging dysfunction. By the time lesions reached the MIA stage, this pattern became less consistent, with greater variability among patient samples. Once the disease progressed to fully invasive adenocarcinoma, mitochondrial transcripts dropped broadly, fitting with at least partial metabolic shift toward glycolysis known to accompany invasion. Taken together, these patterns point toward early mtDNA instability and evolving mitochondrial transcription as features that accompany and possibly shape the stepwise development of LUAD. Acknowledgements: We extend our special thanks to patients and clinical teams at Johns Hopkins, supported by NCI EDRN grant U01CA271896 . We also acknowledge ANID for providing scholarship funding (21222011, 242230375, 752230204) and Swiss Cancer League grant (BIL KLS-3649-02-2015).

#6808 Targeting metabolism in BRCA-deficient tumors.

M. Di Tano[1], M. Ahmed[2], L. Shiri[2], M. Lyashenko[2], N. Ruthen[3], E. Tse[3], D. Pradella[3], C. Echeverria-Andrade[1], I. Nathoo[1], J. Sanford[1], E. Dantas[1], J. Kim[1], A. Saleh[2], R. Kyu[2], E. Reznik[3], L. C. Cantley[4], M. D. Goncalves[1];

[1]NYU Langone Health, New York, NY, [2]Weill Cornell Medical Center, New York, NY, [3]Memorial Sloan Kettering Cancer Center, New York, NY, [4]Dana-Farber Cancer Institute, Boston, MA

Up to 10% of all cancers are attributed to genetic predisposition, with inherited mutations in *BRCA1* and *BRCA2* being the most significant risk factors for developing breast and ovarian cancers. These mutations also increase susceptibility to other malignancies, including prostate, pancreatic, and colorectal cancers. The BRCA1 and BRCA2 proteins play essential roles in homologous recombination (HR), an error-free DNA repair process. When cells lack functional BRCA1 or BRCA2, they become reliant on alternative, error-prone DNA repair mechanisms, which drive genomic instability and tumorigenesis. Although Poly (ADP-ribose) polymerase (PARP) inhibitors have revolutionized targeted therapy for tumors with *BRCA1/2* mutations, the emergence of resistance limits their long-term efficacy, highlighting the urgent need for novel therapeutic strategies. Cancer metabolism of BRCA1/2-deficient tumors remains largely uncharacterized and poorly understood.To address this gap, we analyzed 10,619 tumors representing 33 cancer types using data from The Cancer Genome Atlas (TCGA). Our findings revealed that tumors with HR deficiency signatures exhibit distinct metabolic profiles compared to HR-proficient tumors. Further validation in BRCA2-/- cancer cell models confirmed that BRCA2-deficient tumor cells rely heavily on the activity of pyruvate kinase (PK), an enzyme that catalyzes the final step of glycolysis. Pyruvate kinase exists as two splice isoforms: PKM1, which is constitutively active, and PKM2, which is allosterically regulated. Most cancer cells predominantly express PKM2, as its low activity state enables metabolic flexibility by redirecting glucose-derived carbons from energy production to biosynthesis for growth and survival. Remarkably, we showed for the first time that BRCA1/2-deficient tumor cells and mouse-derived tumors, not only express PKM2, but also the constitutively active PKM1. Therefore, we targeted PKM, and we found that PKM activators selectively kill BRCA2-deficient cancer cells, but not BRCA2-proficient ones, by inducing DNA damage, reducing lactate production, and decreasing glucose oxidation. Notably, PKM1 overexpression in BRCA2-proficient cells phenocopies the sensitivity of BRCA2-deficient cells to PKM activators, suggesting that PKM1 mediates, at least in part, this effect. Our results also reveal that the toxic impact of PKM activators in BRCA2-deficient cancer cells involves impaired mitophagy and mitochondrial dysfunction.
Together, these findings provide a strong rationale for targeting pyruvate kinase in BRCA1/2 deficient and potentially other HR-deficient tumor subtypes.

: Population Sciences at the Forefront 2: Molecular and Genetic Epidemiology of Cancer Risk and Outcomes
Minisymposium

#6811 Plasma proteomic signature for persistent smoking effects and its association with risk of smoking-related cancers among former smokers.
D. Le, Q. Cai, J. Long, S. M. Nguyen, W. Zheng, X.-O. Shu;
Vanderbilt University School of Medicine, Nashville, TN

Background: Previous studies have identified circulating protein signatures associated with smoking, which were associated with cancer risk and reduced with years of smoking cessation. A protein signature for persistent smoking effects after quitting smoking is not available. Our study aims to fill this research gap.
Methods: Included in the study are 47,166 UK Biobank participants, aged from 39 to 70 years at baseline without any cancer history, with proteomics and complete smoking history. A total of 2,911 plasma proteins with less than 20% missing values were analyzed. Linear regression analyses were conducted to identify smoking-related proteins among current (N=4,036) and never smokers (N=32,664), adjusting for age, sex, race, alcohol consumption, body mass index, and Townsend deprivation index. To identify protein biomarkers capturing persistent smoking effects, we analyzed smoking-related proteins among former (N=10,466) and never smokers (N=32,664) using similar linear regression analyses. Proteins with significant associations with former smoking status at FDR-corrected p-value < 0.05 were retained for further analysis. We then applied elastic net regression to the regression residuals of proteins to develop a protein signature for persistent smoking effect (PSPSE), using a 70% training and 30% testing sets, which were randomly split between former and never smokers. The PSPSE was derived by a weighted sum of the selected proteins using their coefficients from the elastic net analysis. We used Cox proportional hazard regressions to examine associations between the PSPSE and risk of 12 smoking-related cancers (SRC), including lung cancer (LC) and upper aerodigestive tract cancer (UATC).
Results: Of 2,911 proteins tested, 2081 proteins were associated with current smoking status at FDR p<0.05. Among them, 1,039 proteins were associated with former smoking status at FDR p<0.05. Of them, 242 proteins were selected to develop the PSPSE among 10,466 former smokers. The PSPSE achieved an area under the curve (AUC) of 0.73 in the training set and 0.70 in the testing set. The PSPSE was significantly associated with the elevated risk of SRC (Hazard ratio (HR)=1.33, 95%CI: 1.17-1.51), LC (HR=1.94, 95%CI: 1.52-2.48), and UATC (HR=1.48, 95%CI: 1.06-2.07) independently of smoking pack-year and quitting duration among former smokers. The PSPSE was not related to an increased risk of non-smoking-related cancers.
Conclusions: We developed a proteomics signature capturing the persistent smoking effect among former smokers, which was associated with elevated risks of SRC, particularly LC. If validated, the PSPSE can be used to identify former smokers at high risk of developing cancer for close surveillance and primary prevention. Updated results will be presented at the meeting.

#6812 Adult height and prostate cancer in the Health Professionals Follow-Up Study: Integrating epidemiologic, genetic, and transcriptomic evidence.

A. Wang[1], M. J. Ro[2], M. R. Shanahan[3], D. Fu[3], H. E. Guard[3], J. B. Vaselkiv[3], S. A. Smith-Warner[3], K. H. Stopsack[4], D. Baynes[5], M. Loda[6], A. Pettersson[7], E. L. Giovannucci[3], S. Sutcliffe[8], S. Tyekucheva[9], B. F. Darst[10], L. A. Mucci[3];

[1]University of Southern California, Los Angeles, CA, [2]Harvard College, Boston, MA, [3]Harvard T.H. Chan School of Public Health, Boston, MA, [4]Leibniz Institute for Prevention Research and Epidemiology, Bremen, Germany, [5]Massachusetts Institute of Technology, Boston, MA, [6]Weill Cornell Medicine, New York, NY, [7]Karolinska Institute, Stockholme, Sweden, [8]Washington University in St. Louis, St. Louis, MO, [9]Dana-Farber Cancer Institute, Boston, MA, [10]Fred Hutchinson Cancer Center, Seattle, WA

Taller height has been associated with increased risk of incident and fatal prostate cancer, potentially through hormonal and growth factor activity during early life. We investigated this association by integrating early-life diet, germline genetics, and tumor biology. We included 49,370 men in the Health Professionals Follow-up Study who were cancer-free at study enrollment in 1986 and were followed through 2020. Cox models with age as the time scale estimated hazard ratios (HRs) and 95% confidence intervals (CIs) for height and total and fatal prostate cancer, adjusting for demographics, BMI, smoking, and PSA screening. To decompose height into its determinants, we derived two residual height measures: genetic residual height from regressing observed height on the height polygenic risk score, and dietary residual height from regressing height on teenage dairy intake to isolate early-life dietary influences. To assess prostate tissue-specific effects of height, transcriptomic profiling was performed on prostate tumor (n = 418) and adjacent normal tissue (n = 209) using Affymetrix GeneChip arrays, and on stromal tissue (n = 272 tumor-adjacent, n = 120 tumor-distant) using RNA sequencing. Differential gene expression was analyzed with *limma*, and pathway enrichment with *CAMERA* using Gene Ontology Biological Process annotations. At enrollment, median age was 54 years (IQR 46-62) and median height was 70 inches (IQR 68-72). Over a median of 28 years of follow-up, 8326 prostate cancer cases were diagnosed, including 1189 fatal cases. Taller height was associated with increased risk of fatal (HR per 5 cm: 1.06, 95% CI 1.01-1.11) but not total prostate cancer (HR 1.00, 95% CI 0.98-1.01). The association for genetic residual height with fatal disease was null (HR ≈ 1), suggesting germline genetics largely explains the observed association. Associations using dietary residual height were similar to those for observed height, indicating minimal contribution from early-life diet. Transcriptomic analysis identified 82 height-associated pathways in tumor and 77 in adjacent normal tissue (FDR < 0.05), with top pathways enriched for mRNA splicing regulation and fatty acid metabolism. In stromal tissue, 63 and 15 pathways were identified in tumor-adjacent and tumor-distant stroma, enriched for cytoplasmic translation and sensory perception/stimuli detection. Taller height was associated with increased risk of fatal prostate cancer during up to 34 years of follow-up. The attenuated association after accounting for genetic determinants of height suggests shared genetics between height and prostate cancer, while early-life dairy intake showed minimal impact. Transcriptomic evidence revealed differentially enriched pathways in the tumor and stroma, suggesting potential height-associated downstream biological processes in prostate cancer development.

#6813 Characterization of high-grade serous ovarian cancer copy number alterations in Black and White Women.

I. M. Vlasac[1], B. M. Reid[2], C. Johnson[3], A. R. Richards[2], C. M. Colin Leitzinger[2], S. J. Yoder[2], D. Roeber[4], T. Mesa[2], A. Berchuck[5], B. Fridley[6], J.-Y. Chern[4], J. A. Doherty[7], K. Haller[3], S. Tworoger[8], J. R. Marks[9], J. M. Schildkrau[3], B. C. Christensen[1], L. C. Peres[2], L. A. Salas Diaz[1], on behalf of the African American Cancer Epidemiology Study;
[1]Dartmouth Geisel School of Medicine, Hanover, NH, [2]Moffitt Cancer Center, Tampa, FL, [3]Emory University, Atlanta, GA, [4]Moffit Cancer Center, Tampa, FL, [5]Duke University School of Medicine, Durham, NC, [6]Children's Mercy Hospital, Kansas City, MO, [7]The University of Utah, Salt Lake City, UT, [8]Oregon Health & Science University, Portland, OH, [9]Duke University, Durham, NC

Background: High-grade serous ovarian cancer (HGSC) is a deadly gynecologic cancer and is characterized by widespread copy number alterations (CNA). However, knowledge of racial differences in HGSC CNA is limited. Using methylation-inferred CNA, we defined and characterized CNA-based tumor clusters to assess patterns by self-reported race.
Methods: Tumor CNA were calculated using Illumina EPIC v1/v2 methylation data for 678 cohort participants (African American Cancer Epidemiology Study, North Carolina Ovarian Cancer Study, Nurses' Health Study) compared to 296 blood samples. Probes were binned (≥10; ≥100 kb), segmented using circular binary methods, autocorrected, and filtered (|mean log R ratio|≥0.3; >4 markers), to define cytoband-level copy number states (-1-loss /0-neutral /+1-gain). CNA were clustered with Ward's method. For each cluster, we computed length-weighted cytoband burden (% genome in gain, loss, or neutral states) and region-level ORs to identify CNA-enriched regions. Models clustered by race were then fit to assess differences.
Results: Combined analysis of HGSC samples from 403 White (59%) and 275 Black women (41%), identified three CNA clusters: C1 (27%), C2 (57%), and C3 (15%). Clusters showed distinct genomic burdens (Kruskal-Wallis $p<10^{-55}$). C1 showed widespread losses, notably in 4q (~75% vs 14% in C2/C3, q<10-45), which has been reported in HGSOC, and 17p (71% vs 13% in C2/C3, q<10-46), which includes TP53. C3 exhibited extensive chromosomal gains, including 20p/q (~82%/72%, q <10-38), 1q/1p (~64%/39%, q<10-32), and 2p/2q (~56%/42%, q <10-31). Gains on 2p/q have been linked to advanced stage and poor prognosis, potentially via overexpression of AURKA, GNAS, and TPD52L2. Amplified 1q may enhance DHX9 expression, a regulator of genomic stability, while BARD1 (2q) interacts with BRCA1 in DNA repair; aberrant BARD1 expression correlates with poor outcomes. Cluster membership was similar between Black and White women (C1: 30% vs 26%, C2: 53% vs 59%, C3: 17% vs 15%). However, arm-level copy number racial differences were observed. Overall, 21q loss was more frequent in tumors from Black women (28%) than White women (16%; OR=0.5, 95% CI=0.34-0.73, q=0.02). This difference was most pronounced in C2, where 21q loss occurred in 27% of Black women compared to 10% in White women (OR = 0.31, 95% CI=0.17-0.56, qcluster=0.002).
Conclusion: Broad arm-level CNAs define molecularly distinct HGSC subgroups with characteristic gain/loss patterns. Race-associated genomic alterations, including 21q loss among Black women, appear to be cluster-dependent genomic events suggesting underlying biological heterogeneity related to focal genomic instability or selective pressures rather than the result of wide-spread changes in overall copy number burden.

#6814 Tumor-stroma spatial context of T cell infiltration and exhaustion as determinants of ovarian cancer survival in Black women.

B. M. Reid[1], A. C. Soupir[1], A. J. Alberg[2], E. V. Bandera[3], M. L. Bondy[4], M. L. Cote[5], K. Haller[6], T. Hastert[7], C. Moran Segura[1], J. V. Nguyen[1], E. S. Peters[8], P. D. Terry[9], A. B. Lawson[10], J. R. Marks[11], B. L. Fridley[12], J. M. Schildkraut[6], L. C. Peres[13];

[1]Moffitt Cancer Center, Tampa, FL, [2]University of South Carolina, Columbia, SC, [3]Rutgers, New Brunswick, NJ, [4]Stanford Cancer Institute, Stanford, CA, [5]IUPUI Fairbanks School of Public Health, Indianapolis, IN, [6]Emory University, Atlanta, GA, [7]Wayne State University, Detroit, MI, [8]University of Nebraska Medical Center, Omaha, NE, [9]University of Tennessee, Memphis, TN, [10]The Medical University of South Carolina, Charleston, SC, [11]Duke University, Durham, NC, [12]Children's Mercy Kansas City, Kansas City, [13]H. Lee Moffitt Cancer Center, Tampa, FL

Background: Tumor-infiltrating lymphocytes are associated with improved ovarian cancer (OC) survival in White women but not Black women despite similar T cell abundance. We evaluated whether exhaustion or localization of T cell infiltration may attenuate the survival advantage among Black women using a spatially informed compartment-specific approach to account for heterogeneity of whole tissue sections (WTS).

Methods: Among 221 Black OC cases in the African American Cancer Epidemiology Study, multiplex immunofluorescence and HALO image analysis quantified total (CD3+) and cytotoxic (CD3+CD8+) T cells, along with exhausted (TIM3+) and terminally exhausted (TIM3+PD1+) subsets in FFPE WTS. PANCK-defined tumor and stroma were refined by excluding mixed interface regions detected using point-pattern intensities. Logit-transformed proportions were compared with paired t-tests. Cox proportional hazards estimated associations of compartment features with overall survival, adjusting for clinical factors.

Results: Black OC cases were primarily advanced stage (58%) and high-grade serous carcinoma (HGSC; 69%); mean follow-up was 6.4 years. In tumor, 60% were T cell infiltrated (≥2% of tumor cells), and the median proportion of cytotoxic cells was 30%. Stroma contained 50% more T cells ($p=9.1x10^{-12}$) but lower cytotoxic fractions (ΔT-S = -8%; $p=3.9x10^{-19}$). Immune-excluded tumors (<2% tumor T cells) displayed strong stromal enrichment of total and cytotoxic T cells. Exhausted T cells were rare (1%) with tumors showing higher exhaustion (ΔT-S=1%, $p=1.6x10^{-3}$) and terminal fractions (ΔT-S=15%, $p=8.8x10^{-18}$) than stroma. Neither tumor nor stroma T cell abundance was associated with survival in univariate models. However, in compartment-adjusted models, tumoral cytotoxic T cells were associated with improved survival (hazard ratio [HR]=0.72, 95% confidence interval [CI]=0.53, 0.97), whereas stromal cytotoxic T cells were associated with worse survival (HR=1.65, CI=1.14, 2.37). A larger tumor-stroma gradient in cytotoxic T cells (> tumor) was similarly protective (HR=0.65, CI=0.48, 0.89). In HGSC, that had higher infiltration and exhaustion, infiltrated tumors had improved survival with higher exhaustion (HR=0.83, CI=0.70, 0.98) and terminal exhaustion (HR=0.88, CI=0.79, 0.99), while immune-excluded tumors did not.

Conclusion: Distinct compartment-specific T cell and exhaustion patterns with divergent survival implications were observed in Black women with OC. Cytotoxic T cells confer a survival benefit only when tumor-dominant rather than stroma-dominant, highlighting the importance of characterizing an immune-exclusion phenotype. Improved survival with tumor T cell exhaustion likely indicates active antitumor immunity. WTS-based spatial profiling is essential for accurate interpretation of immune-survival relationships in Black women with OC.

#6815 Biologic processes enriched in the primary tumors of invasive breast cancer patients with disseminated tumor cells.

K. A. Lawson-Michod[1], T. Ahsan[1], K. Malone[1], B. Harmon[1], M. Stackouse[1], P. Seth[1], M. C. Haffner[1], M. Fitzgibbon[1], A. Zevin[1], A. P. Wiita[2], J. Debnath[3], K. E. Varley[4], A. L. Welm[4], S. Riddell[1], C. M. Ghajar[5], C. I. Li[1];

[1]Fred Hutchinson Cancer Center, Seattle, WA, [2]UCSF, San Francisco, CA, [3]UCSF - University of California San Francisco, San Francisco, CA, [4]University of Utah Huntsman Cancer Institute, Salt Lake City, UT, [5]Fred Hutchinson Cancer Research Center, Seattle, WA

Background: Disseminated tumor cells (DTCs) can persist despite systemic therapy and drive distant recurrence, a major cause of breast cancer-related mortality.
Objective: To identify biologic processes enriched in the primary tumors of invasive breast cancer patients with DTCs detected at the time of their breast cancer diagnosis.
Methods: We performed tumor-normal whole-genome sequencing and bulk RNA sequencing on matched tumor and blood specimens from 65 patients with newly diagnosed invasive breast cancer who underwent bone marrow biopsy at diagnosis to assess DTC status. Mutational signatures were identified using *SigProfilerExtractor*. Differential expression and gene set enrichment analyses were conducted with *DESeq2*. Pathways were defined using MSigDB hallmark gene sets. Genes with Bonferroni-adjusted $p < 0.05$ and $|\log_2 \text{fold change}| > 1$ were considered significantly differentially expressed. Analyses were adjusted for tumor purity, tissue source, stage, age, and neoadjuvant therapy.
Results: Among 41 DTC-positive and 24 DTC-negative patients, DTC-positive tumors were more likely to harbor intronic somatic mutations in *MARCHF1* (78.7% vs 56%, $p = 0.001$) and *MARCHF4* (31.9% vs 4%, $p = 0.007$). Mutations in genes within the WNT and RTK-RAS signaling pathways were more frequent in DTC-positive tumors (WNT: 43.5% vs 27.1%, $p = 0.037$; RTK-RAS: 43.5% vs 27.1%, $p = 0.011$). Gene set enrichment revealed upregulation of E2F targets and G2M checkpoint pathways in DTC-positive tumors (normalized enrichment score = 2.12, $p = 0.01$; 2.04, $p = 0.01$, respectively). Individual genes enriched in DTC-positive patients included HAVCR1, TRIM55, MUC13, and KCNJ12. Recurrent somatic mutations in canonical breast cancer genes (*PIK3CA*, *TP53*, *GATA3*, *CHD1*, *MAP3K1*) and mutational signatures associated with APOBEC activity and homologous recombination deficiency occurred similarly across DTC-positive and DTC-negative patients.
Conclusion: Primary tumors of patients with bone marrow DTCs at diagnosis exhibit upregulation of proliferative programs and increased mutation burden in WNT and RTK-RAS signaling genes. These findings highlight candidate biological pathways in the primary tumor that may facilitate early dissemination and persistence of DTCs.

#6816 Germline genetic impact on risk of colorectal cancer according to birth cohorts.

X. Wang[1], C. Turman[1], Y. Chen[1], C. Qu[2], L. Hsu[2], W. J. Gauderman[3], J. D. Potter[2], U. Peters[2], M. Song[1];
[1]Harvard T.H. Chan School of Public Health, Boston, MA, [2]Fred Hutchinson Cancer Research Center, Seattle, WA, [3]University of Southern California, Los Angeles, CA

Background: The incidence of colorectal cancer (CRC) has been rising globally among adults aged under 50 years, particularly those born after the 1950s. We hypothesized that the polygenic risk score (PRS) may show stronger associations with CRC risk in more recent birth cohorts, reflecting interactions between genetic susceptibility and increasingly prevalent life-time environmental exposures such as obesity and sedentary behaviors.
Methods: Among 37,313 CRC cases and 35,891 controls with available birth year information and genetically defined European ancestry from the Genetics and Epidemiology of Colorectal Cancer Consortium, we calculated the PRS as the weighted sum of risk alleles across 205 CRC-associated genetic variants identified so far. We used multivariable logistic models to estimate odds ratios (ORs) and 95% confidence intervals (CIs) of CRC risk associated with PRS across different birth cohorts. We assessed the interaction between PRS and birth cohorts using Wald test and performed subgroup analysis according to age at diagnosis, family history, endoscopic screening, and CRC molecular subtypes.
Results: PRS showed a generally stronger association with risk of CRC across successive birth cohorts (p for interaction = 0.005). The OR for CRC per 1-standard deviation increase in PRS was 1.62 (95% CI: 1.48, 1.78) among individuals born before 1920, 1.55 (1.49, 1.60) for 1920-1929, 1.60 (1.55, 1.65) for 1930-1939, 1.67 (1.61, 1.74) for 1940-1949, 1.64 (1.55, 1.73) for 1950-1959, and 1.79 (1.65, 1.95) for those born in 1960 or later. The birth cohort effect was primarily observed among participants without a first-degree family history of CRC, with ORs of 1.62 (1.45, 1.80) for those born before 1920 and 1.91 (1.73, 2.12) for 1960 or later (p for interaction <0.001). The birth cohort effect did not differ by age at diagnosis or history of screening. Across CRC subsites, the birth cohort effect was observed for distal (p for interaction = 0.003) and rectal CRC (p = 0.002) but not proximal CRC (p = 0.82). For tumor molecular subtypes, we observed no interactions between PRS and birth cohorts for subtypes classified by microsatellite instability, *BRAF* and *KRAS* mutations, or CpG island methylator phenotype, although only 9.7-12.3% CRC cases had molecular data, limiting statistical power.
Conclusions: PRS is more strongly associated with CRC risk in more recent birth cohorts, suggesting the role of gene-environment interaction in the rise in early-onset CRC and highlighting the increasing utility of genetic risk stratification in contemporary populations.

#6817 *STARD13-LATS2* Axis as a potential genetic modifier of BRCA2 in breast cancer.

Shiv Prakash Verma, Mitul Waghmare, Sanchari Bhattacharyya, Catherine Fanjoy, Shao Hong, Xu Zhang, Jonathan Amsalem, Yelena Kemel, Minna Lee, Matthew Buas, Zsofia Stadler, Pedram Razavi, Mark Robson, Sarat Chandarlapaty, Kenneth Offit*, Vijai Joseph*

Memorial Sloan Kettering Cancer Center, New York, NY

Background: Germline *BRCA2* mutations substantially increase breast cancer risk, but penetrance varies, indicating a role for genetic modifiers. These modifiers can influence tumor initiation and progression even among individuals with the same *BRCA2* variant, and their discovery and characterization can improve risk prediction and therapeutic stratification. For many GWAS-identified *BRCA2* modifiers, the biological mechanisms are still unclear. We examined *STARD13*, a cytoskeletal regulator and putative tumor suppressor identified in prior *BRCA2* GWAS signals, may intersect functionally with the Hippo pathway through effects on RhoA-actin dynamics that influence *LATS2* activity, which in turn regulates *YAP/TAZ*-mediated proliferation and genomic stability. Because *LATS2* supports genomic integrity and suppresses oncogenic signaling, we hypothesized that disruption of the *STARD13* and *LATS2* axis may modify *BRCA2*-associated phenotypes in breast epithelial cells.

Methods: *BRCA2* mutants were generated in breast epithelial cell lines using CRISPR/Cas9 genome editing. Allele-specific regulatory effects of the SNPs were assessed by luciferase reporter assays. To investigate *STARD13* as a genetic modifier, siRNA- and shRNA-mediated knockdown was performed in wild-type and *BRCA2* mutant cells. *LATS2* expression was quantified by qRT-PCR. Functional assays measuring proliferation, apoptosis, and DNA damage sensitivity evaluated the impact of *STARD13* knockdown in different *BRCA2* contexts.

Results: In wild-type *BRCA2* cells, *STARD13* knockdown upregulated *LATS2* expression, indicating activation of a compensatory tumor suppressor pathway. In contrast, In BRCA2-mutant cells, loss of STARD13 fails to induce the compensatory increase in LATS2 seen in BRCA2-wild-type cells, identifying STARD13 as a modifier of the BRCA2-deficient state. These data implicate *LATS2* as a modifier of *BRCA2* via *STARD13*-dependent mechanisms. Ongoing experiments in *BRCA2* mutant cell lines and organoids are examining effects on DNA damage, repair, colony formation, gene expression, and responses to PARP inhibitors using shRNA and CRISPR knockouts.

Conclusions: Our findings support *STARD13* as a potential genetic modifier of *BRCA2*, influencing the activity of *LATS2* tumor suppressor and linking cytoskeletal signaling with DNA repair pathways. The differential regulation of *LATS2* in wild-type versus *BRCA2* mutant backgrounds suggests a novel axis that may underlie variation in *BRCA2* penetrance and cancer risk. These studies aim to elucidate the *STARD13-LATS2-BRCA2* interaction network as a determinant of *BRCA2* penetrance, as a potential biomarker to allow targeting to decrease penetrance of hereditary breast cancer in affected kindreds.

(Supported by Breast Cancer Research Foundation and Niehaus Center for Inherited Cancer Genomics).

: Spatial Biomarkers at Single-Cell Resolution: Mapping Tumor Ecosystems with Proteomics, Transcriptomics, and AI
Minisymposium

#6749 Spatial transcriptomics profiling of colorectal cancer tumors in Alaska Native peoples: Discovery of prognostic biomarkers.

G. Chang[1], D. Redwood[2], A. L. Koehne[1], M. Fitzgibbon[3], C. Qu[1], H. Yin[4], E. Donato[1], M. Lin[1], C. Yeung[1], J. J. Tiesinga[2], S. Thomas[1], L. Hsu[1], C. I. Li[1], T. K. Thomas[2], R. Peters[1], J. Huyghe[1]; [1]Public Health Sciences Division, Fred Hutchinson Cancer Center, Seattle, WA, [2]Alaska Native Tribal Health Consortium, Anchorage, AK, [3]Genomics and Bioinformatics, Fred Hutchinson Cancer Center, Seattle, WA, [4]Department of Medicine, Massachusetts General Hospital, Boston, MA

Colorectal cancer (CRC) is the third most commonly diagnosed cancer and has the second-highest mortality rate overall in the United States (US). Appreciable population differences in incidence and mortality rates persist in the US. These differences are particularly pronounced among Alaska Native peoples who, for over 40 years, have experienced the highest incidence and mortality rates, despite dedicated screening efforts. The reasons underlying these high rates are not understood. A key knowledge gap is the lack of studies characterizing the molecular features of colorectal tumors in Alaska Native patients. This study aims to identify tumor and tumor microenvironment (TME) features present at time of diagnosis that are associated with CRC mortality, and that may contribute to the elevated mortality rate.We analyzed treatment-naïve tumor tissue samples from 217 Alaska Native participants with stage I-III CRC diagnosed at the Alaska Native Medical Center from 2000 to 2017. Participants who died from CRC (n=60) were matched 1:2 to participants who did not die from CRC and who lived at least as long after diagnosis as the participant they were matched to (n=157). Matching was based on age at diagnosis, sex, year of diagnosis, and tumor site and stage. The present study included 139 females (64.1%) and 78 males (35.9%). The median age at diagnosis was 68 years (range: 36-85). At diagnosis, 33 participants (15.2%) had stage I, 93 (42.9%) had stage II, and 91 (41.9%) had stage III CRC. We constructed tissue microarrays (TMAs) from formalin-fixed paraffin-embedded (FFPE) tumor tissue blocks (2 tumor center cores and 1 invasive margin core per tissue) and performed spatial transcriptomics profiling using the GeoMx DSP platform and the Whole Transcriptome Atlas panel. We measured gene expression separately in epithelial and stromal tissue compartments. After quality control, adjustment for batch effects, and normalization, we used DESeq2 to find genes associated with CRC mortality. Analysis was stratified by tissue compartment and tumor location. We performed gene set enrichment analyses using the fgsea R package. Differential gene expression results showed significant downregulation of SPINK4 (3.2-fold decrease, false discovery rate [FDR]-adjusted p=4.72e-3) and MUC2 (2.6-fold decrease, FDR-adjusted p=1.37e-3) genes in the tumor center epithelial compartment in participants who died from CRC. Gene set enrichment analyses showed that upregulation of interferon gamma response hallmark genes was associated with favorable prognosis across tissue compartments and tumor locations, while upregulation of epithelial-mesenchymal transition hallmark genes in the tumor margin was associated with worse prognosis (all FDR-adjusted p<0.05). Additional ongoing work includes cell type deconvolution analyses and expansion of the study size to over 400 Alaska Native participants with CRC.

#6750 Highly multiplexed immunoassays enable discovery of multimarker EV surface signatures as novel biomarkers.

L. Hebert[1], M. Al-Ameen[1], E. A. Gizzie[1], C. Nelson[1], J. H. Butler[1], J. C. Brady[2], J. L. Franklin[3], R. J. Cote[4], R. J. Coffey[3], A. B. Nixon[2], **D. A. Routenberg**[1];
[1]Meso Scale Diagnostics, LLC, Rockville, MD, [2]Duke Univ. Medical Ctr., Durham, NC, [3]Vanderbilt University Medical Center, Nashville, TN, [4]Washington University in St. Louis School of Medicine, St. Louis, MO

Extracellular vesicles (EVs) are lipid bilayer particles that mediate cell communication by carrying molecules that reflect their cell of origin. Their enrichment in disease states and accessibility via minimally invasive sampling make them promising biomarkers. EV heterogeneity remains a challenge as single surface markers are often insufficient to define disease-related EV subpopulations, underscoring the need for technologies enabling single-vesicle resolution and multiplexed detection of composite marker signatures. We developed a highly multiplexed immunoassay technique to count combinations of three surface markers on individual, intact EVs. EVs are captured on magnetic beads using antibodies against tetraspanin proteins broadly expressed on EV surfaces, enabling selective EV enrichment and automation. Plasma is pre-processed using a mixed-mode resin that removes >99.5% of proteins while recovering >60% of EVs, followed by immune-depletion of platelet-derived EVs to improve sensitivity for non-platelet EVs. A panel of barcoded antibodies for different cell-surface proteins is used to bind EV surface antigens. When three antibodies co-localize on an EV, barcodes associated with the antibodies are linked to form a DNA product encoding the three target antigens. A library of probes targeting 63 EV surface markers, selected to distinguish circulating EVs from major cell lineages, enables broad phenotyping. DNA products are PCR-amplified and sequenced, quantifying thousands of 3-marker combinations on individual EVs. We applied our technique to 366 plasma samples provided by collaborators from those with colorectal (CRC), breast, and gastric cancer, alongside 47 healthy controls and cell-line-derived EV samples. Technical precision assessed using replicate controls yielded average inter-plate and intra-plate CVs of 19% and 16%, respectively. Spiking defined EV populations into plasma established a detection limit of 1 part in 10^7. Across all cancer types, differential expression analysis identified elevated 3-marker combinations involving cancer-associated markers (e.g., CEA, CD10, CD13 and N-cadherin) relative to controls. Selected EV populations were validated using ultrasensitive electrochemiluminescence (ECL) assays, showing strong correlation with sequencing results (Pearson's $r > 0.8$). In two longitudinal CRC groups, elevated levels of several 3-marker EV signatures were significantly associated with shorter overall and progression-free survival. This multiplexed single-EV assay offers a powerful, sensitive platform for high-throughput profiling of disease-associated EV populations. Its modular design enables flexible selection of marker panels tailored to specific biological questions. Additionally, it can be integrated with ultrasensitive ECL immunoassays for cost-effective, large-scale validation of selected EV signatures.

#6751 Differences in survival outcomes among metastatic colorectal cancer patients across fibroblast growth factor receptor 2 and 3 expression levels.

S. Soto Trujillo[1], Y. Yang[1], M. Bartolini[1], S. Soni[1], P. Mittal[1], F.-S. Ou[2], L. Torres-Gonzalez[1], U. Shah[1], J. H. Lo[1], Y. Goretsky[1], W. Zhang[1], A. Venook[3], S. Algaze[1], J. Millstein[1], H.-J. Lenz[1]; [1]Norris Comprehensive Cancer Center, Keck School of Medicine, Los Angeles, CA, [2]Mayo Clinic, Rochester, MN, [3]University of California, San Francisco, San Francisco, CA

Introduction: Fibroblast growth factor receptor 2 and 3 (FGFR2 and FGFR3) are metabolic genes overexpressed in malignant epithelia. In colorectal cancer (CRC), intimate crosstalk between FGFR2/3 and epidermal growth factor receptor (EGFR) pathways has been suggested but is not fully elucidated. As a result, this study investigated associations between FGFR2/3 expression levels and clinical outcomes in patients with metastatic CRC (mCRC) enrolled in the phase III clinical trial CALGB /SWOG 80405.

Methods: Data from 433 patients with mCRC enrolled in the CALGB/SWOG 80405 trial were analyzed. Patients received either bevacizumab (bev, n = 226) or cetuximab (cet, n = 207) plus chemotherapy as first-line treatment. Tumor RNA was extracted from FFPE samples and processed through the HiSeq 2500 (Ilumina) platform. Median overall survival (OS) and progression-free survival (PFS) curves were evaluated in all treatment subgroups and stratified according to high (H), medium (M), and low (L) FGFR 2 and 3 gene expression levels. Likelihood ratio tests, hazard ratios (HRs), and 95% confidence intervals (CIs) were calculated using Cox proportional hazards multivariate models, adjusting for age, sex, ECOG performance status, tumor location, number of metastatic sites, *KRAS* status, consensus molecular subtypes, and treatment arm.

Results: Both FGFR2 and FGFR3 expression levels were associated with outcomes in patients treated with cetuximab. FGFR2-L tumors showed significantly longer OS compared to the M (HR = 1.04; 95%CI 0.71-1.51) and H (HR = 1.56; 95%CI 1.06-2.28) expression groups (35.7 vs. 31.2 vs. 23.7 months, p = 0.017). In contrast, FGFR3-L tumors were associated with shorter OS compared to the M (HR = 0.63; 95%CI 0.44-0.92) and H (HR = 0.59; 95%CI 0.41-0.85) expression groups (24.7 vs 32.4 vs 37.1 months, p = 0.0009). Significant differences in PFS were not observed. A nominally significant interaction was found between treatment and FGFR3 expression for both PFS (p = 0.02) and OS (p = 0.0003), but no interaction with FGFR2 expression. No significant associations were detected in patients treated with bev. Neither FGFR2 nor FGFR3 suggested to be prognostic markers after multivariate adjustment analyses.

Conclusions: Our findings suggest a predictive role of FGFR3 in patients with mCRC undergoing anti-EGFR treatment. Differences in survival within the cet subgroup suggest that EGFR inhibitor efficacy may be modulated by FGFR2/3 signaling activity. Interestingly, FGFR2 and FGFR3 expressions were inversely and positively correlated with improved OS. The findings suggest that FGFR2 signaling minimizes the specific effects of cetuximab, while FGFR3 signaling amplifies its therapeutic effects. Further studies should determine whether these associations are seen in other anti-EGFR inhibitors and detail the mechanistic interaction between FGFR and EGFR pathways.

#6752 Mapping the spatial organisation of B cells and immune signalling in TNBC to characterise response to immunotherapy.

L. Ahmad[1], X. Wang[1], N. Masque-Soler[1], E. Schrader[1], C.-S. Huang[2], D. Egle[3], M. Callari[4], M. Dugo[5], B. Bermejo[6], C. Zamagni[7], M. Thill[8], A. Anton[9], S. Russo[10], E. Sevillano[11], E. Ciruelos[12], R. Greil[13], B. Győrffy[14], V. Semiglazov[15], M. Colleoni[16], C. M. Kelly[17], L. Del Mastro[18], G. Mariani[19], G. Viale[16], L. Gianni[4], G. Bianchini[20], R. Ali[1];

[1]University of Cambridge, Cambridge, United Kingdom, [2]National Taiwan University Hospital and Taiwan Breast Cancer Consortium, Taipei, Taiwan, [3]Medical University Innsbruck, Innsbruck, Austria, [4]Fondazione Michelangelo, Milan, Italy, [5]IRCCS San Raffaele Hospital, Milan, Italy, [6]Hospital Clinico Universitario de Valencia, Biomedical Research Institute INCLIVA, Valencia, Italy, [7]IRCCS Azienda Ospedaliero-Universitaria di Bologna, Bologna, Italy, [8]Agaplesion Markus Krankenhaus, Frankfurt am Main, Germany, [9]Hospital Universitario Miguel Servet, Zaragoza, Spain, [10]Azienda Sanitaria Universitaria Friuli Centrale, Udine, Italy, [11]Instituto de Investigacion Sanitaria HM Hospitales, Madrid, Spain, [12]Hospital Universitario 12 de Octubre, Madrid, Spain, [13]Paracelsus Medical University of Salzburg, Salzburg, Austria, [14]Semmelweis University, Budapest, Hungary, [15]NN Petrov Research Institute of Oncology, St. Petersburg, Russian Federation, [16]Istituto Europeo di Oncologia, IRCCS, Milan, Italy, [17]Mater Private Hospital and Cancer Trials, Dublin, Ireland, [18]UO Clinica di Oncologia Medica, Genoa, Italy, [19]Fondazione IRCSS - Istituto Nazionale Tumori, Milan, Italy, [20]Fondazione Michelangelo and San Raffaele Hospital, Milan, Italy

In recent years, B cells and tertiary lymphoid structures (TLS) have emerged as key predictors of immunotherapy response across multiple cancers. B cells exist in various states of spatial organisation within the tumour microenvironment (TME), likely supporting many of their functional roles. However, the landscape of B cell spatial organisation in cancer, and specifically in triple-negative breast cancer (TNBC), is poorly characterised. Organisation and function are processes that are likely orchestrated by a diverse set of immune signalling, but the interplay between organisation and its underlying signalling remains largely uncharacterised in cancer, underscoring the need for a comprehensive and systematic investigation. To characterise the spatial landscape of B cells and immune signalling, we implemented a novel approach for the simultaneous detection of protein and RNA in situ using imaging mass cytometry. We applied this assay to a randomised immunotherapy clinical trial, NeoTRIP, where patients with TNBC were treated with neoadjuvant chemotherapy with or without atezolizumab. Samples were collected from 268 patients at three timepoints: baseline, on-treatment and post-treatment. This study identified that germinal centre B, B and plasma cell densities were significantly associated with response to immunotherapy on-treatment. We identified distinct B and plasma cell niches in TNBC, and showed that B activated niche cell densities were also strong predictors of response to immunotherapy. Additionally, we found that many B and plasma to TME interactions were enriched among immunotherapy responders. These findings were complemented by strong treatment-induced cellular dynamics. Strikingly, the most marked increase in TME cell phenotype abundance in immunotherapy responders was observed in B cells - particularly naïve B cells and broader B cell populations, suggesting that effective immunotherapy induces their expansion following treatment. We subsequently showed that cytokines likely behave in a spatially coordinated manner in the TME, being significantly enriched in the vicinity of the observed B and plasma cell niches. Cytokine expression mirrored the observed immune expansion on-treatment and was also associated with immunotherapy response. Specifically, cytokine-enriched niches appeared to be a feature of immunotherapy responders, suggesting that together organisation and signalling play a central role in treatment responses. Together, these findings highlight a previously unexplored diversity of B cell spatial organisation and its associated immune signalling in TNBC, suggesting that B cell features may serve as on-treatment predictors of immunotherapy response.

#6753 AI-powered Deep Visual Proteomics (DVP) links pancreatic precursor biology to PDAC survival phenotypes.

J. Min[1], L. Schweizer[2], G. Zonderland[2], B. C. Selvanesan[3], J. H. Thomsen[2], L. Oldenburg[2], E. Chelebian[2], B. J. Swanson[4], M. A. Hollingsworth[5], P. M. Grandgenett[6], I. Ummat[2], M. Strauss[2], **A. Mund**[2], A. Maitra[1];

[1]Perlmutter Cancer Center, New York, NY, [2]OmicVision Biosciences, Copenhagen, Denmark, [3]MD Anderson Cancer Center, Houston, TX, [4]University of Nebraska Medical Center, Omaha, NE, [5]UNMC Eppley Institute, F&P Buffett Cancer Center, Omaha, NE, [6]UNMC Eppley Institute for Cancer Research, Omaha, NE

Pancreatic ductal adenocarcinoma (PDAC) exhibits 70-80% post-resection recurrence, yet how the earliest molecular events in PanIN precursors connect to divergent survival outcomes remains unclear. We previously established a spatially resolved proteomic atlas of PanINs that revealed molecular reprogramming preceding histological transformation, using Deep Visual Proteomics (DVP). This work mapped acinar-to-ductal metaplasia, incidental ("iPanIN") and cancer-associated ("cPanIN") lesions, and normal ducts into a continuous trajectory to invasive carcinoma and identified four core programs (stress adaptation, immune engagement, metabolic reprogramming, and mitochondrial dysfunction) evident in morphologically normal ducts and low-grade PanINs, alongside cancer-associated field effects. Our MS-based peptide profiling identified KRAS polyclonality at the protein level, independent of genetic sequencing[1] .We now extend this approach using tile-level Deep Visual Proteomics (TileDVP[2]) to analyze a first-of-its-kind, multi-institutional FFPE biobank of matched primary-metastatic tumor pairs from short- and long-term PDAC survivors. Using laser microdissection of ~15 phenotype-matched cells per sample, TileDVP quantifies 3,500-5,000 proteins, enabling high-resolution molecular profiling of tumor cell populations and metastatic niches at the proteomic level. This workflow represents a 300-fold throughput improvement over DVP, while increasing spatial proteomic resolution. We compare proteomic signatures of survival groups across primary tumors, regional and distant metastases, and metastatic niches, and link precursor biology to recurrence patterns, to define how these programs evolve across metastatic sites within and between organs.By unifying precursors, recurrent tumors, and survival phenotypes in a single spatial proteomics framework, this study identifies potential biomarkers for risk stratification and therapeutic targets for earlier intervention in PDAC.

1. Min, J. *et al.* AI-powered Deep Visual Proteomics reveals critical molecular transitions in pancreatic cancer precursors. *bioRxiv* 2025.07.07.663528 (2025) doi:10.1101/2025.07.07.663528.
2. Mathian, É. et al. Clinical Image-Based Procedures, 14th International Workshop, CLIP 2025, Held in Conjunction with MICCAI 2025, Daejeon, South Korea, September 23, 2025, Proceedings. Lect. Notes Comput. Sci. 21-31 (2025) doi:10.1007/978-3-032-05479-1_3.

#6754 Spatial-immune multiomics refines prognostication in early-stage, estrogen receptor-positive breast cancer.

Z. Kinsella[1], A. Chowdhury Jahangir[2], H. N. Nyarko[1], D. Kalinska-Lysiak[3], C. A. Gonzalez[2], V. Murphy[4], A. O'Grady[5], J. Fay[6], K. Sheehan[6], A. Rahman[7], J. Crown[8], C. Kelly[4], S. S. McDade[9], J. Prehn[3], W. M. Gallagher[2], D. P. O'Connor[3];

[1]Royal College of Surgeons in Ireland (RCSI), Dublin, Ireland, [2]University College Dublin, Dublin, Ireland, [3]Royal College of Surgeons in Ireland, Dublin, Ireland, [4]Mater Hospital, Dublin, Ireland, [5]Royal College of Surgeons in 4190, Dublin, Ireland, [6]Beaumont Hospital, Dublin, Ireland, [7]UCD Conway Institute of Biomolec. & Biomed. Res., Dublin, Ireland, [8]St Vincent's Hospital, Dublin, Ireland, [9]Queen's University Belfast, Belfast

Introduction: Despite a strong 5-10 year prognosis, in $ER^{+}HER2^{-}$ breast cancer relapses are common beyond 10 years. Genomic assays employed to determine recurrence risk at diagnosis, and subsequently the required adjuvant treatment, are still ambiguous for a significant proportion of patients with Intermediate risk (i.e. Oncotype Dx Recurrence Score (RS) 16-25). Contemporary management relies on menopausal status as a risk stratifier, which is a source of inaccuracy for the assessment and prescription of personalised treatment regimens.

Methods: We sought to refine risk stratification by incorporating features of the tumour-immune microenvironment. We employed a spatial multiomics workflow to a tissue microarray of Irish patients previously enrolled on the TAILORx trial (whole-transcriptome, ROI-based spatial transcriptomics n=410, 7-plex spatial proteomics n=442). We subsequently validated CD8 IHC in whole-resection specimens of the same patient cohort (n=453). Our primary endpoint was invasive disease-free survival.

Results: Modelling immune infiltration agnostic of underlying genomic risk produced data congruous with the consensus view of ER+HER2- breast cancer immunogenicity. No tumour-infiltrating lymphocyte (TIL) was independently prognostic across the entire cohort, and the distribution of TILs mirrored the categorical 'hot or not' definition of an immunologically "cold" disease (< 10% TILs). However, modelling by underlying genomic risk revealed monotonic trends of increasing TILs and increased risk. We further demonstrated that macrophage and T-helper cells facilitate and impede cytotoxic T-cells, are associated with extracellular matrix remodelling, M2-like macrophage (SPP1) genes, and cytotoxicity (GZMA, GZMB, PRF1), checkpoints (LAG3, PD-1, PD-L2), and exhaustion (TOX) genes respectively, consistent with restrained T-cell activation. Survival analyses underscored how high cytotoxic T-cell infiltrates were associated with poorer 15-year iDFS in patients receiving additional chemoendocrine therapy (CD8 density: High RS $p = 0.017$, FDR < 0.1. CD8%: Intermediate RS $p=0.027$, FDR>0.1). Critically, in randomised treatment arms of the Intermediate RS, a treatment-biomarker interaction indicated chemotherapy inferiority at higher stromal CD8 density (ΔLR-χ^2: 7.36, $p = 0.007$), which was validated orthogonally on whole-resection specimens from the same cohort (ΔLR-χ^2: 7.48, $p = 0.006$).

Conclusions: To our knowledge for the first time, we have outlined a predictive biomarker of chemotherapy inferiority in the Intermediate RS, suggesting a potential treatment change for up to 50% of patients. This discovery requires validation in the larger TAILORx trial before clinical adoption.

#6755 Unbiased phenotyping of CRISPR-edited tumors with Perturb-map and subcellular imaging of the mouse whole transcriptome (22,000-plex).

M. Dhainaut[1], L. Zhang[2], M. Meister[1], A. Mavropoulos[1], A. Benz[1], I. Lee[2], S. McKinzie[2], D. Millman[1], D. Tran[1], D. Ovando[1], L. Cavalcante[1], K. Mitchell[1], E. Margalit[1], D. Antonio[1], A. Mahajan[1], A. Salm[1], E. Siefkas[1], F. Fernandez[1], H. Kaplan[1], H. Winters[1], J. Schmidt[1], J. Tea[1], J. Decalf[1], L. Ryan[1], M. Zolanvari[1], N. Snell[1], R. Schiemann[1], R. Collins[1], R. Huang[1], Y. Xie[1], Y. Falanga[1], S. Virani[1], L. Padron[1], E. Corse[1], S. He[2], D. Bear[1], J. M. Beechem[2], R. W. Alfa[1];
[1]Noetik, San Francisco, CA, [2]Bruker Spatial Biology, Seattle, WA

The heterogeneity of tumor phenotypes in patients, and the lack of a holistic definition of tumor subtypes, are major barriers to achieving clinical success. Many clinical programs have been halted for failing to refine the patient population that would benefit from treatment. Our OCTO suite of machine learning models, trained on multi-modal data generated from 1000s of patient samples, provides a unified and unbiased classification of patient subtypes that does not solely rely on genotypes or expression of specific biomarkers. Though OCTO enables us to identify target populations for active clinical programs, predicting response for preclinical assets is still an unmet need.In contrast to patient tumors, traditional preclinical models are by design homogeneous, and often do not represent an actual patient populations. Using a scaled in vivo CRISPR perturbation platform, Perturb-map, we have generated 600+ mouse model variants of NSCLC. Each tissue section from Perturb-map contains hundreds of individual tumors, each carrying a specific genetic perturbation, spatially resolved with a molecular barcode. We built a multi-modal (H&E, mIF, transcriptomics) dataset profiling 100,000s of individual tumors. A subset of samples was profiled using the mouse Whole Transcriptome (WTx) panel (22,000-plex) using the Cosmx Spatial Molecular Imager, providing the first data set coupling high-throughput CRISPR perturbations in vivo with unbiased phenotyping at subcellular resolution.Leveraging the unique combination of throughput from Perturb-map and depth of phenotyping from the WTx panel, we mapped genetic perturbations to their impact on tumor development at an unprecedented scale. Comprehensive phenotyping of hundreds of CRISPR-edited tumors revealed the impact of each gene perturbation on relevant signaling pathways within tumor cells and on the composition of the tumor microenvironment, including deep characterization of the immune compartment. Specifically, we found significant overlap among the molecular footprints of known tumor drivers in NSCLC (including EGFR, KRAS and STK11 mutations) in preclinical models and in patients. We also linked tumor phenotypes with their sensitivity to specific treatments, including to immune checkpoint blockade.Altogether, we present a unique dataset generated by profiling hundreds of NSCLC preclinical model variants, each carrying a specific genetic perturbation, using a comprehensive Whole Transcriptome (WTx) panel. A subset of mouse tumor archetypes presented characteristics of specific patient tumor subtypes, and could be used to evaluate population-specific drug responses.

: Targeted Protein Degradation and Non-cannonical Oncogenic Signaling
Minisymposium

#6776 Targeting non-enzymatic *HDAC*-mediated repression reveals a selective stress-adaptive mechanism for cancer therapy.

O. Debnath[1], J. Olivet[2], S. Choi[1], Y. Bramerloo[1], J. Blavier[3], T. O'GRADY[3], F. Laval[1], V. Botchkarev, Jr.[1], B. Hu[1], A. Varca[1], J. Bruyr[3], S. Ibrahim[4], T. Jivanjee[4], J. Bromley[4], S. Nyquist[4], N. Calonghi[5], A. Stefan[5], A. Hochkoeppler[5], M. Baietti[6], E. Leucci[6], M. Calderwood[1], T. Hao[1], A. K. Shalek[4], D. E. Hill[1], S. J. Buhrlage[1], S. Dhe-Paganon[1], F. Dequiedt[3], J. Twizere[3], M. Vidal[1]; [1]Dana-Farber Cancer Institute, Boston, MA, [2]Rega Institute for Medical Research, KU Leuven, Leuven, Belgium, [3]University of Liege, Liege, Belgium, [4]Broad Institute of Harvard and MIT, Cambridge, MA, USA, Cambridge, MA, [5]University of Bologna, Bologna, Italy, [6]KU Leuven, Leuven, Belgium

Purpose: Enzymatic pockets, such as those found in histone deacetylases (HDACs), have long served as attractive targets for drug discovery. However, conventional HDAC inhibitors often lack selectivity and cause systemic toxicity due to paralog redundancy and their incorporation into multi-subunit transcriptional regulatory complexes. To identify more selective modulators, we performed an unbiased yeast genetic screen of ~52,000 compounds by interrogating the activity of the conserved HDAC/Rpd3L complex. Follow-up mechanistic studies uncovered hits that do not directly inhibit HDAC catalytic activity but instead modulate repression through alternative mechanisms. We subsequently evaluated the lead compound, E6R, in human neuroblastoma cells and mouse xenografts, benchmarking against the enzymatic inhibitor TSA in vitro and Vorinostat (SAHA) in vivo. These studies demonstrate that E6R, a first-in-class non-enzymatic SIN3-HDAC modulator, achieves comparable anti-tumor efficacy with far greater selectivity and minimal global transcriptional disruption.
Methods: E6R was evaluated in yeast and SK-N-BE(2)-C neuroblastoma cells using bulk and single-cell RNA-seq (Seq-Well S3), SIN3A ChIP-seq, viability and invasion assays, and mouse xenografts.
Results: In yeast, E6R disrupts Sin3/Rpd3L-dependent transcriptional repression without inhibiting HDAC catalytic activity. In human neuroblastoma cells, E6R produced anti-tumor activity comparable to TSA. Transcriptomically, E6R modulated ~14-fold fewer genes than TSA and caused minimal global perturbation. Interestingly, E6R selectively activated stress- and senescence-associated programs governed by the ATF4-driven integrated stress response (ISR), including *GDF15*, *DDIT3*, *ATF3*, and *FGF21*, while inducing minimal off-target effects. SIN3A ChIP-seq revealed promoter-proximal loss of SIN3A binding at several ISR loci, most notably *GDF15* (~55 bp upstream of the TSS), consistent with direct de-repression through dissociation of the SIN3-HDAC complex. Although both compounds shared repression of *E2F*, *MYC*, and glycolytic targets and activation of p53, TNFα/NF-κB, and apoptotic signaling, E6R induced a distinct stress-adaptive state through an HDAC-independent mechanism. Functionally, E6R significantly reduced neuroblastoma cell invasion and tumor growth with limited cytotoxicity. In vivo, E6R inhibited neuroblastoma xenograft growth comparably to Vorinostat, supporting non-enzymatic HDAC modulation as a therapeutic alternative.
Conclusions: Together, these data strongly suggest that E6R is a selective, non-enzymatic SIN3-HDAC modulator that reprograms chromatin from a repressive to a stress-adaptive, anti-proliferative state, offering a mechanistically distinct and potentially safer framework for HDAC-targeted cancer therapy.

#6777 Targeting HIF-2a pathway with a novel and potent ARNT molecular glue degrader for the treatment of renal cell carcinoma.

J. Fathman, C. Sanchez, N. Cruz, Z. Naiman, J. Lee, M. Cruz, I. Tran, K. Chiu, J. Griffin, A. Hernandez, K. Januszyk, X. Liu, B. Lee, A. Burt, J. Tellew, M. Wu, L. Watson, A. Dominguez-Andres, L. Huang, R. Soriano, D. Knece, M. FitzGibbon, A. Grant, M. Matyskiela, R. Beckwith, K. Wagner, B. Wen, P. Chamberlain;
Neomorph, Inc., San Diego, CA

Clear-cell renal cell carcinoma (ccRCC) is often characterized by the inactivation of the von Hippel-Lindau (VHL) gene, leading to the stabilization of hypoxia-inducible factor-2α (HIF-2α) and HIF-1α. HIF-2/1α drive expression of key oncogenic pathway genes involved in angiogenesis, proliferation, metastasis, and tumor immunity; vascular endothelial growth factor (VEGF) being one of these genes. Aryl hydrocarbon receptor nuclear translocator (ARNT), also known as hypoxia-inducible factor-1β (HIF-1β), forms heterodimers with HIF-1/2α and plays an integral role in driving HIF mediated target gene expression. Current therapies targeting HIF-2α in ccRCC and VHL diseases have shown good anti-cancer activity in the clinic. Here we describe NEO-811, an orally bioavailable, potent, selective, cereblon (CRBN)-dependent molecular glue degrader of ARNT as a novel way to target this key pathway in disease progression. NEO-811 showed dose proportional plasma exposure and good bioavailability in mice. Utilizing 786-O xenografts, a human VHL-deficient ccRCC cell line, we show NEO-811 demonstrated deep and sustained degradation of ARNT and modulation of HIF-2α target genes, VEGF and NDRG1. We observed robust efficacy after daily oral dosing of mice bearing 786-O xenografts and showed that NEO-811 was well tolerated and displayed dose dependent tumor regression. Tumor growth inhibition of 786-O xenografts with our ARNT degrader was comparable to treatment with a HIF-2α inhibitor. Importantly, NEO-811 still retained activity in 786-O xenografts that expressed a HIF-2α mutant (i.e., G323E) that conferred resistance to inhibitors. These data provide preclinical evidence and scientific rationale to further investigate NEO-811, a potent and selective ARNT molecular glue degrader, clinically in patients with ccRCC VHL deficient tumors.

#6778 Selective targeting of CCNE1 using molecular glue degraders for the treatment of *CCNE1* amplified cancers.

W. Tahaney[1], Y. Liu[1], A. Abdullah[1], V. Massafra[2], V. Lang[2], M. Baumann[2], A. Dubois[2], A. Osmont[2], X. Lucas[2], C. Quan[1], A. Kostikova[2], A. Diesslin[2], F. Harvey[2], C. Bianda[2], K. Larpenteur[1], K. Jones[1], A.-C. D'Alessandro[2], C. Perdomo Ortiz[2], H. Farine[2], M. Cabanski[2], M. Korpal[1], B. Demarco[1], D. Bonenfant[2], M. Warmuth[1], F. Janku[1], M. Walter[2], S. Townson[1], B. Fasching[1], S. Totoioli[2], C. King[1], L. McAllister[2], B. Ranieri[2], S. Gkountela[2], **R. Tiedt**[2], N. Ilic Widlund[1];

[1]Monte Rosa Therapeutics, Inc., Boston, MA, [2]Monte Rosa Therapeutics AG, Basel, Switzerland

Cyclin E1 (CCNE1) is a critical driver of cell cycle progression and cell proliferation. It acts as the regulatory subunit for the CCNE1-CDK2 holoenzyme, which coordinates cell cycle progression through the G1/S phases and effectively drives cell proliferation via RB phosphorylation and repression. *CCNE1* is frequently amplified or overexpressed across multiple cancer types, including ovarian, endometrial, gastric, breast, and others, and thus pharmacological targeting of CCNE1 is expected to benefit patients whose cancers bear these alterations. Despite the clear therapeutic promise of directly targeting CCNE1 in these patients, CCNE1 has been considered undruggable by conventional means as it is a regulatory non-enzymatic protein. Hence, we sought to identify molecular glue degraders (MGDs) that selectively target CCNE1 for proteasomal degradation. Using our MGD discovery engine QuEEN^{TM} encompassing biochemical and cellular assays as well as *in silico* modelling, we identified and optimized molecules that potently degrade CCNE1. Leveraging a cryptic pocket, our CCNE1 MGDs selectively degrade the cyclin E1/CDK2 holoenzyme complex, while sparing other proteins such as closely related cyclins or CDKs. In *CCNE1* amplified cancer cell lines CCNE1 MGDs selectively inhibit cellular proliferation, while sparing cell lines without amplification, in line with the “oncogenic addiction” paradigm. These anti-proliferative effects were determined to be governed by downmodulation of RB phosphorylation and E2F-driven gene expression, attesting to the on-target function of our CCNE1 MGDs. When assessed *in vivo*, orally dosed CCNE1 MGDs induced robust tumor growth suppression and regression as a monotherapy in *CCNE1* amplified ovarian, breast, and gastric models. We further established that clinical stage CDK2 inhibitors exhibit significant off-target activity through kinome profiling and genetic modeling, demonstrating the superior selectivity of CCNE1 MGDs. Owing to their exquisite selectivity, we expect that CCNE1 MGDs will avoid dose-limiting toxicities associated with less selective CDK2 inhibitors. CCNE1 MGDs represent a first in class opportunity and a paradigm shift due to their ability to directly target a frequently amplified non-enzymatic driver oncogene in distinct populations of cancer patients with high unmet medical need. With their distinctive ability to spare other proteins whose inhibition is associated with dose-limiting toxicities, CCNE1 MGDs offer a unique precision medicine angle for populations in desperate need of treatment options.

#6779 Molecular glue degraders of the RNA binding protein HuR to treat BRAF-mutant colorectal cancer.

Z. Yang[1], X. Lu[2], X. Wang[2], X. Wang[2], L. Wang[1], C. Xu[1], C. Geng[1], L. Wang[2], Y. Pu[2], Z. Zhu[2], L. Ye[2], J. Huang[2], X. Wei[2], F. Bai[2], Y. Zhu[3], X. Qian[4], H. Dou[1], H. Su[1], Y. Cang[1];
[1]Degron Therapeutics Co., Ltd, Shanghai, China, [2]ShanghaiTech University, Shanghai, China, [3]Zhejiang University, Hangzhou, China, [4]Degron Therapeutics, San Diego, CA

BRAF gain-of-function mutations, particularly BRAF(V600E), occur in approximately 10% of colorectal cancer (CRC) patients and are associated with poor prognosis and limited therapeutic options. While combined BRAF and EGFR inhibition is a standard of care, its efficacy is transient, often leading to rapid resistance and relapse. HuR is a key driver of tumor growth, invasion, and therapy resistance but was thought to be “undruggable” in the past. Here we identify novel molecular glue degraders. dHuR, as a representative, exhibited strong CRBN binding affinity and HuR degradation potency by recruiting the CRL4-CRBN ubiquitin ligase to target the RNA-binding protein HuR for degradation. Cryo-EM structural analysis revealed that dHuR created a unique benzofuran-tethered interface on CRBN, engaging a β-hairpin G-loop degron on HuR and recruiting it as a neo-substrate. Functionally, degradation of HuR by dHuR induced skipping of exon 18 in the *BRAF* transcript, leading to reduction in BRAF protein levels. This mechanism resulted in more effective suppression of BRAF-mutant CRC tumor growth *in vitro* and *in vivo*, including in models resistant to BRAF inhibitors. In vitro studies showed dHuR potently reduced viability in all 6 BRAF-mutant lines, while BRAF-WT cell lines remained unaffected. Mice bearing Colo205 tumors were treated with dHuR via oral gavage for 28 days. The treatment resulted in dose-dependent tumor growth inhibition. No significant changes in body weight or adverse clinical observations were reported. Furthermore, a comprehensive kinome-wide CRISPR screen identified EGFR and MEK inactivation as potent enhancers of dHuR cytotoxicity, establishing a strong rationale for combination therapy in refractory disease. Based on this compelling preclinical profile, we have advanced a clinical candidate, DEG6498. We are pleased to report the successful clearance of Investigational New Drug (IND) applications from both the U.S. FDA (IND 174949) and China's NMPA (CXHL2500454). A Phase I clinical trial has been initiated to evaluate the safety, tolerability, pharmacokinetics, and preliminary efficacy of DEG6498 in patients with advanced solid tumors, including BRAF-mutant CRC as an expansion cohort. This trial marks a significant milestone as the first-in-human study of a HuR-targeted molecular glue degrader, offering a novel therapeutic strategy with a distinct mechanism of action to overcome the limitations of current targeted therapies for this aggressive cancer subset.

#6780 The RAS: PI3Kα breaker BBO-10203 inhibits PI3Kα/AKT activity in HER2+ models through non-canonical RAS signaling blockade.

S. Feng[1], C. Feng[1], M. Cabanski-Dunning[2], C. Zhang[1], M. Chen[1], E. Riegler[1], D. J. Czyzyk[3], Y. Yang[1], R. Xu[1], E. M. Wallace[1], D. K. Simanshu[3], D. V. Nissley[3], F. McCormick[2], K. W. Sinkevicius[1], **J. P. Stice**[1], P. J. Beltran[1];

[1]BBOT, South San Francisco, CA, [2]UCSF, San Francisco, CA, [3]Frederick National Laboratory for Cancer Research, Frederick, MD

BBO-10203 is a first-in-class clinical stage small molecule that disrupts the interaction between RAS and PI3Kα resulting in blockade of RAS-driven PI3Kα pathway activation. Unlike PI3Kα kinase inhibitors, BBO-10203 inhibits PI3Kα signaling without directly targeting the kinase domain, thereby preventing hyperglycemia, as insulin receptor signaling does not rely on RAS proteins. BBO-10203 suppresses PI3Kα activation in preclinical models harboring oncogenic KRAS and/or PIK3CA mutations and exhibits complete suppression of AKT phosphorylation (pAKT) in most HER2 amplified or overexpressing cell lines (HER2+). Importantly, this potent inhibitory effect on pAKT drives robust efficacy in HER2+ xenograft models *in vivo*. Although much is known about HER2 and RAS signaling in tumor cells, it is not clear how inhibiting the interaction of RAS and PI3Kα results in pAKT inhibition in HER2+ cells. Using the HER2+ KYSE-410 esophageal cancer cell line we demonstrate that BBO-10203 inhibits PI3Kα /AKT signaling in HER2+ cells via a mechanism that is mainly driven through non-canonical RAS proteins. CRISPR-mediated knock-in of the PIK3CA RAS-binding domain (RBD) mutations (T208D/K227A), which disrupt the interaction of RAS with PI3Kα, significantly reduced pAKT in the KYSE-410 model, strongly supporting the role of RAS proteins in driving pAKT signaling. Treatment with the panRAS inhibitor RMC-6236 showed little effect on pAKT, suggesting that canonical RAS (K-, H- and N-RAS) may not be important players in pAKT signaling. Among individual RAS isoforms screened via siRNA knockdown, only RRAS/RRAS2 knockdown significantly reduced pAKT, whereas knockdown of other RAS members either elevated pAKT (consistent with compensatory expression) or had no effect. Through co-immunoprecipitation experiments, we identified that RRAS2 is present in the same protein complex as HER2 and HER3, providing mechanistic evidence that this association may contribute to pAKT activation in HER2+ cells. Current efforts are focused on elucidating how BBO-10203 affects the interaction of HER2/3, p85/110α and RRAS2 in HER2+ and other RTK-overexpressing cell line models. Given its orthogonal method of pAKT inhibition and potent activity in HER2+ models, we hypothesized that BBO-10203 would show combination activity with standard-of-care HER2-targeted therapies in HER2+ xenograft models. Indeed, BBO-10203 enhanced the anti-tumor activity of HER2-targeted therapies (tucatinib, trastuzumab, or Enhertu) *in vivo*, leading to tumor regression, even in the trastuzumab-resistant JIMT-1 model. BBO-10203 has entered phase 1 clinical trials (NCT06625775) and is being evaluated in HER2+ breast cancers, both as a monotherapy and in combination with trastuzumab.

#6781 First in class catalytic inhibitor of KAT2A/B demonstrates anti-tumor activity in multiple myeloma.

K. Jensen-Pergakes, S. O'Connell, S. Ninkovic, N. Miller, C. Restaino, A. Ranjan, S. Linker, D. J. Ramms, H. Lam, A. Rohner, P. Alan, R. Visswanathan, E. C. Greenwald, P. Shelton, D. Sandoval, J. Hoffman, J. Donaldson, G. Rescourio, K. Abayasiriwardana, A. Udyavar, T. A. Paul;
Pfizer, Inc., San Diego, CA

KAT2A/B are lysine acetyltransferases that function as catalytic members of the SAGA and ATAC protein complexes, which are lineage dependencies in several tumor types including multiple myeloma (MM). Here we describe a first-in-class, small molecule catalytic inhibitor targeting the lysine acetyltransferases KAT2A and KAT2B. KAT2 inhibition disrupts oncogenic transcriptional programs, including MYC and E2F pathways, leading to growth arrest in multiple myeloma. KAT2 catalytic inhibition reduces chromatin accessibility through the loss of H3K9ac and shows single-agent activity across a panel of MM cell lines. KAT2 inhibition demonstrates tumor growth inhibition as a monotherapy in both immune modulatory drug (IMiD) sensitive and resistant multiple myeloma tumor models with good correlation with reduction of H3K9ac in vivo. KAT2 inhibition has synergistic effects with IMiDs in vitro and demonstrates increased tumor growth inhibition in combination with pomalidomide and dexamethasone in vivo. Additionally, KAT2 inhibition enhances tumor immunogenicity by activating interferon regulatory factors (IRFs) and upregulating interferon-stimulated genes (ISGs). Using a syngeneic mouse model of MM, KAT2 inhibition alters the tumor microenvironment through increased infiltration of pro-inflammatory immune cells, resulting in tumor growth inhibition and enhanced survival in combination with a mBCMA-CD3 bispecific antibody. KAT2 catalytic inhibition represents a novel therapeutic approach targeting epigenetic regulation of tumor intrinsic and immune pathways in hematologic malignancies.

#6782 Discovery of a new class of mutant-targeted catalytic RAS(ON) inhibitors with retained antitumor activity in setting of emergent resistance due to elevated RAS flux.

K. Seamon[1], J. Yin[1], O. Onguka[1], O. Lai[1], C. Blaj[1], L. Jiang[1], J. Liu[1], Y. Huang[1], A. Marquez[1], J. Knox[1], J. Cregg[1], Y. Zhuang[1], Y. Yang[1], U. N. Wasko[1], Q. Liu[1], J. A. Roth[2], M. G. Rees[2], M. Ronan[3], B. J. Maldonato[1], M. Al-Radhawi[1], K. Jayashankar[1], Z. Wang[1], M. Flagella[1], E. Quintana[1], E. S. Koltun[1], M. Singh[1], Z. Wang[1], A. L. Gill[1], D. Wilds[1], J. Jiang[1], **J. A. M. Smith**[1], M. Holderfield[1];

[1]Revolution Medicines, Inc., Redwood City, CA, [2]Broad Institute, Cambridge, MA, [3]Broad Institute of MIT and Harvard, Cambridge, MA

RAS family proteins regulate cell growth by transitioning between GTP-bound (ON) and GDP-bound (OFF) conformations. Transition to the OFF state is facilitated by endogenous GTPase activating proteins (GAPs). Oncogenic mutations in RAS - among the most prevalent genetic events in human cancer - perturb this regulatory cycle by disrupting GAP-mediated stimulation of GTP hydrolysis, leading to sustained RAS activation. The investigational RAS(ON) multi-selective inhibitor daraxonrasib has a dual mechanism of RAS(ON) inhibition: disrupting RAS(ON) effector binding and activating RAS(ON) GTPase activity. Daraxonrasib has demonstrated encouraging response rates and durable antitumor activity with acceptable tolerability in patients with RAS-addicted cancers. Additional strategies are needed to counter emergent drug resistance and further extend clinical benefit. The majority of acquired genomic resistance mechanisms to daraxonrasib converge on reactivation of RAS(ON) and, in particular, RAS gene amplification, highlighting a potential opportunity for RAS(ON) inhibitors less sensitive to such resistance mechanisms. We have leveraged our understanding of tri-complex RAS(ON) inhibitors to design a new class of inhibitors that mimic the catalytic activity of natural GAPs. These compounds bind non-covalently to cyclophilin A to form a binary complex that selectively engages RAS(ON) proteins, including mutant and wild-type variants. The primary mechanism of action of these catalytic RAS(ON) inhibitors is to markedly accelerate the GTPase activity of oncogenic RAS mutants and promote conversion of RAS(ON) to RAS(OFF). Importantly, a single CYPA:catalytic RAS(ON) binary complex can inactivate multiple RAS(ON) proteins. In G12-mutant cell lines the catalytic RAS(ON) inhibitors more efficiently reduced RAS-GTP levels and exhibited more potent inhibition of RAS(ON) signaling and cell proliferation compared to daraxonrasib. In vivo oral administration of the catalytic RAS(ON) inhibitor RM-055 preferentially suppressed RAS pathway activation in G12-mutant tumors relative to normal tissues. At well-tolerated doses RM-055 demonstrated robust antitumor activity represented by deep and particularly durable responses across a panel of G12-mutant xenograft and syngeneic models of PDAC, NSCLC, and CRC, including models refractory to daraxonrasib monotherapy. Furthermore, RM-055 overcame acquired resistance to RAS(ON) inhibition, driving deep and durable regressions in models with elevated oncogenic RAS signaling, such as those with RAS amplification. Collectively, these preclinical data support evaluation of the potential of this new class of mutant-targeted catalytic RAS(ON) inhibitors to sustain clinical antitumor activity in the setting of emergent resistance mechanisms that rely on enhanced RAS pathway flux.

: Targeted Therapies
Minisymposium

#6731 CQ-0736, a new polysaccharide-based therapeutic modality, targets pan-KRAS tumors with robust antitumor activity via macropinocytosis.

Jinghua Hu, Si Wang, Yikang Shi, Xiaohai Li, Weiping Jia, Maoxu Ge, Tingchao Liu, Li Yang, Meng Huo, Anny Wang, Ling Zhao

Santolecan Pharmaceuticals LLC, Jupiter, FL

Oncogenic RAS mutations are among the most prevalent and intractable drivers of human cancer, present in nearly 20% of cases. These mutations not only fuel uncontrolled tumor growth but also reprogram cellular metabolism by dramatically increasing macropinocytosis. This unique “nutrient scavenging” pathway is critical for RAS-driven cancer cells yet largely dispensable in normal tissues and presents a powerful and underexploited therapeutic opportunity.

To address this unmet need, we developed CQ-0736, a first-in-class “Trojan horse” therapeutic that exploits macropinocytosis to selectively co-deliver two synergistic drugs into the pan-KRAS tumors. CQ-0736 is a polysaccharide-based dual-drug conjugate consisting of a 100 kDa dextran backbone covalently grafted with docetaxel (DTX) and gamma-linolenic acid (GLA). This drug construct converts the RAS-driven tumor cell membrane from a “natural barrier” into an “active transport interface”, enabling unprecedented levels of intracellular drug accumulation specifically at tumor sites.Preclinical studies demonstrate the highly transformative potential of CQ-0736. *In vitro*, it exhibited markedly greater cytotoxicity than parent DTX across multiple pan-KRAS cancer cell lines harboring $KRAS^{G12D,}$ $KRAS^{G12C}$, and $KRAS^{WT}$ mutations. Several *in vivo* xenograft models showed that CQ-0736 achieved more than 95% tumor growth inhibition without weight loss or observed toxicity, regardless of KRAS mutation status. Remarkably, the direct head to head *in vivo* comparisons revealed that CQ-0736 significantly outperformed the world-class pan-RAS inhibitor RMC-6236 and the marketed KRAS targeted drug Krazati, displaying superior efficacy, longer durability, and much less drug resistance.Mechanistic analyses confirmed that CQ-0736 robustly suppresses proliferation (decreasing PCNA and Ki-67) while driving apoptosis (elevating cleaved PARP), producing superior effects to parent DTX. These findings underscore the conjugate’s dual impact on tumor biology and highlight its potential to overcome key limitations of both conventional chemotherapy and next-generation targeted RAS inhibitors, including systemic toxicity and acquired resistance.

Conclusion: CQ-0736 represents a highly innovative and clinically promising therapeutic strategy for RAS-driven cancers, a disease with devastating prognosis and few effective options. By turning a fundamental vulnerability of RAS-driven tumors into a drug delivery advantage, CQ-0736 opens a new therapeutic paradigm with the potential to significantly improve outcomes for patients with some of the most aggressive and treatment-resistant malignancies.

#6732 Potent, orally bioavailable small molecules that inhibit c-Myc translation and suppress tumor growth *in vivo*.

M. Kriner, C. Hwang, F. Koyanagi, B. Israels, T. Phan-Everson, W. Kratzman, I. Gupta, J. Fontana, D. Sparkman-Yager;
Wayfinder Biosciences, Seattle, WA

Dysregulation of c-Myc is implicated in over half of all cancers, making it the most important undrugged oncogene. As a transcription factor, the c-Myc protein is not amenable to traditional small molecule inhibition. Recent attempts to reduce c-Myc activity with novel modalities have had limited success in the clinic, highlighting the need for Myc-targeted therapeutics with improved potency and cell permeability. We previously reported discovery of small molecules that bind to structured elements in the 5' UTR of the c-Myc mRNA and repress translation of the c-Myc protein. Here, we describe our hit-to-lead campaign, in which we dramatically improved the potency (>70x), selectivity (>5x) and oral bioavailability (>13x) of our c-Myc RNA-targeting small molecules, yielding a lead series that suppresses tumor growth in an in vivo cell line-derived xenograft (CDX) model of small cell lung cancer (SCLC).

Using a ligand-based approach, we designed and synthesized over 150 analogs of our top hit series and characterized their ability to repress c-Myc protein levels and reduce viability of the highly MYC-amplified SCLC cell line NCI-H82. Notably, we observe excellent correlation between c-Myc protein repression and compound potency, supporting an on-target mechanism. Our compounds demonstrate rapid (~30 min half-life), selective and reversible protein knockdown, consistent with inhibition of c-Myc translation initiation followed by normal protein turnover. We have now achieved single-digit nanomolar potency and continue to make improvements thanks to the establishment of a strong structure-activity relationship for our lead series.

In parallel, we dramatically improved the ADME/PK properties of our series by identifying and correcting a structural liability for liver metabolism. The resulting tool molecule achieved >60% oral bioavailability and exposure above the in vitro IC50 for extended periods, enabling twice-daily oral dosing. This compound achieved significant tumor growth inhibition in a SCLC CDX model and, importantly, dosing was well tolerated by all animals. Beyond SCLC, we observe in vitro efficacy against cell lines from a range of solid and heme cancers, opening the door for xenograft studies in additional indications.

Together, our results validate an RNA-targeted small molecule approach to repress c-Myc. Our promising in vivo data, coupled with sustained oral exposure and favorable tolerability, highlight the potential of this modality to overcome long-standing barriers in MYC drug discovery. Ongoing xenograft and mechanistic studies are expected to further expand the clinical opportunities for treating MYC-driven solid and hematologic cancers.

#6733 Discovery and characterization of CBL-B intramolecular glue inhibitors that increase T cell activation and suppress tumor growth.

S. Gajewski, A. Taherbhoy, B. Bravo, K. Dhamnaskar, J. Sheung, D. Haria, A. Tenn-McClellan, J. Gosling, M. C. Clifton, M. Cardozo, P. A. Barsanti, J. R. Perkins, K. Boyle, T. Cummins, M. Lawrenz, M. Gallotta, J. T. Mihalic, N. O'Connell, S. Prakash, A. Saha, R. Rountree, C. Wang, D. R. Weiss, C. W. Zapf, **F. Cohen**;
Nurix Therapeutics, Brisbane, CA

Background. CBL-B, a RING-type E3 ubiquitin ligase, is a master regulator of peripheral T-cell activation and a promising immuno-oncology (IO) target. Genetic ablation of CBL-B in mice leads to enhanced T-cell activation and spontaneous tumor rejection, suggesting that pharmacological inhibition of CBL-B could reverse immunosuppression in the tumor microenvironment and potentiate anti-tumor immunity. This work describes the rational discovery of intramolecular glue inhibitors targeting the auto-inhibited conformation of CBL-B.
Methods. We designed and executed a high-throughput screening (HTS) campaign using a homogeneous time-resolved fluorescence (HTRF) assay to identify small-molecule inhibitors that stabilize the autoinhibited, closed conformation of CBL-B. Hits were validated through orthogonal HTRF and surface plasmon resonance (SPR) assays. The binding mode was elucidated by X-ray co-crystal structure. The series was optimized for affinity and properties through iterative cycles of medicinal chemistry. Lead compounds were evaluated for their ability to enhance T-cell activation and cytokine secretion in primary human T cells and for anti-tumor efficacy in a syngeneic mouse model.
Results. HTS of >250,000 compounds yielded a singleton hit that inhibited CBL-B activation with K_D = 24.12 ± 8.90 μM. Structure-guided optimization resulted in NRX-8766, with a K_D of 0.033 ± 0.001 μM for CBL-B. Treatment of human peripheral blood mononuclear cells (hPBMCs), with NRX-8766 results in 3- to 4-fold increases in T-cell activation markers (CD25, CD69) and 2- to 25-fold increases in cytokine secretion (IL-2, IFN-γ, TNF-α) when stimulated with α-CD3 or α-CD33/α-CD28. In vivo, oral administration of NRX-8766 to mice bearing syngeneic CT26 tumors significantly increased T-cell activation and suppressed tumor growth.
Conclusions. These studies demonstrate that pharmacological inhibition of CBL-B reproduces the reported mouse knockout phenotype. NX-1607, a first-in-class CBL-B inhibitor, is now in clinical development as a potential cancer immunotherapy.
Keywords: Immuno-oncology, CBL-B, molecular glue, T-cell activation, small-molecule inhibitor, high-throughput screening, tumor immunity

#6734 Discovery and optimization of NEO-811, a first-in-class molecular glue degrader of ARNT, utilizing structure-based drug design.

J. Griffin, A. Hernandez, X. Liu, K. Januszyk, B. Lee, A. Burt, J. Tellew, J. Lee, M. Cruz, I. Tran, K. Chiu, M. Wu, L. Bateman, A. Dominguez-Andres, L. Huang, J. Fathman, C. Sanchez, N. Cruz, R. Soriano, D. Knece, M. Fitzgibbon, A. Grant, M. Matyskiela, R. Beckwith, P. Chamberlain;
Neomorph, Inc., San Diego, CA

ARNT (HIF-1β), a member of the HIF family of transcription factors, heterodimerizes with HIF-2α to regulate the transcription of the hypoxic-response pathway. pVHL mutation leads to constitutive overactivation of HIF transcription, driving cancers such as clear cell renal cell carcinoma (ccRCC). Targeted degradation of ARNT represents a novel therapeutic approach to targeting this oncogenic pathway. Herein we disclose a structure-based drug design approach which afforded NEO-811, a first-in-class ARNT molecular glue degrader. Biochemical and cellular mechanism of action studies revealed ARNT degradation mediated by the CRL4-CRBN E3 ligase. A cryo-EM structure confirmed direct ARNT recruitment to CRBN and revealed opportunities to enhance the depth of degradation and selectivity against neosubstrates. A medicinal chemistry campaign incorporating structure-based drug design enabled the development of NEO-811, a potent and selective degrader of ARNT entering clinical trials for treatment of ccRCC.

#6735 DNA-templated, spatially controlled proteolysis targeting chimeras enable coordinated degradation of the Cyclin D1-CDK4/6 complex.

R. Zheng, A. Prasad, D. Satyabola, Y. Xu, S. Roy, Y. Yan, P. Sulc, H. Yan;
Arizona State University, Tempe, AZ

Background: Hyperactivation of the Cyclin D-CDK4/6 complex drives tumor proliferation across cancers. Although CDK4/6 inhibitors provide clinical benefit, durability is limited by resistance and by Cyclin D1's CDK-independent oncogenic functions that are not addressed by kinase blockade. A strategy that removes the entire Cyclin D1-CDK4/6 complex could suppress both kinase-dependent and independent signaling; however, Cyclin D1 lacks a druggable active site, and prior PROTACs have degraded CDK4/6 individually rather than the intact complex. These gaps motivated the development of DNA templated degraders to program geometry and enable synchronous complex degradation.
Methods: This study engineered DNA-templated proteolysis-targeting chimeras (DTACs) by positioning a CDK4/6 binder and an E3 ligase recruiter on complementary oligonucleotides, enabling systematic variation of intermolecular distance and orientation. A panel of DTACs was profiled for target engagement and degradation (Cyclin D1, CDK4, CDK6), cell-cycle distribution, and antiproliferative activity across cancer cell models. Lead constructs were evaluated for in vivo target degradation and antitumor activity in xenograft models.
Results: Spatial programming dictated degrader performance: DTAC variants exhibited distance- and orientation-dependent degradation of the Cyclin D1-CDK4/6 complex. The optimized construct induced synchronous loss of Cyclin D1 together with CDK4 and CDK6, yielding pronounced G1 arrest and suppression of cellular proliferation. In a xenograft mouse model, lead product exhibited potent therapeutic efficacy by effectively degrading Cyclin D1–CDK4/6 and suppressing tumor growth.
Conclusions: DNA templating provides a modular strategy to control degrader geometry and achieve synchronized degradation of multi-protein complexes. DTACs enable coordinated Cyclin D1-CDK4/6 degradation with functional pathway blockade and antitumor activity. Overall, these findings demonstrate the feasibility of DTAC as a rapid, scalable, and modular platform for the spatial control of functional inhibitors for optimal effectiveness, making it a promising method for proximity-based therapeutics.

#6736 Discovery and characterization of BH-501284: A non-covalent, pan-KRAS inhibitor for treatment of diverse *KRAS*-mutant tumors.

Nancy Ling, Evan Rogers, Eugene Rui, Wei Deng, Ping Jiang, Zhenping Wang, Yue Hu, Joshua Choi, Danan Li, Anindya Sarkar, Levan Darjania, Geoffrey Oxnard, **Jean Cui**

BlossomHill Therapeutics, Inc., San Diego, CA

KRAS mutations are among the most prevalent oncogenic drivers, representing 25% of human cancers. While recently approved covalent KRAS G12C inhibitors have demonstrated meaningful clinical benefit, no targeted therapies are currently approved for other KRAS variants. Consequently, a large portion of the KRAS-driven patient population, including those with pancreatic carcinoma (PDAC), colorectal cancer (CRC), and non-small cell lung cancer (NSCLC), remain underserved. Furthermore, available G12C inhibitors have modest potency and limited durability of effect in clinic. Research attributed these modest outcomes to adaptive resistance mechanisms associated with secondary KRAS mutations or activation of bypass pathways. This resistance, along with unmet medical needs, has driven the development of new KRAS-directed therapies capable of targeting multiple KRAS mutants. Here, we describe BH-501284, a potent, selective, orally available, non-covalent, pan-KRAS inhibitor, targeting the allosteric switch-II pocket of KRAS. BH-501284 inhibited cell viability and suppressed ERK phosphorylation in KRAS-mutant cells (G12D/C/V/S, G13D) and KRAS WT amplified cells with low to sub-nanomolar activity. BH-501284 also demonstrated greater than 300-fold selectivity against both HRAS and NRAS and showed no anti-proliferative activity in non-RAS driven cells. Raf1 effector binding assay data showed BH-501284 to bind KRAS mutants in the inactive (OFF) state, with binding affinity in the picomolar range as measured by SPR. Cellular wash off studies confirmed that BH-501284 tightly engaged KRAS, similar to covalent inhibitors. This unique target engagement allows BH-501284 to more comprehensively reduce active KRAS proteins than other reversible KRAS (ON) inhibitors. Importantly, the anti-proliferation activity of BH-501284 was only minimally affected by growth factors (e.g. EGF) that drive KRAS into the active state and lead to resistance. Durable and potent activity of BH-501284 was also observed in cell-derived xenograft (CDX) tumor models with KRAS G12D, G12V, and G12C mutations, covering NSCLC, CRC, and PDAC. PK profiling revealed good oral bioavailability of BH-501284 in multiple species and dose dependent plasma exposures in mouse xenograft tumor models. Lastly, BH-501284 showed synergistic effects with inhibitors of EGFR, FAK/SRC, and others in combination studies. Altogether, these findings position BH-501284 as a strong candidate for further development.

#6737 Selective degradation of pathologic multimers via a novel TRIM21-engaging molecular glue and PROTAC platform.

N. Huang[1], **A. Yu**[2], Y. Liu[2], N. Zheng[2], T. Han[1];
[1]Tsinghua University, Beijing, China, [2]DeepKinase Biotechnologies Ltd., Beijing, China

Background: Targeted protein degradation (TPD) holds great promise for cancer therapy, but its application is often constrained by the limited repertoire of E3 ligases and the challenge of selectively eliminating pathologic protein assemblies, such as those driving oncogenesis, while sparing monomeric forms. The E3 ligase TRIM21 is a compelling yet underexplored effector, as its activation is hypothesized to require substrate multimerization, potentially conferring intrinsic selectivity for diseased-associated protein complexes.
Methods and Results: We report a novel TPD strategy centered on the activation of TRIM21. Initially, we discovered that (S)-ACE-OH, a metabolite of acepromazine, functions as a molecular glue by inducing a productive interaction between TRIM21 and the multimeric Nuclear Pore Complex (NPC) component NUP98. To systematically map the specificity and scope of this degradation event, we employed quantitative and TurboID proteomics. This analysis confirmed the potent and selective degradation of multiple NPC proteins, consistent with the disruption of a large multiprotein complex. Crucially, monomeric proteins remained unaffected, validating the hypothesized multimer-selectivity of TRIM21-based degradation. This selectivity was further demonstrated by engineering acepromazine-based PROTACs, which effectively degraded diverse multimeric client proteins, including components of biomolecular condensates.
Conclusion: Our work establishes TRIM21 as a promising new E3 ligase for TPD, capable of selectively targeting multimeric proteins and pathologic assemblies. The proteomic analyses were pivotal in unequivocally defining this unique selectivity profile, providing a robust experimental foundation for this platform. This TRIM21-based degradation strategy opens a new therapeutic avenue for directly targeting undruggable, multimeric oncoproteins, with broad implications for cancer treatment.

: Targeted Therapy: Data Driven Approaches and Novel Drugs
Minisymposium

#6758 MUlti-epitope Targeting Tetravalent Antibody (MUTTA™) platform for developing NexGen ADCs with an improved therapeutic window.

Sunil Bhakta, Jiang Liu, Levi Blazer, Jarrett Adams, Vasu Jammalamadaka, Anbalagan Jaganathan, Shane Miersch, Viswanatham Katta, Anay Limaye, Ying-Ping Jiang, Vidya S. Jonnalagadda, Reva Raghupathi, Pradeep Fernandes, Sean Givens, Paul Polakis, Sachdev S. Sidhu, **Jagath R. Junutula**

Aarvik Therapeutics, Inc., Hayward, CA

Antibody-drug conjugates (ADCs) are a class of targeted chemotherapeutic precision medicines that became available to oncology clinical practice in 2000. In the 25 years since, >450 ADCs have progressed into the clinic, of which only 15 ADCs have been approved by the FDA, while >130 have been discontinued or are inactive. The high failure rate (~90%) of ADCs in the clinic is often associated with factors such as low tumor antigen copy number, heterogenous expression of tumor targets in solid tumor cancers, target antigen escape, poor internalization, efficacy-limiting off-target toxicity, and developability risks. Aarvik Therapeutics has developed a novel MUlti-epitope Targeting Tetravalent Antibody (MUTTA™) platform to engineer NextGen ADCs with multifunctional properties to tackle difficult-to-treat solid tumor cancers. The MUTTA™ ADC platform is designed to overcome many of the limitations described above and to broaden the therapeutic window of ADCs. MUTTA™ ADCs apply an OR-gate approach and can address therapeutic limitations such as antigen escape seen with monospecific ADCs in the treatment of solid tumors. We focused initially on developing tetravalent antibody formats with optimal manufacturing properties by screening several tetravalent antibody formats using few hundred constructs and successfully identified MUTTA™ formats specifically suitable for the ADC drug development. To develop and validate the MUTTA™ platform and to test its utility to generate multifunctional therapeutic antibodies, we initially applied this technology to well-validated tumor targets such as Her2 and EGFR for which clinically proven function-blocking antibodies (e.g., trastuzumab, pertuzumab, cetuximab) are available. We successfully engineered a MUTTA™ antibody with 4 different antibody functionalities (4-in-1) and demonstrated functional synergy in blocking-ERK phosphorylation in a trastuzumab-resistant cancer cell line. We demonstrated that multi-target MUTTA™ antibodies display superior internalization over single-target antibodies. In addition, MUTTA™ ADCs exhibited superior cellular potency compared to single-target ADCs and exhibited normal IgG-like pharmacokinetic properties. We further applied the MUTTA™ platform to several solid tumors such as Breast, Colon, Lung, Ovarian, Prostate and Pancreas by first identifying complementary tumor antigens based on co-expression profiles in these solid tumor cancers and then engineering optimally-designed multi-target MUTTA™ ADCs based on this analysis. We will present data that demonstrate *in vitro* and *in vivo* validation of multi-target MUTTA™ ADCs and their improved therapeutic window compared to single-target ADCs, as well as the broad applicability of the MUTTA™ platform across several tumor antigens.

#6759 High-throughput drug screening and single-cell network analysis identify rational combination therapies in IDH-mutant glioma.

Patrick Kerwin, Luca Zanella, Andrea Califano

Columbia University, New York, NY

IDH-mutant gliomas are lethal brain tumors marked by multiple coexisting malignant cell states, likely to elicit heterogeneous drug sensitivities thus limiting the effectiveness of monotherapy. To address this challenge, we integrated multimodal single-cell analysis and functional high-throughput drug screening to identify and pharmacologically target state-specific vulnerabilities, thus supporting rational combination therapy development. Single-nucleus RNA sequencing (snRNA-seq) of 20 treatment-naïve, low-grade IDH-mutant gliomas, followed by Master Regulator (MR) analysis, identified key proteins representing mechanistic determinants of three established malignant states: astrocyte-like (AC), oligodendrocyte-like (OC), and neural progenitor cell-like (NPC). The analysis revealed that the AC state is transcriptionally orthogonal to OC, whereas the OC and NPC share substantial regulatory architecture. OncoMatch analysis identified patient-derived models (SF10417, SU-A03) that optimally recapitulate the MRs of these malignant subpopulations, supporting screening of a 374 oncology-focused compounds (FDA-approved and investigational) followed by transcriptional profile analysis at 24h, using the PLATE-seq technology, resulting in a comprehensive drug perturbational compendium for IDH-mutant gliomas. OncoTreat analysis prioritized compounds based on their ability to invert the aberrant MR activity signatures of each malignant state, revealing highly cell-state-specific drug sensitivities, supporting the design of rational combination strategies targeting tumor plasticity. For example, we found that AC-like cells may first be primed with the mTOR inhibitor temsirolimus to reprogram them toward a more drug-sensitive OC-like state, thereby converting a resistant lineage into one that is more vulnerable, including to the new class of IDH1 inhibitors. A second-line agent such as the HDAC inhibitor romidepsin or the topoisomerase inhibitor irinotecan can then be used, possibly in combination with IDH1 inhibitors, to target the resulting OC-like and pre-existing OC/NPC cells, thus implementing a two-step, sequential treatment strategy. In parallel, barcode-based lineage tracing in SF10417 and SU-A03 is being used to monitor cell-state stability and plasticity under drug treatment, while top candidate agents and combinations are being validated in patient-derived *ex vivo* glioma slice cultures that preserve the native microenvironment. Single-cell and spatial transcriptomic profiling (10x Genomics Xenium) of treated slices will map the reprogramming and elimination of malignant subpopulations in situ. Together, this framework provides a blueprint for discovering state-specific dependencies in IDH-mutant glioma and for guiding rational, combination-based strategies to overcome intratumoral heterogeneity.

#6760 Age-dependent lung vulnerability identifies serum hyaluronic acid as a predictive biomarker of ADC-induced interstitial lung disease.

Liming Jin[1], Ye Lu[2], Qing Wei[3], Peng Guo[2], Liu Yang[4], Dawei He[5]

[1]Hangzhou Institute of Medicine, Hangzhou, China,[2]Hangzhou Institute of Medicine, Chinese Academy of Sciences, Hangzhou, China,[3]Zhejiang Cancer Hospital, Hangzhou, China,[4]Zhejiang Provincial People's Hospital, Hangzhou, China,[5]Children's Hospital of Chongqing Medical University, Chongqing, China

Background: Interstitial lung disease (ILD) is a serious and unpredictable toxicity associated with antibody-drug conjugates (ADCs) such as trastuzumab deruxtecan (T-DXd). However, the cellular origins, age-specific susceptibility, and actionable biomarkers of ADC-induced ILD remain undefined. Here, we combined animal modeling, single-cell transcriptomics, functional assays, and clinical validation to elucidate the mechanistic basis of ILD susceptibility and identify circulating biomarkers predictive of ADC-induced ILD.
Methods: Age-stratified mouse models (postnatal, adolescent, adult) were treated with T-DXd, followed by lung pathology evaluation and pulmonary function analysis. Single-cell RNA sequencing profiled the lung microenvironment across age groups. Functional assays assessed the maturity and phagocytic capacity of alveolar macrophages. Endothelial injury was evaluated by immunohistochemistry, TEM, and analysis of hyaluronidase expression. Plasma hyaluronic acid (HA) levels were quantified, correlated with ILD severity, and tested in a clinical validation cohort consisting of 20 ADC-induced ILD patients and non-ILD controls.
Results: ILD susceptibility was strongly age-dependent, with only adult mice developing interstitial thickening, inflammatory infiltration, and impaired lung function, whereas postnatal and adolescent mice remained protected. Single-cell profiling revealed an adult-specific inflammatory ecosystem with expansion of ILD-associated immune populations absent in immature lungs. Postnatal mice were protected by immature alveolar macrophages with low phagocytic activity and reduced inflammatory signaling, contrasting with the mature, pro-inflammatory macrophages in adults that facilitated ILD onset. Endothelial cells emerged as the earliest and most vulnerable targets of T-DXd, showing the greatest transcriptional perturbation and induction of HYAL2/TMEM2, supported by protein-level and ultrastructural evidence of injury. HYAL2/TMEM2 activation drove excessive HA release into circulation, and plasma HA correlated with ILD severity across mouse models. Importantly, clinical validation in 10 ILD patients showed significantly elevated HA levels compared with 10 ADC-treated controls, with ROC analysis confirming HA as a predictive biomarker consistent with preclinical findings.
Conclusions: Using age-stratified models and single-cell resolution, we identify endothelial injury and hyaluronidase upregulation as early, age-dependent drivers of ADC-induced ILD. We further show that circulating HA is a clinically validated biomarker capable of predicting ILD risk. This integrated preclinical-clinical study provides a new understanding of ILD susceptibility and establishes serum HA as a promising biomarker for early ILD detection and risk stratification in ADC therapy.

#6761 Antitumor activity of datopotamab deruxtecan in a co-clinical trial with patient derived xenografts.

Dhruv Chachad[1], Kurt W. Evans[1], Ming Zhao[1], Erkan Yuca[1], Ran Zhang[1], Yasmeen Rizvi[1], Gabriela Raso[2], Argun Akcakanat[1], Stephen Scott[1], Justin M. Roberts[1], Ming Sun[1], Nakul Shah[3], Hong Zebger-Gong[4], Gunnar Klauss[4], Yui Tanaka[4], Daisuke Okajima[4], Funda Meric-Bernstam[1]

[1]Investigational Cancer Therapeutics, UT MD Anderson Cancer Center, Houston, TX,[2]Translational Molecular Pathology, UT MD Anderson Cancer Center, Houston, TX,[3]Division of Cancer Medicine, UT MD Anderson Cancer Center, Houston, TX,[4]Daiichi Sankyo, Inc., Berlin, Germany

Trophoblast cell-surface antigen-2 (TROP2) is expressed in multiple cancers. Datopotamab deruxtecan (Dato-DXd) is an antibody drug conjugate (ADC) consisting of a humanized anti-TROP2 IgG1 monoclonal antibody covalently linked to a highly potent topoisomerase I inhibitor payload. Dato-DXd is FDA approved for hormone receptor-positive, HER2-negative breast cancer and *EGFR*-mutated non-small cell lung cancer following EGFR-directed therapy and platinum based chemotherapy. However, determinants of response and optimal combinations need further study. We performed a co-clinical trial, to determine the concordance of anti-tumor activity of Dato-DXd in patient derived xenografts (PDX) and matched patients treated with Dato-DXd (TP01) and to assess potential of combinations.We generated 23 PDX models of different cancer types: breast invasive ductal carcinoma, lung adenocarcinoma, urothelial carcinoma, esophageal adenocarcinoma, head and neck carcinoma and pancreatic adenocarcinoma (PDAC). Nineteen models were created from biopsies performed just before Dato-DXd treatment of patients and 4 models were generated after the patients acquired resistance to Dato-DXd. The antitumor efficacy of Dato-DXd and the isotype control-DXd (IgG-DXd) were tested. Antitumor activity was assessed by objective response and event-free survival (time to tumor doubling) per PDXNET metrics. Based on our results from a previous synergy screen *in vitro*, four PDAC cell lines were also treated with a combination of Dato-DXd and gemcitabine. A total of 49 models were implanted, and 23 PDX models generated across 6 tumor types (PDX take rate of 47%). Of 13 pretreatment PDXs tested for Dato-DXd efficacy: 5 (38.5%) had a partial response, 3 (23%) had stable disease, and 5 (38.5%) had progressive disease. Antitumor activity in PDXs was concordant with matched patients treated with Dato-DXd and assessed by RECIST V1.1. in 10 out of 13 (77%) models. Ten of 13 (77%) PDXs had significant prolongation of event-free survival (EFS). Among 4 PDAC PDXs tested 2 (50%) had prolongation of EFS. We sought to identify chemotherapy combinations that enhance activity of Dato-DXd in PDAC cell lines *in vitro*, and determined that the combination of Dato-DXd and gemcitabine was synergistic. A pretreatment PDX model was generated from a patient with PDAC who had received topoisomerase inhibitor treatment (FOLFIRINOX) as well as gemcitabine/abraxane, and had PD as best response to Dato-DXd. The PDX model progressed on both Dato-DXd and gemcitabine monotherapy, but the combination therapy showed tumor regression, and significantly prolonged event-free survival compared to monotherapy ($p = 0.0067$ for both comparisons). Dato-DXd has antitumor activity in several tumor types. Combinations may further enhance antitumor activity. Further studies are needed to explore the mechanisms of resistance and potential combinations.

#6762 A novel therapeutic approach for targeting p53-mutant cancers by leveraging DNA damage response vulnerabilities.

Mohammed M. Alruwaili[1], Yanqi Guo[2], Justin Zonneville[2], Thomas Melendy[3], Robert M. Straubinger[4], Barbara A. Foster[5], Priyanka Rajan[2], Henry G. Withers[6], Sarah Chatley[7], Renuka V. Iyer[7], Christos Fountzilas[7], **Andrei V. Bakin**[2]

[1]Medical Laboratory Technology, Northern Border University, Arar, Saudi Arabia,[2]Department of Cancer Genetics and Genomics, Roswell Park Comprehensive Cancer Center, Buffalo, NY,[3]Department of Microbiology and Immunology, University at Buffalo, Buffalo, NY,[4]Department of Pharmaceutical Sciences,, University at Buffalo, Buffalo, NY,[5]Department of Pharmacology and Therapeutics, Roswell Park Comprehensive Cancer Center, Bufflo, NY,[6]Department of Biostatistics and Bioinformatics, Roswell Park Comprehensive Cancer Center, Buffalo, NY,[7]Department of Medicine, Roswell Park Comprehensive Cancer Center, Buffalo, NY

The tumor suppressor gene TP53 is frequently mutated in most solid malignancies, including colorectal and pancreatic cancers, driving tumor progression and metastasis. However, existing treatments often lack selectivity for p53-mutant (p53mut) cancers and are associated with high toxicity. To address this clinical challenge, we developed a two drug therapeutic approach that selectively targets p53-mutant cancers by combining TAS102, with a PARP inhibitor (PARPi). Mechanistically, incorporation of TFT into DNA triggers post-replicative repair, generating single-strand break intermediates. While PARP facilitates their repair, inhibition of PARP converts these intermediates into lethal double-strand breaks. In p53 wild-type (WT) cells, TAS102 and PARPi activate a p53-dependent G1/S checkpoint, enabling DNA repair and preventing excessive damage. In contrast, p53mut cells, lacking this checkpoint, experience uncontrolled DNA damage accumulation, leading to cell death. This combination demonstrated superior anti-tumor efficacy in p53-mutant cell lines and patient-derived xenograft (PDX) models compared to either agent alone, and was well tolerated in preclinical studies. This two-drug strategy is now being tested in Phase I clinical trial (NCT04511039) in advanced CRC patients showed no significant toxicity and improved PFS relative to historical TAS102 monotherapy. To further elucidate its mechanism, we investigated the DNA damage response (DDR) and checkpoint signaling in p53mut cancer cells. Our findings show that TAS102-PARPi induces a p53-independent G2/M checkpoint mediated by ATR kinase, which activates downstream kinases CHK1 and WEE1 to inhibit CDK1, thereby halting entry into mitosis. Our transcriptomic profiling revealed a marked induction of homologous recombination (HR)-associated double-strand break repair genes, including BRCA1, BRCA2 and RAD51, in p53-deficient cells following TAS102-PARPi treatment. This pronounced upregulation likely reflects enhanced DNA repair activity at the G2 checkpoint, orchestrated by ATR kinase. Based on this mechanistic, we tested whether the TAS102-PARPi regimen could be potentiated by targeting G2-checkpoint kinases. We developed a triple-drug therapeutic strategy that combines our two-drug regimen with a G2-checkpoint kinase inhibitor. Subsequent inhibition of checkpoint kinases such as WEE1 or ATR releases the G2-arrested cells into mitosis, resulting in mitotic catastrophe and cell death. Importantly, sequential administration, delaying the G2-kinase inhibitor after TAS102-PARPi, allows p53WT cells time to repair DNA, thereby minimizing toxicity to normal tissues. This sequential triple-drug strategy acts through a synthetic lethality mechanism, producing massive cell death in p53mut cancer models. In PDXs models, this regimen achieved robust tumor suppression without detectable toxicity.

#6763 KBD111 is a highly selective, long-acting and brain-penetrant PARP1 inhibitor.

Jing Zhang, Yang Chen, Yonggang Wei, Fei Ye, Zhiyong Li, **Xiaoke Liu**, Jiannan Cui

Kangbaida (Sichuan) Biopharmaceutical Technology Co., Ltd, Chengdu, China

Background: Currently, several pan-PARP inhibitors such as olaparib, niraparib, and rucaparib are approved for the treatment of cancers with homologous recombination deficiency (HRD). While these inhibitors have demonstrated significant clinical efficacy, their use is frequently limited by severe toxicities, especially hematological side effects associated with PARP2 inhibition. These adverse effects constrain the potential for combining PARP inhibitors with other anticancer therapies, underscoring the need for selective PARP1 inhibitors.

Methods: An enzymatic evaluation was performed to assess the activity and selectivity profile of KBD111 against major PARP family members. Cell proliferation was evaluated in the DLD-1 $^{BRCA2-/-}$ cell line. Pharmacokinetic studies were conducted in mice, rats, and dogs. The antitumor efficacy of KBD111 was investigated in DLD-1 $^{BRCA2-/-}$ and MDA-MB-436-luc mouse xenograft models. Mechanistic analysis revealed that PARP1 activity was reduced in DLD-1 $^{BRCA2-/-}$ tumor-bearing tissues. In addition, hematological toxicity was evaluated in vitro in $CD34^+$ hematopoietic stem cells and in vivo in rats.

Results: KBD111 exhibited over 5,000-fold selectivity for PARP2 by DNA-trapping assays, demonstrated potent anti-proliferative activity against BRCA-mutant cancer cell lines, while showing markedly reduced cytotoxicity toward normal $CD34^+$ hematopoietic stem cells (IC_{50} >10,000 nM) compared to talazoparib (IC_{50} = 27 nM). In addition, KBD111 exhibited excellent pharmacokinetic properties in different preclinical species and high blood-brain barrier (BBB) permeability. Furthermore, KBD111 achieved superior tumor growth inhibition compared to AZD5305 in DLD-1 $^{BRCA2^{-/-}}$ xenograft models following once every two weeks oral dosing. In an intracranial MDA-MB-436-luc model, KBD111 also demonstrated enhanced efficacy relative to AZD9574 under QW oral dosing. Notably, in vivo studies demonstrated that weekly (QW) treatment exhibited a better safety profile than QD dosing. Moreover, KBD111 was well tolerated in the 14-day toxicity studies in SD rats with 60-fold therapeutic window.

Conclusions: KBD111 is a highly potent, long-acting and brain-penetrant PARP1 inhibitor with superior PK properties in different species, supporting its development as a promising candidate for once every two weeks (Q2W) dosing. KBD111 demonstrated much less hematotoxicity than Olaparib and was well-tolerated in 14-day toxicity studies. A Phase 1 trial is planned for 2026.

#6764 Comparative profiling of TEAD palmitoylation and YAP-TEAD protein-protein interaction inhibitors as combination agents with KRAS inhibitors.

Danielle J. Sanchez[1], Jacob A. Gordon[1], Cynthia Xu[1], Alex Koers[2], Sarah Ross[2], James E. Brownell[1], Simon T. Barry[2], Carla P. Martins[2]

[1]Early Oncology R&D, AstraZeneca, Waltham, MA,[2]Early Oncology R&D, AstraZeneca, Cambridge, United Kingdom

TEAD proteins are the transcriptional effectors of the Hippo pathway that bind coactivators YAP/TAZ to activate genes involved in cell survival, proliferation, and drug resistance. Deregulation of the Hippo pathway leading to increased TEAD activity occurs in multiple cancers, including as an adaptive resistance mechanism to targeted therapies. TEAD transcriptional signatures are elevated in KRAS inhibitor-resistant cell lines, and genome wide CRISPR screens have identified multiple hits in the Hippo pathway which sensitize or confer resistance to KRAS inhibitors. Therefore, targeting the YAP/TAZ-TEAD axis has the potential to inhibit tumor growth as a monotherapy or combination strategy across diverse indications. TEAD inhibitor modalities being investigated clinically include TEAD “central pocket” palmitoylation inhibitors (CPIs) and YAP-TEAD protein-protein interaction inhibitors (PPIs). However, limited data exist on how targeting TEAD with these different classes of inhibitors compare in combination studies. We profiled the activity of a TEAD CPI and PPI alone and as combination agents with $KRAS^{G12C}$ and $KRAS^{G12D}$ inhibitors, assessing effects on TEAD-dependent transcription, proliferation, and tumor growth inhibition. In long-term *in vitro* outgrowth studies in six $KRAS^{G12C}$ and $KRAS^{G12D}$ cell lines, the TEAD PPI demonstrated increased growth inhibition compared to the CPI when combined with KRAS inhibitors. Additionally, the PPI re-sensitized $KRAS^{G12C}$-mutant NCI-H2122 cells resistant to AZD4625, a $KRAS^{G12C}$-selective inhibitor. Combination efficacy was observed across KRAS-mutant but not WT lines, confirming on-target activity of dual TEAD and MAPK pathway suppression. Mechanistically, the PPI suppressed TEAD-dependent transcription to a greater extent than the CPI *in vitro*, while reduced MAPK signaling was driven by KRAS inhibitors and not further enhanced by TEAD inhibition. Given the differences between CPI and PPI activity *in vitro*, combination efficacy was evaluated *in vivo* in three KRAS-mutant tumor models. In contrast to the *in vitro* results, CPI and PPIs drove equivalent regression of NCI-H2122 NSCLC xenografts when combined with the $KRAS^{G12C}$ inhibitor sotorasib, followed by similar outgrowth once dosing was stopped. However, the robust combination efficacy observed *in vitro* did not translate to significant tumor growth inhibition with either TEAD modality in two $KRAS^{G12D}$-mutant pancreatic models, Panc04.03 and Panc10.05. Collectively, these findings suggest that while differential activity was observed between TEAD CPI and PPIs *in vitro*, the two modalities drove similar therapeutic benefit *in vivo* when combined with KRAS inhibitors. Careful exploration of the long-term benefit of TEAD and KRAS inhibitor combinations is warranted due to the disconnect between *in vitro* and *in vivo* data.

Wednesday, April 22, 2026

: Mathematical Modeling and Statistical Methods
Poster Session

#6830 State-transition model of time-series single-cell RNA-seq identifies gene-level origins of disease microstate stability in chronic myeloid leukemia (CML).

David Eugene Frankhouser[1], Anupam Dey[2], Jennifer Rangel Ambriz[1], Ziang Chen[1], Denis O'Meally[1], Yu-Hsuan Fu[1], Jihyun Irizarry[1], Tiffany Kanesa Ybarra[3], Ryan Sathianathen[3], Jeffrey Trent[4], Stephen J. Forman[1], Kathleen M. Sakamoto[3], Ya-Huei Kuo[1], Bin Zhang[1], Adam L. MacLean[2], Guido Marcucci[1], Russell Rockne[1]

[1]City of Hope National Medical Center, Duarte, CA,[2]University of Southern California, Los Angeles, CA,[3]Stanford University, Stanford, CA,[4]Translational Genomics Institute, Phoenix, AZ

CML is defined by evolution from chronic phase (CP) to increased disease burden during blastic phase, but the cellular mechanisms that create these disease states and produce the transition between states is not understood. We previously used state-transition models to show that CML evolution is not encoded in single-cell transcriptional microstates but instead emerges only when gene expression is aggregated into population-level macrostates where distinct phenotypic disease states emerge. Here, we extend this framework to ask how antagonistic teams of genes and their regulatory network defined steady states give rise to these macrostates. Using weekly time-series single-cell RNA sequencing from both CP and blast crisis (BC) inducible CML mouse models, we assessed the origin of phenotypic disease macrostates in each cell type by identifying antagonistic teams of genes. We identified these teams for each cell type lineage by selecting the genes where their eigenvalue in the state-space construction and their observed expression change combine to indicate that the gene either strongly promoted (pro-CML) or strongly opposed (anti-CML) leukemia. To coarse grain the large number of resulting of genes per lineage, we applied weighted gene coexpression network analysis (WGCNA) to define gene modules and module eigengenes that define coordinated transcriptional programs. Each module produced by this process were strongly enriched for either pro- or anti-CML which suggests that they define functional units in leukemia development. We then inferred gene regulatory networks for these modules using Bayesian network inference constrained by prior knowledge from curated interaction and regulatory databases. This produced module-level networks that were unique for each of the B, T, myeloid, and stem cell compartments. For each inferred network, we computed steady states (attractors) and projected the stable transcriptional configurations into the state-space to determine whether the gene derived attractors align with lineage-specific macrostates in the state-space. Preliminary analyses reveal that module networks can reproduce the early, transitional, and late CML macrostates observed from our previous study. Further, we performed in silico perturbations of the networks to predict shifts in attractor occupancy and recapitulate our previous findings that the dominant contributions of B and myeloid compartments to disease progression observed previously. These results support a mechanistic view of leukemia where CML macrostates arise from cell type-specific teams of genes organized into low-dimensional regulatory networks. These network level attractor states could provide a new approach to identify therapeutic targets that are directly related to disease phenotypes and, therefore, new approaches for preventing CML disease evolution.

#6831 Virtual clinical trials of BMP4 differentiation therapy.

Nicholas Harbour[1], Lee Curtin[2], Loizos Michaelides[3], Matthew E. Hubbard[4], Pamela Jackson[2], Vinitha Rani[3], Rajappa Kenchappa[3], Virginea Farias[3], Anna Carrano[3], Markus Owen[1], Alfredo Quinones-Hinojosa[3], Kristin Swanson[2]

[1]Centre for Mathematical Medicine and Biology, The University of Nottingham, Nottingham, United Kingdom,[2]Mathematical Oncology Systems Analysis of Imaging Center (MOSAIC), Cedars-Sinai, LA, CA,[3]Department of Neurosurgery, Mayo Clinic Florida, Jacksonville, FL,[4]School of Mathematical Sciences, The University of Nottingham, Nottingham, United Kingdom

Glioma stem cells (GSCs) are considered a major driver of glioblastoma (GBM) progression and are highly resistant to standard cytotoxic treatments. BMP4 has been shown to promote GSC differentiation, enhance radiosensitivity, slow tumor growth, and extend survival in animal models. Despite this promise, BMP4 has yet to achieve clinical impact, owing largely to heterogeneous and nonlinear responses across preclinical experimental systems. To elucidate how BMP4 could function as an effective targeted differentiation therapy in GBM, we develop a mathematical model that describes the growth of a GBM tumor via a hierarchy of GSCs, progenitor and terminally differentiated cells. We parameterize our model using new radiotherapy and proliferation assay data (with and without BMP4 exposure) from twelve patient-derived GSC lines. This integration of model and data allows us, for the first time, to quantitatively capture patient-specific heterogeneity in BMP4 sensitivity. We perform global sensitivity analysis on the model, identifying proliferation rate and GSC self-renewal sensitivity as key determinants of BMP4 efficacy. These parameters act as model-derived biomarkers that distinguish BMP4-responsive tumors from non-responsive ones. In an in silico analysis across a broad cohort of virtual patients, we find that continuous BMP4 delivery from surgical resection through radiotherapy consistently outperforms a single-dose strategy. Virtual clinical trials further show that, without stratification using these model-derived biomarkers, BMP4 yields little observable therapeutic benefit. In contrast, selecting patients with more proliferative, BMP4-responsive GSCs markedly increases the likelihood of observing a significant treatment effect.

#6832 Toward personalized rotational multi-agent therapies to overcome treatment resistance in pancreatic cancer: A virtual trial framework in mice.

Krithik Vishwanath[1], Hoon Choi[2], Mamta Gupta[2], Rong Zhou[3], Anna G. Sorace[4], Thomas E. Yankeelov[5], Ernesto A.B.F. Lima[6]

[1]Oden Institute for Computational Engineering and Sciences, The University of Texas at Austin, Austin, TX,[2]Department of Radiology, The University of Pennsylvania, Philadelphia, PA,[3]Department of Radiology, Abramson Cancer Center, The University of Pennsylvania, Philadelphia, PA,[4]Department of Radiology, Department of Biomedical Engineering, The University of Alabama, Birmingham, Birmingham, AL,[5]Oden Institute for Computational Engineering and Sciences, Department of Biomedical Engineering, The University of Texas at Austin, Austin, TX,[6]Oden Institute for Computational Engineering and Sciences, Texas Advanced Computing Center, The University of Texas at Austin, Austin, TX

Introduction. Pancreatic ductal adenocarcinoma (PDAC) is highly lethal in part because tumors rapidly evolve resistance to potent regimens. Rotational, multi-agent schedules have emerged as a promising approach to outpace this adaptive escape. To attack this problem, we propose a mechanistic “virtual-trial” framework that couples an ordinary differential equation model with patient-specific data to quantify responses to three first-line chemotherapies (cisplatin, paclitaxel, gemcitabine), stromal-modulating agents (calcipotriol, losartan), and an immune-checkpoint inhibitor (anti-PD-L1). Using an estimated dynamic resistance, our model provides an in-silico testbed for generating and ranking rotational-therapy hypotheses before clinical translation, supporting more adaptive treatment design for pancreatic cancer.

Methods. Longitudinal tumor volume measurements for five distinct combinations of therapy agents were acquired in 49 mice over 14 days. Our mathematical model captures key physiological features such as tumor proliferation, drug efficacy, and temporal treatment resistance to emulate the progression and regression of pancreatic tumors to predict variation in tumor growth. Bayesian calibration of model parameters is derived on data from *in vivo* experiments conducted on mice with a genetically engineered model (GEM) of pancreatic cancer (KPC). We use adaptive optimization to develop personalized rotational therapy regimes across a 2-week simulation of 1000 patients.

Results. The model successfully mimics tumor growth in both control and treatment cases, with an average concordance correlation coefficient (CCC) of 0.99 ± 0.01 when comparing observed and predicted changes in tumor volumes. We extend our analysis by conducting leave-one-out predictions (average CCC = 0.7 ± 0.06), mouse-specific predictions (average CCC = 0.75 ± 0.02), and group-informed, mouse-specific predictions (CCC = 0.85 ± 0.04). Group-informed, mouse-specific predictions show an 82.17 ± 15.07% accuracy in discerning responders from non-responders. Our optimization predicts that switching to a personalized, adaptive schedule would cut median tumor burden by 30.5% and shrink final tumor volume by a median 65.9% relative to any fixed protocol in simulated mice.

Conclusion. Our modeling framework reproduces the experimental tumor-growth data and demonstrates strong predictive power for how pancreatic tumors respond to varied therapeutic combinations. By correctly classifying most responders versus non-responders and by forecasting sizable reductions in tumor burden with individually optimized rotational schedules, the approach offers a practical in-silico tool for designing adaptive treatment regimens. Our framework lays the groundwork for adaptive clinical trials poised to finally outmaneuver PDAC resistance and improve outcomes.

#6834 Modeling the role of homeostatic T-cell reconstitution in durable response to CAR T-cell therapy.

Philipp Martin Altrock[1], Alvaro Martinez-Rubio[2], Maria Rosa[3], Arne Traulsen[4], Michael D. Jain[5], Frederick L. Locke[6]

[1]Hematology & Oncology, Universitatsklinikum Schleswig-Holstein, Kiel, Germany,[2]Computational Oncology Unit, Institut Curie, Paris, France,[3]Biomedical Research and Innovation Institute of Cadiz, Puerta del Mar University Hospital, Cadiz, Spain,[4]Department of Theoretical Biology, Max Planck Institute for Evolutionary Biology, Ploen, Germany,[5]H. Lee Moffitt Cancer Center & Research Institute, Tampa,, FL,[6]H. Lee Moffitt Cancer Center & Research Institute, Tampa, FL

Anti-CD19 Chimeric Antigen Receptor (CAR) T-cell therapy is a promising option for relapsed or refractory lymphoma patients, yet our mechanistic understanding of response heterogeneity remains incomplete. Using retrospective longitudinal data from 21 patients treated with axicabtagene ciloleucel (including CAR T counts, absolute lymphocyte counts, tumor burden, and survival), we developed a computational modeling approach to distinguish between two expansion mechanisms: homeostasis- and antigen-driven. For each patient, we trained and compared three-compartment models to describe the dynamics of normal T-, CAR T-, and tumor cells. Comparisons revealed two distinct patient groups: patients who can be exclusively characterized by homeostatic proliferation as the CAR T expansion mechanism (homeostatic expanders, 10/21) and those of mixed type (mixed homeostatic/antigen-driven expanders, 11/21). These groups were distinguished by differences in the relationship between baseline metabolic tumor volume (taken one to two weeks before CAR T) and the inferred tumor burden at dosing. Notably, homeostatic expanders demonstrated significantly better overall survival (60% vs. 10% beyond day 180, $p = 0.011$), with 6 of 7 patients in this group achieving long-term responses. Our findings highlight how the ability of CAR T-cells to function in a homeostatic reconstitution context and the ability to quantify tumor burden at CAR T dosing influence the predictability of long-term responses. Our personalized mathematical modeling approach provides novel insights into optimizing CAR T-cell therapy and understanding the dynamics of cellular immunotherapy. Importantly, the absence of antigen-driven expansion increases the negative impact of high tumor burden at the time of infusion.

#6835 Multiomic state-transition framework reveals chemotherapy-induced metabolic reprogramming in acute myeloid leukemia.

Jennifer Rangel Ambriz[1], Ziang Chen[1], Yu-Hsuan Fu[1], David Eugene Frankhouser[1], Denis O'Meally[1], Lianjun Zhang[1], Ying-Chieh Chen[1], Sergio Branciamore[1], Jihyun Irizarry[1], Bin Zhang[1], Guido Marcucci[2], Russell Rockne[1], Ya-Huei Kuo[1]

[1]Beckman Research Institute of The City of Hope, Duarte, CA,[2]City of Hope National Medical Center, Duarte, CA

Acute myeloid leukemia (AML) is a highly lethal hematological malignancy with a long-term survival below 32%, largely due to disease relapse driven by treatment-resistant leukemia stem cells and metabolic reprograming. This poor prognosis underscores the need for frameworks that can predict disease dynamics and treatment effects. We previously applied state-transition theory to model AML disease evolution as trajectories of the mRNA and microRNA (miRNA) transcriptomes in their respective AML state-space, characterized by a leukemogenic potential with three critical points representing health, transition, and leukemia states. Here, we apply state-transition theory to characterize chemotherapy-induced transcriptomic and metabolic changes and test the hypothesis that chemotherapy alters the leukemogenic potential landscape by promoting transitions towards health while inducing metabolic shifts. Using a CBFB::MYH11 knock-in murine model of AML, we collected weekly peripheral blood samples before and after a “5+3” chemotherapy regimen consisting of cytarabine and daunorubicin, modeling the standard-of-care “7+3” regimen. All blood samples were subjected to bulk RNA-seq and miRNA-seq and we used PCA to construct mRNA- and miRNA-based state-spaces. Analyzing the mRNA and miRNA transcriptome trajectories over time, we observed that both transcriptome trajectories transitioned towards a health state post-chemotherapy but ultimately relapsed. Notably, the miRNA trajectories exhibited a delayed response of 2 or more weeks after treatment, revealing desynchronized mRNA-miRNA dynamics. To assess metabolic implications, we performed a Gene Set Variation Analysis (GSVA). This analysis revealed that oxidative phosphorylation, glycolysis and fatty acid metabolism pathways were downregulated during remission, indicating a low metabolic state, but were upregulated during relapse, consistent with metabolic reprogramming as a hallmark of AML recurrence. Finally, we extended the state-transition framework to two-dimensions (2D) to characterize how chemotherapy affects the mRNA-miRNA interplay and multiomic potential landscape. The multiomic state-space revealed a strong mRNA-miRNA correlation during AML progression, which is altered after chemotherapy. Further, the 2D state-transition model enables us to capture the effects of chemotherapy on multiomic potential and simulate how the mRNA-miRNA interplay changes over time. Importantly, model simulations capture response followed by relapse similar to the mRNA and miRNA time-series data trajectories. Together, our findings demonstrate that a mathematically grounded, multiomic state-transition framework captures chemotherapy-induced transcriptomic and metabolic dynamics, offering a systematic approach to predict response and identify metabolic vulnerabilities in AML.

#6836 Mechanistic modeling platform predicts patient response to guide antibody-drug conjugate clinical development.

NING Wang, Nathan Siemers

Decode Origin, Palo Alto, CA

To address the critical translational gap in predicting patient responses to novel antibody-drug conjugates in preclinical or early clinical stages, we developed a mechanistic modeling platform integrating drug mechanism and patient genomic profiles to predict response rates before mature clinical data becomes available.

Methods: We developed PatientMatrix, a systems pharmacology modeling-machine learning hybrid platform, and built a specialized platform for antibody-drug conjugates (PatientMatrix-ADC). The platform comprises three components: a mechanistic ADC model employing systems pharmacology to convert drug properties into patient response predictions, a machine learning model, and a combination model integrating both outputs. This platform enables prediction of ADC monotherapy or combination with PD(L)1 inhibitor. We applied this framework to sacituzumab govitecan, a TROP2-targeted ADC. The mechanistic model captures three critical properties: antigen target, payload sensitivity, and resistance mechanisms. The platform was trained on harmonized patient genomic data and clinical trials including ASCENT, then applied to TCGA reference cohorts to predict patient responses.

Results: PatientMatrix-ADC accurately predicted sacituzumab govitecan plus pembrolizumab responses in the EVOKE-02 trial (metastatic NSCLC), achieving accuracy across PD-L1 subgroups: 77.6% predicted vs 75.0% observed (PD-L1 ≥50%), 50.6% predicted vs 44.0% observed (PD-L1 <50%), and 58.1% predicted vs 54.0% observed (ITT population). The model demonstrated qualitative concordance beyond fitted indications, with first-line predictions of 29.0% (endometrial) and 54.3% (urothelial) appropriately trending higher than second-line reports (22.2% and 27.4%, respectively), as expected for treatment-naive patients. Indication prioritization across TCGA identified several candidate tumor indications missed by TROP2 target expression-based approaches. Esophageal cancer emerged as a potential opportunity despite low TROP2 expression, driven by favorable SN38 sensitivity scores. Critically, PatientMatrix-ADC predicted target expression-stratified responses (TROP2 high, medium, and low) learned from ASCENT clinical trials. This enabled the model to estimate TROP2-stratified patient responses in ASCENT-03.

Conclusions: The PatientMatrix modeling platform uses genomic, clinical, and mechanistic data to predict patient response rates to novel therapeutics in preclinical and early clinical stage, and guide indication selection and patient stratification for agents in clinical development. Case studies with sacituzumab govitecan clinical trials demonstrated the utility of the approach as well as broader ability to predict response in adjacent clinical settings or indications.

#6837 Scalable cell type and spatial domain modeling using spatially informed topic inference of cancer niches.

Jeongbin Park, Tingrui Zhang, Cong Ma

University of Michigan, Ann Arbor, MI

Spatially resolved transcriptomics (SRT) has revealed the heterogeneity of cancer samples. Yet, the capability of computationally identifying the full hierarchy of spatial organization in modern large-scale SRT data remains limited. Although many computational methods have been developed to identify spatial domains and cell types, most of them do not consider the entire hierarchy of spatial organization or explicitly model the relationships among adjacent hierarchical layers. Only a few models (BASS, CytoCommunity, and SpaTopic) model the relationship between spatial domains and their cell type composition. However, BASS is not scalable to the latest SRT data, and both CytoCommunity and SpaTopic require user-provided cell-type annotations and assume that these annotations are accurate. Our goal is to infer the hierarchical spatial organization of tissues from large-scale high-dimensional SRT data, which requires uncovering hidden multi-scale structure in the measurements. To achieve this, we use a variational autoencoder (VAE) framework to learn low-dimensional latent variables that explain the observed gene expression, and we place biologically motivated prior distributions on these variables so that the inferred hierarchy remains close to reality. Concretely, our model consists of three coupled artificial neural networks: (1) multiple graph convolutional networks (GCNs) for modeling spatial domains with Gaussian Markov Random Field (GMRF) and Dirichlet prior, (2) a VAE for reconstructing gene expression and revealing cell types and cell-type-wise gene expression profiles, and (3) a feed-forward multi-layer perceptron for modeling cell types from spatial domains. Our model required 4 minutes for inference when applied to a Xenium data of 17K cells. We found that the domain annotations in breast cancer tissue separated the SRT data into three clear structural groups: invasive regions, DCIS type 1, and DCIS type 2. Furthermore, when we compared our predictions with the ground truth, the inferred cell types revealed malignant subpopulations that were not captured by the original labels, highlighting additional layers of tumor heterogeneity. Importantly, we also identified niches where immune cells and cancer cells were co-localized; these niches differed in their proportions of T cells, plasma B cells, pDCs, and monocytes/macrophages. Our method explicitly models the relationship between adjacent layers in the hierarchy, thus revealing the co-varying relationships among cell types and the cell type compositions within spatial domains, which cannot be directly identified by many previous methods that model cell types and spatial domains separately. We expect that this study can be used to identify distinct pathophysiological features in cancer tissues, which will help uncover biological heterogeneity closely associated with cancer progression.

#6838 Most severe adverse events in approved combination therapies occur at rates consistent with independent action.

Kunhee Kim[1], Rishi Bollapalli[2], Adam C. Palmer[2]

[1]Univ. of Connecticut School of Medicine, Farmington, CT,[2]University of North Carolina at Chapel Hill, Chapel Hill, NC

Introduction: Cancer combination therapies are widely used, but tolerability may limit their application. Although ~95% of approved combination therapies show additive or less-than-additive effects on Progression-Free Survival (Hwangbo et al. (2023)), it remains unclear whether severe AEs follow similar patterns. Since grade 3-4 AEs are consistently reported in clinical trials and critical determinants of clinical trial outcomes, we assessed whether grade 3-4 combination AE incidence follows independent action of individual drugs or by a model of maximum-monotherapy-incidence (MMI), in which the expected combination incidence equals the greater monotherapy value.

Methods: We systematically identified 29 phase III trials of combination therapy that included matching monotherapy arms and extracted all grade 3-4 AEs reported (A vs. B vs. A+B). Combination AE incidences were calculated under the null hypothesis of independent action: P(A+B) = 1 - (1-P(A))(1-P(B)) (Palmer et al. (2017)). Deviations from independent action were quantified using Wald z-scores with Benjamini-Hochberg adjustment. We also compared the number of AEs better explained by independent action versus MMI model, and whether monotherapy AE incidence affected the results, and performed subgroup analyses by cancer type, drug class, and AE category.

Results: Across all grade 3-4 AEs, 6% (12/198) largely exceeded expected incidence, 23% (45/198) fell below it, and 71% (141/198) remained within a 0.5-2.0 fold range of expectation. Deviation from the null, measured as mean squared error (MSE), varied markedly by drug class: immunotherapy combinations showed the least MSE (0.0003), solid cancers without immunotherapy were intermediate (0.0028), and hematologic cancers deviated most (0.0121). Independent action explained more AEs (130) than the MMI model (68), and accuracy did not depend on monotherapy AE incidence. Many hematologic AEs were below independence, consistent with shared mechanisms such as bone marrow suppression, whereas immunotherapy AEs aligned with independence, suggesting distinct pathways to toxicity.

Conclusions: The incidences of serious adverse events from combination therapies are predominantly explained by independent action, similar to prior findings on efficacy of combination therapies. The proportion of AEs with ‘more than expected’ (6%) or ‘less than expected’ (22%) incidence are interestingly similar to rates of ‘more than expected’ efficacy (5%) and ‘less than expected’ efficacy (27%) (Hwangbo et al. (2017)). These results indicate that toxicity, like efficacy, is driven mainly by independent drug action and inter-patient heterogeneity, with synergistic or antagonistic toxicities being uncommon. The predictability of combination AEs supports integrating toxicity modeling into trial design to improve combination selection and escalation or de-escalation strategies.

#6839 Structural vulnerabilities of the breast tumor-draining lymph node to radiotherapy-induced fibrosis and lymphedema risk.

Laia Vancells, Leopold Green, Nan Kong

Purdue University, West Lafayette, IN

Lymphedema is a significant survivorship burden in breast cancer, associated with chronic morbidity, diminished quality of life, and increased susceptibility to locoregional recurrence. Radiotherapy to the axillary lymph node, the principal drainage and immune-surveillance hub for the breast, is the dominant late driver of this condition, producing lymphocyte loss, stromal injury, and progressive fibrosis that restricts normal lymphatic flow. Yet the specific intranodal structures that fail first under radiotherapy stress, and how their collapse contributes to impaired antitumor immunity, remain unclear. To date, direct experimental resolution is limited, as lymph nodes cannot be repeatedly imaged after radiotherapy, and existing animal studies lack the spatial resolution and sex-specific depth needed to map structural collapse. This challenge is further compounded by the lymph node's highly nonlinear stromal-sinus architecture, where even small disruptions can propagate unpredictably across the transport network, making computational modeling essential. To address this gap, we developed an agent-based model of the breast tumor-draining lymph node that integrates established fibroblastic reticular cell microanatomy with the broader sinus architecture. To our knowledge, this is the first structural model capable of identifying radiotherapy-induced failure modes within the draining lymph node. Radiotherapy injury was modeled as progressive fibrosis, introducing targeted removal of stromal-sinus connections, local increases in flow resistance, and reduced HEV-paracortex communication based on published radiotherapy injury profiles. Across injury scenarios, radiotherapy consistently produced early nonuniform disruption at stromal-sinus junctions that serve as conduits for lymph inflow and immune-cell entry. Loss of these regions impaired drainage, prolonged antigen transit, and reduced T-cell delivery to antigen-rich compartments, revealing a selective degradation of the LN's core transport axis. Together, these failures define a reproducible intranodal "collapse axis" whose breakdown forecasts diminished antitumor surveillance and generates a radiotherapy immune-risk map that pinpoints the pathways most vulnerable to fibrotic injury. These insights represent a paradigm shift toward structure-guided radiotherapy planning, enabling lymph-node-sparing treatment strategies, more precise recurrence-risk stratification, and targeted interventions to prevent chronic morbidity in breast cancer survivors.

#6840 Developing a data assimilation framework to forecast patient-specific tumor burden in low-grade glioma.

Sophia Ty[1], Devika Shankar[2], Bikash Panthi[2], Mohamad El-Jammal[2], Victoria White[2], Holly Langshaw[2], Eleni Konstantinopoulou[2], Hannah Green[2], Ashi Jain Chakresh[2], Vishantan Kumar[2], Thomas E. Yankeelov[3], Caroline Chung[2], David A. Hormuth[3]

[1]Oden Institute for Computational Engineering and Sciences, The University of Texas at Austin, Austin, TX,[2]The University of Texas, M.D. Anderson Cancer Center, Houston, TX,[3]The University of Texas at Austin, Austin, TX

Low-grade gliomas (LGG) typically grow gradually for years with limited clinical symptoms but may later exhibit erratic growth patterns and undergo transformation to high-grade glioma. This presents challenges to disease management creating a need for novel methods to simulate and predict LGG behavior. Towards this goal, we implemented a data assimilation framework utilizing a previously developed biophysical model capable of spatiotemporally forecasting patient-specific tumor dynamics. The study cohort includes nine LGG patients treated with radiation therapy at the MD Anderson Cancer Center. All patients were longitudinally monitored using magnetic resonance imaging (MRI) to assess tumor cellularity (diffusion-weighted MRI) and extent of disease (T_1-weighted MRI with & without gadolinium-based contrast, T_2-fluid attenuated inversion recovery). MRI was acquired before treatment and approximately at the 4, 5, 6, and 12-month post-treatment visits. Brain and tumor regions were segmented using a semi-automated algorithm. Our biophysical model is a reaction-diffusion equation that explicitly accounts for tumor cell proliferation, invasion, and treatment response. The model focuses on changes in non-enhancing tumor regions, a hallmark of LGG. Total tumor cell count (TTC) derived from spatiotemporal tumor response forecasts was used to quantify tumor burden. The data assimilation framework incorporates MRI data acquired with each subsequent visit then updates its forecast. Predictive accuracy was quantified via the concordance correlation coefficient (CCC) between the observed and predicted TTC for both short (e.g., 1 - 3 months) and longer-term predictions (e.g., 6, 12-months). A Mann-Whitney U test compared short and longer-term prediction performance. The median and interquartile range (IQR) of the model parameters describing tumor cell proliferation and invasion are reported for each follow up visit. The tumors experienced a median volumetric change of -36.4% over 12 months. The model accurately forecasts TTCs at short (CCC: 0.71) and longer interval times (CCC: 0.96) with no statistically significant difference (p-value: 0.34) in performance between groups. The model estimated tumor cell proliferation rate had a median and IQR of 0.10 (0.06) at the 4-month visit, 0.07 (0.04) for the 5-month visit, 0.04 (0.05) at the 6-month visit, and 0.04 (0.04) $days^{-1}$ at the 12-month visit. Similarly, the model estimated tumor diffusion coefficient had a median and IQR of 0.15 (0.10), 0.16 (0.10), 0.18 (0.06), and 0.16 (0.09) mm^2/days for the 4, 5, 6, and 12-month visit. Our preliminary findings demonstrate the model's ability to predict patient-specific LGG behavior and offers a step towards the development of a personalized decision support tool for managing LGG care.

#6842 ctDNA precedes imaging: A predictive model for real-time treatment adaptation in HPV-associated anal squamous cell carcinoma.

Phebe M.A Havor[1], Brandon M Huffman[2], James Cleary[2], Renee Brady-Nicholls[1]

[1]Integrated Mathematical Oncology, H. Lee Moffitt Cancer Center, Tampa, FL,[2]Dana-Farber Cancer Institute, Boston, MA

Background: Real-time assessment of treatment response in HPV-associated anal squamous cell carcinoma (ASCC) remains challenging. Traditional tumor volume measurements require serial imaging that is costly, time-intensive, and delays clinical decision-making. Consequently, patients may receive prolonged suboptimal therapy or unnecessary toxicity from over-treatment. Circulating tumor DNA (ctDNA) offers a more accessible, real-time alternative biomarker—yet its predictive value and clinical utility for guiding treatment adaptation remain undefined.

Methods: We developed a mechanistic mathematical model of tumor volume-ctDNA dynamics which we parameterized and calibrated to longitudinal data from 32 HPV-associated ASCC patients who received immunotherapy (pembrolizumab, once every 3 weeks, up to 2 years). The model was fit across three clinical scenarios: simultaneous measurements (8 patients), volume preceding ctDNA (14 patients), and ctDNA preceding volume (2 patients). We quantified ctDNA's predictive capacity for early treatment response assessment.

Results: ctDNA demonstrated strong positive correlation with tumor burden (SLD) and predicted clinical response status within 4 weeks of treatment initiation. Critically, ctDNA kinetics *preceded* volume changes in multiple patients, providing early signal for response assessment before imaging confirmation. The mathematical model robustly captured heterogeneous patient dynamics across all measurement scenarios, validating its predictive framework.

Conclusions: ctDNA functions as a leading indicator biomarker enabling early identification of treatment response in HPV-associated ASCC. Our quantitative framework translates this biomarker into actionable clinical predictions, allowing clinicians to make real-time decisions on treatment escalation, maintenance, or de-escalation. This approach enhances precision oncology by replacing burdensome imaging with accessible blood-based monitoring—particularly impactful for underserved populations with limited imaging access. Future studies will prospectively validate this model to inform personalized, adaptive treatment strategies.

#6843 A joint model for integrating serial methylation-based tumor fraction and *ESR1* assessment to forecast overall survival in patients with ER+/HER2- metastatic breast cancer.

Christopher Pretz[1], Matthew Ellis[2], Mitchell J. Elliott[3], Caroline Weiport[2], Amar Das[2], Carin Espenschied[4], David Cescon[3]

[1]Guardant Health, Redwood City, CA,[2]Guardant Health, Palo Alto, CA,[3]Princess Margaret Cancer Centre, Toronto, ON, Canada,[4]Guardant Health, Spokane, WA

Background: Methylation-based tumor fraction (TF) dynamics are highly associated with outcomes in metastatic ER+/HER2- breast cancer. Gain-of-function *ESR1* mutations frequently arise under therapeutic pressure and serve as actionable biomarkers. Because TF reflects tumor burden and *ESR1* mutations reflect clonal evolution, jointly modeling their trajectories may improve understanding of biomarker co-evolution and strengthen outcome prediction. We developed a statistical framework that simultaneously characterizes serial *ESR1* mutation burden and TF, capturing both genetic adaptation and epigenetic quantification of tumor fraction.

Methods: A joint model (JM) was applied to serial liquid biopsy data from ER+/HER2- mBC patients enrolled in a prospective plasma-collection study while receiving endocrine therapy (ET) and CDK4/6 inhibitors (CDK4/6i). Patients contributed baseline and ≥ 2 on-treatment samples. TF was measured using Guardant Reveal and *ESR1* alterations were assessed using Guardant360 Liquid. TF and *ESR1* variant allele frequency (VAF) using the *ESR1* alteration with the highest VAF were logit-transformed for modeling and back-transformed for interpretation. A hierarchical cubic spline mixed-effects sub-model captured longitudinal TF and *ESR1* patterns, paired with a Cox regression sub-model for overall survival (OS). Baseline covariates, incorporated in both sub-modules, included age, CDK4/6i agent, line of therapy, and prior treatment.

Results: Forty-nine patients (279 ctDNA timepoints) met inclusion criteria. After covariate adjustment, current TF and *ESR1* values were significantly associated with OS ($p < 0.05$). Rising TF or *ESR1* trajectories corresponded to poorer survival, whereas decreasing trajectories delineate improved outcomes. The model also captures interactions between TF and *ESR1*, showing how molecular signals evolve together and impact outcome. Individualized survival predictions, informed by the dynamic biomarker trends, are visualized through patient-level dynamic prediction plots.

Conclusions: Joint modeling of TF and *ESR1* mutation dynamics provides an integrated view of tumor evolution, capturing both clonal adaptation and tumor burden over time. This approach yields continuously updated, patient-specific survival predictions that may support real-time clinical decision-making. Integrating genomic and epigenomic biomarkers within a unified dynamic model represents a meaningful advance in disease monitoring. Future work should validate this framework in larger, more diverse cohorts and assess feasibility in routine clinical use.

#6844 Functional data analysis of spatial protein imaging data using spatial trajectories with application to ovarian cancer.

Brooke L. Fridley[1], Alex C. Soupir[2], Daisy Liao[3], Chase Sakitis[1], Joellen Schildkraut[3], Andrew B. Lawson[4], Mary K. Townsend[5], Shelley Tworoger[5], Kathryn L. Terry[6], Julia Wrobel[3], Lauren Cole Peres[7]

[1]Children's Mercy Kansas City, Kansas City, MO,[2]Moffitt Cancer Center, Tampa, FL,[3]Emory University, Atlanta, GA,[4]Medical University of South Carolina, Charleston, SC,[5]Oregon Health Sciences University, Portland, OR,[6]Asst. Professor, Dept. of OB/GYN, Brigham and Women's Hospital, Boston, MA,[7]H. Lee Moffitt Cancer Center, Tampa, FL

Background: Researchers can study both the abundance and spatial architecture of cell types within the tumor microenvironment (TME) using spatial technologies. Often, Ripley's K or nearest-neighbor G are used to measure spatial clustering of cells. These measures can be computed at various radii to assess clustering at different spatial ranges. We propose the use of functional principal component analysis (FPCAs) to model the association of the spatial clustering of T cell populations in the TME with survival from high grade serous ovarian cancer (HGSOC).

Methods: We applied FPCA to study the clustering of CD3+ and CD3+CD8+ cells in the ovarian TME with survival. Five ovarian cancer studies were included in the analysis: Nurses' Health Study (N=239), Nurses' Health Study II (N=68), New England Case Control Study of Ovarian Cancer (N=175), African American Cancer Epidemiology Study (N=155), and the North Carolina Ovarian Cancer Study (N=136). Protein imaging data was collected using AKOYA Biosciences OPAL™ IHC Kit with image analysis completed using Vectra®3 Automated Quantitative Pathology Imaging System. Spatial trajectories using G statistic were computed for samples with at least 8 positive cells for a cell type. FPCA was applied to the spatial curves with the top two components (FPC1, FPC2) associated with survival, adjusting for stage, age of diagnosis, and abundance of the cell population (high vs low using 1% threshold). A second model was fit to assess interaction between the abundance and spatial clustering. Analyses were completed for each study with results combined using a random-effect meta-analysis.

Results: From the model without spatial information, we observed that high abundance of CD3+ (hazard ratio (HR): 0.81, 95% confidence interval (0.66, 0.98)) and CD3+CD8+ cells (HR: 0.64 (0.52, 0.79)) were associated with improved survival. The model with both abundance and spatial clustering detected a significant effect for CD3+CD8+ clustering (FPC1 HR: 1.17 (1.04, 1.33)) and a borderline association for CD3+ cells (FPC1 HR: 1.06 (0.99, 1.14)). When fitting a model with interactions for abundance and spatial clustering, a significant interaction for CD3+ cells (HR: 1.23 (1.07, 1.42)) and a borderline interaction for CD3+CD8+ cells (HR: 1.19 (0.98, 1.43)) was observed. Hence, we estimated the HRs for 4 tumor types (high/low abundance and high/low spatial clustering). We observed that patients with high abundance but low spatial clustering of CD3+ and CD3+CD8+ cells had the improved survival, with HRs for the high abundance / low spatial clustering group being 0.74 and 0.41, respectively.

Discussion: In studying the HGSOC TME using spatial proteomics and FPCA, we found that not only is the abundance of T cell populations related to survival, but also the spatial clustering of these cell populations, with improved survival for women with tumors with diffuse T cell infiltration.

#6845 Using cell-type-specific nucleosome patterns to improve cell-free DNA fragmentation models in lung cancer.

Brian Sun Liu, Mengran Zhang, Mohammad Shahrokh Esfahani

Department of Radiation Oncology, Stanford University School of Medicine, Stanford, CA

Background: Cell-free DNA (cfDNA) profiling has emerged as a promising tool in cancer detection. Methods include the identification of circulating tumor DNA (ctDNA), the profiling of cfDNA methylation, and the analysis of cfDNA fragments, including fragment size and position. We previously showed that fragment size diversity is strongly correlated with gene expression (Esfahani et al, 2022). We subsequently developed a mechanistic model for the cfDNA fragmentation process to enhance gene expression inference from cfDNA (Liu et al, 2025).
However, analysis of cfDNA fragment size distribution alone leaves out useful information about fragment position. Since fragment position arises from nucleosome position, we incorporate prior knowledge about nucleosome positioning to improve our cfDNA fragmentation models. We hypothesize that incorporating cell-type-specific nucleosome patterns can progress cfDNA models towards cell-type deconvolution.
Methods: In order to incorporate prior knowledge about cell-type-specific nucleosome organization into our cfDNA fragmentation model, we use Micrococcal Nuclease sequencing (MNase-seq) data from (Valouev et al, 2011) and MNase-Transcription Start Site Sequence Capture method (mTSS-seq) data from (Druliner et al, 2016). For each transcription start site (TSS), we leverage this prior knowledge about nucleosome organization to simulate well-positioned nucleosomes. Then, we generate additional nucleosomes given the gene's strand information and cell type. Next, we generate cuts, and generate a mixture of simulated fragments from various cell types.
Results: In order to evaluate the efficacy of our updated cfDNA fragmentation model, we calculate the coverage over 10 bp intervals within a window of the TSS, and compare it with the coverage for cfDNA control samples. We also calculate the coverage for simulated cfDNA fragments using our previous model, and compare it with the coverage for cfDNA control samples. Our updated model incorporating prior knowledge about nucleosome organization outperformed our previous model in simulating cfDNA fragmentation.
Conclusions: We show that integrating cell-type-specific nucleosome patterns improves cfDNA fragmentation models. Further improvements can be made given nucleosome organization information from additional cell types. We envision that this model-based approach will enhance tissue-of-origin classification and cancer detection.

#6846 Using physiologically-based pharmacokinetics-quantitative systems pharmacology model to optimize peptide-drug conjugates design.

Yuezhe Li, Cole Zmurchok, Daniel C. Kirouac

Metrum Research Group, Boston, MA

Introduction: Peptide-drug conjugates (PDCs) are being developed as new cancer treatments. Compared to larger antibody-drug conjugates (ADCs), they retain the advantage of a targeted therapy, binding to tumor-associated antigens (TAA) to deliver payload, while having better tumor penetration than ADCs. PDCs typically exhibit faster plasma clearance than ADCs, and therefore potentially have less tumor exposure to the drug. The pharmacokinetics is influenced by the molecular weight (MW) of the peptide used in the PDC. A physiologically-based pharmacokinetics (PBPK)-quantitative systems pharmacology (QSP) model would be useful to understand the interplay of pharmacokinetics (PK), tissue disposition, and tumor drug exposure of PDCs.
Methods: A platform PBPK-QSP model was developed based on a published PBPK model (Li et al., 2019) and a genetic tumor QSP model (Scheuher et al., 2024) by coupling these two models with a MW-based tumor penetration relationship. Through calibrated model simulations and sensitivity analysis, we interrogate how parameters of the peptide (e.g., molecular weight, binding affinity towards TAA) impact the PK, tissue disposition, and tumor drug exposure.
Results: The model predicted higher tumoral PDC concentration when the peptide was small, corresponding to the knowledge that smaller peptides resulted in better tumor penetration. However, a bell-shaped relationship was predicted between peptide size and PDC or payload exposure. The model predicts that a peptide with MW of approximately 86 kDa results in maximum tumor PDC or payload exposure despite exhibiting more rapid PK clearance than a 150 kDa ADC. This is in contrast with tissue disposition, as larger peptides led to higher non-tumoral tissue exposure. Further sensitivity analysis indicated this relationship is insensitive to tumor characteristics, such as TAA expression, or PDC binding affinity towards the TAA, but is sensitive to the peptide size.
Conclusions: This work demonstrated that this platform PBPK-QSP model can be a useful tool to guide PDC design and lead selection by optimizing peptide size for PDCs.

#6848 HPlot: A novel quantitative framework for spatial profiling of Immune heterogeneity in tumor microenvironments.

Chao Hui Huang[1], Jadwiga Renata Bienkowska[2], Diane Fernandez[1], Sara Beth Linker[1], Xinmeng Jasmine Mu[2], Robbin Nameki[2], Jennifer Kinong[1], Michelle Saul[1], Aakash Sur[3], Mehmet Tekman[1], Alexander Trageser[1], Wenjing Yang[1], Daniel Chawla[1], Greg Szeto[3], Arne Schmidt[4], Alberto M. Gonzalo[5], Srishti Munjal Mehta[5], Rosemarie Krupar[4], Nina Kozar-Gillan[4], Sophie Laturnus[6], Cornelius Bohm[4], Marija Pezer[4], Gloria H.Y. Lin[1], Darlan Conterno Minussi[1], Keith Ching[1], Thomas Powles[7], Craig Davis[8]

[1]Pfizer Inc., San Diego, CA,[2]Pfizer, Inc., San Diego, CA,[3]Pfizer Inc., Bothell, CA,[4]Aignostics, Berlin, Germany,[5]Aignoistics, Berlin, Germany,[6]AIgnoistics, Berlin, Germany,[7]Barts Cancer Centre, London, United Kingdom,[8]Sage Healthcare Insights, Albany, NY

Spatial organization of immune and tumor cells plays a critical role in disease progression and therapeutic response. Existing spatial analysis methods often treat tissue regions as uniform compartments and fail to quantify how immune composition and functional states change across tumor boundaries. This limits the ability to detect spatial biomarkers associated with treatment outcomes.

We developed H-Plot, a quantitative framework for profiling spatial immune heterogeneity with high resolution. The method is compatible with whole-slide imaging and modern single-cell spatial biology platforms. H-Plot integrates three components:

(1) Cell prediction and classification using machine-learning-based single-cell image analysis or spatial transcriptomics-derived cell subtyping to generate a high-fidelity cellular map;

(2) Cell-function enrichment analysis to identify biologically meaningful structures such as tumor regions, lymphoid aggregates, and tertiary lymphoid structures (TLS) through localized functional program detection; and

(3) Cell spatial profiling, which measures spatial relationships and computes layer-wise distances from biological structure boundaries (e.g., tumor margins) to capture spatial gradients across the tumor-immune interface.

Applying H-Plot to the ABACUS bladder cancer dataset revealed that treatment responders exhibited higher lymphocyte enrichment adjacent to tumor borders and smoother immune-layer transitions, whereas non-responders showed shallow or fragmented infiltration. In the TEMPUS mCRPC cohort, reduced pre-treatment lymphocyte proximity and weaker enrichment layers were associated with poorer clinical outcomes and aligned with RNA-based immune signatures and histological assessments.H-Plot provides a reproducible, interpretable, and visualization-ready framework for quantifying tumor-immune spatial heterogeneity. By converting complex spatial arrangements into layer-wise quantitative profiles and intuitive visualizations, H-Plot enables systematic comparison across patients, treatments, and tumor types. This framework supports spatial biomarker discovery and offers a scalable tool for translational oncology research.

#6849 Tumor microenvironment gene expression dynamics: Keystone cell types and non-cancer cell driver genes.

Yongzhong Zhao, Yixiao Cui, Ji Zheng, Cody Stevens, Jenny Bundy, Eranga Wettewa, Christopher Edwards, Victoria Thilker, Donald Carpenter, Zhongqiang Qiu, Zhijiu Zhong, Eric Zhao, Lili Liao, Qiang Xu, Nan Zhang, John Lin

Frontage Laboratories, Exton, PA

Cancer is not a disease, rather, of multi-scale heterogeneity, i.e., each victim of cancer is of unique evolutionary dynamics at distinct levels. Indeed, cancer therapeutics has been evolving from non-specific chemo and radiation therapy, mutation-specific targeted therapy, immunotherapy, as well as combination therapies, to ongoing tumor microenvironment (TME) specific interventions, in a broader sense, targeting tumor ecosystems. However, the critical schemata of TME with cell-type specific gene expression dynamics underpinning mechanistic druggable key driver genes remains largely obscure. Here, we present an integrated approach of AI-powered modeling TME gene expression dynamics via borrowing ecology models, namely, treating cell types as the counterpart of species in ecological settings. We represent each TME as a tensor with public non-small cell lung cancer (NSCLC) data settings, mainly focusing on lung adenocarcinoma (LUAD) and lung squamous cell carcinoma (LUSC) with scRNA-seq, snRNA-seq, and spatial transcriptomics data. Given that up to 72 distinct cell types/states were found in LUSC and 57 in LUAD, we validated these distinct cell types/states with the uniLung database via wavelet-transformed cell cluster analysis. Furthermore, we treated these cell types as species via incorporating a network ecology model (40 spatial transcriptomics data for NSCLC study, E-MTAB-13530, among other data settings). We found distinct keystone cell types in driving cancer progression in addition to key driver gene sets. These patient specific keystone cell types are not limited to cancer cells, rather many immune and stromal cell types are indeed ecology drivers, such as certain subtypes of cancer associated fibroblast (CAF). Distinct to LUAD, LUSC is of more loss of function of tumor suppressors, such as chromatin remodeling genes *SMARCA4* and *PBRM1*. Of note, *DNMT3A*, *TET2* and *ASXL1* are of immune cell driver genes, much individualized. Thus, tumor driver genes are not limited to cancer cells, yet to discover more non-cancer cell tumor driver gene sets. We propose validation and qualification strategies with our available bioassay platforms, spanning from genomics, cell-based assays and biomarkers. We continue to cross-validate this ecology network model with expanded distinct data setting. Of particular interest, we have been examining these complex interactions via cancer organoid models. Taken together, targeting tumor ecosystems with individualized biologics alongside geography ecology modeling of TME, we advocate integrated AI-powered single-cell level temporospatial analytics infrastructure as we have been building central laboratory logistics for fresh and frozen cancer samples, clinical pathology, automation, high throughput biomarker assays, scRNA-seq and snRNA-seq, spatial transcriptomics, flow cytometry, Elispot assay, cell potency, as well as organoid platforms.

#6850 Dynamic modeling of invisible tumor growth with simulated residual disease and PDX data.

Bryan A. Hawickhorst, Daniel J. McWilliams, Jonathan M. Baker, Amy H. Tang

Old Dominion University, Norfolk, VA

Tumor dormancy, early relapse, and treatment resistance remain poorly understood. After neoadjuvant or adjuvant therapy, the locally advanced and systemically disseminated invisible tumor cells may persist undetected for months or years despite clean MRI or CT scans. Reported detection thresholds and residual tumor sizes vary in the literature, further complicating prognostic accuracy in patient risk stratification. To address this unmet clinical need, we developed mathematical models and generated a computational algorithm to predict the time course of invisible tumor relapse, improve predictive accuracy, and model the invisible-to-visible tumor transition within the detection limits of the MRI/CT tumor imaging tools. We simulated remission-to-relapse trajectories for invisible residual tumors beginning with 1, 10, 10^2, 10^3, and 10^4 cells, and calculated the time for each to progress into a 3 cm^3 visible tumor. Exponential growth models with unrestricted doubling times from 2 to 30 days were used to capture rapid, unimpeded tumor growth. A modified logistic model was then used to model the time course of invisible tumor growth *in vivo*, with doubling times of 5 to 30 days to reflect varying aggressiveness, tumor and tumor microenvironment interactions, and tempo-spatial-context-treatment dependence in response to varied tumor remission and extended tumor latency. To improve mathematical modeling, we refined, verified, and authenticated several variable factors/clinicopathological parameters in experimental biology by fitting our hypothetical tumor growth models to the real-time TNBC tumor growth curves from six patient-derived xenograft (PDX) TNBC models in NSG mice. By varying the clinically invisible residual tumor sizes from 10^{-6} mm^3 to 10^{-2} mm^3, we found that tumors relapsed rapidly once tumor growth resumed, often exceeding the clinical detection thresholds before the regularly scheduled follow-up appointments and allowable MRI/CT-imaging intervals could capture them. Our results highlight the hidden risk of residual diseases, the major challenge of invisible tumor modeling, and the lack of accuracy in relapse prediction in the clinic. Exponential and logistic model fits to the PDX tumor implantation data were complete; the model authentication, relapse prediction augmentation, and correct interpretation of these fitted models will be augmented with the new chemo-resistant PDX models in NSG mice. This work underscores the unmet need and critical importance of modeling invisible tumor growth to improve the accuracy of tumor relapse prediction and patient risk stratification. Future work will focus on transforming this mathematical model into a companion prognostic tool in combination with our selected biomarker panel to predict tumor relapse risk, quantify therapeutic efficacy, and assist and support oncologists' decision-making in real time in the future.

#6851 Multi-cell type model for analyzing spatial single-cell protein imaging data with application to ovarian cancer.

Chase Sakitis[1], Jose Laborde[2], Julia Wrobel[3], Alex C. Soupir[4], Christelle M. Colin-Leitzinger[5], Benjamin G. Bitler[6], Mary K. Townsend[7], Andrew B. Lawson[8], Joellen M. Schildkraut[9], Shelley S. Tworoger[7], Kathryn L. Terry[10], Lauren C. Peres[5], Brooke L. Fridley[1]

[1]Health Services & Outcomes Research, Children's Mercy Kansas City, Kansas City, MO,[2]Biostatistics and Bioinformatics, Moffitt Cancer Center, Tampa, FL,[3]Biostatistics, Emory University, Atlanta, GA,[4]Biostatistics and Bioinformatics/Genitourinary Oncology, Moffitt Cancer Center, Tampa, FL,[5]Cancer Epidemiology, Moffitt Cancer Center, Tampa, FL,[6]University of Colorado Anschutz Medical Campus, Aurora, CO,[7]Division of Oncological Sciences and the Knight Cancer Institute, Oregon Health and Science University, Portland, OR,[8]Public Health Sciences, Medical University of South Carolina, Charleston, SC,[9]Epidemiology, Emory University, Atlanta, GA,[10]Asst. Professor, Dept. of OB/GYN, Brigham and Women's Hospital, Boston, MA

Background: Understanding the tumor immune microenvironment (TIME) is essential for advancing cancer research and improving treatment strategies. Multiplex immunofluorescence (mIF) is a spatial proteomics imaging technique enabling simultaneous analysis of multiple markers in preserved tissues. However, mIF-derived cell abundance data pose statistical challenges, such as zero-inflation, over-dispersion, hierarchical cell relationships, and repeated measures, that must be addressed to extract meaningful insights and enhance translational impact.
Methods: We developed a novel Bayesian multi-cell type analysis model that simultaneously models the relationship of immune cell abundances with clinical and epidemiological factors, while incorporating the biological relationships between immune cell populations. We applied this model to three large studies assessing the TIME of high-grade serous ovarian cancer: Nurses' Health Study I/II (NHSI/II) (N=321), African American Cancer Epidemiology Study (AACES) (N=92), and University of Colorado Ovarian Cancer Study (UCOCS) (N=103). The mIF staining for these studies was performed using the AKOYA Biosciences OPAL™ 7-Color Automation IHC Kit with the Vectra®3 Automated Quantitative Pathology Imaging System (0.499µm/pixel) utilized for image collection. InForm and HALO were utilized for spectral unmixing and cell phenotyping, respectively. Our analysis examined associations between immune cell infiltration (T-cells, B-cells, macrophages) and clinical variables (cancer stage, age at diagnosis, debulking status) with comparisons to the single-cell type model.
Results: In the NHSI/II analysis, our multi-cell type model detected a positive association between age at diagnosis and abundance levels of 6 of the 7 cell types in the analysis while the single-cell type model only detected 2 of the 7. This indicates improved association detection, with our multi-cell type model. We also observed that our multi-cell type model had narrower credible intervals (CIs) for all 7 cell types demonstrating higher accuracy in the association estimation. With cancer stage as the predictor in the NHSI/II analysis, neither model detected an association although our multi-cell type model had narrower CIs for 3 of the 7 cell types compared to the single-cell type model. Despite not capturing any associations between the predictors (age, stage, debulking status) and immune cell populations in the AACES or UCOCS, our Bayesian multi-cell type model had narrower CIs for every cell type in both studies for each predictor.
Discussion: Our Bayesian multi-cell type model offers a flexible framework for incorporating immune cell relationships and is well-suited for cancer studies of the TIME utilizing TMAs, regions of interest, or whole-slide imaging data.

#6852 Measure of three cell population co-localization for spatial protein imaging data analysis.

Kirill Sabitov[1], Alex Soupir[2], Lauren C. Peres[2], Brooke L. Fridley[1]

[1]Children's Mercy Research Institute, Kansas City, MO,[2]Moffitt Cancer Center, Tampa, FL

Background: Spatial protein imaging technologies enable detailed study of the tumor microenvironment (TME) to characterize cell abundance and spatial architecture. Pairwise colocalization metrics (e.g., Ripley's K) miss higher-order patterns, while enumerating all triangles for three cell populations is computationally infeasible on whole-slide images. Metrics using a triangle's longest edge poorly distinguish compact triples from elongated or dispersed arrangements. Thus, we propose a new trivariate colocalization measure using triangle area.

Methods: We developed a Horvitz-Thompson Monte Carlo estimator and benchmarked the unweighted and isoperimetrically weighted area variants against a longest-edge analogue on simulated data. These metrics were applied to a study of primary high-grade serous carcinoma (n=101) to quantify colocalization among T cells (CD3+), cytotoxic T cells (CD3+CD8+), B cells (CD19+), and macrophages (CD68+). Cox PH models evaluated associations between normalized clustering metrics and overall survival at radii of 15 and 25 µm - adjusted for diagnosis age, stage, and debulking.

Results: Simulations showed unbiased, consistent colocalization estimates with lower small-radius variance for area-based measures. Monte Carlo sampling achieved a $>10^5$-fold runtime reduction versus full enumeration. In the ovarian study, lower three-cell colocalization levels of lymphocytes with macrophages corresponded to small improvements in overall survival, though not significant (Table 1). Narrower confidence intervals were also observed for area-based estimators, with weighted and unweighted area variants performing similarly.

Discussion: Our framework enables scalable quantification of higher-order spatial organization in the TME. Despite comparable associations across estimators in the ovarian study, the greater stability of area-based measures supports their use as surrogates of complex cellular architecture in future spatial studies.

Table 1: Cox model hazard ratios and 95% confidence intervals for study cell triples at chosen radii

Cell Triple	Radius	Longest-Edge	Unweighted Area	Weighted Area
T Cell B Cell Macrophage	15	0.83 (0.61, 1.14)	0.93 (0.66, 1.31)	0.89 (0.65, 1.21)
	25	0.90 (0.65, 1.23)	0.91 (0.67, 1.23)	0.93 (0.68, 1.27)
Cytotoxic T Cell B Cell Macrophage	15	0.95 (0.73, 1.23)	0.90 (0.68, 1.17)	0.93 (0.73, 1.20)
	25	0.85 (0.65, 1.12)	0.86 (0.66, 1.11)	0.84 (0.64, 1.09)

#6853 A segmentation-free method for modeling high-resolution spatial transcriptomics at the molecule level.

Xiao Wang[1], Nan Zhang[2], Chi Zhang[3], **Sha Cao**[4]

[1]Indiana University, Bloomington, IN,[2]Fudan University, Shanghai, China,[3]Knight Cancer Institute, Oregon Health & Science University, Portland, OR,[4]Biomedical Engineering, Oregon Health and Science University, Portland, OR

Modern platforms such as Xenium and Visium HD measure the spatial coordinates and identities of millions of individual RNA molecules per tissue section, providing unprecedented resolution to study tumor heterogeneity and the spatial organization of cellular compartments. However, most current analyses rely on cell segmentation, which can be error-prone in densely packed or morphologically complex tumors. Here, we introduce a segmentation-free statistical framework for modeling RNA molecules in high-resolution spatial transcriptomics data using Log-Gaussian Cox Processes (LGCPs). Building on our recently developed efficient variational method for fitting LGCPs, we treat each RNA molecule as a point in continuous space and model gene-specific log-intensity surfaces with a latent Gaussian random field prior. This framework enables us to (i) infer smooth intensity fields for selected genes, (ii) estimate spatial cross-covariance between these fields as a direct measure of gene-gene co-localization, and (iii) perform direct association analyses quantifying how the local abundance of one gene varies as a function of genes or spatial features, all without requiring cell boundaries. These quantities define molecule-level association scores that capture local enrichment or exclusion of RNA species, facilitating the discovery of ligand-receptor hotspots, metabolic niches, and immune-tumor interaction zones at subcellular resolution. By aggregating molecule-level association patterns over marker gene sets, our approach further supports inference of cell type and subtype-level spatial organization and interactions. Simulation studies demonstrate that our segmentation-free LGCP approach accurately recovers underlying intensity surfaces and spatial associations with favorable runtimes. Overall, this work provides a scalable, model-based tool for leveraging the full richness of high-resolution spatial transcriptomics to map RNA molecule associations in cancer tissues without relying on cell segmentation.

: Network Biology and Precision Medicine
Poster Session

#6857 Sex differences in the gene regulatory mechanisms of lung aging and their implications in lung cancer risk.

Enakshi Saha

University of South Carolina, Columbia, SC

Lung cancer is the leading cause of cancer-related deaths worldwide. While disease risk increases with age in both sexes, there is significant difference in prevalence between males and females, even after adjusting for smoking history. We use novel computational models to infer individual-specific gene regulatory networks integrating transcriptomic and epigenomic data. These networks represent gene regulatory interactions between transcription factors, DNA methylation levels and target gene expression at individual-level resolution. We use sex-specific transcription factor motif and protein-protein interaction data as prior information in our network estimation to further highlight sex-specific regulatory interactions. Comparing gene regulatory networks from healthy normal lung tissue from the Genotype Tissue Expression Project across varying ages, we observe that genes involved in immune response , cell proliferation, and cancer-related pathways are differentially regulated with age in a sex-differential manner. Aging-related gene regulatory changes are influenced by estrogen receptor and androgen receptor transcription factors in females, with significant inflection points between ages 40 and 60. Examining individual-specific networks from lung adenocarcinoma samples from The Cancer Genome Atlas, we observe that aging-related gene regulatory changes converge with cancer-associated regulatory patterns. Critically, at any given age, regulatory patterns of immune and cell proliferation pathways in females without a history of smoking resemble disease-related patterns significantly more than their male counterparts. This finding highlights the role of aging-related gene regulatory changes in elevating cancer risk with age, and disproportionately so in females. Individuals with a history of smoking have regulatory signatures more akin to accelerated aging, resembling patterns observed in older never-smokers, and show greater similarity with disease states. These findings underscore age- and sex-specific mechanisms of lung cancer susceptibility, independent of smoking exposure, and highlight the need for tailored prevention strategies, informed by individual age and sex.

#6858 Single-cell elucidation of molecularly distinct states and therapeutic vulnerabilities in IDH-mutant glioma.

Luca Zanella[1], Patrick M. Kerwin[1], Mikko Turunen[1], Peter A. Sims[2], Peter D. Canoll[3], Andrea Califano[4]

[1]Department of Systems Biology, Columbia University Irving Medical Center, New York, NY, New York, NY,[2]Department of Systems Biology and Department of Biochemistry and Molecular Biophysics, Columbia University Irving Medical Center, New York, NY,[3]Department of Pathology and Cell Biology and Department of Neurological Surgery, Columbia University Irving Medical Center, New York, NY,[4]Dept. of Systems Biology and Dept. of Medicine and Dept. of Biomedical Informatics and Dept. of Biochemistry & Molecular Biophysics, and HICCC, Columbia University Irving Medical Center; Chan Zuckerberg Biohub, New York, NY

IDH-mutant gliomas, including oligodendrogliomas (IDH-O) and astrocytomas (IDH-A), are a molecularly defined class of fatal primary brain tumors characterized by mutations in the IDH1 and IDH2 genes. Despite advances in standard-of-care approaches, prognosis remains poor with median survival rates of 5-15 years. Substantial inter- and intra-tumor heterogeneity limits the efficacy of current monotherapies and necessitates *ad hoc* combination strategies targeting distinct tumor subpopulations. To comprehensively characterize the cellular landscape of IDH-mutant gliomas, we generated >250k high-quality single-nucleus transcriptomic profiles from 20 IDH-mutant glioma tumors (grade II and grade III; 10 IDH-O; 10 IDH-A) obtained from the Molecular Pathology Shared Resource (MPSR) Tumor Bank at Columbia University. Gene expression analysis revealed glioma cells, microglia, neurons and mature oligodendrocytes as the predominant cell types in both IDH-O and IDH-A, with a striking depletion of microglia in IDH-O. Network-based VIPER analysis of single-nucleus profiles identified Master Regulator (MR) proteins representing molecular dependencies of three previously described glioma states: astrocyte-like (AC), oligodendrocyte-like (OC) and neural-progenitor-like (NPC). Notably, the AC state was transcriptionally orthogonal to OC, whereas OC and NPC largely shared their regulatory architecture. To predict rational combination therapy candidates, we employed NYS CLIA-certified OncoTarget and OncoTreat algorithms. OncoTarget identifies small molecule inhibitors targeting individual state-specific MRs, while OncoTreat predicts candidate drugs by assessing their ability to invert the activity of glioma-specific MRs, leveraging large-scale drug perturbation assays generated by PLATE-seq. Specifically, we generated a library of genome-wide RNA-seq profiles from patient-matched *in vitro* models, one adherent cell line (SF10417) and one neurosphere (SUA03), 24 hours after treatment with 374 compounds from a library of FDA approved and investigational compounds. OncoTarget uncovered distinct pathway dependencies across glioma states, including STAT3/PI3K/AKT in AC cells, PDGFRA in OC, and RTK/EGFR/MET signaling in NPC cells. OncoTreat identified CNS-permeable agents predicted to invert glioma-specific MR programs. Future work will include validation of candidate compounds in patient-derived acute slice cultures to assess single-cell responses within an intact microenvironment. Complementary Xenium spatial profiling will map the microenvironmental context and cell-cell communication of molecularly distinct subpopulations, informing rational therapeutic strategies. Overall, our study establishes a generalizable framework for precision oncology in transcriptionally complex tumors and provides actionable targets for clinical translation.

#6859 Targeting master regulators to reprogram neutrophils and enhance PD-1 blockade efficacy in castration-resistant prostate cancer.

Melania Franchini[1], Florencia Picech[2], Cory Abate-Shen[3], Andrea Califano[4]

[1]Department of Systems Biology, Columbia University, New York, NY,[2]Department of Molecular Pharmacology and Therapeutics, Columbia University Irving Medical Center, New York, NY,[3]Department of Molecular Pharmacology and Therapeutics, Department of Urology, Columbia University Irving Medical Center, New York, NY,[4]Dept. of Systems Biology and Dept. of Medicine and Dept. of Biomedical Informatics and Dept. of Biochemistry & Molecular Biophysics, and HICCC, Columbia University Irving Medical Center; Chan Zuckerberg Biohub, New York, NY

Introduction: Neutrophil-mediated immunosuppression limits immunotherapy in Castration-Resistant Prostate Cancer (CRPC), but its mechanisms are unclear. This study aims to identify the drivers of this immunosuppression and evaluate whether targeting Master Regulator (MR) proteins can reprogram neutrophils, remodel the tumor microenvironment (TME), and enhance PD-1 blockade efficacy.
Methods: We used orthotopic CRPC models treated with MR inhibitors and anti-PD-1 therapy to assess neutrophil depletion and immune remodeling. Spatial profiling with the 5,000-plex Xenium panel along with cell types annotation via a curated scRNA-seq atlas, revealed a detailed map of tissue organization. Treatment effects on immune populations and spatial reorganization, particularly neutrophils, were quantified. VIPER-based analysis defined MR-driven neutrophil functional states, and spatial mapping was conducted using Xenium data. Finally, ligand-receptor interactions between neutrophils and tumor cells were explored through cell-cell communication network analysis.
Summary of unpublished data: We conducted a pilot Xenium study across four treatment arms (vehicle, Trametinib, anti-PD1, and combination) to assess MR inhibition's effect on immune responses through cell abundance and spatial reorganization. Anti-PD1 induced broad immune recruitment, especially neutrophils, while Trametinib had minimal effect. Combination therapy reduced neutrophil abundance below baseline, attenuating checkpoint blockade-induced neutrophil accumulation. NK/T cells, monocytes, and dendritic cells increased, while macrophages remained stable. Spatial analysis showed that anti-PD1 caused tumor cells to marginalize, while combination therapy partially restored integration. Neutrophils transitioned from marginalization to forming an immunological barrier around tumor cells, and NK/T cells interacted mainly with stromal/myeloid cells, indicating immune exclusion. Despite upregulating PD-L1 in all treatments, combination therapy induced PD-L1 expression without barrier formation, suggesting that spatial organization, not just ligand expression, drives neutrophil-mediated immune exclusion.
Conclusion: Treatments reshape tumor-immune architecture without disrupting tissue organization, relying on both immune cell abundance and their spatial distribution within the TME. Anti-PD1 induces broad immune infiltration, but neutrophils form a barrier limiting tumor penetration, which is relieved by the MR-inhibitor Trametinib. Neutrophils upregulate PD-L1 across all treatments, peaking after anti-PD1, while Trametinib and combination therapy drive PD-L1 expression without barrier formation.

#6860 Ensemble somatic variant calling and transcript reconstruction for high-fidelity neoantigen discovery in mRNA cancer vaccine design.

Po-Yuan Chen[1], Mi-Hua Tao[2], **Tai-Ming Ko**[3]

[1]Academia Sinica, Taipei, Taiwan,[2]Research Fellow, Academia Sinica, Taipei, Taiwan,[3]National Yang Ming Chiao Tung University, Hsinchu, Taiwan

Personalized neoantigen vaccines require accurate identification of tumor-specific epitopes with clinical-grade confidence. However, pipelines that rely on single-caller somatic variant detection and reference-based transcript reconstruction often inflate false-positive neoantigens and mishandle complex mutations such as frameshifts and stop-codon disruptions, limiting the fidelity of candidates for mRNA cancer vaccines. We developed a GPU-accelerated workflow integrating whole-exome sequencing (WES) and RNA-seq, implemented on NVIDIA Parabricks to achieve more than a tenfold reduction in preprocessing time compared with conventional CPU-based pipelines. Somatic variants are identified using an ensemble consensus (≥2 of DeepSomatic, Strelka2 and VarScan), reducing inter-caller discordance while preserving biologically plausible events; germline variants are called with GATK HaplotypeCaller. To support neoepitope generation, we implemented a transcript reconstruction module that integrates all germline and somatic variants into patient-specific, strand-aware open reading frames, applies context-dependent peptide trimming (for example, ±20 amino acids for SNVs and dynamic windows for indels), and validates candidate coding changes against sequencing evidence, resolving multi-isoform usage and early terminations. Benchmarked on clinical solid tumor samples, the ensemble strategy improved reproducibility across technical replicates and showed high concordance with orthogonal variant validation. The reconstruction module robustly recovered mutant transcripts in diverse genomic contexts and enabled precise neoepitope extraction and HLA-binding prediction. Integrated with HLA genotyping and MHC binding models, this reproducible pipeline mitigates upstream sources of epitope inflation and provides a scalable bioinformatics framework for high-fidelity neoantigen discovery in personalized mRNA cancer vaccine design.

#6861 NeonDisco: A Nextflow orchestration framework for in silico discovery and prioritization of recurrent neoantigen candidates.

Mohd Suffian Azizan, Min Hui Tan, Jia Wern Pan, Sok Ching Cheong

Cancer Research Malaysia, Subang Jaya, Malaysia

Neoantigen-based cancer immunotherapy necessitates discovery of tumor-specific antigens that elicit clinically observable response in patients. Advances in bioinformatics have allowed in silico predictions of neoantigens, yet cancer vaccine development have been limited by low discovery rate of immunogenic neoantigens. This is primarily due to the restricted search space from which neoantigens are predicted, namely single-nucleotide variations (SNVs) or insertion-deletion mutations (indels), the prevalence of which also varies across different cancer types. Therefore, expanding the neoantigen landscape beyond SNVs/indels is imperative, both to improve novel neoantigen detection and to make universal, off-the-shelf cancer vaccine development possible. We have implemented NeonDisco, a multimodal bioinformatics pipeline in Nextflow to facilitate discovery of recurrent, immunogenic neoantigens from RNA-seq data. The pipeline incorporates state-of-the-art bioinformatics tools, with a focus on modularity to enable predictions from expanded neoantigen sources. We have prototyped a gene fusion neoantigen discovery module in NeonDisco and analyzed RNA-seq libraries of 990 patient samples from the Malaysian breast cancer cohort, MyBrCa. We identified 96 recurrent fusion breakpoints found across 208 unique samples out of 886 fusion-positive samples, translating to a cohort coverage of 23%. Neopeptide prediction part of the pipeline identified 2,827 unique neoepitope sequences predicted to have IC50 <500 nM to 5% top common MHC-I alleles in the MyBrCa cohort. Future works would focus on extending the discovery modules into alternative-splicing-derived and RNA-editing-derived neoantigen search space, as well as validating gene fusion prediction shortlist in vitro. NeonDisco attempts to consolidate innovative neoantigen discovery algorithms into one streamlined, automated pipeline, and this effort constitute our first step in an optimized strategy to develop off-the-shelf cancer vaccines.

#6862 A scalable workflow for *in silico* TMA construction and groupwise comparison of spatial transcriptomic data for analyzing tumor microenvironment.

Dongjoo Lee, Sungwoo Bae, Yeonjae Jung, Kwon Joong Na, Hongyoon Choi

Portrai, Inc., Seoul, Korea, Republic of

Background:
Spatial transcriptomics provides high-resolution characterization of the tumor microenvironment (TME), offering insights into cellular architecture, spatial interactions, and molecular heterogeneity. However, integrating data across multiple tissue sections or multiple samples from tissue microarrays (TMAs) remains a substantial challenge, particularly for bioinformatics workflows requiring scalability and flexible cohort design. The difficulty is amplified in high-density platforms such as Visium HD, where datasets contain large numbers of cells and preserving spatial relationships during multi-slide integration is critical. Consequently, there is a growing need for a scalable computational framework that enables efficient in silico TMA construction and supports groupwise comparisons for robust TME analysis.
Methods:
We developed a flexible and modular computational workflow enabling in silico TMA construction and groupwise comparison of gastric cancer Visium HD data. From a total of 48 samples (2 mm core), yielding over 3.1 million 8-μm bins of spatially resolved expression data, was used for the integration and scalable group-wise comparison. Selected cores from different slides were digitally reassembled into new TMA-like layouts with automatically re-registered H&E images reflecting updated spatial coordinates. For batch correction and large-scale integration, the workflow employs stratified subsampling and the scArches model, allowing efficient harmonization of datasets containing millions of spatial bins. Interactive visualization modules support region-level comparison and cross-core analysis of cellular composition.
Results:
Preliminary groupwise analyses of the reconstructed TMA revealed reproducible spatial patterns across tumor regions. Areas with dense stromal activation exhibited enrichment of fibroblast and endothelial-related signatures, whereas immune hotspots showed localized $CD8^+$ T-cell and macrophage co-accumulation near the tumor invasive front. Gene expression-based metabolic pathway analysis revealed subtle gradients (glycolytic vs oxidative) between core groups with distinct histopathologic features. The entire integration pipeline processed 3.1 million spatial bins in under 2hours on a single NVIDIA A6000 GPU(48GB VRAM), demonstrating the framework's potential to detect spatially resolved tumor-stroma interactions and immune heterogeneity at scale.
Conclusions:
This workflow provides a scalable approach for constructing virtual TMAs and comparing spatial transcriptomic data. By integrating >3 million Visium HD bins from gastric cancer slides, it enables systematic TME profiling and identification of spatially resolved biomarkers relevant to tumor progression and therapeutic response.

#6863 Integrating computational and experimental approaches to optimize RNA fusion identification in BRCA associated breast cancer.

Janvi Sandhu[1], Anjana Bhardwaj[1], Chathurani Ranathunge[2], Dilshan C. Adhikari[2], Shiyanth Thevasagayampillai[2], Jamal Hill[3], Abhijit Mazumdar[3], Preethi H. Gunaratne[2], Isabelle Bedrosian[1]

[1]Department of Breast Surgical Oncology, UT MD Anderson Cancer Center, Houston, TX,[2]Department of Biology and Biochemistry, University of Houston, Houston, TX,[3]Department of Clinical Cancer Prevention, UT MD Anderson Cancer Center, Houston, TX

Background: Germline testing has improved detection of high-risk breast cancer patients but risk reduction in germline BRCA carriers is limited to surgical intervention with no chemoprevention options. RNA fusions, somatic events from chimeric transcripts, generate neoantigens that can serve as targets for preventative vaccines but its presence in BRCA associated breast cancer is unknown. While these fusions can be predicted from RNA sequencing by tools like *Arriba*, the prediction pipelines need in-vitro validation to optimize target identification. We hypothesize RNA fusions can be identified *in silico* in BRCA associated cancers and validated at high frequency.

Methodology: For identification of fusions in BRCA tumors, public repertoire of RNA sequencing of 34 BRCA associated breast cancers was utilized. Mammary tissue from 21 cancer free subjects were used as controls. For validation of in silico predictions, RNA sequencing was performed on mammary tissues or tumors from 7 normal-like BRCA $c^{o/co}$ Cre $^{+\backslash+}$ p53 $^{+\backslash+}$ controls and 23 BRCA $c^{o/co}$ Cre $^{+\backslash+}$ p53 $^{+\backslash-}$ mice. RNA fusions in both human and mouse samples were detected using Arriba pipeline, followed by post-Arriba filters excluding fusions in normal controls, intra-genic, non-coding RNA and fusion without coding or splice-site breakpoints. Mouse fusion candidates were validated using PCR and Sanger Sequencing.

Results: In human BRCA tumors 338 fusions were detected by *Arriba*; with post- *Arriba* filters, 33 noncanonical, 251 noncoding genes & 3 fusions in CDS/CDS splice sites were removed with 51 patients specific fusions remaining. Fusions were detected in 50% of patient tumors. In 23 BRCA mouse samples, *Arriba* initially detected 352 fusions ; 157 noncanonical, 107 noncoding genes and 22 fusions present in normal control samples were excluded, yielding 69 fusions. Five recurrent mouse fusions- *Thoc1-Usp14* (2 breakpoints), *Tmcc-Raf1*, *Usp14-Thoc1*, *Krt5a-Krt6* (5 breakpoints), *Runx2-Tmem191c* with read counts of 4-21, 31-49, 2-4, 1-3 and 1 respectively were selected for validation. Four of these (except *Runx2-Tmem191c)* were validated by PCR followed by Sanger sequencing. In *Krt5a-Krt6a* fusions, three of five fusion junctions with >1 read count were confirmed. Notably, *Usp14-Thoc1* showed fusions in 8 more samples, suggesting isoforms in common gene partners missed due to low sequencing depth. Overall validation rate of integrated *Arriba*-post *Arriba* pipeline was 80% reaching 100% with >1 supporting reads.

Conclusion: RNA Fusions were successfully detected in both human and mouse samples using *Arriba*. Computational predictions using *Arriba* plus stringent post-filtering, reliably predicts RNA fusions when supported by >1 read count underscoring the importance of integrating computational prediction with *in vitro* validation to accurately characterize fusion landscapes in BRCA-associated breast cancer models.

#6865 A knowledge graph screen of innovative versus incremental lung cancer trials for need-aligned designs.

Mahitha Simhambhatla[1], Maya Ylagan[1], Praneeth Sajja[1], Daruka Mahadevan[2], Erik S. Ferlanti[1], James Carson[1], Boone Goodgame[3], Ehsan Irajizad[4], Samir M. Hanash[4], Jeanne Kowalski[1]

[1]The University of Texas at Austin, Austin, TX,[2]UT Health Science Center at San Antonio, San Antonio, TX,[3]The university of Texas at Austin, Austin, TX,[4]UT MD Anderson Cancer Center, Houston, TX

Background. ClinicalTrials.gov lists >500,000 studies, raising the question of how often “new” trials are truly novel versus incremental design variants. Lung cancer remains a leading cause of cancer-related death worldwide, underscoring the need for innovative over incremental trials. Prior work has used clinical trial knowledge graphs (KGs) to support design recommendations. Here, we apply a small cell lung cancer (SCLC) patient-anchored KG to classify lung cancer targeted therapy trials as “novel additions” versus “aggregate similarity” and to identify gaps where new, need-aligned trial designs are warranted.
Methods. We curated 286 adult lung cancer targeted therapy trials from ClinicalTrials.gov that were retrieved as matches to a SCLC case. We built a trial-to-trial KG by linking each trial to key entities (e.g., tumor type, genomic alterations, targets/pathways, drug classes) and learned graph-based embeddings to obtain trial-level representations. Cosine similarity was used to quantify trial similarity between embeddings; community detection was used to define trial clusters. Clusters with ≥5 trials and median within-cluster similarity ≥0.80 were labeled “aggregate similar.” A novelty score (1 – maximum similarity to any other trial) and betweenness centrality were combined to label “novel additions”. A predefined set of SCLC molecular report-matched trials was cross-referenced to characterize their distribution across identified clusters.
Results. Altogether, we defined 4 trial clusters (median size 67), three of which met our criteria for aggregate similarity, comprising 74% (n=212) of large community trials of highly similar designs. Across all 286 trials, median pairwise (0.74) and nearest-neighbor similarity (0.98) were consistent with dense replication of existing biomarker- and line-of-therapy-defined templates. Only 38 trials (13%) were classified as novel additions based on combined novelty (median=0.070) and betweenness centrality (median 0.004) thresholds, and showed significantly ($p < 0.01$) higher median scores in both as compared to non-novel trials. Novel additions were enriched in a single aggregate similarity cluster (24/74 trials) that contained most case molecular report-matched trials (65/68). The remaining trial clusters had 1-10% novel additions, indicating that case-level matching occurs within dense targeted therapy communities, whereas a KG analysis can surface structurally distinctive, novel addition trials.
Conclusions. KG analysis of lung cancer trials provides a principled way to operationalize “novel addition” versus “aggregate similarity” at the portfolio level. This patient-anchored framework can support sponsors, investigators, and regulators in prioritizing innovative trials, reducing redundancy in an already crowded lung cancer trial landscape, and ultimately aligning trial development with unmet patient needs.

#6866 Mapping cancer-relevant genetic interactions with functional module prediction and in4mer enCas12a platform.

Chenchu Lin[1], Veronica Gheorghe[1], Juihsuan Rosalind Chou[1], Sabriyeh Alibai[1], Subin Kim[1], Nazanin Esmaeili Anvar[1], Yixin Xu[1], Xingdi Ma[1], Lori L. Wilson[1], Russell Moser[2], Junjie Chen[1], Christopher J. Kemp[2], Scott Kopetz[1], Glen Traver Hart[1]

[1]UT MD Anderson Cancer Center, Houston, TX,[2]Fred Hutchinson Cancer Center, Seattle, WA

Genetic interaction (GI), particularly synthetic lethality, is essential to functional genomics and cancer therapy. In yeast, systematic GI mapping has produced a near-complete network covering ~90% of genes, establishing core principles of GI network architecture and defining major functional modules. However, translating this success to human cells has been far more challenging due to the larger genome, greater complexity, and extensive cellular heterogeneity. Even the million-scale CRISPR Cas9 combinatorial screens sample only ~0.1% of the possible search space, highlighting the need for predictive models and more efficient multiplex perturbation technologies. To address this challenge, we leveraged insights from the yeast GI network to prioritize human gene modules predicted to be enriched for genetic interactions. Through this strategy, we identified five densely gene modules, including receptor tyrosine kinase (RTK) signaling and the DNA damage response (DDR) pathway, providing a tractable search space for systematic GI mapping. Using our optimized CRISPR enCas12a-based in4mer platform, which enables compact, high-fidelity multiplex perturbations, we performed all-by-all GI screens within these modules. With a single 88k construct library, we performed all pairwise combinations of 206 RTK genes, 167 DDR genes, and 4,435 curated paralog pairs, along with positive and negative controls, across 12 cancer cell lines. Consistently, paralogs remained the dominant source of strong genetic interactions across screens, while integrated multi-line analysis revealed weaker but consistent synthetic lethal and suppressor interactions. Notably, we identified a dense GI network within the ER-localized protein glycosylation pathway and validated key interactions in 3D organoid and patient-derived xenograft, demonstrating that 2D GI screens are robust predictors of GI dependencies in more physiologically relevant systems. In conclusion, combining functional-module prioritization with enCas12a multiplex screening provides an efficient strategy for uncovering meaningful subsets of the human GI landscape and supports discovery of therapeutically relevant vulnerabilities at scale.

#6867 Uncovering the systems-level mutational landscape of intrinsically disordered regions in cancer.

Kivilcim Ozturk[1], Hannah K. Carter[2]

[1]UC San Diego School of Medicine, La Jolla, CA,[2]UC San Diego, La Jolla, CA

Biological functions and cellular behaviors arise from interactions among proteins and other molecules within cells, and cancers often act to perturb these interactions, resulting in disease phenotypes. Many proteins contain intrinsically disordered regions (IDR) that perform biological functions without relying on a single well-defined conformation. While IDRs of several cancer drivers have emerged as central mediators of oncogenic signaling and post-translational modifications, their role in protein-protein interactions (PPI) is less clear. Here, we set out to characterize the mutational landscape of IDRs in how they contribute to perturbation of underlying protein interaction networks in cancer. A comprehensive analysis of our structurally resolved PPI network showed that IDRs mediating protein interactions are significantly targeted by cancer missense mutations. Furthermore, proteins containing IDRs are more centrally located in the PPI network, especially cancer drivers, where disordered drivers are significantly more central than ordered ones, suggesting that the inherent conformational heterogeneity of IDRs might enable them to interact with a wider range of molecular partners, allowing them to easily propagate signals through the cell and the mutations targeting them to generate a larger impact on cellular activity and phenotypes. Overall, our work demonstrates the importance of uncovering the systems-level mutational landscape of IDRs to identify mechanisms driving cancer development and progression, enabling more effective selection and development of cancer therapeutics.

#6868 Understanding molecular mechanisms of prostate cancer via transcriptome-wide causal gene regulatory networks.

Min Zhang, Zhongli Jiang, Xiaolin Zi, Danni Liu, Yan Li, Dabao Zhang

UC Irvine, Irvine, CA

Background: Prostate cancer remains the most common malignancy among men and a leading cause of cancer-related death worldwide, with an estimated 313,780 new cases expected in 2025. Despite recent advances in screening and treatment, the molecular mechanisms driving prostate cancer are not fully understood. The growing availability of multi-omics data from the same patients provides an unprecedented opportunity to reveal disease pathways and identify novel therapeutic targets. However, integrating these large-scale, multi-modal, and heterogeneous omics profiles poses substantial statistical and computational challenges.

Methods: Transcriptomic and genomic data were obtained from prostate tumor samples in GEO (GSE70768). After pre-processing and quality control, the dataset included 17,426 genes and 272,564 single nucleotide polymorphisms (SNPs) from 90 patients. We applied SIGNET to identify instrumental variables (IVs), yielding 7,806 gene-IV pairs for 3,309 genes. Using these IVs, we then applied SIGNET to conduct causal inference and construct transcriptome-wide gene regulatory networks for prostate cancer based on the integrated genomic and transcriptomic data, supported by 100 bootstrap datasets.

Results: We identified 1,840 gene regulations that were repeatedly recovered in ≥80% of the bootstrap datasets, of which 369 appeared in ≥95% of the constructions. Within these robust subnetworks, we detected hub genes including DDX51, PNPT1, FARSLB, and IFI6. Using data from the Cancer Genome Atlas (TCGA) project, we validated that IFI6 is highly correlated with its predicted targets (correlation coefficient 0.52 ~ 0.90, $p < 0.01$). IFI6 is a negative regulator of innate immunity and has been reported to be overexpressed in multiple cancers, with emerging evidence supporting its role in tumorigenesis and drug resistance. Our findings nominate IFI6 as a candidate regulator in prostate cancer, warranting further functional studies to define its role in tumor proliferation, metastasis, therapy responses, and the immune tumor microenvironment. Finally, Ingenuity Pathway Analysis (IPA) of top subnetworks with high bootstrap frequency highlighted several significant pathways, including primary immunodeficiency signaling and communication between innate and adaptive immune cells.

Conclusion: Using multi-omics data from prostate cancer tissues coupled with transcriptome-wide causal inference, our data-driven detection of regulator-target pairs provides new insights into the molecular mechanisms of prostate cancer and may ultimately facilitate the development of personalized treatment strategies.

#6869 Multi-omic profiling identified three molecular clusters in urothelial carcinoma: A path towards clinical precision.

Nils Cornelis Hendricus van Creij[1], Piotr Tymoszuk[2], Florian Handle[3], Andreas Seeber[4], Teresa Sellemond[1], Agnieszka Martowicz[4], Eva Comperat[5], Hamed Wafa[1], Steffen Ormanns[6], Michael Gunther[6], Walther Parson[7], Maxim Noeparast[8], Frederic Romain Santer[9], Jose Daniel Subiela[10], Petros Grivas[11], Roger Li[12], Zoran Culig[1], Renate Pichler[13]

[1]Experimental Urology, Medical University of Innsbruck, Innsbruck, Austria,[2]Data Analytics As a Service Tirol, Worgl, Austria,[3]XPseq Analytics GmbH, Innsbruck, Austria,[4]Internal Medicine V (Hematology and Oncology), Medical University of Innsbruck, Innsbruck, Austria,[5]Pathology, Medical University of Vienna, Vienna, Austria,[6]General Pathology, Medical University of Innsbruck, Innsbruck, Austria,[7]Legal Medicine, Medical University of Innsbruck, Innsbruck, Austria,[8]Translational Oncology, II. Med Clinics Hematology and Oncology, University of Augsburg, Augsburg, Germany,[9]Gynecology and Obstetrics, Medical University of Innsbruck, Innsbruck, Austria,[10]Urology, Instituto Ramon y Cajal de Investigacion Sanitaria, Hospital Universitario Ramon y Cajal, Madrid, Spain,[11]Fred Hutchinson Cancer Center, University of Washington, Seattle, WA,[12]GU Oncology, Moffitt Cancer Center, Tampa, FL,[13]Urology, Medical University of Innsbruck, Innsbruck, Austria

Introduction: Urothelial carcinoma (UC) is a molecularly heterogeneous disease, and transcriptome-based classification systems have given important insights into its biology. The current consensus classifications for UC represent a major step toward biological stratification; however, its prognostic and predictive relevance remains uncertain, limiting use in clinical guidelines. Furthermore, most molecular schemes have been developed either for non-muscle invasive (NMIBC) or muscle-invasive disease (MIBC), relying only on bulk transcriptomic data. This fragmentation hinders comparability across studies and integration with proteomic or single-cell datasets. A simplified molecular framework is therefore needed to capture UC heterogeneity more comprehensively and to support personalized therapeutic approaches.

Materials & Methods: Using the TCGA bulk bladder cancer transcriptome dataset, we developed three distinct molecular UC clusters, which were validated using 18 transcriptome, 3 proteome and 33 UC cell line datasets. Making use of *in silico* predictions, we selected promising treatment strategies, which were further screened *in vitro* using the IncucyteS3 live-cell imaging system and RNA-sequencing on representative cell lines.

Results: Our transcriptomic and proteomic analyses revealed three UC clusters with distinct molecular, biological and clinical features. Each cluster showed specific mRNA and protein expression patterns, metabolic profiles, and driver gene alterations, translating into divergent prognoses and predicted therapeutic sensitivities. Novel approaches, like liquid biopsy-based stratification using ECM-derived urinary peptides or IHC-based profiling of the proposed distinct markers, are currently being investigated. The stroma-rich, high-risk cluster #1 was associated with responsiveness to ferroptosis inducers and PARP inhibition. Cluster #2, which is highly proliferative and immune-infiltrated with basal/squamous traits, showed predicted benefit from cytotoxic agents and inhibition of EGFR or MEK signaling pathways. Cluster #3, dominated by luminal papillary, low-risk tumors with minimal stromal and immune components, appeared susceptible to epigenetic therapies and EGFR/FGFR inhibition.

Conclusion: Our new integrative molecular classification scheme provides a practical framework for patient stratification, personalized transcriptome- and proteome-based risk assessment, preclinical research and clinical trial design, including both NMIBC and MIBC.

#6870 Quartet: A database of robust somatic mutations in tumor cell lines.

Daniel Halmos[1], Trey Ideker[2]

[1]UCSD Medical Ctr., San Diego, CA,[2]UC San Diego, La Jolla, CA

Introduction: Current collections of tumor cell lines, and their genomic, proteomic, and phenotypic reference data, have been vastly important to cancer research. Given the centrality of these datasets, it is paramount that they be of the highest quality. Here we show that up to 20% of mutations identified within these collections are erroneous, owing to sequencing artifacts, misaligned reads, in addition to other sources of error. To achieve a high-quality set of mutation profiles for all 329 tumor cell lines sequenced by the Cancer Cell Line Encyclopedia (CCLE), we processed all genomes using the consensus of four complementary mutation identification tools, yielding an online resource we call Quartet. We demonstrate considerable benefit from its use compared to currently used mutation profiles across a variety of tasks.
Methods: We retrieved raw sequence data previously generated by the Cancer Cell Line Encyclopedia. We filter for short sequences that disproportionately contribute to noise in mutation profiles, identify candidate mutations using 4 mutation identification tools, and then filter those candidate mutations to the subset with agreement from at least 3 tools. Using a HCC1395 cancer cell-line sequenced at ultra-high depths as a positive control, we attribute roughly 1/5 of mutations originally generated by CCLE to technical artifacts and demonstrate enrichment of True-Positive mutations from Quartet. These artifactual mutations persist at the gene-level, where we observe divergence between predicted variant effects from our ground truth and those expressed in CCLE, a divergence which is significantly recovered through Quartet. When aggregated across all cell lines and viewed with respect to Variant Allele Fraction (VAF) in original CCLE mutations, we observe a bimodal distribution of variants whose lesser mode is enriched for technical artifacts which Quartet effectively filters. We demonstrate these artifactual mutations cannot be removed post-hoc through either VAF thresholds or Variant Effect Prediction, nor through use of alternate databases such as DepMap. We then leverage this recalled CCLE dataset to train pharmacogenomics models and show significant improvement to predictive performance across 10 anti-cancer drugs.
Conclusion: Quartet presents a public resource of cancer cell lines which use consensus support of mutation callers. Quartet demonstrates depletion of artifactual mutations and their deleterious effects in a variety of downstream tasks. These results highlight the potential to enhance cancer biological discovery through Quartet, and we expect these benefits to compound as additional cell lines are incorporated. Quartet data are made publicly available through zenodo and source code is made available at https://github.com/digitaltumors/quartet.

#6871 Real-world analytical concordance of four next-generation sequencing assays: Impact of assay methodology and bioinformatics on clinical decision-making.

Liudmila Zhukova, **Sergei Smolin**, Svetlana Smolina, Nikolai Karnaukhov

Moscow Clinical Scientific Center, Moscow, Russian Federation

Background: Broad tumor genomic profiling is increasingly required for selecting targeted therapies, yet analytical concordance across next-generation sequencing (NGS) assays used in routine practice remains uncertain. We conducted a real-world comparison of four NGS platforms to evaluate variability in key clinically relevant metrics, including tumor mutational burden (TMB), driver SNVs, and driver CNVs.
Methods: Ten patients provided four matched FFPE eppendorfs each. Each aliquot contained at least 10 FFPE sections of 5-7 µm thickness, and all blocks met a ≥20% tumor cell requirement, ensuring uniform pre-analytic quality across all submitted material. All aliquots were analyzed in parallel across four laboratories: FMI (reference CGP), Private Lab 1, Private Lab 2, and Private Lab 3. For the primary comparison, assays were evaluated for patient-level reporting success (≥1 analyzable aliquot per patient), tumor mutational burden (TMB), driver SNVs, and driver CNVs.
Results: FMI and Private Lab 1 successfully generated complete reports for 10/10 patients, Private Lab 3 reported 9/10. Private Lab 2 produced reports for 2/10 patients, an analyzability rate insufficient for inclusion in comparative metrics. TMB was reported for 10/10 patients by FMI and Private Lab 1 and 9/9 evaluable patients by Private Lab 3. For clinically actionable SNVs, FMI identified 6 variants; concordance was Private Lab 3 100% (6/6) and Private Lab 1 67% (4/6). For driver SNVs, FMI detected 31 variants; Private Lab 3 showed strong concordance across analyzable patients (83-100%), whereas Private Lab 1 showed markedly lower concordance (0-33%). For driver CNVs, FMI detected 14 alterations; Private Lab 3 identified 6/14, while Private Lab 1 detected none. Even within the two patients analyzed by Private Lab 2, concordance with FMI was inconsistent. Driver SNVs showed partial overlap, and several FMI-confirmed alterations were not detected. Driver CNVs were not identified in either patient, despite their presence in the reference assay.
Conclusions: Concordance across NGS assays was suboptimal even among aliquots that were successfully processed, indicating substantial assay-to-assay variability. The markedly limited analyzability of the fourth platform further demonstrates that test performance in real-world settings is driven not only by the biological material but also by pre-analytic workflow, laboratory methodology, and the robustness of bioinformatic pipelines. Our findings show that results from different assays can diverge significantly, which may directly affect therapeutic decisions for patients. These observations underscore the need for independent analytical validation of every NGS assay before its results are used to guide clinical management.

#6872 Assessing the Impact of Variant Calling Pipelines on *De Novo* SBS Mutational Signature Extraction.

Zichen Jiang[1], Jessica Nghi Au[1], Mariya Kazachkova[2], Marcos Diaz-Gay[3], Raviteja Vangara[1], Ludmil B. Alexandrov[1]

[1]Department of Cellular and Molecular Medicine, Department of Bioengineering, Moores Cancer Center, University of California San Diego, La Jolla, CA,[2]Department of Cellular and Molecular Medicine, Moores Cancer Center, Biomedical Sciences Graduate Pr, University of California San Diego, La Jolla, CA,[3]Digital Genomics Group, Cancer Genomics Program, Spanish National Cancer Research Center, Madrid, Spain

Deconstructing the mutational processes in a tumor's genome, known as mutational signatures, provides critical insights into cancer etiology and evolution. However, how the upstream variant-calling strategies propagate to affect the accuracy of *de novo* signature extraction remains underexplored. Here, we systematically evaluate how mutation-calling algorithms influence single-base substitution (SBS) signature analysis using over 8,900 whole-exome sequences from The Cancer Genome Atlas and 1,800 whole genomes from the Pan-Cancer Analysis of Whole Genomes study. We demonstrate that consensus variant-calling strategies produce remarkably stable mutational signatures across different reference genomes and pipeline versions. In contrast, individual variant callers introduce systematic false-positive mutations that manifest as stable, artifactual signatures, detectable by three signature extraction tools. A minimal consensus approach, requiring agreement between just two variant callers, successfully eliminates technical signatures while preserving genuine biological signals and is especially important for high SBS mutational context analysis. Our findings establish consensus variant calling as essential for robust mutational signature analysis and provide a clear framework for distinguishing biological processes from technical artifacts.

#6873 Knowledge graph driven insights and drug repurposing opportunities for neuroendocrine prostate cancer.

Pawan Verma, Prasanna Kumar Sekar Sekar, Dharani Dadi, Manimala Sen, Nobal Dhruw, Abhishek Jha

Elucidata Corporation, San Francisco, CA

Biomedical Knowledge Graphs (BKGs) have emerged as powerful tools for integrating, managing, and exploring this complex information landscape. Elucidata has built a knowledge graph that integrates 20+ high-quality, well-curated knowledge sources. Additionally, we have developed a GUI-based application that enables users to derive insights in a no-code manner. This facilitates the discovery of drugs that modulate a target's activity through upstream or downstream network effects.Neuroendocrine prostate cancer (NEPC) represents a highly aggressive histologic subtype of prostate cancer. Literature review shows that the “true biological problem” for drug repurposing in NEPC is not the disease state itself, but the underlying causal process of treatment-induced lineage plasticity. This transition is initiated by RB1 and TP53 loss and sustained by a mutually reinforcing MYCN-AURKA-EZH2 regulatory axis. The outcome of this shift is the loss of conventional therapeutic targets (such as AR and PSMA) and the emergence of new, actionable vulnerabilities—including AURKA, EZH2, BCL2, and DLL3.Its poor clinical outcomes stem from a combination of delayed detection, rapid disease progression, and the absence of effective therapeutic options. Additionally, the number of publicly available NEPC datasets is very low, hampering early-stage R&D. We demonstrate how knowledge graphs can be queried to identify genes with dependency profiles similar to MYCN’s essentiality. Genes with similar essentiality profiles are almost always functionally related (e.g., belonging to the same complex or pathway). We further provide evidence for drugs approved for other diseases that share molecular underpinnings with NEPC and may be advanced into clinical trials to treat NEPC.

#6874 A transcriptome-based AI meta-model for immunotherapy response classification in hepatocellular carcinoma.

Jimin Seo[1], Na Young Kwon[2], Ki Wook Lee[1], Han-En Lo[1], Young-Jun Jeon[1]

[1]Department of Integrative Biotechnology, Sungkyunkwan University, Suwon, Korea, Republic of,[2]Department of MetaBioHealth, Sungkyunkwan University, Suwon, Korea, Republic of

Immune checkpoint inhibitor (ICI) is frequently selected as first-line therapy in advanced hepatocellular carcinoma (HCC), yet current biomarkers that predict therapeutic response show limited accuracy. Robust and clinically applicable predictors of ICI response in HCC need to be established. We performed tissue RNA-seq on ICI-treated HCC patients (Atezolizumab plus Bevacizumab, Nivolumab, or Ipilimumab plus Nivolumab) and developed an AI stacking-based meta-model to classify responders (R, n=32) and non-responders (NR, n=57). To address class imbalance, 80% of samples were distributed into three balanced training sets, and the remaining 20% were used as an internal test set. Gene-feature selection performed with six tree-based algorithms (AB, ERT, GB, LGB, RF, and XGB) improved mean AUC from 0.58 to 0.73 and mean MCC from 0.25 to 0.43. The stacking meta-model, incorporating 14 algorithms (AB, CB, ERT, GB, LGB, RF, XGB, four SVM kernels, LR, NB, and MLP), further increased mean AUC to 0.95 and MCC to 0.79. The meta-model achieved an AUC of 0.92 and MCC of 0.62 in the internal test set, and an AUC of 0.84 and MCC of 0.82 in an external ICI-treated HCC cohort (Table 1). Meta-scores derived from the model clearly stratified clinical outcomes. Patients with high scores showed improved PFS (HR 0.27, 95% CI 0.17-0.45; p<0.0001) and OS (HR 0.37, 95% CI 0.22-0.62; p<0.0001). Feature selection identified 11 AI-important gene (AIG) sets (10-173 genes each), and each set overlapped with at least two others through shared AIGs, reflecting convergent biological signals. Analysis of AIG sets in immune-cell populations from an external single-cell RNA-seq cohort revealed enrichment patterns consistent with known mechanisms of immune activation and resistance. These findings demonstrate that the AI meta-model can help to classify immunotherapy response in HCC and stratify survival outcomes, while revealing biologically relevant AIG signatures.

Table 1. Performance of the final AI meta-model for immunotherapy response classification in HCC

	MCC	**ACC**	**AUC**	**Sensitivity**	**Specificity**
Training	0.88	0.94	0.96	0.96	0.93
Internal Test	0.62	0.76	0.92	1.00	0.64
External Validation	0.82	0.90	0.84	1.00	0.80

#6875 Mapping convergent neurodegenerative and oncogenic pathways in ALS using a multi-scale knowledge-graph framework.

Vasileios Alevizos[1], Sabrina Edralin[2], Clark Xu[3], George A. Papakostas[4], **Zongliang Yue**[5]

[1]Department of Learning, Informatics, Management and Ethics, Karolinska Institutet, Solna, Sweden,[2]Department of Crop Sciences, University of Illinois Urbana-Champaign, Urbana, IL,[3]Mayo Clinic Artificial Intelligence & Discovery, Rochester, MN,[4]Department of Informatics, Democritus University of Thrace, Kavala, Greece,[5]Health Outcomes Research and Policy, Auburn University, Auburn, AL

Amyotrophic lateral sclerosis (ALS) affects approximately 1.5 per 100,000 person-years in the United States, with a point prevalence of 3.8-5.6 per 100,000. ALS arises from the intersection of diverse pathogenic mechanisms spanning genetic mutations (C9orf72, SOD1, FUS, TARDBP), protein misfolding, RNA-metabolism defects, nucleocytoplasmic transport failure, prion-like propagation, mitochondrial dysfunction, and neuroinflammation. Increasing evidence from plasma proteomics and machine-learning studies indicates that these perturbations emerge years prior to clinical onset, highlighting an urgent need for mechanistically grounded patient stratification. At the same time, epidemiologic and molecular studies suggest unexpected parallels between ALS and cancer—including dysregulated DNA-damage responses, cell-cycle control, metabolic rewiring, and aberrant immune signaling—yet these cross-disease links remain fragmented and poorly mapped. We developed a multi-scale ALS-cancer knowledge graph integrating genetic, transcriptomic, proteomic, neuropathological, and longitudinal clinical datasets. Knowledge-graph completion approaches, including link prediction, graph embeddings, and embedding-based reasoning, were applied to infer missing edges and reveal latent modules connecting ALS-associated genetic lesions to oncogenic pathways implicated in genome instability, altered proliferation, metabolic remodeling, and immune dysregulation. This approach enables systematic interrogation of shared molecular programs across ALS and cancer, exposing under-characterized immune, metabolic, and axonal-transport circuits whose dual roles have been suggested but never comprehensively mapped. Predicted associations were evaluated using enrichment for established ALS genes, overlap with curated oncogenic and neurodegenerative pathways, and their ability to stratify patients by site of onset, progression rate, and biomarker signatures. These analyses generated patient-specific pathway fingerprints that (i) resolve dominant biological mechanisms across clinical subgroups, (ii) illuminate mechanistic intersections between neurodegeneration and malignancy, and (iii) prioritize repurposed oncology targets with potential relevance to ALS. This knowledge-graph framework provides a scalable and mechanistically informed strategy for classifying ALS patients, uncovering ALS-cancer pathway convergence, and supporting targeted therapeutic discovery across traditionally siloed disease domains.

#6877 Chromatin networks inform the development of prognostic gene expression signatures in human cancers.

Lucio R. Queiroz[1], Shreyas Rajaram[1], Karnika Singh[1], Angelo Corso Faini[1], Erika Minonne[1], Nicola Barbaro[2], Scarfo Federico[3], Pushpita Roy[1], Wikum Dinalankara[1], **Luigi Marchionni**[1]

[1]Pathology and Laboratory Medicine, Weill Cornell Medicine, New York, NY,[2]Universita di Torino, Torino, Italy,[3]Universita San Raffaele, Milano, Italy

Chromatin architecture is a fundamental determinant of transcriptional regulation across cancer types, yet its integration into biomarker development has been limited. Here, we leverage DNA methylation as a surrogate for large-scale 3D genome structure to reconstruct A/B chromatin compartments and derive chromatin interaction networks that capture spatially coordinated gene organization. Using these methylation-informed networks, we define gene communities that reflect shared regulatory environments and potential co-functional behavior. We apply this framework to two prototypical epithelial malignancies—prostate cancer (PCa) and breast cancer (BCa)—using publicly available DNA methylation and transcriptomic datasets to identify chromatin-constrained modules whose coordinated dysregulation marks aggressive disease biology.

Across both cancer types, chromatin-driven gene communities show stronger coherence with known biological pathways than modules derived solely from expression data, underscoring the value of incorporating 3D genome context into molecular profiling. Using machine-learning approaches, we develop chromatin-informed prognostic signatures that integrate network topology with transcriptional alterations to predict metastasis and lethal outcome.

These signatures demonstrate robust performance across independent datasets and consistently outperform baseline expression-only predictors, highlighting the generalizability of chromatin context as a key source of prognostic information.

Functional analyses reveal that signature genes in both PCa and BCa are enriched for processes implicated in tumor progression, including lineage plasticity, hormone receptor signaling adaptation, disruption of chromatin insulation, and loss of compartmental integrity. Although the specific pathways differ in lineage-specific ways—such as androgen receptor signaling in PCa and estrogen receptor circuitry in BCa—the unifying mechanism lies in perturbations of higher-order genome organization that facilitate oncogenic rewiring.

Together, these findings demonstrate that methylation-derived A/B compartment structure provides a powerful and generalizable framework for reconstructing chromatin networks and identifying biologically coherent regulatory modules. By embedding transcriptomic alterations within their 3D genome context, we advance chromatin-informed gene expression signatures with strong prognostic utility across multiple cancer types, illustrated here through prostate and breast cancer.

Disclosures: AI was used to assist the preparation of this abstract.

#6878 AI-driven structural variant annotation expands therapeutic stratification in breast cancer.

Kriti Shukla[1], Yue Wang[2], Philip M. Spanheimer[3], Elizabeth Brunk[2]

[1]Department of Chemistry, University of North Carolina at Chapel Hill, Chapel Hill, NC,[2]Department of Pharmacology, University of North Carolina at Chapel Hill, Chapel Hill, NC,[3]Department of Surgery, University of North Carolina at Chapel Hill, Chapel Hill, NC

Interpreting variants of unknown significance (VUS) remains a critical barrier to precision oncology, particularly in breast cancer, where the majority of somatic mutations are rare and lack functional annotation. We developed VAMOS (Variant Annotation through Multi-Omics and Structural Biology), a machine learning framework that integrates genomic, transcriptomic, and protein structural data to predict the regulatory impact of coding variants on cancer-driving pathways.

Applied to >14,000 mutations across 1,000+ breast tumors, VAMOS identified 395 variant clusters in 346 proteins associated with dysregulated ESR1 and EZH2 activity, which are two key regulators of endocrine response and epigenetic reprogramming. Spatially resolved clustering revealed that 36% of rare variants co-localize with known oncogenic hotspots, enabling functional reclassification of clinically ambiguous mutations. These predictions were validated using CRISPR dependency and drug response datasets, revealing subtype-specific vulnerabilities. For example, distinct PIK3CA and TP53 clusters were differentially associated with response to mTOR, AKT, and DNA repair inhibitors.

This structure-informed approach expands the set of potentially actionable variants by over 30%, offering new biomarkers for patient stratification and rational therapeutic targeting. By linking variant positions in 3D protein space to transcriptional phenotypes and drug sensitivity, VAMOS provides a scalable framework to bridge molecular profiling and clinical decision-making. These findings support the integration of AI-driven structural genomics into translational oncology pipelines to improve precision treatment strategies.

#6879 Integrating omics-driven digital avatars with patient-derived experimental models to accelerate precision oncology.

Bulak Arpat[1], Amel Bekkar[1], Michelle Barnard[2], Mark Eccleston[3], Ioannis Xenarios[1], Kevin Buyens[1], Michael Prosser[1]

[1]TwinEdge Bioscience SA, Epalinges, Switzerland,[2]ValiRx plc, Nottingham, United Kingdom,[3]Inaphaea Biolabs Ltd., Nottingham, United Kingdom

Precision oncology increasingly depends on linking patient-specific molecular profiles to experimentally validated therapeutic response models. ValiRx and Inaphaea BioLabs are developing advanced patient-derived functional cancer models, while TwinEdge Bioscience is building large-scale Digital Avatar collections that mechanistically represent individual tumours across genomics, transcriptomics, proteomics, regulatory-network dynamics, and drug-response modules. By combining these complementary capabilities, we established a closed-loop translational framework for predicting, testing, and refining precision-treatment strategies, integrating (i) omics profiling of ValiRx's patient-derived cancer models, and (ii) construction of mechanistic Digital Avatars using TwinEdge's modelling engine.

Methods: Avatars are formed by integrating gene expression patterns, pathway activity states, inferred regulatory network, and compound-response modules. We generated digital avatars by integrating matched multi-omics datasets - transcriptomic, genomic, proteomic, and phenotypic layers - into large-scale, mechanistic network models that capture cell-state dynamics. Each individual avatar was then embedded within a population of thousands, allowing systematic comparison to identify subgroups that respond to a given intervention through shared mechanistic signatures. These mechanistically aligned avatars were then analysed to uncover repurposing opportunities and novel biomarker candidates.

Results: Across breast, ovarian, and colorectal cancer models, the Digital Avatars were shown to faithfully recapitulated tumour-specific regulatory features, including pathway activation, metabolic rewiring, and stress-response signatures. Avatar-based predictions revealed compound-specific vulnerabilities across multiple patient-derived models and uncovered previously uncharacterised mechanisms underlying differential responses to both targeted and broad spectrum agents. For certain models, observations pointed to the loss of regulation around VEGF-A, network rewiring around DNA/damage and some loss of c-Myc regulatory feedback. Together, these findings highlight the likelihood of a partial or full response, and allow suggestion of potential therapeutic intervention that would convert partial responders into full responders.

Conclusion: The TwinEdge-ValiRx translational program demonstrates the power of integrating computational Digital Avatars with patient-derived functional models. This combined framework enhances mechanistic interpretability, improves drug response prediction, and accelerates preclinical decision making. These early results form a concrete proof-of-concept that Avatar based loop dynamics capture treatment specific regulatory rewiring and can guide downstream therapeutic evaluation.

#6880 Optimization of a urine based NGS assay for detecting minimal residual disease in bladder cancer.

Yujia Zheng[1], Philip H. Abbosh[1], Muhammed Murtaza[2], Rhea Arya[3]

[1]Fox Chase Cancer Center, Philadelphia, PA,[2]University of Wisconsin Carbone Cancer Center, Madison, WI,[3]University of Florida, Gainesville, FL

Background: Current clinical tools struggle to accurately distinguish minimal residual tumor from benign bladder tissue following neoadjuvant chemotherapy in radicl cystectomy patients. Identification of complete responders might permit avoidance of radical cystectomy. To address this need, we developed an NGS-based urine assay to support non-invasive detection of chemotherapy response. This study focuses on optimizing key pre-analytical factors, including preservative selection and DNA extraction methods.
Methods: To overcome the logistical constraints of immediate -80 °C freezing, multiple urine preservatives were evaluated for their ability to maintain DNA integrity. Two DNA extraction strategies were compared: Sepharose-based extraction and a popular commercial kit. DNA from each condition was subjected quality control testing and to shallow pass whole-genome sequencing, followed by fragmentomics analysis, fragment end-motif profiling, and copy-number alteration (CNA) estimation.
Results: Sepharose extraction combined with a specially designed salt buffer yielded the highest DNA recovery. Commercial products did not promote fragment stability. Fragmentomics analyses showed that cancer patients exhibited higher fraction of aberrant fragments (FAF) than healthy controls when processed with Sepharose extraction. Distinct fragment end-motif patterns were also observed between the two groups. CNA analysis demonstrated that buffer-preserved samples produced higher estimated tumor fractions than samples processed with immediate freezing, indicating improved tumor signal retention. Unexpectedly, Sepharose extraction yielded improved signal-to-noise ratio as well.
Conclusions: The assay shows strong potential for detecting minimal residual bladder cancer and supporting non-invasive evaluation of complete response after chemotherapy. Salt buffer effectively enhances urinary DNA preservation and improves tumor-derived signal detection compared with immediate freezing. We are continuing to collect more urine samples to further refine and clinically validate the assay for clinical use.

#6881 Fast and cost-effective cloud-based pipelines to analyze cancer sequencing data.

Sam Wiseman[1], Samantha Van Seters[1], Saveliy Belkin[1], David I. Heiman[1], Vasuki Narasimha Swamy[1], Antonia Kowalewski[1], Scott Ritterbush[1], Zachary Everton[1], Ron Solan[1], Chip Stewart[1], David Lehotzky[1], Luis Antonio Corchete Sanchez[1], Xavi Loinaz[1], Haruna Tomono[1], Andrew D. Cherniack[1], Gengchao Wang[1], Brian P. Danysh[1], Young Seok Ju[2], Esther Rheinbay[1], Gad Getz[1]

[1]Broad Institute, Cambridge, MA,[2]Inocras Inc., San Diego, CA

With the release of high-quality resequencing of the TCGA cohorts, the scientific community has gained an opportunity to deepen its understanding of cancer's underlying causes and create paths forward for its treatment. Well-experienced with these cohorts, we have developed (i) state-of-the-art computational pipelines that accurately characterize variants in sequenced cancer data, as well as (ii) the infrastructure to run these pipelines quickly and cost-effectively in the cloud. Using a combination of established tools and specialized filters that reduce the likelihood of false calls, our pipelines have been honed over years of use and run extensively in numerous cancer studies. The TCGA cohort presented a unique challenge of >8,000 deep coverage, PCR-free whole-genome-sequenced (WGS) tumor-normal pairs, requiring a massive upscaling of our pipeline infrastructure. Enhancements to individual tools and refinements of our cloud-based workflow engine have reduced the time and cost of our pipeline execution by more than 50% since the start of 2025, allowing us to characterize more than 8,000 of the pairs in less than 1 month. This undertaking detected more than 262 million mutations and 1.17 million structural variants that we believe will provide deep insight into cancer biology and potential therapeutic targets.

#6882 Mechanism-concordant cell-line selection: Bridging real-world tumor drivers and *in vitro* models for target validation.

Aviva G. Beckmann, Phillip Comella, Qi Pan, Jonathan Tyler, Enrique Podaza, Veronica Calvo-Vidal, Mark Fereshteh, Iker Huerga, Eric E. Schadt

Pathos AI, New York, NY

Cancer cell lines remain workhorses for mechanistic studies and preclinical drug prioritization, but their transcriptional programs can shift as they move from in vivo to in vitro conditions and drift under prolonged culture. Selection for growth advantage and stress tolerance can alter lineage and resistance programs, yet these models are still used to infer mechanisms of action and project efficacy to patients, often without a rigorous link to patient-level disease biology.

We leveraged multimodal real-world data comprising longitudinal clinical records, tumor DNA and RNA sequencing, to infer in vivo driver mechanisms that impact outcomes under standard of care. We then developed an integrative framework that connects these patient-level mechanisms to in vitro systems where they can be perturbed and pharmacologically modulated. For each disease context, we construct predictive network models of cancer progression and identify cell type-localized “mechanism programs” whose activity associates with survival and progression. In parallel, we build matched network models for cancer cell lines using multiomic and perturbation data, deriving corresponding mechanism programs in vitro.

The key step is establishing mechanistic and phenotypic concordance between patients and models. For each patient-inferred driver mechanism, we search the in vitro network space for subnetworks with similar structure and activity, defining mechanism-concordant lines and tissue cultures. In phenotypically concordant systems, perturbing the mechanism program shifts molecular state and cell viability in a manner consistent with the direction of the patient-level outcome association; in discordant systems, the same program either fails to respond or drives phenotypes inconsistent with clinical benefit, revealing culture-induced artifacts.

We illustrate this framework in ovarian cancer. Multimodal real-world data reveal distinct driver mechanisms across the disease course, including hormone signaling, lineage plasticity, and platinum resistance networks. A restricted subset of ovarian cell lines and ex vivo cultures are mechanistically and phenotypically concordant for these programs; in these models, genetic or drug perturbation of implicated subnetworks reduces viability, whereas non-concordant models show limited effects. Future work aims to prospectively test modulators nominated by the integrated system in patient-derived ex vivo cultures and assess whether agents targeting concordant mechanisms shift molecular programs and viability as predicted, while agents predicted to be inactive do not. This patient-to-model mechanism bridge enables systematic selection of appropriate in vitro systems, prioritization of targets with both outcome-level and perturbation support, and calibration of preclinical effect sizes against clinically meaningful benefit.

#6883 An RNA-based survival model predicting real-world response to trastuzumab deruxtecan.

Klemen Ziberna, Anze Lovse, Zan Kuralt, Janez Kokosar, Marcel Levstek, Luka Ausec, Miha Stajdohar, Rafael Rosengarten, Mark Uhlik, **Joshua Wheeler**

Genialis, Inc., Boston, MA

Antibody-drug conjugates (ADCs) such as trastuzumab deruxtecan (T-DXd, Enhertu) have redefined therapy for HER2-expressing breast cancer, yet clinical benefit remains unpredictable across HER2-positive, -low, and -ultralow disease. Current IHC/FISH diagnostics quantify receptor abundance but fail to capture the molecular state that governs ADC sensitivity.To address this gap, we developed an RNA-based survival model for Enhertu using the Genialis Supermodel, a large molecular foundation model. The Supermodel maps gene expression into hundreds of biomodules, algorithmic representations of biology that capture diverse oncologic hallmarks including signaling pathways, stress responses, and drug-target mechanisms. We used biomodules specific to ADC mechanisms-of-action as input features in predictive models that learn biological patterns associated with T-DXd response.In a real-world clinical cohort (n≈90 T-DXd-treated patients) from the Tempus real-world multimodal database, we performed survival modeling of time-to-next-treatment (rwTTNT). Stratified nested cross-validation was used to assess model robustness and predictive performance. Prognostic specificity was assessed in prior-line rwTTNT and in an independent clinically matched cohort. The model showed statistically significant discrimination (C-index 0.632, HR 2.22 [95% CI 1.14-4.35], p = 0.017). Predicted-benefit patients had longer rwTTNT (345 vs 245 days), and no prognostic signal appeared in control cohorts (C-index ≈ 0.5), suggesting predictive specificity. Top predictive features aligned with ADC biology, including TOP3B and TOP2A (topoisomerase payload), ATM and TP53 (DNA damage response), HIF1A (hypoxia), ESR1 (hormone signaling), and XBP1/NFATC1 (stress and immune regulation).This Enhertu survival model applies biologically structured AI to real-world RNA-seq data to reveal treatment-specific patterns of response. Integrating large-scale embeddings, mechanistic biomodules, and survival modeling, we identified biological programs related to DNA repair and stress response associated with T-DXd benefit.

#6884 Quantum mechanics-based multi-tensor AI/ML correctly predicts — glioblastoma patients' overall survival, gene targets to sensitize the tumors, and the tumors' response to their targeting — from their whole genomes.

Orly Alter[1], Sri Priya Ponnapalli[2], Marissa Coppola[3], Angela C. Gushue[3], Tessa O. House[3], Penelope L. Miron[4], Kristy L. S. Miskimen[4], Kristin A. Waite[5], Sarah Pollock[6], David Bogumil[6], Nika Iremadze[6], Samantha Hernandez[6], Nadiya Sosonkina[7], Sara E. Coppens[8], Anthony C. Bryan[8], Estevan P. Kiernan[9], Huanming Yang[10], Jay Bowen[8], Ghunwa A. Nakouzi[7], Doron Lipson[6], Jill S. Barnholtz-Sloan[5], Andrew E. Sloan[11], Tiffany R. Hodges[4], Asaf Zviran[12], Jessica W. Tsai[3]

[1]University of Utah and Prism AI Therapeutics, Inc., Salt Lake City, UT,[2]Scale AI, Inc., San Francisco, CA,[3]Children's Hospital of Los Angeles and University of Southern California, Los Angeles, CA,[4]Case Western Reserve University School of Medicine, Cleveland, OH,[5]Winship Cancer Institute of Emory University, Atlanta, GA,[6]Ultima Genomics, Inc., Fremont, CA,[7]HudsonAlpha Clinical Services Lab LLC, Huntsville, AL,[8]The Abigail Wexner Research Institute at Nationwide Children's Hospital, Columbus, OH,[9]Illumina, Inc., San Diego, CA,[10]Complete Genomics, Inc., San Jose, CA,[11]Wright State University, Dayton, OH,[12]Prism AI Therapeutics, Inc., Salt Lake City, UT

Despite the growth in targeted therapy development, the drug failure rate has increased to ~95%. As clinical trials demonstrated, the targeted gene alone does not predict whether patients would have longer life expectancy in response to a drug. As studies with model organisms showed, the effect of the drug, and the mechanisms underlying it, depend on the entire multi-ome. But multi-omic data are small-cohort, noisy, and high-dimensional, i.e., extremely difficult to model.

We have developed our quantum mechanics-based artificial intelligence and machine learning (AI/ML) to overcome these challenges [doi: 10.1158/1538-7445.AM2025-CT227].

We demonstrated our algorithms in the unsupervised modeling of, e.g., whole genomes of 85 astrocytoma patients. Mechanistic interpretation showed that the model blindly removed batch effects, separated normal demographic variations, and discovered a disease-specific genome-wide pattern of DNA copy-number alterations. This pattern was used to derive an actionable predictor of patients' overall survival (OS) and gene targets to sensitize their tumors.

We computationally validated both the predictor and the modeling in federated studies of mutually-exclusive sets of ~50-250 patients. The modeling repeatedly discovered a representation of the predictor in every study, in astrocytoma grades II, III, and IV, i.e., glioblastoma (GBM), patients.

We experimentally validated the predictor in a clinical trial in 79 GBM patients, initially retrospectively, and, in a four-year follow up, also prospectively [doi: 10.1063/1.5142559, 10.1145/3624062.3624078]. In all the cohorts, the predictor, with 75-95% concordance with survival, was more accurate than all standard-of-care indicators. With 100% reproducibility among Complete Genomics, Illumina, and Ultima whole-genome sequencing, and >99% when including Affymetrix and Agilent DNA microarrays, the predictor was also the most precise.

Here, we describe functional genomics experimental validation of both a gene target predicted to sensitize the tumors, as well as the predicted tumors' response level. Guide RNAs were designed and a lentiviral CRISPR-Cas9 all-in-one vector was utilized to knock out the candidate target. Knockout validation at the protein level was performed using Western blot. Knockout in patient-derived GBM cell lines resulted in significantly attenuated cell viability and proliferation. The level of attenuation was significantly different between the cell lines, in agreement with their whole genome-based predicted response.

We conclude that our quantum mechanics-based multi-tensor AI/ML solved the 75-year-old problem of correctly predicting — GBM patients' OS, gene targets to sensitize the tumors, and the tumors' response to their targeting — from their whole genomes.

: New Algorithms and Computational Methods
Poster Session

#6888 scDeBussy: Cohort-level pseudotime alignment reveals recurrent dynamic gene programs in histological transformation.

Meng Wang[1], Jose Meza-Llamosas[2], Xinjun Wang[3], Joseph Chan[1]

[1]Human Oncology & Pathogenesis Program, Memorial Sloan Kettering Cancer Center, New York, NY,[2]Tri-Institutional PhD Program in Computational Biology & Medicine, New York, NY,[3]Department of Epidemiology & Biostatistics, Memorial Sloan Kettering Cancer Center, New York, NY

Introduction: Lineage plasticity and histological transformation are key drivers of therapeutic resistance in cancer. However, recurrent dynamic transcriptional programs are hard to model across patients due to intertumoral heterogeneity and uneven cell-state representation. Existing trajectory alignment methods rely on pairwise comparisons, predefined topologies, or batch correction, limiting detection of shared cohort-level transitions. To address this, we developed scDeBussy, a cohort-level trajectory alignment method that identifies shared dynamic gene programs across samples.
Methods: scDeBussy uses dynamic time-warping barycenter averaging to derive a unified reference trajectory from patient-specific probabilistic pseudotime, enabling cross-sample comparison of gene trends. We modeled aligned pseudotime with generalized additive models, clustered gene trends into early, intermediate, and late transcriptional modules, and quantified recurrence across patients while controlling for clinical covariates. Latent-Factor Multi-Output Gaussian Process simulations show scDeBussy recovers the global latent pseudotime and aligns cells derived from patients sampled at disparate stages of the underlying trajectory. We applied scDeBussy to new and published single-cell RNA-seq datasets of histological transformation, including lung adenocarcinoma (LUAD) to small cell lung cancer (SCLC) and lung adenosquamous cancer, to identify recurrent transcriptional dynamics of lineage plasticity.
Results: scDeBussy aligned patient-specific trajectories despite heterogeneous sampling. In LUAD-to-SCLC neuroendocrine (NE) transformation, it revealed a reproducible continuum from alveolar/secretory states through basal/mesenchymal intermediates to terminal NE states. Early module was enriched for JAK/STAT inflammatory signaling, intermediate module for basal and squamous programs marking a stem-like bottleneck, and late module for NE commitment. In lung adenosquamous cancer, scDeBussy inferred a continuous adeno-to-squamous transition, with early module enriched for LUAD-associated transcription factors (FOS, FOXA1/2) and late module dominated by LUSC drivers (TP63, E2F). Projecting matched scATAC-seq profiles onto pseudotime uncovered epigenetic priming events along the transition, including signatures of epigenetic reprogramming (EZH2), stemness (KLF4, JUN/FOS), and EMT (ZEB1, SMAD2-4).
Conclusion: scDeBussy enables cohort-level pseudotime alignment to detect recurrent dynamic gene programs underlying state transitions. Applied to LUAD-to-SCLC and adeno-to-squamous transformation, it reveals key transitional modules toward distinct terminal fates. By resolving these conserved dynamics, it offers a generalizable approach to dissecting disease processes marked by plasticity and divergent lineage outcomes.

#6889 AI-empowered virtual immunopeptidomics uncovers novel regulators of neoantigen immunogenicity.

Yuhao Tan, Ziqi Yang, Julia Fleming, Hailong Hu, Bo Li

University of Pennsylvania, Philadelphia, PA

Adaptive immunity is governed by both qualitative and quantitative features of antigen presentation. In anti-cancer T cell responses, 'quality' reflects peptide-MHC binding, whereas 'quantity' reflects how abundantly each epitope is displayed. Although binding has been studied extensively, the contribution of peptide abundance to neoantigen immunogenicity remains poorly understood, mainly because of limited immunopeptidome datasets. To bridge this gap, we developed epiVIP, a novel virtual immunopeptidomics method that predicts HLA-I peptide abundance. We first established that mass spectrometry (MS) intensity provides a robust and scalable approximation of absolute epitope abundance. Leveraging this, we curated and uniformly quantified 1.7 million HLA-I peptides from 254 tumors with paired transcriptomes, creating the largest quantitatively standardized immunopeptidome resource to date. We then developed epiVIP, a deep neural network that integrates peptide and HLA sequences with the expression of the peptide's source gene and 472 putative regulators of antigen presentation. To minimize batch effects, we used a pairwise ranking loss strategy. epiVIP achieved high prediction accuracy and generalizability for within-sample abundance, with AUC>0.8 for 20 held-out samples and 24 independent samples.

Applying epiVIP to 33,782 neoantigens from four studies, we observed that higher predicted abundance was strongly associated with increased immunogenicity. Importantly, the effect was conditional on self-discrimination, defined as the sequence similarity between the neoantigen and its wild-type counterpart. Neoantigens with low self-discrimination required high abundance to elicit T cell responses, whereas those with high self-discrimination were immunogenic regardless of abundance. In three immune-checkpoint blockade cohorts, the summed abundance of low self-discrimination neoantigens outperformed tumor mutational burden in predicting response and survival ($p = 4.7*10^{-4}$ vs $1.3*10^{-3}$ in one cohort).

To identify regulators of epitope abundance, we first validated that the predicted abundance changes accurately recapitulated antigen-repertoire remodeling after PSME4 knockdown in A549 cells. We then extended predictions to 409 regulatory gene knockdowns in HCT116 and HEK293T using pseudobulked perturb-seq profiles. We observed that perturbation effects clustered by C-terminus amino acid properties and identified 32 regulators with C-terminal-specific effects, including PSME4 and PSMF1.

In summary, epiVIP establishes epitope abundance as a key quantitative determinant of neoantigen immunogenicity, provides a model to predict abundance when immunopeptidomics is unavailable, and offers a framework to identify gene perturbations that enhance presentation of desired epitopes for TCR-T and cancer vaccine development.

#6890 Subcellular 3D multi-omic models of CDH1-mutant diffuse gastric cancer improve recapitulation of tumor microenvironment structure and reveal precancer signature niches.

Jean R. Clemenceau[1], Yunhe Liu[2], Idania Carolina Lubo Julio[3], Soyoung Im[4], Seock-Jin Chung[1], Sam C. Wang[5], Paul F. Mansfield[6], Luisa Maren Solis Soto[3], Linghua Wang[2], Tae Hyun Hwang[1]

[1]Section of Surgical Research, Vanderbilt University Medical Center, Nashville, TN,[2]UT MD Anderson Cancer Center, Houston, TX,[3]Department of Translational Molecular Pathology, UT MD Anderson Cancer Center, Houston, TX,[4]Department of Pathology, The Catholic University of Korea St. Vincent's Hospital, Suwon, Korea, Republic of,[5]Department of Surgery, UT Southwestern Medical Center, Dallas, TX,[6]Department of Surgical Oncology, UT MD Anderson Cancer Center, Houston, TX

Diffuse-type gastric adenocarcinoma (DGC) presents as the more invasive and aggressive gastric cancer subtype with poorer prognosis. Hereditary germline CDH1 mutations are known to drive DGC in 1-3% of cases in what is known as hereditary diffuse gastric cancer (HDGC). Despite the genomic characterization of HDGC, the mechanisms of onset are still poorly understood, given that evidence suggests it can bypass the classic cascade of gastric intestinal metaplasia (IM) to dysplasia to cancer. Additionally, HDGC presents a complex tumor microenvironment (TME) given by its highly infiltrative distribution with increased immune and stromal interactions, as well as IM and dysplastic marker gene expression. These factors present an opportunity to better understand the complex cellular dynamics to elucidate the etiology of this disease. New advances in spatial transcriptomics and fluorescence imaging have reduced per-sample costs of spatial biology assays, allowing the scale necessary for studying serial sections.

HDGC samples were collected as formalin-fixed, paraffin embedded blocks. Samples were serially sectioned at 5µm thickness into G4x gel pads. Regions of interest (10mm x 10mm) were isolated from the gels pads and transferred to a G4x X2 spatial flow cell. Samples were processed using Singular Genomics G4x spatial multi-omic assay with a custom pre-gastric cancer panel consisting of 16 proteins, 341 transcripts, and fluorescent-based H&E images for every section of tissue. Data was processed following quality control, implementing cell type annotation, followed by registration of cell coordinates, incorporation of histopathological tissue annotations by a board-certified pathologist, and cell neighborhood analysis.

Two models were produced with 7 and 9 serial sections (16 total) representing a tissue depth of 35 µm and 45 µm and populations of 1.6M and 3.4M cells, respectively. The models recapitulate 3D morphology of known tissue structures, such as non-neoplastic epithelial glands, vasculature, and tertiary lymphoid structures. We observed TFF2, a SPEM cell IM marker, expression in the tumor-adjacent gastric mucosa. We also found small clusters of TFF2+ cells within the superficial tumor-invasive area, only present in a few of the total tissue layers.

We successfully built two 3D spatial multi-omic, subcellular resolution models for CDH1-mutant HDGC representing 35-45µm of tissue thickness that recapitulate the samples' histological structures. We show the spatial distribution of metaplastic markers expressed in tumor-adjacent epithelium. Our 3D models allowed for the identification of rare-cell events, such as small TFF2+ cell clusters within tumor-infiltrated tissue regions. These results show the promise that high-resolution 3D models present for improving our understanding of complex TMEs, such as HDGC.

#6891 Context dependent functional aneuploidy in cancer.

Polly L. S. Hung, Stephanie S. Liu, Tina N. Wei, Lesley S. K. Lau, Kui Liu, Karen K. L. Chan, Haonan Lu

Department of Obstetrics & Gynaecology, The University of Hong Kong, Hong Kong SAR, China

Background: Aneuploidy shows strong cancer-type specificity, yet its mechanistic basis remains unclear. Classic events like 8q gain in ovarian cancer or 17p loss in breast cancer highlight recurrent patterns, but the standard 98% arm-coverage rule obscures meaningful CNV boundaries. We hypothesised that recurrent breakpoints across tumours provide a more functional definition of aneuploidy. To address this, we developed BAGEL, which quantifies copy-number alterations by defining CNV segments using BISCUT breakpoints rather than fixed chromosome-arm thresholds.
Methods: We mapped recurrent CNV breakpoints across 38 cancer types using BISCUT and validated them across nine datasets spanning multiple sequencing platforms and segmentation algorithms (APOLLO, CPTAC3, CGCI, TARGET, DepMap, PCAWG, TCGA and two in-house cohorts). BAGEL-derived aneuploidy scores were tested for prognostic value using Cox and Kaplan-Meier analyses in TCGA high-grade ovarian cancer, with validation in PCAWG. Functional effects were assessed by integrating DepMap CRISPR screens and modelling essentiality differences using mixed-effects models. Chromatin constraints were quantified using TAD penetration scores from colorectal tumours and breast and lung cancer cell lines.
Results: BAGEL replaced the arbitrary 98% arm rule by defining CNV segments directly from shared breakpoints. Breakpoints were highly reproducible (mean deviation = 0.089), including 34 nearly identical sites across eight HGSOC cohorts. Prognostic modelling by multivariate cox showed that Breakpoint-defined aneuploidy strongly predicted survival in both HGSOC and breast invasive carcinoma, with TCGA dataset-built model $p<0.0001$ for both and showed consistent trend in PCAWG dataset (5 year OS $p = 0.085$ for HGSOC and $p = 0.026$ for breast invasive carcinoma). Mixed-effects modelling between 584 cancer-pairs showed significant interaction between cancer type and presence of breakpoint event in 123 arms (FDR < 0.05), indicating that the CRISPR essentiality difference between aneuploid and non-aneuploid samples varies substantially across cancer types. Hi-C-derived TAD penetration scores demonstrated consistent structural constraints across tumour and cell-line datasets. Breakpoints showed a subtle but reproducible bias toward TAD boundaries, particularly for negatively selected events, indicating that 3D genome architecture shapes permissible CNA breakpoint positions.
Conclusions: Breakpoint-defined aneuploidy captures recurrent, biologically constrained CNV segments, reveals cancer-type-specific selective pressures, identifies aneuploidy-linked gene-essentiality shifts, and exposes a reproducible positional bias toward TAD boundaries. These findings demonstrate that aneuploidy evolution is shaped jointly by selective fitness pressures and 3D chromatin architecture.

#6892 A pan-cancer atlas of telomere length in tissues and plasma cell-free DNA.

Junming Shi, Leslie Espinoza, Mengran Zhang, Mohammad Shahrokh Esfahani

Stanford University School of Medicine, Stanford, CA

Background:
Telomeres shorten with age because of incomplete replication and limited telomerase activity, and their dysfunction promotes genomic instability in cancer. Existing estimators rely on strict repeat counts and often miss error-affected or biologically shortened fragments. This is problematic in plasma cfDNA where most fragments are ~170 bp and ctDNA is even shorter (Cristiano et al., 2019; Chabon et al., 2020). Nanopore-based assays provide precise measurement (Sanchez et al., 2024; Karimian et al., 2024), but an accurate, error-tolerant short-read approach remains unmet.
Methods:
We developed VERACITY, a machine-learning method that estimates telomere length (TL) from short-read WGS by modeling telomeric-repeat patterns and sequencing-error profiles. VERACITY also computes a Telomere Ambiguity Index (TAI) that quantifies heterogeneity in telomere maintenance. We applied VERACITY to 10,363 TCGA WGS samples (4,847 tumors; 5,089 matched normals; ages 14-85) across 27 cancer types, 3 deep (~200×) cfDNA genomes with systematic down-sampling, and 462 low-pass (2-3×) cfDNA genomes from the DELFI cohort (233 cancers; 229 healthy; ages 14-86), generating an atlas of telomere biology in tissues and plasma.
Results:
Down-sampling showed reliable TL estimation down to ~2.5× coverage, supporting low-pass cfDNA application. Tissue and cfDNA trends were highly concordant. Across cancers, TL declined with age in tumors and matched normals, with tumors showing far steeper erosion (tissue tumor: β_{age} = -62.5*, β_{age^2} = 0.5* vs. normal: -10.8, 0.02; cfDNA cancer: -13 vs. healthy: 0 bp). Male tumors showed greater loss (TCGA: -90.0*, 0.66*; cfDNA: -99.1*, 0.8) than female tumors (TCGA: -15.5, 0.16; cfDNA: -0.9, -0.1).
Age-associated trajectories varied widely: GBM, TGCT, and STAD showed steep nonlinear declines, whereas CESC, KICH, and LGG showed minimal or positive slopes, consistent with adjusted TL residuals. Although stomach tissues show the weakest TL-age correlation (Demanelis et al., 2020), gastric cancers exhibited one of the strongest declines in both tissue (β_{age} = -135.2 bp) and cfDNA (-63.5 bp) and among the lowest Gini and ATR values. Several cancers, including PRAD and TGCT, displayed elevated TAI, suggesting diverse or unstable maintenance strategies.
Conclusions:
VERACITY provides an accurate and scalable framework for TL estimation from standard and low-pass sequencing, enabling the most comprehensive atlas to date of telomere dynamics across cancers in tissues and plasma. The analysis reveals accelerated, sex-stratified, and cancer-type-specific telomere erosion, substantial inter-tumor heterogeneity, and distinct maintenance mechanisms. cfDNA TL patterns closely mirror tissue-derived trends and highlight the potential of telomere metrics as minimally invasive biomarkers of telomere dysfunction, tumor biology, and treatment-relevant telomere states.

#6893 MambaSV: Accurate germline and somatic structural variant calling from long-reads with deep sequence model.

Zhihan Zhou, Tong Zhu, Pankaj Vats

Nvidia Corporation, Santa Clara, CA

Somatic structural variants (SVs) are difficult to detect from long-read sequencing due to the inherent complexity of tumor genomes characterized by low variant allele fractions (VAFs), variable tumor ploidy/purity, and highly complex rearrangement patterns. Deep learning models are underexplored in this problem due to the lack of labeled data. To leverage it, we introduce a novel data simulator that generates paired normal-tumor BAM files with accurate haplotype-aware SV labels to facilitate model training and benchmarking. Built on this, we present MambaSV, a GPU-native deep sequence model for haplotype-resolved somatic SV calling. The scalable, end-to-end, and haplotype-aware data simulator for long read sequencing (PacBio and ONT) is designed to capture real-world somatic SV complexities. It simulates SVs across five SV classes (INS, DEL, DUP, INV, BND) following empirically derived length distributions, partition them by haplotype and sample, and inject them together with SNPs and INDELs into CHM13 to create synthetic genomes. Longreads are simulated from the synthetic genomes with real statistics (e.g., length, error rate, etc.). For Fusions we generate artificial sequence constructs in FASTA format by concatenating relevant sequence fragments to reproduce true breakpoint signatures. To model tumor heterogeneity, we mix reads from SV and SNP-only genomes to achieve per-event VAFs from 0-100%, simulate copy-neutral loss of heterozygosity (cnLOH) in tumor, and haplotag both BAMs with third-party tools to mirror practical workflows. MambaSV is trained to discover SVs from matched tumor and normal alignments. MambaSV formulates SV discovery as a per-base multi-class classification task. At each base, a 30-feature vector (mapping qualities, supplementary evidence, etc.) is computed across three channels (hap1, hap2, unphased) and both samples. Haplotype-specific inputs combine each haplotype with the unphased channel. Leveraging a Siamese network with shared weights, MambaSV jointly processes tumor and normal samples with a bi-directional Mamba-2 backbone that preserves megabase-scale context without loss of single-base resolution. A lightweight decoder outputs haplotype-resolved somatic predictions, which are post-processed to merge contiguous signals and emit VCFs. Trained solely on HiFi BAMs and tested on held-out samples (~23 k SVs), MambaSV achieves F1 = 92.27 (HiFi) and 89.32 (ONT), outperforming Severus (69.18/70.31), Svision-pro (53.92/54.24), SAVANA (56.37/53.93), and Nanomonsv (42.42/42.20). To conclude, our comprehensive simulation framework fuels MambaSV's development by enabling rigorous training and broad generalizability in challenging real-world scenarios, while MambaSV unifies base-level features, haplotype structure, and long-range genomic context in a single deep model to set a new standard for somatic SV calling from long-read data.

#6894 Predict, perturb, and process: A systems biology pipeline for identifying synthetic lethality.

Juihsuan Chou[1], Chenchu Lin[1], Iulia Veronica Gheorghe[1], Sabriyeh Alibai[1], Subin Kim[1], Lori Wilson[1], Xingdi Ma[2], Junjie Chen[3], Glen Traver Hart[3]

[1]Systems Biology, The University of Texas MD Anderson Cancer Center, Houston, TX,[2]Genitourinary Medical Oncology, The University of Texas MD Anderson Cancer Center, Houston, TX,[3]UT MD Anderson Cancer Center, Houston, TX

The synthetic lethality principle holds great promise for cancer therapy, but identifying synthetic lethals presents enormous challenges. Synthetic lethality, where loss of two genes causes cell death, but loss of either gene alone does not, is difficult to assay because combinatorial perturbation technologies are inefficient and because the search space is well beyond the capacity of current experimental systems: 19,000 protein coding genes offer more than 180 million candidate gene pairs. To address this, we combine network-driven predictive models with the In4mer CRISPR/Cas12a combinatorial knockout platform to conduct tractable pairwise knockout screens with high probability of identifying synthetic lethals.Even with these advances, effective methods for quantifying GIs in these screens remain limited. To address this gap, we developed GRAPE (Genetic interaction Regression Analysis of Pairwise Effects), a novel regression-based method for analyzing GIs in all-by-all gene knockout (KO) library designs. GRAPE infers single-gene KO fitness from multiplex CRISPR arrays, predicts combinatorial gene KO fitness, and identifies synthetic lethals that deviate from this expectation. Since no gold-standard exists for benchmarking, we built a simulation framework to systematically evaluate GRAPE, demonstrating improved computational efficiency, adaptability, and precision-recall performance over existing methods.Using the network-driven experimental design, In4mer screening, and GRAPE analysis, we screened all pairwise combinations of 206 genes involved in receptor tyrosine kinase (RTK) signaling, all pairs of 167 genes in DNA damage response (DDR) pathways, and over 4,000 paralog pairs across 12 diverse cancer cell lines. Our DDR results closely align with findings reported by other studies, while our RTK network provides novel insight into ER-mediated protein modification and oncogenic signaling dependencies. Overall, our efforts confirm that we can predict and detect both global and background-specific genetic interactions, advancing the state of the art in functional genomics and cancer target finding.

#6895 DISSECT integrates cytological images and spatial transcriptomics for cell segmentation.

Yufeng He[1], Yanping Zhao[2], Rui Zhang[1], Heli Yang[3], Zhaode Bu[3], Yuan Luo[4], Deng Pan[5], Zexian Zeng[1]

[1]Peking-Tsinghua Center for Life Sciences, Academy for Advanced Interdisciplinary Studies, Peking University, Beijing, China,[2]Tsinghua-Peking Center for Life Sciences, School of Life Sciences, Tsinghua University, Beijing, China,[3]Center of Gastrointestinal Cancer, Peking University Cancer Hospital & Institute, Peking University, Beijing, China,[4]Department of Preventive Medicine, Feinberg School of Medicine, Northwestern University, Chicago, IL,[5]Tsinghua-Peking Center for Life Sciences, Department of Basic Medical Sciences, Tsinghua University, Beijing, China

Advances in both imaging- and sequencing-based spatial transcriptomics technologies have significantly increased panel size and resolution, enabling the measurement and analysis of spatially resolved single-cell transcriptomics. However, challenges remain in accurately segmenting cells due to variability in cell morphology, tissue processing, and staining methods, leading to reduced accuracy and poor generalization of existing cell segmentation algorithms. To address this, we propose DISSECT, a novel cell segmentation model that combines cytological image segmentation with transcriptome-guided fine-tuning. DISSECT leverages a pre-trained deep generative model to identify cell nuclei or membrane boundaries, unifies the gradient fields of both images and transcriptomics to refine cell boundaries, and reconstructs spatial single-cell transcriptomes. We benchmarked DISSECT using the ground-truth dataset profiled by the Visium HD, Stereo-seq, Xenium 5k, and CosMx 6k platforms, demonstrating higher mean average precision than other tools. Furthermore, evaluations on independent 10x Xenium 1k, Nanostring CosMx 1k, and Stereo-seq datasets further validate that DISSECT achieves superior segmentation accuracy, especially in densely packed cell regions. Additionally, DISSECT was applied to three paired gastric adenocarcinoma samples, which we collected before and after PD-1 treatment and sequenced using Stereo-seq, a transcriptome-wide NGS-based sequencing technology, showcasing its potential for driving in-depth biological discoveries.

#6896 ELEVATE: Axis-coupled mapping of co-varying gene programs in single-cell transcriptomic data.

Kourosh Kouhmareh[1], Richard L. Klemke[2]

[1]UC San Diego School of Medicine, La Jolla, CA,[2]UCSD Moores Cancer Center, La Jolla, CA

Differential expression analysis has long been the standard for identifying genes that distinguish one condition from another. However, it is inherently binary and static (comparing X vs Y, high vs low), offering only a snapshot of differences rather than revealing how expression programs develop. Pseudotime algorithms address this by reconstructing *inferred* trajectories that model temporal progression, yet these paths are manifold driven rather than anchored to a defined biological axis, which can allow for dominant sources of variation to mask processes of interest. To directly interrogate how a gene or gene set is upregulated and which associated processes rise alongside it, we developed *ELEVATE (Expression LEVEL-based Variational Analysis of Transcriptional Evolution)*, a trajectory-agnostic framework that orders cells by an anchor gene or signature, partitions them into equal, ascending single-cell Variational Inference (scVI) expression-based percentile bins, and performs sequential adjacent-rising comparisons to identify genes that rise or decline monotonically with the anchor. We additionally define an inflection bin, the percentile interval where anchor gene induction triggers the largest aggregate transcriptomic shift. Applying this framework to single-cell RNA-sequencing data from primary human tumors, we show that *ELEVATE*-based profiling provides finer resolution than discrete clustering, disentangling genes that rise continuously with the anchor from those that don't fully contribute to the end-state expression profile. *ELEVATE* provides actionable, pathway-level insights clarifying how expression programs evolve, and prioritizes candidate drivers and targets for experimental validation.

#6897 A bi-partition function algorithm to evaluate inferred subclonal structures in single-cell sequencing data.

Farid Rashidi Mehrabadi[1], Erfan Sadeqi Azer[2], **John D. Bridgers**[3], Teresa M. Przytycka[3], Salem Malikic[1], Funda Ergun[4], Cenk Sahinalp[1]

[1]National Cancer Institute, National Institutes of Health, Bethesda, MD,[2]Google LLC, Sunnyvale, CA,[3]National Library of Medicine, National Institutes of Health, Bethesda, MD,[4]Computer Science Department, Indiana University, Bloomington, IN

Clonal evolution of cancer results in intratumor heterogeneity, making treatment and cure challenging. Single-cell sequencing has advanced our understanding of intratumor heterogeneity, but tracing subclonal evolution using mutational profiles of cells is limited by scale and noise. Moreover, available tumor progression tree inference methods usually offer a single tree to explain the progression of a tumor, and do not inform about alternative evolutionary scenarios.

We introduce the bi-partition function for a tumor progression tree, to assess the reliability of any proposed subclonal structure in a single-cell sequenced tumor. By using the bi-partition function, we calculate the probability that any given subset R of mutation-profiled single cells from a tumor forms a clade rooted by a specified mutation ρ across all possible tumor progression trees. This provides the means to evaluate whether R forms a subclone with ρ as a possible subclonal driver, which is especially useful if the cells of R are biologically or clinically significant, e.g., have aggressive growth, therapy resistance, or metastatic potential.

We also introduce an algorithm to estimate the bi-partition function, which treats the ground truth as a probability distribution derived from mutational profiles of single cells and samples a tumor progression tree from this distribution independently in each iteration. We prove that our algorithm's estimate of the bi-partition function asymptotically approaches the ground truth and demonstrate its accuracy on simulated data.

Applying our algorithm to the tumor progression tree inferred from single-cell-derived melanoma sublines revealed that, while major clades and their root mutations are robust, (i) the placement of one clade in the tree is unreliable, which we later observed to be a result of Loss of Heterozygosity, and (ii) some of the mutations identified as false positives in the tree are unreliable, which later turned out to be the result of a doublet - a subline which has contamination from another subline. Interestingly, bootstrapping, a technique commonly employed for species trees, failed to point out any of these issues. After correcting the input data for these issues, the reliability of the progression tree improved substantially, demonstrating how our bi-partition function algorithm can aid studies on tumor evolution and intratumor heterogeneity.

#6898 Identifying robust subclonal structures through tumor progression tree alignment.

Jacob Gilbert[1], **Chih Hao Wu**[2], Marina Knittel[3], Alejandro Schaffer[4], Salem Malikić[2], S. Cenk Sahinalp[2]

[1]Department of Computer Science, University of Maryland, College Park, MD,[2]Cancer Data Science Laboratory, NIH-NCI, Bethesda, MD,[3]Department of Computer Science and Engineering, University of California, San Diego, CA,[4]National Cancer Institute, Bethesda

Understanding and comparing tumor evolutionary histories is fundamental to cancer genomics, with direct implications for tracking subclonal population dynamics, treatment resistance, and tumor heterogeneity. Clonal trees, widely used to model tumor progression, are rooted, unordered trees in which each node represents a subclone labeled by a set of distinct mutations. Various principled and efficient methods have been developed for inferring clonal trees from either bulk or single-cell sequencing data. However, no existing computational approach offers a method that is both efficient and principled to fully align clonal trees and to compare their subclonal architectures, which limits the robustness of any downstream analysis based on inferred clonal trees. We introduce omlta, the optimal multi-label tree alignment of two clonal trees, which removes the minimum number of mutation labels, so that the remaining trees are isomorphic. Computing omlta is NP-hard. Here, we present a fixed-parameter tractable algorithm to compute the omlta, with a running time of O(L^3 log L 2^k) where L is the number of mutation labels shared between the input trees and k is the minimum possible number of mutation labels that need to be removed for the alignment - which we call omltd, the optimal multi-label tree edit distance. Our approach provides an exponentially better (in k) asymptotic runtime than the state-of-the-art algorithm by Akutsu et al. for computing the classic tree alignment and edit distance, concepts similar to what omlta/omltd optimizes on clonal trees. We applied omlta to 126 multi-sample bulk-sequencing data from the TRACERx study on non-small cell lung cancers by comparing clonal trees inferred by CONIPHER and PairTree. Despite the theoretically exponential runtime, we could compute the tree alignment for each tumor quickly, often within seconds. The omltd between CONIPHER and PairTree clonal trees on the same tumor varies substantially across tumors and the distances are negatively associated with the mean cancer cell fraction among mutations. For the tumors characterized by mutations with low cancer cell fractions, it is thus advisable not to use a single tree, but rather the alignment of multiple alternative trees, so that downstream inferences are informed only by robustly placed mutations.
We further evaluated our algorithm on an in-house melanoma sample with clonal trees inferred by PhISCS and ScisTree, highlighting the utility of omlta on trees inferred from single-cell sequencing data. On these datasets, our algorithm completed all analyses in practical wall-clock times and showed that it can identify common evolutionary trajectories among clonal trees representing (i) distinct tumors, (ii) distinct samples from the same tumor, (iii) distinct sequencing data from the same sample. Additional supplementary results demonstrate the robustness of our approach in comparison to alternatives on simulated data.

#6900 Wakhan: Reconstruction of chromosome-scale copy number profiles of tumor genomes with long-read sequencing.

Tanveer Ahmad[1], Ayse Keskus[2], Mikhail Kolmogorov[2], Sergey Aganezov[3], Michael C. Dean[4], Midhat S. Farooqi[5], S. Cenk Sahinalp[2], Benedict Paten[6], Karen H. Miga[7], Salem Malikić[2], Yuelin Liu[2], Byunggil Yoo[8], Ataberk Ataberk Donmez[9], Anton Goretsky[9]

[1]National University of Science and Technology (NUST), Islamabad, Pakistan,[2]NIH-NCI, Bethesda, MD,[3]Oxford Nanopore Technologies, Cambridge, MA,[4]National Cancer Institute - Cancer Genomics Research Laboratory (CGR), Rockville, MD,[5]Children's Mercy Research Institute, Kansas City, MO,[6]University of California, Santa Cruz, Santa Cruz, CA,[7]Biomolecular Engineering Department, University of California, Santa Cruz, Santa Cruz, CA,[8]Children's Mercy Kansas City, Kansas City, MO,[9]University of Maryland, College Park, MD

Introduction. Copy number alterations (CNA) is a phenomenon during cancer evolution where some regions of the genome may be amplified or deleted. This results in heterogeneous collections of cancer cells. Profiling and classification of CNA profiles play a vital role in understanding the cancer heterogeneity and evolution to better inform diagnosis and treatment. There are several short-reads haplotype-specific CNA profiling tools but short reads provide a limited phasing range. Long-reads facilitate the direct phasing of genomic variants into megabase-scale haplotypes, which supports the reconstruction of longer, up to chromosome-scale, CNA profiles. Here we present Wakhan, a tool to analyze haplotype-specific chromosome-scale somatic copy number aberrations using long reads. Leveraging high-quality genome assembly coverage profiles, we show that Wakhan significantly outperforms other common short- and long-read CNA callers in achieving chromosome-level CNA consistency.

Methods. Wakhan uses tumor-normal long-read BAMs and phased germline SNP calls as input. It first extends the input phasing to be chromosome-scale by exploiting haplotype coverage imbalance. Wakhan detects those phase switch regions and corrects them by taking into consideration the changes in haplotype-specific coverage. Next, Severus utilizes this enhanced phasing to generate phased structural variant (SV) calls. Finally, Wakhan's integrated CNA algorithm uses the SV calls as boundaries and employs a haplotype coverage model to assign integer copy-number states to the resultant CNA regions.

https://github.com/KolmogorovLab/Wakhan

Results. We sought to compare Wakhan's performance against several state-of-the-art haplotype-specific CNA calling tools. The tools selected for short-read analysis included: Purple, Hatchet, Battenberg and for long-read analysis Purple and Savana are included. As benchmarks for small variants and SV calling are available but no similar benchmarks for somatic CNA calls are available. We designed a CASTLE panel based CNA calling benchmark, consisting of 6 pairs of tumor/normal cell lines sequenced with multiple short- and long-read sequencing technologies. We define *segment error* (SE) as for each CNA segment, we calculate the haplotype-specific mean squared distance between expected and reference coverage at heterozygous SNPs. This is then used to compute a weighted chromosomal average, normalized by the tumor haplotype's mean coverage. Similarly, for *chromosome error* (CE), compare the phase of the whole chromosome against the reference coverage. In the five CASTLE datasets, Wakhan and PURPLE had the lowest SE50 and SE75, indicating high accuracy in reconstructing individual CNA segments. We also evaluated Wakhan on a tumor-only dataset. Both Wakhan and PURPLE handled the absence of normal samples well and accurately reflected the expected tumor/normal profiles.

#6901 Hierarchical Dorfman screening for robust pathway-aware feature selection identifies predictors of MEK-inhibitor response in NSCLC.

Wanru Guo, Juan Xie

University of Maryland, Baltimore, Baltimore, MD

Background: Gene expression predictors of targeted therapy response often exhibit strong within-pathway correlation, heavy-tailed noise, and contamination from batch effects. Such structure severely degrades performance of conventional feature selection methods (LASSO, elastic net, SIS) and existing group-regularized approaches including group LASSO, sparse group LASSO, and group SIS/AR2.
Methods: We introduce Dorfman Screening, a computationally efficient hierarchical feature selection framework for pathway-structured genomic data. The method (1) groups genes into biological pathways using Hallmark annotations and dynamic tree cut clustering, (2) performs global pathway-level testing, (3) conducts within-pathway gene screening, and (4) applies a final regularized selection (Dorfman-LASSO or Dorfman-EN). Robust Dorfman variants additionally incorporate Huber-weighted regression to handle heavy-tailed errors, outliers, leverage points, and batch contamination. All tuning is data-driven through cross-validated RMSE.
Results: In extensive simulations (p=1000, n=200) with varying correlation structures and severe contamination, Dorfman methods consistently outperformed LASSO/EN, SIS, SIS-LASSO, group-LASSO, sparse-group-LASSO, and group-AR2-gpLASSO. Dorfman-EN achieved the highest accuracy under strong correlations (ρ=0.8), while Dorfman-LASSO excelled at lower correlation levels. Robust variants showed marked resilience under nonlinear distortions and heavy-tailed noise, maintaining the lowest false discovery rates. Applied to Genomics of Drug Sensitivity in Cancer (GDSC) RNA-seq data for trametinib response in non-small cell lung cancer (NSCLC), Dorfman methods achieved substantially improved predictive accuracy (RMSE=2.41-2.45) compared to LASSO/EN (RMSE=2.53-2.59) and group-regularized methods (RMSE=2.63-3.66). When genes were stratified into literature-supported biomarker tiers, Dorfman selections were significantly enriched for high-confidence genes and revealed previously unreported candidates not discovered by competing methods.
Conclusions: Dorfman Screening provides a scalable, robust, and biologically interpretable approach for pathway-structured genomic data, yielding improvements in both prediction performance and biomarker discovery for MEK-inhibitor response in NSCLC.

#6902 Remodeling of cancer cell architecture by chemotherapy.

Gege Qian[1], Xiaoyu Zhao[2], Leah V. Schaffer[3], Kyung-Mee Moon[2], Jiahao Gao[2], Emma Lundberg[4], Leonard Foster[2], Trey Ideker[5]

[1]UC San Diego School of Medicine, La Jolla, CA,[23]University of California San Diego - UCSD, San Diego, CA,[4]Schools of Engineering and Medicine, Stanford University, Stanford, CA,[5]UC San Diego, La Jolla, CA

How chemotherapy reshapes tumor cells—and how these changes influence outcomes such as drug resistance—remains largely unclear. Here, we present a multimodal, global characterization of tumor subcellular organization and its reorganization by chemotherapy. We use self-supervised learning to encode protein coordinates across four orthogonal data modalities: proteome-wide size-exclusion chromatography fractionation (before and after treatment with cisplatin or vorinostat), native-state immunofluorescence imaging, affinity purification, and primary sequence information covering 7,579 proteins. This integrated map resolves 174 subcellular components, spanning molecular assemblies from protein complexes to organelles across a size range of ~10-9 to10-5nm. 58 components undergo significant remodeling upon treatment, recapitulating known mechanisms of action and revealing previously unrecognized alterations in pathways such as cytoskeletal organization and metabolic rewiring. We systematically validate these “chemotherapy-response assemblies” using genome-wide CRISPR knockout drug-sensitivity profiling, identifying which assemblies confer drug sensitivity versus resistance. Chemotherapy-remodeled components serve as convergence points for cancer mutations that predict therapeutic response—including those involved in homologous recombination repair, chromatin remodeling, and double-strand break repair.

#6903 A transcript-only framework for pseudocell boundary inference in high-resolution spatial transcriptomics.

Sungwoo Bae, Hongyoon Choi, Dongjoo Lee, Daeseung Lee

Portrai, Inc., Seoul, Korea, Republic of

Background: High-resolution spatial transcriptomics (ST) enables subcellular expression profiling, yet cell-level analysis remains critical for understanding tissue organization. Current cell segmentation methods in ST like bin2cell rely on H&E-based nuclear expansion, making them susceptible to image quality issues, 2D nuclear overlap artifact, bias caused by transcript contamination from neighboring cells, and dependent on histological staining. To address this, we developed HIPSTER (Hotspot-guided Inference of Pseudocell boundaries in Spatial Transcriptomics), a method that delineates cell boundaries solely using transcript density, and validated its accuracy against bin2cell.

Methods: HIPSTER was applied to a human colorectal cancer Visium HD data (2 μm bin). Total UMI counts were normalized using a destripping algorithm to correct for irregularities of ST bin. Transcriptionally dense hotspots were identified by calculating the Getis-Ord Gi* Z-scores to localize maxima (threshold of 0.125). Initial seed regions from local maxima were expanded based on gene-specific transcript distributions to refine cell boundaries. Segmented cells were filtered by size (excluding >144 bins) and total counts (<10). The tissue was divided into 60 segments: 48 (80%) for parameter optimization and 12 (20%) for testing. Performance was assessed via Leiden clustering quality on segmented cells using Average Silhouette Width (ASW), Calinski-Harabasz Index (CHI), and Davies-Bouldin Index (DBI).

Results: Parameter optimization showed that Gaussian smoothing provided no benefit, whereas an 8-bin radius to capture seed regions from local maxima offered the optimal balance between cell clustering performance and cell detection count. In the independent test set (n=12), HIPSTER demonstrated statistically significant and superior clustering performance compared to bin2cell across all three metrics (ASW, CHI, and DBI). Notably, HIPSTER achieved a higher CHI score, reflecting superior cluster separability, in every single paired comparison without exception. Although HIPSTER detected fewer total cells than bin2cell, this reduction reflects a selective focus on transcriptionally meaningful hotspots, resulting in cleaner boundaries and more biologically coherent clustering.

Conclusion: HIPSTER is a robust and effective transcript-only segmentation tool for high-resolution ST data. By defining cells via functional transcriptomic activity rather than H&E-derived nuclear staining, it significantly outperforms the bin2cell method in distinguishing cell clusters by their expression profiles. This improved separation presents a clear trade-off, as HIPSTER's focus on transcriptional hotspots may result in the non-detection of cells characterized by very low local transcript density.

#6904 OTTER: Optimal transport-based transcriptomics and genomics representation fusion for T-ALL subtyping.

Lusheng Li, Jieqiong Wang, **Shibiao Wan**

University of Nebraska Medical Center, Omaha, NE

T-lineage acute lymphoblastic leukemia (T-ALL) is an aggressive pediatric malignancy that hasn't been fully characterized, partly due to the high prevalence of noncoding genomic alterations driving oncogenic deregulation. Identifying T-ALL subtypes is essential for downstream risk stratification and therapeutic strategy selection. Conventional methods for T-ALL characterization, such as immunophenotyping, cytogenetic analysis, fluorescence in situ hybridization (FISH), and targeted molecular assays, are often labor-intensive, time-consuming, and costly. Furthermore, many T-ALL cases harbor alterations in noncoding genomic regions, which are difficult to detect by standard diagnostic workflows. To address these challenges, we present OTTER (Optimal Transport-based Transcriptomics and gEnomics Representation), a novel multi-modal learning framework that integrates transcriptomics data and genomics data for accurate and cost-effective T-ALL subtyping. OTTER first processed single nucleotide variations (SNVs) and gene expression profiles, respectively, through attention modules to capture the most informative features. Then, it leveraged an optimal transport (OT) method to align and fuse heterogeneous omics modalities, capturing complementary biological information across data types. Based on this, the OT-derived cost matrix learned the cross-modal interdependencies by quantifying the cost of aligning one modality to the other. In this way, OTTER generated a shared latent representation that integrated both omics data, enabling a more comprehensive and coherent representation of each patient sample. Experimental results based on >1,300 T-ALL patients demonstrated that multi-omics integration via OTTER significantly outperformed single omics approaches in subtype classification across performance matrices. In addition, OTTER achieved a substantially higher performance than the baseline models (e.g., ensemble learning models and attention-based models). Furthermore, the embeddings derived from OTTER could more clearly separate different T-ALL subtypes in tSNE visualization compared to approaches without OT, highlighting its ability to uncover subtype-specific molecular features for T-ALL. In summary, OTTER is an accurate and cost-effective framework for T-ALL subtyping that could leverage multi-omics data for improved T-ALL characterization performance. Based on this, we believe OTTER will significantly improve downstream T-ALL patient risk assessment and personalized treatment design.

#6905 Reconstruction of Tumor Clonal Trees with Multi-Sample Bulk Sequencing Data by Integrative Combinatorial Optimization.

Salem Malikic[1], Hamza Iseric[2], Chih Hao Wu[1], Erin Molloy[2], S. Cenk Sahinalp[1]

[1]Cancer Data Science Laboratory, Center for Cancer Research, National Cancer Institute, Bethesda, MD,[2]Department of Computer Science, University of Maryland, College Park, MD

Multi-sample bulk DNA sequencing enables reconstruction of a tumor's clonal history, but scalable methods often rely on heuristic search and provide no optimality guarantees. We present CITUP2, an integrative combinatorial optimization framework that reconstructs clonal trees from descendant cell fractions (DCFs) of mutational clusters. CITUP2 formulates tree inference as a mixed-integer quadratic program (MIQP) that jointly determines the tree topology and clone prevalences across samples. It minimizes a weighted discrepancy between observed and inferred DCFs, with options to prioritize trees exhibiting consistency in the presence-absence patterns of parent-child clones. Under this formulation, CITUP2 returns provably optimal solutions (with respect to the model) and avoids the combinatorial explosion of exhaustive topology enumeration used by existing methods with optimality guarantees. In addition, CITUP2 can report a user-specified number of best trees. In simulations and analyses of a large, recently published multi-sample TRACERx cohort, CITUP2 scales to trees with tens of clones (approximately 30) and matches or improves on the fit attained by state-of-the-art approaches, while providing clear optimality certificates.

#6906 Test-time compute for subtype classification in pediatric T-cell acute lymphoblastic leukemia using transcriptomics.

Tarun Karthik Kumar Mamidi, Irina Pushel, Byunggil Yoo, Midhat S. Farooqi, Keith J. August

Clinical Genetics, Children's Mercy Research Institute, Kansas City, MO

Background: T-cell Acute Lymphoblastic Leukemia (T-ALL) represents a highly aggressive hematologic malignancy characterized by profound molecular and clinical heterogeneity. While current T-ALL subtype classifications may not yet be universally integrated into clinical decision-making, the potential for accurate and rapid classification holds significant promise for future prognostic stratification and guiding targeted therapies. Traditional classification methods can be time-consuming and labor-intensive, highlighting the need for efficient, data-driven approaches. Leveraging transcriptomic data alone, we aimed to overcome these limitations by developing a novel approach for precise T-ALL subtype classification.

Methods: We developed a machine learning pipeline for T-ALL subtype classification from RNA-seq data, introducing test-time compute paradigm. Initially, a Random Forest model was trained on a large discovery cohort (Polonen et al., 2024; 1,112 samples, 24,619 genes) to identify top predictive features by selecting the top 100 genes per subtype. At prediction time, the pipeline dynamically executes: (1) filtering preselected features from both training and test datasets (e.g., TARGET cohort, 264 samples, 22,688 genes); (2) batch correction via pycombat; (3) re-training of the Random Forest classifier on the processed training set; and (4) prediction on processed test data. This test-time pipeline is accessible via a Streamlit WebApp and Command Line.

Results: We used F1 score to evaluate the performance of our classifier. Random Forest on initial training with discovery cohort achieved 93% classifying TAL-like, TLX-like, NKX2-1, ETP-like and 'other' subtypes. Selecting the top 100 features from each subtype yielded 478 features. Benchmarking the performance of our model using these selected features resulted in a 96% F1 score. We then applied our test-time pipeline on the independent TARGET cohort with 264 samples. The final model achieved 83% accuracy across 5 subtypes. Performance was highest for clinically relevant subtypes: TAL-like (F1: 0.96), TLX-like (F1: 0.94), and NKX2-1 (F1: 0.89). The “other” category scored moderately (F1: 0.60), while ETP-like was absent in the validation set.

Conclusion: Our RNA-seq-based model delivers robust, scalable T-ALL subtype classification by leveraging test-time compute, integrating dynamic batch correction and real-time model retraining with a curated 478-gene feature set. Strong performance on an independent cohort highlights its clinical utility as a rapid, reliable tool for precision oncology.

#6907 ecSegCls: Deep learning-based method for detecting extrachromosomal DNAs in both interphase and metaphase cancer cells.

Se Young Chun[1], Hoigi Seo[1], Yoonjoo Nam[2], Dong Un Kang[1], Hyewon Bae[1], Ruda Lee[3], Hoon Kim[4]

[1]Department of Electrical and Computer Engineering, Seoul National University, Seoul, Korea, Republic of,[2]Department of Biopharmaceutical Convergence, Sungkyunkwan University, Suwon, Korea, Republic of,[3]Institute of Industrial Nanomaterial (IINa), Kumamoto University, Kumamoto, Japan,[4]Pharmacy, Sungkyunkwan University, Suwon, Korea, Republic of

Extrachromosomal DNA (ecDNA) is an acentric circular DNA element that derives from but exists independently of chromosomes. EcDNAs often carry oncogenes with high copy numbers, contributing to tumor heterogeneity, and poor patient outcomes. Whole genome sequencing provides genome-wide detection of ecDNAs but lacks spatial resolution, while imaging methods such as fluorescence in situ hybridization (FISH) capture spatial context but rely on labor-intensive manual annotation by experts. Existing tools for automated detection of ecDNAs from FISH, such as ecSeg, partially address this limitation but remain restricted to metaphase cells, demonstrating modest classification performance. Here, we present ecSegCls, an automated pipeline for segmenting and classifying ecDNA in FISH and DAPI images with high accuracy. Our proposed method exploits both deep learning-based segmentation model and its extracted features, as well as XGBoost-based classification model, leading to the pipeline of segmenting nuclei, chromosomes, and ecDNA regions, and predicting the presence of ecDNA in both metaphase and interphase cells. Data augmentation and noise simulation were used for improved robustness and segmentation-derived features were used for training an XGBoost classifier. Ablation studies further identified key predictive features, enhancing interpretability. Using a public dataset of 483 FISH images from cancer cell lines as a model training set and a dataset of 776 FISH images internally generated 8 cancer cell lines as a classification set, we assessed and compared the performance of our model with those of previously published architectures, including UNet, UNet++, DeepLabV3+, Swin UNet, FATNet, HiFormer, DAEFormer, and ecSeg. Our proposed ecSegCls has achieved remarkable qualitative and quantitative performance, yielding high performance on diverse regions with diverse metrics in both segmentation and classification benchmarks, thus establishing ecSegCls as a robust and scalable automated framework for accurate ecDNA detection, advancing imaging-based research and clinical applications with ecDNA.

#6908 Large-scale patient cohorts integration via a novel Bayesian transfer learning framework identifies robust drug response signatures in AML.

Dharani Thirumalaisamy[1], Evan F. Lind[2], Elie Traer[3], Jeffrey W. Tyner[4], Mehmet Gonen[5], Olga Nikolova[6]

[1]Biomedical Engineering, Oregon Health & Science University, Portland, OR,[2]Molecular Microbiology and Immunology, Oregon Health & Science University, Portland, OR,[3]Division of Hematology/Medical Oncology, Oregon Health & Science University, Portland, OR,[4]Cell and Developmental Biology Program, Oregon Health & Science University, Portland, OR,[5]College of Engineering, Koc University, Istanbul, Turkey,[6]Division of Oncological Sciences, Oregon Health and Science University, Portland, OR

Introduction: Transfer learning considers distinct but related tasks defined over heterogeneous domains like patient or organoid data, and improves generalization and predictive performance through knowledge transfer between tasks. It can be especially advantageous in applications where training data is limited (i.e. small patient cohorts), where joint learning across domains can enable inference in otherwise underpowered datasets.
Methods: We present a novel Bayesian transfer learning framework that supports multi-task and multi-modal learning across scales, from bulk to single-cell resolution. Our approach is generative and learns latent space representation within each domain, simultaneously across multiple domains, using a feature-wise prior (e.g. genes, drugs, cellular programs) to model complex non-linear relationships. Our model can be pre-trained on an unlimited number of patient cohorts or new approach methodology (NAM) datasets from diverse assay bulk or single-cell platforms to make predictions in previously unseen samples.
Results: We apply our method to predict drug response and identify gene signatures for therapy stratification in acute myeloid leukemia (AML). We benchmark our model's performance in a battery of experiments and compare to five existing approaches. By integrating disjoint large-scale patient cohorts, we enable robust statistical inference in an otherwise underpowered dataset (N=29). Our model successfully transferred information even from cohorts with molecularly characterized samples that lacked matched drug response to inform and improve predictions in other cohorts with statistical significance and impactful effect size. Our approach was especially effective in modeling multi-kinase inhibitors, where our feature-wise priors captured multi-target interactions.
Conclusion: Our novel approach enables joint learning across unlimited number of patient cohorts and other multi-omic and functional data domains and scale. In AML we achieve significant improvements in drug response accuracy and gene signature identification and enable robust statistical inference in very small patient cohorts. Our framework is scalable, interpretable, and adaptable across target phenotypes, offering a robust solution for a wide range of heterogeneous problems.

#6909 Dimensionless, null-calibrated spatial indices from Xenium RNA and protein in breast IDC and lung adenocarcinoma.

Jinghao Tian[1], Tommy Tran[2], Elim Cheung[2], Rikita Gakhar[2], Vidyodhaya Sundaram[2]

[1]Johns Hopkins University, Baltimore, MD,[2]BioChain Institute, Inc., Newark, CA

Spatial features of the tumor-immune microenvironment, including immune exclusion at tumor borders, tertiary lymphoid structures, and checkpoint engagement, shape local control and treatment response, yet routine single-marker IHC or bulk assays miss single-cell context and cell-cell interactions. Same-section spatial multi-omics now measure transcriptome (RNA) and proteome (protein) in interacting cells. Compact metrics are designed from these data to compare regions and cases. Two Xenium slides from FFPE tissue were profiled, each including paired primary tumor (PT) and adjacent normal (PN) regions from breast invasive ductal carcinoma and lung adenocarcinoma using a Human Immuno-Oncology panel plus six protein subpanels. Regions of interest (ROIs) were the analysis unit. Cell types were annotated with SingleR against public single-cell references, and spatial morphologies were inspected. Segmentations showed expected differences: PT breast was dominated by luminal epithelium with stromal and immune heterogeneity, whereas PN breast was fibroblast rich. Lung samples contained epithelial, fibroblast, endothelial, and immune populations with shifts between PT and PN, providing diverse microenvironments on which spatial indices were computed. Three dimensionless indices quantified complementary features of the tumor-immune microenvironment. The Exclusion Index (EI) integrates reduced CD8 T-cell penetration into tumor nests with peritumoral macrophage enrichment and diminished antigen-presenting-cell ingress. The TLS Score identifies B/T aggregates consistent with tertiary lymphoid structures, supported by local chemokine signal and simple maturity surrogates. The Checkpoint Contact Index (CCI) quantifies adjacency between PD-1-positive T cells and PD-L1-positive tumor or myeloid neighbors within a small radius compared with ROI label-shuffle spatial nulls. For all indices, values were centered on PN regions within each case, converted to z-scores within tumor type, and scaled 0-1. The pipeline produced coherent cell-typing and index summaries that aligned with visible histology and tumor-normal heterogeneity, providing a quantitative complement to descriptive reads. Grounding the indices in same-section RNA and protein and explicit spatial nulls yields a practical framework for reporting tumor-immune microenvironment on small-N slides and a common language transferable across studies and pathology teams.

#6910 Consistency-guided diffusion reconstruction enhances peri-hepatic tumor visibility in magnetic particle imaging.

Gen Shi[1], Ziwei Chen[1], Yimeng Li[1], Zeyu Zhang[1], Xin Feng[2], Jie Tian[3]

[1]Beihang University, Beijing, China,[2]Institute of Automation，Chinese Academy of Sciences, Beijing, China,[3]Key Lab of Molecular Imaging, Chinese Academy of Sciences, Chinese Academy of Sciences, Beijing, China

Background: Magnetic Particle Imaging (MPI) is radiation-free and highly sensitive, enabling quantitative tracking of superparamagnetic tracers, which makes it attractive for tumor imaging. In abdominal applications, SPIO tracers accumulate in the liver via hepatic metabolism, creating dominant background that obscures nearby lesions and suppresses tumor contrast. To address this from the reconstruction side, we propose a consistency-guided diffusion method that couples a learned prior with the MPI forward model to recover concentration-faithful peri-hepatic images, without altering hardware or tracer formulation.
Methods: We implement a consistency-guided diffusion procedure that alternates two steps: (i) denoising by a generative diffusion prior trained on abdominal slices, and (ii) a lightweight projection that enforces agreement with measured signals under the MPI forward operator u=Sx. A null-space stabilization term moderates trajectories when liver-tumor concentration disparity is large. Training data are synthesized from public abdominal datasets by extracting liver and tumor masks, deriving concentration maps, and forming z-axis slices; simulated signals are generated with additive white Gaussian noise. Evaluation covers (a) peri-hepatic simulation cases and (b) 3D-printed liver-tumor phantoms filled with SPIOs on an in-house MPI system. Baselines include Kaczmarz, conjugate gradient, ADMM, and a deep-equilibrium reconstruction.
Results: The proposed approach improves fidelity and structure preservation versus classical solvers (higher PSNR/SSIM and lower error) and reduces the over-smoothing typical of equilibrium-based methods. In phantom studies with 5 mm and 2 mm tumor-liver separations, reconstructions exhibit suppressed background streaks/rings and clearer lesion edges, yielding consistent visual detectability across separations. Runtime overhead is modest: a single CG update per diffusion step suffices to maintain consistency. We also applied the method to in vivo human stem-cell MPI imaging experiment, yielding encouraging results and suggesting potential utility for stem cell-based cancer therapies.
Conclusions: Consistency-guided diffusion reconstruction improves peri-hepatic lesion visibility in MPI under strong liver background while remaining software-only and system-agnostic. Its low operational cost and compatibility with existing scanners and tracers support translational potential for liver-adjacent oncologic imaging.

#6911 Frequency-domain signal separation network improves dual-tracer detection of aneurysm regions in magnetic particle imaging.

Ziwei Chen[1], Yimeng Li[1], Gen Shi[1], Jian'an Ye[1], Zeyu Zhang[1], Xin Feng[2], Yu An[1], Jie Tian[1]

[1]Beihang University, Beijing, China,[2]Institute of Automation, Chinese Academy of Sciences, Beijing, China

Aneurysms are vascular abnormalities characterized by marked structuralheterogeneity, and their rupture risk is closely associated with regional dilation, focalweakening, and inflammatory activity. Therefore, reliably distinguishing normalvessels from aneurysm-affected regions is essential for aneurysm detection, regionalvisualization, and lesion assessment. Compared with existing medical imagingtechniques such as magnetic resonance imaging (MRI) and computed tomography(CT), Magnetic Particle Imaging (MPI) offers unique advantages including zero tissuebackground, high sensitivity, real-time imaging, and excellent quantitative capability,making it well suited for multi-tracer vascular imaging. Different superparamagneticiron oxide (SPIO) tracers exhibit inherent differences in magnetic properties andmagnetization dynamics, providing the physical basis for multi-tracer MPI; however,noise, cross-talk, and signal imbalance in practical measurements can obscure thesedifferences and hinder accurate dual-tracer separation. To enhance the reliability ofmulti-tracer MPI, we propose a frequency-domain dual-tracer separation framework,the Frequency-Domain Signal Separation Network (FSS-Net).FSS-Net maps raw MPI signals into a two-dimensional harmonic-frequencyrepresentation, predicts tracer-specific masks through a separation module, andreconstructs interference-free dual-channel harmonic signals using afrequency-domain decoder. To validate its performance, we constructed a dual-traceraneurysm phantom in which normal vessel regions and aneurysm lesions were labeledwith different SPIO tracers, simulating heterogeneous nanoparticle distribution indiseased versus healthy vasculature. FSS-Net was compared with two establishedmulti-color MPI methods—System Matrix Concatenation (SM Cat) and MKZ.Quantitative evaluation using PSNR and SSIM showed that FSS-Net significantlyoutperformed both methods in signal fidelity and structural preservation, effectivelyreducing cross-talk and improving visualization of normal vessels andaneurysm-affected regions.Overall, FSS-Net enables high-quality dual-tracer MPI signal separation and offers areliable approach for aneurysm region detection, regional visualization, andnanoparticle distribution analysis, demonstrating strong potential for vascularpathology imaging and nanoparticle-based biomedical research.

#6912 Phasing tumor clones by timing point mutations using bulk long-read sequencing.

Ataberk Donmez, Mikhail Kolmogorov

National Cancer Institute, Bethesda, MD

Cancer cells differ from healthy cells due to somatic aberrations (e.g., somatic mutations or structural variations). Studying these mutations helps us better understand tumor evolution and opens the way to more effective treatment strategies. Cancer cells exhibit heterogeneity across different populations, even within a single tumor, and these populations are defined by their unique somatic mutations. Given a set of somatic mutations -some shared across different clones and some unique- determining which mutations co-occur enables phasing of tumor clones. Ultimately, phasing these mutations from bulk sequencing data is crucial for studying tumor evolution.

SNVs and short indels are the most common somatic mutations in tumor cells and even though these mutations can be effectively detected with short reads, linking nearby mutations remains challenging due to the nature of these reads. On the other hand, long reads have been successfully used in direct phasing of germline variants into megabase-scale phase blocks by enabling linkage of distant SNVs and thus shows promise for phasing somatic variants.Reconstruction of tumor clones is a multi-allelic phasing problem. Obtaining a phylogeny of detected somatic point mutations (PM) is a first step in phasing these mutations into different clones where nodes in the constructed phylogeny correspond to possible clonal haplotypes. For this purpose, we propose timing pairs of PMs against each other based on their co-occurrences in the reads that cover both locations and whether these reads support the reference or alternate allele. Given two point mutations and a set of reads that cover these two positions; it is possible to deduce whether these two mutations occurred one after the other in the same branch, co-occurred together, or occurred in different branches (i.e., divergent). Since timing of PM pairs are transitive, it is possible to obtain longer chains by timing PM pairs that are not connected by reads. We represent these relationships as a graph where PMs are nodes and each type of relationship is represented by a different edge.

We applied our approach to H2009 and H1437 cell lines from the CASTLE collection (https://github.com/CASTLE-Panel/castle) with regular and ultra-long (100kb+) Oxford Nanopore reads. Although these cell lines are less heterogeneous compared to typical real tumor samples, phasing somatic mutations can also distinguish duplicated chromosome copies. For H1437 and H2009 cell lines, we detected a total of 87,999 and 162,334 somatic SNPs. The graphs constructed with these SNPs contained connected components with median spans of 102Kb and 55Kb (maximum: 9.5Mb and 6.4Mb). For both cell lines, connected components had a median of 2 (maximum: 56 and 80) haplotypes. Of these detected haplotypes, median of 1 for both cell lines (maximum: 23 and 46) consists of multiple SNPs. We plan to extend our approach to include timing of structural variations.

#6913 Unbiased cell type identification and biological interpretation of spatial molecular data.

Filippo Pullara[1], Raymond Yan[1], Brian Falkenstein[1], A. Burak Tosun[1], S. Chakra Chennubhotla[2]

[1]PredxBio, Inc., Pittsburgh, PA,[2]PredxBio, Inc. / University of Pittsburgh, Pittsburgh, PA

Background: While pre-defined, or biased, phenotyping algorithms are a popular approach for analyzing spatial molecular data, offering ready biological interpretation (e.g., CD8+ T-cells, CD68+PD-L1+ macrophages) and reproducibility across labs with consistent threshold choices, they suffer from subjectivity, coarseness, and an inability to capture emergent biology. Conversely, unbiased phenotyping algorithms have the potential to address these limitations, but they currently lack straightforward biological interpretability.
Methods: Our SpaceIQ™ multi-omics platform performs recursive cell typing (RCT) instead of standard hierarchical clustering and other graph-based algorithms for unbiased cell identification. RCT leverages the wide dynamic range (variance) in spatial proteomics, transcriptomics, and morphology data, driven by protein abundance and other technical factors, as biologically insightful. Unlike normalized standard methods, RCT allows markers with larger variances to drive early differentiation, with smaller-variance markers defining subsequent subpopulations.
Results: We demonstrate the broad applicability of RCT using the SpaceIQ™ platform across three publicly available spatial datasets, including proteomics, transcriptomics, and brightfield pathology. To facilitate biological interpretation of the resulting unbiased cell populations, RCT approach: (i) identifies discriminatory biomarker signatures for annotating each RCT; (ii) calculates the probability of pre-defined phenotypes within any unbiased cell type; and (iii) generates a minimal marker panel that can approximate any given unbiased cell type with high probability.
Conclusions: Unbiased cell typing, achieved through RCT, is critical in cancer research. This approach ensures the representation of all cell states—rare, abundant, positive, negative, and transitional—regardless of antigen expression. By not relying on extensive cell-type specific training, it is uniquely suited to capture the full spectrum of cellular heterogeneity.

#6914 STCS: Spatial transcriptomics cell segmentation outperforms existing methods on multiple slides.

Xinyu Hu[1], Fengwei Zhan[1], Lixia C. Wu[1], Jose Gonzalez[1], Chuhanwen Sun[1], Rachel Ofer[1], Tyler Tran[2], Michael Verzi[1], Jiekun Yang[1]

[1]Department of Genetics, Rutgers University, New Brunswick, NJ,[2]Quantitative Biomedicine Program, Rutgers University, New Brunswick, NJ

Spatial transcriptomics (ST) has long been recognized as an advanced technique that provides insights on spatial information beyond what can be obtained from single-cell RNA sequencing. However, widely used sequencing-based ST approaches cannot provide cell level data because their results are aggregated into discrete bins rather than assigned to individual cells. With the advent of Visium HD and other subcellular-resolution platforms, accurate cell segmentation has become essential for extracting biologically meaningful, cell-level information.Here, we present STCS (Spatial Transcriptomics Cell Segmentation), a segmentation framework tailored for high-resolution ST data. We benchmarked STCS against several existing methods—including STHD, bin2cell, and Space Ranger—using a slide with both Visium HD and Xenium results. Evaluation using ground-truth Xenium cell boundary annotations demonstrated that STCS delivers the best performance, achieving 40% accuracy in cell-type prediction and showing the lowest spatial chaos score, a metric that quantifies how spatially continuous clusters are. We also applied STCS to another Visium HD slide from mouse intestinal regeneration model which contains tissue from different time points after radiation. Compared to default Visium HD binning, STCSsegmented cells show clear transcriptional differences by timepoints and identify several rare immune cell types. As a result, downstream analyses such as spatial cell-cell interaction inference and regional pattern characterization can be done in cell level which include more cell types and more immune related pathways like JAK-STAT pathway with STCS.
In addition, STCS is versatile and can be applied to other sequencing-based ST methods like Stereo-seq, which offers nanometer-scale resolution. And it's also an open-source tool with adjustable parameters for different tissue types.In summary, STCS is a robust and flexible cell segmentation tool that provides a one-stop solution for deriving biologically meaningful, cell-level information from high-resolution sequencing-based ST datasets.

#6915 Investigating the role of the conserved notch pathway in glioblastoma cells.

Larissa Barroso[1], Megan E. Keniry[2]

[1]University of Texas Rio Grande Valley - UTRGV, Edinburg, TX,[2]University of Texas Rio Grande Valley, Edinburg, TX

Glioblastoma (GBM) remains the most aggressive primary brain cancer, representing nearly 50% of all brain malignancies, with a median survival of less than 15 months. Our lab has identified a role for the FOXO4 transcription factor in maintaining a stem-like phenotype in GBM. To further investigate this novel role, we performed RNA sequencing on *FOXO4* knockout U87MG cells generated in our laboratory using CRISPR Cas9 mutagenesis. We found that loss of *FOXO4* in U87MG cell lines altered the expression of *NOTCH3* and its downstream targets, such as *CCND1*. Furthermore, exogenous *NOTCH3* induced *CCND1* expression in U87MG cells. These preliminary findings suggest that FOXO4 transcriptional activity may influence glioblastoma aggressiveness at least in part by modulation of *NOTCH3* activation. Ongoing studies aim to confirm whether the FOXO4–NOTCH3 axis is essential for maintaining stem-like states in GBM cells. Elucidating this interaction could uncover novel molecular targets for therapeutic intervention and advance our understanding of GBM pathogenesis.

: Antibody-Drug Conjugates 2
Poster Session

#6920 Preclinical development of a first-in-class CD64-ADC to target leukemic monocytes and tumor-associated macrophages.

Lia Buffa[1], Cintia Garro[1], Constanza Marin[2], Alejandra Garcia[2], Diego Andino[1], Melisa Capitanelli[2], Laura Bertoldi[2], Florencia Villafanez[2], Natalia Monjes[2], Agustina Garcia-Melani[2], Laura Guantay[2], Daniela Arroyo[2], Alejandro Moyano[2], Gimena Ferreira[3], Belkys Marelli[4], Tarek Zaki[1], Gerardo Gatti[2], Candelaria Llorens de los Rios[2], **Gaston Soria**[1]

[1]OncoPrecision, New York, NY,[2]OncoPrecision, Cordoba, Argentina,[3]Sanatorio Allende, Cordoba, Argentina,[4]ICIVET-LITORAL, CONICET-UNL, Esperanza - Santa Fe, Argentina

Cells of the monocytic lineage are involved in the pathophysiology of several human cancers. In myeloid hematologic malignancies such as chronic myelomonocytic leukemia (CMML) and monocytic AML (M4/M5 FAB subtypes), leukemic monocytes display poor response to standard of care treatments and dismal complete remission rates. In solid tumors, tumor-associated macrophages (TAMs) are critical cells of monocytic origin that promote an immunosuppressive tumor microenvironment in malignancies such as TNBC, PDAC, and GBM, thereby driving tumor growth and resistance to PD-1/PD-L1 blockade. Interestingly, both leukemic monocytes and TAMs share a highly differentiated phenotype and a low proliferative capacity, which render them refractory to the mechanism of action (MOA) of established chemotherapeutic regimens. Therefore, identifying druggable targets with broad expression across the monocytic maturation lineage is a promising strategy for designing antibody-drug conjugates (ADCs) aimed at overcoming monocyte-driven resistance.
In this work, we leveraged OncoPrecision's Patient Micro-Avatar (PMA) ex vivo platform to validate novel targets and the optimal payload to develop an ADC to target leukemic monocytes and TAMs. This screening campaign identified CD64 as a target with high expression and druggability in patient-derived monocytic-cells and unveiled PNU-159682 (PNU) as the payload with the optimal MOA to deplete monocytic cells. Intriguingly, payloads with proven clinical success in other malignancies, such as Exatecan and MMAE, displayed poor/null activity against leukemic monocytes and TAMs, thus highlighting a non-obvious vulnerability of monocytic cells to PNU.
ONC001, our first-in-class ADC conjugated to PNU through a non-cleavable linker displays picomolar activity against a panel of monocytic cell lines in vitro and against patient-derived leukemic monocytes and TAMs ex vivo. Multiple in vivo models of leukemia and solid tumors also confirmed a remarkable efficacy and selectivity of ONC001, including a humanized mouse model in which TAMs from the TME of established xenografted tumors were efficiently depleted after a single injection of the ADC. Importantly, we extensively investigated the safety of ONC001 by evaluating its on-target and off-target activity in multiple animal models, and observed remarkable tolerability with no signs of toxicity. Together, these preclinical findings demonstrate a favorable therapeutic index for ONC001, supporting its potential as a powerful agent for depleting pathogenic monocytes in cancer treatment.

#6921 Phosphonate-antibody-drug conjugates, a novel immunostimulatory class of ADCs driving inside-out activation of Vγ9Vδ2 T cells leading to selective tumor cell killing.

Mary J. van Helden, Genny Filliciotto, Wendela A. Kappers, Diels van den Dobbelsteen, Panagiota I. Spantidea, Marga Gunnewijk, Myrthe Rouwette, Anja Scholzen, Seline A. Zwarthoff, Stefanie J. J. Bartels, Sebastiaan Birkedal, Sanne H. C. van den Ouweland, Ellen W. H. Santegoeds-Lenssen, Robbin Tebes, Menno Winkel, Marc C. B. Parade, Lilian Driessen-Engels, Karin de Laat-Arts, Ivan Faraho, Inge M. J. Reinieren-Beeren, Giel Verhagen, Dorian van Kuijk, Daphne W. J. van Kuppeveld, Benny de Wit, Gijs Verheijden, Ruud Ubink, Benno Ingelse, Miranda M. C. Van der Lee, **Wim H. A. Dokter**

Byondis B.V., Nijmegen, Netherlands

Gamma delta (γδ) T cells are cytotoxic effectors capable of recognizing and eliminating tumor cells independently of major histocompatibility complex (MHC) presentation. Their presence within tumors correlates with improved clinical outcomes across various cancer types. Vγ9Vδ2 T cells, the predominant γδ subset in human blood, recognize intracellular phosphoantigens (pAgs) through inside-out activation of the butyrophilin (BTN)3A/BTN2A complex. Clinical trials have previously been conducted using aminobisphosphonates or synthetic pAgs, either alone or in combination with low-dose interleukin-2 (IL-2); however, these compounds lack tumor specificity and are limited by a very short plasma half-life *in vivo*. To address the lack of tumor targeting and short half-life, we engineered antibody-drug conjugates (ADCs) that selectively deliver phosphonates to tumor cells, enabling inside-out activation of Vγ9Vδ2 T cells. These phosphonate-ADCs consist of a monoclonal antibody directed against a tumor-associated antigen (TAA), conjugated to a phosphonate payload via a linker that is cleavable by lysosomal proteases. We applied this strategy to various TAA-targeting antibodies, including CD123, CD20, TROP2 and HER2 directed IgG1-based monoclonal antibodies. TAA-positive tumor cell lines pretreated with phosphonate-ADCs effectively triggered Vγ9Vδ2 T cell activation through a BTN3A-dependent mechanism. This activation led to robust cytokine secretion, degranulation, and efficient tumor cell lysis. Vγ9Vδ2 T cell activation was successfully replicated with *ex vivo* patient tumoroids (EVPTs) and autologous peripheral blood mononuclear cells (PBMCs), supporting the translational relevance of this approach. In an acute myeloid leukemia (AML) adoptive transfer mouse model, Vγ9Vδ2 T cells significantly reduced the tumor burden in the presence of the tumor-targeting phosphonate-ADC. In cynomolgus monkeys, the lead phosphonate-ADC candidate displayed excellent tolerability at a single dose of up to 100 mg/kg, with no clinical signs of cytokine release syndrome (CRS). Immunostimulatory phosphonate-ADCs represent a novel strategy for targeted, physiologically relevant activation of Vγ9Vδ2 T cells by delivering phosphonates directly to tumor cells. This modular platform can be combined with virtually any tumor-targeting monoclonal antibody with the possibility to preserve Fcγ receptor-mediated effector functions. The resulting dual mechanism, integrating the antibody's direct anti-tumor activity with the immune-stimulatory properties of the phosphonate payload, offers a versatile and powerful therapeutic modality. Overall, this platform holds significant promise not only for targeted cancer immunotherapy but also for potential applications in other disease areas.

#6922 BHB810: A novel site-specific CDH17-directed VHH-Fc ADC for gastric cancer.

Ryan Henrici, Timothy Park, Melanie Montgomery, Barbara Steurer, Danielle Barreras, Natalie Alba, Srujan Vadlamudi, Hunter Elliott, Jon Wojciak, John Corbin, Peyton Greenside

BigHat Biosciences, Inc., San Mateo, CA

Background: Gastric cancer remains a significant and growing cause of morbidity and mortality globally, with nearly 1 million newly diagnosed patients each year. Treatment paradigms are limited to checkpoint inhibitors, angiogenic blockade, and conventional chemotherapy, with few patients achieving durable responses. HER2 and CLDN18.2 directed therapies represent breakthroughs but substantial unmet need remains. CDH17 represents one of the most widely expressed tumor-associated antigens, offering the potential to treat 50-60% of patients with gastric cancer, including a substantial population of those without HER2 or CLDN18.2 expression.

Methods: A single domain VHH anti-CDH17 antibody was engineered using BigHat's Milliner platform for optimal internalization, humanized, and subsequently conjugated to MMAE via a site-specific and serum-stable, enzyme-cleavable linker using GlycoConnect SYNstatin E technology. The antibody drug conjugate (ADC) was subsequently interrogated in vitro and in vivo, including in cynomolgus macaques as part of a comprehensive preclinical therapeutic research program.

Results: BHB810 is fully cross-reactive to human, cyno, and rodent orthologues and features robust and maximized internalization within 24 hours. The VHH-Fc fusion was conjugated to achieve a homogeneous DAR 4 with remarkable serum stability, providing a significantly enhanced therapeutic window compared to typical maleimide-vedotin conjugates. Compared to a benchmark clinical-stage CDH17-directed IgG ADC that rapidly loses payload via retro-Michael addition, BHB810 features no detectable deconjugation, payload transfer, or payload loss in human serum. The humanised VHH-Fc fusion backbone of BHB810 is 50% smaller than a typical IgG, resulting in superior tissue penetration. In PDX models, BHB810 leads to complete or near-complete tumor clearance in a panel of 13 different primary gastric cancers, including those with low and heterogeneous antigen densities. Preclinical modeling of pharmacokinetics and safety demonstrate a multi-day half-life, superior tolerability, and no evidence of on-target toxicities in non-malignant organ systems compared to benchmarks. In vivo imaging demonstrates robust target engagement and on-target ADC accumulation with reduced plasma exposure. BHB810 was evaluated in a 1 month GLP primate toxicity study exploring doses up to 5 mg/kg q2w (10 mg/kg of a conventional IgG ADC). No MTD was reached.

Conclusion: BHB810 is a novel, potentially best-in-class CDH17-directed ADC for the treatment of advanced gastric and other GI malignancies. The molecule was engineered on BigHat Biosciences's AI/ML-powered antibody design platform to maximise ADC internalization and potency against cells that express CDH17. First-in-human studies are planned for 2026, prioritizing patients with gastric cancer.

#6923 Targeting tumor-specific Tn-glycoforms of MUC1 and MUC4 with first-in-class antibody-drug conjugates: Preclinical efficacy and translational potential of GO-M100B and GO-M400.

Nisha Shrestha[1], Aaron Christopher Groen[1], Boris Klebanov[1], Constantine Theodoropulos[1], **Hans H. Wandall**[2]

[1]GO Therapeutics, Cambridge, MA,[2]University of Copenhagen, Copenhagen, Denmark

Aberrant O-glycosylation in epithelial cancers generates tumor-specific neoepitopes absent from normal tissues. GO Therapeutics has developed monoclonal antibodies that selectively recognize these Tn-glycoforms on mucins, including GO-M100B, targeting Tn-MUC1, and GO-M400, targeting Tn-MUC4. These antibodies bind aberrantly truncated O-glycans presented on mucin backbones with sub- to low-nanomolar affinity and exceptional site-specificity. These programs exemplify our “clean target” approach that exploits cancer-restricted glycoepitopes to enhance selectivity and therapeutic index. Structural and biochemical characterization revealed that M100B and M400 recognize proprietary glycopeptide neoepitopes unique to malignant epithelial cells, enabling precise tumor targeting. Immunohistochemistry confirmed broad reactivity across epithelial cancers. This includes breast, lung, ovarian, pancreatic, and gastrointestinal tumors. Negligible binding was seen to normal tissues. Both antibodies were engineered as site-specific antibody-drug conjugates (ADCs) using an mc-vc-PAB-MMAE linker to generate homogeneous DAR2 conjugates. These ADCs exhibited potent, selective cytotoxicity against Tn-positive cell lines, achieving sub-nanomolar IC_{50} values, while showing no measurable activity in Tn-negative or primary normal cell models. In vivo, M100B-vedotin and M400-vedotin induced marked tumor regression in both cell-derived (CDX) and patient-derived xenograft (PDX) models, with favorable pharmacokinetics and clean toxicology profiles in cynomolgus monkeys and mice. By targeting cancer-specific glycosylation patterns on mucins, M100B and M400 expand the therapeutic frontier of “clean target” oncology. These next-generation ADCs demonstrate exceptional tumor selectivity, strong preclinical efficacy, and favorable safety, supporting advancement into IND-enabling studies and clinical development for multiple epithelial malignancies.

#6925 Leveraging AI-enhanced multi-omics discovery of novel tumor-selective targets for ADC development.

Daniel Montoro, **Christoph Muus**, Karthik Jagadeesh, Cecile Rouleau, Yueyue Shi, Sho Takahashi, James Meador, Ritika Singh

Research and Development, TenSixty Biosciences, Cambridge, MA

TenSixty Biosciences employs an innovative AI-enhanced multi-omics discovery framework to enable the development of next-generation antibody-drug conjugates (ADCs). This integrated approach identified novel tumor-selective targets with high therapeutic potential by combining:
1. Multi-dimensional omics analysis integrated with advanced AI analytics to uncover therapeutically relevant cancer targets
2. Specialized proteomic profiling focused on unique post-translational modifications (PTMs) that reveal tumor-specific variants of targets, enabling enhanced tumor-selective targeting
3. Proprietary antibody discovery and engineering generates tumor-selective antibodies directed against these variants, yielding highly potent ADC candidates
Applied to small cell lung cancer (SCLC), this framework identified a novel therapeutic target exhibiting tumor-specific hypoglycosylation. Antibodies directed against the epitope exposed by altered glycosylation showed exceptional tumor selectivity and markedly enhanced ADC efficacy. AI-driven integration across discovery and development stages further accelerated target validation and candidate optimization.

#6926 An AI-guided biparatopic DLL3-targeting ADC demonstrates enhanced preclinical efficacy.

Chuan Chen, Yue Wu, Chenpeng Su, Zhaohui Chen, Dandan Liu, Jiyuan Tian, Xiaoqian Chen, Yang He, Yongxin Shang, Rongmei Yan, Liang Tian, Jian Peng, Zhenping Zhu

Earendil Labs, Wilmington, DE

Purpose This study aimed to develop a novel biparatopic antibody-drug conjugate (ADC) targeting delta-like ligand 3 (DLL3) for small cell lung cancer (SCLC) and other neuroendocrine neoplasms, addressing limitations of previous DLL3-targeted therapies.
Methods Leveraging our AI-guided antibody development platform, we engineered a biparatopic anti-DLL3 antibody with optimized binding and internalization properties. The antibody was conjugated with various linker-payload combinations. In vitro cytotoxicity of the ADCs were evaluated using DLL3-expressing cell lines and in vivo efficacy were assessed using CDX mice models. Safety was assessed in transgenic mice and non-human primates.
Results The biparatopic antibody demonstrated higher internalization efficiency compared to the monoclonal antibody counterparts. The ADC showed potent cytotoxicity across multiple DLL3-expressing cell lines and achieved significant tumor suppression in CDX models. Toxicological studies revealed a favorable safety profile in both transgenic mice and non-human primates.
Conclusion This biparatopic ADC represents a promising therapeutic candidate for DLL3-expressing tumors, demonstrating enhanced efficacy and favorable preclinical safety compared to previous approaches.

#6927 ADCE-T02 - A clinical stage antibody drug conjugate targeting tissue factor demonstrates strong efficacy in preclinical models of head and neck squamous cell carcinoma.

Thomas Tuxen Poulsen[1], Olga Ilina[1], Pernille Barkholt[1], Daniela Pontieri[1], Jette Bomholt Lange[1], Jonathan Henry Wardman[1], Christophe Come[1], Christina Hjaresen[1], Shu-Hui Liu[2], Xun Meng[3], Yue Zhang[3], Dominik Mumberg[1]

[1]Adcendo ApS, Frederiksberg, Denmark,[2]Multitude Therapeutics, Redwood City, CA,[3]Multitude Therapeutics, Shanghai, China

Tissue Factor (TF, F3, coagulation factor III, thromboplastin, or CD142), a membrane protein involved in blood coagulation, demonstrates confined expression to the perivascular compartment in healthy tissues but is over-expressed in many solid tumors, making it an attractive target for Antibody Drug Conjugates (ADC). The TF-targeted ADC Tisotumab vedotin is approved for treatment of cervical cancer and has demonstrated efficacy in Head and Neck Squamous Cell Carcinoma (HNSCC)[1], but treatment is limited by substantial side effects including ocular toxicities, peripheral neuropathy, and bleeding warranting development of a more efficacious and better tolerated modality.

ADCE-T02 is a clinical stage TF-targeted ADC composed of a humanized anti-TF antibody specifically designed to limit the impact on blood coagulation, conjugated via a novel T1000 linker moiety to the Topoisomerase-1 inhibitor Exatecan payload at a drug-to-antibody ratio of ~4.

The expression level of TF was evaluated in patients with HNSCC, confirming broad and high TF expression in the majority of tumors, regardless of Human Papilloma Virus (HPV) status. *In vitro,* the efficacy of ADCE-T02 was evaluated and confirmed in a panel of HNSCC tumor cell lines with varying TF expression levels. *In vivo,* ADCE-T02 also demonstrated strong anti-tumor activity in both cell line and patient derived HNSCC xenograft models with varying TF expressions. Intriguingly, strong efficacy of ADCE-T02 (dosed from 1 mg/kg) was observed in HNSCC tumors expressing high levels of Epidermal Growth Factor Receptor (EGFR) but with limited response to anti-EGFR therapy. Furthermore, administration of a single dose of ADCE-T02 to mice bearing large tumors (≥1000mm^3) caused remarkable tumor shrinkage often resulting in complete tumor eradication. In addition, strong antitumor responses of a single dose of ADCE-T02 were observed in large tumors growing out following anti-EGFR therapy.

In summary, ADCE-T02 demonstrates broad efficacy in HNSCC models with varying levels of TF expression including models resistant to EGFR targeted agents. A phase I clinical study of ADCE-T02 in patients with advanced solid tumors is currently ongoing and actively recruiting (Clinical Trial ID NCT06597721).

[1]Sun et al., J. Clin. Oncol.; 42 (16 suppl.); 2024

#6928 Dual-payload antibody drug conjugate targeting TROP2: Multi-Payload Conjugates™ targeting orthogonal mechanisms of cell killing.

Marco Lobba[1], Samantha Brady[1], Devin Trinter[1], Maxwell Nguyen[1], Chanez Symister[1], Andrew Lau[1], Derek Garcia-Almedina[1], Charlotte Choi[1], Saurabh Johri[1], Matthew Francis[2], Richard Kendall[1]

[1]CatenaBio, Berkeley, CA,[2]Chemistry, University of California at Berkeley, Berkeley, CA

Introduction: Antibody-Drug Conjugates (ADCs) have a tremendous impact on patient outcomes in breast and other cancers. Dato-DXd, for example, is a 2nd-line therapy for stage IV, HR+/HER2 negative metastatic breast cancer and EGFR mutant non-small cell lung cancer (NSCLC). Sacituzumab govitecan (SG), is approved as a 3rd line therapy in metastatic HER2 negative breast cancer. Many patients fail to respond or relapse after treatment with these ADCs due to tumor heterogeneity and resistance to the mono payload ADC. Dosing in patients is further limited by off-target toxicity due to instability of the maleimide bond between the antibody and linker. Combination therapies have historically outperformed monotherapies across most solid tumors, pointing to a potential for improvement of ADC efficacy. CatenaBio is developing next generation Multi-Payload Conjugates™ (MPCs™) with dual payloads and a more stable C-Y bond, that deliver targeted combination chemotherapies within a single molecule with reduced toxicities to address shortcomings in current ADCs.

Method: CatenaBio has developed highly stable, dual-payload ADC combination therapies, with tunable payload ratios. Our selective conjugation platform allows the attachment of distinct payloads targeting different mechanisms of action at three unique sites on antibody scaffolds replacing the unstable maleimide bond with a more stable C-Y bond.

Results: Catena's lead TROP2 targeting dual payload MPC, CATB-101, features an optimized combination and ratio of tubulin and TOP1 inhibitors. CATB-101 demonstrates superior tumor growth inhibition and excellent tolerability in multiple TROP2 expressing CDX and PDX models of TNBC, gastric, and lung cancers. In head-to-head comparisons, CATB-101 outperforms T-DXd, SG and Dato-DXd with full tumor elimination at low doses. CATB-101 eliminates tumors in models following progression on SG treatment, demonstrating potential in ADC relapsed patients. Non-GLP non-human primate (NHP) toxicology trials with CATB-101 demonstrate a remarkable safety profile, by eliminating or reducing off-target toxicity.

Conclusion: Advances have been made in the design of ADCs to expand to previously unaddressed populations. High patient relapse and the failure of recent mono-payload ADCs in late-stage trials indicate a need for next generation multi-payload conjugates. Catena's MPCs™ offer a next step in ADC design and allow for targeted delivery of multiple mechanisms of action with a single MPC™ while reducing off-target toxicity. CATB-101 is highly efficacious at eliminating tumors across multiple CDX and PDX models of cancer that display a range of target surface expression. Validated in early NHP toxicology studies with a significantly enhanced therapeutic window, these molecules offer the potential to circumvent tumor resistance pathways to deliver more durable patient responses.

#6929 Targeting intracellular KRAS^{G12D}/HLA-A11 pMHC with a novel TCR-mimic antibody-drug conjugate (TCRm-ADC) demonstrates potent antitumor activity in preclinical models.

Chia-Chun Chao[1], Wei-Ze Hong[1], Hsin-Yu Chang[2], Jhen-Yu Chen[3], Yi-Wen Jiang[3], K.S. Clifford Chao[3], Kevin Chih-Yang Huang[3]

[1]NDV Therapeutics Corp., Hsinchu, Taiwan,[2]National Yang Ming Chiao Tung University, Hsinchu, Taiwan,[3]China Medical University, Taichung, Taiwan

Antibody-drug conjugates (ADCs) targeting tumor-associated antigens (TAAs) frequently cause on-target, off-tumor side effects. TCR-mimic antibodies (TCRms) imitate the capacity of T cell receptors (TCRs) to interact with peptide-MHC complexes (pMHCs), offering a solution to target previously undruggable intracellular cancer antigens, such as KRAS mutations. Here, we screened and identified a TCRm with high specificity and affinity for the KRAS^{G12D}/HLA-A*11 pMHC complex using phage display, ELISA, and cell-based assays. We further confirmed the specificity and safety of the TCRm antibody *in vitro* and *in vivo*. Furthermore, the TCRm-ADC, NDV-ADC01-exatecan, which targets the KRAS^{G12D}/HLA-A*11 pMHC complex, mediated specific antitumor activity *in vitro* and *in vivo* without obvious toxicity in xenograft models of lung, pancreatic, and colorectal cancer. Additionally, NDV-ADC01-exatecan significantly elicited antitumor immunity and reshaped the tumor microenvironment when combined with low-dose radiotherapy in a humanized HLA-A*11/hB2M transgenic model. Together, these screening and engineering processes provide a novel therapeutic strategy to target undruggable KRAS^{G12D}-mutated cancers.

#6930 Preclinical efficacy of BCG018, an ADC targeting ITGB6 and incorporating a topoisomerase I inhibitor payload, was demonstrated to be effective in PDX models.

Yi Yang, Mengran Li, Chengzhang Shang

Biocytogen, Waltham, MA

Integrin αvβ6 is a heterodimer composed of αv and β6 subunits that is primarily found on the surfaces of epithelial cells and is known to be upregulated during the epithelial-mesenchymal transition (EMT). Its overexpression in various solid tumors, which correlates with poor patient prognosis, makes it a promising target for ADC therapy. However, the large size and complexity of the integrin family present significant challenges in developing specific antibodies.

In our studies, we identified the anti-ITGB6-B antibody, which selectively binds to ITGB6 over other beta integrins. This specificity was established using fully human common light chain RenLite mice with ITGB6 knockout. The anti-ITGB6-B antibody demonstrated good binding affinity for both ITGB6 and its heterodimer αvβ6, outperforming the benchmark, as confirmed by SPR and ELISA experiments.

Furthermore, anti-ITGB6-B exhibited excellent binding characteristics across multiple tumor cell lines, effectively targeting cells with varying levels of ITGB6 expression. Importantly, its internalization activity was found to be comparable to or greater than that of the benchmark, enhancing its potential for therapeutic applications. Notably, the anti-ITGB6-B did not block the interaction of ITGB6 with its ligand LAP in ELISA assays, indicating its potential as a targeted therapy without disrupting critical signaling pathways. The anti-ITGB6-B also exhibited excellent physicochemical properties and developability, making it a promising candidate for further development in ADC therapy.

The anti-ITGB6-B was then conjugated to vcMMAE. The resulting conjugate demonstrated superior efficacy to that of the benchmark ADC in PDX models, regardless of ITGB6 expression levels. Additionally, the BCG018, which is anti-ITGB6-B conjugated with a novel topoisomerase I inhibitor (BLD1102), showed superior efficacy to benchmark ADC in models of pancreatic, colorectal, and NSCLC PDX or CDX xenografts. Overall, BCG018 conjugates offer a promising strategy for targeting integrin αvβ6 in solid tumors with specific and potent efficacy.

#6931 Preclinical study of BCG044, a novel bispecific ADC targeting EpCAM and HER3 for the treatment of colorectal and other tumors.

Jeremy Lee, Zhuolin Li, Chengzhang Shang, Yi Yang

Biocytogen, Waltham, MA

Colorectal cancer (CRC) is the third most common cancer and the second leading cause of cancer-related deaths. Unfortunately, current therapies have limited effectiveness on long-term survival. Antibody-drug conjugates (ADCs) represent an emerging class of treatments with potential in oncology, but their efficacy in colorectal cancer has been limited thus far. Therefore, identifying new drug targets and developing ADCs are essential for improving treatment outcomes. Epithelial cell adhesion molecule (EpCAM) is a transmembrane glycoprotein widely expressed in various cancers, notably colorectal, gastric, ovarian, and lung cancers. However, its presence in normal tissues has led to adverse effects from previous biologic therapies, including gastrointestinal toxicity and pancreatitis associated with systemic administration.
In this study, we developed an innovative approach to generate a bispecific ADC targeting both EpCAM and HER3, another antigen that is widely overexpressed in various solid tumors, including gastrointestinal cancers, breast cancer, and NSCLC. By employing a "1+1" format, we aimed to mitigate EpCAM-related toxicity while enhancing tumor selectivity. The BCG044 bispecific antibody (bsAb) effectively bound to a diverse range of gastrointestinal tumor cell lines. Notably, the monovalent form of EpCAM and HER3 resulted in decreased internalization within tumor cells. In contrast, simultaneous engagement of both targets by bsAbs maximized internalization. This suggests that bsAb requires targeting of tumor cells with bivalency. When conjugated with BLD1102, a novel TOP1 inhibitor linker-payload, BCG044 exhibited potent efficacy comparable to the EpCAM benchmark ADC and demonstrated stronger effects than the HER3 benchmark ADC in colorectal, breast, and NSCLC PDX models. Subsequently, we utilized humanized EpCAM mice to test a surrogate ADC that contained the same EpCAM arm, along with a HER3 arm that cross-reacted with mouse HER3. The surrogate ADC demonstrated better tolerance compared to both the parent EpCAM ADC. In summary, BCG044 exhibited the potential to enhance tumor selectivity while maintaining potent efficacy against colorectal and other solid tumors.

#6932 BCG045: A first-in-class bispecific ADC targeting TROP2 and MUC1 demonstrates promising tumor efficacy and potentially reduced toxicity in preclinical studies.

Jeremy Lee, Yifu Zhang, Chengzhang Shang, Yi Yang

Biocytogen, Waltham, MA

Although TROP2 ADCs provide clinical benefits, they face challenges with on-target toxicity and resistance. MUC1 is another crucial biomarker in oncology. In cancer cells, MUC1 loses its normal polarity and redistributes across the cell surface and cytoplasm. It consists of two subunits: the transmembrane domain (MUC1-C), which activates key oncogenic signaling pathways, and the extracellular domain (MUC1-N), which can be shed into circulation. Both TROP2 and MUC1 are overexpressed in various epithelial tumors and are linked to poor prognosis. Furthermore, the induction of TROP2 expression can occur through the binding of galectin-3 to MUC1.

In this study, we developed a bispecific ADC that targets both TROP2 and MUC1, aiming to enhance efficacy while reducing target-related toxicity. To minimize the on-target toxicity associated with TROP2, we identified a TROP2 binder designed to reduce its internalization in a monovalent format with low affinity. To prevent the neutralization of antibodies/ADC by circulating shed MUC1, thereby affecting efficacy and pharmacokinetics, we developed a MUC1 binder that specifically recognizes the MUC1-N/C junction of membrane-bound MUC1 on tumor cells. This membrane-bound MUC1 binder demonstrated high specificity for MUC1 and robust affinity for both human and monkey MUC1. In tumor-bearing mouse models, the MUC1 binder exhibited an improved pharmacokinetic profile compared to benchmark antibodies, as well as strong anti-tumor efficacy. Notably, the performance of the MUC1 binder was unaffected by the presence of shed MUC1, suggesting its potential for effective therapeutic use in targeting MUC1-overexpressing tumors.

The TROP2×MUC1 bispecific antibody (bsAb) demonstrated broad binding capabilities across a range of tumor cell lines with varying expressions of TROP2 and MUC1. Notably, the bsAb exhibited efficient internalization in tumor cells, while also showing reduced internalization activity in TROP2 single-positive cells, which is an important feature for minimizing on-target toxicity. When conjugated with a TOP1 inhibitor (TOP1i) linker-payload, designated as BLD1102, to form BCG045, the bispecific ADC displayed potent efficacy in various patient-derived xenograft (PDX) models.

BCG045 outperformed the benchmark ADCs in certain models, indicating its enhanced therapeutic potential. Overall, the data suggest that BCG045 could be a promising new treatment option for multiple tumors, offering improved efficacy and safety.

#6933 GQ1035: First-in-class ADC against novel targets for gastric cancer and ovarian cancer discovered via high-throughput screening.

Shanshan Xie, Meijun Xiong, Lina Wang, Yajun Sun, Chong Liu, Zhongsheng Hu, Xinju Gao, Yanwen Feng, Yu Han, Zengyan Mu, **Paul H. Song**, Gang Qin

GeneQuantum Healthcare (Suzhou) Co., Ltd., Suzhou, China

Background: Antibody-drug conjugates (ADCs) constitute a breakthrough in gastric cancer (GC) and ovarian cancer (OV) therapy; however about over 50% of patients remain ineligible for existing options, underscoring the urgent need for next-generation ADCs against novel targets. Among these, Target A has emerged as a promising candidate due to its high expression in GC and OV, with no significant correlation to CLDN18.2 or FRα—supporting its potential for ADC development. The iScreener™ platform's high-throughput conjugation capability, rooted in iLDC™/iGDC™ technologies, enables a screening-based strategy for the rapid identification of lead ADCs against Target A.

Method/Results: To develop ADCs against Target A, we constructed a diverse library of ~150 candidates on the iScreener™ platform by combining 11 antibodies with varied linker-payloads. The ADC library was screened using gastric cancer patient-derived organoid (PDO) models. In this screen, Topoli-ADC and Exatecan-ADC demonstrated superior anti-tumor activity compared to other payload-based ADCs (e.g., DXd, MMAE, Eribulin). During in vivo screening, Topoli-ADCs and Eribulin-ADCs emerged as the top candidates by demonstrating potent anti-tumor efficacy in a model resistant to a Topo1 inhibitor-based ADC. Through further refinement in PDX models, GQ1035 was selected based on its ability to induce significant tumor regression across models with varying target expression levels, while maintaining a good safety profile with no significant body weight loss. Safety study for lead candidate is currently ongoing in non-human primates (NHPs).

Conclusion:GQ1035 shows a promising efficacy profile against gastric and ovarian cancers in preclinical PDO and PDX models. This positions GQ1035 as a potential breakthrough therapy in an area of high unmet medical need. It stands as a pioneering example of the strategic shift in biomedicine from “by design” to “by screening”.

#6934 Integrated evaluation of payload-, Fc-, and target-mediated mechanisms of ADCs using streamlined complementary platforms.

Alpana Prasad[1], Surekha Bonasu[1], Radhika Venkatnarayanan[1], Jennifer Lin-Jones[1], Jane E. Lamerdin[1], Gaurav Agrawal[1], Nguyen Ly[2], Jesus A. Diaz de Leon[2], Venkatesh Chari[1]

[1]Eurofins DiscoverX, Fremont, CA,[2]Biosensing Instrument, Tempe, AZ

This study demonstrates an integrated approach for comprehensive characterization of antibody-drug conjugates (ADCs) using complementary bioanalytical platforms. The objective was to evaluate target binding, internalization, and both payload- and Fc-mediated cytotoxic mechanisms to generate a holistic understanding of ADC mode of action.ADC binding affinity and kinetic parameters were characterized by surface plasmon resonance microscopy (SPRm) to assess cell-surface receptor engagement. Internalization was measured in engineered tumor cell lines expressing relevant antigens (e.g., BCMA, CD33) using enzyme-fragment complementation (EFC)-based PathHunter® internalization assays. Functional cytotoxicity was quantified using the KILR® Cytotoxicity platform, providing direct readouts of target-cell death. Fc-effector functions, including antibody-dependent cellular cytotoxicity (ADCC) and phagocytosis (ADCP), were evaluated using effector cell models to distinguish immune-mediated from payload-driven mechanisms.Here we show characterization data for 2 different ADCs which demonstrated high-affinity binding by SPRm and efficient internalization by PathHunter assays. In KILR assays, the ADC produced a concentration-dependent cytotoxic response distinct from its unconjugated parental antibody. Comparative analysis revealed that payload-mediated killing dominated overall cytotoxicity, while measurable ADCC and ADCP activities reflected retained Fc function. Integration of biophysical and cell-based results provided mechanistic resolution of ADC function at multiple levels. Combining SPRm, PathHunter internalization assays, and KILR cytotoxicity enables comprehensive ADC characterization encompassing binding, uptake, and multi-mechanistic cytotoxicity. This integrated workflow supports discovery, optimization, and lot-release testing by linking molecular properties to functional outcomes, enhancing mechanistic understanding critical for ADC development.

#6935 BCG029: An ADAM9-Targeting ADC Featuring a Novel Topoisomerase I Inhibitor Payload Demonstrated Potent Efficacy in PDX Models.

Yong Xie, Mengran Li, Chengzhang Shang, Yi Yang

Biocytogen, Waltham, MA

ADAM9 (A disintegrin and metalloprotease 9) is a membrane-anchored protein that is crucial for various physiological functions, mainly through its disintegrin domain for adhesion and metalloprotease domain for ectodomain shedding of cell surface proteins. Its overexpression in various cancers, including pancreatic, esophageal, breast, gastric, lung, and colorectal cancers, is linked to increased tumor aggressiveness and poor prognosis. Although ADAM9 is a promising target for ADC development, its expression in human tissues and immune cells, such as monocytes, macrophages, and neutrophils, poses challenges. This overlapping expression raises the risk of off-target effects and toxicity to normal tissues, which may hinder the efficacy and safety of ADC therapies targeting ADAM9.

Therefore, we have developed an ADAM9 clone, Ab.01, utilizing the fully human RenLite ADAM9 knockout (KO) mice. Ab.01 specifically binds to the membrane-proximal region of ADAM9-L while disregarding the secreted isoform, ADAM9-S. This clone targets ADAM9 without cross-reactivity to other ADAM family members, a specificity confirmed using an ADAM9 KO cell line. Additionally, Ab.01 demonstrated broad binding activity to a panel of cancer cell lines. Ab.01 also showed effective internalization activity. Furthermore, in a PBMC binding assay, Ab.01 demonstrated minimal binding activity to myeloid cells compared to the benchmark antibody. This observation suggests that Ab.01 may reduce off-target interactions, underscoring its potential for improved specificity in therapeutic applications.

Ab.01 conjugated to vcMMAE showed superior efficacy in several PDX models compared to benchmark antibodies conjugated with the same payload. Ab.01 was then conjugated with BLD1102, a novel Top1 inhibitor, resulting in BCG029, which demonstrated potent efficacy in PDX models. Ongoing *in vivo* studies are continuing to evaluate the performance of BCG029.

These findings underscore the therapeutic potential of BCG029 in targeting solid tumors that express ADAM9. By targeting ADAM9 specifically, BCG029 could provide a safer and more effective treatment option for patients with ADAM9-expressing tumors.

#6936 A novel MSLN×CDH3 bispecific antibody-drug conjugate (BsADC) demonstrates promising anti-tumor efficacy.

Haochen Wei, Zihao Wang, Weiqiu Lan, Xi Yang, Kunying Hao, Jinhua Zhao, Yang Chen, Baihong Liu, Chengzhang Shang, Yi Yang

Biocytogen, Waltham, MA

Background Mesothelin (MSLN) and P-cadherin (CDH3) are cell-surface proteins and co-expressed in multiple solid tumor types (e.g., ovarian, pancreatic) with restricted normal-tissue accessibility, supporting their selection for targeted therapeutics. Their co-expression or spatial complementarity of MSLN and CDH3 in solid tumors provides a mechanistic basis to mitigate antigen escape and enhance internalization-driven delivery. Recent advances suggest that bispecific ADCs (bsADCs) can improve internalization and payload delivery in co-expressing tumors.

Method We developed a fully human anti-human MSLN×CDH3 bsAb using our proprietary common light chain RenLite® mouse platform. Our bsADC employs a monovalent “1+1” architecture with two linker-payload options: monomethyl auristatin E (MMAE), a clinically validated microtubule inhibitor, and BLD1102, a newly developed DNA topoisomerase inhibitor.

Results The anti-MSLN×CDH3 bsAb demonstrates good physicochemical and developability. In vitro, bsAb showed higher binding activity to various types of cancer cell lines, as well as enhanced internalization activity compared to parental antibodies. Next, the bsAb was conjugated with MMAE to generate an anti-MSLN×CDH3 bsADC. This bsADC displayed stronger antigen-dependent cytotoxicity than parental ADC controls across different cell lines, consistent with enhanced internalization. In vivo, we also tested the efficacy of the MSLN×CDH3 bsAb conjugated to BLD1102. Both anti-MSLN×CDH3 bsADC (MMAE) and anti-MSLN×CDH3 bsADC (BLD1102) exhibited superior efficacy in patient-derived ovarian and pancreatic ductal adenocarcinoma xenograft models.

Conclusion Together, these results suggest that anti-MSLN×CDH3 bsADC has the potential to be a novel therapeutic alternative for MSLN and CDH3-expressing tumors.

#6937 BCG046, a CDCP1 ADC that targets CTF, has demonstrated potent *in vitro* and *in vivo* efficacy.

Haochen Wei, Na Zhang, Chengzhang Shang, Yi Yang

Biocytogen, Waltham, MA

Background CUB domain-containing protein 1 (CDCP1) is a type I transmembrane glycoprotein that is associated with tumor progression, drug resistance, and a poor prognosis. CDCP1 is highly expressed in various types of cancer, including pancreatic, breast, prostate, ovarian, colorectal, and lung cancers. It is closely tied to patient prognosis. CDCP1 can be cleaved by extracellular proteases, resulting in the shedding of the protein. The presence of these shedding CDCP1 in the serum of cancer patients raises concerns regarding the neutralization of biologic therapeutics.
Results Thus, we developed the antibody clone Ab.168, which specifically targets the C-terminal fragment (CTF) of CDCP1, utilizing our fully human RenMice platform. Ab.168 exhibited cross-reactivity with human, monkey, and mouse CDCP1, demonstrating a strong affinity for and effective binding to a variety of tumor cell lines. This broad reactivity underscores its potential for use in preclinical development and transition. Additionally, it displayed efficient internalization in cell lines with varying levels of CDCP1 expression, with performance comparable to or better than both the CTF and amino-terminal fragment (ATF) benchmarks. Moreover, Ab.168 exhibited robust development potential, as its binding activity remained unaffected by stress conditions, and it showed no nonspecific binding in polyreaction assays. When conjugated to vcMMAE, Ab.168-vcMMAE demonstrated superior or comparable efficacy to benchmark ADCs in NSCLC and colorectal patient-derived xenograft (PDX) models.
Conclusion These findings underscore the therapeutic potential of Ab.168 in developing an ADC as a promising strategy for treating colorectal cancer and other solid tumors characterized by CDCP1 expression. Further preclinical studies are underway.

#6938 BCG026: FAP × GPC1 bispecific ADC - A novel targeting approach for stromal and tumor cells in pancreatic cancer and other solid tumors.

Haochen Wei, Na Zhang, Kunying Hao, Chengzhang Shang, Yi Yang

Biocytogen, Waltham, MA

Background Pancreatic adenocarcinoma (PAAD) is a highly aggressive cancer that urgently needs new therapeutic strategies. Characterized by a dense fibrotic and desmoplastic stroma, PAAD leads to rapid disease progression, treatment resistance, and poor clinical outcomes. The primary components of this stroma are cancer-associated fibroblasts (CAFs), which accumulate within the tumor and increase the expression of collagen and fibronectin, thereby remodeling the extracellular matrix. CAFs also facilitate the desmoplastic response, contributing to early invasion, high recurrence rates, and resistance to treatment in PAAD. As a result, CAFs represent a promising therapeutic target not only in PAAD but also in other solid tumors. Fibroblast activation protein (FAP) is selectively expressed by CAFs in the majority of human epithelial cancers. Glypican 1 (GPC-1) is aberrantly expressed and plays a significant role in various cancers. It is notably increased in PAAD and has also been found at elevated levels in colorectal, prostate, and breast cancers.
We have confirmed that the PAAD tissue microarray (TMA) showed high expression levels of both FAP and GPC1. In response, we developed BCG026, a novel bispecific ADC that targets both stromal and tumor cells. This approach aims to deplete the tumor stroma, thereby improving efficacy against the stroma barrier and tumor heterogeneity, as well as overcoming resistance associated with traditional single-target therapies. A fully human bispecific antibody against FAP and GPC1 was generated using Biocytogen's RenLite® transgenic mice. The bsAb backbone demonstrated high affinity for both FAP and GPC1, effectively binding to a diverse panel of tumor cells.
Results Furthermore, it exhibited robust binding activity in both stromal and tumor cells, regardless of their varying expression levels of FAP and GPC1. Notably, the bsAb also showed efficient internalization in both stromal and tumor cells, indicating its capacity to deliver therapeutic payloads effectively to stroma and tumor cells. We then conjugated the bsAb with TOP1i linker-payload (BLD1102) to create BCG026. This novel bsADC exhibited a CAF-dependent bystander killing effect *in vitro*, suggesting its ability to induce cytotoxicity in FAP-positive stroma and tumor cells that may not express the target antigens, but are present in proximity to CAFs. Furthermore, BCG026 demonstrated potent efficacy in pancreatic and lung cancer PDX models, as well as a superior synergistic effect to that of the parent ADCs in certain models.
Conclusion These findings underscore its significant potential as a powerful therapeutic agent for targeting PAAD and other tumors. Further preclinical studies are currently underway.

#6939 Tri-specific ADC platform offers potential therapeutic advantage over bi-specific ADC.

Yang Wang, Lixia Cao, Cui Feng, Fangdun Jiang, lixia Gu, Chen Li, Yifan Yang, Qi Zhang, Ming Zhou, Cancan Li, Wei Huang, Bonan Yan, Ziping Wei, Yuhong Zhou

Preclinical Research & Development, Bliss Biopharmaceutical Co., Ltd., Hangzhou, China

Co-expression of EGFR and HER3, along with other tumor-associated antigen (TAA such as c-MET, HER2, B7H3, PD-L1, or others), is frequently observed across diverse human tumors. Targeting more than two TAAs simultaneously presents engineering challenges but offers distinct advantages: increased tumor cell avidity for ADCs, circumvention of antigen-loss-driven resistance, synergistic blockade of cross-talk between signaling pathways, mitigation of tumor heterogeneity, and broadened applicability across cancer types. A tri-specific ADC platform has been developed by combining one arm with both HER3 and EGFR affinities and another arm with affinity for a third TAA. Binding and internalization were assessed in cell lines with varying TAA expression levels to evaluate uptake efficiency. *in vitro* cytotoxicity was measured via dose-response assays across multiple lines with modest expression of each TAA. *in vivo* efficacy was tested in murine xenograft models representing diverse target antigen profiles, in comparison with benchmarks Izalonatamab brengitecan (BL-B01D1, EGFR/HER3 bispecific ADC) and an Amivantamab (EGFR/c-MET bispecific mAb)-derived ADC. Our results show that tri-specific ADCs exhibit significantly faster and more efficient internalization than the EGFR/HER3 bispecific ADC, particularly in cells with medium-to-low EGFR and HER3 expression. *in vitro*, tri-specific ADCs achieved lower IC50 values, indicating enhanced cytotoxic potency across a broad panel of tumor lines. In xenograft models, tri-specific ADCs delivered superior tumor growth inhibition relative to the bispecific benchmark, irrespective of heterogeneous target antigen expression. In conclusion, tri-specific ADCs offer a robust advantage *in vitro* and *in vivo* over EGFR/HER3 or c-MET bispecifics by enabling enhanced tumor cell binding, improved internalization, and more effective delivery of cytotoxic agents. This strategy holds promise for broader clinical application in tumors with varied receptor expressions and may address resistance in heterogeneous cancers.

#6940 A first-in-class PD-L1/B7-H3/VEGF tri-specific ADC achieves enhanced preclinical antitumor efficacy through direct cytotoxicity, immune checkpoint blockade and VEGF inhibition.

Jiajia Pan, Pengfei Wang, Hongwang He, Mengfan Peng, Meng Cheng, Jie Zhang, Chengyi Ju, Jun Wang, Li Li, Hui Feng

Allink Biotherapeutics, Shanghai, China

PD-L1 is an established immunotherapy target highly expressed in various solid tumors, while B7-H3 is another extensively investigated target overexpressed on a wide range of tumor cells. ADCs targeting PD-L1 or B7-H3 have entered clinical development and shown promising efficacy. PD-L1-directed ADCs may combine direct cytotoxicity and immunotherapy, demonstrating antitumor activity even in PD-L1-negative patients. However, ADC-related toxicity may limit their clinical dosing and thus restrict the full immune-mediated effects. Meanwhile, VEGF/PD-(L)1 bispecific antibodies are emerging as next-generation immunotherapies, with multiple trials exploring their combination with ADCs. Here, we developed ALK208, a trispecific ADC targeting PD-L1, B7-H3, and VEGF, conjugated to a topoisomerase I inhibitor payload. It is designed to integrate direct tumor cell killing, immune checkpoint blockade, and anti-angiogenic activity for maximal antitumor efficacy. Through optimized linker-payload design and DAR, ALK208 exhibited an improved safety profile, enabling higher dose levels to support robust PD-L1 blockade and VEGF neutralization. In preclinical studies, ALK208 simultaneously bound B7-H3, PD-L1, and VEGF with affinity comparable to monospecific antibodies. It effectively blocked VEGF/VEGFR and PD-1/PD-L1 interactions in reporter assays. Concurrent binding of B7-H3 and PD-L1 enhanced cellular binding and internalization in B7-H3/PD-L1 double-positive tumor cells, leading to more potent cytotoxicity than monospecific ADCs. VEGF-mediated crosslinking further strengthened binding, internalization, and cell-killing activity compared to a PD-L1/B7-H3 bispecific ADC. In the presence of VEGF homodimer, ALK208 also showed enhanced PD-L1 blockade in functional assays. Importantly, it did not kill activated T cells or APCs in vitro, suggesting a favorable immune safety profile. In xenograft models, ALK208 outperformed clinical-stage PD-L1 and PD-L1/B7-H3 ADCs. In summary, ALK208 is a first-in-class PD-L1/B7-H3/VEGF trispecific ADC that integrates multiple complementary mechanisms to maximize antitumor efficacy while maintaining a promising safety profile.

#6941 Bi- and tri-specific ADCs that target two distinct growth factor receptor forms of MUC1* and HER2 or alpha-v-beta-6 inhibit tumor recurrence and overcome acquired resistance.

Cynthia Carol Bamdad, Benoit J. Smagghe, Scott Moe, Mark G. Carter, Kevin R. Yi, Michael J. Nash, Robert McDermott, Trevor J. Grant, Salvatore Marchese, Daniel S. Miller, Natalie K. Miller, Andrew K. Stewart

Minerva Biotechnologies, Woburn, MA

Purpose: Develop more effective cancer therapeutics by simultaneously targeting multiple drivers of growth, metastasis and resistance.
Methods: MUC1 is aberrantly expressed on over 75% of solid tumor cancers. Although cloned 30 years ago, there is still no approved MUC1-targeted drug. Previous attempts, including those targeting trapped glycans, targeted the tandem repeat domain, which is shed after cleavage by cancer-associated enzymes. MUC1* with a 45-amino acid ecd (extracellular domain) is the only form that has been shown to function as a growth factor receptor via dimerization of ecd by embryonic growth factors. We show that where MUC1 is cleaved determines the conformation of the remaining ecd. Even within a truncated 45-amino acid ecd, there are distinct conformations that only exist on cancer cells and others that are only on progenitor cells. All these species have been mistakenly grouped together as “MUC1-C”. We developed monoclonal antibodies that specifically bind to each conformation and mapped their expression on cancer vs normal tissues vs progenitor cells. We then generated bi- and tri-specific ADCs that simultaneously bind to 2 or 3 cancer targets.
Results: Data show there are 2 distinct MUC1* receptors that drive tumor growth and metastasis. Targeting one and not the other led to tumor recurrence. We developed bi- and tri-specific antibodies that simultaneously bind to both MUC1* growth factor receptors, and HER2 or alpha-v-beta-6. In antibody internalization experiments, multi-specific antibodies were internalized faster and more completely than mono-specifics. In ADC format, bi-specific antibodies that hit both MUC1* growth factor receptors inhibited tumor recurrence in animals. ADCs incorporating both a MUC1* antibody and Trastuzumab killed Trastuzumab-resistant cancer cells with an IC50 of 0.05 nM compared to 0.73 nM on Trastuzumab sensitive parent cells. Indeed, in Phase I huMNC2-CAR44 trial, patients who had acquired resistance to Trastuzumab or Fam-Trastuzumab Deruxtecan-nxki were best responders in our trial with 75% DCR, 11-month OS, 11.3 month increased survival in patients with high MUC1* expression. In animals, our novel linker payload out-performed industry gold standard Deruxtecan.
Conclusions: It is critical that MUC1-targeted therapeutics hit the cancer-specific forms of MUC1*. Therapeutics that incorporate antibodies that bind to hematopoietic stem cells, for example, would be disastrous if given to cancer patients. Therapeutics that target full-length MUC1, whether aberrantly glycosylated or not, could give initial positive responses via ADC bystander killing. However, the hypothesis is that by killing cells expressing full-length MUC1, which plays no role in cell growth, the MUC1*-positive cell population would be enriched and would accelerate tumor growth and metastasis.

#6942 Validation of HER2, TROP2, and NECTIN4 IHC prediction algorithms for the ADC MATCH trial.

Kyle A. Beauchamp[1], Elizabeth Mauer[1], Kaveri Nadhamuni[1], Elizabeth morency[1], Alia Zander[1], Xingyu Zheng[1], Katherine Mclean[1], Sayantoni Mukhopadhyay[1], Seung Won Hyun[1], Chithra Sangli[1], Kate Sasser[1], Halla Nimeiri[1], Charles Koyias[1], Michelle Ting-Lin[1], Funda Meric-Bernstam[2]

[1]Tempus AI, Inc., Chicago, IL,[2]UT MD Anderson Cancer Center, Houston, TX

Introduction

Antibody-drug conjugates (ADC) have recently emerged as a leading class of targeted oncology therapies. Their usage remains complex, with approvals ranging from broad, tumor-agnostic immunohistochemistry (IHC) companion diagnostic approvals to narrower indication-specific labels. The ongoing ADC MATCH clinical trial (NCT06311214) examines whether a treatment algorithm defined by reflex RNA/IHC testing of the HER2, TROP2, and NECTIN4 gene/proteins can lead to successful biomarker-directed treatment of advanced solid tumors. This study describes the validation of an RNA-seq algorithm for identifying likely IHC-positive patients as required by the ADC MATCH study.

Methods

Three retrospective, de-identified RNA+IHC datasets were collected to enable accuracy studies of CAP/CLIA lab-developed tests for HER2 IHC prediction, TROP2 IHC prediction, and NECTIN4 IHC prediction. RNA-seq was performed by Tempus AI, Inc (Tempus xR), while IHC was performed by Neogenomics, Inc (HER2; clone 4B5), Tempus AI, Inc. (TROP2; clone SP294), or Histologix (NECTIN4; AB192033). IHC positivity was defined as 2+/3+ score groups (i.e., approximately an H-score > 100). High expressors were defined as binary thresholds using log2 gene tpm values of 7.9 (HER2), 4.9 (TROP2), and 6.8 (NECTIN4).

Results

The sample sizes for the three accuracy studies were 2,018 (HER2), 184 (TROP2), and 478 (NECTIN4), respectively. The performance of IHC prediction was assessed for these three targets using positive percent agreement (PPA) and negative percent agreement (NPA). The PPA of each target was found to be 47% (HER2; n=545), 93% (TROP2; n=146), and 35% (NECTIN4; n=71). The corresponding NPA of each target was found to be 89% (HER2; n=1473), 55% (TROP2; n = 38), 92% (NECTIN4; n=407). PPA and NPA varied among cancer types; for example, the TROP2 PPA in colorectal cancer was substantially lower than other cancers (62% vs 95%; $p < .05$).

Conclusion

IHC prediction using RNA-seq data is a promising approach to identify patients who are likely to test positive for specific protein biomarkers, potentially aiding in clinical trial screening and treatment decisions. Future studies, such as the ADC MATCH clinical trial, will assess the clinical value and outcomes of this approach.

#6943 Bispecific antibody with dual-payload ADC for metastatic castration-resistant prostate cancer.

Wenkai Zhao, Xiaofei Zhou, Ting Wang, Furong Guo, Huijie Zhao, Ning Wang, Teddy Yang, Ying Lei, Li Tong, **Fei Peng**

Hongcheng Biopharma, Shanghai, China

Treatment of metastatic castration-resistant prostate cancer (mCRPC) remains a significant clinical challenge. While monospecific ADCs have shown promise, target heterogeneity often leads to treatment resistance and relapse. To address this, we developed a bispecific ADC (BsADC) targeting both Prostate-Specific Membrane Antigen (PSMA) and Six-Transmembrane Epithelial Antigen of the Prostate 1 (STEAP1). The BsADC is armed with two distinct payloads with different mechanism of action: designed to enhance antitumor efficacy through dual antigen targeting and synergistic payload mechanisms. A humanized bispecific antibody against PSMA and STEAP1 was generated. The antibody was site-specifically conjugated with tubulin inhibitor and a topoisomerase 1 inhibitor. The PSMA/STEAP1 BsADC demonstrated optimal affinity, simultaneous binding to both targets, with no observable cross-reactivity to unrelated antigens. Unlike monospecific ADC, the BsADC was efficacious against cell lines expressing either or both antigens. The combination of MMAE and TOP1i payloads induced synergistic cell killing. In vivo, the dual-targeted, dual-payload BsADC achieved robust and durable tumor regressions in both homogeneous (PSMA+STEAP1+) and critically, in heterogeneous xenograft models. We have successfully developed a novel BsADC that co-targets PSMA and STEAP1 and delivers two mechanistically distinct warheads. This approach mitigates the issue of antigen escape and leverages synergistic payload activity, resulting in superior efficacy against heterogeneous prostate tumors. Our compelling preclinical data warrant further clinical development, and this BsADC represents a promising therapeutic candidate for patients with mCRPC, including those resistant to current ADC therapies.

#6944 Preclinical evaluation of a novel and highly differentiated FGFR2b-targeting ADC with low risk of ocular toxicity.

Zhaojun An[1], Jia Ge[1], Zhiqiang Xu[1], Yuhao Wang[2], **Barry Duplantis**[2], Quan Yu[1], Xiangyu He[1], Yi Li[1]

[1]Shanghai Ailux Biotechnology Co., Ltd., Shanghai, China,[2]Ailux Inc, Somerville, MA

Background: Fibroblast growth factor receptor-2 isoform IIIb (FGFR2b) plays a crucial role in the tumorigenesis and disease progression of several solid tumors, its overexpression is associated with poor prognosis. About 30% of gastric and gastroesophageal junction (G/GEJ) adenocarcinomas express FGFR2b with limited overlap with current biomarkers, this makes FGFR2b an attractive target. Bemarituzumab, an ADCC-enhanced FGFR2b antagonist, has demonstrated efficacy in patients with FGFR2b-overexpressing G/GEJ cancer. However, its therapeutic benefit appears to be limited by corneal adverse events, likely resulting from the strong blockade of FGFR2b ligands FGF7 and FGF10. Here we developed a novel FGFR2b-targeting ADC based on a highly differentiated antibody, ALX007, which completely spares ligand-receptor interaction and showed an encouraging ocular safety profile in preclinical models.
Methods: Hit antibodies were generated by hybridoma, triaged using a proprietary structural modeling algorithm, and humanized. Antibody binding and internalization were evaluated, and blockade of FGF7 and FGF10 binding to FGFR2b-overexpressing cells was analyzed by flow cytometry. The lead antibody was conjugated to a topoisomerase I inhibitor via a stable and enzyme cleavable linker. Anti-tumor efficacy of the resulting ADC was assessed using FGFR2b-positive xenograft mouse models. PK profile and ocular toxicity were evaluated in relevant mouse models.
Results: The naked antibody ALX007 demonstrated selective, high-affinity FGFR2b binding and rapid internalization in cell lines with varying levels of FGFR2b protein expression. Importantly, ALX007 did not inhibit the interaction between FGF7/FGF10 and FGFR2b even at high concentrations, distinguishing it from Bemarituzumab and several other reference antibodies with potent ligand blockade (IC_{50} < 5 nM). Both structural modeling and epitope binning experiments revealed that ALX007 recognizes a novel, non-ligand-blocking epitope. Functional studies further confirmed that ALX007 did not inhibit FGF7/FGF10-induced FGFR2b phosphorylation. In the SNU-16 gastric cancer xenograft model, a single dose of the FGFR2b-targeting ADC showed sustained and superior anti-tumor efficacy compared with repeated doses of Bemarituzumab. Both the ALX007 naked antibody and its ADC exhibited significantly lower corneal dystrophy than Bemarituzumab in mice. In a human FcRn transgenic mouse model, no apparent difference in serum concentrations was observed between conjugated and total antibodies, indicating a stable antibody-linker conjugation.
Conclusion: Together, these data demonstrate preclinical efficacy and low risk of ocular toxicity of a FGFR2-targeting ADC utilizing ALX007 as a highly differentiated antibody backbone. Further development for the treatment of FGFR2b-expressing tumors is warranted.

#6945 HDM2024: A novel EGFR and HER3 bispecific antibody-drug conjugate exhibits superior antitumor activity and favorable toxicological profile.

Qingyu Shu, Yan Xia, Zhaofeng Qin, Shengxing Zhao, Yang Chen, Rongrong He, Hao Pan, Hongwen Li, Dongzhou Jeffrey Liu

Huadong Medicine Co., Ltd., Hangzhou, China

Introduction: The epidermal growth factor receptor (EGFR) and human epidermal growth factor receptor 3 (HER3) are frequently co-expressed in a variety of solid tumors and play crucial roles in driving tumor growth, therapeutic resistance, and metastasis. To overcome the limitations of single-target approaches, we developed a novel bispecific antibody-drug conjugate simultaneously targeting EGFR and HER3.
Methods:HDM2024 was engineered using single-valency design, consists of a clinically validated HER3 antibody paired with an EGFR-targeting VHH antibody. The antibody was conjugated with exatecan via a cleavable linker, drug-antibody ratio (DAR) is 4. The efficacy and safety of HDM2024 were tested in xenograft and patient derived xenograft (PDX) models and monkeys, respectively.
Results:HDM2024 was designed with balanced affinity towards EGFR and HER3 antigen. In vitro, HDM2024 demonstrated high-affinity binding to both EGFR and HER3 expressing tumor cells, efficient internalization, and potent cytotoxicity across a panel of cancer cell lines with varying expression levels of EGFR and HER3. In vivo, HDM2024 exhibited robust antitumor efficacy in multiple xenograft and patient-derived xenograft (PDX) models, achieving complete or durable tumor regressions at well-tolerated doses. In GLP toxicity study, HDM2024 showed favorable safety with the highest non-severely toxic dose (HNSTD) reaching up to 40mg/kg administered every 2weeks (Q2W) for three cycles.
Conclusion: Collectively, these results support HDM2024 as a promising therapeutic candidate for solid cancer treatment. A differentiated ADC drug design endows HDM2024 with enhanced pharmacological efficacy and safety advantages, giving it the potential to become a best-in-class drug candidate. HDM2024 is expected to start the clinical trial in Mar 2026.

#6946 Preclinical evaluation of BCG017, a novel bispecific ADC targeting PTK7 and EGFR.

Zipeng Zeng, Na Zhang, Chengzhang Shang, Yi Yang

Biocytogen, Waltham, MA

Background: The long-term effectiveness of targeting the key oncogenic driver EGFR can be limited by acquired drug resistance, along with concerns related to on-target toxicity. PTK7, a member of the receptor tyrosine kinase (RTK) family, plays a significant role in Wnt signaling and influences cancer progression and metastasis. PTK7 is overexpressed in various types of solid tumors and has been shown to interact with the extracellular region of EGFR. BCG017, a first-in-class bispecific ADC specifically designed to target both EGFR and PTK7, aims to overcome the resistance mechanisms associated with EGFR while enhancing tumor selectivity through its dual targeting approach.The BCG017 backbone (PTK7×EGFR bsAb) was developed using the fully human common light RenLite® mouse platform, and it exhibits a higher affinity for PTK7 than for EGFR. The bsAb showed strong binding activity and effective internalization in various cancer cell lines, while the monovalent EGFR antibody had reduced capabilities. Furthermore, the bsAb exhibited efficacy comparable to that of monovalent antibodies in cell lines expressing either target alone, suggesting that optimal function relies on the simultaneous binding of both arms.

Results: The bsAb was then conjugated to vcMMAE. The MMAE conjugate exhibited enhanced efficacy in PDX models compared to both benchmark treatments and parental ADCs, even when PTK7 expression levels were low. These findings suggest that the PTK7×EGFR bsADC has a synergistic effect by targeting two distinct antigens, which may help to effectively address tumor heterogeneity in comparison to single-target ADCs. Moreover, while the MMAE conjugate displayed optimal activity, its monovalent ADC counterparts showed reduced efficacy in PDX models. These results highlight the importance of engaging both arms of the bsADC to achieve maximal therapeutic effectiveness. Additionally, the findings indicate a high degree of tumor selectivity, which could potentially minimize EGFR-related toxicity in normal tissues.Then, BCG017 was conjugated with BLD1102, a proprietary topoisomerase 1 inhibitor (TOP1i) linker-payload. BCG017 demonstrated potent in vivo efficacy in PDX models representing various tumor types expressing both EGFR and PTK7, including gastric, colorectal, esophageal, breast, and lung cancers. BCG017 consistently showed superior efficacy to MMAE conjugate using the same bsAb backbone in PDX models. BCG017 exhibited favorable pharmacokinetics in mice, effective tumor delivery in a xenograft model, and good plasma stability.

Conclusion: These results highlight the promising efficacy of BCG017 in preclinical models, indicating improved tumor selectivity and suggesting that it could address the limitations of EGFR-targeting therapies while expanding treatment options for PTK7 and EGFR co-expressed settings.

#6947 A novel bispecific antibody-drug conjugate, BCG016, that targets 5T4 and MUC1, demonstrates robust preclinical antitumor activity.

Zipeng Zeng, Yangyang Xu, Chengzhang Shang, Yi Yang

Biocytogen, Waltham, MA

BackgroundTrophoblast glycoprotein (5T4) is significantly overexpressed in a variety of cancers, including breast, lung, ovarian, endometrial, bladder, pancreatic, esophageal, and colorectal cancers, while demonstrating minimal expression in normal tissues. Its presence in cancer stem cells is correlated with poor prognoses, possibly contributing to metastasis, resistance, and recurrence. MUC1, a highly glycosylated member of the transmembrane mucin family, is also overexpressed across a range of solid cancers. Abnormalities in MUC1 expression and glycosylation in cancer activate multiple pathways that drive tumor migration, invasion, and accelerated growth. Importantly, 5T4 and MUC1 are frequently co-expressed in various solid tumors, such as lung, breast, ovarian, colorectal, and pancreatic cancers.
ResultsIn our study, we generated and evaluated antibodies targeting 5T4 and MUC1 using fully human common light chain RenLite mice. The 5T4 parental antibody demonstrated stronger and specific binding and greater efficacy than the benchmark in vivo. We previously generated the MUC1-C parental antibody, which was identified as targeting membrane-bound MUC1 on cancer cells. The anti-5T4×MUC1 bsAb demonstrated good binding to tumor cells with varying levels of 5T4 and MUC1 expression, with enhanced binding observed in cases of high expression of both 5T4 and MUC1. The bsAb demonstrated efficient internalization activity in the 5T4/MUC1 co-expression cell line, performing either as well as or better than benchmark antibodies. Notably, the anti-5T4×MUC1-vcMMAE demonstrated improved efficacy compared to parental ADCs, outperforming benchmark ADCs in patient-derived xenograft (PDX) models. BCG016, in combination with a TOP1 inhibitor linker-payload (BLD1102), exhibited enhanced efficacy in PDX models compared to parental ADCs, significantly outperforming benchmark ADCs targeting 5T4 and MUC1.
ConclusionIn summary, we have developed a novel bispecific ADC that targets both 5T4 and the membrane-bound MUC1-C. BCG016 showed superior anti-tumor efficacy in PDX models, underscoring its potential as a new therapeutic option for tumors that co-express 5T4 and MUC1.

#6948 A novel bispecific antibody-drug conjugate targeting CEACAM5 and CDH17 exhibits potent anti-tumor activity and enhanced tumor-selectivity.

Jinxiu Hou, Tingting Gu, Lisha Dong, Jiyuan Tian, Xiaoqian Chen, Dandan Liu, Yongxin Shang, Rongmei Yan, Kezhen Ye, Liang Tian, Jian Peng, Zhenping Zhu

Earendil Labs., Wilmington, DE

CEACAM5 and CDH17 are preferentially expressed in gastrointestinal tumors, including more than 95% of colorectal cancers, 80% of gastric and pancreatic cancers, and 70% of cholangiocarcinomas. Moreover, these two molecules are frequently co-expressed in gastrointestinal cancers. Recent advancements in CEACAM5 and CDH17 research have unveiled their potential as the promising targets for developing novel cancer therapeutics. Here we engineered a bispecific antibody (bsAb) capable of simultaneously binding to both CEACAM5 and CDH17. The cell binding and internalization activities of the bsAb were compared to a panel of monoclonal antibodies, including M9140 analog (an anti-CEACAM5 monoclonal antibody) and TORL-3-600 analog (an anti-CDH17 monoclonal antibody), using multiple colorectal and pancreatic cancer cell lines, The bsAb was conjugated to various topoisomerase I inhibitor payloads to generate several bispecific ADC molecules (bsADCs). The activity of these bsADC was studied in vitro in tumor cell-killing assay, and in vivo in multiple CDX models of GI malignancies. We further investigated the bsADC stability in human and cynomolgus monkey plasma over a three-week period, its pharmacokinetic profile and tolerability in both SD rats and cynomolgus monkeys. The results demonstrated that the bsAb exhibits excellent developability, and the resulting bsADCs maintained high purity after conjugation with different linker-payloads. The lead bsADC candidate showed superior bystander killing activity. In GI cancer CDX models with varying CEACAM5/CDH17 expression levels, it showed tumor inhibition comparable or superior to M9140a and TORL-3-600a, suggesting a broad application in GI cancer patients. Furthermore, the candidate exhibited favorable stability in human/cynomolgus plasma and good pharmacokinetic profile and tolerability in SD rats and cynomolgus monkeys. Taken together, these data support further development and broad utility of this bsADC for GI cancer treatment.

#6949 A novel multi-modal PD-L1-ADC could be a potential BIC candidate treatment for pan-solid tumors with enhanced tumor-specificity.

Tao Yang, Hang Ke, Feiyu Peng, Jialin Li, Cen Chen, Lei Zhang, Faming Zhang, **Henry Li**

Hanx Bio, Wuhan, China

PD-L1 is an immune-checkpoint frequently over-expressed oon the surface of many tumor cells, as compared to normal tissues, and it may thus be considered a tumor-associated antigen (TAA), although usually not considered a good one due to wide expression among many normal tissues. Immuno-checkpoint inhibitors (ICIs), *e.g.* mAbs against PD-L1 and its binding partner, PD1 on effector T-cells within tumors ($TIL\text{-}T_{eff}$), become powerful modality to treat cancers. However, only 15~30% of patients across different cancers responded to PD-(L)1 ICIs whereas most of them eventually relapse and become resistant. Combination therapies, *e.g.* ICIs plus chemotherapies, have been proven productive with significant clinical benefit in overall survival (OS) and have become standard practice. Chemotherapy usually comes with severe side-effects with narrow therapeutic window (TW). In recent years, ADC, as a new generation of chemo-modality with significantly improved TW due to tumor targeting specificity, witnessed great success in clinics. We hypothesized that an ADC targeting PD-L1, combining specific tumor-targeting and/or ICI, could become a new powerful multi-modality treatment of cancers, superior to existing single-modal chemotherapy or ICI. To test this, we have created a novel ADC, a PD-L1-mAb conjugated with a topoisomerase-I inhibitor as payload, which is being tested for its anti-tumor activity in preclinical settings. Specifically, although specifically binds to several PD-L1-expressing tumor cell lines with high affinity, its naked antibody exhibited poor internalization in PD-$L1^+$ cells. The ADC showed poor cytotoxicity induction in these cells as compared to FIC SGN-PDL1V that internalized efficiently. However, in contrast, the ADC demonstrated robust cytotoxicity in PD-$L1^+$ 3D-tumor organoids *in vitro*, as well as robust antitumor activity in xenograft models *in vivo*, even stronger than SGN-PDL1V and significantly superior to the cytotoxicity seen in 2D-cell culture. This interesting discrepancy seen between 2D cell culture and “tumor” (3D-organoid or xenograft tumor) may imply added tumor-specificity, in addition to the differential PD-L1 expression between tumors and normal tissues. It is believed that this ADC maximized its immunomodulation as well as cancer cell killing, along with the observed “tumor-specificity”, which may implicating a potential “BIC” PD-L1-ADC for treating pan-solid tumors with enhanced TW.

Reference Xu, X., et al., *A living biobank of matched pairs of patient-derived xenografts and organoids for cancer pharmacology.* PLoS One, 2023. **18**(1): p. e0279821.

: High-Dimensional Immune Profiling and Preclinical Modeling for Cancer Immunotherapy
Poster Session

#6954 Comprehensive immune profiling using a validated high-parameter flow cytometry assay to advance pharmacodynamic biomarker discovery for solid tumor immuno-oncology clinical trials.

Angelina Bisconte[1], Vaishali Shinde[2], Jackie Benko[1], Jorge Pardo[1], Samantha Splitt[1], Rachel Owen[1], Deborah J. Phippard[1]

[1]Precision for Medicine, Frederick, MD,[2]Corbus Pharmaceuticals, Inc., Norwood, MA

Immuno-oncology (IO) research demands robust tools to characterize immune responses in solid tumors and peripheral blood. High-dimensional flow cytometry enables simultaneous assessment of lineage, activation, exhaustion and functional markers, providing critical insights into mechanisms of response and resistance to immunotherapies. Precision for Medicine developed and validated a 32-parameter flow cytometry assay to advance translational research and biomarker discovery in IO clinical trials.

This high-parameter panel profiles major immune subsets in cryopreserved PBMCs - including T cells, memory T cell subsets, regulatory T cells, B cells, NK cells and myeloid populations - while assessing activation (CD25, CD69, CD86), exhaustion (PD-1, LAG-3, TIM-3), proliferation (Ki67), and functional markers (Granzyme B, TCF-1), alongside cytokine expression (IL-2, IL-4, IFNγ, TNFα). Validation followed CLSI guidelines for precision, accuracy, and sensitivity using cryopreserved PBMCs from healthy donors.

The assay demonstrated reproducibility (CV less than 15% for major immune populations), sensitivity for low-frequency subsets such as TCF-1+ stem-like T cells, and robust functional readouts post-stimulation. Clinical relevance was confirmed through profiling of exhaustion and activation states critical for IO trials and solid tumor studies.

This validated high-parameter flow cytometry assay enables scalable immune monitoring in IO clinical trials, supporting biomarker discovery, mechanism of action studies and pharmacodynamic endpoint assessment longitudinally in patients receiving novel immunotherapies. Its reproducibility and functional depth make it suitable for multi-site implementation and integration with computational pipelines, facilitating patient stratification and advanced biomarker insights for solid tumor research.

#6955 Development of a 32-color spectral flow cytometry panel for comprehensive immunophenotyping of PBMCs from cancer patients receiving immunotherapy and radiotherapy.

Yao-Hui Sun[1], Logan Vick[2], Jonathan E. Van Dyke[3], Andrea L. Gompers[2], Sohan Dhar[1], Emanual M. Maverakis[2], Sean J. Judge[4], Robert J. Canter[4], Megan E. daly[1], William J. Murphy[2], Arta M. Monjazeb[1]

[1]Radiation Oncology, UC Davis Medical Center, Sacramento, CA,[2]Dermatology, UC Davis Medical Center, Sacramento, CA,[3]UC Davis Flow Cytometry Shared Resource, UC Davis Medical Center, Sacramento, CA,[4]Surgical Oncology, UC Davis Medical Center, Sacramento, CA

Background: High-dimensional immune profiling is essential for understanding how radiotherapy (RT) and immunotherapy (IO) reshape systemic immunity. Spectral flow cytometry offers major advantages over traditional flow by enabling >30 markers to be measured simultaneously in a single tube, which is critical when PBMC samples are limited and multiple panels are not feasible. This approach also improves detection of rare or functionally important immune subsets that cannot be reliably captured with smaller conventional panels. Using Sony ID7000, we developed a 32-color spectral flow cytometry panel to profile PBMCs from cancer patients enrolled in an ongoing RT/IO clinical trial.

Methods: A 32-color panel was designed to resolve major immune populations (T cells, B cells, NK cells, monocytes, dendritic cells) and key functional markers of differentiation (CD45RA, CCR7, CD27), activation (CD69, HLA-DR, CD38), proliferation (Ki-67), and exhaustion (PD-1, TIGIT, TIM-3, CTLA-4). Panel development incorporated fluorochrome similarity assessments and spectral signature analyses from the five-laser, 147-detector Sony ID7000. Single-color controls, FMOs, and fully stained references were used for spectral unmixing. Validation included both unstimulated PBMCs and anti-CD3/CD28-stimulated samples to assess activation and exhaustion profiles. Data was analyzed with Sony Spectral Analysis Software and FlowJo.

Results: The panel reliably identified all major PBMC lineages and resolved fine T-cell differentiation states, including naïve, memory, regulatory, and exhausted subsets. Myeloid subsets and dendritic cell populations were consistently distinguished with minimal spectral spreading. Stimulation assays produced expected functional changes—such as increased activation/proliferation marker expression—confirming panel sensitivity and functional applicability. Spectral unmixing, gating strategies, and marker resolution were highly reproducible across acquisition days and sample batches.

Conclusion: We developed and validated a robust 32-color spectral flow cytometry panel capable of comprehensive immunophenotyping of PBMCs from cancer patients. The spectral platform provides substantial advantages for limited clinical samples, enabling deep single-panel profiling and improved detection of rare populations. This panel is now being implemented in an active clinical trial (UCDCC#272) involving combined radiotherapy and immunotherapy, supporting immune monitoring and biomarker discovery in translational RT/IO research.

#6956 A 61-parameter CyTOF panel for comprehensive profiling of human PBMC to characterize immune activation, checkpoint expression and cytokine signatures with applications in cancer immunology.

Michael Cohen, Stephen Li, **Lauren Janette Tracey**, Katrina Thomson, Christina Loh

Standard BioTools, Markham, ON, Canada

Understanding the complexity of immune responses in cancer is critical for developing effective immunotherapies and predicting patient outcomes. High-parameter cytometric analysis enables deep profiling of immune cell phenotypes and functional states, revealing mechanisms of tumor immune evasion and therapeutic resistance. CyTOF™ technology is a single-cell analysis platform that uses metal-tagged antibodies to resolve 50-plus markers in a single tube. Unlike fluorescence-based cytometry, spectral unmixing and single-stain controls are not required. Therefore, it is uniquely possible with CyTOF technology to rapidly design high-parameter panels enabling simultaneous assessment of lineage, activation, exhaustion and intracellular signaling pathways. This study aimed to design a 61-parameter CyTOF panel optimized for functional immune profiling of human PBMC to support cancer immunology research. The panel incorporates lineage markers for major immune subsets and an extensive set of T cell phenotyping targets including activation, differentiation, immune checkpoints (for example, PD-1, CTLA-4, TIGIT) and intracellular cytokines relevant to tumor immunity. Untreated and stimulated PBMC were barcoded, pooled and stained. Samples were cryopreserved and later acquired using a CyTOF XT PRO system to minimize technical variation. High-dimensional analysis of stimulated PBMC demonstrated the panel's ability to resolve extensive immuno-functional diversity at the single-cell level. Co-expression patterns of activation markers, immune checkpoints and intracellular cytokines were detected across effector, memory, cytotoxic, regulatory and exhausted immune cell subsets. These findings highlight the panel's potential to uncover signatures relevant to tumor immunity and immunotherapy response when applied to cancer patient samples or tumor-associated immune cells. CyTOF systems enable the highest number of simultaneous measurements in a single panel, allowing for comprehensive immune profiling alongside high resolution of intracellular targets to interrogate functional potential. Overall, studying functional immunology using CyTOF technology can elucidate the complex nature of immune responses to provide an understanding of how they relate to disease and treatments. For Research Use Only. Not for use in diagnostic procedures.

#6957 GAS-Luc2 reporter cell lines enable sensitive detection of interferon-gamma signaling for immune activation and CAR-T evaluation across 2D and 3D systems.

Hyeyoun Chang[1], John G. Foulke[1], Luping Chen[1], Catherine McManus[2], Meghan Sikes[1], Fang Tian[2]

[1]ATCC, Gaithersburg, MD,[2]ATCC, Manassas, VA

Background: Interferon-gamma (IFN-γ) is a key cytokine regulating cellular immune activation and is widely used as a functional biomarker in immunotherapy development. Standard ELISA method has limited sensitivity for early, low-level IFN-γ detection and does not effectively capture paracrine signaling in three-dimensional (3-D) models. To address these limitations, we developed IFN-γ-responsive luciferase reporter cell lines driven by a gamma-interferon activation site (GAS) promoter.
Methods: Three cancer cell lines with high endogenous expression of checkpoint ligands (PD-L1, CD155, B7-H3) were engineered with a GAS-Luc2 construct. An additional GAS-Luc2 reporter cell line was generated from THP-1 cells for monocyte- and macrophage-related applications. Reporter activity was evaluated after stimulation with recombinant IFN-γ, T cell-conditioned media, and co-culture with primary T or NK cells. Assays were performed in 2-D and 3-D systems and compared with IFN-γ ELISA. CAR-T cells were also evaluated using both methods.
Results: Reporter cells showed strong dose-dependent luciferase expression, with 100- to 250-fold increases after recombinant IFN-γ treatment and 50- to 100-fold induction with T-cell conditioned media. Co-cultures with primary immune cells produced 3- to 12-fold activation. Reporter signals remained robust in 3-D models and detected IFN-γ levels below the ELISA detection limit. In CAR-T assays, reporters identified early and low-level cytokine signaling not measurable by ELISA.
Conclusions: GAS-Luc2 reporter cell lines provide a sensitive, quantitative, and scalable platform for monitoring IFN-γ signaling. Their superior performance over ELISA, especially for early activation and 3-D applications, supports their utility in immunotherapy evaluation, immune checkpoint studies, and CAR-T functional assessment.

#6958 Donor source-dependent B cell receptor repertoire patterns visualized by the pGen-SHM plot reveal differences in adaptive immune reconstitution after hematopoietic stem cell transplantation.

Sakuya Matsumoto[1], Yohei Funakoshi[1], Kimikazu Yakushijin[1], Goh Ohji[2], Takaji Matsutani[1], Hidetomo Takakura[1], Yuri Okazoe-Hirakawa[1], Rina Sakai[1], Yumiko Inui[1], Taiji Koyama[1], Yoshiaki Nagatani[1], Keiji Kurata[1], Shiro Kimbara[1], Shinichiro Kawamoto[1], Naomi Kiyota[1], Hironobu Minami[1]

[1]Division of Medical Oncology/Hematology, Department of Medicine, Kobe University Hospital and Graduate School of Medicine, Kobe, Japan,[2]Division of Infection Disease Therapeutics, Department of Microbiology and Infectious Diseases, Kobe University Hospital and Graduate School of Medicine, Kobe, Japan

Background A reliable method to monitor adaptive immune reconstitution after allogeneic hematopoietic stem cell transplantation (HSCT) has not been established, leaving many aspects of donor-source-dependent differences in immune reconstitution unclear. Here, we developed a new method, "probability of generation (pGen)-somatic hypermutation (SHM) plot (pGen-SHM plot)", to objectively and visually monitor long-term immune reconstitution after HSCT.

Methods We conducted longitudinal B cell receptor (BCR) repertoire analysis on peripheral blood mononuclear cells (PBMCs) from six cord blood transplantation (CBT) (21 samples) and six bone marrow transplantation (BMT) patients (14 samples) from two months to approximately two years post-HSCT. PBMCs from 12 healthy adults were used as controls. pGen value, representing the probability of sequence generation by the recombination process, was calculated using OLGA. SHM rates were determined by nucleotide-level identity to the reference V gene. Maturation of repertoire was visualized by plotting the two-dimensional probability density distribution of pGen and SHM rates using Kernel density estimation, which we termed the pGen-SHM plot.

Results After CBT, the proportions of both high pGen (> 1e-15) and low SHM (< 4%) strongly correlated with post-HSCT days ($r = -0.86$ and $r = -0.91$, respectively) and gradually approached levels observed in healthy adults. Furthermore, the plot analysis revealed a continuous transition from the $pGen^{high}SHM^{low}$ to $pGen^{low}SHM^{high}$ population during the post-CBT period. This finding was validated using publicly available datasets of healthy individuals aged 0 to 15 years, which showed a similar age-related shift. In contrast, the proportions of high pGen (> 1e-15) and low SHM (< 4%) after BMT were already close to healthy adult levels by Day 67 and showed little change over two years. Remarkably, the plot analysis identified two distinct populations in the early post-BMT, $pGen^{high}SHM^{low}$ and $pGen^{low}SHM^{high}$; the latter disappeared at around six months while the former gradually shifted toward $pGen^{low}SHM^{high}$, resembling the pattern observed after CBT. We then performed a detailed analysis of the two populations identified in the pGen-SHM plot after BMT. The $pGen^{low}SHM^{high}$ population showed a lower frequency of IgG1-switched sequences and higher frequency of IgG2-switched sequences compared with the $pGen^{high}SHM^{low}$ population. These findings suggest that $pGen^{low}SHM^{high}$ represents graft-derived mature B cells, whereas $pGen^{high}SHM^{low}$ corresponds to newly generated and maturing B cells derived from hematopoietic stem cells.

Conclusion The pGen-SHM plot objectively and visually captured distinct patterns of adaptive immune reconstitution after HSCT, depending on the donor source.

#6959 Functional evaluation of immuno-oncology drug candidates targeting lymphoid and myeloid cells using *in vitro* assays.

Christoph Schifflers, Martijn Vlaming, Sofie Pattyn

IQVIA Laboratories, Gosselies, Belgium

The growing understanding of the complexity of anti-tumor immunity provides novel targets for the development of cancer immunotherapies. However, lead selection methods can be costly and time-consuming and often rely on animal models associated with ethical considerations and limitations. In addition, new drug designs and modes of action can require the development of new or customized assays for functional screenings. In this context, IQVIA Laboratories developed a variety of *in vitro* assays relying on primary immune cells to enable accelerated cost-effective functional characterization of candidate drugs and lead selection. Leveraging optimized PBMC isolation and cryopreservation protocols, a large biobank of quality-controlled and well-characterized samples was generated, providing a critical component for the reliable and reproducible functional screening of drug candidates. Another critical element consists of well-established functional *in vitro* assays involving cultures of specific lymphoid (e.g. T cells, NK cells) and myeloid cell populations (e.g. Macrophages, Neutrophils) or complex co-cultures (e.g. cancer cells, stem cells). These assays can be used to assess immunogenicity (e.g. Neoepitopes), antigen presentation (e.g. Immunopeptidomics), macrophage phenotypes/function (e.g. M2-Suppression Assay), T cell activation (e.g. Suppressive MLR Assay, Priming Assay), Fc-functions (ADCC, ADCP and CDC), Neutrophil function (e.g. NET Formation, Trogocytosis). Several assays can also be performed with primary immune cells of animal origin (e.g. cyno, mouse, dog) with the aim of reducing animal requirement for *in vivo* studies. The combination of well-characterized high-quality PBMCs and a diverse panel of robust functional *in vitro* assays provides a useful tool for cost-effective accelerated lead selection of immuno-oncology drug candidates.

#6960 Improving immune checkpoint blockade efficacy using combination therapy with bioactive molecules.

Dhanir Tailor[1], Arpit Dheeraj[1], Sushil Kumar[2], Wendy Li[2], Bailey F. Keefe[3], **Annah S. Rolig**[4], Shivaani Kummar[4], Lisa M. Coussens[5], Sanjay V. Malhotra[1]

[1]Knight Cancer Institute, Oregon Health & Science University, Portland, OR,[2]OHSU, Beaverton, OR,[3]OSU, Corvallis, OR,[4]OHSU Knight Cancer Institute, Portland, OR,[5]OHSU Knight Cancer Institute, Lake Oswego, OR

Immune checkpoint blockade (ICB) therapies, such as aPD-1 and aPD-L1, reactivate T cells to fight tumors. While these therapies have transformed cancer treatment, with nearly half of U.S. cancer patients eligible for ICB therapy, their efficacy is limited, with highly variable and generally low response rates. Significant investments aimed at improving ICB response rates have primarily focused on combining therapies with ICB, as demonstrated by the thousands of clinical trials testing anti-PD-1 or anti-PD-L1 with additional agents. However, this significant investment has only resulted in marginal improvements, underscoring a critical unmet need for an innovative, streamlined approach to identify compounds that enhance ICB efficacy. To address this gap, we developed a high-throughput screen (HTS) drug discovery platform that efficiently screens compounds for synergy with ICB. One primary mechanism that limits ICB efficacy is the complex tumor microenvironment (TME), which includes tumor-associated macrophages (TAMs) that take on an immunosuppressive (M2) phenotype and suppress T cell recruitment, proliferation, and function. The abundance of TAMs correlates with poor prognosis in numerous cancers, making TAMs a prime target for compounds that synergize with ICB. To identify potential targets that can reduce TAM immunosuppression, our validated HTS uses an *ex vivo* co-culture system of bone marrow-derived macrophages and spleen-derived $CD4^+$ and $CD8^+$ T cells. After incubation with small molecule libraries, cultures are evaluated for increased T cell activity; thus, this assay aims to identify small molecules that diminish myelomonocytic cell-dependent T cell suppression and enhance T cell activity when combined with ICB. Using this HTS, we screened over 3270 bioactive small molecules, identifying 128 that showed TAM-modulating activity. Of those 128 compounds, seven synergized with anti-PD1 and six with anti-PD-L1. One compound synergized with both anti-PD-1 and anti-PD-L1. These compounds were evaluated *in vivo* in syngeneic murine breast cancer models to assess anti-tumor effects. Indeed, combining these agents with anti-PD-1/anti-PD-L1 significantly slowed tumor growth in triple-negative breast cancer (TNBC) models (EMT6), which are generally resistant to anti-PD-1/anti-PD-L1 monotherapy. By tackling the challenges posed by the TME and immune evasion, in a target- and tumor-agnostic manner, our platform has the potential to uncover novel, transformative ICB combination therapies with broad translational potential across multiple malignancies.

#6961 Patient matched organoid-immune co-culture model as a predictive platform for immunotherapy response in precision oncology.

Maryam Nakhjiri[1], Sraboni Chaudhury[1], Youssel Kriko[1], Mohamad Orabi[1], Liwei Bao[1], Mary Horn[1], Rudnick Avery[1], Albana Grajqevci[1], Andrew Chang[1], David Odell[1], Udit Singhal[1], Rishindra M. Reddy[2], Tudor Borza[1], Tasha Hughes[1], Michael Sabel[1], Lesly Dossett[1], Joshua Piche[1], William Aibinder[1], Sofia Merajver[1], Nathan Merrill[1]

[1]Rogel Cancer Center, Ann Arbor, MI,[2]University of Michigan, Ann Arbor, MI

Background: Immunotherapy (IO) is increasingly integrated into cancer treatment, with checkpoint inhibitors (anti-CTLA-4, anti-PD-1/PD-L1) improving progression-free and overall survival in subsets of patients. However, many across cancer types do not respond, highlighting the need for predictive preclinical models to test and tailor IO-based therapies. Traditional in vivo models and 2D cultures fail to replicate the complexity of the human tumor-immune microenvironment. To bridge this gap, we refined a patient-derived organoid (PDO) and immune cell co-culture platform for rapid drug screening of IO combinations, aligning with the NIH directive to reduce animal use. PDOs can be tested within 10-15 days, providing a personalized system to evaluate treatment response and tumor-immune interactions across solid tumors.
Methods: We established a rapid (<7-day) PDO-peripheral blood mononuclear cell (PBMC) co-culture integrating short-term organoid generation, immune activation, and checkpoint blockade assays. PBMCs were isolated, cryopreserved, and reactivated prior to co-culture using optimized cytokine cocktails (IL-2, IL-7, IL-15, IL-21) and tested in multiple media (AIM-V, X-VIVO, HPLM, RPMI). Cell viability was measured using CellTiter-Glo 3D and apoptosis via Caspase-Glo 3/7 assays. Activated PBMCs were co-cultured with PDOs at 5:1 and 10:1 effector-to-target ratios under IO or combination chemotherapy.
Results: We developed a rapid workflow to generate immune-competent PDOs from breast, bladder, and lung cancers co-cultured with autologous PBMCs. Mono- and combination therapies were tested across tumor types, including various IO agents, platins (cisplatin, carboplatin), taxanes, antibody-drug conjugates, and targeted therapies. Multiple functional parameters were measured, and an apoptotic effectiveness index (AEI) is being developed to rank treatment responses. Across all tumor types, IO combined with platinum or taxane agents produced the highest AEI, reflecting strong synergy in standard-of-care regimens and validating the model's predictive potential. AEI-based ranking identified differential apoptotic responses among tumor types, supporting the model's utility in predicting patient-specific responses.
Conclusions: We established and validated a platform that rapidly assesses whether a patient's immune cells can be activated to kill their tumor organoids in the presence of specific immunotherapy or chemotherapy combinations. We anticipate identifying key biomarkers, including immune phenotypes and cytokine signatures, that distinguish immunotherapy-responsive from non-responsive PDO co-cultures across breast, bladder, and lung cancers. These findings lay the groundwork for predictive tools and future clinical correlations.
AI disclosure: AI was used only for language editing; content was verified by the authors.

#6962 Expanding multiplexing capabilities with TrailBlazer StarBright Dye antibody conjugation kits.

Sharon Sanderson[1], Leon Huang[2], Yoon-Tae Kang[3], Ryan Mendoza[2], Errile Pusod[3], Michael Blundell[1], Tracey Long[1]

[1]Bio-Rad Laboratories, Oxford, United Kingdom,[2]Bio-Rad Laboratories, Hercules, CA,[3]Bio-Rad Laboratories, Ann Arbor, MI

Imaging, western blotting, and flow cytometry multiplexing experiments are often constrained by the availability of suitable fluorophores for some antibodies, hindering panel size and optimal experimental design. Here we address those issues using TrailBlazer™ StarBright™ Dye Antibody Labeling Kits. Custom antibody-dye conjugates can be generated using labeling kits, however options are typically restricted to standard fluorophores, such as FITC, which can be suboptimal and limit panel expansion. The newly introduced TrailBlazer Tag and Label Kits have been launched to enable antibody conjugation to superior StarBright Dyes, with 32 options spanning the five main laser lines. Our data shows that antibodies conjugated with TrailBlazer Kits are stable for up to one year, owing to the novel SpyTag-SpyCatcher technology used. This makes them ideal for long-term storage and eliminates the need for repeated labeling reactions, giving reproducible data particularly in longitudinal studies. We also present new data illustrating the versatility of these conjugates in various applications. This includes immunocytochemical (ICC) staining microscopy data, where they provide additional options when multiplexing by using kit-conjugated primary or secondary antibodies. In addition, flow cytometry data show that panels can be expanded to include antibodies that have limited fluorophore options, without compromising optimal panel design and without the use of secondary antibodies. In summary, TrailBlazer Kits offer a significant advance for researchers, delivering an easy self-conjugation method and enabling the generation of robust, reproducible multiplexing data in complex biological studies in multiple applications.

#6963 Empowering IL-2 therapy development: A novel humanized mouse model with functional IL-2 and IL-15 receptors.

Fengqian Chen, Zhenlan Niu, Zhi Zhang, Linlin Wang, Xiaofei Zhou

Biocytogen, Waltham, MA

The efficacy of immuno-oncology therapies, particularly those involving cytokines like IL-2 and IL-15, is often limited by their species-specificity and complex receptor interactions, which are poorly recapitulated in wild-type mice. To establish a robust preclinical platform for evaluating novel human-specific immunotherapies and their combinations, we developed a comprehensive seven-gene humanized mouse model.

The B-hPD-1 plus/hIL2/hIL2RA/hIL2RB/hIL2RG/hIL15/hIL15RA mouse model was engineered on a C57BL/6 background by co-integrating seven key human genes: PD-1, IL2, IL2RA, IL2RB, IL2RG, IL15, and IL15RA. Humanization and cell surface expression of the encoded proteins were confirmed via flow cytometry. The IL2 and IL15 were detected by ELISA. Comprehensive immune cell profiling was performed. The model's functionality was validated *in vivo* using syngeneic tumor models treated with human IL-2 (hIL-2), an anti-human PD-1 antibody (Ketruda), and their combination.

Flow cytometry and ELISA confirmed successful expression of the membrane proteins and the secreted protein, respectively. Immune phenotyping demonstrated the presence of key lymphocyte populations capable of responding to human cytokines. In therapeutic studies, monotherapy with hIL-2 or Ketruda significantly inhibited tumor growth compared to control groups. Notably, the combination of hIL-2 and Ketruda resulted in superior, synergistic antitumor efficacy, significantly outperforming either agent alone. Ongoing histopathological (H&E) and clinical pathology (hematology and serum biochemistry) analyses to date indicate no overt toxicity, supporting the model's utility for safety and efficacy assessments.

We have successfully developed and validated a novel seven-gene humanized mouse model that robustly expresses human PD-1, IL-2, IL-15, and their complete receptor complexes. This model supports functional *in vivo* evaluation of human-specific mono- and combination therapies, as demonstrated by the enhanced efficacy of hIL-2 plus anti-PD-1. It represents a unique and powerful preclinical tool for the screening and mechanistic study of next-generation immunotherapies, including cytokines, checkpoint inhibitors, and their synergistic combinations.

#6964 A novel NSG-SGM3xIL15xDKO-based PBMC humanized mouse model to evaluate efficacy and cytokine release of immunotherapies.

Xiaoqing (Nancy) Zheng, Guoxiang Yang, Beau Parry, James G. Keck, Li-Chin Yao

The Jackson Laboratory, Sacramento, CA

We have observed better engraftment of human peripheral blood mononuclear cells (PBMCs) in NSG-SGM3xIL15xDKO (SDKO) mice compared to NSG-MHC I/II DKO (DKO) mice without irradiation. Irradiation is a way to stimulate immune responses. We examined how irradiation affects human PBMC engraftment in SDKO mice and compared engraftment in irradiated SDKO and DKO mice with and without cancer cells. Efficacy and toxicity of anti-CD3xCD19 BiTE were also tested in Raji model of irradiated SDKO and DKO. **Methods** SDKO and DKO mice were intravenously injected with PBMCs with/without irradiation. Retro-orbital (RO) bleeding was performed to check engraftment with flow cytometry. SDKO and DKO mice were also injected with cancer cells prior to intravenous injection of PBMCs after irradiation. RO blood and spleen were collected to check engraftment of various cell types. Raji-luc-bearing SKO and DKO mice with irradiation were treated with PBS or anti-CD3xCD19 BiTE. Xenogen was performed to measure tumor burdens, and plasma was collected to measure cytokine levels with Luminex assay. **Results** Irradiation accelerated human CD45 (hCD45) cells engraftment in SDKO mice. On day 10 or 14, SDKO mice after irradiation showed 3 folds of hCD45 engraftment compared to SDKO mice that didn't receive irradiation. CD3+ T cells, CD19+ B cells and CD56+ nature killer (NK) cells were engrafted at 2-6 fold higher in irradiated SDKO mice at early timepoints compared to non-irradiated mice. Irradiation significantly improved B cells and NK cells in SDKO mice compared to no irradiation. PBMCs were engrafted at higher levels in SDKO compared to DKO after irradiation. It included CD4+T cells, CD8+T cells, B cells and NK cells in the blood and spleen. On day 9, T cells, B cells, NK cells, dendritic cells (DC) and macrophages in the spleen were 2-10 fold higher in irradiated SDKO compared to DKO. B cell lymphoma Raji cells stimulated PBMCs to engraft after irradiation, including T cells, NKs and macrophages in the spleen. More importantly, SDKO was engrafted at significantly higher cell counts compared to DKO with Raji cells stimulation, including DCs and macrophages. Lastly, we found SDKO supported Raji growth with higher tumor burden on three days after implantation compared to DKO. At the same time, Raji-bearing SDKO responded to anti-CD3xCD19 BiTE faster than DKO, making SDKO a more sensitive model to test BiTE efficacy than DKO. In addition, cytokines production after anti-CD3xCD19 BiTE was much higher in SDKO than DKO in the Raji model. **Conclusion** Irradiation not only expediates engraftment of human PBMCs in SDKO mice. Various cell types, including B cells, NK cells, DCs and macrophages, plus T cells are engrafted at higher cell counts in SDKO than DKO with/without cancer cells stimulation with irradiation. In addition, SDKO implanted with cancer cells is a more sensitive platform than DKO to test drug efficacy and toxicity.

#6965 Utilizing a humanized CD8 mouse model for non-clinical studies of cancer immunotherapy.

Hannah Horton[1], Zhi Zhang[1], Zhiyuan Shen[2], Zhenlan Niu[1], Xiaofei Zhou[1]

[1]Biocytogen, Waltham, MA,[2]Biocytogen, Beijing, China

Background: The CD8 is a cell surface glycoprotein found on most cytotoxic T lymphocytes that mediates efficient cell-cell interactions within the immune system. The CD8 acts as a coreceptor with the T-cell receptor on the T lymphocyte to recognize antigens displayed by an antigen-presenting cell in the context of class I MHC molecules. The coreceptor functions as either a homodimer composed of two alpha chains or as a heterodimer composed of one alpha and one beta chain. Both alpha and beta chains share significant homology to immunoglobulin variable light chains. Cytotoxic CD8+ T cells of the adaptive immune system are the most powerful effectors in the anticancer immune response and constitute the backbone of cancer immunotherapy.
Methods: To more accurately evaluate the efficacy of drugs targeting the human immune system, Biocytogen generated a CD8 humanized mouse model that expresses the human CD8 protein.
Results: Protein expression analysis of this novel humanized CD8 mouse strain indicates that the model exclusively expresses human CD8 protein without mouse CD8 protein detection. Immunoprofilling analysis demonstrates that the proportions of various immune cell subsets remain unaffected following CD8 humanization. This model possesses normal T cell immunogenic function, as confirmed by OVA-induced immune responses. *In vivo* efficacy studies show that CD8+ T cells in this model can effectively kill tumor cells. These findings indicate that the CD8 mouse model serves as a powerful research tool, which can not only be used to study and validate the *in vivo* efficacy of anti-human CD8 agonistic antibodies, but also to investigate CD8-targeting drugs or their synergistic effects with other therapies (such as checkpoint inhibitors).
Conclusion: We have established a promising preclinical research model using CD8 humanized mice. This model serves as a powerful preclinical tool for assessing the efficacy of CD8+ T cell-based immunotherapies, including immune checkpoint blockers, neoantigen vaccines, CAR-T, and TCR-T cell therapies.

#6966 A novel humanized mouse model for evaluating anti-human IL23R drugs.

Qiurong Wang, Chun Wang, Chong Li, Xiaofei Zhou, Linlin Wang, Jing Guo

Biocytogen, Waltham, MA

Background: Numerous clinical studies have found increased levels of IL-23 in various autoimmune diseases, including psoriasis, inflammatory bowel disease (IBD), rheumatoid arthritis (RA), and multiple sclerosis (MS). Targeted therapy against IL-23 has made significant progress in the field of autoimmune diseases, becoming a research hotspot and a key therapeutic target. However, new research indicates that the role of IL-23 is not limited to autoimmune diseases; its potential in tumor immunotherapy is equally noteworthy. Preclinical studies have shown that IL-23 exhibits tumor-promoting properties in various cancer models and is associated with poor patient prognosis. Therefore, ablation of IL-23 or its receptors could reduce tumor burden. Most currently developed drugs targeting human IL23R do not recognize mouse IL23R, therefore mouse models cannot be used for preclinical efficacy or safety evaluations.

Methods: To conduct preclinical evaluation of anti-human IL23R-based therapies, Biocytogen developed a novel humanized mouse model, B-hIL23R/hIL12RB1 plus/hIL12RB2 ad mice, expressing human IL23R, IL12 receptor β1, and IL12 receptor β2. The function of the humanized IL12 receptor complex was validated by stimulating isolated mouse CD4+ T cells with recombinant mouse IL12 and human IL12 and measuring mouse IFN-γ secretion. The function of the humanized IL23 receptor complex was validated by stimulating isolated mouse CD4+ T cells with recombinant mouse IL23 and human IL23 and measuring mouse IL17A secretion. The effect of the test article TA1 (provided by the client) on the humanized IL23 pathway was validated *in vitro*.

Results:*In vitro* stimulation with mouse IL12 and human IL12 induced the secretion of mIFN-γ by CD4+ T cells of C57BL/6 mice, while human IL12 induced the secretion of mIFN-γ by CD4+ T cells of B-hIL23R/hIL12RB1 plus/hIL12RB2 ad mice, confirming the function of the humanized IL12 receptor complex. *In vitro* stimulation with mouse IL23 and human IL23 induced the secretion of mIL17A by CD4+ T cells of C57BL/6 mice and B-hIL23R/hIL12RB1 plus/hIL12RB2 ad mice, confirming the function of the humanized IL23 receptor complex. *In vitro* use of the test article TA1 (provided by the client) significantly inhibited the secretion of mouse IL17A in the humanized IL23 pathway of B-hIL23R/hIL12RB1 plus/hIL12RB2 ad mice.

ConclusionThe humanized IL12 receptor complex and humanized IL23 receptor complex in B-hIL23R/hIL12RB1 plus/hIL12RB2 ad mice are functional and provide a valuable preclinical evaluation mouse model for assessing therapies targeting human IL23 and human IL12 receptors.

#6967 Humanized HLA-A11.1 mice: A preclinical platform for novel vaccine evaluation.

Qiurong Wang, Zhenlan Niu, Shuaiqiang Zhang, Xiaofei Zhou

Biocytogen, Waltham, MA

The Major Histocompatibility Complex (MHC) plays a critical role in the immune defense by presenting antigenic peptides and initiating T cell-mediated immunity. Due to significant genetic differences between animal MHC and the human leukocyte antigen (HLA) system, HLA-humanized mouse models provide a valuable platform for investigating HLA-A-restricted immune responses and facilitating vaccine development.

In this study, we established a novel B-HLA-A11.1 humanized mouse model and systematically characterized its phenotypic and immunological profiles. Blood routine examination and biochemical analysis revealed that B-HLA-A11.1 mice exhibited parameters comparable to those of wild-type controls, indicating that HLA-A11.1 humanization did not adversely affect erythrocyte composition, hematocrit morphology, or the health of major organs such as the heart, liver, and kidneys. Overall, these results support the normal development of B-HLA-A11.1 mice and the absence of spontaneous pathology attributable to HLA humanization. To assess HLA-restricted immunogenicity, HLA-A11.1 and wild-type mice were immunized with a KRAS*G12V peptide. ELISPOT analysis confirmed the induction of peptide-specific T-cell responses exclusively in HLA-A11.1 mice, underscoring the model's HLA-restricted functionality. Furthermore, immunization of the mice with the candidate peptide, followed by tetramer staining flow cytometry, demonstrated that the peptide activated antigen-specific CD8+ T cells. These activated T cells can be utilized for subsequent T cell receptor (TCR) screening.

We further evaluated the efficacy of an mRNA vaccine targeting KRAS*G12V in B-HLA-A11.1 mice. The vaccine significantly suppressed tumor growth compared to the control group. Furthermore, we investigated the combination of the mRNA vaccine with an anti-PD-1 antibody in this model. The experimental data revealed that the combination therapy induced a significantly greater inhibition of tumor growth than either monotherapy.

In summary, our findings demonstrate that the B-HLA-A11.1 humanized mouse model serves as a robust preclinical platform for the *in vivo* and *ex vivo* assessment of novel peptide- and mRNA-based vaccines.

#6968 Preclinical assessment of cell, gene, and antibody therapies using humanized mice.

Audrey Wetzel, Emilie Bayon, Sebastien Tabruyn, **Dan Georgess**

TransCure bioServices, Archamps, France

The preclinical assessment of cell, gene, and antibody therapies is substantially more predictive when performed in humanized immune system (HIS) mice engrafted with human tumors than in immunodeficient or syngeneic models. Here, we present a series of studies illustrating how HIS mice enable evaluation of efficacy, persistence, biodistribution, and safety for diverse therapeutic modalities in ways not achievable in other mouse systems.In the therapeutic antibody category, we first show that HIS mice reconstituted with hematopoietic stem cells from different donors recapitulate the inter-patient heterogeneity observed in responses to immune checkpoint inhibitors (ICIs), and that combining ICIs with macrophage-targeting antibodies markedly enhances antitumor efficacy. In complementary studies, we used HIS mice to rank three engineered variants of T-cell engagers (TCEs) and, separately, three variants of antibody-drug conjugates (ADCs) on the basis of both efficacy (tumor growth inhibition) and safety (systemic IFN-γ, body-weight loss, and survival), identifying the top-performing lead in each class. We also compared the activity of a TCE as a single agent versus a tumor-targeting antibody (TTA) and their combination. Finally, we conducted dose-response efficacy studies of a natural killer cell engager (NKCE). None of these investigations would be feasible in models lacking sufficient reconstitution of human T lymphocytes, macrophages, and NK cells. In the cell therapy category, we evaluated CAR-T, CAR-NK, and TCR-T cells across multiple tumor types. We show that HIS mice enable de-risking of immunogenicity by revealing rapid clearance of allogeneic CAR-T cells that are insufficiently stealthy, yet would otherwise persist for days-to-weeks in immunodeficient mice. Through adoptive cell-transfer experiments, we further demonstrate that CAR-NK cells can be durably supported in HIS mice and exhibit potent antitumor activity, and that iterative optimization of TCR-T constructs can fully suppress growth of an aggressive tumor model. Across these studies, HIS mice reproduced clinical, cellular, and molecular features of immune-related adverse events (irAEs) and cytokine release syndrome (CRS), while concurrently enabling assessment of biodistribution, target engagement, long-term persistence, and therapeutic efficacy. In conclusion, HIS mice constitute a powerful platform for reducing false-positive and false-negative outcomes in the preclinical evaluation of novel therapeutics, thereby improving predictivity and supporting more informed clinical-trial decision-making.

#6969 Analysis of 1000 secreted proteins in functional genomics and compound screens reveals cytotoxic and immunomodulatory targets.

Nathaniel Robichaud[1], Amy Johnson[1], Alistaire Sherman[1], **Eric Miller**[2], Narges Rashidi[1], Milad Dagher[1]

[1]Nomic Bio Inc, Montreal, QC, Canada,[2]Sales and Marketing, Nomic Bio Inc, Montreal, QC, Canada

The identification of novel cancer immunotherapies and the characterization of their immunomodulatory effects is complicated by the plasticity of immune cells and the wide range of phenotypes they may adopt. However, the high cost of capturing this diversity at scale limits typical drug discovery efforts to simple readouts. The Nomic platform is a novel proteomics tool capable of quantifying thousands of proteins at high-throughput and low cost, leveraged here in functional genomics and compound screens, simultaneously characterizing immunomodulatory and cytotoxic effects.

We collected supernatants for secretome analysis from the CPJUMP1 dataset, in which U2OS osteosarcoma cells were perturbed with matched ORF, CRISPR KO, and compound libraries targeting 161 genes, and quantified 191 cytokines using a Nomic Flex panel. Overexpression of upstream kinases induced an inflammatory phenotype, consistent with established oncogene-induced inflammation. Furthermore, as seen in morphological analyses, CRISPR KO phenotypes were poorly matched with the phenotypes of compounds targeting corresponding genes due to poor specificity of compounds for individual targets.

To further characterize on-target and off-target immunomodulatory effects of compounds, we quantified 1000 proteins in supernatants from hepatocytes treated with 510 compounds at three concentrations for 48h, using the Omni 1000. Cytotoxic compounds such as staurosporine resulted in intracellular proteins leaking out of cells and being detected in the supernatant, whereas resiquimod, a TLR7/8 agonist, induced the expression of a variety of cytokines. Clinically-relevant immunotoxicity was captured: thus, methylprednisolone was generally anti-inflammatory, but with paradoxical increases in SAA and IL-6, consistent with paradoxically inflammed livers seen in patients. Actinomycin D was cytotoxic while inducing IL-1b and TNFa, consistent with the immune contribution to this compound's anti-cancer properties. Finally, we demonstrated the capacity of secretome analysis to probe pathways regulating cytokine expression. For example, comparison of a set of 11 mTOR inhibitors identified on-target immune modulation and off target effects at increasing doses, enabling characterization of compound potency and specificity.

Our results demonstrate the value of high-throughput proteomics to identify new immunomodulatory targets and compounds, evaluate potential toxicities, and characterize potency and specificity.

: Novel Models of Immunotherapy Response
Poster Session

#6973 B-NDG hIL15, FcγR KO mice: An optimized humanized model for evaluating T cell-modulating antibodies.

Jiyue Chen, Yanhui Nie, Dexuan Huang, Qingqing Xu, Qiang Liu, Xiaofei Zhou

Biocytogen, Waltham, MA

Background:
Immune checkpoint inhibitors targeting PD-1, PD-L1, and CTLA-4 have achieved remarkable clinical success, but preclinical validation using human immune system (HIS)-reconstituted mice remains challenging. Conventional immunodeficient models often fail to reproduce the efficacy observed in target humanized or immunocompetent mice. The poor antibody pharmacokinetics and suboptimal immune function in HIS models contribute to these discrepancies. In particular, murine innate immune cells expressing Fc gamma receptors (FcγRs) can bind therapeutic antibodies, accelerate their clearance, and induce nonspecific antibody-dependent cellular phagocytosis (ADCP), confounding efficacy assessment. Moreover, insufficient reconstitution and activation of human T cells limit the evaluation of the immune response. Human IL-15 is known to enhance T-cell survival and function following human PBMC engraftment in immunodeficient mice.
Methods:
To address these limitations, Biocytogen developed B-NDG hIL15, FcγR KO mice by expressing human *IL15* and knocking out the murine FcγR genes on the B-NDG background lacking mature T, B, and NK cells. Flow cytometry confirmed the absence of all four FcγRs in splenocytes. After injection of human IgG1 antibody, binding of IgG1 to CD45+ cells was detected in B-NDG mice and B-NDG hIL15 mice, but not in B-NDG hIL15, FcγR KO mice, confirming successful gene deletion. Serum human IL-15 concentration was approximately 112 pg/mL. The distribution and frequency of granulocytes, monocytes, macrophages, and dendritic cells were comparable between B-NDG hIL15 mice and B-NDG hIL15, FcγR KO mice.
Results:
Pharmacokinetic analysis after intravenous injection of an anti-human CTLA-4 IgG1 antibody revealed that antibody clearance was fastest in B-NDG mice and slowest in B-NDG hIL15, FcγR KO mice, indicating significantly prolonged serum half-life. To evaluate antibody efficacy, human PBMCs were engrafted into B-NDG hIL15, FcγR KO mice, followed by subcutaneous implantation of three human PD-L1-high tumor cell lines (HCC827, NCI-H1975, and MDA-MB-231). Treatment with a Keytruda analog (anti-human PD-1 antibody, in-house) via intraperitoneal injection resulted in significant tumor growth inhibition across all models, demonstrating improved immunotherapeutic responsiveness.
Conclusion:
The huPBMC-B-NDG hIL15, FcγR KO mice provide a superior platform for evaluating the efficacy of therapeutic antibodies that modulate human T-cell functions, including immune checkpoint inhibitors.

#6974 A CD3/CD19 double-humanized mouse model for preclinical evaluation of CD19-targeted T-cell engagers.

Shuang Li, Lei Ci, Yi Li, Ruilin Sun

GenoBioTX LLC, Sugar Land, TX

Background: Immunotherapy has transformed the treatment landscape for cancer and autoimmune diseases, with T-cell engagers (TCEs) emerging as a highly promising therapeutic modality. Among them, CD19-targeting TCEs have achieved notable clinical success in B-cell malignancies such as leukemia and lymphoma. However, despite these advances, the development of more sophisticated preclinical models remains essential to better recapitulate human immune responses and to deepen our understanding of TCE efficacy and safety. To address this need, we established a novel CD3/CD19 double-humanized mouse model specifically designed to provide a more accurate and comprehensive in vivo platform for evaluating CD19-directed TCE therapies.

Methods: The CD3 humanized mouse model was generated via ES cell-based gene targeting, in which full-length mouse *Cd3e/Cd3d/Cd3g* gene clusters were replaced with the corresponding human *CD3E/CD3D/CD3G* coding sequences. Separately, we developed the CD19 humanized mice using CRISPR/Cas9 engineering and subsequently crossed them with hCD3 strain to obtian the CD3/CD19 dual humanized mouse model. The expression of human CD3 and CD19 protein in hCD3/hCD19 dual knockin mice was confirmed by flow cytometry. We further characterized the model by examining immune cell subsets—including T and B cell populations—as well as basic physiological and biochemical parameters to ensure normal baseline health status. Finally, the hCD3/hCD19 dual knockin mice were treated with Blinatumomab, a first-in-class CD19-targeting BiTE used clinically for B cell malignancies, to evaluate its efficacy in depleting B cells in vivo.

Results: As expected, the expression profiles of human CD3 and CD19 in hCD3/hCD19 dual knockin mice were consistent with those observed in human. Additionally, the CD3/CD19 humanized mice displayed a fully functional immune system with well-developed T and B cell populations, and their physiological parameters were comparable to those of wild-type controls. Following Blinatumomab administration, the hCD3/hCD19 mice exhibited robust B cells depletion, confirming the model's suitability for assessing CD19-directed therapeutic activity. Furthermore, in hCD3/hCD19 mice with induced systemic lupus erythematosus (SLE), Blinatumomab treatment reduced anti-dsDNA antibody levels in parallel with B cell depletion, indicating the utility of this dual humanized model for preclinical evaluation of anti-CD19 therapies for autoimmune disease.

Conclusion: Our CD3/CD19 double-humanized mouse model represents an advanced and reliable tool for preclinical evaluation of CD19-targeted immunotherapies, including TCEs.

#6975 Endogenous retrovirus-derived neoantigens enable a personalized cancer vaccine strategy for glioblastoma.

Megan Campbell Benz[1], Kenan Zhang[2], David M. Ashley[3], Christian Garde[4], Kirit Singh[3], Ohrt Andersen Rasmus[4], Birgitte Rono[4], Daniela Kleine-Kohlbrecher[4], Stine Friis Thorsen[4], Kelly M. Hotchkiss[1], Jose R. Conejo-Garcia[1], Mustafa Khasraw[5]

[1]Duke University School of Medicine, Durham, NC,[2]Duke University, Durham, NC,[3]Duke University Medical Center, Durham, NC,[4]Evaxion Biotech, Horsholm, Denmark,[5]Duke Cancer Institute, Durham, NC

Introduction/Rationale: Glioblastoma is refractory to immunotherapy because of low mutational burden and paucity of canonical neoantigens. Aberrant expression of endogenous retroviral elements (ERVs), reactivated genomic remnants of ancient viral insertions, may provide an alternative, tumor-specific antigen source suitable for personalized vaccines incorporating both mutation- and ERV-derived epitopes.
Methods: Tumor and matched normal tissues from 25 glioblastoma patients, including 18 long-term survivors (>5 years) and 7 short-term survivors (<18 months), underwent whole-genome and RNA sequencing. Candidate antigens were predicted using AI-based pipelines to identify mutation-derived neoantigens and to derive ERV-encoded epitopes. AI-identified tumor-specific vaccine candidates were ranked by expression, predicted MHC class I and II binding affinity, clonality, and immunogenicity. Top candidates informed design of a personalized DNA vaccine encoding ten patient-specific sequences with a CCL19 molecular adjuvant to enhance dendritic-cell recruitment. ERV-derived immunogenicity was assessed by IFN-γ ELISpot using peripheral blood mononuclear cells (PBMCs) from HLA-typed healthy donors stimulated with synthetic peptides.
Results: High-quality mutation-derived neoantigens were rare (median 3 per patient). In contrast, all tumors expressed abundant, patient-specific ERV transcripts independent of mutation load, with several loci showing clonal, tumor-restricted expression. ERV-derived peptides demonstrated strong predicted MHC class I and II binding, and 22 of 25 tumors contained ERV epitopes meeting criteria for vaccine inclusion. These mapped predominantly to HERV-K and HERV-W families and frequently overlapped interferon-stimulated genomic loci, consistent with innate immune or epigenetic activation. Functional validation studies have demonstrated significant ERV-specific IFN-γ responses in certain HLA allele contexts, highlighting the potential for allele-specific immunogenicity. While T-cell responses were observed in selected donor profiles, others exhibited more restricted reactivity despite validated positive controls, underscoring the importance of genetic context in immune response profiles. Additionally, our ongoing analyses are focused on elucidating ERV expression signatures that may correlate with sustained immune control by comparing long-term and short-term survivor cohorts, with the aim of identifying key immunological patterns associated with favorable outcomes.
Conclusion: ERVs are consistently expressed, immunogenic, and largely tumor-restricted in glioblastoma, providing a scalable antigen source that may overcome limitations imposed by low mutational burden. These findings offer a strong proof-of-concept for personalized DNA vaccines incorporating ERV-derived neoantigens.

#6976 B-CDG mice: A novel severe immunodeficient model suitable for radiotherapeutic and radiopharmaceutical evaluation.

Qiurong Wang, Yanhui Nie, Ruili Lv, Chengzhang Shang, Meiqi Zhang, Qingqing Xu

Biocytogen, Waltham, MA

Background:
Radiopharmaceuticals have emerged as an important therapeutic strategy, but their evaluation in preclinical models is limited by the radiosensitivity of commonly used immunodeficient mice. The B-NDG mice (NOD.CB17-*Prkdc*^{scid} *Il2rg*^{tm1Bcgen}/Bcgen), generated via *Prkdc* mutation, lack mature T and B cells but are hypersensitive to DNA damage due to impaired DNA repair, leading to rapid body weight loss and mortality under irradiation.
Methods:
To overcome these limitations, Biocytogen developed the B-CDG mice on a C57BL/6 background by knocking out *Rag2* and *Il2rg*. This strain lacks mature T, B, and NK cells but retains normal DNA repair capability. Comparative analyses of B-CDG mice and B-NDG mice were performed under X-ray irradiation at doses of 1, 2.5, 4, and 7 Gy. Survival, body weight, hematology, and histopathology were assessed. Additionally, multiple human tumor cell lines—LNCap Clone FGC, 22Rv1, BT-474, AsPC-1, and SHP-77—were tested for xenograft formation.
Results:
B-CDG mice demonstrated superior tolerance to radiation. At 1 Gy and 2.5 Gy, all B-CDG mice survived 30 days, while all B-NDG mice exposed to ≥2.5 Gy died within 2 days. At 4 Gy, partial survival was observed in B-CDG mice, with recovery of body weight after initial decline. Hematology revealed dose-dependent decreases in leukocytes, erythrocytes, and platelets, with subsequent recovery at 30 days. Histological analysis showed extramedullary hematopoiesis in the liver and spleen of B-CDG mice, milder cellular injury, and compensatory marrow regeneration compared to B-NDG mice. Moreover, all tested tumor cell lines successfully established xenografts in B-CDG mice.
Conclusion:
B-CDG mice are a novel severe immunodeficient strain that maintains DNA repair competence and radiation tolerance. These characteristics make B-CDG mice an ideal platform for evaluating the efficacy and toxicity of radiopharmaceuticals and other DNA-damaging agents.

#6977 B-NDG MHC I/II DKO mice plus: A refined humanized model for evaluating T cell engager efficacy and toxicity.

Kelvin Yin, Yanhui Nie, Zhi Zhang, Meiqi Zhang, Yanling Wang, Qiang Liu

Biocytogen, Waltham, MA

Background: T cell engagers (TCEs) have demonstrated potent anti-tumor efficacy but can cause severe immune-related toxicities such as cytokine release syndrome (CRS). Accurate preclinical evaluation of TCE efficacy and safety requires an appropriate humanized animal model. Human PBMC-engrafted immunodeficient mice, such as B-NDG mice that lack mature T, B, and NK cells, are commonly used for this purpose. However, in B-NDG mice, human T cells become aberrantly activated due to interspecies MHC incompatibility, leading to severe graft-versus-host disease (GvHD) that confounds TCE efficacy and toxicity assessments.
Methods: To reduce GvHD, B-NDG MHC I/II DKO mice plus were developed by deleting *B2m* and *H2-Ab1* genes encoding MHC class I and II molecules, respectively. Additionally, a fusion of *B2m* and *Fcgrt* genes was introduced to restore expression of heterodimeric FcRn, minimizing the impact of *B2m* deletion on IgG metabolism. Flow cytometric analysis confirmed the absence of MHC I/II expression in splenocytes. After intravenous administration of anti-human CTLA antibody, serum drug concentrations in B-NDG MHC I/II DKO mice plus were comparable to those in parental B-NDG mice, indicating preserved IgG pharmacokinetics.
Results: To assess the effect of MHC deletion on GvHD, B-NDG, B-NDG B2m KO plus, and B-NDG MHC I/II DKO mice plus were irradiated and intravenously injected with human PBMCs from three donors. Most B-NDG and B2m KO mice developed severe GvHD and died within four weeks, whereas B-NDG MHC I/II DKO mice plus exhibited markedly alleviated GvHD with donor-dependent variability. These findings indicate that dual MHC I/II deletion significantly mitigates PBMC-induced GvHD. Furthermore, in PBMC-humanized B-NDG MHC I/II DKO mice plus bearing subcutaneous NCI-N87 gastric tumors, treatment with an anti-human CD3/HER2 bispecific antibody analog (in-house) significantly inhibited tumor growth. Similarly, in SHP-77 small cell lung cancer xenografts, Tarlatamab analog treatment suppressed tumor progression and elevated serum cytokines (IFNγ, TNFα, IL10, IL6, IL4, IL2) following dosing, reflecting robust T cell activation.
Conclusion: B-NDG MHC I/II DKO mice plus effectively alleviate human PBMC-induced GvHD while retaining normal antibody pharmacokinetics and enabling reliable assessment of TCE anti-tumor efficacy and cytokine-mediated toxicity. This model provides a refined and translationally relevant platform for preclinical evaluation of TCE therapeutics.

#6978 HIS models lacking FcγR provide increased predictability and facilitate study design for evaluation of immuno-oncology therapeutics.

Monika Buczek, Philip Dube, Nicholas Smith, Janell Richardson, Louise Baskin, Esther Andino, Debra Freer, Kathleen Bott

Taconic Biosciences, Inc., Rensselaer, NY

Humanized immune system (HIS) mouse platforms that support durable human NK and T cell function are essential for evaluating CAR-NK and CAR-T therapies. Residual murine Fc gamma receptors (FcγRs) can confound interpretation of IgG-based therapeutics and engineered cell products. We compared hIL-15 NOG and FcγR-null FcResolv™ hIL-15 NOG mice engrafted with human NK cells and observed equivalent ≥12-week persistence and stable $CD56^{+}CD16^{+}$ profiles, enabling extended engineered-cell studies. In $CD34^{+}$ HIS tumor models, anti-PD1 efficacy and pharmacodynamics were accurately detected only in FcResolv™ mice. FcγR-null HIS platforms improve predictive assessment of CAR-NK/CAR-T efficacy, trafficking, and off-target responses.

#6979 An immune-competent, durable MB49-Luc orthotopic bladder cancer model demonstrates bladder-specific tumor immunity for translational immunotherapy research.

Melanie He, Mirian Sifuentes, Neo Wang, Zhigang Peng, Minqi Huang

EnquBio Inc., San Diego, CA

Background and Objective: Bladder cancer remains a significant health concern in the United States, with approximately 85,000 new cases and 17,000 deaths annually. Nearly 70% of cases present as non-muscle-invasive bladder cancer (NMIBC), commonly treated with transurethral resection followed by intravesical immunotherapy. However, limited and inconsistent responses to current therapies underscore ongoing clinical challenges. To enable effective therapeutic development, a reliable, immune-competent, and longitudinally trackable preclinical model capable of representing the unique immune and physiological features of bladder cancer is essential. Despite decades of effort to refine syngeneic orthotopic bladder cancer models in mice, low tumor take rates and limited in-life study duration remain major challenges. Here, we present a syngeneic orthotopic bladder cancer model with extended in-life monitoring capacity that recapitulates bladder tumor immunity and enables robust immunotherapy evaluation.

Method and Result: A luciferase-expressing MB49 cell line was generated via lentiviral transduction. Female C57BL/6 mice were implanted intravesically to establish an orthotopic tumor model. In-life bioluminescence imaging (BLI) using IVIS revealed stable and quantifiable bladder-localized tumor signals for more than 21 days, with a 100% tumor take rate. Tumor presence in the bladder lumen was confirmed by H&E histopathology. Tumor-bearing bladders collected on Days 10 and 21 underwent next-generation sequencing (NGS) and subsequent enrichment analysis. Differential gene expression revealed biomarker signatures reflective of early- and late-stage tumor burden, along with dynamic immune-profiling changes. Pathway enrichment analysis linked these gene-level differences to functional networks governing immune regulation, tumor progression, and bladder cancer physiology.

Conclusion: We established an optimized MB49-Luc orthotopic bladder cancer model that preserves immune relevance, provides a prolonged imaging window, and demonstrates distinct molecular transitions during tumor progression. This long-duration, immune-competent platform enables rigorous evaluation of intravesical and immuno-oncology therapeutics and offers meaningful translational insights to support next-generation NMIBC immunotherapy development.

#6980 PDX*ovo*: Avian embryos as hosts for rapid and quantitative modelling of immunotherapy responses in patient-derived xenografts.

Olivia R. Grafinger[1], Kabir A. Khan[1], Esther Matus[2], Ping Xu[1], Sara Mar[2], Yan Li[1], David E. Goertz[1], Wilder Scott[1], Jean Gariepy[1], Katarzyna J. Jerzak[2], Robert S. Kerbel[1], Hon S. Leong[1]

[1]Sunnybrook Research Institute, Toronto, ON, Canada,[2]University of Toronto, Toronto, ON, Canada

The purpose of patient-derived xenograft (PDX) technology as a pre-clinical model for drug sensitivity testing is well established, but this does not include immunotherapies. When mouse hosts are used, the non-cancer cells within the human tumor xenograft are replaced with murine stromal cells. The lack of the patient's tumor-infiltrated lymphocytes (TILs) within these mouse-based xenografts prohibits immunotherapy testing. We show that avian embryos as a host for PDXs are a superior model because of the ability to test a wide range of therapies, including immunotherapies, because TILs from the patient are still present in the xenograft within days of engraftment in the chorioallantoic membrane (CAM) of the avian embryo. To validate this model for immunotherapy drug testing, we engrafted murine tumors sensitive to PD-L1 immunotherapy into CAM of avian embryos and battle-tested this technology in various experimental conditions. By controlling the amount of mouse TILs in these xenografts, we demonstrate the utility of the PDX*ovo* (PDX *ex ovo*) for testing immunotherapies. We then performed feasibility studies on fresh material from kidney, colorectal, and breast cancer human patients, revealing anti-tumor responses concordant with the initial and final number of human TILs. Finally, spatial omics technology was applied to compare the tumour-immune microenvironment of the original murine tumours to their xenograft counterparts grown in the avian embryo. These findings demonstrate compelling evidence supporting the efficacy of the PDX*ovo* system for maintaining the integrity of the original tumour architecture as well as immune cell populations. Additionally, this model offers high tumor take rate of fresh tumor material, all within 10 days of engraftment. The speed of these experiments is also mirrored by their low cost, which points to their potential role for timely drug sensitivity testing and patient eligibility for existing and emerging therapies.

#6981 Involvement of type I interferon signaling in anti-PD-1-induced tumor rejection in a novel humanized NOG-FcγR$^{-/-}$ mouse model.

Tatsuhito Ii[1], Ting-Wei Yu[1], Katsutoshi Sato[1], Hirotaka Inoue[2], Ayumu Tsubosaka[3], Miwako Kakiuchi[3], Daisuke Komura[3], Ikumi Katano[1], Nao Suzuki[1], Iyo Ootsuka[1], Motohito Goto[4], Misa Mochizuki[5], Kenji Kawai[6], Shumpei Ishikawa[3], Masami Suzuki[5], Takeshi Takahashi[1]

[1]Division of Advanced Biomedical Research, Central Institute for Experimental Medicine and Life Science, Kawasaki, Japan,[2]Department of Neurosurgery, Graduate School of Medical Sciences, Kumamoto University, Kumamoto, Japan,[3]Preventive Medicine, Graduate School of Medicine, The University of Tokyo, Bunkyo-ku, Japan,[4]Laboratory Animal Resource Center, Central Institute for Experimental Medicine and Life Science, Kawasaki, Japan,[5]Division of Translational Research, Central Institute for Experimental Medicine and Life Science, Kawasaki, Japan,[6]Central Institute for Experimental Medicine and Life Science, Kawasaki, Japan

Introductory sentence: To investigate the relationship between anti-PD-1 therapy and immune cells, a model that recapitulates the human tumor microenvironment is required. We previously established a humanized NOG-FcγR$^{-/-}$ mouse model, in which anti-tumor effects by anti-human PD-1 anibody can be confirmed in vivo. Among several tested cell lines, the head and neck carcinoma line HSC4 showed the highest sensitivity in this model. In the present study, we grafted HSC4 cells into humanized NOG-FcγR$^{-/-}$ mice and performed single-cell RNA sequencing (scRNA-seq) and spatial transcriptomic analyses to elucidate the molecular and cellular mechanisms of the tumor rejection.

Experimental procedures: Human immune cells were reconstituted in NOG and NOG-FcγR$^{-/-}$ mice by transplantation of human hematopoietic stem cells. One week after grafting HSC4 cells, the mice received intraperitoneal injections of anti-human PD-1 antibody once weekly for two weeks.For scRNA-seq, CD45^{+} cells were isolated from the grafted tumors, whereas FFPE tumor samples were used for spatial transcriptomic analysis following standard protocols.

New, unpublished data: In the scRNA-seq data, human immune cells were clustered into naïve-like CD4^{+} T cells, cytotoxic CD8^{+} T cells, regulatory CD4^{+} T cells, CXCL13^{+} helper T cells, and macrophages. Pseudobulk analysis with GSEA identified the interferon-α (IFN-α) response as a top enriched pathway in nivolumab-treated NOG-FcγR$^{-/-}$ mice. Feature plots showed that IFN-α-related genes were broadly expressed across human immune cell populations. To further explore this response, we analyzed the transcriptional profiles of CXCL13^{+} helper T cells, since their role in tumors remains unclear.In the spatial transcriptomic analysis, after excluding mouse-derived and low-RNA-content spots, five tumor clusters and one immune cluster containing human T cells and macrophages were identified based on marker genes and spatial context. GSEA revealed that tumor cells located near CXCL13^{+} immune cells predominantly exhibited basal-like features, along with upregulation of type I IFN-related pathways. RNAscope analysis confirmed CXCL10, an IFN response marker, in immune cells and tumor cells with basal-like feature but not in tumor cell with squamous differentiation.

Conclusions: Our results suggest that tumor regression in this model is mediated by type I IFNs within the tumor microenvironment. This mechanism parallels the effects of nivolumab in human tumors, suggesting that this model provides a valuable platform for studying immune checkpoint inhibitor therapy.

#6982 Patient-derived uveal melanoma organoids reveal HLA-I-restricted tumor antigens and tumor-reactive T cells.

Alexander Lim, Wei Tian, Zhuoning Li, Mara Monetti, Alexander Noor Shoushtari, James Smithy, Samuel Tischfield, Mark Donoghue, David A. Scheinberg, **Chenyang Zhan**

Memorial Sloan Kettering Cancer Center, New York, NY

Background: Uveal melanoma (UM) is a rare but aggressive melanoma subtype with limited response to immune checkpoint inhibitors. Identifying tumor-specific or associated antigens and tumor-reactive T cells is critical to advancing precision immunotherapy. Patient-derived tumor organoids (PDOs) offer a physiologically relevant *ex vivo* model to study tumor-immune interactions and to uncover novel therapeutic targets.
Methods: PDOs were established from fine-needle aspiration biopsies of five patients with metastatic UM. HLA-I-restricted immunopeptidomes were successfully characterized in three PDOs through immunoprecipitation of HLA-peptide complexes followed by mass spectrometry (MS). Identified peptides were matched against the UniProt human reviewed database. Dissociated tumor cells from one PDOs were treated with IFN-γ to enhance antigen presentation and then co-cultured with autologous peripheral blood mononuclear cells (PBMCs) for sequential stimulations over four weeks. After a third stimulation, $CD8^+$ T cells were analyzed by flow cytometry and subjected to single-cell RNA and paired V(D)J sequencing using the 10x Genomics platform to define phenotypes and clonotypes of activated T cells. Tumor-reactive TCR clonotypes were identified, and their CDR3β sequences were analyzed using the TCRMatch tool in the IEDB database to assess sequence homology and potential antigen specificity.
Results: Immunopeptidomic analysis identified 3,628, 6,735, and 10,407 unique 8-11mer peptides across three PDOs. Shared tumor-associated antigens (TAAs) included CSPG4, TYRP1, SLC45A2, OCA2, PMEL, TYR, MLANA, and SOX10. T-cell activation assays demonstrated that 12.3% of $CD8^+$ T cells exhibited HLA-I-dependent activation upon restimulation with autologous PDOs, which was abrogated by HLA-I blockade. Single-cell RNA sequencing of $CD8^+$ T cells in the co-culture revealed activated cytotoxic clusters unique in the restimulated cells, characterized by high expression of CD137, GZMH, MIR155HG, PKM, and LAG3. TCR clonotype analysis using TCRMatch identified candidate tumor-reactive TCRs possibly recognizing PMEL, MART-1, and MAGEA10.
Conclusions: This study demonstrates the feasibility of using PDOs from metastatic UM to define the HLA-I-restricted immunopeptidome and to identify tumor-reactive T-cell clonotypes through autologous PDO-PBMC co-culture. The integration of immunopeptidomics with single-cell RNA/TCR sequencing provides a robust framework for mapping patient-specific tumor-immune interactions. Identified TAAs and tumor-reactive TCRs represent potential biomarkers and targets for next-generation precision immunotherapies, including personalized tumor vaccines and TCR-based adoptive cell therapies.

#6983 A novel syngeneic model for evaluating the efficacy of MYC-driven liver cancer targeted and immunotherapy.

Lei Ci, Kai Zhou, Jiangyan Liu, Ruilin Sun

GenoBioTX LLC, Suger Land, TX

In liver cancer, MYC and its signaling pathways undergo significant changes, exerting a profound impact on liver cancer progression. These effects include tumor proliferation, metastasis, dedifferentiation, metabolism, immune microenvironment, and resistance to comprehensive therapies. This makes MYC a highly attractive therapeutic target.Our laboratory engineered mice on a C57BL/6 background with hepatocyte-specific expression of mouse c-Myc, resulting in rapid, spontaneous hepatocellular carcinoma (abbr. c-Myc/ALB model). Primary tumors were harvested and cultured to establish a novel spontaneous tumor cell line. In the c-Myc/ALB syngenic tumor model of immunocompetent C57BL/6 mice, the c-Myc inhibitor 10058-F4 significantly inhibited tumor growth in a dose-dependent manner. The PD-1 antibody in combination of 10058-F4 and immune checkpoint inhibitor PD-1 antibody showed better anti-tumor efficiency.

#6984 Modeling late-stage ovarian cancer and validating oncolytic adenoviral tools for transgene expression and tumor monitoring.

Lakshmi Kadkol[1], Eric Gauchat[2], Maria Jose Godoy Calderon[1], Manali Patwardhan[1], VK Gadi[1]

[1]Medicine, University of Illinois at Chicago, Chicago, IL,[2]Cancer Center, University of Illinois at Chicago, Chicago, IL

Purpose: High-grade serous ovarian cancer (HGSOC) is characterized by profound immune exclusion and peritoneal spread, hypothesized to be orchestrated by the TGF-β and GM-CSF cytokines. We established an immunocompetent murine model of advanced HGSOC and evaluated the tumor selectivity and transgene delivery efficiency of hTERT-driven oncolytic adenoviruses encoding GM-CSF and/or a soluble TGF-β receptor Fc fusion (sTGFβR-Fc).

Experimental Procedures: A syngeneic orthotopic model of advanced HGSOC was established by intraperitoneally injecting luciferase-labeled MOE-KRAS/PTEN (MKP) cells into immunocompetent FVB/N mice. Tumor burden was monitored longitudinally by bioluminescence imaging (BLI). Four hTERT-driven oncolytic adenoviruses (Ad.Null, Ad.GM-CSF [Ad.GM], Ad.sTGFβR [Ad.sT], Ad.sTGFβR.GM-CSF [Ad.sT.GM]) were evaluated in vitro for infectivity, cytolytic activity (Incucyte/caspase 3/7), and transgene expression (flow cytometry) in MKP tumor cells, NIH 3T3 fibroblasts, and 3T3-derived cancer-associated fibroblasts (CAFs).

Results: Serial BLI showed consistent peritoneal tumor engraftment and progression by day 26 (n = 14) confirming model fidelity for late-stage disease. In vitro, IncuCyte live-cell imaging revealed strong, selective apoptosis in MKP cells following oncolytic infection, while NIH 3T3 fibroblasts and CAFs (non-tumor controls) showed minimal response. Apoptotic activity in MKP cells rose sharply at 30-35 hours and peaked at 45 hours post-infection (>60-80% fold increase in caspase3/7+ area over untreated but minimal apoptotic activity in 3T3 and CAFs (<8-fold over untreated). Notably, among virus constructs, Ad.GM and Ad. Null induced the most rapid and robust apoptosis, whereas Ad. sT and Ad.sT.GM showed significantly delayed and reduced effects (Ad.GM vs Ad. Null: $p = 0.0042$; Ad. sT vs Ad.GM or Ad. Null: $p < 0.0001$; 2-way ANOVA with Sidak's test). Transgene expression was quantified by flow cytometry following 48-hour infection. Ad.GM and Ad.sT.GM treatments produced GM-CSF positive cells (2.25% and 1.04% gated, mean fluorescence intensity 6217.54 and 5508.2 respectively) while Ad.sT and Ad.sT.GM treatments produced sTGFβR-Fc positive cells (8.04% and 9.75% gated, mean fluorescence intensity 85092.63 and 84097.65 respectively); live cell frequencies decreased in treated groups (61.45-67.83%) compared to untreated (96.32%) controls. These results demonstrate selective transgene expression and cytotoxicity in tumor cells achieved by the engineered oncolytic constructs.

Conclusions: These data confirm the fidelity for advanced-stage HGSOC model and establish oncolytic adenoviral platforms as effective mechanistic tools—functioning both as cytolytic agents and as delivery vehicles for functional transgenes—to mechanistically dissect TGF-β and GM-CSF signaling in ovarian cancer.

#6985 Overcoming pancreatic ductal adenocarcinoma immunoresistance: Microfluidic-primed organoid interacting lymphocytes demonstrate superior infiltration, cytotoxicity, and tumor suppression in patient-derived models.

Eleftherios Makris, Damian Hutchins, Tiefu Liu, Adam Hall, Lance Miller, Shay Soker, Konstantinos Votanopoulos

Wake Forest University School of Medicine, Winston Salem, NC

Background: Pancreatic ductal adenocarcinoma (PDAC) remains refractory to immunotherapy due to its immunosuppressive tumor microenvironment (TME), characterized by dense desmoplasia, immune exclusion, and T cell exhaustion. With 5-year survival <13%, novel strategies are urgently needed. We developed a platform to generate and evaluate tumor-specific cytotoxic lymphocytes using immunocompetent patient-derived organoids (PTOs) that recapitulate the PDAC TME.
Methods: Immunocompetent PTOs (iPTOs) were established by co-culturing resected PDAC tissue with autologous tumor-draining lymph node cells. Autologous PBMCs were primed via microfluidic tumor-on-a-chip circulation, generating Organoid Interacting Lymphocytes (OILs). OILs were expanded for 14 days and co-cultured with patient-matched PTOs at 5× and 10× effector:target ratios. Tumor-immune dynamics were quantified using high-resolution time-lapse microscopy with automated single-cell tracking, flow cytometry (CD45, CK19, viability), and longitudinal tumor area measurements over 96 hours.
Results: Flow cytometry demonstrated robust immune infiltration, with CD45+ cells comprising 26% of OIL-treated cultures versus 0.5% in tumor-only controls. OILs induced 93% tumor cell death compared to 68% with unstimulated PBMCs. Quantitative tracking revealed OILs migrated 6.1 pixels closer to tumor cells versus 0.6 pixels for PBMCs over 24 hours ($P<0.05$). At 27 hours, OIL-treated organoids exhibited consistent tumor area reduction (-2% to -13%), while PBMC-treated wells showed variable responses including tumor expansion (+7%). Longitudinal analysis confirmed sustained suppression with live OILs, whereas heat-killed OILs permitted 15-fold tumor expansion, demonstrating viability-dependent cytotoxicity. Time-lapse microscopy captured direct killing events, immune synapse formation, and tumor clustering consistent with immune evasion. These findings replicate observations in appendiceal and mesothelioma models where OILs outperformed tumor-infiltrating lymphocytes.
Conclusions: OILs represent a potent, patient-specific adaptive cell therapy capable of overcoming PDAC's immunosuppressive TME. This immunocompetent organoid platform enables quantitative real-time assessment of personalized immunotherapies and supports clinical translation of OIL-based therapies for pancreatic cancer.

: Tumor-induced Immune Suppression
Poster Session

#6989 RBM10 loss promotes *KRAS*-mutant non-small cell lung cancer immune tolerance and PD-1 inhibitor resistance via a non-canonical STING/ NF-κB axis.

Minh Truong Do[1], Teng Zhou[1], Mhd Yousuf Yassouf[1], Richard Lee[1], Obada E. Ababneh[1], Yanhua Tian[1], Leticia B. Rodriguez[1], Jayanthi Gudikote[1], Haniel A. Araujo[1], Stephanie T. Schmidt[2], Jing Wang[3], Frank R. Rojas Alvarez[4], Luisa M. Solis Soto[4], Marcelo V. Negrao[1], Alexandre Reuben[1], Don L. Gibbons[1], Jianjun Zhang[1], John V. Heymach[1], Ferdinandos Skoulidis[1]

[1]Thoracic and Head and Neck Medical Oncology, UT MD Anderson Cancer Center, Houston, TX,[2]Genomic Medicine and the Institute for Data Science in Oncology, UT MD Anderson Cancer Center, Houston, TX,[3]Bioinformatics and Computational Biology, UT MD Anderson Cancer Center, Houston, TX,[4]Translational Molecular Pathology, UT MD Anderson Cancer Center, Houston, TX

Loss-of-function mutations in *RBM10*, encoding a protein involved in the regulation of alternative splicing, are observed in ~10% of non-squamous NSCLC and are enriched in tumors harboring activating mutations in *KRAS*, yet little is known about how *RBM10* inactivation promotes lung cancer progression or influences response to standard-of-care systemic therapies. Here, we elucidated the cooperative interplay between oncogenic *KRAS* activation and *RBM10* loss in NSCLC pathogenesis using a novel genetically engineered mouse model with conditional *RBM10* deletion, as well as multiple isogenic syngeneic allograft models that faithfully recapitulate *RBM10*-deficient human lung adenocarcinoma. We found that loss of *RBM10* accelerates *KRAS*-mutant NSCLC progression by fostering the establishment of a tolerogenic, myeloid cell-rich tumor immune microenvironment (TIME). Mechanistically, *RBM10* loss promoted R-loop accumulation and chronic DNA damage signaling that engaged the non-canonical TRAF6-STING pathway in a cGAS-independent manner, leading to sustained NF-κB activation. We identified several cytokines and chemokines, canonical targets of NF-κB signaling, such as IL-1β, IL-6, TNFα, and MCP-1, that were upregulated in *RBM10*-deficient cells. This NF-κB-driven secretome promoted the development of an inflamed, TIME characterized by accumulation of suppressive myeloid cell subsets - most notably monocytes and M2-like macrophages, and dysfunctional tumor infiltrating lymphocytes (TILs) thereby fostering immune evasion and cancer progression. Furthermore, we exploited the RNA-seq database of human lung adenocarcinoma from The Cancer Genome Atlas (TCGA) and again found that *RBM10* loss was significantly linked to impaired DNA damage response, upregulation of the HALLMARK_TNFA_SIGNALING_VIA_NF-κB, and enrichment of M2-macrophages. Strikingly, targeting the CSF1/CSF1R axis with an anti-CSF1R antibody significantly curtailed the growth of *RBM10*-deficient tumors in syngeneic immunocompetent models and synergized with anti-PD-1 therapy to promote tumor regression. In conclusion, our findings uncovered a novel critical role of *RBM10* inactivation in driving immune escape and PD-1 inhibitor resistance in *KRAS*-mutant NSCLC and suggest a potential therapeutic strategy by co-targeting suppressive myeloid cells to improve cancer immunotherapy for patients bearing *KRAS;RBM10* co-mutated tumors.

#6990 Identification of a secretory immune regulatory ligand.

Benjamin Nicholson, Sydney Fisher, Matthew Wren, Weijie Guo, Yuxuan Phoenix Miao

University of Chicago, Chicago, IL

Immunotherapies have transformed cancer treatment, but subsets of patients experience differential responses. Patients with squamous cell carcinomas (SCCs) in various tissues exhibit a high rate of relapse after initial responses to immunotherapies. Recent research highlighted the critical role of a group of stem cell-like tumor-initiating cells (TICs) in driving resistance to anti-tumor immunity and promoting relapse of both cutaneous (CSCCs) and head and neck (HNSCCs) SCCs despite intact antigen presentation. Although TICs drive SCC relapse, they compose less than 5% of the total tumor cell population, so their unique immune resistance mechanisms have been largely overlooked. We analyzed single-cell RNA-seq data profiling the gene signatures of various tumor populations in spontaneous GEMM CSCCs and identified that cytotoxic T lymphocyte-associated protein 2a (*Ctla2a*) was specifically activated in TICs. Ctla2a is a cysteine peptidase inhibitor with high homology to the I29 inhibitory domain of mouse and human cathepsins. Silencing *Ctla2a* in SCC cells reduced tumor growth, increased the frequency of granzyme B+ CD8+ T cells infiltrating the tumor, and sensitized SCC tumors to immunotherapy. We have found that the conditioned medium from SCC cells overexpressing *Ctla2a* is sufficient to blunt granzyme B production in CD8+ T cells and reduce CD8+ T cell antigen-specific cytotoxicity *in vitro*. Taken together, these results suggest that SCC TICs can secrete Ctla2a to modulate CD8+ T cell anti-tumor cytotoxicity. This interaction may serve as a target for next-generation immunotherapy that is able to blunt TIC-specific immune resistance.

#6991 Direct adhesion of activated platelets suppresses anti-tumor activity of CTL through CD62p-PSGL1 binding.

Sae Nishiguchi[1], Masaru Yokomura[1], Yuki Gomibuchi[2], Seiji Nagano[3], Takuo Yasunaga[4], Hiroshi Kawamoto[3], Satoshi Takagi[5], Ryohei Katayama[6]

[1]Japanese foundation for Cancer Reserch, Tokyo, Japan,[2]Department of Physics and Information Technology, Faculty of Computer Science and Systems Engineerin, Kyushu Institute of Technology, Fukuoka, Japan,[3]Institute for Life and Medical Sciences, Kyoto, Japan,[4]Department of Physics and Information Technology, Kyushu Institute of Technology, Fukuoka, Japan,[5]Division of Experimental Chemotherapy, Japanese foundation for Cancer Reserch, Tokyo, Japan,[6]Japanese Foundation for Cancer Research, Tokyo, Japan

T cell-based immunotherapies, such as CAR-T and TCR-T cell therapies, have shown remarkable success owing to their high target specificity and durable efficacy. However, their clinical efficacy is known to be limited by the immunosuppressive tumor microenvironment (TME). In this study, we focused on platelets as one of the immunosuppressive components in the TME. Platelets can extravasate from leaky tumor vessels and infiltrate into tumor tissues, where they directly interact with various types of cells in the tumor tissue. In addition to direct cell-cell interactions, platelets can influence tumor progression and modulate the function of immune cells through the released factors such as EGF, PDGF, and TGF-β upon platelet activation. In this study, we sought to assess the effect of platelets to the cytotoxic T lymphocytes (CTL). To assess this effect, we performed co-culture experiments of CTLs and tumor cells with human platelets. For the CTLs, we used cancer antigen WT1-specific T cells (CTL3-3) re-differentiated from iPS cells. Cytotoxicity of CTL3-3 was evaluated by co-incubate with HLA matched cancer cells expressing luciferase. After incubation of CTL3-3 with cancer cells with or without WT1 peptide, antigen-specific cytotoxicity was evaluated with luciferase assay. When platelets derived from healthy donors were added to this co-culture system, antigen-specific cytotoxicity was significantly suppressed with IFN-γ release suppression. This result indicated that platelets inhibited CTL3-3 activity. Interestingly, supernatant from activated platelets by collagen I treatment, partially suppressed the CTL3-3 cytotoxicity, suggesting that intact platelets interaction contribute significantly to the inhibitory effect. We then evaluated the direct interaction of platelets with cancer cells, and CTL3-3. Flow cytometry analysis revealed that platelets, which express the activation marker CD62p, preferentially adhered to CTL3-3. Immunofluorescence and electron microscopy analysis further confirmed this adhesion. Both flow cytometry and quantification using fluorescence images demonstrated that neutralizing antibodies against CD62p or its known binding partner, PSGL-1 significantly reduced platelets-CTL3-3 adhesion, suggesting that activated platelets adhere to CTL3-3 through CD62p and PSGL-1. In conclusion, our findings revealed a mechanism by which platelets inhibit antigen-specific CTL activity through direct adhesion, in addition to the soluble factor-mediated killing activity suppression of CTLs. These results suggest that targeting platelet-CTL interaction might enhance the efficacy of T cell-based immunotherapies and provide a potential strategy to overcome immunosuppressive barriers within the TME.

#6992 Tumor stem cells reprogram neutrophils to establish a protective niche.

Weijie Guo[1], Jingyun Luan[2], Yuxuan Phoenix Miao[2]

[1]Ben May, University of Chicago, Chicago, IL,[2]University of Chicago, Chicago, IL

The heterogeneous nature of tumor-associated neutrophils (TANs) has been recognized, but how different cell states of TANs emerge, evolve, distribute, and impact cancer immunotherapy efficacy remain elusive. Using single-cell RNA sequencing, spatial transcriptomics, and genetic manipulations, we show that anti-PDL1 + CD40 agonist immunotherapy can induce interferon responses in TANs, allowing them to regain antitumor activities in squamous cell carcinomas (SCC). In contrast, TANs residing at the tumor-stroma interface can preserve their immune suppressive state. Importantly, we identify a group of SOX2 High tumor-initiating stem cells (tSCs) at the tumor-stroma interface that upregulate fatty acid desaturase 1 (Fads1) to produce arachidonic acid (AA). This tSC-specific pathway enhances the prostaglandin E_2 (PGE_2) signaling in TANs, which can disrupt the interferon response and prevent the interferon-induced anti-tumor functions in TANs. By fine-tuning the plasticity of neutrophils, tSCs shape neutrophil heterogeneity and sculpt a protective micro-niche to survive from immunotherapy and drive cancer relapse.

#6993 Targeting PDE4A ablates an immune checkpoint and unleashes STING-Driven anti-tumor immunity.

Yuting Bai[1], Kejia Xu[1], Huimin Liu[1], Haojie Chen[1], Yi Shi[1], **Rong Xiang**[2]

[1]Nankai University, Tianjin, China,[2]Nankai University, Tian jin, China

Dysregulation of the cGAS-STING pathway is a common mechanism of immune evasion. Here, we identify phosphodiesterase 4A (PDE4A) as a pivotal suppressor of this pathway in tumor cells. High PDE4A expression dampens cGAS-STING signaling and type I interferon production, resulting in impaired infiltration of cytotoxic CD8+ T cells into the tumor microenvironment and accelerated metastasis. Strikingly, both genetic knockdown of PDE4A and its pharmacological inhibition with roflumilast reversed this immune-suppressive phenotype, potently enhanced CD8+ T cell infiltration, and suppressed metastatic progression. Our findings unveil PDE4A as a novel therapeutic target to reactivate anti-tumor immunity and combat metastasis, nominating PDE4A inhibition, particularly with the clinically available agent roflumilast, as a promising immunotherapeutic strategy.

#6994 Proline metabolic competition drives CD8⁺ T cell ferroptosis in BRAF-mutated thyroid cancer.

Yuanxing Dong[1], Xinyue Liu[2], Xiangqian Zheng[1]

[1]Department of Thyroid and Neck Tumor, Tianjin Medical University Cancer Institute and Hospital, National Clinical Research Center for Cancer, Key Laboratory of Cancer Prevention and Therapy, Tianjin's Clinical Research Center for Cancer, Tianjin, China,[2]Department of Pancreatic Cancer, Tianjin Medical University Cancer Institute and Hospital, National Clinical Research Center for Cancer, State Key Laboratory of Draggability Evaluation and Systematic Translational Medicine, Tianjin Key Laboratory of Dige, Tianjin, China

Proline metabolism intermediate pyrroline-5-carboxylate (P5C) has been implicated in regulating T-cell signaling and effector activity, yet how proline availability shapes tumor-immune interactions remains poorly understood. Here, we demonstrate that tumor-driven proline depletion induces ferroptosis in CD8⁺ T cells and thereby promotes tumor progression. We identify proline dehydrogenase (PRODH) as a key metabolic regulator that is markedly upregulated in BRAFV600E-mutant thyroid cancer and strongly associated with enhanced tumor aggressiveness and poor prognosis. Elevated PRODH accelerates proline catabolism in tumor cells, creating pronounced metabolic competition with CD8⁺ T cells and resulting in nutrient deprivation, ferroptotic death, and impaired antitumor function. Mechanistically, BRAFV600E activates MAPK signaling, which induces ERK- and JUN-dependent transcriptional upregulation of PRODH. Sustained proline consumption disrupts the “proline-glutamate-GSH” metabolic axis, leading to redox imbalance, excessive ROS accumulation, and ferroptosis-mediated T-cell dysfunction. Notably, pharmacological inhibition of the proline transporter SLC6A20 alleviates proline shortage, restores glutathione biosynthesis, and rescues CD8⁺ T-cell fitness. In addition, functional restoration of this metabolic circuit enhances cytokine production, promotes T-cell persistence within the tumor microenvironment, and significantly suppresses tumor growth in vivo. These findings identify the BRAFV600E-ERK-PRODH axis as a central driver of proline metabolic reprogramming that simultaneously enhances tumor malignancy and undermines antitumor immunity. Moreover, we highlight the essential role of the proline-glutamate-GSH axis in protecting CD8⁺ T cells from ferroptosis and demonstrate that proline supplementation or blockade of SLC6A20 can reestablish this protective pathway and reinforce T-cell-mediated antitumor responses, offering a promising therapeutic strategy for BRAFV600E-driven cancers.

#6995 Spatial immune landscape in metastatic colorectal cancer.

Susrutha Puthanmadhom Narayanan[1], Chien-Wei Peng[1], Adrienne Visani[1], Xiangwei Fang[1], Andre Luiz N. Targino da Costa[1], Jingxian Liu[2], Reyka G. Jayasinghe[1], Ambrose Plante[1], John M. Herndon[1], Jacqueline Mudd[1], Preet Lal[1], Wagma Caravan[1], Kapur B. Dhami[2], Jennifer Ponce[1], Robert S. Fulton[1], Michael Heinz[1], Milan G. Chheda[1], Feng Chen[2], Michael Iglesia[1], Ryan C. Fields[1], Li Ding[2]

[1]Washington University in St. Louis, St. Louis, MO,[2]Washington University School of Medicine in St. Louis, St. Louis, MO

Microsatellite stable (MSS) metastatic colorectal cancer (mCRC) does not respond well to immunotherapy, but clinical trials have shown promise with immunotherapy in MSS mCRC without liver metastases, especially lung only metastatic disease. To understand the underlying reasons for this site-specific difference in response, we investigated the spatial immune landscape in liver and lung metastases using spatial transcriptomics (Xenium) and single nuclear RNA-sequencing (snRNA seq) on immunotherapy naive, MSS tumors (9 primary, 9 liver and 6 lung samples for Xenium and 17 primary, 21 liver and 5 lung samples for snRNA seq). We defined three spatial regions in Xenium samples- tumor region (contains tumor cell nests), peritumor region (stromal and immune cells that separate tumor region from adjacent parenchyma) and adjacent parenchyma (adjacent normal-appearing tissue in the same section). Expressed as a proportion of all immune cells, liver tumor regions had higher macrophage infiltration ($p<0.01$), while lung tumor regions had higher CD8 T cell infiltration ($p=0.03$). CD8 T cell proportion was not different between liver and lung metastases in peritumor regions or adjacent parenchyma, or in the sn-RNA seq data, highlighting the spatial gradient of CD8 T cells in different organ sites. CD8 T cell density (per mm2) in liver tumor regions (but not peritumor region or adjacent parenchyma) was lower than paired primary colon ($p=0.03$) and lung metastasis (not significant). Tumor regions had a higher proportion of exhausted CD8 T cells (expressing at least one exhaustion marker-*PDCD1, HAVCR2, TIGIT, CTLA4, LAG3*) than the peritumor region or adjacent parenchyma in all three organs. Among T cells that infiltrated tumor regions, liver had a higher Treg proportion than lung ($p=0.02$), this did not hold true in peritumor region and adjacent parenchyma. Differential gene expression between Tregs of liver and lung tumor regions revealed upregulation of *ENTPD1* (codes for CD39, which suppresses CD8 T cells) in liver Tregs; this finding was also present in our sn-RNA seq data. To investigate the reasons for organ-specific variability in the immune landscape of mCRC, we compared the expression of chemokine genes in non-tumor cells of liver and lung metastases. Liver samples had markedly higher levels of *CXCL12* (highest in the adjacent parenchyma) than lung metastases. Tregs and CD8 T cells in the liver had higher levels of *CXCR4* (CXCL12 receptor) than the lung. Spatial gradients in CXCL12 (highest in adjacent parenchyma), may impair CD8 T cell infiltration in the tumor. In summary, we identified an immunosuppressive immune microenvironment in liver than lung mCRC with unique spatial patterns of CD8 T cell and Treg infiltration, and chemokine expression. This may explain the differential response of immunotherapy between these two sites. Inhibition of the CXCL12-CXCR4 axis and CD39 may be potential strategies to augment immunotherapy in patients with liver mCRC.

#6996 Immune regulatory functions and therapeutic opportunities of MIF signaling in pancreatic cancer.

Blake Schwettmann, Fei Peng, Angad Kumar, Valli Annamali, Jason Toombs, Rolf Brekken, Ravikanth Maddipati

UTSW, Dallas, TX

Background: Pancreatic ductal adenocarcinoma (PDAC) is projected to become the second leading cause of cancer-related death in the US, yet current treatments remain largely ineffective. The immunosuppressive tumor immune microenvironment (TIME), particularly tumor-associated macrophages, represents a critical barrier to therapeutic success. To identify critical targets and interactions in the PDAC TIME, we cross-referenced RNA sequencing from the KPCX autochthonous mouse model that recapitulates tumor heterogeneity with RNA sequencing from a cohort of PDAC patients. Through this analysis we identified macrophage migration inhibitory factor (MIF) as an important tumor-derived secreted factor whose function in PDAC immune evasion remains to be fully elucidated. This study investigates how MIF signaling regulates immune responses and promotes immune evasion in PDAC.

Methods: To dissect MIF signaling and the relative contribution from tumor and stromal compartments, we utilized orthotopic syngeneic PDAC allografts in wild-type and Mif $^{-/-}$ mice. We also investigated MIF's cognate receptor, CD74, through orthotopic allografts in global CD74$^{-/-}$ mice and cell-type-specific deletion models targeting macrophages/monocytes (CD74f/f;Cx3cr-Cre). We also incorporated pharmacologic inhibition of MIF in our orthotopic PDAC models. Tumor growth and immune composition were quantified by flow cytometry and immunohistochemistry. MIF signaling on macrophages was also characterized *in vitro* using co-cultures with Mif$^{-/-}$ murine PDAC cell lines 6419 and 6694. M1 (iNos, CD86) and M2 polarization (Arg1, CD206) markers were characterized using RT-qPCR.

Results: Loss of MIF profoundly reduced tumor burden. Syngeneic PDAC cells implanted into Mif$^{-/-}$ mice demonstrated a 50% reduction in tumor growth compared to wild-type mice. Reciprocally, Mif$^{-/-}$ tumor cells showed a marked growth reduction in wild-type recipients, indicating MIF functions in both tumor and stromal compartments. Surprisingly, CD74 deletion, either globally or specifically in macrophages, had minimal impact on tumor growth, suggesting that MIF signals through alternative receptors or acts on other immune populations. Pharmacologic MIF inhibition reduced tumor burden by 50%, decreased pro-tumor M2-like macrophages by 50%, and increased CD8+ T cells 2-3 fold.

Conclusions: Our findings demonstrate that tumor-derived MIF promotes immune evasion in PDAC through CD74-independent mechanisms and involves multiple immune cell types. MIF inhibition remodels this immunosuppressive TIME and thus represents a promising therapeutic strategy to enhance the efficacy of immunotherapy or other targeted therapies in PDAC.

#6997 Defining mechanisms limiting NK cell function in the multiple myeloma tumor microenvironment.

Sadia Afrin, Michelle Becker-Hapak, Lyra Morina, Wilbur Song, Jennifer A. Foltz, Alice Zhou, Kunal Shetty, Yeeun Paik, Samuel Ameh, Emily Philips, Timothy Schappe, Mark Foster, Lynne Marsala, Sushanth Pureti, Yoo-Jin Ahn, David Russler Germain, Todd A. Fehniger

Washington University in St. Louis, St. Louis, MO

Natural killer (NK) cells are cytotoxic cells that have an intrinsic ability to mediate anti-tumor responses. However, the immunosuppressive tumor microenvironment (TME) can limit their efficacy. Multiple myeloma (MM) is a hematologic malignancy characterized by clonal proliferation of plasma cells within the bone marrow. There is a growing understanding that the tumor microenvironment (TME) is a critical factor influencing the effectiveness of cellular therapies. A hallmark characteristic of rapidly proliferating cancer cells is the production of a high amount of lactic acid. Myeloma cells also produce metabolites, including lactic acid, that suppress the effector function of T cells. How lactic acid affects NK cell function remains poorly understood. In this study, we hypothesize that increased lactic acid in the TME inhibits NK cell functionality and thereby serves as a key TME checkpoint on NK cell anti-tumor responses. To test this, primary conventional (c)NK cells and ML NK cells were exposed to varying concentrations of lactic acid and assessed for cytotoxicity, proliferation, and cytokine production in vitro. We observed that cNK cell IFN_γ production (P=0.0035) significantly decreased with 15mM lactic acid conditions compared to controls (0mM and 3mM). ML-differentiation resulted in a partial rescue of lactic acid-induced reductions in IFN_γ production (p=0.0417) observed in cNK cells. Next, we found that degranulation (measured via sCD107a) was significantly (P=0.0018) reduced in both cNK and ML NK cells under 15mM lactic acid treatment conditions compared to controls (0mM and 3mM). cNK and ML NK cytotoxicity were significantly decreased in 15 mM lactic acid compared to controls, with ML NK cells again exhibiting partial resistance to lactic-acid compromised killing. To investigate the impact of lactic acid on NK cell proliferation, we activated the NK cells with IL-12, IL-15, and IL-18 overnight and labeled them with cell trace violet (CTV) . CTV-labeled cells were incubated in media with lactate conc. By day 7, NK cell proliferation was abrogated with exposure to 15 mM lactic acid, while 40% of NK cells proliferated in control conditions (0mM or 3mM lactic acid). This data suggests that NK cell proliferation are suppressed with high lactic concentration. Our data further revealed that lactic acid (15mM) markedly suppressed IL-15-induced pSTAT5 signaling in cNK cells. In contrast, ML NK cells maintained higher pSTAT5 levels in response to IL-15 under high lactic acid (15mM) conditions, demonstrating greater resilience to this TME stress. Finally, we identified the acidity as the major driver of NK cell dysfunction induced by lactic acid by comparing it to sodium lactate and matched pH control conditions. These data suggest that lactic acid is a metabolic checkpoint on NK cells, and ML differentiation and strategies to insulate NK cells from lactic acid effects may improve NK cell anti-tumor responses.

#6998 Use of non-steroidal anti-inflammatory drugs, acetaminophen and somatic immune profiles in breast tumors.

Clara Bodelon[1], James Hodge[1], Daniel G. Stover[2], Melissa A. Troester[3], Lauren E. McCullough[4], Alpa V. Patel[1], Lauren R. Teras[1]

[1]American Cancer Society, Atlanta, GA,[2]OSUCCC - James, Columbus, OH,[3]Assistant Professor of Epidem., UNC Lineberger Comp. Cancer Center, Chapel Hill, NC,[4]Emory University, Rollins School of Public Health, Atlanta, GA

Background. Tumor-infiltrating lymphocytes (TILs) represent a prognostic biomarker in several cancers, including breast cancer. Enrichment of TILs may help to identify highly immunogenic and immune-vulnerable tumors that may be more responsive to immune-mediated mechanisms and are associated with improved outcomes. Recent data suggest that the use of acetaminophen may have immunosuppressive effects. In this study, we investigated the relationship between the use of common analgesics and immune profiles in breast tumors from patients within a population-based prospective cohort study.
Methods. This analysis was conducted among females with invasive breast cancer enrolled in the Cancer Prevention Study 3 (2006-2013). Use of non-steroidal anti-inflammatory drugs (NSAIDs), and acetaminophen was assessed at enrollment and follow-up surveys (2015 and 2019). Analgesic information came from the survey prior to, but closest in time to, their cancer diagnosis. Eligible patients were required to have formalin-fixed paraffin-embedded breast tumor samples available. Immune profiles were generated from tumor RNA using a previously published method to derive ten immune cell-type-specific scores plus a cytotoxic cell score from breast tumors. Linear regression was used to estimate the associations between each type of analgesic use and the immune scores, adjusting for age at diagnosis, stage, and estrogen receptor (ER) status. Multiple testing was addressed using the false discovery rate (FDR), with FDR<0.05 considered statistically significant.
Results. This analysis included 887 breast cancer patients with a median age at diagnosis of 58 years (interquartile range: 51, 63). At the time of diagnosis, most of the women were post-menopausal (61%), had ER positive tumors (80%) and localized disease (65%). Among the breast cancer survivors included in the analysis, 450 (51%) reported NSAID use and 137 (15%) acetaminophen use. Patients who reported use of NSAID had similar immune profiles to non-users (FDR>0.05). However, acetaminophen users had lower scores for T-cells, T helper cells, Treg cells, natural killer (NK) cells, neutrophils, eosinophils and cytotoxic T cells compared with non-users (FDR<0.05). Results among patients with ER-positive tumors were similar to the overall results with the exception that the CD8+ T cell score was also significantly lower among acetaminophen users (FDR<0.05). Among women with ER-negative tumors, there was no difference in immune profiles between NSAID users and non-users. Only NK cell, neutrophil, and eosinophil scores were significantly lower among acetaminophen users compared with non-users (FDR<0.05).
Conclusions. NSAID use does not appear to influence the breast tumor immune microenvironment. In contrast, we observed that acetaminophen use lowers the scores of multiple immune cell types, including those related to improved prognosis.

#6999 GDF-15 inhibition overcomes treatment resistance to platinum- and taxane-based cytotoxic chemoimmunotherapy.

Neha Vashist[1], Amelie Kohler[1], Daniel Schatzlein[1], Sabrina Gen?ler[1], Katja Rungger[2], Hubert Hackl[2], Matthias Kist[1], Sarah Lutzenberger[1], Julia Weigandt[1], Jose Medina-Echerverz[1], Christine Schuberth-Wagner[1], **Thorsten Ross**[1]

[1]CatalYm GmbH, Planegg, Germany,[2]Institute of Bioinformatics, Medical University of Innsbruck, Innsbruck, Austria

Background: GDF-15 is a stress-induced cytokine that restricts $CD8^+$ T cell infiltration, drives immunotherapy resistance, and mediates chemotherapy-induced nausea, emesis, anorexia, and cancer cachexia. Durable responses to GDF-15 blockade have been reported in PD-1-refractory NSCLC and UC, supporting its role as a clinically relevant mediator of immune escape. Because platinum agents and other DNA-damage-inducing therapies strongly upregulate GDF-15, we investigated whether therapy-induced GDF-15 limits the antitumor activity and tolerability of combined PD-1 blockade and cytotoxic chemotherapy.
Methods: Human tumor cell lines were treated with platinum compounds, docetaxel, and a panel of DNA-damage inducers, DNA-damage-repair inhibitors, and cell-cycle and transcriptional stress-inducing agents, and GDF-15 secretion was quantified. Syngeneic MBT-2 and MC-38 models received cisplatin or docetaxel plus anti-PD-1, with or without a GDF-15-neutralizing antibody. Tumor growth, survival, body weight, serum GDF-15, intratumoral immune populations, and peripheral CD8+ T cell activation were analyzed by ELISA, flow cytometry, bulk RNA sequencing, and single-cell RNA sequencing.
Results: A broad range of DNA-damage-inducing, DNA-damage-repair-inhibitory, and cell-cycle stress-inducing agents robustly induced GDF-15 in vitro. In vivo, cisplatin plus anti-PD-1 markedly increased systemic GDF-15 but yielded limited tumor control. Adding GDF-15 blockade substantially delayed tumor growth, extended survival, and fully prevented cisplatin-associated weight loss. Single-cell RNA sequencing demonstrated increased intratumoral $CD8^+$ T cell infiltration. scRNA-seq and bulk RNA sequencing together showed enrichment of activation, co-stimulation, cytotoxicity, and TCR-signaling programs (Lck, Fyn, Zap70, Lat; Gzmb, Prf1; CCL5). Flow cytometry confirmed increased peripheral $CD8^+$ T cell proliferation ($Ki67^+$) and a higher proportion of activated effector $CD8^+$ T cells, including increased PD-1 expression. Bulk RNA-seq revealed an M2-like macrophage signature (CD163, Chil3, Retnla, Marco, Rnase2a) in chemoimmunotherapy-treated tumors, and flow cytometry showed reduced cDC1 activation; both were reversed by GDF-15 blockade.
Conclusions: These findings suggest that therapy-induced GDF-15 contributes to resistance to platinum- and taxane-based PD-1 combinations and may exacerbate treatment-related toxicity. Neutralizing GDF-15 restores antitumor $CD8^+$ T cell immunity, reprograms suppressive myeloid states, and improves the overall activity and tolerability of combined PD-1 blockade and cytotoxic chemotherapy. GDF-15 inhibition therefore holds potential to enhance responses to first-line chemoimmunotherapy in tumors such as NSCLC and UC.

#7000 Genome-wide CRISPR screening reveals tumor-intrinsic immune evasion mechanism in ovarian cancer.

Junyong Park[1], Jiho Lee[1], Hyun Ju Kang[2], Jin-Ku Lee[1]

[1]Department of Biomedical Sciences, Seoul National University, Seoul, Korea, Republic of,[2]Genomic Medicine Institute, Medical Research Center, Seoul National University, Seoul, Korea, Republic of

Ovarian cancer is the most lethal gynecologic malignancy. Previous studies demonstrated high levels of tumor-infiltrating T cells in ovarian cancer, which predict benefit from immunotherapy. However, clinical trials such as KEYNOTE-100 report only ~10% overall response to pembrolizumab. This discrepancy indicates that ovarian cancers harbor heterogeneous, tumor-intrinsic mechanisms of immune evasion.To distinguish immune-resistant cancer cell lines, we established a reporter-based co-culture platform in which pre-activated human T cells were directly co-cultured with ovarian cancer cell lines. We profiled 24 ovarian cancer cell lines engineered with a real-time cytotoxicity reporter to quantify tumor-cell death. Pre-activated T cells from two healthy donors were co-cultured with each cancer cell line, and reporter readouts stratified the set into 11 immune-sensitive and 6 immune-resistant lines. To uncover genetic determinants of resistance, we selected the two most resistant cell lines for whole-genome CRISPR screening. Following co-culture of CRISPR-edited cancer cells with pre-activated T cells, sgRNA abundances were sequenced and analyzed using the MAGeCK-MLE pipeline. Focusing on concordant depletions, we identified 56 genes ($P < 0.05$; $\beta < -0.5$) whose loss augments T-cell-mediated tumor killing in both cell lines. Among these, we prioritized ITGA8 (integrin α8) as a promising surface target. ITGA8 heterodimerizes with β1 to form α8β1, which engages extracellular-matrix ligands and activates adhesion- and survival-linked signaling axes, including FAK/Src. Given that integrins regulate immune-cell infiltration into tumors and pathways such as TGF-β signaling, we hypothesize that ITGA8 sustains pro-survival signaling that constrains T-cell activity. Accordingly, pharmacologic or biologic blockade of ITGA8 may offer a surface-accessible strategy to convert immune-resistant ovarian tumors into immune-sensitive disease.

#7001 Tumor-intrinsic suppression of phagocytosis by RRP1 (ribosomal RNA processing 1) in glioblastoma.

Eshika Kudaravalli, Amr Elkholy, Mostafa Mohamed, Hasan Alrefai, Saeed Zakakhosravi, Satoru Osuka, Christopher D. Willey, Erin Ahn

University of Alabama at Birmingham, Birmingham, AL

Glioblastoma (GBM) is the most aggressive and common malignant brain tumor in adults, with a median survival of just 14.6 months. Standard treatment, comprising maximal surgical resection followed by radiation and temozolomide, offers limited long-term benefit, highlighting the urgent need for more effective therapies. While other cancers have seen promising advances through T-cell immunotherapy, GBM has remained stubbornly resistant, largely due to its immunosuppressive microenvironment dominated by tumor-associated macrophages (TAMs). These macrophages, instead of engulfing tumor cells, are often hijacked to support tumor growth and evade immune clearance. GBM evades immune clearance in part by expressing “don’t eat me” signals such as CD47; however, clinical trials of anti-CD47 therapy in leukemia faced challenges, including toxicity and limited therapeutic efficacy. This gap in effective TAM-targeted therapies highlights an urgent need to uncover new, safer targets that could restore macrophage function.

To address this, we performed a genome-wide CRISPR knockout screen in GBM cells (MGG18-RR) using human peripheral blood-derived macrophages polarized by GBM-conditioned media to identify tumor-intrinsic genes that inhibit macrophage phagocytosis. Our cytometry imaging results demonstrated that tumor-conditioned macrophages adopted distinct polarization profiles relative to unpolarized macrophages, thus establishing them as a more reliable experimental model. Our screen revealed RRP1 (ribosomal RNA processing 1) as a key regulator suppressing macrophage clearance of GBM cells. Proteomic data from the Clinical Proteomic Tumor Analysis Consortium (CPTAC) and the International Cancer Proteogenome Consortium (ICPC) showed that the RRP1 protein was increased in GBM tumors compared to normal brain tissue, indicating RRP1 upregulation as a feature of the GBM proteome. However, RRP1’s role in GBM phagocytosis remains unknown. Thus, to validate RRP1 as a therapeutic target in-vitro, we engineered RRP1 KO GBM cells (JX14P-RT) labeled with pHrodo dye which emits fluorescence when cells are phagocytosed. We performed this in-vitro phagocytosis assays with human peripheral blood-derived macrophages and RAW 264.7 macrophages, co-culturing a ratio of 200K macrophages per 1 million JX14P-RT cells for 20 hours. Co-cultures of CD47-KO-JX14P-RT tumor cells and macrophages were used as a positive control, and co-cultures of CD47-KO-JX14P-RT tumor cells and macrophages with Cytochalasin D, a known phagocytosis inhibitor, were used as negative control. Phagocytosis was quantified by the total Texas Red fluorescent signals. We found that loss of RRP1 significantly increased tumor cell engulfment ($p < 0.05$).

Together, these findings highlight RRP1 as a promising immunotherapeutic target and support further investigation of RRP1 inhibition in vivo using syngeneic murine GBM models.

#7002 Immune evasive characteristics of the KRAS mutant colorectal cancer tumor microenvironment.

Elizabeth A. Boeree[1], Katherine A. Johnson[1], Cheri A. Pasch[1], Dustin A. Deming[2]

[1]Univ. of Wisconsin Madison Sch. of Med. & Public Health, Madison, WI,[2]University of Wisconsin Carbone Cancer Center, Madison, WI

Background: Recent clinical trials have indicated that KRAS mutant colorectal cancer (CRCs) are more resistant to combination immunotherapy approaches compared to KRAS wild-type (WT) microsatellite stable (MSS) CRCs, potentially related to an immune suppressive tumor microenvironment (TME). Here, we investigate the TME of MSS KRAS mutant CRCs to characterize the immune-related signaling pathways and factors that modulate the immune evasive TME associated with KRAS mutant CRCs.
Methods: A gene-set enrichment analysis (GSEA) on the Colorectal Adenocarcinoma (TCGA, PanCancer Atlas) dataset was performed to identify differential gene expression patterns between patients with MSS CRCs with or without a KRAS mutation. A second GSEA analysis explored RNA expression data from the NCI Patient-Derived Models Repository (PDMR) database of matched patient organoid and whole tumor samples from KRAS mutant and WT CRCs.
Results: A total of 496 MSS CRC subjects were identified in the TCGA dataset. KRAS mutant CRCs (195) were compared to a WT cohort consisting of patients lacking a KRAS, NRAS, or BRAF mutation (255). KRAS enriched gene sets (FDR q-value<0.25) included hallmark mitotic spindle, p53 pathway, glycolysis, oxidative phosphorylation, reactive oxygen species pathway, and estrogen response late. The WT cohort had enrichment of immune-related gene sets, including hallmark allograft rejection, inflammatory response, and IL6 JAK STAT3 signaling. Significantly expressed genes (q-value<0.05) in the KRAS enriched gene sets were involved in TGF-beta signaling (TGFB1 (Log2FC: 0.85), EPHA2 (0.4), KLK11 (1.47), INHBE (0.51)), M2-macrophage recruitment (KLK10 (1.24), CA12 (0.75), KLK8 (0.79), and immune exclusion (CD44(0.35), LAMC2 (0.43), KLK8 (0.79), NT53/CD73 (0.66)). Genes upregulated in the WT cohort were associated with immune cell activation and T-cell regulation (GZMB (0.83), MERTK (0.66), PROCR (0.59), CD40 (0.48)), M1-macrophages (AK4 (0.65)), and immune infiltration (SPAG4 (0.49)). RNA expression data from the PDMR database was analyzed from patients with APC and TP53 mutations with or without a KRAS mutation (three patients/cohort). GSEA revealed that immune-related gene sets were significantly enriched in WT tumors including interferon gamma/alpha response, TNFA signaling via NFKB, complement, allograft rejection, and inflammatory response. When immune TME signaling was isolated by separating gene expression present in the organoid data from the original tumor samples, similar results were observed.
Conclusion: KRAS mutant CRCs are characterized by an immune suppressive TME. Further analysis of the pathways and genes driving this phenotype will help identify actionable therapeutic targets to improve immunotherapy responses for these patients.

#7003 The RKIP-HER2 axis regulates breast cancer immune evasion.

Ania Khachikian, Mai Ho, Benjamin Bonavida

Microbiology, Immunology & Molecula Genetics, UCLA - University of California Los Angeles, Los Angeles, CA

Introduction: Breast cancer (BC) is a prevalent malignancy worldwide among women. HER2 overexpression in a subset of BC (HER2+ BC) serves as a critical oncogenic driver and contributes to immune evasion. The Raf Kinase Inhibitor Protein (RKIP), a metastasis suppressor and an immune enhancer, is under-expressed in HER2+ BC. Treatment of HER2+ BC with anti-HER2 mAbs or chemical inhibitors has resulted in significant clinical responses in a subset of patients. However, acquired and induced resistance in HER2+ BC patients highlights the need for new effective therapies.
Procedure: We have analyzed the signaling pathways mediated by both RKIP and HER2 and have found that RKIP and HER2 inductions and downstream signaling showed inverse cross-talks.
Findings: The inverse cross-talks enabled us to establish a dysregulated RKIP-HER2 axis in HER2+ BC. The role of this dysregulated axis in immune evasion was examined. HER2 expression positively regulates immune evasion as it is involved in the expression of PD-L1, the polarization of TAMs, the infiltration of suppressor cells (Tregs, MDSCs), the inhibition of anti-tumor CD8T cells, and an overall immunosuppressive TME. In contrast, RKIP inhibits critical signaling pathways that regulate HER2 expression, including the Raf-MEK-ERK, NF-κB, and PI3K/Akt pathways, thereby preventing immune evasion. The inverse functional relationship between RKIP and HER2 was further supported by bioinformatic analyses that examined expressions and correlations by proteomics and survival analyses.
Conclusion: Various therapeutic strategies are proposed aimed at targeting the dysregulated RKIP-HER2 axis in HER2+ BC to circumvent resistance and immune evasion.

#7005 Tumor cell CEBPB expression contributes to T cell-mediated immune evasion of microsatellite stable colorectal cancer.

Hye Jeong Yun[1], Chan Ho Park[2], Dahye Yun[1], Hye-Ri Shin[3], Naeun Park[1], Changhee Park[4], Jeong Dong Lee[1], Kiyeon Kim[2], Heejun Shim[2], Hyejin Sim[1], Se Min Kim[1], Min Jung Kim[5], Ji Won Park[5], Seung-Bum Ryoo[5], Yoojoo Lim[6], Seung-Yong Jeong[5], Kyu Joo Park[5], Tae-You Kim[4], Junil Kim[2], Jae-Kyung Won[3], Sae-Won Han[4]

[1]Cancer Research Institute, Seoul National University Hospital, Seoul, Korea, Republic of,[2]Department of Bioinformatics, Soongsil University, Seoul, Korea, Republic of,[3]Department of Pathology, Seoul National University Hospital, Seoul, Korea, Republic of,[4]Department of Internal Medicine, Seoul National University Hospital, Seoul, Korea, Republic of,[5]Department of Surgery, Seoul National University Hospital, Seoul, Korea, Republic of,[6]Lunit, Seoul, Korea, Republic of

Background: Microsatellite stable (MSS) colorectal cancer (CRC), which accounts for approximately 80-85% of all colorectal cancer cases, exhibits a poor response to immune checkpoint inhibitors. Tumor protein 53 (*TP53*) mutations are frequently observed in colorectal cancer and may contribute to tumor-driven immunosuppression. In this study, we aimed to investigate the immunosuppressive mechanisms associated with *TP53* mutations in MSS CRC.

Methods: We performed single-cell RNA sequencing (scRNA-seq) on tumor samples from 30 CRC patients and *Trp53*- knockout (KO) CT26 tumors in syngeneic mice to profile the tumor microenvironment and analyze tumor cell gene expression profiles based on *TP53* mutation status. We identified CCAAT enhancer-binding protein beta (*CEBPB*) as a potential immunosuppressive factor associated with *TP53*-mutant CRC. To demonstrate the role of *CEBPB* in T cell immunosuppression, we analyzed T cell-tumor cell co-cultures and *CEBPB*-overexpressing (oe) tumor-injected syngeneic mouse models by flow cytometry.

Results: scRNA-seq analysis of 30 CRCs revealed increased proportions of $CD4^+$ T cell subsets, including Treg, Th17, and Tcm cells, in *TP53* mutant tumors. Immune activation pathways, such as the immune system and interferon-gamma response, were down-regulated in T cells compared to *TP53* wild-type tumors, suggesting that *TP53* mutations might contribute to immune evasion by negatively affecting T cells. scRNA-seq analysis of *Trp53*-KO CT26 tumors identified *CEBPB* as notably upregulated, and we confirmed that loss of *Trp53* WT led to increased *CEBPB* mRNA expression and protein stability in CRC cell lines. *CEBPB* expression was associated with reduced $CD4^+$ T cell infiltration and positively correlated with cytotoxic T lymphocyte-associated protein 4 (*CTLA4*) expression in regulatory T cells (Treg) and exhausted T cells (Tex). *CEBPB*-oe CT26 tumors in syngeneic mice showed reduced $CD4^+$ T cell infiltration and upregulation of CTLA-4 expression on $CD4^+$ T cells *in vivo*. Consistently, spleen T co-cultured with *CEBPB*-overexpressing CT26 cells showed increased CTLA-4 expression and decreased proliferation of $CD4^+$ T cells.

Conclusion: Tumor cell *CEBPB* expression, upregulated by *TP53* mutation, may mediate T cell-mediated immunosuppression and is considered as potential therapeutic target for regulating immune evasion in MSS CRC.

#7006 Inhibiting intracellular cPLA2α in cervical cancer cells enhances antitumor immunity and facilitates the efficacy of anti-PD1 checkpoint immunotherapy.

Yuchao He, Xiangdong Tian, Liwei Chen, Yi Luo, Yu Wang, Lu Chen, Hua Guo

Tianjin Medical Univ. Cancer Inst. & Hospital, Tianjin, China

Immunotherapy has emerged as a breakthrough in treating cancer. However, only a limited subset of patients responds to the treatment and maintain a long-term response. Hence, there is an urgent need to explore the mechanisms of tumor resistance to immune checkpoint blockade (ICB) to identify effective targets and develop efficient combination therapies. Here, we demonstrate genetic ablation of cPLA2α in tumor cells profoundly inhibits tumor growth and prolongs survival in immunocompetent mice but shows minimal effect in immunodeficient mice, implicating the critical role of the adaptive immune system. Wild-type (WT) and cPLA2α-knockout (KO) tumors are profiled by single-cell RNA sequencing, revealing significant differences in genome-wide transcription and the presence of cancer cells, macrophages, and T cells. To elucidate the multifaceted regulatory functions of cPLA2α, we performed multiple functional perturbations, uncovering that: cPLA2α-high tumor cells drive ferroptosis-associated oxidative lipid metabolism via the SLC7A11/ALOX12 axis, leading to 12-HETE accumulation; these lipids are taken up by macrophages via GPR31 to induce M2-like polarization; concurrently, ferroptosis processes in tumor cells suppress the levels of effector factors GZMB in $CD8^+$ T cells. Both effects exert potent immunosuppressive activity, collectively forming a barrier against T cell attack. In contrast, cPLA2α-KO cancer cells downregulate 12-HETE production, promote the polarization of $MKi67^+$ M1-like macrophages, accompanied by upregulation of CXCL16 expression; meanwhile, cPLA2α-KO facilitates the differentiation of T cells into effector memory $CD8^+$ T cells with elevated CXCR6 level. Cell-cell communication analysis reveals that M1-like macrophages and T cells primarily interact via the CXCL16-CXCR6 axis, which facilitates $CD8^+$ T cell recruitment and activation. Furthermore, cPLA2α-KO increases the infiltration of effector memory $CD8^+$ T cells into tumors, triggers $CD8^+$ T cell-mediated control of tumor growth, enhances their cytotoxic functions (e.g., IFNG, GZMB), and reduces the proportion of naïve $CD8^+$ T cells. Loss of cPLA2α enhances T cell proliferation, activation, and the sensitivity of tumor cells to $CD8^+$ T cell cytotoxicity *in vitro*. Depleting $CD8^+$ T cells *in vivo* largely rescues the tumor growth induced by cPLA2α-KO, confirming that $CD8^+$ T cells are responsible for the antitumor effect. Notably, the cPLA2α cancer signature serves as a prognostic indicator for survival and shows an inverse correlation with T cell infiltration intensity in cervical cancers, consistent with its immunosuppressive effects, and targeting cPLA2α synergistically enhances anti-PD1 immunotherapy efficacy. Therefore, disrupting cancer cell cPLA2α-mediated immune escape may offer potential therapeutic strategies to enhance antitumor immunity.

#7007 Hypoxia-mediated suppression and memory of IFI44L and its interaction with STING in breast cancer metastasis and immune evasion.

Rebecca Marker[1], Aidan Moriarty[2], Remi Klotz[3], Min Yu[4]

[1]University of Maryland, Baltimore, Baltimore, MD,[2]University of Maryland School of Medicine, Baltimore, MD,[3]University of Maryland Baltimore, Baltimore, MD,[4]University of Maryland, Baltimore, MD

Solid tumors often contain patches of hypoxic regions that yield aggressive, pro-metastatic phenotypes. Prevention and understanding of metastases is critical for the future of breast cancer research, as metastatic cancer is extremely difficult to manage and treat. Recent work in our lab has shown that long-term hypoxia suppresses type I interferon (IFN) signaling in breast cancer cells. Even upon reoxygenation, these gene expression changes are maintained, indicative of “hypoxic memory.” Breast cancer cells that have disseminated from the primary tumor as circulating tumor cells with this “post-hypoxic” memory phenotype show enhanced metastatic potential. IFNs typically boost and enhance immune cell activity through interferon-stimulated genes (ISGs); thus, hypoxic suppression of IFN signaling yields an immunosuppressive tumor microenvironment. More research is needed to understand how ISGs are downregulated in hypoxia and how those changes in gene expression contribute to immunosuppressive ability of hypoxic and post-hypoxic cells. Interferon-inducible 44-like (IFI44L) is an ISG that has been associated with tumor-suppressive properties, and correlated with presence of tumor-infiltrating lymphocytes in other cancers, but its role in breast cancer has not been studied. We found that IFI44L is significantly suppressed in breast cancer cells in hypoxia and maintained after reoxygenation as a hypoxic memory. To understand the implications of hypoxic memory and suppression of IFI44L, we generated IFI44L overexpression and knockdown models in MCF7 and NT2.5 breast cell lines, and Brx68s, a circulating tumor cell line. We discovered that in adherent MCF7 cells, IFI44L OE significantly increases STING expression, whereas in suspension circulating tumor cells, IFI44L OE suppresses STING expression. We see that IFI44L does not impact canonical STING signaling molecules, pIRF3 and pTBK1. The consequences and mechanisms of STING regulation by IFI44L are unknown and experiments are ongoing in the lab to address these questions; in vivo studies of IFI44L are ongoing to elucidate the impact this gene has on tumor formation and metastasis. We expect to see that IFI44L OE has a tumor suppressive mechanism, and expect the opposite with IFI44L KO. Additionally, we plan to investigate STING regulation by IFI44L and the possible impact that this has on immune evasion and metastasis.

#7008 Multi-omic analysis nominates SPP1-IL10 axis as a novel immunotherapeutic target in gastric peritoneal carcinomatosis.

Turcios Lilia[1], Neelima Hosamani[1], Ellen Beswick[2], Joseph Kim[1], **Mautin Barry-Hundeyin**[1]

[1]University of Kentucky, Lexington, KY,[2]University of New Mexico, Albuquerque, NM

Gastric cancer is 3rd leading cause of cancer-related mortality worldwide. The peritoneum is the most common site of metastasis, accounting for 60% of recurrences. Peritoneal carcinomatosis results in 65% of gastric cancer-associated deaths, resulting in a median overall survival of 6-9 months. Therefore, identifying novel therapies remains a clinically unmet need. SPP1 (osteopontin) is a glycoprotein involved in diverse biological functions. It is secreted by benign and malignant cells. Its role in gastric carcinomatosis is not well defined. Utilizing publicly available transcriptomic datasets, we show that SPP1 is overexpressed in gastric peritoneal metastasis and malignant ascites. Bulk and single-cell analysis demonstrated that SPP1 expression positively correlated with macrophage infiltration in the tumor microenvironment. SPP1 mutant tumors were enriched for macrophage-excluded phenotype. In conjunction with the human data, cytokine array analysis identified elevated SPP1 secretion by murine gastric tumor cells. Recombinant SPP1 promoted macrophage migration and inhibited the secretion of IL-10 in-vitro. Intercellular signaling networks from single-cell sequencing data sets of human malignant ascites revealed SPP1+ epithelial cells regulate macrophage expression of IL-10. Using syngeneic murine models of gastric peritoneal carcinomatosis, we observed that targeted SPP1 blockade diminished tumor growth as demonstrated by a 50% decrease in tumor weight and number of peritoneal nodules. In addition, in-vivo macrophage trafficking and secretion of IL-10 were inhibited by SPP1 blockade. In summary, we have uncovered a novel mechanism of cancer-macrophage crosstalk, suggesting that targeting SPP1 may be effective for reprogramming of the tumor microenvironment in gastric peritoneal carcinomatosis

#7009 From correlation to causation: SOX11 drives a coordinated immune-suppressive network that represses antigen presentation in triple-negative breast cancer.

Salomat Abdulkhuseynova[1], Ashok Pullikuth[2], Lance D. Miller[2]

[1]Wake Forest Institute for Regenerative Medicine, Wake Forest University School of Medicine, Winston Salem, NC, [2]Wake Forest University School of Medicine, Winston Salem, NC

Background: Triple-negative breast cancer (TNBC) is an aggressive subtype with no targeted therapies and limited response to immunotherapy. TNBC evades immune surveillance by repressing antigen presentation machinery (APM) genes, reducing MHC Class I expression. Using bioinformatics, we identified SOX11 as a potential transcriptional regulator associated with APM suppression and immune evasion in TNBC.
Methods: We analyzed gene expression data from basal breast cancer (BRCA) tumors (n = 189) in TCGA and cancer cell lines (n = 1,189) in DepMap. Spearman correlation coefficients were used to evaluate associations between a T-cell infiltration signature and an APM signature. SOX11 was prioritized as it was strongly negatively correlated with both signatures. To identify downstream effectors, we performed RNA-seq analysis on SOX11 knockdown (KD) CAL-148 cells (high endogenous SOX11) and integrated these results with publicly available SOX11-overexpression and KD datasets. To validate key targets, SOX11 KD and MEX3A KD were performed using siRNA, followed by flow cytometry to measure surface MHC Class I (HLA-ABC) expression.
Results: SOX11 was strongly inversely correlated (rho < -0.4, adjusted $p < 0.01$) with APM and T-cell infiltration signatures in basal BRCA and DepMap datasets. In basal BRCA tumors, SOX11 expression was enriched in T-cell cold tumors ($p < 0.01$). Analysis of our SOX11 KD RNA-seq data, integrated with public SOX11-modulated datasets, revealed a highly reproducible SOX11-driven gene signature. This signature was notably enriched for known suppressors of innate immunity. Among the most consistent SOX11 targets were genes implicated in **destabilizing HLA-A (MEX3B)**, **degrading innate immune sensors (MEX3A)**, activating **immunosuppressive signaling (SBK1)**, and facilitating **epigenetic silencing of interferon pathways and APM (RCOR2, NELL2)**. Consistent with this, SOX11 KD in CAL-148 cells significantly increased surface HLA-ABC expression. Furthermore, targeted knockdown of its effector, **MEX3A**, also resulted in a significant increase in APM gene expression.
Conclusions: SOX11 suppresses HLA-A/B/C expression and contributes to immune evasion in TNBC. Its high expression in T-cell cold tumors and its regulation of multiple APM-suppressive targets highlight its potential as a therapeutic target. We hypothesize that SOX11-mediated APM repression is not driven by a single gene but by the concerted activity of this multi-effector network. Targeting SOX11 or its key effectors could restore antigen presentation, promote immune recognition, and enhance immunotherapy responses in TNBC.

#7010 Trogocytosis-orchestrated CLDN18.2-dressed CD8$^+$ T cells drive pancreatic cancer progression via glucose metabolic reprogramming-induced cytotoxicity debilitation and systematic immune senescence-cascade.

Jingrui Yan[1], Tianxing Zhou[2], Jun Yu[1], Jihui Hao[1]

[1]Tianjin Medical Univ. Cancer Inst. & Hospital, Tianjin, China,[2]Tianjin Medical Univ. Cancer Inst. & Hospital, He Xi Qu, China

Background: CLDN18.2 is an established therapeutic target in gastrointestinal cancers; however, a significant proportion of CLDN18.2-positive tumors do not respond to treatment. While its expression has been extensively studied in epithelial cells, the expression, functional role, and regulatory mechanisms of CLDN18.2 in immune cells remain unexplored.

Results: Challenging the conventional paradigm that CLDN18.2 is exclusively epithelial, we report for the first time the presence of CLDN18.2 protein on CD8$^+$ T cells within tumors. Tumor-derived CLDN18.2 is transferred to T cells via ALCAM-CD6-mediated trogocytosis, a process requiring cell-cell contact. Its acquisition correlates with poor prognosis and resistance to immunotherapy in PDAC. In T cells, trogocytosed CLDN18.2 binds directly to β-catenin, recruits the CK1α/GSK3β complex, and promotes β-catenin phosphorylation, recognition by β-TrCP, and subsequent ubiquitin-proteasome degradation, thereby attenuating Wnt/β-catenin signaling. This suppression induces metabolic reprogramming characterized by reduced glucose uptake and glycolytic activity, resulting in impaired T-cell proliferation, activation, granzyme B and IFN-γ production, and overall cytotoxic function. Furthermore, CLDN18.2$^+$ CD8$^+$ T cells exhibit enhanced homing to the bone marrow via CXCL12/CXCR4 signaling, secrete IL-1α, promote hematopoietic stem cell myeloid skewing (expanding GMP/MDP populations), and contribute to systemic immune senescence, collectively dampening antitumor immunity. Based on the CLDN18.2-β-catenin interaction, we developed a peptide inhibitor, PC18.1, which disrupts this signaling axis, reverses glycolytic suppression, restores effector T-cell function, mitigates immune senescence, and synergizes with anti-PD-1 therapy to inhibit PDAC progression in vivo.

Conclusions: Our findings reveal CLDN18.2 as a metabolic immune checkpoint transmitted via trogocytosis from tumor to T cells: transfer of CLDN18.2 inhibits β-catenin signaling, suppresses glycolysis, compromises T-cell cytotoxicity, and induces systemic immune senescence. Therapeutic targeting of the CLDN18.2-β-catenin interface—for instance, with PC18.1—reinvigorates T-cell function and represents a promising strategy for improving treatment outcomes in CLDN18.2-high solid tumors.

#7011 ROCK2-regulated LIF-STAT3 drives immunosuppression in pancreatic cancer.

Varunkumar Krishnamoorthy[1], Sudhakar Jinka[1], Siddharth Mehra[1], Phuong Hong Ngoc Tao[2], Daysi Daniela Manrique[3], Rimpi Khurana[4], Yuguang Ban[4], Vineet Kumar Gupta[1], Austin Dosch[1], Nagaraj Nagathihalli[1]

[1]Department of Surgery, University of Miami Miller School of Medicine, Sylvester Comprehensive Cancer Center, Miami, FL,[2]Department of Microbiology and Immunology, University of Miami, Miami, FL,[3]Department of Biochemistry and Molecular Biology, University of Miami Miller School of Medicine, Miami, FL,[4]Department of Public Health Sciences, University of Miami Miller School of Medicine, Miami, FL

Background: Immunosuppression is a key characteristic of pancreatic ductal adenocarcinoma (PDAC), contributing to metastasis and poor survival. Our studies have identified tumor cell intrinsic Rho-associated coiled-coil containing protein kinase-2 (ROCK2) as a key regulator of extracellular matrix remodeling. In this study, we investigated how ROCK2 regulates immunosuppression in PDAC by modulating Leukemia inhibitory factor (LIF) and its effects on STAT3.

Methods: TCGA PDAC patient dataset was used to compare the ROCK2 and LIF expression in normal and PDAC tissues. CIBERSORT analysis of the PDAC dataset estimated the proportion of tumor infiltrating immune cell subsets. Genomic editing using the CRISPR/Cas9-system in LSL-$Kras^{G12D/+}$; $Trp53^{R172H/+}$; $Pdx1^{Cre/+}$ (KPC) cells was performed to generate KPC Rock2 knockout ($Rock2^{KO}$) cells. Cytokine array was performed on $Rock2^{EV}$ and $Rock2^{KO}$ conditioned media and ELISA was used to validate the results. Flow cytometry was used to profile LIF receptor (LIFR) expression in different cell types from KPC orthotopic tumors. Bone marrow-derived macrophages from C57BL/6 mice were treated with recombinant LIF (rLIF) and LIFR inhibitor (EC359), then analyzed for polarization by flow cytometry. KPC orthotopic tumors were generated, and Immune cell profiling was performed to evaluate alterations in immune cell subsets following treatment with EC359. Findings from ROCK2 and ROCK2-regulated LIF-STAT3 targeting, both in vitro and in vivo were validated using Immunoblotting and immunohistochemistry.

Results: Analysis of the TCGA dataset revealed that Human PDAC tissues have increased expression and correlation of ROCK2 and LIF. Further analysis showed that macrophages constitute a substantial proportion of the immune cell infiltrate. Cytokine array and ELISA-based studies revealed decreased LIF secretion with ROCK2 knockout, providing evidence for ROCK2 dependent regulation of LIF. KPC orthotopic tumors demonstrated higher LIFR expression in tumor-associated macrophages (TAMs) and EC359 treatment reduced ARG1 and PD-L1 expression on these cells. Additionally, EC359 treatment led to a significant increase in the activated effector and effector memory T cell populations. Furthermore, rLIF treatment increased pSTAT3 levels in macrophages, while EC359 lowered its expression, highlighting the role of ROCK2-regulated LIF-LIFR in STAT3 activation.

Conclusion: These findings demonstrate that tumor cell-intrinsic ROCK2 regulates LIF-STAT3, which mediates immunosuppression and can serve as a potential therapeutic target for PDAC.

#7012 Single-cell multi-omics identifies MRD-associated Tr1-like CD4 cells in B-ALL.

Qianyun Luo, Rebecca LaRue, Enoc Granados Centeno, Kyra Bergerud, Michael Farrar, Sean Tracy

University of Minnesota, Minneapolis, MN

Background: The persistence of measureable residual disease (MRD) after frontline chemotherapy in B-cell acute lymphoblastic leukemia (B-ALL) predicts relapse, yet the mechanisms allowing leukemic persistence remain unclear. Despite endogenous leukemia-specific T-cell response, these effector populations fail to eliminate MRD, suggesting active immune evasion. A major unmet need is to define immune programs that enable MRD survival and relapse after chemotherapy and CD19-directed immunotherapies. We aim to delineate the immune mechanisms underlying leukemic immune escape, leveraging a ~350,000-cell single-cell multiomics dataset generated from early-treatment bone marrow aspirates containing residual leukemia.

Methods: Bone marrow aspirates from 11 patients (collected within 100 days of diagnosis; MRD 0-20%) and 2 healthy controls were profiled using the 10x Chromium Flex platform with TotalSeq-C antibodies. Samples were enriched for $CD19^+$ blasts, $CD3^+$ T cells, and non-B/non-T populations, uniquely barcoded, fixed, probe-hybridized, and multiplexed into four captures, yielding ~350,000 cells with RNA + protein profiles. Data were processed with Cell Ranger and analyzed in Seurat. TCR-driven activation was quantified using the TCAT Antigen-Specific Activation (ASA) score.

Results: Across all samples, we observed that all major immune cell lineages in leukemia samples segregated distinctly from healthy controls. Two subsets of highly activated CD4+ T-cells were observed, and both subsets corresponded to known regulatory/suppressive populations. These included a FOXP3+ T-regulatory (Treg) subset, and a FOXP3- IL10+ Type-1 regulatory (Tr1) like population. While FOXP3+ Tregs were also observed in healthy control samples, Tr1 like cells were found only in samples from patients with leukemia. Among CD8+ T-cells, we predominantly observed transcriptomic signatures of early activation and effector/memory features. Only small frequencies (0.01%) of CD8+ T-cells expressed an exhausted phenotype (PD1+/TIM3+/LAG3+), and cells in this subset continued to express TCF7, consistent with an early-progenitor-exhausted state, rather than terminal exhaustion.

Conclusion: At an early-treatment timepoint, the MRD microenvironment undergoes extensive immune remodeling. Activated CD4+ T-cells are dominated by regulatory/suppressive subsets including transcriptionally distinctive FOXP3+ Treg subsets and a unique population of Tr1 like population that expands with increasing MRD, suggesting a dynamic role in immunosuppression. Conversely, CD8+ T-cell display signatures of suboptimal activation, without evidence of terminal exhaustion. Overall, suppressive $CD4^+$ programs appear to limit effective anti-leukemia immunity and may facilitate relapse.

#7014 SPIN1 drives PD-1 immunotherapy resistance in gastric cancer by inducing M2 macrophage polarization and suppressing CD8⁺ T-cell immunity.

Beibei Lyu[1], Zijun Yidan Xu-Monette[2], Xiaoyan lin[1]

[1]Shandong Provincial Hospital Affliated to Shandong First Medical University, Jinan, China,[2]Duke University Medical Center, Durham, NC

Introduction: Resistance to anti-PD-1 therapy remains a major obstacle to improving outcomes in gastric cancer (GC). Although the chromatin reader SPIN1 has been implicated in tumor progression, its contribution to shaping the tumor immune microenvironment (TIME) and driving immunotherapy resistance is not well understood. This study aimed to elucidate how SPIN1 modulates immune components within the TIME to promote resistance to PD-1 blockade.

Experimental Procedures: SPIN1 expression and immune infiltration patterns—including CD8⁺ T cells, CD163⁺ and CD206⁺ macrophages, and TIM-3⁺ exhausted lymphocytes—were assessed by multiplex immunohistochemistry (mIHC) in GC patients treated with anti-PD-1 therapy. Mechanistic studies were performed using GC cell lines with stable SPIN1 knockdown or overexpression in macrophage co-culture assays, metabolic profiling, and flow cytometric characterization of M1/M2 markers. Antitumor efficacy was evaluated in syngeneic mouse models treated with a SPIN1 small-molecule inhibitor, anti-PD-1 antibody, or the combination.

Data Summary: Clinically, SPIN1 expression was significantly higher in non-responders than in responders to PD-1 blockade. Elevated SPIN1 levels strongly correlated with increased infiltration of immunosuppressive M2 macrophages (CD163⁺/CD206⁺) and reduced CD8⁺ T-cell presence in tumor tissue. In vitro, SPIN1 silencing diminished, whereas SPIN1 overexpression enhanced, M2-associated gene expression and surface markers. Flow cytometry confirmed that SPIN1 drives macrophage polarization toward an M2 phenotype. SPIN1-conditioned macrophages subsequently suppressed CD8⁺ T-cell proliferation and cytotoxic function while inducing T-cell exhaustion, evidenced by increased PD-1, TIM-3, and LAG-3 expression. In vivo, pharmacologic inhibition of SPIN1 reshaped the TIME by reducing M2 macrophage accumulation and restoring CD8⁺ T-cell infiltration and effector activity. Notably, combining a SPIN1 inhibitor with anti-PD-1 therapy produced a synergistic antitumor response and significantly reversed acquired resistance compared with either single agent.

Conclusions: This study identifies SPIN1 as a key regulator of immune suppression and therapeutic resistance in GC. By promoting M2 macrophage polarization and driving CD8⁺ T-cell exhaustion, SPIN1 establishes a TIME that limits the efficacy of PD-1 blockade. These findings highlight SPIN1 as both a predictive biomarker for immunotherapy response and a promising therapeutic target for sensitizing gastric tumors to PD-1-based immunotherapy.

#7015 USP5 suppresses MRE11 endonuclease function to facilitate tumor immune escape.

Chuan-Chun Lee[1], Wan-Rong Wu[2], Liang-Chih Liu[1], Ting-Yi Liao[1], You-Zhe Lin[2], Fang-Ying Lin[2], Yi-Chun Shen[2], Yuan-Liang Wang[1], Chih-Hao Lu[3], Wei-Chung Cheng[2], Wei-Chao Chang[1], Yi-Chuan Li[1], Chih-Tung Lin[1], Chung-Yu Chen[2], Sheng-Wen Chen[2], Hsin-An Shih[4], Steven Lin[4], Chen-Yuan Lin[1], Chang-Fang Chiu[1], **Shao-Chun Wang**[2]

[1]China Medical University Hospital, Taichung City, Taiwan,[2]China Medical University, Taichung City, Taiwan,[3]National Yang Ming Chiao Tung University, Hsinchu, Taiwan,[4]Academia Sinica, Taipei City, Taiwan

Replication stress is a hallmark of cancer that generates abnormal cytosolic DNA, thereby activating intrinsic immune pathways that constrain tumor growth. To survive, malignant cells must counteract these immune surveillance mechanisms, yet the underlying regulatory processes remain incompletely understood. The MRE11 nuclease plays a dual role in maintaining genome stability and processing stalled replication forks, where its endonuclease activity produces single-stranded DNA (ssDNA) capable of activating the cGAS-STING axis to induce anti-tumor immunity. In this study, we uncover a ubiquitin-dependent mechanism that connects DNA replication stress to immune evasion. Loss of tyrosine 211 phosphorylation on PCNA (pY211-PCNA) induces endogenous replication stress and promotes site-specific polyubiquitination of MRE11. This modification enhances MRE11 endonuclease activity, resulting in cytosolic ssDNA accumulation, activation of innate immune signaling, and increased susceptibility to natural killer (NK) cell-mediated cytotoxicity. Conversely, in cells expressing pY211-PCNA, the deubiquitinase USP5 is recruited to replication forks, where it removes ubiquitin from MRE11, thereby attenuating its endonuclease activity and suppressing cytosolic ssDNA formation and immune activation. Clinically, elevated USP5 expression correlates with tumor metastasis and poor prognosis in breast cancer. Genetic ablation or pharmacologic inhibition of USP5 restores MRE11-dependent ssDNA production, promotes NK cell infiltration, and suppresses tumor growth in immune-competent but not immune-deficient mouse models. An unbiased drug screen identified two FDA-approved compounds as potent USP5 inhibitors, which mimic USP5 depletion by enhancing cytosolic ssDNA accumulation, triggering NK- and PBMC-mediated killing of patient-derived tumor organoids (PDTOs), and suppressing tumor growth in syngeneic mouse models. These results identify USP5 as a critical negative regulator of MRE11-driven immunogenic DNA processing and reveal a therapeutic strategy to potentiate anti-tumor immunity through targeted USP5 inhibition.

#7016 Targeting sialylation promotes anti-tumor immunity in small cell lung cancer.

Alex D. Doan[1], Kelly Heard[1], Jackson Fatherree[1], Mallika Yalangi[1], Pritha Chanana[2], Mitchell Kluesner[1], Daniel S. Hippe[3], Cody Jenkins[1], Hannah Kerbyson[1], Shivani Srivastava[1], David MacPherson[1]

[1]Human Biology Division, Fred Hutchinson Cancer Center, Seattle, WA,[2]SR Bioinformatics, Fred Hutchinson Cancer Center, Seattle, WA,[3]Clinical Biostatistics, Fred Hutchinson Cancer Center, Seattle, WA

Small cell lung cancer (SCLC) is a highly lethal subtype of lung cancer with a 5-year relative survival rate of less than 10%, even with the addition of immune checkpoint blockade to standard of care therapy. The tumor immune microenvironment of SCLC has been characterized as highly immunosuppressive, and SCLC suppresses the expression of antigen presentation machinery, likely contributing to the lack of effective prolonged immunotherapy responses. Our project investigates the targeting of sialic acid, a sugar molecule overexpressed in many cancers, to increase anti-tumoral immune responses. Studies in other malignancies have shown that cancer cells can hijack this axis as a mechanism of immune evasion through interactions with the SIGLEC family of inhibitory receptors on infiltrating immune cells. We hypothesize that SCLC also utilizes sialic acids for immune masking, and that tumor desialylation would improve anti-tumor responses and could be a potential novel therapeutic approach for SCLC.

Using SCLC lines that we derived from genetically engineered mouse models harboring *Rb1/Trp53* inactivation, we performed genome wide CRISPR deletion screens and identified *Gne* as a top gene regulating SCLC sialylation. We then deleted *Gne* and confirmed robust decreases in sialylation. Under interferon-γ stimulated conditions, *Gne*-deleted cells exhibited elevated MHC-I expression and IFNγ signaling pathway, suggesting that loss of sialylation leads to increased antigen presentation and intrinsic immunogenicity. These results are relevant as recent clinical data revealed SCLC patients with low MHC-I expression respond poorer to anti-PDL1 therapy. When the *Gne*-deleted cells were propagated into mice as flank tumors or as a disseminated metastatic model, we observed delayed tumor kinetics and prolonged survival in syngeneic immunocompetent hosts, but not in immunocompromised recipients, suggesting that the observed effects are immune dependent. Immunophenotyping of syngeneic tumors by flow cytometry revealed increased tumor MHC-I expression and higher infiltration of tumor antigen specific CD8+ T cells upon *Gne* deletion. Furthermore, co-culturing of *Gne*-deleted cells expressing ovalbumin with ovalbumin antigen (OT-I) specific CD8+ T cells showed increased tumor cell killing and T cell activation. Lastly, analysis of patient SCLC samples in the IMpower133 clinical trial revealed a survival benefit with chemo-immunotherapy for patients expressing lower transcriptional levels of key sialic acid biosynthesis genes, while this effect is absent in the chemotherapy only group. Altogether, our data suggests that desialylation improves immunogenicity and anti-tumor immunity in SCLC.

Ultimately, our work improves the understanding of the mechanisms behind immune responses in SCLC and has potentially uncovered a novel glyco-immunotherapeutic approach to develop new treatments for SCLC in the clinical setting.

#7017 EMP2 is a potential immunotherapeutic target to modulate macrophage-induced phagocytosis in glioblastoma.

Amr Elkholy[1], Eshika Kudaravalli[1], Mostafa Mohamed[1], Hasan Alrefai[2], Saeed Zakakhosravi[1], Satoru Osuka[1], Christopher D. Willey[2], Ahn Erin[1]

[1]University of Alabama at Birmingham, Birmingham, AL,[2]O'Neal Comprehensive Cancer Center at UAB, Birmingham, AL

Glioblastoma (GBM) is the most aggressive primary brain tumor. Despite advances in immunotherapy for other solid tumors, T-cell checkpoint blockades have failed to improve overall survival in GBM patients, largely due to low T-cell infiltration. In contrast, tumor-associated macrophages (TAMs) comprise 82-97% of the immune cell population in newly diagnosed GBM. TAMs, however, often fail to engulf tumor cells, partly due to the phagocytosis inhibitory “do not eat me" signals such as CD47, which interacts with macrophage SIRPα to suppress phagocytosis. Although, CD47 blockade enhances phagocytosis in preclinical models, clinical trials of anti-CD47 therapies such as magrolimab were halted due to increased mortality and limited efficacy in acute myeloid leukemia patients, highlighting the need for alternative phagocytosis-inducing therapies. To identify novel tumor-expressed genes that inhibit macrophage phagocytosis, we performed a genome-wide CRISPR screen using two rounds of coculture of radioresistant GBM tumor cells (MGG18-RR) and tumor-conditioned human peripheral blood (hPBMCs)-derived macrophages. Tumor-conditioned hPBMCs macrophages were considered more reliable, as our cytometry imaging results revealed distinct polarization states compared to unpolarized (M0) macrophages. In the first round, MGG18-RR GBM cells were co-cultured with tumor-conditioned hPBMCs-derived macrophages at a 1:5 ratio for 7 days, with media refreshed every 2 days. Parallel tumor-only cultures served as controls. Tumor cells that survived this first co-culture were pooled and subjected to a second 7-day co-culture with freshly differentiated and polarized macrophages. After the second round, the remaining tumor cells were collected, and genomic DNA was extracted for library prep and sequencing. Among the top 100 hits, several known regulators of phagocytosis, including CD47 and KRAS were enriched, validating the reliability of the screen. We identified Epithelial Membrane Protein 2 (EMP2) as a novel tumor-expressed gene that suppresses macrophage phagocytosis. EMP2 showed high expression in glioma cells in publicly available single-cell sequencing data for GBM patients. EMP2 is highly expressed in GBM and associated with tumor progression and poor survival. Functional validation using the pHrodo in-vitro phagocytosis assay demonstrated a significant increase in the engulfment of EMP2-knockout GBM cells (JX14P-RT) by both hPBMCs-derived macrophages and RAW246.7 macrophages ($p < 0.05$), compared to wild-type tumor cells, suggesting that EMP2 acts as an anti-phagocytic regulator in GBM. Ongoing studies aim to validate that EMP2 knockout enhances macrophage phagocytosis in syngeneic murine GBM model. Collectively, our findings highlight EMP2 as a novel regulator of macrophage-mediated tumor clearance and a promising therapeutic target for macrophage-based immunotherapy in GBM.

#7018 The CBS-CXCL10 signaling axis supports tumor progression by driving immune suppression within the tumor microenvironment.

Fanghui Chen, Fan Yang, Jianqiang Yang, Nabil Saba, **Yong Teng**

Emory University, Atlanta, GA

Cystathionine β-synthase (CBS), a key enzyme in the transsulfuration pathway, is overexpressed in cancer cells and promotes tumor progression in part through hydrogen sulfide-mediated metabolic reprogramming. However, its role in shaping the tumor microenvironment and antitumor immunity is not well defined. Here, we show that CBS is highly expressed in head and neck cancer (HNC) tissues and cell lines, and that CBS knockdown slows tumor growth while enhancing antitumor immune responses in orthotopic syngeneic mouse models. Mechanistically, CBS silencing downregulates PSAT1 transcription, a key enzyme in the serine biosynthesis pathway, leading to intracellular serine depletion, DNA damage, and increased oxidative stress. These stress responses activate the cytosolic DNA-sensing pathway, triggering the cGAS-STING axis with phosphorylation and nuclear translocation of IRF3 and subsequent transcription of the chemokine CXCL10. Elevated CXCL10 functions as a potent chemoattractant for cytotoxic T cells, enriching the tumor microenvironment with effector lymphocytes and enhancing tumor control in vivo. Immunophenotyping and functional assays support a reprogrammed microenvironment consistent with heightened antitumor immunity upon CBS knockdown. Importantly, these effects are observed in an immunocompetent, orthotopic model, suggesting that CBS-driven signaling intersects with innate DNA sensing to modulate adaptive immunity in HNC. Collectively, these findings reveal a previously unrecognized immunomodulatory role for CBS in HNC and identify CBS as a potential metabolic-immune-target to augment tumor-reactive immunity and improve immunotherapy outcomes

: Drug Resistance 2: Tyrosine Kinase Inhibitors
Poster Session

#7022 Investigating PRMT5 as a therapeutic target in EGFR TKI resistant NSCLC and assessing the role of mucins in NSCLC as blood biomarkers.

Aditya Krishnan[1], James Jin[2], Usama Altayeh[3], Jessica Hindenburg[1], Neelu Puri[4]

[1]University of Illinois College of Medicine (Rockford), Rockford, IL,[2]College of Medicine, University of Illinois College of Medicine (Rockford), Rockford, IL,[3]Department of Biomedical Sciences, University of Illinois College of Medicine (Rockford), Rockford, IL,[4]University of Illinois at Chicago, Rockford, IL

Lung cancer is on track to cause over 124,000 U.S. deaths in 2025, and about 10-15% of all lung cancers in the United States involve EGFR-resistant NSCLC. Patients with EGFR-mutant NSCLC are initially responsive to TKIs but frequently relapse within 19 months. PRMT5, a type II arginine methyltransferase, drives oncogenic and inflammatory signaling primarily through P13K-Akt signaling, which may be increased by cigarette smoke. We hypothesize that inhibiting PRMT5 by using siRNA will modulate these pathways and restore EGFR-TKI sensitivity. PRMT5 expression was analyzed in EGFR-mutant NSCLC parental cell lines (H3255P, H1975P, PC9) and resistant cell lines (H3255OR, H1975OR, PC9OR) using qPCR and Western blotting following cigarette smoke extract (CSE) exposure and siRNA knockdown using DharmaFECT. Cytokine expression was profiled using qPCR to assess downstream inflammatory effects. Immunohistochemistry (IHC) was performed on normal and tumor tissues from smokers and non-smokers to evaluate PRMT5 levels. The PRMT5 levels were analyzed using a Keyence microscopic software (BZX-800 Analyzer) and statistical analysis was done using Fisher's Exact test. CSE increased PRMT5 mRNA across EGFR-mutant lines by 1.2-11.5 fold at 48 h ($p<0.01–0.001$). Immunoblotting confirmed PRMT5 upregulation at 24–48 h in resistant cells by 1.3-2.5 fold ($p<0.01–0.001$). In H3255-OR and PC9-OR cells, siPRMT5 reduced the 48-h CSE–induced cytokine surge (170-760%) by 10-20%. Compared to Mock plus CSE, siPRMT5 plus CSE reduced IL-8 (60–75%), TNF-α (30–50%), and IL-1β (35–55%). Downregulation of these cytokines was also seen after combinatory treatment with osimertinib and siPRMT5. In PC9-P/OR cells, siPRMT5 lowered PRMT5 transcripts by 35–50% compared to Mock and siPRMT5 plus CSE reduced by 15–45% relative to Mock plus CSE. IHC on 21 smoker and 20 non-smoker lung tissues from lung cancer patients showed PRMT5 expression was higher in smokers versus non-smokers ($p<0.05$). Studies were also conducted on normal lung tissue from 25 smokers and 19 non-smokers and PRMT5 expression was found to be higher in smokers compared to non-smokers using Fisher's exact test ($p<0.001$). In conclusion, PRMT5 is upregulated by CSE in osimertinib-resistant EGFR-mutant cells and is upregulated in smokers. PRMT5 knockdown suppresses inflammatory cytokines and supports the rationale that inhibiting PRMT5 could help restore EGFR-TKI sensitivity.

#7023 ENPP1 inhibits the cGAS-STING pathway to mediate immune evasion in EGFR-TKI resistant NSCLC.

Chao Zhou[1], Yuqing Liu[2], Jun Lu[1], Baohui Han[1]

[1]Shanghai Chest Hospital, Shanghai, China,[2]Shanghai Jiao Tong University School of Medicine, Shanghai, China

Third-generation EGFR tyrosine kinase inhibitors (TKIs), such as osimertinib, have demonstrated promising clinical efficacy in EGFR-mutant non-small cell lung cancer (NSCLC). Despite substantial progress with EGFR-TKIs, the development of acquired resistance remains a major clinical challenge. Notably, the addition of immunotherapy after TKI resistance has not resulted in significant survival benefits compared to chemotherapy. In this study, single-cell RNA sequencing analysis of key immune cell subpopulations and tumor immune features revealed an immunosuppressive shift in the tumor microenvironment of TKI-resistant tumors, characterized by an increased proportion of M2 macrophages, reduced dendritic cells (DCs) and M1 macrophages, and immune function scores indicative of an immunosuppressive state. Comprehensive transcriptomic profiling of established osimertinib-resistant NSCLC cell lines (HCC827OR, H1975OR, PC9OR) demonstrated a significant upregulation of ENPP1 expression compared with their parental, TKI-sensitive counterparts. Given that ENPP1 functions as a cGAMP hydrolase and is implicated in STING pathway suppression and immune evasion, we first assessed cGAMP hydrolysis activity and found that resistant cells exhibited enhanced cGAMP-degrading capacity. Co-culture experiments of tumor cells with antigen-presenting cells (APC) revealed that resistant tumor cells more effectively suppressed cGAS-STING signaling in APCs, thereby attenuating T-cell activation and cytotoxicity. Both genetic silencing of ENPP1 via siRNA and pharmacological inhibition using the ENPP1 inhibitor ENPP-1-IN-1 enhanced STING pathway activation in APCs and restored T-cell activation and cytotoxic functions in co-culture systems. Bioinformatic prediction and dual-luciferase assays identified SP1 as a direct transcriptional regulator of ENPP1. Finally, immune reconstitution mouse models confirmed that ENPP-1-IN-1 potentiated the efficacy of anti-PD-1 therapy in HCC827OR xenografts by increasing immune infiltration and T-cell activity. Collectively, our study highlights a critical role for ENPP1 in mediating immune evasion through suppression of the cGAMP-STING pathway in the EGFR-TKI resistant tumor, supporting ENPP1 as a promising therapeutic target to enhance immunotherapy efficacy in EGFR-TKI resistant NSCLC.

#7024 Simultaneous targeting of CHI3L1 and PD-1/PD-L1 axis to overcome drug resistance and immune tolerance of EGFR non-small cell lung cancer.

Suchitra Kamle[1], Bing Ma[2], Brianna Pham[3], Isabella Fish[3], Marlo Hulnick[3], Taka Sadanaga[2], Hanseok Jeong[2], Mara Hofstetter[4], Hina Khan[5], Christopher Azzoli[5], Katerina A. Politi[6], Roy S. Herbst[6], Chun Geun Lee[2], Jack Elias[1]

[1]Molecular Microbiology & Immunology, Legorreta Cancer Center at Brown University, Providence, RI,[2]Molecular Microbiology & Immunology, Brown University, Providence, RI,[3]Brown University, Providence, RI,[4]University of Zurich, Zurich, Switzerland,[5]Legoretta Cancer Center at Brown University, Providence, RI,[6]Yale Cancer Center, New Haven, CT

Background: Lung cancer is the leading cause of cancer deaths worldwide. Non-small cell lung cancer(NSCLC) accounts for 85% of all lung cancers. The overall prevalence rate of NSCLC with epidermalgrowth factor receptor (EGFR) mutations are significantly increasing in US. Oncogenic EGFR is atransmembrane protein which gets auto-phosphorylated to cause EGFR mutations (L858R, T790M, exon-19-deletion) in exon 18-21. Tyrosine kinase inhibitors (TKIs) are effectively targeted to treat mutated EGFRlung cancer. These TKIs showed favorable responses on patient's treatments for 9-18 months but duringthe treatment, patients acquired EGFR mutations which results into the TKIs drug resistance and at thatpoint TKIs stops its efficacy for further treatment. Thus, there is a high medical unmet need for a newtherapeutic strategy to overcome drug resistance in patients with EGFR mutations. CHI3L1 expressed bymacrophages, neutrophils, epithelial cells, smooth muscle cells, chondrocytes including other immune cells.The levels of circulating CHI3L1 are increased in many malignancies including cancers of the prostate,colon, rectum, ovary, kidney, breast, glioblastomas, malignant melanoma, and lung cancer. CHI3L1contributes to pulmonary metastasis and spread via the regulation of immune-checkpoint (ICP) molecules.Our studies showed that CHI3L1 regulates and is a potent stimulator of PD-1/PD-L1 and PD-L2. CHI3L1stimulates the EGFR physiologic ligands EGF or TGF-a, a well-defined growth factors that stimulate EGFRphosphorylation. EGFR-YAP/TAZ signaling plays a growth-promoting role in cancers harboring EGFRalterations, and that inhibition of YAP/TAZ in combination with EGFR might be beneficial to prevent TKIdrug resistance and cancer recurrence.
Methods: We analyzed EGFR mutant and resistant cells using techniques qPCR, protein accumulation,immuno-pull-down assay, immunofluorescence, FACS and therapeutic effect of YAP inhibitors in-vitroand in-vivo.
Results: We identified that CHI3L1 augments YAP/TAZ nuclear translocation in EGFR mutant and TKIresistant cells. Also, YAP/TAZ inhibitors and agonists (Verteporfin, K-975) able to block YAP/TAZactivation and that suppress PD-1/PD-L1 in EGFR mutant and TKI resistant cells.
Conclusion: These findings led us to understand that CHI3L1 and PD-1/PD-L1 axis mediated throughactivation of Hippo-YAP/TAZ signaling pathways play an essential role in TKIs drug resistance andimmune tolerance that enhances the progression of EGFR NSCLC. Additionally, simultaneous targeting ofCHI3L1 and PD-1/PD-L1 axis employing bispecific antibody (CHI3L1xPD-1) may provide a bettertherapeutic option to overcome TKI resistance and immune tolerance of EGFR NSCLC.

#7025 Mechanisms of zongertinib resistance in HER2-mutant non-small cell lung cancer and potential strategies to overcome resistance.

Yuji Shibata[1], Monique B. Nilsson[2], Ximeng Liu[2], Li (Lily) Cai[2], Hong Jiang[2], Linghzi Hong[2], Alvaro Guimaraes Paula[2], Hibiki Udagawa[2], Jacqulyne Ponville Robichaux[3], Junqin He[2], Xiaoxing Yu[2], John V. Heymach[2]

[1]Thoracic Head & Neck Medical Oncology, UT MD Anderson Cancer Center, Houston, TX,[2]UT MD Anderson Cancer Center, Houston, TX,[3]AstraZeneca Oncology, Houston, TX

Activating mutations in HER2 are found in approximately 2-4% of non-small cell lung cancer (NSCLC). Zongertinib is currently the only FDA-approved tyrosine kinase inhibitor (TKI) for patients with HER2-mutant NSCLC. However, the mechanisms underlying acquired resistance remain unclear, and understanding zongertinib-resistance mechanisms is essential for developing subsequent effective therapeutic strategies in HER2-mutant NSCLC. To identify candidate genomic alterations in HER2 mediating zongertinib resistance, we analyzed HER mutation profiles in clinical samples from NSCLC patients after progression on zongertinib, reviewed previously reported resistance mutations from other HER2 TKIs, and employed the LentiMutate scanning mutagenesis system. Candidate HER2 resistance mutations identified through these approaches were then transduced into Ba/F3 cells and the effect on drug sensitivity was assessed. We detected secondary HER2 mutations including S783C, C805S, and T862A in post-zongertinib clinical samples in combination with the originally observed activating HER2 mutations or NRG1 fusions. Our LentiMutate analysis identified HER2 alterations including C805S, T862A, S783P as well as T798I and L726F as being enriched in zongertinib resistant cells. We next engineered Ba/F3 cells to express HER2 activating mutations (e.g. Y772dupYVMA) alone or in combination with potential secondary HER2 resistance mutations including S783C, T798I, C805S, or T862A, and observed that expression of these mutations rendered cells resistant to zongertinib in vitro. However, S783C and C805S mutations did not impact in vitro sensitivity to the HER2 TKI sevabertinib. Structural analysis revealed that T798I acts as a gatekeeper mutation, whereas S783C and T862A disrupt hydrogen bonds between the drug and HER2, and C805S disrupts a covalent bond, thereby weakening zongertinib-HER2 binding. Next, we implanted mice with tumor cells expressing HER2 activating mutations alone or in combination with S783C or C805S and evaluated the anti-tumor activity of zongertinib and sevabertinib. Consistent with our in vitro findings, tumors bearing C805S or S783C secondary mutations were resistant to zongertinib but sensitive to sevabertinib. Our findings identify novel HER2 mutations that mediate zongertinib resistance and indicate that sevabertinib may be effective against a subset of these genomic alterations.

#7026 IL-1 alpha expression induces drug resistance to all generations of EGFR inhibitors in HNSCC.

Nafis Md Irfan[1], Ishrat Nourin Khan[2], Nurgul Koyuncu[2], Krishna Awasthi[2], Andrean L. Simons-Burnett[1]

[1]Free Radical and Radiation Biology Program, Department of Radiation Oncology, University of Iowa, Iowa City, IA,[2]University of Iowa, Iowa City, IA

Epidermal Growth Factor Receptor (EGFR) expression is upregulated in the majority of head and neck squamous cell carcinomas (HNSCC) and is associated with poor clinical outcomes. Unfortunately, the incorporation of EGFR inhibitors (EGFRIs) into the management of HNSCC has not improved long term survival rates in HNSCC patients despite high EGFR expression. Additionally, EGFR tyrosine kinase inhibitors (TKIs) in particular, have failed to show clinical benefit for HNSCC patients in clinical trials. Therefore, the identification and understanding of strategies that will improve the efficacy of EGFRIs may improve patient treatment and survival. Previous work in our lab has shown that HNSCC cells treated with erlotinib, a first-generation EGFR TKI, increased expression and release of the proinflammatory cytokine interleukin-1 alpha (IL-1α) resulting in inflammation and the development of drug resistance. The goal of this study is to determine if IL-1α-induced drug resistance is maintained across second, third and fourth generation EGFR TKIs.EGFR wildtype-positive HNSCC cells (FaDu, Cal-27 and SQ20B) were treated with the IC_{50} doses of erlotinib (first generation), afatinib (second generation), osimertinib (third generation), and silevertinib (fourth generation) EGFR TKIs for 48 h. Cell viability responses to EGFR TKIs were assessed using MTT assays. IL-1α and IL-6 cytokine expression was detected by ELISA and Western blot. Manipulation of IL-1 expression and signaling was performed using neutralizing antibodies to human IL-1α antibody (nIL-1α) and IL-1β (nIL-1β), and the human IL-1 receptor antagonist - anakinra. Results showed that all four EGFR TKIs triggered the release of IL-1α but not IL-1β from all 3 HNSCC cell lines. Additionally, all four EGFR TKIs increased IL-6 (IL-1α signaling endpoint) release, which was suppressed by nIL-1α and anakinra (but not nIL-1β) implying that IL-1α, rather than IL-1β, acts upstream of IL-6 activation. Overexpression of IL-1α in Cal-27 cells resulted in resistance to all four generations of EGFR TKIs. Lastly, erlotinib-resistant Cal 27 and SQ20B cells also demonstrated resistance to all other generations of EGFR TKIs. Collectively, these findings identify IL-1α expression as a central mediator of poor response and resistance to all EGFR TKIs via an EGFR mutation-independent mechanism. Hence, targeting IL-1α expression/signaling could be a promising strategy to improve long term tumor response to EGFR TKIs in HNSCC.

#7027 Multi-lineage evolution of drug resistance via a novel keratin 17+ drug tolerant persister population in *EGFR*-mutant NSCLC.

Benjamin B. Morris[1], Monique B. Nilsson[1], Ethan Earlie[2], Eric E. Gardner[3], Hong Chen[1], Santiago G. Trevino[1], Alexa J. Halliday[4], Yuanxin Xi[4], Jing Wang[4], Natalie Vokes[1], Don Gibbons[1], Jianjun Zhang[1], Ashley M. Laughney[2], Yasir Y. Elamin[1], Xiuning Le[1], John V. Heymach[1]

[1]Thoracic/Head and Neck Medical Oncology, UT MD Anderson Cancer Center, Houston, TX,[2]Department of Systems and Computational Biomedicine, Weill Cornell Medicine, New York, NY,[3]Weill Cornell Medicine, New York, NY,[4]UT MD Anderson Cancer Center, Houston, TX

Background: EGFR mutant lung cancers initially respond to frontline targeted therapy. However, resistance inevitably develops through diverse mechanisms. Resistant tumors universally emerge from drug tolerant persister cells (DTPCs) that survive initial treatment. Despite this knowledge, the biology of EGFR mutant DTPCs is not well understood. This study was conducted to interrogate DTPC phenotypes that enable evolution of therapy resistance.

Methods: DTPC models were generated by treating EGFR mutant cell lines with >IC90 concentrations of osimertinib for 14 days. After 14 days, cells were profiled with 10X 3' single cell RNA sequencing (scRNAseq). Seurat was used to integrate data, normalize data, cluster cells, and conduct differential expression analyses. UCell was used to score cells for activity of biology pathways. scanpy was used to analyze scRNAseq data from the Gardner et al. ERPMT mouse model. Human patient samples were collected from lung cancer patients treated at MD Anderson Cancer Center using IRB approved protocols. Samples were profiled with 10X 5' scRNAseq. scanpy was used to integrate data, normalize data, and cluster cells. Palantir was used to perform trajectory analyses.

Results: Differential expression (DE) analysis comparing DTPCs and control cells were conducted for cell line pairs. Using DE results, we generated consensus gene signatures capturing genes universally upregulated or downregulated across DTPC models. Review of these genes identified that *KRT17* was highly upregulated in osimertinib DTPCs. We found *KRT17*+ DTPCs upregulate epithelial-to-mesenchymal (EMT), stemness, and aberrant basaloid signatures compared to *KRT17*- DTPCs. Subclustering showed that *KRT17* DTPCs are heterogeneous and label non-overlapping EMT, proliferative, and *MET* expressing populations. To validate our *in vitro* findings, we analyzed scRNAseq datasets from multiple in vivo sources. In GEMM models, *Krt17*+ cells populate minimal residual disease (MRD) following suppression of mutant EGFR. *Krt17*+ cells were a stem-like population that emerged as residual tumor cells lost alveolar epithelial identity prior to neuroendocrine transformation. Lastly, we confirmed the clinical relevance of our findings by investigating human patient clinical specimens. Compared to treatment naïve samples, *KRT17*+ cells were significantly enriched in osimertinib-treated MRD samples. Trajectory analyses demonstrated that *KRT17* expression characterized cell populations that preceded development of resistance through several known mechanisms, including *MET* amplification and histologic transformation (HT).

Conclusions: Our data demonstrate that EGFR-mutant cells surviving initial treatment converge onto a novel *KRT17*+ DTPC state which serves as a multipotent progenitor population capable of leveraging diverse mechanisms to resist therapy, including HT.

#7028 Investigating the role of PLK4 and GDF15 in NSCLC tumorigenicity and EGFR-TKI resistance.

Subaranjana Saravanaguru Vasanthi[1], Georgia Kapetaneas[2], Meet Patel[3], Neelu Puri[1]

[1]Department of Biomedical Sciences, University of Illinois College of Medicine (Rockford), Rockford, IL,[2]College of Medicine, University of Illinois College of Medicine (Rockford), Rockford, IL,[3]Cancer Biology, University of Alabama at Birmingham, Birmingham, AL

Background: Non-small cell lung cancer (NSCLC) accounts for nearly 85% of all lung cancers, and the development of resistance to Epidermal Growth Factor Receptor (EGFR) Tyrosine Kinase Inhibitors (TKIs) remains a major clinical challenge, limiting long-term therapeutic success. Emerging evidence shows that PI3K/Akt and TGF-β-signaling are key drivers of EGFR-TKI resistance. Polo-like kinase 4 (PLK4), a serine/threonine kinase, regulates centriole duplication and maintains genomic stability, while its overexpression can promote oncogenic transformation and tumor progression through PI3K/Akt activation. Notably, PLK4-driven signaling intersects with stress-responsive pathways, creating a cellular environment conducive to survival and therapeutic resistance. Within this context, Growth differentiation factor 15 (GDF15), a stress-responsive cytokine and member of the TGF-β superfamily, is significantly upregulated in NSCLC, particularly in patients with a history of smoking. GDF15 promotes metastasis, epithelial-mesenchymal transition (EMT), and therapy resistance through TGF-β and ErbB crosstalk. Moreover, GDF15 is also emerging as a novel biomarker and potential therapeutic target in NSCLC, playing a key role in EGFR-TKI resistance and enhancing tumorigenicity.
Hypothesis/Aims: We hypothesize that overexpression of PLK4 and GDF15 drives tumorigenesis and EGFR-TKI resistance through PI3K-Akt-mTOR, TGF-β and ErbB signaling in NSCLC, and that modulating these key biomarkers may help reduce tumorigenicity and overcome resistance.
Study Design: We examined PLK4 and GDF15 expressions in drug-resistant - Osimertinib-resistant (OR) and Erlotinib-resistant (ER) and drug-sensitive (parental) NSCLC cell lines after 24- and 48-hour CSE treatment using qPCR, western blotting, and immunofluorescence.
Results: Immunoblot analyses revealed that PLK4 protein expression levels were upregulated by ~2.0- to 4.0-fold in both OR and ER NSCLC cell lines compared with parental controls ($p < 0.05$) also supported by strong immunofluorescence signals. Quantitative PCR further showed significant GDF15 upregulation from 1.4- to 3.4-fold in both Osimertinib and Erlotinib resistant cells particularly after 48 h of cigarette-smoke-extract exposure, suggesting that smoking-related stress may further enhance its expression. These findings indicate that both PLK4 and GDF15 contribute to enhanced proliferative capacity, survival signaling, and the maintenance of resistant phenotypes.
Conclusion: Collectively, our data suggests that overexpression of PLK4 and GDF15 activates PI3K/Akt/mTOR, TGF-β, and ErbB pathways, promoting EGFR-TKI resistance and NSCLC progression. Targeting these key biomarkers may help overcome resistance and limit tumor growth, particularly in smoking-associated NSCLC cases.

#7029 Engineering isogenic models harboring resistance mechanisms to the latest-generation EGFR inhibitor in non-small cell lung cancer.

Hyeyoun Chang[1], Florencia M. Rowdo[2], Kirsty Wienand[2], John G. Foulke[3], Paul Lovell[1], Francisca Vasquez[2], **Fang Tian**[4]

[1]American Type Culture Collection (ATCC), Manassas, VA,[2]Broad Institute of MIT and Harvard, Boston, MA,[3]ATCC, Gaithersburg, MD,[4]ATCC, Manassas, VA

Background: EGFR-mutant lung cancer was among the first epithelial cancer subsets where directly targeting an oncogene yielded significant clinical benefit. While improved inhibitors, such as third-generation EGFR inhibitor Osimertinib, have significantly improved clinical outcomes of non-small lung cancer (NSCLC) patients, acquired resistance to targeted therapies remains a major barrier to durable responses. To address this challenge, we developed three sets of isogenic NSCLC cell models harboring clinically resistant mutations to EGFR targeted therapy through genetic engineering approach.
Method and Results: To systematically investigate resistance mechanisms and associated vulnerabilities, we engineered isogenic NSCLC cell lines to model clinically relevant mechanisms of acquired resistance. Using CRISPR gene editing, three sets of resistant cell lines were generated from three osimertinib-sensitive parental lines (HCC827, HCC4006, and NCI-H292). The engineered alterations included *BRAF V600E*, *KRAS G12D*, *PIK3CA E545K*, *EGFR C797S*, and additional fusion genes such as *TPM3-NTRK1*. Sequence verification and osimertinib sensitivity assays were performed for all models. The engineered cell lines exhibited reduced osimertinib sensitivity consistent with the introduced resistance mechanisms. Initial genomic validation confirmed the intended edits and additional genetic screening will be performed to further characterize the isogenic cell lines. Selected models were further evaluated in 3D culture systems to assess phenotypic impact.
Conclusion: These validated novel models provide a robust platform for the research community and industry to dissect mechanisms of drug resistance, identify therapeutic vulnerabilities and develop combination therapy strategies. This ATCC and Broad institution collaborative effort will also support the establishment of the Resistance Map (ResMap) within DepMap to systematically characterize vulnerabilities in EGFR-driven NSCLC.

#7030 Tumor-macrophage crosstalk promotes resistance to EGFR targeted therapy in lung adenocarcinoma.

Philippe Gui, Victor Olivas, Tiffany Li, Whitney Tamaki, Hannah Bergo, D. Lucas Kerr, Wei Wu, Collin M. Blakely, Trever G. Bivona

UCSF Helen Diller Family Comprehensive Cancer Ctr., San Francisco, CA

Lung cancer remains the leading cause of cancer-related mortality worldwide. Non-small cell lung cancer (NSCLC) is the predominant histologic subtype, with lung adenocarcinoma the most common form of NSCLC. Approximately 15-20% of lung adenocarcinomas harbor activating mutations in the tyrosine kinase domain of the epidermal growth factor receptor (EGFR). Although targeted therapies have substantially improved clinical outcomes for patients with EGFR-mutant NSCLC, most patients do not achieve complete response, underscoring the need to elucidate mechanisms of resistance to EGFR tyrosine kinase inhibitors (TKIs). We hypothesize that, in addition to tumor-cell-intrinsic mechanisms, interactions between cancer cells and the tumor microenvironment could contribute to treatment resistance. Leveraging clinical sequencing data alongside cell co-culture systems, organoid models, and in vivo studies, we show that TKI-treated EGFR-mutant cells upregulate cytokines and chemokines that promote recruitment and maintenance of tumor-infiltrating macrophages, a population associated with poor clinical outcomes. Moreover, interactions between therapy-treated cancer cells and newly recruited macrophages support tumor survival by enhancing cancer cell viability and reducing phagocytic clearance. Genetic and molecular profiling further reveal that soluble pro-inflammatory mediators secreted by macrophages, including TNF-α and IL-1β, engage the NF-κB signaling pathway in EGFR-mutant cells, thereby driving residual disease and resistance. Together, these findings provide a rationale for disrupting microenvironmental crosstalk between EGFR-mutant tumor cells and tumor-infiltrating macrophages as a strategy to limit residual disease. Targeting these interactions may enable a new class of microenvironment-directed therapies to overcome resistance to EGFR TKIs.

#7031 Intra-tumoral *Porphyromonas gingivalis* mediates osimertinib resistance in EGFR-mutant lung adenocarcinoma through gingipain-mediated IGF1R activation.

Wendong Li[1], Mahima Raul[1], Keqiang Zhang[1], Jan Potempa[2], Yuanyuan Gao[1], Dan Raz[1]

[1]City of Hope National Medical Center, Duarte, CA,[2]University of Louisville School of Dentistry, Louisville, KY

Background: Epidermal growth factor receptor tyrosine kinase inhibitors (EGFR-TKIs) are the main therapy for advanced EGFR-mutant lung adenocarcinoma LUAD, but treatment response varies widely and options are limited once resistance develops. Mechanisms of primary EGFR-TKI resistance remain inadequately understood. We found that multiple bacteria of the Bacteroidetes phylum, including the periodontal pathogens *Porphyromonas gingivalis* (Pg), lead to EGFR-TKI resistance in vitro. Pg infection is implicated in the pathogenesis and progression of several malignancies, including lung cancer, likely through secreted virulence factors and immune modulation. This led us to investigate the effect of Pg on EGFR-TKI sensitivity in EGFR mutant lung cancer.

Methods: EGFR-mut LUAD cells were treated with Pg preconditioned medium (PCM) under EGFR-TKI or control conditions, followed by evaluation of drug response, IGF1R signaling activation, and the contribution of Pg gingipains through mutant analyses and treatment with purified gingipains. The presence of Pg in human lung cancer was investigated using Fluorescence In Situ Hybridization (FISH) probes specific to Pg. Human EGFR-mut lung tumor tissue slices were used to assess the Pg effect on osimertinib resistance. Direct interaction between gingipains and IGF1R were analyzed by dot-blot and co-immunofluorescence assays. The equilibrium binding constants (Kd) for IGF1R binding to Kgp and RgpA were determined to quantify the strength of their non-covalent, reversible protein-protein interactions.

Results: Infection with Pg significantly decreased the sensitivity of multiple EGFR-mut LUAD to EGFR-TKIs including osimertinib and lazertinib in both human and mouse EGFR-mutant lung cancer cells through activation of the IGF1R pathway. Pg infection with osimertinib showed higher pIGF1R levels and lower cleaved caspase-3 levels in human lung tumor slice versus osimertinib alone. Mutant gingipain-deficient Pg abolished the activation of IGF1R signaling and restored TKI sensitivity. Clinical isolates of Pg derived from individuals with periodontal disease were also led to dramatic decreases in EGFR-TKI sensitivity. Purified gingipains RgpA and Kgp both activate IGF1R pathway by directly binding to IGF1R protein. The K_d value showed strong binding interaction between IGF1R and RgpA, and moderate binding interaction between IGF1R and Kgp.

Conclusion: Pg, commonly identified within LUAD tissues, induces EGFR-TKI resistance in EGFR-mut LUAD via Pg gingipain-dependent activation of IGF1R. Gingipains directly interact with IGF1R, revealing a new bacterium-tumor crosstalk mechanism that promotes drug resistance and suggesting potential therapeutic benefits of targeting bacterial enzymes or the IGF1R pathway. Additional studies on the effect of Pg on EGFR-TKI response in humans are needed.

#7032 GLAST (SLC1A3), a novel therapeutic target for overcoming osimertinib resistance in lung cancer.

Sara Bernstein[1], Sophie Kim[1], Clara Takanohashi[1], Beatriz P. Peixoto[1], Kathy Nguyen[2], Hiromi Inoue Wettersten[3]

[1]UCSD, La Jolla, CA,[2]Western University of Health Sciences, Pomona, CA,[3]Pathology, UCSD, La Jolla, CA

Lung cancer is the leading cause of cancer-related death in the U.S. with EGFR-mutant non-small cell lung cancer (NSCLC) as the second most common subtype. Although osimertinib, a third-generation EGFR inhibitor, is the preferred first-line treatment and significantly improves outcomes, resistance inevitably develops. The mechanisms driving this resistance are not fully understood, with current research primarily focused on genetic alterations while non-genetic, metabolic factors remain largely unexplored. This knowledge gap limits our ability to design effective therapies to overcome resistance. The objective of this study is to investigate the metabolic pathways that EGFR-mutant NSCLC cells exploit to develop osimertinib resistance. Prior studies with earlier EGFR inhibitors suggest that cancer cells rewire glutamine metabolism to survive EGFR inhibition; therefore we hypothesize that upregulation of glutamine metabolism enables lung cancer cells to acquire osimertinib resistance. To test this hypothesis, osimertinib-resistant and -naive NSCLC cell lines were established from xenograft tumors in mice, and levels of enzymes and transporters in glutamine metabolism were compared. Osimertinib-resistant cells exhibited increased expression of GLAST (SLC1A3), a glutamate transporter, compared to naive cells. Both genetic and pharmacological inhibition of GLAST selectively reduced viability of osimertinib-resistant but not -naive cells. Additionally, patient whole exome sequencing data showed that high GLAST expression correlates with poor prognosis in osimertinib-treated patients.These findings identify GLAST as a novel therapeutic target to overcome osimertinib resistance in EGFR-mutant NSCLC.

#7033 Inhibition of PGC1b/mitochondrial biogenesis as a critical event in mediating therapeutic response of EGFR mutant NSCLC to third generation EGFR inhibitors.

Zhen Chen[1], Dongsheng Wang[2], Songqing Fan[3], Qiming Wang[4], Suresh S. Ramalingam[1], Shi-Yong Sun[5]

[1]Emory Winship Cancer Institute, Atlanta, GA,[2]Research Associate, Dept. of Hem./Onc., Emory University, Atlanta, GA,[3]The Second Xiangya Hospital, Central South University, Changsha, China,[4]The Affiliated Cancer Hospital of Zhengzhou University & Henan Cancer Hospital, Zhengzhou, China,[5]Emory University, Atlanta, GA

Third generation EGFR tyrosine kinase inhibitors (EGFR-TKIs) such as osimertinib are used for the treatment of advanced non-small cell lung cancer (NSCLC) harboring activating EGFR mutations. However, despite robust clinical efficacy of these agents, the inevitable issue of acquired resistance needs to be urgently addressed. Here we reported *PPARGC1B* expression was downregulated, and its regulated mitochondrial biogenesis was inhibited by osimertinib as well other EGFR-TKIs in EGFR mutant (EGFRm) NSCLC cells through a previously unidentified FOSL1/AP-1-mediated transactivation of the *PPARGC1B* gene. Once cells or tumors became resistant to osimertinib, PGC1β encoded by *PPARGC1B* showed rebound elevation and was resistant to downregulation by osimertinib. Enforced overexpression of *PPARGC1B* in osimertinib-sensitive EGFRm NSCLC cell lines conferred resistance to osimertinib, whereas knockdown of *PPARGC1B* in osimertinib-resistant cells restored sensitivity to osimertinib. Moreover, osimertinib combined with a mitochondria-targeting agent such as CPI-613 synergistically decreased cell survival with enhanced suppression of mitochondrial biogenesis and induction of apoptosis in osimertinib-resistant cells and effectively inhibited the growth of osimertinib-resistant tumors. Hence, it is apparent that the modulation of PGC1β/mitochondrial biogenesis critically impacts the therapeutic outcomes of osimertinib in the treatment of EGFRm NSCLC. Our findings not only reveal a novel mechanism underlying osimertinib acquired resistance, but also suggest a potential therapeutic strategy for overcoming acquired resistance to osimertinib via co-targeting PGC1β, particularly mitochondrial biogenesis.

#7034 The potential of dequalinium chloride and osimertinib combination in overcoming osimertinib acquired resistance in EGFR-mutant non-small cell lung cancer.

Jing Sun[1], Dongsheng Wang[2], Suresh S. Ramalingam[3], **Zhen Chen**[4], Shi-Yong Sun[5]

[1]Peking University Cancer Hospital & Institute, Beijing, China,[2]Research Associate, Dept. of Hem./Onc., Emory University School of Medicine, Atlanta, GA,[3]Emory University School of Medicine, Atlanta, GA,[4]Emory Winship Cancer Institute, Atlanta, GA,[5]Emory University, Atlanta, GA

Third-generation EGFR tyrosine kinase inhibitors (TKIs), such as osimertinib, have significantly improved outcomes for patients with EGFR-mutant non-small cell lung cancer (NSCLC). However, nearly all patients eventually develop acquired resistance after an initial response, highlighting the urgent need for novel therapeutic strategies to overcome this challenge. Dequalinium Chloride (DQC) is a clinically used cationic amphiphilic antimicrobial agent with low toxicity that selectively accumulates in mitochondria and induces mitochondrial dysfunction. Leveraging these properties, we investigated the therapeutic potential of combining DQC with osimertinib to overcome resistance in EGFR-mutant NSCLC models. The DQC-osimertinib combination synergistically reduced cell viability, suppressed colony formation, and induced Bim-mediated apoptosis in resistant cell lines. In xenograft models, the combination markedly inhibited tumor growth without increasing systemic toxicity. Mechanistically, in osimertinib-sensitive cells, osimertinib alone increased reactive oxygen species (ROS) levels and decreased mitochondrial membrane potential, whereas these effects were absent in resistant cells, indicating mitochondrial adaptation during acquired resistance. Co-treatment with DQC and osimertinib induced profound mitochondrial dysfunction, characterized by elevated ROS accumulation, loss of mitochondrial membrane potential, and increased γ-H2AX foci formation indicating ROS-dependent DNA damage. The ROS scavenger N-acetylcysteine (NAC) attenuated mitochondrial dysfunction and apoptosis, confirming a ROS-mediated mechanism. Moreover, DQC combined with osimertinib synergistically reduced the survival of EGFR-mutant NSCLC cell lines with primary resistance to osimertinib. In osimertinib-sensitive models, the combination also suppressed proliferation and delayed the onset of acquired resistance. Collectively, these findings demonstrate that targeting mitochondrial homeostasis with DQC enhances osimertinib efficacy and delays resistance, supporting a mitochondria-targeted therapeutic approach for EGFR-mutant NSCLC.

#7035 CD24 as a therapeutic vulnerability in osimertinib-induced drug-tolerant persister cells of EGFR-mutant NSCLC.

Ji Ae Ko[1], Ji Hyung Moon[1], Youwon Lee[2], Minyeop Kim[2], Eun Ji Lee[2], Seung Yeon Oh[2], JI WOO LIM[2], So Young Park[2], Sujin Choi[2], Jii Bum Lee[2], Min Hee Hong[3], Jae-Hwan Kim[4], Sun Min Lim[2], Byoung Chul Cho[2], **Mi Ran Yun**[1]

[1]Severance Biomedical Science Institute, Seoul, Korea, Republic of,[2]Yonsei University College of Medicine, Seoul, Korea, Republic of,[3]Yonsei University College of Medicine SBSI, Seoul, Korea, Republic of,[4]Yonsei University Hospital Cancer Center, Seoul, Korea, Republic of

Drug-tolerant persister (DTP) cells survive therapeutic pressure and drive residual disease, limiting the long-term efficacy of targeted therapies. The third-generation epidermal growth factor receptor (EGFR) tyrosine kinase inhibitor (TKI) osimertinib has markedly improved outcomes for patients with EGFR-mutant non-small cell lung cancer (NSCLC). However, resistance inevitably emerges. This resistance is largely driven by the persistence and adaptive evolution of DTP cells. Nevertheless, the molecular mechanisms underlying the formation and maintenance of osimertinib-induced DTP cells remain poorly understood. To better define these mechanisms, we performed single-cell RNA sequencing (scRNA-seq) on resected tumor specimens from patients with EGFR-mutant NSCLC treated with neoadjuvant osimertinib. Analyses included paired pre-treatment biopsy samples and post-treatment surgical specimens, stratified by pathological response (major pathological response [MPR] vs. non-MPR). Key findings were validated using TCGA/GTEx, public scRNA-seq datasets, IHC of clinical residual tumors, and functional assays in CRISPR/Cas9-edited cell lines and long-term drug-treatment models. Pre-treatment epithelial cells in non-MPR tumors exhibited markedly higher CD24 expression and $CD24^+$ fractions compared with MPR tumors, and these levels remained stable post-treatment, indicating a pre-existing $CD24^+$ state associated with reduced initial response. In contrast, MPR tumors displayed a robust post-treatment increase in CD24 expression and $CD24^+$ epithelial subsets, consistent with public EGFR-TKI DTP datasets. Re-clustering of MPR epithelial cells revealed seven subclusters, among which C1, C3, and C5 were enriched for post-treatment cells and classified as DTP-like. CD24 expression peaked in C1 and C6, with C6 containing balanced pre/post cells. Pseudotime analysis identified three transcriptional trajectories, placing CD24-high clusters C1 and C6 at terminal states enriched for post-treatment cells, with CD24 expression progressively increasing toward this endpoint. Notably, pre-treatment cells within C6 were exclusively CD24-high, suggesting selective preservation of a pre-existing $CD24^+$ subset. CD24-high clusters were enriched for ferroptosis, ROS signaling, and autophagy—canonical DTP programs. *In vitro* DTP models also demonstrated significant upregulation of CD24 following osimertinib treatment, while CD24 depletion reduced basal proliferation, enhanced the antiproliferative effect of osimertinib, and delayed regrowth after drug withdrawal. Together, these results identify CD24 as a marker of both pre-existing and therapy-induced epithelial states that sustain DTP survival and regrowth, highlighting CD24 as a potential therapeutic vulnerability for achieving more durable responses to osimertinib in EGFR-mutant NSCLC.

#7036 EcDNA-mediated oncogene amplification underlies EGFR TKI resistance in NSCLC.

Boyoon Kim[1], Sujin Kim[2], Jeonghee Cho[3], Hoon Kim[4]

[1]Department of Biohealth Regulatory Science, Sungkyunkwan University, Suwon, Korea, Republic of,[2]Department of Biomedical Sciences & Biosystems, Dankook University, Cheonan, Korea, Republic of,[3]Department of Biomedical Sciences & Biosystems, Department of Nanobiomedical Science, Dankook University, Cheonan, Korea, Republic of,[4]Department of Biopharmaceutical Convergence, Department of Pharmacy, Sungkyunkwan University, Suwon, Korea, Republic of

Extrachromosomal DNA (ecDNA) drives oncogene amplification and therapeutic resistance in multiple cancers, but its contribution to acquired resistance to EGFR inhibitors (EGFRi) in EGFR-mutant non-small cell lung cancer (NSCLC) is not well defined. While EGFR TKI resistance frequently arises through acquisition of the EGFR T790M mutation, many cases remain unexplained. We therefore aimed to determine whether ecDNA represents an additional mechanism associated with EGFR TKI resistance. We analyzed whole-genome sequencing datasets from TCGA, PCAWG, and the Hartwig Medical Foundation, encompassing 536 NSCLC tumors, and detected ecDNA structures using AmpliconArchitect. Across these public cohorts, ecDNA prevalence was markedly elevated in EGFR TKI-treated tumors (50%, 10/20) compared with primary tumors (14%, 20/147; OR≈6.35, $p<0.001$) and advanced untreated tumors (25%, 92/369; OR≈3.01, $p=0.02$), indicating a significant association between EGFR TKI exposure and increased ecDNA prevalence. Notably, all ecDNAs detected in the EGFR TKI-treated group harbored oncogenic drivers, underscoring their potential functional relevance. To investigate whether this enrichment reflects resistance-associated events, we established an isogenic PC9 resistance model by generating WGS and RNA-seq data from resistant subclones derived from a single EGFR TKI-sensitive clone following long-term erlotinib exposure. Analysis of 25 resistant PC9 samples revealed ecDNA acquisition in approximately 20% of clones (5/25), all of which contained oncogenes. These ecDNA-positive clones were mutually exclusive with EGFR T790M-positive samples (also 20%, 5/25), suggesting that ecDNA emergence represents an alternative resistance route rather than a secondary event downstream of T790M. Functional analyses demonstrated activation of EGFR downstream signaling pathways in ecDNA-positive resistant cells. For example, in one resistant subclone harboring a newly formed RAF1 ecDNA (copy number ~24), we observed over 100-fold RAF1 overexpression and marked MAPK/ERK pathway activation, as supported by GSEA (NES = 1.39, $p < 0.01$). Functional RAF1-inhibition experiments further confirmed that suppressing RAF1-driven signaling restored erlotinib sensitivity, providing strong evidence that ecDNA-mediated RAF1 amplification leads to EGFR-independent MAPK pathway activation. EcDNA may promote the development of EGFR TKI resistance by enabling alternative signaling pathways that bypass EGFR activity. EcDNA-mediated oncogene amplification represents an important feature of EGFR TKI-resistant NSCLC and a potential therapeutic vulnerability, providing a foundation for strategies aimed at overcoming ecDNA-driven resistance.

#7037 Phospho-reprogramming mitochondrial respiration underlies sunitinib resistance in renal cell carcinoma.

Gianna Lee Mochi[1], Samhitha Adavikolanu[2], Julia K. Burkacki[2], Mark R. Woodford[3]

[1]Urology, Biochemistry & Molecular Biology, SUNY Upstate Medical University, Syracuse, NY,[2]SUNY Upstate Medical University, Syracuse, NY,[3]Urology, SUNY Upstate Medical University, Syracuse, NY

Clear cell renal cell carcinoma (ccRCC) is the most common type of kidney cancer. While surgery is effective for localized ccRCC, advanced disease necessitates the use of additional therapies such as immune checkpoint inhibitors or tyrosine kinase inhibitors (TKIs). Emergent resistance limits TKI efficacy, and prognosis in patients with refractory disease is poor. Recent work indicates that metabolic reprogramming underlies TKI resistance, however the details are poorly understood. Phosphoproteomics study has shown that sunitinib-resistant ccRCC tumors exhibit differential phosphorylation of the electron transport chain Complex II subunit SDHA and the mitochondrial chaperone TRAP1. TRAP1 controls metabolic flux by regulating the activity of the mitochondrial respiratory machinery, indicating a role for TRAP1 phosphorylation in tuning this activity. The objective of our work was to determine the impact of SDHA & TRAP1 phosphorylation on metabolism and TKI resistance.Transient transfection of SDHA phospho-mutants in wild-type 293 or TRAP1 phospho-mutants in TRAP1 knockout 293 cells was used to model phosphorylation changes in SDHA and TRAP1. Immunoblotting and immunoprecipitation were used to evaluate protein expression and interaction. Seahorse Mito stress test analysis was used to measure the respiratory capacity of 293 cells expressing TRAP1 and SDHA phospho-mutants, while MTT assay was used to measure the viability of 293 cells expressing TRAP1 phospho-mutants in response to TKI treatment. MTT assay was additionally used to measure proliferation of naïve and TKI-resistant normal kidney and ccRCC cell lines upon TRAP1 inhibition with Gamitrinib-TPP. We observed that expression of TRAP1 and SDHA phospho-mutants modulated respiration and impacted sensitivity to the TKIs sunitinib and cabozantinib, suggesting a common resistance mechanism. Furthermore, sunitinib-resistant ccRCC cell lines exhibited differing sensitivity to a small molecule TRAP1 inhibitor, suggesting a potential therapeutic intervention. Post-translational modifications regulate the activity of many metabolic proteins, including TRAP1 and SDHA, thereby tuning cellular metabolic flux. Differential phosphorylation of these proteins is correlated with ccRCC sensitivity to sunitinib, and metabolic dysregulation underlies TKI resistance. We found that blocking phosphorylation of SDHA and TRAP1 suppressed respiration, and TRAP1 phospho-null mutation decreased cell sensitivity to TKIs. Furthermore, we observed that sunitinib-resistant ccRCC cell lines demonstrated increased sensitivity to TRAP1 inhibition. Collectively, our work demonstrates the potential for novel combination therapies for targeting TKI-resistant ccRCC.

#7038 SIPA1L3 loss induces TKI resistance via Rap1-MAPK activation in ALK-/RET-fusion positive NSCLC.

Xinzhao Wei[1], Jun Adachi[2], Ryohei Katayama[3]

[1]Division of Experimental Chemotherapy, Cancer Chemotherapy Center, Japanese Foundation for Cancer Research, Tokyo, Japan,[2]Laboratory of Proteomics for Drug Discovery, Center for Drug Design Research, National Institutes of Biomedical Innovation, Health and Nutrition, Osaka, Japan,[3]Japanese Foundation for Cancer Research, Tokyo, Japan

ALK-/RET-fusion-positive non-small cell lung cancer (NSCLC) accounts for 3-5% and 1-2% of total NSCLC cases, respectively. Selective tyrosine kinase inhibitors (TKIs) against ALK or RET have demonstrated remarkable efficacy, and six ALK-TKIs and two RET-TKIs have been approved for the treatment of ALK- or RET-rearranged NSCLC. However, resistance can occur even in patients who initially achieve marked tumor shrinkage. To date, many investigators have reported mechanisms of ALK- or RET-TKI resistance, focusing on secondary mutations, activation of bypass signaling pathways, or EMT transition. Still, in a significant number of cases, the mechanism of resistance remains unknown.To discover additional potential resistance mechanisms, we conducted a genome-wide CRISPR/Cas9 screening under floating culture condition culture conditions in CCDC6-RET fusion positive LC2/ad cells treated with selpercatinib or pralsetinib for nine days. sgRNAs in surviving drug-tolerant cells were then analyzed by NGS. We identified multiple candidate genes, including MED12 and SIPA1L3, that contribute to drug-tolerant persister (DTP) cell survival during RET-TKI treatment. SIPA1L3 encodes a Rap1 GTPase-activating protein (GAP) that promotes the conversion of the active GTP-bound form of Rap1 to its inactive GDP-bound form. Knockout of SIPA1L3 induced significant increase of Rap1-GTP, leading to resistance through activation of the MAPK and PI3K/Akt/mTOR pathways. Phosphoproteomic analysis confirmed upregulation of phospho-Raf, -ERK, and -S6, indicating enhanced MAPK signaling in SIPA1L3-deficient LC2/ad cells after selpercatinib treatment as compared to control cells after the same treatment.These findings highlight the critical regulatory role of SIPA1L3 on Rap1 activation in bypassing RET inhibition through MAPK activation. Notably, combining RET-TKIs with MAPK pathway inhibitors —particularly the Raf-MEK dual inhibitor avutometinib—markedly reduced DTP cell survival *in vitro,* and induced tumor shrinkage in SIPA1L3-knocked-out tumors that relapsed on selpercatinib single treatment *in vivo*, suggesting a promising strategy to overcome such resistance. Furthermore, loss of SIPA1L3 also conferred ALK-TKI resistance in the ALK-fusion H3122 cell line, accompanied by increased Rap1-GTP expression. Co-treatment with alectinib and avutometinib effectively suppressed DTP formation.In conclusion, this study identifies SIPA1L3 as a critical mediator of ALK- or RET-TKI resistance in NSCLC from genome-wide CRISPR screening and underscores the therapeutic potential of avutometinib in combination with ALK-/RET-TKIs to overcome drug-tolerant persistence and improve treatment outcomes in ALK-/RET-rearranged NSCLC.

#7039 FER drives drug-tolerant persister cell survival in EGFR-mutant lung cancer.

Bobak Parang[1], Rabia Khan[2], Ariana Kupai[1], Yuyun Huang[1], Sungyun Cho[2], Michal J. Nagiec[2], Eric E. Gardner[2], Florencia M. Rowdo[2], Benjamin D. Hopkins[2], Qin Fu[3], Sheng Zheng[3], Timothy F. Burns[1], John Blenis[2]

[1]The Ohio State University College of Medicine, Columbus, OH,[2]Weill Cornell Medicine, New York, NY,[3]Cornell University, Ithaca, NY

Approximately 20% of patients with metastatic non-small cell lung cancer (NSCLC) harbor an EGFR-mutation (EGFRm). Osimertinib, a third generation EGFR inhibitor, has dramatically improved patient outcomes, but invariably, residual disease or drug-tolerant “persister” (DTP) cells survive treatment, eventually giving way to resistant or progressive disease. Eradicating DTPs remains a key challenge. Although DTPs have been characterized at the transcriptional level, a major gap in our understanding is how the tyrosine kinome is perturbed. We hypothesized that defining the phospho-tyrosine landscape of DTPs would uncover kinases that could be exploited therapeutically.

We generated DTPs by treating EGFRm cell lines with osimertinib (IC90) for 14 days and performed tyrosine-enriched, phospho-proteomics. Analysis using Kinase Library revealed that FER, a non-receptor tyrosine kinase that has been implicated in regulating a variety of pathways, is highly active in DTPs. To validate our findings, we confirmed that FER is auto-phosphorylated in DTPs. We then demonstrated that FER and its known substrates are phosphorylated within hours of osimertinib treatment, suggesting FER is activated early and throughout treatment. Next, we tested the functional impact of FER. FER knockdown had no effect on baseline phenotypes such as morphology or proliferation, but FER knockdown markedly decreased DTPs after 14 days of osimertinib treatment.

We thus evaluated inhibiting FER as a therapeutic strategy. Alectinib, a well-tolerated FDA approved drug designed to target the ALK kinase, potently inhibits FER. We hypothesized that inhibiting FER using alectinib would eliminate DTPs and prevent osimertinib resistance. We first confirmed that 1) alectinib inhibits FER kinase activity and 2) ALK is not expressed in EGFRm NSCLC, consistent with prior reports. We subsequently treated cells with alectinib at 500nM, the physiologic concentration achievable using low dose alectinib in patients. Combining alectinib with osimertinib dramatically reduced DTPs in four EGFRm cell lines. Phospho-proteomics and RNA-sequencing revealed that alectinib and osimertinib suppressed FER phosphorylation and RHO GTPase signaling, a pathway known to drive DTP survival. Combining alectinib with osimertinib also significantly enhanced osimertinib sensitivity in patient-derived, EGFRm organoids. To test the strategy *in vivo*, we treated EGFRm xenografts with osimertinib or osimertinib and alectinib for only 21 days. After stopping treatment, 100% of the osimertinib-only treated mice had to be euthanized while 33% of mice treated with combination osimertinib and alectinib were disease-free after 150 days of observation. Collectively, our data show that FER is a key tyrosine kinase that is activated in DTPs and that targeting it with alectinib, an FDA approved drug, could be an effective strategy to enable durable remission in patients with EGFRm NSCLC.

#7040 Cancer persister cells are sensitized to copper-mediated death.

Anna Elizabeth Stuhlfire, August (Gus) Finley Williams, Masayoshi Higuchi, Ariel H. Nguyen, David A. Gervasio, Claire Turkal, Janani Nagasubramanya, Michael Nguyen, Suejean Chon, Matthew Hangauer

Dermatology, UC San Diego, La Jolla, CA

Drug-tolerant cancer persister cells survive drug treatments and contribute to acquired resistance. Elimination of persister cells may increase the durability of treatment responses but there are currently no clinically approved therapies targeting persister cells. We previously showed cancer persister cells which survive oncogene-targeted therapy are selectively vulnerable to ferroptosis induced by GPX4 inhibition. While nontoxic bioavailable GPX4 inhibitors have yet to be developed, the recent emergence of bioavailable FSP1 inhibitors allows for induction of ferroptosis in FSP1-dependent tumor cells in vivo. However, we recently found persister cells are more dependent on GPX4 than FSP1 in cell culture and it remains to be determined whether FSP1 inhibition alone is sufficient to kill persister cells in vivo. Here, we considered other clinically available drugs which may selectively kill persister cells. It was previously reported that persister cells are sensitized to disulfiram, an FDA-approved treatment for alcohol use disorder based on disulfiram's aldehyde dehydrogenase (ALDH) inhibition activity. However, we found disulfiram-mediated persister cell killing is independent of ALDH inhibition. Disulfiram also depletes glutathione and we found glutathione replenishment protects persister cells from disulfiram, but glutathione depletion alone is insufficient to kill persister cells because near complete inhibition of glutathione biosynthesis with buthionine sulfoximine is not consistently toxic to persister cells. Furthermore, we found that persister cells are variably rescued from disulfiram treatment by soluble antioxidants or caspase inhibition, and are not rescued by anti-ferroptosis lipophilic antioxidants. However, in all tested persister cell models, disulfiram-induced killing is inhibited by treatment with copper chelator tetrathiomolybdate. Indeed, disulfiram is also a copper ionophore recently demonstrated to induce cuproptosis. We found another clinically tested copper ionophore elesclomol also selectively kills persister cells. Furthermore, other groups have previously shown that co-treatment of EGFR mutant non-small cell lung cancer tumors with disulfiram or elesclomol improves response durability. Therefore, though disulfiram and elesclomol have failed to produce robust clinical benefit when paired with genotoxic chemotherapies or radiation in treatment-refractory tumors, no prior trials have applied either drug to targeted therapy treated tumors or minimal residual disease. Our observations support repurposing copper ionophores to target minimal residual disease in the context of oncogene-targeted therapy treatments.

#7041 Integrated multi-omics and spatial transcriptomics reveal tumor stroma co-evolution driving dabrafenib resistance in BRAF-V600E cholangiocarcinoma.

Nai-Jung Chiang[1], Ya-Chin Hou[2], Chi-Che Hsieh[3], Chao-Chun Cheng[4], Che-Hung Shen[4]

[1]Department of Oncoloy, Taipei Veterans General Hospital, Taipei, Taiwan,[2]Institute of Clinical Medicine, College of Medicine, National Cheng Kung University, Tainan, Taiwan,[3]School of Dentistry, Taipei Medical University, Taipei, Taiwan,[4]National Institute of Cancer Research, National Health Research Institutes, Tainan, Taiwan

Background: BRAF-V600E mutation represents one of the most therapeutically actionable oncogenic alterations in cholangiocarcinoma (CCA). Although BRAF inhibitors such as Dabrafenib have demonstrated clinical benefit, responses in CCA are often transient, with rapid disease recurrence and high invasiveness compared to melanoma or thyroid cancer. The mechanisms underlying such therapy-induced adaptation remain poorly understood.

Methods: We established a Dabrafenib-resistant BRAF-V600E CCA model and its drug-sensitive counterpart, followed by integrated transcriptomic, proteomic, and metabolomic profiling. In parallel, spatial transcriptomics (ST) was performed on paired pre-treatment and post-recurrence CCA patient specimens to spatially dissect malignant cells, cancer-associated fibroblasts (CAFs), and $CD45^+$ immune cells within the tumor microenvironment (TME).

Results: Multi-omics integration identified 3,562 differentially expressed genes, 1,986 proteins, and hundreds of metabolites that collectively revealed a TME-driven resistance phenotype. Resistant malignant cells displayed activation of epithelial-mesenchymal transition (EMT) and xenobiotic detoxification pathways, while CAFs underwent profound PPAR-driven fatty acid metabolic reprogramming and CYP450 enrichment, transforming the stroma into a nutrient-rich and drug-inactivating niche. Concurrently, the $CD45^+$ compartment exhibited transcriptional signatures of KRAS/E2F signaling, chronic inflammation, and metabolic exhaustion. Strikingly, Complement and Coagulation Cascades were spatially co-localized and synchronously activated across all three compartments, suggesting a unified mechanism of immune evasion and stromal barrier formation.

Conclusions: Our findings reveal that acquired Dabrafenib resistance in BRAF-V600E CCA arises from the co-evolution of intrinsic EMT and extrinsic TME remodeling. The CAF metabolic axis and shared TME-Coagulation pathway emerges as actionable vulnerabilities, offering a mechanistic rationale for combination strategies to overcome therapeutic resistance in recurrent CCA.

#7042 Missense mutant p53 regulates DNA replication and damage response to promote resistance to targeted therapies in ALK fusion lung adenocarcinoma.

Esther Redin, Barbara P. Mello, Yingian A. Zhan, Nicholas Socci, Samuel Tischfield, Alexander Lim, Hong Zhong, Mark Donoghue, Richard Koche, Elisa De Stanchina, Alexander Drilon, Alvaro Quintanal-Villalonga, Charles M. Rudin

Memorial Sloan Kettering Cancer Center, New York, NY

ALK gene fusions drive oncogenesis in ~5% of lung adenocarcinomas (LUADs), and ALK tyrosine kinase inhibitors (TKIs) such as lorlatinib have improved outcomes. However, acquired resistance remains a challenge, with >30% of mechanisms unknown. To uncover novel drivers of resistance, we performed multi-omic profiling of clinical samples and PDXs. Genomic analysis of 83 ALK+ LUADs revealed frequent co-occurring alterations, including CDKN2A deletion (34%), TP53 mutation (32%), and MYC amplification (13%). Transcriptomic profiling highlighted enrichment of DNA replication and repair pathways, MYC targets, epithelial-to-mesenchymal transition, and TGF-β signaling in resistant tumors. scRNAseq of matched sensitive and resistant PDXs revealed extensive heterogeneity and diverse resistance pathways, mirroring those in clinical samples. Notably, elevated DNA replication and repair activity strongly correlated with TP53 missense mutations in clinical samples. Analysis of MSK clinical cohort showed that 80% of TP53 mutations in ALK+ LUAD occur in the DNA-binding domain, predominantly missense variants with potential gain-of-function (GOF) properties. The presence of TP53 missense mutations predicted worse prognosis in ALK-fusion LUAD patients treated with TKIs.To assess the role of mutp53 in resistance, we overexpressed R175H and R273H in ALK+ H3122 and H2228 cells. Co-immunoprecipitation and mass spectrometry revealed that mutp53 associates with DNA repair, cell cycle, and chromatin remodeling proteins. Mutp53-expressing cells were refractory to lorlatinib compared to isogenic p53-deficient clones. Overexpression of mutp53 upregulated DNA replication proteins, including ORC and MCM family members, as well as DNA repair proteins such as BRCA1, ATM, CHEK1, and MSH6. Notably, mutp53-expressing cells maintained DNA replication and repair protein levels following lorlatinib-induced DNA damage, unlike p53-deficient counterparts. Immunofluorescence of the DNA damage marker pH2A demonstrated complete repair of lorlatinib-induced lesions in the presence of mutp53, revealing a novel GOF role for these mutants. Furthermore, mutp53 enhanced DNA synthesis by promoting origin firing, thereby facilitating cellular survival under targeted therapy. Similar effects were observed in EGFR-driven LUAD cells, indicating that mutp53 contributes to resistance across oncogene-driven LUADs.To target this axis, we tested the proteasome inhibitor carfilzomib which inhibited mutp53 proteins and promoted the degradation of DNA replication proteins. Carfilzomib synergized with lorlatinib in resistant ALK+ p53 mutant cells and induced robust tumor response in TP53 mutant ALK+ PDX models resistant to lorlatinib, demonstrating therapeutic potential. In summary, missense mutp53 promotes ALK TKI resistance by enhancing DNA replication and repair.

#7044 Resistance to sorafenib leads to epithelial-to-mesenchymal transition and alterations in cell phenotype in HCC.

Paulina Marona[1], Anna Ferenc[1], Isabel Fabregat[2], Ester Gonzales Sanchez[2], Esther Bertran[2], Javier Vaquero[2], Jolanta Jura[1], Katarzyna Miękus[1]

[1]Jagiellonian University, Faculty of Biochemistry, Biophysics and Biotechnology, Krakow, Poland,[2]TGF-β and Cancer Group, Oncobell Program, Bellvitge Biomedical Research Institute IDIBELL, Barcelona, Spain

Introduction: Hepatocellular carcinoma (HCC) remains a highly aggressive malignancy with limited therapeutic options, and the development of resistance to sorafenib—the first-line systemic treatment for advanced disease—significantly compromises clinical outcomes. Understanding the mechanisms underlying the acquisition of sorafenib resistance is crucial, as it not only limits the drug's therapeutic efficacy but also promotes tumor progression and treatment failure in patients with advanced HCC. Previously, we demonstrated that MCPIP1 can partially reverse sorafenib resistance in clear cell renal cell carcinoma. Therefore, the main aim of our research is to investigate the molecular basis of sorafenib resistance in HCC and the potential protective role of MCPIP1 during this process.
Material and Methods: We used two HCC cell lines—HUH7 and SNU449—continuously treated with sorafenib. We analyzed cell proliferation, migration, and invasion. Next, we performed mass spectrometry analysis and validated the obtained results using western blotting and real-time PCR. To determine changes in cell phenotype, we conducted a series of immunohistochemical stainings. To examine the effect of MCPIP1, wild-type and sorafenib-resistant cell lines were transduced to overexpress MCPIP1 along with appropriate controls.
Results and Discussion: Exposure to sorafenib induces notable phenotypic changes in HCC cell lines. In HUH7 cells, which normally display an epithelial phenotype, prolonged treatment is commonly associated with a shift toward a more mesenchymal-like state, characterized by reduced cell-cell adhesion and pronounced morphological alterations, including the formation of membrane protrusions such as filopodia and lamellipodia. SNU449 cells, which already exhibit relatively mesenchymal features, further reinforce this phenotype under sorafenib pressure, displaying increased motility and a more invasive appearance. Consistent with these observations, we detected substantial reorganization of the actin cytoskeleton as well as elevated levels of structural and regulatory proteins such as vimentin, RhoA, RhoB, and Ras. Together, these changes reflect a transition toward epithelial-to-mesenchymal characteristics. Interestingly, all resistant cells exhibited a significantly decreased level of MCPIP1. Following MCPIP1 overexpression, we observed a reduction in EMT-related markers, including vimentin and Snail, suggesting a potential suppressive role of MCPIP1 in the development of sorafenib resistance.
Conclusions: In conclusion, our results indicate that sorafenib resistance in HCC is associated with EMT and cytoskeletal remodeling, and that MCPIP1 may act as a suppressor of this process, representing a potential therapeutic target to overcome resistance.
This study was supported by National Science Center grant no. 2022/47/B/NZ5/02724.

#7045 Multi-omics identifies EMT and PI3K/AKT pathways as mechanisms for Astragalus membranaceus polysaccharide-mediated reversal of osimertinib resistance.

Kenneth K.W. To[1], Longling Wang[1], Zhong Zuo[1], William C. Cho[2]

[1]School of Pharmacy, The Chinese University of Hong Kong, Hong Kong, China,[2]Department of Clinical Oncology, Queen Elizabeth Hospital, Hong Kong, China

Background and Aim: Osimertinib is the only 3rd generation epidermal growth factor receptor (EGFR) tyrosine kinase inhibitor approved for the 1st line therapy of advanced NSCLC patients with EGFR mutations. However, drug resistance severely hinders its efficacy. There is limited therapeutic option after osimertinib failure. *Astragalus membranaceus* (AM) is a medicinal plant long used in traditional Chinese medicine. When combined with chemotherapy, AM has been shown to enhance anticancer efficacy and reduce side effects. The beneficial biological effects of AM are mainly attributed to its polysaccharides (AMP). However, the underlying mechanisms remain elusive. This study employed a multi-omics approach to investigate the mechanism by which AMP overcome osimertinib resistance, focusing on key genetic abnormalities and alterations in critical signaling pathways.

Method: The extraction of AMP from the dry roots of AM has been optimized and standardized. The crude herb and AMP were authenticated based on morphological and chemical properties as per the Chinese Pharmacopoeia. The circumvention of osimertinib resistance by AMP was investigated in NSCLC cell lines *in vitro* and patient-derived tumor xenograft (PDX) in NSG mice. In PDXs that demonstrated promising drug combination effect, RNA sequencing was conducted on total RNA extracted from the tumor tissues to evaluate the dynamic gene expression profile changes. Moreover, mass spectrometry (MS)-based phosphoproteomic analysis was conducted to identify the proteomic signatures and signaling pathway alterations associated with the circumvention of osimertinib resistance by AMP.

Results: Among the tested osimertinib-resistant NSCLC cell lines, AMP was the most effective at potentiating osimertinib in EGFR T790M mutated and *MET* amplified H820 cells. AMP also significantly inhibited tumor migration and invasion. AMP was further shown to remarkably potentiate the antitumor effect of osimertinib in two drug refractory PDX models, without causing notable toxicity. By RNA-seq analysis, GSEA results indicate significant enrichment of EMT-related gene sets in AMP-treated PDX tumors. Using connectivity mapping, AMP was found to share a highly similar transcriptomic signature with PI3K/mTOR inhibitors, suggesting a putative mechanism of action. Global quantitative MS revealed a characteristic proteomic signature of EMT reversal by AMP. MS for phosphorylated proteins further revealed enrichment of ErbB and Rap 1 (KEGG database) and PI3K/AKT signaling pathways (REACTOM database) following AMP treatment. Taken together, our study identified novel mechanisms by which AMP overcome osimertinib resistance at transcriptomic, global proteomic, and phosphoproteomic levels.

Conclusion: The findings support clinical evaluation of AMP for treating osimertinib refractory NSCLC.

#7046 BRAF/EGFR inhibition induces ERBB2 as a targetable tolerance mechanism in *BRAF*-mutant colorectal cancer.

Sara Peltola, Kari J. Kurppa, Klaus Elenius

MediCity Research Laboratories and Institute of Biomedicine, University of Turku, Turku, Finland

Acquired drug resistance remains a major limitation to the long-term efficacy of targeted cancer therapies. The development of acquired resistance can involve the emergence of drug-tolerant persister (DTP) cells, which survive treatment through nongenetic adaptations such as activation of compensatory signaling pathways. Notably, Neuregulin 1 (NRG1) is a growth factor known to promote resistance to targeted therapies across multiple cancer types. This ligand engages the receptor tyrosine kinases ERBB3 and ERBB4, which bind it directly and signal through dimerization with ERBB2. This study aims to define the functional role of NRG1/ERBB signaling in DTPs arising from targeted inhibition of their oncogenic drivers and to evaluate strategies to inhibit this pathway to prevent acquired drug resistance.

NRG1/ERBB pathway activity following targeted therapy was evaluated in a panel of oncogene-addicted cancer cell lines. CRISPR-Cas9-mediated ERBB knockouts were employed to assess the dependency of DTPs on these receptors. The efficacy of NRG1/ERBB axis inhibition with pan-ERBB inhibitors or ERBB-targeting antibody-drug conjugates was evaluated by Incucyte live-cell imaging and colony formation assays.

Upregulation of the NRG1/ERBB signaling axis on transcriptional and protein level was observed in most tested oncogene-addicted cell lines upon therapy against their driver oncogene. Marked upregulation of ERBB2 was detected in drug-tolerant *BRAF*-mutant colorectal cancer (CRC) cell lines treated with dabrafenib and cetuximab. Our flow cytometry data suggest a shift from EGFR to ERBB2/ERBB3 signaling upon treatment in this cancer context. Furthermore, preliminary results using ERBB2 knockout cells demonstrate a dependency of ERBB2 in *BRAF*-mutant CRC DTPs under BRAF/EGFR inhibition. Combination of dabrafenib with a pan-ERBB inhibitor resulted in an improved treatment response *in vitro* compared to dabrafenib with cetuximab.

Taken together, our data imply that drug tolerant *BRAF*-mutant CRC cells upregulate ERBB2/ERBB3 to resist BRAF/EGFR inhibition. Targeting the NRG1/ERBB signaling axis with a pan-ERBB inhibitor in combination with dabrafenib offers a potential strategy to prevent the emergence of resistance.

#7047 Characterization of TKI-induced drug-tolerant persister cells from patient-derived cell lines.

Floriane Braye[1], Inmaculada Alonso Garcia[1], Vincent Boursier[1], Ludovic Bigot[1], Kristi Beshiri[2], FRANCESCO FACCHINETTI[2], Jean-Paul Thiery[2], Benjamin Besse[2], Ken A. Olaussen[3], Luc Friboulet[4]

[1]INSERM U981 (Gustave Roussy), Villejuif, France,[2]Gustave Roussy, Villejuif, France,[3]Inserm U981, Institute Gustave Roussy, Villejuif, France,[4]INSERM U981 (Gustave Roussy), villejuif, France

Introduction: Targeted therapies provide substantial clinical benefit in oncogene-driven cancers, yet relapse remains inevitable. Increasing evidence suggests that a small population of drug-tolerant persister (DTP) cells survives initial therapy and ultimately gives rise to resistance. Understanding the vulnerabilities of these DTP cells is therefore essential for developing strategies that could prevent resistance before it emerges.
Materials and Methods: Patients-derived cell lines (PDC) were established from NSCLC patients included in two prospective clinical trials: MATCH-R study (2015 to 2022) and the ongoing STING trial. The two main models used were MR57, harboring EML4-ALK fusion and ALK C1156Y/G1269A mutation and sensitive to the 3rd generation ALK inhibitor lorlatinib, and ST6566, carrying an EGFR L858R mutation and highly sensitive to osimertinib.
Results and Discussion: DTP cells are characterized by marked phenotypic plasticity. In two PDC models, we observed the co-expression of epithelial and mesenchymal markers, supporting a hybrid EMT state. This plasticity is supported by BRD4, which regulates EMT-associated transcriptional programs, and by FGFR signaling, through pathway rewiring. Phospho-RTK and phosphokinase arrays revealed increased IGF1R and STAT3 phosphorylation level, consistent with adaptative signaling in DTP cells. In parallel, DTP cells displayed elevated γH2AX foci relative to treatment-naive cells, consistent with TKI-induced genomic instability that may induce a dependency on DNA-damage response pathways. *In vitro* models also enable to functionally assess these features, as well as other key DTP cells hallmarks, using long-term survival readouts, including crystal-violet clonogenic assays and IncuCyte live-cell imaging. These experiments revealed that targeting EMT-associated transcriptional control with the BRD4 inhibitor JQ1, inhibiting FGFR-driven signaling with erdafitinib, or blocking DNA-damage repair via the ATM inhibitor AZD-0156 each significantly delayed DTP regrowth. Together, these findings underline multiple actionable weaknesses emerging during the DTP state.
Conclusion: Overall, our results demonstrate that DTP cells regrowth can be delayed *in vitro*, suggesting exploitable vulnerabilities. While further validation is required, they provide a rational for testing these strategies *in vivo*, with an ultimate goal of informing patient therapeutic approach.

#7048 Neuregulin-1(NRG1*)*-directed therapies induce alkaline phosphatase placental (ALPP) expression in *NRG1*-fusion positive cancers: Preclinical data and therapeutic perspective.

Manon Barre[1], Clarisse Thiollier-Schmitt[1], Marie Issenmann[1], Celia Cortay[1], Emeline Cros-Perrial[1], Sandra Ortiz-Cuaran[1], Nicolas Gadot[2], Elodie Voilin[2], Sylvie Lantuejoul[3], Anthony Ferrari[4], Eric Cumunel[4], Charles Dumontet[1], Lars Petter Jordheim[1], Michael Duruisseaux[5]

[1]Cancer Research Center of Lyon (CRCL), Lyon, France,[2]Research pathology platform East, Cancer Research Center of Lyon (CRCL), Lyon, France,[3]UNICANCER Centre Leon Berard, Lyon, France,[4]Gilles Thomas bioinformatics platform, Cancer Research Center of Lyon (CRCL), Lyon, France,[5]Hospices Civils de Lyon, Bron, France

Background: *NRG1*-fusion positive (*NRG1+*) cancers define a new molecular subtype of solid tumors. NRG1 chimeric proteins signal through ERRB3/ERRB2 dimerization, activating PI3K/AKT and MAPK signalling pathways, promoting pro-tumoral properties. *NRG1+* cancers targeting relies on bispecific anti-ERBB2/ERBB3 antibodies such as zenocutuzumab (zeno) or ERBB2 inhibitors such as afatinib (afa). These therapies have limited clinical efficacy, suggesting that the biology of the NRG1/ERBB3 pathway is not totally understood. Our objective is to understand the mechanisms of resistance to NRG1-directed therapies in *NRG1+* cancers.
Material and Methods: We have generated afa-resistant models by continuous exposure to increasing concentrations of afa, using MDA-MB-175 cells. They grew in presence of 256 nM afatinib. Afa-sensitivity was assessed by Prestoblue test. MDA-MB-175 cells exhibit an endogenous *PPP6R3-TENM4-NRG1* fusion and are sensitive to afa, zeno and other NRG1-directed therapy. Bulk RNA sequencing data from afa-naive and afa-resistant MDA-MB-175 were subjected to unsupervised and comparative analysis. Characterization of these models was completed by quantitative RT-PCR and western blotting.
Results: Five afa-resistant MDA-MB-175 models were generated, showing 10-to-100-fold increase in IC50 as compared to sensitive cells. RNA-seq data unsupervised analysis showed that afa-resistant (n=5) and afa-naive (n=5) MDA-MB-175 formed two distinct clusters. *ALPP* was one of the ten most differentially expressed genes in afa-resistant models (log2FoldChange = 8.1, $p = 2.46.10^{-20}$) and the only one with a confirmed lack of expression in afa-naive and expression in afa-resistant MDA-MB-175 at the RNA and protein levels. In afa-resistant models, ALPP expression disappeared after 2-8 weeks when cultured without afa. In afa-naive and afa-resistant MDA-MB-175, an increase of ALPP expression was observed after one or two days of afa exposure. Investigation of NRG1-ERBB3 pathway in afa-resistant models showed a decrease of phospho-ERBB3 and phospho-ERK with no variation of total ERBB3 and ERK.
Conclusion: Afa induced early *ALPP* expression in *NRG1+* MDA-MB-175 cells, and afa-resistance was associated with high ALPP expression and a decrease of ERBB3 and ERK phosphorylation. Validation of ALPP as a relevant target is ongoing using ALPP KO and overexpressing NRG1+ models, including NRG1+ engineered preclinical models and NRG1+ patient-derived models from patients exposed to NRG1-directed therapies. Zeno and zongertinib impact on ALPP expression in preclinical models as well as ALPP expression in a cohort of *NRG1+* non-small cell lung cancer and pancreatic ductal adenocarcinoma is ongoing. Overall, ALPP may represent an attractive target in NRG1+ cancers that may prevent resistance to NRG1-directed therapies.

#7049 Genome-wide CRISPR-Cas9 screen identifies genes conferring lenvatinib resistance in hepatocellular carcinoma.

Ayumu Taguchi[1], Shuang Zhou[1], Hisanori Isomura[1], Haruki Mori[2], Toru Miyake[2], Yuichi Abe[3], Miyako Tanaka[4], Seiji Natsume[3], Masataka Okuno[3], Waki Hosoda[3], Masaji Tani[2], Takayoshi Suganami[4]

[1]Nagoya City Univ. Medical School, Nagoya, Japan,[2]Shiga University of Medical Science, Otsu, Japan,[3]Aichi Cancer Center, Nagoya, Japan,[4]Nagoya University, Nagoya, Japan

Background: Tyrosine kinase inhibitors (TKIs), such as lenvatinib, sorafenib, and regorafenib, form a key component of current systemic therapy for advanced hepatocellular carcinoma (HCC). However, intrinsic and acquired resistance significantly diminish their clinical benefit. Although multiple signaling pathways have been implicated in TKI response, the molecular determinants that sustain broad TKI resistance remain incompletely defined. To uncover these mechanisms, we performed an unbiased genome-wide genetic interrogation in a mouse HCC cell line.
Materials and Methods: We established a murine HCC cell line from melanocortin-4 receptor-deficient mice fed a high-fat diet. These cells exhibited pronounced intrinsic resistance to lenvatinib. To identify genes underlying this resistance, we performed a genome-wide CRISPR-Cas9 knockout screen using a pooled sgRNA library. Top candidates were prioritized by guide depletion scores and validated using siRNAs and shRNAs. Transcriptomic and proteomic analyses were conducted to define downstream pathways. To assess therapeutic relevance, we tested inhibitors targeting enzymes within this network and evaluated their combinatorial effects with lenvatinib and other TKIs across multiple cancer cell lines.
Results: The CRISPR screen identified PCIF1, an mRNA methyltransferase responsible for installing m6Am modification at the 5′ cap, as a leading determinant whose loss markedly sensitized human HCC cells to lenvatinib in both in vitro assays and in vivo tumor models. Integrative multi-omics analysis revealed that PCIF1 regulates a MYBL2-driven transcriptional program that converges on nucleotide metabolic pathways. Within this downstream network, a rate-limiting enzyme in nucleic acid biosynthesis (Molecule A) emerged as a key effector. Pharmacological inhibition of Molecule A exhibited potent synergistic effects not only with lenvatinib but also with additional TKIs, enhancing drug sensitivity and suppressing proliferation across human HCC and other cancer cell lines. Expression of Molecule A was significantly associated with lenvatinib resistance, underscoring its potential relevance as a biomarker and therapeutic target beyond the PCIF1-MYBL2 regulatory axis.
Conclusion: Our findings demonstrate that, even when proliferation appears unchanged, TKI exposure imposes a metabolic stress that drives a rewiring of nucleotide biosynthesis and a pronounced dependency on Molecule A. This adaptive shift is observed across distinct TKIs and cancer types, indicating that altered nucleotide metabolism represents a broadly conserved mechanism of drug resistance. Because clinically approved inhibitors of Molecule A are already available, these results provide a strong rationale for therapeutic repositioning strategies aimed at overcoming TKI resistance in hepatocellular carcinoma.

#7050 A novel 149-amino acid protein encoded by circSOD2 inhibits ferroptosis and promotes cisplatin resistance in bladder cancer.

Shanqi Guo[1], Zhihong Lv[2], Nan Wang[3], **Xingkang Jiang**[2]

[1]First Teaching Hospital of Tianjin University of Traditional Chinese Medicine, Tianjin, China,[2]The Second Hospital of Tianjin Medical University, Tianjin, China,[3]Wake Forest Baptist Comprehensive Cancer Ctr., Winston-Salem, NC

Circular RNAs (circRNAs) play pivotal roles in bladder cancer (BCa) tumorigenesis, metastasis, and chemoresistance, but their functional involvement in cisplatin-induced ferroptosis remains poorly defined. Herein, we identified circSOD2 as a significantly upregulated circRNA in cisplatin-resistant BCa cell lines and clinical specimens via RNA sequencing. Functional assays demonstrated that circSOD2 overexpression enhanced BCa cell proliferation and cisplatin resistance in vitro (CCK-8, colony formation, and ferroptosis detection assays) and in vivo (xenograft mouse models). Mechanistically, ribosome profiling and Western blot analyses confirmed the protein-coding potential of circSOD2, which translates into a novel 149-amino acid peptide (SOD2-149aa). Co-immunoprecipitation (Co-IP) and glutathione S-transferase (GST) pull-down assays verified that SOD2-149aa directly binds to the RING domain of tripartite motif 26 (TRIM26), a ubiquitin E3 ligase. This interaction activates TRIM26-mediated K63-linked polyubiquitination of glutathione peroxidase 4 (GPX4) — a key anti-ferroptotic enzyme — at lysine residue 148, thereby preventing GPX4 proteasomal degradation and enhancing its protein stability. Stabilized GPX4 efficiently scavenges lipid reactive oxygen species (ROS) and reduces iron-dependent lipid peroxidation, ultimately mitigating cisplatin-induced ferroptosis and conferring cisplatin resistance in BCa. Conversely, circSOD2 silencing or SOD2-149aa knockout abrogated TRIM26-GPX4 interaction, diminished GPX4 stability, and restored BCa cell sensitivity to cisplatin. Collectively, our findings uncover a novel circRNA-encoded peptide that regulates ferroptosis and chemoresistance via the TRIM26-GPX4 axis, highlighting circSOD2/SOD2-149aa as a promising prognostic biomarker and therapeutic target for overcoming cisplatin resistance in BCa.

: Epigenetic Modulators 2
Poster Session

#7054 BET domain functions in IDH1^{R132H}/p53$_{mut}$/ATRX$_{loss}$ astrocytoma malignancy.

Leyi Xie, Qingzhu Gao, Jayden Zhang, Lopez-BertoniHernando, John Laterra, **Yunqing Li**

Hugo W. Moser Research Institute at Kennedy Krieger, Baltimore, MD

Grade II/III astrocytomas are the most common primary brain cancer in young adults and are increasingly recognized as epigenetically driven tumors. Their defining mutational background IDH1^{R132H},p53$_{mut}$, and ATRX$_{loss}$ (triple-mut) establishes a hypermethylated and chromatin-disrupted state that reshapes transcriptional networks and creates unique therapeutic vulnerabilities distinct from primary glioblastoma (GBM). This epigenetically altered landscape suggests that tumor progression and treatment response in triple-mut astrocytoma are strongly influenced by chromatin-based mechanisms that can be targeted pharmacologically. BET proteins as epigenetic readers that regulate gene transcription by binding acetylated histone and recruiting master transcription factors to chromatin, yet the specific roles of individual BET family members and their bromodomains remain poorly understood. Analysis of TCGA datasets revealed that BRD3 and BRD2 expressions are significantly elevated in clinical triple-mut gliomas compared to IDH1 wild-type gliomas. Consistently, the immunoblot analysis showed that BRD3 expression is induced by the triple-mut and further enhanced by ionizing radiation (IR) and temozolomide (TMZ) treatment**.** Functionally, inhibition of BET proteins using either pan-BET inhibitors (JQ1, OTX015) or bromodomain 1 (BD1)-selective inhibitor GSK778—but not bromodomain 2 (BD2)-selective inhibitor GSK620— markedly reduces triple-mut glioma cell growth and impairs neurosphere self-renewal**,** and enhances TMZ-induced cell death**.** Moreover, BD1 inhibition significantly suppresses PD-L1 induction triggered by the triple-mut, IR/TMZ treatment, or IFN-γ stimulation. Mechanistically, we find that BD1 inhibition decreases YAP1 and TAZ expression and disrupts YAP1/TAZ transcriptional signaling, whereas BD2 inhibition does not. These findings identify a BD1-dependent transcriptional network that regulates astrocytoma cell phenotype and contributes to an immunosuppressive microenvironment. Targeting BD1 represents a rational therapeutic strategy by simultaneously suppressing tumor cell-intrinsic oncogenic signaling (e.g.,YAP1/TAZ signaling) and reshaping the immunosuppressive microenvironment.

#7055 Synergistic effects of HM97662 as an EZH1/2 dual inhibitor combined with DNA-damaging agents on malignant lung cancers harboring SMARCA4-deficiency.

Seung Hyun Jung, Jaeyul Choi, Aran Park, Seungheon Baek, Jooyun Byun, Young Gil Ahn

Hanmi R&D Center, Hanmi Pharmaceutical Co., Ltd., Gyeonggi-do, Korea, Republic of

EZH (enhancer of zeste homolog) is a histone methyltransferase that catalyzes the trimethylation of H3K27 and functions as a catalytic subunit of the polycomb repressive complex 2 (PRC2). Through epigenetic regulation, EZH modulates the transcription of tumor suppressor genes, thereby contributing to cancer cell survival, proliferation, metastasis, and drug resistance. In particular, the enzymatic activity of EZH2 is strongly associated with poor clinical outcomes, indicating that EZH2 has high therapeutic potential in cancer treatment. Under normal conditions, EZH1 and EZH2 function complementarily to support PRC2 and maintain epigenomic homeostasis. However, inhibiting EZH2 alone can trigger compensatory activation of EZH1, reducing benefit and enabling resistance. Thus, dual inhibition of EZH1 and EZH2 is a rational strategy to overcome resistance *via* broad PRC2 suppression across the tumor microenvironment. Thoracic SMARCA4-deficient undifferentiated tumor (TSDUT) which has been classified in 2021 by World Health Organization (WHO) at first, is a newly defined, high-grade malignancy with undifferentiated/rhabdoid features, marked aggressiveness, and poor prognosis. It is molecularly characterized by SMARCA4 deficiency or concurrent loss of SMARCA2, which are key subunits of the SWI/SNF complex that are often mutated and show synthetical lethal relationships in various cancers. Owing to its rarity and histological heterogeneity, diagnosis is challenging, and standard treatments are lacking; TSDUT frequently recurs after surgery, shows radio-resistance, and responds poorly to chemotherapy. Notably, EZH1/2 inhibition may enhance SLFN11-mediated sensitivity to DNA-damaging agents, offering a promising therapeutic avenue through combination. Herein, we introduce a novel EZH1/2 dual inhibitor, HM97662, which concurrently suppressed the methyltransferase activity not only wild-type EZH1, but also wild-type and gain-of-function mutant EZH2 at nanomolar concentrations. Furthermore, HM97662 demonstrated robust antitumor efficacy in DMS114 and SBC-5 xenograft mouse models of multiple SMARCA4-deficient cancers, including TSDUT. HM97662 synergized with chemotherapies especially topoisomerase 1 inhibitors and other DNA-damaging agents. Collectively, these findings indicate that combining HM97662 with DNA-damaging agents can drive enhanced *in vivo* tumor regression at well-tolerated doses in malignant lung cancers. In conclusion, this preclinical study demonstrated that HM97662, an EZH1/2 dual inhibitor, has promising therapeutic potential against advanced solid tumors, either alone or in combination with DNA-damaging agents. HM97662 is currently underway in a Phase 1 clinical trial, and these results will further support its clinical development.

#7056 Telomir-1: A novel metal ion modulator targeting aging-related disorders and cancer.

Itzchak Angel, **Erez Aminov**

Telomir Pharmaceuticals, Inc, Miami, FL

Background: Telomir-1 is a first-in-class small-molecule metal modulator engineered to selectively regulate intracellular iron and copper homeostasis. It is being developed as a therapeutic candidate for aging-related diseases and cancer, leveraging a dual mechanism of action involving metal balance and epigenetic regulation.
Rationale: Aggressive tumors—including triple-negative breast cancer and prostate cancer—often display an 'iron addiction' phenotype, characterized by excessive iron uptake, storage, and utilization to sustain rapid proliferation and survival. Telomir-1 targets this metabolic vulnerability by reducing the labile intracellular pools of iron and copper required for malignant cell growth, while sparing normal tissues.
Mechanism of Action: Through coordinated modulation of metal-driven redox biology and chromatin-mediated gene control, Telomir-1 addresses two fundamental hallmarks of cancer: 1. Disrupted metal metabolism (iron/copper overload and oxidative stress) 2. Epigenetic repression of tumor-suppressor pathways This integrated mechanism positions Telomir-1 as a novel therapeutic strategy for malignancies driven by metal-dependent metabolic and epigenetic dysregulation. Molecular Insights: Many epigenetic enzymes—particularly iron- and copper-dependent histone demethylases (KDMs)—are overactive in aggressive cancers and require these metal cofactors for catalytic function. This creates a metabolic-epigenetic dependency, whereby malignant cells rely on elevated iron and copper to maintain an epigenetic state favorable to proliferation and survival. Telomir-1 precisely regulates labile metal pools, disrupting the activity of metal-dependent epigenetic enzymes and reactivating silenced tumor-suppressor programs, while simultaneously reducing oxidative stress and tumor metabolism.
Conclusions: By bridging metal biology and chromatin control, Telomir-1 introduces a new therapeutic paradigm with potential applications in iron-dependent and epigenetically dysregulated cancers, including triple-negative breast cancer and prostate cancer, as well as broader aging-related pathologies.

#7057 Therapeutic potential of PCNA and HDAC inhibitor combinations in cutaneous T-cell lymphoma and other cancers.

Caroline M. Li, Robert G. Lingeman, Long Gu, Robert J. Hickey, Linda H. Malkas

Beckman Research Institute of The City of Hope, Duarte, CA

AOH1996, a small molecule inhibitor designed to target protein binding of proliferating cell nuclear antigen (PCNA) in cancer, was previously shown to inhibit cell growth across the NCI-60 human tumor cell line screen with minimal toxicity to nonmalignant cells. Guided by post-translational modification signature enrichment analysis of phosphorylated proteins after AOH1996 treatment, we tested its combination with histone deacetylase inhibitors (HDACi) belinostat and vorinostat. Treatment with AOH1996 and HDACi showed synergistic growth inhibition in neuroblastoma, breast, colon, and cutaneous T-cell lymphoma (CTCL) cell lines. A CRISPR interference screen and selective HDACi studies suggested that the synergy with AOH1996 involved HDAC3 and HDAC6. Furthermore, AOH1996 combined with vorinostat or romidepsin, both FDA-approved for treatment of CTCL, showed synergistic growth inhibition in four cell lines derived from CTCL. Mechanistic studies revealed enhanced DNA damage response, cell cycle arrest, and apoptosis in CTCL cells treated with AOH1996 and HDACi. These findings support the therapeutic potential of combining AOH1996 with HDACi for the treatment of cancers, including CTCL.

#7058 Highly selective HDAC6 inhibitors: Are they the answer for immunomodulation?.

Silvia Rizzo, Edoardo Cellupica, **Chiara Ripamonti**, Grazia Rovelli, Barbara Vergani, Valeria Spadotto, Michela Bottani, Christian Steinkuhler, Gianluca Fossati

Italfarmaco S.p.A., Milan, Italy

Pan-HDAC inhibitors have been approved for the treatment of hematologic malignancies, but their use in solid tumors remains limited due to poor efficacy and significant side effects although direct and immune mediated antitumor effects can be triggered. To overcome these limitations, attention has been focused on the development of selective HDACi. In particular, the generation of selective HDAC6 inhibitors (HDAC6i) has gained interest, since its involvement in tumor progression and immune regulation. HDAC6 knockout mice are viable and fertile, suggesting that selective inhibition could offer therapeutic benefits with minimal toxicity. Among HDAC6i, hydroxamic acid-based compounds such as ITF3756 and ACY-1083 have shown high potency and selectivity, although off-target effects resulting from the binding to other HDACs or non-HDAC targets cannot be ruled out at high concentrations. More recently, difluoromethyl-1,3,4-oxadiazole (DFMO) -based HDAC6i have emerged, offering unprecedented selectivity, prolonged residence time and lack of hydroxamic acid-related limitations. Our group synthesized various DFMO-based HDAC6i and investigated their immunomodulatory potential by evaluating PD-L1 expression and cytokine production in activated human monocytes and CD3 T cells. However, only ITF3756 significantly reduced PD-L1 expression and modulated cytokine release, including TNF-α, IL-1β, IL-10, IFN-γ, and IL-17. DFMO compounds did not exhibit significant effects on these immune responses. These findings suggest that specific HDAC6 inhibition may fail to reproduce the immunomodulatory effects observed with less selective inhibitors or in HDAC6 knockout models. To further explore this discrepancy, we tested PROTAC-DFMO compounds designed to degrade HDAC6, using either Cereblon (CRBN) or Von Hippel-Lindau (VHL) recruiters. Both PROTACs effectively and selectively degraded HDAC6 and increased α-tubulin acetylation. However, only the CRBN-linked PROTAC reduced cytokine production in monocytes, an effect that we determined being attributable to the pomalidomide recruiter itself. In contrast, VHL-linked PROTACs had limited impact. None of the PROTACs significantly modulated cytokine production in T cells. These results indicate that HDAC6 degradation alone is not sufficient to modulate certain immune cell functions, suggesting that broader HDAC inhibition may be required to achieve effective immunomodulatory activity. Furthermore, our results point-out that the effects of degraders in an immunological context may be influenced by their recruiter moiety, rather than being solely driven by target degradation. Overall, this work highlights the complexity of HDAC6's contribution to immune regulation and suggests that while high selectivity may reduce toxicity, it could limit therapeutic efficacy in immuno-oncology contexts.

#7060 Targeting KMT2C induces paralog synthetic lethality in KMT2D null DLBCL through DREAM targets regulation.

Hsiangyu Hu[1], Neeraj K. Aryal[1], Tim Nieuwenhuis[2], Daniel Barrell[3], Ultan McDermott[3], Laura B. Prickett[4], Ming Tang[2], Derek Oien[1], Laura Pasqualucci[5], Anas Younes[6], Lisa Drew[1], Omid Tavana[1]

[1]Hematology Discovery Research and Early Development, AstraZeneca, Waltham, MA,[2]Oncology Data Science & AI, AstraZeneca, Waltham, MA,[3]Functional Genomics Centre, AstraZeneca UK, Cambridge, United Kingdom,[4]Dynamic Omics, Centre for Genomic Research, Discovery Sciences, BioPharmaceuticals R&D, AstraZeneca, Waltham, MA,[5]Inst. for Cancer Genetics, Dept. of Pathology & Cell Biology, & HICCC, Columbia University, New York, NY,[6]Hematology Discovery Research and Early Development, AstraZeneca, New York, NY

KMT2D is a histone methyltransferase that regulates enhancer activation by catalyzing H3K4 mono/di-methylation, in part through a cooperative interaction with CBP/p300. Epigenetic regulation is commonly perturbed in cancer due to recurrent genetic alterations. In particular, KMT2D inactivating mutations are the most common genetic alterations in germinal center-derived B cell lymphoma, including ~30% of diffuse large B cell lymphoma and up to 80% of follicular lymphoma. To identify novel synthetic lethal targets in KMT2D mutant lymphoma, we performed a genome-wide CRISPR knock-out screen in a panel of KMT2D-wt vs -null DLBCL cell lines and revealed the paralog histone methyltransferase KMT2C as a top hit in KMT2D-null cell lines. Interestingly, KMT2C is rarely mutated in KMT2D mutant lymphoma and its protein expression is well-conserved across DLBCL cell lines, suggesting KMT2C may compensate for the loss of KMT2D methyltransferase activity.To validate KMT2C dependency, we knocked out KMT2C in KMT2D proficient or mutant/deficient DLBCL cell lines as well as in KMT2D isogenic knockout models. KMT2C loss leads to G0/G1 cell cycle arrest and apoptotic induction in the KMT2D deficient but not in KMT2D proficient context. To gain mechanistic insights into the preferential sensitivity of KMT2D-null cell lines, we performed RNA-seq in cell lines with varying phenotypic response to KMT2C knockout. In line with the observed cell cycle arrest phenotype, we identified the DREAM (Dimerization partner, RB-like, E2F, and MuvB) complex targets as significantly downregulated upon KMT2C loss. The DREAM complex is a key regulator of cell cycle progression by repressing multiple genes particularly during cell cycle exit. Epigenetic profiling revealed that KMT2C binds to promoters of specific DREAM targets, suggesting a direct regulatory mechanism. Additionally, the protein DYRK1B is known to promote DREAM complex assembly at target promoters. We noticed KMT2C knockout upregulates DYRK1B protein expression only in KMT2D mutant cell lines. Further, overexpression of DYRK1B in KMT2D mutant lines induced anti-proliferative effects, suggesting dual mechanisms by which KMT2C regulates DREAM targets. These results provide mechanistic rationales into how KMT2C loss induces paralog lethality. Lastly, to identify potential combination partners with KMT2C knockout, we performed a combination screen using different small molecules for DLBCL treatment. We observed that inhibitors targeting CBP/p300 and chemotherapy agents like vincristine and doxorubicin combined with KMT2C loss drive deeper responses in KMT2D mutant models. Taken together, our data demonstrate that B cell lymphoma carrying KMT2D mutations are addicted to the residual KMT2C activity and suggest that targeting KMT2C as a monotherapy or in combination may benefit patients with KMT2D loss.

#7061 Mechanistic understanding of a novel CBP/p300 inhibitor in fusion-positive rhabdomyosarcoma.

Md Imdadul H. Khan, Matthew Chang, Yaw Asante, Maya Al-Haddad, Jordyn Kelly, Bhavatharini Udhayakumar, Carrietta Farma-Hai, Berkley Gryder

Genetics and Genome Sciences, Case Western Reserve University School of Medicine, Cleveland, OH

Fusion-positive rhabdomyosarcoma (FP-RMS) is a pediatric soft tissue carcinoma characterized by poor survival rate and limited therapeutic options. The fusion oncoprotein PAX3-FOXO1 (P3F) is the key driver for FP-RMS, and its transcriptional activity is dependent on histone acetyltransferase CBP/p300. Given the challenge of directly targeting the transcription factor P3F, CBP/p300 represents an attractive therapeutic target in treating FP-RMS. Through a focused screening of different epigenetic-modifying agents against FP-RMS, the inhibition of CBP/p300 emerged as the most effective strategy in selectively suppressing P3F-driven transcriptional activity. To overcome the limitations, such as toxicity and efficacy of the existing CBP/p300 inhibitors, we employed structure-based drug design to develop a potent CBP/p300 dual inhibitor, IHK-44. We used chemical genetic approaches to enable precise and temporal control of its function in investigating the underlying mechanism of CBP/p300 in the context of FP-RMS. In studying the basis of IHK-44's selectivity and potency in FP-RMS compared to other CBP/p300 inhibitors and degraders, we conducted a comprehensive series of studies, including luciferase reporter assays, live-cell imaging, RNA-seq, ChIP-seq, and proteomics. These studies revealed that FP-RMS exhibits unique epigenetic dependencies, particularly at 3D clusters of histone acetylation lacking CpG islands. The predictor of gene responsiveness to CBP/p300 inhibition with IHK-44 is to be found by mapping the 3D enhancer/promoter loops into clusters and quantifying the extent of CpG island involvement in the elements that make up clusters. Genes driven CpG-poor clusters, often very rich in enhancers, are hypersensitive to IHK-44, while CpG-rich clusters, usually promoter-rich, are recalcitrant. This allows us to define clear categorization to distinct types of gene regulation hubs in the cancer epigenome. High-throughput screening across 900 cell lines revealed that FP-RMS is one of the cancer subtypes most sensitive to IHK-44, whereas normal cell lines and fusion-negative RMS were resistant. In summary, our findings suggest a novel therapeutic strategy for FP-RMS by targeting CBP/p300 and highlight the potential of IHK-44 as a promising candidate for further preclinical development.

#7062 EP102: Pharmacological inhibition of METTL3 is effective as a monotherapy and potentiates radiation therapy in pancreatic adenocarcinoma via DNA damage and stemness modulation.

Andrea Casazza, Nicolas Parmentier, Catherine Sorlet, Killian Oukoloff, Guillaume Dutheuil, Graeme L. Fraser

EPICS Therapeutics, Charleroi, Belgium

N^6-methyladenosine (m^6A) is the most abundant internal mRNA modification, regulating RNA stability, splicing, and translation. METTL3, the RNA methyltransferase predominantly responsible for the addition of m^6A, is frequently overexpressed in solid tumors and acts as an oncogenic driver by promoting proliferation, survival, and therapy resistance. In pancreatic ductal adenocarcinoma (PDAC), METTL3 upregulation correlates with aggressive disease and poor prognosis. Mechanistic studies implicate METTL3 in PDAC progression through m^6A-dependent regulation of oncogenic transcripts and pathways such as DNA damage repair, contributing to chemoresistance and tumor stemness. Radiotherapy is an established treatment modality for pancreatic cancer, used in neoadjuvant, adjuvant, and locally advanced settings, often combined with chemotherapy. The aim of this work was to evaluate EP102, a selective METTL3 inhibitor, for its efficacy and synergy with radiation therapy in PDAC xenografts and to explore underlying mechanisms. Two independent studies were conducted in Balb/c nude mice bearing PANC08.13 tumors. EP102 was administered alone (47 mg/kg PO, TIW) or combined with radiation (3 Gy × 3) in Study 1 and EP102 alone at 30 mg/kg (PO, TIW) or combined with radiation (2 Gy x 3) in Study 2. Both studies confirmed significant dose dependent tumor growth inhibition by EP102 and marked tumor shrinkage with the combination, supporting synergy across doses. Blood profiling after 4 days of treatment indicated minimal hematologic impact with EP102 alone, supporting its tolerability. Radiation alone and in combination with EP102 led to a pronounced decrease in lymphocytes; notably, the combination suggested a compensatory shift toward innate immunity, where myeloid cells may transiently expand or activate to maintain host defense under genotoxic stress. Mechanistic analysis by Western blot revealed that METTL3 inhibition impairs the expression of key DNA repair and survival genes leading to accumulation of DNA damage: γH2AX and p-CHK2 were upregulated, indicating double-strand break accumulation and checkpoint activation. Importantly, when combined with radiation, EP102 markedly amplified these effects: γH2AX and p-CHK2 surged, BRCA1 and MCL-1 were strongly downregulated, and the expression of stemness marker OV-6 dropped significantly. This combination triggered robust apoptosis and pronounced HR deficiency, correlating with dramatic tumor regression. Together, these findings support a model where EP102 impairs m^6A-dependent repair and survival pathways, and radiation potentiates this disruption, driving synergistic antitumor activity. These findings validate METTL3 as a therapeutic target and provide a strong rationale for combining EP102 with radiotherapy in pancreatic cancer.

#7063 p300 bromodomain inhibitors impair cell proliferation by inducing senescence in HPV positive head and neck squamous cell carcinoma.

Jessica Catarine Frutuoso do Nascimento[1], Wendi Quinn O'Neill[2], Quintin Pan[2]

[1]Case Western Reserve University School of Medicine, Cleveland, OH,[2]University Hospitals Cleveland Medical Center, Cleveland, OH

The incidence of human papillomavirus (HPV)-associated head and neck squamous cell carcinoma (HNSCC) has risen sharply in recent decades and now accounts for most new oropharyngeal cancers diagnosed in the United States. Standard of care therapies are effective but cause significant toxicities and long-term morbidities, highlighting a critical need for alternative treatment strategies. HPV-associated cancers, including oropharyngeal tumors, present a unique opportunity for targeted therapeutic intervention since their pathogenesis depends on the inactivation of major tumor suppressor pathways by the viral oncoproteins E6 and E7. One key oncogenic mechanism is the ability of HPVE6 to bind the transcriptional co-activator p300/CBP, thereby blocking p53 acetylation and activation. Therefore, we hypothesized that p300/CBP bromodomain inhibitors (BDIs) may disrupt the HPVE6-p300/CBP interaction and restore the p53 tumor suppressor program. We evaluated the effect of two p300/CBP BDIs, CCS1477 and GNE-781, on the HPV16+ HNSCC cell line, UM-SCC-47. Cell proliferation was assessed by Incucyte® live cell imaging, clonogenic survival by colony formation assays, and cell-cycle distribution by flow cytometry with propidium iodide. Senescence was measured by β-galactosidase staining, and protein levels of key p53 targets were analyzed by immunoblot. Both p300/CBP BDIs markedly reduced cell proliferation and colony formation. Proliferation decreased in a dose-dependent manner, with an IC50 of 23.66 nM for CCS1477 and 9.06 nM for GNE-781. At 100 nM, CCS1477 and GNE-781 reduced colony formation by 94% ($p<0.0001$) and 97.9% ($p<0.0001$), respectively. p300/CBP BDIs induced G1 arrest, reflected by a 15% ($p<0.0001$) increase in the proportion of cells in G1 and a 30% ($p<0.0001$) reduction in S phase. Both inhibitors triggered a >8-fold ($p<0.0001$) increase in the number of senescent cells. Immunoblot analysis showed increased levels of p53, acetylated p53 (K382Ac), and p21 with no change in caspase 3, supporting senescence, not apoptosis, as the main mechanism responsible for the anti-proliferative effects. In summary, the p300/CBP BDIs, CCS1477 and GNE-781, show anti-tumor activity in HPV16+ UM-SCC-47 cells, reactivating the p53 program and inducing senescence. These findings support further evaluation of p300/CBP BDIs in other HPV+ cancer model systems.

#7064 Development of a new class of KAT6A/B inhibitors with *in vivo* efficacy.

Antonius ter Laak[1], Roman Hillig[2], Steven Ferrara[3], Daniel Korr[2], **Peter Staller**[2], Naomi Barak[1], Philip Lienau[1], Simon Herbert[1], Amaury Fernandez[1], Roland Neuhaus[2], Matyas Gorjanacz[1], Vera Puetter[2], Volker Badock[2], Wilhelm Bone[2], Craig Strathdee[3], Franziska Siegel[1], Christoph Schatz[1], Nowak-Reppel Katrin[2], Olaf Doehr[1], Stefan Gradl[1], Ingo Hartung[1], Matthew Meyerson[3], Lea Bouche[1]

[1]Bayer Pharma AG, Berlin, Germany,[2]Nuvisan ICB GmbH, Berlin, Germany,[3]Broad Institute of MIT and Harvard, Center for the Development of Therapeutics, Boston, MA

KAT6A and KAT6B encode lysine acetyltransferases that catalyse the transfer of acetyl groups from acetyl-CoA to lysine residues on histone proteins, thereby influencing chromatin structure and gene expression. Amplification of these genes is observed in several cancers, with the 8p11-p12 chromosomal region—containing KAT6A—being increased in copy number in approximately 12-15% of breast cancer cases, leading to higher expression of chromatin-modifying enzymes. In this study, we introduce a novel series of acylsulfonamide-benzofuran compounds that function as selective inhibitors of KAT6A and KAT6B. These inhibitors were first identified via high-throughput screening and subsequently refined through computational modelling and co-crystallization studies. The lead compound from this series, BAY-184, demonstrated efficacy in an in vivo proof-of-concept experiment, confirming its potential as a tool for targeting KAT6A/B activity.

#7065 Targeting MTAP-deleted/KRAS mutant cancers using RAS inhibitors in combination with AMG 193, an MTA-cooperative PRMT5 inhibitor.

Katherine Slemmons[1], Siyuan Liu[1], Chun Su[2], Raul Lazaro[1], Tao Osgood[1], Rati Verma[1], Brian Belmontes[1], Paul E. Hughes[1]

[1]Oncology Research, Amgen, Thousand Oaks, CA,[2]Automation, Research Data Systems, Informatics & AI, Amgen, South San Francisco, CA

AMG 193 is a clinical stage MTA-cooperative PRMT5 inhibitor designed to exploit the metabolic vulnerability created by homozygous *MTAP* deletion in tumors. By binding PRMT5 in the presence of accumulated methylthioadenosine (MTA), AMG 193 selectively inhibits PRMT5 activity in MTAP-deleted cells resulting in alternative RNA splicing, DNA damage, and cell cycle arrest. In patients, AMG 193 has demonstrated single-agent antitumor activity and a favorable tolerability profile, supporting its potential as a precision therapy for MTAP-deleted cancers (Rodon et al, 2024).

To further understand the potential for AMG 193 activity, we evaluated combination strategies using AMG 193. We previously demonstrated that AMG 193 synergizes with standard of care chemotherapy by increasing DNA damage, a strategy currently under clinical investigation (NCT06360354, NCT06333951). Given that *MTAP* deletions frequently co-occur with KRAS mutations in pancreatic ductal adenocarcinomas (PDAC; ~30%) and non-small cell lung cancer (NSCLC; ~4%), we hypothesized that dual inhibition of PRMT5 and RAS signaling could further enhance antitumor activity.

Here, AMG 193 was evaluated in combination with the KRAS G12C inhibitor sotorasib or the pan-RAS inhibitor RMC-6236 (daraxonrasib). In the KRAS G12C mutant PDAC cell line MIAPACA2, all RAS inhibitor combinations exhibited similar levels of synergy (Combination Index < 0.5). Nuclear counts confirmed a greater cell growth inhibition in the combination groups and immunoblots confirmed inhibition of both PRMT5 and RAS signaling. RNA-seq analysis revealed synergistic regulation of the RAS pathway and an inhibition of translation and rRNA processing after sotorasib combination treatment. *In vivo*, combination treatment of AMG 193 with sotorasib in MIAPACA2 PDAC xenografts resulted in 28% tumor regression.

In addition, AMG 193 combined with RMC-6236 produced robust synergy across a variety of KRAS G12X mutant PDAC and NSCLC cell lines *in vitro*. *In vivo* efficacy studies evaluating AMG 193 in combination with RAS inhibitors is ongoing in a variety of MTAP-deleted/KRAS mutant tumor models. We also observed that AMG 193 monotherapy efficacy was independent of KRAS mutational status in a NSCLC PDX mouse clinical trial. Overall, AMG 193 displays synergy with RAS targeted agents *in vitro*, and combination treatment with sotorasib *in vivo* substantially inhibits tumor growth. A clinical study evaluating AMG 193 in combination with RMC-6236 in MTAP-deleted PDAC is ongoing (NCT06360354).

#7066 Comparative *in vivo* evaluation of RG-7388, CM-272, and SGI-1027 to determine epigenetic targeting as an effective strategy for treating high-risk neuroblastoma.

Umamaheswari Natarajan[1], Shyam S. Jaganathan[2], Appu Rathinavelu[2]

[1]Rumbaugh-Goodwin Institute for Cancer Research, Barry and Judy Silverman College of Pharmacy, Nova Southeastern University, Fort Lauderdale, FL,[2]Rumbaugh Goodwin Institute for Cancer Research, Barry and Judy Silverman College of Pharmacy, Nova Southeastern University, Fort Lauderdale, FL

Background: High-risk neuroblastoma remains a therapeutic challenge due to its chemoresistance, epigenetic modification, and TP53 pathway dysregulation. SK-N-AS cells, which harbor *TP53* mutations and exhibit highly aggressive behavior, provide a clinically relevant model for evaluating novel epigenetic and apoptotic pathway-targeting agents. This study investigated the therapeutic efficacy of the MDM2 inhibitor (RG-7388), the dual DNMT1/G9a inhibitor (CM-272), and the DNMT inhibitor (SGI-1027) in an SK-N-AS xenograft mouse model.

Methods: Athymic Nu/Nu mice bearing subcutaneous SK-N-AS tumors were randomized into treatment groups and administered RG-7388, CM-272, SGI-1027, or vehicle control (DMSO) according to an optimized dosing schedule. Tumor volumes, body weight, survival rate, and treatment-related toxicity were monitored over the study period. Excised tumors were analyzed for cell-cycle arrest markers, DNA-methylation regulators, apoptotic mediators, and histone acetylation/methylation levels *via* qRT-PCR and Western blot.

Results: Treatment of Cell Derived Xenograft (CDX) animals with CM-272 significantly reduced tumor growth compared to control. Interestingly, treatment with RG-7388 also induced potent tumor suppression but exhibited a less durable response compared to CM-272. The anti-cancer effects produced by CM-272 was robust by showing significant reduction in tumor volume with minimal toxicity, accompanied by marked up-regulation of cell-cycle arrest markers, apoptotic mediators. In addition, a significant increase in the histone acetylation levels, which often serve as DNA/histone methylation regulators, indicated strong epigenetic reprogramming. Mechanistically, both CM-272 and SGI-1027 exhibited strong apoptotic activation, while RG-7388 primarily removed MDM2-associated stress signaling, despite the mutant/null status of *TP53* in SK-N-AS cells. Survival analysis showed that CM-272 prolonged survival the most, followed by RG-7388 and SGI-1027.

Conclusion: Epigenetic targeting of DNMT and G9a *using* CM-272 produced the strongest anti-tumor and survival benefit in the SK-N-AS CDX model, outperforming both RG-7388 and SGI-1027. CM-272's ability to simultaneously inhibit DNMT1 and G9a, appears to reduce repressive chromatin marks, and activate apoptosis cascade that highlights its translational potential for treating *TP53*-mutant and epigenetically driven neuroblastoma. These initial findings suggest advancing preclinical optimization and combination-therapy strategies involving CM-272 for high-risk neuroblastoma.

Acknowledgements: This work was supported by the National Pediatric Cancer Foundation (NPCF), the Florida Department of Health through a Bankhead-Coley Infrastructure Grant, and the Royal Dames of Cancer Research, Inc., Ft. Lauderdale, Florida.

#7067 Synergistic cytotoxicity through combination of DNA methyltransferase (DNMT) inhibitors in cancer cells.

Angelo B. A. Laranjeira[1], Dat Nguyen[1], Michael Difilippantonio[2], Alice P. Chen[3], **Sherry X. Yang**[1], James H. Doroshow[4]

[1]Division of Cancer Treatment and Diagnosis, National Cancer Institute, Bethesda, MD,[2]NCI/NIH, Bethesda, MD,[3]National Cancer Institute, Bethesda, MD,[4]NCI Division of Cancer Treatment and Diagnosis, Bethesda, MD

A new class of DNA methyltransferase inhibitors (DNMTi) including 4'-thio-5-aza-2'-deoxycytidine (aza-TdC) and 4'-thio-2'-deoxycytidine (TdC) demonstrated anti-tumor activity, with IC_{50s} largely in the nanomolar range in DNMTi-sensitive cancer cells, and single to two-digit micromolar spans in DNMTi-resistant cells. In an aza-TdC phase I clinical trial of patients with solid tumors, a best response of stable disease was achieved in eleven (78.6%) of the 14 patients evaluable for response (J Clin. Oncol. Vol 39, No15_suppl). Adverse effect and low clinical activity against human solid tumors remain the limiting factors for their progress in clinical development and application. To overcome the limitations, we investigated synergistic anti-tumor activity by combining either aza-TdC or TdC with a fixed low dose of another DNMTi and antimetabolite - 5-fluoro-2'-deoxycytidine (FdC) - in colorectal and ovarian cancer cells. IC_{50} by aza-TdC, TdC or FdC alone was >10 μM, >10 μM or ~10 μM in DNMTi-resistant/ *DNMT1* knockout colorectal HCT116 cells. In the presence of 0.5 μM FdC, the cytotoxicity of aza-TdC and TdC was dramatically potentiated, showing IC_{50} of 0.24 μM for aza-TdC and <0.001μM for TdC in the DNMTi-resistant cells. The IC_{50} by aza-TdC, TdC or FdC alone was 0.8 μM, 6.29 μM or 0.67 μM in ovarian cancer OVCAR3 cells. The cytotoxicity of aza-TdC and TdC in the presence of 0.5 μM FdC was similarly enhanced, and IC_{50s} were about 0.001 μM for aza-TdC and < 0.001 μM for TdC. In addition, the synergistic potentiation through the combination of 0.5 μM FdC with either aza-TdC or TdC was also observed in other colorectal and ovarian cancer cell lines such as parental HCT116 and SKOV3 cells. Thus, low dose FdC substantially potentiated the cytotoxic effects of novel DNMT inhibitors in DNMTi-resistant and DNMTi-sensitive cancer cells. It warrants to investigate the underlying mechanism of this type of cytotoxic synergy.

#7069 Co-targeting menin and LSD1 dismantles oncogenic programs and restores differentiation in MLL-rearranged acute myeloid leukemia.

Tulasigeri Totiger[1], Mina Tayari[1], Claudia Cabrera Pastrana[1], Florencio Munoz-Legarre[1], Anna Kingham[1], Helena Gomes Dos Santos[1], Felipe Beckedorff[1], Eduardo Bravo[1], Katarzyna Ciurko[1], Declan Foley[1], Efe Karaca[1], Daniel Bilbao[1], Claude-Henry Claude-Henry Volmar[2], Shaun P. Brothers[2], Ramin Shiekhattar[1], Justin Watts[1], Justin Taylor[1]

[1]Univ. of Miami Sylvester Comprehensive Cancer Ctr., Miami, FL,[2]University of Miami Miller School of Medicine, Center for Therapeutic Innovation and Department of Psychiatry & Behavioral Sciences, Miami, FL

Acute myeloid leukemia (AML) with KMT2A-rearrangement carries a poor prognosis, underscoring the urgent need for new therapeutic approaches. Menin inhibitors demonstrate promising anti-leukemic activity in KMT2A-r AML; however, their efficacy as monotherapy may be limited by partial responses and emerging resistance mutations. Combination strategies using epigenetic modulators may enhance their therapeutic potential. In this study, we performed a combination drug screen using an epigenetic compound library in KMT2A-r AML cells to identify synergistic agents that could potentiate menin inhibitor activity.

MV4-11 cells were treated with DSP-5336 (menin inhibitor) to optimize assay performance ($Z' > 0.5$). Cells were then screened with a 932-compound epigenetic library to assess drug effects alone or with DSP-5336. Follow-up studies used ORY-1001 (LSD1 inhibitor) and SNDX-5613 (menin inhibitor) across dose ranges. Viability, IC_{50}, and synergy were evaluated using SynergyFinder 2.0. Mechanistic analyses included Western blotting, co-IP, ChIP-qPCR, CUT&RUN, and mass spectrometry to examine LSD1 binding, interactions, and genome-wide occupancy with the Menin-MLL complex. Patient-derived xenograft cells were implanted in NSG mice.

The combination screen performed robustly and identified LSD1 inhibition as the strongest synergistic enhancer of menin inhibitor activity. LSD1 blockade substantially increased DSP-5336-mediated killing in KMT2A-rearranged AML cells. Mechanistically, LSD1 depletion disrupted key leukemic transcriptional programs and reduced chromatin occupancy at Menin-MLL target loci. LSD1 immunoprecipitation revealed the known MLL interactor PSIP1(LEDGF) as a novel LSD1 interacting partner via mass spectrometry, suggesting cooperative roles of these epigenetic targets in maintaining leukemic gene expression and stem-like properties. The combination of menin and LSD1 inhibition promoted differentiation, shown by an increased proportion of $CD11b^+$ cells compared with either single agent. In an aggressive MLL-AF6 AML PDX model, co-treatment with SNDX-5613 and ORY-1001 produced superior in vivo efficacy. Mice receiving the combination showed markedly reduced leukemia burden and significantly prolonged survival relative to monotherapies, as evidenced by decreased $hCD45^+$ levels and improved survival.

This study identifies LSD1 inhibition as a top synergistic partner for menin-directed therapy in KMT2A-r AML. These findings suggest that combining menin inhibitors with epigenetic modulators such as LSD1 inhibitors may overcome resistance and strengthen anti-leukemic effects. Ongoing in vivo studies aim to further elucidate the underlying mechanisms and therapeutic potential of this combination. Ultimately, this work may guide the development of innovative combination treatment strategies for KMT2A-r AML patients.

#7070 Butyrate modulates key oncogenic pathways in oral squamous cell carcinoma: Insights from transcriptomic profiling.

Oscar A. Loperena Gonzalez[1], Ariana S. Garcia- Lopez[2], Liah M. Roman-Calderon[1], Gabriel Borges Velez[1], Esther Peterson Peguero[2], Josue Perez Santiago[1]

[1]University of Puerto Rico Comprehensive Cancer Center, San Juan, PR,[2]University of Puerto Rico Rio Piedras, San Juan, PR

Introduction: Oral squamous cell carcinoma (OSCC) is a highly aggressive epithelial malignancy that accounts for 90% of oral cancer. Due to late detection, therapeutic resistance and lacking targeted therapies the survival rate for OSCC is below 60%, therefore there is a need for identifying molecular drivers that can be therapeutically targeted. Short chain fatty acids, particularly butyrate has anti-inflammatory, immunomodulatory, and antineoplastic effects in several cancers. We have observed that butyrate treatment reduces cell viability, inhibits migration, and proliferation on OSCC. Thus, to identify the molecular mechanisms related to butyrate treatment and investigate its therapeutic potential in OSCC, we measured transcriptomic changes after butyrate treatment of OSCC.
Methods: OECM-1 (OSCC cell model) were treated with 5 mM butyrate for 24 hours. RNA was extracted, quantified and sequenced on the Illumina NextSeq 550 (PE 2x75 bp). Following quality control (FastQC and Trimmomatic), high-quality reads were aligned to the human genome (GRCh38) using STAR and quantified with RSEM. Differential gene expression was analyzed using R statistical software (tximport and DESeq2 packages). Genes were considered significant if the adjusted p-value was <0.001 and had a log2 fold change >2 or <-2. Functional annotation and protein interaction analyses of significant differentially expressed genes were conducted using Metascape and STRING.
Results: Butyrate treatment had a distinct transcriptomic profile than untreated cells, characterized by a significant alteration of the expression of 1,975 transcripts in OECM-1. The most upregulated transcript (11-fold increase) was NPPB, involved in cell apoptosis and anti-proliferative signaling. Conversely, CCNA2, controls both G1/S and G2/M transition phases of the cell cycle, showed a 3-fold decrease. Additionally, SYC, a modulator of epithelial cell growth, cell proliferation and differentiation, showed a 3.7-fold decrease. Enrichment analysis showed biological processes involved in oncogenesis, including cell proliferation, differentiation, apoptosis, and survival. Protein-protein interaction network identified clusters associated with cell cycle regulation, protein phosphorylation, cell death and transcription factors, with several gene hubs (≥15 connections) including CCNA2, BIRC5, KIF20A and CDCA8, known prognostic markers for cancer.
Conclusions: Our results demonstrate that butyrate modulates the transcriptome of OECM-1 cells, targeting pathways involved in oncogenic processes such as cell cycle, proliferation signaling, genetic regulators and apoptosis, consistent with our cellular results. NPPB is a novel marker for gastric cancer, showing butyrate's capacity to regulate antiproliferative pathways. These findings support butyrate's potential as a microbiome-derived therapeutic for OSCC.

#7071 CRISPRi screening identifies epigenetic vulnerabilities and an ARID1A-PRC2 synthetic-lethal axis sensitizing cutaneous T-cell lymphoma to combined JAK/STAT and EZH2 inhibition.

Yan-Jin Liu[1], Laura Pincus[2], Yu-Ru Chang[3], Frank McCormick[4], Weiyun Z. Ai[5]

[1]Department of Medicine (Hematology/Oncology), UCSF, San Francisco, CA,[2]Department of Dermatology, UCSF, San Francisco, CA,[3]Human Biology, UC Davis, Davis, CA,[4]UCSF Helen Diller Family Comprehensive Cancer Ctr., San Francisco, CA,[5]Asso. Clinical Professor, Dept. of Medicine, UCSF, San Francisco, CA

Advanced-stage cutaneous T-cell lymphoma (CTCL) is life-threatening and has limited treatment options. Aberrant JAK/STAT activation is a defining molecular feature, and a phase II trial demonstrated that ruxolitinib, a JAK1/2 inhibitor, is efficacious in T-cell lymphomas. However, responses are modest and short-lived, highlighting the need for mechanism-based combination strategies.Polycomb repressive complex 2 (PRC2), driven by its catalytic subunit EZH2, regulates H3K27me3-mediated transcriptional repression and functions as a key oncogenic driver in T-cell lymphomas. ARID1A, a core SWI/SNF subunit, physiologically counteracts PRC2-mediated chromatin silencing. Loss or reduction of ARID1A disrupts this antagonism, increasing cellular reliance on PRC2 and sensitizing cells to EZH2 inhibition.To identify genetic modifiers of ruxolitinib response, we performed a genome-wide CRISPR interference screen in CTCL cell lines (HH and Hut78) exposed to JAK/STAT blockade. Ruxolitinib treatment enriched a coherent epigenetic network directly linked to PRC2 function, suggesting that epigenetic modifiers may act synergistically with ruxolitinib.To assess clinical relevance, we analyzed published transcriptomic data from advanced CTCL skin biopsies (n = 70) and normal skin (n = 29). EZH2 expression was significantly elevated in CTCL (P = 0.0014), suggesting heightened PRC2 dependence in advanced-stage disease. We then evaluated the combined inhibition of JAK and EZH2 in primary CTCL PDX-derived tumor cells using a matrix of drug concentrations, yielding 15 paired combinations. This combination produced strong, dose-dependent synergy in growth inhibition and apoptosis induction across three PDX samples, with Loewe synergy scores of 17.54, 27.27, and 20.597, respectively.Mechanistically, CRISPRi profiling revealed depletion of ARID1A sgRNAs under ruxolitinib selection pressure (Hut78: –27.5%, P = 0.0071; HH: –14%, P = 0.069), indicating that JAK/STAT blockade increases CTCL dependence on EZH2 for survival. This ARID1A–PRC2 synthetic-lethal interaction provides a biological basis for the observed drug synergy.Together, these findings demonstrate that JAK/STAT inhibition drives CTCL cells into a PRC2-dependent, EZH2-high epigenetic state, creating a therapeutically actionable vulnerability. These data provide a strong rationale for combining JAK and EZH2 inhibition, and ongoing CTCL PDX in vivo studies will further define the translational potential of this strategy.

#7073 Targeted inhibition of PRC1 in acute leukemia models induces prominent cell growth and differentiation effects.

Sydney Musser, Yiwu Yao, Se Ra Park, Miranda Simes, Hongzhi Miao, Alyssa Winkler, Trupta Purohit, Jolanta Grembecka, Tomasz Cierpicki

University of Michigan, Ann Arbor, MI

Background: Polycomb repressive complex 1 (PRC1) is an epigenetic regulatory complex that silences genes important for cellular identity, stemness and differentiation. All PRC1 complexes contain a RING1A or RING1B protein core which elicits E3 ligase activity to monoubiquitinate histone H2A lysine 119 (H2Aub). PRC1 complex binding and H2Aub deposition induces chromatin compaction and repression of target genes. Previous studies have emphasized the role of PRC1 activity in the maintenance of a leukemic stem cell phenotype, and implicated RING1A/B ubiquitination activity as an important driver of leukemogenesis. Indeed, knockdown of RING1A/B in acute myeloid leukemia (AML) stem cells impairs proliferation and induces myeloid differentiation. Therefore, the development of small molecule inhibitors of PRC1 presents a valuable therapeutic strategy for acute leukemia treatment.

Results: Here, we report the biological activity and molecular mechanisms of a novel small molecule inhibitor of PRC1, RB-231, in acute myeloid and lymphoblastic leukemia (ALL) models. RB-231 is a lead compound among the first-in-class PRC1 small molecule inhibitors developed in our lab, which bind directly to RING1A/B at the nucleosome interface to prevent PRC1 complex binding and H2Aub deposition. RB-231 has shown potent sub-micromolar activity across panels of both AML and ALL cell lines harboring a variety of chromosomal translocations and mutational drivers. Treatment of acute leukemia cell lines with RB-231 results in significant cell growth inhibition, apoptosis, and differentiation, as demonstrated by increased cell surface and gene expression of lineage-associated maturation markers (CD11b, CD14, CD20 and CD86). Treated cells also exhibit morphological changes resembling mature hematopoietic cells and a reduction of leukemic blast populations. Notably, colony formation assays with RB-231 treated primary AML patient samples display reduced colony number, smaller size, and differentiated morphology, while normal human CD34+ bone marrow cells are unaffected by treatment, suggesting selectivity towards a leukemic stem cell phenotype. RNA-sequencing analyses of RB-231 treated acute leukemia cell lines reveal significant upregulation of PRC1 target gene *CDKN1A*, encoding for the p21 cell cycle inhibitor. This effect is also observed in p53-mutant AML cell lines. Indeed, CUT&RUN analysis shows significant reduction of H2Aub enrichment at *CDKN1A*, demonstrating direct de-repression at this locus and RB-231 on-target activity.

Conclusions: Overall, our studies have shown that acute leukemia models are sensitive to PRC1 inhibition and demonstrate significant mechanistic and developmental changes upon treatment. Based on these findings, PRC1 inhibition may offer a novel therapeutic approach for leukemia treatment.

#7074 PLX-61639, a potent and orally bioavailable SMARCA2-selective monovalent direct degrader, enhances efficacy of standard of care agents in SMARCA4 mutant tumor models.

Greg Parker[1], Geoffray Leriche[2], Aleksandar Jamborcic[1], Taylor Kampert[1], Linette Yang[1], Julia Toth[1], Kenneth Steadman[1], Jay Chung[1], Duc Tran[1], Luis Lopez[2], Farhana Barmare[2], Kyohei Hayashi[2], Gang Liu[2], Jianguo Ma[1], Alex Campos[1], Meg McCarrick[2], Kevin Freeman-Cook[2], Peggy Thompson[1]

[1]Biology, Plexium, San Diego, CA,[2]Chemistry, Plexium, San Diego, CA

SMARCA2 and SMARCA4 are mutually exclusive, essential catalytic subunits of human BAF complexes, which are involved in controlling gene expression through the remodeling of chromatin structure. In a subset of solid tumors, SMARCA4 is frequently mutated, rendering cancer cells with SMARCA4 loss-of-function (LOF) mutations highly dependent on SMARCA2 for proliferation and survival. This synthetic lethal dependency offers an opportunity to develop safe and effective treatment options for patients with SMARCA4^{MUT} tumors through the development of selective SMARCA2 degraders. Here we describe the *in vitro* and *in vivo* properties of PLX-61639, a potent, selective, and orally bioavailable SMARCA2 degrader currently in clinical development. PLX-61639 was developed utilizing a monovalent direct degrader strategy where small molecules are designed to bind the target protein and induce its degradation through the recruitment of an E3 ligase complex. PLX-61639 elicits potent and selective degradation of SMARCA2 by inducing a ternary complex with the E3 ligase DCAF16. An electrophilic moiety of PLX-61639 promotes the formation of a covalent drug-E3 ligase adduct and enables extended degradation kinetics and prolonged pharmacodynamic effects. The selective degradation profile of PLX-61639 leads to robust anti-proliferative activity in SMARCA4^{MUT} tumor models and demonstrates the synthetic lethal dependency. *In vivo*, daily oral administration of PLX-61639 in SMARCA4^{MUT} mouse xenograft models exhibits sustained target degradation and dose-dependent tumor growth inhibition and regression at well-tolerated doses. In addition to single agent activity, rational combination strategies were explored, guided by SMARCA2-dependent transcriptionally regulated gene sets and/or specific co-mutations often observed in SMARCA4^{MUT} tumors. PLX-61639 demonstrates robust combination benefit with multiple standard of care agents utilizing different modalities, suggesting potential effective treatment options for future development. The results disclosed here highlight the development of PLX-61639, a potent and selective SMARCA2 monovalent direct degrader, and demonstrate its utility in the treatment of SMARCA4^{MUT} solid tumors.

#7075 Preclinical characterization of FHT-171, a first-in-class degrader targeting CREB-binding protein (CBP) in CBP-dependent solid tumors.

Darshan Sappal[1], Molly M. Wilson[1], Laura La Bonte[1], Meiyun Lin[1], Breanna Bullock[1], Shawn Schiller[2]

[1]Foghorn Therapeutics, Watertown, MA,[2]Orionis Biosciences, Waltham, MA

The paralog lysine acetyltransferases CREB-binding protein (CBP) and E1A-binding protein P300 (EP300) function as transcriptional coactivators that regulate diverse cellular programs. Functional screens have revealed a bidirectional synthetic relationship between these two paralogs in tumor cell biology. This synthetic lethal relationship offers a therapeutic opportunity in selectively targeting CBP in *EP300*-mutant as well as other CBP-dependent cancers. Herein, we present a comprehensive preclinical evaluation for a first-in-class, selective CBP degrader, FHT-171, designed to target transcriptional co-activator dependencies in solid tumors. Through a series of in vitro and in vivo studies, we characterize the compound's biochemical selectivity, cellular degradation kinetics, transcriptional impacts, antitumor efficacy and tolerability across multiple solid tumor models. These findings provide mechanistic and non-clinical translational insight into the therapeutic potential of CBP degradation and support further development of this novel modality for the treatment of CBP-dependent malignancies.

#7076 Discovery of a highly potent and selective KAT6A degrader ATH-002 that demonstrates robust anti-tumor activity with a low risk of hematotoxicity in preclinical studies.

Hanyu Wang, Lei Jiang, Youxi Chen, Baoying Chen, Yuyao Zhang, Nianfeng Huang, Fan Yang, **Feng Zhou**

Atheron therapeutics, Ltd., Shanghai, China

KAT6A, a member of the MYST family of histone acetyltransferases, regulates gene transcription by acetylating histone H3K23 and thereby participates in multiple cellular processes, such as proliferation and differentiation. Amplification or overexpression of KAT6A have been observed in various cancers, including breast cancer, where it is amplified in approximately 15% of patients, highlighting its potential as a promising target for therapy. PF-07248144, the first KAT6A/6B dual inhibitor to enter the clinic, demonstrates durable anti-tumor activity in ER+HER2− metastatic breast cancer, especially in combination with fulvestrant. However, Phase 1 data also revealed hematologic dose-limiting toxicities of neutropenia and anemia. The on-target toxicities resulting from the simultaneous inhibition of KAT6A/6B, which synergistically promote hematopoietic stem cell development. Furthermore, studies have suggested that KAT6A has non-enzymatic functions by its role in DNA damage repair via interaction with PARP and by the observation that depletion of KAT6A more efficiently suppresses the proliferation of KMT2A-rearranged AML cells than blocking its acetyltransferase activity alone. These evidences provide the rationale to develop a KAT6A-specific degrader with the potential for improved efficacy and reduced hematotoxicity. Here we report a potent and oral KAT6A degrader, ATH-002. It effectively induced KAT6A degradation with DC_{50} <1nM, and the degradation could be abolished when E3 was inactive, suggesting a direct mediation by the ubiquitin-proteasome system via E3-ligase binding. Global proteome analysis demonstrated an excellent selectivity against proteins, including KAT6B and other MYST family members. ATH-002 robustly inhibited proliferation in KAT6A amplified cell lines, but not in cells with low KAT6A expression, indicating the activity was driven by the specific KAT6A degradation. Mechanism studies further showed that ATH-002 dose-dependently blocked the H3K23 acetylation, down-regulated ER expression, and concurrently reduced BRPF-1 level, which might be induced by a bystander degradation effect. In contrast to KAT6A/6B inhibitors, ATH-002 significantly decreased hematotoxicity, especially in the myeloid lineage with EC_{50}>30 μM. In a KAT6A amplified xenograft model, ATH-002 effectively inhibited tumor growth, which correlated with KAT6A degradation. Besides monotherapy, ATH-002 displayed an enhanced anti-proliferation effect in combination with SERDs or CDK4/6 inhibitors without overlapping hematotoxicity, implying a potential application of KAT6A degrader and SOC therapy. Collectively, our findings support ATH-002 as a clinical candidate for the treatment of KAT6A-amplified tumors.

#7077 ISM1745, an MTA-cooperative PRMT5 inhibitor for the treatment of MTAP-deleted cancer.

Yilin Yang[1], Zhongying Cao[1], Meng Zhang[1], Xiaoyu Ding[1], Hongfu Lu[1], Qingchuan Zhao[1], Xiaoxia Lin[1], Jiaojiao Yu[1], David Gennert[2], **Suguna Rachakonda**[2], Xiao Ding[1], Xin Cai[1], Man Zhang[1], Feng Ren[1], Alex Zhavoronkov[2]

[1]Insilico Medicine, Shanghai, China,[2]Insilico Medicine, Cambridge, MA

MTAP deficiency is observed in approximately 15% of human cancers and leads to accumulation of methylthioadenosine (MTA), which competes with the methyl-donor S-adenosylmethionine (SAM) to partially inhibit post-translational methyltransferase activity of PRMT5. This molecular context creates a vulnerability in MTAP-deleted tumors, rendering them particularly susceptible to PRMT5 inhibition. MTA-cooperative PRMT5 inhibitors preferentially bind to PRMT5 when MTA occupies the SAM-binding pocket of PRMT5, thus increasing inhibitory specificity to MTAP-deficient cells. Here, we characterize ISM1745, a novel, orally bioavailable MTA-cooperative inhibitor.

ISM1745 potently inhibits formation of symmetric dimethylarginine (SDMA), the PRMT5-catalyzed methylation product, and impairs cell growth in MTAP-deficient HCT116 cancer cells *in vitro* (IC_{50} = 1.1 nM), with 272-fold selectivity over MTAP wild-type HCT116 cells. In addition, Safety44 and methyltransferase panel screening indicated minimal off-target activity for ISM1745. Mechanistically, ISM1745 induces apoptosis, cell cycle arrest, and DNA damage specifically in MTAP-deleted cells, as indicated by an increased proportion of annexin V-positive cells, accumulation in the G1 phase, and elevated expression of DNA damage markers such as γH2AX. Once-daily oral administration of ISM1745 results in marked and sustained tumor growth inhibition in MTAP-deleted xenograft models. Moreover, when combined with ISM3412, an inhibitor of MAT2A, which catalyzes formation of SAM, ISM1745 exhibits significant synergistic anti-tumor activity, highlighting its promise as part of a combinatorial strategy for targeting MTAP-deficient cancers.

In addition to its robust biological potency and high selectivity, ISM1745 exhibits favorable drug-like properties, including optimal in vitro ADMET profiles, excellent in vivo exposure, low clearance (CL<30% Qh in non-rodent species), and moderate to high oral bioavailability across multiple preclinical species. Taken together, these findings support ISM1745 as a potent and selective MTA-cooperative PRMT5 inhibitor with robust anti-tumor efficacy, providing potential therapy for treatment of MTAP-deleted cancers.

: Novel Antitumor Agents 3
Poster Session

#7081 Enzyme hyperactivation to target isocitrate dehydrogenase mutations.

Erick Gonzalez[1], Shengqi Hou[1], Andrew M. Intlekofer[2]

[1]Human Oncology and Pathogenesis Program, Memorial Sloan Kettering Cancer Center, New York, NY,[2]Human Oncology and Pathogenesis Program and Department of Medicine, Memorial Sloan Kettering Cancer Center, New York, NY

Somatic mutations in isocitrate dehydrogenase (IDH) enzymes are hallmarks of acute myeloid leukemia (AML), glioma, and several other cancers. Mutations in IDH result in the neomorphic ability to convert alpha-ketoglutarate (α-KG) into the oncometabolite 2-hydroxyglutarate (2HG), which competitively inhibits α-KG-dependent enzymes and locks malignant cells in a stem cell-like state. Targeted inhibition of mutant IDH enzymes effectively shuts off production of the oncometabolite 2HG and benefits some patients with IDH-mutant cancers. However, the majority of IDH-mutant tumors are impervious to 2HG inhibition. Even for those cases that respond to mutant IDH inhibition, drug resistance invariably develops. Thus, there is an unmet need for novel therapeutic approaches beyond simple inhibition of mutant IDH. Based on mechanistic studies of an unusual drug resistance mutation identified in patients with acquired resistance to IDH inhibitors, we discovered that genetic hyperactivation of mutant IDH2 converts the activity of mutant IDH2 into a lethal metabolic liability. Using chemical screens, we identified small molecules that hyperactivate mutant IDH2, unleash metabolic toxicity, and selectively eliminate IDH2-mutant cancer cells. Thus, we propose that hyperactivation (rather than inhibition) of mutant IDH offers an unexpected and effective new therapeutic approach for targeting IDH-mutant cancers.

#7082 Pseudoginsenoside F11 enhances YBX1-mediated transcriptional repression of PRPS2 to inhibit the stemness and pulmonary metastasis of triple negative breast cancer.

Kejia Xu[1], Huimin Liu[1], Yuting Bai[1], Haojie Chen[1], Yi Liu[1], Yimeng Liu[2], Xing Wan[2], Rong Xiang[1]

[1]Nankai University, Tianjin, China,[2]Tianjin Medical University Cancer Institute and Hospital, Tianjin, China

Background: Hyperactive de novo nucleotide synthesis is a metabolic hallmark of pulmonary metastatic triple-negative breast cancer (TNBC), largely driven by the upregulation of phosphoribosyl pyrophosphate synthetase 2 (PRPS2). The absence of specific PRPS2 inhibitors represents a significant unmet therapeutic need for preventing TNBC metastasis.**Methods:** We screened a library of 320 traditional Chinese herb-derived compounds using a PRPS2-promoter-driven luciferase reporter assay in TNBC cells. The lead compound was evaluated in vitro for effects on PRPS2 expression and cancer stemness, and in vivo using a murine pulmonary metastasis model. The direct target of PF11 was identified via biotin-conjugated pull-down assays. Mechanistic insights were gained through chromatin immunoprecipitation (ChIP) and reporter assays.**Results:** Pseudoginsenoside F11 (PF11) was identified as a potent inhibitor of PRPS2 transcription. Treatment with PF11 significantly suppressed PRPS2 expression, cancer cell stemness, and pulmonary metastasis in murine models. We identified the transcription factor YBX1 as the direct binding target of PF11. PF11 binding enhanced YBX1's affinity with the PRPS2 promoter, enabling it to compete with and displace the transcriptional activator c-Myc. Subsequently, YBX1 recruited the NuRD corepressor complex to the promoter, leading to transcriptional repression of PRPS2.**Conclusion:** Our findings unveil a novel mechanism by which PF11 activates a YBX1-NuRD corepressor complex to downregulate PRPS2, thereby attenuating TNBC stemness and metastasis. We propose PRPS2 as a druggable target and PF11 as a promising natural compound for the targeted therapy of TNBC.

#7083 ABSK211, a highly potent and orally available pan-KRAS inhibitor, demonstrates robust antitumor efficacy in combination with multiple agents.

Qianqian Chen, Bin Shen, Xiao Chen, Jie Wang, Jie Zhang, Manqi Liu, Hongping Yu, **Nannan Zhang**

Abbisko Therapeutics Co., Ltd., Shanghai, China

Background: KRAS mutations are prevalent oncogenic drivers in pancreatic, lung, and colorectal cancers. Although current KRAS inhibitors have shown promising clinical activity, rational combination strategies may yield greater therapeutic benefit. ABSK211, a highly potent and orally available pan-KRAS inhibitor discovered by Abbisko, represents a promising therapeutic candidate targeting a broad spectrum of KRAS-driven tumors. This study evaluates the preclinical combination potential of ABSK211 with mechanistically diverse agents to enhance anti-tumor efficacy.

Methods: *In vitro* synergistic anti-proliferative effects of ABSK211 were assessed in combination with the MTA-cooperative PRMT5 inhibitors, the EGFR monoclonal antibody (mAb), and chemotherapies across KRAS-mutant pancreatic, lung, and colorectal cancer models. Synergy was quantified using combination index analysis. *In vivo* efficacy of the combination regimens was assessed in various tumor models to determine tumor growth inhibition and response durability.

Results: ABSK211 demonstrated *in vitro* synergy with the evaluated combination partners in anti-proliferation assays. Pronounced synergy was observed with PRMT5 inhibitor across diverse KRAS mutation contexts. Similarly, combinations with cetuximab or chemotherapy agents showed strong synergy in KRAS G12D and G12V colorectal and pancreatic models. *In vivo*, combinations of ABSK211 with ABSK131, cetuximab, immunotherapy, or chemotherapy produced markedly enhanced tumor growth inhibition compared with monotherapies in various tumor models.

Conclusions: These findings provide a strong preclinical rationale for advancing these combinations of ABSK211 into clinical development to improve outcomes for patients with KRAS-mutant cancers.

#7084 β-Caryophyllene induces apoptosis and inhibits angiogenesisin colon cancer models.

Loiy Ahmed Hassan, Saad Sabbar, Yasser Tabana

School of Pharmaceutical Sciences - USM, Penang, Malaysia

Beta-Caryophyllene (BCP), a naturally occurring sesquiterpene abundantly found in cloves, hops, and cannabis, is the active candidate of a relatively new group of vascular-inhibiting compounds that aim to block existing tumor blood vessels. The present study aimed to investigate the effects of BCP on *in-vitro*, *ex vivo*, and *in-vivo* models of anti-angiogenic assays and evaluate its anti-cancer activity in xenograft tumor (both ectopic and orthotopic) mice models of human colorectal cancer. Computational structural analysis and an apoptosis antibody array were also performed to understand the molecular players underlying this effect. BCP exhibited strong anti-angiogenic activity by blocking the migration of endothelial cells, tube like network formation, suppression of vascular endothelial growth factor (VEGF) secretion from human umbilical vein endothelial cells and sprouting of rat aorta microvessels. BCP has a probable binding at Site#0 on the surface of VEGFR2. Moreover, BCP significantly deformed the vascularization architecture compared to the negative control in a chick embryo chorioallantoic membrane assay. BCP showed a remarkable reduction in tumor size and fluorescence molecular tomography signal intensity in all the mice treated with BCP, in a dose-dependent relationship, in ectopic and orthotopic tumor xenograft models, respectively. The histological analysis of the tumor from BCP-treated mice revealed a clear reduction of the density of vascularization. In addition, BCP induced apoptosis through downregulation of HSP60, HTRA, survivin, and XIAP, along with the upregulation of p21 expressions. These results suggest that BCP acts at multiple stages of angiogenesis and could be used as a promising therapeutic candidate to halt the growth of colorectal tumor cells.

#7085 Obscurin-PH as a chemo-sensitizer in triple-negative breast cancer.

Kelly Griffiths, Matthew Eason, Aikaterini Kontrogianni-Konstantopoulos

Biochemistry and Molecular Biology, University of Maryland School of Medicine, Baltimore, MD

Triple-negative breast cancer (TNBC) is the most aggressive subtype of breast cancer due to its proclivity to migrate, invade, and metastasize. Given the lack of targetable cell surface markers, the standard of care for TNBC is systemic chemotherapy and surgery. The anthracycline doxorubicin (dox) is an efficacious mainstay chemotherapy for TNBC despite its toxicity, as it triggers dilated cardiomyopathy in up to 20% of patients. Thus, tolerable targeted therapeutics for TNBC are an urgent priority. Obscurin is a giant cytoskeletal protein richly expressed in normal breast epithelium; its expression is often lost in breast cancer, leading to lower survival and reduced responsiveness to anthracyclines. Intriguingly, administration of sublethal dox in TNBC cells upregulates the oncogenic PI3K/AKT axis, potentially conferring a survival advantage. Obscurin's pleckstrin homology domain (obscurin-PH) tightly binds and sequesters the p85 regulatory subunit of PI3K, suppressing PI3K/AKT activation and preventing migration, invasion, and metastasis. We hypothesized that obscurin-PH may act as a chemo-sensitizer by synergizing with dox, improving its efficacy and allowing for lower, less toxic doses to be used for TNBC treatment. The potency of a cocktail combining obscurin-PH and dox was evaluated across 3 TNBC cell lines with distinct PI3K activation patterns (Table 1). Excitingly, our data shows a strong synergy between obscurin-PH and dox across all cell lines, allowing for the use of sub-cardiotoxic dox doses, with the minimal effective synergistic dose varying based on the PI3K activity in each cell line. Mechanistically, the dox-induced survival advantage is blunted via inhibition of the pro-survival/metastatic PI3K/AKT/NF-κB axis. This data underscores the potential of obscurin-PH as a novel non-chemical PI3K inhibitor exhibiting anti-growth, anti-metastatic, and chemo-sensitizing properties. Moreover, it highlights the importance of precision medicine to avoid overtreatment and toxicity.

Table 1. Obscurin-PH synergizes with dox in TNBC cells with varying modes of PI3K activation.

Cell line	**PI3K pathway mutation(s)**	**Clinical significance**	**$IC50_{DOX}$ (μM)**	**$IC50_{OBSCURIN-PH}$ (MOI)**	**Relative Inhibition $(RI)_{DOX}$**	**Relative Inhibition $(RI)_{OBSCURIN-PH}$**	**Combination Sensitivity Score (CSS)**	**CSS > RI = synergy; CSS < RI = antagonism**
MDA-MB-231	N/A	N/A	3.82	941.48	15.43	-2.47	30.58	Synergy, CSS > RI
BT-549	*PTEN* mutant [pVal275fs*1]	Pathogenic, oncogenic	4.33	1765.09	23.2	6.3	30.46	Synergy, CSS > RI
SUM159	*PIK3CA* mutant [p.His1047Leu]	Pathogenic, oncogenic	5.0	8549.62	42.43	13.81	49.74	Synergy, CSS > RI

#7086 Preclinical characterization of a potent and selective Werner helicase (WRN) inhibitor with activity in low-TA repeat microsatellite instability-high (MSI-H) cancers.

Pablo E. Hollstein[1], Daniel A. Aiello[1], Anne Y. Saiki[1], Keegan S. Cooke[1], Petia Mitchell[1], Xiang Yi[2], Ishwar N. Kohale[3], Matthew J. Rardin[3], John Rodgers[4], Mauro Poggio[5], Chun Su[6], Sigurgeir Olafsson[7], Doruk Beyter[7], Jennifer A. Roth[8], Nuria A. Tamayo[9], Kevin L. Greenman[9], Andrew J. Holland[1], Paul E. Hughes[1]

[1]Oncology Research, Amgen, Inc., Thousand Oaks, CA,[2]LD&TPD, Amgen, Inc., South San Francisco, CA,[3]Discovery Proteomics, Amgen, Inc., South San Francisco, CA,[4]PKDM-BA, Amgen, Inc., South San Francisco, CA,[5]Precision Medicine, Amgen, Inc., South San Francisco, CA,[6]Automation, Research data systems, Informatics & AI (ARIA), Amgen, Inc., South San Francisco, CA,[7]Amgen deCODE Genetics, Amgen, Inc., Reykjavik, Iceland,[8]Broad Institute, Cambridge, MA,[9]Small Molecule Therapeutic Discovery, Amgen, Inc., Thousand Oaks, CA

Werner syndrome helicase (WRN), a member of the RecQ family of DNA helicases, is a synthetic-lethal dependency in DNA mismatch repair-deficient cancers that exhibit high microsatellite instability (MSI-H). Here, we characterize Compound 1, a potent and selective small molecule WRN inhibitor. Compound 1 binds within an allosteric pocket in the helicase domain of WRN and forms an irreversible covalent interaction with cysteine 727 (C727), a residue not conserved in other RecQ helicases. *In vitro*, Compound 1 potently inhibited WRN's helicase activity and was confirmed to be a highly selective covalent inhibitor of WRN C727 by mass spectrometry-based cysteine profiling in human MSI-H cancer cells. Consequently, Compound 1 potently impacted the viability of a broad panel of MSI-H cell lines, including colorectal SW48 and RKO (IC50 = < 10 nM and < 100 nM, respectively), and ovarian TOV-21G (IC50 < 300 nM) cells. Treatment with Compound 1 elicited robust induction of pharmacodynamic (PD) biomarkers including sensors of DNA damage and the proteasome-dependent degradation of WRN across the panel. Notably, these responses were selective for MSI-H cells and were not observed in microsatellite-stable (MSS) cells nor in cell lines derived from normal tissues up to the highest concentration tested (5 μM).

In vivo, Compound 1 treatment resulted in a dose-dependent modulation of PD biomarkers, which correlated with strong anti-tumor efficacy in SW48, RKO, and TOV-21G MSI-H cell line-derived xenograft (CDX) models. Covalent engagement of WRN by Compound 1 was measurable in tumor tissue and in peripheral blood monocytes. The exposure and target occupancy of Compound 1 required for efficacy strongly correlated with the expansion of repetitive thymine-adenine (TA) nucleotide DNA microsatellites. These repeats form non-canonical secondary structures that interfere with DNA replication in MSI-H cells and require unwinding by WRN. Long-read DNA sequencing confirmed that the extent of TA-repeat expansion was associated with Compound 1 activity in MSI-H CDX models. An analysis of primary MSI-H tumor cohorts revealed that the majority of patient tumor samples exhibited TA-repeat expansions within the range of Compound 1 efficacy observed in cell-based models. Importantly, dosing of Compound 1 was sufficient to elicit tumor regression in low-TA repeat CDX MSI-H models (RKO, TOV-21G), which have proven to be refractory to WRN inhibitors advanced previously. Together, these data demonstrate that covalent inhibition of WRN by Compound 1 is an effective strategy to selectively kill MSI-H tumor cells with expanded TA repeats.

#7087 Optimizing the linker of venetoclax-artemisinin conjugates to improve water solubility and antileukemia effects.

Jingyi Zhang[1], Linghui Hou[1], Zhenwei Zhang[1], Samuel Waxman[2], Linxiang Zhao[1], Yongkui Jing[1]

[1]Shenyang Pharmaceutical University, Shenyang, China,[2]Samuel Waxman Institute for Aging and Cancer, New York, NY

Venetoclax based combination therapy is utilized as the first-line treatment for elderly acute myeloid leukemia (AML) patients with short remission time due to resistance and relapse. Previously, we reported that artesunate enhanced venetoclax-induced apoptosis by promoting NOXA-mediated degradation of Mcl-1. By employing a chemical conjugation approach, we linked dihydroartemisinin (DHA) to venetoclax using a two-carbon methylene spacer, yielding the conjugate A1. A1 maintains Bcl-2 inhibitory activity and overcomes Mcl-1/Bcl-xL-mediated resistance. However, due to its large molecular size, A1 has limited bioavailability and solubility. To address these limitations, we incorporated various polyethylene glycol (PEG) units between venetoclax and DHA, generating conjugates A18-A20. These derivatives exhibited approximately two-fold greater solubility than A1, and more potent activity to inhibit colony formation of U937 cells in soft agar assays. Moreover, A19 and A20 significantly suppressed tumor growth in vivo. The tumor growth inhibition rates for A19 and A20 (75.6% and 65.8%, respectively) were significantly higher than that of venetoclax alone (33.9%). We further modified the PEG backbone of A20 by incorporating nitrogen-containing polar groups, resulting in compounds A21-A23. These modifications led to further increased aqueous solubility and colony-forming inhibitory activity. These novel conjugates represent promising next-generation venetoclax derivatives capable of overcoming resistance.

#7088 NAD(P)H: Quinone oxidoreductase 1 (NQO1): Is it a potential molecular target in colorectal cancer?.

Chaithanya Ganji[1], Raasil R. Basha[2], Karthikeya Ganji[3], Mehmet Akce[4], Bassel F. El-Rayes[5]

[1]Hematology and Oncology, O'Neal Comprehensive Cancer Center at UAB, Birmingham, AL,[2]Missouri Southern State University, Fort Worth, TX,[3]Harrison High School, Kennesaw, GA,[4]University of Alabama at Birmingham, Birmingham, AL,[5]University of California San Diego, La Jolla, CA

Background: Colorectal cancer (CRC) is the third most frequent cancer in the United States, and it is linked to poor outcomes. NAD(P)H: Quinone Oxidoreductase 1 (NQO1) is an enzyme that has been demonstrated to help in chemoprotection in CRC. The purpose of this meta-analysis is to investigate the relationship between NQO1 C609T polymorphisms and the risk of CRC. The study also investigates the binding ability and efficacy of BBI 608 against NQO1 in CRC using molecular docking.

Methods: Google Scholar, PubMed, and Web of Science were utilized for bibliographic searches. The NQO1 C609T analysis included 18 studies. Data was collected and then calculated using the pooled odds ratio (OR) with a 95% confidence interval. Molecular docking, Western Blot, and QRT-PCR were utilized to determine BBI 608 and NQO1's molecular function.

Results: The NQO1 polymorphism was significantly associated with CRC risk (OR = 1.19, 95% CI = 1.06-1.34, $p < 0.001$). A stratified examination by ethnicity found a significant connection between the NQO1 polymorphism and CRC risk (TT + CT vs. CC: OR = 1.17, 95% CI = 1.08-1.27, $p < 0.001$). This study demonstrates that the NQO1 C609T polymorphism increases the risk of CRC in both Asians and Caucasians. Computational techniques were used to explore the molecular characteristics of BBI 608 (an NQO1 inhibitor) and determine the precise mechanism of NQO1 in CRC. This study provides a deep insight into the interplay between NQO1 and BBI 608, as well as its implications for CRC treatment. *In vitro* experiments were conducted to supplement this computational analysis. BBI 608 causes dose-dependent cytotoxicity in CRC cell lines. BBI 608 treatment significantly ($p < 0.001$) decreased NQO1 expression at protein and RNA levels in both CRC cell lines (HCT116 and RKO).

Conclusion: According to a meta-analysis and computational technique, NQO1 is a valid biomarker and possible molecular target in CRC. *In vitro* studies revealed that suppressing NQO1 with BBI 608 reduced cell growth in both CRC cell lines. Knockout, overexpression, and site-directed mutagenesis are necessary for a deeper understanding of BBI 608-targeted NQO1 and its amino acid residues.

#7089 Diphyllin induces autophagy-mediated ferroptosis in liver cancer.

Jinfang Zhang[1], Zhanghao Li[1], Zheng CHEN[1], Chao Wang[2], Aiping Lu*[1]

[1]Hong Kong Baptist University, Hong Kong, Hong Kong,[2]Guangdong Pharmaceutical University, Guangzhou, China

Background: Liver cancer is one of the most prevalent malignancies and a leading cause of cancer-related mortality worldwide, underscoring the urgent need for novel therapeutic strategies. Ferroptosis, a newly discovered form of regulated cell death characterized by iron accumulation and lipid peroxidation, has emerged as a significant mechanism in cancer biology and a potential therapeutic target. Diphyllin, a natural compound and potent V-ATPase inhibitor, displays promising anticancer activity in preliminary liver cancer studies. However, the molecular mechanism underlying the anti-tumor efficacy of diphyllin remains unclear, thus elucidating these mechanisms may not only deepen our understanding of liver cancer pathogenesis but also provide a scientific foundation for developing diphyllin-based therapies.
Methods: The proliferative effect and cell death of diphyllin on liver cancer cells were quantitatively assessed using the EdU assay and Annexin V-FITC/PI staining followed by flow cytometry. To visualize the morphological alterations induced by diphyllin, the ultrastructure of treated cells was examined using transmission electron microscopy (TEM). For mechanistic exploration, transcriptomic analysis was performed to capture global gene expression changes. The western blotting and confocal immunofluorescence staining were used to measure the ferroptosis key proteins and autophagy markers. Furthermore, pharmacological autophagy inhibitors were applied to determine the dependency of ferroptosis on autophagy.
Results: Treatment with diphyllin significantly suppressed the proliferation activity and increased the cell death rate in liver cancer cell lines. Transcriptomic profiling and western blot analysis revealed that diphyllin triggered ferroptosis, as evidenced by a marked downregulation of GPX4 protein expression. Furthermore, TEM analysis and immunofluorescence staining demonstrated that diphyllin induced autophagy, characterized by an elevated LC3B-II/LC3B-I ratio and a reduction in p62. Notably, the suppression of GPX4 expression was partially reversed upon treatment with an autophagy inhibitor, suggesting a functional link between diphyllin-induced autophagy and ferroptosis. Together, these results indicate that diphyllin promotes ferroptosis in liver cancer cells through an autophagy-dependent pathway. These findings provide a mechanistic basis supporting further preclinical investigation of diphyllin as a potential therapeutic agent for liver.
Conclusions: This study demonstrates that diphyllin suppresses liver cancer by inducing both ferroptosis and autophagy. Mechanistic investigations revealed that diphyllin induced ferroptosis is an autophagy-dependent process, evidenced by the restoration of GPX4 upon autophagy inhibition. These findings establish autophagy-mediated ferroptosis as the novel mechanism underlying diphyllin's anti-tumor efficacy.

#7090 Preclinical characterization of ABSK211: A highly potent, orally bioavailable and selective pan-KRAS inhibitor with broad and robust activity in KRAS-driven tumors.

Yongxian Zhang, Fei Yang, Zhigang Feng, Meimei Sun, Xinyan Huang, Haibing Deng, Hongping Yu, **Haiyan Ying**

Abbisko Therapeutics, Shanghai, China

KRAS is frequently mutated in human cancers, including pancreatic (~90%), colorectal (~35%), and lung cancers (~25%). Several selective pan-KRAS inhibitors have advanced into clinic but their potency against KRAS mutations remained to be further improved. Here we describe that ABSK211, discovered by Abbisko, is a highly potent, and orally bioavailable small-molecule inhibitor with broad activities against multiple KRAS mutations. ABSK211 exhibited strong target engagement *in vitro* against a range of KRAS mutations. Treatment with ABSK211 effectively impaired cell viability at sub-nanomolar to nanomolar concentrations across a diverse panel of cancer cell lines with different KRAS alterations, including G12 mutation, G13 mutation, Q61 mutation and WT amplification. Meanwhile ABSK211 displayed marginal inhibition in normal cell proliferation. *In vivo* daily oral dose of ABSK211 induced deep tumor regression in several KRAS G12V CDX models across different human cancer types. Strong target engagement *in vivo* was also observed. Additionally, ABSK211 exhibited robust anti-tumor activity in xenograft models with other KRAS mutations, such as KRAS G12D/S and KRAS G13D. ABSK211 is currently undergoing IND-enabling studies; its superior preclinical profile supports its advancement into clinical studies.

#7091 DWP216, a TEAD1/2 inhibitor, enhances efficacy of diverse KRAS inhibitors by reversing resistance mechanisms in RAS-dependent cancers.

Bora Yoo, Ye Gi Han, Hye-Been Yoo, Ahreum Kwon, Jiyoon Seok, Youngwoo Choi, Ji-Duck Kim, Hyounmie Doh

Innovative Drug Discovery Center, Daewoong Pharmaceutical Co., Ltd., Yongin-si, Gyeonggi-do, Korea, Republic of

YAP-TEAD pathway plays critical in regulating cell proliferation, tissue regeneration, and organ size control, and it promotes tumor progression and metastasis in cancer. Additionally, YAP-TEAD pathway not only reinforces anti-apoptotic signaling but also remodels the tumor microenvironment into an immune-evasive state, representing a key mechanism driving drug resistance.DWP216 is a selective TEAD1/2 inhibitor with high selectivity over TEAD3, a TEAD form associated with renal toxicity, conferring a more favorable safety profile than pan-TEAD inhibitors. DWP216 has demonstrated superior efficacy in NF2-deficient tumor models and is currently in the final stages of GLP toxicology studies.KRAS mutations are a major oncogenic target, occurring in approximately 95% of pancreatic cancers and 40% of lung cancers. KRAS mutations also promote YAP-TEAD activation and, when KRAS signaling is inhibited, YAP-TEAD frequently functions as a key adaptive bypass pathway.In this study, we evaluated the combinatorial potential of DWP216 with various KRAS inhibitors. We observed that Hippo pathway gene set is upregulated in KRAS inhibitor-resistant cancer cells. DWP216 demonstrated in vitro combinatorial efficacy not only with a G12C inhibitor but also with a G12D inhibitor and a pan-RAS inhibitor. Resistance-associated mechanisms to KRAS inhibition such as activation of MAPK signaling and the PI3K/mTOR pathway, were observed in KRAS inhibitor-resistant cancer cells. Treatment with DWP216 reduced Hippo pathway activation and restored sensitivity to KRAS inhibition by reversing these compensatory mechanisms. Combination treatment with DWP216 and KRAS inhibitors also increased pro-apoptotic markers. In vivo CDX models harboring KRAS mutations showed strong combinatorial activity of DWP216 with KRAS inhibitor. In conclusion, DWP216 can be effectively combined with various KRAS inhibitors and may be extendable as a combination strategy against RAS-dependent cancers such as PDAC.

#7092 Highly potent and mutant-selective p53 Y220C reactivators with best-in-class potential.

Chiou-Hong Lin[1], Benjamin C. Milgram[2], Brendon Ladd[2], Weixue Wang[2], John P. Vu[1], Jun Jacob Hu[2], Yemin Lan[2], Keyur Gada[2], Heidi Koldsoe[2], Stephanie M. Reeve[2], Robert Hicklin[2], Mint Sirisawad[1], Brendan J. Hilbert[2], Jack A. Henderson[2], Simon A. Roberts[2], Gregory Kryukov[2], Hsu-Ping Kuo[1], Natasja Brooijmans[2], Angel Guzman-Perez[2], Darrin D. Stuart[2], Erica L. Jackson[1]

[1]Antares Therapeutics, South San Francisco, CA,[2]Antares Therapeutics, Boston, MA

Background: The tumor suppressor p53, encoded by the *TP53* gene, is a transcription factor that regulates genes involved in DNA repair, cell cycle arrest, senescence, and apoptosis. *TP53* is the most frequently altered tumor suppressor gene with mutations occurring in over 50% of human cancers. *TP53* mutations result in a loss of function, rendering cells incapable of responding to a variety of cellular stresses, making them susceptible to tumorigenesis. The Y220C hotspot mutation accounts for 1.8% of all p53 mutations, occurring in ~1% of all solid tumors. p53 Y220C is a structural mutation that causes destabilization of the p53 protein. Small molecules that bind to a pocket formed by the Y220C mutation, but absent in the p53 wild-type protein, can stabilize the protein to restore normal function. Rezatapopt (PC14586) is the first p53 Y220C reactivator to enter clinical trials, where it is showing clinical benefit. However, because this molecule has modest potency, its efficacy may be limited by insufficient p53 reactivation despite a high RP2D (2000 mg QD), particularly in KRAS mutant patients.

Materials and Methods: Antares's p53 Y220C reactivators were evaluated biochemically in SPR binding and thermal shift assays. Cellular activity was assessed in target engagement, target gene expression and cell proliferation assays across a panel of p53 Y220C mutant cell lines. Additionally, chromatin binding and target gene expression conferred by p53 Y220C reactivation were analyzed by ChIP-seq and RNA-seq. Finally, the *in vivo* efficacy was studied in several human CDX and PDX p53 Y220C models.

Results: Antares's orally bioavailable p53 Y220C reactivators demonstrated a ≥10-fold improvement in *in vitro* potency over rezatapopt in target engagement, ChIP-seq and RNA-seq assays, with corresponding potency improvements in cell proliferation assays across a panel of p53 Y220C mutant cell lines. *In vivo*, these compounds were effective in inhibiting tumor growth in multiple p53 Y220C CDX models at a significantly lower dose than rezatapopt. Importantly, these p53 reactivators exhibit a marked improvement in activity in a KRAS mutant model, both *in vitro* and *in vivo*.

Conclusions: The significantly improved potency of the novel p53 reactivators described here offers the opportunity to restore p53 function in less sensitive patient populations and meaningfully improve upon the clinical response profile of rezatapopt.

#7093 Potential use of MYCN and AURKA dual inhibitors for the treatment of pediatric cancers.

Nur Awaliyah Mentari Sukma, Wan-Ping Wang, Cheng-Ping Jheng, Chung-Chi Lee, Teng-Kuang Yeh, Jyh-Haur Chern, **Ya-Hui Chi**

National Health Research Institutes (NHRI), Zhunan, Taiwan

Aberrant activation of MYCN through genomic copy gain is a defining feature of high-risk neuroblastoma, which continues to have poor clinical outcomes despite intensive therapy. In MYCN-amplified tumors, AURKA contributes to malignant progression by stabilizing MYCN via a protein-protein interaction. Transcriptomic analysis of the St. Jude Children's Research Hospital database revealed that neuroblastomas co-overexpressing high levels of MYCN and AURKA exhibit significantly worse progression outcomes compared with tumors overexpressing either gene alone. We also identified a subset of pediatric soft-tissue tumors with concurrent MYCN and AURKA overexpression, among which Ewing's sarcoma showed a strong negative correlation between co-overexpression and overall survival. Across neuroblastoma and Ewing's sarcoma cell lines, MYCN expression level positively correlated with sensitivity to dual MYCN/AURKA inhibitors, including alisertib and 6K465. To evaluate translational potential, we compared the antitumor efficacy of alisertib and DBPR728 (the prodrug of 6K465) in the SK-N-BE(2) CDX model. DBPR728 administered at 300 mg/kg once weekly produced more durable tumor suppression than alisertib at 50 mg/kg once daily for three weeks. These findings define MYCN/AURKA coactivation as a therapeutic vulnerability and support the further development of dual MYCN/AURKA-targeting agents for pediatric cancers with elevated MYCN and AURKA expression.

#7094 Discovery of QLS1303, a potent and selective KIF18A inhibitor with robust anti-tumor activity in CIN+ preclinical cancer models.

Fei Chen, Wei Wei, Xiaobing Lv, Xiaoping Zheng, Chen Yang, Lili Fan, Fang Zhang, Junguo Hao, Xinrui Shao, Yan Wu, Ling Li, Ping Chen, Dong Yang, Hua Dong, Guqing Shi, Dongdong Wu, Yanling Xu, Weimei Sun, **Liang Xie**, Wenyuan Qian, Daqing Sun, Weikang Tao

Shanghai Qilu Pharmaceutical Research and Development Center LTD., Shanghai, China

Background: Chromosomal instability (CIN) underlies the aneuploidy present in ~90 % of solid tumors and engenders a persistent requirement for the plus-end kinesin KIF18A to silence mitotic checkpoints and align extra chromosomes. Consequently, KIF18A inhibition triggers catastrophic mis-segregation exclusively in CIN-high cells, inducing mitotic arrest or apoptosis, while sparing normal diploid cells. This synthetic-lethal interaction makes KIF18A as an attractive, cancer-selective therapeutic target, which prompted multiple drug-discovery programs, including AMG 650, a clinical-stage KIF18A inhibitor. Here we report the discovery and preclinical profiling of QLS1303, a novel, potent and orally bioavailable KIF18A inhibitor engineered to against aneuploid cancers with CIN-specific vulnerability.
Experimental Procedures: The inhibitory activity of QLS1303 was assessed through biochemical (KIF18A motor activity) and cellular proliferation assays using CIN+ and near-diploid cancer cell lines. In vivo efficacy and tolerability were evaluated in TP53mut/aneuploidy-high CDX models following once-daily oral administration. Selectivity and safety were profiled against a panel of 46 safety targets.
Results: QLS1303 potently inhibited KIF18A motor activity (IC_{50} = 13 nM) with a good selectivity over known toxic kinesin family members. It selectively suppressed proliferation of CIN+ cell lines (IC_{50} = 4-14 nM) with minimal effects on near-diploid cells. Once-daily oral administration of QLS1303 at 3 and 10 mg/kg was well-tolerated and induced tumor regression in multiple TP53mut/aneuploidy-high CDX models, and achieved tumor stasis at one-tenth of AMG 650 dosage in OVCAR3 xenograft model. A clean selectivity and safety profile were confirmed with no significant inhibition (IC_{50} > 10 μM) across the 46-target panel. In addition, QLS1303 exhibits favorable drug-like properties and a promising predicted therapeutic window.
Conclusion: QLS1303 is a highly potent, selective, and orally bioavailable KIF18A inhibitor, demonstrating robust anti-tumor activity in CIN+ preclinical models and a compelling safety profile. These data strongly support its advancement into clinical studies.

#7095 QLS1403, a novel and potent PARG inhibitor with robust anti-tumor efficacy in homologous recombination deficient cancer models.

Tingting Xia, Wei Wei, Xiaobing Lv, Jianfei Wang, Shengnan Zhang Zhang, Jun Chen, Xianyun Huang, Guozhi Liang, Lan Zhang, Ling Li, Ping Chen, Dong Yang, Fangfang Chen, Guqin Shi, Jiahua Chu, Dongdong Wu, Weimei Sun, **Liang Xie**, Wenyuan Qian, Daqing Sun, Weikang Tao

Shanghai Qilu Pharmaceutical Research and Development Center LTD., Shanghai, China

Background: Cancer cells experience high levels of endogenous replication stress due to persistent proliferative signaling. Poly (ADP-ribose) polymerase (PARP) is a first responder to DNA damage, catalyzing the synthesis of poly (ADP-ribose) (PAR) chains that serve as docking platforms for DNA repair proteins. The hydrolysis of these PAR chains, a critical step for the turnover of repair complexes, is primarily mediated by poly (ADP-ribose) glycohydrolase (PARG). Pharmacological inhibition or genetic loss of PARG prevents PAR chain hydrolysis, which results in persistent stalling of replication fork, nucleolytic degradation of nascent and parental DNA and ultimately cell death. IDE-161, a first-in-class PARG inhibitor has entered clinical trials. This study reports the discovery and characterization of QLS1403, a proprietary PARG inhibitor designed to selectively treat homologous recombination deficient (HRD) cancers, particularly those resistant to PARP inhibitors (PARPi) or T-Dxd.
Experimental Procedures: The activities of QLS1403 were characterized by biochemical PARG inhibition assay, cellular viability assessment in HRD-positive and PARPi-resistant or T-Dxd-resistant cancer cell lines and *in vivo* evaluation of efficacy in ovarian and breast cancer xenograft models. In addition, the pharmacodynamic effect, i.e., the PAR chain accumulation and its pharmacokinetic properties were assessed in both cells and animals.
Results: QLS1403 demonstrated exceptional PARG inhibitory activity (IC_{50} = 0.35 nM) and remarkable cellular activity in HRD-positive cancer cell lines, showing approximately 10-fold greater potency than IDE-161. Notably, QLS1403 showed strong activity in PARPi- or T-Dxd-resistant cell lines. Also, QLS1403 caused tumor regression at lower doses across multiple xenograft models with intrinsic PARPi resistance, accompanied by dose-dependent PAR accumulation in tumors. In addition, QLS1403 exhibited a clean selectivity and safety profile *in vitro*, with no significant off-target activity observed in safety assessment panels.
Conclusion: QLS1403 demonstrates superior potency, sustained efficacy in PARPi-resistant and T-Dxd-resistant cancer cell lines, while displaying favorable safety. These compelling data support its clinical evaluation as a new therapeutics for patients with HRD-positive cancers with acquisition of resistance to PARPi or potentially other existing treatments, such as T-Dxd.

#7096 Design and development of a biparatopic antibody-drug conjugate against CDH17.

Jinxiu Hou, Lisha Dong, Tingting Gu, Jiyuan Tian, Dandan Liu, Yongxin Shang, Rongmei Yan, Lifeng Pan, Liang Tian, Jian Peng, Zhenping Zhu

Earendil Labs., Wilmington, DE

CDH17 is overexpressed in various adenocarcinomas, including colorectal, gastric, and pancreatic cancers. High levels of CDH17 are associated with metastatic disease and poor prognosis in patients with these malignancies, In normal tissues, the expression of CDH17 is limited. Currently, various CDH17-based therapeutics, including bispecific antibodies, ADCs, and CAR-T, are under clinical investigation for treating CRC. Here, we describe the discovery and optimization of a novel biparatopic anti-CDH17 antibody. The biparatopic antibody exhibits efficient CDH17-directed cell binding and promotes rapid internalization at a much higher efficiency than the mono-epitope targeting ADCs. Next, we conjugated the biparatopic antibody to various cytotoxic payloads. The ADCs showed selective cytotoxicity towards multiple tumor cell lines with varying levels of CDH17 expression in vitro, and potently inhibited the growth of CDH17-expressing tumor xenografts in animal models. Together, these findings indicate that our lead biparatopic anti-CDH17 ADC is a promising candidate for the treatment of cancers that overexpress CDH17.

#7097 Non-clinical characterization of GSK5764227, a novel B7-H3-directed antibody-drug conjugate (ADC).

Jeremy Waight[1], Yuanfeng Zhou[2], Danni Sun[2], Lu Zhang[2], Michael Adam[1], Dawson Knoblock[1], Wenjin Zhou[2], Pengchao Qiu[2], Jifa Fan[2], Hannah Chenoweth[3], Johannes Breuning[3], Huifeng Niu[2], Srujana Neelam[1], Juan Liu[1], Shannon McKearnan[4], Natacha Steinckwich-Besancon[1], Takahiro Sato[1], Derek Poore[1], Alexander Cocks[3], Prajna Behera[5], Chris Hopson[1], Kenneth W. Hance[1], Klaas Bakker[3]

[1]GSK, Collegeville, PA,[2]Hansoh Pharmaceutical Group Co., Ltd., Shanghai, China,[3]GSK, London, United Kingdom,[4]GKS, Collegeville, PA,[5]GSK, Waltham, MA

B7-H3 (B7 homolog 3 protein), also known as CD276, is an important immunoregulatory ligand and member of the B7-CD28 family. Despite being widely expressed across tissues at the RNA level, the expression of B7-H3 protein is limited, where it can be found in cell-expressed and soluble forms. Notably, B7-H3 protein is found to be overexpressed in a variety of tumor tissues, including gastric, lung, prostate, kidney, oral, and bladder cancer, as well as osteosarcoma and hematologic malignant diseases - making B7-H3 an attractive target for tumor-selective approaches, such as antibody drug conjugates (ADCs). The expression of B7-H3 in tumor tissues is most prevalent on tumor epithelial and stromal cells (e.g., cancer associated fibroblasts and endothelial cells) but has also been described on tumor infiltrating dendritic cells (DCs), macrophages and monocytes. Consistent with its described immunoregulatory and tumor promoting role, B7-H3 is closely associated with poor prognosis and negative clinicopathological features, including metastasis, disease recurrence, and resistance to certain chemotherapeutics.

GSK5764227 is a novel ADC developed by Shanghai Hansoh Biomedical Technology Co., Ltd that is comprised of a fully human anti-B7-H3 monoclonal antibody (mAb) conjugated to an exatecan-derived topoisomerase I (TOPO1) inhibitor (SHR-9265, GSK5757810A, average DAR of 4).

Here we describe various non-clinical characteristics of GSK5764227, including biophysical, functional, and mechanistic attributes of the ADC. In vitro, GSK5764227 demonstrated binding to and internalization into B7-H3-expressing tumor cells, resulting in concentration-dependent tumor cell cytotoxicity. GSK5764227 also elicited cell cycle arrest (S-phase) and bystander killing capability.

In vivo, GSK5764227 exhibited significant and dose-dependent tumor growth inhibition (TGI) towards multiple CDX models, including the small cell lung cancer (SCLC) tumor cell line NCI-H146. Similar anti-tumor activity was observed in human PDX models of SCLC. Importantly, the strong antitumor activity in SCLC models align with early phase clinical data (ARTEMIS-001), where GSK5764227 demonstrated >60% ORR in extensive stage SCLC patients [Wang, 2025]. Collectively, these non-clinical observations, in tandem with emerging clinical data, support GSK5764227 as a promising cancer therapy and its rapidly progressing global clinical development.

#7099 Novel Ect2-Rac inhibitor CPV-337 in breast and pancreatic cancer.

Jessica Colon Gonzalez[1], Nilmary Grafals-Ruiz[1], Anamaris Torres-Sanchez[1], Cornelis Vlaar[2], Suranganie Dharmawardhane[1]

[1]Department of Biochemistry, School of Medicine, University of Puerto Rico Medical Sciences Campus, San Juan, PR,[2]Department of Pharmaceutical Sciences, School of Pharmacy, University of Puerto Rico Medical Sciences Campus, San Juan, PR

Metastasis is the leading cause of treatment failure and poor prognosis in cancer patients; however, there are few metastasis targeted therapies. The homologous Rho GTPases Rac and Cdc42 are viable targets in metastatic cancer due to their central role in cancer cell proliferation, viability, survival, migration, and invasion. In cancer, Rac and Cdc42 are not generally mutated but activated by oncogenic guanine nucleotide exchange factors (GEFs), which exchange the GDP for a GTP. We developed the clinical-stage compound MBQ-167, a Rac and Cdc42 inhibitor, as a metastasis inhibitor. CPV-337 is an MBQ-167 derivative that is specific for Rac (Rac1,2, 3, Rac1b) with an IC50 of ~50nM (i.e., 2X more effective than MBQ-167) in HER2++ breast cancer and an IC50 of <100nM in pancreatic cancer. CPV-337 has a GI50 of 57nM in metastatic breast cancer cells without affecting mammary epithelial cells. In a mouse model of HER2++ breast cancer experimental metastasis, treatment with 5mg/kg CPV-337 resulted in ~90% reduction in mammary tumor growth and metastasis, to the same extent as 10 mg/kg MBQ-167. The objective herein was to characterize the mechanism by which CPV-337 acts as an anticancer agent. We show that CPV-337 inhibits the phosphorylation of Rac downstream effectors PAK and Cofilin, which regulate actin cytoskeletal structures, such as lamellipodia. A significant reduction of the Rac downstream effector WAVE protein that also regulates the actin cytoskeleton, was also observed following CPV-337 treatment. Accordingly, CPV-337 inhibits lamellipodia formation, invasion, and migration of HER2++ breast cancer cells. To identify the mechanism by which CPV-337 inhibits Rac1, pulldowns were conducted using the Rac1(G15A) nucleotide-free mutant, which has a higher affinity for activated GEFs. Of the GEFs tested, Ect2 (Epithelial Cell Transforming 2) was identified as the major Rac.GEF inhibited by CPV-337. To date there are no known Rac-Ect2 specific inhibitors, despite Ect2 being a critical oncogene that regulates cytokinesis and cell cycle progression. Overexpression of Ect2 in different types of cancer has been associated with poor prognosis and reduced overall survival. Ongoing studies are evaluating the inhibitory mechanism of CPV-337 and its specificity using CRISPR-Cas9 Rac-1 knockout breast cancer cells. In conclusion, CPV-337 is a promising anti breast and pancreatic cancer drug with a unique and specific mechanism of inhibition.

#7100 VS-7375: An oral, selective KRAS G12D dual ON/OFF inhibitor with potent anti-tumor activity as a single agent and in combination with other agents.

Silvia Coma[1], Ian Smith[2], Cristina Caffarra Malvezzi[3], Clint A. Stalnecker[4], Emilia Berardelli[3], Enrico Patrucco[3], Fusheng Zhou[5], Channing Der[4], Chiara Ambrogio[3], David G. DeNardo[2], **Jonathan A. Pachter**[1]

[1]Verastem Oncology, Needham, MA,[2]Department of Medicine, Washington University School of Medicine, st louis, MO,[3]Department of Molecular Biotechnology and Health Sciences, University of Torino, Torino, Italy,[4]University of North Carolina at Chapel Hill, Chapel Hill, NC,[5]Genfleet Therapeutics, Shanghai, China

KRAS G12D is the most prevalent KRAS mutation in human cancers, present in 40%, 15%, and 5% of pancreatic, colorectal and lung cancers, respectively. Currently, there are no FDA-approved RAS inhibitors for patients with KRAS G12D-mutated (mt) cancers. VS-7375 (GFH375) is an oral, selective KRAS G12D dual ON/OFF inhibitor exhibiting extremely high affinity (K_D = 12-18 pM) and long residence time (18-24 hours) for the ON and OFF states of human KRAS G12D. VS-7375 has shown potent single agent anti-tumor efficacy with oral dosing across multiple KRAS G12D mt xenograft models representing pancreatic, colorectal and lung cancers. To assess potential benefits of dual ON/OFF inhibition relative to ON-only RAS inhibitors, we compared efficacy in KRAS G12D mt in vivo models relative to the KRAS G12D ON-only inhibitor zoldonrasib (RMC-9805) and the pan-RAS ON-only inhibitor daraxonrasib (RMC-6236). In the KP4 KRAS G12D pancreatic cancer model, VS-7375 (50 mg/kg twice daily orally) showed similar initial tumor regression (through day 9) relative to zoldonrasib (100 mg/kg once daily orally) and daraxonrasib (25 mg/kg once daily orally). However, by approximately 20 days of dosing, zoldonrasib and daraxonrasib progressively lose their anti-tumor activity with associated tumor outgrowth (mean tumor volume >850 mm^3 by day 30) in contrast to those treated with VS-7375 which showed sustained tumor regression (mean tumor volume ~80 mm^3 by day 30). Accordingly, pharmacodynamic analysis with pathway-specific gene signatures showed that whereas all three KRAS inhibitors inhibited MAPK, MYC and PI3K signaling at day 6, only the G12D ON/OFF inhibitor VS-7375 maintained inhibition of these signaling pathways by day 20. VS-7375 also showed deeper tumor regression compared to these RAS ON-only inhibitors in KRAS G12D mt lung and colorectal xenograft models. Currently, we are assessing the anti-tumor efficacy of VS-7375 in combination with other anti-cancer agents including EGFR, PRMT5 and FAK inhibitors. Briefly, the combination of the anti-EGFR antibody cetuximab with VS-7375 induced strong tumor growth inhibition in KRAS G12D mt cancer models. Furthermore, addition of a PRMT5 inhibitor with VS-7375 increased duration of tumor regression in KRAS G12D mt;MTAP-deleted pancreatic cancer models. Lastly, addition of a FAK inhibitor with VS-7375 increased duration of tumor regression in KRAS G12D mt cancer models, altogether supporting the potential clinical evaluation of novel combination strategies with VS-7375 in patients with KRAS G12D mt cancers for maximal anti-tumor efficacy and durability. VS-7375 is currently in phase 1/2 clinical evaluation in the US (VS-7375-101; NCT07020221) and in advanced clinical evaluation in China (NCT06500676) as monotherapy and in combination with cetuximab or chemotherapy ± pembrolizumab for patients with KRAS G12D mt cancers.

#7101 Discovery of first-in-class YTHDC1 small molecule inhibitors for the treatment of MYC-driven cancers.

Richard C. Centore[1], Mark Charles[2], Mansi Arora[1], Marius Rebmann[2], Michael J. Rawling[2], Jerome Cattin[2], Xuejing Yang[3], Emily Batchelor[3], Matthew Watson[2], Nagakumar Bharatham[2], Alexander Howarth[2], Seema Qamar[2], Laura Andraghetti[2], Andrew Seeber[1], Michael G. Kharas[3], Sam Cohen[2], Martin Kulander[2], Tuomas Knowles[2], **Shilpi Arora**[1]

[1]Transition Bio, Inc., Cambridge, MA,[2]Transition Bio Ltd., Cambridge, United Kingdom,[3]Memorial Sloan Kettering Cancer Center, New York, NY

The m6A reader protein YTHDC1 is essential for cancer cell survival, through its ability to form nuclear biomolecular condensates that stabilize oncogenic transcripts such as *MYC*. Here, we report a new class of potent, selective, orally bioavailable small-molecule inhibitors of YTHDC1. These compounds occupy the RNA binding pocket of YTHDC1 and disrupt its interaction with m^6A-modified RNA at nanomolar potency in both biochemical and cellular assays. They display high selectivity for YTHDC1 over other YTH family members, selectively dissolve m6A-dependent YTHDC1 condensates without affecting unrelated condensate systems, and exhibit clean profiles across broad kinase and safety panels. The optimized leads are drug-like, orally bioavailable and possess favorable ADME and *in vivo* properties. Pharmacological inhibition of YTHDC1 disrupts oncogenic YTHDC1 condensates and robustly suppresses MYC signaling resulting in growth arrest, differentiation, and apoptosis of acute myeloid leukemia (AML) and additional cancer cell types, while sparing normal hematopoietic cells. These optimized inhibitors display strong single-agent anti-tumor activity across heme and solid tumor models including AML, small cell lung cancer and neuroendocrine prostate cancer. Moreover, YTHDC1 inhibition shows pronounced synergy with standard of care agents such as venetoclax in AML. Collectively, these findings establish YTHDC1 as a tractable therapeutic target for MYC-driven malignancies.

#7102 Overcoming cytidine deaminase (CDA) mediated resistance via EO-4426 dual DNA-replication targeting: Implications for CDA-high solid tumors and mesenchymal GBM.

Jeffrey Bacha[1], Denni M. Brown[2], Richard Daniels[1], Sarath Kanekal[3], John Langlands[4]

[1]Edison Oncology Holding Corp., Menlo Park, CA, CA,[2]Edison Oncology Holding Corp., Menlo Park, CA,[3]President, Regulatory Strategy Consulting, San Diego, CA,[4]Valent Technologies LLC, Menlo Park, CA, CA

Background: EO-4426 (tezacitabine) is a brain-penetrant, deamination-resistant cytidine analog that uniquely inhibits both DNA polymerase-α (Polα) and ribonucleotide reductase (RNR), leading to dNTP-pool depletion, replication-fork collapse, and DNA-damage accumulation in rapidly proliferating tumor cells. Unlike gemcitabine and hydroxyurea, EO-4426 resists cytidine deaminase (CDA)-mediated inactivation. Tumors with high CDA expression or APOBEC3G-linked cytidine-metabolism activity—including mesenchymal GBM, TNBC, NSCLC, and ovarian cancer—are predicted to exhibit heightened dependence on Polα/RNR function and may therefore be particularly susceptible to dual-targeting strategies.

Methods: Ongoing invitro studies are assessing EO-4426 across engineered and naturally CDA-high cancer cell models to define mechanistic pharmacology and biomarker-enrichment hypotheses. Experimental approaches include: (i) LCMS quantification of EO-4426-induced dNTP-pool depletion; (ii) evaluation of replication-stress and DNA-damage biomarkers (γH2AX, pRPA32, pCHK1) by immunoblot and high-content imaging; (iii) characterization of APOBEC3G→CDA pathway activity and its impact on drug sensitivity; (iv) flow cytometric analysis of S-phase arrest and replication-fork perturbation; and (v) combinatorial studies with ionizing radiation and DDR-targeting agents, including ATR inhibition.

Preliminary Findings: Prior nonclinical studies demonstrate that EO4426 retains potent activity in CDA-high tumor environments and is not susceptible to rapid deamination, distinguishing it from gemcitabine, which is efficiently converted to inactive dFdU. Published work also reports enhanced antitumor activity in combination with DNA-directed agents and fluoropyrimidines, consistent with strong replication-stress induction and dNTP-depletion biology. Clinically, EO4426 has been evaluated in multiple third-party sponsored Phase I/II trials, showing predictable myelosuppression as the principal toxicity and evidence of antitumor activity, including objective responses and durable disease stabilization, in heavily pretreated solid-tumor populations.

Conclusions: New data are being developed to support further investigation of EO-4426 in cytidine metabolism-driven tumor contexts and biomarker guided clinical development strategies for CDA-high solid tumors and mesenchymal/APOBEC3G-enriched GBM. Comprehensive in vitro mechanistic data, biomarker correlations, and combination treatment findings will be presented at the Meeting.

#7103 Evaluation of anti-parasitic agents as potential therapeutics in ovarian cancer.

Aneth Ochoa Negrete[1], Tiffany Duque[1], Adithi Kankanala[1], Gisel Gutierrez[1], Riyaz Basha[2]

[1]UNT Health, Fort Worth, TX,[2]University of North Texas Health Science Center, Fort Worth, TX

Ovarian cancer is projected to claim approximately 13,000 lives in the United States in 2025. Current treatment options remain limited and often insufficiently effective, underscoring the need for alternative therapeutics that may improve survival outcomes. To explore such possibilities, we screened two anti-parasitic drugs: ivermectin (IV) and fenbendazole (FZ). These drugs have been reported to exhibit anti-cancer properties. Both drugs were tested on the ovarian cancer cell lines SKOV3 and ES-2 using a luminescence-based CellTiter-Glo cell viability assay kit (Promega). Previous studies indicate that these compounds can inhibit proliferation and promote apoptosis in some cancer cell lines and mouse xenograft models. FZ in particular has been reported to alter the expression of *MYC*, a gene involved in cancer cell growth, proliferation, and survival. Using the open-access cancer database, we retrieved data from The Cancer Genomic Atlas and found that high *MYC* expression in ovarian cancer patients significantly correlates with decreased survival ($p = 0.044$). Our cell viability assays revealed cell line-dependent anti-proliferative responses. ES-2 cells displayed a clear dose-dependent decrease in viability following IV or FZ treatment, whereas SKOV3 cells were comparatively less sensitive. For ES-2, IV at 8, 4, 2, and 1 µM doses at 48-hour post-treatment, yielded viabilities of 0.88%, 4.91%, 18.82%, and 78.97%, respectively; for SKOV3, the corresponding viabilities were 8.92%, 56.62%, 76.61%, and 100.0%. FZ produced a similar trend: ES-2 viabilities at 5, 2.5, 1.25, and 0.625 µM were 6.97%, 27.02%, 50.52%, and 69.46%, while SKOV3 viabilities were 17.32%, 19.46%, 20.49%, and 50.54%, respectively. IC_{50} calculations further highlighted these differences. In SKOV3, the IC_{50} for FZ (1.02 µM) was lower than that for IV (3.678 µM). In ES-2, both drugs produced similar IC_{50} values (IV: 2.5345 µM; FZ: 2.3285 µM). These findings suggest the potential anti-cancer activity of these anti-parasitic agents and further testing their efficacy as therapeutic candidates for ovarian cancer. Our laboratory is currently investigating the combination therapies involving these drugs with standard chemotherapeutics and other agents shown to modulate MYC and other emerging anti-cancer compounds to improve treatment efficacy for ovarian cancer patients.

#7104 BBO-11818: An orally bioavailable, highly potent and selective non-covalent pan-KRAS(ON) and (OFF) inhibitor with robust anti-tumor activity in KRAS-mutant preclinical models.

Carlos E. Stahlhut Espinosa[1], Anna E. Maciag[2], Kyle A. Sullivan[1], Kanchan Singh[1], Nadege Gitego[1], Zuhui Zhang[1], Albert H. Chan[2], Alok K. Sharma[2], Patrick Alexander[2], Jin Shu[1], Yue Yang[1], Megan Rigby[2], Roger Ma[2], Molly Grandcolas[1], Saman Setoodeh[1], Brian P. Smith[2], Jun Pei[3], Dana Rabara[2], Erik K. Larsen[2], David Turner[2], Cathy Zhang[1], Cindy Feng[1], Siyu Feng[1], James P. Stice[1], Rui Xu[1], Ken Lin[1], Andrew G. Stephen[2], Felice C. Lightstone[3], Chunmei Ji[1], Keshi Wang[1], Dhirendra K. Simanshu[2], Dwight V. Nissley[2], Eli Wallace[1], Bin Wang[1], Kerstin Sinkevicius[1], Frank McCormick[4], Pedro J. Beltran[1]

[1]BridgeBio Oncology Therapeutics, South San Francisco, CA,[2]NCI RAS Initiative, Frederick National Laboratory for Cancer Research, Frederick, MD,[3]Physical and Life Sciences (PLS) Directorate, Lawrence Livermore National Laboratory, Livermore, CA,[4]UCSF Helen Diller Family Comprehensive Cancer Ctr., San Francisco, CA

KRAS is commonly mutated in human cancer. Inhibitors of $KRAS^{G12C}$ have shown promising clinical efficacy; however, there are currently no approved targeted therapies against other KRAS variants, and a significant underserved patient population across several major cancer types, including pancreatic carcinoma (PDAC), colorectal cancer (CRC), and non-small cell lung cancer (NSCLC), remains. We discovered BBO-11818: a potent, selective, orally bioavailable small molecule KRAS inhibitor with activity against multiple KRAS mutants, including $KRAS^{G12D}$ and $KRAS^{G12V}$, in both their active GTP-bound (ON) and inactive GDP-bound (OFF) states. BBO-11818 binds the switch II pocket with high affinity and selectivity, locking the active form in the signaling-incompetent state 1 to disrupt the association of GTP-bound KRAS with its key effector RAF1, and sequestering the inactive form. BBO-11818 potently inhibits several oncogenic KRAS mutants in cell-based assays, resulting in the suppression of MAPK signaling and inhibition of cell proliferation with single-digit nanomolar EC_{50} values. The selectivity of BBO-11818 for KRAS is demonstrated by its >1000-fold lower potency against NRAS- and BRAF-mutant cell lines. BBO-11818 exhibits favorable pharmacokinetic (PK) and pharmacodynamic (PD) properties in mouse models of cancer. Single dose, oral administration results in strong dose- and time-dependent inhibition of pERK in $KRAS^{G12D}$ and $KRAS^{G12V}$ cell-derived xenograft (CDX) models. BBO-11818 monotherapy induces strong anti-tumor responses, including regression at well-tolerated doses in CDX and patient-derived xenograft (PDX) models of KRAS-mutant PDAC, NSCLC, and CRC. Combination treatment with BBO-10203, a clinical-stage (NCT06625775), selective RAS:PI3Kα breaker that blocks RAS-mediated activation of the PI3Kα-AKT pathway, results in decreased cellular proliferation, increased apoptosis, and enhanced efficacy in CDX and PDX models harboring $KRAS^{G12D}$ or $KRAS^{G12V}$ mutations. Similarly, combination treatment with BBO-11818 and cetuximab, an approved anti-EGFR monoclonal antibody, results in enhanced anti-tumor activity in a $KRAS^{G12D}$ CDX model. Finally, BBO-11818 shows combination benefit with anti-PD-1, resulting in complete tumor regressions in the $KRAS^{G12D}$ CT-26 syngeneic tumor mouse model. BBO-11818 is a potent pan-KRAS inhibitor with activity against both the GTP- and GDP-bound states of KRAS, presenting the opportunity to address a large fraction of KRAS-mutant tumors currently lacking targeted therapeutic options. BBO-11818 has entered Phase 1 clinical trials for patients with various KRAS mutations in colorectal, pancreatic, and lung cancers (NCT06917079).

#7105 Therapeutic targeting of ADAR1 p150 splicing activity impairs CD44$^+$ TNBC cell populations in preclinical studies.

Wenxue Ma[1], Jessica Pham[1], Emma Klacking[1], Kendale Wirtjes[1], Inge van der Werf[1], Peggy Wentworth[1], Sheldon Morris[1], James La Clair[1], Michael Burkart[2], Catriona Jamieson[1]

[1]University of California San Diego, La Jolla, CA,[2]Department of Chemistry and Biochemistry, University of California San Diego, La Jolla, CA

Background: Triple-negative breast cancer (TNBC) remains clinically challenging due to the lack of targeted therapies and the presence of therapy-resistant tumor-propagating cells. CD44 and ADAR1 contribute to TNBC progression and therapeutic resistance. Rebecsinib is a small-molecule inhibitor designed to block splicing-mediated activation of ADAR1 (adenosine deaminase acting on RNA 1). This study evaluates its efficacy in selectively targeting CD44$^+$ and ADAR1$^+$ cells in preclinical humanized TNBC models.

Methods: MDA-MB-231 TNBC cell line-derived xenograft (CDX) models were established in Rag2$^{-/-}\gamma c^{-/-}$ and NSG-SGM3 mice. MDA-MB-231 ADAR-nanoluciferase-GFP expressing cells enable tracking of ADAR1 activity by IVIS imaging. Engrafted mice received vehicle, Rebecsinib IV (10 mg/kg), or Rebecsinib PO (15mg/kg), twice a week for two weeks. Tumor burden was measured by IVIS and single-cell suspensions from peripheral blood, and tissues (lung, liver, spleen, and bone marrow) were analyzed by flow cytometry to quantify CD44$^+$ and ADAR1$^+$ cells.

Results: Rebecsinib significantly reduced CD44$^+$ cells in peripheral blood ($p < 0.05$), lung ($p < 0.01$), liver ($p < 0.01$), and spleen ($p < 0.05$) in Rag2$^{-/-}\gamma c^{-/-}$ models (Student *t* test). Corresponding decreases in ADAR1$^+$ cells was observed in the lung ($p < 0.05$), liver ($p < 0.01$), and spleen ($p < 0.01$) in NSG-SGM3 mouse models (Student *t* test). IVIS imaging demonstrated tumor bioluminescence in Rebecsinib-treated groups ($p = 0.02$, student *t* test). Combination with Fedratinib further suppressed tumor growth, indicating a synergistic effect ($p < 0.05$, student *t* test).

Conclusion: Rebecsinib selectively reduces CD44$^+$ and ADAR1$^+$ TNBC cell populations and inhibits tumor progression in humanized preclinical models. These findings support further evaluation of Rebecsinib alone and in combination, as a targeted therapeutic approach for TNBC.

Keywords: TNBC, ADAR1, CD44, Rebecsinib, targeted therapy, preclinical models.

#7106 Q-2361, a treatment for skin cancer prevention in organ transplant recipients.

Rebecca Pouwer[1], **Kimberley Beaumont**[1], Margaret Veitch[2], Maria Parra Reyes[2], Bhanu Chintala[2], Hui Yi Chew[2], Peter Soyer[3], Scott Campbell[4], James Wells[2], Andrew Harvey[1], Terrie-Anne Cock[1], Brian Dymock[1]

[1]QEDDI, UniQuest, University of Queensland, Brisbane, Australia,[2]Frazer Institute, Faculty of Medicine, University of Queensland, Brisbane, Australia,[3]Frazer Institute, Dermatology Research Centre, University of Queensland, Brisbane, Australia,[4]Faculty of Medicine, University of Queensland, Brisbane, Australia

Solid organ transplant recipients require life-long immunosuppression in order to prevent the immune-mediated rejection of their transplanted organs. Tacrolimus, a mainstay in immunosuppressive therapy, acts systemically to suppress the activity of T cells within and around transplanted organs. Consequently, however, these patients suffer a 65- to 250-fold increased risk of developing cutaneous malignancies including squamous cell carcinoma (SCC) and Kaposi's Sarcoma. SCC is the most prevalent cancer in solid organ transplant recipients, with a more aggressive clinical course compared to the general population and is a significant contributor to morbidity and mortality. We have identified a small molecule drug candidate (Q-2361), to locally inhibit the unwanted effects of tacrolimus on T cells and ketatinocyes in the skin. Q-2361 potently blocked the interaction between tacrolimus and FKBP12 and rescued both mouse and human T cell activation and proliferation in the presence of tacrolimus *in vitro*. Functional studies in multiple 'regressor' mouse models of skin cancer showed that the local administration of Q-2361 induced tumor regression in mice that had been systemically immune-suppressed with tacrolimus. Mechanistically, Q-2361 treatment permitted CD8 T cell activation, proliferation, and effector function, and Q-2361 could not induce tumor regression when CD8 T cells were depleted, demonstrating that Q-2361 induces tumor regression through the reactivation of cytotoxic T cells. In separate studies, Q-2361 blocked multiple effects of tacrolimus on UV-damaged keratinocytes, and prevented the formation of SCC tumours in UV-treated nude mice fed a tacrolimus-diet. A simple solution-based Q-2361 topical formulation achieved high and sustained residence in skin with negligible drug in the blood. Thus, topically applied Q-2361 shows high potential for the reactivation of T cells and the rescue of keratinocyte function locally in the skin but not at other body sites, which paves the way to clinical trials of topical Q-2361 treatments for skin malignancies in immunosuppressed organ transplant recipients.

#7107 Dual FLT3/BRAF inhibitor PHI3 overcomes RAS-driven resistance in FLT3-mutant AML.

Shikhar Sharma[1], Anna Skwarska[1], Evangelia Matenoglou[1], Sovira Chaudhry[1], Selvam Murugan[2], Catherine Smith[3], Pamela Sung[2], Eunice Wang[2], Donald Small[4], **Evripidis Gavathiotis**[1], Marina Konopleva[1]

[1]Albert Einstein College of Medicine, Bronx, NY,[2]Roswell Park Comprehensive Cancer Center, Buffalo, NY,[3]University of California San Francisco, San Frncisco, CA,[4]John Hopkins, Sidney Kimmel Comprehensive Cancer Center, Baltimore, MD

Background: FLT3 mutations define a high-risk subset of AML, and FLT3 inhibitors are routinely used in combination with induction chemotherapy in fit patients, and with a low-intensity HMA/Venetoclax backbone in older patients. However, the majority of relapses arise from activation of bypass signaling, most commonly through the RAS/MAPK pathway. RAS mutations emerge in ~20% of patients who progress on gilteritinib or other FLT3 inhibitors, driving sustained MAPK activation and therapy resistance. We hypothesized that simultaneous inhibition of FLT3 and the downstream RAS effector RAF would suppress MAPK reactivation and overcome this dominant resistance mechanism. Here, we characterize PHI3, a novel dual BRAF/FLT3 kinase inhibitor, and evaluate its preclinical activity in FLT3-mutant and RAS-mutant AML models.
Results: Biochemical assays and nanoBRET target-engagement studies showed that PHI3 potently inhibits wild-type BRAF, BRAFV600E, and FLT3 at nanomolar concentrations. Immunoblot analysis confirmed robust suppression of FLT3, MEK, and ERK phosphorylation by PHI3 in FLT3-ITD+ MOLM13 and MOLM14 cells (IC50 ~35 nM), with activity also observed in OCI-AML2 and OCI-AML3. In contrast to gilteritinib, PHI3 effectively inhibited MAPK signaling in MOLM14 NRASG12C cells (IC50 ~125 nM). FLT3-ITD AML lines were most sensitive to PHI3 (IC50 31-90 nM) and underwent apoptosis within 24 h. RAS-mutant cell lines showed variable but meaningful sensitivity: OCI-AML2/3 (IC50 ~330-340 nM), SKM1 KRASK117N (61 nM), and THP-1 NRASG12D (2.6 µM). MOLM14 isogenic NRAS mutants, resistant to gilteritinib (IC50 1 µM), retained marked sensitivity to PHI3 (IC50 276-690 nM). PHI3 also reduced clonogenic growth, viability (IC50 ~190 nM), and MAPK signaling in primary FLT3/RAS-mutant AML specimens (n=9). PHI3 combined with venetoclax produced additive activity in FLT3-ITD models. In vivo, PHI3 and gilteritinib both reduced tumor burden and prolonged survival in MOLM13 xenografts compared with vehicle control (median of 29 vs 20 days). PHI3 had superior efficacy compared with Gilteritinib in mice engrafted with MOLM14 NRASG12C, with a median survival of 20 days in vehicle-treated mice, 24 days in gilteritinib and 38 days in PHI3-treated mice. Leukemic cells from MOLM14-engrafted mice showed MAPK suppression with both PHI3 and gilteritinib, whereas in MOLM14 NRASG12C mice, MAPK signaling was reduced only with PHI3. No weight loss or other side effects were noted in mice that received PHI3 therapy.
Conclusions: PHI3 is a potent dual BRAF/FLT3 inhibitor that effectively suppresses MAPK pathway reactivation and overcomes RAS-driven resistance to FLT3 inhibitors in AML. Its strong in vivo efficacy and tolerability positions PHI3 as a promising therapeutic candidate. These findings provide a clear mechanistic and translational rationale for advancing dual FLT3/BRAF targeting in patients with FLT3-mutant and FLT3/RAS co-mutant AML.

#7108 Polyamine depletion via ivospemin and doxorubicin combination treatment leads to alterations in the ovarian tumor immune microenvironment.

Cassandra E. Holbert[1], Ashley C. Nwafor[2], Lauren J. Imasa[1], Robert A. Casero[2], Tracy Murray Stewart[2]

[1]Loyola University Maryland, Baltimore, MD,[2]Johns Hopkins Sidney Kimmel Comprehensive Cancer Center, Baltimore, MD

Polyamines are protonated alkylamines that influence many cellular processes including growth, transcription, and survival. Cancer cells are fully reliant on elevated polyamine pools to sustain their continual proliferation and survival. As such, pharmacological modulation of polyamine metabolism is promising as a cancer metabolic therapeutic strategy. Previous work has linked DFMO-mediated polyamine depletion with pro-inflammatory changes in the tumor microenvironment. Our work aims to evaluate ivospemin, a spermine analogue, in ovarian cancer. Considering nearly three-quarters of late-stage ovarian cancer patients develop resistance to platinum-based chemotherapies and these tumors are usually immunotherapy-insensitive, the aim of our study is to determine the combinatorial efficacy and potential immune-priming properties of ivospemin and doxorubicin. We previously demonstrated that ivospemin treatment decreases viability in a variety of cancer cell lines through depletion of intracellular polyamines via downregulation of the polyamine biosynthetic enzyme ornithine decarboxylase (ODC) and induction of the polyamine catabolic enzyme spermidine/spermine-N^1-acetyltransferase (SSAT). Additionally, ivospemin increases the efficacy of gemcitabine and topotecan *in vivo* by delaying tumor onset and reducing overall tumor burden. Here we examine the potential of combining ivospemin with doxorubicin, a common chemotherapeutic used in platinum-resistant ovarian cancer. Ovarian adenocarcinoma lines treated with ivospemin and doxorubicin exhibit an additive decrease in survival that is associated with changes in polyamine metabolic enzyme activity and depleted overall polyamine levels. Using the syngeneic VDID8+ ovarian model, we evaluated the efficacy of combination treatment *in vivo*. Co-treated animals exhibited increased median survival, delayed tumor onset, and decreased tumor burden. Polyamine analysis of ascites fluid confirmed decreased polyamine content and N^1-acetylated spermidine accumulation, consistent with upregulation of SSAT activity. The survival benefit was completely absent in an immunocompromised NSG model indicating significant reliance on the immune system for response. Compared to single agent treatment, ascites from co-treated animals showed an increased presence of CD45+ lymphocytes. While treatment did not influence peritoneal macrophage numbers, the polarization of macrophages was altered with a transition from a predominately M2-like phenotype to an M1-like phenotype following treatment. Additionally, an upregulation of PD-L1 was observed suggesting that treatment may increase sensitivity to immune checkpoint inhibitors (ICIs). Future studies will evaluate ivospemin/doxorubicin in combination with various immunomodulatory drugs such as ICIs, TGFβ blockade, and CD-40 agonists.

: Novel Strategies to Reverse Drug Resistance
Poster Session

#7112 Understanding and overcoming resistance of triple-negative breast cancer brain metastases to RET monotherapy.

Phi-Long Tran[1], Elissa Bloom[1], Angelina Regua[2], Shivani Bindal[2], Mariana Najja[1], Sham Syed[2], Hui-Wen Lo[1]

[1]Department of Cell Biology and Genetics, Naresh K. Vashisht College of Medicine, Texas A&M University Health Science Center, College Station, TX,[2]Vivian L. Smith Department of Neurosurgery, McGovern Medical School, The University of Texas Health Science Center at Houston, Houston, TX

Breast cancer is the most common cancer among American women, with over 315,000 new cases and more than 42,000 deaths projected in 2025. Triple-negative breast cancer (TNBC), the most aggressive subtype, has a high incidence of brain metastasis (BrainMet)—up to 45%. Clinical studies show that TNBC patients with BrainMet have the shortest survival times (4-6 months) compared to those with lung, liver, or bone metastases. This poor prognosis is mainly due to a lack of actionable therapeutic targets and blood-brain barrier (BBB)-permeable drugs. No effective TNBC-BrainMet therapeutics have been identified, underscoring the urgent need for novel treatment modalities. Rearranged during transfection (RET) is implicated in tumorigenesis and metastatic progression in non-small cell lung cancers, thyroid carcinoma, and breast cancers. The orally FDA-approved RET inhibitors, Pralsetinib and Selpercatinib, demonstrated brain penetration, with 70-91% intracranial response rates in lung cancer patients with BrainMet, suggesting their possible utility in treating TNBC-BrainMet. In this study, we investigated the role of RET in TNBC-BrainMet and assessed the therapeutic efficacy of these selective RET inhibitors as a TNBC-BrainMet treatment. Our datamining analyses revealed that RET is hyperactivated in TNBC-BrainMet patients and is associated with worsened survival outcomes. Overexpression of RET in TNBC cells promoted brain metastasis in our intracardiac injection and intracranial inoculation mouse models. Treatment with RET inhibitors reduced tumor burden and brain metastasis in the BrainMet prevention mouse study in *vivo*. However, we observed drug resistance to RET inhibitors in the BrainMet treatment model *in vivo*. We also found lower sensitivity to RET inhibitors in brain-tropic TNBC cells compared to parental TNBC cells. To identify the potential mechanisms of resistance, we further investigated whether RET pathway is co-activated with other oncogenic pathways in breast cancer brain metastasis using the TCGA database analyses. We observed that RET is concurrently activated with multiple signaling pathways, including t-GAS, VEGF, AKT, and ERK. Notably, co-inhibition of RET and these signaling pathways produced synergistic effects in suppressing the proliferation of brain-tropic TNBC cells. Our findings suggested that these co-inhibitions may overcome RET monotherapy resistance in TNBC-BrainMet. In summary, targeting RET is promising for preventive therapy; co-inhibition of RET and its associated pathways may overcome RET monotherapy resistance and advance TNBC-BrainMet treatment, providing preclinical evidence to support future clinical evaluation and development of new effective therapies for TNBC patient with brain metastasis.

#7113 Targeting breast cancer brain metastasis through novel combination of FDA-approved orally active BBB-permeable RET and tGLI1 inhibitors.

Joshua Cha[1], Angelina Regua[2], Mariana Najjar[1], Shivani Bindal[3], Elissa Bloom[1], Hui-Wen Lo[3]

[1]The University of Texas MD Anderson Cancer Center UTHealth Houston Graduate School of Biomedical Sciences, Houston, TX,[2]Vivian L. Smith Department of Neurosurgery, McGovern Medical School, The University of Texas Health Science Center at Houston, Houston, Houston, TX,[3]Department of Cell Biology and Genetics, Naresh K. Vashisht College of Medicine, Texas A&M University Health Science Center, College Station, TX

Breast cancer is the most diagnosed cancer in American women, and breast cancer brain metastasis (BCBM) exhibits the worst prognoses, with a life-expectancy averaging 8 months. The short survival stems largely from the lack of effective treatment. Major challenges remain, including the limited number of actionable targets for targeted therapy and the scarcity of effective blood-brain barrier (BBB)-permeable drugs. Hence, identifying new therapeutic targets and BBB-permeable agents is urgently needed. Our lab identified the Rearranged during Transfection receptor tyrosine kinase (RET) as a potential BCBM target. RET inhibitors Pralsetinib and Selpercatinib, FDA-approved for lung and thyroid cancers, exhibit intracranial activity. We previously reported overexpression of RET in BCBM and found that RET monotherapy significantly suppressed BCBM incidences in mouse models but failed to halt the progression of established BCBM. Thus, we sought to identify potential secondary pathways contributing to the observed resistance to RET monotherapy. Through pathway correlation analysis using publicly available breast cancer datasets, Truncated Glioma-Associated Oncogene Homolog 1 (tGLI1) was identified as positively correlated with RET. tGLI1 is an alternatively spliced, gain-of-function variant of the GLI1 transcription factor that is overexpressed in and promotes BCBM. Consequently, we examined IHC-stained patient samples of matched primary and BCBM tumors and observed concurrent elevation in RET activation and tGLI1 expression in over 80% of BCBM tumor samples. Western blot analysis also revealed increased activated RET and tGLI1 levels in brain-tropic breast cancer cell lines compared to parental counter parts. Datamining analysis with patient-derived datasets indicated significantly higher RET and tGLI1 co-activation in patients with brain metastasis, associated with worse clinical outcomes. Finally, tGLI1-knockdown via antisense oligonucleotides sensitized resistant BCBM subline to Pralsetinib. Thus, we hypothesized that RET and tGLI1 functionally crosstalk to mediate BCBM progression and co-targeting them with FDA-approved orally active BBB-permeable inhibitors overcomes the RET monotherapy resistance and synergistically inhibits BCBM. *In vitro* cell proliferation assays using tGLI1-overexpressing BCBM sublines demonstrated increased Pralsetinib resistance but enhanced sensitivity to tGLI1 inhibitor, Ketoconazole. Pralsetinib+Ketoconazole combination treatment yielded synergistic inhibition of BCBM cell viability and migration *in vitro*. The underlying mechanism is under analysis through RNA-sequencing, and *in vivo* efficacy of the Pralsetinib+Ketoconazole combination therapy on BCBM remains to be validated with mouse models. Together, we report a novel mechanism and combination treatment for BCBM patients.

#7114 Therapeutic potential of BTK targeted degrader in B-cell malignancies harboring ibrutinib-resistant mutation.

Shuai Zhao[1], Xiujuan Wu[1], Ting Ni[2], Jian Xiang[3], Zhixiang Zhang[3]

[1]In Vivo Pharmacology Unit, WuXi AppTec, Suzhou, China,[2]WuXi AppTec, Suzhou, China,[3]WuXi AppTec, Shanghai, China

The long-term efficacy of Ibrutinib is limited by the emergence of resistance mutations (e.g., C481S, L528W). These mutations preclude formation of a covalent bond with BTK, leading to diminished drug efficacy and disease progression. Therefore, novel therapeutic strategy is urgently needed for patients who have acquired resistant mutations of Ibrutinib. Targeted protein degradation represents a potential and powerful means to overcome Ibrutinib resistance. To evaluate BTK degradation as a strategy to overcome ibrutinib resistance, we characterized Bexobrutideg (NX-5948), a novel cereblon E3 ligase-engaging small molecule that induces BTK protein degradation. *In vitro*, NX-5948 exhibited potent antiproliferative effects against ibrutinib-sensitive and -resistant B-cell malignancy models (including BTK-C481S and BTK-L528W mutants). *In vivo*, NX-5948 achieved significant tumor growth inhibition in xenografts harboring these resistance mutations, demonstrating its potential to overcome clinical resistance to Ibrutinib. In summary, we have validated the anti-tumor activity of NX-5948 in Ibrutinib-resistant cell lines, both in vitro and in vivo. These findings support targeting BTK degrader could be as a promising strategy to bypass resistance by eliminating mutant BTK in patients with B-cell malignancies.

#7117 Pharmacological disruption of YAP1/TEAD and NF-kappa B crosstalk suppresses prostate cancer.

Sebnem Unlu[1], Abdulrahman M. Dwead[2], Marwah M. Al-Mathkour[2], **Bekir Cinar**[1]

[1]Center for Cancer Research and Therapeutic Development and Department of Biological Sciences, Clark Atlanta University, Atlanta, GA,[2]Clark Atlanta University, Atlanta, GA

Patients with advanced prostate cancer have poorer prognoses, characterized by persistent morbidity and mortality, primarily due to the development of metastatic castration-resistant disease. Recent studies indicate that crosstalk between the YAP1/TEAD and NF-kappa B pathways is critical for cellular biology and disease pathogenesis, including cancer progression, metastasis, and therapeutic relapse. However, the functional association of these oncogenic pathways in prostate cancer remains insufficiently characterized. This study aims to evaluate the effects of two pharmacological inhibitors: TED-347, a selective YAP1/TEAD inhibitor, and genistein, a phytoestrogen that inhibits NF-kappa B signaling, on prostate cancer growth in both cell culture and animal models. Both TED-347 and genistein result in substantial reductions in prostate tumor cell growth in vitro and in vivo. Mechanistically, TED-347 and genistein decrease the expression and activity of YAP1/TEAD and NF-kappa B/RELA in prostate xenografts. These reductions are accompanied by decreased expression of cancer stem cell markers CD44, CXCR4, and ALDH1A1, as shown by immunohistochemistry, suggesting impaired self-renewal and tumor-initiating capacity. Treatment with these agents also increased CDKN1A expression, reduced Ki-67 staining, and significantly elevated cleaved caspase-3 levels. Notably, our data also reveal that genistein attenuates the interaction between RELA and TEAD, a process mediated by YAP1. These findings provide mechanistic insights into how TED-347 and genistein suppress prostate cancer cell growth and induce cell death, directly linking these agents to reduced tumor progression, metastasis, and therapeutic relapse. The molecular reprogramming induced by TED-347 and genistein leads to increased apoptosis and reduced tumor viability, supporting their potential as therapeutic strategies for treatment-resistant prostate cancer and justifying further investigation in preclinical and clinical settings.

#7118 TNKS inhibition rewires AMOT-YAP signaling to overcome YAP-driven therapy resistance in solid tumors.

Jae Sung Kim, Young-Ju Kwon, Dong Young Kim, Yuna Kim

Korea Institute of Radiological & Medical Sciences (KIRAMS), Seoul, Korea, Republic of

Therapy-resistant tumors frequently rely on hyperactivated YAP signaling, particularly in KRAS-mutant contexts, where YAP serves as a major bypass survival pathway. Because direct pharmacologic inhibition of YAP remains challenging, strategies that modulate its upstream regulatory networks are required. Here, we demonstrate that tankyrase (TNKS) inhibition attenuates YAP oncogenic output by stabilizing angiomotin (AMOT), a core scaffold protein that promotes YAP cytoplasmic sequestration. In YAP-high colorectal cancer (CRC) models, TNKS inhibition increased AMOT abundance, strengthened AMOT-YAP complex formation, and restricted YAP nuclear localization, leading to a global reduction in YAP-dependent transcriptional activity. This reprogramming of YAP signaling sensitized KRAS-mutant CRC cells to MEK inhibition, indicating that the TNKS-AMOT axis directly intersects adaptive resistance mechanisms. In CRC models with established MEK inhibitor resistance driven by YAP reactivation, TNKS inhibition restored therapeutic sensitivity in vitro and in vivo. Similar combinatorial enhancement was observed across additional YAP-activated solid tumors, including pancreatic, lung, and breast cancers, while YAP-inactive tumors showed minimal response, highlighting pathway specificity. Together, these findings support TNKS inhibition as a mechanistically grounded approach to constrain YAP-driven oncogenic signaling through AMOT stabilization, offering a promising therapeutic strategy to overcome YAP-mediated resistance and improve targeted or radiation-based treatment responses in YAP-dependent cancers.

#7119 Large-scale drug screening identifies clinically actionable combinations to overcome BTK/PI3K inhibitor resistance in marginal zone lymphoma.

Alberto J. Arribas[1], Elena Mariotto[2], Eleonora Cannas[1], Giampietro Viola[2], **Francesco Bertoni**[1]

[1]Institute of Oncology Research, Universita della Svizzera italiana, Bellinzona, Switzerland,[2]Dipartimento di Salute della Donna e del Bambino - SDB, Universita degli Studi di Padova, Padova, Italy

Background. BTK inhibitors (i), and, more recently, BTK degraders have become clinically relevant drugs for patients with B-cell malignancies, including marginal zone lymphoma (MZL). PI3Ki are also active drugs, although the first- and second-generation molecules are now less used due to toxicity. Here, we present data from a large pharmacological screen involving over 3,500 compounds in 2 MZL models with secondary resistance to BTK/PI3Ki, developed through prolonged exposure to idelalisib (Arribas 2022) or ibrutinib (Arribas 2025).

Methods. Parental VL51 and resistant derivatives were exposed to DMSO or a library of 3,527 compounds (Mariotto 2023) as single agents (5μM) or in combination with either PI3Ki idelalisib (1μM) or BTKi ibrutinib (500nM) for 72 hours. Spatial and intra- and inter-plate effects were corrected. Robust Z-values were then DMSO-normalized. Highly active compounds across parental and resistant lines, as well as those with improved responses in either idelalisib-resistant or ibrutinib-resistant lines, were selected for further validation by combination with idelalisib or ibrutinib (MTT assay, 72 hours). Synergy of combinations was evaluated according to the Chou-Talalay combination index (CI) and to the MuSyC, HSA and ZIP algorithms.

Results. We identified 127 highly active compounds as single agents in both parental and the 2 resistant ($Z<0.5$), 10 compounds with higher activity in both resistant lines ($Z<0.3$), and 27 and 54 with increased response in BTKi and PI3Ki resistant ($Z<0.3$), compared to the parental counterpart, respectively. The identified molecules targeted apoptosis, cell cycle, PI3K/AKT/mTOR, chromatin/epigenetics, GPCR, DNA damage and repair, and immune signaling. Among these compounds, we selected those more advanced in the clinical setting for further testing in combination with BTKi and PI3Ki. The AChE/cytochrome-P450-i acetylshikonin was synergistic when combined with idelalisib or ibrutinib in six cell lines. The addition of the PAK4/NAMPTi KPT-0247 or the antibiotic diclazuril restored sensitivity to BTKi and improved the potency of BTKi in resistant cells, but not in the parental cells. Adding the alisertib (AURKAi), rigosertib (PLKi), fimepinostat (PI3K/HDACi), lanatoside-C (Na+K+ATPase), astragalin (apoptosis), astragaloside-I (WNT) and oridonin (AKT) was of benefit (additivity or synergism) in both parental and resistant cells.

Conclusions. This large-scale screen identifies multiple actionable vulnerabilities in BTKi- and PI3Ki-resistant MZL. Several clinically advanced agents—particularly PAK4/NAMPT, AURKA, WNT, and Na^+/K^+-ATPase inhibitors—enhanced or restored the activity of BTKi/PI3Ki. These findings highlight new therapeutic strategies for relapsed/refractory MZL and support clinical evaluation of targeted combinations to overcome acquired resistance.

#7120 Rinzimetostat, an allosteric EED inhibitor with best-in-class properties for the treatment of prostate cancer, is effective in PRC2 methyltransferase-resistant settings in preclinical studies.

Xi Chen, Livia Ulicna, Eunice Lopez-Fuentes, Anjana Ramnath, Ashley Pereira, Archana Kumar, Robert Warne, Kyle A. Edgar, Aleksandr Pankov, Jason E. Long, Ajit Narang, Lori S. Friedman, Anneleen Daemen, **Melissa R. Junttila**

ORIC Pharmaceuticals, Inc., South San Francisco, CA

Polycomb repressive complex 2 (PRC2) regulates transcription by trimethylating histone H3 at lysine 27 (H3K27me3) to impact cell growth and differentiation. PRC2 dysregulation is a poor prognostic in prostate cancer and promotes lineage plasticity and therapeutic resistance. The key PRC2 subunits, EED, SUZ12, and EZH1 or EZH2, are required for chromatin recruitment and histone methyltransferase activity. In vivo prostate cancer studies have shown PRC2 inhibitor combinations with AR inhibitors prolong survival and inhibit tumor growth. Rinzimetostat (ORIC-944) is a next-generation allosteric PRC2 inhibitor targeting EED, with best-in-class drug properties in preclinical studies including solubility, ADME/PK, and excellent half-life. In assessing rinzimetostat as a potential best-in-class PRC2 inhibitor, further preclinical studies investigated targeting EED vs EZH2 or EZH1/2 in the context of potential acquired resistance mechanisms.

EZH1 paralog compensation has the potential to be a tumor escape mechanism for EZH2 inhibitors, therefore inhibitors of EED, EZH2, and EZH1/2 were assessed in biochemical assays on PRC2 complexes that contained either EZH1 or EZH2 as the enzymatic subunit. Rinzimetostat had comparable potency on PRC2 with either EZH1 or EZH2 in the complex, while other PRC2 inhibitors had reduced activity on EZH1-containing complexes. In prostate cancer cells engineered to overexpress EZH1, the EZH2 inhibitors tazemetostat and mevrometostat lost potency whereas rinzimetostat, an EED inhibitor, retained activity.

We next investigated the activity of PRC2 inhibitors in the context of an EZH2 inhibitor acquired resistance mutation observed in the clinic. As predicted from drug binding sites, EZH2 Y666N mutant-expressing prostate cancer cells were impervious to H3K27me3 reduction by EZH2 inhibitors mevrometostat or tazemetostat; however, rinzimetostat inhibited H3K27me3 in EZH2 Y666N mutant cells.

Cells engineered with an EZH1/2 inhibitor acquired resistance mutant, EED H213R, demonstrated loss of effectiveness upon treatment with EZH1/2 inhibitor valemetostat, whereas rinzimetostat equally inhibited H3K27me3 in the EED mutant and wildtype settings. Together, these data suggest that rinzimetostat, as an EED inhibitor, has the potential for superiority in EZH2 and EZH1/2 inhibitor-acquired resistance contexts.

In summary, preclinical results demonstrate potential best-in-class drug properties of rinzimetostat, as well as the potential superiority of targeting EED to address paralog compensation and avoid acquired resistance mechanisms that may be liabilities for EZH2 or EZH1/2 inhibitors. Rinzimetostat is under clinical evaluation in combination with AR inhibitors in a global Phase 1b study (NCT05413421).

#7121 CRISPR druggable-genome screen identifies BRD4 as a synergistic vulnerability with the natural product cerberin in pancreatic cancer organoids.

Md Shahadat Hossan[1], Lauryn E. Flannagan[1], Michela Cadarso[1], Molly A. Nellen[2], Ethan S. Lin[1], Austin Stram[3], Dustin Rubinstein[4], Derek Pavelec[4], Mark E. Berres[5], Sean Ronnekleiv-Kelly[3], Jeremy D. Kratz[1]

[1]Department of Medicine, University of Wisconsin-Madison, Madison, WI,[2]OVCR, UWBC Advanced Genome Editing, University of Wisconsin-Madison, Madison, WI,[3]SMPH, Department of Surgery, University of Wisconsin-Madison, Madison, WI,[4]OVCR, UWBC Administration, University of Wisconsin-Madison, Madison, WI,[5]OVCR, UWBC Bioinformatics, University of Wisconsin-Madison, Madison, WI

Background: Pancreatic ductal adenocarcinoma (PDAC) acquires resistance to systemic therapy, requiring novel therapeutic combinations. Our prior work demonstrated that cardiac glycosides including cerberin can inhibit PI3K/AKT/mTOR signaling yielding low nanomolar potency in PDAC viability. We recently optimized pooled CRISPR-Cas9 “druggable-genome” screening in 3D PDAC patient-derived organoids (PDOs). Here, we used this platform to define genetic dependencies under cerberin pressure and to nominate synthetic lethal combinations.

Methods: The $KRAS^{G12D}$-mutant PDO line Pan21 was transduced with a lentiviral CRISPR-Cas9 library targeting 2,312 druggable genes (~10,000 sgRNAs; Millipore-Sigma) using optimized viral particle: cell ratios and 6-day puromycin selection. Baseline samples were collected following. PDOs were expanded using media control and cerberin 10nM for 6 days, followed by 2 days of recovery. Guide representation was assessed by next-generation sequencing, and gene-level dropout was analyzed with MAGeCK robust rank aggregation (RRA). For functional validation, dose-response combination matrices were generated for cerberin or digoxin in combination with the BET inhibitor ZEN-3694 in Pan21 PDOs. Viability was measured at 144h using 3D CellTiter-Glo (CTG, 50% v/v), and synergy was quantified in SynergyFinder 3.0.

Results: Library QC confirmed stable Cas9 expression, recovery of more than 95% of sgRNAs, and similar $\log_2$ read-count profiles across baseline, control, and cerberin-treated samples. Cerberin treatment generated a consistent dropout pattern enriched for signaling and metabolic regulators; among the highest-ranked negative-selection hits were CYGB, ANXA2, NR1I2, PIK3R1, TWF2, ENPP2, FDX1, PRG2, and the epigenetic reader BRD4. Although this pilot was limited to stringent FDR thresholds, these genes showed low RRA scores at nominal p-values < 0.005. BRD4 was selected among the top 10 depleted genes (RRA score ~6×10^{-4}; nominal $p \approx 0.003$) due to availability for synthetic inhibitors from NCI’s Cancer Therapeutics Evaluation Program. In Pan21 PDOs, dose-response combinations of cerberin with ZEN-3694 produced robust synergy (HSA 26.2, Bliss 23.3, ZIP 23.6), with values in a range generally interpreted as strong positive drug-drug interaction and clear synergy “hot spots” at submaximal concentrations of both agents. Similarly, digoxin with ZEN-3694 exhibited a synergistic landscape (HSA 25.3, Bliss 24.7), supporting a cardenolide class effect.

Conclusions: Adopting a CRISPR/Cas9 druggable screen in 3D PDAC PDO models, we provide proof-of-concept for synergy between cardiac glycosides and BRD4/BET inhibitors. This work links a PDO-based CRISPR platform with natural-product pharmacology to provide a framework for mechanistic partners to advance the use of cardiac glycosides for clinical translation.

#7122 Nanoparticle-mediated restoration of pomalidomide sensitivity in multiple myeloma.

Joseph Uche Ogbede[1], Kaiqi Long[2], Michael S. Rogers[1], Jinjun Shi[2], Robert J. D'Amato[1], Bruce R. Zetter[1]

[1]Vascular Biology, Boston Children's Hospital, Harvard Medical School, Boston, MA,[2]Nanomedicine and Anesthesiology, Brigham and Women's Hospital, Harvard Medical School, Boston, MA

Multiple myeloma (MM), a plasma cell malignancy, is the second most common hematologic malignancy in the United States after non-Hodgkin lymphoma. Treatment options include immunomodulatory imide drugs (IMiDs). FDA approved IMiDs (thalidomide, lenalidomide, and pomalidomide) have remained among the primary treatments for MM and have helped extend the lifespan of patients up to several years after diagnosis. IMiDs bind to cereblon (CRBN), a component of E3 ubiquitin ligase, to exert their anti-proliferative effect on myeloma cells. While the majority of newly diagnosed myeloma patients respond to treatment with IMiDs, most eventually develop resistance. Cereblon genetic alterations contribute about one-third of acquired resistance observed in the clinic. We aim to restore sensitivity to pomalidomide-resistant cells through nanoparticle-mediated delivery of wildtype cereblon mRNA to cells. We designed lipid nanoparticles and used it to deliver in vitro transcribed cereblon mRNA to pomalidomide-resistant MM1.S cells. We showed that the lipid nanoparticle efficiently delivered cereblon mRNA to the resistant cells with subsequent restoration of pomalidomide sensitivity. Next, delivery of cereblon mRNA-loaded nanoparticles precisely to malignant plasma cells is important to ensure the desired outcome. Among cell surface proteins, B-cell maturation antigen (BCMA) and CD38 are known to be highly expressed by multiple myeloma cells. We therefore screened for peptides that bind to BCMA and CD38 using phage display libraries. Following DNA sequencing, three clones containing cyclic peptides with affinity for these proteins were identified. These peptides have been synthesized and are being tested; they will be conjugated with the nanoparticle-coated cereblon mRNA for targeted delivery to the malignant plasma cells. Our results show that delivery of cereblon mRNA to pomalidomide-resistant cells using lipid nanoparticles led to substantial restoration of pomalidomide sensitivity.

#7123 QW-5-70 targets the colchicine site to overcome multidrug resistance and shows potent antitumor activities.

Yang Xie[1], Ruida Hou[1], Najah Albadari[1], Hao Chen[1], Darcie J. Miller[2], Judith Quadrozzi Gruntz[2], Michael L. Oldham[2], Mir Shahriar Kamal[1], Jianxiong Jiang[1], Zhongzhi Wu[1], Duane D. Miller[1], Wei Li[1]

[1]University of Tennessee Health Science Center, Memphis, TN,[2]St. Jude Children's Research Hospital, Memphis, TN

Drug resistance driven by efflux transporters and altered tubulin dynamics limits the clinical efficacy of taxanes and vincristine in high-risk neuroblastoma (NB) and castration-resistant prostate cancer (CRPC). We developed QW-5-70, a colchicine-binding-site inhibitor (CBSI), engineered to retain subnanomolar potency in both parental and drug-resistant cancer cells by evading P-glycoprotein (P-gp)-mediated efflux. QW-5-70 binds to the colchicine site, inhibits tubulin polymerization, disrupts microtubule networks, and induces mitotic arrest. Across a panel of NB and prostate cancer lines, QW-5-70 maintained subnanomolar activity and remained effective in vincristine-resistant BE2C/VCR and paclitaxel-resistant PC-3/TxR cells. Unlike vincristine and paclitaxel, its activity was unchanged by co-treatment with verapamil, suggesting its ability to circumvent P-gp-mediated drug resistance. In vitro, QW-5-70 significantly reduced colony formation and impaired migration in both parental and resistant cancer cells, and induced G2/M cell cycle arrest and mitochondrial apoptosis. In vivo, QW-5-70 significantly suppressed tumor growth in drug-resistant PC-3/TxR and BE2C/VCR xenografts, with modest weight loss and no evident histopathology in the major organs. Combination testing revealed strong quantitative synergy with DFMO in viability assays and marked increases in apoptosis with reduced clonogenic survival when paired with DFMO or the Aurora A inhibitor MLN8237. Collectively, QW-5-70 is a potent CBSI that circumvents P-gp-associated resistance, triggers mitotic arrest and apoptosis, and achieves robust antitumor activity in multidrug-resistant tumor models with acceptable tolerability, supporting its further preclinical development alone and in combination with other drugs.

#7124 Resistance to the SFK inhibitor NXP900 in cholangiocarcinoma is characterized by IL13RA2-AKT signaling and can be overcome by combination therapy.

Shelby K. Yee[1], Hendrien Kuipers[1], Danielle M. Carlson[2], Jack W. Sample[1], Enis Ozmert[1], Hidemi Nishi[1], Erik Jessen[3], Dong-Gi Mun[4], Aushinie M. Abeynayake[2], Jennifer L. Tomlinson[1], Amro M. Abdelrahman[1], Nathan W. Werneburg[2], Binbin Li[2], Mitesh J. Borad[5], Mark J. Truty[1], Sumera I. Ilyas[2], Gregory J. Gores[2], Rory L. Smoot[1]

[1]Department of Surgery, Mayo Clinic, Rochester, MN,[2]Department of Gastroenterology and Hepatology, Mayo Clinic, Rochester, MN,[3]Department of Biomedical Statistics and Informatics, Mayo Clinic, Rochester, MN,[4]Department of Laboratory Medicine and Pathology, Mayo Clinic, Rochester, MN,[5]Department of Hematology-Oncology, Mayo Clinic Cancer Center, Phoenix, AZ

Introduction: Src Family Kinases (SFKs) have a crucial role in tumor proliferation, survival, and metastasis. NXP900 is a highly selective SFK inhibitor with a novel mechanism of action that locks SFKs in a closed, inhibited conformation, providing sustained suppression of catalytic and non-catalytic functions, which is distinct from other SFK inhibitors like dasatinib. A phase I clinical trial of NXP900 in patients with advanced solid tumors is ongoing. Our preclinical studies showed therapeutic efficacy of NXP900 in cholangiocarcinoma (CCA) through decreased YAP, RAF-MAP and PI3K-AKT signaling. Multiomic profiling (RNA-seq, proteomics, phosphoproteomics) of CCA patient-derived xenografts implicated AKT pathway activation in primary NXP900 resistance. NXP900-resistant CCA cell lines generated via prolonged sublethal dose escalation showed a strong IL13RA2-AKT signature on multiomic analysis. Thus, we hypothesized that IL13RA2-AKT signaling was a mechanism of NXP900 resistance. We aimed to define this mechanism and demonstrate that the combinatorial targeting of IL13RA2 or AKT resensitizes to NXP900 treatment.

Methods: HuCCT1 or HuCCT1-Resisant (HuCCT1-R) cells were injected bilaterally into the flanks of NOD/SCID mice and were allowed to grow for 3 months prior to tumor collection and analysis. Tumor engraftment and growth between HuCCT1 and HuCCT1-R groups were compared. To delineate the mechanisms for acquired NXP900 resistance, in-vitro treatment studies were performed using siRNAs targeting IL13RA2 as well as combination treatment with capivasertib, a pan-AKT inhibitor.

Results: The HuCCT1-R cell line exhibited a higher rate of tumor engraftment and formed significantly larger tumors compared to the parental HuCCT1 cell line, indicating enhanced tumorigenic potential associated with acquired resistance. Silencing of *IL13RA2* in HuCCT1-R cells resulted in pronounced reduction of cell proliferation and partially restored sensitivity to NXP900 treatment. Immunoblot analysis demonstrated a corresponding reduction in phosphorylated AKT (Thr308), consistent with suppression of downstream PI3K-AKT signaling. Furthermore, combination treatment of HuCCT1-R cells with the AKT inhibitor capivasertib, and NXP900 led to a significant increase in cell death and a greater inhibition in cell proliferation compared to either agent alone, indicating enhanced responsiveness and improved therapeutic efficacy.

Conclusion: These findings confirm the central role of IL13RA2 signaling and the PI3K-AKT pathway in mediating acquired resistance to NXP900, consistent with our previous multiomics analysis. Importantly, this study identifies combination strategies that may be able to overcome NXP900 resistance, supporting the development of combinatorial approaches to restore therapeutic efficacy in resistant tumors.

#7125 Mechanistic basis of resistance to HDAC6 inhibitors reveals proteasome inhibition as a rational combination strategy in breast cancer.

Jose Silva[1], Tizita Zewde Zeleke[2], Qingfei Pan[3], Jiyang Yu[3]

[1]Icahn School of Medicine at Mount Sinai, New York, NY,[2]Pathology, Icahn School of Medicine at Mount Sinai, New York, NY,[3]St. Jude Children's Research Hospital, Memphis, TN

Introduction: Cancer treatment is increasingly driven by personalized medicine approaches, where targeted therapies are favored over traditional chemotherapy due to improved specificity and reduced toxicity. Although pan-histone deacetylase inhibitors show antitumor activity in several cancers, their clinical use is limited by toxicity. In contrast, HDAC6-specific inhibitors such as ricolinostat are well-tolerated and demonstrate clinical activity in subsets of breast cancer (BC) patients. However, intrinsic resistance restricts their broader therapeutic utility. Here, we present new evidence identifying proteasomal function as a critical determinant of resistance to HDAC6 inhibitors and show that combinatorial targeting of HDAC6 and the proteasome can overcome this resistance.
Methods: We performed multi-omics analyses comparing the response to HDAC6 inhibitors of sensitive and resistant BC models. These studies led us to hypothesize that enhanced proteasomal capacity drives therapeutic resistance. To test this, we quantified steady-state proteasomal activity using fluorometric assays that measure chymotrypsin-like, trypsin-like, and caspase-like proteolytic functions in vitro. We also conducted therapeutic studies treating sensitive and resistant BC cells with HDAC6 inhibitors alone or in combination with proteasome inhibitors.
Results: Omics profiling revealed that HDAC6 inhibition in sensitive cells induces the unfolded protein response (UPR), downregulates MYC, and upregulates ER-stress markers (BiP, CHOP) in both BC cell lines and MMTV-Neu tumors, indicating activation of a stress-adaptive transcriptional program. Given HDAC6's role in the aggresome-autophagy pathway and the proteasome's role in protein degradation, we assessed whether resistant cells compensate through elevated proteasomal activity. Our data revealed that resistant BC cells exhibited significantly higher basal activity across all three proteolytic subunits. Consistent with this, ricolinostat combined with the proteasome inhibitor bortezomib induced growth inhibition in resistant cells, reversing the resistance to HDAC6i/s. Conversely, chemically enhancing proteasomal function with oleuropein reduced sensitivity to ricolinostat in previously sensitive lines, supporting a mechanistic dependence on limited proteasomal activity for the responses to HDAC6 inhibition.
Conclusions: These findings identify elevated proteasomal capacity as a key driver of resistance to HDAC6 inhibitors, supporting a therapeutic strategy that combines HDAC6 and proteasome inhibition to overcome resistance in breast cancer.

#7126 Targeting Aurora A kinase together with alternative survival signaling overcomes resistance to endocrine and CDK4/6 therapies in ER+ breast cancer.

Chia-Chia Liu[1], Alekya Raghavan[1], Lanfang Qin[1], Sarmistha Nanda[1], Fu-Tien Liao[1], Georg F. Bischof[2], Mothaffar F. Rimawi[1], C. Kent Osborne[1], Jamunarani Veeraraghavan[1], Rachel Schiff[1]

[1]Lester & Sue Smith Breast Center; Dan L Duncan Comprehensive Cancer Center; Department of Medicine, Baylor College of Medicine, Houston, TX,[2]Puma Biotechnology Inc., Los Angeles, CA

Background: Endocrine therapy (ET) in combination with CDK4/6 inhibitors (i) is the standard-of-care for estrogen receptor (ER)+ metastatic breast cancer (BC). Though effective, resistance is inevitable. Aurora A kinase (AURKA) drives mitotic entry and spindle assembly for proper cell division. Clinically, high AURKA levels have been linked to cancer aggressiveness, poor prognosis, and CDK4/6i resistance. A recent phase II trial (NCT02860000) reported clinically meaningful benefit of the AURKAi, alisertib (ALS), in advanced, endocrine-resistant ER+ BC. Identifying biomarkers and key signaling pathways involved in AURKA inhibition is essential to optimize ALS use and guide effective combination strategies to enhance sensitivity and overcome resistance in ER+ BC.
Methods: ER+ BC cell models naïve or resistant (R) to various ET (EndoR) and/or palbociclib (PalboR, a CDK4/6i) were used. ALS-resistant (ALSR) derivatives were developed via long-term exposure to gradually increasing ALS concentrations (≥150 nM). Molecular changes associated with growth and survival signaling, senescence, and apoptosis were assessed by Western blot upon short-term ALS treatment (72 hr) and at resistance. Signaling profiles guided the choice of specific drug combinations, which were then evaluated by cell growth assays.
Results: Morphological changes, characterized by flattened, enlarged giant cells, slowed growth, senescence, and elevated p21, γH2AX, and c-PARP levels were observed in the ALSR derivatives of EndoR and/or PalboR models. In general, induction of various components of the HER/PI3K/MAPK pathways was seen across all ALSR models, with a specific increase in phosphorylated AKT levels in some models. Indeed, AKTi plus ALS was the most effective combination to overcome resistance in the ET-naïve/PalboR and the estrogen-deprivation (ED)R/PalboR/ALSR models. In the tamoxifenR/PalboR model and its ALSR derivative, in line with the signaling changes, EGFRi, pan-HERi (Neratinib, Nrb), or MEKi together with tamoxifen+Palbo+ALS showed strong efficacy. In the dual fulvestrantR/PalboR model, ALS+Nrb was highly effective, and adding Palbo further enhanced this effect, while in its ALSR derivative, fulvestrant+Palbo+ALS+Nrb regimen was needed to achieve substantial growth inhibition.
Conclusions: Our findings highlight the potential of combining ALS with AKT, MAPK, and HER pathway inhibitors, to enhance efficacy or overcome ALS resistance in ET- and CDK4/6i-resistant ER+ BC, inferred by ALS-induced signaling changes. The presence of flattened and enlarged giant cells may reflect ongoing endoreplication, potentially indicating a dormant or persister cell state that may eventually support relapse and disease progression. Additional studies are underway to determine how these cell states can be targeted to induce cell death and overcome resistance.

#7127 RalBP1 inhibition: A novel therapy for prostate cancer.

Sharad S. Singhal, Madhu Krishna, Prakash Kulkarni, David Horne, Ravi Salgia

Beckman Research Institute of The City of Hope, Duarte, CA

Prostate cancer is a predominant cause of cancer related death in men and in most cases, it is difficult to diagnose and adequately monitor. Cancer cells entail targets for effective therapy; however, non-malignant cells do not because they are not expressed in the same way in a cancer cell as in normal cells. RalBP1 functions as a crucial mercapturic acid transporter, playing an essential role in cancer cell survival and therapy resistance. RalBP1 has been identified as the key to radiation and chemotherapy resistance as it is an overexpressed, multi-specific ATP-dependent transporter. Therefore, we investigated its involvement in modulating critical signaling proteins that influence upstream survival pathways and mechanisms responsible for chemo-radiotherapy resistance in prostate cancer. Evidence from *in vitro* cell cultures and *in vivo* tumor models suggests that cancer cell survival depends on RalBP1, as its inhibition or depletion results in selective toxicity toward malignant cells. By generating glutathione-electrophile conjugates (GS-Es) within cells, RalBP1 induces apoptosis in cancer cells. *In vivo* studies revealed that treatment of DU145 prostate cancer xenograft-bearing mice with RalBP1-directed agents; antibodies, siRNA, or antisense oligonucleotides that led to a marked suppression of tumor growth, even in already established subcutaneous tumors, and did so without signs of systemic toxicity. Interestingly, both RalBP1 antibodies, which block RalBP1-mediated transport function, and gene-silencing approaches such as siRNA and antisense, which diminish RalBP1 expression, demonstrate nearly equivalent tumor-regressive effects. This equivalence suggests that disrupting RalBP1 transport function at the cell membrane is sufficient to elicit an anticancer response. Collectively, these findings uncover a novel therapeutic potential for RalBP1 inhibition or depletion in prostate cancer and underscore its promise as a target for new treatment strategies. (This work was supported in part by the Department of Defense grant HT9425-25-1-0500. Funding from the Beckman Research Institute of City of Hope is also acknowledged).

#7128 The rise of YAP: A new hope in glioblastoma treatment.

Shuhan Cao, Ethan C. L. Wong, Gilberto K. K. Leung, Karrie M. Y. Kiang

Department of Surgery, Li Ka Shing Faculty of Medicine, Hong Kong, Hong Kong

Despite advances in cancer treatment, glioblastoma (GBM) remains the most malignant subtype of adult brain tumours, with an overall prognosis of only approximately 18 months. The first-line treatment and current standard of care for GBM, aside from maximum surgical resection, is temozolomide (TMZ). Yet, despite TMZ's initial promising results in improving survival, drug resistance and tumour relapse remain nearly unavoidable. Yes-associated protein (YAP) is a key downstream effector of the Hippo pathway that can translocate to the nucleus to induce the transcriptional enhanced associated domain (TEAD)-mediated expression of genes related to cell growth and proliferation. This makes the Hippo signalling pathway critical in tumorigenesis. Through both in vitro and in vivo models, we investigated the role of YAP in GBM. We found upregulation of YAP in GBM to be associated with poor clinical outcomes, with TMZ-resistant GBM showing greater YAP upregulation compared to chemotherapy-sensitive strains, suggesting its role in driving chemoresistance. When YAP is knocked down, there is a decrease in GBM malignant phenotype, including decreased cell proliferation and colony formation in vitro, and decreased tumour growth in vivo. Finally, we elucidated that YAP mediates GBM chemoresistance by inducing tumour cell stemness, which can be overcome by using the YAP inhibitor verteporfin, increasing GBM susceptibility to TMZ in both sensitive and resistant cell lines. In conclusion, this highlights the importance of YAP in driving GBM cell stemness and chemoresistance, a significant clinical problem, and underscores the potential YAP inhibitors hold as a promising and novel adjuvant or combination therapy in the treatment of chemoresistant GBM.

#7129 Targeting PARPi drug tolerant persistence and progression on treatment with clinical stage ATM inhibitors in advanced prostate cancer.

Akshaya Karthikeyan[1], Bryan Correa Gonzalez[1], Jose G. Torres-Gonzalez[2], Love A. Moore[3], Anamitra Bhaumik[4], Ethan Sandoval[4], Alan P. Lombard[5]

[1]UC Davis Medical Center, Sacramento, CA,[2]UC Davis Medical School, Sacramento, CA,[3]UC Davis, Davis, CA,[4]UC Davis, Sacramento, CA,[5]Urologic Surgery, UC Davis Medical Center, Sacramento, CA

Background: PARP inhibitors (PARPi) have improved prostate cancer management, but progression is inevitable. Drug tolerant persistence (DTP) is characterized by tumor cells which survive treatment and drive failure through transient acquisition of insensitivity. Cycling DTP cells may adapt and expand, giving rise to drug tolerant expanded persister (DTEP) populations which are thought to model progression on treatment. Emerging evidence supports a critical role for DTP in promoting PARPi progression. Identifying and targeting DTP and DTEP vulnerabilities may provide therapeutic strategies to combat disease progression.
Methods: Viability assays, western blots, and additional assays defined treatment response in PARPi-sensitive C4-2B metastatic castration-resistant prostate cancer cells and C4-2B abiraterone-resistant derivative AbiR cells. DTP and DTEP models were developed through prolonged PARPi exposure. NGS profiled DTP cells. Clinical stage ATM inhibitors were tested for their effects on both DTP and DTEP populations.
Results: Response to PARP inhibition is heterogeneous, characterized by cell death and emergence of a largely cytostatic, persistent population. C4-2B and AbiR cells exposed to clinically relevant PARPi dosing for 9 days followed by drug holiday regain normal, parental cell morphology and become re-sensitized to treatment in line with acquisition of a DTP phenotype. DTP cells display differential sensitivity to other classes of drugs compared to parental cells. DTP cells may be broadly stratified into two classes; 1) a minority which cycle and 2) those which don't. Prolonged PARPi treatment is observed to result in drug tolerant expanded persisters (DTEP) derived from cycling-DTP cells. DTP and DTEP cells display increased phospho-ATM levels suggesting constitutive DNA damage response activation. Utilization of clinical stage ATM inhibitors both prevent DTP progression into DTEPs and resensitize DTEPs to PARP inhibition.
Conclusions: Our data suggest that drug tolerant persistence may mediate survival of tumor cells which drive progression on treatment. ATM inhibition may be used to prolong time to progression or to treat progressive disease. Future studies will focus on translating these strategies.

#7130 GRN-300 restores PARP inhibitor sensitivity through inhibition of the HDAC-MEF2A-RAD51 pathway in BRCA2-revertant ovarian cancer.

Carlos Flores Suarez, Janice M. Santiago-O'Farrill, Weiqun Mao, Hailing Yang, Zhen Lu, Robert C. Bast

UT MD Anderson Cancer Center, Houston, TX

Genomic instability is a hallmark of cancer. Germline mutations in DNA repair genes such as BRCA1 and BRCA2 predispose to tumor development but also confer vulnerabilities exploitable by therapy. Poly ADP-ribose polymerase (PARP) inhibitors selectively target tumors with homologous recombination deficiency (HRD) caused by BRCA1/2 mutations and elicit strong responses in ovarian cancer. However, resistance frequently emerges through secondary BRCA1/2 reversion mutations that partially restore DNA repair function, underscoring the need for strategies to overcome PARP inhibitor resistance. Salt-inducible kinase 2 (SIK2), an AMPK-related kinase, is required for ovarian cancer cell proliferation and metastasis. The selective SIK2 inhibitor GRN-300 induces DNA double-strand breaks (DSBs) in HR-proficient cells and synergizes with PARP inhibitors to produce synthetic lethality. Here, we investigated whether GRN-300 can restore PARP inhibitor sensitivity in BRCA2-revertant ovarian cancer. GRN-300 markedly reduced the IC_{50} of olaparib in both PARP-sensitive PEO1 cells (1.98 to 0.64 μM) and resistant BRCA2-revertant PEO1-C4-2 (6.87 to 0.92 μM) and PEO4 (3.47 to 1.17 μM) ovarian cancer cells, restoring responsiveness. GRN-300 increased ROS production, enhanced caspase-3/7 activation, and promoted olaparib-induced apoptosis while suppressing colony formation. In PEO1-C4-2 xenografts, GRN-300 plus olaparib significantly inhibited tumor growth without affecting body weight. Combination treatment increased γ-H2AX and comet-tail formation, indicating enhanced DNA damage accumulation. Mechanistically, GRN-300 reduced RAD51 expression and RAD51 foci formation. SIK2 inhibition decreased phosphorylation of class IIa HDAC4/5/7, abrogating HDAC class II-MEF2A transcriptional activity. ChIP-qPCR revealed reduced MEF2A binding to regulatory regions of DNA repair genes, including RAD51 and RAD50, thereby suppressing DSB end resection and strand invasion mediated by the MRN complex. In summary, GRN-300 restores PARP inhibitor sensitivity in BRCA2-revertant ovarian cancer through inhibition of the HDAC-MEF2-RAD51 pathway, providing a promising therapeutic strategy to overcome PARP resistance.

#7131 Targeting oxidative phosphorylation with lixumistat overcomes PARP inhibitor resistance in ovarian cancer.

Sa deok Hong[1], Min Sil Kang[1], Nar Katuwal[1], Mithun Ghosh[1], Seong Min Park[1], Kim Ju Hyeon[1], Seul-Gi Kim[2], Yong Wha Moon[2]

[1]CHA University, Seongnam-si, Korea, Republic of,[2]CHA Bundang Medical Center, Seongnam-si, Korea, Republic of

Ovarian cancer remains the leading cause of gynecologic cancer-related mortality worldwide. Although poly(ADP-ribose) polymerase (PARP) inhibitors show remarkable efficacy in BRCA1/2-mutated ovarian cancer, nearly half of patients eventually develop resistance. In this study, we investigated whether lixumistat, a novel oxidative phosphorylation (OXPHOS) inhibitor, could overcome PARP inhibitor resistance in preclinical BRCA1/2-mutated ovarian cancer models. Long-term olaparib exposure generated olaparib-resistant BRCA-mutated ovarian cancer cell lines and patient-derived tumor xenograft (PDTX) models. Lixumistat, alone or combined with olaparib, was evaluated in vitro and in vivo. Olaparib-resistant cells exhibited elevated OXPHOS activity, and combining lixumistat with olaparib produced synergistic antitumor effects in both olaparib-sensitive and -resistant cell lines and PDTX models. Switching from olaparib monotherapy to combination therapy markedly suppressed tumor growth in partially resistant and acquired-resistant PDTX models. These results suggest that early integration of lixumistat could enhance efficacy and delay PARP inhibitor resistance. Mechanistically, lixumistat inhibited the OXPHOS-NAD^+-poly(ADP)-ribosylation (PARylation) axis, thereby reducing NAD^+ availability and PARylation to restore PARP inhibitor sensitivity. Notably, exogenous NAD^+ supplementation reversed these effects. Additionally, lixumistat downregulated the SNAIL-phosphorylated RB pathway, impairing cell-cycle progression and further enhancing PARP inhibitor efficacy. Together, these findings identify a novel OXPHOS-associated mechanism underlying PARP inhibitor resistance and establish lixumistat as a promising combinatorial strategy to potentiate PARP inhibitors in both PARP inhibitor-naïve and -resistant ovarian cancer.

#7132 Rinzimetostat blockade of PRC2 activity, a key mechanism of treatment resistance, improves response of androgen receptor pathway inhibition across a spectrum of prostate cancer models.

Aleksandr Pankov, Amber W. Wang, Natalie Yuen, Livia Ulicna, Jason E. Long, Xi Chen, Gina Andretta, Lori S. Friedman, Melissa R. Junttila, Anneleen Daemen

ORIC Pharmaceuticals, South San Francisco, CA

Prostate adenocarcinoma is driven by the lineage-specific transcription factor androgen receptor (AR), with androgen deprivation and AR pathway inhibitors (ARPIs) being highly effective treatments that are a mainstay in the clinic. However, therapeutic resistance that bypasses ARPIs eventually develops due to emergence of tumor heterogeneity highlighted by the acquisition of AR alterations and diverse phenotypic states, including cells with heightened plasticity and divergent lineage features.

The availability of genomic datasets across the prostate cancer treatment continuum enables unprecedented insight into the molecular alterations underpinning disease progression and treatment resistance. We explored the transcriptomes of >1,000 patients with primary prostate cancer, metastatic castration-resistant prostate cancer (mCRPC) and neuroendocrine prostate cancer (NEPC). Analysis of these data and projection along a pseudotime axis revealed gene expression patterns driving prostate cancer progression.

Pseudotime analysis showcased that AR signaling and luminal marker expression increase during primary tumor formation and remain elevated in the early stages of mCRPC. The eventual reduction in AR expression, AR signaling and luminal identity during mCRPC may facilitate lineage plasticity and cell state reprogramming. Integrated analysis of prostate tumors across treatment lines additionally identified cell cycle-associated genes and epigenetic regulators whose expression increase from primary to mCRPC and NEPC tumors, suggesting that they play a key role in driving molecular heterogeneity necessary to circumvent ARPI treatments. One such epigenetic regulator identified, the polycomb repressive complex 2 (PRC2), is a compelling and tractable target for prostate cancer.

Rinzimetostat (ORIC-944) is a next-generation, potent, highly selective, orally bioavailable small molecule inhibitor of PRC2 that allosterically targets the EED subunit, with potential best-in-class drug properties including reduced drug-drug interaction liabilities and superior half-life as compared to other clinical compounds. Rinzimetostat in combination with the ARPI darolutamide demonstrated antitumor activity across a breadth of in vivo models representing the prostate cancer continuum and capturing a broad spectrum of treatment resistance settings including castration-sensitive and -resistant, ARPI-sensitive and -resistant, and AR-mutant and -wildtype. Thus, rinzimetostat represents a promising therapy to re-sensitize resistant tumors to ARPIs and block prostate tumor adaptation. Rinzimetostat is under clinical evaluation in combination with AR inhibitors in a global Phase 1b study (NCT05413421).

#7133 Combined anti-CSF-1R and anti-TIM-3 overcome macrophage-mediated mechanisms of PARP inhibitor (PARPi) resistance in BRCA1-associated triple negative breast cancer.

Adam Nelson[1], Anita K. Mehta[1], Madeline G. Townsend[1], Daniel E. Michaud[1], Madisson Oliwa[1], Kelly F. Zheng[1], Carlos W. S. Wanderley[1], Alex P. Gottlieb[1], Kenichi Shimada[2], Patrice A. Lee[3], Nicholas A. Saccomano[3], Filipa Lynce[4], Nabihah Tayob[4], Geoffrey I. Shapiro[4], Jennifer L. Guerriero[5]

[1]Department of Surgery, Brigham and Women's Hospital, Boston, MA,[2]Harvard Medical School, Boston, MA,[3]Pfizer-Boulder Research and Development, Boulder, CO,[4]Dana-Farber Cancer Institute, Boston, MA,[5]Brigham and Women's Hospital, Boston, MA

Background: Poly (ADP-Ribose) polymerase inhibitors (PARPi) have improved outcomes for *BRCA*-associated triple negative breast cancer (TNBC); however, resistance develops, resulting in lack of durable responses. Our prior work demonstrated that PARPi activates cGAS/STING signaling, driving CD8+ T-cell recruitment, essential for tumor clearance. These studies led to clinical trials testing PARPi plus immune checkpoint blockade (ICB). However, clinical trials demonstrated no benefit compared to PARPi monotherapy, indicating T-cells in the tumor microenvironment (TME) are inhibited. We previously showed that PARPi induce suppressive tumor-associated macrophages (TAMs) which contribute to PARPi resistance. Removing TAMs with anti-CSF-1R therapy significantly enhanced overall survival (OS) when combined with PARPi and is now being tested in clinical trials (NCT03604692). Here, we test if ICB can enhance the CSF-1R +PARPi combination in both treatment naïve and PARPi-resistant tumors.

Methods: Mice bearing naïve or PARPi-resistant BRCA1-deficient TNBC (*K14-Cre;Brca1*$^{f/f}$*;Trp53*$^{f/f}$) tumors were treated with PARPi ± CSF-1R inhibition (CSF-1Ri) ± ICB and followed for tumor size and OS. Flow cytometry was employed to define immune mechanisms of response.

Results: In PARPi-naïve tumors, PARPi + CSF-1Ri significantly increased OS compared to PARPi monotherapy. The combination of PARPi + CSF-1Ri + anti-PD-1 led to a modest improvement in efficacy compared to PARPi + CSF-1Ri treatment. In contrast, the addition of anti-TIM3 to PARPi + CSF-1Ri resulted in durable therapeutic benefit, with a significant increase in OS compared to PARPi + CSF-1Ri. The combination of PARPi + CSF-1Ri + anti-TIM-3 significantly increased CD8+ T-cell infiltration, granzyme B production, and reduction in Tregs indicating an increased anti-tumor immune response. Additionally, anti-TIM-3 induced a pro-inflammatory phenotype in TAMs. In PARPi-resistant tumors TAMs expressed higher levels of CSF-1R compared to PARPi-naïve tumors. Additionally, PARPi-resistant tumors had increased infiltration of Tregs, and higher expression of PD-1 on T-cells, strongly indicating an increased immunosuppressive TME. In PARPi-resistant tumors, anti-CSF-1R therapy restored PARPi efficacy and significantly increased OS. Furthermore, addition of anti-TIM-3 to the anti-CSF-1R + PARPi combination significantly increased OS in PARPi-resistant tumors, whereas anti-PD-1 did not enhance therapy efficacy.

Conclusion: PARPi-resistant tumors have increased T-cell exhaustion and infiltration of immunosuppressive TAMs. Importantly, our data shows that targeting TAMs through the CSF-1R axes can overcome acquired PARPi resistance, which can be further enhanced with anti-TIM3 therapy, defining a novel strategy addressing a critical unmet medical need.

#7134 Developing drug combinations with AMG 193, a novel MTA-cooperative PRMT5 inhibitor, using patient-derived xenograft models of *MTAP*-deleted non-small cell lung cancer and mesothelioma.

Florence T. H. Wu[1], Nhu-An Pham[1], Yu-Hui Wang[1], Ming Li[1], Nikolina Radulovich[1], Katrina Hueniken[1], Quan Li[1], Siyuan (Claret) Liu[2], Brian Belmontes[2], Paul Hughes[2], Ming-Sound Tsao[3], Adrian Sacher[4]

[1]Princess Margaret Cancer Centre, University Health Network, Toronto, ON, Canada,[2]Amgen Research, Thousand Oaks, CA,[3]Princess Margaret Cancer Centre, University Health Network; Departments of Laboratory Medicine & Pathobiology and Medical Biophysics, University of Toronto, Toronto, ON, Canada,[4]Princess Margaret Cancer Centre, University Health Network; Departments of Medicine and Immunology, University of Toronto, Toronto, ON, Canada

BACKGROUND: AMG 193 is an MTA-cooperative PRMT5 inhibitor designed for preferential selectivity against *MTAP*-del tumor cells. AMG 193 is currently being investigated in phase I-II clinical trials in *MTAP*-del solid tumors (MTAPESTRY-101,104, 201). *In vivo* testing in patient-derived xenograft (PDX) models has significant potential to inform focused clinical development of AMG 193.

OBJECTIVES: Using *MTAP*-del PDX models from our institutional biobank, we sought to: (i) identify promising drug combination partners for AMG 193 across lung adenocarcinomas (LUAD), lung squamous cell carcinomas (LUSC), and mesotheliomas (MESO); and (ii) investigate mechanisms of primary or acquired resistance to AMG 193.

METHODS: We identified 21 PDX models with *MTAP* deep deletion by SNP array or MTAP loss by immunohistochemistry - including 7 LUAD (including 2 *KRAS* G12C; 1 *EGFR* L858R + *MET* amp), 10 LUSC, and 6 MESO. *In vivo* AMG 193 activity was characterized in 7 models subcutaneously implanted in NOD SCID or NSG mice (n=5-7 per group).

RESULTS: Four models (2 *KRAS* G12C LUAD; 1 LUSC; 1 MESO) showed sustained sensitivity to AMG 193. Two models (1 *KRAS*-wildtype LUAD; 1 MESO) exhibited primary resistance to AMG 193. One LUSC model showed acquired resistance to AMG 193 after initial sensitivity. Interestingly, the two *KRAS* G12C LUAD models demonstrated additive/synergistic activity with AMG 193+sotorasib despite exhibiting resistance to sotorasib monotherapy.

CONCLUSIONS: A spectrum of AMG 193 activity was demonstrated across *MTAP*-del LUAD, LUSC, MESO PDX models, recapitulating the range of response & resistance seen clinically. Combination therapy with AMG 193 overcame sotorasib resistance in *KRAS* G12C LUAD models. Other drug combinations will be evaluated in primary or acquired resistance models. Acute dosing studies are underway to further characterize response to AMG 193 in these models.

Summary of 7 MTAP-deleted PDX models

PDX model	**Drug Activity†**	**Doubling time in weeks, from linear mixed-effects modeling** (N.R. = not reached due to complete response)
***KRAS* G12C LUAD#239**	Sotorasib monotherapy: resistant. AMG 193 monotherapy: sensitive. Sotorasib + AMG 193: sensitive with accelerated deep response	On-treatment (d10-21), Vehicle 2.3 vs. Sotorasib 3.6 P=0.20, AMG 193 N.R. P<0.001 ***, Combo N.R. P<0.001 ***.
***KRAS* G12C LUAD#256**	Sotorasib monotherapy: resistant. AMG 193 monotherapy: partial sensitivity. Sotorasib + AMG 193: sensitive with accelerated deep response	On-treatment (d0-45), Combo N.R. vs. Sotorasib 5.9 P=0.04*, AMG 193 5.3 P=0.04 *.
***KRAS* WT LUAD#196**	AMG 193: partial resistance	On-treatment (d0-24), Vehicle 1.8 vs. AMG 193 2.3 P=0.04 *
LUSC#410	AMG 193: sensitive (d0-48) with eventual acquired resistance (d49-91)	On-treatment (d0-15), Vehicle 0.9 vs. AMG 193 19.3 P<0.001 ***
LUSC#470	AMG 193: sensitive	On-treatment (d0-20), Vehicle 1.1 vs. AMG 193 2.8 P<0.001 ***
MESO#7	AMG 193: sensitive	On-treatment (d0-49), Vehicle 3.4 vs. AMG 193 N.R. P<0.001 ***
MESO#18	AMG 193: partial resistance	On-treatment (d0-24), Vehicle 1.8 vs. AMG 193 2.9 P=0.003 **
	† Drug activity assessed based upon tumor growth curve kinetics and doubling time.	

#7135 A first-in-class orally bioavailable small molecule to overcome treatment resistance in hormone receptor-positive breast cancer.

Hee-Sung Park, Chakrapani Subramanyam, Kyu-kwang Cho, Se Hee Hyun, Yeonjee Kahm

Promedigen, Daejeon, Korea, Republic of

CDK4/6 inhibitors combined with antiestrogens such as fulvestrant represent frontline therapy for hormone receptor-positive (HR+) breast cancer; however, therapeutic resistance inevitably emerges in a substantial subset of patients through diverse molecular mechanisms. To address this challenge, we developed PMG-A9, a novel, orally bioavailable small molecule designed to restore the function of a key tumor suppressor frequently inactivated across cancers. PMG-A9 potently downregulates major resistance drivers, including Cyclin D1 and c-Myc, in a dose-dependent manner at sub-nanomolar concentrations, while upregulating cell-cycle inhibitors and pro-apoptotic proteins, demonstrating its potential to overcome resistance to CDK4/6 inhibitors and/or fulvestrant. In preclinical HR+ breast cancer xenograft models, PMG-A9 exhibits robust single-agent antitumor activity and pronounced synergy when combined with these agents. These findings highlight tumor-suppressor reactivation as a promising and broadly applicable therapeutic strategy with the potential to address resistance not only in HR+ breast cancer but also across a wide range of tumor types.

#7137 Targeting RRM2 to enhance PARP inhibitor sensitivity in TNBC.

Tamanna Islam[1], Howard L. Elford[2], Jesika S. Faridi[1]

[1]University of the Pacific, Stockton, CA,[2]Molecules for Health, Inc., Richmond, VA

Triple-negative breast cancer (TNBC) remains one of the most aggressive and therapeutically refractory breast cancer subtypes, primarily due to the absence of hormone receptors and HER2 expression. Poly ADP-ribose polymerase (PARP) inhibitors such as olaparib have demonstrated substantial efficacy in BRCA1/2-mutated TNBC by exploiting synthetic lethality in tumors with defective homologous recombination repair. However, the emergence of acquired resistance to olaparib significantly limits its long-term clinical utility. Ribonucleotide reductase (RR), the rate-limiting enzyme responsible for converting ribonucleotides to deoxyribonucleotides, plays a pivotal role in DNA synthesis and cell-cycle progression. Didox (3,4-dihydroxybenzohydroxamic acid) is a ribonucleotide reductase inhibitor with additional iron-chelating and free-radical scavenging activities. Our previous work identified that the RRM2 subunit is upregulated in TNBC cells and contributes to the development of chemoresistance. The present study investigates whether pharmacologic inhibition of RRM2 using Didox can potentiate olaparib activity and mitigate PARP inhibitor resistance in TNBC models. Four TNBC cell lines—MDA-MB-231, MDA-MB-468, MDA-MB-436, and HCC1937—were utilized to encompass both BRCA-wild-type and BRCA-mutant backgrounds. Cytotoxic responses to olaparib and Didox were quantified by MTS-based IC_{50} determination, followed by combination index (CI) analysis using the Chou-Talalay method to assess potential drug synergy. Our data show that MDA-MB-436 (BRCA1-mutant) cells were highly sensitive to olaparib, whereas MDA-MB-231 and MDA-MB-468 (BRCA1-wild-type) exhibited marked resistance. Didox displayed moderate single-agent cytotoxicity, however substantially enhanced olaparib sensitivity in resistant lines. Western blot analyses revealed increased DNA damage signaling under combination treatment, indicating that RRM2 inhibition augments PARP inhibitor-induced genotoxic stress. Collectively, these findings support the therapeutic potential of adding an RR inhibitor to overcome PARP inhibitor resistance in TNBC and warrant further in-depth mechanistic and *in vivo* evaluation.

#7138 Acquired saruparib (AZD5305) resistance in BRCA1-deficient triple negative breast cancer is vulnerable to DNA damage response-targeted therapeutics.

Matthew R. Jordan[1], Pamela S. VanderVere-Carozza[1], Jessica Lynn Kersey[1], Katherine Pawelczak[2], John J. Turchi[1]

[1]Indiana University School of Medicine, Indianapolis, IN,[2]Nerx Biosciences, Inc., Indianapolis, IN

The development of poly (ADP)-ribose polymerase (PARP) inhibitors (PARPi) for the synthetic lethal killing of BRCA1/2-deficient cancers revolutionized BRCA1/2-deficient patient outlook and survival. PARPi are now commonly used to treat BRCA1/2-deficient or homologous recombination (HR)-deficient breast, ovarian, prostate, and pancreatic cancers. Despite this clinical success, 30-40% of BRCA1/2-deficient patients do not respond to PARPi and the vast majority that do initially respond, ultimately develop PARPi resistance. This represents a major challenge limiting the clinical impact of PARPi treatment. Understanding PARPi resistance mechanisms is essential for developing better treatment strategies for intrinsic and acquired PARPi-resistant cancers. Recent efforts to better treat BRCA1/2-deficient cancers and combat PARPi resistance led to the development of saruparib (AZD5305), a PARP1-specific inhibitor with significantly improved safety profiles due to limited off-target inhibition of other PARP family members and hence reduced toxicity. Saruparib is currently undergoing phase 3 clinical trials and is anticipated to be the standard of care PARPi for BRCA1/2- and HR-deficient cancer patients. We have generated 5 saruparib-resistant (SR) cell lines from parental BRCA1-deficient MDA-MB-436 triple negative breast cancer (TNBC) cells that are >1000-fold resistant to saruparib but exhibit differential sensitivity to other nonspecific clinical PARPi. SR cell lines exhibit altered inhibition of cellular PARP activity and PARP trapping in response to saruparib and the nonspecific PARPi talazoparib. Whole genome sequencing identified PARP1 active site mutations in each SR cell line, and *in vitro* reconstitution of these mutants suggests that they are driving resistance to saruparib and altered sensitivity to other nonspecific clinical PARPi. Importantly, despite acquired saruparib resistance, SR cell lines retain sensitivity to other DNA damage response targeted therapeutics. Collectively, this work characterizes what we believe to be the first BRCA1-deficient models of acquired saruparib resistance and uncovers vulnerabilities that may inform rational combination strategies and novel therapeutic approaches for patients who progress on saruparib in the clinic.

#7139 Uncovering PGRMC1-PARP interaction: A novel combination therapeutic strategy in triple-negative breast cancer.

Mahalakshmi Vijayaraghavan[1], Ramadevi Subramani[2], Michel Rojo Amador[1], Kyle Nguyen[1], Kariina Garcia[1], Poornima Devi Narayanan[1], Alfredo Roman[1], Abigail Ramirez[1], Jazmin Lopez[1], Rajkumar Lakshmanaswamy[1]

[1]Texas Tech Univ. Health Sciences Ctr. El Paso, El Paso, TX,[2]Postdoc. Research Assoc., Dept. of Biomed. Sci., Texas Tech University Health Sciences Center (El Paso, TX), El Paso, TX

Background: Triple-negative breast cancer (TNBC) is an aggressive subtype characterized by altered DNA repair pathway with insufficient therapeutic options. Poly (ADP-ribose) polymerase (PARP) is a key enzyme involved in DNA repair, and has emerged as an effective treatment for TNBC and BRCA-associated cancers in clinical trials. Despite these advances, 40-70% of patients ultimately develop resistance to PARPi, highlighting the need to identify additional modulators of therapeutic response. Previous work from our laboratory has shown that Progesterone Receptor Membrane Component 1 (PGRMC1) plays a critical role in regulating cancer cell growth by modulating PI3K/AKT/mTOR and EGFR signaling pathways in both ER-positive and TNBC cells. However, the mechanisms driving PGRMC1 overexpression in TNBC and its potential role in influencing PARP function remains unexplored. To address this challenge, we investigated the unexplored interaction between PARP inhibition and PGRMC1 inhibition in TNBC models.
Methods: TNBC cell lines (BRCA-wild type: MDA-MB-231, MDA-MB-468; BRCA-mutant: HCC1395, MDA-MB-436) were treated with chemical inhibitors targeting PGRMC1 and PARP. Basal expression levels of PARP and PGRMC1 were compared between normal breast cells and TNBC cells by western blotting, and treatment-induced changes were quantified using western blot and qRT-PCR. Cell viability was measured by MTS assay and colony formation assay following inhibitor treatment across TNBC models. DNA damage was evaluated by γ-H2AX and RAD51 immunofluorescence staining. Ferroptosis induction was assessed through intracellular iron quantification and flow cytometry.
Results: We observed markedly elevated PGRMC1 expression in both BRCA-wild-type and BRCA-mutant TNBC cell lines compared with normal controls. Chemical inhibition of PGRMC1 or PARP led to increased DNA damage, evidenced by enhanced γ-H2AX staining and reduced RAD51 levels. Modulating PGRMC1 significantly altered PARP expression, and reciprocal regulation was also observed. These treatments further induced DNA damage markers (γ-H2AX, phospho-RAD51) and altered intracellular heme levels, promoting ferroptosis. The combination strategy effectively reduced cell survival regardless of BRCA mutation status, highlighting a strong dependence on PGRMC1 for survival under PARP inhibitor treatment.
Conclusion: Targeting PGRMC1 may enhance PARPi response in TNBCs. This work identifies PGRMC1 as a promising therapeutic target and supports combination strategies for improving TNBC treatment. Future studies will dissect the mechanistic crosstalk between PGRMC1 and PARP using PGRMC1 knockdown and overexpression models.

#7140 Synthetic lethality of Hsp90beta-selective inhibition with PARPi in homologous recombination repair proficient ovarian cancer.

Sanket Mishra

Grannus Therapeutics, Indianapolis, IN

A significant unmet need exists for cancer patients who are ineligible for PARP inhibitor (PARPi) therapy due to their genetic makeup and/or acquired PARPi resistance. Synthetic lethality occurs when PARP inhibition is combined with an agent that disrupts the DNA double-strand breakage (DSB) repair mechanisms, causing apoptosis and cell death. Inhibition of the Heat Shock Protein 90 (Hsp90) represents an ideal candidate to disrupt DSB repair and induce synthetic lethality with PARP inhibitors, as multiple Hsp90 client proteins are involved in the DSB repair pathways including homologous recombination (HR) repair pathway. Unfortunately, no Hsp90 inhibitor is FDA approved for use due to dose-limiting and on-target toxicities. Hsp90 exists as four isoforms in the cell, Hsp90α, Hsp90β, Grp94 and Trap-1. The cytosolic isoforms Hsp90α and Hsp90β significantly contribute to cancer growth and progression. Interestingly, inhibition of Hsp90α by non-selective (pan-Hsp90) inhibitors can cause cardiac and ocular toxicities. Additionally, inhibitor binding to the inducible isoform, Hsp90α, can also contribute to dosing-challenges associated with previously evaluated pan-Hsp90 inhibitors. Therefore, Hsp90β-selective inhibition has been proposed as safer alternative to pan-Hsp90 inhibition for cancer treatment. This presentation will contain results from mechanistic, efficacy and safety studies of the orally bioavailable and efficacious Hsp90beta-selective inhibitor in combination with a PARP inhibitor.

: Overcoming Microenvironmental and Delivery Barriers in Cancer Therapy
Poster Session

#0485 ML-016: A silicon “plateloid”-based phenotype targeting platform for lung and liver malignancies.

Qingxin Mu, Lorenzo Pradella, Brian Sapp, Mauro Ferrari

BrYet US, Inc, Houston, TX

The treatment of metastatic and drug-resistant tumors in the lungs and liver remains a major challenge for conventional chemotherapeutic agents, including doxorubicin. ML-016 is a novel injectable Phase I drug product developed by BrYet using a proprietary silicon “plateloid” technology designed to exploit distinct vascular and microenvironmental phenotypes. The platelet-shaped silicon microstructures (~2.6 µm in diameter and ~700 nm in thickness) are engineered to optimize hemodynamic behavior and endothelial interaction. The targeting mechanism of ML-016 integrates multiple phenotype-driven nodes acting sequentially across the tumor vasculature and microenvironment: enhanced margination under tumor-associated shear stress; preferential transmigration via polyglutamic acid-doxorubicin (pDox) conjugation; formation of pDox “exosomoids” and efficient internalization into tumor cells; local drug release through pH-mediated cleavage; and intracellular trafficking of released doxorubicin beyond the active range of multidrug-resistance pumps, yielding high perinuclear and nuclear accumulation. This multi-node phenotype targeting approach enhances tumor penetration, reduces systemic toxicity, and overcomes drug resistance. Our preclinical studies have shown strong antitumor efficacy in triple-negative breast cancer models with a 50% long-term functional cure (Nature Biotechnology, 2016, 34(4), 414-418). In a current lung metastasis model of soft-tissue sarcoma, ML-016 has produced durable tumor suppression and markedly prolonged survival, with 50-80% of treated animals surviving beyond five months after tumor inoculation, whereas all vehicle- or free-doxorubicin-treated animals succumbed within the same period. ML-016 has recently received Phase I/II Human Research Ethics Committee (HREC) approval in Australia, marking the initiation of first-in-human evaluation. Overall, ML-016 represents an innovative application of silicon plateloid technology that coordinates vascular, microenvironmental, and intracellular mechanisms to enable efficient phenotype-targeted therapy for resistant tumors in the lung and liver, supporting its continued development toward multi-cancer clinical validation.

#7144 A general method to overcome the binding site barrier in antibody-based therapeutics.

Yuanzheng Li[1], Shili Yao[2], Peng Guo[2]

[1]University of Science and Technology of China, Hefei, China,[2]Hangzhou Institute of Medicine, Chinese Academy of Sciences, Hangzhou, China

Background: Insufficient intratumoral penetration remains a major limitation of antibody-based therapeutics in solid tumors. The binding site barrier (BSB), driven by high-affinity interactions near perivascular regions, restricts deeper tissue distribution of ADCs and bispecific antibodies and thereby limits their therapeutic index. Current strategies such as co-dosing with parental antibodies or engineering lower-affinity variants are constrained by target specificity and require redesign of each therapeutic. A broadly applicable, novel approaches that transiently modulates BSB without altering antibody structure is needed to improve tumor penetration.

Methods: We evaluated DSPE-PEG2000, an FDA-approved amphiphilic phospholipid-polymer conjugate, as a general BSB modulator. Using HER2-, TROP2-, and PD-1/VEGF-targeted therapeutics, we quantified changes in cell-surface engagement, receptor accessibility, and internalization across multiple cancer cell models via flow cytometry, confocal microscopy, and live-cell imaging. In subcutaneous xenograft models, we assessed the intratumoral distribution of Cy3-labeled ADCs and a PD-1/VEGF bispecific antibody using longitudinal IVIS imaging and spatial analysis of tumor sections. Antitumor efficacy was evaluated by tumor growth suppression, treatment durability, and survival. Biosafety assessments included serum chemistry and histopathology of major organs.

Results: DSPE-PEG2000 rapidly incorporated into tumor cell membranes and generated a short-range PEG layer that transiently reduced antibody-antigen interactions by 40-60% across diverse targets (e.g., HER2, TROP2, and PD-1/VEGF). This surface modulation did not impair antibody internalization or downstream trafficking. In vivo, DSPE-PEG2000 substantially broadened the intratumoral distribution of ADCs and bispecific antibodies, enabling deeper penetration beyond perivascular regions. The improved spatial delivery translated into greater tumor growth inhibition and prolonged survival, consistent across multiple ADC payloads and antibody architectures. Co-administration did not increase systemic exposure or off-tumor tissue accumulation, and no treatment-related toxicity was observed.

Conclusions: DSPE-PEG2000 provides a generalizable, target-independent strategy to overcome the binding site barrier and enhance the distribution and functional efficacy of antibody-based therapeutics in solid tumors. By transiently modulating BSB through membrane-anchored PEG grafting without modifying antibody affinity or structure, DSPE-PEG2000 offers a practical and clinically compatible approach to improve tumor penetration of current and next-generation antibody therapeutics.

#7145 A spatial PK/PD framework predicts ADC response in solid tumors by integrating drug delivery, target engagement, and microenvironmental readiness.

Corinne Ramos[1], Martha Baydoun[1], Sandra Delebecq[2], Amandine Gerstenberg[2]

[1]R&D, Aliri, Loos, France,[2]Aliri, Loos, France

Background: Antibody-drug conjugates achieve their effect only when payload delivery, target accessibility, and microenvironmental readiness align within the tumor. Conventional biomarkers capture fragments of this biology, but not the spatial interplay that ultimately determines response. To address this gap, we conducted a translational spatial PK/PD study to determine whether high-resolution tissue mapping could predict early ADC activity in solid tumors.

Methods: Tumor biopsies from patients and PDX models treated with a clinically relevant ADC were analyzed using an integrated spatial PK/PD workflow. Quantitative payload imaging by mass spectrometry imaging was combined with spatial proteomics and transcriptomics to map antigen distribution, stromal architecture, vascular organization, immune niches, and early pharmacodynamic activation. All data modalities were spatially registered and modeled using AI-based neighborhood analysis to generate a continuous delivery-engagement score for each tumor region. Importantly, pharmacodynamic readouts such as cleaved caspase-3 and γH2AX were evaluated in a blinded manner.

Results: Across fourteen matched tumor samples, the analysis revealed a consistent pattern linking spatial drug behavior with early biological response. Regions showing strong spatial convergence between payload localization and antigen-rich tumor pockets exhibited significantly higher apoptotic signaling. Tumors displaying coherent payload influx along perfused vascular corridors were more likely to show downstream pharmacodynamic activation, regardless of their bulk target expression. In addition, microenvironments enriched for dendritic cells, $CD8^+$ T cells, and interferon-responsive stromal states demonstrated enhanced sensitivity to the ADC even before radiographic change. When integrated into a unified spatial competency score, these features correctly classified early responses in eleven of fourteen samples.

Conclusion: This study shows that a spatial PK/PD framework can predict ADC response by capturing the coordinated alignment of delivery, target engagement, and microenvironmental readiness within tissue. These findings provide a mechanistically grounded, clinically relevant approach for improving patient selection and advancing predictive biomarker strategies for next-generation ADCs.

#7146 Targeting tumor macrophage TGF-β signaling overcomes immunotherapy resistance in hepatocellular carcinoma.

Hui Yue, Yan Liu, Han Wang, Yalin Tu, Yaxian Wang, Siyuan Huang, Haoran Wu, Xiaohang Long, Carol Tong, Alfred Sze-Lok Cheng

The Chinese University of Hong Kong, Hong Kong, Hong Kong

Background: Immune checkpoint blockade (ICB) has improved outcomes in hepatocellular carcinoma (HCC), but its response rates remain limited. We aimed to investigate the role of transforming growth factor-beta (TGF-β) signaling in ICB resistance and develop a targeted strategy to enhance therapeutic efficacy.

Methods: We analyzed our in-house clinical single-cell RNA sequencing (scRNA-seq) data (NCT03419481) from HCC patients. An ICB-resistant mouse model was used for therapeutic validation. *In vivo* phage display screening was employed to identify a tumor-associated macrophage (TAM)-homing peptide, which was then conjugated to nanoparticles for targeted delivery of the TGF-β receptor inhibitor (TGFBR1) Vactosertib.

Results: Our scRNA-seq revealed a broad upregulation of TGF-β ligand and pathway activity within the tumor microenvironment (TME) of ICB non-responders compared to responders. Further analysis identified TREM2+ macrophages as the dominant recipients of TGF-β signaling, a finding corroborated by their significant abundance in non-responders, suggesting their central role in a TGF-β-driven resistance pathway. To functionally validate this clinical observation, we employed an ICB-resistant HCC mouse model. Treatment with Vactosertib, in combination with anti-PD-1, markedly restored tumor growth control and significantly prolonged survival, effectively reversing the resistant phenotype. To definitively establish the causal role of macrophage-specific TGF-β signaling in driving resistance, we developed a targeted nanomedicine strategy. Using an *in vivo* phage display screening, we identified a peptide with high specificity and affinity for TAMs. By conjugating this TAM-homing peptide to nanoparticles, we achieved precise delivery of Vactosertib to the TAM population. This targeted intervention not only recapitulated the synergistic anti-tumor effect observed with systemic Vactosertib administration but also more potently reversed the immunosuppressive TME signature, providing direct evidence that TGF-β acts primarily through TAMs to mediate ICB resistance.

Conclusions: Our study establishes TGF-β signaling in TAMs as a key mechanism of ICB resistance in HCC. The TAM-homing nanoparticle platform provides a powerful tool for dissecting macrophage-specific mechanisms and represents a versatile strategy for developing precision immunotherapies that target specific cellular niches within the immunosuppressive TME.

Acknowledgements: This study is supported by RGC GRF14119023, LiKaShing Foundation, and Strategic Seed Funding for Collaborative Research Scheme.

#7147 CAR T-Cell therapy efficacy evaluation inTumorGraft3D tri-culture platform with reconstructed tumor microenvironment.

Stefano Cairo[1], **Fu-Ju Chou**[2], Sumanun Suwunnakorn[2], Annamaria Rapisarda[2], Marianna Zipeto[2], Michael Ritchie[2], Markus Hippich[2], Daniel Ciznadija[3], Veena Jagannathan[2], Brandon Walling[2], Mara Gilardi[2], Haoting Hsu[2], BanuPriya Sridharan[2]

[1]Champions Oncology, Inc. (Hackensack, NJ), Rockville, MD,[2]Champions Oncology (Rockville, MD), Rockville, MD,[3]Champions Oncology, Hackensack, NJ

Chimeric antigen receptor (CAR) T-cell therapy represents one of the most transformative innovations in cancer immunotherapy, offering the ability to redirect a patient's own immune cells toward malignant targets through genetic engineering of tumor-recognizing receptors. While clinical successes in hematologic malignancies such as B-cell acute lymphoblastic leukemia & diffuse large B-cell lymphoma have validated the concept of CAR T-cell-mediated cytotoxicity, extending this efficacy to solid tumors has proven significantly more challenging due to the immunosuppressive nature of the tumor microenvironment (TME), the heterogeneity of antigen expression, &the presence of physical & biochemical barriers that limit CAR T-cell infiltration & persistence. To address these limitations, we developed the TumorGraft3D-Tri-Culture platform, a physiologically relevant ex-vivo system capable of recapitulating the complex interactions that occur among tumor cells, cancer-associated fibroblasts (CAFs), & immune suppressive components such as M2 macrophages. In this study, CD70-directed CAR T-cells were evaluated in a renal cell carcinoma with high CD70 expression. Standard targeted CAR T-cells expressing the CD27 receptor were compared to armored CAR T-cells incorporating a dominant-negative TGFβ receptor II (dnTGFβRII) designed to resist TGFβ-mediated immunosuppression. The tri-culture system consisted of tumor cells, cancer-associated fibroblasts (CAFs), & M2 macrophages, providing a physiologically relevant TME that supported tumor proliferation & cytokine-driven immune suppression. Addition of CAR T-cells enabled a quad-culture system used to assess therapeutic efficacy under suppressive conditions. Tumor cells were seeded at a 1x baseline ratio, with CAFs at 0.5x & M2 macrophages at 0.1-0.5x. Both targeted & armored CAR T-cells reduced tumor viability compared with controls, but armored CAR T-cells showed enhanced cytotoxicity & sustained activation. CD69 expression was markedly elevated in both CAR T-cell types, indicating robust activation, while CD70 surface expression on tumor cells decreased following treatment, reflecting target engagement & selective killing. Brightfield imaging & luminescence analyses confirmed significant tumor lysis, especially in armored CAR T-cell groups. The 3D platform successfully recapitulated stromal & immune-mediated resistance mechanisms absent in conventional two-dimensional systems, validating its translational relevance. These findings demonstrate that TGFβ-resistant armored CAR T-cells maintain effector function within an immunosuppressive TME & highlight CD70 as a viable & selective therapeutic target. Collectively, this work establishes the TumorGraft3D tri-culture platform as a robust preclinical tool for evaluating & advancing next-generation CAR T-cell therapies in solid tumors.

#7148 Stress adaptation defines therapeutic response to CDK4/6 inhibitors in sarcoma.

Jinfen Xiao[1], Emily Ko[1], Ashley Smith[1], Roberta Piras[2], Annaliese Fowler[1], Kristin Ishaya[2], **Jlenia Guarnerio**[1]

[1]Genetics, University of Texas MD Anderson Cancer Center, Houston, TX,[2]Biomedical Science, Cedars-Sinai Medical Center, Los Angeles, CA

CDK4/6 inhibitors are under active clinical evaluation in sarcoma, yet the mechanisms that determine therapeutic sensitivity and resistance remain poorly understood. Here, we show that the CDK4/6 inhibitor abemaciclib not only suppresses tumor cell proliferation but also induces a robust type I interferon (IFN-I) response driven by intracellular double-stranded RNA accumulation—an effect essential for its antitumor activity. Abemaciclib further remodels the sarcoma immune microenvironment by enhancing T cell infiltration and increasing interferon-producing monocytes. Through integrated transcriptomic and proteomic analyses, we identify a stress-adaptive signaling program that is selectively upregulated in tumor cells upon treatment and correlates with poor patient prognosis. Functionally, this pathway mitigates IFN-induced mitochondrial stress, limiting reactive oxygen species accumulation and apoptosis, whereas its suppression exacerbates mitochondrial dysfunction and promotes tumor cell death. In vivo, targeting the adaptive stress-response program synergizes with abemaciclib to inhibit tumor growth and extend survival. These findings define a previously unrecognized mechanism of stress adaptation to CDK4/6 inhibition and highlight a promising strategy to potentiate interferon-driven antitumor responses in sarcoma.

#7150 ICA-1S targets protein kinase C-iota to inhibit the WNT/β-catenin signaling in hepatocellular carcinoma.

Abigail Oluwafisayo Olatunji, Nuzhat Nowshin Oishee, Abiral Hasib Shourav, Grazielly Teodoro, Mildred Acevedo-Duncan

University of South Florida, Tampa, FL

Liver cancer is one of the leading causes of cancer-related mortality in the United States and a significant threat to public health. Despite the projection of the World Health Organization that the global deaths from liver cancer would exceed one million by 2030, liver cancer continues to receive limited attention in oncology drug development. The activation of the WNT/β-catenin signaling pathway is a key molecular event in hepatocellular carcinoma (HCC), and the canonical pathway is activated in approximately one-third of HCC cases. However, therapeutic targeting of this pathway has been limited by challenges in specificity. In this study, we investigated the role of atypical protein kinase C-iota (PKC-ι) and its specific inhibitor, 5-amino-1-((1R,2S,3S,4R)-2,3-dihydroxy-4-methylcyclopentyl)-1H-imidazole-4-carboxamide (ICA-1S), in regulating β-catenin stability and suppressing its signaling in liver cancer cells. We assessed the pathways affected by PKC-ι inhibition by cell proliferation assays, Western blotting, Co-immunoprecipitation, and siRNA knockdowns. HepG2 liver cancer cells were seeded 8×10^4 per well and treated with ICA-1S (10-50 μM) for 72 hours. Untreated wells served as controls. In comparison, we achieved PKC-ι gene knockdown with 80 nM siRNA using polymer-based transfection reagent siTran 2.0. We then assessed protein expression by Western blotting and normalized it to beta-actin. The dose-response curve of ICA-1S showed a 15%, 35%, 53%, 55%, and 63% reduction in proliferation at concentrations of 10 μM, 20 μM, 30 μM, 40 μM, and 50 μM, respectively, after three days of treatment. Moreover, treatment with 20 μM ICA-1S increased cytochrome C (39%), Bcl-2 Interacting Mediator of cell death (BIM) (25%), cleaved Caspase-3 (24%), and cleaved Poly (ADP-ribose) polymerase (PARP) (24%), while reducing total PARP (35%), indicating an intrinsic apoptotic response. ICA-1S reduced β-catenin stability, suggesting that PKC-ι maintains the anti-β-catenin degradation complex. We also observed the downstream effectors of the WNT/β-catenin signaling pathway in response to 20 μM ICA-1S, which resulted in 53% upregulation of Axin-1, 37% downregulation of disheveled segment polarity protein-3 (DVL3), and 55% and 63% downregulation of Low-density lipoprotein receptor-related protein-6 (LRP6) and phospho-LRP6 levels, respectively. Epithelial cadherin and tumor protein p53 were upregulated by 41% and 13%. We have shown in this study that ICA-1S could inhibit proliferation and induce apoptosis in liver cancer cells by destabilizing β-catenin and disrupting the WNT/β-catenin signaling pathway. Our findings identify PKC-ι as a promising therapeutic target, supporting the further development of ICA-1S or related compounds as potential anti-HCC agents that can overcome pathway-specificity challenges in liver cancer therapy.

#7151 Targeted inhibition of atypical PKC isoforms PKC-ι and PKC-ζ by ICA-1S and ζ-Stat suppresses oncogenic signaling and cytokine-mediated bone metastasis in prostate cancer.

Grazielly Teodoro, Wishrawana Sarathi Ratnayake, Luke Lajmi, Sloan Breedy, Aaron Todman, Shreejana Rimal, Mildred Acevedo-Duncan

University of South Florida, Tampa, FL

Bone metastatic prostate cancer (BMPC) remains the leading cause of mortality among prostate cancer patients due to its resistance to current therapeutics and its reliance on the osteogenic microenvironment. The atypical protein kinase C (aPKC) isoforms PKC-ι and PKC-ζ have emerged as pivotal regulators of prostate cancer progression, metastasis, and inflammatory signaling. In this study, we investigated the molecular effects of two selective small-molecule inhibitors, ICA-1S (targeting PKC-ι) and ζ-Stat (targeting PKC-ζ), in DU-145 and PC-3 prostate cancer cells, as well as their interactions with the human osteoblast line hFOB 1.19. Our results demonstrated that both inhibitors effectively suppressed phosphorylation and activity of PKC-ι/ζ and downstream effectors, including Stat3, NFκB, and JNK/c-Jun, leading to marked reductions in cell migration and survival. Cytokine array analysis revealed that ICA-1S and ζ-Stat treatment significantly downregulated pro-metastatic and pro-inflammatory cytokines, including IL-6, IL-8, and CXCL-1, while upregulating IL-18 and ICAM-1, indicating a shift toward apoptotic and pyroptotic signaling. Immunofluorescence confirmed a decreased nuclear localization of Stat3. At the same time, co-immunoprecipitation assays demonstrated a reduced interaction between 14-3-3 and PKC-ι/ζ, supporting the disruption of key scaffold assemblies required for metastatic signaling. Collectively, our findings suggest that dual aPKC inhibition attenuates critical oncogenic cascades and reprograms the osteogenic niche to suppress prostate cancer survival and colonization in bone. These results identify ICA-1S and ζ-Stat as promising lead compounds for precision targeting of aPKC-driven prostate cancer metastasis.

#7152 ICA-1S targets PKC-ι and Cx43 to inhibit glioblastoma multiforme progression.

Grazielly Teodoro, Shreejana Rimal, Wishrawana Sarathi Ratnayake, Gaurab Raj Khanal, mildred acevedo-duncan

University of South Florida, Tampa, FL

Glioblastoma multiforme (GBM) is an aggressive brain cancer, characterized by poor therapeutic outcomes. Atypical protein kinase C iota (PKC-ι) plays a critical role in GBM progression by regulating cell proliferation, motility, and invasion. Connexin 43 (Cx43), a key gap junction protein, mediates intercellular communication between glioma and surrounding astrocytes, promoting tumor growth, invasion, and chemoresistance. Targeting the PKC-ι and Cx43 represents a novel approach to disrupt oncogenic interactions and inhibit GBM progression. This study evaluates the therapeutic potential of ICA-1S ((-Amino-1-[(1R,2S,3R,4R)-2,3-dihydroxy-4-[(phosphonooxy)methyl]cyclopentyl]-1H-imidazole-4-carboxamide), a selective PKC-ι inhibitor, on GBM cell proliferation, signaling, and Cx43 regulation. Treatment of T98G and U87MG cells with ICA-1S resulted in significant reductions in cell proliferation by about 50% in T98G and 40% in U87MG ($p < 0.001$). Co-immunoprecipitation experiments demonstrated that PKC-ι directly interacts with Cx43. Treatment with ICA-1S led to decreased expression of both PKC-ι and Cx43, as shown by Western blot analysis. In addition, ICA-1S promoted autophagy and inhibited critical oncogenic signaling pathways, including PI3K/AKT, while also reducing the expression of proteins involved in epithelial-mesenchymal transition. These results indicate that ICA-1S is a promising candidate for targeted GBM therapy.

#7153 Selective atypical protein kinase C inhibitor reduces proliferation and promotes apoptosis in malignant endometrial cancer cells.

Gaurab Raj Khanal[1], Shreejana Rimal[2], Grazielly Teodoro[2], Mildred Acevedo-Duncan[2]

[1]Chemistry, University of South Florida, Tampa, Florida, US, Tampa, FL,[2]University of South Florida, Tampa, FL

Endometrial cancer is a type of uterine cancer. It starts in the inner lining of the uterus, known as the endometrium. Endometrial cancer is the most commonly diagnosed type of cancer that affects the gynecologic organs in the United States. Globally, endometrial cancer accounts for about 420,000 new cases and nearly 98,000 deaths annually (as of 2022), making it one of the most common gynecologic cancers worldwide. Endometrial cancer primarily affects postmenopausal women, with peak incidence between 60 and 70 years of age. Overall, it remains a disease largely associated with older, postmenopausal women. Among the Protein Kinase C (PKC) family, the atypical PKC (aPKC) subgroup, consisting of Protein Kinase C-iota (PKC-ι) and Protein Kinase C-zeta (PKC-ζ), has been implicated in cancer cell proliferation and survival. PKC-ι, in particular, is frequently overexpressed in various malignancies, including endometrial cancer. 5-amino-1-((1R, 2S, 3S, 4R)-2, 3-dihydroxy-4-methyl cyclopentyl)-1H-imidazole-4-carboxamide (ICA-1S), an inhibitor selective for PKC-ι, has demonstrated anticancer activity in multiple tumor types such as glioblastoma, prostate, ovarian, and lung cancers. In our study, 50,000 Hec1A endometrial cancer cells were seeded in six-well plates and treated with various concentrations of ICA-1S. A concentration-dependent decrease in cell proliferation was observed, with reductions of 17%, 22%, 52%, 38%, and 58% at 1 µM, 5 µM, 10 µM, 20 µM, and 50 µM ICA-1S, respectively. The 10 µM concentration, which produced a significant inhibitory effect, was selected for subsequent experiments. Sodium dodecyl sulfate-polyacrylamide gel electrophoresis (SDS-PAGE) followed by Western Blot analysis showed a marked reduction in the expression and phosphorylation of PKC-ι. Similarly, there was a significant reduction in the levels of PKC-ζ and phosphorylated PKC-ζ. Additionally, expression of key apoptotic markers such as survivin, caspase-3, and poly (ADP-ribose) polymerase (PARP) was significantly decreased in ICA-1S-treated cells compared to untreated controls, suggesting induction of apoptosis. Future experiments will focus on identifying the signaling pathways affected by ICA-1S treatment through more Western Blotting, Immunofluorescence, Co-Immunoprecipitation, and Flow Cytometry to elucidate further the molecular mechanisms underlying the reduced proliferation and enhanced apoptosis observed in Hec1A cells following PKC-ι inhibition.

#7154 The role of TNIK and MINK1 in TNBC tumorigenesis and invasion.

Caroline McCauley, Bruce Bunnell

University of North Texas Health Science Center, Fort Worth, TX

Introduction: TRAF2- and NCK-interacting kinase (TNIK) and Misshapen-like kinase 1 (MINK1) are implicated in MAP kinase signaling cascades, including Wnt signaling. These kinases play a role in cancer-associated processes, like migration and epithelial-to-mesenchymal transition (EMT). Migration and EMT are hallmarks associated with poorer cancer outcomes, specifically in breast cancer patients. Triple-negative breast cancer (TNBC) is more aggressive and challenging to treat, making the identification of novel targets of the utmost importance. TNIK and MINK1 are relatively understudied in TNBC; therefore, our group is studying the effect of TNIK and MINK1 knockdown on TNBC tumorigenesis, invasion, and migration.

Methods: To better understand the role of TNIK and MINK1 in TNBC, an shRNA-mediated knockdown of TNIK and MINK1 was performed in a patient-derived xenograft-derived TNBC cell line: TU-BcX-4IC (4IC). Using pre-validated shRNAs that were pre-packaged in lentiviral particles and specifically target TNIK and MINK1, the expression of these genes was diminished. We confirmed knockdown at the transcript level, as well as by monitoring GFP expression via fluorescent microscopy. We then assessed the effects of knockdown on 4IC cell spheroid formation and invasion, as well as EMT marker gene expression, using a collagen-embedded sphere migration assay and quantitative real-time PCR (qRT-PCR), respectively.

Results: TNIK and MINK1 expression were diminished after stable transduction. TNIK expression was reduced by 82% compared to the scrambled shRNA control. MINK1 expression was decreased by 92%. shTNIK and shMINK1 cell lines were unable to form as tightly compact tumor spheroids as their scrambled shRNA control counterparts. Upon characterizing the spheroids, the area and perimeter of the shMINK1 spheroids were significantly larger, while the circularity and solidity were diminished considerably compared to the control. There was no significant difference in these parameters for the shTNIK spheres, but a biological difference appears to exist. There was no significant difference in spheroid migration through collagen in either group, despite the spheres being much larger and less compact.

Conclusions: Overall, MINK1 and TNIK knockdown have an effect on TNBC cells' spheroid-forming capacity, despite no significant difference in migration being observed compared to the scrambled control. This suggests that MINK1 and TNIK may play a role in tumorigenesis, but not in migration, from a central tumor. However, further research is needed. In the future, we plan to repeat these experiments, as well as stain sectioned spheroids for extracellular matrix (ECM) markers to assess if TNIK and MINK1 are associated with changes in the ECM that may be driving the inability to aggregate. We also plan to generate a double knockdown cell line, which could provide clearer insight into the roles of both proteins simultaneously.

#7155 Therapeutic potential of a selective protein kinase Ciota inhibitor, in suppressing PI3K/AKT driven pancreatic ductal adenocarcinoma proliferation.

Shreejana Rimal[1], Grazielly Teodoro[2], Gaurab Raj Khanal[1], Abigail Oluwafisayo Olatunji[3], Abiral Hasib Shourav[2], Mildred Acevedo-Duncan[4]

[1]Chemistry, University of South Florida, Tampa, FL,[2]University of South Florida, Tampa, FL,[3]University of South Florida - Upward Bound, Tampa, FL,[4]University Of South Florida, Tampa, FL

Pancreatic cancer remains one of the most lethal malignancies due to its late-stage diagnosis and pronounced chemoresistance, ranking as the third leading cause of cancer-related deaths in the United States. Atypical Protein Kinase C (aPKC) isoforms, Protein Kinase C-iota (PKC-ι) and Protein Kinase C- zeta (PKC-ζ), are critical regulators of oncogenic signaling pathways that drive cancer cell proliferation, metastasis, and survival. In this study, we investigated the therapeutic potential of ICA-1S [5-amino-1-((1R,2S,3S,4R)-2,3-dihydroxy-4-methylcyclopentyl)-1H-imidazole-4-carboxamide], a selective PKC-ι inhibitor, in pancreatic adenocarcinoma cell lines AsPC1 and PANC1. Dose-response analyses revealed maximal inhibitory effects at 10 μM ICA-1S, reducing cell proliferation by 52% in AsPC1 and 49.8% in PANC1 cells. Western blot analysis performed on AsPC1 cell line confirmed downregulation of PKC-ι and PKC-ζ protein expression following treatment. Mechanistic studies demonstrated that ICA-1S (10 μM) significantly attenuated the Phosphatidylinositol 3-Kinase (PI3K)/Protein Kinase B (AKT) signaling cascade, phosphorylated Phosphatidylinositol 3-Kinase (pPI3K) by 51%, and total PI3K by 18%. This suppression led to a 39% decrease in phosphorylated AKT (pAKT) and an 18% decrease in total AKT, demonstrating inhibition of downstream PI3K pathway signaling. Additionally, ICA-1S treatment induced apoptosis in AsPC1 cells, as evidenced by increased expression of Cleaved Caspase-9 by 10%, increased Cytochrome c release by 17%, and decreased expression of the anti-apoptotic protein Survivin by 42%. Wound-healing assays further demonstrated the anti-metastatic effect of ICA-1S, with treated AsPC1 cells failing to close wounds even after five days, while control cells achieved complete closure.Collectively, these findings indicate that ICA-1S effectively suppresses PKC-ι-mediated PI3K/AKT signaling and promotes apoptosis in pancreatic cancer cells, underscoring its potential as a promising targeted therapeutic agent for pancreatic adenocarcinoma. Ongoing studies will employ Water-Soluble Tetrazolium (WST) assays, immunoprecipitation, immunofluorescence, and extended Western blot analyses to further delineate the downstream molecular effects of ICA-1S.

#7156 Inhibition in the proliferation of pediatric glioblastoma facilitated with atypical protein kinase c inhibitors.

Shreejana Rimal[1], Grazielly Teodoro[2], Gaurab Raj Khanal[3], Mildred Acevedo-Duncan[4]

[1]Chemistry, University of South Florida, Tampa, FL,[2]University of South Florida, Tampa, FL,[3]University of South Florida - Upward Bound, Tampa, FL,[4]University Of South Florida, Tampa, FL

Pediatric glioblastoma (pGBM) is an aggressive brain tumor with a five-year survival rate of approximately 5%. Current therapeutic options are limited, primarily due to poor blood-brain barrier penetration of available drugs. Atypical Protein Kinase C (aPKC) isoforms, Protein Kinase C- iota (PKC-ι) and Protein Kinase C- zeta (PKC-ζ), play crucial roles in tumor cell proliferation and survival. In this study, we investigated the effects of ICA-1S [5-amino-1-((1R,2S,3S,4R)-2,3-dihydroxy-4-methylcyclopentyl)-1H-imidazole-4-carboxamide], a selective PKC-ι inhibitor, and ζ-Stat [8-hydroxy-1,3,6-naphthalenetrisulfonic acid], a PKC-ζ inhibitor, on pediatric glioblastoma SF188 cells. SF188 cells (50,000/well) were seeded in 6-well plates and treated with varying concentrations of ICA-1S and ζ-Stat for three days. On the fourth day, cell viability was determined to generate a dose-response curve. ICA-1S showed maximal inhibition at 75 μM, while ζ-Stat decreased proliferation by approximately 50% at 20 μM. These results suggest that both PKC-ι and PKC-ζ contribute to SF188 cell proliferation. To explore the molecular mechanisms underlying this inhibition, protein lysates from treated and untreated cells were analyzed via Sodium Dodecyl Sulfate-Polyacrylamide Gel Electrophoresis (SDS-PAGE) and Western blotting. Both ICA-1S and ζ-Stat treatments resulted in downregulation of PKC-ι and PKC-ζ protein expression compared to control samples. Furthermore, expression of the apoptotic marker Caspase-3 was found to be decreased in drug-treated cells, suggesting activation of apoptotic signaling following inhibition of aPKCs. These findings indicate that selective inhibition of aPKCs suppresses proliferation and induces apoptosis in pediatric glioblastoma cells. Ongoing and future studies will employ immunoprecipitation, immunofluorescence, and WST assays to elucidate downstream signaling pathways and validate ICA-1S and ζ-Stat as potential therapeutic candidates for pediatric glioblastoma.

#7157 Programmable RNA-triggered cancer cell elimination using CRISPR-Cas12a2.

Jared Thompson[1], Paul Scholz[2], Kadin Crosby[3], Nathan Krah[4], Grant Schlauderaff[1], Alivia Jolley[1], Emily Wilson[5], Xiaoyang Zhang[5], Ryan Jackson[3], Chase Beisel[6], Yang Liu[1]

[1]Department of Biochemistry, University of Utah School of Medicine, Salt Lake City, UT,[2]Akribion Therapeutics GmbH, Zwingenberg, Germany,[3]Department of Chemistry and Biochemistry, Utah State University, Logan, UT,[4]Department of Internal Medicine, University of Utah, Salt Lake City, UT,[5]Department of Oncological Sciences, Huntsman Cancer Institute, Salt Lake City, UT,[6]Helmholtz Institute for RNA-based Infection Research (HIRI), Helmholtz Centre for Infection Research (HZI), Wurzburg, Germany

Selective eradication of cancer without harming healthy tissue is vital to precision oncology. Although traditional interventions such as chemotherapy or ionizing radiation are broadly applicable across many cancer types, they often exhibit off-target cytotoxicity; conversely, targeted small molecules and biologics improve specificity by binding to protein mutations, yet may not be as broadly applicable. Developing a therapeutic approach with both high specificity and broad applicability thus remains a major challenge in modern cancer care. Here, we show that Cas12a2, a recently discovered CRISPR nuclease exhibiting RNA-triggered DNA shredding, enables programmable sequence-specific elimination of mammalian cells expressing a target transcript. Target-expressing cultures electroporated with NLS-tagged Cas12a2 undergo massive cell death within five days. Activating Cas12a2 elicits widespread double-strand DNA breaks in the nucleus, leading to mitotic catastrophe, cellular inflammation, and apoptosis. We demonstrate that Cas12a2 distinguishes different RNA targets within heterogeneous cultures and induces cell death without observable off-target activity. Leveraging this approach, we eliminate NCI-H23 cancer cells harboring the prevalent oncogenic *KRAS*(G12C) point mutation, including cells with resistance to the FDA-approved *KRAS*(G12C) inhibitor Sotorasib. Taken together, these findings present Cas12a2 as a specific and broadly applicable therapeutic platform for personalized cancer treatment. These findings further establish the basis for use of Cas12a2 as a potent cell ablation tool across disciplines of basic and applied research.

#7158 Human sialidase-armed anti-B7-H3 antibody that enhances innate and adaptive antitumor immune responses.

Wayne Gatlin[1], Jen-Kuan Chang[2], Lizhi Cao[1], Hui Xu[1], Hrishikesh Metha[1], Maryann Timins[1], Mark Yang[1], Jim Broderick[1], Yanling Wang[2], Wilbert Tam[2], Grace Chung[2], Chunlei Ge[3], Lixin Feng[2], Li Peng[1]

[1]Palleon Pharmaceuticals, Waltham MA, MA,[2]Henlius USA, Milpitas, CA,[3]Shanghai Henlius Biotech, Shanghai, China

Tumor hypersialylation, overexpression of sialoglycans on cancer cell surfaces, plays a critical role in cancer progression by suppressing both innate and adaptive anti-tumor immunity. Previously, we demonstrated that an untargeted engineered human sialidase enzyme exhibited single agent and T cell-dependent antitumor activity in preclinical tumor models, a favorable safety profile in non-human primates (NHPs) and cancer patients, and proof-of-mechanism of immune modulation and antitumor signals in cancer patients in a clinical trial (NCT05259696). These findings enabled the development of a platform technology in which the engineered human sialidase is fused to tumor-associated antigen (TAA)-targeting antibodies to achieve deeper and longer tumor desialylation, enhancing both antibody-mediated effector cell cytotoxicity (innate immunity) and T-cell-mediated tumor killing (adaptive immunity). Here we report that fusion of the engineered human sialidase to anti-B7-H3 nanobody, designated E-688 (also called HLX316) significantly improves tumor desialylation depth, durability, and efficacy *in vitro* and *in vivo*, while maintaining a favorable safety profile. In assays using hypersialylated, B7-H3-expressing cancer cell lines, E-688 demonstrated markedly increased potency and pharmacodynamic (PD) effects compared with the untargeted sialidase, showing > 1,000-fold improvement in desialylation. *In vivo*, E-688 also exhibited increased durability of desialylation compared with the untargeted sialidase, extending the PD effect in disease models. Furthermore, desialylation of tumor cell surfaces with E-688 was shown to potentiate antibody-dependent cellular cytotoxicity (ADCC) and antibody-dependent cellular phagocytosis (ADCP), enhancing antibody-mediated effector cell-killing of tumor cells. Single-agent *in vivo* efficacy was observed in multiple mouse tumor models. In an A375 humanized mouse model, E-688 was superior to the B7-H3 antibody, untargeted sialidase, and anti-PD-1 antibody. E-688 was also well tolerated with no toxicity findings in a Good Laboratory Practice (GLP) one-month repeat-dose toxicity study in NHPs, with the NOAEL (no observed adverse effect level) determined to be 150 mg/kg. In summary, E-688 represents a first-in-class cancer therapy, a human-sialidase-armed anti-tumor antibody, that desialylates immunosuppressive tumor-surface sialoglycans to enhance innate and adaptive antitumor immunity. By enabling deeper and more sustained tumor desialylation, E-688 enhances antibody-mediated NK- and macrophage- killing of tumor cells and adaptive antitumor immune responses, while maintaining a favorable tolerability profile. Its clinical development is supported by strong *in vitro, in vivo*, and GLP toxicology data. Additional targets are currently in development to support a platform-based approach.

#7159 Antitumor activity of Avaren-Fc, a novel high-mannose-glycan-targeting immunotherapy, in ovarian cancer.

Katarina Mayer[1], Noel Verjan-Garcia[2], Nobuyuki Matoba[3]

[1]Pharmacology and Toxicology, University of Louisville School of Medicine, Louisville, KY,[2]Center for Predictive Medicine, University of Louisville, Louisville, KY,[3]Pharmacology and Toxicology, Center for Predictive Medicine, Brown Cancer Center, University of Louisville, Louisville, KY

Ovarian cancer (OVCA) is the most lethal and eighth most common gynecological cancer worldwide. Current standard-of-care treatments lack tumor specificity and fail to effectively manage chemoresistant disease recurrence, highlighting the need for new therapeutics. Avaren-Fc (AvFc) is a novel lectin-Fc fusion protein designed to target aberrant *N*-linked high-mannose-type glycans, an underutilized OVCA biomarker. After binding to cancer-associated high-mannose glycans, AvFc can activate Fcγ receptors and induce cytotoxic effector functions. Our previous work showed that AvFc binds to and induces antibody-dependent cell-mediated cytotoxicity (ADCC) activity against multiple human OVCA cells lines (A2780, CAOV3, SKOV3, and SW626) in an *in vitro* luciferase-based ADCC reporter assay using a FcγRIIIa-expressing cell line. AvFc also selectively recognized stage I high-grade serous OVCA tumors over adjacent normal tissue by immunohistochemistry. In the present study, we assessed the anti-OVCA activity of AvFc using the murine ID8 cell line in *in vitro* experiments and a syngeneic orthotopic challenge model in C57BL/6 mice. Flow cytometry analysis demonstrated that AvFc binds to ID8 cells in a dose-dependent manner at nanomolar concentrations, with negligible binding to isolated murine reproductive cells. AvFc binding to ID8 cells significantly increased following treatment with kifunensine, a class I α-mannosidase inhibitor, and this enhanced binding was abolished following high-mannose glycan digestion with endoglycosidase H, confirming high-mannose dependence. AvFc also induced surrogate ADCC activity against ID8 cells by activation of FcγRIIIa. AvFc's antitumor efficacy was assessed in the ID8 OVCA model, where mice were intraperitoneally (i.p.) challenged with $2x10^6$ ID8 cells and treated with 15 doses of AvFc (25 mg/kg, i.p., every other day), a non-sugar binding AvFc mutant, or vehicle beginning one-week post-challenge. AvFc treatment significantly prolonged median survival from 46 to 70 days compared with the vehicle control (p adj=0.0216, Log-rank [Mantel-Cox] test with Bonferroni's correction). Cytometry by time-of-flight (CyTOF) analysis performed one day after the final dose revealed that AvFc treatment uniquely led to the expansion of total spleen leukocytes, including Tbet+ Th1 cells, and increased $CD8^+$ T cells expressing the degranulation marker CD107a in the peritoneal fluid, suggesting that AvFc's anticancer efficacy was partially mediated by adaptive immunity. Imaging mass cytometry analysis of ID8 tumors is ongoing. Taken together, these findings highlight AvFc's promising potential as an immunotherapeutic agent for OVCA.

#7160 NEK2 drives pathogenesis, drug resistance, and LMP1 expression in EBV-positive non-Hodgkin lymphoma.

Maria C. White[1], Philip T. Lange[1], Blossom A. Damania[2]

[1]University of North Carolina at Chapel Hill, Chapel Hill, NC,[2]Associate Professor, Lineberger Cancer Ctr., University of North Carolina at Chapel Hill, Chapel Hill, NC

Non-Hodgkin lymphoma (NHL) is one of the most common cancers worldwide, representing 90% of malignant lymphomas. NHL is a diverse group of malignancies, and a subset of these lymphomas are caused by infection with the human gammaherpesvirus, Epstein-Barr virus (EBV). Many EBV-positive lymphomas are highly aggressive and rapidly develop resistance to treatment, leading to poor patient outcomes. Here, we identify the cellular kinase, NEK2, as a therapeutic target for EBV-positive NHL. We demonstrate NEK2 protein expression is increased in primary lymphocytes following EBV infection, NEK2 expression is significantly upregulated in EBV-positive NHL, and that NEK2 is necessary for the growth and survival of EBV-positive NHL. Inhibition of NEK2 resulted in lymphoma-specific cell death characterized by reactive oxygen species accumulation and gasdermin D cleavage. Additionally, protein levels of the major EBV oncoprotein, LMP1, were decreased following NEK2 inhibition. Furthermore, we demonstrate that MRP1 is the major drug resistance transporter protein in EBV-positive NHL. NEK2 inhibition reduced the expression and activity of cellular drug resistance transporter proteins including MRP1, leading to increased lymphoma cell chemosensitivity. Finally, using a humanized mouse model of EBV-driven lymphomagenesis, we demonstrate that NEK2 inhibition significantly decreased tumor burden and tumor incidence while prolonging survival *in vivo*. Taken together, our data suggest NEK2 inhibition as a promising treatment strategy for EBV-positive NHL.

#7161 A novel StarLinker™-based, CLDN18.2/PD-L1 bispecific dual-payload ADC (CAN017) overcomes tumor heterogeneity.

Pengqi Xu[1], Shaoshan Wang[1], Sanlong Wang[1], Ya Luo[1], Yili Yang[1], Wanping Geng[1], Weihao Li[1], Liying Li[1], Qin Pan[2], Xiangdong Qu[2], Henry N. Yu[1]

[1]CanWell Pharma Inc., Woburn, MA,[2]Qure Biotechnology (Shanghai) Co., Ltd., Shanghai, China

Introduction: Antibody-drug conjugates (ADCs) against the tumor-specific antigen Claudin18.2 (CLDN18.2) have now reached the clinic to treat gastrointestinal (GI) cancers (gastric, pancreatic, esophageal). PD-L1 is an immune checkpoint inhibitor and its antibodies have been approved mainly for lung and hepatocellular cancers. However, their utilities are limited by tumor heterogeneity and resistance leading to disease progression. Now we report to employ the StarLinker™ technology to engineer a first-in-class bispecific ADC (CAN017) targeting CLDN18.2 and PD-L1 bearing two different cytotoxic payloads, and assessed its antitumoral effects in vivo compared with mono-payload ADCs or single-target ADCs.

Methods: CanWell's StarLinker™ technology, which ensures stable conjugation, controlled drug-to-antibody ratio (DAR), and efficient on-target release via a cleavable linker, was used to construct an ADC by conjugating a humanized bispecific antibody targeting CLDN18.2 and PD-L1 with two distinct cytotoxic payloads. The binding, cytotoxicity of this ADC against tumor cell lines expressing CLDN18.2 only, PD-L1 only, and both targets were separately tested. The DMPK profiles of CAN017 were measured *in vivo* and *in vitro*. Furthermore, the antitumor efficacy of CAN017 was evaluated in mouse CDX and PDX tumor models, which overexpress only CLDN18.2, PD-L1 or both targets. We also compare CAN017 with single-target ADCs as references and unconjugated bispecific antibody.

Results: *In vitro* studies confirmed the high-affinity binding of CAN017 to both CLDN18.2 and PD-L1 expressing cells, and potent cytotoxic activity across all tested cell lines. CAN017 demonstrated superior cell-killing activity over single-payload or single-target ADC controls. The compound also exhibited excellent plasma stability and a favorable pharmacokinetic (PK) profile. Moreover, CAN017 showed outstanding anti-tumor activities in all tested CDX and PDX models. Notably, it achieved superior tumor growth inhibitions not only in CLDN18.2+/PD-L1+ tumor models with complete tumor regression and significantly prolonging progression-free survival, but also surprisingly in the models in which tumor cells only express single target (CLDN18.2 or PD-L1). CAN017 has demonstrated its potential to overcome tumor heterogeneity and enhance therapeutic efficacy. The results from non-human primate (NHP) toxicology studies will be presented.

Conclusion: The CLDN18.2/PD-L1 bispecific dual-payload ADC (CAN017), enabled by the StarLinker™ technology, shown superior antitumoral effects in various preclinical tumor models. Coupling with its preliminary excellent DMPK and safety profiles, it provides a strong path to become a potent next-generation ADC for the treatments of advanced solid tumors, particularly pancreatic and GI cancers.

#7162 CD180-targeting ADCs with a topoisomerase I inhibitor payload achieve strong efficacy in AML tumors.

Garima Kaushik[1], Marina Bell[1], Bandana Vishwakarama[2], Abdul Mondal[1], Maxwell Hilbert[1], Arnab Mukharjee[3], Michael Ritchie[1], Kakajan Komurov[1]

[1]Corellia AI, Rockville, MD,[2]Champions Oncology, Rockville, MD,[3]Champions Oncology (Rockville, MD), Rockville, MD

CD180 (RP105) is a type I single-pass transmembrane protein that heterodimerizes with MD-1 or MD-2 to enable stable surface expression. Characterized as an orphan Toll-like receptor predominantly expressed on mature B cells, dendritic cells, and macrophages, CD180 is also upregulated in multiple hematologic malignancies, including diffuse large B-cell lymphoma, mantle cell lymphoma, and acute myeloid leukemia (AML). Here, we identify CD180 as a novel and promising therapeutic target for AML and describe the development of a CD180-directed antibody–drug conjugate (ADC) along with its biochemical properties, antitumor activity across AML models, and pharmacokinetic and safety characteristics in non-human primates.Consistent with emerging datasets, we observed high, homogeneous CD180 expression on AML blasts, including leukemic stem and progenitor compartments, across a large cohort of primary AML specimens, with minimal to no expression on healthy hematopoietic stem cells, common myeloid progenitors, or normal tissues. We generated a fully human monoclonal antibody with high-affinity, selective binding to the human and cynomolgus CD180/MD-1 complex and no reactivity to rodent CD180.This antibody was conjugated to a topoisomerase I inhibitor with a drug-to-antibody ratio (DAR) of 8, selected for its potency and favorable stability profile in hematologic malignancies. The ADC demonstrated rapid internalization, high specificity for CD180-expressing cells, and potent cytotoxicity in AML cell lines, primary ex vivo samples, and patient-derived xenograft models, with therapeutic response strongly correlating with CD180 expression levels.In an exploratory toxicity study in cynomolgus monkeys (10, 30, and 60 mg/kg), the ADC was well tolerated, with no target-related toxicities or cytopenias observed at any dose. All clinical and histopathological findings were mild and reversible, establishing a maximum tolerated dose of 60 mg/kg. The ADC also demonstrated excellent physicochemical stability and developability properties.Together, these findings support advancement of CD180-targeted ADC therapy into clinical development for patients with CD180-positive AML.

#7164 Preclinical characterization of TRO-01, a novel CLDN18.2-targeting ADC, with potent anti-tumor efficacy and favorable PK and safety.

Young Hun Lee, Jeongho Kim, Hyun Ju Lee, Sunhwa Lee, Dong Hoon Seo, Myoungki Baek, Sung Ho Woo

TriOar Inc., Daejeon, Korea, Republic of

Claudin 18.2 (CLDN18.2) is a tight junction protein normally restricted to the gastric mucosa. Loss of epithelial polarity during malignant transformation exposes CLDN18.2 on the surface of gastric and gastroesophageal junction (G/GEJ) adenocarcinoma cells. As CLDN18.2 is highly expressed in 30–40% of G/GEJ cancers and is associated with poor prognosis, it has emerged as a promising therapeutic target for gastric cancer, where effective targeted therapies remain limited. We developed TRO-01, an antibody-drug conjugate (ADC) composed of a fully human anti-CLDN18.2 monoclonal antibody conjugated to a topoisomerase I inhibitor via the proprietary TROSIG^{TM} linker. This cleavable, highly stable, and hydrophilic linker enables a high and uniform drug-to-antibody ratio (DAR) of 8. In vitro studies demonstrated that TRO-01 specifically binds to CLDN18.2 but not to CLDN18.1, exhibiting enhanced affinity compared with competitor antibodies, with cell binding affinities in the single nanomolar range across tested cell lines. Additionally, TRO-01 showed efficient internalization and potent cytotoxicity in CLDN18.2-positive cell lines, with IC_{50} values ranging from sub-nanomolar to double-digit nanomolar depending on the cell type. In vivo, TRO-01 treatment resulted in significant tumor growth inhibition (TGI) in both cell line-derived xenograft (CDX) and patient-derived xenograft (PDX) models. In the Patu8988s CDX model, a single dose of 3 or 6 mg/kg resulted in 86% and 101% TGI, respectively. In the SNU-601 CDX model, BIW x 4 dosing at 0.3 or 0.5 mg/kg resulted in 109% and 111% TGI. In two gastric and two pancreatic PDX models, TRO-01 treatment (QW x 2, 2.7 mg/kg) resulted in 89% and 93% TGI in gastric, and 75% and 84% TGI in pancreatic PDXs, with no significant body weight loss. Pharmacokinetic studies in monkeys demonstrated favorable PK properties ($t_{1/2}$ = 7.2 days, AUC = 13,800 hr·μg/mL, CL = 0.364 mL/hr/kg, Vd = 0.082 L/kg at 5 mg/kg). Toxicology studies in cynomolgus monkeys revealed a favorable safety profile, with a highest non-severely toxic dose (HNSTD) of 40 mg/kg after single dosing. Collectively, these findings highlight TRO-01 as a promising therapeutic candidate for the treatment of CLDN18.2-expressing gastrointestinal cancers.

#7165 The role of NEK2 and AURKB on triple-negative breast cancer progression.

Elliott Rodriguez-Lopez, Alexandra Aquino-Acevedo, Joel Orengo-Orengo, Gretchen Albarran-Acosta, Katiushka Berrocales, Harold Saavedra

Basic Sciences, Ponce Health Sciences University, Ponce, PR

Triple-negative breast cancer (TNBC) is the most aggressive subtype of breast cancer, accounting for 10-20% of all cases. TNBC's aggressiveness is mostly attributed to its high rates of chromosomal instability, proliferation, and metastatic potential. Molecular subtyping has revealed that overexpression of mitotic kinases NEK2 and AURKB is implicated in chromosomal instability and epithelial-to-mesenchymal transition (EMT). Recent studies have shown that the mitotic kinases NEK2 and TTK (a kinase regulated by AURKB) are involved in early metastatic signaling by promoting EMT, cell migration, and invasion through distinct transcriptional pathways. Despite their clinical relevance, no co-targeting therapeutic strategy exists to interrupt the distinct mitotic signaling pathways driven by these kinases. Thus, our study aims to investigate the functional convergence of NEK2 and AURKB signaling pathways as drivers of EMT and metastatic progression in TNBC. We hypothesize that NEK2 and AURKB cooperatively regulate mitotic and EMT-associated phosphorylation events that fuel early metastasis. Our approach leverages TNBC cell models representing ancestrally distinct origins (MDA-MB-231 and MDA-MB-157) and utilizes genetic knockdown to dissect how individual and dual suppression of NEK2 and AURKB alters the phosphorylation state and functional behavior of TNBC cells. Preliminary findings using Kaplan-Meier survival analysis confirm that high expression of NEK2 or AURKB is significantly associated with overall survival and relapse-free survival. STRING (Search Tool for the Retrieval of Interacting Genes/Proteins) protein-protein interaction analysis showed that both AURKB and NEK2 may converge on EMT-related processes, while STRING-based GO enrichment suggested that their inhibition may impair metastatic progression by disrupting EMT signaling in TNBC. Western blot analysis confirmed a decrease in EMT biomarkers Vimentin and Slug after individual and dual knockdown of NEK2 and AURKB. Moreover, invasion assays demonstrated a statistically significant reduction after individual and dual knockdown of both kinases. Overall, these results suggest that suppression of the mitotic kinases NEK2 and AURKB could disrupt EMT-associated metastatic potential in TNBC MDA-MB-231 cells. Ongoing experiments will further confirm and expand these findings. This project may advance the development of more effective precision-targeted approaches for TNBC, particularly for African American and Caribbean Hispanic/Latino women who are disproportionately affected.

: Role of the Microenvironment in Therapeutic Response
Poster Session

#7169 Longitudinal single-cell profiling of breast tumors reveals immune and epigenetic mechanisms of sensitivity and resistance to aromatase inhibitors.

Ilayda Altinonder[1], Villads Winton[1], Quy Khang Le[2], Marie Fongaard[1], Paal M. Bjornstad[3], Elin Edda Seland Agustsdottir[4], Stephanie Geisler[5], Kamilla Fjermeros[5], Manouchehr Seyedzadeh[6], Unn-Cathrin Buvarp[5], Marianne Lyngra[7], Arnoldo Frigessi[8], Diether Lambrechts[9], Vessela N. Kristensen[3], Anthony Mathelier[8], Victor Greiff[2], Jurgen Geisler[5], **Xavier Tekpli**[1]

[1]Department of Pathology, Oslo University Hospital, Oslo, Norway,[2]Department of Immunology, Oslo University Hospital, Oslo, Norway,[3]Department of Medical Genetics, Oslo University Hospital, Oslo, Norway,[4]Department of Breast and Endocrine Surgery, Akershus University Hospital, Oslo, Norway,[5]Department of Oncology, Akershus University Hospital, Oslo, Norway,[6]Department of Radiology, Akershus University Hospital, Oslo, Norway,[7]Department of Pathology, Akershus University Hospital, Oslo, Norway,[8]University of Oslo, Oslo, Norway,[9]KU Leuven, Leuven, Belgium

Background. Aromatase inhibitors like letrozole and exemestane play a pivotal role in the treatment algorithms for estrogen receptor (ER) positive breast cancer in all phases of the disease. However, resistance to such therapies is not fully understood and remains a major clinical challenge.
Methods. To investigate the mechanisms of sensitivity and resistance to aromatase inhibitors in ER-positive HER2-negative breast cancer, we conducted single-cell RNA (scRNA-seq), T cell receptor (scTCR-seq), and B cell receptor (scBCR-seq) sequencing on tumor biopsies obtained before and during neoadjuvant therapy with letrozole and exemestane given in a randomized sequence for 6 months.
Results. We examined 472,737 single cells from 73 biospecimens collected at baseline (n=25), at mid-therapy (n=24) and at the end of neoadjuvant treatment (n=24). We identified transcription start site usage at single cell level to study the role of enhancer activity in the evolution of breast tumors under treatment pressure. Malignant cells that were sensitive to treatment exhibited elevated ER-signaling and increased activity in enhancers containing ER binding sites. Conversely, resistant malignant cells showed upregulated androgen receptor (AR) signaling, cellular de-differentiation, and neuroendocrine-like characteristics. The activity of AR cis-regulome increased under treatment in non-responders, suggesting a role of epigenetic modifications in treatment resistance. Treatment-naïve tumor microenvironment was predictive of response. Non-responders displayed high proportions of naive lymphoid and undifferentiated myeloid cells, indicating an ineffective immune landscape. In contrast, responders were characterized by clonal expansion of T cells.
Conclusions. Taken together our longitudinal single-cell analyses delineate the genetic, epigenetic and cellular mechanisms that drive sensitivity and resistance to aromatase inhibitors in ER positive breast cancer, opening avenues for improved treatment strategies. Footnotes. Ilayda Altinönder and Villads Winton are shared first authors. Jürgen Geisler, Xavier Tekpli have jointly supervised this work.

#7170 AKT inhibition with capivasertib counteracts tumor microenvironment remodeling and enhances AR-targeted therapy in PTEN-deficient prostate cancer.

Marco A. De Velasco[1], Kazuko Sakai[1], Daiki Nakatsu[1], Mamoru Hashimoto[1], Saizo Fujimoto[1], Shingo Toyoda[1], Takafumi Minami[1], Kazuhiro Yoshimura[1], Simon T. Barry[2], Cath Eberlein[2], Claire Rooney[2], Kazuto Nishio[1], Hirotsugu Uemura[1], Kazutoshi Fujita[1]

[1]Kindai University Faculty of Medicine, Sakai City, Japan,[2]AstraZeneca, Cambridge, United Kingdom

Background: PTEN loss in prostate cancer activates PI3K/AKT/mTOR signaling, driving extensive tumor microenvironment (TME) remodeling characterized by stromal desmoplasia, angiogenesis, and immune suppression. Capivasertib (AZD5363), a potent pan-AKT inhibitor, has shown therapeutic benefit in PTEN-deficient tumors when combined with androgen deprivation therapy (ADT) and abiraterone, as demonstrated in preclinical studies and the Phase III CAPItello-281 trial.
Objective: To investigate how AKT inhibition modulates TME dysregulation in PTEN-deficient prostate cancer following AR-targeted therapy.
Methods: Conditional Pten-knockout mouse tumors underwent baseline transcriptomic profiling to characterize AKT-driven changes and ADT effects. TME responses were evaluated in conditional Pten/Trp53 knockout mice after four weeks of ADT and abiraterone (Abi), with or without capivasertib. Analyses included qRT-PCR panels, flow cytometry, and quantitative immunohistochemistry (IHC).
Results: PTEN deletion induced AKT hyperactivation and upregulated MSigDB hallmark pathways associated with TME remodeling, including hypoxia, angiogenesis, inflammatory response, IL6-STAT3, and TGFβ signaling. ADT amplified these changes, while abiraterone further increased extracellular matrix (ECM) remodeling gene expression. Capivasertib co-treatment significantly downregulated ECM and angiogenesis-related genes. Histological evaluation revealed reduced dense, haphazard collagen deposition and fewer inflammatory infiltrates in capivasertib-treated tumors. IHC confirmed decreased stromal p-S6 and p-PRAS40, lower Ki67-positive stromal cell counts, and reduced microvessel density (CD31). Gene signatures for PMN cells, MDSCs, and TAMs—key mediators of ECM remodeling—were diminished, particularly in mice showing strong antitumor responses to capivasertib. Flow cytometry and IHC corroborated the reduction of PMN/MDSC populations in treated tumors.
Conclusion: Capivasertib enhances tumor growth inhibition achieved by ADT plus abiraterone and mitigates TME remodeling associated with PTEN loss and AR-targeted therapy. These findings highlight AKT inhibition as a strategy to counteract TME-driven disease progression and improve therapeutic outcomes.

#7171 Antitumor and antiangiogenic activities of E7386 in combination with lenvatinib in human endometrial carcinoma xenograft models.

Yusuke Adachi, Yudai Narita, Shogo Yamaguchi, Taro Semba

Tsukuba Research Laboratories, Eisai Co., Ltd., Ibaraki, Japan

Background: E7386 is an inhibitor of the protein-protein interaction between CREB-binding protein (CBP) and β-catenin. Currently, a clinical study of E7386 in combination with lenvatinib (LEN), a multiple receptor tyrosine kinase inhibitor mainly targeting VEGFRs and FGFRs, is ongoing for the treatment of advanced solid tumors including endometrial carcinoma (EC) (NCT04008797). We previously reported that E7386 in combination with LEN showed greater antitumor activity and reduction of tumor microvessels than each agent alone in preclinical hepatocellular carcinoma tumor models. In this study, we investigated the antitumor and antiangiogenic activities of E7386 plus LEN in multiple human EC xenograft models.
Methods: Human EC cell lines (HEC151, HEC251, JHUEM2, and HEC50B) were subcutaneously inoculated into female nude mice. Mice with EC xenograft tumors were treated with E7386 at 6.25-50 mg/kg (orally [PO], once daily [QD]) and/or LEN at 10 mg/kg (PO, QD) for 7-14 days. Tumor microvessel analysis of formalin-fixed and paraffin-embedded tumor samples was performed by immunohistochemistry staining using the anti-CD31 antibody.
Results: E7386 in combination with LEN showed enhanced antitumor activity compared with either monotherapy alone without severe body weight loss (>20% body weight loss) in all EC xenograft models tested. Notably, tumor regression was observed by the combination treatment in HEC251 and HEC50B models. The enhancement of antitumor activity was consistently observed across models with E7386 doses at 25 and 50 mg/kg. Tumor microvessel analysis in the HEC151 model revealed that LEN monotherapy decreased the microvessel density, and the combination treatment showed more potent antiangiogenic activity compared with LEN monotherapy.
Conclusion: These results suggest that the combination of E7386 with LEN exerted enhanced antiangiogenic activity against tumor microvessels compared with LEN-alone, and demonstrated potent antitumor activity in preclinical EC xenograft models.

#7172 Combination of B7-H4-TOP1i ADC, PD-1/TIGIT bispecific antibody, and PARP inhibition orchestrates angiogenesis suppression and interferon-program activation in a syngeneic mouse model.

Octavio Morante-Palacios[1], Jon Chesebrough[2], Yoshimi Johnson[3], Raymond Rothstein[3], Varsha Shankarappa[4], Joseph Boland[5], Elizabeth Galery[5], Anna Dominika Staniszewska[6], Mark R. Albertella[6], Alex Cazes[2], Paul Chariou[3], Bilal Omar[3]

[1]Early Oncology Data Science, Oncology Data Science & AI, Oncology R&D, AstraZeneca, Barcelona, Spain,[2]Early Oncology- Oncology Targeted Delivery-Drug Conjugates, Oncology R&D, AstraZeneca, Gaithersburg, MD,[3]Clinical IO Discovery, IO Discovery & Cell Therapy Oncology, Oncology R&D, AstraZeneca, Gaithersburg, MD,[4]Oncology Data Science Platforms, Oncology Data Science & AI, AstraZeneca, Barcelona, Spain,[5]Translational Medicine, Oncology R&D, AstraZeneca, Gaithersburg, MD,[6]Bioscience, Oncology R&D, AstraZeneca, Cambridge, United Kingdom

Purpose: To define the pharmacodynamic mechanisms and synergies of a B7-H4 antibody-drug conjugate (ADC) with a topoisomerase I inhibitor (puxitatug samrotecan; AZD8205), a PD-1/TIGIT bispecific antibody (rilvegostomig; PD-1 arm engineered for murine binding), and a PARP1-selective inhibitor (saruparib), using single-cell RNA sequencing (scRNA-seq) in the MC38 hB7-H4 P1A9 murine syngeneic model.
Methods: C57BL/6J mice bearing MC38 hB7-H4 P1A9 tumors received vehicle, NIP228 (7 mg/kg ADC control), AZD8205 (7 mg/kg), rilvegostomig (10 mg/kg), saruparib (0.1 mg/kg), or doublet combinations. Tumors were collected on day 11 post-treatment and analyzed through scRNA-seq. scRNA-seq data underwent quality control, log normalization, dimensionality reduction, and clustering. After filtering, 356,930 high-quality cells across 38 samples were selected for downstream analyses (n = 4-5 per group). Gene set enrichment analysis (GSEA) using MSigDB Hallmark pathways was performed on pseudobulk differential expression analysis (DEA) profiles for each annotated cell type, comparing treatment groups. Enrichment was considered significant at FDR < 0.01 with |NES| > 1.5, and multiple testing correction was applied across all gene sets per cell type.
Results: All treatment groups showed increased immune infiltration versus vehicle. Pseudobulk DEA showed the most pronounced transcriptional changes occurred with AZD8205 in tumor cells, rilvegostomig in CD8+ T cells, and saruparib in macrophages. Doublet treatments suppressed epithelial-mesenchymal transition, hypoxia, and angiogenesis hallmarks in tumor cells, with decreased *Vegfa* expression, particularly in the AZD8205+ rilvegostomig group. CD8+ T cells from combination groups displayed heightened interferon response programs, and macrophages exhibited concordant interferon-response activation compared to single treatments. Further T cell sub-clustering revealed that rilvegostomig boosts effector T cells and reduces regulatory T cell representation, especially in combination with AZD8205.
Conclusions: scRNA-seq results indicate that the studied drug combinations produce a transcriptomic remodeling characterized by coordinated tumor-cell program suppression and system-wide interferon response amplification in immune cells. AZD8205 doublet treatments deliver the most extensive tumor-intrinsic transcriptional changes, while rilvegostomig or saruparib each add orthogonal immune activation, yielding complementary and potentially synergistic pharmacodynamics that are not observed with individual drugs. The ongoing BLUESTAR clinical trial (NCT05123482) is exploring these combinations in patients. Our preclinical findings suggest potential mechanisms of action and support further investigation.

#7173 Mechanistic studies of fibroblast activation protein activated prodrug AVA6000 in pancreatic and liposarcoma models.

Lisa Pickard[1], Ekta Paranjape[1], Brian Cunningham[2], **Udai Banerji**[2]

[1]The Institute of Cancer Research, London, United Kingdom,[2]The Institute of Cancer Research, London, London, United Kingdom

Background: This study shows single agent and combinatorial activity of AVA6000 (Faridoxorubicin, FAP-Dox), in pancreatic cancer and liposarcoma, cancer associated fibroblast co-culture models. Fibroblast activation protein (FAP) is a transmembrane serine protease and present in cancer associated fibroblasts and some cancer cells. AVA6000 is a FAP cleavable peptide drug conjugate comprised of doxorubicin and a dipeptide that is selectively cleaved by FAP to release active doxorubicin within the tumour microenvironment. We aimed to study a) FAP-specific release of doxorubicin b) combinatorial activity of AVA6000 with DNA damage repair inhibitors, in preclinical models.

Methods: Cancer cells, labelled with GFP, were co-cultured with pancreatic stellate cells (PSCs) showing features of myofibroblastic cancer associated fibroblasts (such as alpha smooth muscle antigen expression) which expressed FAP. Cancer cell growth was quantified by counting the number of GFP labelled cancer cells per well, with cancer cells alone (i.e. no CAFs) used as controls. In addition, we studied the effects of the FAP inhibitor Talabostat (PT100) in reversing the effects of AVA6000 in co-culture conditions. Further, we tested the effects of the combination of an ATR inhibitor BAY1895344 in combination with AVA6000 in the coculture system.

Results: The GI_{50} of AVA6000 in two pancreatic cancer cell lines ASPC-1 and Mia-Paca-2 in the co-culture system with PSCs was 58±21.4nM, (Stdev,n=3) and 66.5±16.3nM (Stdev, n=3). No GI_{50} was obtained in both cell lines at the highest concentration of AVA6000 studied in both cell lines (>100nM n=3) if PSCs were not included in the culture. In addition, we demonstrated that the FAP inhibitor talabostat at 100μM reversed any growth inhibition by AVA6000 (highest concentration of AVA6000 tested 100nM) confirming AVA6000 activation was FAP dependent. We further studied the growth inhibition of AVA6000 in the liposarcoma cell line SW872-GFP in co-culture with FAP expressing fibroblasts GI_{50} 30.6±6.7 nM (StdevD, n=4). The GI_{50} of AVA6000 was not achieved in the absence of fibroblasts at >100nM and the FAP inhibitor talabostat reverses this growth inhibitor effect in the co-culture system. The combination of AVA6000 and BAY1895344 in the co-culture yielded a 2 fold shift in GI_{50}.

Conclusions: AVA6000, is selectively activated by FAP expressing PSCs and is active in pancreatic and liposarcoma co-culture models. It also exhibits synergistic growth inhibition activity with ATR inhibitors in liposarcoma co-culture models. Clinical trials of AVA6000 are ongoing (NCT04969835).

#7174 Restoring antitumor immunity and improving immunotherapy outcomes in KRAS-mutant NSCLC through MYC inhibition by OMO-103.

Inigo Gonzalez-Larreategui[1], Silvia Casacuberta-Serra[2], Magda Arnal[2], Daniel Capitan-Leo[1], Sandra Martinez-Martin[2], Vera Adradas[3], Melina Peressini[3], Laura Vera[4], Lorena Sansegundo-Barbosa[2], Fabio Giuntini[1], Manuel Lillo-Valero[1], Manrique Valdes-Bango Martin[1], Erika Serrano del Pozo[1], Judit Grueso[1], Laia Foradada[2], Sergio Lopez-Estevez[2], Hugo Thabussot[2], Jonathan R. Whitfield[1], Marie-Eve Beaulieu[2], Jon Zugazagoitia[3], Silvestre Vicent[4], Laura Soucek[1]

[1]VHIO Vall D'Hebron Institute of Oncology, Barcelona, Spain,[2]Peptomyc S.L., Barcelona, Spain,[3]H12O-CNIO Lung Cancer Clinical Research Unit, Health Research Institute Hospital 12 de Octubre (imas12)/Spanish National Cancer Research Center (CNIO), Madrid, Spain,[4]Center for Applied Medical Research (CIMA), Pamplona, Spain

Background: MYC is a key oncogenic driver that promotes tumor progression, immune evasion, and therapy resistance. In KRAS-mutant non-small-cell lung cancer (NSCLC), where effective treatments remain limited, MYC functions as a major downstream effector of RAS signaling. High MYC expression in KRAS-mutant NSCLC patient samples is associated with reduced immune engagement and suppression of Tumor Necrosis Factor (TNF) superfamily pathway, suggesting a role for MYC in shaping the tumor immune microenvironment (TIME). We investigated whether MYC inhibition using OMO-103 (Omomyc), the first clinically viable direct MYC inhibitor, could reprogram the TIME and enhance immunotherapy response.

Methods: We performed transcriptomic analysis of KRAS-mutant NSCLC patient samples and generated a $KRAS^{G12D}$-driven transgenic mouse model exhibiting MYC-dependent immunosuppression. Using cell lines derived from this model, we evaluated the effects of MYC inhibition on proliferation and immune-related signaling. *In vivo* studies were conducted in multiple KRAS-driven NSCLC mouse models to assess tumor growth, immune infiltration, and TNF receptor pathway activation. Clinical relevance was examined through analysis of patient samples from the MYCure Phase I trial (NCT04808362).

Results: MYC inhibition impaired cell proliferation and upregulated multiple immune-activating pathways *in vitro. In vivo*, OMO-103 halted tumor progression, increased immune cell infiltration, and enhanced activation of TNF receptor family members—including OX-40 and 4-1BB—on tumor-infiltrating T cells, driving secretion of interferon-γ and TNF-α. Combining OMO-103 with TNFR-targeting immunotherapies resulted in significantly greater tumor regression and overall response rate than monotherapy. Analysis of MYCure patient samples confirmed that OMO-103 induces a more immune-active TIME, with increased interferon response and antigen presentation. Notably, patients with clinical benefit displayed increased expression of TNF superfamily members in tumors and serum, with the KRAS-mutant NSCLC patient showing the highest induction.

Conclusions: MYC inhibition with OMO-103 not only suppresses tumor growth but also reprograms the TIME to promote anti-tumor immunity and enhance response to immunotherapy. These findings support MYC blockade as a promising therapeutic strategy to overcome immunotherapy resistance in KRAS-mutant NSCLC.

#7175 Targeting spatial patterns of CAFs and tumor cells for precision stroma-targeted radionuclide therapy.

Yuning Sun[1], Ye Yang[2], Guanyu Zhu[3], Jiangang Zhang[1], Xiaowei Fan[4], Jian Wang[1], Yang Liu[1], Shaoyan Liu[1], Yansong Lin[5], Xi-Yang Cui[6], Zhibo Liu[7], **Ziren Kong**[1]

[1]Department of Head & Neck Surgery, National Cancer Center/National Clinical Research Center for Cancer/Cancer Hospital, Chinese Academy of Medical Sciences and Peking Union Medical College, Beijing, China,[2]Department of Pathology, National Cancer Center/National Clinical Research Center for Cancer/Cancer Hospital, Chinese Academy of Medical Sciences and Peking Union Medical College, Beijing, China,[3]Chinese Academy of Medical Sciences and Peking Union Medical College, Beijing, China,[4]Changping Laboratory, Beijing, China,[5]Department of Nuclear Medicine, Peking Union Medical College Hospital, Chinese Academy of Medical Sciences and Peking Union Medical College, Beijing, China,[6]Institute of Radiation Medicine, Chinese Academy of Medical Sciences and Peking Union Medical College, Tianjin, China,[7]Beijing National Laboratory for Molecular Sciences, Radiochemistry and Radiation Chemistry Key Laboratory of Fundamental Science, NMPA Key Laboratory for Research and Evaluation of Radiopharmaceuticals, Key Laboratory of Bioorganic Chemistry and Molecular, Beijing, China

Stroma-targeted imaging, particularly fibroblast activation protein inhibitor (FAPI) PET-CT, has demonstrated remarkable diagnostic success across multiple cancer types. In contrast, stroma-targeted radionuclide therapy using ^{177}Lu-labeled compounds showed limited clinical efficacy (response rate: 10%-20%), despite achieving sufficient macroscopic accumulation within tumor lesions. We therefore hypothesize that the microscopic spatial organization between cancer-associated fibroblasts (CAFs) and tumor cells critically influences intratumoral distribution and radiation dose deposition of ^{177}Lu at the microscale. The primary objective of this study is to investigate how spatial pattern affects ^{177}Lu distribution and dose deposition, and to experimentally validate the differential therapeutic outcomes across different spatial patterns.Using medullary thyroid carcinoma (MTC) as a representative model, we performed quantitative histopathological analysis of 279 tissue sections from 15 patients through co-registration, automated image segmentation, and spatial distribution profiling. This identified two recurrent spatial patterns: a "surrounding" type, where CAFs form a continuous ring around tumor clusters, and an "infiltrative" type characterized by a reticular CAF network with dispersed tumor nests. These patterns were consistently observed across primary tumors, lymph node metastases, and invasive foci.Monte Carlo simulations revealed highly heterogeneous ^{177}Lu dose distributions across spatial patterns. While infiltrative lesions showed effective dose delivery, surrounding lesions exhibited dose deposition primarily confined to CAF-rich peripheries. We established biologically relevant 3D bioprinted models mimicking both patterns using 6% GelMA 30 hydrogel, which matches human thyroid mechanical properties (10-20 kPa). Immunohistochemical and immunofluorescence analyses confirmed biological fidelity. Autoradiography with [^{177}Lu]Lu-FS-86 demonstrated distinct uptake patterns - concentrated in CAF rings (surrounding) versus homogeneous distribution (infiltrative) - validating functional relevance.

These models confirmed that the infiltrative pattern allowed homogeneous dose distribution of ^{177}Lu and significant cell death, whereas the surrounding type exhibited limited penetration and limited response. Importantly, we observed consistent therapeutic outcomes across multiple cancer types including lung, liver, breast, and medullary thyroid carcinomas, indicating that stroma-targeted radionuclide efficacy is spatial pattern-dependent rather than tumor type-dependent. The establishment of this spatial classification system provides a framework for identifying optimal stroma-targeting radionuclides based on distinct spatial patterns, demonstrating significant potential for clinical translation.

#7176 Next-generation human vascularized tumor models reveal HER2-independent efficacy and reduced vascular toxicity of T-DXd.

Francesco Bonollo[1], Soheila Zeinali[1], Sabine Schneider[1], Christian Moser[2], Olivier Thierry Guenat[1]

[1]ARTORG Center, University of Bern, Bern, Switzerland,[2]vitronco AG, Bern, Switzerland

Purpose: Antibody-drug conjugates (ADCs) elicit complex responses that conventional 2D assays fail to capture, especially in HER2-low and HER2-negative tumors. We developed human vascularized 3D tumor models to assess the efficacy of HER2-targeting ADC, their mechanism of action, and vascular toxicity with improved physiological relevance.
Methods: Vascularized 3D breast cancer microtissues (HER2-positive and HER2-negative) were generated using human breast cancer cell lines and microvascular networks. Trastuzumab deruxtecan (T-DXd) or Trastuzumab-emtansine (T-DM1) treatment was performed for four days. Real-time monitoring was performed to assess anti-tumor efficacy and vascular toxicity by quantifying the tumor cell-associated fluorescent signal and vascular area density.
Results: T-DXd showed significant cytotoxicity in both HER2-positive and HER2-negative vascularized tumors, whereas in 2D monocultures, T-DXd cytotoxicity against HER2-negative cells was not detected. T-DM1 was effective only in HER2-positive vascularized tumors. T-DM1, unlike T-DXd, induced a strong vascular toxicity in both HER2-positive and HER2-negative tumor models with vascularization.
Conclusions: Human vascularized tumor models capture key pharmacodynamic features of ADCs, including the HER2-independent mechanism of action, extracellular payload activity, and vascular toxicity, which are not recapitulated in 2D systems. HER2-independent efficacy of T-DXd, but not of T-DM1, has also been reported in in vivo breast cancer xenograft models in agreement with these findings. Furthermore, real-time monitoring enabled quantification of tumor regression and vascular remodelling, underscoring the functional relevance and predictive performance of the platform. This platform offers a rapid, quantitative, and predictive approach for evaluating next-generation ADCs, thereby enhancing translational alignment with in vivo outcomes.
AI disclosure: AI-assisted text generation was used to revise this abstract.

#7178 Targeted modulation of the blood-tumor barrier enhances drug delivery and survival in glioblastoma models.

Philippa C. Vaughn-Beaucaire[1], William Hawkins[2], Jasmine S. Clark[2], Jorge Luis Jimenez Macias[3], Bin Wu[4]

[1]Pathology and Laboratory Medicine, Brown University, Providence, RI,[2]Legorreta Cancer Center at Brown University, Providence, RI,[3]Brown University, Providence, RI,[4]Cytodigm, Natick, MA

Efficient drug delivery in glioblastoma (GBM) remains a major therapeutic challenge due to the restrictive properties of the blood-brain and blood-tumor barriers (BBB/BTB). We previously identified a BTB-associated transcriptional signature highlighting CDH5 (vascular endothelial cadherin) as a critical regulatory molecule highly expressed in GBM vasculature. Using bulk RNA sequencing and spatial transcriptomics, we confirmed that CDH5 and its associated genes are selectively enriched in tumor-associated endothelial cells compared with healthy brain tissue. Mechanistically, we show that the indirubin derivative 6-bromoindirubin acetoxime (BIA) significantly downregulates CDH5 and additional BTB-signature genes, including ACVRL1, ENG, and CD93. This molecular modulation disrupts endothelial barrier integrity, demonstrated by reduced trans-endothelial electrical resistance and increased dextran permeability in vitro, as well as enhanced intratumoral sodium fluorescein and cisplatin accumulation in vivo in murine GBM xenograft models. BIA treatment further augments cisplatin efficacy by increasing DNA damage, resulting in significantly extended survival compared with monotherapy. To investigate underlying mechanisms, we are assessing the effects of BIA on transcription factors involved in BBB regulation (including CREB and ERG) and on cytoskeletal dynamics. Given that BIA is a broad-spectrum kinase inhibitor with limited translational potential, we are actively evaluating FDA-approved kinase inhibitors, such as dasatinib. as clinically viable alternatives for rapid translation. Preliminary data indicate that dasatinib similarly disrupts BTB integrity and enhances chemotherapeutic penetration into GBM tumors. Ongoing studies are testing dasatinib's preclinical efficacy, specifically its impact on drug delivery, safety, and therapeutic effectiveness. Collectively, these findings position targeted BTB modulation as a promising therapeutic strategy. Leveraging both novel agents such as BIA and repurposed FDA-approved drugs like dasatinib may significantly enhance drug delivery, improve therapeutic outcomes, and ultimately benefit patients with GBM.

: Targeted Radiopharmaceuticals and Combination Strategies in Cancer Therapy
Poster Session

#7182 Development and evaluation of a novel high affinity PSMA-targeted radioligand ^{177}Lu-PSMA-3D1015 for prostate cancer.

Lu Hou[1], Quanpeng Wang[1], Haitian Fu[1], Chuang Xi[1], Wanggui Yang[2], Fangqiang Tang[2], Qing Gao[2], Lan Qin[2], Wenhua Huang[2], Henry Ho[2], Chunjing Yu[3], **John Gong**[2]

[1]Department of Nuclear Medicine, Affiliated Hospital of Jiangnan University, Wuxi, China,[2]3D Medicines Co., Ltd., Shanghai, China,[3]Department of Nuclear Medicine, Affiliated Hospital of Jiangnan University; Jiangnan University, Wuxi, China

Background: The clinical efficacy of PSMA targeted RLT for metastatic PCa has been well established by Pluvicto®. However, the suboptimal characteristics of existing agents, such as short tumor retention and rapid clearance, may limit the efficiency of radiation energy from ^{177}Lu decay. The small molecular compound, 3D1015, is a newly designed PSMA-targeted ligand with high affinity. Its radiolabeled product, ^{177}Lu-PSMA-3D1015 (hereafter "3D1015"), has been developed to prolong its retention in the tumor tissue, and has shown excellent tumor inhibition effect at low dose, along with great safety profile.
Method: The binding affinity of ligand to PSMA was evaluated using LNCaP cells via FACS-based competition assay, with PSMA-617 as a reference. In vivo biodistribution and efficacy were assessed in LNCaP xenograft B-NDG mice by calculating uptake (%ID/g) and measuring TGI (%) across dose groups. A single-dose toxicity study in SD rats was conducted to determine the dose tolerance and identify target toxic organs. An exploratory study further investigated the dosimetry and safety of 3D1015 in patients with PSMA-positive mCRPC who had failed SOCs. Eligible patients received a single administration of 3D1015 (10 mCi, *i.v.*) then underwent qSPECT/CT at different timepoints.
Results: IC_{50} values were 1.47 nM for 3D1015 ligand and 4.11 nM for PSMA-617. Radiolabeling with ^{177}Lu under mild conditions achieved >97% RCP. Biodistribution studies revealed rapid and sustained tumor uptake of 3D1015, reaching 36.50 %ID/g at 120 h, with renal excretion indicated by high kidney exposure (max: 59.47 %ID/g at 72 h). Efficacy studies demonstrated dose-dependent efficacy (TGI: 80.0%, 98.3%, and 99.8% at 0.1, 0.5, and 1.0 mCi/mouse, respectively). A dose of 0.5 mCi 3D1015 achieved superior TGI versus 1.0 mCi ^{177}Lu-PSMA-617 (TGI: 94.0%). Toxicity study identified the spleen as the primary target organ, with a MTD of 15 mCi/kg; transient toxicities in body weight, food intake, and hematology were fully reversible. Two patients received a single dose of 10 mCi of 3D1015. SPECT/CT imaging indicated that the drug was primarily excreted via the hepatobiliary/intestinal route rather than the renal excretion pathway as shown in the previous animal toxicity research. Uptake of *3D1015* was observed in all pre-identified lesions till 216 h. Mean absorbed dose in kidneys, submandibular and parotid glands, liver, spleen, and bone marrow was 0.80, 1.35, 0.44, 1.12, and 0.12 mGy/MBq, respectively. No > G2 TRAEs occurred. A 14% decline of PSA was observed in 1pts after one dose of 10mCi infusion.
Conclusion: ^{177}Lu-PSMA-3D1015 exhibits high PSMA affinity and prolonged retention in tumor, potentially driving potent efficacy at lower doses. Its distinct hepatobiliary excretion profile differentiates it from existing therapies. These findings address key limitations of current RLTs, and further clinical trials are ongoing.

#7183 SCN-PYTA: A new bifunctional chelator (BFC) for trivalent radiometals to develop target-specific radiopharmaceuticals for imaging and therapy.

Shankar Vallabhajosula[1], Nikki A. Thiele[2], Kyu J. Son[1], Vicente Navarro[1], Md Faizul Islam[2], Alex Brown[1], Neil H. Bander[1], Phillip W. Kantoff[1]

[1]Convergent Therapeutics, Inc., Cambridge, MA,[2]Chemical Sciences Division, Oak Ridge National Laboratory, Oak Ridge, TN

Introduction: The 18-membered macrocycle PYTA is a universal chelator that can complex trivalent radiometals (e.g., ^{225}Ac, ^{177}Lu, ^{111}In and ^{44}Sc) useful for imaging and targeted therapy (Chemical Sci 2024;15:11279-11286). The investigators at ORNL synthesized a BFC, SCN-PYTA, which contains an amine-reactive thiocyanate (SCN) group appended to the pyridine in the PYTA chelator. To establish PYTA as a platform to prepare theranostic radiopharmaceuticals, we investigated the conjugation characteristics of SCN-PYTA to monoclonal antibodies (mAb) and radiometals (^{111}In and ^{225}Ac) to define the chelation properties of PYTA-mAb conjugates. For direct comparison, labeling studies were performed using two other BFCs: SCN-DOTA and SCN-Macropa.

Materials and Methods: Anti-PSMA mAb, rosopatamab and anti-TROP-2 mAb, sacituzumab solutions at 10 mg/mL were prepared in sodium carbonate buffer, pH 9.0±0.2. The BFC solutions (at 5-10 mg/mL) were prepared in metal-free water. Different molar ratios of BFC to mAb were incubated at 37^{o}C for 90 min. The chelate conjugated mAbs were purified by gel chromatography and 0.05 M HEPES buffer, pH 7.5. The chelator:antibody ratios (CAR) were determined using a modified colorimetric arsenazo assay. Chelate-antibody conjugates (0.025-2.0 mg) were incubated (at RT or 37^{o}C) with 0.05-0.5 mCi of ^{225}Ac or ^{111}In chloride in sodium acetate or tetramethylammonium acetate buffer, pH 6±0.3. Radiolabeled mAbs were purified using PD-10 gel permeation chromatography and saline solution containing 1% albumin, and assessed for radiochemical purity (RCP), stability, and immunoreactivity.

Results: PYTA and Macropa conjugated mAbs complex ^{225}Ac or ^{111}In radionuclides very efficiently at RT within 5 min with labeling yields of >97%. The radiochemical purity (RCP) of purified ^{225}Ac-chelator-mAb preparations were >99%. In contrast, DOTA-conjugated mAbs do not label efficiently at RT. Higher labeling yield (80-95%), however, can be obtained at 37^{o}C with longer incubation of 1-2 hours. ^{225}Ac-PYTA-mAbs showed remarkably high in vitro stability at 2-8^{o}C for >10 days (with >99% RCP). Similar stability was observed when challenged with serum or excess chelate (EDTA and DTPA) concentrations. Based *on in vitro* cell binding studies using PSMA+ LNCaP cells and TROP-2+ MCF-7 cells, the immunoreactive fraction (IRF) of ^{225}Ac-PYTA-Rosopatamab and ^{225}Ac-PYTA-Sacituzumab at an infinite antigen concentration (Lindmo assay) was >99%.

Conclusion: SCN-PYTA is an ideal BFC and a suitable platform to develop target specific imaging and therapeutic radiopharmaceuticals based on trivalent radiometals, peptides, proteins, and small molecules. Our preliminary data also suggests that radiolabeled sacituzumab has significant potential as a theranostic radiopharmaceutical for imaging and targeted therapy of TROP-2 positive cancers.

#7184 GT-008: A monoclonal antibody enabling selective radionuclide delivery to a tumor-associated glycosylation form of CD24 - Preclinical proof-of-concept study.

Johanna Gellert, **Andreas Franz**, Manon Weis, Evelyn Hartung, Stephanie Gurka, Lydia Verlaat, Sophie Marinoff, Antje Danielczyk, Patrik Kehler, Dirk Pleimes

Pentixapharm AG, Berlin, Germany

Aberrant O-glycosylation is a hallmark of cancer and many tumor-associated proteins carry truncated O-glycans like Tn or TF antigens. CD24 is a glycoprotein with a fundamental role in tumorigenesis, expressed on solid tumors, but also on selected normal cell types. We developed a humanized IgG1 mAb (GT-008) which binds CD24 only in presence of tumor-associated TF (core-1) glycosylation with limited abundance on normal tissues. This glycoform-selective recognition enables GT-008 to distinguish tumor from normal CD24 and mediate its mode of action in a tumor-selective manner. Unlike protein-specific anti-CD24 antibodies that block the “don’t-eat-me” checkpoint, GT-008 exploits its glycosylation-dependent binding of CD24 for direct cytotoxic activity, including selective radionuclide delivery to tumors. Binding specificity and tumor selectivity of GT-008 was analyzed by ELISA, FACS and immunohistochemistry. After bioconjugation and radiolabeling, *in vitro* validation comprised binding and internalization assays with breast cancer cell lines. The pharmacokinetic profile of GT-008 was analyzed in athymic nude mice. Biodistribution and efficacy studies were performed in a cell-line derived xenograft breast cancer model. GT-008 demonstrated selective recognition of cancerous tissues, including including female cancers of the breast, endometrium and ovaries. It exhibited high-affinity binding in the low nM range and internalization in breast cancer cells, while showing no internalization in healthy CD24+ immune cells. Biodistribution studies showed specific and stable uptake in MCF7 tumors and clearance from other organs resulting in high tumor-to-organ ratios. Therapeutic single doses of GT-008 labeled with alpha or beta radiation emitting isotopes (^{225}Ac-GT-008, 10 + 3 kBq; ^{177}Lu-GT-008, 10 + 3 MBq) resulted in robust control of MCF7 breast tumors. Due to the high linear energy transfer and potent DNA-damaging capacity of α-emitters, ^{225}Ac-GT-008 achieved superior tumor growth inhibition and a higher rate of complete remissions compared with ^{177}Lu-GT-008. All treatments were well tolerated. These findings supports the development of GT-008 as a theranostic radioligand for solid tumors, including female cancers, while supporting its broader potential across CD24-directed modalities such as ADCs, bispecifics, and cellular CAR therapies.

#7185 ^{225}Ac-RAX104: A novel PSMA-targeted radioligand optimized for actinium-225 demonstrates enhanced tumor retention and superior efficacy.

Xupeng Hu, Yang Cao, Min Hong, Shuanglong Liu, **Guangzhou Han**, Gang Chen

RadAlliance Therapeutics Inc, San Diego, CA

Prostate cancer is the second most common malignancy in men and remains a significant cause of cancer-related mortality worldwide. Although the clinical success of ^{177}Lu-PSMA-617 (Pluvicto) has established PSMA-targeted radioligand therapy (RLT) as an effective treatment for metastatic castration-resistant prostate cancer (mCRPC), emerging clinical evidence indicates that ^{225}Ac-based RLT can deliver even greater therapeutic efficacy owing to the high linear energy transfer of α-particles and the radionuclide's 9.92-day physical half-life. To fully exploit these properties, ^{225}Ac-RAX104 was rationally designed to enhance PSMA affinity and tumor retention, thereby kinetically matching the physical and radiobiological characteristics of ^{225}Ac to maximize antitumor potency. RAX104 was successfully synthesized and radiolabeled with ^{225}Ac at a molar activity of up to 3 μCi/nmol, achieving radiochemical purity greater than 95% and maintaining stability for more than 110 hours. Surface plasmon resonance analysis revealed that the RAX104 precursor exhibited approximately 22-fold higher affinity for PSMA than PSMA-617, primarily driven by slower dissociation kinetics. In PSMA-overexpressing PC3 cells, ^{225}Ac-RAX104 showed markedly enhanced cellular uptake and internalization compared with ^{225}Ac-PSMA-617. In PSMA-low 22Rv1 xenografts, ^{225}Ac-RAX104 achieved more than 3-fold higher tumor-absorbed activity ($AUC_{0-\infty}$) and a significantly prolonged biological half-life in tumors relative to ^{225}Ac-PSMA-617, while both radioligands showed comparable blood pharmacokinetics. Consistent with these pharmacokinetic advantages, ^{225}Ac-RAX104 demonstrated superior antitumor efficacy: a single 14.8 kBq dose produced greater tumor growth inhibition and longer survival than 74 kBq (fivefold higher activity) of ^{225}Ac-PSMA-617 in the 22Rv1 model. Toxicity evaluation in normal ICR mice revealed only transient and reversible reductions in white blood cell, neutrophil, and reticulocyte counts, without clinical chemistry abnormalities, indicating a favorable safety profile. An investigator-initiated trial (IIT) of ^{225}Ac-RAX104 has been proposed in mCRPC patients to generate human dosimetry data to inform the design of subsequent clinical studies. Collectively, these results demonstrate that ^{225}Ac-RAX104 achieves optimal kinetic alignment with ^{225}Ac's physical decay and biological action, delivering enhanced tumor exposure and potent therapeutic efficacy at one-fifth the dose of ^{225}Ac-PSMA-617. These findings support ^{225}Ac-RAX104 as a promising next-generation PSMA α-radioligand therapy with the potential to improve outcomes in mCRPC and warrant further clinical development.

#7186 Characterization of LY4257496, a novel GRPR antagonist radiolabeled with lutetium-177.

Shreyas Lingadahalli[1], Gabriela Krivdova[1], Kate Huang[1], David Rodriguez[1], Matt Alteen[1], Chun Ping Yu[2], Chantal Trieu[1], Loredana Puca[3], Robin Hallet[1]

[1]Eli Lilly Canada, Toronto, ON, Canada,[2]Eli Lilly, China R&D Center, Shanghai, China,[3]Eli Lilly and Company, New York, NY

Background: Gastrin-releasing peptide receptor (GRPR) is a G protein-coupled receptor overexpressed in HR+ breast cancer and other solid tumors while having low expression in normal tissues. Although first generation GRPR antagonists have demonstrated utility in diagnostics, their therapeutic potential is limited by poor *in vivo* stability. Here, we present the preclinical profile of LY4257496, a novel GRPR antagonist labeled with lutetium-177, which shows favorable biodistribution, resistance to systemic cleavage, and promising tumor-to-healthy tissue uptake ratio.
Methods: The binding affinity of LY4257496 was evaluated by a competitive binding assay in CHO cells engineered to express human, mouse, and rat specific GRPR isoforms. Biodistribution of LY4257496 (10MBq, 100MBq/nmol) was evaluated in T47D-tumor bearing and non-tumor bearing female mice. Efficacy of LY4257496 was evaluated as mono- and combination therapy in T47D xenografts and clinically relevant HR+ breast cancer PDX models.
Results: A competitive binding assay revealed that LY4257496 specifically bound to GRPR in human, mouse, and rat at comparable nanomolar potency of 8.5, 7.2, and 10.6 nM respectively. In biodistribution analyses, LY4257496 exhibited favorable pharmacokinetics with rapid tumor targeting and prolonged retention (% ID/g 22.6 at 1h, 11.6 at 24h), fast clearance from normal organs (all tissues below 3.5 % ID/g at 24h), and > 50% renal excretion. LY4257496 was well tolerated at 10, 20 and 30MBq (Q14DX2), and efficacy was dose dependent in T47D xenografts (26, 72, and 72 % TGI, respectively). Efficacy was additive when 20MBq (Q14DX2) LY4257496 dose was given in combination with standard-of-care (SoC) therapies including imlunestrant, fulvestrant, and abemaciclib resulting in 40, 32, and 38% tumor regression, respectively at end of treatment (day 28). No tumor regression was observed with SoC therapies alone. LY4257496 also potently inhibited tumor growth in 3 HR+ breast cancer PDX models; 92% TGI (HER2+, PIK3CA:H1047R, and ESR1:Y537S), 58% TGI (HER2-), and 56% TGI (HER2+). These findings demonstrate that LY4257496 is a promising targeted radioligand therapy for tumors with GRPR expression. OMNIRAY, a phase 1 study evaluating LY4257496 in patients with GRPR+ advanced or metastatic disease is ongoing (NCT07114601).

#7187 Preclinical evaluation of BRP-020063, a first-in-class peptide based radiopharmaceutical for the treatment of nectin4-positive cancers.

Maoyi Lei, Lei Peng, Bo Shan

Boomray Pharmaceuticals, Co., Ltd., Suzhou, China

Background: Nectin-4 is aberrantly overexpressed in multiple solid tumors (e.g., bladder, breast, and non-small cell lung cancers, etc.), while showing limited expression in normal tissues. This specific expression reveals that it is a promising drug target for Radionuclide Drug Conjugates (RDC). Here, we describe the preclinical evaluation of BRP-020063, a novel peptide binder based RDC with excellent drug-like properties.
Methods: The protein binding affinity and selectivity of BRP-020063 were determined by surface plasmon resonance (SPR). Cell binding and internalization were characterized in PC3 cells engineered to express human Nectin4 (PC3-Nectin4) by radioligand binding assays using ^{177}Lu[Lu]-BRP-020063. Both of SPECT/CT imaging and *ex vivo* biodistribution studies in PC3-Nectin4 tumor-bearing mice were performed to evaluate the pharmacokinetics of ^{177}Lu[Lu]-BRP-020063. In addition, in vivo antitumor efficacy studies of ^{177}Lu[Lu]-BRP-020063 were also performed in the same cell derived xenograft (CDX) model to assess the therapeutic effect.
Results: SPR studies showed BRP-020063 exhibited picomolar to nanomolar binding affinity to Nectin4 protein of human, mouse, rat, and cynomolgus monkey, and no binding to other members of the human Nectin-family (hNectins1-3, K_D > 10 μmol/L). Potent cellular binding was confirmed in PC3-Nectin4 cells with nanomolar affinity. Cell uptake studies on PC3-Nectin4 cells and parent PC3 cells (PC3-WT) showed ^{177}Lu[Lu]-BRP-020063 specific bound to Nectin4. Meanwhile, ^{177}Lu[Lu]-BRP-020063 gave efficient internalization on PC3-Nectin4 cells. The SPECT/CT imaging of ^{177}Lu[Lu]-BRP-020063 demonstrated high tumor uptake and long-term tumor retention. The tumor uptake reached the peak (54.91±6.43% ID/g) at 24 h post-injection, and still remained 6.22±1.31% ID/g at 240 h post-injection. *Ex vivo* biodistribution studies further confirmed the remarkably robust and sustained tumor uptake of ^{177}Lu[Lu]-BRP-020063, the tumor uptake reached the inspiring 61.18±9.96% ID/g at 24 h post-injection, and maintained 25.50±5.10% ID/g at 72 h post-injection. The resulting tumor-to-kidney ratios were 2.34 at 24 h and 2.15 at 72 h post-injection. In addition, a single dose of 0.5 mCi or 1 mCi ^{177}Lu[Lu]-BRP-020063 per mouse led to robust and sustained tumor regression and prolonged animal survival.
Conclusion: The preclinical *in vitro* and *in vivo* data demonstrate that ^{177}Lu[Lu]-BRP-020063 possesses excellent target specificity, favorable pharmacokinetic properties, and potent antitumor efficacy. These findings strongly support further investigation of the novel therapeutic ^{177}Lu[Lu]-BRP-020063 as a treatment for patients with Nectin4-positive solid tumors.

#7188 Theranostics targeting the calcitonin gene-related peptide receptor (CGRPR) demonstrate efficacy in a preclinical mouse model of human cancer.

Prabhakar Eeka[1], Darpan N. Pandya[1], Andrew F. Russo[2], Yusuke Shiozawa[3], Thaddeus J. Wadas[1]

[1]Radiology, University of Iowa, Iowa City, IA,[2]Molecular Physiology and Biophysics, University of Iowa, Iowa City, IA,[3]Cancer Biology, Wake Forest University Health Sciences, Winston-Salem, NC

Introduction: Recent literature demonstrates that the CGRPR, and its primary ligand, calcitonin gene-related peptide (CGRP) are implicated in 9 of the 14 hallmarks of cancer and contribute to the development of multiple primary cancers. Here, we developed a theranostic strategy for the SPECT imaging and targeted radiotherapy of CGRPR-positive tumors.

Methods: The CGRPR-specific bioconjugate DOTA-Bn-NCS-FV-Tic-TDVGPFAF (ACP) was radiolabelled with ^{111}In (SPECT: $t_{1/2}$ = 2.8 d; $E_{e\text{-}max}$ = 0.245 MeV) or ^{177}Lu (β - emitter: $t_{1/2}$ = 6.7d; $E_{\beta\text{-}max}$ = 0.497 MeV). Biodistribution studies in CGRPR+ HTB-10 tumor-bearing mice were conducted using [^{111}In]In-ACP and radioactivity in tissue was quantified against a known radioactivity standard. Therapy studies with [^{177}Lu]Lu-ACP in the same tumor bearing model were also completed. As animals reached clinical endpoints, the animals were euthanized and processed for histology. QuPath software was used to quantify immunohistochemistry images, while survival and statistical analysis was accomplished using GraphPad Prism v.10.2.

Results: The acute biodistribution of [^{111}In]In-ACP revealed rapid excretion from blood, liver, kidney and bone suggesting effective clearance that may lead to acceptable dosimetry in dose-limiting organs such as the kidney and bone marrow. A tumor-to-muscle ratio of 39 at 4 h p.i., which was reduced to 12 with peptide blockade suggests that the radiopharmaceutical interacts with the CGRPR through a receptor mediated mechanism. Radiotherapy studies revealed that CGRPR+ HTB-10 tumor bearing mice injected with [^{177}Lu]Lu-ACP experienced a survival benefit when compared to animals receiving control treatments ($p = 0.036$). When analysed histologically, tumor sections from animals receiving the radiotherapy exhibited decreased Ki-67 staining (proliferation marker) but higher caspase-3 (apoptosis marker) staining when compared to tumor sections of untreated animals.

Conclusion: Although the CGRPR/CGRP axis is implicated in cancer development, no theranostic strategies exist currently that target this receptor for imaging and therapy. Available data with [^{111}In]In-ACP revealed effective tumor targeting and rapid clearance from normal tissues, while radiotherapy studies with [^{177}Lu]Lu-ACP demonstrated effective tumor growth control. These results suggest targeting the CGRPR/CGRP axis warrants further exploration as a promising new strategy for the imaging and therapy of cancer.

#7189 Innovative theranostic Trop2 antibody-radionuclide conjugates (ARCs) for precision medicine.

Shih-Hsien Chuang[1], Wei-Ting Sun[1], Michael Evans[2], Haibo Xu[2]

[1]HoneyBear Biosciences, Inc., Taipei, Taiwan,[2]University of California San Francisco, San Francisco, CA

Theranostic antibody conjugates are an emerging class of therapeutics that combines an antibody with radionuclides that can both diagnose and treat disease. We have developed a site-specific Trop2 antibody-radionuclide conjugate (ARC), incorporating 89Zr for imaging and 225Ac for therapy. The imaging ARC, leveraging the long half-life of 89Zr, demonstrates strong tumor accumulation and favorable tumor-to-normal tissue (T/N) ratios across multiple xenograft models, including triple-negative breast cancer and non-small cell lung cancer. The therapeutic ARC, carrying an alpha-emitting radionuclide, effectively suppresses tumor growth in the corresponding xenograft models. This ARC is currently in preclinical development, with an investigational new drug (IND) application planned for 2026.

#7190 Novel peptide radioligands targeting CAIX for theranostic applications in clear cell renal cell carcinoma (ccRCC).

Weiliang (Timo) Xu, Jin Zhang

PepLib, Metuchen, NJ

Carbonic anhydrase IX (CAIX) is a hypoxia-inducible transmembrane enzyme highly expressed in clear cell renal cell carcinoma (ccRCC) and several other solid tumors, making it an attractive target for radiotheranostic development.Using PepLib's peptide discovery and optimization platform, we identified a monocyclic peptide ligand, 4B043 (19 amino acids, one disulfide bond) as a high-affinity CAIX binder. 4B043 exhibited sub-nanomolar affinity to human CAIX ($K_D \approx 86$ pM) and strong cross-species binding to canine, mouse, and cynomolgus monkey CAIX. In Balb/c nude mice bearing VMRC-RCW tumor models, ^{68}Ga-4B043 showed high tumor uptake (~55 %ID/g) with a tumor-to-kidney (T/K) ratio ≈ 0.5 at 4 h post-injection. After structural optimization, ^{68}Ga-2B002 maintained high tumor uptake while significantly reducing kidney accumulation (T/K ≈ 2 at 4 h). Encouraged by these preclinical data, ^{68}Ga-4B043 was advanced into a human IIT. In ccRCC patients, ^{68}Ga-4B043 demonstrated high uptake in renal tumor lesions. Due to CAXI expression in normal gastric and small intestinal tissues, ^{68}Ga-4B043 also showed notable uptake in these organs in patients. Notably, kidney uptake was remarkably low in patients, with a tumor-to-kidney ratio > 8 at 2 h, in clear contrast to the CDX model.4B043 and its optimized derivative 2B002 represent a novel class of CAIX-targeted peptide radioligands with excellent tumor uptake, favorable biodistribution, and promising translational potential. These data support their further development as theranostic agents for imaging and targeted radioligand therapy in CAIX-expressing tumors, including ccRCC.

#7191 6-thio-dG enhances standard-of-care radiation therapy by reprogramming the tumor microenvironment in glioblastoma multiforme.

Anthony Alexander Grichuk[1], Merve Yilmaz[1], Summer Barron[1], Priya Darbha[1], Shannon M. McCabe[2], Jerry W. Shay[3], Kristin Huntoon[4]

[1]Cell Biology, UTSW, Dallas, TX,[2]Neurosurgery, University of Arizona, Tucson, AZ,[3]Professor, Dept. of Cell Biology, UT Southwestern Medical Ctr., Dallas, TX,[4]UA faculty member, Neurosurgery, University of Arizona, Tucson, AZ

Background/Objectives - Glioblastoma multiforme (GBM) remains highly lethal, with a five-year survival rate of only 6.9%. Standard-of-care treatments such as ionizing radiation (IR) and temozolomide frequently fail to produce durable responses due to poor drug penetration across the blood-brain barrier (BBB) and the immunosuppressive tumor microenvironment (TME). 6-thio-2'-deoxyguanosine (6-thio-dG) is a telomerase-mediated telomere-targeting guanine analog that induces telomeric DNA damage selectively in telomerase-positive tumor cells. This process activates the cGAS-STING pathway, triggers innate and adaptive immune responses and has previously resensitized resistant tumors to immunotherapy in a Phase 2 NSCLC clinical trial. We hypothesized that 6-thio-dG penetrates the BBB and enhances the therapeutic efficacy of IR by reprogramming the GBM TME.
Methods - GBM models were treated with 6-thio-dG alone, IR alone, or sequential 6-thio-dG followed by IR. Immune signaling, microglia/macrophage phenotypes, and tumor responses were assessed via molecular, histological, and functional analyses.
Results - Sequential 6-thio-dG + IR treatment significantly increased type I interferon (IFN-I) activation and shifted microglia/macrophages toward a pro-inflammatory M1 phenotype. This TME reprogramming resulted in a statistically significant anti-tumor effect relative to monotherapy.
Conclusions - 6-thio-dG enhances IR efficacy in GBM by inducing telomere-driven immune activation and promoting an anti-tumor TME. These findings support 6-thio-dG as a promising adjuvant to standard-of-care and justify further investigation of telomere-targeted combination strategies.

#7192 FLASH reduces radiation-induced oral mucositis in a mouse model of Fanconi anemia.

Phoebe Loo[1], Margaret Pan[1], Man Zhao[1], Stavros Melemenidis[2], Dixin Chen[1], Kerriann M. Casey[1], Michael Epperly[3], Joel S. Greenberger[4], Billy W. Loo[1], Erinn Rankin[1]

[1]Stanford University School of Medicine, Stanford, CA,[2]University of Colorado Anschutz, Aurora, CO,[3]University of Pittsburgh, Pittsburgh, CA,[4]University of Pittsburgh Shadyside Medical Center, Pittsburgh, PA

Patients with Fanconi anemia (FA) are particularly susceptible to developing squamous cell carcinomas of the head and neck regions due to impaired DNA repair pathways. However, their hypersensitivity to DNA damaging agents can limit effective treatment with standard radiotherapy due to severe side effects and complications. In pre-clinical models, ultra-rapid FLASH radiotherapy (FLASH) has been demonstrated to reduce radiation-induced toxicity to multiple normal tissues while maintaining similar tumor control compared to conventional dose rate radiotherapy (CONV) in a wild-type background. Here, we investigated the safety of FLASH for treatment of the head and neck region in a mouse model of FA. The oral cavity of 129/Sv wild-type (WT) and Fanca-knockout (KO) mice was irradiated with a single dose of electron beam FLASH or CONV to evaluate radiation-induced toxicity in non-tumor bearing mice. Fanca WT and KO mice were irradiated with 25 and 18 Gy, respectively, of FLASH (190 Gy/sec) or CONV (0.2 Gy/sec), and tongues were harvested at 12 hours (hpi) and 10 days (dpi) post-irradiation. Following excision, tongues were stained with toluidine blue to visualize ulceration. At 10 dpi, FLASH-irradiated tongues in both genetic backgrounds demonstrated a reduced area of ulceration, expressed as a fraction of total tongue area, at the dorsal surface compared to CONV-irradiated counterparts. Histopathological analysis of the tongue revealed lower mucositis severity scores, reflected by decreased epithelial thinning and ulceration, in FLASH-irradiated tongues compared to CONV-irradiated ones. Analysis of γ-H2AX foci formation at 12 hpi demonstrated a decreased number of foci in the WT background with FLASH compared to CONV and a similar trend in the KO background. These findings suggest a potential normal tissue sparing effect with FLASH and hold important clinical implications for the treatment of patients with Fanconi anemia and head and neck cancers.

#7193 Short exposure to TTFields potentiates radiation response in glioblastoma via downregulation of DNA repair pathways.

Anat Klein-Goldberg[1], **Tali Voloshin**[1], Aviv Meir[1], Efrat Zemer-Tov[1], Hila Ene[1], Lena Lifshitz[1], Kerem Wainer-Katsir[1], Adi Haber[1], Moshe Giladi[1], Uri Weinberg[2], Yoram Palti[1]

[1]Novocure Ltd, Haifa, Israel,[2]Novocure GmbH, Baar, Switzerland

Background: Tumor Treating Fields (TTFields) therapy, which delivers low-intensity, alternating electric fields to disrupt cellular processes crucial for cancer cell division, is an FDA-approved modality for patients with newly diagnosed and recurrent glioblastoma (GBM). Beyond its established antimitotic effects, TTFields have been shown to interfere with DNA damage repair pathways, suggesting potential synergy with radiation therapy (RT). In this study, we explored whether brief exposure to TTFields can sensitize GBM cells to radiation.
Methods: U87-MG GBM cells were exposed to 2 Gy radiation, to TTFields (200 kHz, 2h), or to TTFields followed by radiation, and colony formation was tested. RNA extracts from control and TTFields-treated cells were examined by PCR for changes in DNA damage response genes. Western blot analyses assessed changes in protein levels of DNA repair genes FANCD2, FANCJ, FANCA, FANCB, BRCA1, and BRCA2. C57BL/6 mice were intracranially implanted with GL261-mCherry glioma cells and tumor growth was confirmed by MRI on day 17 post-implantation. Mice were then randomized into treatment groups receiving TTFields (200 kHz), RT (6 Gy) or the two modalities together with various sequencing: TTFields pre-RT, TTFields post-RT, or TTFields both pre- and post-RT. Tumors were harvested for single-cell suspension preparation, and DNA damage was quantified by flow cytometry using γH2AX staining.
Results: Short exposure to TTFields alone was insufficient to reduce colony formation of the cells. However, when TTFields were applied prior to RT, colony formation was decreased relative to that for RT alone. The TTFields-treated cells demonstrated downregulation of genes and proteins associated with DNA damage repair. In mice, while TTFields post-RT had negligible effects on tumor DNA damage levels relative to application of RT alone, TTFields prior to RT resulted in increased DNA damage and reduced expression of DNA repair protein within tumor cells, with no elevation of DNA damage in tumor infiltrating immune cells. When TTFields were applied both pre- and post-RT, increased DNA damage was demonstrated in the tumor.
Conclusions: Our findings demonstrate that GBM can be radiosensitized by short exposure to TTFields, and that timing and sequencing are important for maximizing the effect.

#7194 Inhibiting glutamine metabolism in combination with radiation disrupts mitochondrial function and impairs homologous recombination.

Scott Bright[1], Yogesh Rai[1], Rishab Kolachina[2], Hadil Elldakli[1], Mark D. Wasley[1], Gabriel O. Sawakuchi[1]

[1]UT MD Anderson Cancer Center, Houston, TX,[2]Augusta University, Augusta, GA

A mainstay of lung cancer treatment is radiotherapy. With our ever-increasing ability to genomically stratify patients, it is now possible to identify biomarkers that contribute to radioresistance or radiosensitivity. Mutations in the gene Kelch-like ECH-associated protein 1 (KEAP1) are associated with resistance to radiotherapy resulting in greater local recurrence and poorer patient outcomes. Mutations in KEAP1 lead to Nuclear Factor (erythroid-derived) 2-like Factor (Nrf2) nuclear translocation where it acts as a transcription factor promoting the formation of antioxidant proteins. However, while tumors harboring KEAP1 mutations are more resistant to therapy, they also rely heavily on the amino acid glutamine, which is processed by the enzyme Glutaminase-1 (GLS1) to meet the metabolic demands associated with the constitutive activation of Nrf2. Disrupting glutamine metabolism in KEAP1 mutant cells and tumors using small molecule inhibitors has shown promise as a radiosensitizing strategy. At a basic mechanistic level this has been attributed to a reduced glutamate level, leaving cells unable to produce the antioxidant glutathione, therefore increasing oxidative stress following radiotherapy. This in turn contributes to greater levels of DNA damage and more cell death. Our data support the radiosensitizing effect of GLS1 inhibition in KEAP1 mutant cells, for both photons and protons, with associated increases in oxidative stress, specifically mitochondrial superoxide. In addition to this basic concept, we hypothesize that the profound metabolic disruption induced by inhibiting glutamine metabolism has implications for not only DNA damage induction but also DNA repair. To investigate this, we first explored DNA damage response (ATM) and pathway specific DNA repair (Rad51) proteins, alongside the comet assay to measure total DNA damage. Our results identified that the inhibitor IACS-6274, which inhibits GLS1, increased total DNA damage measured by the alkaline comet assay but abrogated foci formation for both phosphorylated-ATM and Rad51 (homologous recombination [HR]). We also observed significant synergy when IACS-6274 was combined with PARP or ATR inhibitors in the absence of radiation. In parallel, we determined that mitochondrial membrane potential measured using the dye, TMRM, is significantly reduced along with reduced ATP production in GLS1 inhibited cells.

In summary, our results show that KEAP1 mutant lung cancer cells treated with a GLS1 inhibitor can be significantly radiosensitized to radiotherapy, and this in part maybe attributable to reduced HR proficiency. We propose that either bioenergetic crisis prevents fueling of HR processes or that impaired TCA cycle anaplerosis reduces α-ketogluterate levels, which is an important co-factor for chromatin remodeling preventing DNA end resection and resulting Rad51 foci formation.

#7195 Blocking hERG1 enhances radiation sensitization in glioblastoma.

Hannah E. Goen[1], Naya Ohuabunwa[2], Jonathan D. Rodgers Gochicoa[3], Tingting Huang[4], Kelli B. Pointer[4]

[1]Mount Holyoke College, South Hadley, MA,[2]Washington University in St. Louis, St. Louis, MO,[3]Dartmouth College, Hanover, NH,[4]Dartmouth Cancer Center, Lebanon, NH

Background: Glioblastoma (GBM) is the most aggressive primary brain tumor in adults, with a median survival of less than two years. Poor outcomes are driven in part by glioma stem cells (GSCs) that resist radiation and repopulate the tumor. The voltage gated potassium channel hERG1 (KCNH2) is upregulated in GBM and linked to therapy resistance, suggesting that its inhibition might improve radiotherapy efficacy.
Methods: Human GBM cell line LN-229 and patient derived GSC line GNS144 were cultured as spheres. IC_{50} values for the selective hERG1 inhibitor E-4031 were determined (192.9 µM for LN-229, 94.23 µM for GNS144). Cells were treated with the respective IC_{50} concentration of E-4031 (or vehicle) and irradiated with a single fraction of 0 Gy or 10 Gy. Sphere formation assays were performed and quantified 7-14 days later. Cell-cycle distribution was assessed by flow cytometry. All experiments were performed in triplicate; statistical significance was evaluated with Tukey's or Fisher's LSD tests ($p < 0.05$).
Results: In LN-229 spheres, combination therapy with E-4031 and radiation reduced sphere formation more than radiation alone (+14.4 %, $p = 0.0041$) or E-4031 alone (+23.56 %, $p = 0.0002$). In GNS144, the combination also performed better than radiation alone (+25.80 %, $p = 0.0303$) and E-4031 alone (+26.15 %, $p = 0.0283$). Cell cycle analysis of LN-229 showed that E-4031 decreased the S-phase population by 5.95 % ($p = 0.0054$) compared with controls, and when combined with radiation it reduced the S-phase population by an additional 7.36 % ($p = 0.0016$).
Conclusions: Selective blockade of hERG1 with E-4031 markedly radiosensitizes GBM cells, producing synergistic reductions in sphere forming capacity, a surrogate for stemness. Moreover, hERG1 inhibition decreases the radioresistant S-phase cell population. These findings suggest that hERG1 blockade may be beneficial for radiosensitization in GBM, and further exploration of hERG1 targeted strategies could improve outcomes for patients diagnosed with glioblastoma.

#7196 Detection of radiopharmaceuticals and their cold surrogates by Imaging Mass Cytometry enables assessment of single-cell functional response, therapeutic biodistribution, and modulation of the immune microenvironment.

Jennifer L. Gorman[1], Felix B. Salazar[2], Kevin Wyszatko[3], Michael J. Geuenich[1], Smriti Kala[4], Thom G. A. Reuvers[5], Matthew Watson[1], Daniel Majonis[4], Hang Zhou[4], Bao Ying Chen[2], Christopher Heskett[2], Marjolijn Hameetman[6], Qanber Raza[4], Sheila Singh[7], Christina Loh[4], James Mansfield[4], Julie Nonnekens[5], Erik de Blois[8], Kieran R. Campbell[1], Saman Sadeghi[3], Anna M. Wu[2], **Hartland W. Jackson**[1]

[1]Lunenfeld-Tanenbaum Research Institute, Toronto, ON, Canada,[2]Department of Immunology and Theranostics, Beckman Research Institute of City of Hope, Duarte, CA,[3]Department of Chemistry & Chemical Biology, McMaster University, Hamilton, ON, Canada,[4]Standard BioTools, Markham, ON, Canada,[5]Department of Molecular Genetics and Radiology & Nuclear Medicine, Erasmus Medical Center Cancer Institute, Rotterdam, Netherlands,[6]Flow Cytometry Core Facility, Leiden University Medical Center, Leiden, Netherlands,[7]Centre for Discovery in Cancer Research, McMaster University, Hamilton, ON, Canada,[8]Radiology & Nuclear Medicine, Erasmus Medical Center, Rotterdam, Netherlands

Radiopharmaceuticals (RPT) can improve therapeutic responses while decreasing adverse reactions through targeted radiation delivery to the tumor. While localized radionuclide uptake can currently be measured, these techniques lack the resolution to examine biodistribution at the single-cell level or capacity to simultaneously assess multiple measures of response. Here, we show that Imaging Mass Cytometry (IMC), a technique combining immunostaining with laser ablation-enabled inductively coupled plasma mass spectrometry, can measure the spatial distribution of RPT metal, as well as the therapeutic response within multiplexed measurements. Testing the abilities and limitations of this approach, we benchmarked IMC and autoradiography readouts, compared isotope-labelling approaches and dosing necessary for IMC detection, and provide examples of a variety of unique single cell readouts of RPT distribution and cellular response. Using both hot and cold labelling strategies, we measured the distribution of either carrier-added metal or cold surrogate and matched target for two tumor-directed RPTs, seeing clear differences in on- and off-target distributions within the tumor. Metal from carrier added [^{177}Lu]Lu-DOTA-RW03, a fully humanized CD133 antibody, co-localized with CD133 expression in certain regions of the tumor, with CD133^{+} RPT metal^{-} regions interspersed. A cold analog of an engineered antibody fragment against the prostate stem cell antigen (^{169}Tm-PSCA A2DM) was observed in both the tumor mass and peripheral areas of collagen-rich stroma in a syngeneic model using human PSCA expressing cells. Over a 28-day time course, on- versus off-target ratios improved with time, and varying therapeutic dose was shown to change single cell RPT amounts with analog doses as low as 10 µg detected by IMC, highlighting its sensitivity. Diving deeper, IMC enabled functional assessments of response showing higher single-cell positivity for markers of DNA damage and apoptosis in regions with higher RPT exposure. Finally, we show the ability of IMC to assess the RPT-initiated immune response and impact of radioisotope selection by comparing lymphocyte and myeloid cell infiltration in response to alpha or beta emitters conjugated to the same targeting reagent. These findings show the potential of IMC quantification of RPT dose, distribution, and response, which will expand our understanding of localized absorbed dose, how radioisotope selection impacts response, and inform future pre-clinical therapeutic design.

#7197 Molecular characteristics of MP0712, a clinical stage ^{212}Pb-based Radio-DARPin candidate for targeted anti-DLL3 radiotherapy of small cell lung cancer (SCLC).

Stefanie Riesenberg[1], Amal Saidi[2], Francesca Malvezzi[1], Aaron Schatzmann[2], Christian Reichen[1], Tania Stallons[2], Nicole Pina[1], Aline Eggenschwiler[1], Amy Wong[2], Madlaina Mettier[1], Jitka Rantanen[1], Marcela Guzman-Ayala[1], Julien Torgue[2], Daniel Steiner[1]

[1]Molecular Partners AG, Zurich-Schlieren, Switzerland,[2]Orano Med, Plano, TX

Introduction

Delta-like ligand 3 (DLL3) is an inhibitory Notch ligand aberrantly expressed on SCLC cells and largely absent in healthy tissues, making it a promising therapeutic target. However, low DLL3 surface density may limit tumor accumulation of a targeted radiopharmaceutical. MP0712, a half-life extended DLL3-targeting DARPin (Designed Ankyrin Repeat Protein) molecule combined with the short-lived alpha-emitting therapeutic isotope ^{212}Pb, showed favorable safety, biodistribution, and antitumor efficacy in mice (Croset et al. AACR 2025). Under South Africa's Section 21 compassionate care framework, MP0712 was administered for imaging with ^{203}Pb to patients with SCLC and other DLL3-positive neuroendocrine cancers (NECs). Initial human imaging data indicate specific tumor uptake, supporting MP0712's intended mode of action (Steiner et al. TRP EU 2025). Here, we describe MP0712's molecular features, focusing on binding properties, internalization, and circulatory half-life.

Methods

DLL3-expressing SCLC cell lines and xenograft models were used to evaluate MP0712 biodistribution *in vivo*. Internalization was assessed using flow cytometry and confocal microscopy. PK/PD properties were determined in mice. The affinity to DLL3 protein was determined by Surface Plasmon Resonance.

Results

We identified sub-nanomolar affinity as a critical parameter for achieving efficient tumor uptake. MP0712 comprises a high-affinity, DLL3-specific DARPin (K_D of 0.2 nM) that binds efficiently and selectively to DLL3+ SCLC cells. Given the low surface density of DLL3, we reasoned that to maximize accumulation in tumor, rapid and repeated internalization of a Radio-DARPin would be beneficial. Consistent with this hypothesis, we could demonstrate that up to 80% of surface-bound DLL3-DARPin internalizes within 30 min into SCLC cells *in vitro*. Importantly, we observed progressive intracellular accumulation over time upon continuous supply of DLL3-targeting DARPins, suggesting that repeated cycles of internalization occur. Finally, we hypothesized that extending systemic exposure of the DLL3-targeting DARPin would further enhance tumor uptake by leveraging these internalization dynamics. Indeed, we observed that intermediate half-life extension with an albumin-binding moiety improved tumor accumulation in xenograft models compared to non-half-life extended molecules.

Conclusions

MP0712 demonstrates a compelling preclinical profile that suggests it may benefit from rapid receptor turnover-mediated intracellular accumulation, offsetting the effects of low DLL3 surface density. Together with emerging ^{203}Pb-imaging data from compassionate care, these findings support further clinical evaluation of MP0712 therapeutic application with ^{212}Pb-payload in patients with SCLC and other DLL3-positive NECs.

#7198 Synergistic effects of next-generation Tumor-Treating Fields technology and cinnamaldehyde/cinnamon oil on apoptosis, cell cycle arrest and growth suppression in triple-negative breast cancer cells.

Saqib N. Peracha[1], Joseph M. Rohde[2], Margaux A. Santos[2], Emma C. Higgins[2], Lexa M. Campbell[2], Wageesha T. Mallehevidana[3], Juliana R. Seide[2], Aidan Hollister[2], Therese M. Annulis[2], Abdu Mohammed[1], Kiran Khurshid[1], Noor U. Huda[1], Aaron P. Provenzano[4], Jason R. Henderson[5], Daniel Kuebler[2], Joseph A. Pathakamuri[2], John J. O'Connell[6]

[1]Trinity Health System, Steubenville, OH,[2]Department of Biology, Franciscan University of Steubenville, Steubenville, OH,[3]Department of Bioengineering, Swanson School of Engineering, University of Pittsburgh, Pittsburgh, PA,[4]Hillman Cancer Center, University of Pittsburgh Medical Center, Pittsburgh, PA,[5]Quiverent, LLC., Greenville, SC,[6]University of South Carolina School of Medicine Greenville, Greenville, SC; Department of Medicine, Prisma Health Cancer Institute, Greenville, SC

Background: Triple-negative breast cancer (TNBC), one of the most aggressive subtypes of breast cancer, accounts for 10-20% of breast cancers. Tumor-Treating Fields (TTF), disrupt mitotic spindle formation and induce apoptosis in TNBC cells. Cinnamaldehyde (CA), the active component of cinnamon, inhibits TNBC proliferation and promotes apoptosis. This study evaluated whether CA or cinnamon oil (CO) acts in synergy with TTF to enhance growth suppression, apoptosis, and cell-cycle arrest in TNBC cells.

Methods: MDA-MB-231 TNBC cells were seeded at 75,000 cells/mL and treated with CA (150 μM), CO (1:300 dilution), or vehicle controls. Frequency-modulated TTF (FM-TTFields) were applied continuously for 72 hours at 150 kHz (±10 kHz modulation using an 8.3 mHz triangle wave), 1.2 V_{RMS}/cm. Cell proliferation was assessed by CyQUANT assay and Celigo imaging; apoptosis and cell-cycle distribution were analyzed by Annexin V/PI flow cytometry. Synergy was quantified using Bliss independence and Highest Single Agent (HSA) models.

Results:
Cell death synergy: Cell death from combined treatments TTF+CA (96.7%) and TTF+CO (96.3%) exceeded single agents CA (93.6%), CO (86.1%), and TTF (40.0%). Synergy analysis by HSA and Bliss models confirmed synergy, stronger for TTF+CO (HSA Δ = +10.3 ± 2.5 points (pts), p = 0.02; Bliss Δ = +4.7 ± 1.7 pts, p = 0.042) than TTF+CA (HSA Δ = +3.2 ± 1.4 pts, p = 0.06; Bliss Δ = +0.9 ± 1.0 pt, p = 0.27). Combining TTF with CA or CO yields synergistic benefits, with TTF+CO showing the greatest effect.

Apoptosis synergy (Annexin V/PI): TTF+CO (49.9%) and TTF+CA (65.5%) greatly surpassed CA (20.6%), CO (13.9%), and TTF (1.4%). Combinations increased apoptosis ~36-fold (TTF+CO) and ~48-fold (TTF+CD). Synergy was highest for TTF+CA (HSA Δ = +44.3 pts; Bliss Δ = +43.2 pts) versus TTF+CO (HSA Δ = +35.1 pts; Bliss Δ = +33.9 pts). Combining TTF with CA or CO substantially enhances apoptosis, with TTF+CA most effective.

Cell-cycle modulation: CA and CO enriched the S phase relative to DMSO (Δ%: CO +10 pts; CA +8 pts). TTF induced strong G2/M accumulation (+18 pts). Combining TTF with CO further increased G2/M (+12 pts) with minimal S-phase change (+1 pt), while CA+TTF produced only a small G2/M shift (+2 pts). These patterns suggest mechanistic complementarity: CA and CO primarily arrest cells in the S phase, whereas TTF induce mitotic arrest (M phase).

Conclusions: Combining FM-TTFields with cinnamon oil or cinnamaldehyde enhances TNBC cell death and apoptosis through complementary mechanisms—S-phase arrest and mitotic disruption—resulting in significant synergy for FM-TTFields combined with cinnamon oil or cinnamaldehyde. These findings support a novel, combinatorial strategy for treating TNBC. Future studies should validate these results *in vivo* and explore clinical translation.

#7199 From simulation to reality: Evidence supporting safe high-dose TTFields delivery with the LB10000.

Ze'ev Bomzon[1], Scott Krywick[1], Matthew Travers[1], Kenneth L. Watkins[1], Martin Pribula[1], Michael Winegar[2], Peter Travers[1]

[1]Lifebridge Innovations, Longwood, FL,[2]Winegar Consulting Inc, Maple Grove, MN

Introduction: Tumor Treating Fields (TTFields) are a noninvasive cancer therapy that employ alternating electric fields in the 100-500 kHz range to disrupt tumor cell division. TTFields are clinically approved for glioblastoma, mesothelioma, and non-small cell lung cancer. The LB10000 is a novel TTFields device designed to deliver high-dose fields adaptively across large body regions. Unlike existing systems that use four fixed transducer arrays, the LB10000 employs a large matrix of programmable transducers whose phases can be dynamically switched between 0°, 180°, and off. This enables dynamic field shaping, targeted delivery to multiple anatomical sites, and effective thermal management. We present both in-vivo and in-silico evidence demonstrating the safety of this new system.

Methods: Six female Yucatan pigs were treated with the LB10000. Arrays were removed daily between 7-9 a.m. and reapplied between 12-3 p.m., targeting ≥16 hours of active treatment per day for 24-32 days within a period of 40 days from treatment initiation. If a pig reached the desired quota of per-protocol days, treatment was stopped and the animal euthanized. During treatment, skin temperature, treatment duty cycle, current, and voltage were continuously monitored, and animal well-being was evaluated daily by a veterinarian. Following euthanasia, gross examination of major organs was performed. To assess safety in humans, computational modeling was performed using the Sim4Life (ZMT Zurich, Switzerland) ohmic solver. Virtual LB10000 arrays were applied to anthropomorphic phantoms—DUKE (adult male), ELLA (adult female), and FATS (obese male)—and electric field delivery simulated at 200 Vpp, the device's maximum output. Specific Absorption Rate (SAR) distributions were calculated to evaluate potential heating.

Results: In vivo, the LB10000 delivered fields continuously at 130 V and 6 A (~100 W) with 78-90 % on-time per animal. Five of six pigs completed the full protocol(24-32 day with 16hr/day treatment), totaling 2,780 hours of treatment without adverse events or tissue injury. Gross examination revealed no abnormalities. In silico, SAR values in superficial skin layers were 10-100× higher than in internal organs, indicating that any potential heating is localized beneath the transducers. The risk of thermal damage to tissues increases drastically when tissue temperatures exceed 109°F (43°C). The LB10000 continuously monitors skin temperature below the transudcers and controls delivered power to maintain skin temperature below a safety threshold of 105 °F. Together, these findings demonstrate that the LB10000 operates safely at high doses in vivo and that the risk that the device will cause thermal damage in humans is negligible.

Conclusion: These results provide key evidence supporting advancement toward first-in-human clinical evaluation.

#7200 High-dose adaptive tumor treating fields (TTFields): Expanding the boundaries of electric field therapy.

Ze'ev Bomzon[1], Scott Krywick[1], Matthew Travers[1], Kenneth L. Watkins[1], Martin Pribula[1], Michael Winegar[2], Peter Travers[1]

[1]Lifebridge Innovations, Longworrd, FL,[2]Winegar Consulting Inc/, Maple Grove, MN

Introduction: Tumor treating fields (TTFields) are a non-invasive cancer therapy employing alternating electric fields in the 100-500 kHz range to disrupt mitosis. Current TTFields systems use four fixed transducer arrays positioned on the skin near the tumor. This static configuration imposes two critical limitations: (1) electric fields remain confined between arrays, precluding treatment of multifocal or metastatic disease. (2) Delivery of TTFields through the skin leads to localized heating of the skin below the transducers. To avoid thermal damage to tissue, the power delivered must be controlled in a manner that maintains skin temperature below a safety limit of around 105°F, and if skin temperature exceeds this threshold, the device must temporarily halt field delivery until the skin cools to a safe temperature, leading to a reduction in delivered dose. The LB10000 system was engineered to overcome these barriers. It comprises a large array of individually addressable transducers whose phases can be dynamically modulated between three states (0°, 180°, off). This enables adaptive field steering, effective heat dispersion, and targeted energy delivery across the body. We present experimental and computational evidence demonstrating that the LB10000 delivers TTFields to multiple targets at doses substantially exceeding those achievable with existing systems.

Methods: The LB10000 was applied to six female Yucatan pigs for 30-40 days to assess sustained high-dose delivery. Arrays were removed daily between 7-9 a.m. and reapplied between 12-3 p.m., targeting ≥16 hours of treatment per day. Skin temperature, treatment duty cycle, and current-voltage output were continuously recorded. To assess dose-delivery in humans, simulations were performed using the Sim4Life (ZMT Zurich, Switzerland) platform. Virtual arrays were applied to the DUKE (adult male), ELLA (adult female), and FATS (obese male) anatomical phantoms, with power levels matched to those measured in vivo. Electric field distributions were computed for tumors in multiple organ sites.

Results: In vivo, the LB10000 delivered continuous fields at 130 V and 6 A (≈100 W[SK1]) with 78-90[SK2] [3ב] % on-time, maintaining skin temperatures within safety limits and confirming robust thermal control. Simulations demonstrated that the LB10000 achieved mean intratumoral field intensities exceeding 2 V/cm in lung and liver targets—representing at least a two-fold increase over reported values from existing TTFields devices.

Conclusions: The LB10000 enables adaptive, high-dose TTFields delivery with effective thermal regulation and extended coverage, supporting treatment of disseminated or multifocal disease. This technology represents a new paradigm for TTFields therapy, with the potential to significantly broaden its clinical impact.

#7201 Preclinical evaluation of click-cleavable radioimmunoconjugates for enhanced treatment efficacy in radioimmunotherapy.

Marleen H. M. E. van Stevendaal[1], Kim E. de Roode[1], Luc H. M. Zijlmans[1], Jenne T. Meinema[1], Hendrina M. de Wert-Wattimury[1], Renate C. van Daalen-Bruens[1], Bianca Matthee[1], Mark W. Konijnenberg[2], James Nagarajah[3], Raffaella Rossin[1], **Marc S. Robillard**[1]

[1]Tagworks Pharmaceuticals, Nijmegen, Netherlands,[2]Erasmus Medical Center, Rotterdam, Netherlands,[3]Radboud University Medical Center, Nijmegen, Netherlands

Targeted radiotherapy (TRT) with radiolabeled antibodies is hampered by long circulation times, resulting in dose-limiting toxicity. Tagworks developed a novel TRT approach based on its Click-to-Release platform, comprising an internalizing mAb functionalized with a chelator via a click-cleavable trans-cyclooctene (TCO) linker, and a small-molecule trigger (tetrazine). The radiolabeled mAb is administered and allowed to internalize into tumor cells. Then, a non-cell permeable trigger is injected that selectively reacts with the residual circulating mAb, releasing a small fast-clearing radioactive fragment. This approach is envisioned to unlock the treatment benefits of TRT with long-lived potent beta- (^{177}Lu) and alpha (^{225}Ac) radionuclides, minimizing toxicity to the patient's marrow and kidney while delivering a high therapeutic radioactive dose to the tumor. Tagworks' TGW211 program in Phase 0/1 aims at increasing the therapeutic index of radiolabeled trastuzumab (TGW211-DC), targeting HER2+ tumors. In addition, this approach is being applied to mAbs directed to various other targets in a preclinical setting. Chelate-conjugated mAbs were radiolabeled with ^{111}In or ^{177}Lu and release of the radiolabeled-DOTA was measured upon reaction with trigger. Binding and internalization were characterized using BT-474 cells. Pharmacokinetics and biodistribution were determined in nude mice +/- BT-474 xenografts. Patient dosimetry with different radionuclides was modelled using clinical data for [^{89}Zr]Zr-trastuzumab using IDAC-Dose 2.1 and OLINDA. The trigger rapidly released ^{111}In/^{177}Lu-labeled DOTA in PBS and plasma (e.g. 91.8% in 5 min for [^{111}In]In-TGW211-DC). [^{111}In]In-TGW211-DC demonstrated high-affinity in vitro (KD = 8.4 nM), and efficient internalization. In healthy mice, [^{111}In]In-TGW211-DC was highly stable with >20d TCO isomerization half-life, while trigger effectively released the fast-clearing ^{111}In-fragment in blood. In tumor bearing mice, radioactivity was largely retained inside tumor cells, but cleared from blood by the trigger, reaching maximum tumor-to-blood-ratios (T/B) of 16.3, 24h p.i. and 34.8, 72h p.i. Similar results were obtained for [^{177}Lu]Lu-TGW211-DC. Dosimetry projections indicate maximal healthy tissue dose decrease when trigger is administered 24 hrs post TGW211-DC, reaching up to 92% for ^{225}Ac and 88% for ^{177}Lu in marrow. In kidney this resulted in 89% dose decrease for ^{225}Ac. Finally, this click-cleavable TRT approach could be effectively applied to other internalizing mAb-target combinations. In conclusion, the click-cleavable TRT approach has demonstrated strong platform potential and markedly improved the T/B in mice for TGW211. Moreover, beneficial dosimetry of click-cleavable TRT was projected for TGW211. A First-in-human Phase 0/1 study with HER2+ cancer patients has recently been initiated.

#7202 Comparative evaluation of ^{225}Ac-PSMA-Trillium with other ^{225}Ac-PSMA-SMOL assets in a preclinical prostate cancer xenograft model.

Urs B. Hagemann[1], Maria Spelling[1], Shankari Nair[1], Martin Kohs[1], Meike Fehder[1], Stefan Stargard[1], Sabine Zitzmann-Kolbe[2], Dmitry Zubov[1], Ming Xu[1]

[1]Bayer AG, Berlin, Germany,[2]Life Molecular Imaging, Berlin, Germany

Prostate-specific membrane antigen (PSMA) is a transmembrane glycoprotein highly expressed on prostate cancer cells, making it an ideal target for novel prostate cancer therapies. Currently, there are several actinium-225 (^{225}Ac)-PSMA-targeting small molecules (SMOL) in clinical development for treating patients with metastatic castration-resistant prostate cancer. ^{225}Ac-PSMA-Trillium (BAY 3563254), is a novel PSMA-targeting molecule which comprises a highly specific PSMA-binding motif, an albumin-binding domain to optimize tumor uptake and retention, and a Macropa™ chelator complexed with the alpha-emitter ^{225}Ac. Here, we compared ^{225}Ac-PSMA-Trillium with three other ^{225}Ac-PSMA-SMOLs, i.e., ^{225}Ac-PSMA-617, ^{225}Ac-PSMA-R2 and ^{225}Ac-PSMA-I&T, which all utilize a DOTA chelator for complexing ^{225}Ac. All assets were synthesized and radiolabeled at Bayer AG. Binding to PSMA was confirmed using a surface plasmon resonance (SPR) assay. *In vitro* cytotoxicity in LNCaP cells was evaluated using CellTiterGlo®. The antitumor effects of ^{225}Ac-PSMA-SMOLs were investigated in male SCID mice with subcutaneous LNCaP tumors. Mice were randomized and treated with a single i.v injection of ^{225}Ac-PSMA-Trillium or the other ^{225}Ac-PSMA-SMOLs at different dose levels (100-400 kBq/kg, 375 kBq/nmol). Tumor growth and body weights were monitored for 4 weeks post injection. ^{225}Ac activity in various organs and tumors was measured using a high purity germanium detector or autoradiography. ^{177}Lu-PSMA-617 SPECT imaging was performed to evaluate tumor uptake. All PSMA-SMOLs exhibited strong binding affinity to recombinant PSMA as demonstrated by SPR. When radiolabeled with non-radioactive lanthanum as surrogate for ^{225}Ac, the target residence time of PSMA-SMOLs was weakened, except for PSMA-Trillium. All ^{225}Ac-labeled assets induced potent cytotoxicity in LNCaP cells *in vitro*. Radio-HPLC and iTLC confirmed the integrity and high radiochemical purity, respectively. ^{225}Ac-PSMA-Trillium at 400 kBq/kg showed higher tumor uptake compared to other ^{225}Ac-PSMA-SMOLs, homogeneous tumor accumulation 60 hours after injection, and fast clearance from the kidneys based on autoradiography. Furthermore, ^{225}Ac-PSMA-Trillium at all doses inhibited LNCaP tumor growth and decreased tumor weights in a dose-dependent manner, whereas the antitumor response was restricted to the higher doses for all other compounds. In summary, ^{225}Ac-PSMA-Trillium showed the highest tumor uptake and the strongest tumor growth inhibition with a clear dose response compared with the other ^{225}Ac-PSMA-SMOLs. These data support the clinical development of ^{225}Ac-PSMA-Trillium (NCT06217822).

#7203 ^{212}Pb-based CEA pretargeted radioimmunotherapy demonstrates tumor targeting and potent TGI in immunodeficient and humanized mouse models, informing a FIH study in mCRC.

Sofia H. L. Frost[1], Alexandre Pichard[2], Annabelle Mouchotte[2], Agnes Colmont[2], Sara Colombetti[3], Alexander Haas[4], Hans Peter Grimm[3], Birgit Kittel[3], Stephen Fowler[3], Bernhard Reis[3], Vincent Wolowski[3], Uta Sweere[3], Michael Hettich[3], Wolfgang Jacob[4], Frederic Prince[3], Christian Klein[5], Pablo Umana[5], Julien Torgue[6], **Axel Boehnke**[3]

[1]Roche Pharma Research and Early Development, Roche Innovation Center Welwyn, Roche Products Ltd, Welwyn Garden City, United Kingdom,[2]Institut Roche, Roche S.A.S., Boulogne-Billancourt, France,[3]Roche Pharma Research and Early Development, Roche Innovation Center Basel, F. Hoffmann-La Roche AG, Basel, Switzerland,[4]Roche Pharma Research and Early Development, Roche Innovation Center Munich, Roche Diagnostics GmbH, Penzberg, Germany,[5]Roche Pharma Research and Early Development, Roche Innovation Center Zurich, Roche Glycart AG, Schlieren, Switzerland,[6]Orano Med LLC, Plano, TX

Background: Alpha particles (α) are exceptionally cytotoxic, inducing complex DNA damage and bystander effects. Targeted α-therapy demonstrated a favorable therapeutic index (TI) in certain cancers. To improve the TI and expand to other indications, we developed a ^{212}Pb-based carcinoembryonic antigen-related cell adhesion molecule 5 pretargeted radioimmunotherapy (CEA-PRIT 2.0), involving two complementary SeParated v-domains LInkage Technology antibodies (SPLIT Abs) and ^{212}Pb-DOTAM. Each CEA-targeted SPLIT Ab carries half of a DOTAM binding v-domain that, when combined upon target binding, forms concentration-dependent stable complexes with ^{212}Pb-DOTAM. While unbound ^{212}Pb-DOTAM undergoes rapid renal clearance, ^{212}Pb-DOTAM captured by the SPLIT Abs leads to α emission at CEA-expressing cells with minimal systemic irradiation. Here, we report key preclinical data informing a planned first-in-human (FIH) CEA-PRIT 2.0 study in metastatic colorectal cancer (mCRC) patients.

Methods: We assessed CEA-PRIT 2.0-induced tumor growth inhibition (TGI), biodistribution, and tolerability in 3 CEA-expressing human xenograft models. SCID mice bearing BxPC3 (pancreatic) or LS174T (colorectal) tumors received up to 5 treatment cycles, and BRGS-CD47 mice (humanized and non-humanized) bearing HPAF-II (pancreatic) tumors received up to 3 cycles. Each cycle consisted of the two SPLIT Abs (1-5 mg/kg each) given on day 1 to allow for accumulation on CEA-expressing cells before giving ^{212}Pb-DOTAM (20 µCi) on day 8.

Results: Average ^{212}Pb tumor uptake in all models was 10-43% injected activity per gram of tissue (IA/g) at 24 h, with low blood and kidney retention (<3% IA/g). In the BxPC3 model, TGI was SPLIT Ab dose-dependent, while the LS174T model showed potent TGI already at the lowest dose (1 mg/kg). The SPLIT Ab dose-dependence of the TGI in the HPAF-II model was abrogated in huBRGS-CD47, suggesting secondary immune responses contribute to the therapeutic effect.Manageable body weight (BW) loss was observed in the SCID BxPC3 model. More pronounced BW loss in LS174T (SCID) and HPAF-II (BRGS-CD47/huBRGS-CD47) models was observed, but minimal BW gain or actual BW loss in controls suggests tumor burden toxicity or strain-specific sensitivity were contributing factors.Utilizing the preclinical data, we designed a FIH study, starting with ^{203}Pb-DOTAM as a surrogate for therapeutic ^{212}Pb-DOTAM tumor uptake and healthy tissue distribution, SPLIT Ab pharmacokinetics, and tumor CEA expression to inform optimal SPLIT Ab dosing and interval to ^{212}Pb-DOTAM, before initiating the ^{212}Pb-DOTAM activity escalation and potential cancer immunotherapy combinations.

Conclusions: CEA-PRIT 2.0 showed favorable tumor-to-healthy tissue radiation exposure and potent TGI with a favorable toxicity profile. A FIH study in mCRC is planned in H1 2026.

#7205 A universal duplex sequencing approach for accurate detection of somatic mutations.

Shuvro Prokash Nandi[1], Yuhe Cheng[2], Shams Al-azzam[3], Safa Saeed[2], Isabella R Stuewe[1], Zichen Jiang[2], Luka Culibrk[4], Maria Zhivagui[5], Xiaoxu Yang[6], Rachel M. Wise[7], Foster C. Jacobs[8], Berenice Chavanel[9], Michael Korenjak[9], Mia PETLJAK[10], Silvia Balbo[11], Laurie G. Hudson[12], Ke Jian Liu[13], Jiri Zavadil[9], Joseph G. Gleeson[14], Ludmil B. Alexandrov[3]

[1]Cellular and Molecular Medicine, UCSD Moores Cancer Center, La Jolla, CA,[2]UCSD, La Jolla, CA,[3]UC San Diego Health, San Diego, CA,[4]Department of Pathology, Grossman Medical School, New York, NY,[5]University of Nevada, Las Vegas (UNLV), Las Vegas, NV,[6]Department of Human Genetics, University of Utah, Salt Lake City, UT,[7]Department of Pharmaceutical Sciences, University of New Mexico, Albuquerque, NM,[8]University of Minnesota, Minneapolis, MN,[9]International Agency for Research on Cancer WHO, Lyon, France,[10]NYU Langone Health, New York, NY,[11]Postdoctoral Fellow, Masonic Cancer Ctr., University of Minnesota Masonic Cancer Center, Minneapolis, MN,[12]Professor, Dept. of Pharmaceutical Sci., Univ. of New Mexico Health Sciences Ctr., Albuquerque, NM,[13]Stony Brook Cancer Center, Stony Brook, NY,[14]Rady Children's Institute for Genomic Medicine, San Diego, CA

Somatic mutations arise from endogenous and exogenous mutagenic processes, accumulating over time and contributing to aging and disease. Detecting these rare mutations in non-clonal tissues remains a significant challenge due to the high error rates, limited genome coverage, and substantial DNA input requirements of existing sequencing approaches. Here, we introduce UDSeq, a high-accuracy, cost-effective, single-molecule duplex sequencing protocol designed to overcome these limitations. We place UDSeq in the context of existing duplex sequencing approaches, demonstrating that it achieves an exceptionally low error rate of ~2.5×10^{-9} per base pair, supports whole-genome and targeted capture sequencing from as little as 100 picograms of DNA, and delivers up to four times more usable duplex molecules than current state-of-the-art methods from the same input. We demonstrated the broad applicability of UDSeq through a series of in vitro and in vivo mutagenesis experiments, accurately capturing known mutational signatures induced by environmental carcinogens in human cell lines, rodents, and non-model organisms. We further applied UDSeq to normal tissues from a 70-year-old individual, revealing organ-specific mutational burdens and the activity of distinct mutational processes. With its high accuracy, low input requirements, and wide applicability, UDSeq provides a powerful and scalable tool for studying mutational processes across diverse biological contexts. Its versatility supports applications in cancer research, aging, and environmental exposure, expanding our capacity to characterize somatic mutations in both healthy and diseased tissues.

: Tumor Diagnostics, Prognostics, and Therapeutic Outcomes
Poster Session

#7209 Chromosome 3p mutations drive unique and non-redundant transcriptional programs in primary ccRCC.

Parker D. Mathews[1], Eric Knoche[2], Martin W. Schoen[3], Russell Pachynski[2]

[1]Internal Medicine Residency Program, Washington University in St. Louis School of Medicine, St. Louis, MO,[2]Division of Oncology, Washington University in St. Louis School of Medicine, St. Louis, MO,[3]Saint Louis University & St. Louis VAMC, Saint Louis, MO

Background: Chromosome 3p genes (tumor suppressor VHL and chromatin modifiers BAP1, SETD2, PBRM1) are frequently altered in ccRCC and may have prognostic significance, though the mechanism by which they drive ccRCC pathogenesis is incompletely understood. Therapies with novel mechanisms, for example belzutifan targeting hypoxia via HIF, increase the relevance of these mechanisms.
Methods: The Tempus Lens Platform (Tempus AI, Chicago, IL) was used to identify a cohort of de-identified ccRCC cases. Data was analyzed in Tempus Workspaces using the tempusverse suite of R packages. GSEA was applied to differential RNAseq expression data using the msigdbr (“hallmarks”) and clusterprofiler R packages. GSEA pathways are presented as normalized enrichment score with adjusted Q-value.
Results: We identified 166 ccRCC pts with solid tumor DNA and wtRNAseq genomic profiling, excluding biopsies from distant metastatic sites. Median age at diagnosis was 57 (IQR 47.2-66.0). The cohort was 63% male (n=101). Within the cohort, VHL SNV/indels were present in 52% (n=86), PBRM1 in 24% (n=39), BAP1 in 7% (n=12), and SETD2 in 10% (n=17). Copy number changes and structural alterations were not included. As expected, BAP1 and PBRM1 mutations were mutually exclusive (Fisher’s p = 0.037). VHLmut tumors demonstrated a clear hypoxic phenotype (hypoxia 1.50, q 2.27e-02, G2M checkpoint -2.37, q 4.00e-09). The other 3p mut tumors showed distinct phenotypes. BAP1mut was notable for an “immune-hot” signature (allograft rejection 2.83, q <7.37e-10, IFN-g response 2.49, q<7.37e-10, E2F targets 2.33 q<7.37e-10). PBRM1mut tumors were “immune-cold” with hallmarks of metabolic dysregulation (allograft rejection -2.13, q 1.96e-7, inflammatory response -1.92, q 1.22e-5, fatty acid metabolism 1.54, q 6.00e-3). Interestingly, SETD2mut tumors were notably distinct from VHLmut tumors, with downregulation of hypoxia, NFKB, and p53, and upregulation of cell cycle hallmarks, necessitating further investigation (hypoxia -2.15, q 1.57e-7, TNFa signaling -2.43, q 3.05e-9, G2M cell cycle 1.96, q 3.82e-6, p53 pathway -1.73, q 5.25e-4).
Conclusions: New treatments are emerging via rational design efforts enabled by a more detailed understanding of ccRCC pathogenesis. Here we leveraged real-world genomic data to characterize the landscape of 4 common, related genetic alterations known to be pivotal to ccRCC biology. Non-VHL altered patients were overrepresented in our cohort relative to prior studies, though only SNV/indels were captured here. We observed that non-VHL cases frequently have alterations in other chromosome 3p genes, which may drive ccRCC development, progression, and resistance via cellular processes distinct from the classic VHL-HIF-hypoxia axis. As HIF directed therapies become more widely utilized, chromosome 3p alterations have the potential to provide additional predictive and prognostic value to ccRCC patients.

#7210 Frequent intra-regional PLAP expression heterogeneity in gastric adenocarcinomas.

Morton Freytag[1], Eike C. Burandt[1], Florian Viehweger[1], Viktor Reiswich[1], Christina Tsourlakis[1], Ronald Simon[1], Claudia Hube-Magg[1], Martina Kluth[1], Waldemar Wilczak[1], Fiete Gehrisch[1], Thorben W. Fruendt[2], Thomas Roesch[3], Philip Dautel[3], Guido Sauter[1], Till S. Clauditz[1], Nina Schraps[1], Stefan Steurer[1], Clara Luehr[1]

[1]Institute of Pathology, University Medical Center Hamburg-Eppendorf, Hamburg, Germany,[2]Gastroenterology and Hepatology, University Medical Center Hamburg-Eppendorf, Hamburg, Germany,[3]Department of Interdisciplinary Endoscopy, University Medical Center Hamburg-Eppendorf, Hamburg, Germany

Placental alkaline phosphatase (PLAP), also known as alkaline phosphatase, placental type (ALPP) is a membranous protein which is thought to play a role in guiding migratory cells and transport specific molecules over the plasma membrane. In normal tissues, PLAP expression is almost exclusively seen in the placenta. In cancer, PLAP expression is a hallmark of testicular germ cell tumors but can also be found in up to 38% of gastric adenocarcinomas. The membranous location of PLAP in combination with the absence or only very low levels of PLAP expression in vital normal tissues of (non-pregnant) humans, makes PLAP a potentially useful therapeutic target. For targeted therapy, both the therapeutic success and the quality of the diagnostic assessment generally may critically depend on the degree of heterogeneity of target protein expression in a cancer. To study the extent of intratumoral heterogeneity of PLAP expression in gastric cancer, a gastric cancer heterogeneity tissue microarray was analyzed by immunohistochemistry (IHC). The TMA contained 0.6 mm tissue samples from 9 areas each of the primary cancers of 113 gastric cancer patients and 3-9 samples from matched lymph node metastases from 61 of these patients. There were 59.0% of 113 evaluable cancers without any PLAP positivity in all samples while a heterogeneous PLAP positivity was seen in 38 (34.0%) of patients. In most of the samples, heterogeneity occurred within individual TMA spots (intraregional heterogeneity) while only few cancers had a combination of distinctly negative spots and spots with a majority of unequivocally positive cells (regional heterogeneity). Intraregional heterogeneity was mostly caused by an admixture of cancer areas with a glandular growth pattern showing apical/luminal PLAP staining while solid areas of the same cancers were PLAP negative. The PLAP status of metastases was often comparable to the respective primary tumor. PLAP positivity of at least one metastasis spot was observed in 74.0% of 27 PLAP positive, but in only 6.3% of 34 PLAP negative primary tumors. Discrepancies in individual cases were again mostly caused by differences in the growth patterns. Metastases with a more solid tumor growth than seen in the primary tumors, tended to be less PLAP positive, than metastases with a glandular growth pattern. To what extent the common intraregional heterogeneity of PLAP expression will disturb the efficiency of targeted anti-PLAP therapies in gastric cancer remains to be seen.

#7211 High intratumoral homogeneity and tumor specificity makes uroplakin 3b (Upk3b) a promising therapeutic targetin malignant mesothelioma.

Sonke von Weihe[1], Frank Elsholz[1], Philipp Busch[2], Fiete Gehrisch[3], Nina Schraps[3], Martina Kluth[3], Maria C. Tsourlakis[3], Katharina Moller[3], Maximilian Lennartz[3], Veit Bertram[3], Florian Viehweger[3], Florian Lutz[3], Birgit Hantzsch-Kuhn[1], Till Olchers[1], David B. Ellebrecht[1], Christoph Fraune[3], Ronald Simon[3], Guido Sauter[3], Martin Reck[1], **Stefan Steurer**[3]

[1]Department of Thoracic Oncology, Airway Research Center North, German Center for Lung Research, LungenClinic, Grosshansdorf, Germany,[2]General, Visceral and Thoracic Surgery Department and Clinic, University Medical Center Hamburg-Eppendorf, Hamburg, Germany,[3]Institute of Pathology, University Medical Center Hamburg-Eppendorf, Hamburg, Germany

Uroplakin 3B (Upk3b) is one out of 5 known uroplakin (Upk) proteins that cooperatively form the apical asymmetrical unit membrane (AUM) plaques which play a pivotal role in the stabilization and strengthening of epithelial cells that line organs exposed to mechanical stress. In a previous study involving 608 normal tissues and 17,693 cancers we had found that Upk3b expression was limited to membranes of only three cell types which are all subjected to periodical massive distension. These include the apical membrane of the most superficial cell layer of the urothelium (umbrella cells), amnion cells covering the membrane that forms a part of the amniotic sac surrounding the developing fetus in the uterus during pregnancy, and mesothelial cells. Among cancers, Upk3b expression was largely limited to malignant mesothelioma and - less commonly - ovarian carcinomas. The combination of membranous expression in tumor cells and a lack of expression in drug-accessible vital normal cells makes Upk3b a potential therapeutic drug target in malignant mesothelioma. For targeted therapy, both the therapeutic success and the quality of the diagnostic assessment are likely to critically depend on the degree of heterogeneity of target protein expression in individual cancers. Cancers with Upk3b expression in all cancer cells are most likely to be correctly diagnosed as “Upk3b positive” in small biopsies and these tumors may also respond optimally to therapy as all tumor cells carry the drug target. To study the extent of intratumoral heterogeneity of Upk3b expression in malignant mesothelioma, all tumor containing tissue blocks from 58 consecutive patients with a diagnosis of malignant mesothelioma were examined for Upk3b expression by immunohistochemistry. A total of 109 tissue blocks was analyzed (average 2.02 per patient, range 1 - 9). With respect to their Upk3b staining 39 patients (72.2%) were homogeneously positive, 4 (7.4%) were heterogeneously positive and 11 (20.4%) were homogeneously negative. It is concluded from our data that a homogeneous Upk3b expression occurs in about 70.0% of patients with a malignant mesothelioma. This finding supports the notion that UpK3b may represent a promising therapeutic target for malignant mesothelioma, warranting further efforts in drug development.

#7212 MRE11 deficiency occurs in a small group of cancers from various different tumor entities.

Viktor Reiswich[1], Henry Recksiek[1], Katharina Moller[1], Florian Lutz[1], Florian Viehweger[1], Nina Schraps[1], Fiete Gehrisch[1], Christina Tsourlakis[1], Georgia Makrypidi-Fraune[1], Martina Kluth[1], Claudia Hube-Magg[1], Christian Bernreuther[1], Guido Sauter[1], Andreas H Marx[2], Ronald Simon[1], Till Krech[1], Stefan Steurer[1], Christoph Fraune[1], Sarah Minner[1], Viktoria Chirico[1], Bertram Veith[1], Clara Luehr[1], Cosima Volkel[1], Morton Freytag[1], Natalia Gorbokon[1], Maximilian Lennartz[1], Eike C. Burandt[1], Anne Menz[1], Clara von Bargen[1]

[1]Institute of Pathology, University Medical Center Hamburg-Eppendorf, Hamburg, Germany,[2]Department of Pathology, Academic Hospital Fuerth, Fuerth Germany, Fuerth, Germany

The double-strand break repair protein MRE11 forms the core of the MRE11/RAD50/NBS1 (MRN) complex. The MRN complex acts as an early DNA damage response element which is involved in different repair pathways including homologous recombination (HR), non-homologous end joining (NHEJ) and microhomology-mediated end joining (MMEJ) repair. In cancers, altered MRE11 expression has been described in various tumor entities (e.g. carcinoma of the prostate, colon and stomach) and both up- and downregulation was associated with adverse tumor features. Most of the clinical interest comes from studies highlighting the predictive role of MRE11 expression. MRE11 overexpressing cancers have been described to be more radioresistant while low-expressors were more sensitive to radiation and chemotherapy with camptothecin and gemcitabine. Several MRE11 inhibitors are currently being investigated in clinical trials as radiosensitizers. To better understand the role of MRE11 expression in cancer, a tissue microarray containing 14,966 samples from 134 different tumor entities was analyzed. In normal tissues, a strong nuclear MRE11 staining occurred in almost all cell types. Most cancers had a nuclear MRE11 staining that was strong in 11,797 (91.0%), moderate in 1,018 (7.9%), weak in 86 (0.7%), and completely absent (MRE11 deficiency) in 55 (0.4 %) of the 12,956 informative tumor samples. More than one case of MRE11 deficiency was only seen in 6 tumor entities including hepatocellular carcinoma (10 of 292; 3.4%), gastric adenocarcinoma, intestinal type (4 of 208; 1.9%), endometrioid endometrial carcinoma (5 of 268; 1.9%),pulmonary adenocarcinoma (2 of 165; 1.2%), colorectal adenocarcinoma (CRC, 16 of 2,183; 0.7%), and clear cell renal cell carcinoma (ccRCC, 7 of 1,011; 0.7%). Reduced MRE11 staining was associated with mismatch repair deficiency (dMMR) in CRC ($p<0.0001$ each) and in gastric adenocarcinoma ($p<0.0001$), advanced pT stage ($p=0.0003$) and L1 status ($p=0.0019$) in testicular seminoma, high grade ($p<0.05$), advanced pT ($p<0.0001$), and high UICC stage ($p=0.0014$) in ccRCC, advanced pT stage in high-grade serous ovarian carcinoma ($p=0.0396$), and nodal metastases in papillary thyroid cancer ($p=0.0332$). High MRE11 expression was linked to nodal metastasis in hepatocellular carcinoma ($p=0.0258$). It is concluded that MRE11 is highly expressed in most cancers and its reduced expression is associated with an aggressive phenotype in multiple cancer types. The potential to exploit MRE11 deficiency as a target for synthetic lethality deserves to be further explored.

#7213 Evaluation of folate receptor-alpha antibody-drug conjugate mirvetuximab soravtansine-gynx in ovarian cancer PDXs.

Daniel Ciznadija[1], Hsiu-Wen Tsai[2], Marianna Zipeto[2], Markus Hippich[2], Gilad Silberberg[2], **Stefano Cairo**[2], Michael Ritchie[2]

[1]Champions Oncology, Hackensack, NJ,[2]Champions Oncology (Rockville, MD), Rockville, MD

Epithelial ovarian cancer (EOC) remains one of the most lethal gynecologic malignancies, with approximately 20,000 new cases and over 12,000 deaths annually in the United States. Despite initial responsiveness to platinum-based combination chemotherapy, most patients relapse with platinum-resistant disease. Folate receptor-alpha (FRα), a membrane glycoprotein responsible for folate transport, is minimally expressed in normal tissues but highly expressed in ovarian and certain other epithelial cancers, making it an attractive therapeutic target. Elevated FRα expression correlates with reduced overall survival across tumor types, reinforcing its clinical relevance. Mirvetuximab soravtansine-gynx (Elahere®) is an FRα-targeting Antibody-drug conjugate (ADC) that couples an anti-FRα antibody with the cytotoxic maytansinoid derivative DM4. Preclinical models and clinical trials have demonstrated its potent activity in FRα-positive ovarian tumors, leading to regulatory approval in 2022. To evaluate Elahere® in translational preclinical systems, FRα RNA expression was profiled across Champions' patient-derived xenograft (PDX) models. Expression patterns mirrored clinical data, with the highest levels detected in ovarian, kidney, and non-small cell lung cancers. Immunohistochemistry confirmed that models with high FRα RNA display strong membrane staining, whereas FRα-negative models lack detectable expression. Selected ovarian PDX models were treated intravenously with Elahere®. Tumor growth inhibition analyses revealed no response in the FRα-negative model, while FRα-positive tumors displayed variable degrees of sensitivity consistent with patient outcomes, where roughly 43% of FRα-positive individuals respond to therapy. These findings confirm that FRα expression is a strong negative predictor for response when absent, but expression level alone does not discriminate responders from non-responders. To explore potential resistance mechanisms, single-sample gene set enrichment analysis of RNA sequencing data identified enrichment of gene ontology terms related to glutathione and xenobiotic transport in non-responding FRα-positive models, implicating ATP-binding cassette (ABC) transporters such as ABCC1 and ABCC2 in drug efflux-mediated resistance. Additionally, upregulation of cell-cycle checkpoint regulators in non-responders suggests a possible mechanism of mitotic evasion that limits Elahere®'s microtubule-disrupting activity. Collectively, these studies highlight the value of Champions' PDX and bioinformatics platforms in modeling ADC activity. Such translational approaches are essential for optimizing ADC development and improving outcomes for patients with platinum-resistant ovarian cancer.

#7214 LymphGen-based stratification of DLBCL PDX models mirrors clinical tumor complexity.

Marianna Zipeto[1], Mike Ritchie[1], Markus Hippich[1], Daniel Ciznadija[2], Gervaise Henry[1], **Stefano Cairo**[1], Gilad Silberberg[1]

[1]Champions Oncology (Rockville, MD), Rockville, MD,[2]Champions Oncology, Hackensack, NJ

Diffuse Large B-Cell Lymphoma (DLBCL) is a highly heterogeneous malignancy whose biological diversity is best captured by modern molecular classifications. The Cell of Origin (COO) system divides tumors into Germinal Center B-cell-like (GCB) & Activated B-cell-like (ABC) groups, reflecting fundamental differences in differentiation state, signaling reliance, & clinical behavior. Building on COO, the LymphGen classification provides a more granular view by defining genetically coherent subtypes such as MCD, driven by MYD88L265P & CD79B lesions that promote chronic active BCR signaling; BN2, characterized by BCL6 translocations & NOTCH2 mutations typical of marginal-zone-like biology; N1, marked by NOTCH1 activation; A53, enriched for TP53 loss & chromosomal instability; EZB, defined by EZH2 mutation, BCL2 rearrangement, & germinal-center-associated epigenetic rewiring; & additional groups such as ST2, harboring SOCS1 mutations & JAK-STAT pathway alterations. These genomic clusters reveal distinct oncogenic circuits, & potential therapeutic vulnerabilities. In this study, the LymphGen 2.0 classifier integrates somatic mutations, copy-number alterations, & structural variants to assign samples to seven genomic subtypes. To molecularly characterize Champions Oncology's lymphoma PDX & ex vivo models, we applied LymphGen to generated mutation, CNV, & fusion data.

Forty lymphoma models with complete genomic profiling were formatted according to LymphGen 2.0 requirements & submitted via the online data portal. Models were assigned to the following categories: MCD, BN2, N1, EZB, ST2, A53, hybrid subtypes, or Other/Unclassified. Subtype assignments were examined in the context of available clinical metadata & functional datasets.

Among the 40 lymphoma models analyzed, the distribution demonstrate a remarkable ability to reproduce not only the full distribution of LymphGen subtypes but also the detailed combinations of structural variants, driver mutations, & pathway lesions observed in clinical tumors. The presence of multiple hybrid calls reflects either overlapping genomic features or incomplete rule satisfaction, consistent with prior reports on LymphGen behavior in heterogeneous or partially altered samples. This stratification highlights biologically representative diversity across the lymphoma models cohort, enabling subtype-aware selection of models for translational studies, including evaluation of BTK inhibitors in MCD-like backgrounds & EZH2-directed therapies in EZB-assigned models.

Application of LymphGen to Champions Oncology's lymphoma models provides robust subtype resolution that mirrors clinically observed molecular heterogeneity. This integration supports rational preclinical model selection, enhances interpretability of drug-response studies, & lays the foundation for expanded multi-omic subtype refinement across the hematologic pipeline.

#7215 The OTP, CD44, Ki67 biomarker panel predicts prognosis in preoperative lung NET biopsy specimens.

Tijmen JJ van Weert[1], Laura Moonen[1], Lisa M. Hillen[1], Jan von der Thusen[2], Michael A. den Bakker[3], Lisa MV Lap[1], PALGA Group[4], Ronald A. Damhuis[5], Wieneke A. Buikhuisen[6], Anne-Marie C. Dingemans[2], Jules L. Derks[2], **Ernst Jan M. Speel**[2]

[1]Maastricht University, Maastricht, Netherlands,[2]Erasmus MC Cancer Institute, Rotterdam, Netherlands,[3]Maasstad Hospital, Rotterdam, Netherlands,[4]PALGA Foundation, Utrecht, Netherlands,[5]Comprehensive Cancer Association, Utrecht, Netherlands,[6]Netherlands Cancer Institute, Amsterdam, Netherlands

Introduction: Previously OTP, CD44 and Ki-67 have been identified as prognostic biomarkers in resected lung neuroendocrine tumors (lung NETs, also known as lung carcinoids (LCs)).
Aims: We aimed to examine the prognostic value of biomarkers OTP, CD44 and Ki-67 in preoperative LC biopsies.
Methods: Patients with LC (reclassified TNM 8 stage I-III, 2003-2022) who underwent a curative resection were selected from Dutch pathology archives (PALGA). Matching resection (Rx) and biopsy (Bx) specimens were identified and immunohistochemistry (IHC) for OTP, CD44 and Ki-67 was performed. Pathology revision was carried out by three pathologists according to the WHO 2021 classification. OTP and CD44 immunostaining were assessed (H-score), and Ki-67 proliferation index (PI) by eyeball estimation with hot-spot scoring. Bx cases diagnosed as typical carcinoid (TC) or carcinoid not otherwise specified (NOS) were grouped as low risk (i.e. non-atypical carcinoid or non-AC). The biomarker panel was classified as low-risk (OTP≥50, CD44≥30, Ki-67<5%) or high-risk (all others).
Results: In total 98 patients were eligible, including 19 patients with a relapse after a median follow-up of 83.3 months. The biomarker panel correctly identified high-risk in 89% (n=17/19) of relapses, outperforming WHO classification, which assigned only 11% (n=2/19) of relapses as AC. Negative predictive value (NPV) of the biomarker panel was 0.96 compared to 0.82 for WHO. Biomarker risk stratification also showed higher inter-rater agreement (biomarker panel: κ=0.673; WHO: κ=0.276, both $p<0.001$) and improved inter-specimen concordance (biomarker panel: κ=0.584, $p<0.001$; WHO: κ=0.169, $p=0.037$).
Conclusion: An OTP, CD44 and Ki-67 IHC biomarker panel substantially improves identification of patients with low-risk LCs and is applicable on biopsy specimens, outperforming the prognostic value of WHO classification. This may influence the choice of surgical treatment strategy.

#7216 HMGB1 expression is linked to unfavorable tumor features and poor prognosis in colorectal cancers.

Nina Schraps[1], Katharina Moller[1], Viktor Reiswich[1], Florian Viehweger[1], Maria Christina Tsourlakis[1], Georgia Makrypidi-Fraune[1], Claudia Hube-Magg[1], Martina Kluth[1], Till Krech[1], Christoph Fraune[1], Andreas H Marx[1], Fiete Gehrisch[1], Baris Mercanoglu[2], Nathaniel Melling[2], Thilo Hackert[2], Ronald Simon[1], Guido Sauter[1], Morton Freytag[1]

[1]Institute of Pathology, University Medical Center Hamburg-Eppendorf, Hamburg, Germany,[2]General, Visceral and Thoracic Surgery Department and Clinic, University Medical Center Hamburg-Eppendorf, Hamburg, Germany

High-mobility group box 1 (HMGB1) is a chromatin-associated protein with a key role in DNA damage repair and genome stability, involved in DNA replication, transcription, and chromatin remodeling. The translocation of HMGB1 from the nucleus to the cytoplasm may confer additional functions regarding the interplay between autophagy, apoptosis and mitochondrial function. By regulating multiple signaling pathways HMGB1 contributes to critical characteristics of cancer cells including inflammation, angiogenesis, proliferation, migration and invasion, as well as tumor energy metabolism. Both increased and reduced expression of HMGB1 have been found to be linked to unfavorable tumor features, presumably depending on its cellular location and tissue type. To gain further insight into the potential significance of HMGB1 in colorectal cancer, a tissue microarray containing 3,456 colorectal cancers was analyzed by immunohistochemistry for nuclear and cytoplasmic HMGB1. A significant nuclear HMGB1 immunostaining was seen in all normal cells of the colorectal epithelium. However, the level of nuclear HMGB1 was variable in cancers. Among 2,601 interpretable cancers, nuclear HMGB1 was completely lost in 8 cases (0.3%) while the staining was 1+ in 179 (6.9%), 2+ in 684 (26.3%), and 3+ in 1,730 (66.5%) tumors. Strong nuclear HMGB1 was significantly linked to distant metastasis (p<0.0001), lymph node metastasis (p=0.0438), blood vessel invasion (p=0.0365), absence of BRAF V600E mutations (p=0.0107), and shortened overall survival (p=0.0118). Nuclear HMGB1 was markedly reduced in mismatch repair (MMR) deficient (43.8% strong) as compared to MMR proficient tumors (73.4%, p<0.0001). Within MMR proficient tumors, high nuclear HMGB1 was linked to V+ (p=0.0089) and L1 status (p=0.0054). Cytoplasmic HMGB1 was less common (16.7%) and unrelated to the histopathologic tumor phenotype. In summary, our data demonstrate that HMGB1 expression is variable in colorectal cancer and that a high nuclear HMGB1 staining level is associated with aggressive tumor features and poor outcome while reduced nuclear HMGB1 is strongly linked to MMR deficiency.

#7217 Homogeneity of mesothelin expression is tightly linked to its levels of expression in non-small cell lung cancer.

Philipp Busch[1], Fiete Gehrisch[2], **Nina Schraps**[2], Katharina Moller[2], Seyma Buyucek[2], Maximilian Lennartz[2], Florian Viehweger[2], Christoph Fraune[2], Christian Bernreuther[2], Ronald Simon[2], Guido Sauter[2], Till Olchers[3], Florian Lutz[2], Martina Kluth[2], Georgia Makrypidi-Fraune[2], Stefan Steurer[2], Martin Reck[3], Sonke von Weihe[3]

[1]General, Visceral and Thoracic Surgery Department and Clinic, University Medical Center Hamburg-Eppendorf, Hamburg, Germany,[2]Institute of Pathology, University Medical Center Hamburg-Eppendorf, Hamburg, Germany,[3]Department of Thoracic Oncology, Airway Research Center North, German Center for Lung Research, LungenClinic, Grosshansdorf, Germany

Mesothelin is a membrane protein which is commonly expressed in lung cancer as well as in other cancer types while it is only rarely seen on the surface of normal cells. Therefore, mesothelin represents an attractive molecule for targeted cancer therapies employing CAR-T cells, monoclonal antibodies, recombinant immunotoxins, antibody-drug conjugates and other drugs. For targeted therapy, both the therapeutic success and the quality of the diagnostic assessment generally may critically depend on the degree of heterogeneity of target protein expression in each individual cancer. Cancers with mesothelin expression in all cancer cells are most likely to be correctly diagnosed as “mesothelin positive” in small biopsies and may also respond optimally to therapy as all tumor cells carry the critical target signature. To study the extent of intratumoral heterogeneity of mesothelin expression in non-small cell lung cancer (NSCLC), a NSCLC heterogeneity tissue microarray was analyzed by immunohistochemistry (IHC) in a tissue microarray (TMA) format. The TMA contained 0.6 mm tissue samples from 8 areas each of the primary cancers of 130 patients and up to 4 samples (1 sample per nodal metastasis) from matched lymph node metastases from 60 of these patients. Mesothelin positivity was observed in 411 of 1,007 (40.8%) evaluable samples. On a patient level, mesothelin positivity occurred in 56.2% (n=73) while the highest mesothelin staining intensity was strong in 30.0% (n=40), moderate in 9.2% (n=12), and weak in 16.2% (n=21) of patients. Heterogeneity analysis was based on 7.7 samples per patient on average (range 2-12) and revealed a homogeneous mesothelin positivity (observed in all evaluable samples) in 21.5% (n=28), a heterogeneous mesothelin positivity in 34.6% (n=45), and a homogeneous lack of mesothelin staining in 43.8% (n=57) of patients. Homogeneous mesothelin positivity was tightly linked to a high level of mesothelin expression. Among 73 patients with detectable mesothelin positivity in their cancers, positivity was homogeneous in 67.5% (27 out of 40) of patients with at least one strongly positive sample, 8.3% (1 out of 12) with only moderate positivity and not seen (0 out of 21) in patients with only weak mesothelin positivity ($p<0.0001$). It is concluded that NSCLC patients with high level mesothelin expression do mostly exhibit a homogeneous positivity across their cancer while the likelihood for heterogeneous findings increases in patients with a more equivocal mesothelin positivity. These findings could further support the concept that a high level of mesothelin staining could be related to a favorable response to anti-mesothelin drugs in NSCLC patients.

#7218 Preliminary exploration of the synergistic mechanism between EBV LMP1 and MYD88 L265P mutation on the efficacy of PD-1 Inhibitors in ABC-DLBCL.

Chang Wang, Yingtao Lin, Jiesong Wang

Lymphoma, Fujian Cancer Hospital, Fuzhou, China

Background: Activated B-cell-like diffuse large B-cell lymphoma (ABC-DLBCL) is aggressive with poor prognosis. Epstein-Barr virus (EBV) infection and the MYD88 L265P mutation are key molecular drivers in ABC-DLBCL, typically exhibiting mutual exclusivity, potentially due to functional overlap. PD-1 inhibitors show limited efficacy in unselected relapsed/refractory DLBCL patients. However, our retrospective analysis of relapsed/refractory non-GCB DLBCL patients suggested that rare "double-positive" (EBV-positive/MYD88 L265P mutant) patients had higher response rates to PD-1 inhibitors.
Objective: This study investigated how EBV LMP1 modulates intracellular signaling in the context of MYD88 L265P mutation (causing constitutive JAK/STAT activation) and evaluated its synergistic effect with the PD-1 inhibitor tislelizumab.
Methods: Clinical data from 54 relapsed/refractory non-GCB DLBCL patients treated with PD-1 antibodies were analyzed. Patients were stratified by EBER ISH (EBV) and MYD88 sequencing. The HBL-1 cell line (MYD88 L265P mutant, EBV-negative) was used. LMP1 was overexpressed via transfection. Groups: control, tislelizumab alone, LMP1 overexpression, LMP1+tislelizumab. qPCR measured mRNA levels of NF-κB p65, MMP9, c-Myc, TLR3, STAT3, JAK3, LMP1, PD-1, PD-L1. Western blot detected protein expression and phosphorylation of key molecules.
Results: Among 21 patients with complete molecular data, both "double-positive" patients achieved an objective response (100%), compared to 22.2% in EBV-negative/MYD88 mutant (n=9) and 60.0% in EBV-positive/MYD88 wild-type (n=5) groups. HBL-1 cells showed high baseline p-JAK3 and p-STAT3. LMP1 overexpression suppressed p-JAK3 and p-STAT3. HBL-1 cells expressed tumor cell-intrinsic PD-1 mRNA. Tislelizumab alone inhibited p-JAK3/p-STAT3 phosphorylation. The combination of LMP1 overexpression and tislelizumab showed the strongest inhibition, indicating synergy.
Conclusion: MYD88 L265P mutation may cause tumor cell addiction to STAT3 activation maintained by tumor cell-intrinsic PD-1 signaling. LMP1 co-existence adds inhibitory pressure, potentially enhancing this dependency. Tislelizumab blockade may yield a synthetic lethal effect. Combined EBV status and MYD88 profiling could predict PD-1 inhibitor sensitivity in DLBCL, requiring further validation.

#7219 Nectin-4 expression is abundant in many different cancer entities.

Luehr Clara[1], Pia Lehmke[1], Katharina Moller[1], Florian Lutz[1], Florian Viehweger[1], Georgia Makrypidi-Fraune[1], Martina Kluth[1], Claudia Hube-Magg[1], Nina Schraps[1], Fiete Gehrisch[1], Christian Bernreuther[1], Guido Sauter[1], Andreas H Marx[2], Ronald Simon[1], Stefan Steurer[1], Christoph Fraune[1], Viktoria Chirico[1], Till S. Cauditz[1], Bertram Veit[1], Clara Von Bargen[1], Cosima Volkel[1], Morton Freytag[1], Nathalia Gorbokon[1], Maximilian Lennartz[1], Eike C. Burandt[1], Anne Menz[1], Till Krech[1], Maria C. Tsourlakis[1], Sarah Minner[1]

[1]Institute of Pathology, University Medical Center Hamburg-Eppendorf, Hamburg, Germany,[2]Department of Pathology, Academic Hospital Fuerth, Fuerth, Germany

Nectin-4 is a type I transmembrane protein with a crucial role in calcium-independent cell-cell adhesion and a critical involvement in several signaling pathways including the PI3K/AKT and the JAK2-STAT5a pathways. Based on these interactions, Nectin-4 is involved in the regulation of migration, adhesion, and proliferation of tumor cells. In several cancer entities, unfavorable prognosis has been described for Nectin-4 positive cancers. Most of the current significance of Nectin-4 is driven by its role as a drug target for enfortumab vedotin (EV) which has been FDA approved for advanced urothelial carcinoma. EV and several other anti-Nectin-4 drugs are currently being investigated in clinical trials on bladder cancer as well as in several other tumor entities. To better comprehend the prevalence of Nectin-4 expression in different cancer types, Nectin-4 was analyzed by immunohistochemistry (IHC) on tissue microarrays (TMAs) containing 2,418 samples from 43 different tumor types. A total of 35 of 43 tumor categories showed Nectin-4 expression in at least one case, and 22 tumor categories contained at least one strongly positive case. A moderate or strong Nectin-4 positivity was most seen in basal cell carcinoma of the skin (50.0%), squamous cell carcinomas of the larynx (45.8%), vulva (44.3%), anal canal (41.0%), penis (39.0%), floor of the mouth (36.5%), skin (32.5%), pharynx (27.6%), uterine cervix (24.4%), vagina (23.3%), esophagus (20.0%), and the lung (14.5%), muscle-invasive urothelial carcinoma (39.1%), clear cell carcinoma of the ovary (33.3%), pulmonary adenocarcinoma (22.9%), endometrioid carcinoma of the ovary (17.2%), lobular carcinoma of the breast (16.7%), invasive breast carcinoma of no special type (13.3%), carcinosarcoma of the uterus (10.5%) and the ovary (6.3%), ductal adenocarcinoma of the pancreas (9.9%), mucinous carcinoma of the ovary (9.1%), gastric adenocarcinoma of diffuse (5.6%) and intestinal type (2.9%), and prostatic adenocarcinoma (2.6-4.3%). It is concluded from these data that Nectin-4 expression occurs commonly in a broad range of different cancer entities. Thus, anti-Nectin-4 cancer drugs may be applicable in multiple applications beyond bladder cancer.

#7220 Claudin-6 (CLDN6) expression is abundant in many different cancer entities.

Veit Bertram[1], Anin Sharifi[1], Katharina Moller[1], Florian Lutz[1], Florian Viehweger[1], Christina Tsourlakis[1], Georgia Makrypidi-Fraune[1], Martina Kluth[1], Christian Bernreuther[1], Guido Sauter[1], Andreas H. Marx[2], Ronald Simon[1], Fiete Gehrisch[1], Nina Schraps[1], Stefan Steurer[1], Christoph Fraune[1], Viktoria Chirico[1], Clara von Bargen[1], Cosima Volkel[1], Morton Freytag[1], Natalia Gorbokon[1], Maximilian Lennartz[1], Eike C. Burandt[1], Anne Menz[1], Till Krech[1], Sarah Minner[1]

[1]Institute of Pathology, University Medical Center Hamburg-Eppendorf, Hamburg, Germany,[2]Department of Pathology, Academic Hospital Fuerth, Fuerth, Germany

Claudin-6 (CLDN6) is a member of the claudin membrane protein family, which are crucial components of tight junctions, regulating paracellular permeability and maintaining cell polarity. CLDN6 is early expressed in embryonic stem cells and in specific fetal tissues such as kidney, lung, pancreas, and stomach, but is not expressed in corresponding adult tissues. While CLDN6 expression is largely lacking on normal tissues, it is highly expressed in several cancers. Therefore, CLDN6 is considered a potential therapeutic target. Studies evaluating CLDN6 as a target for monoclonal antibodies, antibody-drug conjugates, bispecific antibodies, and CAR-T cells are underway. To better comprehend the prevalence of CLDN6 expression in different cancer types, CLDN6 was analyzed by immunohistochemistry (IHC) on tissue microarrays (TMAs) containing 4,464 samples from 101 different tumor types. A total of 39 tumor categories showed CLDN6 expression in at least one case, and 21 tumor categories contained at least one strongly positive case. At least weak CLDN6 positivity was most commonly seen in embryonal carcinoma (100%), seminoma (97.8%), and yolk sac tumor of the testis (97.6%), serous high-grade (76.4%), endometrioid (41.0%) and clear cell carcinoma (31.6%) of the ovary, carcinosarcoma of the ovary (66.7%) and the endometrium (36.0%), basal cell carcinoma of the skin (44.4%), adenocarcinoma of the ampulla Vateri (20%), endometrioid endometrial carcinoma (18.9%), adenocarcinoma of the cervix uteri (17.4%), adenocarcinoma of the esophagus (13.9%), gastric adenocarcinoma, intestinal type (11.6%), mucinous carcinoma of the ovary (9.1%), ductal adenocarcinoma of the pancreas (8.9%), muscle-invasive urothelial carcinoma (6.9%), cholangiocarcinoma (5.9%), squamous cell carcinomas of the esophagus (4.5%), vulva (4.3%), skin (4.1%), larynx (3.1%), penis (2.8%), pharynx (2.3%), anal canal (1.7%), oral cavity (1.2%), and the cervix uteri (1.2%), Brenner tumor of the ovary (3.6%), invasive breast carcinoma of no special type (3.5%), hepatocellular carcinoma (2.0%), gastric adenocarcinoma, diffuse type (1.8%), colorectal adenocarcinoma (1.7%), and diffuse large B cell lymphoma (1.0%). Our tumor cohorts were large enough to compare CLDN6 expression with tumor phenotype in ovarian, endometrial and pancreatic cancer. CLDN6 positivity was associated with advanced pT stage ($p<0.0001$) and high grade ($p=0.0003$) in ovarian cancer and with high grade in endometrial carcinoma ($p=0.0179$) but was unrelated to phenotype in pancreatic ductal adenocarcinoma. It is concluded that CLDN6 is expressed at significant levels in many different tumor types. Once anti-CLDN6 drugs are approved as safe and efficient, patients with many different cancer types may benefit from these new therapies.

#7221 LncRNA SNHG14 remodels cholesterol metabolism to inhibit pancreatic ductal adenocarcinoma via recruiting USP20 and down-regulating miR-105-5p through IRF1-SNHG14-USP20-HMGCR axis.

Zhu Ke[1], Dong Yan[2], Yingying Tong[1], Yurong Cheng[1], Chan Zhang[1]

[1]Beiijing Luhe Hospital Affiliated to Capital Medical University, Beijing, China,[2]UT MD Anderson Cancer Center, Beijing, China

Introduction: Lipid metabolism disorders are closely linked to pancreatic cancer progression, with intricate interactions underlying this association. Small nucleolar RNA host gene 14 (SNHG14), a long non-coding RNA with oncogenic properties, has been implicated in the progression of various malignant tumors including pancreatic cancer. However, its specific contribution to tumor lipid metabolism, particularly in pancreatic cancer, remains unclear.

Methods: Pancreatic cancer models with SNHG14 overexpression or knockdown were established to assess its effects in vitro. Quantitative RT-PCR and Western blotting evaluated SNHG14's influence on the downstream target USP20, while cholesterol detection assays examined its role in regulating intracellular cholesterol. In vivo, a nude mouse subcutaneous xenograft model was used to study tumor growth following SNHG14-knockdown cell injection, confirming its role in pancreatic cancer progression. Tumor tissues were analyzed for USP20 expression and cholesterol content, further supporting SNHG14's regulatory function. Molecular mechanisms were explored via dual luciferase reporter assays and RIP, confirming the interaction between SNHG14 and miR-105-5p, and its regulation of USP20 mRNA stability through the ceRNA pathway. Co-IP revealed the USP20-HMGCR interaction, while ChIP identified IRF1's binding to SNHG14, elucidating its nuclear regulatory pattern.

Results: SNHG14 significantly upregulated USP20 mRNA and protein expression, consistent with its effects in vitro and in vivo. SNHG14 overexpression promoted pancreatic cancer cell proliferation, invasion, and xenograft growth, while SNHG14 knockdown inhibited these effects, confirming SNHG14's oncogenic role via USP20 upregulation. In vivo, SNHG14 knockdown reduced cholesterol levels in pancreatic tumors, identifying SNHG14 as a key regulator of cholesterol metabolism linked to cholesterol accumulation in pancreatic cancer. In the cytoplasm, SNHG14 acts as a molecular sponge for miR-105-5p, competing with it to regulate USP20 mRNA stability and enhance USP20 expression. As a deubiquitinating enzyme, USP20 promotes HMGCR stability and activates the cholesterol synthesis pathway. In the nucleus, IRF1 binds to the SNHG14 promoter, facilitating its transcription. SNHG14 amplifies HMGCR expression via the miR-105-5p/USP20 axis, remodeling cholesterol metabolism and accelerating disease progression.

#7223 Evaluating treatment-related estrogen signaling and molecular subtype heterogeneity in a racially diverse HR-positive breast cancer cohort.

Abigail M. Fielder[1], Gregory Dyson[1], Julie Ruterbusch[1], David Carr[2], Julie Boerner[1], Ann G. Schwartz[1], Kristen S. Purrington[1]

[1]Oncology, Wayne State University School of Medicine, Detroit, MI,[2]Pathology, Wayne State University School of Medicine, Detroit, MI

African American women (AAW) with hormone receptor-positive (HR+) breast cancer have ~50% higher mortality than European American women (EAW), and AAW are twice as likely to have weakly HR+ tumors (1-10% positivity). Although women with weakly HR+ tumors have 60% higher mortality and may still benefit from endocrine therapy (ET), they are less likely to receive ET. Clinical HR staining may not consistently reflect endocrine activity, and better characterization across HR positivity could help ensure optimal treatment.

We performed targeted RNA sequencing on 118 tumors (54 EA, 64 AA) enrolled in the Detroit Research on Cancer Survivorship (ROCS) cohort and the Karmanos Cancer Institute Biobank to assess functional estrogen signaling with the Sensitivity to Endocrine Therapy (SET) index and heterogeneity in molecular subtypes using the Breast Cancer Consensus Subtype (BCCS) panel. Clinical HR staining was grouped as strongly (>90%), moderately (11-90%), and weakly (1-10%) HR+. RNA-seq data were normalized and $\log_2$-transformed. SET values were grouped into low, intermediate, and high tertiles. BCCS subtypes were assigned using the BCCSclassifier R package, yielding five subtypes: ER-negative (ER-) non-basal, ER- basal, ER+ proliferative, ER+ stromal infiltration, and ER+ strong tumor signaling. Relationships between gene expression, SET score, HR categories, and race were evaluated using ANOVA and chi-square tests. Subtype distribution across HR categories and race was tested with multinomial logistic regression ($\alpha = 0.05$).High SET scores were enriched among strongly HR+ tumors ($\chi^2 = 11.9$, $p = 0.018$). Further, 7% of weakly HR+ tumors had high SET scores, while 15% of strongly HR+ tumors had low SET scores, indicating discordance between clinical staining and treatment-related endocrine activity. Tumors from EAW vs. AAW had higher median SET values among those with intermediate (AA median= -0.21 vs. EA median= 0.017, p=0.028) and high (AA median=0.97 vs. EA median=1.88, p=0.16) SET scores. Considering BCCS, weakly HR+ tumors were more likely to have the ER-negative basal subtype compared to strongly HR+ tumors (OR=38.5, p=0.002) and to moderately HR+ tumors (OR=4.9, P = 0.044). Moderately HR+ tumors were also more likely to be classified as ER- basal (OR = 7.9, p = 0.024) compared to strongly HR+ tumors. The proportion of HR+ tumors assigned an ER-negative subtype differed significantly in AA vs EA patients overall (48.3% vs. 26.1%, p = 0.035), and similar trends were seen among the 1-10% (94% vs 67%, p=0.18) and 11-90% (52% vs 20%, p=0.11) HR groups. We observed meaningful differences in hormone signaling phenotypes between AAW and EAW, suggesting that clinical HR staining may not fully capture the underlying endocrine activity. This emphasizes the need for deeper molecular characterization to guide targeted treatment strategies and address disparities.

#7224 Nuclear/cytoplasmic translocation of β-Catenin protein is a strong predictor of unfavorable patient prognosis in ERG negative but not in ERG positive prostate cancer.

Florian Lutz[1], Osman Gokalp[1], Ronald Simon[1], Hans Heinzer[2], Alexander Haese[3], Sarah Minner[1], Guido Sauter[1], Thorsten Schlomm[4], Martina Kluth[1], Claudia Hube-Magg[1]

[1]Institute of Pathology, University Medical Center Hamburg-Eppendorf, Hamburg, Germany,[2]Martini-Clinic, Prostate Cancer Center, University Medical Center Hamburg-Eppendorf, Hamburg, Germany,[3]Martini-Clinic, Prostate Cancer Center, University Medical Center Hamburg-Eppendorf, Hamburg, Germany,[4]Department of Urology, Charite - Universitatsmedizin Berlin, Hamburg, Germany

β-Catenin (CTNNB1) alterations are of potential interest as a prognostic feature and an option for therapeutic targeting in cancer. β-Catenin (CTNNB1) is a dual function protein with roles in cell cohesion and gene transcription as a critical intracellular signal transducer in the Wnt signaling pathway. Cytoplasmic and nuclear translocation of the β-Catenin protein results in an increased transcription of multiple cancer promoting genes. Aberrant nuclear β-Catenin translocation is especially caused by loss of function mutations of genes encoding proteins of the β-Catenin destruction complex or by gain of function mutations of CTNNB1. Affected cancers can be recognized by immunohistochemistry (IHC) due to their aberrant nuclear/cytoplasmic β-Catenin staining. To study the prevalence and the potential role of aberrant β-Catenin staining patterns, more than 6,000 adenocarcinomas of the prostate were analyzed by immunohistochemistry (IHC) in a tissue microarray format. All patients had been treated by radical prostatectomy. Clinical follow-up data were available for 4,895 patients. Among 6,114 evaluable cancers, membranous β-Catenin staining was considered strong in 2,893 (47.3%), moderate in 2,737 (44.8%), and weak in 326 (5.3%) while additional 158 (2.6%) showed unequivocal nuclear/cytoplasmic translocation of β-Catenin protein. Strong membranous β-Catenin staining was more common in 1,926 tumors with (61.4%) than in 2,617 tumors without (37.7%) *TMPRSS2:ERG* fusion ($p<0.0001$). Strong membranous β-Catenin staining was significantly associated with advanced pT stage as well as a high traditional ($p<0.0001$) and quantitative Gleason grade ($p<0.0001$). A comparison of β-Catenin staining data with PSA recurrence revealed only minimal differences between tumors with weak, moderate, and strong membranous staining but a significantly increased risk for PSA recurrence for patients with nuclear/cytoplasmic β-Catenin translocation ($p=0.0448$). A subgroup analysis of 1,258 ERG positive and 1,672 ERG negative cancers revealed that the unfavorable prognostic impact of nuclear/cytoplasmic β-Catenin translocation was only seen in the ERG negative group ($p<0.0001$) while there was even a tendency towards better patient outcome in case of nuclear/cytoplasmic β-Catenin translocation in ERG positive cancers. It is concluded that nuclear/cytoplasmic β-Catenin translocation as detected by IHC is rare in prostate cancer and occurs in about 3% of patients. Only in ERG negative cancers, nuclear/cytoplasmic translocation of β-Catenin is strongly linked to unfavorable disease course. The strong prognostic role of the β-Catenin status could potentially be exploited for clinically relevant disease course prediction.

#7225 TROP2 expression is abundant in primary and recurrent prostate cancer.

Joanthan Jeutner[1], **Ronald Simon**[2], Maximilian Lennartz[2], Sarah Minner[2], Eike Burandt[2], Fiete Gehrisch[2], Nina Schraps[2], Martina Kluth[2], Guido Sauter[2], Natalia Gorbokon[2], Florian Viehweger[2], Hans Heinzer[3], Alexander Haese[3], Thorsten Schlomm[1], Markus Graefen[3], Stefan Steurer[2], Ria Schlichter[2], Christian Bernreuther[2], David Dum[2], Andreas Lubcke[2], Neele Heckmann[3]

[1]Department of Urology, Charite - Universitatsmedizin Berlin, Corporate Member of Freie Universitat Berlin, Humboldt-Universitat zu Berlin and Berlin Institute of Health, Berlin, Germany,[2]Institute of Pathology, University Medical Center Hamburg-Eppendorf, Hamburg, Germany,[3]Martini-Clinic, Prostate Cancer Centre, University Medical Center Hamburg-Eppendorf, Hamburg, Germany

The membrane glycoprotein Trophoblast cell surface antigen 2 (TROP2) is the molecular target of sacituzumab govitecan (SG), an antibody-drug conjugate that has been approved for treatment of breast cancer and urothelial carcinomas. To assess the prevalence and clinical significance of TROP2 expression in primary and recurrent prostate cancer, a tissue microarray containing 17,627 primary and 258 recurrent prostate cancer samples was analyzed by immunohistochemistry (IHC). A positive TROP2 immunostaining was seen in 100% of 12,807 interpretable primary prostate cancers and was rated strong in 94.5%, moderate in 3.5%, and weak in 2.0% of cases. The intensity of TROP2 staining decreased significantly with high tumor stage and Gleason grade. Among 12,669 evaluable primary prostate cancers, TROP2 staining was strong in 95.3% of pT2, 94.0% of pT3a, and 93.2% of ≥pT3b (p=0.0011) as well as in 95.2% of Gleason 3+3, 95.8% of Gleason 3+4, 92.7% of Gleason 4+3, and 90.2% of Gleason ≥8 (p<0.0001). Among 250 evaluable recurrent prostate cancers, TROP2 staining was strong in 57.6%, moderate in 31.6%, weak in 8.4%, and negative in 2.4%. Accordingly, TROP2 staining was significantly less intense in recurrent prostate cancer than in primary tumors (p<0.0001) and also less intense than in Gleason ≥8 primary cancers (p<0.0001). Among primary prostate cancers, TROP2 staining was significantly more intense in cancers harboring the *TMPRSS2:ERG* fusion (98.8% moderate or strong positivity) than in ERG fusion negative tumors (97.5%; p<0.0001). Low TROP2 expression was significantly linked to early biochemical (PSA) recurrence in ERG positive (p=0.0165) but not in ERG negative cancers (p=0.3271). A comparison with 11 of the most frequent genomic deletions (*PTEN*, 3p13, 5q21, 6q15, 13q14, 18q21, 8p21, 12p13, 12q24, 16q24, 17p13) did only reveal marginal associations of reduced TROP2 expression with deletions of 6q15 and 8p21 in ERG negative and with 17p13 and *PTEN* in ERG positive cancers. It is concluded from our data, that TROP2 is always expressed at significant levels in newly diagnosed prostate cancers and that a significant expression is retained in most recurrent cancers although reduced levels of TROP2 expression occur commonly after systemic therapy. Absence of strong associations with chromosomal deletions argues against a relationship between TROP2 expression levels and genomic instability.

#7226 Tumor cell ICAM-1 expression is frequent in many tumor entities and linked to unfavorable tumor phenotype in renal cell carcinomas.

Clara von Bargen[1], Finn Wickel[1], Katharina Moller[1], Florian Lutz[1], Florian Viehweger[1], Georgia Makrypidi-Fraune[1], Martina Kluth[1], Claudia Hube-Magg[1], Christina Tsourlakis[1], Christian Bernreuther[1], Guido Sauter[1], Andreas H Marx[2], Ronald Simon[1], Stefan Steurer[1], Christoph Frauen[1], Nina Schraps[1], Fiete Gehrisch[1], Viktoria Chirico[1], Bertram Veith[1], Clara Luehr[1], Cosima Volkel[1], Morton Freytag[1], Natalia Gorbokon[1], Maximilian Lennartz[1], Eike C. Burandt[1], Anne Menz[1], Till Krech[1]

[1]University Medical Center Hamburg-Eppendorf, Hamburg, Germany,[2]Academic Hospital Fuerth, Furth, Germany

Intercellular Adhesion Molecule 1 (ICAM-1; CD54) is a transmembranous glycoprotein with roles in immune surveillance, inflammation, cell signaling, and apoptotic processes. ICAM-1 is considered a stemness marker in cancer which is often expressed on cancer cells. It can modulate anti-cancer immune response or facilitate metastasis through interactions with immune cells and the extracellular matrix. Because of its surface expression, ICAM-1 is also being explored as a therapeutic target. To better comprehend the role of ICAM-1 expression on tumor cells in different cancer types, ICAM-1 was analyzed by immunohistochemistry (IHC) on tissue microarrays (TMAs) containing 5,946 samples from 105 different tumor types. A total of 85 of 105 tumor categories showed ICAM-1 expression in at least one case, and 70 tumor categories contained at least one strongly positive case. Strong ICAM-1 positivity was most seen in several subtypes of lymphomas (up to 98.0%), metastatic malignant melanoma (87.7%), clear cell renal cell carcinoma (ccRCC; 79.8%), clear cell (tubulo) papillary RCC (75.0%), squamous cell carcinomas of the penis (68.5%), oral cavity (62.8%), esophagus (56.7%), pharynx (54.5%), larynx (54.0%), anal canal (53.4%), urinary bladder (47.6%), cervix (46.3%), and the vulva (43.0%), hepatocellular carcinoma (55.3%), muscle-invasive urothelial carcinoma of the bladder (47.4%), papillary RCC (pRCC; 40.6%), cholangiocarcinoma of the liver (27.3%), intestinal type gastric adenocarcinoma (25.7%), and in serous high-grade ovarian carcinoma (25.4%). Within 1,337 evaluable ccRCCs, ICAM-1 positivity was considered strong in 79.7%, moderate in 11.7%, weak in 6.7%, and absent in 1.9%. High ICAM-1 expression was associated with unfavorable ISUP grade ($p<0.0001$), advanced pT stage ($p<0.0001$), high UICC stage ($p=0.0002$), and distant metastasis (M1, $p=0.0181$). Within 370 pRCCs, ICAM-1 positivity was strong in 40.0%, moderate in 21.1%, weak in 25.9%, and absent in 13.0%. High ICAM-1 positivity was associated with poor ISUP grade ($p<0.0001$) and also tended to correlate with high pT stage ($p=0.0861$) and UICC stage ($p=0.0890$). It is concluded that ICAM-1 expression on tumor cells occurs commonly in many cancer entities. That high ICAM-1 expression was linked to unfavorable tumor features in RCCs supports the concept of a role of ICAM-1 expression for cancer progression.

#7227 *NECTIN4*-amplified breast cancer targeted by Zelenectide Pevedotin: Amplification and expression are frequent, concordant, and stable.

Alexander Azizi[1], Niklas Klumper[2], Emma Colliver[1], Alexander Quaas[3], Birgid Schoemig-Markiefka[3], Arndt Hartmann[4], Christoph Kuppe[5], Manuel Ritter[2], Viktor Grunwald[6], Michael Holzel[7], Chris Bailey[1], Gustavo Arruda Bezerra[8], Nicholas Guthertz[8], Sergey Nikolaev[9], Fabrice Andre[9], Charles Swanton[1], Johannes Braegelmann[3], Markus Eckstein[10]

[1]The Francis Crick Institute, London, United Kingdom,[2]University of Bonn, Bonn, Germany,[3]University of Cologne, Cologne, Germany,[4]Inst. of Pathology, University Hospital Erlangen, Erlangen, Germany,[5]RWTH Aachen, Aachen, Germany,[6]Essen University Hospital, Essen, Germany,[7]University Medical Centre Bonn, Bonn, Germany,[8]Bicycle Therapeutics, Cambridge, United Kingdom,[9]Gustave Roussy, Villejuif, France,[10]FAU Erlangen-Nurnberg, Nurnberg, Germany

Background

NECTIN4 amplification (amp) can predict response to Nectin4-targeted therapy. In the Phase I/II Duravelo-1 trial (NCT04561362), *NECTIN4*-amp breast cancer (BC) showed higher response rates to the Bicycle® Drug Conjugate (BDC™) zelenectide pevedotin (zele, formerly BT8009) versus non-amp tumors (57.1% vs. 6.3%) (Klümper et al, SABCS 2024). These findings led to FDA Fast Track designation and the Phase II Duravelo-3 trial in *NECTIN4*-amp BC (NCT06840483). To further characterize *NECTIN4* and its targetability, we assessed its prevalence, biology across BC datasets, and describe its structure-activity based targeting.

Methods

Public, multi-omic primary BC data from METABRIC (n=2173), TCGA (n=1079), and TRANSNEO (n=166) were analyzed. Proprietary primary tissue data (Cologne cohort, n=252) linked high *NECTIN4* copy number (CN; amp/polysomy via FISH) with expression and BC subtypes. Metastatic analyses were conducted on META-PRISM (n=59). High *NECTIN4* CN was defined as >2× ploidy (amp) or ≥6 copies (polysomy). Structural and biophysical studies (crystallography, SPR) assessed zele's binding.

Results

High *NECTIN4* CN was observed in 21.1% (METABRIC), 30.8% (TCGA), and 29.5% (TRANSNEO) of cases, ranking in the 97.5th percentile for amp (TCGA, all genes). By subtype, HR+, HER2+, and TNBC tumors exhibited high CN in 21%, 19%, and 20% (METABRIC) and 30%, 29%, and 36% (TCGA), respectively. CN correlated with elevated mRNA ($p < 2 \times 10^{-16}$) and protein expression ($p = 2 \times 10^{-6}$). No differences were observed by immune infiltrate or germline BRCA status. In the Cologne cohort, high *NECTIN4* CN (19.1%) strongly correlated with membranous Nectin-4 expression (median H-score 150 vs 0, $p = 8.8 \times 10^{-28}$). In META-PRISM metastases, high CN prevalence was similar (29%) and correlated with RNA expression ($r^2 = 0.34$, $p < 0.00001$). Zelenectide pevedotin binds Nectin-4 domain 1 with high affinity (Kd 2.5 ± 1.5 nM) and minimal conformational change (RMSD 0.435 Å). Its compact bicyclic scaffold (4.2 kDa, surface area 1900 Å^2) provides a smaller footprint than conventional antibodies while maintaining strong target engagement, and rapid renal clearance (t½ <1 h), which should support rapid tumor penetration, and efficient delivery of the MMAE payload.

Conclusions

NECTIN4 amplification is frequent, concordant with high RNA and protein expression, and stable in frequency between primary and metastatic BC. Nectin-4 can be effectively engaged by the BDC zelenectide pevedotin with high affinity. The frequency and stability of *NECTIN4* amplification across breast cancer subtypes supports its evaluation as a biomarker for patient selection in Nectin-4-targeted trials.

#7228 A novel digital PCR assay can detect MLH1 variants in patients with hereditary colorectal cancer.

Matthew Moldenhauer[1], Aditya Mahadevan[2], Cameron Hom[3], Valeria Rangel[3], Sophie Hasson[4], Farshid Dayyani[3], Ning-Hsiang Hsu[3], Deepika Nathan[3], Vishal Chandan[5], Selma Masri[6], Feng Qiao[3], Nicholas Pannunzio[3], **Jennifer Brooke Valerin**[3]

[1]UC San Diego, La Jolla, CA,[2]UCSF, San Francisco, CA,[3]UC Irvine, Orange, CA,[4]Ohio State University, Columbus, OH,[5]University of California, Irvine, Orange, CA,[6]University of California, Irvine, Irvine, CA

Background: Lynch syndrome significantly increases the risk of developing colorectal cancer (CRC) due to an inherited defect in mismatch repair (MMR). Early detection relies on identification of pathogenic mutations in patients, but few canonical Lynch mutations exist. We describe two separate colon cancer patients with identical mutations in the *MLH1* gene (*MLH1* c.2054C>T) and later determined to be cousins as well as a third relative diagnosed with several cancers with the same mutation. Despite a strong family history of cancer, the *MLH1* mutation was labeled discordantly on different NGS panels and required several weeks to obtain results delaying patient care. This highlights a need for improved diagnostics with faster turn-around time, increased cost effectiveness, and ability to screen for non-canonical Lynch variants. We designed a novel, customizable digital PCR (dPCR) assay to rapidly detect *MLH1* gene variants. We also conducted in-depth molecular modeling, mutational signature analyses, and *Saccharomyces cerevisiae* based functional assays to demonstrate that the *MLH1* mutation likely disrupts the interaction with binding partner PMS2, impairing MMR; defining a novel *MLH1* mutation.

Methods: NGS: DNA was isolated. The NovaSeq platform was used for sequencing. Data analysis was performed on the RTA software. Digital PCR: TaqMan probes were created for *MLH1* using a FAM labeled probe for wild type alleles and a HEX labeled probe for mutants. Quantification of fluorescent signal used Thermo Quantstudio software with total signal converted to a percentage to determine the VAF. Yeast assay: In *S. cerevisiae*, *mlh1* and *pms1* knockout (*mlh1Δ* and *pms1Δ)* strains were obtained through the fragment insertion technique. Yeast expression plasmids encoding the human versions of *mlh1-2054*, *MLH1*, and *PMS2* were obtained via the LR clonase technique. Plasmids were transformed into the heterozygous diploid knockout yeast strain to make the genetic construct for the assay CHT8 and CHT9 in which fresh segregants are dissected into haploids for our 5-FOA assays.

Results: We designed two fluorescently labelled probes, one that recognizes the wild-type *MLH1* allele and one specific for c.2054C>T (*mlh1-2054).* We can detect *MLH1* and *mlh1-2054* alleles in equal amounts, consistent with a heterozygous germline mutation in all 3 patients. We observed a significant increase in mutation frequency in yeast transformed with the *mlh1-2054* variant compared with *wild-type hMLH1*, which reflected the difference in mutation frequency we observed in comparing *MLH1 PMS1* yeast and *mlh1Δ pms1Δ* yeast. This suggests the *mlh1-2054* variant present in all patients is pathogenic due to the resulting MMR defect we see in our yeast genetic model.

Conclusion: This study emphasizes the need for improved diagnostic tools to identify pathogenic mutations in diverse populations and establishes a novel *MLH1* hereditary mutation.

#7229 TM-PAP, everywhere you need it: Cross-species, multi-host panel for fast readouts.

Yue Huang, Xiaomeng Gou, Yao Peng, Jinying Ning, **Feng Hao**

Kyinno Biotechnology Co., LTD, Beijing, China

Prostatic acid phosphatase (PAP, a.k.a. ACP3) is a convenient, druggable antigen for rapid assay development when displayed on the cell surface as TM-PAP (membrane-localized PAP). Compared with ad-hoc antigen systems, a standardized, cross-species TM-PAP panel enables reliable head-to-head testing of antibody and small-molecule formats across hosts and species barriers. Such models accelerate mechanism confirmation (binding, internalization), effector biology (ADCC/ADCP/CDC), payload delivery (ADC, RIC), and analytical assays (qFACS titering, IHC controls), while providing clean negative controls via isogenic ACP3-KO backgrounds.We assembled 15 engineered models spanning four species variants (human, mouse, rat, cynomolgus) across eight host lineages: human cancer and producer lines (LNCaP, VCaP [pools], PC3, HT-1080, 293T) plus bioproduction/rodent oncology backbones (CHO-K1, MC38, CT26). The panel includes LNCaP-ACP3-KO (isogenic negative control); human TM-PAP in PC3, HT-1080, 293T, CHO-K1, MC38, and CT26; ortholog panels in 293T/CHO-K1 for mouse, rat, and cynomolgus TM-PAP; and LNCaP-ACP3 and VCaP-ACP3 for rapid screening when single-cell cloning is unnecessary. The platform now supports both in vitro and in vivo workflows: multiple hosts (e.g., LNCaP, PC3, HT-1080, MC38, CT26) are established for murine xenograft/syngeneic studies, and the remaining lines are compatible with in-vivo deployment or serve as system controls, enabling end-to-end evaluation from binding/internalization to pharmacology and efficacy.Species-matched TM-PAP cDNAs were integrated to generate stable lines (clones or pools), with expression verified by flow cytometry (FACS) and routine QC (mycoplasma-free, STR-authenticated where applicable). The ACP3-KO line was created by CRISPR/Cas9. Typical readouts include high-throughput binding EC_{50}, pH-sensitive internalization, and Fc-mediated functions using human or rodent effectors, plus analytic controls for IHC/ELISA. This panel lets teams (i) standardize antigen-centric screening across species, (ii) de-risk cross-reactivity and matrix effects before animal work, and (iii) compress assay setup time from weeks to days—bringing “TM-PAP, everywhere you need it” to early discovery, CMC-adjacent analytics, and translational method development.

#7230 A paclitaxel-induced rat model of chemotherapy-induced alopecia.

Simonetta I. Gaumond[1], Joaquin Jimenez[2]

[1]Department of Biochemistry and Molecular Biology, University of Miami Miller School of Medicine, Miami, FL,[2]University of Miami Miller School of Medicine, Miami, FL

Chemotherapy-induced alopecia (CIA) is one of the most visible and distressing toxicities of cancer therapy, disproportionately affecting women with breast and ovarian cancers, where paclitaxel remains a cornerstone treatment. Despite its widespread use, no standardized animal model exists to study paclitaxel-induced alopecia or evaluate protective strategies. Here, we report the first reproducible rat model of paclitaxel-induced alopecia. Fourteen-day-old Sprague-Dawley rats were randomized to control (n = 20), low-dose paclitaxel (n = 10), or high-dose paclitaxel (n = 10), administered subcutaneously for three consecutive days. Animals were monitored daily, with peak alopecia observed after two weeks. Alopecia severity was graded by blinded assessors using a quintile grading scale (0 = no hair loss, 4 = complete alopecia). Safety endpoints (weight, grooming, activity) were recorded. On day 28, animals were euthanized and a representative biopsy from each group was acquired, formalin-fixed, paraffin-embedded, and stained with H&E. Alopecia severity differed significantly across treatment groups ($p < 0.0001$, Kruskal-Wallis). Median alopecia scores were 3 in controls, 1 in low-dose paclitaxel ($p = 0.0015$, Dunn's post hoc), and 1 in high-dose paclitaxel ($p < 0.0001$), with no significant difference between paclitaxel doses. Dermoscopy demonstrated localized alopecia at the medial rump injection site. Histopathology revealed reduced follicular density and follicular miniaturization, consistent with classical CIA. Paclitaxel administration reliably induced localized alopecia replicating key clinical and histologic features of CIA. This represents the first standardized paclitaxel rat model of CIA and addresses a critical gap in preclinical dermatology and oncology research. This model provides a biologically relevant platform for mechanistic studies and therapeutic testing, particularly relevant to women, for whom alopecia carries substantial psychosocial burden and may influence treatment adherence.

: Chromatin Architecture and Regulatory Landscapes
Poster Session

#7234 A SWI/SNF-specific Ig-like domain, SWIFT, is a transcription factor binding hub.

Siddhant U. Jain[1], Kaylyn E. Williamson[1], Alexander Ying[1], Aasha M. Turner[1], Jerry R. Jiang[2], Shaunak Raval[3], Kevin So[1], Maxwell J. Allison[1], Akshay Sankar[1], Daniel Guerra[1], Nazar Mashtalir[1], Henry H. Rohrs[2], Cheryl F. Lichti[4], Malvina Papanastasiou[3], Joao A. Paulo[5], Steven Gygi[5], Michael L. Gross[2], Cigall Kadoch[1]

[1]Pediatric Oncology, Dana-Farber Cancer Institute and Harvard Medical School, Boston, MA,[2]Department of Chemistry, Washington University in St. Louis, St. Louis, MO,[3]Broad Institute of MIT and Harvard, Cambridge, MA,[4]Washington University at St. Louis, St. Louis, MO,[5]Department of Cell Biology, Harvard Medical School, Boston, MA

Mammalian SWI/SNF (BAF) chromatin remodeling complexes modulate DNA accessibility and gene expression, however, the mechanisms by which they are targeted on chromatin remain incompletely understood. Here, we define SWIFT (SWI/SNF Ig-Fold for Transcription Factor Interactions), found on the SMARCD family of subunits within the mSWI/SNF core module as an evolutionarily conserved, universal transcription factor (TF) binding platform. SWIFT is necessary and sufficient for direct interaction with the transactivation domain of a lineage-specific TF, PU.1, in vitro and in cells, with a single amino acid mutation in SWIFT able to disrupt PU.1-mSWI/SNF binding, inhibit site-specific complex targeting and activity, and attenuate oncogenic gene expression and proliferation of PU.1-dependent acute myeloid leukemia (AML) cancer cells. Further, dominant expression of the SWIFT domain in isolation sequesters TFs from mSWI/SNF complexes and “poisons” TF-addicted cancer cells across different lineages. Finally, we uncover striking preferences of lineage-specific TFs for the SWIFT domains of specific SMARCD subunit paralogs. These SMARCD paralog-specific affinities of TFs align with their tissue- and differentiation state-specific expression patterns across human cells and tissues, suggesting that that switches in mSWI/SNF subunit composition fine-tune affinities for TFs that govern specialized cell state transitions during normal differentiation and tumorigenesis.In conclusion, this work unmasks a novel mSWI/SNF biochemical interface amenable to targeted therapeutic modulation in a diverse collection of transcriptionally addicted cancers.

#7235 Integrated spatial multiomic profiling of 3D genome architecture and transcriptome-wide gene expression in breast cancer models.

Yi Cui[1], Huy Nguyen[2], Andrea Floris[2], David King[2], Serdar Tulu[2], David Castillo[2], Shanshan He[1], Shyamtanu Chattoraj[2], Jude Dunne[2], Mirko Corselli[1], John Lyssand[1], Joseph M. Beechem[1]

[1]Bruker Spatial Biology, Seattle, WA,[2]Bruker Spatial Genomics, San Jose, CA

Disruption of 3D genome organization profoundly influences gene expression, driving disease and cancer progression. Mechanisms such as oncogene amplification, deletion, and chromatin domain misfolding are key contributors to tumorigenesis. However, conventional approaches like whole-genome sequencing (WGS), RNA-seq, and Hi-C typically assess these changes at the bulk level, masking cell-to-cell heterogeneity. To dissect these mechanisms with single-cell and spatial resolution, we leverage the PaintScape™ system to visualize 3D genome architecture in situ, within single cells. We then correlate changes in genome structure to gene expression and phenotype measured in parallel samples using a spatial multiomic assay on the CosMx® Spatial Molecular Imager (SMI) to generate a comprehensive multi-modal dataset. Using normal (MCF10a) and cancerous (MCF7) breast cell lines, the PaintScape assay enabled high-resolution visualization of chromosomal territories and gene regions involved in cancer-associated pathways, including cell cycle regulation, apoptosis, and chromatin remodeling. We identified cell type-specific structural alterations such as translocations, extrachromosomal DNA (ecDNA) formation, locus copy number variation and shifts in topologically associating domain (TAD) boundaries. Parallel CosMx SMI multiomic imaging revealed transcriptome-wide signatures and subcellular localization patterns of key molecular markers. Upon exposure to Estradiol, an estrogen receptor (ER) agonist, we observed transcriptional upregulation of MYC, CCND1, and E2F1 in ER+ MCF7 cells, contrasting with minimal response in ER- MCF10a cells. PaintScape profiling further revealed spatial clustering of distant estrogen response elements (DEREs) near Chr17q and Chr20q, while CosMx SMI quantified local transcriptional activation, highlighting complementary insights from the two platforms. Together, the PaintScape system and CosMx SMI enable an integrated, single-cell, and spatially resolved interrogation of genome architecture, transcriptomics, and proteomics. This multi-modal approach uncovers cell populations with distinct genomic and phenotypic states, offering a powerful framework to elucidate how 3D genome organization and transcriptional regulation jointly drive cancer heterogeneity and progression.

#7236 Defining and targeting drivers of lineage plasticity in stem cell-like prostate cancer.

Chen Khuan Wong[1], Dan Li[1], Ekta Khurana[2], Yu Chen[1]

[1]Memorial Sloan Kettering Cancer Center, New York, NY,[2]Weill Cornell Medicine, New York, NY

Prostate cancer depends on androgen receptor (AR) signaling for growth, which is why androgen deprivation (castration) therapy is effective at early stages. However, many tumors eventually progress to a lethal form known as castration-resistant prostate cancer (CRPC). A subset of CRPC tumors bypass dependency on AR signaling by acquiring lineage plasticity, where prostate cancer cells transdifferentiate into alternate cellular states through epigenetic reprogramming. Neuroendocrine (NE) prostate cancer represents one well-known lineage plasticity phenotype. Nevertheless, most AR-independent tumors do not exhibit NE features and are defined as AR-negative/NE-negative or “double-negative prostate cancer” (DNPC). In a collaboration with Dr. Ekta Khurana’s computational genomics lab at Weill Cornell Medicine, we recently classified CRPC into four epigenetic subtypes, including the well-established 1) AR and 2) NE, as well as the novel DNPC subgroups 3) WNT and 4) stem cell-like (SCL) (PMID: 35617398). We focused on the SCL subtype as it is the second most common group in CRPC patients and lacks therapeutic targets. Using functional genomic approaches, we found that YAP/TAZ/TEAD cooperates with FOSL1 to drive the SCL lineage and growth of SCL models. We therefore hypothesize that the heightened dependency on the YAP/TAZ/TEAD/FOSL1 transcriptional program represents a therapeutic vulnerability in CRPC-SCL. To test this, we exposed CRPC models to TEAD inhibitors and found robust growth suppression in SCL cells compared to non-SCL cells in vitro. To evaluate whether the TEAD inhibitors are on-target, we performed transcriptomic profiling in SCL models and observed downregulation of YAP/TAZ gene signature as well as FOSL1 expression, which phenocopies the effects of YAP/TAZ double knockdown. To define the cistromes of these factors upon TEAD inhibition, we performed ChIP-seq and observed reduced co-occupancy at consensus sites, suggesting the disruption of the YAP/TAZ/TEAD/FOSL1 transcriptional circuit by the small molecule compound. To determine whether these phenotypes are recapitulated *in vivo*, we will treat mice harboring CRPC-SCL xenografts with TEAD inhibitors to assess growth response and evaluate epigenetic and transcriptional response using single-nucleus Multiome (ATAC+RNA). These studies will establish whether small molecule inhibition of TEAD is a promising strategy for the treatment of CRPC-SCL and allow high-resolution analysis of cell state transitions, with a focus on loss of SCL-specific signatures and potential emergence of AR/NE programs as adaptive resistance mechanisms.

#7237 LDB1-dependent enhancer connectivity constrains a metabolic synthetic lethality in T-cell acute lymphoblastic leukemia.

Rahul S. Bhansali[1], Juan S. Long[2], Siqing Wang[2], Ahnaf Tausif[2], Shuo Zhang[3], Petri Polonen[4], Sarah Skuli[1], Nicholas Aboreden[5], Zhuangzhuang Geng[2], Belinda M. Giardine[6], Cheryl A. Keller[6], Ross C. Hardison[6], Charles G. Mullighan[4], Gerd A. Blobel[2]

[1]Hospital of the University of Pennsylvania, Philadelphia, PA,[2]Children's Hospital of Philadelphia, Philadelphia, PA,[3]University of Pennsylvania, Philadelphia, PA,[4]St. Jude Children's Research Hospital, Memphis, TN,[5]Dana Farber Cancer Institute, Boston, MA,[6]Penn State University, University Park, PA

LDB1 and LMO2, two proteins frequently overexpressed in T-cell acute lymphoblastic leukemia (T-ALL), form a chromatin architectural complex that promotes chromatin looping between enhancers and/or promoters. Here, we defined LDB1-driven oncogenic enhancer connectivity in T-ALL and examined its impact on therapeutic vulnerabilities.

To identify proximal LDB1 targets in T-ALL, we engineered isogenic T-ALL cell lines (LOUCY [ETP-ALL] and KOPT K1 [non-ETP-ALL]) with dTAG degrons at the endogenous LDB1 loci. Treatment with dTAG-V1 ligand for 4 hours reduced LDB1 protein levels and chromatin occupancy by >90%. Acute LDB1 loss disrupted spatial enhancer connectivity at critical leukemic oncogenes in both LOUCY (e.g. *HHEX, MYB, MYCN*) and KOPT K1 (e.g. *DUSP6, STAT4*), resulting in their downregulation and subsequent reduction in cell growth. CRISPRa-mediated restoration of select LDB1-dependent oncogenes, such as *MYB*, in LDB1-depleted cells rescued cell expansion.

Nascent transcript profiling further revealed that acute LDB1 loss affected distinct gene sets in LOUCY and KOPT K1, consistent with their distinct identities. Notably, however, several cholesterol biosynthetic genes (*HMGCS1, MVD, MVK*) were upregulated in both cell types. These changes were not driven by altered expression or subcellular localization of SREBP2—the canonical transcriptional regulator of these genes. Instead, they were caused by altered enhancer-promoter connectivity in the absence of LDB1. Specifically, LDB1 loss disrupted connectivity of nearby enhancers for different genes, thereby liberating them to form de novo contacts with *HMGCS1, MVK,* and *MVD* gene promoters to activate them. Hence, by clustering regulatory elements, LDB1 not only enables the expression of genes but also constrains enhancers from making inappropriate contacts. Importantly, the native LDB1-dependent loops are detected in primary samples from patients with T-ALL based on published H3K27ac HiChIP data.

Functionally, we found that cholesterol flux and expression of upstream regulators, like *SREBP2*, increased with prolonged LDB1 depletion, suggesting a feed-forward regulatory mechanism on cholesterol homeostasis in T-ALL. Using both LDB1 degron and knockout models, we observed that LDB1 loss sensitizes leukemic cells to rosuvastatin and pitavastatin by 2-5-fold. This was recapitulated in several T-ALL cell lines with distinct molecular drivers upon LDB1 knockout. Furthermore, statin sensitization was rescued by spike-in of mevalonate or geranylgeranyl pyrophosphate, confirming that this phenotype is driven by altered cholesterol metabolism.

Together, our study illustrates a paradigm by which LDB1 loss enables illegitimate spatial connections of enhancers with cholesterol biosynthetic gene promoters. This, in turn, creates a new metabolic addiction in leukemic cells, which may be targeted with statins.

#7238 Cis-regulatory role of alternative promoters in cancer.

Emily R. Wilson, Xiaoyang Zhang

University of Utah Huntsman Cancer Institute, Salt Lake City, UT

Alternative promoters are increasingly recognized as critical regulators in cancer, with differential promoter usage driving transcriptional shifts that can support oncogenic activity. While promoters are traditionally viewed as transcription initiation sites, emerging evidence suggests they can also act as cis-regulatory elements, enhancing or compensating for the expression of neighboring genes. Our 3D genomics data reveal that alternative promoters of the same gene interact with each other at the chromatin level, yet it remains unknown whether these interactions play a functional cis-regulatory role in regulating the gene's expression. Through analysis of TCGA data, we discovered that minor alternative promoters exhibit enhancer-like histone modification signatures and cancer-type-specific chromatin accessibility. To mechanistically interrogate their cis-regulatory potential, we employed CRISPR interference (CRISPRi) and CRISPR activation (CRISPRa) to modulate minor promoter activity and assess the impact on major isoform expression in cancer-related genes such as EGFR. We also found that this cis-regulatory enhancer function of minor promoters is driven by lineage-specific transcriptional master regulators. Additionally, CRISPRi-mediated repression of the major promoter led to increased minor isoform expression, suggesting a compensatory function of minor promoters. We will further investigate this compensatory activity using high-resolution chromatin interaction mapping (HiChIP) to determine whether shifts in enhancer interactions contribute mechanistically to compensation. Currently, the field lacks a clear understanding of how alternative promoters function as cis-regulatory elements, limiting our ability to define how cancer cells exploit these promoters to promote oncogenic activity. These studies will delineate mechanisms by which alternative promoters regulate oncogenic gene expression through enhancer-like and compensatory functions and will generate a resource of cancer-type-specific alternative promoters with cis-regulatory activity, offering potential therapeutic targets and a new framework for modulating oncogene expression.

#7239 A genomic deletion variant controls super-enhancer-driven overexpression of LINC00636 and CD47 to promote tumor cell survival in breast cancer.

Carolina Di Benedetto, Amelia Tsark, Alysia Thach, Anmol Singhal, Anthony Rodriguez, **Paola Betancur**

University of California, San Francisco, San Francisco, CA

Dysregulated gene expression in cancer is often driven by epigenetic reprogramming of non-coding regions such as super-enhancers (SEs). These large enhancer clusters are rarely active in normal tissues but can drive overexpression of genes that promote malignant traits, including immune evasion. Previously we have shown that SEs are linked to chemotherapy resistance and anti-apoptotic gene expression in triple-negative breast cancer (TNBC). Although SEs are promising therapeutic targets, their large size makes them difficult to target effectively in cancer therapy. This limitation underscores the need to identify smaller, functionally critical regions within SEs that can serve as precise therapeutic entry points.The goal of this research is to define and functionally validate core elements within breast cancer–specific SEs that are necessary and sufficient to drive immune escape. We hypothesize that these core elements, alone or in combination, act as molecular drivers of malignancy by aberrantly activating the immune-suppressive gene *CD47* and the regulatory long non-coding RNA *LINC00636*.Our rationale stems from the discovery of a breast cancer–specific SE harboring a germline insertion/deletion (InDel) variant that regulates *CD47* and *LINC00636* expression. CRISPR deletion of this variant in engineered breast cancer cells increased chromatin accessibility of the SE region, leading to upregulation of *CD47* and *LINC00636*, enhanced resistance to nutrient-deprivation–induced apoptosis (via *CD47*), activation of senescence (driven by elevated *LINC00636*), and delayed cell death. RNA-seq analyses of cells lacking the insertion and cells with high *LINC00636* expression revealed a shared immunosuppressive and pro-survival transcriptional program, including increased *CXCL17, STAT1, CXCL8*, and *ANGPTL4*—genes associated with tumor immune signaling, senescence and apoptosis resistance. In macrophage-competent xenograft models, deletion of the variant reduced anti-tumor macrophage infiltration, supporting activation of an immune-evasive state. Clinically, breast cancer patients carrying the insertion allele show improved progression-free survival when compared to patients homozygous for the deletion—demonstrating the clinical relevance of discrete SE elements.Together, our findings identify a common InDel variant as a minimal core element that fine-tunes the regulatory activity of a bifunctional SE controlling *CD47* and *LINC00636*. Our work provides new insight into SE-mediated gene dysregulation in breast cancer and highlights the therapeutic potential of targeting discrete SE components rather than entire enhancer clusters.

#7240 Multi-omic analysis identifies BACH2 transcription factor as key epigenetic and transcriptional repressor driving drug-tolerance to targeted therapy in EGFR-mutant lung adenocarcinoma.

Yoshimasa Kudo[1], Althaf Singhawansa[2], Yong Zeng[2], Catherine O'Brien[3], Scott Bratman[4], Geoffrey Liu[1]

[1]Department of Medical Biophysics, University of Toronto, Toronto, ON, Canada,[2]Princess Margaret Cancer Center, University Health Network, Toronto, ON, Canada,[3]Department of Laboratory Medicine and Pathobiology, University of Toronto, Toronto, ON, Canada,[4]Department of Radiation Oncology, University of Toronto, Toronto, ON, Canada

RATIONALE Drug resistance poses a significant challenge for EGFR-mutant lung cancer patients treated with osimertinib, a 3rd-generation EGFR tyrosine kinase inhibitor. Non-mutational mechanisms, particularly epigenetic alterations in drug-tolerant persister (DTP) cells, enable survival under lethal drug pressure and seed resistance. A deeper understanding of these mechanisms is required to evaluate whether targeting epigenetic changes in DTP cells may represent a promising therapeutic strategy.

METHODS We conducted a preclinical multi-omic study to map the epigenetic and transcriptional changes driving DTP in EGFR-mutant lung cancer. Using PC9-DTP cell line exposed to osimertinib for 14 days, we employed a combination of single-cell and bulk omics assays to profile genome-wide DNA methylation, chromatin accessibility, and transcriptomic landscapes defining the DTP state. Top epigenetic regulators were nominated from integrative analyses, and public datasets from other EGFR-mutant lung cancer models were analyzed for validation.

RESULTS DTP cells displayed global DNA hypermethylation across the vast majority (88.7%) of differentially methylated regions. Hypermethylation in cis-regulatory regions were strongly associated with closed chromatin and reduced transcription ($R=-0.64$, $p<2.2e-16$), reflecting coordinated epigenetic silencing. Gene regulatory network analysis and *in silico* perturbation, leveraging paired transcriptomic and chromatin features from single-cell multi-omic assay, identifies BACH2 - transcriptional and epigenetic repressor - as the top repressive transcription factor in DTP-specific networks. Additionally, chromatin remodeler HMGA1 was among the target genes most strongly repressed by BACH2. Based on motif enrichment analysis, BACH2-specific DNA-binding motifs were enriched in hypermethylated ($p<1e-4$) and closed chromatin regions ($p<1e-6$), accompanying the downregulation of corresponding target genes, including HMGA1. Furthermore, pathway analysis of BACH2-repressed target genes revealed enrichment in oxidative phosphorylation and ATP synthesis, indicating a metabolic shift. Finally, analyzing public transcriptomic datasets from other cell line models, patient-derived organoids (PDOs), xenografts (PDXs), and patient tumor samples confirmed consistent BACH2 upregulation in DTP and residual disease state, as well as downregulation of HMGA1 and other target genes.

CONCLUSION These findings position BACH2 as a key contributor of epigenetic silencing and metabolic reprogramming in osimertinib-induced DTP state. Overall, our multi-omic approach provides high-resolution insight into drug-tolerance mechanisms and nominates BACH2 as a priority target, potentially informing novel therapeutic strategy for improved patient outcome.

#7241 Decoding 3D enhancer architecture identifies hierarchical oncogenic regulatory programs in prostate cancer.

Huan Cao, Zexun Wu, Baixi Ji, Seolyn Yang, Leonardo Gonzalez-Smith, Andrew Vu, Suhn K. Rhie

Department of Cancer Biology, Keck School of Medicine of USC, Los Angeles, CA

Aberrations in non-coding DNA regions, particularly those located in regulatory elements, are increasingly implicated as a hallmark of prostate cancer. Yet, mapping enhancers that underpin tumor-specific transcription remains challenging. Here, we developed an integrative workflow to prioritize prostate cancer-specific enhancers (PSEs) by analyzing 204 H3K27ac ChIP-seq datasets from prostate tumor and normal tissues, alongside prostate cell lines. We connected the differentially activated enhancer landscape to three-dimensional (3D) chromatin organization in prostate cancer by identifying key oncogenic topologically associating domains (TADs) from Hi-C datasets. We selected a previously uncharacterized but high-priority locus at chr6q24.1 for in-depth study. To define cancer-specific 3D architecture at chr6q24.1, we generated Region-Capture Micro-C (RCMC) maps at nucleosome resolution in RWPE-1 (normal) and 22Rv1 (cancer) cells. This revealed highly nested enhancer-promoter (E-P) interactions, which we termed multi-connected enhancer hubs, that were prominent in cancer but absent in normal, exceeding the sensitivity of conventional Hi-C for enhancer-centered contacts. CRISPR/Cas9 deletion of individual enhancers across the locus, followed by multi-omic profiling, revealed two distinct enhancer classes. Central PSEs (cPSEs) function as core regulatory organizers, whose deletions weakened activities of other PSEs, collapsed locus-wide chromatin interactions, reduced target gene expression, and impaired cancer cell proliferation without broadly altering CTCF/cohesin architecture. In contrast, redundant PSEs (rPSEs) are buffered by neighboring rescuing enhancers to preserve transcription via compensatory rewiring that strengthens alternative E-P contacts. Our data also suggest that these two classes of enhancer behaviors are associated with differential activity of FOXA1, a pioneer transcription factor in prostate cancer. Together, our study revealed cancer-specific, multi-connected enhancer hubs essential for prostate tumorigenesis and uncovered the regulatory hierarchy of enhancers, providing a framework to functionally characterize and validate oncogenic non-coding DNA regions that sustain prostate cancer phenotypes. This study advances our understanding of non-coding regulatory regions and offers future opportunities for developing novel precision epigenome-based clinical interventions for prostate cancer.

#7243 In-situ direct single-cell visualization of 3D genome architecture in ER+ and HER2+ breast cancer cell lines using PaintScape™ system.

Huy Nguyen[1], Sophie Pribus[2], Zhicheng Ma[2], David King[1], Johnson Huynh[1], Serdar Tulu[1], Marc Glazer[1], Brian Smart[1], David Castillo[1], Kenny Chung[1], Shyamtanu Chattoraj[1], Jude Dunne[1], Doug Werner[1], Christina Curtis[2], Mark Munch[1]

[1]Bruker Spatial Genomics, San Jose, CA,[2]Stanford University, Stanford, CA

Breast cancer (BC) is highly heterogeneous, and classification based on ER, PR, and HER2 expression alone does not fully capture its clinical diversity or therapeutic vulnerabilities. In particular, the aggressive HER2 positive (HER2+) and estrogen receptor positive (ER+) subtypes are driven by complex genomic and cellular dynamics-including epithelial to mesenchymal transition (EMT), chromosomal instability, and 3D genome reorganization that contribute to metastasis, therapy resistance, and poor prognosis. Bulk studies such as WGS and Hi-C have revealed key genomic features in BC sub-types such as focal amplifications (e.g. CCND1-HER2 co-amplification in HER2+ BC; Chr 20q alterations in ER+ BC), A/B compartment switching, TAD boundary disruptions and associated oncogenic rewiring. However, these approaches remain ex-situ and bulk-based obscuring the spatial and cellular heterogeneity and fail to capture the full spectrum of structural and functional interactions within individual cells which is critical to understanding disease progression. To overcome these limitations, in-situ single-cell technologies capable of resolving dynamic 3D genome changes are essential for uncovering resistance mechanisms and enabling precision therapies tailored to the unique genomic landscape of each tumor cell.

Here we present the PaintScape™ system enabling simultaneous in-situ visualization of the 3D genome structure in single BC cells. Over 1,000 targets relevant in several important cancer pathways including Cell Cycle and Apoptosis, Transcriptional Regulation and Chromatin Structure are visualized across all chromosomes using our OncoPaint™ Oncogenic Pathways Panel in ER+ MCF7 and HER2+ HCC 1954 cell lines. We identified common and cell line specific unique 3D genome alterations between MCF7, HCC 1954 and other breast cell lines, and relate these to patterns of genomic rearrangement inferred from patient samples. In ER+ MCF 7, we identified distributions in copy gain/loss of specific chromosome arms e.g. Chr 20q, individual targets including regions of clustered breakpoints, unique ecDNA and distal estrogen response elements (DEREs), at the single cell, and sub-population level. In HER2+ HCC 1954, we identified focal amplification of Chr 8q and directly visualized ecDNA amplification, rearrangement and nuclear localization of key oncogenes such as MYC and CCND1. We simultaneously show A/B compartment switching and TAD boundary disruption of key oncogenic regions in MCF7 and HCC 1954 in-situ, showing consistency with up/down regulation of genes between the cell lines.

The PaintScape system enables simultaneous in-situ 3D genome mapping within single cells revealing structural differences linked to gene dysregulation across BC sub-types, offering an integrated view of how genome architecture influences cellular processes during disease progression.

#7244 AMPK interacts with PRC1.1 complex on chromatin to regulate NADK expression in response to metabolic stress in acute lymphoblastic leukemia.

Anna Shvab[1], Guy J. Leclerc[1], Julio C. Barredo[2]

[1]Pediatrics, University of Miami Miller School of Medicine, Miami, FL,[2]Div. Director, Pediatric Hem./Onc., University of Miami, Miami, FL

Acute lymphoblastic leukemia (ALL) remains a leading cause of pediatric cancer-related mortality. ALL cells are particularly vulnerable to metabolic stress following activation of AMP-activated protein kinase (AMPK), a master regulator of cellular energy homeostasis. We and others have demonstrated that AMPK interacts with chromatin-associated proteins to modulate gene expression in response to energy stress. A comprehensive AMPK interactome analysis using TurboID proximity labeling proteomics identified the non-canonical Polycomb Repressive Complex 1.1 (PRC1.1) as an AMPK-associated complex. Co-immunoprecipitation confirmed interactions between AMPK and PRC1.1 components (PCGF1, RING1, KDM2B, BCOR, BCORL1, USP7, SKP1, and RYBP) in KASUMI-2 (Bp-ALL) and KE-37 (T-ALL) cells, which were enhanced following treatment with allosteric AMPK activators (PF-06409577, 991). To evaluate the functional consequence of AMPK activation on PRC1.1 activity, we measured H2AK119ub levels under metabolic stress and observed a marked increase. In contrast, AMPKα1/α2 double knockout (DKO) HEK293T cells treated with AMPK activators exhibited no change, confirming AMPK dependency. ChIP-seq analysis in KASUMI-2 and KE-37 cells identified *Nicotinamide adenine dinucleotide kinase* (*NADK*) as an AMPK-associated chromatin target. ChIP-qPCR demonstrated accumulation of AMPK, BCOR, and KDM2B at the *NADK* promoter under metabolic stress, correlating with increased H2AK119ub and reduced RNA polymerase II occupancy, indicative of transcriptional repression. RT-qPCR and immunoblot analyses confirmed NADK downregulation in ALL cells exposed to metabolic stress, while pharmacological inhibition of AMPK (BAY-3827) or RING1 (PRT4165) upregulated NADK expression. Similarly, NADK repression was abrogated in HEK293T AMPKα1/α2-deficient cells, and pharmacological inhibition of USP7 (CDDO-Me and Eupalinolode B) increased NADK expression in ALL cells. NADK catalyzes phosphorylation of NAD^+ to $NADP^+$, supporting NADPH generation essential for anabolic metabolism and redox homeostasis. NADK inhibition depletes NADPH, induces oxidative stress, and suppresses proliferation. We propose that AMPK-mediated transcriptional repression of NADK represents an adaptive mechanism to enforce metabolic homeostasis under energy stress. Consistently, combined treatment with the AMPK activator ASP4132 and the NADK inhibitor thionicotinamide induced synergistic cytotoxicity in ALL cells, suggesting a potential therapeutic strategy targeting AMPK-PRC1.1-NADK signaling.

#7245 Mechanistic dissection of ABI1 as DNA-binding transcriptional regulator in cancer cells.

Kate Livingston[1], XIANG Li[2], Kevin M. Lin[1], Leszek Kotula[1]

[1]SUNY Upstate Medical University, Syracuse, NY,[2]UT Southwestern Medical Center, Dallas, TX

Background: ABI1 (Abelson interactor-1) is classically recognized as a multifunctional adaptor protein with homeostatic roles in cancer biology. It functions as a tumor suppressor in some cancer such as prostate cancer, yet exhibits oncogenic activity in other cancers such as for example breast cancer. Historically, ABI1 has been studied for its actin-cytoskeleton-associated functions—including cell-cell adhesion, cell motility, and lamellipodia formation—as well as its role in regulating major signaling hubs such as c-Abl, PI3K, and Src. Our recent findings reveal an unanticipated function of ABI1: direct DNA binding mediated by a conserved homeodomain homology region (HHR). This discovery led us to hypothesize that ABI1 may act as a previously unrecognized transcriptional regulator. Here, we sought to define the molecular mechanisms through which ABI1 contributes to transcriptional control.
Methods: To determine sequence specificity and genomic occupancy, we performed ChIP using HHR-intact and HHR-mutant ABI1 constructs, complemented by in vitro DNA binding assays using purified proteins. Subcellular fractionation and chromatin enrichment assays assessed ABI1 nuclear localization and association with chromatin. ABI1-interacting transcriptional machinery was identified through co-immunoprecipitation (co-IP). RNA-seq comparing cells expressing wild-type ABI1 versus an HHR-defective DNA-binding mutant defined ABI1-dependent transcriptional outputs.
Results: ABI1 binds DNA both in vitro and in vivo and displays reproducible sequence motifs from integrated ChIP and in vitro binding analyses. ABI1 variants containing an intact HHR domain localize preferentially to the nucleus and chromatin fractions. Co-IP studies identify ABI1 as a component of a defined transcriptional complex. RNA-seq analyses reveal that HHR-mediated DNA binding is required for a discrete ABI1-dependent transcriptional program.
Conclusions: We identify ABI1 as a novel DNA-binding protein with sequence preference and transcriptional regulatory capacity mediated through its HHR domain. These findings expand the functional repertoire of ABI1 beyond actin regulation and kinase signaling, providing the first mechanistic framework for ABI1-driven transcriptional control.

#7246 Transcriptional control of myeloid differentiation trajectories in AML.

Sagarajit Mohanty, Jieun Jeong, Soumya Sharma, Daniel Cizin, Jun Ho Lee, Wenbin Xiao, Richard Koche, Thomas Norman, Hans-Guido Wendel

Memorial Sloan Kettering Cancer Center, New York, NY

Across different subtypes, Acute myeloid leukemia (AML) is a malignancy of proliferating myeloid cells that fail to differentiate. The failure of AML cells to respond to physiological differentiation cues remains a critical challenge despite extensive efforts, with few exceptions. We performed a CRISPR screen for transcriptional and epigenetic regulators of differentiation in AML cells. Our findings identified the roles of multiple components of the mediator complex, STAGA complex, and different transcription factors. We applied a Perturb-seq strategy which revealed how each lesion affects differentiation trajectories, uncovering shared and unique pathways in AML. Interestingly, we found multiple distinct transcriptional trajectories of differentiation in AML cells. We have validated these findings through additional in vitro and in vivo evaluations and are exploring their therapeutic relevance. Together, our results highlight key components of transcription regulatory complexes that are required to maintain the differentiation block in AML and pinpoint new targets for interventions.

#7247 BPTF regulates androgen receptor activity in prostate cancer.

Hee-Young Jeon[1], Sudeep Khadka[1], Majid Pornour[1], Hyunju Ryu[1], Hegang Chen[1], Arif Hussain[1], Hung-Ming Lam[2], Eva Corey[3], Htoo Zarni Oo[4], Martin E. Gleave[5], Xiaofang Che[6], Christopher E. Barbieri[7], **Jianfei Qi**[1]

[1]University of Maryland School of Medicine, Baltimore, MD,[2]University of Washington Medical Center, Seattle, WA,[3]University of Washington, Seattle, WA,[4]Department of Urologic Sciences, Vancouver Prostate Centre, BC Cancer Agency Vancouver Center, Vancouver, BC, Canada,[5]Distinguised Professor, Dept. of Urological Sciences, University of British Columbia, Vancouver, BC, Canada,[6]Department of Medical Oncology, The First Hospital of China Medical University, Shenyang, China,[7]Resident, Weill Cornell Medical College, New York, NY

BPTF, the scaffolding subunit of the nucleosome remodeling factor (NURF) complex, has been implicated in the progression of several malignancies, but its role in prostate cancer (PCa) remains unclear. Here, we show that BPTF is upregulated in aggressive PCa and promotes disease progression. BPTF knockdown inhibits PCa cell proliferation, while CRISPRa-mediated upregulation promotes androgen-independent growth. To investigate BPTF function, we performed RNA-seq, ChIP-seq and ATAC-seq analyses in BPTF-knockdown PCa cells. RNA-seq analysis reveals that BPTF primarily upregulates androgen receptor (AR) target gene expression. ChIP-seq data show that BPTF facilitates AR binding to enhancers, super-enhancers as well as promoters. ATAC-seq data indicates that BPTF enhances chromatin accessibility at AR-binding sites, partly via SMARCA1, a catalytic subunit of the NURF complex. Notably, BPTF ChIP-seq peaks exhibit strong enrichment of FOXA1 motifs but weak enrichment of AR motifs. We find that BPTF interacts with both FOXA1 and AR to form a protein complex in which FOXA1 anchors BPTF-AR to chromatin, while BPTF stabilizes the AR-FOXA1 interaction. Importantly, BPTF interacts with AR through its bromodomain, and a bromodomain inhibitor disrupts this interaction, leading to impaired AR signaling and suppressed PCa cell growth. In summary, our findings establish BPTF as a key regulator of AR activity by enhancing chromatin accessibility and stabilizing the AR-FOXA1 complex, highlighting BPTF as a potential therapeutic target for prostate cancer.

#7249 RUNX1T1 as an early driver in treatment-induced neuroendocrine transdifferentiation .

Yuchao Ni[1], **Mingchen Shi**[2], Dong Lin[2], Yen-Yi Lin[3], Hui Xue[4], Xin Dong[4], Liangliang Liu[3], Funda Sar[3], Rebecca Wu[4], Tunc Morova[3], Anne Hargert[3], Robert Bell[3], Xinyao Pang[2], Adam Classen[2], Yu Wang[2], Junru Chen[5], Stephan Le Bihan[3], Wei Dong[6], Vickie Wang[7], Ning Xu[8], Nathan Lack[3], Martin E. Gleave[3], Christopher J. Ong[9], Gang Wang[10], Hao Zeng[11], Colin Collins[3], Yuzhuo Wang[2]

[1]Vancouver Prostate Centre; University of British Columbia; Urology Research Institute, The First Affiliated Hospital, Fujian Medical University, Vancouver, BC, Canada,[2]Vancouver Prostate Centre; BC Cancer; University of British Columbia, Vancouver, BC, Canada,[3]Vancouver Prostate Centre; University of British Columbia, Vancouver, BC, Canada,[4]Vancouver Prostate Centre; BC Cancer, Vancouver, BC, Canada,[5]Vancouver Prostate Centre; BC Cancer; University of British Columbia; Institute of Urology, West China Hospital Sichuan University, Vancouver, BC, Canada,[6]Vancouver Prostate Centre; University of British Columbia ; Union Hospital, Tongji Medical College, Huazhong University of Science and Technology, Vancouver, BC, Canada,[7]University of British Columbia, Vancouver, BC, Canada,[8]Urology Research Institute, the First Affiliated Hospital, Fujian Medical University, Fuzhou, China,[9]Surgery, Vancouver Prostate Centre; University of British Columbia, Vancouver, BC, Canada,[10]BC Cancer; University of British Columbia, Vancouver, BC, Canada,[11]Institute of Urology, West China Hospital, Sichuan University, Chengdu, China

Treatment-induced neuroendocrine prostate cancer (t-NEPC) is a lethal form of castration-resistant variant arising primarily through neuroendocrine (NE) transdifferentiation of prostate adenocarcinoma following androgen deprivation therapy (ADT) and androgen receptor pathway inhibitors (ARPI). Despite its clinical relevance, the early molecular events initiating this transition remain poorly defined. Leveraging the first and only longitudinal patient-derived xenograft (PDX) model capturing adenocarcinoma-to-NEPC transdifferentiation (LTL331/331R), we performed single-cell RNA sequencing (scRNA-seq) across seven key stages spanning pre-castration, post-castration/ transitional phases, and relapsed NEPC.Clustering analysis identified 15 major cell populations and revealed a previously unrecognized intermediate transitional cell state enriched for epithelial-mesenchymal transition (EMT), stemness, metabolic activity, and HDAC-related regulatory signatures, highlighting a unique window of lineage plasticity. Two terminal NEPC subclusters with reciprocal ASCL1/FOXA2 expression patterns reflected intratumoral heterogeneity at relapse.Transcriptional interrogation of the transitional population identified **RUNX1T1** as a central regulator emerging early during plasticity. Functional assays revealed that RUNX1T1 overexpression markedly accelerates AR pathway inhibition-induced NE transdifferentiation and confers resistance to ARPI therapy in prostate adenocarcinoma models. Conversely, RUNX1T1 knockdown reduces NE-related pathway expression, suppresses NEPC cell growth, and induces apoptosis. These findings position RUNX1T1 as an essential factor for both NEPC development and progression.Mechanistically, rapid immunoprecipitation and mass spectrometry (RIME) uncovered that RUNX1T1 interacts with multiple repressive epigenetic factors including HDAC-containing complexes and heterochromatin-related genes. These results support a role for RUNX1T1 in mediating transcriptional silencing and regulatory network reprogramming during NEPC development.In summary, this study delineates the temporal evolution of t-NEPC at single-cell resolution, identifies an intermediate transitional state during NE transdifferentiation, and reveals heterogeneity within terminal NEPC. The identification of RUNX1T1 as an early and persistent driver of this trajectory positions RUNX1T1 and its associated repressive complexes as promising candidates for therapeutic intervention.

#7250 SYMPK regulates *AR* alternative polyadenylation and AR variant expression in advanced prostate cancer.

Kiel T. Tietz, Conor R. Miller, Jamie L. Van Etten, Scott M. Dehm

Masonic Cancer Center, University of Minnesota, Minneapolis, MN

Localized prostate cancer can be cured by radiation or surgery but advanced prostate cancer continues to be a clinical challenge. Advanced prostate cancer can initially be controlled by endocrine therapies that target the androgen receptor (AR), however, these tumors will inevitably develop resistance. This stage of the disease, termed castration-resistant prostate cancer (CRPC), is responsible for practically all prostate cancer-specific deaths. Truncated AR variant (AR-V) proteins are expressed in CRPC cells, and can function as ligand-independent, constitutively active transcription factors that promote resistance to endocrine therapies. Several well-characterized AR-Vs, such as AR-V7 and AR-V9, arise from splicing of *AR* exon 3 to different cryptic exons (CEs) located within *AR* intron 3. Splicing of these CEs is coordinated by a consensus AAUAAA poly(A) site located at the end of *AR* exon CE3. To define sequence elements in *AR* pre-mRNA required for usage of the CE3 poly(A) site, we designed inhibitory antisense oligomers to target regions upstream and downstream of the core AAUAAA motif. We found that sequences directly flanking the AAUAAA motif positively regulated AR-V expression, whereas sequences ~50 nucleotides downstream of the CE3 poly(A) site negatively regulated AR-V expression. To identify trans-acting factors that recognize and drive usage of the CE3 poly(A) site, we performed RNA-immunoprecipitation (RIP) using an RNA bait containing the CE3 poly(A) site or an RNA bait with the AAUAAA motif mutated. Proteins that preferentially bound the CE3 poly(A) site in RIP experiments were identified using mass spectrometry. We identified the scaffold protein SYMPK as a factor that bound specifically to RNA bait containing the CE3 poly(A) site. Consistent with a functional role for this binding event, knockdown of SYMPK reduced AR-V expression and inhibited growth of CRPC cell lines. We have also found SYMPK regulates the growth of AR negative prostate cancer cell lines, demonstrating AR-independent functions for SYMPK in regulating the growth of prostate cancer cells. This work highlights SYMPK as a novel regulator of AR-V expression and a therapeutic target for the treatment of multiple subtypes of advanced prostate cancer.

#7251 Pioneer round of translation factor CTIF regulates tumor immunity in drug-tolerant persister cells.

Yuqing Wang[1], Mengyao Wang[2], Kaixiu Li[2], Shensi Shen[2]

[1]Institute of Thoracic Oncology and Department of Thoracic Surgery, National Clinical Research Center for Geriatrics, Frontiers Science Center for Disease-related Molecular Network, West China Hospital, Sichuan University, Chengdu, China,[2]Institute of Thoracic Oncology and Department of Thoracic Surgery, National Clinical Research Center for Geriatrics, West China Hospital, Sichuan University, Chengdu, China

Background: Tumor cell plasticity enables cancer cells to alter their phenotype through coordinated epigenetic, transcriptional, and translational changes. Drug-tolerant persister cells (DTPs) represent a key plastic state associated with therapy resistance and minimal residual disease (MRD). Newly synthesized mRNAs undergo a pioneer round of translation (PRT) for quality control, yet how PRT influences tumor plasticity and immune evasion remains unknown. We hypothesize that the PRT-associated initiation factor CTIF, a core component of CBP80-CBP20-dependent translation machinery, regulates the immunosuppressive phenotype of DTPs and contributes to MRD-associated immune escape.

Methods: We integrated the bulk RNA-seq datasets across LUAD, BRCA, SKCM and COAD to define cross-cancer DTP transcriptional features. DTP models and isogenic CTIF-knockdown (KD) cells were established across multiple cancer types. We examined PRT-related factor expression, drug IC50, proliferation, and translational output via polysome profile and ribosome sequencing (Ribo-seq). Functional relevance of CTIF was evaluated in vivo using syngeneic immunocompetent and immunodeficient models.

Results: Cross-cancer analyses revealed treatment-specific DTP signatures with convergence on shared pathways, including altered expression of CTIF and additional PRT-related factors. CTIF-KD had minimal effects on drug resistance or proliferation in vitro, but polysome profiling and Ribo-seq indicated altered ribosome translation landscape. Integrated RNA-seq and Ribo-seq demonstrated that CTIF-KD selectively upregulated immune-related transcripts at the translational level, suggesting a previously unrecognized role in immune modulation. In vivo, CTIF-KD did not affect tumor growth in immunodeficient mice but significantly impaired tumor progression in immunocompetent hosts, consistent with enhanced immune recognition.

Conclusions: Our study uncovers a non-canonical, immune-regulatory role of CTIF. Although dispensable for proliferation and drug tolerance in vitro, CTIF is essential for tumor growth in vivo in an immune-dependent manner. We propose that CTIF shapes the tumor translatome to sustain immune evasion, and that targeting PRT, particularly CTIF, may offer a novel strategy to overcome immune suppression and eliminate MRD-associated persister states within the tumor immune microenvironment.

#7252 The landscape of alternative splicing in hepatocellular carcinoma and its association with TP53 mutation.

Xueqing Fang[1], Kui Wu[2], Man Tong[1]

[1]The Chinese University of Hong Kong, Hong Kong, China,[2]BGI Genomics, Shenzhen, China

Alternative splicing (AS) is a key mechanism of post-transcriptional regulation and is crucial for the formation of proteomic diversity in eukaryotes. Splicing dysregulation is increasingly recognized as a new hallmark in cancer development and progression. These aberrant splicing events are not only promising biomarkers for diagnosis and prognosis, but also novel targets for drug development. Hepatocellular carcinoma (HCC), which is the most common primary liver tumor, is characterized by significant tumor heterogeneity, which poses a major challenge for effective treatment. Therefore, there is a need to explore post-transcriptional mechanisms, such as AS, as a novel approach to identify new prognostic biomarkers and therapeutic targets. To explore post-transcriptional mechanisms, we uncovered the landscape of AS in HCC, investigated its clinical implications, and explored its association with key driver gene mutations. Differential AS events between HCC and adjacent normal samples were identified, which enabled patient stratification into two subgroups with different prognoses. The poor-prognosis subgroup exhibited a higher *TP53* mutation frequency and lower AS values. Through cross-dataset analysis, we identified three consensus differential events that were distinct between *TP53*-mutant and wild-type samples. These consensus differential AS events were highly correlated with differentially expressed splicing factors between the *TP53* groups. In conclusion, our study demonstrates that alternative splicing is extensively dysregulated in HCC and has significant prognostic implications. We provide evidence that *TP53* mutation, a key genetic driver in HCC, is associated with distinct AS patterns, potentially through the transcriptional regulation of specific splicing factors.

#7253 Regulation of TbRIII expression and ectodomain shedding via the sheddase, PRSS8, and ERG transcription factor.

Benjamin Michael Greulich, Kaitlyn Eidson, Logan Baker, Hannah Fitzgibbons, Shreya Sudakar, Emma Teng, Cion Kim, Huy Lam

Biology, Mercer University, Macon, GA

TGF-β signaling is frequently dysregulated in cancer and can contribute to cancer-associated phenotypes including immune evasion, migration, and metastasis. Unfortunately, attempts to inhibit TGF-β have had limited success, likely due to the critical roles of TGF-β in normal tissue. For this reason, this work aims to more fully understand the regulation of TGF-β signaling. The co-receptor, TβRIII, can bind ligand and stimulate the TβRI/TβRII complex. Conversely, TβRIII can be shed from the cell surface where it can sequester TGF-β ligand and prevent TβRI/TβRII activation. However, the identity of the enzyme that sheds TβRIII and the regulatory mechanisms that govern TβRIII shedding are unknown. This work aims to address two aspects of TβRIII shedding regulation: firstly, what enzyme is responsible for producing shed TβRIII, and secondly, what novel transcriptional networks are responsible for regulating the expression of TβRIII and its sheddase. PRSS8 increased TβRIII shedding, decreased expression of TGF-β target genes and EMT markers, and decreased TGF-β associated phenotypes of EMT, migration, and invasion. PRSS8 overexpression also sensitized cells to chemotherapy. Furthermore, PRSS8 expression could be induced pharmacologically with lovastatin to elicit similar reductions in TGF-β associated phenotypes. Treatment with cholesterol was able to increase migration of these cells, but PRSS8 overexpression prevented this effect of cholesterol. These data suggest cholesterol homeostasis pathways may regulate PRSS8 expression and therefore alter TGF-β signaling activity. Taken together, this establishes a novel cholesterol-PRSS8-TGF-β axis of regulation. Current work aims to identify novel transcriptional networks that are regulating TβRIII and its shedding. RNA-seq data between prostate cell lines with and without ERG overexpression has revealed ERG increased expression of pro-TGF-β signaling genes and suppressed genes associated with down-regulating TGF-β. In cervical cancer cell lines, knockdown of ERG has reduced phenotypes such as migration, invasion, and chemoresistance. ERG knockdown has also increased TβRIII shedding. ERG ChIP-seq in cervical cancer is being performed in the presence and absence of TGF-β activation to determine the effect of TGF-β on ERG binding. SMAD2/3 ChIP-seq will be performed with and without ERG knockdown to reveal if ERG affects SMAD2/3 binding to the genome. By discovering new transcriptional regulators of TβRIII, such as ERG, new possibilities for rescuing TβRIII expression and reducing dysregulated TGF-β signaling are revealed. Therapies directed at cholesterol homeostasis or ERG may be able to be repurposed and applied to cancers experiencing TGF-β dysregulation.

#7254 Post-transcriptional upregulation of GPC3 via CSTF2-driven 3'UTR remodeling promotes hepatocellular carcinoma progression.

Suk Woo Nam, Soyoung Jeon, Jin Woong Ha, Min jeong Na, Sang Yean Kim

Catholic University of Korea, College of Medicine, Seoul, Korea, Republic of

Alternative polyadenylation (APA) is a widespread post-transcriptional mechanism that generates mRNA isoforms with variable 3′ untranslated regions (3′UTRs), influencing transcript stability and translation. Aberrant 3′UTR shortening frequently occurs in cancer, allowing oncogenic transcripts to evade microRNA (miRNA)-mediated repression. However, the global landscape and functional impact of APA alterations in hepatocellular carcinoma (HCC) remain incompletely defined. We performed transcriptome-wide APA profiling across a multistage human liver cancer cohort to identify genes exhibiting significant 3′UTR alterations during hepatocarcinogenesis. Differential Poly(A) Site Usage Index (ΔPDUI) analysis was applied to detect APA-driven isoform shifts. Candidate genes were validated using independent HCC datasets and correlated with clinical outcomes. Functional assays—including RNA interference, overexpression, and proliferation/apoptosis measurements—were conducted in HCC cell lines to define mechanistic and phenotypic consequences. Approximately 77% of APA-affected mRNAs displayed 3′UTR shortening in HCC compared to normal liver tissue. Among these, Glypican-3 (GPC3) emerged as one of the most prominently upregulated transcripts, with high expression levels strongly associated with poor patient prognosis. Manipulation of GPC3 expression confirmed its oncogenic role, as silencing GPC3 suppressed proliferation and enhanced apoptosis, whereas ectopic expression promoted growth. Among core APA regulators, Cleavage Stimulation Factor 2 (CSTF2) was markedly upregulated in HCC and positively correlated with both GPC3 expression and poor clinical outcomes. CSTF2 overexpression induced 3′UTR shortening of GPC3 and elevated its protein levels, while CSTF2 knockdown lengthened the GPC3 3′UTR and decreased expression. Mechanistically, truncation of the GPC3 3′UTR eliminated binding sites for miR-96-5p and miR-140-5p, relieving translational repression and sustaining oncogenic GPC3 expression. Our findings reveal that CSTF2-driven APA remodeling serves as a key post-transcriptional mechanism promoting GPC3 activation in HCC. CSTF2 overexpression shortens the GPC3 3′UTR, abrogating miRNA-mediated repression and enhancing tumorigenic potential. This CSTF2-GPC3 axis underscores APA dysregulation as a pivotal driver of hepatocarcinogenesis and highlights CSTF2 as a promising therapeutic target for liver malignancies.

#7255 RNA binding proteins mediated oncogenic adaptions in cancer cells.

Jasmine George, Pradeep Chaluvally Raghavan

Medical College of Wisconsin, Wauwatosa, WI

Introduction: Ovarian cancer remains a major contributor to cancer-related deaths in women, underscoring the urgent need for novel therapeutic strategies. Fragile X-related protein 1 (FXR1), frequently amplified and overexpressed in ovarian and other malignancies, plays a central role in driving oncogenesis through translational regulation of multiple cancer-promoting genes. We have determined that the oncogene c-MYC is a direct target of FXR1 both in ovarian cancer cells and in cells within the tumor microenvironment. Tumor-derived extracellular vesicles (EVs) are known to play a critical role in reprogramming the tumor microenvironment (TME). We observed that FXR1 mRNA enriched EVs are taken up by surrounding stromal and immune cells, where they modulate protein translation in ways that promote tumor progression. Building on this background, we aim to investigate the mechanism by which FXR1 mRNA is incorporated into EVs and to elucidate its functional impact on the TME.
Methods: We performed a Surface Sensing of Translation (SUnSET) assay to demonstrate that FXR1 enhances global protein translation in cancer cells. RNA electrophoretic mobility shift assays (REMSA) and proximity ligation assays were conducted to show that FXR1 binds to the AU rich elements (ARE) within the 3′UTR of c-MYC. Intriguingly, we found that FXR1 mRNA is packaged into EVs derived from ovarian cancer cells. RNA immunoprecipitation assays also showed that FXR1 interacts with the exosomal markers TSG101 and CD63. Finally, flow cytometry-based immunophenotyping and single-cell RNA sequencing (scRNA-seq) of tumor-derived ascites from mice were performed to characterize how FXR1 influences overall translation in tumor cells and reshapes the TME.
Results: Our previous data demonstrated that FXR1 plays a crucial role as an oncoprotein and is significantly involved in the pathophysiology of ovarian cancer. We identified that FXR1 stabilizes cMYC mRNA by binding to specific sequences of AREs within its 3′UTR. We further demonstrated that FXR1 mRNA is highly enriched in tumor-derived exosomes, which are transferred into macrophages in the TME. In a corollary, FXR1 enriched EVs resulted into the reprogramming of cells in the tumor microenvironment, favoring tumor growth by inducing macrophage polarization and T-cell inactivation.
Conclusion: Our studies have identified that FXR1 promotes oncogenic translation in cancer cells and in the cells in tumor microenvironment. Our data suggest that FXR1 mediated macrophage polarization and T-cell inactivation is an important mechanism for cancer growth and metastasis.

#7256 Enhancer reprogramming establishes ETS1-RUNX1-FOSL1 as an oncogenic and immunosuppressive transcriptional circuitry in gallbladder carcinoma.

Jiaxi Sun[1], Xing He[2], Yuntan Qiu[1], Zhenyu Zhou[3], Daning Lu[1], Shiru Tang[1], Wenbin Li[2], Dong Yin[1], **Lehang Lin**[1]

[1]Guangdong Provincial Key Laboratory of Malignant Tumor Epigenetics and Gene Regulation, Sun Yat-Sen Memorial Hospital, Sun Yat-sen University, Guangzhou, China,[2]Department of Biliary and Pancreatic Surgery, Sun Yat-Sen Memorial Hospital, Sun Yat-sen University, Guangzhou, China,[3]Department of Hepatobiliary Surgery, Sun Yat-Sen Memorial Hospital, Guangzhou, China

Background: Gallbladder carcinoma (GBC) is a highly aggressive malignancy with poor prognosis and limited therapeutic options. Enhancers and super-enhancers (SEs) are critical regulators of cell type-specific transcription and oncogenic programs, yet their roles in GBC progression remain poorly defined.
Objective: We aimed to map enhancer and SE reprogramming in GBC and identify master transcription factors (TFs) driving these transcriptional programs. Design: Chromatin immunoprecipitation sequencing and RNA sequencing were performed on normal, inflammatory, and tumorous gallbladder tissues, as well as GBC cell lines. Integrative analyses of enhancer remodeling, TF motif enrichment, expression, and transcriptional connectivity were conducted to identify SE-driven master TFs. Functional assays and immunohistochemistry were used to evaluate their oncogenic and immunomodulatory functions.
Results: GBC exhibited extensive enhancer and SE reprogramming relative to non-tumorous gallbladder tissues, with gained enhancers and SEs preferentially enriched in oncogenic pathways. ETS1, RUNX1, and FOSL1 were identified as SE-driven master TFs that form an interconnected regulatory circuitry co-occupying SEs, including those of *CD274* (encoding PD-L1), to promote oncogenic transcription and immune evasion. Perturbation of this circuitry suppressed GBC cell proliferation, migration, and tumor growth *in vitro* and *in vivo*. Clinically, elevated expression of these master TFs correlated with reduced $CD8^+$ T cell infiltration, poorer patient survival, and diminished responsiveness to immunotherapy in GBC.
Conclusion: This study delineates enhancer and SE reprogramming during gallbladder malignant transformation, identifies an ETS1-RUNX1-FOSL1 master TF circuitry, and highlights FOSL1 as a key driver of oncogenic transcription and immune evasion, providing mechanistic, prognostic, and therapeutic insights into GBC.

#7257 Identification of KDR as a novel effector downstream of ETS variant transcription factor 4 in NSCLC.

Su Hyeon Yu, Jiyoon Kang, Ji Won Kim

Jeju Research Institute of Pharmaceutical Sciences, College of Pharmacy, Jeju National University, Jeju, Korea, Republic of

The ETS family comprises transcription factors characterized by a highly conserved DNA-binding domain that recognizes a central GGA(A/T) motif. Among these, ETV4, the predominant member of the PEA3 subfamily, has been strongly associated with advanced disease stage and poor prognosis in multiple malignancies, including non-small cell lung cancer (NSCLC) and hepatocellular carcinoma (HCC), largely through its MAPK-dependent transcriptional activity. Despite its clinicopathologic significance, the downstream effectors and genome-scale regulatory circuitry governed by ETV4 remain incompletely defined. Here, we aimed to define the ETV4-driven transcriptional landscape. We identified KDR/VEGFR2 as a direct ETV4-promoted target, with ETV4 overexpression markedly elevating KDR transcripts and protein levels. Through chromatin immunoprecipitation and complementary binding assays, we demonstrated physical occupancy of ETV4 at the KDR promoter. Although KDR/VEGFR2 is classically characterized as an endothelial receptor that amplifies angiogenic signaling, accumulating evidence indicates that cancer cell-intrinsic KDR supports vasculogenic mimicry and aggressive structural remodeling through VEGF/VEGFR2 paracrine and autocrine circuits. Pharmacologic suppression of ETV4 significantly attenuated KDR expression and impaired epithelial-mesenchymal transition, migration, and invasion, phenotypes that were recapitulated by genetic silencing of either ETV4 or KDR. Collectively, these findings define a previously unrecognized transcriptional axis in which ETV4 directly activates KDR/VEGFR2 to potentiate malignant behavior, positioning the ETV4-KDR pathway as a targetable therapeutic vulnerability across ETV4-high tumors.

: Genomic Approaches to Define Tumor Biology and Clinical Stratification
Poster Session

#7261 Comprehensive multi-omics profiling reveals molecular heterogeneity and developmental signatures in solid pseudopapillary neoplasm of the pancreas.

Dong-Ju Shin[1], Jin Ho Choi[2], Sang Hyub Lee[2], In Rae Cho[2], Kyung-Min Lee[2], Ji Kon Ryu[2], Woo Hyun Paik[2], Jin-Ku Lee[1]

[1]Department of Anatomy and Cell Biology, Seoul National University College of Medicine, Seoul National University, Seoul, Korea, Republic of,[2]Department of Internal Medicine and Liver Research Institute, Seoul National University Hospital, Co, Seoul National University, Seoul, Korea, Republic of

Solid pseudopapillary neoplasm (SPN) of the pancreas is a rare, low-grade malignant tumor that predominantly affects young women. Although previous studies have applied omics approaches, including whole-exome sequencing, transcriptomics, and DNA methylation profiling to characterize SPN, its tumorigenesis and cell of origin remain elusive. Apart from the recurrent *CTNNB1* hotspot mutation, which is currently considered the only canonical driver, SPN is typically diploid and exhibits few recurrent genomic alterations. Moreover, because of its low incidence, previous small-cohort studies have been insufficient for robust molecular subtyping or integrative analysis.

To comprehensively characterize the molecular landscape of SPN, we performed multi-omics analyses on 80 tumors using whole-genome sequencing (WGS), whole-transcriptome sequencing, and whole-genome enzymatic methyl-sequencing (EM-seq). Unsupervised hierarchical clustering based on the top 1,000 genes ranked by median absolute deviation (MAD) across transcriptomes identified two robust molecular subtypes: a *developmentally reprogrammed* type and an *immune-enriched* type: The immune-enriched subtype exhibited significant activation of immune-associated pathways, including immunoglobulin-mediated and adaptive immune responses, whereas the developmentally reprogrammed subtype showed enrichment of embryonic skeletal system development and morphogenesis signatures. Furthermore, SPN tumors displayed a genome-wide hypermethylated pattern compared with normal pancreatic tissues, highlighting their distinct epigenetic state. Beyond expression-based stratification, we systematically examined fusion events, genome-wide somatic mutations, structural variants, mitochondrial genome alterations, numtogenesis, retrotransposon activity, and methylation entropy across the cohort. Notably, a recurrent *TVP23C-CDRT4* fusion was detected in 61% of cases, suggesting a potential novel genomic hallmark of SPN. This study represents the largest integrative multi-omics analysis of SPN to date, revealing distinct transcriptomic and epigenomic subtypes, a recurrent fusion event, and marked molecular heterogeneity. Ongoing integrative analyses aim to clarify the developmental origin and oncogenic evolution of this rare pancreatic neoplasm.

#7262 A fully automated walkaway system programmed with a novel library prep target enrichment protocol for detection of ultra-low frequency mutations in liquid biopsy and tumor samples.

Saharnaz Bigdeli[1], Jan Godoski[1], Bernd Buehler[1], Bahram Arezi[1], Brandyn Clark[1], Denise Rhodes[1], schryl castaneda[1], Bonita Lam[2], Yun Bao[2], ji zhu[1], Gilbert Amparo[2], Neelima Mehendale[2], Khine Win[2], Karen Chapman[1]

[1]Agilent Technologies, La Jolla, CA,[2]Agilent Technologies, Santa Clara, CA

Liquid biopsy has transformed oncology through high sensitivity detection of genomic alterations from circulating cell-free DNA (cfDNA). Issues such as sensitivity, PCR bias, contamination, reproducibility, and long and laborious workflows are yet to be resolved. Here, we have fully automated the workflow for a novel library preparation and target enrichment probe technology, Agilent Avida, that tackles some of the existing challenges by being highly optimized to work with circulating tumor DNA (ctDNA). Our automated protocol using pre-aliquoted reagents, was developed on the Agilent Magnis NGS Prep System for a wide range of DNA inputs (1-100 ng) and various sample types (intact, FFPE DNA, and cfDNA). Using this platform, we construct libraries with a high sample recovery that scales linearly with the input amount and is capable of high sensitivity variant detection without a need for pre-enrichment PCR, minimizing the GC bias. Our automated protocol generates up to eight target-enriched Illumina sequencing-ready DNA libraries in about 8 hours without the need of any user intervention, thus minimizing potential contamination. We have generated data using both Avida catalog and custom panels covering a broad range of target sizes to determine assay sensitivity. Using these probes, we were able to reliably detect cancer-associated genomic alterations, including SNVs, indels, CNVs, and translocations across key oncogenes using well characterized cfDNA and formalin compromised reference standards as well as real ctDNA samples. For example, using 15 ng of SeraCare V4 ctDNA sample enriched with Avida DNA Onco LB panel (1.17 Mb covering 164 pan-cancer-associated genes) and sequenced with a budget of 100 M read pairs, we were able to detect SNP frequencies down to 0.25%. Furthermore, in our automated runs, we obtained high reproducibility across 8 technical replicates. For example, for 5 independent Magnis runs (40 samples) of various sample types and inputs per run using the Avida DNA Onco LB panel, the % Coefficient of Variation (CV) ranged from 0.8 to 2.3% for on-target rate, 1.9 to 8.2% for library complexity (unique molecular identifier UMI recovery), 1 to 3.2% for base coverage, and 0.03 to 0.09% for uniformity.

#7263 Identification of molecular alterations in soft tissue sarcoma patients with combined pan-cancer CGP and bespoke sarcoma fusion detection testing.

Chaugiang Duong[1], Ryan Bender[2], Nathan Montgomery[3], Fernando J. Lopez-Diaz[2]

[1]NeoGenomics, Aliso Viejo, CA,[2]NeoGenomics, San Diego, CA,[3]NeoGenomics, Durham, NC

Introduction: The genomic characterization of soft tissue sarcomas is increasingly applied in patient care to help understand the pathogenesis of these diseases. However, most pan-cancer comprehensive genomic profiling (CGP) tests cover few gene fusions of clinical relevance in sarcomas. Hence, the contribution of all classes of genomic alterations to the pathogenesis of sarcomas often has a methodological bias.
Objective: This study investigates all actionable genomic variants present in soft tissue sarcoma patients using a sarcoma-targeted CGP approach that also interrogates most sarcoma-relevant gene fusions.
Methodology: We screened 20660 test orders for cancer patients with available diagnosis tested by either of two complementary tests: a pan-cancer CGP panel and a sarcoma fusion panel, both routinely performed in our clinical laboratory. The first detects SNV/Indels in 517 genes, CNA in 59 genes, MSI and TMB, and common solid tumor RNA fusions in 55 genes. The second analyzes additional known and novel RNA fusions in 97 genes with high diagnostic, prognostic, and therapeutic value in sarcomas, utilizing fusion enrichment-based RNA-seq. Out of 12885 CGP tested patients, 346 had sarcoma, while 1406 sarcoma patients were tested with the sarcoma fusion panel. Of those, 62 patients were characterized using both tests.
Results: From the 346 sarcoma patients tested with the pan-cancer CGP test, 268 patients had pathogenic DNA alterations, and 22 patients had RNA fusions. Conversely, among 1406 sarcoma patients tested with the sarcoma fusion panel, fusions were detected in 399 patients, with 207 distinct fusions identified. The top 5 genes rearranged were EWSR1, HMGA2, FUS, FLI1, and SS18. We next analyzed the data from the 62 sarcoma patients tested with both assays and found that pathogenic alterations (DNA/RNA) were detected in 56 cases. DNA alterations were found in 54 of them. SNV/indels were present in 53 patients with 86 genes harboring pathogenic mutations, most frequently in TP53, TERT, LRP1B, NF1, TET, and CDKN2A. CNAs were identified in 15 patients, of whom one had only CNAs (KRAS, MDM2, PDGFRA, and KIT). The most frequent CNAs were in MDM2 (n=5), followed by CCND1, CDK4, EGFR, KRAS, and MYC (n=3). Gene fusions were detected in 10 patients. Three (3) patients had fusions detected by both panels, 2 had fusions detected by the CGP panel but not covered by the sarcoma panel, and 5 patients had a fusion only detected by the Sarcoma fusion panel.
Conclusions: Comprehensive genomic profiling of sarcomas with pan-cancer targeted panels unveiled the pathogenic molecular landscape in sarcoma patients from the community. Additional testing with a sarcoma-targeted fusion panel significantly enhanced the identification of pathogenic fusions, enabling a more comprehensive evaluation of the contribution of gene fusions to both pathogenesis and patient care.

#7264 Molecular differences between ovarian and uterine carcinosarcomas.

Kwong-Kwok Wong, Yvonne Tsang

The University of Texas MD Anderson Cancer Center, Houston, TX

Carcinosarcomas, also known as malignant mixed Müllerian tumors (MMMTs), are rare and aggressive neoplasms characterized by the coexistence of both carcinomatous (epithelial) and sarcomatous (mesenchymal) components. These tumors primarily arise in the uterus and less frequently in the ovary. Despite histological similarities, ovarian and uterine carcinosarcomas differ in epidemiology, clinical presentation, prognosis, and treatment strategies. Understanding the molecular differences between ovarian and uterine carcinosarcoma is essential for accurate diagnosis, effective treatment planning, and improved patient outcomes.In this study, whole-exome sequencing (WES) was performed on three ovarian and three uterine carcinosarcomas, along with matched normal blood or tissue DNA. Sequencing libraries were prepared using the Twist Library Preparation and Capture Kit and sequenced on NovaSeq X 25B with 150 bp paired end reads, generating an average of >900 million reads per sample.Somatic variants (missense and indels; n = 1,971-2,542) were identified across samples. Notably, a novel germline mutation in TBC1D32 (p.Thr375Lys) was detected in five of the six carcinosarcomas. TBC1D32 is primarily associated with genetic disorders such as ciliopathies and hypopituitarism, and although mutations have been reported in various cancers, its role as an oncogene or tumor suppressor remains unclear. While the overall number of variants did not differ significantly between ovarian and uterine carcinosarcomas, several somatic variants were unique to ovarian carcinosarcoma, including alterations in ANKDD1A and RPL10. ANKDD1A functions as a tumor suppressor; frequently silenced in glioblastoma via hypermethylation. RPL10 influences cancer through protein synthesis and extra-ribosomal functions; overexpression and mutations linked to tumor development. Validation of these variants in additional carcinosarcoma samples is ongoing. Furthermore, RNA sequencing using the Illumina Stranded Total RNA Prep Ligation with Ribo-Zero Plus Kit and NovaSeq X 25B (100 bp paired-end reads) is being conducted to identify differentially expressed genes between ovarian and uterine carcinosarcomas. Data analysis is currently in progress. In conclusion, we identified a recurrent germline mutation in TBC1D32 (p.Thr375Lys) across both ovarian and uterine carcinosarcomas, as well as somatic variants unique to ovarian carcinosarcoma. Further investigation of these genes may provide insights into carcinosarcoma pathogenesis and inform the development of differential treatment strategies for ovarian versus uterine disease.

#7265 MBCproject: multi-omic profiling of metastatic breast cancer evolution through patient-partnered research.

Diana Garcia-Cortes[1], Esha Jain[2], Mary McGillicuddy[2], Beena S. Thomas[2], Dewey Kim[2], Sara Balch[2], John Navarro[2], Jakob H. Weiss[2], Tania G. Hernandez[2], Michael Dunphy[2], Brett N. Tomson[2], Colleen M. Nguyen[2], Jeremy Johnson[2], Parker S. Chastain[2], Sarah Winnicki[2], Elana Anastasio[2], Diane M. Diehl[2], Todd R. Golub[2], Corrie A. Painter[2], Nikhil Wagle[1], Daniel L. Abravanel[1], Jorge Gomez Tejeda Zanudo[1]

[1]Breast Oncology Program, Dana-Farber Cancer Institute, Boston, MA,[2]Broad Institute, Cambridge, MA

The Metastatic Breast Cancer project (MBCproject) is a patient-partnered research study that has collected clinical, genomic, and survey data through online enrollment. The cohort includes whole exome sequencing from 379 tumor biopsies (bxs) with matched germline from 301 patients (pts) and RNA-seq from 200 bxs (141 pts). In addition to confirming prior observations, this multi-omics cohort has enabled the discovery of novel MBC characteristics. Tumor evolutionary analysis was performed for 56 pts with multiple bxs from different timepoints and sites (115 bxs). Acquired *ESR1* mutations were observed in six pts, all of whom received endocrine therapy between bxs. Mutations in *TP53*, *GATA3*, and *PTEN* were almost always truncal. However, mutations in *PIK3CA*, *CDH1*, and *KMT2C* exhibited complex clonal dynamics with gain/loss events across paired bxs, contrary to the common assumption that such mutations are truncal. For pts with distinct *CDH1* mutant status across bxs, the presence of *CDH1* mutations at the bx level is associated with lobular histology (ILC), and the lack of *CDH1* mutations is associated with ductal histology (IDC). The cohort includes three pts with bilateral breast cancers, which we found to be phylogenetically unrelated. Only one pt harbored a pathogenic germline mutation (*CHEK2*). In one pt, bilateral bxs had distinct histology yet shared copy number variations (CNVs) such as 1q gain and 6q loss. In another, left and right ILCs had distinct *PIK3CA* and CDH1 mutations and dissimilar CNV profiles. The shared altered genes and CNVs from independent tumors in the same pt suggest convergent evolution through tumorigenesis. To further explore evolution over disease progression, we compared treatment-naive primary and treatment-exposed metastatic bxs in the full cohort. *TBX3* mutations were enriched in metastatic bxs ($p=0.024$, FDR<0.25), driven by higher prevalence in HR+/HER2- and HER2+ subtypes, and co-occurred with *CDH1* ($p=0.0016$) and *ERBB2* oncogenic mutations ($p=0.039$). All MBCproject *TBX3-ERBB2* mutant bxs were from pts with ILC and had *CDH1* mutations. MSK IMPACT confirmed *TBX3-CDH1* ($p=4.4e-8$) and *TBX3-ERBB2* ($p=6.1e-5$) co-occurrence and showed *TBX3-ERBB2* mutations also co-occurred in IDC bxs without *CDH1* mutations ($p=9.2e-4$), suggesting that *TBX3-ERBB2* mutations are independent of ILC and *CDH1* status. *TBX3*-only mutant bxs had a proliferation RNA-seq signature score higher than Luminal A bxs ($p=0.032$ MBCproject, $p=0.0047$ TCGA) and more similar to that of IDC than ILC tumors. Overall, this indicates that *TBX3* mutations drive distinct tumor behavior independent of histology and *CDH1* alterations. The MBCproject demonstrates the power of patient-partnered research and multi-omics evolutionary analysis to uncover novel insights into metastatic breast cancer biology.

#7266 Advancing insights into disease biology of non-muscle invasive bladder cancer (NMIBC) through comprehensive multi-omics analysis.

Siew Kee Low[1], Yoshiyuki Nagumo[2], Xuesong Lyu[1], Jiarui Zhang[3], Jie Zhao[1], Kozaburo Tanuma[2], Satoka Kinase[2], Karen Urtishak[3], Neil Beeharry[3], Shibu THOMAS[3], **Longen Zhou**[3], Hiroyuki Nishiyama[2]

[1]Johnson & Johnson, Shanghai, China,[2]Department of Urology, Institute of Medicine, University of Tsukuba, Tsukuba, Ibaraki, Japan,[3]Johnson & Johnson, Spring House, PA

Non-muscle invasive bladder cancer (NMIBC) accounts for approximately 75% of all bladder cancer cases and has high rate of recurrence and potential progression to muscle-invasive disease. Treatment strategies for NMIBC include transurethral resection of bladder tumor (TURBT) followed mainly by Bacillus Calmette-Guérin (BCG) immunotherapy or chemotherapy. Although NMIBC management has progressed, understanding its molecular basis and changes after treatment remains critical for better prognosis, patient stratification and informed treatment strategies. Here, we conducted whole exome and transcriptomic sequencing to elucidate molecular landscape and tumor microenvironment and uncover potential prognostic biomarkers associated with BCG response. Three distinct BCG response subtypes (BRS) were assessed by BCG response subtype predictor using transcriptomic sequencing data. Comparison of genomic alterations' prevalence and transcriptomic signatures in Kyoto Encyclopedia of Genes and Genomes (KEGG) via ssGSEA (single sample Gene Set Enrichment Analysis) between high vs low/intermediate risk were evaluated. Data from 37 pre-treatment NMIBC patients were analyzed (N = 37); including patients treated with TURBT followed by BCG [N = 16], and with TURBT only [N= 21]. Genomic profiling of 37 patients demonstrated mutation frequencies consistent with published literature, with highest prevalence observed in Telomerase Reverse Transcriptase (TERT) (78.4%), followed by Tuberous Sclerosis Complex 1 (TSC1) (64.9%) and Lysine (K)-Specific Methyltransferase (KMT)2D (51.4%). Notably, mutation frequency of Fibroblast Growth Factor Receptor 3 (FGFR3) was higher among low- and intermediate-risk groups (66.7%, N = 15) compared to high-risk groups (36.4%, N = 22). Pathway score calculated using ssGSEA from transcriptomic profiling revealed a markedly higher gene expression profile enriched in cell-cycle pathway in among high- compared to low- and intermediate-risk groups (p = 0.033). Patients with BRS3 tumors exhibited significantly reduced progression free survival (PFS) versus BRS1/2 (p= 0.0095, HR = 5.92), following BCG treatment. BRS3 tumors demonstrated elevated expression of epithelial-mesenchymal transition and basal markers and were characterized by an immunosuppressive profile. We identified that FGFR3 mutation rate is higher among low- and intermediate risk. Cell cycle dysregulation is known to contribute in tumor progression and aggressiveness of bladder cancer; our pathway analysis identified cell cycle pathway enrichment among high-risk NMIBC, which enhances our understanding of NMIBC disease biology. Our data validated BRS3 subtyping in predicting poor BCG response, demonstrating robustness of this classification approach. Further investigation is warranted to confirm these findings, considering smaller cohort in this study

#7267 Genomic architecture of prostate cancer in *BRCA1/2*germline carriers.

Taylor B. Crawford[1], Heena Desai[1], Jiannong Li[2], Ryan Hausler[1], Candace L. Haroldsen[3], Martin W. Schoen[4], Timothy R. Rebbeck[5], Brent S. Rose[6], Michael J. Kelley[7], Bruce Montgomery[8], Nicholas G. Nickols[9], Matthew B. Rettig[10], Kosj Yamoah[11], Isla P. Garraway[12], Kara N. Maxwell[13]

[1]University of Pennsylvania, Philadelphia, PA,[2]Research Scientist, Moffitt Cancer Center, Tampa, FL,[3]University of Utah, Salt Lake City, UT,[4]Saint Louis University School of Medicine, St. Louis, MO,[5]Dana-Farber Cancer Institute, Boston, MA,[6]University of California, San Diego, San Diego, CA,[7]Duke Cancer Institute, Durham, NC,[8]University of Washington, Seattle, WA,[9]University of California Los Angeles, Los Angeles, CA,[10]Professor, UCLA David Geffen School of Medicine, Los Angeles, CA,[11]H. Lee Moffitt Cancer Center, Tampa, FL,[12]UCLA, Manhattan Beach, CA,[13]Perelman School of Med. Univ. of Pennsylvania, Philadelphia, PA

Background: Inherited pathogenic germline variants (PGVs) in *BRCA1 and BRCA2* are significant risk factors for the development of prostate cancer (PCa). Individuals with *BRCA2* PGVs have a 3-4-fold increased risk of developing PCa and demonstrate higher Gleason scores, increased nodal metastases, and overall poorer survival. However, the mechanisms by which *BRCA1/2* loss promotes PCa development is unknown. In this study we aim to summarize somatic genomic alterations of *BRCA1* and *BRCA2* carriers with PCa.

Methods: Germline carriers of PGV or putative PGV *BRCA1/2* variants with PCa were identified in the Veteran Affairs National Precision Oncology Program (VA-NPOP) by either clinical genetic testing or by sequencing of liquid biopsies (VAF≥30%). Controls were patients with no PGV in any cancer risk gene on germline genetic testing. Somatic mutations were identified from tumor tissue or liquid biopsy tests as PCa patients were stratified by hormone sensitive prostate cancer (HSPC) and castration resistant prostate cancer (CRPC) clinical status. Fishers' exact tests were used to compare mutation frequencies in 30 genes, tumor mutational burden (TMB), and microsatellite instability (MSI) scores in *BRCA1* or *BRCA2* carriers vs. germline negative controls.

Results: A total of 85 patients with *BRCA1/2* variants were included in the study (n=70 *BRCA2*, n=15 *BRCA1*) with 1,124 control patients including 844 and 365 PCa patients who had HSPC and CRPC, respectively. Of the HSPC patients who received a tumor tissue test, *BRCA2* carriers had a significantly higher mutation frequency of the *PRKCI* gene compared to controls (13% (n=16) vs n=1% (n=560), p=0.023, respectively). Of the CRPC patients who received a liquid biopsy test, *BRCA2* carriers had a significantly higher mutation frequency of the *KDM6A* gene compared to controls (13% (n=38) vs 2% (n=318), p=0.005, respectively). Additionally, mutations in the *APC* gene were found at a higher frequency in *BRCA1* carriers (22% (n=9) vs 3% (n=318), p=0.027). There was no significant difference in tumor mutational burden and microsatellite instability measurements between *BRCA1* and *BRCA2* carriers and controls regardless of the type of somatic test and sensitivity to hormone therapy. Further work is required to understand mechanisms that contribute to these genomic differences, therefore, we have expanded this study to understand transcriptomic differences between *BRCA2* carriers (n=30) and non-carriers (n=60) with localized PCa by performing bulk DNA and RNA-sequencing and single cell RNA sequencing of fresh *BRCA2* (n=10) prostate tissues and clinically matched control patients (n=20).

Conclusions: We report differences in genomic alteration frequencies in *PRKCI*, *KDM6A*, and *APC* between *BRCA1* and *BRCA2* germline carriers and controls in VA-NPOP. Further work is needed to determine the functional role of genomic and transcriptomic differences in *BRCA1/2* carriers and non-carriers.

#7268 AI-Driven stratification of cancer patients using The Cancer Genome Atlas whole-genome sequencing data.

Jonghoon Lee[1], Chunyang Bao[1], Hansol Park[1], Gang-Hee Lee[1], Yoonsuh Lee[1], Beomki Lee[2], David Lehotzky[3], Ron Solan[3], Antonia Kowalewski[3], Xavi Loinaz[3], Vasuki Narasimha Swamy[3], David I. Heiman[3], Samantha Van Seters[3], Saveliy Belkin[3], Sam Wiseman[3], Andrew D. Cherniack[3], Luis Antonio Corchete Sanchez[3], Brian P Danysh[3], Zachary Everton[3], Chip Stewart[3], Haruna Tomono[3], Gengchao Wang[3], Esther Rheinbay[3], Gad Getz[3], Young Seok Ju[3], Won-Chul Lee[3], Ryul Kim[1]

[1]Inocras, San Diego, CA,[2]Korea Advanced Institute of Science and Technology, Daejeon, Korea, Republic of,[3]Cancer Program, Broad Institute of MIT and Harvard, Cambridge, MA

Recent genomic foundation models have advanced DNA sequence interpretation, yet most remain constrained to local sequence patterns and fail to produce the patient-level insights required for clinical decision-making. To address this limitation, we developed a framework that extends beyond sequence-level inference, enabling robust patient stratification through a Cancer Foundation Model. Our approach begins with “DNAChunker”, which employs a dynamic H-net-based tokenization strategy that divides the genome into variable-length segments, preserving high-resolution detail in regulatory and coding regions while efficiently compressing repetitive sequences. When evaluated on the Nucleotide Transformer and Genomic Benchmarks, DNAChunker achieved performance comparable to the state-of-the-art GENERator (1.2 billion parameters) while using only 156 million parameters. To translate these genomic embeddings into patient-level insights, we implemented a transformer-based Cancer Aggregation Model that integrates mutation embeddings with somatic copy-number alteration (SCNA) features. The framework was evaluated on large whole-genome sequencing (WGS) cohorts, including PCAWG (n=2,040) and CUBRICS breast cancer samples (n=1,053), with TCGA-BRCA (breast cancer; n=920) serving as an external validation cohort. The model effectively stratified patients by cancer type (accuracy, 96.89%), homologous recombination deficiency (HRD; accuracy, 92.83%), and PAM50 subtype (accuracy, 84.05%). Notably, it classified PAM50 intrinsic subtypes using only DNA-level information, eliminating the conventional reliance on RNA-based expression profiling. The Cancer Foundation Model demonstrates that patient-level representation learning from whole-genome data can achieve clinically meaningful stratification across diverse tumor types. By bridging the gap between genomic sequence interpretation and actionable phenotypic classification, this framework establishes a foundation for AI-based precision oncology. With further validation, it will facilitate biomarker discovery and patient stratification in clinical trials directly from WGS data.

#7269 Development and validation of an optimized, bead-based dual nucleic acid extraction method for high-yield genomic profiling of scarce FFPE tumor specimens.

Nripesh Prasad, Rebecca Beatty, Rachel Marshall, Chan-Ho Lee, Elizabeth Coffey, Annamaria Szanto

Discovery Life Science, Huntsville, AL

Formalin-fixed, paraffin-embedded (FFPE) tumor tissues are crucial for retrospective oncology studies, but recovering high-quality nucleic acids (NA) from these samples—especially scarce core needle biopsies (CNBs)—is challenged by chemical crosslinking, fragmentation, and low input volume, often compromising next-generation sequencing (NGS) success. To meet the demand for reliable NGS from limited FFPE material, we developed and validated a Modified Proprietary Dual Extraction Method specifically optimized for low-input and highly degraded FFPE tissues, including CNBs. This novel, bead-based chemistry utilizes a Xylene-free deparaffinization step, followed by Covaris UltraSonication to achieve optimized lysis and de-crosslinking conditions. The method focused on refining key technical parameters, namely lysis buffer concentration and de-crosslinking time/temperature, and was benchmarked against our Internal Standard and a commercial column-based standard (Qiagen AllPrep FFPE Dual Kit). FFPE samples across multiple tumor types (kidney, head and neck, bladder, lung) and varying tissue inputs (0.5 mm^3 to 4.0 mm^3) were tested, including a cohort of known low-quality (LowQ) FFPE samples. We evaluated DNA/RNA yield, integrity (DIN/RIN), and reproducibility across all three methods. The Modified Method demonstrated significantly superior performance: DNA Yield and Recovery: The protocol delivered a dramatic increase in usable DNA yield, with 98.83% of samples meeting the minimum 100 ng NGS threshold, compared to only 73.50% using the commercial kit. DNA Quality: The Modified Method achieved higher DNA yields without compromising DNA integrity and notably improved the quality metrics of challenging LowQ FFPE specimens. RNA Quality: RNA integrity also significantly improved over the AllPrep Kit, enhancing the suitability of the resulting RNA for complex downstream applications like RNA sequencing (RNA-seq) workflows. The protocol exhibited high reproducibility with minimal operator or lot-to-lot variability. This Modified Dual Extraction Method, leveraging optimized bead-based chemistry and sonication, enables superior, high-quality, and reproducible recovery of nucleic acids from the most challenging FFPE tumor specimens. Its validated performance over conventional protocols is critical for advancing reliable genomic profiling in cancer research and precision oncology using archived or limited tissue specimens.

#7270 Comprehensive mutation profiling from The Cancer Genome Atlas (TCGA) whole-genome sequencing datasets.

Chunyang Bao[1], Hansol Park[1], Gang-Hee Lee[1], Ryul Kim[1], Won-Chul Lee[1], Jonghoon Lee[1], Yoonsuh Lee[1], Beomki Lee[2], David Lehotzky[3], Ron Solan[3], Antonia Kowalewski[3], Xavi Loinaz[3], Vasuki Narasimha Swamy[3], David I. Heiman[3], Samantha Van Seters[3], Saveliy Belkin[3], Sam Wiseman[3], Andrew D. Cherniack[3], Luis Antonio Corchete Sanchez[3], Brian P. Danysh[3], Zachary Everton[3], Chip Stewart[3], Haruna Tomono[3], Gengchao Wang[3], Esther Rheinbay[3], Gad Getz[3], Young Seok Ju[1]

[1]Inocras Inc., San Diego, CA,[2]Graduate School of Medical Science and Engineering, Korea Advanced Institute of Science and Technology, Dajeon, Korea, Republic of,[3]Cancer Program, Broad Institute of MIT and Harvard, Cambridge, MA

Cancer arises from the progressive accumulation of genomic alterations. The Cancer Genome Atlas (TCGA), a landmark consortium project, has comprehensively characterized 33 cancer types through multi-omics profiling of over 11,000 tumor-normal pairs. However, most TCGA-based studies had relied on whole-exome sequencing (WES), which covers only ~1-2% of the genome, leaving the majority of the genomic landscape unexplored. To achieve a more comprehensive understanding of cancer genomes, the Broad Institute and Inocras collaboratively analyzed TCGA whole-genome sequencing (WGS) data encompassing over 8,000 tumors across more than 30 cancer types, which were initially analyzed by whole-exome sequencing. To fully leverage this resource, we applied CancerVision, an automated and streamlined bioinformatics pipeline developed by Inocras for clinical-grade WGS interpretation. CancerVision detects diverse genomic variants, including single-nucleotide variants (SNVs), insertions/deletions (indels), somatic copy number alterations (SCNAs), structural variants (SVs), and germline mutations, while also inferring homologous recombination deficiency (HRD) and mutational signatures. Using CancerVision, we performed a comprehensive, harmonized reanalysis of the TCGA WGS dataset and benchmarked our results against the bioinformatics pipelines from the Broad Institute and the official TCGA exome data. Across representative cohorts, ovarian cancer (CNV-driven), thyroid cancer (SNV-driven), and glioblastoma (mixed), CancerVision achieved high concordance, often uncovering additional high-confidence genomic alterations not captured in the existing TCGA resource. By integrating these results, we expand the known landscape of somatic variants, improve driver gene detection, and demonstrate the power of whole-genome-based analytics for actionable insights in precision oncology.

#7271 Clinical genomic and functional genomic support for a role of ARID1A loss in progression of desmoplastic small round cell tumor.

Tom Zhang[1], Andrea Gazzo[1], Christopher A. Febres-Aldana[2], Juan Luis Gomez Martis[1], Lee Spraggon[3], Romel Somwar[1], Marc Ladanyi[1]

[1]Memorial Sloan Kettering Cancer Center, New York, NY,[2]Laboratory of Pathology, National Cancer Institute, National Institute of Health, Bethesda, MD,[3]UCSF READY Center, San Francisco, CA

Background. Desmoplastic small round cell tumor (DSRCT) is a rare, lethal sarcoma defined and driven by the *EWSR1::WT1* fusion. DSRCT has a very low tumor mutational burden (TMB) and few recurrent secondary somatic mutations. Often, the *EWSR1::WT1* fusion is the sole identifiable genetic alteration. We leveraged the Memorial Sloan Kettering Cancer Center (MSK) sarcoma sequencing cohort to conduct a comprehensive profiling of 110 DSRCT cases to better define the genomic landscape and evolution of DSRCT.

Methods. DSRCT samples underwent matched tumor:normal DNA sequencing on the MSK-IMPACT platform (01/2014-12/2023). All cases harbored the *EWSR1::WT1* fusion. A genome-wide, pooled CRISPR-cas9 loss-of-function screen was conducted in 2 DSRCT cell lines (Brunello library, 4 sgRNAs per gene, targeting 19,114 genes). Immunohistochemistry (IHC) was used to assess ARID1A protein expression.

Results. We identified 110 DSRCT samples from 82 patients (pts) after robust filtering and quality control from a starting cohort of 198 samples (123 pts). Pts were predominantly male (85.4%) with a male-to-female ratio of 5.8:1 and a median age of 21.5 yrs (range: 6.5-55.9 yrs). At diagnosis, 50% had localized disease (stage I-II), 28.05% had liver metastasis (stage III), and 21.95% presented with extra-abdominal disease (stage IV). DSRCT samples had a median TMB of 0.8 mutations/Mb (range: 0.0-6.6); indeed, 47.3% had no detectable mutations (muts) among the 505 genes profiled. The most frequent secondary alterations were *ARID1A* inactivating muts (12.2%), followed by *FGFR4* activating muts (7.3%), *TERT* promoter muts (6.1%), and *TP53* muts (4.9%). In the knockout screen, *ARID1A*, *TP53*, and *PTEN* ranked among the top positively selected hits, providing functional genomic support for the clinical genomic findings. Notably, *ARID1A* muts were more common in metastatic lesions (18.5%) than in primary intraabdominal tumors (9.8%), suggesting a role in disease progression. To explore their evolutionary timing, we performed clonal decomposition using cancer cell fraction (CCF) analysis: metastatic samples had significantly higher CCF values (p=0.0067), and clonal muts were predominantly found in metastases (5/7), while subclonal variants were mainly observed in primary tumors (6/8; p=0.021) and their subclonality confirmed by IHC for ARID1A. Two *ARID1A*-mutated patients had both primary and metastatic samples; in one, an *ARID1A* nonsense mutation shifted from subclonal (CCF=0.286) in the primary to clonal (CCF=1.0) in the metastasis. In the 2nd patient, an ARID1A frameshift mutation appeared only in the metastatic lesion.

Conclusions. Late acquisition and metastatic selection of *ARID1A* mutations point to a role for loss of this BAF complex component in DSRCT progression. Future studies will investigate the pathobiology and therapeutic vulnerabilities associated with ARID1A loss in DSRCT.

#7273 Genomic Concordance Patterns Distinguish Multiple Primary Tumors from Metastatic Recurrences.

Brandie Taylor, **Samuel Rivero-Hinojosa**, Sandro Satta, Nicole Scott, Faraz Salmasi, Kevin Manage, Stephanie Woods, Charuta C. Palsuledesai, Ekaterina Kalashnikova, Angel Augusto Rodriguez, Minetta C. Liu

Oncology, Natera, Inc., Austin, TX

Background

Multiple primary cancers (MPC), wherein two or more synchronous or metachronous malignant tumors in the same or different organs are present within a single patient (pt), are observed in ~10-25% of pts with cancer. Differentiating MPCs from metastatic disease has implications for staging, treatment selection and prognosis. Here, we evaluated whole exome sequencing (WES) data of tumor tissues from pts known to have MPCs and metastatic recurrence (MR).

Methods

Pairs of distinct primary tumors from 76 pts with MPCs and primary/metastatic site tumor pairs from 134 pts with MR were compared. Tumor tissue WES was performed as part of either commercial circulating tumor DNA testing (Signatera™, Natera, Inc) or Altera™ Comprehensive Genomic Profiling (Natera, Inc). To enable intertumor comparison, normalization involved restricting variants to shared genomic regions (defined by a BED file) and normalizing variant allele frequencies in each sample by their respective median. Concordance analyses included shared variants (Jaccard index), VAF correlation coefficients, TMB comparisons (mut/Mb) and single-base substitution (SBS) mutational profile. Outlier pairs were identified by >5 mut/Mb TMB difference or Pearson VAF correlation <0.3.

Results

MPC and MR cohorts had 44.7% and 48.9% males, respectively; median pt ages were 69 (40-90) years and 72 (39-90) years, respectively. No primary tumor pairs were from the same organ. MPC tumor pairs exhibited minimal somatic mutation overlap [median Jaccard index = 0.00 (0.00-0.43)], with only 5% of patients having >1 shared driver mutations. Nearly 77% (59/76) MPC tumor pairs had >2-fold differences in TMB. Additionally, the cosine similarity distribution of SBS mutational profiles across MPC tumor pairs was broad and relatively low [median: 0.49 (0-0.95)], indicating distinct mutagenic processes. In contrast, MR tumor pairs demonstrated markedly higher genomic similarity, with high proportion of shared mutations [median Jaccard index = 0.352 (0- 0.965)], high VAF correlations (mean Pearson r = 0.62) in shared mutations, and >1 shared driver mutations in 61.9% of tumor pairs. Further, MR presented a strongly right-skewed distribution of SBS mutational profiles cosine similarity [median: 0.77 (0-0.98)]. TMB was largely concordant between MR paired tumors, though 15% of pairs exhibited divergence >5 mut/Mb.

Conclusions

MPC and MR tumor pairs showed markedly distinct patterns of genomic concordance. MPC tumors have low mutation sharing and minimal similarity in mutational profiles, suggesting independent mutagenic processes. Conversely, MR tumors display high clonal continuity across all genomic metrics, indicating a shared origin. VAF correlation and mutational signature profiling provides a robust framework to molecularly distinguish MPCs from MR, addressing a critical unmet need in tumor classification and precision oncology.

#7274 Structural variant signature discovery across >8,000 TCGA whole genomes using QuantHDP.

Gregory Raskind[1], Youyun Zheng[1], Anthony Zhao[2], Julia Sun[2], Simona Dalin[2], Siyun Lee[2], Chunyang Bao[3], Antonia Kowalewski[2], Ron Solan[2], Sam Wiseman[2], Samantha Van Seters[2], Saveliy Belkin[2], David I. Heiman[2], Chip Stewart[2], David Lehotzky[2], Vasuki Narasimha Swamy[2], Brian P. Danysh[2], Luis Antonio Corchete Sanchez[2], Andrew D. Cherniack[2], Haruna Tomono[2], Gengchao Wang[2], Xavi Loinaz[2], Zachary Everton[2], Gang-Hee Lee[3], Won-Chul Lee[3], Hansol Park[3], Ryul Kim[3], Young Seok Ju[3], Gad Getz[4], Esther Rheinbay[2], Rameen Beroukhim[2]

[1]Department of Biomedical Informatics, Harvard Medical School, Boston, MA,[2]Cancer Program, Broad Institute of MIT and Harvard, Cambridge, MA,[3]Inocras Inc., San Diego, CA,[4]Massachusetts General Hospital, Charlestown, MA

Many cancers have inherent defects in DNA damage response (DDR) which influence their sensitivity to tumor-targeting therapies. Examples include increased activity of immunotherapies in cancers with mismatch-repair deficiency and sensitivity to PARP inhibitors and platinum-based therapies in the context of homologous recombination (HR) deficiency. However, we are currently unable to reliably determine which DDR defects are present in a given cancer sample, which severely limits our ability to exploit these therapeutic vulnerabilities. Structural variants (SVs), or genomic rearrangements formed as a product of aberrant double strand break repair, hold promise as biomarkers of DDR state. Indeed, SVs affect a larger proportion of the cancer genome than any other form of genetic alteration and have features that reflect their mechanism of formation. Here, we develop QuantHDP, a novel computational method for detecting SV signatures which leverages complex modeling of genetic features to distinguish between cancers with different DDR alterations and potentially identify clinically relevant biomarkers. QuantHDP models SV features with probability distributions that reflect our knowledge of the biological mechanisms that generate them, accounts for expected differences in signature content by cancer type, and automatically infers the number of signatures present in a given dataset. In addition to recapitulating multiple previously established associations with defects in DDR - including signatures of BRCA1, BRCA2, and CDK12 alterations — we also uncover novel signatures that warrant further investigation.

#7275 Molecular characterization of Latino gastric adenocarcinomas identifies homologous recombination deficiency and TGF-beta pathways as targets for aggressive genomically stable tumors.

Dennis J. Montoya[1], Ana Patricia Estrada-Florez[2], Paul Lott[3], Katherine Chiu[4], Javi Villalpando[2], Shriveda Reddy[2], Jasmine Diaz Sezati[5], Fabian Castro[6], Guadalupe M Polanco-Echeverry[7], Magdalena Echeverry de Polanco[6], Javier Torres[8], Mabel Bohorquez[6], Luis G. Carvajal-Carmona[5]

[1]Biochemistry and Molecular Medicine, UC Davis School of Medicine, Davis, CA,[2]UC Davis, Davis, CA,[3]Genome Center and Department of Biochemistry and Molecular Biology, UC Davis, Davis, CA,[4]Genome Center, UC Davis, Davis, CA,[5]Biochemistry and Molecular Medicine, UC Davis, Davis, CA,[6]Universidad del Tolima, Ibague, Colombia,[7]The Health Equity Leadership, Science, and Community Research Laboratory, UC Davis, Davis, CA,[8]Instituto Mexicano del Seguro Social, Mexico City, Mexico

Background: Gastric cancer (GC) disproportionately affects Latino populations, yet genomic data from these patients remain scarce. This underrepresentation limits understanding of ancestry-specific molecular features that could inform targeted therapies. Tumors characterized by a genomically stable (GS) subtype are associated with worse outcomes and is more prevalent among Asians and Hispanics than among non-Latino White (NLW) and Black populations.

Methods: We analyzed 192 gastric adenocarcinoma tumors from Latino patients (Colombia, Mexico, and U.S.) using low-pass whole-genome sequencing (LP-WGS), or whole-exome sequencing. Molecular subtypes were classified, and somatic alterations were assessed and compared to the NLW cohort from the cancer genome atlas (TCGA).

Results: Similar to previous studies, the GS subtype was predominant (57.8%) in this Latino cohort, significantly higher than the mostly NLW, TCGA-STAD (11.5%, $p < 10^{-29}$). GS tumors had frequent alterations in cadherin/catenin complex genes (CDH1, CTNND1) as well as the DNA damage repair gene ATM, and TGF-β related pathway members TGFBR2 and ELF3. We identified six novel significantly mutated genes in non-hypermutated tumors and subtype-specific drivers that differ in frequency based on self-identified race. Comparative analysis revealed genetic ancestry-linked differences, including greater Indigenous American (IA) ancestry in diffuse histology tumors and higher CDH1 mutation frequency. Analysis of the therapeutically actionable biomarkers were limited in GS tumors (65% lacked targets), but ATM mutations suggest potential benefit from PARP inhibitors.

Conclusions: Latino GC tumors are enriched for GS subtype and harbor unique genomic alterations, including novel drivers and HRR pathway defects. These findings underscore the need for ancestry-informed therapeutic strategies and highlight PARP inhibition as a promising avenue for GS tumors.

#7276 Understanding cutaneous immune-related adverse events at single-cell resolution.

Olivia J. Cheng[1], Nabeela Khan[2], Terri Clister[2], Rebecca Nichols[2], Khanh Doan[2], Connor Hall[2], Rajan Kulkarni[2], Aik Choon Tan[1]

[1]University of Utah Huntsman Cancer Institute, Salt Lake City, UT,[2]OHSU, Lake Oswego, OR

Background: Immune checkpoint inhibitor (ICI) treatment has demonstrated clinical efficacies in various cancers. However, alongside the benefits of ICI's anti-tumor effect, a subset of patients experience immune-related adverse events (irAEs) that could lead to the termination of treatment, and in severe cases, morbidity and mortality. Cutaneous irAEs often occur early and are among the most common irAE in patients treated with ICIs. In particular, combinations of ICI with other anti-cancer agents can heighten the frequency and severity of irAEs. The goal of this study is to understand the molecular factors of immune-related rash (ir-Rash) and identifying biomarkers for early risk prediction and mechanism-based management.

Method: Five prostate cancer patients were treated with pembrolizumab and enzalutamide (androgen receptor blocker), and skin samples were collected for longitudinal single cell RNA sequencing (scRNA-seq) at various post-treatment timepoints: Week 0, Week 12, and Rash for those who developed ir-Rash. Cell type annotation, gene set enrichment, cell proportion and cell-cell interaction analyses were performed to identify cell types and biological pathways associated with ir-Rash risk and temporal development. To identify predictive biomarkers correlated with the risk of ir-Rash, baseline Week 0 samples were compared between the rash (R) and no-rash (NR) groups. To understand the temporal changes and mechanisms of actions through ir-Rash onset and resolution, we compared samples from patients with rash at the three timepoints.

Results: Cell proportion analysis revealed a higher baseline proportion of dendritic cells (DCs) in ir-Rash patients compared to NR patients. Among ir-Rash patients, cytotoxic cell abundance increased at rash timepoint relative to baseline. Single sample gene set enrichment analysis (ssGSEA) of 50 MSigDB hallmark gene sets across 5 conditions (Week0-NR, Week0-R, Rash, Week12-NR, and Week12-R) showed enrichment of pathways including interferon responses and PI3K-AKT-MTOR signaling at Rash. Week0-Rash samples additionally exhibited enrichment of MYC targets, IL2-STAT5 signaling, hypoxia, mTORC1 signaling, and E2F targets. Particularly in DCs, interferon-gamma response was enriched at both Week0-Rash and Rash timepoints. And among cytotoxic cells, notch signaling, MTORC1 signaling, WNT-BETA-Catenin signaling were enriched at the Rash timepoint.

Conclusions: Our results suggest that immune-related rash is associated with an increase in dendritic cell frequency at baseline and an increase in cytotoxic cells at onset, accompanied by enrichment of pathways including interferon responses. These results may help elucidate potential mechanisms underlying cutaneous toxicity during ICI treatment.

#7278 Single-cell RNA-seq analysis reveals distinct tumor and immunosuppressive T-cell phenotypes in CLL patients treated with ibrutinib..

Shanmugapriya Thangavadivel[1], Jami Shaffer[1], Shrilekha Misra[1], Samon Benrashid[1], Britten Gordon[1], Alexander He[1], Wantong Li[1], Konur Oyman[1], Annika Chura[1], Shelby Cabrera[1], Altan Turkoglu[1], Tzung-Huei Lai[1], Kerry Rogers[2], Seema Bhat[2], John C. Byrd[3], James S. Blachly[4], Jennifer A. Woyach[5], Bradley Blaser[6]

[1]The Ohio State University Comprehensive Cancer Center, Columbus, OH,[2]The Ohio State University, Columbus, OH,[3]UPMC Hillman Cancer Center, University of Pittsburgh, Pittsburgh, PA,[4]Duke University (Columbus, OH), Columbus, OH,[5]Assistant Professor of Internal Medicine, Division of Hematology, Ohio State University College of Medicine, Columbus, OH,[6]Division of Hematology, Department of Internal Medicine, The Ohio State University, Columbus, OH

The development of Bruton tyrosine kinase inhibitors and their introduction into clinical practice represents a major advance in the treatment of chronic lymphocytic leukemia (CLL). However, monotherapy with ibrutinib or other BTKis generally does not induce complete remissions or undetectable minimal residual disease even with extended therapy. Therefore, there is a need to understand the differences between ibrutinib sensitive and resistant CLL cells along with the immune microenvironment to identify novel therapeutic approaches for controlling residual disease during BTKi treatment. Here, we investigated the cellular heterogeneity of peripheral blood mononuclear cells from patients with CLL treated with ibrutinib using single-cell RNA sequencing. We identified unique transcriptional heterogeneity within the B cell cluster in the ibrutinib-sensitive and resistant patients. Ibrutinib sensitive cells showed enrichment of B cell populations with upregulation of MHC I molecules and TNF family members. Additionally, we observed that inflammatory response and metabolism related pathways were decreased, whereas cellular response to stress and DNA repair programs were increased in the ibrutinib resistance samples. T cells in ibrutinib-resistant patients showed expansion of Tregs and an exhausted CD8 effector T cell compartment. Furthermore, CD14+ and CD16+ monocytes from ibrutinib resistant patients preferentially expressed a gene expression program of antiviral immunity. At the single-cell level, our findings demonstrate a picture of transcriptional heterogeneity in the tumor compartment and immune milieu. Overall, these findings highlight transcriptional changes in circulating immune cells associated with ibrutinib resistance, suggesting that T cells exhaustion and monocyte polarization accompany, rather than directly drive, resistance during long-term BTKi therapy.

#7279 Beyond HLA LOH: Alternative modes of HLA loss are common and vary by cancer type.

Qidi Yang, Michael Brodie Mumphrey, Wenjin Gu, Taylor Harding, Ariane Lozac'hmeur

Bioinformatics, Tempus AI, Inc., Chicago, IL

The human leukocyte antigen (HLA) genes play a pivotal role in immune surveillance of tumors by presenting tumor-derived antigens to cytotoxic T cells, enabling immune recognition and elimination of malignant cells. Loss of heterozygosity (LOH), somatic mutations, epigenetic silencing and structural variations at the HLA locus are well-characterized mechanisms by which tumors evade immune detection, contributing to disease progression and resistance to immunotherapies. However, those mechanisms are rarely considered in conjunction. A comprehensive understanding of these diverse modes of HLA loss is critical for elucidating tumor-immune escape and optimizing immunotherapeutic strategies.

We developed an integrated workflow leveraging the Tempus xT assay to detect somatic alterations in HLA genes. Germline HLA alleles were first genotyped using a validated proprietary assay. Patient-specific HLA alleles and decoy sequences were used to realign sequencing reads. The realigned reads were fed into standard variant calling and RNA expression quantification workflows to establish HLA variants and HLA expression. HLA variants were filtered to remove artifacts. HLA expression was normalized and bias corrected using machine learning models trained on over 2,000 samples. Total HLA expression loss was defined as the trimmed mean of M values (TMM) being more than 2 standard deviations below the gene- and tumor-purity-stratified mean. HLA LOH was determined using the validated Tempus HLA LOH device. We applied our workflow to 11,000 cancer samples, assessing HLA genotypes, LOH, somatic variants, and expression.

Our HLA loss detection methods showed a high level of concordance, with DNA-based alterations evident at the RNA level. 61% of HLA alleles with LOH and/or loss of function (LOF) variants also displayed loss of HLA RNA expression, which included both allele-specific expression (ASE) and total expression loss from both HLA alleles. 12% of tumors without any DNA loss events displayed RNA-level HLA loss, potentially due to epigenetic regulation, or other causes. The prevalence and molecular mechanisms of HLA loss varied by cancer type. LOH was the dominant mechanism for HLA loss in most cancers, with exceptionally high rates of LOH in head and neck squamous cell carcinoma (46%, 92% of loss events) and lung squamous cell carcinoma (32%, 87% of loss events). Conversely, somatic LOF variants were the dominant mechanism in MSI-H colorectal cancer (22%, 51% of loss events), and expression loss dominated in prostate cancers (21% of cases, 84% of loss events).

As HLA-restricted immunotherapies expand, accurate and comprehensive characterization of HLA gene alterations in tumors is increasingly important. Our findings highlight that, beyond LOH, LOF variants and transcriptional silencing are significant contributors to HLA loss in certain cancers and should be routinely assessed to inform immunotherapeutic decision-making.

#7280 Pan-cancer single-cell RNA sequencing analysis refines multiorigin monocyte and macrophage lineages.

Truc Do Thanh Nguyen[1], Andrew J. Lee[2], Hyun Jung Park[3], Nameeta Shah[4], Bayrta Mandzhieva[1], Dong-Sup Lee[5], Inkyung Jung[2], Woong-Yang Park[1]

[1]School of Medicine, Sungkyunkwan University, Suwon, Korea, Republic of,[2]Department of Biological Science, Korea Advanced Institute of Science and Technology, Daejeon, Korea, Republic of,[3]The Research Institute for Veterinary Science, College of Veterinary Medicine, Seoul National University, Seoul, Korea, Republic of,[4]Translational Genomics Center, Samsung Medical Center, Seoul, Korea, Republic of,[5]Seoul National University, Seoul, Korea, Republic of

Tumor-associated macrophages (TAMs) are central regulators of tumor progression, influencing tissue homeostasis, immune suppression, and angiogenesis. To define their diversity and developmental organization across human cancers, we analyzed a unified single-cell and spatial transcriptomic atlas of myeloid cells from healthy tissues and multiple tumor types. This analysis delineated two principal trajectories of tumor-associated macrophages (TAMs): a resident macrophage-aligned C1QC$^+$ lineage and a monocyte-derived lineage comprising SPP1$^+$ and ISG15$^+$ TAMs. We further identified THBS1$^+$ immature myeloid cells as a precursor population that transitions toward the SPP1$^+$ TAM state and underlies a strongly immunosuppressive and pro-angiogenic program. Clinically, enrichment of C1QC$^+$ TAMs was associated with more favorable outcomes, whereas activation of the THBS1$^+$ MDSC-SPP1$^+$ TAM axis correlated with poor survival and diminished response to immunotherapy. These findings refine the developmental framework of myeloid cells in cancer and underscore a pathogenic macrophage trajectory with potential therapeutic relevance.

#7281 Immune senescence and antigen presentation defects define a pre-existing state of BCG unresponsiveness in bladder cancer.

KyounJun Lee[1], Jee Soo Park[2], Myung Eun Lee[2], Jongchan Kim[3], Hyoung-oh Jeong[1], Minseo Kim[1], Won Sik Ham[2], Semin Lee[1]

[1]UNIST, Ulsan, Korea, Republic of,[2]Yonsei University College of Medicine, Seoul, Korea, Republic of,[3]Yonsei University Health System, Seoul, Korea, Republic of

Background: Bacillus Calmette-Guérin (BCG) is standard therapy for high-risk non-muscle invasive bladder cancer (NMIBC), yet a substantial proportion of patients fail to respond. Although T-cell dysfunction and impaired antigen presentation have been implicated in BCG resistance, their pre-treatment presence and clinical relevance remain unclear. We aimed to define a reproducible, treatment-specific transcriptomic signature of BCG unresponsiveness centered on antigen presentation machinery (APM) deficiency.

Methods: We performed single-cell RNA sequencing (scRNA-seq) on 10 pre-treatment NMIBC tumors to identify cellular programs associated with BCG outcomes. Tumor-intrinsic APM activity and interferon pathway status were quantified at the independent bulk transcriptomic cohorts (UROMOL and BRS). Pre-treatment urine samples were assessed for a targeted chemokine panel (IL-6, IL-8, IFN-γ, CXCL10, CXCL13, CCL5, CCL21) to determine concordance between transcriptomic IFN/APM activity and protein-level immune signaling.

Results: Single-cell profiling revealed that BCG-unresponsive tumors exhibited markedly reduced epithelial APM expression accompanied by suppression of type I/II interferon signaling and loss of plasmacytoid dendritic cell activity. These transcriptomic features were reflected at the protein level: non-responders displayed significantly lower urine chemokine levels prior to BCG instillation. Bulk transcriptomic validation across >350 patients demonstrated that high APM activity robustly predicted improved recurrence-free survival in BCG-treated patients ($p < 0.05$).

Conclusions: BCG-unresponsive NMIBC is defined by a pre-existing antigen presentation defect coupled with suppressed interferon signaling, detectable at both the transcriptomic and urine protein levels. The APM signature exhibits strong, treatment-specific predictive value across multi-cohort datasets and provides a biologically compelling rationale for APM-restoring or IFN-enhancing intravesical immunotherapies as alternatives for patients unlikely to benefit from BCG.

Acknowledgments: The results shown here are in part based upon data generated by the TCGA Research Network: https://www.cancer.gov/tcga. We thank the staff of the Department of Urology and Laboratory Medicine at Yonsei University College of Medicine for their technical assistance. We also thank all the patients who participated in this study. This study was supported by grants from the National Research Foundation of Korea (NRF) grants funded by the Korean government (MSIT) (grant numbers: 2022R1A2C2003831). This work was also supported by the National Research Foundation of Korea (NRF) funded by the Ministry of Education (RS-2018-NR031072).

#7282 A comprehensive multiomics atlas of treatment-naïve breast cancer uncovers co-occurring tumor-immune ecosystems driving immune hot and cold phenotypes.

Hani Jieun Kim[1], Beata Kiedik[1], Kate Harvey[1], Sehrish Kanwal[2], James Douglas[1], John Reeves[1], Alexander Lobanov[3], Daniel L. Roden[1], Sophie Van Der Leij[1], Mun N. Hui[4], Aziz Al'Khafaji[5], Elgene Lim[1], Sean M. Grimmond[2], Joakim Lundeberg[6], Charles M. Perou[3], Alexander Swarbrick[1]

[1]Garvan Institute of Medical Research, Darlinghurst, Australia,[2]University of Melbourne, Victoria, Australia,[3]UNC Lineberger Comprehensive Cancer Center, Chapel Hill, NC,[4]Chris O'Brien Lifehouse, Camperdown, Australia,[5]Broad Institute of MIT and Harvard, Cambridge, MA,[6]Science for Life Laboratory, KTH Royal Institute of Technology, Stockholm, Sweden

Breast cancer is a clinically and genetically heterogeneous disease. Whilst single-cell studies have advanced our understanding of the underlying biological diversity of this disease, a major limitation in previous studies is that they fail to capture the broad spectrum of breast cancer subtypes and lack the statistical power to resolve subtype-specific differences. To address this gap, we generated a comprehensive breast cancer single-cell atlas designed to robustly characterise transcriptomic and genomic heterogeneity across all major clinical subtypes.

Focusing on treatment-naïve tissues to capture disease biology prior to therapeutic intervention, we profiled nearly 200 patient samples to generate a comprehensive multiomics atlas of scRNA-seq, whole transcriptome sequencing (WTS), whole genome sequencing (WGS), and clinicopathological data, such as age, histological grade and type, ER/PR/HER2 measurements, and stromal tumour-infiltrating lymphocyte (sTIL) and PD-L1 status.

To quantify inter- and intra-tumoral heterogeneity, we developed a framework of breast cancer archetyping that positions malignant epithelial cells along axes capturing the cancer intrinsic properties. Archetyping successfully resolves biologically meaningful gradients and systematically quantifies transcriptomic heterogeneity. Our results show that luminal cancers—particularly Luminal B—exhibit the largest degree of intra- and inter-tumoural diversity. We define the key gene programs that contribute to this variability and identify immune programs among luminal cancers. Using sTIL status as a measure of immunogenicity, we identified an underappreciated subset of luminal tumours exhibiting high immune infiltration—challenging the prevailing view that luminal cancers are uniformly “immune cold.” Leveraging our single-cell data, we performed integrative analysis to uncover the distinct co-occurring tumour-immune ecosystems associated with immune-hot versus immune-cold phenotypes. These observations were further validated using our matched multimodal WGS, WTS, and spatial transcriptomics data.

Our single-cell multiomics breast cancer atlas spanning all major clinical subtypes provides a high-resolution framework for dissecting the multilayered heterogeneity of breast cancer. By maximizing patient representation and integrating rich clinical and genomic metadata, this resource enables robust identification of subtype-specific biology and reveals striking diversity within luminal breast cancers, including a substantial subset with immune-hot characteristics. Ongoing work will leverage this atlas and our deeply curated metadata, including survival outcomes, to refine breast cancer stratification and identify clinically actionable tumour ecosystems.

#7283 Genomic landscape of IDH-wild-type glioblastoma in a patient treated with TNF-alpha inhibitor: Implications for risk stratification and therapeutic decision-making.

Suryanarayan Mohapatra[1], **Natarajan Ganesan**[2]

[1]Internal Medicine, Kaiser Permanente - Mid-Atlantic Permanente Medical Group, Silver Spring, MD,[2]Biomedical and Anatomical Sciences, New York Institute of Technology, College of Osteopathic Medicine (NYITCOM) at Arkansas State University, Jonesboro, AR

Background:
TNF-α inhibitors, such as adalimumab, are widely used for autoimmune diseases, yet their long-term impact on tumorigenesis in genetically susceptible individuals remains unclear. Glioblastoma multiforme (GBM) is an aggressive IDH-wild-type tumor with well-defined molecular drivers, but genomic characterization of GBM arising in TNF-α inhibitor-treated patients remains extremely limited. We investigated the genomic profile of a GBM that developed after sequential methotrexate, sulfasalazine, adalimumab, and tofacitinib therapy to explore possible mechanistic links between immunomodulation and tumor evolution.
Methods:
Tumor tissue underwent immunohistochemistry, targeted next-generation sequencing, and copy-number analysis at two independent clinical laboratories. Genomic results were interpreted in the context of TNF-α pathway biology, tumor microenvironment (TME) interactions, and known molecular pathways associated with GBM progression.
Results:
The tumor demonstrated GFAP and OLIG positivity, Ki-67 of 45%, and strong p53 expression (>90%). Genomic profiling revealed hallmark alterations of IDH-wild-type GBM, including CDKN2A/B deletions, PTEN deletion, and TP53 mutation. Some unusual variants included a KDM6A frameshift variant, an unexpected ATRX mutation with uncertain pathogenicity, and PDPK1 loss. Notably, the tumor lacked a TERT promoter mutation—present in the majority of IDH-wild-type GBMs—suggesting alternative telomere-maintenance pathways. The combination of PTEN loss, TP53 mutation, and CDKN2A/B deletion indicated a highly aggressive molecular phenotype associated with immune evasion within the TME. Several altered pathways intersect with TNF-α signaling, raising the possibility of altered tumor-immune interactions under TNF-α blockade.
Conclusions:
This analysis identifies both canonical and atypical genomic alterations in a GBM arising after prolonged TNF-α-targeted therapy. The absence of a TERT promoter mutation and the presence of an unusual ATRX variant suggest a nonstandard evolutionary trajectory. Although causality cannot be established, the temporal association with TNF-α inhibitor exposure, combined with pathway overlap between TNF-α biology, PTEN/TP53 signaling, and immune regulation, warrants further investigation. These findings highlight the importance of genomic risk stratification and consideration of germline predisposition before initiating TNF-α inhibitors, as well as the need for systematic genomic profiling of tumors emerging during biologic therapy.

#7284 Clinically significant cancer variants detected by comprehensive genomic profiling test PGDx elio tissue complete.

Kenneth C. Valkenburg[1], Jesse Fox[1], Jennifer Jackson[1], Robert Auber[2], Ann L. Carr[2], Eric Severson[1], Taylor Jensen[3], Shakti Ramkissoon[1], Marcia Eisenberg[1], Brian Caveney[1], Christopher Coldren[2]

[1]Labcorp Corporation of America, Burlington, NC,[2]PathGroup, Brentwood, TN,[3]Labcorp, Fuquay-Varina, NC

PGDx elio® tissue complete (ETC) is an FDA-cleared kitted IVD class II tumor profiling assay that detects somatic cancer-associated genomic alterations in formalin-fixed paraffin embedded (FFPE) tissue from all solid tumors. ETC is a hybrid capture 505-gene next-generation sequencing (NGS) test that reports single nucleotide variants (SNVs), insertions and deletions (indels), copy number amplifications, translocations, microsatellite instability (MSI), and tumor mutation burden (TMB). Tumor-specific variants are reported based on AMP/ASCO/CAP guideline-supported clinical significance. The size and design of the gene panel enable reporting of recognized variants with evidence of clinical significance across 16 tumor types (bladder, breast, cholangiocarcinoma, CNS, colon, gastric, GIST, IMT, melanoma, NSCLC, ovarian, pancreatic, prostate, rectal, thyroid, uterine), including variants that are indicated for all solid tumors, empowering comprehensive clinical utility. These variant classes include the following: SNVs and/or indels in 36 genes (*AKT1*, *ATM*, *ATR*, *BARD1*, *BRAF*, *BRCA1*, *BRCA2*, *BRIP1*, *CDK12*, *CHEK1*, *CHEK2*, *EGFR*, *ERBB2*, *ESR1*, *FANCA*, *FANCL*, *FGFR3*, *IDH1*, *IDH2*, *KRAS*, *KIT*, *MET*, *MLH1*, *MRE11A*, *NBN*, *NRAS*, *NTRK3*, *PALB2*, *PDGFRA*, *PIK3CA*, *PTEN*, *RAD51B*, *RAD51C*, *RAD51D*, *RAD54L*, and *RET*), translocations in 4 genes (*ALK*, *RET*, *NTRK2*, and *NTRK3*), amplifications in *ERBB2*, and 2 genomic signatures (MSI and TMB). In addition, resistance mutations in *ALK*, *EGFR*, *BRAF*, *KIT*, *MET*, and *PTCH1* that impact treatment decisions with targeted therapies are reported. Analytical validation studies assessed the specificity for each variant and the sensitivity, accuracy, and reproducibility for many of them, yielding competitive analytical performance. Clinical validation has been performed for *BRAF* V600E/K in melanoma, demonstrating comparable performance relative to other on-market FDA-approved companion diagnostic tests. Analysis of real-world evidence for approximately 20,000 cases reveals that ETC detects clinically significant variants at expected rates when compared to available cancer variant databases. ETC, due to its large gene panel, provides a more comprehensive view of patients' mutational profile, enabling physicians to make treatment decisions that are more precisely tailored to individual needs. Overall, these results demonstrate the exceptional performance of ETC in FFPE tissue and the power of comprehensive genomic profiling over single gene tests in standard testing workflows and discovery studies.

#7285 Gene expression-based subtypes associated with prognosis in Colombian colorectal cancer.

Wendy Johana Montero Ovalle[1], Diego Felipe Ballen-Lozano[2], Liliana Lopez-Kleine[3], Silvia Juliana Serrano-Gomez[4]

[1]Instituto Nacional de Cancerologia, Bogota, Colombia,[2]Oncology, Instituto Nacional de Cancerologia, Bogota, Colombia,[3]Universidad Nacional de Colombia, Bogota, Colombia,[4]Instituto Nacional de Cancerologia, Bogota, Colombia

In Colombia, colorectal cancer (CRC) is the fifth leading cause of cancer-related death. Molecular alterations linked to clinical-pathological variables are useful for prognosis and guiding treatment. However, current gene expression-based classifications have been developed mostly in non-Latin American populations, leaving Latin Americans underrepresented. To date, no gene expression studies have been conducted in Colombian CRC patients.

Objective: Identify and characterize gene expression profiles and evaluate their association with the prognosis in Colombian patients with CRC.

Methodology: FFPE tumor (n=35) and non-tumor (n=17) samples from CRC patients treated at the National Cancer Institute, Bogotá-Colombia between 2010-2014 were analyzed by RNA-seq. Differential gene expression was assessed with DESeq2 (FDR-adjusted ≤0.05, lfc of 2 and p-value ≤0.05)K-means, NFM and clusGap were used to clustering. Functional enrichment was performed using the ClusterProfiler and KEEG. WGCNA identified hub genes. Differences in the presentation of clinical-pathological variables were evaluated with chi-square and Fisher's tests ($p<0.05$ considered statistically significant). Recurrence-free survival (RFS), metastasis-free survival (MFS), and overall survival (OS) were estimated by Kaplan-Meier method and the log-rank test.

Results: From 1642 differentially expressed genes in tumor samples, 3 clusters were identified. Cluster 1, enriched in protein folding/translation pathways, was associated with more advanced disease p-value=0.019) and Right-sided tumors(p-value=0.026). Cluster 2(DNA replication, mitotic nuclear division, chromosome organization and chromatid segregation pathways), as a possible proliferative subtype, with all cases in early stages (I-III:100%) and predominantly left-sided tumors (76.9%). Cluster 3(metabolic and oxidative response pathways), showed shortest RFS (p=0.026), while Cluster 1 had a shortest MFS follow by Cluster 3p=0.005). No statistically significant differences were observed in OS. 19 Hub genes associated with CRC progression were identified (including TMEM150A, HNF1A, SNTB1, CLOCK, CCND1, ITGA2).

Conclusions and perspectives: This first transcriptomic profiling of Colombian CRC patients reveals potential molecular subtypes associated with prognosis. These findings highlight potential biomarkers for personalized management and underscore the importance of including Latin American populations in CRC molecular studies to improve global equity in cancer care.

: Hypoxic and Proteotoxic Stress Response
Poster Session

#7289 Activation of toll-like receptors promotes the expression of XBP1s in CLL cells.

Chih-Hang Anthony Tang, **Chih-Chi Andrew Hu**

Houston Methodist Research Institute, Houston, TX

Toll-like receptors (TLRs) are a family of transmembrane proteins found in nearly all immune cells and are responsible for recognizing a broad range of pathogenic molecular patterns, including DNA, RNA, sugars, and lipids. Mouse and human B cells express TLRs, contributing to activation of both the innate and adaptive immune responses. Several studies have shown crosstalk between TLR and B cell receptor (BCR) signaling, indicating an important role for TLRs in B cell survival, proliferation, and differentiation. Chronic lymphocytic leukemia (CLL) is the most common B-cell cancer in adults and is known for its variable clinical outcomes. CLL is defined by the accumulation of leukemic cells in the blood, spleens, lymph nodes, and bone marrow. Signals from the lymphoid microenvironment contribute to proliferation of malignant CLL clones, especially in those whose BCR signaling is more pronounced. TLR signaling may amplify BCR-induced cell proliferation and thus accelerate CLL progression. Spliced X-box binding protein 1 (XBP1s) is a transcription factor responsible for endoplasmic reticulum (ER) stress response. XBP1s is vital to plasma cell differentiation and antibody production. Previously, we observed that B cells produce XBP1s in response to treatment with TLR4 ligand lipopolysaccharide (LPS) and TLR9 ligand methylated CpG-DNA (CpG). It is possible that these and other TLR ligands may induce proliferation of specific CLL populations, illuminating the unique role of each TLR in the development of CLL. In this study, we showed that TLR agonists, other than LPS and CpG, were capable of mediating increased expression of XBP1s in mouse splenic B cells. Next, we utilized the Eμ-TCL1 mouse model to investigate the effects of TLR stimulation in CLL cells because CLL developed in these mice resembles the aggressive IGHV-unmutated type of human CLL. When compared to mouse B cells, mouse CLL cells were shown to drastically increase XBP1s expression after TLR stimulation. Consistently, when compared with precancerous B cells isolated from the same mouse, CLL cells expressed higher XBP1s levels in response to TLR ligands. Malignant CLL cells frequently downregulated their expression of stimulator of interferon genes (STING) protein, leading to increased surface expression of the BCR. CLL cells purified from $STING^{KO}$/Eμ-TCL1 mice indeed responded to TLR activation by expressing higher levels of XBP1s than those from their control littermates. We thus hypothesize that TLR-induced expression of XBP1s can further modulate BCR signaling in STING-deficient CLL cells to promote malignant progression.

#7290 Tumor treating fields (TTFields) enhance chemotherapy-induced proteotoxic stress in pancreatic cancer cells.

Ruben M. Munoz[1], Naama Flint-Brodsly[2], Yaara Porat[2], Daniel D. Von Hoff[1], Haiyong Han[1]

[1]TGen (The Translational Genomics Research Institute), Phoenix, AZ,[2]Novocure (Israel) Ltd, TIRAT CARMEL, Israel

Tumor Treating Fields (TTFields) have recently demonstrated a clinically meaningful survival benefit when added to first-line gemcitabine and nab-paclitaxel for unresectable, locally advanced pancreatic cancer (PANOVA-3). Pancreatic tumors are highly dependent on the unfolded protein response (UPR) to survive endoplasmic reticulum (ER) stress induced by hypoxia, nutrient deprivation, and cytotoxic chemotherapy. TTFields along with gemcitabine, nab-paclitaxel, and cisplatin (the Triple regimen) is under clinical investigation (NCT04605913) and may enhance antitumor efficacy by overwhelming the tumor's proteostasis mechanisms. In this study, we examined whether TTFields synergize with the Triple regimen to amplify ER stress and UPR signaling to trigger cell death in pancreatic cancer cells. TTFields showed frequency-dependent inhibition of cell proliferation (100-200 kHz) and significantly enhanced chemotherapy-induced cytotoxicity, with maximal effects at 150 kHz with a treatment duration of 72 hours. Western blot analysis revealed that both TTFields and the Triple regimen increased GRP78 expression, with significant greater induction observed when applied together, indicating augmented UPR activation. Immunofluorescence staining further demonstrated that TTFields elevated phospho-PERK and total PERK protein levels. In addition, RT-PCR analysis showed significant enhancement of XBP1 mRNA splicing by TTFields and chemotherapy. Collectively, these findings suggest that TTFields potentiate the antiproliferative effects of the Triple chemotherapy by amplifying UPR signaling through the IRE1α/XBP1 and PERK/eIF2 pathways. These results provide mechanistic insight into how TTFields may enhance the efficacy of chemotherapy in pancreatic cancer and support further clinical evaluation of this concomitant treatment approach.

#7291 Hypoxia selects for early PI3K pathway alterations and drives clonal complexity in HPV-positive oropharyngeal cancer.

Bill Diplas, Xin Pei, Yingjie Zhu, Shu Yazaki, Luc G.T. Morris, Richard J. Wong, Sean M. McBride, Heiko Schoder, Yao Yu, Alan L. Ho, Eric Sherman, Nora Katabi, Nancy Lee, Nadeem Riaz

Memorial Sloan Kettering Cancer Center, New York, NY

Purpose: Tumor hypoxia drives treatment resistance in head and neck cancer, yet its molecular determinants remain unclear. We previously demonstrated that HPV-related oropharyngeal cancer (OPC) exhibiting hypoxia is more aggressive necessitating escalated treatment. Here, we investigated the genetic drivers of tumor hypoxia and their impact on tumor evolution.
Methods: We analyzed 152 patients with early-stage HPV-related OPC from a prospective hypoxia-directed dose de-escalation trial (NCT03323463). Comprehensive genomic profiling included WES (n=122) and RNA-seq (n=91). Tumor hypoxia was assessed using 18F-FMISO PET with a standardized hybrid method incorporating qualitative assessment of four image characteristics and quantitative tumor-to-background ratios (TBR >1.3 considered hypoxic). Clonal architecture was reconstructed using PhylogicNDT. We validated molecular correlates of hypoxia in two independent cohorts of HPV-related oropharyngeal cancer from the TCGA and JAVELIN-HN. Hypoxia in validation cohorts was determined using three established mRNA-based hypoxia signatures (Buffa, Winter, Toustrup).
Results: Hypoxia as determined by FMISO PET was present in 72% of tumors at baseline, and correlated with well-established RNA-based signatures of hypoxia. Mutational profiling showed that hypoxic tumors were enriched for PI3K pathway alterations, most notably PIK3CA mutations (OR=5.45, adjusted p=0.05). Critically, this association was restricted to clonal PIK3CA mutations—subclonal mutations showed no hypoxia association, suggesting early selection under hypoxic conditions. This hypoxia-PI3K relationship was validated in independent cohorts of HPV-OPC (TCGA, JAVELIN-HN) using expression-based signatures of hypoxia (adjusted $p<0.05$ for Winter, Buffa and Toustrup hypoxia signatures). Lastly, clonal mapping further revealed that hypoxic tumors exhibited significantly greater clonal complexity ($p < 0.05$; Shannon diversity). Multi-region sequencing in a subset of 41 tumors confirmed extensive spatial heterogeneity, strongly linked to hypoxic tumors.
Conclusions: Our findings show that hypoxia drives early selection for PI3K pathway alterations and promotes clonal complexity, demonstrating how the microenvironment directs tumor evolution in HPV-related OPC.

#7292 Hypoxia-driven HIF-1α/YAP-AXL signaling drives adaptive resistance to TKIs in NSCLC.

Yuki Katayama[1], Tadaaki Yamada[2], Tomoko Yasuhiro[2], Ryohei Kozaki[3], Shigekuni Hosogi[2], Eishi Ashihara[4], Koichi Takayama[2]

[1]Department of Pulmonary Medicine, Kyoto Prefectural University of Medicine, Kyoto, Japan,[2]Kyoto Prefectural University of Medicine, Kyoto, Japan,[3]Ono Pharmaceutical Co., Ltd., Osaka, Japan,[4]Kyoto Pharmaceutical Univ., Kyoto, Japan

Background: Intratumoral hypoxia is a hallmark of solid cancers and promotes invasion, metastatic progression, and drug resistance. However, the mechanisms by which hypoxia contributes to resistance against tyrosine kinase inhibitors (TKIs) in driver-mutant non-small cell lung cancer (NSCLC) remain insufficiently defined. To address this gap, we systematically examined how hypoxic conditions reprogram signaling networks that undermine TKI responses.

Methods: EGFR-mutant PC-9 and HCC4011 and ALK-rearranged H2228 cells were cultured under normoxia (21% O_2) or hypoxia (1% O_2) and treated with osimertinib or brigatinib. Drug response and signaling were assessed by MTT assays, immunoblotting, and phospho-RTK arrays. Bulk RNA-seq (PC-9; normoxia vs hypoxia, 72 h) supported pathway-level analyses. Mechanistic perturbations included siRNA knockdown, co-immunoprecipitation, nuclear/cytoplasmic fractionation, and immunofluorescence. For spatial analysis of human tumors, multiplex immunofluorescence (HIF-1α, AXL, α-SMA, DAPI) was performed on FFPE EGFR-mutant lung adenocarcinoma specimens and quantified with whole-slide single-cell segmentation and tumor/cancer-associated fibroblast (CAF) classification; CytoMAP nearest-neighbor and 50-μm neighborhood metrics assessed CAF proximity to hypoxic tumor cells.

Results: Hypoxia reduced sensitivity to osimertinib in PC-9 and HCC4011 and to brigatinib in H2228. RNA-seq in PC-9 highlighted enrichment of hypoxia and PI3K/AKT pathways, indicating RTK network rewiring under hypoxia. Integrative phospho-RTK profiling and downstream validation pinpointed AXL as the dominant hypoxia-responsive node. AXL knockdown restored TKI growth inhibition and the suppression of downstream AKT signaling under hypoxia, and the AXL inhibitor ONO-7475 phenocopied these effects. Mechanistically, hypoxia decreased LATS1/YAP phosphorylation, promoted nuclear YAP, and enhanced HIF-1α-YAP interaction; silencing HIF-1α or YAP inhibited hypoxia-induced AXL expression. In patient specimens, HIF-1α-high tumor cells showed higher AXL intensity and closer proximity to α-SMA$^+$ CAFs within 50-μm neighborhoods, linking hypoxia, AXL upregulation, and CAF-enriched niches.

Conclusions: Hypoxia induces adaptive resistance to TKIs via HIF-1α/YAP-AXL signaling, linking oxygen stress to RTK reprogramming. Spatial analyses of patient tumors reveal CAF-proximal hypoxic niches with elevated AXL, providing tissue context for this mechanism. These findings support AXL inhibition as a rational combination partner to TKIs to suppress hypoxia-driven adaptive resistance in NSCLC, and motivate future studies to define the clinical conditions under which targeting this axis improves treatment durability.

#7293 The impact of oxygen exposure on clinical biomarkers - an underrecognized source of pre-analytic variability.

Ruizhong Wang, Adedeji Adebayo, Stephanie Adama, Steven M. Westphal, Hala Fatima, Carla S. Fisher, Hongyu Gao, Yunlong Liu, Ryla G. House, GEORGE SANDUSKY, Sean D. McCabe, Zhongping He, Jamunabai M. Prakash, Amber Roberts, Matt E. Thomas, Mohammad Al-Haddad, Sujani Yadlapati, Pam Rockey, William Berry, Mary B. James, Rana German, Emily M. G. Nelson, April M. Giron, Troy Moeller, Noah Xique, Kathy D. Miller, Harikrishna Nakshatri

Indiana University School of Medicine, Indianapolis, IN

When preclinical research fails to replicate human biology, scientific progress stalls, clinical trials falter, and patients continue to suffer. While many factors contribute to these failures, lack of attention to pre-analytic variability is a seminal issue. We recently reported that even short-term exposure to ambient air is sufficient to trigger signaling changes in tumor and non-malignant biospecimens. Those changes in turn alter their biology and responsiveness to targeted therapies. Thus, characterization of tumors collected and processed under physioxia (3% O_2) instead of current practice of collection and processing under ambient air (21% O_2) will help to identify clinically relevant biomarkers that are affected by O_2 tensions. This approach may help to reduce clinical trial failure rates and increase clinical translation of preclinical studies. Towards this goal, we collected human specimens (biopsies, ascites and pleural effusions from 94 donors) under physioxia, then divided the same specimen into two groups; one group maintained under physioxia, the other group exposed to ambient air. Both were for 45-60 minutes before fixing/processing. Samples were subjected to various biomarker analysis using IHC/IF, Western blotting to measure proteins, and nanopore sequencing for DNA methylation. We found the levels of pAKT, a clinically used biomarker of targeted therapy, were constantly higher in clinical samples under physioxia compared to ambient air. Similar effects of O_2 tension on pERK and MDM4 levels occurred in cells isolated from ascites or pleural effusion in a time-dependent manner. A significant decrease in pEGFR and p53 levels were observed in cells under physioxia. Moreover, O_2 tension-dependent differences extended to key epigenetic regulators including TET2. TET2 levels were lower under physioxia compared to ambient air. Consistently, nanopore sequencing revealed distinct differences in DNA methylation patterns under physioxia and ambient air. The observed differences in signaling pathways extended to cultured cells from ascites fluids and pleural effusions. However, there is a specificity in the effects of O_2 tensions on biomarkers as we did not observe significant differences in pPDGFR$_\beta$, ATE1 and many other biomarkers under two O_2 conditions. These results imply that the O_2 tension affects specific biomarkers and epigenome. Collectively, O_2 tension could result in dynamic and extensive changes in cell membrane, cytoplasmic and nuclear biomarkers. Observable changes of biomarkers could occur within an hour following exposure to ambient O_2, and some changes could last for prolonged period. Thus, our current study lays out a new physiologically relevant biomarker validation/discovery platform, which may accelerate evaluation of physiologically relevant signaling networks, new drug discovery, and enhance clinical translation of preclinical observations.

#7294 SDHA isoform expression modulates reverse electron flow during hypoxia.

Kaveri Goel, Katie Pepper Lee, Nicholas Hill, Weiqi Lee, Neil Pfister

Radiation Oncology, University of Alabama at Birmingham, Birmingham, AL

Succinate dehydrogenase (SDH, also known as complex II) is a mitochondrial enzyme complex that directly connects the TCA cycle to the electron transport chain (ETC) via reductions of succinate to fumarate, leading to the reduction of coenzyme Q to high energy UQH2. The SDH complex is composed of four different subunits. SDHA and SDHB are the enzymatic subunits of SDH that forms the mitochondrial matrix-facing hydrophilic head whereas SDHC and SDHD are the hydrophobic mitochondrial inner membrane anchor subunits. When oxygen is present, electrons flow through the ETC, generating ATP, with oxygen serving as the terminal electron acceptor. However, hypoxic niches exist during a variety of physiological states including cancer where fumarate acts as an additional electron acceptor to regenerate CoQ for additional biological processes including pyrimidine biosynthesis. When SDH is utilized in reverse to recapture electrons onto fumarate, succinate is regenerated, leading to succinate accumulation in cancer cells in hypoxic conditions. It has been previously discovered that some tissues favor forward SDH activity (heart, lung) whereas other tissues (brain, kidney) favor the reverse flow. We hypothesized that different isoforms of SDHA, which contains the active site for the succinate to fumarate enzymatic reaction, could favor or disfavor forward and reverse flow of electrons through SDH and serve as a mechanistic basis for the previously observed experimental findings. We analyzed human tissue datasets and identified 3 major SDHA isoforms. We found tissue-specific differences in SDHA isoform expression with high expression of SDHA isoforms in kidney tissue, and low expression of SDHA isoforms in heart tissue, consistent with our hypothesis. We overexpressed SDHA isoforms in cancer cell lines and analyzed 13C15N-glutamine tracing to provide experimental support of our hypothesis that specific SDHA isoforms prioritize reverse electron flow under hypoxic conditions. We are currently assessing how CRISPR-Cas9 engineered cells to expression only one SDHA isoform (rather than combination of wild-type and variant transcript) affect cell responses to cancer therapy under normal and hypoxic conditions including epigenetic regulation of gene expression via the fumarate and succinate oncometabolites. This study will help us in identifying how SDHA isoforms contribute to cancer initiation and treatment strategies for hypoxic tumors.

#7295 The role of PHD2 inhibition in melanoma progression, metabolic adaptation, and therapy resistance.

Claire Erdaje Palma, Stephen M. F. Jamieson, Tet-Woo Lee, Dean Singleton

Auckland Cancer Society Research Centre, University of Auckland, Auckland, New Zealand

Therapy-resistant melanoma poses significant challenges due to its diverse phenotypes and limited treatment options. A strong dependency of melanoma cells on *EGLN1*, which encodes prolyl hydroxylase domain protein 2 (PHD2)—a key regulator of HIF-α degradation— is evident in large-scale dependency datasets, prompting us to investigate *EGLN1*/PHD2 as a potential therapeutic vulnerability. Melanoma cell lines were engineered using CRISPR-Cas9 to generate knockout (KO) models of *EGLN1*, *HIF1A*, and *HIF1AN*. Pharmacologic assays were performed using the PHD inhibitor roxadustat and the FIH inhibitor tool compound DM-NOFD. Proliferation was assessed in short- and long-term assays. Protein expression was analyzed by immunoblotting, and transcriptional changes were evaluated by RT-qPCR. Metabolic consequences were assessed by measuring NADH/NAD$^+$ ratios. To model resistance to BRAF + MEK inhibition (BRAFi+MEKi), two systems were generated: (1) TGFβ1-induced adaptive resistance and (2) drug-acquired resistance following continuous BRAFi+MEKi exposure. Resistance was confirmed by phosphorylated ERK immunoblotting and IC_{50} analysis.*EGLN1* KO reduced melanoma proliferation by 70–80% relative to control cells ($p < 0.05$). Roxadustat inhibited growth in a HIF-1α–dependent manner, with IC_{50} values of 40–80 μM in wild-type cells versus >100 μM in *HIF1A* KO cells. Long-term treatment with 10–20 μM roxadustat reduced wild-type proliferation by 30–70%, but only 0–10% in *HIF1A* KO cells. Disruption of *HIF1AN* or treatment with DM-NOFD enhanced roxadustat sensitivity, decreasing proliferation by 40–60%, an effect absent in *HIF1A* KO models. Roxadustat increased PHD2 protein levels and induced *EGLN1* transcription in wild-type cells, accompanied by upregulation of canonical HIF-1 targets (*LDHA, PDK1, BNIP3*). A 20–50% increase in the NADH/NAD$^+$ ratio after 4 h of roxadustat treatment indicated a metabolic shift toward reductive stress. In BRAFi+MEKi-resistant models, roxadustat enhanced BRAFi+MEKi potency and inhibited ERK phosphorylation, reversing MAPK pathway reactivation in A375 acquired-resistant cells, but had no effect in A375 *HIF1A* KO resistant models, demonstrating a requirement for HIF-1α. In TGFβ1-induced adaptive resistance, *HIF1A* was necessary for the development and maintenance of resistance phenotypes, indicating that HIF-1α signaling contributes to early adaptive BRAFi+MEKi tolerance. These studies demonstrate that PHD2 inhibition suppresses melanoma growth through HIF-1α stabilization and can be enhanced by concurrent FIH inhibition. The requirement of HIF-1α for both adaptive and acquired BRAFi+MEKi resistance and for roxadustat-mediated re-sensitization highlights a functional link between hypoxia signaling and therapeutic tolerance. These findings support continued evaluation of PHD2-directed strategies, including combination approaches, in melanoma.

#7296 A KRAS G12V-mutant patient-derived organoid model of brain metastasis as a target discovery platform.

Dena Panovska[1], Yao Lulu Xing[2], Maria Dolan[3], Helena C. M. Oft[4], Alexa Gwyn[5], Emon Nasajpour[6], Michitaka Nakano[7], John Newman[8], Calvin Kuo[7], Pardes Habib[2], Claudia K. Petritsch[6]

[1]Neurology, Stanford University, Stanford, CA,[2]Neurosurgery, Stanford University, Stanford, CA,[3]University of Virginia, Charlottesville, VA,[4]Neurology, University of Pittsburgh, Pittsburgh, PA,[5]Vassar College, Poughkeepsie, NY,[6]Neurology and Stanford Cancer Model Development Center, Stanford University, Stanford, CA,[7]Medicine-Hematology, Stanford University, Stanford, CA,[8]Pathology, Stanford University, Stanford, CA

Brain metastasis (BM) is the most common brain tumor, with annual incidence rates ranging from 8 - 14 cases per 100,000 people. In the past decade, eligibility criteria have broadened, advancing treatments for BM with molecular targeted therapies and immune checkpoint inhibitors. Unfortunately, this progress has not yet reached patients with rare forms of BM, such as those originating from colorectal cancer (CRC), which is the second leading cause of cancer death worldwide. BM from CRC (BM-CRC) have the poorest prognosis amongst metastatic CRCs, due to their inherent resistance to chemotherapy and radiation, underscoring the need for new therapeutic approaches. Drug development faces in oncology faces significant challenges and has a high attrition rate, largely due to tumor diversity and the limitation of traditional models, such as 2D cell cultures and animal testing, which often fail to replicate human tumor behavior. Additionally, the small patient cohorts for BM-CRC impede molecular studies necessary for development of evidence-based therapies and clinical guidelines We recently identified elevated levels of transcriptomic signatures for unfolded protein response (UPR) in BM-CRC, by analyses of a public dataset of single cell RNA sequencing data from 8 patients with BM-CRC. CellChat performed with these single cell data revealed interaction between tumor and tumor microenvironment (TME), which underlined the dependency of the tumor on specific components of the TME. We confirmed that the UPR, activated by endoplasmatic reticulum (ER) stress in cancer cells, is upregulated in BM-CRC compared to parental CRC, using multi-omic analyses. To investigate the UPR as a potential therapeutic vulnerability in patients, we generated a novel patient-derived organoid (PDO) from a therapy-resistant KRAS G12V mutant BM-CRC. PDOs reliably forms intracranial tumors in xenografts models and mirror the phenotypic and genetic features of the original malignant tumor reliably BM-CRC. Our preclinical data showed that pharmacologic inhibition of an ER stress-related pathway more effectively reduced PDO viability than MAPK inhibition alone. We furthermore conducted molecular analyses how the upregulation of the UPR influences cell states of BM-CRC, correlating with their poor prognosis. Taken together, our new PDO model was generated as a platform for drug discovery and to evaluate targeted therapies for treatment-refractory BM-CRC. Our preclinical and multi-omics data puts forward UPR as a therapeutic vulnerability.

#7297 HIF-1α pathway is a therapeutic vulnerability in mucinous colorectal cancer.

Yoojeong Seo, Jinho Jang, Kyung-Pil Ko, Jie Zhang, Sohee Jun, Jae-Il Park

Experimental Radiation Oncology, UT MD Anderson Cancer Center, Houston, TX

Mucinous colorectal cancer (muCRC) represents an aggressive and histologically distinct subtype of CRC characterized by abundant extracellular mucin, right-sided predominance, and poor therapeutic response. Despite its clinical relevance, muCRC-specific therapeutic options are not available.Through comparative single-cell transcriptomic profiling of over 360,000 cells from muCRC and non-muCRC tumors, we identified a hypoxia-inducible factor-1α (HIF-1α)-centered regulatory program as a defining transcriptional hallmark of muCRC.Regulon reconstruction revealed that HIF-1α activity coincides with SPDEF- and TFF3-driven mucinous lineage programs, linking hypoxia signaling to secretory differentiation. Immunohistochemical and spatial transcriptomic analyses confirmed marked elevation of HIF-1α protein and target gene expression in murine and patient-derived mucinous CRC models compared to non-mucinous counterparts.Functionally, pharmacologic inhibition of HIF-1α using PX-478 completely prevented mucinous tumor formation in the genetically engineered mouse models, restoring normal crypt architecture and markedly extending survival. Likewise, PX-478 treatment abolished mucin accumulation and tumor growth in cecum orthotopic patient-derived organoid xenografts. Mechanistically, HIF-1α inhibition suppressed SPDEF and MUC2 expression, indicating that hypoxia signaling sustains mucinous differentiation and tumorigenic capacity. Collectively, these findings identify HIF-1α as a molecular dependency and therapeutic vulnerability in muCRC. Together, these results provide a strong translational rationale for HIF-targeted therapy in mucinous and related serrated CRC subtypes.

#7298 Extracellular acidosis modulates calcium signaling and adaptive resistance mechanisms in acute myeloid leukemia.

Eva Gez[1], Sofia Titah[1], Aurelie Guillemette[1], Celine Berthon[1], Laure Goursaud[1], Nathalie Jouy[2], Loic Lemonnier[3], Salomon Manier[1], Carine Brinster[1], Suman Mitra[1], Bruno Quesnel[1], Yasmine Touil[1]

[1]Univ. Lille, CNRS, Inserm, CHU Lille, Institut Pasteur de Lille, UMR9020-U1277-CANTHER-Cancer Heterogeneity Plasticity and Resistance to Therapies, F-59000 Lille, France., Lille, France,[2]Univ. Lille, CNRS, Inserm, CHU Lille, Institut Pasteur de Lille, US 41 - UAR 2014 - PLBS, F-59000 Lille, France, Lille, France,[3]Univ. Lille, Inserm, U1003 - PHYCELL - Physiologie Cellulaire, F-59000 Lille, France., Lille, France

Acute Myeloid Leukemia (AML) is a malignant hematological disease with a high relapse rate linked to multiple resistance mechanisms, including leukemic stem cells, apoptosis resistance, and efflux pump activation. Previous work in the host laboratory demonstrated that calcium signaling contributes to these resistance pathways**.** At the same time, the Warburg effect induces extracellular acidosis, a hallmark of aggressive cancer phenotypes. This study investigates whether an acidic extracellular pH alters calcium signaling and thus participates in AML resistance mechanisms.

The MOLM-13 AML cell line was exposed to acidic (pH 6.5) or neutral (pH 7.4) conditions for various durations (“real-time,” 24 h, and 72 h). Cell proliferation and cycle distribution (Ki-67/IP), viability and apoptosis (Annexin V/IP), leukemic stem-like subpopulations ($CD34^+/CD38^-$), and efflux pump activity (rhodamine exclusion) were analyzed by flow cytometry. Expression of genes regulating pH and calcium homeostasis (STIM, ORAI, SERCA, PMCA families) was quantified by qPCR, and intracellular pH and Ca^{2+} fluxes were assessed by flow cytometry using fluorescent probes.

Preliminary results show that exposure to pH 6.5 transiently slows proliferation and induces G_1 arrest without loss of viability or apoptosis. Acidic pH rapidly increases multidrug resistance (MDR) activity, suggesting an adaptive response, but does not enrich for $CD34^+$ stem-like cells. At the signaling level, acidity downregulates STIM2, SERCA2, ORAI1, and PMCA1 expression and transiently inhibits store-operated calcium entry (SOCE), an effect that diminishes after 72 h, indicating cellular adaptation to the acidic environment.

These findings demonstrate that extracellular acidosis reshapes calcium signaling and efflux activity, enabling rapid metabolic and signaling adaptation in AML cells. Future work will include precise intracellular pH measurements, exploration of TRP channels and STIM2 isoforms, and single-cell RNA-seq to map transcriptional heterogeneity in acidic conditions, using both cell lines and patient-derived PBMC samples.

#7299 A new approach to lung cancer treatment: Targeting endoplasmic reticulum stress.

Chang Zou, Huibin Song, Sixiao He

Shenzhen People's Hospital, Shenzhen, China

Endoplasmic reticulum stress plays a pivotal role in responding to external stimuli, which is closely involved in cancer cell survival. However, its upstream regulatory mechanism has not been well elucidated. Previously we have reported that the methyltransferase like protein METTL7B promoted lung adenocarcinoma progression and TKI resistance mainly via its regulation of ROS metabolism, which may related to its mRNA methylation function. However, whether METTL7B could work as a mRNA methylator remains not clear. Our latest data indicated that the expression of METTL7B in LUAD cell lines was significantly negatively correlated with GRP78, IRE1 and XBP-1s, which are key signaling cohort in endoplasmic reticulum stress and the sensitivity of cells to anticancer drugs. On the other hand, METTL7B can up-regulate the mRNA methylation level and reduce the mRNA stability of GRP78, IRE1 and XBP-1s. Moreover, we also identify Proflavine Hemisulfate, a clinically used preservative agent, as a novel METTL7B inhibitor that potently suppresses its m^6A methyltransferase activity and inhibit the proliferation of lung adenocarcinoma cells in a dose-dependent manner. These findings provide a scientific basis for elucidating the RNA methyltransferase activity of METTL7B and new therapeutic target for lung adenocarcinoma.

#7300 SMARCA4 loss in endometrial cancer induces cell fate chaos concomitant with the senescence associated secretory phenotype and aberrant regulation of mTOR.

Hannah Plummer-Doherty[1], Mackenzie Coatham[2], Julia Vassalakis[1], Farzaneh Afzali[1], Bianca Dauber[1], Einav Renert[1], Tyler Cooper[3], Ivan Topisirovic[4], Cheng Han-Lee[5], Lynne-Marie Postovit[1]

[1]Department of Biomedical and Molecular Sciences, Queen's Univ. Cancer Research Inst., Kingston, ON, Canada,[2]Department of Oncology, University of Alberta, Edmonton, AB, Canada,[3]Department of Obstetrics and Gynecology, Centre de recherche du Centre hospitalier de l'Universite de Montreal, Montreal, QC, Canada,[4]Assistant Professor, Dept. of Onc., McGill University Lady Davis Institute, Montreal, QC, Canada,[5]Department of Pathology and Laboratory Medicine, University of Alberta, Edmonton, AB, Canada

Endometrial cancer is the most common gynecological malignancy worldwide, and incidence has been steadily on the rise. While the prognosis for localized endometrial cancer is excellent, some patients develop dedifferentiated endometrial cancer (DDEC), wherein the five year survival rate is less than 25%. DDEC is an advanced, rare subtype of endometrial cancer characterized pathologically by the mix of dedifferentiated and well differentiated tissue. We have discovered that the loss of *SMARCA4*, the catalytic subunit in the SWI/SNF complex, causes well differentiated endometrial cancer cells to form histologically undifferentiated lesions. SWI/SNF is a critical epigenetic modifier, which remodels chromatin by sliding and evicting nucleosomes. Evidence from our lab suggests that SMARCA4 loss causes epigenomic dysfunction in endometrial cells, leading to cell state chaos and the emergence of tissue that appears dedifferentiated. Interestingly, this chaos occurs only upon passaging *in vivo*, following an initial period wherein cells manifest a senescent-like phenotype. This phenotype is indicated by reduced growth, expression of B-galactosidase, and manifestation of the Senescence Associated Secretory Phenotype (SASP). This suggests that features of the growing tumor, such as hypoxia, may enable cell state chaos and that the SASP may characterize a transitional cell state. The mTOR pathway, which regulates metabolism, survival, and mRNA translation, has been shown to promote the SASP and is normally inactivated in response to cell stress, such as hypoxia. We hypothesize that SMARCA4 loss promotes the senescent-like phenotype by altering mTOR signaling, and that by enabling adaptations in mRNA translation, aberrant mTOR signaling underpins the emergence of cell state chaos and disease progression. We have shown that, in contrast to other cell types, SMARCA4 deficient cells do not respond to hypoxia with a reduction in mTOR activity. SMARCA4 KO cells maintain high levels of phosphorylation of many key effectors, like 4EBP1, under hypoxia. Interestingly, phosphorylation of eIF4E (a cap binding protein involved in translation initiation) is significantly decreased with SMARCA4 KO, under hypoxia and in normoxia. These results suggest there may be modulation to the translational machinery upon SMARCA4 KO. Indeed, SMARCA4 deficient cells maintain high levels of protein synthesis in hypoxia, suggesting a strong resistance to stress-induced reductions in mRNA translation. In conclusion, our results suggest that dysregulated mTOR activity, leading to uncontrolled mRNA translation, may underpin the emergence of cell fate chaos an aggressive dedifferentiated histopathology in endometrial cancers.

#7301 Effect of chronic exposure to acidic pH on the MOLM-13 acute myeloid leukemia cell line.

Aurelie Guillemette[1], Eva Gez[1], Sofia Titah[1], Celine Berthon[1], Laure Goursaud[1], Nathalie Jouy[2], Loic Lemonnier[3], Salomon Manier[1], Carine Brinster[1], Suman Mitra[1], Bruno Quesnel[1], Yasmine TOUIL[1]

[1]University of Lille, CNRS, Inserm, CHU Lille, Institut Pasteur de Lille, UMR9020-U1277-CANTHER-Cancer Heterogeneity Plasticity and Resistance to Therapies, Lille, France,[2]University of Lille, CNRS, Inserm, CHU Lille, Institut Pasteur de Lille, US 41 - UAR 2014 - PLBS, Lille, France,[3]University of Lille, Inserm, U1003 - PHYCELL - Physiologie Cellulaire, Lille, France

Acidification of the extracellular microenvironment (pHe ≈ 6.4-6.8) constitutes a major metabolic stress in cancers, promoting immune evasion, tumor progression, and therapy resistance. In our laboratory, we previously demonstrated the pivotal role of calcium signaling in the resistance mechanisms of leukemic cells. Acute myeloid leukemia (AML), a malignant hematologic disorder with a high relapse rate, exemplifies this issue through the persistence of leukemic stem cells, resistance to apoptosis, and enhanced efflux pump activity. Furthermore, the Warburg effect drives extracellular acidosis, favouring the emergence of aggressive, therapy-resistant phenotypes and altering intracellular metabolic and signaling pathways that support survival and proliferation.

This study aimed to determine whether prolonged exposure to acidic extracellular pH modifies the calcium signature of leukemic cells and contributes to adaptive resistance mechanisms in AML. Experiments were conducted on the MOLM-13 cell line, derived from a relapse case harboring an FLT3 tandem duplication. Cells were cultured for three weeks at acidic (pHe ≈ 6.5) or neutral (pHe ≈ 7.4) pH conditions to induce phenotypic adaptation. Flow cytometry analyses assessed viability and apoptosis (Annexin V/IP), cell-cycle distribution (Ki67/IP), and the leukemic stem cell fraction ($CD34^+/CD38^-$). Intracellular calcium dynamics and intracellular pH were monitored in real time using specific fluorescent probes, while efflux pump activity was quantified by rhodamine exclusion. Gene expression related to calcium homeostasis and pH regulation was evaluated by qPCR to assess transcriptional adaptations to chronic acid stress.

Preliminary results indicate that chronic exposure to acidic pH does not impair viability nor induce apoptosis or necrosis. Cell-cycle analysis shows increased G_0 and S phases with G_1 predominance, accompanied by a reduction in the stem-like fraction. Intracellular pH, calcium stores, and capacitive calcium influx are reduced, whereas efflux pump activity declines by approximately 10%. At the transcriptional level, NFATc1, STIM2, and PMCA4 are downregulated, whereas ORAI1 is overexpressed, suggesting the activation of adaptive or resistance mechanisms in response to sustained acidosis, which may support the survival of residual leukemic cells under metabolic stress.

Although preliminary, these findings highlight the significant impact of chronic extracellular acidification on calcium signaling and the adaptive capacities of leukemic cells. Further investigations, including precise intracellular pH quantification, extended acid exposure, and analyses of primary AML samples from diverse mutational backgrounds, will refine these observations and may ultimately facilitate the identification of novel calcium-related functional biomarkers and potential therapeutic targets to overcome resistance in AML.

#7302 Critical involvement of PRELID2 in the regulation of mitochondrial homeostasis in renal carcinogenesis.

Renpei Kato[1], Daiki Ikarashi[1], Shigekatsu Maekawa[1], Mitsugu Kanehira[1], Yosuke Matsushita[2], Tetsuro Yoshimaru[2], Tomoya Fukawa[3], Toyomasa Katagiri[2], Wataru Obara[1]

[1]Iwate Medical Univ., Iwate, Japan,[2]Laboratory of Biofunctional Molecular Medicine, National Institute of Biomedical Innovation, National Institutes of Biomedical Innovation, Health and Nutrition, Osaka, Japan,[3]Tokushima Univ., Tokushima, Japan

Background: Mitochondrial homeostasis is critical for tumor adaptation to oxidative stress in clear cell renal cell carcinoma (ccRCC). PRELID2, a mitochondrial intermembrane space protein involved in lipid trafficking, has not been studied in renal carcinogenesis. We identified PRELID2 as a novel regulator of mitochondrial function and potential therapeutic target in ccRCC.
Methods: RNA sequencing was performed on 178 ccRCC patient samples. In vitro and in vivo studies established PRELID2's functional roles in ccRCC proliferation and progression. Mitochondrial proteomics, lipidomics (LC-MS), oxidative stress assays, co-immunoprecipitation, and mass spectrometry were conducted for comprehensive analysis.
Results: PRELID2 was significantly elevated in ccRCC and correlated with poor prognosis in metastatic cases. Unlike other PRELI family proteins, PRELID2 specifically interacted with Prohibitin 2 (PHB2), a mitochondrial scaffolding protein. PRELID2 depletion increased mitochondrial oxidative stress, resulting in elevated oxidized peptides and reduced cytochrome c under stress conditions. Lipidomics revealed altered phosphatidylglycerol composition, a cardiolipin precursor. Xenograft experiments showed PRELID2 overexpression significantly enhanced tumor growth.
Conclusion: PRELID2 is a critical regulator of mitochondrial lipid homeostasis and oxidative stress resistance in ccRCC. The PRELID2-PHB2 interaction represents a potential therapeutic target for novel interventions in renal tumorigenesis.

#7303 Activation of HIF1α drives oxidative stress and promotes deep senescence in *EGFR*-mutant NSCLC drug tolerant persister cells.

Radhika Koranne[1], Avishai Wizel[2], Aimee J. Gleason[1], Justine Bellier[1], Heidie Cabanos[1], Sarah Reeves[1], Luke Boland[1], Yotam Drier[2], Aaron N. Hata[1]

[1]Krantz Family Center for Cancer Research, Mass General Brigham Cancer Institute, Boston, MA,[2]The Hebrew University of Jerusalem, Israel, Jerusalem, Israel

Non-small cell lung cancers with oncogenic mutations in EGFR (exon 19 deletions or L858R substitutions) are sensitive to EGFR tyrosine kinase inhibitors (TKIs), which induce deep and durable responses in the majority of patients. However, despite these responses, the development of acquired resistance to EGFR TKIs is inevitable. Preclinical studies have implicated a role for drug-tolerant persister (DTP) cells in the development of acquired drug resistance. DTPs are a subpopulation of cancer cells that survive initial TKI therapy by entering a reversible, slow-cycling or quiescent state. Mechanistically, DTPs leverage reversible, non-genomic mechanisms, including epigenetic plasticity, activation of survival signaling pathways, and lineage switching, to maintain a drug-tolerant state. Importantly, DTP cells can undergo further evolution and acquire mechanisms of drug resistance that drive disease relapse. To identify vulnerabilities of DTP cells, we characterized DTP cells in patient-derived xenograft models of *EGFR*-mutant NSCLC and malignant pleural effusions from patients treated with EGFR TKIs. We observed that HIF1-α (hypoxia-inducible factor 1 alpha) signaling was consistently downregulated in DTP cells across models and patients. Unexpectedly, stabilization and reactivation of HIF-1α with the prolyl hydroxylase inhibitor, resensitized DTP cells to EGFR TKIs and suppressed the emergence of drug-resistant clones. Mechanistically, HIF-1 αreactivation increases oxidative stress in DTPs and promotes entry to an irreversible deep senescence state. These results add to a growing body of evidence that mitigation of oxidative stress is critical for DTP survival and suggest that reactivation of HIF-1α signaling may provide a therapeutic strategy to prevent emergence of resistance in *EGFR*-mutant NSCLC.

#7304 Lactate mediated suppression of tumor intrinsic type I interferon response in luminal breast cancer cells.

Yaminisree Nagidi[1], Aidan Moriarty[1], Min Yu[2]

[1]University of Maryland School of Medicine, Baltimore, MD,[2]University of Maryland, Baltimore, MD

Tumor hypoxia significantly contributes to cancer development, promoting tumor growth and metastasis. Previous work in our lab has shown that long term hypoxia leads to a marked suppression of type I interferon (IFN) signaling within luminal breast tumor cells. Notably, this suppression was persistent even when hypoxic precultured cells were reoxygenated which is indicative of hypoxic memory. Understanding the basis of IFN pathway suppression is important, as diminished IFN signaling weakens antitumor immune response and can promote tumor cell proliferation and survival. Hypoxia is also known to induce metabolic reprogramming which results in lactate accumulation, acidifying the tumor microenvironment (TME), and function as a signaling metabolite that suppresses antitumor immunity. While lactate's role in inhibiting immune response within TME is well established, its role within tumor cells in regulating interferon signaling remains poorly understood. In this study, we aim to explore the mechanisms of lactate mediated suppression of type I IFN response in tumor intrinsic manner. We found that long term hypoxia increases lactate accumulation and reduced type I IFN signaling. We also observed that addition of extracellular lactate to cells cultured under normoxia is sufficient to suppress type I IFN signaling, whereas pharmacological inhibition of lactate dehydrogenase A (LDHA) activity restores IFN signaling in hypoxia. Recent discoveries show that lactate can directly alter gene expression through histone lactylation, a novel epigenetic modification. However, its role in breast cancer immune escape remains largely unexplored. We observed that increased lactate levels under hypoxia correlate with elevated histone lactylation. Determining whether histone lactylation alters gene expression that can enhance the activity of suppressors of type I IFN signaling would elucidate the mechanisms of how lactate mediate suppression of IFN signaling. By uncovering this mechanism, our findings may reveal new therapeutic strategies to restore interferon signaling and enhance immunotherapy efficacy in breast cancer.

#7305 Evaluating the unfolded protein response as a therapeutic target in clear cell renal cell carcinoma patients.

Timothy Shaw[1], Thushara Madanayake[2], Darwin Chang[3], Jay Mandula[4], Alyssa Obermayer[3], George J. Weiner[5], Dan Spakowicz[6], Bodour Salhia[7], Martin McCarter[8], Susanne Arnold[9], Aakrosh Ratan[10], Sheri L. Holmen[11], Stephen B. Edge[12], Julian Acevedo[13], Ayanambakkam Attanathi[14], Robert J. Rounbehler[15], Michelle Churchman[16], Ahmad Tarhini[3], Jose R. Conejo-Garcia[17], Brandon J. Manley[18], Paulo C. Rodriguez[3]

[1]Biostatistics and Bioinformatics, Moffitt Cancer Center, Tampa, FL,[2]Yale School of Medicine, New Haven, CT,[3]Moffitt Cancer Center, Tampa, FL,[4]The Ohio State University, Columbus, OH,[5]Director, University of Iowa Holden Comp. Cancer Center, Iowa City, IA,[6]The Ohio State University College of Medicine, Columbus, OH,[7]USC Norris Comprehensive Cancer Center, Los Angeles, CA,[8]University of Colorado Anschutz, Aurora, CO,[9]University of Kentucky, Lexington, KY,[10]The University of Virginia, Charlottesville, VA,[11]University of Utah Huntsman Cancer Institute, Salt Lake City, UT,[12]Roswell Park Comprehensive Cancer Center, Buffalo, NY,[13]Indiana University Simon Comprehensive Cancer Center, Indianapolis, IN,[14]University of Oklahoma Health Sciences Center, Oklahoma City, OK,[15]Aster Insights, Tampa, FL,[16]Aster Insights, Hudson, FL,[17]Duke University School of Medicine, Durham, NC,[18]H. Lee Moffitt Cancer Center & Research Institute, Tampa, FL

Metastatic clear cell renal cell carcinoma (ccRCC) is an incurable and lethal disease. While treatment of ccRCC has shifted toward antiangiogenic and immunotherapy combinations, long-term response is rare, underscoring the urgent need for novel therapeutic targets. We previously demonstrated in a murine model that therapeutic targeting of the unfolded protein response (UPR) via the mediator PKR-like ER kinase (PERK) can reverse tumor progression, immune suppression, and resistance to immune checkpoint blockade (ICB) (Mandula et al. Cancer Cell. 2022). Early-phase clinical studies are now evaluating PERK inhibition as a therapeutic strategy in solid tumors, including ccRCC. Here, we performed a retrospective analysis of patients with ccRCC using an analytical framework to estimate PERK activity from transcriptome data. We evaluated three independent ccRCC patient data sets - iATLAS patients treated with ICB (n = 296), ORIEN AVATAR patients treated with ICB (n = 85), and a TCGA treatment-naive cohort (n = 534). Across these datasets, PERK expression was associated with increased progression risk and worse overall survival. To evaluate the role of PERK in the context of endoplasmic reticulum (ER) stress, we generated a PERK knockout model using CRISPR gRNA in ccRCC cell lines and then challenged the cells with an ER stressor, thapsigargin. Interestingly, we found cytoplasmic vacuolization reminiscent of an unresolved unfolded protein response, ER swelling, and proteostasis disruption. Moreover, joint treatment with the PERK inhibitor AMG44 and thapsigargin significantly reduced viability in ccRCC cells. To further assess the therapeutic potential of PERK inhibition during standard-of-care therapy, we evaluated its impact during VEGF blockade. We observed decreased cell viability in PERK-silenced cells following cabozantinib (VEGF inhibitor) exposure, either through drug inhibition or genetic deletion. In summary, as clinical interest in PERK inhibition (PERKi) grows across multiple solid tumors, our findings highlight PERK as a potential therapeutic target in ccRCC and identify associated biomarkers that may inform future clinical strategies.

#7306 Does ribosomal protein haploinsufficiency induce cell competition in mammalian epithelia?.

Neha Joshi[1], Nicholas Baker[2], Eyemen Kheir[1]

[1]School of Medicine - Microbiology and Molecular Genetics, Uc-Irvine, Irvine, CA,[2]Uc-Irvine, Irvine, CA

Cell competition is a mechanism in which cells can be eliminated by neighboring cells with higher cellular fitness. Cell competition was discovered in Drosophila where heterozygosity for Ribosomal protein (Rp) gene mutations leads to elimination by cell competition with wild type cells. Rp gene haploinsufficiency is a common feature of aneuploid cells, and in Drosophila is largely responsible for the elimination of sporadic aneuploid cells. In mammals, Rp gene haploinsufficiency activates p53 through the nucleolar stress pathway. Cells with higher relative p53 activity are eliminated from mammalian epithelia, and p53 is also required for the selective removal of aneuploid cells from embryos. It has yet to be determined whether Rp gene haploinsufficiency leads to cell competition in mammals, how this depends on p53, and whether this contributes to aneuploid cell surveillance or tumor suppression. It is also not certain how Rp gene haploinsufficiency affects cells, other than activating the nucleolar stress pathway. We seek, using Crispr-based modification, to investigate the cellular effects of Rp gene haploinsufficiency, and to use epithelioid culture of mouse esophageal epithelium to measure cell competition in mosaic epithelia. We expect to gain insight into the contribution of Rp gene haploinsufficiency to tumor development and or cell competition to tumor suppression.

#7307 Cyclin-dependent kinase 5 (CDK5) contributes to Bruton tyrosine kinase inhibitor (BTKI) resistance via IRE1α/Xbp1s axis in mantle cell lymphoma (MCL).

Sonia Rodriguez-Rodriguez, **Keika Yan**, Andrew Chen, Dan Voung, Carly Roleder, Haifeng Shen, Tycel Phillips, Alexey Danilov

City of Hope, Duarte, CA

Resistance to BTKI is inevitable in MCL. While it may be partially driven by BTK mutations, full mechanisms are not understood. Here we evaluated the role of CDK5 in acquired BTKI resistance. We generated ibrutinib-resistant (IR) MCL cell lines (JeKo and Mino). RNA-seq of JeKo-IR cells showed that CDK5 was one of the upregulated genes with a fold change of 2.15 vs. parental cells, and findings were confirmed by IB. CDK5 is a proline serine/threonine protein kinase that modulates cell cycle proteins in neuronal tissue, however its role in cancer is not known. We established CDK5 overexpression (OE; by sgRNA) in JeKo and Mino cells. CDK5-OE cells exhibited enhanced proliferation and partial resistance to ibrutinib. By contrast, knockdown (KD; shRNA) of CDK5 in JeKo-IR and Mino-IR cell lines re-sensitized cells to ibrutinib. Treatment with GFB-12811, a selective CDK5 inhibitor, reduced proliferation of IR and CDK5-OE MCL cell lines in a dose dependent manner. We next evaluated CDK5 expression following activation of B-cell receptor signaling. IgM and BAFF crosslinking resulted in rapid increase in BTK phosphorylation which was accompanied by upregulated CDK5 protein levels. Furthermore, primary MCL cells cultured in BAFF- or CD40L-expressing stromal conditions (which induce ibrutinib resistance) upregulated CDK5. NSG mice xenografted with CDK5-OE JeKo cells exhibited inferior survival compared with mice xenografted with control cells. Mass spectrometry analysis of cell lines with manipulated CDK5 revealed >1000 differentially expressed proteins and >300 phosphosites, with cell cycle and metabolism-related pathways affected by CDK5. Kinase activity profiling revealed that 29 kinases were differentially active in CDK5-altered cells. In particular, Src kinase activation directly correlated with CDK5 expression. These findings were supported by RNA-seq and validated by immunoblotting. Furthermore, GSEA analysis of RNA-Seq revealed upregulation of the Unfolded Protein Response (UPR), Inflammatory response, Myc targets, p53 pathway and OxPhos in JeKo-IR cells. We next focused on the UPR. Both IR and CDK5-OE JeKo and Mino cells exhibited increased phosphorylation of IRE1α at Ser724 residue and upregulation of Xbp1, compared with control cell lines. By contrast, both pIRE1α and Xbp1 were decreased following CDK5-KD. Immunoprecipitation demonstrated a novel direct interaction between CDK5 and IRE1α. Finally, Xbp1-KD in JeKo-IR and Mino-IR cells led to reduced proliferation and viability, comparable to cells with CDK5-KD. In sum, CDK5 is overexpressed in MCL cells with acquired resistance to BTKi. Genetic or pharmacologic targeting CDK5 partially abrogates ibrutinib resistance. CDK5 contributes to BTKi resistance via modulation of the XBP1/IRE1α axis of the UPR pathway. Thus, CDK5 is a potential therapeutic target in MCL.

#7308 Older statins reduce metastatic potential in ccRCC: Mechanistic validation of SIM (selective inhibitor of metastasis) development.

Lily Wu[1], Junhui Hu[2], Moe Ishihara[1], Glen Brodie[3], Aino Siltari[4], Jimin Kim[1], Stuart Conway[3], Robert Damoiseaux[5], Teemu J. Murtola[6], Michael E. Jung[3]

[1]Molecular & Medical Pharmacology, University of California, Los Angeles, Los Angeles, CA,[2]Molecular & Medical Pharmacology, University of Califonia, Los Angeles, Los Angeles, CA,[3]Chemistry, University of California, Los Angeles, Los Angeles, CA,[4]Tampere University, Helsinki, Finland,[5]Department of Molecular & Medical Pharmacology, University of California, Los Angeles, Los Angeles, CA,[6]University of Tampere, Tampere, Finland

Purpose: Metastasis is the primary cause of mortality in clear cell renal cell carcinoma (ccRCC), and no current therapy prevents metastatic progression. We sought to define mechanism driving metastasis and develop small molecules capable of blocking dissemination.

Methods: Co-culture assays and xenograft models demonstrated that metastasis are promoted by interactions between VHL-deficient HIF1α-high (VHL$^-$HIF1α+) and VHL-proficient (VHL+) ccRCC cells, with the VHL$^-$HIF1α+ cells driving the metastasis by inducing proliferative and migratory programs in neighboring VHL+ cells. A high-throughput screen of over 18,000 small molecule compounds was undertaken to identify drugs selectively toxic to VHL$^-$HIF1α+ cells. Amongst the 2500 FDA approved drugs, 7 hits were identified, with 4 of them being older statins. Fluvastatin, being the most potent, was further tested for metastasis prevention in vivo. Transcriptomic and proteomic analyses compared older versus newer statins to assess HIF1α-dependent mechanisms. A population-based study of 17,792 RCC patients from the Finnish Cancer Registry linked cancer records with prescription data (1998-2018). Statins were classified as older (fluvastatin, simvastatin, lovastatin) or newer (atorvastatin, pravastatin, rosuvastatin). Logistic regression evaluated odds of metastatic presentation, and time-dependent Cox models assessed RCC-specific mortality, adjusting for demographics, comorbidities, tumor extent, and treatments.

Results: Screening identified fluvastatin (SIM-1) as a selective inhibitor, and medicinal chemistry yielded SIM-2 with >4-fold higher potency. Pre-treatment with fluvastatin reduced metastatic burden in vivo. Older statins showed more potent selective cytotoxicity against VHL$^-$HIF1α+ ccRCC cells than newer statins despite lower HMGCR affinity. HIF1α knockout abrogated fluvastatin sensitivity, suggesting its HIF1α dependence. Population analysis showed that pre-diagnostic use of older statins was associated with reduced odds of metastatic RCC at diagnosis, while newer statins did not reduce the risk of metastasis.

Conclusions: Mechanistic, pharmacologic, and epidemiologic data converge to identify older statins as inhibitors of metastasis acting through the HIF1α pathway. These findings support further development of SIMs towards achieving metastasis-preventive therapy for ccRCC.

#7309 Chronic extracellular acidosis drives metabolic plasticity and adaptive survival in multiple myeloma.

Hua-Ling Chen[1], Pei-Chu Tsai[1], Sheng-Chieh Lin[1], Fang-Yu Tsai[1], Shih Sheng Jiang[1], Chieh-Lin J. Teng[2], **Wun-Shaing Wayne Chang**[1]

[1]National Institute of Cancer Research, National Health Research Institutes (NHRI), Zhunan, Taiwan,[2]Division of Hematology/Medical Oncology, Taichung Veterans General Hospital, Taichung, Taiwan

Multiple myeloma (MM) is a plasma cell malignancy that evolves within the complex bone marrow microenvironment, where persistent extracellular acidosis exerts significant biological influence but remains insufficiently investigated. To elucidate the long-term impact of acidotic stress, we developed MM cell models chronically cultured under mildly acidic conditions, mimicking the gradual acidification seen during disease progression. This approach revealed a biphasic MM cellular response: early acidic exposure impaired proliferation, triggered apoptosis, and disrupted metabolic activity, whereas prolonged acidification induced a dynamic, reversible state marked by metabolic recovery, mitochondrial remodeling, and restored growth. Further transcriptomic profiling uncovered distinct gene expression programs associated with this chronic adaptation, including a set of acid-acclimated genes strongly correlated with disease stage and overall survival in MM patients. These findings suggest that extracellular acidosis is not a passive consequence of tumor metabolism, but a key determinant of MM progression by promoting adaptive metabolic plasticity and clonal evolution.

#7310 Interplay between HIF-1α and HIF-2α modulates TNBC phenotypes.

Aleksandra K. Kurowska, Long Chi Nguyen, Madeline Henn Bungert, Marsha Rich Rosner

The University of Chicago, Chicago, IL

Hypoxia-driven adaptation is a central feature of triple-negative breast cancer (TNBC) and contributes to its aggressive behavior. TNBC lacks ER, PR, and HER2 expression, which limits targeted treatment options. Hypoxia-inducible factors (HIFs), particularly the HIF-1α and HIF-2α isoforms, orchestrate the transcriptional response to low oxygen to maintain survival and metabolic programs, making them attractive therapeutic targets. HIF-1α is the main hypoxic responder in TNBC, but efforts to target it have failed in the clinic. The FDA approval of the HIF-2α inhibitor belzutifan for kidney cancer makes it urgent to determine whether inhibition may be effective in other solid tumors. Although HIF-1α and HIF-2α share some targets, their functions vary by cancer type, and the significance of HIF-2α in TNBC remains unclear. To address this, we investigated the individual and combined contributions of HIF-1α and HIF-2α in TNBC. Here, we show that HIF-2α is an important regulator in TNBC, in part due to previously unrecognized redundant or compensatory interactions between the two isoforms. Dual knockout of HIF-1α and HIF-2α did not further inhibit tumor growth compared to single knockouts, indicating functional overlap. Notably, HIF-2α acted antagonistically to HIF-1α and limited pro-metastatic effects, as HIF-2α knockout tumors showed increased metastatic burden in a syngeneic mouse model. This phenotype was supported by scRNA-seq analysis, which revealed elevated EMT hallmark signatures in HIF-2α-deficient xenograft tumors, and by *in vitro* observations where HIF-2α-deficient cells displayed a more invasive morphology. Some HIF-2α functions are context-specific and further shaped by the tumor microenvironment. Together, our findings reveal that HIF-1α and HIF-2α engage in redundant, compensatory, or antagonistic interactions dependent on the specific pathway. Thus, both factors contribute to stress responses, but HIF-2α also exhibits cancer-intrinsic functions that may potentially counteract the pro-metastatic effects of HIF-1α. Overall, these findings reveal the nuanced roles of HIF isoforms in tumor progression and highlight the need for careful consideration of HIF-2α targeting in TNBC therapy.

#7311 Characterization of PERK-positive polyploid-like breast cancer cells and their association with unfolded protein response signatures.

LUIS DEL POZO-YAUNER[1], Veronica Ramirez-Alcantara[2], Elba A. Turbat-Herrera[3], Hector Chavarria Bernal[1], Maha Babker[1], **Huseyin Kilic**[1], Rosetta Campbell[1], Bahaaeldin Youssef[1], Ajay Singh[4], Julio Isael Perez-Carreon[5], Wei Yang[6], Guillermo A. Herrera[1]

[1]Pathology, University of South Alabama College of Medicine, Mobile, AL,[2]USA Health Mitchell Cancer Institute, Mobile, AL,[3]University of South Alabama College of Medicine, Mobile, AL,[4]SOM-Cell and Molecular Biology, University of Mississippi Medical Center and Cancer Center and Research Institute, Jackson, MS,[5]National Institute of Genomic Medicine, Mexico City, Mexico,[6]Bruker Spatial Biology, Seattle, WA

Endoplasmic reticulum stress activates the unfolded protein response (UPR), a pathway linked to breast cancer (BC) progression, chemoresistance, and the formation of polyploid giant cancer cells (PGCCs). In a preliminary study, we identified a small subpopulation of breast cancer cells that were strongly positive for the phospho-PERK antibody in immunohistochemistry (IHC), some of which showed atypical mitosis and PGCC-like morphology. Because PGCCs are associated with tumor aggressiveness and poor outcomes, we hypothesize that the strongly PERK-positive BC cells represent PGCCs or their precursors and are enriched in tumors with active unfolded protein response (UPR) signaling. This study aimed to define the frequency of PERK-positive BC cells in BC, assess their association with UPR activation, and identify transcriptomic and proteomic features linked to tumors containing these cells. FFPE tissues from 131 BC patients (96 TNBC, 35 non-TNBC) were analyzed by IHC using antibodies against phospho-PERK, ATF6, and phospho-IRE1. All samples were collected before treatment. PERK-positive BC cells were defined as tumor cells with strong (3+) cytoplasmic and nuclear phospho-PERK staining. The IHC indicates an association between PERK-positive BC cells and tumors with a TNBC phenotype. These cells represent an heterogeneous population with broad variation in cell morphology and size, and mitosis status. Based on IHC results, 21 tumors (13 TNBC, 8 non-TNBC) were selected for nCounter multiomics, using BC360 and MO protein panel for transcriptomic and proteomic analysis, respectively. Eleven tumors contained abundant PERK-positive BC cells, while ten had few or none. Three normal breast tissues were included as controls. When breast cancer tumors with abundant PERK-positive BC cells were compared with those without, 388 genes were differentially expressed (p-value threshold 0.05), of which 296 had p-values < 0.01. Of them, SLPI, S100A7, SERPINB5, KIT, and PHGDH showed the most significant increase in expression (log fold-change >2.0), while 132 genes, including TFF1, PIP, TFF3, CDCA8, PAX5, IL24, and VEGFD, showed the most significant decrease in expression (log fold-change <-2.0). When BC tumors with abundant PERK+ cells were compared with normal breast tissue, 315 genes were differentially expressed (p-value threshold 0.05), of which 184 had p-values < 0.01. Of them, 28, including SPP1, KIFC1, CDK1, TOP2A, RRM2, CENPF, and MYBL2 had a log fold-change >2.0, while 94 genes, including APOD, ZBTB16, PDK4, RELN, TFF3, TIMP4, EGF, and VEGFD had a log fold-change <-2.0. Tumors containing abundant PERK-positive BC cells show clear evidence of unfolded protein response activation and a transcriptomic profile associated with aggressive behavior, metabolic reprogramming, and loss of differentiation.

This study was funded by a grant from the Breast Cancer Research Foundation of Alabama (BCRFA) to LPY.

: Metabolic Vulnerabilities in Pancreatic, Hepatic, and Renal Cancers
Poster Session

#7315 Polysulfides contribute to persulfidation of FSCN-1 to accelerate development of pancreatic ductal adenocarcinoma.

Makoto Suematsu[1], Takehiro Yamamoto[1], Minako Takizawa[1], Chiyoko Nishime[1], Masami Suzuki[1], Nobuyoshi Hiraoka[2]

[1]Central Institute for Experimental Medicine and Life Science, Kawasaki city, Japan,[2]Pathology, National Cancer Center Japan, Tokyo, Japan

We previously reported polysulfides (PS) are overgenerated in ovarian and breast cancers that contribute to worsening prognosis and chemoresistance (1, 2), while molecular mechanisms remain unknown. In this study, expression of PS-generating enzymes in post-operative pancreatic ductal adenocarcinoma (PDAC) tissues were examined immunohistochemically using FFPE samples from 120 Japanese patients. Analyses revealed that cystathionine γ-lyase (CSE) expressed in cancer-associated fibroblasts (CAF) serves as an independent factor worsening post-operative disease-free and overall survivals. CSE-positive CAF predominantly occurs in regions adjacent to cancer cells and activated glycolysis to deliver C1 units towards transsulfudation as judged by elevated methylation of PFKFB3 and PKM2 that activates the carbon delivery for serine-cysteine synthesis. Gold nanoparticle-based surface-enhanced Raman spectroscopy (SERS) imaging (3) using frozen PDAC tissues unveiled PS generation over the cancer tissues. PS renders cancer cells to induce site-specific persulfidation of fascin-actin-bundling protein (FSCN)-1 to stimulate the ability of cancer cells to migrate, while PS-degrading ambroxol or gemcitabine canceled the effects through their action to scavenge PS in vitro. These results suggest that PS serves as a marker inducing CAF-mediated cancer invasiveness.References
(1) Yamamoto T, et al. Cancer Res (2024)(2) Honda K, et al. Redox Biol (2021)(3) Shiota M, et al. Nature Commun (2018)

#7316 Targeting sulfatide metabolism as a therapeutic vulnerability in pancreatic pre-cancer lesions.

Riccardo Ballaro[1], Yihui Chen[1], Marta Sans[1], Fredrik Ivar Thege[1], Rongzhang Dou[1], Jimin Min[1], Michele Yip-Schneider[2], Jianjun Zhang[3], Ranran Wu[1], Ehsan Irajizad[1], Yuki Makino[1], Kimal Rajapakshe[1], Mark Hurd[1], Ricardo A. Leon-Letelier[1], Jody Vykoukal[1], Jennifer B. Dennison[1], Kim-Anh Do[1], Samir M. Hanash[1], Robert Wolff[1], Paola A. Guerrera[1], Michael Paul Kim[1], C. Max Schmidt[1], Anirban Maitra[1], Johannes Fahrmann[1]

[1]UT MD Anderson Cancer Center, Houston, TX,[2]Indiana University School of Medicine, Indianapolis, IN,[3]Indiana University, Indianapolis, IN

Asymptomatic precursor lesions that predate invasive pancreatic ductal adenocarcinoma (PDAC) by years provide a compelling opportunity for cancer interception. One such precursor is the intraductal papillary mucinous neoplasm (IPMN). Using Matrix-Assisted Laser Desorption/Ionization Mass Spectrometry (MALDI-MS) imaging and spatial transcriptomics, we discovered long-chain hydroxylated sulfatide species and their biosynthetic enzymes as selectively enriched in IPMN. Genetic ablation of UGT8 and Gal3st1, the key enzymes catalyzing the synthesis of the sulfatide precursor galactosylceramide (GalCer) and sulfatides, respectively, suppressed sulfatide production and triggered mitochondrial ceramide accumulation in mutant Kras;Gnas IPMN cells. These metabolic disruptions led to reduced proliferation and invasiveness, alongside increased caspase-dependent apoptosis. Pharmacologic UGT8 inhibition also caused profound impairments in mitochondrial function and morphology. Integrated lipidomic and proteomic analyses on mitochondrial fractions revealed remodeling of lipid composition and dysregulation of proteins involved in mitochondrial translation, oxidative phosphorylation, mitophagy and sphingolipid metabolism, corroborating the phenotypic changes observed in our functional studies. In vivo, UGT8 inhibition suppressed tumor growth in IPMN allograft models. Collectively, our findings identify enhanced sulfatide metabolism as an early metabolic alteration of cystic pre-cancerous lesions and demonstrate that targeting UGT8 perturbs mitochondrial homeostasis and function, revealing a potential strategy for pancreatic cancer interception.

#7317 Dual targeting of SLC6A14 and autophagy/macropinocytosis enhances therapeutic efficacy in pancreatic ductal adenocarcinoma.

Mosharaf Mahmud Syed[1], Devaraja Rajasekaran[1], Souad R. Sennoune[1], Tanima Sharker[1], Oscar Sanchez[1], Mary Katherine Jurek[2], Longfa Kou[3], Ruijie Chen[3], Vadivel Ganapathy[1], Yangzom D. Bhutia[1]

[1]Cell Biology and Biochemistry, Texas Tech University Health Sciences Center, Lubbock, TX,[2]Psychiatry, Tufts Medical Center, Boston, MA,[3]Pharmacy, Wenzhou Municipal Key Laboratory of Pediatric Pharmacy, The Second Affiliated Hospital and Yuying Children's Hospital of Wenzhou Medical University, Wenzhou, China

PDAC is highly desmoplastic and undergoes metabolic reprogramming to sustain their growth and proliferation. Our laboratory has identified SLC6A14, an amino acid transporter, as a novel drug target for PDAC. Genetic deletion of SLC6A14 or its pharmacological blockade with α-MLT attenuates PDAC growth by inducing amino acid deprivation. However, nutrient stress, particularly amino acid deprivation, can induce nutrient scavenging mechanisms like autophagy and macropinocytosis, thereby undermining the full anticancer potential of SLC6A14 blockade. To address this, the current work was conducted to test if SLC6A14 blockade induces autophagy and/or macropinocytosis and to further investigate if dual inhibition of SLC6A14 (α-MLT) and autophagy/macropinocytosis (HCQ) would yield a better therapeutic outcome in PDAC as opposed to targeting SLC6A14 alone. In vitro assays (MTT and colony formation) revealed that the combination treatment significantly reduced PDAC cell viability and clonogenic potential as opposed to monotherapy. Treatment model subcutaneous xenograft in athymic nude mice demonstrated a superior therapeutic outcome with the combination regimen. Collectively, our study demonstrates that the afore-described combination therapy creates a metabolic trap wherein α-MLT induces nutrient stress, while HCQ prevents autophagic and macropinocytosis compensation, thus culminating in a more potent tumor attenuation. This dual blockade represents a hitherto unexplored treatment strategy for PDAC.

#7318 Pancreatic ductal adenocarcinoma causes altered whole-body iron distribution.

Amit Roopan, Subin Pyo, Yichi Zhang, Anna Barbeau, ChiHin Feng, Matthew G. Vander Heiden

Koch Institute for Integrative Cancer Research at MIT, Cambridge, MA

Anemia of chronic disease is a prevalent form of anemia that occurs in patients with acute or chronic immune activation associated with multiple diseases, including cancer. A hallmark of anemia of chronic disease is disturbed iron homeostasis, where iron uptake and retention within the reticuloendothelial system and within peripheral tissues is increased to divert iron away from circulation and into storage sites, limiting availability for erythropoiesis. We observe in PDAC mice and patients that they exhibit anemia of chronic disease and find in different mouse models of PDAC that iron availability is decreased in circulation and that instead iron is being stored in peripheral tissues such as muscle, pancreas, liver, spleen, and many other organs and tissues. Our laboratory has shown that impaired exocrine function is a key driver of peripheral tissue wasting in PDAC and that decreased pancreatic enzyme secretion can be used for early diagnosis of PDAC. Therefore, we wondered whether intestinal iron absorption is decreased in PDAC and surprisingly found increased intestinal iron absorption in PDAC due to upregulation of the enterocyte iron importer DMT1 and iron exporter Ferroportin. Iron uptake from diet and iron sequestration into peripheral tissues can be studied through isotope tracing experiments. Fe56 is the predominant naturally abundant iron isotope so we used an Fe57-infused diet to study the kinetics of Fe57 intake and found that Fe57 is less abundant in the serum from PDAC mice compared to wildtype mice, suggesting that iron is quickly sequestered from circulation and into peripheral tissues. We are now focusing on identifying the regulators of increased intestinal iron absorption and iron sequestration in the context of PDAC.

#7319 Targeting HDAC1 activity presents vulnerabilities in pancreatic cancer metabolism.

Don-Gerard C. B. Conde[1], Evan J. Zhou[2], Soren Jensen[1], Maximillian Farma[2], Chiamaka Joy Ezeh[2], Alexander N. Behram[1], Phuong T. N. Pham[1], Nabila N. Binti[1], Laiba Shiekh[2], Matthew C. Cheung[2], Zeribe Nwosu[2]

[1]Molecular Biology and Genetics, Cornell University, Ithaca, NY,[2]Cornell University, Ithaca, NY

Pancreatic cancer is a lethal disease with significant metabolic reprogramming, which promotes tumor growth, therapy resistance, and adaptation to stress. These alterations are largely attributed to mutations in the KRAS oncogene but with limited progress in therapeutic discovery. Despite the recent focus on metabolism in pancreatic cancer, the major mediators of altered metabolism remain unknown. Our differential gene expression analyses in multiple patient cohorts' pancreatic tumors versus normal tissues identify histone deacetylase 1 (HDAC1) as a consistently upregulated epigenetic gene. HDAC1-high tumors correlate strongly with metabolic pathways, including glycolysis, redox metabolism, and nucleotide biosynthesis. Using CRISPR/Cas9 gene editing, we found that the deletion of HDAC1 in pancreatic cancer cell lines triggers metabolic shifts, notably in glucose metabolism, and led to a distinct growth phenotype in a cell context-dependent manner. Similarly, treatment with class I selective HDAC inhibitors was selectively effective in suppressing pancreatic cancer cell growth. Furthermore, our drug screenings demonstrate profound synergies that overlap across the HDAC1-deleted and HDACi treated cell lines that present under-explored avenues for therapeutics. Our data provides evidence of compensatory metabolic alterations upon HDAC1 inhibition, which could broaden the opportunities for therapeutic intervention in pancreatic cancer.

#7320 KRAS-PIP5K1A-SDC1 axis regulates nutrient scavenging in pancreatic cancer.

Sommer H. Ramos, Oisun Jung, Suyong Choi

Eppley Institute For Cancer Research, University of Nebraska Medical Center, Omaha, NE

Pancreatic ductal adenocarcinoma (PDAC) is a lethal malignancy with limited treatment options and a five-year survival rate of 13%. A defining characteristic of PDAC is its ability to survive and proliferate in nutrient-deprived environments. This is driven by metabolic reprogramming induced by mutant KRAS, which is present in over 90% of cases. However, the mechanism by which mutant KRAS coordinates the metabolic adaptation remains incompletely understood. We have discovered recently that mutant KRAS directly interacts with Phosphatidylinositol-4-Phosphate 5-Kinase Type I Alpha (PIP5K1A), a lipid kinase responsible for generating phosphoinositide phosphatidylinositol 4,5-bisphosphate ($PI4,5P_2$) and enhances its enzymatic activity. Upon activation by mutant KRAS, PIP5K1A generates elevated levels of $PI4,5P_2$ at the plasma membrane, allowing $PI4,5P_2$ to associate with Syndecan-1 (SDC1), a transmembrane heparan sulfate proteoglycan. The goal of this study is to define the roles of SDC1 and PIP5K1A in two major nutrient acquisition pathways: macropinocytosis-mediated uptake of extracellular proteins and SDC1-dependent regulation of Glucose Transporter 1 (GLUT1), to promote enhanced glucose uptake in pancreatic cancer cells. In CFPAC-II cells, we observed the co-localization of $PI4,5P_2$, PIP5K1A, KRAS, and SDC1 at membrane ruffles, consistent with macropinocytic structures. In-vitro binding assays demonstrated a direct interaction between the SDC1 extracellular domain and nutrient transporters GLUT1 and CD98. Additionally, glucose uptake assays showed that knockdown of either SDC1 or PIP5K1A significantly decreased glucose uptake in KPC cells. Together, these findings identify a novel KRAS-PIP5K1A-SDC1 signaling axis that regulates nutrient acquisition in PDAC, highlighting a potential therapeutic strategy to disrupt nutrient scavenging in KRAS-driven pancreatic cancer.

#7321 The link between metabolism and inflammation in Black African pancreatic ductal adenocarcinoma patients.

Nnenna Elebo[1], Dupe Ojo[2], Jones A.O. Omoshoro-Jones[1], Stefano Cacciatore[2], John Devar[1], Ekene E. Nweke[1]

[1]Surgery, University of Witwatersrand, Johannesburg, South Africa,[2]Bioinformatics, International Centre for Genetic Engineering and Biotechnology, Capetown, South Africa

Background: Pancreatic Ductal Adenocarcinoma (PDAC) remains one of the most lethal cancers globally, with increasing incidence among Black African populations. Emerging evidence suggests that the interplay between metabolic dysregulation and inflammation may play crucial roles in the pathogenesis and progression of PDAC. However, this relationship remains underexplored in African cohorts.

Methods: We conducted an untargeted metabolomics study using Nuclear Magnetic Resonance (NMR) spectroscopy on plasma samples obtained from consenting participants comprising 81 PDAC patients (57 resectable, 15 locally advanced, and 9 metastatic), 6 chronic pancreatitis patients, and 6 healthy controls. Reactive oxygen species (ROS) levels were quantified using the OxiSelect™ In Vitro ROS/RNS Assay Kit (Green Fluorescence). Group comparisons were performed using Wilcoxon and Kruskal-Wallis rank-sum tests, while Spearman's correlation and Kaplan-Meier analyses were applied for correlation and survival assessment. A p-value < 0.05 was considered statistically significant.

Results: Total bilirubin (p = 0.004), conjugated bilirubin (p = 0.003), alanine aminotransferases (p = 0.01) and aspartate aminotransferases (p = 0.03) levels were significantly altered across the groups. Metabolomic profiling revealed elevated levels of 2-hydroxybutyrate (2-HB, p = 0.004) and acetoacetate (p = 0.009) with advancing tumor stage. PDAC patients were stratified into "high" and "normal/low" 2-HB groups, with the top 25% representing the "high" group. Furthermore, lower 2-HB concentrations were associated with longer survival outcomes. Although not statistically significant, patients with high 2-HB exhibited increased ROS/RNS levels compared to those with low 2-HB. There was a positive correlation between 2-HB and inflammatory markers: GlycA (rho=0.07, p=0.64), GlycB (rho=0.07, p=0.66), CRP (rho=0.49, p=0.08) and White cell count (rho=0.48, p=0.08).

Conclusion: This study demonstrates a potential link between altered metabolic pathways and oxidative stress in Black African PDAC patients. Elevated 2-HB and acetoacetate may serve as metabolic indicators of tumor progression and poor prognosis. These findings highlight the importance of integrating metabolic and inflammatory profiling to better understand PDAC biology in African populations.

#7322 Vav1 promotes pancreatic tumor cell invasion via GLS1-dependent glutamine metabolism.

Mustafa Emre Gedik[1], Omar L. Gutierrez-Ruiz[2], Katherine M. Johnson[1], Ella Rose D. Chianis[1], Jing Chen[3], Alex Bittner[4], Adam Zahm[1], Ankit Chhoda[1], Taro Hitosugi[5], Mark A. McNiven[3], Gina Razidlo[1]

[1]Department of Biochemistry and Molecular Biology, Mayo Clinic, Rochester, MN,[2]Division of Hematology, Mayo Clinic, Rochester, MN,[3]Division of Gastroenterology and Hepatology, Mayo Clinic, Rochester, MN,[4]St. Olaf College, Northfield, MN,[5]Department of Oncology, Mayo Clinic, Rochester, MN

Pancreatic ductal adenocarcinoma (PDAC) is an aggressive malignancy due in part to metabolic rewiring and a high rate of metastasis. Pancreatic tumors are particularly dependent upon glutamine (Gln) as a nutrient source for multiple metabolic pathways. To adapt to low levels of glutamine, PDAC cells upregulate the Rac1 dependent process of macropinocytosis, which internalizes extracellular macromolecules to scavenge them as a glutamine source. The proto oncogene Vav1 is an activator of the potent Rac/Cdc42 signaling cascades that regulate actin dynamics. While Vav1 is normally restricted to hematopoietic cells, Vav1 expression is significantly increased in PDAC, with high Vav1 correlating with worse overall survival. Here we uncover a novel Vav1 mediated regulation of glutamine metabolism in PDAC cells. While Vav1 is a potent activator of Rac1, surprisingly, Vav1 expression inhibited macropinocytosis in PDAC cells. Intriguingly, genomic and metabolomic analysis revealed that high Vav1 expression correlates with increased dependence on glutamine and glutamate (Glu) metabolism. Indeed, Vav1 dependent macropinocytosis was rescued by cell permeable glutamate, confirming disrupted Gln/Glu balance in Vav1 knockdown cells. RPPA screening indicated a Vav1 dependent effect on glutaminase 1 (GLS1, KGA isoform), which converts glutamine to glutamate. Mechanistically, we discovered that Vav1 modulates GLS1 localization to the mitochondria through regulation of GLS1 posttranslational modification. Disrupting GLS1 localization by deleting its mitochondrial targeting motif phenocopied loss of Vav1 in reducing the invasive potential of tumor cells. Investigation of Vav1 dependent metabolic consequences showed that knockdown of Vav1 alters 13C Gln derived metabolic flux into the TCA cycle, as well as a deficiency in the level of the antioxidant glutathione (GSH), which utilizes glutamate for its synthesis. Consequently, targeting Vav1 resulted in increased levels of cellular and mitochondrial reactive oxygen species (ROS) and increased sensitivity to lipid peroxidation. Notably, dual targeting of both glucose and glutamine pathways showed significant synergistic effects on cellular viability in Vav1 expressing cells. Here we established a new tumor promoting role for Vav1 via Gln/Glu regulation and uncover a novel subcellular regulation of mitochondrial glutamine metabolism. Our findings establish Vav1 as a critical regulator of metabolic rewiring in PDAC and orchestrates glutamine metabolism by controlling the KGA isoform of GLS1 mitochondrial localization. Importantly, Vav1 functions as a signaling adapter in glutamine metabolism, providing a potential therapeutic vulnerabilities for PDAC patients with high Vav1 expression.

#7323 ACADS-dependent fatty acid oxidation drive mitochondrial remodeling in pancreatic cancer cells.

Madison Brown-Blackshear, Divine Asamoah, Nadiya Harris, Mengistu Lemecha

Hampton University, Hampton, VA

Pancreatic ductal adenocarcinoma (PDAC) is a highly aggressive cancer projected to become the second leading cause of cancer-related deaths by 2030. While PDAC cells rely primarily on glycolysis, emerging evidence indicates that mitochondrial metabolism also contributes to tumor survival. The metabolic impact of stromal fibroblasts on pancreatic cancer mitochondria, particularly through fatty acid oxidation (FAO), remains poorly understood. Here, we investigated whether fibroblast exposure alters mitochondrial remodeling in PDAC cells and if this remodeling depends on mitochondrial fatty Acyl-CoA Dehydrogenase (ACADS) mediated FAO. Mitochondrial changes were assessed in Panc1 cells cultured alone and co-cultured with 3T3-L1 fibroblasts. MitoTracker Red staining and confocal microscopy were used to visualize mitochondrial content. Mitochondrial and metabolic proteins were quantified with Western blotting. Carnitine Palmitoyltransferase 1 (CPT1) was inhibited using Etomoxir (5-100 μM, 24 hrs). Compared with fibroblasts grown separately, Panc1 cells showed lower baseline mitochondrial mass. However, when direct co-cultured, Panc1 cells exhibited increased mitochondrial content and elevated expression of ACADS and Mitochondrially Encoded Cytochrome c Oxidase (MTCO1), suggesting mitochondrial adaptation in response to fibroblast interaction. To test whether this remodeling required downstream short-chain FAO, we inhibited CPT1, the rate-limiting enzyme for mitochondrial fatty-acid import. Although CPT1 does not directly regulate ACADS, Etomoxir-mediated CPT1 inhibition significantly decreased ACADS levels, consistent with reduced FAO flux. CPT1 blockade also triggered metabolic stress, evidenced by increased phosphorylated AMP-activated protein kinase alpha (p-AMPKα), and resulted in a dose-dependent increase in Dynamin-Related Protein 1 (DRP1), indicating enhanced mitochondrial fission and dysfunction. Collectively, our preliminary data suggests that PDAC cells depend on intact fatty-acid oxidation to maintain mitochondrial integrity.

#7324 HER3 mediates metabolic reprogramming in metastatic colorectal and pancreatic cancer.

Moeez Ghani Rathore, Chao Wei, Kimberly Curry, Mehrdad Zarei, Zhenghe Wang, Jordan Winter, Rui Wang

Case Comprehensive Cancer Center, Cleveland, OH

Background: Liver metastasis occurs in ~80% of all metastatic colorectal cancer (mCRC) and metastatic pancreatic cancer (mPC), and the liver has a unique microenvironment that promotes cancer cell survival. Prior studies from our group and others have reported that the liver endothelium and hepatocytes secrete soluble factors (NRG1 and LRG1) that activate the cancer-associated HER3 signaling pathway and promote cancer growth. This study examines the impact of HER3 signaling on the metabolism of mCRC and mPC, aiming to identify a novel therapeutic approach.

Methods: We performed mass spectrometry to profile the metabolic changes in mCRC and mPC tumors with/without HER3 inhibition in a syngeneic, orthotopic mouse model with hepatic injection. We also performed in vitro metabolic assays to determine the effect of HER3 ligands on the metabolism of CRC and PC. To further define the role of HER3 in metabolic reprogramming, we used siRNA silencing of HER3 and pharmacological inhibition of HER3 downstream signaling proteins to identify the key mediator(s) of HER3-induced metabolic shift. We performed in vitro synergy studies combining HER3i (Sapitinib) with oxidative phosphorylation (OXPHOS) inhibitors (metformin and ivosedinib). To further determine the synergistic efficacy *in vivo*, we established syngeneic, orthotopic metastases of mCRC/mPC in the liver via hepatic injection and treated the mice with HER3 and OXPHOS inhibitors.

Results: We found that HER3 ligands increase cell acidification and lactate secretion (as measured by Seahorse FX and ELISA, established readouts of glycolysis) while simultaneously reducing oxygen consumption and mitochondrial membrane potential (as measured by Seahorse FX and TMRE, key indicators of oxidative phosphorylation metabolites, OXPHOS). We found that PFK2 is activated by HER3 signaling, as determined by phosphorylation, and that the HER3-AKT/RSK-PFK2 signaling axis is the key mediator of HER3-induced glycolysis. We then determined that HER3 inhibition decreased glycolysis readouts but induced an adaptive survival strategy by causing a metabolic shift towards OXPHOS. Thus, we found that simultaneous inhibition of HER3 and OXPHOS synergistically blocked the growth of cancer cells *in vitro* and led to an unprecedented 70% complete response in mouse models with orthotopic mCRC/mPC liver metastases.

Conclusions: We identified the HER3-AKT/RSK-PFK2 axis as a promoter of glycolysis and growth in CRC/PC liver metastases. Leveraging the discovery of metabolic shifting towards OXPHOS caused by HER3 inhibition, we identified a potential therapeutic strategy of combining HER3 inhibitors and OXPHOS inhibitors for treating patients with mCRC/mPC.

#7325 Cytosolic transport of citrate protects nutrient-austere pancreatic cancer from ferroptosis.

Adam Kneebone[1], Kailey Lindaur[1], Ata Abbas[2], Joel Cassel[3], Sarah Graff[4], Caudia Rose Keating[1], Gerard Abood[1], Xianzhong Ding[1], William Small[5], Clodia Osipo[1], Wei Qiu[1], Curtis Tatsuoka[6], Simone Sidoli[4], Costas Andreas Lyssiotis[7], Joseph M. Salvino[3], Ali Vaziri-Gohar[1]

[1]Loyola University Chicago Stritch School of Medicine, Maywood, IL,[2]Case Western Reserve University, Cleveland, OH,[3]The Wistar Institute, Philadelphia, PA,[4]Albert Einstein College of Medicine, New York, NY,[5]Professor, Loyola University Medical Center, Maywood, IL,[6]University of Maryland, Baltimore, MD,[7]University of Michigan, Ann Arbor, MI

Pancreatic cancer (PDAC) cells experience nutrient starvation in a poorly perfused tumor microenvironment. Metabolic dependencies that protect PDAC cells from detrimental oxidative stress in a nutrient-restricted niche represent as tumor-specific targets. While the role of mitochondria in supporting energy production and biosynthetic requirements of cells has been well investigated, their contribution to maintaining intracellular redox homeostasis when PDAC cells are exposed to nutrient deprivation is unknown. Our results demonstrate that cytosolic transport of citrate via SLC25A1 confers a survival advantage to PDAC cells by protecting them from ferroptosis, a well-established iron-dependent cell death mechanism, under nutrient-limited conditions. Employing selective SLC25A1 inhibitor or targeting mitochondrial OXPHOS dramatically reduced GPX4 expression and PDAC cell viability. Rescuing GPX4 expression with the products of both ACLY and ACO1-dependent pathways uncovered their critical role in conferring survival advantage under metabolic stress. Importantly, exogenous expression of GPX4 reversed redox imbalance and metabolic discordance resulting from the lack of SLC25A1 activity, indicating the requirement of citrate-induced GPX4 expression to support mitochondrial health and function. As observed with cultured cells under nutrient limitation, SLC25A1 function was revealed to be indispensable in pancreatic tumor microenvironment, and the reduced growth, due to the lack of SLC25A1 activity, was rescued with antioxidant NAC in preclinical models of PDAC. Lastly, SLC25A1 suppression was accompanied by elevated glutamine metabolism, and combination therapy with pharmacologic inhibitors of SLC25A1 and glutaminase inhibitor CB-839 dramatically suppressed tumor growth, highlighting this combinatorial approach as a potential therapeutic strategy in PDAC.

#7326 PU-H71 alters metabolism to suppress growth in pancreatic cancer.

Chiamaka J. Ezeh, Darren Binder, Leo Li, Zeribee C. Nwosu

Molecular Biology and Genetics, Cornell University, Ithaca, NY

Pancreatic ductal adenocarcinoma (PDAC) is a deadly cancer with limited therapeutic options. Oncogenic KRAS signaling, mainly via the mitogen-activated protein kinase (MAPK) pathway, is the key driver of PDAC. To sustain its growth and resist therapy, PDAC tumors continuously reprogram their metabolic activities. To identify therapeutic agents capable of disrupting these adaptive survival activities, we performed a high-throughput drug screen of >2,000 compounds in two PDAC cell lines. This screen identified PU-H71, a selective epichaperome and heat shock protein 90 inhibitor, as a potent suppressor of PDAC viability. PU-H71 reduced short-term cell growth and impaired clonogenic survival across multiple PDAC models. Metabolomics profiling revealed that treatment with PU-H71 consistently altered intracellular amino acid levels, metabolites in key biochemical pathways, and caused a significant shift in extracellular metabolites, suggesting coordinated changes in metabolite flux and utilization. Further, treatment of PDAC cells with PU-H71 reduced the phosphorylation of mTOR-associated signaling components and suppressed the MAPK signaling pathway. Together, these findings indicate that PU-H71 disrupts PDAC survival by simultaneously perturbing metabolic programming and growth signaling networks. Our results identify PU-H71 as a promising therapeutic agent for targeting the crosstalk between metabolism and signaling programs that promote PDAC growth and therapeutic resistance.

#7327 Dissecting lysosomal metabolic dependencies in pancreatic cancer through functional genomics.

Caleb Cheng[1], Ruya Pakkan[1], Jasmine Wisniewski[1], Sydney Peters[2], Yuanyuan Qiao[2], Costas Andreas Lyssiotis[1], Arul Chinnaiyan[1]

[1]University of Michigan, Ann Arbor, MI,[2]University of Michigan Medical School, Ann Arbor, MI

BACKGROUND:Lysosomal nutrient recycling and acquisition pathways employed at an elevated capacity in pancreatic cancer cells in response to the harsh metabolic microenvironment in which they subsist. We have others have previously studied autophagy or lysosomal inhibition strategies and identified the metabolic adaptations they effect on cancer cells. These studies have thus suggested that the lysosome plays a role in regulating iron, lipids, nucleotides, and amino acids, among other nutrients. However, these studies have differed in their experimental approaches, pharmacological agent, and molecular targets, and it is unclear whether these multiple conclusions are broadly generalizable across all autophagy or lysosome inhibition strategies.
METHODS AND RESULTS:To address these issues, here we perform parallel metabolism-focused CRISPR activation and knockout screens using 8 different autophagy or lysosome inhibitors in pancreatic cancer cell lines. From these, we determined that iron homeostasis is primarily affected by agents that affect lysosomal pH, such as bafilomycin A1 and Ammonium, but not by other inhibitors of lysosomal function such as apilimod, ESK981, or chloroquine, or by ULK1 inhibitors ULK101, SBI-0206965, or DCC-3116. Pairing the CRISPR screen data with transcriptomics, we further identified that lipid homeostasis was affected by all lysosome inhibitors but not ULK inhibitors. These multi-omics approaches specifically highlighted Farnesyl Diphosphate Synthase (FDPS), a gene involved in cholesterol synthesis as a prominent metabolic vulnerability revealed upon lysosome inhibition, whether with chloroquine, bafilomycin A1, or apilimod.
DISCUSSION:Our study demonstrates a clear metabolic distinction between inhibiting autophagy compared to inhibiting the lysosome. Our data further highlight that disturbances in lipid metabolism are a general effect of lysosome inhibition, while disruptions in iron homeostasis may primarily be due to disturbances in lysosomal pH.

#7328 EPR imaging of oxygen consumption driven by NQO1-activated compounds in FH-deficient renal tumors.

Yuki Shibata[1], Shun Kishimoto[2], Ye Yang[1], Ming-Hui Wei[1], Julia Medina-Velazquez[1], Burchelle Blackman[3], Jeeva Munasinghe[4], Viraj Chegu[1], Vaishnavi S. Srirama[1], Tyler A. On[1], Nallathamby Devasahayam[2], Chandramouli V. Gadisetti[5], Jeffrey R. Brender[6], Murali C. Krishna[2], **Daniel R. Crooks**[1], William Marston Linehan[7]

[1]Urologic Oncology Branch, National Cancer Institute, Bethesda, MD,[2]National Cancer Institute, Bethesda, MD,[3]Chemical Synthesis Center, National Heart Lung and Blood Institute, Bethesda, MD,[4]National Institute of Neurological Diseases and Stroke, Bethesda, MD,[5]President, GenEpria Consulting Inc., Columbia, MD,[6]Radiation Biology Branch, National Cancer Institute, Bethesda, MD,[7]National Cancer Institute, Berhesda, MD

Patients with hereditary leiomyomatosis and renal cell carcinoma (HLRCC), characterized by mutations in the *fumarate hydratase* (FH) gene, are at risk for development of aggressive FH-deficient RCCs. FH-deficient tumor cells undergo a pronounced and irreversible metabolic shift to lactate fermentation due in part to loss and mutation of mitochondrial DNA. Fumarate accumulation in FH-deficient tumor cells leads to increased expression of NAD(P)H-quinone oxidoreductase 1 (NQO1) through activation of the NRF2 transcription factor. Although several therapeutic agents have shown promise in the treatment of FH-deficient RCC, clinical outcomes in patients remain unsatisfactory. In this study, we examined the mechanism and therapeutic efficacy of isobutyl-deoxynyboquinone (IB-DNQ), which undergoes futile redox cycling in the presence of NQO1 and oxygen, leading to sustained generation of the highly reactive and toxic superoxide anion. First, we found that patient-derived FH-deficient tumor cells exhibit minimal oxygen consumption in vitro, and EPR oxygen mapping of FH-deficient tumor xenografts in vivo revealed that tumor oxygen levels were elevated relative to other genetically defined in vivo models of RCC. Infusion of IB-DNQ in tumor-bearing animals resulted in rapid and robust non-mitochondrial oxygen consumption in FH-deficient tumor xenografts as measured by both EPR oxygen imaging and photoacoustic mapping of tumor hemoglobin saturation. Repeated doses of IB-DNQ resulted in reduced tumor growth rates. Metabolomic analyses revealed that IB-DNQ treatment strongly suppressed glycolysis and reduced cellular ATP levels by rapidly depleting NADH and NADPH in FH-deficient tumor cells. Finally, [1-^{13}C]pyruvate hyperpolarized MR spectroscopy revealed decreased conversion of pyruvate to lactate in FH-deficient tumor xenografts following IB-DNQ treatment, providing a direct measurement of the impact of IB-DNQ on lactate fermentation in vivo. The combination of these in vivo imaging techniques and metabolite measurements demonstrate that NQO1-activated quinones can effectively target aerobic glycolysis in FH-deficient tumors which rely heavily on lactate fermentation for growth.

#7329 Host organ environment shapes clear cell renal cell carcinoma metastatic metabolism.

X. Alex Guo[1], Lina P. Calderon[2], Andrea L. Sanmiguel[2], Anirudh Sridharan[1], A. Ari Hakimi[2], Ed Reznik[1]

[1]Computational Oncology, Memorial Sloan Kettering Cancer Center, New York, NY,[2]Department of Urology, Memorial Sloan Kettering Cancer Center, New York, NY

Primary clear cell renal cell carcinoma (ccRCC) is characterized by profound metabolic rewiring which adapts as tumors evolve to become more aggressive, yet the evidence showing whether those programs are preserved versus reshaped at distant metastatic sites in humans remains limited. To investigate the determinants of ccRCC metastatic metabolism, we performed mass-spectrometry-based metabolomic profiling on quartets of primary tumor, adjacent normal kidney, distant metastasis, and normal adjacent to metastasis, from 14 patients with metachronous metastases. We find three key results. First, through unpaired comparisons of ccRCC metastases versus primaries, we observe decreases in glutathione metabolism in metastatic tissues. Second, using linear models, we find that metabolic profiles of metastatic tumors more closely resemble those of the normal tissue at the metastatic site than those of the patient's original kidney tumor. Third, we show that several metabolites in metastases can be approximated as simple mixtures of the primary tumor and the local normal tissue. Together, these results suggest that ccRCC metastases are strongly reshaped by the metabolic environment of the metastatic organ.

#7330 Hypoxia enhances sensitivity to RAS inhibition in PDAC.

Anna Shevzov-Zebrun[1], Darius Sinha[1], Muhammad Bin Munim[1], Keene Abbott[2], Matthew G. Vander Heiden[1]

[1]Koch Institute for Integrative Cancer Research at MIT, Cambridge, MA,[2]Dana Farber Cancer Institute, Boston, MA

Pancreatic ductal adenocarcinoma (PDAC) is one of the most lethal malignancies, in part due to acquired therapy resistance. As ~90% of PDAC tumors harbor activating *KRAS* mutations, direct inhibition of RAS has emerged as a promising therapeutic strategy. The RAS(ON) multi-selective inhibitor daraxonrasib has demonstrated clinical activity in PDAC and is currently being evaluated in Phase 3 trials; however, monotherapy resistance still emerges underscoring the need to identify biological processes that enable tumor cell survival following RAS inhibition. As RAS signaling regulates cancer metabolism, we hypothesized that metabolic remodeling contributes to RAS inhibitor sensitivity and resistance. To test this, we profiled polar metabolites in PDAC cells treated with RMC-7977, a tool RAS(ON) multi-selective inhibitor. RAS(ON) inhibition led to broad alterations in metabolite levels, including decreased levels of glycolytic and pentose phosphate pathway intermediates. In line with these findings, RMC-7977 treatment reduced glucose uptake and increased lactate secretion, suggesting that RMC-7977 treatment reduces glycolysis and promotes a shift toward increased oxidative metabolism. Given this shift toward oxidative metabolism, which requires mitochondrial respiration, we hypothesized that hypoxia, a hallmark of PDAC, may increase sensitivity to RAS inhibition. Indeed, PDAC cells exhibited enhanced growth inhibition in response to RMC-7977 in low oxygen conditions. RMC-7977 also suppressed glucose uptake and lactate secretion similarly under normoxic and hypoxic conditions. Pharmacologic inhibition of mitochondrial respiration under normoxia also enhanced RMC-7977 sensitivity. Together, these findings reveal that RMC-7977 reduces glucose uptake and shifts cells toward oxidative metabolism and uncovers a potential metabolic vulnerability involving the PDAC tumor microenvironment that has the potential to enhance the impact of RAS inhibition.

#7331 Hepatic proton conductance as a bioenergetic vulnerability and therapeutic target in MASH-associated HCC.

Elizabeth Rachel Marie Zunica[1], Kim Pedersen[2], Anan L. Cole[3], Analisa L. Taylor[3], Elizabeth C. Heintz[3], Megan D. Dousay[4], Bolormaa Vandanmagsar[3], Monika Sharma[5], Odinakhon Shamieva[6], Lucas Kniess Debarba[6], Marcus DaSilva Goncalves[7], Tomislav Jelesijevic[8], Rees G. Matthew[9], Jennifer A. Roth[9], Martin J. Ronis[2], Christopher L. Axelrod[3], John P. Kirwan[1]

[1]Pennington Biomedical Research Ctr., Baton Rouge, LA,[2]Department of Pharmacology and Experimental Therapeutics, School of Medicine, Louisiana State University Health Sciences Center New Orleans, New Orleans, LA,[3]Integrated Physiology and Molecular Medicine Laboratory, Pennington Biomedical Research Ctr., Baton Rouge, LA,[4]Integrated Physiology and Molecular Medicine Laboratory, Pennington Biomedical Research Center, Pennington Biomedical Research Ctr., Baton Rouge, LA,[5]OrsoBio Inc, Menlo Park, CA,[6]Department of Medicine, New York University Langone Health, New York City, NY,[7]NYU Langone Health, New York, NY,[8]School of Veterinary Medicine, Louisiana State University, Baton Rouge, LA,[9]Broad Institute of MIT and Harvard, Cambridge, MA

Metabolic dysfunction-associated steatohepatitis (MASH) is the fastest growing cause of hepatocellular carcinoma (HCC), yet the metabolic dependencies underlying MASH-HCC remain poorly defined. Here, we identify mitochondrial proton conductance as a central determinant of HCC progression and therapeutic vulnerability. Human HCC exhibited increased mitochondrial efficiency and glycolytic flux with reduced oxidative flux, consistent with large-scale HCC dependency datasets showing strong enrichment for downregulated mitochondrial pathways. To functionally interrogate this bioenergetic liability, we performed an unbiased PRISM barcoded-cell-line screen using the mitochondrial uncoupler BAM15. Lineage-level analysis revealed broad cytotoxicity with marked enrichment of sensitivity in HCC, which was validated in HepG2 cells, where BAM15 demonstrated greater potency than sorafenib, a frontline therapy for advanced HCC. We next evaluated mitochondrial uncoupling in vivo using two MASH-HCC models: (1) high-fat, fructose, and cholesterol diet with thermoneutral housing plus low-dose DEN, and (2) cocoa-butter diet plus DEN, each recapitulating metabolic injury and tumor development. In both models, BAM15 significantly reduced tumor burden and improved liver function. These effects persisted in PPARα-null mice, indicating that uncoupling exerts its efficacy through direct disruption of mitochondrial efficiency rather than secondary activation of fatty acid oxidation. To assess translational relevance, we tested the long-acting liver-targeted mitochondrial uncoupler TLC-1180, which similarly decreased tumor burden and improved hepatic function. Finally, liver-specific deletion of Ucp2 reduced hepatic proton conductance, increased tumorigenesis, and impaired liver function, establishing a mechanistic link between diminished uncoupling capacity and enhanced carcinogenic progression. Together, these data demonstrate that suppressed proton conductance is a fundamental metabolic adaptation that promotes HCC growth, and that enforced mitochondrial uncoupling directly counteracts this program. These findings position hepatic proton conductivity as a mechanistically grounded therapeutic target and support mitochondrial uncoupling, particularly liver-directed approaches, as a rational strategy for treating MASH-HCC.

#7332 Targeting a DYRK1A-regulated lipogenesis-STING axis alleviates hepatic metabolic dysfunction and lipotoxicity in metabolic steatohepatitis.

Wen Yan Huang[1], Kyunghee Noh[2]

[1]Bionanotechnology Research Center, Korea Research Institute of Bioscience and Biotechnology, Daejeon, Korea, Republic of,[2]Bionanotechnology Research Center; Department of Nanobiotechnology, Korea Research Institute of Bioscience and Biotechnology, Daejeon, Korea, Republic of

Background Metabolic dysfunction-associated steatohepatitis (MASH) is a progressive liver disease marked by lipid accumulation, inflammation, and fibrosis that can advance to hepatocellular carcinoma. While both *de novo* lipogenesis (DNL) and innate immune activation drive disease progression, their mechanistic connection remains unclear. Here, we identified DYRK1A as a novel kinase that activates STING-dependent inflammatory signaling and links metabolic and immune dysregulation in MASH.

MethodsMASH and fibrosis models were established in both cellular and animal systems. DYRK1A expression was modulated through knockdown, overexpression, and pharmacological inhibition. Lipogenesis, STING activation, lipotoxicity, and fibrosis were assessed using molecular assays, histopathology, and serum injury markers.

ResultsDYRK1A expression was elevated by approximately 40% in cellular models of MASH compared with controls. Further, we confirmed DYRK1A overexpression reduced phosphorylation of AMPK and ACC, enhancing lipogenic flux and elevating lipid accumulation, supporting its potential involvement in metabolic regulation. Conversely, DYRK1A silencing or inhibitor treatment suppressed DNL, destabilized STING, and mitigated lipotoxicity by reducing the phosphorylation of STING, TBK1 and IRF3, as confirmed by Oil Red O staining and immunoblotting. *In vivo*, DYRK1A was markedly elevated in MASH-associated fibrosis, whereas its inhibition reduced hepatic triglyceride deposition (~30%), collagen remodeling (~30%), and serum AST/ALT levels (~40%), indicating improved liver function. Consistent with *in vitro* results, inhibitor-treated livers exhibited diminished DNL- and STING-related proteins expression, underscoring DYRK1A as a newly identified key driver of metabolic inflammation and fibrosis.

ConclusionsThis study defines a novel DYRK1A-mediated lipogenic-inflammatory cascade linking metabolic stress to innate immune activation and fibrosis in MASH. Targeting DYRK1A may provide a therapeutic strategy to disrupt the lipogenesis-STING axis, alleviate chronic metabolic liver injury, and potentially prevent progression to hepatocellular carcinoma.

#7333 Disrupting tumor lipid homeostasis by MUFA depletion drives cell death in HCC.

Justyna J. Gleba, Victoria N. Rios, Brian M. Necela, Skyeler M. Klinge, Matt L. Pawlush, Mike J. Redig, Aylin Alasonyalilar-Demirer, Han W. Tun and John A. Copland III

Mayo Clinic Comprehensive Cancer Center, Jacksonville, FL

Background: The cellular balance between saturated and monounsaturated fatty acids is a defining feature of tumor lipid metabolism, with SCD1 functioning as a key modulator through the production of MUFAs. Elevated SCD1 activity and MUFA accumulation have been documented in hepatocellular carcinomas, although the consequences of restricting MUFA synthesis have not been fully clarified.
Methods: A selective SCD1 inhibitor, SSI-4, was evaluated across established human HCC cell lines and xenograft models. Measurements included cell viability, lipid compositional analyses, and characterization of stress response pathways at both molecular and biochemical levels. The effects of MUFA depletion were studied *in vitro* and *in vivo*, with attention to ER stress, apoptosis, ferroptosis markers, and autophagy induction.
Results: SSI-4 treatment led to marked reduction in cellular MUFA content and an increase in saturated fatty acid pools. The resulting metabolic stress correlated with activation of unfolded protein response components, caspase-mediated cell death, and the upregulation of ferroptosis-associated genes. Triglyceride and MUFA levels declined precipitously, as confirmed by mass spectrometry-based lipidomics. Tumor growth was suppressed in PDX models and evidence of autophagic flux was apparent in sensitive cell lines. Variability in response highlights metabolic heterogeneity in HCC.
Conclusions: Targeted disruption of MUFA biosynthesis inflicts metabolic vulnerability on HCC cells, precipitating membrane alterations and activation of multiple cell death programs. These findings recommend further investigation into metabolic interventions exploiting MUFA depletion, with consideration for stratifying patients according to lipid metabolic phenotypes.
Funding: This work is supported by Mayo Clinic Comprehensive Cancer Center and the Jay and Deanie Stein Career Development Award for Cancer Research at Mayo Clinic Jacksonville and the Mayo Clinic Translational Hepatobiliary Cancer SPORE P**50CA210964** Career Enhancement Program (CEP) and Florida Department of Health/Florida Cancer Innovation Fund C25C23.

#7334 Mitochondrial creatine kinase promotes hepatocellular carcinoma progression.

Nusrat Israr Khan, Luke Jordan, Olayinka David, Shreya Pattisapu, Kyle Schachtschneider, Kejia Cai, Ron Gaba, **Lobna Elkhadragy**

Radiology, University of Illinois at Chicago, Chicago, IL

Background: Hepatocellular carcinoma (HCC), the most common type of liver cancer, is an aggressive malignancy with limited therapeutic options and poor prognosis, underscoring the need for novel therapeutic targets. Emerging evidence implicates dysregulated creatine metabolism in HCC pathogenesis. Serum creatine levels inversely correlate with HCC progression and mitochondrial creatine kinase (MtCK), encoded by *CKMT1*, has been identified as a potential diagnostic biomarker. MtCK catalyzes the reversible transfer of a phosphate group from ATP to creatine to generate phosphocreatine, a key energy buffer that supports cellular bioenergetics. However, the functional role of *CKMT1* in HCC progression remains poorly understood.

Methods: We investigated the role of *CKMT1* in HCC progression using both human (Hep3B) and porcine (Oncopig A272) HCC cells. *CKMT1* overexpression was achieved by lentiviral transduction of human *CKMT1* followed by antibiotic selection, and *CKMT1* knockout (KO) clones were generated by CRISPR/Cas9 and single-cell clone isolation. Altered CKMT1 expression was confirmed by Western blotting. Cell proliferation and migration were assessed by MTS and wound-healing assays, respectively. Intracellular creatine levels were quantified using colorimetric method, and *in vivo* tumor growth was evaluated by subcutaneous injection into both flanks of SCID mice (n=6 mice/group).

Results: *CKMT1* overexpression significantly decreased intracellular creatine levels and increased Hep3B cell proliferation and migration. A272 cells, which exhibit higher endogenous *CKMT1* expression compared to Hep3b, did not show further increase in proliferation or migration upon overexpression. Conversely, A272 *CKMT1* KO clones exhibited significantly elevated intracellular creatine levels and reduced proliferation and migration. *In vivo,* xenografts derived from *CKMT1*-overexpressing A272 cells exhibited significantly increased tumor growth rate compared to parental controls ($p < 0.001$), whereas *CKMT1* KO tumors grew at rates comparable to the parental line.

Conclusions: These findings identify *CKMT1* as a promoter of HCC progression, linking altered creatine metabolism to HCC growth. Targeting mitochondrial creatine kinase or its metabolic network may represent a promising therapeutic strategy. Ongoing studies focus on developing porcine HCC models with modulated creatine metabolism to enable integrated metabolic and molecular imaging approaches for improved diagnosis, risk stratification, and treatment monitoring in a physiologically relevant large-animal model.

#7335 Spatio-temporal interactome of fructose-1,6-bisphosphate aldolase B in hepatocellular carcinoma.

XIANGNAN CHEN, Hongfei WANG, Shanshan Zhong, Huiyong YIN

Biomedical Engineering, City University of Hong Kong, Hong Kong, Hong Kong

Hepatocellular carcinoma (HCC) is a prevalent and aggressive form of malignancies with limited therapeutic options. Understanding the molecular mechanisms underlying HCC development and progression is crucial for the identification of novel therapeutic targets. Fructose-1,6-bisphosphate aldolase B (ALDOB) is a key enzyme in glycolysis which has been implicated in HCC pathogenesis. Metabolic reprogramming is a core hallmark of cancer, and downregulation of ALDOB in HCC leads to alterations in glucose metabolism. Our previous studies identified multiple enzymatic and non-enzymatic roles of ALDOB in HCC through protein-protein interactions in different cellular locations including cytosol and nucleus. In this study, to better understanding the precise role and the network of interacting proteins of ALDOB in HCC, we aim to reveal the potential regulatory mechanisms of ALDOB in HCC through a combination of proteomics and metabolomics. By performing subcellular proteome fractions and combine with APEX proximity labeling, we identified the ALDOB function in nuclear of different cell stage and conditions. To be more comprehensively understand the underlying pathway and mechanism, we possess RNA-seq to identify how ALDOB functional units associated pathways. We propose to perform comprehensive analyses to identify proteins that physically interact with ALDOB and their dynamic changes under various biological stimuli and across different stages of HCC, shedding light on its functional associations and molecular pathways in liver cancer in an attempt to enhance the understanding of HCC biology. This project will lay the ground for developing novel therapeutic strategies targeting ALDOB and its interactors in the fight against this deadly disease.

#7336 Harnessing lipid metabolism to treat drug-tolerant persister cells.

Mumina Sadullozoda, Patrick Jonker, Erin Szuromi, Asha Bozicevich, Alexander Muir

Ben May Department for Cancer Research, University of Chicago, Chicago, IL

Pancreatic ductal adenocarcinoma (PDAC) remains one of the most lethal cancers, with a five-year survival rate of only 13% and limited response to current therapies. A major contributor to treatment failure is the emergence of drug-tolerant persister cells (DTPs), a slow-cycling subpopulation that survives targeted and systemic therapy and drives relapse. Here, we aimed to determine whether the metabolic dependencies of DTPs could be exploited to eliminate these cells. Through analysis of publicly available transcriptomic datasets across multiple malignancies, including PDAC, colorectal, breast, and non-small cell lung cancers, we identified consistent downregulation of *SREBF1*, a master regulator of de novo lipid synthesis, in DTPs. We previously demonstrated that PDAC cells with impaired lipogenesis are selectively vulnerable to exogenous polyunsaturated fatty acids (PUFAs) due to their inability to balance saturated and monounsaturated fatty acid pools, resulting in ferroptotic death. Based on these findings, we hypothesized that DTPs can be targeted through PUFA overload. To test this, we induced DTPs in murine PDAC cell lines using the KRAS-targeted therapy RMC-7977 and treated them with PUFAs, including alpha-eleostearic acid (ESA). ESA supplementation was sufficient to eradicate PDAC DTPs at dietarily achievable concentrations. We are now evaluating whether this approach can limit relapse by targeting minimal residual disease in animal models of PDAC treated with KRAS inhibitors. These findings reveal a diet-based strategy that exploits metabolic vulnerabilities of therapy-persistent PDAC cells and may reduce the risk of disease recurrence.

#7337 Estrogen-related receptor gamma maintains oxidative metabolism via glutamine-derived anaplerosis.

Samantha A. McLaughlin[1], Zelia M. Correa[1], J. William Harbour[2], Daniel Pelaez[1]

[1]Bascom Palmer Eye Institute, University of Miami Miller School of Medicine, Miami, FL,[2]Ophthalmology, UT Southwestern Medical Center, Dallas, TX

Glutamine (Gln), traditionally considered a nonessential amino acid, becomes essential in cancer cells as the rate of Gln consumption exceeds that of endogenous biosynthesis. This metabolic dependency constitutes a unique “glutamine addiction”. Although many factors, both genetic and environmental, have been shown to contribute to the control of Gln metabolism, the precise regulation of Gln utilization in cancer still remains largely unclear. Here, we identify estrogen-related receptor gamma (ERRγ) as a critical regulator of glutaminolytic enzymes and cellular Gln utilization. RNA-sequencing of four primary retinoblastoma cells lines with or without shRNA-mediated ERRγ knockdown showed that, relative to shGFP controls, shERRγ downregulated genes were enriched for hypoxic adaptation and glycolysis pathways (*FDR < 0.05*), with no change in oxidative phosphorylation, indicating a shift toward lactate-producing glucose flux. Consistent with this, key genes in lactic acid fermentation (PDK1, LDH, MCT1) were significantly reduced ($p < 0.05$). shERRγ also decreased expression of glutaminolysis-related genes (*FDR < 0.05*), suggesting reliance on Gln-derived carbon to sustain TCA activity in a “Warburg-like” state. Functionally, RB006, a model cancer cell line with high basal ERRγ expression, requires exogenous Gln for viability, exhibiting marked cell death upon Gln withdrawal and a dose-dependent increase in proliferation, with ≥ 4mM required for maximal growth. Mesenchymal stem cells (MSCs), which express low ERRγ, were Gln-independent; however, ERRγ overexpression (MSC[ERRγ]), induced both Gln dependence and dose-responsive proliferation. To further assess Gln utilization, cells were supplemented with increasing Gln, and TCA intermediates (glutamate, α-KG, citrate, pyruvate, ATP) were quantified. All lines converted Gln to glutamate in a dose-dependent manner, but only RB006 and MSC[ERRγ] showed parallel increases in α-KG and citrate, consistent with ERRγ-mediated control of GLUD1/2 and downstream reductive carboxylation. High- ERRγ cells demonstrated strong correlations between Gln levels and all metabolites ($r > 0.9$), produced greater metabolite output per unit Gln than MSCs, and exhibited larger stepwise increases in Gln-derived flux, reflecting enhanced glutamine-handling capacity. Our results indicate ERRγ may be necessary to support oxidative phosphorylation via glutamine-derived anaplerosis. We provide evidence that ERRγ is required for glutaminolytic pathways, suggesting that ERRγ may be a key player in the metabolic adaptation of highly proliferative cell lines.

#7338 Elucidating the interplay between phospholipid biosynthesis and oxidative stress responses in the tumorigenesis of Clear Cell Renal Cell Carcinoma.

Rento Ito[1], Renpei Kato[1], Yosuke Matsushita[2], Toyomasa Katagiri[2], Wataru Obara[1]

[1]Iwate Medical Univ., Iwate, Japan,[2]Laboratory of Biofunctional Molecular Medicine, National Institute of Biomedical Innovation, National Institutes of Biomedical Innovation, Health and Nutrition, Osaka, Japan

Background: Phospholipids are essential components of biological membranes that regulate diverse cellular processes. Cardiolipin (CL) is a mitochondria-specific phospholipid crucial for maintaining mitochondrial structure and function. However, its role in clear cell renal cell carcinoma (ccRCC) remains unclear. **Methods:** Comprehensive phospholipidomic profiling of paired tumor and normal kidney tissues from ccRCC patients was performed using LC-TQMS. Quantitative data were integrated with immunoblotting, immunohistochemistry, and transcriptomic analyses from both TCGA and an institutional RNA-seq cohort. **Results:** CL levels were significantly reduced in tumor tissues compared with normal renal cortex, whereas other phospholipids (PA, PI, PS and PG) showed no significant differences. Reduced CL content paralleled decreased VDAC1 expression, indicating lower mitochondrial abundance. Lipidomic analysis revealed selective suppression of unsaturated CL species in tumors, suggesting mitochondrial membrane remodeling induced by oxidative stress. Analyses of gene expression showed a consistent increase in the expersiion of enzymes involved in CL synthesis and remodeling, namely TAMM41 and TAZ, in both TCGA and in-house datasets, with ACSL5 being the only gene that was significantly increased in fatty acid activation. **Conclusions:** ccRCC is characterized by quantitative and qualitative cardiolipin remodeling, reflecting mitochondrial reduction and adaptation to oxidative stress. Altered CL metabolism may represent a key mechanism of mitochondrial reprogramming in tumor cells and a potential therapeutic target in renal cancer.**Statement of significance:** This study identifies cardiolipin remodeling as a hallmark of mitochondrial reprogramming in clear cell renal cell carcinoma, revealing a potential therapeutic vulnerability in mitochondrial lipid metabolism.

#7339 Transcriptomic features associated with tumoral metabolites characterizing the immune microenvironment in clear cell renal cell carcinoma.

Sei Naito, Takafumi Narisawa, Hiromi Ito, Norihiko Tschiya

Urology, Yamagata University Faculty of Medicine, Yamagata, Japan

Abstract: Objectives: Previous studies have demonstrated that the metabolic milieu plays a pivotal role in shaping the immunological landscape of cancer tissues. This study aimed to characterize the immune microenvironment of clear cell renal cell carcinoma (ccRCC) in relation to intratumoral metabolite levels.

Methods: Metabolomic and transcriptomic analyses were performed on frozen tumor samples and their paired formalin-fixed paraffin-embedded (FFPE) specimens from 31 ccRCC surgical cases. Five metabolites previously implicated in immune modulation—lactate, glutamine, adenosine, arginine, and tryptophan—were quantified and compared against transcriptomic profiles using pre-ranked gene set enrichment analysis (GSEA). The analysis incorporated hallmark gene sets (h.all.v2025.1.Hs.symbols) and immune-related gene sets (c7.immunesigdb.v2025.1.Hs.symbols).

Results: Lactate levels positively correlated with gene sets related to *glycolysis*, *hypoxia*, *interferon gamma response*, and *unfolded protein response*, as well as immune signatures derived from monocytes and dendritic cells stimulated by influenza A virus and HPV antigens. Negative correlations were observed with *mitotic spindle* and *oxidative phosphorylation* pathways. Glutamine showed positive associations with *glycolysis*, *RORgammat-deficient CD4+ T cells under Th17-polarizing conditions*, *SPHK1 knockout inflammatory responses*, and *type I interferon-treated endothelial cells*, while negatively correlating with *coagulation*. Adenosine was positively linked to *glycolysis*, *hypoxia*, *xenobiotic metabolism*, *mTORC1 signaling*, and *reactive oxygen species pathways*, as well as immune signatures involving memory CD4+ T cells, IL-4 stimulation, and monocyte activation. Negative correlations included *mitotic spindle*, *FOXP3-mutant Tconv cells*, and *plasmacytoid dendritic cell responses*. Arginine was positively associated with gene sets reflecting monocyte culture dynamics, memory CD8+ T cell differentiation, and thymocyte maturation.

Conclusions: These findings highlight distinct transcriptomic programs associated with specific metabolites in ccRCC, suggesting that intratumoral metabolic states—particularly elevated lactate and adenosine—are linked to immunosuppressive and inflammatory transcriptional profiles. The enrichment of immune gene sets derived from viral stimulation contexts implies that tumor metabolism may mimic or modulate immune activation pathways typically seen in infection. Overall, this integrative metabolomic-transcriptomic approach provides insight into how metabolic reprogramming in ccRCC contributes to shaping the immune microenvironment, with potential implications for immunotherapeutic strategies and metabolic targeting.

#7340 Exploring the role of PNPLA3 I148M in cancer using the selective small molecule degrader NUV-244.

Katrin Juenemann, Patrick Steigemann, Ralf Lesche, Tamara Kanashova, Hanna Meyer, Claudia Noack, Barbara Nicke, Peter Staller, Charlotte Kopitz, **Martin Lange**

Nuvisan ICB GmbH, Berlin, Germany

The patatin-like phospholipase domain-containing protein 3 (PNPLA3) I148M variant is a well-established genetic determinant of fatty liver disease, yet emerging evidence suggests broader implications in cancer biology, particularly in hepatocellular carcinoma and metabolic reprogramming of tumor cells (Tavaglione et al., 2024). We recently identified NUV-244 as a potent and selective small-molecule degrader of PNPLA3 I148M (Steigemann et al., 2025). These findings provided the first pharmacological and molecular framework to directly interrogate PNPLA3 I148M´s function in liver cells. Building upon these insights, we sought to investigate the potential oncogenic or tumor-modulatory role of PNPLA3 I148M in cancer, and to evaluate how pharmacologic inhibition by NUV-244 influences cancer cell metabolism, proliferation, and survival. We performed a comparative analysis of cancer cell lines harboring endogenous PNPLA3 I148M mutations versus wild-type counterparts and generated isogenic cell line models using a PNPLA3 I148M overexpression approach. These models were used to assess transcriptomic and proteomic modulation, mitochondrial function and cell viability with and without NUV-244 treatment. Using these experimental systems, we aim to define how PNPLA3 I148M contributes to cancer cell metabolic plasticity and whether its pharmacologic inhibition creates selective vulnerabilities. In summary, these studies establish a mechanistic basis for PNPLA3 I148M´s potential role in tumor biology and highlight NUV-244 as a chemical tool to probe its function in cancer.

: Transcription Factor Function in Cell Identity, Signaling, and Post-Transcriptional Control
Poster Session

#7344 NRG1 knock out in cancer cell lines decreases their aggressiveness.

Marie Issenmann[1], Clarisse Thiollier-Schmitt[1], **Manon Barre**[1], Emeline Cros-Perrial[1], Michael Duruisseaux[2], Lars Petter Jordheim[1]

[1]Cancer Research Center of Lyon (CRCL), Lyon, France,[2]Hospices Civils de Lyon, Bron, France

Introduction Neuregulin-1 (NRG1) is a growth factor which can bind to the ErbB/human epidermal growth factor receptors (HERs), especially to HER3, and activate the downstream signalling pathways. The *NRG1* gene has the potential to form oncogenic gene fusions with diverse gene partners leading to the emergence of cancer. Several therapeutic approaches targeting more or less directly *NRG1*'s signalling pathway exist, but patients tend to respond poorly to treatments or rapidly develop resistances. A better understanding of the NRG1- and *NRG1*-fusion-dependent cell biology could allow us to propose new treatment options to these patients. Here our objective is to study NRG1-dependent cell biology parameters in various cancer cell lines, with or without genetic alterations of NRG1.

Methods A CRISPR-Cas9-based deletion of *NRG1* was obtained in the A549 and SW1573 Non-Small Cell Lung Cancer (NSCLC) cell lines which highly express wild type NRG1, in the HCC95 NSCLC cell line which has an amplification of *NRG1*, and in the MDA-MB-175 breast cancer cell line which bears a complex *PPP6R3-TENM4-NRG1* fusion. The modified cell lines were grown as either or both polyclonal and monoclonal populations and were characterized using classic cell biology techniques such as western blot and flow cytometry to monitor protein expression, confluence assay and Cell-Trace CFSE to study proliferative capacities, scratch wound assay and Boyden chamber to monitor migratory capacities, and soft agar and clonogenic assay to study stemness characteristics.

Results The NRG1-deficient A549 clones (n=5) clustered into two distinct behavioural groups. One of them showed a loss of HER3 expression, a 3-fold increased sensitivity to afatinib, and up to 2-fold decreased migratory capacities. As for the other group, there was an induced expression of mesenchymal markers and a loss of FGFR1 expression. For other parameters, all A549 clones behaved in a similar manner as control clones. Preliminary results in NRG1-deficient HCC95 (n=2) suggest they have slightly reduced proliferative capacities and NRG1-deficient MDA-MB-175 (n=2) have a 2-fold higher sensitivity to several treatments including afatinib. All clones for the SW1573 cell line (n=4) exhibited no difference within all performed experiments.

Conclusion Overall, NRG1-deficiency decreases cancer cells' aggressiveness, although in a cell-specific manner. Upcoming transcriptomic assay of our different models will give us a better insight in NRG1-related molecular modifications. Further analyses of all models are ongoing (clones of MDA-MB-175 and HCC95, 3D bioprinting experiments, *in vivo* tumour growth⋯) and results will be included in the poster.

#7345 Synergistic targeting of mSWI/SNF and UTX reveals a novel combination therapy in T-cell acute lymphoblastic leukemia.

Shi Hao Tan[1], Hyoju Kim[1], Ziyang Lee[1], Lee Hui Chua[1], Sanda Takaomi[2], Allen Eng Juh Yeoh[1]

[1]Cancer Science Institute of Singapore, Singapore, Singapore,[2]Nagoya City Univ. Medical School, Nagoya, Japan

Dysregulated expression of oncogenic transcription factors (TFs) is a critical hallmark of T-cell acute lymphoblastic leukemia (T-ALL). These aberrations disrupt the tightly regulated spatial-temporal expression of downstream target genes and rewire transcriptional programs, culminating in a state of “transcription addiction”. We show that oncogenic factors such as RUNX1 and NOTCH1 in T-ALL recruit the mSWI/SNF chromatin-remodeling complex to modulate chromatin accessibility at target gene loci to initiate and maintain oncogenic transcriptional networks. Inhibiting mSWI/SNF function with SMARCA2/4 ATPase inhibitors (FHD-286) or PROTAC degraders (ACBI-1) targeting the SMARCA protein induces apoptosis and impairs T-ALL cell growth. To further dissect the functional dependencies of T-ALL cells on the mSWI/SNF complex, we performed genome-wide CRISPR knockout (KO) screens in T-ALL cells treated with FHD-286 or ACBI-1. These screens revealed that multiple members of the Mediator complex were high-confidence targets whose individual knockout was sufficient to rescue T-ALL cells from inhibitor-induced cell death. In contrast, knockout of the histone demethylase UTX sensitized T-ALL cells to mSWI/SNF inhibition. Notably, the IC50 of FHD-286 treatment decreased significantly in UTX KO cells compared to wild-type (WT) controls. Furthermore, UTX KO T-ALL xenograft mice showed improved survival when treated with FHD-286 compared to FHD-286-treated WT xenografts. A synergistic effect emerged when T-ALL cells or patient-derived xenografts (PDXs) were co-treated with GSK-J4, a histone demethylase inhibitor, and FHD-286. Transcriptomic analyses indicated that genes promoting ribosomal and mitochondrial function were substantially downregulated in UTX KO T-ALL cells treated with FHD-286 but not in similarly treated WT cells, suggesting a previously unrecognized role of UTX in gene regulation. Overall, these findings demonstrate that simultaneously targeting the mSWI/SNF complex and UTX may represent an innovative combinatorial strategy for T-ALL treatment.

#7346 RNA-seq analysis confirms post-thaw transcriptomic stability in ThawReady (TM) THP-1 assay-ready cells.

Ajeet P. Singh, Utsav Sharma, Lucas Underwood, Noah Wax, Steve King, Nilay Chakraborty, Jonathan Jacobs

ATCC, Manassas, VA

Cryopreserved cell lines have become essential for high-throughput screening and assay development, offering convenience and consistency across experiments. However, the freeze-thaw process can induce cellular stress, potentially affecting gene expression and compromising functional reliability. To ensure consistent assay performance, it is crucial to verify that cryopreserved cells retain their transcriptomic and functional integrity after thawing. In this study, we evaluated the transcriptomic stability of ThawReady™ THP-1 (TIB-202-AR™) cells using RNA sequencing (RNA-seq). Cells were analyzed immediately after thawing (0-hour) and following 2-hour and 8-hour recovery intervals and were compared to freshly cultured THP-1 cells. Principal component and hierarchical clustering analyses revealed that post-thaw samples closely grouped with fresh controls, demonstrating preservation of cellular identity and global gene expression patterns. Gene expression profiles showed strong concordance across key immune and inflammatory pathways characteristic of THP-1 cells. Differential expression analysis identified 178 genes altered at 0 hours, 951 at 2 hours, and 713 at 8 hours post-thaw relative to fresh culture, using a threshold of absolute fold change >5 and FDR-adjusted p-value <0.05. Despite these transient changes, pathways related to cell survival and proliferation remained stable. Notably, phagosome formation was the top-enriched pathway, suggesting adaptive recovery responses that support cell viability. Overall, these results confirm that ThawReady™ THP-1 cells maintain robust transcriptomic integrity post-thaw, supporting their reliability and reproducibility for downstream immune and inflammation-related functional assays.

#7347 Leptin-driven transcriptional reprogramming in triple-negative breast cancer: Exploring biological drivers of racial disparities.

Sarabjeet Kour Sudan[1], Amod Sharma[1], Shashi Anand[1], Jasleen Kaur[2], Lavanya Challagundla[2], Ajay P Singh[1], Seema Singh[1]

[1]Cell and Molecular Biology, Cancer Center and Research Institute, University of Mississippi Medical Center, Jackson, MS,[2]Cell and Molecular Biology, University of Mississippi Medical Center, Jackson, MS

We recently demonstrated that obesity is a significant risk factor for breast cancer (BC) diagnosis with triple-negative and Luminal A subtypes, especially in Black women. Furthermore, obesity was linked to earlier disease onset in Black women, who also demonstrated elevated serum leptin levels, an obesity-associated hormone, that showed a similar epidemiologic association. In this study, we investigated leptin-induced transcriptomic alterations in two triple-negative breast cancer (TNBC) cell lines derived from White (MDA-MB-231) and Black (MDA-MB-468) patients by performing mRNA sequencing, followed by bioinformatic and pathway analyses to identify differentially-expressed genes (DEGs) and their impact on biological pathways. Leptin treatment resulted in widespread gene expression alterations, with 1,857 DEGs identified in MDA-MB-231 and 1,242 DEGs in MDA-MB-468 cells ($P < 0.05$). Of these DEGs, 1030 and 827 were upregulated, and 617 and 625 were downregulated in MDA-MB-231 and MDA-MB-468, respectively. A comparison of DEGs between MDA-MB-231 and MDA-MB-468 showed only 177 DEGs to be commonly altered, suggesting a diverse and cell line-specific transcriptional impact of leptin signaling. Interestingly, the comparison of sequencing reads from vehicle-treated MDA-MB-231 and MDA-MB-468 cells identified significant transcript-level differences between the two lines. In leptin-treated MDA-MB-231 cells, KEGG pathway analysis revealed enrichment of the spliceosome, steroid biosynthesis, protein export, and basal transcription factor pathways, accompanied by suppression of AMPK signaling, focal adhesion, longevity regulation, and insulin signaling. Conversely, in MDA-MB-468 cells, leptin induced the activation of the ECM-receptor interaction, Notch, PI3K-AKT, and transcriptional misregulation in cancer pathways, while downregulating oxidative phosphorylation, mRNA surveillance, the TCA cycle, and AMPK signaling. Together, these findings suggest that leptin induces distinct, cell line-specific transcriptional reprogramming in TNBC, engaging proliferative signaling pathways, while suppressing energy-sensing and metabolic regulatory networks. Overall, our study highlights that targeting leptin-driven pathways may offer novel therapeutic and preventive opportunities to mitigate the obesity-associated risk of early-onset aggressive breast cancer.

#7348 Chronic e-cigarette aerosol exposure dysregulates NF-kB signaling and alters IRF-dependent innate immune signaling in human lung epithelial cells.

Vengatesh Ganapathy[1], Sulfath Thottungal Parambil[1], Jimmy Manyanga[1], Gautham Chengizkhan[1], Mayilvanan Chinnaiyan[1], Adele Hammoudi[1], Balaji Sadhasivam[2], Ilangovan Ramachandran[3], David Rubenstein[4], Lurdes Queimado[1]

[1]Departments of Otolaryngology Head and Neck Surgery, The University of Oklahoma Health Sciences Center, Oklahoma City, OK,[2]Occupational and Environmental Health, The University of Oklahoma Health Sciences Center, Oklahoma City, OK,[3]University of Madras, Chennai, India,[4]Biomedical Engineering, Stony Brook University, Stony Brook, NY

Background: Although electronic cigarettes (e-cigarettes) are marketed as safer alternatives to combustible tobacco, accumulating evidence indicates that chronic use may impair respiratory health. E-cigarette aerosols contain harmful constituents, including nicotine, carbonyl compounds, metals, carcinogens, and reactive oxygen species (ROS). Excess ROS can overwhelm antioxidant defenses, driving oxidative stress and chronic inflammation. NF-κB is a central regulator of inflammation and antiviral immunity, yet its modulation by chronic exposure to e-cigarette aerosol remains poorly defined. **Objective:** To determine how chronic exposure to e-cigarette aerosols alters NF-κB signaling and downstream inflammatory and antiviral pathways in lung epithelial cells.
Methods: Normal human bronchial epithelial cells (NuLi-1) were exposed to aerosol extracts generated from two commercial tobacco-flavored e-cigarette products every other day for 2 weeks. Exposure delivered approximately 30 ng/ml of nicotine to mimic the median levels observed in the plasma of e-cigarette users. NF-κB mRNA levels were measured by real-time RT-qPCR. Protein expressions of NF-κB, TLR3, TLR4, IRF1, IRF3 and IRF7 were quantified by Western blotting. Statistical significance was evaluated by Student's *t*-test.
Results: Chronic e-cigarette aerosol exposure significantly upregulated NF-κB mRNA and protein levels. TLR3, TLR4, and IRF7 proteins were also elevated after chronic exposure to e-cigarette aerosols, indicating activation of stress- and pathogen-sensing pathways. In contrast, IRF1, and IRF3 protein expression were significantly decreased, consistent with suppression of key antiviral transcription factors. This pattern reflects an inflammatory shift characterized by NF-κB activation with concurrent impairment of IRF-dependent innate immune signaling.
Conclusion: Chronic e-cigarette aerosol exposure induces a dysregulated inflammatory phenotype in human lung epithelial cells, marked by NF-κB activation and suppression of IRF-mediated antiviral pathways. These findings suggest that chronic e-cigarette use may compromise epithelial innate immunity and increase susceptibility to respiratory infections and inflammatory disease.
Grant support: NIH/NCI (R01CA242168, Queimado); TSET HPRC (Ganapathy); NHI/NIGMS (U54GM104938-140).

#7350 DPF3a-YY1 cooperation drivesimmunosuppression in renal cell carcinoma by activating CSF2 transcription.

Xin-Ru Yu, Haodong Liu, Zeyun Mi, **Kexin Chen**

Tianjin Medical Univ. Cancer Inst. & Hospital, Tianjin, China, Tianjin, China

Background: Renal cell carcinoma (RCC) is among the most aggressive and therapy-resistant malignancies, characterized by extensive vascularization and profound immune evasion. Genome-wide association studies have identified the SNP rs4903064 as a key variant regulating the expression of DPF3a, a chromatin remodeling factor that interacts with HIF signaling in RCC. Although the DPF3 gene encodes two isoforms (DPF3a and DPF3b), the biological significance of DPF3a in RCC initiation and progression remains largely unexplored.
Methods: The expression of DPF3 isoforms in RCC cell lines and clinical tumor specimens was examined by Western blotting (WB), quantitative PCR (qPCR), and immunohistochemistry (IHC). Multi-omics approach integrating RNA-seq, CUT&Tag, and ATAC-seq were applied to define DPF3a-dependent transcriptional and chromatin accessibility landscapes. TurboID-based proximity labeling assays were used to identify interactors of DPF3a,and co-immunoprecipitation (Co-IP) were performed to validate these interactions. Single-cell RNA sequencing (scRNA-seq) and flow cytometry were used to evaluate the impact of DPF3a on the tumor immune microenvironment.
Results: In this study, we found DPF3a, but not DPF3b, was markedly overexpressed in RCC tissues and cell lines. Integrated multi-omics analysis revealed that DPF3a binds to the promoter of the CSF2 gene and promotes its transcriptional activation, consequently leading to increased CSF2 secretion. Mechanistically, the PHD1/2 domains of DPF3a mediate its interaction with the transcription factor YY1, which collaboratively facilitates CSF2 transcription. Furthermore, single-cell RNA sequencing analysis indicated that DPF3a-driven CSF2 upregulation promotes neutrophil infiltration and $CD8^+$ T-cell exhaustion, thereby contributing to the suppression of anti-tumor immunity.
Conclusions: Our findings identify DPF3a as a previously unrecognized oncogenic isoform in RCC. By forming a complex with YY1 and activating CSF2 transcription, DPF3a drives neutrophil recruitment and $CD8^+$ T-cell exhaustion, thereby fostering an immunosuppressive microenvironment and promoting RCC progression.
Keywords: DPF3a; YY1; CSF2; Renal Cell Carcinoma; Tumor Immune Microenvironment

#7352 CYLD mediated non-canonical RelB NF-κB transcription axis in multiple myeloma.

Uday Aditya Sarkar[1], Lalit Kumar[2]

[1]National Institute of Immunology, New Delhi, India,[2]Department of Medical Oncology, All India Institute of Medical Sciences, New Delhi, India

Introduction: Multiple myeloma (MM), a plasma B cell neoplastic disease, has been studied widely for its dependency on NF-κB signaling, yet the crosstalk between canonical (RelA/p50) and non-canonical (RelB/p52) arms remains incompletely defined. Tumor suppressor protein CYLD, an established negative regulator of canonical NF-κB, emerged in our studies as an enforcer of RelB-driven transcription. We define a CYLD-mediated RelB enforced signaling that promotes the disease pathogenesis by supporting survival and migration in tumor cells.

Methods: Primary CD138+ plasma cells were isolated from bone marrow aspirates of 74 patients with MM using MACS based separation. Cells were used for NF-κB DNA binding assay (n=15) and quantitative RT-PCR based gene expression studies (n=42). For *in vitro* studies, patient derived MM cell lines (MMCLs) JIM3 and KP-6 were used for biochemical studies. CYLD deficient isogenic MMCLs were generated using CRISPR-Cas9 gene editing. The RNA-seq metadata available with the Multiple Myeloma Research Foundation (MMRF) database IA13a were used for *in silico* transcriptomic analyses.

Results: In our study, using primary myeloma cells, we established the presence of increased nuclear RelB (nRelB) activity in newly diagnosed patients with MM. This increased nRelB activity was shown to be positively correlated with high RelB expression. MMRF transcriptomic data allowed us to show association of high RelB expression with poor prognosis. With NEMO kinase activity assay and NF-κB DNA binding assay on MMCLs, we showed that CYLD deficient KP-6 has higher canonical NF-κB activity as compared to CYLD sufficient JIM3 cells. This absence of deubiquitinase CYLD was associated with high RelB mRNA and protein levels at basal state that were further augmented by stimulation with BAFF, a non-canonical NF-κB activating cytokine. The re-enforced RelB activity in the absence of CYLD also provided advantage to CYLD deficient cells in survival and migration activities. This phenotypic advantage was mapped onto RelB mediated transcription of pro-survival factors such as BCL2, BIRC2, BIRC3, TRAF1 & c-FLIP and pro-migratory chemokine receptors such as CXCR4 & CXCR7. Deletion of CYLD using CRISPR-Cas9 editing to generate JIM3^{sgCYLD} cells, provided the causal role of CYLD mediated RelB enforced transcriptional axis that supports survival and migration in these malignant plasma cells.

Conclusions: The tumor microenvironment and cancer-associated mutations activate both canonical and non-canonical NF-κB pathways in MM. More so, these NF-κB pathways are intimately interlinked via a number of biochemical mechanisms. Our data signifies that RelB plays a role in the survival and migration of myeloma cells and mutational inactivation of CYLD exacerbates this disease-associated RelB phenotype, thus suggesting that NF-κB crosstalk mechanisms may provide prognostic evidence and therapeutic opportunities in the future.

#7354 ETS1 orchestrates a hybrid EMT program to drive metastasis and immune evasion in UASCC.

Chehyun Nam[1], Talia Wenger[1], Benjamin Ziman[2], Daniel Arnaudov[1], Thomas Tilton[1], Ethan Pan[1], Young Min Park[3], Uttam K. Sinha[4], De-Chen Lin[1]

[1]University of Southern California, Los Angeles, CA,[2]Biocare Medical, LLC, Walnut Creek, CA,[3]Yonsei University of College of Medicine, Seoul, Korea, Republic of,[4]Keck School of Medicine at USC, Los Angeles, CA

Intratumoral transcriptional heterogeneity (ITH) is a defining feature of aggressive cancers, yet the mechanisms by which distinct ITH programs drive metastasis and immune escape in upper aerodigestive squamous cell carcinoma (UASCC) remain poorly understood. Using single-cell RNA sequencing of cancer cell lines and patient tumors, we identified a hybrid epithelial-mesenchymal transition (hEMT) program strongly associated with metastatic potential. We determined that the transcription factor ETS1 functions as a master regulator of this hEMT state, directly activating pro-invasive and pro-metastatic gene networks and promoting distant dissemination in vivo. Beyond its role in metastasis, ETS1 unexpectedly established an immune-cold microenvironment by transcriptionally inducing STAT1 and PD-L1 (CD274), leading to reduced T-cell infiltration and elevated immune checkpoint expression. Clinically, ETS1-high tumors were consistently linked to poor survival and diminished responses to immune checkpoint blockade across multiple independent cohorts. Through a focused drug screen, we found that ETS1-high cancers exhibit selective vulnerability to HSP90 inhibition (e.g., Alvespimycin), which reduces ETS1 expression via disruption of HIF1A-driven transcription. Together, these findings define ETS1 as a central driver of both metastatic progression and immune evasion in UASCC and nominate HSP90 inhibitors as a promising therapeutic strategy for ETS1-driven disease states.

#7355 Investigating the interplay of transcription factor, ERG, and TGF-beta signaling in cervical cancer cells.

Kaitlyn Marie Eidson, Hannah Mckinsey Fitzgibbons, Logan J. Baker, Benjamin M. Greulich

Biology, Mercer University, Macon, GA

In healthy cells, TGF-β signaling is crucial to the cell cycle. The pathway promotes apoptosis, suppresses cellular proliferation, and stimulates immune cell activation. In malignant cells, however, TGF-β signaling has been shown to drive the proliferation of cancer through migration and metastasis, immune evasion, and angiogenesis. The effects of TGF-β signaling shift from tumor-suppressing to tumor-promoting as cancer progresses. Using TCGA data, we identified genes coexpressed with TβRIII. After determining which genes had the highest correlation, we used Enrichr to conduct pathway analysis. Pathway analysis indicated a relationship with ERG, leading us to hypothesize that ERG regulates TβRIII and other related genes. ERG seems to share many cancer behaviors with TGF-β, such as proliferation, invasion, and overall cell survival in cervical cancer. Kaplan-Meier Survival plots of TCGA data support decreased survival rates with high ERG expression in several other cancers as well, for the scope of this study, cervical cancer specifically. However, ERG has not been extensively investigated in this context. Western Blot analysis confirmed the presence of ERG expression in HeLa cells. Functional assays demonstrated that manipulating HeLa cells to express a knockdown of ERG led to a significant decrease in cell migration. The addition of TGF-β to HeLa cells with ERG knockdown (shERG) partially restores migration, suggesting that TGF-β could potentially compensate for the loss of ERG expression. To further investigate the effects of ERG on TGF-β, galunisertib, a known inhibitor of TGF-β signaling, was used. Analysis of scratch assays showed that in control HeLa cells, migration rates significantly reduced when exposed to galunisertib. In HeLa-shERG cells, migration was reduced as well; however, galunisertib failed to have the same decreased migration pattern in HeLa-shERG cells, suggesting that ERG and TGF-β pathways may converge in some way. HeLa-shERG significantly reduced the expression of TGFβ-I as well as decreasing the activation of SMAD2, a transcription factor that plays a significant role in TGF-β signaling. Invasion assays exposed HeLa cells' ability to travel throughout the extracellular matrix when manipulating TGF-β and ERG to measure metastasis. ChIP-seq is being done to investigate the possible interactions between TGFB signaling and ERG occupancy on the genome in cervical cancer, which will be compared to ERG sites in extensively studied cancers. Together, these findings suggest that ERG promotes cervical cancer cell migration and invasion, at least in part by regulating TGF-β signaling.

#7358 MYB expression increases progressively in pancreatic cancer, correlating with advancing tumor grade, metastasis, and poor patient survival.

Shashi Anand[1], Kunwar Somesh Vikramdeo[1], Mohammad Aslam Khan[2], Lingling Xian[3], Paul M. Grandgenett[4], James Elliot Carter[5], Moh'd Khushman[6], Seema Singh[1], Ajay Pratap Singh[1]

[1]Department of Cell and Molecular Biology, Cancer Center and Research Institute, University of Mississippi Medical Center, Jackson, MS,[2]Department of Pharmacy and Pharmaceutical Sciences, St. Jude Children's Research Hospital, Memphis, TN,[3]Department of Pathology, Yale School of Medicine, New Haven, CT,[4]Eppley Institute for Research in Cancer and Allied Diseases, University of Nebraska Medical Center, Omaha, NE,[5]Department of Pathology, Frederick P. Whiddon College of Medicine, University of South Alabama, Mobile, AL,[6]Division of Hematology and Oncology, Washington University in St. Louis and Siteman Cancer Center, St. Louis, MO

The transcription factor MYB plays a pivotal role in regulating cell proliferation, differentiation, and survival. Although it is amplified in a subset of pancreatic cancers, emerging evidence indicates that MYB overexpression may also arise through diverse regulatory mechanisms. We have previously demonstrated multiple oncogenic roles of MYB in pancreatic cancer pathogenesis; however, the temporal dynamics of its dysregulation during tumor progression remain poorly understood. Here, we investigated MYB expression across a spectrum of tissue samples representing normal, precancerous, and malignant stages of the pancreas, as well as matched liver metastases, by performing immunohistochemical analysis. The differential expression of MYB and its correlation with advancing tumor grade and patient survival were assessed using appropriate statistical analyses. We observed negligible expression of MYB in the normal pancreas, and its aberrant expression became noticeable in precancerous lesions, increasing progressively as the disease advanced. A high expression of MYB was also reported in metastatic lesions. Elevated MYB levels were positively correlated with higher tumor grade and significantly associated with reduced survival of pancreatic cancer patients. Interestingly, functional enrichment analyses of genes regulated by MYB overexpression suggested its involvement in key oncogenic programs, including proliferation, survival, epithelial-mesenchymal transition, and metastatic signaling pathways. These findings demonstrate that MYB dysregulation occurs early in pancreatic tumorigenesis and intensifies with disease progression, underscoring its potential as a biomarker for tumor aggressiveness and a potential target for therapeutic intervention.

#7359 The role of USP21 in prostate cancer.

Cheng Zhang

University of Kentucky, Lexington, KY

The Ubiquitin-specific protease 21 (USP21) is a deubiquitinase with pro-carcinogenic effects in various cancers. While its role and molecular mechanism in prostate cancer remain elusive. To investigate the role of USP21 in promoting prostate cancer, we evaluated that USP21 shows the highest mRNA expression in prostate cancer patients, and high USP21 levels predicted a poor prognosis in patients with prostate cancer. Additionally, suppression of USP21 significantly inhibited prostate cancer cell proliferation. *In vivo*, USP21 depletion significantly suppressed tumor growth in xenograft models. Moreover, we identified the androgen receptor (AR) as a potential substrate of USP21 by tandem affinity purification. Mechanistically, i) USP21 directly interacted and stabilized AR by deubiquitinating its K48-linked polyubiquitination, which is a main driver for prostate cancer. Silencing of USP21 enhances polyubiquitination of AR, promotes its proteasomal degradation, and ultimately attenuates PSA, while these effects could be largely restored by reintroduction of AR. ii) USP21 regulates transcriptional activity of AR according to our RNA-seq studies, we revealed that siUSP21 decreases both androgen response and AR-induced pathways, and knockdown USP21 decreases mRNA level of AR target genes. In conclusion, our project gives insight into the mechanism underlying how USP21 regulates AR to promote the progression of prostate cancer , therefore providing a novel approach for prostate cancer treatment.

#7360 Side-by-side evaluation of STAT3 targeted agents in oncology.

Xiaolan Su, Yue Zhai, Zhu Meng, Mingying Li, Tanfeng Zhao, Zhaoxia Yin, Qian Wang, Yanan Zhao, Lili Chai, Qiang Xia, **Tj (Tiejun) Bing**

ICE Bioscience, Beijing, China

Signal transducer and activator of transcription 3 (STAT3) is a critical transcription factor, which is aberrant activated in hematological malignancies, including acute myeloid leukemia (AML) and chronic lymphocytic leukemia (CLL), as well as solid tumors of the lung, breast, and others. Yet no selective STAT3 inhibitor has reached the clinic owing to disparate chemical matter, binding sites (SH2, DBD, CCD), and mechanisms (pY705 blockade, dimer disruption, DNA binding inhibition, degradation). We established a standardized integrated analytics platform that directly compares 5-10 chemically diverse STAT3 agents—including covalent SH2 ligands, allosteric DBD antagonists and PROTAC degraders—using harmonized biochemical (FP, TR-FRET etc), biophysical (SPR, SPS etc), and cellular (pSTAT3, reporter gene, HiBiT, proliferation) assays. Family and species selectivity, together with resistance panels, reveal distinct vulnerability windows and mechanism-based liabilities for each modality. The same matrix is screened in combination with JAK, SRC, EGFR, and chemotherapy partners to quantify synergy landscapes; By providing a comprehensive molecular-evaluation platform, the program streamlines hit-to-lead decisions, propels STAT3-directed drug discovery and accelerates the path to the clinic.

: Biological Mechanisms of Tumor and Normal Tissue Response and Clinical Studies
Poster Session

#7364 Candidate identification for SBRT versus surgery in early-stage NSCLC with interlobar pleural involvement: A multicenter retrospective study.

Zhengkun Cai, Zhiyong Yuan, Yue Wang

Tianjin Medical Univ. Cancer Inst. & Hospital, Tianjin, China

Purpose: This study aimed to compare survival outcomes between surgery and stereotactic body radiation therapy (SBRT) for early-stage non-small cell lung cancer (ES-NSCLC) with interlobar pleural involvement (ILPI), and to further identify patients who benefit more from SBRT.

Methods: This retrospective study analyzed 573 ES-NSCLC patients with ILPI, treated with surgery (n=379) or SBRT (n=194) across four centers. Propensity score matching (PSM) was employed to minimize confounding factors between treatment groups. Survival outcomes, including cancer-specific survival (CSS), disease-free survival (DFS) were estimated using the Kaplan-Meier method and compared with the log-rank test. Subgroup analyses utilized Cox proportional hazards models. We also conducted a comparative analysis of treatment-related adverse events (TRAEs) and assessed health-related quality of life (HRQoL) using the EORTC QLQ-C30.

Results: In the entire cohort, 3-year CSS was comparable between surgery and SBRT (HR, 1.48, 95% CI, 1.0-2.3; $P = 0.075$). In the PSM-matched cohort, CSS and DFS showed no significant differences (CSS: HR, 1.02, 95% CI, 0.6-1.5; $P = 0.822$; DFS: HR, 1.38; 95% CI, 0.8-2.5; $P = 0.374$). Multivariate Cox analysis identified several independent prognostic factors for CSS, including IPI features (site: HR, 0.48, 95% CI, 0.3-0.8; $P = 0.009$; location: HR, 2.05, 95% CI, 1.2–3.6; $P = 0.014$; type: HR, 8.00, 95% CI, 1.8–35.1; $P = 0.006$) and patient characteristics (age: HR, 1.88, 95% CI, 1.1–3.3; $P = 0.027$; smoking history: HR, 2.28 95% CI, 1.4–3.7; $P = 0.001$). Crucially, in the subgroup of patients over 70 years of age, SBRT was associated with significantly superior CSS compared to surgery (HR, 0.37, 95% CI, 0.2-0.8; $P = 0.007$). Specifically, CSS was improved in SBRT patients over 70 years with ILPI characterized by: Abutment-type ILPI (HR, 0.36, 95% CI, 0.1-1.0; $P = 0.045$), left lung oblique fissure (OF) involvement (HR, 0.21, 95% CI, 0.1-0.7; $P = 0.011$), or central ILPI location (HR, 0.10, 95% CI, 0.0-0.6; $P = 0.012$). Conversely, surgery showed better DFS in patients < 70 years and those with peripheral ILPI or right OF involvement. Regarding TRAEs, surgery was predominantly associated with pain (28.5%), while the SBRT cohort experienced fatigue (22.7%). The HRQoL showed SBRT was associated with significantly better preservation of emotional function and avoided the worsening of pain observed after surgery, which showed greater improvements in role and social function.

Conclusions: SBRT offers survival outcomes comparable to surgery for ES-NSCLC with ILPI without increasing the burden of TRAEs or compromising HRQoL. Patient age and ILPI characteristics are critical factors in guiding treatment selection. SBRT is particularly beneficial for patients over 70 years, especially those presenting with abutment-type ILPI, left OF involvement, or central ILPI.

#7365 Potential role of Lipocalin 2 as a biomarker of radio resistance in head and neck squamous cell carcinoma (HNSCC).

Smriti Suri[1], Sushmita Ghoshal[2], Jaimanti Bakshi[3], Arnab Pal[1]

[1]Biochemistry, Postgraduate Institute of Medical Education & Research (PGIMER), Chandigarh, India,[2]Radiotherapy, Postgraduate Institute of Medical Education & Research (PGIMER), Chandigarh, India,[3]Otolaryngology and Head & Neck Surgery (ENT), Postgraduate Institute of Medical Education & Research (PGIMER), Chandigarh, India

Background: HNSCC has significant burden with high morbidity and mortality. Majority of the HNSCC patients receive Radiotherapy (RT), which is associated with development of radiation resistance and disease-recurrence, which needs in-depth evaluation. Lipocalin2(LCN2), found to be dysregulated in the saliva of HNSCC patients in our previous study using LC/MS shotgun proteomics, is also found associated with radio resistance (RR). To establish the potential role as a predictor of RR, we evaluated LCN2 in HNSCC patients.

Methodology: 356 biopsy-proven treatment-naïve HNSCC, 26 Oral Pre-Malignant Diseases (OPMDs) and 118 healthy subjects were recruited for the study. The patients were treated with curative intent with 66Gy of RT. 5ml of unstimulated saliva and 3ml of whole blood were collected at baseline and during follow-ups in No evidence of disease (NED) and Residual Disease (RD)patients post therapy completion. To evaluate the role LCN2 as a marker of RR, radioresistant cells were generated by repeated sub-lethal exposure of Cal27 cells to γ-rays from radioactive Co^{60}. The RR phenotype was confirmed by phosphorylated H2AX(γH2AX) expression using Western Blot (WB) and Immunofluorescence (IF). Various RR assays such as clonogenic survival assay, apoptosis assay and cell cycle analysis, were performed on the successfully generated RR cells, which were later analysed for the expression of LCN2.

Results: Significantly higher($p \leq 0.0001$) levels of LCN2 in saliva and serum (median- 609.15ng/ml & 186.18ng/ml) of patients compared to OPMD (median-358.47ng/ml & 124.05ng/ml) and healthy controls (median-95.70ng/ml & 85.53ng/ml) respectively. The increased level of these proteins also correlated with patients' response post therapy completion with significantly higher($p \leq 0.0001$) LCN2 in RD (median-1919.61ng/ml & 133.48ng/ml) group compared to NED (median-537.27ng/ml & 90.68ng/ml), indicating that the increased LCN2 level estimated after therapy completion is associated with therapy resistance. Poorly differentiated patients had significantly higher($p \leq 0.0001$) LCN2(H-score148.12) as compared to moderately(H-score34.04) and well differentiated(H-score17.12) on IHC analysis. In the generated RR cell line, on IF analysis γH2AX foci was significantly higher validated by western blot. Further using clonogenic survival assay, apoptosis and cell cycle analysis assay it was henceforth proven that the cell lines generated had RR characteristics. The proven RR cell lines were further checked for LCN2 expression, which had significantly higher (3.6 fold) expression as compared to wild type cell lines. The results were validated with western blot.

Conclusion: LCN2 is proposed as a predictive biomarker to prognosticate resistance to radiation in patients with HNSCC.

#7366 Survival outcomes with concurrent systemic therapy in patients with a medical contraindication to cisplatin in the non-operative management of locally advanced HNSCC, an NCDB Study.

Deniz C. Demircioglu[1], Sohil Singh[1], Johnny Belcher[1], Joseph Zenga[2], Stuart J. Wong[3], Musaddiq Awan[4]

[1]Medical College of Wisconsin, Wauwatosa, WI,[2]Department of Otolaryngology, Medical College of Wisconsin, Wauwatosa, WI,[3]Department of Medicine, Division of Hematology and Oncology, Medical College of Wisconsin, Wauwatosa, WI,[4]Department of Radiation Oncology, Medical College of Wisconsin, Wauwatosa, WI

Standard-of-care non-operative management for locally advanced head & neck squamous cell carcinoma (HNSCC) is definitive radiation with concurrent cisplatin. NRG-HN004 demonstrated the benefit of concurrent cetuximab in patients with a medical contraindication to cisplatin including those older than 70 with a Charleson-Deyo (CD) score ≥ 1 and those under 70 with a CD score ≥ 2. In these populations, the survival benefits of concurrent systemic therapies may be limited due to medical co-morbidities. We evaluated overall survival (OS) of these populations in the National Cancer Database (NCDB) comparing radiation-treated patients who received concurrent chemotherapy against concurrent immunotherapy (most likely cetuximab given it is the only FDA-approved immunotherapy for this indication). The NCDB was queried for data from 2015-2023 to include stage III, IVa, and IVb non-metastatic HNSCC patients that met the HN-004 criteria. Histological subtypes of squamous cell carcinoma (SCC) were identified using ICD-O-3 codes 8070-8078. Patients with clinical T3-T4 and/or clinically node-positive disease with a known primary were included. Patients who received less than 60 Gy were excluded. Groups were stratified based on radiation with chemotherapy (RT-C) or radiation with immunotherapy (RT-I) without overlap. Concurrent systemic therapy was defined as having started within 30 days of the initiation of radiation. OS was evaluated using Kaplan-Meier (KM) statistics and differences were evaluated using log-rank testing. A $p < 0.05$ was considered statistically significant. To minimize the effect of informative censoring, patients without documented follow-up after January 1, 2023 were counted as deaths unless they had greater than 5 years of observed follow-up. Additionally, KM estimates were capped at 5 years. A total of 6299 patients were identified: 5657 treated with RT-C and 642 treated with RT-I. 2-year OS was 65.0% (95% CI, 63.8-66.3) and 52.9% (95% CI, 49.2-57.0) for RT-C and RT-I, respectively. 5-year OS was 20.7% (95% CI, 19.6-21.9) and 21.8% (95% CI, 18.7-25.5) for RT-C and RT-I, respectively. KM analysis ultimately showed no significant difference between the two treatment cohorts (log-rank p=0.059). In a subgroup of patients with medical contraindications to cisplatin, there was no statistically significant improvement in OS with concurrent chemotherapy over concurrent immunotherapy (likely cetuximab) for locally advanced HNSCC in this real-world dataset. Critically, early survival benefits seen with concurrent chemotherapy dissipate with long-term follow-up possibly due to deaths from other causes in this population with extensive co-morbidity. Further prospective study is needed to evaluate the benefit of concurrent chemotherapy over cetuximab in this frail population.

#7367 Proton versus photon VMAT craniospinal irradiation for hematologic leptomeningeal disease: A comparative study.

Brianna Hostler[1], Gene Lamanilao[2], Tam Le[2], Tara Austin[3], Caitlin L. Costello[4], Ah-Reum Jeong[4], Kaitlyn Dykes[4], Ayad Hamdan[4], Nadeem Tabbara[4], Iain Macewan[2], Jona A. Hattangadi-Gluth[2], Parag Sanghvi[2], Kathryn R. Tringale[2]

[1]Department of Psychology, San Diego State University, San Diego, CA,[2]Department of Radiation Medicine and Applied Sciences, University of California San Diego, La Jolla, CA,[3]Department of Psychiatry, University of California San Diego, La Jolla, CA,[4]Department of Medicine, University of California San Diego, La Jolla, CA

Craniospinal irradiation (CSI) is an effective treatment option in the treatment of hematologic leptomeningeal disease (LMD), a challenging condition seen in a variety of hematologic malignancies. Comparative outcomes between CSI delivered with protons (“pCSI”) versus modern photon-based volumetric modulated arc therapy (VMAT, or “xCSI”) have not been described in hematologic LMD. It is hypothesized that pCSI may reduce hematologic toxicity compared to xCSI due to the more favorable dose distribution regarding bone marrow sparing. This study compares acute toxicities and survival between xCSI and pCSI, hypothesizing higher toxicity with xCSI but similar survival after adjusting for performance status. Adult hematologic LMD patients treated with CSI between 2020 and 2025 were identified. Acute hematologic toxicities were graded using CTCAE v.5.0 at baseline, during treatment, and at 1- and 3-months post-CSI. Overall survival (OS) and CNS progression-free survival (CNS-PFS) were evaluated from CSI end to death and progression event, respectively, using Kaplan-Meier. OS was further analyzed using Cox proportional hazards models adjusted for ECOG performance status. Of 34 patients (median age 38), 26 (76%) received xCSI and 8 (24%) received pCSI. The delivered radiation dose ranged from 7.2 Gy-30.6 Gy in 4-17 fractions. Baseline clinicodemographic variables were similar between pCSI and xCSI: most patients had an ECOG score of 1 (p=.802), and acute lymphoblastic leukemia (58.8%) and non-Hodgkin lymphoma (17.6%) were the most common histologies (p=.517). Grade ≥3 lymphopenia was significantly higher during xCSI (p=0.006) but resolved by the 1-month post-CSI follow-up (p=.202). No other significant differences in acute hematologic toxicities were observed. Median OS was 28.3 months and did not significantly differ between the groups (28.26m; 95%CI, 21.19-35.33; p=.228) and remained nonsignificant after adjustment for ECOG (HR 0.16; 95% CI, 0.02-1.45; p=.103). Median CNS-PFS was not reached (p=.212). pCSI and xCSI demonstrated similar survival and acute hematologic toxicity profiles in hematologic LMD, supporting the safety of VMAT xCSI. However, patients who received xCSI were more likely to have severe lymphopenia, which is a particularly relevant endpoint for patients with hematologic malignancies who often have vulnerable bone marrow. These data are important to add to the existing literature on CSI for solid tumor LMD, as hematologic malignancies are a particularly at-risk population. While this study is limited by small cohort size and patient selection, it is an important first step toward optimizing the management of hematologic LMD.

#7368 Dynamic molecular and immune characterization for personalized treatment in locally advanced rectal cancer.

Fiza Ishaqwala[1], Ashley McCulloch[1], Lily Hillson[1], Liang Tang[2], Leonor Schubert Santana[1], Chia Yew Kong[1], Ross McMahon[1], Lynsey Devlin[3], Walaiphorn Woraharn[1], Noori Maka[4], Timothy Mitchell[3], Sean O'Cathail[1], Jean Quinn[1], Simon WF Milling[1], Philip Dunne[5], Colin W. Steele[1], **Joanne Edwards**[1], Campbell S. Roxburgh[1]

[1]University of Glasgow, Glasgow, United Kingdom,[2]Varian Medical Systems, Salt lake city, UT,[3]NHS Greater galsggow and Clyde, Glasgow, United Kingdom,[4]Queen Elizabeth University Hospital, Glasgow, United Kingdom,[5]Queen's University Belfast, Belfast

Background: Locally advanced rectal cancer (LARC) shows highly variable responses to neoadjuvant radiotherapy with a minority of patients achieving complete tumor regression. Existing clinical tools cannot reliably predict responders using pre-treatment samples. Understanding the dynamic molecular and immune changes occurring during and after radiotherapy is initiated is therefore critical to guide personalized treatment strategies and improve outcomes.
Aims/Objectives: This study employed a serial rectal tumor sampling protocol during neoadjuvant treatment. We aim to characterize longitudinal transcriptomic changes in LARC tumors during radiotherapy and to identify early molecular and microenvironmental features associated with treatment response.
Methods/Results: Tumor biopsies were collected from 38 patients at baseline, week 2, week 6, and week 12 during short-course or long-course radiotherapy. Bulk RNA-seq was used to profile gene expression across time. PCA and differential expression analyses showed that most transcriptional reprogramming occurred between baseline and week 2, with minimal changes at later time points. Responders exhibited early downregulation of proliferation-related genes alongside sustained activation of immune pathways. Divergence from non-responders was most evident by week 2, highlighting a critical window for treatment response. Consensus Molecular Subtype (CMS) classification showed enrichment of CMS2 in non-responders and CMS4 in responders. Tissue composition further influenced transcriptional patterns, with stromal-rich samples in responders displaying stronger immune signatures. Based on Cell deconvolution tools, responders showed pronounced week-2 activation of myeloid and lymphoid populations, while non-responders exhibited delayed immune activation.
Conclusions: This study shows that radiotherapy response in LARC is determined early, with week 2 emerging as a key point where responders and non-responders clearly diverge. Responders rapidly suppress proliferation and activate strong immune programs, while non-responders show delayed or minimal immune engagement. These early molecular and microenvironmental shifts highlight an important role for early immune activation in directing successful RT responses. These features, present early during therapy suggest that on-treatment predictive biomarker development should be pursued to support development of adaptive, personalized treatment strategies.

#7369 Hypofractionated prostate and pelvic nodal radiotherapy with androgen deprivation therapy for high-risk prostate cancer: A retrospective analysis of oncologic outcomes and toxicity.

Eashwer Reddy[1], **Affan Ahmad Ansari**[2], Inamul Haque[1], Dunia Khaled[3], John Park[4]

[1]Medical/Radiation Oncology, Kansas City VA Medical Center, Kansas City, MO,[2]University of Missouri - Kansas City, Kansas City, MO,[3]Urology, Kansas City VA Medical Center, Kansas City, MO,[4]Radiation Oncology, North Kansas City Hospital, Kansas City, MO

Purpose: This study evaluated the clinical outcomes and toxicity of hypo-fractionated prostate radiotherapy combined with elective pelvic nodal irradiation and androgen deprivation therapy (ADT) in patients with unfavorable intermediate-risk, high-risk, and very high-risk localized prostate cancer.
Methods: A retrospective analysis was conducted on 152 consecutively treated patients from 2014 to 2024. After excluding 21 deaths unrelated to prostate cancer, 131 patients formed the study cohort. All patients received volumetric modulated arc therapy (VMAT) with daily cone-beam CT image guidance. Treatment consisted of prostate hypo-fractionation delivered with a simultaneous integrated boost and pelvic nodal irradiation to 46-50 Gy in 20-25 fractions. ADT was administered for 6-24 months according to disease risk. Patients were followed for biochemical relapse-free survival (bRFS), disease-free survival (DFS), overall survival (OS), and genitourinary (GU) and gastrointestinal (GI) toxicity.
Results: With a median follow-up of 55 months, the cohort demonstrated a DFS rate of 93.8% and an OS rate of 97.7%. Eight patients experienced progression, including five metastatic deaths and three biochemical failures. Cumulative grade III or higher GU toxicity was 3.8%, including one grade IV event; no grade III or higher GI toxicity occurred. Toxicity remained low despite pelvic treatment, likely attributable to modern VMAT planning, daily image guidance, and consistent bowel and bladder preparation.
Conclusions: Hypo-fractionated prostate radiotherapy with elective pelvic nodal coverage and ADT produced excellent long-term disease control with minimal severe toxicity in high-risk and very high-risk prostate cancer. These findings support the safety and effectiveness of elective pelvic nodal irradiation when delivered with contemporary image-guided radiotherapy techniques and reinforce its potential role in the modern management of high-risk disease.

#7370 End-to-end *in vitro* and *in vivo* evaluation of radiopharmaceuticals in patient-derived models.

Anita Liu[1], Bryan Miller[2], Antonella di Mambro[2], Prabhakar Panday[1], Rosemary Shoop[1], Esther Kingma[2], Chiara Da Pieve[1], Bhushan Rai[2], Juliana Maynard[1], Elisabet Fernandez-Potente[1], Tatiane Takahashi[1], Bram Herpers[2], Lucy Harris[2], Lynne Braidwood[1], Ludovic Bourre[2], **Benedetta Arno**[1]

[1]Medicines Discovery Catapult Limited, Macclesfield, United Kingdom,[2]Crown Bioscience Inc, San Diego, CA

Background & Rationale Targeted radionuclide therapy (TRT) using alpha- and beta-emitting agents offers a precision approach to cancers treatments, with improving outcomes while minimizing systemic toxicity. The development and clinical translation of novel radiopharmaceuticals depend on the integration of robust *in vitro* and *in vivo* assays throughout the drug discovery process, critical for assessing target specificity, pharmacokinetics, biodistribution, drug resistance mechanism and therapeutic index. 3D cell lines and cell line-derived xenograft (CDX) provide fast and cost-effective means to assess drug effects, whereas patient-derived (xenograft) organoid (PD(X)O) and patient-derived xenograft (PDX) models preserve heterogeneity, tumour architecture, and enable more clinically predictive assessment of therapeutic efficacy across diverse patient populations. In this study, the theranostic pairing of [^{68}Ga]Ga-PSMA-617 and [^{177}Lu]Lu-PSMA-617 were prepared and tested in 2D and 3D in vitro assays using CDX and PDXO, followed by *in vivo* testing in PDX models to evaluate target expression, therapeutic efficacy, and translational relevance across heterogeneous PSMA expression profiles.

Methods PSMA-617 was radiolabelled with ^{68}Ga and ^{177}Lu using standard manual procedures. The RCP was confirmed by RP-HPLC and TLC analysis. Viability was measured on prostate cancer models with differential PSMA expression levels upon treatment with [^{177}Lu]Lu-PSMA-617. DNA damage (γH2AX) was assessed by immunofluorescence to evaluate radiobiological effects. PDX mouse models were imaged with [^{68}Ga]Ga-PSMA-617 PET to assess target density and heterogeneity prior to therapy and monitor treatment response. Prostate PDX models received a single dose of 50 MBq [^{177}Lu]Lu-PSMA-617. Subcutaneous tumour growth, survival and body weight were monitored over time. CBC (WBC, RBC, platelets, neutrophils, lymphocytes) was analysed prior to treatment and regularly after treatment to assess bone marrow toxicity.

Results Radiolabelling of PSMA-617 with ^{68}Ga and ^{177}Lu yielded products with an RCP≥95%, as determined by HPLC analysis, with no further purification. The specific activities of [^{68}Ga]Ga-PSMA-617 and [^{177}Lu]Lu-PSMA-617 were 10 and 17.5 MBq/nmol, respectively. Both *in vitro* and *in vivo* findings demonstrate distinct responses to [^177Lu]Lu-PSMA-617 treatment, consistent with varying PSMA expression levels, evidenced by diagnostic PET imaging and comprehensive PDX models characterization.

Conclusions Our results highlight the importance of integrating radiochemistry expertise with clinically relevant patient-derived models to thoroughly characterize novel radiopharmaceuticals. This holistic approach enhances the predictive accuracy of preclinical studies and ensures that emerging therapeutic strategies are closely aligned with clinical demand.

#7371 High-definition spatial and single-cell multiomics reveal immunological remodeling and radiation resistance mechanisms in colorectal cancer.

Junbum Kim[1], Olivier Elemento[2], Christina Montagna[3], Nir Ben Chetrit[1], Silvia C. Formenti[1], Liron Yoffe[1]

[1]Weill Cornell Medicine, New York, NY,[2]Weill Cornell Medical College of Cornell Univ., New York, NY,[3]Radiation Oncology, Rutgers University, New Brunswick, NJ

Radiation therapy remains central to colorectal cancer care, yet many patients experience incomplete response or recurrence. Understanding why tumors adapt instead of regress requires mapping how radiation reshapes both local and systemic immunity. The ImmunoRad ROBIN initiative addresses this need by integrating high definition spatial and single cell profiling to identify biological processes that sustain radiation resistance.Our cohort included six patients sampled before treatment, after radiation, and at surgery across tumor, adjacent mucosa, and lymph nodes. Using VisiumHD at 2 × 2 µm resolution, we generated more than one and a half million spatial spots, providing a near cellular view of therapy induced remodeling. A dominant pattern emerged at the tumor stroma boundary, where radiation triggered extracellular matrix activation, fibroblast signaling, and wound repair programs. These regions were enriched for M2 like macrophages expressing profibrotic and angiogenic genes. Their expansion suggests that a macrophage dependent repair niche forms at the invasive front and creates conditions that support tumor persistence.These stromal changes aligned with localized epithelial stress responses, showing that adaptation occurs through coordinated tissue level remodeling. Epithelial compartments displayed DNA damage repair, interferon signaling, and partial plasticity, especially near M2 rich zones. Adjacent mucosa showed weaker shifts in antigen presentation and barrier pathways. These patterns indicate that radiation injury extends across tumor and non-tumor tissue, generating new gradients that may influence treatment outcome.To assess systemic adaptation, we performed single cell RNA sequencing on matched blood. Early after radiation, circulating lymphocytes and dendritic cells showed transient interferon signatures. By surgery, these activated populations contracted and were replaced by suppressive myeloid subsets with reduced cytotoxic T cells, suggesting that initial immune activation shifts into a suppressive state. Lymph nodes exhibited disrupted follicular structure, reduced germinal center polarity, and expansion of mantle zones. Integrated analysis showed enrichment of regulatory T cells and exhausted CD8 T cells, consistent with impaired antigen driven immunity.Together, these findings support a model in which radiation triggers acute injury and immune activation that rapidly transitions into macrophage driven repair and systemic immune suppression. This coupled remodeling allows tumor cells to survive therapy and regain growth potential. The ImmunoRad ROBIN framework offers a scalable strategy for decoding treatment induced ecosystem changes and highlights stromal remodeling and lymph node dysfunction as central contributors to radiation resistance in colorectal cancer.

#7372 HOXA1 promotes radioresistance via activation of the ERK/HIF1A signaling pathway.

Tae-Jun Kim, Hyun-Jin Shin, Jong Kuk Park

Korea Institute of Radiological & Medical Sciences (KIRAMS), Seoul, Korea, Republic of

Oral squamous cell carcinoma (OSCC), the most common subtype of head and neck squamous cell carcinoma (HNSCC), remains a major clinical challenge due to treatment resistance, particularly radioresistance. Despite advances in surgery, radiotherapy, chemotherapy, targeted therapy, and immunotherapy, the 5-year survival rate for HNSCC patients has improved only marginally. HOXA1, a member of the homeobox (HOX) gene family, has been implicated in tumor progression and prognosis across several cancer types. However, its specific role in OSCC and its potential involvement in radioresistance remain unclear. In this study, we analyzed HOXA1 expression in OSCC patient samples with diverse clinicopathological features and generated HOXA1-deficient OSCC cell lines using CRISPR/Cas9 technology. Following validation of stable knockout, we assessed the expression of genes associated with proliferation, migration, and invasion at both mRNA and protein levels. HOXA1-deficient cells exhibited markedly decreased colony formation and cell viability after irradiation compared with control cells, indicating that HOXA1 contributes to radioresistance. Transcriptomic enrichment analysis further revealed an upregulation of focal adhesion-related genes in HOXA1-deficient OSCC cells. Mechanistically, HOXA1 was found to activate a focal adhesion via the ERK/HIF1A signaling pathway, underscoring its pivotal role in OSCC progression and therapeutic response.

#7373 An integrated bioinformatic and experimental analysis of radiation-induced epigenetic reorganization in colorectal cancer.

Megan Tandar, Allison Pittman, Christine E. Eyler

Duke University, Durham, NC

Colorectal cancer is the second-leading cause of cancer-related deaths in the US. Resistance to radiation therapy - known as radioresistance - often develops during treatment, leading to metastases and death. Current research overlooks the dynamic epigenetic changes that occur during therapy, limiting the development of effective therapeutics.

My project aims to profile and interrogate these radiation-induced epigenetic alterations across multiple in vitro colorectal cancer models. To study this phenomenon across diverse colorectal cancer subtypes, I integrated high-throughput sequencing analyses with wet-lab CRISPR screens to identify radiotherapy-affected epigenetic regions and validate them in biologically relevant models.

I performed RNA Sequencing (RNA-Seq), Gene Set Enrichment Analysis (GSEA), and Assay for Transposase-Accessible Chromatin Sequencing (ATAC-Seq) on radiation-treated colorectal cancer cell lines to characterize radiation-induced epigenetic changes. I administered two courses of radiation treatments on HCT116, SW480, MDST8, and RKO lines to mimic clinically relevant radiation courses: (1) a single-dose treatment of 0, 2, or 5 Gy, and (2) a fractionated-dose treatment of 0 or 2 Gy administered daily for five consecutive days. To validate these bioinformatic analyses, I employed dual whole-genome-wide CRISPR knockout screens in both HCT116 and MDST8 colorectal cancer cell lines to experimentally identify radiation-induced epigenetic alterations, screening 180 million cells under 0 Gy control and 2 Gy multi-dose irradiation conditions.

RNA-Seq revealed consistent post-radiation transcriptional changes in all four cell lines. The 5 Gy-irradiated RKO lines showed regions of the genome that had increases in gene expression with increasing radiation treatment, suggesting a potential radiation-induced epigenetic regulatory mechanism. In multi-radiation dose experiments, volcano plot analysis revealed increased expression of immune-related genes such as IFIT1 in HCT116 cells and similar lines. I ran additional GSEA analyses, which confirmed alterations in immune-sensing pathways following radiation treatment and suggest a potential link among immune response, radiation treatment, and epigenetic regulation in colorectal cancer. I am currently analyzing CRISPR and ATAC-Seq data, but anticipate overlap in radiation-altered epigenetic regions between datasets.

We aim to integrate CRISPR-screen data with RNA-Seq, GSEA, and ATAC-Seq analyses. I expect these results to contribute to the novel characterization of key radiation-induced colorectal epigenetic alterations and provide a robust framework for studying radioresistance in colorectal cancer. Ultimately, we hope to use these results to develop personalized, time-sensitive therapies that may improve patient outcomes and quality of life.

#7374 Molecular imaging guided precision radiotherapy and quantitative assessment of metastatic colorectal cancer.

Yunwen Huang[1], Jiahao Chen[1], Ning Zhao[2], Yidong Yang[1]

[1]University of Science and Technology of China, Hefei, China,[2]Raycision Medical Technology Co. Ltd., Hefei, China

Early detection and intervention of metastasis remain challenging and contribute significantly to cancer mortality. This study developed a molecular image-guided precision radiotherapy system that can early detect, precisely irradiate, and quantitatively assess metastatic tumors. Using the highly aggressive orthotopic HCT116 colorectal cancer model, we validated the system's detection sensitivity for primary and metastatic tumors and the efficacy of BLT/CT-guided radiotherapy (32 Gy in 4 fractions). The system detected metastatic tumors as small as 300 μm, with BLT-derived tumor size strongly correlating with histopathology ($R^2 = 0.91$, $p < 0.001$). γ-H2AX immunofluorescence staining revealed DNA damage foci predominantly localized within the tumor volume, confirming precise targeting. At 23 days post-treatment, the irradiation group exhibited reduction in bioluminescence intensity to 0.61-fold and tumor volume to 0.57-fold of initial values, whereas the control group showed increases to 86.62-fold and 5.89-fold, respectively ($p < 0.001$). FITC-dextran permeability assay and histological analysis of the entire intestine confirmed preserved intestinal barrier function and structural integrity. With precise targeting and minimal toxicity, the radiation group achieved >2-fold prolonged survival. This multimodal image-guided system enables accurate localization, precise treatment, and quantitative assessment of early-stage and metastatic tumors, offering significant potential for malignancies within complex soft tissue environments or with disseminated spread.

#7375 Efficacy of irreversible electroporation as treatment for hepatocellular carcinoma based on liver explants.

Michael Lauricella, Gauri Kelekar, Olufoladare Olorunsola

California Pacific Medical Center, San Francisco, CA

Introduction: Hepatocellular carcinoma (HCC) commonly develops in the context of cirrhosis. In these patients, liver transplantation remains the therapeutic approach with the highest likelihood of achieving cure. Local treatments such as ablation may be used to control HCC in patients awaiting a suitable organ. Irreversible electroporation (IRE) is a nonthermal ablation modality often considered for tumors in locations not amenable to thermal ablation, such as those near bile ducts, bowel, and other vulnerable structures. Previous studies investigating IRE have assessed efficacy primarily based on surveillance imaging. To these authors' knowledge, this is the largest study to examine HCC response to IRE in liver explants.

Methods: This single-institution retrospective study includes 18 patients who received IRE for HCC between 2018 and 2025 and subsequently underwent liver transplantation. Among liver transplantation candidates with HCC requiring a bridging locoregional therapy, IRE was selected as the treatment modality for tumors less than 3 cm located within 1 cm of heat-vulnerable structures. IRE treatments were performed in a single session. Procedural complications were recorded and classified according to the Society of International Radiology (SIR) grading system. Surveillance imaging (CT or MRI) was obtained at one month post-IRE, and every three months subsequently. A board-certified radiologist specialized in abdominal imaging interpreted all surveillance imaging according to LI-RADS treatment response criteria, with binary categorization of the treated lesion as viable or nonviable. One of several board-certified pathologists evaluated each liver explant with respect to viability of the IRE-treated lesion.

Results: Mean patient age was 62 (SD: 54-70). 72% were male. Their race/ethnicity were 61% white, 27% hispanic, 5% asian, 5% black. The etiology of their cirrhosis was either hepatitis C (61%), hepatitis B (11%), or alcohol use disorder (27%). Barcelona Clinic Liver Cancer (BCLC) classification was either A (78%) or B (22%). Child-Pugh classification was either A (78%) or B (22%). The average pre-ablative alpha-fetoprotein (AFP) was 33 (SD: 0-100). Mean size of treated lesions was 2.3 cm (SD: 1.3-3.3). Mean time between IRE and liver transplantation was 540 days (SD: 300-780). Two patients had IRE procedural complications, one classified as SIR 1 and the other as SIR 2. 16 of the 18 patients (89%) had complete tumor necrosis of the treated lesion on pathological review of the explanted liver. There was 100% correlation between viability assessment on surveillance imaging and that on explant histopathology.

Conclusions: IRE is a safe and effective method for treating HCC in the pre-transplant setting. Surveillance imaging has high accuracy in assessing HCC response after IRE relative to histopathologic assessment.

#7376 HMGB2-mediated radioresistance of glioblastoma stem cells.

Sara Nalina Barcik Weissman[1], Cheol Park[1], Connor Mork[1], Khoi Huynh[1], Yingwen Ding[2], Ze-yan Zhang[2], Eric L. Chang[1], Erik P. Sulman[2], Aram S. Modrek[1]

[1]Radiation Oncology, Keck School of Medicine of USC, Los Angeles, CA,[2]Radiation Oncology, NYU School of Medicine, New York, NY

Glioblastoma (GBM) is the most common and deadly adult central nervous system cancer. Despite surgical resection combined with DNA-damaging radiation and chemotherapy, GBM almost invariably recurs, becoming more resistant to radiation. To investigate the drivers of this radioresistance, we conducted a knockout radiosensitization screen and identified the High Mobility Group B2 (HMGB2) protein as a potential contributor. To elucidate HMGB2's role in GBM radioresistance, we performed viability, clonogenic survival, extreme limiting dilution (ELDA), and deletion mutant assays on patient-derived glioblastoma stem cells (GSCs) treated with a combination of radiotherapy (RT) and either HMGB2 knockdown or inhibition using Inflachromene (ICM), a small molecule inhibitor of HMGB2. Without radiation, ICM showed IC-50 values ranging from 8.43 μM to 10 μM across three GSC lines. Both ICM treatment and HMGB2 knockdown significantly reduced neurosphere formation compared to cultures treated with only RT and vehicle. Knockdown of endogenous HMGB2 combined with overexpression of an Acidic Tail-deleted HMGB2 mutant produced distinct puncta under fluorescence microscopy, unlike other deletion mutants. These findings implicate HMGB2 in GBM radioresistance and suggest that the Acidic Tail region mediates chromatin binding, possibly playing a role in HMGB2's mechanism of action. Together, these results provide a foundation for clarifying HMGB2's role in GBM biology and it's potential relevance to improving therapeutic response.

#7377 Radiation-mediated complement cascade activation within the lung tumor microenvironment diminishes the efficacy of radiation therapy.

Harendra Shah[1], Minakshi Saikia[1], Xiaobo Wu[2], John P. Atkinson[2], Abhay K. Singh[2], **Vaishali Kapoor**[2]

[1]Department of Radiation Oncology, Washington University In St. Louis School of Medicine, St. Louis, MO,[2]Washington University In St. Louis School of Medicine, St. Louis, MO

Non-small cell lung cancer (NSCLC) is the primary cause of cancer-related mortality worldwide, necessitating novel interventions to improve survival rates. Current treatment modalities for locally advanced NSCLC involve cytotoxic chemotherapy with concurrent external beam radiation therapy (XRT), followed by immunotherapy. However, the impact of XRT on the complement system, a crucial component of innate immunity, remains unclear. The complement regulatory proteins (CRPs), including CD46, CD55, and CD59, tightly control complement activation mediated by the three pathways. In this study, we investigated the surface expression of CRPs in NSCLC cell lines *in vitro* and within the tumor microenvironment (TME) *in vivo*. We assessed the activation of the three complement pathways in the TME and monitored tumor growth and survival in C57BL/6 wild-type, $C3^{-/-}$, and $C3AR^{-/-}$ mice following XRT. Following XRT, NSCLC cell lines A549 and H460 exhibited a significant increase in the cell surface expression of CD46, CD59, and CD55 compared to controls ($p<0.05$), whereas normal lung epithelial cells (MRC5) did not display such upregulation. Irradiated Lewis lung carcinoma (LLC) tumors in wild-type mice demonstrated elevated levels of C3 and C5 mRNA and protein ($p=0.0013$). Also, C3AR and C5AR were significantly upregulated in the irradiated LLC tumor as compared to the sham. Additionally, the alternative complement pathway components, factor B and factor D, were significantly upregulated ($p<0.001$) in the LLC TME following XRT. However, the membrane attack complex (MAC) did not form in XRT-treated LLC tumors compared to sham. Deficiency of the central C3 and C3AR complement components in $C3^{-/-}$ and $C3AR^{-/-}$ mice delays LLC tumor growth in combination with XRT. Our findings suggest that XRT increases the expression of CRPs in NSCLC, potentially facilitating immune evasion by tumor cells. We also found activation of the alternative pathway of the complement system. Targeting C3 and C3AR effectively delayed tumor growth, highlighting the potential of complement pathway modulation to enhance the efficacy of XRT in NSCLC treatment. These results underscore the importance of elucidating the intricate interplay between radiation-induced complement activation and tumor survival for devising novel therapeutic strategies in NSCLC.

#7378 Prolonged radiation exposure alters cellular proteome network in human hepatocellular carcinoma cells.

Mohammed Sikander, Shabnam Malik, Rajasekhar Baru, Daniel Zubieta, Iris Enriquez, Mirza S. Baig, Murali M. Yallapu, Subhash C. Chauhan

The University of Texas Rio Grande Valley, Edinburg, TX

Background: Hepatocellular carcinoma (HCC), leading cause of cancer-related mortality globally, presents a major challenge as majority of patients are diagnosed at later stages, rendering them ineligible for effective interventions such as liver resection and transplantation. Radiation therapy (RT) is growing as a well-tolerated non-invasive local ablative treatment option; however, its effectiveness is restricted by therapy-induced radioresistance, resulting in tumor recurrence, enhanced invasion, and alterations in the extracellular matrix. This study aims to examine the impact of prolonged radiation exposure on the molecular dynamics and cellular behavior of HCC cells, with particular emphasis on the function of invadopodia in acquired resistance and increased invasiveness, to pave the way for development of novel therapeutic strategies for improved patient outcomes.
Methodology: Radioresistant HCC cell lines were created by exposing them to a cumulative dose of 20 Gy of radiation (2 Gy daily for ten-days) followed by functional assays to measure colony formation, invasion, and migration. LC-MS was used to identify and quantify proteins in both the radiation-treated and control groups. Western blotting and immunofluorescence analysis were carried out to verify the differentially expressed proteins.
Results: Functional assays showed a significant increase in colony formation which indicates radioresistant HCC cells had enhanced proliferation capabilities as compared to normal cancer cells. In addition, these cells demonstrated a significant increase in their invasive and migratory abilities, suggesting that radioresistant cells not only exhibit improved survival but also have a higher potential for metastatic spread. Proteomic profiling analysis showed a differential expression of proteins between the radiation-treated and control groups. When compared to the control group, which included 5,201 proteins, the radiation-treated cells contained a total of 5,342 proteins. Additionally, 5,007 proteins were found to be present in both groups. Significant differences were observed, especially in proteins related to cell proliferation, cellular organization, metabolism, stress response, signal transduction, and other biological processes. Drebrin, plectin, and filamin-A were selected for further analysis due to their considerable upregulation among the differentially expressed proteins. Microscopic investigation revealed the existence of invadopodia, actin-rich protrusions, in radioresistant cells compared to control HCC cells. F-actin staining demonstrated more prominent invadopodia structures in radioresistant specimens compared to the control group.
Conclusion: This study suggests that prolonged radiation exposure influences multiple cellular and proteome level changes to promote aggressive tumorigenic and metastatic behavior of HCC cells.

#7379 FDXR expression is a rectal cancer biomarker of radiation resistance and confers resistance through ferroptosis.

Sara Soltani Tehrani, May Zin Hlaing, Joseph Fedro, Rami-James Aoun, Karishma Kundu, Sylvain Ferrandon, Matthew F. Kalady

The Ohio State University College of Medicine, Columbus, OH

Purpose: Treatment of locally advanced rectal cancer is multimodal and includes total neoadjuvant therapy (TNT) with chemoradiation and chemotherapy. Response to TNT is highly variable and correlates with oncologic outcomes. There are limited biomarkers for rectal cancer radiation response, and there is also a critical need to identify potential therapeutic targets that could improve radiation sensitivity. The gene *FDXR* encodes a mitochondrial flavoprotein involved in electron transport, iron metabolism and ferroptosis. This study evaluates the role of *FDXR* in rectal cancer radiation response.

Methods: Pretreatment biopsies from 33 rectal cancer patients were analyzed previously, identifying *FDXR* as differentially expressed among different AJCC Tumor Regression Score (TRS). *FDXR* expression was examined in public datasets. FDXR expression was measured by RT-qPCR in ten colorectal cancer (CRC) cell lines and correlated with radiosensitivity parameters (IC50, D10, SF2). Stable *FDXR* knockdown lines (HCT116, SW480) were generated using lentiviral shRNA. Knockdown was confirmed by Western blot. To assess mitochondrial morphology and structural integrity, Transmission electron microscopy (TEM). Clonogenic survival after irradiation, viability (CCK-8), lipid peroxidation (Image-iT), mitochondrial iron (MitoFerroGreen), and ROS levels were assessed before and after irradiation.

Results: *FDXR* was significantly overexpressed in rectal tumors compared with normal tissue in TCGA and GSE87211. In our patient cohort, higher *FDXR* expression correlated with poorer response (TRS 2-3) and showed strong predictive ability (AUC=0.8577). Across CRC cell lines, *FDXR* expression correlated positively with IC50, D10, and SF2. *FDXR* knockdown caused loss of mitochondrial structural integrity on TEM and significantly reduced clonogenic survival while increasing radiation-induced cell death. Knockdown lines exhibited higher mitochondrial iron, increased ROS, and elevated lipid peroxidation.

Conclusions: *FDXR* is a strong biomarker of rectal cancer radiation response. Loss of *FDXR* enhances ferroptosis through iron accumulation, ROS generation, and lipid peroxidation, increasing radiosensitivity. These results suggest that targeting *FDXR* could enhance radiation efficacy, offering a novel strategy for radiosensitization in rectal cancer.

#7380 TP53 mutants cooperate with H3K27M to enhance survival after DNA damage and drive radioresistance in DIPG.

Karol A. Arizaca Maquera, Viral Oza, Andrew Gaines, Colin Williams, Jessica Blackburn

Molecular and Cellular Biochemistry, University of Kentucky, Lexington, KY

Diffuse intrinsic pontine glioma (DIPG) is driven by the H3K27M oncohistone and frequently co-occurs with TP53 mutations, a genetic combination closely associated with radiation failure. Because H3K27M globally reprograms chromatin and alters promoter accessibility, we hypothesized that it creates a permissive epigenetic environment that enhances the stability and activity of specific TP53 mutants to promote radioresistance. To test this, we expressed TP53 wild-type (WT) or DNA-binding-domain hotspot mutants, including contact mutants (R273C, R273H, R248W) and a conformational mutant (R175H), in TP53-knockout HEK293 cells with either H3.3 or H3K27M. Sequence-specific DNA binding was first assessed using a transcription factor assay. Several mutants (R273H, R273C) retained DNA-binding activity, which increased substantially in the H3K27M context, whereas R175H remained low. Because these results suggested enhanced promoter engagement after DNA damage, we next performed ChIP-qPCR after 8 Gy irradiation. In the presence of H3K27M, multiple mutants (R273H, R273C, R248W) maintained occupancy at p53 target genes (MDM2, CDKN1A/p21), in contrast to reduced binding when H3.3 WT was expressed. Western blot analysis further revealed that several TP53 mutants, including R175H, were selectively stabilized in H3K27M-expressing cells, while WT p53 levels and transcriptional output were unchanged. We then examined transcriptional programs influenced by H3K27M in each TP53 background. Although several chaperone and chromatin-remodeling genes (HSPA14, BRD4, KDM7A) showed modest changes in R273C_H3K27M cells, the most prominent alterations were in stress-signaling pathways, including induction of the NKG2D stress-ligand RAET1E (logFC = +1.14, p = 0.0627). These gene-level changes indicate that H3K27M rewires cellular programs that cooperate with mutant p53 under genotoxic stress. Finally, we tested whether these chromatin-driven molecular effects translate into a functional phenotype. H3K27M provided only a modest proliferative advantage to WT TP53 cells, but markedly increased the survival and regrowth of TP53-mutant cells over 24-72 hours after irradiation. Taken together, these findings support a model in which H3K27M enhances mutant p53 DNA binding, stabilizes mutant p53 proteins, and reprograms stress-responsive pathways to amplify pro-survival responses after DNA damage. This cooperation between H3K27M and specific TP53 mutants provides a mechanistic explanation for radioresistance in DIPG and underscores the importance of considering both TP53 genotype and histone context when designing targeted radiosensitization strategies.

: Functional and Spatial Regulation of Immune Evasion and Anti-Tumor Immunity
Poster Session

#7384 Electrical activity powered neural circuit sustains systemic immune evasion in gastric cancer.

Puran Zhang[1], Feijing Wu[2], Yi Zeng[2], Shuang Li[2], Jin Qian[2], Hualong Zheng[2], Biyun Zheng[2], Juli Lin[2], Hiroki Kobayashi[2], Junya Arai[2], Yosuke Ochiai[2], Masahiro Hata[2], Leah B. Zamechek[2], Timothy C. Wang[2]

[1]Herbert Irving Comprehensive Cancer Ctr., New York, NY,[2]Columbia University Irving Medical Center, New York, NY

Background: Nociceptive sensory nerves are emerging as active regulators of tumor progression and immune suppression within the tumor microenvironment (TME). We previously showed that gastric cancer cells establish a bi-directional electrical circuit with CGRP⁺ sensory neurons, in which cancer depolarization triggers neuronal firing and CGRP release. Given that sensory afferents serve as the afferent limb of the inflammatory reflex transmitting peripheral signals to the brainstem, we hypothesized that cancer may similarly exploit neural circuits and neuropeptide signaling to regulate systemic immunity.
Methods: A chemogenetic receptor (PSAM4-$5HT_3$) was introduced into a syngeneic murine (ACKP) gastric cancer cell line to evoke cancer depolarization in vivo. Cancer-activated neuronal projections were mapped in TRAP2 (Fos-CreERT2) mice using Cre-dependent AAV reporters. Immune profiling was performed to characterize antigen-experienced T cells in the tumor-draining lymph node (TDLN) and various CD8⁺ T-cell subsets within the TME. In vivo imaging was used to monitor T-cell motility dynamics, and GCaMP6s was expressed in immune cells to visualize neuron-triggered calcium flux.
Results: Cancer depolarization activated nociceptive sensory neurons, which established synapse-like contacts with CD8⁺ TILs preferentially at the perivascular niche and tertiary lymphoid structures. The cancer-coupled sensory nerves upregulated Cxcl10, attracting T cells toward their terminals to form these connections. In a 3-D co-culture system comprising cancer spheroids, dorsal root ganglia, and CD8⁺ TILs, optogenetic stimulation of cancer cells induced a calcium flux in sensory nerve-connected T cells, confirming functional transmission. Local activation of this cancer-nerve-T-cell circuit enhanced T-cell migration toward nerve terminals but diminished effector capacity, evidenced by reduced TNFα and IFNγ expression and limited infiltration into the tumor core. Sensory afferents relayed signals to higher brainstem areas, including the nucleus tractus solitarius (NTS) and rostral ventrolateral medulla (RVLM), eliciting sympathetic output to the TDLN. This afferent-brain-efferent loop retained and immobilized antigen-experienced CD44⁺PD-1⁺ T cells within the TDLN, thereby restraining systemic immunity in a norepinephrine-Adrb2-dependent manner. Anti-PD-1 therapy paradoxically strengthens the cancer-sensory nerve coupling. Ablatio of this cancer-evoked neural circuit restored T-cell effector function systemically and synergized with anti-PD-1 therapy.
Conclusions: These findings reveal that cancer depolarization activates CGRP⁺ sensory neurons to form synaptic contacts with CD8⁺ T cells, linking local peptidergic signaling to systemic immune suppression via the NTS-RVLM-TDLN axis. Disrupting this circuit restores T-cell function and enhances anti-PD-1 response.

#7385 Cholesterol-associated immune cell dysfunction across lung cancer progression.

Jiwon Hwang, Ajay Tosh, Satyanarayana Rachagani

University of Missouri, Columbia, MO

Lung cancer progression occurs through tumor microenvironment (TME) transformation, leading cells to modify their metabolic patterns to support tumor growth. Research has recently focused on cholesterol metabolism because it shows promise to affect tumor cell behavior and immune system responses. The TME contains elevated cholesterol levels which lead to $CD8^+$ T-cell exhaustion through a process that results in increased inhibitory receptor expression and decreased antitumor activity. Previous studies have produced conflicting results about cholesterol effects on T-cell function because some studies found cholesterol builds up in tumor-infiltrating T cells whereas others showed that low cholesterol levels can impair T-cell performance. The current understanding lacks information about how cholesterol-related genes change between different cell types and different stages of lung cancer development. In this study, we analyzed single-cell RNA-seq data from a GEO dataset representing multiple stages of lung cancer progression to characterize stage-specific changes in cholesterol-related gene expression across major cell populations. To understand how these metabolic shifts relate to $CD8^+$ T-cell exhaustion, this study investigates the progression of cholesterol metabolism during lung cancer and its potential influence on antitumor immunity.

#7386 Estradiol-responsive niches drive immune exclusion in the tumor microenvironment.

Minsung Kim[1], Kwanghwan Lee[2], Hyun Ju Kang[2], Jin-Ku Lee[1]

[1]Department of Biomedical Sciences, Seoul National University, Seoul, Korea, Republic of,[2]Genomic Medicine Institute, Medical Research Center, Seoul National University, Seoul, Korea, Republic of

Epithelial ovarian cancer (EOC) presents marked molecular diversity, which is largely influenced by the tumor microenvironment (TME). However, the specific factors driving this diversity remain unclear. We established a multi-omics platform integrating growth factor-omics profiling with transcriptomic analysis of patient-derived ovarian tumor tissues. Using samples from 31 EOC patients, we identified the responsiveness of 128 factor combinations and analyzed through integrated bulk and single-cell RNA sequencing. Two main clusters were identified, one responsive to estradiol and Wnt and the other to R-spondin. These results were further validated by a pan-cancer analysis of 11,000 TCGA tumors across 33 cancer types, confirming the conservativeness and clinical relevance of this response program. Estradiol exposure induced robust proliferation characterized by mesenchymal and stem cell-associated transcriptional signatures, leading to tumor growth. Single-cell analysis identified two estradiol-responsive niches: a malignant PDCD5+ subtype and a TNFSF10-expressing fibroblast population, both of which increased after estradiol stimulation. MAL.PDCD5 cells exhibited impaired antigen presentation and metabolic suppression via reduced oxidative phosphorylation, whereas FB.TNFSF10 fibroblasts exhibited increased TGF-beta and CAF.S1 signaling, consistent with immunosuppressive reprogramming. Spatial transcriptomic analysis revealed a distinct spatial segregation between FB.TNFSF10 fibroblasts and T/NK cells, providing direct evidence for hormone-induced immune exclusion. Across various tumor types, elevated FB.TNFSF10 expression correlated with elevated stromal cell and regulatory T cell scores and was an independent predictor of reduced response to immune checkpoint blockade, independent of PD-L1 expression or tumor mutation burden. These findings demonstrate a preserved estradiol-responsive architecture that remodels the tumor microenvironment, preventing immune infiltration. These findings suggest novel biomarkers and therapeutic targets that could enhance the efficacy of immunotherapy across diverse cancers.

#7388 Distinct immune crosstalk axes define the tumor microenvironment across EGFR mutation status in NSCLC by single-cell profiling.

Yoojin Kim[1], Hyunsu Kim[2], Kyungjong Lee[3], Bo Mi Ku[2], Hae-Ock Lee[4], Jinyong Kim[2], Hyun Ae Jung[2], Jong-Mu Sun[2], Se-Hoon Lee[2], Jin Seok Ahn[2], Myung-Ju Ahn[2], Sehhoon Park[2]

[1]Department of Health Sciences and Technology, Samsung Advanced Institute of Health Sciences and Technology, Sungkyunkwan University, Seoul, Korea, Republic of,[2]Division of Hematology-Oncology, Department of Medicine, Samsung Medical Center, Sungkyunkwan University School of Medicine, Seoul, Korea, Republic of,[3]Division of Pulmonary and Critical Care Medicine, Department of Medicine, Samsung Medical Center, Sungkyunkwan University School of Medicine, Seoul, Korea, Republic of,[4]Department of Biomedicine and Health Sciences, Graduate School, The Catholic University of Korea, Seoul, Korea, Republic of

Background: Epidermal growth factor receptor (EGFR) is a major oncogenic driver in non-small cell lung cancer (NSCLC). Patients with EGFR-mutant NSCLC show limited responses to immune checkpoint inhibitors (ICIs) compared with those with EGFR-wild-type tumors, as previously reported. The mechanisms underlying primary ICI resistance and distinct tumor microenvironment (TME) characteristics in EGFR-mutant NSCLC remain poorly understood.

Methods: We performed single-cell RNA sequencing of treatment-naïve NSCLC samples from 88 patients (31 EGFR-mutant, 57 EGFR-wild-type) to characterize TME. Data processing, normalization, dimensional reduction, and clustering were conducted with *Seurat* package. Cell types were annotated with canonical marker genes, and transitional epithelial populations were further identified through consensus non-negative matrix factorization (cNMF). Cell-cell communication networks were computationally inferred, and the identified interactions were supported through differential expression and pathway enrichment analyses.

Results: By profiling 241,333 high-quality single cells, we identified 33,628 epithelial cells. cNMF revealed an inflammatory transitional epithelial (Epi_inflammatory) subset based on interferon-driven immune programs. In EGFR-wild-type tumors, these Epi_inflammatory cells showed dominant interactions with CD8+ tissue-resident memory T (Trm) cells through MHC class I-CD8 signaling. The epithelial cells exhibited higher expression of key antigen-presentation genes (*B2M, TAP1, PSMB8/9*), while CD8+ Trm cells showed elevated expression of cytotoxic markers (*GZMB, PRF1, NKG7*) and differentially expressed TCR repertoire-associated genes, indicating enhanced T-cell activation. GSEA showed enrichment of the "*Cell killing*" pathway in CD8+ Trm cells and "*Antigen processing and presentation of endogenous peptide antigen*" in epithelial cells, supporting dominant MHC class I-mediated interaction in EGFR-wild-type tumors. In contrast, intensified crosstalk between tumor-associated macrophages (TAMs) and CD8+ Trm cells was inferred in EGFR-mutant tumors, predominantly driven by the SPP1-CD44 ligand-receptor axis. Hypoxic and STAB1+ TAMs displayed upregulated SPP1 levels and reduced antigen-presentation genes expression, while CD8+ Trm cells expressed higher CD44 levels. Notably, expression of SPP1 in macrophages positively correlated with the exhaustion score of CD8+ Trm cells ($p = 0.041$).

Conclusion: Our findings suggest distinct immune landscapes; EGFR-mutant tumors showed macrophage-driven immunosuppressive TME via SPP1-CD44 axis, leading to CD8+ Trm dysfunction, whereas EGFR-wild-type tumors exhibited epithelial-CD8+ Trm crosstalk, establishing a cytotoxic niche. This divergence may explain the limited benefit of ICI therapy in EGFR-mutant NSCLC.

#7389 Evaluation of tumor-infiltrating γδ T cells across solid tumor indications.

Shawn P. Fahl, Cavin Ott, Kerri Colwell, Kayla Williams, Audrey Kleeman, Jessica Maxwell

Discovery Life Sciences, Huntsville, AL

The tumor microenvironment is a complex heterogeneous cellular mixture containing not only tumor cells, but also immune cells, fibroblasts, and endothelial cells. Based on numerous factors, including cellular subtype and activation, these cell types can have both tumor-promoting and tumor-eradicating activities. We have previously analyzed both intra-tumoral αβ T cells and B cells using a combination of flow cytometry and single cell transcriptomics across solid tumor indications such as bladder, colorectal, endometrial, lung, ovarian, prostate, and renal cancer using human dissociated tumor cells (DTCs). αβ T cells represented the largest tumor-infiltrating lymphocyte (TIL) subset, and the majority of αβ T cells were in an exhausted state based on high surface expression of inhibitory receptors such as PD1 and TIGIT. Across all indications, B cells were the next most prevalent TIL subset, although indication-specific differences were observed. Overall, like αβ T cells, intra-tumoral B cells had an exhausted phenotype, and a high proportion of these B cells were plasmablasts.γδ T cells represent an attractive candidate for immunomodulation as they recognize their cognate antigens in an HLA-independent manner and have intrinsic cytotoxic potential. Previous studies utilized large scale bulk transcriptomics inferred a substantial percentage of γδ T cells across several solid tumor indications. Further studies in melanoma and colorectal cancer analyzed the activation status and Vδ1/2 usage of intra-tumoral γδ T cells; however, a fully comprehensive evaluation and comparison of γδ T cell activation status, Vγ/Vδ usage, and putative γδ T cell ligand expression across numerous indications remains unstudied. We have now utilized DTCs across twelve solid tumor indications to analyze the relative percentages of γδ T cells, including their Vγ chain and Vδ chain usage. The naïve versus memory phenotype of the γδ T cells and the surface expression of exhaustion and natural cytotoxicity receptors were also evaluated. Finally, the expression of γδ T cell ligands, such as stress receptors and butyrophilins, on the tumor cells was assessed. Collectively, these studies provide crucial insight into the indication-specific γδ T cell composition to inform future γδ T cell-mediated immunotherapies.

#7391 A pd-l1 acetylation switch coordinates chromosome cohesion and antitumor immunity.

Meijie Wang[1], Jia Yu[2], Liewei Wang[3]

[1]Molecular Pharmacology & Experimental Therapeutics, Mayo Clinic Hospital-Rochester, Rochester, MN,[2]Mayo Clinic, Rochester, MN,[3]Mayo Clinic College of Medicine, Rochester, MN

Background: PD-L1 is best known for suppressing antitumor immunity at the cell surface, yet emerging evidence suggests additional nuclear functions. Previous studies from our laboratory demonstrated that nuclear PD-L1 interacts with the cohesin complex to maintain chromosomal stability. However, the upstream regulatory mechanism governing this interaction and its immunological consequences remain unknown.
Methods and Results: Using acetylation-site prediction, mutagenesis, and structural modeling, we identified lysine 178 (human) / 177 (mouse) as a conserved acetylation switch regulating PD-L1 function. Deacetylation of PD-L1 (K178R/K177R) disrupted PD-L1-PDS5B/cohesin binding without affecting subcellular localization. This led to defective sister chromatid cohesion, micronuclei formation, and cytosolic DNA accumulation. RNA-seq, qPCR, and immunoblotting demonstrated robust activation of the cGAS-STING-IFN-γ signaling axis and enhanced MHC-I antigen-presentation machinery in PD-L1 K178R cells. Functionally, K178R cells proliferated more slowly and were highly susceptible to PBMC-mediated killing in co-culture assays, with further enhancement upon anti-PD-L1 antibody treatment. In xenograft models (NSG mice), tumors expressing PD-L1 K178R grew significantly slower than WT. In immunocompetent C57BL/6 syngeneic models, PD-L1 K177R tumors showed reduced growth and heightened responsiveness to PD-L1 blockade. Structural and biochemical analyses confirmed that PD-L1 acetylation at K178/K177 stabilizes its interaction with the cohesin complex, thereby preventing chromosomal instability-induced immune activation.
Conclusions: We identify a conserved PD-L1 acetylation switch that couples cohesin stability to innate immune activation. PD-L1 deacetylation promotes chromosomal instability, activates cGAS-STING-IFN-γ signaling, enhances antigen presentation, and sensitizes tumors to PD-L1 immunotherapy. These findings uncover a previously unrecognized regulatory axis linking tumor genomic integrity to immune recognition, providing a mechanistic foundation for targeting PD-L1 acetylation in cancer treatment.

#7392 A cancer cell-intrinsic PAR1/MALT1/PD-L1 signaling pathway drives immune evasion in triple-negative breast cancer.

Dong Hu[1], Prasanna Ekambaram[2], Zheqi Li[3], Linda Klei[2], Maria L. Beecher[4], Yi Liu[5], Zongyou Cai[6], John Little[7], Jeffrey A. Meridew[7], Jia-Ying Lee[8], E. Aubrey Thompson[9], Tullia C. Bruno[10], Lidija Covic[11], Seung-Oe Lim[12], Anushka Dongre[13], Heide L. Ford[14], Mien-Chie Hung[15], Adrian V. Lee[16], Steffi Oesterreich[16], Linda McAllister-Lucas[17], Peter C. Lucas[18]

[1]Department of Laboratory Medicine and Pathology, Mayo Clinic, Rochester, MN,[2]Department of Pediatrics, University of Pittsburgh School of Medicine, Pittsburgh, PA,[3]Department of Medicine, Harvard Medical School, Boston, MA,[4]Department of Pathology, University of Pittsburgh School of Medicine, Pittsburgh, PA,[5]Department of Cancer Biology, Mayo Clinic, Jacksonville, FL,[6]Tsinghua University School of Medicine, Beijing, China,[7]Laboratory Medicine and Pathology, Mayo Clinic, Rochester, MN,[8]Pathology, University of Pittsburgh School of Medicine, Pittsburgh, PA,[9]Cancer Biology, Mayo Clinic, Jacksonville, FL,[10]Department of Immunology, University of Pittsburgh School of Medicine, Pittsburgh, PA,[11]Department of Medicine, Tufts Medical Center, Boston,, MA,[12]Department of Medicinal Chemistry and Molecular Pharmacology, Purdue University, West Lafayette, IN,[13]Department of Biomedical Sciences, Cornell University College of Veterinary Medicine, Ithaca, NY,[14]Department of Pharmacology, University of Colorado Anschutz Medical Campus, Aurora, CO,[15]Institute of Biochemistry and Molecular Biology, China Medical University, Taichung, Taiwan,[16]Department of Pharmacology and Chemical Biology, University of Pittsburgh School of Medicine, Pittsburgh, PA,[17]Department of Pediatrics and Adolescent Medicine, Mayo Clinic Comprehensive Cancer Center, Mayo Clinic, Rochester, MN,[18]Department of Laboratory Medicine and Pathology, Mayo Clinic Comprehensive Cancer Center, Mayo Clinic, Rochester, MN

Background: Triple-negative breast cancer (TNBC) is the most aggressive subtype of breast cancer and remains difficult to treat due to the absence of targeted therapies. While recent advances in immunotherapy, particularly with immune checkpoint inhibitors (ICIs), have transformed the treatment landscape for many cancers, response rates to ICIs remain low for TNBC, largely due to tumor-intrinsic immune evasion mechanisms.

Objective: We identify and characterize a novel immune evasion pathway in TNBC driven by deregulation of cancer cell-intrinsic protease-activated receptor 1 (PAR1), a thrombin receptor frequently upregulated in aggressive tumors.

Methods and Results: Through integrative bioinformatic analyses, genetic perturbations, xenograft models (immunodeficient and immunocompetent), flow cytometry-based tumor immune profiling, and RNA-seq, we demonstrate that PAR1 activation enhances immune evasion in TNBC. Mechanistically, we show that the paracaspase MALT1 acts as a critical downstream effector of PAR1 signaling and promotes immune escape by driving PD-L1 expression in TNBC cells. Functional assays reveal that genetic depletion of MALT1 or PD-L1 increases TNBC cell susceptibility to T cell-mediated cytotoxicity *in vitro* and significantly suppresses tumor growth *in vivo*. Notably, through knock-in and rescue experiments using a catalytically inactive MALT1 mutant, we reveal that MALT1's scaffolding - rather than protease - function is essential for PD-L1 regulation. Immune cell depletion assays further identify CD4+ T cells, CD8+ T cells, and natural killer (NK) cells as key mediators of the anti-tumor immune response suppressed by the PAR1-MALT1 axis. These findings are supported by human TNBC specimen analyses, where MALT1 expression inversely correlates with T cell activation and positively associates with PD-L1 in PAR1-high, but not PAR1-low, tumors.

Conclusion: Our study reveals immune evasion as a novel mechanism of PAR1-driven breast cancer pathogenesis, mediated by a PAR1/MALT1/PD-L1 signaling cascade. These findings bridge a critical gap by positioning MALT1 at the interface between tumor-intrinsic signaling and the immune microenvironment - two areas of CARMA-BCL10-MALT1 (CBM) complex research that have largely evolved in parallel over the years. Importantly, targeting MALT1 may enhance immunotherapy efficacy in TNBC. Given the availability of MALT1 inhibitors in clinical development, our work supports combining MALT1 inhibition with ICIs or other immune-oncology agents as a promising strategy to overcome immune resistance in TNBC.

#7394 Cytokine-driven CD38$^+$HLA-DR$^+$ CD8$^+$ T cells define a bystander program predicting poor prognosis in hepatocellular carcinoma.

Wei-Ting Ku[1], Chien-Hao Huang[1], Cheng-Heng Wu[1], Wei Teng[1], Po Ting Lin[1], Tsung-Han Wu[2], Jian-He Fang[1], Chan-Keng Yang[3], Yen-Chun Liu[1], Wen-Juei Jeng[1], Yung-Chang Lin[3], Chun-Yen Lin[1]

[1]Department of Gastroenterology-Hepatology, Linkou Chang Gung Memorial Hospital, Taoyuan, Taiwan,[2]Department of General Surgery, Linkou Chanf Gung Memorial Hospital, Taoyuan, Taiwan,[3]Department of Hematology-Oncology, Linkou Chang Gung Memorial Hospital, Taoyuan, Taiwan

Hepatocellular carcinoma (HCC) exhibits poor immunotherapy responses despite CD8$^+$ T cell infiltration, suggesting critical gaps in understanding tumor-reactive versus bystander immunity. While CD8$^+$ T cells can mediate anti-tumor effects through TCR engagement, their effector function may be subverted by immunosuppressive programs. Here, we identified a distinct CD38$^+$HLA-DR$^+$ CD8$^+$ T cell population whose expansion associates with adverse HCC outcomes independent of tumor-specific immunity. We integrated data from ex vivo cytokine (IL-12/15/18)-stimulated CD8$^+$ T cells, bulk RNA-seq and CITE-seq of matched peripheral blood (PB), non-tumor liver (NT), and tumor (T), and TCR clonotype mapping from an HCC cohort. We further projected cytokine-driven versus mutation-associated neoantigen (MANA) signatures onto TCGA-LIHC and integrated these with clinical flow cytometry, serum cytokines, and survival modeling in this cohort. IL-12/15/18 maximally drove bystander CD8$^+$ proliferation and effector function. Bulk RNA-seq distinguished cytokine- from TCR-driven activation, with strong *MKI67* upregulation and lower exhaustion transcripts (*PDCD1, CTLA4, LAG3*) in the former. Co-expression of CD38 and HLA-DR reliably identified these IL-12/15/18-induced bystander-activated CD8$^+$ T cells. Comparative profiling indicated that cytokine-activated CD38$^+$HLA-DR$^+$ CD8$^+$ T cells adopt an NK-like killing program. CITE-seq across PB/NT/T confirmed an in-vivo CD38$^+$HLA-DR$^+$ subset, whose state shifts from circulating bystander-like to tumor-adapted effector; TCR mapping showed extensive PB-tumor clonotype sharing. Gene-set analyses revealed an E2F-dominated proliferation/DNA-repair program in CD38$^+$HLA-DR$^+$ CD8$^+$ T cells ("risk" genes), versus an IRF-driven TCR/IL2-STAT5/IFN-γ effector program in MANA-specific "protective" genes. In TCGA-LIHC, the CD38$^+$HLA-DR$^+$ signature associated with higher *IL12A/IL15/IL18* expression and immunosuppressive signatures (Foxp3^{high} Tregs, MDSCs), indicating a cytokine-rich suppressive milieu. Clinically, peripheral CD38$^+$HLA-DR$^+$ CD8$^+$ T cells were enriched in HCC versus healthy donors and were highest in tumors; concomitant elevation of serum IL-12p70, IL-15, and IL-18 tracked with increased CD38$^+$HLA-DR$^+$ frequencies. Higher peripheral CD38$^+$HLA-DR$^+$ proportions associated with worse survival and remained an independent prognostic factor after adjustment for tumor burden and liver function. Together, cytokine-driven bystander activation generates a transcriptionally and functionally distinct CD38$^+$HLA-DR$^+$ CD8$^+$ population with NK-like features. Unlike MANA-specific T cells linked to favorable outcomes, this cytokine-driven program aligns with proliferative, immunosuppressive networks, leading to poor prognosis and nominating CD38$^+$HLA-DR$^+$ CD8$^+$ T cells as a biomarker and potential therapeutic target in HCC.

#7396 Osteopetrosis-associated transmembrane protein1 modulates CD8⁺ T-cell responses during immunotherapy in hepatocellular carcinoma.

Yixin Chen, Jie Luo, Nanzhou Yu, Yu Zhang, Ming Zhu, Yuma Yang, Lanqi Gong, Xin-Yuan Guan

University of Hong Kong, Hong Kong, Hong Kong

Background: Hepatocellular carcinoma (HCC), the most common form of primary liver cancer, is the third leading cause of cancer-related deaths worldwide. Although atezolizumab plus bevacizumab (Atezo+Beva) has shown some efficacy in the treatment of advanced HCC, its therapeutic benefit remains limited. Systematically identifying these regulatory factors is crucial for recognizing predictive biomarkers and therapeutic targets in HCC.

Methods: An *in vivo* genome-wide CRISPR/Cas9 knockout screen was performed in a murine HCC model treated with anti-programmed death ligand 1 (anti-PD-L1) and anti-vascular endothelial growth factor a (anti-VEGFa) antibodies to identify key regulators of immunotherapy resistance. Osteopetrosis-associated transmembrane protein 1 (OSTM1), an uncharacterised oncogene, was identified as a leading candidate. It was subsequently validated through tumour-cell–specific knockout in both orthotopic and hydrodynamic tail-vein injection (HDTVi) mouse models. Bulk RNA sequencing was performed on tumour tissues from OSTM1-knockout and control groups.

Results: The screening nominated OSTM1 as a key mediator of resistance to anti-PD-L1 and anti-VEGFa. Knockout of OSTM1 in tumour cells improved response to therapy and reduced tumour growth in both orthotopic and HDTVi mice models. Clinically, elevated OSTM1 levels have been demonstrated to be associated with diminished survival rates in patients with HCC who have been treated with Atezo+Beva. Mechanistically, OSTM1 fostered an immunosuppressive microenvironment by impairing CD8⁺ T-cell infiltration and multiple effector functions, including Interferon gamma (IFN-γ) production, and by reducing markers of proliferation and cytotoxicity such as kiel 67 (KI67), granzyme b (GZMB), and Perforin. Moreover, we merged differentially expressed genes from both the orthotopic and HDTVi OSTM1-knockout models consistently revealed PRELI domain containing 2 (PRELID2) as a downstream gene suppressed by OSTM1. Given that PRELID2 is involved in mitochondrial regulation and there is a new link between mitochondrial function and immune cell activity, this finding suggests that OSTM1 may indirectly influence immune cell infiltration and function in the tumor microenvironment through a potential axis.

Conclusion: OSTM1 contributes to poor immunotherapy response in HCC, suggesting its utility as a biomarker and candidate therapeutic target during Atezo+Beva therapy. Future research will investigate how targeting OSTM1 may enhance CD8⁺ T-cell infiltration and function in the tumour microenvironment.

#7397 Intercellular transfer of hepatocellular carcinoma-derived RNAs via tunneling nanotubes educates macrophages and enhances antigen presentation.

Yutao He, Lin Wang, Zhitian Shi

The Second Affiliated Hospital of Kunming Medical University, Kunming, China

Despite significant progress in immunotherapy for hepatocellular carcinoma (HCC), effective therapeutic targets remain limited, highlighting the urgent need for novel immunotherapeutic strategies. Intercellular communication is fundamental for maintaining homeostasis and responding to external stimuli, and while various modes such as ligand-receptor interactions and extracellular vesicle transfer are known, the potential role of tunneling nanotubes (TNTs) in macrophage-HCC cell communication has been unclear. In this study, using peritoneal macrophages from C57BL/6J mice co-cultured with Hepa1-6 HCC cells in vitro, we observed via field emission scanning electron microscopy and confocal microscopy that macrophages and HCC cells form TNTs—slender, straight, and suspended structures with vesicle-like protrusions indicative of cargo transport, composed of F-actin, α-tubulin, and Sec5. By physically inhibiting TNT formation using 0.4 μm transwell inserts and applying single-cell RNA sequencing, we found that in the TNT system, the HCC cell phenotype did not change significantly, but the proportion of MHC II⁺ macrophages greatly increased, and OT-II T cell activation assays further demonstrated enhanced antigen presentation ability in macrophages. Using specific markers for proteins, mitochondria, DNA, and RNA (CellTracker Blue, MitoTracker, Hoechst 34580, Click-iT RNA) and corresponding inhibitors (metformin, DNase, RNase), we obtained direct evidence that HCC cell-derived RNAs are transferred via TNTs to
macrophages, leading to increased antigen presentation capability. Moreover, blocking macrophage RNA sensors with hydroxychloroquine suppressed the TNT-induced increase in MHC II⁺ macrophages, and in an orthotopic HCC mouse model, intratumoral injection of hydroxychloroquine-pretreated macrophages resulted in significantly larger tumor diameters by day 7 compared to the untreated group. In summary, our study reveals that macrophages and HCC cells establish a novel form of intercellular communication—TNTs—through which HCC cells transfer RNAs to macrophages, mediating an increase in MHC II⁺ macrophage proportion and enhanced antigen presentation capacity, thereby suppressing tumor progression. We propose that promoting efficient transfer of HCC-derived RNAs to macrophages by TNTs and enhancing macrophage recognition of these RNAs may provide novel insights and potential therapeutic targets for innovative anti-HCC treatments.

#7398 Senescent regulatory T cells retain potent suppressive function in clear cell renal cell carcinoma.

Temitope Mary Ogunmola[1], Myung-Chul Kim[2], Zeng Jin[1], Umasankar de[3], Lina Cui[4], Guangrong Zheng[4], Ryan Kolb[4], Weizhou Zhang[4]

[1]University of Florida College of Medicine, Gainesville, FL,[2]Kyungpook National University, Daegu, Korea, Republic of,[3]Pharmacy, Sungkyunkwan University (SKKU), Suwon, Korea, Republic of,[4]University of Florida, Gainesville, FL

Clear cell renal cell carcinoma (ccRCC) is an aging-associated malignancy characterized by a highly immunosuppressive, immune-rich tumor microenvironment and variable response to immune checkpoint blockade. Regulatory T cells (Tregs) are dominant orchestrators of immune suppression in ccRCC, yet the functional consequences of cellular senescence in these cells remain unknown and are widely presumed to be impairing. Single-cell RNA sequencing of treatment-naïve human ccRCC tumors revealed a distinct tumor-infiltrating Treg (TI-Treg) subpopulation co-expressing classic senescence markers (p16^INK4a, p21), senescence-associated β-galactosidase activity (SA-β-gal), BCL-xL, and robust immunosuppressive effector programs. Contrary to the prevailing view that senescence attenuates Treg function, we hypothesized that senescent TI-Tregs retain potent suppressive capacity. To functionally characterize these senescent TI-Treg subsets, we used a novel activity-based fluorescent senescence probe that labels SA-β-gal and employed p16-tdTomato reporter mice for the isolation of viable senescent TI-Tregs. Additionally, using an in vitro co-culture system in which naïve Tregs are driven into senescence by ccRCC cell-derived factors, suppression assays demonstrated that senescent Tregs maintain strong inhibitory activity against $CD4^+$ T-cell proliferation, comparable to non-senescent Tregs. Concomitant RNA sequencing confirmed persistence of canonical immunosuppressive pathways and acquisition of a senescence-reinforced suppressive transcriptome. These findings challenge the assumptions that senescence Tregs are dysfunctional in cancer and establish senescent Tregs as critical contributors to immunosuppression in aging-associated ccRCC. This work unravels senescent TI-Tregs as therapeutic targets/vulnerabilities for their selective elimination to restore antitumor immunity.

#7399 Eosinophils promote an immunosuppressive bone marrow microenvironment in multiple myeloma.

Haley du Bois[1], Alberto Chaves[2], Ryan Bishop[1], Dina Atta[3], Jeremy Steven Frieling[1], Karl Nyman[1], Tao Li[1], Mostafa Nasr[4], Conor C. Lynch[1]

[1]Moffitt Cancer Center, Tampa, FL,[2]College of Engineering, University of South Florida, Tampa, FL,[3]H. Lee Moffitt Cancer Center and Research Institute and the University of South Florida, Tampa, FL,[4]Tumor Microenvironment & Metastasis, Moffitt Cancer Center, Tampa, FL

Multiple Myeloma (MM) is an incurable malignancy characterized by the expansion of plasma cells within the bone marrow, leading to structural disruption, osteolytic lesions, and profound immune dysregulation. Although therapeutic advances have improved initial responses, nearly all patients eventually develop relapsed or refractory disease. Understanding the cellular mechanisms that drive tumor immune escape and MM progression remains a critical unmet need, particularly as patients become candidates for cellular therapies (CAR-T) or T-cell engagers (TCEs), which currently achieve a median progression-free survival of only ~1 year. This limited durability is largely attributed to the MM-induced immunosuppressive microenvironment and T-cell exhaustion. Identifying cellular mediators of immunosuppression within the bone marrow is therefore essential to improving the efficacy of immunotherapies.To address this gap in knowledge we leveraged spatial transcriptomics (10x Visium) to interrogate the MM bone marrow microenvironment in an unbiased manner and revealed that eosinophils are enriched within the tumor bed of MM-bearing mice. Eosinophils have not previously been investigated in MM and are underrepresented in scRNA-seq datasets due to their labile nature and high RNAase content. To test the functional role of eosinophils, we used a syngeneic MM model (5TGM1 cells in immunocompetent C57BL/6-KaLwRij mice) that recapitulates key features of human disease. We found that depletion of eosinophils (α-SiglecF antibody; IP) prior to the establishment of MM significantly reduces tumor growth *in vivo*. We then compared KaLwRij versus C57BL/6 RAG2 (B and T cell deficient) mice and observed that eosinophil-mediated MM progression requires an intact adaptive immune system. Using flow cytometry, we determined that eosinophil depletion decreases $CD8^+$ T-cell exhaustion ($TIM\text{-}3^+$ $PD\text{-}1^+$) while enhancing T-cell activation ($CD69^+$ $CD25^+$). *In vitro*, we used primary eosinophils and found that exposure to 5TGM1 MM cells is sufficient to induce eosinophil PD-L1 expression. We also observed that MM-educated eosinophils can induce exhaustion (PD1+ CTLA4+) in pre-activated CD8 T cells.Together, our findings identify eosinophils as previously unrecognized mediators of immunosuppression in the MM bone marrow microenvironment and highlight them as a potential therapeutic target to enhance the durability of existing immunotherapies.

#7400 UHRF1 as an epigenetic driver of tumorigenicity and immune evasion in triple negative breast cancer.

Marina Suarez Pizarro[1], Ahhyun Kim[2], Jaime-Jean De La Torre[1], Xiyu Chen[1], Roberto Tinoco[1], Claudia A. Benavente[1]

[1]University of California Irvine, Irvine, CA,[2]University of California San Diego, San Diego, CA

Ubiquitin-like with PHD and RING Finger Domains 1 (UHRF1) is a multidomain epigenetic regulator essential for the maintenance of DNA methylation and repressive histone marks during cell division. As a downstream effector of the RB/E2F pathway, frequently deregulated in cancer, UHRF1 is aberrantly overexpressed in several malignancies, including triple-negative breast cancer (TNBC). Clinical datasets reveal that high UHRF1expression correlates with poor overall survival in TNBC, underscoring its clinical relevance.Using CRISPR/Cas9-mediated gene editing, we demonstrate that UHRF1 loss significantly impairs TNBC cell tumorigenicity. UHRF1-deficient TNBC cells exhibited reduced clonogenicity, migration, and invasion in vitro. In orthotopic xenograft models, tumors with low UHRF1 expression displayed significantly reduced growth and metastatic potential compared to controls. Transcriptomic profiling revealed that UHRF1 loss led to widespread depression of immune-related genes, suggesting that UHRF1 orchestrates an epigenetically repressed, immune-evasive state. To validate these findings in an immunocompetent context, Uhrf1 knockout (KO) TNBC cell lines were generated from mouse 4T1 cells.Consistent with human models, Uhrf1 KO cells displayed reduced tumorigenic potential and formed significantly smaller tumors in Balb/cJ mice. Importantly, Uhrf1 KO tumors showed increased infiltration of activated cytotoxic T cells (CD8+ CD44hi) and plasmacytoid dendritic cells (pDCs), alongside a higher cytotoxic-to-regulatory T cell ration, indicating an enhanced anti-tumor immune landscape following loss of UHRF1-mediated repression.Together, these results establish UHRF1 as a master epigenetic regulator linking the RB/E2F axis to tumor progression and immune modulation in TNBC. Targeting UHRF1-dependent chromatin regulation may represent a promising strategy to simultaneously suppress tumor growth and overcome immune evasion in aggressive breast cancers.

#7401 STING proton channel function controls T cell survival and tumor immune evasion.

Cong Xing, Kun Song, Zhen Tang, Antonina Araszkiewicz, Nicole Dobbs, Wanwan Huai, Nan Yan

Department of Immunology, University of Texas Southwestern Medical Center, Dallas, TX

Background The cGAS-STING pathway is a central sensor of cytosolic DNA that activates type I interferon (IFN-I) responses. In cancer, cGAS-STING signaling can promote antitumor immunity by enhancing antigen presentation and T cell priming. However, intrinsic STING activation in T cells also triggers T cell death within the tumor microenvironment in an IFN-independent manner, thereby limiting antitumor T cell immunity. The precise mechanisms underlying this dichotomous behavior remain unknown. Recent work has revealed that, beyond its canonical role in IFN induction, STING also acts as a proton channel that mediates IFN-independent processes such as autophagy, lysosome biogenesis, and cell death. Yet the physiological relevance of STING proton channel in vivo—particularly in shaping T cell fate in tumors—has remained unclear due to the lack of genetic models that selectively disrupt it.

Methods We performed targeted mutagenesis of conserved residues in mouse and human STING to identify mutations that selectively abolish proton channel activity while preserving IFN-I signaling. The effects of the mutations on STING trafficking, signaling, autophagy induction, and antiviral responses were evaluated using biochemical assays, imaging, and flow cytometry. To define the physiological role of STING's proton channel in vivo, we generated a knock-in mouse model carrying the channel mutation. T cell death and antitumor function were assessed using syngeneic tumor models.

Results We identified a conserved STING mutation in mouse and human that eliminated proton channel activity and Golgi deacidification while preserving STING trafficking, TBK1-IRF3 activation, and IFN-I induction. Functional assays revealed that the channel mutation abolished STING-mediated autophagy, lysosome biogenesis, and impaired antiviral defense. Splenic T cells from the channel-deficient-STING knock-in mice lost channel-dependent activities and were resistant to STING-induced cell death in vitro. In vivo, STING channel deficiency protected $CD8^+$ T cells from STING-driven cell death in an IFN-independent manner. We further showed that STING channel deficiency enhanced T cell persistence in the tumor microenvironment and significantly reduced tumor growth in the MC38 colon adenocarcinoma model, demonstrating a previously unrecognized role for the STING proton channel in modulating T cell survival and antitumor immunity.

Conclusions We establish the first genetic model that selectively disrupts STING proton channel activity while preserving IFN-I signaling. This model uncovers a critical IFN-independent role for the STING proton channel in driving T cell death and promoting tumor immune evasion. Our findings demonstrate distinct, separable outputs of STING signaling and identify the proton channel activity of STING as a potential therapeutic target to improve T cell-mediated antitumor immunity.

#7402 Tumor-intrinsic miR-21a orchestrates Treg-mediated immunosuppression through Pag-1 repression.

Yufei Deng[1], Wenyan Han[2], Zhaoyang Jia[2], Lujing Wu[2], Na Li[2], Lingling Wang[2], Tariq M. Rana[2], Zhouting Zhu[3]

[1]Cancer and Cell Biology program, Graduate School of Biomedical Science, Baylor College of Medicine, Houston, TX,[2]Department of Cellular and Molecular Medicine, University of California San Diego, La Jolla, CA,[3]Graduate School of Biomedical Sciences, Sanford Burnham Prebys Institute, La Jolla, CA

Immune checkpoint blockades (ICBs) such as anti-PD-1 and anti-CTLA-4 achieve durable responses in some cancers but fail in many patients, highlighting the need for additional immune modulators. Through comparative small RNA profiling of ICB-treated mouse tumors, we identified miR-21a as highly upregulated during combination immunotherapy. To define its tumor-intrinsic function, we generated CRISPR-Cas9 miR-21a knockout (KO) models in melanoma (B16F10, YUMM1.7), colorectal (MC38, CT26), and triple-negative breast cancer (4T1). Despite unchanged in vitro proliferation, miR-21a KO tumors exhibited markedly reduced growth in vivo, even without anti-PD-1 therapy, demonstrating its broad pro-tumorigenic role across cancer types. Single-cell RNA sequencing of MC38 KO tumors revealed reprogramming of regulatory T cells (Tregs) toward a less suppressive phenotype. Mechanistically, Pag-1 (phosphoprotein associated with glycosphingolipid microdomains 1) was identified as a direct target of miR-21a, and its de-repression in KO tumors contributed to enhanced immune activation. These findings uncover miR-21a as a conserved tumor-intrinsic immune regulator that orchestrates Treg-mediated immunosuppression through Pag-1, providing a promising therapeutic axis to improve immunotherapy efficacy.

#7403 Clinical impact of intraepithelial versus stromal immune cells in kidney cancer.

Zhihao Huang[1], Jan H. Muller[1], Ronald Simon[1], Christian Bernreuther[1], Nina Schraps[2], Fiete Gehrisch[2], Natalia Gorbokon[1], Florian Viehweger[1], Frank Jacobsen[1], Guido Sauter[1], Katharina Moller[1], Andreas Lubke[1], Andrea Hinsch[1], Till S. Clauditz[1], Eike C. Burandt[1], Elena Bady[1]

[1]Institute of Pathology, University Medical Center Hamburg-Eppendorf, Hamburg, Germany,[2]General, Visceral and Thoracic Surgery Department and Clinic, University Medical Center Hamburg-Eppendorf, Hamburg, Germany

Although renal cell carcinoma (RCC), has become an important target for immune checkpoint therapies, the role of specific immune cell populations and checkpoint expression within its tumor microenvironment remains poorly understood. To learn more on the role of different immune cell populations and their expression of checkpoint proteins, we analyzed a tissue microarray containing 646 RCC samples using a 14-marker multiplex immunohistochemistry approach. Immune cell composition, checkpoint expression, and spatial distribution (stromal vs. intraepithelial) were quantified across 55 spatial immune parameters and evaluated for associations with clinicopathological features. With respect to individual cell types, high densities of FOXP3$^+$ regulatory T-cells (Tregs) were significantly associated with advanced pT stage ($p < 0.001$), whereas other cell types or overall inflammatory infiltration showed no such association. Increased immune infiltration - specifically CD3$^+$ and CD4$^+$ T-cells - correlated with nodal metastasis ($p < 0.05$). Both associations were predominantly driven by stromal rather than intraepithelial immune cells. The expression of several checkpoint proteins in multiple cell types was associated with unfavorable tumor phenotype. Higher PD-1 expression on CD4$^+$ ($p < 0.001$) and CD8$^+$ T-cells ($p = 0.03$) and higher TIM-3 expression on FOXP3$^+$ T-cells ($p = 0.04$) and CD11c$^+$ dendritic cells ($p = 0.04$) were associated with advanced pT stage. High levels of PD-L1 expression on macrophages ($p = 0.008$), CTLA-4 expression on CD4$^+$ ($p = 0.04$) and CD8$^+$ ($p = 0.005$) T-cells, TIM-3 expression on FOXP3$^+$ T-cells ($p = 0.04$), and PD-1 expression on CD4$^+$ T-cells ($p = 0.04$) were linked to nodal metastasis. These immune checkpoint associations were likewise predominantly stromal in nature. It is concluded, that Immune cell composition and checkpoint pathway activity correlate with tumor progression and metastatic behavior in kidney cancer. These clinically relevant interactions arise primarily in the stromal compartment, highlighting the stroma as a key immune regulatory niche within the tumor microenvironment of kidney cancer.

#7404 MTAP loss reshapes the immune and proliferative landscape of pancreatic ductal adenocarcinoma.

Nicolaus F. Debatin[1], **Elena Bady**[2], Jan H. Muller[2], Ronald Simon[2], Christian Bernreuther[2], Nina Schraps[3], Fiete Gehrisch[3], Natalia Gorbokon[2], Florian Viehweger[2], Frank Jacobsen[2], Guido Sauter[2], Katharina Moller[2], Andreas Lubke[2], Andrea Hinsch[2], Till S. Clauditz[2], Eike C. Burandt[2], Zhihao Huang[2]

[1]Department of Otorhinolaryngology, University Hospital Hamburg-Eppendorf, Hamburg, Germany,[2]Institute of Pathology, University Medical Center Hamburg-Eppendorf, Hamburg, Germany,[3]General, Visceral and Thoracic Surgery Department and Clinic, University Medical Center Hamburg-Eppendorf, Hamburg, Germany

S-methyl-5′-thioadenosine phosphorylase (MTAP) is encoded by the MTAP gene located at 9p21 and is often homozygously co-deleted in cancer together with cyclin dependent kinase 2A (CDKN2A). As a result, MTAP deficiency results in a critical vulnerability of cancer cells towards drugs targeting multiple pathways. MTAP deficiency has also been found to predict poor response to immune checkpoint inhibitors. Ductal adenocarcinoma of the pancreas belongs to a group of tumors with a particularly high rate of MTAP deficiencies. To learn more on potential differences in the tumor-microenvironment and proliferative activity between MTAP deficient and proficient cancers, a tissue microarray containing 378 pancreatic ductal adenocarcinomas were analyzed by an 8-marker multiplex immunohistochemistry approach. With respect to innate immune infiltration, MTAP loss was associated with significantly higher densities of $CD68^+$ macrophages compared to MTAP-retained tumors ($p = 0.010$), an effect predominantly driven by stromal $CD68^+PanCK^-$ macrophages ($p = 0.005$). In contrast, total lymphocyte densities ($CD45^+CD68^-PanCK^-$) showed only a mild, non-significant increase in MTAP-loss tumors. However, proliferative lymphocytes within the tumor compartment ($CD45^+CD68^-MCM3^+Ki67^+PanCK^+$) were significantly enriched in MTAP-loss cases ($p = 0.018$), while proliferative intraepithelial lymphocytes lacking Ki67 ($CD45^+CD68^-MCM3^+PanCK^+$) showed a trend toward higher density ($p = 0.052$). Tumor cell proliferative activity was consistently elevated in MTAP-loss tumors, reflected by significantly increased labeling indices in very early ($Ki67^+MCM3^+$; $p = 0.004$), early ($MCM3^+$; $p = 0.007$), and intermediate ($Ki67^+MCM3^+$; $p = 0.030$) cell-cycle phases. Clinicopathological parameters further modulated these associations. Early-stage tumors (pT1-2) displayed higher lymphocyte densities than pT3-4 tumors ($p = 0.025$), particularly in MTAP-loss cases, whereas MTAP-retained tumors showed higher densities of proliferating macrophages in pT1-2 than in pT3-4 lesions ($p < 0.001$). Nodal-negative tumors (pN0) exhibited higher intraepithelial lymphocyte ($p = 0.044$) and proliferative lymphocyte ($p = 0.036$) densities than pN^+ tumors, most prominently in MTAP-retained cases. Similarly, lower-grade tumors (Grade 1-2) demonstrated significantly higher intraepithelial proliferative lymphocyte densities ($p < 0.005$) compared to Grade 3 tumors, again largely restricted to MTAP-retained cancers. It is concluded, that MTAP deficiency impacts the immune microenvironment of pancreatic ductal adenocarcinoma by promoting stromal macrophage accumulation and increased proliferation within immune and tumor compartments.

#7405 Targeting cysteine cathepsins to boost gemcitabine in PDAC.

Nika Mazej Jeram[1], Biljana Mileva Mileva Boshkoska[2], Ales Tomazič[3], Stanislav Gobec[4], Damijan Knez[4], Janko Kos[4], **Milica M. Perisic Nanut**[1]

[1]Biotechnology, Jozef Stefan Institute, Ljubljana, Slovenia,[2]Jozef Stefan Institute, Ljubljana, Slovenia,[3]Dept of Abdominal Surgery, Ljubljana University Medical Centre, Ljubljana, Slovenia,[4]Faculty of Pharmacy, University of Ljubljana, Ljubljana, Slovenia

Cysteine cathepsins are increasingly recognized as important regulators of lysosomal function and autophagy, two processes that help cancer cells survive under treatment-induced stress. In pancreatic ductal adenocarcinoma (PDAC), where gemcitabine is still widely used as first-line chemotherapy, growing evidence indicates that drug-induced autophagy contributes to the development of resistance. In this study, we asked whether autophagy triggered by gemcitabine depends on cysteine cathepsins and whether blocking these proteases can improve gemcitabine's antitumor activity. We focused on cathepsins L, B, and V, major lysosomal proteases with established roles in proteolysis and emerging functions in survival signalling. Using three PDAC cell lines with distinct genetic backgrounds and chemosensitivity (PANC1, Capan2, BxPC3), we treated cells with sublethal LC30 and LC60 concentrations of gemcitabine to trigger stress responses without inducing extensive cell death, thereby allowing us to dissect adaptive autophagy from direct cytotoxicity. Using western blot analysis and immunocytochemistry, we examined expression, processing, and subcellular localization of cathepsins and key autophagy markers, and we quantified autophagic flux and lysosomal function in the presence or absence of selective inhibitors of cathepsins V, L, and B. In parallel, cell viability and apoptosis assays were used to assess treatment responses, and 3D patient-derived organoids and NK cell co-culture systems were employed to validate our findings in more physiologically relevant models. Our results show that gemcitabine-induced autophagy is at least partly dependent on cysteine cathepsin activity, and that pharmacologic inhibition of these enzymes interferes with autophagic processing and makes PDAC cells more sensitive to gemcitabine. We confirmed these findings in patient-derived organoids, where the combination of gemcitabine and cathepsin inhibition reduced tumour cell viability more effectively than either treatment alone. In addition, we tested how this combination affects immune recognition and found that natural killer (NK) cell–mediated killing was increased in gemcitabine- and cathepsin inhibitor–treated tumour cells. Overall, our data identify cathepsins L, B, and V as key modulators of gemcitabine-induced autophagy and immune susceptibility in PDAC and support their further exploration as therapeutic targets to overcome chemoresistance and improve clinical responses.

#7406 FcRn and macropinocytosis promote albumin uptake in tumor-associated macrophages.

Huiyu Hu[1], Xinying Ge[1], Thomas Sc Ng[1], Ralph Weissleder[2], Christopher S. Garris[1], Miles Aaron Miller[3]

[1]Massachusetts General Hospital, Boston, MA,[2]Director, Ctr. for Systems Bio., Massachusetts General Hospital, Boston, MA,[3]Graduate Student, Biological Engineering, Massachusetts General Hospital, Boston, MA

Background: Serum albumin, the most abundant and long-circulating protein in serum, has been successfully used as a drug delivery vehicle for cancer therapy. We have previously demonstrated that albumin accumulates at high levels in tumors, including anaplastic thyroid cancer (ATC), pancreatic cancer and prostate cancer. Oncogene-driven macropinocytosis in cancer cells plays a major role in albumin uptake. However, little is known about the level of albumin uptake and the mechanisms that contribute to its accumulation in tumor-infiltrating immune cells. We hypothesized that tumor-infiltrating immune cells, particularly tumor-associated macrophages (TAMs), efficiently take up albumin via macropinocytosis and FcRn-mediated endocytosis.

Methods: We assessed the *in vivo* uptake of mouse serum albumin by fluorescent reflectance imaging, and cellular albumin uptake by flow cytometry in the immunocompetent ATC TBP3743 ($Braf^{V600E}$ $p53^{-/-}$) in B6129SF1/J mice and melanoma YUMM1.7 ($Braf^{V600E/wt}$ $Pten^{-/-}$ $Cdkn2^{-/-}$) in C57BL/6J mice. We further identified tumor and cellular albumin uptake in neonatal Fc receptor (FcRn)- and caveolin 1 (Cav1)-deficient mice. *In vitro* cellular uptake of serum albumin was quantified in bone marrow-derived macrophages (BMDM) isolated from wildtype, $FcRn^{-/-}$ ($Fcgrt^{-/-}$) and $Cav1^{-/-}$ mice. We further treated BMDM with Na+/H+ exchanger (NHE) inhibitor 5-(N-ethyl-N-isopropyl)amiloride (EIPA) to block macropinocytosis, and fucoidan to block scavenger receptor-mediated endocytosis.

Results: TBP3743 tumors and YUMM1.7 tumors accumulated serum albumin at 9%ID/g (% injected dose per gram tissue) and 11%ID/g, respectively, in mice 24 hrs after intravenous albumin administration. Although TAMs comprised only 4% of cells in ATC tumors and 5% in melanoma tumors, they accumulated a disproportionately high proportion (22% and 19%, respectively) of total fluorescent albumin in the tumor microenvironment. Tumors in $Cav1^{-/-}$ and $FcRn^{-/-}$ mice accumulated only 10% and 29%, respectively, of the albumin uptake observed in wildtype mice. The mean fluorescence intensity of the serum albumin in TAMs in $Cav1^{-/-}$ and $FcRn^{-/-}$ hosts was 78%and 32% of the level in wildtype hosts. *In vitro* $Cav1^{-/-}$ and $FcRn^{-/-}$ BMDM accumulated albumin 107% and 44% of wildtype BMDM. EIPA reduced albumin uptake by 68%, 76% and 84% in wildtype, $Cav1^{-/-}$ and $FcRn^{-/-}$ BMDM. Fucoidan didn't alter albumin uptake in either BMDM.

Conclusion: TAMs exhibit the highest albumin uptake, on a per-cell basis, among cells within ATC and melanoma tumor microenvironments. Importantly, our data show that macropinocytosis and FcRn-mediated endocytosis are responsible for albumin uptake in TAMs. Thus, albumin accumulates efficiently in TAMs via FcRn and macropinocytosis, providing rationale for albumin as a drug delivery vehicle for TAM-targeted therapeutics.

#7407 The NAT10-PBX1 ac4C axis disables MHC Class II antigen presentation to promote immune-cold cholangiocarcinoma.

Kai Luo[1], Yuhan Fang[2], Yinzhao Chen[2], Yuting Zhao[2], Jialin Qu[3], Dong Shang[3], **Caiming Xu**[4], Guixin Zhang[1]

[1]The Second Hospital of Dalian Medical University, Dalian, China,[2]Institute (College) of Integrative Medicine, Dalian Medical University, Dalian, China,[3]The First Affiliated Hospital of Dalian Medical University, Dalian, China,[4]Beckman Research Institute of The City of Hope, Monrovia, CA

Background: Intrahepatic cholangiocarcinoma (ICC) is an aggressive malignancy with poor prognosis, partly driven by an inherently immune-cold tumor microenvironment. N4-acetylcytidine (ac4C) is a conserved RNA modification that regulates RNA stability and translation, and NAT10-mediated ac4C remodeling has been implicated in tumor metastasis and immune cell infiltration. Here, we investigate how ac4C modification promotes ICC progression and immune evasion to identify potential therapeutic vulnerabilities.

Methods: We quantified ac4C modification and NAT10 expression in ICC using publicly available cohorts and clinical tissue samples, and performed single-cell transcriptomic profiling to investigate the impact of NAT10 expression on immune cell infiltration. CRISPR-Cas9-based genetic manipulation of NAT10 in ICC cell lines and mouse models enabled functional interrogation of its contribution to tumor initiation and progression. Mechanistic insights were obtained through an integrated multi-omics and molecular approach, including RNA-seq, acRIP-seq, CUT&Tag, RIP, ChIP, FISH, dual-luciferase reporter assays and RNA stability assays.

Results: We found that both ac4C modification and NAT10 expression were significantly elevated in ICC tissues compared with adjacent non-tumor tissues ($P < 0.05$). Clinically, high NAT10 expression was associated with shorter mOS (17.3 vs 26.7 months; log-rank $P = 0.021$). In cellular models, NAT10 knockdown reduced ac4C levels and ICC cell proliferation (EdU-positive HUCCT1 and RBE cells decreased by 11.7% and 15.6%, respectively) and impaired invasion and metastasis, with Transwell migration reduced by 45.2% and 38.7%. In vivo, NAT10 knockout suppressed tumor growth in murine xenografts; tumor volumes were reduced by 67% ($P < 0.05$). Mechanistically, NAT10 knockdown diminished ac4C modification on PBX1 mRNA, leading to reduced mRNA stability and downregulation of PBX1 protein. PBX1 was identified as a transcriptional repressor of CIITA: NAT10 silencing increased CIITA expression via PBX1 downregulation, subsequently elevating transcript and protein levels of MHC class II genes. Conversely, PBX1 overexpression reversed these effects. Single-cell transcriptomic analysis demonstrated that ICC tumors with high NAT10 expression exhibited reduced infiltration levels of $CD4^+$/$CD8^+$ T cells, which was validated by multiplex immunofluorescence and flow cytometry in murine models.

Conclusion: Our study reveals that NAT10 promotes ICC progression and immune exclusion by ac4C-modifying PBX1 to repress the CIITA-MHC class II pathway, thereby limiting T-cell infiltration. Targeting NAT10 may restore antigen presentation and improve immunotherapy responsiveness in ICC.

#7408 *Brca2*-deficiency promotes increased cGAS-STING pathway activation and an immunosuppressive tumor immune microenvironment in prostate cancer.

Kimberly A. Rickman[1], Irena Q. Sun[2], Ramya Parameswaran[1], Xuxu Gou[2], Morgan E. Diolaiti[2], Harish N. Vasudevan[3], Alan Ashworth[2]

[1]Divsion of Hematology and Oncology, Department of Medicine, University of California, UCSF Helen Diller Family Comprehensive Cancer Ctr., San Francisco, CA,[2]UCSF Helen Diller Family Comprehensive Cancer Ctr., San Francisco, CA,[3]Department of Radiation Oncology and Neurological Surgery, University of California, San Francisco, San Francisco, CA

Background: Combined germline and somatic tumor profiling of advanced metastatic prostate cancer has revealed that ~20% of metastatic tumors have mutations in DNA repair genes such as *BRCA2*. Germline variants in *BRCA2* predispose to aggressive high-risk prostate cancer and more advanced disease at diagnosis. BRCA2 is vital to the repair of DNA double-strand breaks (DSB) by homologous recombination (HR) and deficiency leads to genomic instability which has been shown to drive inflammation via the cGAS-STING pathway. The implications of loss of *BRCA2* function in prostate cancer on immune activation and the tumor microenvironment (TME) are unknown. This represents a significant knowledge gap towards devising therapies that effectively target the immunosuppressive TME of HR-deficient prostate cancer.

Methods: We have engineered an immunocompetent *Brca2*-deficient prostate cancer model with loss of function frame shift (fs) mutations (*Brca2*^{fs}) using CRISPR/Cas9 to address the critical gap in current preclinical models. We validated BRCA2 loss of function and characterized innate immune signaling through the cGAS-STING pathway. We performed spectral flow cytometry and single-cell RNA sequencing (scRNA-seq) on *Brca2*^{WT} and *Brca2*^{fs} tumors from immunocompetent mice to assess the TME. Mice bearing *Brca2*^{fs} tumors were treated with anti-CCR8 monoclonal antibodies with and without anti-PD-1 to test the effectiveness of targeting the CCR8-axis in *Brca2*-deficient prostate tumors.

Results: *Brca2*^{fs} cells show hallmarks of increased DNA damage and cGAS-STING pathway activation compared to *Brca2*^{WT} cells. Analysis of implanted *Brca2*^{fs} tumors demonstrated enrichment of CD4+ T cells and immunosuppressive CCR8+ regulatory T cells (Treg) compared to *Brca2*^{WT} tumors. scRNA-seq of *Brca2*^{fs} tumors implanted in immunocompetent mice showed a significant increase in the interferon expression signature that is likely the result of increased cGAS-STING pathway activation in tumor cells. Additionally, tumor associated macrophages (TAMs) from *Brca2*^{fs} tumors showed a greater immunosuppressive phenotype with an increase in M2 polarization (pro-tumor) and high expression of *Ccl8*, the CCR8 receptor ligand. Combination anti-CCR8 and anti-PD-1 therapy significantly reduced tumor growth in mice bearing *Brca2*^{fs} tumors.

Conclusions: Our analysis has revealed enrichment of immunosuppressive CCR8+ Tregs and *Ccl8*-high expressing TAMs in *Brca2*-deficient but not *Brca2*-proficient prostate cancer tumors. Anti-CCR8 therapy, to deplete CCR8+ Tregs, in combination with anti-PD-1 therapy significantly reduced *Brca2*^{fs} tumor growth in our immunocompetent mouse model. These findings present the exciting possibility of targeting the CCR8-axis in *BRCA2*-deficient prostate tumors to overcome these immunosuppressive mechanisms and enhance activity of tumor-reactive T cells.

#7409 CD4 T cells regulate B and plasma cells to restrict tumor growth in Medulloblastoma.

Tanja Eisemann[1], **Alexander Thomas Wenzel**[2], Jill P. Mesirov[2], Robert Wechsler-Reya[3]

[1]SBP Medical Discovery Institute, La Jolla, CA,[2]Medicine, University of California, San Diego, La Jolla, CA,[3]Neurology, Columbia University, New York, CA

Medulloblastoma is the most common pediatric brain cancer. While survival has improved in recent years, some subtypes, such as “Group 3”, still have a poor prognosis, and due to the lifelong side effects of standard chemotherapy and radiation, new treatments with less toxicity are greatly needed. Further, immunotherapy, while beneficial for other cancers, has not impacted brain cancer treatment, and immune system dynamics and interactions with tumor cells in the brain are poorly understood. We created a mouse model of Group 3 Medulloblastoma in which transformed, orthotopically transplanted neural stem cells form tumors in syngeneic, immune-competent mice, allowing us to study the effects of immune system modulation on Medulloblastoma tumor growth. Though they comprised a relatively small subpopulation of immune cells in the brain, depleting CD4+ T cells resulted in rapid tumor growth and worse survival. An analysis of tumor and control cells profiled with single cell RNA-sequencing (scRNA-seq) showed that, in addition to a loss of CD4+ T cells, B cells and plasma cells were also substantially reduced. In a pseudotemporal model of B cell to plasma cell differentiation, tumor cells from treated mice were absent from differentiated plasma cells and from a plasmablast population. These results indicate that brain-resident CD4+ T cells play a key role in controlling Medulloblastoma tumor growth by regulating B and plasma cells, and that immunotherapy may play a role in future Medulloblastoma treatments.

#7410 Antiviral therapy reverses CMV-induced oncogenic signaling and enhances NK cell cytotoxicity in glioblastoma with associated PD-L1 upregulation and ilmmune modulation.

Vida Tajiknia[1], Wafik S. El-Deiry[2], Connor Purcell[2], Sean E. Lawler[2]

[1]Legorreta Cancer Center,Brown University, Providence, RI,[2]Brown University, Providence, RI

Background: Cytomegalovirus (CMV) has been implicated in glioblastoma (GBM) pathogenesis by promoting stemness, angiogenesis&immune evasion. Clinical trials targeting CMV in GBM have shown preliminary promise, However, the molecular mechanisms remain unclear. We hypothesized that CMV enhances oncogenic signaling and immune resistance in GBM, and that antiviral therapy may reverse these effects and increase susceptibility to immune-mediated cytotoxicity

Materials and Methods: Human GBM cell lines (U251, U87, U138, T98G, LN229) & normal astrocytes were infected with a mCherry-human CMV TB40 strain (MOI 0.5). Phenotypic assays including spheroid & colony formation were performed. A 60-plex cytokine panel and Western blotting were used to evaluate cytokine profiles & signaling pathway activation (IL-6/STAT3, Akt, SOX2, Survivin, p-RB). Co-culture experiments with NK-92mi cells were conducted using CMFDA and Eth-homodimer dyes to assess cytotoxicity.

Results: CMV infection upregulated IL-6/STAT3, SOX2, Survivin, p-AKT, and p-RB, promoting GBM cell proliferation, stemness, and resistance to apoptosis. Infected cells exhibited a tumor-supportive cytokine profile and, after ganciclovir treatment, reduced VEGF and Angiopoietin-2 levels. CMV-infected astrocytes also showed increased oncogenic signaling and colony formation, suggesting a role in early transformation. Ganciclovir partially reversed these effects, shifting cytokine expression toward an immune-permissive state. While NK cells alone failed to lyse GBM cells, ganciclovir-treated, CMV-infected cells showed significantly enhanced NK-mediated cytotoxicity. PD-L1 expression increased after CMV infection and remained elevated post-treatment, indicating immune modulation and potential for checkpoint blockade.

Conclusions: CMV infection reprograms both glioblastoma cells and normal astrocytes toward a more aggressive, immune-evasive phenotype through activation of IL-6/STAT3, p-AKT, SOX2, and angiogenic pathways. Ganciclovir treatment partially reverses these effects, reducing VEGF and Angiopoietin-2 levels, shifting cytokine profiles, and—critically—enhancing NK cell-mediated cytotoxicity. Persistent PD-L1 upregulation following infection suggests a novel immune checkpoint vulnerability, opening the door for synergistic antiviral and immunotherapy approaches. These findings identify CMV not only as a driver of tumor progression but as a tractable therapeutic target in GBM.

#7411 Proteotranscriptomic dissection of breast cancer T cell states identifies CD103+ Tfh-derived cytotoxic CD4+ cells linked to immunotherapy response.

Ghamdan Al-Eryani[1], Sophie van der Leij[2], Etienne Masle-Farquhar[2], Alma Andersson[3], Kate Harvey[2], Sunny Wu[2], Tony Wang[2], John Reeves[2], Cindy Ma[2], Daniel L. Roden[2], Charles M. Perou[4], Nir Hacohen[1], Aziz Al'Khafaji[1], Mats Nilsson[5], Joakim Lundeberg[3], Marcel Batten[2], Simon Junankar[2], Alexander Swarbrick[2]

[1]Broad Institute, Cambridge, MA,[2]Garvan Institute of Medical Research, Darlinghurst, Australia,[3]Science for Life Laboratory, KTH Royal Institute of Technology, Stockholm, Sweden,[4]UNC Lineberger Comprehensive Cancer, Chapel Hill, NC,[5]Stockholm University, Stockholm, Sweden

While cancer immunotherapies have primarily focused on activation of cytotoxic CD8 killing, CD4 T cell activity is also associated with survival and immunotherapeutic response in numerous cancers. We applied integrated single-cell RNA sequencing and multiplexed protein epitope profiling to breast cancer samples to resolve the complexity of immune cell states within the tumor microenvironment. This approach enhanced phenotypic resolution, identifying three distinct states within the T follicular helper (Tfh) cell cluster. A CXCR4high progenitor state gave rise to two differentiated states: an IGFL2high subset resembling conventional Tfh cells and localised to B cell-rich lymphoid aggregates, and a CD103+ subset, exhibiting features of tissue residency, exhaustion, and cytotoxicity, which co-localised with tumor foci. CD103+ Tfh-like cells were found to interact with CXCL10+ macrophages through production of CCL chemokines and CSF1. A higher CD103+ Tfh to IGFL2high Tfh ratio correlated with improved patient survival and enhanced responses to anti-PD1 checkpoint blockade. These findings integrate Tfh and CD4 with cytotoxic potential in breast cancer, offering new insight into anti-tumor immunity and response to checkpoint blockade.

#7412 ANXA1 and MYADM regulate CD4$^+$T cell differentiation and exhaustion in non-small cell lung cancer (NSCLC).

Minyeop Kim[1], Youwon Lee[1], **Seung Yeon Oh**[2], Eun Ji Lee[1], Ji Ae Ko[1], Jihyoung Mun[1], Byoung Chul Cho[1], Mi Ran Yun[1]

[1]Yonsei University College of Medicine, Seoul, Korea, Republic of,[2]Yonsei University College of Medicine SBSI, Seoul, Korea, Republic of

Introduction: CD4$^+$ T cells have primarily been known for their helper function with the tumor microenvironment (TME), and recent studies have demonstrated their ability to directly exert cytotoxic activity against tumor cells. Despite this functional potential, their cytotoxic activity can be compromised by exhaustion within the immunosuppressive TME. Therefore, preventing CD4$^+$ T cell exhaustion may be critical for promoting an anti-tumor immune responses. In this study, we aimed to identify potential target that contribute to CD4$^+$ T cell exhaustion in the TME.

Method: To analyze CD4$^+$ T cell in NSCLC, we performed single-cell RNA sequencing (scRNA-seq) on samples from 83 lung adenocarcinoma (LUAD) patients using the 10X genomic platform. After excluding B cells, lymphoid populations were annotated by canonical marker genes as CD8$^+$ T cells, CD4$^+$ T cells, NK cells, and proliferating cells. Subsequently, CD4$^+$ T cells were re-clustered to identify functional subtypes. Differential gene expression and pathway analyses were than performed to characterize the molecular feature of each cluster.

Result: CD4$^+$ T cells were identified as 10 distinct clusters and further categorized into early, intermediate, and late states based on state-specific marker gene expression. Clusters within the same state showed high transcriptional similarity. Interestingly, the tissue-resident memory (TRM) cluster (intermediate state), and ITGAE$^+$ Tfh-like clusters (late state) exhibited notable transcriptional similarity despite representing different functional states. Pathway enrichment analysis revealed that both clusters share certain effector and adhesion-related features, with TRM displaying stronger effector functions. In contrast, ITGAE$^+$ Tfh-like cells appeared more exhausted. Consistent with this, TRM cells were enriched in normal tissues, whereas ITGAE$^+$ Tfh-like cells predominated in tumors, reflecting activation- versus suppression- associated profiles. Trajectory analysis further revealed differentiation pathway from TRM cells to ITGAE$^+$ Tfh-like T cells. This transition was accompanied by reduced inflammatory response and regulation of T cell proliferation pathways, indicating progression toward an exhausted state. Notably, ANXA1, SMAD7, and MYADM were identified as key genes potentially regulating these processes, with ANXA1 and MYADM especially showing positive correlations with the T cell activation pathway as well as with each other.

Conclusion: These findings suggest a potential differentiation of TRM into ITGAE$^+$ Tfh like T cells, accompanied by transcriptional and functional changes indicative of progressive exhaustion. Such alterations likely contribute to the formation of an immunosuppressive TME. ANXA1 and MYADM play pivotal roles in regulating this process and may serve as potential targets for modulating T cell function in the tissue microenvironment.

#7413 CD36 influences leukemia progression in MLL-AF9-driven AML by modulating the leukemia immune microenvironment.

Yiting Meng, Wenda Zhu, Mateusz Pospiech, Long Huynh, Kalyani Divgi, Yiyu Xiao, Qianqian Peng, Nicholas A. Graham, **Houda Alachkar**

USC - University of Southern California, Los Angeles, CA

CD36, a fatty acid translocase, is recognized as a potential therapeutic target in acute myeloid leukemia (AML), where its overexpression is associated with disease progression, yet its role in leukemogenesis remains to be elucidated. This study investigates the role of CD36 in leukemia initiation using the MLL-AF9 mouse model, where hematopoietic stem progenitor cells (HSPCs) from Cd36 knockout (KO) or wild-type (WT) mice were transduced with MLL-AF9 virus and evaluated for leukemogenic potential through in vitro and in vivo assays, and comprehensive transcriptomic, metabolomic, and immune profiling. Both Cd36KO and Cd36WT HSPCs transformed into leukemic cells, but Cd36 deletion led to a less aggressive leukemia phenotype, with reduced leukemia burden and extended median survival in sublethaly irradiated mice (15 vs. 22 days, P = 0.001). Leukemia engraftment was significantly higher in Cd36WT-MA9 compared with Cd36KO-MA9 transplanted mice in spleen (74.99% vs. 38.67%, P = 0.008) and blood (85.49% vs. 26.84%, P < 0.001) relative to bone marrow (BM). Increased CD4 (13.93% vs. 36.78%, P = 0.025) and CD8 T cells (7.62% vs. 16.06%, P = 0.02) and less CD4CD25 T cells (34.53% vs. 19.24%, P = 0.006) were observed in mice engrafted with Cd36KO-MA9 cells compared with Cd36WT-MA9 mice. qPCR analysis shows elevated *Gzmb* (2.43-fold, P < 0.001), and *Tim3* (5.88-fold, P = 0.002) mRNA expression in Cd36WT-MA9 compared with Cd36KO-MA9 mice, while *Foxp3*, *Lag3*, and *Pd1* showed no significant differences. A more pronounced phenotypic was observed in immunocompetent, non-irradiated mice; Cd36WT-MA9 cells displayed significantly greater leukemia engraftment (BM: 98.58% vs. 0.73%, P < 0.0001; spleen: 64.60% vs. 0.79%, P < 0.001, and blood: 89.08% vs. 10.20%, P = 0.014) compared with Cd36KO-MA9 cells. Cd36KO-MA9 mice showed enhanced immune responses with higher CD3+ (10.87% vs. 37.82%, P < 0.001), CD4 (27.77% vs. 55.19%, P = 0.008), CD8 T cells (17.84% vs. 31.24%, P < 0.001), and NK1.1 cells (14.47% vs. 29.83%, P < 0.0001), but lower CD4CD25 (11.11% vs. 5.55%, P = 0.045), DN-T cells (51.95% vs. 10.46%, P < 0.001), and CD25 DN T cells (17.77% vs. 4.00%, P < 0.001) compared with Cd36WT-MA9 mice, suggesting Cd36 deletion reduces leukemia progression by enhancing anti-leukemic immunity. RNA-sequencing and gene set enrichment analysis indicated enrichment of inflammatory (TNFA, FDR < 0.001) and metabolic pathways (oxidative phosphorylation, FDR < 0.001) in Cd36WT-MA9 cells compared with Cd36KO-MA9 mice. Metabolomic analysis identified 124 metabolites, with Cd36KO-MA9 cells showing a significant increase in asparagine (10.00-fold, unadj P = 0.009) and a decrease in purine (7.68-fold, unadj P < 0.0001) compared with Cd36WT-MA9 cells. While Cd36 deletion does not prevent leukemogenesis, it alters the leukemia immune microenvironment and slows leukemia progression, highlighting its role in modulating leukemia development.

: Microenvironmental Determinants of Therapy Response and Resistance 2
Poster Session

#7417 Immune system state shapes clinical response to CAR-T therapy in mantle cell lymphoma.

Vivian Jiang, Qingsong Cai, Hong Kim, Lei Nie, Chengtai Yu, Yang Liu, Yijing Li, Jovanny Vargas, Michael Wang

UT MD Anderson Cancer Center, Houston, TX

Background:
CAR-T therapy has transformed treatment for relapsed/refractory mantle cell lymphoma (MCL), yet a significant subset of patients relapses or fails to respond. The biological mechanisms driving relapse and refractoriness remain poorly defined, particularly the influence of systemic immune dynamics in shaping CAR-T efficacy.
Methods:
Single-cell RNA sequencing (scRNA-seq) was performed on 56 blood samples from 44 MCL patients treated with brexucabtagene autoleucel, including 24 long-term responders (pre-CAR-T samples), 17 relapsed patients (13 with paired pre-CAR-T and post-relapse samples), and 3 refractory patients (paired pre- and post-CAR-T samples). Integrative computational analysis was conducted to define immune system state (ISS) at single-cell resolution and correlate them with clinical outcomes. An AI-assisted predictive model is under development for clinical application.
Results:
scRNA-seq analysis of 156,852 cells in total revealed three major ISS categories strongly associated with clinical outcomes: immune surveillance (low-risk), immune equilibrium (intermediate-risk), and immune suppression (high-risk), based on cytotoxicity and immunosuppressive profiles. Low-risk patients exhibited robust cytotoxic activity and durable remission, whereas relapse involved evolution to high-risk states characterized by T-cell and NK-cell exhaustion and monocyte enrichment. All refractory patients displayed high-risk ISS prior to CAR-T. Exhaustion scores and checkpoint expression (e.g. TIGIT, LAG3) were elevated in T-cell subsets (CTL, Tex, TCM) and NK cells post-relapse or in refractory cases. These findings establish ISS as a predictive framework for CAR-T response and relapse risk in MCL.
Conclusions:
ISS provides a clinically actionable framework for predicting CAR-T response in MCL by capturing systemic immune dynamics. ISS-guided risk stratification may inform CAR-T optimization and rational combination strategies in MCL.

#7418 Evaluation of chemo-radiation therapy's effect on the senescence status of tumor microenvironment of HNSCC.

Lan Gao[1], Alanna Sun[1], Ruomin Xin[1], Daniel John[1], Wei Tse Li[2], Weg M. Ongkeko[1]

[1]University of California San Diego, San Diego, CA,[2]University of California San Francisco, San Francisco, CA

Background: Cellular senescence is a stress-induced, irreversible arrest of cell proliferation accompanied by a senescence-associated secretory phenotype (SASP), which may impair the immune system's ability to detect and eliminate cancer cells. Chemotherapy and radiation therapy (RT) are standard treatments for head and neck squamous cell carcinoma (HNSCC) by inducing DNA damage. Despite their therapeutic utility, studies have shown that chemotherapy and RT-induced DNA damage may also cause immune cell senescence in other cancers. The effect of these therapies on the senescence state of the tumor microenvironment (TME) in HNSCC has not been elucidated. We hypothesized that chemoradiation treatment results in the immunosenescence of TME in HNSCC. In this study, we analyzed how chemotherapy and radiation therapy influence the senescence-associated gene programs in the TME of HNSCC.

Methods: Bulk immune-targeted RNA sequencing data were obtained from 30 HNSCC patients before and after chemoradiotherapy (GSE193445 from GEO). Single-cell RNA sequencing data were obtained from oral cancer tumor samples of 4 patients with HNSCC (GSE280982) at 3 time points of RT treatment. Filtering, normalization, integration, and clustering were performed on the sequencing data. Generative AI was used for assistance in debugging analyses.

Results: Gene Set Enrichment Analysis (GSEA) of bulk RNA-seq data shows that, post-chemoradiation, myeloid cell activation involved in immune response was upregulated (NES = +1.93, padj = 0.0056), while cytokinesis was downregulated (NES = -2.32, padj = 0.0037). Differential expression analysis identified interferon-stimulated genes ISG15 (log2FC = -1.48, padj = 4.9e-07) and IFI6 (log2FC = -1.46, padj = 2.2e-07) were strongly downregulated after chemoradiation. Additional immune-modulatory genes expression such as IGFBP3 (log2FC = -1.56, padj = 6.0e-08) and GAGE family genes (log2FC = -1.79, padj = 0.022) also decreased post-treatment. Single-cell RNA-Seq data show that in individual cell clusters after RT, in CD8+ T cells, the p53 pathway was upregulated (NES = 1.8, padj = 0.0038) and IL-2/STAT5 signaling pathway was suppressed (NES = -1.8, padj = 0.02). In B cells, TNFα signaling (NES = 2.6, padj = 4.1e-07) and apoptosis pathway (NES = 1.66, padj = 0.03) is upregulated. In Tregs, oxidative phosphorylation (NES = 2.6, padj = 6.1e-05) and MYC signaling is upregulated in Tregs (NES = 3.2, padj = 2.5e-08).

Conclusion: Preliminary data suggest that innate immune pathways in the TME of HNSCC were suppressed after chemoradiation therapy; the proliferative and survival pathways of CD8+ T cells, B cells, and Tregs are altered as a response to RT.

#7419 Comprehensive profiling of primary and metastatic prostate tumors reveals distinct tumor and fibroblast cell states associated with androgen resistance.

Aleksandar Obradovic[1], Kwangmin Yoo[2], Chang Liu[3], Patrick McCann[4], Casey R. Ager[5], Matthew C. Dallos[4], Samir Zaidi[6]

[1]Columbia University, New York, NY,[2]Korea University College of Medicine, Seoul, Korea, Republic of,[3]Columbia University Irving Medical Center,[4]Memorial Sloan Kettering, New York, NY,[5]Mayo Clinic, Phoenix, AZ,[6]Yale University, New Haven, CT

Prostate cancer requires continual escape from immune surveillance, but mechanisms underlying this escape in the transition from androgen sensitivity to resistance and metastasis remain incompletely understood. Androgen-deprivation therapy (ADT)—the treatment backbone—induces tumor cell apoptosis but also remodels the tumor microenvironment (TME). We have assembled a single-cell RNA-seq atlas from >800,000 cells across 68 patients treated at Columbia University and Memorial Sloan Kettering. The resource includes 33 primary tumors (16 treatment-naïve, 17 post-ADT) annotated with time to PSA recurrence, and 31 metastases, including longitudinal pre- and post-ADT data in 14 castration-sensitive tumors (CSPC), 17 castration-resistant tumors (CRPC), and 4 neuroendocrine tumors (NEPC). This dataset spans the spectrum of prostate cancer disease progression.Using ARACNe and VIPER to infer activity of transcriptional regulatory and signaling proteins, we detect conserved cell state programs while minimizing batch effects. Several significant features emerged. Immune infiltration—both lymphoid and myeloid—is significantly higher in CSPC metastases than in primary or CRPC tumors and increases further after ADT. T cells constitute ~15% of cells in primary tumors versus 30% in treatment-naive CSPC (40% post-ADT), falling to 13% in CRPC and <1% in NEPC ($p<1e-32$), consistent with an initially "hot" CSPC TME that progressively excludes T cells with disease progression.Among ~350,000 epithelial/tumor cells, trajectory analysis reveals two differentiation pathways from normal epithelium. Pathway 1—dominant in primary tumors—shows androgen receptor (AR) activity with three sub-phenotypes (T1-T3): T1 exclusive to primary tumors; T2 shared by primary and CSPC; and T3 restricted to CRPC, with high ERG expression, and very strong AR activity. Pathway 2 (clusters T4-T6), present in NEPC and a subset of CRPC, lacks AR activity and displays SOX2, FOXA2, PRKD1. These aggressive states uniformly overexpress AURKA, RET, and TOP2A, suggesting druggable targets for combination therapy.We further define five cancer-associated fibroblast (CAF) subtypes. CAF1-3 track with advanced, treatment-resistant disease—enriched in NEPC versus CRPC (25% vs 18% of CAFs) and in CRPC versus CSPC (18% vs 11%)—while CAF4-5 predominate in primary tumors. We identify druggable proteins and receptor-ligand interactions linking CAF1-3 with T4-T6 tumor states; in vivo perturbations are underway.This atlas provides a resource profiling tumor and immune ecosystems across prostate cancer progression. It highlights MR programs and stromal-tumor-immune interactions that underlie immune evasion and ADT resistance, yielding actionable targets and combination-therapy hypotheses for aggressive disease.

#7420 Mechanistic study of CX3CL1 promoting T cell exhaustion in ESCC via the JAK/STAT3 axis.

Jiayi Huang[1], Beilei Liu[2], Licheng Tan[1], Hongyu Zhou[3], Bowen Yao[1], Shuang Zhang[1], Xin-Yuan Guan[1]

[1]Clinical Oncology, The University of Hong Kong, Hong Kong, Hong Kong,[2]City University of Hong Kong, Hong Kong, Hong Kong,[3]Shanghai Cancer Center, Shanghai, China

Despite the transformative impact of T cell therapy on hematologic cancers, its efficacy in solid tumors such as esophageal squamous cell carcinoma (ESCC) is hampered by T cell exhaustion and poor tumor infiltration. By establishing an immunocompetent ESCC mouse model and conducting single-cell RNA sequencing (scRNA-seq), we have generated a dynamic single-cell atlas of tumor evolution across four distinct phases: immune surveillance, immune equilibrium, immune suppression, and immune escape. We found that CX3CL1 is highly enriched in the immune suppression stage and associated with T cell exhaustion. Further GO analysis demonstrated that CX3CL1$^+$ tumor cells activate the JAK/STAT3 signaling pathway. Both in vitro co-culture systems and in vivo studies showed that treatment with CX3CL1-neutralizing antibodies and JAK inhibitors effectively enhances T cell cytotoxicity and promotes tumor cell apoptosis. Combined therapy with PD-1 inhibitors and CX3CL1-neutralizing antibodies/JAK inhibitors significantly suppressed the growth of subcutaneous ESCC tumors in mice. Our findings indicate that CX3CL1 is a potential therapeutic target in ESCC, and targeting the CX3CL1/JAK/STAT3 axis in combination with immune checkpoint inhibitors may confer potential benefits to ESCC patients.

#7421 Palmatine modulates tumor microenvironment and improves gemcitabine efficacy in PDAC via HOXA10-STAT3 axis suppression.

Meagan Marie Ybarra[1], Xiaoyu Yang[1], Siri Borra[1], Chia-Nung Hung[2], John Baer[3], Ramya Chengalvala[3], Rolando Trevino Jr[4], Shaye Hagler[3], Sung-Jen Wei[4], Joel Michalek[5], Zhao Zhang[1], Sukeshi A. Patel[6], Danielle Fritze[7], Glenn Halff[7], Zhao Lai[8], Yuji Ikeno[9], Yidong Chen[10], Rita Ghosh[11], Addanki Pratap Kumar[11]

[1]Molecular Medicine, UT Health Science Center at San Antonio, San Antonio, TX,[2]UT Health Science Center at San Antonio, San Antonio, TX,[3]Bruker Spatial Biology, St. Louis, MO,[4]Radiation Oncology, UT Health Science Center at San Antonio, San Antonio, TX,[5]Population Health Sciences, Mays Cancer Center, UT Health Science Center at San Antonio, San Antonio, TX,[6]Mays Cancer Center, Medicine, UT Health Science Center at San Antonio, San Antonio, TX,[7]Surgery, UT Health Science Center at San Antonio, San Antonio, TX,[8]Greehey Children's Cancer, San Antonio, TX,[9]Pathology & Laboratory Medicine, UT Health Science Center at San Antonio, San Antonio, TX,[10]Population Health Sciences, Mays Cancer Center, Greehey Childrens Cancer Institute, UT Health Science Center at San Antonio, San Antonio, TX,[11]Molecular Medicine, Urology, Pharmacology, UT Health Science Center at San Antonio, San Antonio, TX

Pancreatic ductal adenocarcinoma (PDAC) is a highly aggressive malignancy with a five-yearsurvival below 12%. This poor prognosis stems from the late diagnosis, intrinsicchemoresistance, immunosuppression, and a dense desmoplastic stroma that promotes tumorprogression and therapeutic resistance. Current first-line treatments, including gemcitabine/nab-paclitaxel and FOLFIRINOX, are limited due to patient-specific responses, highlighting the needfor broadly effective therapies. Our previous work identified palmatine, a naturally occurringisoquinoline alkaloid, as a potent inhibitor of pancreatic stellate cells (PSCs) and PDAC cellgrowth. In this study, we evaluated the therapeutic efficacy of palmatine in combination withgemcitabine using an orthotopic KPC syngeneic mouse model. Combination treatmentsignificantly reduced tumor volume compared to vehicle or gemcitabine alone. Spatial immuneprofiling and transcriptomics of excised tumors revealed that combination treatment wasassociated with marked reduction in macrophage density, whereas gemcitabine alone displayedclear presence of macrophage-enriched immune neighborhoods not distinctly observed in thecombination group. Additionally, gemcitabine treated tissues exhibited a higher frequency ofneutrophil and dendritic cell-rich aggregates. Notably, the predominant immunemicroenvironment in combination-treated samples demonstrated a reduction in dendritic cellpopulations, alongside modest increases in $CD4^+$ and $CD8^+$ T cell subsets. Integration of bulkRNA-sequencing and spatial transcriptomics identified elevated *Hoxa10* expression andactivation of the IL-6/STAT3 signaling axis in mesenchymal cells. CyTOF analysesdemonstrated increased HOXA10, phosphorylated STAT3, and epithelial-mesenchymaltransition (EMT)-associated proteins in PSCs co-cultured with PANC-1 cells, which wereattenuated by combination treatment. Functional assays, including colony formation, confirmedthat combination therapy was more effective in suppressing clonogenic growth than gemcitabinealone. ChIP-seq data with HOXA10 pull-down from ENCODE project identified STAT3 as apotential HOXA10 target. These findings suggest that palmatine enhances gemcitabine efficacyby mitigating the immunosuppressive tumor microenvironment by targeting the HOXA10-STAT3 axis, and disrupting EMT programs. This combination represents a promising strategy toovercome PDAC chemoresistance and improve therapeutic outcomes. Supported in part throughZachry Endowment and VA Merit Award BX003876 (APK).

#7422 Investigation of acquired resistance to atezolizumab-bevacizumab in hepatocellular carcinoma: Paired tumor microenvironment analysis in a mouse model and human subjects.

Tsung-Hao Liu[1], Li-Chun Lu[1], Yu-Yun Shao[2], Shu-Han Yang[1], Chi-Yuan Yao[1], Chia-Lang Hsu[3], Ying-Chun Shen[4], Ann-Lii A. Cheng[5], Chih-Hung Hsu[1]

[1]National Taiwan University Hospital, Taipei, Taiwan,[2]National Taiwan University, Taipei, Taiwan,[3]Department of Medical Research, National Taiwan University Hospital, Taipei, Taiwan,[4]National Taiwan University Cancer Center (NTUCC), Taipei, Taiwan,[5]Professor, Dept. of Internal Medicine, National Taiwan University Hospital, Taipei, Taiwan

Background Immunotherapy combinations are the standard first-line treatment for advanced hepatocellular carcinoma (HCC), yet most responders eventually develop resistance. No standard second-line therapy exists post-progression, and elucidating mechanisms of acquired resistance is essential to guide future strategies.

Methods Hep53.4 murine HCC cells were subcutaneously implanted into C57BL/6 mice and treated with anti-programmed death-ligand 1 (PD-L1) monoclonal antibody (mAb) (clone 6E11, 5 mg/kg) and anti-vascular endothelial growth factor (VEGF) mAb (clone B20-4.1.1, 5 mg/kg). Tumors were harvested at baseline, responding, and resistant phase (n=6 per group) for analysis using NanoString nCounter® Pan-Cancer IO 360™, bulk RNA sequencing (RNA-seq), and immunohistochemistry (IHC) staining. Paired human tumor samples (n=4) at pre- and post-progression on atezolizumab-bevacizumab were analyzed with RNAseq. Immune cell fractions were estimated using CIBERSORT.

Results NanoString analysis of different response phases - baseline, responding, and resistant phase of murine Hep53.4 HCC tumors treated with anti-PD-L1 and anti-VEGF mAb revealed distinct tumor-immune microenvironment (TME) changes. Total tumor-infiltrating lymphocytes and cytotoxic T cells increased in responding tumors but declined in resistant ones, whereas exhausted and regulatory T cells showed the opposite trend. No significant changes were observed in B cells or dendritic cells. Notably, mast cells decreased in responding tumors but increased significantly in resistant ones. RNA-seq with CIBERSORT and IHC validated immune dynamics, including mast cell fluctuations, in murine tumors. Paired human tumors also showed mast cell enrichment at progression versus baseline.

Conclusion TME profiling of a murine HCC model treated with anti-PD-L1/VEGF mAbs demonstrated a dynamic shift in immune contexture, mirroring the immune response-resistance phenomenon. Mast cells decreased in response but increased upon resistance—a trend confirmed in human samples. Further investigation of the role of mast cells in acquired resistance is warranted.

#7423 Longitudinal tumor microenvironment analysis to predict immunochemotherapy response in salivary duct carcinoma.

Boseung Choi[1], Hyunsu Kim[2], Dongryul Oh[3], Myung-Ju Ahn[2], Hyun Ae Jung[2], Junhun Cho[4], Han-Sin Jeong[5], Se-Hoon Lee[2], Kyungmi Yang[3], Nayeon Choi[5], Eun-hye Kim[5], Sehhoon Park[2]

[1]Department of Health Sciences and Technology, Samsung Advanced Institute of Health Sciences and Technology, Sungkyunkwan University School of Medicine, Seoul, Korea, Republic of,[2]Division of Hematology-Oncology, Department of Medicine, Samsung Medical Center, Sungkyunkwan University School of Medicine, Seoul, Korea, Republic of,[3]Department of Radiation Oncology, Samsung Medical Center, Sungkyunkwan University School of Medicine, Seoul, Korea, Republic of,[4]Department of Pathology and Translational Genomics, Samsung Medical Center, Sungkyunkwan University School of Medicine, Seoul, Korea, Republic of,[5]Department of Otorhinolaryngology-Head and Neck Surgery, Samsung Medical Center, Sungkyunkwan University School of Medicine, Seoul, Korea, Republic of

Background:
Salivary duct carcinoma (SDC) is a rare but highly aggressive malignancy. Although neoadjuvant cytotoxic chemotherapy followed by surgery is standard for locally advanced high-grade SDC, recent studies suggest potential benefit from immune checkpoint inhibitors (ICIs) in the perioperative setting. To characterize treatment-related tumor microenvironment (TME) features, we analyzed paired pre- and post-immunochemotherapy samples from a perioperative clinical trial (ONO-4538-X78).
Method:
A total of 42 tumor samples from 30 SDC patients were analyzed using whole-transcriptome sequencing (WTS). Samples were collected at diagnosis (T1) and at surgery (T2) after three cycles of immunochemotherapy. Patients with <10% residual viable tumor were classified as major pathologic responders (MPR). Samples were classified into T1 non-MPR (n=7), T1 MPR (n=15), T2 non-MPR (n=11), and T2 MPR (n=9), and TMEs were compared across time points and response groups.
Result:
To characterize TME differences, we inferred cell states for each response group. At baseline (T1), non-MPR tumors exhibited a pro-angiogenic TME driven by malignant epithelial cells, consistent with EMT and angiogenesis pathways. In contrast, T1 MPR tumors showed a more immune-infiltrated TME with interferon-related signaling.
From the surgical samples (T2), direct comparison of MPR and non-MPR revealed distinct antitumor immune patterns, indicating robust T- and B-cell-mediated adaptive immunity in MPR, whereas non-MPR displayed chronic inflammatory signatures rather than effective antitumor responses. ssGSEA using core enrichment genes from T- and B-cell-related GOBP pathways confirmed significantly higher immune activation in the T2 MPR group compared with T2 non-MPR (p=0.001).
Longitudinal comparison further highlighted divergent trajectories. In non-MPR tumors, T2 non-MPR tumors were inferred to retain malignant epithelial features with minimal immune cells; DEG analysis supported this with inflammatory responses at T2 and EMT programs at T1.Conversely, T2 MPR tumors were inferred to lose malignant epithelial signatures and show immune activation, consistent with T cell-mediated adaptive responses pathways, whereas T1 MPR displayed epithelial cell-cycle pathways.
Conclusion:
In this study, we found that MPR tumors exhibited a pre-existing interferon-activated tumor microenvironment at baseline, which transitioned into an adaptive immune response after immunochemotherapy. These findings suggest that an interferon-primed TME is a prerequisite for effective post-treatment immune activation and may serve as a predictive biomarker for immunochemotherapy responsiveness.

#7424 Longitudinal and spatial heterogeneity of intra-tumoral TCR repertoires during immunotherapy in metastatic cancers.

Asimina Zoitou[1], Stefan Velculescu[2], Gavin Pereira[3], Archana Balan[3], Mimi Najjar[3], Amna Jamali[3], James R. White[3], Rachel Karchin[3], Noushin Niknafs[3], Hyunseok Kang[4], Patrick M. Forde[3], Christine L. Hann[3], Jody E. Hooper[5], Julie R. Brahmer[3], Valsamo (Elsa) Anagnostou[3]

[1]Department of Biomedical Engineering, Johns Hopkins University, Baltimore, MD,[2]Department of Chemistry, Princeton University, Princeton, NJ,[3]Department of Oncology, Johns Hopkins University, Baltimore, MD,[4]Stanford University, Palo Alto, CA,[5]Department of Pathology, Stanford University, Palo Alto, CA

Introduction: Spatial and temporal heterogeneity and evolution of the T cell receptor (TCR) landscape may influence immunotherapy outcomes. Studying TCR repertoires and their antigen specificities, together with T cell dynamics, could provide important insights into the quality of anti-tumor immune responses and their impact on cancer immunotherapy effectiveness.
Methods: We performed serial and multi-region sampling at critical timepoints (n=52 samples) during the clinical course of 7 patients with metastatic lung and head and neck cancer, who received immunotherapy-containing regimens. To study the TCR repertoire, we performed bulk TCR sequencing of TCR-β CDR3 regions and recovered 69,135 unique productive clones (ImmunoSeq assay, Adaptive Biotechnologies). To determine differential responses to immunotherapy across tumor sites and patients, we evaluated TCR repertoire similarity using Morisita's overlap index (MI) based on clonotype frequency and identity. Next, we clustered TCR clones of similar antigen specificities using GIANA (15,476 clusters) and performed differential T cell abundance analyses at the clone- and cluster-level to assess T cell dynamics. Statistically significant TCR expansions and regressions were determined using Fisher's exact test ($p \leq 0.05$). We used the VDJDB and CEDAR databases to de-orphanize 2,019 TCR clusters, mapping to TCRs with known antigen specificities.
Results: We found significant TCR repertoire heterogeneity between patients ($MI_{between\ patients} \approx 0$), suggesting private TCR landscapes at a patient level. In individual patients, a higher heterogeneity was noted between primary and metastatic sites ($MI_{baseline\text{-}metastatic} = 0.01 - 0.34$) while TCR repertoires of metastatic sites from proximal anatomic locations shared similarities ($MI_{proximal\ metastasis} = 0.47 - 0.96$). Despite the largely private expanded clusters and clones in each patient, similar dynamics were observed in regressing compared to progressing tumors in the context of immunotherapy, while at the autopsy sites, significantly expanded clusters dominated their respective TCR repertoires (14-28% abundance). TCR sequences recognizing viral antigen epitopes, such as GLCTLVAML (EBV), KLGGALQAK (CMV) and RAKFKQLL (EBV) were identified across patients and were part of the significantly expanded clusters in progressing metastatic sites. Several significantly expanding TCR clusters (FDR $p \leq 0.05$) were detected; while these had unmapped antigen specificity, they could recognize tumor antigens and mutation-associated neoantigens relevant for mounting anti-tumor immune responses.
Conclusions: Spatial and temporal TCR repertoire analyses provided a better understanding of the patients' immune landscape during therapy and offered insights that can be used to further dissect the heterogeneity of adaptive immune responses in the context of immunotherapy.

#7425 Histologic and tumor microenvironmental features as prognostic markers in mantle cell lymphoma: A digital pathology-based study.

Hyungjin Kim[1], Sei Na[1], Jeong-Ok Lee[2], Ji Yun Lee[2], Sang-A Kim[2], Jin Ho Paik[1]

[1]Department of Pathology, Seoul National University Bundang Hospital, Seongnam-si, Korea, Republic of,[2]Department of Internal Medicine, Seoul National University Bundang Hospital, Seongnam-si, Korea, Republic of

Mantle cell lymphoma (MCL) is a mature B-cell non-Hodgkin lymphoma with limited histopathologic markers for prognostication. We aimed to characterize histologic pattern and tumor microenvironment (TME) of MCL and evaluate their prognostic significance. A total of 33 cases of MCL (17 excisional biopsy and 16 needle biopsy specimens) were reviewed with pathologic slides and medical records. Survival outcomes including overall survival (OS) and progression-free survival (PFS) were calculated for 28 patients. CD4+, CD8+, and FoxP3+ T-lymphocytes, oncogene p53 expression patterns and Ki-67 proliferative index were assessed by immunohistochemistry, and quantified using Qupath digital image analysis. The median age of patients with MCL (n=33) was 69 years (range, 47-84), and 25 cases were male (75.8%). The majority of cases presented with advanced Ann Arbor stage (III-IV; 24/29, 82.8%). According to the Mantle Cell Lymphoma International Prognostic Index (MIPI), patients were categorized into low-risk (n=14, 46.7%), intermediate-risk (n=9, 30.0%), and high-risk (n=7, 23.3%) groups. Histologic patterns were evaluable in 30 cases, with 16 cases (53.3%) exhibiting a diffuse histologic pattern and 14 cases (46.7%) showing multinodular/mantle zone patterns. The diffuse histologic pattern was significantly associated with inferior PFS (p=0.011) and higher Ki-67 index (>30%, p=0.022). CD3+ cell density, defined as the number of CD3+ cells per square millimeter (cells/mm2), ranged from 576.2/mm2 to 8104.4/mm2 (median=1829.6/mm2). Higher CD3+ cell density was associated with worse OS (p=0.018). CD4+ cell density ranged from 0/mm2 to 6169.7/mm2 (median=508.5/mm2), and lower CD4+ cell density correlated with aberrant p53 expression, higher Ki-67 index and high-risk MIPI (p=0.012, 0.027 and 0.009, respectively). FoxP3+ cell ratio, defined as the proportion of FoxP3+ cells among total nucleated cells, ranged from 0% to 7.62% (median=1.20%). Higher FoxP3+ cell infiltration trended toward better PFS, without reaching statistical significance (p=0.099). Aberrant p53 expression (null/overexpression patterns; 5/33, 15.2%) was correlated with worse OS and PFS (p=0.005 and 0.038, respectively), and also with higher Ki-67 index (p=<0.001). CD4+/CD8+ cell ratio was highly variable (range, 0.01-7.53; median=0.77). In excisional biopsy specimens, cases with bone marrow involvement (4/17, 23.5%) exhibited higher CD4+/CD8+ cell ratio (p=0.028). Histologic pattern, tumor immune microenvironment and p53 expression pattern appear to have prognostic value in MCL. Quantitative assessment of TME using digital pathology methods may provide additional tools for predicting clinical behavior of MCL.

#7427 Genomic analysis of microenvironment composition by breast cancer molecular subtype using an integrated single-cell RNA sequencing cohort.

Constandina (Dina) E. O'Connell[1], Alexander V. Lobanov[2], Kevin R. Mott[3], Daniel P. Hollern[4], Brian C. Miller[5], Charles M. Perou[3]

[1]Department of Pathology and Laboratory Medicine, University of North Carolina at Chapel Hill, Chapel Hill, NC,[2]Department of Genetics, University of North Carolina at Chapel Hill, Chapel Hill, NC,[3]Lineberger Comprehensive Cancer Center, University of North Carolina at Chapel Hill, Chapel Hill, NC,[4]Salk Institute Cancer Center, La Jolla, CA,[5]Division of Oncology, University of North Carolina at Chapel Hill, Chapel Hill, NC

Breast cancer is a heterogeneous disease clinically classified by expression of three key biomarkers, namely ER, PR, and HER2. Between clinical subtypes, the prognostic value of immune cell infiltration varies significantly. In triple-negative/basal-like tumors, tumor infiltrating lymphocytes (TILs) are positively prognostic, while in ER+/luminal tumors, TILs are less prognostic and sometimes associated with worse outcomes. This opposing, subtype-specific behavior suggests different roles for the immune system and is important to understand as immunomodulatory treatments are increasingly tested and utilized across breast cancer subtypes. Previous work using TCGA Breast Cancer bulk RNA sequencing data determined that among highly immune infiltrated tumors, there is significant variation in the immune microenvironment according to PAM50 molecular subtype. High-TIL luminal tumors were enriched for innate immune features, while high-TIL HER2-enriched and basal-like tumors had elevated expression of B and T cell features, respectively. To extend these findings, we curated an integrated dataset of single-cell RNA sequencing from 115 human breast tumors and 17 normal tissue specimens. Samples spanning all clinical subtypes came from four publicly available datasets, and common bioinformatic approaches were used to guide cell type annotation. Cell type frequencies in each sample were calculated and compared by PAM50 subtype. Basal-like tumors were enriched for multiple effector T cell and macrophage populations, while HER2-enriched exhibited increased frequency of IgG-secreting plasma cells. Conversely, luminal A tumors were enriched for various stromal cell types, including fibroblasts, endothelial cells, and perivascular-like cells; interestingly, a macrophage subset expressing the immunosuppressive marker TREM2 was also more abundant in luminal A. We identified highly immune infiltrated tumors from our cohort and compared cell type frequencies in these tumors by PAM50, finding that many baseline differences in microenvironment composition by subtype persist into the immune-high setting. Finally, we analyzed a subset of tumors from Bassez *et al.* (PMID: 33958794) that included T cell expansion data as a proxy for anti-PD1 immunotherapy response. In pre-treatment basal-like tumors, increased proportions of plasma cells, effector T cells, and regulatory T cells were associated with T cell expansion following anti-PD1. Ongoing work is exploring tumor-microenvironment crosstalk using ligand-receptor interaction prediction, with a focus on stromal cells in luminal tumors and B cell-T cell crosstalk in basal-like; for the latter, CD40-CD40LG interaction has emerged in preliminary analysis as a potential target for clinical intervention to improve patient outcomes and is currently being tested in mouse model systems.

#7428 Tumors induce a NR4A1 transcriptional program in dendritic cells leading to immune tolerance and cancer progression.

Michael P. Plebanek, Mahere Rezazade Bazaz, Y-Van Nguyen, Balamayooran Theivanthiran, Brent A. Hanks

UNC Lineberger Comprehensive Cancer Center, Chapel Hill, NC

The induction of effective anti-tumor immune responses is reliant upon efficient dendritic cell (DC)-mediated activation of T cells. Furthermore, DCs are necessary for the efficacy of checkpoint inhibitors. However, during tumor progression, transcriptional reprogramming of DCs occurs leading to the development of dysfunctional DCs which potentiates tolerance within the tumor microenvironment (TME). This process is facilitated by the release of metabolites and soluble factors by tumor cells leading to the activation of transcriptional states that suppress the capacity of DCs to stimulate T cells. In prior studies, we have demonstrated that tumor-derived lactate activates SREBP2 in DCs within the TME, promoting the development of pro-tolerogenic mature regulatory DCs (mregDCs) that can inhibit antigen cross-presentation and facilitate tumor progression. Despite this work, our understanding of the exact transcriptional programs that govern the development of immunotolerant DC states, the mechanisms driving the suppressive functions of DCs, and the importance of intersecting transcription factor networks remain unclear. Insights into these mechanisms hold great promise for the development of novel immunotherapeutic strategies. In this project, we investigated DC regulatory programs that are induced during tumor progression using transgenic mouse models of melanoma. Single cell assay for transposase accessible chromatin sequencing (scATACseq) and transcription factor binding motif analysis of DCs isolated from the tumor-draining lymph nodes (TDLNs) of $BRAF^{V600E}PTEN^{-/-}$ transgenic melanoma mice revealed an enrichment in the accessibility of NR4A1 transcription factor motifs in mregDCs relative to other conventional DC populations. *Nr4a1*-GFP reporter mice show increased expression of *Nr4a1* in cDCs of tumor bearing mice, particularly in mregDCs that have developed from cDC1s. We proceeded to characterize the role of DC-expressed NR4A1 in regulating anti-tumor immunity using both *in vitro* and *in vivo* models. Zbtb46-restricted *Nr4a1* knockout mice show that loss of *Nr4a1* in DCs suppresses tumor progression and promotes $CD8^+$ T cell tumor infiltration. Furthermore, we determined that lactic acid released by tumor cells via monocarboxylate transporter 1 (MCT1) induces DC *Nr4a1* gene expression in a SREBP2-dependent manner. We went on to verify that SREBP2 binds to the *Nr4a1* promoter using ChIP-qPCR. Additional studies found NR4A1 inhibition to suppress DC expression of *Ido1* and *Il4i1* while also inhibiting mregDC-dependent $FoxP3^+$ regulatory T cell development and activation. Collectively, this data demonstrates a previously unknown role for NR4A1 in DCs. Ultimately, we have identified a DC regulatory program centered around a lactate-SREBP2-NR4A1 signaling axis that represents a promising strategy for overcoming anti-PD-1 resistance in treatment refractory tumors.

#7429 Characterizing the spatial tumor microenvironments of therapy-induced and hereditary mismatch-repair-deficient hypermutated gliomas.

Chae Yun (Kate) Cho[1], Bo Zhao[1], Lingqun Ye[1], Ines Martin-Barrio[1], Yonathan Lissanu[2], Kadir C. Akdemir[1]

[1]Department of Neurosurgery, UT MD Anderson Cancer Center, Houston, TX,[2]Department of Thoracic and Cardiovascular Surgery, UT MD Anderson Cancer Center, Houston, TX

Hypermutation in gliomas is observed in some recurrent tumors and hereditary cancer syndromes; however, the extent to which elevated tumor mutational burden influences the tumor microenvironment and contributes to a more aggressive clinical phenotype remains unclear. We comprehensively define the spatial tumor microenvironments in 49 glioma tissues from 32 patients by mapping the transcriptional and spatial organization of 2.3 million single cells *in situ*. Longitudinal analyses reveal an enrichment of proliferating, stem-cell-like malignant states in both therapy-induced and hereditary mismatch-repair (MMR)-deficient hypermutated tumors, consistent with the increased proliferative activity observed with hypermutation. Additionally, despite a shared MMR-deficiency, malignant cells from chemotherapy-induced and hereditary origin hypermutated tumors exhibit distinct transcriptional programs, underscoring the influence of mutation etiology on malignant cell states. Hypermutation at recurrence does not consistently correlate with increased lymphocytic infiltration or response to immune checkpoint blockade, despite clear transcriptional changes. Together, our single-cell spatial maps illustrate how hypermutation of distinct origins drives divergent cellular transcriptional programs and tissue architecture in gliomas, highlighting the role of tumor-immune microenvironment in shaping cancer evolution and informing therapeutic strategies.

#7430 Transcriptional programs of precursor-exhausted CD8$^+$ T cells associated with checkpoint blockade response in NSCLC.

Ethan Daniel Littlestone, Md Roungu Ahmmad, **Xiaoli Zhang**

University of South Florida, Tampa, FL

Immune checkpoint blockade (ICB) benefits only a subset of patients with non-small cell lung cancer (NSCLC), and the immune determinants of major pathologic response (MPR) remain incompletely defined. Recent studies suggest that precursor-exhausted CD8$^+$ T cells (Tpex) are critical for sustaining anti-tumor immunity and generating the effector pool reinvigorated by PD-1 blockade. Although Tpex cells tend to be enriched in responders, the mechanisms by which they contribute to improved therapeutic outcomes remain unclear. In this study, we profiled Tpex transcriptional states in patients with MPR versus non-responders using a publicly available single-cell RNA-sequencing dataset (GSE243013). Differential gene expression analysis revealed that Tpex cells from responders showed upregulated expression of genes involved in metal-ion homeostasis (e.g., MT2A) and adaptive stress tolerance (e.g., MTRNR2L12, SLPI, ITGA6). In contrast, Tpex cells from non-responders preferentially expressed interferon-stimulated and proliferative-stress programs (e.g., TYMS, HMOX1, LINC01480). Pathway enrichment analysis supported these findings, identifying metallothionein-associated processes in responders and enriched cytokine/interferon signaling in non-responders. Cox proportional hazard regression modeling of Tpex differentially expressed genes further demonstrated that MYB proto-oncogene like 2 (MYBL2), which was upregulated in non-responders, was associated with poorer recurrence-free survival (HR ≈ 1.28; 95% CI: 1.12-1.44; adjusted P = 0.016). Additional genes linked to proliferative or interferon-driven dysfunction (RRM2, GEM, PKMYT1, ISG15) showed nominal associations with adverse outcomes, reinforcing the presence of a cycling, IFN-high, shift towards terminal exhaustion in patients who experienced recurrence. Taken together, our study provides important information for linking Tpex functional states to therapeutic response and disease recurrence, with potential implications for refining immunotherapy strategies in NSCLC. Generative AI assistance was used and limited to improving clarity of methodological descriptions.

#7431 Metabolic correlates of measurable residual disease following high dose melphalan conditioning for autologous stem cell transplant in multiple myeloma.

Qualia Hooker, Timothy Triche

Van Andel Institute (VAI), Grand Rapids, MI

In Multiple Myeloma (MM) high dose melphalan (HDM) conditioning followed by autologous stem cell transplant (ASCT) yields durable remissions, but measurable residual disease (MRD) is the strongest predictor of early relapse. Metabolic plasticity of malignant plasma cells and immune subsets are emerging as key determinants of MRD, potentially contributing to differences in transplant outcomes. However, the metabolic programs that separate MRD+ from MRD- patients remain poorly understood. As an alkylator, HDM induces oxidative stress and DNA damage that selects for malignant plasma cells with enhanced metabolic features, while simultaneously impairing reconstitution of protective T-cell subsets. Importantly, germline genetic variation may prime for distinct metabolic fates and immune reconstitution post-ASCT. Thus, we posit that MRD reflects the dual pressure of metabolically adapted MM clones and impaired immune recovery. We performed a retrospective analysis of paired 5′ scRNA-seq and TCR-seq from CD138- bone marrow aspirates of 28 MM patients (progressors n=13 vs. non-progressors n=15 and MRD-positive n=17 vs. MRD-negative n=11) collected pre- and post-ASCT. MRD status was independent of progression. BCR analysis revealed clonal restriction patterns in plasmablasts consistent with biochemical relapse. We used METAflux to analyze B-cell flux activities and determined that MRD is correlated with oxidative stress (OR:1.62, 95% CI:1.06-2.48), while progression was linked to upregulation of oxidative and biosynthetic metabolism pathways. Plasmablasts from MRD+ progressors exhibited enhanced proliferative metabolism signatures consistent with active MM clones. Progression in the T cell compartment was strongly linked to oxidative phosphorylation (OR:2.46, 95% CI:1.44-4.20), while there were no significant MRD associations. However, MRD+ progressors displayed clonal restriction patterns in CD8+ T cells signifying defective immune reconstitution. This study identifies cell-type specific metabolic alterations distinguishing MRD-positive from MRD-negative patients post-ASCT. Enrichment of antioxidant metabolism in B-cells coupled with altered T-cell metabolism and recovery demonstrates dual vulnerabilities: metabolic plasticity and immune deficits. These results identify potential immunometabolic dependencies that may serve as therapeutic targets that can be used to eliminate MRD and improve transplant outcomes.

#7432 Spatial protein profiling of irradiated ER positive breast cancer lymph nodes suggests nodal irradiation modulates immune function.

Stephanie O. Dudzinski[1], **Elizve N. Barrientos-Toro**[2], Benjamin D. Smith[3], Simona F. Shaitelman[4], Sharia Hernandez[2], Alejandra Serrano[2], Khan Khaja[2], Larisa Kostousov[2], Wei Lu[2], Rensi Zacharia[1], Nathan Comeaux[1], Solis M. Luisa[2], Aysegul A. Sahin[4], Maria Gabriela Raso[2], Jing Wang[5], Karen Hoffman[3], Wendy A. Woodward[3]

[1]Radiation Oncology, UT MD Anderson Cancer Center, Houston, TX,[2]Translational Molecular Pathology, UT MD Anderson Cancer Center, Houston, TX,[3]Breast Radiation Oncology, UT MD Anderson Cancer Center, Houston, TX,[4]UT MD Anderson Cancer Center, Houston, TX,[5]Bioinformatics & Comp Biology, UT MD Anderson Cancer Center, Houston, TX

Background: We hypothesized that the systemic benefit of regional nodal irradiation (RNI) for breast cancer derives from immune stimulation in involved nodes. We compared involved lymph nodes (ILN) from patients treated on a prospective trial of pre-operative and post-operative conventional (2 Gy/fx) versus hypofractionated (2.67 Gy/fx) RNI regimens (SAPHIRE NCT02912312).
Methods: 17 patients ILNs with ER+, pN+ BC were Digitally Spatially Profiled with immune-related proteins. 6 post-op cases had no neoadjuvant chemotherapy (NACT) (untreated controls). All others had NACT +/- RNI. 4 pre-operative RNI short-course (RNI_NACT-2.67Gy/fx); 5 pre-op standard RNI (RNI_NACT-2 Gy/fx); 3 post-op RNI after NACT. 5 Regions of Interest (ROIs) were selected and categorized as “Tumor” (PanCK+) or “Immune” (CD45+) compartments. Cell density and spatial analysis were assessed in selected cases. Pearson’s correlations, T-Test and KS tests were performed on protein expression in all ROIs, FDR < 0.1, P value < 0.05. Signals with Log2 differences between -1 and 1 were analyzed using adjusted LMM for patient-level variation, and PCA of ROIs by compartment was performed.
Results: Nearest neighbor analysis shows increasing median distance between tumor and immune cells from untreated, to NACT, and NACT+RNI, and no differences between short and standard pre-operative RNI. Proximity analysis reveals the distribution of CD3+ cells from the CK+ cells changes with increasing therapy, favoring frequency of closer immune cells, although the average number of cells around each CK+ cell diminishes with increasing therapies. CK+ cell density remains stable, suggesting migration rather than cell death. Differences in expression profiles of immune ROIs suggest more immune signaling in pre-op short. Considering all RT, 27 differentially expressed proteins (DEP) were significantly upregulated in Post tumor ROIs. None were significantly downregulated. After correction by LMM, 11 markers were up in Post cases and none downregulated. We found lower expression of SMA , CD4, CD45RO, CD14, CD11c, TIM-3, and B7-H3 in the Pre nodes. No significant DEPs remain in immune ROIs after LMM correction. The first two principal components accounted for 45.8% of the total variance, with PC1 largely separating samples based on Pre RNI. Pre-short vs Pre-standard showed 9 increased and 0 decreased proteins in Pre-short including CD27, Sting, CD40, CD11c, CD25.
Conclusions: Pre-operative radiation contributes to Immune microenvironment remodeling, complementing neoadjuvant chemotherapy in ILN, without altering immune cell density. Different immune signals in irradiated ILN suggest a less immunosuppressive phenotype in RNI, and potential immune activation in Pre-short RNI. Small sample size limits conclusions, immune studies will follow to optimize radiation regimens.

#7433 Dual stromal and tumoral origins of TWEAK drive CSC maintenance in ovarian cancer relapse.

Mikella Robinson, Luisjesus S. Cruz, Carrie House

San Diego State University, San Diego, CA

Serous ovarian cancer (OC) has one of the highest relapse rates of all cancers, with around 85% of patients relapsing following chemotherapy. Evidence suggests that cancer stem-like cells (CSCs) exhibit chemoresistance, sustained self-renewal, and tumor-initiating potential to drive recurrence. We have previously identified TWEAK, an inflammatory cytokine enriched in OC tumors post-chemotherapy, promotes CSC maintenance and survival. Furthermore, antagonism of TWEAK-Fn14 signaling following chemotherapy in a murine relapse model significantly prolonged survival. Because Fn14 is broadly expressed within the tumor microenvironment, we sought to identify sources of TWEAK. Conventionally, TWEAK is secreted by macrophages, and although single cell sequencing of treatment-naive human OC tumors suggests that infiltrating tumor associated macrophages (TAMs) primarily express TWEAK, recent work in relapsing pancreatic cancer identified cancer cells as an additional source of TWEAK. We therefore hypothesized that TWEAK in ovarian cancer is derived from multiple sources, including macrophages and cancer cells. Since macrophages are the predominant immune cell type found in OC tumors, we used an interperitoneal xenograft nude mouse bearing human CAOV4 OC cells to model relapse. Inhibition of macrophage recruitment using a CSF-R1 inhibitor BLZ945 during chemotherapy significantly reduced CSC expression and improved survival, compared to chemotherapy alone. Using a 14-marker flow cytometry panel, we profiled TWEAK expression in relapsed tumors across macrophage (CD45, F4-80, CD11b, LyVe1, CD80, CD206, CD273, MHC Class II), endothelial (CD31), fibroblast (PDGFRa), and CSCs (CD117) populations. We identified 12 distinct cell populations, representing four TAM (CD45+/F4-80+/CD11b+) clusters including two high in MHC Class II, one tissue-resident macrophage (TRM) cluster (CD45+/F4-80+/LyVe1+), two fibroblast clusters, one endothelial cluster, and four cancer cell clusters. Four clusters expressed TWEAK, included one TAM, TRM, fibroblast, and OC cluster. The highest baseline TWEAK expression was in the TAM and TRM clusters; however, these decreased after chemotherapy. The OC cluster, comprised of CSCs, significantly increased (twofold) TWEAK expression following chemotherapy and were BLZ945 responsive, suggesting their chemotherapy-dependent TWEAK expression was also macrophage-dependent. Preliminary in vitro studies of gene expression, imaging, and flow cytometry further indicate that OC-derived TWEAK increases in response to chemotherapy. Future studies will investigate how macrophages regulate OC-derived TWEAK and the contribution of this signaling to relapse. Defining the stromal and tumoral cell sources of TWEAK and delineating their roles in TWEAK-Fn14 mediated tumor recurrence may facilitate development of targeted therapies for patients at risk of recurrence.

#7434 Metabolic dependence of prostate cancer subtypes and its association with the tumor-immune microenvironment.

Tonatiuh A. Gonzalez[1], Anisha Tehim[2], Inna Serganova[1], Roberta Zappasodi[3], Ekta Khurana[3]

[1]Weill Cornell Grad. School of Medical Sci., New York, NY,[2]Cornell University, Ithaca, NY,[3]Weill Cornell Medicine, New York, NY

Due to the rising use of androgen deprivation therapy (ADT) and AR signaling inhibitors (ARSIs), metastatic castration-resistant prostate cancer is expanding and although it is known that its subtypes provide predictive utility, their individual tumor-immune microenvironments are woefully underexplored mechanistically. Careful investigation of these subtypes of mCRPC may provide insights into therapeutic resistance beyond mCRPC. Using both publicly available and in-house single-cell RNA-sequencing and spatial transcriptomics datasets, we have characterized mCRPC cells and their accompanying tumor-immune microenvironment using established marker genes and verified their identity using inferred copy-number variation status. Firstly, we have explored metabolic profiles of the various cell-types in our samples by calculating scores based on transcription of genes involved in metabolic processes. We have performed ligand-receptor pair analysis to predict which cell types are interacting and through which inflammatory and metabolic axes these interactions are occurring. Finally, we have demonstrated interaction feasibility by measuring distance in space via our spatial transcriptomics data. Our preliminary results indicate that these subtypes have significantly different metabolic profiles. Additionally, the immune cells near to these different subtypes have shown differential immunosuppressive programs and metabolic reprogramming. These findings suggest the potential role of tumor metabolic forces in the induction of an immunosuppressive tumor microenvironment and point to a promising utility of metabolic perturbations in mCRPC as a neoadjuvant to enhance response to immune checkpoint blockade (ICB). This work highlights novel lenses in which to analyze tumors in the hopes of suggesting combination therapies that may overcome treatment obstacles.

#7435 Spatial transcriptomics unveils tumor microenvironment changes in murine glioblastoma upon EGFRvIII suppression.

Fabio de Mello[1], David Eisenbarth[1], Feng Guo[1], Yamei Chen[2], Kun Huang[2], Chunhai Hao[3], Y. Alan Wang[1]

[1]Brown Center for Immunotherapy, IU Simon Comprehensive Cancer Center, Indianapolis, IN,[2]Department of Biostatistics & Health Data Science, Indiana University School of Medicine, Indianapolis, IN,[3]Indiana University School of Medicine, Indianapolis, IN

EGFRvIII, a tumor-specific in-frame deletion of exons 2-7 that generates a constitutively active EGFR mutant, drives potent oncogenic signaling in a molecularly defined subset of glioblastoma (GBM) and is implicated in altered invasion, therapy resistance and immune modulation; because EGFRvIII occurs in a substantial fraction of GBMs we asked how suppression of this mutation in established tumors reshapes tumor cells and immune microenvironment in order to reveal treatment opportunities. We used an inducible EGFRvIII GBM mouse model to perform single-cell RNA sequencing and spatial transcriptomics on established with and without transcriptional suppression of EGFRvIII. Findings were validated in spatial transcriptomic profiles from human GBM specimens stratified by EGFR status. EGFRvIII suppression increases infiltration of myeloid and lymphoid cells into core tumor regions, slowing most tumor growth and increasing mouse survival. However, it also promotes invasion and proliferation in EGFRvIII-independent tumor-subpopulations, due to loss of EGFRvIII-driven communication between EGFRvIII-positive and -negative subpopulations. These observations are consistent with prior literature knowledge that direct EGFR inhibition often leads to resistance by vIII-negative populations, and complements it with insights into its mechanistic bases. Overall, our data argue for approaches that exploit the immune microenvironment changes to enhance direct EGFRvIII-targeted strategies for vIII-positive GBM.

#7436 Dissecting the spatial architecture of plasmacytoid urothelial carcinoma to inform therapeutic strategies.

Kathryn H. Gessner, Jeffrey S. Damrauer, Siyao Liu, Mi Zhou, David Corcoran, Sara E. Wobker, William Kim

UNC Lineberger Comprehensive Cancer Center, Chapel Hill, NC

Plasmacytoid urothelial carcinoma (PUC) is an aggressive histologic subtype of bladder cancer that frequently co-exists with conventional urothelial carcinoma (CUC). Patients with PUC have worse response to cisplatin-based neoadjuvant chemotherapy and worse outcomes than patients with CUC, emphasizing the importance of therapeutic development. Elucidating the biology of plasmacytoid urothelial carcinoma (PUC) may reveal therapeutic vulnerabilities specific to this variant. PUC is defined by loss of E-cadherin protein expression, and evidence from other cancer types suggests a complex relationship between E-cadherin signaling, epithelial-to-mesenchymal transition (EMT), tumor microenvironment (TME) remodeling, and responsiveness to immune checkpoint blockade. This study seeks to understand the impact of E-cadherin loss on TME composition in PUC and the crosstalk between cell types. Archival formalin-fixed paraffin embedded tissue samples from patients with urothelial carcinoma who underwent surgical intervention was obtained. Hematoxylin and eosin stains were performed and reviewed by a GU pathologist to identify areas of histology consistent with conventional or plasmacytoid UC. Immunohistochemistry for E-cadherin confirmed loss of E-cadherin in histologic areas of PUC. The 10X Genomics Xenium In Situ assay was utilized to perform spatial transcriptomics. The expression of 477 genes was profiled in situ using a combination of the 10X Genomics Human Multi-Tissue and Cancer panel and a custom 100-gene panel, designed to evaluate the expression of bladder cancer specific genes. Xenium data analysis was performed using a combination of the 10X Genomics Xenium Explorer and R-based packages, including Seurat and HoodScanR. Analysis focused on a mixed histology tumor with histologic areas of PUC and CUC. Within areas of PUC histology, CDH1 (gene encoding E-cadherin) RNA expression was absent, and genes associated with EMT signaling (Snail, vimentin) were upregulated. Relative proportions of immune cells were characterized and PUC-specific cellular neighborhoods were identified. In the area of PUC histology, increased infiltration of macrophages was identified, with different macrophage phenotypes identified between PUC and CUC areas. Using spatial transcriptomics at single cell resolution, this study delineates PUC architecture and demonstrates the interplay between E-cadherin loss, EMT, and macrophage activation. Further characterization of PUC-specific expression and TME components will identify potential therapeutic vulnerabilities.

#7437 Decoding tumor microenvironment heterogeneity through spatial microdomains and network biology to predict immunotherapy outcomes.

A. Burak Tosun[1], Raymond Yan[1], Brian Falkenstein[1], Filippo Pullara[1], S. Chakra Chennubhotla[2]

[1]PredxBio, Inc., Pittsburgh, PA,[2]PredxBio, Inc. / University of Pittsburgh, Pittsburgh, PA

Background: Spatial niches, often quantified through the co-occurrence or colocalization of various cell types, are a common measure of tissue organization in health and disease. However, a clear link is missing between how these spatial measures quantify tissue heterogeneity, how that heterogeneity relates to functional organization within the tissue, and how the functional organization impacts patient outcomes.
Methods: The SpaceIQ™ multi-omics analysis platform addresses tissue heterogeneity through a formal analysis of spatial cell-cell communication from a mutual information perspective. This methodology allows for the virtual dissection of tissue into distinct tumor microenvironment (TME) programs. Inter-patient heterogeneity is then revealed by clustering these spatial TME programs based on their compositional fractions, a process independent of patient outcomes. Crucially, these spatial TME programs serve as highly effective "microdomains" that provide critical local context for cell-to-cell interactions and spatially modulated "network biology," demonstrating strong predictive power for patient outcomes.
Results: We analyzed a publicly available 51-plex immunofluorescence based spatial proteomics data (CODEX platform) from checkpoint-treated cutaneous T-cell lymphoma patients, using spatial analysis based on microdomains and network biology. Our findings demonstrate that: (i) checkpoint expressions alone are poor predictors of patient response; (ii) spatial interactions between different cell types moderately improve prediction accuracy compared to multi-marker phenotypes; and (iii) microdomains significantly outperform non-spatial methods and checkpoint expression-based approaches in predicting response.
Conclusions: Spatial analysis leveraging microdomains and network biology significantly enhance prediction accuracy compared to non-spatial or checkpoint expression-based methods. This advancement enables improved biomarker-driven patient selection and targeted therapy optimization.

#7438 Residual disease on a dish: A practical approach to deep intrinsic resistance in melanoma.

Balraj Singh, Vanessa N. Sarli, Nikil Erry, Anthony Lucci

UT MD Anderson Cancer Center, Houston, TX

Cancer is an evolution like process; wherein genetically abnormal cells persist despite a variety of mechanisms designed to kill such cells. Immune checkpoint and targeted therapies have significantly improved outcomes in melanoma. However, residual disease remaining after treatment, as indicated by a lack of complete pathological response or as detected by other sensitive methods, often evolves further leading to recurrence/metastasis. Thus, there is a need to inhibit or eradicate residual disease to prevent recurrence. In this regard, there is a lack of good preclinical models of residual disease, particularly for testing new therapies that would inhibit quiescent or slow-growing melanoma cells. This is important since opportunistically switching to quiescence and to survive in deep quiescence are major hurdles in improving outcomes. Our approach to a cell culture model of residual disease aligns with the idea that selection pressures are important in enforcing cancer cell quiescence. A selection pressure involving a severe and extended metabolic change, such as a lack of glutamine in culture medium, is an excellent choice for eliminating bulk of sensitive cells that proliferate in artificially rich medium. We subjected two highly metastatic melanoma cell lines, A375SM (representing undifferentiated melanoma with a common BRAF V600E mutation and homozygous CDKN2A deletion) and B16-BL6 (suitable for syngeneic mouse model), to glutamine deficiency in two ways: 1) culture in Gln-free medium (with low 27 μM Gln coming from serum, instead of 4 mM Gln in complete medium), and 2) culture in stringent Gln-free medium (near zero Gln with the use of dialyzed serum in medium). More than 99% cells died in Gln-free medium; rare cells survived in deep quiescence, and then gradually exited quiescence after 4-5 weeks and proliferated indefinitely. We extended the quiescence to 7 weeks and beyond by culturing A375SM cells in stringent Gln-free medium. In these experiments, we replaced medium with fresh medium every 2-3 weeks. Interestingly, if we did not replace medium for an extended period (50 days), we found that A375SM cells did not exit quiescence. We interpret that rare cells surviving in deep quiescence gradually develop an ability to exit quiescence; however, this exit or/and proliferation requires some glutamine. By not changing medium for an extended period, low level of Gln got exhausted, and cells stayed quiescent. We refer to the cells selected in this manner as metabolically adaptable (MA); they are broadly adaptable. The MA cells were much more resistant to paclitaxel than were their parental cell lines. Our results support the feasibility of the approach for modeling residual disease. In conclusion, when we approach deep intrinsic resistance in melanoma with a new perspective (abnormal quiescence besides abnormal proliferation leading to recurrence), new insights and fresh solutions are likely to emerge.

#7439 SPP1 positive macrophage spatial feature correlation to stage III-IV colon cancer multiple pathology parameters.

Shaojun Xu[1], Hongzhe Sun[2], Shuo Han[2], Lin Zhu[2], Yan Wu[1], Qisong Zhang[1], Aiwen Wu[1], Zhifu Zhang[2], Enkai Zhang[3], Na Li[3], **Zhongwu Li**[1]

[1]Key Laboratory of Carcinogenesis and Translational Research (Ministry of Education), Department of Pathology, Peking University Cancer Hospital & Institute, Beijing, China,[2]Beijing PhenoVision Bio Co., ltd, Beijing, China,[3]Hangzhou PhenoVision Bio Co., ltd, Hangzhou, China

Colorectal cancer (CRC) is a frequent gastrointestinal malignancy with high rates of morbidity and mortality. Our previous studies have shown macrophages exhibited significant variations in stage III-IV colon cancer compared to other immune cells. Current study reviewed 11 stage III-IV CRC patient archived FFPE samples carried varied pathology and treatment conditions to investigate macrophage cell features. IHC control, multiplex immunofluorescence (mIF) panel control and the followed mIF staining were conducted using PN 7-Plex Detection Kit (PhenoVision Bio Co., ltd) targeted CD68, CD163, HLA-DR, panCK, SPP1 and PD-L1. The QC procedures made sure each marker from mIF results exhibited identical location and density of the same marker from IHC staining. The 11 staining slides were scanned, tumor areas were lined out by pathologist based on H&E staining from the serial section of each sample. Non-tumor region, tumor parenchyma and tumor stromal region were analyzed using PhenoVision mIF AI analysis system trained from Oncotopix Discovery system (Visiopharm). Positive cell percentage were analyzed in 11 samples. Statistical analysis exhibited correlation of CD68+/SPP1+ co-positive cell to the pathology parameter of PCR/non-PCR (p=0.05), dMMR/pMMR (p=0.024), with or without mucin pool (p=0.022) in tumor stromal region based on binary logistic regression. PD-L1 correlated to dMMR/pMMR in tumor parenchyma region. The co-positive marker did not show correlation to treatment (p=0.069) and necrosis (p=0.313) groups. There was lower CD68+/SPP1+ cell percentage in tumor stromal region in PCR *vs.* non-PCR group (0.46% *vs.* 2.01%, p=0.049) and non-cellular mucin pool group *vs.* with cellular mucin pool group (0.47% vs. 2.39%, p=0.022). Interestingly, there were more CD68+/SPP1+ cells in pMMR *vs.* dMMR group (1.94% *vs.* 0.24%, p=0.027). CD68+/SPP1+ co-positive cell distribution did not exhibit variations among necrosis groups (with *vs.* without necrosis, p=0.254), different treatment strategies (Chemoradiotherapy + Immunotherapy *vs.* Immunotherapy, p=0.066) and pathology stages (III *vs.* IV, p=0.460) in tumor, stromal, and normal region. Besides CD68+/SPP1+ co-positive marker in tumor stromal region, PD-L1 positive cell percentages were higher in tumor parenchyma region of dMMR patient samples compared to pMMR samples (10.09% *vs.* 1.04%, p=0.024). Current study indicates that CD68+/SPP1+ cell spatial feature correlates to PCR stage, MMR stage and mucin pool conditions of stage III-IV colon cancers. Increased sample number may lead to correlation of the marker to treatment variation which suggests the marker distribution characteristics may be utilized for stage III to IV CRCs patients' health monitoring plans.

#7440 Characterization of the metastatic TIME via spatial transcriptomics reveals unique cellular phenotypes post anti-CSF-1R and immuno-chemotherapy.

Diego Armando Pedroza[1], Sung Wook Kang[1], Xiang H.-F. Zhang[1], Bora Lim[2], Hyun-Sung Lee[1], Jeffrey M. Rosen[1]

[1]Baylor College of Medicine, Houston, TX,[2]UT MD Anderson Cancer Center, Houston, TX

Metastatic breast cancer is the main cause of breast cancer related deaths amongst diagnosed women. Current standard-of-care therapies with chemotherapy (CTX) and T cell activating immune checkpoint inhibitors (ICIs) are limited against metastatic disease. Clinical trials have revealed that the tumor immune microenvironments (TIME) with high levels of tumor associated macrophages (TAMs) are associated with ICI treatment failure. We have developed and extensively characterized several genetically engineered mouse models that lack the p53 gene that is most frequently altered in TNBC. These “claudin low” models closely phenocopy the high EMT/TAM subtype observed in patients. We previously showed that TAM ablation by anti-CSF1R mAb therapy coupled with CTX alters the TIME of multiple p53 null GEMMs. This new immunologically “hot” environment displayed elevated levels of IL-17, IL-5 and type II interferon response with residual inflamed- MHCII+ macrophages. A long-term anti-tumor adaptive immune response was accompanied by the infiltration of CD4+/CD8+ T and B cells. However, in lung metastases adjacent micro-metastases persisted and continued to display a “cold” TIME now with elevated PD-L1 indicative of intra-tumoral heterogeneity (ITH). The addition of ICB to SNDX-ms6352 and CTX resulted in sustained loss of TAMs, tumor cells, decreased PD-L1/PD-1 expression and was accompanied by B- and T cell infiltrations in both lung and liver tissues. To understand the differences within the metastatic TIME between single agent and combination treatments, we applied Vizgen’s MERSCOPE platform that encompasses Multiplex Error-Robust Fluorescence in situ Hybridization (MERFISH) technology. Using a unique 500 gene mouse specific immuno-oncology panel we conducted spatial transcriptomics (SP) on lung and liver tissues from mice treated with IgG, SNDX-ms6352, CTX, CTX+SNDX-ms6352+/-aPD1. To study the TIME in depth we have pre-selected up to 8 regions of interest (ROIs) from each tissue, spanning both tumor macro- and micro-metastases, stromal and normal tissue. Collectively across 5 tissues we have been able to capture approximately 2 million single cells that have been identified as cancer, immune and stromal. With uniform manifold approximation and projection (UMAP) uncovering up to 60 cellular phenotypes. Strikingly the combination groups illustrate loss of *Trem2, Arg1, Mcr1*- TAMs with dense accumulation of *Cd19*- B, and activated *Gzma*, *Nkg7*-NK and *Gzmb*, *Cd3g*-T cells compared to single agent treatment. Lymphoid, stromal and CAFs where spatially closer to tumor cells within combination treated neighborhoods. Thus, this novel combination treatment turns immunologically “cold” lung and liver metastases “hot”. We will compare our mouse SP to spatially resolved datasets from the NewSTART Clinical trial (NCT06959537).

#7441 Mapping immune clonotypes in prostate cancer using spatial V(D)J to resolve cancer vaccine response.

Eirik Hoye[1], Karishma Sajnani[2], Reetta Natkin[2], Sini Hakkola[2], Antti Kiviaho[2], Thomas Cecchetto[2], Anthony Mathelier[1], Matti Nykter[2], Wolfgang Lilleby[3], Sini Eerola[2], Alfonso Urbanucci[2], Tapio Visakorpi[2], Heini Kallio[2]

[1]Norwegian Centre for Molecular Biosciences and Medicine (NCMBM), Nordic EMBL Partnership, University of Oslo, Oslo, Norway,[2]Faculty of Medicine and Health Technology, Tampere University and Tampere University Hospital Cancer Center, Tampere, Finland,[3]Department of Oncology, Oslo University Hospital, Oslo, Norway

Purpose: The prostate tumor microenvironment (TME) is immunologically “cold,” limiting the efficacy of immunotherapy. Vaccine-induced immune activation has shown promise, but the spatial distribution and function of immune clones within the TME remain poorly understood.
Methods: We applied spatial V(D)J sequencing, combining long- and short-read analysis of the CDR3 region, to map T and B cell clonotypes alongside gene expression signatures directly in prostate tissue while preserving spatial context. Prior data from a phase 1/2a clinical trial (NCT01784913) of the telomerase (hTERT) peptide vaccine UV1, administered in combination with radiation therapy, used TCRseq to investigate changes in the TME and T cell repertoires before and after vaccination, as well as factors distinguishing the cancer vaccine non-responders from the responders who had a very favourable outcome.
Results: TCRseq data revealed distinct profiles in tissue prior to vaccination that differentiated responders from non-responders. Notably, a T cell receptor motif signature in pre-vaccination tissue was associated with patients who mounted an early immune response to the vaccine. Differences in transcriptomic profiles and T cell repertoires were observed among patients with early, late, or no immune response, linking immune contexture to clinical outcomes.
Conclusions: Our findings provide high-resolution insights into immune-tumor interactions in prostate cancer, demonstrating that specific immune clonotypes underlie effective vaccine responses and may inform future immunotherapy strategies, and that spatial V(D)J analysis can be leveraged to explore the spatial contexture of the prostate cancer tumor microenvironment.

#7442 Cancer chemotherapy-induced accelerated aging is mitigated by activation of the altruistic stem cell defense response.

Lekhika Pathak[1], Partha Jyoti Saikia[1], Upasha Sarmah[2], Rupam Das[3], Chayanika Das[3], Tulika Sarma[3], Bikul Das[1]

[1]Department of Cancer and Stem Cell Biology, KaviKrishna Laboratory, Guwahati, India,[2]Department of Stem Cell and Infectious Diseases, KaviKrishna Laboratory, Guwahati, India,[3]KaviKrishna Telemedicine Care, Sualkuchi, India

Introduction: Accelerated biological aging (ABA) is increasingly recognised as a driver of poor survivorship outcomes in cancer. Conventional aging biomarkers including epigenetic clocks, inflammatory signatures, and frailty scales are descriptive and lack mechanistic specificity. We hypothesized that the Altruistic Stem Cell (ASC) Defense (ASD) response (1) of mesenchymal stem cells (MSCs) represents protective pathway against chemotherapy and tumor-induced ABA at both systemic and tumor-microenvironment (TME) levels.

Methods: A cisplatin-induced accelerated aging mouse model (2) was used to evaluate whether activation of the ASD response mitigates ABA. MCF-7 breast cancer-bearing mice received cisplatin with or without squalene supplementation, a nutritional geroprotectant predicted to enhance ASD activity. ABA was quantified in BM-derived MSCs ($CD271+/CD45^-$ progenitors) and tumor-derived $CD271^+$ MSCs using two canonical aging hallmarks: DNA double-strand breaks (γH2AX) and heterochromatin loss (H3K9Me3). The ASC phenotype of MSCs were measured as described (1). 20 PBMC samples from breast, lung, and ovarian cancer patients (N=10) treated with cisplatin (KaviKrishna HealArt cohort) were analyzed. $CD45^-$ MSCs were isolated and expanded under naïve MSC conditions (3). The ASD response was measured by quantifying the ASC phenotype of the CD45- MSCs (3).

Results: Cisplatin induced a robust accelerated aging phenotype in tumor-bearing mice, characterized by elevated γH2AX and reduced H3K9Me3 in BM-derived MSCs. Notably, TME-derived $CD271^+$ MSCs also exhibited pronounced aging features, indicating that chemotherapy accelerates aging locally within the tumor niche. This aging TME correlated with increased tumor burden in cisplatin-treated mice. Although the ASD was activated, it was not sustained. Squalene supplementation sustained the ASD response, evidenced by the mobilization of ASCs to the circulation. Activation of ASD reversed aging hallmarks in both BM-MSCs and tumor-derived $CD271^+$ MSCs, reducing DNA damage and restoring heterochromatin integrity. Importantly, squalene-treated mice displayed reduced tumor growth, suggesting that preventing aging of the TME suppresses tumor-supportive signals. In the human study, we identified a subset of patients (n=4) with ASD-positive MSCs showed significantly lower γH2AX ($p < 0.05$) and higher H3K9Me3 CTCF values compared to patients (n=6) having ASD-negative MSCs.

Conclusion: Chemotherapy accelerates aging in circulating progenitors and in tumor-derived $CD271^+$ MSCs, creating an aging TME that may foster tumor progression. Clinically, ASD can be quantified from PBMC-derived MSCs and may serve as a biomarker to stratify patients at highest risk of ABA.

References:1. Pathak L, et al PMID: 33887214.2. Das B, et al. PMID: 18813359.3. Talukdar J et al. https://doi.org/10.1158/1538-7445.AM2016-920.

#7443 Low hypoxia microenvironment and impaired T cell maturation drive immunotherapy resistance in premenopausal triple negative breast cancer.

Vidya Prasad Nimbalkar[1], Snijesh V P[1], Anupama CE[1], Mahalakshmi S[1], Annie Alexander[1], Rakesh Ramesh[2], Srinath BS[3], Jyothi S. Prabhu[1]

[1]Division of Molecular Medicine, St. John's Research Institute, Bangalore, India,[2]Department of Surgical Oncology, St. John's Medical College and Hospital, Bangalore, India,[3]Department of Surgical Oncology, Sri Shankara Cancer Hospital and Research Centre, Bangalore, India

Purpose: Triple-negative breast cancer (TNBC) often show limited response to immune checkpoint blockade (ICB) therapy, but the mechanisms underlying this resistance remain unclear. This study aimed to investigate how menopausal status associated changes in the tumor microenvironment influence antitumor immunity, particularly T-cell differentiation and activation, and how these factors may contribute to ICB resistance.

Methods: Spatial transcriptomic profiling (NanoString GeoMx DSP) was performed on 19 TNBC tumors across 59 tumor and immune regions. These data were integrated with publicly available bulk RNA seq datasets from METABRIC and SCAN-B, as well as single-cell RNA seq data (GSE176078) including pre and postmenopausal TNBC samples. Gene Set Enrichment Analysis (GSEA) was used to identify pathway-level differences, and T-cell subtypes from the single-cell dataset were assessed for distribution and functional state. Findings were further investigated using immunotherapy response data from the I-SPY2 clinical trial.

Results: Premenopausal TNBC tumors showed consistent downregulation of hypoxia and angiogenesis pathways across both spatial and bulk transcriptomic datasets. These pathways were positively correlated ($r = 0.61$, $p = 5.8e-05$) and associated with reduced immune signaling. Single-cell profiling showed an enrichment of naïve and progenitor-like $CD8^+$ T cells in premenopausal tumors, lacking exhaustion markers such *as PDCD1, TOX,* and *TIGIT*. In contrast, postmenopausal tumors contained more cytotoxic $CD8^+$ T cells expressing granzyme and perforin, indicative of enhanced effector activity. Although premenopausal tumors had higher proportions of M1 macrophages and follicular helper T cells, these populations did not appear to drive effective cytotoxic responses. Importantly, the hypoxia-low transcriptional profile of premenopausal TNBC resembled that of ICB non-responders in the I-SPY2 trial.

Conclusions: Reduced hypoxia-related signaling and impaired maturation of cytotoxic T-cell responses may contribute to weak antitumor immunity and poor ICB efficacy in premenopausal TNBC. These findings point to the need for tailored therapeutic strategies to improve immunotherapy responses in premenopausal TNBC.

#7444 Tetraspanin-driven metabolic plasticity and chemoresistance in disseminated breast cancer cells.

Alexia Brunel*[1], Kristin Decker*[2], Suvendu Das[1], Praveen Neel[1], Asad Ullah[1], Jasmin Meier[2], Ganesan Ramamoorthi[3], Flavio Palma[4], Jacob Torrez[5], Duy Nguyen[5], Marcelo Bonini[4], Brian Czerniecki[3], Thordur Oskarsson[1]

[1]Department of Molecular Oncology, Moffitt Cancer Center, Tampa, FL,[2]Heidelberg Institute for Stem Cell Technology and Experimental Medicine (HI-STEM), Heidelberg, Germany,[3]Department of Breast Oncology, Moffitt Cancer Center, Tampa, FL,[4]Department of Metabolism and Physiology, Moffitt Cancer Center, Tampa, FL,[5]Department of Bioengineering, Moffitt Cancer Center, Tampa, FL

Breast cancer (BC) is a major cause of cancer-related death in women, largely due to metastasis. Therapy-resistant Disseminated Cancer Cells (DCCs) can persist in a dormant state for long periods and serve as latent seeds of relapse. Their ability to evade detection and withstand treatment, such as chemotherapy, underscores the need to better understand DCC biology and to develop strategies to eliminate them before metastatic outgrowth.

Across multiple orthotopic BC mouse models, including cell-line based or patient-derived xenografts, we observed extensive dissemination of tumor cells to multiple organs. DCCs persisted in a quiescent state for weeks yet retained metastatic capacity. Notably, whereas primary tumors and growing lung metastases responded to chemotherapy, DCCs remained resistant, indicating distinct survival mechanisms.

To investigate the molecular properties of DCCs, we isolated the cells from secondary organs by flow cytometry and subjected them to transcriptomic profiling to uncover mechanisms underlying their biological function and resistance to chemotherapeutics. DCCs were analyzed across multiple secondary sites, including bone, kidney, and pancreas. This revealed specific differences between DCCs and mammary tumor cells, as well as remarkably conserved adaptive programs among DCCs from distinct organs, highlighting common survival strategies that may represent shared therapeutic targets. Gene signature analysis identified various cellular functions altered in DCCs. We observed reduced apoptotic responses, accompanied by enhanced DNA repair and striking metabolic rewiring as hallmarks of DCC persistence. Specifically, DCCs repressed glycolysis while inducing oxidative phosphorylation and fatty acid metabolism to establish a bioenergetic state that supports survival under therapeutic stress.

Among the most highly upregulated genes in DCCs, we identified TSPAN8 and TSPAN1, which emerged as essential mediators of DCC metabolic adaptation and chemoresistance. These two members of the tetraspanin superfamily are transmembrane proteins that lack intrinsic enzymatic activity but organize membrane microdomains via interactions with partner receptors and signaling molecules. Their expression was strongly correlated in DCCs, suggesting a shared regulatory mechanism. Functional studies *in vitro* and *in vivo* demonstrated that ectopic TSPAN1/8 expression promotes metabolic adaptation and chemoresistance, whereas their knockdown disrupts the rewired metabolic network and sensitizes DCCs to chemotherapy.

Collectively, our study establishes TSPAN1 and TSPAN8 as mediators of metabolic plasticity and chemoresistance in dormant DCCs. These findings provide a rationale to investigate combinatorial therapies integrating metabolic inhibitors with standard-of-care chemotherapy to eradicate dormant DCCs, the root drivers of metastatic recurrence.

#7445 Effector regulatory T-cell infiltration, ARID1A status, and *Ex Vivo* anti-PD-1 response in ovarian clear cell carcinoma: Insights from a comparative high-grade serous ovarian cancer cohort.

Junsik Park[1], Eun Kyung Kim[2], Jung Chul Kim[1], Nari Kim[3], JooHyang Lee[3], Sunghoon Kim[3], Sang Wun Kim[3], Yong Jae Lee[3], Jung-Yun Lee[3]

[1]Department of Obstetrics and Gynecology, Soonchunhyang University Hospital Bucheon, Bucheon, Korea, Republic of,[2]Department of Pathology, National Health Insurance Service Ilsan Hosp., Goyang, Korea, Republic of,[3]Department of Obstetrics and Gynecology, Yonsei University College of Medicine, Seoul, Korea, Republic of

Recent trials suggest potential benefit of immune checkpoint blockade (ICB) in ovarian clear cell carcinoma (OCCC), but the immune contexture and biomarkers that modulate ICB response remain poorly understood. We characterized tumor-infiltrating lymphocytes (TILs) in OCCC and explored associations with clinical features, ex vivo anti-PD-1-based ICB responsiveness, and biomarker expression. Peripheral blood mononuclear cells (PBMCs) and TILs were obtained from patients with OCCC (n=55). Immune checkpoint receptor and transcription factor expression were analyzed by multicolor flow cytometry. TILs were stimulated ex vivo with anti-CD3 plus anti-PD-1 with or without anti-CTLA-4, and proliferation was assessed by T-cell division. HER2, ARID1A, and L1CAM expression were evaluated by immunohistochemistry on tumor tissue. Twenty of 55 patients had stage III/IV or recurrent disease, and most tumors were grade 3. Among evaluable tumors, 9/38 exhibited HER2 2+/3+, 24/41 showed loss of ARID1A, and 29/41 showed high L1CAM expression. In flow cytometric analysis, CD8 T cells and regulatory T cells (Tregs) were enriched in tumors compared with peripheral blood. $CD8^+$ TILs showed a profoundly exhausted phenotype, with higher PD-1, CTLA-4, and TOX and lower TCF-1 expression than $CD8^+$ T cells in blood, while tumor-reactive $CD39^+CD103^+$ CD8 TILs were also more enriched. Tregs exhibited highly suppressive features with increased immune checkpoint receptors, CD39, and CCR8, and effector Tregs ($CD45RA^-$FoxP3high) were more abundant in stage III/IV or recurrent tumors than in stage I/II disease. In ex vivo assays, CD8 TILs from a subset of patients showed robust anti-PD-1-induced proliferation, and effector Treg frequency was inversely associated with anti-PD-1-induced CD8 T-cell reinvigoration. ARID1A-deficient tumors exhibited significantly lower effector Treg infiltration, whereas HER2 and L1CAM expression were not clearly associated with T-cell phenotypes or anti-PD-1 response. When compared with our previously reported cohort of advanced-stage high-grade serous ovarian cancer (HGSOC), the percentage of tumor-infiltrating Tregs, particularly $4\text{-}1BB^+$ Tregs, was lower in advanced/recurrent OCCC than in HGSOC. In conclusion, OCCC exhibits profound exhaustion of CD8 TILs alongside infiltration of highly suppressive Tregs. Effector Treg frequency was inversely associated with anti-PD-1-induced CD8 T-cell reinvigoration, and ARID1A loss may be linked to a tumor microenvironment more permissive to anti-PD-1-based immune checkpoint blockade. This hypothesis may help explain the high ICB response rate reported in OCCC compared with HGSOC and requires confirmation in larger clinical cohorts and mechanistic studies elucidating how ARID1A loss in OCCC reprograms the tumor immune microenvironment.

#7446 Inflammation and chemotherapy induce immune mimicry in PDAC and promote crosstalk between fibroblasts and tumor cells.

Carson Cable[1], Qinlin Jiang[2], Kourosh Kouhmareh[3], Richard L. Klemke[4], Ryan Matthew Shepard[5], Alejandro D. Campos[4], Sara M. Weis[5], David A. Cheresh[5]

[1]Pathology, University of California, San Diego, La Jolla, CA,[2]University of California, San Diego, La Jolla, CA,[3]UC San Diego School of Medicine, La Jolla, CA,[4]UCSD Moores Cancer Center, La Jolla, CA,[5]UCSD Medical Ctr., San Diego, CA

Pancreatic ductal adenocarcinoma (PDAC) is a leading cause of cancer-related mortality partly due to refractory responses to chemotherapeutics. Factors secreted by immune cells and cancer-associated fibroblasts (CAFs) like interleukin (IL)-6 family members can activate Signal transducer and activator of transcription 3 (STAT3) in PDAC cells, driving drug resistance. We developed a STAT3 effector gene signature induced by inflammatory mediators that strongly correlates with poor relapse-free survival in PDAC. One of the signature genes, *IL7R*, encoding interleukin-7 receptor alpha (IL7Rα), is commonly associated with lymphoid cells. Importantly, we observed *IL7R* enrichment in tumor cells from chemotherapy-treated patients compared to treatment-naïve patients that correlates with an increased epithelial-to-mesenchymal transition (EMT) score. Furthermore, we identified high expression of the IL7Rα ligand thymic stromal lymphopoietin (TSLP) primarily restricted to CAFs from PDAC patients. PDAC cells exposed to an IL-6 family member gained IL7Rα expression leading to hyperactivation of the tumor-promoting transcription factors, STAT1, STAT3, and STAT5 in response to TSLP. We contend that *IL7R* expression represents an “immune mimicry” response leveraged by tumor cells to gain stress tolerance, drug resistance, and EMT through crosstalk with CAFs, leading to an aggressive cancer phenotype.

: Therapeutic Modulation of the Tumor Microenvironment: New Targets and Approaches 2
Poster Session

#7450 TGF-β heterogeneity in cancer cells might be associated with tumor progression in gastric cancer.

Daiki Imanishi[1], Masakazu Yashiro[1], Hinano Nishikubo[1], Tomoya Sano[1], Dongheng Ma[1], Canfeng Fan[1], Takashi Sakuma[1], Yurie Yamamoto[1], Kiyoshi Maeda[2]

[1]Department of Molecular Oncology and Therapeutics, Osaka Metropolitan Univ. Graduate School of Med., Osaka, Japan,[2]Department of Gastroenterological Surgery, Osaka Metropolitan Univ. Graduate School of Med., Osaka, Japan

Background: It has been reported that tumor heterogeneity is frequently found in various types of human carcinomas. Tumor heterogeneity may exist in not only human tumors but also cancer cell lines. Analysis of tumor heterogeneity might be useful to understand the mechanisms of tumor development. In this study, we examined the heterogeneity of gastric cancer using a gastric cancer cell line and human gastric tumor samples.
Materials and Methods: A gastric cancer cell line OCUM-12 and a total of 530 gastric cancers were used in this study. The heterogeneity of cancer cell line was examined after subcloning of OCUM-12 cells using limiting dilution. mRNA expression levels of *TGF-β1* and *TGF-β2* in each subclone cell were examined by RT-PCR. Next, we performed immunohistochemical study of TGF-β using 530 gastric cancers specimens. TGF-β expression was evaluated both at cancer cells and at cancer-associated fibroblasts (CAFs). Immunohistochemical staining level was evaluated by not only manual but also using digital QuPath. Correlation between TGF-β1 expression and clinicopathological features were analyzed.
Results: mRNA expression levels of *TGF-β1* and *TGF-β2* was different among 12 OCUM-12 subclones. Immunohistochemical staining level of TGF-β was also different among tumor specimens. Five-year recurrence-free survival rate of high TGF-β expression group tended to be a poor prognosis ($p = 0.0913$) in Stage 2, while the survival rate showed a better prognosis in Stage 3.
Conclusion: TGF-β heterogeneity in cancer cells might be associated with tumor progression in gastric cancer.

#7451 Integrated bulk and single cell transcriptomics reveal *PARL* as a mitochondrial regulator associated with immunometabolic reprogramming and favorable prognosis in lung squamous cell carcinoma.

Jaber H. Jaradat[1], Zaid Alwarawrah[2], Laith Alomari[3], Anwaar Saeed[4], Azhar Saeed[5]

[1]Faculty of Medicine, Mutah University, Al-Karak, Jordan,[2]Griffin Hospital, Derby, CT,[3]Department of Medicine, Jefferson Einstein Philadelphia Hospital, Philadelphia, PA,[4]UPMC Hillman Cancer Center, Pittsburgh, PA,[5]University of Vermont Medical Center, Colchester, VT

Background: Lung squamous cell carcinoma (LUSC) lacks reliable prognostic biomarkers. Given the growing recognition of mitochondrial dysfunction as a driver of cancer metabolism and immune regulation, we investigated the mitochondrial protease presenilin-associated rhomboid-like (PARL) gene expression as a potential modulator of tumor progression and immune microenvironment in LUSC.
Methods: TCGA-LUSC bulk RNA-seq was analyzed with DESeq2 to evaluate PARL differential expression. Univariate and multivariate Cox models were performed to evaluate association with overall survival (OS). Limma was used to assess pathway-level differences using Hallmark MSigDB gene sets. Functional enrichment was performed using GO and GSEA. CIBERSORTx was utilized to assess immune infiltration. Single-cell analysis of the 10x Genomics NSCLC Tumor 1 dataset included quality control, normalization, clustering, automated annotation (SingleR), and pseudotime trajectory analysis to examine lineage-specific PARL patterns.
Results: Low *PARL* expression correlated with shorter OS (median OS: 39 vs. 61 months; log-rank $p = 0.008$) and remained an independent favorable prognostic factor (HR = 0.75, $p = 0.003$). The survival benefit of high *PARL* expression persisted across early and late disease stages. Functional enrichment analysis indicated that high-*PARL* tumors were enriched for mitochondrial organization, oxidative phosphorylation, and apoptotic regulation, whereas *PARL*-low tumors favored proliferative and cell cycle pathways. Key pathways downregulated in high-*PARL* tumors included KRAS signaling, complement, IL6/JAK/STAT3, and TGF-β signaling, while DNA repair, MYC targets, Oxidative Phosphorylation, and G2M checkpoint pathways were upregulated, suggesting enhanced metabolic activity and cell cycle regulation. Furthermore, Pearson's chi-squared test showed a significant association between *PARL* expression and TP53 mutations ($\chi^2 = 8.04$, $p = 0.0046$). CIBERSORTx analysis revealed that *PARL*-high tumors exhibited lower infiltration of immunosuppressive and pro-inflammatory cells, including Tregs, M2 macrophages, and neutrophils suggesting a role for *PARL* in shaping a less suppressive immune microenvironment. Single-cell trajectory analysis revealed *PARL* expression peaked in progenitor and stromal populations, implying an early role in mitochondrial quality control and immune differentiation, influencing tumor-immune dynamics and clinical outcomes.
Conclusions: *PARL* emerges as a candidate gene expression-based biomarker associated with mitochondrial homeostasis, reduced immunosuppression and favorable prognosis in LUSC. These findings highlight a potential role of *PARL* in immune metabolic adaptation and support further validation to establish its clinical relevance.

#7452 Claudin 18.2 targeted proapoptotic peptide for early pancreatic diagnosis and tumor-target killing.

Poongkavithai Vadevoo Sri Murugan[1], Gunassekaran Gowri Rangaswamy[2], Byungheon Lee[1]

[1]Kyungpook National University, Daegu, Korea, Republic of,[2]Biochemistry and Cell Biology, Kyungpook National University, Daegu, Korea, Republic of

Pancreatic adenocarcinoma is a lethal condition with a rising incidence, predicted to become the second leading cause of cancer-related deaths worldwide by 2030. One major hurdle in the treatment of this disease is the predominantly elderly patient population and clinically silent and aggressive nature. Early detection of pancreatic neoplasms and novel treatment for highly aggressive and metastatic conditions is of great need in pancreatic tumor therapy.Claudins are crucial components of tight junctions. They are transmembrane proteins and are the keeper of the “fence function”. Claudins in tumor are like the fall of the soldiers entrusted to protect the gate. Claudin 18.2 is a member of the claudin family, commonly expressed in multiple cancers, including Gastric cancer and Pancreatic cancer. Claudin-18.2 expression on cancer cells is increased and exposed on surface of the cells. The development of malignant tumors leads to the disruption of tight junctions, exposing the Claudin 18.2 epitope on the surface of tumor cells as a specific target. Also, claudin 18.2 is transcriptionally upregulated with the binding of cyclic AMP-responsive element binding protein to the methylated CLDN18.2 promoter region. Claudin 18.2 is considered an early stage marker of pancreatic carcinogenesis. Claudin 18.2 is considered a ‘dark horse’ in anti-tumor therapy. Thus, Claudin 18.2 could be a good “target” for early detection and target-specific treatment of pancreatic tumor.Construction of phage peptide library and bio panning for claudin18.2-binding peptides using claudin18.2 overexpressing cells : After five rounds of screening, phage titers that bind to transfected cells were enriched higher-fold compared to phage titers isolated in the first round. 2 phage clones displaying peptides that selectively bound to transfected cells were chosen and sequenced for further study. The two peptides showed selective binding to claudin 18.2 expressing cells as analyzed by Immunofluorescence. Pull down assay further confirmed selective binding of peptide to claudin 18.2. Bioaccumulation study in vivo showed significant accumulation of peptide in tumor tissue. Treatment of KPC transgenic pancreatic tumor bearing mice with claudin 18.2 peptide conjugated to proapoptotic peptide enhanced the survival of the mice. In summary, Claudin 18.2 peptide can specifically target the tumor cells and conjugation with proapoptotic peptide can induce tumor targeted apoptosis with increased survival in pancreatic tumor bearing mice. Claudin 18.2 targeted tumor killing can be a promising approach for pancreatic tumor treatment.

#7456 PCSK1 and PCSK7 orchestrate immune checkpoints to amplify anti-tumor immunity.

Marta Martin-Bornez[1], Chloe Porcheron[1], Geraldine Siegfried[1], Serge Evrard[2], John Creemers[3], Nabil Seidah[4], Simon Pernot[2], **Abdel-Majid Khatib**[1]

[1]INSERM, Bordeaux, France,[2]Bergonie, Bordeaux, France,[3]KU Leuven, Leuven, Belgium,[4]IRCM, Montreal, QC, Canada

Background: Immune-checkpoint receptors (ICPs) such as PD-1, CTLA-4, and TIGIT restrain T-cell activation and enable tumor immune evasion. Although ICP-targeting antibodies have transformed cancer therapy, many patients exhibit incomplete or transient responses, underscoring the need to identify upstream regulators that control ICP expression and function. Proprotein convertases (PCSKs) have recently emerged as modulators of immunity, but their roles in T-cell checkpoint regulation remain poorly defined.
Methods: We investigated the functions of Furin and PCSK7 using CRISPR/Cas9-mediated gene deletion, antisense oligonucleotides (ASOs), overexpression systems, mouse knockout models, patient-derived tumor samples, paired PBMCs, and ex vivo T-cell activation assays. Immune-checkpoint expression and trafficking were assessed using flow cytometry, transcriptomic profiling, and imaging. Functional consequences were evaluated through cytokine secretion, proliferation assays, cytotoxicity measurements, chemotaxis analyses, and tumor-organoid co-culture systems.
Results: Furin and PCSK7 emerged as complementary and essential regulators of ICP biology in T cells. Furin controls ICP expression at the transcriptional level, reducing mRNA abundance of PD-1, CTLA-4, and TIGIT upon deletion. In contrast, PCSK7 functions as a non-enzymatic chaperone, stabilizing newly synthesized ICPs and directing them to the cell surface. Loss of either convertase significantly diminished surface checkpoint levels and reduced the fraction of T cells co-expressing multiple inhibitory receptors. In human tumors and corresponding PBMC-derived T cells, decreased Furin or PCSK7 expression correlated with enhanced T-cell proliferation, cytokine release, and cytotoxic function. Organoid models, ex vivo patient tumor assays, and tumor-bearing mouse models demonstrated that targeting Furin and PCSK7 enhances the efficacy of chemotherapy and immunotherapy.
Conclusions: Furin and PCSK7 constitute key upstream regulators of immune checkpoints, controlling both transcriptional abundance and cell-surface availability through distinct mechanisms. Their inhibition enhances T-cell activation and anti-tumor function, representing a promising therapeutic strategy to potentiate immune responses and overcome resistance to current checkpoint-blocking therapies.

#7457 IL-33-mediated control of myeloid immunity in glioblastoma progression.

Tala-Maria Mouannes, Shyam V. Menon, Peipei Zeng, Jianbo Zhang, Isabelle Carrier, Eduardo Diez, Stephen M. Robbins, Donna L. Senger

Lady Davis Institute at Jewish General Hospital, Montreal, QC, Canada

Glioblastoma (GB) is the most lethal primary brain cancer in adults, characterized by a profoundly immunosuppressive microenvironment dominated by tumor-associated macrophages and microglia (TAMs). We previously identified Interleukin-33 (IL-33), a dual-function cytokine with nuclear and extracellular roles, as a key modulator of this innate immune landscape. While full-length IL-33 accelerates GB progression by recruiting immunosuppressive myeloid cells, a nuclear-deficient variant lacking the nuclear localization sequence (ND-IL-33) potently halts tumor growth and prolongs survival. This growth-restrictive state is marked by the emergence of a distinct pro-inflammatory, anti-tumor myeloid population. Secretome profiling reveals that ND-IL-33-expressing glioma cells produce a unique repertoire of immune-stimulatory factors, consistent with enhanced innate immune activation, suggesting that loss of IL-33 nuclear activity reshapes tumor-intrinsic signaling to drive myeloid reprogramming. The clinical relevance of this biology is supported in patient-derived GB specimens, where high IL-33 expression is associated with increased immunosuppressive TAM infiltration and reduced overall survival. Ongoing bulk and single-cell RNA sequencing, integrated with functional co-culture assays, aims to define the transcriptional programs that distinguish tumor-inhibiting from tumor-promoting myeloid populations and to uncover therapeutic pathways capable of inducing this anti-tumor state. Together, these findings position IL-33 activity as a targetable regulator of myeloid plasticity in GB and offers a promising avenue to leverage innate immunity for improved therapeutic outcomes in glioblastoma.

#7458 Examining OST4's impact on tumorigenesis and immune microenvironment in ovarian cancer.

Mengyi Gu[1], Michelle K.y. Siu[1], Ruiqian Zhang[2], Luqi CHEN[1], Ling Shan HUNG[3], Kui Liu[1], Yuen Sheung Hextan Ngan[4], Haonan Lu[1], Annie NY Cheung[5], Karen K.l. Chan[1]

[1]University of Hong Kong, Hong Kong SAR, China,[2]University of Hong Kong, The - Li Ka Shing Faculty of Medicine, Pok Fu Lam, China,[3]Universtiy of Hong Kong, Hong Kong SAR, China,[4]University of Hong Kong, Hong Kong, SAR, China,[5]Clinical Professor, Dept. of Pathology, University of Hong Kong, Pokfulam, China

IntroductionOvarian cancer remains one of the deadliest malignancies in gynecology, characterized by a high tendency for metastasis, strong drug resistance, and limited response to immunotherapy. Protein glycosylation plays a critical role in these processes, making it an attractive target for therapeutic development. The oligosaccharidyltransferase (OST) complex, which catalyzes a central step in N-linked glycosylation, is of particular importance. Among OST subunits, OST4 serves as a key regulatory element. Previous studies indicate that OST4 expression modulates the efficiency of protein N-glycosylation and has been recognized as a prognostic marker in head and neck cancers, with connections to PD-L1 expression. However, the role of glycosylation-related genes such as OST4 in ovarian cancer development and immune cell activity within the tumor microenvironment remains unclear. This study explores the function of OST4 in ovarian cancer and assesses its potential as a therapeutic target.MethodsWe employed comprehensive data mining of The Cancer Genome Atlas (TCGA) and single-cell RNA sequencing datasets to identify pathways linked to OST4 in ovarian cancer and its immune-related effects. OST4 expression was knocked down in ovarian cancer cell lines (OVCAR4 and OVCAR8) using siRNA. Cell migration and invasion were measured to evaluate metastatic potential, and proliferation was assessed via XTT assays. Western blot analysis was performed to examine associated signaling pathways and downstream effectors. Tumor Conditioned Medium (TCM) was collected from ovarian cancer cells transfected with OST4 siRNA and scRNA, incubated in complete medium for 48 hours. The transwell migration assay was used to determine the infiltration of T cells cultured with the TCM. ResultsOST4 was found to be highly expressed in ovarian cancer. Patient stratification based on OST4 expression levels revealed associations with macrophage and T-cell infiltration. Pathway analysis indicated that OST4 may regulate the unfolded protein response (UPR). Silencing OST4 suppressed ovarian cancer cell migration, invasion, and proliferation. Western blot analysis further demonstrated that OST4 knockdown decreased the expression of IRE1α, a central component of the UPR pathway. The number of infiltrated $CD8^+$ T cells increased in the presence of TCM derived from OST4-silenced OC cells compared to control TCM.ConclusionIn conclusion, OST4 influences ovarian cancer progression and $CD8^+$ T cell infiltration, potentially through activation of the UPR pathway. Targeting OST4 may offer a promising therapeutic approach for ovarian cancer.

#7459 Localized co-delivery of hyaluronidase enhances CSPG4 CAR-T cells cytotoxicity against chordoma.

Maoyang Qi[1], Giulia Cattaneo[2], Zan Chen[3], Cristina Ferrone[2], Joseph Schwab[1]

[1]The Department of Orthopaedics, Cedars-Sinai Medical Center, Los Angeles, CA,[2]The Department of Surgery, Cedars-Sinai Medical Center, Los Angeles, CA,[3]The Department of Neurosurgery, Xuanwu Hospital, Beijing, China

Background: Chordoma is a rare malignant bone tumor characterized by a dense extracellular matrix (ECM) and an immunologically “cold” microenvironment that limits immune cell infiltration and therapeutic efficacy. Chondroitin sulfate proteoglycan 4 (CSPG4) has emerged as a promising tumor-associated antigen in chordoma. However, the hyaluronan-rich ECM forms a physical and biochemical barrier that hampers CAR-T cell trafficking and function. We hypothesized that localized co-delivery of hyaluronidase (PH20) could remodel the ECM and enhance the cytotoxic activity of CSPG4-directed CAR-T cells.
Methods: CSPG4 CAR-T cells were generated using a third-generation lentiviral construct containing CD28-Ox40-CD3ζ signaling domains. Human chordoma cell lines and patient-derived 3D organoids were used to evaluate cytotoxicity and infiltration. Electrical impedance assays were applied to monitor real-time changes in surface charge and cell-matrix interactions following PH20 treatment. Transwell migration assays and 3D organoid co-cultures were used to assess CAR-T infiltration, and cytokine secretion was quantified by ELISA. In vivo efficacy and safety were examined in xenograft models following localized co-delivery of PH20 and CAR-T cells.
Results: CSPG4 CAR-T cells exhibited antigen-specific cytolytic activity against chordoma cells, but their infiltration was markedly restricted in hyaluronan-rich environments. Electrical impedance analysis revealed that PH20-mediated ECM degradation significantly altered the charge distribution and impedance profile, indicating reduced matrix density and improved accessibility for CAR-T cells. In Transwell assays, PH20 enhanced CSPG4 CAR-T transmigration across hyaluronan-containing barriers. Similarly, in 3D chordoma organoids, PH20 co-treatment promoted deeper CAR-T infiltration and led to greater cytotoxicity with elevated IFN-γ and Granzyme B production. Consistent findings were observed across multiple patient-derived organoid models. In xenograft studies, localized co-delivery of PH20 with CSPG4 CAR-T cells resulted in stronger tumor regression and prolonged survival compared with CAR-T monotherapy ($p < 0.01$), without observable systemic toxicity.
Conclusion: ECM degradation through localized hyaluronidase co-delivery effectively enhances CSPG4 CAR-T cell infiltration and cytotoxicity against chordoma. This combinatorial approach overcomes stromal barriers, reshapes the tumor microenvironment, and represents a feasible strategy to improve CAR-T efficacy in solid tumors with dense ECM architecture.

#7460 Logic-gated T cell engager linked with mutant IL-2 for safer and better effective solid tumor immunotherapy.

Yang-Xin Fu

tsinghua University, Beijing, China

T cell engagers (TCEs) have achieved transformative success in B-cell malignancies but show limited efficacy in solid tumors with severe toxicity. Here, we identify insufficient IL-2 signaling as a key bottleneck for sustaining TCE-induced T-cell function. Although exogenous IL-2 enhances TCE efficacy, its systemic administration causes more severe toxicity. To overcome this limitation, we engineered a protease-activatable dual-variable-domain (DVD) as Pro-TCE to reduce its off-tumor toxicity. Furthermore, we designed a mutant IL-2 (3E) with markedly reduced receptor affinity that is inactive in periphery. The construct (DVD-3E) remains inert in circulation and becomes locally activated only upon tumor-specific protease cleavage, coupling T-cell engagement with cis IL-2 signaling. This logic-gated design restricts both TCE and cytokine activity to the tumor microenvironment (TME), enabling potent antitumor responses without systemic toxicity. Mechanistically, DVD-3E enhances the persistence and effector function of preexisting intratumoral T cells, expands $TCF1^{+}$ progenitor and antigen-specific T cells populations, mitigates exhaustion, and establishes durable immune memory. Notably, DVD-3E treatment increased the frequency of antigen-specific T cells in draining lymph nodes, which were capable of controlling distant tumors and mediating effective tumor regression upon adoptive transfer. These findings define a new design principle for logic gated TCEs that achieve a favorable balance between safety and efficacy, offering a strategy to overcome current therapeutic resistant.

#7461 Inhibitory effects of induction of massive apoptosis (PRIMA-1^{MET}) on tumorigenic chemokines in ovarian cancer cells.

Audene B. Wilkinson, Deok-Soo Son

Department of Biochemistry and Cancer Biology, Meharry Medical College, Nashville, TN

Background/Purpose: Ovarian cancer is the most lethal gynecologic malignancy, with TP53 mutations present in >95% of high-grade serous cases, representing a prime molecular target for therapy. In addition to disrupted p53 signaling, elevated pro-inflammatory chemokines drive tumor progression by enhancing proliferation and distant metastasis. This study investigates the therapeutic potential of PRIMA-1^{MET}, a small-molecule reactivator of mutant p53, to suppress tumorigenic chemokine production in ovarian cancer cells.

Methods: OVCAR3 cells (harboring TP53^{R248Q} mutation) were cultured under standard conditions. Cell viability was quantified by MTT assay to determine IC50 values. Protein levels and phosphorylation status were assessed by Western blotting. The transcriptional activity of p53 was measured in cells transiently transfected with p53-responsive luciferase reporter plasmids ± wild-type and mutant p53 expression vectors, followed by measurement of luciferase activity. Chemokine profiling was performed using a Human XL Cytokine Array.

Results: PRIMA-1^{MET} reduced OVCAR3 viability in a dose-dependent manner (IC50 ≈ 30 μM), and significantly down-regulated chemokines CXCL1, CXCL8, and CCL20, indicating attenuated pro-inflammatory and pro-metastatic signaling. PRIMA-1^{MET} markedly decreased phosphorylated NF-κB, implicating suppression of this master regulator of chemokine transcription. Consistent with p53 reactivation, PRIMA-1^{MET} enhanced p53-driven luciferase reporter activity while concomitantly inhibiting CXCL8 promoter activity—containing an NF-κB binding site—at both basal and IL-1β-induced levels.

Conclusion: PRIMA-1^{MET} restores mutant p53 function and inhibits NF-κB-driven chemokine signaling, thereby restraining ovarian cancer progression and metastasis. These findings highlight its promise as targeted therapy.

#7462 DAPK3-DCAF1 pathway regulates ZBP1 protein stability to orchestrate innate immune responses and PANoptosis.

Zhiqi Liao[1], Linghui Wang[1], Wenjian Gong[1], Ziyan Zhang[1], Gordon B. Mills[2], Ding Ma[1], Guangnian Zhao[1], Qinglei Gao[1], Yong Fang[1]

[1]Department of Gynecological Oncology, Tongji Hospital, Tongji Medical College, Huazhong University of Science and Technology, Wuhan, China,[2]OHSU Knight Cancer Institute, Portland, OR

Background: Z-DNA binding protein 1 (ZBP1) is an interferons (IFN)-stimulated cytosolic sensor of Z-nucleic acids (Z-NA) that regulates PANoptosis (pyroptosis, apoptosis, and/or necroptosis) and thereby drives potent anti-tumor immune responses. However, the mechanisms controlling ZBP1 protein stability in tumors—and whether they can be therapeutically manipulated to induce ICD—remain unclear. We sought to define regulatory pathways that govern ZBP1 abundance in ovarian cancer and to test strategies that exploit ZBP1 activation for antitumor therapy.

Methods & Results: Here we demonstrate that the reduced ZBP1 expression in ovarian cancer and correlated with poorer survival. Type I IFN (IFN-β) rapidly increased ZBP1 levels by inhibiting its proteasome-dependent ubiquitination. Proximity labeling and biochemical assays identified DCAF1 as a key interactor that mediates ZBP1 ubiquitination and degradation. Furthermore, IP-MS and LC-MS/MS identified DAPK3 as an IFN-induced DCAF1 kinase, which phosphorylates DCAF1-pS1328 to promote its turnover, thereby stabilizing ZBP1. Genetic ablation of DCAF1 impaired tumor cell proliferation *in vitro*, reduced tumor burden and promoted anti-tumor immunity *in vivo*. Pharmacological targeting of this pathway using the DCAF1 inhibitor B32B3 and—when combined with the Z-NA activator CBL0137—effectively reactivated ZBP1 signaling, promoted PANoptosis, and enhanced antitumor immunity, thereby suppressing tumor growth in two chemotherapy-resistant ovarian cancer patient-derived xenograft (PDX) models and providing a promising therapeutic strategy for refractory malignancies.

Conclusion: Overall, this study delineates a novel DAPK3-DCAF1 signaling axis that governs ZBP1 stability, unveiling an integrated regulatory framework that connects interferon signaling, post-translational modification, and immunogenic cell death. Combining DCAF1 blockade with Z-NA activation elicits ZBP1-mediated PANoptosis and augments anti-tumor immunity, representing a promising therapeutic approach for refractory ovarian cancer.

#7463 Targeting S100A7/RAGE-driven Stat3/Serpin-E1 signaling for immunotherapy in metastatic breast cancer.

Pratyusha Ghanta[1], Ajeet K. Verma[1], Cho-Hao Lin[1], Manish Charan[1], Ganesh R. Koshre[2], Tanisha Mukherjee[1], Wayne O. Miles[2], Sanjay Mishra[1], Ramesh Ganju[1]

[1]Pathology, Ohio State University, Columbus, OH,[2]Cancer Biology and Genetics, Ohio State University, Columbus, OH

Background: Triple-negative breast cancer (TNBC) is an aggressive type that lacks targeted therapies, with immunosuppressive variants resistant to checkpoint blockade. Elevated S100A7 expression is reported in these immune-ignored, anti-PD1-refractory tumors; yet S100A7 mechanisms, which shape the immune tumor microenvironment (iTME), remain unclear. Here, we investigated how S100A7 activates the RAGE/Stat3 axis to induce Serpin-E1, reshaping the iTME, and assessed therapeutic potential in immunosuppressive TNBC.

Method: Expressions of S100A7, RAGE, Stat3, and Serpin-E1 were analyzed in TNBC cells by Western blotting, cytokine arrays, and ELISA. Functional assays evaluated the impact of S100A7 overexpression (OE) or knockdown (KD) and pharmacologic inhibition of RAGE and Stat3, alone or combined, on viability, migration, and colony formation. Pre-clinical models, including doxycycline (DOX)-inducible mammary gland-specific S100A7-OE bitransgenic mice treated with RAGE and Stat3 inhibitors ± Serpin-E1 neutralizing antibody (nAb) were utilized for *in-vivo* studies. Multi-color flow cytometry determined macrophage polarization and T-cell activation. CD4/CD8 depletion assays and *in-silico* analyses evaluated T-cell dependency and prognostic significance.

Results: S100A7 upregulation enhanced phosphorylation of Stat3 (Ser727) and Serpin-E1 expression, whereas its downregulation suppressed pStat3/Serpin-E1. Dual inhibition of RAGE and Stat3 produced synergistic suppression of TNBC cell viability, migration, and colony formation and markedly inhibited downstream pStat3 signaling. Mechanistic studies revealed that S100A7/RAGE signaling activates Stat3, which binds to the Serpin-E1 promoter and enhances its transcription. *In-vitro* assays demonstrated a potential role for Serpin-E1 in modulating macrophage polarization. Next, *in-vivo* treatment of RAGE and Stat3 inhibitors ± Serpin E1 nAb led to significant reductions in primary tumor growth and distant metastasis in female NSG mice. Significantly decreased tumor burden in S100A7-OE mice treated with the combination of RAGE/Stat3 inhibitors was observed compared to alone treatment groups alone. Additional immune profiling within tumor tissues revealed a significant abundance of antitumor iNOS and $MHCII^{high}$ TAMs and increased activation of CD4+ and CD8+ T cells with elevated effector markers in combinatorial treatment compared to a single regimen. These effects were abrogated by CD4/CD8 depletion. Clinically, high co-expression of S100A7 and Serpin-E1 correlated with poorer outcomes, particularly in basal and immunomodulatory TNBC subtypes.

Conclusions: This study identifies the S100A7/RAGE/Stat3/Serpin-E1 axis as a key regulator of tumor growth and iTME suppression in TNBC and its potential for a targeted therapeutic strategy for immune-ignored TNBC subtypes.

#7464 Inhibiting interferon-gamma-stimulated melanoma progression by disrupting the crosstalk between nNOS/NO and COX-2.

Anika Patel[1], Kate Alison Lozada[1], Moom Roosan[1], Basir Syed[1], Jennifer Totonchy[1], Amardeep Awasthi[2], Richard B. Silverman[2], **Sun Yang**[1]

[1]Chapman University, Irvine, CA,[2]Northwestern University, Evanston, IL

Interferon gamma (IFN-γ) in the melanoma tumor microenvironment plays opposing roles, orchestrating both pro-tumorigenic activity and anticancer immune responses. Our previous studies demonstrated the role of neuronal nitric oxide synthase (nNOS) in IFN-γ-stimulated melanoma progression. However, the underlying mechanism has not been well defined. Bioinformatic analysis of patient and cellular proteomic data was conducted to identify proteins of interest associated with IFN-γ treatment in melanoma. Our omics analysis revealed that the induction of COX-2 was significantly predictive of IFN-γ treatment in melanoma cells. In the presence of IFN-γ, PGE_2 further enhanced PD-L1 expression and amplified the induction of nNOS, which increased intracellular NO levels. Cotreatment with celecoxib, a selective COX-2 inhibitor, effectively diminished these changes induced by PGE_2. nNOS blockade using a selective small molecule inhibitor (HH044) efficiently inhibited IFN-γ-Induced PGE_2 production and COX-2 expression in melanoma cells. STAT3 inhibitor napabucasin also inhibited COX-2 expression both in the presence and absence of IFN-γ. *In vivo*, HH044 treatment significantly reduced tumor PGE_2 levels in a human melanoma xenograft mouse model (A375/Nu/Nu). Combination treatment with HH044 and celecoxib yielded the greatest tumor suppression in the syngeneic murine melanoma model (Cloudman S91/DBA/2), reducing tumor volume to 19% of control, compared to 38% and 52% with HH044 or celecoxib alone, respectively. Furthermore, transcriptomic analysis revealed significant changes in genes involved in matrix remodeling and metastasis after HH044 treatment. *Ex vivo* co-culturing human PBMCs with melanoma cells inhibited T cell activation, decreasing IL-2-secreting T cells in the presence and absence of IFN-γ. PBMCs from a significant portion of donors (64%) were reactivated by HH044 pretreatment, displaying a significant increase in IL-2+ T cells after coincubation with melanoma cells.Our study reveals a positive feedback loop linking nNOS-mediated NO signaling to the COX-2/PGE_2 signaling axis in melanoma, thereby further enhancing the pro-tumorigenic activity of IFN-γ. Disrupting crosstalk between nNOS/NO and COX-2 with selective inhibitors effectively suppressed melanoma tumor growth, possibly by modulating the tumor immune microenvironment.

#7465 Chemically regulated STING-activating prodrugs of deoxyribose cyclic dinucleotides elicit robust immune activation and durable antitumor immunity.

Huimin Liu, Zhiqiang Xie, Kejia Xu, Rong Xiang, Shibo Li, Zhen Xi

Nankai University, Tianjin, China

Background: Prodrugs derived from deoxyribose cyclic dinucleotides (dCDNs) exhibit enhanced cellular permeability, stability, and sustained STING activation. However, the impact of phosphotriester chirality on their bioactivity remains underexplored. This study systematically evaluates the stereochemistry-dependent pharmacology of alkyne-conjugated, esterase-sensitive dCDN prodrugs in vitro and in vivo. Methods: Three diastereoisomers of the dCDN prodrug: (Rp,Rp)-10, (Sp,Sp)-10, and (Rp,Sp)-10—were synthesized, purified by chiral HPLC, and confirmed by NMR and HRMS. Cellular uptake and stability were assessed in THP1-Lucia ISG cells. STING pathway activation was measured by IFN-β reporter assays and phospho-TBK1/IRF3 immunoblots. In vivo efficacy was evaluated in CT26 colon carcinoma-bearing BALB/c mice following intravenous administration. Immune memory was assessed by tumor rechallenge. Results: Among the isomers, (Rp,Rp)-10 exhibited the most potent STING activation (EC50 = 1.7 nM), superior cellular uptake, and prolonged TBK1/IRF3 signaling. In mice, all three prodrugs induced stronger systemic cytokine responses than ADU-S100 or the parent CDN 3′,3′-c-di-dAMP. In the CT26 model, (Rp,Rp)-10 achieved complete tumor regression in 9/10 mice (90% CR), significantly improved survival ($p < 0.001$), and established long-term immunological memory with 100% rejection upon rechallenge. No overt toxicity was observed. Conclusion: Phosphotriester chirality is a critical determinant of dCDN prodrug activity. (Rp,Rp)-10 represents a promising next-generation STING agonist with potent systemic antitumor immunity and durable therapeutic effects. These findings underscore the importance of stereochemical control in the rational design of STING-targeted cancer immunotherapies.

#7466 Epiregulin drives immunosuppressive TAM programming and is negatively regulated by miR-19a-3p in colorectal cancer.

Ah Ran Yu[1], Ju Yeon Park[1], Jeong Eun Kang[1], Sang Hyuk Moon[2], Hey Kyung Hong[3], **Yong Beom Cho**[4]

[1]Institute for Future Medicine, Samsung Medical Center, SEOUL, Korea, Republic of,[2]Department of Biopharmaceutical Convergence, SEOUL, Korea, Republic of,[3]Samsung Medical Center, SEOUL, Korea, Republic of,[4]Department of Health Sciences and Technology, SAIHST, Sunkyunkwan University, Seoul, Korea, Republic of

Colorectal cancer (CRC) is one of the most prevalent malignancies worldwide and remains a leading cause of cancer-related mortality. Its clinical challenge is compounded by the presence of a highly immunosuppressive tumor microenvironment (TME), which not only facilitates tumor growth and metastasis but also contributes to poor responses to immunotherapy. Among the cellular components of the TME, tumor-associated macrophages (TAMs) play a central role in supporting tumor progression, largely through their polarization into an M2-like, immunosuppressive phenotype. Despite their importance, the upstream regulators and downstream signaling pathways that maintain the tumor-promoting state of TAMs in CRC remain insufficiently defined. We performed single-cell RNA sequencing and transcriptomic profiling of CRC patient samples, which led to the identification of epiregulin (EREG) as a TAM-enriched gene, with predominant expression in SPP1^{+} macrophage clusters. Functional studies using EREG knockdown in murine CT26-derived TAMs and human M2-polarized macrophages demonstrated that EREG promotes M2-like polarization, elevates the secretion of pro-tumoral cytokines and enhances the proliferation and migration of co-cultured CRC cells. Mechanistically, we found that EREG signals through the JAK/STAT3 pathway, as its silencing led to reduced STAT3 phosphorylation and downregulation of associated target genes involved in immune suppression and tumor progression. Furthermore, miRNA screening and validation assays revealed that miR-19a-3p directly binds to the 3′UTR of EREG mRNA, as confirmed by RIP (Ago2) enrichment analysis. Introduction of miR-19a-3p mimics led to a significant reduction in EREG expression, suppression of JAK/STAT3 signaling, and reprogramming of TAMs toward an M1-like, anti-tumor phenotype. Collectively, our findings uncover the miR-19a-3p–EREG–JAK/STAT3 axis as a critical regulatory mechanism of TAM programming in colorectal cancer and highlight its potential as a therapeutic target for reprogramming the immunosuppressive tumor microenvironment.

#7467 Real-time detection of ADC internalization kinetics using a pH-sensitive fluorescent dye.

An Ouyang[1], Linlin Ma[2], Di Shi[2], Siwen Wang[1], Tianfu Zhang[2], Zhicheng Dong[2], YuehChun Hsieh[2]

[1]ACROBiosystems Inc., Newark, DE,[2]ACROBiosystems Co., Ltd., Beijing, China

BACKGROUND Monitoring antibody-drug conjugate (ADC) internalization demands highly sensitive and specific methods to differentiate surface-bound from internalized molecules. To address this need, we developed an internalization detection reagent based on pH-sensitive fluorescent dyes that enable real-time visualization of endocytosis events in live cells. This assay allows quantitative monitoring of dynamic parameters such as initiation rate, uptake duration, and total internalization, providing critical insights for understanding ADC mechanisms of action, optimizing dosing regimens, and refining administration strategies.

METHOD AND MATERIALS The primary antibody (2 μg/mL) and Internalization Detection reagent (1μg/mL) were prepared in cell culture medium, mixed, and incubated at room temperature for 10 min to form the labeling complex. For suspension cells, 50 μL of cell suspension (1×10^6 cells/mL) was seeded into each well of a 96-well plate and combined with 50 μL of the labeling complex. For adherent cells, 5,000-10,000 cells were plated per well and allow to attach. The medium was then replaced with 50 μL of fresh medium prior to the addition of 50 μL of the labeling complex. Cells were incubated with the labeling complex for 0.5-24 h, followed by analysis via flow cytometry or high-content imaging at designated time points.

RESULTS SK-BR-3 (HER2+) cells were incubated with various Anti-HER2 mAbs and our internalization detection reagent. Throughout the incubation period, there was a time-dependent increase in fluorescence across all tested primary antibodies, with signal intensity gradually increasing over time. In contrast, no positive signal was detected in the negative control cell line MDA-MB-468(HER2-). SK-BR-3(HER2+) cells were also incubated with anti-HER2 mAbs and their corresponding ADC drugs in presence of the internalization detection reagent. The intensity of the internalization detection signal showed a dose-dependent upward trend with increasing reagent concentration. The internalization detection signal for anti-HER2 antibody in SK-BR-3 cells increased gradually over the initial 7 hours, then the signal reached a plateau and maintained stable for up to 18 hours. Upon removal of the reagent and antibody mixture at the 7-hour mark, the internalization signal in the 2 nM anti-HER2 antibody group showed a gradual decline over the next 24 hours.

CONCLUSION The developed internalization detection reagent enables real-time, quantitative monitoring of antibody and ADC internalization kinetics with high sensitivity, reproducibility, and specificity. The reagent demonstrates consistent performance across different targets such as HER2 and CD20, offering a robust and versatile platform for studying endocytosis mechanisms, comparing candidate antibodies, and accelerating ADC development and optimization.

#7468 Calcium homeostasis modulator GRIN2D activates cancer-associated fibroblast for desmoplasia and promotes neutrophil infiltration for neutrophil extracellular trap formation in pancreatic ductal adenocarcinoma.

Chi Hin Wong[1], Yip Kan Kwan[1], Ka-Fai To[2], Yangchao Chen[1]

[1]School of Biomedical Sciences, The Chinese University of Hong Kong, Shatin, Hong Kong,[2]Department of Anatomical and Cellular Pathology, The Chinese University of Hong Kong, Shatin, Hong Kong

Pancreatic ductal adenocarcinoma (PDAC) is recognized as a “cold tumor” due to its poor response to immunotherapy, which is greatly contributed by the dense and complicated tumor microenvironment. Calcium ions (Ca^{2+}) are important signaling molecules for various biological processes. Dysregulated calcium channels and transporters greatly contribute to abnormal calcium homeostasis and, in turn, promote cancer progression. However, its roles in the PDAC tumor microenvironment and therapeutic resistance are still largely unknown. We previously demonstrated the importance of calcium transporters glutamate ionotropic receptor NMDA type subunit 2D (GRIN2D) in promoting PDAC tumor growth and liver metastasis. Here, we studied the importance of GRIN2D in the tumor microenvironment and therapeutic resistance. The upregulated GRIN2D activated cancer-associated fibroblast (CAF) and promoted neutrophil infiltration, contributing to an oncogenic tumor microenvironment. Mechanistically, transcriptome profiling after GRIN2D knockdown in PDAC cells identified fibronectin 1 (FN1) and interleukin-1 beta (IL-1β) as GRIN2D downstream targets under calcium signaling. The GRIN2D-FN1 pathway activated CAF for tumor desmoplasia, while the GRIN2D-IL-1β pathway promoted neutrophil infiltration and neutrophil extracellular traps formation. Furthermore, we revealed the epigenetic mechanism leading to the upregulation of GRIN2D in PDAC. We identified a hypermethylated Exon-CpG island at GRIN2D, promoting GRIN2D expression in PDAC tumors. Targeting GRIN2D in the tumor microenvironment enhances the efficacy of both chemotherapies and immunotherapies in inhibiting tumor growth and metastasis. Knowledge gained from this project uncovers the importance of GRIN2D and calcium homeostasis in PDAC progression and contributes to novel therapeutic targets in PDAC.

#7469 Targeting the tumor immune microenvironment to promote efficacy of chemo agents against breast cancer.

Alexander J. Krusell[1], Yi Le[2], William G. Richards[3], Deborah A. Dillon[4], Zhenglun Zhu[2]

[1]Massachusetts Institute of Technology, Cambridge, MA,[2]Department of Medicine, Brigham and Women's Hospital, Boston, MA,[3]Department of Surgery, Brigham and Women's Hospital, Boston, MA,[4]Department of Pathology, Brigham and Women's Hospital, Boston, MA

Breast cancer (BC) is the most common cancer worldwide and the second leading cause of cancer related death for women in the US. Despite significant advances in mechanistic exploration and therapeutic intervention, improving the overall survival rate (OS), treating metastatic breast cancer remains an urgent challenge. Estrogen, progesterone and human epidermal growth factor 2 (HER2) receptor triple negative BC (TNBC), for example, has a 5-year OS of 11% and a median OS of only 11 to 13 months. Due to the lack of a feasible target or biomarkers for targeted therapy, chemo agents serve as a limited therapeutic option for metastatic TNBC. Currently, clinical application of chemotherapy has been significantly limited by age-related and dosage-dependent cytotoxicity of chemo agents. While recent studies have suggested that the tumor immune microenvironment (TIME) plays an important role in chemoresistance, how to target the TIME to improve the efficacy of chemotherapy against TNBC has remained largely unknown. In this study, we characterized the immune cell profile in the TIME of BC and found that the expression level of the homeobox protein VentX, a transcription factor implicated in macrophage plasticity, is significantly downregulated in BC tumor associated macrophages (TAMs). We found that down-regulated VentX expression in BC-TAMs is associated with their pro-tumor M2-like phenotype and is accompanied by the increased population of immune suppressive T_{reg} cells in the BC-TIME. We also demonstrated that ectopic expression of VentX in BC-TAMs converted its pro-tumor M2-like phenotype into an anti-tumor M1 phenotype. Using an *ex-vivo* TIME enabling model system (TIME-EMS) developed in the lab, we showed that elevated expression of VentX in BC-TAMs led to transformation of the BC-TIME from an immune suppressive state into an immune activated state. Using the TIME-EMS models of BC, we explored the effects of chemo agents on cancer cells in BC-TIME. We discovered that conversion of BC-TIME from an immune suppressive state into an immune activated state drastically increased the sensitivity of cancer cells to the chemotherapeutic agent paclitaxel. Besides TNBC, we showed that reversal of immune suppression of BC-TIME also improves chemosensitivity of paclitaxel on other sub-groups of BC. We also demonstrated that elevated expression of VentX in BC-TAMs did not increase the cytotoxicity of paclitaxel on normal breast epithelial cells. In summary, our work demonstrates the utility of the TIME-EMS models as an *ex-vivo* model system to explore treatment options for BC in the context of the TIME. Our results suggest that VentX may serve as a potential therapeutic target to improve the efficacy of chemo agents against BC and improve prognosis of TNBC patients who have limited therapeutic options.

#7470 Uncovering the role of XPO6 in nasopharyngeal carcinoma.

Ziye Lu[1], Ziyang Qi[1], Lanqi Gong[2], Yuma Yang[1], Jie Luo[2], Qin Liu[2], Xin-Yuan Guan[2]

[1]The University of Hong Kong, Shenzhen Hospital, Shenzhen Shi, China,[2]The University of Hong Kong, Hong Kong, Hong Kong

Nasopharyngeal carcinoma (NPC) is a geographically prevalent malignancy, especially in southern China and Southeast Asia, with over 95% of cases in endemic regions linked to Epstein-Barr virus (EBV) infection. Despite advances in screening and chemoradiotherapy, advanced and treatment-resistant NPC remains a significant clinical challenge, characterized by high recurrence rates and limited therapeutic options. While immunotherapy, including anti-PD-1/PD-L1 agents, has been proposed to address this unmet need, responses are often suboptimal, underscoring the need to understand EBV-specific immune evasion mechanisms intrinsic to tumor cells.

Our study focuses on Exportin-6 (XPO6), a nuclear export protein identified as a candidate mediator of immune resistance in EBV-positive NPC through a comprehensive CRISPR-Cas9 screen. The screen targeted 19,114 genes in the EBV-positive C666 NPC cell line and the EBV-negative HK1 NPC cell line. Both cell lines were subjected to cytotoxic pressure from NY-ESO-1-specific TCR-engineered T cells, a model that recapitulates antigen-specific antitumor immune responses. Analysis with MAGeCK highlighted XPO6 as an EBV-positive NPC-specific regulator, with its deletion significantly sensitizing tumor cells to T cell-mediated killing. To validate these findings, we generated XPO6 knockout (KO) and overexpression (OE) derivatives of the C666 cell line. Functional co-culture assays confirmed that XPO6 KO markedly reduced NPC cell viability in the presence of TCR-engineered T cells, directly demonstrating enhanced susceptibility to T cell-mediated cytotoxicity. Consistent with this, XPO6 KO C666 cells also exhibited increased secretion of T cell-derived proinflammatory cytokines, including IFN-gamma and TNF-alpha, indicating that XPO6 deletion amplifies the anti-tumor immune response beyond direct cytotoxicity. Conversely, XPO6 OE in C666 cells conferred increased resistance to T cell killing, confirming that XPO6 expression is sufficient to drive immune evasion in EBV-positive NPC. The precise molecular mechanism by which XPO6 mediates these effects remains to be fully elucidated and warrants further investigation.

This study identifies XPO6 as a pivotal regulator of immune resistance specifically in EBV-positive NPC. Targeting XPO6 not only enhances tumor cell sensitivity to T cell cytotoxicity but also promotes a more robust T cell cytokine response, highlighting its potential as a therapeutic target to improve immunotherapeutic outcomes. Further exploration of the underlying molecular pathways through which XPO6 enables immune escape will be undertaken in the future.

#7471 Identification and characterization of compounds that block heterocellular adhesion between diffuse-type gastric cancer cells and cancer-associated fibroblasts.

Hideki Yamaguchi[1], Yuko Nagamura[1], Makoto Miyazaki[2]

[1]Department of Cancer Cell Biology, Sasaki Institute, Sasaki Foundation, Tokyo, Japan,[2]Laboratory of Pediatric and Refractory Cancer, Chiba Cancer Center Research Institute, Chiba, Japan

The phenotypes of cancer cells are profoundly influenced by reciprocal interaction with the tumor stroma within the tumor microenvironment. Among stromal components, cancer-associated fibroblasts (CAFs) are the most abundant and play pivotal roles in shaping the tumor milieu. CAFs promote cancer progression through the secretion of pro-tumorigenic factors and remodeling of the extracellular matrix. In addition to these paracrine effects, recent studies have emphasized the critical role of direct heterocellular adhesion between cancer cells and CAFs in tumor progression. Diffuse-type gastric cancer (DGC) is the most aggressive subtype of gastric cancer with an extremely poor prognosis. DGC is characterized by rapid infiltrative growth and frequent peritoneal metastasis. DGC is commonly accompanied by desmoplastic stroma, which results from the extensive proliferation of CAFs. We previously demonstrated that direct interactions with CAFs are essential for the invasion and peritoneal metastasis of DGC cells. To further elucidate the biological significance of this interaction, we established a high-throughput screening system to identify molecules that disrupt DGC cell-CAF adhesion. Using this screening system, we successfully obtained monoclonal antibodies that block this heterocellular adhesion and suppress peritoneal metastasis of DGC in vivo. In the present study, we aimed to identify small-molecule compounds that inhibit heterocellular adhesion between DGC cells and CAFs. High-throughput screening of a chemical library led to the identification of several hit compounds. Notably, one compound not only inhibited DGC cell-CAF adhesion but also suppressed the proliferation of DGC cells. Furthermore, this compound markedly reduced peritoneal metastasis of DGC in a mouse xenograft model. These findings suggest that targeting the heterocellular adhesion between cancer cells and CAFs represents a promising therapeutic strategy, and that small molecules disrupting this interaction may serve as novel anti-cancer agents.

#7472 Taraxasterol suppresses *H. pylori*-induced gastritis and gastric cancer by targetingPTP1B/PKM2/NF-κB signaling pathway.

Liting Zhou

Zhengzhou University, Zhengzhou, China

Chronic *Helicobacter pylori* infection is a primary cause of gastritis, peptic ulcers, and gastric cancer (GC), creating a demand for novel therapeutic agents that address both inflammation and tumor progression. Taraxasterol (TAX) has demonstrated significant therapeutic potential against both gastritis and gastric cancer (GC). *In vitro*, TAX effectively alleviated H. pylori-induced gastritis by reducing intracellular bacterial load and attenuating the inflammatory response, specifically by decreasing TNF-α levels and reactive oxygen species, and inhibiting the NF-κB signaling pathway (IKKα and P65 phosphorylation). TAX did not directly inhibit H. pylori growth, suggesting its mechanism is primarily anti-inflammatory. Beyond gastritis, TAX exhibited potent anti-cancer effects on GC cell lines (AGS and MGC803), dose-dependently inhibiting their proliferation and colony formation. Mechanistically, computational and experimental analyses (SPR, DARTS, CETSA) identified Protein Tyrosine Phosphatase 1B (PTP1B) as a direct target of TAX. PTP1B, found to be highly expressed in gastritis and GC tissues and associated with poor prognosis, had its phosphatase activity inhibited by TAX. Further studies showed that PTP1B knockdown inhibited GC cell proliferation and that TAX's anti-proliferative effects were partially mediated through PTP1B, modulating the PTP1B/PKM2/NF-κB signaling pathway. *In vivo*, TAX successfully inhibited H. pylori and/or alcohol-induced gastritis in mice, reducing inflammation, lymphocyte infiltration, and cytokine levels. Crucially, TAX also suppressed tumor growth in gastric cancer patient-derived xenograft (PDX) models. These findings collectively highlight TAX as a promising therapeutic agent for both gastritis and gastric cancer, primarily through its anti-inflammatory properties and its targeted inhibition of PTP1B.

#7473 A novel dual-target strategy against TNBC: Combining EZH2 inhibition and dopamine D1 receptor activation to restore immune balance.

Rajni Kant Shukla[1], Kate Ormiston[2], Gautam Sarathy[2], Shivani Dhekne[2], Dionisia Marie Quiroga[2], Sanjay Gupta[3], Daniel G. Stover[4], Pierre Giglio[5], Christian Rolfo[2], **Eswar Shankar**[2]

[1]Oklahoma State Health Science Center, Oklahoma, OK,[2]Division of Medical Oncology, Department of Internal Medicine, Wexner Medical Center, The Ohio State University, Columbus, OH,[3]Department of Urology, School of Medicine, Case Western Reserve University School of Medicine, Cleveland, OH,[4]OSUCCC - James, Columbus, OH,[5]Department of Neurology, School of Medicine, Wexner Medical Center, The Ohio State University, Columbus, OH

Triple-negative breast cancer (TNBC) remains one of the most aggressive and therapeutically challenging breast cancer subtypes, characterized by high heterogeneity, intrinsic resistance, and poor immune infiltration. There is a critical unmet need for less toxic approaches that can both suppress tumor growth and remodel the tumor microenvironment (TME). EZH2, a histone methyltransferase, is frequently overexpressed in TNBC, associated with immunosuppression, and disease progression. We previously reported combining GSK126 (an EZH2 inhibitor) with A77636 (a dopamine D1 receptor [DRD1] agonist) produced superior antitumor effects compared to monotherapies. We hypothesized synergistic targeting of EZH2 and DRD1 would convert the immunologically “cold” TNBC microenvironment into a “hot,” immune-permissive state, thereby enhancing therapeutic efficacy and overcoming resistance mechanisms. Female NSG mice (4-6 weeks old) were orthotopically implanted with MDA-MB-231 cells, randomized into four treatment groups (n=8): vehicle, GSK126 (2 mg/kg), A77636 (50 mg/kg), or combination. Treatments were administered intraperitoneally weekly for four weeks. Tumor volume was measured weekly and at endpoint. Tumors and immune tissues were analyzed by flow cytometry. Combination therapy significantly reduced tumor weight (mean difference = 0.278g, 95% CI: 0.109-0.446, p=0.0018) and volume (mean difference = 101 mm³, 95% CI: 51.7-151, p<0.0001) compared with vehicle and single agents. Notably, the combination markedly decreased monocyte populations in both blood and tumor tissue and downregulated EZH2 expression in tumor-associated monocytes and neutrophils. Kinetic profiling revealed a biphasic monocyte response-initial Ly6C^hi recruitment followed by Ly6C^lo transition. The combination suppressed Ly6C^hi infiltration (0.32 vs. 0.92; 65% decrease, p=0.0138) while promoting Ly6C^lo accumulation (2.5 vs. 1.5; 1.67-fold increase, p=0.5126). By using a combinational treatment strategy to redirect monocyte phenotypes, we were able to suppress the pro-inflammatory IL-1β environment while simultaneously enhancing anti-inflammatory IL-10 signaling-ultimately creating a tumor-suppressive immune milieu. In summary, dual modulation of EZH2 and DRD1 effectively halts TNBC progression by reshaping the immunological landscape. These findings uncover a distinctive therapeutic avenue that integrates epigenetic regulation with dopaminergic activation to restore immune responsiveness in TNBC. *(This work was supported by DOD W81XWH2010065 to Eswar Shankar).*

#7474 M4N as a potential anti-inflammatory therapy for KDM6A-deficient bladder cancer.

Nobuhito Muramoto[1], Masayuki Iwasaki[1], Yasuyuki Sera[1], Kohei Kobatake[2], Kyosuke Iwane[2], Tsuyoshi Fukushima[3], Kotohiko Kimura[4], Ru Chih C. Huang[4], Hiroaki Honda[1]

[1]Tokyo Women's Medical University, Tokyo, Japan,[2]Hiroshima University, Hiroshima, Japan,[3]Assistant Professor, Dept. of Pathology, University of Miyazaki, Miyazaki, Japan,[4]Johns Hopkins University, Baltimore, MD

Introduction and Objective: Histone modifications are important for tissue homeostasis, and their mutations are involved in carcinogenesis. Mutations in an X-linked histone demethylase KDM6A are most frequently observed in bladder cancer (BCa) among human malignancies. We previously demonstrated that loss-of-function of KDM6A contributes to BCa development by promoting inflammation through activating the JAK-STAT pathway. Tetra-O-methyl-nordihydroguaiaretic acid (M_4N), a methylated derivative of nordihydroguaiaretic acid, inhibits transcription factor Hypoxia-Inducible Factor (HIF) and Specificity protein 1 (Sp1) and exerts anti-inflammatory activities through inhibiting the JAK-STAT pathway. Here, we investigated the therapeutic efficacy of M_4N against KDM6A-deficient BCa using a subcutaneous syngeneic model.

Methods: To investigate the anti-proliferative effect of M_4N on KDM6A-deficient BCa, we used CRISPR-Cas9 genome editing and established *Kdm6a*-deficient sublines from mice BCa cell lines, MB49 and MBT2. *Kdm6a*-deficient and *control parental* cells were subcutaneously implanted into syngeneic mice and tumor growth on the recipients fed either a normal diet and an M_4N-supplemented diet was continuously monitored. Resected tumors were subjected to pathological, molecular, and cellular analyses using real-time PCR and immunohistochemical staining.

Results: In subcutaneous syngeneic models, *Kdm6a*-deficient cells formed significantly larger tumors compared to *control* cells. M_4N efficiently suppressed tumor growth of *Kdm6a*-deficient cells but showed no effect on tumors of *control* cells. By performing RNA sequencing and pathway analyses using resected tumors, we found that M_4N suppressed inflammatory pathways such as chemokine signaling and JAK-STAT pathways. In *Kdm6a*-deficient tumors, M_4N significantly suppressed the expression of pro-inflammatory cytokines and chemokines, such as *Il-6* and *Ccl2*, and also reduced the expression of *Vegfa* and *Nampt*, the downstream targets of Sp1 and HIF, involved in inflammatory pathways. Moreover, immunostaining of the tumors with F4/80, a macrophage marker, and with p-STAT, a JAK-STAT pathway marker, revealed significant macrophage accumulation and activation of the JAK-STAT pathway, specifically in tumors lacking *Kdm6a*, which was efficiently suppressed by M_4N.

Conclusions: M_4N may serve as a novel therapeutic approach for patients with BCa bearing *Kdm6a* mutations by suppressing inflammation.

#7475 Combinations of grape seed procyanidin extract and milk thistle silymarin extract additively decrease recruitment of THP-1 derived M2 macrophages into the lung tumor microenvironment..

Jenny T. Mao[1], Diego Oliva[1], Jessica Schilter[1], Lauren Rollin[1], Lily Jih[2]

[1]Pulmonary, Critical Care & Sleep Medicine, VA Medical Center, San Diego/UCSD, San Diego, CA,[2]Pathology and Laboratory Medicine, VA Medical Center, San Diego/UCSD, San Diego, CA

Introduction: Grape seed procyanidin extract (GSE) and milk thistle silymarin extract (MTE) are widely used as health food supplements to promote cardiovascular and hepatobiliary health, respectively. Both GSE and MTE contain high levels of structurally distinct polyphenols and each agent has been shown to exert antineoplastic effects against lung cancer. Previously we have shown that the combinations of GSE and MTE decreased production of the tumor promoting, M2 macrophage polarizing CCL2 chemokine by lung cancer cells. CCL2 is a key chemokine in the tumor microenvironment that facilitates recruitment and polarization of macrophages toward the tumor promoting M2c phenotype, which promotes tumor progression by creating a pro-tumorigenic environment. Targeting recruitment to and M2c macrophage polarization in the lung tumor microenvironment with GSE + MTE may represent a novel immunotherapeutic strategy against lung cancer.
Methods:THP-1 cells were differentiated into M0 cells with phorbol-12-myristate-13-acetate (PMA), then to M2c macrophages using interleukin (IL)-10 priming as previously described. M2c phenotype was then confirmed using qPCR profiling with CD163 and CD206 primers. The effects of GSE and MTE conditioning, alone or in combination, on the ability of A549 cells to recruit M2c cells were assessed using co-culture migration/invasion assay of THP-1 derived M0 and M2c macrophages with A549 cells and conditioned cell culture supernatants, simulating the lung tumor microenvironment.
Results: Conditioning of A549 cells with GSE and MTE additively reduced CCL2 production by A549 cells and co-culture with GSE $\pm$ MTE conditioned A549 cells/supernatants additively decreased migration/invasion of M2c cells.
Conclusions: In the present study, we report on the additive effects of GSE and MTE on reducing the migration/invasion of tumor promoting M2c cells in the lung tumor microenvironment. Our findings illustrate a potential novel immunomodulatory mechanism of GSE combined with MTE against lung cancer and support the continued investigation of the combinations for lung cancer prevention and treatment.

#7476 Role of AOC1 in modulating the ovarian cancer tumor microenvironment and malignant phenotype.

Sammy Ferri-Borgogno, Chun Wai (Oscar) Ng, Basant T. Gamal, Erin H. Seeley, Yadira Pacheco, Christopher D. Pacheco, Jared K. Burks, Samuel Mok

UT MD Anderson Cancer Center, Houston, TX

Ovarian cancer can be subdivided into different histologic types. Among them, clear cell ovarian cancer (CCOC), which constitutes 8% of ovarian cancer, differs from the other types with respect to its clinical characteristics. Most of CCOC frequently presents at an early stage compared to high-grade serous ovarian cancer (HGSOC), with most cases diagnosed at Stage I or II, which offers a favorable prognosis. However, those diagnosed with advanced disease experience poorer clinical outcomes compared to those with HGSOC, since CCOC is usually more resistant to systemic chemotherapy than other types. Despite multiple studies showing promise of immune checkpoint inhibitors (ICIs) treatment in patients with CCOC, the molecular mechanisms by which CCOC confers improved response to ICIs, and biomarkers that can predict treatment response to these ICIs in CCOC have not been thoroughly explored. In addition, it remains unclear whether the immune microenvironment plays a role in the early presentation and in metastatic potential of CCOC.Recent spatial transcriptomics (ST) analyses demonstrated that increased AOC1 expression was found in the epithelial cell cluster of early stage CCOC than in HGSOC, which was subsequently validated by sequential immunofluorescence (seqIF) analysis on 17 CCOC and 34 HGSOC patient samples. Increased AOC1 expression is associated with improved overall survival in HGSOC patients. Functional studies showed that despite the lack of a direct effect on the growth of ovarian cancer (OC) cells, syngeneic mouse cells transfected with full-length AOC1 had significantly lower tumor burden than the control mice, suggesting that the tumor microenvironment (TME) mediates the effect of AOC1 on tumor growth. Integrating ST and mass spectrometry imaging (MSI) revealed significantly inverse correlation between AOC1, and histamine and cell membrane VISTA expression levels in cancer cells and/or macrophages in the TME of CCOC and HGSOC, which was confirmed by seqIF. These findings suggest that histamine and VISTA mediate the tumor suppressive effect of AOC1. Indeed, our in vitro studies demonstrated that AOC1 abrogates the growth promoting effect of histamine in OC cells expressing high levels of histamine receptor HRH1, and AOC1 attenuates histamine induced OC proliferation and enhance T cell-mediated anti-tumor immunity via the histamine/HRH1/VISTA axis. Further studies demonstrated that in addition to VISTA, histamine can upregulate PD-L1 in both macrophages and OC cells. AOC1 may increase immune surveillance through attenuating histamine-induced VISTA and PD-L1 expression in the OC TME. Studies to further delineate the immune modulation role of AOC1 and exploring whether enhancing circulating AOC1 levels or targeting histamine with repurposed drugs to improve the efficacy of ICIs as a new strategy in the treatment of OC patients are warranted.

#7477 Angiogenic profile associated with KRAS dependency upon modulation of TIMP1.

Ilamathi M-Thirusenthilarasan[1], Pankaj Kumar Ahluwalia[2], Bilal Siddiqui[3], Ravindra Kolhe[2], Amyn M. Rojiani[4], Mumtaz V. Rojiani[5]

[1]Pathology, Penn State College of Medicine/Penn State Cancer Institute, Hershey, PA,[2]Pathology, Medical College of Georgia/Augusta University, Augusta, GA,[3]Pathology, Penn State College of Medicine, Hershey, PA,[4]Pathology, Penn State College of Medicine/Penn State Health Hershey Medical Center, Hershey, PA,[5]Pathology, and Neuroscience and Experimental Therapeutics, Penn State College of Medicine/Penn State Cancer Institute, Hershey, PA

Non-small cell lung carcinoma (NSCLC) remains a leading cause of cancer-related deaths, with KRAS mutations conferring oncogene addiction and chemoresistance to therapy. Our previous work demonstrated that Tissue Inhibitor of Metalloproteinase-1 (TIMP-1) inversely correlates with KRAS dependency and promotes epithelial-mesenchymal transition (EMT). Given the role of TIMP-1 in tumor progression, we investigated how TIMP-1 modulation impacts the expression of angiogenic mediators in NSCLC cells.KRAS-dependent (H441) and KRAS-independent (H460) NSCLC cell lines were modulated to overexpress (OE) or knock down (KD) TIMP-1, respectively. Serum free conditioned media from these cells was analyzed using angiogenesis proteome profiler array (R&D systems). We found that the levels of pro-angiogenic factors VEGF1 and CXCL8 increased upon TIMP1 overexpression and decreased upon knocking down TIMP1. On the other hand, Thrombospondin-1, an angiogenic inhibitor was downregulated when TIMP1 was over-expressed and upregulated when TIMP1 was knocked down. Additionally, TIMP-1 overexpression in H441 cells increased Angiogenin and decreased Endostatin, Angiostatin, Serpin E1, and Platelet Factor 4 (PF4). Conversely, TIMP-1 knockdown in H460 cells showed the opposite trend, indicating that TIMP1 is pro-angiogenic. RNA-seq data analysis across five NSCLC lines revealed a reciprocal TIMP1:THBS1 expression pattern with strong CXCL8 induction under TIMP1 overexpression, most pronounced in H441. The TIMP1-THBS1 inverse relationship supports a CXCL8-dominant angiogenic axis.As studies have shown that KRAS dependency is associated with upregulation of c-Myc and ERK, leading to a decrease in TSP-1 levels, we assessed c-Myc levels in the lysates using Western blot. We found that the levels of c-MYC were high in KRAS-dependent parental cells and further increased upon TIMP-1 overexpression. In KRAS-independent cells however, TIMP-1 knockdown did not significantly alter c-MYC levels. Ongoing studies continue to evaluate the effects of TIMP-1 modulation on angiogenic responses under normoxic and hypoxic conditions.Our findings highlight TIMP-1 as a potential regulator of tumor angiogenesis in NSCLC in a KRAS dependency specific manner, incorporating a CXCL8-dominant axis.

#7478 Targeting the extracellular matrix in Wilms tumor.

Wilson Yeung[1], Hripsime Chomoyan[1], Matthew E. Thornton[2], David S. Koos[1], Valentina Villani[1], Justin Sunwoo[1], Brendan H. Grubbs[2], Roger E. De Filippo[3], Laura Perin[3], Astgik Petrosyan[3]

[1]Children's Hospital Los Angeles, Los Angeles, CA,[2]Keck School of Medicine of USC, Los Angeles, CA,[3]Children's Hospital Los Angeles/Keck School of Medicine of USC, Los Angeles, CA

Introduction: Wilms tumor (WT) represents approximately 90% of pediatric renal malignancies. While standard treatments are effective for many patients, those with relapse or unfavorable histopathology experience poor survival and severe long-term toxicities. The extracellular matrix (ECM) plays a critical role in driving cancer progression and drug resistance. Our comprehensive profiling of WT revealed type II collagen alpha 1 (COL2A1), absent in normal kidney, to be highly expressed in high-risk tumors, highlighting its potential as a novel biomarker and therapeutic target.
Methods: We utilized WT cancer stem cell (CSC)-like progenitors, 3D cultures, and patient-derived xenografts (PDXs) with metastatic and chemoresistant phenotypes to investigate COL2A1-mediated signaling. Comparative transcriptomics were performed on WT CSCs cultured on WT-versus normal kidney-derived decellularized ECM. Functional assays assessed epithelial-mesenchymal transition (EMT), tumor suppressor expression, and chemotherapy response following COL2A1 inhibition.
Results: COL2A1-enriched substrates activated AKT signaling, induced EMT, downregulated tumor suppressors, and promoted chemoresistance. Transcriptomic analysis revealed COL2A1 upregulation alongside its transcriptional regulator SP1, correlating with enhanced tumorigenic pathways and reduced drug sensitivity. Notably, COL2A1 blockade using a specific antibody reversed EMT (i.e., increased cytokeratin and decreased vimentin), restored tumor suppressor expression, and enhanced chemotherapy response.
Conclusions: COL2A1 is a critical ECM component driving therapy resistance in WT. Targeting COL2A1 offers a promising ECM-directed strategy to overcome treatment resistance and improve outcomes in high-risk WT patients. These findings highlight ECM-directed interventions as a new frontier in the treatment of pediatric kidney cancer.

#7479 A CCL20-high chemokine program defines a CCR6⁺ immune-myeloid niche in gastric cancer.

Kurtay Ozuner[1], Jaewon Kim[2], Sandra W. Ryeom[3]

[1]Herbert Irving Comprehensive Cancer Ctr., New York, NY,[2]Albert Einstein College of Medicine, New York, NY,[3]Columbia University Irving Medical Center, New York, NY

Introduction: Gastric cancer remains one of the leading causes of cancer mortality worldwide and is characterized by an aggressive clinical course and a profoundly immunosuppressive tumor microenvironment with limited therapeutic options. Chemokine signaling has emerged as an important regulator of gastric tumor progression, and among these pathways, the CCL20-CCR6 axis is a validated driver of epithelial to mesenchymal transition, invasion, and metastasis, and is associated with poor patient survival. However, the upstream signals that generate high levels of CCL20 within gastric tumors, and the specific CCR6⁺ immune compartment that respond to this signal remain poorly understood. Understanding the source and downstream signaling for this axis may offer novel therapeutic options for gastric cancer. Here, we identify a previously unrecognized CCL20 high chemokine signature and a dynamically regulated CCR6⁺ immune and myeloid niche in gastric cancer.

Methods:

Chemokine profiling of murine gastric cancer cell lines, multiplex immunohistochemistry of gastric tumors isolated from preclinical models of gastric cancer, and integration with human gastric single-cell RNA-seq confirmed CCL20 expression by gastric cancer cells and CCR6 expression in myeloid and B lineage clusters in the gastric tumor microenvironment.

Results:

Gastric cancer murine organoids exhibited a distinct chemokine signature marked by high CCL20 together with CCL22 and M-CSF. Confocal imaging confirmed abundant CCL20 protein within gastric tumors and organoids. Analysis of TCGA stomach adenocarcinoma data demonstrated that high CCR6 expression correlates with reduced overall survival. Multiplex immunohistochemistry revealed that substantial CCR6 positive CD11c⁺ MHCII⁺ immune cells infiltrate into the gastric cancer tumor microenvironment, including B220⁺ plasmacytoid DC-like (pDC-like) subset. pDC-like cells increased with tumor burden and was modulated by anti-PD-1 and 5-fluorouracil treatment, indicating dynamic regulation of CCR6⁺ myeloid subsets. Human gastric single-cell RNA-seq datasets identified CCR6 expression on myeloid clusters capable of responding to CCL20 through the CCR6 receptor.

Conclusions:

These findings define a previously unrecognized CCL20-high, CCR6⁺ immune-myeloid population in gastric cancer that offers insight into the source of chemokines that drive recruitment of immune cells into the gastric cancer tumor microenvironment. Targeting this axis may reveal actionable vulnerabilities in gastric cancer progression.

: Tumor Adhesion
Poster Session

#7483 Adhesion plasticity and bidirectional paracrine signaling cooperatively drive glioblastoma invasion.

Abhinaba Banerjee[1], Audrey Iwashita[1], Afsheen Banisadr[2], Frank Furnari[3], Adam Engler[1]

[1]Bioengineering, University of California San Diego, San Diego, CA,[2]Biomedical Sciences Program, University of California San Diego, San Diego, CA,[3]Department of Medicine, University of California San Diego, San Diego, CA

Glioblastoma (GBM) lethality stems from diffuse invasion beyond surgical margins. EGFR amplification is frequent, and constitutively active mutant EGFRvIII co-exists with wild-type EGFR (wtEGFR) cells in ~50% of tumors, yet cell-intrinsic and extrinsic mechanisms coupling this heterogeneity to invasion remain unresolved. Murine astrocytes engineered with wtEGFR or EGFRvIII expression were interrogated across complementary 2-D, 3-D, and in-vivo platforms. Here, we found that EGFRvIII cells were ~40% less adherent, enabling faster migration than their wtEGFR counterparts. EGFRvIII conditioned media reduced adhesion strength of wtEGFR cells, but direct co-culture showed bidirectional signaling, with both populations experiencing a two-fold decrease in adhesion strength. Cooperative adhesion reduction was induced by a secretome unique to co-cultured cells, further suggesting bidirectional communication. Adhesion changes also cause post-"education" differences in invasion mode; EGFRvIII cells alone disseminate in a follow-the-leader mode but switch to single cell scattering when co-cultured with wtEGFR (and similar to the wt cells only condition). In addition to mode, the extent of migration is impacted by co-culture; mixed co-culture spheroids invade the matrix more extensively (>2-fold) than spheroids of either population alone, mirroring how patient tumors heterogeneity scales with invasiveness and prognosis. Moreover, RNA-seq, cytokine-arrays, and intracranially injected in vivo mouse models identified transcriptional and signaling alterations that could drive GBM adhesion. Heterotypic interaction between wtEGFR and EGFRvIII induces remodeling of focal adhesions through a distinct paracrine program, highlighting cooperative invasion. Targeting this adhesion-modulating axis offers a strategy to limit diffuse GBM spread. Together, these data show that both intrinsic and extrinsic signaling propel glioma migration and nominate new therapeutic entry points to improve patient outcomes.

#7484 Self-made matrix: Tumor-derived Laminin-α5 supports pancreatic cancer cell survival and metastatic persistence.

Annant Bir Kaur, Nivedeta Krishna Kumar, Pratima Raut, Kirtana Arikath, Venkatesh Varadharaj, Zahraa Wajih Alsafwani, Jesse Cox, Poompozhil Mathivanan, Surindar K. Batra, Moorthy P Ponnusamy

University of Nebraska Medical Center, Omaha, NE

This study investigates how pancreatic cancer cells utilize LAMA5 to build an autonomous niche that promotes survival and metastasis, revealing novel therapeutic vulnerabilities. A stiff and fibrotic extracellular matrix (ECM) is a defining feature of pancreatic ductal adenocarcinoma (PDAC). This dense microenvironment impedes drug penetration, contributing to pronounced therapeutic refractoriness and poor patient survival. While stromal cells are classically regarded as the primary source of ECM, recent evidence suggests that tumor cells themselves can generate matrix components, establishing an autonomous survival niche. Laminin-α5 (LAMA5), a key basement membrane protein, regulates epithelial adhesion, polarity, and migration, yet its tumor-intrinsic role in PDAC remains unexplored. Our comprehensive interrogation of bulk, single-cell RNA sequencing, and spatial transcriptomics datasets revealed selective enrichment of LAMA5 within malignant epithelial cells rather than the stromal compartment. In a clinical context, immunohistochemistry of human PDAC patient samples showed marked upregulation compared with adjacent normal pancreas, and further elevation in metastatic cell clusters in the liver. Next, in murine PDAC progression models (KC: *Kras; PdxCre* and KPC: *Kras; p53; PdxCre*), the ductal cell-derived contribution of LAMA5 increased progressively with disease severity, surpassing stromal expression. KPC-derived organoids similarly exhibited enhanced luminal LAMA5 expression compared with normal ducts, as confirmed by multiplex immunofluorescence, indicating robust secretion by tumor ductal epithelium. Long-term LAMA5 depletion in primary and metastatic human PDAC cell lines impaired proliferation, cell adhesion, anchorage-independent growth, and survival under non-adherent conditions, indicating a role in protecting against anoikis (apoptosis due to loss of attachment to ECM). Interestingly, supplementation with extracellular LAMA5 restored these phenotypes, establishing LAMA5 as a key mediator of adhesion-dependent survival. Tumor cells also exhibited elevated expression of LAMA5-binding receptors ITGA6, ITGB4, and BCAM, supporting an autocrine survival loop that reinforces epithelial adhesion and stress tolerance. To uncover therapeutic vulnerabilities, connectivity mapping through the iLINCS platform identified an FDA-approved compound, Lomustine, which reduced LAMA5 expression and markedly inhibited the growth of mouse and human PDAC organoids. Our findings collectively show that PDAC cells secrete LAMA5 to build a self-made matrix microenvironment that supports survival, adhesion, and metastatic persistence. Tumor-intrinsic LAMA5 redefines the tumor-stroma paradigm, enabling microenvironmental autonomy and anoikis-resistance, and highlights potential targets for intervention in PDAC.

#7485 RNA modification control of platinum sensitivity via ADAM23-dependent pathway.

Hao Huang[1], Ujin Kim[1], junzui li[2], Daniela E. Matei[3]

[1]Department of Obstetrics and Gynecology, Feinberg School of Medicine, Northwestern University, Chicago, IL,[2]Northwestern Univ. Feinberg School of Medicine, Chicago, IL,[3]Northwestern University - Chicago, Chicago, IL

N6-methyladenosine (m6A) is the most common modification involved in post-transcriptional regulation of RNA, affecting stability, splicing, and translation. M^{6}A modifications are regulated by methyltransferases (“writers”) and demethylases (“erasers”). Methyltransferase-like 3 (METTL3) is one of the m^{6}A writer complexes, catalyzing the m6A modification by transferring a methyl group to the N6 position of adenosine. METTL3 has been implicated in tumor development by modulating m^{6}A distribution and promoting the translation of oncogenic transcripts. Overcoming platinum resistance in ovarian cancer is a significant clinical challenge; therefore, we hypothesized that METTL3-mediated m^{6}A methylation contributes to resistance by altering cellular response to platinum drugs. We assessed m^{6}A and METTL3 expression after cisplatin treatment using RT-qPCR and western blotting. To evaluate their functional role, we measured the IC_{50} of cisplatin in ovarian cancer cell lines with METTL3 overexpression or knockdown. Additionally, the METTL3 inhibitor STM2457 was utilized to investigate the role of METTL3 in ovarian cancer, both in vitro and in vivo. Cisplatin treatment upregulated m^{6}A and METTL3 levels. METTL3 overexpression enhanced platinum resistance. Conversely, METTL3 knockdown or STM2457 treatment sensitized cells to cisplatin. RNA-seq analysis identified ADAM23 as a downstream target of METTL3. ADAM23 is a member of the ADAM (a disintegrin and metalloprotease) family involved in cell adhesion and extracellular matrix interactions. The protease is silenced in various tumors, including breast, gastric, pancreatic cancers, and gliomas. In ovarian cancer cell lines, ADAM23 expression was inversely correlated with METTL3 levels, showing decreased expression upon METTL3 overexpression and increased expression following METTL3 knockdown. Notably, cisplatin treatment led to reduced ADAM23 expression through METTL3 upregulation. Further analysis using SRAMP identified several very high confidence m6A modification sites on ADAM23 mRNA in human. These findings suggest that METTL3-mediated m^{6}A modifications, through regulation of ADAM23, may represent a novel therapeutic target in ovarian cancer.

#7486 SORL1 promotes mesothelial clearance and migration of ovarian cancer cells through regulating integrin trafficking.

Jasmine Jathan, Viktoriia Kolesnyk, Samantha Goncalves Novo, Miranda Mansolf, Yang Yang-Hartwich

Yale School of Medicine, New Haven, CT

Background: Peritoneal dissemination is a hallmark of advanced ovarian cancer and leading cause of poor patient prognosis. Ovarian cancer metastasis involves adhesion, invasion, and dynamic remodeling of cell-matrix interactions, where integrin trafficking plays a central role. The intracellular sorting receptor, SORL1 regulates receptor recycling and intracellular trafficking, with evidence linking its activity to oncogenic signaling in various cancers. Building on our prior findings that SORL1 modulates endosomal trafficking and recycling of EGFR1 and FGFR4 in ovarian cancer, this study aimed to investigate how SORL1 regulates ovarian cancer invasion and metastasis by modulating integrin trafficking and endosomal recycling. The therapeutic potential of inhibiting tumor peritoneal dissemination and metastasis in recurrent ovarian cancer by targeting SORL1 was also evaluated.
Methods:SORL1 expression was knocked down in patient-derived ovarian cancer cells using siRNA/shRNA. Tumor spheroid co-cultured with mesothelial cells were used to quantify cancer cell clearance efficiency. Integrin localization was examined by immunofluorescence co-staining with endosomal markers and confocal microscope imaging. Flow cytometry measured cell surface integrin levels with and without activation by fibronectin as an extracellular matrix ligand. Co-immunoprecipitation and proximity assays assessed SORL1-dependent interactions between integrins α3/β1 and the trafficking adaptor GGA1. Finally, the activity of a SORL1-blocking protein on inhibition of ovarian cancer migration and mesothelial clearance was evaluated.
Results:SORL1 knockdown significantly reduced ovarian cancer invasion and mesothelial clearance. Immunofluorescence staining analysis revealed enhanced internalization of integrin-a3 upon SORL1 inhibition, showing a shift from the plasma membrane to intracellular endosomal compartments. Consistently, the decreased surface levels of integrins after fibronectin activation in SORL1-knockdown cells indicated impaired integrin recycling. Increased interaction of integrins with GGA1 in SORL1 knockdown cells suggested accumulation in early and recycling endosomes. SORL1-blocking antibody inhibited ovarian cancer migration and mesothelial clearance. These findings demonstrate that loss of SORL1 disrupts integrin trafficking and surface expression, thereby impairing integrin-mediated adhesion and invasion in ovarian cancer.
Conclusion:SORL1 regulates integrin trafficking and recycling to maintain integrin-mediated adhesion and invasion in ovarian cancer cells. Loss of SORL1 disrupts these processes, limiting peritoneal dissemination. Targeting SORL1-dependent trafficking pathways may offer therapeutic potential to inhibit ovarian cancer metastasis.

#7488 C-Met and Integrin-αV regulated the response of desmoid cells to sorafenib.

Tianjie Pu[1], Jia Hu[1], Vladislav Tsiperson[2], Lakshana Senthilkumar[3], Narasimhan P. Agaram[1], Marco Vincenzo Russo[1], Ralph Garippa[1], Samuel Singer[1], Meera Hameed[1], Aimee Marie Crago[1]

[1]Memorial Sloan Kettering Cancer Center, New York, NY,[2]SUNY Downstate Health Sciences University, New York, NY,[3]Metropolitan Hospital Center, New York, NY

Background: The basis of sorafenib activity in desmoid tumors (DT) is poorly understood and predictive markers have not been defined. Activation of β-catenin transcription target c-ABL by PDGFRβ is associated with accumulation of EGR1 and increased sorafenib sensitivity in vitro, but in tumors, elevated EGR1 is associated with sorafenib resistance. Here we evaluate whether environmental signaling pathways outside of PDGFRβ modify EGR1 levels in DT and regulate sorafenib response.

Methods: A lentiviral shRNA screen targeting genes highly expressed in DT was performed in primary DT cell line (DES9525T). Potentially mitogenic genes encoding cell surface receptors were validated in DES8163T. Following treatment with drugs, shRNA directed at MET/ITGAV, HGF or vitronectin, cell proliferation, gene expression and protein analysis were assayed using CyQuant, RT-PCR and immunoblot, respectively. Synergy to drug treatments was assessed using Synergyfinder web (v3.0).

Results: The custom screen identified both MET and ITGAV as affecting DT cell proliferation (35 and 31% decrease in knock-downs [KDs], respectively, $p \leq 0.01$). Supplementation of DT cell cultures with HGF or vitronectin conversely promoted desmoid proliferation (1.9 and 1.7-fold, respectively, $p \leq 0.01$) and increased the IC_{50} of sorafenib in DT cells (from 5.2 and 5.7μM to 7.3 and 7.6μM). Growth of DT cells on vitronectin-coated plates was associated with increased phosphorylation of FAK but also PDGFRβ, ERK1/2 and the canonical c-ABL target CrkL; vitronectin exposure led to EGR1 accumulation in cells. ITGAV KD or treatment of cells with the FAK inhibitor defactinib abrogated this response and increased cell sensitivity to sorafenib with combined sorafenib/defactinib treatment having a synergistic effect on DT proliferation (HAS synergy score 19). Stimulation of cells with HGF also resulted in phosphorylation of c-MET, AKT, ERK1/2, and CrkL, led to EGR1 accumulation and increased FAK phosphorylation consistent with reported HGF/c-MET role in integrin signaling regulation; this was inhibited by MET KD. Treatment of DT cells with MET inhibitor tivantinib was additive with sorafenib while HGF supplementation was associated with increased synergy score when assessing combined sorafenib and FAK inhibitor defactinib (HAS synergy score 12 vs. 15).

Conclusions: Together, these findings demonstrate that HGF/MET and integrin-αV/FAK signaling each promote DT proliferation and sorafenib resistance. This is likely related to activation of downstream ERK/EGR1 in a manner not targetable by the PDGFRβ inhibitor. C-MET and integrin signaling pathway components may represent appropriate molecules to assess as markers predictive of sorafenib response in DT patients.

#7489 Unraveling a new ECM stiffening function of the axon guidance molecule Netrin-1.

Gaetan THIVOLLE LIOUX, Laurent Fattet, PATRICK MEHLEN

Cancer Research Center of Lyon, Lyon, France

State of the art The extracellular matrix (ECM) is a complex and dynamic network composed of core structural proteins and matrisome-associated components. Under physiological conditions, ECM homeostasis contributes to the maintenance of natural tissue stiffness. However, disruption of this balance can lead to abnormal stiffening, a hallmark observed in various pathological conditions, including fibrosis and cancer. Our laboratory investigates the role of the dependence receptor ligand Netrin-1 (NTN1), a neuronal guidance protein predominantly expressed during early developmental stages. Intriguingly, NTN1 is frequently re-expressed in tumors, where its presence has been correlated with increased ECM stiffness. As such, our research aims to elucidate the role of NTN1 in ECM remodelling and stiffening.
Methodology and resultsUsing atomic force microscopy (AFM) on inert Matrigel matrices, we observed a marked increase in stiffness upon supplementation with recombinant Netrin-1 (rNTN1). This stiffening effect was reversed by NP137, a monoclonal antibody targeting NTN1. Structural analyses via immunofluorescence staining for laminin-111 and rNTN1, alongside scanning electron microscopy (SEM), revealed a significant reduction in pore size in the presence of rNTN1. Complementary in silico analysis using PEPPI software indicated strong interactions between NTN1 and key ECM components such as Nidogen and Laminin.
PerspectivesTo validate these predicted interactions, we performed biolayer interferometry with various ECM proteins. Furthermore, 3D cultures models of MCF10A normal mammary epithelial cells exposed to NTN1 displayed a phenotypic transition toward a more mesenchymal and invasive state. Interestingly, knockdown of NTN1 receptors did not prevent this phenotypic shift, suggesting a novel receptor-independent function for NTN1 in promoting cell invasiveness through direct modulation of ECM stiffness. Ongoing structural analyses are being conducted on fibroblast-derived matrices, with and without endogenous Netrin-1 expression, to evaluate its potential remodeling effects on collagen IV and fibronectin networks. In parallel, these matrices are utilized in functional assays to investigate how Netrin-1 ECM impact, influences cellular behaviours and transcriptional activity, using a range of experimental approaches.

#7490 MYBBP1A is part of a mechanically modulated system that alters breast cancer metastatic potential by regulating focal adhesion.

Xi Chen, Kent W. Hunter

National Cancer Institute, Bethesda, MD

MYB binding protein 1a (MYBBP1A) was first identified for its ability to bind and repress the proto-oncogene c-MYB. Most research focuses on its role in regulating ribosomal RNA (rRNA) transcription; However, its impact on metastasis remains unclear. Analysis of TCGA breast cancer patient data reveals higher MYBBP1A levels are associated with shorter survival times in breast cancer patients, while a Mybbp1a knockdown (KD) gene signature, generated by machine learning, indicates significantly improved patient survival outcomes. Using mouse spontaneous metastasis model, we confirmed that MYBBP1A loss suppresses breast cancer cell metastasis. Further analysis revealed that Mybbp1a KD cells exhibit robust abnormalities in cell morphology, which is associated with reduced cell invasion and disrupted F-actin organization. Cell morphological changes are partially rescued in type I collagen-coated high stiffness extracellular matrix (ECM) culture, indicating MYBBP1A could be part of a mechanically modulated system that alters breast cancer metastatic potential. This is supported by the observation that MYBBP1A levels exhibit a gradually increase in response to the increases of ECM stiffness, which is coupled with increased cell invasion capacity. Mechanical stimuli from the tumor microenvironment play an important role in mediating breast cancer metastasis. The pathways that cancer cells use to sense and leverage mechanical cues are largely driven by the assembly and disassembly of focal adhesions, which regulate the dynamics of F-actin stress fibers and couple F-actin with the extracellular matrix (ECM) to transduce mechano-signaling to nucleus and regulate cell motility. Focal adhesion can be visualized by immunofluorescence (IF) staining of phospho-FAK (focal adhesion kinase) plaques at the points of F-actin filaments and be measured by FAK level. Our data shows focal adhesion is reduced in Mybbp1a KD cells, evidenced by weakened level and number of phospho-FAK clustering at the points of F-actin. In parallel, overexpression of FAK rescues breast cancer cell phenotypes and partially restores the reduced cell metastasis capacity observed in Mybbp1a KD. In exploring the function of MYBBP1A in regulating mechanosignal transduction, we found that SUN2, an important component of the Linker of Nucleoskeleton to the Cytoskeleton (LINC) complex, was stripped from nuclear envelop and relocated to heterochromatin dense areas, upon Mybbp1a KD. That breaks the connection between nucleus and cytoskeleton and could explain the reduced focal adhesion assembly following Mybbp1a KD. In the future, we will keep studyingFuture work will focus on the role of MYBBP1A as part of a mechanically modulated complex that is important in promoting breast cancer metastasis.

#7492 Preclinical osimertinib-resistant mouse models for advancing third-generation EGFR-TKI drug development.

Hongyan Sun, Yinuo Wang, Shiying Guo, Yujing Zhang, Huixin Yang, Xiang Gao

GemPharmatech Co., Ltd., Nanjing, China

The efficacy of Osimertinib, a third-generation EGFR tyrosine kinase inhibitor used in non-small cell lung cancer (NSCLC), is well established through clinical trials showing prolonged patient survival with EGFR-TKI therapy. However, a key clinical challenge arises from acquired resistance, frequently mediated by EGFR C797 mutations—notably the triple mutations Del19/T790M/C797S and L858R/T790M/C797S. To systematically investigate Osimertinib resistance and enable the testing of new therapeutic candidates, we have developed a panel of resistant models in both in vitro and in vivo settings. Using the human lung adenocarcinoma NCI-H1975 cell line—which carries the dual EGFR L858R/T790M mutations, we employed precise gene editing to introduce the C797S mutation, generating an isogenic triple-mutant subline (H1975 L858R/T790M/C797S). This model recapitulates the genetic profile of patients who have developed resistance following Osimertinib treatment. In addition to C797S-mediated resistance, we applied prolonged in vitro exposure of multiple cell lines to escalating Osimertinib concentrations, inducing acquired resistance independent of C797 mutations. Resistance was quantitatively confirmed through IC50 assays, which revealed a marked increase in Osimertinib tolerance. These models were further validated in vivo for tumor growth and drug response, confirming their functional resistance. We now possess well-characterized Osimertinib-resistant cell lines, including triple-mutant NCI-H1975 and PC-14 variants, providing essential platforms for dissecting resistance mechanisms and accelerating the development of next-generation treatments.

#7493 Novel preclinical models for evaluating checkpoint inhibitor resistance.

Hongyan Sun, Yan Wang, Fang Zhu, Yujing Zhang, Huixin Yang, Xiang Gao

GemPharmatech Co., Ltd., Nanjing, China

Cancer immunotherapy targeting the PD-1/PD-L1 axis has revolutionized oncology, producing durable responses in a range of malignancies. However, a significant number of patients either fail to respond or develop resistance following initial success. There is a critical need for robust preclinical models of anti-PD-1 resistance to elucidate underlying mechanisms and inform new therapeutic strategies. Known resistance mechanisms include impaired tumor antigen presentation, downregulation of MHC class I molecules, alterations in IFN-γ signaling, and an immunosuppressive tumor microenvironment. To address this need, GemPharmatech has developed three distinct preclinical models of anti-PD-1 resistance:

Drug-Induced Resistance Model: CT26 tumors were engrafted in BALB/c-hPD-1 mice and subjected to repeated cycles of anti-PD-1 treatment (KEYTRUDA®) and re-implantation of non-responding tumors. This iterative in vivo selection pressure generated a stable anti-PD-1 resistant model.

Genetically Engineered Model: Isogenic anti-PD-1 resistant models were created by knocking out genes associated with resistance (B2Mor STK11) in the CT26 cell line.

Primary Resistance Model. Characterization of the drug-induced model confirmed a stable resistant phenotype in vivo, with resistant CT26 cells exhibiting accelerated tumor growth compared to parental cells. RNA sequencing identified differentially expressed genes, offering insights into potential resistance pathways. In the engineered STK11knockout model, loss of STK11 abrogated the response to anti-PD-1 therapy. This was associated with a reduced infiltration of CD8+ T cells, a significant accumulation of myeloid-derived suppressor cells (MDSCs) in the tumor microenvironment, and decreased PD-L1 expression on tumor cells, implicating immunosuppressive mechanisms in the resistance phenotype. In summary, these validated preclinical models of anti-PD-1 resistance serve as powerful tools for deconstructing resistance mechanisms, facilitating biomarker identification, and guiding the development of novel combination therapies.

#7494 Development of enhanced enhertu-resistant HER2-positive breast cancer models for ADC resistance research.

Hongyan Sun, Yuan Fang, Fang Zhu, Yujing Zhang, Huixin Yang, Xiang Gao

GemPharmatech Co., Ltd., Nanjing, China

Antibody-drug conjugates (ADCs) combine the precision of a monoclonal antibody with a potent cytotoxic payload to selectively target cancer cells and represent a promising strategy for targeted cancer therapy. Enhertu (trastuzumab deruxtecan, DS-8201), an ADC targeting HER2-positive cancers, has achieved remarkable clinical efficacy and set a new benchmark for anti-HER2 ADCs, yet acquired resistance remains a major challenge. To elucidate resistance mechanisms and support development of next-generation ADCs, we established a stepwise preclinical platform for Enhertu resistance using the HER2-positive breast cancer cell line JIMT-1. JIMT-1 tumor bearing mice were first subjected to repeated *in vivo* Enhertu dosing, and subsequent residual tumors were harvested to derive a resistant cell line. This resistant cell line exhibited stable resistance to Enhertu both *in vitro* and *in vivo. In vitro*, resistant cells showed a right-shifted IC50 to the DXd payload, while flow cytometry and immunohistochemistry demonstrated the line maintained HER2 expression. RNA sequencing and whole-exome sequencing revealed upregulation of ABCG2 and other transporters, indicating a payload-centric resistance mechanism driven by altered payload sensitivity and enhanced drug efflux rather than target downregulation. To generate a more stringent model that better reflects long-term, high-intensity clinical exposure, the resistant cell line was re-implanted and serially passaged *in vivo* under high-dose Enhertu treatment, yielding an “enhanced” high-dose resistant tumor model. These enhanced tumors remained HER2-positive by IHC and displayed transcriptional changes similar to the resistant cell line, including pronounced ABCG2 upregulation and broader alterations in genes related to drug transport and cell-cycle regulation. Together, these Enhertu-resistant models offer a practical system to investigate resistance mechanisms that may not yet be evident in clinical samples and to identify candidate biomarkers and therapeutic targets. These cell lines also enable preclinical testing of biomarker-guided combination therapies and next-generation ADCs designed to overcome Enhertu resistance in HER2-positive malignancies.

#7495 Modeling of de novo and experimentally induced acquired resistance to trastuzumab deruxtecan in HER2-positive patient-derived xenografts.

Hongyan Sun, Xiaoliu Yang, Shiying Guo, Yujing Zhang, Huixin Yang, Xiang Gao

GemPharmatech Co., Ltd., Nanjing, China

Trastuzumab Deruxtecan (T-DXd) has improved outcomes for HER2-positive cancers, yet intrinsic and acquired resistance present significant clinical hurdles. The mechanisms of resistance are diverse and incompletely understood, and optimal subsequent therapies for T-DXd-resistant patients remain undefined. To address this, we established a matched pair of patient-derived xenograft (PDX) models that recapitulate these critical clinical scenarios. Through in vivo efficacy screening of our HER2-positive PDX bank, we identified a unique model demonstrating de novo resistance to T-DXd, showing minimal tumor regression upon treatment. Separately, we generated a model of acquired resistance by subjecting an initially sensitive HER2-positive PDX to repeated cycles of T-DXd in vivo. This model recapitulated the clinical progression from initial response to treatment failure. This paired set of models provides a powerful, controlled system for a direct comparative analysis of resistance mechanisms. These well-characterized PDX models represent a critical resource for the oncology community. They enable the direct comparison of molecular mechanisms driving both intrinsic and treatment-induced resistance in a controlled, in vivo setting. This platform is immediately applicable for investigating alterations in HER2 biology, payload delivery, and bypass signaling pathways, and is ideally suited for evaluating novel therapeutic strategies aimed at overcoming T-DXd resistance.

: Tumor Heterogeneity
Poster Session

#7499 Genetic evolution of sarcomatoid/rhabdoid de differentiation in renal cancers..

Natalie R. Abuelsamen, Kate I. Glennon, Mustafa Soytas, Madeleine Arseneault, Peixi Liu, eleonora scarlata, fadi brimo, Simon Tanguay, Yasser Riazalhosseini

Human Genetics, McGill University, Montreal, QC, Canada

Background: The presence of sarcomatoid and rhabdoid (SR) differentiation is associated withpoor prognosis in renal cell carcinomas (RCCs), yet molecular underpinnings of SR patterns areunderstudied. While advances in cancer genomics have shed light on substantial intratumoralheterogeneity (ITH) in RCC, the evolutionary dynamics fueling disease progression, andemergence of SR dedifferentiation has remained poorly understood.
Methods: We conducted multi-region whole-exome sequencing (WES) of 156 tumor samples,representing S/R histological features and matched clear-cell or papillary tumor areas from 46RCC patients. Somatic variant and copy number analysis was performed to identify distinctsubclonal populations within each sample. Using PyClone and ClonEvol, we modeled thetrajectories of subclonal evolution within each patient, capturing the emergence and progressionof shared and site-specific subclones across tumor regions and metastatic sites.
Results: We observed significant ITH across RCC subtypes. Each individual sample exhibitedseveral cell populations with distinct profiles of subclonal somatic mutations. Temporal orderingof subclones revealed the emergence of new subclonal cell populations during the transition to S/Rdifferentiation. We constructed phylogenetic trees for each individual patient, in which theemergence of subclones driving S/R features exhibited both monoclonal and polyclonal seedingpatterns, suggesting that there may be several evolutionary routes to these changes.
Significance: Monoclonal tumors showed a more uniform path of evolution, while polyclonaltumors exhibited greater genetic complexity, reflecting the diversity of tumor progressionpatterns. These findings underscore the importance of targeting truncal mutations in early-stagetumors and monitoring subclonal evolution in aggressive phenotypes.
Disclosures: The authors have no conflicts to disclose.

#7500 Dependent lineage regulatory programs in TP53-mutated acute myeloid leukemia revealed through deep single-cell multi-omic profiling of patient samples.

Felix A. Radtke[1], Bijay S. Jaiswal[2], Gonzalo Lopez[3], Junfei Zhao[4], Sagnik Banerjee[5], Daiane Hemerich Brennan[4], Yilin Zhao[6], Verena Korber[1], Marlen Metzner[1], Rachel Moore[1], Bilyana Stoilova[1], Batchimeg Usukhbayar[1], David Cruz Hernandez[1], Maria Ortiz Estevez[7], Aimee O'Donohue[8], Daniel Lopes de Menezes[2], Rajasekhar NVS Suragani[9], Anita K. Gandhi[8], Paresh Vyas[1]

[1]MRC Molecular Haematology Unit, Radcliffe Department of Medicine, Weatherall Institute of Medicine, University of Oxford, Oxford, United Kingdom,[2]Translational Development, Bristol Myers Squibb, Brisbane, CA,[3]Informatics and Predictive Sciences, Bristol Myers Squibb, Cambridge, MA,[4]Informatics and Predictive Sciences, Bristol Myers Squibb, Summit, NJ,[5]Informatics and Predictive Sciences, Bristol Myers Squibb, San Diego, CA,[6]Informatics and Predictive Sciences, Bristol Myers Squibb, Seattle, WA,[7]Informatics and Predictive Sciences, Bristol Myers Squibb, Sevilla, Spain,[8]Translational Development, Bristol Myers Squibb, Summit, NJ,[9]Translational Development, Bristol Myers Squibb, Cambridge, MA

TP53-mutated (*TP53*m) Acute myeloid leukemia (AML) represents a clinically intractable and biologically distinct disease. To study the molecular basis of this disease through hemopoiesis, we integrated single-cell RNA-seq (10x and long-read Oxford Nanopore sequencing) with open chromatin profiles (scATAC-seq), whole-genome (WGS) to capture structural variants and copy number alterations, and deep panel DNA sequencing from bone marrow samples taken from a cohort of 49 *TP53*m AML patients, 7 *TP53* wild type (WT) AML patients, and 4 healthy donors.

Phased genotyping plus WGS revealed biallelic loss to be associated with intrachromosomal breakage, whereas monoallelic loss favored numerical chromosomal alterations. *TP53*m clones pervaded stem/progenitors and myeloerythroid lineages but were proportionally depleted in mature lymphocytes. While co-occurring AML driver mutations influence the lineage biases of *TP53m* clones, we observed expansion of HSC/MPP, LMPP, and late erythroid compartments.

In HSC/MPP dominant disease, *TP53m* cells displayed suppression of translational and mitochondrial-respiratory programs, with enrichment of a “p53-LSC” signature linked to chronic inflammatory stress. This suggests adaptation through metabolic quiescence, conferring persistence under inflammatory pressure. In LMPP-dominant expansion, we observed enriched MYC/E2F targets. Transcriptomic neighborhood analysis with pseudotime showed the erythroid compartment to be heterogeneous, with less mature basophilic cells enriched for *TP53*m clones, whereas more mature orthochromatic cells were enriched for *TP53*wt clones, nominating this transition as a tipping point for differentiation delay/arrest. Consistently, in erythroid dominant patients, late-stage erythroid cells demonstrated impaired GATA-1 and KLF1 (erythroid TFs) activities, and *TP53*m clones showed heightened GATA2, SPI1, and CEBPD regulon activity. *TP53*m versus *TP53*wt clones in erythroid differentiation showed heightened transcriptional activity of the EIF2AK1(HRI)→eIF2α mediated integrated stress response (ISR). Differential expression analysis within the aforementioned erythroid compartment showed ISR activation in *TP53m* clones; *SESN2*, *DDIT4*, and *DDIT3*/CHOP significantly up, with *ATF3*, and *XBP1*, up-trending, together with increased *GATA2*. Replication/mitochondrial-handling components (*GINS2*, *RPA3*, *ABCB8*) were significantly downregulated. These data together support a model in which deficient GATA-1/KLF1 function underpins the intra erythroid arrest of *TP53*m clones possibly due to activated HRI-ISR circuitry.

These detailed molecular differentiation stage specific analyses of *TP53*m AML provide mechanistic insights and a platform for functional and synthetic lethal studies to specifically target *TP53*m leukemic cells.

#7502 Spindle assembly checkpoint integrity determines sensitivity to KIF18A inhibition in small-cell lung cancer.

Chiori Tabe, Rajesh Kumar, Yang Zhang, Yue Huang, Ajit Kumar Sharma, Roshan L. Shrestha, Anish Thomas

National Cancer Institute, National Institutes of Health, Bethesda, MD

Small-cell lung cancer (SCLC) is characterized by extensive chromosomal instability (CIN) and rapid proliferative turnover, yet the cellular vulnerabilities arising from these features remain insufficiently defined. KIF18A, a kinesin-8 family motor protein that regulates microtubule plus-end dynamics and facilitates chromosome alignment at metaphase, has been recently emerged as a selective dependency in CIN-high tumors. Here, we investigated the role of KIF18A in SCLC, a prototypical CIN-high malignancy. Transcriptomic analyses revealed that KIF18A expression was markedly higher in SCLC compared with non-small-cell lung cancer (NSCLC) subtypes and positively correlated with CIN-related gene signatures (CES, CIN70) and proliferation markers such as MKI67 and PCNA. However, neither KIF18A transcript nor protein levels were predictive of responsiveness to the selective KIF18A inhibitor AM-9022 across a diverse panel of SCLC cell lines, indicating that dependency is not governed by expression levels. Comparative RNA-sequencing of AM-9022-sensitive and -resistant SCLC cell lines demonstrated distinct mitotic gene-expression programs. Sensitive cells showed enrichment of pathways associated with mitotic spindle assembly kinetochore organization, and spindle assembly checkpoint (SAC) activation. Consistently, immunofluorescence analysis revealed that resistant cells exhibited diminished expression and impaired kinetochore localization of the SAC components MAD1 and BUBR1, indicative of defective SAC signaling. Live-cell imaging confirmed that KIF18A inhibition induced pronounced mitotic arrest and apoptotic cell death in SAC-proficient cells, whereas SAC-deficient lines bypassed prolonged arrest and proceeded through aberrant mitosis with chromosome segregation errors, thereby escaping cell death. Collectively, these findings establish SAC competency as a critical determinant of vulnerability to KIF18A inhibition in SCLC. KIF18A blockade triggers catastrophic mitotic arrest and apoptosis in SAC-proficient, CIN-high SCLC cells, while SAC deficient counterparts tolerate spindle perturbations and continue proliferating despite persistent chromosomal errors. This study defines mitotic checkpoint integrity as both a mechanistic basis and a predictive biomarker for therapeutic response to KIF18A inhibition, providing a conceptual framework for exploiting mitotic control in chromosomally unstable SCLC.

#7503 Spatio-temporal analysis of EGFR inhibitor resistant tumor epithelial clusters.

Shuichi Watanabe[1], Yoshiyuki Suehara[1], Masachika Ikegami[1], Soohwan Park[1], Yo Kimura[1], Toshihide Ueno[1], Takuo Hayashi[2], Hiroyuki Mano[3], Kazuya Takamochi[4], Shinji Kohsaka[1]

[1]Division of Cellular Signaling, National Cancer Center Japan, Tokyo, Japan,[2]Department of Diagnostic Pathology, Juntendo University Hospital, Tokyo, Japan,[3]National Cancer Center Japan, Tokyo, Japan,[4]General Thoracic Surgery, Juntendo University Hospital, Tokyo, Japan

[Background]Drug-tolerant persister (DTP) cells are a reversible drug-insensitive tumor subpopulation implicated in minimal residual disease (MRD) and recurrence. However, their emergence mechanisms and therapeutic vulnerabilities remain unclear. We previously tracked clonal dynamics in vivo using genetic barcodes and showed that expansion of specific clones contributes to the resistance of EGFR inhibitors. Here, we analyzed non-small cell lung cancer treated with EGFR inhibitors to (1) identify treatment-resistant tumor cell populations and (2) elucidate spatial mechanisms underlying DTP cell emergence.
[Methods]Tumor samples from the PIT3 trial (UMIN000026197) were analyzed before and after the neoadjuvant EGFR inhibitor therapy. Single-cell (sc) RNA-seq (n = 8) and Visium HD spatial transcriptomics (n = 10) were performed. Spatial datasets were processed using HueTracer (https://github.com/MANO-B/HueTracer), enabling extraction of single-cell-level expression profiles and integration with scRNA-seq.
[Results]Integrated scRNA-seq analysis (8 specimens, 16,419 cells) identified multiple tumor epithelial clusters, including an EGFR-resistant subcluster enriched in poor responders. This subcluster showed a higher proportion of G1-phase cells, reduced EGFR, and elevated EMT-related genes, suggesting treatment-resistant phenotypes. Rare cells with similar transcriptional features were also detected in responders, indicating the presence of surviving DTP-like cells.
Spatial transcriptomic analysis (20 specimens, 2,415,876 cells) identified tumor clusters and treatment-responsive regions characterized by island-like residual lesions with necrosis and desmoplasia. Small numbers of surviving cells were designated as DTP candidates and compared with other tumor epithelial cells. Across five cases, meta-analysis of differentially expressed genes revealed consistent upregulation of inflammation- and plasticity-related genes, including *ILR-X*, *TF-X*, *LAMB3*, and *TXLNB* (FDR < 0.05). GSEA showed enrichment of TNF-α/NFκB signaling, interferon response, EMT, and tissue remodeling pathways, indicating a shared inflammatory and plasticity-enhanced state in DTP candidates.
[Conclusion]Single-cell and spatial analyses demonstrate that DTP-like cells persisting after EGFR inhibitor therapy exhibit a shared molecular phenotype characterized by heightened inflammation and epithelial plasticity. These features may underlie microscopic residual disease capable of driving post-treatment recurrence, supporting the concept of DTP cells as a potential therapeutic target.

#7504 Do secondary MSH3/MSH6 alterations define an immune-modulatory subtype of MSI gastric cancer?.

Marika Milan[1], Daniela Conticelli[1], Marco Volante[2], Claudia Orru[2], Emanuela Boccuni[2], Simona Corso[2], Silvia Giordano[2]

[1]Candiolo Cancer Institute-IRCCS, Candiolo, Italy,[2]University of Turin, Turin, Italy

Gastric cancer (GC) is one of the leading causes of cancer-related morbidity and mortality worldwide. Molecular classification stratifies GC into four major subtypes: Epstein-Barr virus-positive, microsatellite instability (MSI), genomically stable, and chromosomal instability. Among these, MSI GC—representing approximately 8-25% of cases—is characterized by high mutational burden resulting from defects in the mismatch repair (MMR) system. For early-stage cancer the main therapeutic approaches include surgery, along with chemotherapy. Recently, immune checkpoint inhibitors, administered alone or in combination with other treatments, have demonstrated potent antitumoral activity in some subgroups of GC; among the responders are MSI tumors, which are associated with a better clinical prognosis compared with microsatellite-stable (MSS) ones. However, only around 50% of MSI GC obtain a benefit from immunotherapy. This study aims to elucidate the molecular mechanisms underlying the different ability of MSI CG to respond to immunotherapy, focusing on how alterations in mismatch repair genes can contribute to mutational burden, neoantigen formation, and immune activation. Taking advantage from our molecularly annotated platform including around 1000 primary tumors and 250 patient-derived xenografts (PDXs), we performed a multilevel molecular characterization to define MMR status and to functionally evaluate how specific MMR alterations influence immune responsiveness in vivo. Our preliminary data indicate that gastric cancers are characterized by intratumoral heterogeneity of the MMR, which may manifest as primary heterogeneity, defined by the coexistence of MSS and MSI regions, or as secondary heterogeneity, where MLH1 silencing is frequently accompanied by the additional loss of another MMR component, typically MSH3 or MSH6.This loss often results from frameshift mutations at mononucleotide repeat hotspots. These alterations, potentially reversible, have been linked to immune evasion. Notably, our findings indicate that secondary MSH3 and MSH6 mutations represent a frequent event in gastric MSI tumors (56% of MSI GCs display MSH3/MSH6 frameshift mutations), and we aim to explore their potential clinical implications. Future directions include dissecting the molecular pathways through which alterations in MMR genes generate subclonal neoantigenic diversity, ultimately shaping tumor-immune system interactions. A deeper understanding of these processes may inform the development and refinement of immunotherapeutic strategies for MSI gastric cancer.

#7505 Single-cell transcriptomics identifies distinct EPCAM-low and EPCAM-negative epithelial populations with aggressive phenotypes in hormone-receptor positive breast cancer.

Elise Di Lena[1], Alyssa Victoria Francis[2], Atilla Omeroglu[1], Sarkis Meterissian[1], Luke McCaffrey[1]

[1]McGill University, Montreal, QC, Canada,[2]Medicine, McGill Univ. Goodman Cancer Ctr., Montreal, QC, Canada

The intra-tumoral heterogeneity of hormone-receptor positive (HR+) breast cancers is incompletely known. The purpose of this study was to perform an unbiased characterization of the epithelial landscape in untreated, early-stage hormone-receptor positive (HR+) breast cancers. We performed single-cell RNA sequencing on over 60,000 unsorted cells from 6 primary HR+ tumors. A standardized bioinformatic pipeline was used for clustering, differential gene expression, and pathway analysis. Key findings were validated spatially using multiplexed immunofluorescence and Imaging Mass Cytometry. Our unbiased analysis revealed a complex epithelial landscape. The EPCAM-high cells, representing the largest luminal compartment, were highly heterogeneous and clustered into multiple patient-specific ("private") phenotypes that were strongly ER-positive and made up a tumor fingerprint unique to each patient. In contrast, we identified two distinct "public" phenotypes, present across multiple patients, with significantly reduced or absent EPCAM expression. The first population (EPCAM-low) expressed a unique pro-inflammatory signature enriched for interferon-gamma response and KRAS signaling pathways. The second population (EPCAM-negative) clustered distantly from all other epithelial cells and was enriched for aggressive, stem-like pathways, including TNF-alpha signaling via NF-kB and Hedgehog signaling. Both EPCAM-low/negative populations were hormone-receptor low. The EPCAM-high compartment is a heterogeneous mix of patient-specific populations, while the EPCAM-low/negative compartment contains distinct, shared populations with aggressive, non-targetable phenotypes. These findings reveal a pre-existing cellular reservoir that may drive de novo resistance to endocrine therapy and contribute to late recurrence. This work also highlights that common marker-based epithelial sorting methods may fail to capture the full heterogeneity of HR+ breast cancer.

#7506 CEACAM1-dominant molecular program drives immune escape in EGFR-mutant lung adenocarcinoma.

Jianyu Li, Qinglin Wang, Tongyan Liu, Siwei Wang, Rong Yin

Department of Thoracic Surgery, Jiangsu Cancer Hospital, The Affiliated Cancer Hospital of Nanjing Medical University, Nanjing, China

Background: In East Asian populations, EGFR-mutant lung adenocarcinoma (LUAD) represents the predominant molecular subtype, yet even the two most common variants, exon 19 deletions (19del) and L858R, exhibit substantial molecular and clinical heterogeneity whose determinants of malignant progression remain poorly defined. A subset of EGFR-mutant LUADs exhibits an immune-escape phenotype with poor tyrosine kinase inhibitor (TKI) response, highlighting the need to define EGFR-driven malignant programs and intercellular mechanistic crosstalk.

Methods: We performed single-cell RNA sequencing (scRNA-seq) on $EGFR^{19del}$ and $EGFR^{L858R}$ genetically engineered mouse models (GEMMs; n = 20) and on an in-house human EGFR-mutant LUAD cohort spanning early to advanced stages (n = 33), of which a subset had paired spatial transcriptomics (n = 8). Consensus non-negative matrix factorization (cNMF) was applied to derive metaprograms, which were correlated with immune composition, spatial niches, and clinical outcomes. Mechanistic and therapeutic relevance were evaluated using organoid co-cultures, blocking CEACAM1, and *in vivo* studies combining the anti-CEACAM1 antibody CM24 with TKIs and immune checkpoint inhibitors in TKI-resistant models.

Results: Analyses revealed immune-related malignant programs and a proliferation-associated program. Intriguingly, a CEACAM1-dominant metaprogram, termed CEACAM1-MP, emerged as an invasive subtype indicator independent of EGFR mutant status and was consistently associated with early progression and immune escape. A high CEACAM1-MP score correlated with worse overall survival (HR = 2.39, $P < 0.001$) in multiple datasets. CEACAM1-MP^{high} tumor cells showed reduced effector $CD8^+$ T-cell infiltration but strong interactions with $SPP1^+TIM3^+$ tumor-associated macrophages (TAMs), predominantly via CEACAM1-TIM3. Spatial transcriptomics revealed that CEACAM1-MP^{high} tumor cells localized to perivascular regions where they co-accumulated with $SPP1^+TIM3^+$ TAMs, forming an immunosuppressive niche that promoted M2-like polarization. The anti-CEACAM1 antibody CM24 impaired CEACAM1-MP^{high} tumor cell proliferation. In TKI-resistant models, CM24 combined with TKIs and PD-1 blockade significantly delayed tumor growth, with a tumor growth inhibition rate of 68% ($P < 0.01$).

Conclusions: This study identifies a CEACAM1-MP as an important driver of early invasion and immune escape in EGFR-mutant LUAD, defined by a perivascular niche and tight crosstalk with $SPP1^+TIM3^+$ TAMs. CEACAM1-MP provides a novel indicator to identify high-risk EGFR-mutant patients, while targeting CEACAM1 represents a promising strategy for refractory lung cancer.

#7507 Genomic evolution and heterogeneity of von Hippel-Lindau (VHL)-associated clear cell renal cell carcinoma revealed by multi-region whole-genome sequencing.

Francesca Corea[1], Husayn A. Pallikonda[2], Scott T. C. Shepherd[2], Isaline Rowe[3], Alessandro Larcher[3], Andrea Salonia[1], Samra Turajlic[2], Thomas J. Mitchell[4], Rosa Bernardi[5], Umberto Capitanio[3]

[1]Universita Vita-Salute San Raffaele, Milano, Italy,[2]The Francis Crick Institute, London, United Kingdom,[3]Comprehensive Cancer Center/Unit of Urology; URI, IRCCS San Raffaele Hospital, Milano, Italy,[4]Early Cancer Institute, University of Cambridge, Cambridge, United Kingdom,[5]Comprehensive Cancer Center, IRCCS San Raffaele Hospital, Milano, Italy

Intra-tumor heterogeneity (ITH) of somatic mutations is a hallmark of sporadic clear cell renal cell carcinoma (ccRCC). In contrast, the extent and nature of ITH in hereditary (VHL-associated) ccRCC remain poorly characterised, primarily due to the rarity of these tumors. This study aims to comprehensively characterise this heterogeneity and elucidate its evolutionary dynamics and biological relevance. To investigate intra- and inter-tumor heterogeneity in VHL-associated ccRCC, we performed multi-region whole-genome sequencing (WGS) of 23 primary tumor biopsies obtained from four spatially distinct regions of six small (≤3 cm) renal tumors across two patients carrying pathogenic germline *VHL* mutations. Somatic single-nucleotide variants (SNVs) and copy number alterations (CNAs) were analysed to reconstruct the genomic histories of these tumors. We found that all tumors were clonally independent, each harboring distinct sets of somatic variants and chromosomal copy number alterations, including the characteristic chromosome 3p loss. Within individual tumors, copy number profiles were homogeneous across regions, suggesting early acquisition of these events. Subclonal diversification of somatic SNVs was detected in all tumors. Notably, in one patient, two of the three analysed tumors displayed pronounced ITH, with most mutations being unique to a single region. Moreover, markedly distinct patient-specific molecular profiles emerged, characterised by divergent driver events and copy number landscapes that correlated with differences in their clinical grades. Although preliminary, these findings provide new insights into the genomic heterogeneity of VHL-associated ccRCC, advancing our understanding of how inherited kidney cancers develop and diversify, and potentially informing improved clinical management of patients with VHL disease.

#7509 A spatiotemporal cancer cell trajectory underlies glioblastoma heterogeneity.

Grant De Jong[1], Fani Memi[1], Tannia Gracia[1], Olga Lazareva[2], Richard Mair[3], Sam Behjati[1], Oliver Stegle[2], **Omer Bayraktar**[1]

[1]Wellcome Sanger Institute, Cambridge, United Kingdom,[2]German Cancer Resarch Centre, Heidelberg, Germany,[3]Cancer Research UK Cambridge Institute, Cambrige, United Kingdom

Cancer cells display highly heterogeneous and plastic states in glioblastoma, an incurable brain tumour. However, how these malignant states arise and whether they follow defined cellular trajectories across tumours is poorly understood. Here, we generated a deep single cell and spatial multi-omic atlas of human glioblastoma that pairs transcriptomic, epigenomic and genomic profiling of 12 tumours across multiple regions. We identify that glioblastoma heterogeneity is driven by spatially-patterned transitions of cancer cells from developmental-like states towards those defined by a glial injury response and hypoxia. This cellular trajectory regionalises tumours into distinct tissue niches and manifests in a molecularly conserved manner across tumours as well as genetically distinct tumour subclones. Moreover, using a new deep learning framework to map cancer cell states jointly with clones in situ, we show that tumour subclones are finely spatially intermixed through glioblastoma tissue niches. Finally, we show that this cancer cell trajectory is intimately linked to myeloid heterogeneity and unfolds across regionalised myeloid signalling environments. Our findings define a stereotyped trajectory of cancer cells in glioblastoma and unify glioblastoma tumour heterogeneity into a tractable cellular and tissue framework.

#7510 Molecular and clinical correlates of extrachromosomal DNA in oral squamous cell carcinoma.

Lucas Penny[1], Hugh Kim[2], Jeffrey Bruce[1], Matthew Waas[1], Meinusha Govindarajan[1], Christopher Yao[2], Thomas Kislinger[1], Laurie Ailles[1], Scott V. Bratmn[1]

[1]Department of Medical Biophysics, University of Toronto, Toronto, ON, Canada,[2]Department of Otolaryngology, University of Toronto, Toronto, ON, Canada

Introduction: Extrachromosomal DNA (ecDNA) consists of circularized chromosomal fragments generated through structural instability. In solid tumors, ecDNA amplifies oncogenes, reshapes cis-regulatory architecture, and alters therapeutic response. Its role in HPV-negative oral cavity squamous cell carcinoma (OSCC) remains poorly defined, with only limited tumor-specific analyses to date. Clarifying its contribution to transcriptional dysregulation and tumor phenotypes may identify drivers of carcinogenesis of OSCC.

Methods: We evaluated OSCC cases from Canada's Marathon of Hope Cancer Centres Network (MOHCCN). Whole-genome (~80X depth) and bulk whole-transcriptome sequencing (~80M reads) were performed on 131 primary tumors. ecDNA architecture was resolved using AmpliconArchitect and AmpliconClassifier. Differential gene expression was performed by DESeq2, and immune cell type deconvolution was performed by Cibersort. Matched patient-derived xenografts (PDXs) were generated to assess downstream functional effects.

Results: All OSCC cases were surgically treated with 16% stage I-II and 84% stage III-IVB. ecDNA was detected in 33 of 131 (25.2%) tumors. ecDNA positivity showed a significantly different subsite distribution compared with ecDNA-negative cases, with ecDNA positivity enriched in floor-of-mouth and tongue tumors (Fisher's exact $p = 1.7\times10^{-4}$). Smoking status, drinking history, and stage were not significantly associated with ecDNA burden. Recurrent ecDNA structures harbored key oncogenes and co-amplified partners, including CCND1, FGF19, FGF3, FGF4, MYEOV, PPFIA1, CTTN, and ANO1, with the highest enrichment on chromosomes 11 (n=14) and 7 (n=9). Transcriptomic analysis demonstrated marked up-regulation of ecDNA-enriched genes, with expression levels elevated by approximately six-fold relative to non-ecDNA counterparts (Wilcoxon test, $p < 1\times10^{-16}$). Correlation of ecDNA copy number with RNA expression supported direct dosage effects and regulatory augmentation; promoter-like element density showed a positive association with expression ($R=0.36$, $p=0.046$). Immune deconvolution demonstrated a significant reduction in resting natural killer cells in ecDNA-positive tumors (FDR < 0.05), while M1 macrophages (FDR = 0.065) and CD8 T cells (FDR = 0.096) showed similar downward trends. Additionally, matched PDX models were generated and profiled for transcriptome and proteome on 88 of the 131 patients; 26/88 (29.5%) tumors were ecDNA positive.

Conclusion: This work delineates the landscape and functional impact of ecDNA in OSCC, linked to transcriptional amplification, regulatory element activity, and shifts in immune contexture. These findings establish ecDNA as a correlate of tumor biology and a potential therapeutic target.

#7511 Extrachromosomal *MDM2* amplifications define an ecDNA-permissive tumor cell state that impacts intercellular tumor heterogeneity and treatment response across cancers.

Rachel Schmargon[1], Giulia Montuori[1], Elias Rodriguez-Fos[1], Lotte Bruckner[1], Dennis Gurgen[2], Anton George Henssen[1], Jan-Rafael Dorr[1]

[1]Department of Pediatric Oncology/Hematology, Charite-Universitatsmedizin Berlin, corporate member of Freie Universitat Berlin and Humboldt Universitat zu Berlin, Berlin, Germany, Berlin, Germany,[2]Experimental Pharmacology and Oncology Berlin-Buch GmbH, Berlin, Germany

Extrachromosomal DNA (ecDNA) amplifies oncogenes with high copy-number variability, promoting heterogeneity, rapid tumor evolution and treatment failure. MDM2, a key negative regulator of TP53, is frequently amplified on ecDNA, yet its impact on ecDNA dynamics and ecDNA dosage-driven treatment responses remains unclear. We integrated pan-cancer ecDNA reconstructions (TCGA + PCAWG), single-cell DNA FISH and ImmunoFISH, scRNA-seq, scG&T-seq from cell lines and PDX models with acute drug perturbations to analyze the impact of extrachromosomal *MDM2* amplifications on ecDNA maintenance, TP53 function and treatment response. Consistent with prior work, our analysis of pan-cancer ecDNA reconstructions (TCGA + PCAWG) revealed that *MDM2* is the most frequently amplified oncogene on ecDNA and is predominantly amplified extrachromosomally rather than on homogeneously staining regions (HSRs). Among over 100 recurrently amplified oncogenes, we found *MDM2* to be one of the strongest ecDNA-biased drivers and to be associated with increased amplicon size and complexity. In contrast to *MDM2* amplifications on HSR, *MDM2* ecDNA almost exclusively arose in *TP53*-wildtype tumors and frequently co-occurred with additional ecDNA oncogenes, suggesting that *MDM2* ecDNA creates a phenotypically *TP53*-deficient state that supports ecDNA maintenance and diversification. In neuroblastoma and astrocytoma models, *MDM2* ecDNA copy number tightly correlated with protein and transcript abundance, generating pronounced single-cell heterogeneity. In this way *MDM2* copy number determined TP53 activity and differentially affected treatment outcome in response to cytotoxic or targeted therapies at single-cell level as determined by combined fluorescence-in-situ hybridization and immunofluorescence (FISH/IF) and G&T sequencing data. Whereas chemotherapy rapidly enriched for ecDNA-high cells with reduced TP53 signaling, pharmacologic MDM2 inhibition (Nutlin-3a/Idasanutlin) selectively eliminated ecDNA-high subclones through TP53-dependent apoptosis. Similarly, MDM2 inhibition also reduced *MYCN* copy numbers in neuroblastoma cell lines and PDX with *MYCN* amplification, indicating that TP53 activation disrupts ecDNA-permissive states across different oncogenes. Our study demonstrates that *MDM2* ecDNA is the predominant ecDNA oncogene in human cancers and defines an ecDNA-permissive state in *TP53*-wildtype tumors which facilitates rapid adaptation to different therapeutic pressures. These results identify *MDM2* ecDNA copy number variation as a functional determinant of acute treatment responses and reveal MDM2-regulated TP53 function as a vulnerability in ecDNA-carrying cancers that may be exploited through rational treatment sequencing.

#7513 Integrated clonal and single-cell analyses uncover progenitor-driven tumor diversification in early-stage endometrioid endometrial carcinoma.

Suguru Miyata[1], Hiroshi Yoshida[2], Toyoyuki Hanazawa[3], Masahito Kawazu[4]

[1]Chiba Cancer Center, Chiba, Japan,[2]Gastrointestinal Oncology Division, National Cancer Center Hospital, Tokyo, Japan,[3]Chiba University, Chiba, Japan,[4]Chiba Cancer Center Research Institute, Chiba-shi, Japan

Background and Objectives

The normal endometrium undergoes cyclical regeneration and frequently contains somatic mutations, yet the earliest steps of endometrioid endometrial carcinoma (EEC) development remain poorly defined. Although tumor heterogeneity arises from both genomic evolution and diversity in epithelial cell states, how these two axes interact during early tumorigenesis is not well understood. To address this question, we focused on early-stage EEC and performed an integrative analysis linking clonal architecture with cell-state heterogeneity.

Methods

We performed multi-region whole-exome sequencing (WES) of uterine samples from 37 patients with early-stage EEC to map the anatomical distribution of tumor clones. Representative cases covering POLE-mutated, microsatellite instability-high, and copy-number-low subtypes underwent single-cell RNA sequencing to characterize epithelial differentiation states and reconstruct lineage relationships. Somatic mutations identified by WES were used to infer clonal structures at single-cell resolution. Patient-derived organoids were established to functionally evaluate distinct progenitor-like tumor populations.

Results

Single-cell RNA sequencing revealed a spectrum of epithelial differentiation, ranging from mature ciliated and secretory cells to undifferentiated progenitor-like tumor cells. The proportions of these states varied widely not only between patients but also across regions within the same uterus. By integrating WES-derived mutations with single-cell profiles, we showed that individual tumor clones contained both progenitor-like and differentiated cells, recapitulating a hierarchical epithelial organization reminiscent of the normal endometrium.

Subclonal populations differed markedly in epithelial composition and proliferative activity, indicating that clone-specific genomic alterations influence cell-state output. Notably, we identified two transcriptionally and functionally distinct progenitor-like tumor cell types, suggesting multiple differentiation routes in early tumor evolution.

Conclusions

Early-stage EEC exhibits coordinated heterogeneity at genetic and cellular levels. The discovery of two progenitor-like tumor populations provides evidence for parallel differentiation programs that drive early tumor diversification. By integrating clonal evolution driven by genetic alterations with single-cell phenotypes, this study refines current EEC classification frameworks such as ProMisE and offers new biological insights into the origins, propagation, and therapeutic vulnerabilities of early-stage endometrial cancer.

#7514 Spatial multimodal and functional dissection reveal a UCHL1-driven malignant program in clear cell renal cell carcinoma.

Yize Li[1], Wagma Caravan[1], Xiyi Wei[1], Kapur B. Dhami[1], Kazuhito Sato[1], Xiangwei Fang[1], Preet Lal[1], Hongyi Liu[2], Lijun Chen[2], Cody Weimholt[1], Hui Zhang[2], Li Ding[1], Feng Chen[1]

[1]Washington University in St. Louis, Saint Louis, MO,[2]Johns Hopkins University, Baltimore, MD

Clear cell renal cell carcinoma (ccRCC), the most common subtype of kidney cancer, exhibits substantial molecular and spatial heterogeneity that contributes to therapeutic resistance and poor clinical outcomes. Our previous work identified UCHL1 as a marker of aggressive ccRCC, but its mechanistic role in tumor progression remained unclear. To further elucidate UCHL1 function, we integrated single-nucleus RNA sequencing (snRNA-seq) from 67 tumors with bulk proteogenomics and spatial assays addressing molecular coverage and spatial specificity. Our refined tumor-intrinsic UCHL1 classification identified a distinct ccRCC subgroup characterized by elevated UCHL1 mRNA and protein abundance. The UCHL1-high subgroup, comprising 19% of tumors in this cohort, was significantly associated with BAP1 mutants, immune infiltration, and poor prognosis. The spatial mapping in Xenium indicated UCHL1-high tumors displayed enhanced interactions with an immune-inflamed tumor microenvironment (TME), whereas UCHL1-low tumors were enriched for immune-desert regions dominated by endothelium and VEGF signaling. Furthermore, we observed spatial dynamics in UCHL1 expression arising from distinct subclones within the same tumor, reflecting the intratumoral heterogeneity in the UCHL1-high subgroup. Our functional studies demonstrated that UCHL1 knockout and downregulation markedly suppressed ccRCC cell proliferation and tumorigenicity in vitro and in cell line-derived xenograft (CDX) models. Pharmacological inhibition of UCHL1 consistently reduced tumor growth in ccRCC cell lines. The corresponding cell line proteomics and post-translational modification profiling, including phosphorylation and ubiquitination, delineated that UCHL1 regulated key tumor-promoting pathways of inflammation and epithelial-mesenchymal transition (EMT) through NF-κB activation. Notably, the RESL9 patient-derived xenograft (PDX) model responded robustly to the UCHL1 inhibitor, exhibiting pronounced tumor growth suppression. Collectively, these findings establish UCHL1 as a critical molecular driver and therapeutic target in ccRCC, supporting the potential of UCHL1-directed monotherapies or combination regimens to improve outcomes for patients with advanced ccRCC.

#7515 Uncovering transdifferentiation mechanisms underlying heterogeneity in neuroblastoma.

Michele Tomanelli[1], Jennifer Hoti[2], Ilaria Medici[2], Chaimae Sellak[2], Tullio Florio[3], Aldo Pagano[4]

[1]Department of Experimental Medicine, University of Genoa, Genoa, Italy,[2]University of Genoa, Genoa, Italy,[3]Department of Internal Medicine, University of Genoa, Genoa, Italy,[4]IRCCS Ospedale Policlinico San Martino, Genoa, Italy

Neuroblastoma is the most prevalent extracranial tumor in newborns and originates from neural crest-derived cells. Using selected Neuroblastoma cell lines, we generated clones engineered to express the non-coding RNA NDM29. This approach allowed us to investigate the function of NDM29 in tumor cell differentiation and to identify potential new therapeutic targets aimed at limiting tumor aggressiveness. Additional analyses, including single-cell sequencing, revealed the existence of distinct cellular subpopulations within this model. These subsets were subsequently separated through FACS sorting. The cellular heterogeneity observed in this system mirrors the complexity found in neuroblastoma patient samples. The clonal nature of our model and the presence of multiple subpopulations suggest that the observed heterogeneity arises from transdifferentiation processes. The plasticity of these subpopulations is a central focus of our study. The ability of cancer cells to undergo transdifferentiation is a key aspect in cancer research. In our model, we identified a subpopulation capable of responding to VEGF signaling and potentially able to regulate the angiogenic process within the tumor nodule. Understanding the plasticity mechanisms involved in this model, which lead to the generation of this and other subpopulations, may enable us to develop targeted therapeutic strategies aimed at counteracting tumor cell transdifferentiation.

: Tumor Models and Assays: In Vitro, In Vivo
Poster Session

#7520 Developing patient-derived organoid and xenograft models for preclinical assessment in ovarian cancer.

Choong-Jae Lee[1], Jubi Heo[1], Joo Hang Jeong[1], Ha-eun Lee[1], Jinyoung Park[1], Wonyoung Choi[2], Sang Yoon Park[3], Yo Han Woo[3], Myong Cheol Lim[3], Sun-Young Kong[1]

[1]Targeted Therapy Branch, National Cancer Center - Korea, Goyang-si, Gyeonggi-do, Korea, Republic of,[2]Department of Cancer biomedical science, National Cancer Center - Korea, Goyang-si, Gyeonggi-do, Korea, Republic of,[3]Center for Gynecologic Cancer, National Cancer Center - Korea, Goyang-si, Gyeonggi-do, Korea, Republic of

Background: Ovarian cancer (OC) is a highly lethal malignancy, characterized by late-stage diagnosis, marked tumor heterogeneity, and poor overall prognosis. Preclinical models of OCs, including patient-derived organoids (PDO) and xenografts (PDX), has been investigated for drug development and precision medicine. In this study, we established OC PDOs and PDX models
Methods: Tumor tissue were collected from multiple sites (ovary, omentum, diaphragm, and peritoneum) or ascites during surgery. After tissue dissociation, single cells were embedded in basement membrane extract for PDO culture and injected either intrabursally or subcutaneously into immunodeficient mice (NOD/Shi-scid IL-2Rv^{null}) to generate PDXs. PDOs were successfully cultured beyond five passage, and drug screening across 14 drugs including platinum-based agents, taxanes, topoisomerase inhibitors, and PARP inhibitors was performed using the CellTiter-Glo 3D viability assay. PDXs tumor growth were monitored three times a week, and analyzed the time points to reach 100 mm^3.
Results: A total of 18 PDOs were successfully established from 14 advanced-stage OC patients with diverse histological and genetical characteristics. Drug screening demonstrated a variable range of responses with the area under the curve ranging from 0.29 to 1.00, especially to platinum-based drugs and PARP inhibitors. The OC PDX model was successfully established in 9 (26.5%) out of 34 patients. Overall, the duration until 100 mm^3 tumor growth was shorter in intrabursal models compared to subcutaneous models with mean times of 90.3 days (n = 4) and 149.8 days (n = 9), respectively. Notably, tumor formation accelerated with successive passages, suggesting enhanced engraftment efficiency and growth kinetics in later generations.
Conclusions: We successfully developed OC PDO and PDX models that preserve tumor heterogeneity. These models enable detailed investigation of tumor biology offering critical insights for the development of novel treatment strategies. This research was supported by the Bio&Medical Technology Development Program of the National Research Foundation (NRF) funded by the Korean government (MSIT): RS-2025-19542979, RS-2025-25437292

#7521 Optimization of tumor tissue enzymatic dissociation for rapid and viable tumoroid generation.

Colin D. Paul, Anthony Chatman, **Logan Wilson**, Chris Yankaskas, Pradip Shahi Thakuri, Matt Dallas, David Kuninger

Thermo Fisher Scientific, Frederick, MD

Patient-derived tumoroids, or 3D organoid cultures from dissociated tumor tissue, are a powerful translational tool that bridge molecular profiling with functional drug testing. However, the success of tumoroid derivation is critically dependent on preanalytical variables—tissue handling, transport, and enzymatic dissociation—that influence viable cell recovery and culture performance. Here, we report an optimized workflow and enzyme formulations to maximize cell yield and fitness for downstream tumoroid culture and functional assays.Fresh surgical resections from colorectal, endometrial, breast, lung, and head and neck cancers were processed to assess the impact of dissociation on downstream culture. Tissues were collected in Hibernate™-A-based transport buffer supplemented with GlutaMAX™ and B-27™ supplements, antibiotics, and the ROCK inhibitor Y-27632, to ensure stability during overnight transport on ice. Upon receipt, samples were washed in Advanced DMEM/F-12-based tissue processing buffer and mechanically minced before enzymatic dissociation. A designed experimental framework evaluated enzyme type, concentration, and interactions across donors, measuring outcomes of viable cell yield (cells/mg tissue) and tumoroid formation at day 7 post-plating in OncoPro™ Tumoroid Culture Medium.Optimization revealed that initial viable cell yield was not predictive of subsequent culture success, necessitating dual metrics of viability and tumoroid growth. Collagenases, DNase, dispase, and hyaluronidase were beneficial depending on tissue type. While higher yields were obtained in some dissociation conditions, tumoroid formation was compromised, demonstrating a trade-off between digestion of tissue and stress on cells. Approximately 90% of dissociated samples generated tumoroids within 7 days, demonstrating both speed and reproducibility of the optimized workflow. Next-generation sequencing of paired solid tissue, dissociated cells, and day 7 tumoroids revealed >85% correlation in cancer-related gene expression and >95% overlap in single nucleotide variants, confirming preservation of tumor identity throughout processing. We further explored whether long-term tumoroid derivation success could be improved by spike-in of additional supplements and growth factors to OncoPro medium and identified several candidates that potentially contribute to line establishment. This integrated workflow of tumor transport, dissociation, and culture led to optimal viable cell recovery and tumoroid formation efficiency across multiple cancer indications. These results establish a practical and scalable framework for generating high-quality patient-derived tumoroids.

#7522 Ex vivo drug sensitivity and in silico evaluation of phytochemicals in gynaecological cancers.

Maria Nomusa Sikhakhane[1], Deepak Govindaraj[2], Mutsa Monica Takundwa[2], Xavier Siwe Noundou[1]

[1]Pharmaceutical Sciences, Sefako Makgatho Health Sciences University, Pretoria, South Africa,[2]CSIR South Africa, Pretoria, South Africa

Background: Gynaecological cancers—including cervical, ovarian, endometrial, and vulvar cancers—pose significant therapeutic challenges due to late-stage diagnosis, therapeutic resistance, and the presence of cancer stem cells. Dietary phytochemicals are emerging as potential modulators of cancer-related pathways, but their clinical utility is often limited by poor pharmacokinetics. Integrating in silico ADMET (Absorption, Distribution, Metabolism, Excretion, and Toxicity) profiling, molecular docking, and ex vivo drug sensitivity screening may facilitate the identification of effective therapies.
Methods: Primary tumor cells were isolated from 22 patients (age range 29-83 years) undergoing surgery for cervical (n=13), ovarian (n=2), endometrial/uterine (n=4), and vulvar (n=3) cancers. Cell yields ranged from 15.9×10^6 to 3.05×10^9 with viability between 14-99%. Cells were cryopreserved for downstream assays. Six dietary phytochemicals (quercetin, curcumin, resveratrol, EGCG, genistein, ursolic acid) were evaluated using SwissADME and pkCSM to predict pharmacokinetic and toxicity profiles. Boiled-egg plots assessed gastrointestinal absorption and blood-brain barrier permeability. Molecular docking was performed against key enzymes implicated in gynecological cancer pathways (EGFR, VEGFR-2, PI3K, TOP2A) using AutoDock Vina. Ex vivo drug sensitivity screening compared FDA-approved chemotherapeutics with the selected phytochemicals to identify compounds with higher cytotoxic potential.
Results: ADMET profiling revealed high gastrointestinal absorption for quercetin, curcumin, resveratrol, and genistein (HIA 77-93%), with limited BBB penetration except for resveratrol. Ursolic acid and EGCG demonstrated poor absorption. P-glycoprotein efflux and CYP inhibition were minimal for most compounds, though EGCG showed hERG II inhibition, and ursolic acid presented hepatotoxicity risk. Molecular docking showed favorable binding of EGCG to EGFR (-9.3 kcal/mol), curcumin to VEGFR-2 (-9.4 kcal/mol), and ursolic acid to TOP2A (-9.1 kcal/mol), comparable to FDA-approved inhibitors. Preliminary ex vivo drug screening indicated that FDA-approved chemotherapeutics exhibited higher cytotoxicity across patient-derived cells compared to the dietary phytochemicals.
Conclusions and Future Directions: Our integrated approach demonstrates that ex vivo drug sensitivity screening complements in silico ADMET and molecular docking, providing a platform to prioritize therapeutic candidates. Preliminary data suggest FDA-approved chemotherapeutics outperform dietary phytochemicals in patient-derived models. Future work will incorporate biostatistical and genomic analyses to predict optimal drug combinations for individualized therapy, potentially enabling precision oncology strategies for gynecological cancers.

#7523 A vascularized glioblastoma tumor spheroid model for studying tumor invasion and therapeutic response.

Anagha Shreesha[1], Sheridan Ke-Wing Fok[2], Brendan Harley[3]

[1]Bioengineering, University of Illinois, Urbana-Champaign, Urbana, IL,[2]University of Illinois at Urbana-Champaign, Champaign, IL,[3]University of Illinois at Urbana-Champaign, Urbana, IL

Introduction: GBM is characterized by its extensive invasiveness; its highly infiltrative cells penetrate surrounding brain tissue and often cannot be completely removed through surgery, leading to tumor recurrence and poor survival. The extent of vascularization directly correlates with GBM malignancy. Previous studies have demonstrated that sequentially adding fibroblasts to a pre-formed spheroid resulted in their peripheral concentration and enhanced vascularization in a SN12C kidney cancer model. We are interested in investigating whether sequentially adding fibroblasts promote vasculature formation in vitro and induces angiogenesis in the presence of endothelial cells. The objective of this experiment is to develop a representative model of the GBM tumor spheroid, with a focus on how vascularization and stromal cell populations could affect invasion and therapeutic response.

Materials & Methods: Sequential spheroids are synthesized by adding $2.5x10^3$ U87-MG cells to an ultra-low attachment plate and incubated at 37°C for 24 hours to allow spheroid aggregation. After 24 hours, an equal amount of NHLFs are added to the preformed spheroids at a 1:1 ratio. Cells were incubated at 37°C for an additional 24 hours to allow complete spheroid formation. Co-mixed spheroids are synthesized using a similar method but adding U87-MG and NHLFs concurrently. NHLF and HUVECs were resuspended in 5% GelMA solution at a ratio of 2: 1 ($2x10^6$ NHLF:$1x10^6$ HUVEC). Individual spheroids were pipetted into each well of a 20 µL hydrogel mold and polymerized using UV radiation.

Results: We observed distinct patterns in fibroblast distribution and spheroid behavior. In sequential spheroids, fibroblasts localized primarily at the periphery, whereas the co-mixed method produced a more uniform distribution throughout the spheroid. When sequential and co-mixed spheroids are encapsulated with endothelial cells (HUVECs) and NHLFs, sequential spheroids demonstrated more vessel formation around the spheroids, while limited network development occurred around co-mixed spheroids. Additionally, AlamarBlue data confirmed significant higher metabolic activity in hydrogels containing sequential spheroid on Day 5. We also observed that sequential spheroid outgrowth correlated to fibroblast density, while co-mixed spheroid outgrowth was more evenly distributed around the spheroid. Temozolomide treated sequential spheroids showed no significant difference compared to untreated controls, suggesting a reduced response to TMZ.

Conclusion: Future work will focus on understanding how spheroid organization influences population dynamics. We plan to track changes in cellular populations and investigate whether spheroid organization affects cytokine release in a 3D model. Finally, we aim to validate the effects of fibroblasts on tumor invasion using different cancer cell lines.

#7524 Genetically defined organoid systems uncover PIK3CA-mediated suppression of an oral-immune program during early squamous neoplastic evolution.

Hua Zhao[1], Young Min Park[2], Yueyuan Zheng[3], Qiong Mao[1], Hao Wu[1], Fanyi Mo[1], Uttam K. Sinha[1], Parish Sedghizadeh[1], De-Chen Lin[1]

[1]USC - University of Southern California, Los Angeles, CA,[2]Yonsei University Health System, Seoul, Korea, Republic of,[3]Hong Kong University of Science and Technology, Hong Kong, Hong Kong

Head and neck squamous cell carcinoma (HNSCC) is an aggressive and lethal neoplasm, yet its early neoplastic transformation mechanisms remain poorly defined. Despite extensive genomic characterization, translation of these molecular insights into clinical practice has been limited. A critical barrier has been the absence of physiologically relevant human models capable of faithfully recapitulating the stepwise progression from precursor lesions to invasive tumors while enabling rigorous interrogation of genotype-phenotype relationships. Here, we developed two complementary, cross-species, genetically defined organoid systems—a genome-sequenced patient-derived platform spanning normal tissue, precursor lesions, and tumors, and a CRISPR/Cas9-engineered human and mouse organoid platform targeting key HNSCC drivers (*TP53*, *CDKN2A*, *PIK3CA*) to reconstruct the continuum of squamous malignant transformation. Using these models, we uncovered critical insights into early neoplastic evolution. *TP53*/*CDKN2A* double-knockout (DKO) organoids exhibited morphological dysplasia, hyperproliferation, loss of squamous differentiation, and tumorigenicity—phenotypes further exacerbated by introducing mutant *PIK3CA*^{E545K} (DKOP). Single-cell RNA sequencing of DKO and DKOP organoids revealed expansion of quiescent basal and proliferative squamous populations and depletion of differentiated cells. Notably, an Oral-Immune transcriptional program characteristic of normal squamous epithelium was attenuated in DKO organoids and further diminished in DKOP. The Oral-Immune program was strongly correlated with intratumoral T-cell infiltration in HNSCC, marked by enrichment of cytotoxic and proliferative CD8$^+$ subsets and upregulation of IFN-pathway and cytotoxic effector genes. Strikingly, across 46 ICB-treated cohorts, its strongest association with therapeutic response occurred in an HNSCC cohort, where it outperformed 17 established immune gene-expression signatures, including *IFNG* and *PD-L1*. Both CD8$^+$ T-cell scores and the Oral-Immune score were inversely correlated with PIK3CA mutation status. Mutant *PIK3CA*^{E545K} suppressed Oral-Immune program genes in HNSCC, and this effect was reversible with PI3K inhibition. Functionally, *PIK3CA* mutations reduced CD8$^+$ T-cell infiltration in both in vitro CD8$^+$ T cell-organoid coculture assays and in vivo orthotopic allograft models. Together, these findings identify the Oral-Immune program as a key determinant of immune-inflamed tumor states, reveal *PIK3CA* mutations as drivers of immune evasion and diminished immunotherapy responsiveness through suppression of this program, and underscore the power of genetically defined organoid models for dissecting early cancer evolution.

#7525 Drug screening using patient-derived tumoroids harboring diverse mutations to identify effective therapeutics for metastatic cancer patients.

Seyoum Ayehunie[1], Dylan Bryda[1], Alex armento[1], Groves Megan[2], Anthony Tolcher[2]

[1]Sartorius, Ashland, MA,[2]NextOncology, San Antonio, TX

Patient-derived primary tumors (PDPTs) are emerging as physiologically relevant and translational in vitro models for predicting human responses to cancer therapeutics. Compared to conventional 2D cell lines, PDPTs more accurately recapitulate the tumor microenvironment, enable high-throughput drug screening, and support precision medicine. However, widespread adoption has been limited by challenges in large-scale expansion without phenotypic changes. We developed a novel system for in vitro expansion and biobanking of colorectal cancer tumoroids derived from four metastatic donors with distinct mutations. Our approach integrates matrix-coated plates with microwell technology to scale up tumoroid growth. Two assay platforms were established: (a) Tumoroids generated by seeding 5000 single tumor cells as a stand-alone model, and (b) Complex 3D tissues created by co-seeding 500 tumor cells with fibroblasts, endothelial cells, and immune cells to mimic the tumor microenvironment (TME). Tumoroids were treated with five chemotherapeutic agents—Cisplatin, Doxorubicin, Oxaliplatin, Fluorouracil, and Cetuximab—at six concentrations over a 7-day period (three doses). For tumoroids grown in TME, microscopic and histological analyses confirmed uniform-sized tumoroids and glandular-like structures. Epithelial origin and fibroblast presence were validated by CK19+ and vimentin staining, respectively. Live/dead staining using calcein AM and PI revealed dose- and time-dependent drug responses in both platforms. Notably, Doxorubicin, previously unused in these patients, demonstrated significant activity—highlighting the assay's potential to identify drugs for precision therapy and enable patient-specific drug ranking. In summary, scalable PDPT expansion combined with physiologically relevant assay systems offers a cost-effective, predictive, and non-animal approach for metastatic cancer drug screening, advancing the concept of precision medicine.

#7526 Breast cancer organoids as a complementary preclinical model to PDX, enabling immunotherapy evaluation.

Olivier Deas[1], Emilie Indersie[1], Amandine Prioux-Quartier[2], Philippe Lluel[2], **Emilie Decaup**[2]

[1]Xentech, Evry-Courcouronnes, France,[2]Urosphere, Toulouse, France

Background : Breast cancer (BC) remains a major global health challenge, with increasing incidence and mortality rates. Given the genetic, pathological, and clinical heterogeneity of BC subtypes, preclinical models that accurately reproduce tumor complexity are essential. To address this need, we established patient-derived xenograft (PDX) models alongside matched organoids (PDXO). This study aimed to demonstrate the high degree of similarity between PDX and their corresponding PDXO models in genomics and pharmacology. We validated organoids as a relevant platform for immunotherapy assessment, illustrated by the evaluation of trastuzumab, monoclonal antibody directed against HER2, in a co-culture system with immune cells.

Methods: PDX models were generated by xenografting patient's tumors tissues in immunodeficient mice and serially passages into mice after the first engraftment. To generate matched PDXO models, PDX tumors were minced and enzymatically digested before murine cells depletion. Then, human epithelial isolated cells were seeded in Matrigel® and cultured in optimized medium. Molecular characterization was performed by whole exome and transcriptome sequencing. PDXs and PDXOs were subjected to equivalent pharmacological treatments. For trastuzumab efficacy evaluation, organoids were co-cultured with activated peripheral blood mononuclear cells (PBMCs) from healthy donors at several Effector:Target ratios. Organoid viability was evaluated after 72 hours of treatment.

Results : PDXs and their corresponding PDXOs exhibited comparable responses to standard chemotherapies. Omics analyses revealed a high degree of mutational concordance between paired models, including shared oncogenic driver mutations such as TP53 and ATM. We further evaluated responses to HER2-targeted therapies using trastuzumab-emtansine (T-DM1) in two pairs of PDX and PDXO models differing in HER2 expression. T-DM1 demonstrated efficacy in both a HER2-positive PDX and its matched PDXO, resulting in tumor growth inhibition and organoid mortality. Furthermore, using a co-culture system of PBMCs and HER2-expressing organoids, we assessed the activity of trastuzumab. The antibody showed a clear antibody-dependent cell-mediated cytotoxicity effect against HER2-positive organoids, confirming the relevance of these models for evaluating immunotherapeutic responses.

Conclusion: The establishment of a mirror biobank comprising matched PDX and PDXO models enables acceleration of early-stage drug screening and seamless in vivo validation using corresponding PDXs. Beyond pharmacological testing, organoids offer an advantage by facilitating the evaluation of immunotherapeutic strategies. Together, these complementary models provide powerful translational tools for the development of novel breast cancer therapies and open new avenues for advancing immunotherapy research.

#7527 Sequential 3D functional profiling shows preserved drug resistance and sensitivity profiles after neoadjuvant treatment in an ovarian cancer patient.

Chiara Maestri, Ivan Trus, Rajeshwar Nitiyanandan, Ricardo J. Parker, Chris Apfel

SageMedic Corp., Redwood City, CA

Background
Despite standard platinum-based doublet therapy, most patients with advanced ovarian cancer do eventually relapse[1], and subsequent therapies exhibit variable benefit. Functional precision assays can guide treatment selection and reduce exposure to ineffective therapies. Here we used a multiplexed 3D functional profiling platform on specimens collected before and after neoadjuvant treatment, capturing evolving cytotoxic and antiproliferative responses and identifying effective treatment options.
Methods
Fresh specimens were obtained from a patient with high-grade serous ovarian carcinoma: a baseline ascites sample from stage III disease, and a surgical biopsy sample collected at stage IV disease after neoadjuvant carboplatin-paclitaxel treatment. Specimens were processed to obtain ex-vivo microtumors[2] and exposed to NCCN-recommended therapies. After 4 days of drug exposure, multiplexed viability and proliferation profiling was performed[3]. Four-parameter logistic dose-response curves were fitted, and differences (Δ) in cytotoxic and antiproliferative efficacies at standardized drug concentrations between the baseline and post-treatment samples were calculated.
Results
The carboplatin paclitaxel combination showed moderate cytotoxic (0.37, estimated 95% CI [0.34-0.41]) and antiproliferative effects (0.37 [0.36-0.39]) before and after neo-adjuvant treatment (0.30 [0.25-0.36] and 0.33 [0.31-0.36]), aligning with the limited objective tumor response. VAC (vincristine, actinomycin, and cyclophosphamide) demonstrated high cytotoxic and antiproliferative efficacy before (0.85, [0.75-0.90], and 0.97 [0.92-0.99]) and after therapy (0.73 [0.64-0.78], and 0.99 [0.94-1.00]). Interestingly, the PARP-inhibitors olaparib and rucaparib showed limited cytotoxicity (0.10 [0.08-0.12] and 0 [0-0.08]) but pronounced antiproliferation (0.60 [0.53-0.70] and 0.58 [0.49-0.74]) before the treatment with no material change after it.
Conclusions
Sequential ex-vivo multiplexed profiling of this advanced ovarian cancer revealed that neoadjuvant carboplatin paclitaxel minimally altered cytotoxic and antiproliferative drug response sensitivity and resistance patterns to VAC and PARP inhibitors. Thus, pre-treatment functional profiling, when tumor tissue is readily available, might provide useful follow-on treatment options to avoid exposure to ineffective regimens in the future.
[1] Pignata S et al., Treatment of recurrent ovarian cancer. Ann Oncol. 2017 [2] Apfel C. Preparation of cells, cell aggregates and tissue fragments. Published October 2014 [3] Apfel C et al., High-throughput multiplexed sensitivity and resistance assay. US Patent US 12,312,631 B1

#7528 Utilizing confocal live-cell imaging for evaluating therapeutic efficacy and toxicity in complex oncology models.

John Rauch[1], Jasmine Trigg[2], Kirsty McBain[2], Jonathan Bezenah[1], Libuse Oupicka[1], Richard Lister[1], Laura Skerlos[1]

[1]Sartorius, Ann Arbor, MI,[2]Sartorius, Royston, United Kingdom

Oncology research continues to progress towards utilizing more complex, translational cellular models to improve clinical outcomes. The need for complementary bioanalytical tools to enable clear insights from increasingly complex data has evolved in parallel. The Incucyte® CX3 enables multiplane, spinning disk confocal imaging of complex tumor models and organoids under physiologically relevant conditions. This poster will highlight the application of this technology, paired with integrated analysis tools, to evaluate the efficacy and off-target toxicity of therapeutic compounds. The effects of chemotherapeutic compounds were first evaluated in solid tumor models. For example, MCF7 cells stably expressing a nuclear-restricted green fluorescent protein were embedded in extracellular matrix and plated in the presence of a fluorescent dye to monitor apoptosis. Spheroid formation was monitored for 3 days, then the effects of camptothecin (0.3 - 10 µM) or cisplatin (3 - 100 µM) were tested. Automated analysis performed on confocal max projection images revealed a concentration-dependent decrease in spheroid growth and complementary increase in apoptosis. Many chemotherapeutic agents have been observed to induce hepatotoxicity in clinical cases. Therefore, the effects of compounds were also measured in a model of liver toxicity. Mouse hepatic organoids stably expressing a nuclear-restricted orange fluorescent protein were plated in a similar manner to cancer spheroids. Confocal multiplane images were acquired every 8 hours during formation (1 day) and for an additional four days following drug treatment. Camptothecin and cisplatin induced a concentration-dependent decrease in growth over time, with high concentrations (5-10 µM or 50-100 µM, respectively) inducing apoptosis. Importantly, fluorescent readouts of toxicity enabled by confocal imaging were more sensitive, as cellular debris can be difficult to distinguish from healthy organoids via brightfield readouts. Immune- and cancer-cell coculture models were also evaluated. SKOV-3 Nuclight Orange spheroids were seeded with a density range of activated (10 ng/mL CD3/CD28 for 72 hours) or non-activated PBMCs in the presence of Fabfluor-488-CD45 or Fabfluour-488-IgG1 and optigreen background suppressor. Co-cultures were imaged over 6 days using confocal multiplane acquisition. The results showed a density-dependent decrease in orange area with increasing PBMC density for activated PBMCs, indicating target cell death. Additionally, following immune-mediated tumor killing, we observed a density-depending increase in green area with PBMCs expansion. Taken together, these data highlight the ability of multiparameter, multiplane confocal live cell analysis to provide clear, rapid insights from a variety of complex pre-clinical models, including immuno-oncology and organoid-based toxicity readouts.

#7529 Reproducible 3D bioprinting of patient-derived tumors enables high-fidelity preclinical drug testing.

H. Nikki March, Ben Kennedy, Olivia Matthews, Andrew McCormack, Abby McSorley, Laura Nixon, Lorna Ewart

Carcinotech Ltd., Edinburgh, United Kingdom

Traditional 2D cancer cell culture systems have substantially advanced our understanding of tumor biology but fail to recapitulate the architectural organization, ECM composition, and spatial nutrient and oxygen gradients present in vivo. Consequently, they show weak correlation between in vitro drug sensitivity and clinical response. This translational gap contributes to high attrition in cancer drug development, with many therapies performing well preclinically but failing clinically due to the insufficient predictive power of early models, including in vivo systems that lack patient-specific biology and exhibit species-specific differences. Developments in 3D bioprinting enable reconstruction of tumor tissues containing epithelial, stromal, and immune populations embedded within physiological matrix analogs, more accurately reproducing the tumor microenvironment and retaining cell-cell and cell-matrix interactions. Bioprinting allows standardized, scalable tumor models while maintaining biologically relevant complexity. Early studies established feasibility, but systemic validation using fresh human tumor tissue, including compositional and functional fidelity, remains incomplete. We demonstrate that patient-derived ovarian and HER2+ breast tumors can be dissociated, bioprinted, and maintained in 3D culture while preserving key cellular populations and functional behaviors, and that treatment responses in these models correlate with known patient outcomes and standard-of-care drug efficacy. Constructs were generated using biomimetic hydrogels supplemented with ECM-derived proteins and primary tumor cells, and evaluated for viability, structural stability, and microarchitecture by live/dead imaging, histology, flow cytometry, and quantitative microscopy. Drug-response assays with standard-of-care chemotherapies and targeted anti-HER2 agents were performed. Optimized initial cell density supported sustained survival, proliferation, and hierarchical reorganization. Evaluation of our printing strategy showed we can achieve constructs with coefficients of variation below 10% for both bioprint structural integrity and cell viability at one day post-print and that this could be maintained over prolonged culture. This degree of reproducibility permitted attribution of drug responses to the treatment and supported investigation of optimal pre-treatment culture duration. Drug-response profiles differed from those in 2D cultures, indicating greater physiological relevance. Collectively, these findings highlight the predictive validity of bioprinted tumor constructs as a promising tool for preclinical efficacy assessment. Ongoing work will expand multicellular complexity, incorporate immune components, and benchmark against clinical datasets.

#7530 Comparative analysis of therapy responses and stem cell marker expression in glioblastoma neurospheres verus monolayer cultures using imaging, cytotoxicity assays, and flow cytometry.

Daniel S. Costa, **Joseph P. Kolb**, Olivia Mankos, Karsten E. Fynboe, Stephanie M. Fogerson, William D. Culp, Kathryn R. Meshaw

Powered Research LLC, Durham, NC

Background: Glioblastoma (GBM) is an aggressive and lethal primary brain tumor that is resistant to conventional therapies. Despite advances in treatment strategies, the standard of care and median patient survival have remained largely unchanged for nearly two decades. One major obstacle to therapeutic progress is the complexity of the GBM tumor microenvironment, which is poorly recapitulated by most GBM cell lines when used in animal models and in vitro screening assays. Three-dimensional (3D) neurosphere cultures of GBM cell lines are thought to improve model performance over traditional two-dimensional (2D) monolayer systems by enriching for glioblastoma stem-like cells (GSC), which, when implanted orthotopically, produce tumors that more closely resemble human disease. Consequently, in vitro drug screens using neurospheres more accurately reflect the spatial architecture, cell-cell interactions, and diffusion gradients improving predictive values of these types of studies. Here, we sought to further characterize the phenotype of U-87 MG-Luc2 cells grown in 2D or as neurospheres and to assess their drug sensitivity in vitro and as xenografts.
Methods: U-87 MG-Luc2 cells grown in 2D or as neurospheres were treated with temozolomide, lomustine, and bortezomib, individually and in combination, to assess drug sensitivity in vitro. In addition, these cells were stained for the GSC markers CD133, CD15, CD49f, and CD44 and analyzed by flow cytometry before and after intracranial implant. Orthotopic cell growth was tracked by IVIS imaging.
Results: Cytotoxicity assays revealed that neurospheres were significantly less sensitive to treatment compared to monolayers, consistent with enhanced resistance mechanisms supported by 3D architecture and GSC. Flow cytometry indicated differences in cell size, granularity, and GSC markers between the two models. Importantly, both culture types successfully engrafted and proliferated as murine orthotopic xenografts.
Conclusion: These findings suggest that 3D neurosphere models more accurately reflect the in vivo tumor environment and drug response, while 2D monolayers remain a valuable tool for initial therapeutic screening. Neurosphere culture conditions impacted U-87 MG-Luc2 GSC surface marker expression. Tracking changes in frequency and expression of GSC markers after drug treatment may be useful for selecting promising drug candidates. Head-to-head comparisons underscore the importance of model selection in preclinical GBM research.

#7531 Autoimmunity in a Dish: A 3D human orbital fibroblast platform for inflammatory biomarker discovery and fibrotic stromal biology.

Mengling Liu, Gene Lin, Noel Derecki, Lily Li, Paula Pellon, Calvin Ha

Immunology and Biomarker, EnquBio, San Diego, CA

Thyroid eye disease (TED) is an autoimmune inflammatory disorder and the most common cause of orbital disease in adults. Often associated with Graves' disease, TED can lead to debilitating visual impairment due to bulging of the eyes (proptosis) from severe swelling of the extraocular muscles and orbital tissues. The pathophysiology of TED is thought to involve activation of periorbital fibroblasts, triggering an inflammatory cascade that results in local accumulation of lipids and glycosaminoglycans and, ultimately, fibrosis. Fibroblast-driven extracellular matrix remodeling and fibrosis are also hallmarks of the stromal compartment in many solid tumors, linking TED biology to broader questions in tumor microenvironment research. To better understand the mechanistic pathophysiology of TED and to support discovery of agents that target fibrotic stroma, we have developed an in vitro 3D culture model using primary human orbital fibroblasts. In this system, fibroblasts form spheroidal 3D structures that provide a more physiologically relevant context than conventional monolayer culture. Using this platform as a bridge between clinic and bench, we assay surface, intracellular, and secreted inflammatory biomarkers following IGF-1 stimulation—a signaling axis with established roles in both autoimmunity and cancer—using ELISA, MSD, JESS, and flow cytometry. Endpoint data are integrated through a bespoke AI- and machine-learning-based pipeline to identify and rank multidimensional biomarker signatures. Taken together, these data strongly validate our 3D human orbital fibroblast culture as a useful model to investigate the molecular mechanisms underlying the pathogenesis of TED and to screen potential therapeutics via assays developed in-house with clients and partners in the autoimmune space. More broadly, this IGF-1-responsive 3D human stromal platform provides a tractable model of fibrotic, inflammatory fibroblast biology that is directly relevant to the tumor microenvironment and can be extended to future co-culture studies with tumor and immune cells to support preclinical oncology drug discovery.

#7532 Multi-cancer patient-derived organoid platform for translational cancer research.

JUBI HEO[1], Choong-Jae LEE[1], Eun Joo LEE[1], Sung Weon Choi[2], Sang-Jae Park[3], Sang Myung Woo[3], Sang Yoon Park[4], Myong Cheol Lim[4], So-Youn Jung[5], Bo Hyun Kim[3], Jung Won Chun[3], Joohyun Hong[6], Wonyoung Choi[1], Sun-Young Kong[1]

[1]Targeted Therapy Branch, National Cancer Center(NCC), Goyang, Korea, Republic of,[2]Department of Oral and Maxilofacial Surgery, National Cancer Center(NCC), Goyang, Korea, Republic of,[3]Center for Liver and Pancreatobiliary Cancer, National Cancer Center(NCC), Goyang, Korea, Republic of,[4]Center for Gynecologic Cancer, National Cancer Center(NCC), Goyang, Korea, Republic of,[5]Center for Breast Cancer, National Cancer Center(NCC), Goyang, Korea, Republic of,[6]Center for Colorectal Cancer, National Cancer Center(NCC), Goyang, Korea, Republic of

Purpose Patient-derived organoids (PDOs) are useful cancer models because they reflect important features of each patient's tumor. In Korea, however, researchers have not had enough PDO samples with clear clinical information. To improve this situation, the National Cancer Center created a platform to collect organoids from different cancers and provide reliable models that can be used for research.
Methods Tumor specimens were obtained through surgical resection, image-guided biopsy, and malignant body fluids. All samples were processed using a unified workflow covering tissue handling, enzymatic dissociation, organoid culture, and criteria for long-term growth. PDOs that continued to grow for more than five passages were classified as successfully established. Quality checks included STR profiling, mycoplasma testing, and histologic and genomic evaluation to ensure accuracy and safety. Clinical and pathological information was linked to each PDO, and biobanking procedures were used for long-term storage. Selected models were evaluated in drug-response assays using a 384-well screening format.
Results The platform currently maintains 122 PDO models across multiple cancer types, including oral (n = 33), pancreatic (n = 20), tongue (n = 16), gastric (n = 16), ovarian (n = 9), gallbladder (n = 8), biliary tract (n = 8), breast (n = 5), liver (n = 4), and colorectal cancers (n = 3). These PDOs preserved key histopathologic, genetic, and phenotypic characteristics of their matched tumors and were successfully cryopreserved for long-term use. Drug-response profiling of 42 PDOs with 46 therapeutic agents revealed substantial inter-tumoral variability, and several investigational compounds demonstrated notable antitumor activity. In representative cases, ex vivo cytotoxic responses corresponded with clinical treatment outcomes, underscoring the translational relevance of the platform.
Conclusions This PDO platform provides a centralized and high-quality resource that reflects the biological and clinical diversity of human cancers. By supporting systematic drug screening, mechanistic studies, and biomarker-based precision approaches, the platform offers essential infrastructure to advance translational oncology research and promote the development of personalized therapeutic strategies in Korea. This research was supported by the Bio&Medical Technology Development Program of the National Research Foundation (NRF) funded by the Korean government (MSIT) (No. RS-2025-19542979)

#7533 The protease MALT1 is required for chronic lymphocytic leukemia genesis in Eμ-TCL1 mice.

Delia Carlino[1], Julia Boehling[1], Terri Rasmussen[2], Van Hoang[1], Carole Bitar[3], Matthew Burow[1], Nakhle Saba[1]

[1]Hematology/Oncology, Tulane School of Medicine, New Orleans, LA,[2]Tulane School of Medicine, New Orleans, LA,[3]Dermatology and Dermatopathology, Tulane School of Medicine, New Orleans, LA

The Bruton's Tyrosine Kinase inhibitors, such as ibrutinib, acalabrutinib, and zanubrutinib, are leading the frontline treatment in Chronic lymphocytic leukemia (CLL), but acquired resistance represents a significant clinical challenge. Our group has previously shown that targeting Mucosa-Associated Lymphoid Tissue 1 (*MALT1*) *in vitro* induces apoptosis in ibrutinib-sensitive and -resistant CLL cells, suggesting the involvement of the MALT1 axis in CLL progression and survival. Here, we generated a mouse model crossbreeding the Eμ-*TCL1* transgenic C57BL/6 system of spontaneous CLL with CRISPR-mediated *MALT1* knockout (KO) mice to test the requirement for *MALT1* in CLL development. Through genotyping, we established four cohorts with at least 25 mice per cohort: Eμ-TCL1^{wt}/*MALT1*^{wt}, Eμ-TCL1^{wt}/*MALT1*$^{+/-}$, Eμ-TCL1^{wt}/*MALT1*$^{-/-}$, and Eμ-TCL1$^{-/-}$/*MALT1*$^{-/-}$. We measured leukemia burden in these groups by measuring splenomegaly and collecting cells from the bone marrow, spleen, and peritoneal fluid following euthanasia and analyzed cell populations using flow cytometry. Our results show low/negligible CLL burden in the Eμ-TCL1$^{-/-}$/*MALT1*$^{-/-}$ and Eμ-TCL1^{wt}/*MALT1*$^{-/-}$ cohorts. Conversely, the Eμ-TCL1^{wt}/*MALT1*^{wt} and Eμ-TCL1^{wt}/*MALT1*$^{+/-}$ groups showed higher levels of CLL cell populations in each compartment. The largest median number of cells that were positive for CLL markers were in the peritoneal fluid and were 43% and 53% respectively. There was no statistical significance between the Eμ-TCL1^{wt}/*MALT1*^{wt} and Eμ-TCL1^{wt}/*MALT1*$^{+/-}$ cohorts in terms of CLL positive cells or levels of splenomegaly. There were significant differences between the Eμ-TCL1$^{-/-}$/*MALT1*$^{-/-}$ and Eμ-TCL1^{wt}/*MALT1*$^{-/-}$ cohorts versus the Eμ-TCL1^{wt}/*MALT1*^{wt} cohort in both the peritoneal fluid (p-value = 0.0162 and 0.0161 respectively) and the bone marrow (p-value = 0.0016 and 0.0017 respectively), but not the spleen. Using the Kaplan-Meier method to compare overall survival of the four groups, we showed that all cohorts survived longer than the Eμ-TCL1^{wt}/*MALT1*^{wt} cohort. The majority of mice in the Eμ-TCL1$^{-/-}$/*MALT1*$^{-/-}$ and Eμ-TCL1^{wt}/*MALT1*$^{-/-}$ cohorts expired due to non-CLL-related complications, namely the development of dermatological lesions and ocular ulcers. These complications led to the Eμ-TCL1wt/MALT1+/- cohort having the largest median survival at 435 days. Therefore, we were able to show that MALT1 knockout mice experienced lower leukemia burden, as defined by positive CLL cells and splenomegaly. Our data concerning the dermatopathological complications associated with the Eμ-TCL1$^{-/-}$/*MALT1*$^{-/-}$ and Eμ-TCL1^{wt}/*MALT1*$^{-/-}$ cohorts highlights potential side effects of MALT1 inhibition and are of note due to the frequent clinical presentation of cutaneous lesions in CLL patients. Overall, our data suggest that MALT1 is required for CLL leukemogenesis and may represent a critical component in therapeutic targeting.

#7534 Novel mouse models for cancer research.

Jason Beckwith, Jen Merriam, Darcy Pomerleau, Crystal Davis, Jennifer Kelmenson, Hiroaki Onda

The Jackson Laboratory, Bar Harbor, ME

The Jackson Laboratory (JAX) is a centralized resource of genetically defined mutant and transgenic mice to support the scientific research community. This poster will highlight new models available for specific cancers, xenograft recipients, immunodeficient platforms for PDX studies and multi-purpose tool strains having CRISPR utility, conditional/inducible expression (Cre-lox, FLP-frt, Tet-On/-Off), optogenetic function and calcium-sensing technologies. The NSG (NOD scid IL2rγc-/-) portfolio of strains for transplantation/engraftment and humanized mouse research continues to grow, with recent humanized alleles (*e.g.*, IL6, TSLP) expanding the options for immune-oncology studies. New mouse lines for cancer immunology and antibody therapeutic studies combine humanized FCGRT and ALB alleles for human preclinical pharmacokinetics (HuPK), as well as humanized PD-1 and PD-L1 alleles. Novel fluorescent strains include Gene Editing Reporters for visualizing homology-directed repair (HDR) and non-homologous end joining (NHEJ) repair events, as well as several CRISPR Editing, Bxb1 Integrase Editing, Base Editor, Prime Editor and DNA repair pathway tools. In addition to cryopreserving each strain, JAX employs a genetic quality control program that confirms mutation identity and genetic background, and screens for common unwanted alleles (via testing for neo, Cre, FLP, GFP, RFP, etc.). Cancer researchers are encouraged to query the collection of innovative mouse models using the JAX Mouse Search website (mice.jax.org). This resource includes models created by many generous donating institutions. Researchers are encouraged to donate their mouse lines via a very short Strain Submission form (jax.org/donate-a-mouse). Please also visit the JAX Oncology webpage for cancer research related strains and resources (jax.org/jax-mice-and-services/solutions-by-therapeutic-area/oncology). JAX is supported by the NIH, The Howard Hughes Medical Institute and other private charitable foundations.

#7535 Over 800! Establishment of an ADC payload efficacy database across diverse tumor cell lines: Foundation for optimized in vitro ADC evaluation and drug development.

Guoqian Wang, Yao Tang, Jingxiao Xu, Tingduo Lv, jinying ning, **Feng Hao**

Kyinno Biotechnology Co., LTD, Beijing, China

Ever since the first antibody-drug conjugate (ADC), Mylotarg, received approval back in 2000, the ADC market has expanded to include 15 approved products so far, while more than 210 others are currently in clinical trials. This indicates that ADC drug development has stepped into a thriving phase—especially when targeting molecules like HER2, EGFR, Trop2, CLDN18.2, and Nectin-4, ADCs have demonstrated notable efficacy and favorable safety profiles. As such, ADC therapy holds extremely broad application prospects in the field of cancer treatment.Antibody-drug conjugates (ADCs) consist of three core components: a monoclonal antibody, a linker, and a toxin. Among these, the ADC toxin—also referred to as the ADC payload—is a critical element of ADC drugs, as it serves as the key factor determining the drug's potency. The payloads used in approved ADCs are highly toxic; major examples include MMAE/MMAF, calicheamicin, DM1/DM4, and SN38/Dxd. Compared with traditional chemotherapy drugs, these payloads are 1 to 2 orders of magnitude more toxic, and some even reach toxicity levels in the picomolar (pM) range. For payloads currently under development, their mechanisms of action mainly fall into four categories: DNA alkylating agents, DNA topoisomerase inhibitors, microtubule disruptors, and RNApolII inhibitors.We have established an extensive cell bank, which houses over 800 human tumor cell lines and 100 animal tumor cell lines, covering all types of cancers. Leveraging this rich cell resource, we are constructing an ADC screening platform. Through comprehensive testing, we collect efficacy data of different ADC payloads across various cell lines—this data then guides us in selecting appropriate cell lines for in vitro ADC evaluation. Up to now, we have already finished over 700 commonly used cell lines using several ADC payloads, such as MMAE, SN38, Dxd, and exatecan. As a large-scale initiative, the ADC screening platform is expected to play a positive and supportive role in the screening and evaluation of ADC drugs.

#7536 In vitro and in vivo screening platform for discovery of JAK2 inhibitors.

Na Li, Hao Huang, Xinyu Zhong, Guoqian Wang, Xuyang Duan, Yue Huang, Jinying Ning, **Feng Hao**

Kyinno Biotechnology Co., LTD, Beijing, China

Background: The JAK-STAT signaling pathway, activated by cytokine receptors, plays a central role in regulating cell proliferation, differentiation, apoptosis, and immune responses. JAK2, a key kinase in this pathway, transduces signals from hematopoietic growth factor receptors such as thrombopoietin (TPO), erythropoietin (EPO), and granulocyte-macrophage colony-stimulating factor (GM-CSF). Dysregulation of JAK2 is implicated in the pathogenesis of myeloproliferative neoplasms (MPNs), including polycythemia vera (PV), myelofibrosis (MF), and essential thrombocythemia (ET).
Objectives: This study aimed to evaluate the efficacy of JAK2 inhibitors, elucidate their mechanisms of action, and identify optimal dosing strategies to maximize therapeutic benefit while minimizing adverse effects.
Method: An *In vivo*, a murine model of JAK2-driven myeloproliferative disease was established by intravenous transplantation of JAK2-activated cell lines into BALB/c nude mice. Disease progression was monitored using bioluminescent imaging. Terminal analyses included evaluation of splenomegaly, serum biochemistry (ALT and AST), and splenic histopathology (hematoxylin and eosin staining).For *in vitro* analysis, a panel of cell lines was treated with increasing concentrations of JAK inhibitors (Ruxolitinib, Fedratinib, and Tofacitinib) to evaluate compound efficacy. Inhibition of downstream JAK2-STAT5 signaling was quantified using an α-LISA for phosphorylated STAT5 (p-STAT5). Dose-response profiles were generated, and IC_{50} values were calculated to determine the relative sensitivity of the cells to each agent.
Results:*In vivo*, our model mice displayed progressive increases in bioluminescent signal, marked splenomegaly and hepatomegaly, decreased survival, and elevated serum ALT/AST levels. Ruxolitinib treatment significantly suppressed bioluminescent signal progression, reduced hepatic and splenic tumor burden, and extended survival.*In vitro*, Ruxolitinib potently and dose-dependently inhibited JAK2-STAT5 signaling, with IC_{50} values confirming target sensitivity. The cell lines exhibited differential sensitivity to the JAK2 inhibitors Ruxolitinib, Fedratinib, and Tofacitinib.
Conclusion: We established integrated *in vivo* and *in vitro* screening platforms for the discovery and evaluation JAK2 inhibitors. This model provides a valuable tool for optimizing treatment regimens against JAK2-driven pathologies.

#7537 From BTK in-situ mutation (C481S, A428D, etc.) to in vivo screening: A comprehensive platform to address drug resistance in BTK-targeted therapy.

Yao Tang, Guoqian Wang, Hao Huang, Yue Huang, Jinying Ning, **Feng Hao**

Kyinno Biotechnology Co., LTD, Beijing, China

Bruton's tyrosine kinase (BTK) is a core regulatory molecule in the B-cell receptor (BCR) signaling pathway. It is constitutively expressed in myeloid and lymphoid cells and plays a decisive role in the proliferation, survival, differentiation, activation, and apoptosis of B cells. Abnormal activation of BTK is closely associated with B-cell malignancies such as chronic lymphocytic leukemia (CLL) and mantle cell lymphoma (MCL). In hematologic tumors, BTK inhibitors block key steps in the BCR signaling pathway, thereby inhibiting the proliferation and survival of tumor cells. Ibrutinib is the first effective covalent Bruton's tyrosine kinase inhibitor (BTKi), approved by the U.S. Food and Drug Administration (FDA) in 2013, ushering in an era of chemotherapy-free treatment for B-cell malignancies. Second-generation covalent BTK inhibitors, including acalabrutinib, zanubrutinib, and orelabrutinib, have also been approved for marketing in China. The advent of BTK inhibitors has had profound significance for the treatment of B-cell malignancies, improving the treatment modalities and prognosis for patients with B-cell lymphoma. However, traditional BTK inhibitors exhibit poor kinase selectivity and a high incidence of off-target adverse reactions. Moreover, in recent years, although BTK inhibitors (such as ibrutinib and acalabrutinib) have significantly improved patient survival, the issue of drug resistance has become increasingly prominent—approximately 30% of patients develop resistance due to BTK gene mutations (e.g., C481S, T474I, L528W, etc.), limiting therapeutic efficacy. Through breakthroughs in in-situ mutation technology, kyinno has precisely introduced specific BTK mutations directly into the genome of TMD8 cells, preserving the natural expression regulatory mechanisms. This provides a more clinically relevant "touchstone" for analyzing BTK resistance mechanisms and developing targeted therapies. Kyinno has developed over 20 BTK in-situ mutant cell lines (including single mutations such as C481S, T474I, A428D, L528W, and compound mutations). These novel cell models, based on in-situ mutation technology, enable systematic evaluation of the dynamic impact of different mutations on drug binding and guide the structural optimization of next-generation inhibitors. Additionally, we have developed in vitro and in vivo screening platforms based on these mutant cell lines, enabling rapid validation of lead compounds from the molecular to the organism level, thereby accelerating BTK inhibitor development.

#7538 Establishment of a translational research ecosystem: A globally networked PDX model platform to accelerate oncology drug development.

Alyssa Simonson[1], Anna Stackpole[1], Amy Fredrickson[1], Johnnie Mitchell[1], Jennifer Garcia[1], Natalia Banos Herraiz[1], Jim Lund[1], Ashley Jamison[1], Andrew Cunningham[1], Kyriakos P. Papadopoulos[2], Victor Moreno Garcia[3], Emiliano Calvo[3], Chris Takimoto[2], Michael J. Wick[2]

[1]The START Center for Cancer Research- XenoSTART, San Antonio, TX,[2]The START Center for Cancer Research, San Antonio, TX,[3]The START Center for Cancer Research- Madrid, Madrid, Spain

Background: Patient-derived xenograft (PDX) models continue to play a critical role in translating novel oncology drug innovation from discovery through late-stage development. The START Center for Cancer Research is a global translational and clinical trials oncology network that includes XenoSTART, a PDX development and testing division. XenoSTART offers end-to-end capabilities, beginning with the establishment of PDX models directly from conventional and trial patients across diverse indications, reflecting current treatment landscapes with the added ability to support a full suite of in vivo study capabilities, provide models and data under license, and tailored model development. Strategic partnerships allow for extended service capabilities which include orthotopic imaging, radioligand therapy (RLT), and humanized systems capabilities, enabling mechanistic depth and modality-specific translational insights rarely available through a single platform.

Methods: XenoSTART PDX (XPDX) models are collected from primary or metastatic patient tumor samples and engrafted into immunocompromised mice under standardized workflows; a curated extraction of clinical details and treatment histories from donor patients ranging from newly diagnosed through heavily pretreated is performed for all collected samples. Resulting models are serially passaged and further developed until growth stabilization. Established models are profiled using integrated molecular and pathological analysis including WES and RNAseq, receptor expression, and advanced bioinformatics to support biomarker discovery or mechanistic insights and further characterized through in vivo responses to standard-of-care and emerging therapies. Bioinformatic analyses are conducted using validated pipelines to evaluate molecular signatures and biomarker associations. In vivo studies following harmonized protocols align with clinically relevant dosing schedules.

Results: The XenoSTART platform generates a diverse and deeply characterized XPDX repository reflecting contemporary treatment landscapes, with high rates of molecular and phenotypic fidelity. Treatment benchmarking replicates known clinical response patterns to standard-of-care agents. Integrated clinical and molecular datasets revealed biomarkers associated with treatment sensitivity and resistance. Specialized collaborations enable innovative translational studies including orthotopic imaging, RLT, and humanized immune-oncology evaluation.

Conclusion: XenoSTART's globally connected PDX ecosystem provides a clinically focused, best-in-class translational resource that enhances predictive accuracy, informs patient-stratification strategies, and drives more confident decision-making from early discovery through late-stage clinical development.

#7539 *In vivo* metastatic prostate tumor model development and follow-up progression using *in vivo* bioluminescence imaging.

Vincent Faugeroux, Nicolas Hoffmann, Sarah Belderbos, Maeva Albanese, Kenny Herry, Nicolas Ancellin, Caroline Mignard, **Marc Hilairet de Boisferon**

Oncodesign Services, Dijon, France

Prostate cancer is the most frequently diagnosed malignancy in men and the second leading cause of cancer-related death after lung cancer. Its incidence is highest in high-income regions. Although widespread screening allows approximately 80% of cases to be detected while still organ-confined, 15–20% of patients present with locoregional or distant metastases. In the United States, the proportion of men diagnosed with metastatic disease has been rising in recent years, particularly among younger patients. Clinical outcome strongly correlates with tumor grade and stage at diagnosis; men with metastatic disease have significantly reduced overall survival compared with those with localized tumors. The primary metastatic sites are lymph nodes and bone, followed by liver and lung. However, few preclinical models effectively recapitulate these advanced stages, creating a critical gap for evaluating novel therapeutics.

Here, we describe the establishment of liver and lung metastases in immunodeficient male mice using 22Rv1-Luc-mCherry prostate cancer cells delivered via intratibial or intra-arterial injection. Mice were monitored three times per week for clinical condition and body weight. Tumor progression was assessed by in vivo bioluminescence imaging once per week for five weeks. At euthanasia, major organs were collected for ex vivo imaging to confirm metastatic localization.

Following intratibial inoculation, bioluminescence increased initially at the injection site during the first two weeks, then predominantly in the liver and lungs from days 15 to 42. These findings were confirmed by ex vivo imaging. After intra-arterial inoculation, early bioluminescence was detected primarily in bone through day 28, followed by a marked increase in the liver between days 28 and 35. Ex vivo imaging verified metastatic dissemination to the liver, limb bones, spinal column, and seminal vesicles.

In summary, we report a reproducible metastatic prostate cancer model that mimics key features of late-stage disease, providing a valuable platform for preclinical evaluation of new therapeutic compounds

#7540 Integrated multi-omics analysis reveals conserved tumor-associated antigens (TAAs) profiles in PDX and organoid models for advancing ADC development.

Xiaolong Tu[1], Likun Zhang[1], Jie Lin[1], Hengyuan Liu[1], Jun Zhou[1], Marrit Putker[2], Ludovic Bourre[2], Julie Myer[2]

[1]Crown Bioscience, Taicang, China,[2]Crown Bioscience, Inc., San Diego, CA

Introduction The development of antibody-drug conjugates (ADCs) requires reliable tumor-associated antigens (TAAs) expression for efficacy, necessitating predictive preclinical models. Patient-derived xenografts (PDXs) preserve patient tumor characteristics, which serve as a mainstay in translational oncology research, while patient-derived organoids (PDOs) and PDX-derived organoids (PDXOs) have recently emerged as powerful *in vitro* 3D systems that offer enhanced scalability while retaining key biological features of the original tissue. However, their fidelity in maintaining TAA profiles requires multi-omics validation. This study evaluates TAA consistency across platforms and between PDXs and matched organoids.

Methods We analyzed 18 clinically relevant TAAs using IHC on ~1000 PDX models across 18 cancer types. IHC quantification was analyzed using HALO AI platform to generate H-Score, this data was integrated with RNA-seq and MS-mass spectra-proteomics from Crown Bioscience's database to determine the correlation coefficients. To assess model translatability, a focused panel of 10 key TAAs was selected for IHC assessment between a subset of ~400 characterized PDXs and their paired PDOs/PDXOs, enabling a cross-model comparison.

Results Our integrated multi-omics analysis within the extensive PDXs cohort demonstrated a high degree of concordance between protein expression (H-Score) and both transcriptomics and proteomics data for the 18 investigated TAAs, including HER2(R_{RNAseq}=0.871,$R_{Proteomics}$=0.765), TROP2(R_{RNAseq}=0.852, $R_{Proteomics}$=0.775), Nectin-4(R_{RNAseq}=0.679, $R_{Proteomics}$=0.861), DLL3(R_{RNAseq}=0.75, $R_{Proteomics}$=0.698), CEACAM5(R_{RNAseq}=0.799, $R_{Proteomics}$=0.743). Critically, a remarkably high degree of concordance was observed in TAAs protein expression patterns between PDXs and their paired PDOs/PDXOs models, including TROP2(R=0.946, P<0.0001), Nectin-4(R=0.772, P<0.0001), DLL3(R=0.819, P<0.0001), HER3(R=0.659, P<0.0001), Claudin 18.2(R=0.775, P<0.0001). The consistency of IHC intensity and heterogeneity characteristics between organoids and their in vivo counterparts further supports this molecular fidelity.

Conclusion This study validated TAAs expression concordance across multi-omics platforms in a large PDX cohort. More significantly, we deliver compelling evidence that PDOs/PDXOs models exhibit exceptional fidelity in maintaining the TAA expression landscape of their corresponding PDX tumors, demonstrating PDOs/PDXOs as highly reliable and invaluable tools from initial target validation and lead antibody characterization to the formulation of biomarker-driven patient selection strategies in clinical trials.

#7541 Comprehensive preclinical *in vivo* oncology platform for rational drug candidate nomination.

Amandine Alard, Marie Lafitte, Nizar Serhan, Giuseppina Claps, Frederique Dol-Gleizes, Pascale Lejeune

Evotec, Toulouse, France

Introduction: Robust in vivo pharmacology is critical to de-risk oncology drug candidates and guide translational decision-making. Evotec's integrated preclinical platform combines scientific and animal welfare expertise with AAALAC and My Green Lab accreditations to accelerate candidate nomination.
Methods and Results: Leveraging multidisciplinary capabilities such as chemistry, early formulation, ADME/DMPK (LC-MS/MS), in vitro biology, and translational biomarker analysis is essential to support projects at any stage of drug discovery and whatever the therapeutic modality: small molecules, degraders, ADCs, antibodies, oligonucleotides, cell therapies, vaccines, and oncolytic viruses. Our extensive tumor model repertoire covers multiple cancer indications and includes CDX and syngeneic models implanted SC, orthotopically or as metastatic model in a variety of mice backgrounds, immunocompetent, immunosuppressed or humanized for the immune system. We describe here case studies illustrating flexible study designs that include:•Target validation with engineered cancer cells•PK/PD studies (single/repeated dosing)•Tolerability for chronic dosing derisking•Efficacy studies assessing anti-tumor activityReadouts encompass tumor growth inhibition, PK/PD correlation, target engagement, transcriptomics, proteomics, metabolomics, and tumor microenvironment characterization.In addition, deciphering the relationship between PK, PD markers modulation and antitumor efficacy is of great value to model and predict human dose. Experts at Evotec have access to several modeling and simulation softwares from PK, PK/PD, PBPK, statistical and mathematical analysis to optimize dosing for best efficacy while minimizing toxicity.
Conclusion: Our platform enables tailored strategies that integrate PK/PD and biomarker-driven endpoints to optimize dosing and predict efficacy. Over 5 years, our multidisciplinary expertise delivered comprehensive in vivo solutions that accelerated oncology drug discovery with the nomination of nine preclinical drug candidates progressing in the clinic.

#7542 *In vitro* and *in vivo* evaluation of bortezomib using the 5TGM1 cell line and a syngeneic mouse model of multiple myeloma.

Mari I. Suominen, Katja M. Fagerlund, Justyna Zdrojewska, Jukka P. Rissanen, Jenni H. E. Maki-Jouppila

Pharmatest Services Ltd., Turku, Finland

Multiple myeloma (MM) is the second most prevalent hematologic cancer, originating from plasma cells (differentiated B-cells) and accounting for approximately 2% of cancer-related deaths. Clinical manifestations often include bone pain due to osteolytic lesions, pathologic fractures, and hypercalcemia. MM typically exhibits a low proliferative index and relies heavily on its surrounding microenvironment, making it resistant to conventional chemotherapy. However, these same characteristics present opportunities for emerging therapies, such as stroma-targeting agents and immunotherapies. The success of these novel strategies depends on robust preclinical models that accurately reflect both immune function and the tumor microenvironment. To support the relevance of the syngeneic 5TGM1 murine model in drug development, we evaluated the sensitivity of 5TGM1 cells to bortezomib both *in vitro* and *in vivo*.

In vitro, 5TGM1 cells were cultured for six days, and cell viability was assessed using the CellTiter-Glo assay on days 0, 3, and 6. The EC50 value for bortezomib was determined, confirming its cytotoxic effect on 5TGM1 cells. *In vivo*, female C57Bl/KaLwRij mice (6-8 weeks old) were intravenously inoculated with 5TGM1 cells. Bortezomib treatment was initiated one day post-inoculation and administered intraperitoneally. The study included an untreated control group, a group receiving bortezomib twice weekly, and a group receiving bortezomib thrice weekly. Additionally, untreated satellite animals were included to evaluate disease progression and were sacrificed on day 35, prior to the termination of the main study. Mice were monitored daily for clinical condition, with body weight recorded twice a week. Sacrifice criteria included ≥20% weight loss or paraplegia. Serum IgG2b levels, which indicate disease progression, were measured from samples collected before inoculation, on day 21, day 35, and at sacrifice. Gross necropsy was performed to assess metastases, and *ex vivo* microCT scans of both tibias were conducted to analyze osteolytic lesions.

Bortezomib was well tolerated, with no significant differences in body weight between groups. The termination day was determined based on disease progression in the vehicle control group; 40% of the vehicle group was sacrificed on day 41, and the remaining animals were sacrificed the following day. IgG2b levels were reduced in treated groups, particularly in the thrice-weekly regimen. However, bortezomib did not prevent the progression of bone lesions, which increased notably in the final week of the study.

These findings support the use of bortezomib as a reference compound *in vitro* and *in vivo* in the 5TGM1 model, demonstrating its efficacy in reducing tumor burden as indicated by IgG2b levels. However, its protective effect on bone integrity remains limited.

#7544 Validation of a bone metastasis technology platform against clinically used standard-of-care therapies.

Tiina E. Kahkonen[1], Jie Wen[2], Ru Yang[2], Jussi M. Halleen[1]

[1]OncoBone Ltd, Kiviniemi, Finland,[2]PharmaLegacy LLC, Shanghai, China

Bone metastases are a significant clinical problem in many major cancers, especially in breast and prostate cancer where 70-90% of advanced patients develop bone metastases. Myeloma bone disease is associated with similar clinical problems than bone metastases. Current cancer therapies can only partially decrease tumor growth in bone, resulting in only 5% of bone metastatic patients being alive 5 years after the diagnosis. Bone metastases decrease the quality of life of patients due to cancer-induced bone loss that leads to increased risk of fractures and bone pain. Bone metastases are therefore a high unmet medical need with a high demand for effective therapies.

Lack of appropriate preclinical bone metastasis models that would exhibit the same clinical features and responses to therapies that are observed in bone metastatic patients has made it difficult to advance therapy development at early stages. In this study, we validated our previously established Bone Metastasis Technology Platform (BMTP©) against standard-of-care (SOC) therapies in triple-negative breast cancer (TNBC) and castration-resistant prostate cancer (CRPC) bone metastasis models, and in a multiple myeloma (MM) bone disease model.

In this study, we used the following cell lines and mouse strains: 4T1 mouse TNBC cells in BALB/c mice, RM-1 mouse CRPC cells in C57BL/6 mice, and human RPMI 8226 MM cells in immunodeficient NPG mice. Intratibial inoculation into the bone marrow was used to model tumor growth in bone. Tumor growth was monitored by bioluminescence imaging, cancer-induced bone changes by X-ray imaging, and bone pain by Von Frey filaments (mechanical allodynia). SOC treatments included doxorubicin (4 mg/kg, ip, BIW) in the TNBC model, docetaxel (10 mg/kg, ip, BIW) in the CRPC model, bortezomib (0.5 mg/kg, ip, BIW) in the MM model, and zoledronic acid (0.1 mg/kg, QW) in all models as an inhibitor of cancer-induced bone loss.

In the TNBC model, doxorubicin decreased tumor growth and both doxorubicin and zoledronic acid decreased bone loss. Neither therapy was effective in reducing bone pain. In the CRPC model, docetaxel decreased tumor growth and zoledronic acid decreased bone loss, but no effects were observed on bone pain. In the MM model, bortezomib decreased tumor growth and zoledronic acid decreased bone loss.

These results demonstrate that BMTP shows the same clinical features and responses to therapies that are observed in patients with TNBC, CRPC and MM. We conclude that BMTP is a clinically relevant translational tool for evaluating efficacy of cancer therapies on bone metastasizing cancers.

#7548 Mechanistic insights into reactive oxygen species (ROS) homeostasis in ovarian cancer chemoresistance.

Minjun HE[1], Michelle K.Y. SIU[1], Mingo M.H. YUNG[1], Crystal TANG[1], Ruiqian ZHANG[1], Cui CAN[1], Xiaoyan ZHONG[1], Haonan LU[1], Kui LIU[1], Annie N.Y. CHEUNG[2], Hextan Y.S. NGAN[1], David W. CHAN[1], Karen K.L. CHAN[1]

[1]Department of Obstetrics & Gynaecology, The University of Hong Kong, Hong Kong SAR, China,[2]Department of Pathology, The University of Hong Kong, Hong Kong SAR, China

Background: Ovarian cancer remains one of the most lethal gynecologic malignancies, with disease recurrence and platinum resistance representing major therapeutic challenges. Reactive oxygen species (ROS) homeostasis and cancer stem cells (CSC) contribute critically to chemoresistance; however, the molecular mechanisms that sustain CSC expansion under oxidative stress remain insufficiently defined. This study investigated how ROS regulation in ovarian cancer spheroids engages NOTCH1/HES1 and IL11/STAT5-mediated signaling to drive stemness and resistance to cisplatin.

Methods: Ovarian cancer cell-derived spheroids and/or patinum-resistant patient-derived organoids were used to evaluate ROS homeostasis, antioxidant enzyme expression, and CSC phenotypes. ROS levels and MnSOD/HO-1 expression were assessed by fluorescence detection and immunoblotting. Expression, promoter activity and/or activation of P38/NRF2, NOTCH1/HES1, and IL11/STAT5 signaling were examined by qPCR, Western blotting, and reporter assays. Gene silencing of MnSOD, HO-1, HES1 or NRF2 was achieved using siRNA. Pharmacologic inhibition was performed using GSI-MK0752 (NOTCH1/HES1) and CYT387 (JAK2/STAT5). CSC activity was quantified by ALDH assays, CD44 expression, and spheroid formation capacity. An orthotopic ovarian cancer xenograft model was used to evaluate therapeutic efficacy of cisplatin given alone or in combination with pathway inhibitors.

Results: Ovarian cancer spheroids maintained a low-ROS environment through induction of key antioxidants MnSOD and HO-1. Cisplatin activated spheroids P38/NRF2 signaling, which consequently upregulated NOTCH1/HES1 signaling. Silencing of MnSOD, HO-1, or NRF2 impaired spheroids NOTCH1/HES1 activation. Pharmacologic inhibition of either NOTCH1/HES1 or IL11/STAT5 signaling confirmed the NOTCH1/HES1 and IL11/STAT5 signaling axis and decreased spheroids CSC markers and $ALDH^+/CD44^+$ CSC subpopulations, while dual inhibition produced synergistic effects. Moreover, CSC subpopulations enhanced cisplatin responsiveness. Cisplatin induced organoids NOTCH1 activation and promoted STAT5 signaling and expanded $ALDH^+/CD44^+$ CSC subpopulations. In vivo, combined pathway blockade with cisplatin significantly reduced tumor burden and ascites formation compared with monotherapies.

Conclusion: A ROS-responsive NOTCH1/HES1 and IL11/STAT5 signaling axis plays a central role in maintaining CSC populations and promoting platinum resistance in ovarian cancer. Dual targeting of these signaling pathways disrupts the redox-regulated circuit and enhances cisplatin efficacy, supporting further investigation of this combinatorial strategy as a potential therapeutic approach for platinum-resistant ovarian cancer.

Acknowledgement: HMRF (18191641).

#7549 Development of personalized medicine strategies for rectal cancer.

Kiki Lianos[1], Kelly Olsen[1], Aleksandra Edmundson[2], Danielle Siganto[2], Matthew Burge[3], David Clark[2], Vicki Whitehall[1]

[1]Conjoint Gastroenterology Laboratory, QIMR Berghofer, Brisbane, Australia,[2]The Department of General Surgery, Royal Brisbane and Women's Hospital, Brisbane, Australia,[3]The Department of Medical Oncology, Royal Brisbane and Women's Hospital, Brisbane, Australia

Background: Standard of care treatment for patients with locally-advanced rectal cancer includes neoadjuvant chemoradiotherapy followed by surgery. However, this treatment is toxic affecting the patient's quality of life. Additionally, 20% of patients achieve a complete response, 15% show no response and 30-40% may develop metastasis post treatment. Therefore, predicting patient response to treatment would be beneficial to inform clinicians if treatment is not optimal. 3D patient-derived tumor organoids (PDTOs) have been used to predict patient response to treatment due to their ability to replicate the biology and drug responsiveness of the original tumor. My project aims to use rectal cancer PDTOs to develop a personalized medicine strategy to accurately predict patient clinical response prior to therapy to inform clinicians of their treatment options. Patient-derived normal organoids (PDNOs) will also be used for toxicity assessment.

Methods: Rectal cancer patients that meet the required criteria were recruited. Biopsies were collected via flexible-sigmoidoscopy and processed immediately in the laboratory for PDO establishment. Post establishment, patient-derived organoids (PDOs) were tested using a chemoradiation assay to determine sensitive, partial and resistant responders. On day 0, PDOs were seeded on a 384 well plate in 5% matrigel. On day 2, PDOs were exposed to Fluorouracil (0.412uM) followed by radiation (2 and 4 Grays). On day 7, live cells were measured using CellTiter Glo 3D Cell Viability Assay (Promega) on the Cytation 5 multiplate reader. Treatment sensitivity was investigated by calculating 50% growth rate (GR50) using Graphpad Prism.

Results: To date, 14 patients have been recruited and 11 (78.5%) patient biopsy samples have been collected. Out of the collected biopsy samples, 7 out of 10 (70%) have been established with one currently in progress. Chemoradiation assays have been completed for 5 of the 7 established PDOs (RC-001, RC-003, RC-006, RC-008 and RC-010). RC-001 PDTOs exhibited a cytotoxic effect indicating complete response to treatment. The remaining PDTOs illustrated a partial effect indicating partial response to treatment. RC-001, 003, 008 and 010 PDNOs achieved GR50 at 4Gy whereas RC-006 PDNOs achieved GR50 at 2.2Gy. These results indicate that the complete responder could potentially benefit from chemoradiation treatment and the partial responders and could potentially benefit from additional treatment strategies with one partial responder potentially more susceptible to adverse treatment effects.

Conclusion: This project is the first of its kind in Australia to predict patient response to chemoradiotherapy using PDOs. We demonstrate varied patient response to treatment and the important information that could potentially be garnered. Our work has the potential to inform selection of optimal therapy for patients and improve rectal cancer outcomes.

: Psychosocial and Behavioral Epidemiology, Health Services Research, Implementation Science, Pharmacoepidemiology, and Other Topics
Poster Session

#7553 Digital access, health literacy, and cancer beliefs: Findings from a multi-region community survey.

Tingyu Zou[1], Monica L. Albertie[1], Emelina Asto-Flores[1], Manisha Salinas[1], Farhia Omar[2], Adeline Abbenyi[3], Noreen Stephenson[1], Nuwanthi Heendeniya[2], James R. Cerhan[4], Kathleen J. Yost[3], Folakemi T. Odedina[1]

[1]Mayo Clinic, Jacksonville, FL,[2]Mayo Clinic, Phoenix, AZ,[3]Mayo Clinic, Rochester, MN,[4]Mayo Clinic College of Medicine and Science, Rochester, MN

Background: Digital access, health literacy, and confidence in obtaining cancer information are well-known factors that influence cancer beliefs and behaviors. However, less is understood about whether these information-related factors vary across regions within a cancer center's catchment area and how they collectively relate to cancer beliefs in large community samples. This study investigated regional differences in digital access, health literacy, and confidence in seeking information, and examined the connections between these factors and cancer risk perceptions, fatalistic beliefs, prevention confusion, and willingness to participate in cancer clinical trials.
Methods: Data (N=2,334) from the 2023 Mayo Clinic Comprehensive Cancer Center's Cancer-Focused Needs Assessment, conducted across catchment areas in Arizona, Florida, and the Midwest (Minnesota, Wisconsin, Iowa). Regional differences in digital access (Internet use and device ownership), health literacy, and confidence in obtaining cancer information were analyzed using multivariable ANCOVAs and logistic regressions, adjusting for sociodemographic covariates. Follow-up models examined whether these information precursors are associated with perceived cancer risk, fatalistic beliefs, confusion about recommendations, and willingness to participate in cancer clinical trials, adjusting for the same covariates.
Results: Regions showed minimal differences in digital access and health literacy. Health literacy was instead associated with ethnicity, age, gender, and education (all $p<.001$). Confidence in obtaining cancer information followed similar trends, with significant influences of ethnicity and gender ($p<.01$). Internet use was strongly associated with sociodemographic factors (all $p<.01$). Additionally, the information precursors consistently correlated with cancer beliefs across the full sample: Higher health literacy and greater confidence in obtaining cancer information were associated with increased perceived cancer risk, reduced cancer fatalism, and less confusion regarding prevention guidelines (ps $< .001$). Internet use and device access were significantly related to a greater willingness to participate in clinical trials (ps $< .01$). These relationships persisted even after controlling for sociodemographic covariates.
Conclusions: Regional differences in digital access and health literacy were minimal, indicating a consistent information environment. Within this context, individual sociodemographic and information-related factors played a larger role, strongly shaping cancer beliefs. These findings underscore technology access and information empowerment as key targets for enhancing cancer prevention knowledge and research engagement, and indicate that the effects of information empowerment are primarily driven at the individual rather than the geographic level.

#7554 Strengthening the future cancer workforce: Factors influencing STEM career interest among high school students in Puerto Rico.

Natalie Alamo- Rodriguez[1], Jacquelinee Rojas-Livia[1], Xavier Lopez-Leon[2], Vivian Colon- Lopez[1]

[1]Cancer Control and Population Sciences, University of Puerto Rico Comprehensive Cancer Center, San Juan, PR,[2]Community Outreach and Engagement Office, University of Puerto Rico Comprehensive Cancer Center, San Juan, PR

Introduction: National data indicate a decline in student interest in science and biomedical research, posing risks to the future research and clinical workforce. This is especially concerning in cancer, given the rising incidence of the disease and the growing population of survivors.
Objective: This study aimed to evaluate among public high school students in Puerto Rico, the factors associated with the interest in pursuing careers in STEM. Methods: Two public high schools were randomly selected from among the seven educational regions defined by the Puerto Rico Department of Education (n=14). Following school authorization, teachers distributed parental consent forms and invited students in grades 9-12 to participate in the study. After parental informed consent received, students completed a survey via REDCap. The instrument assessed five domains: sociodemographic characteristics, academic self-efficacy, school climate, perceived social support, and science career motivation. Main dependent variable was students' interest in pursuing careers in STEM, dichotomized as (1) students who intend to or may consider following STEM careers, and (2) students who are not interested or reported not having sufficient knowledge about STEM careers. Student's t-test, Wilcoxon rank-sum test, and Pearson's Chi-square test examined associations between student interest in STEM and potential covariates. Logistic regression was used to estimate odds ratios (OR) and 95% CI. Model selection based on Akaike Information Criterions, Bayesian Information Criterions and likelihood ratio tests.
Results: A total of 197 students were recruited, the majority (62.1%) identified as female and 65% expressed interest in or were considering pursuing a STEM career. In the best-fitting logistic model, higher levels of academic self-efficacy and greater science career motivation significantly increased the odds of students being interested in pursuing STEM careers (OR = 1.71, 95% CI: 1.09-2.80; OR = 2.66, 95% CI: 1.55-4.89, respectively), after adjusting for science self-determination and use of tutoring services.
Conclusions: Our findings show that academic self-efficacy and science career motivation are key drivers of STEM interest among Puerto Rican high school students. Understanding these factors can inform the design of targeted programs that provide early exposure to engaging science experiences, while strengthening students' confidence in their academic abilities, ultimately supporting the development of a skilled workforce capable of meeting the growing demands of cancer research and care. Funding: This work was supported by the NIH (R25MD007607). Ethical approval for the study was secured from the UPR-CCC IRB (20503011465). Declaration of Generative AI and AI-assisted technologies in the writing process: During the preparation of this work the authors used AI for editing.

#7555 Association of political ideology and fatalistic cancer beliefs.

Chinenye M. Okafor[1], Chinenye C. Egwuonwu[2], Onyema Chido-Amajuoyi[3], Henry Onyeaka[4]

[1]The Medical University of South Carolina (MUSC), Florence, SC,[2]Piedmont Athens Regional, Athens, GA,[3]Fred Hutchinson Cancer Center, Seattle, WA,[4]Geisinger Health, Moosic, PA

Introduction: Cancer fatalism is linked to lower adherence to cancer screening and poor preventive health behaviors. Race, health information and social factors have been associated with cancer fatalism, however there is limited research on association with political orientation.

Methods: Data from the National Cancer Institute's Health Information National Trends Survey (HINTS) 7, conducted from March 25 - September 16, 2024, was used. This is a publicly available, de-identified, nationally representative survey of non-institutionalized civilian US adults and is thus exempt from institutional review board review. Survey response rate was 27.3%, with over 86% responding to the specific questions on fatalistic cancer beliefs and political ideology. Primary outcome was fatalistic cancer beliefs assessed using four items in the HINTS survey, each re-coded into a dichotomous variable of strongly agree/somewhat agree vs. strongly disagree/somewhat disagree for this study. Political ideology and race were self-reported. Multivariable logistic regression (adjusted for age, sex, race/ethnicity, educational level, household income, personal cancer history and rural-urban residence) was carried out for each fatalistic belief and political ideology. Statistical analyses were performed using Stata 18.0 software (StataCorp LLC) with 2-sided significance at $p < .05$

Results: The study sample included 6267 adults [3708 (48.3%) women, 3386 non-Hispanic White (61%), and 5400 (87.2%) urban residents. 2033 (31.9%) self-reported as conservative, 2232 (37.5%) as moderate, and 2002 (30.6%) as liberal. Adjusted logistic regression models showed that conservative participants, compared with liberals and moderates were more likely to say they strongly agree/somewhat agree that it seems everything causes cancer [adjusted odds ratio (aOR), 1.47; 95% CI, 1.27-1.69 and 1.29; 95% CI, 1.12-1.49 respectively]. Similarly, when statements on "there is not much you can do to lower your chances of getting cancer" and "there are so many different recommendations about preventing cancer, it's hard to know which ones to follow" were analyzed, conservative participants were more likely to strongly agree/somewhat agree compared with liberal participants [aOR 1.46; 95% CI, 1.26-1.70 and 1.51; 95% CI, 1.32-1.78 respectively] and moderate participants [aOR 1.41; 95% CI, 1.22-1.63 and 1.57; 95% CI, 1.36-1.81 respectively]. There was no significant difference in the statement "When I think about cancer, I automatically think about death" across political ideologies.

Conclusions: In this nationally representative survey of US adults, significant association exists between political ideology and cancer fatalism statements. Given that cancer fatalism has been linked to decrease in screening uptake and health behaviors, political ideologies should be considered as a factor for culturally appropriate interventions, and health promotion strategies.

#7556 Association between health literacy and cancer history with medical trust among adults in the United States.

Huda Haque[1], Morgan Byrd[2], Joab O. Odera[1], Nosa Osazuwa-Peters[2]

[1]Duke University, Durham, NC,[2]Duke University School of Medicine, Durham, NC

Introduction: Health literacy, or the ability to understand health information, shapes health-seeking behaviors. Among those with a history of cancer, low health literacy is associated with poor outcomes. In an era of disinformation, examining how health literacy and cancer history interact with trust in sources of health information can elucidate individuals' health decisions.
Methods: We analyzed data from the Health Information National Trends Survey (HINTS), a nationally representative dataset, for the 2014, 2018, 2020, 2022, and 2024 cycles. Health literacy (Low: never, rarely, sometimes; High: always), personal cancer history (ever vs. never), and age (18-39, 40-64, 65+) were examined in relation to trust in doctors, family, and religious organizations for health information (Low: not at all, a little, some; High: a lot). All variables were self-reported. Survey-weighted logistic regression models accounted for complex sampling and replicate weights using the jackknife method in R. Models included health literacy, cancer history, age category, and survey cycle as predictors. Interactions between age and health literacy, and age and cancer history were tested using Rao-Scott likelihood ratio tests; significant interactions were explored with stratified odds ratios.
Results: Higher health literacy was significantly associated with greater trust in doctors for health information (aOR 4.50, 95% CI 3.61-5.60). When stratified by age, the association varied (ages 18-39: aOR 4.78, 95% CI 2.89-7.91; ages 40-64: aOR 4.00, 95% CI 2.91-5.50; ages 65+: aOR 5.34, 95% CI 3.68-7.75). Cancer history was not associated with doctor trust (aOR 1.17, 95% CI 0.91-1.51), and trust did not vary meaningfully by cycle. For trust in family for health information, the association with health literacy differed by age (interaction p = 0.03). In stratified analyses, higher health literacy showed a trend towards greater trust among younger adults (ages 18-39: aOR 2.02, 95% CI 0.91-4.51), while associations were weaker for middle-aged (ages 40-64: aOR 0.71, 95% CI 0.43-1.16) and older adults (65+: aOR 1.02, 95% CI 0.56-1.87). Cancer history was not associated with family trust, but trust was lower in later cycles (2022 vs. 2017 aOR 0.58, 95% CI 0.42-0.81; 2024 vs. 2014 AOR 0.56, 95% CI 0.41-0.76), suggesting shifting trust in family after the COVID-19 pandemic. Trust in religious organizations for health information was higher in older adults (ages 40-64 vs. 18-39 aOR: 1.95, 95% CI 1.36-2.79; 65+ vs. 18-39 aOR: 1.55, 95% CI 1.13-2.15) and lower among cancer survivors (aOR 0.61, 95% CI 0.43-0.87). Health literacy was not associated with trust in religious organizations and trust remained stable across cycles.
Conclusion: These findings emphasize the importance of targeted outreach for different patient and trust contexts to promote informed health decisions, especially for older adults and cancer survivors.

#7557 Perceived stress and immigration-related demands in a Haitian immigrant community: Descriptive findings from a cancer disparity registry.

Jovanka Ravix[1], Maurice Chery[1], Sandy St. Hilaire[1], Mame Dioum[1], Lauren Smith[1], Twyla Murphy[1], Ivana Saborit[1], Johnathon Penso[1], Nadege Jacques[2], Sonide Cherise[2], Loukencia Jean[2], Priscila Barreto Coelho[1], Rimsky Denis[2], Sophia Hl George[3]

[1]University of Miami, Miller School of Medicine, Miami, FL,[2]Center for Haitian Studies, Miami, FL,[3]Univ. of Miami Sylvester Comprehensive Cancer Ctr., Miami, FL

Introduction: Psychosocial stress plays a critical role in shaping cancer-related outcomes, influencing both health behaviors and biological processes such as inflammation and immune function. Among immigrant populations, stress is often compounded by migration-related challenges and structural barriers. This study provides a descriptive profile of perceived stress and immigration-related demands among Haitian adults participating in the Florida Cancer Health Disparity Registry.

Methods: Seventy-five Haitian adults residing in South Florida completed a cross-sectional survey. The Perceived Stress Scale (PSS-10) was used to assess global stress levels, while the Immigration Demand Scale captured migration-related stressors. Participants also provided sociodemographic data, including age, education, income, employment status, and family history of cancer. Descriptive statistics were used to summarize responses.

Results: The mean age was 43.45 years (±13.47), with the majority aged 31-45 (40.0%) and 46-60 (29.3%). Most participants reported low income (66.7% earning < $10,000/year), and 56.8% were not employed. Only 19.7% reported a family history of cancer. On the Immigration Demand Scale (0-3 scale), the most strongly endorsed stressors included “Job market disadvantage” (1.96 ±0.21), “Missing people from country of origin” (1.92±0.31), and “Not feeling accepted” (1.81±0.16), with additional concerns about accent discrimination and language barriers. On the PSS-10, the mean stress score was 2.26 (±0.50). The most frequently reported experiences were feeling “nervous and stressed” (2.82 ± 0.89), being “upset by something unexpected” (2.47±1.10), and feeling “unable to control important things” (2.33±1.13). Positively framed items such as “Felt things were going your way” (1.47 ± 1.12) and “Felt on top of things” (1.80 ± 1.04) scored lowest, suggesting limited perceived control and optimism.

Conclusions and Implications: Participants reported high levels of perceived stress and immigration-related adversity, highlighting the psychosocial burden faced by Haitian immigrants. These stress exposures are important to understand in the context of cancer outcomes, as they may influence healthcare engagement, risk perception, and biological vulnerability. Future analyses will explore the relationship between stress and other cancer-relevant outcomes, including potential impacts on immune and inflammatory biomarkers, to inform culturally grounded prevention strategies.

#7558 Burden of non-vaccine high-risk oral HPV in updated cohort of people with HIV: Implications for public health strategies.

Jurelis Torres-Reyes[1], Juliana Mary Serrano-Rodriguez[2], Gabriel Borges-Velez[1], Jeannette L. Salgado Montilla[1], Maria M. Sanchez-Vazquez[1], Magaly Martinez-Ferrer[3], Ramon F. Gonzalez-Garcia[3], Josue Perez-Santiago[1]

[1]Comprehensive Cancer Center of University of Puerto Rico, San Juan, Puerto Rico,[2]University of Puerto Rico - Rio Piedras, San Juan, PR,[3]University of Puerto Rico School of Medicine, San Juan, Puerto Rico

Introduction/Background: Human papillomavirus (HPV) is the most common sexually transmitted infection and is considered the second infectious agent related to cancer. People with HIV (PWH) are at a higher risk of acquiring oral HPV infection, despite antiretroviral therapy, increasing their risk for oropharyngeal cancer (OPC). While there are more than 200 HPV genotypes, about 15 of them are classified as high-risk (hr) and responsible for HPV-related cancers. Currently, a nine-valent HPV vaccine is recommended in the US, providing protection against (6,11,16,18,31,33,45,52,58) HPV types. HPV vaccination is recommended for females, and males aged 13-26 years; for adults ages 27-45 years might get the HPV vaccination based on discussion with their clinician. In 2023, HPV vaccination rates among US Hispanics were 60%, but in Puerto Rico (PR) remain limited, particularly among PWH. Here, we described the prevalence of oral HPV infection by HPV genotypes among PWH, investigated HPV vaccination rates, and nonmedical factors associated with HPV infection.

Methods: We evaluated 184 sexually active PWH with a median age of 48 years. Oral rinse samples were collected and analyzed for HPV and genotyped using the DNA ELISA kit HPV SPF10 and RHA kit HPV SPF10-LiPA25. An administered questionnaire collected sociodemographic characteristics and lifestyle variables. Statistical analyses were performed in R-statistical software.

Results: The prevalence of oral HPV infection was 33%, of which 62% were hr genotypes, with HPV-18 being the most abundant (30%). Also, the prevalence of other hr HPV was 14% (HPV-35), 11% (HPV-33, HPV-16), 5% (HPV-39, HPV-51, HPV-53, HPV-56, HPV-59, HPV-74), and 3% (HPV-44, HPV-43, HPV-70). The prevalence of hr HPV genotypes not covered by the current nine-valent vaccine were more prevalent (57%) than vaccine covered hr genotypes (41%). There are not significantly difference between hr HPV, and socio-behavioral factors as current smokers (p=0.35), more than fifty sexual partners in lifetime (p=0.40), and education level (p=0.53).

Conclusion: PWH exhibited an elevated prevalence of oral HPV infection, with rates higher than those previously documented in PR. Although current HPV vaccines offer broad protection to some hr HPV oncogenic genotypes, limited vaccination rates may contribute to the persistence of oral HPV infection. Additionally, we have observed several other hr HPV oncogenic genotypes which are not currently covered by the existing vaccines, highlight the need for novel improved HPV vaccines.

#7559 Implementation of an interactive clinical trials education and decision tool for Florida cancer patients at an NCI Center.

Susan T. Vadaparampil, Lindsay N. Fuzzell, Elliott S. Tapia-Kwan, Yayi Zhao, Rossybelle Amorrortu, Dana Rollison, **Margaret Byrne**

Moffitt Cancer Center, Tampa, FL

Background: CHOICES Decision Aid (DA) is an evidence-based, interactive, education and decision-making support tool (available in English and Spanish) for cancer patients about participation in cancer clinical trials (CCTs). As part of the ACT WONDERS study, a multi-level intervention aimed at increasing referral and enrollment of diverse patients to CCTs, the website was made accessible to new Moffitt Cancer Center patients residing in seven geographically defined study intervention zones in the catchment area. CHOICES DA features education content such as facts about CCTs, values clarification tools on CCT participation, and patient narratives about CCT participation.
Method: Eligible patients were able to access the site via patient portal and received an email with a description and website link. Upon site exit, patients were asked to complete an optional 5-item survey about subjective CCT knowledge (1-7 scale), preparedness to talk with providers about CCTs (1-7), CCT decision readiness (1-7), and usefulness (1-10), and satisfaction with the site (1-10). Mean scores were re-scaled to 100% for comparison. Usage metrics were continuously monitored.
Results: In the first year following intervention launch (September 17, 2024 - October 2, 2025), 550 of 2,340 eligible patients (24%) visited CHOICES DA. Of 550 eligible patients who viewed the site, race demographics were: white 37% (n=203); Black 4% (n=27); other race 4% (n=23); not reported 54% (n=297). Ethnicity was 11% (n=61) Hispanic/Latino, 33% (n=181) non-Hispanic/Latino, and 56% (n=308) unknown. Mean age was 65 (range 56-73). 10% of users returned to the site at least once. 13% of patients viewed the Spanish site. 45 (8%) patients completed the survey. Mean self-rated CCT knowledge was 84%, readiness to decide about CCTs was 83%, and readiness to discuss CCTs with a doctor was 88.6%. Mean website usefulness and satisfaction were 86% and 85%, respectively.
Conclusion: Findings suggest CHOICES DA could be readily implemented in a high-volume oncology care setting leveraging existing communication channels available to patients. Survey completers gave high ratings to their CCT knowledge and readiness to discuss and make decisions about participation in CCTs, as well as website satisfaction and usefulness. CHOICES DA will also be evaluated at the two-year post-implementation time point, and future analyses will examine the impact on CCT enrollment at the cancer center.

#7561 Understanding beliefs about hereditary susceptibility for cancer: An analysis of HINTS 2020.

Ashley Hatch[1], Heidy N. Medina[2], Nicholas A. Borja[2], Matthew Schlumbrecht[3], Patricia I. Moreno[2]

[1]Department of Public Health Sciences, University of Miami, Miami, FL,[2]University of Miami, Miami, FL,[3]Miller School of Medicine - University of Miami, Miami, FL

Purpose: Cancer is driven by a complex interplay of genes and environment. However, little is known about the public's beliefs about hereditary susceptibility to cancer. This study characterized beliefs about hereditary susceptibility to cancer in a nationally representative survey of US adults. We also identified who is more likely to want to know if they had a genetic predisposition to cancer.**Procedures:** We analyzed data from the NCI Health Information National Trends Survey (HINTS) 2020 Cycle 5 Wave 4 using SAS 9.4 for weighted survey analysis. Adjusted linear regression models assessed predictors of (1) how much respondents believe genes that are inherited determine whether or not a person will develop cancer and (2) how much respondents would want to know if they had a genetic change that increases their chance of getting cancer (these items were reverse coded). Individuals with a previous cancer diagnosis were excluded.**Results:** Most respondents (N=3,253) were female (46.9%), non-Hispanic White (57.4%), married (44.4%), and were 46.6 years old (SE=.58). On average, respondents endorsed between "somewhat" and "a lot" for how much hereditary susceptibility determines a person's cancer risk and their desire to know if they had a genetic predisposition to cancer. Respondents believed that hereditary susceptibility to cancer (M=1.8, SE=.02), cardiovascular disease (M=1.8, SE=.02), and diabetes (M=1.8, SE=.02) were similar (p's >.6), but believed hereditary susceptibility to obesity was significantly lower (M=2.2, SE =.02, p<.0001). Individuals with health insurance (versus those who were uninsured, β = –.42 - –.37, p = .017 - .021) and those who had previously sought cancer information (β = –.19, p < .001) were more likely to believe that hereditary susceptibility determines a person's cancer risk. Individuals who believe in greater hereditary susceptibility to cancer were more likely to want to know if they had a genetic predisposition to cancer (β = .14, p = .001). Hispanic (β = –.25, p = .0098) and non-Hispanic Black (β = –.47, p < .0001) respondents, and individuals with a family history of cancer (β = –.20, p = .0051), who previously sought cancer information (β = –.19, p = .0019), and were less fatalistic (β = –.08, p = .036) were also more likely to want to know about their genetic predisposition to cancer. **Conclusions:** Individuals who believe in greater hereditary susceptibility to cancer are more likely to want to be informed if they have a genetic predisposition to cancer. Importantly, Hispanic and Black individuals were more likely than non-Hispanic Whites to want to know about their genetic risk to cancer, which highlights the critical need to overcome barriers related to access and cost and ensure equitable access to genetic testing. Outreach and educational efforts are needed to address fatalistic beliefs and lack of information or misinformation.

#7562 Evaluating the effectiveness of the C.H.A.N.G.E. training: A community-based tobacco cessation program for community health workers.

Andres Mauricio Garcia-Sierra, Victoria Nassar Abuabara, Tianqu Lu, Cynthia Tang, Anna Veluz-Wilkins, Marcia Tan

University of Chicago, Chicago, IL

Background: Commercial tobacco use drives approximately 30% of cancer-related deaths and remains disproportionately high among low-socioeconomic-status (SES) populations. Community health workers (CHWs) are uniquely positioned to promote tobacco cessation within this communities. The C.H.A.N.G.E. (Community Health Allies Nicotine Guidance Education) training was developed to enhance CHWs' capacity to deliver culturally responsive cessation counseling. This study evaluated its effectiveness in improving CHWs' tobacco-related knowledge, motivation, readiness, and confidence.
Methods: We conducted a secondary analysis of pre-, post-, and six-month follow-up data from CHWs (N=155) in Chicago, IL, recruited through a public health department, community-based organizations, and a CHW degree program. Of these, 144 completed post-training and 98 completed six-month assessments. The participatory curriculum, adapted from the WHO 5A's and 5R's Toolkit, emphasized motivational interviewing (MI), culturally tailored communication, and the social determinants of tobacco use. Changes across time points were analyzed using paired-sample t-tests.
Results: Significant improvements were observed from pre- to post-training (all $p<.05$): knowledge (Mean=4.89 to 7.91 out of 10), motivation (Mean=7.81 to 8.71 out of 10), readiness (Mean=6.09 to 8.25 out of 10), confidence in delivering cessation support (Mean=6.48 to 8.39 out of 10), and MI confidence (Mean=6.96 to 8.57 out of 10). At six months, all mean scores declined relative to post-training ($p\leq.05$) but remained significantly higher than pre-training for all domains except motivation ($p\leq.05$).
Conclusions: The C.H.A.N.G.E. training effectively improved CHWs' competence and self-efficacy in delivering tobacco cessation counseling. Findings support community-driven, culturally adapted models to extend evidence-based cessation interventions beyond clinical settings. Ongoing booster sessions and train-the-trainer approaches may enhance long-term skill retention and contribute to reducing tobacco-related cancer disparities in low-SES populations.

#7565 Psychological distress, antidepressants, and sympathetic-immune profiles in cancer survivors.

Ji E. Park[1], Andrew Ray[1], Rikki Cannioto[1], Kathryn Glaser[1], Han Yu[2], Karen Hulme[1], Susan LaValley[1], Orla Maguire[3], Hans Minderman[3], Krystin Mantione[4], Nicolas Schlecht[1], Shipra Gandhi[5], Elizabeth Bouchard[1], Elizabeth Repasky[6], Christine Ambrosone[1], Chi-Chen Hong[1]

[1]Cancer Prevention and Control, Roswell Park Comprehensive Cancer Center, Buffalo, NY,[2]Biostatistics and Bioinformatics, Roswell Park Comprehensive Cancer Center, Buffalo, NY,[3]Flow and Immune Analysis Shared Resource, Roswell Park Comprehensive Cancer Center, Buffalo, NY,[4]Pharmacology and Therapeutics, Roswell Park Comprehensive Cancer Center, Buffalo, NY,[5]Medicine, Winship Cancer Institute of Emory University, Atlanta, GA,[6]Immunology, Roswell Park Comprehensive Cancer Center, Buffalo, NY

Background: Psychological distress, including perceived stress, anxiety, and depression, can activate the sympathetic nervous system and increase norepinephrine (NE) and epinephrine (E). These catecholamines may impair anti-tumor immunity through β2-adrenergic effects on CD8+ T-cells and myeloid-derived suppressor cells (MDSCs). Antidepressants that alter NE reuptake may further modify sympathetic signaling and immune regulation in cancer survivors.

Methods: This analysis included 152 cancer survivors who completed the Perceived Stress Scale (PSS), PROMIS Anxiety (PROMIS), and Center for Epidemiological Studies Depression (CES-D) surveys and reported clinical diagnosis of anxiety or depression and current antidepressant use. Plasma NE, E, 3,4-dihydroxyphenylglycol (3,4-DHPG), and dopamine (DA) were quantified by LC-MS/MS, and CD8+ T-cell and MDSC subsets were assessed by flow cytometry as percent cell-subset events over total cell type events. Antidepressant use was classified as none (N=120), selective serotonin reuptake inhibitor (SSRI, N=11), or serotonin-NE or NE-DA reuptake inhibitors (SNRI/NDRI, N=21); five clinically diagnosed individuals not taking antidepressants were excluded. Associations of distress measures, clinical diagnoses, and medication class with catecholamines and immune profiles were evaluated using ANCOVA adjusted for age, education, and smoking history, with reciprocal adjustment for PROMIS or CES-D in clinical diagnosis models.

Results: Catecholamine levels were not associated with PSS, PROMIS, or CES-D. Higher perceived stress was associated with altered CD8+ T-cell distributions: naïve CD8+ T-cells were 30.7% higher in the highest vs lowest quartile (62.2 vs 47.6%, p=0.03), while memory CD8+ T-cells were 28.5% lower (36.6 vs 51.2%, p=0.01). Clinical anxiety (N=23) was not related to catecholamine levels, but clinical depression (N=24) was associated with higher NE (22.2%; 663.0 vs 542.2 pg/mL, p=0.01) and DA (41.8%, 20.5 vs 14.5 pg/mL, p=0.002). Neither diagnosis was associated with CD8+ T-cells or MDSCs. Antidepressant class showed expected physiologic patterns: SNRI/NDRI users had higher NE (37.7%; 485.3 vs 352.4, p=0.04), lower 3,4-DHPG (19.9%; 912.7 vs 1139.4 pg/mL, p=0.0004), and higher DA (64.5%, 16.1 vs 9.8 pg/mL, p=0.001) than SSRI users. PMN-MDSCs trended 32.2% higher (1.15 vs 0.87%, p=0.11) and M-MDSCs 54.8% higher (4.32 vs 2.79%, p=0.09) among SNRI/NDRI users vs SSRI users, consistent with increased adrenergic-linked immunosuppressive myeloid activity.

Conclusion: Clinical depression was associated with higher sympathetic catecholamines, and NE-reuptake-inhibiting antidepressants produced expected catecholamine shifts. Corresponding increases in PMN-MDSC and M-MDSC among SNRI/NDRI users suggest adrenergic signaling may contribute to immunosuppressive myeloid abundance in cancer survivors.

#7566 Use of supportive care medications is associated with pancreatic cancer tumor location at diagnosis.

Hussein Khalil[1], Kourtney A. D. Byrd[1], Yi Guo[2], Shuang Yang[3], Xiwei Lou[3], Lisa Scarton[4], Sherise C. Rodgers[5], Diana J. Wilke[4], John M. Allen[1]

[1]Purdue University, West Lafayette, IN,[2]University of Florida College of Medicine, Gainesville, FL,[3]College of Medicine, University of Florida, Gainesville, FL,[4]University of Florida, Gainesville, FL,[5]Brown University, Providence, RI

Background: Pancreatic cancer (PC) often presents with non-specific symptoms that vary by tumor location. Tumors in the body and tail often present later and are more commonly associated with pain, nausea, or cachexia. Supportive care medications (SCMs) such as psychotropics, pain relief medications, antinausea agents, and appetite stimulants ae commonly used to manage these symptoms yet little is known about whether prescribing patterns differ by tumor location. We evaluated whether pancreatic tumor location at diagnosis is associated with subsequent use of SCMs among older adults with pancreatic cancer.
Methods: We conducted a retrospective cohort study using Surveillance, Epidemiology, and End Results (SEER)-Medicare data (2007-2019). The study included patients aged ≥65 years old with incident pancreatic cancer and continuous Medicare parts A, B, and D coverage for 3 months before diagnosis. Patients with another cancer diagnosis within 6 months or missing baseline data were excluded. Pre-diagnosis SCM use was ascertained from Medicare Part D prescription claims. Tumor location at diagnosis were categorized as pancreatic head (C250), body (C251), tail (C252), or other (C253, C254, C257, C258, C679). We used multivariable logistic regression to evaluate the association between SCM use and tumor location adjusting potential confounders.
Results: Compared to tumors in the pancreatic head, tumors in the body were associated with higher odds of receiving most SCM classes including psychotropic medications (OR for any psychotropic: 1.13; 95% CI: 1.08-1.19), pain medications (OR for any pain medication: 1.25; 95% CI: 1.19-1.31), anti-nausea agents (OR: 1.08; 95% CI: 1.03-1.13), appetite stimulants (OR: 1.16; 95% CI: 1.11-1.21). Tail tumors were associated with increased use of anxiolytics (OR: 1.07; 95% CI: 1.00 - 1.14) and non-opioid analgesics (OR: 1.25; 95% CI: 1.15-1.37), but lower odds of anti-nausea use (OR: 0.85; 95% CI: 0.81-0.89). Tumors in other locations generally had lower odds of SCM use across nearly all categories.
Conclusion: Pancreatic cancer tumor location at diagnosis is associated with distinct patterns of supportive care medication use. Patients with tumors in the body of the pancreas were more likely to receive symptom-directed therapies than those with head tumors while those with tail or other locations had more variable patterns. These findings suggest that tumor location may influence supportive care needs and should be considered when tailoring symptom management strategies.

#7567 Predictors of antidepressant use in older adults after pancreatic cancer diagnosis: A SEER-Medicare analysis.

Hussein Khalil[1], Kourtney A. D. Byrd[1], Yi Guo[2], Shuang Yang[3], Lisa Scarton[3], Xiwei Lou[3], Diana J. Wilkie[4], Sherise C. Rodgers[5], John M. Allen[1]

[1]Purdue University, West Lafayette, IN,[2]University of Florida College of Medicine, Gainesville, FL,[3]Department of Health Outcomes & Biomedical Informatics, University of Florida, Gainesville, FL,[4]Biobehavioral Nursing Science, University of Florida, Gainesville, FL,[5]Brown University Warren Alpert Medical School, Providence, RI

Depression is highly prevalent among patients with pancreatic cancer (PC), driven by both the biological effects and the profound psychosocial burden of the diagnosis. Untreated depression contributes to poorer quality of life, reduced treatment adherence, increased symptom burden, and worse survival. Prior work suggests sociodemographic inequities may shape access to supportive care medications, yet little is known about how these factors operate specifically within older adults with PC. We aimed to characterize predictors of antidepressant use following pancreatic cancer diagnosis, with the goal of identifying inequities and informing patient-centered approaches to supportive care delivery in this high-risk population.

We conducted a retrospective cohort study using SEER-Medicare data among patients aged ≥65 years diagnosed with primary PC between 2007 and 2019. Antidepressant use was identified from Medicare Part D claims up to 24 months post-diagnosis. We compared patient characteristics by antidepressant use status. Multivariable logistic regression models estimated adjusted odds ratios (ORs) and 95% confidence intervals (CIs).

Among 81,535 patients with PC, 23.5% (N=19,181) received antidepressants post-diagnosis. Compared with those living in the highest-SES neighborhoods, patients in the lowest SES quintile had 19% lower odds of receiving antidepressants (aOR: 0.81; 95% CI 0.74-0.88). Increasing age was strongly associated with reduced use (≥80 vs. 65-69 years: aOR:0.60; 95% CI 0.57-0.63), while female sex was associated with higher odds (aOR:1.19; 95% CI 1.15-1.23). Marked racial/ethnic disparities were observed: non-Hispanic Black (aOR:0.63; 95% CI 0.59-0.67) and Asian (aOR:0.60; 95% CI 0.56-0.65) patients were substantially less likely to receive antidepressants compared with non-Hispanic White patients. Higher comorbidity modestly increased use (CCI per point: aOR:1.07; 95% CI 1.06-1.08). Strong associations were observed for prior supportive care medication use (aOR: 2.02; 95% CI 1.94-2.09) and hospice enrollment (aOR: 1.73; 95% CI 1.67-1.80).

In our study, nearly a quarter of older adults with PC received antidepressants, with substantial variation by socioeconomic status, race/ethnicity, age. The markedly lower use among racial/ethnic minority and lower-SES patients indicates potential inequities in mental health treatment access and potential cultural influences. Increased use among those with higher comorbidity burden and hospice enrollment suggests that antidepressants are more often introduced in the context of advanced symptom burden or end-of-life care rather than early in the cancer course. These findings underscore the need for systematic depression screening across all demographic groups and proactive integration of mental health services into routine pancreatic cancer care.

#7568 The STANDOUT program: A model for undergraduate training and career development in behavioral cancer prevention and control.

Joel Erblich[1], Jennifer S. Ford[1], Guy H. Montgomery[2]

[1]Department of Psychology and Center for Cancer Health Disparities Research, Hunter College, New York, NY,[2]Center for Behavioral Oncology, Icahn School of Medicine at Mount Sinai, New York, NY

The potential for behavioral science to make meaningful strides in cancer prevention and control is significant, yet more behavioral scientists focused on cancer prevention and control are desperately needed to achieve this end. Unfortunately, progress in behavioral cancer prevention and control (BCPC) research is hampered by several key barriers. These include: 1) the relatively small fraction of scientists who focus on BCPC, 2) limited awareness of BCPC career opportunities when college students consider their advanced educational options, 3) limited opportunities to receive formal early training in BCPC research, and 4) a lack of stewardship of outstanding college students to transition from research labs to successful graduate education. The objective of STANDOUT (Summer Training Accelerating and Nurturing the Development of Outstanding Undergraduate Trainees; R25CA260125) is to address institutional challenges head-on, by providing multifaceted, immersive summer training and career development opportunities to talented undergraduates attending Hunter College, a large diverse urban university in New York City. Now in its third year, we report on trainee outcomes to date. Undergraduate Trainees (n=41, 16-18/cohort) completed a 10-week summer research internship program. The program includes: 1) formal mentored BCPC research training with scientists at either Hunter College of the City University of New York or the Center for Behavioral Oncology at the Icahn School of Medicine at Mount Sinai, 2) biweekly research and career development seminars, 3) research and networking conferences, and 4) continued outreach and mentoring as students advance in their education and training. We conducted pre-post assessments of key outcomes, as well as program satisfaction, and annual follow-ups to track student advancement and accomplishments. Findings indicated that trainees consistently endorsed high levels of satisfaction across multiple program elements, including mentor quality, research experience, and seminars and conferences. Trainees also exhibited significant increases in a number of key research-related skills, including conducting literature reviews, writing, generating and refining hypotheses, conducting quantitative analyses, and presenting research. Notably, trainees' interest in pursuing cancer research increased significantly following the program. Finally, annual follow-up data revealed continued interest in BCPC research, increases in related professional activities, presentations, publications, attendance at scientific conferences, and career and academic advancement (e.g., successful application to graduate programs). STANDOUT is an example of a program that can both train and inspire students early in their academic trajectories to pursue careers aimed at advancing research in behavioral cancer prevention and control.

#7569 Health literacy and beliefs about cancer causation and prevention in a Haitian immigrant population.

Maurice J Chery[1], Jovanka Ravix[1], Sandy St. Hilaire[1], Mame Dioum[1], Lauren Smith[1], Twyla Murphy[1], Ivana Saborit[1], Johnathon Penso[1], Nadege Jacques[2], Sonide Cherise[2], Loukencia Jean[2], Priscila Barreto Coelho[1], Rimsky Denis[2], Sophia Hl George[3]

[1]University of Miami Miller School of Medicine, Miami, FL,[2]Center for Haitian Studies, Miami, FL,[3]Univ. of Miami Sylvester Comprehensive Cancer Ctr., Miami, FL

Introduction: Cancer prevention efforts are influenced by individuals' beliefs about disease causation and their ability to access, understand, and use health information. This descriptive study presents interim findings on health literacy, cancer causal beliefs, and cancer prevention attitudes among Haitian immigrants. The data come from a subsample in the Florida Cancer Health Disparity Registry.
Methods: We conducted a cross-sectional survey among 75 Haitian adults residing in South FL. Health literacy was assessed using the HLS19-Q12 and the BRIEF HL Screening Tool. Additional items evaluated beliefs about the causes and preventability of cancer. Descriptive statistics summarized sociodemographic data, literacy levels, and thematic patterns in belief systems. No inferential testing was performed at this stage.
Results: Mean age of participants was 43.45 years (+/-13.47). Over half (52.7%) had never been married. Educational attainment varied, 44.0% having intermediate education, 32.0% low, and 24.0% high. Two-third reported earning less than $10,000 annually, and 56.8% were unemployed. Family history of cancer was reported by 19.7% of respondents. On the HL, 44.1% of participants had inadequate HL, and 33.9% had problematic HL, totaling 78% with suboptimal skills. On the BRIEF, 82.0% had trouble learning from written health materials, 80.3% struggled to understand spoken explanations, and 77.1% required help reading hospital materials. Only 53.2% felt confident completing forms, while 46.8% lacked confidence. Overall, 60.7% demonstrated “not sufficient” health literacy. Regarding cancer causation, participants listed 188 beliefs, the most frequent being diet and nutrition (35.1%), referencing processed foods, sugar, red meat, and chemical additives. Other belief categories included environmental exposures (14.4%), genetic/biological factors (12.8%), behavioral factors (11.7%), infections (10.6%), physical causes (8.0%), and cosmetic products (4.3%). When analyzed by controllability, 47% listed three controllable causes, and 36% listed two, suggesting widespread belief in individual agency over cancer risk. In terms of prevention beliefs, 76.6% disagreed with the statement "Everything causes cancer," and 65.6% disagreed with "Not much you can do to prevent cancer," reflecting positive attitudes toward preventability. However, 40.6% agreed that cancer means death, and 54.8% found cancer prevention recommendations confusing.
Conclusions: Our results highlight limited health literacy alongside strong beliefs in cancer preventability and personal control over risk among Haitian immigrants. Findings support the need for tailored education addressing literacy gaps and cancer-related misconceptions. Further analyses will examine associations between literacy, beliefs, and sociodemographic factors to guide targeted intervention development.

#7570 Expanding digital access to cancer immunotherapy trials: Nationwide engagement and high match rates among 21,000 patients.

Cynthia L. Neben, Wendy Weise, Samik Upadhaya, Alicia Y. Zhou

Cancer Research Institute, New York, NY

Clinical trials are essential to advancing cancer care and precision medicine. They provide access to innovative treatments and are fundamental to validating new therapies, generating evidence for regulatory approval and improved care. Yet participation remains limited - only 9% of U.S. patients report being invited to a clinical trial, and one in five adult cancer trials fail to finish due to low enrollment. Increasing patient and provider awareness and helping patients navigate their best options are key to closing this gap.

To help address these barriers, the Cancer Research Institute (CRI) provides a free, online Clinical Trial Finder designed to connect patients with cancer immunotherapy trials. The tool uses a short survey to match users to open studies based on cancer type, location, and other eligibility criteria. Users can access the full portfolio of clinical trials sourced from the ClinicalTrials.gov and search by cancer type, drug type, trial phase, and sponsor. Additional one-on-one trial navigation support is available by phone or email.

Over nine months, more than 21,300 individuals visited the CRI Clinical Trial Finder webpage (https://cri.careboxhealth.com/en-US/). Nearly all individuals who completed the survey did so online (95.6%, 3,651) rather than by phone or email (169, 4.4%). Survey completion rates were also higher for online users (2,510, 68.7%) versus phone or email (87, 5.1%). Among all individuals who completed the survey (n=2,597), 97.2% matched to at least one open clinical trial. This match rate is substantially higher than published reports and may reflect broad eligibility of cancer-type-agnostic and genomically-driven immunotherapy trials.

Users came from 49 U.S. states and the District of Columbia, with the largest numbers in California (157), Texas (74), and Florida (74) (n=1,036 who provided location); there were no users in Wyoming. These data mirror general U.S. population distribution and demonstrate nation-wide reach.

About one-third (1,210) of users reported a diagnosis of pancreatic, breast, or ovarian cancer. While breast cancer is the most commonly diagnosed cancer among women in the U.S., pancreatic and ovarian cancers are lower incidence and often detected in later stages, with fewer treatment options, making clinical trials particularly relevant for these patients. Individuals with sarcoma (118), kidney (66), skin (16), thyroid (8), or testicular (4) cancer had a 100% match rate. Melanoma had the lowest (87.3%, 48).

Our findings demonstrate how online, patient-friendly tools supplemented with personalized navigational support can help bridge the gap between patients and cancer research. By lowering barriers to access and empowering patients, digital trial-matching services can help advance clinical trial participation and make more life-saving immunotherapies available to more people.

AI was used to review abstract text.

#7571 Health literacy and colorectal cancer: A targeted review of screening, outcomes, and challenges in vulnerable populations.

Nijole P. Tjader[1], Brigette Waldrup[2], Hyoshin Kim[1], **Enrique I. Velazquez Villarreal**[2]

[1]Biomedical Informatics, The Ohio State University Wexner Medical Center College of Medicine, Columbus, OH,[2]Integrative Translational Science, City of Hope, Duarte, CA

Health literacy is increasingly recognized as a critical determinant of cancer prevention, treatment adherence, and survivorship outcomes. In colorectal cancer (CRC), its importance is pronounced, in part because early detection through screening can significantly reduce incidence and mortality. Persistent disparities in CRC-related health literacy may contribute to lower screening uptake, suboptimal treatment decisions, and reduced quality of life, especially among populations experiencing disproportionate health burdens. To characterize the scope and impact of health literacy in CRC, we conducted a targeted literature review examining its relationship with clinical, behavioral, and psychosocial outcomes across the CRC care continuum. Using PubMed, we identified peer-reviewed studies that evaluated associations between health literacy and outcomes such as screening participation, treatment adherence, patient-reported experiences, and quality of life. Studies were included if they addressed CRC and incorporated measurable health literacy constructs. Thirty-nine studies met inclusion criteria. We synthesized approaches and key findings, with particular attention to implications for disproportionately affected populations. Across diverse geographic and clinical settings, limited health literacy was consistently associated with lower CRC screening rates, reduced knowledge of guideline recommendations, greater perceived barriers, and more fatalistic beliefs. Among individuals diagnosed with CRC, lower health literacy was linked to poorer treatment adherence, reduced health-related quality of life, and increased mortality, with especially strong effects in early-stage disease. Challenges were amplified among individuals with both limited literacy and limited English proficiency. Interventional studies demonstrated the promise of culturally-tailored interventions, including educational materials, patient navigation, and community-based outreach, in mitigating literacy-related disparities. Recent studies identified the influence of health literacy on financial toxicity, communication preferences, and care satisfaction, particularly among rural, immigrant, and low-income populations. Overall, this review identified key ways that health literacy is a significant, modifiable determinant of CRC outcomes and a contributor to persistent disparities. Targeted interventions to address literacy gaps, especially among vulnerable populations, should be prioritized in CRC across prevention, diagnosis, and survivorship. Future research should focus on scalable, culturally and linguistically appropriate strategies, including the integration of artificial intelligence and digital health tools, to strengthen informed decision-making and improve outcomes across all populations throughout the CRC care continuum.

#7572 Personalized counseling on cancer prevention at the National Cancer Prevention Center's Prevention clinic: Bridging the gap between research, application, and individual implementation.
Ursula Melanie Christel Will

DKFZ German Cancer Research Center, Heidelberg, Germany

The prevention of non-communicable diseases is becoming an increasingly important focus of modern health systems. In addition to population-based strategies, approaches that consider genetic, biological, and lifestyle-related risk factors are becoming important for individualized prevention. The National Cancer Prevention Center (NCPC) is being established in Germany through a long-term strategic partnership between the German Cancer Research Center (DKFZ) and the German Cancer Aid. The NCPC brings together all key components of cancer prevention under one roof: from fundamental research and prevention trials to evidence-based counseling for the public and training for prevention specialists and multipliers. A central element is the Prevention Outpatient Clinic (POC), a unique model facility in Germany that maximizes the potential of cancer prevention and makes it accessible to everyone. In the POC, risk profiles are systematically created based on identified cancer risk factors, including family history, genetic predispositions, lifestyle factors, previous illnesses, and medication use. With these risk profiles, we create individualized prevention pathways that link health promotion counseling with recommendations for early detection and lifestyle changes. There is a strong focus on health literacy and sustainable behavior change because prevention only works when it is feasible in everyday life. Thus, the POC serves as an active partner in behavior modification. At the same time, the POC functions as a research platform for epidemiological, implementation, and translational trials. Standardized data on risk profiles, adherence, effectiveness, and acceptance of preventive measures provides insight into the success factors and barriers of cancer prevention. Linking research and application creates a bidirectional knowledge loop in which findings from science are translated into practice and re-translated from application to new research questions. Additionally, the POC fosters interdisciplinary collaboration among oncology, human genetics, nutrition and sports medicine, psychology, and public health. Digital tools and AI-supported algorithms offer new perspectives for more precise risk assessment and personalized prevention planning for specific risk reduction. The POC exemplifies a paradigm shift in oncology, moving away from solely treating disease and toward a proactive, personalized, and accessible health strategy nationwide. The POC combines research and application, strengthens health literacy and self-efficacy, and establishes prevention as an integral part of modern society.

#7573 Evaluation of a training intervention for primary care providers to prepare patients for cancer discussions with their oncologists.

Carma Bylund[1], Alyssa Crowe[1], Margo Michaels[2], Domenic Durante[1], Maria Sae-Hau[3], Andrea Cassells[4], Jason Arnold[1], Ana Natale-Pereira[5], Raymond Mailhot Vega[6], Zhongyue Zhang[1], Ji-Hyun Lee[1], Elisa S. Weiss[3]

[1]University of Florida, Gainesville, FL,[2]Health Care Access & Action, Boston, MA,[3]Blood Cancer United, Rye Brook, NY,[4]Clinical Directors Network, New York, NY,[5]Rutgers New Jersey Medical School, Newark, NJ,[6]University of Florida, Jacksonville, FL

We examined the impact of an online training intervention, “Preparing Patients for Cancer Treatment Discussions,” on primary care providers’ knowledge, attitudes/beliefs, and communication/referral behavior.

We partnered with Clinical Directors Network (CDN), Florida Academy of Family Physicians, and U.S. Residency Program Directors to recruit primary care providers (MDs, DOs, NPs, and PAs), Family Medicine residents, Internal Medicine residents and Geriatric fellows. The 1-hour, asynchronous online training was hosted by three faculty members: a primary care provider, radiation oncologist, and cancer clinical trials expert. Participants engaged in simulated patient and clinical scenarios to practice communication about oncology referrals and cancer clinical trials. Pre- and post-training surveys measured knowledge, attitudes, beliefs, and willingness to discuss trials. Further, a 3-month follow-up survey measured the sustained impact of the training on communication behavior about clinical trial referrals.

135 primary care providers (91 residents, 44 practicing clinicians) participated in the training intervention (84% retention at 3-month follow-up). Knowledge improved from a mean of 51.8% to 82.4% correct (p<.001) immediately after training and was sustained with a mean score of 77.7% correct (p<.001) at 3-month follow-up. Mean belief scores concerning the primary care provider's role in assisting patients with decisions about clinical trials increased from 4.1 to 4.6 (1-5 scale; p<.001) immediately following training. This improvement was sustained at a score of 4.5 (p<.001) during the 3-month follow-up. Additionally, mean scores for the willingness to communicate about clinical trials increased from 4.3 to 4.6 (1-5 scale; p<.001) immediately after training. This improvement was sustained at a score 4.5 (p<.001) during the 3-month follow-up. Behavior measures increased significantly at 3-month follow-up. Providers were asked the percentage of patients they educated about receiving treatment with a cancer clinical trial and encouraged to inquire about receiving treatment from a cancer clinical trial prior to making a referral. Education (15.1% to 52.9%) and inquiry encouragement (17.6% to 62.4%) both increased (p<0.001). Providers were asked the same questions regarding patients that returned after their oncology visit to discuss treatment options. Education (13.9% to 49.5%) and inquiry encouragement (20.7% to 47.8%) both increased significantly (p<0.001).

Significant improvements in knowledge, attitudes, beliefs, communication and referral behavior demonstrate the online course was effective. Future plans for dissemination and sustainability include integrating the online course into curricula for medical and nursing education.

#7574 A single arm clinical trial evaluating the impact of patient education on cancer clinical trials knowledge and beliefs.

Diana Laura Morales, Trista A. Beard, Chanita Hughes Halbert

Population and Public Health Sciences, Keck School of Medicine of USC, Los Angeles, CA

Background: Racial and ethnic minorities remain underrepresented in cancer clinical trials (CCTs), limiting the generalizability of findings and equitable access to new therapies. Barriers include limited trial access in diverse communities, low referral rates among medically underserved groups, and lack of awareness or understanding of CCTs. Educational interventions may help address these gaps by improving knowledge and engagement among disparity populations.

Objective: Evaluate patient knowledge and beliefs of CCTs after an education intervention at an NCI-designated cancer center.

Methods: Patients being treated for any type of cancer were invited (by mailer and posted pamphlets) to participate in a Clinical Trial Social Determinants Survey to characterize their social determinants of health and preferences for clinical trials education. A secondary validated instrument (CHEKS) evaluated patients' knowledge and beliefs about CCTs, before and after exposure to educational stimuli (written and video) detailing the purpose and characteristics of CCTs.

Results: A total of 51 cancer patients observed the educational stimuli and completed pre and post surveys. The mean score for positive '*knowledge and beliefs*' (out of 100) increased from 86.1 pre-intervention to 90.9 post-intervention. The sample was 60.8% female and 39.2% male. One third (33%) reported prior enrollment in a CCT; 47.1% reported annual household income <$75K and 51% reported >$75K; 78% reported education as some college or beyond and 21.6% reported a high school degree or lower; and 62% reported being in a domestic partnership and 37.3% were single. Because 65% of patients were White, and other groups were represented in small numbers, no results by race/ethnicity are reported. For every subgroup (male/female, education low/high, income low/high, previous CT yes/no, coupled yes/no), the educational intervention showed a positive effect, meaning the knowledge score increased post stimuli. Males' knowledge (mean) score increased +5.75 points, while females increased +4.2; married or coupled patients' score increased significantly (+6.59) while single persons had the lowest increase of all subgroups (+1.79). The highest increase in knowledge scores was the high-income group (+6.8), and the low-income group increase was +2.83; high school graduate or less increased +4.09, some college and beyond increased +5; for those who have previously enrolled in a clinical trial the score increased +4.59, and those with no clinical trial experience increased +4.91.

Conclusions: Specific and high quality CCT educational material that explains the purpose and phases of CCTs, the need for diverse populations, safety protocols, costs, and patient rights can impact patients' views and understanding of CCTs. By reducing the knowledge barrier, we hope to improve enrollment of underrepresented groups in CCTs.

#7575 Characterizing radiation oncologist work patterns with a time-motion study.

Sophie C. Chang, Kenya Ochoa, Maryum Haidari, Van Nguyen, Johan Carrascoza-Bolanos, Phillip Schofield, Melody K. Schiaffino

UC San Diego School of Medicine, La Jolla, CA

Oncologists face increased demands in their workload from growing administrative and technology-related burdens such as charting and responding to messages. In radiation oncology, where care involves multiple multidisciplinary care touchpoints, these tasks can detract from patient-facing time needed for essential assessments of increasingly complex patients. Pressure to multitask will likely increase without effective workflow optimization. While previous literature has explored system- or process-level workflows in radiation oncology, we sought to characterize physician work patterns in an ambulatory setting to support improved workflow management and patient care. We used an observational time-motion study design to characterize the work patterns of seven attending radiation oncologists and two PGY5 residents at a large urban academic medical center. Each physician was observed for at least nine hours by a trained observer across two to three shifts for a total of 90 hours of observation. Observers recorded the number and type of activities performed within each five-minute interval. Intervals with more than one recorded activity were considered instances of multitasking. To estimate the total amount of time spent performing each activity, we divided the duration of each five-minute interval equally among its recorded activities. Patient visit duration was calculated as the length of an uninterrupted block of patient-facing time. On average, radiation oncologists spent 37.4 ± 9.5% of their time directly interfacing with patients, 39.9 ± 7.4% on patient-adjacent tasks, 10.6 ± 7.9% on administrative work, 2.6 ± 2.2% on personal time, and 9.5 ± 5.4% on tasks categorized as research/other. Patient-adjacent tasks included computer-based work such as charting and responding to messages (18.5 ± 5.1%), interacting with clinical staff (11.3 ± 4.7%), making consults (8.0 ± 6.9%), and interfacing with medical physicists (1.6 ± 2.1%). Physicians multitasked in 53.7% of five-minute intervals. Patient-adjacent tasks contributed to 85.9% of instances of multitasking. Durations of 121 patient visits ranged from 5 to 65 minutes (median 15 minutes). Visits with at least one family member present (n=53) were significantly longer than visits without (n=68) (median 20 vs 10 minutes, $p < 0.01$, Mann-Whitney U). This preliminary time-motion study reveals a significant burden of patient-adjacent tasks in radiation oncologist workflow. Physicians spent more time on these tasks than on direct patient interactions on average and multitasked in more than half of the observed time intervals. Longer patient visit durations in the presence of family underscore the need to optimize patient-adjacent workload to support complex visits, improve efficiency, and reduce physician burden.

#7576 Evaluating a community-focused approach to increase representation of understudied populations in clinical studies.

Kimlin Ashing[1], Virginia Savage[1], Diana Tam[1], Gaole Song[1], Brenda Gascon[1], Alyssa Cardenas[2], Sophia Yeung[1]

[1]City of Hope National Medical Center, Duarte, CA,[2]TGen, Phoenix, AZ

Background: Our Community Scientist Advocate (CSA) program aimed to address the critical underrepresentation of ethnic minority populations in cancer-focused clinical trials by preparing health leaders to promote clinical research engagement in their communities. We developed and implemented an evidence-based training curriculum with six modules that discussed the role and benefit of clinical studies, research ethics, barriers to participation, social drivers of health, cancer care, and research engagement promotion strategies.

Methods: CSAs are community health leaders and educators recruited via community health services or advocacy organizations. We delivered modules through Zoom and Teams with six CSA cohorts serving diverse communities in California. CSAs were encouraged to conduct community science and clinical study dissemination and log their activities. We assessed CSA preparedness to promote clinical research engagement through analysis of 12 items gathered in pre- and post-surveys. We evaluated the scope and reach of participants' community outreach activities, as well as barriers to study participation, through analysis of activity tracking forms and surveys.

Results: A total of 103 participants, 83% female and 14% male, completed pre- and post-program surveys (n=103). Participants represented diverse communities, with 50% self-identifying as Latinx, 37% as Asian, 12% as African American/Black, and 2% as Pacific Islander. The mean score of participant preparedness increased from 24.7 at baseline to 31.3 post-intervention. 72 community outreach activities were reported through tracking forms and were estimated to serve more than 1662 community members. Activities consisted of 40 informal health research education and 32 formal health research education events such as community presentations, health fairs, etc. Participants noted that ongoing barriers to clinical study participation include concerns about research or health system trustworthiness; concerns about privacy or data use; language barriers; lack of information tailored to communities, cost barriers, lack of doctor referral, and embarrassment/cultural stigma.

Conclusions: The CSA program offered an impactful approach to increase representation in clinical research through advocacy development. Further efforts are needed to continue building trust between clinical researchers and underrepresented communities, develop close partnerships between multisectoral stakeholders, and address structural barriers to research participation.

#7577 Advancing the science, practice and impact of COE.

Kimlin Ashing[1], CHARNITA ZEIGLER-JOHNSON[2], Hayley S. Thompson[3], Kim Rhoads[4], Nadine Barrett[5], Lisa Carter Bawa[6], Timiya S. Nolan[7], Monica Baskin[8], Vanessa B. Sheppard[9], Marvella E. Ford[10], Erica Phillips[11], Lorna H. McNeill[12], Folakemi T. Odedina[13]

[1]City of Hope National Medical Center, Duarte, CA,[2]Fox Chase Cancer Center, Philadelphia, PA,[3]Wayne State University School of Medicine, Huntington Woods, MI,[4]University of San Francisco, San Francisco, CA,[5]Wake Forest University, Winston-Salem, NC,[6]Georgetown University, Washington DC, WA,[7]University of Alabama at Birmingham, Birmingham, AL,[8]UPMC Hillman Cancer Center, Pittsburgh, PA,[9]Virginia Commonwealth University, Richmond, VA,[10]Associate Director of Cancer Disparities, Medical University of SC Hollings Cancer Center, Charleston, SC,[11]Division of General Internal Medicine, Weill Cornell Medicine, New York, NY,[12]UT MD Anderson Cancer Center, Houston, TX,[13]Mayo Clinic Florida, Jacksonville, FL

Introduction: COE has become the gold standard in addressing health disparities. COE's value is emphasized by NIH and leading cancer-related organizations e.g., AACR. The Alliance for COE (The Alliance) mission is to advance the art, science, and impact of COE; promote community health and wellness; and reduce cancer burden and disparities. Methods: This abstract builds on the Alliance's Science of Community Outreach and Engagement (SoCOE) Conference a NCI R13 funded series. SoCOE Conference is organized by 10 NCI-designated Cancer Centers to provide a platform for COE academic-clinical-policy-community stakeholders to share best practices for solution-focused community responsive cancer prevention, diagnostics, therapeutics and survivorship research and practice. Results: > 500 researchers, clinicians, policymakers, healthcare administrators, with >12% being survivors and/or advocates, participated in our SoCOE Conferences. The delegates' recommendations are:

Decentralize who/entities that hold all the power in science and clinical research (trials). Communities hold valuable, necessary wisdom and resources to inform and guide science

Include multisectoral partners early and always

Community capacity building and compensation with gratitude

Mentoring of junior COE researchers, clinicians, policymakers, healthcare administrators, survivors and advocates with humility is a must

Develop virtual communities to share best practices across cancer centers and within regions

Develop working groups to identify and explore commonalities across COE work in rural/urban, diverse/homogenous spaces

Publish Science of COE papers on various topics related to COE Frameworks and evidenced-solutions

Provide community reports on best practice guide that can be widely available to be shared locally and in-person, and digitally

Partner and learn from COE teams working with other cultural/ethnic groups

Attend to, measure and remedy societal/social drivers of health disparities that mirror barriers to care, and research engagement and participation.

Discussion: Informed by our community advisory boards and the findings for our SoCOE Conferences, we present the pillars of the Alliance to tackle population cancer burden and disparities: Training future COE leaders/advocates, Advocating for public health policies/guidelines, Increasing access to cancer prevention and care that will also increase access to studies, Engaging and partnering with multisectoral stakeholders and communities, Building community capacity, Advancing COE science through catchment-relevant research, and Leading bi-directional communication and information and resource sharing between catchment area communities and cancer centers. The expectation and impact of COE can only be achieved if COE teams are valued, supported cancer center members with community advisory boards and community as cancer centers' priority population.

: Risk Prediction Modeling, Screening, Early Detection, and Preneoplastic and Tumor Markers
Poster Session

#7581 Loss of the duffy antigen receptor for chemokines (DARC/ACKR1) expression in ductal carcinoma in situ is associated with immune dysregulation and progression to invasive ductal carcinoma.

Dana Franklin[1], Ni-Chun Tsai[2], Hyejin Cho[3], Yate-Ching Yuan[2], Yuqi Zhao[3], Padmashree Rida[4], Nikita Jinna[1]

[1]Population Sciences, City of Hope Comprehensive Cancer Ctr., Duarte, CA,[2]Computational and Quantitative Medicine, City of Hope Comprehensive Cancer Ctr., Duarte, CA,[3]Integrative Genomics, City of Hope Comprehensive Cancer Ctr., Duarte, CA,[4]Science, Rowland Halll, Salt Lake City, UT

Ductal carcinoma in situ (DCIS) is a non-invasive precursor of breast cancer, characterized by malignant epithelial proliferation confined within the ducts. DCIS accounts for 20-25% of all breast cancer cases. Majority of DCIS lesions are treated with highly invasive surgeries and cytotoxic radiotherapy. Left untreated, 25-60% of DCIS lesions progress to invasive ductal carcinoma (IDC). Discerning which DCIS lesions will progress to IDC, to circumvent over- or under- treatment, remains a major clinical challenge. Accumulating evidence suggests that immune dysregulation within the tumor microenvironment (TME) plays a pivotal role in DCIS progression. Altered immune composition—reduced antigen presentation, T cell activation, and immune surveillance—can create a permissive environment that supports tumor growth and invasion. The Duffy Antigen Receptor for Chemokines (DARC/ACKR1), a decoy chemokine receptor expressed on erythrocytes, binds and sequesters pro-inflammatory chemokines for lysosomal degradation to maintain tissue immune homeostasis. Thus, ACKR1 regulates TME immune cell infiltration and the immune response. Loss of ACKR1 expression may disrupt chemokine gradients and impair immune cell recruitment to the TME, contributing to tumor immune evasion and progression. We hypothesize that ACKR1 influences DCIS progression by modulating immune cell composition and activation within the breast TME. We analyzed the influence of ACKR1 on the tumor immune response and DCIS TME in RNA-seq data derived from breast cancer patients in multiple independent publicly-available gene-expression datasets (GEO, Oncohuman, METABRIC) via the OmicSoft platform. We observed significant downregulation of ACKR1 expression from DCIS to IDC lesions in both the Oncohuman and METABRIC datasets, and this loss correlated with loss of E-cadherin expression in DCIS lesions. GEO analysis uncovered significant differences in a chemokine signaling network and cytokine expression profiles between ACKR1-low and ACKR1-high DCIS cases. CIBERSORT immune cell deconvolution revealed that relative to ACKR1-high lesions, ACKR1-low lesions exhibit significantly reduced proportions of naïve B cells, activated dendritic cells, $CD4^+$ memory-activated T cells, and T follicular helper cells in DCIS. Our findings support the role of ACKR1 in shaping immune signaling within the DCIS TME by demonstrating distinct immune response profiles based on ACKR1 status. Our work suggests that loss of ACKR1 expression in DCIS supports an “immune-cold” TME, further highlighting its role as a suppressor of tumor invasion and potential biomarker of disease progression. Thus, ACKR1 may improve clinical decision making and DCIS patient management by providing insight into patient immune response profiles and predisposition for progression.

#7584 Tumor microRNA expressions associated with prostate cancer aggressiveness across independent cohorts.

Huiyi Lin[1], Jong Y. Park[2], Masuma Mannan[1]

[1]Lousiana State Univ. Health Ctr., New Orleans, LA,[2]Moffitt Cancer Center, Tampa, FL

Introduction: Tumor microRNAs (miRNAs) play a critical role in prostate cancer (PCa) biology and may serve as biomarkers for disease aggressiveness. However, robust identification and validation of tumor miRNA expressions across independent datasets remain challenging. This study aimed to discover and validate miRNAs associated with PCa aggressiveness using three independent cohorts.
Methods: We analyzed tumor miRNA expression profiles from three datasets: our cohort (discovery set, 268 Whites), TCGA-PRAD (406 Whites), and GSE135535 (GSE, 320 men). In our cohort, we identified the top 25 miRNAs significantly associated with PCa aggressiveness ($p < 0.01$) using univariate logistic models. Using these 25 miRNAs, stepwise selection was performed in the 1,000 bootstrap samples based on our cohort. Among the 9 miRNAs selected in >20% of 1000 bootstrap runs, many miRNA expressions are highly correlated. Therefore, we further performed stepwise selection to identify the most informative miRNAs associated with PCa aggressiveness. Then, the selected miRNAs were tested in the other two validation sets.
Results: Two tumor miRNA expressions were significantly associated with PCa aggressiveness in our cohort (hsa-miR-145-5p, $p<0.001$, and hsa-miR-182-5p, $p = 0.001$, AUC=0.74). In the GSE135535 cohort, the p-values were 0.003 and 0.099 for hsa-miR-145-5p and hsa-miR-182-5p, respectively (AUC=0.621). In the TCGA set, the p-values were 0.024 and 0.059 for hsa-miR-145-5p and hsa-miR-182-5p, respectively (AUC=0.591). Thus, these two miRNAs represent distinct biological clusters, suggesting complementary roles in PCa aggressiveness.
Conclusion: Our multi-cohort analysis identified and validated two miRNAs associated with PCa aggressiveness. Other previous studies have supported the biological function of these two miRNAs. It has been shown that hsa-miR-145-5p significantly inhibits PCa cell growth and metastasis by negatively regulating metadherin (MTDH) expression and acts as a tumor suppressor. hsa-miR-182-5p acts as an oncogenic miRNA to contribute to poor prognosis for PCa patients. Up-regulation of miR-182 is significantly associated with PCa risk, progression, and treatment response. Functional enrichment analysis in previous studies revealed a significant association between miR-182 and its target genes, MITF (melanocyte inducing transcription factor) with epithelial-to-mesenchymal transition (EMT). Our findings support their potential utility as prognostic biomarkers and warrant further functional studies to elucidate underlying biological mechanisms.

#7585 Fatty liver index and AST/ALT ratio for hepatocellular carcinoma prediction in low-risk Korean men: Results from the HEXA-G cohort.

So Yoon Lee[1], Hyobin Lee[1], Sukhong Min[1], Sinyoung Cho[2], Jeongheon Kim[1], Ji-Yeob Choi[3], Daehee Kang[4]

[1]Seoul National University, Seoul, Korea, Republic of,[2]Seoul National University Hospital, Seoul, Korea, Republic of,[3]Assistant Professor, Seoul National Univ. College of Medicine, Seoul, Korea, Republic of,[4]Dean, Professor, Dept. of Molecular Medicine And Biopharmaceutical Sciences, Seoul National University, Seoul, Korea, Republic of

Background: The prognostic utility of the fatty liver index (FLI, a steatosis index derived from BMI, waist circumference, triglycerides, and GGT) and AST/ALT (De Ritis) ratio for hepatocellular carcinoma (HCC) risk in low-risk Asian populations is not well defined. We evaluated their independent and incremental predictive value in a large Korean cohort.
Methods: We analyzed 43,981 Korean men (376 HCC cases) from the Health Examinees-Gem (HEXA-G) cohort (2004-2013). A low-risk subcohort (n = 39,033) was defined by excluding individuals with diabetes or chronic hepatitis. Multivariable Cox models assessed associations with log-transformed FLI and the AST/ALT ratio after adjusting for demographic, lifestyle, socioeconomic, and metabolic factors. Incremental predictive value was evaluated using likelihood ratio tests (LRTs), changes in C-statistics, and Bayesian Information Criterion (BIC). Sensitivity analyses using penalized regression produced similar results.
Results: In univariable analyses, the AST/ALT ratio showed crude associations with HCC, whereas FLI did not. After adjustment, this pattern reversed: the AST/ALT ratio became non-predictive—consistent with confounding by age, alcohol consumption, smoking, and metabolic factors—while log(FLI) emerged as a modest independent predictor in the low-risk subcohort (adjusted HR 1.08; 95% CI, 1.01-1.16; p = 0.04). Discrimination improved minimally (C-statistic 0.715 to 0.719), and conventional FLI categories failed to stratify risk. In the full cohort, log(FLI) remained independently associated with HCC (adjusted HR 1.11; 95% CI, 1.03-1.20; p = 0.009) and modestly improved model fit (LRT p = 0.011) without meaningfully improving discrimination (C-statistic 0.795 to 0.797). The De Ritis ratio added no independent or incremental value in any model.
Conclusions: Across low-risk and mixed-risk Korean men, FLI remained an independent predictor of HCC after adjustment, although the effect size was modest. In contrast, the AST/ALT ratio lost all prognostic value after accounting for demographic, lifestyle, and metabolic confounding. The reversal of crude versus adjusted associations underscores substantial confounding for AST/ALT and a small, metabolically related signal for FLI. Overall, these findings highlight that FLI provides some independent information in low-risk settings, but substantial improvement in HCC risk prediction will require more robust biomarkers.

#7586 The impact of COVID-19 on sexual minority women seeking breast cancer screenings and treatment: An analysis of the OUT national cancer survey data.

Kristi Tredway[1], Melissa S. Camp[2], Vered Stearns[3]

[1]Cancer Population Science, OHSU Knight Cancer Institute, Portland, OR,[2]Sidney Kimmel Comprehensive Cancer Center, Johns Hopkins University, Baltimore, MD,[3]Oncology, Weill Cornell Medicine, New York, NY

Breast cancer is the most frequently diagnosed female cancer in the U.S. and now globally. Early detection of breast cancer through screening is well established to reduce mortality. Despite the substantial benefits, sexual minority women (e.g., lesbians and bisexual women) are significantly less likely to access breast cancer screenings, have lower lifetime prevalence of screening mammography, and undergo less timely screening as compared to sexual majority women (i.e., heterosexual women). Some reasons for the low utilization of screenings include negative beliefs about care, lower perceived severity, lack of health insurance, costs of care, and perceptions of heterosexism and homophobia among providers. Hesitancy in breast cancer screenings for sexual minority women is compounded by culturally-specific risk factors that place many sexual minority women at higher risk for breast cancer. Risk factors identified as those sexual minority women are more subject to include: tobacco use and smoking, higher alcohol consumption, drug use, obesity, low levels of physical activity, less likely to undergo routine preventive screenings, less likely to have insurance coverage, less satisfaction with medical interactions, higher rates of psychological distress (likely due to the fear of homophobia and bias), and nulliparity or not bearing offspring. Hesitancy and delays were increased during the COVID-19 era even with the temporary transition to telehealth (online, virtual) appointments with healthcare practioners. Using data from the National LGBT Cancer Network's OUT National Cancer Survey, this study analyzes the experiences of sexual minority women who faced breast cancer diagnoses. This dataset is the first large, nationwide sample to target LGBTQ+ populations regarding their cancer diagnoses. Survey items included demographics, behavioral questions about cancer treatment and social support, and structural and psychosocial barriers to or facilitators of seeking care. A total of 2,700 respondents completed the National LGBT Cancer Network survey. Of those 2,700 respondents, 503 had had breast cancer diagnoses. The sample for this study included the 490 females (since birth), 359 were lesbian or gay and 62 were bisexual, of those 503 respondents. Findings highlight experiences with social isolation, levels of optimism versus pessimism, whether doctors or medical clinics delayed cancer screenings, experiences and satisfaction with telemedicine, and other impacts of COVID-19.

#7587 Cervical cancer screening and prevention among Latinas in the U.S. among a network of community health centers.

Selena Rushton[1], Tahlia Hodes[2], Jennifer A. Lucas[2], John Heintzman[2], Cirila Estela Vasquez Guzman[3]

[1]ASHA-American Sexual Health Association, Lacey, WA,[2]OHSU, Portland, OR,[3]OHSU Knight Cancer Institute, Portland, OR

Introduction: Timely cervical cancer screenings are critical for middle to older aged Latinas, who have high morbidity and mortality from cervical cancer, but we currently know less about screening in this population. Efforts to engage middle to older-age Latina immigrants need to be tailored to recognize their distinct experiences with coming to the US that may set them apart from other groups. Latinas tend to receive disproportionate care in Community Health Centers (CHCs) and CHCs are a vital component for cancer screening and prevention. This study leverages a national network of CHCs to assess disparities in and utilization of cervical cancer screening among middle to older age Latinas.
Methods: Retrospective analysis of electronic health record data from a multistate network of CHCs across the United States. Data were extracted on Latina and non-Hispanic White (NHW) women age >45 with known birth country and at least one in-person primary care visit in a CHC between January 1, 2014, and September 14, 2022, across 527 community-based primary care clinics in 15 states. To examine the receipt of at least one Pap Smear and/or Human papilloma Varus (HPV) test ever during the study period, generalized estimating equations (GEE) logistic regression were conducted, overall and disaggregated by country of origin.
Results: Among 34,135 patients, we found that all Latina groups aside from US born Latinas and those from other countries with sample sizes too small to analyze individually had higher odds of receiving either an HPV or Pap test compared to non-Hispanic Whites. When disaggregated by country of origin, all Latina groups born in Central America have higher odds than non-Hispanic Whites. All three of the models showed that Latinas had higher odds of receiving either an HPV or Pap test at least once during the study period compared to non-Hispanic White patients.
Conclusion: CHCs may have unique strengths to address diverse and underserved populations such as Latinas; however, rates remain less than optimal, and work is still needed

#7588 Addressing the immigrant screening gap: A systematic review on interventions to increase colorectal cancer screening among immigrants in the United States.

Taylor McCready[1], Ethan Cohen[2], Delaney Gordon[3], Perla Chebli[4], Peter S. Liang[4], Audrey Renson[1]

[1]Department of Population Health, NYU Grossman School of Medicine, New York, NY,[2]Allegheny Health Network, Pittsburgh, PA,[3]Bucknell University, Lewisburg, PA,[4]NYU Langone Health, New York, NY

Introduction Colorectal cancer (CRC) screening rates are lower among immigrants in the United States (US) than the general population. Immigrant communities face structural barriers that disincentivize engagement in CRC screening. A growing body of literature has evaluated the effects of interventions aimed at increasing CRC screening engagement among immigrants, but findings have not been systematically synthesized. We systematically evaluated quantitative studies of interventions to increase CRC screening among immigrants in the US.

Methods We searched English-language peer-reviewed and grey literature on interventions to improve CRC screening rates among immigrants, published between January 1, 2000 and April 30, 2025 in seven databases: PubMed, Cochrane Library, CINAHL (EBSCO), ClinicalTrials.gov, Embase, Scopus, and Web of Science and imported into Covidence. Two reviewers independently screened records and extracted data. Risk of bias was assessed using the Cochrane Risk of Bias 2 (ROB2) tool for randomized controlled trials, and the Risk of Bias in Non-Randomized Studies of Interventions (ROBINS-I) tool for other study designs. Quantitative synthesis was restricted to studies that explicitly defined immigrants in their population. The protocol was registered in PROSPERO (CRD42023488183) and published in PLOS One.

Results The primary outcome was CRC screening completion. Of 1,824 unique records screened, 45 studies were included (39 randomized trials, 6 non-randomized studies), representing over 21,000 participants. Individualized education (n=12), navigation-based interventions (n=17; including patient navigation alone and navigation plus culturally targeted materials), and non-individualized educational campaigns (n=7) were the most evaluated strategies, alongside mailed outreach with fecal tests and telephone reminders (n=4). Across trials reporting screening outcomes for both intervention and control arms (n=19), interventions increased screening by an average of 20% compared with control, with culturally tailored navigation-based approaches generally yielding the largest gains. Substantial heterogeneity in immigrant group definitions, settings, and outcome measures, coupled with limited and inconsistently collected immigration-related variables, constrained cross-population comparisons and precluded a formal meta-analysis.

Conclusions Culturally and linguistically tailored patient navigation emerged as the most effective approach. Limited and inconsistently collected immigration-related information and heterogeneity across immigrant groups restricted inference but the findings still offer concrete guidance for practitioners and policymakers developing tailored programs and policies to improve CRC screening uptake among immigrant populations in the US.

#7589 On the road to early detection: A survey of barriers and facilitators to community participation in mobile lung cancer screening.

Cherell Cottrell-Daniels[1], Najy Sadig[2], Sofia Haddan[2], Sashanna Roman[2], Vani N. Simmons[2], **Matthew B. Schabath**[2]

[1]Health Choice Network, Miami, FL,[2]Moffitt Cancer Center, Tampa, FL

Introduction: Mobile screening units (MSUs) are an innovative strategy to mitigate barriers to community access to cancer screening modalities. A pivotal step in implementing an MSU is identifying potential barriers that may impact community utilization. Therefore, the goal of this study was to conduct a community-wide cross-sectional survey to assess barriers and facilitators to mobile lung cancer screening using validated survey measures.

Methods: Patient eligibility included have undergone any cancer screening at Moffitt Cancer Center (MCC) between Jan 1, 2023 and Dec 1, 2024, or patients who visited MCC during the same time and met current lung cancer screening guidelines. The web-based survey was administered from May 2025 to June 2025 and included items derived from validated measures, existing literature, and questions developed by the study team. The survey collected data on health behaviors, barriers, facilitators, screening preferences, and demographics. Participants were offered a $10 Amazon gift card upon survey completion. Descriptive statistics and exploratory stratified analyses were used to quantify survey responses.

Results: Among the 218 participants who completed the survey, 33% reported a prior clinician discussion about lung cancer screening. Most participants (73.4%) reported no concerns about getting screened in a mobile screening unit, but 67.9% reported concerned about the cost or if insurance covered mobile lung cancer screening, and 84.4% reported they would be screened if a voucher or insurance would pay for it. Regarding preferences, 54.1% reported no preference for the time of year for a mobile screening event, 59.6% reported they will be willing to wait up to 30 minutes to get screened, 44% would travel more than 20 minutes to get screened, and 44% preferred only Monday-Friday 9 am to 5 pm to get screened in a mobile unit. There were only few statistically significant differences found in stratified analyses by smoking status (ever vs. never), race/ethnicity (non-Hispanic Whites vs. all other groups), age (<67 vs. ≥67), and veteran status (former/active vs. no).

Conclusions: In this community-wide survey study, mobile lung cancer screening was broadly acceptable. Actionable preferences included: daytime weekday events, indoor waiting, short waits, proximity to home, clear cost coverage, and streamlined clinician recommendation. Implementation strategies that focus on provider prompts/referrals, financial transparency (vouchers/coverage), and hybrid workflows (vouchers/coverage) may enhance uptake.

#7590 Calibration of the US breast cancer risk assessment tool in 114,533 Mexican women: Evidence from the Mexican Teachers' Cohort.

Liliana Gomez-Flores-Ramos[1], Mario Arturo Aguilar[2], Dalia Stern[1], Adrian Cortes-Valencia[2], Marion Brochier[2], Ariadna Gutierrez[2], Gabriela Torres-Mejia[2], Salvador Zamora[3], Pabel Miranda-Aguirre[4], Patricia Perez-Escobedo[5], Alejandro Mohar[6], Ruth Pfeiffer[7], Martin Lajous[8]

[1]Secihti, National Institute of Public Health of Mexico, Mexico City, Mexico,[2]National Institute of Public Health of Mexico, Mexico City, Mexico,[3]UNAM, Mexico City, Mexico,[4]ISSSTE, Mexico City, Mexico,[5]Direccion medica, ISSSTE, Mexico City, Mexico,[6]Instituto de Investigaciones Biomedicas, UNAM, Mexico City, Mexico,[7]National Cancer Institute, NIH, Bethesda, MD,[8]National Institute of Public Health, Harvard T.H. Chan School of Public Health,, Bethesda, MD

Background: Breast cancer risk prediction models are increasingly used to identify women for risk-based screening and chemoprevention. The US Breast Cancer Risk Assessment Tool (NCI-BCRAT/Gail) is a widely used model, yet its performance in Mexican women is unknown. The Mexican Teachers' Cohort (MTC), a prospective cancer cohort in Mexico, is a unique resource that can be leveraged to assess the usefulness of breast cancer risk models in this understudied population. Thus, we evaluated calibration and discrimination of this model in a large, diverse cohort of Mexican women.

Methods: Absolute invasive breast cancer risk was calculated from enrollment to December 31, 2019, in 114,533 cancer-free women aged 25-80 years. Missing model predictors were assigned to the lowest-risk category. We compared expected and observed cases overall and by 5-year age groups and Indigenous ethnicity using expected-to-observed (E/O) ratios with 95% confidence intervals (95% CI). Discrimination was assessed with the area under the ROC curve (AUC). We quantified the proportion of women with a predicted risk above the 5-year high-risk threshold among those who developed and those who did not develop breast cancer.

Results: Over a mean follow-up period of 11.2 years, we identified 1,490 women with invasive breast cancer among cohort participants. The NCI-BCRAT/Gail model predicted that 2,115 women would develop breast cancer, leading to an expected-to-observed (E/O) ratio of 1.40 (95% CI 1.35-1.49). Overestimation was most pronounced in the 50-54 age group (E/O = 1.62; 95% CI 1.41-1.87). Among Indigenous women, 79 developed breast cancer compared to 135 women who were predicted to develop the disease (E/O = 1.71;95% CI 1.35-1.49), and for age 50-54 E/O ratio was 2.71 (95% CI 1.29-5.86). The model's discriminatory accuracy was 63% (95% CI, 62%-65%). Yet, 82% of women who developed breast cancer did not reach the 5-year high-risk threshold. Also, 7% of non-cases had a predicted risk above the 5-year high-risk threshold. Further, results using different breast cancer incidence estimates for Mexico and 5-year high-risk thresholds will also be presented.

Conclusions. The NCI-BCRAT/Gail model overestimated invasive breast cancer risk in Mexican women from the MTC. Overestimation was particularly salient in older women and Indigenous women. Using this model "as is", most women who developed breast cancer would have been classified as average risk. These findings suggest that the NCI-BCRAT/Gail should be recalibrated and validated before clinical use in this population.

#7591 Identification of a multi-protein signature to predict 5-year stomach cancer risk using high-throughput proteomics and machine learning.

Jessica Chadwick[1], Clare Paterson[1], Sama Shrestha[1], Hannah Biegel[1], Jessica Kuzma[2], Stephen Williams[2], In collaboration with the EPIC - Proteomic investigators

[1]Illumina, San Diego, CA,[2]SomaLogic, Boulder, CO

Introduction: Stomach cancer is the fifth most common cancer worldwide, and the fourth leading cause of cancer death, with an average 5-year relative survival rate of only 20%-30%. This low survival rate is largely due to late diagnosis, which often occurs after the cancer has spread and is more difficult to treat. There is currently no guidance from the US Preventive Services Task Force around screening for stomach cancer or *Helicobacter pylori* (*H pylori*) infection, a primary risk factor for stomach cancer. This study investigated whether high-throughput proteomics could be used to develop a stomach cancer susceptibility model that may help stratify individual risk and direct screening procedures.

Methods: Samples from the European Prospective Investigation into Cancer and Nutrition study were assayed using modified-aptamer proteomics technology (SomaScan™ 7K assay). Following data QC, 14,787 citrate plasma samples had clinical and proteomic data (totaling ~103 million protein measurements), which included n=56 and n=219 stomach cancer diagnosis within 5 years and over 20-year follow-up period, respectively. Machine learning techniques were used to identify a model that predicts risk of stomach cancer diagnosis within 5 years of blood draw using an 80% training split of the data. Discrimination was assessed via C-index and 5-year AUC. A post-hoc subset analysis was performed in individuals with H pylori infection status (n=286).

Results: An abundance of proteomic signal was detected with 922 proteins significantly associated with incident stomach cancer at FDR <0.1. An 8-protein accelerated failure time model was identified that accurately predicted stomach cancer risk with a 5-year AUC of 0.742 and C-Index of 0.697 in the hold-out validation dataset. Performance of the protein model was higher than the average performance of the Polygenic Risk Score-based models used to predict lifetime stomach cancer risk. The model included proteins known to be up or downregulated in stomach cancer (75%), although only a subset of these proteins (37.5%) are predictive of stomach cancer risk, and novel proteins (25%). In the subset of individuals positive for H pylori infection (n=214), the stomach cancer risk model had a 5-year AUC = 0.698 and C-Index of 0.599 suggesting the model can still accurately predict risk in individuals with H pylori infection.

Conclusions: We successfully developed a multi-protein model to predict 5-year risk of stomach cancer in individuals with and without H pylori infection, highlighting the potential utility of high-throughput proteomics as a novel screening tool for assessing cancer risk.

#7592 Machine learning enables accurate prediction of patient outcomes for immune checkpoint blockade using real-world clinical data.

Alyssa Pybus[1], Isis Yanina Narvaez-Bandera[2], Tosin Jolaogun[1], PAULO CILAS MORAIS LYRA JR[2], Khai Dang[2], Jeremy Goecks[2]

[1]Machine Learning, H. Lee Moffitt Cancer Center, Tampa, FL,[2]H. Lee Moffitt Cancer Center, Tampa, FL

Background: While immune checkpoint blockade (ICB) therapy can produce durable clinical responses and substantially improve patient outcomes, accurate predictors of outcomes are critical as up to half of patients with advanced disease derive limited or no benefit. Accurate ICB outcome prediction will improve treatment stratification, reduce unnecessary toxicity, and enhance outcomes for cancer patients.
Methods: We used state-of-the-art machine learning survival models to accurately predict patient survival after ICB therapy in our large multi-cancer institutional cohort. This retrospective study included 2,090 patients with advanced melanoma (n=908), advanced non-small cell lung cancer (NSCLC, n=878), or metastatic renal cell carcinoma (RCC, n=304) who underwent anti-PD-1/PD-L1 and/or anti-CTLA-4 ICB therapy at Moffitt Cancer Center from 2011-2025. Over 50 pre-treatment clinical and laboratory features were abstracted from electronic health records and analyzed against overall and progression-free survival. We trained and tested survival support vector machine models to predict patient outcomes with a 75/25 random split.
Results: Cox PH analysis identified 11-44 statistically significant features per data set for inclusion into each model, including serum albumin, neutrophil-to-lymphocyte ratio, blood pressure, heart rate, and ECOG scores. Our models achieved AUC values of up to 0.83 in melanoma, 0.80 in NSCLC, and 0.85 in RCC, with enhanced performance in progression models trained on multi-cancer data. Our models outperformed PD-L1 and TMB at each time point where data is available.
Conclusions: Our work demonstrates the promise of machine learning with accessible clinical and laboratory features to predict ICB patient outcomes with improved performance versus current biomarkers.

Time-dependent receiver operating characteristic area under the curve (AUC) for our model vs PD-L1

Real-world data set	Sample size	Model AUC at 6mo, OS	PD-L1 AUC at 6mo, OS	Model AUC at 24mo, OS	PD-L1 AUC at 24mo, OS	Model AUC at 6mo, PFS	PD-L1 AUC at 6mo, PFS	Model AUC at 24mo, PFS	PD-L1 AUC at 24mo, PFS
Melanoma	n = 908	**Melanoma: 0.80**, Multi: 0.79	0.60	**Melanoma: 0.72**, Multi: 0.70	0.51	Melanoma: 0.72, **Multi: 0.79**	0.64	Melanoma: 0.73, **Multi: 0.83**	N/A
Non-small cell lung cancer	n = 878	**NSCLC: 0.77**, Multi: 0.70	0.56	**NSCLC: 0.71**, Multi: 0.62	0.59	NSCLC: 0.66, **Multi: 0.69**	0.57	NSCLC: 0.67, **Multi: 0.80**	0.61
Renal cell carcinoma	n = 304	RCC: 0.79, **Multi: 0.85**	0.62	**RCC: 0.80**, Multi: 0.74	0.56	**RCC: 0.78**, Multi: 0.77	N/A	**RCC: 0.82**, Multi: 0.68	N/A

#7593 Personalized risk assessment of breast cancer using administrative health data.

Fidela Mushashi[1], Shi-ang Qi[2], Parveen Bhatti[3], Andrew Roth[1], Russell Greiner[2], Rachel A. Murphy[4]

[1]University of British Columbia, Vancouver, BC, Canada,[2]University of Alberta, Edmonton, AB, Canada,[3]British Columbia Institute of Cancer Research, Vancouver, BC, Canada,[4]School of Population and Public Health, University of British Columbia, Vancouver, BC, Canada

Breast cancer screening programs are one-size-fits-most approaches with suboptimal participation rates. Population-level administrative health databases provide a unique opportunity to build scalable, data-driven risk assessment tools capable of identifying women who may benefit from more personalized screening strategies. We assembled nearly two decades of longitudinal health data, including mammographic screening history, medication use, physician visits, and hospital discharge abstracts, for 1.74 million women in British Columbia, among whom 39,211 incident breast cancers were diagnosed. Our team is developing new breast cancer risk assessment models to predict each woman's individual time until Breast Cancer Onset (BCo) using administrative health data from Canada's publicly funded healthcare system. We are applying machine learning Individual Survival Distribution (ISD) models, which identify each subject x with a distribution S (t | x), showing the probability that x's time until BCo is at least t more years, for all t > 0. We can then use these models to estimate each woman's expected time until BCo, as well as her risk score. In preliminary models using 25 features with known/suspected links to breast cancer, random survival forest (RSF) achieved the highest concordance index (CI = 58.9%), while multitask logistic regression (MTLR) achieved a competitive 5-year Brier score (BS = 0.0068) and a low mean absolute error (MAE = 30.4 months). These early results demonstrate the feasibility of leveraging administrative health data for personalized breast cancer risk prediction. Ongoing work will substantially expand the feature sets to improve model discrimination.

#7594 Combining electronic health records, environmental, and genomics data for lung cancer risk prediction in Southern California.

Gianni Pucillo[1], Sanye Naqvi[2], Allison Jue[3], Chandler Law[3], Sandip Patel[2], Uduak Z. George[1]

[1]Computational Science Research Center, San Diego State University, San Diego, CA,[2]UC San Diego, San Diego, CA,[3]San Diego State University, San Diego, CA

Background: Lung cancer risk reflects intersecting clinical, environmental, and genomic factors, yet these data types are rarely integrated at the individual level. We assembled an EHR-based cohort in Southern California to build a predictive model of incident lung cancer diagnosis and to characterize the clinical, genomic, and neighborhood features that drive risk.
Methods: We constructed a retrospective cohort of 7,151 adults from UC San Diego Health electronic health records (50.4% female, 65% ≥ 65 years) and linked approximately 40 clinical features to census-tract-level environmental and socioeconomic indicators from CalEnviroScreen, as well as genomic mutation status for ALK and EGFR. We compared 14 classifiers (logistic regression, random forest, XGBoost, and 11 PyTorch neural networks) using stratified five-fold cross-validation to predict lung cancer diagnosis. Hyperparameters for top performing models were optimized using Bayesian search in Optuna. Model performance was summarized using AUROC, accuracy, precision, recall, and F1, and feature importance was assessed using Shapley (SHAP) values.
Results: Optimized XGBoost achieved the best cross-validated discrimination (AUROC 0.879), with accuracy 0.802, precision 0.744, and F1 0.694, outperforming linear and deep-learning baselines. Top-ranked features by SHAP included smoking intensity, cardiometabolic comorbidity, and age, with neighborhood unemployment, pesticide burden, and ozone levels contributing additional, though smaller, predictive signal, reinforcing the contribution of neighborhood disadvantage and pollution to lung cancer vulnerability in this regional cohort. Among genomically profiled patients, ALK-positive cases were diagnosed at a significantly younger age than ALK-wildtype cases (mean 56 vs 71 years, p=0.016), underscoring biologically distinct disease courses.
Conclusion: An integrated gradient-boosting model leveraging EHR, environmental, and genomic data can meaningfully stratify individual lung cancer risk in a diverse regional cohort and elevate both clinical and neighborhood drivers of vulnerability. These findings support the use of routinely collected health and environmental data to guide targeted lung cancer screening and prevention efforts and motivate future work on external validation, time-varying exposures, and explicit fairness constraints across racial and socioeconomic groups.

#7595 Survival outcomes in chemotherapy patients using a multi-institutional risk model. A retrospective analysis.

Aswanth Reddy[1], Arpana Ashok[1], Yang Wang[2], Jay Carlson[2]

[1]Mercy Hospital, Fort Smtih, AR,[2]Mercy Hospital, St. Louis, MO

Background: Patients with cancer who are receiving chemotherapy have a high risk of complications due to the disease and from adverse events due to therapy. The Chen Model, a proprietary risk stratification tool (multivariable analysis) developed by Mercy Health, St. Louis, identifies chemotherapy patients at risk for adverse outcomes. The Chen Model stratifies patients into high risk (score>=90), moderate high risk (80 to 89), and low risk groups (<80). From our multi-institutional analysis, we aim to identify the 6- and 12-month mortality rates among adult chemotherapy patients (non-leukemia, age >18) stratified by the Chen model.
Methods: We conducted a retrospective analysis of 18,854 chemotherapy patients treated between July 2023 and August 2025 at the Mercy Hospital system, which includes multiple hospital sites and oncology practices across three states (Missouri, Arkansas, and Oklahoma). Patients were assigned to cohorts based on their maximum Chen model score during the 7-day post-chemotherapy period. A total of 2139 patients were in the high-risk group, 2449 in moderate high-risk, and 14266 in the low-risk group. Kaplan-Meier estimates and Cox proportional hazards models were used to assess 6- and 12-month mortality, with hazard ratios (HR) and 95% confidence intervals (CI) calculated.
Results: Six-month mortality rates were 39.96% (95% CI: 37.85%-42.14%) for the high-risk group, 22.59% (95% CI: 20.91%-24.40%) for the moderate high-risk group, and 11.65% (95% CI: 11.12%-12.21%) for the low-risk group. Twelve-month mortality rates were 51.63% (95% CI: 49.31%-54.00%), 31.44% (95% CI: 29.36%-33.62%), and 19.54% (95% CI: 18.84%-20.26%), respectively. Cox models showed significantly elevated hazard of death for high-risk (HR=4.4 at 6 months, HR=3.7 at 12 months; $p<0.005$) and moderate high-risk (HR=1.5 at 6 months, HR=1.4 at 12 months; $p<0.005$) groups compared to the low-risk group. Further analysis on composite palliative care and hospice services utilization was identified to be 23.2% in high risk and 15.6% in moderate high-risk groups.
Conclusions: The Chen model effectively stratifies chemotherapy patients by mortality risk, with high-risk patients facing substantially worse outcomes at 6 and 12 months. We also identified a lower palliative care utility in the higher-risk groups. These findings support the model's utility in identifying patients who may benefit from intensified monitoring and early involvement of supportive services, particularly palliative care services. Further studies are needed to validate these results and assess the impact of targeted interventions.

#7596 Risk factors and prediction models for colorectal cancer in older US individuals.

Chen Yuan[1], Qiao-Li Wang[2], Sara K. Char[3], Wenjie Ma[4], Brian M. Wolpin[3], Jeffrey A. Meyerhardt[3], Shuji Ogino[5], Mingyang Song[6], Andrew T. Chan[4], Edward L. Giovannucci[6], Kimmie Ng[3]

[1]Cedars-Sinai Medical Center, Los Angeles, CA,[2]Lund University, Malmo, Sweden,[3]Dana-Farber Cancer Institute, Boston, MA,[4]Massachusetts General Hospital, Boston, MA,[5]Brigham and Women's Hospital, Boston, MA,[6]Harvard T.H. Chan School of Public Health, Boston, MA

Background: Colorectal cancer (CRC) has high incidence and mortality in older adults, yet routine screening after age 75 is generally not recommended and current guidelines are limited. Risk factors for CRC diagnosed after age 75 and the subgroups of older individuals at highest risk are not well defined.
Methods: We conducted a prospective cohort analysis within the Nurses' Health Study and the Health Professionals Follow-Up Study among participants free of CRC through age 75. Established CRC risk factors were assessed up to age 75, with modifiable factors averaged across repeated questionnaires. We calculated age- and sex-standardized incidence rates (standardized to the 2000 US standard population) and used Cox proportional hazards regression to estimate associations and build a risk prediction model. Model discrimination was evaluated using the C-statistic.
Results: Among 92,773 participants, 848 developed CRC after age 75. A history of lower endoscopy by age 75 was associated with substantially lower CRC risk (incidence, 113 vs 237 per 100,000), and this association was consistent regardless of indication (screening or symptoms). When considering endoscopy timing by age 75, participants whose last endoscopy occurred between ages 66 and 75 had lower CRC incidence than those whose last endoscopy was before age 66 (i.e., missing at least one recommended endoscopy; 102 vs 163 per 100,000). Risk was higher in men and in those with a family history of CRC. Modifiable factors showed positive associations for heavy smoking, alcohol consumption, body mass index (BMI), and processed meat intake. Some subgroups had incidence rates comparable to those without prior endoscopy, such as individuals with ≥2 affected first-degree relatives, >2 alcoholic drinks/day, and BMI ≥35 kg/m^2 (210 to 243 per 100,000). No significant associations were observed for height, waist circumference, history of diabetes, physical activity, unprocessed red meat, dietary fiber, or whole grain intake. Compared to a model including only prior lower endoscopy, adding last-endoscopy timing, sex, family history, and modifiable factors significantly improved discrimination (C-statistic from 0.55 to 0.66; $p < 0.001$).
Conclusion: In two large prospective cohorts, lower endoscopy by age 75, particularly between ages 66 and 75, was associated with substantially lower CRC incidence after age 75, and family history and modifiable factors further stratify risk. Incorporating these factors improved risk prediction and may guide individualized prevention beyond age 75.

#7599 HOUSES as a screening tool for cancer screening: Patient-level housing-based socioeconomic status and breast and cervical cancer screening adherence.

Eunice Y. Park[1], Madison Beenken[2], Dave Watson[2], Chung Il Wi[3], Tufia Haddad[4], Gladys Asiedu[5], Karla BALLMAN[2], James R. Cerhan[2], Carolyn Flock[6], Brian Lynch[3], Folakemi T. Odedina[4], Scott H. Okuno[4], Young J Juhn[3]

[1]Radiation Oncology, Mayo Clinic, Rochester, MN,[2]Quantitative Health Sciences, Mayo Clinic, Rochester, MN,[3]Pediatric and Adolescent Medicine, Mayo Clinic, Rochester, MN,[4]Oncology, Mayo Clinic, Rochester, MN,[5]Kern Center for the Science of Health Care Delivery, Mayo Clinic, Rochester, MN,[6]Mayo Clinic Health System Research, Mayo Clinic, Rochester, MN

Introduction: The National Cancer Institute estimated almost 317,000 new breast cancer and over 13,000 new cervical cancer cases in 2025. While the National Breast and Cervical Cancer Early Detection Program has served millions of women over the past two decades, inequities in cancer screening, subsequently delayed diagnosis, and timely and appropriate treatment remain a public health challenge in the United States. Despite the substantial impact of social determinants of health (SDOH) on cancer screening, few studies have accounted for SDOH at the individual level when assessing breast and cervical cancer screening adherence. The primary objective of this study is to examine whether the individual-level SDOH, measured using HOUsing-based SocioEconomic Status (HOUSES) index, is associated with breast and cervical cancer screening non-adherence (not current on respective USPSTF recommendations for age and frequency).

Methods: In this retrospective study, patients were identified as those receiving primary care in the Mayo Clinic Health System and Mayo Clinic (Rochester, MN). The Midwest Quality Metrics panel was then used to assess patients due for screening for breast or cervical cancer in July 2023. The HOUSES, using home address and publicly available data on the residence which measures and categorizes housing status into quartiles, was obtained using the electronic health records (EHRs)-linkable patient-level information. Logistic regression analyses were conducted, controlling for Census block group-level adverse social exposome from the Area Deprivation Index, age, and comorbidities. Results are presented as odds ratios (OR) with corresponding 95% confidence intervals (CI).

Results: For breast cancer, among 128,462 eligible patients, 20.1% (n= 25,857) were non-adherent. Compared to the highest HOUSES quartile (Q4), lower HOUSES groups showed significantly higher odds of non-adherence: Q3 OR=1.20 (95% CI=1.15, 1.25), Q2 OR=1.45; (95% CI=1.40, 1.53), and Q1 OR=1.90 (95% CI=1.81, 1.99). For cervical cancer, among 175,712 eligible patients, 29.9% (n=52,533) were non-adherent. Compared to the highest HOUSES quartile (Q4), lower HOUSES groups showed significantly higher odds of non-adherence: Q3 OR=1.07 (95% CI=1.03, 1.10), Q2 OR=1.16; (95% CI=1.12, 1.20), and Q1 OR=1.36 (95% CI=1.31, 1.41).

Conclusions: A clinically meaningful association between the HOUSES index and cancer screening adherence was observed. A lower HOUSES index was associated with higher odds of non-adherence for both breast and cervical cancer screening, even after accounting for neighborhood-level risk, age, and comorbidities. Incorporating HOUSES into EHRs can be a practical “screening-for-screening” tool that enables close monitoring of higher-risk patients without additional burden of surveys.

#7600 Thirty years of breast cancer screening and socioeconomic inequalities: A national register-based study in Finland.

Peng Li[1], Pekka Martikainen[2], Mikko Myrskyla[1]

[1]Population Health, Max Planck Institute for Demographic Research, Rostock, Germany,[2]Population Research Unit, University of Helsinki, Helsinki, Finland

Background: The national wide Finnish breast cancer screening program has operated since 1992, yet the long-term effects of screening and socioeconomic inequalities remain incompletely characterized. This study examines 30 years of screening invitations, participation, diagnostic stage, and mortality, with a focus on educational disparities.

Methods: We used data from the Mass Screening Registry, which contains more than 8 million screening invitations issued to 1.2 million women aged 50-69 during 1992-2022. These data were linked with demographic information from Statistics Finland and cancer diagnosis records from the Finnish Cancer Registry. All invited individuals and participation were stratified by education. Survival differences by educational level and screening participation status were assessed using Kaplan-Meier survival curves. Overall mortality was analyzed using Cox proportional hazards models adjusted for education, marital status, urbanization level of residence, and stage at diagnosis. Effects of screening and education on early-stage detection (stage I-II vs. III-IV) were assessed using logistic regression models.

Results: Screening participation displayed a clear socioeconomic gradient (low education 80.2%, medium 84.7%, high 85.7%) and slightly decreased by year. Mean age at death was higher among screened than unscreened women overall (+2.65 years, 81.73 vs. 79.08), and the survival advantage was largest in the lower-educated group (+3.51 years, 81.12 vs. 77.61) than in the higher-educated group (+1.56 years, 82.38 vs. 80.82). Screening participation was associated with a 54% reduction in mortality (HR = 0.46, 95% CI 0.45-0.46) after full adjustment. Screened women had more than double the odds of early-stage diagnosis (OR = 2.31, 95% CI 2.00-2.68). Higher-educated women were more likely to receive an early-stage diagnosis (OR = 1.80, 95% CI 1.52-2.13) than lower-educated women.

Conclusions: Participation in the national breast cancer screening program is strongly associated with improved survival, markedly earlier detection, and substantially reduced mortality risk. Although women with lower education gain the largest absolute survival benefit when they attend screening, their lower participation rates contribute to persistent socioeconomic inequalities. Targeted efforts to increase screening uptake among disadvantaged groups may reduce these disparities.

Main messages: Overall, the national breast cancer screening program demonstrates strong effectiveness in improving survival and promoting earlier detection, while highlighting persistent socioeconomic inequalities that require targeted attention.

#7602 Effectiveness of initiating FIT screening at age 45: Comparative yield with adults aged 50-54 years.

Le Wang[1], Chen Zhu[1], Yu Qiu[1], Weimiao Wu[1], Dong Hang[2], Ni Li[3], Partha Basu[4], Lingbin Du[1]

[1]Zhejiang Cancer Hospital, Hangzhou Institute of Medicine (HIM), Chinese Academy of Sciences, Hangzhou, China,[2]Nanjing Medical University, Nanjing, China,[3]National Cancer Center/National Clinical Research Center for Cancer/Cancer Hospital, Chinese Academy of Medical Sciences and Peking Union Medical College, Beijing, China,[4]International Agency for Research on Cancer (WHO), Lyon, France

Background and aim: Over the past two decades, the incidence of early-onset colorectal cancer (CRC) has risen in several high-income countries. To address this trend, the United States Preventative Services Task Force recommended lowering the starting age for CRC screening from 50 to 45 years based on estimates from microsimulation models. However, real-world evidence on the screening yield across diverse populations remains limited.

Methods: A population-based CRC screening program has been implemented since 2020 in a region with high CRC incidence (Zhejiang Province, China). The program primarily targeted individuals aged 50-74 years but also included those aged 40-49 years. Screening consisted of two-sample fecal immunochemical testing (FIT), with colonoscopy offered to individuals testing positive on either sample. We compared screening outcomes between participants aged 45-49 years and 50-54 years, including: (1) FIT positivity (threshold of 20 μg hemoglobin per gram of feces); (2) colonoscopy completion; and (3) positive predictive values (PPV, cases detected among those with a positive FIT and available colonoscopy) for neoplasia. Advanced neoplasia included CRC, advanced adenoma and advanced serrated lesion. Variables with standardized mean differences greater than 0.1, including sex, fruit intake, and year of participation, were included in the propensity score model for 1:1 matching between age groups. Risk ratios (RRs) were estimated using a Poisson mixed-effects model.

Results: After propensity score matching, 89 446 subjects aged 45-49 and 89446 subjects aged 50-54 who completed the FIT test were selected, with comparable baseline characteristics. The FIT positivity in the 45-49 age group was 10.61%, which was lower than 11.02% in the 50-54 age group (RR, 0.96; 95% CI, 0.94-0.99), with similar colonoscopy adherence (46.75% vs 47.43%; RR, 0.99; 95% CI, 0.95-1.03). Compared with the 50-54 age group, the 45-49 age group had significantly lower PPVs for any adenoma (15.82% vs 19.91%; RR, 0.79; 95% CI, 0.72-0.88) and advanced neoplasia (6.06% vs 8.25%; RR, 0.73; 95% CI, 0.63-0.86).In subgroup analyses of 45-49 age group, the PPVs for advanced neoplasia among participants with smoking, BMI ≥28 kg/m^2, frequent alcohol drinking, personal history of adenoma or a family history of CRC exceeded that observed in the 50-54 age group.

Conclusions: Individuals aged 45-49 years had comparable colonoscopy adherence to those aged 50-54 years but a lower yield for adenomas and advanced neoplasia. Higher yields among younger individuals with risk factors highlight the potential of risk-stratified approaches. These findings contribute population-specific evidence to inform ongoing discussions on optimal screening initiation age, but further longitudinal, cost-effectiveness, and programmatic evaluations are warranted.

#7603 Type-2 Diabetes, medications, and risk of multiple colorectal polyps: A colonoscopy-based study using natural language processing.

Jessica van Onselen[1], Ryzen Benson[2], Stephanie Richardson[3], Maci Winn[1], Candace Winterton[3], Svenja Pauleck[3], Ainhoa Gomez-Lumbreras[3], Polly A. Newcomb[4], Cornelia M. Ulrich[1], John Inadomi[5], Sheetal Hardikar[1]

[1]University of Utah Huntsman Cancer Institute, Salt Lake City, UT,[2]Department of Radiation Oncology, University of California, San Fransico, San Francisco, CA,[3]Huntsman Cancer Institute, Salt Lake City, UT,[4]Fred Hutchinson Cancer Center, Seattle, WA,[5]Department of Internal Medicine, University of Utah, Salt Lake City, UT

Introduction: Colorectal polyps are known precursors to colorectal cancer (CRC), and a higher polyp count is associated with an increased CRC risk. This study aimed to investigate the impact of type-2 diabetes (T2D) and its treatments on polyp count.

Methods: We leveraged pathology reports from the University of Utah (UofU) Enterprise Data Warehouse (EDW) to develop a rule-based natural language processing pipeline, to extract polyp diagnoses and features (site, count) for 38,038 patients who underwent colonoscopy at the UofU Gastroenterology clinic from 2011-2020. We identified 6,556 patients with T2D via ICD codes and anti-diabetes medication prescriptions. Patient characteristics were extracted from the EDW, including age, sex, race, smoking, BMI, anti-inflammatory medication use, and active prescriptions for insulin, metformin, sulfonylureas, GLP-1 agonists, and DPP-4 inhibitors. Polyp count was categorized as none, one, or multiple. Adjusted odds ratios (OR) and 95% confidence intervals (CI) for polyp counts were calculated using multinomial logistic regression.

Results: Patients were on average 56 years old, 84% White, 51% female, with a mean BMI of 30 kg/m^2. 73% of patients with T2D used anti-diabetes medications. T2D alone was not associated with multiple polyps, but patients with T2D taking anti-diabetes medications had a lower risk of polyps overall, irrespective of polyp count. Insulin use was associated with an increased risk of one or multiple polyps [OR(95%CI)=1.29(1.08-1.54) and 1.40(1.18-1.66), respectively], compared to other medications. Metformin and GLP-1 agonists were both associated with a decreased risk of one [Metformin OR(95% CI)=0.71(0.59-0.85), GLP-1=0.79(0.64-0.99)] or multiple polyps [Metformin OR(95% CI)=0.71(0.52-0.73), GLP-1=0.63(0.51-0.77)], compared to patients taking medications other than metformin or GLP-1 agonists, respectively. Compared to patients taking no anti-diabetes medications, those on insulin, metformin, DPP-4 inhibitors, or sulfonylureas had an increased risk of at least one polyp, while patients taking GLP-1 agonists had a lower risk of multiple polyps [OR(95%CI)=0.81(0.63-1.03)]. DPP-4 inhibitors and sulfonylureas also had a lower risk of multiple polyps [OR(95%CI)=0.79(0.64-0.97) and 0.80(0.68, 0.96), respectively].

Conclusion: Overall, T2D alone was not associated with polyp count, but medication use modified this relationship. Insulin use was associated with increased risk, whereas the use of metformin, GLP-1 agonists, DPP-4 inhibitors, and sulfonylureas was associated with decreased risk of one or multiple polyps, compared to patients taking other anti-diabetes medications. These results highlight the potential role of T2D medication choice in altering colorectal polyp risk, underscoring the need for more research into underlying mechanisms to guide potential interventions.

#7604 Disaggregating Latino nativity using machine learning on electronic health records: Insights for colorectal cancer screening disparities.

Miguel Marino[1], Jun Hwang[1], Jennifer A. Lucas[1], Wyatt Bensken[2], Matthew P. Banegas[3], John D. Heintzman[1]

[1]Oregon Health & Science University, Portland, OR,[2]OCHIN Inc., Portland, OR,[3]Cancer Prevention Fellow, UC San Diego, San Diego, CA

Background: Advancements in colorectal cancer (CRC) prevention have not been equitable with studies showing reduced CRC screening rates and later-stage diagnoses among Latino patients. Latino subgroups vary in their cancer-related risk factors but also differ widely in their sociodemographic characteristics, migration histories, insurance coverage, and health care access patterns that may impact cancer prevention. However, large-scale datasets seldom contain granular data needed to study Latino subgroup-specific differences in cancer risk and outcomes. This study evaluated a machine learning approach designed to infer nativity and country of birth and advance cancer prevention research to better evaluate health equity among Latinos.

Methods: We used comprehensive electronic health record data from 1,500,191 Latino patients receiving care at 1,876 community health centers across 28 states, along with geocoded census-tract-level neighborhood composition data, and surname-based data to develop machine learning models of Latino subgroups. Multiple supervised learning algorithms were trained and tested to predict nativity and country of birth. Model predictive performance was evaluated using area under the receiver operating curve (AUC). As a case example, we used model-predicted probabilities of Latino subgroups and nativity to evaluate CRC screening disparities by foreign-born status, both known and predicted.

Results: Among 1,500,191 Latinos in the network, country of birth was self-reported by Latino patients for only 173,278 (11.6%), underscoring the challenges of using existing EHR data for studying Latino heterogeneity. Prediction models for nativity showed excellent discriminatory prediction performance across all groups (US-born vs. foreign-born: AUC=0.90; Mexican vs. non-Mexican: AUC=0.87; Guatemalan vs. non-Guatemalan: AUC=0.84; Cuban vs. non-Cuban: AUC=0.84). In our case example, using known foreign-born status of Latino patients, we observed that US-born Latinos had lower odds of CRC screening compared to foreign-born Latinos (OR=0.55, 95% CI=0.50-0.617). We observed high concordance between known and model-predicted estimates of CRC screening odds ratios.

Conclusion: National calls for data disaggregation, including among Latinos, have numerous challenges. We developed and validated novel prediction models to infer Latino nativity and country of birth for use in population-based cancer disparities research. These methods present an opportunity to evaluate cancer disparities in data where Latino nativity is not collected.

#7605 Multilevel determinants of hepatocellular carcinoma surveillance in eligible Hispanic and Asian American patients: Language concordance and ethnic enclaves.

Caroline A. Thompson[1], Enyao Zhang[1], Mindy C. Hebert-DeRouen[2], Alison J. Canchola[2], Alyssa Cortella[2], Terri Rice[2], Pushkar P. Inamdar[2], Mai Vu[3], Pragati Kenkare[3], Janet N. Chu[4], Anna D. Rubinsky[5], Chanda Ho[6], Su-Ying Liang[3], Hashem B. El-Serag[7], Michele M. Tana[4], Ma Somsouk[4], Mark Segal[2], Mi-Ok Kim[2], Iona C. Cheng[2], Scarlett L. Gomez[5], Salma Shariff-Marco[2]

[1]Epidemiology, University of North Carolina at Chapel Hill, Chapel Hill, NC,[2]Epidemiology and Biostatistics, University of California San Francisco, San Francisco, CA,[3]Palo Alto Medical Foundation Research Institute, Palo Alto, CA,[4]Medicine, University of California San Francisco, San Francisco, CA,[5]University of California San Francisco, San Francisco, CA,[6]California Pacific Medical Center, San Francisco, CA,[7]Baylor College of Medicine, Houston, TX

Low hepatocellular carcinoma (HCC) surveillance uptake among high-risk Hispanic and Asian American populations may be influenced by provider communication and/or neighborhood context. We investigated associations between patient-provider language concordance, neighborhood ethnic enclave and HCC surveillance in a large, diverse California health system. We analyzed electronic health record data from Sutter Health (2000-2016) appended to census tract-level ethnic enclave indices (% recent immigrants, Spanish/Asian language-speaking households and limited English proficiency, % Hispanic/Asian residents). Eligible adults had an assigned primary care provider (PCP), ≥1 encounter, valid address, no liver cancer history, surveillance indication (cirrhosis or chronic hepatitis B/C), ≥18 months follow-up, and self-identified as Hispanic (HA) or Asian American (AA). Surveillance was ultrasound every 6 months and/or contrast-enhanced CT/MRI (with/without alpha-fetoprotein). We defined uptake as ≥1 test and adherence as percent time up-to-date (PTUDS) among those surveilled. We assessed language concordance (PCP spoke patient's non-English language) and ethnic enclave (quintiles; Q5=highest). Hierarchical logistic/linear regression with facility clustering estimated ORs (uptake) and betas (PTUDS), adjusting for demographics, follow-up time, utilization. N=11,311 patients were included (3,444 HA, 7,867 AA); 19% of HAs and 28% of AAs were non-English speakers; 38% of HAs and 55% of AAs lived in Q5 enclaves. Overall, 36% of HAs and 43% of AAs were surveilled (median PTUDS: 0.16 HA, 0.15 AA). Among AAs, compared to English speakers, language-concordant non-English speakers had higher uptake (OR=1.35, 95%CI 1.12-1.62) and adherence (beta=0.024, 95%CI 0.009-0.039), while non-concordant non-English speakers had similar uptake (OR=1.01, 95%CI 0.88-1.16) but higher adherence (beta=0.020, 95%CI 0.008-0.032). Among HAs, language-concordant non-English speakers showed similar uptake/adherence to English speakers, but non-concordant non-English speakers had higher uptake (OR=1.43, 95%CI 1.16-1.76). Ethnic enclave showed no AA association (p-trend=0.46) but HA uptake was inversely associated with enclave (OR=0.79 comparing Q1 vs. Q5, 95%CI 0.59-1.07, p-trend=0.01). Adherence was not associated with enclave. Patient-provider language concordance and neighborhood ethnic enclave influenced HCC surveillance differently by race/ethnicity. AA surveillance was associated with language-concordant providers but not enclave; HA surveillance was associated with enclave but not provider language. These differential patterns suggest tailored intervention targets: multilingual provider recruitment for Asian languages, and community-based outreach leveraging existing networks in Hispanic neighborhoods.

#7606 Tumor and Host Determinants of the Breast Tumor Immune Microenvironment in Kenyan Breast Cancer Women.

Li Feng[1], Amber N. Hurson[1], Shahin Sayed[2], Hela Koka[1], Viviane Oluoch[2], Veronica Ngundo[2], Alfred Mburu Githuka[2], Zaitun Ajuoga[2], Shaoqi Fan[1], Kristine Jones[3], Belynda Hicks[3], Amy Hutchinson[3], Maria Brown[3], Petra Lenz[3], Aaron M. Rozeboom[3], Difei Wang[3], Francis Makokha[4], Stefan Ambs[5], Jonine D. Figueroa[1], Ruth M. Pfeiffer[1], Xiaohong Rose Yang[1]

[1]Division of Cancer Epidemiology and Genetics, National Cancer Institute, Bethesda, MD,[2]Aga Khan University Hospital, Nairobi, Kenya,[3]Cancer Genomics Research Laboratory, Frederick National Laboratory for Cancer Research, Frederick, MD,[4]Mount Kenya University, Nairobi, Kenya,[5]Center for Cancer Research, National Cancer Institute, Bethesda, MD

Background: The tumor immune microenvironment (TIME) reflects both tumor-intrinsic biology and host-modifiable factors. Characterizing how tumor features, body mass index (BMI), and reproductive history relate to immune activity may help explain heterogeneity in breast cancer and inform precision prevention and survivorship strategies.**Methods:** We analyzed 461 invasive breast tumors from Kenyan patients using a custom NanoString nCounter® immune-focused gene panel. Intrinsic subtypes were assigned with PAM50, and immune cell composition (relative proportions for 22 immune cells) was estimated by CIBERSORTx. Composite immune activity scores were derived to represent functional modules: *z_hot* (CD8+, M1 macrophages, NK activated, T follicular helper) and *z_suppression* (Treg + M2 macrophages) from CIBERSORTx; *z_cytotoxic (GZMB, PRF1), z_exhaustion (PDCD1, LAG3, CTLA4)*, and *z_checkpoint* (*PDCD1, PDCD1LG2, CTLA4, LAG3*) from GSVA signatures. Associations between immune scores and tumor features (PAM50 subtypes, risk of recurrence (ROR), RNA-based TP53 status, tumor grade) or host factors (BMI, menopausal status, parity, breastfeeding) were evaluated in age-adjusted linear regression models. Independent effects of host factors were further examined in multivariable regression models adjusted for tumor characteristics and lifestyle covariates. Multiple testing was accommodated using a false discovery rate adjusted *p*-values.**Results:** Participants had a mean age of 50.3 years; 43.8% of tumors were luminal A and 21.5% basal-like. Most women were overweight/obese (BMI ≥ 25, 73.1%) and 65.7% had ≥ 3 children. High-grade, basal-like, high-ROR, and TP53 mutant-like tumors showed strong evidence of elevated *z_hot*, *z_cytotoxic*, *z_checkpoint*, and *z_exhaustion* scores (BH-adjusted $p < 0.001$), along with modestly lower *z_suppression* in basal-like and TP53 mutant-like tumors ($p < 0.05$), indicating an active TIME characteristic of aggressive tumors. In contrast, established BC risk factors showed weaker influence on TIME. Overweight/obese patients were more likely to have cold TIME (lower CD8 ($p = 0.09$), T follicular helper ($p < 0.05$), and *z_hot* score ($p < 0.05$)), while patients with longer duration of breastfeeding had more active TIME (higher T follicular helper and *z_cytotoxicity;* lower M2 macrophages and *z_suppression* (all $p < 0.05$)).**Conclusions:** Tumor-intrinsic subtype classification remains the dominant determinant of immune heterogeneity, while established BC risk factors (BMI and reproductive risk factors) may modulate immune responsiveness. Integrating tumor, reproductive, and lifestyle data can help clarify immune variation across diverse populations.

#7607 CT-assessed body composition and tumor immunologic characteristics in patients with endometrial cancer.

Yidan Zhang[1], Cuthbert Mario Mahenge[1], Jordan Krull[2], Rand Talal Akasheh[1], Laura Chambers[3], Xuan Nguyen[4], Ting-Yuan David Cheng[1]

[1]Department of Internal Medicine, The Ohio State University Wexner Medical Center, Columbus, OH,[2]Pelotonia Institute for Immuno-Oncology, The Ohio State University Comprehensive Cancer Center, Columbus, OH,[3]Division of Gynecologic Oncology, The Ohio State University Comprehensive Cancer Center - James Cancer Hospital and Solove Research Institute, Columbus, OH,[4]Department of Radiology, The Ohio State University College of Medicine, Columbus, OH

Background: Variations in the body composition, specifically fat and muscle mass, may influence tissue immune infiltration. However, the relationships between these components and the tumor immune microenvironment in endometrial cancer remain poorly defined. We aimed to investigate whether CT-assessed body composition is associated with tumor immune cell infiltration in endometrial cancer.
Methods: We analyzed 63 patients with endometrial cancer from The Cancer Genome Atlas (TCGA) and the Clinical Proteomic Tumor Analysis Consortium (CPTAC) who had pre-treatment CT body composition measurements at the L3 vertebral level and bulk RNA-seq-based immune deconvolution. Approximately 75% of these patients had endometrioid adenocarcinoma. Immune cell abundances for 22 CIBERSORTx-derived subsets were estimated in absolute mode; subsets with ≥75% zero values were excluded, leaving 14 immune cell types plus the CIBERSORT total immune score for analysis. Eight CT-derived body composition metrics were evaluated, including visceral adipose tissue (VAT), subcutaneous adipose tissue (SAT), intermuscular adipose tissue (IMAT), skeletal muscle areas, and corresponding Hounsfield unit (HU)-based density measures. Linear regression models assessed associations between body composition metrics and log1p-transformed immune abundances. Analyses were conducted using univariable and multivariable models adjusting for age and cohort. P-values were corrected for multiple testing using the Benjamini-Hochberg false discovery rate (FDR).
Results: Immune cell abundances were generally low (median<0.10 for most subsets). In univariable models, higher VAT was nominally associated with lower total immune score and reduced abundances of several innate immune subsets, including NK-cell (resting and activated), and macrophage (M0/M1) (all $p<0.05$). In contrast, several HU-based density metrics, including SATHU and IMATHU, showed nominal positive associations with CD8 T cells. However, no associations remained statistically significant after FDR correction (all FDR ≥0.32). Multivariable models adjusting for age and cohort yielded similar patterns.
Conclusion: In this exploratory cohort, CT-derived body composition metrics showed heterogeneous associations with immune cell infiltration. Visceral adiposity showed potential inverse associations with innate immune infiltration, whereas higher subcutaneous adipose tissue showed potential positive associations with CD8 T-cells. These heterogeneous innate and adaptive immune patterns suggest potential differences in how body composition relates to immune infiltration, warranting further investigation in larger cohorts.

#7608 Characterizing myoepithelial marker loss in young-onset DCIS through integrated mouse and human studies.

Zhenzhen Zhang[1], Tanya Russell[2], Elizabeth Elizabeth Mitchell[1], SONALI JINDAL[1], Solange Bassale[1], Jayasri Narasimhan[1], Emily Guinto[3], Alison Fraser[3], Ken Smith[3], Pepper Schedin[1]

[1]Knight Cancer Institute, Oregon Health & Science University, Portland, OR,[2]University of Colorado, Aurora, CO,[3]Pedigree and Population Resource, Population Sciences, Huntsman Cancer Institute, Salt Lake City, UT

INTRODUCTION: Postpartum breast cancer (PPBC), diagnosed within 5-10 years after recent childbirth, is associated with increased metastasis, but postpartum status's impact on mortality among young women diagnosed with Ductal Carcinoma in Situ (DCIS) remains unclear. This study investigates how the postpartum environment may influence DCIS behavior in young women (≤45 years) diagnosed with DCIS and explores biological mechanisms through myoepithelial markers that could promote postpartum DCIS progression.

METHODS: Young women diagnosed with DCIS and invasive breast cancer were identified through the statewide Utah Population Database (UPDB) and SEER Utah Cancer Registry data (diagnosis year 1996-2017 with a median follow-up of 12.5 years, and mortality outcomes were evaluated in relation to DCIS diagnosis time since recent childbirth. Patterns of postpartum status among women diagnosed with DCIS versus invasive breast cancer were compared. To identify underlying biological mechanisms, we examined myoepithelial integrity in normal human breast tissues collected at defined post-weaning intervals and used mouse models of DCIS to evaluate how postpartum mammary gland involution influences tumor progression.

RESULTS: Of 597 women with DCIS, 23 deaths occurred during follow-up. DCIS was less frequent in the <5-year postpartum group (12.4%) compared to nulliparous (17.6%) and 5-<10 years group (17.6%), and invasive BC more frequent in the <5-year group. ER-negative DCIS was higher in the <5-year group (18%) compared to other groups (7%, 6%, 9%). Mortality outcomes were similar between postpartum and nulliparous women, with no clear evidence of increased all-cause mortality associated with recent childbirth. In normal human breast, postpartum breast involution is associated with reduced expression of the myoepithelial markers p63 and calponin, hallmarks of DCIS-to-invasive transition. Mouse models of postpartum DCIS confirmed increased tumor progression in involuting glands compared to nulliparous controls. Moreover, calponin loss in murine mammary myoepithelium correlated with increased tumor dissemination.

CONCLUSION: In young onset DCIS patients, BC-specific mortality was very low during the follow-up, implicating standard care as largely curative. We observed lower frequency of DCIS in the <5-year postpartum group suggesting potential progression of DCIS to invasive carcinoma during the early postpartum period. We find that recent childbirth, specifically weaning, reduces myoepithelial cell calponin expression, potentially facilitating DCIS progression to invasive disease. Calponin loss in a DCIS mouse model confers tumor advantage. These results highlight the importance of reproductive history and the postpartum breast microenvironment in early breast cancer prognosis and may inform risk-stratified management strategies for young women with DCIS.

#7609 Emotional functioning and NR3C1 and FKBP5 expression in multiple myeloma.

Mark Aaron Fiala[1], Steven Cole[2], Judith E. Carroll[2]

[1]Washington Univeristy School of Medicine, St. Louis, MO,[2]UCLA - University of California Los Angeles, Los Angeles, CA

Introduction: Emotional distress is common following a cancer diagnosis, and for some cancers it has also been associated with worse outcomes. However, the impact of emotional distress in patients with multiple myeloma (MM) remains relatively understudied. Methods: This study utilized data from CoMMpass (IA22), a longitudinal study of over 1000 patients who provided biospecimens, clinical data, patient reported outcomes (PROs). In this analysis, we aimed to determine if patient-reported and/or biomarker-based indicators of emotional distress at MM diagnosis were associated with patient outcomes. Patients completed the EORTC QLQ-C30 at diagnosis. The emotional functioning subscale was calculated, with scores ranging 0-100 and lower scores indicating higher distress. CoMMpass lacks data on common biomarkers for distress such as cortisol and cytokines. Therefore, we used mRNA expression (mRNA-seq on CD138-enriched MM cells) of two genes that play an important role in stress response and are dysregulated in people with emotional distress, NR3C1 and FKBP5.

Analysis: Patient reported emotional functioning and NR3C1 and FKBP5 expression were classified into quartiles. Patients in the lowest quartile of emotional functioning were classified as having emotional distress. Associations between emotional functioning, stress biomarkers, and relevant clinical factors were assessed using ANOVA and x^2. Associations with progression-free and overall survival were assessed using Cox Regression and adjusted for patient age, sex, race, and stage (International Staging System [ISS]). Results: 572 patients had baseline PROs and mRNA-seq data. The median age was 64 [IQR 57-71], 59% were male, 78% were White, 15% were Black, and 7% were another race. The median emotional functioning score was 75 [IQR 58.3-91.7]. There was an association between patient reported emotional functioning and higher FKBP5 expression ($p = 0.043$), but not NR3C1 ($p = 0.932$), despite a strong positive association between FKBP5 and NR3C1 ($p < 0.001$). Emotional functioning was also associated with age ($p = 0.023$), sex ($p = 0.006$), and race ($p = 0.003$), but not ISS stage ($p = 0.980$). In multivariable models, both emotional distress and FKBP5 expression were independently associated with prognosis. Patients with emotional distress had a 39% increase in hazard for progression (aHR 1.39; 95% CI 1.07-1.79; $p = 0.012$), but emotional distress was not associated with overall survival. Patients in the highest quartile of FKBP5 expression had a 53% increase in hazard for progression (aHR 1.53; 95% CI 1.16-2.03; $p = 0.003$) and 64% increase in hazard for death (aHR 1.64; 95% CI 1.14-2.36; $p = 0.007$).

Conclusion: Emotional Functioning and FKBP5 expression are both independently associated with MM prognosis. In further analyses, we aim explore the mechanisms underlying these associations and to evaluate potential interventions to mitigate the adverse effects on MM outcomes.

#7610 Tumor-intrinsic programs of epithelial-mesenchymal transition and immune deregulation are linked to disease recurrence in papillary thyroid carcinoma.

Emma Su[1], Amanda E. Garza[1], Jihye Park[1], Himanshu Patankar[2], Brendan Reardon[1], Yutaro Tanaka[1], Jingxin Fu[1], Sabrina Y. Camp[1], Erica Maria Pimenta[1], Helena Jun[1], Josephine Yates[1], Gerard Doherty[3], Justine Barletta[4], Erik Alexander[4], Eliezer M. Van Allen[1], **Theodora Pappa**[5]

[1]Dana-Farber Cancer Institute, Boston, MA,[2]Mass General Hospital, Boston, MA,[3]Surgery, Mass General Brigham, Boston, MA,[4]Mass General Brigham, Boston, MA,[5]Mass General Brigham and Dana-Farber Cancer Institute, Boston, MA

Introduction: Papillary thyroid carcinoma (PTC) is the most common subtype of differentiated thyroid cancer, predominantly affecting females and young adults. Current clinical models fail to capture its marked molecular heterogeneity and integrate this information into prognostic algorithms that would enable personalized care plans. Here, we identify tumor-intrinsic molecular programs contributing to thyroid cancer progression that may inform risk stratification.

Methods: We performed single nuclei multiome (RNA and ATAC) sequencing of 16 fresh frozen samples from a PTC clinical cohort with varying risks of disease recurrence, as determined by the 2025 American Thyroid Association guidelines. Programs with distinct cellular activity were identified with consensus non-negative matrix factorization (cNMF). Cell-cell communication between the tumor and its microenvironment was assessed with MultiNicheNET. Active regulons within cell types of interest were identified using SCENIC. Chromatin accessibility analysis was performed using Signac.

Results: We identified a novel, tumor-specific transcriptional program, defined by composite upregulation of epithelial-to-mesenchymal-transition (EMT) and TNF-alpha signaling, that was enriched in high-risk PTC. Top active regulons in this program included molecules involved in inflammatory response and immune modulation. Chromatin accessibility analysis revealed a significantly differentially accessible peak near CCL20, previously shown to promote thyroid cancer invasion via NF-kB signaling, in tumor cells with highest expression of the program. In thyroid cancer lines from the Broad Institute's Cancer Cell Line Encyclopedia (CCLE), expression of this program was significantly higher in the presence of BRAFV600E mutation ($p<0.001$). Similarly, when projecting this program onto the Thyroid Cancer Genome Atlas (TCGA) database of 496 PTC samples, we observed a significant association between usage of this transcriptional program and both higher risk of recurrence and presence of BRAFV600E mutation ($p<0.001$). This association remained independent in a multiple linear regression model and after adjusting for sex and tumor purity. Cell-cell interaction analyses demonstrated increased activity of thrombospondin-1, a key EMT mediator, signaling from cancer associated fibroblasts to tumor cells, that was unique to high-risk PTC samples.

Conclusions: We identified a new, tumor-intrinsic transcriptional program through integrative multi-omic analysis that is characterized by EMT and immune deregulation, enriched in high-risk PTC, and validated its clinical relevance in TCGA. Evaluating the performance of this program in larger thyroid cancer cohorts will be essential to establish its prognostic value and potential to incorporate into clinical risk stratification models.

: Cancer and Cancer Related Alterations, Detection Approaches, and Molecular Characterization
Poster Session

#7614 Early cancer detection using early-access Illumina protein prep 6K assay and machine learning.

KAMEL LAHOUEL, **Mete Mulazimoglu**, Kameron Bates, Candice Wike, Kunjur Manasa Upadhyaya, Victoria Zismann, Kamawela Leka, Payton Smith, Gracyn Benck, Kianna Martos Rupp, Chaney Jambor, Matteo Munini, Sophie Penisson, Stephanie Pond, Jeffrey Trent, Patrick Pirrotte, Cristian Tomasetti

TGen (The Translational Genomics Research Institute), Phoenix, AZ

Background:
Studies in cancer early detection have revealed circulating proteins to be powerful and informative biomarkers. We further aimed to develop a machine-learning framework robust to batch effects across independently processed datasets and to identify a subset of proteins capable of detecting cancer at its earliest stages. In this study, we sought to evaluate the early-access Illumina protein prep proteomic assay not only for its technical reproducibility but also for its ability to yield biologically informative protein signatures relevant to cancer early detection.
Experimental Procedures:
Proteomic profiles from six plates were analyzed, encompassing approximately 217 normal and 206 cancer plasma samples. The first four plates contained samples collected from Eastern European sources and were used for model training and feature selection, while the remaining two plates contained samples collected in the United States from populations with diverse ancestry backgrounds and served as an external test set. These two plates included samples from bladder, breast, gastric, and lung cancers, representing diverse biological and technical conditions.
Feature selection was performed using the Minimum Redundancy-Maximum Relevance (MRMR) method, which ranks proteins by maximizing mutual information with cancer status while minimizing redundancy. The top 200 proteins were used to train a Support Vector Machine (SVM) classifier with a radial-basis kernel.
Results:
The model achieved a mean AUC of 0.89 across the two independent test plates, demonstrating strong cross-batch and cross-ancestry reproducibility and confirming that informative, generalizable protein features can be extracted from the Illumina platform. At 95% specificity, the classifier achieved an overall sensitivity of 65% (95% CI: 51-77%), with particularly strong performance in Stage II cancers at 82% (95% CI: 52-95%), underscoring its potential utility for early detection. Performance was consistent across cancer types, with highest sensitivities observed in lung. Importantly, a six-fold leave-one-plate out cross-validation yielded an average sensitivity of 82% at 99% specificity, demonstrating that integrating diverse data sources will likely strengthen model generalizability.
Conclusions:
A machine-learning framework applied to large-scale proteomic data identifies a compact and biologically meaningful subset of proteins capable of early cancer detection. The results highlight the robustness of the Illumina Protein Prep, 6K assay, and the feasibility of developing batch-insensitive protein classifiers for population-scale cancer screening.

#7615 Multiplex detection of BCR-ABL1 fusion transcripts in a streamlined single-tube workflow using PCR-based single molecule counting.

Vladyslava Ratushna, Jung won Keum, Christina Fan

R&D, Countable Labs, Palo Alto, CA

Accurate quantification of *BCR-ABL1* fusion transcripts is essential for monitoring minimal residual disease (MRD) in chronic myeloid leukemia (CML), where distinguishing between isoforms (p210, p230, p190) is clinically important for diagnosis, prognosis, and treatment monitoring. Traditional detection methods rely on two-step workflows involving reverse transcription (RT) followed by PCR amplification, either via qPCR or digital PCR (dPCR). While dPCR enables absolute quantification without standard curves, its limited dynamic range and multi-step workflow present challenges for streamlined isoform detection. We developed a one-step multiplex RNA assay for the direct detection and molecular counting of p210, p230, and p190 isoforms, even amid abundant wild-type *ABL1* molecules, within a single tube. The entire workflow, including RT-PCR and counting, occurs without sample transfers, reducing hands-on time and contamination risk. Using 3D light-sheet microscopy, molecules are directly counted by imaging the complete 50 µL reaction volume, eliminating dead volume and partitioning statistics. When *BCR-ABL1* RNA containing each isoform was serially diluted into wild-type *ABL1* background at varying ratios, wild-type *ABL1* counts remained stable, near one million molecules, while *BCR-ABL1* counts decreased proportionally with dilution.This highlights the highly sensitive and specific detection of RNA isoforms across a 6-log dynamic range with low variance (<10% CV), enabling monitoring of both abundant and rare transcripts within a single tube. This single-tube approach provides a streamlined alternative for sensitive detection of all *BCR-ABL1* isoforms in one multiplexed reaction, with potential applications in clinical assessment and therapeutic decision-making in CML.

#7616 Early detection of pancreatic cancer with a multi-omic liquid biopsy.

James M. Cameron, Holly J. Butler, David S. Palmer, Rose G. McHardy, Matthew J. Baker

Dxcover Ltd., Glasgow, United Kingdom

Background: Early diagnosis is the central challenge in pancreatic ductal adenocarcinoma (PDAC) and the successful development of an early detection biomarker test would revolutionize the field. PDAC is the 3rd leading cause of cancer-related deaths in the United States with 66,400 new diagnoses in 2024. The five-year survival is only 12.8% because 80% of patients are diagnosed in advanced stages limiting the potential for curative surgical resection. There is an urgent need to facilitate the triage of high-risk groups into the diagnostic pathway, particularly those with pancreatic cysts, chronic pancreatitis and new-onset diabetes over the age of 50. However, the incidence of PDAC in these at-risk populations is ~1% over the next 3 years. Imaging modalities, such as CT/MRI and endoscopic ultrasound with fine-needle aspiration, are too expensive and invasive to serve as primary screening tools.

Methods: Here the ability of a spectroscopic blood test as an alternative strategy for PDAC detection is assessed. The technology utilizes infrared (IR) spectroscopy, and interrogates a blood sample with IR light to produce a distinctive signature that is sensitive to the hallmarks of cancer. When combined with machine learning, the test detects PDAC by monitoring of all biomolecular components of the sample. In this proof-of-concept study, 166 PDAC patients were classified against 459 symptomatic patients with a non-cancer diagnosis.

Results: The receiver operating characteristic (ROC) curve reported an area under the curve (AUC) value of 0.84. The diagnostic algorithm reported 92% sensitivity with 52% specificity. Importantly, the model did not seem to be affected by cancer stage. The detection rates with the sensitivity-tuned model were 88% stage I, 94% stage II, 99% stage III and 95% stage IV.

Conclusions: The detection of PDAC in early stages would improve prognosis and survival rates of affected patients. Advancements in genetic sequencing have opened opportunities for tumor-derived biomarkers, using genomics, epigenomics, and transcriptomics to isolate circulating tumor DNA, exosomes, and/or microRNA. However, these biomarkers are limited in PDAC at early stages due low release and near-undetectable signals. A spectroscopy-based multi-omic blood test represents an alternative strategy, particularly for high-risk populations, that may address the gap in PDAC diagnostics.

#7617 A multi-omic liquid biopsy for the earlier detection of ovarian cancer.

James M. Cameron, Holly Butler, David Palmer, Rose McHardy, Matthew Baker

Dxcover Ltd., Glasgow, United Kingdom

Background: Ovarian cancer has one of the highest mortality rates among gynecologic cancers, largely because more than 70% of cases are diagnosed at more advanced stages. Early-stage ovarian cancer, by contrast, has a five-year survival rate above 90%. Currently, there are no approved population-wide screening tests for ovarian cancer, due to ineffective testing options highlighting the urgent need for better early detection tools. Novel liquid biopsy technologies offer a promising path to identify ovarian cancer early, when treatment is far more effective.
Methods: This study explored the ability of a multi-omic liquid biopsy as an alternative strategy for ovarian cancer detection. The technology utilizes infrared (IR) spectroscopy and interrogates a blood sample with IR light to produce a distinctive signature that is sensitive to the signals of cancer. In this proof-of-concept study, 125 ovarian cancer patients were classified against 260 female symptomatic patients with a non-cancer diagnosis. Blood was obtained from patients before surgical resection or the start of other anti-cancer therapies. Blood serum samples were analyzed by the Dxcover® Liquid Biopsy Platform and classified with machine learning algorithms. These trained algorithms are then independently tested on an additional clinical dataset.
Results: The receiver operating characteristic (ROC) curve reported an area under the curve (AUC) value of 0.86. The sensitivity-tuned algorithm reported 92% sensitivity with 54% specificity, and the specificity-tuned model reported 58% sensitivity with 90% specificity. Importantly, the diagnostic algorithm was unaffected by cancer stage. The detection rates were 97% stage I, 86% stage II, 92% stage III and 100% stage IV, for the high sensitivity model. Validation testing provided additional confirmation of diagnostic ability in the intended use population.
Conclusions: Detecting ovarian cancer earlier improves prognosis and survival rates of affected patients. There is a low barrier to integrating the blood test into existing diagnostic pathways since the technology is simple to use, minute sample volumes are required, and results can be provided rapidly. This liquid biopsy represents an alternative strategy, particularly for high-risk populations, that may address the gap in ovarian cancer diagnostics.

#7619 PanGIA Analysis System, a novel machine learning platform for non-invasive diagnosis of oral cancer through an oral sample.

Francis Lim, Abhignyan Nagesetti, Nick Gonzalez, Miguel Javiel, Pablo Hernandez, Kyle Ambert, Robert Cardwell, **Obdulio Piloto**

PanGIA Biotech Inc., Miami, FL

The PanGIA Analysis System (PAS) is an advanced diagnostic platform designed to characterize complex biological systems through machine learning-assisted biochemical profiling. Powered by trained algorithms and proprietary hydrogel microarrays known as NuTec Slides, PAS enables unbiased capture and analysis of biomolecular signatures from diverse biofluids. Oral samples represent a particularly valuable yet underexplored matrix for noninvasive disease assessment, offering insight into both local and systemic health conditions. In this study, a commercialization-ready PAS prototype was evaluated for its capacity to differentiate between cancer-spiked and unspiked oral samples. Oral fluid from healthy volunteers was pooled with TruSample Oral Buffer Cell and spiked with literature-validated analyte panels representative of oral cancer. Following incubation of NuTec Slides with both spiked and unspiked control samples, heat-based signal development and high-resolution scanning were performed. Extracted image feature data were analyzed by principal component analysis (PCA). This proof-of-concept study indicates that PAS can distinguish between control and spiked human oral samples containing literature supported oral cancer analytes. Conclusion: These findings establish proof-of-concept for the use of PAS in noninvasive cancer detection through oral fluid profiling. Further clinical validation is warranted to expand its diagnostic applications across additional cancer types and to explore its potential in longitudinal monitoring, risk stratification, and personalized medicine.

#7620 PanGIA Analysis System, a novel machine learning platform for non-invasive diagnosis of multiple cancers through urine.

Abhignyan Nagesetti, Francis Lim, Nick Gonzalez, Miguel Javiel, Pablo Hernandez, Kyle Ambert, Robert Cardwell, **Obdulio Piloto**

PanGIA Biotech Inc., Miami, FL

The PanGIA Analysis System (PAS) represents a novel machine learning-driven platform for the interrogation of complex biological systems through biochemical signature profiling. Analogous to advanced language models such as Google Gemini or ChatGPT, PAS employs trained algorithms to interpret multidimensional data derived from biological samples. The system utilizes proprietary hydrogel-based microarray substrates, termed NuTec Slides, designed to capture unbiased biomolecular profiles from diverse liquid matrices. Among these, urine offers a particularly informative yet underutilized medium for assessing physiological and pathological states. In this study, a commercialization-ready prototype of PAS was evaluated for its ability to discriminate urine samples containing cancer-associated analytes from non-spiked controls. First-morning urine from healthy volunteers was pooled and spiked with literature-validated analyte panels representing hematological cancers, breast, bone, and brain cancers. Following incubation of NuTec Slides with both spiked and unspiked samples, heat-based signal development, and scanning, extracted image feature data were analyzed by principal component analysis (PCA). This proof-of-concept study indicates that PAS can distinguish between control and spiked human urine samples containing literature supported analytes. Furthermore, we observe distinct clustering between individual cancers. Conclusion: These findings demonstrate the feasibility of PAS as a non-invasive diagnostic tool for cancer detection using urine-based biomolecular profiling. Continued clinical validation is warranted to establish its broader utility in diagnostics, prognostics, companion diagnostics, and monitoring of minimal residual disease.

#7621 Early-onset colorectal cancer detection through a non-invasive label-free electrochemical immunosensor probe.

Ruma Paul[1], Md Zahirul Islam Khan[2], Soumya Nair[2], Alicia I Loya[1], Sourav Roy[2], Carlos R. Cabrera[1]

[1]Chemistry and Biochemistry, The University of Texas at El Paso, El Paso, TX,[2]The University of Texas at El Paso, El Paso, TX

Early-onset colorectal cancer (CRC; <50 years) is rapidly increasing in the United States and disproportionately affects Hispanic and African American patients. Since survival rates are positively associated with early detection, the absence of reliable and accessible screening tools for younger adults remains a significant unmet need. Liquid-biopsy diagnostics offer a practical alternative to invasive tests; however, the risk of false negatives is too high. Using gene-expression datasets, cDNA arrays, tissue-microarrays, and tissues from CRC patients, we have identified and validated the elevated expressions of CCNB1 and MCM10, at the transcript and protein levels, in Hispanic early-onset CRC patients when compared to their Non-Hispanic White counterparts. We are developing a label-free electrochemical immunosensor for point-of-care (POC) detection of these early-onset CRC biomarkers. As a prototype, we designed a sensor targeting the early CRC biomarker CCSP-2. A gold working electrode (Au) was functionalized with cysteine-modified recombinant Protein G, which selectively binds the Fc region of hIgG to achieve controlled orientation of CCSP-2 antibodies (Ab) on the Au surface. After Ab immobilization, bovine serum albumin (BSA) was used as a blocker, and each modification step was characterized by cyclic voltammetry and electrochemical impedance spectroscopy (EIS). EIS quantified CCSP-2 antigen (Ag) through changes in relative charge-transfer resistance ($\Delta R_{ct}/R_{ctl}$). The resulting calibration curve ($\Delta R_{ct}/R_{ctl}$ vs Ag) demonstrated strong linearity (R^2 = 0.95) from 10-100 ng/µL, with a detection limit of 0.71 ng/µL.

To further enhance stability and antifouling performance in complex biofluids, we are integrating a porous BSA-glutaraldehyde-gold nanowire (BSA-GA-AuNW) hydrogel onto Au interdigitated microelectrodes, followed by antibody immobilization and testing of early-onset CRC biomarkers. This conductive, hydrophilic matrix is expected to improve sensitivity and specificity while enabling reliable blood-based measurements. This non-invasive, low-cost electrochemical probe has strong potential to expand screening and improve early detection of CRC, especially among younger and underserved populations, thereby improving the survival rates.

#7622 Breaking barriers to scalable multi-cancer early detection (MCED).

Bahram G. Kermani

Crystal Genetics, Inc., Los Altos, CA

In recent years, MCED via liquid biopsy has risen to prominence for its potential to shift the paradigm of cancer detection from one to many, and from late to early stages. Yet, realizing this promise requires addressing several fundamental challenges, without which MCED risks remaining confined to expensive niche markets rather than becoming a broadly practical clinical tool. These challenges comprise technical, methodological, psychological, and economic factors. While detection at all early stages is challenging, detecting solid cancers at Stage I is significantly more demanding compared to Stage II. For the four most common solid cancers, volumetric measurements suggest that Stage I is roughly 5 to 30 times harder to detect than Stage II. This nonlinear challenge, compounded by the inherent nature of some cancer types, highlights the demanding sensitivity requirements of a true early detection scheme and the limitations faced by many advanced molecular platforms. Specificity poses a parallel challenge. Maintaining high specificity while simultaneously preserving strong Stage I sensitivity is intrinsically difficult because early cancer signals can closely resemble healthy baselines. A compromise in Stage I sensitivity, for instance, could translate to apparent increased specificity. This, in turn, could lead to a perceived exaggeration of the positive predictive value (PPV) if not interpreted with caution. Rigorous cohort design is essential to prevent distortion of accuracy. Careful consideration of age, comorbidities, and related variables is crucial to avoid significant consequences. For example, an older-skewed cohort could falsely inflate the perceived PPV. Similarly, age differences between cancer and healthy groups can mislead metrics, as older individuals' non-cancer signals may falsely raise apparent sensitivity. Psychological factors can hinder cancer screening, with fear and anxiety particularly high in MCED, which targets multiple cancers simultaneously. Employing MCED as a triage rather than a definitive screening test can reduce these concerns, as positive results prompt confirmatory screening. However, while this approach makes MCED an accessible entry point, it would demand high sensitivity, particularly at the earliest cancer stages. Lastly, cost remains a critical consideration. For MCED to achieve widespread adoption, it must be economically viable, ensuring cost-effectiveness, accessible reimbursement pathways, and consequently affordability at the population level. These economic factors will be key to its real-world feasibility. In this work, we present a low-cost, high-sensitivity/specificity MCED leveraging proteomics and machine intelligence, initially targeting breast, lung, prostate, and colon cancers. By addressing the key challenges, we demonstrate how MCED can evolve from a costly niche market to a clinically actionable tool for large-scale early cancer detection.

#7623 Non-invasive detection of early colorectal neoplasia using red blood cell DNA profiling: a prospective clinical validation.

Chengcheng Liu[1], Xingyun Yao[2], Haobo Sun[2], Yurong Jiao[1], Xiangxing Kong[1], Jie Jin[3], Kefeng Ding[1], Jun Li[1], Xiaofei Gao[4]

[1]Department of Colorectal Surgery and Oncology, Key Laboratory of Cancer Prevention and Intervention, Ministry of Education, The Second Affiliated Hospital, Zhejiang University School of Medicine, Hangzhou, China,[2]Westlake University, Hangzhou, China,[3]Timing Biotech, Hangzhou, China,[4]Research Center for Industries of the Future and School of Life Sciences, Westlake University, Hangzhou, China

Background: Colorectal cancer (CRC) is a major cause of cancer mortality, yet early detection markedly improves outcomes. Current screening tools like colonoscopy and fecal immunochemical test (FIT) face limitations in accessibility, participation, and sensitivity, particularly for advanced adenomas (AA). Emerging evidence indicates that tumor-derived systemic stress can induce genomic and epigenetic abnormalities in bone marrow, thereby remotely reprogramming hematopoiesis. Consistent with this phenomenon, our previous work revealed that colorectal tumors remotely disrupt the genomic integrity of hematopoietic stem and progenitor cells, and that these alterations presist through erythroid differentiation to generate distinct DNA signatures in mature red blood cells (rbcDNA). Leveraging these rbcDNA signatures, we developed a CRC-rbcDNA based classifier for early detection of CRC and AA. Following multi-center validation, this study presents the first prospective clinical evaluation of the classifier and a head-to-head comparison with quantitative FIT (qFIT), aiming to assess its performance in detecting both early CRC and AA.

Methods: We conduct a prospective cohort clinical study (NCT05875584) designed to validate the locked rbcDNA classifier and to benchmark its performance against qFIT. A total of 598 individuals were enrolled, of which 585 samples were available for analysis. These comprised 299 non-CRC controls (non-neoplastic findings, non-advanced adenomas, and limited non-CRC malignancies), 206 AAs (high-grade dysplasia, villous features, or lesions ≥10 mm), and 80 CRCs. All samples underwent rbcDNA isolation, purification, and low-coverage whole-genome sequencing to generate rbcDNA profiles. For each participant, the locked classifier generated an rbcDNA-based predictive score, and qFIT results were collected in parallel.

Results: Using the predefined threshold, the rbcDNA assay reached 90% sensitivity for CRC, including over 90% of stage I-II tumors, and detected 60% of AA cases. Among 299 controls, specificity was 90% and remained consistent across clinical subgroups. Performance in the prospective cohort closely matched that of the multi-center validation set and remained consistent across demographic, clinical, and pathological characteristics. Compared with qFIT, the rbcDNA assay achieved similar CRC sensitivity (90% vs. 88%) but substantially improved AA sensitivity (60% vs. 18%). Overall, the rbcDNA assay showed substantially higher sensitivity than qFIT for early-stage CRC and AA, which typically present with low tumor burden, while maintaining similar specificity.

Conclusions: This prospective clinical study demonstrated rbcDNA can be a highly sensitive and non-invasive method for early detection of colorectal neoplasia, supporting its promise for integration into clinical screening practice.

#7624 Liquid biopsy MCED enabled by a novel 800K-locus bimodal amplicon sequencing technology.

Kamel Lahouel, **Kameron Bates**, Victoria Zismann, Candice Wike, Kunjur Manasa Upadhyaya, Matteo Munini, Mete Mulazimoglu, Gracyn Benck, Kianna Martos Rupp, Payton Smith, Chaney Jambor, Sophie Penisson, Stephanie Pond, Jeffrey Trent, Cristian Tomasetti

TGen (The Translational Genomics Research Institute), Phoenix, AZ

Background:
Multi-cancer early detection (MCED) from plasma liquid biopsy has advanced rapidly, demonstrating that diverse cfDNA features can reveal early tumor signals. Most current assays rely on whole-genome or methylation sequencing, which are costly and require deep coverage. EarlySeek is a novel, highly multiplexed cfDNA amplicon-based alternative that targets ~800,000 SINE-enriched loci using long and short amplicons, generating a bimodal insert-size distribution and requiring as little as 0.25 ng of DNA input. This design captures complementary signals such as fragmentation, aneuploidy, genomic abundance shifts, and sequence motif patterns. We evaluated a multi-signal framework integrating these features using artificial intelligence and machine learning.
Methods:
Three datasets were analyzed: a training set (237 cancers, 463 normals), a calibration set (72 cancers, 140 normals), and an independent test set with tissues present in training (78 cancers, 192 normals). EarlySeek output yields six biological scores: fragment length, two aneuploidy scores, two coverage/abundance scores, and a 6-mer motif score. Scores were generated using representation and deep learning architectures, including autoencoders that compress amplicon-level and binned genomic information into informative latent features, combined with machine learning classifiers such as support vector machines and gradient-boosted trees. Each score was calibrated via quantile-to-quantile regression, and a predefined multi-signal rule was applied to generate final scores for the test cohort.
Results:
Across 270 independent test samples, the combined six-score framework achieved 51% sensitivity at 99% specificity (95% CI: 40%-62%). Sensitivity by stage showed meaningful early detection: 45% for stage I (CI 26%-66%), 58% for stage II (CI 39%-74%), 57% for stage III (CI 37%-67%), and 100% for stage IV (2/2; CI 34%-100%). Performance varied by cancer type, with strongest detection in colorectal (61%), gastric (71%), liver (80%), ovarian (75%), and pancreatic cancer (64%). Lower sensitivities in breast, and prostate cancers reflected known low cfDNA shedding.
Conclusions:
EarlySeek's bimodal amplicon design enables extraction of diverse cfDNA signals from a single sequencing assay. Integrating these orthogonal features through artificial intelligence and machine learning supports high-specificity MCED detection and yields meaningful early-stage performance. This approach offers a scalable, cost-effective MCED test, a desirable feature for population-level cancer screening.

#7625 Development of a blood-based tumor hypoxia detection assay.

Azemat Jamshidi-Parsian[1], Ruud Petrus Dings[1], Rajshekar A. Kore[1], Narasimhan Rajaram[2], Varsha Karunakaran[3], **Robert J. Griffin**[1]

[1]University of Arkansas for Med Sci, Little Rock, AR,[2]Biomedical Engineering, University of Arkansas, Fayetteville, AR,[3]University of Arkansas, Fayetteville, AR

We have developed a method designed for detection of hypoxia-based markers in the vesicles shed from tumor cells in vitro and in vivo to non-invasively assess the degree of hypoxia present in a patient (patent pending). Our initial studies indicated that vesicle proteins can be labeled by various nitroimidazoles and detected by western blotting of exosome lysates from blood samples or tissue culture. In addition, vesicles secreted from 4T1 murine breast tumor cells incubated with pimonidazole in hypoxia (0.5% O_2) could be detected using flow cytometry or plate-reader fluorescence quantification of purified exosome samples assayed with a fluorescent anti-pimonidazole primary antibody. There was a 2.4-fold elevation in binding signal in exosomes sampled from hypoxic vs oxic culture. Recently, we have also studied the production of pimonidazole-labeled exosomes in the U118 human brain tumor cell line and found a marked difference in signal between exosomes isolated from aerobic culture vs. exosomes isolated in hypoxic culture. In 4T1 tumor tissue lysates, hypoxia induced a maximum over 8-fold increase in pimonidazole adducts by day 11 of tumor growth. However, at day 4 of tumor growth there was a maximum of 3.95-fold increase in adducts from exosomes isolated from a blood sample, and the signal decreased, yet remained elevated compared to samples from non-tumor bearing mice, in blood samples taken at day 7, 11 or 14 or tumor growth. We theorized that the more advanced the tumor becomes, the less blood circulation and more necrosis are present which prevents hypoxic exosomes from entering the circulation. In U118 brain tumor cell exosomes from in vitro culture, there were similar distinct signal enhancements found, where there was a 3.8 fold enhancement of pimonidazole adduct bands in exosomes harvested from U118 cells cultured in 0.5% O_2 overnight compared to exosomes from cells cultured in normoxia. We have most recently investigated a click-chemistry based detection of nitroimidazoles in biological samples, thereby avoiding the need for antibody detection and thus improving the sensitivity and specificity. We have observed marked hypoxia-specific binding of the click-compatible dye in cells cultured in hypoxia and found a distinct reduced azido-aza associated peak using Raman spectroscopy, which could be a more efficient and rapid test for clinically obtained samples. Finally, a dot blot approach we developed has demonstrated that vesicles obtained from the blood of tumor bearing mice indicate an average signal increase of 40% in tumor-bearing mouse exosomes vs. animals without tumor. We surmise that the detection of vesicles being shed from a hypoxic niche could lead to a non-invasive blood test for tumor or ischemia presence, as well as a surrogate marker for treatment success or tumor recurrence. Efforts to correlate individual tumor hypoxic fraction and the exosome signal are ongoing to verify the specificity of the approach.

#7626 A gene expression classifier to predict progression risk of ductal carcinoma in situ to invasive breast cancer.

William Joseph Harley[1], Maria Roman-Escorza[2], Jelle Wesseling[3], Elinor Sawyer[2], Renee X. de Menezes[4], Esther Lips[3]

[1]The Netherlands Cancer Institute, Amsterdam, Netherlands,[2]King's College London, London, United Kingdom,[3]Moleculaire Pathologie / Molecular Pathology, The Netherlands Cancer Institute, Amsterdam, Netherlands,[4]Biostatistics Center, The Netherlands Cancer Institute, Amsterdam, Netherlands

Background: Ductal carcinoma in situ (DCIS) is a non-obligate precursor to invasive ductal carcinoma. A minority of DCIS cases will ever progress to ipsilateral invasive breast cancer (iIBC), but almost all are treated with breast-conserving surgery and radiotherapy. Reliable biomarkers of progression risk are needed to prevent overtreatment of low-risk lesions. We present a DCIS gene expression classifier to predict the risk of iIBC occurring within the first 5 years of diagnosis.
Methods: The model was trained on a dataset of pure primary DCIS RNA-seq samples from a Dutch population-based cohort collected from 1989 to 2005. Samples from 188 patients treated with breast-conserving surgery only were retained for the training data to remove radiotherapy as a confounding factor in iIBC risk. The classifier is a logistic regression model with elastic net penalization, trained in a nested 5x5 cross-validation scheme. The final model was validated on an external, independent dataset of 91 British DCIS samples from the NHS Sloane project.
Results: The classifier achieved an overall AUC of 0.642 on the outer loop test sets in the Dutch training set, and 0.694 in the Sloane independent validation set. The classifier risk score is shown in a logistic model to be associated with an increased risk of iIBC within 5 years in the Sloane validation dataset [OR: 1.16; CI: 1.05-1.27; p = 0.0496] where HER2 status, ER status, histopathological grade and age at diagnosis were not. A threshold to categorize risk scores into low- and high-risk categories was chosen on the training set by selecting the cut-point that maximized balanced accuracy. Gene set enrichment analysis showed enrichment of cell cycle and proliferation gene sets in the high-risk category (HALLMARK_E2F_TARGETS, HALLMARK_G2M_CHECKPOINT, GNF2_MKI67).
Discussion: The performance of this classifier on an external, independent validation dataset shows that signals of risk of developing iIBC within 5 years of diagnosis can be detected within the gene expression profile of pure primary DCIS lesions. That the classifier was trained and validated on samples from patients who received the least aggressive treatment available without the confounding factors of radiotherapy or mastectomy brings us closer to an understanding of the biology underlying the risk of progression to iIBC in DCIS untreated at diagnosis. Such an understanding could be valuable information for including DCIS patients in active surveillance trials, and a step forward in preventing women having to undergo unnecessary surgery and radiotherapy.

#7627 Multi-omics integration reveals evening circadian preference as a causal risk factor for cancer-depression comorbidity through shared neuro-endocrine-immune pathways.

Liansha Tang, Wenbo He, Handan Hu, Jiayao Wang, Jiyan Liu

West China Hospital of Sichuan University, Chengdu City, China

Background: The comorbidity of cancer and depression leads to substantially poor prognosis, yet its shared mechanisms remain elusive. Circadian disruption, particularly evening circadian preference, is a plausible link but its role and underlying pathways in comorbidity warrant further investigation.

Methods: We conducted an integrative multi-omics analysis. Utilizing prospective UK Biobank data (N=299155), we assessed the association of evening chronotype with cancer-depression comorbidity risk across distinct transition pathways (baseline to comorbidity, cancer to comorbidity, depression to comorbidity). Mendelian randomization (MR) and polygenic risk scores (PRS) for morning chronotype were performed for causal inference and genetic stratification. To uncover molecular mechanisms, we integrated summary-data-based MR (SMR) and colocalization analyses using GWAS and eQTL data to identify circadian clock-related genes (CRGs) consistently associated with breast (BCa), prostate (PCa), colorectal cancer (CRC), and depression. Pathway enrichment analysis and immune cell infiltration analysis were also conducted to investigate shared mechanisms.

Results: Evening chronotype significantly increased the risk of transitioning from a healthy baseline state to comorbidity for overall cancer, CRC, and BCa (fully adjusted HRs = 1.30, 1.55, and 1.43, respectively), and on the transition from cancer to comorbidity (HRs=1.29, 1.50, and 1.34, respectively). The effect was more pronounced in subgroups such as women, smokers, individuals with higher levels of education, and those with a lower socioeconomic status. Genetically, morning chronotype PRS showed protective effects, and individuals with both evening chronotype and low PRS constituted the highest-risk subgroup. Two-sample MR confirmed a causal protective effect of morning chronotype on BCa, CRC, and depression. Multi-omics integration identified five key CRGs (GAL, ALAS1, SUCNR1, PTK2, DDIT3) with consistent causal effects on both cancer and depression. Pathway enrichment analysis revealed that these genes were significantly clustered in neuroendocrine regulation and metabolic pathways. GAL and SUCNR1/PTK2 were significantly correlated with mast cells and CD8+ T cells infiltration, respectively, revealing a pathway from circadian disruption to comorbidity through neuro-endocrine-immune dysregulation.

Conclusion: Our study elucidates evening chronotype as a significant and modifiable risk factor for cancer-depression comorbidity. We identify a high-risk genetic subgroup and delineate shared biological mechanisms, providing a foundational framework for targeted circadian-based interventions to mitigate comorbidity risk.

#7628 Sensitive detection of microRNAs from human melanoma cell lines and FFPE tissue using fluorescent nitrogen-vacancy center nanodiamonds.

Isaac Rampersaud[1], Charles Fletcher[1], Colin Angell[2], William E. Carson[3], **Arfaan Rampersaud**[1]

[1]Columbus NanoWorks, Inc., Columbus, OH,[2]The Ohio State University, Columbus, OH,[3]Professor of Surgery, The Ohio State University, Columbus, OH

Diamond magnetometry (DM), using fluorescent nitrogen-vacancy center nanodiamonds (FND), is an enzyme-free, quantum-based platform that can detect and monitor cancer biomarkers, such as microRNAs. Fluorescence is due to the nitrogen vacancy center (NV-center), a crystallographic defect where a nitrogen atom is adjacent to a vacant (empty) site within the diamond lattice. Importantly, NV-center fluorescence can be optically manipulated and is sensitive to nanoscale magnetic fields. In the present study, we used diamond magnetometry to rapidly detect picomolar amounts of microRNAs in human melanoma cell lines without requiring the Polymerase Chain Reaction (PCR) or amplification or preamplification steps. Method. FNDs and magnetic nanoparticles were functionalized with biomolecules to create NV-Biosensors for miR-486-5p, miR-363-3p, miR-196-5p, miR-135b-5p, and miR-21-5p. Synthetic RNA and DNA oligonucleotides were synthesized by IDT and quantified on a Nanodrop spectrophotometer. Total RNA was prepared from the melanoma cell lines A375, MEL-39, CHL-1 HT-144, 18105 Mel, and MEL1174. Following isolation, nucleic acid sensors were mixed with 2 µL of total RNA in TBS reaction buffer containing 0.05% SDS, 5 mM $MgCl_2$, and 1 nM of a random 50-mer DNA sequence. Reactions were run for 15 minutes, then spotted onto a glass coverslip, gently rinsed, then mounted on a widefield fluorescence microscope set-up, and analyzed by a technique called optically detected magnetic resonance (ODMR). In the absence of a microRNA target, the FND and magnetic particle are associated with DNA hybridization and show low ODMR contrast. If a microRNA target is present, it displaces the FND-MNP hybrid, and the FND shows increased ODMR contrast. Results were collected in a few minutes at room temperature, with between 200 and 600 independent ODMR data points recorded for each sample. The large number of data points allowed robust data analysis. Results. We demonstrated the specific detection of synthetic RNA and DNA oligonucleotides for miR-21-5p and miR-486-5p down to a concentration of 1 pmole. Our NV-Biosensors also detected miR target molecules in total RNA preparations from cell lines. We could not detect miR-486-5p in total RNA from HT-144 and this was consistent with Reverse Transcription-Polymerase Chain Reaction (RT-PCR) results. We used total RNA from HT-144 in spiking studies to demonstrate specific detection of miR-486-5p. Finally, we benchmarked our technology against the gold standard, RT-PCR, and showed that DM was as sensitive as RT-PCR for microRNA detection. DM has the advantage of using single microliter sample volumes and is a simple, accurate assay that can be performed in a fraction of the time needed for RT-PCR

#7630 Shear wave elastography and photoacoustic imaging to non-invasively identify resistant regions in the tumor microenvironment.

Sarah K. Burris[1], Caroline O'Riordan[2], Peter Kesa[2], Philippe Trochet[2], Dieter Fuchs[2]

[1]FUJIFILM VisualSonics Inc., Toronto, ON, Canada,[2]FUJIFILM VisualSonics Inc., Amsterdam, Netherlands

Increased stiffness is a hallmark of malignant tumors and can impede chemotherapy delivery due to elevated interstitial pressure. Clinically, tumor stiffness is assessed using Shear Wave Elastography (SWE); however, small animal imaging systems combining SWE with anatomical, functional, and molecular information have been lacking. Here, we present, for the first time, high-frequency ultrasound with ultrafast plane wave acquisition combined with assessments of capillary function and tumor oxygenation, offering non-invasive, detailed insight into the tumor microenvironment.CT26 murine colorectal carcinoma cells were implanted subcutaneously into the flanks of Balb/C mice to establish solid tumors. Two weeks later, tumor imaging was performed using the Vevo® F2 LAZR-X system. During a single imaging session, tumor structure, vascularization (after intravenous injection of the MicroMarker contrast agent), oxygenation/hypoxia (via photoacoustic imaging), and stiffness (via SWE) were evaluated without moving the animals. An oxygen challenge identified regions responsive to changing conditions (potentially treatable “responder” regions), which were compared with SWE-measured stiffness and vascular data.Our results demonstrate that combining SWE with ultrasound and photoacoustic imaging provides real-time, non-invasive insights into the tumor microenvironment. Regions of high stiffness, identified by SWE, are linked to increased interstitial pressure, which may restrict drug delivery and affect treatment efficacy. By mapping vascular and hypoxic features alongside stiffness, this multimodal approach revealed intra- and inter-tumor heterogeneity. Areas with higher stiffness correlated with non-responsive oxygen regions and lower vascular density, providing a non-invasive representation of evolving tumor characteristics.This study establishes SWE as a powerful tool for non-invasively assessing tumor stiffness and its relationship with hypoxia and vascularity. Integrating SWE with photoacoustic and ultrasound imaging provides a comprehensive, multidimensional method to characterize the tumor microenvironment, moving beyond traditional measures based solely on tumor volume. This advancement enhances understanding of tumor heterogeneity and supports the development of personalized therapeutic strategies, ultimately improving treatment planning and outcomes

#7631 Predicting and preventing cancer stemness in low Earth orbit.

Jessica Pham[1], Wenxue Ma[1], Claire Engstrom[1], Patrick Chang[2], Shuvro P. Nandi[3], Inge van der Werf[1], Emma Klacking[1], Teresa Sposito[1], Kendale Wirtjes[1], Thomas Frias[1], Antonio Ruiz[1], Jane Isquith[2], Luisa Ladel[1], Christina N. Wu[1], Jana Stoudemire[2], Pinar Mesci[4], Kay T. Yeung[5], Rebecca A. Shatsky[5], Anna A. Khachatrian[6], James J. La Clair[7], Michael D. Burkart[7], Peggy Wentworth[2], Curtis L. Scribner[8], Sheldon R. Morris[2], Thomas Whisenant[9], Karla Mack[2], Ludmil B. Alexandrov[10], Catriona H. M. Jamieson[2]

[1]Department of Medicine, Division of Regenerative Medicine, UC San Diego, La Jolla, CA,[2]Sanford Stem Cell Institute, UC San Diego, La Jolla, CA,[3]Department of Cellular and Molecular Medicine, Department of Bioengineering, UC San Diego, La Jolla, CA,[4]Axiom Space, Houston, TX,[5]Department of Medicine, UC San Diego, La Jolla, CA,[6]Scripps Health, La Jolla, CA,[7]Department of Chemistry and Biochemistry, UC San Diego, La Jolla, CA,[8]Aspera Biomedicines, La Jolla, CA,[9]Center for Computational Biology and Bioinformatics, UC San Diego, La Jolla, CA,[10]Sanford Stem Cell Institute, Dept. of Cellular and Molecular Medicine, Depart. of Bioengineering, UC San Diego, La Jolla, CA

Cancer stemness properties, including enhanced survival, malignant regeneration, telomere deregulation, genomic and epitranscriptomic instability, fuel metastases, and have been linked to stress, retrotransposon and inflammatory cytokine activation, which can occur in low earth orbit (LEO). In NASA Axiom 1, 2 and 3 missions to the ISS, confocal imaging, WGS, RNA-seq and scRNA-seq of lentiviral FUCCI2BL cell cycle and ADAR1-GFP reporter transduced erythroleukemia (TF-1a), colorectal (Caco-2) and metastatic breast cancer (MBC; MDA-MB-231 and patient samples) revealed proliferation, significant genomic instability, HERV and LINE-1 retrotransposon deregulation, and APOBEC3C and ADAR1 activation. Moreover, in Axiom 2 and 3 missions with ADAR1-reporter expressing MBC organoids and in humanized MBC mouse models, an ADAR1p150 splicing modulator, rebecsinib (IND 153126), prevented tumor propagation. Thus, cancer studies in LEO may accelerate the development of innovative cancer therapeutics and countermeasures for long-term spaceflight.

#7632 Plasma proteomics for risk prediction of lung cancer.

Tej Pandya[1], Maria Zagorulya[1], Michelle M. Leung[2], Marcellus Augustine[1], Lydia Y. Liu[1], Oleg Blyuss[3], Jincheng Wu[4], Marc Pelletier[4], Vernon Burk[5], Neil Wright[6], David Muller[7], Ka Hung Chan[8], Ekaterina Pazukhina[3], Marc Gunter[9], Elizabeth A. Platz[5], Karl Smith-Byrne[10], Nuno Rocha Nene[1], Eva Camilla Gronroos[1], Nicholas McGranahan[11], William Hill[1], Clare Weeden[1], Charles Swanton[1]

[1]Francis Crick Institute, London, United Kingdom,[2]University College London, London, United Kingdom,[3]Centre for Prevention, Detection and Early Diagnosis, Wolfson Institute of Population Health, Queen Mary, University of London, London, United Kingdom,[4]Novartis (Cambridge, MA), Cambridge, MA,[5]Johns Hopkins Bloomberg Sch. of Public Health, Baltimore, MD,[6]Nuffield Department of Population Health, University of Oxford, Oxford, United Kingdom,[7]Department of Epidemiology and Biostatistics, School of Public Health, Imperial College London, London, United Kingdom.[8]University of Oxford, Oxford, United Kingdom,[9]Cancer Epidemiology and Prevention Research Unit, School of Public Health, Imperial College London, London, United Kingdom,[10]University of Oxford, Cancer Epidemiology Unit, United Kingdom,[11]UCL London Cancer Institute, London, United Kingdom

Background: Current lung cancer screening programs rely heavily on age and smoking history, excluding never-smokers and those with minimal smoking exposure. Such criteria have a low positive predictive value (PPV), limiting molecular prevention strategies. Our previous work identified interleukin-1β (IL-1β) as a mediator of lung cancer initiation through environmental particulate matter (PM) exposure, suggesting potential targets for therapeutic cancer prevention. Here, we sought to identify circulating signals predictive of lung cancer prior to clinical diagnosis and determine if they were useful for clinical trial stratification of IL-1β therapy.
Methods: Using human plasma proteomic data from the UK Biobank (n=48,099 individuals; 375 lung cancer cases), we developed a machine-learning framework to identify proteins predictive of lung cancer diagnosis. We validated this model in eight independent human cohorts (2,176 cases, 54,324 controls). We further analysed plasma proteomic murine data from EGFR-mutant mice exposed to PM as well as from baseline samples from the CANTOS trial which previously had demonstrated reduction of lung cancer incidence with IL-1β inhibition.
Results: Our machine-learning approach identified a plasma signature of 14 proteins, predictive of lung cancer diagnosis up to 6 years before clinical detection, significantly outperforming current lung cancer risk models ($p<0.01$ by de Long's test). Validation across eight external human cohorts confirmed consistent associations for all proteins. Mouse experiments demonstrated a sustained increase in circulating signature proteins following PM exposure specifically in EGFR-mutant mice, linking environmental PM exposure directly to the alveolar niche as an early tumour-promoting microenvironment. Retrospective analysis of the CANTOS trial showed the protein signature stratified individuals deriving benefit from IL-1β inhibition, reducing the number needed to treat from 1516 to 55.
Discussion: Our findings indicate that a circulating plasma signature derived from alveolar niche remodelling and induced by PM and EGFR-driven oncogenesis can effectively identify individuals at high risk of lung cancer two years before clinical onset. The identified proteins may enable targeted stratification for molecular prevention trials. Future research should focus on extending this approach and developing absolute quantification assays to for clinical translation.

#7633 Dynamic monitoring and identification of reliable biomarkers to predict efficacy of bireociclib and fulvestrant: An exploratory ctDNA analysis of the BRIGHT-2 study.

Yan Wang[1], Hangcheng Xu[1], Yiran Zhou[1], Liang Cui[2], Qiang Sa[1], Hong Cheng[1], Renchi Gao[1], Qingyuan Zhang[3], HHiping Li[4], Zhongsheng Tong[5], Quchang Ouyang[6], Xinxin Tan[7], Jing Bai[2], Li Wang[8], Xianghui Duan[8], Fan Yang[8], Jiayu Wang[1], Binghe Xu[1]

[1]Cancer Hospital Chinese Academy of Medical Sciences, Beijing, China,[2]Geneplus-Beijing Institute, Beijing, China,[3]Harbin Medical University Cancer Hospital, Harbin, China,[4]Beijing Cancer Hospital, Beijing, China,[5]Tianjin Medical University Cancer Institute and Hospital, Tianjin, China,[6]Hunan Cancer Hospital, Hunan, China,[7]Geneplus-Shenzhen Clinical Laboratory, Shenzhen, China,[8]Xuanzhu Biopharmaceutical Co.Ltd., Beijing, China

Background Although the novel cyclin-dependent kinase 4 and 6 (CDK4/6) inhibitor bireociclib demonstrated potent efficacy for hormone receptor -positive, human epidermal growth factor receptor 2 (HER2)-negative advanced breast cancer in the BRIGHT-2 study (NCT05077449), patient exhibited substantial heterogeneity in therapeutic efficacy—some demonstrated high sensitivity, while others rapidly developed resistance. Consequently, a critical research aim is to ascertain sensitivity before treatment initiation and define biomarkers that can dynamically detect therapeutic outcomes earlier than imaging.

Methods Based on the BRIGHT-2 study, longitudinal circulating tumor DNA (ctDNA) analysis was performed using a 1021-gene panel at baseline, on-treatment, and end-of-treatment timepoints. Somatic mutations were identified and molecular tumor burden index (mTBI) was calculated. Survival analyses employed Kaplan-Meier curves with log-rank tests and Cox proportional hazards models, while the interaction analysis between treatment and gene alternations were conducted using False Discovery Rate (FDR) method. All the analyses were performed using R software, with statistical significance set at $p<0.05$.

Results The bireociclib group collected 197, 139, and 86 ctDNA samples from three timepoints, compared with 79, 46, and 49 from placebo group. The most frequently mutated genes were *PIK3CA* (48%), *TP53* (37%), and *ESR1* (23%). Patients with ctDNA-positive or high mTBI had conspicuously shorter progression-free survival (PFS) and overall survival (OS) than those with ctDNA-negative or low mTBI. The gene alterations in CCND1 and FGF19 were associated with a greater PFS benefit with bireociclib versus placebo (FDR-adjusted P values of 0.030 and 0.002, respectively). The *gBRCA* and homologous recombination repair genes mutation indicated poorer prognosis compared to wild-type in bireociclib group. Dynamic clearance of ctDNA or specific gene mutations was correlated with improved efficacy and survival outcomes for CDK4/6 inhibitor.

Conclusions Both baseline and dynamic monitoring of ctDNA demonstrated salient predictive value for treatment response and survival outcomes in hormone receptor-positive, HER2-negative breast cancer patients receiving bireociclib plus fulvestrant. These potential biomarkers warrant further validation through larger clinical trials and basic researches.

Key words: CDK4/6 inhibitor, advanced breast cancer, biomarkers, bireociclib, prognosis.

#7635 Elucidating the molecular interaction between RELT and Filamin A and the physiological role of this interaction in breast cancer cells.

Samantha Wong[1], Ashley Ko[1], Yashar Pourmoghadam[1], Hunter Hudgins[1], Maryann Batiste[1], Bethany Joy[1], Ashley Christensen[1], Eslam Mohamed[2], John K. Cusick[3]

[1]College of Medicine, California Northstate University, Elk Grove, CA,[2]California Northstate University, Elk Grove, CA,[3]Department of Medical Education, University of California, Merced, Merced, CA

Receptor Expressed in Lymphoid Tissues (RELT) is a member of the Tumor Necrosis Factor Receptor Superfamily that was previously shown to be upregulated in breast cancer. A proteomic screen identified Filamin A (FLNA), an actin-binding scaffold protein involved in various cell processes, including DNA repair, signal transduction, and cell migration, as a potential RELT-interacting partner. FLNA is implicated to play a vital role in breast cancer, as its expression correlates with tumor grade and stage, and it has been shown to bind both BRCA1 and BRCA2. This study aimed to further explore the novel interaction between RELT and FLNA and to characterize its physiological significance.

A yeast two-hybrid screen was utilized to identify a carboxy-terminal fragment of FLNA (C-FLNA) as a potential RELT-binding partner. Transient overexpression of C-FLNA and deletion mutants of RELT in HEK-293 cells, followed by co-immunoprecipitation (co-IP) and western blotting, was performed to identify the binding site on RELT for FLNA. Immunofluorescence (IF) microscopy was used to evaluate RELT-FLNA subcellular colocalization in MDA-MB-231 (231) breast cancer cells. To examine the impact of C-FLNA on RELT's ability to induce cell death, 231 cells, a model for triple-negative breast cancer, were transiently transfected with varying combinations of RELT, FLNA mutants, and empty vector control plasmids. Consequently, these cells were analyzed for apoptosis via flow cytometry, using Annexin V/Propidium Iodide (AV/PI) staining.

Co-IP experiments performed with deletion mutants demonstrated that C-FLNA binds within amino acids 340-400 of RELT's intracellular domain. IF studies confirmed cytosolic colocalization of RELT and FLNA, supporting a direct interaction between these two proteins. Flow cytometry data revealed that co-expression of RELT and C-FLNA induced significantly higher AV/PI staining in 231 cells, indicating greater levels of apoptosis, compared to cells expressing either protein alone.

These findings define an intracellular binding region on RELT for FLNA binding. Furthermore, co-expression of RELT and C-FLNA resulted in significantly enhanced apoptosis in breast cancer cells, suggesting a potentially synergistic effect. Current studies are examining whether RELT expression influences breast cancer cell migration given FLNA's established role in cytoskeletal dynamics and motility. Collectively, these results enhance our understanding of the interaction between RELT, a protein that is upregulated in breast cancer, and FLNA, a protein whose importance for breast cancer has been well established.

#7636 A rare multipotent peg-like epithelial cell is a candidate cell-of-origin for high-grade serous ovarian cancer.

Megan L. Ritting[1], Wenmei Yang[2], Syed Mohammed Musheer Aalam[2], Hui Zhao[2], Liang Feng[2], Jianning Song[2], Mihai G. Dumbrava[1], Wazim M. Ismail[3], Kenneth Schaufelberger[2], S. John Weroha[4], Scott H. Kaufmann[5], Alexandre Gaspar-Maia[3], Mark E. Sherman[6], Jamie N. Bakkum-Gamez[7], Nagarajan Kannan[2]

[1]Mayo Clinic College of Medicine and Science, Rochester, MN,[2]Department of Laboratory Medicine and Pathology, Mayo Clinic, Rochester, MN,[3]Center for Individualized Medicine, Mayo Clinic, Rochester, MN,[4]Department of Medical Oncology, Mayo Clinic, Rochester, MN,[5]Department of Oncology, Mayo Clinic, Rochester, MN,[6]Quantitative Health Sciences, Mayo Clinic, Jacksonville, FL,[7]Department of Obstetrics and Gynecology, Mayo Clinic, Rochester, MN

High-grade serous ovarian cancer (HGSOC), the most prevalent and lethal ovarian cancer subtype, is typically diagnosed at an advanced stage due to the absence of effective early detection strategies. Mounting evidence indicates that HGSOC originates from the fallopian tube (FT), particularly from secretory epithelial cells in the fimbria. However, incomplete understanding of the cellular and molecular origins of HGSOC continues to hinder early interception efforts. To address this, we established a clinically and genetically annotated living FT organoid biobank at Mayo Clinic, representing over 200 patient donors. Using optimized enrichment protocols, we isolated FT epithelial stem/progenitor cells from tissue and Tao brushings, generating organoids independent of anatomical site or laterality that recapitulate native FT epithelial architecture and lineage differentiation. We applied integrated multi-omic analyses, including single-cell RNA sequencing, single-nucleus RNA/ATAC sequencing, and bulk RNA-seq, across fresh cells and organoids. Integration with public datasets produced the largest single-cell atlas of normal and high-risk FTs to date. This analysis defined high-specificity gene signatures for secretory and multiciliated lineages that outperform canonical lineage markers (e.g. *PAX8, FOXJ1*), identified lineage-defining transcription factors and regulatory networks, and showed concordant protein expression in the human FT epithelium. Notably, subcluster-level analysis revealed a rare hybrid epithelial-mesenchymal population transcriptionally and proteomically aligned with the mesenchymal-like subtype of HGSOC. Spatial immunoprofiling demonstrated that these cells express multiple defining markers and reside above the basement membrane, intercalated between epithelial cells and lack luminal contact, reminiscent of the histologically described peg cell population. Comparative analyses with fetal mesonephric tissues uncovered developmental parallels, and this population was stably maintained in 3D organoid cultures, providing a robust *ex-vivo* model to study early transformation. Together, our findings identify a rare, multipotent epithelial population with mesenchymal features as a candidate origin for mesenchymal-like HGSOC and establish the FT organoid biobank as a powerful platform for mechanistic and translational studies in ovarian carcinogenesis.

#7637 Genome-wide CRISPR screening reveals a PKA-driven resistance mechanism to metformin for oral cancer prevention that can be exploited by combination with NSAIDs.

Thomas S. Hoang[1], Farhoud Faraji[2], Amaya Mendez-Molina[1], Sendi R. Adame-Garcia[1], Kuniaki Sato[1], Tomohiko Ishikawa[1], Pham Thuy Vo[1], Sydney Ramirez[3], Paola Y. Anguiano Quiroz[1], Tracy Guo[1], Katie Fan[1], Xingyu Wu[1], Alfredo Molinolo[4], Ezra E. W. Cohen[5], Prashant Mali[6], Scott M. Lippman[5], J. Silvio Gutkind[1]

[1]Pharmacology, UCSD Moores Cancer Center, La Jolla, CA,[2]Otolaryngology-Head and Neck Surgery, UCSD, La Jolla, CA,[3]La Jolla Institute for Immunology, La Jolla, CA,[4]Pathology, UCSD Moores Cancer Center, La Jolla, CA,[5]UCSD Moores Cancer Center, La Jolla, CA,[6]UCSD, La Jolla, CA

Head and neck squamous cell carcinoma (HNSCC) is among the ten most common cancers worldwide and is associated with high morbidity and poor survival. Diminished HNSCC outcomes are often related to delayed diagnosis and treatment of occult progression of premalignant lesions, underscoring the need for effective and low risk chemoprevention strategies. In this regard, metformin has shown promising clinical activity for HNSCC prevention. Here, we performed a genome-wide CRISPR/Cas9 screen of metformin-treated HNSCC cells and identified activation of PKA signaling as the top resistance pathway. We show that metformin mediates PKA activation in HNSCC cells, and that PKA inhibition (PKAi) when combined with metformin treatment synergistically inhibits HNSCC growth. We found that metformin-induced PKA activation is mediated by a prostaglandin E2 (PGE2) autocrine loop, which can be blocked using cyclooxygenase-2 (COX2) inhibitors. Importantly, COX2 inhibition using non-steroidal anti-inflammatory drugs (NSAIDs) combined with metformin treatment synergistically inhibits of HNSCC cell growth and prevents progression of oral premalignant lesions (OPLs) into invasive HNSCC in a model of tobacco driven oral carcinogenesis. Together, these findings demonstrate that metformin and NSAID combination therapy may represent a promising therapeutic strategy for HNSCC chemoprevention.

#7639 Primate comparative oncology reveal humans' unique cancer susceptibility.

Zachary Taylor Compton[1], Walker Mellon[2], Lisa M. Abegglen[3], Tara Harrison[4], Joshua D. Schiffman[5], Amy M. Boddy[6], Carlo C. Maley[7]

[1]University of Arizona Cancer Center, Tucson, AZ,[2]University of Arizona College of Medicine - Phoenix, Phoenix, AZ,[3]University of Utah Huntsman Cancer Institute, Salt Lake City, UT,[4]North Carolina State College of Veterinary Medicine, Raleigh, NC,[5]Peel Therapeutics, Inc, Salt Lake City, UT,[6]UCSF Medical Ctr., Goleta, CA,[7]Arizona State Univ. Biodesign Institute, Tempe, AZ

Studying cancer from an evolutionary perspective can yield important theoretical and applied insights; however, little is known about the prevalence of cancer among non-human primates. Non-human primates are our closest living relatives, yet the primate lineage is phenotypically diverse, exhibiting wide variation in evolutionary and life-history characteristics. By integrating comparative phenotypic data with prevalence records of neoplastic disease, we assembled a dataset of 2,095 individuals from 36 species across nine primate families to examine cross-species cancer risk. Additionally, functional in vitro studies using isolated and cultured primary fibroblast cell lines from representative species show that resistance to cellular death correlates with certain life-history traits. Comparative phylogenetic modeling of human cancer risk, situated within the broader primate phylogeny, demonstrates a drastic reduction in cancer risk even among primates most closely related to humans (e.g., the great apes). Together, large-scale cancer prevalence records and functional assays provide valuable insights into the ecological and cellular dynamics of cancer in our closest living relatives—and in ourselves.

#7640 Ciliated cells drive critical STING-mediated tumor suppression in fallopian tube epithelium.

Jose Colina[1], Maria Sol Recouvreux[2], Alex Sobeck[3], Benjamin K. Johnson[4], Yinzhi Lin[5], Sreeja C. Sekhar[6], Rita A. Avelar[5], Gabriela Rivera[5], Yali Zhai[6], amber fatima[5], Paula DiBenedetto[5], Justin Baldassarre[5], Grace McIntyre[5], Jessica Teitel[5], Michele Cusato[6], Harini Ram[5], Noah Puleo[6], Karan Bedi[5], Jane Miglo[7], Hui Shen[8], Dafydd G. Thomas[9], Jutta Huvila[10], Dawn R. Cochrane[11], Ronny I. Drapkin[12], Yu Lei[13], Joanna E. Burdette[14], David G. Huntsman[15], Kathleen Cho[6], Sandra Orsulic[16], **Analisa DiFeo**[5]

[1]George Washington University, Washington, DC,[2]UCLA, Los Angeles, CA,[3]Washington University in St. Louis, St. Louis, MO,[4]Van Andel Research Institute, Grand Rapids, MI,[5]University of Michigan, Ann Arbor, MI,[6]University of Michigan Medical School, Ann Arbor, MI,[7]University of Chicago, Chicago, IL,[8]Graduate Student, Van Andel Research Institute, Grand Rapids, MI,[9]Lecturer/Research Investigator, University of Michigan, Ann Arbor, MI,[10]University of Turku, Turku, Finland,[11]BC Cancer Agency, Vancouver, BC, Canada,[12]University of Pennsylvania, Merion Station, PA,[13]MD Anderson Cancer Center, Houston, TX,[14]Assistant Professor, Dept. of Medical Chemistry, University of Illinois at Chicago, Chicago, IL,[15]University of British Columbia, Vancouver, BC, Canada,[16]David Geffen School of Medicine, Los Angeles, CA

Mitigating DNA damage in the fallopian tube epithelium (FTE) is essential for preventing tubo-ovarian high-grade serous carcinoma (HGSC). Here we demonstrate that STING is abundantly expressed in the ciliated cells of the FTE and functions as a critical immune-independent tumor suppressor. Using patient samples, mouse models, and organoid systems, we demonstrate that ciliated cells mount a dual protective response to ovulation-associated genotoxic stress: intrinsic STING-driven apoptosis and extrinsic clearance of neighboring damaged secretory cells via TNFα secretion. This surveillance mechanism markedly limits DNA damage accumulation within the epithelial microenvironment. Crucially, while these mechanisms are vital for maintaining homeostasis and reducing genomic instability, they fail to impact p53-deficient precursor lesions as both intrinsic and extrinsic pro-apoptotic processes rely on functional p53 signaling. This study uncovers a previously unrecognized, immune-independent role for STING-high ciliated fallopian tube cells as active guardians of genomic integrity, whose loss creates a permissive niche for HGSC initiation.

CONFLICT OF INTEREST STATEMENT: R.D. serves on the scientific advisory board of VOC Health and Repare Therapeutics. DGH is a previous founder and Chief Medical Officer of Imagia Canexia Health. The other authors declare that they have no competing interests.

#7641 Decoding the spatial architecture of the immune microenvironment in mismatch repair-deficient colorectal carcinogenesis.

Abel Martel-Martel[1], Nan Deng[1], Melissa W. Taggart[2], Araceli Garcia-Gonzalez[1], Jacklyn V. Thompson[1], Luigi Ricciardiello[3], Y. Nancy You[4], Selvi Thirumurthi[4], Krishna M. Sinha[1], Eduardo Vilar[1]

[1]Clinical Cancer Prevention, The University of Texas MD Anderson Cancer Center, Houston, TX,[2]Pathology, The University of Texas MD Anderson Cancer Center, Houston, TX,[3]Gastroenterology, Hepatology and Nutrition, The University of Texas MD Anderson Cancer Center, Houston, TX,[4]Colorectal Surgery, The University of Texas MD Anderson Cancer Center, Houston, TX

Introduction: Lynch Syndrome (LS) is the most common hereditary colorectal cancer syndrome and is secondary to germline mutations in the mismatch repair (MMR) genes. Upon acquiring a second somatic hit, epithelial cells become MMR-deficient (MMRd) and accumulate high number of indel mutations in microsatellite loci, generating frameshift peptides (mutated neo-antigens). These neo-antigens activate robust immune responses and promote the expansion of specific T-cell clonotypes. However, the spatial organization of immune-epithelial compartments, and how MMR loss shapes early immune surveillance and escape, remains unclear.

Methods: We dissected the immune microenvironment across the LS carcinogenesis axis using spatial transcriptomics to interrogate over 5,000 genes and 27 LS neoantigen-specific TCR clonotypes from our LS cohort at MD Anderson. We studied a total of 41 colorectal biopsies from 23 LS and 15 sporadic cases that were arranged in tissue microarrays and analyzed according to MMR status and malignancy, thus representing the largest spatial transcriptomic dataset generate to date in the context of LS.

Results: Spatial profiling using Xenium platform identified distinct epithelial, immune, and stromal domains across LS and sporadic samples. Relative to normal mucosa, adenomas showed expansion of proliferating transit-amplifying epithelium, cancer stem-like cells, REG4^{+} epithelia, and a shift toward M2b-enriched macrophages, consistent with signs of early immune modulation. Neo-antigen-specific TCRs increased along the pathology axis and localized near dysplastic glands. MMRd adenomas displayed enrichment of activated monocytes/macrophages, plasma cells, inflammatory epithelium, and broad induction of interferon-responsive and cytokine-mediated pathways, thus reflecting strong innate and adaptative immunity. CD8^{+} T cells in MMRd lesions also expressed higher CTLA-4 levels, indicating activation-induced inhibitory signaling and early exhaustion. Compared to sporadic samples, LS tissues showed stronger immune activation, larger inflammatory and remodeling neighborhoods, and increased macrophage and plasma-cell infiltration. Multiple neo-antigen-specific TCR clones appeared exclusively in LS lesions, supporting enhanced immune surveillance.

Conclusions: Spatial transcriptomics reveals coordinated remodeling of epithelial, immune, and stromal neighborhoods driven by pathology progression, MMR loss, and LS background. These spatial patterns provide insights into immune-epithelial interactions during LS neoplasm progression, establishing spatial biomarkers that may inform surveillance and immune interception strategies in hereditary gastrointestinal syndromes, such neo-antigen-based vaccination for boosting the expansion, infiltration, and effector function of tumor-specific T cells in MMRd cancers.

#7642 Nicotine dependence partially mediates the association between *IP6K3* genetic variation and risk of lung squamous cell carcinoma among smokers.

Jing Jin[1], Yasir Rahmatallah[2], Horacio Gomez-Acevedo[2], Yong-Moon (Mark) Park[3], David Ussery[2], Mohammed Orloff[3]

[1]Biostatistics, University of Arkansas for Medical Sciences, Little Rock, AR,[2]Biomedical Informatics, University of Arkansas for Medical Sciences, Little Rock, AR,[3]Epidemiology, University of Arkansas for Medical Sciences, Little Rock, AR

INTRODUCTION: Nicotine dependence is a heritable trait that may mediate genetic susceptibility to lung cancer. Building on a prior integrative genomic study that identified significant SNPs and their annotated genes located within tracts of homozygosity (TOH) overlapping differentially methylated regions (DMRs) in lung tissue, we investigated whether these SNPs and haplotypes within these methylation-driven genes were associated with Non-Small Cell Lung Cancer (NSCLC) risk through pathways involving nicotine dependence among smokers.

METHODS: The study included individuals with lung adenocarcinoma (LUAD), lung squamous cell carcinoma (LUSC), and population-based controls from a genome-wide association study (GWAS). Genes exhibiting differential expression with an absolute $\log_2$ fold-change ≥2 between tumor and adjacent normal tissues were retained as candidate loci for SNP- and haplotype-based mediation models. Within candidate genes, linkage disequilibrium blocks were defined to construct haplotypes. Multivariable logistic regression models adjusted for age and sex were used to estimate SNP- and haplotype-level associations with NSCLC risk by subtypes. Individuals carrying a significant haplotype were coded as exposed. Causal mediation analyses were used to estimate the proportion of each SNP or haplotype's effect on NSCLC risk that was mediated by nicotine dependence, measured by the Fagerström Test for Nicotine Dependence (FTND). Structural equation modeling (SEM) further quantified direct and indirect associations among age, sex, cancer status, smoking cessation status, smoking pack years, nicotine dependence (FTND), and carrier status for the significant haplotypes.

RESULTS: The *IP6K3* haplotype "GTGTG" (rs649775-rs2966-10947433-rs4713668-rs6457740) was inversely associated with LUSC risk, with approximately 39% of its protective association mediated by nicotine dependence (average causal mediation effect [ACME]=-0.023, 95% CI: -0.039, -0.010). Consistent with this pattern, *IP6K3* rs2966 (TT vs CC; CT vs CC) and rs4713668 (TT vs CC; CT vs CC) exhibited significant indirect effects via nicotine dependence (ACME ranges from -0.023 to -0.027; *p*-values between 0.004 and 0.024), accounting for 33-38% of their total protective effects on LUSC risk.

CONCLUSION: These findings identify *IP6K3* as a potential candidate gene in nicotine-related lung carcinogenesis and highlight the relevance of neurobiological dependence pathways in personalized smoking cessation and lung cancer prevention strategies.

#7643 A novel pH-sensitive probe to quantify autophagy on high throughput/content imaging platforms.

Giuseppe D. Ciccotosto[1], Lorenzo Lorenzo[2], David L. Hare[3], **Peter J. Wookey**[1]

[1]Medicine-Austin, University of Melbourne, Heidelberg, Australia,[2]Fox Chase Cancer Center, Philadelphia, PA,[3]University of Melbourne, Melbourne, Australia

Autophagy is deregulated in various pathological conditions including cardiovascular, neurological, neoplastic, autoimmune and degenerative disorders. However, clinically relevant pharmacological modulators of autophagy remain elusive, calling for the development of novel screening approaches, amenable to high throughput/content applications. Cellular responses were imaged with the novel CalRexin^{TM}:pHrodo^{TM} Red (CalRexin^{TM}, Apop Biosciences Pty Ltd) reagent on the Operetta high content screening platform. Human cervical carcinoma HeLa cells, and mutants *RB1CC1-/- (FIP200)* and *ATG5-/-* were induced for autophagy with rapamycin, torin-1 and serum deprivation and inhibited with 3-methyladenine, MRT68921, chloroquine and bafilomycin A1. The co-localisation with pixel definition between CalRexin^{TM}:pHrodo^{TM} Red and markers of early and late endosomes and autolysosomes was studied with high resolution confocal microscopy and Fiji software. Pixel co-localization analysis demonstrated significant overlap between CalRexin^{TM}:pHrodo^{TM} Red and markers of early and late endosomes, as well as LysoTracker^{TM}, a marker of autolysosomes.CalRexin^{TM}:pHrodo^{TM} Red is accumulated via the endosome-amphisome-autolysosome (low pH ~4.5) pathway, thus connecting to canonical autophagy and yielding a bright fluorescent signal. CalRexin^{TM}:pHrodo^{TM} Red provides a novel approach for imaging autophagy on high throughput/content platforms and is adaptable for screening large chemical libraries for the identification of novel autophagy-modulators as potential drugs for treatment of chronic diseases.

: Multi-Omics, Systems Biology, and Biological Mass Spectrometry
Poster Session

#7647 Ecotype-guided multi-omics profiling identifies potential cell-surface therapeutic targets in gastric cancer.

Yuefan Wang[1], Lindsey K. Olsen[2], Hui Zhang[1], Bing Zhang[2], Clinical Proteomic Tumor Analysis Consortium (CPTAC)

[1]Pathology, Johns Hopkins University, Baltimore, MD,[2]Baylor College of Medicine, Houston, TX

Gastric cancer (GC) exhibits marked heterogeneity, complex molecular alterations, and limited therapeutic options. To comprehensively define its biology and vulnerabilities, we performed 15-layer multi-omics profiling of 159 gastric adenocarcinomas and 30 matched normal adjacent tissues, encompassing genomics, epigenomics, transcriptomics, proteomics, post-translational modifications, protein–protein interactions, metabolomics, and microbiome analyses, yielding more than 385,000 features. By integrating cell-state deconvolution, we defined gastric tumor ecotypes based on cellular states, providing a new framework for multi-omics integration. These ecotypes captured distinct tumor ecosystems and stromal–immune compositions and offered deeper mechanistic insight than conventional genomic or histologic classifications.Leveraging machine learning and large-scale AI models, we identified ecotype-specific molecular features and linked them to clinical outcome. To prioritize therapeutic opportunities, we applied high-outlier analysis to proteins and glycoproteins. Multiple cell-surface–associated targets showed strong high-outlier expression, including several known or emerging therapeutic candidates. Extracellular matrix (ECM) components were significantly enriched among high-outlier proteins, underscoring their central role in tumor growth, invasion, and potential therapeutic targeting. We further characterized altered cell-surface glycosylation patterns in high-outlier glycoproteins, revealing changes in immune regulation and ECM engagement. Phosphosite-resolved analysis identified key signaling signatures associated with aggressive tumor behavior.Importantly, embedding these high-outlier events within ecotype and genomic subtype frameworks revealed distinct, ecotype-specific patterns that were not apparent from genomic classification alone. Single-cell analyses localized many targets to specific stromal compartments, particularly fibroblast-rich ecosystems, suggesting that targeting fibroblast-driven niches may provide new therapeutic strategies for aggressive GC subsets. Overall, this study establishes an ecotype-guided proteogenomic approach to nominate cell-surface proteins, glycoproteins, and signaling nodes as precision therapy candidates in gastric cancer, and offers a broadly applicable model for dissecting heterogeneity in other complex malignancies.

#7648 Plasma proteo-transcriptomic integration identifies molecular signatures and circulating biomarkers in ependymomas.

Rafat Malik[1], Ritu Kulshreshtha[2], Amandeep Kumar[3], Vaishali Suri[1], Mehar Chand Sharma[1]

[1]Neuropathology, Neurosciences Centre, All India Institute of Medical Sciences (AIIMS), New Delhi, India,[2]Department of Biochemical Engineering and Biotechnology, Indian Institute of Technology Delhi, New Delhi, India,[3]Neurosurgery, All India Institute of Medical Sciences (AIIMS), New Delhi, India

Background: Ependymomas (EPNs) are heterogeneous central nervous system (CNS) tumors that lack reliable blood-based biomarkers for diagnosis, prognosis, treatment monitoring, and recurrence detection. We generated the first plasma proteo-transcriptomic atlas of pediatric EPN to define circulating signatures across tumor subtypes, grades, treatment states and recurrence.
Methods: Plasma from 33 EPN patients and seven controls was analyzed using quantitative label-free untargeted LC-MS/MS and integrated with 44 tumor Total RNA sequencing and six control (differentially expressed genes (DEGs); $|\log_2 FC| \geq 1$, FDR < 0.05). Differentially expressed proteins ($|\log_2 FC| \geq 0.58$, FDR < 0.05) were examined via GO/KEGG/Reactome enrichment, STRING protein-interaction networks, and multi-omics concordance analyses. Biomarkers correlated with Cyclin D1 positivity, 1q gain, ZFTA-RELA fusion, and CDKN2A loss. CancerMine contextualizes known oncogenic roles.
Results: We identified 270 dysregulated plasma proteins that delineated a systemic pattern of ECM activation, coagulation complementation, lipid metabolic reprogramming, and humoral immune suppression. FN1 was the top marker, elevated 26.36-fold in subependymoma, 7.66-fold in supratentorial, and 6.37-fold in posterior fossa tumors, sharply decreasing post-treatment (1.64-fold), reflecting tumor dynamics. APOE (3.29-fold), APOD, APOH, APOA4, and TMEM198 (2.12-fold) were consistently elevated and decreased after therapy. Immune suppression was evident, with JCHAIN reduced to 0.32-fold, immunoglobulins (IGHD 0.07-fold), and complement proteins (C1QB, C4A/B) downregulated. IGHV3-35 was elevated pre-treatment (2.03-fold) and at recurrence, serving as a dual biomarker. LPA and SERPINF1 were recurrence-specific, and CD5L was supratentorial-specific. Transcriptomics identified 1,286 DEGs, of which 132 mapped to plasma proteins (57 upregulated, 75 downregulated). FN1, TMEM198, and IGKC showed RNA-protein concordance, whereas APOE, APOD, and JCHAIN showed secretion-driven discordance. STRING analysis revealed dense ECM and coagulation-lipid interaction hubs (PPI $p < 1 \times 10^{-16}$). CancerMine validated oncogenic roles of FN1, APOE/APOD, JCHAIN, C1QB, and TTR in other cancers, novel to EPN. Biomarkers were strongly correlated with aggressive genotypes.
Conclusion: This plasma proteo-transcriptomic atlas revealed a robust systemic signature in pediatric EPN, defined by ECM remodeling, coagulation dominance, metabolic rewiring, and immune suppression. Key biomarkers, such as FN1, TMEM198, APOE/APOD, IGHV3-35, JCHAIN, LPA, and SERPINF1, offer strong potential for non-invasive diagnosis, stratification, therapy monitoring, and early recurrence detection, establishing plasma proteomics as a transformative precision oncology platform.

#7649 Urinary arsenic speciation and metabolic indices associate with exposure chemistry and prostate cancer aggressiveness.

Sithembiso S. Msibi[1], MinJae Lee[2], Ping-Ching Hsu[3], L. Joseph Su[1]

[1]UT Southwestern Medical Center, Dallas, TX,[2]UT Health, Houston, TX,[3]University of Arkansas for Medical Sciences, Little Rock, AR

Background: Prostate cancer (PCa) is the second most common type of cancer among men worldwide. Environmental exposure to arsenic has been implicated in PCa carcinogenesis and progression through various pathways. This study assessed arsenic species and methylation indices and their association with aggressive PCa.

Methods: We analyzed data from 1,497 men (722 Black and 775 White) enrolled in the North Carolina-Louisiana Prostate Cancer Project (PCaP), including 396 with high and 1,101 with low aggressive PCa. Urinary arsenic species concentrations were quantified using HPLC-ICPMS and adjusted for urine dilution using creatinine. We assessed the arsenic species including inorganic arsenic (iAs), monomethylarsonate (MMA), and dimethylarsinate (DMA) and methylation indices (Primary Methylation Index and Secondary Methylation Index) between low vs. high aggressive groups using univariable tests. We also performed multivariable logistic regression models, adjusting for screening history, waist-to-hip ratio (WHR), age, smoking status, study site and race.

Results: Univariable comparisons showed no significant difference in individual arsenic species and methylation indices with low vs. high aggressive PCa (all p>0.10). However, median concentrations of total inorganic arsenic (iAs+DMA+MMA) showed a marginal difference between low vs. high aggressive PCa (1.34[0.39-2.68] vs. 1.49[0.62-3.02], p=0.06). When comparing race, Black and White men had similar levels of total iAs (1.35[0.42-2.86] vs. 1.39[0.46-2.68]; p=0.83). Multivariable logistic regression models showed overall positive association with elevated arsenic concentrations, with tertile 2 and 3 showing significantly higher odds of aggressive PCa (OR: 1.39, 95% CI: 1.01-1.91, p = 0.04 and OR: 1.45, 95%CI: 1.07-1.97, p = 0.02, respectively). A significant linear trend was also observed across increasing total iAs tertiles (p-trend=0.02). Race-stratified models showed significant association for White men (OR: 1.68, 95% CI: 1.05-2.67, p = 0.03) and not statistically significant association for Black men (OR: 1.34, 95% CI: 0.89-2.03, p = 0.16). Race did not modify the association between total iAs and aggressive PCa (p-interaction = 0.76). PMI and SMI were not significantly associated with aggressive PCa in adjusted models (OR: 1.01, 95% CI: 0.81-1.25, p = 0.91; and OR: 1.13, 95% CI: 0.96-1.33, p = 0.14).

Conclusions: Our findings show that elevated urinary inorganic arsenic levels are associated with increased odds of aggressive prostate cancer, independent of race and methylation efficiency. The results point to inorganic arsenic, rather than its methylated metabolites, as the key chemical driver of prostate cancer progression. This connection between arsenic speciation and prostate cancer aggressiveness underscores the translational importance of environmental chemistry in cancer prevention.

#7650 High-resolution detection of post-translational modifications using single-molecule protein sequencing.

Natchanon Sittipongpittaya[1], Khanh (Kendrick) Dinh Quoc Nguyen[2], Andrey Reshetnyak[3], Muriel Priault[4], Ajay Vashisht[5], John Vieceli[5], **Meredith Carpenter**[5], Nidhi Sahni[6], Gloria Sheynkman[1]

[1]Molecular Physiology and Biological Physics, University of Virginia, Charlottesville, VA,[2]Quantum-Si, San Diego, CA,[3]Structural Biology, St. Jude Children's Hospital, Memphis, TN,[4]IBGC, University of Bordeaux, Bordeaux, France,[5]Quantum-Si, Branford, CT,[6]Neurosurgery, Baylor College of Medicine, Temple, TX

Post-translational modifications (PTMs) play a critical role in regulating protein function and cellular processes. However, due to the diversity and complexity of the proteome, detecting and quantifying PTMs remains challenging. While conventional mass spectrometry and antibody-based methods provide valuable information, they are limited in their capacity to resolve and quantify PTMs at the amino acid level, particularly for PTMs with minimal differences in mass. The Quantum-Si Platinum® and Platinum® Pro sequencers are benchtop instruments designed for high-resolution, single-molecule protein sequencing. These instruments use engineered N-terminal amino acid recognizers to accurately determine the sequence composition of proteins, enabling the detection of PTMs and making advanced proteomic analysis accessible in a standard laboratory setting. In addition to leveraging the recognizer binding patterns, the recent development of PTM-specific binders further enhances the instrument's ability to detect and quantify PTMs by selectively targeting modified residues. This combined approach improves sensitivity and specificity, allowing researchers to quantify PTMs and obtain even more detailed PTM profiles on a single run. In this study, we investigated the application of single-molecule protein sequencing on Platinum Pro to detect and quantify multiple PTMs across diverse protein types. We demonstrate the detection of phosphorylation order at several sites within the anaplastic lymphoma kinase (ALK) protein, citrullination events on vimentin, asparagine deamidation as a marker of molecular ageing, and the identification and differentiation of aspartic acid stereoisomers in calmodulin sequences. This is the first study demonstrating the ability to resolve and quantify multiple PTMs on the Platinum Pro, enabling differentiation of chemical changes and stereochemical variants that, while subtle, can nevertheless have significant biological impacts. Platinum Pro can also be used to add proteoform characterization to biomarker studies, providing additional resolution not readily available in broad biomarker screening panels. We expect this technology to democratize advanced protein characterization, making the high-resolution detection of PTMs available to a broader scientific community.

#7652 Two-way proteogenomics identifies tumor-specific, immune-visible peptides for immunotherapy development in triple-negative breast cancer.

Moran Chen, Jong Min Choi, Zhiao Shi, Wenrong Chen, Bing Zhang

Baylor College of Medicine, Houston, TX

Introduction: Triple-negative breast cancer (TNBC) is an aggressive disease with limited treatment options. Despite its frequently inflamed tumor microenvironment, TNBC exhibits poor and inconsistent responses to immunotherapy, highlighting the need for alternative strategies, such as TCR-based therapy and cancer vaccines. These approaches depend on robust identification of HLA-presented, tumor-specific peptides that are visible to the immune system. To address this need, we applied immunopeptidomics together with a new proteogenomic integration framework to a panel of TNBC cell lines to establish a foundation for a comprehensive antigen resource to support peptide-based immunotherapy development.

Methods: Five TNBC cell lines were profiled with and without IFN-γ stimulation. Whole-genome sequencing, whole-exome sequencing, RNA-seq, Ribo-seq, and immunopeptidomic data were jointly analyzed using NeoFlow2, a next-generation two-way proteogenomics framework. In addition to the conventional forward approach, in which genomic and transcriptomic data inform proteogenomic database searches, NeoFlow2 introduces a reverse direction by mapping de novo-sequenced peptides back to the transcriptome to reveal unannotated translation events. NeoFlow2 further assesses tumor specificity using PepQueryMHC, which evaluates peptide-level transcript support in tumor versus normal RNA-seq data across TCGA and GTEx cohorts.

Results: NeoFlow2 revealed a markedly expanded repertoire of both canonical and non-canonical peptides across the profiled TNBC cell lines, with IFN-γ stimulation further enhancing antigen diversity. Among these, the pipeline identified hundreds of non-reference peptides arising from diverse genomic and transcriptomic origins, including missense mutations, frameshifts, alternative splicing, UTRs, intron retention, non-coding RNAs, and alternative ORFs. Leveraging TCGA and GTEx datasets, we prioritized peptides presented in TNBC tumors but absent from normal tissues, yielding a focused set of TNBC-specific antigens with strong immunotherapeutic potential.

Conclusions: NeoFlow2 provides an effective framework for integrating multi-omics and immunopeptidomic data to systematically identify canonical and non-canonical tumor antigens. In TNBC cell lines, this framework revealed a set of TNBC-specific antigens with potential relevance for peptide-based cancer immunotherapy.

#7653 Novel therapeutic opportunities in POU2F3 transcription factor-driven small cell lung cancer.

Lily L. R. Rix[1], Hayley D. Ackerman[1], Nicole R. Hackel[1], Xueli Li[1], Rachel Leigh O'Rourke[2], Juhyeon Son[1], Michelle A. Reiser[1], Arianna Nenci[1], Bin Fang[1], Eric A. Welsh[1], Brandon J. C. Klein[1], John M. Koomen[1], Eric B. Haura[1], Florian Karreth[1], Amanda Garner[2], Elsa R. Flores[1], **Uwe Rix**[1]

[1]H. Lee Moffitt Cancer Center & Research Institute, Tampa, FL,[2]University of Michigan, Ann Arbor, MI

Small cell lung cancer (SCLC) is a recalcitrant cancer characterized by loss of *TP53* and *RB1*. POU2F3+ SCLC cells are uniquely dependent on IGF1R signaling although this has not yet led to clinical translation. We therefore aimed to identify efficacious pharmacological targeting approaches for POU2F3+ SCLC and elucidate the underlying mechanisms.Cell viability was measured by CellTiter-Glo and soft agar assays. Drug targets and signaling pathways were identified by quantitative mass spectrometry-based proteomics and validated by Western blot. POU2F3 mutants were cloned to determine the kinase responsible for phosphorylation of POU2F3 the cellular effects of POU2F3 phosphorylation. Loss- and gain-of-function experiments were done using CRISPR, RNAi, chemical probes, or protein expression. Xenograft tumors were obtained by subcutaneous injection of POU2F3+ H526 cells into athymic nude mice. *POU2F3* overexpressing, transgenic $Rb1^{fl/fl}Trp53^{fl/fl}(Myc^{LSL/LSL})$ (RP/RPM) mice are being generated by genetic engineering and transfer of embryonic stem cells.Combination drug screening identified synergistic combinations between ALK-inhibitors with cross-reactivity for IGF1R and WEE1 inhibitors abrogating cell growth *in vitro* and in *in vivo*. Efficacy differences between the IGF1R inhibitors suggested the presence of additional druggable targets. Merging proteome-wide drug targets with changes in protein signaling and expression highlighted mTOR and cell cycle pathways and RSK1/2 as a relevant off-target. Interestingly, changes in both POU2F3 phosphorylation itself and expression of downstream POU2F3 transcriptional targets were identified upon individual or combination drug treatment and confirmed by immunoblotting. Rescue by overexpression of POU2F3 phospho-mutants upon CRISPR knockout of endogenous POU2F3 suggest an inhibitory function for pPOU2F3. Brigatinib and ceritinib, two potent FDA approved ALK/IGF1R inhibitors, were found to synergize with WEE1 inhibitors, in POU2F3+ SCLC. Quantitative, global chemical proteomics analysis found overlapping target profiles indicating favorable polypharmacology beyond IGF1R inhibition. Furthermore, quantitative phospho- and expression proteomics and subsequent genetic validation identified a novel regulatory mechanism of the oncogenic transcription factor POU2F3 by loss-of-function phosphorylation, which is strongly induced by drug combination treatment. This modification may indicate a new actionable vulnerability, which could be targeted to benefit the greatly underserved SCLC patient population.

#7654 Unique oncogenic mechanisms of ultrahigh-frequency mutant PTEN^{R130G}in endometrial cancer.

Xiangyi Kong[1], Li Wang[2], Md Kamrul Hasan Khan[2], Jidong Wang[3], Huaijun Zhou[1], Xinyan Wu[2]

[1]Nanjing Drum Tower Hospital Affiliated to Nanjing University Medical School, Nanjing, China,[2]Mayo Clinic Cancer Center Minnesota, Rochester, MN,[3]Jinan Central Hospital Affiliated to Shandong University, Jinan, China

Phosphatase and Tensin Homolog (PTEN) is a critical tumor suppressor frequently mutated in cancers, notably endometrial cancer (EC), where it drives early carcinogenesis. PTEN mutations disrupt lipid phosphatase activity, causing PI3K/AKT/mTOR pathway hyperactivation. However, clinical trials targeting this pathway in advanced EC yield suboptimal outcomes, with PTEN loss showing poorly predictive value for therapeutic response, indicating other mechanisms are involved. TCGA Pan-Cancer Atlas data show a 39.1% co-mutation rate of PTEN and PIK3CA in EC, much higher than the 3.6% pan-cancer rate, challenging the idea of mutual exclusivity in driver mutations within the same pathway. PTEN missense mutations are most common in EC (41.44%), with R130 as a hotspot, especially among PIK3CA-mutant patients (45.28%), while other cancers with frequent PTEN mutations show much lower R130 rates. These findings suggest PTEN R130 missense mutants undergo positive selection and may have unique oncogenic effects in EC.To characterize these mutants, a Tet-on inducible system in PTEN-null SPAC-1-S EC cells compared wild-type PTEN (PTEN^{WT}), loss of function mutant PTEN^{R173C}, and ultrahigh frequency mutant PTEN^{R130G}. PTEN^{WT} suppressed proliferation, PTEN^{R173C} showed reduced tumor suppressive activity, while PTEN^{R130G} increased proliferation, indicating a PTEN^{WT}-independent tumor-promoting function. In MFE 296 cells with PTEN $^{R130Q/N332fs}$ mutations, knockdown of PTEN^{R130Q} suppressed proliferation, providing functional evidence that PTEN^{R130G} has PTEN^{WT}-independent oncogenic activity in EC.

To elucidate the underlying mechanisms, we performed quantitative proteomic and BioSITe analyses in SPAC-1-S cells inducibly expressing PTEN^{WT} or PTEN^{R130G}, enabling comprehensive mapping of the unique signaling alterations specific to this ultrahigh-frequency PTEN^{R130G} mutant. Our initial analysis revealed that PTEN^{WT} induction caused broad transcriptional suppression of oncogenic and structural pathways, including MAPK/ERBB, focal adhesion, ECM-receptor interaction, and lysosomal function, consistent with restored tumor-suppressive activity. In contrast, PTEN^{R130G} induction led to a distinct transcriptional response; while partially repressing lysosomal and adhesion pathways, stress-adaptive and metabolic programs like TGF-β signaling and glutathione metabolism remained active or were reactivated. These results suggest PTEN^{R130G} not only loses PTEN's inhibitory functions but may gain new transcriptional and metabolic activities that promote cell survival and tumor progression. Overall, our analysis indicates wildtype PTEN restores signaling restraint, while PTEN^{R130G} reprograms the transcriptome toward a pro-cancer, stress-resilient state, suggesting a gain-of-function oncogenic role.

#7655 Defining molecular interfaces of glyco-immune checkpoint ligands using tandem mass spectrometry and ion-ion reactions.

Tim S. Veth, Haley M. Schramm, **Nicholas M. Riley**

Chemistry, University of Washington, Seattle, WA

The Siglec (sialic acid-binding immunoglobulin-like lectin) family of glycan-binding immune receptors are emerging as attractive targets for cancer immunotherapy. Siglecs recognize cell surface glycoproteins through complex interactions with various glycans containing sialic acid residues, which are upregulated in numerous malignancies. Engagement of Siglecs by their sialoglyco-ligands elicits an inhibitory signaling cascade using the same immunoreceptor tyrosine-based inhibitory motif (ITIM) signaling domains shared by established immune checkpoint receptors (e.g., PD-1, CTLA-4, and SIRPα). Our understanding of the mechanisms behind Siglec-mediated immune evasion has been rapidly improving, largely due to efforts to define transcriptional and metabolic programs that promote Siglec ligand expression. Even so, unknown combinations of glycan and protein epitopes (i.e., the glycocode) that guide Siglec ligand recognition are a major hurdle for exploiting Siglecs as therapeutic targets. Molecular details of specific glycocode patterns that contribute to Siglec ligand recognition are needed to target immune modulatory glycoforms in tumor-specific microenvironments while minimizing off-target effects, but these heterogenous modifications states challenge traditional analytical approaches. Here, we describe our efforts to develop cutting-edge mass spectrometry (MS) data acquisition technologies that incorporate electron transfer dissociation (ETD) and proton transfer charge reduction (PTCR) ion-ion reactions to profile highly complex Siglec ligand glycoproteins. We use online and offline MS workflows in combination with bottom-up glycoproteomics to profile highly heterogeneous intact glycoproteoforms of Siglec ligands that have emerged as attractive targets for next-generation glyco-immunotherapies. PTCR readily isolated and charge-reduced proteoforms of interest, generating pseudo-native spectra. PTCR scans of interest were identified, and spectra were cleaned using in-house software, PTCRcleaner. Analysis of both intact approaches was supported by bottom-up mass spectrometry data collected using a sceHCD-pd-EThcD approach. We also applied this workflow to characterize other glycosylated immune checkpoint ligands, e.g., PD-L1. Altogether, our novel tandem MS approaches that uniquely leverage ion-ion reactions enable the characterization of highly heterogeneous glycoproteoform repertoires, contributing to a deeper understanding of the complexity of the glycocode and how these proteins contribute to heterogeneity in the tumor-immune synapse.

#7656 Comprehensive investigation of stool metaproteomes among patients with precancerous lesions and colorectal cancer.

Emmalee J. Northrop-Albrecht, Vinod K. Gupta, William R. Taylor, Jason P. Sinnwell, Doug W. Mahoney, Patrick H. Foote, Kelli N. Burger, Jaeyun Sung, John B. Kisiel

Mayo Clinic, Rochester, MN

INTRODUCTION: Colorectal cancer (CRC) is the 2nd most fatal cancer in the U.S.; most benefits of CRC screening are from detection of advanced pre-cancerous lesions (APLs). With a goal to improve non-invasive stool test APL sensitivity, we sought novel APL signatures in stool metaproteomes (host- and gut microbiome-derived proteins) among cancer-free controls (CTRL), APL, and CRC patients. Since dysbiosis in gut microbiota is associated with CRC initiation, we also examined the microbial source of differentially expressed proteins (DEPs).
METHODS: Mass spectrometry was performed on archival stool supernatants (n=63 patients; 15 CTRL, 32 APL [16 adenomas & 16 sessile serrated lesions], 16 CRC). A sectioning and database-enrichment strategy was applied for peptide-spectrum matching. Microbial and human-derived proteins were searched against the Integrated Gene Catalogue (IGC) and UniProt human reference proteome. DEPs were identified using thresholds of $P < 0.05$ and fold-change ≥ 1.5. Pathway annotation of human DEPs was performed with the REVIGO webserver, while gut microbial DEPs were functionally categorized using the KEGG Automatic Annotation Server (KAAS). To assess the taxonomic distribution of microbial DEPs, sequences were aligned against the NCBI non-redundant database using BLASTP.
RESULTS: Mass spectrometry detected 879 human and 32,514 microbiome-derived proteins. When limiting detection to proteins present in ≥ 75% of patients, only 117 human and 204 microbial proteins remained. There were 17 (4,875), 288 (9,638), and 63 (3,053) unique human (microbial) proteins detected in CTRL, APL, and CRC groups, respectively. When the protein presence cutoff was set at >30% of patients, there were 52 (13 human [11 upregulated, 2 downregulated], 39 microbial [28 upregulated, 11 downregulated]) DEPs detected for the CRC + APL vs CTRL comparison. Some pathways associated with upregulated human DEPs included: inflammatory response, cellular response to iron, and endothelial cell migration. The top upregulated microbial DEPs were derived from the Phocaeicola, Lachnospiraceae, and Oscillospiraceae genera. The top downregulated microbial DEPs belonged to the Bacteroides, Eubacterium, Agathobacter, Coprococcus, and Blautia genera.
CONCLUSION: This work highlights the biological diversity and molecular heterogeneity of the stool proteome. We identified several host and microbial protein markers that differentiate APLs and early CRC from controls. These results provide a foundation for future validation studies, which are necessary to determine the clinical utility of these protein biomarkers prior to their integration into a noninvasive stool test.

#7657 An AFA assisted workflow for mass-spectrometry based proteomics of FFPE samples.

Dong-Gi Mun[1], Kiran Mangalaparthi[1], Daigo Gunji[2], Amy J. French[1], Raghavendra Pasupuleti[3], Cristine Charlesworth[1], Sameer Vasantgadkar[4], DEB BHATTACHARYYA[4], Akhilesh Pandey[5]

[1]Mayo Clinic, Rochester, MN,[2]Mayo Clinic Cancer Center Minnesota, Rochester, MN,[3]Mayo CLinic, Rochester, MN,[4]Covaris, Woburn, MA,[5]Mayo Clinic, Rochseter, MN

Introduction: The intricate cellular structure is a constantly evolving environment where cells interact, communicate, and adapt to their surroundings. The fate, role, and actions of each cell are shaped by its specific location within the tissue. Therefore, studying the spatial proteome is crucial for gaining a deeper understanding of physiological or pathological processes. With significant advancements in microscopy and mass spectrometry, it has become feasible to explore the cellular proteome at low or even single cell numbers. However, spatial proteomics is an evolving field with scope for newer sample preparation and data analysis techniques. Our objective was to develop a sample preparation workflow for analyzing proteome from limited cells extracted from formalin fixed paraffin embedded (FFPE) tissue using laser capture microdissection (LCM).

Methods: One hundred cells from the FFPE normal colon tissue were extracted by LCM and collected into an AFA-compatible 96-well plate. Decrosslinking was performed at 90ºC for 50 minutes followed by lysis in a buffer composed of 100 mM triethylammonium bicarbonate and 0.1% n-dodecyl-β-D-maltoside using adaptive focused acoustic (AFA) energetics in scanning mode for 5 minutes. After lysis, the proteins were digested using Trypsin/Lys-C mix using AFA energetics for 1 hour. The resulting peptides were acidified with trifluoroacetic acid and analyzed on a timsTOF Ultra 2 mass spectrometer coupled to a nanoElute 2 liquid chromatography system using a 15 cm (75 µm) IonOpticks column, in DDA-PASEF mode for a total run time of 34 minutes. The data were searched against the UniProt Human Reviewed protein database using MSFragger.

Results: We utilized AFA energetics to extract and digest proteins from a limited number of cells isolated from FFPE tissue using LCM. This experiment was conducted with technical replicates to ensure accuracy and reliability. A total of 3,723 proteins were identified across the three replicates, with replicate 1 identifying 3,895 proteins, replicate 2 identifying 3,754 proteins, and replicate 3 identifying 3,519 proteins. In total, we identified 21,005 peptides, with replicate 1 identifying 22,896 peptides, replicate 2 identifying 22,377 peptides, and replicate 3 identifying 17,741 peptides from 100 colon cells. Notably, we observed a 70% overlap in the proteins identified across the three replicates, which highlights the reproducibility of the approach.

Conclusion: The entire sample preparation process, after cell collection, was completed within a concise four-hour timeframe, demonstrating the efficiency of this methodology for analyzing protein profiles from small cell populations. Further, this approach is highly adaptable to automation and high-throughput applications. Its adaptability and scalability make it a promising strategy for spatial proteomics applications.

#7658 Mapping mutation-specific interaction and signalling networks across FGFR1-4 to understand cancer-associated rewiring.

Iftekhar Mahmud Chowdhury, Xiaonan Liu, Markku Varjosalo

University of Helsinki, Helsinki, Finland

Fibroblast growth factor receptors (FGFR1-4) are essential receptor tyrosine kinases that play a crucial role in controlling cellular fate, guiding tissue development, and maintaining physiological balance. Cancer-driving mutations in FGFRs are found in many tumour types, but exactly how each mutation alters receptor behaviour, protein interactions, and signalling pathways is still not fully understood. In this study, we systematically analysed wild-type, kinase-dead, and two cancer driver mutants for each FGFR paralogue by generating stable, isogenic Flp-In™ T-REx™ 293 cell lines which were engineered under inducible expression for each FGFR variant. We performed affinity purification-mass spectrometry (AP-MS) and proximity-dependent biotinylation (BioID) to generate high-confidence mutation-level map of FGFR interactomes, integrating both stable and transient protein associations. To understand the functional implications of the altered interactome we performed phosphoproteomics on both global lysates and affinity-purified complexes. This enabled quantification of pathway-specific signalling changes and differentiation between the catalytic and scaffolding roles of mutant receptors. Distinct signalling rewiring patterns were observed between wild-type and mutant FGFRs such as preferred activation of MAPK versus PI3K-AKT signalling pathway and revealed mutation-specific signalling biases consistent with recent models of RTK signalling divergence. Functional assays in NIH3T3 and U2OS cells, including colony formation, immunofluorescence, cell cycle profiling, and reporter assays, validated the differential oncogenic potential and subcellular localisation of each variant. We further evaluated the effects of clinically relevant FGFR inhibitors on the viability and signalling pathway activity across all mutants, identifying both drug-sensitive and drug-resistant classes linked to specific mutations, including gatekeeper substitutions (e.g., FGFR4-V550L) and extracellular loop alterations (e.g., FGFR2-S252W). Together, our findings establish the first paralogue-wide, mutation-resolved signalling atlas of the FGFR family. This integrative approach of structural, functional and pharmacological analysis provides systematic insight into oncogenic mechanism and therapeutic sensitivity and establishes a broadly applicable framework for the functional annotation of kinase driver mutations in cancer.

#7660 Altered cell surface N-glycosylation implicates hypersialylation in breast cancer brain metastasis.

Judith Nwaiwu, Wenjing Peng, Akhila Reddy, Xue Dong, Parisa Ahmadi, Jingfu Zhao, Yifan Huang, Peilin Jiang, Waziha Purba, Oluwatosin Daramola, Yehia Mechref

Department of Chemistry and Biochemistry, Texas Tech University, Lubbock, TX

Breast cancer is the second most common cause of brain metastasis, often in advanced-stage disease. The mechanisms underlying breast cancer brain metastasis (BCBM), particularly how tumor cells cross the blood-brain barrier and adapt to the brain environment, remain unclear. Cell surface glycosylation plays diverse roles, and its dysregulation in cancer can disrupt signaling and promote metastasis. We investigated how changes in cell surface N-glycans contribute to BCBM by analyzing N-glycans released from human breast cancer cell lines (MDA-MB-231, MDA-MB-361, HTB-131, HTB-22), a brain-seeking variant (MDA-MB-231BR), and glioblastoma cells (CRL-1620) using nano liquid chromatography-tandem mass spectrometry (LC-MS/MS). Surface N-glycans were enzymatically released from live cells with PNGase F without compromising membrane integrity. Results showed the 231BR cell line expressed higher levels of sialylated N-glycans than other cells, with N-glycan 4502 as the most abundant. Four sialylated structures (4501, 4502, 3501, 5602) were significantly elevated in 231BR, suggesting a role in brain metastasis. This study expands understanding of altered N-glycan profiles in BCBM and highlights potential molecular features linked to brain colonization. Further research on these N-glycans could clarify their function in mediating metastasis and identifying therapeutic targets.

#7661 Integrated multiomics profiling of lysates using nCounter® protein and RNA panels for comprehensive oncology insights.

Brian Filanoski, Lori Hamanishi, Giang Ong, Terence C. Theisen, Erin Piazza, Christina Bailey, Prajan Divakar, Margaret L. Hoang, Joseph M. Beechem

Research and Development, Bruker Spatial Biology, Seattle, WA

Multiomic approaches combining transcriptomic and proteomic data are critical for understanding complex biological systems in oncology. The nCounter® platform enables simultaneous quantification of RNA and protein targets from the same sample, reducing variability and maximizing biological insight. This innovation builds upon the demonstrated clinical utility of classic nCounter mRNA assays in translational and clinical research, including Prosigna®(FDA-cleared), Lymph2Cx, and Merck's Tumor Inflammation Signature (TIS). Lysates were prepared from eight different cancer cell lines (HT-29, Daudi, PC-3, U-937, LNCaP, HeLa, PANC-1, MCF-7) following optimized protocols for nCounter multiomics. Protein targets were profiled using the new nCounter Tumor Signaling Panel plus Immune Pathways (500+ Abcam RabMab monoclonal antibodies) and combined with IO360 gene expression panel for integrated analysis. Using 5,000 - 20,000 lysed cells, we find high reproducibility between replicate lysate, with low coefficient of variation (CV) for RNA and protein across replicates. Sensitivity of detection was maintained down to 50 ng of RNA and 200 ng protein per lysate. As expected median Pearson correlation between RNA and protein expression for overlapping markers was $R < 0.5$, highlighting the high multiomics assay information content. In addition, integrated analysis of transcript and protein levels uncovered concordant activated pathways, including key post-translational modifications (PTMs). This study demonstrates the feasibility and utility of lysate-based multiomics using nCounter panels for oncology research. The approach provides a streamlined workflow for comprehensive molecular profiling, supporting translational studies and biomarker discovery.

#7662 A high-throughput, automated, and reproducible mIF workflow for spatial biology enabled by ZEISS slide stream and Vizgen's InSituPlex® assays.

Cassandra Kysilovsky[1], Kevin Hwang[1], Susanne Pfeifenbring[2], Michael Downing[1], Sherry Derakhshani[2], Moritz Widmaier[2], Jiang He[1], Angela Vasaturo[1]

[1]Vizgen, Cambridge, MA,[2]Zeiss, Jena, Germany

Multiplex immunofluorescence (mIF) has become a cornerstone technique in spatial biology for investigating the tumor microenvironment. Despite its widespread use, existing mIF workflows are often hindered by variability in image acquisition and dependence on labor-intensive manual steps. To overcome these limitations, we developed a fully integrated, high-throughput spatial biology workflow combining the highly standardized and automated ZEISS spatial biology platform with Vizgen's pre-optimized InSituPlex assay. Together, these deliver high-throughput, fully automated, and reproducible biomarker detection across a broad dynamic range, enhancing both efficiency and scalability. To validate these claims, we conducted a multisite verification study. A 4-plex OmniVUE panel including CD3, Ki67, Granzyme-B and CK/Sox10 was utilized to stain multiple tissue indications on formalin-fixed paraffin-embedded (FFPE) sections. On all sites, the slides underwent the same predefined and automated routine for staining using Leica Bond RX instruments and imaging using ZEISS Axioscan 7 spatial biology slide scanners. Acquired images were seamlessly uploaded to Mindpeak and analyzed with integrated STARVUE algorithms optimized for Vizgen InSituPlex assays imaged on Axioscan scanners, providing quantitative analysis for densities and fluorescence intensities of positive cells. Analysis of the results demonstrated excellent concordance between sites, confirming the precision and accuracy of the combined workflow across multiple operators and instruments. Qualitatively, staining was highly comparable across all sites, and the limited variations in fluorescence signal and background did not affect the accuracy of the STARVUE™ AI algorithms. Quantitatively, the presented workflow exhibits high reproducibility and repeatability of results across locations, providing a reliable solution for translational research with amplified speed and quality of data generation. As a result, it offers significant potential to advance spatial biology from translational research to clinical applications

#7663 Discovery of tumor-specific and neoantigenic peptides in cancer tissue samples using mass spectrometry-based immunopeptidomic.

Cameron Ellis[1], Arhur Viode[2], Anamarija Pfeiffer[2], Lucy Yang[2], Monika Pepelnjak[2], George Rosenberger[2], Polina Shichkova[2], Kristina Marx[3], Christopher Below[2], Roland Bruderer[2]

[1]PreOmics Inc., Billerica, MA,[2]Biognosys AG, Schlieren, Switzerland,[3]Bruker Daltonics GmbH & Co. KG, Bremen, Germany

Therapeutic peptide-based vaccination is a promising strategy for cancer immunotherapies. The identification of tumor-specific antigens is key to developing therapies. Mass spectrometry has emerged as the primary technique for the identification of peptides presented on human leukocyte antigen (HLA), i.e., immunopeptides. While tremendous progress has been made, the analysis of immunopeptides remains challenging. This is especially true for scarce clinical tissue, with amounts below 20mg. Here, we present a robust and scalable workflow utilizing the BeatBox tissue homogenizer that enables deep immunopeptidomics profiling of clinically relevant samples, facilitating the discovery of tumor-specific and neoantigenic peptides for therapeutic development. A total of 33 tissue samples from 11 donors are homogenized under native conditions with the BeatBox tissue homogenizer using the BeatBox Tissue Kit 24x kit (PreOmics). Immunopeptides are isolated using a pan anti-HLA class 1 antibody (W6/32) coupled to magnetic protein A beads in a semi-automated manner on the KingFisher (Thermo Fisher). Peptides are eluted under acidic conditions and filtered using a 10kDa MWCO plate. The immunopeptides are loaded onto Evotips (Evosep) for analysis using the Whisper Zoom method from Evosep coupled to a timsUltra AIP (Bruker) mass spectrometer. Data analysis is performed using Spectronaut 20 (Biognosys) using directDIA. For the RNA sequencing, total RNA was extracted from fresh frozen tissue samples and sequenced using Illumina 2×150 bp paired-end reads (~100M reads per sample). We analyzed matched tissue samples from 11 HLA-typed colorectal cancer donors, including healthy tumor-adjacent tissue, primary tumors, and metastatic tumors (n = 33). We profiled over 80,000 peptides with an average of 10,000 per sample using directDIA. Overall, more than 70% of the peptides were predicted to be binders (MHCFlurry). Integration of MS-based immunopeptidomics data with RNA sequencing enabled the identification of key antigens that could be used for the development of immunotherapy. We identified neoepitopes shared between tumors and metastatic tumors within patients as well as unique neoepitopes in tumors. Amongst detected neoepitopes, multiple patented or previously established immunotherapy targets were observed. Taken together, we have developed a robust workflow for the immunopeptidome profiling of clinically relevant samples and identification of neoepitopes. These findings demonstrate the potential of this workflow to support personalized cancer vaccine development and advance precision immunotherapy strategies.

#7664 An automated sequential protein/DNA/RNA extraction workflow for comprehensive multiomics analysis from cells and tissue.

Laure Jobert[1], Charmaine Hinahon[2], Leigh Foster[3], Marie Holter-Sorensen[1], Samri Michael[1], Iwona Grad[1], Lina Zheng[4], Berit Reed[1]

[1]Thermo Fisher Scientific, Oslo, Norway,[2]Thermo Fisher Scientific, Austin, TX,[3]Thermo Fisher Scientific, Rockford, IL,[4]Thermo Fisher Scientific, Carlsbad, CA

Introduction: The integration of proteomics, genomics, and transcriptomics is crucial for comprehensive biological insights. We have developed an automated sequential Protein/DNA/RNA workflow designed to reproducibly isolate high-quality protein, DNA, and RNA from the same sample using the KingFisher™ SamplePrep Purification System, enhancing the efficiency, through-put and depth of multiomics studies.
Methods: Our sequential Protein/DNA/RNA extraction workflow utilizes a magnetic bead-based approach, leveraging the well renowned Dynabeads™ and MagMAX™ magnetic beads technologies. This enables efficient isolation of protein, DNA, and RNA from as few as 1,000 cells or 1 mg of tissue. The workflow is compatible with both manual and automated processing on the KingFisher™ sample purification system, accommodating a wide range of sample numbers from low to high throughput.
Results:

- Mass Spectrometry (MS): The workflow produces high-quality proteins suitable for MS analysis. Comparative studies with the EasyPep™ MS Sample Prep Kit show similar chromatograms, peptide properties, and distribution profiles among biological processes and cellular components, as well as absence of incompatible reagents.
- Next-Generation Sequencing (NGS): The workflow yields high-quality nucleic acids compatible with NGS. Whole genome sequencing and rRNA depletion sequencing demonstrate excellent molecular depth, coverage and uniformity, with robust QC metrics across various sample types.

Conclusion: The sequential Protein/DNA/RNA workflow offers a versatile and efficient solution for multiomics research, providing high-quality analytes compatible with both MS and NGS. This magnetic bead-based workflow, utilizing Dynabeads™ and MagMAX™ magnetic beads, is ideal for precious and small samples, enabling reproducible data and high throughput capabilities. For Research Use Only. Not for use in diagnostic procedures.

#7665 Multi-step antibody validation for nCounter high-plex multiomics panels.

Giang Ong, Terence C. Theisen, Brian Filanoski, Lori Hamanishi, Erin Piazza, Christina Bailey, Prajan Divakar, Margaret L. Hoang, Joseph M. Beechem

Research and Development, Bruker Spatial Biology, Seattle, WA

Expanded development on the nCounter® Analysis System now enables simultaneous quantification of over 500 proteins and up to 800 transcripts from a single FFPE tissue sample. With the introduction of two high-plex protein panels used in combination with any prebuilt nCounter® RNA Panel this new capability brings a novel non-destructive FFPE assay with new depth, simplicity and reliability for immuno-oncology multiomics research. The nCounter® platform has long been known as the gold standard for oncology and immunology studies including diagnostic development. Confirming performance in support of translational and clinical applications is essential part of this capabilityTo ensure high data integrity in this complex environment, we developed a rigorous multi-step antibody validation pipeline. The process begins with an initial IHC screening, performed by our antibody partner AbCam, to confirm specificity in known positive and negative tissues. These single-plex IHC validated antibodies are individually conjugated to nCounter-compatible UV-cleavable oligonucleotides. Functional performance of the high-plex protein panels was assessed using more than 90 cell lines and more than 100 tissue cores from over 30 tissue types featuring cancerous and healthy FFPE samples. Sensitivity and specificity are benchmarked against available orthogonal RNA-Seq and mass spectrometry datasets for the cell lines. The specificity of phospho-specific antibodies was also tested in a phosphatase treatment assay, confirming that >90% of signal is reduced with treatment.To demonstrate the compatibility of these antibodies in a high-plex panel, we show antibody performance remains robust when our protein panels are stacked together or run independently. Finally, reproducibility is confirmed across users and runs. This validation framework ensures high specificity, sensitivity, and reproducibility, enabling confident multiomic profiling of complex tissue samples and accelerating translational insights in cancer biology.

#7666 Comprehensive surfaceome profiling reveals tumor specific targets in osteosarcoma.

Snehal D. Ganjave[1], Kevin K. Leung[1], Leanne C. Sayles[2], Alejandro Sweet-Cordero[1], James A. Wells[3]

[1]UCSF - University of California San Francisco, San Francisco, CA,[2]Lab Manager, Pediatrics Cancer Biology, University of California, San Francisco, CA,[3]UCSF Comprehensive Cancer Ctr., San Francisco, CA

Osteosarcoma (OS) is an aggressive bone cancer characterized by significant genomic alterations. Despite recent efforts to study OS, the extracellular proteins driving tumorigenesis and metastasis in xenograft models remain understudied due to technical limitations in enriching low-abundance surface proteins. Here, we employed quantitative surfaceome profiling via Wheat Germ Agglutinin (WGA)-HRP mediated cell surface protein enrichment to map the dynamic surface protein landscape of primary and metastatic OS, uncovering clinically actionable targets. We applied an integrated proteomics approach combining WGA-HRP-based cell surface capture and deep offline peptide fractionation coupled with DIA-PASEF mass spectrometry to achieve deep and accurate surfaceome coverage. Primary and metastatic OS cell lines (n = 9) and PDX tumors (n = 4-5), along with controls (n = 3), were analyzed using WGA-HRP mediated surface enrichment followed by Neutravidin based pulldown. PDX tumors were mechanically dissociated to obtain single suspensions. Enriched proteins were fractionated offline, and a deep spectral library was generated using high-pH fractionation and DDA-PASEF, enabling high-resolution, quantitative mapping of the OS surfaceome across diverse samples. The optimized workflow identified ~6,000 total proteins, of which over 600 were validated as druggable surface proteins through Surfy database (FDR < 0.01). PCA revealed clear separation of samples by disease state and phenotype, demonstrating the high reproducibility and biological fidelity of the surfaceome profiles. Comparative analysis of all metastatic OS cell lines vs. controls identified numerous highly dysregulated surface proteins ($log_2FC \geq 5$). The surfaceome profile revealed both reported & novel targets, including a pronounced and coordinated upregulation of proteins critically involved in enhanced nutrient transport and metabolic reprogramming, key cell-cell adhesion and structural maintenance molecules, and prominent growth signaling receptors. These upregulated functional classes are critically implicated in enhanced metastatic capacity and aggressive tumor progression. These findings provide a comprehensive surfaceome map of OS remodelling, revealing interconnected, tumor-specific dysregulation and actionable surface targets. The identified protein classes highlight potential biomarkers for early diagnosis, prognosis, and monitoring therapeutic response, and can guide the rational development of targeted biologics and immunotherapies to improve outcomes for OS patients.

Acknowledgement: This project is supported by the OCE, FDA of the U.S. Dept of Health and Human Services (HHS) as part of a financial assistance award [CERSI grant to UCSF, U01FD005978] totaling $1,257,392. The contents are those of the author(s) & do not necessarily represent the official views of, nor an endorsement by FDA/HHS, or the U.S. Govt.

#7667 Integrating multi-omics and AI-driven approaches into STEMM education to advance cancer research training.

Shixia Huang

Baylor College of Medicine, Houston, TX

Preparing future scientists to address the complexity of cancer requires early exposure to advanced analytical methods and transdisciplinary thinking. We developed scalable STEMM education programs that integrate multi-omics and artificial intelligence into cancer research training across multiple learner levels. Central to this effort is the Biotechnology Research Incubator for Teachers (BRITE), an NIH R25 Science Education Partnership Award program providing secondary-school teachers with hands-on multi-omics training rooted in cancer biology. By incorporating genomics, proteomics, and data-driven interpretation, BRITE equips teachers to translate authentic cancer research practices into classroom learning. Building on this foundation, the NCI-funded P20 Cancer Research Education Program (C-REP) engages undergraduate and graduate/PharmD trainees in multi-omics workflows, tumor signaling pathways, and computational analyses. We also established the IMPACT Medical Scholar Program, which introduces medical students to cancer research methodologies, advanced analytics, and patient-centered communication. To broaden the early pipeline, we created high-school programs that use AI-assisted adapted primary literature and culminate in a student research symposium. Collectively, these programs provide a scalable model for integrating advanced technologies into STEMM education to strengthen participation in cancer research.

#7668 Characterization of outer membrane vesicles (OMVs) from *pks+*NC101 and *pks-*DH10B *E. coli* strands.

Lissette Marie Perez-Rovira[1], Grace Enid Velez Crespo[2], Luis A. Prieto-Costas[2], Jeremy J. Colon-Morales[2], Abel Baerga-Ortiz[2]

[1]University of Puerto Rico Comprehensive Cancer Center, San Juan, PR,[2]UPR Molecular Science Research Center, San Juan, Puerto Rico

Background & Objectives: Colibactin is a genotoxin encoded by the *pks* genomic island in pathogenic Gram-negative bacteria and has been implicated in colorectal cancer. Colibactin synthesis and activation occur in a two-step process in which pre-colibactin is produced in the bacterial cytoplasm and subsequently activated into colibactin within the periplasmic space. However, the mechanism by which *pks*$^+$ bacteria export colibactin to host cells remains unclear. We hypothesize that outer membrane vesicles (OMVs), nanosized proteoliposomes released by Gram-negative bacteria capable of transporting diverse biomolecules, serve as a delivery system for this toxin to host cells.

Methods: To investigate this, OMVs were isolated from *pks*$^+$ NC101 and *pks*$^-$ DH10B *E. coli* strains using the exoEasy Maxi Kit and quantified with a BSA-based protein assay on a Synergy H1 microplate reader.

Results: Yielding concentrations consistent with typical OMV preparations. The stability and morphological characteristics of the extracted OMVs will be evaluated using dynamic light scattering (DLS). Metabolites extracted from OMVs will be examined via mass spectrometry to confirm the presence of known colibactin-related intermediates. Additionally, OMVs will undergo proteomic analysis to identify proteins involved in OMV-host interaction mechanisms. Finally, we aim to assess the effects of OMV exposure on large intestinal epithelial cells to better understand their contribution to colibactin-associated toxicity and colorectal cancer development.

Conclusion: Ultimately, this research seeks to clarify how OMVs mediate colibactin transport and cytotoxicity, providing new insights into bacterial factors that promote colorectal carcinogenesis.

Acknowledgements: This research was funded by the National Institute of Allergy and Infectious Diseases (NIAID) Grant #5R25AI183304-02.

#7669 Automated multiplex profiling of human cytokines and autoantibodies using an Automated Assay Workstation.

Wen-Rong Lie, Brooke Gilliam, Laura Marquardt, Mark Pawlicki, Ernest Mueller, Xiuyuan Zhang, Nathanael Ellis, Todd Hendrich, Linda Meeh, Scott Keefer, Qiang Xiao

MilliporeSigma, Burlington, MA

Automated multiplex bead-based immunoassays were performed using an AAW™ Automated Assay Workstation for high-throughput profiling of immune factors and cancer autoantibodies. Human serum cytokine analysis was conducted with MILLIPLEX Human Cytokine Panel A and Panel B kits (48-plex, overnight protocol), and across cytokines spanning a broad dynamic range, automated-to-manual correlation coefficients (R^2) were greater than 0.95 with regression slopes between 0.80 and 1.20. Cancer autoantibody profiling used a 15-plex antigen-coated bead multiplex panel on sera from various cancer types and healthy donors (n=96 total samples). The AAW™ workstation automates all critical liquid handling, standard curve preparation, sample transfer, reagent dispensing (matrix solution, Assay Buffer, Standards, QCs, samples, and Beads), and plate setup with robotic lidding. Assay plates were washed off-deck on an automatic plate washer and analyzed with a Luminex instrument. The automated protocol enabled processing of 2-3 plates daily, with streamlined setup which significantly reduce hands-on time. Minimizing manual interventions reduced opportunities for human errors, resulting in greater reliability and efficiency for high-throughput applications. The AAW™ performance confirms robust, reproducible, and scalable multiplex analysis for cancer and immunology research.

#7670 Integrated mass spectrometric workflows enabling next-generation conjugate therapeutics in cancer research.

Min Fang, Nilesh Sonawane, Wenchuan Ma, Benjamin Wei, Qingcong Lin

Medicilon, Lexington, MA

Antibody-drug conjugates (ADCs) and the broader class of Antibody-X Conjugates (AXCs)—including emerging Antibody-Oligonucleotide Conjugates (AOCs)—are rapidly advancing as therapeutic modalities in oncology and autoimmunity. Their expanding impact increases the need for robust bioanalytical strategies capable of quantifying total and conjugated antibodies, released payloads, and associated biotransformation pathways.LC-MS/MS has become an essential platform for addressing the analytical complexity of AXCs, supporting hybrid LBA-LC-MS workflows for total and conjugated antibodies, as well as direct measurement of free payloads and payload metabolites. Click-chemistry-enabled drug systems, designed for tumor-selective activation, present similar analytical challenges that require high sensitivity and specificity. The platform described here meets these demands through enhanced sensitivity, selectivity, and comprehensive biotransformation characterization.We developed an integrated LC-MS/MS workflow tailored for ADC, AXC, and AOC programs. Optimized controlled-reduction and selective-extraction methods enabled accurate quantification of diverse payload classes—including auristatins (MMAE/MMAF), topoisomerase-I inhibitors (DXd, SN-38, exatecan), and associated linker-drug species—while minimizing artificial payload release. These assays demonstrated high sensitivity, linearity, and matrix robustness across plasma, tumor, tissue, and cell-based systems, supporting reliable pharmacokinetic, stability, and biotransformation assessments.A complementary bioorthogonal click-chemistry workflow using azide-alkyne and TCO-tetrazine reactions was also established to selectively tag precursor and product species, enhancing MS detectability and enabling quantitative analysis of activation behavior.Together, these LC-MS/MS-based approaches provide a unified analytical solution for ADCs, AOCs, AXCs, and click-activated therapeutics. The platform supports comprehensive in vitro, ex vivo, and in vivo pharmacokinetic studies across plasma and tissue matrices, facilitating robust PK/PD correlation and exposure profiling for these emerging modalities.

#7671 Integrated proteogenomics of primary tumoroid models for precision oncology.

Shawn P. Fahl, Audrey Kleeman, Jessica Maxwell, Yukta Bhurke, Jessica Moore, Jaison Arivalagan, Kerri Colwell, Cavin Ott, Kayla Williams, Danielle Gutierrez

Discovery Life Sciences, Huntsville, AL

The availability of scalable primary oncology models remains an impediment to preclinical evaluation of new therapeutic strategies. Recently, primary tumoroid models have been developed to aid in early-phase evaluation of drug compounds. These models are generated from dissociated primary tumors and can be expanded through numerous passages, from a conventional, embedded dome stage through a suspension state, which allows for the generation of a large number of tumoroids for comprehensive studies. The tumoroid lines maintain the underlying genomic and transcriptomic signatures of the parent tumor from the initial, early-passage embedded stage to later-passage suspension cultures. These models are highly amendable to in vitro evaluation of cell-intrinsic therapeutic interventions, as well as cell-extrinsic modalities, since tumor-resident immune and stromal cells from the parent tissue are preserved in the cryopreserved dissociated tissue. Proteogenomics is the integration of genomic, transcriptomic, and proteomic datasets to uncover novel biological insights that cannot be uncovered with a single data set alone. Tumoroids represent the most physiologically relevant oncology models to understand the relationship between DNA variants, RNA expression, and protein expression. Mass spectrometry-based proteomic data were generated from the tumoroid models and searched against sample-specific databases generated from whole exome sequencing as well as whole transcriptome data for a comprehensive overview of the biology of the tumoroids. This robust analysis was further supported by drug response data of the tumoroids exposed to a standard set of classical chemotherapeutic compounds and small-molecule inhibitors. We identified a colorectal cancer tumor model with a pathogenic KRAS-G12C mutation, and how treatment with the clinical KRAS-G12C inhibitor sotorasib altered global protein expression was further evaluated. Additionally, high mutational burden tumoroids generated from deficient DNA mismatch repair endometrial tumors were analyzed to better understand how DNA hypermutation affects global protein expression. Collectively, these studies establish a pipeline to generate a holistic view of tumor cell biology, enabling for the discovery of new biomarkers and drug targets.

#7672 Automated, flexible multiplex immunofluorescence for tumor microenvironment profiling using HCR™ Gold IF and clinically-relevant antibody clones.

Wudy Yang[1], Randy Chen[1], Harry Choi[1], Aneesh Acharya[1], Anne Hellebust[2], Will Howat[3]

[1]Molecular Instruments, Inc., Los Angeles, CA,[2]Indica Labs, Albuquerque, NM,[3]Abcam, Cambridge, United Kingdom

Background: Multiplexed immunofluorescence (mIF) is central to oncology research but is often limited by fixed panels, antibody modification requirements, harsh stripping, and workflows that risk epitope damage. HCR™ Gold IF enabled by HCR™ HiFi Encoders addresses these constraints by providing enzyme-free amplification with universal compatibility to unmodified rabbit IgG and mouse IgG1 primaries. Here, we evaluated a complete, interoperable workflow combining automated HCR™ Gold IF on Leica Biosystems' BOND RX staining instrument, validated Abcam antibodies, and quantitative image analysis using Indica Lab's HALO platform for tumor microenvironment (TME) profiling.

Methods: FFPE tissue sections from healthy tissues and tumors were stained via HCR™ Gold IF on the BOND RX staining instrument. Panels included epithelial, proliferation, immune, and checkpoint markers (e.g., panCK, Ki67, CD3, CD8, CD68, PD-1, PD-L1). All primary antibodies were obtained from Abcam and qualified in a single-plex experiment prior to multiplex assembly. Slides were imaged with whole-slide scanners and analyzed in the HALO® platform to quantify biomarker expression and interrogate spatial relationships between cell populations.

Results: The automated, protease-free workflow generated high signal-to-background with crisp subcellular localization and clean channel separation across tissues and targets. Universal compatibility with unmodified Abcam antibodies streamlined panel design and minimized assay development time. Single-plex to multiplex concordance met predefined acceptance criteria, indicating minimal epitope masking or channel cross-talk. Across tumor cohorts, we observed expected and quantifiable TME shifts versus matched healthy tissues, including elevated PD-L1 on tumor/myeloid compartments and increased CD8+ and CD68+ densities at tumor-stroma interfaces.

Conclusions: Integrating HCR™ Gold IF, powered by the HiFi Encoders, on the BOND RX staining instrument and analyzing in the HALO platform delivers an automated, plug-and-play mIF solution that couples superior, enzyme-free amplification with true bring-your-own-antibody flexibility. This end-to-end workflow lowers barriers to custom, high-plex TME studies, preserves tissue integrity, and enables standardized generation of spatial biomarkers to inform immune-oncology research and patient stratification. The approach is readily extensible to larger panels and to combined RNA/protein co-detection for deeper, multi-omic context. For Research Use Only. Not for use in diagnostic procedures.

#7673 9-channel spatial co-detection of clinically relevant protein and RNA targets in FFPE tumors with HCR™ Gold and MoxiePlex.

Wudy Yang[1], Randy Chen[1], Harry Choi[1], Aneesh Acharya[1], Minakshi Singh[2], Quyen Vu[3]

[1]Molecular Instruments, Inc., Los Angeles, CA,[2]Hamamatsu Photonics Europe GmbH, Herrsching am Ammersee, Germany,[3]Hamamatsu Corporation, Bridgewater, NJ

Background: High-plex spatial profiling of protein & RNA in FFPE tumors is increasingly important for characterizing tumor-immune interactions, but existing methods often limit exploration to predefined antibody panels, harsh stripping/eluting steps, and iterative cycles that compromise sample and target integrity and make assay development and validation burdensome. HCR™ Gold IF, enabled by the HiFi Encoder, supports enzyme-free fluorescent detection using unmodified, user-supplied primary antibodies and operates on the same amplification platform as HCR™ Gold RNA-FISH. Combined with the Hamamatsu MoxiePlex multispectral tissue imaging platform, which enables whole-slide single-round imaging of 7-9-plex panels without the need for cyclic-staining, this workflow offers a practical route to flexible, 7-9-plex protein and RNA co-detection in FFPE specimens.

Methods: FFPE human tumor sections were stained with HCR™ Gold IF using encoded, clinically validated primary antibodies alongside HCR™ HiFi Probes. Two parallel multiplex configurations were tested on the MoxiePlex:1. 7-plex panel: DAPI, 425, 488, 546, 594, 700, 7502. 9-plex panel: DAPI, 425, 488, 514, 546, 594, 633, 700, 750Panels incorporated antibodies specific to cancer-relevant proteins (e.g., pan-CK, Ki-67, PD-L1, CD8, CD68) & RNA targets representing tumor and immune biology (e.g., EPCAM, CXCL9, CD274). For each fluorophore-target combination, single-stain reference slides were generated to establish exposure settings, verify filter performance, and quantify spectral bleed-through to enable spectral unmxing. Multiplex slides were imaged in a single acquisition round, and data were evaluated for signal intensity, channel crosstalk, expected biological localization, and concordance with single-stain references. Spectral unmixing was carried out automatically for the whole- slide image, following acquisition, as part of the imaging process.

Results: HCR™ Gold IF & HCR™ Gold RNA-FISH produced bright, robust signals with preserved tissue architecture. In whole- slide multiplex imaging, protein and RNA targets localized to expected tumor and stroma regions highlighting immune infliltration in the tumor microenvironment, the expression of which. closely matched single-stain reference patterns. The MoxiePlex platform delivered consistent, whole-slide imaging performance with reproducible acquisition settings appropriate for routine 7-9-plex scanning.

Conclusions: HCR™ Gold IF & HCR™ Gold RNA-FISH can be combined in a single-round workflow on the MoxiePlex to achieve up to 9-plex imaging of clinically relevant protein and RNA targets in FFPE tissue. This approach avoids stripping or photobleaching, maintains compatibility with validated antibodies and standard filter sets, and provides a practical path for flexible, 7-9-plex spatial assays in translational and clinical research.

#7674 Formaldehyde-free fixation for safe, scalable and flexible single-cell multiomics studies.

Joseph Olives, Hongduan Huang, Zhiqi Zhang, Lin Chen, Rosary Nguyen, Hye-won Song, Aruna Ayer

Single Cell Multiomics, Becton Dickinson Biosciences, San Diego, CA

The development and commercialization of flexible single-cell multiomics methods has allowed for investigator selection and implementation of assays which provide the desired biological depth and context for their disease model of interest. Multiomic methods generally achieve best results with fresh, high-quality samples for efficient recovery of the native biological state. These dynamic samples, however, pose logistical challenges for larger clinical studies, limiting scope and reproducibility. Formaldehyde (PFA) fixation has been the standard for tissue preservation, due to its accessibility and stability enabling simplified clinical sample preparation and biobanking from large patient cohorts. The implementation of PFA, however, predates common knowledge of its carcinogenicity and nucleic acid crosslinking, limiting future transcriptomic and genomic study. Unlike tissue, fixation of single cell suspensions has not yet been standardized to this extent, offering a valuable opportunity to survey more safe and flexible solutions for sample preservation. To address this, we evaluated fixatives that have increasingly been investigated for these advantages over PFA with the goal of suggesting an alternative single-cell fixative solution for further investigation. We optimized each alternative fixation solution using various cellular and molecular analysis tools suggesting broad multiomic and clinical compatibility. Optimal formulations were used to treat peripheral blood monocytes (PBMCs) and their nuclei and analyzed by genetic (ATAC-seq), transcriptomic (WTA) and proteomic (CITE-seq) assays for multiomic evaluation against live and PFA controls. Our data identified a safe and stable novel fixative formulation for preserving PBMC samples throughout a mock biobanking process and gave broad multiomic compatibility comparable or exceeding that of PFA.This alternative and its novel preparation are underrepresented in academic and industry studies on single-cell fixation solutions at a critical time for large cohort studies. Further development, optimization and demonstration of this safer alternative is needed as these large single cell atlas and clinical studies become increasingly common. Such studies' data are shaping new virtual cell models and clinical standard operating procedures foundational to this field and necessitate further review of safer alternatives with more flexible assay compatibility.

: Proteomics: Biomarker Discovery and Signaling Networks
Poster Session

#7677 High-throughput plasma proteomics enables sarcopenia stratification and identifies the IGFBP axis as a key mediator of muscle impairment in cancer patients.

Filippo Gustavo Dall'Olio[1], Wael Salem Zrafi[1], Xinran Song[1], Littisha Lawrance[1], Fei Chen[1], Pierre Busson[1], Catherine Brenner[1], Rebecca Ibrahim[1], Marie Guinhut[1], Caroline Even[1], Nathalie Lassau[1], Diana Cardenas-Braz[1], Fabrice Barlesi[2], Yohann Loriot[1], Fabrice Andre[1], Mariam Jamal-Hanjani[3], Antoine Italiano[1], Yegor Vassetzky[1], Benjamin Besse[1]

[1]Gustave Roussy, Villejuif, France,[2]Gustave Roussy, villejuif, France,[3]University College London (UCL) Cancer Institute, London, United Kingdom

Background: Cancer-related sarcopenia, defined by progressive loss of skeletal muscle mass and function, worsens outcomes but lacks a single universally accepted diagnostic criteria. Current assessments are time-consuming. We aimed to identify a plasma proteomic signature of sarcopenia and uncover soluble mediators involved in muscle decline.
Methods: Two MATCH-R cohorts (NCT2517892) were analyzed: advanced cancers treated with immunotherapy (training) and metastatic castration-resistant prostate cancer (mCRPC) treated with enzalutamide (validation). An external validation cohort came from TRACERx (NCT01888601, resected and relapsed NSCLC). In MATCH-R, skeletal muscle index (SMI) at L3 level was measured on CT/PET within 42 days of blood draw; ECOG PS was used as a surrogate for muscle function. Plasma proteomics was performed using Olink Explore 1536/3072. Bulk and, for selected cases, single-cell RNA-seq were available for paired biopsies. In TRACERx, skeletal muscle area (SKM) was quantified via an automated deep-learning pipeline (PMID: 37045997). An XGBoost classifier was trained on high-contrast cases (low sarcopenia, LS: high SMI, ECOG 0; high sarcopenia, HS: low SMI, ECOG ≥2) using neuromuscular-related proteins enriched in LS. The model generated sarcopenia probability (SP, 0-100%) applied to all cohorts.
Results: The training cohort included 99 patients (36 high-contrast: 21 HS, 15 LS). Using a 50% SP cutoff, the model showed an accuracy of 0.889 in 18 high-contrast validation cases. SP correlated with ECOG PS when available ($p < 0.001$) and SMI in training and mCRPC cohorts (training: $\rho = -0.39$, $p = 0.004$ for male and ρ -0.42 for female; mCRPC: $\rho = -0.41$, $p = 0.008$), with SKM in TRACERx baseline ($\rho = -0.29$, p 0.01 and ρ -0.24 p 0.07 for male and female), recurrence $\rho = -0.42$, p 0.002 and ρ -0.36 p 0.04 for male and female). A change in SP was associated with a corresponding changement in SKM in paired samples (ρ -0.32 , $p=0.006$). SP > 50% was associated with poorer survival across datasets (training: OS 5 vs 25.8 months, $p < 0.0001$; mCRPC: 8.9 vs 21.9 months, $p < 0.0001$; TRACERx baseline: DFS 10.7 vs 20.2 months, $p = 0.007$; OS 25 vs 48 months, $p < 0.001$; TRACERx recurrence: OS 44 vs 30.5, $p = 0.043$). Transcriptomic analyses in both training and mCRPC cohorts showed convergent upregulation of inflammatory pathways and suppression of muscle-related programs in patients with high SP. Across all cohorts, amongst others, plasma IGFBP1, IGFBP2, and IL6 were consistently higher in sarcopenic patients. Functional assays showed that IGFBP1/2 (1µg/mL) markedly impaired human myoblast differentiation (reduced fusion index and decreased MHC/β-actin expression)
Conclusions: Plasma proteomics offers a scalable, imaging-free diagnostic for sarcopenia and identifies IGFBP1/2 as actionable drivers of cancer-associated muscle dysfunction

#7678 Ultra-low-abundance cancer biomarker discovery: Multiplexed protein profiling with attomolar sensitivity.

Malcolm MacKenzie[1], Ilya Alexandrov[2], Matthew Preimesberger[2]

[1]ActivSignal, Natick, MA,[2]ActivSignal, NATICK, MA

Introduction: There is a great potential for utilizing ultra-low-abundance biomarkers in numerous applications across oncology research. These biomarkers, including many cancer-related signaling proteins and their post-translationally modified (PTM) isoforms, may provide key biological indicators, yet remain technically challenging to measure, particularly in multiplex. The leading discovery platforms available in the market lack the necessary sensitivity to reliably detect sub-fM biomarkers, and, therefore, do not include PTM isoforms in their panels. Based on published third-party assessments, 1,000+ plex platforms can return non-detects on over half of the targets in their panels for a given sample, due to insufficient sensitivity. **Methods and Results:** We have developed and validated a multiplex protein profiling technology, BlueSCAI™ (Background Lowering using Serial-Capture, Adapter-Insertion), which can increase technical sensitivity down to the attomolar level. BlueSCAI is a proximity-based platform with a capture-release-recapture mechanism. We conducted a head-to-head comparison with an industry leading proximity profiling platform, encompassing an overlap of 21 randomly selected biomarkers, for which there were i. published LODs available for other commercial platform; and ii. the required reagents, and iii. the target antigens, were readily available from vetted vendors**.** Across numerous protein targets, BlueSCAI demonstrated limits of detection that are several logs lower than those of high plex protein platforms, representing a substantial improvement in analytical sensitivity. In addition, in comparisons with commercial ELISA assays, using the same antibody pairs, BlueSCAI demonstrated LODs almost 1,000 fold lower for multiple biomarkers. For example, BlueSCAI's integrated CA19-9 biomarker has an improved sensitivity of ~ 3 logs compared to CA19-9 measured using a leading clinical lab platform (<0.0001 U/mL vs 0.6 U/mL). Analysis of dose-response curves indicated that almost half of the target panel exhibited 4+ logs of linear dynamic range, with an equal fraction showing maximal signal above background of greater than 10,000. Cross-reactivity (1-signal specificity) was measured with a leave-out mixed antigen pool approach. Signal specificities exceeded 99.9% across ¾ of the target panel, and over 98% specific on the remaining 25% of targets.**Conclusion:** BlueSCAI's specific, high sensitivity, multiplex detection shows great promise for profiling new oncology-related, biologically informative, ultra-low-abundance biomarkers, which includes cancer signaling proteins, PTM isoforms, and extracellular vesicle cargo, across diverse cancer research applications.

#7679 Advanced proteomic profiling of patient-derived tumor models reveals high cross-model concordance and improved translational fidelity.

Jia Xue[1], Hengyuan Liu[1], Xiaobo Chen[2], Sheng Guo[1]

[1]Crown Bioscience, Inc., Suzhou, China,[2]Crown Bioscience, Inc., Beijing, China

Introduction: High-throughput proteomic profiling of preclinical tumor models is increasingly critical in oncology studies and translational research for anti-cancer drug development. However, the murine stromal compartment in patient-derived xenografts (PDXs) confounds accurate proteomic quantification, as previously demonstrated. For instance, 30% of PDX tumor samples contain over 25% mouse stromal cells, which causes false results in downstream proteomic analysis.
Methods: To overcome this issue, we developed an optimized "separate-then-run" methodology that effectively separates human and mouse cells before proteomics profiling by mass spectrometry, thus enabling the acquisition of precise human tumor proteomic signatures from PDX samples. For organoid models, no mouse cell removal was performed before the mass spectrometry experiment.
Results: Using an optimized data-analysis pipeline, we profiled 418 PDX models and 89 organoids, including 59 patient-derived organoid (PDO) and 30 PDX-derived organoid (PDXO) models, quantifying a median of 9,916 human proteins per sample (range: 8,514-11,206) with high reproducibility after batch correction and normalization (Pearson correlation coefficient range: 0.93-0.98). To evaluate cross-platform fidelity, we also start to perform proteomic profiling of paired *in vivo* and *in vitro* tumor models; preliminary results show high consistency of proteome expression between paired models. For example, Pearson correlation coefficients are 0.93-0.96 for 3 PDO-PDOX pairs and 0.91-0.96 for 7 PDX-PDXO pairs; both are much higher than inter-model correlation within PDO, PDOX, PDX, and PDXO (Wilcox test p-value < 0.01). Further ongoing studies will provide more evidence on within/between tumor model proteome similarity.
Conclusions: In summary, we have established an advanced proteomic profiling platform that significantly enhances protein detection coverage in preclinical tumor models over conventional methods and validates the high concordance of protein expression between paired *in vitro* and *in vivo* tumor models.

#7680 Pre-diagnostic plasma proteomic signatures associated with early-onset colorectal cancer in two large prospective cohorts.

Mengyao Shi[1], Xiaoyu Zong[1], Ruiyi Tian[2], Daniel Hong[3], Xinyuan (Cindy) Zhang[4], Yichen Sun[1], A. Heather Eliassen[5], Edward L. Giovannucci[6], Gong Yang[7], Andrew T. Chan[8], Wei Zheng[7], Yin Cao[9]

[1]Washington University School of Medicine, St. Louis, MO,[2]Washington University In St. Louis, St. Louis, MO,[3]Washington University School of Medicine in St. Louis,[4]Brigham and Women's Hospital and Harvard Medical School, Boston, MA,[5]Assistant Professor, Harvard University, Boston, MA,[6]Professor of Nutrition & Epidem., Harvard TH Chan School of Public Health, Boston, MA,[7]Vanderbilt University Medical Center, Nashville, TN,[8]Massachusetts General Hospital, Boston, MA,[9]Washington University in St. Louis, St Louis, MO

Objective: Early-onset colorectal cancer (EOCRC) has been rising globally, yet its molecular pathways and mechanisms have not been fully explored. Large-scale proteomic studies suggest circulating proteins can illuminate key biological pathways and early markers of carcinogenesis, but robust evidence on pre-diagnostic protein biomarkers specific to EOCRC is still scarce.
Design: We measured 3,072 pre-diagnostic plasma proteins using the Olink Explore platform in EOCRC (<age 55 at diagnosis) cases and matched controls, in two prospective studies, the Nurses' Health Study II (NHSII, 1989-2015; 43 pairs; 98.8% White) and Southern Community Cohort Study (SCCS, 2002-2015; 109 pairs; 78.9% Black), as well as 59 pairs of advanced adenoma (<age 50) in NHSII. Controls were matched on age and year at blood draw, sex, and race. Cohort-specific multivariable logistic regression models were used to estimate odds ratios (ORs) and 95% confidence intervals (CIs) per standard deviation (SD) increase by protein. Inverse variance-weighted fixed-effect meta-analyses estimated pooled ORs. We additionally generated plasma protein-based estimates of organ-specific biological aging to assess differences in accelerated aging between cases and controls.
Results: The mean (SD) age at blood draw was 43.7 (4.7) years in NHSII and 45.5 (3.6) years in SCCS. Meta-analysis identified 13 proteins associated with EOCRC that met replication criteria (consistent effect direction, $I^2 \leq 40\%$, FDR < 0.25). Top replicated proteins implicate immune regulation (IL7 [OR per SD increase: 1.67; 95% CI 1.25-2.25; ANK2 [1.35; 1.02-1.80]; PTX3 [1.33; 1.03-1.72]), cellular structural pathways (PRSS53 [1.31; 1.00-1.71]; FSTL1 [0.67; 0.50-0.92]; MMP13 [0.75; 0.56-0.99]), and metabolic pathways (GHRL [1.33; 1.02-1.74]; GIPR [0.73; 0.55-0.96]). Cohort-specific analyses revealed additional distinct protein associations. In NHSII, TLR4, VEGFA, PGLYRP2, PXDNL, KRT17, and HRC were associated with EOCRC risk, implicating disrupted host-microbiome interactions, angiogenic signaling and altered epithelial biology as potential pathways. Some associations (KRT17 and HRC) were also observed in advanced adenoma compared with controls, highlighting their potential roles in initiation of precancerous changes. In SCCS, proteins positively associated with EOCRC risk suggested alterations in matrix and cytoskeletal remodeling (AFAP1, CORO6, ARAF) and immune activation (WAS). Organ-specific aging analyses suggested higher accelerated aging levels in EOCRC cases for multiple organs, including brain, the immune system, and intestine.
Conclusion: In this prospective, multi-cohort proteomic profiling study, we identified pre-diagnostic circulating proteins associated with EOCRC risk, highlighting immune and inflammatory signaling, and metabolic dysregulation as key biological pathways.

#7681 Chemical proteomics identifies a transcription-related network of proteins that interact with the next-generation poly(ADP-ribose) polymerase inhibitor saruparib.

Rachael H. Martin[1], Lindsey Nguy[2], Thales Da Costa Nepomuceno[2], Ou Deng[2], John M. Koomen[2], Uwe Rix[2], Alvaro N. Monteiro[2]

[1]Moffitt Cancer Center/University of South Florida, Tampa, FL,[2]Moffitt Cancer Center, Tampa, FL

Introduction: Ovarian cancer is one of the leading causes of gynecological-related mortality rates, often due to late-stage diagnosis. Poly(ADP-ribose) polymerase 1 inhibitors (PARPi) have been FDA approved for treatment in ovarian, breast, pancreatic, and prostate cancers. PARPi's lead to synthetic lethality in cells deficient in homologous recombination repair. Although PARPi's are a promising cancer therapeutic, drug resistance as well as side effects like hematological toxicity remain unmet clinical challenges.

Methods: In this study we utilized *PARP1*-proficient and generated CRISPR *PARP1*-deficient isogenic HEYA8 and HAP1 cell lines to perform chemical proteomics using derivatized Olaparib and a next-generation PARPi, Saruparib. Proteins and protein complexes engaged with the drug were pulled down after click chemistry in cell lysates, followed by LC-MS/MS to identify new targets of Saruparib.

Results: The subsequent analysis revealed a statistically significant set (p-value ≤ 0.03) of 247 unique proteins that were ≥2-fold enriched when compared to the unmodified PARPi competition. Within those 247 proteins, we compared the different conditions in both cell lines to identify proteins that interacted with Saruparib as well as its canonical target, PARP1. 182 were found exclusively in the Saruparib pulldown, 192 were found only in PARP1-proficient conditions regardless of drug, and 159 were found in both the Saruparib pulldown and PARP1-proficient conditions. Several proteins associated with the TFIID complex, composed of pre-initiation transcription factors, were shown to be enriched only in the Saruparib pulldown regardless of PARP1-proficiency, indicating a potential deregulation of the transcriptional machinery. However, one protein of the TFIID complex, BRD2, was shown to have enrichment dependent on PARP1-proficiency, indicating both potential drug and PARP specificity. BRD2 is a member of the BET family of proteins, which plays a role in transcriptional regulation and gene expression. We further validated the interaction between endogenous BRD2 and PARP1 through co-immunoprecipitation experiments with HEK293T whole cell lysates.

Conclusions: Our findings have uncovered a novel landscape of transcription-related proteins, including BRD2, that might provide targets for combination therapy with the PARPi Saruparib.

#7682 Integrative Blood Proteomics Reveals the HuBP Atlas of over 10,000 Proteins Informing Human Physiology and Disease..

Zhenyu Sun, Tung-Shing M. Lih, Yuanyu Huang, Yingwei Hu, Yuefan Wang, Hui Zhang

Department of Pathology, Johns Hopkins University School of Medicine, Baltimore, MD

Blood provides a rich and accessible source of clinical information, yet no centralized resource systematically documents which proteins are detectable across blood sample types, analytical workflows, and disease states. To address these needs, we developed the Human Blood Proteome (HuBP) database that links protein detectability, abundance, and reproducibility across analytical workflows, sample types, and disease contexts.Using data-independent acquisition, we profiled healthy plasma with complementary workflows, including direct analysis, high-abundance protein depletion, low-abundance protein enrichment, and extracellular vesicle enrichment and identified 9,965 proteins in total. HuBP enables users to query protein detectability across methods and provides standardized performance metrics and detailed standard operating procedures (SOPs) to support reproducibility and cross-laboratory implementation.To characterize disease-associated alterations, we further analyzed 140 pancreatic ductal adenocarcinoma (PDAC), 111 clear cell renal cell carcinoma (ccRCC), and 82 lung adenocarcinoma (LUAD) whole-blood samples, identifying 8,002, 8,006, and 8,009 proteins, respectively. Across these cancers, 8,021 proteins were detected, including 498 proteins absent in healthy controls, highlighting disease-specific blood proteomic signatures.In total, HuBP assembles 10,463 nonredundant blood proteins, representing the most comprehensive blood proteome resource to date. By providing an integrated and quantitative atlas across workflows, sample types, and disease contexts, HuBP offers a valuable platform for optimizing experimental designs in both large-scale blood proteomics studies and targeted analyses of disease-specific proteins, ultimately supporting the discovery of non-invasive biomarkers and the advancement of precision medicine.

#7683 A proteomic analysis of differential protein expression between platinum-sensitive and platinum-resistant high grade serous ovarian cancer.

Nujsaubnusi Cassandra Vue[1], Kyla Frenia[2], Xi Peng[3], Eirwen Miller[1], John Nakayama[1], Sharon Liang[1], Sarah Crafton[1], Alyssa Wield[1], Christopher Morse[1], Thomas Krivak[1], Qiangmin Zheng[3], Kunhong Xiao[3]

[1]Western Pennsylvania Hospital, Pittsburgh, PA,[2]University of Pittsburgh, Pittsburgh, PA,[3]Allegheny Health Network, Pittsburgh, PA

Introduction: Ovarian cancer is the most lethal gynecologic malignancy. Platinum-based therapy is the mainstay of treatment, with 70% chance of treatment sensitivity. Resistance to platinum therapy is the leading cause of mortality in advanced ovarian cancer. There are limited studies using proteomics to evaluate platinum resistance in ovarian cancer. This study aims to perform proteomic evaluation of treatment naive tissue from high grade serous ovarian cancer (HGSOC) tumors that are platinum-sensitive (PS) versus resistant (PR).
Methods: Formalin-fixed paraffin-embedded (FFPE) tumor tissue collected from 63 patients with HGSOC were analyzed, including 40 PS & 23 PR. Platinum sensitivity was defined as disease response without evidence of recurrence after 6 months of treatment. Samples were analyzed using a high-throughput liquid chromatography-tandem mass spectrometry (LC-MS/MS) protocol. Differential expression (DE) analysis was performed to identify proteins distinguishing between the two groups. Unsupervised machine learning techniques such as least absolute shrinkage and selection operator (LASSO) regression analysis, linear discriminant analysis (LDA), and weighted gene co-expression network analysis (WCGNA) were employed to create a differentially expressed protein profile between PS and PR.
Results: Among 4048 proteins identified, 1,604 met quality thresholds for further analysis, appearing in >50% of samples. Thirty-seven proteins were significantly differentially expressed with four upregulated in PS and 33 upregulated in PR. With LASSO regression analysis, an additional 61 DE proteins were identified. LDA revealed 7 proteins (DPM1, INF2, ISYNA1, RBM12B, ATP5F1C, GNL1, UBA7) to have a predictive potential with 85% sensitivity and 100% specificity. Functional enrichment analysis implicated pathways related to RNA binding, epigenetic regulation, spliceosome activity, glutathione metabolism, and metabolic reprogramming in platinum sensitivity.
Conclusion: With the combination of traditional statistics and unsupervised machine learning, this study generated a list of DE proteins and facilitated a 7-protein panel that can be used to further investigate and understand the complex tumor dynamics behind platinum sensitivity and resistance.

#7684 Absolute quantification of 400 plasma proteins using a novel NGS-based immunoassay: Analytical validation and biomarker discovery in breast cancer.

David Aaron Routenberg[1], Evan A. Gizzie[1], Annamaria Szabolics[1], Lucie Hebert[1], Somnath Paul[2], Anthony Williams[2], Richard J. Cote[2], Jacob N. Wohlstadter[1]

[1]Meso Scale Diagnostics, LLC, Gaithersburg, MD,[2]Washington University in St. Louis School of Medicine, St. Louis, MO

Next generation sequencing (NGS)-based immunoassays have enabled multiplex, sensitive, wide dynamic range protein measurements, but existing platforms lack absolute quantitation and a clear path for translating proteomic hits into focused assay panels on platforms suitable for down-stream studies. We introduce a novel high multiplex immunoassay platform from ProteinXI, a division of Meso Scale Diagnostics, LLC. (MSD), with accurate and reproducible absolute quantification, and demonstrate simultaneous measurement of hundreds of targets in human biofluids. We also show strong concordance with analogous assays on MSD's high-throughput electrochemiluminescence (ECL) platform, providing an efficient route to focused validation panels. The ProteinXI Discovery 400 panel was evaluated for analytical sensitivity, precision, reproducibility and dilution linearity using a set of 40 commercially sourced plasma samples from healthy donors. Concordance with well-established commercial immunoassays was assessed for over one hundred analytes by measuring the same sample set using MSD V-PLEX or U-PLEX assays. To assess translational relevance, we measured plasma samples from a cohort of 387 subjects with breast cancer of varying stages and molecular subtypes monitored during neoadjuvant therapy (NAT). Samples were collected at baseline (pre-treatment), on day 1 of the second therapy cycle (C2D1), and prior to surgery. Tumor and lymph node biopsies were obtained before and after NAT, and treatment response was evaluated using the MD Anderson Residual Cancer Burden (RCB) score. The platform showed high dynamic range, with 90% of assays spanning at least 4 logs between lower limit of detection (LLOD) and upper limit of quantitation (ULOQ). Analytical sensitivity exceeded 1 fg/mL for some assays, with a median LLOD of 0.48 pg/mL. Most (80%) analytes were within the quantifiable range in at least 75% of healthy plasma samples. Dilution linearity was between 70% and 130% for 85% of quantifiable analytes. Median intraplate CVs of calculated concentrations across all quantifiable samples and analytes was 6.8% (IQR=3.1%-13.3%). Median Interplate and inter-run CVs of calculated concentrations were 10.3 and 11.7% respectively. Concordance with U-PLEX and V-PLEX immunoassays was high with Pearson correlations >0.8 for 84% of assays. In breast cancer samples, classical markers CA15-3, CEA, CA125 and Cytokeratin 8 were elevated relative to healthy controls and correlated with tumor stage, as did VEGF-A, VCAM-1, MMP-7 and Osteopontin. High baseline Ki67 and Leptin levels were associated with lower RCB score. PDGF-AA and PDGF-AB both decreased with NAT, while BAFF and GDF-15 increased. These results demonstrate the ProteinXI platform's robust analytical performance and ability to reproduce expected biological patterns, supporting its translational utility.

#7685 Absolute quantification of aqueous humor proteins for prognostic stratification in uveal melanoma.

Donny Liang[1], Elaine Huang[1], Yilin Chen[2], Chen-Ching (Patrick) Peng[3], Jesse Berry[3], Liya Xu[3]

[1]USC - University of Southern California, Los Angeles, CA,[2]Children's Hospital Los Angeles,[3]Children's Hospital Los Angeles, Los Angeles, CA

Background: Uveal melanoma (UM) is the most common primary intraocular malignancy in adults and carries a high risk of metastatic progression, particularly in tumors with high-risk gene expression profiles or advanced clinical stage. Direct tumor biopsy provides valuable prognostic information but carries procedural risk, highlighting the need for minimally invasive approaches to capture tumor-derived biomarkers. Aqueous humor (AH) contains detectable molecular material released by intraocular tumors, yet absolute quantification of protein biomarkers has not previously been performed. This study aims to establish the first calibrated AH proteome map for UM and to identify protein biomarkers associated with molecular classification and disease stage.
Methods: AH samples from 70 UM eyes were collected before plaque brachytherapy. Fine needle tumor aspiration provided gene expression profiling (GEP1, GEP2) and PRAME status. All samples underwent NGS based high-plex proximity extension assay (PEA), and 27 samples with remaining volume underwent qPCR-based PEA targeting 92 proteins. Regression models derived from 66 overlapping proteins enabled extrapolation of absolute pg/mL concentrations across the full cohort. Proteins with median concentrations >5 pg/mL were assessed for differences by GEP class, PRAME status, and AJCC stage. Pathway enrichment and upstream regulators were identified using Ingenuity Pathway Analysis.
Results: Twenty-three proteins were present at clinically quantifiable concentrations. The lowest protein levels were observed in GEP1/PRAME- tumors, with progressive increases seen across advanced AJCC stages. Significant elevations were noted in Stage IV disease for CXCL8 ($p=0.00024$), IL10 ($p=0.00049$), and PDCD1 ($p=0.00094$). Pathway analysis demonstrated enrichment in immune and tumor-associated signaling pathways. VEGFA ($z=3.1$) and CCL2 ($z=1.7$) were identified as predicted upstream regulators and were elevated in advanced-stage tumors.
Conclusions: This study provides the first absolute quantitative map of AH proteins in UM and identifies a panel of 23 clinically detectable biomarkers associated with tumor biology, molecular classification, and stage. These findings position AH proteomics as a minimally invasive liquid biopsy platform capable of capturing stage-linked immune activity in UM and supporting the development of standardized biomarkers for prognostic stratification.

#7686 Identification of a first-in-class therapeutic target using machine learning enabled translational-optimized proteomics system (TPS).

Catherine Wong[1], Ning Li[2], Shuaixin Gao[1], Nan Zhang[1], Jiming Yin[2], Yonghong Zhang[2]

[1]Foreseen Biotechnology (Beijing) Co., Ltd., Beijing, China,[2]Beijing You-An Hospital, Capital Medical University, Beijing, China

Background:
At Foreseen, we built a translational-optimized proteomics system (TPS) and assembled a vast collection of well-characterized human clinical samples. Our platform can extract actionable insights from complex proteomics and clinical datasets to accelerate the discovery of clinically relevant targets for drug discovery and for diagnostic applications.
Methods:
Chronic hepatitis B (CHB) infection may lead to progressive liver diseases including fibrosis, cirrhosis, and ultimately hepatocellular carcinoma (HCC). An optimized plasma proteomics analysis using parallel accumulation-serial fragmentation combined with data-independent acquisition (DIA-PASEF) on a large liver cohort was performed. This cohort (N=340) consists of healthy individuals (n = 48), patients with either CHB (n = 39), liver fibrosis (n = 47), liver cirrhosis (LC, n = 56), and HCC (4 subgroups based on TNM staging system: HCC1-4; n = 36, 38, 39, and 37). Highly abundant proteins were removed from plasma prior to proteomic preparation. Samples were processed and analyzed using DIA-MS for high-throughput protein quantification. Our TPS can identify potential biomarkers and stage-specific molecular drivers associated with liver disease and liver cancer progression. Expression analysis using tissue microarrays (TMA), followed by validation through in vitro (cell lines) and in vivo (cell-derived xenograft models) studies were conducted on selected candidate targets.
Results:
Integrin alpha-2 (ITGA2) was among the seven tumor-associated antigens (TAAs) identified in hepatocellular carcinoma (HCC) we selected as final drug candidates after screening. It is a cell surface membrane receptor and may function as a regulatory factor in cancer, responsible for driving tumorigenesis, inducing chemoresistance, regulating genomic instability and remodeling the tumor microenvironment. In this study we demonstrated that the protein expression of ITGA2 is low in patients' groups of CHB, fibrosis and cirrhosis, but significantly upregulated in HCC. Furthermore, ITGA2 is overexpressed in multiple solid tumors, including pancreatic, gastric, and colorectal cancers using TMA analyses. We discovered and developed an antibody targeting ITGA2 with nM binding affinity and good internalization properties. We advanced FS001(IPN60300) into the final stages of preclinical development. This a first-in-class antibody drug conjugate comprised of (i) Foreseen's proprietary antibody targeting ITGA2 and (ii) linker-payload with excellent pharmaceutical features developed by Shanghai Escugen Biotechnology. Foreseen has granted an exclusive worldwide license of FS001(IPN60300) to Ipsen in July 2024.
Conclusion:
Our translational-optimized proteomics system (TPS) has led to the discovery of ITGA2, a novel tumor-associated antigen (TAA) and enabled the development of FS001(IPN60300).

#7688 Blood-based proteomic profiling reveals novel biomarkers of neuroendocrine prostate cancer.

Tatiana Erazo[1], Ethan S. Barnett[1], Amanda Weaver[2], A. Zara Herskovits[1], Alisa Valentino[1], Howard I. Scher[1], Gary A. Pestano[2]

[1]Memorial Sloan Kettering Cancer Center, New York, NY,[2]Biodesix, Inc., Broomfield, CO

Neuroendocrine prostate cancer (NEPC) is an aggressive, AR-indifferent subtype of metastatic prostate cancer, with a median survival of 7-15 months. Trans-differentiation from prostate adenocarcinoma to NEPC occurs through a mechanism termed lineage plasticity. Diagnosing NEPC remains a major clinical challenge due to the lack of robust biomarkers and pronounced spatial and temporal heterogeneity. There is an urgent need for diagnostic biomarkers of NEPC before clinical manifestation. To characterize the proteomic landscape of NEPC, we first performed a bottom-up proteomic analysis using LC-MS/MS in NEPC (H660) and adenocarcinoma (VCaP) cell lines. An average of 10,230 proteins were identified in both cell lines, with over 1,300 proteins significantly enriched in NEPC compared to VCaP. NCAM1, a clinical marker of NEPC, was among the significantly enriched proteins (*adjusted p*=0.004; Log2FC=6.5), supporting the biological significance of our findings. Pathway analysis revealed enrichment in E2F, EMT, and p53 signaling pathways, consistent with established mechanisms of lineage plasticity. Next, we conducted a prospective pilot study using plasma from patients with pathologically confirmed NEPC or concurrent *RB1/TP53* loss (n=21) and from patients with *RB1/TP53wt* prostate adenocarcinoma without evidence of histological transformation (n=20). To enhance the detection of low-abundance proteins, we applied sequential enrichment and elution (SEER) followed by Proteograph XT digestion and high-resolution mass spectrometry. Putative proteoforms were identified using data-independent acquisition-neural network (DIA-NN) processing. A total of 6,619 proteins were identified in both cohorts, 93 of which were significantly enriched in the NEPC samples, including NCAM1, validating the approach in plasma. In addition, potential new markers were detected such as methionine adenosyltransferase 2A (MAT2A) (*adjusted p*=2.59E-09; Log2FC=2.8), a critical metabolic driver of androgen-independent cellular state. Neuronal-specific enolase (NSE/ENO2), a glycolytic enzyme associated with poor prognosis and tumor dedifferentiation in prostate cancer, was exclusively expressed in H660 cells and NEPC patient samples. Pathway analysis revealed co-enrichment of neuroendocrine and mitotic germ cell-associated programs, reflecting extensive phenotypic reprogramming that enhances metastatic capacity during lineage plasticity. These findings demonstrate the utility of blood proteomic profiling for the discovery of prognostic and predictive NEPC biomarkers. These markers may help elucidate molecular mechanisms underlying lineage plasticity. Furthermore, high-resolution plasma proteomics offers a promising approach to overcome the limitations of tissue biopsy, which is often restricted by high intra-tumoral heterogeneity and the lack of specificity of current pathological markers.

#7689 Absolute quantification by targeted proteomics identifies BRCA1 hypomorphs and other PARP inhibitor resistance mechanisms in patient-derived xenografts.

Beom-Jun Kim[1], Alba Llop-Guevara[2], Steve M. Sweet[1], Camille Lombard-Banek[1], Robert Hanson[3], Chris Richardson[1], Violeta Serra[2], Elizabeth A. Harrington[3], Josep Forment[3], Yeoun Jin Kim[1]

[1]Cancer Biomarker Development, AstraZeneca, Gaithersburg, MD,[2]Translational Medicine, AstraZeneca, Barcelona, Spain,[3]Translational Medicine, AstraZeneca, Cambridge, United Kingdom

Introduction: BRCA1 is a tumor suppressor required for homologous recombination repair (HRR) of DNA double-strand breaks. BRCA1 loss-of-function mutations cause HRR deficiency and sensitize tumors to platinum-based chemotherapy and PARP inhibitors (PARPi). Standard gene-level testing may miss other mechanisms affecting BRCA1 protein functionality, such as BRCA1 promoter methylation, or other PARPi response molecular determinants, such as hypomorphic protein expression that partially restores HRR, leading to PARPi resistance. Current standard assays suitable for formalin-fixed paraffin-embedded (FFPE) tissue, such as immunohistochemistry, are limited in their ability to characterize BRCA1 protein levels - highlighting the need for new approaches for protein-level quantification.
Methods: Targeted proteomics was performed on an Orbitrap Exploris 480 mass spectrometer coupled to an Evosep One nanoLC to quantify BRCA1 peptides spanning the N-terminal RING domain, Exon 11 and C-terminal BRCT domain, enabling BRCA1 hypomorph detection based on domain-specific peptide abundance. The targeted panel assay also included additional DNA repair proteins. This assay was applied to 56 FFPE tumors from 26 patient-derived xenografts (PDX), including 7 samples collected at acquired olaparib resistance.
Results: PDX tumours from BRCA1 wild-type, BRCA2-mutant, or PALB2-mutant models (n=10), had a median BRCA1 peptide expression level of 45.8 amol/µg (range 20.7-120.9), consistent with a normal-expression reference range. In contrast, PDX tumors with BRCA1 promoter hypermethylation (n=4) exhibited low BRCA1 peptide levels (< 1.8 amol/µg). At acquired olaparib resistance, tumours from the same models showed a ~25-fold BRCA1 protein increase, consistent with demethylation and restored BRCA1 expression. Among BRCA1-mutant PDX models (n=15), most models exhibited low expression, consistent with loss-of-function mutations (n=8 with < 5 amol/µg). Targeted proteomics further identified seven candidate BRCA1-mutant PDX hypomorphic cases in which at least one BRCA1 domain peptide exceeded the ~5 amol/µg threshold; their BRCA1 peptide levels ranged from 6.2 to 31.7 amol/µg. Six out of seven hypomorph cases (86%) were PARPi resistant. Low 53BP1 expression was observed in four PARPi-resistant PDX models; three of these had known 53BP1 dysregulation or mutation. However, one model showed low 53BP1 despite the absence of a known TP53BP1 mutation, implicating 53BP1 loss as a plausible contributor to resistance.
Conclusion: These data support this targeted proteomic assay as a practical approach to distinguish normal from low BRCA1 expression at the protein level, nominate hypomorphic BRCA1 variants linked to PARPi resistance, and identify deficiency in additional resistance biomarkers.

#7690 Extracellular kinome network reveals secretory kinase FAM20C as a key driver of recurrence in oral squamous cell carcinoma.

Mi Rim Lee[1], Yu-Sun Lee[1], Sumin Kang[1], Jiyoung Lee[1], Hye Won Shon[1], Sun Il Choi[1], Gyeongmin Kang[1], Kyung-Hee Kim[2], Jong-Ho Lee[3], Ik-Jae Kwon[4], Sung Woen Choi[3], Yun-Hee Kim[1]

[1]Research Institute of National Cancer Center, Goyang-si, Gyeonggi-do, Korea, Republic of,[2]Kookmin University, Seoul, Korea, Republic of,[3]National Cancer Center, Goyang-si, Gyeonggi-do, Korea, Republic of,[4]Seoul National University Dental Hospital, Seoul, Korea, Republic of

Oral squamous cell carcinoma (OSCC) is a highly aggressive malignancy with a recurrence rate of 40-60%, frequently exhibiting locoregional relapse and lymph node metastasis even after definitive treatment. Tumor progression and recurrence are driven not only by intrinsic characteristics of cancer cells but also by complex interactions with the surrounding tumor microenvironment (TME). To explore recurrence-associated regulatory pathways, we performed LC-MS/MS-based phosphoproteomic profiling of plasma from 34 OSCC patients and identified 113 phosphoproteins harboring 261 phosphosites enriched in lipid binding, complement activation, extracellular matrix (ECM) organization, and calcium-binding functions. Principal component and correlation analyses distinguished patients with recurrence from those without, and consensus clustering revealed three phospho-secretory subtypes. Notably, the subtype with the poor prognosis exhibited a enrichment of phospho-serine within the S-x-E motif. This pattern suggested activation of the secreted serine kinase FAM20C, which phosphorylates ER/Golgi-localized secretory proteins and membrane ectodomain substrates. Public datasets confirmed that high FAM20C expression correlates with increased recurrence risk and reduced overall and progression-free survival. To validate these findings, we examined patient-derived organoids (PDOs) and cancer-associated fibroblasts (CAFs) established from our cohort. Both FAM20C expression and secretion were markedly elevated in PDOs derived from recurrent tumors, and CAFs from recurrent patients also exhibited increased FAM20C secretion. Functionally, FAM20C overexpression enhanced invasion, ECM remodeling, and EMT activation, while FAM20C knockdown suppressed mesenchymal markers, reduced TGF-β-SMAD2/3 signaling, and suppressed stemness-associated genes including SOX2, OCT4, CD44, NANOG, MYC, and CD133. Together, these findings identify FAM20C as a key regulator of recurrence-associated extracellular signaling and highlight its potential as a prognostic biomarker for recurrence in OSCC.

#7691 A magnetic bead-based workflow for streamlined and quantitative mass spectrometry sample preparation in cancer proteomics.

Mike Rosenblatt[1], Zhiyang Zeng[2], Atul Deshpande[3], Marjeta Urh[4], **Wenhui Zhou**[5]

[1]Research & Development, Promega Corporation, Fitchburg, WI,[2]Research and Development, Promega Corporation, San Luis Obispo, CA,[3]Marketing, Promega Corporation, Fitchburg, WI,[4]Research and Development, Promega Corporation, Fitchburg, WI,[5]Research and Development, Promega, San Luis Obispo, CA

Background: Efficient and reproducible sample preparation is essential for robust mass spectrometry (MS)-based proteomics, particularly in oncology applications where input materials can be limited. We developed a Magnetic Particle-based Sample Preparation (MPSP) platform leveraging magnetic bead-based protein capture from diverse lysis conditions, enabling integration with automated workflows and downstream proteomic analysis.

Methods: Human K562 cells and other cancer cell lines were lysed using various buffers. Proteins were captured via magnetic beads and organic solvent-induced precipitation, followed by on-bead digestion with optimized protease combinations (e.g., trypsin, Lys-C, Arg-C). Peptide recovery and digestion efficiency were benchmarked against precipitation and filter-based methods. The workflow was automated using an Agilent AssayMAP Bravo system, and performance was assessed using LC-MS/MS, SDS-PAGE, and high-pH reversed-phase HPLC fractionation. Application-specific adaptations included quantitative PROTAC analysis and phospho/enrichment strategies.

Results: MPSP enabled efficient surfactant removal with minimal protein loss, achieving higher protein identifications (5,794 proteins) than precipitation (5,413) or filter-based (5,567) methods. The approach was compatible across bead surface chemistries and cell lines (HEK, HeLa, K562) and demonstrated scalability to low-input samples (<10,000 cells). Digestion optimization via Design of Experiments (DOE) established ideal parameters: 1:16 enzyme-to-substrate ratio, 16-hour digestion at 40°C, yielding improved peptide recovery (94% digestion efficiency). MPSP reduced sample prep time by ≥1 day and supported quantitative accuracy in PROTAC screens, enabling BRD4 ubiquitination detection and enhanced peptide enrichment using K-ε-GG, pY antibodies, and IMAC/TiO_2. Automated exosome processing using MPSP identified 697 proteins versus 256 by manual methods, with a 2,861-protein overlap.

Conclusions: MPSP offers a scalable, automation-compatible solution for cancer proteomics sample preparation. It supports robust quantitation, high sensitivity, and reproducibility across diverse sample types and workflows. This platform is positioned to enhance throughput and analytical depth in translational and discovery oncology research.

#7692 Proteomic analysis of immune synapses by high-precision microscopy-guided photo-biotinylation.

Jung-Chi Liao, Chantal Hoi Yin Cheung, Weng-Man Chong, Harry Huang, Hsiao-Jen Chang, Chia-Wen Chung

Syncell Inc., Taipei City, Taiwan

An immune synapse (IS) is essential for lymphocyte recognition and cytotoxic response against tumor cells. Although numerous proteins involved in IS formation, stability, and signaling pathways have been characterized, the complete proteomic composition of the synapse remains unknown. A significant challenge involves the purification of proteins at a nanoscale organization with adequate specificity and sensitivity. In this context, we employed an integrated workflow using Syncell's Microscoop® Mint platform, an advanced technology integrating microscopy-guided automated photo-biotinylation, pulldown, and mass spectrometry to isolate and identify proteins localized between T-lymphocytes (Jurkat) and B cells (Raji B). IS formation between T-B cells was recognized using a convolutional neural network-based deep learning algorithm based on CD3 (T-lymphocyte surface marker) signal at the T-B cell synapses. Automated photo-induced biotinylation was performed across thousands of fields of view so that sufficient proteins were biotinylated for the subsequent pulldown and LC-MS/MS-based proteome identification. We precisely identified canonical proteins linked to critical components of T-cell receptor (TCR) signaling pathways, including the TCR/CD3 complex, Src and Tec family tyrosine kinases, and essential NF-kB signaling molecules, thereby validating the specificity of our spatial proteomics methodology. Furthermore, we observed enrichment of proteins not previously associated with the T-B cell immune generating testable hypotheses for advancing the functional dissection of the immunological synapse. Microscoop couples optics and proteomics to enable the precise enrichment of the IS proteins at the Raji-Jurkat interface, and can be readily applied to studies of other types of ISs or ISs from patient tissue samples. Together, these data demonstrate that resolving the nanoscale proteomic architecture of the IS is essential for uncovering how lymphocytes recognize and sometimes fail to recognize tumor cells. By enabling precise, unbiased enrichment of IS proteins, this approach opens new avenues to identify immune-evasion mechanisms and novel therapeutic targets in cancer.

#7693 Unlocking the surfaceome: Nanoscale spatial proteomics for biomarker and target discovery using Synlight-Rich and Synlight-Pure.

Jung-Chi Liao[1], Po-Chao Chan[1], Weng-Man Chong[1], Hsiao-Jen Chang[2], Michelli Faria de Oliveira[3], Elate Huang[1], Daniel Dlugolenski[3]

[1]Syncell Inc., Taipei City, Taiwan,[2]Syncell Inc, Taipei City, Taiwan,[3]Syncell Inc., Livermore, CA

Cell surface proteins mediate essential signaling, trafficking, and cell-cell interactions, representing key biomarker and drug target classes. Yet, comprehensive characterization of human cells surfaceome remains challenging due to the limited spatial precision and labeling specificity of existing proteomic methods. We present an integrated workflow using Syncell's Microscoop® Mint platform in combination with Synlight-Rich and Synlight-Pure reagents to achieve nanometer-scale, unbiased surfaceome discovery with exceptionally high specificity. Synlight-Rich employs two-photon photo-biotinylation to covalently tag proteins within user-defined microscopy regions of interest (ROI) at ~350 nm lateral resolution, enabling deep proteomic interrogation of subcellular domains with high spatial control. Labeled proteins are recovered via the Synpull kit and analyzed by LC-MS/MS. Building on this, Synlight-Pure introduces antibody-mediated proximity labeling, restricting biotinylation to within ~25-50 nm of the target structure. This dual-precision approach—image-guided and chemistry-confined—enables selective, high-specificity enrichment of membrane-associated and interaction-proximal proteins. In HeLa cells, Microscoop with Synlight-Rich identified >3,500 proteins, including >1,000 known plasma-membrane proteins, with >50% showing ≥1.5-fold enrichment ($P < 0.05$) over unlabeled controls. Gene Ontology analysis revealed that ~55% of the top 200 enriched proteins localized to plasma-membrane compartments. Integration of Synlight-Pure increased membrane-specific identifications to ~70% within the same enrichment group, highlighting substantial improvement in labeling specificity and the discovery of previously uncharacterized surface components involved in receptor- and transporter-mediated signaling. By extending spatial proteomics from the micrometer to nanometer scale, Synlight-Rich and Synlight-Pure together unify unbiased discovery and targeted molecular precision within a single workflow. This platform enables comprehensive cell surfaceome mapping with unparalleled specificity, accelerating biomarker and therapeutic target identification across oncology, neurodegeneration, and immunology.

#7694 Proteomic analysis of BRAF-V600E mutant metastatic colorectal cancer FFPE tissues reveals potential involvement of WEE1 expression in therapeutic resistance.

Shotaro Yamaguchi[1], Satoshi Muraoka[2], Yosui Nojima[3], Toshiharu Hirose[1], Hidekazu Hirano[1], Natsuko Okita[1], Atsuo Takashima[1], Jun Adachi[2], Hirokazu Shoji[1], Ken Kato[4]

[1]Gastrointestinal Medical Oncology, National Cancer Center Hospital, Tokyo, Japan,[2]Laboratory of Proteomics for Drug Discovery, Center for Drug Design Research, National Institute of Biomedical Innovation, Health and Nutrition, Osaka, Japan,[3]Center for Mathematical Modeling and Data Science, The University of Osaka, Osaka, Japan,[4]Head and Neck, Esophageal Medical Oncology / Department of Gastrointestinal Medical Oncology, National Cancer Center Hospital, Tokyo, Japan

Background and Aims: Approximately 10% of metastatic colorectal cancers (mCRC) harbor the *BRAF*-V600E mutation. Although targeted therapies such as encorafenib plus cetuximab with or without binimetinib (BEACON regimen) have been developed for this subtype, clinical outcomes remain poor, and overcoming therapeutic resistance represents a critical unmet need. To elucidate the molecular mechanisms underlying this resistance, we performed a proteomic analysis using formalin-fixed paraffin-embedded (FFPE) tissues obtained from patients with *BRAF*-V600E mutant mCRC. The aim of this study was to identify proteins potentially associated with resistance to *BRAF*-targeted therapy and to explore therapeutic targets for this population.

Methods: FFPE tumor samples were collected from patients with *BRAF*-V600E mutant mCRC prior to any systemic treatment. Sections (5 μm thick) were mounted on PEN glass slides, and macro-dissected tumor areas (12-130 mm^2 per sample) were processed for protein extraction. Proteins were purified and digested using the Single-pot, solid-phase-enhanced sample preparation (SP3) protocol, followed by mass spectrometric analysis on an Orbitrap Exploris 480. Furthermore, we retrospectively analyzed clinical data from patients who received the BEACON regimen as second-line treatment for mCRC at our hospital between December 2020 and April 2024. Correlations between quantitative protein expression and clinical outcomes, including progression-free survival (PFS), were assessed using the log-rank test.

Results: A total of 15 patients were included, and protein quantification was successfully achieved in samples of 12 patients. Across these samples, 9,078 proteins were quantitatively profiled, and correlations between protein expression and PFS were examined. The median PFS (mPFS) for patients who received the BEACON regimen as second-line therapy was 6.9 months (95% CI, 2.6-11.0). Among the quantified proteins, 13 proteins showed a negative correlation with PFS (correlation coefficient [r] < -0.8), with WEE1 demonstrating the strongest correlation (r = -0.94). In contrast, no significant correlation was observed between WEE1 expression and PFS during first-line treatment (r = -0.48). When patients were stratified by WEE1 expression levels for the second-line setting, the high-WEE1 group exhibited significantly shorter PFS than the low-WEE1 group (mPFS: 3.6 months vs 10.8 months [HR, 21.88, 95% CI, 3.84-124.6]; $p = 0.0005$).

Conclusion: Our proteomic analysis identified WEE1 expression as a potential biomarker associated with poor clinical outcomes in patients with *BRAF*-V600E mutant mCRC treated with the BEACON regimen. These findings suggest a context-dependent resistance mechanism as a promising therapeutic target warranting further investigation in preclinical and clinical settings.

#7695 Blood-based proteomics analysis for uveal melanoma prognosis.

Abarajithan Chandrasekaran[1], Nikhil Nayee[2], Jerome Lacombe[1], Timothy Karr[3], Frederic Zenhausern[4], Justin Moser[5]

[1]University of Arizona College of Medicine - Phoenix, Phoenix, AZ,[2]Department of Medical Oncology, HonorHealth Research Institute, Scottsdale, AZ,[3]Biosciences Mass Spec/Proteomics Core, ASU-Banner Neurodegenerative Disease Research Center, Phoenix, AZ,[4]Center for Applied NanoBioscience and Medicine, University of Arizona College of Medicine - Phoenix, Phoenix, AZ,[5]HonorHealth Research Institute, Scottsdale, AZ

Background: Uveal melanoma (UM) is the most common intraocular tumor of the eye in adults. About 50% of cases become metastatic, indicating poorer prognosis and survivability. There is currently no well-established blood-based method to accurately predict the risk of metastasis and disease progression of UM using proteomic analysis. This study aimed to test the efficacy and utility of proteomics in the risk assessment of UM.

Methods: Proteomic analysis from serum and extracellular vesicles (EV) of 49 samples from 27 unique patients was performed to classify metastatic and non-metastatic disease. Controls were taken from 5 patients with cutaneous melanoma. Initial serum depletion was completed using the ProteoSpin Abundant Serum Protein Depletion Kit. EVs were extracted via the qEV Concentration Kit IZON system. Proteins from depleted serum and EVs were analyzed via Mass Spectrometry (MS) using a standard trypsin-based workflow. A data-dependent MS^2 method on Thermo Fisher Orbitrap Lumos generated MS data. Orbitrap MS^1 spectra was followed by MS^2 fragmentation via ion trap using collision-induced dissociation. Machine learning was used to develop a predictive proteomic signature for metastasis. Models were trained with 3052 EV and serum protein levels and 906 serum only levels. Model sensitivity and positive predictive value (PPV) were calculated using out-of-bag bootstrap sampling conducted 500 times. Candidate models for classification of disease vs controls were used to classify holdout surveillance samples from 9 unique patients. Additionally, differential abundance analysis of each sample classification used the log(2) ratio of protein abundances with a cut off >1 and <-1, indicating increased and decreased abundance, respectively. Statistical significance of abundance was set at $p<0.05$.

Results: Machine learning models revealed EVs showed higher sensitivity and PPV than serum. EV proteins with the strongest signals for disease (primary, surveillance, metastatic) vs controls include immunoglobulin (Ig) lambda variable 3-10, Ig mu heavy chain, 14-3-3 protein zeta/delta, heat shock cognate 71 kDa protein, and fibrinogen beta chain. Serum proteins include trypsin-3, mitochondrial ATP synthase complex subunit C1, type 2 cytoskeletal keratin, and polymeric Ig receptor. Dopamine beta-hydroxylase was most prominent in metastatic vs non-metastatic (primary, surveillance) in serum. Differential expression analysis of EV and serum revealed significant abundance of proteins related to metabolism, cellular organization and biogenesis, and cell proliferation in disease groups vs controls.

Conclusion: This preliminary analysis demonstrates that blood-based proteomic analysis of various UM stages can be useful in providing diagnosis or prognosis of disease course for such patients. Further work with a larger sample size and repeated sampling at different disease progression stages is warranted to advance this work.

#7696 Quantitative plasma proteomics on stellar MS enables discovery of clinically relevant cancer biomarkers.

Stephanie Samra, Qingling Li, Cristina Jacob, Philip Remes, Jared Deyarmin

Thermo Fisher Scientific, San Jose, CA

Quantitative plasma proteomics is essential for discovering circulating biomarkers that enable early cancer detection and patient stratification. However, existing assays often lack the scalability, reproducibility, and sensitivity required for large clinical studies. To overcome these limitations, we developed a high-throughput targeted proteomics workflow on the Thermo Scientific™ Stellar™ mass spectrometer, enabling rapid and precise quantification of plasma proteins. The platform's fast acquisition speed and robust retention time stability allow comprehensive analysis of hundreds of peptides within a 30-minute gradient, while MS^3 fragmentation enhances selectivity for low-abundance targets. Using the Biognosys PQ500 reference peptide kit, we quantified 804 peptides representing 322 plasma proteins, including 57 FDA-approved biomarkers, in plasma from patients with colorectal and lung cancer and healthy donors. More than 94% of peptides showed coefficients of variation below 25%, with linear responses across six orders of magnitude and limits of quantitation down to the attomole range. In colorectal cancer plasma, 29 proteins were significantly altered (adjusted $p < 0.05$, > 2-fold change) compared with controls. Notably, serum amyloid A2 (SAA2), alpha-2-glycoprotein-like (A2GL), and complement component C9 (CO9) were elevated—proteins implicated in inflammatory and immune pathways driving tumor progression. This study demonstrates that quantitative plasma proteomics on Stellar MS provides the sensitivity, reproducibility, and throughput needed to identify clinically relevant biomarker signatures in cancer. The workflow offers a robust and scalable foundation for translational proteomics and precision oncology applications, bridging the gap between discovery and clinical validation.

#7697 Machine learning-based plasma proteomic signatures for diagnosis and prognosis of cholangiocarcinoma.

Chongming Zheng[1], Yi Wang[2], Gang Chen[1]

[1]The First Affiliated Hospital of Wenzhou Medical University, Wenzhou, China,[2]Wenzhou Medical University, Wenzhou, China

Background: Cholangiocarcinoma (CCA) lacks reliable non-invasive biomarkers for early diagnosis and individualized prognostic assessment. Circulating proteomic profiling offers an opportunity to develop clinically actionable molecular signatures.Methods: A total of 320 plasma samples were collected across two centers, including patients with CCA, benign biliary disease, and healthy controls. Proteins were quantified using the Olink Explore Oncology II panel. Machine-learning pipelines integrating LASSO feature selection and ensemble classifiers were used to construct diagnostic and prognostic models. Model robustness and discrimination were evaluated in independent test cohorts. Integration with bulk RNA sequencing and single-cell datasets was performed to determine the cellular origins and tumor microenvironment context of candidate proteins.Results: A five-protein diagnostic classifier (5-PCM) accurately distinguished CCA from non-CCA controls, achieving AUCs of 0.917-0.930 across cohorts and outperforming conventional serum biomarkers. A seven-protein prognostic model (7-PPC) stratified overall survival with concordance indices of 0.726 and 0.853 in the derivation and validation cohorts, respectively. Multi-omics analyses demonstrated that these diagnostic and prognostic proteins were enriched in malignant epithelial cells, immune subsets, or stromal compartments, supporting their biological relevance in CCA.Conclusions: Plasma proteomics combined with machine learning enables accurate, non-invasive diagnosis and prognostic stratification of CCA. These protein signatures show strong translational potential for early detection and precision clinical management of cholangiocarcinoma.

#7698 Advancing plasma proteomics: A next-generation nanoparticle enrichment workflow for deep and quantitative biomarker discovery in colorectal cancer.

Cameron Ellis[1], Katharina Limm[2], Sandra Schar[3], Roland Bruderer[3], Nils Kulak[2]

[1]PreOmics Inc., Billerica, MA,[2]PreOmics GmbH, Planegg/Martinsried, Germany,[3]Biognosys AG, Zurich, Switzerland

Human plasma provides a minimally invasive source of circulating cancer biomarkers, yet its extreme protein dynamic range and interindividual heterogeneity hinder the detection of low-abundance, tumor-derived markers. In colorectal cancer (CRC), where early detection, risk stratification, and therapy monitoring remain major unmet needs, these analytical barriers limit clinical translation. Here, we present a single-particle enrichment workflow that combines P2 nanoparticles with iST sample preparation and Spectronaut® 20 DIA analysis to enable deeper proteome coverage, improved quantitative precision, and enhanced biological insights in human EDTA-plasma biomarker discovery. Human EDTA-plasma samples from a pilot study of CRC and healthy specimens (n = 6 per group) were processed using the P2-iST Plasma workflow (PreOmics), employing proprietary nanoparticles that selectively capture low-abundance proteins while depleting high-abundance species. Enriched samples were subsequently digested and purified using the optimized iST technology (PreOmics), ensuring standardized peptide generation. Peptides were analyzed on a timsTOF HT (Bruker) operated in dia-PASEF® mode and data processed in Spectronaut® 20 (Biognosys) using the directDIA+ framework for deep, quantitative profiling. Compared with non-enriched plasma samples, the integrated workflow yielded deeper proteome coverage and high quantitative precision (median protein-level CV <15% across replicates). Principal-component and hierarchical clustering analyses demonstrated clear discrimination between CRC and control samples. Functional enrichment revealed distinct biological pathways differentiating disease from control groups, highlighting the sensitivity and discriminative potential of the workflow. The P2-iST Plasma workflow integrates nanoparticle-based enrichment, standardized digestion, and advanced DIA analysis to generate deep, precise, and reproducible plasma proteomes that reflect disease-relevant biology in colorectal cancer. By unlocking new possibilities in circulating biomarker discovery, it supports research in early detection, molecular subtyping, prognosis, and treatment monitoring. Its scalable, automation-friendly design further enables large-cohort validation and longitudinal studies in colorectal and other cancers.

#7699 Quantitative TMT-based proteomic profiling reveals stage-specific protein dysregulation in colorectal cancer.

Camille N. Zenon Melendez, Gabriel Borges Velez, Josue Perez-Santiago, Yakshi Ortiz Maldonado, Liliana Castro Jimenez, Hilmaris Centeno Girona, Sheila N. Lopez Acevedo, Elba V. Caraballo

University of Puerto Rico Comprehensive Cancer Center, San Juan, Puerto Rico

Background: Colorectal cancer (CRC) is a leading cause of cancer-related deaths in the U.S. and its territories, with incidence increasing particularly early-onset CRC, and is often diagnosed at advanced stages. Quantitative proteomics using Tandem Mass Tag (TMT) provides an opportunity to characterize stage-associated molecular alterations. This study aimed to profile the proteomic landscape of CRC in a cohort of Hispanics living in Puerto Rico (HPR) and identify molecular differences across disease stages.
Methods: Tissue samples from healthy controls (n=21), early-stage CRC (n=11), and advanced-stage CRC (n=12) were obtained from the Puerto Rico Familial Colorectal Cancer Registry (PURIFICAR). Samples underwent TMT-based quantitative proteomics followed by liquid chromatography- tandem mass spectrometry (LC-MS/MS). Normalized protein abundance was processed in MetaboAnalyst 5.0. Compositional differences across study groups were evaluated using principal component analyses (PCAs) and PERMANOVA permutation testing for statistical evaluation. Differential protein abundance was assessed using a one-factor analysis with |fold change| ≥1.5 and p≤0.05. Dysregulated proteins were annotated using UniProt and Ingenuity Pathway Analysis (IPA).
Results: PCA showed significant proteomic differentiation among all pairwise comparisons, confirmed by PERMANOVA testing: early-stage CRC versus healthy controls (p=0.001), advanced-stage CRC versus healthy controls (p=0.001), and advanced versus early-stage CRC (p=0.021). Early-stage CRC had 203 differentially abundant proteins relative to healthy controls (72 upregulated, 131 downregulated), with 55.2% unique to this stage. Advanced-stage CRC showed 131 (77 upregulated, 54 downregulated), of which 33.6% were unique. Only twenty-eight (28) proteins were differentially abundant between advanced and early-stages. Venn diagram revealed no proteins common to all three contrasts (0 in the three-way intersection). Early-stage CRC showed dysregulation of DEF1, AZU1, and FCGBP, while advanced-stage CRC demonstrated changes in MMP9, ANXA3, and DEF1. Pathway analysis of classified dysregulated proteins predominantly as enzymes, transporters, and membrane-associated proteins.
Conclusion: Quantitative proteomic profiling identified distinct proteomic profiles associated with CRC stage within this HPR cohort. Early- and advanced-stage CRC demonstrated different dysregulation patterns, with early-stage disease showing greater overall proteomic remodeling and a unique protein composition compared with advanced-stage disease. These stage-associated differences warrant further validation to determine their relevance for early CRC detection and biological characterization.

#7700 Secretomic profiling of triple-negative breast cancer media using Mag-Net™ HP.

Antolize Deetlefs[1], Charne Scully[1], Hafiza Parkar[1], Andrea Ellero[1], Amy van Graan[2], Melissa Vorster[2], Justin Jordaan[2], **Previn Naicker**[2]

[1]Department of Pharmacology, University of Pretoria, Pretoria, South Africa,[2]ReSyn Biosciences, Pretoria, South Africa

Introduction: Secretomics provides a real-time view of tumor biology by profiling proteins that cancer cells release into their microenvironment and circulation. In breast and other cancers, secreted factors can serve as predictive and prognostic markers of disease state and treatment response. However, conventional mass-spectrometry workflows often miss low-abundance cytokines, growth factors, and signalling mediators masked by highly abundant plasma proteins. *Ex vivo* secretome analyses in controlled culture conditions allow reproducible characterization of secreted proteomic signatures, which can then guide targeted validation in larger clinical cohorts. Mag-Net™ enrichment, as demonstrated by Wu et al., offers cost-effective capture of extracellular vesicle-linked, low-abundance proteins from plasma and other biofluids, enhancing downstream MS sensitivity. Here, we present Mag-Net™ HP enabled secretome profiling to sensitively track dose responses to doxorubicin in an *in vitro* model of triple-negative breast cancer (TNBC).

Methods: BT-20 cells (1×10^5 cells/well) were cultured in 24-well plates and treated in triplicate with doxorubicin (0.1, 0.3, 0.7 or 1.5 µM), or DMSO. After 72 h, conditioned media were collected and incubated with Mag-Net™ HP beads for secretome enrichment. Vesicle capture, clean up and digestion was performed in a semi-automated manner on a KingFisher™ Flex using the Mag-Net™ HP kit. Peptides were loaded onto Evotips and analysed using an Evosep One coupled to a Bruker timsTOF HT system.

Results: Mag-Net™ HP yielded substantial improvements in secretomic proteome coverage compared with conventional methods i.e. ~4-fold improvement compared to protein aggregation capture. Approximately 300 proteins were significantly (FDR<0.05) changed proportional to dose—mostly decreasing, negative correlations and others increasing, positive correlations. Gene set enrichment analyses of proteins positively correlated with dose showed, consistent with doxorubicin's mechanism of action, induction of pathways related to DNA damage, p53-related and checkpoint networks (via ATM/ATR, RB1, and MECP2 pathways) potentially indicative of cell-cycle arrest and apoptosis initiation. Together, these results show that Mag-Net™ HP -enhanced secretome profiling enables coherent, reproducible, and biologically interpretable proteomic readouts of drug response that may warrant further investigation in clinical applications.

Conclusion: Mag-Net™ HP enrichment markedly improves detection of low-abundance secretome proteins in doxorubicin-treated TNBC cells in which doxorubicin drives a clear, dose-graded shift in the secretome. This streamlined approach enhances MS-based secretome workflows and supports discovery of clinically relevant biomarkers. Ongoing studies extend this pipeline to additional cell lines and patient-derived organoids.

#7701 Potential clinical utility of small extracellular vesicles derived from head and neck tumors.

Abolfazl Jangholi[1], B. W. M. Thilini Basnayake[1], Omar Breik[2], Liz Kenny[3], Sarju Vasani[2], Riccardo Dolcetti[4], **Chamindie Puyadeera**[1]

[1]Griffith University, Nathan, Australia,[2]Royal Brisbane and Women's Hospital, Brisbane, Australia,[3]The University of Queensland, Brisbane, Australia,[4]University of Melbourne, Melbourne, Australia

Small extracellular vesicles (EVs) carry selective protein cargo that reflect the physiological state of their parent tumor cells, making them a promising source of biomarkers for head and neck cancer (HNC). HNC-derived small EVs are known to contribute to key pathological processes, including immunosuppression, therapy resistance, and metastatic potential. Saliva and plasma, as accessible and minimally invasive biofluids, represent surrogates for tumor-derived biomarkers to enhance clinical monitoring. However, it remains unclear whether small EVs enriched from these fluids accurately represent tumor-derived EVs. This study optimised small EV isolation from HNC tumor tissue and evaluated proteomic overlap between tumor-, saliva-, and plasma-derived EVs.

Small EVs were isolated from tumor tissue and saliva by ultracentrifugation and from plasma using size exclusion chromatography. The morphology, size and concentration of small EVs were assessed by cryogenic Transmission electron microscopy (cryo-TEM) and nanoparticle tracking analysis (NTA). The proteome of small EVs was profiled and quantified using SWATH mass spectrometry. Functional analysis of overlapping and unique proteins was performed to determine their biological relevance.

Small EVs isolated from tumor tissue, saliva and plasma exhibited typical lipid bilayer morphology with sizes ranging from 40 to 200 nm. More than 60% of the identified protein cargoes were shared across all three sources. These shared proteins were significantly enriched in pathways associated with cancer progression, including mTORC1 signalling, coagulation, complement, epithelial-mesenchymal transition, and PI3K/AKT/mTOR signalling. To support the reliability of the proteomic results, a subset of proteins was further validated by immunoblotting.

The substantial proteomic overlap between small EVs from tumor tissue, saliva, and plasma supports the feasibility of using biofluid EVs as surrogates for tumor EVs. Saliva and plasma, being easily accessible, represent viable, non-invasive sources for biomarker discovery and clinical monitoring. These findings provide a strong foundation for advancing liquid biopsy approaches in HNC.

#7702 Integrin αvβ3-driven secretome remodeling uncovers THBS1 as a potential prognostic mediator in cutaneous T-cell lymphoma.

Maria Mercedes Debernardi[1], Lucero Alvarado[1], Ingrid Souza[2], Alejandro Cagnoni[3], Karina Formoso[1], Graciela Cremaschi[1], Alejandro Correa Dominguez[2], Florencia Cayrol[1]

[1]Instituto de Investigaciones Biomedicas (BIOMED-UCA-CONICET), Buenos Aires, Argentina,[2]Instituto Carlos Chagas, Curitiba, Brazil,[3]IBYME-CONICET (Institute of Biology and Experimental Medicine), CABA, Argentina

Cutaneous T-cell lymphomas (CTCL) are a heterogeneous group of T-cell non-Hodgkin lymphomas whose progression depends on dynamic interactions with the tumor microenvironment. Thyroid hormones (THs), at physiological concentrations, act through the membrane receptor integrin αvβ3 to activate oncogenic signaling such as MAPK and JAK/STAT, promoting proliferation and dissemination in T-cell lymphomas. However, the impact of this pathway on the CTCL secretome and its contribution to disease progression remain poorly characterized. Here, we analyzed how integrin αvβ3 activation modulates the CTCL secretome using Mycosis Fungoides (MJ) and Sézary Syndrome (HuT78) cell lines treated with THs (T4=100 nM, T3=1 nM) with or without the αvβ3 inhibitor cilengitide (1.5 µM). Proteins secreted into supernatants were analyzed by LC–MS/MS, and differential expression was evaluated using *limma* and ShinyGO. Under basal conditions, HuT78 secretome displayed a more aggressive profile, enriched in angiogenesis, metabolic reprogramming, and immune evasion pathways compared to MJ. TH treatment significantly altered the secretome composition in both models, with 66 proteins upregulated and 54 downregulated in HuT78 (FDR <0.1). Enriched pathways included VEGFA–VEGFR2, focal adhesion, and TGF-β signaling, all of which are associated with tumor dissemination and immunosuppressive remodeling. THBS1, FN1, FLNA, FLNB, and TLN1 were among the top upregulated proteins and are functionally related to extracellular matrix organization, endothelial activation, and inhibition of antitumor immunity. Importantly, integrin αvβ3 blockade with cilengitide reversed the TH-induced upregulation of these proteins, demonstrating integrin dependence. Transcriptomic analysis of CTCL patient datasets (GSE113113, GSE168508) revealed that the expression of protein THBS1 positively correlates with ITGB3 ($p<0.05$) and is significantly increased in advanced disease stages, consistent with poorer survival. Together, our results show that physiological activation of integrin αvβ3 by THs reshapes the CTCL secretome toward a pro-tumorigenic and immunosuppressive state. THBS1 emerges as a potential prognostic mediator within this network, underscoring how systemic factors like hormones can influence lymphoma progression and revealing new molecular targets with diagnostic and therapeutic relevance.

#7703 Proteomic profiling of Neem (Azadirachta indica) leaves.

Abigail Kahsay, Basir Syed, Dorna Davani, Aftab Ahmed

Pharmaceutical science, Chapman University, Irvine, CA

Modern scientific studies have contributed largely to creating well -validated research data for the holistically rooted use of the Neem *(Azadirachta Indica)* tree in disease management. Neem's astonishing historical and modern relevance reveal more evidence as to why Neem is the target of our study.Valuable studies have shown that the whole parts of the Neem tree are are markable natural source of more than 130 bioactive compounds, which are highly responsible for many therapeutic applications. Historically, Neem has been used as a source of complementary and traditional medicine Ayurvedic and Unani medicine for over 4,500 years. The mystical tree Neem originated from southern Asian countries. This research focuses on the proteomic profiling of Neem leaves and tests their anticancer potential on breast cancer cells. Recent Cancer studies have ranked breast cancer among the most rapidly increasing cancer types in women. Despite consistent advancements in therapies, breast cancer remains a concerning health issue and a deadly disease among women. Many of the existing and emerging Cancer therapies come with numerous drawbacks, increasing the thirst to find better the rapeutics from plant sources with safer and efficacious outcomes. Neem has shown a remarkable potential against cancer due to its wide range of biologically active compounds, including proteins. Studies on the proteins present in Neem remain largely unexplored. The reviewed SwissProt database in UniprotKB shows only three proteins reported from the Neem tree.Therefore, this study has great potential to explore the global proteomic profiling of Neem leaves. Further analysis has also evaluated the cytotoxic potential of proteins from Neem leaves against MDA-MB 231 breast cancer cell lines. The defatted Neem leaves were extracted in n -hexane, followed by extraction in a 20 mM Tris/HCl buffer, pH 8, and then precipitated using 80% ammonium sulfate. The crude extract was dialyzed in water using a 3.5MWCO dialysis tubing and then lyophilized. The anticancer assay of Neem leaves Crude protein at different concentrations was evaluated against MDA-MB-231 cells by using MTS assay, where cells were incubated for 24hours, followed by the treatment with Crude protein for 48 hours, and absorbance was measured at 490 nm. Concentration ranges (6.4- 0.2 mg/mL) showed inhibitory effects on MDA - MB 231 cells. Further, the downstream proteomics was achieved by purification of Crude using gel filtration chromatography first on Hiload Superdex-200 column. The electrophoretic profile was developed by SDS-PAGE electrophoresis using a 10% Tris/Glycine gel, confirmed the presence of proteins with MW ranging from 10 to 37 kDa. The Proteomic profiles were established by peptide mass fingerprinting using Q-tof LC-MS/MS. The bioinformatic analysis using PEAKS Studio X and the UniProtKB TrEMBL Viridiplantae database revealed 17 proteins in 11 groups at an FDR ≤ 1% with a minimum of two unique peptide matches.

#7704 Proteome-wide high throughput perturbation screening of microglial response to oncologic compounds reveals distinct immunomodulation and toxicity profiles.

Alyssa Rosenbloom, Kiran Edwardson, Nathaniel Robichaud, Narges Rashidi, Milad Dagher

Nomic Bio, Montreal, QC, Canada

Microglia are critical for maintaining neural homeostasis. However, under pathological conditions, they can adopt a pro-inflammatory M1 phenotype characterized by the release of IL12, IL1β, TNFα, and IL6. Chronically, the M1 state contributes to neurodegenerative diseases including Alzheimer's, Parkinson's, and multiple sclerosis (MS). M1-polarized microglia are of particular interest in glioblastoma (GBM) because their pro-inflammatory cytokine programs can both suppress antitumor immunity and promote tumor growth; influencing disease progression and shaping effectiveness of emerging therapeutic strategies. Identifying potential therapies requires capturing the breath of inflammatory proteins produced by microglia, and signals of potential toxicities to minimize adverse events (AEs).

The high cost of capturing these diverse signals at scale limits typical drug discovery efforts to simple low-plex readouts. To address this, we previously described the Nomic platform, a proteomics tool capable of quantifying >1000 proteins simultaneously. Here, we leverage Nomic's Omni 1000 to screen 510 bioactive small molecules in microglia stimulated with LPS to mimic a pro-inflammatory state., generating >6,500 samples and >6.5 million data points.

LPS led to expected increased expression of TNFα, IL1β, and IL6, as well as ISG15 and IL12 p40, indicators of chronic inflammation associated with neurodegenerative diseases. Approximately 1/3 of the compounds screened blocked inflammation, of which ¼ presented clear signs of toxicity, characterized by leaking of intracellular content into the supernatant. To further assess potential toxicities, we treated cardiomyocytes and hepatocytes with these compounds, identifying expected and novel drugs with promising properties. For example, Berberine (BBR) is being developed to revert M1 microglia to M2 by blocking NF-κB signaling. We observed significantly reduced IL12 p40, IL10, and CXCL6 upon addition of BBR, with minimal signs of toxicities. Methylprednisolone (MP), a synthetic glucocorticoid, is used for inflammatory flares in MS. Here, MP significantly reduced TNFα, IL6, IL1β, and IL12 p40 in LPS-treated microglia. However, in hepatocytes, MP led to increased SAA, and IL6, consistent with clinical reports of hepatic AEs with high MP exposure. In addition, several compounds under clinical investigation for GBM, including proteasome inhibitors (Bortezomib), and topoisomerase inhibitors (Doxorubicin, Camptothecin derivatives), showed distinct immunomodulatory and toxicity profiles, revealing microglial cytokine programs that may inform potential therapeutic outcomes or combinatorial strategies

Our results demonstrate the value of high-throughput proteomics to simultaneously identify immunomodulatory compounds and characterize their efficacy and safety profile.

#7705 Simultaneous quantitation and discovery of cancer-related proteins in plasma using a fast, high-resolution accurate mass spectrometry-based assay provides insight into precision oncology and drug discovery.

Dominique Figueroa[1], Qingling Li[1], Jared Deyarmin[1], Sophia Steigerwald[2], Matthew R. Dallas[3], Stephanie Samra[1]

[1]Thermo Fisher Scientific, San Jose, CA,[2]Thermo Fisher Scientific, Bremen, Germany,[3]Thermo Fisher Scientific, Frederick, MD

The inherent heterogeneity of cancer has spurred significant technological advancements to enhance the detailed study required to characterize this complex disease, predominantly defined by uncontrolled changes. Efforts to address and treat this multi-faceted variability are executed as investigation of plasma - a readily accessible biological fluid rich in information regarding physiological states. This work seeks to present robust and standardized methods for the quantitation and discovery of known cancer-related proteins found in plasma. Specifically, our methods aim to reduce variability and labor across workflows and spur the adoption of next-generation plasma proteomic and mass spectrometry methods in discovery and development research. PQ500 peptides were prepared per manufacturer instructions, and human plasma samples from BioIVT Inc were digested using the AccelerOme automated platform and pooled as the sample matrix. Two experiments evaluated hybrid-DIA performance. The first tested different targeted peptide numbers (30-300) in SureQuant and tMS2 hybrid-DIA methods using PQ500 peptides spiked into pooled plasma. The second assessed linearity, limit of detection, and limit of quantification using serial dilutions analyzed on the Orbitrap Astral Zoom MS. LC-MS analysis was performed on a Vanquish Neo UHPLC with an EASY-Spray column and optimized gradients, with samples analyzed using both hybrid-DIA methods on the Orbitrap Astral Zoom mass spectrometer. This analysis spans 144 proteins identified as cancer-associated. Key tumor suppressors include TP53 and PTEN, while major oncogenic drivers such as EGFR, ERBB2, KIT, and SHH promote cell proliferation and survival. Proteins like VEGFA, MMP2, and MMP9 regulate angiogenesis and metastasis, and immune modulators such as PVR, VTCN1, and B2M support tumor immune evasion. Metabolic and redox enzymes including PKM2, LDHA, and TXN drive cancer cell metabolism and stress adaptation. Clinically relevant biomarkers—CEACAM5 (CEA), KLK3 (PSA), MUC16 (CA125), WFDC2 (HE4), and MSLN—aid in diagnosis and monitoring. Overall, these proteins cover major cancer hallmarks including proliferation, angiogenesis, immune escape, invasion, and metabolic reprogramming, representing both established and emerging therapeutic targets. Future directions will leverage the unique capabilities of mass spectrometry-based proteomics to investigate post-translational modifications, including phosphorylation and glycosylation, which are crucial in signaling and cancer. By integrating plasma proteomics studies, quantifiable reference peptides, and the Orbitrap Astral Zoom mass spectrometer, we aim to streamline precision oncology and drug discovery by minimizing variability in these dynamic models.

#7706 Phase-separated RTK fusion condensates orchestrate oncogenic signaling through extensive protein recruitment and RTK crosstalk.

Wei Yang[1], Thomas C. Whisenant[2], Daniel J. Donoghue[1]

[1]Chemistry and Biochemistry, University of California San Diego, La Jolla, CA,[2]Center for Computational Biology and Bioinformatics, University of California San Diego, La Jolla, CA

Liquid-liquid phase-separated RTK (Receptor Tyrosine Kinase) fusion condensates represent a newly identified category of biomolecular assemblies that play a key role in driving the oncogenic functions of RTK fusion proteins. In this study, we isolated the NACC2-NTRK2 (Nucleus Accumbens-Associated Protein 2 - Neurotrophic Receptor Tyrosine Kinase 2) fusion condensate and applied LC-MS/MS along with IMAC (Immobilized Metal Affinity Chromatography) to profile its total proteome and phospho-proteome. Our analyses revealed that the condensate selectively recruits 190 proteins via kinase activation, impacting essential cellular pathways such as signal transduction, transcriptional regulation, cell division, cell-cycle progression, and metabolic control. Fluorescence microscopy further demonstrated that proteins with distinct cellular roles interact with the condensates in different ways. Phospho-proteomic profiling showed that the kinase active condensates bring phosphorylation to 1,399 proteins and facilitate RTK crosstalk, particularly with ephrin receptor tyrosine kinases, enabling ligand-independent activation of EPHA2 (Ephrin Receptor A2) and EPHB4 (Ephrin Receptor B4).

: Biomarkers Predictive of Therapeutic Benefit 6
Poster Session

#7710 Extracellular vesicle immunopeptidomics recovers immunogenic neoantigen peptides from cancer patient plasma.

Todd Hembrough[1], Alan Mark Ezrin[1], Zackary Opheim[1], Cheryl Bandoski[1], Sarah Bennett[2], Kate Fagan-Solis[2], Benjamin G. Vincent[3], William Hoos[2]

[1]Nexosome Oncology, Durham, NC,[2]Pathfinder Oncology, Chapel Hill, NC,[3]University of North Carolina at Chapel Hill, Chapel Hill, NC

Personalized immunotherapy using patient-specific neoantigens is a critical strategy in immuno-oncology. DNA/RNA sequencing and MHC affinity modeling are used to select optimal neoantigen peptides for development. Tissue-based peptide-MHC (pMHC) mass spectrometry (MS) immunopeptidomics studies have been used to confirm MHC presentation of neoantigen peptides. Since these pMHC analyses are tissue intensive, novel ways to identify MHC presentation of patient-specific neoantigen peptides are needed. Extracellular vesicles (EV) are constitutively expressed by all tumor and immune cells and represent a potential plasma source of patient specific pMHC complexes. Using a proprietary EV purification method, we report detection and characterization of patient specific neoantigen pMHC complexes from very small volumes of patient plasma using targeted proteomics. Methods: Consented patient plasma was used in this study, and patient metadata (DNA/RNA sequencing, HLA haplotyping, and neoantigen peptide binding predictions) was used to define potential neoantigens. EV were purified from plasma (0.5 mL) using proprietary size exclusion chromatography (SEC) methods. Class I MHC-presented peptides were enriched from samples using a pan-MHC antibody column, and enriched peptides were analyzed by high-resolution targeted LC-MS/MS with heavy peptide standards**.** Single chain trimers (SCT) for pMHC complexes were used to evaluate neoantigen-specific T cell frequencies in the peripheral blood, sort T cells for TCR sequencing, and engineer TCR-T cells for further neoantigen characterization. Results: EVs purified from patient plasma using proprietary SEC methods surprisingly yielded ~20 greater amounts of total class I MHC protein based on ELISA than standard EV preps, illustrating a potential for pMHC detection. Plasma enriched EVs from two patients (advanced CRC and osteosarcoma (OST)) were used in subsequent experiments. Multiple patient-specific pMHC were recovered from each patient, 3 peptides from OST and 5 peptides from CRC. Expression of multiple pMHC were confirmed in tumor tissue by MS. Peptides represent candidate neoantigens based upon expression and MHC presentation. Immunogenicity was confirmed for multiple peptides (4 CRC/ 2 OST) by identification of neoantigen-specific CD8+ T cells in peripheral blood using SCT staining and flow cytometry. Subsequent studies will be reported with engineered TCR-T's. Conclusions: Identification of patient-specific tumor antigens is a prerequisite for personalized immunotherapy. We have developed a workflow for Extracellular Vesicle Immunopeptidomics (EV-IMPX) to validate neoantigen presentation using small-volume patient plasma samples. We expect that peptide selection based on EV-IMPX will enhance immunotherapy by narrowing neoantigen selection to MHC-presented peptides with the highest likelihood of tumor killing.

#7712 Wnt-driven chromosomal instability as a biomarker for PORCN inhibition.

Diego Garcia-Lopez[1], Azedine Zoufir[1], Hector De Galard Terraube[1], Laura Madrid[1], Amy Cullen[1], Ania Piskorz[1], Nicola Wallis[1], Ruth Plummer[2], Steven Jackson[3], Jackie Walling[1], James D. Brenton[4], Florian M. Markowetz[5], Jason Yip[1], Jose Teles[1], **Geoff Macintyre**[6]

[1]Tailor Bio Ltd, Cambridge, United Kingdom,[2]Newcastle University, Newcastle, United Kingdom,[3]Cancer Research UK Cambridge Insitute, University of Cambridge, Cambridge, United Kingdom,[4]University of Cambridge, Cambridge, United Kingdom,[5]University of Cambridge, CRUK Cambridge Institute, Cambridge, United Kingdom,[6]Spanish National Cancer Research Ctr. (CNIO), Madrid, Spain

Targeting Porcupine (PORCN), a key regulator of the WNT-signalling pathway, has shown therapeutic potential in multiple cancers. However, clinical responses to PORCN inhibitors have so far been limited despite strong target engagement data and a favourable safety profile. Given that Wnt signaling can drive tumorigenesis by inducing chromosomal instability (CIN), we hypothesised that CIN signatures might serve as a novel predictive biomarker to improve PORCN inhibitor response rates. Using a combination of CIN signatures capturing diverse Wnt-driven CIN processes including replication stress, error-prone non-homologous end joining repair, and whole genome duplication, we established proof-of-concept of a biomarker predictive of PORCN inhibition response. We found that CIN signature activity significantly correlated with both knockdown and pharmacological inhibition of PORCN across 180 and 24 cancer cell lines, respectively (Kendall's Tau=-0.16, P-value=0.001,Tau=-0.22, P-value=0.065). We performed a meta-analysis of 25 studies of in vivo patient-derived or cell-line xenografts treated with PORCN inhibitors, and found that biomarker activity was quantitatively associated with response to PORCN inhibition, (CIN signature activity versus tumour over control ratio, Pearson's R=-0.66, P-value=0.009). Using these data to determine an optimised threshold for clinical application (specificity=100%, 95%CI:54.07%-100% and sensitivity=100%, 95%CI:29.24%-100%), we showed concordance between predicted and observed efficacy in previous PORCN inhibitor clinical trials. The quantitative nature of the CIN signature biomarker offers an opportunity to widen the therapeutic index of existing clinical stage PORCN inhibitors and analysis of biomarker prevalence across 6,335 patient tumours from The Cancer Genome Atlas study identifies esophageal and gastric cancers as optimal indications for future clinical development.

#7713 Biomarker-guided treatment approach For advanced bladder cancer.

Dhasarathan Ganesan[1], Karina Aguilar[1], Tianyu yang[1], Bal L. Lokeshwar[1], Vinata B. Lokeshwar[2]

[1]Augusta University, Augusta, GA,[2]Associate Professor, Dept. of Urology, University of Miami, Miller School of Medicine, Augusta, GA

INTRODUCTION AND OBJECTIVE: We previously discovered a first-in-class human Chondroitinase (Chase) that degrades chondroitin sulfate. This Chase is a splice variant of HYAL4 (V1) and promotes a malignant phenotype and chemoresistance in bladder cancer (BC) cells. We evaluated the diagnostic and prognostic potential of V1-Chase and its functions in driving treatment resistant BC in preclinical models.
METHODS: Efficacy of the V1 (qPCR) and Chase (ELISA-like assay) was evaluated in three test and validation cohorts (total n = 925; BC=239; non-BC = 686). 40 cystectomy specimens from MIBC patients who received adjuvant Gemcitabine plus cisplatin (G+C) treatment. V1 was expressed in BC cell lines or silenced and the transfectants were analyzed for sensitivity to Gemcitabine (Gem) and Cisplatin. The mechanism of Gem resistance was evaluated in preclinical *in vitro* and *in vivo* models.
RESULTS: Chase levels were 7-10-fold elevated in patients with BC compared to patients with benign genitourinary conditions, history of BC, or other cancers. In all three cohorts, Chase test detected BC with > 92% sensitivity and > 85% specificity. Chase test correctly diagnosed atypical cytology inferences. V1 induced an invasive stem cell phenotype. V1's Chase activity induced Gem resistance in BC cells by cleaving CD44 and promoting intracellular JAK2/Stat3 signaling which caused up-regulation of cytidine deaminase (CDA). CDA induces Gem metabolism and efflux of dFdU, an inactive Gem metabolite. In patients with MIBC, V1/p-JAK2/CDA signature predicted failure to G+C adjuvant/salvage treatment (P<0.0001). STAT3 and CDA inhibitors re-sensitized V1-expressing cells to Gem. Transcriptome and gene enrichment analyses showed V1 induces JAK-Stat3, inflammatory and invasion/metastasis gene signatures, which were validated in clinical specimens. V1-expressing tumors were Gem resistant but were re-sensitized to Gem treatment in combination with a CDA inhibitor.
CONCLUSION: V1/Chase is a potential diagnostic and prognostic biomarker for bladder cancer and drives muscle-invasion, metastasis, and Gem resistance in BC. Inhibitors of the Chase signaling pathway overcome V1-induced Gem resistance, suggesting a precision-based treatment approach to improve treatment response.
Support: 1R01CA283699-03
Key words: prognostic marker; HYAL4; invasive bladder cancer

#7714 Extracellular vesicle glycosylation profilepredictsand affectstherapeutic outcomes ofCLDN18.2-targeted CAR-T cell therapyagainst gastrointestinal cancers.

Wenran Li, Min Tao, Changsong Qi, Lin Shen, Cheng Zhang

Department of Gastrointestinal Oncology, Peking University Cancer Hospital & Institute, Beijing, China

CLDN18.2-targeted CAR-T cell therapy has shown promising potential against gastrointestinal cancers (GIC). However, biomarkers for its patient selection and outcome prediction are urgently needed. This study aims to analyze plasma extracellular vesicle (EV) glycosylation profile and select key features to predict and monitor survival outcomes and therapeutic response of CLDN18.2-targeted CAR-T cell therapy and further investigate the underlying potential mechanisms. We depicted EV glycosylation profile via a 56-lectin array in 91 dynamic plasma samples from 53 GI cancer patients received CLDN18.2-CAR-T therapy (CT041-CG4006 trial). Based on the baseline EV glycosylation profile, we found that GalNAc/Gal related glycosylation on total EVs correlated with patients' survival outcomes. We selected the binding intensity of plasma total EVs to four key lectin features using machine learning methods which simultaneously predicted progression-free survival (PFS), overall survival (OS) and therapeutic response at baseline and all specifically recognized GalNAc/Gal. Besides the baseline analysis, dynamic changes in the binding intensity of key lectins were also related to treatment response and survival outcomes. Furthermore, high binding intensity of the key lectins to total EVs and high expression of genes mediating GalNAc/Gal glycosylation were associated with weaker anti-tumor immunity represented by fewer circulating CD8+CD28+ T cells, and correlated with poorer tumor progression indicated by elevated expression of abdominal tumor biomarkers. Mechanistically, decreasing the level of GalNAc on the surface of EVs and tumor cells could strengthen killing capability of CAR-T cells in vitro. Collectively, our work provided novel biomarkers for GIC patients undergoing CLDN18.2 CAR-T cell therapy in view of plasma EV glycosylation and revealed the potential mechanism by which the EV glycosylation affects the efficacy of CAR-T therapy.

#7715 Elevated baseline DKK1 plasma is a biomarker for sirexatamab treated colorectal cancer patients.

Zongzhong Tong[1], Scott Patton[1], Patty Ormonde-Hanson[1], Calvin Jia[2], Cyndi Sirard[2], Jay Baum[2], **Mike Kagey**[2]

[1]ARUP Laboratories, Salt Lake City, UT,[2]Leap Therapeutics, Cambridge, MA

Sirexatamab is an IgG4 monoclonal antibody that potently neutralizes dickkopf-related protein 1 (DKK1). DKK1 is a secreted protein that has been implicated as a poor prognostic marker and as an oncogenic driver for colorectal cancer (CRC). The DeFianCe (NCT05480306) Phase 2 randomized, global, open-label, multicenter study was conducted to evaluate the efficacy and safety of sirexatamab plus the current standard of care (SOC) treatment regimen (FOLFIRI/FOLFOX and bevacizumab) versus SOC as second-line treatment for participants with advanced CRC (n=188). A retrospective analysis of baseline plasma levels of DKK1 using a research assay identified a significant improvement in progression free and overall survival favoring the experimental arm in patients with elevated levels of DKK1. In order to enable future prospective patient selection, an optimized DKK1 assay using the Meso Scale Discovery (MSD) platform was developed and underwent feasibility at a central laboratory. DeFianCe samples were retested with the optimized assay. Consistent with the research assay, patients whose DKK1 levels were above the median showed improved clinical outcomes in the experimental arm compared to SOC. Furthermore, approximately 500 commercial CRC plasma samples were evaluated to determine the prevalence of patients with elevated DKK1 in a real-world data set and understand the association between demographics and DKK1 levels. Future work will include completing the development and validation of the assay as a potential companion diagnostic and determining the appropriate threshold of DKK1 plasma levels for CRC patients who would be most likely to derive clinical benefit from a sirexatamab-based therapy.

#7716 Tumor-intrinsic MHC-II activation in pancreatic ductal adenocarcinoma enhances immune response and treatment efficacy.

Canping Chen[1], Kyle P. Gribbin[2], Xi Li[3], Tugba Ozmen[4], Furkan Ozmen[4], Shamilene Sivagnanam[2], James Kim[2], Katie E. Blise[5], Xinxing Yang[1], Yi Zhang[2], Dove Keith[5], Mara H. Sherman[6], Mushui Dai[7], Lisa M. Coussens[8], Charles D. Lopez[9], Rosalie C. Sears[7], Gordon B. Mills[10], Katelyn T. Byrne[7], Zheng Xia[10]

[1]Biomedical Engineer, Oregon Health & Science University, Portland, OR,[2]Department of Cell, Developmental and Cancer Biology, Oregon Health & Science University, Portland, OR,[3]Medical, Huazhong University of Science and Technology, Wuhan, China,[4]Division of Oncological Sciences, Knight Cancer Institute, Oregon Health & Science University, Portland, OR,[5]Brenden-Colson Center for Pancreatic Care, Oregon Health & Science University, Portland, OR,[6]Memorial Sloan Kettering Cancer Center, New York, NY,[7]OHSU, Portland, OR,[8]OHSU Knight Cancer Institute, Lake Oswego, OR,[9]Assoc. Professor, Div. of Hemat./Onc., Oregon Health & Science University, Portland, OR,[10]OHSU Knight Cancer Institute, Portland, OR

Pancreatic ductal adenocarcinoma (PDAC) is characterized by an immunosuppressivetumor microenvironment (TME) and poor prognosis. While major histocompatibility complexclass II (MHC-II) expression is traditionally associated with professional antigen-presentingcells, its role in PDAC malignant cells remains underexplored. Herein, we utilized single-cellRNA sequencing (scRNA-seq), spatial transcriptomics, bulk RNA sequencing, multipleximmunohistochemistry (mIHC) and ex vivo studies in culture with both human and murinemodels to investigate the prognostic relevance of MHC-II expression in malignant PDACcells. Elevated MHC-II expression in malignant cells was strongly associated with increasedinfiltration of CD4+ T and CD8+ T cells in human PDAC, and pronounced co-localization withplasma cells, indicative of an antigen-activated immune microenvironment. In the KPCmouse model of PDAC, pharmacologic induction of MHC-II expression by cobimetinibtreatment in malignant epithelial cells significantly enhanced the therapeutic response toimmune checkpoint blockade (ICB). These findings highlight the role of malignant cell-intrinsic MHC-II expression in promoting antigen presentation and fostering an anti-tumorimmune microenvironment. Our results position MHC-II as a promising prognostic biomarkerand therapeutic target in PDAC, paving the way for novel immunomodulatory strategies.

#7717 TRPM4 expression predicts Acetalax sensitivity in prostate cancer.

Yuka Hoshi[1], William C. Reinhold[1], Daiki Taniyama[1], Yoshitaka Inoue[2], Augustin Luna[1], Suresh Kumar[1], NAI-YUN SUN[3], Yoo Sun Kim[1], Yin Juanjuan[1], Nitin Roper[1], Adam G. Sowalsky[1], Naoko Takebe[4], Yves Pommier[1]

[1]National Cancer Institute, Bethesda, MD,[2]Library of Medicine, National Institute of Health, Bethesda, MD,[3]Graduate Institute of Oncology, National Taiwan University, Taipei, Taiwan,[4]Stephenson Cancer Center at the University of Oklahoma, Oklahoma, OK

Background: Advanced and treatment-refractory prostate cancer, including castration-resistant disease, highlights the need for new therapeutic strategies exploiting targetable vulnerabilities. TRPM4, a calcium-activated monovalent cation channel, regulates cell volume and promotes cancer progression. Our research showed that Acetalax induces selective oncosis-like cell death in TRPM4-positive triple-negative breast cancer, suggesting TRPM4-dependent susceptibility. Targeting TRPM4 may offer advantages over existing therapies by disrupting ion-transport and volume-regulatory mechanisms not addressed by current treatments. We examined TRPM4 expression and Acetalax activity in prostate cancer.
Methods: We assessed Acetalax sensitivity in prostate cancer cell lines with high or low TRPM4, including androgen-dependent (LNCaP) and castration-resistant models (PC3, DU145, 22Rv1). TRPM4 dynamics, cellular swelling, and oncosis-associated phenotypes were evaluated by Western blotting and immunofluorescence. Resistant clones were developed by continuous drug exposure. TRPM4 expression in patient samples was analyzed using tissue microarrays (TMAs) and TCGA. Transcriptomic changes following TRPM4 loss were examined by RNA sequencing. Antitumor activity and tolerability were tested in TRPM4-positive PDX models.
Results: TRPM4-high prostate cancer cells exhibited rapid swelling, membrane blebbing, and TRPM4 degradation after Acetalax, whereas TRPM4-low cells and resistant clones lacking TRPM4 were unaffected. Resistant clones showed TRPM4 depletion, confirming TRPM4 is required for responsiveness. In patient samples, TRPM4 protein was higher in adenocarcinoma than benign hyperplasia, and TCGA datasets confirmed increased TRPM4 transcripts in tumors relative to normal tissue, with minimal differences across stage or Gleason grade. Transcriptomic profiling revealed gene-expression changes associated with TRPM4 loss, including alterations in ion transport, cytoskeletal organization, and cell-death-related pathways, with a shift toward proliferative programs and reduced stress and inflammatory signaling consistent with disrupted volume-regulatory networks. In vivo, Acetalax significantly suppressed growth of TRPM4-positive PDX tumors in a dose-dependent manner without systemic toxicity.
Conclusions: TRPM4 functions as a target and predictive biomarker for Acetalax response in prostate cancer. These findings highlight a TRPM4-dependent therapeutic vulnerability and support biomarker-guided development of Acetalax for TRPM4-expressing, treatment-refractory prostate cancer, including CRPC.

#7718 Stearic acid-macrophage crosstalk identifies MIF-CD44 signaling as a therapeutic target in lung cancer initiation.

Amrita Roy[1], Greta Forbes[1], Dikshaya Prabhakara[1], Tyler Faith[2], Apurva Mallisetty[3], Samuel Weinberg[4], Alicia Hulbert[2], Frank D. Weinberg[5]

[1]Department of Medicine, University of Illinois at Chicago, Chicago, IL,[2]University of Illinois at Chicago, Chicago, IL,[3]University of Illinois, Chicago, IL,[4]Northwestern University, Chicago, IL,[5]University of Illinois Cancer Center, Chicago, IL

Background: Lung cancer (LC) is the leading cause of cancer-related mortality, yet the process of tumor initiation is poorly understood. Prior work from our group indicated that biomolecules like stearic acid (SA) and proinflammatory cytokines like MIP1α and MIP1β were selectively elevated in the tumor bearing lung lobes of early-stage LC patients. Hence, we hypothesized that a SA-macrophage (MΦ) inflammatory axis contributes to neoplastic transformation in lung epithelium.

Method: Plasma cytokine profiles were compared between early-stage LC patients (n=5) and healthy controls (n=6). Cytokine production following SA exposure at transcriptional and translational level were assessed in PBMC-derived MΦs and human monocytic cell lines (U937) to establish synchrony between two systems. Conditioned media (CM) from SA-treated MΦs (SA-CM) was applied to BEAS2B epithelial cells (non-transformed lung epithelial cells), with transformation measured by soft agar and spheroid assays. Receptor expression for MIP1α (CCR5) and MIF (CD44) was quantified by mRNA/protein analyses. Functional blockades of CCR5 and CD44 were performed using small-molecule antagonists (Maraviroc and Verbascoside respectively) to identify critical cytokine driving transformation.

Results: Elevated MIP1α were observed in plasma samples from early-stage LC patients compared to healthy individuals. SA treatment augmented MIP1α and MIF expression from both PBMC and U937 derived MΦs. Simultaneously, SA-CM from both PBMC and U937 derived MΦs induced significantly greater colony formation in soft agar matrix and robust spheroid growth under low-attachment conditions, indicating neoplastic transformation. Receptor analysis revealed abundant CD44 but limited CCR5 expression on BEAS2B cells. Blockade of CD44 with Verbascoside abrogated SA-CM-induced spheroid formation, whereas CCR5 inhibition had no effect.

Conclusion: Based on these observations we conclude that SA reprograms MΦ transcriptional states promoting a MΦ driven proinflammatory environment that induces MIF-CD44-dependent neoplastic transformation of lung epithelial cells. These findings implicate a novel immunometabolic axis involved in the early oncogenic events of LC initiation and support therapeutic targeting of SA-MIF-CD44 signaling as a potential preventive strategy.

#7719 Exploring biomarker predictors of response to nintedanib and bevacizumab combination therapy in advanced cancer patients: Correlative studies from Phase 1b study.

Ravi Kumar Paluri[1], Anup Kasi[2], Francisco Robert[1], Gagan Deep[3], Ashish Manne[4]

[1]Wake Forest Baptist Health, Winston Salem, NC,[2]The University of Kansas Cancer Center, Kansas City, KS,[3]Wake Forest University School of Medicine, Winston-Salem, NC,[4]Ohio State University, Columbus, OH

Background: Bevacizumab and other VEGF inhibitors provide clinical benefit across multiple cancers but are limited by resistance driven largely by revascularization through alternate pro-angiogenic pathways, including PDGFR and FGFR. Nintedanib, a triple kinase inhibitor targeting VEGFR, PDGFR, and FGFR, may overcome these escape mechanisms. The safety and efficacy of nintedanib plus bevacizumab was previously explored in our phase 1B study and published. We are presenting correlative biomarker studies on the plasma samples acquired at prespecified endpoints.
Methods: Plasma samples were obtained from patients enrolled in a phase 1 dose-escalation study evaluating nintedanib in combination with bevacizumab for advanced solid tumors (lung n=9, colon n=8, cervical n=1). Baseline plasma biomarkers—including IL-8, ICAM-1, Angiopoietin-2, KDR/VEGFR2, E-selectin, VEGF, and SDF-1α—were analyzed and correlated with clinical outcomes. Biomarker quantification was performed using multiplex bead-based immunoassays (Luminex), with select analytes validated by ELISA.
Results: Nintedanib 200 mg twice daily was well tolerated with no dose-limiting toxicities. . Among bevacizumab-pretreated patients, 55% achieved durable disease control, including one complete response and four stable diseases. Higher baseline levels of KDR/VEGFR2 and E-selectin and lower SDF-1α were associated with improved outcomes. ANOVA identified several biomarkers significantly linked to disease control, including KDR/VEGFR2 ($p=0.004$), PDGF-AA ($p=0.037$), and Endoglin ($p=0.020$).
Conclusion: Nintedanib combined with bevacizumab was safe, well tolerated, and demonstrated meaningful clinical activity in heavily pretreated patients. Baseline KDR/VEGFR2, E-selectin, and SDF-1α emerged as potential predictive biomarkers. These data support further validation in larger cohort as a strategy to refine biomarker-driven patient selection for treatments in lung and colorectal cancers.

#7720 Differences in FGFR2 fusion detection between DNA and RNA NGS in a large Chinese lung cancer cohort.

Wenxue Chen[1], Xinlin Yu[1], Lipeng Bai[1], Can Wen[1], Wennan Zhang[1], Wanwan Zou[1], Zhiliang Liu[1], Ruijia Sun[2], Mengli Huang[2]

[1]Jiangxi Key Laboratory of Translational Cancer Research Jiangxi Cancer Hospital, Nanchang, China,[2]Department of Medical Affairs, 3D Medicines Inc., Shanghai, China

Background: Fibroblast growth factor receptor 2 (FGFR2) fusions are rare driver gene alterations in non-small cell lung cancer (NSCLC), with an overall incidence of approximately 0.02%. FGFR2 fusion breakpoints typically occur within exons 17-19, and numerous fusion partner genes have been identified. While next-generation sequencing (NGS) is the primary method for fusion detection, the differences in the detection spectrum between DNA- and RNA-based NGS for FGFR2 fusions remain inadequately characterized in large-scale cohorts.
Methods: This retrospective study analyzed a large Chinese lung cancer cohort comprising 12,974 tumor samples. Among these, 3,578 samples were tested by DNA-NGS for fusion detection, and 9,396 samples were tested using RNA-NGS. Only FGFR2 fusions classified as pathogenic or likely pathogenic were included in the final analysis.
Results: A total of 18 FGFR2 fusion events were identified, yielding an overall detection rate of 0.14%. The patient cohort was predominantly male (72.22%), with a median age of 65 years (range: 52-78). Histologically, most cases were diagnosed as lung adenocarcinoma (44.44%) and lung squamous cell carcinoma (38.89%), with 3 cases of undetermined pathology. All FGFR2 fusions were characterized by 5'-3' rearrangements. DNA-NGS identified 5 FGFR2 fusions (0.14%), all in lung adenocarcinoma, with heterogenous fusion partners including FGFR2-INPP5F, FGFR2-TACC2 (non-canonical breakpoints: exon 6), FGFR2-PCAT2, FGFR2-KCNH5, and one complex fusion involving FGFR2-NME9 and NME9-FGFR2. Meanwhile, RNA-NGS detected 13 FGFR2 fusions (0.14%), with a partner distribution distinct from DNA-NGS: 11 cases of FGFR2-ATE1 (84.62%) involving non-canonical breakpoints (exon2/5/6/9), as well as FGFR2-BICC1 and FGFR2-TACC2. All FGFR2-ATE1 fusion patients were male, and 7 of the 8 cases with specified pathology were lung squamous cell carcinomas, indicating a potential enrichment. Importantly, the FGFR2-ATE1 fusion lacked the FGFR2 kinase domain, and the vast majority (90.91%) had supporting reads <100, suggesting low expression levels. These features imply that FGFR2-ATE1 may exert oncogenic effects via kinase-independent mechanisms, and such fusions are unlikely to respond well to FGFR kinase inhibitors. The pathogenicity of atypical, low-expressed fusion transcripts requires cautious evaluation and reclassification.
Conclusions: This study reveals distinct FGFR2 fusion detection patterns between DNA and RNA NGS. When interpreting complex or atypical fusions for targeted therapy guidance, integrating results from both DNA and RNA NGS is recommended to optimize patient stratification and treatment decisions.

#7721 Correlation between PD-L1, desmocollin 3, and stromal lymphocytes in recurrent head and neck squamous cell carcinomas.

Vedanti Newaskar[1], Shivani Sharma[1], **Bakulesh M. Khamar**[2]

[1]Core Diagnostics, Delhi, India,[2]Cadila Pharmaceuticals, Ahmedabad, India

Introduction: Immune checkpoint inhibitors has improved outcome of recurrent /metastatic head and cancer (rmHNSCC) . Benefit is seen in around 20% pf patients and is proportionate to PD-L1 expression. We evaluated correlation between PD-L1, Desmocollin-3 (DSC3) and stromal tumor infiltrating lymphocytes (TIL) to explore possibility of using DSC3 specific therapy along rmHNSCC . DSC3 is a predictive biomarker for an investigational product CADI-05.

Methods: Samples from patients with rmHNSCC were evaluated PD-L1 expression using standard protocol and expressed as combined proportion score (CPS) and tumor proportion score (TPS) . DSC3 expression was evaluated as tumor proportion score (TPS) by immunohistochemistry, using mouse anti-DSC3 monoclonal antibody (Progen, Heidelberg, Germany Cat#61093 dilution: 1:50) following removal of paffinization of formalin-fixed, paraffin-embedded tissue. TIL was evaluated after staining with hematoxylin and eosin and expressed as a percentage of total cells. All evaluated samples were received after informed consent of patients.

Results: Total of seventy (70) samples were evaluated between September 2023 to May 2025 for PD-L1, DSC3 and TIL. PD-L1 expression as CPS and TPS was observed in 77% and 51% of samples. PD-L1 values ranged from 0-95% (CPS) and 0-95%(TPS). DSC3 expression was observed in 93% of samples. DSC3 (TPS) values ranged from 0-80%. No correlation was found between PD-L1(CPS) and DSC3 expression (Spearman correlation coefficient r = -0.1432, p = 0.3846; 95% Confidence interval = -0.4389 to 0.1805). There was a moderate negative correlation (r= -0.3) between PD-L1(TPS) and DSC3. All PD-L1 negative samples expressed DSC3.Mean and median DSC3 expression values were not different between PD-L1 positive and negative samples. Based on expression level TIL were grouped as samples having TIL ≥ 10% and <10%. TIL ≥ 10% were observed in 40% of evaluated samples. All samples expressing PD-L1(CPS and TPS) as well as DSC3 had TIL ≥ 10% . TIL were absent in five samples and all expressed DSC3 from 10-40%.

Conclusion: DSC3 is expressed in 93% of rmHNSCC , irrespective of PD-L1 and TIL expression suggesting DSC3 specific therapy may be useful in management of patients with rmHNSCC with absent/low PD-L1 and or TIL .

#7722 Biomarkers of nelmastobart efficacy: BTN1A1 expression and tumor microenvironment dynamics in colorectal cancer.

Bong-Ki Hong[1], Soohyeon Lee[2], Andrew H. Park[1], Young-Seung Kim[1], Chunai Wu[1], Seung-Hoon Lee[1], Jong-Su Park[1], **Stephen S. Yoo**[1]

[1]STCube Pharmaceuticals Inc., Rockville, MD,[2]Korea Univ. Medical Center, Seoul, Korea, Republic of

Background: Butyrophilin 1A1 (BTN1A1) is an immune regulatory protein expressed in various tumors and immune cell populations, playing a role in shaping the tumor microenvironment (TME). Our previous tissue microarray (TMA) analysis demonstrated that high BTN1A1 expression in colorectal cancer is associated with reduced intratumoral $CD8^+$ T-cell infiltration, suggesting BTN1A1's role in promoting an immunosuppressive TME. The Phase 1 clinical study of Nelmastobart, a BTN1A1-targeting antibody, showed acceptable safety and preliminary antitumor activity. Additionally, early findings from the ongoing STCUBE-IIT Phase 1b/2 trial (ClinicalTrials.gov: NCT05990543) suggest a potential link between BTN1A1 expression and therapeutic response. To further investigate the biological significance of BTN1A1 and identify reliable biomarkers predictive of Nelmastobart efficacy, we conducted a deep, multiplexed tissue analysis using the CellDIVE platform on baseline tumor specimens from patients enrolled in the STCUBE-IIT Phase 1b/2 clinical trial.
Methods: Baseline colorectal tumor tissues were analyzed using the CellDIVE multiplex imaging system. Quantitative profiling included BTN1A1, CD8, FoxP3, and additional TME- and tumor-intrinsic markers. TME composition and spatial organization were compared between responders and non-responders. Baseline BTN1A1 expression and pathway activity scores were integrated to assess correlations with objective response rate (ORR) and progression-free survival (PFS). The primary endpoint was the association between BTN1A1 expression and immune cell composition; the secondary endpoint examined composite molecular features predictive of response to Nelmastobart.
Results: High BTN1A1 expression was associated with lower intratumoral $CD8^+$ T-cell infiltration and increased immunosuppressive cellular populations. Integrated analyses revealed that combining exhausted $CD8^+$ T-cell abundance and spatial distribution with tumor-intrinsic DNA damage repair activity more strongly correlated with treatment response than BTN1A1 expression alone.
Conclusions: BTN1A1 expression is linked to key immunological alterations in the colorectal cancer TME. A composite biomarker incorporating exhausted $CD8^+$ T-cell features and tumor DNA damage-related repair activity provides superior predictive value for Nelmastobart response compared with BTN1A1 alone. These findings support a multidimensional biomarker strategy for optimizing BTN1A1-targeted therapies and warrant validation in larger clinical cohorts.

#7723 Implementation of a novel immune monitoring strategy for multicenter clinical trials to enable equity in cancer prognosis for individuals from remote settings of Australia.

Natalie J. Smith[1], Michael Cohen[2], Lauren J. Tracey[2], Julie Alipaz[3], Christina Loh[3], David A. King[4], Neha Pulyani[5], Rebecca Auzins[5], Elin S. Gray[6], Sandra Taylor[7], Rajat Rai[7], Steven Kao[8], Barbara Fazekas de St Groth[1], **Helen McGuire**[1]

[1]The University of Sydney, Sydney, Australia,[2]Standard BioTools, Markham, ON, Canada,[3]Standard BioTools, San Francisco, CA,[4]Standard BioTools, South San Francisco, CA,[5]Edith Cowan University, WA, Australia,[6]Edith Cowan University, Joondalup, Australia,[7]Dubbo Base Hospital, Dubbo, Australia,[8]Chris O'Brien Lifehouse, Sydney, Australia

Improved cancer prognosis begins with the collection of high-quality data from clinical trials. However, execution of longitudinal immune phenotyping studies by flow cytometry is complex due to logistical challenges that could affect data quality. The challenges of immune monitoring are exacerbated when considering remote and rural communities in Australia, which are burdened by both an increased prevalence and worse prognosis of cancer. Paradoxically, these communities are often underrepresented in clinical trials. Our group has developed a novel blood-based “immune signature” that robustly predicts failure to make a clinical response to checkpoint therapies targeting the PD-1/PD-L1 pathway in melanoma and lung cancer. We have now taken these groundbreaking findings to implement in remote clinical settings, along with an expanded CyTOF™ panel for 50-plus-parameter analysis of cancer patient peripheral blood samples. Recent developments in CyTOF technology facilitate a highly simplified workflow of asynchronous sample collection and staining, compatible with current hospital laboratories, which typically run on unpredictable schedules, to remote settings, which are resource-poor and have limited clinical trial infrastructure. This is uniquely enabled by using a stable, dried-down cocktail of CyTOF antibodies and an easy-to-follow protocol that yields reproducible staining while minimizing sample required. Furthermore, this unique mass cytometry workflow provides flexibility and minimizes technical variation via sample barcoding and freezing of stained samples for shipment to a central site for batch acquisition. As such, this study is designed to demonstrate both clinical impact of the large panel and utility of CyTOF technology for a highly simplified and robust workflow for multi-site clinical trials. Here we present findings from the implementation of this novel workflow through a 100-sample pilot study at three sites across Australia, in a variety of clinical implementation setups. Remote asynchronous sample collection was performed to compare two surface staining approaches on i) PBMC versus ii) plasma-depleted whole blood to suit settings where centrifugation access was readily available or not, respectively. Stained samples were shipped to a central lab for processing. In the case of cryopreserved whole blood, bead-based granulocyte depletion was first performed, with all samples subsequently multiplex barcoded together for intracellular antibody staining of key functional markers. Analysis harmonization was achieved across sample collection sites and staining approaches. Overall, this workflow enables access to underserved communities, facilitating for the first time equity and scalability of immune phenotyping studies to harness truly geographically dispersed clinical centers.

#7724 A circulating GPNMB-based multimodal model integrates tumor-immune crosstalk to predict immunotherapy response in esophageal cancer.

Liang Zhu[1], Xiaoyuan Wang[2], Guoyu Cheng[1], Yancheng Lai[1], Lan Lan[1], Zhenghao Dong[1], Zhixuan You[1], Xinjie Chen[1], Ziyi He[1], Xinyi Xiao[1], Lingxuan Zhu[1], Rucheng Liu[1], Shaosen Zhang[1], Dongxin Lin[1], **Chen Wu**[1], Jiang Chang[3]

[1]Cancer Hospital Chinese Academy of Medical Sciences, Beijing, China,[2]Harbin Medical University Cancer Hospital, Harbin, China,[3]Department of Epidemiology and Biostatistics, Huazhong University of Science & Technology, Wuhan, China

Neoadjuvant immunotherapy improves outcomes in esophageal squamous cell carcinoma (ESCC), yet ~70% of patients fail to respond. Pretreatment biopsies and plasma thus provide critical opportunities for biomarker discovery. Here, we performed plasma proteomic profiling and identified soluble glycoprotein non-metastatic melanoma protein B (sGPNMB) as the most elevated circulating protein in non-responders. Mechanistically, tumor cell-derived sGPNMB suppressed $CD8^+$ T cell receptor (TCR) signaling to induce functional exhaustion, with secretion being required for its immunosuppressive activity. Cancer-associated fibroblast-epithelial (CAF-Epi) niches promoted SOX2 upregulation in tumor cells, transcriptionally activating GPNMB expression. In humanized PDX models, plasma GPNMB levels predicted response to PD-1 blockade, and GPNMB inhibition synergised with therapy. Across retrospective cohorts and a prospective clinical trial, a multimodal model combining plasma GPNMB levels, CAF-Epi niche detection, and clinical-pathological features achieved robust predictive accuracy for immunotherapy response and survival. These findings establish a mechanistically grounded, spatial-circulating biomarker framework for precision immunotherapy in ESCC.

#7725 Integrative molecular profiling identifies predictors of response to sacituzumab govitecan in advanced prostate cancer.

Jacque Lyman[1], Todd Knutson[2], Allison Haaning[2], Braedan M. McCluskey[2], Yingming Li[1], Jamie M. Sperger[3], Rendong Yang[4], Christos Kyriakopolous[5], Susan F. Slovin[6], Scott T. Tagawa[7], Joshua M. Lang[3], Scott M. Dehm[1]

[1]Masonic Cancer Center, Minneapolis, MN,[2]Minnesota Supercomputing Institute, University of Minnesota, Minneapolis, MN,[3]University of Wisconsin-Madison, Madison, WI,[4]Feinberg School of Medicine, Northwestern University, Chicago, IL,[5]University of Wisconsin, Madison, WI,[6]Associate Professor of Medicine, Memorial Sloan Kettering Cancer Center, New York, NY,[7]Weill Cornell Medicine, New York, NY

Prostate cancer is the second leading cause of cancer related death in men. Potent therapies that inhibit the androgen receptor (AR) transcription factor have improved survival of patients with prostate cancer, however many cases progress to lethal castration resistant prostate cancer (CRPC). Resistance to AR-targeted therapies is frequently mediated by reactivation of AR signaling or transition to AR-independent, non-luminal subtypes. Identifying new treatment strategies for patients with CRPC who are resistant to available therapies is critical for improving survival outcomes. One promising therapeutic target for CRPC is the trophoblastic cell surface antigen (Trop-2). Found to be highly expressed in many solid tumors, Trop-2 has oncogenic activities implicated in CRPC progression and could provide a target for treatment of prostate cancer resistant to AR targeted therapies. Sacituzumab Govitecan (SG) is an anti-Trop-2 antibody drug conjugate that provides targeted delivery of the topoisomerase I inhibitor SN-38. As part of a completed phase II clinical trial assessing the efficacy of SG in CRPC, we performed integrative whole exome DNA-seq and RNA-seq on metastatic biopsies obtained from 29 patients at baseline (pre-treatment with SG) and during treatment with SG. We characterized the gene expression profiles and mutational landscapes to evaluate the prognostic value of gene signatures and acquired genetic alterations. Baseline biopsies from patients that responded to SG displayed enrichment for gene signatures that define basal subtypes of CRPC and inflammatory response. Conversely, baseline biopsies from patients that did not respond to SG displayed enrichment for pathways related to high proliferation and AR activity. These findings provide a framework for interpreting response to SG that may inform future clinical development as well as selection of laboratory models to enhance mechanistic knowledge of SG response and resistance.

#7726 Expression profile of therapeutic target CDH17 in gastric cancer.

Fei Chu[1], Jiaxing Zhao[2], Dan Huang[1], Hao Luo[1], Aaron Hong[1], Ye Tian[2], Chang Liu[2], David Chu[3], Jim Lu[1]

[1]Gopath Diagnostics, LLC, Buffulo Grove, IL,[2]Celnovte Biotech, Rockville, MA,[3]Fetchflow Inc, San Francisco, CA

Background:
CDH17 has recently gained attention as a promising therapeutic target in gastric cancer (GC), driven by advances in antibody-drug conjugates and other targeted modalities designed to exploit its highly restricted expression in gastrointestinal tissues. Despite growing therapeutic interest, the real-world prevalence and staining characteristics of CDH17 in clinical GC samples are not well established. A clearer understanding of CDH17 expression patterns may help refine patient selection strategies, guide the development of CDH17-directed therapies, and support biomarker-driven clinical decision-making.
Methods:
Tissue microarrays from 73 patients with histologically confirmed gastric cancer were evaluated by immunohistochemistry (IHC). CDH17 staining was performed using the Celnovte IHC platform with CNT-PolyStacker secondary antibodies (clone C5A5), which enables high-specificity visualization of membrane-associated and cytoplasmic expression. Staining intensity was scored semi-quantitatively, and CDH17 positivity was defined as ≥50% of tumor cells demonstrating 2+ or 3+ intensity. All slides were reviewed independently by board-certified pathologists to ensure consistent interpretation.
Results:
CDH17 expression was identified in 15.1% (11/73) of gastric cancer cases. Positive tumors demonstrated strong, well-defined membranous and cytoplasmic staining, consistent with the known biology of CDH17 as an intestine-specific adhesion molecule. Within this cohort, CDH17-positive cases appeared across both intestinal and diffuse histologic subtypes, and no clear relationship with tumor differentiation, sample location, or patient demographic factors was observed. The overall expression rate aligns with reported ranges from prior smaller studies, suggesting that CDH17 may define a distinct molecular subset of GC patients potentially suitable for targeted therapeutic approaches.
Conclusions:
CDH17 expression was detected in approximately 15% of gastric cancer cases in this real-world cohort, reinforcing the relevance of CDH17 as a potential biomarker for targeted therapy development. As CDH17-directed agents continue to advance in early-phase clinical trials, reliable biomarker prevalence data will be essential for refining clinical trial eligibility criteria and informing market-wide testing strategies. Additional studies with larger and more diverse patient populations are warranted to validate the prevalence, biological implications, and potential predictive value of CDH17 expression in gastric cancer.

#7727 Integrated FHIT and IDH2 biomarkers predict synthetic lethal response to DCPS inhibition in acute myeloid leukemia.

Madhurendra Singh[1], Francesca Grassi[1], Lisa Bast[2], Vladimir Talibov[1], Camilla Silvander[1], Simon Moussaud[1], Matthieu Desroses[1], Angelo De-Milito[1], Julian Walfridsson[2], Andreas Hoglund[1], Martin Andersson[1]

[1]Tumor Biology, Sprint Bioscience AB, Stockholm, Sweden,[2]Karolinska Institutet, Stockholm, Sweden

DCPS (Decapping Scavenger Enzyme) is a critical regulator of RNA metabolism that clears cap structures generated during mRNA decay. At Sprint Bioscience, in the frame of our efforts to develop new modalities in oncology, we have generated, among others, novel selective DCPS inhibitors (DCPSi) with sub-nanomolar activity in cells using our fragment- and structure-based drug discovery platform. Using the clinically validated DCPSi RG3039 across a panel of AML cell models, we identified a synthetic lethal interaction between DCPS and the cap-degrading enzyme Fragile Histidine Triad (FHIT), which shares overlapping substrate specificity. In both *in vivo* and *ex vivo* systems, low FHIT expression emerged as a strong predictive biomarker of therapeutic response to DCPSi, while hydroxyurea pretreatment was identified as a negative confounding factor. Mechanistically, FHIT loss preserves the therapeutic effects of DCPSi, including release of differentiation blockade, induction of cell-cycle arrest, and apoptosis—key vulnerabilities in AML. Interrogation of AML databases (cBioPortal OHSU 2022, total 942 samples) and primary patient samples (Champions Oncology, 30 *ex vivo unpassaged primary AML*) further revealed that IDH2 mutation status correlates with both FHIT expression (FDR=0.002) and sensitivity to DCPSi (p=0.042), identifying IDH2 as an additional predictive biomarker. Primary AML specimens harboring IDH2 mutations demonstrated increased susceptibility to RG3039, consistent with this molecular association. Together, these findings establish DCPS as a safe and efficacious therapeutic target in AML. We propose that FHIT expression, frequently reduced in cancer, provides a biomarker-driven strategy for patient stratification, and that IDH2 mutation status further refines prediction of response to DCPS-targeted therapy.

#7728 Glycogen branching enzyme 1 as a metabolic determinant and prognostic driver of the CMS4 subtype in colorectal cancer.

Fang-Chi Hsu[1], Leila Su[1], Frank Luh[1], Yi-Fan Chen[2], Xin Wang[1], Yun Yen[3]

[1]Sino-American Cancer Foundation, Covina, CA,[2]International Master Program for Translational Science, Taipei Medical University, Taipei, Taiwan,[3]Sino-American Cancer Foundation, Arcadia, CA

Colorectal cancer (CRC) continues to impose a substantial global health burden, ranking among the top causes of cancer incidence and mortality. Despite meaningful advances in screening, surgical techniques, and systemic therapy, patients with biologically aggressive molecular subtypes—particularly consensus molecular subtype 4 (CMS4)—experience limited therapeutic benefit and disproportionately poor outcomes. CMS4 tumors are characterized by a mesenchymal phenotype, pronounced hypoxic signaling, activation of Wnt-driven transcriptional programs, and a proliferative state that contributes to treatment resistance. Identifying actionable metabolic determinants of this phenotype remains an unmet clinical need.Through integrative multi-omics profiling across independent CRC cohorts, we identified glycogen branching enzyme 1 (GBE1) as a central metabolic regulator closely aligned with the CMS4 transcriptional landscape. GBE1 expression is significantly enriched in CMS4 tumors and demonstrates a strong, inverse association with overall survival, underscoring its potential as a subtype-specific prognostic biomarker. Transcriptomic analyses further reveal that GBE1 and its downstream glycogen-synthesis pathways are selectively activated in CMS4 tumors, achieving robust statistical significance.Mechanistically, GBE1 operates as a hypoxia-induced effector downstream of HIF-1α, reshaping carbohydrate metabolism in a manner that reinforces the metabolic rigidity of CMS4 disease. Beyond its canonical enzymatic role, GBE1 influences broader glycosylation and glycosyltransferase networks, and modulates lipid biosynthetic programs through the PPARγ/Wnt/β-catenin axis. This dual control of carbohydrate and lipid metabolism endows CMS4 tumors with a pronounced growth advantage. Functional studies using CRISPR-mediated GBE1 knockout demonstrate marked suppression of tumor cell proliferation and attenuation of Wnt/β-catenin signaling, confirming its mechanistic role in sustaining the pro-invasive CMS4 phenotype.Together, these findings identify GBE1 as a clinically meaningful metabolic vulnerability that defines the CMS4 subtype. GBE1 emerges as both a prognostic marker and a tractable therapeutic target, providing a precision oncology framework for the management of high-risk CRC patients with metabolically and immunologically dysregulated diseases.

#7729 Phosphorylated FRS2 (pFRS2) as a biomarker for FGFR mutation or fusion activity assessment in formalin-fixed paraffin-embedded tumor sections.

Peter Feiszt, Kristopher A. Lofgren, **Paraic A. Kenny**

Gundersen Medical Foundation, La Crosse, WI

Genes encoding the Fibroblast Growth Factor Receptor family (FGFR1, FGFR2, FGFR3 and FGFR4) are a recurrent target of genomic alterations in several solid tumor types. Alteration types include gene amplification, gene fusion and point mutations which can affect both extracellular and intracellular domains. The FGFR inhibitors, pemigatinib, erdafitinib and futibatinib, have FDA approvals to treat selected solid tumors with FGFR pathway alterations. Because FRS2 is a common substrate for each of these kinases, we investigated whether the level and subcellular localization of phosphorylated FRS2 (pFRS2) would be an effective biomarker to read out pathway activity in clinical FFPE tumor specimens.

The Gundersen Precision Oncology Cohort includes 1,046 patients who received next-generation sequencing at Gundersen Health System during their cancer care. A total of 29 patients had FGFR alterations (13 x FGFR1, 9 x FGFR2 and 7 x FGFR3) with fusions, point mutations and gene amplifications represented. The most common tumor types were urothelial (7), lung (7) and biliary tract (6).

Here we report a pFRS2 immunofluorescence assay that permits high-resolution readout of both the level and subcellular localization of the activity of genetically altered FGFRs. This enables quantitative distinction between specimens with high pathway activity (including fusions and some point mutations) from specimens with lower pathway activity (some amplifications), suggesting utility as a companion diagnostic for identification of likely responders to currently approved and newly emerging FGFR therapies. In particular, the ability to determine subcellular localization of pathway activity may prove useful for trials of both antibody-drug conjugates and bispecific antibodies which might be expected to be less effective in tumors where the oncogenic FGFR activity is primarily internal and not cell-surface associated.

#7730 A novel ultra-sensitive qPCR-based liquid biopsy assay: ESR1 mutation detection in peripheral plasma derived cfDNA.

Fei Ma[1], Haili Qian[1], Wenna Wang[1], **Yongpan Yan**[2], Bowen Ji[2], Yuwei Pei[2]

[1]State Key Laboratory of Molecular Oncology, National Cancer Center/Cancer Hospital, Chinese Academy of Medical Sciences & Peking Union Medical College, Beijing, China,[2]RayBio Inc, Beijing, China

Background: ESR1 mutations are a leading cause of acquired resistance to endocrine therapy in HR+/HER2- metastatic breast cancer (mBC). Monitoring of ESR1 mutations' dynamic accumulations is critical for patients to quickly switch to effective selective estrogen receptor degrader (SERD) treatment. Therefore, a rapid and cost-effective assay for ESR1 mutations status monitoring is in urgent demand in clinical practice.
Methods: ESR1 sequence with consecutive mutations poses a major hurdle for conventional qPCR assay development. Here an Innovative Suppression Probe PCR was designed and assay was successfully developed (Eq-PCR). Genomic cell-free DNA samples which were extracted from ESR1 mutated breast cancer cell lines (n=47) and patient-derived peripheral blood samples (n=25) were subjected to Eq-PCR, ddPCR (digital droplet PCR) and Next generation sequencing (NGS covering 78 genes).
Results: Our Eq-PCR assay has a limit of detection of 0.5% mutation frequency for major ESR1 mutations. For 47 cell lines samples (10ng DNA input), overall agreement between Eq-PCR and ddPCR is 100%. For 25 samples collected from mBC patients(cfDNA concentration ranged from 0.2ng-0.8ng/μl), overall agreement between Eq-PCR and NGS is 100.0% of PPV (5 positive samples) and 85.0% of NPV (20 negative samples).
Conclusion: A novel, cost-effective qPCR-based assay for major ESR1 mutations was developed with top accuracy and quick turn-around time. This assay provides an urgently needed clinical tool to monitor critical ESR1 mutation in HR+/HER2- mBC patients in a convenient, timely and cost-effective fashion.

#7731 Tumor immune microenvironment features associated with response to neoadjuvant durvalumab plus gemcitabine, cisplatin, and nab-paclitaxel (DURGAP) in resectable biliary tract cancer.

Huiying Yan[1], Wenxin Li[2], **Linze Xu**[1], Rentao Li[2], Linlin Fu[2], Qi Qi[2], Xihao Zhang[2], Jihui Hao[3], Huikai Li[2], Yang Liu[1]

[1]Department of Hepatobilay Cancer, Liver Cancer Center, Tianjin Medical University Cancer Institute & Hospital, National Clinical Research Center for Cancer, Key Laboratory of Cancer Prevention and Therapy, Tianjin's Clinical Research Center for Cancer, Tianjin, China,[2]Department of Hepatobiliary and Pancreatic Oncology, Tianjin Cancer Hospital Airport Hospital, Tianjin, China,[3]The Pancreas Center, Tianjin Medical University Cancer Institute & Hospital, National Clinical Research Center for Cancer, Tianjin Key Laboratory of Digestive Cancer, Tianjin's Clinical Research Center for Cancer, Tianjin, China

Background: Neoadjuvant DurGAP therapy has shown promising efficacy in resectable biliary tract cancer (BTC). In an updated cohort of 30 patients (2025 The Lancet Summit: Cancer Control in China, Abstract #TLSU2025_0087; NCT05640791), the objective response rate (ORR) was 60%, disease control rate (DCR) 86.7%, and R0 resection rate among resected patients 93.8%. However, mechanisms underlying variable response remain unclear. This study explored the tumor immune microenvironment (TIME) associated with differential tumor regression grades (TRG).

Methods: Four TRG1 (major response) and four TRG3 (minimal response) patients from the DurGAP cohort were analyzed. Multiplex immunofluorescence quantified $CD8^+$ T cells, $CD4^+$ T cells, and regulatory T cells (Tregs). One representative case per group underwent spatial transcriptomic sequencing to assess cellular composition and spatial distribution. Immunofluorescence data were compared using Mann-Whitney U test. Spatial transcriptomic data were processed with the Seurat and sctransform pipelines, normalized and batch-corrected via Harmony, followed by PCA and UMAP-based clustering. Spatial domains were annotated using FindAllMarkers to identify domain-specific genes. Differentially expressed genes ($p<0.05$, $|\log_2 FC|>\log_2 1.5$) were subjected to GO and KEGG pathway enrichment analysis.

Results: TRG1 tumors displayed significantly higher infiltration of $CD8^+$ and $CD4^+$ T cells compared with TRG3, while Tregs were enriched in TRG3. Spatial transcriptomics confirmed these findings, revealing greater T and B lymphocyte density and fewer malignant cells in TRG1, whereas TRG3 exhibited higher tumor cell proportions and reduced effector infiltration. Subset analysis showed that the proportion of Tregs among total T cells was markedly higher in TRG3, while the $CD8^+$/Treg ratio was substantially greater in TRG1. Functional enrichment highlighted immune activation and antigen presentation pathways in TRG1, contrasting with metabolic and proliferative signaling enrichment in TRG3. These spatial and transcriptional patterns indicate that robust effector T-cell infiltration and coordinated immune architecture underlie effective tumor regression, whereas immunosuppressive microenvironments limit therapeutic benefit.

Conclusions: Distinct TIME profiles distinguish responders from non-responders to neoadjuvant DurGAP in BTC. Higher effector T-cell infiltration, an increased $CD8^+$/Treg ratio, and immune-enriched spatial domains are linked to major tumor regression, whereas Treg-dominant microenvironments correspond to poor response. These findings highlight potential immune biomarkers to refine patient selection and improve future therapeutic strategies.

#7732 A stromal-immune spatial transcriptomic signature associated with MUC4 identifies potential biomarkers of trastuzumab resistance in HER2-positive breast cancer.

Maria F. Mercogliano[1], Nadine Schrode[2], Kristin Beaumont[3], Roxana Schillaci[4]

[1]Laboratorio de Inmunologia Tumoral, Instituto de Biologia y Medicina Experimental, Buenos Aires, Argentina,[2]Center for Advanced Genomics Technology, Icahn School of Medicine at Mount Sinai, New York, NY,[3]Icahn School of Medicine at Mount Sinai, New York, NY,[4]Laboratorio de Inmunologia Tumoral, Instituto de Biologia y Medicina Experimental, Buenos Aires, Argentina

Trastuzumab-based therapies are the standard of care treatment for HER2-positive breast cancer. We previously demonstrated that mucin 4 (MUC4) expression is associated with trastuzumab resistance and is an independent biomarker of poor clinical response. The aim of this work was to refine the prognostic and predictive value of MUC4.Five HER2-positive breast cancer samples obtained at diagnosis and classified as either MUC4-positive/non-responder or MUC4-negative/responder to trastuzumab were used to analyze spatial expression of transcripts using the Visium platform from 10X Genomics. Libraries were sequenced on a NextSeq 550 and data were processed with Cell Ranger. To minimize batch effects and to optimize noise-to-signal ratio, data were integrated using different approaches: reciprocal PCA, canonical correlation analysis and Harmony. RPCA was selected for optimal batch correction and preservation of biological heterogeneity.Cell annotation included three approaches: manual annotation using cell specific markers, automated prediction using data from other five spatial transcriptomic experiments and a semi-automated method using Unicell. Cells were annotated when at least two of these methods coincided in cell annotation. Differential gene expression was performed with Seurat and limma, accounting for donor and cell type composition. Notably, downregulated genes included multiple immunoglobulin-related transcripts consistent with previously reported trastuzumab response signatures such as HER2DX.To reduce false positives arising from gene list variability, we applied an elastic net penalized logistic regression which refined the initial set of 267 MUC4-associated genes to 37 high confidence candidates. For each gene, we analyzed structural features, biological function, protein-protein interactions and relevance in cancer using resources such as The Human Protein Atlas, Gene Cards, UniProt and PubMed. The analyzed gene set showed strong enrichment for Gene Ontology Biological Process categories related to extracellular matrix remodeling, stromal activation, epithelial-to-mesenchymal transition, angiogenesis, cell invasion and migration, immune modulation and metabolic reprogramming. Spatial transcriptomics therefore identified 37 differentially expressed genes in MUC4-positive breast cancer associated with stromal and immune transcriptional programs that may contribute to trastuzumab resistance and refine MUC4 predictive and prognostic value improving the identification of patients most likely to benefit from trastuzumab treatment.

#7733 Reliable antibodies for cancer research: TROP2 as a case study of Abcam's enhanced validation framework.

Caroline S. Hirst, JK Tanjore Ramanathan, Nadine Nelson, Antonella Galli, Will Howat, Silvia Sbacchi

Abcam Limited, Cambridge, United Kingdom

Reliable antibody performance is essential for cancer research, particularly when investigating disease-associated targets such as TROP2. Conventional antibody validation methods often fall short in addressing the complexity of human tissue expression and disease heterogeneity. To overcome these limitations, an enhanced validation framework was developed that integrates disease-relevant tissue profiling. This approach combines multiple validation steps, including knock out validation testing and generating detailed IHC expression profiles in selected formalin-fixed paraffin-embedded (FFPE) human tissue microarrays (TMA) using automated immunohistochemistry (IHC) platforms. As a case study, a recombinant rabbit monoclonal antibody (RabMab®) targeting TROP2, clone EPR20043 (ab214488) was validated across multiple IHC automated platforms. The antibody demonstrated high specificity, with no TROP2 detected by IHC in FFPE cell pellets prepared from TACSTD2 knockout MCF7 cells (ab286330). Furthermore, AI-driven expression profiling of multi-cancer TMAs (breast, lung, ovarian and endometrial cancer) revealed high sensitivity for detecting diverse protein expression levels, supporting its potential for biomarker assessment, patient stratification and diagnostic applications across varied disease settings. This study highlights the value of enhanced antibody validation in de-risking reagent selection and ensuring robust, reproducible results in cancer research. The TROP2 case exemplifies how rigorous Abcam's antibody validation can accelerate discovery and translational applications in the oncology research.

#7734 The gap score: A functional biomarker of drug sensitivity.

Sharon B. Cantor, Jenna Whalen, Tokio Sano

MCCB, UMass Chan Medical School, Worcester, MA

Accurate identification of tumors most likely to benefit from DNA damage response (DDR)-targeted therapies remains a major clinical challenge. Current biomarkers, including genomic instability assays and multi-gene HRD panels, rely on “genomic scarring” to infer homologous recombination repair (HRR) defects. While informative, these static measurements capture historical DNA repair events and fail to provide a real-time functional assessment of DDR pathway activity. RAD51 foci assays offer dynamic evaluation but remain intrinsically tied to HDR capacity, thereby overlooking non-HR mechanisms that drive therapeutic vulnerability.Here, we present single-stranded DNA (ssDNA) gaps as a mechanistically grounded and clinically actionable biomarker that reflects the common denominator of DDR dysfunction across tumor types. We developed a robust, scalable ssDNA gap detection assay optimized for clinical specimens, enabling real-time quantification of endogenous replication-associated gaps without prior drug exposure. Using this platform, we demonstrate that ssDNA gaps are intrinsically elevated in BRCA-deficient cancers, independent of genotoxic stress, revealing a native replication vulnerability not captured by HRD scores.AI-assisted imaging analysis enabled fully automated and unbiased quantification of gap burden across tumor sections and xenograft samples. ssDNA gap levels strongly correlated with sensitivity to PARP inhibitors and other replication-perturbing agents, outperforming HRD-score and RAD51-based assays in predicting therapeutic response. Mechanistically, gap formation in BRCA-deficient tumors arises during replication through combined contributions of abasic site accumulation, PrimPol-mediated repriming, and aberrant nuclease processing. These findings establish ssDNA gaps as the functional consequence of impaired genome maintenance, integrating multiple upstream DDR alterations into a single measurable phenotype.Collectively, our data position ssDNA gap burden as a rapid, reliable, and more biologically faithful biomarker than traditional HRD metrics for stratifying patients likely to benefit from DDR-targeted therapies. By shifting biomarker development from HR deficiency to replication gap biology, this approach enables improved patient selection in clinical trials and supports the implementation of precision medicine strategies that directly measure tumor vulnerability rather than relying on genomic proxies.

#7735 *HER2* expression and tumor-infiltrating lymphocytes predict response to tucatinib plus trastuzumab in *HER2*-positive metastatic colorectal cancer (MOUNTAINEER): Exploratory analysis of a multicenter, Phase II trial.

Mitsuho Imai[1], John H. Strickler[2], Woochan Hwang[3], Kara Bonneau[4], Andrew B. Nixon[5], Jongchan Park[3], Chang Ho Ahn[3], Tanios Bekaii-Saab[6], Takayuki Yoshino[7]

[1]National Cancer Center Hospital East, Kashiwa, Japan,[2]Medicine, Duke University Medical Center, Durham, NC,[3]Lunit.Inc, Seoul, Korea, Republic of,[4]Duke University Medical Center, Durham, NC,[5]Duke Univ. Medical Ctr., Durham, NC,[6]Mayo Clinic Arizona, Scottsdale, AZ,[7]National Cancer Center Hospital East, Kashiwa City, Chiba, Japan

Introduction: The HER2-targeted doublet, tucatinib and trastuzumab, recently received FDA approval for previously treated HER2-positive metastatic colorectal cancer (mCRC). While the intensity of HER2 IHC staining and ERBB2 amplification have been proposed as potential markers of response, our understanding of the role of the tumor microenvironment remains limited.
Methods: The phase II MOUNTAINEER Trial (NCT03043313) enrolled patients for tucatinib plus trastuzumab based on HER2 positivity (IHC or NGS amplification). Patients from cohort A with available HER2 IHC and H&E slides were included in this analysis. Previously validated AI-based models (Lunit SCOPE uIHC and SCOPE IO) were used to quantify the percentage of HER2 3+ stained tumor cells (AI-H3+) and the densities of tumor infiltrating lymphocytes (TILs) in the cancer epithelium (iTIL) and stroma (sTIL).
Results: The analyzed cohort (N=30) had an objective response rate (ORR) of 43.4% and median progression-free survival (PFS) of 8.0 months. AI-H3+ percentage showed a strong, dose-dependent association with an ORR of 57.1%, 66.6%, and 80.0% for tumors with AI-H3+ ≥10% (n=14), ≥25% (n=12), and ≥50% (n=10), respectively. This benefit extended to PFS, with the ≥50% cohort reporting a PFS HR of 0.17 (P=0.002) compared to tumors with AI-H3+ <50%. Tumors with below median iTIL or sTIL had significantly shorter PFS. Notably, tumors with sTIL density in the bottom quantile had an ORR of 0% and PFS HR of 4.40 (P=0.002) despite including cases with high AI-H3+. TIL densities and AI-H3+ percentage were not correlated.
Conclusion: These findings confirm AI-quantified HER2 intensity as a marker of response and suggests the importance of TILs, which may have a role through immunogenic cell death. Stratification by HER2 and TIL may be an approach to consider as this regimen progresses into the first-line setting.

	Overall	OverallHigh AI-H3+ percentage			Low iTIL density	Low sTIL density	
Cutoff	n/a	≧ 10%	≧ 25%	≧ 50%	< 2.6 cells/mm^2 (median)	< 131.8 cells/mm^2 (median)	< 52.1 cells/mm^2 (25% quantile)
N	30	14	12	10	15	15	8
ORR	43.4%	57.1%	66.6%	80.0%	26.7%	26.7%	0.0%
PFS	n/a	HR 0.44 [95% CI 0.18-1.10], P=0.071	HR 0.31 [95% CI 0.11-0.85], P=0.017	HR 0.17 [95% CI: 0.05-0.59], P=0.002	HR 3.14 [95% CI: 1.27-7.73], P=0.010	HR 3.57 [95% CI: 1.42-9.00], P=0.005	HR 4.40 [95% CI: 1.55-10.51], P=0.002

#7736 Rare *EGFR* cis compound L833V/H835L mutation in non-small cell lung cancer is oncogenic and a therapeutic target of EGFR tyrosine kinase inhibitors.

Yo Han Jeon[1], **Ahjin Lim**[2], Myung Kyung Choi[3], Hee Seong Choi[3], Yurimi Lee[4], Hyunju Song[2], Hyun-Soo Cho[3], Jeonghee Cho[2], Yoon-La Choi[4]

[1]Kosin University, Busan, Korea, Republic of,[2]Dankook University, Cheonan, Korea, Republic of,[3]Yonsei University, Seoul, Korea, Republic of,[4]Sungkyunkwan University, Seoul, Korea, Republic of

Non-small cell lung cancer (NSCLC) with *EGFR* L833V/H835L in cis mutation remains poorly understood. We retrospectively reviewed the clinicopathologic features NSCLC with either *EGFR* L833V or H835L mutation. The study population includes NSCLC patients (n=3835) at Samsung Medical Center, Seoul, Korea. A total of 8 patients with *EGFR* L833V/H835L in cis mutation were identified. Poorly differentiated histology (either micropapillary or solid patterns) presented in 4 of 5 resected cases. Four patients received EGFR tyrosine kinase inhibitors (TKIs) and achieved a median progression-free survival of 13 months. The oncogenic and therapeutic properties of the mutation were investigated through a combination of functional and biochemical analyses, utilizing both in vitro and in vivo models, and structural modeling. The L833V/H835L mutant exhibited oncogenic potential, transforming NIH-3T3 cells and promoting IL3-independent growth in Ba/F3 cells. Furthermore, EGFR TKIs effectively suppressed the mutant's oncogenic activity in both in vitro and in vivo studies. These phenomena are further supported by its increased kinase activity in structural modeling. Although rare, *EGFR* L833V/H835L in cis mutation, represents a biologically oncogenic and clinically actionable variant in NSCLC.

#7737 Baseline CD16$^+$ NK cells are associated with clinical outcome of nivolumab plus ipilimumab immunotherapy in advanced hepatocellular carcinoma.

Hongjae Chon[1], Narim Lee[2], Hannah Yang[1], Junho Kang[3], Won Suk Lee[1], So Jung Kong[1], Beodeul Kang[1], Jung Sun Kim[1], Ho Yeong Lim[1], Jung Kyoon Choi[3], Chan Kim[1]

[1]CHA Bundang Medical Center, Seongnam, Korea, Republic of,[2]CHA University, Seongnam, Korea, Republic of,[3]Department of Bio and Brain Engineering, KAIST, Daejeon, Korea, Republic of

Background: Combination immunotherapy of nivolumab plus ipilimumab (Nivo/Ipi) has shown durable responses in advanced hepatocellular carcinoma (HCC). However, reliable biomarkers predicting clinical benefit remain limited. CD16$^+$ (FcγRIIIa) NK cells mediate antibody-dependent cellular cytotoxicity (ADCC) and may influence the efficacy of Ipi, a human IgG1 monoclonal antibody. We investigated whether baseline peripheral CD16$^+$ NK cell levels correlate with clinical outcomes in advanced HCC patients receiving Nivo/Ipi.

Method: Patients with advanced HCC were prospectively enrolled from 4 tertiary cancer centers in Korea from Mar 2020 to Aug 2023. Patients received Nivo 1 mg/kg plus Ipi 3 mg/kg every 3 weeks (4 cycles) followed by Nivo maintenance (240 mg every 2 weeks). Peripheral blood mononuclear cell samples were collected at baseline and on day 22 (Cycle 2 Day 1 [C2D1]) and analyzed by flow cytometry. Patients were classified into high and low CD16$^+$ NK groups based on a cut-point determined by maximally selected rank statistics. Single-cell RNA sequencing from 10 responders and 20 non-responders was performed to identify transcriptional correlates of treatment response.

Results: 55 patients were enrolled and analyzed. Most patients were male (82%) with Hepatitis B virus infection (81.8%), and preserved liver function (Child-Pugh A 78.2%, B 21.8%). 74.5% had received ≥2 prior systemic therapies, and 23.6% were immunotherapy naïve. The median follow-up duration was 38.7 months (range, 18.3-50.1). Median progression-free survival (PFS) was 1.3 months (95% CI, 1.2-1.7), and median overall survival (OS) was 4.7 months (95% CI, 3.8-9.1). Although there were no differences in total NK cell numbers between responders and non-responders (p = 0.139), baseline CD16$^+$ NK cells were significantly higher in responders. The high CD16$^+$ NK group showed superior objective response rate (60% vs 17.8%, p = 0.012), disease control rate (70% vs 26.7%, p = 0.023), and longer PFS (14.4 months, 95% CI 1.4-not reached [NR], p = 0.017) and OS (14.7 months, 95% CI 1.4-NR, p = 0.079). High baseline CD16$^+$ NK cell proportion were associated with the decline of regulatory T cells at C2D1, suggesting enhanced ADCC by Ipi. Consistently, single cell analysis also revealed higher baseline CD16$^+$ expression in NK cells at baseline in responders than non-responders. Independent validation of these findings is ongoing.

Conclusion: Baseline peripheral CD16$^+$ NK cell levels were significantly associated with improved clinical outcomes in advanced HCC patients treated with Nivo/Ipi. High CD16$^+$ NK cell frequency correlated with higher response rates and prolonged survival, potentially through enhanced ADCC and suppression of regulatory T cells. These findings suggest that baseline CD16$^+$ NK cells may serve as a predictive biomarker for Nivo/Ipi in HCC, warranting further validation cohorts.

: Immune Response to Therapies
Poster Session

#7741 AI-designed personalized neoantigen vaccine, EVX-01, induces durable *de novo* T-cell responses in advanced melanoma patients.

Mads Lausen[1], Michail Angelos Pavlidis[1], Ohrt Andersen Rasmus[1], Thuesen Nikolas[1], Nadia Viborg[1], Georgina V. Long[2], Adnan Khattak[3], Paolo A Ascierto[4], Carolina Cimminiello[5], Thomas Trolle[1], Christian Garde[1], Michael J. Chisamore[6], Benjamin Wolthers[1], Stine Friis Thorsen[1], Birgitte Rono[1], Daniela Kleine-Kohlbrecher[1]

[1]Evaxion A/S, Hoersholm, Denmark,[2]Melanoma Institute Australia, The University of Sydney, and Mater and Royal North Shore Hospitals, Sydney, NSW, Australia,[3]One Clinical Research, Hollywood Private Hospital & Edith Cowan University, Perth, WA, Australia,[4]Melanoma, Cancer Immunotherapy & Developmental Therapeutics, Istituto Nazionale Tumori - IRCCS - Fondazione Pascale, Neaples, Italy,[5]Divisione di Oncologia Medica del Melanoma, Sarcoma e Tumori Rari, IEO - Istituto Europeo di Oncologia IRCCS, Milano, Italy,[6]Merck & Co., Inc., Wheaton, IL

Cancer vaccines have recently emerged as promising anti-cancer therapies that complement immune checkpoint blockade by stimulating targeted anti-tumor immunity. Their efficacy critically depends on including tumor antigens that can elicit a potent, cancer-specific T-cell response. To achieve this, Evaxion developed the proprietary AI-Immunology™ platform to identify highly immunogenic tumor antigens and design personalized cancer vaccines based on patient-specific sequencing data, optimized for maximal immune activation.The AI-platform identifies somatic mutations and indels in the tumor mutanome, considering tumor expression, clonality and HLA loss to select neoantigens with highest immunogenic potential. EVX-01, the first vaccine candidate generated from this AI-platform, was evaluated in a phase 2 clinical study (NCT05309421) in advanced melanoma. EVX-01 was administered in combination with pembrolizumab, following a 12-week run-in period with pembrolizumab as monotherapy. Patients received in total 10 EVX-01 doses, split into 6 priming and 4 booster immunizations. Primary endpoint was RECIST 1.1-based response improvement of the objective response rate (ORR). For immunogenicity and biomarker analysis peripheral blood was collected before, during and after treatment and processed to peripheral blood mononuclear cells (PBMC). Vaccine-specific T-cell responses were assessed by Interferon-gamma ELISpot and intracellular cytokine staining and flow cytometry, both *ex vivo* and after *in vitro* stimulation. Non-vaccine antigens were tested to investigate potential epitope spreading. At the two-year read out, the ORR was 75% (12/16) in the overall cohort. Of the responders, 92% (11/12) continued to respond at 24 month follow up. The treatment was well-tolerated, and the manufacturing success rate was 100%. Additionally, of 13 patients with stable disease (SD) or partial response (PR) after a the 12-week pembrolizumab induction, 54% (7/13) deepened the response upon initiation of EVX-01. The final immunogenicity analysis showed that EVX-01 priming induced strong vaccine-specific T-cell responses in the 15 assessable patients, with booster doses sustaining response magnitudes until last assessment at week 102. Both CD4+ and CD8+ T cells contributed to the response, with CD4+ T cells predominating. 84% of tested neoantigens elicited a specific immune response and AI-Immunology™ platform-assigned immunogenicity scores correlated with the magnitude of T-cell reactivity. In conclusion, the AI-Immunology™ platform can effectively identify highly immunogenic neoantigens, design manufacturable and safe personalized cancer vaccines with pharmacodynamic activity. Combined with PD-1 blockade, EVX-01 achieves a 75% ORR and induces durable, vaccine-specific T-cell immunity in all treated patients, validating the platforms predictive precision.

#7742 Intratumoral effector T-cells and macrophages underlie prolonged survival after PD-1 axis blockade in metastatic non-small cell lung cancer (mNSCLC).

Daniel Boiarsky[1], Thazin Nwe Aung[2], Anna Wurtz[3], Jianlei Gu[4], Benjamin Y. Lu[5], David L. Rimm[2], Arutha Kulasinghe[6], Katerina A. Politi[7], Scott Gettinger[8], Kurt Alex Schalper[9]

[1]Department of Medicine (Medical Oncology and Hematology), Yale School of Medicine, New Haven, CT,[2]Yale School of Medicine, New Haven, CT,[3]Yale Cancer Center, Yale School of Medicine, New Haven, CT,[4]Department of Pathology, Yale School of Medicine, New Haven, CT,[5]Department of Medicine (Medical Oncology and Hematology), Yale New Haven Hospital, New Haven, CT,[6]University of Queensland, Woolloongabba, Australia,[7]Yale Cancer Center, New Haven, CT,[8]Yale Univ., New Haven, CT,[9]Yale University, Branford, CT

Background: Although PD-1 axis inhibitors have improved outcomes in patients with mNSCLC, only a subset of patients derives long-term benefit. Most studies assessing determinants of sensitivity have relied on short-term endpoints such as response, potentially overlooking biological features underlying durable tumor control. We hypothesized that patients achieving prolonged response after PD-1 axis blockade exhibit distinct tumor microenvironment (TME) features compared with those with primary resistance or limited response.

Methods: We assembled a retrospective cohort of bulk whole-transcriptome data from 342 pretreatment tumor samples from patients with mNSCLC treated with PD-1 axis blockade alone or in combination with anti-CTLA-4 therapy from Yale (n=31), Stand Up To Cancer (n=73), and Samsung Medical Center (n=278). Patients were classified as having primary progression (PP; PFS <3 mo; n=200), non-exceptional response (NER; PFS 6-36 mo; n=116), and prolonged survival (PS; PFS >36 mo; n=26). After batch correction, differential expression (limma) and CIBERSORT were used to identify genes and immune cells associated with PS. Single-cell RNA sequencing from a publicly-available lung cancer immune cell atlas (n=234) was used to refine immune cell signatures and assess their association with outcomes via ssGSEA. Spatial proteomics (Phenocycler-Fusion) performed on baseline samples from patients treated with PD-1 axis blockade (n=55; PP=21, NER=26, PS=8) at Yale and the University of Queensland was used for validation.

Results: Tumors from PP, NER, and PS demonstrated a stepwise increase in HLA class I antigen-presentation machinery (APM) transcripts (PSMB9, ERAP2), memory T-cell markers (CXCR6), and $CD8^+$ T-cell infiltration. PD-L1 expression was markedly higher in NER than PP, but similar between NER and PS. The most significantly enriched genes in PS relative to NER were macrophage-related, with higher absolute M1 (Cliff's δ=0.34, p=0.007) and M2 (δ=0.29, p=0.023) tumor-associated macrophage (TAM) scores. This difference was not observed between NER and PP. Four percent of patients with low (≤ median) calculated $CD8^+$ T-cell and TAM levels were PS, compared with 15% of those with high $CD8^+$/TAM levels (odds ratio=4.5, p=0.0083). Single-cell analysis identified 15 TAM subsets, several enriched in PS but none in PP. Spatial proteomics confirmed an increase in the proportion of stromal TAMs in PS (PS vs NER: δ=0.62, p=0.0079; PS vs PP: δ=0.58, p=0.016) and revealed a stepwise decrease in the proportion SMA^+ fibroblasts across clinical benefit groups.

Conclusion: Prolonged survival after PD-1 blockade in mNSCLC is associated with distinct TME features including increased expression of APM components, and increased CD8 T-cells and TAMs. These insights may inform the development of predictive biomarkers and novel therapeutic strategies.

#7743 Pre-existing T cells drive durable anti-tumor immunity after oncolytic virus therapy in glioblastoma.

Maxime Meylan[1], Ye Tian[1], Lijian Wu[1], Alexander L. Ling[2], Daniel Kovarsky[3], Graham L. Barlow[1], Linh D. Nguyen[1], Jason Pyrdol[1], Lucas Westphal[1], Michel Julius[1], Nicolas L. Gonzalez Castro[4], Sydney D. Dumont[4], Andres Santos[2], Itay Tirosh[3], Mario L. Suva[4], E Antonio Chiocca[2], Kai W. Wucherpfennig[1]

[1]Cancer Immunology and Virology, Dana-Farber Cancer Institute, Boston, MA,[2]Harvey Cushing Neuro-oncology Laboratories, Department of Neurosurgery and Center for Tumors of the, Mass General Brigham Cancer Institute, Boston, MA,[3]Department of Molecular Cell Biology, Weizmann Institute of Science, Rehovot, Israel,[4]Department of Pathology and Krantz Family Center for Cancer Research, Massachusetts General Hospital, Boston, MA

Background: Recurrent glioblastoma (rGBM) remains refractory to immunotherapy due to sparse and suppressed T cell infiltration. We recently reported that survival correlated with immune activation signatures in rGBM patients receiving the oncolytic HSV-1 (oHSV) rQNestin34.5v.2 (CAN-3110). Here, we provide in-situ and molecular evidence that a single oncolytic virus injection can induce durable, tumor-reactive T cell immunity in rGBM.

Methods: We integrated highly multiplexed spatial proteomics (CODEX), spatial transcriptomics (Xenium) with custom probes for viral, immune and TCR targets, and bulk TCR-sequencing on paired pre- and post-treatment specimens from a phase 1 clinical trial (NCT03152318).

Results: T cell densities strongly increased after treatment, with deep infiltration into viable tumor regions persisting up to two years after a single intratumoral oHSV injection. Cytotoxic GZMB+ T cells were located in close proximity with cleaved-caspase 3+ apoptotic tumor cells, and shorter T cell-tumor distance correlated with longer-progression free survival, demonstrating ongoing anti-tumor immunity. Spatial transcriptomics identified CD8+ T cells states expressing early TCR activation (NR4A1, CD69) and tissue residency (ZNF683 [HOBIT], ITGAE [CD103]) programs enriched in the tumor bed while stem-like T cells localized within lymphoid aggregates. Bulk and spatial TCR analyses revealed in-situ expansion of pre-existing tumoral T cell clones whose amplification correlated with survival. Expanded clones featured tissue resident phenotypes and were positioned closer to tumor cells than non-expanded T cells. Viral remnants were limited to necrotic regions and did not co-localize with T cells, suggesting persistent tumor recognition rather than viral antigen.

Conclusion: These results provide in-situ evidence that a single intratumoral oncolytic virus injection can amplify pre-existing T cells clones and induce sustained T cell mediated tumor cytotoxicity even after virus clearance. This suggests that oncolytic virotherapy is as potent T cell activating strategy in rGBM.

#7744 Single-cell and spatial profiling reveal tumor-immune features underlying pathologic complete response to neoadjuvant anti-PD-L1 and chemoradiotherapy in NSCLC.

Jii Bum (Joy) Lee[1], Sang Hoon Lee[2], Haangik Park[2], Seul Lee[3], **Dong Kwon Kim**[2], Jae-Hwan Kim[4], Ju-Hyeon Lee[2], Jaeho Cho[5], Chang Geol Lee[5], Chang Young Lee[6], Jin Gu Lee[6], Dae Joon Kim[6], Hyo Sup Shim[7], Sun Min Lim[8], Hye Ryun Kim[8], Byoung Chul Cho[9]

[1]Yonsei University, Seoul City, Korea, Republic of,[2]Severance Biomedical Science Institute, Seoul, Korea, Republic of,[3]Yonsei University College of Medicine,[4]Yonsei University Hospital Cancer Center, Seoul, Korea, Republic of,[5]Department of Radiation Oncology, Yonsei Cancer Center, Seoul, Korea, Republic of,[6]Department of Thoracic and Cardiovascular Surgery, Seoul, Korea, Republic of,[7]Department of Pathology, Severance Hospital, Seoul, Korea, Republic of,[8]Division of Medical Oncology, Department of Internal Medicine, Seoul, Korea, Republic of,[9]Yonsei University College of Medicine, Seoul

Background: Perioperative chemoimmunotherapy has become standard for resectable non-small cell lung cancer (NSCLC), yet how neoadjuvant anti-PD-L1 and chemoradiotherapy remodel the tumor microenvironment (TME) remains poorly defined.

Methods: Tumors from patients with stage III NSCLC treated with neoadjuvant durvalumab plus concurrent chemoradiotherapy in the NCT03694236 trial were analyzed using single-cell RNA sequencing (scRNA-seq), T cell receptor sequencing (TCR-seq), and spatial transcriptomics to delineate cellular and molecular programs associated with pathologic response.

Results: Neoadjuvant durvalumab combined with concurrent chemoradiotherapy was administered to 30 patients with resectable stage III NSCLC. All patients completed therapy without surgical delay, achieving a major pathologic response (MPR) rate of 74% and a pathologic complete response (pCR) rate of 41%, with R0 resection in all surgical cases. Integrated scRNA-seq, TCR-seq, and spatial analyses of 19 tumors revealed distinct immune architectures between pCR and non-pCR groups. pCR tumors exhibited expansion and spatial clustering of clonally enriched CD8$^+$ effector-memory (T_{EM}) and progenitor-exhausted (T_{PEX}) cells forming a $T_{EM}\rightarrow T_{PEX}\rightarrow T_{EX}$ trajectory with cytotoxic and antigen-processing programs localized adjacent to tumor nests. In contrast, non-pCR tumors accumulated TNFα-producing OLR1$^+$ monocytes and FOLR2$^+$macrophages that promoted TNFR2$^+$ regulatory T cell (Treg) differentiation through TNF-TNFR2 signaling, reinforcing immunosuppression. Chemokine-receptor mapping demonstrated divergent recruitment patterns: antigen-presenting CAFs (apCAFs) and myeloid cells in pCR expressed CCL5 and CCL3, recruiting T_{PEX} cells via CCR5, whereas CCL20-CCR6/CCR4 signaling in non-pCR favored Treg attraction. apCAFs in pCR upregulated antigen-presentation and cytotoxicity-related genes while losing immunosuppressive traits, facilitating CD8$^+$ T cell infiltration and spatial organization of an inflamed TME. Collectively, these findings delineate opposing immune circuits-cytotoxic CD8$^+$ T_{PEX}/T_{EX} activation in pCR versus TNF-TNFR2-driven myeloid-Treg suppression in non-pCR tumors.

Conclusion: Neoadjuvant durvalumab-based chemoradiotherapy reprograms the stage III NSCLC TME toward clonally expanded, cytotoxic CD8$^+$ T cell immunity in pCR, while persistent TNF-TNFR2-Treg signaling sustains immune resistance in non-pCR tumors. Targeting TNFR2 signaling, modulating myeloid polarization, or enhancing CCL5-CCR5-mediated T cell recruitment may further potentiate antitumor efficacy. These findings provide a mechanistic rationale for integrating TNFR2 blockade or chemokine-axis modulation with neoadjuvant immunotherapy to improve pathologic response and long-term outcomes.

#7745 EGFR-TKI enhances anti-CD47 antibody-mediated macrophage phagocytosis in EGFR-mutant non-small cell lung cancer.

Myungja Ro[1], Seung Min Yang[2], **Youngtaek Kim**[3], Min-Hak Lee[4], Eun Ji Lee[3], JuHyeon Lee[2], Mi Ran Yun[1], Ji-Eun Park[5], Jiyea Choi[5], Hyesun Lee[5], Sung Ho Kim[5], Heung Tae Kim[5], Byoung Chul Cho[1]

[1]Yonsei New Il Han Institute for Integrative Lung Cancer Research, Seoul, Korea, Republic of,[2]Department of Research, Yonsei Biomedical Research Institute, Seoul, Korea, Republic of,[3]Yonsei University College of Medicine, Seoul, Korea, Republic of,[4]JEUK Institute for Cancer Research, JEUK Co., Gumi, Korea, Republic of,[5]ImmuneOncia Therapeutics, Inc., Gyeonggi-do, Korea, Republic of

Background: CD47, a “don’t eat me” signal, enables tumor cells to evade macrophage-mediated clearance. EGFR-mutant non-small cell lung cancer (NSCLC) exhibits increased CD47 expression, facilitating immune evasion by inhibiting phagocytosis. Preclinical studies suggest that combining third-generation EGFR TKIs with CD47 blockade can enhance antitumor immunity. Here, we investigated the therapeutic potential of combining the anti-CD47 antibody IMC-002 with lazertinib to enhance macrophage phagocytosis.
Methods: EGFR-mutant and wild-type NSCLC cell lines, patient-derived cells (PDCs), and TKI-resistant derivatives were analyzed for CD47 expression by qPCR, immunoblotting, and flow cytometry. Cells were treated with lazertinib and IMC-002 individually or in combination across a concentration range. Macrophage phagocytosis was quantified by flow cytometry and live-cell imaging (Incucyte). Single-cell RNA sequencing (scRNA-seq) datasets from EGFR-mutant NSCLC patients before and after TKI treatment were analyzed to characterize changes in CD47 expression and resistance-associated pathways.
Results: EGFR-mutant cell lines showed overall higher baseline CD47 expression compared to wild-type controls. Lazertinib treatment induced a dose-dependent increase in surface CD47 expression in H1975 cells. Co-treatment with lazertinib and IMC-002 led to additive to synergistic increases in macrophage-mediated phagocytosis in multiple EGFR-mutant cell lines and in PDCs. In cell lines where lazertinib upregulated surface CD47, IMC-002 blockade elicited substantially greater phagocytosis than lazertinib alone, suggesting that TKI exposure increases target availability and that subsequent antibody blockade acts synergistically by abrogating CD47-SIRPα signaling and promoting macrophage-mediated engulfment. scRNA-seq analyses of EGFR-mutant NSCLC patients before and after third-generation EGFR TKI treatment revealed increased CD47 expression within tumor clusters enriched for drug-tolerant persister signatures, including TGF-β, Wnt, and YAP pathways, providing additional explanations for enhanced anti-CD47 antibody accessibility and phagocytic clearance following combination treatment. Collectively, EGFR-TKI exposure can increase the abundance and accessibility of CD47 on tumor cells, and anti-CD47 antibody treatment synergizes with lazertinib to amplify macrophage-mediated clearance, supporting a rationale for a combination strategy to improve antitumor immunity in EGFR-mutant NSCLC.
Conclusion: Lazertinib induces CD47 upregulation and synergizes with IMC-002 to enhance macrophage-mediated clearance of EGFR-mutant NSCLC cells. These findings provide a mechanistic rationale for clinical evaluation of EGFR-TKI and anti-CD47 combination strategies to improve therapeutic efficacy in EGFR-mutant lung cancer.

#7746 CEACAM5/6+ cancer cell and IL1B+ macrophage-mediated resistance in anti-PD-1 treated gastric cancer.

Liudeng Zhang[1], Jian Chen[2], Yikai Luo[1], Lie Wang[2], Han Liang[1]

[1]Bioinformatics and Computational Biology, UT MD Anderson Cancer Center, Houston, TX,[2]Zhejiang University, Hangzhou, China

Immune checkpoint blockade therapy has shown limited efficacy in gastric cancer, with most patients developing resistance through mechanisms that remain incompletely defined. Here, we generate a comprehensive single-cell RNA sequencing atlas of 526,583 cells from gastric cancer patients treated with anti-PD-1 plus chemotherapy, analyzing paired pre- and post-treatment samples to capture dynamic resistance mechanisms. We identify two distinct resistance pathways that emerge during treatment. First, CEACAM5/6+ cancer cells are markedly enriched in pre-treatment non-responders and predict treatment failure. These CEACAM5/6+ epithelial cells show the highest tumor scores and correlate with increased regulatory T cell infiltration expressing CEACAM1, establishing an alternative checkpoint axis that bypasses PD-1/PD-L1 blockade. External validation in independent cohorts confirms CEACAM5/6 expression as a robust predictor of anti-PD-1 resistance. Second, we uncover a macrophage-driven inflammatory cascade central to treatment resistance. IL-1β+ macrophages serve as the primary source of NF-κB pathway activation across the tumor microenvironment, triggering downstream IL-6 production, Th17 cell differentiation, chronic inflammation and epithelial-mesenchymal transition. This macrophage module is significantly enriched in post-treatment non-responders, with TNF-high expressing monocyte-macrophages absent in responders but prevalent in resistant tumors. The resulting inflammatory milieu drives PD-L1 upregulation across multiple cell types, creating a self-reinforcing immunosuppressive niche. Collectively, these findings nominate CEACAM5/6$^+$ epithelial cells and IL-1β$^+$ inflammatory macrophages as actionable therapeutic targets for overcoming anti-PD-1 resistance in gastric cancer, providing a mechanistic framework and rational blueprint for next-generation combination immunotherapy strategies.

#7747 Comparison of T-cell activation status in patients treated with retifanlimab in combination with anti-LAG3/Anti-TIM3 vs retifanlimab alone.

Robert I. Haddad[1], Denis Soulieres[2], Prakash Neupane[3], Amaury Daste[4], **Zhiwan Dong**[5], Jin Lu[5], Michelle Kinder[5], Jeff Jackson[5], Richard Schaub[5], Nawel Bourayou[5], John Janik[5], Christophe Le Tourneau[6]

[1]Dana-Farber Cancer Institute, Brigham and Women's Hospital, Harvard Medical School, Boston, MA,[2]Centre Hospitalier de l'Universite de Montreal, Montreal, QC, Canada,[3]The University of Kansas Medical Center, Kansas City, KS,[4]Hopital Saint-Andre, CHU Bordeaux-University of Bordeaux, Bordeaux, France,[5]Incyte, Wilmington, DE,[6]DITEP, Gustave Roussy, Villejuif, France

PD-1/PD-L1-targeting antibodies have revolutionized cancer treatment but most pts fail to respond (primary resistance) or lose response (secondary resistance). Anti-PD-1 therapy resistance mechanisms are poorly understood; other checkpoint inhibitor pathways are important investigational targets based on animal model studies. Co-expression of PD-1, LAG3, and TIM3 is associated with functional T-cell exhaustion and may contribute to resistance. Antibodies targeting LAG3 and TIM3 are potential candidates for overcoming anti-PD-1 resistance; LAG3 is also clinically supported as a target for resistance in pts with melanoma. INCAGN2385-203 is a randomized, phase 2 study to evaluate the efficacy and safety of retifanlimab (anti-PD-1) + INCAGN02385 (anti-LAG3) and retifanlimab + INCAGN02385 + INCAGN02390 (anti-TIM3) combinations vs retifanlimab alone in immunotherapy naïve PD-L1-positive (CPS ≥1) recurrent/metastatic SCCHN. Objective response rate was numerically higher in anti-LAG3-containing arms (~30%) vs the retifanlimab monotherapy arm (20%). Median progression-free survival was similar in all 3 arms. To evaluate pharmacodynamic biomarkers associated with LAG3 and/or TIM3 blockade in the context of PD-1 inhibition, flow cytometry was used to evaluate frequency changes of CD4 and CD8 T cells, regulatory T cells, and memory T cells, as well as activation and proliferation markers in whole blood samples. T-cell proliferation and activation were observed in all 3 arms. T-cell proliferation (CD4 and CD8) measured by frequency change of Ki67-positive T cells and HLA-DR expression was more pronounced in both anti-LAG3-containing arms vs the retifanlimab alone arm. No significant difference in regulatory T cells was observed between the 3 arms. Naïve CD4 and CD8 T cells decreased at similar levels at cycle 1, day 8 across all arms. A steady decrease of central memory CD4 and CD8 T cells up to cycle 4, day 1 was observed with retifanlimab alone, whereas retifanlimab + anti-LAG3 showed elevation of central memory T-cell frequencies in both CD4 and CD8 T cells up to cycle 1, day 15, before decreasing steadily up to cycle 4, day 1; there was no obvious change from baseline to cycle 4, day 1 in the triplet arm. Opposite trends were observed in effector memory CD4 and CD8 T cells. Retifanlimab alone produced a steady increase, whereas retifanlimab + anti-LAG3 showed decreases in CD4 (up to cycle 1, day 15) and CD8 (up to cycle 2, day 1) effector memory T cells before increasing steadily. These preliminary results suggest that LAG3 and/or TIM3 blockade may have unique effects on T-cell function. LAG3 with PD-1 blockade may overstimulate T cells and lead to T-cell elimination, highlighting the need for dose optimization. Further evaluation of T-cell responses of PD-1/PD-L1 blockade with other checkpoint inhibitors, including those targeting LAG3 and TIM3, is warranted.

#7748 Immune-related RNA-seq biomarker-based clustering reveals heterogeneous immunotherapy responses and guides subtype-specific strategies in metastatic NSCLC.

Jiyon Lyu[1], Sebastia Franch-Exposito[2], **Sanghwa Kim**[1], Liam Il-Young Chung[1], Ronald Min[1], Sung Hwan Lee[3], Shinkyo Yoon[1], Michelle M. Stein[2], JACOB MERCER[2], Paul Fields[2], Bella Kim[4], Young Kwang Chae[1]

[1]Department of Medicine, Northwestern University Feinberg School of Medicine, Chicago, IL,[2]Tempus AI, Chicago, IL,[3]Department of Surgery, CHA Bundang Medical Center, Seongnam, Korea, Republic of,[4]Northwestern University, Chicago, IL

Metastatic non-small cell lung cancer (mNSCLC) represents a highly heterogeneous disease with variable clinical outcomes under first-line immunotherapy plus chemotherapy. To better understand immune landscape features associated with heterogeneous response to immunotherapy, we performed biomarker-driven RNA-seq molecular clustering using known immune-related markers *TIGIT, FOXP3, CD274* (*PD-L1*), and tumor-associated macrophage (TAM) score.

We analyzed a real-world cohort of 2,235 mNSCLC patients with pre-treatment tumor biopsies in the de-identified Tempus database treated with first-line PD-(L)1 plus chemotherapy. Unsupervised clustering of RNA-seq data defined four distinct immune subtypes. Real-world overall survival (rwOS) and progression-free survival (rwPFS) were assessed via Kaplan-Meier analysis with a log-rank test. Pathway enrichment using hallmark gene sets, tumor mutational burden (TMB), and immune cell composition using QuantiSeq were analyzed.

Expression levels of RNA-seq biomarkers and TAM score were significantly different across identified clusters (ANOVA; p <0.001). These clusters also showed significantly differential prevalence of TMB-high and PD-L1-positive (IHC) (Chi-squared; p < 0.001, respectively), as well as characteristic pathway enrichment and immune profiles. Non-squamous/Never smoker were more frequent in Cluster 2, whereas Squamous/Current smoker were predominant in Cluster 1 (Chi-squared; Histology/Smoking, p <0.05, respectively). Survival differed significantly, being poorest in Cluster 1 and best in Cluster 3 (rwOS/rwPFS, p <0.001) (Table 1).

This biomarker-driven RNA-seq analysis identified four immune clusters of mNSCLC with differential survival outcomes. This study provides a foundation for understanding tumor heterogeneity and supports the use of immune biomarkers to enable patient stratification for therapeutic combinations.

Table 1.

	Cluster 1 (Immune-desert) N=713	**Cluster 2 (TAM-enriched) N=402**	**Cluster 3 (Immune-hot) N=813**	**Cluster 4 (Myeloid-inflamed, PD-L1-high) N=302**	***p*-value**
Median Survival Time (Months) rwOS/rwPFS	11.5/5.95 mo	14.8/7.33 mo	18.1/8.15 mo	16.7/6.84 mo	Log-rank test; p <0.001
RNA-Seq Biomarkers (TIGIT, FOXP3, CD274 (PD-L1)) and TAM Score	Uniformly low expression of all markers	High TAM but low TIGIT/FOXP3/PD-L1	High TIGIT/FOXP3/PD-L1 with elevated TAM	High PD-L1 with low TIGIT/FOXP3	ANOVA test; p <0.001
Pathway Enrichment TME: tumor microenvironment	↑ Oncogenic signalings and proliferation ↓ Immune -related pathways	↑ TME remodeling pathways	↑ Immune/inflammatory signaling (e.g., IFNγ) and TME remodeling pathways	↑ Proliferation and DNA-repair pathways	Welch ANOVA + Games-Howell or Kruskal-Wallis and Dunn (BH) test; adjusted p <0.05
Immune Cell Composition	↓ Lymphoid and myeloid cell infiltration	↑ M1/M2 macrophage	Broad infiltration (↑ CD8, CD4, Treg, B, NK)	↑ Myeloid cell infiltration	Kruskal-Wallis and Dunn (BH) test; adjusted p <0.05
TMB-High (TMB ≥10 mut/Mb)	283 (34%)	92 (20%)	254 (26%)	124 (35%)	Chi-squared test; p <0.001
PD-L1-Positive (IHC; TPS ≥ 1%)	203 (36%)	174 (54%)	421 (68%)	213 (94%)	Chi-squared test; p <0.001
Tumor Histology					Chi-squared test; p <0.001
Squamous	232 (33%)	73 (18%)	221 (27%)	84 (28%)	
Non-Squamous	444 (62%)	315 (78%)	555 (68%)	201 (67%)	
NOS	37 (5.2%)	14 (3.5%)	37 (4.6%)	17 (5.6%)	
Smoking Status					Chi-squared test; p <0.05
Current Smoker	118 (62%)	44 (46%)	113 (55%)	48 (59%)	
Never Smoker	16 (8.4%)	23 (24%)	32 (15%)	12 (15%)	
Ex-Smoker	56 (29%)	29 (30%)	62 (30%)	21 (26%)	
Unknown	523	306	606	221	

#7749 Increased immune activity in patients with high-grade serious ovarian cancer after combination PARPi + ATRi therapy.

Elias Pavlatos[1], Benjamin Tate[1], Austin Nguyen[1], Ian S. Heller[2], Dimitrios Nasioudis[2], Janos L. Tanyi[3], Drew A. Torigian[4], Diego Rodriguez[2], Susan M. Domchek[4], Ronny I. Drapkin[2], Eric J. Brown[5], Gordon B. Mills[6], Fiona Simpkins[2]

[1]Immune Monitoring and Cancer Omics Services, OHSU Knight Cancer Institute, Portland, OR,[2]Division of Gynecologic Oncology, Department of Gynecology and Obstetrics, University of Pennsylvania, University School of Medicine, Philadelphia, PA,[3]Division of Medical Oncology, Perelman School of Medicine at the University of Pennsylvania, Philadelphia, PA,[4]Department of Radiology, Perelman School of Medicine at the University of Pennsylvania, Philadelphia, PA,[5]Department of Cancer Biology & Abramson Family Cancer Research Institute, Perelman School of Medicine at the University of Pennsylvania, Philadelphia, PA,[6]OHSU Knight Cancer Institute, Portland, OR

Introduction: Complete responses to PARP inhibitor (PARPi) monotherapy in recurrent high-grade serous ovarian cancer (HGSOC) are rare. However, preclinical data have demonstrated promising synergy between PARP and ATR inhibitors. Characterizing the immune contexture of the tumor microenvironment and the surrounding stroma during treatment may provide valuable biological insights into the efficacy of this combination therapy and inform future combinations.

Methods: Patients with recurrent HGSOC received ceralasertib 160mg orally daily, days 1-7 and olaparib 300mg twice daily, days 1-28 of a 28-day cycle. 18 tissue samples were collected across archival (resection) and pre-treatment and on-treatment timepoints (core biopsies). Each sample was analyzed using a 25-plex multiplex immunohistochemistry (mIHC) assay, which interrogates cell composition and functional states of neoplastic and immune cell types, including all major lymphoid and myeloid populations. Segmented cells were assigned to either a tumor or stroma compartment using a PanCK mask that was uniformly expanded by 25µm, and average cell densities were calculated for each compartment.

Results: Samples obtained during combination PARPi + ATRi treatment demonstrated widespread increases in immune cell densities including T cells (CD8+, Tregs, and Th1-like cells), B cells, dendritic cells, macrophages, and monocytes. Among the T-cell populations, higher densities of Granzyme B and PD-1 were observed, indicating enhanced cytotoxic activity and immune engagement. Concurrently, there was a decrease in proliferating neoplastic cells (PanCK$^+$Ki67$^+$), consistent with reduced tumor cell proliferation during treatment. Using the PanCK tumor mask, we observed that CD8$^+$ T cells, Th1-like cells, B cells, and dendritic cells increased more prominently within the tumor compartment compared to the surrounding stroma. Samples obtained prior to treatment from patients with stable or progressive disease (SD/PD) exhibited higher macrophage densities, primarily attributable to elevated levels of M2-like (immunosuppressive) macrophages.

Conclusions: The increased immune cell densities measured by mIHC indicate overall activation of the immune system following PARPi + ATRi treatment. Elevated levels of PD-1$^+$ and Granzyme B$^+$ T cells suggest enhanced immune activation and cytotoxic potential, while comparative analysis of the tumor versus stroma compartments demonstrates improved immune cell infiltration into the tumor. Notably, higher baseline densities of M2-like macrophages may influence or limit response to therapy. Collectively, these findings provide evidence that PARPi + ATRi combination therapy promotes anti-tumor immune activity. However, additional data is needed to correlate these immune changes with clinical outcomes.

#7750 Integration of spatial single cell proteomics and spatial metabolomics reveals tumor microenvironment predictive of immunotherapy response in mucosal melanoma.

Jun Wang[1], Priyadharsini Nagarajan[2], Sungnam Cho[3], Yunhe Liu[1], Erin H. Seeley[4], Yibo Dai[1], Yang Liu[1], Jared K. Burks[3], Jennifer L. McQuade[5], Adi Diab[5], Linghua Wang[6], Suhendan Ekmekcioglu[5]

[1]Department of Genomic Medicine, UT MD Anderson Cancer Center, Houston, TX,[2]Department of Pathology, UT MD Anderson Cancer Center, Houston, TX,[3]Hematopoietic Biology & Malignancy, UT MD Anderson Cancer Center, Houston, TX,[4]Mass Spectrometry Imaging Core Facility, UT MD Anderson Cancer Center, Houston, TX,[5]Department of Melanoma Medical Oncology, UT MD Anderson Cancer Center, Houston, TX,[6]UT MD Anderson Cancer Center, Houston, TX

Background: Mucosal melanoma (MuM) is a rare melanoma subtype, accounting for only 1-2% of all melanoma cases, yet is highly aggressive, demonstrating poorer responsiveness to immune checkpoint blockade than the more common cutaneous melanoma. However, the biological mechanisms driving therapeutic resistance in MuM remain poorly understood. This study aims to uncover spatial and molecular mechanisms underlying response and resistance of MuM to immune checkpoint blockade therapies.

Study Design and Methods: An integrative spatial multi-omics framework was applied, which combined single-cell spatial proteomics using COMET platform with high mass resolution spatial metabolomics using imaging mass spectrometry (MALDI-IMS). We comprehensively profiled cellular compositions and spatially defined cellular neighborhoods (CNs) across 97 FFPE tissue cores from 26 MuM patients treated with PD-1/PD-L1 or CTLA-4 inhibitors. Spatial organization, cell-cell interactions, proteomic profiles and metabolomic features of CNs were further compared across responders and non-responders.

Results: The comprehensive approach enabled spatially resolved profiling of 695,444 single cells, which were categorized into 25 cellular phenotypes spanning 9 major cell lineages. Spatial cellar neighborhood analysis revealed 15 biologically distinct CNs that differed in their composition and spatial distribution of tumor, immune, and stromal cell compartments. In patients who responded to immunotherapy, three tumor-associated CNs—the central tumor, invasive tumor, and tumor boundary CNs—were significantly enriched and collectively formed unique spatial organization patterns. Notably, the invasive tumor CN and tumor boundary CN were characterized by spatial proximity among Ki67$^+$ tumor cells, CD163$^+$ macrophages, and CD11c$^+$ dendritic cells. These CD163$^+$ macrophages exhibited reduced expression of IRF4 and Arg1, consistent with lower immunosuppressive activity. Conversely, non-responders exhibited a stromal-dominant CN composed primarily of SMA$^-$ stromal cells and demonstrated reduced immune infiltration in both pre-treatment and post-treatment samples. Spatial metabolomic profiling further revealed a pronounced reduction of tryptophan-derived indole metabolites in responders, which significantly correlated with CD11c and CD163 expression, indicating coordinated immunometabolic remodeling within the tumor microenvironment.

Conclusions: These findings highlight that spatial tumor-immune architecture, stromal exclusion, and metabolic rewiring collectively shape immunotherapy response in MuM. The identified spatially resolved tryptophan-derived metabolite signatures offer promising biomarkers and potential therapeutic targets to improve treatment outcomes in this clinically challenging melanoma subtype.

#7751 Integrative multi-omics and spatial transcriptomics reveal novel immunotherapy targets in hepatocellular carcinoma.

Zihui Zhao[1], Xiaohang Long[2], Siyuan HUANG[2], Yan Liu[3], Alfred S. l. Cheng[4]

[1]School of Biomedical Science, Chinese University of Hong Kong (CUHK), Hong Kong, Hong Kong,[2]CUHK, NT, Hong Kong,[3]The Chinese University of Hong Kong, Shatin, NT,[4]Chinese University of Hong Kong (CUHK), Hong Kong, Hong Kong

Background: Immunotherapy has transformed the management of hepatocellular carcinoma (HCC), yet most patients fail to achieve durable responses. The underlying single-cell-level gene-regulatory mechanisms shaping immune evasion remain poorly understood. To uncover previously unknown therapeutic vulnerabilities, we integrated single-cell multiomic profiling with spatial transcriptomics in a 25-patient HCC immunotherapy cohort.

Methods: Tumor samples underwent 10x multiome sequencing, enabling simultaneous scATAC-seq and scRNA-seq from the *same cells* using shared barcodes. This allowed cell-resolved mapping of chromatin accessibility, transcriptional states, and gene-regulatory relationships. We identified differentially accessible regions and gene-expression changes associated with clinical immunotherapy outcomes. To contextualize these regulatory programs in situ, spatial transcriptomic profiling was performed to map target-gene expression and immune-cell localization within the tumor microenvironment.

Results: Joint scATAC-scRNA integration revealed previously unrecognized regulatory circuits distinguishing responders from non-responders, including chromatin-primed dysfunctional $CD8^+$ T cells and TREM2+ macrophage programs not detectable by single-modality assays. Multiomic analysis identified novel candidate immune-regulatory targets, defined by coordinated shifts in chromatin accessibility and transcriptional activation at the single-cell level. Spatial mapping demonstrated that these targets are enriched in discrete immune-excluded regions and at tumor-myeloid interfaces, revealing new spatially orchestrated mechanisms of immune suppression. Several ligand-receptor pairs and non-canonical transcriptional regulators emerged as high-confidence targets for therapeutic intervention.

Conclusions: By combining shared-barcode single-cell multiomics with spatial transcriptomics, we provide a comprehensive, mechanistic view of gene-regulatory changes driving immunotherapy resistance in HCC. This study uncovers novel, spatially validated immune-regulatory targets and highlights previously unknown cell-state transitions that may be leveraged to improve immunotherapy efficacy. Acknowledgements This research was supported by Li Ka Shing Foundation and internal funding from The Chinese University of Hong Kong. We thank all lab members for their contributions.

#7752 Targeting SOAT1 to Boost NK Cell Mediated Cytotoxicity in High Grade Serous Ovarian Cancer.

Luqi Chen[1], Michelle K.y. Siu[1], Ruiqian Zhang[1], Ling Shan Hung[1], Mengyi Gu[1], Dickson Ngan[1], Xin He[1], Haonan Lu[1], Hextan Y.s. Ngan[1], Kui Liu[1], Annie Ny Cheung[2], Karen K.l. Chan[1]

[1]Department of Obstetrics & Gynaecology, The University of Hong Kong, Hong Kong, China,[2]Clinical Professor, Dept. of Pathology, University of Hong Kong, Pokfulam, China

Rationale: Despite advances in surgery and chemotherapy, high-grade serous ovarian cancer (HGSOC) still carries poor long-term survival, and most patients with advanced disease suffer relapse. Tumor cells exploit cholesterol metabolism, and the enzyme sterol O-acyltransferase 1 (SOAT1/ACAT1), which converts free cholesterol to cholesteryl esters, has emerged as a potential driver of tumor progression and immune evasion. NK cell degranulation, widely monitored via CD107a surface expression, provides a readout of NK cytotoxicity. We sought to identify genes whose loss enhances NK-mediated killing of HGSOC cells.
Methods: We implemented a whole-genome CRISPR/Cas9 screen in OVCAR8 HGSOC cells challenged with allogeneic primary NK cells at an effector:target ratio. Relative guide RNA abundance was measured by next-generation sequencing before and after co-culture to identify genes whose disruption decreased tumor cell survival. Candidate negative genes were prioritized using filters: (1) ovarian cancer DepMap CERES score > -0.3 to avoid highly fitness-essential genes; (2) removal of curated core-essential genes; (3) at least three effective sgRNAs exhibiting consistent depletion; and (4) higher expression in ovarian cancer compared with normal ovary in public transcriptomic cohorts. SOAT1 emerged from this pipeline and was taken forward. OVCAR8 cells were transfected with SOAT1 siRNA and then co-cultured with NK92 cells. Tumor viability was quantified using metabolic/viability assay, while NK92 activation was evaluated by CD107a staining and flow cytometry. To assess clinical relevance, we interrogated independent ovarian cancer datasets (GSE118828, GSE26712) for relationships between SOAT1 expression, NK-related transcriptional signatures, and overall survival.
Results: The CRISPR screen pinpointed SOAT1 as a top metabolic modifier of NK-mediated tumor clearance. SOAT1 silencing produced mRNA knockdown in OVCAR8 and significantly reduced tumor cell survival under NK92 attack, with median viability falling to 50-60% of control conditions. NK92 cells co-cultured with SOAT1-deficient OVCAR8 exhibited increased CD107a surface expression, indicating augmented degranulation and effector activity. Across public datasets, SOAT1 expression was elevated in ovarian tumors versus normal and adjacent tissues and aligned positively with transcriptional scores of NK infiltration and cytotoxic function. Notably, in cases with high NK infiltration, patients with higher SOAT1 expression experienced worse overall survival.
Conclusions: By integrating genome-wide CRISPR screening with functional and bioinformatic analyses, we identify SOAT1 as a cholesterol-metabolic regulator that attenuates NK cell cytotoxicity in ovarian cancer. These findings nominate SOAT1 inhibition as an approach to metabolically reprogram HGSOC and improve the efficacy of NK-directed immunotherapies.

#7753 Circulating thymidine kinase activity (TKa) as a predictive and dynamic biomarker in the metastatic non-small cell lung cancer (NSCLC): Immunoblood study.

Maristella Giammaruco[1], Lorenza Landi[2], **Mattias Bergqvist**[3], Gabriele Minuti[2], Silvia Carpano[1], Francesca Fusco[1], Martina Brandi[1], Fabiana Letizia Cecere[1], Vincenzo Pio Di Noia[1], Livia Tosetto[1], Andrea Torchia[1], Corrado Orciuolo[1], Daniele Marinelli[1], Grisel Maver Militello[1], Diana Giannarelli[4], Federico Cappuzzo[1]

[1]Medical Oncology 2, IRCCS Regina Elena National Cancer Institute, Rome, Italy,[2]Clinical Trials Unit: Phase 1 and Precision Medicine, IRCCS Regina Elena National Cancer Institute, Rome, Italy,[3]Biovica International AB, Uppsala, Sweden,[4]Epidemiology and Biostatistics, Gemelli University Hospital Foundation, IRCCS, Rome, Italy

Introduction: Despite major advances with immune checkpoint inhibitors (ICIs) in treatment of metastatic NSCLC, reliable biomarkers to predict who will benefit from therapy and monitor early treatment response remain limited. Thymidine kinase is an enzyme fundamental in the DNA synthesis, its activity reflects tumor cell proliferation and tumor aggressiveness. This study (NCT06823401) is the first to evaluate plasma TKa levels in NSCLC patients receiving immunotherapy (IT) or chemotherapy-IT (CHT-IT). The objectives were to determine whether baseline TKa levels can predict efficacy of IT and if early on-treatment changes in TKa levels reflect treatment response, thereby supporting TKa as a minimally invasive biomarker for patient therapy selection and early efficacy assessment. The capacity of TKa to evaluate cell proliferation is expected to reflect and predict successful T-cell activation of IT and prolonged efficacy.

Methods: 94 patients (50 males, 44 females) with metastatic NSCLC, had plasma samples collected at baseline (pre-treatment) and at second treatment cycle of whom 93 received first-line systemic therapy. Circulating TKa was measured using the FDA cleared and CE marked DiviTum® TKa assay (Biovica, Sweden), with values reported in DiviTum units of activity (DuA). Analysis was performed blinded to clinical outcomes. TKa was evaluated for its association with response rate (RR), progression-free survival (PFS), overall survival (OS) and was also correlated to other biomarkers, including PD-L1 expression.

Results: 65 pts (70%) received first-line CHT-IT, while 28 pts (30%) received IT alone. PD-L1 expression was <1% in 37 pts (40%), 1-49% in 17 pts (18%), ≥50% in 34 pts (36%), and unknown in 6 pts (6%). The median baseline TKa level was 203 DuA. The RR in the low (<203 DuA) and high-TKa group was 52% and 32% respectively ($p = 0.80$) while the mPFS was not reached in the low TKa group versus 7.3 mos in high TKa group ($p = 0.13$). The 1-year OS rate was similar between the two groups (69.9% vs 62.4%, $p = 0.34$). Using a TKa cutoff of 326 DuA, we observed a statistically significant difference in mPFS; 13.8 months in the low-TKa group (65 pts) versus 3.3 months in the high-TKa group (23 pts) ($p = 0.004$). The 1-year OS rate was 65.6% vs 53.3%, respectively ($p = 0.18$). Further data on patients treated with IT alone and with CHT-IT will be presented at the meeting.

Conclusions: Our study shows a possible association between high plasma TKa levels and shorter PFS and OS in advanced NSCLC treated with first-line IT alone or combined with CHT, supporting the potential role in guiding treatment choice. Further studies are needed to validate the prognostic and predictive value of TKa in this setting.

#7754 Peripheral immune signatures associated with peptide receptor radionuclide therapy in neuroendocrine tumors.

Eriko Katsuta[1], Takuto Nobuhiro[1], Masaru Takeuchi[1], Satoshi Matsui[1], Asano Daisuke[1], Ishikawa Yoshiya[1], Hiroki Ueda[1], Keiichi Akahoshi[1], Noritoshi Kobayashi[2], Yasushi Ichikawa[2], Daisuke Ban[1]

[1]Institute of Science Tokyo, Tokyo, Japan,[2]Yokohama City University, Yokohama, Japan

Background: Peptide receptor radionuclide therapy (PRRT) is an internal radiotherapy for somatostatin receptor (SSTR)-positive neuroendocrine tumor (NET). The tumor microenvironment, particularly cytotoxic T lymphocyte (CTL), is a key determinant of tumor behavior, treatment response, and prognosis, but NET typically shows a “cold” immune microenvironment with sparse immune-cell infiltration, which may contribute to the limited efficacy of ICI-based therapies. External beam radiotherapy can activate systemic antitumor immunity and occasionally induce abscopal effects, in which irradiation of a primary lesion leads to shrinkage of both irradiated and distant metastatic sites; however, the influence of PRRT on systemic immunity has scarcely been studied. We hypothesized that PRRT modulates systemic immunity in NET patients and investigated changes in circulating cytokines.
Methods: We analyzed changes in serum cytokine levels in NET patients treated with PRRT at Yokohama City University. Twelve paired serum samples from 9 patients were collected before and after PRRT and analyzed with a 36-plex cytokine array.
Results: Of the 9 patients, 7 were undergoing their first PRRT course and 2 a second course (retreatment after a prior four-administration PRRT course that had achieved at least partial response with ≥1.5 year of disease control). Primary sites were pancreas (n=6), rectum (n=1), lung (n=1), and thymus (n=1), and target lesions were in the liver (n=7), bone (n=2), primary site (n=1), lymph node (n=1), and peritoneum (n=1). Twelve serum pairs comprised 10 pre- and post-individual PRRT administrations and 2 pre- and post-full-course pairs. Of the 36 examined cytokines, only 12 were detectable. Among these, CD154 showed more than 2-fold changes in 7 pairs, with 6 showing downregulation and 1 showing upregulation after PRRT. IL-1ra was also upregulated in 3 pairs.
Conclusion: We found that PRRT is associated with systemic changes in circulating cytokines in NET patients, notably modulation of CD154 and IL-1ra. These data suggest that PRRT may influence host antitumor immunity; larger studies are required to elucidate the mechanisms and clinical significance of these immune changes.

#7755 Precision immune therapies for cancer developed through understanding the role of myeloid checkpoints as key mediators of adaptive resistance in T-cell checkpoint inhibitor resistant patients.
Ronan O'Hagan, Magali Perderzoli-Ribeil

Bectas Therapeutics, Houston, TX

Background: T-cell immune checkpoint inhibitor (ICI) therapies can deliver cures to cancer patients. However, about 80% of patients show only transient responses or outright resistance to these therapies. Thus, ICI resistance is a major unmet medical need. A key challenge is the lack of precise understanding of which specific resistance mechanism is operative in which specific subset of patients. Moreover, previous studies have demonstrated that molecular signals for clinical response or resistance to ICI therapies are evident only after initiation of treatment and that pre-treatment molecular profiles are poorly predictive. Hence, a precision strategy that accounts for the homeostatic nature of the immune response and the resulting adaptive nature of ICI resistance is key to successfully developing new ICI monotherapy or combination approaches.
Methods: To elucidate adaptive mechanisms of resistance to ICI's and precisely determine which resistance mechanism was relevant in each patient we applied defined machine learning models to analyze serial longitudinal clinical and molecular data from over 400 cancer patients undergoing aPD1/aCTLA4 treatment. This led to the definition of a blood-based biomarker predictive of non-response and the identification of dynamically regulated drivers of resistance that represent targets for precision drug discovery. The newly established links between druggable adaptive resistance targets in ICI resistant patients and blood-based patient selection biomarkers can guide clinical development of agents directed to these targets.
Results: Myeloid driven immune suppression was identified as the dominant mechanism of adaptive resistance in patients treated with ICI's. Specific myeloid checkpoints that drive resistance were indentified in subsets of patients that could be defined by protein signatures detectable in blood. These precision biomarkers identified patients across multiple indications in which ICI resistance is driven by a targetable myeloid checkpoint. Bectas has now developed monoclonal antibody therapies to a series of myeloid checkpoint targets identified through this approach. In each case, the antibody therapy is accompanied by a precision biomarker to enable patient selection.
Conclusions: Our unique multi-dimensional blood-based biomarker strategy enables early detection of resistance to ICI treatment, and identifies specific myeloid checkpoints driving resistance in specific patients. This precision approach, coupled with first in class antibody therapies directed to these myeloid checkpoints has the potential to significantly accelerate the development of new therapeutic regimes to address the 80% of cancer patients who do not benefit currently from immune-based therapies.

#7756 A tumor-targeting IL-12 immunocytokine therapy increases peripheral natural killer (NK) cells with phenotypes associated with increased tumor cell lysis in patients with advanced solid tumors.
Stephanie C. Pitts, Nicole J. Toney, Jennifer L. Marte, James L. Gulley, Jeffrey Schlom, Renee N. Donahue

National Cancer Institute, Bethesda, MD

Background: PDS01ADC (previously designated NHS-IL12) is a tumor-targeting immunocytokine with promising preclinical activity. A first-in-human clinical trial (NCT01417546) showed PDS01ADC monotherapy to be safe and well tolerated in patients with advanced solid malignancies, and preliminary signs of clinical activity (stable disease in 50% of evaluable patients) were observed. Here, we investigate peripheral blood natural killer (NK) cell phenotypes that associate with tumor cell lysis in ex-vivo assays, and evaluate patients treated with PDS01ADC for changes in these NK phenotypes and for correlations with clinical response.
Methods: Healthy donor NK cells (n=12) were evaluated in lysis assays with human SW620 colorectal and H69 small cell lung cancer tumor cells and assessed by flow cytometry. Peripheral blood collected from patients with advanced malignancies before and after 2 and 4 weeks of PDS01ADC treatment (n=28) was also assessed for changes in NK cell phenotypes and for correlations with response.
Results: Total NK cells were not changed upon PDS01ADC treatment; however, several NK cell phenotypes that positively associated with NK cytotoxicity were increased after treatment. For example, Granzyme B^+ NK cells positively correlated with NK cell lysis of SW620 tumor cells ($p=0.0299$, $r=0.6364$) and were increased with PDS01ADC treatment ($p<0.0001$). A more refined phenotype of NK cells, co-expressing both cytotoxic molecules and activating receptors (Granzyme B^+Perforin$^+$NKG2D$^+$NKp46$^+$), showed a stronger correlation with NK cell lysis ($p=0.0002$, $r=0.9021$), and was both increased in patients upon PDS01ADC treatment and associated with clinical response ($p=0.0688$). Other refined NK subsets expressing inhibitory receptors, such as NKG2A$^+$TIGIT$^+$Perforin$^+$ NK cells, negatively correlated with lysis ($p=0.0078$, $r=-0.7413$), and were decreased with PDS01ADC, with greater decreases associated with improved clinical response ($p=0.0224$).
Conclusions: PDS01ADC increased peripheral NK cells with specific phenotypes that positively associated with tumor cell lysis, with increases in some cases correlating with clinical response. These findings highlight the importance of deep interrogation of the peripheral immunome and demonstrate the role of NK cells in the biologic activity of PDS01ADC. Studies combining PDS01ADC with other agents to synergize with these NK cell changes are warranted.

#7757 Investigating the mechanisms underlying regulatory T cell dysfunction in ICI-induced colitis.

Emily Schahrer, Paul Ngai, Mehdi Benjelloun Zahar, Christopher R. Weber, David Zemmour

University of Chicago, Chicago, IL

Immune checkpoint inhibitors (ICIs) have revolutionized cancer therapy but can trigger immune-related adverse events such as colitis. The mechanisms driving these toxicities remain poorly understood. In this study, we analyzed colon biopsies from a patient cohort with ICI-induced colitis using integrated single-cell RNA sequencing and paired spatial transcriptomics and proteomics to define disease mechanisms and model human autoimmunity.Transcriptomic mapping revealed accumulation of proliferative cytotoxic T cells in the colon, suggesting failure of regulatory T cells (Tregs) to restrain effector responses. Tregs displayed upregulation of Th1- and IFN-response genes, including *IL12RB2, IFI6*, and *CXCL9*, distinguishing ICI colitis from patterns observed in Th17-driven inflammatory bowel disease.Within the $CD8^+$ T cell compartment, combined single-cell and TCR analyses identified tissue-resident memory (Trm) cells as key targets of ICIs driving colonic inflammation. Activated $CD8^+$ Trm cells displayed a cytotoxic, IFN-γ-rich profile enriched for granzymes, chemokines, and effector transcriptional modules characteristic of human ICI colitis. Spatial mapping will confirm the co-localization of Trm cell activation, Treg dysfunction, and IFN-driven microenvironments within epithelial and mucosal niches.Together, these results define a pathogenic circuit in which Trm activation, Treg destabilization, and Th1-skewed inflammation converge to drive ICI-induced colitis. This work provides a mechanistic framework for understanding ICI-associated autoimmunity and may guide development of targeted therapeutic strategies that preserve antitumor immunity while limiting tissue toxicity.

#7758 Prediction of pharmacokinetics and pharmacodynamics profile for a fixed dosing and body weight-based dosing of GI-102 based on cell-level pharmacodynamics-mediated drug disposition model in patients with advanced or metastatic solid tumors.

Suemin Park[1], Seung Chan Choi[1], Kwang-Soo Shin[2], Nari Yun[2], **Myoung Ho Jang**[2], Hyeong-Seok Lim[1]

[1]Department of Clinical Pharmacology and Therapeutics, Asan Medical Center, University of Ulsan College of Medicine, Seoul, Korea, Republic of,[2]Clinical development, GI Innovation, Seoul, Korea, Republic of

GI-102 (CD80/IL2v3) is designed to direct IL-2 variant to immune cells and tumor cells, and to block CTLA-4 via CD80. Proliferation of cytotoxic T (T_c) cells and natural killer (NK) cells is enhanced through selective binding to IL-2Rβγ. CD80-CTLA4 binding further inhibits immunosuppressive function of regulatory T (T_{reg}) cells. Based on GI-102 monotherapy dose-escalation data of the phase 1/2 first-in-human study (KEYNOTE-G08), a cell-level pharmacodynamics-mediated drug disposition (PDMDD) model was constructed to assess the relationship between drug exposure, target receptor occupancy, and pharmacodynamic (PD) effect. Historically, IL-2 therapies relied on body-weight-based dosing due to narrow therapeutic windows and high interpatient variability. Leveraging GI-102 safety and tolerability in humans, model-informed simulations compared overall pharmacokinetic (PK) and PD profiles of fixed-dose versus weight-based dosing.The model was constructed by simultaneously fitting drug concentrations (n=1185) and total lymphocyte (n=826), T_c cell, NK cell, and T_{reg} cell counts (n=529 each) from 54 patients with advanced or metastatic solid tumors who received GI-102 intravenously every three weeks at doses of 0.06-0.45 mg/kg. The target-mediated drug disposition (TMDD) model incorporated time-varying PD-mediated disposition at the cellular level. Lymphocyte diapedesis after treatment was described empirically, and time delay between drug concentrations and lymphocyte increase driven by GI-102-IL-2Rβγ stimulation was captured by an indirect response model with the operational model of agonism. Following model diagnostics, Monte-Carlo simulations with 1000 replicates were performed for each scenario using the final model. Modeling was conducted using NONMEM® v7.5.0, and data processing and plotting using R v4.3.3. The two-compartment, cell-level PDMDD model adequately described central tendency of observed PK/PD data. Simulations showed a clear exposure-response relationship across doses. At 0.24-0.45 mg/kg, total lymphocytes and T_c cells, accounting for diapedesis, reached levels around 3640-4136 cells/μL and 515-572 cells/μL, respectively. At the same range, NK cells were predicted to exceed 1000 cell/μL, indicating robust expansion at receptor occupancy < 50%. In addition, simulations for fixed-dose regimen of 10, 20, and 30 mg showed increased immune cell proliferation, largely comparable to corresponding weight-based doses of 0.12, 0.24, and 0.35 mg/kg, respectively. Our modeling and simulation provides preliminary prediction of PD effect at tested doses and fixed-dose regimens, serving as reference for determining optimal dose and dosing regimen.

#7759 Construction of a novel immune gene signature to distinguish immunotherapy responders and non-responders.

Moonyoung Lee[1], Yona Kim[2], Sangjeong Ahn[2], Sung Hak Lee[1]

[1]Department of Hospital Pathology, Seoul St. Mary's Hospital, College of Medicine, The Catholic University of Korea, Seoul, Korea, Republic of,[2]Department of Pathology, Korea University Anam Hospital, College of Medicine, Korea University, Seoul, Korea, Republic of

Introduction: Immune checkpoint therapies (ICT) restore the immune system's ability to fight cancer by blocking inhibitory signals of T cell activation, allowing them to recognize and attack tumor cells. Representative examples include drugs targeting PD-1, PD-L1, and CTLA-4 proteins. Despite active research into ICT, many patients remain untreated. The response to ICT vary across cancer types and even within cancer types, depending on immune subtype. Therefore, we aimed to define a new immune signature to identify responders and non-responders in individual cancer types. We developed a model using data from 11 cancer types from the TCGA as a training dataset and validated this model with other data sets.

Methods: Using TCGA data for 11 cancer types (BLCA, BRCA, COAD, UCEC, ESCA, HNSC, KIRC, LIHC, LUAD, SKCM, STAD), we divided them into immunologically hot group, cold group, and intermediate group, according to the expected effects of ICT. To divide the data into three groups, we used immune-related pathways, immune markers from literature, Cibersort, Ecotype, and Methylation data as features. Lasso was used to select important features, and Kmeans was used for clustering. To test the results, Silhouette score, CH index, and Dunn index were used. The results of these coefficients decreased further when methylation data and ecotype features were added, so these two features were finally removed and clustered. We then created a new gene set signature using leading edge genes/markers that overlapped across these features. We tested this gene set signature on melanoma data and confirmed that it effectively distinguished responders from non-responders.

Results: A total of 5,089 samples corresponding to 11 cancer types were selected, and 38 pathways were selected as features, and it was confirmed through a heatmap that they were well divided into 3 groups. A new signature was discovered with a total of 84 genes, including leading edge genes that appear repeatedly in this pathway and markers corresponding to the signature. This confirmed that the discovered gene set was well-separated across each cancer type. For further validation, we used the GSE91061 dataset to examine whether the new gene set differed between the responder and non-responder groups using a NES plot. The positive enrichment score was biased toward the responder group, and the padj value was significant at 0.028, consistent with the pattern observed in TCGA. When ORA was used with Reactome and GOBP, immune-related pathways were also significantly identified.

Conclusion: Given the close connection between ICT and immunity, we believe this new gene set signature will be helpful in distinguishing between ICT-responsive and non-responsive groups. We plan to conduct validation tests using other cancer type data and WSI on immunologically hot and cold tumor groups to further improve accuracy.

#7761 Tertiary lymphoid structure (TLS) representative cells elicit response to anti-PD-1$^+$ therapy in a cold tumor.

Satish Sankaran[1], Priyanka Chevour[1], Kowshik Jaganathan[1], Biswajit Das[1], Moumita Nath[1], Abdul Haseeb[1], Jobin K Paul[1], Vasanthakumar A[1], Oliyarasi M[1], Rajashekar M[1], Jayaprakash C[2], Venkatesh T[2], MS Ganesh[3], Amritha Prabha[3], Prakash BV[4], Upendra K[1], Mehul Kapur[1], Ritu Malhotra[1], Govindaraj K[1], Pavithira .[1], Mohit Malhotra[1]

[1]Farcast Biosciences India Pvt. Ltd., Bangalore, Bangalore, India,[2]DBR & SK Super Speciality Hospital, Tirupati, Tirupati, India,[3]Vydehi Institute of Medical Sciences and Research Centre, Bangalore, Bangalore, India,[4]Sri Lakshmi Multi Speciality Hospital, Bangalore, Bangalore, India

The composition and activation phenotype of immune cells within the tumor microenvironment (TME) can significantly influence therapeutic response to PD-1 based immunotherapy. Using the Farcast TruTumor histoculture platform, we investigated potential factors contributing to the unexpected anti-PD-1 responsiveness in an immune cold TME. Freshly resected Head and Neck Squamous Cell Carcinoma (HNSCC) samples (n=5) and matched blood were collected from consented patients. Explants were generated from the tumors and treated in culture with anti PD-1 (Nivolumab132 µg/ml) for 72 h. The response was evaluated using histopathology and flow cytometry readouts. Among the five samples analysed, one responder (S2) exhibited elevated cleaved caspase-3 expression (2.5-fold increase) in the tumor relative to the control. Interestingly, this sample (immune content <2%), exhibited a cold tumor immune microenvironment compared with the four non-responder (NR) samples (mean immune content = 4.5%). To investigate factors underlying the observed response, we evaluated the baseline immune profile. Sample S2 exhibited a more heterogenous Lo-SSC compartment compared to NR samples. This was characterized by a high proportion of CD23$^+$ follicular B cells (3.9-fold increase), CD11c$^+$ dendritic cells (1.5-fold increase), and DC-LAMP$^+$ expressing mature dendritic cells (2.9-fold increase) compared to NR samples. These sub-populations are indicative of immune cell subsets typically present in or associated with TLS. Although the responder sample contained a relatively low overall proportion of CD8$^+$T cells, it exhibited 15 fold lower proportions of both early (CD8$^+$PD-1$^+$) and late (CD8$^+$CD39$^+$) exhausted T-cells, while displaying a 12-fold increase in stem-like (CD8$^+$TCF1$^+$) T cells. Upon ex vivo culture of tumor explants on TruTumor platform, the responder sample showed a distinct increase of 1.8-fold in pro-inflammatory M1 macrophages in the treated relative to the untreated control, whereas no appreciable change was observed in the non-responder samples. Interestingly, anti PD-1 treatment led to the emergence of an NKT-cell population (CD3$^+$CD56$^+$) and an increase in NK cells expressing Granzyme B (CD3$^-$CD56$^+$Granzyme B$^+$). In summary, our data reveals that response to anti-PD-1 is not solely dependent on the abundance of CD8$^+$ T cells but also involves substantial contributions from TLS representative immune sub-populations within the TME. Specifically, the presence of follicular B cells, stem-like CD8$^+$ T cells, CD11c$^+$ cells, and DC-LAMP$^+$ dendritic cells may contribute to treatment responsiveness, even in the context of an otherwise immune-poor phenotype. The TruTumor histoculture platform provides a translational model to study tumor response to immunotherapy with insights into how tumor responsiveness, transcends beyond mere presence of CD8$^+$ T cells in the TME.

#7762 PD-L1-dependent 4-1BB costimulation enhances anti-tumor efficacy and T cell persistence as monotherapy or in combination with tarlatamab.

Felipe Vences Catalan[1], Willy Tsai[1], Wendy Chen[1], Anja Henn[2], Kevin Cook[1], Maryam Yousefi[3], Tanya Vagner[3], Andrew Jimena[1], Khushboo Sharma[4], Deepali Sawant[1], Jason DeVoss[1], Matthias Friedrich[2], Mithun Khattar[1], Julie Bailis[1], Andrew Rankin[1], **Sungeun Kim**[1]

[1]Amgen Research, Amgen, Inc., South San Francisco, CA,[2]Amgen Research, Amgen, Inc., Munich, Germany,[3]Research biomarkers, Amgen, Inc., South San Francisco, CA,[4]Precision Medicine, Amgen, Inc., South San Francisco, CA

Bispecific T-cell engagers (TCEs) have demonstrated transformative clinical efficacy by redirecting T cells to eliminate tumor cells. However, clinical outcomes highlight opportunities to further enhance therapeutic benefits, particularly by improving overall response rates and durability of responses. Sustained CD3 engagement by TCEs can lead to T cell exhaustion, resulting in diminished effector function and reduced persistence. To address these challenges, we developed AMG 728, a PD-L1-targeted 4-1BB bispecific molecule designed to enhance T cell anti-tumor activity and persistence. AMG 728 simultaneously blocks PD-1/PD-L1 inhibitory signaling and activates 4-1BB costimulatory signaling in a PD-L1-dependent manner. This dual mechanism is intended to enhance T cell activation and persistence while minimizing the risk of immune activation and off-tumor toxicity associated with systemic 4-1BB agonism. By combining the CD3-mediated signaling from TCEs with 4-1BB costimulation provided by AMG 728, we aimed to fully activate T cells, thereby promoting cytolytic effector differentiation, improving survival, and expanding memory T cell populations. A mouse surrogate PD-L1-4-1BB bispecific molecule demonstrated dose-dependent anti-tumor efficacy as a monotherapy in a human PD-L1/4-1BB double knock-in mouse model bearing syngeneic, human PD-L1-expressing tumors. Mechanistic characterization of this surrogate molecule further revealed several potential pharmacodynamic biomarkers *in vivo*, including increased $CD8^+$ T cell proliferation, expansion of central memory T cells in draining lymph nodes, enhanced cytolytic effector T cell differentiation within tumors, and elevated levels of soluble 4-1BB. Furthermore, AMG 728 was evaluated for its potential to improve the efficacy of tarlatamab, a DLL3-targeted bispecific TCE *in vitro* and in a T cell humanized small cell lung cancer (SCLC) preclinical mouse model. Selective 4-1BB agonism on PD-L1-positive tumors enhanced the cytotoxic activity of tarlatamab *in vitro*. In the human PD-L1-overexpressing SHP-77 SCLC xenograft implanted in NSG mice, combination treatment with AMG 728 and tarlatamab at suboptimal doses resulted in significantly greater tumor growth inhibition, extended survival, and a higher frequency of complete responses, compared with either monotherapy. Notably, AMG 728 treatment led to a significant increase in central memory T cells in the tumors from tarlatamab-treated mice. Collectively, these findings suggest that the addition of AMG 728 to tarlatamab represents a rational combination strategy that enhances T cell activation and longevity, resulting in improved antitumor activity and survival.

#7763 FOXA1 in ovarian cancer: Therapeutic target and immunotherapy enhancer.

Taewan Kim, Baek MooJun, HyoWook Gil, Eunjung Yang, Kwangseock Kim, jaesung Ryu, Kong Hyejeong, Beamjun Park, **Seob Jeon**

Soonchunhyang University Cheonan Hospital, Cheonan, Korea, Republic of

OBJECTIVE
This study aimed to elucidate the oncogenic role of FOXA1 (Forkhead Box A1) in ovarian cancer and to evaluate its potential as both a therapeutic target and a diagnostic biomarker. We further investigated whether FOXA1 inhibition could enhance responsiveness to immune checkpoint blockade and overcome chemoresistance.
METHODS
A total of 76 ovarian tissue samples were analyzed, including 9 normal, 34 benign, and 33 malignant specimens. Immunohistochemical (IHC) staining was performed to assess FOXA1 expression and its correlation with tumor stage. Functional studies were conducted using FOXA1 siRNA in SK-OV3 and HEYA8 cell lines. Changes in cell proliferation, migration, invasion, and wound-healing ability were evaluated following FOXA1 silencing. Quantitative RT-PCR was used to measure FOXA1 and epithelial-mesenchymal transition (EMT)-related gene expression. In addition, the effects of FOXA1 inhibition on sensitivity to carboplatin and the immune checkpoint inhibitor atezolizumab were assessed.
RESULTS
IHC analysis revealed significant differences in FOXA1 expression among normal, benign, and malignant tissues, with expression levels correlating with tumor stage. FOXA1 silencing significantly reduced cell proliferation and decreased migration and invasion by 60-80%. EMT-related genes were markedly downregulated after FOXA1 knockdown. Moreover, FOXA1 inhibition enhanced atezolizumab responsiveness and reduced carboplatin resistance in ovarian cancer cells.
CONCLUSION
FOXA1 acts as an oncogenic driver in ovarian cancer, promoting proliferation, invasion, and EMT activation. Its overexpression correlates with disease progression, supporting its role as a diagnostic and prognostic biomarker. Targeting FOXA1 may enhance immunotherapy efficacy and overcome chemoresistance in ovarian cancer.

#7764 Modeling CRS in humanized immune system mice.

Audrey Wetzel[1], Anais Meynet-Cordonnier[1], Clothilde Philouze[1], Charline Boulot[1], Emilie Bayon[1], Sebastien Tabruyn[2], **Dan Georgess**[1]

[1]TransCure bioServices, Archamps, France,[2]TransCure, Archamp, France

Cytokine release syndrome (CRS) is a major risk during treatment with CAR-T cells, T-cell engagers, and, occasionally, checkpoint inhibitors. Because humanized immune-system mice are frequently used for the preclinical development of such therapies, we sought to provide a platform to derisk CRS before the clinical stage. We therefore characterized CRS induction, immune dynamics, and clinical manifestation in two different humanized mouse models. We humanized the immune system of initially immunodeficient mice by engrafting them either PBMCs or CD34+ hematopoietic stem cells. In the PBMC model, T cells were the only engrafted human immune population and exhibited a chronically induced, partially exhausted (TIM3+, LAG3+, PD1-) phenotype at baseline. At one week post-PBMC engraftment, circulating T-cells were at approximately at 1000 cells per mL, and OKT3 injection depleted them, thereby failing to induce CRS. At three weeks post-engraftment, however, circulating T-cell counts reached one million cells per mL and were no longer depleted by OKT3, which instead induced severe CRS and mortality within 24 hours. CRS induction in PBMC mice was accompanied by increases in circulating TNF-α, IFN-γ, and IL-2, as well as transient (≤6 hours) T-cell proliferation. In contrast, in the CD34 model, a more complete human immune system developed after engraftment, including myeloid, NK, dendritic, B, and non-exhausted T cells. This broader immune reconstitution enabled OKT3 to induce CRS with as few as 10,000 circulating T cells. Although clinical CRS symptoms were milder than those observed in PBMC-engrafted mice, the CRS cytokine signature in the CD34 model included not only the IFN-γ, TNF-α, and IL-2 surges observed in PBMC mice but also substantial increases in hallmark myeloid-derived CRS cytokines such as IL-6, CXCL10, and CCL2. Likewise, the cellular signature of CRS was more complete in CD34 mice, with induction of T-cell activation (CD69+, CD38+, HLA-DR+), exhaustion (PD1+, TIM3+), and proliferation (Ki67) markers, along with increased monocyte mobilization into the blood. In summary, our results demonstrate that the CD34 model displays mild-to-moderate clinical symptoms while more comprehensively recapitulating the hallmark cellular and molecular features of CRS.

#7766 Single-dose neoadjuvant atezolizumab in resectable stage IA-IIIA non-N2 NSCLC: Tumor infiltrate analysis from the PRINCEPS trial.

Antonio Nuccio[1], Lydie Cassard[2], Nathalie Cozic[3], Malek Ben Salah[4], Vesna Lukic[4], Julien Adam[5], Wael Salem Zrafi[3], David Planchard[6], Jordi Remon[7], Pernelle Lavaud[7], Anas Gazzah[8], Vincent Thomas de Montpreville[9], Maria Rosa Ghigna[10], Patrick Dumont[11], Elie Fadel[12], Fabrice Barlesi[1], Caroline Caramella[13], Filippo Gustavo Dall'Olio[6], Olaf Mercier[12], Paul-Henry Cournede[4], Nathalie Chaput[14], Benjamin Besse[1]

[1]Inserm, U981, F-94805, Universite Paris-Saclay, Gustave Roussy, Villejuif, France,[2], INSERM US23, Laboratoire d'immunomonitoring en Oncologie, F-94805,, Universite Paris-Saclay, Gustave Roussy, Villejuif, France,[3]Service de Biostatistique et d'Epidemiologie, Gustave Roussy, Universite Paris-Saclay, Villejuif, France,[4]Lab of Mathematics and Computer Science (MICS), Universite Paris-Saclay, CentraleSupelec, Paris, France,[5]Pathology, Hopital Paris Saint-Joseph, Paris, France,[6]Medical Oncology, Institut Gustave Roussy, Villejuif, France,[7]Institut Gustave Roussy, Villejuif, France,[8]DITEP, F-94805, Universite Paris-Saclay, Gustave Roussy, Villejuif, France,[9]Pathology, Hospital Marie Lannelongue, Le Plessis Robinson, Paris, France,[10]BIOPATH, F-94805, Universite Paris-Saclay, Gustave Roussy, Villejuif, France,[11]Centre Hospitalier de Chauny, Chauny, France,[12]Department of Thoracic Surgery & Heart-Lung Transplantation, Universite Paris-Saclay, Hopital Marie Lannelongue, Paris, France,[13]Radiology Department, Groupe Hospitalier Paris Saint Joseph, Hopital Marie Lannelongue, Paris, France,[14]INSERM US23, Laboratoire d'immunomonitoring en Oncologie, F-94805, Universite Paris-Saclay, Gustave Roussy, Villejuif, France

Phase 2 PRINCEPS trial (NCT02994576) showed that single dose neoadjuvant Atezolizumab (A, 1200 mg IV) was feasible in 30 stage IA-IIIA non-N2 NSCLC patients (treated arm, T). A comparative arm (C) was later added. We report tumor immune profiles and updated survival for T and C arms.
C arm included untreated resected stage IA-IIIA non-N2 NSCLC patients. Surgery samples were profiled for residual viable tumor (RVT) and immune infiltrates. RVT cutoffs were defined with Maximally Selected Rank Test for DFS/OS (Table1). Immune infiltrates (N=316) were compared across groups by Mann Whitney U test.
From 9/2019 to 8/2022, 30 patients were enrolled in C (2 non-NSCLC excluded). Mean age was 64 vs 66, squamous histology 13% vs 26%, PD-L1 neg 63% vs 46%, adjuvant ChT 20% vs 50% (T vs C).
T arm tumors were enriched in CD45+ leukocytes, CD8+ T cells, HLA-DR+ CD163+ myeloids; C arm tumors showed CD115+ CD163+ macrophages and CD16Low immature neutrophils suggesting an immunosuppressive TME.
In T arm, Responders (RVT≤60%) had higher lymphocyte, activated/exhausted PD-1+/TIGIT+ T cell and mature/activated CD16+ CD11bHigh neutrophil rates; Non-Responders (RVT>60%) showed more senescent CD57+ T cells and immunosuppressive (CD16-, CD163+) myeloids.
In C arm, Spontaneous Regressors (RVT≤95%) had proliferating Ki67+ OX40+ T cells, CD69+ NK, exhausted CTLA4+ TIGIT+ T cells and pro-inflammatory CD16+ macrophages vs Non-Spontaneous Regressors (RVT>95%), enriched in highly activated Treg.
In conclusion, neoadjuvant single dose A induced a CD8+/activated-myeloid profile that could relate to durable survival benefit. In T arm Responders showed activated/exhausted T cells and mature pro-inflammatory neutrophils, similar to Spontaneous Regressors in C arm; Non-Responders were enriched in senescent T cells and immunosuppressive myeloids. These results may indicate PD-1+/TIGIT+ exhausted T cells and pro-inflammatory myeloids as predictive biomarkers of A activity.

Table 1. DFS: Disease-free Survival; OS: Overall Survival; MaxStat: Maximally Selected Rank Test

Arm	**Treated [N=30]**	**Comparative [N=28]**
Median follow-up months (95%CI)	80 (74.2-94.5)	50.6 (40.5-60.7)
Overall 5 years DFS	76.3%	55.6%
Overall 5 years OS	83.3%	58.7%
***MaxStat* RVT cutoff predicting best DFS outcome**	60%	95%
***MaxStat* RVT cutoff predicting best OS outcome**	60%	95%
Number of patients achieving ≤RVT *MaxStat* cutoff for DFS	13 (Responders)	19 (Spontaneous Regressors)
5 years DFS in ≤RVT *MaxStat* cutoff	84.6%	61.8%
5 yearsDFS in>RVT *MaxStat* cutoff group	69.7%	41.7%
DFS HR (95% CI) ≤RVT vs >RVT *MaxStat* cutoff groups	0.47 (0.12-1.82)	0.41 (0.13-1.37)
DFS ≤RVT vs >RVT *MaxStat* cutoff groups log-rang p value	0.26	0.13
5 years OS in ≤RVT *MaxStat* cutoff group	100%	63.7%
5 years OS in >RVT *MaxStat* cutoff group	70%	44.4%
OS HR (95% CI) ≤RVT vs >RVT *MaxStat* cutoff groups	NA (no events)	0.52 (0.14-1.94)
OS ≤RVT vs >RVT *MaxStat* cutoff groups log-rang p value	0.01	0.31

#7767 Spatial profiling of the tumor immune microenvironment following oncolytic herpes simplex virus treatment in glioblastoma.

Sophia A. Paxton[1], Corinne H. Strawser[1], Lakshmi Prakruthi Rao Venkata[1], Elizabeth A. R. Garfinkle[1], James M. Markert[2], Katherine E. Miller[1], Kevin A. Cassady[3], Elaine R. Mardis[1]

[1]The Steve and Cindy Rasmussen Institute for Genomic Medicine, The Abigail Wexner Research Institute at Nationwide Children's Hospital, Columbus, OH, [2]Department of Neurosurgery, University of Alabama at Birmingham, Birmingham, AL,[3]Center for Childhood Cancer Research, The Abigail Wexner Research Institute at Nationwide Children's Hospital, Columbus, OH

Glioblastoma (GBM) is the most common and aggressive malignant brain tumor in adults, with an extremely low 5-year survival rate of ~5%. Despite established surgery and chemoradiotherapy treatments, outcomes remain poor due to GBM's profound heterogeneity and highly immunosuppressive tumor immune microenvironment (TIME). Emerging immunotherapies offer new opportunities to overcome these barriers. Among them, oncolytic herpes simplex viruses (oHSVs) stand out for their dual ability to selectively lyse tumor cells while stimulating robust anti-tumor immune responses. Preclinical and early clinical studies demonstrate that oHSVs can profoundly remodel immune cell expression within tumors, but these analyses lack spatial insight. Spatial multi-omics technologies now enable precise mapping of such immune transcriptome and proteome changes, answering how immune reorganization shapes the GBM TIME. The present study utilized 10x Genomics Visium spatial multi-omics to comprehensively map oHSV-induced immune responses in human GBM and explore their association with patient outcomes. Brain tumor samples were obtained from a Phase IA dose-escalation oHSV trial for recurrent glioma, with tissue collected both before treatment and at post-treatment resection. Across four patients, a total of seventeen formalin-fixed, paraffin-embedded samples were profiled using the Visium Spatial Gene Expression (Whole Transcriptome) and Visium Immune Profiling (Protein) panels. Spatial multi-omic data were analyzed in Seurat, leveraging a human brain immune reference integrated with our oHSV single-cell RNA-sequencing data to enhance cell type identification for spatial deconvolution. We characterized key immune cell populations, evaluating how their localization, abundance, and expression varied across treatment status (pre- vs. post-oHSV), spatial context (tumor bed vs. periphery), and clinical response (responders vs. non-responders). We also explored the use of custom viral RNA probes to detect viral presence within tissue; while signal detection was limited, these efforts informed future optimization of viral localization methods. By comparing spatial immune architectures between responders and non-responders, we identified trends that illuminate how immune cell organization shapes therapeutic efficacy. Furthermore, the observed concordance between spatial gene and protein expression of key immune markers reinforces the biological validity of these signatures and suggests their possible association with treatment response. Ultimately, elucidating the mechanisms by which oHSV modulates the GBM TIME advances our understanding of its anti-tumor effect and provides a rationale for its continued clinical development.

#7768 Biological pathways of response to neoadjuvant chemo-immunotherapy in triple-negative breast cancer (TNBC).

Nickolas Stabellini[1], Perrana B. Parthasarathy[2], Iluja Gautam[3], Patricia A. Rayman[2], Monaben Patel[2], Paul G. Pavicic Jr[2], Adam Moen[2], Brian Race[2], Eden Mundell[2], Amanda Trevino[2], Jennifer Powers[2], Tyler Joseph Alban[2], Jennifer Ko[2], Bahar Moftakhar[4], Takae Mizukami[5], Cynthia Owusu[5], Timothy A. Chan[6], Alberto J. Montero[5], C. Marcela Diaz-Montero[2]

[1]Case Western Reserve University School of Medicine, Cleveland, OH,[2]Cleveland Clinic, Cleveland, OH,[3]Cleveland Clinic Lerner College of Medicine, Cleveland, OH,[4]University Hospitals Seidman Cancer Center, Cleveland, OH,[5]University Hospitals Cleveland Medical Center, Cleveland, OH,[6]The Cleveland Clinic, Taussig Cancer Institute, Cleveland, OH

Background: KEYNOTE-522 established neoadjuvant pembrolizumab plus chemotherapy as standard care for early-stage TNBC, improving pathological complete response (pCR) rates. However, up to 45% of patients (pts) do not achieve pCR, and mechanisms driving differential responses are unclear. This study aimed to identify biological pathways distinguishing pCR from non-pCR pts at baseline (BL) and to characterize how these pathways evolve during treatment (DT) and post-surgery (PS).
Methods: Blood samples from TNBC pts were collected at BL, DT, and PS. Peripheral blood mononuclear cells (PBMCs) were isolated by density gradient centrifugation. Single-cell RNA sequencing was performed using the Parse Biosciences platform. Gene Set Enrichment Analysis identified enriched pathways using the Molecular Signatures Database (MSigDB) hallmark (50 gene sets) and Reactome (1,787 gene sets) collections. Comparisons were made between pCR and non-pCR patients at each timepoint and within groups (DT vs. BL).
Results: Among 18 sequenced pts, 11 achieved pCR. A total of 883,183 cells across 17 cell types were analyzed. At BL, responders showed elevated interferon (IFN) and cytokine signaling, mainly from lymphocytes, along with chemokine upregulation in classical monocytes (CM) and increased DAP12 expression in CD8+ T cells. During treatment, responders demonstrated a myeloid-driven TNFα/NFκB inflammatory response and upregulated GPCR signaling in CM. In contrast, non-responders exhibited ineffective myeloid IFN signaling and downregulated TNFα/NFκB activity across all cell types DT.
Conclusions: pCR is distinguished by a coordinated lymphocyte and myeloid immune activation. Non-responders exhibit ineffective signaling and suppressed inflammatory pathways. These divergent mechanisms highlight potential biomarkers to guide patient stratification and therapeutic optimization in TNBC.

Table 1. Most prominent pathways differing between responders and non-responders

Pathway	MSigDB Gene set	Cell Type	Baseline (responders vs non-responders)	On treatment (responders vs non-responders)	Post-Surgery (responders vs non-responders)
Antigen Presentation & Immune Activation					
ANTIGEN_PROCESSING_CROSS_PRESENTATION	Reactome	Classical Monocytes, Non-classical Monocytes	Downregulated	Downregulated	-
BINDING/UPTAKE BY SCAVENGER RECEPTORS	Reactome	CD8+ T-cells	-	Upregulated	Upregulated
REGULATION OF TLR BY ENDOGENOUS LIGAND	Reactome	Plasma cells	-	Downregulated	Upregulated
T-Cell & Cytokine Signaling					
INTERFERON_GAMMA SIGNALING	Reactome	CD8+ T-cells	Upregulated	-	Upregulated
INTERFERON_ALPHA_RESPONSE and INTERFERON_GAMMA_RESPONSE	Hallmark	CD8+ T-cells, CD4+ T-cells, B cells, Plasma cells, regulatory T-cells, NK-cells	Upregulated	Upregulated	Upregulated
INTERFERON_ALPHA_RESPONSE and INTERFERON_GAMMA_RESPONSE	Hallmark	Classical Moncoytes, Non-classical monocytes, Dendritic cells	Upregulated	Downregulated	Upregulated
INTERFERON_GAMMA SIGNALING	Reactome	CD8+ T-cells	Upregulated	-	Upregulated
TNFA_SIGNALING_VIA_NFKB	Hallmark	CD8+ T-cells, CD4+ T-cells, B cells, Plasma cells, regulatory T-cells, NK-cells	Upregulated	Upregulated	Upregulated
CYTOKINE SIGNALING IN IMMUNE SYSTEM	Reactome	CD8+ T-cells, CD4+ T-cells	Upregulated	-	Upregulated
INTERFERON_ALPHA_BETA_SIGNALING	Reactome	Classical Monocytes, CD8+ T-cells	Upregulated	-	Upregulated
INTERFERON_SIGNALING	Reactome	CD8+ T-cells, CD4+ T-cells	Upregulated	-	Upregulated
INTERFERON_SIGNALING	Reactome	Classical Monocytes	-	Downregulated	Upregulated
DAP12_INTERACTIONS	Reactome	CD8+ T-cells	Upregulated	-	Upregulated
Cellular Signaling & Trafficking					
SIGNALING_BY_GPCR	Reactome	Classical Monocytes	Upregulated	Upregulated	-
GPCR_LIGAND_BINDING	Reactome	Classical Monocytes	Upregulated	Upregulated	Upregulated
GPCR_LIGAND_BINDING	Reactome	Plasma cells	-	Upregulated	Upregulated
CHEMOKINE_RECEPTOR_BIND_CHEMOKINES	Reactome	Classical Monocytes	Upregulated	Upregulated	Upregulated
FORMATION OF BETA-CATENIN TCF COMPLEX	Reactome	Classical Monocytes	Upregulated	Upregulated	-
FORMATION OF BETA-CATENIN TCF COMPLEX	Reactome	Non-classical Monocytes	Upregulated	Upregulated	Downregulated
Cell Cycle & DNA Replication					
DNA_METHYLATION	Reactome	Classical Monocytes	Upregulated	Upregulated	-
DNA_METHYLATION	Reactome	Non-classical Monocytes	Upregulated	Upregulated	Downregulated
DNA_METHYLATION	Reactome	Plasma cells	Downregulated	-	Downregulated
CELL_CYCLE_MITOTIC	Reactome	Plasma cells	Downregulated	-	Downregulated
CELL_CYCLE_CHECKPOINTS	Reactome	Plasma cells	Downregulated	-	Downregulated
DNA_REPLICATION	Reactome	Plasma cells	Downregulated	-	Downregulated
Metabolism & Biosynthesis					
RESPIRATORY_ELECTRON_TRANSPORT	Reactome	Non-classical Monocytes	Downregulated	Downregulated	-
HEME_SIGNALING	Reactome	Immature T-cells	Upregulated	Upregulated	-
HEPARAN_SULFATE/HEPARIN METABOLISM	Reactome	Classical Monocytes	Downregulated	-	Downregulated

#7769 IL-12/anti-PD-1 armored oncolytic HSV-1 reprograms CNS immunity: Integrated longitudinal immune, genomic, and metabolic CSF profiling in the MVR-C5252 PuMP Trial.

Elizabeth Owens, Kelly Hotchkiss, Stevie Threatt, Justin T. Low, Monika Anand, Julia Louw, Melody Goldston, Margaret O. Johnson, Claire Bradbury, James E. Herndon, Gerry A. Grant, David M. Ashley, Anoop P. Patel, Annik Desjardins, Michael C. Brown, Mustafa Khasraw

Duke University School of Medicine, Durham, NC

Introduction/Rationale: Glioblastoma (GBM) remains refractory to immunotherapy and exhibits low basal IL-12 and IFN-γ levels relative to other solid tumors, reflecting an immunologically quiescent microenvironment. MVR-C5252 is a replication-competent HSV-1 engineered to deliver IL-12 and an anti-PD-1 antibody fragment, coupling oncolysis with Th1 polarization and localized checkpoint blockade to overcome this resistance.
Methods: Stage 1 of PuMP (NCT06126744) assessed safety in six adults with recurrent IDH-wildtype GBM treated with a single convection-enhanced intratumoral infusion (5×10^8 or 1×10^9 PFU). An Ommaya reservoir enabled CSF sampling at baseline, 1 hour, and 28 days. Serial CSF single-cell RNA sequencing (scRNA-seq) assessed immune cells, and whole-genome sequencing (WGS) quantified ctDNA and viral kinetics. Liquid chromatography-mass spectrometry (LC-MS)-based metabolomics interrogated IFN-γ-linked tryptophan/kynurenine and arginine/NO pathways. Stage 2 (ongoing) incorporates repeat dosing via an implanted pump, and Stage 3 delivers 12 doses in a Bayesian Optimal Interval (BOIN) dose-escalation design, with the selected dose and schedule planned for expansion in Stage 4.
Results: Six patients (3M/3F; 50-59 years; KPS 90 in 5, 80 in 1; MGMT unmethylated in 5) were treated in Stage 1. Median PFS was three months and median OS was 6.1 months, with two patients alive at last follow-up. MVR-C5252 was well tolerated (grade 1-2 only) with no PCR-detectable shedding in urine or saliva. scRNA-seq in four patients with CSF from all three timepoints yielded 14,049 high-quality cells and diverse T-cell and myeloid populations. $CD8^+$ subsets included cytotoxic and exhausted states, while $CD4^+$ subsets spanned naïve, memory, effector, and regulatory states. TAM-like microglia and macrophages were also identified. Rapid early IFN-driven activation and monocyte/dendritic-cell recruitment were observed, followed by sustained cytotoxic and myeloid remodeling at 28 days. $CD8^+$ populations showed increased effector states and fewer exhausted cells, while $CD4^+$ T-cell states spanned naïve and helper lineages. Tumor and viral genome kinetics were characterized by WGS, immune-metabolic pathways were quantified by LC-MS-based metabolomics, and integrated CSF-tumor-blood analyses will be presented.
Conclusions: Stage 1 demonstrates safety and immunobiological activity of MVR-C5252, with a single infusion inducing immune remodeling that was not sustained. Meaningful antitumor activity is expected to require repeated intratumoral dosing, as planned in Stages 2-4. These findings establish a mechanistic human model in which localized IL-12/anti-PD-1 virotherapy shifts the tumor microenvironment from a quiescent to a Th1-polarized, cytotoxic state, providing a foundation for next-phase efficacy evaluation.

: Immunomodulatory Agents and Interventions
Poster Session

#7773 Continuation of immune checkpoint inhibitor therapy after progression in head and neck squamous cell carcinoma: A multicenter study.

Hyun Ae Jung[1], Young Kim[2], Ross Merkin[3], Thomas Roberts[3], Manisha Patel[3], Boram Park[4], Jinyong Kim[1], Sehhoon Park[1], Jong-Mu Sun[1], Se-Hoon Lee[1], Jin Seok Ahn[1], Myung-Ju Ahn[1], Lori J. Wirth[3], Jong Chul Park[3]

[1]Samsung Medical Center, Seoul, Korea, Republic of,[2]New York Medical College, Valhalla, NY,[3]Massachusetts General Hospital, Boston, MA,[4]College of Medicine, Inha University, Incheon, Korea, Republic of

Background: Immune checkpoint inhibitors (ICIs) have significantly improved survival outcomes in recurrent or metastatic head and neck squamous cell carcinoma (HNSCC). However, disease progression after first-line ICI therapy remains a major clinical challenge, and the benefit of ICI continuation or rechallenge after progression has not been fully elucidated.
Methods: In this multicenter retrospective study, we included patients diagnosed with HNSCC between 2016 and May 2025 at Samsung Medical Center and Massachusetts General Hospital. This study included patients who received first-line ICI therapy with or without other agents. Overall survival (OS) was compared between patients who received second-line ICI continuation (ICI-based regimens) and those who received non-ICI treatments.
Results: A total of 278 patients received first-line ICI therapy with or without chemotherapy, including 85 (30.6%) with HPV-positive HNSCC, 133 (47.8%) with HPV-negative disease, and 60 (21.6%) with unknown HPV status. Among them, 242 patients (87.0%) experienced disease progression after first-line ICI ± chemotherapy, and 210 proceeded to second-line treatment. Of these 210 patients, 73(34.8%) received ICI-based therapy — while the remaining 137 (65.2%) received cytotoxic chemotherapy or other non-ICI regimens. The median OS from the start of first-line therapy was 17.0 months (95% CI, 14.5-19.5). Median OS was 21.1 months for patients who received second-line ICI continuation and 14.3 months for those who received non-ICI treatments (HR 0.61, 95% CI 0.43-0.85, P = 0.004). The median OS from the start of second-line therapy was 12.2 months for patients who received ICI with or without other agents and 8.0 months for those who received chemotherapy (P = 0.003). In subgroup analyses stratified by first-line ICI efficacy, patients with a first-line treatment duration of < 6 months showed a modest OS advantage with ICI-based second-line therapy compared with non-ICI regimens (11.2 vs. 8.0 months; P = 0.042). In patients whose first-line treatment duration was ≥ 6 months, the difference was substantially more pronounced, with ICI-based therapy demonstrating a markedly longer OS compared with non-ICI treatment (12.7 vs. 7.8 months; P = 0.035).
Conclusions: ICI continuation was associated with a significant OS benefit compared with non-ICI regimens in patients with recurrent or metastatic HNSCC who progressed after first-line ICIs. These findings indicate that continuing ICI-based treatment may be a feasible option regardless of the duration of first-line PFS, with a more pronounced benefit in patients who initially achieved durable disease control with first-line ICI therapy.

#7774 Blockade of cell-ECM interaction with an oncolytic virus suppresses tumoral STING activation while inducing antitumor immunity.

Upasana Sahu[1], Matthew Mullarkey[2], Kimberly Rivera Caraballo[1], Sergie Bombin[1], Adam Chadli[1], Ravindra Kolhe[3], James M. Markert[4], Bangxing Hong[1], Balveen Kaur[1]

[1]Augusta University, Augusta, GA,[2]The University of Texas Health Science Center At Houston, Houston, TX,[3]Pathology, Medical College of Georgia, Augusta, GA,[4]University of Alabama at Birmingham (UAB), Birmingham, AL

Oncolytic HSV (oHSV) therapy is an emerging immunotherapeutic modality currently approved for melanoma in USA and EU and conditionally approved for recurrent brain tumors in Japan. Several clinical trials are investigating the utility of this approach in patients. To investigate ways to improve its therapeutic index, we analyzed the transcriptomic changes in patients with recurrent brain tumor pre and post CAN-3110 treatment (NCT03152318). Gene set enrichment analysis showed significant enrichment in the pathways of extracellular matrix (ECM) interactions and glycosaminoglycan (GAG) synthesis post virotherapy. CD44, a cell surface receptor, plays a crucial role in cell-cell and cell-ECM interactions. Apart from engaging with ECM components like hyaluronic acid (HA), collagens, fibronectin, osteopontin, matrix metalloproteinases (MMPs), etc., it also partners with several cell surface receptors like growth factor receptor family and integrins to guide cellular responses to ECM and growth factor stimulation. Here we investigated the role of CD44 signaling in regulation of both anti-viral innate immunity and anticancer adaptive immunity by creating an oHSV that encodes for the secreted extracellular portion of CD44 (OV-x44). Our results indicated that OV-x44 destabilized xCT and disrupted cellular redox homeostasis. Increased oxidative stress resulted in tumor selective STING carbonylation, and reduced TBK1 activation, thereby enhancing virus replication. On the contrary, single-cell RNA sequencing uncovered enhanced innate immune responses in immune cells with TLR7 driven activation in T cells in the tumor microenvironment (TME). To our knowledge, this is the first report to describe an oHSV that can inhibit innate intracellular anti-viral immunity in tumor cells and can also stimulate innate immune responses in the TME to guide antitumor immunity. Collectively, this study uncovers the significance of OV-x44 as a potent immune stimulating anticancer therapeutic.

#7775 Pharmacodynamic biomarkers of TGFβR2xPD-1 bispecific antibody INCA33890 in patients with MSS metastatic colorectal cancer (mCRC).

Michelle Kinder[1], Rui Hong[1], Chifei Sun[1], Yunlan Fang[1], **Michael Smith**[1], Cynthia Timmers[1], Chiara Greggio[1], Jordi Rodon Ahnert[2]

[1]Incyte Corporation, Wilmington, DE,[2]The University of Texas MD Anderson Cancer Center, Houston, TX

INCA33890 is an TGFβR2xPD-1 bispecific antibody designed to antagonize TGFβR2/PD-1 signaling in immune cells co-expressing both targets. In the INCA 33890-101 study (NCT05836324) part 1A, 48 patients (pts) across 10 tumor types were evaluated with 7 dose levels (100, 300, 600, 900, 1200, 1500 mg Q2W and 900 mg Q4W). In part 1B, 94 pts with MSS mCRC were treated across 3 dose levels (300, 600, and 900 mg Q2W). During part 1B dose expansion, fresh or archival (≤3 years of first dose) baseline biopsies and on-treatment biopsies (Cycle 2, Day 15 [C2D15] up to Cycle 2, Day 28) were required. We present pharmacodynamic biomarker analyses from pts in part 1A and part 1B with MSS mCRC. Peripheral blood from pts was analyzed by flow cytometry for receptor occupancy, anti-idiotype binding, and T-cell activation (Ki67 and HLA-DR). Cytokines (CXCL9, CXCL10, IFNγ) were measured in plasma using a 4-Plex ELLA or proinflammatory MSD assay. Intratumoral T-cell infiltration was measured at baseline and C2D15 using multiplex immunohistochemistry, which included CD8, Granzyme B, and FOXP3. Multiplex immunofluorescence staining for phosphorylated SMAD (pSMAD) and spatial transcriptomics using the Xenium immuno-oncology panel were also performed. Following INCA33890 treatment, PD-1 competitive binding decreased, demonstrating target engagement. Anti-idiotype binding of INCA33890 increased in both PD-1^{+} effector memory T cells and PD-1^{-} naïve T cells, demonstrating dose-dependent engagement of TGFβR2 at the highest dose levels. At all doses, INCA33890 induced T-cell activation, evidenced by increased Ki67 and HLA-DR expression on peripheral T cells, and increased proinflammatory cytokines IFNγ, CXCL9, and CXCL10. In pts with MSS mCRC, intra-tumoral CD8^{+} T-cell density was significantly increased in matched post-treatment tumor biopsies. pSMAD and T cell TGFβR2 response signatures were decreased in PD-1^{+} T cells in post-treatment biopsies of responding patients. In the INCA 33890-101 study, treatment with INCA33890 resulted in activation of peripheral CD4^{+} and CD8^{+} T cells, and increased T-cell infiltration within the tumor microenvironment. At the recommended doses for expansion, INCA33890 binding was specific for PD-1^{+} T cells, as evidenced by low anti-idiotype binding on naïve T cells, which do not express PD-1. Decreases in pSMAD and T-cell TGFβR2 response signature in intratumoral T cells demonstrated the inhibition of TGFβR2 by INCA33890.

#7776 An exopolysaccharide-containing yogurt preserves CCR6$^+$ CD4$^+$ T Cells: Th7R, and may enhance immunotherapy responses in lung cancer patients.

Hiroshi Kagamu[1], Ayako Shiono[1], Hisao Imai[1], Atsuto Mouri[1], Ou Yamaguchi[1], Kosuke Hashimoto[1], Shota Takei[1], Hirotaka Kawanabe-Matsuda[2], Kyoichi Kaira[1]

[1]Saitama Medical University International Medical Center, Hidaka, Japan,[2]Meiji Holdings Co., Ltd., Hachioji, Japan

Background: Anti-tumor T-cell immunity is strongly influenced by the host immune state, known as the cancer-immune set point, in which gut immunity plays an essential role. Kawanabe-Matsuda et al. demonstrated in tumor-bearing mice that oral intake of purified exopolysaccharides derived from *Lactobacillus delbrueckii ssp. bulgaricus* OLL1073R-1 (R-1 EPS) induces CCR6$^+$ T cells in Peyer's patches and enhances the antitumor efficacy of immune checkpoint inhibitors. A randomized controlled study also reported that 4-week continuous consumption of yogurt containing R-1 EPS increases CCR6$^+$ T-cell subsets in the peripheral blood of healthy volunteers. We previously identified a novel CCR4$^-$CCR6$^+$ CD4$^+$ T-cell cluster, Th7R, enriched in advanced non-small cell lung cancer (NSCLC) patients who responded to PD-1 blockade therapy. Pre-treatment Th7R predicted ICI efficacy, and long-term survivors maintained a high proportion of Th7R after therapy.

Objective: To analyze longitudinal changes in T-cell subsets in patients with histologically confirmed lung cancer who consumed yogurt fermented by *L. bulgaricus* OLL1073R-1 containing R-1 EPS.

Methods: Peripheral blood was collected before intake, after 4 weeks of yogurt consumption, and 4 weeks after discontinuation. Changes in T-cell immune markers were evaluated using the Welch test and correlation analyses. Adverse events and the influence of concurrent cancer treatments were assessed.

Results: By August 15, 2025, 91 NSCLC patients were enrolled (median age 73 years; 70 males). Participants included stage II-III patients who received neoadjuvant therapy plus surgery or chemoradiotherapy, and patients with advanced or recurrent disease receiving systemic therapy. Treatments included targeted therapy (n=5), pembrolizumab (n=15), ipilimumab plus nivolumab (n=51), cytotoxic agents plus pembrolizumab (n=2), chemoradiotherapy (n=3), and neoadjuvant cytotoxic therapy plus nivolumab (n=9). In the PD-1 inhibitor group, an increase in peripheral GZMB$^+$ CD8$^+$ T cells was observed. Moreover, compared with historical data, the pembrolizumab-induced reduction of Th7R cells was attenuated. In the pembrolizumab subgroup with PD-L1 TPS ≥50%, treatment efficacy was favorable relative to historical controls (ORR 58.3%; DCR 91.7%). Notably, the neoadjuvant cohort achieved a 100% response rate.

Conclusion: Intake of yogurt containing R-1 EPS may enhance the efficacy of immuno-oncology therapies by suppressing the decline of Th7R cells.

#7777 Direct *in vivo* activation and functional reprogramming of human TILs using a multifunctional nanoengager in humanized renal carcinoma.

Man Wang[1], Lifu Ruan[1], Xin Wen[2], Tian Zhang[1], Andrew Z. Wang[1]

[1]University of Texas Southwestern Medical Center, Dallas, TX,[2]Xuzhou Medical University, Xuzhou, China

INTRODUCTION: Tumor-infiltrating lymphocytes (TILs) therapy has demonstrated remarkable clinical success in melanoma. However, its application in other cancers has been limited by high manufacturing cost and toxic conditioning regimen. To overcome these limitations, we aimed to develop a novel strategy to directly activate and expand TILs in vivo using a multifunctional nanoengager (TIL-NPs). In this study, we report the validation of TIL-NPs using mouse models of cancer, including a humanized renal carcinoma model that closely recapitulates human immune-tumor interactions.
METHODS: TIL-NPs were generated by conjugating azide-functionalized PEG-PLGA nanoparticles with DBCO-modified anti-CD3, anti-4-1BB, and IL-2. Their ability to activate and expand TILs was assessed using both MC38 and 786-O models. For the MC38 study, mice bearing bilateral tumors received intratumoral TIL-NPs in the right flank tumor only, and TIL activation was further evaluated using isolated MC38 TILs co-cultured with MC38 cells in vitro. To assess human relevance, TIL-NP-mediated expansion of human TILs was tested using renal cell carcinoma (RCC) patient samples, and a humanized RCC model was established by inoculating 786-O cells into NSG mice engrafted with human PBMCs.
RESULTS: We engineered multifunctional nanoparticles (TIL-NPs) displaying anti-CD3, anti-4-1BB, and IL-2, measuring ~126 nm with ~50 μg of immune agonists conjugated per mg NP. In vitro, MC38 tumor-derived TILs stimulated with TIL-NPs showed markedly enhanced cytotoxicity against MC38 cells and produced the highest IFN-γ levels compared with free antibodies or unstimulated TILs. In vivo, intratumoral delivery of TIL-NPs in a bilateral MC38 model induced complete regression of all injected tumors and generated a strong systemic response, with substantial regression of contralateral tumors and improved survival. Using RCC patient-derived TILs, TIL-NPs also enhanced cytotoxicity against 786-O and ACHN cells relative to free antibodies. In a humanized RCC model, TIL-NPs produced near-complete regression of treated tumors and markedly suppressed contralateral tumor growth. Immunohistochemistry confirmed dense $CD8^+$ T-cell infiltration in TIL-NP-treated tumors, indicating enhanced activation and recruitment of cytotoxic T cells. Overall, TIL-NPs strengthened T-cell signaling through receptor clustering, prolonged survival, and elicited potent local and systemic antitumor responses.
CONCLUSION: TIL-NPs potently activate and reprogram TILs in vivo, enhancing cytotoxicity and systemic antitumor immunity, highlighting their translational potential for adoptive T-cell therapy in solid tumors.

#7778 GS24-B047, a potential best-in-class DLL3-targeting T-cell engager with integrated costimulatory signal, for the treatment of small cell lung cancer.

Zeng Qi[1], **Fu Li**[1], Zhiyu Cui[1], Hongmei Xie[1], Sijia Liu[1], Dechen Cao[1], Liang Xu[1], Yihui Lin[1], Lishan Kang[1], Siqin Wang[1], Lei Jin[2], John L. Xu[2]

[1]Changchun GeneScience Pharmaceutical Co., Ltd., Shanghai, China,[2]Changchun GeneScience Pharmaceutical Co., Ltd, Shanghai, China

Background: Small cell lung cancer (SCLC) remains an aggressive malignancy with limited therapeutic options and poor prognosis, particularly in the relapsed/refractory settings. DLL3, a tumor-associated antigen highly expressed on SCLC cells with minimal expression in normal tissues, represents a promising therapeutic target. While T-cell engagers (TCEs) targeting DLL3 and CD3, such as Tarlatamab, have demonstrated clinical activity, maintaining T-cell function in the tumor microenvironment remains challenging, and improvements in progression-free survival (PFS) have been limited. GS24-B047 is a novel DLL3-targeting TCE that incorporates a proprietary costimulatory signal designed to enhance T cell activation and persistence, with the potential to improve clinical efficacy in SCLC patients.

Methods: Binding activity and specificity of GS24-B047 to DLL3, CD3, and the costimulatory target were characterized by surface plasmon resonance (SPR), Octet biosensor, and flow cytometry. *In vitro* functional activity was assessed in co-culture assays with human PBMCs and DLL3-expressing SCLC cell lines, measuring T cell activation, cytokine release, and cytotoxicity. *In vivo* anti-tumor efficacy was evaluated in SCLC cell-derived xenograft (CDX) models with human immune system reconstitution.

Results: GS24-B047 bound to DLL3 with sub-nanomolar affinity, recognizing a distinct, more membrane-proximal epitope as compared to Tarlatamab, and effectively mediated simultaneous engagement of DLL3 on tumor cells and CD3 on T cells. *In vitro*, GS24-B047 induced T cell activation, proliferation, and cytokine secretion, and exhibited potent cytotoxicity against DLL3-expressing SCLC cell lines (with EC_{50} values in the picomolar range). GS24-B047 demonstrated a favorable therapeutic index with a high ratio of tumor cell killing to IL-6 release. The integrated costimulatory signal reduced markers of T-cell exhaustion as compared to a benchmark DLL3xCD3 TCE, supporting a more sustained T-cell response. *In vivo*, GS24-B047 treatment resulted in significant and durable tumor regression in multiple CDX models of SCLC, showing enhanced anti-tumor activity when compared to clinical benchmarks.

Conclusion: GS24-B047 is a novel DLL3-targeting TCE with integrated costimulation that promotes potent and sustained anti-tumor immunity in preclinical SCLC models. Collectively, our data support GS24-B047 as a potential therapeutic candidate for SCLC and warrant further evaluation in IND-enabling studies.

#7779 A tunable interleukin-18 (IL-18) platform engineered for complete escape from the decoy receptor IL-18 binding protein (IL-18BP).

Haiming Huang[1], Wencong Peng[1], Ruohan Zhu[1], Quanxiao Li[1], Liwen Ji[1], Yao Lu[1], Dong Wei[1], Yanling Wu[2], Tianlei Ying[2]

[1]Suzhou Forlong Biotechnology Co., Ltd, Suzhou, China,[2]Key Laboratory of Medical Molecular Virology (MOE/NHC/CAMS), Shanghai Institute of Infectious Disease and Biosecurity, School of Basic Medical Sciences, Fudan University, Shanghai, China

Background: IL-18 is a potent immune cytokine that promotes $CD8^+$ T-cell- and NK-cell-mediated antitumor responses. Its therapeutic potential is limited by rapid neutralization by IL-18BP, poor stability, short half-life, and systemic toxicity. Multiple efforts have attempted to generate IL-18 variants that escape IL-18BP neutralization, but current variants either retain residual IL-18BP binding or require extensive mutations. Our goal was to produce IL-18 variants fully resistant to IL-18BP with minimal mutations while maintaining controlled IL-18 activity via engaging the IL-18 receptor (IL-18R1).
Methods: Using structural modeling with our AI-driven Intelligent Biomolecular Discovery Platform, we identified amino acids critical for IL-18BP and IL-18R1 interactions. A combinatorial IL-18 library was constructed by site-directed mutagenesis and displayed on yeast. Variants that lost IL-18BP binding but retained IL-18R1 interaction were enriched by FACS. DNA coding sequences of positive clones were Sanger sequenced, subcloned into mammalian expression vector. And recombinant proteins were purified. IL-18R1-specific binding and IL-18BP escape were confirmed by ELISA, and binding KDs were determined by bio-layer interferometry. Functional activity was assessed by IFN-γ production from human PBMCs in the presence of 5 μg/mL IL-18BP.
Results: We initially identified a positive clone named E8 which showed reducing binding affinity to IL-18BP. We further obtained more than 200 clones which completely lost binding to IL-18BP from a secondary library based on the sequence of E8. Multiple sequence alignment revealed that clones with few amino acid mutations could fully abolish IL-18BP binding while retaining minimal IL-18R1 interaction. In addition, specific amino acid positions were identified whose single or combined mutation restored IL-18R1 affinity. Combinatorial mutations of specificity-related and affinity-related amino acids yielded a panel of over 100 IL-18 variants with IL-18R1 binding KDs ranging from 10^{-9} to 10^{-7} M and complete loss of IL-18BP binding. Representative variants activated human PBMCs with graded IFN-γ responses despite presence of high IL-18BP levels. One representative variant was fused to a anti-PD-1 IgG and demonstrated a tumor growth inhibition of 98% in mouse MC38 tumor model.
Conclusion: We developed a series of engineered IL-18 variants (IL-18v) that fully escape IL-18BP neutralization while providing tunable IL-18R1 affinity. This IL-18v platform enables customizable cytokine potency and supports diverse research and therapeutic applications, including incorporation into fusion proteins, targeted cytokine therapies, and next-generation immunotherapy strategies.

#7780 The first-in-class covalent peroxiredoxin 3 (PRX3) inhibitor RSO-021 modulates immune phenotypes in mesothelioma.

Victoria Gibson[1], Joanna Dzialo[2], Aida Habibovic[1], Christopher Landry[1], Dean Fennell[2], **Brian Cunniff**[1]

[1]University of Vermont Cancer Center, Burlington, VT,[2]Mesothelioma Research Programme, University of Leicester, Leicester, UK, Leicester, United Kingdom

RSO-021 is the clinical formulation of the first-in-class covalent peroxiredoxin 3 (PRX3) inhibitor thiostrepton (TS). TS covalently inactivates PRX3 active site cysteines leading to increased oxidative stress and apoptotic tumor cell death. RSO-021 was safe and showed early anti-tumor activity in a phase 1 trial in patients with malignant pleural effusion (MPE) arising from mesothelioma or metastatic disease to the lung (Fennell et al. *J Clin Oncol* 42, 3019-3019(2024)). The phase 2 trial is currently ongoing (NCT05278975). In this study we profiled immune signatures of human mesothelioma cell lines and patient derived explants treated with TS, and malignant pleural effusions from patients treated with RSO-021. Treatment of human mesothelioma cell lines showed TS down-regulated expression of PD-L1 and increased MHC class 1 expression. RNA-sequencing of human mesothelioma cells and patient-derived mesothelioma explants treated with TS showed modulation of transforming growth factor beta (TGFβ), tumor necrosis factor (TNFα), interferon alpha, and interferon gamma gene signatures. We performed multiplex ELISA analysis of cytokines in MPE from patients treated with RSO-021 via an intrapleural catheter to the pleural space. The levels of Resistin, a cytokine related to macrophage signaling in mesothelioma, was significantly increased 24 hours and 7-days post RSO-021 treatment. Levels of IL-6 and IL-8 were increased 24 hours after RSO-021 treatment and returned to baseline at 7 days. Lastly, in a syngeneic mouse model of mesothelioma end stage tumor burden was assessed in mice treated with TS, anti-PD1/anti-CTLA4 antibodies, or a combination of TS and anti-PD1/anti-CTLA4 antibodies. TS treated mice showed 30% tumor reduction. Anti-PD1/anti-CTLA4 antibody treated animals showed partial responses with 2 of 6 mice having complete tumor reduction. The combo of TS plus anti-PD1/anti-CTLA4 antibody showed complete tumor reduction in 6 of 6 mice. Together, these data highlight the immunomodulatory activity in cells, mouse models, and human tissue with RSO-021 and support further clinical development of RSO-021 in combination with immune-oncology therapies.

#7781 Patient derived tumor-immune organoids capture the functional and mechanistic interface in predicting response to standard therapeutics and immunotherapeutics in colorectal cancer patients.

Suman Dutta[1], Debarpan Mitra[2], Manoranjan Jha[1], Rimi Mukherjee[2], Juluri Srinivas[3], Kadambari Dixit[1], Krishanu Dey[1], Aswin Pandit[3], Sindu Pilli[1], Chandra C. Ghosh[2], Amjad Hussain[2], Gnaneswar Atturu[4], Ram Shankar Upadhayaya[1], Pradip K Majumder[5], Biswanath Majumder[1]

[1]Aryastha Life Sciences Private Limited, Hyderabad, India,[2]CanFinis Therapeutics, RISE, IISER, Kolkata, India,[3]Renova Century Hospitals, Hyderabad, India,[4]Care Hospital, Hyderabad, India,[5]Aryastha Life Sciences Inc, Cambridge, MA

Background: Colorectal cancer (CRC) is an emerging challenge, with rising early onset incidence and high mortality among younger individuals. Curative outcomes remain difficult due to its complexity. While chemotherapy and targeted drugs remain standard, immune checkpoint inhibitors (ICI) and engineered CAR-T are advancing as promising therapy options.
Objectives: Here we report the development of Aryastha BioSolution®, an integrated patient-derived tumor-immune organoid platform designed to predict therapeutic responses in CRC. The mechanistic interface of this platform enables parallel assessment of agents, ICI, and adoptive cell therapies, while capturing patient specific tumor-immune interaction dynamics that underlie treatment sensitivity and resistance.
Experimental procedure: Patient Derived Tumor Organoids (PDTOs) were established from surgically resected colorectal tumors and maintained in 3D milieu. PDTOs were treated with human equivalent doses of Oxaliplatin and Capecitabine and tumor killing was measured by live/dead staining. PDTOs were also co-cultured with human immune cells (PBMCs or engineered CAR-Ts) for 72 hours. Dynamics of tumor-immune engagement and therapy-induced organoid killing was tracked using time-lapse live imaging. Modulatory effects of ICI and CAR-T and their inflammatory responses were determined 72 hours post-culture by IFN-γ and chemokines levels.
Results: Early passage PDTOs retained the core genomic and phenotypic landscape of parent tumors, including point mutations, copy-number alterations, microsatellite (MSI) profile, as well as viability (Ki67) and histopathology signatures. Evaluation of SOC regimens showed that PDTO sensitivity markedly correlated with clinical treatment outcomes as measured by PET-CT. Co-culture assays showed distinct infiltration and killing trajectories of ICI treated PBMCs and CAR-T, characterized by robust cytolytic activity and close to 50% tumor volume reduction. We identified augmented IFN-γ and proinflammatory chemokines in responder PDTOs. Genomic profile (MSI-H/MMRd, tumor mutational burden, transcriptomic profile) and reactivity of tumor using these functional readouts underscore the mechanism of response and non-response which align with their known clinical trends.
Conclusions: The PDTO platform effectively bridges the translational gap that conventional models fail to overcome. Aryastha BioSolutions® provides a clinically aligned drug-response system that captures the phenotypic diversity of CRC and delineates the biology distinguishing responders from non-responders, enabling rational therapeutic combinations. The platform's high translatability positions it to strengthen clinical trial design and personalize both standard and emerging immunotherapy approaches.

#7782 Cbl-b-Notch1 axis blockers rewire immunosuppressive tumors to drive cytotoxic and anti-angiogenic immune responses.

Zhi Huang[1], Mairah Khan[2], Laura Naldi[3], Brionna King[1], Luis Del Valle[1], Silvana Leit[4], Beth Browning[4], Christine Loh[4], Lucio Miele[1], Giulia Monticone[1]

[1]LSU Health New Orleans, New Orleans, LA,[2]Department of Urology, Northwestern University, Chicago, IL,[3]University of Florence, Florence, Italy,[4]Nimbus Discovery LLC, Cambridge, MA

Background. Immunotherapies aimed at enhancing antitumor immune responses or delay immune cell exhaustion have shown encouraging results across multiple cancer types. However, immunotherapy still presents limited and variable response rates in immunosuppressive solid tumors, where cancer cells develop multiple strategies to evade and block antitumor immune responses. As a result, options to treat immunosuppressive tumors remain limited and this calls for the development of novel targeted immunotherapies to meet this critical need. Our group recently proved that an immunosuppressive pathway, named as the Cbl-b-Notch1 axis, exists in T cells and acts to constrain T cell function by means of increased Notch1 degradation by Casitas B-lineage lymphoma proto-oncogene B (Cbl-b), following T cell activation. We also found that inhibiting Cbl-b using small-molecule inhibitors effectively restores Notch1 level and enhances CD8 and CD4 T cell functions in *in vitro* and *ex vivo* conditions. In this study, we aimed to demonstrate the effectiveness and the underlying mechanisms though which blocking the Cbl-b-Notch1 axis rewires the immunosuppressive tumor microenvironment to mount protective antitumor immune responses.

Experimental procedures and results. This work leveraged a combination of genetic editing, targeted immune cell depletion, *in silico*, *in vivo*, *ex vivo* models and functional assays in primary cells. We found that blocking the Cbl-b-Notch1 axis, via Cbl-b inhibition, is effective in hindering tumor growth in immunosuppressive Triple-Negative Breast Cancer (TNBC) models (C0321 and 4T1) and pre-clinical tumor-derived organoids. We found that Cbl-b inhibition exerts its antitumor effects primarily by conferring a cytotoxic Th9 phenotype to CD4 T cells, via Notch1 stimulation which regulates cytotoxic and Th9 features, including Granzyme B (GZMB) and IL9 secretion. Cbl-b-inhibitor-primed CD4 T cells reshape the tumor microenvironment through multifaceted mechanisms: (i) exert direct cytotoxicity against tumor cells via GZMB, (ii) recruit and enable CD8 T cell cytotoxic responses, (iii) reprogram macrophages to produce Thrombospondin-1 (Thbs1), via Notch1-dependend release of IL9 in the tumor microenvironment and (iv) hence leads to strong anti-angiogenesis effects that cut off the nutrients supply within the tumor. These findings are consistent with TNBC patient data in which increased Notch1, IL9 and Thbs1 expression are predictive of a better prognosis and longer survival.

Conclusions. Overall, our work identifies Cbl-b-Notch1 axis blockers, like Cbl-b inhibitors, as a promising strategy to reprogram anticancer immune responses, remodel the tumor microenvironment, and suppress tumor growth, providing a promising avenue for next-generation targeted immunotherapies.

#7783 Collagen-binding IL-12 remodels immunosuppresive microenvironment and improves survival in recurrent glioblastoma.

Opeyemi Iwaloye[1], Jun Takei[1], Lewis Barr[1], Ken Furudate[2], Koichi Sasaki[3], Haruka Ichie[1], Shunsuke Tsuzuki[1], Jun Ishihara[3], Satoru Osuka[1]

[1]Neurosurgery, University of Alabama at Birmingham, Birmingham, AL,[2]UT MD Anderson Cancer Center, Houston, TX,[3]Bioengineering, Imperial College London, London, United Kingdom

Recurrent GBM (rGBM) is the most aggressive malignant brain tumors, with a median survival of 6 months. rGBM establishes a severe immunosuppressive tumor microenvironment (TME) with increased Tregs and impaired CD8 T cell recruitment, rendering immunotherapies effective in other cancers ineffective. While IL-12 is a potent immunostimulatory cytokine capable of remodeling this immunosuppressive TME, systemic delivery causes severe toxicity, hindering clinical application. Therefore, technology to selectively deliver IL-12 to rGBM tumors is critically needed. rGBM acquires treatment resistance through construction of a unique extracellular matrix (ECM); therefore, we conceived of utilizing this as a reservoir to accumulate IL-12. Through screening, we focused on COL I & III, minimally expressed in normal brain but highly upregulated after radiotherapy and in rGBM. We created CBD-IL-12 by fusing IL-12 with the collagen-binding domain (CBD) of von Willebrand factor (vWF), leveraging vWF's selective binding to COL I & III at sites of vascular disruption, inflammation, and tumors while sparing normal organs. Biodistribution assays in a mouse rGBM model demonstrated selective CBD-IL-12 accumulation in rGBM tumors without accumulation in other COL I & III-high organs. Toxicity studies in mice and dogs showed CBD-IL-12 significantly reduced peripheral IFN-γ levels compared to IL-12 without hepatic or pancreatic dysfunction. Spectral flow cytometry and single-cell RNA-seq revealed that CBD-IL-12 increased effector memory CD8 T cells, M1-like macrophages, and DCs while reducing Tregs, exhausted T cells, M2-like macrophages, and MDSCs, dramatically reversing immunosuppression. CBD-IL-12 (25μg i.v., twice) prolonged survival by 260% with a 13% CR rate in rGBM mice models. Combining CBD-IL-12 with radiotherapy achieved 63% CR. Notably, in our rGBM model where radiotherapy alone provided no survival benefit, combination with CBD-IL-12 achieved dramatic tumor suppression, likely through radiation-induced COL I & III upregulation and enhanced macrophage/microglia recruitment. Long-term survivors demonstrated durable immune memory by rechallenge testing. For clinical translation, we engineered humanized CBD-IL-12 and validated its efficacy in 3D human GBM slice cultures, demonstrating increased CD8 T cells and reduced Tregs. Collagen-binding IL-12 overcomed rGBM immunosuppression with potent antitumor effects, representing a promising novel immunotherapeutic approach.

#7784 Targeting PRMT7 elicits anti-AML immunity by promoting MHC-I expression.

Shuaishuai Ge[1], Kaixiu Luo[2], Lei Zhang[1], Meng Liu[1], Xin He[1], Guohua Wu[1], Yang Li[1], Yadav P. Umesh[1], Haojie Dong[1], Shengli Xue[3], Jian Jin[2], Ling Li[1]

[1]City of Hope National Medical Center, Duarte, CA,[2]Icahn School of Medicine at Mount Sinai, New York, NY,[3]The First Affiliated Hospital of Soochow University, Suzhou, China

Protein arginine methylation regulates several cellular functions, including RNA splicing, translation and DNA damage repair. Protein arginine N-methyltransferase (PRMT) dysregulation is often seen in malignant hematopoiesis. PRMT7, the only type III PRMT, catalyzes monomethyl arginine (MMA) modification, but its role in leukemogenesis is elusive. Re-analysis of a previous genome-wide CRISPR/Cas9 screen revealed PRMT7 to be a crucial negative-regulator of MHC-I, prompting us to ask whether PRMT7 inhibition might promote anti-AML immunity. To assess the potential PRMT7 function in MHC-I presenting, we knocked out PRMT7 in human AML lines including THP-1 and Molm13 and assessed MHC-I levels. Relative to controls, PRMT7 KO remarkably upregulated MHC-I expression in both lines. We also observed MHC-I upregulation was also observed in both cell lines after treatment with the targeted degrader (PRMT7 PROTAC) ex-vivo at relatively low concentrations, while the same dose of either compound spared normal hematopoietic stem/progenitor ($CD34^+$) cells. To confirm MHC-I dynamics in an MLL-AF9 mouse model, we generated a Prmt7 KO MLL-MA9 mouse model from hematopoietic-specific Prmt7 KO mice ($Prmt7^{fl/fl}$;Vav1-Cre) and observed 2-fold upregulation of H-2Kb expression relative to WT MLL-AF9 cells.Given the critical role of MHC-I in $CD8^+$ T cell activation, we next asked whether PRMT7 deletion would enhance $CD8^+$ T cell responses. We evaluated human T cell killing effects in PRMT7-KO/-WT THP-1 or Molm13 cells cocultured with activated $CD8^+$ T cells derived from healthy donors. Post-coculture, we found that PRMT7 KO AML cells were more susceptible to human T cell-mediated killing. In agreement, PRMT7 KO murine AML cells were more sensitive to mouse T cell-mediated killing using a coculture model of MA9 and syngeneic active $CD8^+$ T cells. Moreover, following PRMT7 PROTAC pretreatment, THP1 cells were more sensitive to human T cells mediated killing in a coculture system of THP1 cells and $CD8^+$ T cells.Next, to assess whether PRMT7 deletion impairs normal hematopoiesis, we analyzed total bone marrow cellularity and lineage frequency in Prmt7 KO (Vav1-Cre+) versus Prmt7-WT (Vav1-Cre-) mice via Cytek full-spectrum flow cytometry. While total BM cellularity was comparable, PRMT7 KO slightly increased the number of $CD4^+$ or $CD8^+$
T cells. These results suggest that although PRMT7 function is likely dispensable for normal hematopoiesis, PRMT7 loss may have a modest effect on T cell proliferation or activation. In future studies, we will confirm whether PRMT7 inhibition promotes anti-tumor T cell activity in-vivo, and whether the underlying mechanism is via MHC-I regulation. Overall, we have shown that PRMT7 depletion or pharmacological inhibition enhances T cell function in part by upregulating MHC-I. These findings suggest that combining PRMT7 inhibitors with immunotherapy could be a promising strategy to overcome AML's immune-cold properties.

#7785 Spatial profiling reveals epigenetic and immunotherapy-driven remodeling of the tumor and lymph node microenvironment in HPV-associated HNSCC.

Takeshi Ito[1], Alexander Ladenheim[1], Hans Zhao[1], Ernest Hidalgo Cedeno[1], Benjamin Judson[1], Saral Mehra[1], Ansley Roche[1], Zafar Sayed[1], Avanti Verma[1], Natalia Isaeva[2], Wendell Yarbrough[2], Aarti Bhatia[1], Barbara Burtness[1], **Michael Chiorazzi**[1]

[1]Yale Cancer Center, New Haven, CT,[2]UNC School of Medicine, Chapel Hill, NC

Human papillomavirus (HPV) leads to most oropharynx cancers in the United States, with increasing incidence, significant morbidity from therapy and mortality from metastatic recurrence. HPV+ tumors exhibit a higher cure rate with surgery or chemoradiation but display lower sensitivity to immune checkpoint inhibitors (ICI). Tumor-draining lymph nodes (LNs), crucial for antigen presentation and T-cell priming in the cancer-immunity cycle, remain less well studied with respect to the effects of epigenomic and ICI agents on the LN microenvironment (LNME).

HPV-positive tumors exhibit a distinct hypermethylation pattern compared with HPV-negative tumors, promoting immune evasion and providing rationale for an ongoing window-of-opportunity trial testing the epigenomic agent 5-azacytidine (5-AzaC) in combination with the ICI nivolumab. In this trial, patients with resectable HPV+ head and neck squamous cell carcinoma (HNSCC) are randomized 2:2:1 to nivolumab, nivolumab plus 5-AzaC, or 5-AzaC alone prior to standard-of-care resection and pathology-directed adjuvant therapy.

We assessed the impact of trial therapies on immune infiltration and cell states in the TME and LNME using quantitative multiplex immunofluorescence on tumor and draining LN tissue donated by a subset of trial participants (n=14 patients) as well as untreated controls. We constructed a tissue microarray (TMA) comprising tumor resection tissue and involved LN tissue sampled with four-fold redundancy. Using qIF panels to assay protein expression of CD3, CD4, CD8, CD20, Ki67, GZMB, we investigated immune cell characteristics and activation. Initial analyses reveal the impacts of 5-AzaC vs nivolumab vs 5-AzaC+Nivo on tumor architecture and cell states in HNSCC tumor tissues. Trial therapies display effects on T cell infiltration, as hypothesized, with combination therapy leading to significant increases in CD3+ T cells, including both CD4+ and CD8+ subsets ($p<0.05$).

We next performed spatial gene expression profiling to identify the impacts of trial therapies on architecture and cell states in tumor and LN. Included in our gene panel were HPV probes to mark cells bearing viral transformation. Initial analyses of 462,376 cells assayed in situ demonstrate the presence of varied immune populations, including macrophages, tumor infiltrating CD8 T cells, CD4 T cells, in tumor and LNs, confirming the utility of spatial approaches to correlate gene expression profiles with clinical drug response parameters.

In depth immunologic analyses of patient tissues reveal potent effects of trial therapies on the LNME in HPV-associated HNSCC and suggest that epigenomic alteration may prime the TME for more effective immune responses. Detailed evaluation of the LNME may nominate novel biomarkers of immunotherapy response and identify future druggable targets within this critical anatomic site.

#7786 Targeted, conditionally active interferons, interleukins and CD8 T cell engagers for novel cancer immunotherapies.

Lennart Zabeau[1], Anje Cauwels[1], Leander Huyghe[1], Silvie Taveirne[1], Joris Wauman[1], Alexander Van Parys[1], Jared E. Lopes[2], Erik Depla[1], **Niko Kley**[2]

[1]Orionis Biosciences BV, Ghent, Belgium,[2]Orionis Biosciences Inc., Waltham, MA

Cytokines, including interferons (IFNs) and various interleukins (ILs) such as IL-2 and IL-1, play major roles in the regulation of innate/adaptive immune responses and the emergence and progression of multiple cancer types. This involves both immune and cancer cell intrinsic signaling pathways. For example, IFNs and ILs are potent stimulators of tumor neoantigen processing and presentation by antigen presenting cells, activation of CD8 T and NK cells, and modulation of immune suppressive components of tumor microenvironments (e.g., MDSCs, TAMs). Repression of cancer cell intrinsic IFN signaling is implicated in mechanisms whereby oncogenic signals (e.g., KRAS mutations, MYC overexpression, p53 loss of function) contribute to establishment and maintenance of an immune-suppressive tumor microenvironment. We have established a multifaceted technology foundation for the engineering of vectorized, on-target, conditionally active cytokines to exploit their therapeutic potential and simultaneously avoid systemic toxicities associated with traditional cytokine-based therapies. We will describe applications of our technology innovations for the development of targeted cDC1 dendritic cell activators, immune checkpoint regulatory cell engagers, and potent CD8 T cell-selective engagers with broad spectrum cancer application potential. Examples of these we have recently advanced into clinical trials.

#7787 Phenotype-tailored prophylactic immunomodulation enables safe immune checkpoint inhibitor rechallenge after severe irAEs in high-risk patients.

Lucrezia Mencarelli, Pierre Van Mol, Douglas Daoudlarian, Sofiya Latifyan, Nuria Alfonso Mederos, Hasna Bouchaab, Matteo Torsello, Antonia Stamatiou, Nicolas Etienne, Karim Abdelhamid, Nabila Ferahta, Athina Stravodimou, Keyvan Shabafrouz, Solange Peters, **Michel Obeid**

CHUV, Lausanne, Switzerland

Background: Severe immune-related adverse events (irAEs) frequently lead to permanent discontinuation of immune checkpoint inhibitors (ICIs). Whether phenotype-tailored prophylactic immunomodulation (PTPI) can safely enable ICI rechallenge in such high-risk patients is unknown.
Methods: We retrospectively studied patients with ICI interruption after at least one grade ≥2 irAE who were subsequently rechallenged under prophylactic biologic immunomodulation in a tertiary immuno-oncology toxicity program. Prophylaxis was selected according to the dominant inflammatory phenotype of the index irAE, with or without low-dose steroids. Primary endpoints were ICI discontinuation due to irAEs at 3 and 6 months and incidence of grade ≥3 irAEs during rechallenge. Secondary endpoints included timing and phenotype of recurrent irAEs, an “immune tolerance enabling strategy” (ITES; on ICI at 6 months without grade ≥3 irAEs), disease control rates (DCR) and exploratory comparisons by prophylaxis class
Results: Thirty-eight patients were rechallenged under prophylaxis. irAEs were rheumatologic (39%), colitis (32%) and uveitis (8%); 66% were multi-organ. Twelve patients (32%) had received combination and 26 (68%) anti-PD-(L)1. The main tumour types were lung (39%), melanoma (32%), renal cell carcinoma (13%). Prophylaxis consisted of IL-6R blockade in 61% and TNF blockade in 26%. During rechallenge, 26% developed grade ≥3 irAEs. IrAE-related ICI discontinuation occurred in 16% and 24% at 3 and 6 months, respectively; among 15 patients who discontinued for irAEs, median time to discontinuation was 130 days. Median time to recurrent irAE was 108 days with 50% occurring >90 days. ITES was achieved in 55% of patients, with median ICI duration 201 days. In colitis, TNF-based prophylaxis was associated with rare colitis recurrences (11%) and fewer irAE-related discontinuations than non-TNF strategies. In rheumatologic phenotypes, IL-6R blockade showed lower recurrence (14%) and fewer irAE-related discontinuations than minimal/non-IL-6R prophylaxis. Only one patient (3%) discontinued ICI for an infectious complication, no grade 4 irAEs occurred. DCR at 3, 6, 9 and 12 months were 52%, 63%, 62% and 65%, respectively.
Conclusions: In high-risk patients, PTPI enabled prolonged ICI exposure with acceptable high-grade toxicity, low irAE-driven discontinuation, preserved disease control, supporting organ-tailored prophylaxis as a strategy to be tested in prospective trials.

#7788 Daiad-2/15: A conditionally active, targeted, hyperpotent IL-2/IL-15 immune agonist is safe and effective *in vivo*.

Anu Jayabalu, Mark E. Branum, **Jonathan G. Drachman**, Alexander Astrakhan

StradBio, Inc., Seattle, WA

Although high-dose interleukin-2 (IL-2) has been approved for the treatment of certain cancers since 1992, widespread use has been limited due to systemic toxicity, including cytokine release syndrome and vascular leak syndrome. Versions of IL-2 with reduced potency have been studied, but these variants have reduced efficacy as well as toxicity. In this report, we describe Daiad-2/15, a computationally designed, highly potent IL-2/IL-15 agonist that is delivered specifically to tumor-targeting T cells without systemic immune activation. Using our Daiad^{TM} platform technology, a logic gate was engineered by splitting Neo-2/15 into two separate pieces. The individual split Neo-2/15 domains are unable to bind or activate the IL-2 receptor complex. By fusing each portion of the cytokine mimetic to a targeting domain, two distinct modules are created, which together constitute Daiad-2/15. *In vitro*, Daiad-2/15 activates only T cells that express the targeted antigen, with a 10,000-fold lower threshold for signaling compared to antigen-negative T cells. By targeting two different antigens, the Daiad-2/15 acts as an effective 'AND' gate, only activating T cells that express both antigens. Furthermore, Daiad-2/15 does not trans-activate target-negative cells, even when present in an admixed culture. The Daiad architecture is compatible with both full length and single-domain antibodies and leads to antigen-specific T cell expansion *in vitro*. We designed Daiad-2/15 to activate exhausted T cells in the tumor microenvironment using nanobodies specific for PD1 and LAG3. We evaluated the tolerability and antitumor activity of Daiad-2/15 in a stringent syngeneic tumor model, CT26. Individual checkpoint-specific Daiad-2/15 modules had no impact on tumor growth or weight loss, while the wild-type IL-2 and the parental Neo2/15 cytokine mimetic were toxic *in vivo*. Treating mice with both Daiad-2/15 modules, specific for PD1and LAG3, resulted in significantly improved antitumor activity compared to the two nanobodies alone, with no signs of systemic toxicity. Together, our data suggest that Daiad-2/15 could potentiate the systemic delivery of a highly potent immune agonist to specific immune cells in the tumor microenvironment and draining lymph nodes with a wide therapeutic index. Additional preclinical studies are underway, and clinical testing of Daiad-2/15 is planned.

#7789 ACM-CpG, a polymersome-delivered TLR9 agonist, elicits rapid and broad immune activation in a phase I trial for advanced solid tumors.

Amit Jain[1], Aaron C. Tan[1], Andrea Budiman[1], Nan Jiang[1], Kim Peng Tan[2], Jackwee Lim[2], Loo Ser Yue[3], Jian Hang Lam[3], Yan Jun Lee[3], Teck Wan Chia[3], Katherine Schultheis[3], Madhavan Nallani[3], Daniel Sw Tan[1]

[1]National Cancer Centre Singapore, Singapore, Singapore,[2]A*STAR, Singapore, Singapore,[3]ACM BIolabs Pte Ltd, Singapore, Singapore, Singapore

Background: ACM-CpG is a novel innate immune activator comprising of TLR9 agonist CpG7909 encapsulated within polymer vesicles (“polymersomes”). This formulation enhances in vivo immune activation compared with free CpG. In preclinical animal models, ACM-CpG induced tumor regression, durable antitumor immune memory, and growth inhibition of distal, non-injected tumors. Intramuscular administration also achieved tumor control on abscopal subcutaneous tumors. Based on these findings, a Phase I clinical trial (NCT06587295) was initiated at the National Cancer Centre Singapore to evaluate the safety and early efficacy signals of intramuscular ACM-CpG monotherapy in patients with advanced solid malignancies.

Methods: This is a 3+3 dose-escalation study of ACM-CpG administered intramuscularly as monotherapy. Eligible patients had advanced cancers with prior clinical response to immune checkpoint inhibitors, either alone or in combination with chemotherapy. A total of 8 patients have been treated to date in the monotherapy arm. Subsequent study arms will assess ACM-CpG in combination with immune checkpoint inhibitors or cancer peptide vaccines. Immune responses were profiled using CyTOF, multiplex cytokine assays (Luminex/Olink), IFN-γ ELISPOT, and single-cell RNA/TCR sequencing.

Results: Pharmacodynamic data covering the first treatment cycle of all patients shows that ACM-CpG triggered rapid and coordinated activation across multiple innate and adaptive compartments within 24 hours post-injection. Immune profiling showed expansion of myeloid populations with upregulation of activation markers CD86, CD38, and CD40, accompanied by transient expansion of MDSCs and pDCs, indicating strong antigen-presenting activity. Adaptive immune activation was demonstrated by proliferation and activation of NK cells and $CD4^+$/$CD8^+$ T cells expressing CD69, along with PD-1 upregulation in some patients, consistent with T-cell priming. Cytokine profiling revealed 5-30-fold elevations of MCP-1, MCP-2, CXCL10, and CXCL11, reflecting potent TLR9-driven pro-inflammatory signaling. IFN-γ ELISPOT confirmed a 1.4-3.4-fold increase in antigen-specific IFN-γ-secreting T cells. Single-cell transcriptomics identified strong type I interferon signatures and upregulation of innate and adaptive immune effectors. CpG7909 was rapidly cleared within 24 hours, with no systemic accumulation observed. ACM-CpG was well tolerated with no dose-limiting toxicities observed.

Conclusions: ACM-CpG induces rapid, broad-spectrum immune activation, engaging both innate and adaptive compartments and enhancing cytokine and T-cell responses with a favorable safety profile. These early clinical findings support continued development of ACM-CpG as a potent monotherapy and a versatile immunologic amplifier for combination immunotherapy.

#7790 Peptide-delivered low dose IL-2 reprograms pancreatic cancer immunity to improve survival.

In Hwan Park, Shawn Abeynaike, Ashley Martinez, Jonathan Cho, Daisuke Nishizaki, Gregory P. Botta

UCSD Moores Cancer Center, La Jolla, CA

Metastatic pancreatic cancer (PC) has a dismal 5-year survival of only 2% due to limited chemotherapy efficacy, poor drug penetration, and an immunosuppressive TIME. Dense desmoplasia, inactive anti T-cells, and highly enriched immunosuppressive Tregs hinder immunotherapy responses.IL-2, a dual-function cytokine that promotes T-cell growth at high concentrations while also inducing immunosuppression at lower concentrations. High dose (HD) IL-2 is a highly an active immunotherapy that enhances cytotoxic T-cell activity while attenuating suppressive Tregs with cures in melanoma and renal cell carcinoma. Unfortunately, HD IL-2 has significant systemic toxicities that induce capillary leak syndrome (CLS), severe hypotension, and renal failure. The CendR-peptide (iRGD) binds to av/B3 integrins specifically at the tumor and induces a NRP-1 dependent transcytotic uptake of co-administered drug and is currently being evaluated in Phase 2 metastatic PC clinical trials. We hypothesized that iRGD could direct systemically low dose (LD) IL-2 into mouse PC and concentrate it locally within the tumor as HD IL-2. As such, we immunomodulate the TIME of PC to activate CD8 cytotoxic T-cells, reduce tumor growth and increases survival while reducing systemic toxicity associated with HD IL-2.Orthotopic KPC PC were developed in C57BL6 WT mice. Tumor-bearing mice were treated i.v. with iRGD and titrated concentrations of IL-2 (3/week). Tumors were analyzed for CD8+ T-cell proliferation, activation, and cytotoxicity. CD8 T cell depletion confirmed necessity of cytotoxic T cells. Lung tissue was evaluated for IL-2 induced CLS. Patient-derived PDAC slice cultures were treated ex vivo for translational relevance. iRGD + LD IL-2 significantly reduced tumor weight and increased survival compared with monotherapy or HD IL-2. The median survival in treated mice was significantly increased. iRGD combination treatment avoided cachexia, CLS, and systemic inflammation, with no elevation in IL-6 or TNF-a. iRGD combined with LD IL-2 did not reduce Treg numbers or increase CD8 T-cell infiltration/proliferation, but enhanced resident cytotoxic T-cell activity as demonstrated by increased p-STAT5, Granzyme B, and cl-Caspase 3. CD8+ T-cell depletion abrogated these effects, confirming CD8+ T cell dependence. In patient-derived PDAC slice cultures, iRGD+IL-2 increased Granzyme B, supporting translational relevance. Importantly, the peptide combination therapy avoids the severe side effects of CLS and cachexia commonly associated with HD IL-2. This combination significantly improves anti-tumor responses and prolongs survival in preclinical models of mouse and human PC, highlighting a robust, safe, and sustained anti-tumor immune response. iRGD combined with LD IL-2 has appropriate pre-clinical anti-cancer and safety signals to warrant early Phase 1 clinical trials in PC.

#7791 PAI-1 inhibition attenuates the inflammatory response in a murine model of sclerodermatous chronic graft-versus-host disease.

Sahra Gabure, Yogamaya Divakar Prabhu, Vasantharaja Raguraman, Shanid Mohiyuddin, Yan Ji, William Fay, Senthilnathan Palaniyandi, Gerhard Hildebrandt

University of Missouri, Columbia, MO

Hematopoietic stem cell transplantation (HSCT) is a critical tool for managing malignant and defective disorders of hematopoiesis but is limited by graft-versus-host disease (GVHD). Chronic GVHD (cGVHD) remains a leading cause of non-relapse morbidity and mortality following allogeneic HSCT. Due to its high immunoreactivity, the skin is most commonly affected in cGVHD, where it undergoes aberrant tissue repair and progressive fibrosis. Therapeutic options for sclerodermatous cGVHD are limited and disease progression drives long-term morbidity and functional impairment. Plasminogen Activator Inhibitor-1 (PAI-1) is a mediator of tissue remodeling and fibrosis, regulating extracellular matrix deposition and the migration of fibrogenic cell populations. In this study, we hypothesized that pharmacologic inhibition of PAI-1 may improve clinical and histopathological outcomes in a murine model of sclerodermatous cGVHD by reducing pro-fibrotic signaling. C57BL/6 mice were conditioned with total body irradiation followed by intravenous infusion of bone marrow cells and splenocytes of either syngeneic (C57BL/6) or allogeneic (LP/J) donors. Mice received oral PAI-1 inhibitor PAI-039 (10 mg/kg) or vehicle every other day from day +14 until day +56. Clinical signs of GVHD and survival were monitored throughout this duration. At day +56, tissues and serum were collected for downstream molecular analyses. PAI-039 treatment improved survival and clinical GVHD scores. Serum levels of pro-inflammatory cytokines IFN-γ ($P=0.006$) and TNF-α ($P=0.002$) were significantly reduced in PAI-039 treated mice compared to controls, alongside decreased expression of IFN-γ ($P=0.04$) in skin isolates. These findings indicate that PAI-1 inhibition may provide therapeutic benefit in the treatment of sclerodermatous cGVHD by disrupting pathogenic fibrotic signaling, warranting further investigation.

#7792 PIK3CA activating mutation reshapes the tumor microenvironment to promote immune evasion in squamous cell carcinoma.

Sydney Fisher, Benjamin Nicholson, Weijie Guo, Yuxuan Phoenix Miao

University of Chicago, Chicago, IL

Head and neck squamous cell carcinoma (HNSCC) is a leader in cancer incidence worldwide. Although the introduction of immunotherapy, such as immune checkpoint blockade (ICB), has improved the landscape of cancer treatment in many solid tumors, including HNSCCs, there remain challenges in achieving durable responses with such therapies. Indeed, HNSCC patients often relapse following ICB treatment. While relapse events are high, there is a lack of understanding of the mechanisms underlying cancer immune evasion. These disparities in patient outcomes strongly suggest the existence of genetic variations that underlie their distinct responses to ICB. Although the specific oncogenic mutations responsible for driving relapse in SCC patients remain unclear, it is critical to elucidate the mechanisms of cancer immune evasion in individuals with specific genetic profiles to enhance the precision of immunotherapy. We aim to understand the genetic basis shaping the immune suppressive TME and hypothesize that oncogenic driver mutations play a dominant role in preventing the immune clearance of transformed cells by reprogramming the immune landscape in the tumors. To determine the critical genetic signatures enriched in SCC patients that can impact anti-tumor immunity, we analyzed TCGA data which revealed a strong negative correlation between *PIK3CA* level and CD8+ T cell signatures. We have identified that activating mutations in the *PIK3CA* gene, found in 20% of HNSCCs, promote rapid tumor relapse after initial response to anti-PD-L1 and anti-CTLA-4 ICB treatments. Utilizing single-cell analysis, quantitative immune profiling, and multiplexed imaging, our lab showed that tumor-initiating cells (TICs) in SCCs can have an intricate dialogue with myeloid-derived suppressor cells (MDSCs) where TICs secrete factors to enhance MDSC recruitment and suppressive function on cytotoxic T cells. Our lab also identified that SOX2 amplification in *PIK3CA* mutant SCC could modulate neutrophils and block their interferon responses via activation of fatty acid desaturase 1 (FADS1) to aid neutrophils in maintaining their immune suppressive functions during immunotherapy treatments. As such, this study has led to key mechanistic understanding of how *PIK3CA* mutation allows cancer cells to shape the immune suppressive responses. Thus, our findings uncover a unique mechanism whereby *PIK3CA* mutant SCCs critically shape the tumor microenvironment to survive robust immunotherapy and give rise to tumor relapse.

#7793 Bioelectromagnetic reprogramming of tumor-immune metabolism to selectively destroy NSCLC.

Sunny Huang[1], Jennifer Petssche[2], Danielle Foster[2], Charles Searby[2], Val Sheffield[2], Douglas R. Spitz[3], Calvin Carter[1]

[1]Geminii, Inc., Chicago, IL,[2]University of Iowa, Iowa City, IA,[3]Director, Free Radical & Radiation Bio., University of Iowa, Iowa City, IA

BACKGROUND: Dysregulated oxygen and redox-active metal metabolism create an oxidized tumor microenvironment in non-small cell lung cancer (NSCLC). Tumors accumulate reactive oxygen species (ROS) and labile iron, promoting progression yet creating a vulnerability to iron-catalyzed ROS and lipid peroxidation. This oxidized microenvironment also alters tumor-immune metabolic balance, impeding immune function in the TME. Existing electromagnetic-based therapies such as tumor treating fields and electroporation do not directly target redox-metabolic vulnerabilities and have usability constraints. Building on our recent work published in *Cell Metabolism* showing that orthogonally applied static electromagnetic fields (EMFs) safely reprogram redox and glucose metabolism to treat diabetes, we sought to determine whether a bioelectromagnetic modality applied during convenient treatment times could be engineered to reprogram tumor-immune metabolism for selective killing of NSCLC.
METHODS: We engineered a device to deliver orthogonally oriented static EMFs for ≥6 hours / day. Mice bearing human NSCLC xenografts (H1299 & A549) or syngeneic LLC tumors were randomized to EMF or sham. Tumor growth, survival & combination with chemoradiation therapies were evaluated. Mechanistic studies assessed lipid peroxidation, γH2AX, T-cell activation/exhaustion & antigen-specific $CD8^+$ trafficking, $CD4^+$/$CD8^+$ depletion, and effects of scavenging H_2O_2, labile iron, or lipid peroxides on ferroptotic pathways. Histopathology assessed toxicity.
RESULTS: EMF monotherapy inhibited tumor growth & prolonged survival versus sham and improved chemoradiation efficacy. EMF-treated tumors showed increased lipid peroxides and γH2AX, consistent with lipid peroxidation and DNA damage induced tumor death. In syngeneic tumors, EMF enhanced $CD8^+$ and $CD4^+$ T-cell activation and reduced exhaustion. OT-I and T-cell depletion studies showed EMF efficacy requires antigen-specific adaptive immunity. Genetic scavenging of H_2O_2, iron, or lipid peroxides within tumors attenuated EMF-induced tumor killing, demonstrating ferroptotic tumor death without normal-tissue toxicity.
CONCLUSIONS: Orthogonally applied static EMFs represent a novel bioelectronic strategy to selectively kill NSCLC by exploiting redox-metabolic vulnerabilities and activating antitumor immunity. This bioelectronic modality could be used to safely enhance tumor killing while overcoming adherence challenges of existing field-based modalities.

#7794 When stress spreads: Transmissible ER stress as a driver of immune remodeling in PDAC.

Naveen Chintala Ramulu[1], Shreya Pokharel[1], Nishanthini Pirashanna[2], Basel Abuaita[2], Joseph Francis[1]

[1]Comparative Biomedical Sciences, Louisiana State University, Baton Rouge, LA,[2]Pathobiological Sciences, Louisiana State University, Baton Rouge, LA

Pancreatic ductal adenocarcinoma (PDAC) remains one of the most lethal malignancies, with a 5-year survival rate of only 11%. Within the PDAC tumor microenvironment (TME), rapidly proliferating tumor cells outgrow the vascular supply, creating hostile microenvironmental conditions such as nutrient deprivation, hypoxia, and high metabolic demand. This, in turn, perturbs the protein folding capacity of the endoplasmic reticulum (ER), thereby provoking a cellular state of 'ER Stress'. Also, tumor cells can disseminate ER stress to the stromal cells within the TME in a process known as 'transmissible ER stress'. Although PDAC is considered an immunologically 'cold' tumor, ER stress appears to rewire the host immune system for tumor cell immune evasion. In this regard, we determined if the bone marrow-derived macrophages (BMDM) are susceptible to "transmissible" ER stress. Herein, murine pancreatic Panc02 and KPC cells (transmitter cells) were treated with thapsigargin (Tg), and the ER stress-conditioned medium was used to culture the murine BMDMs (receiver cells). Our preliminary data demonstrated that BMDMs cultured in ER-stress-conditioned medium demonstrated a significant transcriptional upregulation of proinflammatory modulators, including *iNOS*, IRE1α(*Xbp1*, nuclear factor-kappaB (*NF-κB*), and cyclooxygenase-2 (*COX-2*). Strikingly, this inflammatory state co-occurred with increased *Arg1*, consistent with an immunosuppressive, tumor-promoting macrophage phenotype. Altogether, this transcriptional profile reflects a hybrid inflammatory-immunoregulatory state characteristic of PDAC tumor-associated macrophages (TAMs). To delineate the mechanism by which transmissible ER stress modulates the immune profile of BMDMs, we propose genetic ablation and/or pharmacological inhibition of the classical stress pathways, including IRE1α, PERK, and ATF6, to determine their effect on BMDM polarization. In conclusion, our findings provide new insights into the dynamic crosstalk between PDAC cells and BMDMs, highlighting two key aspects: a) the complexity underlying the concurrent pro-inflammatory and immunosuppressive features within the TME following ER stress, and b) raises the possibility that this phenomenon may contribute to the attenuation of intrinsic antitumor T-cell responses..

Key Words: Pancreatic ductal adenocarcinoma, tumor microenvironment, ER stress, bone marrow-derived macrophages.

: Immunotherapies in Pediatric Cancers
Poster Session

#7798 Embryonal and alveolar rhabdomyosarcoma immunotherapy treatment benefit prediction by CURE AI.

Amit Weiss[1], Ofir Landau[1], Tzvi Lederer[1], Gregory Koushnir[1], Radesh P. Nattamai Malli[1], Tal Shor[1], Daniel Khankin[1], Vitalay Fomin[1], **Neil Pfister**[2]

[1]Numenos, New York, NY,[2]University of Alabama at Birmingham; Numenos, Birmingham, AL

Clinical trials are not able to study individual treatment effects as methods to do so have not yet matured into practical use. For decades, we have studied groups of patients enrolled on a trial, comparing groups of patients as large cohorts and losing signal for important, complex features that define individuals. Foundation models take a different approach. Using the CURE AI foundation model generated from clinical and multi-omics data from hundreds of thousands of patients, complex and non-linear biological patterns can be found in new datasets that can provide insights into disease biology. We previously identified a complex signature predictive of immunotherapy treatment benefit compared to chemotherapy benefit by analysis of a set of non-small cell lung cancer clinical trials (Weiss et al., AI in Precision Oncology, 2025). In the current study, we theorized that we could apply predictors of immunotherapy response/nonresponse from adult clinical trials to pediatric cancer patients. If feasible, this approach could dramatically accelerate progress in pediatric cancer treatment development by leading to the development of better treatment strategies that could immediately be assessed on pediatric clinical trials.
We analyzed RNA sequencing from over 50 types of pediatric cancers to predict treatment benefit of immunotherapy relative to chemotherapy. Alveolar and embryonal rhabdomyosarcomas (RMS) stood out as notable case studies as the majority of patients in both rhabdomyosarcoma groups were, based on treatment response prediction from adult immunotherapy clinical trials, predicted to respond favorably to immunotherapy. However, about one-third of both RMS subtypes were predicted to be resistant to immunotherapy. Alveolar RMS had significantly more immunotherapy resistance-related genes upregulated in patients with predicted immunotherapy resistance compared to embryonal RMS, with largely different compositions of immune-related genes between the RMS subtypes. Interestingly, CURE AI identified 36 genes with > 4-fold upregulation that were in common between embryonal and alveolar RMS patients with predicted immunotherapy resistance including many genes not previously associated with RMS or immunotherapy resistance including TLL2 and F2RL2, suggesting that these pathways may be targeted to overcome immunotherapy resistance in RMS. Furthermore, alveolar RMS-specific and embryonal RMS-specific cytokine signatures were identified that could be implemented to guide patient selection for immunotherapy treatment.
These results demonstrate that biological foundation models can be used to analyze adult clinical trials to gain novel insights into different cancer types to generate patient-level pediatric data that could justify accelerated clinical trial concept development in pediatric cancers.

#7801 Preclinical efficacy of DLL3 targeted CAR T cells in neuroblastoma.

Salvatore M. Aspromonte, Tamar Feinberg, Ali Cihan, Samantha Brosius, Armaan H. Siddiquee, Dylan Domenico, Daoqi You, Shakeel Modak, Kevin J. Curran, Andrew L. Kung, Anthony Daniyan, Filemon Dela Cruz

Memorial Sloan Kettering Cancer Center, New York, NY

Background: Neuroblastoma (NBL), the most common extracranial solid tumor in children, accounts for 15% of pediatric cancer deaths, and survival after relapse remains <50%. To expand immunotherapeutic options, we evaluated Delta-like ligand 3 (DLL3), an inhibitory NOTCH ligand normally silenced in healthy tissues but aberrantly expressed in neuroendocrine tumors. NOTCH dysregulation in NBL and emerging datasets indicating DLL3 expression support investigation of DLL3 as a target and assessment of IL-18-armored DLL3-directed CAR T cells originally developed for small-cell lung cancer.
Methods: DLL3 expression was assessed in NBL patient samples and PDX models by RNA sequencing, immunohistochemistry (IHC), and flow cytometry. IL-18-armored DLL3 CAR T cells were tested in vitro against NBL cell lines across multiple effector-to-tumor (E:T) ratios. Cumulative killing was compared using Vardi's test for area-under-the-curve analysis, and Wilcoxon rank-sum tests evaluated differences at individual E:T ratios.
Results: RNA sequencing of pediatric solid tumors treated at MSK (n=540) showed that NBL (n=109) had the highest DLL3 transcript levels relative to other non-CNS tumors (0-19.7 TPM; median 0.38). In NBL patient samples, IHC (n=31) demonstrated DLL3 protein expression (H-score ≥10, range 10-300, median 100) in 52% (16/31) with strong transcript-protein concordance (Spearman $r=0.847$, $p=2\times10^{-9}$). In NBL PDX models, DLL3 protein expression was detected in 63% (19/30), with H-scores ranging 10-123 (median 73). Flow cytometry across five PDX models spanning H-scores 7-105 showed DLL3 surface expression on 25-88% of tumor cells, confirming antigen accessibility. IL-18-armored DLL3-CAR T cells exhibited significantly greater cumulative cytotoxicity than untransduced T cells against two DLL3+ NBL cell lines, SK-N-DZ (51% DLL3+, $p=0.03$) and SK-N-SH (29% DLL3+, $p=0.03$), with activity across multiple E:T ratios ($p<0.05$). To confirm antigen specificity, IL-18-armored DLL3-CAR T cells were compared with a clinical-grade IL-18-armored CD371-directed CAR (CLEAR AML) as a non-DLL3-targeting control. DLL3-CAR T cells exhibited significantly greater cytotoxicity against both cell lines (SK-N-DZ, $p=0.0006$; SK-N-SH, $p=0.0004$) and outperformed the control CAR across all E:T ratios ($p<0.001$).
Conclusions: DLL3 is expressed in a subset of NBL patient tumors and PDX models and is accessible for CAR targeting. IL-18-armored DLL3-directed CAR T cells show strong in vitro cytotoxicity against DLL3+ NBL models. In vivo testing in a DLL3+ NBL PDX is underway. These findings support DLL3 as a promising immunotherapeutic target and justify further development of DLL3-directed CAR T therapy for NBL.

#7802 cGAS-STING pathway agonist plus immune checkpoint inhibitor augments chemotherapy effectiveness in murine osteosarcoma models.

Mayra L. Mendiola, Michele Doucet, Erin E. Resch, Brian H. Ladle

Johns Hopkins University School of Medicine, Baltimore, MD

Osteosarcoma (OS) is the most prevalent pediatric bone cancer, and standard of care treatment includes neoadjuvant chemotherapy, surgery, and adjuvant chemotherapy. Several prognostic factors for overall survival have been identified, including >95% tumor necrosis at the time of primary surgery (surrogate of chemotherapy sensitivity) and the degree of inflammatory immune infiltrates in the tumor at diagnosis. We hypothesize that increasing the immune infiltrates in OS will improve tumor sensitivity to chemotherapy and overall survival. Our group has studied the impact of activating the cGAS-STING pathway in OS via intratumoral delivery of ADU-S100 — a potent STING agonist — in both murine and canine OS. ADU-S100 increases levels of pro-inflammatory cytokines and chemokines, including Tumor Necrosis Factor-α, Interferon-β, Interleukin-6, CCL5 and CXCL10 in the treated tumors. In addition, increased activated macrophage, T-, and B-cell infiltrates are observed. We hypothesized that combining the ADU-S100 STING agonist with chemotherapy could improve outcomes in our models of OS. As we have shown the effects of STING agonist to recruit T-cells into the tumor, we also incorporated immune checkpoint inhibitor (ICI) treatment (anti-PD1 and anti-CTLA4). We used the syngeneic murine OS cell line F420 to establish intratibial tumors in C57BL/6 mice. Once tumors were palpable, cohorts of mice were treated with ADU-S100 followed by carboplatin and ICI, comparing outcomes to the monotherapy and dual therapy control cohorts. ADU-S100 + carboplatin (standard OS chemotherapy in canines) or ADU-S100 + carboplatin + ICI significantly increases ($P<0.05$) median survival compared to any of the treatments given as monotherapy. The addition of ICI to ADU-S100 + carboplatin appears to further extend the survival in responder mice. At day 40 post-tumor challenge, 46% of the ADU-S100 + carboplatin + ICI treated mice continue with disease control compared to 9% in the ADU-S100 + carboplatin treated cohort ($P=0.035$). Ongoing studies include combining ADU-S100 + ICI with doxorubicin, cisplatin, and methotrexate (standard of care chemotherapy agents given for OS in humans) and investigations of the mechanisms determining responder versus non-responder mice.

#7805 Development of a GFRA2-targeting antibody drug conjugate for neuroblastoma (NB), and Ewing sarcoma (EWS).

Amber K. Hamilton[1], Seungmin Shin[2], Raphael D. Lopez[1], Nicholas Hartnett[1], Alexander B. Radaoui[1], Maggie Hines[2], Maria Evancho[1], Rebecca S. Kaufman[1], Khushbu Patel[1], Karina L. Conkrite[1], Dan Martinez[1], Brian Mooney[3], Michelle E. Keyel[4], Elissa Levine[5], Alberto D. Guerra[1], Jarrett Lindsay[1], Yael P. Mosse[1], Jennifer Pogoriler[1], Gregg Morin[6], Poul H. Sorensen[6], Patrick J. Grohar[5], Benjamin A. Garcia[7], C. Patrick Reynolds[4], Wei Li[2], Sharon J. Diskin[1], John M. Maris[1]

[1]Children's Hospital of Philadelphia, Philadelphia, PA,[2]University of Pittsburgh, Pittsburgh, PA,[3]BC Cancer Research Institute, Vancouver, BC, Canada,[4]Texas Tech University Health Sciences Center, Lubbock, TX,[5]University of Michigan Medical School, Ann Arbor, MI,[6]University of British Columbia, Vancouver, BC, Canada,[7]Washington University School of Medicine in St. Louis, St. Louis, MO

Background: We recently defined the NB/EWS surfaceomes using integrative proteogenomics to prioritize proteins as candidate immunotherapeutic targets. GFRA2 was a top ranked candidate for both NB and EWS (*Clin Cancer Res* 2023, *Cancer Cell* 2024).

Aims: (1) Validate and assess mechanism of GFRA2 overexpression; (2) Identify selective antibody binders to GFRA2; (3) Engineer antibody drug conjugates (ADCs) and test for internalization and potency.

Methods: ChIP- and RNA-sequencing of NB and RNA-sequencing following siRNA depletion of EWSR1::FLI1 were used to evaluate mechanisms of GFRA2 overexpression. GFRA2 abundance and cellular localization was evaluated by flow cytometry and immunofluorescence. Phage display was performed with recombinant GFRA2 extracellular domain protein as the bait and the highly conserved GFRA1 and GFRA3 recombinant proteins as counters. In parallel, we humanized the anti-GFRA2 murine HSAN antibody. While we plan on reporting on several linker-payload combinations, here we focus on the initial humanized HSAN antibody conjugated to pyrrolobenzodiazepine (PBD) via a cleavable linker, which was tested for internalization using live cell imaging and cytotoxicity across a panel of human NB and EWS preclinical models.

Results: We identified a proximal super enhancer (Percentile: 97.4%-99.7%) or enhancer (94.4%-97.7%) in all 10 NB cell lines profiled. Depletion of EWSR1::FLI1 resulted in significantly decreased GFRA2 mRNA expression across 6 EWS cell lines ($P<0.0001$), and this was validated via immunoblotting. GFRA2 protein was expressed uniformly and to variable degrees on the cell surface of 10 NB cell lines, 8 NB patient-derived xenografts, and 6 EWS cell lines by flow cytometry and/or immunofluorescence. Patient tumor RNA-Seq showed 92.8% of NB (N=126; median=47.65) and 74% of EWS (N=85, median=11.47) had high expression defined as a GFRA2 TPM > 5. Phage display panning of fully human antibody fragments yielded three Fabs and one VH single domain antibody specific to GFRA2 with moderate binding affinity (50-500 nM). Humanized HSAN (co-hu-HSAN) showed high binding affinity specific to GFRA2 (1-10 nM). We then showed robust internalization of co-hu-HSAN across 6 NB cell lines. A co-hu-HSAN-PBD ADC showed potent and specific cytotoxicity across GFRA2+ cell lines (NB=2; median IC_{50}=1.69;2.92pM, EWS=2; median IC_{50}=9.81;12.43pM) with no cytotoxicity in GFRA2 null cell lines (N=2; median IC_{50}=NA).

Conclusions: GFRA2 is a lineage restricted oncoprotein abundantly expressed in both NB/EWS, as well as other human solid cancers. We show initial proof-of-concept for potent and specific cytotoxicity in both NB/EWS with the co-hu-HSAN-PBD ADC. We will report on efficacy testing of the co-hu-HSAN-PBD ADC across NB/EWS xenograft models. Work to affinity enhance the fully human binders, and progress with additional linker/payload combinations are ongoing and will be reported.

#7806 CAR priming lowers TCR activation threshold to enhance recognition of low affinity tumor antigens.

Chu-Hsuan Chiu[1], Leo D. Wang[2]

[1]Beckman Research Institute of City of Hope, Duarte, CA,[2]Beckman Research Institute, City of Hope, Duarte, CA

Chimeric antigen receptor (CAR)-T cell therapy has shown remarkable efficacy in hematologic malignancies but has achieved limited success in solid tumors due to barriers such as immunosuppressive tumor microenvironments and poor antigen presentation1. Primary brain tumors, across pediatric and adult settings, represent a particularly difficult target: they display profound intratumoral heterogeneity, frequently downregulate MHC class I2, and often present low-avidity or subclonally expressed antigens that are poorly recognized by conventional T cell receptors (TCRs). Prior studies have reported crosstalk between CAR and TCR signaling, suggesting that TCR expression is important for optimal CAR function3, and others indicate that CAR function may be suppressed when encountering low-avidity TCR antigens4. Our preliminary data show that CAR priming enhances TCR responses against weak antigens and promotes a more memory-like, less effector-like phenotype, a state linked to improved persistence and durable tumor control. Together, these findings highlight a key gap: how CAR signaling influences TCR function in the setting of weak antigens. Addressing this question is particularly critical in brain tumors, where recognition of low-avidity and poorly presented antigens limits the efficacy of current CAR T-cell therapies.

#7808 Efficacy of AZD0754, a dominant-negative TGFβRII-armored STEAP2 CAR T-cell therapy, in Ewing sarcoma xenograft models.

Peter Zanvit[1], Brianna Janocha[1], Shannon Breen[1], Christine Fazenbaker[1], Jessica Pezold[1], Lihe Zhang[1], David Clark[1], Nicolas Giraldo[2], Ryan Golden[1], Jonathan Fitzgerald[3], Mark Cobbold[3], Gordon Moody[1], Emily Bosco[1]

[1]Early Oncology, AstraZeneca Pharmaceuticals LP, Gaithersburg, MD,[2]Scientific Affairs, Global Diagnostics, AstraZeneca, Barcelona, Spain,[3]Early Oncology, AstraZeneca Pharmaceuticals LP, Waltham, MA

Background:
Ewing sarcoma (EWS) is a rare, aggressive bone and soft tissue malignancy predominantly affecting children and young adults. Despite advances in multimodal therapy, treatment options remain limited for refractory or relapsed EWS (1). Chimeric antigen receptor (CAR) T-cell therapy has shown marked efficacy in hematologic malignancies and is being developed for solid tumors. AZD0754 is a STEAP2-targeted CAR T-cell therapy incorporating a dominant-negative TGFβRII (dnTGFβRII) armoring strategy and is in Phase 1 clinical development for prostate cancer. Recent published proteomic analyses identified STEAP2 expression in EWS patient samples and cell line-derived xenografts, supporting STEAP2 as a potential candidate immunotherapeutic target (2).
Methods:
STEAP2 surface expression was evaluated across different human EWS cell lines by flow cytometry. AZD0754-mediated cytotoxicity was assessed *in vitro* using the xCELLigence real-time cell analysis platform. Based on *in vitro* results, A673, RD-ES, and SK-NEP-1 xenograft models were selected for *in vivo* efficacy studies. Mice received varying doses of AZD0754, and tumor growth and overall survival were monitored. Blood was collected at different time points for serum cytokine analysis to assess pharmacodynamic activity.
Results:
EWS cell lines expressed detectable cell surface expression of STEAP2 at receptor densities much lower than workhorse prostate cancer cell lines. Despite this, AZD0754 was capable of inducing antigen-dependent cytotoxicity *in vitro* and suppressing tumor growth in EWS xenograft models. AZD0754 exhibited dose-dependent antitumor activity that correlated with serum IFNγ levels, indicating on-target immune engagement.
Conclusions:
AZD0754 demonstrates robust preclinical anti-tumor activity against EWS *in vitro* and *in vivo*, with dose-dependent efficacy and corresponding cytokine levels. These findings support STEAP2 as a potential therapeutic target in EWS. STEAP2 targeting has the potential to address a critical unmet need in EWS by expanding treatment options to biologic and immune-based therapies.
References:
1. National Center for Biotechnology Information (2021). Ewing Sarcoma. NCBI Bookshelf.2. Mooney B, Negri GL, Shyp T, Delaidelli A, et al. Surface and global proteome analyses identify ENPP1 and other surface proteins as actionable immunotherapeutic targets in Ewing sarcoma. Clin Cancer Res.
2024;30(5):1022-1037. doi:10.1158/1078-0432.CCR-23-2187.

#7809 Epitope-encoded mRNA-LNP vaccine to enhance anti-tumor potency and persistence of PHOX2B peptide-centric CAR T cells.

Timothy T. Spear[1], Nicholas Hartnett[1], Elisabeth Posthill[1], David Groff[1], Dana Al-Halawani[1], Minu Samanta[1], Keelan O'Reilly[1], Richa Kapoor[1], Muzamil Want[1], Lingling Liu[2], Tingting Wang[2], Ruoning Wang[3], Richard Madnick[4], Irina Shkundina[4], Kristopher R. Bosse[1], Mohamad-Gabriel Alameh[1], Drew Weissman[4], John M. Maris[1]

[1]Children's Hospital of Philadelphia, Philadelphia, PA,[2]Nationwide Children's Hospital, Columbus, OH,[3]Postdoctoral Fellow, Dept. of Immunology, Nationwide Children's Hospital, Columbus, OH,[4]University of Pennsylvania, Philadelphia, PA

Background: A Phase 1/1b clinical trial testing peptide-centric chimeric antigen receptor (PC-CAR) T cells that recognize a peptide derived from the major neuroblastoma oncoprotein PHOX2B presented in the context of HLA-A*24:02 and 20 other HLA-A alleles is showing early signs of safety and efficacy (NCT07007117). Anticipated barriers to durable cures include poor persistence and a hostile tumor immune microenvironment (TIME). We hypothesize that persistence and potency can be enhanced, without compromising safety, through the deployment of a “CAR boosting” PHOX2B epitope-encoding mRNA-lipid nanoparticle (LNP) vaccine.
Methods: We established a screening platform to test various PHOX2B mRNAs and LNP designs, and here report on the prioritized formulation: a nucleoside-modified PHOX2B 9mer monomer encapsulated by FDA-approved LNP SM-102. In parallel, we established a genetically engineered mouse model (GEMM) of NB to deploy our PHOX2B epitope mRNA-LNP vaccination strategy *in vivo*.

Results: A24$^+$ healthy donor or NB patient monocyte-derived dendritic cells (moDCs) treated with vaccine exhibited log-fold higher PHOX2B 9mer presentation compared to tumor cells and upregulated T cell costimulatory ligands CD80/86 and CD40. PC-CAR T cells exposed to vaccine-treated moDCs had significantly increased proliferation, polyfunctionality, and migratory markers compared to co-cultures with HLA matched NB cell lines. Moreover, vaccine-treated moDCs enriched central, effector, and/or stem cell memory PC-CAR T cell immunophenotypes (donor/patient-dependent) compared to tumor-induced PD1^{hi}CD39^{hi} terminal effectors. PC-CAR T cells primed with vaccine-treated moDCs maintained significantly greater cytotoxicity in serial tumor rechallenges. A comprehensive characterization of the immunobiological effects of mRNA-LNP on DC and PC-CAR T cell function using O-link proteomics and transcriptional profiling are ongoing and will be reported.

GEMM-derived allografts faithfully recapitulate human disease and express a chimeric HLA-A*24:02/H-2K^b MHC that presents a conserved PHOX2B 9mer. Murine (m)PC-CAR T cells engineered with clinical scFv conjoined to murine 41BB- or CD28-CD3ζ were polyfunctional and cytotoxic against A24/H-2K^b allografts. Vaccine-treated A24/H-2K^b knock-in mice presented PHOX2B 9mer by DCs in spleen and lymph nodes, activating PC-CAR T cells. Comprehensive *in vivo* evaluation of mPC-CAR-T expansion, memory formation, and anti-tumor potency with TIME spatialomic profiling are ongoing and will be reported.
Conclusion: These IND-enabling studies will inform our clinical vaccine dosing strategy with the recommended Phase 2 PC-CAR T cell dose in an upcoming trial amendment. This CAR boosting vaccine may not only improve efficacy of PC-CAR T cells for NB but also guide mRNA-LNP enhancement strategies for other adoptive cellular therapies.

#7810 Engineering macrophages as a novel therapeutic approach for high-risk neuroblastoma.

Ke-En Tan[1], Kok Siong Yeo[2], Cheng Zhang[3], Caleb Baker[2], Shyang Hong Tan[3], Alexis M. Sosic[2], Yat-Yuen Lim[1], Choong-Yong Ung[3], Cristina Correia[3], Stephanie F. Polites[4], Yi Lin[5], William A. Weiss[6], Hu Li[3], Shizhen Zhu[2]

[1]University of Malaya, Kuala Lumpur, Malaysia,[2]Department of Biochemistry and Molecular Biology, Mayo Clinic College of Medicine, Rochester, MN,[3]Department of Molecular Pharmacology and Experimental Therapeutics, Mayo Clinic College of Medicine, Rochester, MN,[4]Department of Surgery, Mayo Clinic, Rochester, MN,[5]Division of Hematology, Mayo Clinic, Rochester, MN,[6]University of California, San Francisco, CA

Neuroblastoma (NB) accounts for 10% of pediatric cancer-related deaths. High-risk NB is frequently metastatic at diagnosis and has a poor 5-year survival rate (<50%) despite aggressive treatment. GD2, a disialoganglioside glycolipid that is expressed in nearly all NBs, has been validated as a promising immunotherapy target. Although GD2-CAR-T cells have been clinically evaluated, their efficacy has been limited by poor tumor infiltration and the immunosuppressive tumor microenvironment (TME), highlighting the need for alternative immune-based strategies. With inherent capacity of macrophages to infiltrate tumors, phagocytose cancer cells, and modulate TME, they represent a promising alternative strategy for immunotherapy in NB. In this study, we developed and evaluated GD2-CAR-macrophages (GD2-CAR-Ms) as a novel therapeutic approach for NB. GD2-specific CAR constructs were designed, validated, and introduced into multiple human and murine monocyte/macrophage cell lines via lentiviral transduction. Fluorescent microscopy and flow cytometry confirmed a significant enhancement in the phagocytosis of GD2-high NB cells by GD2-CAR-Ms containing *Hu3F8* single-chain variable fragment (*scFv*). A strong positive correlation was observed between GD2 expression levels on the target cells and phagocytosis efficiency of GD2-CAR-Ms, indicating that the phagocytic activity of GD2-CAR-Ms is antigen-specific. Anti-tumor efficacy was further evaluated *in vivo* using an immunocompetent *Mycn*-expressing NB non-genetically engineered mouse model (MYCN-NGEMM). Mice treated with GD2-CAR-Ms exhibited significantly reduced tumor burden and prolonged survival compared to control groups. Notably, treatment of mice bearing GD2-high tumors resulted in markedly improved survival, including one complete remission among ten treated animals, underscoring the therapeutic potential of GD2-targeted macrophage therapy. Histological analysis showed increased deposition of connective tissues and decreased tumor cells density, suggesting TME remodeling. Furthermore, immunohistochemistry reveals increased immune cell infiltration, particularly of macrophages, neutrophils and T cells, indicating a favorable shift in the immune TME from “cold” to “hot” following GD2-CAR-M treatment. Additionally, inhibition of tumor growth was also observed in our zebrafish NB model after GD2-CAR-Ms treatment, further supporting their therapeutic potential. Together, our findings demonstrate that GD2-CAR-Ms exhibit potent antitumor activity and reshape the tumor immune microenvironment, supporting their translational potential as a therapeutic strategy for high-risk NB.

#7811 Using γδ T cells as a potent adoptive cell therapy platform in models of pediatric sarcoma.

Jessica P. Sanchez[1], Anne-Katrin Urzynicok[1], Gabriella Albert[2], Eduardo Davila[2], Brian H. Ladle[1]

[1]Johns Hopkins University School of Medicine, Baltimore, MD,[2]University of Colorado, Anschutz Medical Campus, Aurora, CO

New treatment approaches for high-risk pediatric sarcomas are desperately needed. Immunotherapy advances with adoptive cell therapy in hematologic malignancies have not yet been translated to pediatric solid tumors including sarcomas. Hallmarks of the immune microenvironment in pediatric sarcomas include the presence of immunosuppressive immune cells and cytokines, and a lack of potent T cell activation. We are seeking ways to overcome these barriers to effective adoptive cell therapy in pediatric sarcomas. γδ T cells are known to have innate anti-tumor activity across many cancers but their activity against pediatric sarcomas remains poorly characterized. Here we detail the anti-tumor activity of γδ T cells against a panel of human and murine models of pediatric sarcomas including human and murine osteosarcoma (OS), human and murine rhabdomyosarcoma (RMS), and human Ewings sarcoma (EWS). Human and murine γδ T cells demonstrated varied anti-tumor activity across the different models of pediatric sarcomas. Co-cultures of varying effector to target ratios (E:T) of γδ T cells to tumor demonstrated strong anti-tumor effects against our models of OS and EWS. Interestingly, RMS, especially the human fusion-positive RMS cell line Rh30 showed significant resistance to γδ T cell killing. We further assessed the γδ T cell potency against pediatric sarcomas in vivo. In our syngeneic and human tumor xenograft models of sarcoma we observed temporary tumor growth control following adoptive transfer with ten million activated γδ T cells highlighting the need to improve in vivo function. We explored the addition of intratumoral STING (stimulator of interferon genes) agonist with the goal of increasing γδ T cell trafficking to the tumor. We show that STING agonist delivery prior to adoptive transfer results in increased numbers of γδ T cells in the tumor. In addition, we are exploring the introduction of a novel synthetic co-receptor, CD8a:MyD88, shown previously to augment αβ T cell effector function, to determine if γδ T cell function can be improved as well. We transduced γδ T cells ex vivo to express the CD8a:MyD88 synthetic co-receptor resulting in improved in vitro tumor lytic function and increased interferon gamma production when co-cultured with osteosarcoma cells compared to control vector-transduced T cells. Ongoing and future work is investigating the in vivo effectiveness of the CD8a:MyD88 expressing γδ T cells in our panel of sarcoma models. These studies further define the obstacles and potential solutions to successful adoptive T cell therapy for pediatric sarcomas.

#7812 Preclinical evaluation of a dnTGFβR-armored GPC3 CAR-T (AZD5851) in pediatric solid tumor PDX models - A report from the Pediatric Preclinical *In Vivo* Testing (PIVOT) Consortium.

Filemon S. Dela Cruz[1], Glorife Ibanez Sanchez[1], Samantha Brosius[1], Kristen Victor[1], Daoqi You[1], Armaan H. Siddiquee[1], Kristina C. Guillan[1], Michael V. Ortiz[2], Jee Young Kwon[3], Emily L. Jocoy[4], Timothy M. Stearns[5], Steven B. Neuhauser[5], Jeffrey H. Chuang[3], Letizia Giardino[6], Eric Tu[7], Carol J. Bult[5], Beverly A. Teicher[8], Andrew L. Kung[9], Malcolm A. Smith[8]

[1]Memorial Sloan Kettering Cancer Center, New York, NY,[2]Pediatrics, Memorial Sloan Kettering Cancer Center, New York, NY,[3]The Jackson Laboratory, Farmington, CT,[4]The Jackson Laboratory, Sacramento, CA,[5]The Jackson Laboratory, Bar Harbor, ME,[6]AstraZeneca, Cambridge, United Kingdom,[7]AstraZeneca, Gaithersburg, MD,[8]National Cancer Institute, Bethesda, MD,[9]Chair, Division of Pediatric Hematology/Oncology, Memorial Sloan Kettering Cancer Center, New York, NY

Introduction

GPC3 is a heparan sulfate proteoglycan aberrantly expressed in pediatric tumors such as hepatoblastoma (HBL), Wilms tumor (WT), germ cell tumors (GCT), malignant rhabdoid tumor (MRT), and rhabdomyosarcoma (RMS). AZD5851 is an armored GPC3-targeted CAR-T incorporating a dominant-negative TGF-β receptor II (dnTGFβRII) to resist TGF-β-mediated inhibition and enhance functionality. AZD5851 was evaluated in pediatric patient-derived xenograft (PDX) models to assess antitumor activity and associations between GPC3 and TGF-β expression.

Methods

PDX models were characterized by IHC for GPC3 (H-score) and TGF-β (% cells ≥1+ staining in tumor and stroma). Stromal TGF-β was classified as low (≤30%), moderate (31-60%), or high (>60%). Nine PDX models (3 WT, 2 HBL, 2 GCT, 1 MRT, 1 RMS) were treated in NSG MHC DKO mice (Jackson Laboratory) with 5×10^6 AZD5851 or untransduced T cells intravenously. Tumor responses were categorized per established PIVOT metrics (Houghton et al., 2007) using an event definition of >4-fold increase in tumor volume. For EFS analyses, a complementary definition of tumor volume >1,000 mm^3 or moribund status was also applied to account for delayed tumor regression typical of CAR-T therapies. EFS distributions were estimated by Kaplan-Meier analysis and compared using the log-rank test.

Results

PDX models demonstrated variable GPC3 expression (median H-score = 90, range 0-254). TGF-β staining was low in tumor cells (<5-20%) but prominent in stroma (40-90%, median ~80%). Only models with GPC3 H-scores >200 (2 HBL, 1 RMS) showed partial responses (PR) or stable disease (SD). One HBL model exhibited initial progression followed by regression after day 21. Models with H-scores <200 showed only PD. EFS analysis showed that AZD5851 significantly prolonged EFS in models with high GPC3 expression (H-score >200; $p = 0.002$-0.01, log-rank) compared with controls, while models with lower expression (≤100) showed no significant differences ($p \geq 0.2$). Responses occurred in models with both moderate (40%) and high (90%) stromal TGF-β, suggesting dnTGFβRII armoring may protect CAR-T cells from TGF-β-mediated suppression.

Conclusions

AZD5851 demonstrated tumor-regressing activity in pediatric PDX models with high GPC3 expression (RMS, HBL). Activity across models was heterogeneous, with evidence of delayed responses following initial progression. As seen with other CAR T-cell therapies, delayed activity may reflect in vivo proliferation and expansion of infused cells, and standard event-based metrics may not fully capture this effect. These findings support clinical evaluation of GPC3 CAR T cells with dnTGFβR armoring for GPC3-expressing pediatric cancers such as RMS and HBL and suggest that GPC3 expression by IHC may serve as a predictive biomarker of response.

#7813 Antitumor activity of a B7-H3 antibody-drug conjugate in osteosarcoma patient-derived and metastatic models.

Wendong Zhang[1], **Adil Bahadir**[1], Zhongting Zhang[1], Yianhua Yi[1], Zhaohui Xu[1], Simon Olivares[1], Harjeet Singh[1], AMER NAJJAR[1], Caterina Longo[1], Xin Zhou[1], Jasbir Kaur[2], Hiroki Torikai[2], Chunhua Shi[2], Jonathan Gill[1], Michael Roth[1], Tim Heffernan[2], Richard Gorlick[1]

[1]UT MD Anderson Cancer Center, Houston, TX,[2]Oncology Research for Biologics and Immunotherapy Translation (ORBIT), MD Anderson Cancer Center, Houston, TX

Background: Osteosarcoma outcomes have not improved in over three decades, and prognosis remains poor for patients with pulmonary metastases. B7-H3 is highly expressed on osteosarcoma with limited normal-tissue expression, making it an attractive therapeutic target. This study evaluated the antitumor activity of a B7-H3-targeting antibody-drug conjugate (B7H3 ADC) in osteosarcoma PDX and metastatic models.
Methods: The B7-H3 antibody (developed by ORBIT, MD Anderson) was conjugated to the tesirine payload SG3249. In vitro, cell viability was assessed in six PDX-derived osteosarcoma cell lines treated with B7H3 ADC (10-point dilution, 1000 nM start) over 120 h using Incucyte imaging. IC_{50} values were calculated by nonlinear regression, and dose-response effects were analyzed by one-way ANOVA with η^2 and Cohen's f. In vivo, six PDX models were treated with a single 1 mg/kg IP dose of B7H3 ADC, isotype-ADC, or PBS. Tumor growth inhibition and EFS were evaluated. Metastatic efficacy was assessed in IV and tibial injection models using luciferase-labeled SJSA LM7 cells, with treatment initiated at ~3×10^6 photons/sec.
Results: B7H3 ADC produced strong, dose-dependent cytotoxicity across all six cell lines (IC_{50} = 0.0795-0.6703 nM), with large effect sizes (η^2 = 0.80-0.93; Cohen's f = 2.01-3.65; $p < 0.001$). In vivo, three of six PDX models achieved maintained complete response (MCR), two showed partial response (PR), and one exhibited progressive disease (PD). In the IV metastasis model, control mice required euthanasia beginning on day 20, whereas all treated mice remained metastasis-free through day 93. In the tibial model, control mice were euthanized by day 25 with lung metastases detected by day 22. Treated mice showed complete tibial tumor regression by day 17 and remained metastasis-free through day 64.
Conclusions: B7H3 ADC demonstrated potent and reproducible antitumor activity in osteosarcoma PDX and metastatic models, inducing durable tumor regression and preventing metastatic progression. These findings support B7-H3 as a promising therapeutic target and justify further development of B7H3 ADC for primary and metastatic osteosarcoma.

#7814 Ganglioside targeting: Exerting sweet revenge on neuroblastoma.

Guillermo Nicolas Dalton[1], Wonju Kim[1], Kevin H. Lu[1], Alessandro Gasparetto[2], haley Ohlson[2], Nathaniel W. Mabe[3], Min Huang[4], Maria Caterina Rotiroti[1], Rebekah Kennedy[5], Susan Ghazarian[5], Araz Marachelian[5], SHAHAB ASGHARZADEH[5], Kimberly Stegmaier[6], Roberto Chiarle[2], Robbie G. Majzner[7]

[1]Pediatric Oncology, Dana-Farber Cancer Institute, Boston, MA,[2]Boston Children's Hospital, Boston, MA,[3]Medicinal Chemistry and Molecular Pharmacology, Perdue University, West Lafayette, IN,[4]Stanford University, Stanford, CA,[5]Children's Hospital Los Angeles, Los Angeles, CA,[6]Dana-Farber Cancer Institute, Boston, MA,[7]Stanford University School of Medicine, Palo Alto, CA

Neuroblastoma (NBL) is the most common extracranial solid tumor diagnosed in children and is responsible for 11% of pediatric cancer deaths. Dinutuximab is an FDA approved monoclonal antibody (mAb) against GD2, used in the treatment of high-risk NBL. Despite integration of dinutuximab into upfront treatment protocols, 40-50% of patients still relapse and eventually die of their disease. Resistance to anti-GD2 therapy is poorly understood. Previously, we have shown GD2 loss in xenografts in response to anti-GD2 immunotherapy. This resistance mechanism is driven by downregulation of one enzyme, ST8SIA1 while other enzymes in the GD2 pathway remain unchanged. We hypothesized that loss of ST8SIA1 leads to reduced GD2 and a compensatory increase in GM2. In the present work, we validate our hypothesis, vetting GM2 as an immunotherapy target for which we engineered GM2-specific chimeric antigen receptors (CAR) and mAbs and tested their efficacy and safety in murine models.First, we tested anti-GM2 mAbs as a monotherapy in 3 metastatic NBL xenograft models. Regardless of initial efficacy, monotherapy fail to provide long-lasting responses and eventually all mice relapsed. However, because each antibody showed partial activity in the GD2-high model, we added a combination-therapy arm in the next experiment. The combination proved to be superior, as all mice receiving it saw tumor eradication and long-term survival.We then tested anti-GM2 CAR T cells, based on the same binder used for mAbs, and saw robust and durable responses. Dual targeting GD2 and GM2, with a tandem GM2-GD2 CAR, was able to eliminate the tumors completely and provided long-term survival.Ganglioside distribution in normal tissue is poorly understood. However, it is known that GD2 is present in peripheral nerves, where it causes neuropathic pain, the main dose-limiting toxicity. To anticipate potential toxicities the combination could present, we optimized ganglioside detection by IHC on frozen tissue and successfully screened healthy tissue microarrays (TMAs). GM2 showed limited tissue distribution, being restricted to the kidneys and thyroid. More importantly, no overlap between GD2 and GM2 was observed.We also screened murine tissues from in search of a safety model. The kidneys of C57Bl/6 mice showed GM2 levels comparable to human kidneys, so were used for toxicity studies. GM2 mAbs were well tolerated with no evidence of off-target toxicity, no weight loss or noticeable pathological features.Finally, courtesy of NANT, we procured viably frozen bone marrow samples from relapsed NBL patients, previously treated with anti-GD2. These samples showed heterogeneous GD2, yet high GM2.Together these data shows, GD2 loss driven by immunotherapy and a concomitant increase in GM2. More importantly, it validates GM2 as an alternative target for GD2 low NBL and because GM2 has limited normal-tissue expression, it can be safely targeted alongside GD2 to prevent antigen escape

#7815 Efficacy of ABBV-706, a SEZ6-targeted topoisomerase 1 inhibitor ADC: A report from the Pediatric Preclinical In Vivo Testing (PIVOT) Program.

Elizabeth A. Stewart[1], Michael A. Dyer[1], Yael P. Mosse[2], John M. Maris[2], Xiao-Nan Li[3], Stefan Atkinson[1], Chen He[1], David N. Groff[2], Alvin Farrel[2], Yuchen Du[3], Jinnan Chen[3], Steven B. Neuhauser[4], Timothy M. Stearns[4], Emily L. Jocoy[5], Jee Young Kwon[6], Jeffrey H. Chuang[6], Emily Faivre[7], Kelly Doyle[7], Kimberly E. Ellison[7], Joshua F. Hernandez[7], Joann P. Palma[7], Michael Barnes[7], Pooja Hingorani[7], Nandini Rudra-Ganguly[7], Beverly A. Teicher[8], Carol J. Bult[4], Malcolm A. Smith[8]

[1]St. Jude Children's Research Hospital, Memphis, TN,[2]Children's Hospital of Philadelphia, Philadelphia, PA,[3]Ann & Robert H. Lurie Children's Hosp. of Chicago, Chicago, IL,[4]The Jackson Laboratory, Bar Harbor, ME,[5]The Jackson Laboratory, Sacramento, CA,[6]The Jackson Laboratory, Farmington, CT,[7]AbbVie Inc, North Chicago, IL,[8]National Cancer Institute, Bethesda, MD

Introduction: ABBV-706 is an antibody-drug conjugate (ADC) composed of a monoclonal antibody targeting the seizure-related homolog 6 (SEZ6) surface protein linked to topoisomerase 1 inhibitor payload. A Phase 1 trial of ABBV-706 is underway in adults with SEZ6 expressing relapsed solid tumors (NCT05599984). ABBV-706 became of interest as SEZ6 is highly expressed in many pediatric cancers. The goal was to evaluate ABBV-706 in models of childhood cancers with notable SEZ6 expression: neuroblastoma (NB), medulloblastoma (MB), retinoblastoma (RB), and alveolar rhabdomyosarcoma (ARMS) and compare the activity to vehicle and isotype non-target control ADC (IC-ADC).

Methods: Pediatric xenograft models were screened for SEZ6 expression. Single agent in vivo studies were completed in NB, MB, RB, and ARMS models with varying SEZ6 expression. After engraftment, 2 total doses of ABBV-706 or IC-ADC were given by IP injection 3 weeks apart at 2 dose levels (DL1, DL2). Efficacy was assessed by median event free survival (KM med, in days) and objective response measure (ORM, Ped Blood Cancer 2007;49:928-940). ORM defines an objective response as partial, complete, or maintained complete response (PR, CR, and MCR) compared to stable disease (SD) or progressive disease, with or without growth delay (PD2 and PD1, respectively).

Results: ABBV-706 showed efficacy in a broad range of SEZ6 expressing non-CNS (NB, RB, ARMS) models. At DL1, PR, CR, or MCR responses were seen in 8 of 11 models. At DL2, 9 of 11 models had PR, CR, or MCR responses. For most models, ABBV-706 was more active than IC-ADC. Survival advantage was observed in 1 of 2 MB models.

Conclusion: We showed high anti-tumor activity for ABBV-706 in multiple SEZ6 expressing models and enhanced efficacy versus IC-ADC. Due to high expression of SEZ6 in several pediatric histologies, ABBV-706 has potential for clinical activity in patients with these cancers.

Model	SEZ6 mRNA (FPKM)	Cancer Type	Vehicle KM med	Vehicle ORM	ABBV-706 DL1 KM med	ABBV-706 DL1 ORM	ABBV-706 DL2 KM med	ABBV-706 DL2 ORM	IC-ADC DL1 KM med	IC-ADC DL1 ORM	IC-ADC DL2 KM med	IC-ADC DL2 ORM
COG-N-424x	46.1	NB	8.6	PD	82.8*	MCR	>99*	MCR	6	PD1	13.6	PD1
COG-N-496x	59.9	NB	11.1	PD	>103*	MCR	>103	MCR	8.3	PD1	>103	MCR
COG-N-561x	13	NB	8.2	PD	78.4*	PR	101*	MCR	13.7	PD1	37	PD2
NB-1691	17.9	NB	7.9	PD	19.4*	PD2	34.3*	PD2	10.7	PD1	10.8	PD1
SK-N-AS	0.06	NB	9.7	PD	9.4	PD1	10.5	PD1	8.74	PD1	12.3	PD1
SJRB012408_X2	53.8	RB	35	PD	126*	MCR	108.5	PR	42	PD1	70	PD1
SJRB063836_X1	78.6	RB	35	PD	140*	MCR	140*	MCR	35	PD1	87.5	SD
SJRHB030765_X1	119.8	ARMS	35	PD	63*	PD1	140*	PR	42	PD1	70	PD1
SJRHB030787_X1	129.3	ARMS	35	PD	105*	CR	91	CR	63	PD1	84	SD
SJRHB031320_X1	21.8	ARMS	35	PD	98*	PR	108.5*	PR	66.5	PD1	91	SD
SJRHB046156_X1	111.7	ARMS	14	PD	84	PR	105*	CR	21	PD1	21	PD1
Icb-2164MB	166.4	MB	69.5	-	76	-	91*	-	77.5	-	72	-
Icb-3130MB	46.1	MB	90	-	137	-	148.5	-	121.5	-	117.5	-

*indicates p-value <0.05 compared to matched IC-ADC

#7816 Spatial profiling identifies tumor-associated stroma enrichment and MIF as potential immunotherapy targets in primary Ewing sarcomas.

Christopher Kuo[1], Krinio Giannikou[1], Nuoya Wang[2], Mikako Warren[1], Andrew E. Goodspeed[3], Nick Shillingford[1], Mas Hayashi[4], Micha S. Raredon[2], James Amatruda[1]

[1]Children's Hospital Los Angeles, Los Angeles, CA,[2]Yale School of Medicine, New Haven, CT,[3]University of Colorado Cancer Center,, Aurora, CO,[4]The University of Colorado School of Medicine, Aurora, CO

Objective: To date, the response rate of immunotherapy in Ewing sarcoma (EwS) has been poor. The vast majority of children with metastatic or relapsed EwS die despite current intensive, multimodal therapy. The tumor immune microenvironment (TME) has a vital role in cancer survival and progression with implications in drug resistance and immune escape. However, there is a lack of understanding of the TME of EwS. Although recent single-cell RNA sequencing of EwS and immune cells have revealed a heterogenous transcriptional landscape with distinct subsets of immune cell populations in EwS, little is known about the spatial organization and spatial microenvironmental niches of the TME of EwS.

Methods: We performed Spatial Transcriptomics (ST) on 16 primary treatment naïve EwS tumor biopsies from patients with localized EwS (L-EwS) or with metastatic EwS (M-EwS), complemented by high-plex spatial proteomic analysis.

Results: Integrated analysis revealed inter- and intra-tumoral heterogeneity. We inferred the stromal regions of tumors transcriptionally and noted that tumors from L-EwS had significantly more stromal signature than M-EwS (p-value <2.2e-16). Gene set enrichment analysis using Hallmark gene sets revealed that L-EwS tumors were enriched in epithelial mesenchymal transition (EMT) and inflammatory signatures (adjusted p-value <0.05) and M-EwS tumors were enriched in proliferative signatures (adjusted p-value <0.05). We identified a set of 46 unique genes enriched in L-EwS that overlapped with genes in EMT hallmark pathways and were predominantly extracellular matrix related (ECM-r) genes such as *COL3A1, COL1A2, ITGB1, MMP2, ACTA2, TNC, TGFB1*. These ECM-r genes spatially overlapped with the stromal regions of individual tumors. Through spatial ligand-receptor analysis, we showed that the stromal enriched regions harbor unique extracellular matrix related cytokines, immune recruitment and proinflammatory microenvironmental signals, implying EwS stroma may play an anti-tumor role by acting as an immune recruitment center. All EwS tumors expressed pro-tumorigenic MIF-CD74 immune signaling connectivity, suggesting a potential immune-evasive mechanism.

Conclusion: L-EwS tumors are enriched in ECM and ECM-related microenvironmental signals compared to M-EwS. Spatial cellular microenvironmental signals reveal the potential immune recruitment role of tumor-associated stroma, our findings provide spatial insight into the TME of EwS and provide a rationale for the preclinical investigation of MIF as a potential target for EwS immunotherapy.

: Liquid Biopsies: Circulating Nucleic Acids 5
Poster Session

#7820 CHIP detection in solid tumors differs between liquid biopsy testing approaches.

Florian Klemm[1], Fuad Mohammad[2], Alex Charles Tuck[1], Grecia Morales[2], Rochelle Awuku[3], Katya Mokretar[3], Alasdair Heasman[3], Gareth Gerrard[4], Persephone du Parcq[3], Zhenyu Xu[1]

[1]SOPHiA GENETICS, Rolle, Switzerland,[2]SOPHiA GENETICS, Boston, MA,[3]Synnovis, Cancer Genetics, Guy's Hospital, London, United Kingdom,[4]South East Genomic Laboratory Hub, London, United Kingdom

Objective: Clonal hematopoiesis of indeterminate potential (CHIP) arises from somatic variants in hematopoietic progenitor cells and is more frequent in older individuals. CHIP can appear as incidental findings in cell-free DNA (cfDNA) from patients with solid tumors, introducing biological background noise that may confound result interpretation. MSK-ACCESS® powered with SOPHiA DDM™ incorporates matched white blood cell (WBC) DNA sequencing to allow filtering of CHIP and germline variants. This study evaluated CHIP detection in patients with solid tumors across different cfDNA testing approaches.
Materials and Methods: We conducted a multicenter, retrospective observational study; results from one center are presented here. Samples from 102 individuals with colorectal, prostate, pancreatic, or breast cancer were analyzed. cfDNA and matched WBC gDNA were processed using MSK-ACCESS® powered with SOPHiA DDM™, which detects SNVs/INDELs, CNVs, and structural variants. Orthogonal results from a centralized, send-out cfDNA-only assay were also available, including annotations for putative germline and CHIP variants. Concordance (percent positive agreement, PPA) was assessed while also focusing on discordant CHIP calls attributable to the inclusion of WBC sequencing.
Results: MSK-ACCESS® powered with SOPHiA DDM™ achieved 95% PPA for all variants with variant allele frequencies (VAF) ≥ 0.5% independent of classification, consistent with its limit of detection. Detected VAF showed strong correlation with the orthogonal assay (R^2 = 0.86). Discordant CHIP and tumor-specific calls were observed between the cfDNA-only approach and MSK-ACCESS® powered with SOPHiA DDM™. These were influenced by factors such as cfDNA-to-WBC VAF ratio thresholds, gene set composition (e.g., *DNMT3A* vs. *TP53*), and statistical filtering criteria. Overall percent agreement (OPA) for CHIP calls is under evaluation.
Conclusion: Incorporating matched WBC sequencing, as implemented in MSK-ACCESS® powered with SOPHiA DDM™, yields a potential advantage in resolving CHIP-related ambiguity compared to tumor-only cfDNA approaches. Continued assessment across methodologies and further evaluation are warranted.

#7821 Plasma-based comprehensive epigenomic profiling enables multiplexed prediction of target gene expression and detection of resistance mechanisms.

Nicole Kramer[1], Jonathan Beagan[1], **Aparna Gorthi**[1], Praful K. Ravi[2], Rashad Nawfal[2], Anthony D'Ippolito[1], Sylvan C. Baca[2], Travis A. Clark[1], Khoi Nguyen[1], Daniel Karl[1], Kristian Cibulskis[1], Karl Semaan[2], Marc Eid[2], Jacob E. Berchuck[3], Corrie A. Painter[1], Matthew L. Eaton[1], J. Carl Barrett[1]

[1]Precede Biosciences, Inc., Boston, MA,[2]Dana Farber Cancer Institute, Boston, MA,[3]Winship Cancer Institute, Emory University School of Medicine, Atlanta, GA

Background: As novel targeted therapies including drug, radio-, and immune-conjugates, advance toward broad clinical implementation, there is an urgent need for scalable, minimally invasive diagnostics capable of resolving gene expression programs to guide patient selection and therapeutic monitoring. We applied a comprehensive epigenomics liquid biopsy and machine learning platform to infer tumor gene expression, delineate lineage plasticity, and reveal therapeutically relevant molecular programs and resistance mechanisms from only 1 mL of plasma.
Methods: 1 mL of plasma from a pan-cancer cohort of patients (95 prostate adenocarcinoma (PRAD), 19 neuroendocrine prostate cancer (NEPC), 45 non-small cell lung cancer, 58 small cell lung cancer, 130 breast cancer, 21 gastroesophageal cancer, and 5 ovarian cancer) was profiled using Precede Biosciences liquid biopsy platform. All samples were assessed for the expression of therapeutically relevant targets. In prostate cancer, samples were further evaluated for the extent of neuroendocrine (NE) transformation, a key mechanism of lineage plasticity and therapeutic resistance.
Results: Plasma-derived NE scores distinguished prostate adenocarcinoma (PRAD, n = 97) from neuroendocrine prostate cancer (NEPC, n = 15) along a continuous axis. Intermediate scores suggested partial or heterogeneous NE differentiation, with concurrent expression of PRAD- and NE-associated markers. Within these prostate cancer samples, predicted gene expression profiles clearly differentiated PRAD (high AR, KLK2, KLK3, FOLH1/PSMA) from NEPC (high CHGA, DLL3, SEZ6). DLL3 expression was further assessed across a multi-cancer cohort, and plasma-based predictions demonstrated a dynamic range consistent with published observations in tissue using both IHC and RNA-seq. For a subset of patients with matched FFPE tissue, immunohistochemistry for key drug targets is being performed to assess concordance with plasma-based expression predictions.
Conclusion: Plasma-based epigenomic profiling resolved tumor gene expression programs of key therapeutic targets such as DLL3 and delineated a continuum of neuroendocrine differentiation, uncovering molecular states associated with therapeutic response and resistance. Collectively, these findings underscore the potential of a minimally invasive, comprehensive epigenomics platform to deliver real-time, gene expression-level insights into tumor evolution and target expression, thereby guiding therapeutic decision-making.

#7822 High-sensitivity cfDNA detection of KRAS amplification subtypes to inform targeted therapy response and resistance mechanisms.

Yong Huang, Lisha Zhu, Binggang Xiang, Pan Du

Predicine, Inc., Hayward, CA

Background: *KRAS* is a key oncogenic driver gene, and both mutations and amplifications serve as important therapeutic targets and resistance biomarkers. Point mutations, amplifications of the wildtype allele, or amplifications of the mutant allele (sometimes via mutant allele-specific imbalance (MASI)) in *KRAS* all may impact cancer therapy greatly. Detection of *KRAS* amplifications in cell-free DNA (cfDNA) samples is particularly challenging because *KRAS* spans a relatively small 45kb region within a highly variable segment on chromosome 12. Achieving sensitive and accurate detection of *KRAS* amplifications in cfDNA and distinguishing the amplification types remains a pressing need in tumor drug development.

Methods: We developed a proprietary algorithm to enhance tumor fraction estimation and CNV calling of large genomic regions. Using 200 plasma samples , we developed a new model for the relationship among tumor fraction, observed copy number and variant allele frequencies. This model enables more comprehensive investigation of *KRAS* amplification events, including differentiation between focal amplification and large genomic fragment level amplification of *KRAS*, and between wild type allele amplification and mutant allele amplification in samples with *KRAS* driver mutations. The refined model also improves sensitivity of *KRAS* amplification calling when the amplification types can be assigned.

Results: Application of the new model allowed accurate determination of *KRAS* amplification types in most of the evaluated samples. In an expanded cohort of 800 cfDNA samples representing diverse solid tumors, *KRAS* amplification positive cases increased by 10% with the use of the refined model. Amplification types (wild-type allele or mutant allele amplification; focal or large genomic level) could be resolved in more than 80% of the cases. KRAS ctDNA dynamics were observed in both baseline and on-treatment samples.

Conclusions: This study provides an in-depth analysis of *KRAS* amplification profiles in cfDNA samples and introduces an improved model for *KRAS* copy number calling. The enhanced method increases detection sensitivity and yields richer biological insights by distinguishing amplification subtypes. These advancements strengthen the clinical utility of cfDNA-based KRAS assessment for therapeutic decision-making and drug development.

#7823 Ultrasensitive abnormal DNA methylation detection in plasma samples from patients with three different childhood sarcomas.

Giancarlo Bonora[1], Ziqi Zhu[1], Binggang Xiang[1], Kemin Zhou[1], Pan Du[1], Soumya Turaga[2], Glenson Samuel[3], Andrew Godwin[2]

[1]Predicine, Inc., Hayward, CA,[2]University of Kansas Medical Center, Overland Park, KS,[3]Children's Mercy Hospital, Kansas City, MO

Introduction: Early and accurate detection of Ewing sarcoma (EWS), Osteosarcoma (OS), Rhabdomyosarcoma (RMS), is critical because these aggressive pediatric and adolescent malignancies progress rapidly, often metastasize at diagnosis, and require timely, targeted therapy to improve survival and reduce long-term morbidity. Aberrant cell-free DNA (cfDNA) methylation pattern profiling holds great promise for the non-invasive detection and monitoring of cancer. However, sarcomas generally shed less DNA into the bloodstream than other cancers, making them particularly challenging cases that require highly sensitive detection methods. Here, we used an ultrasensitive cfDNA methylation assay to detect abnormal methylation patterns in archival plasma samples from seven patients representing three sarcoma subtypes. We observed robust aberrant methylation patterns in all samples, highlighting the potential of epigenetic alterations as a non-invasive indicator of tumor burden.

Methods: Longitudinal plasma samples were obtained from seven sarcoma patients: 3 patients with EWS 2 with OS and 2 with RMS. Samples were variously collected post-surgery and radiation treatment, when there was no evidence of disease, or at the time of relapse. cfDNA methylation was profiled using PredicineALERT™, a panel-based DNA methylation assay designed to detect abnormally methylated genomic fragments relative to a background model constructed from healthy-donor plasma. Importantly, only 1 ml of archival plasma stored in Acid-Citrate-Dextrose was used.

Results: Differentially methylated fragments (DMFs) were detected across the genome in all sarcoma samples, with DMF counts markedly higher than those observed in healthy-donor controls. Sarcoma samples clustered distinctly away from the controls, with patient samples grouping together and showing evidence of subtype-specific DMF patterns. DMF dynamics also corresponded with disease progression in that signal decreased for patients in remission and increased in cases showing relapse.

Conclusion: This study demonstrates the utility of cfDNA methylation profiling for sensitive, non-invasive detection and tracking of disease in childhood sarcoma patients. Future work will include generating corresponding tumor-tissue methylation libraries to confirm that plasma-derived methylation signatures are subtype-specific and biologically representative and evaluation of an extend longitudinal biobank of pediatric sarcoma patients.

#7824 Plasma-only classification of CHIP, low-VAF germline, and somatic variants enables accurate tumor-fraction estimation without matched normal samples.

Tiantian Zheng, Yong Huang, Chao Dai, Junmei Wang, Xiaohong Wang, Pan Du

Predicine, Inc., Hayward, CA

Background: Clonal hematopoiesis (CHIP) and germline variants commonly appear in cell-free DNA (cfDNA) and confound tumor genotyping. We analyzed historical paired plasma and Peripheral Blood Mononuclear Cell (PBMC)/buffy coat samples to (i) quantify CHIP prevalence and variant allele frequency (VAF) distributions, (ii) characterize low-VAF germline signals attributable to copy number variation (CNV) or alignment artifacts, (iii) identify tumor-derived somatic variants by integrating fragmentomics, CNV context, and longitudinal VAF dynamics, and (iv) benchmark plasma-only tumor-fraction (TF) estimation. Data were generated with the PredicineCARE and PredicineATLAS assays.

Methods: We retrospectively profiled ~1,000 plasma samples spanning prostate, breast, colorectal, lung, pancreatic, and other solid tumors with matched PBMC/buffy coat specimens. UMI-aware pipelines called single nucleotide variants/insertions/deletions/CNVs. Variants were annotated for CHIP drivers (e.g., *DNMT3A, TET2, ASXL1, PPM1D, TP53, SF3B1/SRSF2/U2AF1, JAK2*), population AF, hotspots, and an in-house knowledge base. Low-VAF germline events were adjudicated using a genome-wide germline SNP skeleton to explain deviations from the ~50% heterozygous expectation under local CNV. We trained and locked a plasma-only classifier (CHIP/germline/somatic) and estimated mutation-derived TF from tumor-assigned variants, benchmarking both against matched-normal labels. Longitudinal analyses (baseline + follow-up, months apart) assessed VAF dynamics and further improved the tumor fraction detection sensitivity.

Results: CHIP was prevalent and dominated by *DNMT3A/TET2/ASXL1*, with a minority of high-VAF clones; VAF distributions were summarized with and without TF normalization. Low-VAF germline signals were frequent but often CNV-driven, resolved by the SNP-skeleton model. On single-timepoint plasma, >95% of CHIP variants with VAF > 2% were correctly classified. Incorporating longitudinal VAF dynamics further differentiated low-VAF CHIP when TF changed >2-fold between draws, while tumor-derived variants tracked response/progression. The plasma-only TF showed excellent concordance with matched-normal TF (concordance correlation coefficient > 0.95).

Conclusions: CHIP is common and often low-VAF; a non-trivial fraction of apparent low-VAF germline findings reflect copy-number-induced VAF shifts. A plasma-only strategy that integrates CNV-aware germline modeling, CHIP gene context, fragmentomics, and longitudinal VAF dynamics closely reproduces matched-normal truth, enabling accurate somatic calling and tumor-fraction estimation without matched PBMC/buffy coat.

#7825 Ultra-sensitive MRD detection through comprehensive structural variant profiling in solid and hematologic malignancies.

Kemin Zhou, Yong Huang, Abby He, Junmei Wang, Binggang Xiang, Xiaohong Wang, Pan Du

Predicine Inc, Hayward, CA

Background: Structural variants (SVs), including fusions, translocations, large insertions/deletions, inversions and duplications, are highly tumor-specific genomic events and powerful biomarkers for molecular residual disease (MRD) assessment. Detecting SVs with unknown partners using short-read sequencing remains challenging, especially at ultra-low variant fractions. We developed the Predicine DeepSEA SV detection algorithm to enable comprehensive discovery and sensitive tracking of multi-class SVs in tissue and plasma.
Methods: Predicine DeepSEA integrates de novo assembly, refined BWA-based re-alignment, fragment-level molecular quantification, and combined split-read and paired-read evidence to detect and classify five SV subtypes with high accuracy. The workflow was applied to tumor tissue and matched longitudinal plasma samples from 30 patients with solid tumors or hematologic malignancies. PredicineBEACON MRD assays incorporated somatic SV breakpoints identified by whole-genome sequencing of high-tumor-fraction (>20% TF) baseline samples. Personalized SV-based panels were then designed for targeted MRD tracking. Analytical sensitivity was evaluated using titration experiments in which patient-derived cfDNA was spiked into healthy donor cfDNA at defined dilutions down to 1 part per million (ppm).
Results: DeepSEA identified diverse somatic SVs across all tumors, enabling construction of individualized MRD marker sets. In longitudinal plasma analysis, patient-specific SVs were quantifiable at extremely low variant fractions, and integration of multiple SV markers improved detection robustness compared with single-event tracking. In dilution studies, the PredicineBEACON assay achieved reliable MRD detection down to 1 ppm with high specificity, supported by fragment-level consensus filtering and multi-evidence breakpoint calls. SV-derived signals were detectable in both solid and hematologic cancers, underscoring the platform's broad applicability.
Conclusion: The Predicine DeepSEA pipeline provides sensitive and specific detection of structural variants in tissue and plasma. Incorporation of SVs into the PredicineBEACON MRD assay enables highly sensitive, personalized ctDNA tracking with detection limits approaching 1 ppm. This SV-based framework delivers a technically robust and broadly applicable platform for molecular monitoring across diverse cancer types.

#7826 Monitoring molecular residual disease in colorectal cancer using tumor-informed ctDNA analysis.

William C. Cho[1], Qianqian Yao[2], Yingyu Wang[2], Tam Berntsen[2], George Yeung[2], Paul Tang[2], Tobias Wittkop[2], Li Weng[2], Lui Ng[3], Dominic C.C. Foo[3]

[1]Department of Clinical Oncology, Queen Elizabeth Hospital, Hong Kong SAR, China,[2]Department of Research and Development, AccuraGen Inc., San Jose, CA,[3]Department of Surgery, University of Hong Kong, Hong Kong SAR, China

Background: Circulating tumor DNA (ctDNA) has become a critical tool for detecting molecular residual disease (MRD) and predicting recurrence in colorectal cancer (CRC). Tumor-informed ctDNA assays depend on a reference mutation profile from tumor tissue, commonly sourced from formalin-fixed, paraffin-embedded (FFPE) or fresh-frozen (FF) samples. Although FFPE tissues are widely available, they are susceptible to formalin-induced artifacts that may affect mutation calling accuracy. This study evaluated the sensitivity and specificity of ctDNA MRD assays, compared the mutation profiles and ctDNA MRD performance between FFPE and FF tissues, and evaluated the prognostic value of ctDNA.

Methods: We analyzed 28 CRC patients after curative-intent surgery. Whole-genome sequencing of 18 FFPE and 16 FF tumor samples (including six matched pairs) was conducted to assess variant burden, allele frequency, and mutational signatures. Plasma ctDNA was measured pre- and post-operatively using the tandem error-correction sequencing platform (AccuScan). Performance metrics for recurrence were evaluated at a landmark period (2-6 weeks post-surgery) and during longitudinal follow-up. Disease-free survival (DFS) was analyzed with Kaplan-Meier methods.

Results: FFPE samples exhibited a higher median variant count than FF tissues (8,774 vs. 4,906, $p = 0.001$) and lower variant allele frequency (17.54% vs. 21.38%, $p = 0.033$), along with enriched A>T transversions ($p = 0.031$). Despite these differences, ctDNA MRD detection showed 100% specificity and positive predictive value for recurrence across tissue types. FFPE-informed testing showed higher sensitivity during longitudinal monitoring (88.9% vs. 71.4%). MRD positivity was strongly associated with reduced DFS ($p < 0.0001$). In two cases, recurrence detected by FFPE-informed testing was missed with FF-based analysis, suggesting potential false negatives with FF samples.

Discussion: These findings support that FFPE tissues, despite more artifacts, are a clinically practical and often more sensitive source for ctDNA MRD assays after bioinformatic processing. The high specificity of ctDNA underscores its utility in guiding treatment decisions. This study confirms the prognostic value of ctDNA and promotes the use of archival FFPE tissues to improve test accessibility without compromising accuracy, facilitating the integration of liquid biopsy into personalized CRC management.

#7827 Analytical evaluation of tumor-naive ctDNA molecular response detection through baseline informed comprehensive genomic profiling with matched white blood cell analyses.

Cynthia Maddox[1], Cesar Nalvarte[1], Amanda Harvey[1], Vito Caropreso[1], Andrew Georgiadis[1], Aanavi Karandikar[1], Kenneth C. Valkenburg[1], Eric Severson[2], Taylor J. Jenson[2], Shakti Ramkissoon[2], Mark Sausen[1]

[1]Labcorp, Baltimore, MD,[2]Labcorp, Durham, NC

Liquid biopsies can provide an improvement over existing diagnostic modalities to detect, characterize and monitor cancer across the care continuum. Circulating tumor DNA (ctDNA) dynamics have been shown to identify cancer progression earlier than can be achieved with imaging-based assessments, however, can be limited due to low tumor burden together with the biological background associated with germline and clonal hematopoietic (CH) alterations in cell-free DNA. PGDx elio® plasma complete™ (EPC) is a pan-solid tumor hybrid capture, next-generation sequencing (NGS) comprehensive genomic profiling test for the identification of single nucleotide variants (SNVs), insertions and deletions (indels), copy number amplifications, translocations, microsatellite instability (MSI), and blood tumor mutation burden (bTMB) across 521 genes. To optimize EPC for the sensitive and specific detection and quantification of limited ctDNA levels, patient-matched white blood cells (WBCs) were sequenced and a baseline informed bioinformatic approach was implemented, aggregating the tumor-specific mutational signature across the panel. To demonstrate the analytical performance of this strategy, noncancerous donor plasma samples (n=29, 25 ng each) and four contrived reference models were analyzed across seven tumor content levels, with five replicates of each model evaluated at each level (n=140, 25 ng each). These studies demonstrated 100% specificity (116/116) with a limit of detection (95%) of 0.05% tumor and limit of quantification of 0.15% tumor (<20% median CV). Taken together, these data demonstrate that through the integrated analysis of cfDNA and matched white blood cell DNA, with a tumor-naïve approach, EPC can achieve increased sensitivity for the accurate detection and quantification of ctDNA required for the assessment of molecular response in patients with metastatic solid tumors.

#7828 Development of a comprehensive tumor-informed ctDNA workflow for ultrasensitive molecular residual disease detection using diverse tumor profiling inputs.

Leisa Jackson, Helen Halpin, Emma Longshore, Gary A. Pestano

Biodesix, Inc., Louisville, CO

Background: Circulating tumor DNA (ctDNA) analysis represents a transformative approach to molecular residual disease (MRD) surveillance, enabling non-invasive disease monitoring and treatment response assessment. While tumor-agnostic methodologies offer broad applicability, tumor-informed strategies leveraging patient-specific genomic alterations can provide enhanced sensitivity for detecting low-burden disease. We developed an integrated wet lab and bioinformatics workflow capable of identifying and monitoring structural variants (SVs), single nucleotide variants (SNVs), and insertions/deletions (Indels) across multiple genomic profiling platforms.

Methods: Patient-specific variant discovery was performed using whole genome sequencing (WGS), comprehensive genomic profiling (CGP), or whole exome sequencing (WES) using formalin-fixed paraffin-embedded tissue (FFPET) specimens. Our proprietary informatics pipeline annotated, filtered, and prioritized variants based on stringent quality metrics and variant allele frequency. To evaluate WGS inputs, two clinical metastatic castration-resistant prostate cancer (mCRPC) specimens with matched FFPET and plasma were used to design multiplexed droplet digital PCR (ddPCR) assays for detection of up to 12 SVs per reaction well. For cases with CGP inputs, off-the-shelf duplex ddPCR assays were used to monitor 6 unique SNVs detected across clinical mCRPC patients. The informatics pipeline was also employed to identify SVs, SNVs, and small Indels from patients with WES data from tissue.

Results: WGS libraries were successfully generated and passed quality control using as little as 40 ng FFPET DNA. Sequencing identified multiple high-confidence SVs, from which bespoke assays were designed. Assays were pooled and evaluated for cross-reactivity with wild-type genomic DNA and no-template controls. All CGP-derived targets were successfully detected in matched baseline plasma specimens with variant allele frequencies as low as 0.12 percent. WES data analysis from 8 subjects identified multiple SVs, SNVs, and Indels using a proprietary informatics pipeline. However, no WES-identified SVs were suitable for ddPCR assay design, suggesting SNV and Indel targets may be more appropriate for this data input type.

Conclusions: This study demonstrates successful development of a comprehensive ctDNA workflow for MRD detection using mCRPC specimens. The workflow accommodates multiple sequencing input types (WGS, CGP, WES) and successfully detects low-frequency variants in plasma using multiplex ddPCR. These data suggest that WGS-derived SVs and CGP- or WES-derived SNVs/Indels represent complementary strategies for tumor-informed MRD monitoring. Further validation studies with larger cohorts from various cancer types are planned.

#7829 Fragmented plasma cfDNA as a prognostic and surveillance biomarker for locoregional recurrence in oral squamous cell carcinoma.

Jiyoung Lee[1], Mi Rim Lee[1], Sumin Kang[1], Jung-Ah Hwang[2], Hye Won Shon[1], Yu-Sun Lee[1], Sun Il Choi[1], Gyeongmin Kang[1], Jong-Ho Lee[1], Sun-Young Kong[1], Sung Weon Choi[1], Yun-Hee Kim[1]

[1]National Cancer Center, Goyang-si, Korea, Republic of,[2]Geninus Inc., Seoul, Korea, Republic of

Oral squamous cell carcinoma (OSCC) frequently exhibits early locoregional recurrence despite adjuvant therapy. Circulating cell-free DNA (cfDNA) has emerged as a minimally invasive approach for evaluating tumor burden and disease dynamics. While most studies have focused on ctDNA mutations, the prognostic value of cfDNA fragmentomics—particularly mononucleosomal and dinucleosomal DNA—remains unclear in OSCC. Here, we investigated baseline cfDNA characteristics, mutational profiles, and fragmentation patterns, and evaluated their utility for recurrence prediction and longitudinal surveillance. Sixty-eight HPV-negative OSCC patients were prospectively enrolled, and plasma was collected at diagnosis and during follow-up. Baseline cfDNA was detected in 98.5% of patients (mean 6.65 μg/mL). Higher cfDNA levels correlated with aggressive clinical features, including advanced T stage, lymph node metastasis, and TNM III-IV disease, supporting its association with tumor burden. Targeted sequencing identified somatic variants in 30 genes, most commonly NOTCH1 (41%), FBXW7 (25%), and MGA (22%). Pathogenic variants were less frequent and did not correlate with TNM stage, and patients who recurred harbored fewer detectable mutations, indicating limited prognostic value of mutation-based profiling. Fragmentation analysis revealed distinct clinical implications for mono- and dinucleosomal cfDNA. Elevated baseline mononucleosomal cfDNA predicted recurrence, and a 3 ng/mL cutoff identified patients with significantly shorter recurrence-free survival. Dinucleosomal cfDNA, however, demonstrated superior value for longitudinal surveillance. Among 16 patients with locoregional recurrence, 13 (81%) showed detectable dinucleosomal cfDNA at or before radiologic confirmation, often during imaging-negative intervals. Persistent dinucleosomal cfDNA reflected ongoing local tumor activity, whereas metastatic recurrences rarely showed positivity. These results demonstrate that cfDNA fragmentomics provides prognostic information beyond mutation profiling in OSCC. Baseline mononucleosomal cfDNA stratifies patients at increased risk of recurrence, while the presence of dinucleosomal cfDNA offers a sensitive and clinically practical indicator of emerging locoregional disease. Together, these fragment-based biomarkers support the incorporation of cfDNA fragmentation analysis into postoperative surveillance strategies for earlier and more accurate detection of relapse.

#7830 Transport under various conditions: Evaluating blood sample stability across seasons.

Daniel Grolz[1], Markus Wolf[1], Daniela Mancarella-Langer[1], Franziska Kaiser[1], Michelle Walther[2], Eric Provencer[2]

[1]QIAGEN GmbH, Hilden, Germany,[2]BD, Franklin Lakes, NJ

INTRODUCTION: For analysis of circulating cell-free DNA (ccfDNA) in cancer screening or monitoring, specialized blood collection tubes - such as the PAXgene® Blood ccfDNA Tube (PreAnalytiX) - offer a reliable solution for users who are unable to process samples within 4 hours of collection. These tubes stabilize ccfDNA profiles by preventing blood cells from releasing genomic DNA (gDNA) during transport, thereby preserving sample integrity for sensitive downstream ccfDNA analyses. According to international standards and regulations (ISO 20186-3:2019, (EU) 2017/746 on In Vitro Diagnostic Medical Devices) preanalytical conditions like sample collection, transport, and storage must be validated to ensure that the quality of ccfDNA is maintained. Here, we evaluated sample packaging, temperature fluctuations during transit, and the impact of shipment on downstream assay performance to assess whether blood samples in PAXgene tubes can be transported at ambient temperature.

METHODS: Blood was collected from 30 apparently healthy consented donors into PAXgene Blood ccfDNA Tubes. Filled tubes were processed within 4 hours after phlebotomy or stored refrigerated (2-8°C), at 15°C or at room temperature (15-25°C) for 10 days and at 30°C for 7 days. For international transport tubes were shipped from the collection site (QIAGEN, Hilden, Germany) to an external processing site (BD, Franklin Lakes, USA). Samples were placed in insulated boxes compliant with IATA standards and without active temperature control. This included a leakproof triple packaging concept with a primary receptacle, a secondary package, and a rigid outer package. Upon arrival, blood samples were processed directly or subjected to an additional transport simulation test according to requirements defined in the standard ASTM D4169. Plasma and cellular fraction were separated, frozen and shipped back to QIAGEN for ccfDNA and gDNA extraction and analysis.

RESULTS: Temperature fluctuations during transport were in the range of 18-35°C during summer and 7-25°C during winter. Additional drop, vibration and altitude tests to simulate transportation by truck, rail and air did not compromise yield or quality of DNA. The relative yield of ccfDNA from plasma, measured by qPCR, between samples processed immediately and after storage or transport and simulation was only slightly increased with mean values between 1.0- to 1.3-fold. gDNA yield and purity measured by spectrophotometry were high for all conditions in the range of 26 to 55 µg of gDNA per mL of cellular fraction and mean 260/280 ratios between 1.80 and 1.82.

CONCLUSION: Excellent sample stability could be demonstrated in whole blood samples collected into PAXgene Blood ccfDNA Tubes under both controlled storage and real-world transport conditions. The data confirm that sample integrity is maintained following air and ground transportation at ambient temperatures across both summer and winter seasons.

#7831 Diagnostic genomics in retinoblastoma: Aqueous humor outperforms blood for tumor-specific insights.

Elaine Huang[1], Atrey Khoche[1], Sabrina Abed[2], Venkata Yellapantula[3], Laura Kagami[3], Brianne Brown[2], Liya Xu[2], Jesse L. Berry[2]

[1]Keck School of Medicine of USC, Los Angeles, CA,[2]Childrens Hospital Los Angeles, Los Angeles, CA,[3]Center for Personalized Medicine, Childrens Hospital Los Angeles, Los Angeles, CA

Purpose: There remains controversy in ocular oncology over whether blood or AH is a superior liquid biopsy for retinoblastoma (RB). Herein, we compare their diagnostic utility.

Methods: Matched AH and plasma were collected at diagnosis from 13 patients (16 eyes) with RB. Cell-free DNA was sequenced to assess copy number alteration (CNA) amplitude; ichorCNA software was used to estimate tumor fraction (TFx). Paired results were compared using the Wilcoxon test.

Results: SCNAs were detectable in 93.8% of AH samples versus 53.8% of plasma samples. Plasma TFx was significantly lower (4.33-7.84%; average 7.65%) than AH TFx (4.69-99.37%; average 34.19%; p=0.004), with a median difference of 16.73%. Plasma CNAs were detected only in patients with Group D/E eyes, two-thirds of which were enucleated. By contrast, AH enabled CNA detection across all groups. In 75% of patients positive in both substrates, AH identified additional alterations absent in plasma. In bilateral cases (23%), AH revealed eye-specific alterations indistinguishable in plasma. No evidence of metastasis was observed at average follow-up of 4 months.

Conclusion: While blood CNA detection may correlate with advanced disease, AH demonstrates superior sensitivity for intraocular diagnosis.

Clinical Implication: Validated by a CLIA-certified assay (LBSeq4Kids), AH consistently outperforms plasma as a biopsy surrogate.

#7832 Plasma epigenomic profiling captures B-cell lymphoma biology.

Aleem Aamir[1], Steven De Michino[1], Michael Hong[2], Ting Liu[2], Victoria Shelton[2], Benjamin Haibe-Kains[1], Michael M. Hoffman[1], Mathieu Lupien[1], Robert Kridel[2], Benjamin Lok[1], Scott V. Bratman[1]

[1]Medical Biophysics, University of Toronto, Toronto, ON, Canada,[2]Princess Margaret Cancer Center, Toronto, ON, Canada

Background: B-cell lymphomas (BCLs), including diffuse large B-cell lymphoma (DLBCL) and follicular lymphoma (FL), display widespread epigenetic dysregulation. The histone methyltransferase EZH2 catalyzes the repressive mark H3K27me3 and is an important epigenetic regulator for B-cell development. Although previous work has examined H3K27me3 in BCL tumour samples, the landscape of H3K27me3-decorated cell-free chromatin in BCL remains largely unexplored.

Methods: We performed cfChIP-seq targeting H3K27me3 on n=55 DLBCL, n=19 FL, and n=21 non-cancer controls from the Princess Margaret LIBERATE study. For global analyses, reads were counted in 10kb genomic windows and background reads were subtracted using a truncated Poisson MLE and data were library size normalized. BCL scores were computed using leave-one-out NNLS against a healthy reference panel and a high-burden lymphoma archetype. For promoter analyses, reads ±2kb of the TSS were counted and library size normalized.

Results: Global plasma H3K27me3 profiles in advanced-stage BCL separate from limited-stage BCL and non-lymphoma samples. Mean BCL scores were higher in advanced-stage BCL($p<0.0001$) and limited-stage BCL ($p<0.05$) compared to non-lymphoma controls. Moreover, both DLBCL ($p<0.0001$) and FL ($p<0.001$) had higher mean BCL scores than non-lymphoma controls. BCL scores were highly correlated to PC1 ($\rho=0.902$, $p=2.97e-35$) and the orthogonal tumour fraction metrics including mean VAF from targeted sequencing ($\rho=0.850$, $p=4.79e-18$), ichorCNA tumour fraction from ~0.5X WGS ($\rho=0.779$, $p=3.86e-12$), and total lesion glycolysis from FDG-PET/CT ($\rho=0.669$, $p=1.37e-10$). Correlation analysis between H3K27me3 signal at promoters and mean VAF revealed a negative association at B-cell lineage loci such as PAX5 ($r=-0.705$, $p=1.29e-09$) and DTX1 ($r=-0.622$, $p=3.11e-07$), and a positive association at other hematopoietic lineage loci such as MCEMP1 ($r=0.746$, $p=4.1e-11$) and IL6R ($r=0.635$, $p=1.46e-07$), indicating an increased contribution of B-cell lineage contribution with increasing tumour fraction.

Conclusions: These data show that plasma H3K27me3 profiles capture disease burden and reflect underlying tumour biology in BCL. Furthermore, these profiles capture lineage-specific promoter repression patterns, manifesting in negative correlations between H3K27me3 signal B-cell lineage markers and tumour fraction, contrasting positive correlations observed at markers of other hematopoietic lineages. Overall, cfChIP-seq of H3K27me3 provides a non-invasive epigenomic readout of circulating cell-free chromatin in BCL.

#7833 A novel extraction method for enrichment of circulating cell-free DNA.

Seka Lazare, Megan Rivera, Zachary Costliow, Ashley Tellis, Zhuosheng Gu, Michael A. Harmon, Wendy Winckler

Droplet Biosciences, Inc., Cambridge, MA

Proximal biofluids have shown enriched sensitivity for liquid biopsy but present unique preanalytical challenges. Even in plasma, variations in collection or processing can affect cell-free DNA (cfDNA) isolation and size profiles. These differences may affect downstream sensitivity.

Our lab has pioneered the use of lymphatic exudate (“lymph”) from surgical drains as a novel proximal liquid biofluid for MRD detection. We have previously shown that lymph collected 24 hours after surgery identified molecular residual disease (MRD) in head and neck squamous cell carcinoma (HNSCC). This biofluid contains lymphatic fluid, blood, and interstitial fluid, and differs markedly from blood or plasma. cfDNA in lymph displays distinct nucleosomal distribution, including prominent mono- and dinucleosome peaks (“cfDNA fraction”), but most extracellular DNA is >700 bp (“HMW fraction”). Our analysis revealed that tumor-derived DNA is more abundant within the < 700 bp cfDNA fraction.

To negate the signal-diluting effects of the HMW fraction, we developed a novel extraction method that simultaneously maximizes cfDNA recovery and selectively depletes HMW DNA. The method utilizes Proteinase K treatment for protein removal, selective bead-based removal of the HMW fraction, and purification of the enriched cfDNA from the supernatant.

We benchmarked this method against three commercial cfDNA extraction kits. To characterize all size fractions, we also generated a non-depleted extract using a simplified version of our protocol lacking the selective bead-binding step. We refer to this non-depleted material as “raw cfDNA extract.” Lymph was collected in K2EDTA/Streck blood collection tubes, centrifuged to remove cells and debris, and the supernatant stored at -80 °C (n=36). All 36 samples were processed using our novel extraction method; matched subsets were used for commercial kit comparisons. cfDNA concentration and size distribution were analyzed using Qubit dsDNA and Tapestation cfDNA assays respectively, with cfDNA defined as fragments 50-700 bp.

Raw cfDNA extract was highly concentrated (mean 40 ng/µL of extracted lymph, n=9) but displayed variable purity (6-31%). Commercial kits yielded highly variable quantity and purity (cfDNA yield = 0.08-19.88 ng/µL of extracted lymph; purity = 1.3-31%; n = 3, 3 and 2 for kits 1-3). In stark contrast, our novel extraction method delivered high yield and purity consistently across all 36 extractions (mean yield = 1.8 ng/µL, cfDNA purity = 92% [80-98%]).

We present an optimized cfDNA extraction method which consistently yields high purity, concentrated cfDNA from biofluids with substantial HMW fractions, dramatically increasing the effective ctDNA yield compared to standard commercial protocols. This technical advancement resolves a critical preanalytical challenge for assays using lymphatic exudate, enabling sensitive clinical monitoring with this readily available proximal biofluid.

#7834 DNA methylation: A highly accurate biomarker for treatment monitoring - A retrospective case study using cfDNA methylation and machine learning in breast cancer patients.

Jean-Valery Turatsinze[1], Andrea Blum[1], Adrien Godfroid[1], **Ekaterina Gracheva**[2], Matteo Tosolini[1]

[1]Hologic Diagenode, Liege, Belgium,[2]Diagenode LLC, Denville, NJ

DNA methylation plays a critical role in gene regulation and maintaining genomic stability. Abnormal DNA methylation patterns are common in breast cancer and relate to tumor growth and resistance to therapy. Liquid biopsies, especially analyzing cell-free DNA (cfDNA) in plasma, offer a minimally invasive way to monitor tumor-specific molecular changes in real time. This study evaluates the power of DNA methylation analysis to identify biomarkers for monitoring breast cancer treatment. Plasma samples from healthy individuals were used to first determine the reproducibility and robustness of the technology, while plasma from patients with breast cancer at different stages of disease was used for a biological validation study. After cfDNA extraction, all samples have been subjected to EM-seq library preparation followed by capture and next-generation sequencing. Sequenced reads were aligned to the human reference genome (hg38), and the DNA methylation levels were measured and filtered. The most differentially methylated CpGs were used as features for supervised machine learning models to differentiate between four disease states: progressive disease, partial remission, and complete remission, while some patients still showed residual abnormalities. The results of the analytical study demonstrate that the Hologic Diagenode Human Methylome procedure is highly reproducible across operators, input amounts, and technical replicates during the analytical phase. The biological validation demonstrates that, in patients undergoing various treatment regimens, the identified DNA methylation signature can predict their clinical state — ranging from progressive disease to partial and complete remission — with extremely high accuracy (92%). CpGs included in the identified signature were also relevant to the clinical context, as their associated genes were previously associated with cancer. These results underscore the potential of DNA methylation as a powerful molecular biomarker, not only for cancer diagnosis but also for treatment monitoring and potentially for minimal residual disease (MRD) detection.

#7835 Integrated DNA/RNA recovery from 1-20 mL inputs enables sensitive KRAS G12V detection in a liquid biopsy model.

Mayer Saidian, Jason Saenz, Carlos Hernandez, Cameron Van Dieren, Daniel Cedeno, Nafiseh Jafari

nRichDX, Irvine, CA

Introduction: Liquid-biopsy applications increasingly need concurrent access to tumor-derived DNA and RNA, sensitivity at low variant abundance, and support for larger input volumes. Separate cfDNA/cfRNA workflows add hands-on time and can limit sensitivity. We evaluated a single-extraction total nucleic acid (TNA) workflow designed to co-recover circulating DNA and RNA across inputs ranging from 1 to 20 mL.
Methods: Conditioned media from KRAS-G12V-positive H441 cells were pooled, clarified, and filtered to form a uniform tumor-conditioned matrix. Replicate extractions (n = 5 per condition) were performed at 1, 5, 10, and 20 mL using the same silica-magnetic-bead TNA chemistry and a single fixed-volume eluate. Eluate was split post-extraction for DNA (Qubit HS DNA; KRAS-G12V qPCR) and RNA (Qubit HS RNA; RT-qPCR). Metrics included total yield, KRAS-G12V copies/mL, allele fraction, and coefficient of variation (CV). Rare-event performance was tested using a dilution series (100%, 20%, 5%, 1%, 0.2% KRAS-G12V) extracted at 20 mL (n = 5 per level). Fragment integrity for 1 mL vs 20 mL inputs was evaluated by high-sensitivity capillary electrophoresis.
Results: KRAS-G12V copies/mL scaled linearly with input volume for both DNA- and RNA-derived signal ($R^2 \geq 0.98$ across 1-20 mL; within-volume CV≤15%). Increasing input reduced allele-fraction variance, improving quantitative precision without changing chemistry or handling. Split-eluate analysis showed strong concordance between DNA and RNA KRAS-G12V copies/mL across volumes, demonstrating that one extraction supports both genomic (mutation) and transcriptional readouts. In dilution experiments at 20 mL, KRAS-G12V was consistently detected down to 0.2% variant fraction. Fragment analysis confirmed cf-like size profiles (~160-180 bp) with minimal high-molecular-weight carryover at all inputs.
Conclusions: A single-eluate TNA workflow co-recovers DNA and RNA from up to 20 mL input, yields linear signal scaling, preserves cf-like integrity, and maintains detection at low simulated tumor fractions. Larger inputs not only boost recovery but also tighten allele-fraction precision. These data support high-volume, integrated DNA/RNA liquid biopsy workflows for applications such as minimal residual disease monitoring and longitudinal response assessment.

#7836 Automated high-volume cfDNA extraction on a liquid-handling platform achieves analytical equivalence to a manual high-input magnetic-bead workflow with 96-sample throughput.

Nafiseh Jafari, Cameron Van Dieren, Jason Saenz, Carlos Hernandez, Daniel Cedeno, Mayer Saidian

nRichDX, Irvine, CA

Introduction: High-volume cfDNA extraction improves sensitivity for liquid biopsy studies but is limited by manual hands-on time and variability. We evaluated whether implementing a high-volume magnetic-bead cfDNA workflow on an automated liquid-handling platform maintains analytical performance while increasing throughput and reducing labor.
Methods: Human plasma collected in K2EDTA tubes was processed using double centrifugation (low- then high-speed). Urine was preserved in Tris-EDTA pH 8 and clarified by high-speed centrifugation. Plasma and urine inputs (1-20 mL) were extracted manually or on the automated platform using identical magnetic-bead chemistry; only wash/elution steps were automated. Replicates were run across multiple reagent lots and days. Endpoints included cfDNA yield (Qubit HS), fragment metrics (Agilent cfDNA ScreenTape), and locus-specific qPCR. Pre-specified non-inferiority margins were ±10% for yield and fragment attributes. Equivalence was assessed with paired statistics, TOST, Bland-Altman, and variance components. Operational metrics included batch size, hands-on time (HOT), turnaround time (TAT), and walk-away time. Cross-contamination was assessed using checkerboard layouts analyzed by Qubit and qPCR. End-to-end traceability used unique barcodes on capture tubes readable by the automation platform.
Results: Automation preserved analytical performance across matrices and input volumes. The automated/manual yield ratio was 0.93 (95% CI ±7.8%), meeting the ±10% non-inferiority criterion (TOST $p < 0.05$). Fragment metrics—including modal size (~170 bp), 50-700 bp distribution, and mono:di-nucleosome ratios—were equivalent, differing by ~1% with between-run CV ≈1%. qPCR copy numbers showed minimal bias (mean 3.35 copies/reaction) with acceptable limits of agreement; limits of detection were identical for all loci. All 96-sample runs met QC thresholds. Checkerboard assays showed no detectable cross-contamination. Automation increased batch capacity from ~24-48 to 96 samples/run, reduced HOT by ~70-85% (to ~2 hours per batch), and shortened TAT by ~40-60%, providing ~2.5 hours of walk-away time.
Conclusions: Automating a high-volume magnetic-bead cfDNA workflow delivers analytical equivalence to manual processing while enabling 96-sample throughput and major reductions in labor and turnaround time. These findings support automation as a scalable solution for high-volume cfDNA programs requiring consistent, high-sensitivity performance. Portions of this text were generated with AI and were reviewed, edited, and approved by the authors.

#7837 Enhanced sensitivity and scalability in liquid biopsy through integrated high-volume cfDNA extraction and droplet digital PCR mutation detection.

Nafiseh Jafari[1], Andrew Partner[2], Necip Mehmet[2], Nish Kumar[2], Prithwish Pal[2], Jason Saenz[1], Carlos Hernandez[1], Daniel Cedeno[1], Cameron Van Dieren[1], Mayer Saidian[1]

[1]nRichDX, Irvine, CA,[2]Bio-Rad Laboratories, Inc, Pleasanton, CA

Introduction: Detecting rare tumor-derived variants in plasma requires both efficient recovery of cell-free DNA (cfDNA) and highly quantitative mutation analysis. Conventional extraction methods are limited by low input capacity and potential bias toward longer fragments, which can compromise sensitivity for low-frequency alleles.
Methods: Plasma cfDNA was extracted using the nRichDX Revolution cfDNA Max20 Kit, a high-volume magnetic-bead-based system, and then compared with the Qiagen QIAamp Circulating Nucleic Acid Kit. Pooled human plasma (1-15 mL, n = 3) and contrived samples spiked with 1% EGFR E746_A750delELREA (COSM6223) and KRAS G12C (COSM516) mutant gBlocks were processed per manufacturer's protocols. cfDNA concentration was measured by Qubit fluorometry, and mutation fractional abundance was quantified using the Bio-Rad QX600™ Droplet Digital™ PCR System (ddPCR™). Linearity, recovery efficiency, and reproducibility were evaluated across input volumes.
Results: The nRichDX Revolution cfDNA Max20 Kit demonstrated linear cfDNA recovery across 1-15 mL plasma inputs ($R^2 = 0.98$) and maintains scalability up to 50 mL without reconcentration or parallel extractions. When coupled with the Bio-Rad ddPCR System, mutation analysis consistently detected 1% variant allele frequencies, yielding 15-30% higher measured fractional abundance compared to the Qiagen QIAamp Circulating Nucleic Acid Kit, which uses carrier RNA.The nRichDX workflow preserved short cfDNA fragments critical for mutation detection, improving signal-to-background ratios and enhancing analytical sensitivity. Replicate variability remained below 10%, confirming robust precision across input volumes.
Conclusions: Integration of the nRichDX Revolution cfDNA Max20 Kit with the Bio-Rad QX600 ddPCR System enhances analytical sensitivity, recovery accuracy, and scalability for cfDNA-based liquid biopsy applications. By maintaining cfDNA integrity and eliminating carrier RNA interference, this workflow enables the reliable quantification of low-frequency variants, supporting clinical research in early detection, therapy monitoring, and minimal residual disease assessment.

#7838 Innovative biomarker discovery: A non-invasive, comprehensive tumor characterization approach with plasma and urine from breast cancer patients.

Ivonne Nel, Ekaterina Firsova, Laura Weydandt, Bahriye Aktas

Dept. of Gynecology, Leipzig University, Medical Faculty, Leipzig, Germany

Background: Circulating cell-free DNA (cfDNA) profiling from blood plasma has demonstrated considerable potential for clinical applications in breast cancer, yet urinary cfDNA remains less explored. In a previous pilot study of plasma-derived and matching urinary cfDNA (n=30), we have found plasma and urines may be complementary liquid biopsy samples for molecular profiling.
Methods: In this study, we expand to a larger patient cohort. To enhance the sensitivity of the assay, we utilized direct preservation with Urinary Analyte Stabilizer, which led to improved yield and quality of cfDNA from urine samples. We conducted an extensive analysis of 150 matched plasma and urine samples from breast cancer patients utilizing QIAGEN's QIAseq Human Breast Cancer Panel, Element Biosciences' Aviti system, CLC secondary analysis and QCI Interpret bioinformatic solutions.Results: The cfDNA levels in urine were increased compared to plasma but with minimal correlation between the two body fluids. Compared to the pilot study the validation study achieved improved sequencing precision and enhanced variant detection and identification. Both cfDNA sources led to quantitatively and qualitatively comparable results with a median number of 137 vs. 131 somatic variants in plasma vs. urine. Further, 53% of the variants had a super low abundance with VAF< 3%. The variants were similarly distributed in matching plasma and urinary cfDNA samples (5 vs. 4% pathogenic, 15 vs. 17% likely pathogenic, 73 vs. 76% VUS). We found 571 shared variants among both body fluids with a median of 14 shared pathogenic variants per sample.
Conclusion: Unlocking the clinical utility of urinary cfDNA as a non-invasive approach could redefine liquid biopsy strategies, offering a more comprehensive and dynamic view of tumor evolution and therapeutic response.

#7839 EU Instand-NGS4P: Pre-analytical multimodal workflows for NGS research and future precision cancer care.

Franziska Kaiser[1], Daniela Mancarella-Langer[1], Daniel Groelz[1], Jorg Lindenmann[2], Iurii Mykoliuk[2], Paul Swatek[2], Peter Michael Abuja[3], Kurt Zatloukal[3], Kalle Guenther[1], Uwe Oelmueller[1]

[1]QIAGEN GmbH, Hilden, Germany,[2]Division of Thoracic and Hyperbaric Surgery, Medical University of Graz, Graz, Austria,[3]Diagnostic and Research Institute of Pathology, Medical University of Graz, Graz, Austria

INTRODUCTION: The EU-funded Pre-Commercial Research project Instand-NGS4P (GA no. 874719) aims to improve cancer research by developing complete workflows for NGS, from specimen collection through data analysis and reporting. Multimodal testing involves analyzing multiple specimen types from one individual and/or multiple analytes (e.g., RNA, circulating cell-free DNA [ccfDNA], gDNA) from a single specimen. This can improve diagnostics by combining complementary results and increase sensitivity for earlier cancer detection. We developed 23 novel integrated NGS workflows for research purposes. Here, we present six exemplary workflows that may inform future innovation in clinical applications.

METHODS: Different specimen types were obtained from lung cancer patients at the Medical University of Graz (Austria) under local ethics committee approval. Whole blood specimens were collected and stabilized in PAXgene® Blood ccfDNA Tubes. Urine specimens were collected and stabilized using the PAXgene Urine Liquid Biopsy Set. Tumor tissue was preserved by PAXgene Tissue or formalin fixation followed by paraffin embedding (PFPE and FFPE) as well as cryopreservation. Stabilized specimens were shipped to QIAGEN, Hilden, Germany. Blood ccfDNA and gDNA were extracted using the QIAamp® DSP Circulating Nucleic Acid Kit and QIAsymphony® DSP DNA Mini Kit. Urine cell-free DNA (cfDNA) was isolated upon arrival at QIAGEN and after additional storage using the QIAsymphony DSP Circulating DNA Kit. Tissue gDNA was extracted using the PAXgene Tissue DNA Kit for PFPE samples, QIAamp DNA FFPE Advanced UNG Kit for FFPE samples and QIAamp DNA Mini Kit for cryopreserved samples. Mutation analysis of cfDNA was performed with QIAseq® Targeted cfDNA Ultra Human Lung Cancer Panel, while gDNA was analyzed with QIAseq Targeted DNA Pro Human Lung Cancer Focus Panel. Sequencing runs were performed using the Illumina® NextSeq® 500/550 Mid Output Kit v2.5 (300 cycles).

RESULTS: The developed workflows encompass specimen collection, stabilization, storage, analyte isolation, quality control (QC), library preparation, and sequencing. A novel QC concept enables traceability and process standardization through systematic metadata documentation. Specimens yielded high-quality libraries and successful sequencing performance across all analyte runs. Comparative mutational profiling of blood ccfDNA, urine cfDNA, and tissue DNA revealed both overlapping as well as complementary variants in key tumor genes. This gain in molecular information may lead to further development of multimodal liquid biopsy-based approaches with urine as a valuable complementing specimen type.

CONCLUSIONS: Our NGS workflows support multi- and single-mode testing for cancer research. They are developed in alignment with recognized international regulatory principles to enable comprehensive validation from sample collection to assay output.

#7840 Evaluation of somatic mutations in cell-free DNA as noninvasive biomarkers of cancer in asymptomatic pregnant women.

Zhigang Kang[1], Amy E. Turriff[2], Yuelin Jack Zhu[1], Erica Pehrsson[1], Hsein-Chao Chou[1], Jun Wei[1], Kerstin Heselmeyer-Haddad[1], Paul S. Meltzer[1], Javed Khan[1], Liang Cao[1], Diana W. Bianchi[2]

[1]National Cancer Institute, Bethesda, MD,[2]National Human Genome Research Institute, Bethesda, MD

Prenatal cell-free (cf) DNA sequencing for fetal aneuploidy incidentally detects circulating tumor DNA in the plasma of asymptomatic pregnant women. Distinguishing the subset of women with malignant tumors detected by prenatal sequencing from those with benign conditions, such as uterine fibroids, is critical to maternal medical management. In this pilot study, prospectively collected blood samples from 65 pregnant or postpartum women with and without occult cancers were analyzed blindly for cfDNA somatic mutations in 275 cancer-associated genes. Somatic variants were common among all 65 women, however, when stringent mutation analysis criteria were applied, these data could independently differentiate women with cancer with a sensitivity of 80.6% and specificity of 100%. Mutation profiling complements radiographic imaging by clarifying tumor origin, evaluating malignancy in indeterminate cases, identifying actionable genomic alterations, and flagging high-risk patients for urgent intervention. These findings provide preliminary evidence that cfDNA somatic mutations could serve as an additional noninvasive biomarker of malignancy potentially aiding the management of women with prenatal cfDNA findings suspicious for cancer.

#7841 Evaluation of uProcess for detection of oncogene sequences in buffer and urine by qPCR following 3-minute capture and 5- minute purification procedure.

Floyd E. Taub[1], Sean Pearson[1], Suzin E. M. Wright[1], Charles (Preston) Neff[2]

[1]aiGENE, Inc, Aurora, CO,[2]CU Medical Center, Aurora, CO

Cell-free DNA (cfDNA) and circulating tumor DNA (ctDNA), found in blood and urine, have firmly established themselves as key analytes for the diagnosis of various cancers and defining therapy. Primary sequence and epigenetic markers within cfDNA are key in screening and monitoring for cancer. However, both screening and long-term monitoring have two major limitations - test sensitivity and individual participation. Even as NGS, ddPCR, and other methods continue to improve, they require large amounts of cfDNA to reliably detect rare ctDNA fragments. For example, a single BioRad ddPCR reaction can analyze 1 ug of short cfDNA, but a single tube of blood might yield on the order of 10ng, thus cutting potential sensitivity 100x. Additionally, participation is typically a severe impediment to screening and long-term monitoring. Historically, this has been a major obstacle, especially for screening. Travel to clinics, pain/difficulty of phlebotomy, and patient aversion to it limit participation. Urine offers a far more accessible alternative, but ctDNA concentrations are lower and current urine-based cfDNA/ctDNA collection methods have yet to achieve yields adequate for highly sensitive testing. A ug of cfDNA is required for detection at the 0.001% level. Herein, we test and optimize a system (uProcess) designed for at-home urine filtration; it was previously demonstrated to capture over 2 ug of cfDNA from 200 mL of urine on a mail-in filter cartridge. Compared to previous versions, we have reduced the elution volume 5-fold from 2.5 to 0.5 mls, allowing concentrated samples for downstream processing. We demonstrated that the improved device can efficiently concentrate oncogene sequences, in buffer or urine, into a small elution volume in under five minutes vs. typical procedures taking 90-120 minutes. We then detected KRAS and TP53 oncogenes by qPCR, underscoring that the method produces ctDNA suitable for downstream usage. Together, these findings support the potential of uProcess to significantly expand access to cfDNA/ctDNA testing, improve sensitivity, shorten cfDNA purification time, and overcome longstanding barriers to cancer screening or monitoring.

#7842 A new high fidelity PCR master mix with broad NGS workflow compatibility and superior performance in high sensitivity applications.

Margaret R. Heider, Kyle Vrtis, Jian Sun, Bradley W. Langhorst, Chen Song, Yan Wang, Nicole M. Nichols

New England Biolabs, Inc., Ipswich, MA

The widespread adoption of sensitive mutation profiling in precision oncology and the emergence of next-generation sequencing platforms with increasing data quality demand high accuracy library preparation tools. Additionally, PCR master mixes used in NGS library prep are often specialized for specific applications, sometimes necessitating inconveniently distinct library preparation workflows within the same lab depending on the use case. Here we introduce a new PCR master mix that can be used for a wide array of input amounts, sample types, and workflows including whole genome sequencing (WGS), library prep for hybrid capture, and post-hybrid capture amplification. Using whole genome sequencing of different DNA sample types and species, we demonstrate high library yield, uniform genome coverage, and consistent library insert size across a broad range of cycle numbers for both picogram and high nanogram levels of DNA input. Next, we applied this PCR master mix to hybrid capture workflows, achieving sufficient library yield for capture and robust amplification of post-capture libraries in the presence of streptavidin beads. Using tissue-extracted DNA and cell-free DNA (cfDNA) samples, we demonstrated the critical importance of fidelity to enable highly precise single nucleotide variant (SNV) and indel calling. As part of a library prep workflow that maximizes conversion and introduces minimal errors, this PCR master mix can enable more accurate and cost-effective somatic variant detection. This new PCR master mix is designed to be readily applied to most DNA library prep applications with broad input amount and cycle number compatibility. Our data emphasizes the benefits of a high-fidelity PCR master mix as part of a high conversion library prep workflow for sensitive variant detection and high accuracy sequencing platforms.

#7843 Integrated multiomics for deep molecular exploration of prostate cancer from urine.

Bhaven Mehta[1], Andrea O'Hara[1], Ethan Stancliffe[2], Tom Cohen[2], David Corney[1], Haythem Latif[1]

[1]GENEWIZ from Azenta Life Sciences, Burlington, MA,[2]Panome Bio, St. Louis, MO

Background: The omics era has greatly expanded the repertoire of approaches available to unravel the complexity underpinning human health, with the ability to rapidly characterize genomes, epigenomes, transcriptomes, proteomes and metabolomes from a wide range of sample types. Urogenital cancers, including prostate cancer, is the most prevalent cancer in men. Current early detection methods rely on blood screening of prostate-specific antigen (PSA), however, it has a high rate of false positives, resulting in the search for alternative biomarkers. Urine is an ultra-non-invasive analyte ideal for urogenital cancer detection, including prostate cancer. Cell free RNA/DNA (cfRNA/DNA), along with metabolomics directly from urine, is an ideal candidate for biomarker identification for use in diagnostics, treatment monitoring and tumor tissue of origin prediction.
Methods: Here we describe integrated metabolomics and RNA-Seq analysis from a series of prostate cancer affected and control urine samples. First, cfRNA from affected and control samples were isolated using a specialized method with efficient cfRNA recovery rate from urine. The cfRNA was then subjected to highly sensitive RNA-Seq to evaluate a series of prostate cancer biomarkers. The same urine samples were also subjected to metabolite profiling using multiple complementary LC-MS assays to deliver the highest quality untargeted metabolomics data. Both data types were used for integrated multiomics analysis.
Results: Urine proves to be an ideal ultra-non-invasive method for biomarker screening and detection. Integrated analysis across multiple data modalities, including transcriptomics and metabolomics, allows for holistic views of pathways and processes that are highly impacted, with increased statistical significance than any one modality alone.
Conclusion: Biomarker detection and multiomics analyses are critical to assess individuals in both pre- and post-treatment during therapeutic development and early-stage clinical trials. Urine offers a truly non-invasive approach that, when combined with omics tools, can provide comprehensive insight across urogenital patient cohorts.

#7844 Simultaneous identification of methylation and somatic variants can improve sensitivity for cancer detection and monitoring.

Tom Charlesworth, Cillian Nolan, Luke Sarre, Fabio Puddu, Angela Simeone, Aurelie Modat, Ermira Lleshi, Robert Crawford, Robert J. Osborne, **Thao Huynh**

biomodal Ltd, Cambridge, United Kingdom

There is increasing evidence that combining genetic and DNA methylation information in cancer research and diagnostics provides significant utility. For example, bi-allelic inactivation of tumour suppressor genes commonly occurs through a combination of somatic mutation at one allele and epigenetic silencing of the second allele and can be a key driver of cancer progression. In addition, gene fusions have an impact on DNA methylation patterns and DNA methylation changes can provide information on gene fusion status, even where the fusion event itself cannot be confidently identified in genetic sequencing data. Furthermore, combined genetic and epigenetic analysis of individual DNA fragments can increase sensitivity of somatic variant detection, which is particularly important in liquid biopsy applications. Here we analyse cell-free DNA (cfDNA) using 6-base sequencing with duet evoC, which calls genetic mutations and distinguishes between 5-methylcytosine (5mC) and 5-hydroxymethylcytosine (5hmC) with high accuracy. We leverage duet evoC to confidently identify circulating-tumor DNA (ctDNA) fragments in cfDNA, a method that can be generally applied to increase the sensitivity of MRD detection. We also demonstrate that bi-allelic inactivation of tumor suppressor genes in patient samples can be identified in a single assay. Further, we identify methylation patterns that are indicative of gene fusions or chromosomal rearrangements, opening the possibility of improving the sensitivity of gene fusion detection in clinical samples.

#7845 Dynamic plasma *KRAS* and *EGFR* ctDNA profiling identifies treatment response and nascent resistance in metastatic lung cancer.

Valentina Buzzi[1], Greta Berti[2], Michele Santillo[1], Arianna Belli[3], Giulia Favarato[4], Mauro Iannopollo[2], Elisabetta Rosi[3], Federico Lavorini[3], Sara Tomassetti[4], Annarosa Arcangeli[1], **Elena Lastraioli**[1]

[1]Universita degli Studi di Firenze - UniFI (University of Florence), Firenze, Italy,[2]Medical Oncology, S. Jacopo Hospital, Pistoia, Italy,[3]Pulmonology and Intensive Care Unit, Careggi University Hospital, Firenze, Italy,[4]Interventional Pulmonology Unit, Careggi University Hospital, Firenze, Italy

Background: Liquid biopsy enables minimally invasive tumor genomic assessment. We evaluated serial circulating tumor DNA (ctDNA) monitoring for KRAS and EGFR in metastatic lung cancer to characterize mutational dynamics, correlate changes with clinical events, and assess plasma testing for early resistance detection.
Aims: Describe longitudinal KRAS and EGFR plasma patterns during systemic therapy and relate ctDNA kinetics to treatment changes and outcomes.
Methods: Thirty-five metastatic lung cancer patients were prospectively enrolled (31.4% female; median age 70, IQR 41-84). Plasma was collected at baseline and, for 20 patients, at weeks 4, 8, 12 and 24 and thereafter until progression or death. KRAS and EGFR status was assessed with targeted ctDNA assays using the Idylla platform.
Results: Tissue-plasma concordance was fair to moderate for KRAS and EGFR (Cohen's kappa 0.35 and 0.43). Serial monitoring showed marked interpatient heterogeneity and dynamic shifts in mutant allele fractions. Two patients had early KRAS increases at week 4; one died and the other progressed to second-line therapy and developed a second KRAS codon 12 mutation (G12R alongside baseline G12C) at week 8, consistent with clonal diversification. Another patient showed oscillating KRAS detection—present at baseline and week 8 but absent at weeks 4 and 12—suggesting transient clonal suppression and re-expansion related to treatment scheduling. One patient's EGFR levels tracked therapy: high at baseline and week 4, cleared at week 8 after switching to Amivantamab, then reappeared at week 12 after treatment discontinuation for toxicity. EGFR mutations were observed in one patient only (8.3%); others remained EGFR wild type throughout follow-up.
Conclusions: Longitudinal plasma KRAS and EGFR testing captured evolving mutational landscapes that anticipated progression and reflected treatment effects, including emergence of secondary clones and transient suppression of mutant fractions. Serial ctDNA profiling is a pragmatic adjunct to tissue genotyping for early resistance detection and therapeutic guidance. Larger cohorts are needed to quantify predictive performance and integrate ctDNA kinetics into clinical decision algorithms.

: Real World Impact of Prognostic and Predictive Parameters
Poster Session

#7849 Real-world landscape analysis of circulating tumor DNA minimal residual disease as a clinical trial endpoint in breast cancer.

Momo Arai[1], Alaa Khalilaa[1], **Ahmed Elkhanany**[2]

[1]Alfaisal University, Riyadh, Saudi Arabia,[2]Baylor College of Medicine, Houston, TX

Background: Minimal Residual Disease (MRD) assessment via circulating tumor DNA (ctDNA) offers superior sensitivity over imaging for relapse detection and monitoring. In breast cancer, MRD identifies molecular relapse with a median 8.9-month lead time from prior studies, serving as an independent prognostic and potential predictive marker for outcome and therapy escalation.
Methods: A systematic ClinicalTrials.gov search (July 2025) yielded 133 trials; 124 met inclusion. Studies were stratified by endpoint hierarchy (primary vs. secondary), status, and methodology (tumor-informed, panel-based, methylation, or CTC/protein/tissue).
Results: Among 124 trials, MRD was primary endpoint in 56 (45%) and secondary in 66 (53%). Only 4 primary-endpoint trials have published results, while 52 are ongoing. Tumor-informed/patient-specific assays were the dominant modality (38%), followed by CTC/tissue (20%), fixed panels (17%), and methylation (7%); 18% were unreported. Published clinical utility (primary-endpoint trials). In metastatic guidance (NCT05079074), 85% of patients had baseline ctDNA positivity, and those receiving druggable mutation-guided therapy achieved improved progression-free survival (PFS) versus physician's choice (HR 0.45). In a prognostication cohort (NCT03792529), genomic profiling identified frequent TP53 (44%), PIK3CA (28.4%), and ERBB2 (24.8%) alterations; high ctDNA fraction and blood tumor mutational burden (bTMB) predicted shorter PFS in TNBC and HER2+ subtypes. In the relapse-prediction setting (NCT02797652), baseline ctDNA was detected in ~70% (21/30) of operable patients; post-operative ctDNA positivity was 100% predictive of distant metastasis, yielding 71.4% sensitivity for clinical relapses. In an early-detection setting (NCT05227261), among 9,024 individuals screened (0.48% positive), a multi-cancer test demonstrated 99.71% specificity, 70.83% sensitivity, 39.53% positive predictive value, and 99.92% negative predictive value. Monitoring and MRD-adaptive strategies. Serial ctDNA clearance in immunotherapy trials (e.g., NCT02644369) tracked survival, with 100% of patients achieving clearance remaining alive at a median 25-month follow-up. Active MRD-adaptive investigations now deploy randomization to escalation at molecular relapses (e.g., DARE/NCT04567420), single-arm escalation in MRD-positive HER2+ disease (e.g., NCT05388149), and clearance-based de-escalation (e.g., NCT06970912).
Conclusions: ctDNA-MRD integration in breast cancer trials is expanding rapidly, shifting to tumor-informed assays. Published data validate ctDNA as a potent prognostic tool (71.4% relapse sensitivity) and predictive biomarker (HR 0.45 intervention benefit). As evidence matures with ongoing randomized trials, assay standardization and actionability remains critical for clinical translation.

#7850 Real-world concordance analysis of functional drug sensitivity testing in solid cancers with prospective observational case series of pancreatic cancer.

Weng Tong Ho[1], **Masturah Rashid**[1], Jhin Jieh Lim[1], John Seng Hooi Low[2], Yugarajah Asokumaran[2], Shin Yee Wong[2], David Khie Siong Hii[2], Edward Kai-Hua Chow[1]

[1]KYAN Technologies, Singapore, Singapore,[2]OncoCare Cancer Centre, Selangor, Malaysia

Background:
Fluorouracil- and Gemcitabine-based combinations are the preferred early treatments of pancreatic ductal adenocarcinoma (PDAC). However, treatment choice is empirical due to the lack of reliable predictive biomarkers. We report an observational case series using Optim.AI™, a functional drug sensitivity testing (DST) platform, to identify the activity toward standard-of-care regimes and assess concordance with clinical response.
Methods:
Tumor samples from PDAC patients underwent ex vivo analysis using Optim.AI™ platform. Tumor cells were isolated and tested with a customized panel of chemotherapeutic and targeted agents, including standard-of-care treatment. Optim.AI™ assesses all possible combinations and ranks them by sensitivity for individual patients. Clinical responses were obtained from chart review, and concordance with ex vivo findings was assessed. To further evaluate performance across tumor types, 76 solid cancer cases were evaluated for Optim.AI™ functional testing were also analyzed. Retrospective concordance was determined by evaluating tumor cell viability responses generated by Optim.AI™ against the treatments previously administered to the corresponding patients.
Results:
Optim.AI™ reports were successfully generated for 95% of the samples with sufficient yield for testing. Pan-cancer retrospective analysis also demonstrated 91% concordance between Optim.AI™-reported sensitivities and prior clinical responses across the 76 solid tumor cases evaluated. Six PDAC patients underwent functional DST, with Optim.AI™ reports generated within a median turnaround of six days from sample collection. Substantial inter-patient variability in ex vivo drug sensitivity toward the standard-of-care was observed. Across six patients, there were seven assessable clinical outcomes corresponding to the combinations tested ex vivo. Optim.AI™ correctly predicted resistance to the prior or ongoing therapy in six out of seven instances (NCV > 0.5 defined as ex vivo resistance), resulting in a predictive accuracy of 85.7%. Furthermore, Optim.AI™ identified a combination regimen that was more sensitive than the treatments previously administered, underscoring its potential value in guiding more effective therapeutic options for refractory cases.
Conclusions:
This study highlights the feasibility and potential clinical relevance of Optim.AI™ in PDAC. Optim.AI™ revealed individualized drug response profiles, including cases in which standard treatments may be resistant, achieving a predictive accuracy of 85%. These findings are consistent with results from the pan-cancer retrospective concordance analysis.

#7851 Early-phase clinical trial referral and outcomes in breast cancer: A prospective screening cohort and a real-world Phase I program experience at Gustave Roussy..

Alessandra Spata[1], Matthieu Roulleaux-Dugage[2], Berenger Poirier[1], Christophe Massard[2], Sophie C. Postel-Vinay[2], Antoine Hollebecque[2], Madona Sakkal[2], Kaissa Ouali[2], Rastislav Bahleda[2], Yohann Loriot[2], Joana M. Ribeiro[2], Barbara Pistilli[1], Cyril Roussel-Simonin[2]

[1]Departement de Medecine Oncologique, Gustave Roussy Cancer Center, Villejuif, France,[2]Departement des Innovations Therapeutique et des Essais Precoces (DITEP), Gustave Roussy Cancer Center, Villejuif, France

Background: Early-phase clinical trials are increasingly relevant for metastatic breast cancer, but referral timing and benefit remain insufficiently documented.
Methods: We analyzed two complementary cohorts. The first comprised 231 consecutive metastatic breast cancer patients prospectively screened for early-phase trial consideration at Gustave Roussy. The second included all breast cancer patients who initiated treatment in a phase I trial (C1D1 cohort) since 2009. Baseline characteristics, treatment history, referral decisions, RECIST outcomes, progression-free survival (PFS), and overall survival (OS) were collected.
Results: In the prospective cohort (n=231), most patients had HR+/HER2- (54%) or TNBC (40%) disease. Only 18% underwent molecular profiling before referral review. Overall, 39% were referred to a phase-I trial, while the main reasons for non-referral were absence of available trial slots (37.3%), excessive prior treatment lines (36.4%), lack of measurable disease (7.4%) and brain metastases (6.2%). Patients entering phase I screening had received fewer prior therapies (median 3 vs 6) than those excluded, highlighting that late referral frequently precluded eligibility.In the C1D1 cohort (n=343), median age at treatment start was 52 years and patients had received a median of 3 prior lines of therapy. TNBC accounted for 48% of treated cases, followed by HR+/HER2- (45%) and HER2+ (7%). Most patients received targeted therapy (66%), immunotherapy (20%) or intratumoral therapy (8.1%). Median PFS and OS were 3.2 and 11.5 months. HER2-positive disease achieved the longest PFS (4.24 months), followed by HR+/HER2- (3.19 months) and TNBC (2.86 months). The overall response rate was 13.4% and the clinical benefit rate was 52.8%. The highest responses were observed in HER2-positive tumors (31.8%), whereas TNBC demonstrated the lowest (~7%). Targeted therapies achieved the best outcomes (median PFS 3.7 months), while intratumoral approaches showed limited benefit (2.1 months).
Conclusions: Most patients in the prospective cohort were referred late and became ineligible due to protocol-defined treatment history or disease burden. Early molecular profiling and proactive referral are essential to preserve eligibility. Patients who receive phase I treatment derive meaningful benefit, particularly with targeted approaches, supporting earlier integration of phase I programs in the breast cancer therapeutic sequence.

#7852 Tobacco, nicotine, cannabis, and alcohol use among LGBTQ+ patients with cancer: Real-world analysis at an NCI-Designated Comprehensive Cancer Center.

Min-Jeong Yang[1], Shahrzad A. Zamani[2], Matthew B. Schabath[2]

[1]Rutgers University - New Brunswick, New Brunswick, NJ,[2]H. Lee Moffitt Cancer Center and Research Institute, Tampa, FL

Background: Prior studies have described patterns of substance use, such as tobacco and alcohol use, that are elevated among sexual and gender minority (SGM) individuals with cancer. However, the findings have been limited to specific cancers and study designs (e.g., population-based survey). Real-world data can reveal important insights into the substance use behaviors among SGM cancer patients to meet the patients' needs and provide tailored cancer care. In this study, we conducted a real-world analysis on the association between substance use (tobacco, nicotine, cannabis, and alcohol) by SGM status.

Methods: This study included 110,072 cancer patients who completed a standard-of-care electronic patient questionnaire (EPQ) during their initial visit at the Moffitt Cancer Center (Tampa, FL). The EPQ captures patient-reported information on demographics (including sexual orientation and gender identity [SOGI]), medical history, family cancer history, lifestyle factors, use of complementary and alternative medicine, and quality of life. SGM and non-SGM patients were identified using the SOGI items. The outcome variables included (1) past and current tobacco and nicotine product use, (2) recent alcohol use, and (3) recent substance and non-medically indicated prescription medication use. Pearson's Chi-Square test was utilized; significance was determined by $p<0.05$.

Results: Approximately 3.1% of the population self-identified as an SGM. Compared to non-SGM patients, SGMs reported higher rates of current cigarette smoking (14.8% vs 10.7%; $p<.001$), smoking their first cigarette after waking up (within 5 minutes: 5.6% vs 4.7%; 6-30 minutes: 13.1 vs. 10.8%, $p<.001$), current pipe smoking (0.2% vs 0.1%, $p<.001$), current and former electronic cigarette use (4.0% vs 1.7% and 9.6% vs 4.3%, respectively, $p<.001$), alcohol use in the past year ($p<.001$), more number of drinks on the days of alcohol use ($p<.001$), and past 3-months cannabis use (4.7% vs 2.1%) along with sedatives and stimulants use ($p<.001$). However, SGM reported lower use of ever pipe (2.0% and 2.8%, $p<.001$), ever and current cigar ($p<.01$), ever and current smokeless tobacco ($p<.001$), and alcohol more than 9 days per month ($p<.01$).

Discussion: These data suggest that SGM cancer patients, compared to non-SGM cancer patients, present with higher use of tobacco, nicotine, cannabis, and alcohol. These results add to the existing literature by elucidating patterns of substance use among SGM cancer patients with heterogeneous cancer types. Further research is warranted on the patterns of substance use among subgroups of SGM patients and the potential need for systematic assessment and early intervention.

#7853 A seven-gene mutation signature predicts immunotherapy benefit in bladder cancer.

I-Cheng Huang, Chun-Nan Kuo

School of Pharmacy, College of Pharmacy, Taipei Medical University, Taipei, Taiwan

Introduction: Immunotherapy plays an important role in advanced bladder cancer. However, no mutation-based biomarker has been established to reliably predict immunotherapy benefit in bladder cancer. This study aimed to identify the gene mutation signature predicting immunotherapy efficacy.
Method: We retrieved genetic and clinical data of patients with bladder cancer and immunotherapy treatment from MSK-TMB cohort. We selected targeted mutation genes if they occurred in more than three patients, with a higher incidence rate in survival patients, and belonged to non-synonymous mutation. Based on the selected genes, we categorized patients into three groups: compound mutation, single mutation and wild-type group. We compared the efficacy on overall survival (OS) among the three groups. Tumor mutation burden (TMB) was then integrated with the selected gene mutation information for further survival analysis.
Result: A total of 215 patients from MSK-TMB cohort were included. The mean age was 67.1-year-old. The cohort consisted 116 (80.6%) males and the mean TMB was 11.7/megabase. Among 468 identified genes, seven genes were found following the selection criteria.The median OS was not reached, 19, and 11 months in compound mutation group, single group and wild-type group ($p < 0.001$ for compound mutation vs. wild-type group, 0.0063 for single mutation vs. wild-type group, respectively). After integrating TMB status, a survival advantage was observed among patients in the compound mutation with low TMB (compound-L) group. The median OS was NR, 13.5, and 9.0 months in the compound-L, single mutation with low TMB (single-L), and wild-type with low TMB (WT-L) groups ($p = 0.055$ for compound-L vs. single-L; $p < 0.001$ for compound-L vs. WT-L, respectively).
Discussion: These findings provide evidence that the seven-gene mutation signature has potential as a predictive biomarker for the efficacy of immunotherapy in metastatic bladder cancer. Furter validation and functional studies are warranted.

#7854 Prognostic impact of gain-of-function TP53 mutations on outcomes in HER2-negative advanced gastric cancer.

Jong-Ho Kim[1], Jwa Hoon Kim[2], Ji Won Lee[2]

[1]Korea University Research Institute for Medical Bigdata Science, Korea University College of Medicine, Seoul, Korea, Republic of,[2]Korea University College of Medicine, Seoul, Korea, Republic of

Background:
TP53 alterations are among the most prevalent genomic events across solid tumors, yet the biological and clinical heterogeneity of TP53 mutation types—particularly gain-of-function (GOF) variants—remains poorly defined in advanced gastric cancer (AGC). GOF mutations involving the DNA-binding domain can confer oncogenic properties beyond simple loss of tumor suppressor activity. We aimed to characterize the landscape of GOF and non-GOF TP53 mutations and evaluate their prognostic relevance in patients with HER2-negative AGC treated with first-line oxaliplatin-based chemotherapy.
Methods:
From 2017-2021, tumor tissues from 675 patients with AGC were sequenced. Among these, 409 patients with HER2-negative AGC receiving first-line FOLFOX (n=188) or XELOX (n=221) were included. Targeted sequencing was performed using CancerSCAN or K-MASTER v1.0/v1.1 NGS panels. GOF TP53 variants were prespecified (R175H, R248W, R248Q, R249S, R273H, R273L, R282W), with all remaining alterations classified as non-GOF. PFS and OS were assessed using Kaplan-Meier methods.
Results:
Among 675 patients, 409 patients with HER2-negative AGC were treated with first-line FOLFOX (n=188) or XELOX (n=221). TP53 mutation was identified in 115 (28.1%) of 409 patients; GOF (n=21, 5.1%) and non-GOF (n=94, 23.0%). The most common hotspot of GOF TP53 mutations was R175H (n=8), followed by R248W (n=7), R248Q (n=4), and R273H (n=2). With a median follow-up duration of 22.7 months, the median progression-free survival (PFS) with FOLFOX/XELOX and overall survival (OS) of 409 patients were 5.1 and 21.8 months, respectively. Patients with TP53 mutated AGC showed significantly shorter PFS than those with wild-type TP53 mutation (median 4.8 vs. 5.3 months, *P*=0.049). There were no significant differences in PFS between GOF TP53 and non-GOF TP53 mutated AGC (median 4.9 vs. 4.8 months, *P*=0.680). There were no significant differences in OS between TP53 mutated and wild-type AGC (18.4 vs. 22.0 months, *P*=0.261). Median OS seemed to be numerically shorter in patients with GOF TP53 mutated AGC compared to those with non-GOF TP53 mutated and wild-type AGC (15.7 vs. 19.3 vs. 22.0 months, *P*=0.442).
Conclusions:
TP53 mutations—including biologically aggressive GOF variants—were identified in nearly one-third of HER2-negative AGC patients. Although statistical significance was not achieved, GOF TP53 mutations demonstrated a consistent pattern toward inferior survival, suggesting their potential role as poor-prognostic genomic biomarkers in chemotherapy-treated AGC. Larger prospective analyses integrating molecular subtypes and immunologic signatures are warranted to clarify the therapeutic and biological relevance of TP53 functional subclasses.

#7855 Transcriptomic profiling of Ki67 expression in melanoma patient specimens reveals distinct immune signatures.

Eleanor A. Fallon[1], Kei Kawashima[2], Kazuaki Takabe[2]

[1]Surgical Oncology, Roswell Park Comprehensive Cancer Center, Buffalo, NY,[2]Roswell Park Comprehensive Cancer Center, Buffalo, NY

Background: The Ki67 gene (MKI67) is clinically relevant as a marker of high cellular activity in melanoma among other cancer subtypes. We hypothesized that transcriptomic profiling of human melanoma tissue as stratified by MIK67-high and MKI67-low expression may correlate with immune signatures of biologic activity and with clinical outcomes.
Methods: Analyzed tumor tissue included subcutaneous melanoma metastatic sites and lymph nodes (GSE22153 n=57), tumor biopsies (GSE65904 n=214), The Cancer Genome Atlas (TCGA n=443), pre-ICB biopsies (GSE78220 n=28), and pre-treatment plus on-treatment mixed Immune Checkpoint Blockade (ICB) cohorts (GSE91061 n=65). Median MKI67 expression was utilized to stratify the groups. The xCell platform was utilized to analyze cellular subsets. Hallmark gene sets within the Molecular Signatures Database (MSigDB) were utilized for the Gene Set Enrichment Analysis (GSEA). The immune subtype classification as described by Thorsson *et al.* was utilized.
Results: The MKI67 transcriptomic expression correlated with highly proliferative genesets including E2F targets, G2M checkpoint, mitotic spindle, and MYC targets v1/v2 (|NES|>1.5 and FDR < 0.25 for all pathways). Within the TCGA cohort, the proliferative and wound healing pathways were enriched ($p<0.05$), further supporting the concept that Ki67-high is indeed indicative of greater cell turnover and activity. Interestingly, silent and non-silent mutation rates were higher in the MKI67-high group ($p=0.00187$ and 0.00262, respectively) but this was not the case for neoantigens ($p=0.163$). On Chi-squared analysis, the TCGA dataset (n=441) demonstrated an association between MKI67-high expression (n=220) and KIT mutations (n=13, $p=0.043$), as well as CDKN2A mutations (n=20, $p=0.004$). On xCell analysis, Th1 cells demonstrated MKI67-high expression was associated with Th1 cell infiltration in the TCGA and GSE65904 cohorts ($p<0.05$), but this associated was weaker for Th2 cells. There were no statistically significant differences across the groups in terms of clinical features such as race, gender, anatomic site or melanoma stage (e.g. T, N) as relating to Ki-67 expression. Overall Survival (OS) and Disease-Free Survival (DFS) were both associated with lower MKI67 expression at the 100-month time point ($p=0.0004$ and $p=0.0177$, respectively), but this difference was lost on later clinical follow-up.
Conclusions: We have herein utilized analysis of the MKI67 transcriptome as a means to interrogate the underlying molecular biology of melanoma tumors as they relate to the tumor immune microenvironment and clinical outcomes. MKI67 expression correlates with a unique constellation of gene enrichment and immune infiltration as well as tissue mutations and warrants further investigation as a potential tool for clinical decision-making.

#7856 Prevalence and association of clonal hematopoiesis with cardiovascular health in patients of the Avera sequencing and analytics protocol (ASAP) Study.

Mikayla Bendix[1], McKenna Perrin[2], Ryan Vaca[2], Padmapriya Swaminathan[2], Crystal Hattum[2], Shakeel Mir[3], Lucia Speroni[3], Emily Teslow[3], David Starks[2], Benjamin Solomon[2], William Spanos[2], Rachel Elsey[2], Tobias Meissner[2]

[1]Sanford School of Medecine, University of South Dakota, Vermillion, SD,[2]Avera Cancer Institute, Sioux Falls, SD,[3]Tempus AI, Chicago, IL

Introduction: Clonal Hematopoiesis (CH) refers to age-associated somatic mutations in hematopoietic stem cells. CH may be incidentally discovered in oncology patients via next-generation sequencing. Cancer therapies such as cytotoxic chemotherapy and radiation can accelerate the development or expansion of CH, particularly in genes associated with therapy-related myeloid neoplasms. Certain CH variants are also linked to increased cardiovascular (CV) risk. Understanding which patients are at higher risk of poor CV outcomes is an underrecognized threat to long-term cancer survivorship.

Methods: This retrospective cohort study of Avera Sequencing and Analytics Protocol (ASAP; NCT05142033) patients used Tempus xF+, a cell-free DNA liquid biopsy panel (~1.8 Mb) that detects single-nucleotide variants and insertions/deletions across 523 genes, including all tests completed prior to March 2025. CH classification was based on mutations in 17 commonly associated genes. Data on demographics, CV outcomes, (e.g., stroke, hypertension, angina, myocardial infarction, heart failure, arrhythmias, valvular heart disease, and venous thrombosis), cancer characteristics, and labs were extracted from the EMR using ICD-10-based SQL queries. Statistical analyses evaluated differences by presence of CH.

Results: A total of 456 patients were included in the final analysis. 197 (43%) patients were identified as CH-positive. The most frequently mutated genes were DNMT3A, TP53, and PPM1D. Results supported that CH is an age-associated condition, with prevalence rising from 11% in patients under 50 years old, to 30% among those aged 50-59, 42% in the 60-69 age group and reaching 56% in patients over 70. CV events were observed in 72.6% of CH patients, compared to 57.5% of non-CH patients. Among CH-positive individuals, the average VAF was 8.4% (0.3% - 77.0%) for those with CV events, versus 7.6% (0.3% - 51.6%) for those without. Consistent with existing literature, TET2 and ASXL1 mutations conferred the highest probabilities of developing CV outcomes. Pancreatic (OR 5.9, $p = 0.2$), lung (OR 4.1, $p = 0.02$), and esophageal (OR 3.5, $p = 0.6$) cancers exhibited strong but variably significant associations with CV risk, potentially limited by sample size.

Conclusion: Our findings are consistent with previously reported data showing higher rates of CV outcomes in patients with CH in this oncology patient cohort. Some limitations of this study include the retrospective, single cohort design, the use of correlational data, and potential selection bias for study inclusion. This data supports the need for development of cardiology referral guidelines to reduce morbidity and mortality of CV outcomes in oncology patients where CH mutations are identified by liquid biopsy testing.

#7857 Multi-modal real-world data uncovers predictors of clinical response to TOP1i and optimizes ADC strategies in colorectal cancer.

Alireza Tafazzol[1], Sebastian Cruz-Gonzalez[1], Xu Shi[1], Zoltan Dezso[1], Douglas E. Kline[2], Jack Chen[3], Peter J. Ansell[4], Relja Popovic[5], Rong Chen[5], Josue Samayoa[5], Xi Zhao[1], Weilong Zhao[1]

[1]Quantitative Medicine and Genomics, AbbVie, South San Francisco, CA,[2]Oncology Discovery Research, AbbVie, North Chicago, IL,[3]Precision Medicine, AbbVie, South San Francisco, CA,[4]Precision Medicine, AbbVie, North Chicago, IL,[5]Quantitative Medicine and Genomics, AbbVie, North Chicago, IL

Real-world data (RWD) encompassing diverse treatment regimens offers a valuable opportunity to identify predictive biomarkers of response and resistance across broad patient populations. Although data from clinical trials with antibody-drug conjugate (ADC) therapies remains limited, analysis of large standard-of-care cohorts offers valuable insight into chemotherapy resistance. For example, irinotecan—a widely used topoisomerase I inhibitor (TOP1i) in metastatic colorectal cancer (CRC) regimens—serves as a model to infer potential resistance to ADCs that utilize TOP1i payloads and the feasibility of combination strategies.

We analyzed ConcertAI PT360® electronic health records linked to Caris Life Sciences genomic data for 810 CRC patients with available clinical responses and pre-treatment samples to investigate irinotecan response and resistance mechanisms. Patients were classified into responder (R; n = 241), non-responder (NR; n = 308), acquired resistance (AR; n = 181, transition from R to NR), and stable disease (SD; n = 80). Response to irinotecan was associated with significantly better overall survival ($p < 0.0001$), with median OS of 106, 87, 73, and 47 months for R, SD, AR, and NR, respectively. Response classifications and transcriptomic data were independent of covariates such as ECOG score, diagnostic stage, ethnicity, sex, or age. Most patients were microsatellite stable with low tumor mutational burden.

Gene expression and mutation profiling revealed upregulation of mucins (*MUC5AC*, *MUC2*) and enrichment of *KRAS* mutations in NR, indicating a mucinous CRC subtype resistant to irinotecan. Conversely, *TOP1* gene amplification and increased expression were more frequent in R. Pathway analysis indicated higher inflammation and pre-existing immune activity in R/AR versus NR, especially B cell immunity. Gene signatures of tertiary lymphoid structures were also elevated in R/AR, further linking to B-cell immunity. Longitudinal samples revealed enhanced anti-tumor immune signatures post treatment, including dendritic cell activation, upregulated antigen presentation, and elevated interferon-gamma signaling. Additionally, we utilized an innovative *in silico* CRISPR knockout machine learning model on curated RWD to identify potential novel targets to overcome irinotecan resistance.

This study leveraged a rigorously curated multi-modal RWD cohort of CRC patients treated with irinotecan to elucidate mechanisms of clinical response and resistance. Enrichment of immune activation pathways in irinotecan responders suggests that baseline tumor microenvironment may predict outcome, while increased immune signatures post-treatment indicate that combining immunotherapy could enhance responses. These findings provide insights into the biomarkers associated with systemic TOP1i and may inform further clinical development of TOP1i-ADCs.

#7858 Machine learning predicts retinoblastoma (Rb) function in real-world small cell lung cancer patients.

Sana Parveen[1], Neshatul Haque[2], Emma T. Corcoran[3], Sebastia Franch-Exposito[3], Prerna Jain[3], Jacob Mercer[3], Anthony J. Trimboli[4], Gustavo W. Leone[4], Navonil de Sarkar[4], Abdul R. Naqash[5], Christine M. Lovly[6], Paul Fields[3], Hui-Zi Chen[1]

[1]Division of Hematology & Oncology, Department of Medicine, Medical College of Wisconsin, Wauwatosa, WI,[2]Linda T. and John A. Mellowes Center for Genomic Sciences and Precision Medicine, Medical College of Wisconsin, Wauwatosa, WI,[3]Tempus AI, Chicago, IL,[4]Department of Pathology, Medical College of Wisconsin, Wauwatosa, WI,[5]Department of Medicine, The University of Oklahoma, Oklahoma City, OK,[6]Department of Medical Oncology & Therapeutics Research, City of Hope Comprehensive Cancer Ctr., Duarte, CA

Inactivation of the retinoblastoma (Rb) tumor suppressor has long been considered a molecular hallmark of small cell lung carcinoma (SCLC), an aggressive form of bronchogenic, smoking-induced lung cancer with an extremely poor prognosis. Currently, SCLC can be classified into the following molecular subtypes: ASCL1, NEUROD1, POU2F3, and Inflamed. We analyzed a real-world cohort of ~1,400 SCLC tumors sequenced with both Tempus xT (DNA sequencing) and xR (RNA sequencing) and assigned them to molecular subtypes based on non-matrix factorization. Interestingly, we determined that *RB1* alterations (e.g. single nucleotide variants, insertions/deletions) were not detected in approximately 30% of the Tempus SCLC cohort, regardless of tumor molecular subtype. However, absence of *RB1* genomic alterations does not guarantee Rb protein function in SCLC, as alternate mechanisms such as *RB1* promoter hypermethylation may result in gene silencing and loss-of-function (LOF), along with intronic splicing mutations that may not be well captured in probe-based methods. Therefore, we developed a machine learning model (Nested Random Forest) to predict Rb LOF in the Tempus SCLC cohort. We trained our model using 21,656 features including genomic, transcriptomic and clinical variables from 409 Tempus SCLC patients (cross-validation AUC 0.924 ± 0.020), whose tumors were either (1) *RB1*-altered and had low *RB1* expression (defined as less than 25th percentile of expression of *RB1*-altered samples) or (2) *RB1* wild-type and had high *RB1* expression (defined as greater than 75th percentile of expression of *RB1* wild-type samples). We then applied the model to remaining N=1,224 SCLC tumors in the Tempus dataset. Surprisingly, our model predicted that ~30% (N=241) of *RB1*-altered tumors (N=837) had an Rb wild-type or functional phenotype. This finding contradicts the notion that all *RB1* genomic aberrations lead to loss of Rb pathway activity. Conversely, our model predicted that a proportion of *RB1* wild-type tumors had Rb LOF, due to mechanisms such as *CDKN2A* (*p16^{INK4a}*) deletion. Furthermore, we evaluated the frequency of predicted Rb function in the four SCLC subtypes. Our results showed that approximately one half of POU2F3 and Inflamed tumors had predicted Rb function, while approximately only 20% of ASCL1 and NEUROD1 tumors had predicted Rb function. In conclusion, our machine learning model predicted that a considerable number of real-world SCLC patients may contain a functional Rb pathway despite having genomic alterations in *RB1*. The impact of our finding on clinical outcomes including response to first-line chemotherapy and immunotherapy in real-world SCLC patients is currently being evaluated.

#7859 Exploring multilevel risk factors for metabolic dysfunction-associated steatotic liver disease (MASLD) in an electronic health record (EHR)-based cohort.

Janet N. Chu[1], Mindy Hebert-Derouen[2], Alison Canchola[3], Alyssa Cortella[3], Pushkar Inamdar[3], Hashem B. El-Serag[4], Scarlett L. Gomez[5], Salma Shariff-Marco[6]

[1]Medicine, UCSF- University of California, San Francisco, San Francisco, CA,[2]Department of Public Health Sciences, New Mexico State University, Las Cruces, NM,[3]Epidemiology & Biostatistics, UCSF- University of California, San Francisco, San Francisco, CA,[4]Baylor College of Medicine, Houston, TX,[5]Epidemiology & Biostatistics, UCSF - University of California San Francisco, San Francisco, CA,[6]Epidemiology and Biostatistics, UCSF - University of California San Francisco, San Francisco, CA

Background: MASLD is a growing risk factor for liver cancer. Few studies have examined multilevel risk factors contributing to MASLD disparities, particularly the impact of neighborhood attributes. Elucidating multilevel risk factors can help identify groups relevant for targeted interventions to mitigate liver disease, including liver cancer.
Methods: Our EHR-based cohort included adults with at least one in-person visit between 2000-2017 to Kaiser Permanente Hawai'i. From the EHR, we extracted data on patient sociodemographic characteristics; diagnostic codes; medication prescriptions; and lab results. Patient observations were appended to census tract-level neighborhood SES (nSES). The outcome was incident MASLD, defined using ICD-codes with follow-up until 12/31/2017. We used multivariable Cox proportional hazards regression to explore factors associated with incident MASLD; models were adjusted for baseline year and decile of number of encounters. Model 1 included sociodemographic variables (i.e., sex, race/ethnicity, English proficiency); in Model 2 we retained sociodemographic variables which were multivariably statistically significant and added clinical characteristics (i.e., body mass index [BMI], smoking history, hypertension, diabetes, and hyperlipidemia); and in Model 3 we retained clinical characteristics which were multivariably statistically significant and added nSES.
Results: Of 439,709 patients, 8,339 had incident MASLD during 18,350 person-years of follow up. In Model 1, males had higher risk of developing MASLD than females. Compared to non-Hispanic White individuals, those who identified as Chinese, Japanese, Korean, multiracial, or Hispanic had higher risk (HR range 1.08-1.83), and as Native Hawaiian, Pacific Islander, or Black had lower risk of MASLD (HR range 0.54-0.78). Limited English proficiency was associated with increased MASLD risk (HR= 1.52, 95% CI 1.30-1.78). In model 2, overweight and obese BMI, ever smoking, elevated triglycerides, low HDL, and diabetes were associated with higher MASLD risk (HR range 1.02-1.99). In Model 3, nSES was not statistically significantly associated with MASLD risk when added to sociodemographic and clinical factors. Significant factors in prior models remained independently associated with MASLD risk, except for smoking.
Discussion: Our study provided critical disaggregated data on MASLD risk for ethnic groups that are typically understudied. We found that among this diverse cohort, disparities in MASLD incidence persist, despite adjusting for other sociodemographic, clinical, and neighborhood SES. Future efforts to reduce MASLD burden may consider focusing on these ethnic groups at higher risk. Furthermore, future studies should explore the role of other neighborhood social and built attributes such as food environment and access to parks.

#7860 Fusion gene machine learning models improve clinical outcome prediction of hepatocellular carcinoma.

Jian-Hua Luo[1], Silvia Liu[1], Yanping Yu[2]

[1]University of Pittsburgh, Pittsburgh, PA,[2]Assistant Professor, Dept. of Pathology, University of Pittsburgh, Pittsburgh, PA

Hepatocellular carcinoma is one of the most lethal malignancies for humans. Assessing the clinical outcomes of HCC remains challenging. In this study, we analyzed a panel of 20 fusion genes in 200 hepatocellular carcinoma (HCC) samples to predict the recurrence and survival rates of HCC patients undergoing surgical interventions using machine learning models. The results showed that fusion genes, Milan criteria, serum α-fetal protein (AFP), and pathology grade had moderate predictive accuracy for HCC recurrence. However, the combination of selected fusion genes with these clinical parameters significantly enhanced the prediction accuracy of each parameter. When models of fusion genes were applied to predict the 3-year survival rate of HCC patients, they outperformed the Milan criteria, pathology grade, and serum AFP. The combination of a fusion gene panel with Milan criteria, pathology grade, or serum AFP yielded significantly improved results compared to those produced by these clinical parameters alone. As a result, examining the fusion gene status of HCC samples may hold promise as a new and improved approach to assessing the clinical outcomes of this disease.

#7861 Translating temporal multi-disease pathways in multiple cancer types using real-world clinical data.

Md Ashad Alam

Ochsner Health System, New Orleans, LA

Although several pre-cancer comorbidities have been described, the role of medically interpretable preceding diagnoses as multi-disease pathways (MDPs) remains underexplored in the U.S. population. We analyzed electronic health record data from Ochsner Health (Louisiana) spanning 2013-2022, encompassing more than 4.1 million patients. Disease trajectories were identified by analyzing pairs of diagnoses that exhibited significant temporal correlations. To construct three-diagnosis trajectories, we merged overlapping pairs (e.g.,D1→D2 and D2→C (cancer) were combined to form D1→D2→C). For each patient, all three-step diagnostic sequences were extracted, and the pairs within each triplet were tested for directiona lsignificance. We applied this analysis to ten high-burden cancers, breast, melanoma, lung, prostate, pancreatic, liver, bladder, leukemia, ovarian, and colorectal, which yielded 501 (11 significant), 507 (10),194 (2), 349 (8), 49, 132 (3), 111, 84, 39, and 155 directional associations, respectively. Significant directional trajectories to cancer included breast lump → abnormal breast imaging, joint disorder → overuse/soft-tissue disorder, joint disorder → shoulder lesion, acute sinusitis → acute upperrespiratory infection, osteoporosis → other bone disorder, knee osteoarthritis → joint disorder, majordepression → anxiety disorder, acute pharyngitis → acute upper respiratory infection, cough → breathingab normality, joint disorder → other soft-tissue disorder, and finger/toe deformity → bonedensity/structure disorder preceding breast cancer; acute viral hepatitis → liver fibrosis/cirrhosis, chronicviral hepatitis → liver cirrhosis (unspecified), and liver fibrosis/cirrhosis → other liver disease precedingliver cancer; urinary frequency → sexual dysfunction, joint disorder → shoulder lesion, benign prostatichyperplasia → abnormal tumor markers, knee osteoarthritis → joint disorder, erectile dysfunction →abnormal tumor markers, joint disorder → other soft-tissue disorder, obstructive/reflux uropathy →benign prostatic hyperplasia, and osteoarthritis → joint disorder preceding prostate cancer; osteoarthritis of knee → joint disorder → soft-tissue disorder preceding lung cancer; and actinic keratosis → seborrheickeratosis, osteoarthritis → joint disorder, allergic/vasomotor rhinitis → chronic sinusitis, and joint disorder→ soft-tissue disorder preceding melanoma cancer. An important consideration in this approach is that while these MDPs are statistically significant, they may not represent causative associations. For example, conditions such as erectile dysfunction may lead to age-appropriate screening in a high cancer risk population. Likewise, a diagnosis of breast lump may directly imply cancer prior to formal diagnosis. Biologically plausibility of all significant MDPs should be investigated individually.

#7862 Population analysis and immunologic landscape of melanoma in people living with HIV.

Lindsay Barger[1], Derek Wang[2], Ashley Saravia[1], Valeria Mezzano-Robinson[3], Gyles Ward[3], Cynthia Loomis[3], Carly Feldman[4], Madalina Tuluc[4], Rino S. Seedor[4], Peter J. Gaskill[1], Anna E. Coghill[5], Gita Suneja[6], Iman Dehzangi[2], Jenna Hope[1], George Jour[3], **Gabriele Romano**[1]

[1]Drexel University College of Medicine, Philadelphia, PA,[2]Rutgers University, Camden, NJ,[3]NYU Langone Health, New York, NY,[4]Thomas Jefferson University, Philadelphia, PA,[5]Moffitt Cancer Center, Tampa, FL,[6]Huntsman Cancer Institute, Salt Lake City, UT

Purpose: To dissect the clinical and immunological features of people living with HIV (PLWH) diagnosed with melanoma, who have consistently shown worse outcomes than HIV-negative individuals (PLw/oH) with the same cancer.
Experimental Design: We analyzed electronic health records from 1,087 PLWH and 394,437 PLw/oH with melanoma. Demographic and clinical characteristics were compared. Spatial immune transcriptomics (72 immune-related genes) was performed on melanoma tumor samples (n=11), with downstream validation using multiplex immunofluorescence (n=15 PLWH, n=14 PLw/oH).
Results: PLWH were diagnosed at a younger age, had greater representation of Hispanic and Black individuals, and showed reduced survival. They also had a markedly increased risk of brain metastases. PLWH experienced significant delays in initiating immune checkpoint inhibitor (ICI) therapy and had worse post-ICI survival, even after balancing covariates. Spatial transcriptomics revealed a more immunosuppressive tumor microenvironment in PLWH, with increased transcription of immune checkpoints (PD1, LAG3) and reduced antigen-presentation markers (HLA-DRB, B2M), with distinct spatial distributions in tumors and surrounding microenvironments. Multiplex immunofluorescence demonstrated features of an exhausted $CD8^+$ T cell compartment, including enrichment of $PD1^{int}LAG3^-$ and $PD1^{int}LAG3^+$ subpopulations, and a significant accumulation of myeloid-derived suppressor cells ($CD11b^+$ $HLA\text{-}DR^-$ $CD33^+$).
Conclusions: Melanoma in PLWH is associated with distinct clinical and immunological features, including delayed ICI treatment, reduced survival, and an immunosuppressive microenvironment with exhausted $CD8^+$ T cells and expanded myeloid-derived suppressor cells. These findings suggest that chronic HIV infection may impair antitumor immunity in melanoma. Targeting the pathways identified here may improve therapeutic responses and outcomes in this population.

#7863 Aspirin and celecoxib use and overall survival in ER+/HER2- metastatic breast cancer: A large real-world cohort analysis.

Mostafa Eysha[1], Mohanad Elchouemi[1], Harshitha Popuri[1], Gaurav Periapattanam[1], Arsalaan Asad[2], Yasmin Youssef[3], Ahmed Elkhanany[4], Sumit Gaur[5]

[1]Texas Tech Univ. Foster School of Medicine, El Paso, TX,[2]University of Texas Medical Branch John Sealy School of Medicine, Galveston, TX,[3]Mansoura university, faculty of medicine, Mansoura, Egypt,[4]Baylor College of Medicine, Houston, TX,[5]Texas Tech Univ. Foster School of Medicine,, El Paso, TX

Background: Endocrine resistance in ER+/HER2- breast cancer (BC) is frequently linked to PI3K-AKT-mTOR pathway dysregulation. While aspirin benefits *PIK3CA*-mutant colorectal cancer, randomized trials of adjuvant endocrine therapy ± COX inhibition in BC failed to demonstrate survival benefits, potentially due to lack of biomarker selection. Given that ER+/HER2- metastatic disease is clinically enriched for PI3K pathway activation, we hypothesized that real-world aspirin and celecoxib (COXI) use might be associated with improved survival in this population. This study evaluated the association between COXI use and survival in ER+/HER2- metastatic BC, utilizing this subtype as a clinical proxy for *PIK3CA* pathway activation.

Methods: Using the TriNetX US Collaborative Network, we identified patients with ER+/HER2- metastatic BC via ICD-10 codes and biomarker fields. Patients were grouped into three prevalent-user cohorts based on post-diagnosis medication use: (1) control (no use); (2) single-agent COXI; and (3) combination COXI (aspirin and celecoxib). Propensity score matching (1:1) was utilized to balance cohorts for demographics, comorbidities, cardiovascular risk factors, and concomitant systemic therapies (endocrine agents, chemotherapy, and CDK4/6 inhibitors). We estimated Hazard Ratios (HRs) for overall mortality and Major Adverse Cardiovascular Events (MACE: myocardial infarction, stroke, and cardiovascular death).

Results: After matching, 14,955 patient pairs (Single-agent vs. Control) and 1,913 patient pairs (Combination vs. Control) were analyzed. The Combination cohort demonstrated the lowest mortality hazard (HR, 0.429; 95% CI, 0.379-0.486; $p < 0.0001$). The Single-agent cohort also showed a significantly lower mortality hazard compared to controls (HR, 0.629; 95% CI, 0.604-0.656; $p < 0.0001$). Conversely, the hazard of MACE was significantly higher in both treated groups compared to controls (Combination: HR, 1.492; Single-agent: HR, 1.641; both $p < 0.0001$).

Conclusion: In this large real-world cohort of ER+/HER2- metastatic breast cancer, aspirin and/or celecoxib use was associated with a graded improvement in overall survival. This association persisted despite the treated groups showing a significantly higher risk of MACE. This difference, even after PSM, reflects residual confounding due to bias by indication. This suggests the survival improvement is driven by a genuine oncologic effect, mitigating concerns about "healthy user" bias. However, findings must be interpreted cautiously given the observational design and potential for biases such as immortal time bias and residual confounding. *PIK3CA* genomic data was sparse in this dataset, precluding genotype-stratified analyses. These results support further investigation via prospective, biomarker-driven trials specifically targeting *PIK3CA*-associated ER+/HER2- disease.

#7864 Real-world overall survival and healthcare utilization with CDK4/6 inhibitor based regimens versus chemotherapy in previously treated HR+/HER2+ metastatic breast cancer: A TriNetX Global Collaborative Network analysis.

Mostafa Eysha[1], Usman Hussain[1], Mohanad Elchouemi[1], Mariah Black[1], Sharon Siby[1], Wanyu Zhang[2], Arsalaan Asad[3], Ahmed Elkhanany[4]

[1]Texas Tech Univ. Foster School of Medicine, El Paso, TX,[2]Duke Universoty, Durham, NC,[3]UTMB John Sealy School of Medicine, Galveston, TX,[4]Baylor College of Medicine, Houston, TX

Background: In the phase II monarcHER trial, abemaciclib plus trastuzumab with or without endocrine therapy improved overall survival (OS) versus chemotherapy plus trastuzumab in heavily pretreated hormone receptor-positive (HR+)/HER2+ metastatic breast cancer. Robust real-world evidence (RWE) comparing CDK4/6 inhibitor-based regimens with chemotherapy in this setting remains limited.
Methods: We conducted a retrospective cohort study using de-identified electronic health records from the TriNetX Global Collaborative Network to compare two regimens in adults with highly pretreated HR+/HER2+ metastatic breast cancer: (1) CDK4/6 inhibitor plus endocrine and anti-HER2 therapy, and (2) chemotherapy plus anti-HER2 therapy. Prior exposure to anti-HER2 regimens was present, but explicit progression events and line counts were unavailable. The primary endpoint was overall survival (OS) up to 1200 days; secondary endpoints included neutropenia, heart failure (as a proxy for cardiotoxicity), and emergency department (ED) visits. Propensity score matching (1:1) was used to balance cohorts on demographics and comorbidities. Survival probabilities and hazard ratios (HRs) were estimated using Kaplan-Meier methods, log-rank tests, and Cox proportional hazards models.
Results: PSM resulted in 140 patients per cohort with balanced baselines. Median follow-up was 573 days for chemotherapy and 479 days for CDK4/6 inhibitor therapy. Over 1200 days, death occurred in 36.4% (51/140) of the chemotherapy cohort and 17.1% (24/140) of the CDK4/6 inhibitor cohort, a 19.3% absolute risk reduction (95% CI, 9.2-29.4) favoring CDK4/6 inhibitors. Over the 1200-day, CDK4/6 inhibitor-based regimens significantly lowered the hazard of death compared to chemotherapy (HR, 0.52; 95% CI, 0.32-0.84; p=0.007). Neutropenia and heart failure were similar, but ED visits were more frequent with chemotherapy (HR 1.59; p=0.012).
Conclusions: In this real-world, propensity-matched analysis of previously treated HR+/HER2+ metastatic breast cancer, CDK4/6 inhibitor-based endocrine and anti-HER2 therapy was associated with substantially lower mortality risk (HR 0.52; 19.3% absolute risk reduction) and reduced ED utilization compared with chemotherapy plus anti-HER2 therapy over a 1200-day window. These findings support the OS benefit seen in monarcHER and reinforce targeted endocrine strategies as clinically relevant alternatives to chemotherapy in heavily pretreated HR+/HER2+ metastatic breast cancer, despite the limitations of retrospective, non-randomized real-world evidence.

#7865 Survival profile of patients presented at technology-enhanced multidisciplinary cancer conferences.

Opuruiche Ibekwe[1], Carmelo Gaudioso[1], Quratulain Sabih[2], Han Yu[3], Peter Frederick[4], Ellis G. Levine[5], Chukwumere E. Nwogu[1]

[1]Thoracic Surgery, Roswell Park Comprehensive Cancer Center, Buffalo, NY,[2]Breast Surgery, University of Pittsburgh Medical Center, Pittsburgh, PA,[3]Biostatistics & Bioinformatics, Roswell Park Comprehensive Cancer Center, Buffalo, NY,[4]Gynecologic Oncology, Roswell Park Comprehensive Cancer Center, Buffalo, NY,[5]Breast Medical Oncology, Roswell Park Comprehensive Cancer Center, Buffalo, NY

Background: Emerging research suggests that multidisciplinary cancer conferences (MCCs) positively impact survival in cancer patients. This study aimed to assess the survival outcomes in technology-enhanced thoracic, gynecology and breast tumor boards.
Methods: We conducted a prospective study, pre vs post implementation of a tumor board technology platform, September 2020 to February 2022 in a comprehensive cancer center. Using data sourced from the cancer registry, we compared the survival rates of patients presented at the thoracic, gynecology, and breast MCCs with matched cases not presented at the MCCs. Comparisons were made using the Mann-Whitney U and Fisher's Exact test. Survival outcomes were summarized using Kaplan-Meier methods.
Results: A total of 214, 75, and 52 cancer patients presented at the thoracic, breast and gynecology MCCs, respectively, were matched with corresponding numbers of non-MCC cohorts. Patients in the thoracic MCC cohort had an increased overall survival compared with that of the non-MCC cohort (median time = 47.8 vs 37.2 months, p=0.013) and cancer-specific survival (median time = 77.9 vs 51.5 months, p=0.019). We found no significant survival benefit in the breast and gynecology MCCs or after implementation of the technology platform.
Conclusion: MCCs lead to improved survival outcomes in thoracic cancer patients. A larger sample size would be required to fully assess any potential survival impact in breast and gynecologic oncology patients. Our study did not show that the digital tumor board platform had an impact on the survival outcome for patients presented at any of the MCCs.

#7866 BMI- and subtype-specific molecular clusters reveal distinct obesity mechanisms in breast cancer across Nigerian and U.S. cohorts.

Oyomoare Osazuwa-Peters[1], Jovita Kokwesiga Byemerwa[1], Omolola Salako[2], Adetola Daramola[2], Olusegun Isaac Alatise[3], Gabriel Ogun[4], Tomi Akinyemiju[5]

[1]Population Health Sciences, Duke University School of Medicine, Durham, NC,[2]College of Medicine, University of Lagos, Lagos, Nigeria,[3]Obafemi Awolowo University, Ile-Ife, Nigeria,[4]University College Hospital, University of Ibadan, Ibadan, Nigeria,[5]Duke University School of Medicine, Durham, NC

Background: Obesity is a major breast cancer risk factor, yet its biological mechanisms remain poorly characterized in African populations. We hypothesized that distinct obesity-associated molecular signatures would differentiate obese from normal-weight Nigerian women and reveal subtype-specific patterns in U.S. women.
Methods: Targeted gene expression profiling (NanoString, 785 genes) was performed on tumors from 46 Nigerian women (MEND), and publicly available gene expression data from Women's Circle of Health Study (WCHS; n=367; African and European ancestry) were analyzed. Enrichment scores for obesity-related pathways (glycolysis, inflammation, Extracellular matrix (ECM) remodeling, adipokine signaling, insulin/IGF1 signaling, hypoxia, cholesterol biosynthesis) were computed using Gene Set Variation Analysis in R (v4.5.0) with KEGG and Reactome gene sets. Bipartite network clustering identified co-occurring mechanism clusters. Associations were tested for cluster membership with BMI using Firth logistic regression for MEND, and with subtype and ancestry using standard logistic regression for WCHS, adjusting for covariates (MEND: age, subtype, menopausal status; WCHS: age).
Results: MEND participants averaged 48.7 (10.6) years; WCHS averaged 54.07 (11.99) years. In MEND, three clusters emerged (Q=0.14, p<0.05): Cluster 1 (hypoxia, cholesterol biosynthesis), Cluster 2 (ECM remodeling, adipokine, insulin/IGF1 signaling), and Cluster 3 (glycolysis, inflammation). Overweight/obese women had higher odds of Cluster 2 (aOR=5.4, 95% CI: 1.3-31.3), while normal-weight women were enriched for Cluster 1 (0.12, 0.02-0.54). In WCHS, six enrichment scores yielded three clusters (Q=0.10, p<0.05): Cluster 1 (inflammation, hypoxia), Cluster 2 (ECM remodeling, insulin/IGF1 signaling), and Cluster 3 (adipokine signaling, glycolysis). Cluster membership did not differ by ancestry, but subtype associations (Luminal A reference) were striking: Cluster 1 strongly associated with Luminal A (Luminal B: 0.33, 0.18-0.61; HER2: 0.15, 0.06-0.34; Triple Neg: 0.19, 0.11-0.34), Cluster 2 with Luminal B (3.47, 1.8-6.9) and HER2 (4.09, 1.9-8.99), and Cluster 3 with Triple Negative (3.15, 1.78-5.73).
Conclusions: Obesity-linked mechanisms differ by BMI and subtype. ECM remodeling and growth factor signaling dominate obesity-related tumors, while hypoxia and lipid metabolism characterize normal-weight tumors. Subtype-specific clustering suggests heterogeneity beyond BMI. Findings highlight opportunities for precision prevention and treatment, including metabolic pathway targeting and potential use of GLP-1 receptor agonists in high-risk subtypes.
Disclosure: Generative AI (Microsoft Copilot) was used to assist with language editing; authors reviewed and verified all content.

#7867 Independent effects of genetic risk, socioeconomic status, and lifestyle factors in melanoma: A large-scale gene-environment analysis.

Elle Kim[1], Nilanjan Chatterjee[2]

[1]Johns Hopkins Medicine, Baltimore, MD,[2]Johns Hopkins Kimmel Comp. Cancer Ctr., Baltimore, MD

Background: Melanoma is the 5th most common cancer with an increasing incidence in the younger population. Prior literatures have shown that melanoma incidence paradoxically increases with socioeconomic affluence. Yet, the mechanisms underlying this pattern remains unclear. Prior gene-environment studies have focused primarily on sun exposure and phenotypic traits, with socioeconomic context largely unexplored. Our study integrates genetic, socioeconomic, and lifestyle data from the United Kingdom Biobank (UKBB) to disentangle the independent and joint effects of genetic risk and socioeconomic factors on melanoma incidence.

Methods: We analyzed 303,880 UKBB participants using Cox proportional hazards models to estimate hazard ratios (HRs) and 95% confidence intervals (CIs) for incident melanoma in an unrelated White British ancestry. We adjusted for sex, body mass index, smoking, skin color, alcohol intake frequency, vitamin D levels, sun-protection behavior, and assessment center (proxy for home location). We modelled the effects of the Index of Multiple Deprivation (IMD) by quartiles and polygenic risk score (PRS) on incident melanoma: IMD and PRS independently, additive model (IMD + PRS), and an interaction model (IMD × PRS).

Results: In the IMD-only model, compared to the least deprived (Q1), participants in Q3 and Q4 had significantly lower risk of melanoma incidence (Q3: HR = 0.84 [95% CI = 0.72 - 0.98]; Q4: HR = 0.84, [95% CI = 0.71 - 1.00]). In the PRS-only model, each unit increase in PRS was associated with a 2.16-fold increased melanoma risk (HR = 2.16 [95% CI = 1.99 - 2.34]). In the additive model, PRS and IMD effect remained largely unchanged. The interaction model showed no evidence of IMD-PRS interaction (HR 1.0; $p > 0.6$).

Conclusions: Greater genetic susceptibility and higher socioeconomic status was associated with increased melanoma risk through independent and non-interacting pathways. Even after accounting for lifestyle factors, socioeconomic differences remained, suggesting that melanoma risk is shaped by factors extending beyond individual lifestyle and behavior. Our findings highlight that there is no evidence that socioeconomic disparities reflect differences in genetic susceptibility, reinforcing the need for prevention and early detection strategies that address both inherited risk and social and structural contexts.

#7868 Skin and systemic interplay in immune checkpoint inhibitor therapy: Evidence of global immune activation.

Elle Kim[1], Joel Chaim Sunshine[2]

[1]Johns Hopkins Medicine, Baltimore, MD,[2]Johns Hopkins University School of Medicine, Baltimore, MD

Background: Immune-related adverse events (irAEs) from immune checkpoint inhibitor therapies (ICI; PD-1/L1, CTLA-4, and/or LAG3) are non-trivial. Cutaneous irAEs (cirAEs) are some of the earliest to occur, but their implication as markers of broader systemic immune activation remains unclear.
Objective: To evaluate the association between cirAEs and systemic irAEs in melanoma patients receiving ICI.
Methods: We performed a retrospective cohort study of 18,886 (aged 18 or older) primary melanoma patients (C43) using the TrinetX network. We performed 1:1 propensity score matching (PSM) between patients who developed cirAEs within 6 months of ICI initiation (cirAE group) and those that did not (non-cirAE group). Time-to-event analyses for 13 organ-systems (cardiac, endocrine, renal, pulmonary, neurologic, hepatic, hematologic, musculoskeletal, ocular, gastrointestinal (GI), rheumatologic, and electrolyte abnormalities) involving 54 distinct irAE categories were performed using Kaplan-Meier curves and Cox models. To approximate temporal ordering, we applied a dual index-date framework: a primary analysis anchoring both cohorts at ICI initiation, and a secondary analysis re-anchoring the cirAE cohort at the onset of cirAE. For each outcome, equality of hazard ratios (HRs) across anchors was tested using a Wald chi-square test with a false discovery rate correction to evaluate for coherence between the frameworks.
Results: In the matched cohort, the cox model showed significantly higher hazards in patients who developed cirAEs in the first year post-ICI. 32 distinct conditions were significantly associated with cirAEs. HRs ranged from 1.4 to nearly 5-fold higher vs. the matched non-cirAE cohort. The strongest signals were in GI (mucosal and secretory disorders; HR=5.06[3.54-7.23]), joint disorders (musculoskeletal conditions including pain, stiffness, and bursopathy, HR=2.67[2.08-3.42]), and esophagitis (HR=2.64[1.41-4.97]). Nine out of the 32 conditions including hypo-osmolality and hyponatremia and acute kidney injury showed non-coherence, marked by attenuated HRs and loss of significance in the cirAE-anchored analysis compared to the primary. As expected, the cirAE group showed improved survival (HR=0.61[0.54-0.70]) in the cirAE cohort (86%) compared to 79% in the non-cirAE group at the end of the 1-year time window, corresponding to approximately 171 additional survivors in the cirAE cohort.
Conclusions: cirAEs are associated with increased 1-year risk of numerous systemic irAEs across multiple organ systems, whereas others show reduced effect sizes in the secondary analysis, suggesting that their risk is concentrated pre-cirAE. The robustness of associations across temporal anchors suggests that cirAEs may serve as early markers of broader immune activation, warranting enhanced monitoring and multidisciplinary management.

: Targeted Therapies, Predispositions, and Survivorship in Pediatric Cancers
Poster Session

#7870 Targeting the MYC-SUMO axis with TAK-981 reverses immune suppression and restores antigen presentation in osteosarcoma.

Bikesh Kumar Nirala[1], Jeffrey Ritzenthaler[2], Tajhal Patel[3], Taku Yamamichi[1], Ryo Tsukada[1], Lyazat Kurenbekova[3], Juan Dou[2], Heath Bradley[2], Atreyi Dasgupta[4], Jason T. Yustein[2]

[1]Pediatrics, Emory University, Atlanta, GA,[2]Emory University, Atlanta, GA,[3]Baylor College of Medicine, Houston, TX,[4]Texas Children's Hospital Cancer & Hematology Ctr., Houston, TX

Background: Osteosarcoma (OS), the most common primary bone cancer in adolescents, remains difficult to treat due to aggressive growth, early metastasis, and poor response to immunotherapy. About 20-30% of OS harbor 8q24 amplification, causing MYC overexpression and an immune-cold tumor microenvironment (TME). To investigate MYC-driven immune evasion, we generated an osteoblast-specific Myc-knockin GEMM and performed complementary mechanistic studies.
Methods: The Myc-knockin model was characterized through histopathology, growth kinetics, immune profiling (flow cytometry, IHC), Western blotting, and RNA-seq. Antigen-presentation machinery (APM) gene expression was assessed in GEMM tumors, OS PDXs, and public datasets. MYC dependence was tested using dTAG degradation and siRNA knockdown. Because MYC is linked to SUMO-dependent repression, we examined the SUMO pathway using the SAE inhibitor TAK-981 and SAE1 knockdown. SUMO-interactome profiling (SUMO-IP/MS) identified MYC-associated SUMO substrates.
Results: The MYC-knockin GEMM developed rapidly progressive and highly metastatic OS that transcriptionally resembled MYC-high human OS. MYC activation produced a strongly immunosuppressive TME with reduced CD45⁺ cells and broad APM repression. MYC loss restored APM expression, establishing MYC as a key inhibitor of antigen presentation. SUMOylation machinery (SUMO1/2, SAE1/2, UBC9) was elevated in MYC-high models and inversely correlated with APM. TAK-981 showed potent MYC-selective cytotoxicity in vitro, with MYC-high cells far more sensitive than MYC-low counterparts across mouse and PDX lines. TAK-981 also reduced proliferation, migration, and sphere formation. In vivo, TAK-981 significantly suppressed tumor growth across syngeneic and PDX models. Transcriptomics revealed reduced MYC targets, EMT, glycolysis, and G2/M signaling, alongside induction of IFN-α/γ pathways, inflammatory responses, and APM genes. SUMO-IP/MS identified MYC-regulated SUMO-interacting proteins, including G3BP1/2, TARDBP, EIF3D, and PSMD4, implicating SUMO-dependent immune-evasion mechanisms. Combining TAK-981 with a STING agonist produced synergistic tumor control, achieving near-complete responses.
Conclusions: MYC drives immune suppression in OS through SUMO-dependent repression of antigen-presentation and innate immune pathways. Targeting the MYC-SUMO axis with TAK-981 converts the TME from immune-cold to immune-inflamed and enhances immunotherapy responses, supporting TAK-981-based combinations as a promising strategy for MYC-driven OS.

#7871 Onvansertib-mediated PLK1 inhibition reduces cell viability in neuroblastoma cells.

Aileen A. Yasukochi[1], Susanna Kim[2], CARLA SAMPAIO[3], Peter E. Zage[3]

[1]San Diego State University, San Diego, CA,[2]University of California San Diego, San Diego, CA,[3]UCSD Moores Cancer Center, San Diego, CA

Background: Neuroblastoma is the most common extracranial solid tumor of childhood and accounts for a significant proportion of pediatric cancer-related mortality. Despite advances in multimodal therapy including intensive chemotherapy, radiotherapy, stem cell transplantation, patients with high-risk disease continue to experience poor long-term survival. Consequently, there is an urgent need for rationally designed targeted therapies that selectively impair oncogenic proliferation while minimizing systemic damage. Polo-like kinase 1 (PLK1), a serine/threonine kinase essential for mitotic entry, spindle assembly, chromosome alignment, and cytokinesis, is aberrantly overexpressed in neuroblastoma and contributes to unchecked cell-cycle progression and evasion of apoptotic cues. Onvansertib, a highly selective PLK1 inhibitor, has emerged as a promising therapeutic candidate due to its ability to disrupt mitotic fidelity and induce programmed cell death.
Method: In this study, we evaluated the therapeutic potential of Onvansertib across multiple neuroblastoma cell lines using cell viability assays and molecular analyses. CCK-8 assays demonstrated a clear dose-dependent decrease in cell viability following 24-72 hours of treatment, indicating significant suppression of proliferation. To uncover the mechanisms underlying reduced viability, we conducted Western blot analyses assessing markers of DNA damage, apoptosis and cell-cycle disruption.
Results: Onvansertib treatment resulted in substantial downregulation of PLK1 protein levels, consistent with effective pathway inhibition. Concurrently, we observed increased phosphorylation of H2AX, a hallmark of double-strand DNA breaks, indicating activation of DNA damage responses. Apoptotic signaling was strongly induced, as evidenced by elevated levels of cleaved PARP and cleaved caspase-3 across cell lines. Additionally, decreased phosphorylation of Cdc25c, a downstream regulator of mitotic entry, further supported disruption of normal mitotic progression.
Conclusion: Together, these findings demonstrate that Onvansertib effectively compromises neuroblastoma cell survival through a multifaceted mechanism involving mitotic disruption, DNA damage accumulation and apoptotic activation. By targeting a fundamental regulator of the cell cycle, PLK1 inhibition represents a compelling therapeutic strategy for high-risk neuroblastoma. These data support further exploration of Onvansertib in preclinical models and provide a strong rationale for its advancement toward clinical evaluation in this very prevalent malignancy.

#7872 CDK7 inhibition mitigates AZD1775 resistance via chromatin reprogramming in MYC-MB.

Kiara Smart, Bethany Veo, Rajeev Vibhakar

The University of Colorado School of Medicine, Aurora, CO

Medulloblastoma (MB) is the most common malignant brain tumor in children, comprising ~20% of pediatric brain tumors. MB is a heterogeneous disease, with clinical outcomes heavily influenced by molecular subgroups. Among these, Group 3 MB, characterized by MYC amplification, exhibits the poorest prognosis, with a high propensity for metastasis and recurrence. Our previous research identified WEE1 as a critical regulator of MB cell survival and found that Myc-driven MB is particularly sensitive to the WEE1 inhibitor AZD1775. Although AZD1775 has demonstrated efficacy, especially when combined with genotoxic agents, resistance to small molecule inhibitors often emerges, limiting its therapeutic potential.CDK7, a kinase essential for transcriptional initiation via phosphorylation of RNA Pol II's C-terminal domain, plays a critical role in Myc-driven malignancies and is frequently enriched at super-enhancers. AZD1775-resistant cells undergo chromatin reorganization to establish alternate cis-acting elements that promote transcription of DNA repair and proliferation genes, circumventing treatment. We hypothesized that targeting CDK7-mediated transcriptional reprogramming could overcome AZD1775 resistance.Using the CDK7 inhibitor THZ1, we performed western blot analysis of DNA repair proteins and observed inhibition of ATM pathway activation, a key component of the DNA damage response. Proliferation assays in both parental and AZD1775-resistant cell lines demonstrated that combining AZD1775 with THZ1 significantly suppressed cell growth. These findings suggest that THZ1 may reverse adaptive chromatin reorganization, sensitizing resistant MB cells to AZD1775 and enhancing the overall therapeutic response.Future studies will investigate the potential of combining CDK7 inhibitors with other epigenetic modulators to further disrupt resistance mechanisms and improve treatment outcomes in aggressive MB subtypes, particularly Group 3 MB. This approach offers a promising avenue for overcoming therapeutic resistance and advancing precision medicine in medulloblastoma.

#7873 *In vivo* preclinical efficacy of a novel "payload-bearing" peptide LX-101 targeting IGF-1R in Ewing sarcoma.

Roberto Cardenas-Zuniga, Jiaqian Fan, Asmaa G. Ahmed, Marcus Thurm, Kien Ryan Cao, Clement Agyemang, Danh Truong, Joseph A. Ludwig

UT MD Anderson Cancer Center, Houston, TX

Ewing sarcoma (ES) is an extremely aggressive and highly metastatic bone cancer in children and young adults, ranked as the second most frequent bone tumor in pediatric patients. With a survival of ~80% for localized and regional tumors, which can drop down to ~40% for metastatic cases, standard treatment for ES usually includes radiotherapy, surgery, and chemotherapy based on the VDC/IE regimen. Alternative therapeutic approaches targeting critical pathways with recognized roles in tumorigenesis, such as IGF-1, PI3K, and mTOR, have also demonstrated remarkable clinical activity as single agents or in combinations for several cancer types. For this reason, it is imperative to confirm and generate preclinical evidence of anticancer activity in ES. Here, we tested the *in vitro* and *in vivo* efficacy of LX-101, a next-generation therapy targeting IGF-1R, which couples a proprietary IGF-1 variant to a cytotoxic MTX payload, as a single agent or in combination with alpelisib (a PI3K inhibitor) and temsirolimus (an mTOR inhibitor) in various ES models. We tested the *in vitro* activity of LX-101 on the proliferation and viability of A-673, ES-8, and TC-71 cell lines. Once anti-proliferative activity was confirmed, we evaluated the sensitivity of all three ES cell lines to the combination of LX-101 with alpelisib and temsirolimus, estimating synergistic effects on the viability of the ES cultures. To consolidate that the cytotoxic effect on ES is mediated by on-target impact, we examined the changes in the expression and activation of IGF-1 downstream effectors by western blot, which were clearly reduced after LX-101 exposure in all three cell lines when compared with non-exposed cells, confirming that LX-101 inhibits the activation of IGF-1R, and indicating the suppression of the IGF-1 pathway. Finally, we tested the in vivo activity using three different PDX Ewing sarcoma models, with and without alpelisib or temsirolimus to assess synergistic preclinical efficacy. The pharmacodynamic effects were evaluated using a custom tissue microarray (TMA) analysis, using sequential multiplex immunofluorescence of 40 proteins related to the IGF/PI3K/mTOR signaling pathway.Our results indicate that LX-101 exhibits potent single-agent activity in the preclinical setting as an anti-cancer agent for ES, and even stronger activity when combined with agents that inhibit PI3K or mTOR. Collectively, the preclinical efficacy demonstrated provides a strong rationale for advancing LX-101 into clinical trials for ES.

#7874 Dose-response efficacy of cell adhesion molecule 1 (CADM1)-GGFG-Exatecan vs CADM1-PEG3-VC-Exatecan in preclinical osteosarcoma models.

Zhongting Zhang[1], Caterina Longo[1], Wendong Zhang[1], Yifei Wang[2], Yanhua Yi[1], Zhaohui Xu[1], Xin Zhou[1], Adil Bahadir[1], Michael Roth[1], Jonathan Gill[1], Richard Gorlick[1]

[1]UT MD Anderson Cancer Center, Houston, TX,[2]Orthopaedic Oncology, UT MD Anderson Cancer Center, Houston, TX

Background: Osteosarcoma is the most common primary bone malignancy in children and young adults. Despite multimodal therapy, survival rates have remained unchanged since the 1980s. Antibody-drug conjugates (ADCs) targeting CADM1 show promise as targeted treatments. This study compares the dose-response effectiveness of two CADM1-targeted ADC formulations, CADM1-GGFG-Exatecan and CADM1-PEG3-VC-Exatecan, in preclinical osteosarcoma models. Both ADCs are conjugated with Exatecan, a potent topoisomerase I inhibitor, but differ in their linker structures (GGFG vs PEG3), which may affect payload release and tumor penetration.

Methods: We assessed the cytotoxicity of both ADCs in osteosarcoma cell lines (HOS, OS17, OS31) to determine IC_{50} values. Internalization studies compared uptake kinetics in the same lines. In vivo testing evaluated both ADCs in six patient-derived xenograft (PDX) osteosarcoma models (OS1, OS2, OS9, OS17, OS31, OS33) at doses of 3 mg/kg and 6 mg/kg. Human-IgG1-GGFG-Exatecan, Human-IgG1-PEG3-VC-Exatecan, and PBS served as isotype and vehicle controls. Tumor growth inhibition and event-free survival (EFS) were measured.

Results: CADM1-GGFG-Exatecan showed significantly greater anti-tumor activity than CADM1-PEG3-VC-Exatecan, with lower IC_{50} values and higher internalization in CADM1-expressing cells. Internalization of CADM1-GGFG-Exatecan reached a steady plateau by day 4, whereas CADM1-PEG3-VC-Exatecan showed minimal uptake. In vivo, both ADCs were well tolerated (≤10% body weight loss). CADM1-GGFG-Exatecan significantly prolonged EFS across all six PDX models ($P < 0.05$), inducing maintained complete responses (MCR) in OS1, OS31, and OS33, a partial response (PR) in OS2, and progressive disease (PD) in OS9 and OS17. In contrast, PEG3-VC-Exatecan and all controls resulted in PD in all models.

Conclusion: CADM1-GGFG-Exatecan demonstrates superior dose-response efficacy versus CADM1-PEG3-VC-Exatecan in both in vitro and in vivo osteosarcoma models. Its enhanced anti-tumor activity, likely driven by improved internalization and potency, supports further development in CADM1-expressing osteosarcoma, including optimization of pharmacokinetics and combination strategies.

#7875 Eflornithine and venetoclax combination therapy: Targeting senescence to induce apoptosis in neuroblastoma.

Tarlan Arjmandi, Jeremy Hengst, Muhammad Younis, Meenakshi Shukla, Mohammad Haque, Katherine McClain, Jonathan Lerch, Thussenthan Walter-Angelo, Giselle Saulnier Sholler

Penn State College of Medicine, Hershey, PA

High-risk neuroblastoma (HRNB) is difficult to cure due to relapses and limited therapeutic durability. Eflornithine, an inhibitor of ornithine decarboxylase, inhibits polyamine synthesis and is clinically effective in preventing HRNB recurrence. Eflornithine induces a stable senescent phenotype that suppresses proliferation. Eliminating these senescent HRNB cells is of therapeutic interest. Venetoclax, a selective Bcl-2 inhibitor approved for hematologic malignancies, has been identified as a potent senolytic that triggers apoptosis in senescent cells. We therefore hypothesized that venetoclax may induce apoptosis in eflornithine-induced senescent HRNB cells, thereby overcoming tumor persistence. HRNB cells (BE2c cell line) were sequentially treated with eflornithine for 4 days to induce senescence followed by the addition of venetoclax for 18 hours to induce apoptosis. Senescence was assessed by β-galactosidase staining and p21, p16, and p27 protein expression. Apoptosis and survival markers were analyzed by Western blotting to detect Mcl-1, BAG3, GLS1, cleaved Caspase-3, and cleaved PARP. Cytokine levels were measured by qPCR. Treatment of NB cells with eflornithine induced a robust senescence response, increasing β-galactosidase activity and expression of p21, p16, and p27 in a time-dependent manner. Venetoclax alone failed to induce apoptosis and instead upregulated the pro-survival protein Mcl-1 (5.5-fold), whereas pre-treatment with eflornithine both reduced basal Mcl-1 (0.5-fold) and prevented venetoclax-induced Mcl-1 elevation (0.03-fold in the combination). Consistent with eflornithine's effect on polyamine-dependent translation, BAG3, a chaperone that stabilizes Mcl-1, was downregulated, providing a mechanistic basis for Mcl-1 destabilization and enhanced venetoclax sensitivity. Eflornithine also decreased expression of GLS1, an enzyme linked to mitochondrial fitness and anti-apoptotic signaling. Sequential treatment of eflornithine followed by venetoclax triggered strong activation of apoptotic markers, increasing cleaved Caspase-3 (1.4-fold) and cleaved PARP (9-fold) compared to vehicle, confirming a synergistic shift from senescence to apoptosis. Cytokine analysis revealed selective remodeling of the SASP, with an increase in IL-1β (33-fold) and IL-6 (6-fold), and IFN-γ (>50-fold). Together, these findings establish a novel mechanistically informed combinatorial strategy in which polyamine depletion converts senescent tumor cells into apoptotically vulnerable targets, offering a promising therapeutic avenue for HRNB. Ongoing in vivo studies will determine the translational potential of eflornithine + venetoclax as a rational senescence-targeting regimen.

#7876 Melatonin protects against long-term doxorubicin-induced cardiotoxicity in a preclinical model of childhood cancer survivors.

Marisol Fernandez Ortiz, Logan Davis, Joseph Schell, Erik Marchant, Blake Rasmussen, David Gius, Gregory Aune

The University of Texas at San Antonio, San Antonio, TX

Cardiovascular disease is the leading cause of early mortality among childhood cancer survivors. Most of these patients receive anthracyclines, particularly doxorubicin (DOX), due to its high efficacy against solid tumors and hematological malignancies. However, DOX is associated with long-term cardiac toxicity, including delayed cardiac dysfunction and irreversible heart failure, making survivorship care a growing concern. A proposed mechanism of long-term doxorubicin-induced cardiotoxicity (DOXIC) is the accumulation of DOX in cardiomyocyte mitochondria, which increases free radical production, promotes oxidative stress, and progressively impairs cardiac function. We hypothesized that melatonin (aMT), a mitochondria-targeted antioxidant, could prevent DOXIC. Melatonin has demonstrated safety at high doses and can enhance chemotherapy efficacy. This study evaluated the cardioprotective effects of aMT in a mouse model mimicking childhood cancer survivorship. Wild-type mice received DOX from 3 to 5 weeks of age and were assessed at 12 months. aMT was administered during DOX treatment and continued for one month afterward. Experimental groups included: (1) Vehicle, (2) DOX, and (3) DOX + aMT. Cardiac function, mitochondrial structure and function, and gene expression were evaluated using echocardiography, TEM, high-resolution respirometry and mRNA sequencing. Gene Set Enrichment Analysis (GSEA) and Ingenuity Pathway Analysis (IPA) were used for transcriptomic analysis. Melatonin preserved cardiac function both during and long after DOX exposure and protected mitochondrial ultrastructure and function. GSEA showed that aMT upregulated genes related to cardiac development, contractility, action potential, sarcomere structure, and energy metabolism. IPA further revealed that aMT suppressed pathways involved in heart disease, among them cardiomyopathy, myocardial dysfunction and hypertrophy of left ventricle, apoptosis and organismal death, while enhancing those linked to cardiac contractility, cell viability and survival, microtubule organization, and DNA repair. These findings provide the first evidence that melatonin can prevent long-term DOXIC, supporting its potential as a cardioprotective agent for childhood cancer survivors.

#7877 Combination of AVA-NP-695 and DDRi demonstrates strong synergy resulting in potent anti-tumor activity in rare pediatric cancers.

Aditya Kulkarni[1], Borja Ruiz-Fernandez de Cordoba[2], Avijit Goswami[3], Sandeep Goyal[3], Kawaljit Singh[3], Princy Khurana[3], Alejandro Sweet-Cordero[4]

[1]Avammune Therapeutics, Levitown, PA,[2]University of California San Francisco, San Francisco, CA,[3]Avammune Lifesciences, Bangalore, India,[4]UCSF - University of California San Francisco, San Francisco, CA

Background: Ectonucleotide pyrophosphatase/phosphodiesterase 1 (ENPP1) overexpression is linked to poor prognosis in various cancers, including astrocyte tumors, triple-negative breast cancer (TNBC), Ewing sarcoma (EWS), and osteosarcoma (OS). Transcriptomics and proteomic analyses highlight the highest ENPP1 expression in EWS, OS, and breast cancer. Importantly, ENPP1 is increasingly implicated in driving lung and bone metastasis, a major clinical challenge for cancers like TNBC, Ewing sarcoma, and osteosarcoma. Overall, ENPP1 is a clinically relevant and druggable target for several hard-to-treat ICB-refractory cancers. Therefore, the therapeutic of ENPP1 inhibition was explored as monotherapy as well as in combination with DDR inhibitors like Ceralasertib and Olaparib.
Methods: The potency of AVA-NP-695, a small-molecule ENPP1 inhibitor, was validated through enzymatic assays using different substrates. Pharmacokinetic profiles were evaluated in mice, rats, and beagle dogs. ENPP1 expression and cGAMP export were evaluated after dsDNA stimulation, and ENPP1 activity was measured using a biochemical assay in OS cell lines, including OSPDX-cell lines. Mono and combination therapy effects of AVA-NP-695 and Olaparib/Ceralasertib were evaluated in OS and EWS models.
Results: AVA-NP-695 demonstrated potent and selective ENPP1 inhibition with no adverse effects in repeat-dose and dose-escalation toxicity studies. In OS models, AVA-NP-695 induced tumor regression in both paratibial (orthotopic) and metastatic (lung) contexts. Interestingly, targeted pharmacological screen revealed synthetic lethality between AVA-NP-695 and both Olaparib/Ceralasertib in osteosarcoma cell lines. In two patient-derived xenograft (PDX) OS models (OS384 and OS526), as well as in a EWS (A673) CDX model, AVA-NP-695 administered as a monotherapy showed similar efficacy as olaparib alone, and the combination of the two agents combination resulted in significant tumour regression. In GS383 intrapulmonary model, it achieved strong tumor shrinkage in lung nodules on post-treatment scans and prolonged progression-free survival. Similar effects were observed in combination with Ceralasertib in case of Osteosarcoma syngeneic model.
Conclusions: These findings underscore the therapeutic potential of AVA-NP-695 across hard-to-treat ICB-refractory pediatric cancers such as OS and EWS. AVA-NP-695 exploits ENPP1 inhibition to exert a strong anti-tumor response and obliviates metastasis. Additionally, AVA-NP-695 also demonstrates strong synergy with DDR inhibitors like Olaparib and Ceralasertib in both these cancers. Overall, these findings demonstrate that AVA-NP-695 has strong potential as a therapeutic modality in OS and EWS as a monotherapy and combination with DDR inhibitors.

#7878 Disrupting the lipid-ETV6 axis: A therapeutic vulnerability in Ewing sarcoma.

Yuan Gao, Hang Zhao

Pharmacology, Case Western Reserve University School of Medicine, Cleveland, OH

Ewing sarcoma is a transcriptionally driven pediatric cancer with few targetable dependencies. Through a gain-of-function metabolic screen, we discovered that Ewing sarcoma cells exhibit lineage-specific hypersensitivity to activation of glycerophospholipid metabolism. Mechanistic studies revealed that phosphatidic acid (PA), a central lipid signaling molecule, directly binds to the transcriptional repressor ETV6, an essential and selective dependency in Ewing sarcoma. PA binding disrupts ETV6 oligomerization and chromatin occupancy, leading to de-repression of its target genes. We further mapped this interaction to a unique five-amino acid motif in the ETV6 ETS domain and generated lipid-insensitive mutants that retain DNA binding but resist PA-induced inactivation. CRISPR activation of endogenous PA-producing enzymes phenocopied the effects of exogenous PA, supporting a direct role for lipid signaling in modulating ETV6 function and tumor cell viability. These findings define a previously unrecognized lipid-sensitive transcriptional state in Ewing sarcoma and reveal the ETV6-PA axis as a novel therapeutic target.

#7879 Opaganib in combination with oxaliplatin and doxorubicin as a novel salvage therapy for relapsed/refractory high-risk neuroblastoma.

Jeremy Hengst[1], Mohammad Haque[1], Muhammad Younis[1], Thussenthan Walter Angelo[1], Anna Bourne[1], Katherine McClain[1], Meenakshi Shukla[1], Jonathan Lerch[1], Tarlan Arjmandi[1], Eric Cochran[1], Lynn Maines[2], Charles D. Smith[2], Vladimir S. Spiegelman[1], Jacqueline M. Kraveka[3], Giselle L. Saulnier Sholler[1]

[1]Penn State College of Medicine, Hershey, PA,[2]Apogee Biotechnology, Hershey, PA,[3]Medical University of South Carolina, Charleston, SC

The combination of oxaliplatin and doxorubicin (OXDOX) has shown efficacy in heavily pre-treated neuroblastoma (NB) patients. Nevertheless, addition of agents that enhance response to OXDOX may improve outcomes. DOX has been shown to up-regulate the expression of the Sphingosine kinases (SphK1 and SphK2) and enhance the production of pro-survival sphingosine-1-phosphate (S1P) at the expense of pro-apoptotic ceramide (Cer) which, in turn, mediates resistance to DOX. Elsewhere, studies have shown that the SphKs regulate the sensitivity of cells to OX. Inhibition of SphK activity decreases S1P production and may reverse OXDOX resistance. The purpose of this study was to determine whether the addition of the SphK2 inhibitor, opaganib, could improve the efficacy of OXDOX salvage therapy for high risk relapsed/refractory neuroblastoma (HRNB) patients. An immunocompetent mouse model of HRNB was utilized with 9464-D M2 cells grown subcutaneously in syngeneic C57BL/6 mice, to evaluate the efficacy of the combined treatment relative to OXDOX and opaganib alone cohorts. Opaganib has been shown to reduce c-Myc and n-Myc expression. Western blot analysis evaluated the expression of n-Myc, Mcl-1, and markers of apoptosis including cleaved Caspase 3 and cleaved PARP in response to single agent and combination treatments. The reduction of MYCN in MYCN amplified NB patients was further explored to examine the ability of opaganib to directly target engage n-Myc using the Cellular Thermal Shift (CETSA) assay and Isothermal Dose-Response Fingerprint (ITDRF) assays. In the immunocompetent 9464-D mouse model, the combination of agents significantly reduced tumor size relative to opaganib alone and OXDOX alone cohorts ($p<0.001$). IHC staining demonstrated that the combination reduced proliferation (Ki-67), enhanced apoptosis (Caspase 3) and, enhanced macrophage infiltration (CD68) into the tumor microenvironment. Western blot analysis revealed that opaganib reduced n-Myc and Mcl-1 expression (> 5-fold). CETSA experiments confirmed direct target engagement of n-Myc by opaganib in live, whole cell assays. ITDRF assays determined that opaganib binds to n-Myc with micromolar affinity, consistent with its IC50 for cell viability. Time course assays demonstrated that opaganib rapidly bound n-Myc within 30 minutes of exposure. Together, these studies indicate that opaganib enhances the therapeutic efficacy of the OXDOX combination by both altering sphingolipid metabolic profiles to enhance the production of pro-apoptotic ceramide and by directly binding to and destabilizing n-Myc, a key oncogenic driver of high-risk NB. Opaganib has been extensively tested in adult COVID patient populations with a favorable toxicity profile. Clinical testing of this novel three-drug combination in NB patients is under evaluation by the Beat Childhood Cancer Research Consortium.

#7881 Hijacking the BRD4-NUT fusion oncoprotein to activate programmed cell death.

Kelly Wang[1], Yanlan Wang[1], Tian Qiu[2], Brendan G. Dwyer[2], Daryl Griffin[3], Geoffrey I. Shapiro[3], Chris A. French[4], Nathanael S. Gray[2], Gerald R. Crabtree[1]

[1]Dept. of Pathology and Developmental Biology, Stanford University, Stanford, CA,[2]Dept. of Chemical and Systems Biology, Stanford University, Stanford, CA,[3]Dept. of Medical Oncology and Medicine, Dana-Farber Cancer Institute, Brigham and Women's Hospital and Harvard Medical School, Boston, MA,[4]Professor, Dept. of Pathology, Brigham and Women's Hospital and Harvard Medical School, Boston, MA

Fusion oncogenes account for about 10-20% of all cancer drivers and generally result from in-frame recombination with specific partners. Cancers driven by fusion oncogenes often occur in young people whose genomes are relatively free of other mutations, providing a singular reliance on the fusion and its underlying mechanisms. Despite this focus, fusion oncogenes — particularly those that arise from transcription factors — have been difficult to target therapeutically. We demonstrate in this study that the fusion oncoprotein BRD4-NUT can be used to specifically activate programmed cell death in an aggressive form of squamous cancer, NUT carcinoma (NC). NC is caused by a translocation of the *NUTM1* gene downstream of the *BRD4* gene. Transcription of the fusion gene is therefore controlled by the *BRD4* regulatory region, leading to high-level expression of the fusion oncoprotein. The NUT protein is normally restricted to the testes, where it is essential for histone hyperacetylation, histone removal and replacement by protamines. NC currently has a mean survival of 6-9 months and no approved treatments. We reasoned that the oncogenic program of BRD4-NUT could be reprogrammed to activate a synthetic death circuit. To selectively inhibit NC, we developed bifunctional molecules that target the BRD4-NUT fusion, BRD4 and PARP. We call the new class of molecules DD-CIPs for DNA Damage-Chemical Inducers of Proximity. The most potent member of this new class (TWQ-184) kills NC cell lines (10-15, SW and 14169) at concentrations between 0.74 nM and 6 nM. TWQ-184 forms a ternary complex with BRD4-NUT and PARP, resulting in cell death. P300 inhibitors partially rescue NC cells from TWQ-184-induced apoptosis, suggesting that transcription at PARP-bound DNA breaks driven by BRD4-NUT is required to initiate cell death. TWQ-184 induces γH2AX deposition and ATM activation within 24 hours, suggesting that PARP-bound single-strand breaks are converted to lethal double-strand breaks in the cancer cells. Exposure to TWQ-184 for one hour gives near-complete NC death at 72 hours, suggesting that intermittent dosing might be effective. TWQ-184 additionally exhibits high specificity for the malignant cells, evidenced by the substantial therapeutic windows between NC cell lines and healthy human lymphocytes and fibroblasts. Based on our current findings, the compound's high efficacy in the cancer cells and low toxicity in healthy cells offer a promising approach to treat NC. This strategy for hijacking a fusion oncoprotein to activate transcriptionally coupled DNA damage-mediated cell death could be applicable to other transcriptional fusion oncogenes.

#7883 Surface CADM1 (Cell Adhesion Molecule 1) abundance predicts payload delivery and in-vitro efficacy of CADM1-GGFG-Exatecan ADC in osteosarcoma, aiding optimal candidate selection.

Caterina Longo[1], Zhongting Zhang[2], Wendong Zhang[2], Yifei Wang[2], Adil Bahadir[2], Yi Yanhua[2], Zhaohui Xu[2], Xin Zhou[1], Michael Roth[3], Jonathan Gill[2], Richard Gorlick[2]

[1]The University of Texas MD Anderson Cancer Center, Houston, TX,[2]UT MD Anderson Cancer Center, Houston, TX,[3]The University of Texas MD Anderson Cancer Center

Background: ADC development in osteosarcoma has been hindered by the absence of effective, targetable surface antigens. We previously identified CADM1, a cell-surface adhesion molecule, as a promising therapeutic target and generated three CADM1-directed ADCs (CADM1-Tesirine, CADM1-PEG-Exatecan, and CADM1-GGFG-Exatecan) with distinct linker-payload combinations. To select the optimal candidate for clinical translation, we evaluated target engagement and target-dependent cytotoxicity across multiple in vitro models.
Methods: Confocal microscopy was used to visualize ADC trafficking through cellular compartments and its lysosomal localization over time. CADM1 knockout (KO) osteosarcoma cell lines (SaOS2 and OS31) were generated using CRISPR/Cas9 and validated by flow cytometry, Western blotting, and mass spectrometry (MS). Cell-surface CADM1 levels were quantified by MS and correlated with ADC cytotoxicity (IC_{50} values) measured by real-time live-cell imaging on the IncuCyte platform. Spearman correlation analyses across nine osteosarcoma cell lines assessed the relationship between CADM1 expression and ADC potency for all three constructs.
Results: Confocal time-course imaging showed ADC trafficking from the plasma membrane (30 min) to lysosomes (6 h) and cytoplasmic dispersion (24 h), absent in CADM1-KO cells, confirming target-mediated internalization and lysosomal processing. CRISPR/Cas9-mediated knockout of CADM1 was achieved in SaOS2 and OS31 osteosarcoma cell lines. Loss of CADM1 expression was confirmed by flow cytometry, Western blotting, and mass spectrometry, showing complete depletion of surface protein. CADM1 loss markedly reduced ADC cytotoxicity (IC_{50} = 77.41 nM in SaOS2 CADM1-KO vs 0.014 nM in SaOS2), confirming on-target activity. Across nine osteosarcoma models, CADM1 surface abundance strongly correlated with drug potency, most notably for CADM1-GGFG-Exatecan (Spearman ρ = -0.98, p = 0.001). These data identify CADM1 as a determinant of ADC efficacy and highlight the contribution of other ADC components.
Conclusions: These data demonstrate potent, target-dependent activity of the generated CADM1-targeted ADCs, validating CADM1 as a rational therapeutic target. Among them, CADM1-GGFG-Exatecan showed the strongest correlation between IC_{50} and target expression, supporting selective cytotoxic delivery. In vivo efficacy and toxicology studies are ongoing to finalize candidate selection.

#7884 Germline genetic testing trends in pediatric cancer patients: A SEER registry analysis.

Claire Johns[1], Minxuan Huang[1], Rebecca Hodan[2], Molly McGuinness[2], Allison W. Kurian[2], Raya Saab[1]

[1]Stanford Children's Health, Palo Alto, CA,[2]Stanford University, Stanford, CA

Germline pathogenic variants (PVs) are reported to occur in 8-16% of pediatric cancer patients, and have important implications for potential treatment modifications, cancer surveillance, and family cascade testing. Data are lacking on the utilization and results of germline testing in pediatric oncology patients. We utilized statewide SEER registry data from California and Georgia to identify patients aged ≤ 19 years diagnosed with cancer between January 1, 2013, and December 31, 2019. Linked germline genetic tests pooled from four laboratories (Ambry Genetics, Bioreference/GeneDx, Labcorp/Invitae, and Myriad Genetics) were reviewed. Results were evaluated by cancer type, demographic information, and year of diagnosis using descriptive and multivariable logistic regression analyses. PV prevalence was assessed by affected gene. Among 16,613 analyzed patients, 344 (2%) underwent germline testing. Testing rate was highest in patients with carcinomas (4.6%) and lowest in those with hematologic malignancies (0.3%). Testing rates increased from 0.7% in 2013 to 4.0% in 2019. Patients in the fifth quintile (highest) socioeconomic level had the highest testing rate (2.9%) (OR 1.58, 95% confidence interval 1.07-2.31, p=0.020 vs. the first quintile (lowest)). Testing was higher in non-Hispanic white and Asian patients compared to other races, however, this was not statistically significant in multivariable analysis. Of the patients who underwent testing, 75/344 (22%) had a germline PV. *TP53* was the most frequently tested gene. *RB1* and *TP53* had the highest yield of PVs amongst patients tested (12/151 and 12/241 respectively). To our knowledge, this is the first population level report of germline genetic testing in pediatric cancer patients. While the rate of germline testing increased significantly from 2013-2019, the rate in 2019 rate remained low at 4%. Higher rates of testing were seen in solid malignancies, which coincides with previous reports of higher germline PV prevalence in solid tumor patients. Germline testing utilization varied by socioeconomic quintile but not by race or ethnicity. These results establish a population-level baseline for germline testing rate and results in pediatric cancer patients; identify testing gaps and disparities; and demonstrate an urgent need for education about germline testing for patients and their families.

#7885 Defining genome-wide cfDNA methylation landscapes in pediatric and adolescent and young adult (AYA) bone and soft-tissue sarcomas.

Lilli J. Greiner, Roman O. Kowalchuk, Jeff Szymanski, Pradeep S. Chauhan, Adam Amundson, Peter J. Schoettler, Wendy Allen-Rhoades, Stephanie F. Polites, Peter S. Rose, Kelly Bailey, Linda McAllister-Lucas, Anita Mahajan, Nadia Laack, Aadel Chaudhuri

Mayo Clinic Hospital-Rochester, Rochester, MN

Background: Pediatric and AYA sarcomas are rare, biologically heterogeneous tumors with limited noninvasive biomarkers to guide diagnosis, personalized treatment, and disease monitoring. Standard-of-care evaluation relies on invasive biopsies that carry procedural risks and imaging modalities with limited sensitivity for detecting minimal residual disease and distinguishing tumor types. Cell-free DNA (cfDNA) methylation profiling offers a minimally invasive alternative capable of capturing tumor-derived epigenomic alterations and has consistently shown strong clinical utility in adult malignancies. However, genome-wide cfDNA methylation patterns across diverse pediatric and AYA sarcoma subtypes remain poorly defined.
Methods: Plasma was collected from 93 pediatric and AYA patients (pediatric <18 years; AYA 15-39 years) representing 27 Ewing sarcoma, 17 rhabdomyosarcoma, 11 liposarcoma, 10 chordoma, 8 synovial sarcoma, 7 chondrosarcoma, 6 osteosarcoma, and 6 fibrosarcoma cases, plus 19 matched healthy donors. cfDNA was isolated from 1 mL plasma, quantified by Qubit, and assessed by Bioanalyzer. Libraries were prepared using the NEBNext EM-seq v2 workflow with PCR cycles scaled to cfDNA input amount. Genome-wide sequencing (15× target depth) was followed by alignment, deduplication, and methylation calling. MultiQC was used to assess depth, duplication rate, conversion efficiency, and CpG coverage. Global methylation summaries were computed, and methylKit was used to generate per-CpG and 1-kb tiling matrices and initiate differential methylation analyses.
Results: Ewing sarcoma patients had significantly higher plasma cfDNA concentrations than age- and sex-matched healthy donors (24.4 vs 4.6 ng/mL, $p < 0.0001$), whereas cfDNA levels for other sarcoma subtypes overlapped with the healthy cohort. Low or undetectable cfDNA concentrations by Qubit were far more common among non-Ewing sarcoma samples (23 of 66) than Ewing sarcoma (1 of 27). All samples achieved sufficient CpG coverage for genome-wide methylation modeling. Global methylation summaries revealed no significant differences in mean β-values across sarcoma subtypes or versus healthy donors. An independent analysis of the Ewing subset identified 299 significant differentially methylated regions (DMRs), supporting the detectability of disease-specific methylation changes.
Conclusions: These results demonstrate the feasibility of high-quality cfDNA methylome profiling across a large and diverse pediatric and AYA sarcoma cohort, including in plasma samples with cfDNA concentrations below the limit of detection. While global methylation levels appear broadly similar across subtypes, proof-of-concept DMR analysis in Ewing sarcoma suggests that subtype-specific epigenomic signatures could enable future noninvasive diagnostic tools for pediatric and AYA sarcomas.

#7886 Therapy-related clonal hematopoiesis in pediatric cancer survivors.

Michael R. Kessler[1], Yash Pershad[2], Robert W. Corty[3], Eric T. Shinohara[1], Debra Friedman[4], Alexander G. Bick[2], Ben H. Park[5], Leo Y. Luo[1]

[1]Department of Radiation Oncology, Vanderbilt University Medical Center, Nashville, TN,[2]Division of Genetic Medicine, Department of Medicine, Vanderbilt University Medical Center, Nashville, TN,[3]Division of Rheumatology and Immunology, Department of Medicine, Vanderbilt University Medical Center, Nashville, TN,[4]Division of Pediatric Hematology and Oncology, Department of Pediatrics, Vanderbilt University Medical Center, Nashville, TN,[5]Division of Hematology and Oncology, Department of Medicine, Vanderbilt University Medical Center, Nashville, TN

Background: Clonal hematopoiesis of indeterminate potential (CHIP) refers to clonal expansion of hematopoietic stem cells due to somatic mutations and is associated with heightened risk of myeloid neoplasms and cardiovascular diseases. Genotoxic therapies such as chemotherapy and radiation therapy are well-recognized contributors to CHIP in adult cancer population. However, CHIP prevalence, mutational patterns, and treatment associations in pediatric populations remain poorly characterized.

Methods: We conducted a retrospective analysis of pediatric patients (age ≤ 18) diagnosed with cancer with blood samples collected after cancer therapy. CHIP was defined as the presence of a pathogenic somatic mutation in an accepted driver gene with variant allele frequency (VAF) ≥2%. CHIP prevalence was estimated overall and stratified by histology and therapeutic exposure. Logistic regression with Firth correction and exposure adjustment was used for multivariable analyses. *TP53* variants with known Li-Fraumeni syndrome association and VAF >40% were considered germline mutations and excluded from analyses.

Results: CHIP mutations were identified in 23 of 1,052 (2.2%) patients in this cohort. Mutations occurred most frequently in the *TET2* (26%), *DNMT3A* (22%), and *KRAS* (13%) genes. CHIP prevalence was numerically higher among patients who received chemotherapy (3.3% vs. 1.4%, p=0.055). Multivariable analysis showed a modest female predominance (OR 0.45, p=0.04) and a trend toward higher CHIP risk with chemotherapy (OR 1.9, p=0.16). Among drug classes, antimetabolite therapy showed the highest CHIP prevalence (OR 3.46, p = 0.048), driven by methotrexate exposure (OR 21.5, p = 0.001). No correlations were found with age, histology, or radiation.

Conclusion: We identified a low overall prevalence of CHIP in pediatric cancer patients and an association with antimetabolite therapy. Further studies are needed to define the long-term clinical implications of clonal hematopoiesis in pediatric cancer survivors.

Baseline characteristics by CHIP status

Characteristic			Overall (n = 1052)	No CHIP mutation (n = 1029)	CHIP mutation (n = 23)	p-value
Age (mean ± SD)			11.5 ± 7.4	11.6 ± 7.4	9.3 ± 5.7	**0.083**
Gender						**0.091**
	Male		516 (49.0%)	509 (49.5%)	7 (30.4%)	
	Female		536 (51.0%)	520 (50.5%)	16 (69.6%)	
Cancer type						**0.5**
	Lymphoid leukemias		225 (21.4%)	216 (21.0%)	9 (39.1%)	
	Sarcoma		179 (17.0%)	177 (17.2%)	2 (8.7%)	
	Glioma		136 (12.9%)	135 (13.1%)	1 (4.3%)	
	Neuroblastoma		72 (6.8%)	71 (6.9%)	1 (4.3%)	
	Renal/Hepatic tumors		62 (5.9%)	61 (5.9%)	1 (4.3%)	
	Hodgkin lymphoma		49 (4.7%)	48 (4.7%)	1 (4.3%)	
	Benign tumor		46 (4.4%)	45 (4.4%)	1 (4.3%)	
	Medulloblastoma / Embryonal tumors		44 (4.2%)	43 (4.2%)	1 (4.3%)	
	Non-Hodgkin lymphoma		43 (4.1%)	42 (4.1%)	1 (4.3%)	
	Other CNS		36 (3.4%)	36 (3.5%)	0 (0.0%)	
	Germ cell tumors		35 (3.3%)	33 (3.2%)	2 (8.7%)	
	Carcinoma NOS		27 (2.6%)	26 (2.5%)	1 (4.3%)	
	Endocrine tumors		25 (2.4%)	25 (2.4%)	0 (0.0%)	
	Myeloid leukemias		22 (2.1%)	22 (2.1%)	0 (0.0%)	
	Ependymoma		20 (1.9%)	20 (1.9%)	0 (0.0%)	
	Retinoblastoma		17 (1.6%)	16 (1.6%)	1 (4.3%)	
	Other tumor		14 (1.3%)	13 (1.3%)	1 (4.3%)	
Chemotherapy						**0.055**
	Yes		430 (40.9%)	416 (40.4%)	14 (60.9%)	
	No		622 (59.1%)	613 (59.6%)	9 (39.1%)	
Chemotherapy type						**0.3**
	Antimitotic Agent		153 (14.5%)	149 (14.5%)	4 (17.4%)	
	Antimetabolite		110 (10.5%)	103 (10.0%)	7 (30.4%)	
		Methotrexate	13 (1.2%)	10 (1.0%)	3 (13.0%)	
	Alkylating Agent		84 (8.0%)	81 (7.9%)	3 (13.0%)	
	Antitumor Antibiotic		55 (5.2%)	55 (5.3%)	0 (0.0%)	
	Plant Alkaloid		26 (2.5%)	26 (2.5%)	0 (0.0%)	
	Miscellaneous Agent		1 (0.1%)	1 (0.1%)	0 (0.0%)	
	Topoisomerase I Inhibitor		1 (0.1%)	1 (0.1%)	0 (0.0%)	
Immunotherapy						**>0.9**
	Yes		6 (0.6%)	6 (0.6%)	0 (0.0%)	
	No		1046 (99.4%)	1023 (97.2%)	23 (100.0%)	
External beam RT						**>0.9**
	Yes		119 (11.3%)	117 (11.4%)	2 (8.7%)	
	No		933 (88.7%)	912 (88.6%)	21 (91.3%)	
Radiopharmaceuticals						**>0.9**
	Yes		36 (3.4%)	36 (3.5%)	0 (0.0%)	
	No		1016 (96.6%)	993 (96.5%)	23 (100.0%)	

#7887 Associations between polygenic risk scores for immune dysregulation and Hodgkin lymphoma in childhood cancer survivors.

Ji Yun Tark[1], Sharon M. Castellino[2], Philip J. Lupo[2], Austin L. Brown[3]

[1]Department of Medicine, Baylor College of Medicine, Houston, TX,[2]Department of Pediatrics, Emory University School of Medicine, Atlanta, GA,[3]Department of Pediatrics, Baylor College of Medicine, Houston, TX

Background: Hodgkin lymphoma (HL) is the most common malignancy diagnosed in adolescents aged 15-19 years. Epidemiologic evidence suggests a link between HL incidence and immune dysregulation, suggesting that genetic variability in immune function may contribute to disease susceptibility. However, the extent of shared genetic overlap between immunologic and oncologic phenotypes has not been fully elucidated. To address this gap, we evaluated associations between HL and polygenic risk scores (PRS) for various immune-related conditions previously implicated in HL risk, to determine whether specific immune predispositions are enriched among cases of HL compared with other non-hematologic malignancies.

Methods: We used the St. Jude Survivorship Portal, which aggregates data on ~8000 childhood cancer survivors from the St. Jude Lifetime (SJLIFE) and the Childhood Cancer Survivor Study (CCSS) cohorts. The portal integrates 1,600 phenotypic variables with ~400 million genetic variants and includes PRS available derived from the PGS Catalog. We summarized demographic characteristics using the Portal's summary tools, then applied logistic regression to estimate odds ratios (OR) and 95% confidence intervals (CIs) for HL versus other non-hematologic malignancies per one-unit increase in PRS for five immune-related traits (dermatitis, asthma, Crohn's disease, rheumatoid arthritis, and systemic lupus erythematosus), adjusting for age at cancer diagnosis and sex. For each trait, we selected one PRS from the Portal's precomputed set, prioritizing those with larger discovery samples, broader variant coverage, and ancestry diversity. Analyses were conducted in the combined cohort (3,322 HL and 14,167 other survivors).

Results: Among 17,489 survivors of HL and other non-hematologic malignancies, the median age at cancer diagnosis was 7.7 years (IQR 2.8-13.9); 52% were male, and 86% were White, 9% Black, and 5% other. In adjusted logistic regression models, a higher dermatitis PRS was significantly associated with higher odds of HL compared with other non-hematologic malignancies (OR 5.3, 95% CI 1.8-15.4, p=0.002). No significant associations were observed for PRS associated with asthma (OR 1.1, 95% CI 0.7-1.9, p=0.656), Crohn's disease (OR 0.9, 95% CI 0.6-1.3, p=0.604), rheumatoid arthritis (OR 1.0, 95% CI 0.9-1.0, p=0.223), or systemic lupus erythematosus (OR 0.9, 95% CI 0.8-1.1, p=0.455) and HL relative to non-hematologic malignancies.

Conclusion: Using the St. Jude Survivorship Portal, we observed that survivors of HL tend to harbor a higher dermatitis PRS compared with survivors of non-hematologic malignancies. Although these findings are exploratory and should be interpreted with caution, they highlight a potential role for immune-related genetic variation in HL etiology and demonstrate a need for further investigation and independent validation.

#7888 Financial hardships and chronic medical conditions in adolescent and young adult cancer survivors.

Diego Del Toro Rivera[1], Qian Li[1], Anne Kirchhoff[2], Salene M. Jones[3], Candice A. M. Sauder[1], Ann M. Brunson[1], Charles P. Quensenberry[4], Lisa M. Moy[4], Renata Abrahao[1], Ted Wun[1], Hazel B. Nichols[5], Lawrence H. Kushi[4], Jessica Chubak[6], Erin E. Hahn[7], **Theresa H. M. Keegan**[1]

[1]UC Davis Comprehensive Cancer Center, Sacramento, CA,[2]University of Utah, Salt Lake City, UT,[3]Fred Hutch Cancer Center, Seattle, WA,[4]Kaiser Permanente Northern California, Oakland, CA,[5]University of North Carolina at Chapel Hill, Chapel Hill, NC,[6]Kaiser Permanente Washington Health Research Institute, Seattle, WA,[7]Kaiser Permanente Southern California, Pasadena, CA

Adolescents and young adult (AYA) cancer survivors face a higher risk of chronic medical conditions and are more likely to delay or forgo health care due to costs compared to same-age individuals without cancer. They also experience greater financial hardship than older adult survivors. However, gaps remain in our understanding of the financial hardships associated with cancer or the lasting health effects of treatment in AYA cancer survivors. In the Valuing Opinions and Insights from Cancer Experiences (VOICE) Study, participants diagnosed during 2016-2022 with 10 common AYA cancers between ages 15-39 years in California completed a survey in 2023-2024. Financial hardship was measured by financial debt due to cancer and 8 questions on the impact of medical expenses in the past year, categorized into trouble meeting needs (e.g., put off major purchases, unable to pay for basic necessities), asset depletion (e.g., took money from savings/retirement, credit card debt) and major financial changes (e.g., needed mortgage against home, thought about bankruptcy). In addition, we assessed whether AYAs were diagnosed after cancer diagnosis with 10 chronic medical conditions (asthma/lung problems, blood clots, bladder dysfunction, diabetes, heart conditions, hypertension, kidney dysfunction, liver problems, osteoporosis, thyroid problems). We examined the association of each financial hardship with 1 or ≥2 (vs 0) medical conditions using multinomial logistic regression, adjusting for age, sex, race/ethnicity, current health insurance and cancer type. Among 3,685 AYAs, most were age 30-39 years at diagnosis (70.6%), of non-Hispanic (NH) White (34.6%) or Hispanic (32.4%) race or ethnicity and had employer-sponsored insurance (66.6%). Breast (25.3%), thyroid (22.4%) melanoma (10.0%), and testicular (10.3%) were the most common cancers. Overall, 18.9% and 7.8% of AYAs developed 1 or ≥2 of the 10 chronic medical conditions, respectively. Nearly one-fifth (18.8%) of AYAs experienced financial debt since their cancer diagnosis. In the past year, approximately one-third of AYAs experienced trouble meeting needs (27.5%) and asset depletion (31.7%), while 6.1% experienced major financial changes. In multivariable models, AYAs with ≥2 conditions were more likely to have financial debt (odds ratio (OR)=1.99, 95% confidence interval (CI) 1.50-2.64 vs. no medical conditions), trouble meeting needs (OR=2.05, CI 1.58-2.67), asset depletion (OR=1.83, CI 1.42-2.37) and major financial changes (OR=2.24, CI 1.49-3.36). Financial hardship impacts one-third of AYA cancer survivors, and those with chronic medical conditions have a substantially greater likelihood of experiencing financial hardship. Our findings highlight the long-term economic impact of cancer in this population and the need to evaluate the effectiveness of targeted interventions, such as financial navigation, to address financial burden.

#7889 Integrating genetic predictors into breast cancer risk stratification among female survivors of childhood cancer.

Aparna Srinivasan[1], Jian Wang[2], Gavriel Matt[2], Lauren J. Mills[1], Yadav Sapkota[2], Zhaoming Wang[3], Tianzhong Yang[1], Joseph P. Neglia[1], Lucie M. Turcotte[1], Melissa M. Hudson[2], Kirsten K. Ness[2], Gregory T. Armstrong[2], Jinghui Zhang[2], Leslie L. Robison[2], Xin Zhou[2], Yutaka Yasui[2], Cindy Im[1]

[1]Pediatrics, University of Minnesota, Minneapolis, MN,[2]St. Jude Children's Research Hospital, Memphis, TN,[3]University of South Florida, Tempa, FL

Background: Childhood cancer survivors are at high risk for developing breast cancer (BC). Existing BC risk stratification tools primarily consider childhood cancer treatment risk factors, but do not assess genetic predictors. The St. Jude Survivorship Portal (https://survivorship.stjude.cloud) is a new open-access online data resource that supports deeper investigations of late effects genetic susceptibility. In this study, we evaluated data available in this portal, specifically common and rare genetic variation, for their relative contributions to subsequent BC risk stratification.
Methods: Five-year female survivors from 2 cohort studies (Childhood Cancer Survivor Study; St. Jude Lifetime Cohort) were analyzed. Common variants were assessed using 99 published general population sporadic BC polygenic risk scores (PRSs), computed using whole-genome sequencing (WGS) or imputed array-based genotype data. Hazard ratios (HRs) were estimated with Cox regression using age as the time scale and adjusted for genetic ancestry, batch, and chest radiotherapy (RT) and anthracycline doses. PRS-RT interactions assessed whether PRSs modified risks conferred by chest RT dose. Rare pathogenic/likely pathogenic (P/LP) variants in BC susceptibility genes examined in general population sequencing studies (BRCA1, BRCA2, CHEK2, PALB2, RAD51C, RAD51D, TP53, ATM) were evaluated.
Results: In this multi-ancestry cohort (N=5388; 88% European, 8% African, 4% Asian ancestry), the median attained age was 38y (IQR 30-46) and 63% were treated with chest RT. 319 survivors developed BC. Overall, 90.1% of sporadic BC PRSs were nominally replicated (P<0.05). No PRS modified chest RT-related BC risk. Notably, the most studied BC PRS (313 variants; evaluated in >70 studies) did not show the strongest risk association in survivors (HR per SD=1.17, 95% CI=1.04-1.31). Instead, PRSs with more variants genome-wide demonstrated effect sizes similar to some treatment predictors (e.g., “best” PRS: ~6.4 million variants, HR per SD=1.71, 95% CI=1.43-2.05; P=4.2x10-9). BC PRSs with the strongest associations (top 25%) were 4.7-times more likely to include variants mapped to multiple (2) DNA repair pathways (P=0.018). Among the 3292 survivors with WGS, 61 (1.8%) carried rare P/LP variants in BC risk genes. Carrying BC P/LP variants was suggestively associated with BC risk (HR=2.40, P=0.055). While the best BC PRS had greater risk stratification potential (top vs bottom 20%: HR=5.94, 95% CI=2.70-13.07, P=8.6x10-6), most (4 out of 6) BC-affected survivors with BC P/LP variants were not captured by this PRS cutoff.
Conclusions: Overall, our results suggest specific published sporadic BC PRSs could be considered in future updates to childhood cancer survivorship care guidelines and in subsequent BC risk prediction models. Further study of targeted BC pathogenic risk variant screening is needed in this population.

#7890 Insights into chemotherapy-related cognitive impairment in childhood acute myeloid leukemia survivors.

Joel Costoya[1], Carolyn Cabrera[2], Joaquin J. Jimenez[3]

[1]Department of Biochemistry and Molecular Biology, University of Miami Miller School of Medicine, Miami, FL,[2]University of Miami Miller School of Medicine, Miami, FL,[3]Phillip Frost Department of Dermatology and Cutaneous Surgery, University of Miami Miller School of Medicine, Miami, FL

Chemotherapy-related cognitive impairment (CRCI) has mainly been explored within the context of childhood ALL survivors, whereas data analyzing for pediatric AML neurocognitive outcomes following chemotherapy remains sparse. Standard induction therapy for pediatric AML involves the use of high dose Ara-C intrathecal chemotherapy for CNS prophylaxis, sometimes combined with Methotrexate, both well-documented causal agents regarding neurotoxicity and their link to CRCI. In order to better understand how standard induction therapy affects neurocognitive outcomes for childhood survivors of AML, we searched PubMed, EMBASE, and PsycINFO (2015-2025) using terms such as “childhood acute myeloid leukemia”, “neurocognitive outcomes”, “ ‘chemo brain’ ”, and “cognitive”. Inclusion criteria were limited to pediatric AML-specific cohorts who had undergone validated neuropsychological testing and/or self-reported outcomes. Exclusion criteria were HSCT/cranial RT unless chemotherapy-only results were separable. Three peer-reviewed studies, and one meeting abstract were found which met the criteria. Across AML-specific cohorts, treatment with conventional therapy was associated with impairment in at least one neurocognitive domain, with the relative risk for impairment in two domains being demonstrably higher in the CCSS AML cohort. These studies revealed broad impairment across all domains, with working memory emerging as being notably affected, and exhibiting lasting negative effects on QoL persisting well into adulthood amongst these cohorts. Other similarly impaired neurocognitive domains corresponded to issues with emotional regulation and efficiency accomplishing tasks. One study found no difference in FSIQ when comparing AML survivors to population means, yet their study had an n=12, and showed time since diagnosis, and age at assessment were significant predictors of FSIQ. Additionally, these studies also support the risk for CRCI independent of HSCT, as large survivorship analysis differentiating intense chemotherapy with or without HSCT still found measurable neurocognitive impairment regardless of treatment modality. Given the current evidence, childhood survivors of AML exposed to standard induction therapies are at risk of developing CRCI, with working memory and executive functioning being likely impaired. A significant fraction of pediatric AML survivors experience CRCI may be suffering from unrecognized health conditions, and as such may largely benefit from increased neurocognitive monitoring and resources. As for future pediatric AML patients, careful consideration of these neurocognitive consequences could inform risk-stratified intensity adjustments and introduce targeted neuroprotective strategies during therapy, minimizing cognitive morbidity and allowing patients to not only live longer, but live better.

#7891 Real world treatment with molecularly matched targeted therapies in the era of pediatric precision cancer medicine: Gaining ground or inching forward?.

Jennifer A. Oberg[1], Jack Boublik-Whiteley[2]

[1]Pediatrics, Division of Pediatric Oncology, Columbia University Medical Center, New York, NY,[2]Los Altos High School, Los Altos, CA

Introduction: Children and adolescents diagnosed with relapsed/refractory or high-risk cancer have a poor prognosis and <20% survival rates for those with recurrent disease. Several pediatric precision cancer medicine programs have been established to inform clinical decision making and provide molecularly matched therapeutic options for patients in need. However, the clinical benefit of these therapies in real-world settings is unknown. A review of the literature and patients sequenced through the Precision in Pediatric Sequencing (PIPseq) program at Columbia University Medical Center (CUMC) was conducted to describe outcomes of patients with solid or CNS tumors treated with a molecularly matched targeted therapy (MTT).

Methods: PubMed and the CUMC medical record were reviewed between 2013-2025. Patient-level molecular and treatment data were extracted for those diagnosed with high-risk or relapsed/refractory disease. Clinical benefit rate (CBR) (percent complete response (CR), partial response (PR), and stable disease (SD) for >/= 6 months) was evaluated. Progression free (PFS) and overall survival (OS) differences were assessed using the log-rank test.

Results: 20 studies and 29 PIPseq patients were identified. 233 CNS and 394 solid tumor (ST) patients were included. 40% (CNS), 23% (ST) and 30% overall derived clinical benefit. Patients with low grade glioma had the highest CBR (69%, n = 36) and medulloblastoma had the lowest CBR (20%, n = 20). CBR for the largest CNS cohort, high grade glioma, was (25%, n = 122). CBR for select ST subtypes were 16% (adrenal, n = 81), 11% (osteosarcoma, n = 65), 16% (rhabdomyosarcoma, n = 55) and 12% (Ewing sarcoma, n = 33). Kaplan-Meier survival analysis was conducted to compare survival distributions across treatment categories, MTT monotherapy, multi agent MTT, and MTT+chemotherapy. By treatment category, median PFS/OS for CNS patients (n = 166/138) were 5.5/32.1, 14/32.2, and 4.8/24 months, respectively. Log-rank tests indicated a significant PFS/non-significant OS difference, $X^2(2) = 7.45/1.12$, $p = .025/.571$ with an estimated median follow-up of 28/32.1 months. Median PFS/OS times for ST patients (n = 263/179) by treatment category were 4.2/11.6, 1.7/32.3, and 4.1/13.7 months, respectively with non-significant differences in survival, $X^2(2) = 4.1/1.72$, $p = .129/.423$. The estimated median follow-up was 22.8/28.2 months.

Conclusions: Overall, 30% of patients treated with MTT derived clinical benefit. There was a significant difference in PFS but not OS for CNS patients with multiagent MTT yielding the longest PFS and OS compared to MTT monotherapy or MTT+chemotherapy. Treatment modality did not reveal a significant difference in survival for ST patients. Longer follow up beyond 2 years is needed to assess survival in pediatric patients treated with MTT.

#7892 Multi-ancestry genome-wide association study (GWAS) of pediatric acute myeloid leukemia (AML) risk identifies four risk loci.

Cindy Im[1], **Lauren J. Mills**[1], Peggy Meng[2], Marijana Vujkovic[3], Jenny N. Poynter[1], Melissa Maria Hudson[2], Kirsten K. Ness[2], Joseph L. Wiemels[4], Logan G. Spector[1], Saonli Basu[5], Zhaoming Wang[6], Richard Aplenc[7]

[1]University of Minnesota, Minneapolis, MN,[2]St. Jude Children's Research Hospital, Memphis, TN,[3]University of Pennsylvania, Philadelphia, PA,[4]University of Southern California, Los Angeles, CA,[5]Masonic Cancer Center, Minneapolis, MN,[6]University of South Florida, Tampa, FL,[7]Children's Hospital of Philadelphia, Philadelphia, PA

Introduction: AML is a relatively rare pediatric hematological malignancy, but its treatment outcomes trail other acute leukemias with a 5-year survival rate at ~70%. While genome-scale susceptibility studies of adult AML risk have been conducted, similar pediatric AML studies have not been published.

Methods: 1854 pediatric AML cases (diagnosis age <25y) were assembled from the Children's Oncology Group (clinical trials AAML-03P1/0531/1031), Hospital for Sick Children (CA), International Berlin-Frankfurt-Münster Study Group (DE), and Royal Alexandra Hospital for Children (AUS). Cases were genotyped with the Illumina HumanOmni 2.5 BeadChip. Using ADMIXTURE-inferred global genetic ancestry, 1355 cases were grouped in African (AFR, N=95), Admixed American (AMR, N=118), East Asian (EAS, N=74) and European (EUR, N=1068) ancestry groups. Sex-/ancestry-matched publicly available adult controls from 3 external cohorts (Age-Related Eye Disease Study, Health and Retirement Study, Long Life Family Study) genotyped with the same platform were identified at a ~4:1 ratio. TOPMed-based imputation (version r3) supported ancestry-specific GWAS with 5.5-10.7 million common variants (minor allele frequency, MAF≥1%). Logistic regression models adjusted for population substructure tested variant risk associations. Multi-ancestry meta-analysis was performed using an inverse variance-weighted fixed effects model.

Results: Four novel genome-wide significant ($P<5x10^{-8}$) pediatric AML risk loci (*PRIM2*, *HERC2*, *AGRN*, *DEFB131A*) were identified in the EUR GWAS (N=5340), with moderate per-allele odd ratios (OR range: 1.9-2.9). *In silico* analyses indicated lead variants at *HERC2*, *AGRN*, and *DEFB131A* loci are in active chromatin regions in blood or bone marrow tissues and overlap transcription factor binding sites, including in leukemia cell lines. The *HERC2* index variant (OR=1.9, 95% CI: 1.5-2.3) is associated with *HERC2* expression in venous blood (GTEx). Multiple variants at known EUR adult AML risk locus *KMT5B* were also nominally replicated ($P=8.7x10^{-3}$). Additional suggestive associations ($P<1x10^{-6}$) in the AFR (N=475) and AMR (N=518) GWAS were seen; among these, putative pediatric AML risk locus *KANK1*, which was characterized by low frequency (MAF=1-5%) AFR-specific effect alleles, i.e., nearly absent in other ancestries, is notable for its large risk effects (OR=5.6, 95% CI: 3.0-10.7). The multi-ancestry meta-analysis did not reveal additional genetic signals shared across ancestry groups.

Conclusion: We report results from the first pediatric AML GWAS (N=6507, 1355 cases) using international data. We identified 4 novel EUR-specific risk loci, a plausible novel AFR-specific risk locus, and replicated *KMT5B*, a risk locus reported in a EUR adult AML meta-analysis. Future work includes replication and functional validation studies.

: Translational Biomarkers and Emerging Molecular Approaches
Poster Session

#7896 Induction of targeted-cytoxicity and immunogenic cell death using an anti-CEA antibody linked to IRDye700Dx.

Simran Mehta[1], Jitender Jitender[1], Teresa Hong[1], Michael Bouvet[2], John E. Shively[1], Paul J. Yazaki[1], **Thinzar Min Lwin**[3]

[1]City of Hope Comprehensive Cancer Ctr., Duarte, CA,[2]UCSD Medical Ctr., La Jolla, CA,[3]Department of Surgery, City of Hope Comprehensive Cancer Ctr., Duarte, CA

Introduction: Near-infrared photoimmunotherapy (NIR-PIT) uses antibody-photosensitizer conjugates to induce spatially controlled and targeted cytotoxicity. The IRDye700DX phthalocyanine photosensitizer undergoes photochemical alterations upon activation with 690 nm light which results in targeted cell death via membrane disruption on cancer cells. This study evaluated the therapeutic efficacy and antigen specificity of a carcinoembryonic (CEA) antigen-targeted NIR-PIT using the humanized anti-CEA antibody (M5A) conjugated to IRDye700Dx (M5A-IR700) in a colon cancer model.
Methods: M5A was conjugated to NHS-IRDye700DX and validated for binding to human colon cancer cell lines with high-CEA (LS174T), low-CEA (HCT116) by flow cytometry. In vitro, cells were exposed to graded NIR irradiation (690 nm), assessed for cell death (MTS) and evaluated for immunogenic cell death markers (ICD, extracellular ATP, HMGB1). In vivo efficacy was evaluated in athymic mice bearing subcutaneous LS174T xenografts. Mice received intravenous M5A-IR700 (75 µg) followed 24 hours later by a 690 nm laser treatment (150 mW/cm², 30 minutes).
Results: Flow cytometry confirmed robust, antigen-dependent binding in high-CEA LS174T cells relative to the weak binding observed in low-CEA HCT116 cells (Figure 1A). NIR-PIT with M5A-IR700 resulted in light fluence-dependent and concentration-dependent cytotoxicity (Figure 1B). Maximal phototoxicity was observed in LS174T at 64 J/cm². In contrast, there was minimal response in low CEA expressing HCT116 cells, confirming antigen-density dependent cytotoxicity. Extracellular ATP and HMGB1 were significantly elevated in LS174T but not HCT116 cells (Figure 1C). Rapid release of extracellular ATP occurred immediately following NIR-PIT in LS174T cells and this response was attenuated in HCT116 cells. These findings indicate an antigen-restricted induction of ICD. Mice treated with M5A-IR700 and laser activation (M5A-IR700 PIT) demonstrate significant suppression of tumor volume over 30 days compared with untreated controls and mice receiving antibody alone ($p<0.01$) (Figure 1E).
Conclusion: CEA-targeted NIR-PIT using M5A-IR700 effectively induced antigen-specific immunogenic cell death in vitro and robust tumor control in vivo. Differential responses between LS174T and HCT116 validate antigen density dependence which is essential for clinical translation. These findings provide strong rationale for clinical development of M5A-IR700-mediated NIR-PIT as targeted therapy for CEA-positive colorectal cancers.

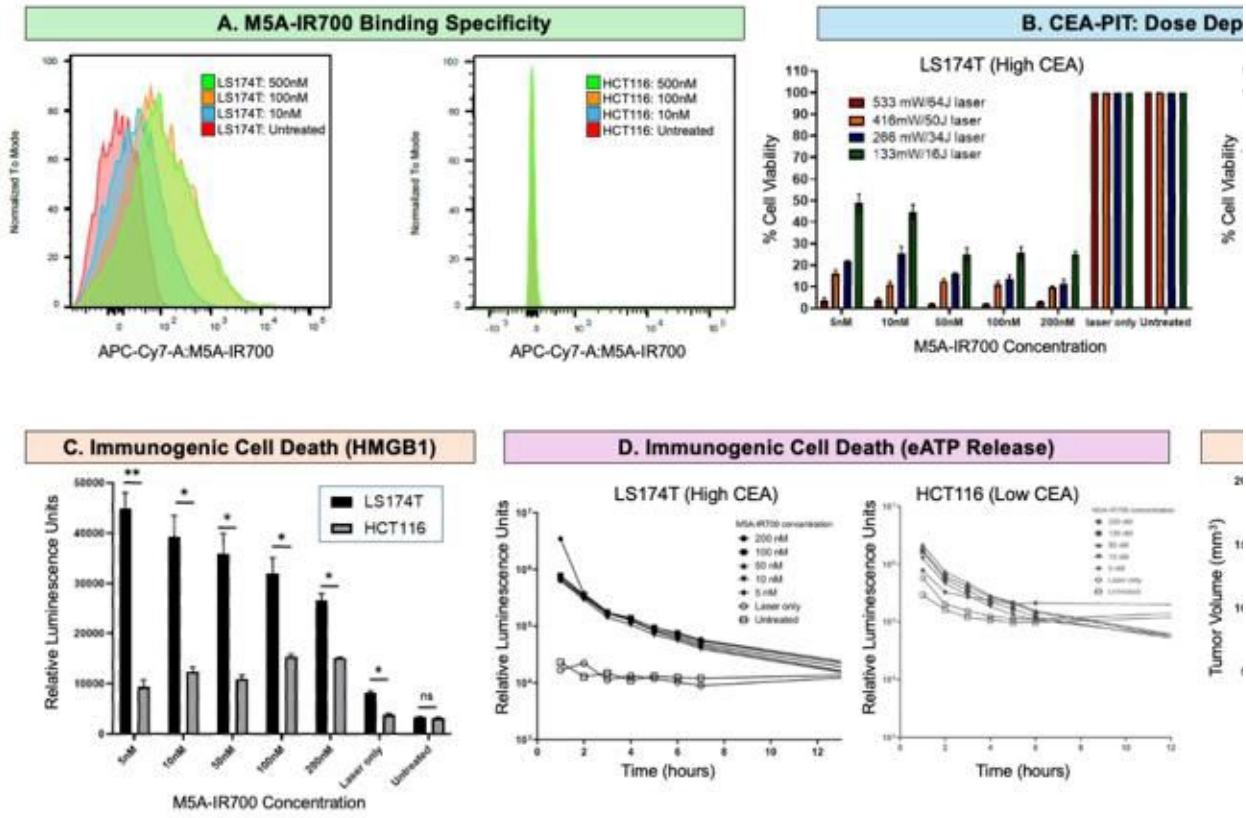

#7897 Novel Rho-GTPase regulatory protein gene family variants are frequent and associate with poor survival in patients (pts) with acute myeloid leukemia (AML).

Ethan Hamp[1], Lorenz Oelschlager[2], Bailee N. Kain[3], Deedra Nicolet[4], Krzysztof Mrozek[1], Katherine E. Miller[5], Audrey Bollas[5], Michael C. Walker[4], Christopher J. Walker[1], Jill Buss[1], Andrea Laganson[1], Andrew J. Carroll[6], William G. Blum[7], Bayard L. Powell[8], Geoffrey L. Uy[9], Wendy Stock[10], Marina Y. Konopleva[11], Richard M. Stone[12], John C. Byrd[13], Martin Carroll[14], Tanmoy Sarkar[14], Akmaljon Salimov[14], Benjamin J. Kelly[5], Electra D. Paskett[1], Jesse J. Plascak[1], Shannon McWeeney[15], Jeffrey W. Tyner[15], Jeffery Klco[16], Nathan Salomonis[3], H. Leighton Grimes[3], Elaine R. Mardis[5], Ann-Kathrin Eisfeld[1]

[1]Ohio State University Comprehensive Cancer Center, Columbus, OH,[2]University Hospital Schleswig-Holstein, Lubeck, Germany,[3]Cincinnati Children's Hospital Medical Center, Cincinnati, OH,[4]Clara D. Bloomfield Center for Leukemia Outcomes Research, Columbus, OH,[5]Institute for Genomic Medicine, Nationwide Children's Hospital, Columbus, OH,[6]University of Alabama, Birmingham, AL,[7]Emory University, Atlanta, GA,[8]Wake Forest University, Winston-Salem, NC,[9]Division of Oncology, Washington University School of Medicine, Saint Louis, MO,[10]College of Medicine, University of Chicago, Chicago, IL,[11]Department of Oncology, Albert Einstein College of Medicine, New York City, NY,[12]Department of Medical Oncology, Dana-Farber Cancer Institute, Boston, MA,[13]Department of Internal Medicine, University of Cincinnati, Cincinnati, OH,[14]University of Pennsylvania, Philadelphia, PA,[15]OHSU Knight Cancer Institute, Portland, OR,[16]St. Jude Children's Research Hospital, Memphis, TN

Introduction: AML is a molecularly heterogeneous disease that is classified by recurrent cytogenetic abnormalities and gene mutations. Recent studies have shown divergent frequencies of several genetic aberrations depending on genetic ancestry and self-reported race/ethnicity, highlighting the need to broaden sequencing efforts to include more diverse pts.
Methods: We performed paired tumor/normal whole exome sequencing (WES) and transcriptome sequencing on 271 ancestry and/or ethnically diverse pts [including 100 African American (AA) and 71 self-identified Hispanic pts; CALGB/Alliance], and a validation cohort of 45 AA pts (University of Pennsylvania).
Results: We identified >20 genes to be mutated in 3-8% of pts that were not seen in previous sequencing efforts of predominantly non-Hispanic White/European ancestry (EA) pts. Notably, variants in genes encoding Rho-GTPase regulatory proteins (*ARHG* family, belonging to the *RAS* gene superfamily) were identified in 12% of pts, placing these genes in the top 5 of recurrently mutated genes in this pt cohort. This frequency was confirmed in the second cohort of AA pts (n=7/45, 15%). In contrast, analysis of 805 EA adults with WES data (BeatAML 2022) and 877 pediatric AML pts (TARGET) found *ARHG* gene family variants in 26/805 (3%) and 17/877 (1.9%) of EA AML pts, respectively. With a median age of 41y, *ARHG*-mutated(m) pts tended to be younger (P=.16) and more often diagnosed with core-binding factor AML (39% vs 19%, P=.02). *ARHG* mutations frequently co-occurred with *NRAS* and *FLT3* mut (each found in 35% of *ARHG*m pts). Notably, survival of *ARHG*m pts was poor, with a median overall survival (OS) of <12 months, thereby mirroring OS of the 2022 European LeukemiaNet (ELN) Adverse risk group. Within the 2022 ELN Favorable risk group in the ancestry diverse cohort, *ARHG*m pts had shorter OS than *ARHG*wt pts (P=.02). The clinical outcome was especially poor in young adolescents and adults (AYA, 18-39y) (mut vs wt; 3y disease-free survival, 10% vs 50%, P<.001; 3y OS, 20% vs 55%, P=.008). RNAseq of 17 *ARHG*m pts showed transcriptomic RAS pathway activation, with 52% displaying a RAS-associated signature, also in the absence of other *RAS* mutations. Furthermore, bulk transcriptomic analyses of 1250 AML pts identified 120 predicted *RAS* signature genes, with the upregulated genes being enriched in metallopeptidases, MAP kinase phosphatases, and *ARHG* genes.
Conclusion: We identified mutations in *ARHG* family genes as frequent yet thus far unrecognized RAS pathway activators in AML associated with poor survival that are not yet included in clinical testing panels. Their lack of recognition is likely due to the heterogeneity of mutationally affected *ARHG* family genes, enrichment in AYA pts and the high frequency in pts of non-European ancestry, both of which are pt populations that were underrepresented in previous sequencing efforts.

#7898 Clinical benefit of the HIF-2α inhibitor casdatifan (Cas) across molecular subtypes in clear cell renal cell carcinoma (ccRCC) patients from the ARC-20 Clinical Study.

Benjamin Weeder[1], Yinghui Guan[1], Jaskirat Singh[1], Brian Rini[2], Toni K. Choueiri[3], Angelo Kaplan[1], Omar Kabbarah[1], Soonweng Cho[1]

[1]Arcus Biosciences, Inc., Hayward, CA,[2]Vanderbilt, Nashville, TN,[3]Dana-Farber Cancer Institute, Boston, MA

Introduction: Recently, casdatifan (Cas), an orally bioavailable small molecule inhibitor of hypoxia-inducible factor-2 alpha (HIF-2α), demonstrated promising efficacy in metastatic ccRCC in the ARC-20 clinical trial (NCT05536141). Despite progress towards the identification of ccRCC molecular subtypes, the relationship between established molecular classifications (Motzer et al., Cancer Cell 2020), HIF-2α transcriptional signatures (Courtney et al., CCR 2020), and clinical benefit from HIF-2α inhibitors has not been investigated. Herein we explore whether patients characterized by these RNA-based molecular subtypes show evidence of HIF-2α activity and whether they derive clinical benefit from Cas monotherapy.
Methods: Archival tumor biopsies were taken from 67 ccRCC patients enrolled in ARC-20 who received daily doses ≥50mg of Cas monotherapy. Molecular subtypes were defined based on the quantile normalized RNA expression of literature-defined molecular signatures. Gene signature assessment across subtypes was performed using ssGSEA on voom-normalized RNA expression levels.
Results: Using literature-based classification of ARC-20 samples, patients were assigned to one of six molecular subtypes (angiogenesis/stromal, angiogenesis, immune/proliferative, proliferative, stromal/proliferative, or unclassified), falling into one of three broader molecular categories (angiogenesis, immune, or other). Cas monotherapy resulted in similar disease control rate (DCR) and progression free survival (PFS) across the previously derived molecular subtypes (χ^2=0.26, p=0.878; Log-rank p>0.9). We further explored the relationship between HIF-2α activity and previously defined ccRCC subtypes using HIF-2α-related gene expression signatures; there was no enrichment of HIF-2α related gene expression signatures in these predefined molecular categories. However, we observed a strong relationship between the expression of HIF-2α transcriptional signatures and clinical benefit in patients treated with Cas monotherapy. In contrast, higher HIF-2α gene signature expression was associated with shorter PFS in patients treated with either sunitinib (Log-rank, p<0.001) or atezolizumab plus bevacizumab (Log-rank p=0.012) in available data from the IMmotion 151 study.
Conclusions: The HIF-2α inhibitor Cas produces similar clinical benefit in all previously described molecular subtypes of ccRCC. While most ARC-20 patients derived benefit from Cas monotherapy, there was a strong relationship between clinical benefit (PFS) and expression levels of HIF-2α transcriptional signatures in tumor samples.

#7899 BGB-21447, a next generation Bcl-2 inhibitor, shows high potential in Bcl-2 overexpressing B cell non-Hodgkin lymphomas (NHL) cancers in preclinical studies.

Haitao Wang[1], Lin Li[1], Yiwen Wang[1], Weiwei Song[1], Shuang Peng[1], Sijia Zhai[1], Ziyu Jia[1], Peng Chi[1], Teiko Sumiyoshi[2], Ting Deng[3], Yang Liu[3], Wei Jin[1], Zhirong Shen[3]

[1]BeOne Medicine (Beijing) Co., Ltd., Beijing, China,[2]BeOne Medicines USA, Inc., San Carlos, CA,[3]BeOne Medicines (Shanghai) Co., Ltd., Shanghai, China

Background: Venetoclax's success in CLL/SLL and AML validates Bcl-2 as a therapeutic target in hematologic malignancies. However, suboptimal efficacy has limited its development in DLBCL and multiple myeloma (MM) , raising uncertainty about whether Bcl-2 is an effective target in these diseases or if a more potent Bcl-2 inhibitor is needed. Biologically, DLBCL has ≥20% BCL2 genetic alterations or ≥50% overexpression in patients, while Bcl-2 overexpression is also commonly observed in MM patients. These findings underscore the relevance of targeting Bcl-2 in both indications. In this study, we evaluate the potential of BGB-21447, a next-generation Bcl-2 inhibitor structurally distinct from sonrotoclax (BGB-11417), mainly in DLBCL/B-NHL via preclinical studies.

Methods: Cell viability was assessed by CTG assay *in vitro*. Xenografts were established by subcutaneously inoculating cancer cells into NCG mice for in vivo efficacy evaluation. Bcl-2 protein levels were quantified using western blot and ELISA.

Results: A panel of 21 DLBCL cell lines (15 GCB-DLBCL and 6 ABC-DLBCL) was tested for sensitivity to BGB-21447. In vitro CTG assays showed that 8/21 DLBCL cell lines responded to BGB-21447 with single-digit nanomolar (nM) potency, while the others were resistant. Sensitivity did not correlate with cell-of-origin subtype, but was enriched in cell lines with BCL2 genetic alterations, such as BCL2 amplification or t(14;18) translocation. Bcl-2 protein expression analysis revealed that these genetic alterations were associated with high Bcl-2 protein levels, as determined by western blot and ELISA. Notably, only cell lines with high Bcl-2 protein level were sensitive to BGB-21447, suggesting Bcl-2 protein expression as a potential predictive biomarker. In vitro studies in Bcl-2-dependent DLBCL and MCL cell lines demonstrated that BGB-21447 is over 50-fold more potent than venetoclax, indicating strong potential in indications where venetoclax efficacy is limited. This was further supported by in vivo studies: BGB-21447, at 4 or 8 mpk QD (clinically achievable doses), showed significant anti-tumor activity in Toledo xenografts, while venetoclax at 50mpk QD (doses relevant to 1200 mg QD in humans) showed only partial efficacy. In SU-DHL-6 xenografts, venetoclax at 50 mpk QD had minimal effect, whereas BGB-21447 at 8 mpk significantly inhibited tumor growth. Similar trends were observed in Minami-1 (FL model) xenografts, where BGB-21447 induced complete tumor regression, while venetoclax at 50 mpk QD showed partial activity.

Conclusions: These findings indicate that BGB-21447 is a Bcl-2 inhibitor with substantially greater potency than venetoclax and strong potential in indications such as DLBCL where venetoclax has suboptimal efficacy. Clinical trials are needed to validate these results.

#7900 Clinical significance of elevated *UBQLN4* expression with resistance to cisplatin in intrahepatic cholangiocarcinoma.

Kodai Abe[1], Kelly K. Chong[1], Yuta Abe[2], Minoru Kitago[2], Motonori Edanami[2], Yosuke Uematsu[2], Yohei Masugi[3], Akihisa Ueno[3], Anton Bilchik[4], Yosef Shiloh[5], Yuko Kitagawa[2], Dave Hoon[1]

[1]Translational Molecular Medicine, Providence Saint John's Cancer Institute, Santa Monica, CA,[2]Surgery, Keio University School of Medicine, Tokyo, Shinjuku-ku, Japan,[3]Diagnostic pathology, Keio University School of Medicine, Tokyo, Shinjuku-ku, Japan,[4]Gastrointestinal and Hepatobiliary Surgery, Providence Saint John's Health Center, Santa Monica, CA,[5]Human Molecular Genetics and Biochemistry, The David and Inez Myers Laboratory for Cancer Research, Tel Aviv, Israel

Backgrounds & Aims: Intrahepatic cholangiocarcinoma (iCCA) is a devastating biliary tract cancer increasing in incidence worldwide with limited treatment options. We previously identified ubiquilin-4 (*UBQLN4*) was associated with prognosis and chemotherapy response in breast and esophageal cancer. *UBQLN4* is a ubiquitinated-binding protein which inhibits homologous recombination repair while promoting non-homologous end-joining repair in DNA damage repair. The objective of this study is to determine the clinical utility of *UBQLN4*, as a potential prognostic biomarker associated with iCCA clinical outcomes.

Methods: The public datasets from TCGA-CHOL (n=32), DepMap, and Fu-iCCA cohort (n=238), GSE107943 (n=30), and GSE32225 (n=148) were assessed for copy number variation (CNV) and/or mRNA expression analysis of *UBQLN4* located on 1q22 chromosome. As validation, an independent cohort of iCCA patients (n=66) were analyzed for clinical significance of *UBQLN4*. We finally investigated *in-vitro* analysis to evaluate the molecular features and cisplatin-resistance (CR) mechanism of UBQLN4.

Results: GISTIC analysis of TCGA-CHOL dataset showed that 1q22 including *UBQLN4* is one of the highest amplifications in all chromosomes. There is high correlation between CNV and mRNA expression of *UBQLN4* gene in iCCA tissues from TCGA-CHOL, DepMap, and FuiCCA cohort. *UBQLN4* was also found to be upregulated in iCCA tissues compared to normal liver tissues or biliary epithelium from TCGA-CHOL, GSE107943 and GSE32225 datasets. In an independent iCCA validation cohort, *UBQLN4* mRNA upregulation was significantly associated with poor recurrence-free survival ($p = 0.025$). *UBQLN4* mRNA high expression was an independent recurrence risk factor in a multivariate cox regression analysis (Hazard risk = 2.26, 95% confidence interval 1.00 - 5.11, $p = 0.048$). In *in-vitro* using iCCA cell lines (RBE and HCCC9810), knockdown of *UBQLN4* lead to high sensitivity for cisplatin compared to controls; however, CR-iCCA cell lines showed high UBQLN4 expression concomitant with increased phosphorylated ATM (pATM). Moreover, 3D spheroid assay revealed UBQLN4 and pATM are expressed significantly higher in CR-iCCA cell lines than respective parental cell lines. In clinically annotated iCCA specimens, non-responders to neoadjuvant chemotherapy including cisplatin had increased UBQLN4 and pATM protein levels in iCCA tissues as assessed by multiplex immunofluorescence, supporting that FuiCCA cohorts showed high UBQLN4 and pATM protein levels lead to worse prognosis (p=0.049).

Conclusions: Upregulated *UBQLN4* expression correlates with postoperative recurrence as well as resistance to cisplatin in iCCA patients, indicating that *UBQLN4* is a strong prognostic biomarker related to cisplatin treatment of iCCA patients.

#7901 Renal cancer early diagnosis using a novel B7-H3 targeted ultrasound contrast imaging.

Arutselvan Natarajan, Jihye Baek, Ramasamy Paulmurugan, Jeremy Dahl

Stanford University, Stanford, CA

Aim: Cost-effective or accessible methods to detect kidney cancers, especially those with renal insufficiency, remain elusive. We propose ultrasound molecular imaging (UMI) using microbubbles (MBs) targeted to cancer-associated vascular endothelial (VE) markers as a diagnostic imaging tool for kidney cancer with high specificity. CD276 (B7-H3), an immune checkpoint (IC) marker and a member of the immunoglobulin superfamily, is overexpressed on the VE cells of different cancers including renal cancer.

Methods: We have developed an engineered affibody (Aby) specifically targeting both mouse and human B7-H3 for imaging renal cancer in vivo using US. In this study, we biotinylated the Aby and linked to MBs that were functionalized with avidin to create B7-H3 targetable MBs (TMBs) or with a scrambled Aby not binding to B7-H3 as a control MBs (non-targeted MBs or NTMBs), yielding (10×10^8 MBs/mL). Balb/C mice (n=4) were implanted with renca kidney cancer cells at the lower flank for in vivo imaging of VE-B7-H3 expression in the tumor. We also performed immunofluorescence (IF) analysis of the tumor tissue for the presence of B7-H3 and CD31 on VE cells at the vessels in the tumor microenvironment (TME).

Results: Mice were imaged after tumor growth reached to 0.8-1.1 mm diameter with UMI, after administration of $1\text{-}2 \times 10^7$ TMBs or NTMBs in 200 µL of saline. Compared to control NTMBs, the UMI signal using B7-H3-targeted TMBs was significantly higher (P= 0.002). IF analysis confirmed a high correspondence between B7-H3 and the universal vascular CD31 marker.

Conclusions: The developed TMBs were able to detect and image the in vivo expression of tumor-associated B7-H3 in the VE cells. The results support the feasibility of these B7-H3-TMBs in translating into human kidney cancer diagnosis using UMI.

#7902 Analytical accuracy and clinical performance of the OncoMate MSI Dx Analysis System in a subset of KEYNOTE-775 endometrial carcinoma classified as MSS (not MSI-H) by the companion diagnostic.

Sam Sibley[1], Matthew Marton[2], Amy Wehn[2], Yiwei Zhang[2], Kathryn Oostdik[1], Ryan Mordini[1], Gary Tarpley[1]

[1]Promega, Madison, WI,[2]Merck & Co., Rahway, NJ

Background: Advanced endometrial carcinoma (EC) presents a major clinical challenge, with poor prognosis and few treatment options. Pembrolizumab (KEYTRUDA®) in combination with lenvatinib (LENVIMA®) has been approved by the FDA for the treatment of adult patients with advanced EC that is mismatch repair proficient (pMMR) or not microsatellite instability high (MSI-H). The OncoMate® MSI Dx Analysis System is a PCR-based assay for MSI determination in FFPE tumor tissue with custom software for automated analysis. Here, we present analytical accuracy and clinical performance data that supported FDA approval of the OncoMate® MSI Dx assay as a companion diagnostic (CDx) to identify patients with advanced EC who may benefit from treatment with pembrolizumab plus lenvatinib.

Design: Analytical accuracy was assessed retrospectively in 255 EC samples from the KEYNOTE-775 clinical trial by comparing OncoMate® MSI Dx assay results with a commercially available immunohistochemistry (IHC) panel. Clinical performance was evaluated in a bridging study (n=489) linking MSI status with outcomes from KEYNOTE-775. The efficacy of pembrolizumab plus lenvatinib versus treatment of physician's choice (TPC) was estimated for progression-free survival (PFS), overall survival (OS), objective response rates (ORR), and duration of response (DOR) for the CDx-defined microsatellite stable (MSS; equivalent to not MSI-H) subpopulation.

Results: Analytical accuracy was high: agreement between MSS vs pMMR results was 99.0% (95% CI, 96.5-99.7%), agreement between MSI-H vs dMMR results was 91.7% (95% CI, 80.4-96.7%), and overall agreement was 97.6% (95% CI, 95.0-98.9%). In the clinical cohort, patients with MSS tumors identified by the OncoMate® MSI Dx assay demonstrated significant benefit from pembrolizumab plus lenvatinib versus TPC, with improvements in PFS, OS, ORR, and DOR consistent with published trial results.

Conclusion: The OncoMate® MSI Dx assay was accurate compared with an established IHC orthogonal method and provided complementary information to IHC about tumor MMR status for some patients. The assay, which directly assesses DNA MMR function via microsatellites, retrospectively identified EC patients who would benefit from combination treatment with pembrolizumab plus lenvatinib compared with TPC. Specifically, pembrolizumab plus lenvatinib efficacy in a subset of KEYNOTE-775 participants with CDx-defined MSS (not MSI-H) tumors was comparable to the efficacy observed in all IHC-defined pMMR participants randomized in the original trial. These results support use of the OncoMate® MSI Dx assay for this indication and validate that PCR- and IHC-based methods identify comparable patient populations who benefit from pembrolizumab plus lenvatinib.

#7903 MiR-362-3p enhances platinum response in breast cancer.

Zhaoji Liu[1], Shizhong Ke[1], Xiaohui Li[1], Catherine Wu[1], Madison M. Uyemura[1], Brian R. Sardella[1], Erica S. Massicott[1], Lin Wang[1], Emily K. Aronson[1], Dimitra Karagkouni[1], Nikolas Kalavros[1], Ioannis S. Vlachos[1], Felipe Batalini[2], Cristina S. Bogsan[1], Jit Kong Cheong[3], Lihan Zhou[3], He Cheng[3], Phillip Munson[3], Erica L. Mayer[4], Judy E. Garber[4], Stuart J. Schnitt[1], Nadine M. Tung[1], Andrea L. Kasinski[5], Frank J. Slack[1], **Gerburg M. Wulf**[1], Yujing J. Heng[1]

[1]Beth Israel Deaconess Medical Center, Boston, MA,[2]Mayo Clinic, Phoenix, AZ,[3]Mirxes, Singapore, Singapore,[4]Dana Farber Cancer Institute, Boston, MA,[5]Purdue University, West Lafayette, IN

The INFORM trial (NCT01670500) was a randomized, two-arm Phase II neoadjuvant study comparing the efficacy of a platinum-based regimen (cisplatin) versus an anthracycline (AC)-based regimen in participants with germline *BRCA1/2* mutations and early-stage, HER2-negative breast cancer. MicroRNAs (miRNAs) are emerging as promising non-invasive biomarkers for disease detection and treatment monitoring. The initial aim of this study was to evaluate whether pretreatment plasma miRNA profiles were associated with treatment outcomes in the INFORM trial cohort. Pretreatment plasma samples from 97 INFORM participants (n=53 cisplatin and n=44 AC) were screened for 352 miRNAs commonly implicated in cancer using the qPCR-based ID3EAL^{TM} Cancer Panel. Twenty out of 53 participants achieved residual cancer burden (RCB) score of 0 or 1 with cisplatin and 20/44 with AC. Higher plasma miR-362-3p expression was associated with a favorable response to cisplatin (1.7-fold; p<0.01), but not to AC. MiR-362-3p expression in paired pretreatment tumor biopsies (n=79) did not significantly correlate with plasma expression and was not associated with RCB 0/1 (p>0.05). In TCGA, miR-362-3p expression was higher in breast tumors than in adjacent normal tissue, and higher in triple negative breast cancers (TNBCs) compared with hormone receptor-positive tumors (both FDR<0.001), independent of *BRCA* mutation or Single Base Substitution Signature 3 (SBS3) status. The miR-362-3p findings in INFORM did not replicate in a sister trial, TBCRC 030 (NCT01982448; 11 out of 46 cisplatin-treated patients achieved RCB 0/1, p=0.46). These results suggest that while miR-362-3p is unsuitable as a circulating biomarker for cisplatin response, it may play an important biological role in mediating cisplatin sensitivity in TNBCs, independent of *BRCA1/2* mutations. Functional studies demonstrated that miR-362-3p is expressed and secreted by TNBC cell lines, operates as a tumor suppressor, and generally correlates with cisplatin sensitivity. Overexpression of miR-362-3p rendered MDA-MB-231 and CAL-51 cells cisplatin sensitive, while knockdown induced resistance in MDA-MB-436 cells. Ongoing studies are testing whether these effects translate in xenograft models. *In* silico and functional assays identified *BCLAF1*, a DNA damage response (DDR) regulator, as a direct target of miR-362-3p. Overexpression of miR-362-3p suppresses *BCLAF1* mRNA and protein levels. Our findings demonstrate that miR-362-3p enhances cisplatin responsiveness by targeting *BCLAF1*. A miR-362-3p-based therapeutic may be useful as a co-agent to enhance tumor responses to platinum-based chemotherapy.

#7904 Galectin-9 as a glycan-modulating adjuvant to enhance Elotuzumab-mediated immunotherapy in multiple myeloma.

Rajib Kumar Shil[1], Guenther Koehne[2], Charles J. Dimitroff[1]

[1]Cellular and Molecular Medicine, Florida International University, Miami, FL,[2]Hematologic Oncology and Benign Hematology, Baptist Health South Florida/Miami Cancer Institute, Miami, FL

Multiple myeloma (MM) is a hematologic malignancy characterized by the clonal expansion of malignant antibody-producing plasma cells within the bone marrow. Despite advances in therapeutic strategies, MM remains incurable, emphasizing the need for innovative approaches to augment current immunotherapies. The surface glycan repertoire or glycome profile of myeloma cells plays a pivotal role in modulating host-tumor immune interactions, influencing both immune recognition and therapeutic responsiveness. Galectin-9 (Gal-9), a β-galactoside-binding lectin, has emerged as a key regulator of immune and tumor cell signaling through its interaction with specific glycan structures. Recent findings from our laboratory revealed a strong binding affinity of Gal-9 for B cell surface glycans, resulting in the upregulation of signaling lymphocytic activation molecule F7 (SLAMF7), a critical immunoregulatory receptor expressed on malignant plasma cells and a validated therapeutic target of the monoclonal antibody Elotuzumab. In this study, we investigated whether Gal-9 treatment enhances Elotuzumab efficacy by modulating SLAMF7 expression and immune responsiveness in MM cells. Using flow cytometry, we quantified Gal-9 binding and SLAMF7 surface expression across B-lymphoblast models and primary MM bone marrow samples. Gal-9 exposure significantly increased SLAMF7 expression (~3-fold) compared to untreated controls. Furthermore, Gal-9-primed MM cells exhibited augmented antibody-dependent cellular cytotoxicity (ADCC) when co-cultured with natural killer (NK) cells in the presence of anti-SLAMF7 antibody Elotuzumab, suggesting (~2.5-fold) functional enhancement of immune-mediated cytotoxicity. All methods were conducted at least 3 times and analyzed for statistical significance using Student's t-test (*$p \leq 0.05$, **$p \leq 0.01$, *** $p \leq 0.001$). Collectively, these findings highlight Gal-9 as a promising combinatorial agent capable of enhancing SLAMF7 expression and amplifying Elotuzumab-induced cytotoxicity in MM. This study underscores the therapeutic potential of integrating glycan-targeting strategies with existing monoclonal antibody-based regimens to improve treatment efficacy and patient outcomes in multiple myeloma.

#7905 Dihydroorotate dehydrogenase (DHODH) inhibition as a promising therapeutic strategy with synergistic targeting of ROR1 in small cell lung cancer.

Bahareh Nourmohammadi[1], Ola A. Elgamal[2], Sandip Vibhute[1], Christopher C. Coss[1], Thomas E. Goodwin[3], Erin Hertlein[2], Joseph M. Amann[1], Ju Hwan Cho[1], Chad E. Bennett[1], John C. Byrd[2], David P. Carbone[1]

[1]The Ohio State University, Columbus, OH,[2]University of Cincinnati, Cincinnati, OH,[3]Hendrix College, Conway, AR

Small-cell lung cancer is an aggressive subtype of lung cancer with poor prognosis and comprises approximately 15% of all lung cancers. The frontline therapy for SCLC is platinum-etoposide chemotherapy. However, patients almost relapse shortly after the start of therapy, and second line therapies typically provide only a few months of benefit. Clearly, better therapeutics are necessary for the treatment of SCLC. Cancer cells often have dysregulated metabolic pathways. These changes are often necessary to enable the continued proliferation of cancer cells. Dihydroorotate dehydrogenase (DHODH), which catalyzes the conversion of dihydroorotate to orotate in the pyrimidine *de novo* synthesis pathway, has a particular role in the survival of multiple cancers including SCLC. Recent studies have shown that SCLC cells are thought to respond to therapy but recur due to a chemotherapy-resistant “stem cell” or “persister” population of tumor cells induced by therapy. Receptor tyrosine kinase-like orphan receptor 1 (ROR1) is a receptor tyrosine kinase that is re-expressed in multiple cancers, including SCLC, where its expression is associated with shorter survival and rapid relapse. Therefore, targeting ROR1 may reduce stem-like tumor cells and improve therapeutic response in SCLC. We evaluated the effect of HOSU-53, a DHODH inhibitor, on SCLC tumor growth *in vitro*. We measured IC50s of 18 SCLC cell lines and most SCLC cells showed promising sensitivity to HOSU-53 treatment. However, some SCLC cells demonstrated resistance to DHODH inhibition. Therefore, we evaluated the synergy between HOSU-53 and KAN0441571C, a ROR1 inhibitor *in vitro*. SCLC cells were treated with the compounds as single agents as well as the combination. Synergy was observed between KAN0441571C and HOSU-53 in SCLC cells. To evaluate the effect of DHODH inhibition on SCLC tumor growth *in vivo*, we treated xenograft models with HOSU-53 alone or in combination with etoposide plus cisplatin. We observed a significant decrease in tumor volume when HOSU-53 was used alone and in combination, without significant animal weight loss. Additionally, to evaluate the effect of HOSU-53 and ROR1 inhibition on tumor burden *in vivo*, a treatment-resistant xenograft SCLC model was treated with HOSU-53 and KAN0441571C as single agents and the combination. We observed a significant reduction in tumor volume in the combination arm compared with the single-agent treatment arms, without significant loss of body weight. Together, these data demonstrated the promising efficacy of HOSU-53 as single agent as well as in combination with KAN0441571C in treatment-resistant SCLC models. These findings support the initiation of a phase I clinical trial to evaluate the preliminary efficacy and tolerability of HOSU-53 and support the strategy of targeting DHODH and ROR1 as a potential therapeutic approach for the treatment of SCLC.

#7906 Integrated multi-omics profiling identifies an immunotherapy vulnerable and prognostic associated subtype in cholangiocarcinoma.

Lu Chen, Xiangdong Tian

Tianjin Medical Univ. Cancer Inst. & Hospital, Tianjin, China

Cholangiocarcinoma (CCA) is an aggressive malignancy with poor prognosis and limited treatment options. This study performed integrated multi-omics profiling as well as immunohistochemical validation on 424 CCA patients, identifying four molecular subtypes with distinct clinical and immunological features: C1 (Proliferative): Driven by *TP53/KRAS* mutations and CpG island methylator phenotype (CIMP+) hypermethylation, showing Th17 cells infiltration and poor outcomes; C2 (Immune-Suppressed Macro_LYVE1, (ISM_LYVE1)): Stroma-rich with LYVE1$^+$ macrophages and epithelial-mesenchymal transition (EMT) activation; C3 (Immune-Activated Macro_C1QC (ISM_C1QC)): Enriched in C1QC$^+$ macrophages, CD8$^+$ T-cells, and metabolic pathways, highly responsive to immune checkpoint blockade (75% Overall Response Rate (ORR)); C4 (Immune-Excluded, (IE)): FGFR2-altered and IDH1-mutant, with an immunologically-cold phenotype. We validated ATP2B1 as a novel prognostic biomarker and developed a 160-gene classifier for subtype prediction. The C3 subtype's exceptional immune checkpoint blockade (ICB) response, independent of conventional biomarkers (PD-L1/microsatellite instability (MSI)/tumor mutational burden (TMB)), highlights the clinical utility of this classification system in guiding precision immunotherapy for CCA.

#7907 Genomic, immune, and clinical characterization of estrogen receptor-positive, HER2-low breast cancer: The NextGIM trial latest updates.

Barbara Cardinali[1], Alice Stella[1], Chiara Molinelli[1], Marco Bruzzone[1], Yanina Lizet Castillo[1], Francesca Pitto[1], Barbara Massa[1], Simona Pigozzi[2], Andrea Sciutto[1], Giorgia Anselmi[1], Maria Dono[1], Virna Maltoni[2], Benedetta Conte[3], Giulia Buzzatti[1], Davide Soldato[1], Gaia Griguolo[4], Valentina Guarneri[4], Mario Giuliano[5], Caterina Marchio[6], Fabio Puglisi[7], Lorenzo Gerratana[7], Francesca Poggio[1], Lucia Del Mastro[1]

[1]IRCCS Ospedale Policlinico San Martino, Genova, Italy,[2]University of Genova, Genova, Italy,[3]University of Piemonte Orientale, Novara, Italy,[4]Institute of Oncology IOV-IRCCS, Padova, Italy,[5]University of Naples "Federico II", Naples, Italy,[6]FPO Istituto Candiolo (IRCCS), Candiolo, Italy,[7]Centro di Riferimento Oncologico IRCCS, Aviano, Italy

Background: Approximately 47-65% of estrogen receptor-positive (ER+)/HER2-negative breast cancers (BC), although classified as HER2-negative due to the absence of HER2 gene amplification, exhibit low levels of HER2 expression (referred to as HER2-low BC) with immunohistochemistry (IHC) 1+ or 2+ without amplification scores. More recently, an additional subclass—HER2-ultralow—has been proposed for tumors with HER2 IHC-0 and <10% tumor cell staining. Emerging evidence indicates that HER2-low and HER2-ultralow BC may represent biologically distinct entities compared with HER2-null BC. Here, the latest updates of the NextGIM trail, a retrospective, multicenter translational study designed to comprehensively characterize ER+/HER2-low BC, are presented.
Methods: Primary tumor samples from patients enrolled in three randomized clinical trials (GIM2, GIM4, and GIM10) of the GIM (Gruppo Italiano Mammella) Investigator Group, underwent re-assessment of HER2 expression and tumor-infiltrating lymphocytes (TILs) in accordance with ASCO/CAP and TILs Working Group guidelines. In parallel, gene expression profiling was performed using the nCounter Breast Cancer 360 Panel on the NanoString platform. Clinical and survival data will be updated and integrated to evaluate potential prognostic markers and to investigate mechanisms of treatment resistance.
Results: To date, from a total of 283 patients selected at participating centres, 208 samples were deemed suitable for molecular analyses after pathological and RNA quality/quantity assessment. HER2 expression has been re-evaluated in 179 samples. At diagnosis, HER2 classification was: 45.8% HER2-negative (IHC not specified), 26.8% HER2-0, 19.6% HER2-1+, and 7.8% HER2-2+. After pathological reassessment, the distribution shifted to 58.7% HER2-null, 20.7% HER2-ultralow, 15.1% HER2 1+, 5.0% HER2 2+, and 0.6% HER2 3+. Notably, HER2-null BC resulted more prevalent in older archival samples (before 2011). TILs levels ≤1% were more frequently observed in HER2-null and HER2-ultralow tumors compared with HER2-1+ and HER2-2+ (59.1% & 67.6% vs. 25.9% & 55.6%).. Genomic profiling has been completed for 208 cases and data analyses are ongoing. An integrated analysis of molecular, pathological and clinical data will be conducted upon completion of the dataset.
Conclusion: The results obtained so far from HER2 re-evaluation has indicated that the interval between sample collection and reassessment can affect tissue antigenicity and immunohistochemistry results, and should be considered when re-evaluating HER2 status for therapeutic purposes. Overall, the study is expected, integrating genomic, immunological, and clinical information, to validate HER2-low and -ultralow expression as prognostic/predictive biomarkers to support personalized treatment.

#7908 Distinct molecular and clinical aggressiveness in very early-onset colorectal cancer: Survival and genomic divergence between patients aged 30-39 vs 40-49 years.

Andrea Pretta[1], Gaia Rebecchi[2], Giulia Maddalena[3], Federica Marmorino[4], Pina Ziranu[5], Federica Manoni[6], Maria Caterina De Grandis[3], Martina Carullo[4], Clelia Donisi[5], Giovanni Randon[6], Eleonora Perissinotto[3], Ada Taravella[4], Vincenzo Nasca[6], Federica Buggin[3], Paolo Ciraci[4], Francesca Bergamo[3], Chiara Cremolini[7], Sara Lonardi[3], Mario Scartozzi[5], Filippo Pietrantonio[6]

[1]Medical Oncology Unit, University and University Hospital of Cagliari, Cagliari, Italy,[2]IRCCS Istituto Nazionale dei Tumori, Milan, Italy,[3]Oncology Unit 1, Veneto Institute of Oncology IOV-IRCCS, Padua, Italy,[4]Unit of Oncology, University Hospital of Pisa, Pisa, Italy,[5]Medical Oncology Unit, University Hospital and University of Cagliari, Cagliari, Italy,[6]Fondazione IRCCS Istituto Nazionale dei Tumori, Milan, Italy,[7]Polo Oncologico - AOUP, Pisa, Italy

Background: Early-onset colorectal cancer (EO-CRC) is rising worldwide and exhibits clinical heterogeneity. Patients under 40 may constitute a biologically distinct subgroup within EO-CRC. We investigated whether “very early-onset” colorectal cancer (VEO-CRC, ages 30-39) exhibits specific clinical and genomic features compared with patients aged 40-49, and whether these differences lead to variations in survival at the point of metastatic diagnosis.

Methods: We analysed metastatic EO-CRC patients from a multi-institutional database, divided into two predefined age groups: 30-39 years (n=65) and 40-49 years (n=199). Overall survival (OS) from metastatic diagnosis was estimated using Kaplan-Meier methods, and hazard ratios (HRS) were calculated with Cox regression. Comprehensive genomic profiling was carried out using the Foundation Medicine next-generation sequencing platform (FoundationOne® CDx / Heme; over 300 cancer-related genes). Key molecular alterations (KRAS, NRAS, BRAF, APC, PTEN, POLE) were compared using odds ratios (ORs), with prespecified one-sided tests for directionality. Baseline clinicopathologic characteristics were assessed with χ^2 or Fisher’s exact tests.

Results: Median OS was notably shorter in patients aged 30-39 years than in those aged 40-49 years (30.0 vs 38.0 months; log-rank p = 0.0269; HR = 0.67, 95% CI 0.48-0.96). A distinct genomic profile appeared in VEO-CRC, characterised by higher KRAS mutation rates (55.4% vs 42.0%; OR=1.71; 95% CI 0.98-3.01; one-sided p=0.041) and lower APC alterations (69.2% vs 82.0%; OR=0.49; 95% CI 0.26-0.94; one-sided p=0.024). NRAS, BRAF, PTEN, and POLE alterations were directionally consistent with a more aggressive biology, although event counts were limited. Clinically, overall ECOG distribution was similar (χ^2 p=0.099), but ECOG 0 was more common in VEO-CRC (89.1% vs 76.8%; p=0.0468). Peritoneal metastases occurred significantly more frequently in patients aged 30-39 (32.3% vs 19.6%; p=0.041). No differences were observed regarding liver, lung, or nodal involvement.

Conclusions: Patients aged 30-39 years constitute a biologically distinct subgroup within EO-CRC, with shorter survival, greater KRAS enrichment, fewer APC alterations, and increased peritoneal involvement, despite similar performance status. These findings support the emerging idea of an “ultra-young,” genomically driven CRC subtype, with implications for disease biology, risk assessment, and treatment development.

#7909 Exploring a LINC00092-associated multiomics signature as a clinically tractable biomarker in colorectal cancer.

Pankaj Kumar Ahluwalia, Alicia Walker, Sade Logan, Denton Lord, Shamia Jordan, Kimya Jones, Ashis Mondal, Ravindra Kolhe

Pathology, Augusta University, Augusta, GA

Colorectal cancer (CRC) exhibits significant inter-patient heterogeneity, limiting the efficacy of modern targeted and immunotherapies. Advances in genomics continue to improve our understanding of CRC. Long non-coding RNAs (lncRNAs) are emerging as key regulators of cancer metabolism and immunity. We evaluated the systems-level role and translational potential of a LINC00092-centered multiomics signature as a clinically tractable biomarker. Under an IRB approved protocol at Augusta University, we profiled 50 paired FFPE CRC tumor and normal-adjacent tissues using a NanoString assay and 8-plex multiplex immunofluorescence spatial imaging. For orthogonal validation, we analyzed 304 TCGA-COAD tumors to identify a LINC00092-centered gene signature, infer pathway flux via PROGENy, characterize metabolic enrichment, and score MHC-I/II, antigen-processing, checkpoint, and immunoproteasome programs. In our paired cohort and TCGA, LINC00092 expression was significantly higher in NAT (normal-adjacent tissue) than in matched tumors, consistent with a NAT-enriched state. LINC00092-high tumors retained elements of this state, whereas LINC00092-low tumors showed a distinct, alternate state. Immune cell profiling and deconvolution revealed distinct immune composition with altered inflammatory signatures in LINC00092-low tumors. LINC00092-high tumors displayed suppression of EGFR/PI3K/MAPK and hypoxia/JAK-STAT signaling with preserved pro-apoptotic (e.g., TRAIL/p53) activity. Concurrently, they exhibited higher MHC-II and checkpoint scores but reduced immunoproteasome activity, defining an antigen-presenting, T cell-modulated, checkpoint-rich state. In contrast, LINC00092-low tumors clustered into a hyperproliferative, hypoxia-adapted, immune-cold/immunoproteasome-high phenotype. Metabolic enrichment supported a lipid- and nucleotide-centric reprogramming in LINC00092-high tumors, with increased fatty acid oxidation, sphingolipid and eicosanoid pathways, and pyrimidine synthesis, indicating a distinct immunometabolic mode rather than purely hyperproliferative growth. In summary, a LINC00092-based multiomics signature, measurable in routine FFPE tissue, separates CRC tumors into groups with distinct signaling, metabolic, and immune profiles. This signature can help stratify patients for pro-apoptotic therapies, immunotherapy, and rational drug combinations.

#7910 Advanced preclinical cancer models and imaging protocols for translational treatment studies in orthotopic prostate, bladder, liver, pancreatic and brain cancer.

Celine Christine Jensen[1], Emilie Garly[1], Rikke Stagaard[1], Michala Nordfalk[1], Sigrid Cold[1], Mette Munk Wessel[1], Tea Kirkegaard Nielsen[1], Margarete Karg[1], Natalia Łopuszyńska[1], Marina Simon Martin[1], Sara Vangsgaard[1], Sebastian Gnosa[1], Ingrid Hunter[1], Emma Papin[1], Camilla Malec[1], Anne Hessellund Langhave[1], Trine Nielsen[1], Andreas Kjaer[2], Esben Christensen[1], Trine Bjoernbo Engel[1], **Lotte Kellemann**[1], Carsten Haagen Nielsen[1]

[1]Minerva Imaging, Oelstykke, Denmark,[2]Cluster for Molecular Imaging, Rigshospitalet & Department of Biomedical Sciences, University of Copenhagen, Copenhagen, Denmark

Introduction: Translatable animal models mimicking and predicting clinical disease outcomes are in high demand to increase the success rate of novel anti-cancer therapies. Orthotopic or metastatic cancer models, where tumors are established in their tissue of origin, have gained significant interest in drug development as they more accurately replicate the tumor microenvironment, metastatic behavior, and treatment response seen in patients. In these studies, we generated advanced orthotopic models of cancer including prostate, bladder and pancreas, as well as disseminated models of cancer spread to liver and brain. Furthermore, we developed imaging protocols to accurately monitor treatment responses and drug targeting engagement in preclinical studies.

Methods: Murine and human prostate cancer cell lines engineered to express human PSMA (RM-1.hPSMA and PC-3.hPSMA, respectively) were injected into the prostate gland of immunodeficient and immunocompetent mice. Human UM-UC-3 bladder cancer cells were intramurally injected into the bladder wall under laparotomy. Human BxPC-3 pancreatic cancer cells were surgically inoculated into the head of pancreas. Seeding in the liver was established by intrasplenic injection of murine 4T1 breast cancer cells. Metastatic seeding in the brain was established by injection of MDA-MB-231 TNBC cells into the intracarotid artery (ICt). Tumor growth was monitored using bioluminescence imaging (BLI), magnetic resonance imaging (MRI), and ultrasound (US), while SPECT/CT imaging was applied for target engagement of [^{177}Lu]Lu-PSMA-617. IHC and light sheet microscopy (LSM) were used to validate *in vivo* findings.

Results: Orthotopic tumors were successfully established in pancreas, bladder and prostate with a take-rate >90%, >60% and >75%, respectively. Intrasplenic inoculation led to numerous liver metastases with a take rate of 100%, while ICt inoculation resulted exclusively in the formation of brain metastases with a take rate >70%. MRI imaging revealed 1-7 metastases per animal with intra- and intersubject variation in BBB permeability. MRI and US provided accurate tumor volumetry, while BLI monitored viable tumor burden with correlation to different modalities across the studies, verified by IHC and LSM.

Conclusion: We successfully developed complex surgical procedures for establishing orthotopic models and models of metastatic spread for cancers with an unmet clinical need. All models presented with key characteristics of human disease. Combined with multimodal, reliable and state-of-the-art imaging readouts, this is an attractive platform to increase the translational value of preclinical studies with novel anti-cancer therapies and combinations.

#7911 Multi-cohort transcriptomic profiling identifies pathways driving high-risk biochemical recurrence in prostate cancer.

Sabrina Yepes-Rodriguez[1], Rafael Parra-Medina[2]

[1]Laboratorio de Patologia Molecular, Instituto Nacional de Cancerologia, Bogota, Colombia,[2]Instituto Nacional de Cancerologia, Bogota, Colombia

Background: Biochemical recurrence (BCR) after radical prostatectomy for localized or locally advanced prostate adenocarcinoma is clinically heterogeneous, and current risk categories only partially capture the underlying biology. Multi-cohort transcriptomic integration may clarify molecular distinctions between European Association of Urology (EAU) low- versus high-risk BCR. Objective: To identify reproducible gene-expression profile associated with high-risk BCR across independent datasets and to determine whether low-risk BCR tumors differ biologically from non-recurrent disease. Methods: Transcriptomic data were analyzed from TCGA-PRAD (n=479), GSE220095 (BCR-No=101, BCR-EAU-Low=45, BCR-EAU-High=30), GSE70768 (No=93, Low=7, High=12), GSE54460 (No=48, Low=29, High=21), and GSE70769 (No=49, Low=21, High=24). Cohorts were reclassified into and adapted EAU-like BCR groups. RNA-seq data were log-transformed. All matrices were then harmonized, filtered, and aligned to curated metadata. Differential expression was performed with limma on R software using contrasts High-vs-No, High-vs-Low, and Low-vs-No. Pathway enrichment was evaluated using preranked GSEA (GO/Reactome). Results: Across cohorts, high-risk BCR tumors consistently upregulated cell-cycle and DNA-replication programs, including G2/M checkpoint activation, sister chromatid segregation, replication-stress signaling, and mitotic spindle assembly. TCGA-PRAD high-risk tumors showed strong activation of ATR-dependent replication-stress pathways. GSE220095 high-risk cases exhibited enrichment of mitotic checkpoint and pre-replicative complex assembly mechanisms. In GSE70768, key differentially expressed genes included *PAGE4, PGM5, SERPINA3,* and *TOP2A*, indicating loss of androgen-regulated stress-response programs and increased proliferative drive. GSE70769 and GSE54460 similarly converged on cell-cycle deregulation, chromatin remodeling, and ECM/EMT-related signaling. The absence of DEGs between low- and high-risk BCR groups—despite marked differences between high-risk and No-BCR—suggests that low-risk tumors form a heterogeneous intermediate state, sharing baseline expression with No-BCR cases while lacking the proliferative and replication-stress programs. Computational workflow and writing support was provided by an AI-based language (ChatGPT, OpenAI). Conclusions: High-risk BCR tumors show a strong, reproducible transcriptional signature driven by replication stress and proliferative pathways, whereas low-risk BCR tumors are molecularly similar to non-recurrent diseases. These results provide biological validation of the EAU risk stratification system and highlight the potential of transcriptomic profiling to refine surveillance and treatment decisions after prostatectomy.

#7912 Performance analysis of a novel PD-L1 CAL10 assay in esophageal cancer.

Ibrahim Abukhiran[1], Matthew G. Hanna[1], Dimitrios Korentzelos[1], Rajiv Dhir[1], Aatur D. Singhi[1], Shubham Dayal[2], Joseph Chiweshe[2], Xiaozhi Zhou[2], Robert Monroe[3], Michelle Wood-Trageser[1]

[1]University of Pittsburgh Medical Center, Pittsburgh, PA,[2]Leica Biosystems, Vista, CA,[3]Danaher Diagnostics, Vista, CA

Background: Esophageal cancer (ESCC) remains a highly lethal disease due to late diagnosis and limited responsiveness to conventional therapies. Recent studies have highlighted the role of immune checkpoint pathways in its pathogenesis, particularly the PD-1/PD-L1 interaction, which enables tumor cells to escape immune surveillance. We have developed a PD-L1 CAL10 assay for immunohistochemical (IHC) detection of PD-L1 in ESCC specimens.
Here, we have compared this novel PD-L1 CAL10 assay for IHC detection of PD-L1 in ESCC specimens with two common research-utilized PD-L1 IHC assays.
Design: The primary objective was to compare the PD-L1 CAL10 assay with other commercially available assays, SP263 and 22C3, at ≥1% tumor proportion score (TPS) and ≥50% TPS cutoffs. Also, we measured interobserver/interpathologist agreement (secondary objective) for each assay type at ≥1% TPS and ≥50% TPS cutoffs. Seventy (70) whole tissue formalin fixed paraffin embedded (FFPE) unique ESCC cases were included in the study. Each case was serially sectioned at 4 µm. Each of these sections was stained with H&E and anti-PD-L1 antibodies: CAL10 on Leica Biosystems BOND RX, SP263 on Ventana BenchMark ULTRA, and Agilent/Dako's 22C3 optimized for use on a Ventana Discovery Ultra. These tissue-mounted glass slides were scored manually by 3 pathologists, with a washout period of two weeks between reads for each clone. In comparison to other assays, the PD-L1 CAL10 stained slides had no significant background or artifacts. Each pathologist scored independently, and the majority score for the PD-L1 status (positive or negative) was recorded.
Results: The PD-L1 CAL10 assay showed comparable interassay and interreader variability (Table 1). Additionally, its scoring pattern was similar to the other two PD-L1 clones.

Table 1. TPS agreement rates

Interassay	**CAL10 vs. SP263**	**CAL10 vs. 22C3**	**SP263 vs. 22C3**
≥1% TPS cutoff	Almost perfect (k= 0.82)	Moderate (k=0.59)	Substantial (k=0.67)
	OPA-91.2%	OPA-79.7%	OPA - 84.1%
≥50% TPS cutoff	Moderate (k= 0.42)	Slight (k=0.19)	Substantial (k=0.65)
	OPA-92.6%	OPA-89.9%	OPA - 97.1%
Interpathologist	**CAL10**	**SP263**	**22C3**
≥1% TPS cutoff	Moderate (k=0.54)	Substantial (k=0.71)	Moderate (k=0.53)
≥50% TPS cutoff	Moderate (k=0.48)	Fair (k=0.37)	Moderate (k=0.42)
k, Cohen's kappa statistic; OPA, Overall percent agreement			

Conclusion: The initial results suggest that the PD-L1 CAL10 assay is comparable to the other tested PD-L1 assays for ESCC specimens and can be a suitable option for further translational research evaluations.

#7913 OXC-101 (karonudib) in canine lymphoma and hemangiosarcoma: Safety, early efficacy, and translational potential.

Kumar Sanjiv[1], Sara Saelstrom[2], Martin Scobie[3], Ulrika warpman Berglung[3], Thomas Helleday[1], Henrik Ronnberg[2]

[1]Oncology and Pathology, Karolinska Institute, Science for Life Laboratory, Solna, Sweden,[2]University Animal hospital (UDS) and HBIO, Swedish University of Agricultural Sciences, SLU, Uppsala, Sweden,[3]Oxcia AB, Solna, Sweden

Background: Canine lymphoma (CL) and hemangiosarcoma (HSA) are aggressive malignancies. Current treatments have limited efficacy, profound toxicity which causes poor quality of life (QoL) in patients. There is strong biological and clinical similarity to human non-Hodgkin lymphoma and human angiosarcoma, which makes dogs an attractive model for translation research. OXC-101 (Karonudib), a dual-function MTH1 inhibitor, induces incorporation of oxidized nucleotides into DNA and inhibits microtubule polymerization and includes the toxicity in cancer cells. OXC-101 is currently being evaluated in two human clinical trials (Phase 1 solid tumors; Phase 1/2 hematologic malignancies) and has received Orphan Drug Designation for acute myeloid leukemia, underscoring its translational relevance.
Methods: We conducted an open-label pilot study to assess safety and preliminary efficacy of oral OXC-101 in nine pet dogs with CL (n=6) or HSA (n=3). Dogs received 8-10 mg/kg orally twice daily every other day for up to eight months. Clinical exams, laboratory analyses, and owner feedback were used to monitor safety, response, and quality of life.
Results: Eight dogs (five CL, three HSA) completed the evaluable portion; two withdrew for reasons unrelated to treatment. Most CL cases enrolled to trial had relapsed disease after Adriamycin-based chemotherapy. Relapsed CL dogs showed stable disease to partial responses lasting up to five months, with improved quality of life and no evident toxicity. One treatment-naïve stage V CL dog showed rapid lymph node reduction and normalization of liver enzymes within 21 days before voluntary withdrawal. In HSA, two out of three splenectomised dogs remain recurrence-free beyond 150 days with good QoL. In all the enrolled patients, OXC-101 was found to be well tolerated, with no gastrointestinal side effects, no neutropenia/ Thrombocytopenia or any significant biochemical abnormalities.
Conclusions: This pilot study shows that OXC-101 is safe and demonstrates early antitumor activity in relapsed CL and post-operative HSA. Given the close parallels between these canine cancers and their human counterparts—and ongoing human trials— these results strongly support further clinical development. OXC-101 may represent a promising new targeted therapy for both veterinary and human oncology.

#7914 Preclinical modeling of plasmacytoid urothelial carcinoma to study cancer mechanisms and therapeutic response.

Kanisha Kar[1], Caroline Dickey[1], William Kim[1], Kathryn Gessner[2]

[1]UNC Lineberger Comprehensive Cancer Center, Chapel Hill, NC,[2]University of North Carolina at Chapel Hill, Chapel Hill, NC

Plasmacytoid urothelial carcinoma (PUC) is an aggressive histologic subtype of bladder cancer with poor patient outcomes and worse response to standard chemotherapies than conventional histology urothelial carcinoma (CUC). The hallmark molecular alteration in PUC is loss of E-cadherin, which can occur through mutations or promoter hypermethylation of *CDH1*, the gene encoding E-cadherin. Aside from E-cadherin loss, the mutational spectrum of PUC is similar to that of CUC, although with higher rates of mutations in RB1 and p53 in PUC. E-cadherin, a transmembrane glycoprotein essential for epithelial adhesion and integrity, is a central regulator of EMT. Decreased expression of E-cadherin promotes EMT through transcriptional repressors (Snail, Slug, Twist, ZEB1/2), a cadherin switch, and epigenetic remodeling, driving enhanced invasiveness and metastatic potential. Despite our knowledge regarding the function of E-cadherin, the precise mechanism by which E-cadherin loss promotes disease progression and therapeutic resistance within urothelial carcinoma is not understood. Additionally, due to the lack of a preclinical PUC model and the limited ability to perform randomized controlled trials in this rare tumor type, clinicians face uncertainty regarding which therapeutic agents are most effective, reinforcing the need for innovative preclinical studies. Therefore, we aim to interrogate the impact of CDH1 loss in PUC on cancer phenotypes, elucidate mechanistic insights, and identify novel therapeutic strategies for PUC through preclinical modeling. To model PUC biology, we utilized CRISPR/Cas9 mediated knockout to generate CDH1 loss in two luminal (UPPL1541, UPPL1595) and one basal (BBN963) previously established murine bladder cancer cell lines using three independent gRNAs. Resulting CDH1 mutations at the CRISPR-Cas9 target site were confirmed by Sanger sequencing and E-cadherin protein loss confirmed by western blot. Compared to non-targeted, CDH1-intact control cells, CDH1-knockout cells demonstrate increased N-cadherin protein expression and increased expression of the mesenchymal markers Snail, Slug, ZEB1, and Vimentin by western blot. CDH1 knockout cells did not demonstrate a difference in cell proliferation compared to non-targeting controls, as determined by cell-titer glo assay. On transwell invasion assay, CDH1 knockout cells demonstrate significantly increased cell invasion compared to nontargeted, CDH1-intact control cells. These findings demonstrate that CDH1 loss is associated with upregulation of the epithelial-to-mesenchymal transition and enhanced *in vitro* cell invasion in urothelial carcinoma. We will continue to advance this work by dissecting tumor-microenvironment interactions and therapeutic responses in syngeneic models, positioning this platform as a novel preclinical resource for the clinically-challenging PUC variant.

#7915 Molecular landscape of colorectal cancer (CRC) with KRAS 13D mutations.

Masango Samuel[1], Yuliang Chen[2], Sarah Castillo[3], Chenbo Sun[2], Natalia Ignatenko[2], Daruka Mahadevan[4], **Ritu Pandey**[5]

[1]University of Arizona Health Sciences, Tucson, AZ,[2]University of Arizona Cancer Center, Tucson, AZ,[3]University of Arizona, Tucson, AZ,[4]UT Health Science Center at San Antonio, San Antonio, TX,[5]University of Arizona Cancer Center, Department of Cellular and Molecular Medicine, Tucson, AZ

Background: Colorectal cancer (CRC) is one of the leading causes of cancer related mortality across the world. Approximately 50% of the CRC patients exhibit mutation in the KRAS gene, most frequently found in codons 12 and 13. KRAS 13D mutation tumors are unique in that they are more aggressive and have different treatment response and outcome than tumors with other KRAS gene mutations. This is attributed to the underlying combination of distinct biology. We report a detailed comparative study of stratified KRAS 13D mutant patients with disease, poor outcome, exceptional response and mutant cell lines for distinct co-occurring mutations and gene expression.

Methods: RNA-Seq, whole exome sequencing and clinical data of CRC patients with known KRAS mutation type were obtained from Genomic Data Commons (GDC) while CRC cell lines data were obtained from NCBI GEO. The patient dataset included 170 KRAS mutated samples in Cancer Genome Atlas with 31 tumors with KRAS 13 mutations and NCI Exceptional responder's initiative with KRAS mutated samples. Normalized log transformed expression profiles and gene variants were statistically analyzed for differential expression, likelihood ratios, enrichment, correlation, odd ratios, deconvolution and log rank test for outcome using R (v4.5.1) and computing platform provided by GDC.

Observations: The KRAS 13 tumors proportionally had higher mutation burden (TMB) and prevalent in ascending colon compared to other location. The KRAS13D tumors were also of mixed CMS (consensus molecular) subtypes. Among the top mutated genes in KRAS mutated tumors there were common co-occurring mutations in both KRAS 12 and KRAS 13 but frequency of mutations in genes RYR2, FAT3, CMSD1 and MUC4 amongst others were enriched more in KRAS 13 mutated tumors. Cell lines expression data identifies specific genes uniquely overexpressed in KRAS 13 mutants and some of them were found to be common with genes over expressed in exceptional responders. The poor outcome patients compared with exceptional responders found differential genes with significance in cellular processes. Log rank test shows few of these genes associated with better or worse outcomes after treatment.

Conclusions and ongoing research: We found that a right combination of mutations could give KRAS 13D mutated tumors advantage to become more aggressive, but a background of unique network of gene expression could make the tumors respond well to treatment or resist therapy. We are currently testing the significance of these unique molecular correlates in KRAS 13D patient derived organoids with specific drugs and RAS inhibitor screens to provide insights into resistance and response of some of the KRAS 13D mutated CRC patients.

#7916 Galectin-2 expression in the tumor microenvironment: A silent pathway of pancreatic ductal adenocarcinoma progression.

Moacyr Jesus B. Melo Rego[1], Richard Tomasini[2], Sophie Vasseur[3], Maira Pitta[4], Maria Clara P. D. Sampaio[1], Amanda P. B. Albuquerque[1], Pascal Finetti[2], Claudio Montenegro[1], Michelly Cristiny Pereira[5], Michelle Rosa[1]

[1]Federal University of Pernambuco (UFPE), Recife, Brazil,[2]CRCM, Marseille, France,[3]INSERM 4624, Marseille, France,[4]UFPE, Recife, Brazil,[5]Federal University of Pernambuco (UFPE), Olinda, Brazil

Background: Pancreatic ductal adenocarcinoma (PDAC) is an aggressive cancer with a complex microenvironment in which galectins play key roles. This study evaluated galectins expression to investigate its potential as a prognostic biomarker.

Methods: Transcriptomic analyses were performed *in silico* on a cohort of 938 individuals with primary PDAC. Laser microdissection, immunohistochemistry, and RT-qPCR were used to assess the expression profile in the tumor and stromal regions of PDAC biopsies. Serum GAL-2 levels were measured by ELISA. GAL2 expression was also evaluated during distinct stages of tumor progression using the KIC murine model.

Results: To analyze the galectin transcriptomic expression profile in human PDAC, transcripts of *LGALS* genes were evaluated in a cohort of 938 individuals diagnosed with primary PDAC tumors. *LGALS2* emerged as a key transcript, exhibiting expression levels two-fold below the median in PDAC samples. Correlation analysis of *LGALS* transcripts revealed a positive cluster among *LGALS2*, *LGALS3*, *LGALS4*, and *LGALS9*, and a negative association between *LGALS1* and *LGALS2*. *LGALS2* expression was downregulated in primary tumors (p = 8.76E-22) and metastatic sites (p = 2.75E-30) compared to both the control group and normal pancreatic tissue. In the KIC mouse model, a progressive reduction in *LGALS2* expression was observed throughout tumor progression, from early lesions to established primary and metastatic tumors. High *LGALS2* expression was associated with classical and well-differentiated epithelial PDAC subtypes, whereas low expression characterized basal-like, squamous, and mesenchymal tumors. Importantly, increased *LGALS2* expression correlated with better disease-free and overall survival. Furthermore, higher *LGALS2* expression was significantly associated with improved overall survival in patients treated with the FOLFIRINOX regimen (p = 4.08E-02). Additionally, low GAL-2 protein expression was observed in biopsies from patients diagnosed with PDAC. Serum GAL-2 levels were significantly lower in PDAC patients, especially those with metastasis when compared to health donors. Promoter hypomethylation (CpG island cpg25247183) was identified as a potential regulatory mechanism underlying its downregulation.

Conclusions: The downregulation of *LGALS2* expression across different stages of PDAC progression underscores its importance in tumor pathogenesis and suggests its potential as a prognostic and therapeutic biomarker.

#7917 RUVBL1 and SPARC as prognostic biomarkers in breast cancer.

Flavia Rotea Mangone[1], Fernando A. Soares[2], Maria Aparecida Nagai[3]

[1]Center for Translational Research in Oncology, Instituto do Cancer do Estado de Sao Paulo and Comprehensive Center for Precision Oncology, Sao Paulo, Brazil,[2]Department of Anatomic Pathology, Instituto D'Or de Pesquisa e Ensino (IDOR), Sao Paulo, Brazil,[3]Center for Translational Research in Oncology, Instituto do Cancer do Estado de Sao Paulo and Comprehensive Center for Precision Oncology/Disciplina de Oncologia do Departamento de Radiologia e Oncologia, Sao Paulo, Brazil

Despite significant progress in elucidating the biology of breast cancer, there remains a need for biomarkers for accurate prognostic stratification and prediction of therapeutic response. In the present study, we sought to determine the protein expression pattern and prognostic value of RUVBL1 alone or in combination with SPARC in breast cancer. We performed IHC analysis using antibodies against RUVBL1 and SPARC on a tissue microarray comprising 319 primary breast tumor samples. RUVBL1, a member of the highly conserved ATPases of the AAA+ superfamily, is involved in key cellular processes related to tumorigenesis. Our previous work has shown that the downregulation of SPARC protein expression, a matricellular protein with pleiotropic functions, is an independent prognostic factor for breast cancer. RUVBL1 expression was positively associated with HER2 positivity (p=0.006), post-menopausal status (p=0.007), and reduced ER/PR expression (p=0.046). Although we did not observe any significant prognostic value of RUVBL1 expression in our population, we observed a strong association between RUVBL1 and SPARC expression (p<0.0001). Moreover, the combined profile of high RUVBL1 and low SPARC expression stratified a subgroup of patients with markedly poorer survival outcomes (HR=2.49, 95% CI: 1.36–4.56, p=0.003), exhibiting a survival rate of 17%. Our results provide novel insights supporting the prognostic significance of RUVBL1 and SPARC in breast cancer. These findings underscore the need for further experimental and clinical investigations to fully understand the clinical implications of RUVBL1 and SPARC expression in breast cancer.

#7918 Suppression of MAGED1 increases sensitivity to PARP inhibitor in BRCA-mutated breast cancer cells.

In Hee Lee, Soo Jung Lee, Byeongju Kang, Jeeyeon Lee, Ho Yong Park, Joon Suk Moon, Ji-Young Park, Yee Soo Chae, Eun Ae Kim, Seol-Hwa Jeong, Jieun Kang

Kyungpook National Chilgok University Hospital, Daegu, Korea, Republic of

Background: MAGED1 (Melanoma Antigen Gene Family, Member D1) is a member of the MAGE gene family and is known to be involved in various cellular processes such as cell death, cell cycle regulation, and differentiation. Furthermore, previous studies indicate that MAGED1 is essential for double-strand break (DSB) repair via homologous recombination repair (HRR), and reduced MAGED1 expression sensitizes cancer cells to DNA-damaging agents. This study aimed to investigate the role of MAGED1 in HRR in triple-negative breast cancer (TNBC) and BRCA1/2 mutant breast cancer.
Methods: In this study, we validated the function of MAGED1 in HRD using siRNA in triple-negative breast cancer (TNBC) and BRCA-mutated breast cancer cell lines. Cell viability was assessed using CytoFLEX after treating Hs578T, HCC-1937 (BRCA1 5382insC), and BT-474 (BRCA2 c.0391C>A) breast cancer cell lines with cisplatin 200 μM, olaparib 200 μM, and niraparib 50 μM, respectively. Cells were transfected with control siRNA (si-Cont) or two independent siRNAs targeting MAGED1 (si-MAGED1 #1, si-MAGED1 #2).
Result: Using cytoFLEX flow cytometry, we investigated siRNA-mediated MAGED1 suppression in BRCA1/2 mutant breast cancer cell lines HCC-1937 (BRCA1 5382insC) and BT-474 (BRCA2 c.0391C>A) exhibited increased sensitivity compared to normal breast cells MCF10A and breast cancer cell lines MCF7 (luminal A) and Hs578T (TNBC). Furthermore, the platinum-based anticancer drug cisplatin was found not to affect MAGED1 inhibition, and the synergistic effect of PARP inhibitors on MAGED1 inhibition was more pronounced in BRCA-mutant cell lines. Additional studies involving RNF8, BARD1, RAD51, and ATM are underway to further elucidate the roles of HRD and MAGED1.
Conclusions: Our study demonstrates that silencing of MAGED1 enhances sensitivity to PARP inhibitors in BRCA1/2-mutant breast cancer cell lines. These results suggest that MAGED1 is involved in HRD and could be a therapeutic target to enhance PARP inhibitor response in breast cancer.

#7919 Clinical, genomic, and therapeutic outcomes of lung squamous cell carcinoma with high *LGR5* expression : A study from the LC-SCRUM-Asia database.

Yu Tanaka[1], Shuji Murakami[2], Kazumi Nishino[3], Motoko Tachihara[4], Ichiro Nakachi[5], Mayu Kawakami[6], Satoshi Hara[7], hitomi Aono[8], Shoichi Kuyama[9], Gaku Yamamoto[1], Eri Sugiyama[1], Tetsuya Sakai[1], Hiroki Izumi[1], Shigeki Umemura[1], HIBIKI UDAGAWA[1], Yoshitaka Zenke[1], Shingo Matsumoto[1], Kiyotaka Yoh[1], Koichi Goto[1]

[1]National Cancer Center Hospital East, Chiba, Japan,[2]Kanagawa Cancer Center, Kanagawa, Japan,[3]Osaka International Cancer Institute, Osaka, Japan,[4]Kobe University Hospital, Hyogo, Japan,[5]Research Scholar, Dept. of Medicine, University of Colorado Denver, Aurora, CO,[6]Saiseikai Imabari Hospital, Ehime, Japan,[7]Itami City Hospital, Osaka, Japan,[8]Tokyo Metropolitan Police Hospital, Tokyo, Japan,[9]National Hospital Organization Iwakuni Clinical Center, Yamaguchi, Japan

Introduction: Petosemtamab, a bispecific antibody targeting LGR5 (Leucine-rich repeat-containing G-protein coupled receptor 5) and EGFR, is under clinical development. Wnt-driven LGR5, a stem cell-associated marker, stabilizes EGFR by preventing lysosomal degradation, thereby promoting cancer cell survival. However, its role in lung squamous cell carcinoma (LUSC) remains unclear. This study evaluates the impact of *LGR5* expression on clinical characteristics, genomic alterations, and therapeutic outcomes in LUSC.

Methods: Using the LC-SCRUM-Asia clinico-genomic database, mRNA levels of *LGR5*, *EGFR*, and other genes were assessed via the AMOY Master Panel. High *LGR5* was defined as above the median. Clinical, genomic characteristics, and treatment outcomes were compared between high and low *LGR5* groups.

Results: *LGR5* expression was evaluated in 233 LUSC patients between June 2021 and February 2022. The median *LGR5* expression was 0.02 FPKM (range: 0.00-5.44), and the median *EGFR* expression was 12.09 FPKM (range: 0.07-572.49). No correlation was observed between *LGR5* and *EGFR* expression (Pearson r = -0.0387, $P = 0.687$). Clinical characteristics, including age, sex, smoking history, ECOG-PS, and clinical stage, did not differ significantly between high and low *LGR5* groups. The prevalence of driver gene alterations (*KRAS* mutation: 6 vs. 3, *EGFR* mutation: 2 vs. 4, *MET* ex14 skipping: 2 vs. 4, *ALK* fusion: 3 vs. 1) also showed no significant differences ($P = 0.816$). Among 103 patients receiving first-line ICI with or without chemotherapy, the median PFS was 8.0 months in the high *LGR5* group and 5.6 months in the low *LGR5* group (HR = 0.91, 95% CI: 0.58-1.44, $P = 0.570$). In 90 patients treated with first-line platinum-based chemotherapy, the median PFS was 5.5 months in the high *LGR5* group and 4.3 months in the low *LGR5* group (HR = 0.99, 95% CI: 0.52-1.91, $P = 0.985$). Wnt (*P*-weighted Log2FC = 0.753), Hedgehog (*P*-weighted Log2FC = 0.877), and Notch (*P*-weighted Log2FC = 0.564) pathways, key regulators of stem cell function, were significantly upregulated in the high *LGR5* group (all $P < 0.05$).

Conclusion: High LGR5 expression does not define a clinically or genomically distinct subgroup of LUSC; however, it is associated with a transcriptionally stemness-activated phenotype characterized by upregulation of Wnt, Hedgehog, and Notch pathways. These findings suggest that LGR5-high LUSC represents a biologically distinct subtype that may inform future development of LGR5×EGFR-targeted therapies.

#7920 Integrated proteogenomics reveals molecular predictors of recurrence beyond HER2 IHC in HER2-positive breast cancer.

Eunjoo Lee[1], Seung Min Park[2], Kyung-Hee Kim[3], So-Youn Jung[4], Gi Yeon Lee[5], Eun-Gyeong Lee[6], Min-Chae Kang[7], Jong Bae Park[8], Kong Sun-Young[1]

[1]National Cancer Center, Goyangsi, Korea, Republic of,[2]Targeted Therapy Branch, National Cancer Center, Goyangsi, Korea, Republic of,[3]Proteomics Analysis Team, Research Core Center, Research Institute, National Cancer Center, Goyangsi, Korea, Republic of,[4]National Cancer Center - Korea, Goyang-si, Korea, Republic of,[5]Targeted Therapy Branch,, National Cancer Center, Goyang, Korea, Republic of,[6]Center for Breast Cancer, National Cancer Center, Goyangsi, Korea, Republic of,[7]Hanyang Univ. College of Medicine, Seoul,[8]Cancer Biomedical Science, National Cancer Center, Goyangsi, Korea, Republic of

Purpose: Breast cancer remains the most common malignancy among women, with about 20% driven by HER2 overexpression. Although HER2-targeted therapies have improved outcomes, acquired resistance and recurrence persist. Clinical HER2 Immunohistochemistry(IHC) often fails to reflect actual HER2 abundance, as seen in both IHC-negative/high-protein and IHC 3+/low-protein cases. Thus we conducted an integrated proteogenomic analysis to define HER2 heterogeneity and identify recurrence-associated signatures.
Methods: Total of 62 patients with a median age of 41.5 years (range, 25-60) were included from National Cancer Center in Korea, and breast tumor tissues analyzed using an integrated proteogenomic workflow combining whole-exome sequencing, whole-transcriptome, global proteomics, phosphoproteomics, and PRM-based HER2 quantification. Differential genomic and proteomic features between the 46 non-recurrence and 15 recurrence patients were compared and validated in TCGA and CPTAC cohorts.
Results: Description between clinical IHC and quantitative HER2 measurement were observed in 10% of low HER2 and in 25% of high HER2 cases. Recurrent patients revealed frequent TP53 mutations, MYC amplification, and ERBB2 hotspot variants (E192* and D844*) in genomic profiling. DEGs analyses integrating RNA and proteomic expression identified a shared set of recurrence-associated genes, including ATXN7L3BM GPRC5A and GPRC5A and WNT5A, which collectively reflected pathways related to extracellular matrix remodeling, metastatic, signaling, metabloic reprogramming, and transcriptional regulation. METABRIC comparison showed similar patterns of ERBB2/MYC amplification, TP53 loss, and genomic instability observed in recurrent tumors. Mutational signature analysis indicated dominant contributions from aging-related, APOBEC-driven, and homologous recombination-defective processes. Copy-number signature profiling further identified five recurrent genomic subtypes (CNV48 A-E), including chromothripsis-like and loss of heterozygosity patterns shared with TCGA and METABRIC HER2-positive tumors.
Conclusions: These findings indicate that recurrence risk in HER2-positive breast cancer is determined more by initial tumor stage than by HER2 IHC status. This underscores the clinical value of quantitative proteogenomic assessment as a complementary tool to improve risk stratification beyond conventional HER2 testing. This work was supported by grant from the National Cancer Center. (Grant No. 2510692-1)

#7921 The development of a novel *PDGFRA* resistance mutation in a recurrent *KIT*-mutant gastrointestinal stromal tumor (GIST).

Rachael S. Lowney[1], Shruthi R. Perati[2], Aaron Dinerman[3], Abraham Hakim[1], Molly A. Sullivan[1], Stephanie N. Canady[1], Diane S. Ahn[1], Michael C. Heinrich[4], Homma Khosroyani[4], Andrew M. Blakely[5]

[1]National Institute for Cancer Research, Bethesda, MD,[2]Rutgers Robert Wood Johnson Medical School, New Brunswick, NJ,[3]University of South Alabama College of Medicine, Mobile, AL,[4]OHSU Knight Cancer Institute, Portland, OR,[5]National Cancer Institute, Bethesda, MD

Background: GISTs are sarcomas of the gastrointestinal tract that classically arise through mutations in *KIT* or *PDGFRA* tyrosine kinases. GISTs can exhibit both temporal and spatial mutational tumor heterogeneity, however, *KIT* and *PDGFRA* mutations are traditionally considered mutually exclusive. To date, only one other case of concurrent mutations exists in the literature. The purpose of this study was to investigate the relationship between primary, metastatic, and recurrent GIST tumors on the genomic level.

Methods: This patient with histologically confirmed GIST was enrolled on NCT04557969 and underwent complete cytoreductive surgery for metastatic GIST. A tissue section of the primary tumor was sent for next-generation sequencing (NGS) via the National Cancer Institute Comprehensive Oncologic Molecular Pathology and Sequencing Service (NCI-COMPASS) that utilized the TruSight Oncology 500 Gene Panel for detection of somatic mutations. NGS was repeated upon tumor recurrence and a peri-sigmoid mesocolic metastasis from the index surgery that was retrospectively noted to have no treatment effect. A detailed chart review, including medical history, operative reports, pathology reports, and NGS was performed.

Results: This patient is a 51-year-old male who presented with 3 large intra-abdominal masses and was discovered to have a *KIT* exon 11 GIST on biopsy. He was initiated on imatinib with significant response over one year of therapy. He then underwent exploratory laparotomy with resection of jejunal primary and multiple peritoneal metastases in November, 2023. NGS of the jejunal primary confirmed previously identified *KIT* exon 11 (p.Val560Asp) mutation. After 1 year of surveillance imaging on adjuvant imatinib, he was found to have an isolated lesion posterior to the left lower rectus. A review of the pathology report from the index surgery identified a peri-sigmoid metastases that demonstrated no treatment effect. A sample of this metastasis was sent for NGS which showed the previously known *KIT* exon 11 (p.Val560Asp) mutation and a new pathologic structural copy number variation (CNV) loss of *CDKN2A* on chr9:21968226. He underwent resection of the recurrent mass in March, 2025. NGS of the recurrence demonstrated the *KIT* exon 11 (p.Val560Asp) mutation, the CNV loss of *CDKN2A,* and a novel *PDGFRA* D842Y (p. Asp842Tyr) mutation that is considered imatinib-resistant.

Conclusion: This case demonstrates a rare example of a *PDGFRA* mutation present in a tumor recurrence that arose as a resistance mutation to a baseline *KIT* mutation. The presence of this CNV loss in both an imatinib -resistant metastasis and the peritoneal recurrence suggests a clonal relationship. This case highlights the geographic and temporal heterogeneity of GIST and underscores the importance of repeat NGS to evaluate GIST recurrences to inform subsequent medical therapy.

#7922 Effect of plasma activated media, with and without chemotherapeutics, on viability of normal and malignant human breast cells.

Jakob Doster[1], Lavanya Sankaran[2], Chuanling Xu[3], Nathalie Gonce[3], Valentyne Thomas[3], Sofia Melendrez[1], Komal Vig[4], Vijay Rangarari[5], Satyanarayana Pondugula[3], Amit Morey[1]

[1]Poultry Science, Auburn University, Auburn, AL,[2]College of Osteopathic Medicine, California Health Sciences University, Clovis, CA,[3]College of Veterinary Medicine, Auburn University, Auburn, AL,[4]Biological Sciences, Alabama State University, Montgomery, AL,[5]Materials Science and Engineering, Tuskegee University, Tuskegee, AL

Chemotherapy used for cancer treatment results in debilitating side effects for patients. Despite decades of research, enhancing drug sensitivity and minimizing toxicity remains a major challenge. Cold atmospheric plasma (CAP) offers a novel, non-thermal strategy to address this gap. CAP can alter biological processes at the cellular levelto amplify the effects of existing chemotherapeutics. However, the comparative impact of plasma-treated media on normal tissues remains poorly understood and represents a critical barrier to clinical translation. Therefore, the goal wasto determine the effect of the plasma-treated media, alone or in combination with chemotherapeutics, on viability of normal and malignant human breast cells. We conducted a series of experiments using malignant breast MCF-7 and MDA-MB-231 cell lines, and the corresponding normal breast MCF-10A cell line to assess the effects of plasma-treated media combined with different chemotherapeutic agents; paclitaxel, docetaxel, doxorubicin, cisplatin, carboplatin, 5-fluorouracil, and gemcitabine. Media were exposed to dielectric barrier discharge (DBD) air plasma for 5, 10, or 20 minutes before drug administration. Our results demonstrated that breast cancer cell lines showed limited responsiveness to plasma-treated media, whereas normal cells were markedly susceptible. Neither MCF-7 nor MDA-MB-231 cells displayed significant changes in viability following 5-minute plasma exposure, and only modest reductions were observed at 10- and 20-minute exposures across most drug conditions. Among the chemotherapeutics tested, docetaxel at 1 μM exhibited the most pronounced plasma-enhanced reduction in cancer cell viability. In contrast, MCF-10A cells demonstrated heightened sensitivity to plasma-treated media, consistently exhibiting approximately twice the loss of viability observed in cancer cells across nearly all treatment groups. These findings suggest that, within the current DBD air-plasma setup, the oxidative burden generated is disproportionately harmful to normal epithelial breast cell lines and does not produce a correspondingly advantageous cytotoxic effect in the malignant breast cell lines tested. Future studies will evaluate the effect of different types of plasma, alone or combined with chemotherapeutics, on both normal and breast cancer cells, and will investigate the underlying mechanisms.

: Tumor Microenvironment Modulators
Poster Session

#7926 Efficacy, *in vivo* safety, and PK/PD studies for novel, oral, highly selective PTPN2/1 inhibitor (ZE00-0388).

Alexei Pushechnikov[1], Ruben Karapetian[2], Stepan Mochalov[2], Sanja Baumann Tomovska[3], Nikolay Savchuk[3], Iain Dukes[3], Ruben Abagyan[4]

[1]Expert Systems, Inc., San Diego, CA,[2]Navegador Biosciences, Cantanhede, Portugal,[3]Mondego Bio, Cantanhede, Portugal,[4]MolSoft LLC, San Diego, CA

PTPN2 inhibition is a novel immuno-oncology approach: by releasing an intracellular “brake” it increases cytokine responsiveness (e.g., IFN-γ/JAK-STAT), boosts antigen presentation, and enhances T-cell cytotoxicity, helping to overcome immune evasion in tumors resistant to PD-1 blockade.
Our development candidate ZE00-0388 demonstrates potential best-in-class profile: Nanomolar potency with high selectivity for PTPN2/1 over other phosphatases, predictable PK/PD with sustained exposure above EC50, and proven target engagement. ZE00-0388 shows favorable bioavailability in all species, with best translation expected from dog to human.
The combination of anti-mPD-1 and ZE00-0388 exhibited remarkable dose-dependent anti-tumor efficacy against the subcutaneous MC38 colon model. Solo treatments with ZE00-0388 demonstrated tumor growth inhibition of 81% and in combination with anti-mPD-1 complete regression of tumor in 50% of animals. ZE00-0388 has a very favorable safety profile with tolerated doses significantly above pre-clinical proof-of-concept efficacious doses, which indicates that ZE00-0388 should have a very broad therapeutic window.

#7927 Exosomes, regulated by SPRED2, reshape tumor microenvironment via activating IL6/ STAT3 signaling.

Tong Gao[1], Akihiro Matsukawa[2]

[1]Department of Pathology and Experimental Medicine, Graduate School of Medicine, Dentistry and Pharmaceutical Sciences, Okayama University, Okayama, Japan,[2]Graduate School of Medicine, Dentistry and Pharmaceutical Sciences, Okayama University, Okayama, Japan

SPRED2 (Sprouty-related, EVH1 domain-containing protein 2) is a negative regulator of Ras-dependent ERK1/2 signaling. Our previous studies revealed that SPRED2 suppresses hepatocellular carcinoma (HCC) progression by limiting cancer stemness through a SPRED2/p53/miR-506-3p/KLF4 signaling axis. Loss of SPRED2 enhanced proliferation, invasion, and chemoresistance in HCC cells, highlighting its tumor-suppressive role.To further elucidate the broader role of SPRED2 in tumor biology, we shifted our focus from intracellular signaling in HCC to intercellular communication within the tumor microenvironment. Using esophageal squamous cell carcinoma (ESCC) as a model, we demonstrated that SPRED2 suppresses exosome secretion by modulating multivesicular body (MVB)-associated proteins VAMP2 and Syntaxin 4 (STX4). Exosomes, nanosized vesicles released upon MVB-plasma membrane fusion, are critical mediators of intercellular signaling in cancer. Loss of SPRED2 markedly increased exosome release, suggesting that SPRED2 negatively regulates exosome biogenesis and secretion. Functionally, ESCC-derived exosomes were found to carry biologically active interleukin-6 (IL-6), which promotes tumor proliferation and metastasis through two major mechanisms: activation of STAT3 signaling in ESCC cells and induction of tumor-associated macrophage (TAM) polarization within the tumor microenvironment. Notably, exosomes derived from SPRED2-deficient ESCC cells enhanced both tumor cell aggressiveness and TAM polarization, whereas exosomes from SPRED2-overexpressing cells exhibited inhibitory effects on M1 and M2 macrophage polarization. The polarized macrophages, in turn, promoted ESCC proliferation and invasion via STAT3 activation, establishing a reciprocal feed-forward loop between tumor cells and immune cells. Furthermore, exosomes from polarized THP-1 cells significantly accelerated tumor progression in vivo, an effect that was effectively attenuated by Tocilizumab, an IL-6 receptor inhibitor.Collectively, our findings identify SPRED2 as a key regulator of exosome biogenesis and secretion through its interaction with VAMP2 and STX4. By controlling IL-6-enriched exosome release, SPRED2 modulates tumor-immune cell communication and suppresses the formation of a pro-tumorigenic microenvironment, extending its role from an intracellular suppressor of cancer stemness to a central coordinator of tumor-immune interactions.

#7928 Immune microenvironmental patterns in rapidly progressive young-onset tongue cancer: A case series analysis.

Alisa Kimura[1], Takahiro Tsujikawa[1], Shota Sugaya[2], Yuna van der Aar[2], Koichi Yoshizawa[2], Sumiyo Saburi[2], Shigeyuki Mukudai[2], Hikaru Nagao[2], Aki Tamura[2], Nana Sakurai[2], Aya Miyagawa-Hayashino[3], Hiroshi Ogi[4], Saya Shibata[4], Eiichi Konishi[2], Kyoko Itoh[3], Shigeru Hirano[1]

[1]Department of Otolaryngology-Head and Neck Surgery, Kyoto Prefectural University of Medicine, Kyoto, Japan,[2]Kyoto Prefectural University of Medicine, Kyoto, Japan,[3]Department of Pathology and Applied Biology, Kyoto Prefectural University of Medicine, Kyoto, Japan,[4]SCREEN Holdings Co., Ltd., Kyoto, Japan

Young-onset tongue cancer is increasingly recognized as a distinct clinical entity, differing from conventional tongue cancer associated with alcohol and tobacco use in terms of risk factors, clinical behavior, and molecular alterations. In rapidly progressive cases, delayed diagnosis and therapeutic challenges have been highlighted. Prior studies have implicated a myeloid-inflamed tumor microenvironment in this subset, suggesting that unique immune landscapes may influence diseases trajectories and treatment response. We analyzed five cases of rapidly progressive young-onset tongue cancer, focusing on clinical characteristics, genetic alterations, and immune tumor microenvironmental features assessed by 14-marker multiplex immunohistochemistry. Patients ranged from 22 to 48 years (median, 40 years), with a median time to recurrence of three months following initial treatment. Three of 5 patients had no history of alcohol or tobacco use. TERT promoter mutation were identified in two cases. All tumors exhibited abundant tumor-associated macrophages. $CD8^+$ T cell infiltration showed inter-case variability, ranging from sparse to dense. However, in contrast to non-young-onset tongue cancer tissues, $CD8^+$ T cells in young-onset cases were frequently excluded from tumor cell nests, even in specimens with high overall infiltration. These findings suggest the presence of immune exclusion mechanisms underlying the rapid progression of young-onset tongue cancer. Immune exclusion may represent a key barrier to effective immunotherapy in this population and warrants further investigation as a therapeutic target.

#7929 DDR2-CAR macrophages reprogram the tumor microenvironment and normalize vasculature to potentiate antitumor immunity.

Dandan WANG

Guangzhou Medical University, Guangzhou, China

The immunosuppressive extracellular matrix (ECM) of solid tumors is a major barrier to effective antitumor immunity, primarily by fostering immune exclusion. Targeting cancer-associated fibroblasts (CAFs), particularly via discoidin domain receptor 2 (DDR2), has emerged as a strategic avenue to overcome this barrier. Here, we engineered DDR2-targeted chimeric antigen receptor macrophages (DDR2-CAR-M) to leverage macrophage infiltration capacity and disrupt ECM-mediated immunosuppression. In vitro studies demonstrated robust DDR2-CAR adenoviral transduction efficiency (>95%) in primary mouse bone marrow-derived macrophages, with flow cytometry confirming M1 polarization within 48 hours post-transduction. In murine models, immunofluorescence and in vivo imaging revealed elevated DDR2 expression in the ECM of LLC subcutaneous tumor, MC-38 subcutaneous tumor, and U87MG orthotopic glioblastoma model. Tumor growth curves demonstrated significant suppression of lung and colorectal cancers following DDR2-CAR-M combination therapy. Mechanistic investigations using single-cell RNA sequencing, pathological analysis, and flow cytometry indicated a marked activation of immune-related signaling pathways in the CAR-M treatment group, characterized by a significant increase in CD8+ T cells and dendritic cells, suggesting that CAR-M-mediated targeting of CAFs can effectively convert immunologically "cold" tumors into "hot" ones. Furthermore, DDR2-CAR-M remodeled the tumor microenvironment by inhibiting aberrant angiogenesis and promoting vascular normalization, enhancing antigen presentation by macrophages, and promoting T-cell infiltration. These findings establish DDR2-CAR-M as a novel immunotherapeutic approach for solid tumors through stromal reprogramming and immune microenvironment optimization.

#7930 Interaction of visceral adiposity and age in shaping the human breast tumor microenvironment.

Anlan Cao[1], Sophia Fuller[1], Jorge Gomez Tejeda Zanudo[2], Wendy Y. Chen[3], Deborah A. Dillon[4], Sandra S. McAllister[5], Rinath M. Jeselsohn[6], Bette J. Caan[1], Adrienne L. Castillo[1], **Elizabeth M. C. Feliciano**[1]

[1]Division of Research, Kaiser Permanente - Northern California, Pleasanton, CA,[2]Department of Medical Oncology, Dana-Farber Cancer Institute, Boston, MA,[3]Breast Oncology Program, Dana-Farber Brigham Cancer Center, Boston, MA,[4]Assistant Professor, Pathology, Dana-Farber Cancer Institute, Boston, MA,[5]Harvard Medical School, Boston, MA,[6]Dana-Farber Cancer Institute, Boston, MA

Background: Preclinical studies suggest that aging and adiposity synergistically impair anti-tumor immunity, but most evidence comes from triple negative breast cancer (TNBC) models. In humans, visceral adipose tissue (VAT), a metabolically active, pro-inflammatory depot not captured by body mass index, has been linked to alterations in the breast tumor microenvironment (TME), with patterns varying by molecular intrinsic subtype. However, the joint impact of aging and adiposity on the human breast TME remains poorly understood.

Methods: We included 1,377 women diagnosed with primary, stage II-III breast cancer who received treatment at Kaiser Permanente Northern California between 2005 and 2015 and had an abdominal computed tomography (CT) scan within 6 months of diagnosis and before systemic therapy. We selected a stratified random sample enriching for HER2+ and ER- tumors and isolated RNA from treatment-naïve specimens collected at biopsy or excision, verified RNA quality, and performed NanoString BC360™ profiling to determine PAM50 subtype and quantify TME-related gene expression levels. VAT area (cm^2) was quantified from CT scans at the third lumbar vertebra. We examined the differential gene expressions associated with high vs. low VAT index (VAT area scaled to height; ≥42.5 vs <42.5 cm^2/m^2) stratified by age as a proxy for menopausal status (≤55 vs >55) and PAM50 subtype.

Results: Patients were on average 56±13 years old at diagnosis. Most had overweight (30%, BMI 25-<30) or obesity (38%, BMI 30+) and stage II (58%) cancer. The PAM50 subtype distribution was: Basal-like (31%), HER2-enriched (25%), Luminal B (22%), and Luminal A (22%). VAT was associated with differential TME gene expression only among patients aged >55: In Basal-like tumors, high VAT was associated with upregulation of CDKN2A, a cell cycle inhibitor that can drive senescence, which in turn, promotes immune modulation, treatment resistance, and poor prognosis in TNBC. In Luminal A tumors, low VAT showed increased expression of genes associated with metabolic adaptation (PCK1) and differentiation regulators (ACVR1C, WIF1, SOCS2), whereas high VAT was linked to SPP1, a pro-inflammatory glycoprotein also related to senescence.

Conclusion: Excess VAT modifies breast TME gene expression in post-menopausal patients with Basal-like and Luminal A breast cancers. The differential expression patterns were suggestive of metabolic shifts and inflammatory reprogramming that could lead to an aggressive, pro-inflammatory and/or immunosuppressive breast TME in menopausal patients, negatively impacting treatment response. These findings highlight the interplay of aging and visceral adiposity in breast cancer biology and prognosis.

#7931 Distinct microbiota composition in anorectal mucosal melanoma is associated with resistance to immune checkpoint inhibition.

Pritika Parmar[1], Morgan MacBeth[2], Mallory Karr[2], Nichole Nusbacher[2], Stacey M. Bagby[2], Phaedra Whitty[2], Kylie Michel[2], Richard P. Tobin[3], Martin McCarter[3], Theresa Medina[2], Catherine Lozupone[2], William A. Robinson[2], Kasey Couts[2]

[1]Dermatology, University of Colorado Anschutz Medical Campus, Aurora, CO,[2]University of Colorado Anschutz Medical Campus, Aurora, CO,[3]Surgery, University of Colorado Anschutz Medical Campus, Aurora, CO

Anorectal mucosal melanoma (AMM) is a rare and aggressive melanoma subtype characterized by poor responses to immune checkpoint inhibitor (ICI) therapy. While cutaneous melanoma metastases to gastrointestinal (GI) sites often retain strong ICI responses, the mechanisms underlying poor responses in AMM remain unclear. Given that AMM arises in microbial rich mucosal environments, we hypothesized that tumor-associated microbiota may contribute to local immune suppression. To investigate this, we performed 16S rRNA gene sequencing on primary AMM tumors and compared their microbial composition with cutaneous melanoma GI metastases (CM-GI-met) and normal mucosal reference samples, including nasal, rectal, and vaginal swabs. AMM tumors were enriched with Firmicutes Clostridia taxa, including Lactospiraceae and Ruminococcaceae, known butyrate producers associated with immunomodulation. In contrast, CM-GI-met tumors exhibited distinct microbial signatures, with a relatively higher abundance of Fusobacteriaceae and Bacteriodaceae. These patients notably had improved ICI responses compared to AMM primaries. Functional profiling suggested that AMM microbiomes had increased butyrate synthesis, known to create an immunosuppressive tumor microenvironment, which may contribute to poor ICI response. These findings are also seen in our orthotopic rectal mouse melanoma model, which showed reduced tumor growth rates, tumor burden, and overall survival in mice treated with combination vancomycin (Gram-positive selective antibiotic which targets Firmicutes Clostridia) and anti-PD-1 therapy compared to controls and monotherapy. Our findings demonstrate that AMM tumors contain a distinct butyrate-rich microbiome that may contribute to local tumor evasion whereas CM tumors contain a more ICI-permissive microbiome.

#7932 FL115, a novel IL-15 superagonist rationally designed to minimize safety risks for cancer immunotherapy.

Quanxiao Li[1], Yaping Cheng[2], Dong Wei[1], Qiang Gao[3], Yanling Wu[2], Tianlei Ying[2]

[1]Forlong Biotechnology, Suzhou, China,[2]Key Laboratory of Medical Molecular Virology (MOE/NHC/CAMS), Shanghai Institute of Infectious Disease and Biosecurity, School of Basic Medical Sciences, Fudan University, Shanghai, China,[3]Department of Hepatobiliary Surgery and Transplantation, Liver Cancer Institute and Key Laboratory of Carcinogenesis and Cancer Invasion (MOE), Zhongshan Hospital, Fudan University, Shanghai, China

Background: Interleukin(IL)-15 is a potent cytokine that activates NK and T cells but has been hampered by a short half-life, systemic toxicity, and dependence on IL-15Rα Sushi domain (IL-15RαSu) trans-presentation. ALT803, an IgG1 Fc-fused IL-15RαSu and IL-15, has been FDA-approved for bladder cancer via intravesical instillation. Nonetheless, no IL-15 agonist has yet been approved for systemic use due to safety concerns and challenging therapeutic index. We developed a novel superagonist, FL115, by fusing IL-15RαSu and IL-15 with a single-chain Fc (sFc). This sFc is half size of human IgG1 Fc and lacks FcγRs binding while retaining FcRn binding, conferring FL115 a distinct and potentially improved profile compared with ALT803 *in vivo*.
Methods: Different mouse models were used to compare the efficacy and safety of FL115 and ALT803. The immunomodulatory mechanism of FL115 was analyzed via single-cell RNA sequencing (scRNA-seq), immune cell depletion, qPCR and flow cytometry. The structure of FL115/FcRn/β2M were elucidated through cryo-electron microscopy (Cryo-EM).
Results: FL115 was rationally designed to eliminate FcγR binding while retaining FcRn interaction. Cryo-EM analysis of FL115/FcRn/β2M complex revealed that sFc aligns with only one chain of Fc but deviated from the other, disrupting the key interface required for FcγR engagement and preventing FcγR-mediated immune activation. Consistent with structural insight, FL115 exhibited markedly improved *in vivo* safety compared with ALT803. At 20 mg/kg, ALT803 caused 100% mortality accompanied by severe liver injury and pro-inflammatory cytokines such as IL-6. In contrast, all FL115-treated mice survived without detectable toxicity. The maximum tolerated dose of FL115 was over 10 times than ALT803. scRNA-seq of liver tissue revealed that ALT803 promotes the activation of neutrophils and macrophages through FcγR signaling, leading to cytokine release and systemic toxicity. FL115, lacking FcγR-binding capacity, did not trigger these inflammatory pathways. Importantly, FL115 showed comparable efficacy to ALT803 in CT26 and B16-F10 tumor models. Single-cell transcriptomics revealed FL115 reshapes the tumor microenvironment by enhancing NK and T cells infiltration, pro-inflammatory macrophage polarization, and dendritic cell expansion.. Immune cell depletion confirmed that FL115's antitumor effect is exclusively NK cell-dependent. Deep analysis further showed FL115 promotes NK cell maturation, cytotoxicity, and intratumoral recruitment.
Conclusion: Our study revealed the mechanism underlying the superior safety of FL115 over ALT803 while exhibiting comparable anti-tumor activities. These findings highlight the rational design strategy of FL115 as next-generation IL-15-based superagonist, supporting its favorable safety and preliminary clinical responses observed in multiple Phase 1 clinical studies.

#7933 Extracellular vesicle-mediated transfer of cortisol-induced miR-143-3p from macrophages promotes angiogenesis.

Amod Sharma, Sarabjeet Kour Sudan, Ajay P. Singh, Seema Singh

Cell and Molecular Biology, Cancer Center and Research Institute, University of Mississippi Medical Center, Jackson, MS

Chronic stress can lead to hormonal imbalance and contribute to cancer risk and progression. We previously reported higher levels of serum cortisol in breast cancer (BC) patients compared to those without a cancer diagnosis. Furthermore, we observed relatively higher levels of serum cortisol in Black patients than their White counterparts. Additionally, we found that cortisol treatment promoted M2 polarization of macrophages by inducing the expression of miR-143-3p, which was also released in extracellular vesicles (EV). Here, we investigated the role of EV-encapsulated miR-143-3p in angiogenesis, considering the fact that Black patients exhibit a higher microvessel density in their breast tumors. Treatment of endothelial cells with EV from cortisol-treated macrophages (Corti-Mφ-EV) increased their proliferation, migration, invasion, and tube formation. Efficient uptake of EV by endothelial cells was confirmed by fluorescence-based imaging, which correlated with an increase in the intracellular levels of miR-143-3p in Corti-Mφ-EV treated endothelial cells. Pre-treatment of endothelial cells with a miR-143-3p inhibitor abrogated Corti-Mφ-EV-induced proliferation and tube formation, whereas transfection with a miR-143-3p mimic promoted these effects. Computational analysis using the web-based platforms (Targetscan and miRDB) identified IGFBP5 as a potential miR-143-3p target. A reduction in IGFBP5 expression was reported in Corti-Mφ-EV or miR-143-3p mimic-treated endothelial cells. siRNA-mediated knockdown of IGFBP5 also increased endothelial cell growth and tube formation. Interestingly, surveying of the TCGA dataset showed a significant positive correlation between the M2 macrophage marker (CD163) and endothelial cell markers (PECAM1 and CDH5). Altogether, these findings reveal a novel mechanism by which cortisol may promote angiogenesis, establishing an additional pathobiological connection of chronic stress with increased cancer risk.

#7934 IL-24 engineered mesenchymal stem cells as a novel therapeutic strategy to remodel the tumor microenvironment in non-small cell lung cancer.

Yuting Zhang[1], Yuxuan Zhang[1], Sai Fung Yeung[1], Chi-Hang Wong[1], Tsz Tung Kwong[1], Connie Wun Chun Hui[1], Stephen Kwok-Wing Tsui[2], Tony S. Mok[1], Desheng Liang[3], Molly Siu Ching Li[1]

[1]The Chinese University of Hong Kong, Hong Kong, Hong Kong,[2]School of Biomedical Sciences, Chinese University of Hong Kong (CUHK), Shatin, Hong Kong,[3]Central South University, Changsha, China

Immune checkpoint inhibitor (ICI) resistance in non-small cell lung cancer (NSCLC) is frequently driven by an immunosuppressive tumor microenvironment (TME). To address this issue, we developed IL-24-iMSC, a novel mesenchymal stem cell-based therapy designed to remodel the immunosuppressive tumor microenvironment through sustained secretion of interleukin 24 (IL-24), an immunomodulatory cytokine with anti-cancer properties. Induced mesenchymal stem cells (iMSCs) were derived from induced pluripotent stem cells (iPSCs) and the IL-24 gene was integrated into iMSC at the B2M locus under the control of the EF1α promoter using CRISPR/Cas. IL-24-iMSCs were confirmed to constitutively secrete IL-24. Metastatic lung cancer models were established by tail vein injection of Lewis Lung Carcinoma cells expressing luciferase (LLC-luc) into immunocompetent C57BL/6 mice. Tumor progression was monitored using an In Vivo Imaging System (IVIS). Treatment was administered 20 days after tumor inoculation, and mice were randomized into three groups: iMSC, IL-24-iMSC, or vehicle control. All mice were sacrificed three days after treatment. Tumor growth was confirmed by bioluminescence imaging using IVIS, and tumor samples were collected for immune profiling. While there was no significant difference in tumor growth among the three groups, tumors exposed to IL-24-iMSC demonstrated a pro-inflammatory phenotype. Multiplex immunohistochemistry confirmed infiltration of MSCs into the TME, with significantly increased IL-24 expression in the IL-24-iMSC arm. Compared with the control group (untreated), tumors treated with IL-24-iMSC showed increased CD8+ T cells, dendritic cells, and memory CD4+ T cells. IFN-γ and TNF-α expressions were also elevated in the IL-24-iMSC treatment arm. On the contrary, regulatory T cells and exhausted T cells (PD1+ TIM3+) were significantly reduced in the IL-24-iMSC group. In conclusion, IL-24-iMSCs demonstrated the ability to modulate immune cell composition within the tumor microenvironment, suggesting their potential to synergize with ICI in NSCLC.

#7935 Multimodal immunotherapy remodels the tumor microenvironment in hepatocellular carcinoma: Integrative spatial and transcriptomic profiling from a Phase II trial.

Lionel Aurelien Kankeu Fonkoua[1], Christopher L. Hallemeier[2], Basim Salem[3], Arina Tkachuk[3], Kaitlynn McCay[3], Panwen Wang[4], Ying Li[5], Thomas D. Atwell[6], Krishan R. Jethwa[2], Caitlin Conboy[1], Nguyen H. Tran[1], Leslie A. Washburn[7], Melody Wu[8], Chen Wu[8], Andre De Menezes Silva Corraes[9], Rondell P. Graham[10], Jose Caetano Villasboas[10], Kevin Regan[10], Zuoyi Shao[10], Rayaan Kamal[9], Nathan R. Foster[10], Haidong Dong[8], Sean Park[10], Yi Lin[11], Lewis R. Roberts[8]

[1]Medical Oncology, Mayo Clinic Cancer Center, Rochester, MN,[2]Radiation Oncology, Mayo Clinic Cancer Center, Rochester, MN,[3]BostonGene Corporation, Waltham, MA,[4]Biomedical Informatics, Mayo Clinic, Scottsdale, AZ,[5]Quantitative Health Sciences, Mayo Clinic, Jacksonville, FL,[6]Mayo Clinic Cancer Center Minnesota, Rochester, MN,[7]Medical Oncology, Mayo Clinic, Rochester, MN,[8]Mayo Clinic College of Medicine and Science, Rochester, MN,[9]Research, Mayo Clinic, Rochester, MN,[10]Mayo Clinic, Rochester, MN,[11]Asst. Professor, Div. of Hemat., Mayo Clinic, Rochester, MN

Background: Hepatocellular carcinoma (HCC) is largely refractory to immune checkpoint blockade due to immune exclusion, stromal barriers, and aberrant vasculature. We evaluated whether multimodal therapy - external beam radiotherapy (EBRT) for antigen release, intratumoral dendritic cell (DC) vaccination for antigen presentation, PD-L1 blockade for immune activation, and VEGF inhibition for vascular normalization - could convert “cold” HCC tumors into sustained immune-inflamed states.

Methods: Serial biopsies (baseline, post-EBRT, end-of-treatment [EOT], and progression [PD] when available) from three patients enrolled in an ongoing phase II trial (NCT03942328) underwent multiplex immunofluorescence, spatial neighborhood analysis, and transcriptomic profiling. Longitudinal changes in cellular composition, immune-stromal architecture, spatial contact networks, and pathway activity were compared.

Results: Baseline tumor microenvironments (TMEs) were strongly immune-excluded, dominated by tumor (PanCK⁺60-70%) and stroma (SMA⁺/Vimentin⁺25-30%) with sparse immune infiltration (<10-15%). Post-therapy, immune complexity and spatial connectivity increased 2-3-fold in all patients. Patient 1 showed robust cold-to-hot conversion with CD8⁺(3x), CD4⁺(2.2x), and DC (2.3x) expansion, increased CD8-DC interactions (2.5x), and reduced tumor fraction (-40%). Transcriptomics showed marked upregulation of IFN-γ (↑3.4x), HLA-DRA (↑2.7x), and reductions in VEGFR2 (↓50%) and HIF1A (↓40%), consistent with vascular normalization. Patient 2 exhibited stromal/vascular remodeling and improved T-cell infiltration but restricted immune diversity, with CD4⁺/CD8⁺ dyads (↑2.2x) and B/NK cells(↓ 60%). Neighborhood diversity rose (3→7 communities) and immune-tumor proximity improved (distance ↓ 35%). Patient 3 showed transient inflaming with CD8⁺(↑3x), DC(↑2x), and new CD4-CD20/CD4-CD56 interactions, followed by relapse marked by stromal/myeloid re-expansion (SMA⁺↑1.8x, CD14⁺↑2.5x), angiogenic resurgence (VEGFR2/CD34⁺↑2.2x), contraction of immune networks, and genomic shift from activating CTNNB1 mutation loss to ATM gain. DCs accumulated but localized mainly to DC-DC or DC-myeloid niches, indicating non-productive antigen presentation.

Conclusions: Multimodal EBRT+DC+PD-L1/VEGF blockade induces four-sided synergistic TME reprogramming - antigen release, immune priming, checkpoint release, and vascular normalization - promoting cold-to-hot conversion in HCC. Durable inflaming correlates with sustained T-cell/DC expansion and vascular remodeling, whereas relapse reflects stromal/myeloid reinforcement and genomic adaptation. These findings define mechanistic trajectories of TME remodeling and highlight actionable barriers to sustained immunotherapy response in HCC.

#7936 Epigenetic reprogramming of stromal-epithelial crosstalk to improve immunotherapy response in pancreatic ductal adenocarcinoma.

Celia Martin-Otal[1], Daire Hanna[1], Kairbaan Hodivala-Dilke[1], Angus J. M. Cameron[2], Oliver Pearce[1], David Propper[1]

[1]Centre for Tumour Microenvironment, Barts Cancer Institute, London, United Kingdom,[2]Centre for Tumour Biology, Barts Cancer Institute, London, United Kingdom

Pancreatic ductal adenocarcinoma (PDAC) is highly aggressive and profoundly resistant to immunotherapy, driven by a dense, desmoplastic, and immunosuppressive stroma dominated by cancer-associated fibroblasts (CAFs). CAFs are genetically stable and abundant, making them attractive targets for epigenetic reprogramming to overcome immune exclusion.We hypothesized that epigenetic modulators could reshape CAF-cancer cell interactions, reduce immunosuppression, and enhance responsiveness to immunotherapies, including immune checkpoint blockade and CAR-T cells. Using a 3D PDAC co-culture spheroid model, we screened a panel of clinically relevant epigenetic agents. Transcriptomic profiling revealed drug-induced changes in both tumor and stromal compartments, focusing on CAF subtype reprogramming, stroma-epithelial crosstalk, tumor growth and invasion, immunosuppression, and matrisome remodeling.The CDK7 inhibitor CT7001 emerged as a promising candidate, profoundly altering CAF phenotype, reprogramming CAF subtypes, and modulating stromal gene expression, while reducing epithelial-mesenchymal transition and cell cycle pathways in cancer cells. In an orthotopic PDAC mouse model, CT7001 combined with Gemcitabine significantly extended survival. Notably, treated tumors exhibited increased T-cell infiltration into the otherwise immunologically “cold” PDAC microenvironment, highlighting its potential to sensitize tumors to immunotherapy. Ongoing spatial multiplex imaging and RNA-seq analyses aim to correlate *in vivo* immune and stromal changes with *in vitro* findings, supporting rational combination strategies. This epigenetic screening platform provides a predictive framework to evaluate compounds that overcome CAF-mediated immune exclusion and modulate the tumor microenvironment, offering new avenues to enhance PDAC responsiveness to diverse immunotherapies.

#7937 Advancing the best-in-class cross-specific LILRB1/LILRB2 antibody IOMX-0675 into clinical development for solid tumors.

Ana Ogrinc Wagner[1], Kristina Heinig[1], Christina Hartl[1], Marisa Stebegg-Wagner[1], Michail Maraslis[1], Carmen Ginzel[1], Thomas Jaquin[2], Bettina Langer[1], Alina Huth[1], Tiantom Jarutat[1], Alexander N. Marziale[1], Stefan Bissinger[1]

[1]iOmx Therapeutics AG, Martinsried, Germany,[2]Proteinea, Cambridge, MA

IOMX-0675 is a fully human, cross-specific immunoglobulin G1 (IgG1) antibody targeting LILRB1 (ILT2) and LILRB2 (ILT4), two key immunosuppressive receptors that drive tumor immune evasion and resistance to T cell checkpoint blockade. LILRB1 and LILRB2 recognize both classical and non-classical MHC-I molecules and are highly expressed on tumor-infiltrating myeloid cells, with LILRB1 also being expressed on lymphoid cells. Molecular profiling revealed concurrent expression of highly homologous immune-activating LILRA1/LILRA3 with inhibitory LILRB1/LILRB2, underscoring the critical need for selective receptor targeting. IOMX-0675 exhibits a unique, superior binding profile defining its best-in-class potential: selective, high-affinity binding to inhibitory LILRB1/LILRB2 with minimal affinity to immune-activating LILRA1/LILRA3. This differentiated selectivity maximizes anti-tumor efficacy by preserving immune activation, while blocking immunosuppression. Comparative functional studies demonstrate IOMX-0675's superior potency in tumor cell phagocytosis as well as a repolarization activity of M2-macrophages compared to competitor compounds. Notably, only simultaneous blocking of LILRB1 and LILRB2 with dual-targeting IOMX-0675 leads to significant T cell activation in co-culture assays. In support of a potential clinical patient selection approach, a donor screening was performed *in vitro* which revealed a distinct IOMX-0675 efficacy profile with clear differences between responsive and non-responsive donors. An integrated multi-omics-based biomarker analysis offers strong potential for a future biomarker-driven patient selection process. Functional assays using stimulated PBMCs demonstrate that IOMX-0675 synergizes with anti-PD-1 treatment, potentiating pro-inflammatory cytokine secretion and driving cytotoxic T cell activation *in vitro*. Co-culture assays modeling patient-relevant tumor or lymph node microenvironments demonstrate that IOMX-0675 repolarizes immunosuppressive milieus and restores T cell function, in a situation where anti-PD-1 monotherapy is ineffective. In summary, IOMX-0675 represents a best-in-class therapeutic antibody that combines selective LILRB1/LILRB2 antagonism with minimal immune-activating receptor binding and demonstrates superior myeloid reprogramming and T cell restoration both *in vitro* and *in vivo*. IOMX-0675 will enter a Phase I/II clinical trial in early 2026 as monotherapy as well as combination therapy with anti-PD1 in patients with previously treated advanced/metastatic solid tumors.

#7938 Identification of a novel lncRNA in pancreatic cancer: Contribution to malignancy through Wnt pathway regulation.

Isshin Narumoto, Keiko Shinjo, Yutaka Kondo, Shu Hirako

Nagoya University, Nagoya, Japan

Long non-coding RNAs (lncRNAs) are non-coding RNAs longer than 200 nucleotides that play essential roles in transcriptional regulation and protein localization through interactions with various proteins. These functions have attracted considerable attention in cancer research.

We identified lnc243, which is highly expressed in mesenchymal-type cells of pancreatic ductal adenocarcinoma (PDAC) and is associated with poor patient survival. Previous studies reported that lnc243 regulates mRNA expression by acting as a competing endogenous RNA through binding to miRNAs. However, the subcellular localization of lnc243 and its function through protein interactions in PDAC remain poorly understood.RNA fluorescence in situ hybridization (RNA-FISH) revealed that lnc243 localization varies depending on the cellular state: it is localized to the cell membrane in adherent cells but translocates into the cytoplasm during invasion. Because lnc243 and β-catenin were found to co-localize on the cell membrane, we next examined their potential interaction using AlphaFold3. This analysis suggested a possible interaction between lnc243 and β-catenin, which was further supported by RNA immunoprecipitation showing that β-catenin binds to lnc243. Moreover, knockdown of lnc243 led to a decrease in the post-translational levels of β-catenin.

Mutations in Wnt pathway genes are rare in PDAC; however, increased lnc243 expression may represent an alternative mechanism for dysregulating β-catenin and promoting malignancy in PDAC.

#7939 Stress-induced anoikis-resistance triggers malignant-like phenotypes in uterine leiomyoma cells.

Roseli da Silva Soares[1], Edmund C. Baracat[2], **Katia C. Carvalho**[3]

[1]University of Sao Paulo, Faculty of Medicine, Sao Paulo, Brazil,[2]Sao Paulo University, Sao Paulo, Brazil,[3]Obstetrics and Gynecology, HCFMUSP, Sao Paulo, Brazil

Background: Uterine leiomyomas (LM) are the most common tumors in women of reproductive age and represent a major clinical burden. Although LM are classically considered benign, a long-standing scientific question concerns whether a subset of these tumors may undergo malignant transformation into leiomyosarcomas (LMS), a rare but highly aggressive uterine sarcoma. To date, this progression has not been conclusively demonstrated, yet it also cannot be fully excluded, and the biological mechanisms that might enable such a transition remain poorly understood. Anoikis resistance - the capacity of cells to survive loss of extracellular matrix attachment - is a hallmark of malignant transformation and early metastatic behavior in several solid tumors. Therefore, experimental models that induce anoikis resistance may offer insight into whether LM cells can acquire malignant-like traits under sustained cellular stress.
Methods: Established cell lines of myometrium (MM; PCS-460-011) and leiomyoma (LM; THESCs; CRL-4003) were cultured (1×10^5 cells/mL) on plates coated with 1% sterile agarose to prevent cell-matrix adhesion and maintained for 96 hours at 37°C and 5% CO_2. Surviving non-adherent spheroids (anoikis-resistant cells) were collected and replated under adherent conditions. This spheroid-formation cycle was repeated four times, generating the derived cell populations LM1C, LM2C, LM3C, and LM4C. Subsequently, spheroids were subjected to limiting dilution to obtain clonal populations. Five clones were randomly selected for expansion and functional/molecular analyses.
Results: Preliminary findings indicate that LM cells progressively lose adhesion capacity and acquire anoikis resistance, accompanied by notable phenotypic alterations. MM cells did not survive repeated adhesion-blocking cycles and were eliminated before cycle 5 (C5), whereas LM cells successfully persisted through all cycles. After clonal expansion, genetic identity was confirmed through sequencing, validating their LM origin. Clonogenic assays demonstrated significant behavioral changes: anoikis-resistant LM derivatives exhibited an increased ability to survive and proliferate independently of cell-cell contact compared with parental LM cells. Ongoing assays of proliferation, migration, and invasion further indicate important phenotypic and behavioral alterations in vitro.
Conclusion: The anoikis-resistance model appears to be a valuable tool for studying uterine leiomyoma biology. Our findings suggest that LM cells may acquire malignant-like traits when subjected to repeated adhesion stress, supporting the hypothesis that anoikis resistance may contribute to malignant transformation in uterine smooth muscle tumors.

#7940 Pharmacokinetics of TNX-1700 in non-human primates and human FcRn/serum albumin transgenic mice.

Mayanka Awasthi[1], Jennifer Cho[1], Nelson Martinez[1], Bernd Meibohm[2], Seth Lederman[3], Christopher Cooper[1], Sina Bavari[1], **Bruce L. Daugherty**[3]

[1]Tonix Pharmaceuticals, Inc., Frederick, MD,[2]University of Tennessee Health Science Center, Memphis, TN,[3]Tonix Pharmaceuticals, Inc., Chatham, NJ

Introduction: TNX-1700 is a novel recombinant fusion molecule of human Trefoil Factor-2 (TFF2) protein and human serum albumin (HSA) that is being investigated as a potential therapeutic for gastric cancer. In syngeneic mouse models of gastric and colorectal cancer, TNX-1700 functions as a CXCR4 partial agonist that activates antitumor immunity in the tumor microenvironment by modulating myeloid cell trafficking to reduce tumor-induced granulopoiesis and accumulation of immunosuppressive neutrophils. TNX-1700 is engineered to extend plasma half-life, enhance systemic exposure, and improve cancer immunotherapy. The HSA domain in TNX-1700 provides a long circulatory half-life (>14 days) and multiple ligand-binding sites. Approved albumin-linked drugs include detemir (Levemir®), liraglutide (Victoza®), and albiglutide (Eperzan®/Tanzeum®) for diabetes, and nanoparticle albumin-bound paclitaxel (nab-paclitaxel) for cancer therapy. TNX-1700 represents a next-generation application of the albumin platform in immuno-oncology.
Methods: The pharmacokinetics (PK) of TNX-1700 were evaluated in non-human primates (NHP; cynomolgus macaques) and double-transgenic mice expressing human neonatal Fc receptor (FcRn) and human serum albumin (HSA). Animals received a single dose of 1 mg/kg or 3 mg/kg TNX-1700, administered intravenously (IV) to NHPs or intraperitoneally (IP) to FcRn/HSA mice. For comparison, untagged human TFF2 (molar equivalent to TNX-1700) was also administered into FcRn/HSA mice. Serial blood samples were collected over 0-35 days and analyzed using the Boster PicoKine™ Human TFF2 ELISA kit. Pharmacokinetic parameters were determined by non-compartmental analysis.
Results: All animals survived without clinical signs or >10% body-weight loss. Comparable PK profiles were observed across species and doses. In cynomolgus macaques, mean terminal half-life (t½) was 7.1 days (%CV = 9.65), clearance (CL) 13.3 mL/day (%CV = 14.3), and volume of distribution (Vz) 135.2 mL (%CV = 18.3). Allometric scaling predicted in humans a t½ of 14.2 days (%CV = 12.9), CL = 105.2 mL/day (%CV = 26.4), and Vz = 2,158 mL (%CV = 34.0). Results from the humanized murine studies provided evidence that untagged human TFF2 is rapidly cleared and that fusion with HSA significantly increased the PK profile similar to that observed in NHPs and to levels supportive for clinical candidates.
Conclusion: TNX-1700 exhibited dose-independent, linear pharmacokinetics with low inter-animal variability, and exposure was consistent across doses and species. Although its half-life is shorter and clearance higher than IgG-based biologics, TNX-1700 substantially extends the half-life of TFF2 and achieves durable systemic exposure, supporting its potential as a therapeutic candidate for gastric cancer.

#7941 The Sphk1-B cell axis as a targetable immunoregulatory pathway in cancer.

Mona Singh[1], Prachi Gupta[2], Arezou Rahimi[1], Sunila Pradeep[1]

[1]Medical College of Wisconsin, Wauwatosa, WI,[2]Earle A. Chiles Research Institute, Portland, OR

Background: The sphingosine kinase 1 (SPHK1)/sphingosine-1-phosphate (S1P) signaling axis regulates tumor progression and immune suppression within the tumor microenvironment (TME). While SPHK1-mediated S1P generation is known to promote ovarian cancer growth, its role in shaping B cell-driven anti-tumor immunity remains unclear.

Methods and Results: Genetic ablation of SPHK1 (SPHK1$^{-/-}$) in murine ovarian cancer (ID8 Trp53$^{-/-}$; Brca2$^{-/-}$), melanoma (B16F10), and colorectal cancer (MC38) models resulted in markedly reduced tumor burden accompanied by ~50% reduction in S1P levels. Tumors from SPHK1$^{-/-}$ mice demonstrated increased immune infiltration, primarily B and T lymphocytes, and enrichment of immunoglobulin-related and antigen presentation gene signatures. Flow cytometry and IHC confirmed enhanced tumor-infiltrating CD19^{+} B cells, plasma cells, and upregulation of activation and antigen-presentation markers (CD69, CD80, CD86, CD40, MHC-II).Mechanistically, SPHK1 deficiency promoted metabolic reprogramming that supported plasma cell differentiation, characterized by elevated unfolded protein response (XBP1, BiP, GRP94), increased oxidative phosphorylation, ATP generation, mitochondrial biogenesis, and FOXO1 activation. Pharmacologic SPHK1 inhibition using PF543 phenocopied genetic knockout, increasing plasma cell frequency, immunoglobulin secretion, and activation-associated transcriptional programs. Taken together, our data suggest that SPHK1 inhibition activates B cells for enhanced anti- tumor immune response.

Conclusion: SPHK1/S1P axis inhibition reprograms B cells toward robust metabolic fitness, plasma cell differentiation, and antibody-mediated anti-tumor immunity. Targeting SPHK1 represents a promising strategy to boost humoral immunity and overcome immune-excluded ovarian cancer phenotypes.

Impact: This study uncovers a previously unrecognized immunometabolism by which SPHK1 controls B cell function, highlighting its therapeutic potential for enhancing anti-tumor immunity and improving immunotherapy responsiveness.

#7942 TAE226 reprograms immune-cold head and neck tumors to immune-hot, augmenting immunotherapy efficacy.

Atish Ranjan Mohanty[1], Dana Do[2], Sharad S. Singhal[3], Haiqing Li[4], Sravani Ramisetty[4], Raju Pillai[4], Sultatna Shoukath[5], Prakash Kulkarni[4], Ellie G. Maghami[6], Ravi Salgia[4], Erminia Massarelli[5]

[1]City of Hope Comprehensive Cancer Ctr., Duarte, CA,[2]City of Hope National Medical Center, Monrovia, CA,[3]Beckman Research Institute of The City of Hope, Duarte, CA,[4]City of Hope National Medical Center, Duarte, CA,[5]University of Texas, Tyler, TX,[6]Faculty, Div. of Surgery, City of Hope, Duarte, CA

Introduction: Current treatment strategies in advanced/recurrent LSCC include chemotherapy, radiation therapy, and immune checkpoint inhibitors (ICI). ICI treatment is associated with durable benefit in about 20% of patients with advanced/incurable platinum-resistant LSCC. There is a clear need to develop strategies to reprogram the tumor microenvironment (TME) from immune-cold to immune-hot to enhance T-cell infiltration and activation that correlate with ICI treatment response. We investigated the therapeutic potential of Focal Adhesion Kinase (FAK) inhibition using a tyrosine kinase inhibitor, TAE226, alone and in combination with anti-PD-1 immune checkpoint blockade, to reprogram the TME and enhance immunotherapeutic responsiveness in a model of platinum-resistant LSCC.
Methods: LSCC cell lines (SQ20B, SCC17A) were used to assess the inhibitory response to FAK inhibitors using the CCK-8 assay. RNA-seq was performed to evaluate global transcriptional changes and pathway enrichment. Syngeneic MOC2 mouse models were used to assess the therapeutic efficacy of TAE226 in combination with anti-PD-1 therapy. Post euthanization, the xenografts were processed for isolating single cells and performing single-cell RNA sequencing.
Results: TAE226 significantly reduced LSCC cell proliferation, viability, and wound-healing capacity, indicating potent anti-tumor activity. Bulk RNA-seq and pathway enrichment analyses revealed robust upregulation of interferon and cytokine signaling pathways, consistent with an immune-stimulatory phenotype, while downregulating proliferative and metabolic programs. This dual modulation suggests that TAE226 exerts both tumor-intrinsic anti-proliferative and tumor-extrinsic immune-activating effects. In the MOC2 syngeneic model, the combination of TAE226 and anti-PD-1 produced a synergistic response, resulting in markedly enhanced antitumor signaling and significantly greater tumor regression compared to either monotherapy. Single-cell RNA-seq further demonstrated that TAE226 treatment induced profound TME remodeling, characterized by expansion of cytotoxic $CD8^+$ T cells, dendritic cells, and activated macrophages, and depletion of proliferative epithelial and fibroblast-rich stromal clusters. Hallmark pathway analyses highlighted activation of interferon-α/γ, IL2-STAT5, TNFA-NFκB, and complement signaling-consistent with broad activation of innate and adaptive immune programs.
Conclusion: These findings indicate that TAE226 disrupts FAK-mediated adhesion and cytoskeletal signaling, converting the TME from immune-cold to immune-hot and enhancing responsiveness to immune checkpoint blockade and offering a promising therapeutic strategy for platinum-resistant laryngeal cancer.

#7943 TP53 mutation reshapes the immune microenvironment in endometrial cancer.

Konrad Snioch, Mahima Rasquinha, Dmitriy Zamarin

The Tisch Cancer Institute, Icahn School of Medicine at Mount Sinai, New York, NY

Gynecologic cancers account for almost 40% of all cancer cases and more than 30% of cancer-related deaths in women globally, with endometrial cancer (EC) being the most prevalent gynecological cancer in the US. Four principal molecular subtypes of EC include POLE-ultramutated, mismatch repair-deficient (dMMR), MMR-proficient (pMMR) copy-number (CN)-low cancers (TP53-wild type), and pMMR CN-high cancers (TP53 mutant). Despite the emergence of immune checkpoint blockade (ICB)as a promising treatment for many cancers, in EC only the first two subtypes (POLE and dMMR) are susceptible to immunotherapy, whereas pMMR CN-low and CN-high cancers are largely resistant. One key problem in understanding the reduced effectiveness and mechanism of action of ICB in EC is the lack of immunocompetent preclinical models that accurately recapitulate the genetics and biology of human ECs. To address this problem, we developed organoids from mice bearing conditional (LoxP-controlled) expression of the mutant genes most frequently mutated in human ECs, representative of CN-Low ($PTEN^{-/-}PIK3CA^{H1047R}$) and CN-high ($PTEN^{-/-}PIK3CAH^{1047R}p53^{R172H}$ and $PTEN^{-/-}PIK3CA^{H1047R}p53^{-/-}$) endometrial cancer subtypes. Using cyclic immunofluorescence (CyCIF), we performed spatially resolved, multiplex profiling of immune populations in TP53-mutant and TP53-wild-type EC samples.TP53-mutant tumors exhibited a myeloid-enriched microenvironment, with abundant macrophages and neutrophils, while lymphoid populations were comparatively sparse. PD-L1 expression was high in these tumors, whereas PD-1 expression was minimal or absent, suggesting an immunosuppressive environment. In contrast, TP53-wild-type tumors showed a more balanced immune composition, with higher lymphoid infiltration. These results indicate that TP53 mutation is associated with a myeloid-dominant, lymphoid-poor, and PD-L1-high immune landscape in EC, highlighting potential mechanisms of immune evasion and possible targets for combination immunotherapy.

#7944 Tumor immune micro-environment (TME) dynamics in longitudinal diffuse large B-cell lymphoma (DLBCL) cases from diagnosis to RCHOP relapse.

Raoul Santiago[1], Raquel Aloyz[2], Stephanie Bianco[1], Svetlana Dmitrienko[2], Nathalie Johnson[2], Andreas I. Papadakis[3], Naciba Benlimame[4], Cynthia Guilbert[2], Alan Spatz[5], Francois E. Mercier[2], Madelyne Abraham[2], Laura Hilton[6], David W. Scott[6], Koren K. Mann[7], Sarit Assouline[2]

[1]Research Center, CHU of Quebec, Laval University, Quebec, QC, Canada,[2]Segal Cancer Centre and Lady Davis Institute for Medical Research, Montreal, QC, Canada,[3]Molecular pathology, Lady Davis Institute for Medical Research, Montreal, QC, Canada,[4]The George and Olga Minarik Research Pathology Facility, Lady Davis Institute for Medical Research, Montreal, QC, Canada,[5]Molecular pathology, Lady Davis Institute for Medical Research, Montreal, QC, Canada, Montreal, QC, Canada,[6]Centre for Lymphoid Cancer, BC Cancer, Vancouver, BC, Canada,[7]Department of Pharmacology and Therapeutics, McGill University, Montreal, QC, Canada

DLBCL gene expression signatures from single-nucleus analyses have recently identified new tumor microenvironment (TME) archetypes (LymphoMAPs) linked to RCHOP and CAR-T cell sensitivity. While some archetypes are enriched at diagnosis or relapse, their stability during disease progression remains unclear. We analyzed longitudinal DLBCL cases using LymphoMAP signatures and histologic annotation to assess archetype switching after RCHOP.

Methods: We utilized two independent well-annotated DLBCL cohorts with paired diagnosis/relapse biopsies:23 in-house (46 samples) and 44 published cases (88 samples). Gene expression in our cohort was profiled using the NanoString Cancer Immune Panel on fixed (FFPE) specimens. The external dataset comprised whole-transcriptome from FFPE or fresh-frozen samples pre- and post-RCHOP. LymphoMapR predicted the archetypes from normalized counts: enriched in fibroblast and tumor-associated macrophages (FMAC), naïve and memory T cell (LN), activated macrophages and exhausted T cell (TEX). Samples with classification probability <0.7 were excluded. Additionally, we correlated the archetypes with histologic annotation from our cohort. Immunohistochemistry (IHC) supported T cell markers (CD3, CD4, CD8) and PDL1 expression. Multiplex OPAL imaging quantified macrophage markers (CD68, CD163) with immune checkpoint (CD47), and chemokines (CXCL9 and CXCL10) with receptor (CXCR3).

Results: In the in-house cohort, 8 patients relapsed following only RCHOP, others received ≥1 relapse regimen. One patient per cohort was excluded for low LymphoMAP confidence. Notably, archetype switching occurred in 13 of 22 patients (59%, 95% CI: 36-79%) in-house and 18 of 43 patients (42%, 95% CI: 28-57%) externally. To gain statistical power, the cohorts were combined, yielding an overall switch rate of 48% (95% CI: 36-60%). Switching was less frequent for patients with LN at diagnosis (38%, 95% CI: 23-57%) than FMAC (59%, 95% CI: 36-78%) or TEX (57%, 95% CI: 33-79%), but no consistent direction of switch or correlation with relapse timing was observed. Germinal center B-cell-like (GCB) DLBCLs were predominantly LN archetype (58%), whereas non-GCB encompassed all LymphoMAP archetypes, suggesting an association with cell-of-origin. Histology was consistent with LymphoMAP prediction: T cell abundance (CD3, CD4, CD8) and CXCR3 expression were highest in TEX, followed by LN and FMAC (p<0.05). IHC also demonstrated a significant decrease in CD3 and CD8 T cells at relapse compared with diagnosis.

Conclusions: Based on our observations, the immune environment of DLBCL is dynamic. Although relapse samples exhibited more T cell-depleted environments, changes in TME archetypes frequently occurred, without a dominant pattern. In the context of patient selection for CAR-T cell therapy, relapsed TME should not be inferred from TME at diagnosis.

#7945 Whole-genome doubling induces chromosomal instability to shape the tumor-immune microenvironment and impair the response to immune checkpoint inhibitors in non-small cell lung cancer.
Cheolyong Joe, Jinyong Kim, Hyemin Kim, Junsu Choe, Miran Jang, Eunjoo Oh, Naeun Lee, Subin Kim, Sehhoon Park, Hyun Ae Jung, Jong-Mu Sun, Jin Seok Ahn, Myung-Ju Ahn, Joo Kyung Park, Se-Hoon Lee

Department of Medicine, Sungkyunkwan University School of Medicine, Samsung Medical Center, Seoul, Korea, Republic of

Introduction: Whole genome doubling (WGD), observed in 30-40% of cancers, drives chromosomal instability (CIN), but its role in modulating the immune landscape in NSCLC remains unclear. We investigated how WGD shapes tumor-intrinsic and -extrinsic features to influence immune checkpoint inhibitors (ICI) response.
Methods: We analyzed 520 baseline NSCLC tumor tissues (WES, n=520; WTS, n=500). WGD was defined from WES-derived copy number profiles as >50% of the autosomal genome having a major copy number ≥2. Tumor-infiltrating lymphocytes (TILs) were quantified in a subset (n=304) via AI-powered spatial analysis of whole slide images (WSIs). Statistical comparisons utilized Fisher's exact and Wilcoxon rank-sum tests.
Results: Among 520 tumors, 202 (38.8%) were WGD+ and 318 (61.2%) were WGD-. TP53 mutations were significantly enriched in WGD+ tumors (57.4% vs WGD-: 40.3%, $p=1.51\times10^{-4}$). While the 17p13.1 (TP53) locus was significantly higher in WGD+ cohort (76.7% vs WGD-:39.9%, $p=8.82\times10^{-17}$). Furthermore, this coupling of TP53 mutation and LOH coupling was particularly prominent in WGD+: 90.3% (93/103 pre-WGD mutants) acquired LOH, vs 64.8% (83/128) in WGD- tumors. WGD+ tumors also exhibited a significantly higher burden of HLA Class I LOH burden (≥2 loci in 16.1% vs 6.3%, $p=8.42\times10^{-4}$). WGD+ tumors also showed significantly lower T cell infiltration. Using ploidy-corrected T cell fractions (n=520), the median T cell fraction was significantly lower in the WGD+ group than in the WGD- group (0.138 vs 0.184, $p=4.28\times10^{-4}$). Gene set enrichment analysis (GSEA) showed WGD+ tumors enriched metabolic/proliferative programs. In contrast, WGD- tumors upregulated immune-activation pathways. This "immune-cold" profile in WGD+ tumors was confirmed by significantly lower immune scores; median cytolytic activity score was 2.53 vs. 3.08 ($p=5.34\times10^{-5}$) and median TLS score was 5.40 vs. 6.51 ($p=1.05\times10^{-12}$). Spatially, AI-powered WSI analysis corroborated this, linking WGD+ tumors to fewer inflamed and more immune-desert phenotypes ($p=2.74\times10^{-3}$). Clinically, WGD status was significantly associated with inferior outcomes. Compared to non-WGD patients, WGD patients demonstrated worse overall survival (HR 1.284, 95% CI 1.050-1.569, $p=1.47\times10^{-2}$) and progression-free survival (HR 1.286, 95% CI 1.057-1.563, $p=1.18\times10^{-2}$).
Conclusion: In NSCLC, WGD promotes high genomic instability through TP53 mutation and critical HLA Class I LOH, enabling immune escape. This genomic landscape shapes an immunosuppressive ecosystem characterized by metabolic reprogramming, lower T cell infiltration, and immune-desert phenotypes. As a result, WGD defines an immune-refractory microenvironment and serves as a robust predictive biomarker for unfavorable ICI response.

#7946 Identification of a highly selective ITK inhibitor which promotes Th1 differentiation and alleviates T cell exhaustion *in vitro* and *in vivo*.

Lei Jiang, Zhiyong Yu, Xin Cheng, Baoying Cheng, Yuyao Zhang, Wenwen Zhao, Youxi Chen, **Feng Zhou**

Atheron Therapeutics, Ltd., Shanghai, China

ITK is a member of the TEC family of kinases, expressed in T, NK, and mast cells. ITK plays important roles in TCR signaling and T cell differentiation. Following TCR stimulation, ITK is recruited to the cell membrane and then leads to phosphorylation and activation of PLCγ1. ITK knockout mice show defects in Th2 differentiation, while retaining the ability to differentiate into Th1 cells, a phenomenon known as Th1 skewing. It is generally accepted that Th1 cells are the primary Th cell subtype associated with tumor elimination. ITK and RLK double knockout in T cells has a more substantial signaling defect, resulting in a profound loss of normal T cell function. Thus, it holds great therapeutic promise to treat cancer with selective ITK inhibitors while sparing RLK.Here, we report that ATH-409 is a highly selective, covalent ITK inhibitor with an IC50 of < 5 nM and more than 300-fold selectivity against RLK and at least 100-fold selectivity against the remaining 10 cysteine-containing kinases. In the kinase panel assay involving 430 kinases, ATH-409 exhibits inhibitory activity against less than 5 of these kinases, with an IC_{50} selectivity of at least 60-fold for all of the non-target kinases. ATH-409 potently suppresses ITK-mediated phosphorylation of PLCγ1 and TCR activation-induced IL2 release in PBMCs. At high concentrations, ATH-409 exerts an anti-proliferation effect on human primary T cells, while showing no impact on T cell viability. Under both polarizing and non-polarizing conditions, ATH-409 does not affect the production of Th1 cytokines, but decreases the release of Th2 cytokines. Additionally, ATH-409 attenuates the occurrence of T cell exhaustion. ATH-409 alone does not suppress the proliferation of CT26 cells *in vitro*, but does inhibit CT26 tumor growth *in vivo*, indicating that the anti-tumor effect of ATH-409 is achieved through regulating the immune system. In *in vivo* model, the ITK occupancy increases with the elevation of ATH-409. Furthermore, when ATH-409 is combined with PD-1 antibody and CTLA-4 antibody, the inhibitory effect on CT26 tumors is further enhanced. Analysis of tumor-infiltrating lymphocytes (TILs) reveals that under the combination treatment, the proportion of Th1 cells in tumors increases and T cell exhaustion is alleviated, which is consistent with the phenomena observed in *in vitro* experiments.

#7947 miR-150 orchestrates immune activation and lymphocyte trafficking in breast cancer.

Masanori Oshi[1], Rongrong Wu[2], Colin J. Rog[3], Li Yan[3], Takashi Ishikawa[4], Itaru Endo[5], Kazuaki Takabe[1]

[1]Roswell Park Comprehensive Cancer Center, Buffalo, NY,[2]Tokyo medical hospital, Tokyo, Japan,[3]Roswell Park Comprehensives Cancer Center, Buffalo, NY,[4]Breast Surgery, Tokyo Medical University, Tokyo, Japan,[5]Yokohama City University Hospital, Yokohama, Japan

Background: Tumor-infiltrating lymphocytes (TILs) are known to relate with response to treatments followed by better survival; however, majority of breast cancer (BC) hardly have any TILs. Thus, discovery of targetable novel mechanism of TIL infiltration is expected to have a major clinical implication. MiR-150 has been reported to promote cell proliferation and migration, but its role in TIL infiltration is not known. The aim of this study is to investigate the role and clinical relevance of tumor miR-150 expression and attraction of TILs in BC patients.
Methods: In silico analyses was conducted on total of 1,961 breast cancer patients from large independent cohorts, The Cancer Genome Atlas (TCGA) and the Molecular Taxonomy of Breast Cancer International Consortium (METABRIC). In Vitro experiments using MDA-MB231 and BT-549 BC cell lines and Jurkart lymphocyte cell line, were repeated three times to ensure rigor and reproducibility.
Results: As expected, miR-150 expression correlated with Nottingham grade and was higher in triple negative subtype in both cohorts (all $p<0.001$). On the other hand, miR-150 expression not only enriched MTORC1 and KRAS signaling, but also multiple immune-related Hallmark gene sets including IFN-Y, TNF-α, IL-2, IL-6, IFN-α, allograft rejection, and inflammatory response by gene set variant analysis (all Spearman's coefficient $r>0.50$ and $p<0.01$). High miR-150 expression significantly correlated with lymphocyte infiltration and TCR-Shannon in TCGA cohort. High miR-150 expression was associated with high infiltration of CD8+, CD4+ memory T cells and dendritic cells, and was strongly correlated with cytolytic activity consistently in both cohorts ($r=0.824$ and 0.786, both $p<0.01$), all suggesting strong relationship with immune cell infiltration and immune response. In agreement, high MiR-150 expression was associated with improved overall survival ($p<0.001$, $p=0.030$), particularly in ER-positive/HER2-negative patients. Surprisingly, mimic overexpression of miR-150 did not promote cell proliferation, migration nor invasion neither in MDA-MB231 or BT-549 BC cell lines. However, mimic overexpression of miR-150 in either MB231 or BT-549 cells significantly increased the migration intensity of Jurkart cells demonstrated by Transwell invasion assay. Further, mimic overexpression of miR-150 in MDA-MB231 cells enriched cell proliferation-related gene sets; E2F Targets, G2M checkpoint, as well as multiple immune-related gene sets including IFN-Y, TNF-α, IL-2, IL-6, allograft rejection and inflammatory response.
Conclusions: MiR-150 expression in patients' breast cancer evoke immune response, attracts lymphocytes to tumor microenvironment and is associated with overall survival.

#7948 Targeting the UFMylation pathway to promote immunotherapy response of breast cancers.

Ciara J. Miller[1], Jackson P. Riffee[1], Danielle R. Cook[2], **Timothy D. Martin**[1]

[1]Pharmacology, University of Virginia, Charlottesville, VA,[2]Hematology & Oncology, University of Virginia, Charlottesville, VA

The immune system puts immense selective pressure on tumors to evolve mechanisms to avoid immune mediated cell death during tumorigenesis. Ultimately, these evolved tumor cells fuel the aberrant growth that leads to metastasis and patient mortality. Immunotherapies have been breakthrough treatments for certain tumor types highlighting just how life-changing reinvigorating the immune system can be in the battle against cancer. Unfortunately, current immunotherapies do not work for all patients and tumor types so we must identify new strategies that can turn non-responding patients into potent responders. To identify candidate drug targets whose inhibition can increase anti-tumor immunity (ATI), we utilized in vivo CRISPR screens in syngeneic mouse breast (BC) cancer models. The results from these screens revealed that inhibition of protein UFMylation, a ubiquitin-like post-translational modification pathway that is most known for its role in promoting protein translational fidelity, results in tumor cell death only in the presence of a fully functioning immune system. We have identified that loss of UFMylation can alter inflammatory gene expression to remodel the tumor microenvironment, promote antigen processing and presentation through the regulation of MHC class I protein levels, and render tumor cells more sensitive to killing by T cells. Using orthotopic in vivo tumor models that fail to respond to immunotherapies, we demonstrate that combining UFMylation inhibition with immune checkpoint blockade leads to potent ATI and a reduction in tumor growth. These data identify protein UFMylation as a drug target whose inhibition generates an anti-tumor immune response in tumors that fail to respond to immunotherapies.

#7949 Pharmacologic wtIDH1 inhibition remodels the PDAC immune landscape and improves checkpoint blockade efficacy.

Priyashree Sunita[1], Shakti Pattanayak[1], Mehdad Zarei[1], Omid Hajihassani, Goutam dey, Hallie Graor, Sami Abul-Khoudoud, Faith Nakazzi, Jordan M Winter[2]

[1]Case Western Reserve University School of Medicine, Cleveland, OH,[2]Case Western Reserve University, Cleveland, OH

Introduction: Pancreatic ductal adenocarcinoma (PDAC) remains one of the most lethal human malignancies, with a five-year survival rate under 3%. Its aggressive biology, early metastasis, and profound resistance to therapy are driven in part by a dense, immunosuppressive tumor microenvironment (TME). Although metabolic inhibitors have shown promise in selecting molecular subtypes, the therapeutic potential of targeting metabolic vulnerabilities in wild-type tumors is less explored. Our earlier work identified that AG-120 (Ivosidenib), an FDA-approved inhibitor of mutant IDH1, also inhibits wild-type IDH1 (wtIDH1) under nutrient-restricted conditions typical of PDAC. Here, we investigate how wtIDH1 inhibition simultaneously disrupts tumor metabolism and reshapes the immune microenvironment.
Methods: Miapaca-2, Panc-1, and KPC cells were cultured in low-glucose (2.5 mM) and low-magnesium (0.08 mM) media to simulate PDAC metabolic stress. Cell viability was measured using Titer-Glo, PicoGreen, and colony-formation assays. Cytoplasmic reactive oxygen species and mitochondrial ROS were quantified via DCFDA and MitoSOX using fluorescence and flow cytometry. Proliferation and cell-cycle regulation were evaluated by CellTrace and BrdU incorporation. Orthotopic and syngeneic mouse models were used to assess therapeutic efficacy, immune-cell infiltration, and synergy with anti-PD-1 therapy.
Results: wtIDH1 inhibition significantly reduced cell proliferation, impaired DNA synthesis, and elevated mitochondrial and cytosolic ROS, leading to apoptosis. In vivo, Ivosidenib increased infiltration of $CD45^+$ immune cells, including $CD4^+$ and CD8+ central-memory T cells, and enhanced M1-like macrophage populations with reduced PD-L1 expression. Treatment group decreased M2-like monocytes and shifting the TME toward an inflammatory, anti-tumor state. Combination therapy with anti-PD-1 improved survival and conferred protection upon tumor rechallenge through robust central- and effector-memory T-cell expansion.
Conclusion: wtIDH1 inhibition offers a dual benefit in PDAC by impairing tumor metabolism and promoting immune activation. This metabolic-immune reprogramming provides a strong rationale for combining wtIDH1 inhibitors with existing immunotherapies.

#7950 Targeting the OSM-OSMR signaling axis to reprogram the tumor microenvironment and overcome immune suppression in pancreatic cancer.

Yuan Sui, Tony Hunter

Salk Institute, La Jolla, CA

Pancreatic ductal adenocarcinoma (PDA) is one of the deadliest malignancies, characterized by a dense, fibrotic, and immune-excluded tumor microenvironment (TME) that resists current therapies. Emerging evidence implicates the Oncostatin M (OSM)-Oncostatin M receptor (OSMR) signaling axis, a member of the IL-6 cytokine family, as a key driver of PDA progression through regulation of tumor-stroma-immune interactions. My research aims to define how OSM-OSMR signaling orchestrates the immune-suppressive microenvironment in PDA and to evaluate whether its inhibition can reprogram tumors toward immune responsiveness.Spatial transcriptomics analysis of treatment-naïve human PDA revealed high OSMR expression associated with cancer-associated fibroblast (CAF) activation, stromal stiffness, and enrichment of macrophage and monocyte gene signatures, alongside reduced $CD8^+$ T-cell infiltration. Integrated transcriptomic analyses identified OSMR-associated genes enriched for NF-κB, JAK-STAT, and IFN-γ pathways. Functional studies showed that OSM-OSMR signaling promotes PDA cell proliferation, migration, and invasion, while driving CAF activation and polarization of monocytes toward immunosuppressive $CD163^+/CD206^+$ macrophages. In *ex vivo* human PDA slice cultures, recombinant OSM enhanced proliferation and STAT3 phosphorylation, effects reversed by OSM or OSMR neutralizing antibodies.To dissect the underlying mechanisms, I employed CRISPR-engineered OSMR knockout and rescue PDA cell lines, OSMR-overexpressing CAFs, and 3D co-cultures with monocyte-derived macrophages, integrated with single-cell RNA-seq, phospho-proteomics, and spatial transcriptomics. Parallel translational studies will test OSM/OSMR-neutralizing antibodies in patient-derived organoids, tumor slice cultures, and genetically engineered mouse models (GEMMs), alone or in combination with FDA-approved chemotherapies. These studies will assess the effects of OSM-OSMR signaling on tumor growth, stromal remodeling, immune infiltration, and metastasis.By defining how OSM-OSMR signaling sustains PDA's fibrotic and immune-suppressive TME and establishing its therapeutic vulnerability, this work aims to develop rational strategies that reprogram the TME, enhance immunotherapy responsiveness, and improve outcomes for patients with pancreatic cancer.

#7951 Ovarian tumor FAK inhibition releases omega-3 fatty acids stimulating GATA6 peritoneal macrophage CXCL13 production augmenting TIGIT immunotherapy.

Xiao Lei Chen[1], Kevin M. Tharp[2], Marjaana Ojalill[1], Duygu Ozmadenci[1], Antonia Boyer[1], Terrance J. Hannen[1], Christine Lawson[1], Hyojae J. Lee[1], Marvin Xia[1], Elise Tahon[1], Yichi Zhang[1], Cray Minor[2], Safir U. Khan[1], Colin C. Anderson[3], Travis Nemkov[3], Michael Rose[4], Monica V. Estrada[4], Alfredo A. Molinolo[4], Elias Warren[4], Patrick Penalosa[1], Ramez N. Eskander[1], Michael T. McHale[1], Shizhen E. Wang[4], Denise C. Connolly[5], Kathleen M. Fisch[4], Dwayne G. Stupack[1], **David D. Schlaepfer**[1]

[1]Obstetrics, Gynecology, and Reproductive Sciences, University of California San Diego, Moores Cancer Center, La Jolla, CA,[2]Sanford Burnham Prebys Medical Discovery Institute, San Diego, CA,[3]Anschutz Medical Campus, University of Colorado Denver, Aurora, CO,[4]University of California San Diego, Moores Cancer Center, La Jolla, CA,[5]Fox Chase Cancer Center, Philadelphia, PA

High grade serous ovarian cancer (HGSOC) is a lethal gynecologic malignancy due to accumulated therapy resistance. Focal adhesion kinase (FAK) expression is elevated in HGSOC, and inhibition of FAK activity (FAKi) in syngeneic ovarian tumors reduced tumor burden with elevated CXCL13 chemokine expression by peritoneal macrophages. Combining FAKi with pegylated doxorubicin chemotherapy and anti-TIGIT immune checkpoint antibody repressed tumors and extended survival with tertiary lymphoid structure formation. Peritoneal macrophage GATA6 inactivation reduced CXCL13 expression *in vivo*, enhanced FAK knockout (KO) tumor growth, and limited ascites B cell infiltration. FAKi-treated or FAK-KO conditioned media contained exosomes enriched with omega-3 fatty acids that stimulated macrophage CXCL13 production. As isolated by paracentesis, FAKi-treated HGSOC tumor cells or purified macrophages treated with eicosapentaenoic acid triggered anti-tumor macrophage reprogramming and CXCL13 expression. Together, our studies define a tumor lipid to macrophage signaling linkage upon FAK inhibition supporting B cell recruitment, survival, and anti-TIGIT immunotherapy enhancement.

#7952 Integrated tissue and secretome profiling identifies an IL-6/IL-8-dominant immune phenotype in peritoneal carcinomatosis.

Christopher Sherry[1], Neda Dadgar[1], Zuqiang Liu[1], Yong Fan[1], Hyun Young Park[2], Ali Zaidi[1], Paige Mirsky[1], Oleksii Kucherenko[1], Albert Donnenberg[1], David L. Bartlett[3], Vera S. Donnenberg[4], Patrick Wagner[1]

[1]Cancer Institute, Allegheny Health Network, Pittsburgh, PA,[2]Allegheny Health Network, Pittsburgh, PA,[3]Allegheny General Hospital, Pittsburgh, PA,[4]Assistant Professor, Surgery & Pharmacy, University of Pittsburgh Cancer Institute, Pittsburgh, PA

Background: Peritoneal carcinomatosis (PC) is a late manifestation of abdominopelvic malignancies, often resistant to current treatments due to an incomplete understanding of its biological drivers within the peritoneal immune microenvironment. This study aimed to identify actionable therapeutic targets for PC by analyzing peritoneal soluble mediators and cellular composition in patients. Building on existing evidence implicating IL-8 as a critical mediator of tumor-associated inflammation and immunosuppression in other cancers and preliminary data in PC, the study also evaluated IL-8 pathway inhibition in a preclinical model.
Methods: Peritoneal tissue and fluid were collected from three patient groups: patients without benign conditions (n=15), cancer without PC (n=30), and confirmed PC (n=41). Immunohistochemistry was used to quantify immune cells in tissue and Luminex panels to analyze immune, inflammatory, and growth factors in peritoneal fluid. Statistical analyses identified group differences, correlations with disease burden (Peritoneal Cancer Index - PCI), and overall survival (OS). To assess therapeutic tractability of IL-8 axis blockade, a bioluminescent CT26-luc murine PC model was treated daily with the CXCR2 antagonist AZD5069 (100 mg/kg) or saline from day 0-9, with serial IVIS imaging, body-weight monitoring, and survival tracking through day 11.
Results: PC tissue exhibited increased immune cell infiltration compared to non-PC groups, including elevated mast cells, neutrophils, $CD4^+$ T cells, $CD14^+$ monocytes, $CD20^+$ B cells, and $CD138^+$ plasma cells. Secretomic analysis of peritoneal fluid in PC revealed a dominant IL-6/IL-8-centered inflammatory signature, with increased GRO, IL-6, IL-8, CXCL10, IL-10, and TGF-β. This pattern supports pro-angiogenic, immunosuppressive, and stromal-activation signaling. Densities of $CD4^+$, $CD14^+$, $CD20^+$, and $CD138^+$ cells positively correlated with PCI, indicating progressive immune-stromal co-evolution with tumor burden. In human samples, neutrophil infiltration correlated with worse OS, while $CD1a^+$ dendritic cell enrichment correlated with improved OS, underscoring the clinical relevance of the immunologic findings. In the murine model, AZD5069 demonstrated a therapeutic effect in 4 of 10 treated mice, suggesting potential efficacy of IL-8-axis targeting in specific patient subsets.
Conclusion: PC is characterized by distinct immune cell infiltration and a significant IL-6/IL-8 cytokine network. Both neutrophil infiltration and the IL-6/IL-8 axis are associated with disease burden and patient survival, highlighting the IL-6/IL-8 axis as a relevant therapeutic target. Preclinical evidence supports its potential in specific patient groups. Further research is needed to identify predictive biomarkers for treatment response and translate these findings into clinical strategies.

#7953 Engineered IL7/IL15 secreting iPSC-derived mesenchymal stromal cells convert the immunosuppressive into immune-activated tumor microenvironments (TME) and potentiate antitumor immunity.

Michael Andreeff[1], Sandeep Singh[1], Andrea Bedoy[1], Muharrem Muftuoglu[1], Li Li[1], Vivek Anand[1], Dipmoy Nath[2], Lauren Ostermann[1], Ivo Vletic[1], Christopher D. Pacheco[1], Mahesh Basyal[1], Taeyun Kim[3], Kyle M. Garland[3], Matthew Angel[2], Sanjeev Luther[2], Robert Pierce[2], Christopher B. Rohde[3]

[1]Leukemia, UT MD Anderson Cancer Center, Houston, TX,[2]Ernexa Therapeutics, Inc., Cambridge, MA,[3]Factor Bioscience, Inc., Cambridge, MA

Mesenchymal stromal cells (MSCs) derived from bone marrow (BM-MSCs) exhibit inherent tumor-tropic behavior (Andreeff M., Cancer Res. 2002, JNCI 2004). However, their finite proliferative lifespan, donor-to-donor variability, and senescence-associated transcriptional drift present barriers to clinical scalability. To address these limitations, we reprogrammed adult dermal fibroblasts into induced pluripotent stem cells (iPSCs) using a synthetic, non-integrating mRNA transfection system. These iPSCs were stably modified to express interleukin-7 and interleukin-15, prior to mesodermal lineage specification into MSCs (hereafter referred to as IL7-IL15-iMSCs). Flow cytometry and transcriptomic profiling confirmed expression of canonical MSC markers (CD73⁺CD90⁺CD105⁺), absence of hematopoietic or endothelial lineage antigens and trilineage differentiation potential. IL7-IL15-iMSCs secreted supraphysiologic levels of cytokines, converting immune-suppressive MSCs into immune-activating MSCs. In vitro, IL7-IL15-iMSCs induced potent T cell proliferation sustaining the long-term expansion of T cells, macrophages and CAR T cells in vitro, and induced tumor cell death in a triple co-culture system comprising IL7-IL15-iMSCs, the ovarian cancer cell line ID8, and human PBMCs. In a syngeneic mouse model of ovarian cancer (ID8 and platinum-resistant ID8 cells in C57BL/6 mice), intraperitoneal administration of IL7-IL15-MSCs resulted in reduced tumor burden and extended survival. Immunohistochemical and CyTOF analyses revealed massive infiltration of activated T cells, macrophages, and other immune cells into the tumor microenvironment (TME) as well as enrichment in tumoricidal M1-type macrophages, with no detection of exhausted or regulatory T cells, in contrast to controls. To mitigate pulmonary first-pass entrapment associated with systemic, intra-venous (IV) MSC delivery, we optimized a fractionated low-dose IV administration regimen in the orthotopic 4T1 triple-negative breast cancer model. Six weeks post IL7-IL15-iMSC IV administration, tissue IHC staining showed robust iMSC localization to the TME, infiltration of immune cells and tumor reduction as observed in ovarian cancer.

Conclusion: These data establish IL7-IL15-iMSCs as a novel, immunologically active stromal cell platform capable of remodeling the TME and amplifying both innate and adaptive anti-tumor responses. IL7-IL15 iMSC convert an immune-suppressed into an immune-activated TME in diverse tumor types. The scalability of iPSC-derived MSCs, combined with synthetic mRNA reprogramming and stable cytokine expression, supports the suitability of this platform for clinical translation. A first clinical trial in ovarian cancer is under development.